Canadian Journal of Chemistry
Published by
THE NATIONAL RESEARCH COUNCIL OF CANADA

Journal canadien de chimie
Publié par
LE CONSEIL NATIONAL DE RECHERCHES DU CANADA

Volume 58 Number 1 January 1, 1980 Volume 58 numéro 1 1 janvier 1980

Isotopic exchanges in the treatment of cyclobutane with tritiated or deuterated trifluoromethanesulfonic acid or with tritiated sulfuric acid

CHOI CHUCK LEE AND ERIC C. F. KO
Department of Chemistry and Chemical Engineering, University of Saskatchewan, Saskatoon, Sask., Canada S7N 0W0
Received May 1, 1979

CHOI CHUCK LEE and ERIC C. F. KO. Can. J. Chem. **58**, 1 (1980).

When cyclobutane (**1**) is shaken at 0°C with $[^3H]CF_3SO_3H$ (**2**-*t*) or with $(^2H)CF_3SO_3H$ (**2**-*d*), incorporation of T or D into the hydrocarbon layer readily occurred. All eight H atoms of **1** can be involved in the exchange since polydeuterated species including octadeuterated hydrocarbons were observed by mass spectrometry. In an experiment with **1** and **2**-*t*, quenching of the acid layer with H_2O gave a mixture of cyclobutanol, cyclopropylcarbinol, and allylcarbinol in the ratio of 61:37:2, respectively, as estimated by isotopic dilution, while vpc analysis of the hydrocarbon layer showed the presence of **1**, methylcyclopropane, and 1-butene in the ratio of 66:30:4. The results are explained by a carbocationic chain mechanism, involving the formation of equilibrating bicyclobutonium ions. Similar but slower incorporation of T into the hydrocarbon layer was observed when **1** was treated with $[^3H]H_2SO_4$.

CHOI CHUCK LEE et ERIC C. F. KO. Can. J. Chem. **58**, 1 (1980).

Quand on agite le cyclobutane **1** à 0°C avec de l'acide trifluorométhane sulfonique tritié $[^3H]CF_3SO_3H$ (**2**-*t*) ou deutéré $[^2H]CF_3SO_3H$ (**2**-*d*) l'incorporation du tritium ou du deutérium dans la phase hydrocarbonée se produit facilement. Tous les huit atomes d'hydrogène de **1** peuvent être impliqués dans l'échange puisqu'on observe par spectrométrie de masse des espèces polydeutérées incluant des hydrocarbures octodeutérés. Dans une expérience avec **1** et **2**-*t* la brusque dilution de la phase acide avec de l'eau donne un mélange de cyclobutanol, de cyclopropylcarbinol et d'allylcarbinol dans un rapport de 61:37:2 respectivement tel qu'évalué par dilution isotopique, tandis que l'analyse par cpg de la phase hydrocarbonée révèle la présence de **1**, du méthylcyclopropane et du butène-1 dans un rapport de: 66:30:4. On explique ces résultats selon un mécanisme en chaîne carbocationique impliquant la formation d'ions bicyclobutonium en équilibre. On observe une incorporation similaire mais plus lente du tritium dans la phase hydrocarbonée quand on traite **1** avec du $[^3H]H_2SO_4$.

[Traduit par le journal]

By analogy with the protonation of cyclopropane with deuterated or tritiated H_2SO_4 (1, 2) to give protonated cyclopropane intermediates, which led to the formation of 1-propyl products with the isotopic label scrambled over all three carbon positions (3, 4), we had attempted to obtain evidence for protonated cyclobutane intermediates by treating cyclobutane (**1**) with tritiated acids such as $[^3H]H_2SO_4$ or $[^3H]CF_3SO_3H$ (5). Since no tritiated butyl product was detectable from the treatment of **1** with $[^3H]H_2SO_4$ and an upper limit of no more than 1% ring cleavage was observed in the treatment of **1** with $[^3H]CF_3SO_3H$, it was concluded that processes via protonated cyclobutane intermediates are not likely to be major reaction pathways (5). In accord with this conclusion, the isotopic scramblings observed in the trifluoroacetolysis of 1-[1-^{14}C]butyl tosylate (6) or 1-[1-^{14}C]butylmercuric perchlorate (7), and in the deamination of 1-[1-^{14}C]butylamine (8), were interpreted by invoking some contribution from protonated methylcyclopropane intermediates rather than from protonated cyclobutane.

In the treatment of **1** with $[^3H]CF_3SO_3H$ (5), after the mixture was shaken at 75°C for 3 days, isotopic H–T exchange was observed and the recovered **1** was found to have the same specific activity as that of the original $[^3H]CF_3SO_3H$. Since treatment of cyclopropane with D_2SO_4 resulted in the formation of monodeuterocyclopropane (9), the H–T exchange was assumed to be due to monotritiation of **1**, giving rise to an active **1** with essentially the same specific activity as the original $[^3H]CF_3SO_3H$. We have now found that this interpretation is incorrect and this paper reports on the results obtained from further studies on isotopic exchanges when **1** is

0008-4042/80/010001-05$01.00/0
©1980 National Research Council of Canada/Conseil national de recherches du Canada

Can. J. Chem. Downloaded from www.nrcresearchpress.com by 210.87.254.5 on 09/05/12
For personal use only.

TABLE 1. Relative compositions of deuterated species with d_0 at m/e 56 for C_4H_8[a]

Reaction time (min)[b]	Composition (%)[c]								
	d_0	d_1	d_2	d_3	d_4	d_5	d_6	d_7	d_8
30	95.2	1.0	1.0	0.2	0.4	0.5	0.7	0.5	0.5
45	96.0	1.1	0.6	0.1	0.3	0.5	0.7	0.5	0.3
60	92.4	0.7	0.7	0.5	0.9	1.5	1.3	1.2	0.7
75	87.0	0.3	4.6	0.8	1.4	2.3	1.9	1.2	0.6
90	80.7	0.6	1.5	2.1	4.1	4.3	3.7	2.2	0.9
210	4.8	10.6	18.6	22.8	20.0	13.6	6.2	2.6	0.8

[a]From mass spectral analysis of 0.2-mL aliquots of the hydrocarbon layer withdrawn periodically from an initial mixture of 2.0 mL of cyclobutane (**1**) and 4.0 mL of CF_3SO_3D (**2**-*d*) being shaken at 0°C.
[b]There was an induction period and no D incorporation into the hydrocarbon was observed at reaction times of up to 25 min.
[c]Corrected for P + 1 and P + 2 due to ^{13}C.

treated with $[^3H]CF_3SO_3H$ (**2**-*t*), $(^2H)CF_3SO_3H$ (**2**-*d*), or $[^3H]H_2SO_4$ (**3**-*t*).

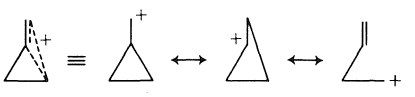
In the earlier work (5), the exchange was measured after **1** was shaken with **2**-*t* at 75°C for 3 days because these were the conditions used in the attempt to obtain open chain butyl products. In the present study, it was found that the H–T exchange can occur under much milder conditions. For example, when a 1:2 (by volume) mixture of **1** and **2**-*t* was shaken at 0°C, after a variable induction period of about 10–30 min, incorporation of T into the hydrocarbon layer took place and the specific activity of the recovered tritiated hydrocarbon rose above the specific activity of the original **2**-*t* in less than an hour. This finding alone suggests that monotritiation is certainly not sufficient to account for the extent of exchange.

It is of interest to note that years ago, Stevenson and co-workers (10, 11) studied the H–D exchange between saturated hydrocarbons and H_2SO_4. For example, when hydrocarbons such as isobutane or isopentane were passed through D_2SO_4, polydeuterated hydrocarbons were obtained and the exchange was interpreted by means of a carbocationic chain mechanism. The mass spectral analysis of the hydrocarbon layer on treatment of **1** with **2**-*d* also showed the occurrence of polydeuteration. A typical set of data, obtained from analyzing sample aliquots withdrawn at different times from a mixture of **1** and **2**-*d* that was being shaken at 0°C, is given in Table 1.

Since exchange could involve all H atoms of **1**, at infinite time, a complete mixing of all H isotopes would result. Under the conditions of the previous experiment reported in 1976 (5), the calculated specific activity of the recovered hydrocarbon at infinite time, x_∞, was 1.76×10^7 dpm/mmol (see Experimental section for illustrations of the calculation). After **1** and **2**-*t* were shaken at 75°C for 3 days, the specific activity of the resulting hydrocarbon, x, was coincidentally the same as that of the original **2**-*t*, namely, 1.42×10^7 dpm/mmol. Thus the ratio x/x_∞ was 1.42/1.76 = 0.81 or the exchange was about 81% complete.

Utilizing the method of data treatment described by Stevenson and co-workers (10) in their study on the exchange between isobutane and H_2SO_4, for the reaction of **1** with **2**-*t*, a plot of $\ln [1 - (x/x_\infty)]$ vs. reaction time would give a straight line the negative slope of which is the initial first order rate constant, k, for the appearance of tritium in the hydrocarbon layer. The observed results from duplicate sets of such experiments, carried out at 0°C, are summarized in Table 2, and these gave k values of $2.4 - 2.5 \times 10^{-4}$ s^{-1}. When **1** was treated with $[^3H]H_2SO_4$ (**3**-*t*), tritium was also incorporated into the hydrocarbon layer, but at a much slower rate than in the reaction with **2**-*t*. A typical set of results obtained from an experiment carried out at 40°C is summarized in Table 3, giving a k value of 1.3×10^{-6} s^{-1}.

If the exchange during the treatment of **1** with **2**-*t* or **3**-*t* were to proceed via a carbocationic mechanism, formation of the cyclobutyl cation would likely result in rearrangements since cyclobutyl, cyclopropylcarbinyl, and allylcarbinyl cations are known to interconvert readily via equilibrating bicyclobutonium ions (**4**) (12–14). Indeed, Olah and Lukas (15) have observed by nmr that treatment of cycloalkanes at low temperature in the super-acids FSO_3H–SbF_5 and HF–SbF_5, with or without SO_2-ClF as diluent, resulted in hydride ion abstraction to give cycloalkyl cations. When a solution of **1** in SO_2ClF–FSO_3H–SbF_5 was quenched with CH_3OH, an 80% yield of a 9:1 mixture of methyl cyclopropylcarbinyl ether and methyl cyclobutyl ether was obtained (15).



4

Can. J. Chem. Downloaded from www.nrcresearchpress.com by 210.87.254.5 on 09/05/12
For personal use only.

TABLE 2. Incorporation of T into the hydrocarbon layer in the treatment of cyclobutane (**1**) with [^{3}H]CF_3SO_3H (**2**-*t*) at 0°C[a]

Reaction time (min)	Specific activity x (10^{-7} dpm/mmol)		x/x_∞	
	Run 1	Run 2	Run 1	Run 2
0[b]	0.35	0.51	0.068	0.098
10	1.08	1.11	0.209	0.214
20	—	1.54	—	0.297
30	2.26	2.16	0.436	0.417
40	2.57	—	0.496	—
		$10^4 k(s^{-1})$	2.5	2.4

[a]Initially, 1.0 mL of **1** and 4.0 mL of **2**-*t* with specific activity of 2.10×10^7 dpm/mmol were shaken at 0°C. The calculated specific activity for the C_4H_8 hydrocarbon layer at complete exchange, x_∞, was 5.18×10^7 dpm/mmol.
[b]The zero time was arbitrarily chosen after an initial induction period of up to 30 min.

TABLE 3. Incorporation of T into the hydrocarbon layer in the treatment of cyclobutane (**1**) with [^{3}H]H_2SO_4 (**3**-*t*) at 40°C[a]

Reaction time (h)	Specific activity x (10^{-5} dpm/mmol)	x/x_∞
0[b]	0.915	0.0134
5	2.85	0.0416
17	6.06	0.0885
24	8.42	0.123
41	12.4	0.181
48	14.4	0.210
	k (s^{-1})	1.3×10^{-6}

[a]Samples each containing 0.25 mL of **1** and 1.0 mL of **3**-*t* with specific activity of 2.82×10^6 dpm/mmol were shaken in sealed tubes at 40°C. The calculated x_∞ was 6.85×10^6 dpm/mmol.
[b]To allow for the induction period, each sample was shaken for 1.5 h before being regarded as having reached its zero time.

In order to ascertain whether rearrangement via bicyclobutonium ions have occurred in the present study, a mixture of 1.0 mL of **1** and 4.0 mL of **2**-*t* was shaken at 0°C for 4 h. After 1.0-mL aliquots of the acid layer were quenched in H_2O containing cyclobutanol (**5**), cyclopropylcarbinol (**6**), or allylcarbinol (**7**) as carrier, the recovered activities in the urethane derivations fo **5**, **6**, and **7**, respectively, were in the ratio of 61:37:2. Similarly, vpc analysis of the hydrocarbon layer showed the presence of three peaks with relative areas of 66:30:4, and these were assigned, respectively, to cyclobutane, methylcyclopropane, and 1-butene.

All the above observations may be accommodated by a carbocationic chain mechanism as was originally suggested by Stevenson and co-workers (10, 11). The initiation step is the formation of the carbocation. In the reaction of isobutane with H_2SO_4, for example, it was suggested (10) that initiation could arise either from oxidation of isobutane to the *t*-butyl cation or from protonation of traces of olefinic impurity such as isobutene. In the present work, **1** was freshly prepared and there is probably no olefinic impurity.. Oxidation, or abstraction of hydride ion, the term used by Olah and Lukas (15), could be responsible for the initiation. The slow initiation could then account for the induction period which was also observed by Stevenson and co-workers (10). It is of interest to note that Setkina *et al.* (16) have also reported the observation of H–D exchanges between saturated hydrocarbons and D_2SO_4. A free radical mechanism was proposed (16); but subsequently, evidence was obtained for the formation of carbocations from the reaction of saturated hydrocarbons with H_2SO_4 (17).

Olah and co-workers (18) have more recently proposed a variant to hydride abstraction, which involves an electrophilic protolysis of a C—H bond, giving a two-electron three-center bonded carbonium ion, which subsequently loses H_2 to give the tricoordinated carbenium ion. The fact that the stronger acid, [^{3}H]CF_3SO_3H, could react with **1** faster than [^{3}H]H_2SO_4 might be regarded as in accord with electrophilic protolysis. However, an attempt to detect the liberated H_2 by mass spectrometry in the reaction of **1** with CF_3SO_3H has failed to give positive results. This is not surprising since the amount of H_2 produced may be very small as its liberation would take place only in the initiation step of a chain mechanism.

As proposed by Stevenson and co-workers (10, 11), the carbocationic chains are propagated through intermolecular transfers of hydride ions between carbocation and hydrocarbon molecules ($R^+ + RH \rightleftharpoons RH + R^+$), and the chains are terminated by some irreversible side reactions of the cations. The hydride ion transfers could take place between the cations and the dissolved hydrocarbon molecules or hydrocarbon molecules in the interface. In the exchange between isobutane and H_2SO_4, it was suggested (10) that during the existence of the *t*-butyl cation, any of its α-hydrocarbons may exchange with the protons of the acid. It was assumed that this exchange occurred at a

Can. J. Chem. Downloaded from www.nrcresearchpress.com by 210.87.254.5 on 09/05/12
For personal use only.

Can. J. Chem. Downloaded from www.nrcresearchpress.com by 210.87.254.5 on 09/05/12
For personal use only.

rate such that equilibrium between carbocation hydrogens and acid hydrogens was established during the life of each ion. Since the *t*-butyl cation does not undergo intramolecular hydrogen shifts, the exchanges will involve only the nine primary hydrogens. Consequently, a maximum extent of deuteration by D_2SO_4 will produce isobutane-d_9, with the tertiary hydrogen unaffected (10).

In the present study with **1**, the bicyclobutonium ion, **4**, will be formed, either directly from **1** or as a result of a rearrangement of the cyclobutyl cation. It is known (13, 14) that different bicyclobutonium ions can arise from 1,2-shifts of neighboring σ-bonds, and equilibration of these bicyclobutonium ions will eventually cause all three methylene groups in **4** to become equivalent. Thus the H atoms are intramolecularly rearranged among the methylene groups. This intramolecular rearrangement, together with the possibility of 1,2-hydride shifts in the cyclobutyl cation, the many cycles of intermolecular hydride transfers between cations and hydrocarbon molecules, and exchanges between the α-H, D, or T of the cation and the H, D, or T of the acid during the lifetime of the cation, will lead to the involvement of all eight hydrogen atoms of the C_4H_8 molecule in the exchange. This mechanism is borne out by the data in Table 1. The intermolecular hydride transfer reactions involving bicyclobutonium ion **4** will also lead to the formation of the rearranged hydrocarbons, methylcyclopropane, and 1-butene, as well as cyclobutane, and this again is in agreement with observation.

The actual mechanism for the exchange between the α-hydrogens of the cation and the acid hydrogens has not been elucidated either in the early work of Stevenson and co-workers (10) or in the present study. One possibility (suggested by a referee and an editor) is the involvement of an olefinic intermediate, $R^+ \rightleftharpoons$ alkene + H^+. In that event, polymerization of the olefinic intermediate followed by fragmentation conceivably might account for some of the d_1 to d_8 species recorded in the mass spectra (Table 1). However, such possible contributions from a polymerization–fragmentation process likely did not account for all of the observed d_1 to d_8 species and would not invalidate the conclusion that polydeuteration occurred during the treatment of **1** with **2**-*d*, especially when the reaction of **1** with **2**-*t* may be reasonably interpreted on the basis of a complete exchange between the eight H atoms of **1** and the *t*-label of **2**-*t*.

Experimental

Reaction of Cyclobutane (1) with (^2H)CF_3SO_3H (2-d)

A mixture of 2.0 mL (26 mmol) of **1**, bp 12–13°C, prepared from 1,4-dibromobutane (19), and 4.0 mL (46 mmol) of **2**-*d*, prepared from trifluoromethanesulfonic acid anhydride and D_2O, was shaken mechanically in a stoppered glass tube kept at 0°C in an ice-water bath. Periodically, 0.2-mL aliquots of the hydrocarbon layer were withdrawn and analyzed by mass spectrometry to give the results recorded in Table 1, showing the presence of polydeuterated species in the hydrocarbon layer. In this experiment, the amount of hydrocarbon relative to the amount of acid in the reaction mixture would decrease as aliquots of the hydrocarbon layer were withdrawn, hence no kinetic treatment was attempted.

Reaction of 1 with [^3H]CF_4SO_4H (2-t)

In preliminary studies, when mixtures of **1** and **2**-*t*, the latter being prepared by adding [^{3}H]H_2O and the calculated amount of trifluoromethanesulfonic acid anhydride to ordinary **2**, were placed in individual sealed tubes and shaken at 0°C for different lengths of time, the incorporation of T into the hydrocarbon layer was found to be not reproducible quantitively. This difficulty arose because of the variability of the initial induction period. To obtain the results recorded in Table 2, the following procedure was adopted.

A mixture of 1.0 mL (718 mg, 12.8 mmol) of **1** and 4.0 mL (6860 mg, 45.7 mmol) of **2**-*t*, with a specific activity of 2.10×10^7 dpm/mmol, was shaken in a stoppered glass tube at 0°C as in the experiment with **2**-*d*. After the induction period has passed, 0.2-mL and 0.8-mL aliquots, respectively, of the hydrocarbon and acid layers were withdrawn at different times and the T incorporation into the hydrocarbon layer was measured. In this way, the relative amounts of hydrocarbon to acid, and hence the theoretical specific activity in the C_4H_8 hydrocarbon layer at complete exchange, x_∞, would remain constant throughout the experiment.

In this experiment, the total amount of activity involved was $45.7 \times 2.10 \times 10^7 = 9.60 \times 10^8$ dpm, and the total amount of H involved was $(12.8 \times 8) + 45.7 = 148$ mg atoms.

When exchange is complete, the specific activity, x_∞, would be $(9.60 \times 10^8)/148 = 6.49 \times 10^6$ dpm/mg atom H or $6.49 \times 10^6 \times 8 = 5.18 \times 10^7$ dpm/mmol C_4H_8.

From the observed specific activities, x, that were incorporated into the hydrocarbon layer at different reaction times, x/x_∞ were calculated and plots of $\ln [1 - (x/x_\infty)]$ vs. time gave the k values of 2.4×10^{-4} and 2.5×10^{-4} s^{-1} for the duplicate runs (Table 2).

In the earlier experiment reported in 1976 (5), 18 mmol of **1** was shaken with 22.8 mmol of **2**-*t* whose specific activity was 1.42×10^7 dpm/mmol. At complete exchange, x_∞ would be $8(1.42 \times 10^7 \times 22.8)/(22.8 + 8 \times 18) = 1.76 \times 10^7$ dpm/mmol C_4H_8.

Quenching and Product Studies

A mixture of 1.0 mL of **1** and 4.0 mL of **2**-*t* (2.10×10^7 dpm/mmol) was shaken at 0°C for 4 h. One-mL aliquots of the acid layer were quenched separately by shaking with 10 mL of H_2O containing 0.5 mL of cyclobutanol (**5**, 461 mg, 6.4 mmol), cyclopropylcarbinol (**6**, 444 mg, 6.1 mmol), or allylcarbinol (**7**, 429 mg, 6.0 mmol) as carrier. The alcohol was then recovered by ether extraction and purified by preparative vpc (1/4 in. × 8 ft copper column packed with 25% β,β′-oxydipropionitrile on chromosorb P at 80°C). The phenylurethanes of **5** and **6** and the α-naphthylurethane of **7** were prepared (12) and these were repeatedly recrystallized to give constant specific activities of 1.83×10^5, 1.19×10^5, and 7.03×10^3 dpm/mmol, respectively, for the derivatives of **5**, **6**, and **7**. Making the reasonable assumption that essentially all the weight of each alcohol was due to the added carrier, the total activities recovered were $1.83 \times 10^5 \times 6.4 = 1.2 \times 10^6$ dpm, $1.19 \times 10^5 \times 6.1 = 7.3 \times 10^5$ dpm, and $7.03 \times 10^3 \times 6.0 = 4.2 \times 10^4$ dpm, respectively, for **5**, **6**, and **7**, corresponding to a ratio of 61:37:2.

The hydrocarbon layer from the above experiment was analyzed by vpc (1/4 in. × 8 ft copper column packed with 15% silicone gum rubber on chromosorb W at 20°C). Three peaks were obtained with retention times of 30, 40, and 75 s and with relative areas of 30:66:4, respectively. Comparison with a sample of **1** showed that the largest peak with retention time of 40 s was **1**, and by analogy with the results from the quenching experiment, the other two peaks are assigned to methylcyclopropane and 1-butene, with a relative ratio of 66:30:4 for cyclobutane:methylcyclopropane:1-butene.

Reaction of ***1*** *with* $[^3H]H_2SO_4$ (***3***-t)

The **3**-*t* was prepared by adding $[^3H]H_2O$ to a calculated amount of fuming H_2SO_4. The reaction was carried out at 40°C in individual sealed tubes each containing 1940 mg (19.8 mmol, about 1.0 mL) of **3**-*t* (2.82×10^6 dpm/mmol) and 180 mg (3.2 mmol, about 0.25 mL) of **1**. From preliminary trials under these conditions, the induction time was about 1.5 h. The reaction mixtures were, therefore, allowed to shake at 40°C for 1.5 h before being regarded as having reached the zero time. At different times after this arbitrarily chosen induction period, the incorporation of T into the hydrocarbon layer was measured to give the results of Table 3. In this experiment, the specific activity at complete exchange, x_∞, would be $8(2.82 \times 10^6 \times 19.8)/(19.8 \times 2 + 2.3 \times 8) = 6.85 \times 10^6$ dpm/mmol C_4H_8.

Acknowledgments

We wish to express our sincere thanks to Professor M. Saunders of Yale University and Professor P. von R. Schleyer of Universität Erlangen-Nürnberg for suggesting to us that the exchange between **1** and **2**-*t* should be further investigated and for their valuable comments. The financial support given by the Natural Sciences and Engineering Research Council of Canada is gratefully acknowledged.

1. R. L. Baird and A. A. Aboderin. J. Am. Chem. Soc. **86**, 252 (1964).
2. C. C. Lee and L. Gruber. J. Am. Chem. Soc. **90**, 3775 (1968).
3. C. J. Collins. Chem. Rev. **69**, 543 (1969).
4. C. C. Lee. Prog. Phys. Org. Chem. **7**, 129 (1970).
5. C. C. Lee and E. C. F. Ko. Can. J. Chem. **54**, 1722 (1976).
6. C. C. Lee, A. J. Cessna, E. C. F. Ko, and S. Vassie. J. Am. Chem. Soc. **95**, 5688 (1973).
7. C. C. Lee and R. Reichle. J. Org. Chem. **42**, 2058 (1977).
8. C. C. Lee, R. Reichle, and U. Weber. Can. J. Chem. **56**, 658 (1978).
9. R. L. Baird and A. Aboderin. Tetrahedron Lett. 235 (1963).
10. J. W. Otvos, D. P. Stevenson, C. D. Wagner, and O. Beeck. J. Am. Chem. Soc. **73**, 5741 (1951).
11. D. P. Stevenson, C. D. Wagner, O. Beeck, and J. W. Otvos. J. Am. Chem. Soc. **74**, 3269 (1952).
12. J. D. Roberts and R. H. Mazur. J. Am. Chem. Soc. **73**, 2509 (1951).
13. R. H. Mazur, W. N. White, D. A. Semenov, C. C. Lee, M. S. Silver, and J. D. Roberts. J. Am. Chem. Soc. **81**, 4390 (1959).
14. R. Breslow. *In* Molecular rearrangements. Vol. 1. *Edited by* P. de Mayo. Interscience Publishers, New York, NY. 1963. pp. 259–265.
15. G. A. Olah and J. Lukas. J. Am. Chem. Soc. **90**, 933 (1968).
16. V. N. Setkina, D. N. Kursanov, O. D. Sterligov, and A. L. Liberman. Probl. Mekhanizma Org. Reaktsii, Akad. Nauk Ukr. S.S.R. Otdel. Fiz-Mat. Khim. Nauk, 199 (1953). Chem. Abstr. **50**, 16314e (1956).
17. V. F. Lavrushin, D. N. Kursanov, and V. N. Setkina. Dokl. Akad. Nauk SSSR, **97**, 265 (1954). Chem. Abstr. **49**, 8890*b* (1955).
18. G. A. Olah, Y. Halpern, J. Shen, and Y. K. Mo. J. Am. Chem. Soc. **95**, 4960 (1973).
19. K. B. Wiberg and D. S. Connor. J. Am. Chem. Soc. **88**, 4437 (1966).

Can. J. Chem. Downloaded from www.nrcresearchpress.com by 210.87.254.5 on 09/05/12
For personal use only.

Photochemistry of selenoketones[1]

NORMAN Y. M. FUNG, PAUL DE MAYO, BERND RUGE, ALAN C. WEEDON, AND S. KING WONG
Photochemistry Unit, Department of Chemistry, University of Western Ontario, London, Ont., Canada N6A 5B7
Received July 3, 1979

NORMAN Y. M. FUNG, PAUL DE MAYO, BERND RUGE, ALAN C. WEEDON, and S. KING WONG. Can. J. Chem. **58**, 6 (1980).

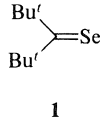
The photochemistry of di-*tert*-butylselenoketone **1** and selenofenchone **2** has been examined. Their photochemical properties resemble those of thioketones rather than ketones in that hydrogen abstraction occurs from an upper excited state and not from the lowest ($n \rightarrow \pi^*$) excited state. Di-*tert*-butylselenoketone, **1**, on irradiation into the S_2 band forms the diselenide **3**. The quantum yield for this process was found to be 0.0055 and was increased in the presence of a good hydrogen atom donor. No reaction was observed following excitation into the S_1 state unless a good hydrogen atom donor was present, and even then the photoreaction was very inefficient. Quenching experiments with biacetyl demonstrated the lifetime of the abstracting state to be in the order of 10^{-11} s. The formation of the diselenide **3** has been rationalized in terms of hydrogen abstraction from solvent by photoexcited **1** and trapping of the radicals produced by ground state **1**, leading to the radical **6**. The mechanism is supported by esr evidence for the existence of **6**. Selenofenchone, **2**, also, did not react following excitation into the S_1 state, but underwent intramolecular cyclization in a similar manner to bicyclic thioketones following excitation into the S_2 state.

NORMAN Y. M. FUNG, PAUL DE MAYO, BERND RUGE, ALAN C. WEEDON et S. KING WONG. Can. J. Chem. **58**, 6 (1980).

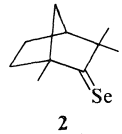
On a examiné la stéréochimie de la di-*tert*-butylsélénocétone **1** et de la sélénofenchone **2**. Leurs propriétés photochimiques sont semblables à celles des thiocétones plutôt qu'à celles des cétones où il se produit une élimination d'hydrogène à partir de l'état excité supérieur et non à partir de l'état excité le plus faible ($n \rightarrow \pi^*$). L'irradiation de la di-*tert*-butylsélénocétone **1** dans la bande S_2 conduit au disélénure **3**. On a trouvé que le rendement quantique de cette réaction est de 0.0055 et qu'il augmente en présence d'un bon donneur d'hydrogène. L'irradiation dans la bande S_1 ne donne pas de réaction à moins qu'un donneur d'hydrogène soit présent et, même dans ces conditions, la réaction photochimique n'est pas efficace. L'interruption brusque des réactions à l'aide du biacétyle a montré que la durée de vie de l'état où il y a élimination d'hydrogène est de l'ordre de 10^{-11} s. On a rationalisé la formation du disélénure **3** en fonction d'une élimination d'hydrogène à partir du solvant par le composé **1** photoexcité et en fonction du piégeage des radicaux produits dans l'état fondamental, conduisant au radical **6**. Les preuves de l'existence du dérivé **6** apportées par la rpe confirment le mécanisme proposé. La sélénofenchone **2** ne réagit pas non plus à la suite d'une excitation dans l'état S_1 mais il subit une cyclisation intramoléculaire de façon similaire aux thiocétones bicycliques après une excitation dans l'état S_2.
[Traduit par le journal]

Introduction

Recently Barton and colleagues (1) reported the preparation of the first isolable selenoketones, namely di-*tert*-butylselenoketone, **1**, and selenofenchone **2**. As is the case with the related thioketones (2), selenoketones possess a low energy electronic transition giving rise to a weak intensity band, $S_1(T_1)$, in the visible region of the absorption spectrum. There are also higher energy electronic transitions which result in strong absorption in the ultraviolet. Whereas ketones abstract hydrogen atoms when excited into the $S_1(T_1; n \rightarrow \pi^*)$ electronic state, thioketones have been shown to abstract hydrogen atoms more efficiently when excited into the S_2 state, which is probably of $\pi \rightarrow \pi^*$ character (2). This ability to abstract hydrogen whilst in a higher excited state is a property deriving, at least in part, from the lifetime of the S_2 state of thioketones (10^{-10}–10^{-11} s) which is long enough to allow both intra- and intermolecular reactions to occur. These lifetimes may owe their longevity to slow internal conversion, itself arising, in part, from the large energy separation between the S_2 and S_1 states; this is of the order of 40–60 kcal/mol for thioketones. The energy separation between the S_1 and S_2 states of selenoketones **1** and **2** is comparable (ca. 60–65 kcal/mol) suggesting that they too might possess comparatively long lived upper excited states despite the presence of the heavy atom. We report here the results of an investigation into the photochemistry of the selenoketones **1** and **2** undertaken to determine if their reactions paralleled those of thioketones, so extending the class of compounds known to react from an upper excited state (3).



1



2

Results and Discussion

Di-tert-*butylselenoketone, 1*

When irradiated in the presence of olefins, thioketones have been shown to undergo cycloaddition to yield thietanes (4*a*). However, irradiation

[1]Contribution number 235 from the Photochemistry Unit, University of Western Ontario.

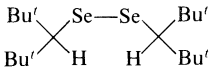
0008-4042/80/010006-09$01.00/0
©1980 National Research Council of Canada/Conseil national de recherches du Canada

Can. J. Chem. Downloaded from www.nrcresearchpress.com by 210.87.254.42 on 09/05/12
For personal use only.

Can. J. Chem. Downloaded from www.nrcresearchpress.com by 210.87.254.42 on 09/05/12
For personal use only.

of the selenoketone **1** into both the S_1 and S_2 states[2] in the presence of any one of acrylonitrile, ethyl vinyl ether, fumaronitrile, and dimethylmaleate failed to produce detectable amounts of adducts, possibly merely a consequence of steric hindrance (4*b*).

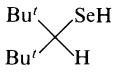
Barton and colleagues (1) reported that irradiation, through quartz, of a solution of selenoketone **1** in benzene gave the diselenide, **3** in high yield. We



3

have found that by irradiation, through both Pyrex and quartz, of **1** in a variety of solvents (cyclohexane, hexanes, dioxane, benzene, and acetonitrile), in all cases formation of the diselenide **3** occurred. The diselenide was identified by comparison with an authentic sample prepared in high yield by lithium aluminium hydride reduction of the selenoketone followed by air oxidation of the intermediate selenol **4**.

In these solvents, excepting benzene, other reactions also occurred, to give substantial quantities of unidentified compounds along with selenium metal, reducing the diselenide yield to less than 50%. However, in benzene as solvent, or in the presence of added selenol **4**, the photochemical reaction to yield diselenide was much cleaner and proceeded in high chemical yield (85%).

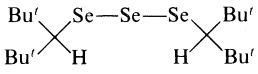


4

In Table 1 the quantum yields of disappearance of **1** in the presence of varying amounts of selenol **4** are shown; increasing the concentration of **4** enhances the quantum yield considerably. The data also demonstrate that the photoreaction is wavelength dependant; reaction of **1** following excitation into the S_1 state is extremely inefficient, indicating that the selenoketone mimics thioketones in that it reacts more readily from an upper excited state. The nature of the "S_1" band is uncertain. In thiones the $S_0 \rightarrow T_1$ transition has about 20% of the strength of the $S_0 \rightarrow S_1$ transition and occurs as a shoulder on the long wavelength side of the latter. In **1** the band is very broad and suggests comparable intensities perhaps and considerable mixing. Hence excitation may well give the triplet directly. The reactive state attained after excitation into the S_2 is assigned only by analogy as $S_2(\pi \rightarrow \pi^*)$.

The quantum yields of disappearance of **1** obtained in the presence of selenol, following excitation into S_1, are very scattered. This is because of a competing ground state reaction between the selenoketone and the selenol which occurs at a rate comparable to that of the photochemical process: correction was made, but the errors are large.

Investigation of the dark reaction showed that in the absence of air the only product is the diselenide **3**, presumably arising from nucleophilic attack by selenol upon the selenoketone; thioketones can also undergo nucleophilic attack at the sulphur atom (5). If the ground state reaction between **1** and **4** was performed in the presence of oxygen, a second product was produced, which was identified as the triselenide **5**. The structure of **5** has been proved by X-ray crystallographic analysis and this, along with a discussion of its mode of formation, has been reported elsewhere (6).



5

In Figs. 1 and 2 are shown the esr signals observed when selenoketone **1** was irradiated in pentane at −110°C under conditions such that the diselenide **3** is formed. These signals are assigned to

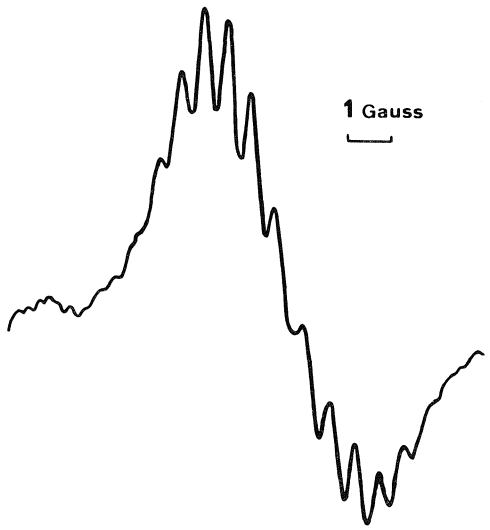


FIG. 1. Hyperfine splitting by γ-protons in radical **6***a*; a_H = 0.50 G.

[2]The electronic spectrum of **1** in hexanes possesses maxima at 698 nm (ε 25), 266 nm (ε 7400), and 229 (ε 3000). The 266 nm band tails to wavelengths beyond 300 nm and consequently irradiation of **1** in Pyrex using a medium pressure mercury lamp allows excitation into both S_1 and S_2 states in the same experiment.

Can. J. Chem. Downloaded from www.nrcresearchpress.com by 210.87.254.42 on 09/05/12
For personal use only.

TABLE 1. Effect of concentration of selenol **4** and of exciting light wavelength upon the quantum yield of disappearance of selenoketone **1** at room temperature in hydrogen atom donating solvents

λ (nm)	[1] (mol/L)	[4] (mol/L)	Solvent	ϕ_{dis}†
278	1.02×10^{-2}	0	Hexanes	0.0054±0.0005
278	2.7×10^{-4}	0	Cyclohexane	0.0055±0.0005
278	1.52×10^{-2}	0	Cyclohexane	0.0056±0.0005
278	2.56×10^{-2}	5×10^{-2}	Hexanes	0.032 ±0.005
278	3.15×10^{-2}	9×10^{-2}	Hexanes	0.08 ±0.01
689	2.13×10^{-2}	0	Hexanes	$<4.8\times10^{-5}$*
689	10^{-2}	0	Cyclohexane	$<6.7\times10^{-4}$*
689	2.45×10^{-2}	5×10^{-2}	Hexanes	0.0012±0.0002
689	3.59×10^{-2}	8×10^{-2}	Hexanes	0.0003±0.0003
689	3.52×10^{-2}	8×10^{-2}	Hexanes	0.0014±0.0003
689	3.52×10^{-2}	8×10^{-2}	Hexanes	0.0014±0.0004

*These values represent upper limits: no conversion of 1 was observed.
†Determined at 5% conversion, or less.

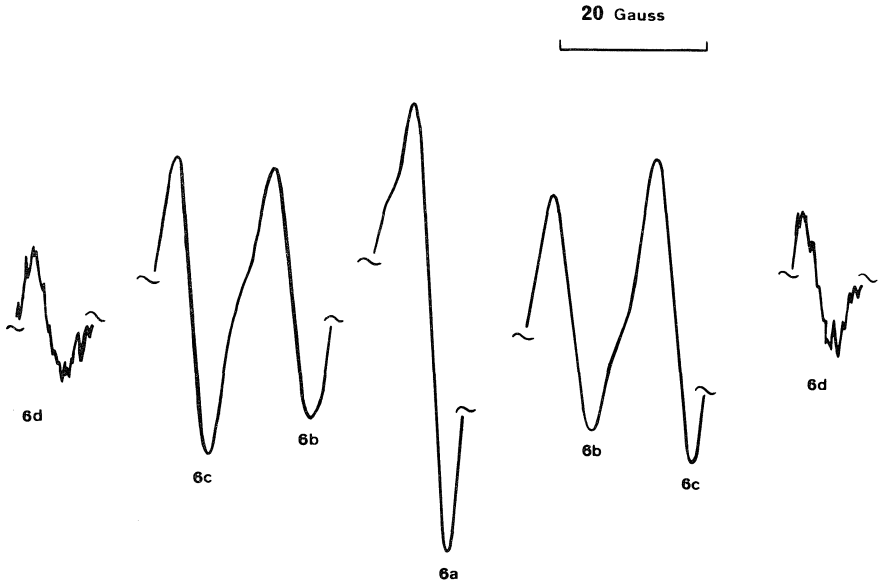
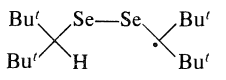


FIG. 2. Hyperfine splittings by ^{77}Se in radicals **6***b*, **6***c*, and **6***d*; a_{Se} = 38.1 and 65.3 G. Discontinuities signify changes in instrument sensitivity (amplification factors 1×, 10×, and 16× for signals assigned to **6***a*, **6***b* and **6***c*, and **6***d* respectively). Assignments for **6***b* and **6***c* may be reversed.

the radical **6** which was subsequently observed by Scaino and Ingold (7). The hyperfine splittings (a_H = 0.50 G, a_{Se} = 38.1 and 65.3 G) are similar to those reported by Scaino and Ingold as is the *g*-factor which was determined to be 2.0021. No signals were observed following irradiation into the S_1 band of **1** (with light of wavelength greater than 460 nm) unless selenol **4** was present. Allowing for the wavelength dependence of the intensity of the irradiation source, the ratio of intensities of the esr signals produced when **1** was irradiated in the S_1 or S_2 bands was approximately 1:60 respectively. Similarly, the esr signal intensities were in the ratio of approximately 20:1 depending upon the presence or absence of the selenol **4** during irradiation into S_2.[3]



6

In the absence of selenol **4**, the esr signal produced upon excitation into the S_2 state decayed in a first order manner ($t_{1/2} \sim 1.8$ s at −110°C), whilst in the presence of **4** the decay was more complex, and, initially, faster. This is consistent with quenching of the radical by solvent (pentane) in the absence of **4** to give apparent first order kinetics of

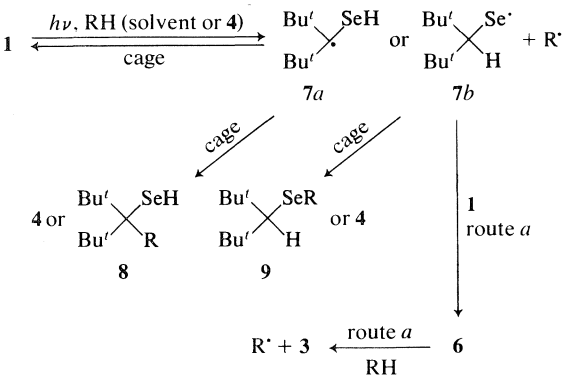
[3]This ratio is concentration dependent; 0.1–0.2 *M* solutions of **1** and **4** were used.

TABLE 2. Comparison of calculated and measured esr signal strengths for all possible ^{77}Se distributions in radical **6**

Parameter	Value			
	6*a*	**6***b*	**6***c*	**6***d*
Calculated abundance (%)*	84.84	7.29	7.29	0.58
(Number of lines expected)	(1)	(2)	(2)	(4)‡
Calculated line intensity	23	1	1	0.04
Measured line intensity†	27	1	0.75	0.04

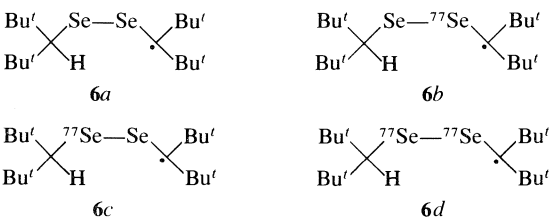
*Based on an ^{77}Se natural abundance of 7.58%.
†Signal height was used. Mean of several determinations.
‡Only the outer two lines were observed.

decay, whereas quenching by **4** may be initially faster but sets up a chain: radical **7***b* is produced, which can generate more of **6** when trapped by **1** (see Scheme 1; Scaino and Ingold (7) have demonstrated the efficiency of **1** as a radical trap).



SCHEME 1

The assignment of the structure **6** to the radical observed is based upon the hyperfine splitting pattern in the esr spectrum. The only stable selenium isotope to possess a nuclear spin (^{77}Se, $I = \frac{1}{2}$) has a natural abundance of 7.58%. Thus coupling of the unpaired electron in **6** can occur with none (structure **6***a* in Fig. 2), one (structure **6***b* or **6***c*), or two selenium atoms (structure **6***d*) to give rise to a set of



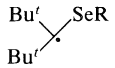
lines with a predictable ratio of intensities. The calculated and measured ratios are given in Table 2 and show reasonable agreement. Only the outer pair of the four lines expected for the radical **6***d* were observed, the inner two presumably being hidden under the stronger signals of **6***b* and **6***c*. That the lines observed were due to the same radical containing different numbers of ^{77}Se atoms was further supported by the observation of identical decay rates for the lines assigned to **6***a*, **6***b*, and **6***c* following irradiation of **1** in pentane at − 110°C.

The results described are rationalized in terms of the processes shown in Scheme 1. By analogy with the reactions of photoexcited ketones and thioketones, and because of the observed acceleration by selenol (ascribed to the presumed good hydrogen atom donating ability of the selenium–hydrogen bond, which has a bond dissociation energy of 90 kcal/mol in H_2Se (13)), the primary act of the photoexcited selenoketone is proposed to be hydrogen abstraction to give either of the radicals **7***a* or **7***b*. Neither of these are observed in the esr spectrum; in the case of **7***b* this is to be expected since the spectrum would be very broad (sulphur centred radicals have never been observed for this reason). In the case of **7***a* the non-observation may reflect its rapid trapping either within or outside the solvent cage in which it is formed. The latter process appears unlikely to be faster than the analogous trapping of radical **6** by hydrogen atom donation from solvent; since **6** *is* observed, this may indicate that **7***a* is not formed or undergoes rapid recombination or disproportionation within the solvent cage. The fates of **7***a*, if formed, within the solvent cage could be disproportionation with the accompanying solvent (or selenol) derived radical to give the selenol **4**, or alternatively combination to give selenol **8**. The latter process should be slow because of steric hindrance. Similarly **7***b* would be expected to disproportionate or combine with its partner radical within the solvent cage to give **4** or the selenide **9**. If **7***b* escapes from its solvent cage then its most probable fates are reaction with selenoketone **1**, a good radical trap (7), or hydrogen abstraction from solvent or selenol **4**. Reaction with **1** yields the observed radical **6**, which can proceed to the isolated product **3**, whilst hydrogen abstraction yields selenol **4**. If **4** reaches a high enough concentration, or if it is added to the system, then a chain sequence may be expected since hydrogen

Can. J. Chem. Downloaded from www.nrcresearchpress.com by 210.87.254.42 on 09/05/12
For personal use only.

Can. J. Chem. Downloaded from www.nrcresearchpress.com by 210.87.254.42 on 09/05/12
For personal use only.

atom abstraction from **4** by photoexcited **1** to give one molecule of **3** yields two **7***b* radicals each of which can be trapped by **1** to give more of **6** and hence more of **3** and **7***b* (path *a* in Scheme 1). It is possible that any selenol **4** produced may all be consumed by ground state reaction with **1** to give diselenide **3**; in this case, and in the absence of added **4**, the solvent derived radical should be trapped by **1** to give radical **10**, which may abstract from



10

solvent and set up a chain sequence. The fact that in the absence of added **4** approximately 50% of the product is diselenide **3** suggests that any chain reactions set up by quenching of solvent derived radicals by **1** must be very short. Selenol **4** generated in the reaction may be partly responsible for this chain terminating step. That none of the radical **10** was observed in the esr experiment may also be relevant, although Scaino and Ingold (7) do report the presence of a second radical, other than **6**, in lower concentration.

More information about the abstracting state of **1** following excitation into the S_2 band was obtained by determinations of relative quantum yields in the presence of a quencher. In Figs. 3 and 4 are shown Stern–Volmer plots for the quantum yields of disappearance of **1** and formation of **3** in the presence of various concentrations of biacetyl. From Fig. 3 the lifetime of the excited state being quenched is $(1.5 \pm 0.6) \times 10^{-10}$ s whilst from Fig. 4 it is $(0.5 \pm 0.2) \times 10^{-11}$ s, which are of the same order as the reactive state of thioketones following excitation into S_2 (2).

The errors in the lifetimes are large and hence the

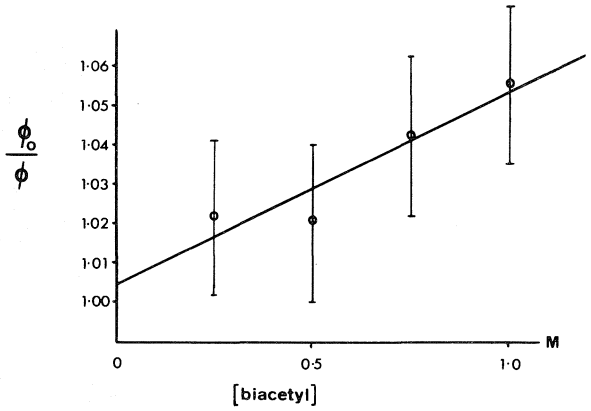


FIG. 3. Stern–Volmer plot for quantum yield of formation of **3** from **1** in hexanes in the presence of biacetyl. Slope = 1.5 ± 0.6 L/mol, whence $\tau = (15 \pm 6) \times 10^{-11}$ s assuming $k_q = 10^{10}$ L/mol s.

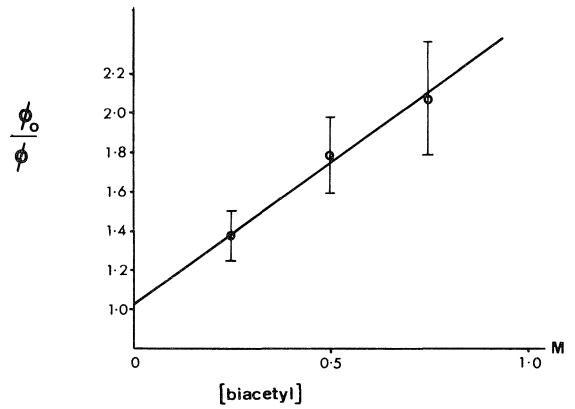


FIG. 4. Stern–Volmer plot for quantum yield of disappearance of **1** in hexanes in the presence of biacetyl. Slope = 0.06 ± 0.02 L/mol, whence $\tau = (0.6 \pm 0.2) \times 10^{-11}$ s assuming $k_q = 10^{10}$ L/mol s.

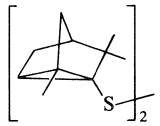
τ are essentially only order of magnitude determinations. Also, quenching of the excited state of **1** only has an indirect effect upon the quantum yields of disappearance of **1** and appearance of **3**, and the exact effect cannot be predicted. Further, the amount of **3** formed was determined by uv spectrophotometry; **3** may have been contaminated by the triselenide **5** whose extinction coefficient at the wavelengths monitored is much greater than that of **3** (ε_{254} for **3** $\approx$ 300; for **5** $>$ 2000), resulting in overestimation of the yield of **3**.

Irradiation of Selenofenchone, 2

Thiofenchone possesses maxima at 490 nm and 235 nm in the electronic absorption spectrum, and irradiation into the S_2 band results in intramolecular hydrogen abstraction and conversion to the thiol **11** and the disulphide **12** in 56 and 38%



11



12

yield respectively. No intermolecular hydrogen abstraction is observed, even in reasonably good hydrogen atom donating solvents such as pentane. The disulphide **12** only appears at high conversion, suggesting that it is a secondary photoproduct (8).

Selenofenchone, **2**, possesses maxima at 616 nm (ε 42), 272 nm (ε 9600), and 224 nm (ε 3700) in hexanes, and thus resembles di-*tert*-butylselenoketone, **1**. When a benzene solution of **2** was irradiated through Pyrex, under which conditions both the S_1 and S_2 states are populated, clean conversion to a mixture of the diselenides **13**, **14**, and possibly **15** was observed. Conversion was high but

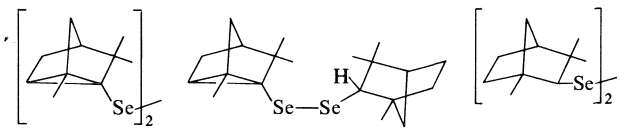
Can. J. Chem. Downloaded from www.nrcresearchpress.com by 210.87.254.42 on 09/05/12
For personal use only.

TABLE 3. Calculated and observed natural isotopic distributions for molecular ions of compounds **13**, **16**, and **17** and for a mixture of **13**, **14**, and **15***

	13 Peak height		**13, 14, 15** Peak height			**16** Peak height		**17** Peak height	
m/e	Obsd	Calcd	Obsd	Calcd†	*m/e*	Obsd	Calcd	Obsd	Calcd
420	0.5	0.5	–	–	224	2	2	–	–
421	0.5	0.6	–	–	225	0.5	0.2	–	–
422	4.5	4	2	2	226	19	18	1.5	2
423	5	6	3.5	3.5	227	18	17.5	1	0.2
424	19.5	20	13.5	12.5	228	48	49	21	18
425	16.5	16	11.5	11.5	229	6	6	21.5	17.5
426	54.5	53	43	37.5	230	100	100	55.5	49
427	38	37	29	27.5	231	14	12	7	6
428	90.5	91	75	74.5	232	18.5	18.5	100	100
429	23	24	32	32	233	2	2	14	12
430	100	100	100	100	234	–	–	20	18.5
431	21	22	24	25	235	–	–	3.5	2
432	32.5	31	72	71.5					
433	7	7	14	16					
434	4	3	22	22.5					
435	0.5	0.7	4.5	5					
436	–	–	3.5	3					

*Assuming natural abundance of each isotope as follows: ^{12}C 98.89%, ^{13}C 1.11%, ^{74}Se 0.87%, ^{76}Se 9.02%, ^{77}Se 7.58%, ^{80}Se 49.82%, ^{82}Se 9.19%.
†Assuming **13**, **14**, and **15** present in the ratio 1:1:0.1.

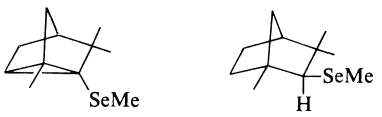
not complete, presumably because of light absorption by the products, and no deposition of selenium metal was observed. Chromatography of the reaction mixture on silica gel did not allow separation of the diselenides, but the mass spectrum confirmed the composition of the mixture. The molecular weights of the diselenides **13**, **14**, and **15** are 430, 432, and 434 respectively (based upon ^{80}Se) and



13 **14** **15**

selenium has six stable isotopes of appreciable natural abundance; analysis of the family of molecular ion peaks ascribed to **13**, **14**, and **15** molecules indicates that they are present in the approximate ratio 1:1:0.1 (Table 3), although the errors are sufficiently large that little, or no **15** may be present.[4] This was supported by the ^1H-nmr spectrum of the mixture of diselenides where the hydrogen atom adjacent to the selenium atom is observed at δ 3.2; the ratio of this signal to all others was approx. 1:50 (a 1:1:0.1 ratio of **13**:**14**:**15** requires 1:54). Whilst the extremely non-polar diselenides could not be separated by normal chromatography on silica gel, repeated, careful high pressure liquid chromatography on a reverse phase column allowed partial separation into fractions from which small amounts of the diselenide **13** could be obtained in pure crystalline form. The mass spectrum of the pure diselenide **13** exhibited the correct molecular ion at 430 mass units and the isotopic pattern was consistent with the presence of two selenium atoms (Table 3). The ^1H-nmr spectrum of **13** was extremely similar to that of the sulphur analogue **12** and the characteristic C—H stretching vibration of a cyclopropyl methine was observed at 3080 cm^{-1} in the infrared spectrum.

Since the diselenides **14** and **15** could not be isolated pure, the mixture of **13**, **14**, and **15** was further characterized by reduction of the Se–Se bond with lithium aluminium hydride (9) and trapping of the resultant selenols with methyl iodide to give the selenides **16** and **17**; these were easily



16 **17**

separable by chromatography. Isolation of the intermediate selenols was not attempted because of their extremely rapid air oxidation to give diselenides. The mass spectrum of the selenide **16** possessed the correct molecular ion and isotopic pattern for one selenium atom (Table 3) and the ^1H-nmr spectrum exhibited the cyclopropyl hydrogen atom at 1.01 ppm. Similarly, the selenide **17** exhibited the correct molecular ion and isotopic

[4]This analysis, of course, assumes that the molecular ion intensities reflect the ratio of **13**, **14**, and **15** present in the crude reaction mixture.

TABLE 4. ^{13}C-nmr chemical shifts relative to tetramethylsilane*

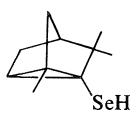
Compound	Chemical shift			
	Primary	Secondary	Tertiary	Quaternary
16	4.8	32.8	28.6	29.1
	16.0	37.9	41.9	39.0
	22.0			48.0
	22.7			
17	5.8	26.3	48.4	40.4
	21.5	29.8	66.9	50.9
	25.6	43.8		
	31.9			

*Degree of substitution on carbon determined by comparison of completely decoupled and partial off-resonance spectra.

Can. J. Chem. Downloaded from www.nrcresearchpress.com by 210.87.254.42 on 09/05/12
For personal use only.

distribution (Table 3) and in the ^{1}H-nmr spectrum the methine adjacent to the selenium atom appeared as a doublet at δ 2.57 (J = 2.5 Hz). Two isomers of **17** are possible (*exo* or *endo*); in the ^{1}H-nmr spectrum of unpurified **17** a second, but lower intensity doublet at 2.47 ppm (J = 2.5 Hz) was observed. If the minor product is an isomer at position 2, then the major product may be the *endo*-isomer by analogy with the relative chemical shift of the hydrogen in position 2 of *exo* and *endo* isomers of fenchol and norborneol (10). The coupling constant of the methine at 2.57 ppm cannot be used reliably for stereochemical assignment; the J values for the corresponding hydrogens in *exo* and *endo* fenchol are 1.85 and 1.35 Hz, respectively (11). Confirmation of the bicyclic and tricyclic structures of **17** and **16** was obtained from the ^{13}C-nmr spectra (Table 4); whilst it is not possible to assign specific positions to the signals unambiguously, the number of quaternary, tertiary, and secondary carbons in each spectrum clearly indicates the structural differences.

As mentioned above, irradiation of thiofenchone gives as the primary product of irradiation the cyclopropylthiol **11**, which, apparently, on further reaction yields the disulphide **12**. In the case of selenofenchone the situation is complicated by the fact that the presumed primary product, the selenol **18** may, by analogy with **1**, undergo a dark reaction with the starting material to give diselenide **14**. If its concentration becomes high enough, **18** may also act as a hydrogen donor for excited **2**. Two experiments were performed to estimate the concentration of **18** at different times during the reaction: an oxygen free solution of **2** was irradiated to 50% conversion and then allowed to stand in the dark.



18

No dark reaction was observed, indicating that little or no **18** was present, or that the dark reaction does not occur. In the second experiment irradiation was continued to ~90% conversion and the reaction mixture was treated with methyl iodide/sodium hydride in the absence of oxygen to trap any **18** formed. Only a trace of the selenide **16** was detected indicating that selenol concentration was very low. These results suggest that the selenol **18** is consumed rapidly during the irradiation, presumably by ground state reaction with **2**, to give **14**. The diselenide **15** may be formed by photolysis of **13** or **14** at high conversion, or it may arise from abstraction from solvent by excited **2** and trapping of the radical produced by ground state **2** in a similar manner to the formation of **3** from **1**. Attempted observation of an esr spectrum during irradiation of **2** under the same conditions used for **1** was unsuccessful, indicating that any radical intermediates, other than those centred on selenium, are either extremely short-lived or formed in concentrations at least 100 times lower than when **1** was irradiated.

From the data and observations described, the formation of **13** as a major product is difficult to explain; it is not formed by air oxidation of selenol **18** during work-up since little **18** was trapped by methyl iodide. Also it cannot be formed by photolysis of diselenide **14** since little of **15** is formed, and photolysis of **14** would lead to a statistical ratio of **13**:**14**:**15** of 1:2:1. Furthermore photolysis of **18**, the presumed primary photoproduct, would appear unlikely since its concentration appears to be low at 50% and 90% conversion and also since the extinction coefficient of **18** should be small in comparison with that of the diselenides.

The state from which selenoketone **2** reacts was also investigated by measuring the absolute quantum yield of disappearance in benzene solution. Irradiating with light of wavelength 602 nm resulted in no conversion of selenoketone requiring a quantum yield of disappearance following excita-

Can. J. Chem. Downloaded from www.nrcresearchpress.com by 210.87.254.42 on 09/05/12
For personal use only.

tion into the S_1 state of less than 6×10^{-4}. Irradiating with light of wavelength 268 nm gave a quantum yield of disappearance of $5.0 \times 10^{-3} \pm 0.2 \times 10^{-3}$; thus selenofenchone resembles thiofenchone in that it undergoes intramolecular H-abstraction following excitation into the S_2 state to give products arising from β-insertion, but not following excitation into the S_1 state. Fenchone itself does not undergo β-insertion, presumably because the $S_2(\pi \rightarrow \pi^*)$ state is too short lived and the $S_1(n \rightarrow \pi^*)$ state possesses the wrong geometry for abstraction to occur (in excited fenchone the n orbital, rendered electrophilic because of its electron deficiency, cannot reach the β C—H bond). In thio- and selenofenchone, if the S_2 state is of $\pi \rightarrow \pi^*$ nature, the partially filled, and hence electrophilic, π orbital is of the right geometry to insert into the β C—H bond.

Experimental

Di-*tert*-butylselenoketone **1** was prepared by the method of Barton and co-workers (1) in 69% yield. Natural fenchone was purified by the literature method (12) and converted to selenofenchone by the method of Barton and co-workers (1) in 31% yield. Di-*tert*-butylselenol **4** and the triselenide **5** were prepared as previously described (6). All irradiations were performed on solutions which had been degassed by at least three freeze–pump–thaw cycles to a residual pressure better than 5×10^{-4} Torr. Quantum yield determination irradiations were performed in a merry-go-round apparatus with a 450 W medium pressure Hg lamp, or in a JASCO spectroirradiator. Light intensities were determined in the latter at 278 nm by ferrioxalate actinometry and related to intensity at 689 nm using a thermopile. The disappearance of the selenoketones **1** and **2** was monitored by decline of the optical density of the visible band at ~698 nm (**1**) and 606 nm (**2**). All ^{1}H-nmr spectra were recorded at 100 MHz on a Varian XL100 spectrometer. ^{13}C-nmr spectra were recorded on the same machine at 25.2 MHz. Electron spin resonance spectra were obtained on a Varian E12 spectrometer equipped with a variable temperature accessory.

High pressure liquid chromatography was performed on a Varian 8500 instrument using a Whatman Partisil PX210/25 ODS-2 reverse phase column and methanol/water (98.2:1.8) as eluent.

Diselenide (3)

Selenoketone **1** (2.0 g) under nitrogen and in ether (15 mL) was added to lithium aluminum hydride (300 mg) in ether (15 mL). After a few minutes the mixture was acidified and the product isolated with methylene chloride (200 mL). Concentrated aqueous ammonia (15 mL) was added and air was bubbled through the stirred solution for 24 h after which time the originally colourless solution had turned yellow. The mixture was neutralized with aqueous hydrochloric acid and the aqueous phase was extracted with methylene chloride. The combined organic phases were dried (Na_2SO_4) and evaporated. The residue was crystallized from methanol to give 1.03 g of **3** as yellow crystals mp 58–59°C (lit. (1) 56.5°C); nmr (CCl_4) 1.22 (s), 3.08 (s) ppm, in the ratio 18:1; uv λ_{max} 319 nm (ε 287).

Irradiation of Selenoketone 1 in Hexanes

A degassed solution of selenoketone **1** (234 mg) in hexanes (mixture of isomers, 5 mL) was irradiated through quartz with a low pressure mercury lamp for 6 days, after which time red selenium metal had begun to deposit upon walls of the reaction vessel. The reaction mixture was diluted to 10 mL and the visible electronic spectrum was recorded; from the optical density at 700 nm it was calculated that 61% (142 mg) of the selenoketone remained. The solvent was removed and unconverted selenoketone was distilled out; the residue was chromatographed (silica gel/petroleum ether) to give a yellow material (48 mg) found by nmr to be the diselenide **3** contaminated to the extent of 15% by the triselenide **5**. Crystallization from methanol gave a sample of the yellow diselenide **3**, identical with an authentic specimen.

Irradiation of Selenoketone 1 in Hexanes in the Presence of Selenol 4

The selenoketone **1** (120 mg) and the selenol **4** (100 mg), each in hexanes (3 mL), were degassed in separate, but connected quartz vessels and mixed directly before being irradiated with a low pressure mercury lamp for 7 h, after which time selenium metal began to be deposited on the vessel walls. The reaction mixture was diluted to 10 mL and the optical density was measured at 700 nm, whence the selenoketone was found to be 60% converted. The solvent was removed and most of the excess selenoketone was distilled out (0.1 mm/50°C). The residue (147 mg) was chromatographed (silica gel/petroleum ether) to give a yellow material (132 mg) found to comprise the diselenide **3** (85%) and the triselenide **5** (15%) by nmr.

Reaction of Selenoketone 1 with Selenol 4 in the Presence of Air

Selenoketone **1** (157 mg) and selenol **4** (127 mg) were dissolved in hexanes (6 mL) and allowed to stand for 15 h during which time the solution changed in colour from blue to green to yellow. The solvent was removed and the nmr spectrum of the residue indicated a 1:1 mixture of diselenide **3** and triselenide **5**. Crystallization from isopentane/methanol gave orange crystals of **5** (55 mg). Recrystallization from ethanol gave pure **5** (27 mg) mp 85–88°C (lit. (6) 86–88°C).

Reaction of Selenoketone 1 with Selenol 4 in the Absence of Air

Selenoketone **1** (124 mg) and selenol **4** (100 mg) each in hexanes (3 mL) were degassed in separate, but connected vessels and mixed together. After 10 days at 70°C and one month at room temperature, the optical density of the solution at 700 nm following dilution to 10 mL indicated that 65% of the selenoketone had been converted. Removal of solvent and distillation of excess **1** and **4** yielded crystalline diselenide **3**, 130 mg. Recrystallization from methanol gave pure **3** (100 mg), identical with an authentic sample.

Irradiation of Selenofenchone 2 in Benzene

Selenofenchone **2** (120 mg) in benzene (10 mL) was irradiated through Pyrex with a medium pressure mercury lamp for 36 h and the resulting green solution was chromatographed (silica gel/pentane) to give unchanged starting material (8 mg) and a yellow oil (105 mg) which travelled near the solvent front. High pressure liquid chromatography of this material indicated the presence of two major components, the faster moving of which was separated in sufficiently pure form to allow crystallization to give a sample of the diselenide **13**, mp 70–77°C; ir (CCl_4) 3080, 2980, 2940, 2890, 1540, 1460, 1360, 1320 cm^{-1}; ^{1}H-nmr ($CDCl_3$) 1.82 (1 H, broad d, $J = 9$ Hz), 1.69 (1 H, broad d, $J = 9$ Hz), 1.57 (1 H, m), 1.41 (3 H, s), 1.28 (1 H, broad d, $J = 9$ Hz), 1.22 (1 H, broad m), 1.16 (1 H, broad d, $J = 9$ Hz), 0.92 (3 H, s), 0.88 (3 H, s); ms *m/e* (for Se containing fragments, the peak corresponding to ^{80}Se is given) 430 (m^+, 27%), 215 (39, containing 1 Se atom), 173 (18, containing 1 Se atom), 159 (34, containing 1 Se atom), 137 (14), 135 (40), 134 (100), 133 (54), 121 (23), 119 (49), 108 (40), 106 (27), 94 (25), 92 (39), 82 (59 $H_2{}^{80}$Se), 80 (54, $H_2{}^{78}$Se), 78 (27, $H_2{}^{76}$Se), for analysis of isotopic distribution of selenium in the

molecular ion see Table 3; precise mass determination: $C_{20}H_{30}{}^{80}Se_2$ requires *m/e* 430.0677; $C_{20}H_{30}{}^{78}Se^{82}Se$ requires *m/e* 430.0687. Found, 430.0682, 430.0687.

Reduction and Alkylation of Diselenides ***13, 14, and 15***

A degassed solution of selenofenchone (185 mg) in benzene (10 mL) was irradiated through Pyrex with a medium pressure mercury lamp for 34 h. The solvent was removed from the greenish yellow solution and the residue was chromatographed (silica gel/pentane) to give the mixture of diselenides (110 mg) which was dissolved in ether and added, under nitrogen, to lithium aluminum hydride (61 mg) in ether. At completion of the addition the yellow colour of the diselenides had disappeared. Methyl iodide (1.4 g) was added and the solution was stirred for 16 h. Following an aqueous work-up the product was chromatographed twice (silica gel/pentane) to give starting material (37 mg), selenide **16** (44 mg), and selenide **17** (25 mg) as oils. For **16**; ^{13}C-nmr see Table 4; ^{1}H-nmr (CDCl) 1.95 (3 H, s), 1.75 (1 H, broad d, J = 10.5 Hz), 1.70 (broad dt, 1 H, J = 10.5, 1.5 Hz), 1.49 (1 H, m, J = 1.5 Hz), 1.41 (3 H, s), 1.28 (1 H, broad dt, J = 10.5, 1.5 Hz), 1.17 (1 H, broad d, J = 10.5 Hz), 1.01 (1 H, broad s), 0.91 (6 H, s); ms, *m/e* (for Se containing fragments, only the largest peak, corresponding to ^{80}Se, is given) 230 (M^+, 31), 215 (25, contains Se), 187 (12, contains Se), 171 (11, contains Se), 159 (4, contains Se), 135 (16), 119 (100), 108 (30), 106 (31), 94 (36), 93 (23), 92 (75), 80 (42), 78 (41), 69 (40); precise mass determination: $C_{11}H_{18}{}^{80}Se$ requires *m/e* 230.0573; found, 230.0577; *Anal.* calcd. for $C_{11}H_{18}{}^{80}Se$: C 57.64, H 7.91; found: C 57.45, H 8.10. For **17**; ^{1}H-nmr ($CDCl_3$) 2.56 (1 H, d, J = 2.5 Hz), 1.95 (3 H, s), 1.78–1.05 (7 H, superimposed multiplets), 1.15 (3 H, s), 1.03 (6 H, s); ^{13}C-nmr, see Table 4; ms, *m/e* (for Se-containing fragments, only the largest peak corresponding to ^{80}Se is given) 232 (M^+, 5.5), 217 (0.5, contains Se), 149 (2, contains Se), 137 (29), 96 (21), 82 (100), 69 (19), 52 (19); precise mass determination: $C_{11}H_{20}{}^{80}Se$ requires 232.0730; found 232.0725.

1. T. G. Back, D. H. R. Barton, M. R. Britten-Kelly, and F. S. Guziec. J. Chem. Soc. Perkin I, 2079 (1976).
2. P. de Mayo. Acc. Chem. Res. **9**, 52 (1976).
3. N. J. Turro, V. Ramamurthy, W. Cherry, and W. Farneth. Chem. Rev. **78**, 125 (1978).
4. (*a*) C. C. Liao and P. de Mayo. Chem. Commun. 1525 (1971); (*b*) A. Ohno, M. Uohama, K. Nakamura, and S. Oka. Tetrahedron Lett. 1905 (1977).
5. A. Ohno, K. Nakamura, M. Uohama, S. Oka, T. Yamabe, and S. Nagata. Bull. Chem. Soc. Jpn. **48**, 3718 (1975) and references therein.
6. B. J. McKinnon, P. de Mayo, N. C. Payne, and B. Ruge. Nouv. J. Chim. **2**, 91 (1978).
7. J. C. Scaino and K. U. Ingold. J. Phys. Chem. **80**, 1901 (1976); J. Am. Chem. Soc. **99**, 2079 (1977).
8. D. S. L. Blackwell, K. H. Lee, P. de Mayo, G. L. R. Petrasiunas, and G. Reverdy. Nouv. J. Chim. **3**, 123 (1979).
9. D. W. Goheen and W. R. Vaughan. J. Org. Chem. **20**, 1019 (1955); S. H. Chu, W. H. H. Gunther, and H. G. Mautner. Biochem. Prep. **10**, 153 (1963).
10. K. M. Baker and B. R. Davis. Tetrahedron, **24**, 1663 (1968); H. J. Schneider and E. F. Weigand. Tetrahedron, **31**, 2125 (1975); E. W. C. Wong and C. C. Lee. Can. J. Chem. **42**, 1245 (1964); J. Paasivirta. Suom. Kemistil. **46**, 159 (1973).
11. J. I. Musher. Mol. Phys. **6**, 93 (1963).
12. O. Wallach. Ann. Chem. **353**, 209 (1907).
13. T. Balkis, A. F. Gaines, G. Özgen, I. T. Özgen, and M. C. Flowers. J. Chem. Soc. Faraday Trans. II, **72**, 524 (1976).

Can. J. Chem. Downloaded from www.nrcresearchpress.com by 210.87.254.42 on 09/05/12
For personal use only.

Preparation and ^{31}P nuclear magnetic resonance studies of chiral phosphines

NICHOLAS C. PAYNE[1] AND DOUGLAS W. STEPHAN

Department of Chemistry, University of Western Ontario, London, Ont., Canada N6A 5B7

Received April 2, 1979

NICHOLAS C. PAYNE and DOUGLAS W. STEPHAN. Can. J. Chem. **58**, 15 (1980).

The reaction of Li metal with alkyldiphenylphosphines generates the alkylphenylphosphide anions, which can undergo subsequent reactions with alkyl halides to give chiral phosphines (RR′R″P). The ^{31}P nmr chemical shifts have been measured for these phosphines, and show greater deviations from the values predicted by the first order additivity model than do those of more symmetrical phosphines (i.e., R_3P and $R_2R'P$). The shifts for these chiral molecules, and for a wide range of other phosphines, can be accurately predicted using a second order pairwise additivity scheme. The dependence of the observed and calculated chemical shifts upon electronegativity and steric factors is discussed.

NICHOLAS C. PAYNE et DOUGLAS W. STEPHAN. Can. J. Chem. **58**, 15 (1980).

La réaction du lithium métallique avec les alkyldiphénylphosphines produit des anions alkylphénylphosphures qui, par des réactions subséquentes avec les halogénures d'alkyle, peuvent conduire à des phosphines chirales (RR′R″P). La mesure des déplacements chimiques du ^{31}P révèle que ces phosphines ont, par rapport aux valeurs prévues du modèle d'additivité de premier ordre, des déviations plus grandes que celles d'autres phosphines plus symétriques (i.e., R_3P et $R_2R'P$). Pour ces molécules chirales et un grand nombre d'autres phosphines, on peut prédire, avec précision, les déplacements chimiques en utilisant un modèle apparié d'additivité de deuxième ordre. On discute du fait que les déplacements chimiques observés et calculés dépendent des facteurs d'électronégativité et stérique.

[Traduit par le journal]

Introduction

Catalytic asymmetric hydrogenation has received considerable attention of late (1–10). The common component in these studies has been the use of metal complexes of chiral phosphines to hydrogenate unsaturated prochiral substrates. It has been shown by both crystallographic studies (2, 11) and chemical modification of the chiral phosphine (12) that the orientation of the substituents on the phosphorus atoms dictates the degree of asymmetric induction. In initiating further research in this area, we have undertaken the preparation of some phosphines containing one phenyl substituent, with the chiral centre at the phosphorus atom. Previously used routes to the racemic modifications of such phosphines are in general tedious, with poor yields (reactions [1] to [4]) (13–16).

$$[1]\quad RR'R''P{=}O \xrightarrow{LiAlH_4} RR'R''P$$

$$[2]\quad RR'R''_2PI \xrightarrow{Na} RR'R''P$$

$$[3]\quad RR'HP \xrightarrow{Li} RR'P^- \xrightarrow{R''X} RR'R''P$$

$$[4]\quad RR'PCl \xrightarrow{R''MgX} RR'R''P$$

In each of these cases the preparation of the starting material is not trivial. In contrast, we have prepared the racemic modifications of chiral phosphines from the commonly available alkyldiphenylphosphines.

Chiral phosphines provide an excellent test for the validity of a ^{31}P chemical shift additivity scheme. The observed chemical shifts for these phosphines deviate from the first order calculation (17) to a greater extent than those of the more symmetrically substituted phosphines (i.e. R_3P and $R_2R'P$). This led us to propose an alternative scheme, a second order pairwise additivity model, which proves to be both more accurate and applicable to a wider range of phosphines.

Experimental

All preparations were done under an atmosphere of dry nitrogen. The ^{31}P nmr spectra were recorded for ether solutions of the purified phosphines and methylene chloride solutions of the phosphonium salt derivatives. Samples were sealed in 10 mm tubes under a nitrogen atmosphere. $(CH_3O)_3PO$ was used as the external reference, though the reported chemical shifts are relative to 85% phosphoric acid. The spectra were recorded on a Varian Associates XL 100 instrument operating at 40.5 Mc s^{-1}, and broad band proton decoupling was employed. Proton nmr spectra were recorded on both the XL 100 and T60 spectrometers. Infrared spectra were obtained on a Perkin-Elmer 621 infrared spectrometer. Melting points were determined on a Gallenkamp melting point apparatus and are uncorrected. Analyses were performed by the Spang Microanalytical Lab., Eagle Harbor, Michigan and Gygli Microanalysis Lab., Toronto, Ontario.

Preparation of Starting Materials

Diphenylmethylphosphine (18) and diphenylcyclohexylphosphine were prepared by the standard Grignard routes, using freshly distilled ether (from $LiAlH_4$), the appropriate Grignard reagent and chlorodiphenylphosphine obtained from Aldrich Chem. Co. Inc.

A. Preparation of Ethylmethylphenylphosphine, PPhMeEt

Diphenylmethylphosphine (30 mL) was dissolved in freshly

[1]To whom all correspondence should be addressed.

0008-4042/80/010015-07$01.00/0

©1980 National Research Council of Canada/Conseil national de recherches du Canada

Can. J. Chem. Downloaded from www.nrcresearchpress.com by 210.87.254.6 on 09/05/12
For personal use only.

Can. J. Chem. Downloaded from www.nrcresearchpress.com by 210.87.254.6 on 09/05/12
For personal use only.

TABLE 1. Characterization of phosphines

Phosphine	$\delta(^{31}P)^a$	Method (yield)	Bp (°C/Torr)[b]	Salt	$\delta(^{31}P)^a$	Mp(°C)[b]	Analysis Calcd. C	Calcd. H	Found C	Found H
1. PPhMeEt	−32.82	A(37%)	108–112/20	$PPhMe_2EtI$	26.90	138–140	40.84	5.48	40.54	5.46
2. PPhMePr	−37.95	A(39%)	116–118/20	$PPhMe_2PrI$	24.34	75–79	42.88	5.89	42.82	5.76
3. PPhMeCy	−25.42	A(33%)	130/5	$PPhMe_2CyI$	27.45	115–117	48.29	6.37	47.71	6.12
4. PPhMeBz	−30.88	B(22%)	120/5	$PPhMe_2BzI$	23.59	158–160	50.58	5.09	51.27	5.07
5. PPhEtCy	−8.10	A(45%)	122/5	PPhEtCyMeI	33.47	168–170	49.74	6.68	49.52	6.37
6. PPhPrCy	−13.56	A(56%)	158–160/10	PPhPrCyMeI	30.78	176–178	51.08	6.97	50.92	7.03
7. $(CyPhPCH_2CH_2)_2$[c]	−13.12	C(10%)				63–66	76.68	9.13	76.22	9.20
8. $PMePr_2$	−45.02	D[d]	60/30	PMe_2Pr_2I	28.52	176–180	35.05	7.35	34.88	7.40
9. $PEtCy_2$	−0.56	D[d]	100/1	$PEtCy_2MeI$	35.80	142–145	48.92	8 21	48.75	8.12
10. $PMeBz_2$	−30.03	D[d]	124–128/011	PMe_2Bz_2I	27.70	113–115	51.91	5.45	51.86	5.29
11. $PPrCy_2$	−6.96	D[d]	115–120/1	$PPrCy_2MeI$	33.81	174–176	50.27	8.44	49.84	8.29

[a]These chemical shifts are reported in ppm relative to 85% H_3PO_4 such that a downfield shift is positive.
[b]Temperatures reported are uncorrected.
[c]Since this phosphine was an air stable solid, no derivative was prepared.
[d]Yields were not recorded.

distilled tetrahydrofuran (from Na/benzophenone) and 2.5 g of Li metal, freshly cut, were added. The mixture was stirred for 5 h. Within the first 15 min an intense red colour appeared. After stirring, the solution was cooled in a salt/ice bath and 24.6 mL of bromoethane (35.9 g) was added dropwise over a 45 min period with stirring. Gradually the solution faded in colour and was allowed to warm to room temperature. It was then stirred for an additional hour. Degassed H_2O (150 mL) was added slowly to the solution which was cooled in an ice bath. After only a few drops were added the colour changed from red to pale yellow. After completion of the hydrolysis, the THF layer was removed and the aqueous layer extracted with ether. The THF layer and the ether extracts were combined and dried overnight over magnesium sulfate. The magnesium sulfate was filtered off and the THF and ether removed by distillation. Vacuum distillation of the remaining solution yielded 9.2 g of ethylmethylphenylphosphine (37%) bp 108–112°C/20 mm.

In an analogous manner methylphenylpropylphosphine, PPhMePr, was prepared by reaction of the phosphide anion with 1-bromopropane. By generating the phenylcyclohexylphosphide anion from diphenylcyclohexylphosphine, the preparations of cyclohexylmethylphenylphosphine, PPhMeCy, cyclohexylethylphenylphosphine, PPhEtCy, and cyclohexylphenylpropylphosphine, PPhPrCy, were achieved. Details are given in Table 1.

B. Preparation of Benzylmethylphenylphosphine, PPhMeBz

Attempts to prepare benzylmethylphenylphosphine from lithium methylphenylphosphide and benzyl chloride were hindered by difficulties in separation of the product from unreacted starting material (i.e. diphenylmethylphosphine). Because of this, an alternative route was used. Benzyldiphenylmethylphosphonium iodide was prepared by the route of Bailey *et al.* (10); 44 g of this salt were dissolved in freshly distilled THF and 3.87 g of lithium aluminum hydride added. The mixture was refluxed for 30 h. The major portion of the THF was then distilled off. Sodium potassium tartrate solution (20%, 385 mL) was added slowly with cooling (ice bath). Following this hydrolysis the solution was stirred for 30 min and extracted with two 325 mL portions of ether. The extracts were combined, dried over magnesium sulfate, filtered, and the ether distilled off. Vacuum distillation gave 9.0 g (41%) benzylmethylphenylphosphine, bp 120°C/5 mm.

C. Preparation of 1,4-Di(cyclohexylphenylphosphino)butane

The starting material was the dimesylate of 1,4-butanediol. This was prepared by analogy to the work of Crossland and Servis (19). 1,4-Butanediol (19.28 g) was dissolved in 450 mL of methylene chloride and 90 mL of triethylamine was added. Methanesulfonylchloride (54 mL) was added dropwise with cooling (ice bath), and the mixture stirred for 4 h. The solution was extracted successively with 250 mL each of water, 10% HCl solution, saturated bicarbonate solution, and saturated brine solution. The methylene chloride layer was dried over magnesium sulfate. The solution was then filtered, the solvent removed by rotary evaporation, and the oil crystallized by addition of ether. The product was filtered and washed with cold THF. The formulation as the dimesylate of 1,4-butanediol was supported by the ^1H nmr and mass spectra.

As before lithium cyclohexylphenylphosphide was prepared from 62.9 g of diphenylcyclohexylphosphine and Li metal (3.25 g). To this solution, 25.8 mL of freshly distilled *tert*-butyl chloride was added slowly over a 50 min period. Dimesylate (19 g) was added over a period of half an hour. The red colour faded to orange-yellow during an additional half hour of stirring. H_2O (125 mL) was added slowly, and the THF was distilled off. The aqueous layer was extracted three times with 125 mL of ether, and the ether layers combined and filtered. To

Can. J. Chem. Downloaded from www.nrcresearchpress.com by 210.87.254.6 on 09/05/12
For personal use only.

the ethereal solution 22.75 g of $Ni(NO_3)_2 \cdot 6H_2O$ in absolute alcohol was added. Sodium thiocyanate (29 g) in absolute alcohol was also added and the resulting mixture stirred overnight. The crude nickel complex (40 g) was filtered off, suspended in 165 mL of ethanol, treated with 19 g of sodium cyanide, and stirred for 24 h. The solution was then extracted with three portions (250 mL) of ether, and the extracts dried over magnesium sulfate. The ether layer was filtered and the solvent removed by rotary evaporation. The resulting coloured oil was passed down a 20 cm column of alumina with ether elution. Removal of the solvent yielded a colourless oil which crystallized in ethanol. The yield was 3.4 g (10%) of 1,4-di(cyclohexylphenylphosphino)butane.

D. Preparation of Dipropylmethylphosphine, Dibenzylmethylphosphine, Dicyclohexylethylphosphine, and Dicyclohexylpropylphosphine

These phosphines were prepared from the appropriate Grignard reagent and either dichloromethylphosphine, chlorodicyclohexylphosphine, or dichloroethylphosphine, which were purchased from the Pressure Chemical Co.

E. Preparation of the Phosphonium Salts

To an ether solution of the appropriate phosphine, excess iodomethane was added. Crystallization occurred rapidly. The solutions were cooled, filtered, the white salt isolated and washed with excess ether.

Results and Discussion

Preparative Route

The chiral phosphines reported here were synthesized via reaction [5].

$$[5]\quad PPh_2R + 2Li \rightarrow PPhR^-Li^+ + Li^+Ph^-$$
$$\downarrow R'X$$
$$PPhRR' \text{ (33–56%)} + LiX + PhR'$$

Cleavage of a phenyl ring from the alkyldiphenylphosphine was accomplished with lithium metal in THF under a dry, oxygen free, nitrogen atmosphere. Subsequent reaction of the alkylphenylphosphide anion with a suitable alkyl halide, followed by distillation, yielded the racemic modification of the trisubstituted phosphine. This route has the advantage that a commonly available starting material exists, whereas previous routes required chiral phosphorus precursors.

Attempts to prepare PPhMeR by the same route, where R is benzyl (Bz) or substituted phenyl groups, proved unsuccessful. ^1H and ^{31}P nmr spectra clearly illustrated the presence of a mixture of product and unreacted starting material in the distillate.

To prepare a sample of PPhMeBz, a method analogous to that used by Bailey *et al.* (16) was employed. The reaction route is shown in reaction [6].

$$[6]\quad PPhCl_2 + BzMgX \xrightarrow{Et_2O} PPhBz_2 \xrightarrow[Et_2O]{MeI} PPhBz_2MeI$$
$$\downarrow LiAlH_4/THF$$
$$PPhMeBz\ (22\%)$$

In addition to the monophosphines, a chiral bidentate phosphine was also prepared by reaction [5]. In order to achieve disubstitution, a better leaving group than a halide ion is required. Use of the dimesylate of 1,4-butanediol resulted in the product $(PhCyPCH_2CH_2)_2$. Purification of the ligand by formation of the nickel thiocyanate complex, followed by subsequent displacement from the metal with cyanide ion was successful, since the desired product is removed from the organic impurities present resulting from incomplete or elimination reactions.

All the phosphines were characterized by their ^{31}P, ^1H nmr, and ir spectra. The purity of the phosphines was indicated by the presence of only singlets in the ^1H decoupled ^{31}P nmr spectra. Observed chemical shifts are given in Table 1. Proton spectral integrations were consistent with the formulated products. Overlapping of signals, particularly when a cyclohexyl group was present, precluded the observation of many of the expected coupling constants. Methyl–phosphorus coupling (J_{P-CH_3}) is reported, as the resonances are sharp and intense doublets. As has been observed for other phosphines (20), the coupling of the phosphorus to the β methyl group in PPhMeEt was observed to be stronger than to the α methyl group. Infrared spectra showed the expected absorptions and in addition indicated that no oxidation had occurred. Analytical data, ^{31}P and ^1H nmr spectra were obtained for the methyl iodide derivatives of the monophosphines. These results are listed in Tables 1 and 2. For the phosphonium salts, ^{31}P nmr spectra showed singlets with the expected downfield shift of the resonances relative to the precursor phosphines. Proton spectra of the phosphonium salts were as expected, with a marked increase in the phosphorus–hydrogen coupling constant relative to those seen for the corresponding phosphines.

The proton spectra of PPhMeBz and $PPhBz_2MeI$ illustrated the magnetic inequivalence of the benzyl protons. With the chiral centre at the phosphorus atom, these protons become diastereotopic and thus geminal coupling is observed.

^{31}P nmr Additivity Schemes to Account for Chemical Shifts

The concept of an empirical additivity scheme has been applied to a variety of spectroscopic parameters (21, 22). Grim *et al.* (17) proposed a first order group contribution additivity scheme for the ^{31}P chemical shifts of trivalent phosphorus species. Tabulated in Table 5 are the observed and calculated ^{31}P chemical shifts for a large number of phosphines. The approach of Grim *et al.* showed significant deviations from the observed ^{31}P chemical shift for phosphines with substituents whose electronegativity

Can. J. Chem. Downloaded from www.nrcresearchpress.com by 210.87.254.6 on 09/05/12
For personal use only.

TABLE 2. Proton nmr data

Species	Chemical shifts (ppm)[a]				Coupling constants (Hz)		
	Ph	CH_2	CH_3	P—CH_3	$J_{P—CH_3}$	$J_{P—CH_2}$	Other
Phosphines							
PPhMeEt	7.35(m)	1.65(m)	1.0(d of t)	1.28(d)	2.5		$J_{CH_2—CH_3} = 7$ $J_{P—CH_3'} = 15$
PPhMePr	7.4(m)	1.60(m)	1.00(m)	1.30(d)	2.7		
PPhMeCy	7.4(m)	1.60(br m)	1.10(m)	1.28(d)	3.0		
PPhMeBz	7.2(m)	2.96(d of d)		1.21(d)	3.3	4.0	$J_{CH—CH'} = 2$
PPhEtCy	7.3(m)	0.85 to 2.0(br m)					
PPhPrCy	7.3(m)	0.80 to 2.0(br m)					
$(CyPhPCH_2CH_2)_2$	7.4(m)	0.90 to 2.0(br m)					
Salts							
$PPhMe_2EtI$	8.2(m) 7.8(m)	3.0(d of q)	1.2(d of t)	2.57(d)	14		$J_{CH_2—CH_3} = 6$
$PPhMe_2PrI$	8.2(m) 7.8(m)	2.9(m) 1.6(m)	1.1(m)	2.56(d)	13		
$PPhMe_2CyI$	8.0(m) 7.75(m)	1.0 to 2.2(br m)		2.46(d)	13		
$PPhMe_2BzI$	7.9(m) 7.6(m) 7.2(m)	4.54(d)		2.49(d)	14	16	
PPhEtCyMeI	8.0(m) 7.75(m)	3.0(m) 1.0 to 2.2(br m)		2.44(d)	12		
PPhPrCyMeI	8.0(m) 7.75(m)	2.6 to 3.4(br m), 1.0 to 2.2(br m)		2.44(d)	13		
$PPhBz_2MeI$	7.7(m) 7.2(m)	4.76(d of d)		2.25(d)	14	15	$J_{CH—CH'} = 5$
$PPrMeCy_2I$		1.1 to 2.9(m)		2.00(d)	12		
$PEtMeCy_2I$		1.1 to 2.9(m)		2.00(d)	12		
PMe_2Bz_2I	7.4(m)	4.36(m)		1.96(d)	12	15	
PMe_2Pr_2I		2.5(m)	1.7(m)	2.16(d)	13		

[a]m = multiplet, d = doublet, q = quartet, t = triplet, br = broad.

Can. J. Chem. Downloaded from www.nrcresearchpress.com by 210.87.254.6 on 09/05/12
For personal use only.

TABLE 3. Pairwise second order chemical shift contributions

Substituent pair	Contribution	Substituent pair	Contribution
Me–Me[a]	−20.5	Cy–Pr	−5.0
Et–Et	−6.5	*t*Bu–*t*Bu	+20.4
Cy–Cy	+2.3	*i*Pr–*i*Pr	+6.6
Ph–Ph	−2.2	H–H	−79.3
Pr–Pr	−11.0	Me–H	−42.1
Bz–Bz	−4.3	Et–H	−24.4
Me–Pr	−17.4	Ph–H	−21.3
Me–Et	−14.2	Me_3Sn–$SnMe_3$	−110.0
Me–Bz	−13.2	Me_3Sn–Ph	−27.5
Me–Ph	−13.0	Me_3Sn–H	−94.9
Me–Cy	−11.3	Ph–*i*Pr	+1.4
Et–Ph	−5.1	Ph–*i*Bu	−9.6
Et–Cy	−1.8	CF_3–CF_3	−0.9
Ph–Pr	−8.0	CF_3–H	−24.5
Ph–Bz	−4.1	Bu–Bu	−10.8
Ph–Cy	−0.7	Bu–H	−29.4
*t*Bu–H	−0.2	*t*Bu–Ph	+9.6
*i*Bu–*i*Bu	−15.1		

[a]Me, methyl; Et, ethyl; Pr, *n*-propyl; *i*Pr, isopropyl; Bu, butyl; *i*Bu, isobutyl; *t*Bu, *tert*-butyl; Cy, cyclohexyl; Ph, phenyl; Bz, benzyl.

is markedly different from that of a typical alkyl or aryl group (i.e. H, CF_3, $SnMe_3$).

The ^{31}P chemical shifts of the common alkyl or aryl phosphines have been observed to be qualitatively dominated by the steric bulk of the substituents (23, 28). An attempt was made to demonstrate this in a quantitative fashion by correlating the first order ^{31}P chemical shift group contribution of a substituent to its cone angle. The substituent cone angles were defined from crystallographic positional parameters. Phosphorus–carbon and carbon–hydrogen bond lengths were assumed to be 1.8 and 1.0 Å respectively, and phosphorus, carbon, and hydrogen atoms were assumed to be spherical with atomic radii of 1.9, 1.4, and 1.2 Å, respectively. The intersections of all atoms of the substituent with planes normal to the P—C bond were calculated at 0.2 Å intervals along the P—C vector in the region between 1.0 Å and 4.0 Å from the phosphorus atom. At 5° intervals about the P—C bond the maximum breadth of intersection was considered to subtend an angle at the phosphorus nucleus. The reported cone angles (Table 4) are an average of the maximum values calculated at each of the 5° intervals. The plot of the substituent cone angles versus the ^{31}P chemical shift group contributions is shown in Fig. 1. In general, a steric dependence of ^{31}P chemical shift for alkyl/aryl phosphines is observed, though significant deviations from linearity occur, which can be attributed to the electronic factors that affect the contribution of a group to the chemical shift.

TABLE 4. Substituent cone angle

Substituent	Average cone angle (deg)
t-Bu	124
i-Pr	116
Cy	118
Ph	107
Et	109
Me	102

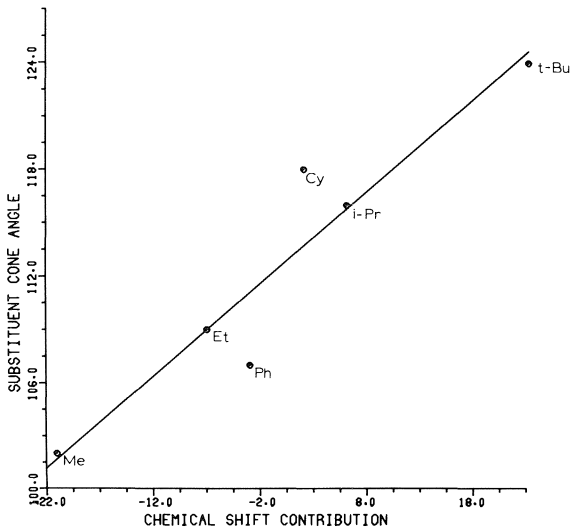


FIG. 1. Substituent cone angle versus chemical shift contribution. The straight line is an unweighted least-squares fit of the plotted data.

When Grim's model is applied to phosphines where the electronic factors affecting the ^{31}P chemical shift become even more significant, then large deviations of the calculated values from the observed are seen. Even in the case of chiral alkyl/

Can. J. Chem. Downloaded from www.nrcresearchpress.com by 210.87.254.6 on 09/05/12
For personal use only.

TABLE 5. Comparison of the two empiricisms for the calculation of phosphine ^{31}P chemical shifts

Phosphine	Chemical shifts[a] Obsd	1st order	2nd order	Phosphine	Chemical shifts Obsd	1st order	2nd order
PCy_3	+7[c]	+6	+6.9	$P(CF_3)_3$	−2.6[c]	−2.6	−2.7
PMe_3	−62[b]	−63	−61.5	$P(CF_3)_2H$	−50.7[c]	−81.1	−50.8
PEt_3	−19.5[b]	−21	−19.5	$P(CF_3)H_2$	−129[c]	−160.3	−128.3
PPh_3	−6.6[b]	−9	−6.6	$P(nBu)_3$	−32.3[c]	−33	−32.4
PPr_3	−33[c]	−33	−33.0	$P(nBu)_2H$	−69.5[c]	−102	−67.6
PBz_3	−12.9[c]	−12	−12.9	$P(nBu)H_2$	−135[c]	−170	−138.1
$PPhMe_2$	−46[b]	−45	−46.5	$P(tBu)_3$	+61.1[c]	+69	+61.2
PPh_2Me	−28[b]	−27	−28.2	$P(tBu)_2H$	+20.1[c]	+33	+20.0
PMe_2Et	−48.5[b]	−49	−48.9	$P(tBu)H_2$	−82[c]	−137	−78.9
$PMeEt_2$	−34[b]	−35	−34.9	$P(iPr)_3$	+19.3[c]	+18	+19.8
$PEtPh_2$	−12.0[b]	−13	−12.4	$P(iPr)_2Ph$	+9.3[c]	+9	+9.4
PEt_2Ph	−16.2[b]	−17	−16.7	$P(iPr)Ph_2$	+0.2[c]	0	+0.6
PPh_2Pr	−17.6[c]	−17	−18.2	$PiBu_3$	−45.3[c]	−45	−45.3
$PPhPr_2$	−27.7[c]	−25	−27.0	$P(iBu)_2Ph$	−34.2[c]	−33	−34.2
PPh_2Cy	−4.4[c]	−4	−3.6	$P(iBu)Ph_2$	−21[c]	−21	−21.4
$PPhCy_2$	+2.5[c]	+1	+0.9	$P(tBu)Ph_2$	+17.1[c]	+17	+17.1
PPh_2Bz	−10.4[c]	−10	−10.6	PH_3	−238[b]	−238	−237.9
$PPhBz_2$	−12.1[c]	−11	−12.7	$PMeH_2$	−163.5[b]	−179	−163.5
$PCyMe_2$	−43.1[d]	−40	−43.1	$PEtH_2$	−128.0[b]	−165	−128.1
$PMePr_2$	−45.02[f]	−43	−45.8	$PPhH_2$	−122[b]	−161	−121.9
PCy_2Et	−0.56[f]	−3	−1.3	PMe_2H	−99.5[b]	−121	−104.7
PCy_2Pr	−6.96[f]	−7	−7.7	PEt_2H	−55.5[b]	−101	−55.3
$PMeBz_2$	−30.03[f]	−29	−31.8	PPh_2H	41.1[b]	−85	−44.8
$P(SnMe_3)_3$	−329.6[e]	−329.6	−330.0	PPhMePr	−37.95[f]	−36	−38.4
$P(SnMe_3)_2Ph$	−165.2[e]	−223	−165.0	PPhCyPr	−13.56[f]	−12	−13.7
$P(SnMe_3)Ph_2$	−58.3[e]	−116	−57.2	PPhMeCy	−25.42[f]	−22	−25.0
$P(SnMe_3)H_2$	−269[e]	−268	−269.1	PPhEtCy	−8.10[f]	−8	−7.6
$P(SnMe_3)PhH$	−131[e]	−192	−123.2	PPhMeEt	−32.82[f]	−31	−32.3
PPhMeH	−72.3[b]	−103	−76.4	PPhMeBz	−30.88[f]	−28	−30.6
PEtMeH	−77.5[b]	−107	−80.7				

[a]Chemical shifts are relative to 85% H_3PO_4 such that a downfield shift is positive.
[b]See ref. 24.
[c]See ref. 25.
[d]See ref. 26.
[e]See ref. 27.
[f]Our measurement.

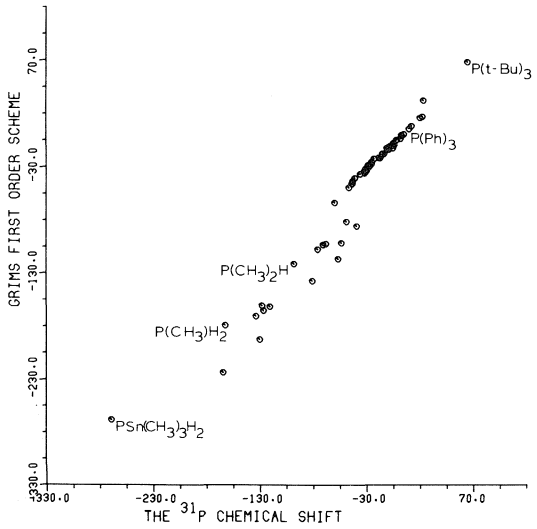


FIG. 2. First order calculation of the ^{31}P chemical shift versus the observed values.

aryl phosphines, the discrepancy between calculated and observed ^{31}P chemical shifts is significantly larger than that seen for the more symmetric phosphines. In light of this we propose an alternative additivity scheme. Our approach considers three substituent pairwise contributions to the chemical shift. Thus, for PPhMeEt the sum of the Ph–Me, Ph–Et, and Me–Et pairwise contributions would yield the observed ^{31}P chemical shift. Pairwise contributions involving the lone pair of electrons as one 'substituent' were not included, so to calculate the R–R′ pairwise contribution constant (PC), eqs. [7] and [8] were solved using the observed chemical shifts (CS) for PR_3 and PR_2R'

$$[7]\quad CS_{PR_3} = 3PC_{R-R}$$

$$[8]\quad CS_{PR_2R'} = 2PC_{R-R'} + PC_{R-R}$$

Repetition of such calculations yielded the pairwise contribution constants tabulated in Table 3.

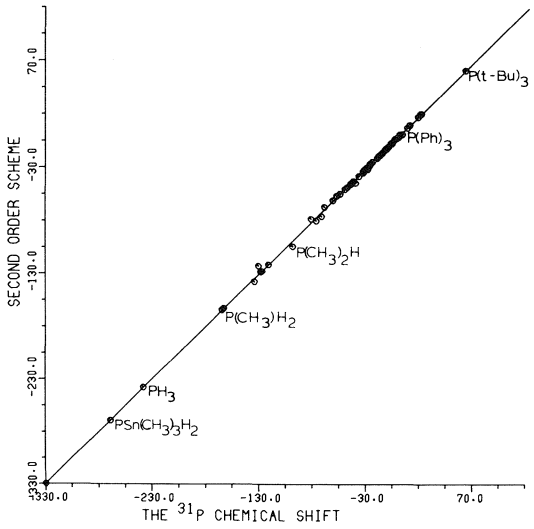


FIG. 3. Second order pairwise calculation of the ^{31}P chemical shift versus the observed values. The straight line is an unweighted least-squares fit of the plotted data. The correlation coefficient here is 1.000.

Table 5 shows the calculated chemical shifts for a wide range of phosphines using this second order approach. These data are also illustrated graphically in Figs. 2 and 3. Not only for alkyl/aryl phosphines or phosphines with electronegative substituents, but even for phosphines that contain a $SnMe_3$ group, for which no consistent group contribution constant could previously be assigned (27), the agreement between observed and calculated ^{31}P chemical shifts is significantly better using the second order pairwise additivity scheme. The improvement can be attributed to the fact that this scheme takes account of the environment of the substituent, and in that way better reflects the steric and electronic factors that alter the ^{31}P chemical shifts.

Acknowledgements

We thank the National Research Council of Canada for financial support of this work and D.W.S. is grateful for the award of an NRCC postgraduate scholarship.

1. H. B. KAGAN and T. P. DANG. J. Am. Chem. Soc. **94**, 6429 (1972).
2. B. D. VINEYARD, W. S. KNOWLES, M. J. SABACKY, G. L. BACHMAN, and D. J. WEINKAUFF. J. Am. Chem. Soc. **99**, 5946 (1977).
3. M. D. FRYZUK and B. BOSNICH. J. Am. Chem. Soc. **99**, 6262 (1977).
4. T. HAYASHI, M. TANAKA, and I. OGATA. Tetrahedron Lett. 295 (1977).
5. K. ACHIWA. J. Am. Chem. Soc. **98**, 8265 (1976).
6. K. ACHIWA. Tetrahedron Lett. 3735 (1977).
7. K. ACHIWA, T. KOGURE, and I. OJIMA. Tetrahedron Lett. 4431 (1977).
8. K. HANAKI, K. KASHIWABARA, and J. FUJITA. Chem. Lett. 489 (1978).
9. B. BOGDANOVIC. Angew. Chem. Int. Ed. **12**, 954 (1973).
10. T. HAYASHI, K. YAMAMOTO, and M. KUMADA. J. Organomet. Chem. **112**, 253 (1976).
11. R. G. BALL and N. C. PAYNE. Inorg. Chem. **16**, 1187 (1977).
12. H. B. KAGAN. Pure Appl. Chem. **43**, 401 (1975).
13. W. E. MCEWEN, K. F. KUMLI, A. BLADE-FONT, M. ZANGER, and C. A. VANDERWERF. J. Am. Chem. Soc. **86**, 2378 (1964).
14. R. C. HINTON, F. G. MANN, and D. TODD. J. Chem. Soc. 5454 (1961).
15. L. HORNER, A. WINKLER, A. RUPP, A. MENTRUP, H. HOFFMAN, and P. BECK. Tetrahedron Lett. 161 (1961).
16. W. J. BAILEY, S. A. BUCKLER, and F. MARKTSCHEFFEL. J. Org. Chem. **25**, 1996 (1960).
17. S. O. GRIM, W. MCFARLANE, and E. F. DAVIDOFF. J. Org. Chem. **32**, 781 (1967).
18. D. J. PETERSON and H. R. HAYS. J. Org. Chem. **30**, 1939 (1970).
19. R. R. CROSSLAND and K. L. SERVIS. J. Org. Chem. **35**, 3195 (1970).
20. J. R. VAN WAZER and J. H. LETCHER. Top. Phosphorus Chem. **5**, 169 (1967).
21. R. G. KIDD and H. G. SPINNEY. Inorg. Chem. **12**, 1967 (1973).
22. P. A. W. DEAN and D. F. EVANS. J. Chem. Soc. A, 1154 (1968).
23. B. E. MANN. J. Chem. Soc. 30 (1972).
24. V. MARK, C. H. DUNGAN, M. M. CRUTCHFIELD, and J. R. VAN WAZER. Top. Phosphorus Chem. **5**, 227 (1967).
25. G. M. KOSOLAPOFF and L. MAIER. Org. Phosphorus Comp. **1**, 1 (1972).
26. M. D. GORDON and L. D. QUIN. J. Magn. Reson. **22**, 149 (1976).
27. W. MCFARLANE and D. S. RYCROFT. J. Chem. Soc. D, 1977 (1975).
28. S. AIME, R. K. HARRIS, E. M. MCVICKER, and M. FILD. J. Chem. Soc. D, 2144 (1976).

Can. J. Chem. Downloaded from www.nrcresearchpress.com by 210.87.254.6 on 09/05/12
For personal use only.

Studies on trifluoromethanesulfonic acid. Part 2. Conductivities of solutions of metal trifluoromethanesulfonates and other bases in trifluoromethanesulfonic acid

DAVID G. RUSSELL AND JOHN B. SENIOR[1]

Department of Chemistry and Chemical Engineering, University of Saskatchewan, Saskatoon, Sask., Canada S7N 0W0

Received May 29, 1979

DAVID G. RUSSELL and JOHN B. SENIOR. Can. J. Chem. **58**, 22 (1980).

Electrical conductivity measurements are reported for solutions in trifluoromethanesulfonic acid of a number of simple and complex bases, including univalent and divalent metal trifluoromethanesulfonates. The univalent metal salts, water, aniline, and acetic acid behave as fully dissociated bases, while the alkaline earth metal salts show considerable ion association. The trifluoromethanesulfonate anion appears to have an abnormally high mobility, as compared to the metal cations, and is believed to conduct by a proton-transfer mechanism. Dissociation constants for some weak organic bases and association constants for strontium and barium trifluoromethanesulfonates are estimated. Sulfuric acid behaves as a weak electrolyte, while sulfur trioxide is effectively a non-electrolyte. The conductivities of potassium nitrate and potassium dihydrogenphosphate are consistent with the formation of the nitryl cation and the phosphate acidium ion, respectively.

DAVID G. RUSSELL et JOHN B. SENIOR. Can. J. Chem. **58**, 22 (1980).

On rapporte les mesures de conductivité électrique d'un certain nombre de bases simples et complexes incluant les trifluorométhane sulfonates de métaux mono et bivalents en solution dans l'acide trifluorométhane sulfonique. Les sels de métaux monovalents, l'eau, l'aniline et l'acide acétique se comportent comme des bases totalement dissociées alors que les sels de métaux alcalino terreux montrent une très grande association d'ions. L'anion trifluorométhanesulfonique semble avoir une grande mobilité qui est anormale si on la compare à celle des cations métalliques et on pense que cette mobilité est due à un mécanisme de transfert de proton. On évalue les constantes de dissociation de quelques bases organiques faibles et les constantes d'association des trifluorométhanesulfonates de strontium et de barium. L'acide sulfurique se comporte comme un électrolyte faible alors que l'anhydride sulfurique est effectivement un non électrolyte. Les conductivités du nitrate et du phosphate diacide de potassium sont en accord avec la formation du cation nitryle et de l'ion phosphate acidium respectivement.

[Traduit par le journal]

Introduction

Trifluoromethanesulfonic acid (HTFMS) was first prepared in 1954 (1). Since that time, and especially since the acid has become commercially available, there has been considerable interest in this very strong acid as a solvent and reaction medium. An extensive review was recently published covering the literature prior to 1976 (2). Since the majority of solutes may be expected to give rise to ionic species in solution in HTFMS, electrical conductivity measurements should prove valuable in studying solute behavior. Although conductivity measurements have been made on mixtures of HTFMS with sulfuric acid (3), carboxylic acids (4), and water (5), no previous systematic study has been made of solutions in HTFMS itself as solvent. In this paper we report the conductivities of solutions in HTFMS of Group IA and IIA metal trifluoromethanesulfonates and of a number of other simple and complex bases.

Experimental

HTFMS (3M Company) was purified by double distillation at atmospheric pressure with rigorous exclusion of moisture. The fraction boiling at 162°C was collected directly in the conductivity cell. This acid was free from H_2SO_4 (a significant impurity in the commercial acid) and all samples had specific conductivities less than 1.6×10^{-4} ohm^{-1} cm^{-1} at 25°C. In later experiments a small amount of P_2O_5 was added prior to the first distillation. This resulted in a significant reduction of the specific conductivity to values within the range 3.48 to 7.0×10^{-5} ohm^{-1} cm^{-1}. Some HTFMS anhydride was produced, it was discarded in the lower boiling fractions.

Barium trifluoromethanesulfonate (3M Company) was recrystallized from water. *Alkali metal and thallium(I) trifluoromethanesulfonates* were prepared by addition of a slight excess of the appropriate metal sulfate to an aqueous solution of barium trifluoromethanesulfonate.. The reaction mixture was allowed to stand for 1 day, and filtered to remove the precipitate of barium sulfate. The filtrate was evaporated to dryness and the product recrystallized from dried acetone. All the salts were

TABLE 1. Analytical data for trifluoromethanesulfonates

M	% M Found	% M Calculated	Melting point (°C)
Li	4.43	4.45[a]	>300
Na	13.3	13.4[a]	255–257
K	20.6	20.8[a]	236–238
Rb	36.2	36.4[a]	252–254
Cs	47.6	47.2[a]	279–281
Tl	58.3	57.8[a]	248–251
Ag	41.9	42.0[a]	>300
NH_4	10.4	10.2[a,c]	—
Ca	11.7	11.9[b]	>300
Sr	22.6	22.7[b]	>300
Ba	31.5	31.5[b]	>300

[a]For CF_3SO_3M.
[b]For $(CF_3SO_3)_2M$.
[c]% NH_3.

[1]To whom all correspondence should be addressed.

0008-4042/80/010022-08$01.00/0

©1980 National Research Council of Canada/Conseil national de recherches du Canada

Can. J. Chem. Downloaded from www.nrcresearchpress.com by 210.87.254.6 on 09/05/12
For personal use only.

TABLE 2. Some physical properties of trifluoromethanesulfonic acid

Parameter	Value	Reference
Boiling point	162°C at 760 mm	1
Melting point	−43.53°C	5
Density (25°C)	1.6980 g cm^{-3}	4
	1.696 g cm^{-3}	5
Viscosity (25°C)	2.87 cP	4
	2.97 cP	5
Specific conductivity (25°C)	2×10^{-4} ohm^{-1} cm^{-1}	4
	6×10^{-5} ohm^{-1} cm^{-1}	5
	3.48×10^{-5} ohm^{-1} cm^{-1}	This work
Hammett acidity function, H_0	−13	21

tested and found to be free from Ba^{2+} and SO_4^{2-} ions. *Ammonium trifluoromethanesulfonate* was prepared by the addition of ammonia to an aqueous solution of HTFMS to give a neutral solution, followed by careful evaporation of the solvent. *Calcium, strontium, and silver trifluoromethanesulfonates* were prepared by the addition of a slight excess of the appropriate carbonate to aqueous HTFMS. After filtration and evaporation to dryness, the calcium and strontium salts were recrystallized from dried acetone and the silver salt was recrystallized from a dried benzene – carbon tetrachloride mixture. All of the salts were dried under vacuum at 110°C.

Analyses: lithium, sodium, strontium, and barium were determined gravimetrically as their sulfates. Potassium, rubidium, caesium, and thallium were precipitated and weighed as their tetraphenylborates. Silver was determined gravimetrically as the chloride. Calcium was precipitated as the oxalate and after ignition was weighed as the carbonate. The ammonium salt was analyzed by determining its ammonia content. Analytical data and melting points are shown in Table 1. Infrared spectra of the salts (Nujol mulls) showed only bands characteristic of the $CF_3SO_3^-$ ion (6). The absence of bands at 1610, 3600, and 3750 cm^{-1} showed that the samples were free from water.

Nitrobenzene was purified by fractional freezing (mp 6°C). *Nitromethane* was fractionally distilled twice (bp 97.5/735 mm Hg). *Aniline* was refluxed with stannous chloride, then distilled. Glacial *acetic acid* was refluxed with acetic anhydride followed by fractional distillation. p-*Nitrochlorobenzene* was recrystallized twice from methanol and stored over P_2O_5 in a vacuum desiccator (mp 83°C). *1,3,5-Trinitrobenzene* was recrystallized from glacial acetic acid, washed with water, then dried and stored over P_2O_5 in a vacuum desiccator (mp 122–123°C).

Reagent grade *potassium nitrate* and *potassium dihydrogenphosphate* were dried at 120°C. Anhydrous *sulfuric acid* was prepared by adding sufficient dilute oleum to minimum-conducting sulfuric acid to increase its conductivity to 1.0439×10^{-2} ohm^{-1} cm^{-1}. *Sulfur trioxide* was distilled from 65% fuming sulfuric acid.

Conductance measurements were made in an oil thermostat at 25 ± 0.002°C using an Industrial Instruments Inc. RC 18 conductivity bridge. Conductivity cells were similar to those described by Barr *et al.* (7), with platinized platinum electrodes. Cell constants were determined using minimum-conducting sulfuric acid as a secondary standard (8). Solid and liquid solutes were added to the conductivity cell from weight burettes, with minimum exposure to the atmosphere.

Densities were measured at 25 ± 0.002°C using a 25 mL specific gravity bottle.

Results and Discussion

Some properties of HTFMS are summarized in Table 2. By analogy with other protonic solvents it may be assumed that HTFMS undergoes autoprotolysis

$$2CF_3SO_3H \rightleftharpoons CF_3SO_3H_2^+ + CF_3SO_3^-$$

The lowest value we measured for the conductivity of HTFMS, 3.48×10^{-5} ohm^{-1} cm^{-1}, is significantly lower than previously reported values (4, 5), and thus represents an upper limit for the conductivity of the pure acid. We provisionally adopt this value for the conductivity of pure HTFMS, due to the autoprotolysis ions. If a sample of HTFMS has a conductivity in excess of this value, the excess must be ascribed to impurities; the most probable of these being water, which acts as a strong base. From the measured initial conductivities of the solvent, we estimate the maximum concentrations of water to be 5×10^{-4} *m* and 2×10^{-3} *m* respectively, for samples prepared with and without P_2O_5 addition in the first distillation step. Conductivities reported in Tables 3, 4, and 6 have been corrected for the conductivity due to impurities in the solvent using the expression:

$$\kappa_{corr} = \kappa_{obs} - (\kappa_{solv} - \kappa_{ap})$$

where κ_{obs} and κ_{corr} are respectively the observed and corrected conductivities of the given solution, κ_{solv} is the initial conductivity of the solvent and $\kappa_{ap} = 3.48 \times 10^{-5}$ ohm^{-1} cm^{-1}.

Bases in HTFMS as solvent may be defined as substances which increase the concentration of the trifluoromethanesulfonate ion, $CF_3SO_3^-$, and acids as substances which increase the concentration of the acidium ion $CF_3SO_3H_2^+$. By analogy with the behavior of the corresponding salts in other strong acid solvents, the Group IA and IIA metal trifluoromethanesulfonates might be expected to behave as strong bases of the HTFMS solvent system.

Univalent Metal Trifluoromethanesulfonates

Interpolated values of the conductivities of solu-

Can. J. Chem. Downloaded from www.nrcresearchpress.com by 210.87.254.6 on 09/05/12
For personal use only.

Can. J. Chem. Downloaded from www.nrcresearchpress.com by 210.87.254.6 on 09/05/12
For personal use only.

TABLE 3. Interpolated values of the specific conductivity of trifluoromethanesulfonates in trifluoromethanesulfonic acid at 25°C

$10^2\ m$ (mol kg^{-1})	$10^4\ \kappa$ (ohm^{-1} cm^{-1})									
	CF_3SO_3Li	CF_3SO_3Na	CF_3SO_3K	CF_3SO_3Rb	CF_3SO_3Cs	$CF_3SO_3NH_4$	CF_3SO_3Tl	CF_3SO_3Ag	$(CF_3SO_3)_2Sr$	$(CF_3SO_3)_2Ba$
1.0	7.0	7.2	7.2	7.2	7.2	7.2	7.2	7.5	8.2	9.4
2.0	13.0	13.4	13.4	13.6	13.6	13.6	13.6	14.2	14.4	16.4
3.0	18.6	19.2	19.3	19.5	19.7	19.7	19.7	20.6	19.3	22.3
4.0	23.9	24.5	24.9	25.2	25.6	25.6	25.6	26.6	23.6	27.8
5.0	28.8	29.7	30.3	30.6	30.8	30.8	30.8	32.3	27.5	32.5
6.0	33.5	34.8	35.4	35.6	36.0	36.0	36.0	37.5	31.0	36.8
8.0	42.2	43.9	44.5	44.8	45.6	45.6	45.6	47.0	—	44.5
10.0	49.6	51.8	52.7	53.1	54.5	54.5	54.5	55.8	—	—
12.0	56.7	59.0	60.1	60.8	62.3	62.5	62.6	63.8	—	—
14.0	63.0	65.2	66.8	67.7	69.4	69.7	70.0	71.1	—	—
16.0	69.1	70.9	72.5	73.7	76.0	76.4	—	77.4	—	—
18.0	—	76.0	78.1	—	—	82.3	—	—	—	—

tions of metal trifluoromethanesulfonates are given in Table 3. The original experimental results are available as supplementary material.[2] The conductivity curves of the univalent metal salts are very similar (Fig. 1), suggesting that these salts do in fact behave as fully dissociated bases of the HTFMS system. The conductivities decrease slightly, at any given concentration, in the order

$$Ag > Tl \sim NH_4 \sim Cs > Rb > K > Na > Li$$

The relatively small dependence of the conductivity on the nature of the cation suggests that the major part of the current is carried by the $CF_3SO_3^-$ anion, which could conduct by a proton-transfer mechanism as well as by the normal ion-migration mechanism, and thus have an abnormally large mobility. This has been shown to be the case for the anions HSO_4^- (9), SO_3F^- (7), and SO_3Cl^- (10) ions in their respective parent solvents. Estimates of normal ionic mobilities in HTFMS using Walden's rule suggests strongly that the $CF_3SO_3^-$ ion does indeed have an abnormally large mobility in HTFMS solution. In fluorosulfuric acid (viscosity 1.56 cP), the limiting ionic mobility of the potassium ion, $\lambda^0_{K^+}$, has been found from transport number measurements to be 17 ohm^{-1} cm^2 equiv^{-1} (7). Using the value of 2.97 cP for the viscosity of HTFMS (5) we estimate $\lambda^0_{K^+}$ in HTFMS to be 9. The limiting equivalent conductance Λ_0 of CF_3SO_3K in HTFMS, obtained by linear extrapolation of the curve of Λ vs. $c^{1/2}$ to zero concentration is 44.5, from which $\lambda^0_{CF_3SO_3^-}$ is 35.5. Similarly $\lambda^0_{Na^+}$ in chlorosulfuric acid (viscosity 2.43 cP) has been reported to be 9 (10), from which we deduce $\lambda^0_{Na^+}$ in HTFMS to be 7. We find $\Lambda_0(CF_3SO_3Na)$ to be 44.8, giving $\lambda^0_{CF_3SO_3^-} = 37.8$. These two estimates agree reasonably well, considering the approximate nature of Walden's rule, and indicate that the $CF_3SO_3^-$ ion carries approximately 80% of the total current in these solutions, about the same fraction carried by the abnormally-conducting hydroxide ion in aqueous solutions of alkali metal hydroxides. At the same time, the mobility of $CF_3SO_3^-$ is considerably lower than those of SO_3F^- and SO_3Cl^- in their parent solvents, which suggests that the proton-transfer mechanism is less effective in HTFMS than in these other solvents. It is possible that the more bulky CF_3 group in some way hinders the reorientation of solvent molecules, which is an essential, and possibly rate-limiting, step in the proton-transfer conduction process. More definite conclusions concerning individual ionic mobilities must await the results of transport

[2]Complete set of data is available, at a nominal charge, from the Depository of Unpublished Data, CISTI, National Research Council of Canada, Ottawa, Ont., Canada K1A 0S2.

TABLE 4. Interpolated values of the specific conductivity of organic bases in trifluoromethanesulfonic acid at 25°C

$10^2 m$ (mol kg^{-1})	$10^4 \kappa$ (ohm^{-1} cm^{-1})					
	Aniline	Acetic acid	Nitrobenzene	*p*-Nitrochlorobenzene	Nitromethane	1,3,5-Trinitrobenzene
2.0	13.8	12.9	12.4	11.3	4.9	1.4
4.0	25.7	23.6	22.5	20.1	8.2	2.2
6.0	36.5	33.8	31.6	27.4	10.9	2.8
8.0	46.6	43.2	39.5	33.3	13.2	3.4
10.0	55.9	52.3	46.5	38.9	15.6	4.1
12.0	64.1	61.1	53.0	43.8	17.7	4.6
14.0	71.8	68.7	58.5	48.0	19.5	5.2
16.0	78.6	75.7	63.7	51.8	21.2	5.9
18.0	—	82.4	68.5	—	23.0	6.5

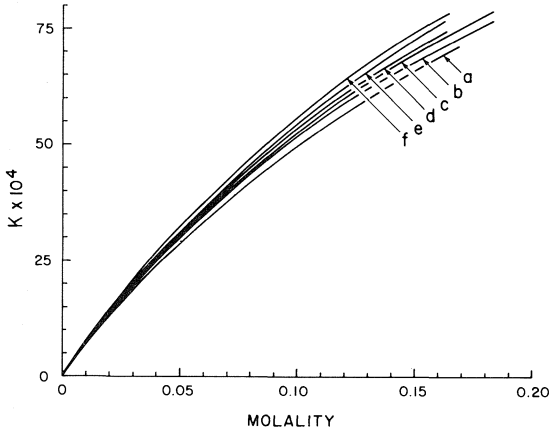


FIG. 1. Specific conductivities of solutions of trifluoromethanesulfonates, CF_3SO_3M. M = *a*, Li; *b*, Na; *c*, K; *d*, Rb; *e*, Cs, Tl, NH_4; *f*, Ag.

number measurements. Fialkov and Ligus (4) have reported transport fractions for some carboxylic acid – HTFMS mixtures. Although these refer to much more concentrated solutions than any studied in the present work, it is perhaps of interest that for an approximately 1.0 *m* solution of acetic acid (a strong base in HTFMS), the transport fraction for the $CH_3COOH_2^+$ ion is reported to be 0.181, which is just the magnitude predicted by our calculations.

The order of conductivities of the univalent salts is similar to that found in other strong acid solvents (7, 9, 10) and may be explained in an analogous manner in terms of an increase in the extent of cation solvation in the order

$$Ag < Tl \sim NH_4 \sim Cs < Rb < K < Na < Li$$

Cation solvation could affect the conductivity in two ways. Firstly, the more highly solvated cations will have larger Stokes radii and thus lower mobilities. Secondly, solvent molecules which are "tied up" in the solvation shells of cations are less available to participate in the proton-transfer mechanism of conduction by the anion, and the most highly solvated cations will interfere with this mechanism to the greatest extent. The latter effect may be the more important, especially at high concentrations, if the cations conduct a rather small fraction of the total current.

Plots of equivalent conductivity, Λ, vs. the square root of the molar concentration, $c^{1/2}$, for the univalent metal trifluoromethanesulfonates were linear up to the highest concentrations studied. Since density data were not available for most of the solutions studied, the conversion from molal to molar concentrations was made assuming the solutions to have the same density (1.696 g cm^{-3}) as the pure solvent. In the case of the potassium salt, for which the following densities were measured: $m = 0.0786, d = 1.705$; $m = 0.169, d = 1.715$ g cm^{-3}, this approximation appeared to be satisfactory and no significant difference was found either in the slope of the Λ vs. $c^{1/2}$ plot or in the value of the limiting equivalent conductance obtained by extrapolation to zero concentration, when interpolated densities of the solution were used instead of that of the pure solvent. Plots of Λ vs. $c^{1/2}$ are not usually linear over such a wide concentration range for fully dissociated electrolytes, and such behavior might be taken to indicate some degree of ion association. However, similar behaviour observed in aqueous hydrochloric acid solutions (11), and for solutions in sulfuric (9) and fluorosulfuric (7) acids has been attributed (7) to interference with the proton-transfer mechanism of conductance, as solvent molecules are increasingly "tied up" in the solvation shells of cations at higher concentrations.

For sufficiently dilute solutions, the variation of equivalent conductivity with concentration is described by the Debye–Hückel–Onsager limiting law

$$\Lambda = \Lambda_0 - AI^{1/2}$$

where I is the ionic strength, and A depends on the temperature, the charges on the ions, and on the viscosity and dielectric constant of the solvent. The

Can. J. Chem. Downloaded from www.nrcresearchpress.com by 210.87.254.6 on 09/05/12
For personal use only.

TABLE 5. Dissociation constants for organic bases in strong acid solvents

Base	$10^2 K_b$			
	HSO_3F	$CFSO_3H$	H_2SO_4	CH_3SO_3H
Acetic acid	Fully ionized	Fully ionized	Fully ionized	0.42
Nitrobenzene	Fully ionized	32	1.0	0.032
p-Nitrochlorobenzene	76	12	0.4	—
Nitromethane	2.7	0.76	0.25	Very feebly ionized
1,3,5-Trinitrobenzene	0.004	0.04	—	—

dielectric constant of HTFMS is not known, so it is not possible to compare the observed slopes of the Λ vs. $c^{1/2}$ curves with that predicted by the above equation. Agreement with the observed slopes can be obtained, for the lithium and sodium salts, by inserting into the limiting law equation a value of 58 for the dielectric constant, and for the salts of the other alkali metals, ammonium and thallium(I) by using values in the range 68–71, along with the value of 0.0297 P for the viscosity. A dielectric constant of this order of magnitude would be reasonable for a solvent of this type, and would be consistent both with essentially complete dissociation of uni-univalent salts and the extensive ion association which is found for the salts of divalent cations.

Other Bases

In interpreting the conductivities of solutions of complex bases, and of incompletely ionized bases, we make the assumption that solutions of different bases having equal conductivities contain equal concentrations of the $CF_3SO_3^-$ anion. The ratio, γ, of the concentrations of a fully dissociated reference base and of a base B, having equal conductivities, then gives the number of moles of $CF_3SO_3^-$ ion produced in solution, per mole of B. This method, which is valid if the mobility of the abnormally conducting anion is sufficiently high that differences in cation mobilities may to a good approximation be neglected, has been used successfully for solutions in related solvents such as sulfuric (12), fluorosulfuric (7), and chlorosulfuric (10) acids. With a suitable choice of reference base, so that cation mobilities are as similar as possible, the method appears to give reasonable results in HTFMS also.

Organic Bases

For a weak, monoprotic base, ionizing according to the equation

$$B + CF_3SO_3H \rightleftharpoons BH^+ + CF_3SO_3^-$$

the degree of dissociation is equal to the value of γ as defined above. The dissociation constant K_b may be calculated from the relation

$$K_b = [BH^+][CF_3SO_3^-]/[B] = \gamma^2 m/(1 - \gamma)$$

Brackets denote actual concentrations in molal units and m is the stoichiometric molal concentration of the weak base.

The results of conductivity measurements at 25°C on solutions of acetic acid, aniline, nitrobenzene, *p*-nitrochlorobenzene, nitromethane, and 1,3,5-trinitrobenzene are given in Table 4 and Fig. 2. Acetic acid and aniline give conductivity curves which are very similar to those for the univalent metal trifluoromethanesulphonates, and evidently behave as strong bases.

The other solutes give lower conductivities, and behave as weak bases. Values of K_b for these bases, calculated from the γ-values obtained using aniline as the reference base, are given in Table 5, along with K_b-values for the same bases in other strong acid solvent systems (7, 12–14). It can be seen that in general, for any given base, the K_b-value decreases in the order

$$FSO_3H > CF_3SO_3H > H_2SO_4 > CH_3SO_3H$$

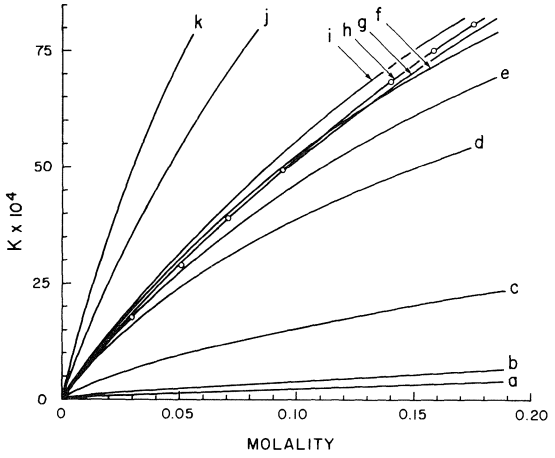


FIG. 2. Specific conductivities of solutions of organic and inorganic bases: *a*, H_2SO_4; *b*, 1,3,5-trinitrobenzene; *c*, nitromethane; *d*, *p*-nitrochlorobenzene; *e*, nitrobenzene; *f*, CF_3SO_3K; *g*, H_2O; *h*, acetic acid; *i*, aniline; *j*, KH_2PO_4; *k*, KNO_3.

Can. J. Chem. Downloaded from www.nrcresearchpress.com by 210.87.254.6 on 09/05/12
For personal use only.

Can. J. Chem. Downloaded from www.nrcresearchpress.com by 210.87.254.6 on 09/05/12
For personal use only.

TABLE 6. Interpolated values of the specific conductivities of inorganic solutes in trifluoromethanesulfonic acid at 25°C

$10^2 m$ (mol kg^{-1})	$10^4 \kappa$ (ohm^{-1} cm^{-1})				
	H_2O	KNO_3	KH_2PO_4	H_2SO_4	SO_3
2.0	12.5	35.4	25.5	1.0	0.38
4.0	23.5	61.8	45.8	1.5	0.42
6.0	33.3	81.5	63.3	1.9	0.45
8.0	42.5	97.5	77.7	2.3	0.48
10.0	51.0	110.3	90.2	2.7	0.51
12.0	59.0	119.6	100.6	3.1	0.53
14.0	66.8	126.3	109.0	3.4	0.56
16.0	74.0	130.4	115.9	3.7	0.60
18.0	81.0	132.6	121.7	—	0.63
20.0	87.5	—	—	—	0.66
25.0	102.4				
30.0	115.5				
35.0	127.0				
40.0	137.4				
45.0	146.5				

We have shown elsewhere (15) that trifluoromethanesulfonic acid behaves as a weaker acid in sulfuric acid than does fluorosulfuric acid, and it appears that this order of acid strengths holds also for the bulk solvents. 1,3,5-Trinitrobenzene, however, appears to behave as a slightly stronger base in trifluoromethanesulfonic acid than it does in fluorosulfuric acid. We have no explanation for this apparent anomaly.

Group IIA Metal Trifluoromethanesulfonates

Conductivity data for calcium, strontium, and barium trifluoromethanesulfonates are given in Table 3 and Fig. 3. These substances are of limited solubility, and in each case conductivities have been measured up to the most concentrated solutions which could be obtained. Solubility decreases in the order

$$Ba > Sr > Ca > Mg$$

It was not possible to obtain a sufficiently concentrated solution of the magnesium salt to give a meaningful conductivity measurement.

If the divalent metal salts were fully dissociated in solution, they would be expected to produce solutions of a given conductivity at about half the molal concentration required for univalent metal salts, i.e. their γ-values should be close to 2.0. In fact, as Fig. 3 shows, the conductivity curves for the barium and strontium salts, while they do indeed lie above that for the potassium salt at lower concentrations, show considerable curvature, and actually fall below the potassium curve at higher concentrations. The curve for the calcium salt, over its very limited solubility range, never rises above that for potassium. It is evident that these salts undergo extensive ion association in solution, and the formation of both ion pairs

$$M^{2+} + CF_3SO_3^- \rightleftharpoons CF_3SO_3M^+$$

and neutral species

$$CF_3SO_3M^+ + CF_3SO_3^- \rightleftharpoons (CF_3SO_3)_2M$$

must be postulated.

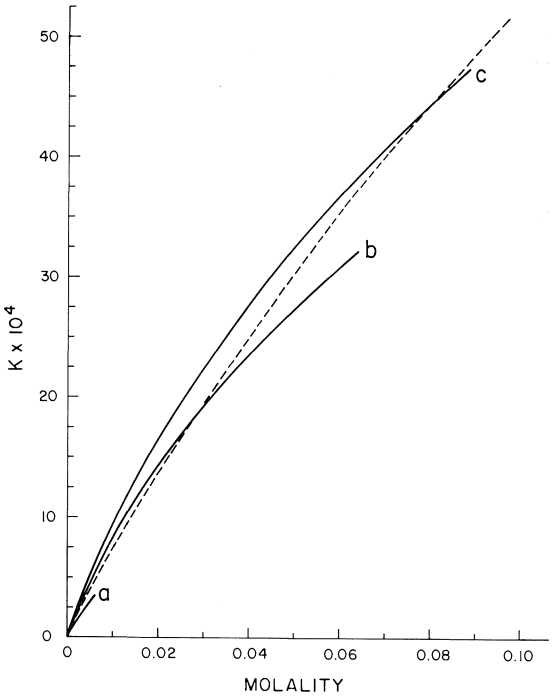


FIG. 3. Specific conductivities of solutions of trifluoromethanesulfonates, $(CF_3SO_3)_2M$. M = *a*, Ca; *b*, Sr; *c*, Ba. Dashed curve, CF_3SO_3K.

The equilibria can be expressed in terms of the association constants as

$$K_1 = [MX^+]/[M^{2+}][X^-]$$

$$K_2 = [MX_2]/[MX^+][X^-] \qquad (X = CF_3SO_3)$$

With γ as defined above, and making the same assumptions, it can be shown that

$$K_1 + \frac{K_1K_2\gamma^2 m}{\gamma - 1} = \frac{2 - \gamma}{\gamma m(\gamma - 1)}$$

Thus a plot of $(2 - \gamma)/\gamma m(\gamma - 1)$ vs. $\gamma^2 m/(\gamma - 1)$ should be a straight line with intercept K_1 and slope K_1K_2. Linear plots were obtained for the barium and strontium salts, using γ-values obtained with CF_3SO_3K as reference base. A least-squares analysis gave the following values for the associa-

Can. J. Chem. Downloaded from www.nrcresearchpress.com by 210.87.254.6 on 09/05/12
For personal use only.

tion constants: $Ba(CF_3SO_3)_2$, $K_1 = 51 \pm 3$, $K_2 = 3.2 \pm 0.2$; $Sr(CF_3SO_3)_2$, $K_1 = 250 \pm 20$, $K_2 = 4.7 \pm 0.5$.

The extent of ion association increases with decreasing crystal radius of the divalent metal cation. This is the same order as found for hydroxides in aqueous solution (16) and for chlorosulfates in chlorosulfuric acid (10) and is what would be expected for purely electrostatic anion–cation interaction, and contact ion-pairs. The reverse order might be expected if solvent molecules separated the anion and the cation, since the crystallographically smaller cations would have the larger solvated radii. It has been pointed out (16) that solvent-separated ion pairs formed by metal hydroxides in aqueous solution, M^{n+},H_2O,OH^- would tend to pass over into M^{n+},OH^-,H_2O by proton transfer along a hydrogen bond, and a similar effect would be expected to occur in the present case, so that solvent-separated ion pairs would not be stable.

Inorganic Solutes

Conductivity data for a number of inorganic solutes are given in Table 4 and Fig. 2. The conductivity curve for water is almost identical to that for potassium trifluoromethanesulfonate. Water thus behaves as a strong base, ionizing according to

$$H_2O + CF_3SO_3H \rightleftharpoons H_3O^+ + CF_3SO_3^-$$

Sulfuric acid is a very weak electrolyte in HTFMS. Since HTFMS has been shown to behave as a weak acid in sulfuric acid (15), it is probable that sulfuric acid in turn behaves as a weak base in HTFMS:

$$H_2SO_4 + CF_3SO_3H \rightleftharpoons H_3SO_4^+ + CF_3SO_3^-$$

The K_b-value for sulfuric acid in this solvent is estimated from the conductivity data to be about 1.0×10^{-4}. In the light of these results, the ionic formulation, $H_3SO_4^+CF_3SO_3^-$, proposed by Fialkov and Ligus (3) for the 1:1 compound found by them in the HTFMS – sulfuric acid system, is most unlikely to be correct.

Sulfur trioxide behaves as an extremely weak electrolyte in HTFMS. By analogy with its reactions with sulfuric, fluorosulfuric, and methanesulfonic acids, sulfur trioxide would be expected to form trifluoromethanedisulfonic acid, $CF_3S_2O_6H$, which is expected to be a very weak acid of the HTFMS solvent system. However, no conductivity minimum could be observed on titration with potassium trifluoromethanesulfonate, and this, plus the very low conductivity of the solutions, shows that $CF_3S_2O_6H$, if formed, is extremely weakly ionized. Preliminary studies of nmr spectra of CF_3SO_3H–SO_3 mixtures suggest that $CF_3S_2O_6H$ is formed initially, but the solutions are unstable and decompose slowly over a period of several days, to give a complicated mixture of products.[3] SO_3 was not studied at a low enough concentration to permit detection of the initial decrease in conductivity which might have been expected due to its reaction with the trace amount of water in the solvent.

In order to test the usefulness of conductance measurements for the study of more complex electrolytes, we studied solutions of potassium nitrate and potassium dihydrogenphosphate. The modes of ionization of these two solutes are well established in other strong acid solvents, and there is no reason to suppose that they would behave differently in HTFMS.

Potassium nitrate gives γ-values close to 3, consistent with ionization to give the nitryl cation

$$KNO_3 + 3CF_3SO_3H \rightleftharpoons K^+ + NO_2^+ + H_3O^+ + 3CF_3SO_3^-$$

Potassium nitrate has been shown to ionize similarly in sulfuric acid (17) and in fluorosulfuric acid (18), and the preparation of a mixture of $CF_3SO_3^-NO_2^+$ and $CF_3SO_3^-H_3O^+$ by the reaction of anhydrous nitric acid with HTFMS has been reported (19).

Potassium dihydrogenphosphate gives γ-values close to 2, consistent with ionization to give the phosphate acidium ion

$$KH_2PO_4 + 2CF_3SO_3H \rightleftharpoons K^+ + H_4PO_4^+ + 2CF_3SO_3^-$$

as found for this solute in sulfuric acid (20).

Conclusions

This work demonstrates that conductivity measurements can play a useful role in studies of solute behavior in HTFMS. So long as only singly-charged cations are present, it is possible both to determine the mode of ionization of simple and complex bases, and to estimate, at least semi-quantitatively, the degree of dissociation of weak bases. Some difficulty may be anticipated in the interpretation of results for complex systems in which doubly-charged cations are produced, because of the occurrence of ion association, the extent of which varies considerably with the nature of the ions involved. It would be most desirable to have a reliable value for the dielectric constant of HTFMS, obtained by direct measurement, as this would permit the use of more sophisticated treatments of the data, taking account of non-ideality effects.

[3]D. Richards and J. B. Senior. Unpublished results.

Acknowledgements

This work was supported in part by an operating grant from the National Research Council of Canada. We thank the 3M Company for a gift of barium trifluoromethanesulfonate.

1. R. N. Haszeldine and J. M. Kidd. J. Chem. Soc. 4228 (1954).
2. R. D. Howells and J. D. McCown. Chem. Rev. **77**, 69 (1977).
3. Yu. Ya. Fialkov and V. I. Ligus. Dokl. Akad. Nauk SSSR, **197**, 1353 (1971).
4. Yu. Ya. Fialkov and V. I. Ligus. Zh. Obshch. Khim. **42**, 267 (1972).
5. R. Corkum and J. Milne. Can. J. Chem. **56**, 1832 (1978).
6. M. G. Miles, G. Doyle, R. P. Cooney, and R. S. Tobias. Spectrochim. Acta, **25**A, 1515 (1969).
7. J. Barr, R. J. Gillespie, and R. C. Thompson. Inorg. Chem. **3**, 1149 (1964).
8. R. J. Gillespie, J. V. Oubridge, and C. Solomons. J. Chem. Soc. 1804 (1958).
9. R. H. Flowers, R. J. Gillespie, E. A. Robinson, and C. Solomons. J. Chem. Soc. 4327 (1960).
10. E. A. Robinson and J. A. Ciruna. Can. J. Chem. **46**, 1719 (1968).
11. R. A. Robinson and R. H. Stokes. Electrolyte solutions. 2nd ed. Academic Press, New York, NY. 1959. p. 372.
12. R. J. Gillespie and C. Solomons. J. Chem. Soc. 1796 (1960).
13. R. C. Paul, K. K. Paul, and K. C. Malhotra. J. Chem. Soc. A, 2712 (1970).
14. R. J. Gillespie and E. A. Robinson. J. Chem. Soc. 4233 (1957).
15. D. G. Russell and J. B. Senior. Can. J. Chem. **52**, 2975 (1974).
16. C. W. Davies. Ion association. Butterworth, London. 1962. p. 84.
17. R. J. Gillespie and D. J. Millen. Q. Rev. **2**, 277 (1948).
18. R. J. Gillespie, J. B. Milne, and J. B. Senior. Inorg. Chem. **5**, 1233 (1966).
19. C. L. Coon, W. G. Blucher, and M. E. Hill. J. Org. Chem. **38**, 4243 (1973).
20. R. J. Gillespie and E. A. Robinson. *In* Non-aqueous solvent systems. *Edited by* T. C. Waddington. Academic Press, New York, NY. 1965. p. 174.
21. G. M. Kramer. J. Org. Chem. **40**, 302 (1975).

Can. J. Chem. Downloaded from www.nrcresearchpress.com by 210.87.254.6 on 09/05/12
For personal use only.

Le comportement électrochimique du magnésium en milieux légèrement alcalins

ROBERT-LOUIS BROSSARD
Centre de Recherches pour la Défense, Ottawa, Ont., Canada K1A 0Z4
ET
DOMINIQUE-LOUIS PIRON
Ecole Polytechnique, P.B. 6079, Station "A", Montréal (Qué.), Canada H3C 2A7

Reçu le 18 juin 1979

ROBERT-LOUIS BROSSARD et DOMINIQUE-LOUIS PIRON. Can. J. Chem. **58**, 30 (1980).

L'étude de l'oxydation anodique du magnésium a été entreprise en milieu légèrement alcalin dont l'eau de mer simulée. Les analyses du produit de corrosion, formé en présence d'une forte concentration en ions chlorures, sont compatibles avec la formation d'un composé dont la formule chimique est voisine de $5\,Mg(OH)_2 \cdot MgCl_2$. Cependant, ce chloro-complexe de magnésium se transforme en $Mg(OH)_2$ après un contact de plusieurs heures avec la solution.

Cette étude a conduit à l'élaboration d'un modèle qui permet d'expliquer le comportement anodique du magnésium sans faire appel à la formation d'intermédiaires. Ce modèle lie étroitement les caractéristiques du comportement anodique aux propriétés du produit de corrosion qui se voit traversé par un réseau de pores dans toute son épaisseur. Le courant et l'hydrogène gazeux circulent par les pores tandis que la nature poreuse de ce film explique qu'il soit faiblement protecteur. Par ailleurs, la surconsommation de magnésium qu'entraine le dégagement d'hydrogène s'explique à partir de la dissolution de fines particules de magnésium prisonnières dans le produit de corrosion. De plus, l'activation de l'électrode dès le retour à l'abandon est attribué à la mise à nu du métal à l'extrémité des pores durant la dissolution anodique.

Enfin, la substitution des chlorures par les sulfates comme électrolyte n'affecte nullement la valeur de la tension corrigée de l'anode pour la chute ohmique qui demeure constante à -1.65 V (/E.C.S.) approximativement.

ROBERT-LOUIS BROSSARD and DOMINIQUE-LOUIS PIRON. Can. J. Chem. **58**, 30 (1980).

This study of the anodic behavior of magnesium in simulated seawater has shown that the corrosion product formed at the surface of the electrode depends mainly on the nature of ions dissolved in the electrolyte. Analyses of the corrosion product, formed in the presence of a high concentration of chloride ions, are compatible with the formation of a compound having approximately the formula $5Mg(OH)_2 \cdot MgCl_2$. However, this complex is gradually transformed over a period of several hours into $Mg(OH)_2$.

A model of the oxidation mechanism is presented in which the characteristics of the anodic behavior of magnesium are related to the structure of the oxidation layer. For example, the activation of the surface of the anode, the kinetics of the hydrogen evolution reaction, and the large difference between values of corrected and uncorrected electrode potential can all be explained by this model. It is the resistance of the film to the flow of current which controls the kinetics of anodic dissolution of magnesium.

Introduction

Le magnésium est l'un des métaux les plus actifs du point de vue électrochimique (1). L'utilisation de ce métal offre donc une alternative intéressante dans les systèmes de protection des structures métalliques où il fait avantageusement office d'anode sacrificielle (2). L'anode de magnésium se rencontre aussi dans les piles qui servent, par exemple, à la propulsion des torpilles ainsi qu'à l'alimentation des circuits électroniques que l'on retrouve dans les détecteurs de sous-marins, les ballons météorologiques et les émetteurs de secours (3–17).

La dissolution anodique du magnésium s'accompagne d'un dégagement d'hydrogène qui consomme une fraction des électrons libérés (18–24). Ceci se traduit par un faible rendement faradaique des anodes de Mg généralement observé.

Un procédé d'oxydation en deux étapes intermédiaires a été imaginé pour expliquer ce phénomène. Il comporte la formation initiale d'un intermédiaire: l'ion de magnésium monovalent (Mg^+) (23, 24) ou le dihydrure de Mg (25, 26). La réaction ultérieure de cet intermédiaire avec la solution génèrent les électrons qui servent au dégagement de l'hydrogène (23–26). Par contre, un dernier groupe de chercheurs (27–34) attribue au phénomène de désintégration de l'anode, la surconsommation de métal tandis qu'ils soutiennent que le dégagement d'hydrogène résulte de la réaction de ces particules avec la solution. Les modèles suggérés dans la littérature ont été élaborés principalement à partir de mesures de dégagement d'hydrogène et de pertes de poids dans des milieux alcalins ou s'approchant de la neutralité. Les solutions contenaient généralement des ions chlorures en faible ou forte concentration.

Ainsi, les modèles proposés dans la littérature traduisent des points de vue fort différents et souvent même contradictoires. Le présent travail se propose donc d'approfondir l'étude de l'oxydation anodique de ce métal à partir d'un éventail de tech-

0008-4042/80/010030-09$01.00/0
©1980 National Research Council of Canada/Conseil national de recherches du Canada

Can. J. Chem. Downloaded from www.nrcresearchpress.com by 210.87.254.5 on 09/05/12
For personal use only.

Can. J. Chem. Downloaded from www.nrcresearchpress.com by 210.87.254.5 on 09/05/12
For personal use only.

niques expérimentales variées dans les solutions qui simulent les milieux réels d'utilisation dont le plus répandu est l'eau de mer.

Programme expérimental

La cellule et ses organes (fig. 1)

La solution (environ 2 L) repose dans une jarre en Pyrex percée latéralement et recouverte d'un couvercle en Téflon. Celui-ci voit de nombreux tubes le traverser: l'hydrogène pénètre par un long tube de verre (E); un thermomètre permet de relever la température; deux électrodes auxiliaires en platine platinisée assurent le passage du courant vers l'électrode de travail en magnésium (T); une électrode au calomel saturé sert de référence. Elle baigne dans l'électrolyte contenu dans la partie supérieure du capillaire de Luggin; le capillaire traverse complètement la cellule et vient à près de 1 mm de la surface de l'électrode de magnésium; l'hydrogène qui se dégage de l'anode de Mg monte dans une burette graduée partiellement remplie d'électrolyte.

C'est à partir du volume d'électrolyte déplacé qu'on déduit la quantité d'hydrogène dégagée.

L'électrode de magnésium (A) se présente sous forme d'une tige de 1 cm de diamètre par 1.5 cm de profondeur (fig. 2). L'électrode est en contact avec une vis d'acier soudée à un fil de cuivre. Un tube de Tygon serre l'électrode de magnésium tandis que l'époxy remplit l'espace vide entre le tube et les conducteurs.

La pureté des échantillons

L'analyse spectrographique[1] des échantillons révèle la présence de quelques impuretés: Cu: 30 ppm, Fe: 116 ppm, Si: 3 ppm tandis que le magnésium est pur à 99.95%.

Par ailleurs, les échantillons n'ont subit aucun traitement thermique ou autre visant à modifier la grosseur des grains. L'examen de quelques échantillons au microscope a révélé que le diamètre des grains était de l'ordre de 1 mm.

Une eau doublement distillée dont la conductivité spécifique était voisine de $10^{-6}\ \Omega^{-1}\ cm^{-1}$ a été utilisée dans la préparation des solutions.

La préparation des essais

De la solution

Les solutions utilisées ont été soigneusement préparées par des méthodes gravimétriques et volumétriques usuelles. La cellule d'électrolyse et ses divers organes ont subit plusieurs rinçage à l'eau distillée avant de recevoir près de 2 L de solutions.

L'hydrogène gazeux barbottait plus de 12 h dans la solution avant l'immersion de l'électrode de travail. Les solutions étaient légèrement alcalines (le pH étant compris entre 8 et 11) et contenaient une forte concentration en ions sulfates ou chlorures. Les chlorures ont surtout été utilisées.

De l'électrode de Mg

La méthode utilisée par Blanchet (35) a été retenue: l'échantillon subissait préalablement un polissage mécanique avant de subir une attaque chimique.

Une immersion de une demi-heure dans la solution de travail précédait l'imposition du courant ou de la tension à l'électrode de magnésium.

Les techniques expérimentales utilisées

Les courbes de polarisation potentiostatiques et galvanostatiques ont été obtenues par les méthodes courantes.

[1]Certificat d'analyse fourni par Ventron Corp., Chem. Div., Congress St., Beverly, MA.

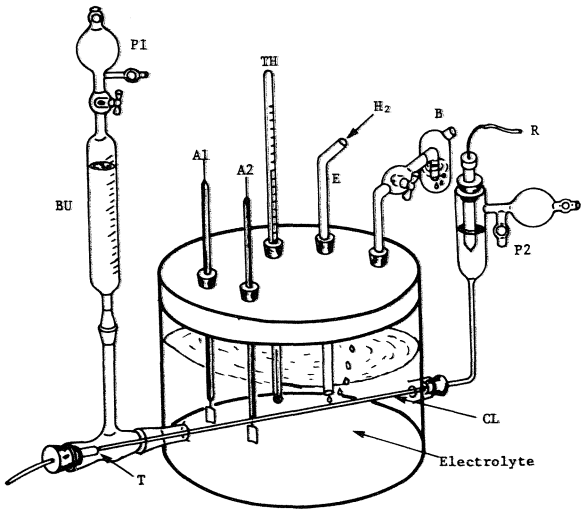


FIG. 1. La cellule et ses accessoires. A1, A2: électrodes auxiliaires; B: bûleur; Bu: burette graduée; C1: capillaire de Luggin; E: entrée du gaz (hydrogène); El: électrolyte; P1, P2: poires; R: électrode de référence au calomel saturé; T: électrode de magnésium; Th: thermomètre.

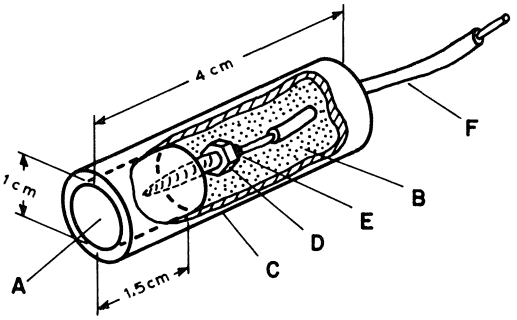


FIG. 2. L'électrode de magnésium et son support. A: disque de magnésium; B: époxy; C: gaine en tygon recouverte extérieurement de ruban de Téflon; D: vis en acier; E: soudure; F: fils de cuivre recouvert d'une gaine de plastique.

En chronopotentiométrie, le courant imposé demeurait constant tandis que la tension d'électrode était enregistrée sur un enregistreur deux plumes Moseley 7100-B de Hewlett-Packard ou à l'aide d'un oscilloscope à mémoire Tektronix No 7623-A pour les variations rapides.

Par ailleurs, la tension d'électrode imposée demeurait constante en chronoampérométrie grâce à l'emploi d'un potentiostat Tacussel PRT 2U-2X tandis que le courant était enregistré en fonction du temps.

Enfin, la tension corrigée de l'électrode a été obtenue par interruption instantanée du courant.

Résultats expérimentaux et discussion

L'analyse des courbes de polarisation potentiostatique, des micrographies montrant les modifications que subit la surface de l'anode et les mesures de la cinétique du dégagement d'hydrogène fournit de précieuses indications sur le processus

Can. J. Chem. Downloaded from www.nrcresearchpress.com by 210.87.254.5 on 09/05/12
For personal use only.

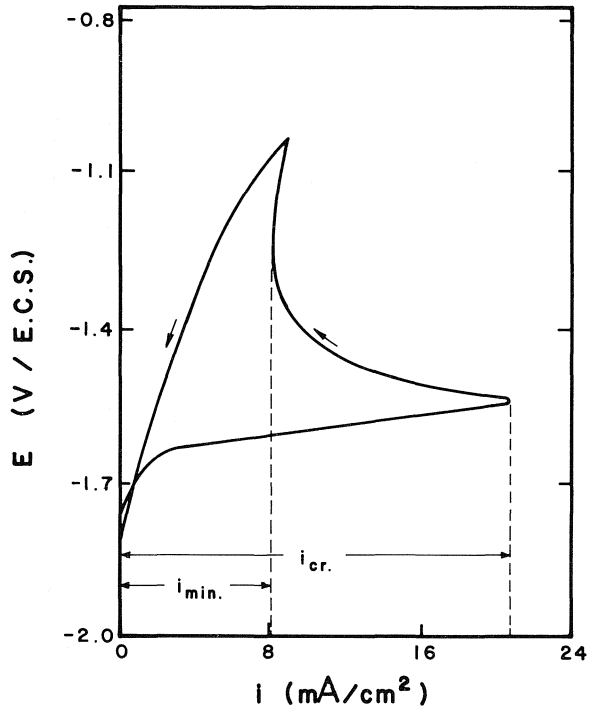


FIG. 3. Courbe de polarisation potentiostatique. E: tension d'électrode; i: densité de courant. Composition de la solution: H_3BO_3: 0.15 M; KOH: 0.086 M; KCl: 1 M; pH: 9.8; T: 25°C; ΔE: +20 mV; Δt: 5 min.

d'électrode. Elles nous ont conduit à l'élaboration d'un modèle qui permet d'expliquer le comportement de l'anode de magnésium.

Elaboration du modèle

L'examen de la courbe de la fig. 3, représentative du comportement anodique du magnésium, révèle un accroissement soudain de la vitesse de dissolution alors que la tension de polarisation est de l'ordre de 100 mV seulement. Pour des valeurs de tension croissantes (convention d'oxydo-réduction) elle passe par un maximum, 20 mA/cm² approximativement, pour décroître ensuite progressivement jusqu'à une valeur voisine de 8 mA/cm². L'allure de cette courbe rappelle la formation de films protecteurs qui sont observés lors de la passivation du nickel (36) et du fer (37) entre autres. Le recouvrement de la surface de l'anode de Mg par un film est nettement visible à l'œil nu.

Cependant, la faible décroissante du courant suggère que la protection offerte par ce dernier est beaucoup moins parfaite que dans le cas du Ni (36) et du Fe (37). Par ailleurs, le phénomène d'hystérésis prononcé (fig. 3) est attribuable à la lenteur ou à l'absence de redissolution du film.

La surface de l'anode a été examinée dans les instants qui précèdent son recouvrement complet par le produit de corrosion. Les examens au microscope optique (50×–300×) révèlent la formation de cavités plus ou moins étendues et profondes où les produits de corrosion ont tendance à s'accumuler. Elles se traduisent par la présence de zones sombres sur les micrographies obtenues (fig. 4). De plus, la portion de surface couverte par ces zones sombres s'accroît avec une augmentation de la quantité d'électricité qui a traversée l'électrode. Par ailleurs, les zones claires sont constituées de petits points d'éclat métallique qui correspondent au magnésium lui-même. Ces observations suggèrent que la dissolution est très localisée tandis que la rugosité de la surface augmente avec la quantité de courant ayant traversé l'anode. La rugosité devient telle qu'il est raisonnable d'envisager que des particules de magnésium se séparent complètement de l'anode pour demeurer captives dans le produit de corrosion.

Ces particules sont sujettes à la corrosion métallique suivant les réactions globales (38):

[1] $Mg \rightarrow Mg^{2+} + 2e^-$

[2] $2H_2O + 2e^- \rightarrow 2OH^- + H_2$

au même titre que la surface de l'anode de Mg en contact avec l'électrolyte. Néanmoins, on a ob-



FIG. 4. Apparence de la surface d'une anode de Mg. Grossissement: 300×; densité de courant imposée: 15 mA/cm²; durée de la polarisation: 3 min. 15 s.

Can. J. Chem. Downloaded from www.nrcresearchpress.com by 210.87.254.5 on 09/05/12
For personal use only.

servé qu'un dégagement d'hydrogène gazeux abondant se produit durant plusieurs secondes sur un flocon d'oxyde qui se détache complètement de l'anode de Mg. Ceci suggère que l'hydrogène gazeux résulte surtout de la dissolution des particules métalliques.

Mentionnons que Hoey et Cohen (39) ont aussi observé la dissolution localisée du magnésium dans des solutions de pH = 10 contenant 110 ppm de NaCl tandis que Staumanis et Bhatia (33) ont observé la présence de particules de Mg dans le film d'oxydation anodique formé en solution neutre ou légèrement alcaline.

Revenons aux réactions [1] et [2]. Le dégagement d'hydrogène qui en résulte explique la consommation de magnésium sans produire d'électrons utiles. De plus, une augmentation de la densité de courant doit se traduire par un accroissement proportionnel de la vitesse de dissolution de l'anode métallique. Ce qui entraîne la séparation d'un plus grand nombre de particules de magnésium par unité de temps et, par conséquent, un dégagement d'hydrogène plus abondant. Les mesures expérimentales de la vitesse du dégagement d'hydrogène à différentes valeurs de densité de courant anodique constantes ($1\,mA/cm^2 \leq i_a \leq 50\,mA/cm^2$) tendent à confirmer cette prévision du modèle. En effet, nous avons observé que la vitesse du dégagement d'hydrogène demeure constante à densité de courant anodique imposée constante ($1\,mA \leq i_a \leq 50\,mA/cm^2$) comme le montre la courbe de la fig. 5. Dans l'exemple choisi, le courant anodique est de 30 mA/cm² tandis que la solution contient plusieurs espèces ioniques dont les ions Na^+ et Cl^- qui prédominent largement en terme de concentration. Par ailleurs, la fig. 6 révèle que l'accroissement du débit d'hydrogène dégagé est approximativement de 0.2×10^{-6} mol/cm² min. pour une augmentation de courant de 1 mA/cm² dans ces solutions. Cette observation est en parfait accord avec le modèle proposé. De plus, la vitesse du dégagement d'hydrogène est indépendante de la concentration en électrolyte (figs 6 et 7). Néanmoins, la substitution des ions Cl^- par les ions $(SO_4)^{2-}$ se traduit par une diminution de la vitesse du dégagement d'hydrogène (fig. 6): elle est respectivement égale à 0.6 et 0.4×10^{-5} mol/min cm² alors que la densité de courant est de 30 mA/cm².

Par ailleurs, le dégagement de l'hydrogène nécessite la présence d'un réseau de pores dans le film formé par l'accumulation des produits de corrosion. Cette couche protectrice serait donc traversée dans toute son épaisseur par un réseau de pores constitué d'une multitude de canaux (fig. 8) tandis que la surface métallique de l'anode est, par

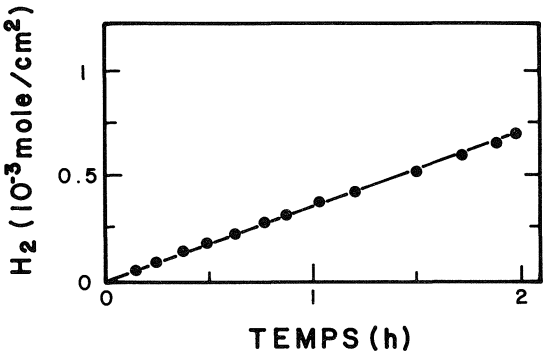


FIG. 5. Quantité d'hydrogène dégagée sur une anode de Mg en fonction du temps. Densité de courant imposée: 30 mA/cm². Composition de la solution: NaCl: 25 g/L; KCl: 0.7 g/L; $MgCl_2$: 5 g/L; Na_2SO_4: 4 g/L; $NaHCO_3$: 0.2 g/L.

ailleurs, fort rugueuse. La formation de multiple cavités entraîne le détachement de particules de magnésium métallique qui demeurent prisonnières du produit de corrosion.

Les résultats chronoampérométriques et chronopotentiométriques commentés plus loin tendent à confirmer et préciser le modèle présenté.

Nature du produit de corrosion

On a observé que le produit de corrosion dépend des espèces ioniques présentes dans l'électrolyte. En solutions fortement concentrées en chlorure, les résultats des analyses au spectromètre Auger sont caractéristiques de la formation d'un chlorocomplexe de magnésium dont la formule chimique est voisine de $5Mg(OH)_2 \cdot MgCl_2$ (40). De plus, pour des durées de polarisation de plusieurs heures, seul l'hydroxyde de magnésium $Mg(OH)_2$ était présent. Enfin, du carbonate, du sulfate et de l'hydroxyde de magnésium ont aussi été détectés dans le film lorsque la solution contenait des carbonates et des sulfates.

Analyse des résultats chronopotentiométriques

Le produit de corrosion fait obstacle au passage de courant d'où l'apparition d'une chute ohmique non négligeable qui coincide avec le recouvrement total de l'anode. Nos mesures indiquent que la chute ohmique est responsable de l'accroissement de la tension d'électrode au-delà de −1.65 V (/E.C.S.) environ alors que le film s'épaissit et que des changements s'y manifestent (fig. 9). La courbe de la fig. 9 montre la valeur de la tension d'électrode non-corrigée pour la chute ohmique en fonction du temps. On observe que la tension d'électrode corrigée pour la chute ohmique est constante à une valeur voisine de −1.65 V (/E.C.S.) tandis que la chute ohmique peut dépasser 2.5 V.

Par contre, l'écaillement du film, souvent ob-

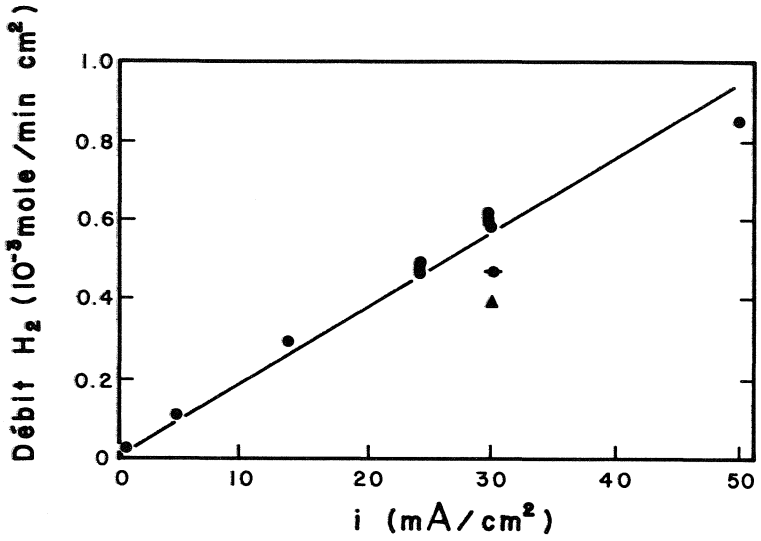


FIG. 6. Débit d'hydrogène dégagé en fonction de la densité de courant anodique pour différents électrolytes: ●, $MgSO_4$, 6.31 g/L, Na_2SO_4, 73.36 g/L, $NaHCO_3$, 4 g/L; △$MgSO_4$, 6.31 g/L, Na_2SO_4, 4 g/L, $NaHCO_3$, 4 g/L; ○ KCl entre 0.5 et 2.5 *M*.

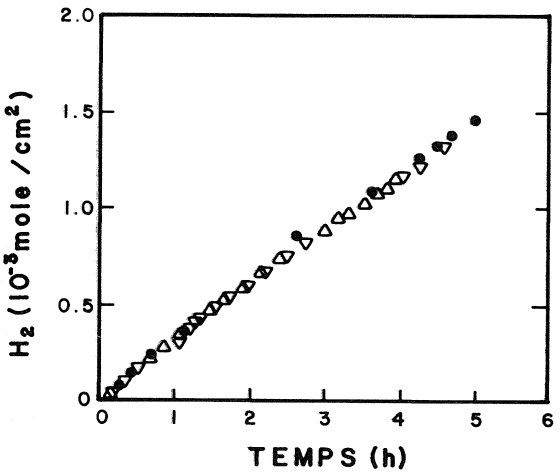


FIG. 7. Quantité d'hydrogène dégagée en fonction du temps écoulé pour différentes concentrations en KCl. Densité de courant imposé: 24.62 mA/cm^2. Composition de la solution: H_3BO_3: 0.15 *M*, KOH: 0.086 *M*; ▽, KCl: 0.5 *M*, ○ KCl: 1 *M*, △, KCl: 2.5 *M*.

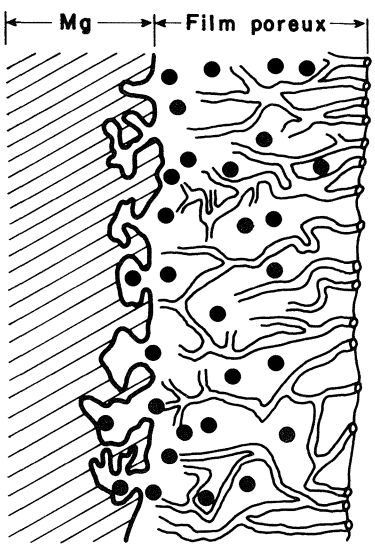


FIG. 8. Coupe schématique du produit de corrosion formé sur l'anode de Mg.

servable à l'œil nu, abaisse la barrière offerte au passage du courant ce qui entraîne des baisses substantielles de la tension d'électrode. Elles peuvent atteindre plusieurs centaines de mV: environ 1200 mV dans l'exemple de la fig. 9. De plus, la chute quasi-instantanée de la tension correspondant au point (*a*) (fig. 9) coïncide avec le détachement complet d'un disque formé par l'accumulation du produit de corrosion à la surface de l'anode. L'épaisseur de ce disque est évaluée à 1 mm approximativement.

On déduit de l'ensemble de ces observations que la résistance offerte par le film tend à freiner considérablement la vitesse de dissolution anodique du magnésium.

Mode de croissance du film poreux

Rappelons que le réseau de pores est considéré comme étant partiellement rempli d'électrolyte. Le chemin le plus facile offert au passage du courant est alors l'électrolyte contenu dans le réseau. Par ailleurs, les densités du courant apparentes im-

Can. J. Chem. Downloaded from www.nrcresearchpress.com by 210.87.254.5 on 09/05/12
For personal use only.

Can. J. Chem. Downloaded from www.nrcresearchpress.com by 210.87.254.5 on 09/05/12
For personal use only.

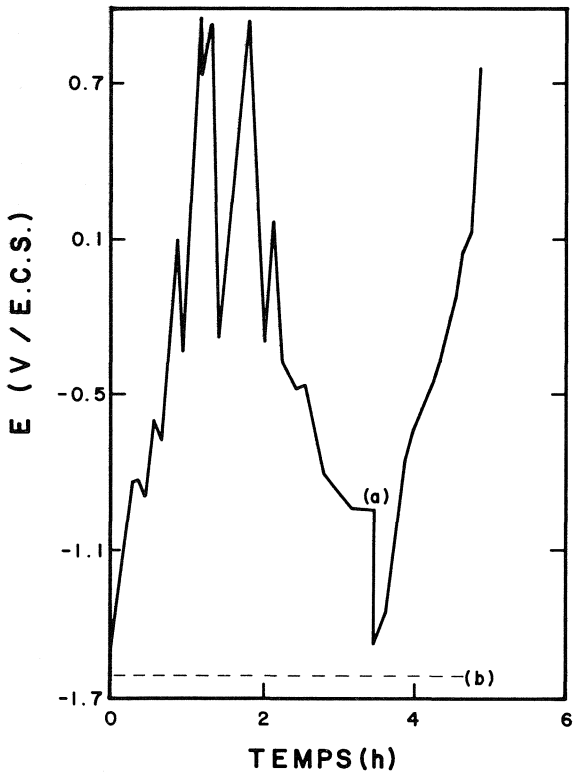


FIG. 9. Allure typique d'un enregistrement chronopotentiométrique. *E*: tension d'électrode; densité de courant: 50 mA/cm²; force ionique: 1.086; *T*: 25°C. Composition de la solution: H_3BO_3: 0.15 *M*; KCl: 1 *M*; KOH: 0.086. (*a*) Correspond à un disque d'oxyde qui se détache de l'électrode; (*b*) valeur de la tension d'électrode corrigée pour la chute ohmique. Elle est égale à −1.65 V.

posées étaient égales ou supérieures à 1 mA/cm² environ. Par conséquent, la densité de courant à l'extrémité des pores est susceptible d'être élevée. La vitesse de dissolution rapide du magnésium devrait donc entraîner la destruction locale d'un mince film protecteur initialement présent à la surface de l'anode de Mg. C'est ainsi que l'on explique l'activation de la surface de l'électrode de Mg dès le retour à l'abandon, qui peut atteindre jusqu'à 300 mV par rapport à la tension de −1.65 V (/E.C.S.) (fig. 10). La tension corrigée de l'anode pour la chute ohmique est voisine de −1.65 V à l'interruption du courant en (*c*).

Le grattage de l'anode de Mg révèle effectivement la présence d'un film qui est en contact direct avec le magnésium; il est très mince et de couleur gris-noir. Bien que Huber et Fleukiger (42) aient fait une observation identique et ait identifié l'oxyde de magnésium (MgO), la nature et le rôle exact de ce mince film demeurent cependant obscurs. Greenblatt (18) considère ce film comme un mauvais conducteur tandis que l'oxyde de magnésium alors identifié pourrait aussi être le résultat du contact du magnésium avec l'air lors du grattage.

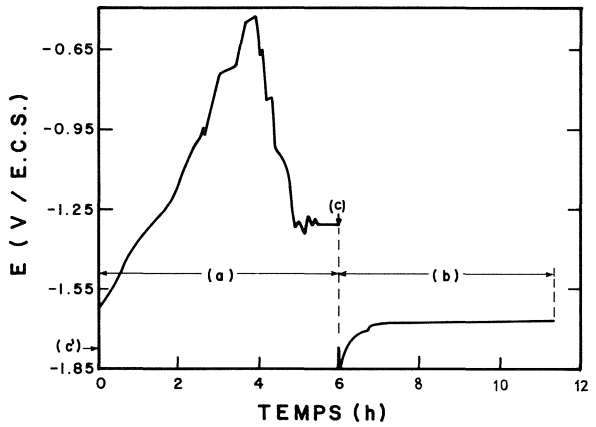


FIG. 10. Tension d'électrode en fonction du temps durant et après polarisation: (*a*) durant la polarisation, (*b*) à l'abandon, (*c*) valeur initiale de la tension d'électrode à l'abandon. *E*: tension d'électrode; densité de courant imposée durant la polarisation: 12 mA/cm²; composition de la solution: KCl: 1 *M*, H_3BO_3: 0.15 *M*, KOH: 0.086 *M*.

L'extrémité des pores est aussi susceptible de s'enrichir notablement en ions Mg^{2+}. Les ions de signe contraire vont donc devoir se déplacer afin de préserver la neutralité électrique. Un précipité est donc susceptible de se former suite à cet enrichissement (un chloro-complexe, par exemple) et de se déposer sur les parois des pores qui se retrouvent alors partiellement bloquées.

Par ailleurs, dans une fourchette de temps comprise entre 200 et 2500 s les courbes chronoampérométrique vérifient les relations suivantes (fig. 11):

$$[3] \quad i = A' t^{-1}$$

ce qui se ramène a

$$[4] \quad \int_{t=t_0}^{t=t} i \, dt = a + 2.303 A' \log_{10} t$$

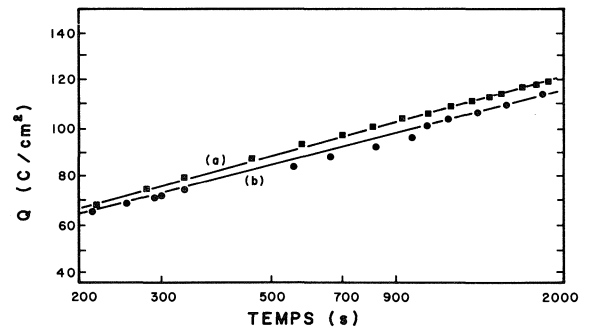


FIG. 11. Quantité d'électricité ayant traversé l'anode de magnésium en fonction du temps: (*a*) $E = -1.32$ V(/E.C.S.), (*b*) $E = -1.2$ V(/E.C.S.). Composition de la solution: KCl: 1 *M*, H_3BO_3:0.15 *M*, KOH: 0.086 *M*.

Can. J. Chem. Downloaded from www.nrcresearchpress.com by 210.87.254.5 on 09/05/12
For personal use only.

TABLEAU 1. Valeurs des constantes A' déduites des courbes chronoampérométriques

E (V/E.C.S.)[a]	A' (C/cm²)[b]
−1.57	22.2
−1.32	24.4
−1.20	22.2
−1.15	23.9
−1.06	25.0
−0.91	24.3

[a]Non corrigé pour la chute ohmique.
[b]$A' = i \cdot t$.

où a et A' sont des constantes avec A' indépendante de la tension anodique imposée (tableau 1).

La pente des droites définies par la relation [4] est de 55 ± 2 C/cm² dans les conditions expérimentales figurant sur la fig. 11. Elle correspond à $2.303A'$.

Un tel comportement est compatible avec le mécanisme du blocage partiel des pores (41). Par conséquent, le mécanisme de croissance du film en serait un de dissolution–précipitation. L'effet d'étranglement créé par l'accumulation du précipité sur les parois des pores contribuerait alors à freiner la dissolution du magnésium.

Influence de l'électrolyte et du courant

Jusqu'ici, l'influence de la concentration en électrolyte et du courant imposé sur le comportement électrochimique de l'anode de magnésium n'a pas encore été abordée. Tel que l'illustre les enregistrements chronopotentiométriques reproduite à la fig. 12, une élévation de la concentration en électrolyte fort, qui est notamment le KCl dans l'exemple choisi, se traduit par une diminution substantielle de la résistance offerte par le film au passage du courant. Cette diminution de résistance est attribuée à une augmentation de la conductivité électrique de l'électrolyte contenu dans les pores.

Par ailleurs, la tension corrigée d'électrode reste constante à une valeur voisine de −1.65 V (/E.C.S.). Cette valeur est inaffectée par une variation de la concentration en électrolyte fort que celui-ci soit un chlorure ou un sulfate.

Enfin, la vitesse avec laquelle le produit de corrosion s'accumule à la surface de l'anode doit être proportionnelle à la vitesse de dissolution des ions Mg^{2+}. De plus, une augmentation de la quantité de produit de corrosion accumulé doit se traduire par un accroissement de la chute ohmique. Par conséquent, la vitesse de croissance de la chute ohmique devient plus rapide avec une augmentation du courant anodique (fig. 13). Cependant, d'autres phénomènes contribuent à diminuer ou à

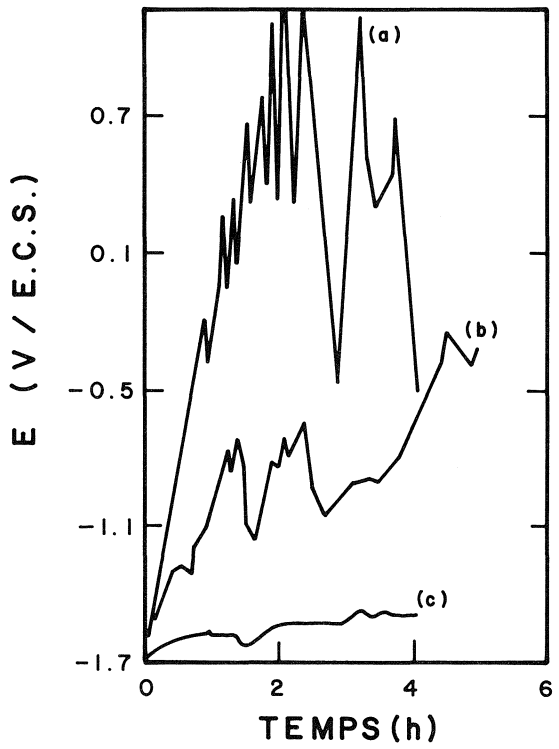


FIG. 12. Enregistrements chronopotentiométriques sur une anode de magnésium pour différentes concentrations en électrolyte fort. (*a*) $I = 0.586$ pour KCl = 0.5 *M*, (*b*) $I = 1.086$ pour KCl = 1 *M*, (*c*) $I = 2.586$ pour KCl = 2.5 *M* où I = force ionique. Densité de courant imposée: 24.62 mA/cm². Sont présents dans ces solutions: H_3BO_3: 0.15 *M*, KOH: 0.086 *M*.

augmenter la valeur de la chute ohmique comme, par exemple, le blocage partiel des pores par l'hydrogène gazeux et l'écaillement du film poreux. C'est à ce dernier que l'on attribue l'allure en dents de scie des courbes chronopotentiométriques.

Conclusions générales

1. La nature du produit de corrosion qui s'accumule à la surface de l'électrode de magnésium dépend de la nature des ions présents dans l'électrolyte. En solution fortement concentrées en chlorure, les analyses du film sont compatibles avec la formation d'un chloro-complexe de magnésium dont la formule chimique est voisine de $5Mg(OH)_2 \cdot MgCl_2$. Au contact prolongé avec la solution, il se transforme en $Mg(OH)_2$ tandis que du carbonate et du sulfate sont aussi présents lorsque l'électrolyte contient des carbonates et des sulfates.

2. Le modèle présenté permet d'expliquer le comportement anodique du magnésium sans faire appel à la formation d'intermédiaires. Ce modèle lie

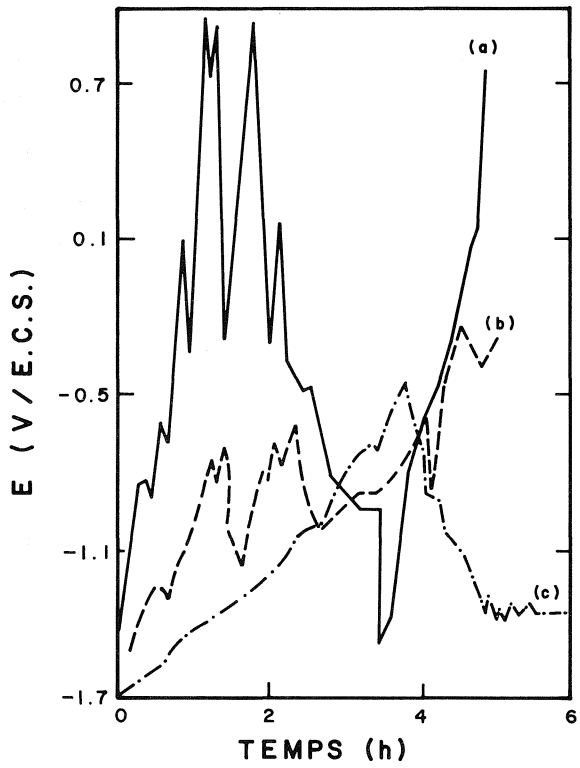


FIG. 13. Enregistrements chronopotentiométriques pour différentes densités de courant anodique. Densité de courant (mA/cm^2): (*a*) 50, (*b*) 24.6, (*c*) 12. Composition de la solution: H_3BO_3: 0.15 *M*, KOH: 0.086 *M*, KCl: 1 *M*. Force ionique: 1.086.

étroitement les caractéristiques du comportement anodique aux propriétés du produit de corrosion. Ce dernier se voit traversé complètement par un réseau de pores par où circule le courant et l'hydrogène gazeux. La nature poreuse de ce film explique qu'il soit faiblement protecteur.

3. Le surconsommation de magnésium qu'entraîne le dégagement d'hydrogène résulte de la dissolution des fines particules de Mg prisonnières du produit de corrosion.

4. L'activation de l'électrode dès le retour à l'abandon est attribuée à la mise à nu du métal à l'extrémité des pores durant la dissolution anodique.

5. Les variations de la tension apparent d'électrode (au-dessus de −1.65 V (/E.C.S.)) sont attribuées à des variations de la chute ohmique conséquente à l'épaississement du film et aux changements qui s'y manifestent dont le blocage partiel des pores et l'écaillement du film. La substitution des chlorures par les sulfates comme électrolyte n'affecte nullement la valeur de la tension corrigée de l'anode de magnésium qui demeure constante à −1.65 V (/E.C.S.) approximativement.

Remerciements

Les auteurs tiennent à remercier les organismes suivant: l'École Polytechnique où les travaux ont été entrepris, le Centre de Recherches pour la Défense (Ottawa) qui a subventionné la présente étude, la compagnie Stelco et le CNRC pour avoir versé une bourse à l'un des auteurs (R.-L.B.).

1. M. B. FONTANA et N. D. GREENE. Corrosion engineering. McGraw-Hill. 1973. Chapt. 3.
2. M. B. FONTANA et N. D. GREENE. Corrosion engineering. McGraw-Hill. 1973. Chapt. 6.
3. J. B. DOE. Characteristics of meta-dinitrobenzene dry cells. Technical Report ECOM-3084. January 1969.
4. S. S. JAFFE. Organic depolarized cells utilizing meta-dinitrobenzene. Reports 1 through 5. 15 June 1965 to November 1968, Contract DA 28-043-AMC-01401 (E) (USAECOM), Bright Star Industries, Inc.
5. J. C. PAWLAK. Organic depolarized primary batteries. Technical Report ECOM-2753 (Progress Report No. 2) (AD 616120). July 1966.
6. J. C. PAWLAK. Organic depolarized primary batteries. Technical Report ECOM-2567 (Progress Report No. 1) (AD 638305). March 1965.
7. J. J. MURPHY et D. B. WOOD. Magnesium battery program. Proc. 21st Annual Power Sources Conference, 100 (1967).
8. J. B. DOE et D. B. WOOD. Meta-dinitrobenzene cell performance. Proc. 22nd Annual Power Sources Conference, 97 (1968).
9. R. L. WIKSTRON. USA ECOM. Unpublished report.
10. J. BLANCHET. Commissariat à l'En. At. France, Rapp.: CEA R 2815 (1965).
11. R.C.A. US Army Electronic Command Contract No. DA 36-039 SC 85340 Rep. Dec. 1962.
12. R. GLICKSMAN. J. Electrochem. Soc. **106**, 457 (1957).
13. D. W. FALETTI, M. A. GACKSTETTER et J. A. ARNE. J. Electrochem. Soc. **116**, 552 (1969).
14. D. W. FALETTI et M. A. GACKSTETTER. J. Electrochem. Soc. **115**, 1210 (1968).
15. D. W. FALETTI et M. A. GACKSTETTER. J. Electrochem. Soc. **114**, 299 (1967).
16. D. W. FALETTI. J. Electrochem. Soc. **117**, 1524 (1970).
17. D. W. FALETTI, I. W. MERRICH et M. A. ADAMS. J. Electrochem. Soc. **116**, 698 (1969).
18. J. H. GREENBLATT. J. Electrochem. Soc. **103**, 539 (1956).
19. J. PRZYLUSKI et E. PALKA. El. Acta, **15**, 539 (1970).
20. J. H. GREENBLATT. Corrosion, **18**, 125t (1962).
21. P. F. KING. J. Electrochem. Soc. **113**, 537 (1966).
22. W. MCEVEN, J. KLEINBERG, D. L. BURDICK, W. D. HOFFMAN et J. Y. YANG. J. Am. Chem. Soc. **78**, 4587 (1956).
23. G. R. HOEY et M. COHEN. J. Electrochem. Soc. **105**, 245 (1958).
24. E. J. CASEY, R. E. BERGERON et G. D. NAGY. Can. J. Chem. **40**, 463 (1962).
25. G. G. PERRAULT. Electrochem. Soc. Meeting, New York, Oct. 1974, Abst. 1.
26. G. G. PERRAULT. J. Electroanal. Chem. **27**, 47#58 (1970).
27. J. W. JOHNSON, C. K. CHI et W. J. JAMES. Corrosion, **23**, 204 (1967).

Can. J. Chem. Downloaded from www.nrcresearchpress.com by 210.87.254.5 on 09/05/12
For personal use only.

28. K. F. LORKING. Report Arl/Met'76, April 1969, Dept of Supply/Austr. Def. Sc. Serv.
29. J. L. ROBINSON et P. F. KING. J. Electrochem. Soc. **108**, 36 (1961).
30. W. J. JAMES, M. E. STRAUMANIS, B. K. BHATIA et J. W. JOHNSON. J. Electrochem. Soc. **110**, 1117 (1963).
31. K. F. LORKING. Rapport No. ARL/111, 512 (1964).
32. P. F. KING. J. Electrochem. Soc. **110**, 1113 (1963).
33. M. E. STRAUMANIS et B. K. BHATIA. J. Electrochem. Soc. **110**, 357 (1963).
34. G. J. DIMASI. Tech. Rep. ECOM-2763, U.S. Army El. Comm. 1966.
35. J. BLANCHET. Rapport CEA(F)-R 2815, 1965.
36. B. MACDOUGALL et M. COHEN. J. Electrochem. Soc. **121**, 152 (1974).
37. J. E. REINOEHL, F. H. BECK et M. G. FONTANA. Corrosion, **36**, 832 (1970).
38. M. POURBAIX. Atlas d'équilibres électrochimiques. Gauthier-Villars, Paris. 1963. p. 139.
39. G. R. HOEY et M. COHEN. J. Electrochem. Soc. **106**, 776 (1959).
40. W. FEITKNECHT et F. HELO. Helv. Chim. Acta, **27**, 1480 (1944).
41. U. R. EVANS. The corrosion and oxidation of metals. E. Arnold Ltd., London. 1960. Chapt. XX.
42. K. HUBER et H. F. FLEUKIGER. International Committee of Electrochemical Thermodynamics and Kinetics, 123 (1951).

Can. J. Chem. Downloaded from www.nrcresearchpress.com by 210.87.254.5 on 09/05/12
For personal use only.

Influence des groupes *tert*-butyle, triméthylsilyle et triméthylgermyle sur la stéréochimie de réactions d'addition en série cyclohexénique. III. Epoxydation de cyclohexènes substitués en position allylique et réduction des époxydes par $LiAlH_4$

JEAN-CLAUDE RICHER ET MARC-ANDRÉ POIRIER

Département de Chimie, Université de Montréal, B.P. 6210, Montréal (Qué.), Canada H3C 3V1

ET

YVETTE MARONI ET GEORGES MANUEL

Département de Chimie, Université Paul Sabatier, 118 Route de Narbonne, 31077 Toulouse France

Reçu le 11 avril 1978[1]

JEAN-CLAUDE RICHER, MARC-ANDRÉ POIRIER, YVETTE MARONI et GEORGES MANUEL. Can. J. Chem. **58**, 39 (1980).

On a étudié la réaction d'époxydation des *tert*-butyl-6 (ou triméthylsilyl-6 ou triméthylgermyl-6) diméthyl-3,3 cyclohexènes; on note que la stéréochimie de ces réactions est gouvernée principalement par des facteurs stériques. On rapporte aussi les résultats obtenus lors de la réduction par l'hydrure double de lithium et d'aluminium des époxydes *cis* ainsi que *trans*; on remarque que la stéréochimie et la régiochimie des réactions de réduction sont influencées par des facteurs stériques ainsi que par les effets électroniques du groupe triméthylsilyle.

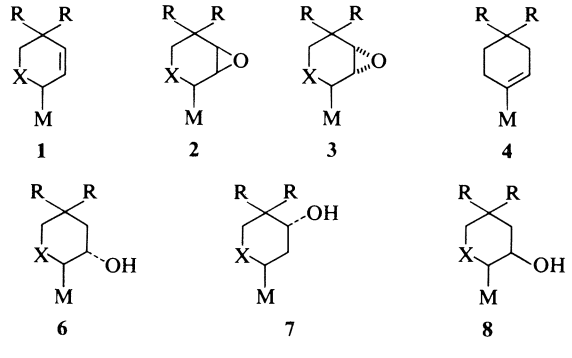
JEAN-CLAUDE RICHER, MARC-ANDRÉ POIRIER, YVETTE MARONI, and GEORGES MANUEL. Can. J. Chem. **58**, 39 (1980).

The epoxidation of allylic alkenes in the 6-*tert*-butyl (or 6-trimethylsilyl or 6-trimethylgermyl) 3,3-dimethylcyclohexenes is examined; it has been found that the stereochemistry of these reactions is governed mostly by steric factors. The results obtained by the reduction of *cis* and *trans* epoxides by lithium aluminium hydride are also reported, the regiochemistry and the stereochemistry of the reactions of reduction are governed by steric factors as well as by the electronic effects of the trimethylsilyl group.

Introduction

Dans un travail antérieur (1), on a décrit la synthèse des alcènes **1***a*, **1***b*, **1***c* et **4***a*, **4***b*, **4***c*. Plus récemment (2), on a examiné la stéréochimie de l'ouverture des époxydes dérivés des alcènes vinyliques du type **4** par différents réactifs. On a montré que ces réactions sont gouvernées, d'une part, par l'influence stérique des divers substituants et, d'autre part, par les effets électroniques des groupes triméthylsilyle et triméthylgermyle.

Dans la première partie de cette communication, on examine la stéréochimie de la réaction d'époxydation, par l'acide *m*-chloroperbenzoïque (AMCP), des alcènes allyliques **1***a*, **1***b* et **1***c*. Dans une seconde partie, on étudie la réduction des époxydes correspondants *cis* (**2***a*, **2***b*, **2***c*) et *trans* (**3***a*, **3***b*, **3***c*) par l'hydrure double de lithium et d'aluminium ($LiAlH_4$). Les résultats obtenus sont regroupés dans le Tableau 2 où figurent aussi ceux rapportés par Richer et Freppel (3) pour les composés **2***d* et **3***d*, ceux obtenus par Rickborn et Lamke (4) pour les composés **2***e* et **3***e*, les résultats de Moir et coll. (5) et Hartman et Rickborn (6) pour les époxydes **2***f* et **3***f* et enfin les résultats de Berti *et al.* (7) pour les composés **2***g* et **3***g*.



1 **2** **3** **4**

6 **7** **8**

9 **10**

a M = $(CH_3)_3C$ R = CH_3 X = CH_2
b M = $(CH_3)_3Si$ R = CH_3 X = CH_2
c M = $(CH_3)_3Ge$ R = CH_3 X = CH_2
d M = $(CH_3)_3C$ R = H X = CH_2
e M = CH_3 R = H X = CH_2
f M = OCH_3 R = H X = CH_2
g M = CH_3 R = H X = O

Résultats et discussion

Les résultats obtenus lors de l'époxydation (3, 8) des alcènes du type **1** sont regroupés dans le Tableau 1. On note, en série carbonée et siliciée, la formation d'un fort pourcentage d'isomère *trans*. Ce fait expérimental doit essentiellement résulter de la présence du groupe *tert*-butyle (ou du groupe triméthylsilyle) et du méthyle pseudo-axial. Ces

[1]La révision reçu le 24 septembre 1979.

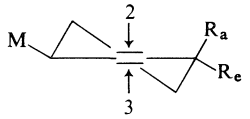
0008-4042/80/010039-06$01.00/0

©1980 National Research Council of Canada/Conseil national de recherches du Canada

Can. J. Chem. Downloaded from www.nrcresearchpress.com by 210.87.254.42 on 09/05/12
For personal use only.

TABLEAU 1. Pourcentages relatifs des produits obtenus lors de l'époxydation des alcènes du type **1**

Alcène	% Epoxyde 2 (*cis*)	% Epoxyde 3 (*trans*)	% Produit de clivage 5
1*a*	6	94	—
1*b*	24	76	—
1*c*	—	—	100



M = Me_3C, Me_3Si, Me ou OMe
R_a = Me_a ou H_a
R_e = Me_e ou H_e

SCHÉMA 1

groupes masquent la face *cis* de la molécule et orientent la réaction d'époxydation vers l'autre face (flèche 3 du schéma 1). On note également une nette augmentation du pourcentage en isomère *cis* quand on passe de la série carbonée à la série siliciée. On peut donner une explication à ce résultat en remarquant que la liaison C—Si, plus longue que la liaison C—C (9), permet une diminution des interactions 1,3 diaxiales dans l'état de transition, entre le réactif et l'un des méthyles du groupe $SiMe_3$. On remarque que les pourcentages relatifs d'addition *cis*/*trans* lors des réactions d'époxydation discutées ici sont similaires à ceux observés lors de l'hydroboration de ces mêmes alcènes (1). En effet, la stéréochimie de l'époxydation ressemble beaucoup à celle de l'hydroboration et les réactions sont contrôlées par des facteurs stériques intervenant dans l'état de transition.

Lors de la réaction de l'acide *m*-chloroperbenzoïque avec l'alcène germylé **1***c*, il n'a pas été possible d'isoler les époxydes **2***c* et **3***c* attendus, même en présence de carbonate de potassium nécessaire à l'obtention des époxydes silylés **2***b* et **3***b*. L'alcool allylique isolé **5** résulte d'une β-décomposition (schéma 2) beaucoup plus prononcée en série germylée qu'en série silylée dans la généralité des cas (10, 11).

Réduction des époxydes par $LiAlH_4$

Les résultats obtenus lors de la réduction par $LiAlH_4$ de mélanges d'époxydes des types **2** et **3** sont résumés dans le Tableau 2. L'interprétation générale des résultats est basée sur le fait que l'ouverture des époxydes se fait toujours d'une façon *trans* et généralement diaxiale selon la généralisation de Furst et Plattner (12) soit sous les formes chaise-croisée ou bateau-croisé conduisant respectivement aux produits d'ouvertures normale (produit diaxial) et anormale (produit diéquatorial). Les résultats sont discutés à l'aide des équilibres conformationnels représentés dans les schémas 3 et 4.

La réduction de l'époxyde *cis* (**2***d*) du *tert*-butyl-3 cyclohexène (X = CH_2, M = Me_3C, R = H) conduit à 100% d'isomère *cis* **8***d*. L'examen du schéma 3 indique que cet époxyde réagit essentiellement sous les formes *A* et *B*. En effet, le conformère *C* comportant des groupes aussi volumineux

TABLEAU 2. Pourcentages relatifs des alcools obtenus par réduction des époxydes par $LiAlH_4$

	Ref.	**2** **3** *cis*/*trans* (%)	X	M	R	Pourcentages relatifs des alcools **6**	**7**	**8**	**9**
2*b*, **3***b*		24/76	CH_2	Me_3Si	Me	0	65	12	23
3*b*		0/100*	CH_2	Me_3Si	Me	0	83	0	17
2*b*		100/0*	CH_2	Me_3Si	Me	0	0	50	50
3*a*		0/100	CH_2	Me_3C	Me	1	82	0	17
2*a*		100/0	CH_2	Me_3C	Me	0	0	65	35
2*d*, **3***d*	3	12/88	CH_2	Me_3C	H	31	44	12	13
3*d*	3	0/100	CH_2	Me_3C	H	35	50	0	15
2*d*	3	100/0	CH_2	Me_3C	H	0	0	100	0
3*e*	4	0/100	CH_2	Me	H	30	61	0	9
2*e*	4	100/0	CH_2	Me	H	9	0	89	2
3*f*	5, 6	0/100	CH_2	OMe	H	52	47	0	1
2*f*	5, 6	100/0	CH_2	OMe	H	0	0	43	57
3*g*	7	0/100	O	Me	H	90	8	2	0
2*g*	7	100/0	O	Me	H	5	0	93	2

*Pourcentages extrapolés du résultat obtenu de la réduction par $LiAlH_4$ du mélange 24/76.

Can. J. Chem. Downloaded from www.nrcresearchpress.com by 210.87.254.42 on 09/05/12
For personal use only.

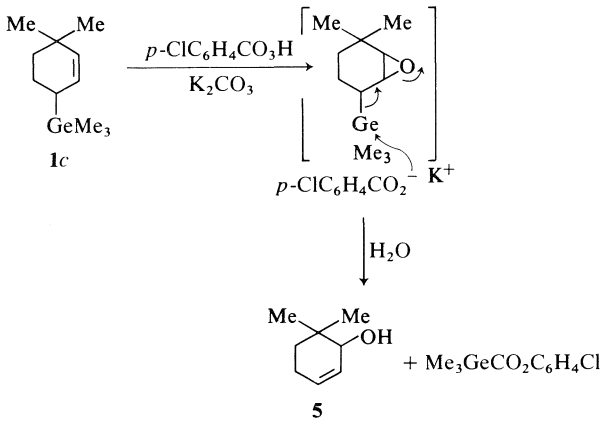


SCHÉMA 2

que $(CH_3)_3C$ ou $(CH_3)_3Si$ en position pseudo-axiale est très improbable. Qui plus est, on peut, dans le cas particulier où R = H, admettre que le conformère *B*, moins stable que le conformère *A*, n'intervient pas. Les interactions entre R (R = H pour l'époxyde **2***d*) et l'hydrure entrant doivent être faibles. Dans ces conditions, l'ouverture de **2***d* se ferait exclusivement selon l'état de transition *A* conduisant à l'alcool **8***d* par une ouverture normale.

La réduction de l'époxyde *cis* (**2***a*) du *tert*-butyl-6 diméthyl-3,3 cyclohexène (X = CH_2, M = Me_3C, R = CH_3) conduit à 35% de l'alcool **9***a* correspondant à une ouverture anormale résultant du conformère *B*. Dans ce cas, l'énergie de l'état de transition *A* doit être suffisamment élevée (par suit des interactions 1,2 qui existent entre le réactif et le méthyle pseudo-équatorial ou comme l'a suggéré un des arbitres, à cause de l'interaction diaxiale-1,3 entre le méthyle axial et l'oxygène négatif qui se développe en axial dans l'état de transition *A*) pour qu'un état de transition différent, impliquant la forme bateau-croisé *B*, puisse devenir compétitif.

La réduction de l'époxyde silylé (**2***b*) conduit à un pourcentage d'ouverture anormale (**9***b*: 50%) plus élevé qu'en série carbonée analogue (**9***a*: 35%). Cette variation du pourcentage peut résulter de l'accroissement de la longueur de la liaison interatomique quand on passe du C—C au motif Si—C. Ce phénomène favorise l'attaque en α du groupe Me_3Si (formation de **9***b*) par rapport à l'attaque en α du groupe Me_3C (formation de **9***a*).

Le comportement de l'époxyde *cis* (**2***e*) issu du méthyl-3 cyclohexène (**1***e*) lors de la réduction par $LiAlH_4$ est analogue à celui de l'époxyde *cis* (**2***d*) formé à partir du *tert*-butyl-3 cyclohexène (**1***d*). L'interprétation des résultats observés dans ce cas est donc, pour l'essentiel, celle déjà indiquée pour le composé **2***d*.

L'époxyde *cis* (**2***f*) du méthoxy-3 cyclohexène (**1***f*) conduit à 57% d'alcool **9***f* provenant d'une ouverture anormale du conformère *B*. Pour interpréter cette régiosélectivité, on peut, à côté des facteurs stériques déjà énoncés pour rendre compte des résultats précédents, suggérer que la conformation *C* (schéma 3) est favorisée par l'association avec une molécule d'hydrure (conformation *C* du schéma 5). Une explication de cet ordre (conformation *A* du schéma 5) pourrait être avancée pour rationaliser les résultats obtenus par Berti *et al.* (7) lors de la réduction de l'époxyde *cis* (**2***g*).

La réduction de l'époxyde silylé *trans* (**3***b*) conduit exclusivement au produit **7***b* issu de l'ouver-

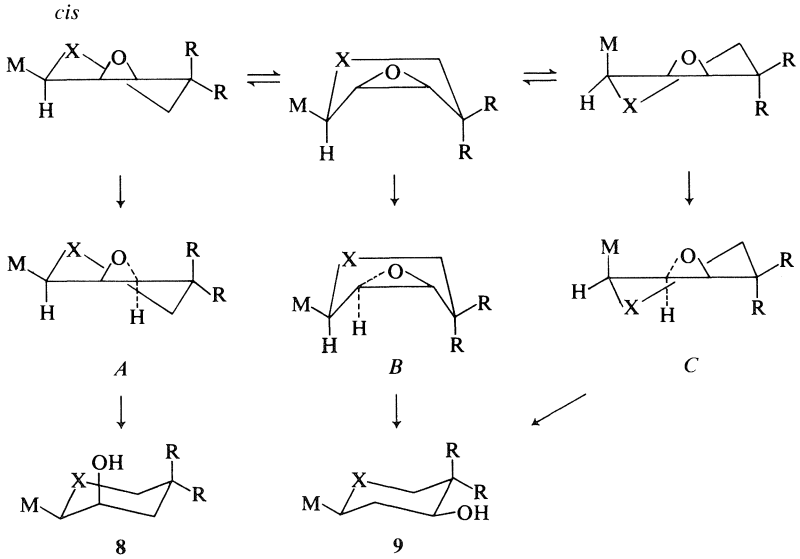


SCHÉMA 3

Can. J. Chem. Downloaded from www.nrcresearchpress.com by 210.87.254.42 on 09/05/12
For personal use only.

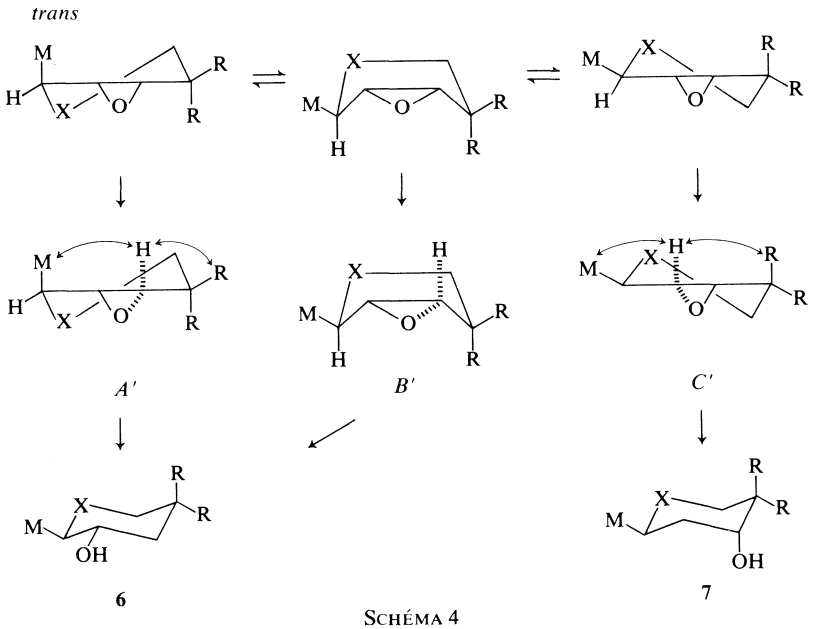


SCHÉMA 4

ture normale du conformère *C'* (schéma 4). L'alcool **9***b* provient vraisemblablement de la réduction de la cétone **10***b* qui pourrait se former par réarrangement (13, 14) de l'époxyde. Pour des raisons d'ordre stérique, la présence du conformère *A'* semble improbable. Le niveau énergétique de l'état de transition *C'* (schéma 4) est élevé car il implique de fortes interactions entre le réactif et l'un des méthyles du groupe triméthylsilyle d'une part et le méthyl pseudo-axial, d'autre part. Le fait qu'une ouverture normale se produise par l'intermédiaire de cet état de transition malgré ces interactions donne une idée de l'ordre de grandeur des énergies nécessaires pour parvenir à la forme bateau-croisé *B'* et forcer l'entrée du réactif en α du groupe méthyl (R) équatorial.

L'époxyde *trans* (**3***a*) du *tert*-butyl-6 diméthyl-3,3 cyclohexène **1***a* a le même comportement que son analogue silylé (**3***b*) et implique les mêmes interactions.

Par contre, l'époxyde *trans* (**3***d*) du *tert*-butyl-3 cyclohexène **1***d* conduit à 35% de l'alcool **6***d* résultant d'une ouverture anormale. Le conformère *A'* n'étant pas plus favorisé dans ce cas que dans les cas mentionnés précédemment, on doit faire l'hypothèse que le produit anormal provient d'une attaque du conformère *B'*. Cette attaque serait favorisée par l'absence de l'interaction entre le réactif et le méthyle (R) en position pseudo-équatoriale.

Pour l'époxyde *trans* (**3***e*) du méthyl-3 cyclohexène, on observe pratiquement les mêmes résultats que pour l'époxyde **3***d*. On ne peut, dans ce cas, exclure une participation du conformère *A'*.

En ce qui concerne l'époxyde *trans* (**3***g*), on invoque à nouveau le fait que le conformère *A'* permet une chélation dans l'état de transition (schéma 5) pour expliquer la formation presque univoque d'alcool **6***g* résultant d'une ouverture anormale.

Dans le cas de l'époxyde *trans* (**3***f*) du méthoxy-3 cyclohexène (**1***f*) pour lequel il n'existe aucun conformère permettant ce type d'association, la réduction conduit à 47% d'alcool (**7***f*) provenant d'une ouverture normale (état de transition *C'* du schéma 5) et 53% de (**6***f*) correspondant à une ouverture anormale (états de transition *A'* ou *B'*). L'effet inductif du groupe OCH_3 favorise la conformation *A'*. Les énergies du même ordre de grandeur impliquées dans les états de transition A' et C'

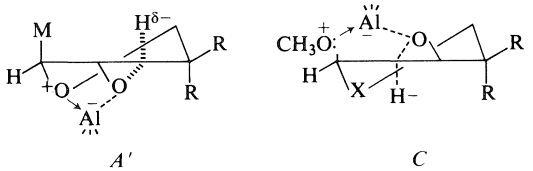


SCHÉMA 5

TABLEAU 3. Temps de rétention (en min) des alcools

Alcool	Série *a**	Série *b*†	Série *c*†
8	5.5	4.3	6.4
6	7.3	5.1	7.2
7	8.3	6.3	9.2
9	10.1	7.4	10.8

*Température de la colonne 115°C; débit d'hélium 37 mL/min.
†Température de la colonne 120°C; débit d'hélium 26 mL/min.

Can. J. Chem. Downloaded from www.nrcresearchpress.com by 210.87.254.42 on 09/05/12
For personal use only.

Can. J. Chem. Downloaded from www.nrcresearchpress.com by 210.87.254.42 on 09/05/12
For personal use only.

TABLEAU 4. Propriétés des alcools obtenus

	Point de fusion (°C) ou point d'ébullition (°C/Torr)	Infrarouge (cm^{-1})	Résonance magnétique nucléaire (CCl_4, δ ppm (multiplicité))		
			C*H*OH	$(CH_3)_2C<$	$(CH_3)_3M$
6*a*	50–52	3360, 1110, 1040	3.67(6)	0.90	1.00
6*b*	45–46	3300, 1240, 1050	3.63(6)	0.99 et 0.93	0.13
6*c*	47–48	3280, 1380, 1360, 1030	3.56(6)	0.93 et 0.89	0.16
7*a*	48–50 (Lit. (18) 47–49.5)				
7*b*	27–29	3400, 1380, 1360, 1240, 950	3.40(3)	0.96 et 0.93	0.06
7*c*	30–31	3440, 1030, 815	3.33(3)	0.89	0.09
8*a*	29–30	3520, 955	4.20(4)	1.10 et 0.85	0.95
8*b*	35/0.3	3670, 3520, 1245, 1010	4.16(4)	1.10 et 0.90	0.03
8*c*†	85/4	3420, 1385, 1365, 830	4.09(4)	1.03 et 0.86	0.13
9*a*	85–86 (Lit. (18) 85.5–86)				
9*b*	64–65	3320, 1240, 1030	3.23(4)	0.93 et 0.79	−0.04
9*c*	66–68	3400, 1035, 815	3.24(4)	0.99 et 0.86	0.14

*n_D^{23} = 1.4625.
†n_D^{23} = 1.4780.

doivent donc permettre la rationalisation de l'ensemble des résultats.

En conclusion, on peut indiquer que la stéréochimie des réactions d'époxydation examinées est essentiellement sous le contrôle de facteurs stériques. D'autre part, la réduction des époxydes par $LiAlH_4$ conduit généralement à des ouvertures *trans* et diaxiales. Dans certains cas, cependant, la coordination d'un hydrure entre deux atomes d'oxygène (bases) orientés favorablement permet de modifier ce comportement.

Partie expérimentale

Les points de fusion ont été mesurés sur un appareil Cole-Parmer de la compagnie Instrument & Equipment.

Les spectres ir ont été enregistrés à l'aide d'un spectrophotomètre Beckman modèle IR-8 à double faisceau et sauf indication contraire, tous les spectres ont été pris entre deux plaques de NaCl.

Les spectres de résonance magnétique nucléaire ont été déterminés sur un spectromètre modèle C-60-H de la compagnie JEOL. Le solvant choisi est le chloroforme deutéré pour les composés carbonés et le tétrachlorure de carbone pour les produits silylés et germylés.

Les indices de réfraction ont été déterminés à l'aide d'un réfractomètre du type Abbé. La pureté de tous les nouveaux produits décrits dans ce travail a été déterminée par chromatographie en phase gazeuse et leur identité confirmée par spectrométrie de masse à l'aide d'un spectromètre Hitachi Perkin-Elmer modèle RMU 6-D opérant avec une énergie de faisceau d'électrons ionisant de 70 eV et d'un spectromètre AEI MS-902 relié à un ordinateur PDP-8; toutes les masses moléculaires expérimentales déterminées correspondent à ± 0.0015 unités de masses aux valeurs calculées.

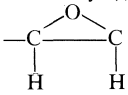
Synthèse de alcènes

La synthèse des alcènes **1***a*, **1***b*, **1***c* est décrite dans un travail antérieur (1).

Epoxydation des alcènes

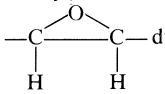
Epoxydation du tert*-butyl-6 diméthyl-3,3 cyclohexène* **1***a*

On obtient les époxydes **2***a* et **3***a* (rendement de 90%) en utilisant le même mode opératoire que pour l'alcène vinylique **4***a* (2).

Les deux époxydes ont été séparés (d'un mélange contenant 6 et 94% respectivement de **2***a* et **3***a*) en faisant appel à la chromatographie en phase gazeuse préparative à 140°C pour un débit de 55 mL/min et utilisant une colonne de 8 pi sur ¼ de po de diamètre remplie de tris-cyanoéthoxypropane à 20% sur Chromosorb R (80–100). A la suite de 25 injections de 50 μL, on isole 500 mg d'époxyde *trans* (**3***a*) ayant les caractéristiques suivantes: pé 52°C/0.2 Torr; n_D^{26} 1.6934; ir: 1255, 915, 695, 645 cm^{-1}; rmn ($CDCl_3$): 0.98 (s, 9H, groupe *tert*-butyle), 1.02 (s, 6H, méthyle), 2.90 (d, 1H) et 2.52 (d, 1H,  du pont époxyde) ppm.

Préparation de l'époxyde cis *2*a

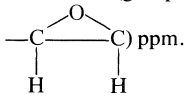
Dans un ballon de 50 mL, muni d'un refrigérant, on introduit 1.66 g d'alcène **1***a* (0.01 mol) dans 40 mL de diméthylsulfoxyde contenant 10 gouttes d'eau (15, 16). Le ballon étant maintenu sous atmosphère d'azote, on ajoute en une seule fois 3.1 g de *N*-bromosuccinimide. On laisse à 50°C pendant deux heures. Le mélange réactionnel est extrait de la manière habituelle et les bromhydrines résultantes sont traitées par 60 mL de *tert*-butylate de potassium dans le DMSO et laissés sous atmosphère d'azote à 50°C pendant une heure (17). Le mélange réactionnel conduit, après extraction à 0.75 g d'un mélange des époxydes **2***a* et **3***a* (40% du rendement théorique).

La séparation du mélange d'époxydes (contenant respectivement 42% et 58% de **2***a* et **3***a*) est effectuée comme précédemment par chromatographie en phase gazeuse préparative. Les caractéristiques de l'époxyde *cis* **2***a* sont les suivantes: pé 56°C/0.3 Torr; n_D^{25} 1.6943; ir: 795, 830, 860, 900 cm^{-1}; rmn ($CDCl_3$): 0.97 (s, 9H, *tert*-butyle), 1.00 (doublet mal résolu, 6H, méthyl), 3.25 (d, 1H) et 2.65 (d, 1H pour les protons  du pont époxyde) ppm.

Epoxydation du diméthyl-3,3 triméthylsilyl-6 cyclohexène **1***b*

Dans un ballon refroidi à −5°C contenant 15 mL de chloroforme et 40 mL de chlorure de méthylène, on ajoute 2.0 g d'alcène **1***b* (11 mmol) suivi de 4.0 g de carbonate de potassium anhydre et 4.0 g d'acide *m*-chloroperbenzoïque (8). On maintient cette température pendant 35 min, puis on filtre. Le filtrat

est lavé avec une solution de soude à 5%, extrait à l'éther selon la méthode habituelle. On obtient ainsi 1.9 g d'un mélange des composés **2***b* et **3***b* (90% du rendement théorique) dans lequel le rapport de **2***b*/**3***b* déterminé par rmn est de 24/76; ir (mélange): 1380, 1360, 1245, 870, 740 cm^{-1}; rmn (CCl_4): 0.06 (s, Me_3Si), 1.06 et 0.93 (groupe *gem*-diméthyle), 2.96 (d, 1H) et 2.56 (d, 1H,



ppm.

Epoxydation du diméthyl-3,3 triméthylgermyl-6 cyclohexène **1***c*

Le traitement de l'alcène **1***c* par la méthode décrite pour le composé **1***b* ne conduit pas aux époxydes **2***c* et **3***c*, mais au composé **5** (rendement 79%); pé 78–79°C/9 Torr; ir: 3380, 3040 cm^{-1}; rmn (CCl_4): 0.93 et 1.00 (groupe *gem*-diméthyle), 4.00 (proton carbinolique) et 5.50 (m, 2H, proton oléfinique) ppm.

Réduction des époxydes et analyse des alcools obtenus

Réduction

La réduction de 5.5 mmol des époxydes des types **2** et **3** par 0.5 g d'hydrure double de lithium et d'aluminium en suspension dans 10 mL d'éther anhydre est effectuée à 0°C. Après avoir chauffé le mélange réactionnel au reflux pendant 20 h, on l'hydrolyse à 0°C par une solution de soude à 50%. On extrait à l'éther et on obtient les alcools correspondants (rendements moyens 85%).

Analyse des produits

Les mélanges d'alcools provenant des réactions de réduction des époxydes **2** et **3** ont été analysés par chromatographie en phase gazeuse à l'aide d'un chromatographe à ionisation de flamme Research Chromatograph 700 de la compagnie F et M muni d'une colonne de 6 pi × $\frac{1}{8}$ de po remplie de Diatoport 5750 (80–100) supportant 6% de son poids de LAC 728. Les temps de rétention (en min) des alcools dans ces conditions sont résumés au Tableau 3. L'identification des pics a été réalisée par superposition avec des échantillons authentiques dont le propriétés sont décrites dans le Tableau 4.

Remerciements

Les auteurs remercient vivement le Conseil National de Recherches du Canada, le CNRS, et les autorités chargées d'administrer les accords Franco–Québécois pour l'aide financière apportée sous forme d'octroi de recherches, de bourse d'études et de frais de mission. Les auteurs tiennent à remercier le Dr Pierre Maroni pour l'accueil chaleureux réservé à M. Marc-André Poirier durant son stage à Toulouse. Les auteurs tiennent aussi à exprimer leur reconnaissance aux Dr Mazerolles et Lesbre pour leur compréhension et leurs discussions utiles.

1. C. Freppel, M. A. Poirier, J. C. Richer, Y. Maroni et G. Manuel. Can. J. Chem. **52**, 4133 (1974).
2. J. C. Richer, M. A. Poirier, Y. Maroni et G. Manuel. Can. J. Chem. **56**, 2049 (1978).
3. J. C. Richer et C. Freppel. Can. J. Chem. **46**, 3709 (1968).
4. B. Rickborn et W. E. Lamke. J. Org. Chem. **32**, 537 (1967).
5. R. A. B. Bannard, A. A. Casselman, E. J. Langstaff et R. Y. Moir. Can. J. Chem. **46**, 35 (1968).
6. B. C. Hartman et B. Rickborn. J. Org. Chem. **37**, 4246 (1972).
7. G. Berti, G. Catelani, M. Ferretti et L. Monti. Tetrahedron, **30**, 4013 (1974).
8. G. Manuel, P. Mazerolles et J. C. Florence. C.R. Acad. Sci. Ser. C, 1553 (1969).
9. R. J. Ouellette, D. Baron, J. Stolfo, A. Rosenblum et P. Weber. Tetrahedron, **28**, 2163 (1972).
10. P. F. Hudrlik et G. P. Withers. Tetrahedron Lett. 29 (1976).
11. M. J. Carter et I. Fleming. Chem. Commun. 679 (1976).
12. A. Furst et P. A. Plattner. Helv. Chim. Acta, **32**, 275 (1949).
13. J. J. Eisch et J. T. Trainor. J. Org. Chem. **28**, 2870 (1963).
14. B. Rickborn et J. Quartucci. J. Org. Chem. **29**, 3185 (1964).
15. D. R. Dalton, V. P. Dutta et D. C. Jones. J. Am. Chem. Soc. **90**, 5500 (1968).
16. D. R. Dalton et R. M. Davis. Tetrahedron Lett. 1057 (1972).
17. D. R. Dalton et V. P. Dutta. J. Chem. Soc. B, 89 (1971).
18. J. Sicher et M. Tichy. Collect. Czech. Chem. Commun. **32**, 3687 (1967).

Can. J. Chem. Downloaded from www.nrcresearchpress.com by 210.87.254.42 on 09/05/12
For personal use only.

A proton magnetic resonance relaxation time study of several vitamin D derivatives

GEORGE KOTOWYCZ, TOM T. NAKASHIMA, M. KIRK GREEN,[1] AND GERDY H. M. AARTS
Department of Chemistry, University of Alberta, Edmonton, Alta., Canada T6G 2G2

Received July 23, 1979

GEORGE KOTOWYCZ, TOM T. NAKASHIMA, M. KIRK GREEN, and GERDY H. M. AARTS. Can. J. Chem. **58**, 45 (1980).

Proton magnetic resonance relaxation time studies at 200 and 400 MHz have been measured for vitamins D_2, D_3, as well as the biologically active 1α,25-$(OH)_2D_3$. A comparison of these relaxation times at the two frequencies allows the evaluation of the dipolar correlation times for the different protons in the molecule. These are very short, and range from $< 0.7 \times 10^{-10}$ s to 1.2×10^{-10} s. Application of the Solomon equation to the relaxation times of the 19*Z* and 19*E* protons allows a calculation of the internuclear distance since these two geminal protons relax each other predominantly by the dipolar mechanism. Using the T_1 values, the calculated distances are 1.98 ± 0.10 Å for 1α,25-$(OH)_2D_3$, 2.01 ± 0.10 Å for D_3, and 1.95 ± 0.10 Å for D_2. The calculated distance based on a neutron diffraction distance for the C—H bond is 1.91 Å. The measurement of the relaxation times also allows a definitive spectral assignment of the 21- and 28-methyl protons for vitamin D_2.

GEORGE KOTOWYCZ, TOM T. NAKASHIMA, M. KIRK GREEN et GERDY H. M. AARTS. Can. J. Chem. **58**, 45 (1980).

On a étudié et mesuré le temps de relaxation pour la résonance magnétique du proton à 200 et 400 MHz des vitamines D_2, D_3 et également du composé biologiquement actif 1α,25-$(OH)_2D_3$. La comparaison de ces temps de relaxation à ces deux fréquences permet une évaluation des temps de corrélation dipolaire des différents protons de la molécule. Les temps sont très courts et s'échelonnent entre $< 0.7 \times 10^{-10}$ s et 1.2×10^{-10} s. L'application des équations de Solomon aux temps de relaxation des protons 19*Z* et 19*E* permet le calcul des distances internucléaires puisque ces deux protons portés par le même carbone relâchent tous deux de façon prédominante selon un mécanisme dipolaire. En utilisant les valeurs de T_1 les distances calculées sont: 1.98 ± 0.10 Å pour 1α,25-$(OH)_2D_3$, 2.01 ± 0.10 Å pour D_3 et 1.95 ± 0.10 Å pour D_2. La distance de la liaison C—H est de 1.91 Å. Cette distance est calculée en se basant sur la distance de diffraction d'un neutron. La mesure des temps de relaxation permet également une identification définitive des protons des méthyles en positions 21 et 28 de la vitamine D_2.

[Traduit par le journal]

Introduction

One of the three most important biological regulators for calcium and phosphorus metabolism is vitamin D (1). Vitamin D and its derivatives have been studied extensively as witnessed by a recent workshop on the biochemical, chemical, and clinical aspects of vitamin D (2). A large number of review articles has now been published on this vitamin and on its metabolism (1–4), to list only a few. Vitamin D is a steroid, whose structure differs from that observed for other steroids. The main difference is the fact that its B ring is cleaved and the preferred conformation about the C6—C7 bond is *S-trans* instead of an *S-cis* (5). The hormonally active form of the vitamin is 1α,25-$(OH)_2D_3$ (1–4). The structural formulae for this molecule as well as for vitamins D_2 and D_3 are given in Fig. 1.

Some conformational studies have been carried out on vitamin D compounds and their derivatives, especially since the development and availability of high-field, nmr cryospectrometers. For example, proton magnetic resonance studies of vitamin D_3, 1α,25-$(OH)_2D_3$, and several structural analogs have established that the A ring exists in solution as an equilibrium mixture of roughly equal populations of two chair conformers (1, 6, 7). Shift reagents have also been used to study this equilibrium in vitamins D_2 (8) and D_3 (7). As Norman and coworkers (1) point out "Thus, while it is definitely a fact that all vitamin D-seco steroids undergo the

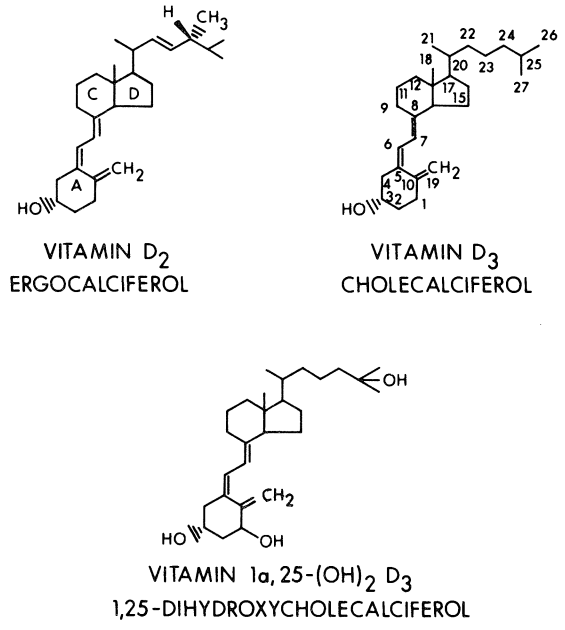


FIG. 1. Structures of vitamins D_2, D_3, and 1α,25-$(OH)_2D_3$.

[1]Present address: Alberta Research Council, Edmonton, Alberta.

0008-4042/80/010045-06$01.00/0
©1980 National Research Council of Canada/Conseil national de recherches du Canada

Can. J. Chem. Downloaded from www.nrcresearchpress.com by 210.87.254.42 on 09/05/12
For personal use only.

Can. J. Chem. Downloaded from www.nrcresearchpress.com by 210.87.254.42 on 09/05/12
For personal use only.

dynamic equilibration between the two conformers, it remains to the future to delineate the implications of this phenomenon of vitamin D-related molecules to their detailed biochemical mode of action. The concept of conformational optimization of biological activity of vitamin D-like compounds is clearly one that bears further examination in the future''.

Other conformational analyses using a variety of techniques have been carried out by Berman *et al.* (ref. 2, pp. 19–28) and Okamura *et al.* (ref. 2, pp. 33–45, 9, 10). Both ^{13}C and ^{1}H nmr techniques have been applied by Mazur and co-workers (5, 11) and ^{13}C nmr techniques have also been applied by Tsukida *et al.* (12). DeLuca and co-workers (ref. 2, p. 927) and Knobler *et al.* (14) have obtained the solid-state conformations of vitamin D and related molecules. Quantum mechanical calculations (15) have also been applied in deriving structure–activity relationships. Finally, Wing (ref. 2, pp. 71–83) has carried out both nmr and force field calculations on vitamin D compounds. His critical analysis of the conformational equilibria data as well as of the theoretical calculations indicates that all of the results are in very good agreement.

We chose to study the vitamin D system, especially the 1α,25-$(OH)_2D_3$ derivative, since this appears to be the hormonally active form of this vitamin. There are many diseases which are known to be related in some fashion to vitamin D. These include (1) chronic renal disease, vitamin D-dependent rickets, hypoparathyroidism, drug induced metabolism of vitamin D as in the case of chronic administration of anti-convulsant drugs, and a host of bone diseases. The above compound is especially important in the kidney, where the biologically active form of this vitamin is produced.

In the present study, we have measured proton magnetic resonance longitudinal relaxation times both at 200 MHz and at 400 MHz. From the frequency dependence of the proton relaxation times, using the Solomon equation (16), the correlation times are obtained for the protons of vitamin D_2, D_3, and 1α,25-$(OH)_2D_3$. Distances in solution between the two C-19 protons for these three vitamins are calculated and compared with the neutron diffraction distance.

Experimental

Solutions of vitamins D_2 (Sigma Chemical Co.) and D_3 (Aldrich Chemical Co.) were prepared by dissolving 20.0 mg and 20.5 mg of each compound, respectively, in 5.0 mL of $CDCl_3$ (Scientific Graphics) so that the vitamin concentration was 0.010 *M*. Before use, the $CDCl_3$ was treated with Al_2O_3 (BDH Chemicals Ltd.) to remove acidic impurities. The solutions for the nmr experiments were vacuum degassed using the freeze–pump–thaw technique and were sealed.

The 1α,25-$(OH)_2D_3$ derivative was a gift from Dr. M. Uskokovic. About 0.9 mg (close to saturation) of this derivative were dissolved in 0.35 mL of degassed $CDCl_3$ and then the sample was vacuum degassed and sealed. Whenever possible, the solutions were prepared in the dark and kept in the freezer right up to the time that the experiments were run. To eliminate paramagnetic materials, all glassware was extensively cleaned following procedures previously reported (17).

The proton magnetic resonance experiments were obtained at 28°C on a Bruker WH-200/DS (200 MHz) and a Bruker WH-400/DS (400 MHz) nmr spectrometer operating in the pulsed Fourier transform mode using the Bruker Aspect 2000 computer, and 16 K data points. The deuterium resonance of the $CDCl_3$ was used as the lock signal. The longitudinal relaxation times (T_1) were obtained using the 180°–τ–90° two-pulse sequence and 9 to 10 τ values were included in the analysis of the T_1 data, based on the initial slope of a plot of $\ln((M_\infty - M_\tau)/(M_\infty))$ vs. τ. In this plot, M_∞ is the equilibrium value of the magnetization, and M_τ is the value of the magnetization at time τ between the 180° and 90° pulse. These *M* values were obtained from the measurement of the peak heights. The T_1 data were obtained from a computer analysis of the intensities as a function of the τ value using a least-squares program. The standard deviations at 400 MHz and 200 MHz were about 2% and 4%, respectively. For two different samples of vitamins D_2 and D_3, T_1 values varied by 5%.

Results

A 400 MHz spectrum of vitamins D_2 and D_3 is shown in Fig. 2 and a spectrum for 1α,25-$(OH)_2D_3$ is given in Fig. 3. Typical 180°–τ–90° inversion recovery spectra are shown in Fig. 4 for 1α,25-$(OH)_2D_3$ and the T_1 data for the isolated proton resonances are given in Table 1, both at 200 and 400 MHz. The proton resonances were assigned according to the work of Wing *et al.* (7). However, for D_2, they assign the C-28 methyl resonance to low field of the C-21 methyl resonance. We have changed this assignment, since the C-21 methyl protons are expected to have the same relaxation times in all three molecules. This can only be true if the C-21 methyl resonances are assigned to low field of the C-28 methyl resonances. In addition, the assignment of the 19*Z* and 19*E* proton resonances is interchanged for vitamins D_2 and D_3, based on proton magnetic resonance nOe difference studies (G. Kotowycz, G. H. M. Aarts, and K. Bock, in preparation). This in no way affects the present results since a distance is calculated only between these two protons.

A comparison of the spectra in Figs. 2 and 3 indicates that the C-19 protons shift to low field in 1α,25-$(OH)_2D_3$ with respect to these protons in D_3. In addition, proton 6 experiences a shift to low field with respect to proton 7. Similar results have been previously observed (7). Chemical shift and coupling constant analyses have been published for vitamins D_3 (7) and D_2 (8).

Can. J. Chem. Downloaded from www.nrcresearchpress.com by 210.87.254.42 on 09/05/12
For personal use only.

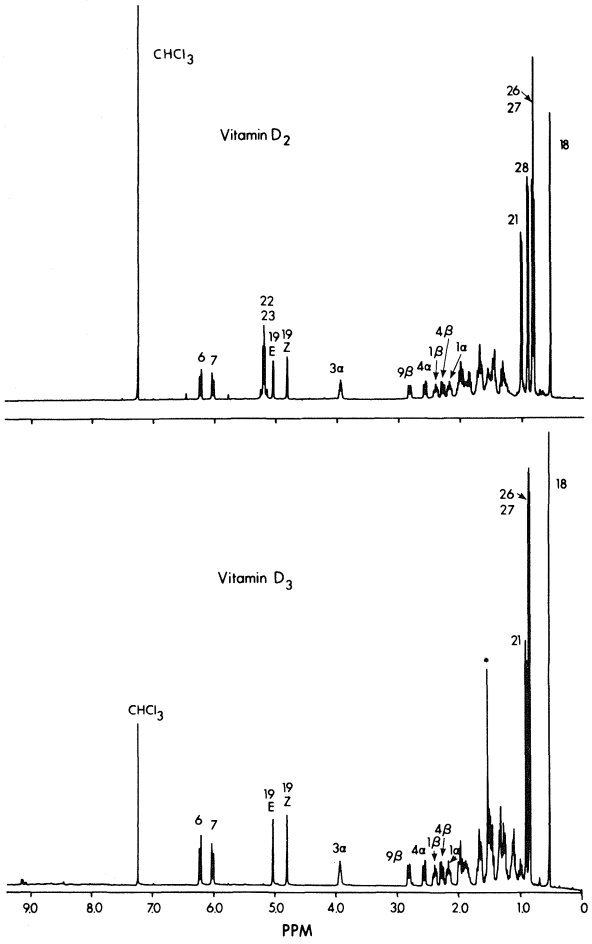


FIG. 2. The 400 MHz proton magnetic resonance spectra of vitamins D_2 and D_3 in $CDCl_3$. The * indicates a water impurity peak.

Discussion

The Solomon equation for the longitudinal relaxation times due to the dipolar interaction is given by (16)

$$[1] \quad \frac{1}{T_{1D}} = \frac{C^6}{r^6}\left(\frac{\tau_R}{1 + \omega_I^2\tau_R^2} + \frac{4\tau_R}{1 + 4\omega_I^2\tau_R^2}\right)$$

In this equation, C is a product of physical constants equal to 74.48 Å $s^{-\frac{1}{6}}$ for two interacting protons (18), r is the interproton distance in Å, ω_I is the proton resonance frequency in rad/s, and τ_R is the rotational correlation time ($C^6 = (3/10)(\hbar^2\gamma_H^4/10^{-48})$ where $\hbar$ is Planck's constant divided by 2π, γ_H is the magnetogyric ratio for a proton, and 10^{-48} converts units of cm to Å). Taking the ratio of this equation at two frequencies, namely 200 and 400 MHz, and rearranging, one obtains eq. [2]:

$$[2] \quad \frac{T_{1D}(400)}{T_{1D}(200)} = \frac{\left(\frac{5 + 8\omega_I^2\tau_R^2}{1 + 5\omega_I^2\tau_R^2 + 4\omega_I^4\tau_R^4}\right)_{200\ MHz}}{\left(\frac{5 + 8\omega_I^2\tau_R^2}{1 + 5\omega_I^2\tau_R^2 + 4\omega_I^4\tau_R^4}\right)_{400\ MHz}}$$

Hence, from a knowledge of the T_1 value at 400 MHz, $T_{1D}(400)$ for a given proton and the corresponding value at 200 MHz, $T_{1D}(200)$, τ_R for any proton can be evaluated. A plot of τ_R vs. the $T_{1D}(400)/T_{1D}(200)$ quotient is shown in Fig. 5. This approach has been previously applied by Fung *et al.* (18) to obtain the correlation times for the propionyl-CoA protons. They worked both at 220 MHz and 100 MHz. However, the form of eq. [2] is slightly different from that quoted in ref. 18.

Using the graph shown in Fig. 5, the correlation times for the protons are given in Table 1 for the three molecules. The correlation times range from $< 0.7 \times 10^{-10}$ s to 1.2×10^{-10} s.

Distance calculations between the 19*Z* and 19*E* protons can now be carried out, as these geminal protons are relaxed foremost by each other by the dipolar mechanism while contributions to their relaxation from neighboring protons are expected to be small. Using the average values of the T_1 results at 400 MHz for both protons for each molecule, and the average correlation times (0.99×10^{-10} s for 1α,25-$(OH)_2D_3$, 0.88×10^{-10} s for D_3, and 0.70×10^{-10} s for D_2), 19*Z* to 19*E* interproton distances were calculated using eq. [1]. These are 1.98 ± 0.10 Å for 1α,25-$(OH)_2D_3$, 2.01 ± 0.10 Å for D_3, and 1.95 ± 0.10 Å for D_2. Using a neutron diffraction value for the C—H bond distance of 1.10 Å (13), and a bond angle of 120°, the calculated distance between these two protons is 1.91 Å. The calculated and measured interproton distances are in excellent agreement, considering the fact that other protons can contribute slightly to the relaxation. The error limits on the measured interproton distances are 5%. Sykes and co-workers (19) have carried out a detailed study of the calculation of absolute interproton distances of *cis*- and *trans*-crotonaldehyde in solution and also present a detailed bibliography of earlier studies.

The data in Table 1 show two additional interesting features. The T_1 value for protons 26 and 27 for 1α,25-$(OH)_2D_3$ at 400 MHz is 0.85 s, whereas for D_3 it is 1.57 s. The former molecule contains an OH group attached to the C-25 carbon. The shorter T_1 values for the 1α,25-$(OH)_2D_3$ molecule are probably due to changes in internal motion due to some steric hindrance arising from the OH group. This effect will decrease the T_1 value for the 26- and

Can. J. Chem. Downloaded from www.nrcresearchpress.com by 210.87.254.42 on 09/05/12
For personal use only.

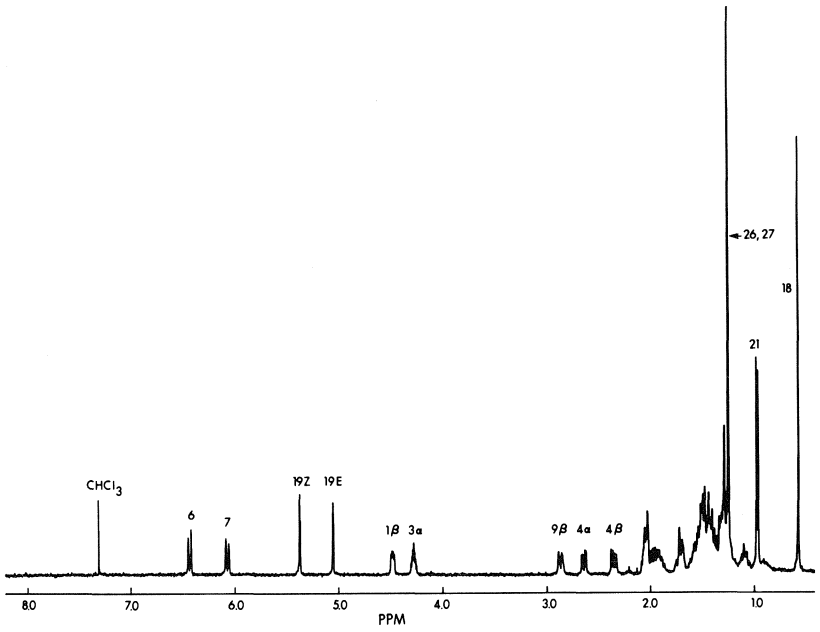


FIG. 3. The 400 MHz proton magnetic resonance spectrum of 1α,25-$(OH)_2D_3$ in $CDCl_3$.

TABLE 1. Summary of the T_1 data obtained at 200 and 400 MHz, together with the correlation times (s)

	D_2			D_3			1α,25-$(OH)_2D_3$		
Proton	200	400	$\tau_R \times 10^{10}$	200	400	$\tau_R \times 10^{10}$	200	400	$\tau_R \times 10^{10}$
6	0.81	0.90	0.85	0.74	0.89	1.18	0.64	0.77	1.18
7	0.89	0.99	0.85	0.88	1.02	1.05	0.74	0.87	1.10
19*E*	0.91	0.97	0.68	0.90	1.01	0.90	0.75	0.86	1.01
19*Z*	0.96	1.04	0.72	0.93	1.03	0.85	0.74	0.84	0.97
3α	1.30	1.53	1.10	1.22	1.38	0.94	1.07	1.19	0.85
9β	0.39	0.40	[a]	0.38	0.40	[a]	0.28	0.33	[a]
4α	0.58	0.64	0.80	0.61	0.62	<0.7	0.48	0.52	[a]
1β	[b]	0.65	—	[b]	0.68	—	1.15	1.29	0.91
4β	[b]	0.68	—	[b]	0.66	—	0.47	0.55	[a]
1α	[b]	0.70	—	[b]	0.61	—	—	—	—
28	1.16	1.13	<0.7	—	—	—	—	—	—
21	0.57	0.61	<0.7	0.62	0.65	<0.7	0.53	0.55	<0.7
26,27	1.09	1.10	<0.7	1.50	1.57	<0.7	0.85	0.85	<0.7
18	0.76	0.81	<0.7	0.76	0.85	0.90	0.68	0.71	<0.7

[a]Since very small changes in these short T_1 values cause extensive changes in the $T_1(400)/T_1(200)$ quotient, τ_R values were not evaluated.
[b]Reliable T_1 values were not obtained due to multiplet overlap.

27-methyl protons in comparison with those for D_3. Secondly, the shorter T_1 value for proton 1β in D_3 with respect to the 1β proton in 1α,25-$(OH)_2D_3$ is due to the substitution of a geminal proton by the OH group in the latter compound. The difference in T_1 for these two values could not give us an accurate distance between the 1α and the 1β protons for D_3.

In the present study, the initial rates have been calculated. The experiments were carried out at the lowest possible concentration (0.01 *M* and less) so that only *intra*molecular dipolar interactions are important. Relaxation mechanisms due to paramagnetic impurities have been minimized by careful cleaning of all glassware, and the degassing of all samples. A deuterated solvent was used to eliminate solute–solvent dipolar interactions. Consequently, the initial rates are very nearly equal to $1/T_{1D}$ providing that other relaxation mechanisms, such as spin–rotation, do not contribute to the T_1. The effects of cross-relaxation are minimized by the initial slope approximation (20). The discussion of cross-relaxation effects has now been well documented (21, 22). Campbell and Freeman (23) investigated the effects of cross-relaxation in weakly and strongly coupled two-spin systems. For

Can. J. Chem. Downloaded from www.nrcresearchpress.com by 210.87.254.42 on 09/05/12
For personal use only.

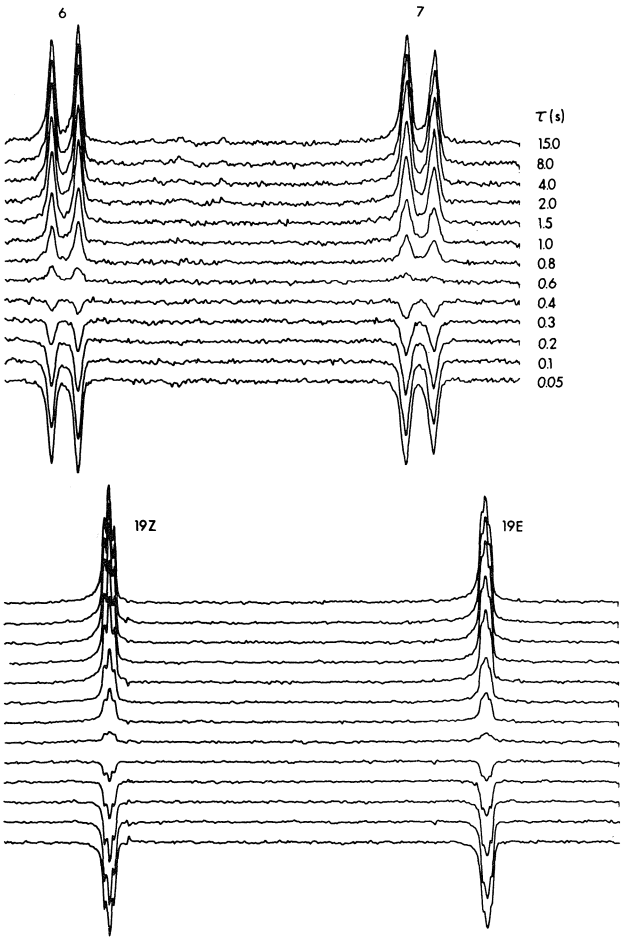


FIG. 4. The 180°–τ–90° inversion recovery spectra obtained at 400 MHz for protons 6, 7, 19*Z*, and 19*E* of 1α,25-$(OH)_2D_3$. The τ values are indicated in the figure. The delay time between the pulse sequences was 15 s; 16 000 data points were used together with 40 scans.

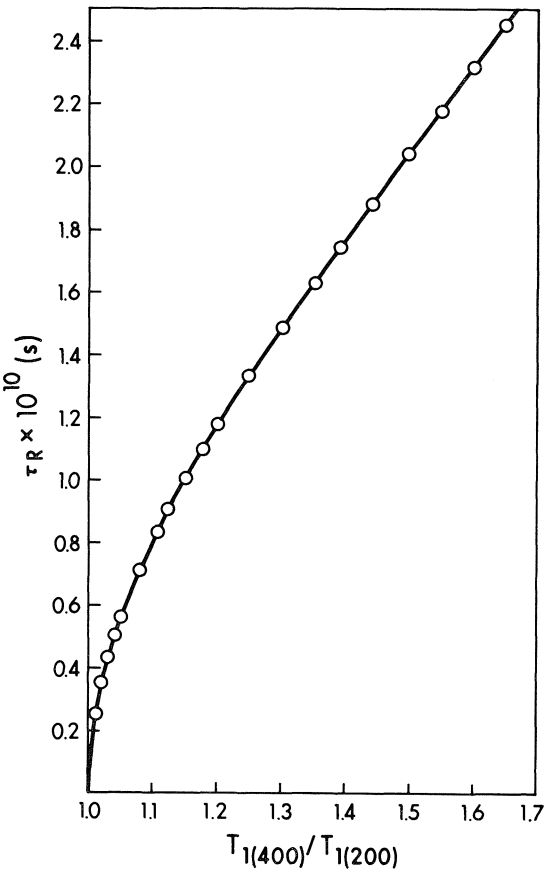


FIG. 5. A plot of τ_R vs. the $T_{1D}(400\ MHz)/T_{1D}$ (200 MHz) quotient. The curve was computed according to eq. [2].

the weakly coupled case, the maximum error in the derived spin–lattice relaxation time is of the order of 10%, and the authors conclude that it may be safely neglected for many applications (23). For the strongly coupled case, deviations from exponential spin–lattice relaxation due to cross-relaxation requires (*a*) strong dipolar relaxation, (*b*) strong spin–spin coupling, and (*c*) asymmetrical external relaxation. As the authors acknowledge (23), these three criteria are not easily satisfied simultaneously. In the systems involved in the present study, because of the high magnetic field strengths employed, many of the protons are weakly coupled. In addition, the small range of T_1 values indicates that condition (*c*) is not fulfilled for any strongly-coupled protons.

In summary, solution geometry based on high resolution proton T_1 values is now being obtained for a range of organic molecules (19, 24, 25), and various selective and non-selective relaxation measurements provide valuable information of the solution conformation. The study of the role of vitamins in nutrition and in health is now increasing, as evidenced by a recent review article (26). The presence of the two extra hydroxyl groups in the active form of vitamin D is extremely important. The cellular mechanism by which 1α,25-$(OH)_2D_3$ increases intestinal calcium absorption in several hours in the rat, while vitamin D_3 takes 12–24 h, is not well understood (27). The results of the present study can be used as a basis for further studies involving the binding of Ca(II) ions, interactions with calcium binding proteins, and 1α,25-$(OH)_2D_3$.

Acknowledgements

The authors are grateful to Dr. Milan R. Uskokovic (Hoffman-LaRoche, Inc.) for a sample of 1,25-dihydroxycholecalciferol, Dr. Klaus Bock for valuable discussions, and the Natural Sciences and

Engineering Research Council of Canada and the University of Alberta for generous financial assistance.

1. A. W. NORMAN, W. H. OKAMURA, E. J. FRIEDLANDER, H. L. HENRY, R. L. JOHNSON, M. N. MITRA, D. A. PROSCAL, and W. WECKSLER. Calcif. Tissue Res. **21**, 153 (1976).
2. A. W. NORMAN, K. SCHAEFER, J. W. COBURN, H. F. DELUCA, D. FRASER, H. G. GRIGOLEIT, and D. V. HERRATH (*Editors*). Vitamin D: biochemical, chemical and clinical aspects related to calcium metabolism. Proceedings of the Third Workshop on Vitamin D, Asilomar, Pacific Grove, CA. Walter de Gruyter, New York. 1977.
3. H. F. DELUCA. Vitamin D. *In* The fat-soluble vitamins. Handbook of Lipid Research. Vol. 2. *Edited by* H. F. DeLuca. Plenum Press, NY. 1978. pp. 69–132.
4. H. F. DELUCA and H. K. SCHNOES. Annu. Rev. Biochem. **45**, 631 (1976).
5. E. BERMAN, N. FRIEDMAN, Y. MAZUR, and M. SHEVES. J. Am. Chem. Soc. **100**, 5626 (1978).
6. R. M. WING, W. H. OKAMURA, M. R. PIRIO, S. M. SINE, and A. W. NORMAN. Science, **186**, 939 (1974).
7. R. M. WING, W. H. OKAMURA, A. REGO, M. R. PIRIO, and A. W. NORMAN. J. Am. Chem. Soc. **97**, 4980 (1975).
8. G. N. LAMAR and D. L. BUDD. J. Am. Chem. Soc. **96**, 7317 (1974).
9. W. H. OKAMURA, M. L. HAMMOND, A. REGO, A. W. NORMAN, and R. M. WING. J. Org. Chem. **42**, 2284 (1977).
10. W. H. OKAMURA and M. R. PIRIO. Tetrahedron Lett. **49**, 4317 (1975).
11. E. BERMAN, Z. LUZ, Y. MAZUR, and M. SHEVES. J. Org. Chem. **42**, 3325 (1977).
12. K. TSUKIDA, K. AKUTSU, and K. SAIKI. J. Nutr. Sci. Vitaminol. **21**, 411 (1975).
13. W. C. HAMILTON and J. A. IBERS. Hydrogen bonding in solids. W. A. Benjamin, Inc., NY. 1968. p. 52.
14. C. KNOBLER, C. ROMERS, P. B. BRAUN, and J. HORNSTRA. Acta Crystallogr. Sect. B, **28**, 2097 (1972).
15. H.-J. HOFMANN, H.-J. KOHLER, and T. WELLER. Tetrahedron, **32**, 1303 (1976).
16. I. SOLOMON. Phys. Rev. **99**, 559 (1955).
17. Y. THERIAULT, Y. MORIO, and G. KOTOWYCZ. Can. J. Biochem. **57**, 165 (1979).
18. C. H. FUNG, R. J. FELDMANN, and A. S. MILDVAN. Biochemistry, **15**, 75 (1976).
19. R. ROWAN III, J. A. MCCAMMON, and B. D. SYKES. J. Am. Chem. Soc. **96**, 4773 (1974).
20. J. H. NOGGLE and R. E. SCHIRMER. The nuclear Overhauser effect. Academic Press, NY. 1971. pp. 45–51.
21. L. G. WERBELOW and D. M. GRANT. Intramolecular dipolar relaxation in multispin systems. *In* Advances in magnetic resonance. *Edited by* J. S. Waugh. Academic Press, NY. 1977. pp. 189–299.
22. R. L. VOLD and R. R. VOLD. Progress in NMR spectroscopy. Vol. 12. *Edited by* J. W. Emsley, J. Feeney, and L. H. Sutcliffe. Pergamon Press, Oxford. 1978. pp. 79–133.
23. I. D. CAMPBELL and R. FREEMAN. J. Magn. Reson. **11**, 143 (1973).
24. L. D. HALL and H. D. W. HILL. J. Am. Chem. Soc. **98**, 1269 (1976).
25. L. D. HALL. Proceedings 18th Experimental NMR Conference, Asilomar, CA. 1977.
26. H. J. SANDERS. Chem. Eng. News, **57**, 27 (1979).
27. H. J. ARMBRECHT, R. H. WASSERMAN, and M. E. H. BRUNS. Arch. Biochem. Biophys. **192**, 466 (1979).

Can. J. Chem. Downloaded from www.nrcresearchpress.com by 210.87.254.42 on 09/05/12
For personal use only.

Acid-catalyzed rearrangement of cyclobutanones. V. Preparation of polycyclic aromatic dihydrofurans and dihydropyrans

PAUL DUPERROUZEL AND EDWARD LEE-RUFF
Department of Chemistry, York University, Downsview, Ont., Canada M3J 1P3

Received July 19, 1979

PAUL DUPERROUZEL and EDWARD LEE-RUFF. Can. J. Chem. **58**, 51 (1980).

Cyclobutanones derived from α-phenyl, α,α-diphenyl, and bisphenyleneketene cycloaddition to dihydrofuran and dihydropyran were rearranged under acidic conditions to polycyclic aromatic dihydrofurans and dihydropyrans respectively. A mechanism for these rearrangements is proposed.

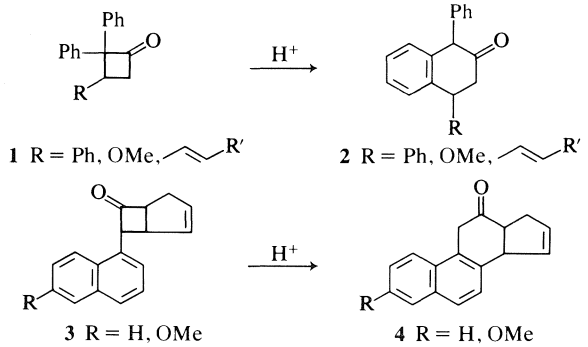
PAUL DUPERROUZEL et EDWARD LEE-RUFF. Can. J. Chem. **58**, 51 (1980).

Les cyclobutanones provenant de la cycloaddition de l'α-phényle, de l'α,α-diphényle et du bisphénylènecétène sur le dihydrofuranne et le dihydropyranne sont transposés en milieu acide respectivement en dihydrofurannes et dihydropyrannes polycycliques aromatiques. On propose un mécanisme pour ces transpositions.

[Traduit par le journal]

Can. J. Chem. Downloaded from www.nrcresearchpress.com by 210.87.254.105 on 09/05/12
For personal use only.

Protonated cyclobutanones undergo a wide variety of ring opening reactions (1–4). The ease of preparation of these derivatives by a number of classical (5) as well as contemporary (6) methods makes this class of compounds potentially useful synthetic intermediates. We have reported (3, 4) that 2-aryl-cyclobutanones possessing positive charge stabilizing groups at carbon-3, i.e., **1** undergo acid rearrangement to β-tetralones, i.e., **2**. By this method steroid derivatives such as **4** were



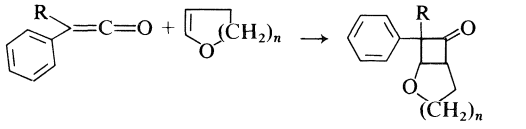
1 R = Ph, OMe, R′ **2** R = Ph, OMe, R′

3 R = H, OMe **4** R = H, OMe

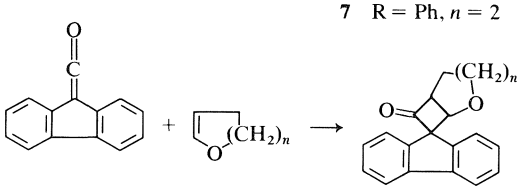
prepared from cyclobutanones **3**. With the increased reactivity of enol ethers towards ketene cycloadditions (7) and the ready availability of dihydrofuran and dihydropyran we were interested in widening the scope of such rearrangement towards the synthesis of polycyclic derivatives incorporating such ring systems.

Cyclobutanones **5–9** were prepared by cycloaddition of dihydrofuran or dihydropyran with the respective ketene. The yields of these derivatives depend on the mode of preparation in instances where the ketene is not stable, however under optimised conditions the yields of cyclobutanones **5–9** exceeded 80%. Due to the extreme reactive nature of phenylketene towards homopolymerization, the preparation of **5** was accomplished by the addition of 1 equiv. of triethylamine to an ethereal solution of phenylacetylchloride containing 3 equiv. of dihydrofuran. In the reverse mode of addition only trace amounts of **5** were obtained with the principal product being a crystalline 2:1 ketene–dihydrofuran adduct. Cyclobutanones **6** and **7** had been previously described (7). Ketones **5**, **8**, and **9** were assigned structures based on the spectral data and comparison of these with those of ketones **6** and **7**.

Cyclobutanones **5–9** were rearranged under acidic conditions using either 1 equiv. of P_2O_5 at ambient temperature in benzene or preferably catalytic amounts of *p*-toluenesulphonic acid at reflux temperature. The principal products of these reactions are the aromatic dihydrofurans **10–12**, **15**, **16** in yields ranging from 30 to 90% (see Table 1). The structural assignments of these compounds were based on their spectral data as well as in



5 R = H, *n* = 1
6 R = Ph, *n* = 1
7 R = Ph, *n* = 2



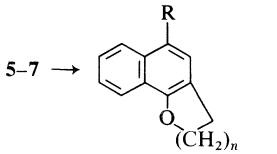
8 *n* = 1
9 *n* = 2

0008-4042/80/010051-04$01.00/0
©1980 National Research Council of Canada/Conseil national de recherches du Canada

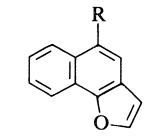
TABLE 1. Yields and mode of preparation of dihydrofurans

Dihydrofurans	Mode of preparation		Yields* (%)	Melting point (°C)
10	P_2O_5/C_6H_6	24 h	0	
	$TsOH/C_6H_6$	2 h	30	Oil
11	P_2O_5/C_6H_6	2 h	65	109–112 (dec.)
	$TsOH/C_6H_6$	24 h	90	109–112
12	P_2O_5/C_6H_6	2 h	94	102–105 (dec.)
15	P_2O_5/C_6H_6	24 h	40	124–126
	$TsOH/C_6H_6$	20 h	70	
16	P_2O_5/C_6H_6	24 h	35	Oil
	$TsOH/C_6H_6$	20 h	60	

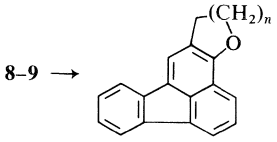
*Yields based on weight of isolated material.



10 R = H, n = 1
11 R = Ph, n = 1
12 R = Ph, n = 2



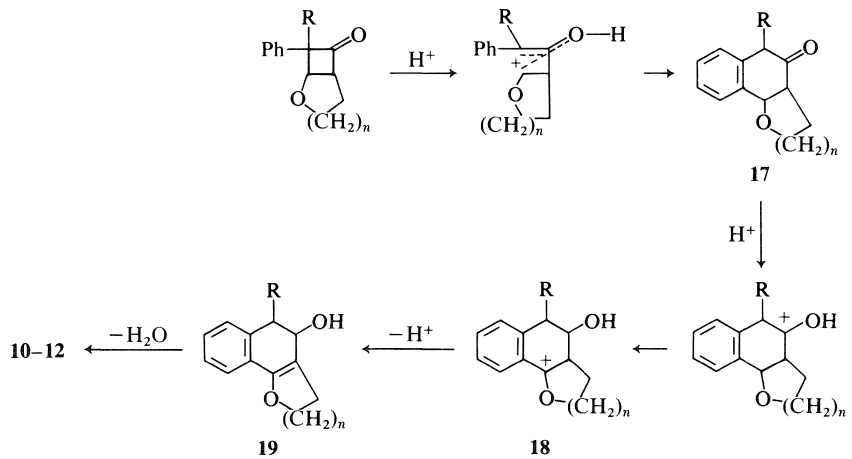
13 R = H
14 R = Ph



15 n = 1
16 n = 2

certain instances, i.e., **10** and **11**, conversion to the aromatic furans **13** and **14** with 2,3-dichloro-5,6-dicyano-1,4-benzoquinone (DDQ) (12). Naphthofuran **13** had an identical uv spectrum and mp of picrate to those reported for **13** obtained by an alternate synthesis (8). The fluoranthene chromophore in **15** and **16** was established by the close correspondence of their uv spectra to that of fluoranthene (see Fig. 1).

The acid rearrangements of cyclobutanones **5–9** appear to follow a different course when compared to ketones **1** and **3** in that β-tetralones are not formed as principal products in the former case. However the formation of aromatic dihydrofurans **12**, **15**, and **16** formally involves a dehydration step and it is conceivable that β-tetralones are precursors to these dihydrofurans. In one study on the acid rearrangement of **16** with *p*-toluenesulphonic acid in benzene solution the ir absorption of the reaction mixture was monitored for carbonyl absorption. Peaks at 1725 and 1620 cm^{-1} appeared in the early stages of the reaction and then decreased in intensity as the reaction progressed. We were not successful in the isolation of any intermediates prior to completion of the reaction. Given that β-tetralones **17** are primary reaction products in these rearrangements and are formed by a mechanism previously reported for ketones **1** and **3** (3), the subsequent dehydration of **17** could involve a hydride shift of the protonated species to form a more



17
18
19
10–12

Can. J. Chem. Downloaded from www.nrcresearchpress.com by 210.87.254.105 on 09/05/12
For personal use only.

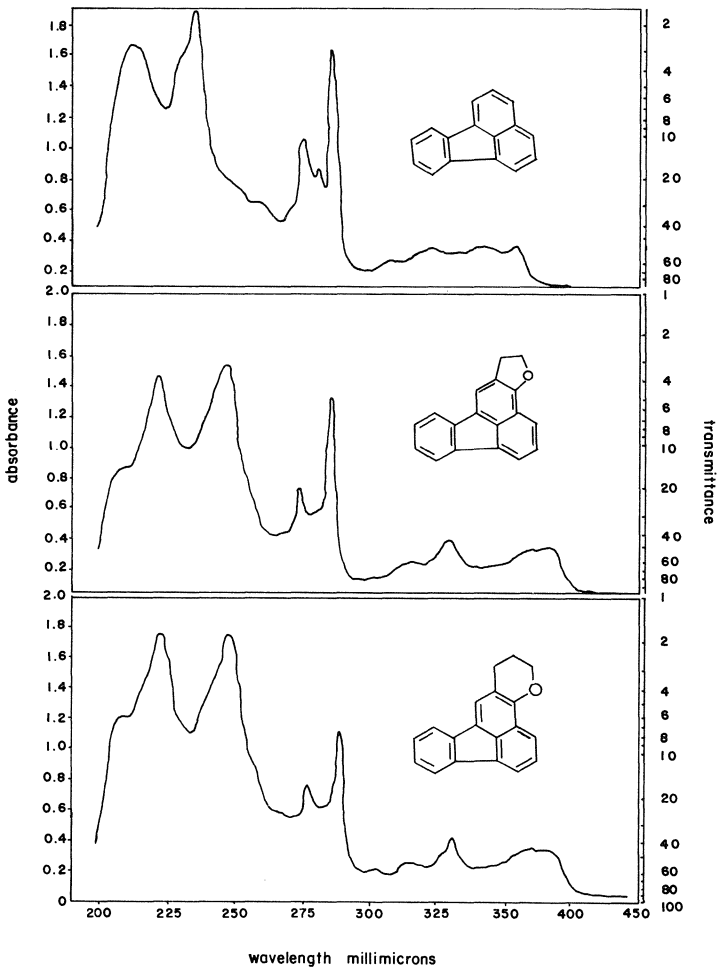


FIG. 1. Ultraviolet spectra of fluoranthenes (for ε values see Experimental).

stabilized carbonium ion **18**. An ensuing proton loss to **19** and dehydration leads to the observed products. Evidence for such a mechanism could be obtained from suitable labelling experiments.

With the current interest in the synthesis of polycyclic aromatic hydrocarbons and their oxidative metabolites, our cyclobutanone rearrangement reactions constitute a novel and useful addition to this area. Furthermore, polycyclic furans such as **13** and **14** posses a "bay region" (8) and may possibly increase the carcinogenic character of naphthalene derivatives. These compounds are currently being screened for mutagenic properties by standard tests.

Experimental

The melting points were determined on a Reichert melting point apparatus and are uncorrected. Infrared spectra were recorded on a Unicam SP1000 instrument as thin films (neat) or KBr pellets. Nuclear magnetic resonance spectra were recorded on a Varian EM-360 instrument in $CDCl_3$ solution containing 1% tetramethylsilane as internal standard. Ultraviolet spectra were obtained on a Unicam SP800A spectrometer using ethanol solutions. All starting materials were obtained from Aldrich Chemicals. Microanalyses were performed by Gygli Microanalysis Laboratories of Toronto.

Preparation of Acid Chlorides

The carboxylic acids were refluxed in 3-fold excess of thionyl chloride for 2–4 hours. The excess thionyl chloride was evaporated. The acid chlorides were crystallized from hexane solutions (9-fluorenylcarbonyl chloride mp 74–75°C (lit. (9) mp 76°C)) or distilled (2-phenylacetyl chloride bp 98°C/12 Torr (lit. (10) bp 100°C/12 Torr)).

Preparation of Cyclobutanones

Cis *7,7-Diphenyl-2-oxabicycloheptan-6-one (**6**) and* Cis *8,8-Diphenyl-2-oxabicyclooctan-7-one (**7**)*

These were prepared according to the procedures of Huisgen (7) with no modifications.

*7-Phenyl-2-oxabicycloheptan-6-one (**5**)*

To a solution containing 2 g of 2-phenylacetyl chloride in 70 mL of anhydrous ether and 5 g of dihydrofuran was slowly added 1.31 g of triethylamine in 10 mL of ether under nitrogen at

Can. J. Chem. Downloaded from www.nrcresearchpress.com by 210.87.254.105 on 09/05/12
For personal use only.

Can. J. Chem. Downloaded from www.nrcresearchpress.com by 210.87.254.105 on 09/05/12
For personal use only.

room temperature. When the addition was complete the solution was stirred for a further 30 min. The reaction mixture was filtered and the filtrate evaporated to give an oily residue. Infrared ν: 1785 (C=O stretch), 1085 (C—O stretch) cm^{-1}; ^{1}Hmr ($CDCl_3$) δ: 7.3 (s, 5H), 5.2 (q, 1H, J = 4 Hz), 4.5 (d, 1H, J = 4 Hz), 3.9 (m, 3H), 2.1 (m, 2H); ms $M^+ - 70$ (C_4H_6O) base peak m/e: 70 ($C_4H_6{}^+O$).

7,7-Bisphenylene-2-oxabicycloheptan-6-one (8)

To 1 g of 9-fluorenylcarbonyl chloride in 50 mL of anhydrous ether cooled to −60°C was slowly added 0.442 g of triethylamine in 10 mL of ether. An orange coloured solution was immediately formed. To this solution was added 3 g of dihydrofuran and the solution was warmed to 0°C and stirred for one hour. The solution was filtered and the precipitate was washed with 3 × 50 mL of distilled water.

The precipitate was recrystallized in ether–methanol mp 114–116°C; ir ν: 1775 (C=O stretch), 1090 (C—O stretch) cm^{-1}; ^{1}Hmr ($CDCl_3$) δ: 7.2–8.0 (m, 8H), 4.9 (d, J = 6 Hz, 1H), 4.0–4.5 (m, 3H), 2.0–2.7 (m, 2H); ms m/e: 262 (M^+), base peak 70 ($C_4H_6O^+$). *Anal.* calcd. for $C_{18}H_{14}O_2$: C 82.44, H 5.34; found: C 82.23, H 5.51.

8,8-Bisphenylene-2-oxabicyclooctan-7-one (9)

The same procedure as for the preparation of ketone **8** was used, except dihydropyran was used in place of dihydrofuran. Ketone **9** was found to be soluble in ether and the following workup procedure was used. The solution was filtered and the filtrate was evaporated to dryness. The residue was crystallized in ether mp 121–123°C; ir ν: 1774 (C=O stretch), 1050 (C—O stretch) cm^{-1}, ^{1}Hmr ($CDCl_3$) δ: 7.3–7.9 (m, 8H), 4.6 (d, J = 6 Hz, 1H), 3.2–4.2 (m, 3H), 1.3–2.5 (m, 4H); ms m/e: 276 (M^+), base peak 84 ($C_5H_8O^+$). *Anal.* calcd. for $C_{19}H_{16}O_2$: C 82.61, H 5.80; found: C 82.58, H 5.75.

Acid-catalyzed Rearrangement. General Procedure

P_2O_5/C_6H_6

The cyclobutanone (200–500 mg) was dissolved in dry benzene (40 mL). To this solution was added 2 equiv. of P_2O_5 and the suspension was stirred from 2–24 h. The suspension was filtered and the solid was washed with benzene and ether. The filtrate and washing were evaporated. In certain instances (**10**, **15**, and **16**) the residue was chromatographed on silica gel thin layer plates. Yields and specific details of the reactions are given in Table 1.

TsOH/C_6H_6

To a solution of benzene (30–40 mL) containing the cyclobutanone (200–500 mg) was added a few crystals of toluenesulphonic acid. The solution was heated to reflux for 2–24 hours. The solution was washed with 10% aqueous sodium bicarbonate, then dried with anhydrous magnesium sulphate and evaporated. The residue in certain instances was chromatographed on silica gel thin layer plates.

Spectral Data of Dihydrofurans and Dihydropyrans

*Derivative **10***

Infrared ν: 1105, 1053 (C—O stretch, bend) cm^{-1}; ^{1}Hmr ($CDCl_3$) δ: 7.1–7.5 (m, 6H), 4.6 (t, J = 8 Hz, 2H), 3.3 (t, J = 8 Hz, 2H); ms m/e: 170 (M^+).

*Derivative **11***

Infrared ν: 1240, 1080, 1010 (C—O stretch, bend) cm^{-1}; ^{1}Hmr ($CDCL_3$) δ: 7.2–7.7 (m, 10H), 4.6 (t, J = 8 Hz, 2H), 3.4 (t, J = 8 Hz, 2H); ms m/e: 246 (M^+). *Anal.* calcd. for $C_{18}H_{14}O$: C 87.81, H 5.71; found: C 87.73, H 5.70.

*Derivative **12***

Infrared ν: 1250, 1115, 1075 (C—O stretch, bend) cm^{-1}; ^{1}Hmr ($CDCl_3$) δ: 7.1–7.7 (m, 10H), 4.2 (t, J = 5 Hz, 2H), 3.1 (t, J = 6 Hz, 2H), 2.0 (t of t J = 5, 6 Hz, 2H); ms m/e: 260 (M^+). *Anal.* calcd. for $C_{19}H_{16}O$: C 87.69, H 6.15; found: C 87.60, H 6.21.

*Derivative **15***

Infrared ν: 1240, 1120, 1000 (C—O stretch, bend) cm^{-1}; uv λ_{max} (log ε): 223 (4.61), 247 (4.65), 275 (4.37), 286 (4.60), 319 (3.76), 329 (4.01), 358 (3.94), 392 (3.97); ^{1}Hmr ($CDCl_3$) δ: 7.2–8.1 (m, 8H), 4.7 (t, J = 8 Hz, 2H), 3.3 (t, J = 8 Hz, 2H); ms m/e: 244 (M^+). *Anal.* calcd. for $C_{18}H_{12}O$: C 88.53, H 4.92; found: C 88.59, H 5.01.

*Derivative **16***

Infrared ν: 1250, 1125, 1070 (C—O stretch, bend) cm^{-1}; uv λ_{max} (log ε): 224 (4.59), 248 (4.61), 278 (4.21), 289 (4.43), 316 (3.72), 331 (3.97), 360 (3.86), 392 (3.83); ^{1}Hmr ($CDCl_3$) δ: 7.3–8.2 (m, 8H), 4.5 (t, J = 5 Hz, 2H), 3.2 (t, J = 6 Hz, 2H), 2.2 (t of t, J = 6 Hz, 5 Hz, 2H); ms m/e: 258 (M^+). *Anal.* calcd. for $C_{19}H_{16}O$: C 88.37, H 5.43; found: C 88.20, H 5.41.

*Dehydrogenation of Dihydrofuran **10***

To a solution of 100 mg of **10** was added 150 mg of DDQ and the solution was heated to reflux for 10 h. The solvent was evaporated and the residue chromatographed on a silica gel column (benzene) to yield 80 mg of furan **13** (oil). Picrate mp 112–113°C (lit (11) mp 113°C); ms m/e base peak 168 (M^+).

*Dehydrogenation of Dihydrofuran **11***

To a solution of 50 mg of **11** was added 55 mg of DDQ and the mixture stirred at reflux overnight. The solution was filtered and washed with 10% $NaHCO_3$ solution, dried over anhydrous $MgSO_4$, and evaporated under reduced pressure. Yield 42 mg of **14**, mp 148°C; ms m/e base peak 244 (M^+). *Anal.* calcd. for $C_{18}H_{12}O$: C 88.53, H 4.92; found: C 88.56, H 4.85.

Acknowledgements

We would like to thank the Natural Sciences and Engineering Research Council as well as the Imperial Oil Company of Canada for financial support of this project.

1. K. E. Hine and R. F. Childs. Can. J. Chem. **54**, 12 (1976).
2. E. Lee-Ruff. Can. J. Chem. **50**, 952 (1972).
3. V. P. Abegg, A. C. Hopkinson, and E. Lee-Ruff. Can. J. Chem. **56**, 99 (1978).
4. L. H. Dao, A. C. Hopkinson, and E. Lee-Ruff. Tetrahedron Lett. 1413 (1978).
5. R. Huisgen and L. A. Feiler. Chem. Ber. **102**, 3391 (1969).
6. B. M. Trost. Acc. Chem. Res. **7**, 85 (1974).
7. R. Huisgen, L. A. Feiler, and P. Otto. Chem. Ber. **102**, 3405 (1969).
8. D. M. Jerina, H. Yagi, R. E. Lehr, D. R. Thakker, M. Schaefer-Ridder, J. M. Karle, W. Levin, A. W. Wood, R. L. Chang, and A. H. Conney. *In* Polycyclic hydrocarbons and cancer. *Edited by* H. V. Gelboin and P. O. P. Tso. Academic Press, New York. 1978.
9. R. Stolle and F. Wolf. Ber. **46**, 2248 (1913).
10. Dictionary of organic compounds. 4th ed. Eyre & Spottiswoode, London. 1965.
11. N. S. Narasimhan and R. S. Mali. Tetrahedron, **31**, 1005 (1975).
12. D. Walker and J. D. Hiebert. Chem. Rev. **67**, 153 (1967).

Réactions d'addition nucléophiles sur les cétones. Mise en évidence d'un effet directionnel d'origine stérique dans l'effet isotopique secondaire du deutérium

BERNARD BOYER, GÉRARD LAMATY ET JEAN-PIERRE ROQUE

Laboratoire de Chimie Organique Physique, Université des Sciences et Techniques du Languedoc, Place Eugène Bataillon, 34060 Montpellier France

ET

PATRICK GENESTE

Laboratoire de Chimie Organique Physique Appliquée, Ecole Nationale Supérieure de Chimie de Montpellier, Rue de l'Ecole Normale, 34075 Montpellier France

Reçu le 30 avril 1979

BERNARD BOYER, GÉRARD LAMATY, JEAN-PIERRE ROQUE et PATRICK GENESTE. Can. J. Chem. **58**, 55 (1980).

L'étude cinétique des réactions d'addition de l'ion borohydrure, de l'ion sulfite et de l'hydroxylamine sur un certain nombre de composés carbonylés stéréospécifiquement deutériés (tétraméthyl-3,3,5,5 cyclohexanone, bicyclo[2,2,1]norbornanone-2 d_2-7,7), a permis de mettre en évidence un effet isotopique secondaire lointain du deutérium. Les résultats obtenus révèlent l'intervention d'un effet directionnel dans l'origine stérique de ces effets isotopiques. En particulier, cette étude montre l'importance de la nature et de l'orientation des vibrations mises en jeu par une liaison C—D au cours du processus réactionnel.

BERNARD BOYER, GÉRARD LAMATY, JEAN-PIERRE ROQUE and PATRICK GENESTE. Can. J. Chem. **58**, 55 (1980).

A kinetic study of the addition reactions of borohydride and sulfite ions and of hydroxylamine to a number of stereospecifically deuterated carbonyl compounds (3,3,5,5-tetramethyl cyclohexanone, 7,7-d_2-bicyclo[2,2,1]-2-bornanone) leads to the observation of a distant secondary deuterium isotope effect. The results obtained reveal the intervention of a directional effect in the steric origin of these isotope effects. In particular, this study shows the importance of the orientation of the vibrations brought into play by a C—D bond during the reaction process.

(Journal translation)

Introduction

Dans un article précédent (1), nous avions remarqué l'absence d'effet isotopique secondaire du deutérium dans la réaction d'addition de BH_4^- sur la bicyclo[2,2,1]heptanone-2 d_2-5,6 *endo* (**1**) et dans la réaction de décomposition de la combinaison bisulfitique de cette même cétone. Sur la base classique de l'origine stérique des effets isotopiques (4, 5), ces résultats sont surprenants. En effet, la réaction de réduction est connue pour avoir un état de transition très tardif (2, 6) entraînant des interactions stériques importantes entre l'oxygène et les hydrogènes (ou deutériums) 5,6 *endo* (fig. 1*a*).

Par ailleurs, la décomposition de la combinaison bisulfitique (fig. 1*b*) passe par un état de transition proche de la cétone (3) dans lequel sont supprimées les interactions de non-liaison entre le groupe hydroxyle et les hydrogènes (ou deutériums) 5,6 *endo*. On pouvait s'attendre à trouver un effet isotopique inverse dans le premier cas ($k^H/k^D < 1$) et direct dans le second ($k^H/k^D > 1$), puisque le deutérium est supposé "moins volumineux" que l'hydrogène (4).

Par contre, nous avons observé que la réduction de la diphényl-2,6 pipéridone-4, (**2**), deutériée en position 2,6 axiale (fig. 2), donne lieu à un effet isotopique secondaire $k^H/k^D = 0.96_3$ (7).

Nous avons suggéré que cette différence de comportement pouvait être due au fait que dans le premier composé (fig. 1) les interactions de non-liaison se produisent "par le flanc" des liaisons C—H (ou C—D) et affectent donc les mouvements de déformation ("bending") de ces liaisons, alors que dans le second (fig. 2) ces mêmes interactions se produisent essentiellement par "la pointe des liaisons" et affectent ainsi leurs mouvements d'élongation ("stretching"). Nous avions conclu qu'il devait exister un effet directionnel dans l'effet isotopique d'origine stérique: les vibrations de déformation seraient peu affectées par la substitution isotopique, seules les vibrations d'élongation le seraient.

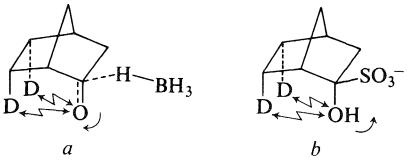


FIG. 1. Bicyclo[2,2,1]heptanone-2 d_2-5,6 *endo*.

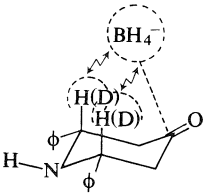


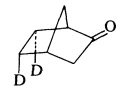
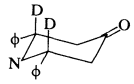
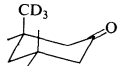
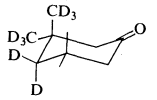
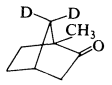
FIG. 2. Diphényl-2,6 pipéridone-4 (**2**).

0008-4042/80/010055-05$01.00/0

©1980 National Research Council of Canada/Conseil national de recherches du Canada

Can. J. Chem. Downloaded from www.nrcresearchpress.com by 210.87.254.6 on 09/05/12
For personal use only.

TABLEAU 1. Valeurs des rapports k^H/k^D pour les réactions d'addition de BH_4^-, NH_2OH et SO_3H^- et pour la réaction de décomposition des combinaisons bisulfitiques

Produits	k^H/k^D			
	BH_4^-	Addition de NH_2OH	SO_3HNa	Décomposition de la combinaison bisulfitique
 **1**	1.00_4[a]	—	—	1.00_5[a]
 **2**	0.96_3[b]	—	—	—
 **3a**	0.98_7[c]	—	—	—
 **3b**[f]	0.96_4[c]	0.97[d]	0.98_4[e]	1.01_3[e]
 **4**	0.95_9[c]	0.97[d]	—	—

[a]Voir réf. 1.
[b]Voir réf. 7.
[c]Effets isotopiques mesurés à 25.0 ± 0.1°C dans le mélange eau–dioxanne 50/50 avec une précision meilleure que 1%.
[d]Effets isotopiques mesurés à 25.0 ± 0.1°C dans des solutions aqueuses d'acides chlorhydrique de concentrations variables, avec une précision meilleure que 2%.
[e]Effets isotopiques mesurés à 25.0 ± 0.1°C dans un tampon acide acétique–acétate de sodium à pH = 5.41 dans le solvant H_2O–EtOH (60/40 en volume). La précision sur les valeurs du rapport k^H/k^D est meilleure que 1%.
[f]La présence de 2 atomes de deutérium en position 4 n'apporte aucune contribution supplémentaire à l'effet isotopique observé. La cohérence des résultats obtenus pour **3***a* et **3***b* (voir texte) montre bien qu'il y a additivité de l'effet isotopique quand on passe du mono-CD_3 au di-CD_3 et que les deux deutériums en 4 ne modifient pas le résultat.

Dans le cadre d'une étude plus générale portant sur l'addition de divers nucléophiles sur les cétones cyclaniques, nous avons utilisé deux modèles qui se prêtent bien à la vérification de cette hypothèse. Il s'agit, d'une part de la tétraméthyl-3,3,5,5 cyclohexanone (**3**) substituée en 3 par un, **3***a*, ou deux groupes CD_3, **3***b*, et d'autre part de la méthyl-1 bicyclo[2,2,1]heptanone-2 (**4**) deutériée en position 7.

Résultats et discussion

Sur toutes ces cétones nous avons mesuré la vitesse d'addition de l'ion borohydrure dans l'eau–dioxanne 50/50 à 25°C, et, pour certaines d'entre elles, la vitesse de décomposition de la combinaison bisulfitique.

Les résultats expérimentaux sont reportés dans le tableau 1.

L'examen des résultats fait apparaître que la substitution isotopique sur le(s) groupe(s) méthyle(s) en position 3 de la tétraméthyl-3,3,5,5 cyclohexanone, composés **3***a* et **3***b*, entraîne un effet isotopique inverse dans les réactions d'addition des trois nucléophiles et un effet isotopique direct dans le cas de la réaction de décomposition de la combinaison bisulfitique.

Ces effets isotopiques sont faibles, comme on pouvait s'y attendre, et avant de les discuter il convient de savoir s'ils sont significatifs ou non. Chaque constante de vitesse est la moyenne de 6 déterminations indépendantes, la déviation standard étant, dans tous les cas, $\leq 0.3\%$; l'incertitude sur le rapport k^H/k^D est donc légèrement inférieure à 0.01. La comparaison des effets isotopiques observés avec **3***a* et **3***b* confirme la confiance que nous pouvons avoir dans nos données; le composé **3***a*, qui ne possède qu'un seul groupe méthyle en position 3 est en réalité un mélange à parties pratiquement égales des deux conformères (fig. 3).

Seule la conformation **3**′*a* donnera un effet isotopique stérique lors de l'addition de l'ion borohydrure car on ne peut raisonnablement envisager

Can. J. Chem. Downloaded from www.nrcresearchpress.com by 210.87.254.6 on 09/05/12
For personal use only.

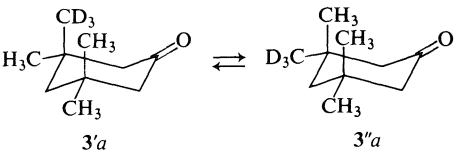


FIG. 3.

que le CD_3 équatorial de **3″*a*** modifie tant soit peu la vitesse de la réaction; la variation de l'énergie libre d'activation due à la substitution isotopique sera donc deux fois plus faible pour **3*a*** que pour **3*b*** et on devra donc avoir

$$(k^H/k^D)_{3b} = (k^H/k^D)^2_{3a}$$

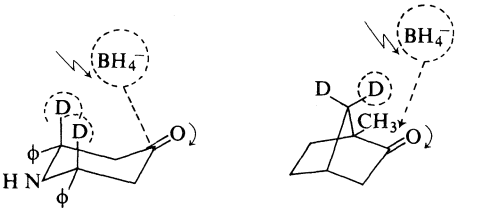
C'est ce que confirme l'expérience puisque $(0.987)^2 = 0.97_3$, compatible avec la valeur trouver pour **3*b*** aux erreurs expérimentales près.

Les réactions conduisent essentiellement aux composés à groupe —OH axial. Au fur et à mesure de l'avancement de la réaction, il y a donc apparition d'un effet stérique de compression dû aux interactions de non-liaison entre l'oxygène de la cétone et les groupes méthyles axiaux; l'existence d'un effet isotopique inverse indique que cette interaction est moindre dans le cas des composés deutériés (**3*a*** et **3*b***). On remarque que l'effet isotopique varie légèrement d'un nucléophile à l'autre; on doit s'attendre à ce qu'il soit d'autant plus important que l'état de transition de la réaction est plus tardif (plus proche des produits finaux). Nous avons montré par ailleurs que l'addition de l'ion sulfite et de l'hydroxylamine conduisait à un état de transition précoce (3, 6, 8) tandis que l'addition de BH_4^- conduit à un état de transition tardif (2, 6); on retrouve bien ici cette différence puisque l'effet isotopique avec l'ion borohydrure est sensiblement plus élevé qu'avec les deux autres nucléophiles.

On peut remarquer également que la décomposition de la combinaison bisulfitique de la cétone, **3*b***, s'accompagne d'un relâchement des interactions 1,3 diaxiales qui se traduit par effet isotopique direct.

Examinons à présent les résultats obtenus lors de l'addition de BH_4^- sur les cétones **1**, **2**, **3*b*** et **4**. Ces 4 modèles peuvent être subdivisés en 2 groupes si l'on considère la nature de la contribution stérique à l'effet isotopique.

Dans le premier groupe, réunissant les composés **2** et **4**, nous pouvons constater (fig. 4) que les liaisons C—H (C—D) en position 3,5 diaxiale pour **2** et la liaison C—H (C—D) en position *syn*-7 pour **4**, se trouvent dans la direction la plus propice à une interaction avec le nucléophile lors de son approche par la face axiale pour **2** et par la face *exo* pour **4** (additions largement prépondérantes).



2 $k^H/k^D = 0.96_3$ **4** $k^H/k^D = 0.95_9$

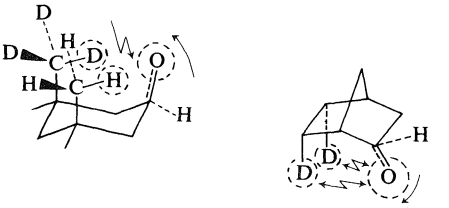
FIG. 4. Effets stériques d'approche dans la réduction par l'ion borohydrure.

Ainsi la présence de 2 atomes de deutérium dans la pipéridone **2** conduit à une diminution de l'énergie d'activation de 22 cal soit 11 cal par deutérium. Par contre, un seul atome de deutérium conduit à $\Delta\Delta G^{\neq}$ égal à 25 cal pour **4**. Bien qu'il s'agisse dans les deux cas d'un effet stérique d'approche, l'orientation de la liaison C—D dans le composé **4** est telle que les interactions stériques mettent davantage en jeu la vibration d'élongation de cette liaison que dans le cas du composé **2**.

Par contre dans le deuxième groupe (**3*b*** et **1**), l'orientation des liaisons C—H (C—D) est favorable à l'intervention d'un "effet stérique de compression" lié au développement, dans l'état de transition tardif, d'interactions de non-liaison entre l'oxygène du carbonyle et, d'une part le groupe CD_3 axial (addition équatoriale) pour **3*b***, et d'autre part les liaisons C—H (C—D) 5,6 *endo* pour **1** (fig. 5).

L'examen des valeurs observées au sein de ce groupe est révélateur de l'importance de l'orientation de la liaison C—D sur l'effet isotopique d'origine stérique.

Dans le cas de la tétraméthyl-3,3,5,5 cyclohexanone **3*b***, un seul atome de deutérium du CD_3 axial apporte une contribution à l'effet isotopique; l'orientation de la liaison C—D est telle que les interactions de non-liaison qui se développent dans l'état de transition affectent essentiellement la vibration d'élongation de cette liaison; ceci conduit à



3 $k^H/k^D = 0.96_4$ **1** $k^H/k^D = 1.00_4$

FIG. 5. Effets stériques de compression dans la réduction par l'ion borohydrure.

Can. J. Chem. Downloaded from www.nrcresearchpress.com by 210.87.254.6 on 09/05/12
For personal use only.

Can. J. Chem. Downloaded from www.nrcresearchpress.com by 210.87.254.6 on 09/05/12
For personal use only.

un effet isotopique de 4% environ, correspondant à un $\Delta\Delta G^{\neq}$ égal à 22 cal, identique à celui observé pour la cétone **4**.

La littérature nous fournit un certain nombre d'exemple de l'influence des interactions de non-liaison liées aux variations des vibrations d'élongation. C'est le cas, en particulier, des résultats obtenus dans la série des dérivés du biphényle par Mislow *et al.* (9), Melander et Carter (10), Carter et Dahlgren (11) pour lesquels la réaction d'inversion configurationnelle donne lieu à un rapport k^H/k^D compris entre 0.87_6 et 0.83_3 selon la température et la nature du substrat.

Un exemple plus récent est celui donné par la solvolyse de *p*-nitrobenzoate de tertiobutyl-2 adamantyle-2 (**5**) qui s'accompagne d'un effet isotopique direct $k^H/k^D = 1.11$ (12) ($\Delta\Delta G^{\neq} = -62$ cal) lorsqu'on substitue les hydrogènes du groupe tertiobutyle par des deutériums. Or, au cours de cette réaction, de type S_N1, il y a suppression des interactions 1,3 diaxiales du groupe tertiobutyle avec deux atomes d'hydrogène. Statistiquement on peut dire qu'en première approximation, la substitution isotopique n'affecte que l'interaction d'un seul hydrogène (ou deutérium) avec deux atomes d'hydrogène (fig. 6).

Pour une seule interaction H(D)–H, on peut donc estimer à 31 cal l'augmentation de l'énergie d'activation provoquée par la substitution isotopique. Cette valeur est dans le même sens bien que légèrement plus élevée que dans le cas des composés **3***b* et **4**.

L'hypothèse d'une dépendance directionnelle de l'effet isotopique stérique semble parfaitement justifiée lorsque l'on considère la nature et l'origine même des interactions mises en jeu au cours du processus réactionnel. En effet, ces interactions de non-liaison, réunissant sous le même vocable les effets stériques d'approche et les effets stériques de compression, représentent en fait des interactions qui se produisent entre atomes non liés lorsqu'ils arrivent à une distance supérieure à la somme de leurs rayons de van der Waals. Ces contacts peuvent se produire selon diverses directions suivant

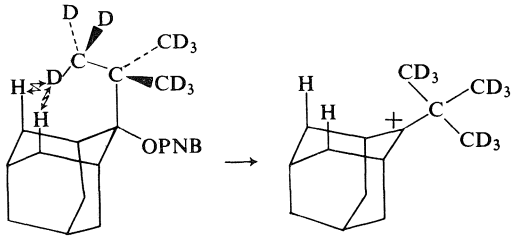


FIG. 6. Solvolyse du *p*-nitrobenzoate de tertiobutyl-2 adamantyle-2 (**5**).

l'orientation dans l'espace des atomes impliqués dans ces interactions de non-liaison.

Or, d'après la représentation de Pauling de la liaison covalente (13), une liaison C—H (ou C—D) est anisotrope et présente un aplatissement sur le flanc du lobe orbitalaire (fig. 7); il sera donc plus facile, pour un autre atome, de s'approcher à une distance donnée d'un atome d'hydrogène par "le flanc" que par "la pointe". En outre, les fréquences de vibration de déformation (bending) étant beaucoup plus faibles que celles d'élongation (stretching), une "gène stérique identique en amplitude" mettra en jeu des énergies moindre lorsqu'elle se produira sur "le flanc" du lobe que sur "la pointe".

C'est en effet ce que l'on observe expérimentalement puisqu'en ne considérant que l'interaction créée par un seul atome de deutérium, les $\Delta\Delta G^{\neq}$ vairent de 0 à 31 cal quand on passe du composé **1**, pour lequel n'interviennent que les vibrations de déformation, au composé **5** où les interactions 1,3 diaxiales mettent en jeu les vibrations d'élongation.

Il est hors de doute que la substitution d'un hydrogène par un deutérium entraîne une variation des contraintes stériques au sein de la molécule. Toutefois, nous pensons avoir montré que cet effet ne peut affecter sensiblement la vitesse d'une réaction que si les atomes qui viennent au contact de la liaison C—H (ou C—D) le font suivant l'axe de cette liaison et non selon une direction perpendiculaire.

Partie expérimentale

Obtention des produits

Le composé **3***b* a été synthétisé selon le schéma réactionnel suivant:

L'isophorone d_8 (14) a été préparé selon la méthode de Starks (15) par échange en milieu basique ($NaOD/D_2O$) en présence de bromure de cétyltriméthylammonium (CTAB). L'addition de ICD_3Mg sur cette cétone éthylénique conduit après hydrolyse au composé **3**. Après dédeutériation sélective ($NaOH/H_2O$) (15), nous avons isolé **3***b* avec un rendement de 63%, pé: 94°C/20 Torr.

Par un procédé analogue au précédent mais en utilisant l'isophorone non deutériée comme produit de départ, nous avons obtenu l'homologue mono-trideutériée en 3 (**3***a*).

Le composé bicyclique **4** a été préparé selon la méthode de Berson et coll. (16) en utilisant comme produit de départ la norbornanone-2 sélectivement deutériée en α du carbonyle par CF_3CO_2D (17) pé: 65°C/20 Torr.

La teneur isotopique a été contrôlée par spectrométrie de masse. Le taux de deutérium est dans tous les cas supérieur à 98%.

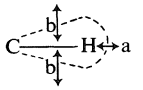
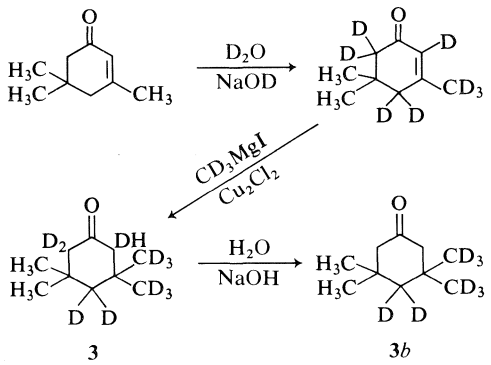


FIG. 7. Liaison C—H selon le modèle de Pauling (13).



3 3*b*

SCHÉMA 1

Mesures cinétiques

Cinétiques de réduction des cétones par l'ion borohydrure

Les conditions de concentration et de solvant sont les mêmes que celles de Geneste et Lamaty (2): eau–dioxanne 50/50 en volume, 0.05 *N* en soude. La réaction est suivie à 25.0 ± 0.1°C par spectrophotométrie uv à une longueur d'onde (285 nm) pour laquelle seule la cétone de départ absorbe (1).

Etude cinétique de la réaction d'oximation

Les conditions de détermination des constantes de vitesse sont identiques à celles décrites par Petitjean et coll. (18).

Etude cinétique de l'addition de l'ion sulfite. Décomposition des combinaisons bisulfitiques

Nous avons utilisé la méthode spectrophotométrique uv mise au point au Laboratoire et décrite par ailleurs (19).

1. B. BOYER, G. LAMATY, J. P. ROQUE et P. GENESTE. Recl. Trav. Chim. Pays-Bas, **93**, 260 (1974).
2. P. GENESTE et G. LAMATY. Bull. Soc. Chim. Fr. 669 (1968).
3. P. GENESTE, G. LAMATY et J. P. ROQUE. Tetrahedron, **27**, 5539 (1971).
4. L. S. BARTELL. Tetrahedron Lett. **6**, 13 (1960).
5. R. E. CARTER et L. MELANDER. Adv. Phys. Org. Chem. **10**, 1 (1973).
6. P. GENESTE, G. LAMATY et J. P. ROQUE. Tetrahedron Lett. 5007 (1970).
7. R. DURAND, P. GENESTE, G. LAMATY et J. P. ROQUE. Tetrahedron Lett. 199 (1977).
8. P. GENESTE, G. LAMATY et J. P. ROQUE. Tetrahedron, **27**, 5561 (1971).
9. K. MISLOW, R. GRAEVE, A. J. GORDON et G. H. WAHL, JR. J. Am. Chem. Soc. **86**, 1733 (1964).
10. L. MELANDER et R. E. CARTER. Acta Chem. Scand. **18**, 1138 (1964).
11. R. E. CARTER et L. DAHLGREN. Acta Chem. Scand. **23**, 504 (1969).
12. J. L. FRY et R. C. BADGER. J. Am. Chem. Soc. **97**, 6276 (1975).
13. L. PAULING. The nature of the chemical bond and the structure of molecular crystals. 3rd ed. Cornell University Press, Ithaca, NY. 1960. p. 264.
14. B. L. SHAPIRO et M. M. CHRYSAM. J. Org. Chem. **38**, 880 (1973).
15. C. M. STARKS. J. Am. Chem. Soc. **93**, 195 (1971).
16. J. A. BERSON, J. S. WALIA, A. REMANICK, S. SUZIKI, P. REYNOLDS-WARNHOFF et J. WILER. J. Am. Chem. Soc. **83**, 3986 (1961).
17. D. A. WEINBERG et C. DJERASSI. J. Org. Chem. **31**, 115 (1966).
18. A. NATAT, A. PETITJEAN, G. LAMATY, J. P. ROQUE, P. GENESTE et B. SCHLICK. Recl. Trav. Chim. Pays-Bas, **95**, 54 (1976).
19. B. BOYER. Thèse de Doctorat d'Etat, Montpellier, 1978; B. BOYER, G. LAMATY et J. P. ROQUE. A paraître.

Can. J. Chem. Downloaded from www.nrcresearchpress.com by 210.87.254.6 on 09/05/12
For personal use only.

N-(*tert*-Butyldimethylsilyl)imidazole and related heterocycles: ^{13}C nuclear magnetic resonance study and reaction with dimethylsulfoxide

ALEXANDER F. JANZEN AND GERALD N. LYPKA
Department of Chemistry, University of Manitoba, Winnipeg, Man., Canada R3T 2N2
AND
RODERICK E. WASYLISHEN
Department of Chemistry, University of Winnipeg, Winnipeg, Man., Canada R3B 2E9
Received July 16, 1979

ALEXANDER F. JANZEN, GERALD N. LYPKA, and RODERICK E. WASYLISHEN. Can. J. Chem. **58**, 60 (1980).

N-tert-Butyldimethylsilyl derivatives of imidazole, 2-methylimidazole, 4-methylimidazole, benzimidazole, pyrazole, 1,2,4-triazole, and benzotriazole were prepared from *tert*-butyldimethylsilyl chloride and the corresponding heterocyclic compound. The products were identified by carbon and proton nmr, mass spectrometry, and elemental analysis. The carbon nmr spectra confirmed the absence of intermolecular silyl exchange at ambient temperature. Silyl exchange did occur at elevated temperatures, 130–160°C.

Reaction of *N-tert*-butyldimethylsilyl or *N*-trimethylsilyl heterocycles with dimethylsulfoxide gave *N*-(methylthio)methyl derivatives of imidazole, 2-methylimidazole, 4-methylimidazole, benzimidazole, pyrazole, and 1,2,4-triazole. The products were characterized by carbon and proton nmr, mass spectrometry, and elemental analysis. A mechanism involving a Pummerer rearrangement is proposed to account for the results.

ALEXANDER F. JANZEN, GERALD N. LYPKA et RODERICK E. WASYLISHEN. Can. J. Chem. **58**, 60 (1980).

On a préparé des dérivés *N-tert*-butyldiméthylsilyles de l'imidazole, de la benzimidazole, des Me-2 et Me-4 imidazoles, du pyrazole, du triazole-1,2,4 et du benzotriazole, à partir du chlorure de *tert*-butyldiméthylsilyle et des composés hétérocycliques correspondants. On a identifié les produits par rmn du ^1H et du ^{13}C, par spectrométrie de masse et par analyse élémentaire. Les spectres rmn du ^{13}C confirment l'absence d'un échange intermoléculaire du groupe silyle à température ambiante. L'échange se produit à température élevée, 130–160°C. Les hétérocycles ayant des substituants *tert*-butyldiméthylsilyle ou triméthylsilyle sur l'azote réagissent avec le diméthylsulfoxyde pour donner des dérivés *N*-(méthylthio) méthyle de l'imidazole, des méthyl-2 et méthyl-4 imidazoles, du benzimidazole, du pyrazole et du triazole-1,2,4. On a caractérisé les produits par rmn du ^1H et du ^{13}C, par spectrométrie de masse et par analyse élémentaire. Tenant compte de ces résultats, on propose un mécanisme réactionnel qui implique une transposition de Pummerer.

[Traduit par le journal]

Silyl exchange in *N*-(trimethylsilyl)pyrazoles occurs with activation energies of 24–32 kcal/mol, except in dilute solutions of diphenyl ether where inordinately low (3–6 kcal/mol) activation energies were observed (1). The low energy pathway of intermolecular silyl exchange in *N*-(trimethylsilyl)imidazole (~7.7 kcal/mol) and *N*-(trimethylsilyl)-2-methylimidazole was attributed to rapid hydrolysis; silyl exchange was slowed down in two ways: firstly, by re-distillation of products under anhydrous conditions and, secondly, by addition of a large excess of triethylamine which presumably inhibited further exchange reactions at silicon (2).

Since bulky substituents are known to inhibit reaction at silicon (3), it seemed reasonable that introduction of the *tert*-butyl group would reduce the problem of catalyzed silyl exchange in *N*-trialkylsilyl heterocycles. Consequently, a variety of *tert*-butyldimethylsilyl derivatives of imidazole, 2- and 4-methylimidazole, benzimidazole, pyrazole, 1,2,4-triazole, and benzotriazole were prepared and investigated by means of ^{13}C and ^1H nmr.

During the course of this work, it was observed that *N*-trialkylsilyl heterocycles interacted with dimethylsulfoxide to give *N*-(methylthio)methyl derivatives. These derivatives were presumably formed via a Pummerer rearrangement.

Experimental

Natural abundance ^{13}C nmr spectra were measured at 20 MHz using a Varian CFT-20 Fourier Transform nmr spectrometer. Gated proton decoupling was used in order to retain nuclear Overhauser enhancements of the proton coupled spectra. Typically, flip angles of 40 to 60° were used with acquisition time > 1 s and a pulse delay of 2–5 s. Proton nmr spectra were obtained on a Varian A-56/60A spectrometer. Mass spectra were obtained on a Finnigan 1015 quadrupole mass spectrometer. Elemental analyses were performed by Micro-Tech Laboratories, Skokie, Illinois.

Imidazole (Aldrich), 2-methylimidazole (Sigma), 4-methylimidazole (ROC/RIC), benzimidazole (Aldrich), pyrazole (Eastman), 1,2,4-triazole (Aldrich), benzotriazole (Aldrich) were used without further purification. Me_2SiCl_2 (PCR) and $(Me_3Si)_2NH$ (MCB) were redistilled prior to use. Methylene chloride, triethylamine, cyclohexane, and dimethylsulfoxide were dried, redistilled, and stored over molecular sieve. *t*-$BuMe_2SiCl$ was prepared from *t*-BuLi and Me_2SiCl_2 (3) and 1-(trimethylsilyl)imidazole, 1-(trimethylsilyl)pyrazole, and 1-(trimethylsilyl)-1,2,4-triazole were prepared from $(Me_3Si)_2NH$ and the corresponding heterocycle (4).

0008-4042/80/010060-05$01.00/0
©1980 National Research Council of Canada/Conseil national de recherches du Canada

Can. J. Chem. Downloaded from www.nrcresearchpress.com by 210.87.254.105 on 09/05/12
For personal use only.

TABLE 1. ^{13}C nuclear magnetic resonance chemical shifts of some *N*-(*tert*-butyldimethylsilyl)heterocycles[a]

	^{13}C chemical shift, ppm						
$(CH_3)_3CSi(CH_3)_2$—R	C-2	C-4	C-5	CH_3Si	$C(CH_3)_3$	$C(CH_3)_3$	Other
1	140.6	130.4	120.7	−5.7	17.7	25.6	
2	149.0	128.9	121.8	−3.8	19.0	26.2	CH_3—C-2 16.8
3	139.2	140.1	117.0	−5.6	17.8	25.8	CH_3—C-4 13.5
4	146.3			−5.0	18.7	25.9	C(ring) 113.4 120.2 121.8 122.5 137.8 146.4[b]
5		105.9	134.0	−5.5	18.2	26.0	C-3 142.8
6			149.4	−5.7	17.8	25.7	C-3 154.1
7				−4.7	19.0	25.9	C(ring) 112.1 115.3 119.8 123.8 125.7 127.4

[a]Negative chemical shifts are upfield from internal TMS.
[b]Peaks at 137.8 and 146.4 are due to carbons without directly bonded protons.

TABLE 2. $^{13}C,H$ coupling constants in some *N*-(*tert*-butyldimethylsilyl)heterocycles

	$^{13}C,H$ coupling constant, Hz[a]
1	$^1J_{(C\text{-}2,H)} = 204.2$ $^3J_{(C\text{-}2,H\text{-}4)} = 11.6$ $^3J_{(C\text{-}2,H\text{-}5)} = 7.9$ $^1J_{(C\text{-}4,H)} = 186.1$ $^2J_{(C\text{-}4,H\text{-}5)} \simeq {}^3J_{(C\text{-}4,H\text{-}2)} = 10.9$ $^1J_{(C\text{-}5,H)} = 186.6$ $^2J_{(C\text{-}5,H\text{-}4)} = 17.1$ $^3J_{(C\text{-}5,H\text{-}2)} = 4.1$ $^1J_{(CH_3\text{—}Si)} = 120.3$ $^1J_{C(CH_3)_3} = 125.4$
2	$^1J_{(C\text{-}4,H)} = 185.3$ $^2J_{(C\text{-}4,H\text{-}5)} = 9.9$ $^1J_{(C\text{-}5,H)} = 185.7$ $^2J_{(C\text{-}5,H\text{-}4)} = 16.4$ $^1J_{(CH_3\text{—}Si)} = 120.1$ $^1J_{(CH_3\text{—}C\text{-}2)} = 127.5$ $^1J_{C(CH_3)_3} = 125.6$
3	$^1J_{(C\text{-}2,H)} = 203.2$ $^3J_{(C\text{-}2,H\text{-}5)} = 8.1$ $^1J_{(C\text{-}5,H)} = 184.8$ $^3J_{(C\text{-}5,H\text{-}2)} = 4.1 \pm 1.0$ $^1J_{(CH_3\text{—}Si)} = 120.3$ $^1J_{(CH_3\text{—}C\text{-}4)} = 126.0$ $^1J_{C(CH_3)_3} = 125.4$
5	$^1J_{(C\text{-}3,H)} = 181.7$ $^2J_{(C\text{-}3,H\text{-}4)} = {}^3J_{(C\text{-}3,H\text{-}5)} = 7.3$ $^1J_{(C\text{-}4,H)} = 174.3$ $^2J_{(C\text{-}4,H\text{-}3)}$ or $^2J_{(C\text{-}4,H\text{-}5)} = 9.3$ $^2J_{(C\text{-}4,H\text{-}5)}$ or $^2J_{(C\text{-}4,H\text{-}3)} = 11.6$ $^1J_{(C\text{-}5,H)} = 182.3$ $^2J_{(C\text{-}5,H\text{-}4)}$ or $^3J_{(C\text{-}5,H\text{-}3)} = 5.2$ $^3J_{(C\text{-}5,H\text{-}3)}$ or $^2J_{(C\text{-}5,H\text{-}4)} = 9.2$ $^1J_{(CH_3\text{—}Si)} = 120.4$ $^1J_{C(CH_3)_3} = 125.5$
6	$^1J_{(C\text{-}3,H)} = 203.8$ $^3J_{(C\text{-}3,H\text{-}5)} = 11.7$ $^1J_{(C\text{-}5,H)} = 206.6$ $^3J_{(C\text{-}5,H\text{-}3)} = 8.5$ $^1J_{(CH_3\text{—}Si)} = 120.6$ $^1J_{C(CH_3)_3} = 125.8$

[a]Error ±0.5 Hz, unless otherwise indicated.

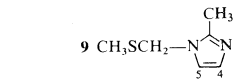
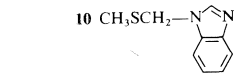
N-tert-*Butyldimethylsilyl Heterocycles*

Compounds **1**–**7** were prepared on a 0.02 mol scale by mixing equimolar amounts of *t*-$BuMe_2SiCl$ and the corresponding heterocycle in the presence of excess triethylamine (5, 6). The reaction mixture was either stirred at room temperature for 3–6 days or refluxed for 5–20 h until reaction was complete, as determined by nmr. $Et_3N{\cdot}HCl$ was filtered off and Et_3N was removed under vacuum. A trace of $Et_3N{\cdot}HCl$ was removed by adding cyclohexane, refiltering and removing cyclohexane under vacuum. All products (except **6**) were purified by distillation at 10^{-2} Torr and were clear, viscous liquids. Recrystallization of **6** from cyclohexane gave a white solid mp 87–89°C. Yields of final products were 50% or greater.

The products **1** to **7** were identified by ^{13}C nmr (Tables 1 and

Can. J. Chem. Downloaded from www.nrcresearchpress.com by 210.87.254.105 on 09/05/12
For personal use only.

TABLE 3. Elemental analyses and ^{13}C nuclear magnetic resonance data of

Compound		Elemental analysis Calcd.	Found	^{13}C chemical shifts, ppm C-2	C-4	C-5	CH_2	CH_3S	$CH_3—C_2$
8 	C	46.85	46.89	136.3	129.0	118.1	48.7	13.4	—
	H	6.29	6.19						
	N	21.85	22.20						
9 	C	50.67	51.15	144.4	126.6	119.3	48.2	13.6	12.7
	H	7.09	7.22						
	N	19.70	21.32						
10 	C	60.64	59.35	142.3	—	—	47.2	13.9	—
	H	5.65	5.69						
	N	15.72	15.27						

2), ^1H nmr, and mass spectrometry. Compound **1** has been studied previously (5, 6) and **6** was identified by elemental analysis.

Anal. calcd. for $C_8H_{17}N_3Si$: C 52.41, H 9.35, N 22.92; found: C 51.69, H 9.27, N 22.64.

Reaction with DMSO

N-(Methylthio)methyl derivatives **8–13** were prepared at 140–180°C for 8–24 h in three ways: (*a*) *N*-trimethylsilyl heterocycle and DMSO, (*b*) *N-tert*-butyldimethylsilyl heterocycle and DMSO, (*c*) hexamethyldisilazane, heterocycle, and DMSO. Yields of products were 40–60%.

In a typical reaction, benzimidazole (15 g, 0.13 mol), DMSO (5.0 g, 0.063 mol), and $(Me_3Si)_2NH$ (10.3 g, 0.064 mol) were refluxed for 20 h. The colourless top layer ($Me_3SiOSiMe_3$) was decanted. CCl_4 was added and a white precipitate (benzimidazole, 8.4 g) was removed. The CCl_4 fraction was washed with 3 × 20 mL portions of H_2O and the CCl_4 layer dried ($MgSO_4$) and rotary evaporated to yield a yellow oil which was extracted once more with CCl_4/hexane and dried under vacuum. The oil was identified as *N*-[(methylthio)methyl]benzimidazole on the basis of elemental analysis, carbon nmr (Table 3), proton nmr, and mass spectrometry.

In another reaction, 2-methylimidazole (10 g, 0.12 mol), DMSO (4.8 g, 0.061 mol), and $(Me_3Si)_2NH$ (10 g, 0.062 mol) were refluxed for 8 h. The colourless top layer ($Me_3SiOSiMe_3$) was decanted. CCl_4 was added and the white precipitate (2-methylimidazole) removed. The CCl_4 fraction was rotary evaporated and the product purified by gas chromatography and identified as *N*-[(methylthio)methyl]-2-methylimidazole on the basis of elemental analysis, carbon nmr (Table 3), proton nmr, and mass spectrometry.

Results and Discussion

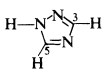
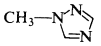
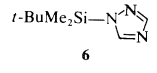
N-(tert-*Butyldimethylsilyl)imidazole and Related Heterocycles*

The ^{13}C nmr spectra (Tables 1 and 2) of compounds **1–7** show clearly that the introduction of the bulky *tert*-butyl substituent gives non-fluxional molecules. In each case, separate signals are observed for non-equivalent ring carbons, as required in the absence of intermolecular silyl exchange. (Only the spectrum of **3** is insensitive to chemical exchange effects.)

The carbon spectra were assigned on the basis of nmr data reported for *N*-methyl analogues of **1–7** (7–9). For the methyl group directly bonded to silicon, $^1J_{C,H}$ = 120.3[5] ± 0.2[5] Hz which is only slightly larger than the value of 118.4 Hz observed for $^1J_{C,H}$ in TMS (10). The $^1J_{C,H}$ values for the methyl carbons of the *tert*-butyl moiety were also the same for all compounds within experimental error, 125.5[5] ± 0.25 Hz, slightly larger than the value of 124.04 ± 0.10 Hz observed in neopentane.[1]

$^nJ_{C,H}$ values involving the ring carbons of **1** and **2** are similar to those reported previously for the corresponding *N*-trimethylsilyl derivatives of **1** and **2** (2), while values for **5** and **6** are similar to those observed in 1-methylpyrazole (7, 8) and 1-methyl-1,2,4-triazole (7).

In order to help confirm the assignment of C-3 and C-5 in 1,2,4-triazole derivatives, INDO-MO-FPT level molecular orbital calculations (11) of the various $^nJ_{C,H}$ values in 1,2,4-triazole were carried out. Atomic coordinates were calculated from the bond lengths and angles derived from an X-ray study (12). The results are summarized below.

Parameter	 (Calcd)	 (Obsd, ref. 7)	*t*-BuMe$_2$Si—  **6** (Obsd, this study)
$^1J_{(C\text{-}3,H)}$	180.7 Hz	205.3 Hz	203.8 Hz
$^3J_{(C\text{-}3,H\text{-}5)}$	14.5	11.9	11.8
$^1J_{(C\text{-}5,H)}$	184.4	210.1	206.6
$^3J_{(C\text{-}5,H\text{-}3)}$	11.8	7.3	8.4

[1]R. E. Wasylishen. Unpublished results.

Can. J. Chem. Downloaded from www.nrcresearchpress.com by 210.87.254.105 on 09/05/12
For personal use only.

some *N*-(methylthio)methyl derivatives

^{13}C,H coupling constants, Hz			
$^1J_{(CH_3)} = 139.4$ $^1J_{(C\text{-}4,H)} = 189.4$ $^2J_{(C\text{-}4,H\text{-}5)} = 10.4$	$^1J_{(CH_2S)} = 152.7$ $^1J_{(C\text{-}5,H)} = 186.5$ $^3J_{(CH_3SCH_2)} = 4.8$	$^1J_{(C\text{-}2,H)} = 203.8$ $^2J_{(C\text{-}5,H\text{-}4)} = 17.4$ $^3J_{(CH_2SCH_3)} = 4.5$	$^3J_{(C\text{-}4,H\text{-}2)} = 10.4$
$^1J_{(CH_3\text{-}C\text{-}2)} = 128.7$ $^1J_{(C\text{-}5,H)} = 188.8$ $^3J_{(CH_3SCH_2)} = 4.5$	$^1J_{(CH_3S)} = 139.2$ $^2J_{(C\text{-}4,H\text{-}5)} = 9.2$ $^3J_{(CH_2SCH_3)} = 4.8$	$^1J_{(CH_2S)} = 151.8$ $^2J_{(C\text{-}5,H\text{-}4)} = 15.9$ $^3J_{(C\text{-}5,CH_2S)} = 3.3$	$^1J_{(C\text{-}4,H)} = 188.8$
$^1J_{(CH_3)} = 139.3$ $^3J_{(CH_3SCH_2)} = 4.7$	$^1J_{(CH_2S)} = 152.2$ $^3J_{(CH_2SCH_3)} = 4.8$	$^1J_{(C\text{-}2,H)} = 206.0$ $^3J_{(C\text{-}2,CH_2S)} = 3.1$	

The relative magnitudes of calculated $^1J_{C,H}$ and $^3J_{C,H}$ values are in agreement with the assignments made on the basis of chemical shifts.

The ^{13}C nmr spectra of **1–7** were recorded at elevated temperature. Compounds **1**, **4**, and **6** showed no broadening of the lines at 150°C but **2** and **3** showed broadening at 130°C. In the case of **5**, no exchange was observed at 125°C, but considerable exchange was evident at 150°C and coalescence of C-3 and C-5 occurred at 175 ± 10°C from which we estimate $\Delta G_c^{\ddagger} = 21.2 \pm 1.0$ kcal/mol (C-4 remained unchanged during this process, as expected).

The proton nmr spectra of **1–7** at 40°C are consistent with rigid structures; however, because of small chemical shift differences the assignment of ring hydrogens could not be made unambiguously.

Reaction of DMSO with N-*Trialkylsilyl Heterocycles*[2]

DMSO was found to react with *N-tert*-butyldimethylsilyl or *N*-trimethylsilyl heterocycles at elevated temperature 140–180°C in the absence of solvent to give the corresponding *N*-(methylthio)-methyl heterocycles **8–13**. Heating a mixture of DMSO, heterocycle, and $(Me_3Si)_2NH$ also gave the same products since, in this case, the *N*-trimethylsilyl heterocycle was formed *in situ* from $(Me_3Si)_2NH$ and heterocycle (4), followed by reaction with DMSO.

[1] $2R_3Si\text{—}N\langle\!\rangle N + (CH_3)_2S{=}O \longrightarrow CH_3SCH_2\text{—}N\langle\!\rangle N + R_3SiOSiR_3 + HN\langle\!\rangle N$

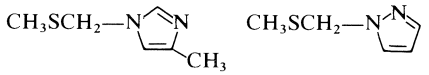
8

The products **8–10** were identified by elemental analysis, carbon nmr (Table 3), proton nmr, and mass spectrometry. Compounds **11–13** were identified by proton nmr and mass spectrometry.

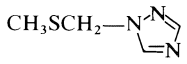
[2]For a preliminary account, see ref. 19.

The mass spectra of **8–13** showed prominent peaks at M^+, $M - SCH_3^+$, and *m/e* 61 ($CH_3SCH_2^+$).

A typical ^{13}C nmr spectrum is shown in Fig. 1. The carbon nmr data confirm the structures of **8–13**



11 **12**



13

since the chemical shifts and coupling constants of the ring carbons (Table 3) are very similar to those of the corresponding *tert*-butyldimethylsilyl heterocycles (Table 1 and 2) while the CH_3SCH_2 group in **8–13** is similar to CH_3SCH_2F (13) and CH_3SCH_2Cl (14). The proton nmr of **8–13** showed the CH_3S group at 1.93 to 2.13 ppm and the CH_2 group at 4.78 to 5.37 ppm.

The formation of **8–13** is an example of a Pummerer rearrangement in which a nitrogen, rather than the more familiar oxygen or halogen (15), substituent migrates to the α-position. A possible mechanism is described in Scheme 1. Insertion of

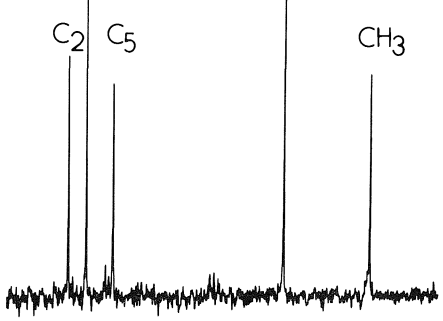
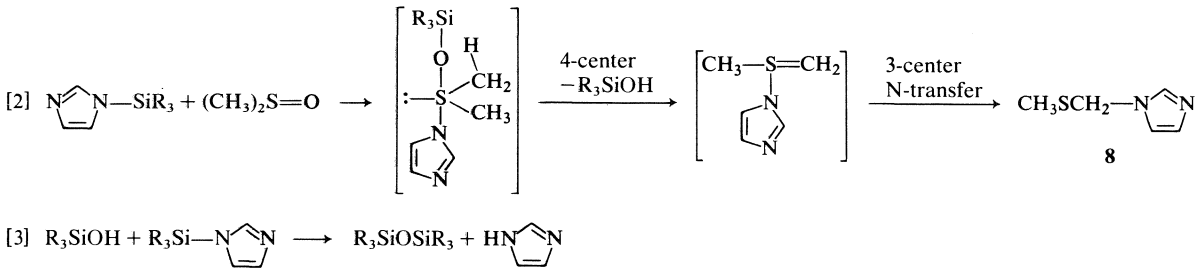


FIG. 1. ^{13}C nmr spectrum of *N*-[(methylthio)methyl]imidazole **8**.

Can. J. Chem. Downloaded from www.nrcresearchpress.com by 210.87.254.105 on 09/05/12
For personal use only.



SCHEME 1

DMSO into the Si—N bond is analogous to SO_2 or SO_3 insertion into Si—N compounds (16) and the 4-center and 3-center steps are similar to the postulated conversion of Me_2SF_2 to $MeSCH_2F$ (13) and Me_2SCl_2 to $MeSCH_2Cl$ (17). Equation [3] is analogous to the reaction of alcohols with Si—N compounds (18).

Acknowledgements

The financial assistance of the National Research Council of Canada and the Research Board of the University of Manitoba is gratefully acknowledged. We thank Dr. J. B. Westmore for a sample of *tert*-butyldimethylsilyl chloride and Mr. R. K. Marat for assistance with the DMSO reactions.

1. D. H. O'Brien and C.-P. Hrung. J. Organomet. Chem. **27**, 185 (1971).
2. R. E. Wasylishen, G. S. Birdi, and A. F. Janzen. Inorg. Chem. **15**, 3054 (1976).
3. L. H. Sommer and L. J. Tyler. J. Am. Chem. Soc. **76**, 1030 (1954).
4. L. Birkofer, P. Richter, and A. Ritter. Chem. Ber. **93**, 2804 (1960).
5. J. Kutschinski. Ph.D. Thesis, University of California, Davis, CA. 1974. p. 87.
6. K. K. Ogilvie, S. L. Beaucage, D. W. Entwistle, E. A. Thompson, M. A. Quilliam, and J. B. Westmore. J. Carbohydr. Nucleosides Nucleotides. **3**, 197 (1976).
7. M. Begtrup. J. Chem. Soc. Perkin Trans. II, 736 (1976).
8. R. E. Wasylishen and H. M. Hutton. Can. J. Chem. **55**, 619 (1977).
9. R. E. Wasylishen and G. Tomlinson. Can. J. Biochem. **55**, 579 (1977).
10. H. Dreeskamp and G. Stegmeier. Z. Naturforsch. Teil A, **22**, 1458 (1967).
11. J. A. Pople and D. L. Beveridge. Approximate molecular orbital theory. McGraw-Hill Book Co., New York, NY. 1970.
12. P. Goldstein, J. Ladell, and G. Abowitz. Acta Crystallogr. Sect. B, **25**, 135 (1969).
13. R. K. Marat and A. F. Janzen. Can. J. Chem. **55**, 3031 (1977).
14. The Sadtler Standard N. M. R. Spectra. Vol. 34. Sadtler Research Laboratories, Inc., Philadelphia, PA. 21619M.
15. T. Durst. *In* Advances in organic chemistry, methods and results. Vol. 6. Interscience Publishers, New York, NY. 1969. pp. 356–365; G. A. Russell and G. J. Mikol. *In* Mechanisms of molecular migrations. Vol. 1. *Edited by* B. S. Thyagarajan. Interscience Publishers, New York, NY. 1968. pp. 157–176; M. F. Lappert and J. K. Smith. J. Chem. Soc. 3224 (1961).
16. M. F. Lappert and B. Prokai. Adv. Organomet. Chem. **5**, 225 (1967).
17. A. Queen, A. E. Lemire, A. F. Janzen, and M. N. Paddon-Row. Can. J. Chem. **56**, 2884 (1978).
18. J. F. Klebe. *In* Advances in organic chemistry: methods and results. Vol. 8. Interscience Publishers, New York, NY. 1972. pp. 97.
19. A. F. Janzen, G. N. Lypka, and R. E. Wasylishen. J. Heterocycl. Chem. **16**, 415 (1979).

Can. J. Chem. Downloaded from www.nrcresearchpress.com by 210.87.254.105 on 09/05/12
For personal use only.

Trifluoromethylsulfonyl aryl derivatives: competitive nucleophilic attack at an aromatic carbon and at the sulfur atom of an aromatic SO_2CF_3 group

FRANÇOIS TERRIER AND JEAN MOREL

Laboratoire de Physicochimie des Solutions (LA CNRS 161), Ecole nationale supérieure de chimie de Paris, 11 rue Pierre et Marie Curie, 75231 Paris Cedex 05 and Faculté des Sciences de Rouen, 76130 Mont Saint Aignan, France

AND

MARIE-JOSÉ POUET AND MARIE-PAULE SIMONNIN

Laboratoire de Spectrographie (ERA CNRS 390), Ecole nationale supérieure de chimie de Paris, 11 rue Pierre et Marie Curie, 75231 Paris, France

Received July 5, 1979

FRANÇOIS TERRIER, JEAN MOREL, MARIE-JOSÉ POUET, and MARIE-PAULE SIMONNIN. Can. J. Chem. **58**, 65 (1980).

The reaction of methoxide ion with 2-nitro-4-trifluoromethylsulfonylanisole, 4-nitro-2-trifluoromethylsulfonylanisole and 2,4-bis(trifluoromethylsulfonyl)anisole in DMSO has been studied by ^1H and ^{19}F nmr. Evidence for the transient formation of *gem*-dimethoxy σ-adducts arising from nucleophilic attack at the aromatic C1 carbon is given. Concurrent methoxide ion attack occurs at the sulfur atom of the SO_2CF_3 group to give the aryl methyl sulfonates $ArSO_3CH_3$, which are slowly converted into aryl sulfonates $ArSO_3^-$. The ^1H chemical shifts of the anisoles are consistent with a greater electron-withdrawing effect of the SO_2CF_3 group compared to the nitro group. In contrast, a 4-nitro group appears to be more efficient than a 4-SO_2CF_3 group in delocalizing the negative charge of the σ-adducts.

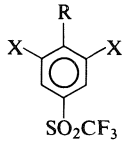
FRANÇOIS TERRIER, JEAN MOREL, MARIE-JOSÉ POUET et MARIE-PAULE SIMONNIN. Can. J. Chem. **58**, 65 (1980).

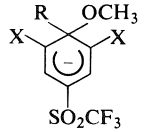
La réaction des ions méthoxyde avec les nitro-2-trifluorométhylsulfonyl-4, nitro-4 trifluorométhylsulfonyl-2 et bis(trifluorométhylsulfonyl)-2,4 anisoles a été étudiée en milieu DMSO par rmn du proton et du fluor. Les résultats mettent en évidence la formation transitoire des complexes-σ *gem*-diméthoxylés résultant de l'attaque nucléophile des ions CH_3O^- sur le carbone aromatique C1. Une attaque nucléophile intervient simultanément sur l'atome de soufre du groupe SO_2CF_3 et conduit aux aryl sulfonates de méthyle $ArSO_3CH_3$ correspondants, qui sont eux-mêmes progressivement transformés en sulfonates $ArSO_3^-$. Les déplacements chimiques δ_H des anisoles confirment que l'effet attracteur d'un groupe SO_2CF_3 est plus important que celui d'un groupe nitro. Par contre, ce dernier présente une aptitude plus importante à délocaliser la charge négative des complexes-σ.

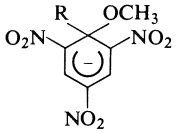
Introduction

The trifluoromethylsulfonyl function is the most powerful neutral electron-withdrawing group known, as evidenced by its Taft and Hammett constants (1–3). Not surprisingly this substituent greatly facilitates formation of Meisenheimer-type complexes from aromatic substrates. Thus, tris-1,3,5-(trifluoromethylsulfonyl)benzene, **1**, gives the monomethoxyl σ-complex, **2**, which is 2×10^6-fold more stable than its trinitro analogue **3** in methanol (4, 5). Similarly, 2,6-dinitro-4-trifluoromethylsulfonylanisole, **4**, reacts with CH_3O^- ion to give the σ-complex **5**, which is about 10^2-fold more stable than the trinitro complex **6** (6).

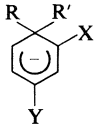
The stability of Meisenheimer adducts is strongly decreased when the parent aromatic substrates are activated by two instead of three electron withdrawing groups (7). As a consequence







1 R = H X = SO_2CF_3 **2** R = H X = SO_2CF_3 **3** R = H
4 R = OCH_3 X = NO_2 **5** R = OCH_3 X = NO_2 **6** R = OCH_3



a R = R′ = OCH_3
b R = R′ = OC_2H_5
7 X = Y = NO_2 *c* R = H R′ = CH_2COCH_3
d R = H R′ = CH_2NO_2

8 X = NO_2 Y = CN, CF_3, SO_2CH_3
9 X = CN, CF_3, SO_2CH_3 Y = NO_2

only 2,4-dinitro adducts **7** have been unambiguously identified (7–10), while 2,4-disubstituted adducts like **8** or **9** could not be observed.

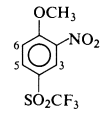
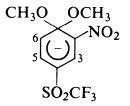
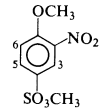
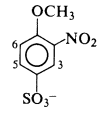
However, the presence of a powerful electron-withdrawing substituent such as SO_2CF_3 might be expected to enhance the stability of such adducts and allow their identification.

We now report an nmr identification of the trifluoromethylsulfonyl σ-adducts **11**, **15**, and **19** which arise from methoxide ion attack at the aromatic C1 carbon of 2-nitro-4-trifluoromethylsulfonylanisole **10**, 4-nitro-2-trifluoromethylsulfonylanisole **14**, and 2,4-bis(trifluoromethylsulfonyl)anisole **18**, respectively. This study also reveals the occurrence of a competitive nucleophilic substitution at the sulfur atom of the SO_2CF_3 group of **10** and **14** to form the methylsulfonates **12** and **16**; these products are unstable and irreversibly converted into the sulfonates **13** and **17**.

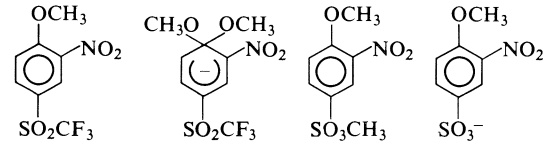
0008-4042/80/010065-07$01.00/0
©1980 National Research Council of Canada/Conseil national de recherches du Canada

Can. J. Chem. Downloaded from www.nrcresearchpress.com by 210.87.254.105 on 09/05/12
For personal use only.

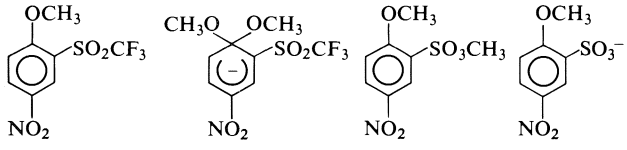
TABLE 1. Nuclear magnetic resonance parameters of anisole **10**, σ-adduct **11**, and compounds **12**, **13**[a]

Compounds	δ(¹⁹F)	δ_{H3}	δ_{H5}	δ_{H6}	δ_{OCH_3}	$\delta_{SO_3CH_3}$	$^4J_{3-5}$	$^3J_{5-6}$	$^5J_{3-6}$
 **10**	−78.1	8.62	8.38_5	7.80	4.16_5		2.4_5 $J_{F-H5}=0.5$	9.0_5	0.4 $J_{F-H3}=0.4$
 **11**	−79.3	8.15	6.55	5.07	2.87		2.4	10	
 **12**		8.39	8.17	7.64	4.06	3.79	2.4	9.0	
 **13**		8.01	7.87	7.33	3.95		2.1	8.7	0.3

[a]δ in ppm relative to internal TMS (¹H) and internal $CFCl_3$ (¹⁹F). Negative values are upfield from the reference compound. *J* in Hz.



10 **11** **12** **13**



14 **15** **16** **17**

Results

The reactions of CH_3O^- with the anisoles **10**, **14**, and **18** in DMSO solution were followed by repetitively scanning ¹H nmr spectra at 100 MHz and ¹⁹F nmr spectra at 94.1 MHz (Varian XL-100). Meisenheimer complexes **11**, **15**, and **19** were observed when less than 1 equiv. of CH_3OK was used. The species have too short a half-life to be observed at higher base concentrations.

The ring protons of all the compounds studied, except **16**, gave an AMX system with coupling constants allowing an unambiguous assignment of individual protons: $^3J_{5-6}=8$–10 Hz, $^4J_{3-5}=2$–3 Hz, $^5J_{3-6}<0.5$ Hz (see Tables 1 and 2). Moreover, a long-range coupling between H6 and the methoxyl protons was observed in aromatic derivatives, so that $^5J_{3-6}$ could be resolved only when irradiating the methoxyl protons.

2-Nitro-4-trifluoromethylsulfonylanisole

The ¹H nmr spectrum of **10** in DMSO-d_6 exhibits a methoxyl singlet at 4.17 ppm, a doublet at 7.80 (H6), a doublet of doublets at 8.39 (H5), and a doublet at 8.62 (H3) (Table 1). The fluorine signal appears as a singlet at −78.1 ppm (upfield from $CFCl_3$).

Addition of less than 1 equiv. of concentrated methanolic potassium methoxide (4.4 *M*) to a DMSO-d_6 solution of **10** resulted in an almost complete disappearance of the signals from **10** and the concomitant appearance of four new products (Fig. 1). One set of signals, which is observed only for a few minutes, consists of a singlet at 2.87 and an AMX system with a high field doublet at 5.07 (H6), a doublet of doublets at 6.55 (H5), and a doublet at 8.15 (H3). Integration showed that the relative intensities are in a 6:1:1:1 ratio. These results point out the formation of the σ-adduct **11**. In agreement with this structure, the ¹⁹F spectrum shows a new singlet at −79.3 ppm, which is at slightly higher field than that of the parent molecule.

The presence of fluoroform is evidenced from both ¹H spectra (quadruplet at δ = 7.28 ppm, $^2J_{FH}$ = 79 Hz) and ¹⁹F spectra (doublet at δ = −78.3 ppm, $^2J_{FH}=79$ Hz).

The two other products are aromatic and contain

Can. J. Chem. Downloaded from www.nrcresearchpress.com by 210.87.254.105 on 09/05/12
For personal use only.

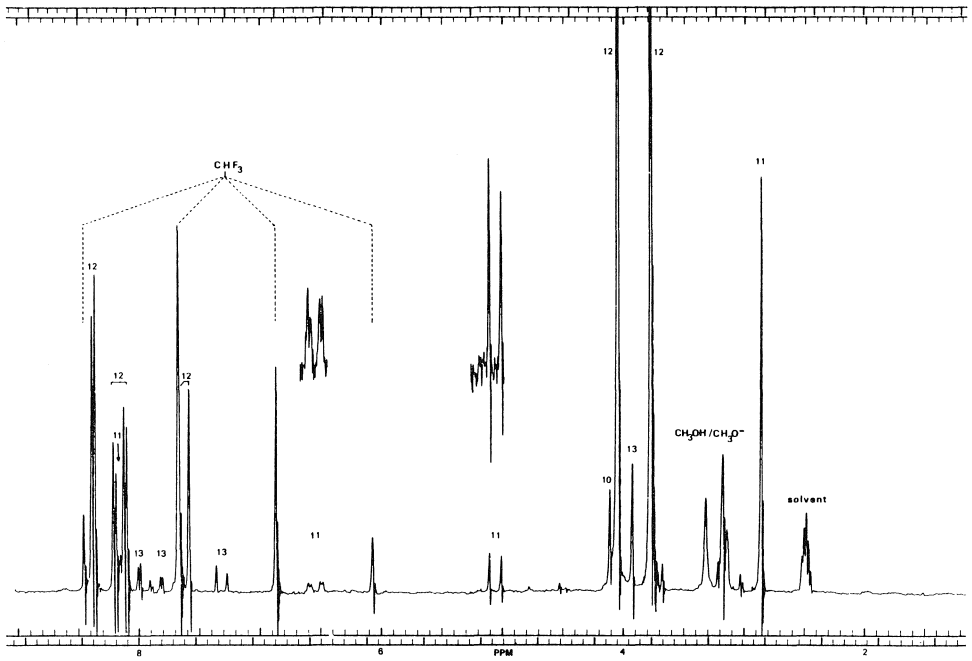


FIG. 1. ^{1}H nmr spectrum of the *in situ* generation of the σ-adduct **11**, the methylsulfonate **12**, and the sulfonate **13**, by addition of methanolic potassium methoxide to the anisole **10** in DMSO-d_6. Resonances are identified by structure numbers.

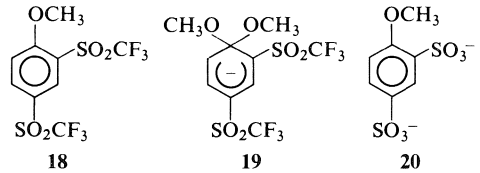
no fluorine, as deduced from ^{19}F spectra. They may be identified as the methylsulfonate **12** and the sulfonate anion **13**, respectively, which both exhibit an AMX pattern in the aromatic region. Moreover, **12** gives two methoxyl singlets at 4.06 and 3.79 ppm, while **13** has only one OCH_3 signal at 3.95 ppm. With time, the signals belonging to **12** decrease while those of **13** increase; after a few days, **13** is the only product in the solution. A definitive proof of the formation of **13** comes from a comparison of its ^{1}H nmr spectrum with that of an authentic sample of the corresponding ammonium salt dissolved in DMSO-d_6 (see Experimental).

4-Nitro-2-trifluoromethylsulfonylanisole

The general features for the reaction of **14** with methoxide ion are similar to those observed with **10**. Four products are also formed with **14**, one of which is CHF_3. Differences in the nmr spectra of the various species are of interest. In the parent anisoles **10** and **14**, H3 has almost identical chemical shifts but H5 is less shielded in **14** than in **10**, leading to an inversion in the field position of H3 and H5 resonances. In a similar way, H5 is less shielded than H3 in the methylsulfonate **16**, but the differences between these shifts is smaller than in **14**. As a result, the spectrum of **16** is of the ABX type and the H6 resonance exhibits a six line pattern. A second order analysis yields the parameters indicated in Table 2 and has been confirmed by a simulation of the spectrum (Fig. 2). Moreover, as can be seen in Fig. 2, the AB part of **16** overlaps with the H3 doublet of **17**.

2,4-Bis(trifluoromethylsulfonyl)anisole

A similar study of the reaction of CH_3O^- with 2,4-bis(trifluoromethylsulfonyl)anisole **18** has been performed, but we were not able to identify all the various species involved in this system. The formation of CHF_3 and the characterization of the disulfonate **20** (Table 3) as the final product show, however, that we are dealing with an analogous sequence of reactions. Indeed, due to the presence of two SO_2CF_3 moieties, up to ten products may be expected to coexist in the solution, explaining the complexity of the observed nmr spectra.

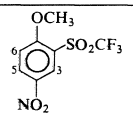
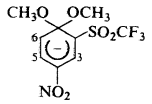
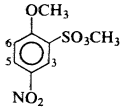
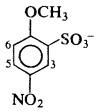


18 **19** **20**

However, immediately after the addition of CH_3O^- to a solution of **18** in DMSO, the high-field part of the ^{1}H spectra exhibits a doublet of doublets at 6.58 ppm, a doublet at 5.17 ppm, and an intense singlet at 2.91 ppm, which can be observed only for a few minutes. Though the low-field signal could not be identified, due to the overlap of many signals

Can. J. Chem. Downloaded from www.nrcresearchpress.com by 210.87.254.105 on 09/05/12
For personal use only.

TABLE 2. Nuclear magnetic resonance parameters of anisole **14**, σ-adduct **15**, and compounds **16**, **17**[a]

Compounds	δ(¹⁹F)	δ_{H3}	δ_{H5}	δ_{H6}	δ_{OCH_3}	$\delta_{SO_3CH_3}$	$^4J_{3-5}$	$^3J_{5-6}$	$^5J_{3-6}$
 **14**	−75.9	8.64	8.77_5	7.72	4.18_5		2.8	9.2	0.3_8
 **15**	−77.8	8.23	7.18	5.14	2.93		2.8	10.2	
 **16**		8.54_5	8.60	7.59	4.11	3.85	2.8_8	9.5	
 **17**		8.55_5	8.25	7.25	3.95		3.0	9.0	

[a]δ in ppm relative to internal TMS (¹H) and internal $CFCl_3$ (¹⁹F). Negative values are upfield from the reference compound. *J* in Hz.

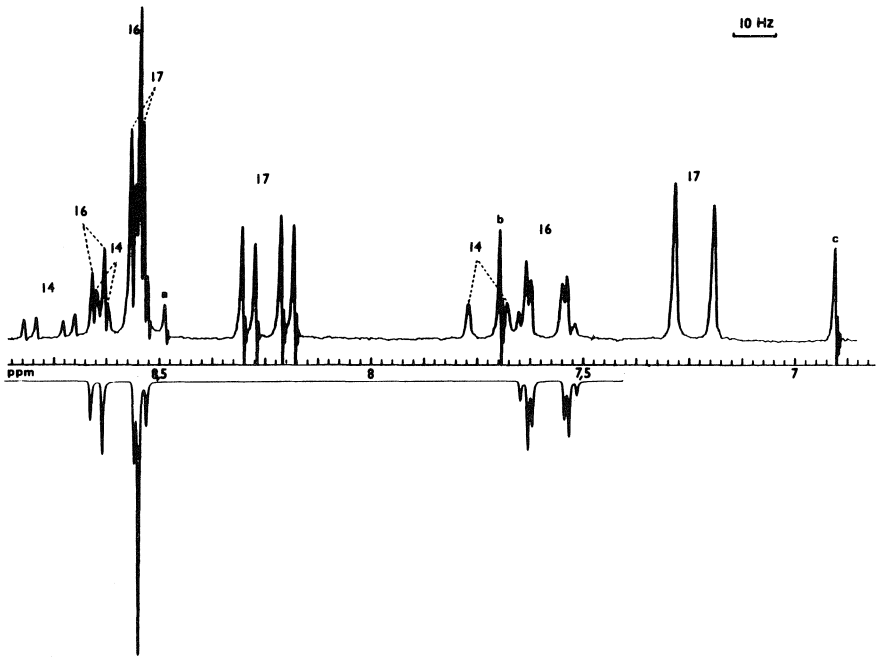
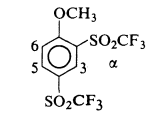
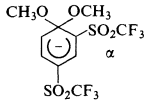
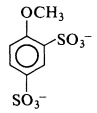


FIG. 2. Low-field part of the ¹H nmr spectrum of the methylsulfonate **16** and the sulfonate **17** and the simulated ABX system of **16**. Resonances are identified by structure numbers. Signals noted *a*, *b*, *c*, are three components of the quartet from CHF_3.

in this region, these results clearly point out the initial formation of the σ-adduct **19**. Further evidence comes from the ¹⁹F spectra: addition of CH_3O^- to a solution of **18** in DMSO-d_6 results in an almost complete disappearance of the signals from **18** at −76.10 and −78.16 ppm and the appearance of two equally intense absorptions at −78.23 and −79.53 ppm, which quickly disappear. These ¹⁹F shifts are in agreement with those expected for the σ-adduct **19**. The formation of CHF_3 and of other fluorinated species can also be observed by ¹⁹F nmr.

Can. J. Chem. Downloaded from www.nrcresearchpress.com by 210.87.254.105 on 09/05/12
For personal use only.

TABLE 3. Nuclear magnetic resonance parameters of anisole **18**, σ-adduct **19**, and disulfonate **20**[a]

Compounds	δ(¹⁹F)	δ_{H3}	δ_{H5}	δ_{H6}	δ_{OCH_3}	$^4J_{3-5}$	$^3J_{5-6}$	$J_{F\beta-H5}$
 **18**	α: -76.1_0 β: -78.1_6	8.40	8.67	7.88	4.23	2.4_5	9.0_5	0.6
 **19**	α: -78.2_3 β: -79.5_3		6.58	5.17	2.91	2.4	10	
 **20**		8.05	7.58	6.93	3.79	2.3	8.5	

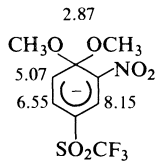
[a]δ in ppm relative to internal TMS (¹H) and internal $CFCl_3$ (¹⁹F). Negative values are upfield from the reference compound. *J* in Hz.

The structure of the final product **20** has been proved by a comparison of its ¹H spectrum with that of an authentic sample of the corresponding barium salt, dissolved in DMSO-d_6 (see Experimental).

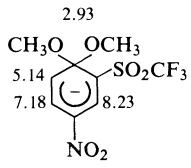
Discussion

Proton Chemical Shifts

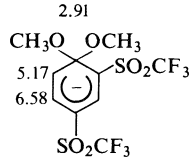
The formation of the σ-adducts **11**, **15**, and **19** from nucleophilic attack of CH_3O^- at the aromatic C1 carbon of the anisoles **10**, **14**, and **18** is confirmed by a comparison of the observed nmr parameters with those previously reported for the dinitro-analogue **7***a* (7).



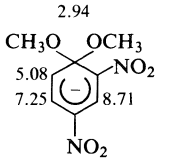
11



15



19



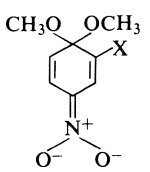
7a

In particular, the high-field shift of H6, which resonates at about 5.1 ppm, appears to be diagnostic of such *gem*-dialkoxyl-2,4-disubstituted adducts. Also, the resonance of the methoxyl protons is seen near 2.9 ppm while it is shifted to ~3 ppm in the *gem*-dimethoxyl trisubstituted adducts.

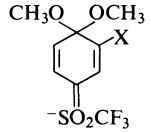
Comparing the OCH_3, H3, and H5 shifts in **11** and ***7a*** shows that the replacement of the SO_2CF_3 substituent by a nitro group at the 4-position results in a low-field shift of all of these resonances. Similarly, the OCH_3 and H5 resonances are at lower field in **15** than in **19**. This suggests that the 4-nitro group is more efficient than SO_2CF_3 in delocalizing the negative charge of the σ-adducts. This result is in agreement with our previous study of 4-X-substituted 2,6-dinitro-1,1-dimethoxyl adducts (11). In this case a linear plot of $\delta_{H3,5}$ versus the σ_R constant of the 4-X substituent was observed; however, to fit the above correlation for X = NO_2, σ_{Rp^-} has to be used. It thus appears that the resonance contributor, **21**, is of a much greater importance than the analogous one, **22**, which involves the *d* orbital participation of the sulfur atom, at least in this type of negatively charged species.

A quite different trend is observed in the parent anisoles **10** and **18**. H5, which is *ortho* to the same SO_2CF_3 substituent, is less shielded when *para* to a SO_2CF_3 group, as in **18**, than when *para* to a nitro group, as in **10**. This shows that SO_2CF_3 is more electron-withdrawing than NO_2 in aromatic substrates, as expected from the σ_p constants: (NO_2: $\sigma_p = 0.778$; SO_2CF_3: $\sigma_p = 0.93$) (12).

A similar comparison of H5 chemical shift in the



21



22

(X = NO_2, SO_2CF_3)

Can. J. Chem. Downloaded from www.nrcresearchpress.com by 210.87.254.105 on 09/05/12
For personal use only.

Can. J. Chem. Downloaded from www.nrcresearchpress.com by 210.87.254.105 on 09/05/12
For personal use only.

sulfonates **13** and **20**, where H5 is *ortho* to the same SO_3^- substituent but *para* to NO_2 in **13** and to SO_3^- in **20**, indicates that, as expected, SO_3^- has a much less electron-attractive influence than NO_2 (SO_3^-: $\sigma_p = 0.090$) (12).

Fluorine Chemical Shifts

Both the anisole **18** and the σ-complex **19** exhibit two fluorine signals which may be assigned to the 2-SO_2CF_3 and 4-SO_2CF_3 groups respectively in the following way. Long range coupling constants $^5J_{F-H5}$ and $^5J_{F-H3}$ are observed in the anisole **10**, where the SO_2CF_3 group is *para* to the methoxyl substituent. No such F—H coupling constant is present in the anisole **14**, where the SO_2CF_3 group is *ortho* to the methoxyl substituent. The spectrum of **18** shows that H5 is spin-coupled with the three fluorines of one of the SO_2CF_3 groups, the ^{19}F resonance of which appears at −78.16 ppm. This allows us to assign this high-field fluorine signal (δ = −78.16 ppm) to the 4-SO_2CF_3 group and the low-field resonance (δ = −76.10 ppm) to the 2-SO_2CF_3 group.

A comparison of the ^{19}F chemical shifts in the three anisoles **10**, **14**, and **18** indicates that the fluorines of 4-SO_2CF_3 groups in **10** and **18** are shielded relative to those of 2-SO_2CF_3 groups in **14** and **18**, suggesting that the donor effect of the methoxyl group is more important in the *para* than in the *ortho* position.

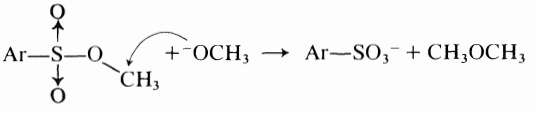
An assignment of the fluorine resonances in the σ-adduct **19** can be made on the basis of the upfield ^{19}F shifts observed on going from anisoles **10** and **14** to σ-complexes **11** and **15** ($\delta_{11} - \delta_{10} = -1.2$ ppm) and ($\delta_{15} - \delta_{14} = -1.9$ ppm), respectively. If the high-field fluorine resonance of **19** is assigned to the 4-SO_2CF_3 group, similar upfield shifts are obtained on going from **18** to **19**: 4-SO_2CF_3, $\Delta\delta = -1.37$ ppm and 2-SO_2CF_3, $\Delta\delta = -2.13$ ppm.

Conclusion

The occurrence of a competitive nucleophilic attack of methoxide ion at the aromatic C1 carbon of the anisoles **10**, **14**, and **18** to give the σ-adducts **11**, **15**, and **19** and at the sulfur atom of the SO_2CF_3 group of **10** and **14** to form the methylsulfonates **12** and **16** is clearly established by our experimental nmr data. This result is fully consistent with the well-known leaving group ability of the CF_3 substituent and the reaction certainly proceeds via a direct bimolecular nucleophilic displacement mechanism. Such a mechanism has been proved to operate in the hydrolysis or methanolysis of sulfonyl derivatives, which have a poorer leaving group, such as chlorine or dialkylamino (13, 14). The identification of **12** and **16** is, however, of interest since several authors have postulated, but not observed, the formation of methylsulfonates as intermediates in the conversion of trifluoromethylsulfonyl aromatic derivatives into benzene sulfonates in strongly basic medium (15, 16).

As to the formation of sulfonates as final products, it may be formulated, in agreement with previous results of Tommila and Lindholm (17), in terms of an Sn2 displacement at the methoxyl carbon of the SO_3CH_3 moiety. The good leaving group ability of the arylsulfonate moiety should favor such a reaction, which may be compared to the methoxide ion Sn2 attack on the methoxyl carbon of activated polynitroanisoles (18–20). In this latter case, the corresponding phenoxides and dimethylether are obtained. The nonobservation of dimethylether in the nmr spectra is probably due to its high volatility at the probe temperature of the nmr spectrometer (32°C).

During the completion of this work, an nmr identification of the σ-adduct **19** has been reported (21). A comparison of the published parameters for **19** with those found in this work for this adduct and for **11** and **15** makes these results (21) somewhat questionable. In particular, the reported OCH_3 and H6 chemical shifts $\delta_{OCH_3} = 3.75$, $\delta_{H6} = 6.61$ from HMDS ($\delta_{OCH_3} = 3.81$, $\delta_{H6} = 6.67$ from TMS) are not consistent with values generally found for *gem*-dimethoxyl-2,4-disubstituted σ-adducts (*vide supra*).



Experimental

2-Nitro-4-trifluoromethylsulfonylanisole **10**, 4-nitro-2-trifluoromethylsulfonylanisole **14**, and 2,4-bis(trifluoromethylsulfonyl)anisole **18** were prepared as previously described (22, 23, 24): **10** mp = 81°C, **14** mp = 71°C, **18** mp = 119°C. The ammonium salt of **13** was prepared from the corresponding acid, which was obtained by sulfonation of *o*-nitroanisole with chlorosulfonic acid, as previously described (25, 26). Its ^1H nmr spectrum was identical to that of the final product obtained in the reaction of CH_3O^- with **10**. An authentic sample of 1-methoxybenzenedisulfonate **20** was prepared according to the method of Svanholm and Parker (27). Its ^1H nmr spectrum was identical to that of the final product obtained in the reaction of CH_3O^- with **18**.

Acknowledgement

The authors are grateful to the Délégation Générale pour la Recherche Scientifique et Technique, Fluorine Chemistry Section, for financial support.

1. L. M. YAGUPOL'SKII and L. N. YAGUPOLS'KAYA. Proc. Acad. Sci. USSR (Engl. Transl.), **134**, 1207 (1960).
2. W. A. SHEPPARD. J. Am. Chem. Soc. **85**, 1314 (1963).
3. P. J. STANG and A. G. ANDERSON. J. Org. Chem. **41**, 781 (1976).
4. L. M. YAGUPOL'SKII, V. N. BOIKO, G. M. SHCHUPAK, N. V. KONDRATENKO, and W. P. SAMBUR. Tetrahedron Lett. 4413 (1975).
5. F. TERRIER, F. MILLOT, A. P. CHATROUSSE, L. M. YAGUPOL'SKII, V. N. BOIKO, G. M. SHCHUPAK, and N. V. IGNATEV. J. Chem. Res. 272, 1979.
6. F. TERRIER, F. MILLOT, and J. MOREL. J. Org. Chem. **41**, 3892 (1976).
7. (*a*) R. FOSTER and C. A. FYFE. Rev. Pure Appl. Chem. **16**, 61 (1966); (*b*) E. BUNCEL, A. R. NORRIS, and K. E. RUSSELL. Q. Rev. Chem. Soc. **22**, 123 (1968); (*c*) M. J. STRAUSS. Chem. Rev. **70**, 667 (1970); (*d*) C. F. BERNASCONI. MTP Int. Rev. Sci. Org. Chem. Ser. I, **3**, 33 (1973).
8. R. FOSTER, C. A. FYFE, P. H. EMSLIE, and M. I. FOREMAN. Tetrahedron, **23**, 227 (1967).
9. W. E. BYRNE, E. J. FENDLER, J. H. FENDLER, and C. E. GRIFFIN. J. Org. Chem. **32**, 2506 (1967).
10. C. A. FYFE. Can. J. Chem. **46**, 3047 (1968).
11. M. P. SIMONNIN, M. J. LECOURT, F. TERRIER, and C. A. DEARING. Can. J. Chem. **50**, 3558 (1972).
12. C. G. SWAIN and E. C. LUPTON. J. Am. Chem. Soc. **90**, 4328 (1968).
13. O. ROGNE. J. Chem. Soc. B, 1294 (1968); 1334 (1971).
14. D. KLAMANN and H. BERTSCH. Chem. Ber. **91**, 1427 (1958).
15. (*a*) S. M. SHEIN, M. I. KRASNOSEL'SKAYA, and V. N. BOIKO. Zh. Obshch. Khim. **36**, 2141 (1966); (*b*) S. M. SHEIN and M. I. KRASNOSEL'SKAYA. Zh. Obshch. Khim. **36**, 2148 (1966).
16. S. M. SHEIN, K. V. SOLODOVA, and V. I. GOVORCHENKO. Zh. Obshch. Khim. **39**, 1634 (1969).
17. E. TOMMILA and M. LINDHOLM. Acta Chem. Scand. **5**, 647 (1951).
18. J. F. BUNNETT and R. H. GARST. J. Org. Chem. **33**, 2320 (1968).
19. G. ILLUMINATI and F. STEGEL. Tetrahedron Lett. 4169 (1968).
20. A. P. CHATROUSSE, F. TERRIER, and R. SCHAAL. J. Chem. Res. (S) 288; (M) 2413 (1977).
21. V. N. BOIKO, G. M. SHCHUPAK, and L. M. YAGUPOL'SKII. Zh. Org. Khim. **14**, 670 (1978).
22. L. M. YAGUPOL'SKII and M. S. MARENETS. Zh. Obshch. Khim. **29**, 278 (1959).
23. S. M. SHEIN, V. A. IGNATOV, L. A. KOZOREZ, and L. F. CHERVATYNK. Zh. Obshch. Khim. **37**, 114 (1967).
24. S. M. SHEIN and M. I. KRASNOSEL'SKAYA. Zh. Vses. Khim. Ova. **10**, 592 (1965).
25. R. GNEHM and O. KNECHT. J. Prakt. Chem. **74**, 92 (1906).
26. L. G. CANNELL. J. Am. Chem. Soc. **79**, 2932 (1957).
27. U. SVANHOLM and V. N. PARKER. J. Chem. Soc. Perkin Trans. II, 962 (1972).

Can. J. Chem. Downloaded from www.nrcresearchpress.com by 210.87.254.105 on 09/05/12
For personal use only.

Unequal primary kinetic isotope effects in the base-catalysed H–D exchange of diastereotopic protons

ROBERT R. FRASER AND PHILIPPE J. CHAMPAGNE
Department of Chemistry, University of Ottawa, Ottawa, Ont., Canada K1N 9B4

Received July 16, 1979

ROBERT R. FRASER and PHILIPPE J. CHAMPAGNE. Can. J. Chem. **58**, 72 (1980).

Primary kinetic isotope effects have been measured for the base-catalyzed exchange reaction of 4′,1″-dimethyl-1,2,3,4-dibenzcyclohepta-1,3-diene-6-one, **1**. It was found that the isotope effects k^H/k^T and k^D/k^T for the faster exchanging protons (13.6 and 3.8 respectively) are significantly larger than the corresponding values for the slower exchanging protons (4.6 and 1.6 respectively). These differences could result from truly unequal isotope effects due to transition state differences or intrusion of a second pathway for exchange of the less reactive proton in the dedeuteration reaction. The data appear to support the latter interpretation. The secondary deuterium isotope effect was found to be 1.18.

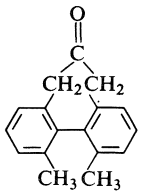
ROBERT R. FRASER et PHILIPPE J. CHAMPAGNE. Can. J. Chem. **58**, 72 (1980).

On a mesuré l'effet isotopique cinétique primaire de la réaction d'échange catalysée par les bases de la diméthyl-4′,1″ dibenz-1,2,3,4 cycloheptadiène-1,3 one-6 **1**. On a trouvé que l'effet isotopique k^H/k^T et k^D/k^T pour les échanges les plus rapides de proton (13.6 et 3.8 respectivement) sont d'une manière significative plus grandes que les valeurs correspondantes pour les échanges les plus lents de proton (4.6 et 1.6 respectivement). Ces différences peuvent provenir d'un effet isotopique vraiment inégal dû à des différences d'état de transition ou à l'intrusion d'un second modèle d'échange du proton moins réactif dans la réaction de dédeutération. Les données semblent confirmer la deuxième interprétation. On a trouvé que l'effet isotopique secondaire du deutérium est de 1.18.

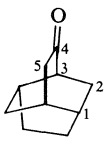
[Traduit par le journal]

Introduction

We have previously described the measurement of markedly different rates of hydrogen–deuterium exchange of the diastereotopic protons α to the carbonyl function in ketones **1** (1) and **2** (2). The reported rate ratios of 73 and 290 were interpreted as evidence for the importance of stereoelectronic control in the reactions of enolates. In order to substantiate the validity of this conclusion it is important to obtain evidence regarding the occurrence of internal return during the exchange reaction. To this end we wish to describe in this paper the measurement of the primary isotope effects k^H/k^T and k^D/k^T for each of the diastereotopic protons of **1**. These isotope effects have been found to



1



2

differ by factors of 3 and 2.5 respectively for the two protons. The difference can be attributed either to unequal proportions of internal return or to intrinsically different primary kinetic isotope effects. Arguments in support of the former interpretation of the data will be presented.

Internal Return

In its simplest form internal return refers to the process by which an anion produced by proton abstraction reverts to starting material. For example, in eq. [1] the reverse reaction defined by k_{-1} represents the internal return process which is expressed quantitatively as the ratio $a^H = k_{-1}/k_2$.

$$[1]\quad R_3C{-}H + SO^- \underset{k_{-1}}{\overset{k_1}{\rightleftharpoons}} R_3C^- \ldots H{-}OS \xrightarrow[SOD]{k_2} R_3CD + SO^- + SOH$$

Tests for the presence of internal return have thus far been of two types. One indication of its occurrence in a stereoselective isotopic exchange reaction is the observation of a significant influence of added crown ether on the stereoselectivity (3, 4). Another clearly predictable consequence of a large value for a^H would be an isotope effect which approaches unity as a^H becomes much greater than one. For smaller values of a^H one expects to observe a decrease from the normal primary isotope effect, whose magnitude cannot be measured. An ingenious solution to this problem was achieved by Streitwieser *et al.* (5) who have utilized the Swain–Schaad relations (6) between hydrogen, deuterium, and tritium exchange rates.

Streitwieser's Equations

The basis for the calculation of internal return is the relationship [2] below derived by Swain *et al.* (6) who assumed all isotope effects arise from zero

0008-4042/80/010072-07$01.00/0
©1980 National Research Council of Canada/Conseil national de recherches du Canada

Can. J. Chem. Downloaded from www.nrcresearchpress.com by 210.87.254.40 on 09/05/12
For personal use only.

Can. J. Chem. Downloaded from www.nrcresearchpress.com by 210.87.254.40 on 09/05/12
For personal use only.

point vibrational energy differences (no tunnelling).

[2] $$k^H/k^T = (k^D/k^T)^{x+1} = (k^H/k^D)^{(x+1)/x}$$

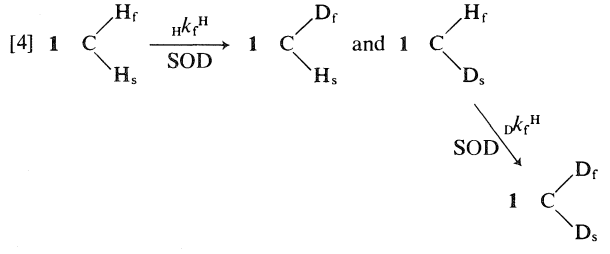
The value assigned to x (2.26) was revised to 2.344 by Streitwieser and co-workers (5) to include the effects of reduced mass. These relations were then used to test for internal return in a number of isotope exchange reactions of aryl, diaryl, and triarylmethanes (5, 7). In essence, the approach was to determine $(k^H/k^T)_{SOD}$ and $(k^D/k^T)_{SOH}$ by experiment. If the difference in isotope effects gave a value for x of 2.344, it could be concluded that internal return was absent. Any diminution in x could be converted, using the quantitative relations given in the Appendix, into a value of a^H. By this method, a significant amount of internal return ($a^T = 0.66$, where a^T refers to internal return during exchange of tritium for hydrogen) was detected in the exchange of triphenylmethane in methanol containing sodium methoxide (5). In contrast, the amount of internal return in the exchange of the same compound in cyclohexylamine (plus lithium amide) was negligible; $a^T = 0.02$ (7). More recently the same method was utilized in our laboratory to establish the absence of internal return in the exchange of the benzylic protons of benzyl methyl sulfoxide (8). The equations derived by Streitwieser appear in the Appendix.

For application of these equations to ketone **1** two additional sets of experimental data are required. One is the equilibrium constant $K^{T'}$ described in eq. [3].

[3] $$\mathbf{1}\,C{-}T + CH_3OH \rightleftharpoons \mathbf{1}\,C{-}H + CH_3OT$$

Tritium analysis of solvent and ketone after equilibration gave a value for $K^{T'} = 1.23 \pm 3\%$. Previously, values of similar magnitude had been observed for 9-phenylfluorene in methanol, $K^{T'} = 1.3$ (5), and for benzyl methyl sulfoxide in methanol $K^{T'} = 1.27$ (8).

The second requirement is a knowledge of the secondary deuterium isotope effect which represents the ratio of the rates of H–D exchange when the diastereotopic partner is hydrogen versus deuterium, i.e., ${}_Hk_f^H/{}_Dk_f^H$ as illustrated in eq. [4].

[4] 

Results and Discussion

Measurement of Secondary Isotope Effect in 1

In the case of the biarylcycloheptadienone, **1**, the high stereoselectivity between abstraction of H_f and H_s of 62:1 in the H–D exchange and the stereoselectivity of 12:1 in the D–H exchange of **1**-d_4 (to be described in detail later) allows preparation of **1**, selectively labelled with deuterium in 50% of the H_s position, and only 4% in the H_f position.

In the H–D exchange of this sample one monitors by ^1H nmr the exchange of both types of fast protons (the extent of exchange of H_s being negligible over the time interval used). The isotope effect ${}_Hk_f^H/{}_Dk_f^H$ was thereby found to be 1.18 (see Table 1) in good agreement with those secondary isotope effects previously reported for fluorene 9,9-d_2, i = 1.18 (5*a*), and for toluene-d_3, i = 1.18 (16). The secondary isotope effect for exchange in the slow position of **1** is not determinable and can only be assumed to have the same magnitude.

Measurements of Isotope Effects in 1

The orientation of the two diastereotopic protons of **1** was established previously to be that shown in Fig. 1. The pro R in R protons, the more labile towards base, will be referred to as the "fast" protons and the pro S in R protons referred to as the "slow" protons. These are labelled H_f and H_s respectively. Their relative rates of exchange k_f/k_s have been measured in methanol-*O*-*d* in the presence and absence of crown ether and found to be about 60:1[1] in both instances. These rate data are given in Table 2. The lack of effect of crown ether can be interpreted as an indication that internal return is not of importance in this exchange reaction. Nevertheless, the more quantitative indications of isotope effects were sought. The very large difference in proton abstraction rates made possible the measurement of isotope effects for each proton. Several examples of the methods used to measure the isotopic exchange rates are given in the Appendix.

Primary Isotope Effects and Internal Return

The rate constants in Table 2 give rise to the following primary isotope effects;

$$(k_f^H/k_f^T)_{CH_3OD} = 13.6 \qquad (k_f^D/k_f^T)_{CH_3OD} \geqq 3.8$$

$$(k_s^H/k_s^T)_{CH_3OH} = 4.6 \qquad (k_s^D/k_s^T)_{CH_3OH} = 1.6$$

From these kinetic isotope effects and $K^{T'}$, the

[1] In our preliminary communication (1) the individual rate constants reported were in error by the conversion factor 2.303. In addition, the rate data has been reanalyzed using the more exact treatment of Sachs (9) thereby leading to the modified rate constants which are included in Table 2.

TABLE 1. Secondary isotope effect measurement for **1** (in CH_3OD, 0.002 *M* in sodium methoxide)*

Time (s)	${}_DA_f^H$	${}_HA_f^H$	A_e^H	B	${}_Dk_f^H$ (s^{-1})	${}_Hk_f^H$ (s^{-1})	i_f
0	0.840	1.080					
60	0.556	0.654	0.028	0.121	7.14	8.61	1.20
120	0.378	0.424	0.034	0.190	7.04	8.16	1.16

*The superscripts denote bond being broken, left hand subscripts denote the nature of the geminal nucleus.

TABLE 2. Kinetics of H–D (D–H) exchange in the ketone **1**

Run	Solvent/base (conc.)	Rate constants (L M^{-1} s^{-1}) Fast position	Slow position
1	CH_3OD/CH_3ONa (2.9×10^{-3} *M*)	$k_f^H = 6.3$	$k_s^H = 0.095$
2	CH_3OD/CH_3ONa-C.E.*(1.6×10^{-3} *M*)	$k_f^H = 6.2$	$k_s^H = 0.10$
3	CH_3OD/CH_3ONa (1.3×10^{-3} *M*)	$k_f^H = 7.1$ $k_f^T = 0.52$	
4	CH_3OD/CH_3ONa (6.0×10^{-3} *M*)		$k_s^H = 0.15$ $k_s^T = 0.033$
5	CH_3OH/CH_3ONa (6.1×10^{-3} *M*)	$k_f^D = 0.65$ $k_f^T = 0.17$	$k_s^D = 0.054$ $k_s^T = 0.033$

*C.E. refers to dicyclohexyl-18-crown-6.

internal return is calculated to be 11.7 for a_f^H and 0.32 for a_s^H. The resultant a_f^H of 11.7 representing 92% internal return is particularly remarkable. Any large amount of internal return in methanol is unexpected, for as Hunter has pointed out (10), previous exchanges in this solvent have indicated little if any internal return. A more disturbing aspect associated with this internal return is the value for the H–D isotope effect for proton abstraction which can be calculated from k_f^H/k_f^T and a_f^H. This value representing the primary H–D isotope effect for step 1, eq. [1], is 36.

Such a high value for a primary isotope effect in base catalysed carbanion formation is without precedence; a number of examples of normal primary kinetic isotope effects are reported by Jones (11). We are therefore led to question the validity of Streitwieser's equations as applied to ketone **1**. The most significant assumption inherent in their application is that there will be no solvent effect on internal return. However, this assumption cannot be tested directly. Tunnelling is assumed to be absent as well (12).[2] Failure of the method could also result from difficulties specific to **1**. For example, since **1** possesses two of each type of diastereotopic proton, the accuracy of the mass spectral analysis is decreased from a normal precision of ±2% to an estimated 4 to 6% due to the measurement of intensity ratios involving five isotopic molecular ions. Since the rate constants are usually the average of only two measurements, due to a practical limitation on the amount of **1** synthesized, the combined errors could lead to uncertainties in isotope effects of up to 8% or more. Also, because of repeated exponential relations between the measured isotope effects and a^H, the uncertainty range calculated for a^H is 3 to 13 for the labile proton and 0.25 to 1.2 for the slowly exchanging proton. Equally important is the question of the proper choice of exponent (12). Errors in temperature, measurement of $K^{T'}$ and i, and additional approximations in the Sachs equation reduce the quantitative assessment of a^H to a qualitative status of indeterminate accuracy.[3]

Nevertheless, the experimentally determined

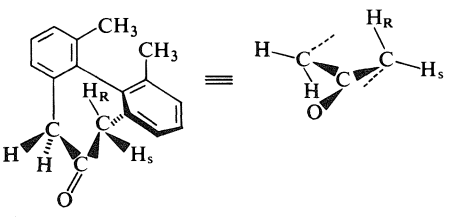


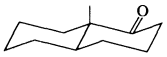
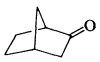
FIG. 1. A three-dimensional representation of 4′,1″-dimethyl-1,2,3,4-dibenzcyclohepta-1,3-diene-6-one, **1**.

[2]Any value for k^H/k^D in excess of ten is considered to require a contribution from tunnelling, and appears to be associated with steric hindrance.

[3]One further uncertainty could not be avoided. It was found that minor amounts of water in the solvent had a substantial effect on the rates of exchange. For the practical consideration of time, runs 3, 4, and 5 could not be performed on the same days. Although all possible precautions were taken to avoid exposure to moisture, small differences in traces of water in the solvent possibly occur.

Can. J. Chem. Downloaded from www.nrcresearchpress.com by 210.87.254.40 on 09/05/12
For personal use only.

TABLE 3. Rate ratios for exchange of diastereotopic protons in ketones

Ketone	k_f/k_s(Solvent)	Ref.
	3.8 (D_2O/dioxane) 1.9 (H_2O/dioxane)	13 13
	740[661](D_2O/dioxane) 100[72](H_2O/dioxane)	13[14,15] 13[14]
1	62 (CH_3OD) 12 (CH_3OH)	1 This work
2	280 (CH_3OD) 51 (CH_3OH)	2 2,17

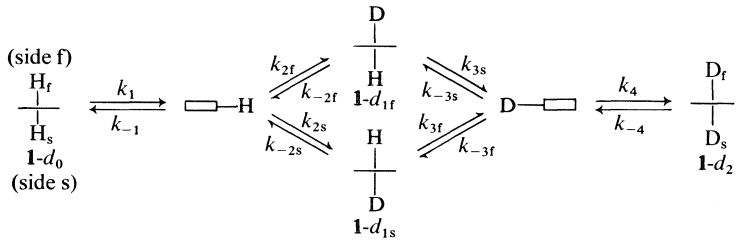


FIG. 2. Proposed pathways and their associated rate constants for the H–D exchange of a pair of diastereotopic protons α to a carbonyl (or for the D → H exchange of **1**-$d_2 \rightarrow d_0$).

kinetic isotope effects do provide some valuable mechanistic information. From k_f^H/k_f^T, *assuming no internal return*, one can calculate the primary isotope effect k_f^H/k_f^D to be 6.2 and, by the same method, k_s^H/k_s^D to be 2.9. This divergence of the two primary isotope effects may be interpreted as either a reflection of intrinsically different isotope effects since any two C—H bonds involving diastereotopic protons are different, *or* the smaller isotope effect exhibited by H_s results from diminution of its true isotope effect by internal return. A special type of internal return has already been proposed independently by two groups. Work by Lamaty (13) and by Banerjee and Werstiuk (14) has clearly established a much greater selectivity in the deuteration of a chiral ketone than in the dedeuteration of the same α,α-dideuterated chiral ketone. Their results and those for ketones **1** and **2** are summarized in Table 3. The scheme, first put forward by Banerjee and Werstiuk (14), is represented in Fig. 2. Essentially, the explanation for the fact that k_f^H/k_s^H on deuteration of norbornanone is 740 but that k_f^D/k_s^D for the dedeuteration of 3,3-dideutero-2-norbornanone is only 100 is as follows. In the reverse exchange, i.e., **1** $d_2 \rightarrow d_0$, the faster exchange (side f) produces d_{1s}. The second dedeuteration step k_{-2s} will experience more effective competition from k_{3f} than in the deuteration process since k_{-2s} will be retarded by the primary isotope effect, whereas in deuteration k_{-2f} experiences the retarded isotope effect. This explanation, involving reversible monodeuteration and resultant exchange with inversion is plausible but contains in it certain questionable assumptions. First, it assumes no secondary isotope effect and no solvent effects on isotope effects. In addition, it utilizes a symmetrical enol or enolate as the intermediate, although the involvement of two enolates or one or more asymmetrically solvated intermediates is also possible.[4] It also assumes no internal return of the type we sought to detect, i.e., formation and collapse of an anion to starting material as indicated in eq. [1].

All of the isotope effects revealed by the data in Table 2 are consistent with the schemes of Werstiuk and Lamaty. Indeed the further reduction in stereoselectivity in the tritium exchange to $k_f^T/k_s^T = 5.1$ is predicted as a result of the inversion pathway in Fig. 2. In addition, the fact that the solvent isotope effect for the rapidly exchanging proton is 2.6 (see runs 3 and 5 and secondary isotope effect) while that for the slow proton is 1.2 (see runs 4 and 5) can also be readily accounted for by the presence of inversion during the exchange of the slow tritium.

There is another possible interpretation[5] that all the observed rate constants represent exchanges in the absence of any inversion. Consequently the

[4]Tidwell and co-workers discuss the difficulties in distinguishing between enol and enolate intermediates (15). Even though the exchange of the fast proton via a mandatory retention pathway must involve an asymmetric intermediate this factor is not represented in the figure.

[5]It is important to note that regardless of the interpretation of these isotope effects the observed stereoselectivity of 63:1 is a minimum value and is not the result of internal return in the slow position. Thus the conclusions of refs. 1 and 2 remain valid.

Can. J. Chem. Downloaded from www.nrcresearchpress.com by 210.87.254.40 on 09/05/12
For personal use only.

primary kinetic isotope effects and solvent isotope effects would differ by surprisingly large amounts for the two diastereotopic protons. Work is in progress to test this interpretation.

Experimental

Heavy water (99.9 at.% D) and methanol-*O*-*d* (99 at.% D) were obtained from Merck, Sharp and Dohme Canada Limited. Tritiated water (25 mCi/mL) and standard tritiated toluene (4.5 × 10^6 dpm/mL) were obtained from New England Nuclear Corporation. Solutions of lower specific activity were prepared by volumetric dilution. Tritiated methanol and methanol-*O*-*d* were prepared by dilution with tritiated water and the respective solvents. Dicyclohexyl-18-crown-6 cyclic polyether obtained from Aldrich was used without further purification.

Diphenyloxazole (PPO) and 2,2′-*p*-phenylene-bis(5-phenyloxazole) (POPOP), liquid scintillation counter grade, were obtained from Baker Co. Scintanalyzed toluene was obtained from Fisher Scientific.

All weighings for scintillation counting were done on an E. Mettler Zurich Type H-16 balance accurate to 0.05 mg. The nmr spectra were taken in deuterochloroform solution (unless otherwise stated) on a Varian T-60 spectrometer or a Varian HA-100 spectrometer equipped with an SD-100 deuterium spin decoupler. Control tests showed the T-60 integration to be as accurate as the HA-100 integration so the T-60 nmr was used for analysis unless otherwise stated. Tritium counting was carried out in a Beckman LS-150 scintillation counter equipped with an external standard channels ratio function. Kinetic samples which involved mass spectrometric analysis were run on an AEI MS-903 mass spectrometer. The experimental conditions reported are those found to give the most accurate and reliable results after a minimum of two pre-trials for each rate determination.

Unless otherwise stated, the experimental data were treated by the Sachs equation (9) for equilibrating pseudo-first order reactions as given below.

$$\frac{d_0 + h_0}{d_0 + h_0 + B} \ln \frac{A_0 - A_e}{A_t - A_e} = kT$$

where d_0 = initial concentration of exchangeable deuterium in solvent, h_0 = initial concentration of exchangeable hydrogen in solvent, B = concentration of hydrogen (or deuterium or tritium) in solvent due to exchange with substrate, A = concentration of hydrogen (or deuterium or tritium) in substrate, A_e = equilibrium concentration of hydrogen (or deuterium or tritium) in substrate.

Preparation of Solutions For Kinetic Measurements

Sodium methoxide solutions in methanol or methanol-*O*-*d* were prepared by adding methanol volumetrically by syringe to the required amount of clean, dry sodium in a cooled serum capped flask which had been flushed with nitrogen. The deuterium gas formed was allowed to escape through a second syringe needle. The base was then titrated with standard hydrochloric acid solution. Alternatively, solutions were prepared by dissolving a weighed amount of fresh, dry sodium methoxide in methanol-*O*-*d*. Both methods gave base solutions which remained clear and colourless and maintained their base strength for periods up to three months when stored in the refrigerator under nitrogen and with the serum caps taped and wrapped with Parafilm.

Toluene scintillation liquid was prepared by dissolving 4 g of PPO and 1 g of POPOP in 1 L of Scintanalyzed toluene.

Sample Preparation

For Nuclear Magnetic Resonance

When extraction was to be used for recovery of the partially exchanged ketone, the reaction mixture was quenched with 0.1 *N* HCl and the resulting suspension was extracted three times with spectral grade methylene chloride. The organic phase was dried over anhydrous magnesium sulphate, filtered, and the solvent removed on the rotary evaporator. Traces of solvent were removed by drying under a vacuum of about 0.2 Torr for at least one hour. Control tests using deuterated acid indicated no isotope exchange due to this work-up procedure.

Since the partially exchanged ketone samples were unstable in their isotope content towards chromatographic purification, and recrystallization resulted in large losses, samples for nmr analysis were prepared as above unless otherwise specified. Ketone **1** was not sublimable below its melting temperature with the available vacuum.

For Mass Spectrometry

Each sample for scintillation counting and for mass spectrometry was prepared in the following way. The aliquot to be quenched was withdrawn from the reaction by syringe and added to three times its volume of distilled water containing hydrochloric acid 10% in excess of the base present. The resulting suspension was covered and stored in the refrigerator overnight, after which time the pure, white ketone had precipitated out. This precipitate was filtered, washed with distilled water, and dried under vacuum to constant weight.

For Scintillation Counting

The purified aliquot (5–25 mg) was weighed out accurately in a 20 mL polyethylene scintillation vial (Fisher) and was dissolved in 10 mL of the toluene scintillation liquid. With each set of quenched samples was included a set of standards for calibrating the counting efficiency of the machine. Samples were counted with an ^3H window for varying times depending on the sample size and specific activity to give maximum 1.0% statistical error except in a few cases where, due to small sample size, the error rose to 1.5%.

Due to a shortage of available ketone **1**, the standard samples used to calibrate the counting efficiency of the scintillation counter were made up by adding increasing amounts (0 to 0.2 mL) of chloroform to solutions of 0.01 mL of standard tritiated toluene in 10 mL of toluene scintillation liquid, such that the range of standard sample quenching was greater than the range involved in tritium counting of quenched samples.

For each standard sample counted, the machine registered an external standard ratio which allows conversion of the counting rate into a specific activity for each sample.

Method of Treatment of Mass Spectral Data

For all measurements of primary isotope effects the proton and deuterium content were determined by mass spectrometric analysis. Each sample was analyzed at least eight times over a range of six *m/e* units above and below the parent molecular ion (M^+). Each set of peak heights was normalized to a total of 100, then averages were taken for each *m/e* value. The spectra of pure **1** showed a large PMI (M^+), and $(M + 1)^+$ and $(M + 2)^+$ peaks which were 20.27% and 2.54% respectively of the M^+ peak. Therefore, each peak height in an analytical sample was corrected accordingly. The concentrations of the d_0, d_1, d_2, d_3, and d_4 species could then be calculated from these corrected peak heights. The details of this treatment of the spectral data appear in the thesis of P.J.C. (17). All proton concentrations (or deuterium for the reverse exchange) are expressed as the number of protons (or deuterons) remaining out of the 4 originally available for exchange.

Can. J. Chem. Downloaded from www.nrcresearchpress.com by 210.87.254.40 on 09/05/12
For personal use only.

Can. J. Chem. Downloaded from www.nrcresearchpress.com by 210.87.254.40 on 09/05/12
For personal use only.

This treatment gives individual rate constants with a precision of ±4–6%. Comparable accuracy is obtained when rate constants are obtained from several quenched aliquots.

*Determination of the Secondary Isotope Effect (*i*) for the Fast Methylene Position in* **1**

Preparation of **1** *Specifically Deuterated in 50% of the Slow Position*

Reaction conditions were based on previous pre-trial estimates of deuteration and dedeuteration rates.

To 100 mg (0.424 mmol) of **1** in 2.46 mL of methanol-*O-d* was added 0.01 mL of sodium methoxide/methanol-*O-d* (0.18 *M*) under nitrogen with stirring. The reaction was stirred at 29.4 ± 0.1°C for 2 780 s, after which time the reaction was quenched and the ketone (76 mg) recovered by extraction. The nmr of this ketone showed only 0.8 protons remaining, all of them in the high field (slow) position. The ketone was redissolved in 1.83 mL of methanol under nitrogen and 0.065 mL of sodium methoxide/methanol solution (0.045 *M*) was added with stirring at 29.0 ± 0.1°C. This reaction was quenched after 6 980 s and the ketone isolated. The nmr of this product showed a total of 3.08 hydrogens in the two methylene positions. The 100 MHz spectrum on 250 Hz sweep width with deuterium decoupling gave the following breakdown for this 3.08 hydrogens: CD_fH_s = 0.08 H; CH_fD_s = 0.84 H; CH_fH_s = 2.16 H (see Table 2).

Measurement of Secondary Isotope Effect, i_f

To 40 mg (0.17 mmol) of the monodeutero **1** from above in 0.99 mL of methanol-*O-d* under nitrogen was added, with stirring, 0.01 mL of sodium methoxide/methanol-*O-d* solution (0.18 *M*) at 29.0 ± 0.1°C. After 60 s 0.5 mL was withdrawn by syringe and quenched. The remainder was quenched after 120 s. The samples of ketone were recovered by extraction and examined by 100 MHz nmr as above. The results of the proton analysis of these samples[6] are presented in Table 1 and show the secondary isotope to be 1.18.

Measurement of Rates in Runs 1 to 5 in Table 2

The details of these rate measurements have been placed in the Depository of Unpublished Data.[7]

Acknowledgement

The authors thank the Natural Sciences and Engineering Research Council of Canada for their financial support.

1. R. R. Fraser and P. J. Champagne. Can. J. Chem. **54**, 3809 (1976).
2. R. R. Fraser and P. J. Champagne. J. Am. Chem. Soc. **100**, 657 (1978).
3. J. F. Bieĺlmann and J. J. Vicens. Tetrahedron Lett. 2915 (1974).
4. (*a*) S. H. Wong, H. D. Fischer, and D. J. Cram. J. Am. Chem. Soc. **93**, 2235 (1971); (*b*) J. Almy, D. C. Garwood, and D. J. Cram. J. Am. Chem. Soc. **92**, 4321 (1970); D. H. Hunter, Y.-T. Lin, A. L. McIntyre, D. J. Shearing, and M. Zvagulis. J. Am. Chem. Soc. **95**, 8327 (1973).
5. A. Streitwieser, Jr., W. B. Hollyhead, H. H. Pudjaatmaka, P. H. Owens, T. L. Kruger, P. A. Rubenstein, R. A. McQuarrie, M. L. Brokaw, W. K. C. Chu, and H. M. Niemeyer. J. Am. Chem. Soc. **93**, 5088 (1971); A. Streitwieser, Jr., W. B. Hollyhead, G. Sonnichsen, A. H. Pudjaatmaka, C. J. Chiang, and T. L. Kruger. J. Am. Chem. Soc. **93**, 5096 (1971).
6. C. G. Swain, E. C. Stivers, J. F. Reuwer, Jr., and L. J. Schaad. J. Am. Chem. Soc. **80**, 5885 (1958).
7. A. Streitwieser, Jr., P. H. Owens, G. Sonnichsen, W. K. Smith, G. R. Zeigler, H. M. Niemeyer, and T. L. Kruger. J. Am. Chem. Soc. **95**, 4254 (1973); A. Streitwieser, Jr., M. R. Granger, F. Mares, and R. A. Wolf. J. Am. Chem. Soc. **95**, 4257 (1973).
8. R. R. Fraser and L. K. Ng. J. Am. Chem. Soc. **98**, 4334 (1976).
9. W. H. Sachs. Acta. Chem. Scand. **25**, 2132 (1971).
10. D. H. Hunter. *In* Isotope effects in organic chemistry. Vol. 1. *Edited by* E. Buncel and C. C. Lee. Elsevier, Amsterdam. 1975. p. 135.
11. J. R. Jones. Prog. Phys. Org. Chem. **9**, 262 (1972).
12. R. P. Bell. *In* The proton in chemistry. Cornell University Press, Ithaca, NY. 1973. p. 281.
13. G. Lamaty. *In* Isotopes in organic chemistry. Vol. 2. *Edited by* E. Buncel and C. C. Lee. Elsevier, Amsterdam. 1976. p. 33.
14. S. Banerjee and N. H. Werstiuk. Can. J. Chem. **53**, 1099 (1975).
15. G. A. Abad, S. P. Jindall, and T. T. Tidwell. J. Am. Chem. Soc. **95**, 6326 (1973).
16. A. Streitwieser, Jr. and D. E. Van Sickle. J. Am. Chem. Soc. **84**, 254 (1962).
17. P. J. Champagne. Ph.D. Thesis, University of Ottawa, Ottawa, Ont. 1978.

Appendix

Determination of k_f^H *and* k_f^T *in Methanol*-O-d

To prepare a sample of **1** selectively tritiated in the fast position an exchange was carried out in tritiated methanol until 5% of the equilibrium tritium content was incorporated in **1**. Under these conditions (see Experimental for details) the distribution between fast and slow positions will still be 63:1.

Exchange of this sample of **1** was carried out in methanol-*O-d* containing sodium methoxide (1.3×10^{-3} *M*). Aliquots for deuterium were taken at times considered optimum on the basis of three previous experiments on the same sample under the same conditions. Only the first two of four aliquots analyzed for deuterium content contained sufficient remaining protons to yield an accurate k_f^H. This exemplifies a problem in reproducing conditions for a given set of rates due to limitations in the accuracy with which a solution of desired base concentration can be prepared and also to the difficulty in maintaining a reproducible water content in the solvent. For the same reason only two of three aliquots subjected to tritium analysis were used in calculating k_f^T.

Determination of k_s^H *and* k_s^T *in Methanol*-O-d

A sample of **1** equilibrated in methanol-*O-t* con-

[6]The measurements were made during simultaneous irradiation using an SD-100 deuterium spin decoupler.

[7]Copies may be obtained, at a nominal charge, from the Depository of Unpublished Data, CISTI, National Research Council of Canada, Ottawa, Ont., Canada K1A 0S2.

taining methoxide catalyst was shown by tritium analysis to be fully labelled in both positions. Exchange of this sample in methanol-*O-d* (6.03 *M* in $NaOCH_3$) was monitored by taking of aliquots at times determined from three previous experiments to be optimum. This required all fast proton and tritium contents to have attained equilibrium values and for aliquots to possess contents of H_s and T_s in the range of 20 to 75% of their starting values. For both k_s^H and k_s^T only two aliquots analysed proved to be in this range.

Determination of k_f^D, k_f^T, k_s^D, *and* k_s^T *in Light Solvent*

Because of the isotope effects being smaller and also the selectivity being reduced to about 12 (observed in preliminary exchanges) it was possible to take aliquots at times optimum for measuring each of the four rate constants during a single reverse exchange reaction. The sample of **1**, fully deuterated (96%) and fully tritiated (11 429 dpm/mg) by exchange to equilibrium in tritiated methanol-*O-d* was exchanged in methanol-*O-h* containing sodium methoxide (6.1×10^{-3} *M*). The results of isotope content determination gave the derived rate constants appearing in Table 2.

Aliquots taken at intermediate times could not be used for calculation of k_s^D since it was not certain that all of D_f had exchanged and also since a significant part of the D_s exchange at these points had taken place under the influence of the secondary isotope effect caused by deuterium in the fast positions. As a result only three of six aliquots were used to obtain the value of $k_s^D = 0.32 \times 10^{-3}\ s^{-1}$ with good agreement between samples (standard deviation = ±2%). For the fast exchange, the first five samples were used in the calculation of $k_f^D = 3.97 \times 10^{-3}\ s^{-1}$, (the sixth sample had exchanged more than 90%) but the agreement between the rate constants calculated from these samples was not as good (standard deviation = ±6.8%). These two results give rise to a stereoselectivity of $k_f^D/k_s^D = 12.1 \pm 9\%$ which has decreased by a factor of 5.1 from the forward exchange stereoselectivity of 63.

Streitwieser's Equations

The value for $a^H = (k_{-1}/k_2)$ (1) can be obtained (5) from the relationships between the following experimental measurements:

$$A = (k_{ex}^D/k_{ex}^T)^{x+1} \cdot k_{ex}^T/k_{ex}^H$$

$$B = (k_{ex}^D/k_{ex}^T)^{x+1} \cdot K^{T'}$$

where $K^{T'}$ represents the equilibrium given in eq. [3],

$$a^T(A - B) = [1 - a^T(B^{1/x+1} - 1)]^{x+1} - A$$

$$a^H = a^T k_{-1}^H/k_{-1}^T$$

$$= a^T K^T k_1^H/k_1^T$$

where k_1^H refers to carbanion formation from light isotope loss, and

$$k_1^T/k_1^H = k_{ex}^T/k_{ex}^H + a^T\left(\frac{k_{ex}^T}{k_{ex}^H} - K^{T'}\right)$$

Similar expressions for k^T/k^D relations appear in ref. 5.

Can. J. Chem. Downloaded from www.nrcresearchpress.com by 210.87.254.40 on 09/05/12
For personal use only.

Transfer free energies of alkali metal chlorides and of some individual ions in glycerol and water mixtures

INDRA N. BASUMULLICK[1] AND KIRON K. KUNDU[2]

Physical Chemistry Laboratories, Jadavpur University, Calcutta – 700032, India

Received May 29, 1979

INDRA N. BASUMULLICK and KIRON K. KUNDU. Can. J. Chem. **58**, 79 (1980).

Standard free energies of transfer, ΔG_t^0, of alkali metal chlorides from water to aqueous mixtures of 10, 30, 50, and 70 wt.% glycerol have been determined from emf measurements of the double cell comprising Ag–AgCl and K(Hg) electrodes at 25°C. These values were divided into individual ion contributions by use of tetraphenyl arsonium tetraphenyl boride (Ph_4AsBPh_4) assumption, the required ΔG_t^0 values of the reference electrolyte (Ph_4AsPh_4B), obtained by measuring solubilities of $KBPh_4$, Ph_4AsPi, and KPi (Pi = picrate) in the solvents. The solvation behaviour of the involved ions, as dictated by their respective $\Delta G_t^0(i)$ values, in this as well as in systems of other similar co-solvents like ethanol, ethylene glycol, and urea, suggests that it is determined by one or several effects of acid–base, Born-type, and dispersion interactions. Moreover, comparable stability of Ph_4B^-, particularly in aqueous glycerol and urea, suggests that "specific interactions" are possibly responsible for the well-known folding–unfolding phenomenon of native conformation of proteins in presence of co-solvents.

INDRA N. BASUMULLICK et KIRON K. KUNDU. Can. J. Chem. **58**, 79 (1980).

On a déterminé les énergies libres normales de transfert ΔG_t^0 des chlorures métalliques alcalins dans l'eau et dans des mélanges aqueux à 10, 30, 50 et 70% en poids de glycérol à partir des mesures fem d'une double cellule comprenant des électrodes Ag–AgCl et K(Hg) à 25°C. Ces valeurs sont divisées en contributions individuelles d'ions en faisant appel à l'hypothèse du tétraphénylborure de tétraphényle arsonium (Ph_4AsBPh_4); on a obtenu les valeurs requises de ΔG_t^0 de l'électrolyte de référence (Ph_4AsPh_4B) en mesurant les solubilités du $KBPh_4$, Ph_4AsPi et du KPi (Pi = picrate) dans les solvants. Les valeurs respectives de $\Delta G_t^0(i)$ obtenues dans ce système de solvants aussi bien que dans d'autres systèmes de cosolvants similaires comme l'éthanol, l'éthylèneglycol et l'urée, suggèrent que du point de vue de la solvatation les comportements des ions impliqués sont dictés principalement par des effets combinés acide–base du type Born ou par des interactions de dispersion. De plus, la stabilité comparable du Ph_4B^-, particulièrement dans le glycérol aqueux et dans l'urée, suggère que des interactions spécifiques sont responsables du phénomène bien connu de plissement–déplissement de la conformation naturelle des protéines en présence de co-solvants.

[Traduit par le journal]

Introduction

It is well recognized that glycerol has a striking ability of stabilizing (1–3) the native conformation of proteins as oppose the well-known destabilizing effect of urea (4–6). The genesis of these differences in the stability of protein is yet a conflicting issue (1). It is, however, widely believed that unfolding action of urea and stabilizing action of glycerol possibly stem from their effects on water structure (1, 3, 7, 8). Dipaola and Belleau (1, 9), from their apparent molar volume and heat capacity studies, increasingly emphasized that "specific interactions" rather than structural changes of water are the key to the stabilizing action of glycerol.

Recent studies of transfer energies of hydrogen halides (HX) and those accompanying the ionization of water in aqueous mixtures of urea (10, 11) and glycerol (12) have revealed that the structural order induced by both glycerol and urea are significantly less compared to those of aqueous alcohols, possibly due to the "specific-site hydration" (13) through hydrogen bonding centres of these co-solvents. Also, while urea acts more like a statistical structure breaker (14), glycerol lies on the border line of the structure making mono-ols (15) and structure breaking poly-ols (9). At any rate the observed differences in the structural order induced by these two co-solvents are not significantly different to be ascribed as the genesis of the converse behaviour of these co-solvents on thermodynamic stability of native proteins. Consequently, it should be of particular interest to investigate further if solvating behaviour of these two co-solvents on the different constituent groups of proteins or interactions of "specific nature" by the respective co-solvents play an important role in dictating the folding–unfolding phenomena of proteins caused by these co-solvents.

Previously, Kundu and co-workers have reported free energies, ΔG_t^0 of H^+X^- (10), H^+OH^- (11), M^+Cl^- (16*a*) and of the individual ions obtained by the Ph_4AsBPh_4 or TATB assumption (16*b*) in aqueous urea solutions and have drawn important reflections on the relative acid–base properties and solvating capacities of the solvents and on the nature of ion–solvent interactions in the solvents (10, 11, 16, 17). As a part of the parallel studies in glycerol and water mixtures we now re-

[1]Holder of a U.G.C. Teacher Fellowship.

[2]To whom all correspondence should be addressed.

0008-4042/80/010079-07$01.00/0

©1980 National Research Council of Canada/Conseil national de recherches du Canada

Can. J. Chem. Downloaded from www.nrcresearchpress.com by 210.87.254.42 on 09/05/12
For personal use only.

Can. J. Chem. Downloaded from www.nrcresearchpress.com by 210.87.254.42 on 09/05/12
For personal use only.

port ΔG_t^0 values of alkali metal chlorides and of the individual ions obtained by using same TATB assumption. It is hoped that comparison of these results with those in aqueous solutions of urea as well as of a mono-ol like ethanol (EtOH) (18) and a di-ol like ethylene glycol (EG) (19) will help reveal the essential differences in the relative stability of these simple hydrophilic ions on the one hand and hydrophobic Ph_4As^+/Ph_4B^- on the other in these solvents. Moreover, since either of the latter ions is often used as a model solute for hydrophobic hydration (20), ΔG_t^0 values of these ions will help reflect the relative interactions between the hydrophobic sites like apolar side chains of protein molecules and hence on the genesis of the relative stabilization of proteins in the respective co-solvent systems.

ΔG_t^0 values of MCl (M = Li, Na, K, Rb, or Cs) have been evaluated at 25°C in aqueous mixtures of 10, 30, 50, and 70 wt.% glycerol from the standard emf's (ΔE^0) of the double cell [1]

[1] Ag–AgCl/MCl(m), solvent/M(Hg)/MCl(m), water/AgCl–Ag

that have been determined by measuring the emf of the cell at different molalities (m) of MCl. ΔG_t^0 values were then divided into individual contributions by the widely used (21) and amply justified (22, 23) "TATB" assumption [2]:

$$[2] \quad \Delta G_t^0(Ph_4As^+) = \Delta G_t^0(Ph_4B^-) = \tfrac{1}{2}\Delta G_t^0(Ph_4AsBPh_4)$$

The ΔG_t^0 values for the reference electrolyte (R.E.) have been determined by equation:

$$[3] \quad \Delta G_t^0(Ph_4AsBPh_4) = \Delta G_t^0(Ph_4AsPi) + \Delta G_t^0(KBPh_4) - \Delta G_t^0(KPi)$$

the corresponding values of the salts Ph_4AsPi, $KBPh_4$, and KPi being evaluated by the solubility method described earlier (16*b*).

Experimental

Purification of the solvents has been described (12). The origin of and pretreatment for alkali metal chlorides (MCl) used and preparation cell solutions were similar to those described earlier (16, 24*a*). Metal amalgams were prepared by the electrolysis of a fairly concentrated solution of the corresponding alkali metal salts: hydroxides (G.R., Merck) in the case of Na and K and carbonates (G.R., Merck) in the case of Rb and Cs. Li amalgam was prepared from a moderately concentrated solution of LiCl (G.R., Merck). Electrolysis was performed at 0.5–1.0 A between a mercury pool cathode and a Pt-foil anode for 30–40 min (less for Li), after which the amalgam was drained off, washed quickly with purified water and then methanol, dried *in vacuo* at about 50°C, and stored in a vacuum desiccator. Before use the amalgam was first diluted with mercury, if required, in a closed vessel, then passed through a long capillary tube fitted at the bottom of the vessel to free it from the scum and transferred directly into the dropping amalgam reservoir. These operations were performed in a dry H_2 atmosphere. The concentration of the metal in the amalgam was estimated by adding excess standard HCl and titrating back with standard alkali. For "Li" amalgam best behaviour was obtained at a concentration of about 0.001 m whereas for the amalgams of other metals, a concentration near 0.005 m was found to be more suitable. While in use the dropping amalgam reservoir (DAR) was disturbed as little as possible to preserve the homogeneity of the amalgam. Before each experiment, time was allowed for the impurities to rise to the surface. While in use, dry H_2 gas was occasionally passed into the DAR to fill the vacant space left by the out-flowing amalgam and thus to ensure easy flow.

The dropping amalgam reservoir consists of a vertical glass cylinder with two parallel tubes fused vertically into its tapering bottom. Each tube ends in a fine capillary with an upcurving tip and is fitted with a stop-cock, as well as a provision for electrical contact. Standard joints provide for smooth and air-tight introduction of the tubes into the cell vessels. A funnel and a stop-cock arrangement at the top allows filling the DAR with amalgam. A water-circulating jacket around the cylindrical body ensures that the amalgam remains at the desired operating temperature. The two glass cell vessels resemble that used by Izmailov and Ivanova (25). Electromotive force values were measured with the help of a Leeds and Northrup K_4-potentiometer in conjunction with a moving coil galvanometer (Cambridge Inst. Co.). General experimental procedures were similar to those of previous measurements (16, 24*a*).

Preparation of the salts viz. $KBPh_4$, Ph_4AsPi, and KPi and measurement of their saturated solubilities by spectrophotometric method were essentially similar to those described earlier (19, 24*b*). Constancy of the absorbance to within 1% was taken as the criterion of the attainment of the saturated solubility of the salts. At least two sets of measurements were made for all the solutes and the results were found to agree to within 1%. The required dilution of the saturated solution of the salts, the molar extinction coefficient (ε) values of the salts in the media, and the wavelength of light used are given elsewhere.[3]

Results

The observed emf (ΔE) values of cell [1] at different molalities m (mol kg^{-1}) of MCl for the different solvent mixtures are given in the Depository.[3] The standard ΔE^0 values (Table 1) were obtained by extrapolating the function $\Delta E^{0\prime}$ described by [4] against m to $m = 0$ (24*a*)

$$[4] \quad \Delta E^{0\prime} = \Delta E - 2k[f_s(m) - f_w(m)] = \Delta E^0 - 2k\Delta bm$$

where

$$f(m) = -A_0B_0m^{1/2}(1 + a^0B_0m^{1/2})^{-1} - \ln(1 + 0.002Mm)$$

Here subscripts s and w indicate the mixed solvents and water respectively, $k = RT/F$, Δb is the differ-

[3]Complete set of the experimental data is available, at a nominal charge, from the Depository of Unpublished Data, CISTI, National Research Council of Canada, Ottawa, Ont., Canada K1A 0S2.

TABLE 1. Values of ΔE^0 (V) and ΔG_t^0 (kJ mol^{-1}) (mole fraction scale) in glycerol + water mixtures at 25°C

	10 wt.% glycerol		30 wt.% glycerol		50 wt.% glycerol		70 wt.% glycerol	
Salt	ΔE^0	ΔG_t^0	ΔE^0	ΔG_t^0	ΔE^0	ΔG_t^0	ΔE^0	ΔG_t^0
HCl*	—	0.16	—	0.55	—	1.25	—	2.40
LiCl	0.0050	0.07	0.0150	0.08	0.0315	0.48	0.0570	1.39
NaCl	0.0060	0.16	0.0200	0.56	0.0350	0.82	0.0520	0.91
KCl	0.0060	0.16	0.0185	0.41	0.0320	0.53	0.0500	0.71
RbCl	0.0060	0.16	0.0175	0.32	0.0305	0.39	0.0495	0.66
CsCl	0.0055	0.12	0.0165	0.22	0.0300	0.34	0.0460	0.33

*Reference 12*a*; maximum uncertainties in ΔE^0 values are ±0.5 mV and in ΔG_t^0 values, ±0.05 kJ mol^{-1}.

ence between the coefficients of the first power of m in the extended Debye–Hückel equation in the two solvents and a constant depending upon the solute and solvent properties and ion-size parameter a^0, and M is the mean or the simple molecular weight of the mixed solvents or water, respectively. A_0B_0 and B_0 are the conventional Debye–Hückel constants as described earlier (12). Since alteration of the value of a^0 caused no significant change in ΔE^0, $a^0 = 0$ was used in all cases. The estimated standard deviation in ΔE^0 values for all the cases lie within ±0.5 mV. Standard free energies of transfer ΔG_t^0 of MCl from water to the mixed solvents on mole fraction scale were derived at 25°C from [5]

$$[5] \quad \Delta G_t^0 = F\Delta E^0 - 2RT \ln (M_s/M_w)$$

where F = Faraday. The values of ΔG_t^0(MCl) are given in Table 1. The average uncertainty is about ±0.05 kJ mol^{-1}.

Since the salts $KBPh_4$, Ph_4AsPi, and KPi are found to be sparingly soluble in these solvents and dielectric constants of these mixed solvents are fairly large, their ΔG_t^0 values were evaluated on mole fraction scale by use of [6], assuming complete ionization.

$$[6] \quad \Delta G_t^0 = 2.303RT[p({}_sK_{sp}{}^c) - p({}_wK_{sp}{}^c)] + 4.606RT \log M_w d_s/M_s d_w$$
$$= 4.606RT \log {}_wS_wY_{\pm}/{}_sS_sY_{\pm} + 4.606RT \log M_w d_s/M_s d_w$$

where $K_{sp}{}^c$ is the solubility product in molar scale, S is the solubility in mol dm^{-3}, and $Y_{\pm}$ is the mean molar activity coefficient of the saturated solutions. The $Y_{\pm}$ values were calculated by [7] using the familiar standard form of the Debye–Hückel equation

$$[7] \quad -\ln Y_{\pm} = \tfrac{1}{2}A_0B_0d_s^{-1/2}S^{1/2} \times [(1 + a_+{}^0B_0d_s^{-1/2}S^{1/2})^{-1} + (1 + a_-{}^0B_0d_s^{-1/2}S^{1/2})^{-1}] + \log [(d_S - 0.001SM + 0.002SM_s)/d_s]$$

where the terms have their usual meaning (19). Density d_s of the solutions were assumed to be approximately equal to that d_S of the respective solvents. Most of the parameters were taken from the previous paper (12*a*). As before (19), the ion-size parameters $a_+{}^0$ and $a_-{}^0$ for the cations and anions, respectively, are taken as (18)

$$a_{K^+}{}^0 = a_{Pi^-}{}^0 = 0.3 \text{ nm}$$

and

$$a_{Ph_4B^-}{}^0 = a_{Ph_4As^+}{}^0 = 0.5 \text{ nm}$$

The observed solubilities, calculated $pK_{sp}{}^c$ and also ΔG_t^0 values are given in Table 2. The $pK_{sp}{}^c$ values were found reproducible to within ±0.01 unit. The ΔG_t^0 values of Ph_4B^-/Ph_4As^+ were then computed by use of [2] and are presented in Table 3. Those of other individual ions were then derived from the ΔG_t^0 values of the appropriate salts listed in Table 1 and those of HX reported earlier (12*a*). These values of $\Delta G_t^0(i)$ with a maximum uncertainty of ±0.1 kJ mol^{-1} are presented in Table 3.

Discussion

Figure 1 illustrates the variation of the ΔG_t^0 values of the individual ions with the co-solvent composition. For the sake of comparison the profile for H^+ obtained by Wells' method (26) is also shown. It is worth noting that the $\Delta G_t^0(H^+)$ values obtained by Wells' method are less than those obtained by the present RE Method. The discrepancy possibly lies in the fact that the equilibrium constant K_c of the reaction

$$[8] \quad H^+(H_2O)_5 + ROH \rightleftharpoons H^+(ROH)(H_2O)_4 + H_2O$$

Can. J. Chem. Downloaded from www.nrcresearchpress.com by 210.87.254.42 on 09/05/12
For personal use only.

Can. J. Chem. Downloaded from www.nrcresearchpress.com by 210.87.254.42 on 09/05/12
For personal use only.

TABLE 2. Solubilities (S), solubility products p(K_{sp}^c), and ΔG_t^0(mole fraction scale) of $KBPh_4$, Ph_4AsPi, and KPi in glycerol–water mixtures at 25°C

	$KBPh_4$			Ph_4AsPi			KPi		
Wt.% glycerol	$S \times 10^4$ (mol dm^{-3})	p(K_{sp}^c)	ΔG_t^0 (kJ mol^{-1})	$S \times 10^4$ (mol dm^{-3})	p(K_{sp}^c)	ΔG_t^0 (kJ mol^{-1})	$S \times 10^4$ (mol dm^{-3})	p(K_{sp}^c)	ΔG_t^0 (kJ mol^{-1})
0*	—	7.53	0.00	—	8.92	0.00	—	3.41	0.00
10	1.78	7.51	−0.42	4.69	8.66	−1.80	2.31	3.42	−0.25
30	1.80	7.50	−1.20	6.39	8.40	−4.00	2.23	3.46	−0.75
50	1.89	7.47	−2.32	9.51	8.06	−6.89	2.17	3.51	−1.41
70	1.92	7.46	−3.70	15.65	7.63	−10.66	2.13	3.55	−2.50

*Reference 21; p(K_{sp}^c) values are correct to within ±0.01 and ΔG_t^0 values to within ±0.05 kJ mol^{-1}.

TABLE 3. ΔG_t^0 values in kJ (g-ion)$^{-1}$ of some individual ions based on the Ph_4AsBPh_4 assumption in glycerol + water mixtures at 25°C (mole fraction scale)*

	ΔG_t^0 for glycerol content			
Ion	10 wt.%	30 wt.%	50 wt.%	70 wt.%
H^+	0.56	1.34	2.30	3.92
Li^+	0.47	0.87	1.53	2.91
Na^+	0.56	1.35	1.87	2.43
K^+	0.56	1.20	1.58	2.23
Rb^+	0.56	1.11	1.44	2.18
Cs^+	0.52	1.01	1.39	1.85
Cl^-	−0.40	−0.79	−1.05	−1.52
Br^-	−0.44	−1.00	−1.78	−2.47
I^-	−0.74	−1.61	−2.88	−4.40
Pi^-	−0.81	−1.77	−2.99	−4.73
Ph_4B^-/Ph_4As^+	−0.98	−2.22	−3.90	−5.93

*Maximum uncertainties in $\Delta G_t^0(i)$ values are ±0.1 kJ (g-ion)$^{-1}$.

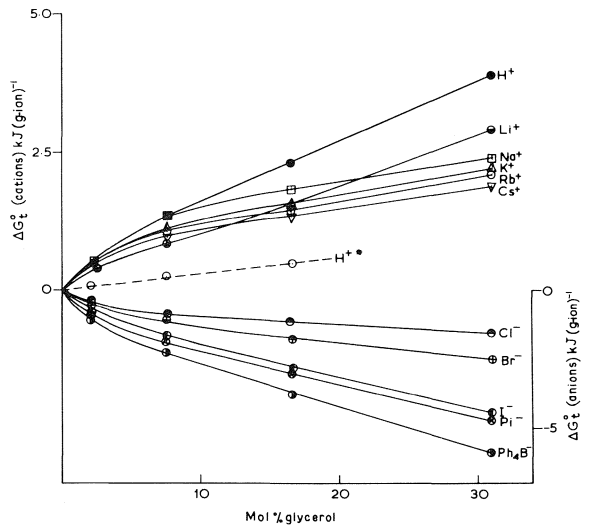


FIG. 1. Variation of $\Delta G_t^0(i)$ of some individual ions from water to glycerol + water mixtures at 25°C. * Wells' data (26).

where ROH denotes co-solvent, is negligibly small for this system, Wells equated $\Delta G_t^0(H^+)$ with the Born-type electrostatic (27) contribution only, neglecting the chemical or basicity effects (27). This leads us to suspect if the very basis of Wells' method is valid for less basic co-solvents like glycerol. However, the small values of K_c for these mixed solvents corroborate that the observed pronounced destabilization of H^+ is the result of decreased basicity of the mixed solvents compared to water.

The observed increasing destabilization of other simple cations and increasing stabilization of simple anions also conform to what is expected from the acid–base type interactions (28, 29), between "anion-acidic H-centre" and "cation-basic O-centre" of these more acidic (30, 31) and less basic (26) co-solvents. For alkali metal cations the observed relative order of destabilization also follows the sequence $Na^+ > K^+ > Rb^+ > Cs^+$, as expected from acid–base type interactions. For Li^+, however, the observed sharp destabilization beyond 50% glycerol can be attributed to the fact that in water-rich regions the smooth exchange of water molecules from the strong hydration cosphere of Li^+ (32) by the added co-solvent molecules is likely to be somewhat difficult. But at co-solvent-rich compositions where glycerol molecules are prone to exchange H_2O molecules from the primary solvation zone, they change the solvation number untowardly, possibly due to steric ef-

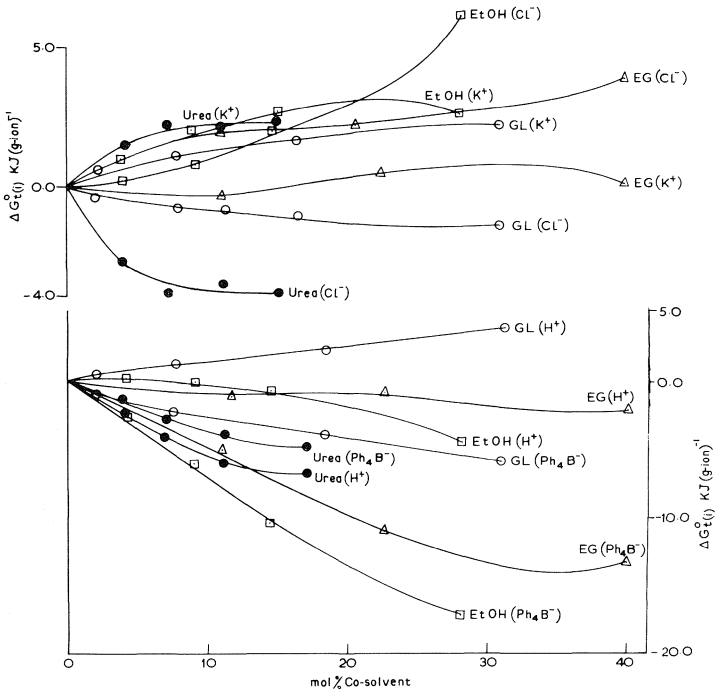


FIG. 2. Comparison of $\Delta G_t^0(i)$ of H^+, K^+, Cl^-, and Ph_4B^- from water to aqueous mixtures of ethanol (EtOH), ethylene glycol (EG), glycerol (GL), and urea (UH).

fect of their large size compared to water. Recently Choi and Criss (33) also contended that the large $\Delta H^0_{TMS \leftarrow AN}$ values (TMS = sulpholane and AN = acetonitrile) for the Li salt are the result of a greater change in solvation number for Li^+ relative to other alkali metal ions when they are transferred from AN to TMS. The large size of TMS molecules compared to ACN brings about the relatively low degree of solvation of Li^+ in TMS than in ACN.

The observed increased stability of the halide ions though conforms to the increased acid–base interaction resulting from the increased acidity of the solvents their order $Cl^- > Br^- > I^-$ does not. This is possibly due to the superimposed effects of dipole-induced polarization of the halide ion as indicated by Wells (26). Alternatively, the feasibility of the crowding of the larger number of co-solvent dipoles or their hydrogen bonded aquo-complexes (29) round the larger sized I^- compared to those round Br^- and Cl^- may be partly responsible for the observed order of stabilization of the halide ions.

In the case of organic ions, however, the observed pronounced stabilization of Ph_4As^+/Ph_4B^- is indicative of the effect of large dispersion interactions of hydrophobic phenyl groups (34). But the increased stabilization of Pi^- is the result of combined effects of increased acidity of the solvents and the increased dispersion interaction with the phenyl group of Pi^- ion. Notably, dispersion interaction effects on four phenyl groups of Ph_4As^+/Ph_4B^- exceed the combined effects of acidity and dispersion interactions on Pi^- ion.

Again, from Fig. 2 where ΔG_t^0–composition profiles of some typical simple ions like H^+, Cl^-, and K^+ and large hydrophobic ion Ph_4B^- have been compared with those in the aqueous mixtures of EtOH (18), EG (19) as well as urea, UH (16*b*), it may be observed that the order of increased stabilization of H^+ is UH + water > EtOH + water > EG + water > glycerol (GL) + water. In fact, this is also the order in which the negative charge density on the basic $\equiv C—O^-$-group of UH or —O-atom of other co-solvents varies. Thus, proton stabilization appears to be so strongly guided by charge densities of basic centres of the co-solvents that other effects including Born-type electrostatic interactions are frequently masked and this provides a firm support to $\Delta G_t^0(H^+)$ as a measure of the Brønsted basicity of the co-solvents relative to water (27).

On the other hand, $\Delta G_t^0(Cl^-)$ composition profiles indicate that while Cl^- is increasingly destabilized in the cases of EtOH and EG, it is increasingly stabilized in GL and UH and relative order of stability increases in the aqueous mixtures of EtOH < EG < GL < UH. Leaving aside UH, since the acidity increases in the same order (27), one should expect that the observed order is the

Can. J. Chem. Downloaded from www.nrcresearchpress.com by 210.87.254.42 on 09/05/12
For personal use only.

Can. J. Chem. Downloaded from www.nrcresearchpress.com by 210.87.254.42 on 09/05/12
For personal use only.

result of increased acidity and decreased Born-type electrostatic effects of the co-solvents. In the case of urea, however, since the dielectric constant increases with the addition of urea, Born-type electrostatic effects augment the stabilization of Cl^- due to the possible ion–dipole interactions through the positive charge centre of the zwitterionic form of urea.

Unlike Cl^-, the behaviour of K^+ and other alkali metal cations in the aqueous mixtures of these co-solvents appears to be somewhat involved, for no regular order in $\Delta G_t^0(K^+)$–composition profiles is discernable. Apparently, as indicated earlier (19), the behaviour of alkali metal cations is guided by the combined effects of pronounced Born-type electrostatic contribution, acid–base type interaction, and also "structural" interaction (35) of the solvents.

As Fig. 2 illustrates, $\Delta G_t^0(Ph_4B^-)$ values for these aqueous co-solvents are increasingly negative, indicating the increased stability of these hydrophobic ions in each of these mixed solvents. Since the Born-type electrostatic effects associated with the transfer of this large hydrophobic ion in all the solvent systems are likely to be fairly small and its relative stability is expected to be chiefly guided by the dispersion forces arising from the hydrophobic propensities of the respective co-solvents, the relative positions of the $\Delta G_t^0(Ph_4B)$–composition profiles suggest that the order of hydrophobicity of the co-solvents is EtOH > EG > UH > GL.

Since the solvation of model hydrophobic solutes Ph_4B^-/Ph_4As^+ in urea–water mixtures exceeds that in glycerol–water mixtures, it appears to suggest that in the latter solvents the hydrophobic solutes are likely to be relatively less solvated and hence more prone to undergo hydrophobic interactions among themselves than in the former solvents. Moreover, if hydrophobic interaction (HI) (36) through the apolar side chain of a protein molecule is a major contributor to protein stabilization, the results of the present study may lead one to conclude that the protein molecules are likely to be more stabilized in glycerol–water mixtures than in urea–water mixtures. Also HI among the apolar side chains of a protein molecule is possibly one of the guiding factors for the relative stabilization of proteins by these two co-solvents.

However, since the $\Delta G_t^0(Ph_4B^-)$ values in these two co-solvent systems do not seem significantly different from each other, one may wonder if the little difference in hydrophobic propensity of these two co-solvents could induce sufficient hydrophobic interactions in the apolar side chains of a protein molecule so as to result in the observed relative stabilization of proteins. Evidently, some other factors, including "specific interactions" as emphasized by Belleau *et al.* (9), possibly serve as the key to the relative stabilization of the native confirmation of proteins.

Acknowledgement

Thanks are due to the University Grants Commission, New Delhi, for granting a Teacher Fellowship to I.N.B.

1. G. DIPAOLA and B. BELLEAU. Can. J. Chem. **53**, 3452 (1975) and references therein for the ealier work.
2. P. H. VON HIPPER and K. Y. WONG. J. Biol. Chem. **250**, 3905 (1965).
3. I. FRIDDOVICH. J. Biol. Chem. **237**, 345 (1962).
4. (*a*) R. B. SIMPSON and W. KAUZMANN. J. Am. Chem. Soc. **75**, 5134 (1953); (*b*) H. K. FRENSDORF, M. T. WATSON, and W. KAUZMANN. J. Am. Chem. Soc. **75**, 5157 (1957).
5. J. JARABAK, A. E. SEEDS, JR., and P. TALALAY. Biochemistry, **5**, 1269 (1966).
6. S. RAJENDER and R. LUMRY. Biopolymers, **9**, 1154 (1970).
7. S. SUBRAMANIAN, T. S. SARMA, D. BALASUBRAMANIAN, and J. C. AHLUWALIA. J. Phys. Chem. **75**, 815 (1971) and references therein.
8. M. J. MASTROIANNI, M. J. PIKAL, and S. LINDENBAUM. J. Phys. Chem. **76**, 3050 (1972).
9. G. DIPAOLA and B. BELLEAU. Can. J. Chem. (*a*) **55**, 3825 (1977); (*b*) **56**, 848 (1978).
10. K. K. KUNDU and K. MAZUMDAR. J. Chem. Soc. Faraday Trans. 1, (*a*) **69**, 806 (1973); (*b*) **71**, 1422 (1975).
11. A. K. DAS and K. K. KUNDU. J. Phys. Chem. **79**, 2604 (1975).
12. I. N. BASUMULLICK and K. K. KUNDU. (*a*) Can. J. Chem. **57**, 961 (1979); (*b*) Ind. J. Chem. **18A**, 1 (1979).
13. M. J. TAIT, A. SUGGETT, F. FRANKS, S. ALBETT, and P. A. QUICKENDON. J. Soln. Chem. **1**, 131 (1972).
14. H. S. FRANK and F. FRANKS. J. Chem. Phys. **48**, 4746 (1968).
15. F. FRANKS and D. J. G. IVES. Q. Rev. Chem. Soc. **20**, 1 (1966).
16. A. K. DAS and K. K. KUNDU. J. Soln. Chem. (*a*) **6**, 431 (1976); (*b*) **8**, 259 (1979).
17. A. K. DAS. Ph.D. Dissertation, Jadavpur University. 1975.
18. O. POPOVYCH, A. GIBOFSKY, and D. H. BERNE. Anal. Chem. **44**, 811 (1972).
19. A. K. DAS and K. K. KUNDU. Ind. J. Chem. **16A**, 467 (1978).
20. S. SUNDER, B. CHAWLA, and J. C. AHLUWATEA. J. Phys. Chem. **78**, 738 (1974).
21. B. G. COX, R. R. HEDWING, A. J. PARKER, and D. W. WATT. Aust. J. Chem. **27**, 477 (1974).
22. J. I. KIM. J. Phys. Chem. **82**, 191 (1978).
23. M. H. ABRAHAM and A. NASEHZADEH. Can. J. Chem. **57**, 71 (1979).
24. K. BOSE and K. K. KUNDU. (*a*) J. Soln. Chem. **8**, 175 (1979); (*b*) Can. J. Chem. **57**, 2470 (1979); **57**, 2476 (1979).
25. N. A. IZMAILOV and E. F. IVANOVA. Zh. Fiz. Khim. **29**, 1422 (1955).
26. C. F. WELLS. J. Chem. Soc. Faraday Trans. I, **71**, 868 (1975).
27. R. G. BATES. *In* Hydrogen-bonded solvent systems. *Edited*

by A. K. Covington and P. Jones. Taylor and Francis, London. 1968. p. 49.
28. D. FEAKINS. *In* Physico-chemical processes in mixed aqueous solvents. *Edited by* F. Franks. Heinemann Educational Books, London. 1967. p. 71.
29. K. KUNDU, A. K. RAKSHIT, and M. N. DAS. Electrochim. Acta, **17**, 192 (1972).
30. E. M. WOOLLEY, J. TOMKINS, and L. G. HEPLER. J. Soln. Chem. **76**, 3050 (1972).
31. P. BALLINGER and F. A. LONG. J. Am. Chem. Soc. **82**, 798 (1960).
32. (*a*) J. E. DESNOYERS, P. R. PHILIP, and J. L. FORTLER. J. Soln. Chem. **3**, 523 (1974); (*b*) J. E. DESNOYERS, G. PERRON, and L. AVEDIKIAN. J. Soln. Chem. **4**, 331 (1975).
33. Y. S. CHOI and C. M. CRISS. J. Chem. Eng. Data, **22**, 297 (1977).
34. O. POPOVYCH. Anal. Chem. **46**, 2009 (1974).
35. N. DESROSIERS, G. PERRON, J. G. MATHIESON, B. E. CONWAY, and J. E. DESNOYERS. J. Soln. Chem. **3**, 789 (1974).
36. A. BEN NAIM. J. Phys. Chem. **78**, 170 (1974).

Can. J. Chem. Downloaded from www.nrcresearchpress.com by 210.87.254.42 on 09/05/12
For personal use only.

Electrostatic effects of substrate charge on base-catalyzed proton exchange in purines. Implications for the involvement of zwitterions

SPENCER E. TAYLOR

Department of Chemistry, Queen's University, Kingston, Ont., Canada K7L 3N6

Received July 26, 1979

SPENCER E. TAYLOR. Can. J. Chem. **58**, 86 (1980).

Rates of detritiation from the C-8 position of various ionized purine molecules have been shown to reflect electrostatic interactions occurring within the transition state of the exchange reaction. The purines are capable of existing as protonated, anionic, neutral, and zwitterionic species in aqueous solution, each of which have been shown previously to undergo specific hydroxide ion-catalyzed detritiation. The effects of substrate charge are quantified as the *proton activating factor*, *anion deactivating factor*, and *zwitterion activating factor*. Localized charge and not net charge is shown to govern the reactivities of the various species, especially the zwitterions.

Estimation of rate constants for the zwitterionic species (hitherto only postulated to account for the observed rate behaviour) has enabled the calculation of the corresponding zwitterionic equilibrium constants (K_{zw}). K_{zw} values calculated in this manner agree with those estimated from suitable literature pK_a data.

SPENCER E. TAYLOR. Can. J. Chem. **58**, 86 (1980).

On a montré que les vitesses de détritiation à partir de la position C-8 de différentes molécules purines ionisées, reflètent les interactions électrostatiques se produisant à l'intérieur de l'état de transition de la réaction d'échange. Les purines peuvent exister en solution aqueuse sous forme d'espèces protonées, anioniques, neutres et hermaphrodites. On a montré antérieurement que chacune de ces espèces subit une détritiation catalysée spécifiquement par l'ion hydroxyde. On a quantifié les effets de la charge du substrat sous forme de facteur activant le proton, facteur désactivant l'anion et facteur activant l'ion hermaphrodite. On a montré que la charge localisée et non la charge résultante, gouverne les réactivités des différentes espèces et spécialement celle des zwitterions.

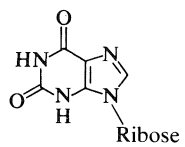
Une évaluation des constantes de vitesse des espèces hermaphrodites (postulée seulement jusqu'à date pour tenir compte du comportement de la vitesse observée) a permis de calculer les constantes d'équilibre (K_{zw}) du zwitterion correspondant. Les valeurs de K_{zw} calculées de cette façon concordent avec celles évaluées à partir des données appropriées de pK_a de la littérature.

[Traduit par le journal]

The specific hydroxide ion-catalyzed isotopic hydrogen exchange from the C-8 position of purines has been shown to involve different ionized species, ranging from the N-7- or 9-protonated molecule through to the mono- and di-anions (ionization having occurred in the pyrimidine ring) (1). In addition, strong evidence has been put forward in favour of the involvement of zwitterionic species (2).

Based solely on a consideration of the coulombic interaction between the reactants, it would be expected that base and nucleophilic catalysis would be facilitated after protonation of the neutral purine molecule; deprotonation, on the other hand, would lead to decreased reactivity. However, complications to this simplified scheme can be envisaged for aromatic systems in which extensive charge delocalization and the presence of several potential protonation/deprotonation sites may preclude a rigorous theoretical treatment. Quantitative data on the effects of the charged state of the substrate can nevertheless be obtained. Stewart and Srinivasan (3) defined the term "proton activating factor" (**paf**) as the relative rate enhancement resulting from protonation (or alkylation (4)) of the substrate molecule, and Jones and Taylor (5) introduced the "metal activating factor" to quantify the similar effects of metal ion co-ordination. These ideas are taken a stage further in the present paper in which the effects of anion formation in purines are also considered, and the "anion deactivating factor" (**adf**) is introduced accordingly.

Few systems possess the capability of the purines to exist in as many different ionized forms within a relatively narrow pH range. The additional involvement of zwitterion species has only served to extend the number of possible structures available in aqueous solution (e.g. the case of xanthosine, **1** (1*a*)).



1

In the present paper, a quantitative examination is made to assess the effects of molecular charge on the rates of the hydroxide ion-catalyzed detritiation of a number of ionized purine species. The discussion is restricted to consequences of protonation or

0008-4042/80/010086-06$01.00/0

©1980 National Research Council of Canada/Conseil national de recherches du Canada

Can. J. Chem. Downloaded from www.nrcresearchpress.com by 210.87.254.42 on 09/05/12
For personal use only.

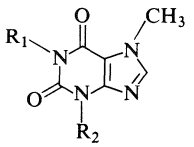
Can. J. Chem. Downloaded from www.nrcresearchpress.com by 210.87.254.42 on 09/05/12
For personal use only.

ionization occurring in the purine base moiety, but the considerations are equally valid for charge modifications in the ribose or ribose-phosphate groups of nucleosides and nucleotides, respectively. The magnitudes of the **paf** and **adf** values are interpreted on the basis of simple electrostatic interactions in the transition state. In addition, a method for the estimation of zwitterionic equilibrium constants from the kinetic data is outlined.

Results and Discussion

Paf and Adf Values in the Detritiation of Xanthines

The detritiation of [8-^{3}H]-labelled xanthines represent the most extensively-studied purine system so far reported (1*a*). Rate constants at 85°C have been obtained for the reactions involving the neutral and several ionic forms of this class of purine, and data for caffeine (**2**), theobromine (**3**), and paraxanthine (**4**) are summarized in Table 1. The two dimethylxanthines **3** and **4** can exist in three



2; $R_1 = R_2 = CH_3$
3; $R_1 = H, R_2 = CH_3$
4; $R_1 = CH_3, R_2 = H$

predominant forms within the pH range 0–12 at 85°C (1*a*), viz. the N-9-protonated (BH_2^+), neutral (BH), and monoanionic (B^-) molecules, each of which have been shown to contribute to the pH-rate behaviour (1*a*). In addition, zwitterionic species ($BH^{\pm}$) formed by proton migration from the pyrimidine to imidazole rings have been implicated as being the major contributors to the rate at intermediate pH (1*a*), following the original suggestion by Tomasz *et al.* (6), such that the measured rate constant (k') is a composite function comprising contributions from the neutral (k_b) and zwitterionic (k_c) molecules, according to the equation (1*a*, 2)

$$[1] \quad k' = k_b + K_{zw}k_c$$

in which K_{zw} is the zwitterionic equilibrium constant (= $[BH^{\pm}]/[BH]$). In view of this complication, the 1,3,7-trimethyl derivative **2** was studied. Owing to the lack of an ionizable proton in the pyrimidine ring, **2** cannot exist as a zwitterion, and thus serves as a suitable "model" for neutral **3** and **4**, assuming the effects of the additional methyl group are similar to those of hydrogen (3), and enables the calculation of satisfactory **paf** values (= k_a/k_b)[1] free from contributions from zwitterionic species. Calculated **paf** and the corresponding **adf** (= k_d/k_b)[1] values are summarized in Table 1. Second-order rate constants for reactions involving the zwitterions of **3** and **4** are calculated from the relationship

$$[2] \quad k_c = k_a \times \mathbf{adf} \quad (\equiv k_d \times \mathbf{paf})$$

which assumes that the **adf** for the protonated molecule is the same as that for the neutral molecule (and that the **paf** for the neutral molecule is the same as for the anion).

The **paf** values found for **2***a*, **3***a*, and **4***a* (9.3×10^7, 1.4×10^8, and 2.0×10^8, respectively) are similar in magnitude to the values found previously (3*a*, 7) for 9-alkylpurines (1.3×10^8) and illustrate the effect of protonation at the site adjacent to the reaction centre (3*b*).

Anion formation at the N-3 position (in **4**) is seen to have a greater influence on the detritiation rate at C-8 than anion formation at N-1 (in **3**) by the larger **adf** value in the latter case (Table 1). Still larger effects of anion formation occur as a result of ionization in the imidazole ring (relevant to purine bases such as adenine (8), guanine (9), hypoxxanthine (9), and xanthine (1*a*), and to imidazole itself (10)). Previous analyses (1*a*, 8–11) have not accounted for an exchange mechanism involving such anions, but it seems reasonable to expect a rate reduction of similar magnitude to the rate enhancement observed for protonation of the imidazole ring (i.e., an **adf** value of $\sim 10^{-8}$); such a value would be difficult to measure experimentally.

Origin of the Paf and Adf Values

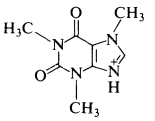
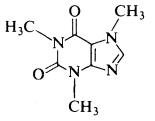
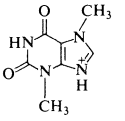
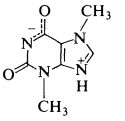
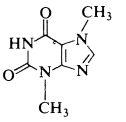
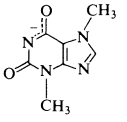
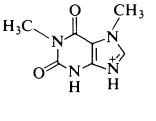
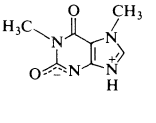
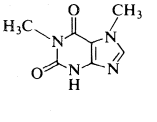
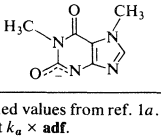
For reactions between ions, electrostatic control of reaction rate is usually the dominant factor. However, where different protonation and/or ionization sites exist within a molecule, it is not possible to treat the reactants as simple charged spheres, nor is it valid to consider overall (net) charge as the major influence on the reaction rate. In consideration of these points, we have constructed a model to illustrate that the observed effects of substrate charge can possibly originate from simple electrostatic interactions within the transition state of the exchange process. Assuming a highly product-like transition state[2] in which virtually complete triton transfer to hydroxide has occurred, with concomitant localization of a full negative charge

[1]The subscripts *a*, *b*, *c*, and *d* refer to the protonated, neutral, zwitterionic, and monoanionic purine species, respectively, corresponding to the symbolism employed in Table 1.

[2]An interpretation consistent with low kinetic isotope effects and near-unity Brønsted β-coefficients (12).

Can. J. Chem. Downloaded from www.nrcresearchpress.com by 210.87.254.42 on 09/05/12
For personal use only.

TABLE 1. Second-order rate constants and derived **paf** and **adf** values for the detritiation of [8-^{3}H]-**2**, **3**, and **4** at 85°C (from ref. 1*a*)

Substrate	Active species, **x**		Detritiation rate constant, k_x (L mol^{-1} s^{-1})	**Paf** ($= k_a/k_b$)	**Adf** ($= k_d/k_b$)
2		a	2.52×10^{6}*	9.26×10^{7}	
		b	2.72×10^{-2}*		
3		a	3.76×10^{6}*	1.38×10^{8}	
		c	2.70×10^{5}†		
			6.34×10^{-2}*		
		b	2.72×10^{-2}‡		7.17×10^{-2}
		d	1.95×10^{-3}*		
4		a	5.50×10^{6}*	2.02×10^{8}	
		c	1.01×10^{5}†		
			98.4*		
		b	2.72×10^{-2}‡		1.84×10^{-2}
		d	5.0×10^{-4}*		

*Experimentally determined values from ref. 1*a*.
†Calculated as the product $k_a \times$ **adf**.
‡Value assumed to be the same as for neutral **2**.

on C-8 (Fig. 1), it is envisaged that protonation of N-7/9 would serve to stabilize the transition state whereas anion formation would produce the opposite effect. In this model, it is assumed that protonation and ionization localizes full charges on the *N* atoms concerned, some justification for which comes from the finding that protonation and alkylation of the imidazole ring produce similar rate-enhancing effects, suggesting a certain independence of the *nature* of the substituent.

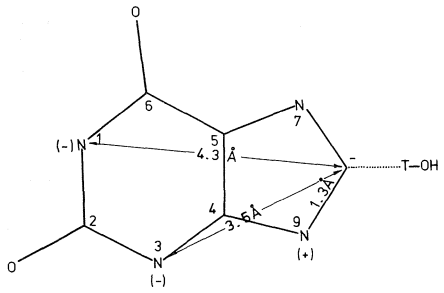


FIG. 1. The geometry of a typical xanthine molecule used for the calculation of intercharge distances in the transition state model.

Electrostatic effects on the rate of detritiation based on the above model can therefore be described by (ref. 13, ref. 14, chapt. 9):

$$[3] \quad \log k_a/k_b = \log (\mathbf{paf}) = \frac{\varepsilon^2}{2.303kTr_{-+}D_{\text{eff}}}$$

for the effect of protonation, and

$$[4] \quad \log k_d/k_b = \log (\mathbf{adf}) = -\frac{\varepsilon^2}{2.303kTr_{--}D_{\text{eff}}}$$

for the effect of ionization, where k is Boltzmann's constant, T the absolute temperature, r_{-+} and r_{--} the distances between the assumed point charges ($-\varepsilon$ and $+\varepsilon$, and $-\varepsilon$ and $-\varepsilon$, respectively, located on C-8 and the relevant N atoms), ε the electronic charge, and D_{eff} the effective (microscopic) permittivity of the region between the charges.

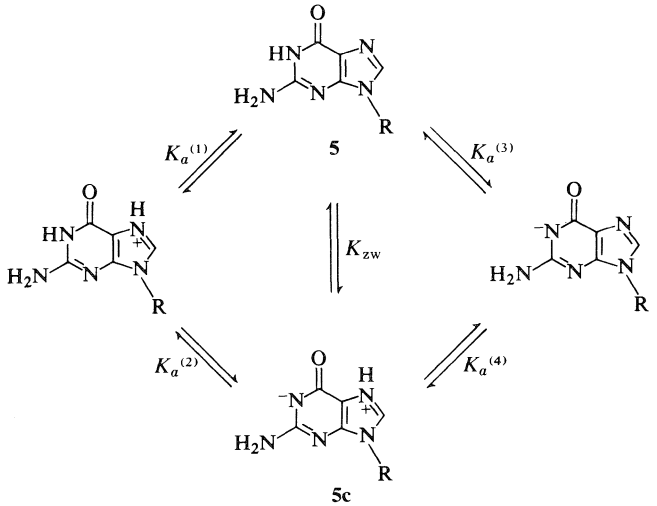
Equations [3] and [4] reduce to [5] at 85°C, after substitution of the various constants, $\mathring{r}_{-\pm}$ being expressed in Ångstroms.

$$[5] \quad \log (\mathbf{paf}) \text{ or } \log (\mathbf{adf}) = \pm\frac{205.8}{\mathring{r}_{-\pm}D_{\text{eff}}}$$

Although a small change in the geometry of the imidazole ring in 7-methylxanthine occurs as a result of N-9 protonation (15), generally the crystal structures of caffeine (16), the xanthine N-3 anion (17), theobromine (18), and theophylline (19) exhibit a reasonably constant geometry of the xanthine ring system. We have therefore arbitrarily chosen the xanthine anion (17) as the geometrical basis of our model xanthine, shown in Fig. 1. Based on this model, the distances $r_{\text{C-8-N-9}}$, $r_{\text{C-8-N-3}}$, and $r_{\text{C-8-N-1}}$ are found to be 1.3, 3.5, and 4.3 Å, respectively. Substitution of these values into eq. [5], together with the corresponding log (**paf**) or log (**adf**) values, permits the calculation of D_{eff} in each case. Thus, D_{eff} values of 19 (C-8 – N-9, based on an average **paf** value for **2**, **3**, and **4**), 34 (C-8 – N-3 for **4**), and 42 (C-8 – N-1 for **3**) are found. These values are intermediate between the permittivity of water at 85°C (60 (ref. 14, p. 178)) and the much lower value generally regarded (14) as typical of a hydrocarbon molecular framework. That D_{eff} appears to vary with intercharge distance may be an inherent feature of this oversimplified model, or it may genuinely reflect the increasing solvent participation with increasing charge separation. The fact that the measured D_{eff} values are found to be of reasonable magnitudes lends support to the transition state model chosen.

*Zwitterionic Equilibrium Constants and the "Zwitterion Activating Factor" (**Zaf**)*

For the purpose of calculating k_c for guanosine from the high pH value of k', Tomasz *et al.* (16) first derived a value for K_{zw} using the method of Tucker and Irvin (21). Since we presently adopt the same approach in the present paper, a brief account of the principles involved will be given at this stage. The ionization sequence of, e.g. guanosine (**5**, R = ribose) is considered to be as shown in Scheme 1.



SCHEME 1

Can. J. Chem. Downloaded from www.nrcresearchpress.com by 210.87.254.42 on 09/05/12
For personal use only.

TABLE 2. Zwitterionic equilibrium constants and zwitterion rate constants calculated from detritiation rate data at 85°C for several purine systems

Substrate	Zwitterion: Proton transferred to	Zwitterion: from	k_c ($L\,mol^{-1}\,s^{-1}$)	K_{zw}*	Reference†
Theobromine	N-9	N-1	2.70×10^{5}‡	1.34×10^{-7}	1*a*
Paraxanthine	N-9	N-3	1.01×10^{5}‡	9.72×10^{-4}	1*a*
Xanthine	N-7/9	N-3	1.14×10^{4}‡	8.10×10^{-3}	1*a*
Xanthosine	N-7	N-3	1.22×10^{6}§	1.69×10^{-2}	1*a*
	N-7	N-1	8.73×10^{4}‖	6.69×10^{-6}	1*a*
Guanosine	N-7	N-1	2.23×10^{5}‡	2.71×10^{-5}	2, 9
Inosine	N-7	N-1	1.12×10^{6}‡	1.50×10^{-5}	2, 9

*Calculated using eq. [1].
†Reference to the original rate data.
‡Calculated from k_a and the relevant **adf** value.
§Calculated from k_d and the mean **paf** value for the xanthines (1.44×10^{8}).
‖Calculated from the preceding k_c value and the relevant **adf**.

TABLE 3. Zwitterionic equilibrium constants calculated using the method of Tucker and Irvin (21) (see text for details)

Substrate	Zwitterion analogue	pK_a	$pK_a^{(2)}$	K_{zw}*†
Theobromine	3,7,9-Trimethylxanthine	0.3‡	7.0§	2.0×10^{-7}
Paraxanthine	1,7,9-Trimethylxanthine	0.5‡	3.2§	2.0×10^{-3}
Xanthine	7,9-Dimethylxanthine	1.2‡	3.2§	1.0×10^{-2}
Guanosine	7-Methylguanosine	2.29‖	6.91‖	1.9×10^{-5}‖

*At 25°C unless otherwise stated.
†Calculated from eq. [9].
‡Reference 23.
§Reference 22.
‖Reference 6, at 37°C.

The measured K_a for N-7 protonation is thus given by:

[6] $K_a = K_a^{(1)} + K_a^{(2)}$

Similarly, the zwitterionic equilibrium constant is given by:

[7] $K_{zw} = K_a^{(2)}/K_a^{(1)} \quad (= K_a^{(4)}/K_a^{(3)})$

Combination of eqs. [6] and [7] leads to [8].

[8] $K_{zw} = K_a^{(2)}/(K_a - K_a^{(2)})$

If $K_a^{(2)}$ is small compared with K_a, K_{zw} can be calculated from the simplified expression,

[9] $pK_{zw} = pK_a^{(2)} - pK_a$

By using the corresponding N-7 methylated compound as a model for the zwitterionic species, a value of $K_a^{(2)}$ can be obtained. Thus Tomasz *et al.* (6) compared the pK_a values for guanosine and 7-methylguanosine in order to estimate K_{zw} for guanosine, a value of 1.9×10^{-5} being obtained at 37°C. These workers then proceeded to evaluate k_c (from eq. [1] with $k_b = 0$).

In addition to this method, however, our present considerations of the quantitative effects of protonation and deprotonation on the rate of detritiation in purine systems provides a measure of k_c which we can use in conjunction with eq. [1] and the known values of k' and k_b to evaluate K_{zw}. A summary of k_c and derived K_{zw} values for the xanthines and other purine systems (assuming the same **adf** for N-1 deprotonation as found for **3**) is presented in Table 2. These K_{zw} values can be compared with those calculated using Tucker and Irvin's method. Although there is a paucity of literature $pK_a^{(2)}$ measurements, suitable data (22) are available for the 9-methyl derivatives of **3** and **4**, and for 7,9-dimethylxanthine (assumed to be a reasonable model for the xanthinium ion), in addition to the data used by Tomasz *et al.* (6). Data from the latter source, together with the K_{zw} values calculated using eq. [9], are given in Table 3.

A comparison of the K_{zw} data given in Tables 2 and 3 calculated using the present "kinetic" approach and Tucker and Irvin's "equilibrium" method shows there to be remarkable agreement, and indicates little change in K_{zw} with temperature. The magnitude of the K_{zw} values deserves some comment. Intuitively, a major determinant of the magnitude of K_{zw} is considered to be the basicity

Can. J. Chem. Downloaded from www.nrcresearchpress.com by 210.87.254.42 on 09/05/12
For personal use only.

Can. J. Chem. Downloaded from www.nrcresearchpress.com by 210.87.254.42 on 09/05/12
For personal use only.

difference between proton donor and acceptor sites. This can be exemplified by comparing the paraxanthine and theobromine systems. Using ΔpK_a (= pK_a (donor site) − pK_a (acceptor site)) as a measure of the difference in basicity, the greater (by $\sim 10^4$) K_{zw} value in the former case can be correlated with a smaller ΔpK_a (by ~2.6 at 25°C (23)).

Even though the concentration of neutral molecules far exceeds the zwitterion concentration, the much greater reactivity of the latter, expressed in terms of the "zwitterion activating factor" (**zaf** = k_c/k_b), accounts for its dominance in the reaction pathway. The **zaf** values are intermediate between the corresponding **paf** and **adf** values, as would be expected, and range from 3.7×10^6 for paraxanthine to 8.9×10^7 for guanosine.

Concluding Remarks

In the present paper it has been shown that it is possible to quantitatively dissect the electrostatic effects of molecular charge on the rate of the hydroxide ion-catalyzed detritiation from purines. This also applies to situations in which more than one localized charged site is present in the molecule, such as for zwitterionic species hitherto only postulated to account for the observed rate behaviour.

In addition, one final point is worthy of note. In adenine and purine derivatives, the major protonation site is N-1 and not N-7 as is the case for most other purines (20), although detritiation is suggested as proceeding via the N-7-protonated molecules (7, 8). Different relative degrees of N-7- and N-1-protonation may therefore exist in solution, which would necessarily make any conclusions based on the effects of single-site protonation hazardous. Such considerations account for the lower-than-average **paf** values observed for adenosine (3*a*, 8).

Acknowledgement

I would like to express my gratitude to Dr. J. R. Jones, University of Surrey, Guildford, U.K., for his help and encouragement which made this study possible.

1. (*a*) J. R. Jones and S. E. Taylor. J. Chem. Soc. Perkin II, 1253 (1979); (*b*) M. Jelinska, J. Szydlowski, and J. Sobkowski. Tetrahedron, **35**, 663 (1979).
2. J. R. Jones and S. E. Taylor. J. Chem. Soc. Perkin II, in press.
3. (*a*) R. Stewart and R. Srinivasan. Acc. Chem. Res. **11**, 271 (1978); (*b*) R. Srinivasan and R. Stewart. Can. J. Chem. **53**, 224 (1975).
4. R. Stewart and R. Srinivasan. Can. J. Chem. **53**, 2906 (1975).
5. J. R. Jones and S. E. Taylor. J. Chem. Soc. Perkin II, in press.
6. M. Tomasz, J. Olsen, and C. M. Mercado. Biochemistry, **11**, 1235 (1972).
7. J. A. Elvidge, J. R. Jones, C. O'Brien, E. A. Evans, and H. C. Sheppard. J. Chem. Soc. Perkin II, 1889 (1973).
8. J. A. Elvidge, J. R. Jones, C. O'Brien, E. A. Evans, and H. C. Sheppard. J. Chem. Soc. Perkin II, 2138 (1973).
9. J. A. Elvidge, J. R. Jones, C. O'Brien, E. A. Evans, and H. C. Sheppard. J. Chem. Soc. Perkin II, 174 (1974).
10. (*a*) J. D. Vaughan, Z. Mughrabi, and E. C. Wu. J. Org. Chem. **35**, 1141 (1970); (*b*) J. L. Wong and J. H. Keck, Jr. J. Org. Chem. **39**, 2398 (1974).
11. J. A. Elvidge, J. R. Jones, C. O'Brien, E. A. Evans, and J. C. Turner. J. Chem. Soc. Perkin II, 432 (1973).
12. J. A. Elvidge, J. R. Jones, C. O'Brien, E. A. Evans, and H. C. Sheppard. Adv. Heterocycl. Chem. **16**, 1 (1974).
13. G. Scatchard. Chem. Rev. **10**, 229 (1932).
14. E. A. Moelwyn-Hughes. Chemical statics and kinetics of solutions. Academic Press, London. 1971.
15. T. J. Kistenmacher and T. Sorrell. Acta Crystallogr. **B31**, 489 (1975).
16. (*a*) D. J. Sutor. Acta Crystallogr. **11**, 453 (1958); (*b*) E. Shefter. J. Pharm. Sci. **57**, 1163 (1968).
17. H. Mizuno, T. Fujiwara, and K. Tomita. Bull. Chem. Soc. Jpn. **42**, 3099 (1969).
18. E. Shefter, T. F. Brennan, and P. Sackman. Chem. Pharm. Bull. **19**, 746 (1971).
19. (*a*) D. J. Sutor. Acta Crystallogr. **11**, 83 (1958); (*b*) E. Shefter. J. Pharm. Sci. **58**, 710 (1969).
20. R. M. Izatt, J. J. Christensen, and J. H. Rytting. Chem. Rev. **71**, 439 (1971).
21. G. F. Tucker and J. L. Irvin. J. Am. Chem. Soc. **73**, 1923 (1951).
22. W. Pfleiderer. Annalen, **647**, 161 (1961).
23. D. Lichtenberg, F. Bergmann, and Z. Neiman. J. Chem. Soc. C, 1676 (1971).

Metal complexes as antioxidants. 7. Kinetics of inhibition of styrene autoxidation by zinc di-isopropyldithiophosphate[1]

J. A. HOWARD AND S-B. TONG[2]

Division of Chemistry, National Research Council of Canada, Ottawa, Ont., Canada K1A 0R9

Received August 14, 1979

J. A. HOWARD and S-B. TONG. Can. J. Chem. **58**, 92 (1980).

Rates of oxygen absorption by styrene (RH) containing 2,2,3,3-tetraphenylbutane and zinc di-isopropyldithiophosphate at 30°C obey the rate law $-d[O_2]/dt \propto [RH]^{1.4} R_i^{0.79}/[Zn[(i\text{-}PrO)_2PS_2]_2]^{0.54}$, where R_i is the rate of free-radical chain initiation. This order with respect to the styrene concentration implies extensive chain transfer from the poly(peroxystyryl)peroxy radical to a radical derived from the inhibitor. Reaction products confirm the displacement of a di-isopropyldithiophosphoryl radical in the chain termination reaction.

Diethyldithiophosphoric acid also inhibits styrene autoxidation by a mechanism which involves extensive chain transfer.

J. A. HOWARD et S-B. TONG. Can. J. Chem. **58**, 92 (1980).

Les vitesses d'absorption de l'oxygène par le styrène (RH) contenant du tétraphényl-2,2,3,3 butane et du diisopropyldithiophosphate de zinc à 30°C obéissent à la loi de vitesse: $-d[O_2]/dt \propto [RH]^{1.4} R_i^{0.79}/[Zn[(i\text{-}PrO)_2PS_2]_2]^{0.54}$, où R_i est la vitesse d'initiation d'une chaîne de radicaux libres. Cet ordre par rapport à la concentration du styrène implique des transferts de chaîne importants du radical polyperoxy(peroxystyryle) au radical dérivé de l'inhibiteur. Les produits de la réaction confirment le déplacement du radical diisopropyldithiophosphoryle dans le blocage de la réaction en chaîne.

L'acide diéthyldithiophosphorique inhibe également l'autoxydation du styrène selon un mécanisme qui implique des transferts de chaîne importants.

[Traduit par le journal]

Introduction

In the first part of this series it was reported (1) that rates of inhibited autoxidation of several hydrocarbons (styrene, cyclohexene, tetralin, etc.) by a number of zinc dialkyldithiophosphates, xanthates, and dialkyldithiocarbamates at 30° and 50°C obey the rate expression

$$[1] \qquad \frac{-d[O_2]}{dt} = \frac{k_p[RH]R_i}{nk_{inh}[ZnL_2]}$$

where $-d[O_2]/dt$ is the inhibited rate of oxygen absorption, k_p is the rate controlling homopropagation rate constant for the hydrocarbon, RH, R_i is the rate of chain initiation, k_{inh} is the rate constant for reaction of the chain-carrying alkylperoxy radical with the metal complex, ZnL_2, and n is the total number of alkylperoxy radicals destroyed by each molecule of ZnL_2.

A linear dependence of $-d[O_2]/dt$ on R_i and an inverse dependence on $[ZnL_2]$ gave support to the following mechanism for the termination reaction

$$[2] \qquad RO_2^{\cdot} + ZnL_2 \xrightarrow{k_{inh}} X$$

$$[3] \qquad (n-1)RO_2^{\cdot} + X \xrightarrow{fast} \text{non-radical products}$$

where X is a transient intermediate. We tentatively concluded at that time that the peroxy radical reacts with the complex at the metal centre either by an electron transfer reaction [4] or an S_H2 process [5]

$$[4] \qquad RO_2^{\cdot} + ZnL_2 \xrightarrow{k_{inh}} RO_2^{-} + ZnL_2^{+\cdot} \longrightarrow RO_2ZnL + L^{\cdot}$$

$$[5] \qquad RO_2^{\cdot} + ZnL_2 \longrightarrow RO_2ZnL_2 \longrightarrow RO_2ZnL + L^{\cdot}$$

which would mean that the ligand radical $L^{\cdot}$ is the transient intermediate X.

Burn had, however, previously argued (2, 3) that inhibition of olefins such as styrene, cyclohexene, and indene by ZnL_2 was not consistent with this mechanism because of the known rapidity with which sulphur radicals add to double bonds (4–6).

Although kinetic electron spin resonance spectroscopy has been used to show that alkylperoxy radicals do indeed react with ZnL_2 (1, 7) the reaction kinetics have not been established. Thus it was originally reported that rates of decay of $t\text{-}BuO_2^{\cdot}$ are first-order with respect to the concentration of the radical *and* the complex (1) while it has since been demonstrated that, although radical decays are exponential, rates of reaction are virtually independent of the complex concentration.

Because of the apparent inconsistencies in the reported kinetics for reaction of alkylperoxy radicals with $Zn[(i\text{-}PrO)_2PS_2]_2$ we decided to reinvestigate the inhibition kinetics using styrene as a model substrate. The results of this work, which are reported here, are consistent with either mechanism [4] or [5] and also with the ability of $(i\text{-}PrO)_2PS_2^{\cdot}$ to add to vinyl compounds.

[1]NRCC No. 17879.

[2]NRCC Research Associate 1977–1979.

0008-4042/80/010092-04$01.00/0

©1980 National Research Council of Canada/Conseil national de recherches du Canada

Can. J. Chem. Downloaded from www.nrcresearchpress.com by 210.87.254.42 on 09/05/12
For personal use only.

Can. J. Chem. Downloaded from www.nrcresearchpress.com by 210.87.254.42 on 09/05/12
For personal use only.

Experimental

Materials

Styrene (Aldrich) was passed down a column of basic alumina to remove stabilizer and trap-to-trap distilled onto the initiator (2,2,3,3-tetraphenylbutane) and the inhibitor from cupric diethyldithiocarbamate. This latter procedure was performed to ensure complete removal of adventitious hydroperoxidic impurities. Chlorobenzene (solvent) and *tert*-butyl hydroperoxide were purified by standard methods. 2,2,3,3-Tetraphenylbutane was obtained from Dr. L. R. Mahoney (Ford Motor Co., Dearborn, MI) and zinc di-isopropyldithiophosphate was obtained from several sources, and it was also prepared in our laboratory, mp 149–150°C. Diethyldithiophosphoric acid (Aldrich) was purified by distillation.

Kinetic Procedure

All rate measurements reported in this paper were performed at 30°C using a previously described apparatus (8).

Products

Polyperoxides produced after autoxidation of styrene (7.8 *M*) containing tetraphenylbutane (4.3×10^{-4} *M*) and inhibitor were isolated by slow addition of the reaction mixture to a large excess of *n*-hexane. The viscous oils which were precipitated were dissolved in benzene and freeze-dried to give white powders which were analyzed for percentage zinc, sulphur, and phosphorus by atomic absorption, a turbidimetric method, and an inductively coupled plasma emission method respectively. Pulsed Fourier transform ^{31}P nmr spectra of the polymeric peroxides in $CDCl_3$ were obtained with a Varian XL-100 spectrometer. Chemical shifts were measured relative to $(MeO)_3P$ in $CDCl_3$.

Results

The Kinetics of Inhibited Autoxidation

Initial rates of oxygen absorption by solutions of styrene in chlorobenzene containing 2,2,3,3-tetraphenylbutane (TPB) and $Zn[(i\text{-}PrO)_2PS_2]_2$ were measured at 30°C and inhibited rates of autoxidation were calculated from the observed rates by subtracting the rate of oxygen absorption by the initiator ($R_i = 2 \times 2 \times 10^{-6}$[TPB]*M* s^{-1}). Inhibited rates were measured over as wide a range of styrene, TPB, and $Zn[(i\text{-}PrO)_2PS_2]_2$ concentrations as possible, and the results are presented as log (inhibited rate) against log (reactant concentration) plots in Figures 1, 2, and 3.

The order with respect to styrene was determined at two concentrations of $Zn[(i\text{-}PrO)_2PS_2]_2$ (0.015 and 0.041 *M*) and the gradients of the log–log plots gave substrate concentration exponents of 1.45 ± 0.13 and 1.36 ± 0.05 respectively. The order with respect to the initiator concentration was also determined at these two inhibitor concentrations and found to be 0.79 ± 0.05. The gradient of the plot of log $(-d[O_2]/dt)$ against log $[Zn[(i\text{-}PrO)_2PS_2]_2]$ gave an inhibitor concentration exponent of 0.54 ± 0.09.

These results indicate that rates of oxidation of styrene containing $Zn[(i\text{-}PrO)_2PS_2]_2$ obey the rate

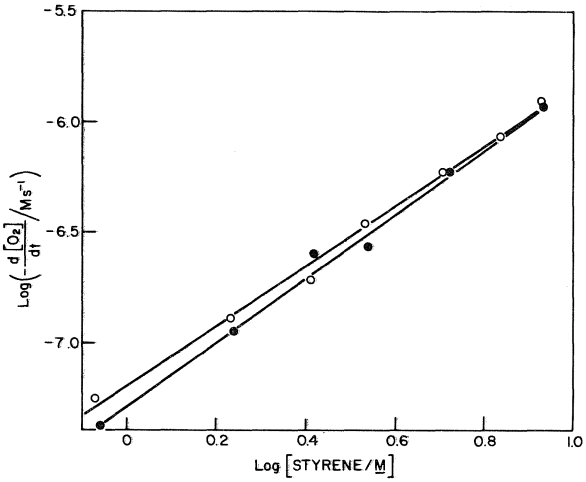


FIG. 1. A plot of the logarithm of the inhibited rate of autoxidation of styrene against the logarithm of the styrene concentration. Open circles, [TPB] = 9.8×10^{-4} *M*, $Zn[(i\text{-}PrO)_2PS_2]_2$ = 0.041 *M*; filled circles, [TPB] = 4.5×10^{-4} *M*, $Zn[(i\text{-}PrO)_2PS_2]_2$ = 0.015 *M*.

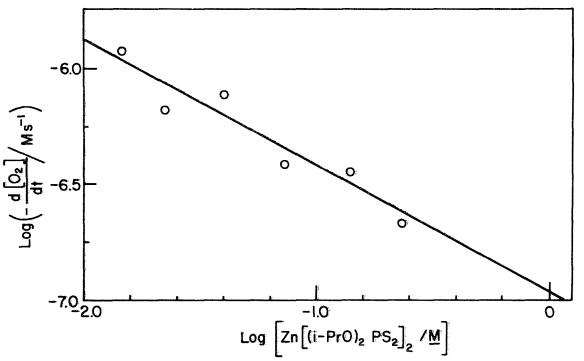


FIG. 2. A plot of the logarithm of the inhibited rate of oxidation of styrene ([TPB] = 4.3×10^{-4} *M*) against the logarithm of the $Zn[(i\text{-}PrO)_2PS_2]_2$ concentration.

expression

$$[6] \qquad \frac{-d[O_2]}{dt} \propto \frac{[RH]^{1.4} R_i^{0.79}}{[ZnL_2]^{0.54}}$$

which is almost identical with the rate laws that have been found for the inhibited autoxidation of 9,10-dihydroanthracene and tetralin by phenol at 60°C (9), tetralin by 1,1′-bis(*N*-phenyl-2-naphthylamine) at 60°C (10), and styrene by 2,4,6-tri-*tert*-butylaniline at 65°C (4).

A rate expression of this form is indicative of a mechanism in which there is extensive involvement of radicals derived from the inhibitor in rate controlling propagation reactions, i.e., extensive chain transfer (11, 12). Based on this kinetic evidence inhibition of autoxidation of styrene by $Zn[(i\text{-}PrO)_2PS_2]_2$ can be represented by the elementary

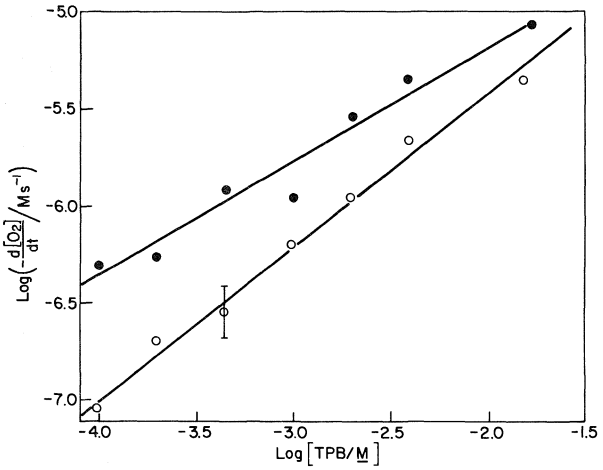


FIG. 3. A log–log plot of the inhibited rate of oxidation of styrene against the TPB concentration. Open circles, $Zn[(i\text{-}PrO)_2PS_2]_2$ = 0.072 *M*; filled circles $Zn[(i\text{-}PrO)_2PS_2]_2$ = 0.015 *M*.

reactions

[7] $R'\text{–}R' \longrightarrow 2R'^{\bullet}$

[8] $R'^{\bullet} + O_2 \xrightarrow{k_0} R'O_2^{\bullet}$

[9] $R'O_2 + RH \xrightarrow{k'_p} R'O_2RH^{\bullet}$

[10] $R'O_2RH^{\bullet} + O_2 \xrightarrow{k_0} R'O_2RHO_2^{\bullet}$

[11] $R'O_2RHO_2^{\bullet} + RH \xrightarrow{k_p} R'O_2RHO_2RH^{\bullet}$

[12] $R'O_2RHO_2^{\bullet} + ZnL_2 \xrightarrow{k_{inh}} R'O_2RHO_2ZnL + L^{\bullet}$

[13] $L^{\bullet} + RH \xrightarrow{k_{13}} LRH^{\bullet}$

[14] $L^{\bullet} + R'O_2RHO_2^{\bullet} \xrightarrow{k_{14}}$ inert products

where R′–R′ represents TPB, RH is styrene, and L• is $(i\text{-}PrO)_2PS_2$.

Making the usual steady state assumptions that the rate of initiation is equal to the rate of termination and that $k_p[R'O_2RHO_2][RH] = k_0[R'O_2RH^{\bullet}][O_2]$ along with the further approximations that $k_p[RH] \gg k_{inh}[ZnL_2]$ and $k_p[RH] \gg k_{14}[RO_2^{\bullet}]$, the inhibited rate is given by

$$[15] \quad \frac{-d[O_2]}{dt} = k_p\left(\frac{k_{13}R_i}{2k_{inh}k_{14}}\right)^{\frac{1}{2}}\frac{[RH]^{\frac{3}{2}}}{[ZnL_2]^{\frac{1}{2}}}$$

Substitution of all the inhibited rates and reactant concentrations into this expression gives $k_{13}/2k_{inh}k_{14} \sim 10^{-11}$ *M* s.

This reaction mechanism does, of course, require a termination reaction between $(i\text{-}PrO)_2PS_2^{\bullet}$ and $RO_2^{\bullet}$ and that the styrene polyperoxide produced in rate controlling propagation reactions contains $Zn(i\text{-}PrO)_2PS_2$ and $(i\text{-}PrO)_2PS_2$ end groups.

Styrene polyperoxide produced after prolonged autoxidation of styrene in the presence of zinc diisopropyldithiophosphate was isolated and found to contain zinc (0.85 ± 0.02%), sulphur (2.19 ± 0.11%), and phosphorus (0.88 ± 0.04%). $Zn[(i\text{-}PrO)_2PS_2]_2$ would, therefore, appear to have been incorporated into the polymer by the inhibition reaction [12] and the chain transfer reaction [13].

Effect of Hydroperoxide

Several groups of workers have shown by radical scavenging (13, 14) and aromatic amine destruction (15, 16) experiments that there is a reaction between $Zn[(i\text{-}PrO)_2PS_2]_2$ and alkyl hydroperoxides which produces free radicals capable of initiating autoxidation. We found, however, that when *tert*-butyl hydroperoxide (0.008 *M*) was added to styrene containing TPB (0.001 *M*) and $Zn[(i\text{-}PrO)_2PS_2]_2$ (0.04 *M*) the inhibited rate was reduced by a factor of ~3.5. Furthermore, the inhibited rate was independent of the hydroperoxide concentration from 0.00005 to 0.001 *M*.

Inhibited rates in the presence of *t*-BuOOH (0.0002 *M*) were found to obey the rate expression

$$\frac{-d[O_2]}{dt} = \frac{[RH]^{1.47\pm0.13}R_i^{0.86\pm0.1}}{[Zn[(i\text{-}PrO)_2PS_2]_2]^{0.58\pm0.1}}$$

which is very similar to the rate in the absence of *t*-BuOOH implying that chain transfer is still important in the presence of hydroperoxide.

Effect of Dialkyldithiophosphoric Acid

Although it has been reported (1) that dialkyldithiophosphoric acids inhibit the autoxidation of styrene and cyclohexene, reactant exponents have not previously been determined. We now report that diethyldithiophosphoric acid is about 5 times more efficient than $Zn[(i\text{-}PrO)_2PS_2]_2$ in styrene and that the order with respect to the substrate concentration is 1.45 ± 0.17 for styrene containing TPB (6×10^{-4} *M*) and $(EtO)_2PS_2H$ (5.6×10^{-3} *M*). This indicates that inhibition of this hydrocarbon by the free acid can probably be described by the elementary reactions [7] to [14], with reaction [12] taking the form

$$RO_2^{\bullet} + (EtO)_2PS_2H \rightarrow RO_2H + (EtO)_2PS_2^{\bullet}$$

This mechanism was substantiated by the observation that the polyperoxide produced by autoxidation of styrene in the presence of $(EtO)_2PS_2H$ contained low percentages of phosphorus and sulphur and that the ^{31}P nmr spectrum in $CDCl_3$ showed a major transition at −51.65 ppm, a somewhat less

Can. J. Chem. Downloaded from www.nrcresearchpress.com by 210.87.254.42 on 09/05/12
For personal use only.

intense transition at −145.35 ppm and minor transitions at −79.41 ppm and −122 ppm relative to $(MeO)_3P$ in $CDCl_3$.[3] The major transition had a chemical shift quite different from the chemical shift for $(EtO)_2PS_2H$ (−61.21 ppm) and is tentatively assigned to the phosphorus nucleus in a diethyldithiophosphoryl end group in polystyrene peroxide. The occurrence of a fairly major peak at $\delta\ ^{31}P = -145.35$ suggests that the polystyrene peroxide contained some type of phosphate group produced by replacement of sulphur by oxygen. This type of reaction, although poorly understood, is common in lubricants containing zinc dialkyldithiophosphates.[4]

Conclusions

There appears to be no doubt that an alkylperoxy radical can displace a di-isopropyldithiophosphoryl radical from zinc di-isopropyldithiophosphate and that this radical has the ability to add to styrene and also to undergo a chain termination reaction. It is, therefore, not surprising that inhibition of styrene autoxidation by diethyldithiophosphoric acid also involves extensive chain transfer. The generality of this mechanism has, however, not yet been demonstrated and work is in progress in our laboratory on the kinetics and products of the inhibition of styrene autoxidation by other dialkyldithiophosphates and dialkyldithiocarbamates.

The influence of *tert*-butyl hydroperoxide on autoxidation of styrene in the presence of zinc di-isopropyldithiophosphate is not at the present time clear. Enhanced inhibition could perhaps be the result of interception of ligand radicals by the hydroperoxide to give *tert*-butylperoxy radicals which are known to be less reactive towards styrene than the poly(peroxystyryl)peroxy radical (17).

$$(i\text{-PrO})_2PS_2^{\cdot} + t\text{-BuOOH} \rightarrow (i\text{-PrO})_2PS_2H + t\text{-BuO}_2^{\cdot}$$

In addition this reaction gives di-isopropyldithiophosphoric acid which is a better inhibitor than $Zn[(i\text{-PrO})_2PS_2]_2$.

[3]Downfield shifts are positive, relative to internal $(MeO)_3P$ using Ξ (^{31}P in $(MeO)_3P$) = 40 486 459 Hz at 100 MHz relative to TMS. Chemical shifts relative to the more familiar but less reproducible standard H_3PO_4 can be calculated from $\delta\ H_3PO_4 = -141$.

[4]We thank a referee for bringing this point to our attention.

Acknowledgements

The authors are indebted to Mr. J. Bornais for nmr spectra and Dr. S. K. Brownstein for advice on the interpretation of these spectra.

1. J. A. Howard, Y. Ohkatsu, J. H. B. Chenier, and K. U. Ingold. Can. J. Chem. **51**, 1543 (1973).
2. A. J. Burn. Tetrahedron, **22**, 2153 (1966).
3. A. J. Burn. Adv. Chem. Ser. **75**, 323 (1968).
4. D. V. Gardner, J. A. Howard, and K. U. Ingold. Can. J. Chem. **42**, 2847 (1964).
5. W. E. Bacon and W. M. LeSuer. J. Am. Chem. Soc. **76**, 670 (1954).
6. S. Oae, A. Nakanishi, and N. Tsiyimoto. Tetrahedron, **28**, 2981 (1972) and refs. cited in ref. 3.
7. J. A. Howard and J. H. B. Chenier. Can. J. Chem. **54**, 382 (1976).
8. J. A. Howard and K. U. Ingold. Can. J. Chem. **47**, 3809 (1969).
9. L. R. Mahoney and F. C. Ferris. J. Am. Chem. Soc. **85**, 2345 (1963).
10. R. F. Bridger. J. Org. Chem. **36**, 1214 (1971); J. A. Howard and K. U. Ingold. Can. J. Chem. **42**, 2324 (1964).
11. W. A. Waters and C. Wickham-Jones. J. Chem. Soc. 812 (1951).
12. A. F. Bickel and E. C. Kooyman. J. Chem. Soc. 2215 (1956).
13. S. K. Ivanov and I. Kateva. Dokl. Bolg. Akad. Nauk, **25**, 645 (1972).
14. G. Brunton, B. C. Gilbert, and R. J. Mawby. J. Chem. Soc. Perkin Trans. II, 650 (1976).
15. S. K. Ivanov and I. Kateva. Neftekhimiya, **11**, 290 (1971).
16. S. K. Ivanov and J. D. Kateva. J. Polym. Sci. Symp. No. 57, 237 (1976).
17. J. A. Howard. Can. J. Chem. **50**, 2298 (1972).

Can. J. Chem. Downloaded from www.nrcresearchpress.com by 210.87.254.42 on 09/05/12
For personal use only.

Canadian Journal of Chemistry
Published by
THE NATIONAL RESEARCH COUNCIL OF CANADA

Journal canadien de chimie
Publié par
LE CONSEIL NATIONAL DE RECHERCHES DU CANADA

Volume 58 Number 2 January 15, 1980

Volume 58 numéro 2 15 janvier 1980

Can. J. Chem. Downloaded from www.nrcresearchpress.com by 210.87.254.6 on 09/05/12
For personal use only.

The molecular and crystal structure of *trans*-dichloro(dimethylformamide)(2,6-lutidine)platinum(II)

F. D. ROCHON, P. C. KONG, and R. MELANSON
Département de chimie, Université du Québec à Montréal, C.P. 8888, Montréal (Qué.), Canada H3C 3P8

Received June 15, 1979

F. D. ROCHON, P. C. KONG, and R. MELANSON. Can. J. Chem. **58**, 97 (1980).

The crystal structure of *trans*-[Pt(DMF)(2,6-lutidine)Cl_2] has been determined by X-ray diffraction. The crystals are orthorhombic, space group *Pbca*, with $a = 11.612(13)$, $b = 26.504(33)$, $c = 9.271(9)$ Å, and $Z = 8$. The structure was refined by full matrix least-squares analysis to a conventional R factor of 0.051 and a weighted $R_w = 0.044$. The coordination around the platinum atom is square planar. The 2,6-lutidine ring is perpendicular to the platinum plane. DMF is bonded to platinum through the oxygen atom. It is planar and makes an angle of 71° with the platinum plane. The *cis–trans* configuration of the [Pt(DMF)(L)Cl_2] (L = pyridine derivative) complexes in DMF solution is discussed.

F. D. ROCHON, P. C. KONG et R. MELANSON. Can. J. Chem. **58**, 97 (1980).

La structure cristalline de *trans*-[Pt(DMF)(lutidine-2,6)Cl_2] a été déterminée par diffraction des rayons-X. Les cristaux appartiennent au groupe spatial orthorhombique *Pbca*, avec $a = 11.612(13)$, $b = 26.504(33)$, $c = 9.271(9)$ Å et $Z = 8$. Les coordonnées et les facteurs thermiques anisotropes ont été affinés par moindres-carrés (matrice entière) jusqu'à $R = 0.051$ et $R_w = 0.044$. La coordination autour de l'atome de platine est plane. Le noyau lutidine-2,6 est perpendiculaire au plan du platine. DMF est lié au platine par l'atome d'oxygène. Le ligand DMF est plan et forme un angle de 71° avec la plan du platine. La configuration *cis–trans* des complexes [Pt(DMF)(L)Cl_2] (L = dérivé de la pyridine) en solution dans le DMF, est discutée.

Introduction

In an attempt to prepare compounds of the type *cis*-[Pt(am)(am′)Cl_2] (am = amine, am′ = amine ≠ am) in a view of increasing the screening range for antitumour properties of platinum complexes, we have isolated a series of compounds [Pt(DMF)(L)Cl_2] where L = pyridine derivative and DMF = dimethylformamide (1). The compounds were first prepared by the following reaction:

$$[1]\quad K[Pt(L)Cl_3] \xrightarrow[DMF]{Ag^+} [Pt(L)(DMF)Cl_2]$$

The compounds were assumed to have the *cis* configuration for two reasons: (*i*) The *trans* effect of chlorine is greater than the *trans* effect of pyridine derivatives. (*ii*) The following reactions were observed (except when L = 2,6-lutidine):

$$[2]\quad \begin{aligned} K[Pt(L)Cl_3] + L &\xrightarrow[DMF]{Ag^+} \textit{cis}\text{-}[Pt(L)_2Cl_2] \\ [Pt(DMF)(L)Cl_2] + L &\xrightarrow{DMF} \textit{cis}\text{-}[Pt(L)_2Cl_2] + DMF \end{aligned}$$

Therefore [Pt(DMF)(L)Cl_2] was assumed to be an intermediate in the above overall reaction [2]. Since [Pt$(L)_2Cl_2$] has the *cis* configuration, [Pt(DMF)(L)Cl_2] was also assumed to be the *cis*-isomer. When L = 2,6-lutidine (2,6-lut), the reaction stops at [Pt(DMF)(2,6-lut)Cl_2]. We have already reported that the steric hindrance of 2,6-lut to its *cis* position is so large that *cis*-[Pt$(2,6\text{-lut})_2Cl_2$] cannot be obtained from the reaction of K[Pt(2,6-lut)Cl_3] and 2,6-lut (2).

In order to confirm our hypothesis, we decided to undertake a crystal structure analysis of one of the compounds. Only [Pt(DMF)(2,6-lut)Cl_2] gave suitable crystals for X-ray analysis. Even we realized that this compound was not necessarily representative of the series, we have decided to determine its structure. We were surprised to find out that it had the *trans*-configuration.

The DMF compounds can also be prepared by dissolving the bridged compounds [Pt(L)$Cl_2]_2$ in DMF (1). Infrared spectroscopy has shown that the products obtained by both methods were identical.

0008-4042/80/020097-05$01.00/0
©1980 National Research Council of Canada/Conseil national de recherches du Canada

Can. J. Chem. Downloaded from www.nrcresearchpress.com by 210.87.254.6 on 09/05/12
For personal use only.

Experimental

[Pt(DMF)(2,6-lut)Cl_2] was synthesized according to ref. 1 and recrystallized as plates from a DMF–ether solution.

The orthorhombic standard centrosymmetric space group *Pbca* was established unambiguously from precession photographs. The cell parameters were calculated by least-squares refinement of the setting angles of 15 independent peaks centered on a Syntex $P\bar{1}$ diffractometer using graphite monochromatized MoKα radiation.

Crystal data are as follows:

$PtCl_2C_{10}H_{16}N_2O$ mw = 446.25
Orthorhombic *Pbca*, a = 11.612(13), b = 26.504(33), c = 9.271(9) Å, V = 2853(5) Å^3, Z = 8, D_x = 2.078 g cm^{-3}, D_m = 2.07(2) g cm^{-3} (flotation), λ(MoKα) = 0.71069 Å, μ(MoKα) = 107.01 cm^{-1}, and T = 22°C.

Collection and Reduction of Intensity Data

The intensity data were collected from a crystal of dimensions 0.76 × 0.358 × 0.076 mm. A total of 4196 independent reflections were measured in the region of $2\theta < 60°$ by the $2\theta/\theta$ scan technique using MoKα radiation. The scan rate was 1° (2θ) min^{-1} for most reflections, but rates as high as 24° min^{-1} were selected for strong reflections by the autocollection program. A 2θ scan range of 1° below $K\alpha_1$ and 1° above $K\alpha_2$ was selected. The background time to scan time ratio was 0.40. Three standard reflections were measured after every 47 reflections. They showed fluctuations of ±3% during the data collection.

The reflections for which the intensity was less than $2.5\sigma(I)$ were considered as unobserved. The standard deviation $\sigma(I)$ was calculated as already described (3). An absorption correction based on the equations of the crystal faces was applied to all the reflections. The transmission factors varied from 0.058 to 0.443. The data were then corrected for the Lorentz and polarization effects. This set of 2125 observed reflections was used for the structure determination.

The atomic scattering factors of Cromer and Waber (4) were used for Pt, Cl, O, N, and C atoms, those of Stewart, Davidson, and Simpson (5) were used for hydrogen. The anomalous dispersion terms (6) of platinum and chlorine were included in the calculations.

Structure Determination

The structure was solved by the heavy atom method. The refinement of the parameters was carried out by full-matrix least-squares methods. In the early stages of refinement, unit weights were assigned to all observed reflections. Later, individual weights $w = 1/\sigma^2(F)$ (7) were applied. The hydrogen atoms on the lutidine ring and the aldehyde hydrogen atom were fixed at their calculated position (C—H = 0.95 Å, angle = 120°) and assigned isotropic temperature factors of β = 6.0 Å^2. An isotropic secondary extinction coefficient (8) was also applied. The refinement of the scale factor, the coordinates and anisotropic temperature factors of all the non-hydrogen atoms converged to $R = \sum ||F_o| - |F_c|| / \sum |F_o| = 0.051$ and $R_w = [\sum w(|F_o| - |F_c|)^2 / \sum w|F_o|^2]^{1/2} = 0.044$. The final difference Fourier map did not show peaks higher than ±0.7 e Å^{-3}. Attempts to find the hydrogen atoms on the methyl groups were not successful.

The calculations were carried out with a Cyber 73 computer and the programs used have already been described (3). A table of observed and calculated structure factors is available from the Depository of Unpublished Data.[1]

[1]Complete set of data (lists of structure factors and anisotropic thermal parameters) is available, at a nominal charge, from the Depository of Unpublished Data, CISTI, National Research Council of Canada, Ottawa, Ont., Canada K1A 0S2.

Results and Discussion

The refined atomic parameters are listed in Table 1. A list of the anisotropic temperature factors is available. A labelled diagram of the molecule is shown in Fig. 1. The bond distances and angles within the molecule are listed in Table 2.

As mentioned earlier, we expected the compound to be the *cis* isomer, but we were surprised to find out that it had the *trans* configuration. The DMF ligand is bonded to platinum through the oxygen atom which confirmed our previous hypothesis based on infrared and nmr spectroscopy (1).

TABLE 1. Final atomic parameters (× 10^4). The estimated standard deviations are given in parentheses

Atom	x	y	z
Pt	1629.5(3)	1167.2(1)	886.9(5)
Cl(1)	2981(2)	1300(1)	−881(4)
Cl(2)	312(2)	1046(1)	2703(5)
O	1970(6)	408(2)	829(10)
N(1)	1259(6)	1909(2)	891(10)
N(2)	3208(7)	−237(3)	1116(13)
C(1)	421(7)	2065(4)	26(13)
C(2)	185(8)	2593(4)	−9(16)
C(3)	765(11)	2907(4)	777(17)
C(4)	1594(11)	2743(4)	1630(15)
C(5)	1876(8)	2215(3)	1720(12)
C(6)	−329(8)	1701(4)	−842(15)
C(7)	2789(8)	2000(3)	2681(15)
C(8)	2937(8)	247(4)	1213(16)
C(9)	4352(9)	−429(4)	1679(21)
C(10)	2369(13)	−597(4)	538(18)

TABLE 2. Bond distances (Å) and bond angles (deg)

Bond	Length	Bonds	Angle
Pt—Cl(1)	2.297(3)	Cl(1)—Pt—Cl(2)	178.3(1)
Pt—Cl(2)	2.297(4)	Cl(1)—Pt—O	90.0(2)
Pt—O	2.051(6)	Cl(1)—Pt—N(1)	89.9(2)
Pt—N(1)	2.013(6)	Cl(2)—Pt—O	90.6(2)
N(1)—C(1)	1.326(13)	Cl(2)—Pt—N(1)	89.6(2)
N(1)—C(5)	1.328(12)	O—Pt—N(1)	178.1(3)
C(1)—C(2)	1.429(14)	Pt—O—C(8)	120.0(7)
C(1)—C(6)	1.529(15)	Pt—N(1)—C(1)	117.4(6)
C(2)—C(3)	1.295(17)	Pt—N(1)—C(5)	118.8(6)
C(3)—C(4)	1.320(18)	C(1)—N(1)—C(5)	123.8(8)
C(4)—C(5)	1.439(14)	N(1)—C(1)—C(2)	117.4(9)
C(5)—C(7)	1.497(15)	N(1)—C(1)—C(6)	122.7(9)
O—C(8)	1.253(12)	C(2)—C(1)—C(6)	119.8(9)
N(2)—C(8)	1.326(13)	C(1)—C(2)—C(3)	121.1(11)
N(2)—C(9)	1.516(15)	C(2)—C(3)—C(4)	120.4(12)
N(2)—C(10)	1.465(16)	C(3)—C(4)—C(5)	121.4(11)
		N(1)—C(5)—C(4)	116.0(9)
		N(1)—C(5)—C(7)	119.6(9)
		C(4)—C(5)—C(7)	124.4(9)
		O—C(8)—N(2)	121.6(10)
		C(8)—N(2)—C(9)	120.7(10)
		C(8)—N(2)—C(10)	119.9(10)
		C(9)—N(2)—C(10)	119.3(10)

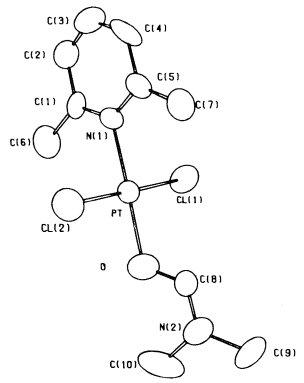


FIG. 1. Labelled view of the molecule *trans*-[Pt(dimethylformamide)(2,6-lutidine)Cl_2].

As expected, the coordination around the platinum atom is square planar. The weighted best plane was calculated through the five atoms. The deviations from this plane are: Pt, 0.0007; Cl(1), −0.026; Cl(2), −0.035; O, 0.033; and N(1), 0.034 Å. The angles around the platinum atom are close to the expected 90° and 180°.

The Pt—Cl bonds (2.297 Å) are normal and agree well with the published values (3, 10, 11). The Pt—O bond of 2.051 Å also seems normal. Infrared spectroscopy has already shown that [Pt(DMF)$_2$Cl$_2$], [Pt(dimethylacetamide)$_2$Cl$_2$] (12), and the analyzed compound (1) were bonded to platinum through the oxygen atom. But to our knowledge, this study is the first structure determination of platinum–DMF complex. Platinum does not usually form bonds with oxygen atoms. For example, DMSO coordinates to platinum through the sulphur atom (3, 10, 11) and not through the oxygen atom like most other metals.

DMF exists as a resonance structure of the two mesomeric forms $(CH_3)_2NCHO$ and $(CH_3)_2N^+CHO^+$. Because of the ionic form, platinum will form bonds more easily with the oxygen atom than with the nitrogen atom. The decrease in multiplicity of the C—O bond and the increased multiplicity of the C—N bond resulting from the resonance structures, have been observed in all published crystal structures involving DMF molecules. Table 3 shows a brief summary of several DMF crystal structure determinations.

Since the ionic form is favored when DMF is coordinated to a metal, a more pronounced decrease in multiplicity of the C—O bond along with an increase of multiplicity of the C—N bond would be expected. But it is interesting to observe that DMF has the same structure, whether it is coordinated to a metal or uncomplexed as a molecule of crystallization. The structure of DMF in the gas phase has been determined in 1962 by electron diffraction (13). The C—O distance (1.20 Å) seems shorter than the distances found in crystal structures of DMF compounds (1.21–1.30 Å). But in many determinations, including DMF, the standard deviations are very high. Therefore the difference might not be significant. The C—N distance in DMF (1.34 Å) is the same as the distances found in crystalline DMF compounds (1.28–1.35 Å). Therefore the structure of DMF seems unaltered whether it is free, crystallized as a molecule of solvent or bonded to a metal.

All the published structures show that DMF is planar. In our study of *trans*-[Pt(DMF)(2,6-lut)Cl_2], DMF is also planar. The deviations from the weighed best plane are: O, −0.01(1); N(2), 0.02(1); C(8), 0.02(1); C(9), −0.03(2); and C(10), 0.00(2) Å. The C(8)—O bond distance of 1.253(12) Å agrees well with the published data (Table 3). It is slightly longer than a normal C=O bond. The N(2)—C(8) bond (1.326(13) Å) also agrees with the data shown on Table 3. It is shorter than a normal N—C bond showing an increase in multiplicity of the bond resulting from the resonance structures. The angles around the nitrogen atom are close to 120° and agree with the data published on DMF structures of Table 3.

The Pt—N(1) distance of 2.013 Å agrees well with published Pt—N distances in pyridine derivative compounds (10, 11). The 2,6-lutidine ligand is planar and is perpendicular to the platinum coordination plane (88.4°). The distances within the ligand are normal and agree with published data (10, 11). The angles are close to the expected 120°.

A stereoscopic view of the packing in the *trans*-[Pt(DMF)(2,6-lut)Cl_2] crystal is shown in Fig. 2. The molecules are packed in planes parallel to the *bc* plane. All the hydrogen atoms being bonded to carbon atoms, no strong hydrogen bonding was expected, but one interaction involving the aldehyde proton with a chlorine atom is worth mentioning. The distances and angles involved are shown in Table 4. The H···Cl(2) distance (2.67 Å) is shorter than the Van der Waals distance (3.0 Å). The angles are good, but the long distance C(8)···Cl(2) (3.62 Å) indicates that this interaction is fairly weak.

Since the *trans* effect of chlorine is greater than pyridine derivatives, the products of reactions [1] and [3] should have the *cis*-configuration, at least, the initial products should be the *cis* isomers.

$$[3]\quad [Pt(L)Cl_2]_2 + 2DMF \xrightarrow{DMF} 2[Pt(L)(DMF)Cl_2]$$

Can. J. Chem. Downloaded from www.nrcresearchpress.com by 210.87.254.6 on 09/05/12
For personal use only.

TABLE 3. Published DMF crystal structures

Compound	Distance (Å) C—O	Distance (Å) C—N	Reference
Free DMF			
DMF (electron diffraction in gas phase)	1.20	1.34(4)	13
NaI—DMF	1.23(4)	1.34(4)	14
Symmetrical cedrone—2DMF	1.235(4)	1.317(4)	15
1,7-Diacetoxy-2,4,6-trinitro-2,4,6-triazaheptane — DMF	1.211(5)	1.327(5)	16
1,3,5,7-Tetranitro-1,3,5,7-tetraazacyclooctane — DMF	1.232(12)	1.345(32)	17
2,5-Pyridinedicarboxylic acid — DMF monohydrate	1.273(5)	1.322(5)	18
HfT_4—DMF	1.242	1.314	19
Bis(quinoxaline-2,3-dithiolato)Ni(II)—2DMF	1.233(6)	1.306(5)	20
trans-5-Amino-3-[2-(5-nitro-2-furyl)vinyl]-1,2,4-oxadiazole — DMF (DMF disordered)	1.29(1) 1.30(1)	1.30(1) 1.41(2)	21
8β-Hydroxy-Δ⁹-tetrahydrocannabinol — DMF	1.233(4)	1.332(4)	22
Bonded DMF			
$[Ni(DMF)_4(NCSe)_2]$	1.26(3)	1.35(4)	23
Dioxodichlorobis(DMF)Mo(VI)	1.29(1)	1.28(1)	24
$(Co\ salen)_2(O_2)(DMF)_2$	1.222(11)	1.310(11)	25
Tetrakis(tropolonato)(DMF)Th(IV)	1.233(11)	1.325(11)	26
Bis(DMF)bis(1,3-diphenyl-1,3-propanedionato)Mg	1.228(5)	1.288(5)	27
Trichloro(DMF)(1,10-phen)Cr(III)	1.28(2)	1.34(2)	28
$(\eta^5\text{-}C_5H_5)_2MoH_2 \cdot ZnBr_2 \cdot DMF$	1.244(20)	1.315(21)	29
$MeSnCl_3 \cdot 2DMF$	1.32(2)	1.35(3)	30
$MeSnBr_3 \cdot DMF$	1.24(6)	1.33(6)	30
$Pt(DMF)(2,6\text{-lut})Cl_2$	1.253(12)	1.326(13)	This work

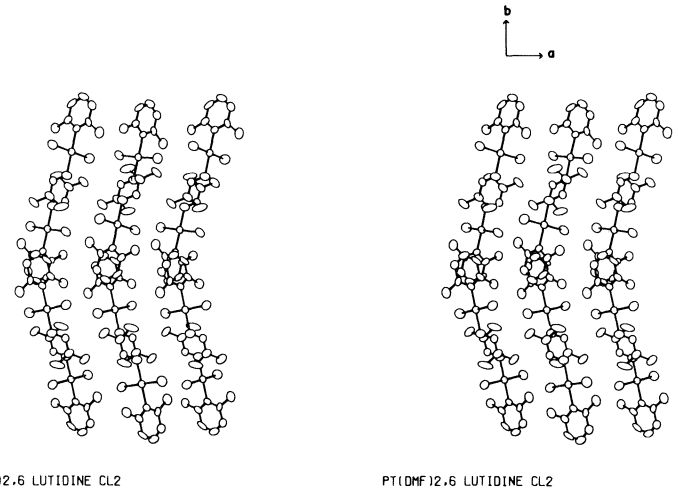


FIG. 2. Stereoscopic view of the packing in the *trans*-$[Pt(DMF)(2,6\text{-lut})Cl_2]$ crystal.

The *trans*-isomers could be formed from the subsequent isomerization of the *cis*-isomers, as is $[Pt(DMSO)(L)Cl_2]$ in dimethylsulphoxide (DMSO) solution (9). The nmr signals of the ortho-protons of $[Pt(DMSO)(4\text{-picoline})Cl_2]$ in DMSO, appeared at 8.52 ppm for the *trans*-isomer and at 8.76 ppm for the *cis*-isomer. The nmr spectrum of $[Pt(2,4\text{-lut})(DMF)Cl_2]$ in DMF-d_6 does not give positive evidence of two isomers in solution (only one doublet for the ortho proton of 2,4-lut with half width of 2.5 Hz). This may be because the *trans* effect of DMF is smaller than the *trans* effect of DMSO. Therefore the influence of the DMF ligand on the ortho proton of 2,4-lut might be the same, whether it is in the *cis* or *trans* position.

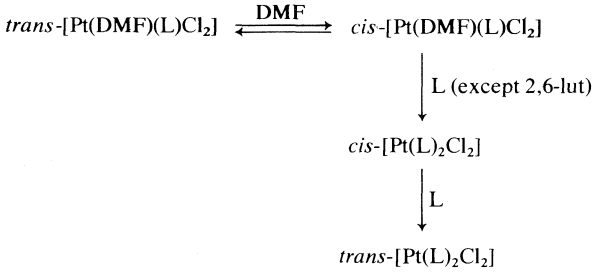
cis-$[Pt(DMF)(L)Cl_2]$ is suggested to exist in solution because of the following observations. No $[Pt(2,6\text{-lut})_2Cl_2]$ can be obtained from the reaction of *trans*-$[Pt(DMF)(2,6\text{-lut})Cl_2]$ and 2,6-lut in DMF. Since 2,6-lut causes no steric hindrance in the *trans* position, the inability to displace DMF is presumably due to the stability of *trans*-[Pt(DMF)(2,6-

Can. J. Chem. Downloaded from www.nrcresearchpress.com by 210.87.254.6 on 09/05/12
For personal use only.

TABLE 4. Possible hydrogen bonds

Atoms	Transformation (on last atom)	Distance (Å)	Atoms	Angle (deg)
C(8)—H...Cl(2)	$\frac{1}{2}+x, y, \frac{1}{2}-z$	3.620(1)	O(8)—C(8)...Cl(2)	124.2(7)
H...Cl(2)	$\frac{1}{2}+x, y, \frac{1}{2}-z$	2.673	N(2)—C(8)...Cl(2)	113.9(7)
			C(8)—H...Cl(2)	167.2(7)

lut)Cl_2]. This explanation should also apply to other *trans*-[Pt(DMF)(L)Cl_2]. However, when L = pyridine, 2-picoline, and 4-picoline, *cis*-[Pt(L)$_2Cl_2$] can be obtained from the reaction of [Pt(DMF)(L)Cl_2] and L in DMF or $CHCl_3$ at room temperature (Pt: L = 1:1, concentration 0.05 *M*, and time = 1.5 h). Since *trans*-[Pt(L)$_2Cl_2$] cannot isomerize to *cis*-[Pt(L)$_2Cl_2$], the formation of the *cis* isomer should come from the direct reaction of *cis*-[Pt(DMF)(L)Cl_2] and L. The failure to obtain [Pt(2,6-lut)$_2Cl_2$] does not contradict the existence of *cis*-[Pt(DMF)(2,6-lut)Cl_2] in solution. It has already been found that the steric hindrance of 2,6-lut to its *cis* position is so large that *cis*-[Pt(2,6-lut)$_2Cl_2$] cannot be obtained from the reaction of K[Pt(2,6-lut)Cl_3] and 2,6-lut (2). Therefore, in DMF solution, [Pt(DMF)(L)Cl_2] should be a mixture of *cis*- and *trans*-isomers. The scheme of the reactions is thus as follows.



Acknowledgments

The authors are grateful to the Natural Sciences and Engineering Research Council of Canada and to the Cancer Research Society Inc. for financial support and to Johnson Matthey & Co. Limited for a loan of potassium chloroplatinite.

1. P. C. KONG and F. D. ROCHON. Can. J. Chem. **57**, 682 (1979).
2. P. C. KONG and F. D. ROCHON. Can. J. Chem. **56**, 441 (1978).
3. R. MELANSON and F. D. ROCHON. Can. J. Chem. **53**, 2371 (1975).
4. D. T. CROMER and J. T. WABER. Acta Crystallogr. **18**, 104 (1965).
5. R. T. STEWART, E. R. DAVIDSON, and W. T. SIMPSON. J. Chem. Phys. **42**, 3175 (1965).
6. D. T. CROMER and D. LIBERMAN. J. Chem. Phys. **53**, 1891 (1970).
7. G. H. STOUT and L. H. JENSEN. X-ray structure determination. Macmillan, London. 1968.
8. P. COPPENS and W. C. HAMILTON. Acta Crystallogr. A**26**, 71 (1970).
9. P. C. KONG, D. IYAMUREMYE, and F. D. ROCHON. Can. J. Chem. **54**, 3224 (1976).
10. R. MELANSON and F. D. ROCHON. Can. J. Chem. **54**, 1002 (1976).
11. R. MELANSON and F. D. ROCHON. Acta Crystallogr. B**33**, 3571 (1977); B**34**, 941 (1978); B**34**, 1125 (1978).
12. J. M. GIORIA and B. P. SUSZ. Helv. Chim. Acta, **54**, 2251 (1971).
13. L. V. VILKOV, P. A. AKISHIN, and V. M. PRESNYAKOVA. J. Struct. Chem. **3**, 3 (1962).
14. Y. GOBILLON, P. PIRET, and M. VAN MEERSSCHE. Bull. Soc. Chim. Fr. 551 (1962).
15. J. A. BEISLER and J. V. SILVERTON. Acta Crystallogr. B**28**, 298 (1972).
16. R. E. COBBLEDICK and R. W. H. SMALL. Acta Crystallogr. B**29**, 1659 (1973).
17. R. E. COBBLEDICK and R. W. H. SMALL. Acta Crystallogr. B**31**, 2805 (1975).
18. KUNIAKI ITO, SETSWO KASHINO, and MASAO HAISA. Acta Crystallogr. B**32**, 511 (1976).
19. D. TRANQUI, A. TISSIER, J. LAUGIER, and P. BOYER. Acta Crystallogr. B**33**, 392 (1977).
20. A. PIGNEDOLI and G. PEYRONEL. Acta Crystallogr. B**33**, 1439 (1977).
21. D. B. HOWE, C. H. ROBINSON, and L. M. AMZEL. Acta Crystallogr. B**33**, 2353 (1977).
22. T. OTTERSEN and E. ROSENQVIST. Acta Chem. Scan. B**31**, 749 (1977).
23. G. V. TSINTSADZE, M. A. PORAI-KOSHITS, and A. S. ANTSYSHKINA. J. Struct. Chem. **8**, 253 (1967).
24. L. R. FLORIAN and E. R. COREY. Inorg. Chem. **7**, 722 (1968).
25. M. CALLIGARIS, G. NARDIN, and L. RANDACCIO. J. Chem. Soc. D, 763 (1969); M. CALLIGARIS, G. NARDIN, L. RANDACCIO, and A. RIPAMONTI. J. Chem. Soc. A, 1069 (1970).
26. V. W. DAY and J. L. HOARD. J. Am. Chem. Soc. **92**, 3626 (1970).
27. F. J. HOLLANDER, D. H. TEMPLETON, and A. ZALKIN. Acta Crystallogr. B**29**, 1289 (1973).
28. J. A. BROOMHEAD, J. EVANS, W. D. GRUMLEY, and M. STERNS. J. Chem. Soc. Dalton, 173 (1977).
29. D. E. CROTTY, T. J. ANDERSON, M. D. GLICK, and J. P. OLIVER. Inorg. Chem. **16**, 2346 (1977).
30. L. A. ASLANOV, V. M. IONOV, V. M. ATTIYA, A. B. PERMIN, and V. S. PETROSYAN. J. Struct. Chem. **19**, 269 (1978).

Can. J. Chem. Downloaded from www.nrcresearchpress.com by 210.87.254.6 on 09/05/12
For personal use only.

Molecular motion and methyl group rotation barriers from ^{13}C nmr relaxation times. Norbornane and adamantane derivatives in solution

HELMUT BEIERBECK, ROBERT MARTINO, [1] AND JOHN K. SAUNDERS
Département de chimie, Université de Sherbrooke, Sherbrooke (Qué.), Canada J1K 2R1

Received June 8, 1979

HELMUT BEIERBECK, ROBERT MARTINO, and JOHN K. SAUNDERS. Can. J. Chem. **58**, 102 (1980).

The carbon-13 relaxation time data for several norbornane and adamantane derivatives are presented. It is shown that the most probable principal axis of the rotational diffusion tensor is an axis which contains the centre of mass of the molecule and the heterosubstituent. The influence of the C—Ĉ—H bond angle on the calculation of methyl group rotation barriers from relaxation time data and on the barrier is discussed.

HELMUT BEIERBECK, ROBERT MARTINO et JOHN K. SAUNDERS. Can. J. Chem. **58**, 102 (1980).

Le temps de relaxation du carbone-13 de plusieurs dérivés de norbornane et d'adamantane sont présenté. On démontre que l'axe principale le plus probable de la tensor de la diffusion rotationnel est celle que contient le centre de masse de la molécule et l'hétérosubstituant. On discute l'influence de l'angle C—Ĉ—H sur le calcul de la barrière de rotation d'un groupement méthyle à partir du temps de relaxation et aussi sur la barrière elle-même.

The analysis of ^{13}C nmr spin lattice relaxation times (T_1) provides insight into the dynamic behaviour of organic molecules in solution, including the overall diffusion constants for the molecules (1) and diffusion constants for rotation about single bonds (2–4). The simplest case of overall motion is isotropic motion. In such a case the diffusion constant can be obtained directly from T_1 data using eq. [1], since most models of molecular reorientation

$$[1]\quad \frac{1}{T_1} = \frac{N\gamma_H{}^2\gamma_C{}^2\hbar^2}{(r_{C-H})^6}\,\tau_c$$

assume that the rotational diffusion constant R_i about the ith axis is related to the correlation time about this axis (τ_{ci}) by the expression $(1/6R_i) = \tau_{ci}$ (5).

The internal reorientation rate of a CH_3 group rotation can be calculated using eq. [2] (6), where

$$[2]\quad \frac{1}{T_1} = \frac{3\gamma_H{}^2\gamma_C{}^2\hbar^2}{(r_{C-H})^6} \times \left[\frac{A}{6R} + \frac{B}{6R + R_{int}} + \frac{C}{6R + R_{int}}\right]$$

A, B, and C are geometrical terms, R is the overall diffusion constant obtained by application of eq. [1] to the T_1 data of rigid carbons, and R_{int} is the diffusion constant for reorientation about the carbon—CH_3 bond. Equation [2] is the stochastic diffusion model. The relaxation rate constant for CH_3 groups jumping between three equivalent positions separated by 120° is given by eq. [3] (7)

$$[3]\quad \frac{1}{T_1} = \frac{3\gamma_H{}^2\gamma_C{}^2\hbar^2}{(r_{C-H})^6}\left[\frac{A}{6R} + \frac{B + C}{6R + R_{int}}\right]$$

In an earlier publication (8) we have shown that the values of R_{int} for CH_3 groups in steroids depend on the number of 1,3 diaxial CH_3–hydrogen interactions to which the CH_3 group is subjected. In order to further explore the factors which influence R_{int}, we have studied several methylated bicyclo-[2,2,1]heptanes and adamantanes, the results of which are presented in Table 1. The T_1 values represent the dipole–dipole contributions since the nOe was 2.0 ± 0.1 for all carbons in all molecules. Inspection of the results given in Table 1 reveals that the T_1 data cannot be analysed by application of eqs. [1] and [2] since the NT_1 values of ring carbons in most compounds are not constant. For example, C-5 has a significantly shorter T_1 than C-6 for compound **1** when $CDCl_3$ is employed as solvent. This implies that the overall motion of the molecules is anisotropic. Previously reported data for norbornene (9, 10) showed non uniform NT_1 values for ring carbons, particularly at C-4, which was interpreted in terms of anisotropic motion (9) and different C—H bond lengths (10). A shorter C—H bond length than normal at C-4 is plausible but it appears very unlikely that the difference in T_1 between C-5 and C-6 in **1**, **2**, and **3** can be attributed to bond length differences.

In systems undergoing anisotropic motion, τ_c of eq. [1] must be replaced by an expression containing the diffusion constants about the various molecular axes. The simplest case of an anisotropic system is that of a symmetric top molecule in which τ_c is expressed in terms of R_1 and R_2, where R_1 describes the rotation about the C_3 axis and R_2 the

[1]Permanent address: Université Paul Sabatier, 118 route de Narbonne, Toulouse, France.

0008-4042/80/020102-08$01.00/0
©1980 National Research Council of Canada/Conseil national de recherches du Canada

Can. J. Chem. Downloaded from www.nrcresearchpress.com by 210.87.254.105 on 09/05/12
For personal use only.

TABLE 1. ^{13}C nmr T_1 data[a] for compounds **1–10**

Compound	Solvent	Concentration	C-1	C-2	C-3	C-4	C-5	C-6	C-7	C-8	C-9	C-10	C-11	C-12
1	$CDCl_3$	3 *M*	—	5.9	3.1	5.8	2.1	2.9	—	4.8	4.8	3.7	—	—
	$CDCl_3$	2 *M*	—	7.3	3.6	6.7	2.4	3.6	—	5.6	5.6	4.3	—	—
	C_3D_6O	2 *M*	—	10.7	5.6	9.7	5.3	5.4	—	6.6	6.4	5.2	—	—
2	$CDCl_3$	2 *M*	—	5.2	2.8	5.6	2.3	1.8	—	4.5	4.7	2.9	—	—
3	$CDCl_3$	2 *M*	—	—	5.8	8.0	4.3	5.2	—	4.9	5.8	5.6	—	—
4	$CDCl_3$	2 *M*	—	8.7	—	6.7	3.9	3.9	4.1	3.3	3.3	3.7	—	—
5	$CDCl_3$	2 *M*	—	—	—	6.3	3.6	3.9	3.8	4.2	3.9	4.5	—	—
6	$CDCl_3$	1 *M*	9.0	—	9.0	4.3	8.6	5.1	6.4	5.0	4.3	5.0	—	4.6
	C_5D_5N	2 *M*	4.3	—	4.3	2.0	4.2	2.3	2.9	2.4	2.0	2.4	—	3.2
	CD_3OD	2 *M*	3.7	—	3.7	1.7	3.9	2.2	2.3	2.4	1.7	2.4	—	2.6
7	$CDCl_3$	2 *M*	9.6	—	9.6	4.8	10.0	5.5	8.5	5.2	4.8	5.2	—	4.4
8	$CDCl_3$	1.5 *M*	5.0	5.1	5.7	—	4.0	2.8	5.7	2.2	2.8	2.4	3.3	3.3
9	$CDCl_3$	1.6 *M*	6.7	7.0	7.1	—	7.3	3.7	6.1	3.7	3.3	3.7	3.8	3.6
10	$CDCl_3$	2 *M*	7.0	—	7.4	—	7.3	3.8	7.4	4.1	4.0	4.0	4.1	3.2

[a] T_1 in seconds; estimated error ± 10%.

rotation about the two mutually perpendicular axes. The equation necessary to convert T_1 data into R_1 and R_2 was developed by Woessner (6) and is shown as eq. [4]. The constants A, B, and C are

$$[4]\quad \frac{1}{T_1} = \frac{N\hbar^2\gamma_C{}^2\gamma_H{}^2}{r_{C-H}} \times \left[\frac{A}{6R_2} + \frac{B}{5R_2 + R_1} + \frac{C}{2R_1 + 4R_2}\right]$$

again geometrical constants which are functions of the angles between the C—H bond vectors and the symmetry axes. The definition of the geometrical constants, together with the equation for determining the three principal values of the rotational diffusion constants for an asymmetric top molecule, can be found in ref. 6.

Woessner's equations have been successfully applied to simple molecules (11), molecules containing only carbon and hydrogen (12), and to molecules containing heterosubstituents (13, 14), where the carbon–heterosubstituent bond is coincident with the symmetry axis of the molecule. Molecules containing heterosubstituents, which are not on the symmetry axis, pose a much more serious problem in that the calculation of diffusion constants about various axes requires *a priori* that the axes have been defined. The normal method based on Woessner's equation assumes that the principal axes of diffusion coincide with the principal axes of the moment of inertia. This is a reasonable assumption for the above mentioned cases, but may not be valid for heterosubstituted molecules, where the substituent is not on an axis (15). First of all, if the motion is controlled by diffusion rather than by inertial properties, it is the volume rather than the moment of inertia that must be considered (10). Secondly, heterosubstituents are often more strongly solvated and can be involved in solute–solute interactions.

We have calculated T_1 values for each carbon by optimizing the diffusion constants using three different principal axes. The first series (*A*) of T_1 values was calculated using the principal axes of the moment of inertia as the principal axes of the diffusion tensor. The second assumption (*B*) also used the moment of inertia but placed the heterosubstituent on the principal axis of rotation. In other words, this method assumes that the rotation of the hydrocarbon moiety is controlled by inertial effects (which correspond to volume effects as this part of the molecule contains only carbon and hydrogen), and that movement of the heterosubstituent is more restricted. The final method (*C*) was to assume that the carbon–heterosubstituent bond is the principal axis of molecular rotation. This method assumes that the heterosubstituent is "fixed" in solution by intermolecular interactions and that the most energetically favored path for molecular rotation is that about the carbon–oxygen bond. The values were calculated by assuming that the molecules behave as symmetric tops in solution. It is evident that the difference between observed and calculated values would be reduced by the use of three axes, since an additional variable would be introduced. However, in view of the experimental error in T_1 measurements and the limited number of C—H bond vectors in some molecules, it was felt

Can. J. Chem. Downloaded from www.nrcresearchpress.com by 210.87.254.105 on 09/05/12
For personal use only.

TABLE 2. Diffusion constants[a] and T_1 values for compounds **1–10**

Compound	Axis[b]	T_1 values C-1	C-2	C-3	C-4	C-5	C-6	C-7	C-8	C-9	C-10	Diffusion constants R_1	R_2
1 ($CDCl_3$ 2 *M*)	Obs		7.3	3.6	6.7	2.4	3.6						
	A		7.4	3.7	7.2	2.4	3.5					8	1
	B		7.6	3.7	7.3	2.4	3.4					7.9	1.2
	C		6.4	3.1	6.2	3.1	3.2					3.0	2.1
1 ($CDCl_3$ 3 *M*)	Obs		5.9	3.1	5.8	2.1	2.9						
	A		6.2	3.1	5.9	2.1	2.9					6.2	1
	B		6.3	3.1	6.0	2.1	2.8					6.2	1
	C		5.3	2.7	5.2	2.7	2.7					2.2	2.0
1($(CD_3)_2CO$)	Obs		10.7	5.6	9.7	5.3	5.4						
	A		10.8	5.5	10.4	5.3	5.4					4.4	4.0
	B		10.8	5.5	10.4	5.3	5.4					4.4	4.0
	C		10.6	5.4	10.4	5.4	5.4					4.3	4.1
2	Obs		5.2	2.8	5.4	2.3	1.8						
	A		5.9	2.7	5.9	2.3	1.8					6.9	0.9
	B		5.7	2.9	5.5	2.2	1.8					7.1	0.8
	C		5.9	2.4	5.1	2.6	1.8					5.6	1.0
3	Obs			5.8	8.0	4.3	5.2						
	A			5.8	9.8	4.4	4.8					7.1	2.8
	B			5.8	9.8	4.4	4.8					7.2	2.7
	C			5.9	9.0	4.3	5.0					8.5	2.4
4	Obs			8.7		6.7	3.9	3.9	4.1				
	A			8.7		7.3	3.9	3.8	4.0			4.5	2.4
	B			8.8		7.2	3.9	3.8	4.1			4.3	2.6
	C			8.4		7.5	3.9	3.8	4.0			3.8	2.7
5	Obs					6.3	3.6	3.9	3.8				
	A					7.1	3.7	3.7	3.8			2.8	2.9
	B					7.1	3.7	3.7	3.8			3.0	2.8
	C					7.0	3.6	3.8	3.8			4.7	2.3
6 ($CDCl_3$)	Obs	9.0	—	9.0	4.3	8.6	5.1	6.4	5.0	4.3	5.0		
	A	8.8	—	8.8	4.6	8.7	4.6	8.6	4.6	4.6	4.6	3.7	3.5
	B	9.2	—	9.2	4.1	9.2	5.0	6.7	5.1	4.1	5.1	7.3	2.3
	C	9.4	—	9.4	4.2	9.1	5.0	6.6	5.0	4.2	5.0	5.8	2.6
6 (Pyridine)	Obs	4.3	—	4.3	2.0	4.2	2.3	2.9	2.4	2.0	2.4		
	A	4.0	—	4.0	2.1	4.2	2.1	4.0	2.2	2.1	2.2	2.1	1.5
	B	4.3	—	4.3	1.9	4.5	2.3	3.1	2.4	1.9	2.4	3.5	1.0
	C	4.4	—	4.4	1.9	4.2	2.4	3.0	2.3	1.9	2.3	2.8	1.2
6 (CD_3OD)	Obs	3.7		3.7	1.7	3.9	2.2	2.3	2.4	1.7	2.4		
	A	3.6		3.6	1.9	3.8	1.9	3.6	2.0	1.9	2.0	2.1	1.3
	B	4.1		4.1	1.6	4.0	2.2	2.5	2.2	1.6	2.2	4.3	0.8
	C	4.2		4.2	1.6	4.0	2.2	2.4	2.2	1.6	2.2	3.3	0.9
7	Obs	9.6		9.6	4.8	10.0	5.5	8.5	5.2	4.8	5.2		
	A	9.4		9.8	4.9	10.2	5.3	8.5	5.2	4.9	5.4	5.5	3.3
	B	9.4		9.8	4.9	10.2	5.3	8.5	5.4	4.9	5.4	5.5	3.3
8	Obs	5.0	5.1	5.7		4.0	2.8	5.7	2.2	2.8	2.4		
	A	4.6	5.6	5.5		4.4	2.5	5.2	2.5	2.8	2.3	3.2	1.5
	B	4.9	5.8	5.5		4.1	2.7	5.4	2.4	2.9	2.3	3.7	1.4
	C	5.2	5.6	5.4		3.9	2.8	5.2	2.3	2.8	2.3	3.2	1.5
9	Obs	6.7	7.0	7.1		7.3	3.7	6.1	3.7	3.3	3.7		
	A	7.1	7.4	6.7		7.0	3.6	6.1	3.6	3.4	3.7	3.7	2.3
	B	6.5	7.4	7.1		7.2	3.6	5.9	3.7	3.4	3.7	4.1	2.1
	C	6.9	7.3	7.0		6.9	3.7	5.8	3.7	3.4	3.7	3.4	2.4
10	Obs	7.0		7.4		7.3	3.8	7.4	4.1	4.0	4.0		
	A	7.6		7.8		7.5	3.9	7.4	4.0	4.0	3.9	3.2	2.9
	B	7.5		7.9		7.5	3.9	7.3	3.9	4.0	3.9	3.2	2.9
	C	7.5		7.8		7.5	3.9	7.4	3.9	4.0	3.9	2.7	3.3

[a]Calculated using Woessner's equations for a symmetric top (6).
[b]Principal axis of the diffusion tensor assumed. *A*, principal axis of the moment of intertia; *B*, passes through hetero atom and centre of mass; *C*, carbon–oxygen bond.

Can. J. Chem. Downloaded from www.nrcresearchpress.com by 210.87.254.105 on 09/05/12
For personal use only.

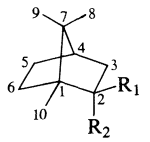
Can. J. Chem. Downloaded from www.nrcresearchpress.com by 210.87.254.105 on 09/05/12
For personal use only.

that more meaningful results would be obtained using the symmetric top model. Verification of this was found by inspection of calculated moment of inertia data and from calculations using an asymmetric top model for several compounds.

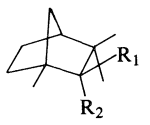
Discussion

Overall Motion

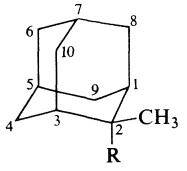
The carbon-13 T_1 values calculated using the three assumptions are compared with those obtained experimentally in Table 2. Compounds **1** and **6** are illustrated in Figs. 1 and 2 as a function of the three principal axes chosen. The T_1 values for **1** calculated by *A* or *B* correlate reasonably well with those observed in $CDCl_3$ whereas those calculated using *C* do not. Inspection of Fig. 1 shows that the position of the principal axis in *B* does not differ significantly from *A* and in both cases the C-5—H_{exo} vector is almost parallel with the principal axis, whereas this is not the case using the C—O bond as the principal axis. In acetone-d_6 isoborneol **1** displays isotropic motion, which is calculated equally well by all three assumptions. For compound **2**, the CH_2 carbon relaxation times increase in the order C-6 < C-5 < C-3, which is reproduced by both *A* and *B*, but not by *C*. Also the difference between calculated and experimental suggests that *B* is the superior assumption. The values for the other compounds are inconclusive, in that each assumption gives much the same values and similar differences. The one possible exception is camphor, in which it appears that the best correlation is obtained by utilizing assumption *C*. The main reason for this is the abnormally short value for C-4. Examination of the data for the other compounds shows that T_1 (C-4) is always smaller than calculated, and in most cases this difference is quite significant. This implies that the C—H bond length



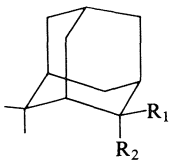
1 R_1 = OH, R_2 = H
2 R_1 = H, R_2 = OH
3 $R_1 + R_2$ = O



4 R_1 = H, R_2 = OH
5 $R_1 + R_2$ = O



6 R = OH
7 R = Br



8 R_1 = OH, R_2 = H
9 R_1 = H, R_2 = OH
10 $R_1 + R_2$ = O

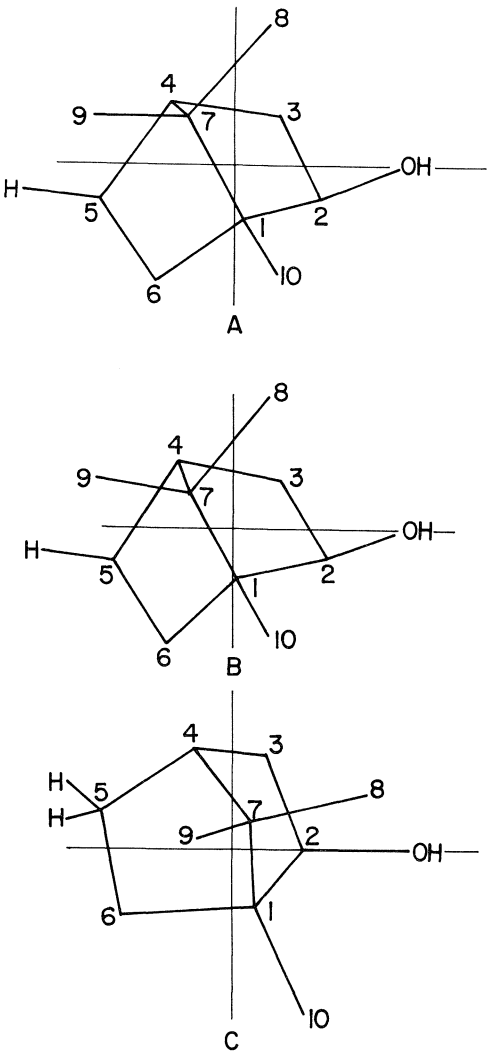


FIG. 1. Representation of isoborneol relative to the various principal axes of rotation tensor. *A*: principal axes of the moment of inertia. *B*: principal axis of rotation tensor passes through oxygen and the centre of mass of the molecule. *C*: principal axis is coincident with the C—O bond.

for C-4 is less than the normally accepted value, as had been suggested earlier (10), and that this shortening is even more pronounced when there is a carbonyl group at C-2. For compounds **3** and **5** the number of different C—H bond vectors is even more limited. The conclusion that can be drawn from the data on compounds **1**–**5** is that both *A* or *B* result in satisfactory correlation of calculated with observed relaxation times, whereas *C* does not give as good a correlation.

The T_1 values for **6** indicate significant anisotropic motion, since C-4 and C-9 have shorter relaxation times than other CH_2 carbons and C-7 has a shorter T_1 value than other CH carbons. The

Can. J. Chem. Downloaded from www.nrcresearchpress.com by 210.87.254.105 on 09/05/12
For personal use only.

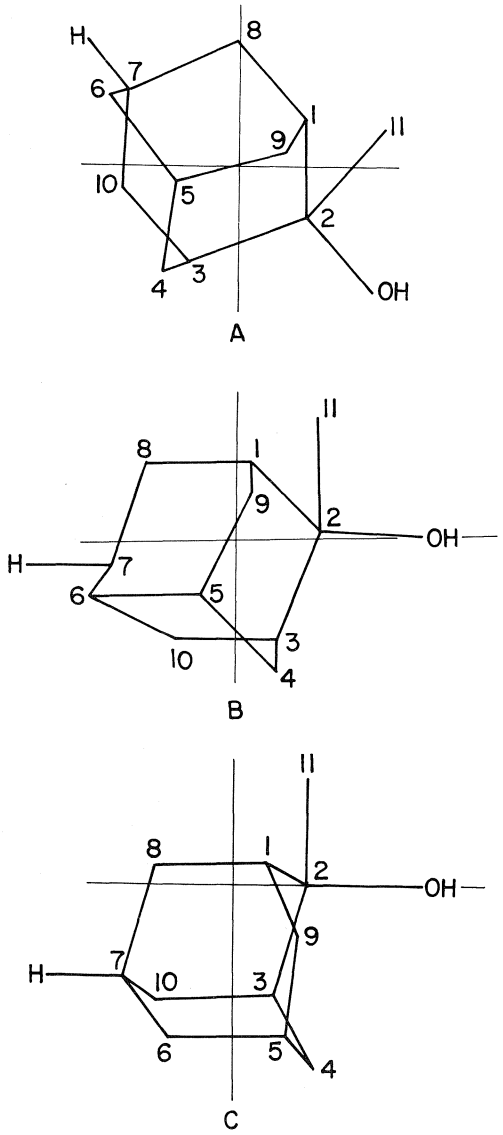


FIG. 2. Representation of 2 methyl adamantan-2-ol relative to the various axes of rotation tensor. *A*: principal axes of the moment of inertia. *B*: principal axis of rotation tensor passes through oxygen and the centre of mass of the molecule. *C*: principal axis is coincident with the C—O bond.

calculations using *A* cannot reproduce these differences. The lack of correlation for *A* is readily explained by inspection of Fig. 2, where it can be seen that the C-7—H bond vector is nowhere near parallel to the principal axis. The results for compounds **8–10** are inconclusive with respect to the choice of a principal axis, although generally *B* and *C* result in slightly better correlations. For example, the differences between observed and calculated values for C-5 and C-9 using *A* are at the limit and just outside the limit of experimental error, respectively. It is of interest to note that the experimental value for an oxygen bearing carbon is always less than that calculated. The rotation rates calculated for **10**, using method *C*, show that the result cannot be interpreted in terms of the C—O bond being the principal axis of rotation. The conclusion that can be drawn from the adamantane derivatives is that *B* and *C* (with the exception of *C* for **10**) give reasonable correlation between calculated and experimental values, whereas *A* fails for compound **6**.

It should be emphasized that a measured T_1 value is an average. For example, the T_1 value of a molecule which forms an associated species will only measure the diffusion constant of the associated species if its lifetime is longer than R^{-1}. If the lifetime is much shorter than R^{-1}, then we will observe the T_1 values of the monomer (14). Intermediate values of lifetime relative to R^{-1} result in both monomeric and associated species contributing to the observed T_1 value. If the results presented here represent the rotation of a monomer (without specific solvation) then the degree of anisotropy from volume considerations would have a maximum value of $R_1/R_2 = 1.5$ and it would be reasonable to assume that the inertia and diffusion axes are coincident. It is possible that **1** (in acetone), **5**, **7**, and **10** rotate essentially as monomers since the degree of anisotropy is small. The compounds **1** (in $CDCl_3$), **2**, and **6** are observed as associated species either due to solute–solute interactions or strong solvation. Both interactions will be centered at oxygen and it is therefore reasonable to assume that oxygen is on the principal axis of diffusion. The actual degree of anisotropy (R_1/R_2) depends on many factors. These include the type of association, the lifetime of the associated species relative to R^{-1}, the barrier to rotation about the C—O bond, and also the strength of solvent–solvent interactions. It is thus not prudent to discuss the type of associated species formed from a simple T_1 measurement.

The conclusion that can be drawn is that the most probable principal axis of the diffusion tensor is that which passes through oxygen and the centre of mass of the molecule. The difference between calculated and experimental values, using this axis, is within experimental error (10%) for all carbons in all molecules. Use of *A* or *B* does not result in a significant variation in R_2 for the compounds **1–5** nor does the use of *B* or *C* result in a large difference for R_2 in **6–10**. The variation in R_1 is more significant (up to 30%).

Methyl Group Energy Barriers

The calculated values of the diffusion constant for internal reorientation, R_{int}, and the energy bar-

TABLE 3. Methyl group diffusion constants (R_{int})[a] and energy barriers (V_R)[b] for internal rotation

Compound	C-8			C-9			C-10			C-11			C-12		
	R_{int}	V_R	V_R^1	R_{int}	V_R	V_R^1	R_{int}	V_R	V_R^1	R_{int}	V_R	V_R^1	R_{int}	V_R	V_R^1
1 ($CDCl_3$)	25	10.1	10.3	25	10.1	10.3	14	11.6	11.8						
($CDCl_3$)	30	9.7	9.9	30	9.7	9.9	16	11.2	11.4						
(C_3D_6O)	25	10.1	10.3	22	10.4	10.5	12	12.0	12.1						
2	26	9.9	10.2	28	9.8	10.0	11	12.2	12.4						
3	17	11.0	11.2	26	10.0	10.3	23	10.3	10.4						
3[c]		12.7	11.6		13.3	12.0		12.9	11.7						
4	5.2	14.1	14.3	5.2	14.1	14.3	8	13.0	13.3						
5	14	11.6	11.7	12	12.0	12.2	17	11.0	11.2						
6										13	11.7	12.0			
										15	11.4	11.6			
										11	12.2	12.4			
7										8.3	12.9	13.0			
8										13	11.7	12.0	14	11.6	11.8
9										12	12.0	12.3	10	12.4	12.7
10										12	12.0	12.1	5.1	14.1	14.4

[a] $R \times 10^{10}$ s^{-1}; calculated for a C—Ĉ—H angle of 109.47°; estimated error ± 15%.
[b] kJ/mol; V_R calculated for C—Ĉ—H angle of 109.47°; V_R^1 calculated for an angle of 112°.
[c] From Zens and Ellis (3).

riers (V_R) to this rotation are given in Table 3. R_{int} was calculated using eq. [3] modified to take into account the anisotropy in the overall motion (16). The barriers were then calculated using $R_{int} = R_0 e^{-V_R/RT}$ where R_0 is given by

$$R_0 = \frac{3}{2}\sqrt{\frac{kT}{I}}$$

and I is the moment of inertia. The barriers are recorded for C—C—H angles of 109.47° and 112° since the latter is the value obtained from a neutron diffraction study of durene (17). Stothers and Blunt (4) have shown the effect of varying this angle on R_{int} and hence on V_R. The effect of angle on the calculated value of R_{int} depends on the ratio $T_1(CH_3)/T_1(CH)$ and becomes more important the larger this ratio becomes. The limit of rapid rotation for an angle of 109.47° is $T_1(CH_3) = 3T_1(CH)$ whereas that for an angle of 112° is $T_1(CH_3) \simeq 4T_1(CH)$.

The barriers to rotation for camphor have been reported previously by Zens and Ellis (3) from a study of T_{ISR} (SR ≡ spin rotation). They obtained a linear plot from a graph of $T_{ISR} = K(1 + \alpha V_R)$ for a number of compounds where V_R was known and then used T_{ISR} to calculate V_R for the CH_3 groups in camphor. More recently, Ellis and co-workers (18) have published a second article in which they showed dependence to be exponential rather than linear. The apparent reason for the difference in behaviour is due to a systematic error in the determination of the nOe in the first publication. The results in the second article do not invalidate the conclusions of the first (18). The results presented by Zens and Ellis (3) for camphor are significantly higher than those presented here. An error in our nOe measurements implies a longer T_{IDD} and hence a smaller V_R, which is opposite to that observed. The calculation of V_R from T_{ISR} data contains a term $I^{3/2}$ which, as shown by Stothers and Blunt (4), will depend on the value of the C—Ĉ—H angle. The values calculated for camphor using an angle of 112° and eq. [13] of ref. 3 are also given in Table 3. The values for C-8 from the two laboratories using 112° as the angle are within experimental error. The calculation from the spin rotation data assumes that the C—Ĉ—H angles of the model compounds are the normal tetrahedral values. Correlation between the values of V_R for C-9 and C-10 occurs at angles of 114° and 113.5°, respectively, with the respective barriers being 10.6 and 10.7 kJ/mol.

It is of interest to compare the T_1 values used in the two sets of calculation. The order is the same, T_1(C-8) < T_1(C-10) < T_1(C-9) as are the dipolar and the spin rotation contributions. An increase in T_{IDD} implies a decrease in V_R. However, an increase in bond angle results in a larger calculated barrier of V_R from T_{IDD} and a smaller barrier when calculated using T_{ISR}. Thus a combination of both T_{ISR} and T_{IDD} will furnish the barrier to rotation about the methyl–carbon bond and the valency angle C—Ĉ—H. The spin rotation contribution becomes more important at higher temperatures and lower

Can. J. Chem. Downloaded from www.nrcresearchpress.com by 210.87.254.105 on 09/05/12
For personal use only.

Can. J. Chem. Downloaded from www.nrcresearchpress.com by 210.87.254.105 on 09/05/12
For personal use only.

TABLE 4. Energy barriers[a] to methyl group rotation in monosubstituted androstanes (8)

Substituent[b]	Carbon	V_R[c]	V_R[d]
2 Keto, 4 keto	C-19	10.2	10.6
2 βOH, 4 βOH	C-19	10.3	10.8
Δ5	C-19	11.7	11.9
3 αOH, 3 βOH, 3 keto	C-19	8.0	8.9
4αOH, 16 keto, 17 keto	C-18	12.7	13.0
11 Keto	C-18	12.7	13.0
16 Keto	C-18	13.5	13.7
[e]	C-18	10.8	10.9

[a]In kJ/mol.
[b]Average value for the given substituents.
[c]Calculated using a C—Ĉ—H angle of 109.47°.
[d]Calculated using a C—Ĉ—H angle of 112°.
[e]Average value for A and B ring substituent.

concentrations. The calculations of R_{INT} and V_R for the compounds reported here are fairly insensitive to variations in the C—Ĉ—H angle, since the ratio $T_1(CH_3)/T_1(CH)$ is in the range 0.4–2.4 (7).

The results for the adamantane derivatives, together with those obtained from steroids (8), given in Table 4, show a decrease in the barrier, as the number of 1,3 diaxial methyl–hydrogen interactions increases. The results for **3** show the same trend in that V_R for C-8 is higher than for C-9, which has an additional *pseudo* 1,3-diaxial methyl–hydrogen interaction. The lower barriers in camphor than in the adamantanes is no doubt due to the C-1—C-7—C-4 angle being significantly less than 109.47° in the former. Inspection of the rotation path of a methyl group implies that the energy difference between the preferred (*gauche*) and highest (eclipsed) energy conformation should be independent of the number of such interactions since the 1,3-diaxial interactions are equivalent in both conformations. It is reasonable to assume, however, that an increase in the number of 1,3-diaxial interactions increases the C—Ĉ—H angle. This will have two consequences on the barrier. First of all the calculated value will increase as the C—Ĉ—H angle increases, which will decrease the differences observed as a function of the number of interactions. Calculation of V_R as a function of angle shows that this is not sufficient, however, to account completely for the differences. Secondly, an increase in the C—Ĉ—H angle will decrease the repulsive interaction in the eclipsed conformation and therefore decrease the barrier.

The methyl group rotation barriers in the rigid compounds are essentially the same, whether the methyl group is subjected to 1,3-diaxial (or *pseudo* diaxial) methyl–hydrogen or methyl–hydroxyl interactions. In the steroids the barrier is higher for the methyl–hydroxyl interaction. Ring A of the steroids is quite flexible. The reduction of a keto group to an alcohol increases the barrier to rotation for a methyl group on the carbon β to the substituted ring carbon.

Experimental

All T_1 measurements and data analyses were performed as described previously (14). Sweep widths of 2000 Hz (8 K data points) were used. The errors are estimated to be ±10%, although the relative accuracy is better (±5%). The errors in R_1, R_2, and R_{int} vary, depending on the relative rates. For example, R_{int} for isotropic motion is given by $R_{int} = (48/X - 6)$ where $X = 3T_1(CH)/T_1(CH_3) - 1$. When $T_1(CH_3)$ approaches $\frac{1}{3}T_1(CH)$, X approaches 8, and the term $48/X$ approaches 6. A small percentage error in T_1 causes a large percentage error in R_{int}. An error of ±5% in the T_1 values can lead to an error in R_{int} of ±50%, when the ratio approaches this limit. Small errors in T_1 also result in large errors in R_{int} when $T_1(CH_3)$ approaches $3T_1(CH)$. In the examples described herein, $T_1(CH_3)$ is in the range 0.8–2.4 $T_1(CH)$ and errors of ±5% in $T_1(CH_3)$ result in average ±10% error of R_{int}. The average overall error in R_{int} is then ±15% and that in V_R ±5%.

The nOe measurements were obtained using the suppressed nOe technique (*1a*). Only hydrogen-bearing carbons were examined and the nOe was in all cases 2.0 ± 0.1. A good indication of a methyl group possessing an nOe of less than 2.0 in reasonably sized molecules can be ascertained from comparisons of peak areas of the signal corresponding to the methyl group carbon to those corresponding to methylene and methine carbons. All nOe and T_1 measurements were performed at 32°C.

The compounds used were either obtained from commercial sources or prepared using literature methods. Compounds **1–3** and **5** were commercial samples. Compound **4** was obtained by $LiAlH_4$ reduction of **5** (19). The preparation of compounds **6** and **7** was reported previously (20). Compounds **9–11** were prepared as described by McKervey *et al.* (21).

The ^{13}C nmr chemical shifts were assigned according to literature values, **1–5** (22); **6**, **7** (20). The spectra for the other compounds were assigned using standard techniques such as off-resonance decoupling, $Pr(fod)_3$ induced shifts, and comparison with other adamantane derivatives. The recorded shifts are found in Table 5.

TABLE 5. Chemical shift data[a] for compounds **8–10**

Compound	C-1	C-2	C-3	C-4	C-5	C-6	C-7	C-8	C-9	C-10	C-11	C-12
8	34.4	77.8	44.1	36.7	36.8	32.8	27.2	32.4	33.3	26.2	27.6	27.6
9	35.0	70.5	44.1	37.0	37.6	32.8	27.0	38.6	28.7	33.4	29.4	29.3
10	46.1	212.0	57.4	39.4	37.1	32.5	27.1	40.6	34.7	34.7	25.7	28.0

[a]In ppm relative to TMS.

Acknowledgments

The authors wish to express their appreciation to Mr N. Pothier for the preparation of compounds used in this study, to the National Research Council of Canada for generous financial support, and to the France–Quebec exchange program for a post-doctoral fellowship to one of us (R.M.).

1. (*a*) J. R. LYERLA and G. C. LEVY. Top. Carbon-13 NMR Spectrosc. **1**, 79 (1974); (*b*) F. WEHRLI. Top. Carbon-13 NMR Spectrosc. **2**, 343 (1975).
2. T. D. ALGER, D. M. GRANT, and R. K. HARRIS. J. Phys. Chem. **76**, 281 (1972).
3. A. P. ZENS and P. D. ELLIS. J. Am. Chem. Soc. **97**, 5685 (1975).
4. J. W. BLUNT and J. B. STOTHERS. J. Magn. Reson. **27**, 515 (1976).
5. D. WALLACH and W. T. HUNTRESS. J. Chem. Phys. **50**, 1219 (1969).
6. D. E. WOESSNER. J. Chem. Phys. **37**, 647 (1962).
7. D. E. WOESSNER and B. S. SNOWDEN. Adv. Mol. Relaxation Processes, **3**, 181 (1972).
8. J. W. APSIMON, H. BEIERBECK, and J. K. SAUNDERS. Can. J. Chem. **53**, 338 (1975).
9. D. M. GRANT, R. J. PUGMIRE, E. P. BLACK, and K. A. CHRISTENSEN. J. Am. Chem. Soc. **95**, 8465 (1973).
10. (*a*) J. GRANDJEAN and P. LASZLO. Mol. Phys. **25**, 695 (1975); (*b*) **30**, 413 (1975).
11. J. R. LYERLA, D. M. GRANT, and R. K. HARRIS. J. Phys. Chem. **75**, 585 (1971); J. R. LYERLA and D. M. GRANT. J. Phys. Chem. **76**, 3213 (1972).
12. K. F. KUHLMANN, D. M. GRANT, and R. K. HARRIS. J. Chem. Phys. **52**, 3439 (1970); S. BERGER, F. R. KREISSL, D. M. GRANT, and J. D. ROBERTS. J. Am. Chem. Soc. **97**, 1805 (1975).
13. G. C. LEVY, J. D. CARGIOLI, and F. A. L. ANET. J. Am. Chem. Soc. **95**, 1528 (1973).
14. H. BEIERBECK, R. MARTINO, and J. K. SAUNDERS. Can. J. Chem. **57**, 1224 (1979).
15. P. STILBS and M. E. MOSELEY. J. Magn. Reson. **33**, 209 (1979).
16. D. E. WOESSNER, B. S. SNOWDEN, and G. H. MEYER. J. Chem. Phys. **50**, 719 (1969).
17. E. PRINCE, L. W. SCHROEDER, and J. J. RUSH. Acta Crystallogr. Sect. B, **29**, 184 (1973).
18. A. TANCREDO, P. S. PIZANI, C. MENDONIA, H. A. FARACH, C. P. POOLE, P. D. ELLIS, and R. A. BYRD. J. Magn. Reson. **33**, 208 (1979).
19. W. F. DANNON and H. O. HOUSE. Org. Synth. **40**, 14 (1960).
20. H. BEIERBECK and J. K. SAUNDERS. Can. J. Chem. **55**, 3161 (1977).
21. M. A. MCKERVEY, D. FAULKNER, and H. HAMILL. Tetrahedron Lett. 1971 (1970).
22. E. LIPPMAA, T. PEHK, J. PAASIVIRTA, N. BELIKOVA, and A. PLATE. Org. Magn. Reson. **2**, 581 (1970).

Can. J. Chem. Downloaded from www.nrcresearchpress.com by 210.87.254.105 on 09/05/12
For personal use only.

Studies in membrane processes. IX. The bilayer structure in mixed dodecanoate/decyltrimethylammonium micelles of a novel type II mesophase

YUNKO LEE,[1] LEONARD W. REEVES,[2] AND ALAN S. TRACEY
Department of Chemistry, University of Waterloo, Waterloo, Ont., Canada N2L 3G1
Received November 21, 1978[3]

YUNKO LEE, LEONARD W. REEVES, and ALAN S. TRACEY. Can. J. Chem. **58**, 110 (1980).

Nematic lyotropic liquid crystalline materials, which spontaneously align in a magnetic field (Type II) have been prepared from a mixed detergent system consisting of potassium dodecanoate and decyltrimethylammonium bromide. This system has an advantage that the charge on the interface of the finite disc micelles can be readily varied. Sodium and bromide ion interactions with the interface have been investigated by nuclear magnetic resonance of the ions. Deuterium magnetic resonance spectra of deuteriated water and specifically deuteriated detergent chains have been obtained. The results show that there is a water structure built around the carboxylate headgroups which ceases to be stable when about 30% of potassium dodecanoate is replaced by decyltrimethylammonium bromide. Bromine magnetic resonance studies show that the bromide ion interacts only weakly with carboxylate but indicates, as would be expected, much stronger interaction with the trimethylammonium groups. The sodium ion in contrast was found to bind strongly with carboxylate and weakly with trimethylammonium. The sodium spectra indicate that the association of sodium with carboxylate is complex, involving two specific binding sites. Deuterium spectra from deuteriated hydrocarbon chains are interpreted in terms of the motional freedom of the individual chains. The results re-emphasize that the motional properties of a particular hydrocarbon chain of an amphiphile in the micellar bilayer is determined to a large extent by its headgroup and that the behaviour of one chemical species cannot be inferred from that of another.

YUNKO LEE, LEONARD W. REEVES et ALAN S. TRACEY. Can. J. Chem. **58**, 110 (1980).

On a préparé des composés à cristaux liquides du type nématique et lyotropique, qui s'alignent spontanément dans un champ magnétique (type II), à partir d'un mélange de détergents formé de dodécanoate de potassium et de bromure de décyltriméthylammonium. L'avantage de ce système réside dans le fait que l'on peut facilement faire varier la charge à l'interface des disques finis de micelles. On a utilisé la résonance magnétique des ions pour étudier les interactions des ions sodium et bromures avec l'interface. On a obtenu les spectres de résonance magnétique du deutérium de l'eau deutérée et des chaînes de détergents deutérées d'une façon spécifique. Les résultats indiquent qu'il se forme un arrangement des molécules d'eau autour du carboxylate de la tête polaire et que cette structure perd sa stabilité quand on remplace 30% de dodécanoate de potassium par du bromure de décyltriméthylammonium. Les études de résonance magnétique du brome montrent que les ions bromures sont en interaction faible avec le carboxylate mais comme on s'y attendait, cette interaction est beaucoup plus forte avec le groupement triméthylammonium. On trouve au contraire que les ions sodium sont liés plus fortement au carboxylate et faiblement au groupement triméthylammonium. On interprète les spectres du sodium obtenus à partir des chaînes hydrocarbonées deutérés, en fonction du mouvement libre des chaînes individuelles. Ces résultats mettent d'avantage l'accent sur le fait que les propriétés de mouvement d'une chaîne hydrocarbonée particulière d'un composé amphiphile dans la double phase micellaire sont déterminés dans une large mesure par la tête polaire et que le comportement d'une espèce chimique ne peut être déduit de celui d'une autre.
[Traduit par le journal]

Introduction

The spontaneous formation of bilayer structures by aqueous dispersions of amphiphiles is a well known phenomenon (1) which was discovered by the colloid chemists (2) interested in soap solutions and their ability to solubilize substances not otherwise soluble in water. The term bilayer has usually been reserved for the lamellar arrangement of two polar interfaces separated by approximately extended hydrocarbon chains (3) between the two interfaces. In this case the bilayer has a plane of symmetry bisecting the distance between the headgroups or polar interfaces. The bilayer concept can be extended to include an axis of symmetry for the bilayer, in which case the interface forms a cylindrical surface, or even a centre of symmetry where there is a spherical shaped interface (4).

Bilayers occur widely in biology (5) and a great deal of current activity derives from this fact. On the one hand chemically homogeneous planar bilayers of lipids (6) or soaps have been studied by physicists (7) interested in the phases formed and state of motion of hydrocarbon chains in these various phases (8). The methods used have with one exception (9) not been addressed, indeed they are often inappropriate, to bilayers which contain more than one chemical component. In this one exception the emphasis of the study was directed toward the provocation of phase changes in bilayer structures where the polar headgroups are homogeneous in chemistry but the chains in a binary mixture have different lengths (9). The biochemical aspects of bilayers are only accessible in systems

[1]Present address: Arthur Amos Laboratory of Chemical Physics, California Institute of Technology, Pasadena, CA 91125.

[2]Author to whom correspondence may be addressed.

[3]Revision received August 1, 1979.

0008-4042/80/020110-14$01.00/0
©1980 National Research Council of Canada/Conseil national de recherches du Canada

Can. J. Chem. Downloaded from www.nrcresearchpress.com by 210.87.254.5 on 09/05/12
For personal use only.

Can. J. Chem. Downloaded from www.nrcresearchpress.com by 210.87.254.5 on 09/05/12
For personal use only.

where there is a wide variety of lipids, and sometimes proteins as well (5).

The shapes and sizes of bilayer architectures lead to a wide variety of liquid crystalline mixtures (4) and thus the work on bilayers has a strong link with the fluid crystalline state, which is otherwise based on positional and orientational order of molecules rather than micelles (4). Most liquid crystalline manifestations of the hydrophobic effect derive their properties from infinitely repeating structures with positional order (4) such as the L_α, H_α, or isotropic phases (4). The extensive studies from our own laboratories have derived from liquid crystals based on micellar units which have an extended but finite bilayer structure where long range orientational but not positional order is maintained. These materials spontaneously align in magnetic fields, the first such system having been reported in 1967 by Lawson and Flautt (10).

An extensive literature now exists from our previous studies, which have been addressed to several different aspects of bilayer and liquid crystal chemistry. These studies include (*a*) synthesis of new lyotropic nematic phases (11–16); (*b*) the discovery of methods to obtain the structure of ions in fluids (17, 18); (*c*) the solution chemistry of micellar bilayers at the level of segmental motions of hydrocarbon chains (19, 20); (*d*) the study of degree of order of solubilized guests (21, 22); (*e*) the behaviour of ions and water at the micelle interface (23, 24); (*f*) investigation of induced chemical shift anisotropy in ions (25); (*g*) a magnetic classification of the new liquid crystalline materials (11), etc.

The present study of a Type II (11) mesophase is directed both toward the structure of the micelle interface as well as the behaviour of hydrocarbon chain motions in a bilayer micelle. The finite micelle unit is a binary solution of two amphiphiles, with decanol a minor component, added in low concentration in order to sustain the integrity of the same phase. The binary bilayer solution is of special interest because it combines both cationic and anionic polar headgroups and because the mesophase is a novel one.

Type II mesophases that spontaneously align in magnetic fields of a few thousand gauss (11) at room temperature are composed of disc shaped lamellar, but finite, micelles which retain orientational order over long distances. They have negative diamagnetic anisotropy (26). The magnetic field tends to align along the polar interface of the micelle which is of course in a dynamical sense in anisotropic motion about this orientation. The mean direction of the normal to the micelles is the director of the liquid crystal. The nature of the Type II nematic phases is suggested by the evidence of diamagnetic anisotropy (13) and studies of phase diagrams near the related L_α phase (27), but it has been confirmed by the low angle X-ray diffraction studies of Queiroz de Amaral *et al.* (28).

The present investigation includes sodium-23, bromine-79, bromine-81, and proton resonance of ions and deuterium magnetic resonance studies of water (DOH) and specifically and massively labelled hydrocarbon chains. In Type II nematic mesophases composed of sodium decylsulphate, decanol, water, and sodium sulphate the disc micelles are 38 Å in bilayer thickness, greater than 1000 Å in extent, and immersed in an aqueous matrix of about 90 Å in average thickness (28).

Results and Discussion

Water and Ions at the Interface of the Micelle

We have been particularly concerned with two aspects of the properties of nematic bilayer systems. One of these has been the mechanism by which quadrupole splittings arise for normally spherical ions at the micelle interface, the other has been the motional properties of the hydrocarbon chains of the constituent detergents of the anisotropic bilayer solution.

Should sodium quadrupole splittings arise from ion-binding to specific sites then a systematic elimination of such binding sites will give rise to a steady decrease in the sodium quadrupole splitting. A chemical variation of the content of the micelles without a phase change occurring provides a means of accomplishing this. We have found that the potassium dodecanoate of the lyotropic mesophase prepared from potassium dodecanoate/NaBr/D_2O can, within rather broad limits, be replaced with decyltrimethylammonium bromide on a mole for mole basis without provoking a phase change. Each bilayer disc-like micelle is thus a binary solution of two amphiphiles with the possibility of variation of composition in a continuous manner. When this replacement was made, it was found that the sodium quadrupole splitting decreased linearly with decrease in mole fraction of potassium dodecanoate. The splitting becomes zero when about 25% of the dodecanoate has been replaced. The magnitude of the splitting then increases to a maximum when somewhat less than 50% replacement of dodecanoate has occurred. That no phase change was responsible for this behaviour was established by observing the deuterium quadrupole splitting of the D_2O in the sample. The results are displayed in Fig. 1. At the point where the sodium

Can. J. Chem. Downloaded from www.nrcresearchpress.com by 210.87.254.5 on 09/05/12
For personal use only.

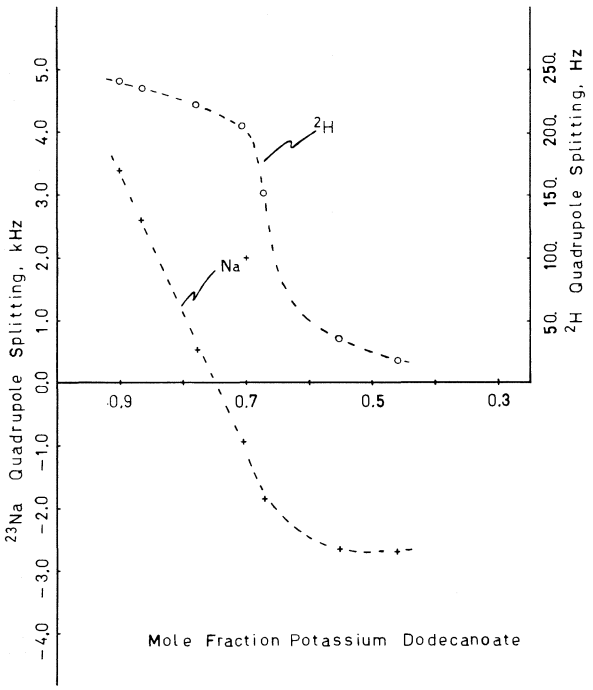


FIG. 1. Sodium and deuterium quadrupole splittings are plotted as a function of the mole fraction of potassium dodecanoate in total detergent where the second component is decyltrimethylammonium bromide. The mesophase was prepared using D_2O.

splitting is zero the deuterium splitting has decreased only slightly from its initial value at high dodecanoate concentration. These results indicate a change in *sign* of the sodium quadrupole splitting. The *absolute* signs of sodium quadrupole splittings have previously been ascertained by utilizing the direction of change in magnitude of the splitting as a function of temperature (29). By using such criteria the sodium splittings in entries 1 and 3 of Table 1 should have opposite signs because the temperature dependencies are opposite. The results displayed in Figs. 1 and 2 show that this is not true because the concentration dependence shows the signs of the sodium splittings to be the same. The mesophases studied here are all Type II nematic liquid crystals made up of disc micelles (11), that is, they align in the magnetic field so that the director is perpendicular to the direction of the field. This means that signs of any splittings are opposite to and the magnitudes one-half as large as those which would normally be assigned for spectra from mesophases which orient with their directors aligned along the magnetic field direction.

A remarkable feature of Fig. 1 is the large decrease in the magnitude of the deuterium quadrupole splitting, from deuteriated water, which begins at about 70 mol% potassium dodecanoate. It is evident that a hydration structure, built around the carboxylate headgroups cannot remain stable after 30% of the dodecanoate in the bilayer has been replaced by the cationic detergent. There follows a rapid decrease to small values of the deuterium splitting. The value obtained at high mole fractions of trimethylammonium in the bilayer, of 18 Hz, is typical of values we have obtained for cationic lyotropic phases prepared from hexadecyltrimethylammonium or hexadecylpyridinium chlorides (14). This small value was found when only about 50% of the dodecanoate had been replaced by trimethylammonium.

With the above results in view it was decided to investigate the behaviour of the hydrocarbon chains in order to study chemical effects on the whole bilayer as well as simultaneously monitoring both the sodium and water splittings. In order to do this, the D_2O in the above phase was replaced with H_2O containing 0.1 wt.% D_2O. Because of deuterium isotope effects, which have not been studied here, the molar proportion of water was varied to accommodate replacement of ^2H with ^1H without causing a phase change. In this second mesophase there was about 18 mol% less H_2O (0.1% D_2O) than D_2O and also there was a 14% decrease in the amount of sodium bromide used. In spite of these changes in the composition of the mesophase, which also change the proportion of K^+ counter- and Na^+ co-ions, the sodium splitting (Fig. 2) goes to zero at the same bilayer composition as in the first phase and the curve follows quite closely that of Fig. 1. This confirms that the integrity of the mesophase has been maintained and indicates that the distribution of sodium and potassium ions between the interface and interstitial water is unchanged.

Since the water deuterium splittings displayed in Fig. 2 appear substantially different from those of Fig. 1, it should be pointed out that the range of stability of this latter mesophase with only two detergents lies in the range of 58 to 78 mol% dodecanoate. Outside this range some decanol is required. The decanol simply stabilizes the type II nematic mesophase, extends its range, and in all cases is a minor component of the constituent micelles. Without decanol an isotropic material is obtained. The sudden decrease in the water splittings of Fig. 1 is obscured in Fig. 2 by the limited range of the stability of the second mesophase.

As indicated by the fifth column of Table 1, the deuterium quadrupole splitting of the water signal for the mesophase composition range of 1.0 to 0.7 mol fraction dodecanoate is insensitive to tem-

TABLE 1. Some parameters[a] obtained for the potassium dodecanoate/decyltrimethylammonium bromide mixed detergent system. Magnitudes of splittings are given and the temperature dependence reflects the direction of change in magnitude as the mesophase warms to magnet temperature

Composition mol% KC_{12}	$\Delta\nu_{Na}$(kHz)	Temperature dependence	DOH $\Delta\nu_D$(Hz)	Temperature dependence	$\Delta\nu_{^{81}Br}$(kHz)	Centre transition half-height width ^{81}Br (kHz)
100	5.04	Decrease	400	None found	10.20	0.54
90	3.81	Increase (small)	327	None found	16.31	0.74
75	0.33	Increase	289	None found	29.22	1.28
74.1	0.00	Decrease	281	None found	30.03	1.35
65.0	1.62	Decrease	224	Increase	29.98	1.45
50.0	2.39	Decrease	118	Increase	73.0	3.32
35.0	1.50	Decrease	47	Increase	—	4.4
					90 mg NaBr in 882 mg H_2O	0.415

[a]Measured parameters are reproducible to better than 2% of the values reported, except the 74.1 mol% sodium splitting which varies about 10 Hz from phase to phase.

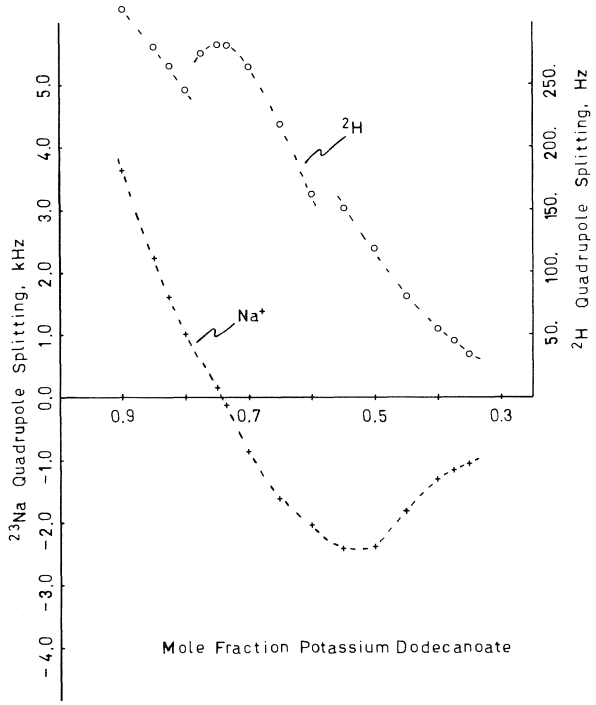


FIG. 2. Sodium and deuterium quadrupole splittings are plotted as a function of the mole fraction of potassium dodecanoate in total detergent. The second detergent is decyltrimethylammonium bromide and the mesophase was prepared using H_2O containing 0.1 wt.% D_2O.

perature changes. This region corresponds to the quadrupole splittings of large magnitude in Fig. 1. The larger magnitude of the D_2O quadrupole splitting throughout this range shows that there is a stable hydration of the carboxylate groups at the bilayer interface. At bilayer compositions less than 65 to 70 mol% dodecanoate, the interface is unable to accommodate tight binding of the water. The water quadrupole splittings decrease substantially in magnitude and simultaneously become quite temperature sensitive with quadrupole splittings increasing 10–20% over a 10° rise in temperature through the range 20–30°C. The headgroup, $-N(CH_3)_3^+$, does not bind the water as strongly because of the more shielded charge and permits water near the interface to tumble in an almost isotropic manner.

In spite of small decanol additions to preserve the Type II nematic phase a rapid drop in water splittings at about 70 mol% dodecanoate in total detergent is still observed (Fig. 2). Increasing the decanol content and slightly extending the range for its usage was sufficient to remove any discontinuity in the nmr parameters, which are plotted in Fig. 2.

The sodium quadrupole splittings on the other hand, (Figs. 1 and 2), are not sensitive to the replacement of D_2O by H_2O. The curves closely follow each other and the zero splitting occurs at the same mole fraction of potassium dodecanoate in the bilayer (~74 mol% in total detergent). The Na^+ and K^+ ions are distributed in the same proportion between the interface and interstitial water and thus the sodium splitting represents the population weighted average for both. Figure 2 shows that there is a decrease in magnitude of the sodium quadrupole splitting in the range 0.5 to 0.3 mol% dodecanoate, a point not evident from Fig. 1 because of restrictions in the range of the desired mesophase.

Changes in the water content of the mesophases have minimal effect on the sodium splittings, but the variation of co-ion concentrations (by using more or less sodium bromide in the preparation of the mesophase) does have a very small but observable effect on the position of zero splitting. With 74.0 mol% potassium dodecanoate and a magnet temperature of 31.4°C a −30 Hz sodium quad-

Can. J. Chem. Downloaded from www.nrcresearchpress.com by 210.87.254.5 on 09/05/12
For personal use only.

Can. J. Chem. Downloaded from www.nrcresearchpress.com by 210.87.254.5 on 09/05/12
For personal use only.

rupole splitting is observed when sodium bromide is 3.1 wt.% of the mesophase. At twice this value (6.0 wt.%) the splitting is −20 Hz, at 8.7 wt.% it is +72 Hz, and at 11.3 wt.% of the mesophase is +250 Hz. Thus a four-fold increase in the amount of sodium bromide present has changed the sodium splitting by +280 Hz, with the major increase in splitting occurring at high salt concentration, which concentration change incidently also induces a phase transition at 31°C. The temperature dependence of the sodium splittings was used in order to suggest their *relative* signs. As seen from Table 1, at 90 and 75 mol% potassium dodecanoate the magnitudes of the sodium splittings increase with temperature. This is determined by placing a room temperature sample in the probe and observing the change in quadrupole splittings with rise in temperature to that of the magnet. At 65 and 50 mol% potassium dodecanoate the magnitude of the splittings decreases with increasing temperature. At 74.0 mol% potassium dodecanoate and 3.1 wt.% sodium bromide the sodium splitting starts at ~ −225 Hz and increases to −30 Hz. In the 6.0 wt.% mesophase the splitting starts at ~ −190 Hz and rises to −20 Hz. For the 8.7 wt.% phase the splitting starts at ~ −75 Hz, passes through zero (a measured line width of about 20 Hz), then rises to +72 Hz. No attempt to determine an accurate temperature dependence was made. Significant observations concerning these results are that an 8–10 degree rise in temperature has as large an effect on the sodium splittings as has a change in sodium bromide concentration from 3.1 to 11.3 wt.% of the mesophase and also that the direction of change is the same in both cases.

The small deviations from zero with large change in concentration of sodium ions shows that sodium ions not residing in the interface region of the micelle, i.e., those located in the interstitial water, have a very small or zero quadrupole splitting corresponding to almost isotropic sodium ion. As a consequence, exchange with those ions located in the interface has a minimal effect on the zero position. In this regard it should be noted from Fig. 2 that when the detergent interface of the micelle has a large positive charge, the sodium quadrupole splittings are about −1 kHz. In cationic mesophases prepared from hexadecyltrimethylammonium bromide or hexadecylpyridinium chloride, sodium splittings are typically in the order of +0.7 to +1.2 kHz (14). Clearly this shows that the induced quadrupole splitting for sodium ions becomes small when the sodium is combined with a micelle structure whose charge limit corresponds to a cationic detergent interface.

The description of the variation of the sodium quadrupole splitting as the amphiphile composition of the bilayer is varied *requires* at least three well designated sites for the location of the sodium ion. We propose that the three sites correspond to the following. In site I the sodium ions are located mainly within the plane of the interface, their location being determined by hydrogen bond interactions between the hydration sphere of the sodium and two carboxylate residues. With the partial replacement of carboxylate by trimethylammonium some of these bridging sites are no longer available and they are replaced by weakly hydrated sites involving a single carboxylate group. In this case the sodium ions are displaced from the plane of the interface but are still bound to it via the single carboxylates. In the third site sodium ions are remote from the interface region in an aqueous environment. The observed quadrupole splitting is then a population weighted average of splittings for the three sites. In the population weighted average the sodium and potassium ions are included because their distribution between interface and interstitial water is the same. The sign of the quadrupole splitting at each site is determined by the average orientation of the constraint axis as in eq. [1]

$$[1] \quad \Delta\gamma_{Na} = 2Q_{Na}\tfrac{1}{2}(3\cos^2\phi - 1)S_{con}$$

where $\Delta\gamma_{Na}$ is the sodium quadrupole splitting, Q_{Na} the sodium quadrupole coupling constant at the site in question, and ϕ is the angle between the constraint axis and direction of the electric field gradient. S_{con} is the order parameter describing the alignment of the constraint axis and is given by $\frac{1}{2} \times \langle 3\cos^2\theta - 1\rangle$ where the angular brackets indicate a value averaged over all θ where θ is the instantaneous angle between the constraint axis and the magnetic field. As the angle ϕ changes, the value of $\frac{1}{2}(3\cos^2\phi - 1)$ can change sign and consequently so will the sodium quadrupole splitting, $\Delta\gamma_{Na}$.

Collecting together the two angular terms of eq. [1] we can rewrite it in a simplified manner as

$$[2] \quad \Delta\gamma_{Na} = 2Q_{Na}S$$

Taking into account a multisite model we have $\Delta\gamma_{Na}$ as a summation over X_i, the fraction of molecules in site i as

$$[3] \quad \Delta\gamma_{Na} = 2\sum_i X_i Q_i S_i$$

or equivalently we can write for the case of the particular situation here that

$$[4] \quad \Delta\gamma_{Na} = X_I\Delta\gamma_I + X_{II}\Delta\gamma_{II} + X_{III}\Delta\gamma_{III}$$

where $\Delta\gamma_I$, $\Delta\gamma_{II}$, and $\Delta\gamma_{III}$ are quadrupole splittings characteristic of the individual sites.

Can. J. Chem. Downloaded from www.nrcresearchpress.com by 210.87.254.5 on 09/05/12
For personal use only.

From Figs. 1 and 2 a value of +5.8 kHz for the value of $\Delta\gamma_{Na}$ in a pure dodecanoate mesophase can be estimated and since X_{II} is assumed to be zero in our model on a pure dodecanoate interface this value is given by

$$[5] \quad \Delta\gamma_{Na} = X_I\Delta\gamma_I + X_{III}\Delta\gamma_{III}$$

From the Experimental it is seen that there are 2.980 sodium and potassium ions for 2.105 carboxylate headgroups. If we make the reasonable assumption that on an average one carboxylate accommodates one sodium or one potassium ion then $X_I = 0.71$ and $X_{III} = 0.29$. We have shown that sodium and potassium ions are sufficiently alike that there is no preference for one over the other in any of the three sites. The sodium quadrupole splitting then monitors the mean location of either ion. $\Delta\gamma_{III}$ must be estimated but it should correspond reasonably closely to the observed splittings for the cationic mesophases prepared from hexadecyltrimethylammonium for which splittings of ~0.90 kHz were obtained (30). Using these numbers we can calculate that the characteristic coupling for site I is +7.8 kHz. A characteristic value for $\Delta\gamma_{II}$ is more difficult to assess. In our model, the replacement of a dodecanoate ion by a decyltrimethylammonium ion should result in two alkali metal ions being displaced to a site II. The model also predicts that there are no alkali metal ions in site I when 50% of the dodecanoate has been replaced by decyltrimethylammonium. It is reasonable to assume an interface of alternating negative and positive charge arrangements rather than any appreciable two dimensional phase separations giving areas of negative and positive charges. Consequently the sodium splitting in the bilayer with no net charge can be written as

$$[6] \quad \Delta\gamma_{Na} = X_{II}\Delta\gamma_{II} + X_{III}\Delta\gamma_{III}$$

From the observed values for $\Delta\gamma_{Na}$ of −2.6 kHz (Figs. 1, 2) and the appropriate X_{II} and X_{III} (Experimental) the characteristic splitting for site II is −5.5 kHz. Thus the characteristic splittings for sites I, II, and III are +7.8, −5.5, and +0.9 kHz respectively. It is possible to test our model by calculating the mole fraction of dodecanoate in total detergent at which a zero sodium splitting occurs, and to compare this to the experimental value. In the general case corresponding to our model, eq. [4] can be rewritten as

$$[7] \quad \Delta\gamma_{Na} = [\Delta\gamma_I C_D(3x - 2) + 2\Delta\gamma_{II}C_D(1 - x) + \Delta\gamma_{III}C_E]/[xC_D + C_E]$$

where x is the mole fraction potassium dodecanoate, C_D is the total number of moles of amphiphile, and C_E is the number of moles of the electrolyte (sodium bromide). With $\Delta\gamma_{Na}$ equal to zero and C_D and C_E equal to 2.105 and 0.875 respectively, from the Experimental, and $\Delta\gamma_I$, $\Delta\gamma_{II}$, and $\Delta\gamma_{III}$ taking the previously derived values, the mole fraction, x, calculated is 0.76. This value agrees extremely well with the value actually obtained (Figs. 1, 2) of 0.74–0.75.

A problem with the model adopted is that it assumes that site I in the pure dodecanoate mesophase is fully occupied with alkali metal ions. However, the sodium splitting in the pure mesophase decreases with rise in temperature (Table 1) indicating that some alkali ions are being displaced into either site II or III. The result is that $\Delta\gamma_I$ could be underestimated.

The model also ignores the possibility that site III actually consists of two sites, one containing truly isotropic cations in the interstitial water and one with cations in a diffuse water layer loosely bound to the interface (31). This should be unimportant since the number of excess alkali metal ions and the amount of water present is constant. The division of site III into two sites would probably be required if an attempt to explain the temperature dependence throughout the complete concentration range were made. As previously discussed some sodium ion concentration studies were made in the mesophase region of zero sodium quadrupole splitting. The number of moles of sodium bromide present was varied by a factor of 4, from 0.437 to 1.75 mmol. A positive shift in quadrupole splitting of nearly 300 Hz was observed. The corresponding calculated shift, using eq. [7], was close to 400 Hz. The agreement is good and the discrepancy can probably be accounted for in terms of a truly isotropic region within site III.

The change in sign of the quadrupole splitting on going from site I to II or II to III is described by eq. [2] where S has changed sign because of the displacement of cations from one site to another. In terms of our model, S and thus the induced quadrupole splitting, in a pure dodecanoate mesophase, should be positive in sign. The signs of the other splittings follow as shown in Figs. 1 and 2. The signs of the water splittings have arbitrarily been assigned as positive.

In the hope that bromine magnetic resonance would provide information concerning the interactions occurring for the bromide ion at the micellar interface, both ^{79}Br and ^{81}Br spectra were obtained. Only ^{81}Br parameters are quoted. ^{79}Br magnetic resonance was used as a check whenever required. As a further check ^{23}Na quadrupole split-

Can. J. Chem. Downloaded from www.nrcresearchpress.com by 210.87.254.5 on 09/05/12
For personal use only.

tings were obtained to ensure they corresponded to those of Fig. 2 assuring us of mesophase integrity. At a concentration of 90 mol% potassium dodecanoate in total detergent, ^{81}Br had a small quadrupole splitting of 15.5 ± 0.1 kHz. As can be seen from Fig. 3, the bromine transitions were well resolved. It is worth mentioning that the chemical shift of this bromide ion is 90 ± 40 Hz from that of the bromide ion in a concentrated aqueous sodium bromide solution. In view of the extreme sensitivity of bromine chemical shifts to solvent environment, this small shift indicates an almost isotropic aqueous environment. At 100, 74, and 65 mol% of dodecanoate, ^{81}Br quadrupole splittings of 10.2 ± 0.1, 30.6 ± 0.2, and 30.4 ± 0.2 kHz respectively were obtained while a 74 mol% mesophase containing one-half the normal sodium bromide concentration gave an ^{81}Br splitting of 21.7 ± 0.2 kHz. Substantial broadening both of the centre and outer transitions over those of Fig. 3 both in ^{79}Br and ^{81}Br was observed as the proportion of decyltrimethylammonium bromide was increased. With 50 and 35 mol% of potassium dodecanoate the central transitions of the triplet were 3.3 and 4.4 kHz wide respectively and the outer transitions extremely difficult to observe (see Table 1). Sodium transitions were, under identical conditions (i.e., nothing changed but the transmitter frequency), as sharp as was normally found. It is known that ^{81}Br quadrupole coupling constants are typically in the order of 300–400 MHz (31, 32) although it has been estimated that $^{81}Br^-$ bound to $-N(CH_3)_3^+$ headgroups has a quadrupole coupling constant of 1.8 MHz (30). In either case the results here indicate that bromine interacts weakly with dodecanoate headgroups, behaving in a near isotropic manner when no decyltrimethylammonium is present but behaving more and more anisotropically as the decyltrimethylammonium content is increased. The increased broadening of the bromine transitions with increased decyltrimethylammonium content can be attributed to more efficient relaxation of the bromine nucleus as interactions with the increasingly positively charged interface become more important (30), a mechanism which leads also to the enhanced quadrupole splittings. These results provide no evidence that the bromide ion undergoes complex interactions similar to those of the sodium ion.

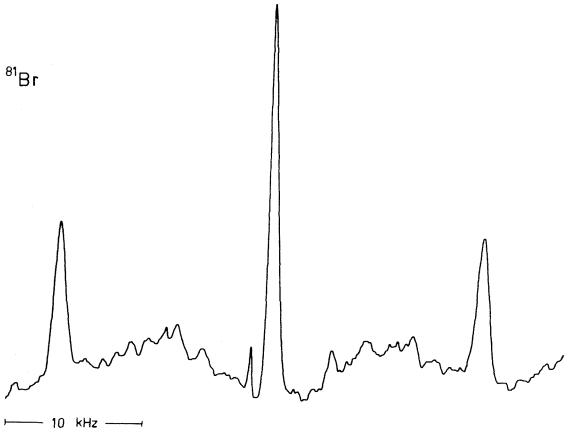


FIG. 3. An ^{81}Br spectrum taken at a mesophase composition of 90 mol% potassium dodecanoate (see Fig. 2) in the total detergent.

Another negatively charged ion which possibly could help resolve the problems of ion-interface binding is acetate. In this case the anisotropic motion of the ion can be measured through the proton–proton or proton–carbon dipolar interactions. The dipolar coupling, D_{HH}, is given by eq. [8].

$$[8] \quad D_{HH} = \frac{h \cdot \gamma_H^2}{4\pi^2 r_{HH}^3} S_{C_3}$$

S_{C_3} is the degree of alignment of the major axis of the acetate ion, γ_H is the magnetogyric ratio for protons, r_{HH} is the proton internuclear distance and h is Planck's constant. In conjunction with the acetate dipolar splittings both ^{23}Na and ^{2}H quadrupole splittings were obtained. The composition of the first set of mesophases studied was potassium dodecanoate/decyltrimethylammonium bromide/sodium acetate of molar proportions 1.17:1.17:1.0 with D_2O content varied between 51.2 and 61.3 wt.% of the mesophase. The results are shown in Fig. 4. Of major significance in these results is the fact that the ratio of quadrupole splittings of sodium to deuterium remains relatively constant, at least to very high water content. On the other hand, the ratio of the sodium or deuterium splitting to the acetate splitting decreases with water content. This is seen from the ratios entered into Table 2. The linearity between the sodium and deuterium quadrupole splittings can be explained if it is assumed that the sodium and the water splittings originate from a common interface interaction involving both species. On the other hand, the results for the 90 mole fraction dodecanoate micelle produced no linearity between any of the parameters measured (Table 3). These results give support to the three-site model for the behaviour of the sodium ions. In this model those ions in site II will behave differently with respect to water than those at site I. There is no evidence that the ^{81}Br splittings undergo a sign change and investigation of ^{13}C acetate unequivocally shows that D_{HH} does not undergo a change in sign.

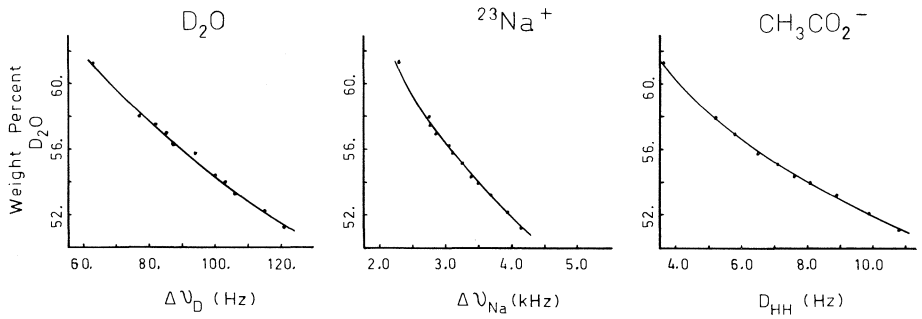


FIG. 4. Quadrupole splittings (^2H, ^{23}Na) and dipolar coupling (D_{HH}) in acetate ion plotted as a function of water content of the mesophase. Absolute values are plotted.

TABLE 2. Nuclear magnetic resonance parameters, $\Delta\nu_D$ deuterium splitting for D_2O, $\Delta\nu_{Na}$ for sodium, and D_{HH} the intramethyl proton dipole–dipole coupling for acetate ions. The values for the splittings at the various concentrations of D_2O were taken from the smooth curves of Fig. 4. The mesophase compositions are given in the text. Ratios of nuclear magnetic resonance parameters are listed in the last columns

	D_2O	$^{23}Na^+$	$CH_3CO_2^-$		
Wt.% D_2O	$\Delta\nu_D$ (Hz)	$\Delta\nu_{Na}$ (kHz)	D_{HH} (Hz)	$\Delta\nu_{Na}/\Delta\nu_D$	$\Delta\nu_D/D_{HH}$
51	122	4.22	11.2	34.6	10.9
52	115	3.98	10.0	34.6	11.5
53	109	3.73	9.0	34.2	12.1
54	103	3.49	8.0	33.9	12.9
55	96	3.26	7.1	34.0	13.5
56	90	3.07	6.4	34.1	14.1
57	84	2.89	5.7	34.4	14.7
58	78	2.74	5.1	35.1	15.3
59	73	2.58	4.6	35.3	15.9
61	63	2.30	3.6	36.5	17.5

In the hope that the acetate ion might provide further information, the vibrationally uncorrected structure of the methyl group has carefully been determined at various molar ratios of potassium dodecanoate to decyltrimethylammonium bromide. The results are given in Table 4 which also includes a structure determined for acetate ion in a cationic phase prepared from decylammonium chloride (24). An HCH angle of 109.9° within the error of all measurements was obtained. This is important because it establishes that the extremely small dipolar couplings observed here derive from a truly small order parameter rather than from an average between two large parameters of opposite sign. This latter averaging often occurs in thermotropic systems and leads to the determination of anomalous geometries, chemical shift anisotropies, and quadrupole coupling constants (33). The absence of such averaging for acetate and the obvious presence of it for sodium indicates clearly that the interaction sites occupied by the positively charged sodium ions are very different from those of the negatively charged acetate.

The Hydrophobic Region of the Micellar Bilayer

Deuterium quadrupole splittings from deuterium labelled hydrocarbon chains provide information concerning the non-aqueous region of the bilayer. Deuterium quadrupole splittings have been assigned to all positions in the dodecanoate, decyltrimethylammonium, and decanol chains. Assignments were made by preparing specifically deuteriated compounds and using those splittings to assign resonances from perdeuteriated species. Four mesophases were thoroughly investigated. They were: (1) 90 mol%, (2) 74 mol%, (3) 50 mol%, and (4) 45 mol%, potassium dodecanoate. Table 5 gives the collected results of the measurements. All values are normalized to an average ^2H splitting for the $—N(CD_3)_3^+$ headgroup of deuteriated decyltrimethylammonium, a small amount of which was incorporated into all mesophases. This was done because the CD_3 splitting varied slightly from sample to sample. The most obvious observation which can be made from Table 5 is that the magnitude of the quadrupole splittings does not change a great deal throughout the range studied, i.e., the average

Can. J. Chem. Downloaded from www.nrcresearchpress.com by 210.87.254.5 on 09/05/12
For personal use only.

TABLE 3. Measured splittings and molar proportion of components in the mesophases are reported as a function of water content. Errors in splittings are estimated to be approximately 5 in the last significant figure

	D_2O	$^{23}Na^+$	$CH_3CO_2^-$		
Wt.% D_2O	$\Delta\nu_D$ (Hz)	$\Delta\nu_{Na}$ (kHz)	D_{HH} (Hz)	$\Delta\nu_{Na}/\Delta\nu_D$	$\Delta\nu_D/D_{HH}$
Potassium dodecanoate/decyltrimethylammonium bromide/sodium acetate = 2.93:0.38:1.0					
54.3	497	2.81	21.6	5.65	23.0
55.2	439	2.71	19.4	6.17	22.6
56.2	384	2.51	15.0	6.54	25.6
57.2	309	2.19	11.3	7.09	27.3
58.3	←		Isotropic		→
Potassium dodecanoate/decyltrimethylammonium bromide/sodium acetate = 2.69:0.35:1.0					
56.1	438	2.85	19.0	6.51	23.1
57.3	382	2.76	13.7	7.23	27.9
58.4	327	2.59	11.4	7.92	28.7
59.2	280	2.38	9.4	8.50	29.8
60.3	217	1.95	6.0	8.99	36.2
60.9	←		Isotropic		→

TABLE 4.[a] Dipolar coupling constants, the corresponding HCH angles and order parameters for 2-^{13}C-acetate ion dissolved in various mesophases

Mesophase composition[b]	Weight %	D_{HH}	D_{CH}[c]	Angle HCH	S_{C_3}[d]
Potassium dodecanoate	31.4	−7.1	−5.1	109.2 ±1.0°	-3.41×10^{-4}
Sodium acetate	1.9				
Sodium acetate ($^{13}CH_3$)	2.8				
Decanol	2.0				
D_2O	61.9				
Potassium dodecanoate	30.4	−4.2	−3.1	109.6 ±1.8°	-2.02×10^{-4}
Decyltrimethylammonium bromide	4.6				
Sodium acetate	0.9				
Sodium acetate ($^{13}CH_3$)	2.5				
D_2O	61.6				
Potassium dodecanoate	10.6	−40.3	−30.9	110.2 ±0.3°	-1.93×10^{-3}
Decyltrimethylammonium bromide	36.6				
Sodium acetate	3.7				
Sodium acetate ($^{13}CH_3$)	2.8				
Decanol	4.3				
D_2O	42.0				
Decylammonium chloride	33.1	−129.4	−96.9	109.85±0.10°	-6.21×10^{-3}
Sodium acetate ($^{13}CH_3$)	5.0				
Decanol	2.4				
D_2O	59.5				

[a]Errors in dipolar couplings are estimated to be less than 0.2 Hz.
[b]The composition for the decylammonium phase is taken from ref. 18.
[c]J_{HH} taken to be +126.2 ± 0.1; measured in aqueous solution to be 126.6 ± 0.1 Hz, ref. 18.
[d]Obtained using the assumption r_{HH} = 1.793 Å.

alignment of the components of the hydrophobic region at 90 mol% dodecanoate is not much different from the alignment at 74, 50, or 35 mol%. A second general observation is that the quadrupole splittings are very sensitive to the nature of the headgroup on the hydrocarbon chain, and that this sensitivity is propagated even down to the terminal position of a chain at least ten carbons long. This is a point well worth stressing since it is clear that if information concerning a particular species in a bilayer is desired one should not base conclusions on observations made on closely related compounds in the same bilayer.

It is interesting in this regard to note the relative change in magnitude of the quadrupole splitting from the decyltrimethylammonium and dodecanoate ions labelled at the α position. The values go in the order of 11, 17, 40, and 50% larger quadrupole splitting of dodecanoate over decyltrimethylammonium for the phases of 90, 74, 50, and 35 mol% dodecanoate respectively. Decanol shows an opposite behaviour being 21% greater at

Can. J. Chem. Downloaded from www.nrcresearchpress.com by 210.87.254.5 on 09/05/12
For personal use only.

Can. J. Chem. Downloaded from www.nrcresearchpress.com by 210.87.254.5 on 09/05/12
For personal use only.

90 mol%, only 96% as large at 50 mol% and dropping to 89% of the dodecanoate splitting at 35 mol%. These results are illustrated by Fig. 5. Only the two extremes are shown, 90 mol% (Fig. 5*A*) and 35 mol% potassium dodecanoate (Fig. 5*B*).

The degree of order S_i, of a carbon–deuterium bond in the hydrocarbon component of the bilayer derives from motions affecting the chain as a whole, as well as from motions particular to the given methylene segment containing that bond. Consequently the order parameter measured is a product of two such parameters which are related to the deuterium quadrupole splitting observed, by eq. [9]

$$[9] \quad \Delta\gamma_i = \tfrac{3}{2}Q_D S_i = \tfrac{3}{2}Q_D S_i(\mathrm{RB}).S_i(\mathrm{I})$$

S_i(RB) is associated with rigid body motion and S_i(I) with the intrinsic degree of alignment. Contributions to rigid body motion are motions such as oscillations of the disc-like micelle, chain diffusion, and chain rotations, which affect all chains of the same chemical identity equally. The major motions reducing S_i(I) from the value of 1 are *trans/gauche* rotations (34, 35) which can in general have a different effect on each methylene segment. The rigid body motion of the chain does not affect individual methylene segments differently and as a conse-

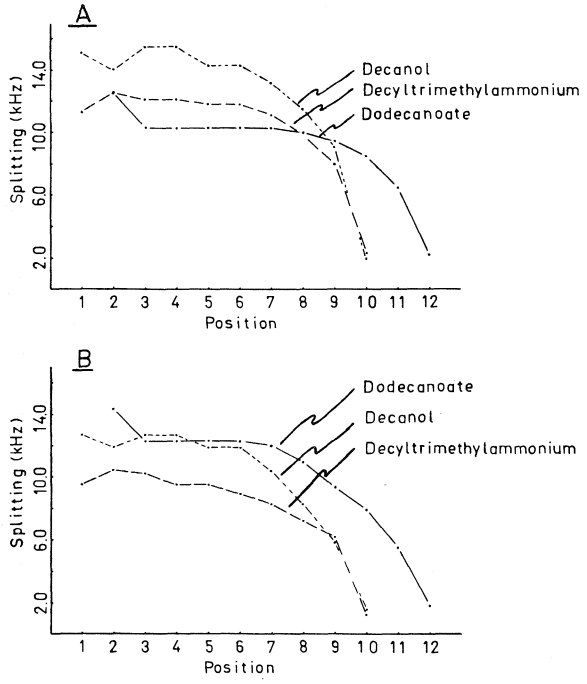


FIG. 5. Deuterium quadrupole splittings are plotted as a function of —CD_2— position along the various hydrocarbon chains. (*A*) Mesophase contains 90 mol% potassium dodecanoate in total detergent (see Fig. 2 for other parameters). (*B*) Mesophase has 35 mol% potassium dodecanoate in total detergent (refer to Fig. 2 for other parameters).

TABLE 5. The measured chain —CD_2— deuterium quadrupole splittings in kHz for the various amphiphile components of the mesophases studied; 90, 74, 50, and 35 mol% potassium dodecanoate should be referred to the appropriate region in Fig. 2

Component	Position												
	1	2	3	4	5	6	7	8	9	10	11	12	—$N(CD_3)_3^+$
90 mol% potassium dodecanoate													
Dodecanoate	—	12.47	10.5	10.3	10.3	10.3	10.3	9.95	9.53	8.55	6.532	2.213	—
Decyltrimethylammonium	11.27	12.49	12.1	12.1	11.8	11.8	11.14	9.91	8.00	2.391	—	—	1.768
Decanol	15.09	14.00	15.45	15.4	14.3	14.3	13.13	11.55	9.070	1.979	—	—	—
74 mol% potassium dodecanoate													
Dodecanoate	—	16.09	13.81	13.4	13.4	13.4	13.4	13.02	11.94	10.56	7.91	2.620	—
Decyltrimethylammonium	13.8	15.15	14.32	13.8	13.8	13.8	12.797	11.432	9.357	2.726	—	—	2.244
50 mol% potassium dodecanoate													
Dodecanoate	—	16.1	13.6	13.3	13.3	13.3	13.3	12.71	11.14	9.62	6.894	2.246	—
Decyltrimethylammonium	11.59	12.81	12.33	11.6	11.6	10.89	10.31	9.08	7.486	2.074	—	—	1.978
Decanol	15.41	14.81	16.0	16.0	14.8	14.8	13.37	10.67	8.061	1.702	—	—	—
35 mol% potassium dodecanoate													
Dodecanoate	—	14.35	12.3	12.3	12.3	12.3	11.9	11.00	9.39	7.99	5.564	1.827	—
Decyltrimethylammonium	9.56	10.4	10.2	9.52	9.52	8.88	8.33	7.267	5.925	1.598	—	—	1.621
Decanol	12.68	11.90	12.68	12.7	11.9	11.9	10.39	8.27	6.200	1.323	—	—	—

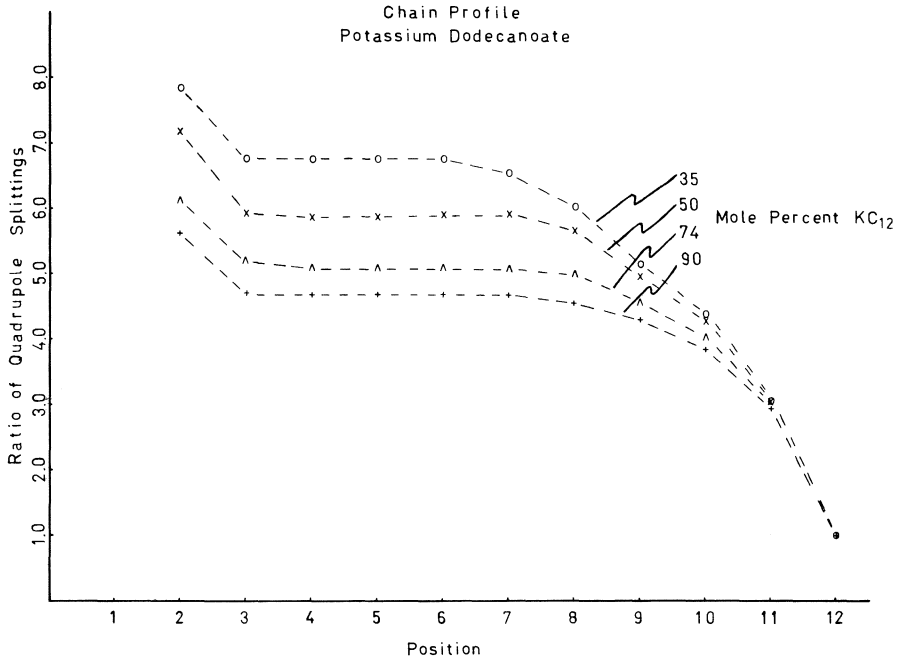


FIG. 6. The chain order profiles for potassium dodecanoate at the various mesophase compositions shown (refer to Fig. 2). KC_{12} refers to potassium dodecanoate and the parameter plotted is $\Delta\nu_x/\Delta\nu_{12}$ versus methylene position (x).

quence, by division of one quadrupole splitting by another from a position within the same hydrocarbon chain, the expression [10] is obtained. Any set of ratios of deuterium splittings provides

$$[10] \quad \Delta\gamma_i/\Delta\gamma_k = S_i(\mathrm{I})/S_k(\mathrm{I})$$

the same information. We use the splitting of the deuteriomethyl group as the reference and compare all the splittings from the same chain to it. The results provide a profile for the relative motions of the various methylene segments of the hydrocarbon chain. This incidentally provides a simple test to determine whether changes in magnitude of quadrupole splittings as a function, say, of water content or temperature variation reflect changes in rigid body motion rather than changes in the internal motions of the individual detergent molecules. In the first case the profile remains constant, and in the second it should change.

Figures 6, 7, and 8 show the chain profiles obtained for the various components of the bilayer. A comparison of the figures shows that there are large differences in the shape of the profiles between the three components. On the other hand, large changes in the composition of the mesophase bilayer have rather small effects on the shape of profiles for chains of the same chemical identity, the major effect being a scaling of all segment splitting values with respect to those of the terminal methyl group. Chain profiles are determined *mainly* by the headgroup and often rather large changes in bilayer composition have minimal effect on the profile as is observed in the figures. We have never observed the same degree of order profile from aliphatic chains with different headgroups. The headgroup of the hydrocarbon chain is anchored more or less securely in the interface region of the micelles of the mesophase by its own peculiar hydration and counter ion interactions. Chemically distinct headgroups are anchored differently. This is an important experimental result bearing on bilayer solution chemistry.

Equal quadrupole splittings, three times greater than for the terminal methyl group, would be obtained for the methylene deuteriums if the hydrocarbon chain were extended, rigid, and rapidly rotating about its long axis. In this case the profile would be perfectly flat until the methyl group is reached. The hydrocarbon chain of course is not rigid and internal rotations about carbon–carbon bonds do occur. It has been shown that a flat chain profile is maintained if rotations occur as complementary *gauche* pairs which cause formation of "kinks" ((±)-*gauche*/*trans*/(∓)-*gauche* sequences) and "jogs" ((±)-*gauche*/multiple *trans*/(∓)-*gauche* sequences), which oscillate along the length of the chain (34, 35). Random single *gauche* rotations produce a rapid decrease in the quadrupole splittings and since they occur most easily near the terminal carbons of the hydrocarbon

Can. J. Chem. Downloaded from www.nrcresearchpress.com by 210.87.254.5 on 09/05/12
For personal use only.

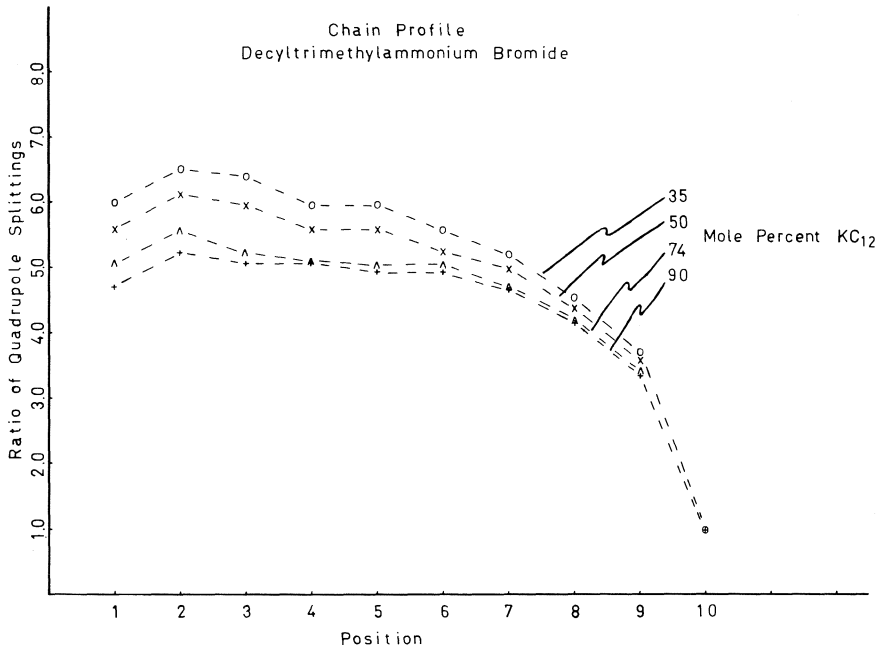


FIG. 7. The chain order profiles for decyltrimethylammonium bromide at the mesophase compositions shown (refer to Fig. 2). $\Delta\nu_x/\Delta\nu_{10}$ versus methylene position (x) is the parameter plotted. KC_{12} refers to potassium dodecanoate.

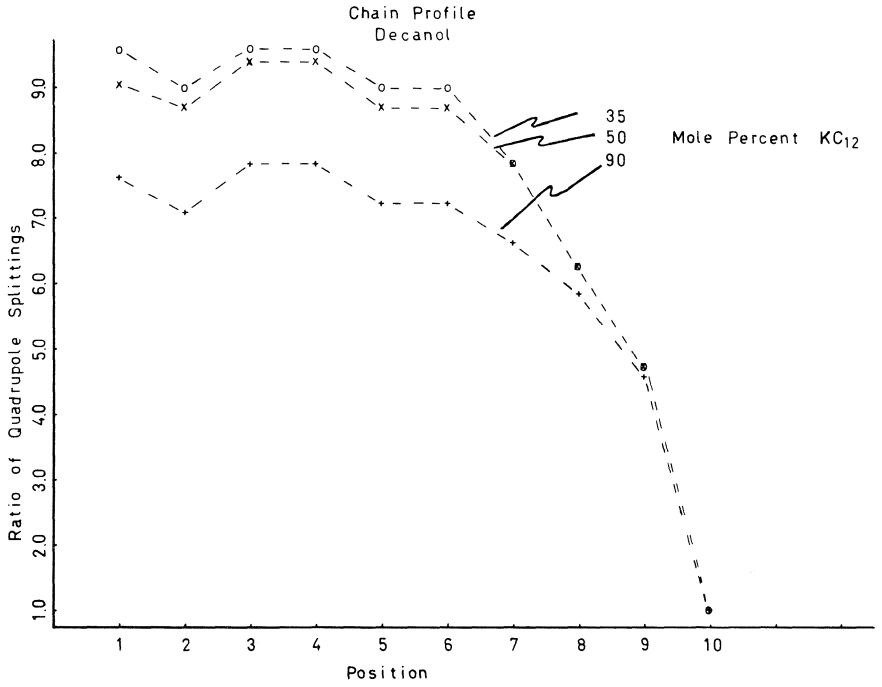


FIG. 8. The chain order profiles for decanol at the various mesophase compositions shown. KC_{12} refers to potassium dodecanoate and the parameter plotted is the methylene position (x) versus $\Delta\nu_x/\Delta\nu_{10}$.

chains the chain profile usually has a plateau-like region extending from the initial methylene group then terminated by a rapid decay resulting in a methyl splitting much less than one-third that of the plateau value. This behaviour is clearly seen for the profiles of Figs. 6, 7, and 8. If the plateau region of the profile is not flat it will be because the "kinks" and "jogs" are preferentially formed at one posi-

Can. J. Chem. Downloaded from www.nrcresearchpress.com by 210.87.254.5 on 09/05/12
For personal use only.

Can. J. Chem. Downloaded from www.nrcresearchpress.com by 210.87.254.5 on 09/05/12
For personal use only.

tion rather than another. Formation of a "kink" results in certain carbon–deuterium bonds being directed at different average angles with respect to the magnetic field of the nmr spectrometer, thus giving rise to varying quadrupole splittings for different deuteriums. These differences will disappear only if averaging over all positions is complete. The most obvious cause of positions of preferential formation of "kinks" or "jogs" is that the initial segments of the hydrocarbon chain are being held by the headgroup at an angle different from that which would be preferred in the absence of such a constraint. The preferred angle is generally accepted to be perpendicular to the interface but this has been questioned (36, 37, 38). In this regard it has been found that increasing the length of the hydrocarbon chain but retaining the same headgroup has only a small effect on the chain profile, within the relevant region (38).

Examination of Fig. 6 provides considerable information concerning the behaviour of the dodecanoate hydrocarbon chain. Characteristic of the four profiles is an initial large value of the quadrupole splitting at position 2 dropping considerably to a plateau of values which extends, in the case of the 90 mol% profile, essentially to carbon 8. With increase in decyltrimethylammonium content, this plateau embraces fewer segments, finally extending to carbon 6 for the 35 mol% profile. These results show that the dodecanoate chain is more constrained (i.e., the ratio of plateau/terminal CD_3 splitting decreases) with respect to neighbouring chains at the higher concentrations of dodecanoate.

The formation of single *gauche* rotations near the nonpolar end of the chains is interpreted as less probable when the chains are more tightly packed. An extended chain which is rotating freely about its long axis has a theoretical ratio of 3 between chain methylene deuterium splittings and the terminal $-CD_3$ doublet separations. A ratio which approaches 3 for the methyl $-CD_3$ group to the $-CD_2$-plateau value indicates a small population of single *gauche* rotamers as does an extension of the plateau region to include more segments. In Fig. 7 the decyl chain of the substituted ammonium ion behaves in a similar manner to the profiles of the dodecanoate chains shown in Fig. 6, a minimum probability of *gauche* rotations in both chains occurring at 90 mol% dodecanoate bilayers.

Experimental

Spectra

Deuterium and sodium nuclear magnetic resonance spectra were obtained either from a Varian VF-16 wide-line nmr spectrometer (results in Figs. 1 and 4, and Table 2) observing at 4.7 and 8.1 MHz respectively, or from a Bruker SXP FT spectrometer (results in Figs. 2, 5, 6, 7, and 8, and Table 4) observing at 9.2 and 15.8 MHz for deuterium and sodium. ^{79}Br and ^{81}Br spectra were obtained using the SXP spectrometer at carrier frequencies of 15.1 and 16.2 MHz respectively. The maximum spectral window on the FT spectrometer is 50 kHz. In the case of large spectral widths, transitions which were folded were unambiguously identified by changing the carrier frequency and observing the relative shifts in peak positions. Proton spectra were recorded using a Varian HA-100 spectrometer operating in the locked mode.

Materials

The lyotropic mesophases which were used to obtain the results in Figs. 2, 3, 5, 6, 7, and 8, and Table 4 had the following composition, in millimoles for each component: total detergent/sodium bromide/water (0.1 wt.% D_2O)/decanol (maximum) = 2.105:0.875:49.0:0.42. The mole fraction of potassium dodecanoate in total detergent was varied from 100 mol% to 35 mol%, consequently the proportion of decyltrimethylammonium bromide varied from 0 to 65 mol%. Decanol was required in the ranges (*a*) 100.0–77.5 mol% potassium dodecanoate, 0.40–0.0 mmol decanol; (*b*) 57.0–35.0 mol% potassium dodecanoate, 0.0–0.42 mmol decanol.

A second series of mesophases containing D_2O instead of H_2O was utilized to obtain the results for Fig. 1. The molar proportions were: total detergent/sodium bromide/D_2O = 2.105:1.02:60. The compositions of all other mesophases are given in the text.

The specifically deuteriated compounds were prepared by standard techniques from commercially available materials (19, 39). Perdeuteriated decanol and decyltrimethylammonium bromide were prepared from perdeuteriated decanoic acid by the following sequence of elementary reactions.

[11] $CD_3(CD_2)_8C(=O)OH \xrightarrow{SOCl_2} CD_3(CD_2)_8C(=O)Cl \xrightarrow{LiAlD_4} CD_3(CD_2)_8CD_2OH$

[12] $CD_3(CD_2)_8CD_2OH \xrightarrow{TsCl/pyridine} CD_3(CD_2)_8CD_2OTs \xrightarrow[MeOH/H_2O]{NaN_3} CD_3(CD_2)_8CD_2N_3 \xrightarrow{LiAlH_4} CD_3(CD_2)_8CD_2NH_2$

[13] $CD_3(CD_2)_9NH_2 \xrightarrow[MeOH/NaHCO_3]{CH_3I} CD_3(CD_2)_8CD_2N(CH_3)_3I \xrightarrow[MeOH]{Ag_2O} CD_3(CD_2)_8CD_2N(CH_3)_3OH \xrightarrow{HBr} CD_3(CD_2)_8CD_2N(CH_3)_3Br$

Overall yields of the pure decyltrimethylammonium bromide (recrystallized from ethylacetate/ethanol (~20/1)), ranged between 50 and 70% from the starting decanoic acid. Where required, steps of the reaction sequence were checked for completion using thin layer chromatography. Iodine vapour or 10% sulfuric acid and heat were used to visualize the plates.

Perdeuteriated decanoic and dodecanoic acids were prepared using an adaption of the process of Stenhagen and Dinh-Nguyen (40) as has been described (14). After one cycle the deuterium enrichment was found to be approximately 90%.

Can. J. Chem. Downloaded from www.nrcresearchpress.com by 210.87.254.5 on 09/05/12
For personal use only.

Acknowledgments

We are thankful to the National Research Council of Canada for its financial support of this work by operating grants to L.W.R.

1. C. TANFORD. The hydrophobic effect: formation of micelles and biological membranes. Wiley, New York. 1973.
2. HARTLEY *et al.* Trans. Faraday Soc. **31**, 31 (1935); **31**, 120 (1935); **31**, 183 (1935); Z. Phys. Chem. **170**, 321 (1934).
3. D. CHAPMAN. *In* Liquid crystals and plastic crystals. Vol. 1. *Edited by* G. W. Gray and P. A. Winsor. Wiley, New York. 1974. p. 288.
4. G. H. BROWN, J. W. DOANE, and V. D. NEFF. A review of the structure and physical properties of liquid crystals. CRC Publishing House, Cleveland, OH. 1971.
5. L. L. M. VAN DEENEN. *In* The molecular basis of membrane function. *Edited by* D. C. Tosteson. Prentice Hall, NJ. 1969. p. 47.
6. V. LUZZATTI, H. MUSTACCHI, and A. E. SKOULIOUS. Discuss. Faraday Soc. **25**, 43 (1958).
7. M. BLOOM, E. E. BURNELL, S. B. W. ROEDER, and M. I. VALIC. J. Chem. Phys. **66**, 3012 (1977).
8. J. CHARVOLIN and P. RIGNY. J. Chem. Phys. **58**, 3999 (1973).
9. J. CHARVOLIN and B. MELY. Mol. Cryst. Liq. Cryst. **41**, 209 (1978).
10. K. D. LAWSON and T. J. FLAUTT. J. Am. Chem. Soc. **89**, 5489 (1967).
11. K. RADLEY, L. W. REEVES, and A. S. TRACEY. J. Phys. Chem. **80**, 174 (1976).
12. K. RADLEY and L. W. REEVES. Can. J. Chem. **53**, 161 (1975).
13. F. FUJIWARA, L. W. REEVES, M. SUZUKI, and J. A. VANIN. *In* Solution chemistry of surfactants. Vol. 1. Proc. Nat. Colloid Symp. Knoxville, TN. 1978. *Edited by* K. Mittall. Plenum Press. 1979. p. 63.
14. L. W. REEVES, A. S. TRACEY, and M. M. TRACEY. Can. J. Chem. **57**, 747 (1979).
15. L. HECKER, L. W. REEVES, and A. S. TRACEY. Mol. Cryst. Liq. Cryst. **53**, 77 (1979).
16. M. E. MARCONDES HELENE, V. R. PAOLI-MONTEIRO, L. W. REEVES, and J. A. VANIN. Abstracts of 1979 meeting of Sociedade Brasileira para o progresso de Ciencia, Fortaleza. July, 1979.
17. L. W. REEVES, J. SANCHES DE CARA, M. SUZUKI, and A. S. TRACEY. Mol. Phys. **25**, 1481 (1973).
18. L. W. REEVES, A. S. TRACEY, and M. M. TRACEY. J. Am. Chem. Soc. **95**, 3799 (1973).
19. L. W. REEVES and A. S. TRACEY. J. Am. Chem. Soc. **97**, 5729 (1975).
20. F. FUJIWARA and L. W. REEVES. J. Am. Chem. Soc. **98**, 6790 (1976).
21. Y. LEE and L. W. REEVES. Can. J. Chem. **54**, 500 (1976).
22. D. M. CHEN, F. Y. FUJIWARA, and L. W. REEVES. Can. J. Chem. **55**, 2404 (1977).
23. D. BAILEY, A. D. BUCKINGHAM, F. Y. FUJIWARA, and L. W. REEVES. J. Magn. Reson. **18**, 344 (1975).
24. D. M. CHEN, L. W. REEVES, A. S. TRACEY, and M. M. TRACEY. J. Am. Chem. Soc. **96**, 5349 (1974).
25. F. Y. FUJIWARA and L. W. REEVES. Mol. Phys. **36**, 1897 (1978).
26. L. POHL, R. EIDENSCHINK, J. KRAUSE, and G. WEBER. Phys. Lett. A, **65**, 169 (1978).
27. F. Y. FUJIWARA and L. W. REEVES. J. Phys. Chem. Submitted.
28. L. QUEIROZ DO AMARAL, C. ALVARENGA PIMENTEL, and M. TAVARES. Private Communication (1977); M. TAVARES. M.Sc. Dissertation. 1978; Suppl. to Acta Crystallogr. Sect. A, **34**, S188 (1978); J. Chem. Phys. **71**, 2940 (1979).
29. G. LINDBLOM, B. LINDMAN, and G. T. T. TIDDY. Acta Chem. Scand. Ser. A, **29**, 876 (1975).
30. G. LINDBLOM, B. LINDMAN, and G. T. T. TIDDY. J. Am. Chem. Soc. **100**, 2299 (1978).
31. B. LINDMAN and S. FRASER. NMR basic principles and progress. Vol. 12. 1976.
32. F. A. C. LUCKEN. Nuclear quadrupole coupling constants. Academic Press, London. 1969.
33. P. DIEHL, M. REINHOLD, A. S. TRACEY, and E. WALLSCHLEGER. Mol. Phys. **30**, 1781 (1975).
34. A. SEELIG and T. SEELIG. Biochemistry, **13**, 4839 (1974).
35. T. SEELIG and W. NIEDERBERGER. Biochemistry, **13**, 1585 (1974).
36. N. O. PETERSEN and S. I. CHAN. Biochemistry, **16**, 2657 (1977).
37. A. S. TRACEY and P. DIEHL. Can. J. Chem. **54**, 2283 (1976).
38. C. DIJKEMA and H. J. C. BERENDSEN. J. Magn. Reson. **14**, 251 (1974).
39. A. F. THOMAS. Deuterium labelling in organic chemistry. Appleton-Century-Crofts, Education Division, New York, NY. 1971.
40. E. A. STENHAGEN and N. DINH-NGUYEN. Chem. Abstr. **67**, 63814 (1971).

Vinyl ether hydrolysis. XIII. The failure of I-strain to produce a change in rate-determining step[1]

Y. CHIANG, W. K. CHWANG, A. J. KRESGE,[2] AND S. SZILAGYI

Department of Chemistry, University of Toronto, Scarborough College, West Hill, Ont., Canada M1C 1A4

Received July 30, 1979

Y. CHIANG, W. K. CHWANG, A. J. KRESGE, and S. SZILAGYI. Can. J. Chem. **58**, 124 (1980).

Rates of hydrolysis of 1-ethoxy-3,3,5,5-tetramethylcyclopentene and 1-methoxy-2,3,3,5,5-pentamethylcyclopentene measured in mineral acid and formic and acetic acid buffer solutions show general acid catalysis and give large kinetic isotope effects in the normal direction ($k_H/k_D > 1$). This indicates that these reactions proceed by the conventional mechanism for vinyl ether hydrolysis in which proton transfer from the catalyzing acid to the substrate is rate-determining, and that the I-strain in these substrates is insufficiently great to shift the reaction mechanism to rapidly reversible substrate protonation followed by rate-determining hydration of the ensuing cationic intermediate.

Y. CHIANG, W. K. CHWANG, A. J. KRESGE et S. SZILAGYI. Can. J. Chem. **58**, 124 (1980).

On a mesuré les vitesses d'hydrolyse de l'éthoxy-1 tétraméthyl-3,3,5,5 et du méthoxy-1 pentaméthyl-2,3,3,5,5 cyclopentène en utilisant un acide minéral et des solutions tampons d'acides formique et acétique. Ces vitesses montrent l'effet d'une catalyse générale par les acides et donnent de grands effets isotopiques cinétiques dans la direction normale ($k_H/k_D > 1$). Ceci indique d'une part que ces réactions se déroulent suivant le mécanisme conventionnel d'hydrolyse d'un éther vinylique dans lequel le transfert d'un proton de l'acide au substrat est l'étape déterminante et d'autre part que la tension I dans ces substrats n'est pas suffisamment importante pour faire évoluer le mécanisme de la réaction vers une protonation réversible du substrat suivie d'une étape déterminante impliquant l'hydratation de l'intermédiaire cationique qui en résulte.

[Traduit par le journal]

The acid-catalyzed hydrolysis of simple vinyl ethers is known to occur through rate-determining protonation of the double bond of the substrate (eq. [1]) followed by rapid hydration of the ensuing carbonium ion (eq. [2]) and subsequent fast breakdown of the hemiacetal intermediate (eq. [3]).

[1] $CH_2{=}CHOR + HA \rightarrow CH_3\overset{+}{C}HOR + A^-$

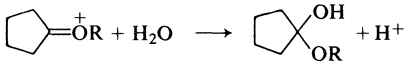
[2] $CH_3\overset{+}{C}HOR + H_2O \rightarrow CH_3\underset{OH}{C}HOR + H^+$

[3] $CH_3\underset{OH}{C}HOR \rightarrow CH_3CHO + HOR$

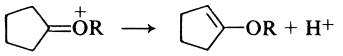
There is reason to believe, however, that the protonation step is close to being reversible (1), and in fact a system has been discovered in which the reaction mechanism appears to change from rate-determining protonation in mineral acid solutions to rate-determining hydration preceded by rapid and reversible protonation in carboxylic acid buffers (2).

In an effort to explore this mechanistic change we have been searching, so far in vain, for other examples of rate-determining hydration in vinyl ether hydrolysis (1, 3). We report here the results of an attempt to bring internal steric effects in cyclic substrates, I-strain (4), to bear upon the problem.

The substrates we used are derivatives of 1-alkoxycyclopentene. It is known that eclipsing strain in saturated five-membered carbocyclic systems impedes chemical processes which convert the hybridization of ring atoms from sp^2 to sp^3, and this effect should therefore make the reaction of 1-alkoxycyclopentyl cations with water (eq. [4])

[4] 

more difficult than it would otherwise be. Eclipsing strain is known also to favour introduction of a carbon–carbon double bond into a cyclopentane ring (5), and this effect should therefore facilitate deprotonation of the cation to regenerate vinyl ether (eq. [5]). These two effects taken together can

[5] 

thus be expected to slow hydration relative to deprotonation, and, if the effects are sufficiently great, the result might be a change in rate-determining step.

Our previous work shows that this does not happen with 1-ethoxycyclopentene itself; all of the available evidence indicates that this substrate hydrolyses by the normal rate-determining proton transfer mechanism (6). Substitution of methyl groups for ring hydrogens in this system, however, might increase eclipsing strain significantly, and we have therefore extended our previous work by

[1]For part XII, see ref. 3.

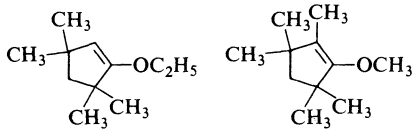
[2]Author to whom correspondence should be addressed.

0008-4042/80/020124-06$01.00/0

© 1980 National Research Council of Canada/Conseil national de recherches du Canada

Can. J. Chem. Downloaded from www.nrcresearchpress.com by 210.87.254.6 on 09/05/12
For personal use only.

examining the behavior of 1-ethoxy-3,3,5,5-tetramethylcyclopentene, **1**, and 1-methoxy-2,3,3,5,5-pentamethylcyclopentene, **2**.



1 **2**

Experimental

Materials

1-Ethoxy-3,3,5,5-tetramethylcyclopentene was prepared from the corresponding ketal, which in turn was made by treating 2,2,4,4-tetramethylcyclopentanone (Chemical Samples Co.) with triethyl orthoformate in ethanol solution in the presence of a catalytic amount of sulfuric acid. Heating this mixture under reflux for one day followed by neutralization of the sulfuric acid (with sodium ethoxide), removal of the solvent, and vacuum distillation of the residue gave a mixture of ketal and vinyl ether which was separated into pure components by gas chromatography. Both products were characterized by nmr and mass spectroscopy; ^{1}H nmr ketal, δ: 3.45 (q, 4H), 1.78 (s, 2H), 1.43 (s, 2H), 1.15 (t, 6H), 1.03 (s, 12H); vinyl ether, δ: 4.02 (s, 1H), 3.63 (q, 2H), 1.55 (s, 2H), 1.25 (t, 3H), 1.05 (s, 12H).

1-Methoxy-2,3,3,5,5-pentamethylcyclopentene was made in a similar fashion from trimethyl orthoformate and 2,2,4,4,5-pentamethylcyclopentanone. In this case, the vacuum distillate contained only the vinyl ether and starting ketone; no ketal was isolated. The starting ketone was prepared by methylating 2,2,-4,4-tetramethylcyclopentanone using methyl iodide and an equivalent amount of sodium hydride. This ketone as well as the vinyl ether were characterized by nmr and mass spectroscopy; ^{1}H nmr ketone, δ: 2.07 (m, 1H), 1.67 (s, 2H), 1.07 (s, 3H), 1.03 (s, 6H), 0.89 (s, 3H), 0.75 (s, 3H); vinyl ether, δ: 3.74 (s, 3H), 1.63 (s, 5H), 1.04 (s, 6H), 1.02 (s, 6H).

Solutions were prepared using best available commercial grades of acids and bases and either deionized H_2O purified further by distillation from alkaline permanganate or D_2O as received (Merck).

Kinetics

Rates of reaction were measured spectroscopically by following the decrease of the intense vinyl ether absorption in the region 200–220 nm. Measurements were made using a Cary 118 C spectrometer with thermostatted cell compartment (25.0 ± 0.02°C). Substrates dissolved in ethanol were added to acid or buffer solutions contained in quartz cuvettes after these solutions had come to temperature equilibrium with the cell compartment; the amount of ethanol used was such that its final concentration in the reaction mixtures was of the order of 0.1%. Both substrates were only very sparingly soluble in water, and care had to be taken to shake the reaction mixtures sufficiently vigorously to effect complete solution.

Data so obtained followed the first-order rate law accurately. Rate constants were evaluated graphically, either using infinite-time readings taken after 10–12 half-lives or, in the case of the slower runs, by the Guggenheim (7) or Swinbourne (8) methods.

Results

1-Ethoxy-3,3,5,5-tetramethylcyclopentene

First-order rate constants for the hydrolysis of this substrate were measured in acetic acid buffer solutions using H_2O and D_2O as the solvents. The data are summarized in Table 1.

These observed first-order rate constants proved to be accurately proportional to acetic acid concentration in buffer solutions of constant hydrogen ion concentration, maintained by keeping the buffer ratio constant, and, when the buffer ratio was changed, the proportionality constant relating observed rate constants to acetic acid concentration remained invariant. This indicates that only the acid component of the buffer and not the buffer base is catalytically effective, which implies that the system is undergoing general acid catalysis. The rate law for such a process is given by eq. [6].

$$[6] \quad k_1 = k_H + [H^+] + k_{HA}[HA]$$

The data were fitted to this expression by linear least-squares analysis, and the results (Table 1) showed good constancy of k_{HA}: $(1.90 \pm 0.05) \times 10^{-1}\ M^{-1}\ s^{-1}$ at a buffer ratio of 1.0 and $(1.91 \pm 0.04) \times 10^{-1}\ M^{-1}\ s^{-1}$ at a buffer ratio of 0.5.

Hydronium ion catalytic coefficients were evaluated from the intercepts of these least-squares

TABLE 1. Rates of hydrolysis of 1-ethoxy-3,3,5,5-tetramethylcyclopentene in acetic acid buffer solutions at 25°C[a]

10^2[Acetic acid](M)	$10^3 k(s^{-1})$
H_2O; [HOAc]/[NaOAc] = 0.96	
0.76	7.67, 7.73, 7.58
1.53	8.92, 8.61, 8.78
1.91	10.0, 10.0, 9.90
2.29	10.8, 11.0, 10.9, 10.6, 10.6
3.06	11.9, 12.0, 12.0, 11.7
3.82	13.5, 13.4, 13.3
$k_1 = (6.21 \pm 0.13) \times 10^{-3} + (1.90 \pm 0.05) \times 10^{-1}$ [HOAc]	
$k_{H^+} = (2.67 \pm 0.06) \times 10^2\ M^{-1}\ s^{-1}$	
H_2O; [HOAc]/[NaOAc] = 0.49	
0.39	4.00, 4.00
0.78	4.74, 4.73, 4.72
1.18	5.67, 5.61, 5.36
1.57	6.29, 6.33
1.96	7.01, 6.95, 6.94
$k_1 = (3.27 \pm 0.05) \times 10^{-3} + (1.91 \pm 0.04) \times 10^{-1}$ [HOAc]	
$k_{H^+} = (2.74 \pm 0.04) \times 10^2\ M^{-1}\ s^{-1}$	
D_2O; [DOAc]/[NaOAc] = 3.3	
0.84	2.32, 2.34, 2.28
1.75	2.78, 2.74, 2.75
2.27	2.98, 2.84
2.57	2.93
3.43	3.44, 3.36, 3.36
4.30	3.66, 3.65
$k_1 = (2.01 \pm 0.03) \times 10^{-3} + (3.90 \pm 0.12) \times 10^{-2}$ [DOAc]	
$k_{D^+} = (8.15 \pm 0.12) \times 10^1\ M^{-1}\ s^{-1}$	

[a]Ionic strength maintained at 0.040 M by adding sodium chloride; indicated error limits are standard deviations of mean values.

Can. J. Chem. Downloaded from www.nrcresearchpress.com by 210.87.254.6 on 09/05/12
For personal use only.

Can. J. Chem. Downloaded from www.nrcresearchpress.com by 210.87.254.6 on 09/05/12
For personal use only.

relationships using hydronium ion concentrations calculated from the thermodynamic dissociation constant of acetic acid and activity coefficients for the hydronium and acetate ions recommended by Bates (9). These catalytic coefficients also showed good consistency: $k_{H^+} = (2.67 \pm 0.06) \times 10^2 M^{-1}$ s^{-1} and $k_{H^+} = (2.74 \pm 0.04) \times 10^2 M^{-1} s^{-1}$, indicating that the system conforms to the rate law of eq. [6] quite well.

The data obtained in D_2O solution were treated similarly. The results (Table 1), when combined with those provided by the H_2O measurements, give the following isotope effects: $k_{H^+}/k_{D^+} = 3.32 \pm 0.07$ and $k_{HA}/k_{DA} = 4.88 \pm 0.17$.

1-Methoxy-2,3,3,5,5-pentamethylcyclopentene

Rates of hydrolysis of this substrate were measured in perchloric and hydrochloric acid solutions as well as in formic and acetic acid buffers. The data are summarized in Tables 2 and 3.

In the mineral acid solutions first-order rate constants proved to be accurately proportional to hydronium ion concentration, with no indication of catalysis by water species. Second-order rate constants were therefore evaluated simply by dividing the first-order constants by acid concentration and taking averages of the values so obtained. The results showed good agreement between perchloric and hydrochloric acid solutions: $k_{H^+} = 3.06 \pm 0.08$ $M^{-1} s^{-1}$ and 2.92 ± 0.10 $M^{-1} s^{-1}$, respectively. The measurements in HCl/H_2O and DCl/D_2O gave the isotope effect $k_{H^+}/k_{D^+} = 2.70 \pm 0.12$.

TABLE 2. Rates of hydrolysis of 1-methoxy-2,3,3,5,5-pentamethylcyclopentene in perchloric and hydrochloric acid solutions at 25°C

10^2[Acid](M)	$10^2 k$(s^{-1})
H_2O; Acid = $HClO_4$	
0.66	1.97, 1.97, 1.96
0.96	2.84, 2.91, 3.16
1.52	4.74, 4.79, 4.74
1.92	5.87, 5.97, 6.15
$k_{H^+} = 3.06 \pm 0.08$ $M^{-1} s^{-1}$	
H_2O; Acid = HCl	
0.40	1.17, 1.20, 1.19
0.80	2.34, 2.33, 2.38
1.20	3.64, 3.54, 3.54
1.60	4.79, 4.73, 4.49
2.00	5.58, 5.35
$k_{H^+} = 2.92 \pm 0.10$ $M^{-1} s^{-1}$	
D_2O; Acid = DCl	
1.20	1.34, 1.22, 1.31
1.72	1.87, 1.87, 1.91
2.34	2.53, 2.53
3.78	4.01, 3.87
4.63	5.11, 4.88
$k_{D^+} = 1.08 \pm 0.03$ $M^{-1} s^{-1}$	

TABLE 3. Rates of hydrolysis of 1-methoxy-2,3,3,5,5-pentamethylcyclopentene in formic and acetic acid buffer solutions at 25°C[a]

10^2[HA](M)	$10^3 k_1$(s^{-1})
H_2O; HA = HCO_2H; [HA]/[NaA] = 2.4	
0.96	1.58, 1.59, 1.60
1.91	1.71, 1.79
2.86	1.75, 1.78, 1.79
3.82	1.85, 1.82, 1.78
4.77	1.88, 1.90, 1.88
$k_{corr} = (1.77 \pm 0.01) \times 10^{-3} + (2.21 \pm 0.38) \times 10^{-3}$ [HA]	
$k_{H^+} = 2.99 \pm 0.02$ $M^{-1} s^{-1}$	
H_2O; HA = CH_3CO_2H; [HA]/[NaA] = 2.4	
0.94	0.179, 0.178
1.89	0.181, 0.182
2.83	0.192, 0.191
3.78	0.194, 0.193
4.72	0.202
$k_1 = (1.72 \pm 0.01) \times 10^{-4} + (6.12 \pm 0.53) \times 10^{-4}$ [HA]	
$k_{H^+} = 2.96 \pm 0.02$ $M^{-1} s^{-1}$	

[a]Ionic strength maintained at 0.040 M by adding sodium chloride; indicated error limits are standard deviations of mean values.

The data obtained in acetic acid buffers were treated as described above for the other substrate; this produced a value of $k_{H^+} = 2.96 \pm 0.02$ $M^{-1} s^{-1}$, which is nicely consistent with the mineral acid results. The formic acid solution data, on the other hand, had to be corrected for "buffer failure", inasmuch as significant ionization of this (stronger) buffer acid occurred at the lowest buffer concentrations used, and actual (as opposed to stoichiometric) buffer ratios, and therefore hydronium ion concentrations, consequently did not remain constant along a series of solutions of constant stoichiometric buffer ratio. This correction was performed as before (6*a*) using activity coefficients recommended by Bates (9) and the hydronium ion catalytic coefficients determined in perchloric and hydrochloric acids. This treatment produced a value of $k_{H^+} = 2.99 \pm 0.02$ $M^{-1} s^{-1}$, in very good agreement with results from the measurements in other acids.

Discussion

Reaction Mechanism

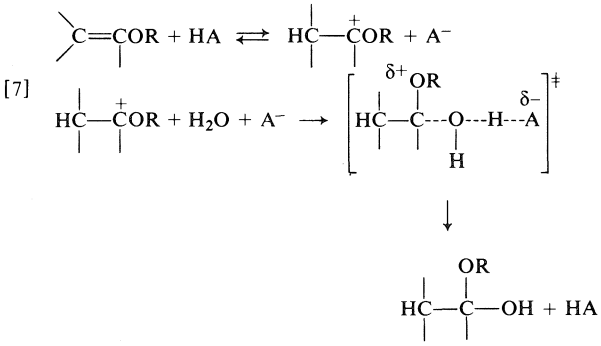
The hydrolysis of both of the vinyl ethers examined here shows general acid catalysis. This is the behavior expected for a reaction in which proton transfer from the catalyst to the substrate (eq. [1]) is rate-determining. A process in which proton transfer is rapid and reversible and hydration of the ensuing carbonium ion (eq. [2]) is the slow step would, on the other hand, lead to specific hydronium ion catalysis. The form of acid catalysis observed therefore suggests that the hydrolysis of these substrates proceeds by the conventional

Can. J. Chem. Downloaded from www.nrcresearchpress.com by 210.87.254.6 on 09/05/12
For personal use only.

mechanism in which substrate protonation is the rate-determining step.

This conclusion is supported by the large kinetic isotope effects found for the hydrolysis of these substrates when the catalyst is the hydronium ion, $k_{H^+}/k_{D^+} \simeq 3$. Isotope effects of this magnitude are to be expected for rate-determining proton transfer from the hydronium ion to a substrate which is a carbon base, and such isotope effects have in fact been found for a number of vinyl ether hydrolyses known to proceed by the conventional, rate-determining proton-transfer mechanism (6*b*). Rate-determining hydration preceded by rapidly reversible protonation, on the other hand, would be expected to give inverse isotope effects, $k_{H^+}/k_{D^+} < 1$, due principally to inverse isotope effects on the reversible pre-equilibrium protonation step. Since this prediction is quite at variance with the experimental findings, reversible protonation followed by rate-determining hydration must be rejected as a mechanistic possibility.

There is, however, a variant of the rejected mechanism which could produce hydronium ion isotope effects of the observed magnitude. In this mechanistic variation, rapidly reversible substrate protonation is followed by a hydration step in which the attacking water molecule gives up one of its protons to a general base simultaneously with C—O bond formation (eq. [7]). The primary isotope effect which such a process might show would offset the inverse isotope effect on the pre-equilibrium step, and the overall isotope effect could well be as great as $k_{H^+}/k_{D^+} = 3$. This scheme would also show overall general acid catalysis, which is consistent with the experimental observation.



[7]

This mechanism, however, is inconsistent with the fact that the isotope effects found for hydration of one of the present substrates, 1-ethoxy-3,3,-5,5-tetramethylcyclopentene, catalyzed by two different acids are both quite large: $k_H/k_D = 3.3$ for the hydronium ion and $k_H/k_D = 4.9$ for acetic acid. It has recently been discovered that isotope effects on proton transfer between electronegative atoms, such as the oxygens of the proton donor and proton acceptor in the scheme of eq. [7] under catalysis by hydronium ion and acetic acid, pass through a very narrow maximum as the pK_a difference between donor and acceptor is changed systematically (10). The width of this maximum is considerably less than the difference of seven pK_a units between the acid strengths of acetic acid and the hydronium ion, and it follows, therefore, that if one of these catalysts shows a large isotope effect in the present reaction operating through the mechanism of eq. [7], the other should not. The mechanism of eq. [7] must thus be inoperative.

Further support for a conventional mechanism with rate-determining substrate protonation comes from the good agreement between the presently observed hydronium ion isotope effects and values expected from a correlation of such isotope effects for a number of other vinyl ether hydrolyses. We found recently that hydronium ion isotope effects for the hydrolysis of some 30 vinyl ethers could be related to the free energies of activation of these reactions using a relationship suggested by Marcus rate theory (6*b*). This correlation predicts $k_{H^+}/k_{D^+} = 3.68$ for the hydrolysis of 1-ethoxy-3,3,5,5-tetramethylcyclopentene, whereas the observed value is $k_{H^+}/k_{D^+} = 3.32$, and it predicts $k_{H^+}/k_{D^+} = 3.06$ for the hydrolysis of 1-methoxy-2,3,3,5,5-pentamethylcyclopentene, whereas the observed value is $k_{H^+}/k_{D^+} = 2.70$.

It can be argued, moreover, that general base-catalyzed hydration of a carbocation such as that shown in eq. [7], would be unlikely in the present situation. Catalyzed hydrations of this kind have been found only in the case of relatively stable cations such as methoxy- or amino-substituted triarylmethyl ions (11), aryltropilium ions (12), and phthalimidinium ions (13). This is presumably because in these cases removal of a proton from the attacking water molecule simultaneously with C—O bond formation avoids generation of an unfavorable reaction intermediate (14); the protonated alcohol which would be formed in the absence of proton removal is less stable than either the carbocation or the alcohol itself, and provision of a route which bypasses this substance removes an unnecessary reaction barrier. The carbocations formed in vinyl ether hydrolysis, however, are considerably less stable than the ions listed above, and it is likely that they are less stable also than the protonated alcohols formed by their hydration. Bypassing these protonated alcohols via general base catalysis would therefore provide no particular mechanistic advantage, and the entropic requirement of a process of higher molecularity would militate against it.

Can. J. Chem. Downloaded from www.nrcresearchpress.com by 210.87.254.6 on 09/05/12
For personal use only.

Relative Reactivities

The arguments presented above show that the hydrolysis of the cyclopentenyl vinyl ethers investigated here occurs by the conventional, rate-determining substrate protonation mechanism which operates in the hydrolysis of most other vinyl ethers, and that I-strain has not succeeded in producing a mechanistic change. This result could not have been predicted beforehand, but it can now be rationalized after the fact using data which this study has provided.

1-Ethoxy-3,3,5,5-tetramethylcyclopentene is only slightly less reactive than its unmethylated analog, 1-ethoxycyclopentene; the rate constants for hydrolysis catalyzed by the hydronium ion are 270 M^{-1} s^{-1} and 454 M^{-1} s^{-1} (6*a*) respectively. This amounts to a rate reduction of only 0.59. The smallness of this change suggests that introduction of these four methyl groups into the system does not raise eclipsing strain very much at all, and that there is no appreciable difference in I-strain between 1-ethoxycyclopentene and its tetramethyl analog.

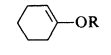
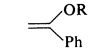
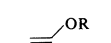
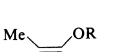
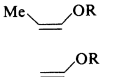
Further substitution of a fifth methyl group has a much greater rate effect: k_{H^+} for 1-methoxy-2,3,-3,5,5-pentamethylcyclopentene is only 2.98 M^{-1} s^{-1}, which makes this substrate 150 times less reactive than 1-ethoxycyclopentene and 90 times less reactive than 1-ethoxy-3,3,5,5-tetramethylcyclopentene. However, not all of this difference can be assigned to an increase in I-strain. The fifth methyl group introduced here is placed on the β-carbon atom of the vinyl ether function where it can stabilize the double bond and reduce the rate of reaction by lowering the free energy of the initial state; such substitution is known to slow vinyl ether hydrolysis in acyclic systems where I-strain is not a factor. Furthermore, the pentamethyl substrate is a methyl vinyl ether whereas the substances with which it is being compared are ethyl vinyl ethers, and methyl vinyl ethers have proved to be less reactive than their ethyl counterparts.

The effect of changing the saturated group from ethyl to methyl can be estimated by comparing rates of hydrolysis of ethyl and methyl vinyl ethers reported in the literature. Data for five such pairs are available; these (Table 4) show rate reductions in the range 0.43 to 0.53 and give an average value of 0.48 ± 0.02.

The effect of β-methyl substitution on double bond stability can also be evaluated by using information from the literature. The data here (Table 5) show significantly different rate retardations for *cis* than for *trans* methyl substitution, which can be understood in terms of unfavorable steric interference between methyl and alkoxy groups in the *cis* isomer. The quantity of interest in the present situation is of course the effect of *cis*-β-methyl substitution, and the data of Table 5 put this rate reduction at 0.31 ± 0.03.

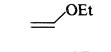
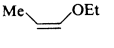
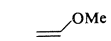
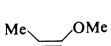
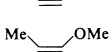
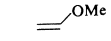
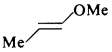
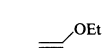
Use of these two factors to correct for the change in saturated alkoxy group and to eliminate the double-bond stabilizing effect gives (1/90)/(0.48 × 0.31) = 0.074 as the rate retardation attributable to the increase in I-strain in 1-methoxy-2,3,3,5,5-pentamethylcyclopentene over that in 1-ethoxy-3,3,5,5-tetramethylcyclopentene. This is considerably greater than the reduction of 0.59 found in

TABLE 4. Comparison of rates of hydronium-ion catalyzed hydrolysis of ethyl and methyl vinyl ethers in aqueous solution at 25°C[a]

Substrate	$k_{H^+}(M^{-1}s^{-1})$ R = Me	$k_{H^+}(M^{-1}s^{-1})$ R = Et	k(Me)/k(Et)
	42.3	80.0	0.53
	53.3	118.	0.45
	0.760	1.75	0.43
	0.255	0.480	0.53
	0.0720	0.160	0.45
			Av. 0.48 ± 0.02

[a]Data from ref. 6*b*; indicated error limits are standard deviations of mean values.

TABLE 5. Comparison of rates of hydronium-ion catalyzed hydrolysis of β-methyl substituted and unsubstituted vinyl ethers in aqueous solution at 25°C[a]

Substrate	$k_{H^+}(M^{-1}s^{-1})$	k(β-Me)/k(H)
	1.75	0.274
	0.480	
	0.760	0.335
	0.255	
	0.0252	0.0988
	0.760	0.0947
	0.0720	
	1.75	0.0914
	0.160	

[a]Data from ref. 6*b*.

going from 1-methoxycyclopentene to 1-methoxy-3,3,5,5-tetramethylcyclopentene. But the effect is still quite small: a rate factor of 0.074 corresponds to a free energy difference of only 1.5 kcal/mol. This could well be too little to effect a mechanistic change even in the present system where the free energies of the two transition states being affected are presumably quite similar.

Acknowledgements

We are grateful to the Natural Sciences and Engineering Research Council of Canada and the Petroleum Research Fund, administered by the American Chemical Society, for their financial support of this research.

1. A. J. KRESGE and H. J. CHEN. J. Am. Chem. Soc. **94**, 2818 (1972); A. J. KRESGE and W. K. CHWANG. J. Am. Chem. Soc. **100**, 1249 (1978).
2. J. D. COOPER, V. P. VITULLO, and D. L. WHALEN. J. Am. Chem. Soc. **93**, 6294 (1971).
3. Y. CHIANG, A. J. KRESGE, and C. I. YOUNG. Can. J. Chem. **56**, 461 (1978).
4. H. C. BROWN. Rec. Chem. Prog. **14**, 83 (1953); J. Chem. Soc. 1248 (1956).
5. R. B. TURNER and R. H. GARNER. J. Am. Chem. Soc. **80**, 1424 (1958); R. B. TURNER. *In* Theoretical organic chemistry. IUPAC Kekule Symposium. Butterworth & Co., London. 1959. p. 79; A. C. COPE, D. AMBROS, E. CIGANEK, C. F. HOWELL, and Z. JACURA. J. Am. Chem. Soc. **82**, 1750 (1960); J. HERLING, J. SHABATAI, and E. GIL-AV. J. Am. Chem. Soc. **87**, 4107 (1965); A. KANKAANPERA, E. TASKINEN, and P. SALOMAA. Acta Chem. Scand. **21**, 2487 (1967).
6. (*a*) A. J. KRESGE, H. L. CHEN, Y. CHIANG, E. MURRILL, M. A. PAYNE, and D. S. SAGATYS. J. Am. Chem. Soc. **93**, 413 (1971); (*b*) A. J. KRESGE, D. S. SAGATYS, and H. L. CHEN. J. Am. Chem. Soc. **99**, 7228 (1977).
7. E. A. GUGGENHEIM. Philos. Mag. **2**, 538 (1926).
8. E. S. SWINBOURNE. J. Chem. Soc. 2371 (1960).
9. R. G. BATES. Determination of pH. John Wiley and Sons, New York. 1973. p. 49.
10. N. A. BERGMAN, Y. CHIANG, and A. J. KRESGE. J. Am. Chem. Soc. **100**, 5954 (1978); M. M. COX and W. P. JENCKS. J. Am. Chem. Soc. **100**, 5956 (1978).
11. C. D. RITCHIE. J. Am. Chem. Soc. **94**, 3275 (1972); C. D. RITCHIE, D. J. WAIGHT, D. S. HUANG, and A. A. KAMEGO. J. Am. Chem. Soc. **97**, 1163 (1975); J. N. RIDE, P. A. H. WYATT, and Z. M. ZOCHOWSKI. J. Chem. Soc. Perkin Trans. II, 1188 (1974).
12. C. D. RITCHIE, R. J. MINASZ, A. A. KAMEGO, and M. SAWADA. J. Am. Chem. Soc. **99**, 3747 (1977).
13. W. P. JENCKS and N. GRAVITZ. J. Am. Chem. Soc. **96**, 489 (1974).
14. W. P. JENCKS. Chem. Rev. **72**, 705 (1972).

Can. J. Chem. Downloaded from www.nrcresearchpress.com by 210.87.254.6 on 09/05/12
For personal use only.

Synthesis and reactions of 1-hydroxy-1-(pyridinyl)-2-propanones

EDWARD E. KNAUS,[1] KAMLAKAR AVASTHI, KINFE REDDA, AND ABRAHAM BENDERLY

Faculty of Pharmacy and Pharmaceutical Sciences, University of Alberta, Edmonton, Alta., Canada T6G 2N8

Received August 28, 1979

EDWARD E. KNAUS, KAMLAKAR AVASTHI, KINFE REDDA, and ABRAHAM BENDERLY. Can. J. Chem. **58**, 130 (1980).

Reaction of pyridinecarboxaldehydes **1** with α-ethoxyvinyllithium **2** affords 2-ethoxy-1-(pyridinyl)-2-propen-1-ols **3** which on hydrolysis with aqueous formic acid give pyridinyl α-hydroxyketones **4**. Selenium dioxide oxidation of **4***a* and **4***b* provides pyridinyl α-diketones **9** which on condensation with *o*-phenylenediamine afford 3-methyl-2-(pyridinyl) quinoxalines **11**. Pyridinyl α-hydroxyketones **4***a* and **4***b* react with hydroxylamines to yield a mixture of *E*- and *Z*-oximes **5** and **6**.

EDWARD E. KNAUS, KAMLAKAR AVASTHI, KINFE REDDA et ABRAHAM BENDERLY. Can. J. Chem. **58**, 130 (1980).

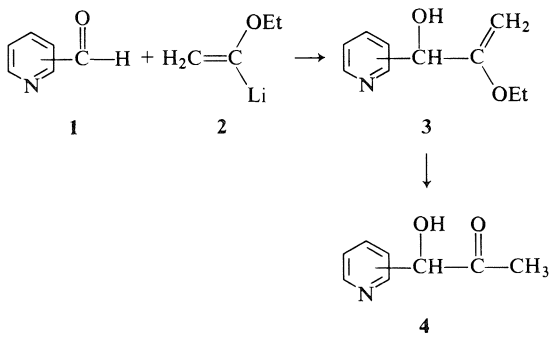
La réaction des pyridinecarboxaldéhydes **1** avec l'α-éthoxyvinyllithium **2** fournit les éthoxy-2 (pyridinyl)-1 propèn-2 ols-1 **3** qui par hydrolyse avec l'acide formique en solution aqueuse conduisent aux pyridinyl α hydroxycétones **4**. L'oxydation de **4***a* et **4***b* par le bioxyde de sélénium conduit aux pyridinyl α dicétones **9** qui condensés sur la *o*-phénylènediamine produisent les méthyl-3 (pyridinyl)-2 quinoxalines **11**. Les pyridinyl-α hydroxycétones **4***a* et **4***b* réagissent avec des hydroxylamines pour donner des mélanges d'oximes *E* et *Z*, **5** et **6**.

[Traduit par le journal]

Can. J. Chem. Downloaded from www.nrcresearchpress.com by 210.87.254.105 on 09/05/12
For personal use only.

The phenethyl group is a common structural feature present in many classes of drugs such as β-adrenergic blocking agents, bronchodilators, CNS stimulants, and vasoconstrictors (1). To date there have been very few studies involving the synthesis of bioisosteric compounds having the pyridinyl ethyl structural feature (2, 3). The reaction of α-methoxy and α-ethoxyvinyllithium with aryl (alkyl) aldehydes and ketones as a method of preparing aryl (alkyl) α-hydroxyketones has been reported (4, 5). It would be of interest, therefore, to prepare medicinal precursors which could subsequently be elaborated to compounds having the pyridinyl moiety as part of a freely rotating, semi-rigid, or rigid conformation. We now describe the synthesis of pyridinyl α-hydroxyketones and α-diketones, and their reaction with amines.

Reaction of 4-pyridinecarboxaldehyde **1***a* with the masked acyl anion α-ethoxyvinyllithium **2**, obtained by treatment of ethyl vinyl ether with *tert*-butyllithium (4, 5), at −65°C under nitrogen afforded 2-ethoxy-1-(4-pyridinyl) -2- propen-1-ol (**3***a*, 82%). Similar reactions of **1***b* and **1***c* with **2** gave the respective hydroxy enol ethers **3***b* (65%) and **3***c* (50%). Hydrolysis of hydroxy enol ethers **3***a* and **3***b* using 44% aqueous formic acid with ether methylene chloride (14:11 v/v) as solvent at 25°C for 4 h gave rise to the respective α-hydroxyketones **4***a* (62.9%) and **4***b* (82.9%). A similar hydrolysis of the 2-substituted pyridine **3***c* resulted in complete cleavage of the enol ether. The ^{1}H nmr spectrum of the unpurified reaction mixture exhibited those absorptions expected for the α-diketone



a 4-Pyridyl, *b* 3-Pyridyl, *c* 2-Pyridyl

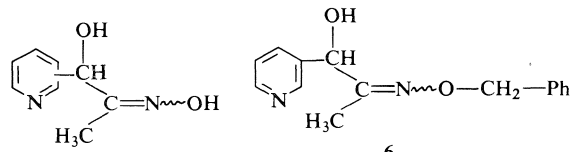
9*c* rather than the α-hydroxyketone **4***c*. All attempts to purify this reaction mixture resulted in extensive decomposition. An impure sample of the α-diketone **9***c* was obtained after neutral alumina oxide column chromatography (about 12% from **3***c*). The mass spectrum of **9***c* exhibited a molecular ion at *m/e* 149 (*Exact Mass* calcd. for $C_8H_7NO_2$: 149.0477; found (high resolution ms): 149.0475) while the ^{1}H nmr spectrum displayed a 3H singlet at 2.58 due to the methyl absorption as well as the absorptions due to those of a 2-substituted pyridine ring. Other hydrolytic procedures investigated indicated that **3***b* was inert to 0.2 *N* aqueous methanolic HCl at 25°C for 12 h whereas treatment with 3 *N* aqueous methanolic HCl afforded a complex mixture of products.

Reaction of α-hydroxyketones **4***a* and **4***b* with hydroxyl amines gave rise to oximes. For example, reaction of **4***a* and **4***b* with hydroxylamine afforded **5***a* (27.6%) and **5***b* (63.3%) respectively, while treatment of **4***b* with *O*-benzylhydroxylamine yielded oxime **6** (62.5%). The respective ^{1}H nmr

[1]Author to whom correspondence should be addressed.

0008-4042/80/020130-04$01.00/0

©1980 National Research Council of Canada/Conseil national de recherches du Canada

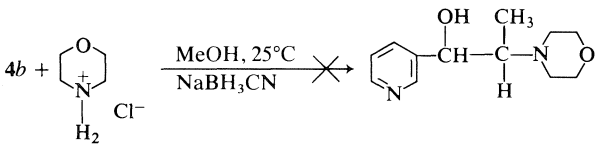


5 6

a 4-Pyridyl, *b* 3-Pyridyl

spectra of **5***a*, **5***b*, and **6** exhibited dual methyl absorptions at δ 1.68 and 1.76, 1.7 and 1.83, and 1.7 and 1.88 in ratios of 5:1, 3:1, and 12:1. These spectral data suggest that oximes **5** and **6** exist as a mixture of *E*- and *Z*-isomers. Oximes **5** and **6** were not elaborated further.

The reductive amination of the α-hydroxyketone **4***b* with morpholine hydrochloride **7** in the presence of sodium cyanoborohydride over the pH range 4–7.5 was investigated as a method to prepare the aminoalcohol **8**. The reaction gave a complex mix-

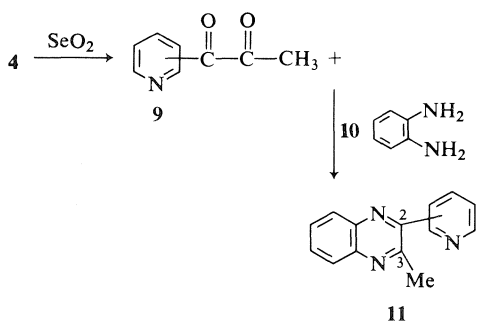


7 8

ture of products which did not contain **8**. Other attempts to generate the iminium species by reaction of **4***b* with morpholine using molecular sieves or titanium tetrachloride as water scavengers were also unsuccessful (6). The failure of **4***b* to react with secondary amines such as morpholine or pyrrolidine may be due to strong hydrogen bonding between the hydroxyl and carbonyl groups of **4***b*.

Oxidation of α-hydroxyketones **4***a* and **4***b* using selenium dioxide afforded the α-diketones **9***a* (42.9%) and **9***b* (32%) respectively. Condensation of the α-diketones **9***a* and **9***b* with *o*-phenylenediamine **10** gave the quinoxalines **11***a* (72%) and **11***b* (79.2%) respectively.

The pyridyl α-hydroxyketones **4** and α-diketones **9** will be used in subsequent studies involving the



9 10 11

a 4-Pyridyl, *b* 3-Pyridyl, *c* 2-Pyridyl

design of new nitrogen heterocycles with pharmacological activity.

Experimental

Melting points were determined with a Büchi capillary apparatus and are uncorrected. Nuclear magnetic resonance spectra were determined in deuterochloroform (unless otherwise noted) with TMS as internal standard with a Varian EM-360 A spectrometer. Infrared spectra (potassium bromide unless otherwise noted) were taken on a Unicam SP-1000 or Perkin Elmer 267 spectrometer. Mass spectra were measured with an AEI-MS-50 mass spectrometer and these exact mass measurements are used almost exclusively in lieu of elemental analyses. All of the products described gave rise to a single spot on tlc using a solvent system less polar and more polar than the specific solvent system described for purification of the reaction mixture. No residue remained after combustion of the products purified by tlc or column chromatography.

*2-Ethoxy-1-(4-pyridinyl)-2-propen-1-ol (***3***a)*

General Procedure A

To a solution of ethyl vinyl ether (5.04 g, 70 mmol) in 30 mL anhydrous tetrahydrofuran, under a nitrogen atmosphere at −65°C, *tert*-butyllithium (3.01 g, 47 mmol) in pentane (29.4 mL) was added dropwise with stirring during 25 min. The cooling bath was removed and the yellow solid slowly redissolved as the temperature was allowed to warm from −65°C to 0°C over a period of 20 min. This solution was cooled to −65°C and a solution of 4-pyridinecarboxaldehyde (5 g, 46.7 mmol) in 30 mL dry tetrahydrofuran was added dropwise over a period of 45 min. The resulting dark brown mixture was allowed to warm gradually to 25°C over a 2 h period. The mixture was then cooled to 0°C and 50 mL of 20% aqueous ammonium chloride was added with stirring for 5 min followed by an additional 50 mL water. The organic layer was separated and the aqueous fraction was extracted with ether – methylene chloride (14:11 v/v) (3 × 30 mL). The combined organic extracts were washed with water and brine. Drying (Na_2SO_4) and removal of the solvent *in vacuo* gave **3***a* along with an impurity as indicated by ^{1}H nmr. Dissolution of the reaction mixture in 20 mL ether – methylene chloride (14:11 v/v) and then washing with 2.5 *N* sodium hydroxide (3 × 20 mL) removes the impurity. Drying the ether – methylene chloride layer (Na_2SO_4) and removal of the solvent *in vacuo* afforded **3***a* as a white solid (6.85 g, 82%); mp: 72–73°C; ir: 1420 and 1660 (s, C=CH_2) cm^{-1}; ^{1}H nmr δ: 1.21 (t, $J_{CH_2CH_3}$ = 7 Hz, 3H, CH_3), 3.72 (q, $J_{CH_2CH_3}$ = 7 Hz, 2H, —CH_2CH_3), 4.11 (d, J_{gem} = 2.5 Hz, 1H, C=C(H)(H)), 4.36 (d, J_{gem} = 2.5 Hz, 1H, C=C(H)(H)), 5.12 (s, 1H, —C*H*), 5.45 (broad s, 1H, OH, exchanges with deuterium oxide), 7.42 (d, $J_{2,3} = J_{5,6}$ = 5 Hz of d, $J_{3,5}$ = 1.5 Hz, 2H, H-3, H-5), 8.5 (d, $J_{2,3} = J_{5,6}$ = 5 Hz of d, $J_{2,5} = J_{3,6}$ = 1 Hz, 2H, H-2, H-6). *Exact Mass* calcd. for $C_{10}H_{13}NO_2$: 179.0946; found (high resolution ms): 179.0954.

*2-Ethoxy-1-(3-pyridinyl)-2-propen-1-ol (***3***b)*

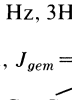
Reaction of 3-pyridinecarboxaldehyde (5 g, 46.7 mmol) with α-ethoxyvinyllithium (47 mmol) and completion of the reaction as described under General Procedure *A* gave **3***b* as a pale yellow semi-solid (5.43 g, 65%); ir (neat): 3300 (br m, OH), 1430, and 1660 (m, C=CH_2) cm^{-1}; ^{1}H nmr δ: 1.2 (t, $J_{CH_2CH_3}$ = 7 Hz, 3H, CH_3), 3.71 (q, $J_{CH_2CH_3}$ = 7 Hz, 2H, —CH_2CH_3), 4.08 (d, J_{gem} = 2.5 Hz, 1H, C=C(H)(H)), 4.35 (d, J_{gem} = 2.5 Hz, 1H,

Can. J. Chem. Downloaded from www.nrcresearchpress.com by 210.87.254.105 on 09/05/12
For personal use only.

Can. J. Chem. Downloaded from www.nrcresearchpress.com by 210.87.254.105 on 09/05/12
For personal use only.

), 5.12 (s, 1H, —CH—), 5.42 (broad s, 1H, OH, exchanges with deuterium oxide), 7.23 (d, $J_{4,5}$ = 8.5 Hz of d, $J_{5,6}$ = 5 Hz, 1H, H-5), 7.82 (d, $J_{4,5}$ = 8.5 Hz of d, $J_{4,6}$ = 1.75 Hz of d, $J_{2,4}$ = 1.75 Hz, 1H, H-4), 8.4 (d, $J_{5,6}$ = 5 Hz of d, $J_{4,6}$ = 1.75 Hz, 1H, H-6), 8.56 (d, $J_{2,4}$ = 1.75 Hz, 1H, H-2). *Exact Mass* calcd. for $C_{10}H_{13}NO_2$: 179.0946; found (high resolution ms): 179.0950.

*2-Ethoxy-1-(2-pyridinyl)-2-propen-1-ol (**3**c)*

Reaction of 2-pyridinecarboxaldehyde (5 g, 46.7 mmol) with α-ethoxyvinyllithium (47 mmol) and completion of the reaction as described under General Procedure *A* gave **3***c* as a pale yellow semi-solid (4.24 g, 50.7%); ir: 1445 and 1630 (m, C=CH_2) cm^{-1}; ^1H nmr δ: 1.23 (t, $J_{CH_2CH_3}$ = 7 Hz, 3H, CH_3), 3.8 (q, $J_{CH_2CH_3}$ = 7 Hz, 2H, —CH_2CH_3), 4.1 (d, J_{gem} = 2.5 Hz, 1H, ), 4.41 (d, J_{gem} = 2.5 Hz, 1H, ), 5.15 (broad s, 2H, —CH—, OH, exchanges with deuterium oxide), 7.1–7.58 (complex m, 2H, H-3, H-5), 7.72 (d, $J_{4,5}$ = 8 Hz of d, $J_{3,4}$ = 8 Hz of d, $J_{4,6}$ = 2 Hz, 1H, H-6). *Exact Mass* calcd. for $C_{10}H_{12}NO$ (M^+ − OH): 162.0873; found (high resolution ms): 162.0922 (base peak).

*1-Hydroxy-1-(4-pyridinyl)-2-propanone (**4**a)*

General Procedure B

To a solution of the enol ether **3***a* (1 g, 5.58 mmol) in 10 mL ether – methylene chloride (14:11 v/v) was added 2 mL 88% formic acid and 2 mL water. Solid sodium carbonate was added until the reaction mixture was just alkaline to litmus paper and the mixture was allowed to stir for a further 30 min. The reaction mixture was eluted from a 2.5 × 20 cm column of sodium sulfate using 600 mL ether – methylene chloride (14:11 v/v) to yield **4***a* as a pale yellow semi-solid (0.531 g, 62.9%); ir (neat): 3400 (m, OH) and 1725 (s, CO) cm^{-1}; ^1H nmr δ: 2.23 (s, 3H, CH_3), 5.28 (s, 1H, —CH—), 6.64 (broad s, 1H, OH, exchanges with deuterium oxide), 7.5 (d, $J_{2,3}$ = $J_{5,6}$ = 5 Hz of d, $J_{3,5}$ = 1.5 Hz, 2H, H-3, H-5), 8.64 (d, $J_{5,6}$ = 5 Hz of d, $J_{3,6}$ = $J_{2,5}$ = 1 Hz, 2H, H-2, H-6). *Exact Mass* calcd. for $C_8H_9NO_2$: 151.0633; found (high resolution ms): 151.0631.

*1-Hydroxy-1-(3-pyridinyl)-2-propanone (**4**b)*

Hydrolysis of the enol ether **3***b* (1 g, 5.58 mmol) using aqueous formic acid and completion of the reaction as described under General Procedure *B* afforded **4***b* as a yellow semi-solid (0.70 g, 82.9%); ir: 3400 (m, OH) and 1725 (s, CO) cm^{-1}; ^1H nmr δ: 2.17 (s, 3H, CH_3), 5.19 (s, 1H, —CH—), 5.4 (s, 1H, OH, exchanges with deuterium oxide), 7.32 (d, $J_{4,5}$ = 8.5 Hz of d, $J_{5,6}$ = 5 Hz, 1H, H-5), 7.71 (d, $J_{4,5}$ = 8.5 Hz of d, $J_{4,6}$ = 2 Hz of d, $J_{2,4}$ = 2 Hz, 1H, H-4), 8.57 (d, $J_{5,6}$ = 5 Hz of d, $J_{4,6}$ = 2 Hz, 1H, H-6), 8.65 (d, $J_{2,4}$ = 2 Hz, 1H, H-2). *Exact Mass* calcd. for $C_8H_9NO_2$: 151.0633; found (high resolution ms): 151.0635.

*1-Hydroxy-1-(4-pyridinyl)-2-propanone oxime (**5**a)*

General Procedure C

To a stirred solution of α-hydroxyketone **4***a* (0.27 g, 1.788 mmol) in 40 mL methanol at 0°C was added sodium acetate (0.149 g, 1.817 mmol) and hydroxylamine hydrochloride (0.124 g, 1.788 mmol). The reaction mixture was allowed to stir for 2 h at 25°C prior to pouring onto 100 mL water. Extraction with chloroform (4 × 100 mL), drying (Na_2SO_4), and removal of the solvent *in vacuo* gave a pale yellow solid which was purified using six 20 cm × 20 cm silica gel G plates, 0.75 mm in thickness, with ethyl acetate as development solvent. Extraction of the fraction having R_f 0.29 using 200 mL warm methanol afforded **5***a* (0.082 g, 27.63%); mp 149–151°C; ir: 3240 (m, C—OH), 2805 and 2680 (m, =N—OH), and 1610 (s, C=N—) cm^{-1}; ^1H nmr δ ($CDCl_3$ + DMSO-d_6): 1.68 and 1.76 (s, 3H, CH_3), 3.34 (s, 1H, =N—OH, exchanges with deuterium oxide), 5.28 (s, 1H, C*H*—OH), 5.88 (broad s, 1H, C—O*H*, exchanges with deuterium oxide), 7.41 (d, $J_{2,3}$ = $J_{5,6}$ = 5 Hz of d, $J_{3,5}$ = 1.5 Hz, 2H, H-3, H-5), 8.6 (d, $J_{2,3}$ = $J_{5,6}$ = 5 Hz of d, $J_{2,5}$ = $J_{3,6}$ = 1 Hz, 2H, H-2, H-6). *Exact Mass* calcd. for $C_8H_{10}N_2O_2$: 166.0743; found (high resolution ms): 166.0745. *Anal.* calcd. for $C_8H_{10}N_2O_2$: C 57.82, H 6.06; found: C 58.02, H 6.02.

*1-Hydroxy-1-(3-pyridinyl)-2-propanone oxime (**5**b)*

Reaction of the α-hydroxyketone **4***b* (0.283 g, 1.87 mmol) with hydroxylamine hydrochloride (0.131 g, 1.87 mmol) in the presence of sodium acetate (0.307 g, 3.74 mmol) and completion of the reaction as described under General Procedure *C* including purification by preparative tlc gave **5***b*, having R_f 0.5, as a white solid (0.197 g, 63.3%); mp 133–135°C; ir: 3250 (m, C—OH), 2720 (m, =N—OH), and 1590 (m, C=N) cm^{-1}; ^1H nmr (DMSO-d_6) δ: 1.7 and 1.83 (s, 3H, C*H*$_3$), 3.48 (s, 1H, =NOH, exchanges with deuterium oxide), 5.3 (s, 1H, —CH—), 5.9 (broad s, 1H, CH—OH, exchanges with deuterium oxide), 7.38 (d, $J_{4,5}$ = 8.5 Hz of d, $J_{5,6}$ = 5 Hz, 1H, H-5), 7.8 (d, $J_{4,5}$ = 8.5 Hz of d, $J_{4,6}$ = 2 Hz of d, $J_{2,4}$ = 2 Hz, 1H, H-4), 8.51 (d, $J_{5,6}$ = 5 Hz of d, $J_{4,6}$ = 2 Hz, 1H, H-6), 8.6 (d, $J_{2,4}$ = 2 Hz, 1H, H-2). *Exact Mass* calcd. for $C_8H_{10}N_2O_2$: 166.0743; found (high resolution ms): 166.0744. *Anal.* calcd. for $C_8H_{10}N_2O_2$: C 57.82, H 6.06; found: C 57.73, H 6.04.

*1-Hydroxy-1-(3-pyridinyl)-2-propanone O-(Phenylmethyl)oxime (**6**)*

O-Benzylhydroxylamine hydrochloride (0.318 g, 1.99 mmol) was added to a solution of α-hydroxyketone **4***b* (0.304 g, 2.01 mmol) in 30 mL methanol at 0°C and the reaction was allowed to proceed at 0°C for 1 h and then at 25°C for 6 h with stirring. The reaction mixture was poured onto 100 mL water. Extraction with chloroform (4 × 50 mL), drying (Na_2SO_4), and removal of the solvent *in vacuo* yielded **6** as a pale yellow solid (0.323 g, 62.5%); mp 92–94°C; ir: 3150–3200 (m, C—OH), 2700 (m, =NOH), 1590, and 1660 (s, C=N) cm^{-1}; ^1H nmr δ: 1.7 and 1.88 (s, 3H, CH_3), 4.56 (s, 1H, OH, exchanges with deuterium oxide), 5.18 and 5.27 (s, 2H, —OCH_2—), 7.32 (m, 6H, H-5, C_6H_5), 7.7 (d, $J_{4,5}$ = 8.5 Hz of d, $J_{4,6}$ = 2 Hz of d, $J_{2,4}$ = 2 Hz, 1H, H-4), 8.55 (m, 2H, H-2, H-6). *Exact Mass* calcd. for $C_{15}H_{16}N_2O_2$: 256.1212; found (high resolution ms): 256.1214.

*1-(4-Pyridinyl)-2,3-propanedione (**9**a)*

General Procedure D

To a solution of selenium dioxide (1.11 g, 10 mmol) in 40 mL dioxane and 1 mL water was added at once a solution of the α-hydroxyketone **4***a* (2.42 g, 16 mmol) in 20 mL dioxane. The reaction mixture changes from white to orange during the addition of **4***a* and a dark red precipitate soon begins to separate. The reaction was allowed to continue 12 h with stirring. The solvent dioxane was removed by decantation and transferred to another flask. The residual dark red solid deposited on the sides of the reaction flask was washed with methylene chloride (2 × 10 mL). Removal of the solvent *in vacuo* from the combined dioxane and methylene chloride fractions gave a dark reddish-black liquid containing suspended solid which was purified on a neutral alumina column (30 g). Elution with benzene – ethyl acetate (1:1 v/v, 100 mL) afforded **9***a* (1.02 g, 42.9%) as a pale yellow solid; mp 86–88°C; ir: 1730 and 1740 (s, CO) cm^{-1}; ^1H nmr δ: 2.57 (s, 3H, CH_3), 7.88 (d, $J_{2,3}$ = $J_{5,6}$ = 5 Hz of d, $J_{3,5}$ = 1.5 Hz, 2H, H-3, H-5), 8.9 (d, $J_{2,3}$ = $J_{5,6}$ = 5 Hz of d, $J_{2,5}$ = $J_{3,6}$ = 1 Hz, 2H, H-2, H-6). *Exact Mass* calcd. for $C_8H_7NO_2$: 149.0477; found (high resolution ms): 149.0477.

*1-(3-Pyridinyl)-2,3-propanedione (**9**b)*

Oxidation of the α-hydroxyketone **4***b* (2.42 g, 16 mmol) using

selenium dioxide (1.11 g, 10 mmol), completion of the reaction and neutral alumina oxide chromatography of the reaction mixture as described under General Procedure *D* gave **9***b* as a pale yellow oil (0.76 g, 32%); ir (film): 1680, 1720, and 1775 (s, CO) cm^{-1}; ^1H nmr δ: 2.52 (s, 3H, CH_3), 7.42 (d, $J_{4,5}$ = 8.5 Hz of d, $J_{5,6}$ = 5 Hz, 1H, H-5), 8.36 (d, $J_{4,5}$ = 8.5 Hz of d, $J_{2,4}$ = 2 Hz of d, $J_{4,6}$ = 2 Hz, 1H, H-4), 8.84 (d, $J_{5,6}$ = 5 Hz of d, $J_{4,6}$ = 2 Hz, 1H, H-6), 9.26 (d, $J_{2,4}$ = 2 Hz, 1H, H-2). *Exact Mass* calcd. for $C_8H_7NO_2$: 149.0477; found (high resolution ms): 149.0478.

*3-Methyl-2-(4-pyridinyl)quinoxaline (**11**a)*

General Procedure E

A solution of the α-diketone **9***a* (0.215 g, 1.44 mmol) and *o*-phenylenediamine **10** (0.16 g, 1.48 mmol) in 20 mL absolute ethanol was boiled under reflux for 6 h. Removal of the solvent *in vacuo* gave a light yellow-green solid which was purified on a neutral alumina column (10 g). Elution with ethyl acetate (25 mL) afforded **11***a* (0.23 g, 72.33%); mp 135–137°C; ir: 1595 (s, C=N) cm^{-1}; ^1H nmr δ: 2.84 (s, 3H, CH_3), 7.55–8.4 (complex m, 6H, phenyl hydrogens, H-3, H-5, pyridine), 8.9 (d, $J_{2,3}$ = $J_{5,6}$ = 5 Hz of d, $J_{2,5}$ = $J_{3,6}$ = 1 Hz, 2H, H-2, H-6, pyridine). *Exact Mass* calcd. for $C_{14}H_{11}N_3$: 221.0953; found (high resolution ms): 221.0948.

*3-Methyl-2-(3-pyridinyl)quinoxaline (**11**b)*

Reaction of the α-diketone **9***b* (0.309 g, 2.08 mmol) with *o*-phenylenediamine (0.227 g, 2.1 mmol) in 30 mL absolute ethanol followed by purification as described under General Procedure *E* gave **11***b* as a pale yellow solid (0.364 g, 79.2%); mp 95–97°C; ir: 1550, 1560, 1575, and 1590 (s, C=N) cm^{-1}; ^1H nmr δ: 2.82 (s, 3H, CH_3), 7.56 (d, $J_{4,5}$ = 8.5 Hz of d, $J_{5,6}$ = 5 Hz, 1H, H-5, pyridine), 7.7–8.3 (complex m, 5H, phenyl hydrogens, H-4, pyridine), 8.78 (d, $J_{5,6}$ = 5 Hz of d, $J_{4,6}$ = 2 Hz, 1H, H-6, pyridine), 9.0 (d, $J_{2,4}$ = 2 Hz, 1H, H-2, pyridine). *Exact Mass* calcd. for $C_{14}H_{11}N_3$: 221.0953; found (high resolution ms): 221.0940.

Acknowledgement

We are grateful to the National Research Council of Canada (Grant A0531) for financial support of this work.

1. C. O. Wilson, O. Gisvold, and R. F. Doerge. Textbook of organic medicinal and pharmaceutical chemistry. 7th ed. J. B. Lippincott Co., Toronto. 1977.
2. C. H. Gnewuch and H. L. Friedman. J. Med. Chem. **15**, 1321 (1972).
3. T. Jen, J. S. Frazee, M. S. Schwartz, C. Kaiser, D. F. Colella, and J. R. Wardell, Jr. J. Med. Chem. **20**, 1258 (1977).
4. J. E. Baldwin, G. A. Hofle, and O. W. Lever, Jr. J. Am. Chem. Soc. **96**, 7125 (1974).
5. U. Schollkopf and P. Hanssle. Justus Liebigs Ann. Chem. **763**, 208 (1972).
6. R. Carlson, L. Nilsson, C. Rappe, A. Babadjamian, and J. Metzger. Acta Chem. Scand. **32**, 85 (1978); R. Carlson, R. P. T. Luu, D. Mathieu, F. A. Ahouande, A. Babadjamian, and J. Metzger. Acta Chem. Scand. **32**, 335 (1978).

Can. J. Chem. Downloaded from www.nrcresearchpress.com by 210.87.254.105 on 09/05/12
For personal use only.

Carbon catalyzed organic reactions: carbon promoted solvolysis of a phosphate ester derived from 1,1′-bi-2-naphthol

YUMIKO Y. HOYANO AND RICHARD E. PINCOCK

Department of Chemistry, University of British Columbia, Vancouver, B.C., Canada V6T 1W5

Received July 11, 1979

YUMIKO Y. HOYANO and RICHARD E. PINCOCK. Can. J. Chem. **58**, 134 (1980).

Active carbons which catalyze the racemization of 1,1′-binaphthyl are not effective in racemizing the 2,2′-dihydroxyl and the 8,8′-dicarbomethoxyl derivatives of binaphthyl. The 2,2′-binaphthyl methyl phosphate ester derived from optically active 1,1′-bi-2-naphthol undergoes slow thermal racemization at 190°C ($t_{1/2}$ 100 min, $\Delta H^{\neq}$ 26.1 kcal/mol, $\Delta S^{\neq}$ −21 cal/mol deg) in triglyme and this racemization rate is also unaffected by active carbon. However, in the hydroxylic solvent 2-(2-ethoxyethoxy)ethanol at 130°C the rate of solvolysis of the phosphate ester is increased ca. tenfold by carbon blacks or decolorizing carbon at 1 mg/mL concentration. Control experiments show that the acceleration is not due to soluble impurities released by the carbons; heterogeneous catalysis, probably by acidic and/or nucleophilic functional groups on the carbon surfaces, is involved.

YUMIKO Y. HOYANO et RICHARD E. PINCOCK. Can. J. Chem. **58**, 134 (1980).

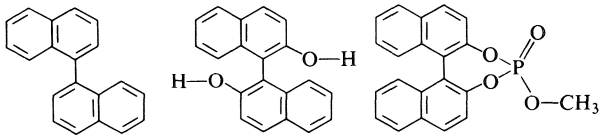
Les charbons actifs qui catalysent la racémisation du binaphtyle-1,1′ ne sont pas efficaces dans le cas des dérivés dihydroxyl-2,2′ et dicarbométhoxyl-8,8′ du binaphtyle. L'ester méthylique du binaphtyl-2,2′ phosphate derivé du bi-2 naphtol-1,1′ optiquement actif subit une racémisation lente à 190°C ($t_{1/2}$ 100 min, $\Delta H^{\neq}$ 26.1 kcal/mol, $\Delta S^{\neq}$ −21 cal/mol deg) dans le triglyme et cette vitesse de racémisation n'est pas affectée par le charbon actif. Cependant dans un solvant hydroxylé comme le (éthoxyéthoxy-2)-2 éthanol à 130°C, le charbon noir ou le charbon décolorant à une concentration de 1 mg/mL augmente d'environ 10 fois la vitesse de solvolyse de l'ester phosphorique. Des expériences de contrôle mettent en relief le fait que l'augmentation de vitesse n'est pas due aux impuretés solubles libérées par les charbons. On pense plutôt à une catalyse hétérogène due probablement à des groupes fonctionnels acides ou nucléophiles présents sur la surface du charbon.

[Traduit par le journal]

1,1′-Binaphthyl, **1**, is sufficiently hindered around the interannular bond so that thermal rotation of this bond is slow at room temperature. However, the rotation can be very effectively promoted by suspensions of carbon blacks or activated carbons and catalytic racemization of optically active binaphthyl is thereby rapidly achieved (1). The kinetics of this heterogeneous catalytic reaction have been presented in some detail (2) but extensions of this interesting reaction type remain unexplored.

We have investigated the possibility that the barrier to rotation in a highly hindered binaphthyl derivative, such as in 1,1′-bi-2-naphthol **2**, where the presence of the two hydroxyl groups prevents rotation except at high temperatures (3), might be lowered by the catalytic power of adsorption on carbon blacks. Also the multitude of functional groups on part of the active carbon surface (4) suggested, in addition, that both electrophilic and nucleophilic catalysis of some reactions (e.g., ester hydrolysis) may occur during adsorption on carbon. Indeed, together with the many examples of catalysis by carbon of inorganic reactions, of oxidations, and of hydrocarbon isomerizations, there are a few reports of solvolysis reactions catalyzed by carbon (5).

We have therefore extended our catalytic studies to the methyl phosphate ester **3** derived from optically active binaphthol **2**. This compound presents the possibilities both of catalyzed racemization related to that of 1,1′-binaphthyl as well as ester solvolysis of the phosphate moiety. It was hoped that a demonstration of solvolytic activity by carbon could supply an initial model for possible catalytic properties of carbon (in addition to its well-known adsorption properties) during removal of pesticides and other contaminates from water (6). The phosphate ester **3** was therefore chosen to be investigated both because of its relationship to binaphthyl and its likely adsorption due to the presence of larger aromatic groups, but also as a model for potential reactions of biological phosphate esters and related insecticides.



1 **2** **3**

Results and Discussion

The 2,2′-dihydroxyl derivative of 1,1′-binaphthyl is optically stable over long periods at 100°C in neutral solvents but is considerably racemized within a day in basic or acidic conditions near this temperature (3). At 150°C in diglyme the compound

0008-4042/80/020134-04$01.00/0

©1980 National Research Council of Canada/Conseil national de recherches du Canada

Can. J. Chem. Downloaded from www.nrcresearchpress.com by 210.87.254.42 on 09/05/12
For personal use only.

Can. J. Chem. Downloaded from www.nrcresearchpress.com by 210.87.254.42 on 09/05/12
For personal use only.

is only 10% racemized after 20 h and, in spite of sensitivity of the racemization rate to acidic and basic catalysis, the addition of active carbons (Norite or Spheron 6) had no effect on this slow racemization.

The phosphate ester **3** derived from bi-2-naphthol, **2**, is also highly optically stable. The phosphate ring compels the rotation to proceed only by passage of the 8 and 8′ positions past each other rather than the less hindering 8′ and 2 (and 8 and 2′) positions as a binaphthyl and its 2,2′-dihydroxyl derivative. Slow racemization of **3** in triglyme proceeds only near 190°C ($t_{1/2}$ 100 min) with $\Delta H^{\ddagger}$ 26.1 kcal/mol, $\Delta S^{\ddagger}$ −21 cal/mol deg. Addition of Norite or Spheron 6 to solutions of the phosphate ester had no effect on the loss of optical activity in this solvent.

Similarly, another derivative of 1,1′-binaphthyl, this one with carbomethoxy groups in the 8 and 8′ positions and a low barrier to rotation corresponding to a half life of 23 min at 50°C (7), showed no catalysis of racemization by Norite under conditions where binaphthyl itself is very rapidly racemized by carbon surfaces.

The lack of any effect of carbon in the racemization of these compounds shows that the catalytic racemization reaction of binaphthyls is not a very general phenomenon. It can be expected that the adsorption process, with a possible flattening of the binaphthyl rings as it approaches the graphitic planes of active carbons (1, 2) should be a rather specific process which is easily disrupted by functional groups on the aromatic rings.

Although the binaphthyl methyl phosphate **3** is not catalytically racemized by suspensions of carbon in nonhydroxylic solvents, it does undergo a reaction promoted by carbon in a hydroxylic solvent. When ester **3** is present in the monoethyl ether of diethylene glycol, a slow loss of optical activity occurs at 130°C due to solvolysis. Addition of a variety of different carbons of both acidic and basic character (i.e., Carbolac 1 "pH 3", Spheron 6 "pH 6", and Sterling FT "pH 9") increased the rate of loss of optical rotation to about the same degree. That solvolysis rather than a simple racemization was occurring was shown by isolation of 1,1′-bi-2-naphthol from a larger scale catalyzed run. The naphthol retained its optical purity but its greatly lower specific rotation results in essentially complete loss of measured activity during a kinetic run.

Figure 1 shows first order plots for the loss of optical activity at three concentrations of ester and with Norite as catalyst at ca. 1.0 mg/mL. The rate

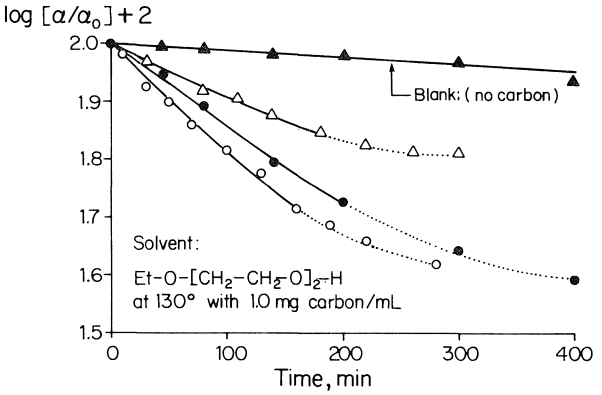


FIG. 1. First order plots of the loss of optical activity at 130°C for phosphate ester **3** in diethyleneglycol monoethyl ether with and without carbon black (Norite) at 0.9–1.1 mg/mL. The ester concentration (× 10^3) and Norite concentration were, respectively, ▲ 5.76 with no carbon, △ 11.6 with 1 mg/mL, ● 5.76 with 0.9 mg/mL, and ○ 2.97 with 1.1 mg/mL.

constants calculated from the initial portions of such plots are collected in Table 1. The initial rate of loss of optical rotation can be over ten times greater with carbon than without. Although this catalytic effect of carbon was reproducible with different batches of ester and of carbon and with measurement by either polarimetry or ultraviolet spectrometry, the results do not allow a satisfying kinetic analysis. Unfortunately the carbon-promoted reaction always slowed and sometimes essentially stopped (see Fig. 1) during a run. This

TABLE 1. Initial first order rate constants for solvolysis of binaphthyl phosphate ester **3** in diethyleneglycol monoethyl ether at 130°C.

Concentration of ester (mol/L × 10^3)	Carbon added[a] (mg/mL)	k_{obs}[b] (s^{-1} × 10^5)
5.76	None	0.40
2.97	1.10	7.03
5.55	0.46	5.39
5.76	0.89	5.29
5.21	1.86	5.22
11.6	1.00	3.16
5.91	None	0.59[c]
5.91	1.04	5.09[c]
5.61	1.00[d]	4.95
5.52	1.00[e]	6.36
5.52	1.00[f]	5.75
5.82	1.12	5.75
5.82	None	0.54[g]
6.04	1.42	4.58
6.04	None	0.62[g]

[a]The carbon was Norite unless mentioned otherwise.
[b]Obtained by measurement of loss of optical rotation (except *c*).
[c]Obtained by measurement of uv absorption at 302 nm.
[d]Carbolac 1.
[e]Spheron 6.
[f]Sterling FT.
[g]Paired runs, each from a side of a U-tube separated by a filter plug.

Can. J. Chem. Downloaded from www.nrcresearchpress.com by 210.87.254.42 on 09/05/12
For personal use only.

deactivation also showed up in a decrease in the initial first order rate constant at higher ester concentration. It is possible that some active sites on carbon, say hydroxyl groups, might be irretrievably covered up and inactivated by transfer of the phosphate group from naphthyl to the carbon surface; this would occur more effectively at high ester concentrations. However, such a noncatalytic, "bimolecular" reaction of functional groups on carbon with the ester can be eliminated as the major reaction since no loss of ester occurred in the similar, but otherwise non-hydroxylic, solvent diglyme at 130°C in the presence of carbon over 13 h. The catalytic reaction in the hydroxylic solvent has a half life of about 3 h under these conditions.

Most disturbing to a more complete kinetic treatment of the reaction was that the rate was very insensitive to the amount and type of suspended carbon. This suggested that an impurity in the carbons, possibly low molecular weight (and soluble) acids or bases, might be extracted into the solvent where it reached a constant saturated concentration. A homogeneous reaction at constant rate rather than a heterogeneous catalytic reaction would then occur. Several experiments were carried out to investigate this possibility.

First a suspension of the carbon in the hydroxylic solvent was held at 150°C, filtered hot, and the filtrate used for a normal kinetic control run (i.e., without carbon present). No especially accelerated rate of solvolysis was found. It is possible, however, that an active soluble agent at 150°C had precipitated and been lost during the preparation of the control solution at room temperature, so a further more definitive test was carried out.

A U-shaped tube with a fine sintered glass filter at the centre bottom, dividing the tube into equal sections, was employed. A normal kinetic solution of the ester complete with suspended carbon was heated and introduced into one side of the U-tube placed in a 130°C bath. By applying a little air pressure above the solution about half of the solution was then filtered into the other section of the tube; samples from both sides of the tube could be taken separately and measured as usual. The reaction in the filtered side, free from carbon, showed the normal, slow, uncatalyzed solvolysis; the reaction in the side with suspended carbon showed the catalytically enhanced rate of loss of ester. The results definitely show that a heterogeneous reaction of the suspended carbon particles is involved in the more rapid loss of ester. The rate of about 10-fold is not large and its origin is unknown, but since some aromatic phosphate esters are subject to nucleophilic, general base and acid catalysis (8, 9), it seems that groups on carbon blacks such as hydroxyl, carboxyl, and phenolic must be involved. Unlike the catalytic effect of carbon in the racemization of 1,1′-binaphthyl (2), the catalysis by carbon of this phosphate ester solvolysis is not inhibited by naphthalene. Relatively nonpolar, graphitic planes, which may competitively adsorb naphthalene, may be involved in the former catalysis while polar functional groups, not influenced by the presence of naphthalene, are active with the latter substrate. The example of catalytic activity reported here at least shows that if a way to prevent the deactivation of the catalyst could be found, and indeed, if an increased activity could be affected by modification of the catalyst, carbon black could be an interesting and useful catalyst of some solvolytic reactions.

Unfortunately, an extension to the reaction of another aromatic phosphate ester with a hydroxylic solvent in the presence of carbon failed to show any catalytic effects. The insecticide Paraoxon (i.e., *p*-nitrophenyl diethyl phosphate) is stable in monomethyl diethylene glycol at 80°C over 4 h with or without Norite at 1 mg/mL. At 130°C slow reaction of Paraoxon occurs, but the rate remains unaffected by the presence of active carbon particles. Therefore, both the catalyzed racemization of binaphthyl and the catalyzed solvolysis of phosphate ester **3** so far remain unique examples of these types of catalytic activity of carbon.

Experimental

The cyclic phosphate diester of 1,1′-bi-2-naphthol was prepared by methods similar to that mentioned (10) except that binaphthol, phosphorus oxychloride, and pyridine (mole ratios 1:1:2) were reacted in benzene and then refluxed overnight. The crude binaphthylphosphorus chloride, isolated by ether extraction, was hydrolyzed in 50% dioxane–water at 50°C until (ca. 30 min) no chloride was detected by thin layer chromatography. After extraction into dichloromethane, the solid was recrystallized from methanol to give the binaphthylphosphoric acid, mp 344–346°C. *Anal.* calcd. for $C_{20}H_{13}PO_4$: C 68.96, H 3.73; found: C 68.44, H 3.90.

Rather than cinchonine (10), strychnine was used in methanol as the resolving agent. After recrystallizations from large volumes of methanol (by concentration through evaporation to bring about crystallization) the salt, mp 245–247°C, was taken up in ethanol and decomposed by treatment at 70°C with Dowex 50W-X12 acid ion exchange resin. Evaporation of the decanted solution gave an oily residue which crystallized from methanol to give a solid, mp 335–337°C, $[\alpha]_D$ −609° (2.4 mg/mL in methanol), (lit. (9) 530°). A private communication from Prof. D. J. Cram and K. P. Shepherd reported $[\alpha]_D$ 601° for the plus enantiomer. *Anal.* calcd. for $C_{20}H_{13}PO_4$: C 68.96, H 3.73; found: C 68.68, H 3.70.

The methylbinaphthylphosphate ester **3** was prepared from the binaphthylphosphoric acid in methanol by treatment with diazomethane in ether. After recrystallization from benzene – petroleum ether it gave mp 210–212°C, $[\alpha]_D$ −490° (1.94 mg/mL

Can. J. Chem. Downloaded from www.nrcresearchpress.com by 210.87.254.42 on 09/05/12
For personal use only.

in methanol), (lit. (10) mp 210°C and $[\alpha]_D$ 544°). Optically active 1,1′-bi-2-naphthol was kindly supplied by Professor D. J. Cram.

1,1′-Binaphthyl-8,8′-dicarboxylic acid was resolved with brucine (11) and reacted with diazomethane to give the diester, mp 125–126°C, (lit. (7) mp 123–125°C). Paraoxon (bp 150–158°C/0.5 Torr) (lit. (12) bp 155°C/0.1 Torr) was prepared by reaction of *p*-nitrophenol with diethylchlorophosphate and triethylamine in benzene. Diglyme (i.e., bis(2-methoxyethyl)-ether) and triglyme (i.e., 1, 2-bis(2-methoxyethoxy)ethane) were refluxed and distilled from calcium hydride or lithium aluminum hydride. Diethyleneglycol monoethyl ether (i.e., 2-(2-ethoxy-ethoxy)ethanol was distilled and a centre portion, bp 210°C, collected for use. Sources of the carbon blacks have been described (2).

For kinetic studies the usual conditions were a suspension of carbon black in 9 mL of solvent containing 18 mg of phosphate ester. The rate of stirring was not critical as the carbon particles were readily suspended by light agitation. The kinetic sample was heated in a constant temperature oil bath and samples periodically withdrawn, cooled, and filtered using a Swinny syringe filter. Polarimetric analysis was with a Bendix type 143A automatic polarimeter. The rate constants were obtained from the initial slopes of the plots of log α/α_0 = log (fraction of reaction) versus time; the optical rotations of infinity samples were essentially zero and negligible. The plots were usually sufficiently straight to the first half-life, but showed considerable slowing thereafter (see Fig. 1). The rate of loss of rotation in a solution of 2.97×10^{-3} *M* ester with 1.1 mg of Norite/mL was unaffected by the presence of 0.134 *M* naphthalene.

The rate of reaction was also measured by loss of uv absorption of ester **3** at 302 nm in filtered aliquots of the kinetic run after dilution with ethanol. At the concentration of ester employed in the kinetic studies there was no measurable loss of the ester by adsorption onto the carbon. This was determined by comparison of uv spectra at room temperature before and after addition (and filtering) of the carbon. Under the higher temperature conditions of the kinetic runs even less ester would be reversibly adsorbed.

The thermal racemization of ester **3** at 0.0046–0.006 *M* in triglyme was determined at 190, 180, and 170°C. Good first order plots with rate constants 11.8, 5.60, and 3.43×10^{-5} s^{-1}, respectively, were obtained. Assuming a 5% error in k_{obs}, values of $\Delta H^{\ddagger}$ 26.1 ± 2.3 kcal/mol and $\Delta S^{\ddagger}$ −21 ± 6 cal/mol deg were calculated.

Product studies were carried out with 150 mg of ester in 7.5 mL of diethyleneglycol monoethyl ether containing 67 mg of Norite at 130°C for 70 h. Addition of water, extraction with benzene, and preparative thin layer chromatography showed 1,1′-bi-2-naphthol (identified by infrared and ultraviolet spectra) as the only noticeable product. For quantitative analysis a sample of ester, 28.6 mg, in 1 mL of solvent with 12 mg of Norite heated 20 h at 130°C showed a rotation of −0.069 in a 1 cm cell. With the specific rotation of binaphthol at −33.8 (3) this measured rotation corresponds to production of binaphthol with 90% retention of activity.

Acknowledgements

We thank the National Research Council of Canada for support of this research and Professor D. J. Cram and Dr. K. P. Shepard, University of California at Los Angeles, for suggestions on the preparation of phosphate ester **3** and a sample of optically active binaphthol.

1. R. E. Pincock, W. M. Johnson, K. R. Wilson, and J. Haywood-Farmer. J. Am. Chem. Soc. **95**, 6477 (1973).
2. R. E. Pincock, W. M. Johnson, and J. Haywood-Farmer. Can. J. Chem. **54**, 548 (1976).
3. E. B. Kyba, K. Koga, L. R. Sousa, M. G. Siegel, and D. J. Cram. J. Am. Chem. Soc. **95**, 2692 (1973).
4. J. S. Mattson and H. B. Mark, Jr. Activated carbon. M. Dekker, New York, NY. 1971; J.-B. Donnet and A. Voet. Carbon black. M. Dekker, New York, NY. 1976. p. 126.
5. V. A. Liferova, Z. D. Skripnik, and G. F. Yankovskaya. Adsorbtsiya Adsorbenty, **2**, 43 (1974); Chem. Abstr. **81**, 104246 (1974). See also Chem. Abstr. **79**, 65808 (1973); **79**, 137681 (1973). For catalysis by carbon see also J. W. Hassler. Purification with activated carbon. Chemical Publishing Company, Inc., New York, NY. 1974. p. 261 and references given therein.
6. D. L. Becker and S. C. Wilson. *In* Carbon adsorption handbook. *Edited by* P. N. Cheremisinoff and F. Ellerbusch. Ann Arbor Science Publishers, Ann Arbor, MI. 1978. p. 167.
7. A. S. Cooke and M. M. Harris. J. Chem. Soc. 2365 (1963).
8. T. C. Bruice and S. J. Benkovic. Bioorganic mechanisms. Vol. II. Benjamin, New York. 1966. p. 29.
9. C. A. Bunton. Acc. Chem. Res. **3**, 257 (1970).
10. J. Jacques and C. Fouquey. Tetrahedron Lett. **48**, 4617 (1971).
11. J. Meisenheimer and O. Beisswenger. Ber. **65**, 32 (1932).
12. J. Cheymol, P. Chabrier, N.-T. Thuong, and H. Choisy. Therapie, **19**, 929 (1964); see Chem. Abstr. **63**, 2242 (1965).

Chemistry of hexamethyldisilazane. Silylation of β-diketones and amination of β-triketones

DANIEL T. W. CHU[1,2] AND STUART N. HUCKIN[3]

Abbott Laboratories, Limited, P.O. Box 6150, Montreal, P.Q., Canada H3C 3K6

Received August 8, 1979

DANIEL T. W. CHU and STUART N. HUCKIN. Can. J. Chem. **58**, 138 (1980).

It is discovered that hexamethyldisilazane, a reagent generally used to silylate amino, hydroxyl, sulfhydryl, and carbonyl groups, reacts with β-diketones to form their trimethylsilyl enol ethers in high yield.

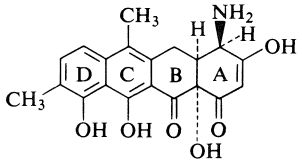
An efficient and simple procedure for aminating β-triketones to their enaminodiketones by the use of hexamethyldisilazane is also described.

DANIEL T. W. CHU et STUART N. HUCKIN. Can. J. Chem. **58**, 138 (1980).

On a découvert que l'hexaméthyldisilazane, un réactif utilisé habituellement dans la silylation des groupements amino, hydroxyle, sulfhydryle et carbonyle, réagit avec les β-dicétones pour former leur éthers énoliques triméthylsilylés avec des rendements élevés, On décrit également une méthode simple et efficace d'amination de β-tricétones en énaminodicétones correspondantes à l'aide de l'hexaméthyldisilazane.

[Traduit par le journal]

During the course of our investigation on chemical modification of 2-deacetylchelocardin (**1**) (1, 2), we were interested in protecting the enolized ketone group of the β-diketone in ring A by a silyl group.

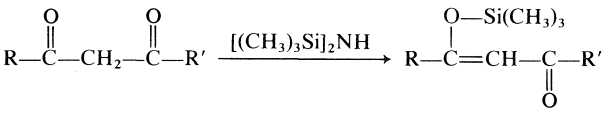


1

β-Diketones, under standard procedures (3, 4) do not undergo silylation readily. Silylation of carbonyl compounds has been reported using chlorotrimethylsilane and strong base (3, 4), bis(trimethylsilyl)acetamide (5), triethylsilylthiobenzene (6), trimethylsilyl trifluoromethanesulfonate (7), and ethyl trimethylsilylacetate and tetra-*n*-butylammonium fluoride (8). Attempted silylation of 1,3-dicarbonyl compounds by standard silylation methods (3, 4) resulted in relatively low yields.

To avoid loss of a substantial amount of 2-deacetylchelocardin (**1**), we used simple β-diketones as model compounds in the search for a mild silylation procedure.

It has now been found that silylation of β-diketones to their corresponding trimethylsilyl enol ethers is effected in very high yield by the use of hexamethyldisilazane as illustrated in Schemes 1

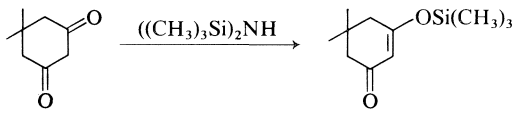


2*a*, *b* **3***a*, *b*

a R = R′ = CH_3
b R = R′ = C_6H_5

SCHEME 1

and 2. This procedure involves the reaction of the β-diketone in an aprotic solvent with a slight excess of hexamethyldisilazane at room temperature. The product is isolated by evaporating the excess hexamethyldisilazane and solvent under reduced pressure, yielding essentially pure residue. The reaction appears to be general for enolizable β-diketones as illustrated in Table 1.



4 **5**

SCHEME 2

While our investigation was in progress, it was claimed that 1,3-dicarbonyl compounds can be silylated by 1-(trimethylsilyl)imidazole (9). This procedure involves heating a mixture of the 1,3-dicarbonyl compound, hexamethyldisilazane, and a catalytic amount of imidazole at refluxing temperature (126°C) for several hours followed by fractional distillation. The authors also reported that reaction of 1,3-dicarbonyl compounds with 1-(trimethylsilyl)imidazole in pentane and ligroin resulted in low yields of the corresponding trimethylsilyl enol ethers. These results may be explained by

[1]Author to whom correspondence may be addressed.

[2]Present address: Abbott Laboratories, D-482, North Chicago, IL 60064, U.S.A.

[3]Present address: Agassiz Research Station, P.O. Box 1000, Agassiz, B.C., Canada V0M 1A0.

0008-4042/80/020138-05$01.00/0

©1980 National Research Council of Canada/Conseil national de recherches du Canada

TABLE 1. Preparation of trimethylsilyl enol ethers from β-diketones

β-Diketone	Product	Reaction time (h at 20°C)	Yield (%)	Physical data of product: Boiling point or melting point (°C)	Nuclear magnetic resonance value ($CDCl_3$)	Mass spectrum
2a	*3a*	30	94	61–63/3 Torr (lit. (4) 66–68/4 Torr)	0.28 and 0.30 (s, 9H) 2.10 and 2.24 (s, 6H) 5.21 and 5.56 (s, 1H)[a]	Calcd. for $C_8H_{16}O_2Si$[b] *m/e*: 172 found: 172
2b	*3b*	16	96	[c]	0.05 and 0.21 (s, 9H) 6.78 and 6.83 (s, 1H) 7.46 and 8.85 (m, 10H)[a]	Calcd. for $C_{18}H_{20}O_2Si$[b] *m/e*: 296 found: 296
4	**5**	1½	98	56–58 (lit. (5) 56–58)	0.29 (s, 9H), 1.05 (s, 6H) 2.19 (s, 2H), 2.21 (s, 2H) 5.38 (s, 1H)	Calcd. for $C_{11}H_{20}O_2Si$ *m/e*: 212.1233 found: 212.1234

[a]The geometric isomers were not separable and similar peaks of the different isomers are placed under the same heading.
[b]A high resolution ms could not be obtained as the compound evaporated very rapidly.
[c]A liquid which hydrolyzes rapidly.

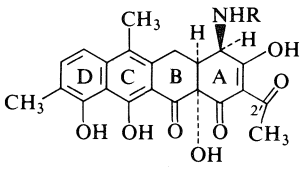
the possibility that the effecting agent in this silylation procedure is hexamethyldisilazane itself.

Since our present procedure involves no heating and all the by-products are highly volatile, it offers the advantage of being mild, efficient, and simple. It is particularly useful when the silylated product is extremely high boiling since it avoids fractional distillation. Purification by chromatographic techniques is not feasible since the silylated β-diketones are very readily hydrolyzed.

Amination of β-Triketones

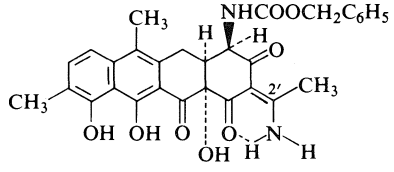
Chelocardin, a broad spectrum antibiotic, was first described in 1961 (10) and subsequently shown to be (**6**) (11). During our investigation on the chemical modification of chelocardin (**6**), it became apparent that protection of the enolized ketone group of the β-triketone system in ring A would yield a versatile intermediate for the synthesis of various chelocardin analogs.

With the discovery of an efficient procedure for silylation of β-diketones by the use of hexamethyl-



6 R = H
7 R = $COOCH_2C_6H_5$

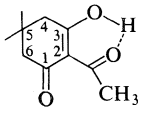
disilazane, we explored the effect of hexamethyldisilazane on β-triketones, particularly on chelocardin derivatives. Successful extension of this silylation procedure on *N*-carbobenzoxychelocardin (**7**) (12) would have produced the desired ring A intermediate. Treatment of *N*-carbobenzoxychelocardin (**7**) with hexamethyldisilazane in methylene chloride gave a crude product having two trimethylsilyl groups in its nmr spectrum. As the phenolic hydroxyl groups were expected to be silylated, it seemed that silylation of the β-diketone system in ring A had not occurred. In order to identify the product further, it was then subjected to hydrolysis to see whether we recovered *N*-carbobenzoxychelocardin (**7**). However, treatment of the crude product with methanolic hydrogen chloride yielded, unexpectedly, 2′-amino-*N*-carbobenzoxychelocardin (**8**), a product which was previously prepared by reaction of (**7**) with ammonium acetate (13). Thus the 2′-enol group in *N*-carbobenzoxychelocardin (**7**) was replaced by an enamine.



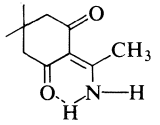
8

2-Acetyldimedone was used as a model compound to study this transformation of the β-triketone to the enaminodiketone by the use of hexamethyldisilazane. 2-Acetyldimedone (**9**) (14) possesses two singlets at δ 2.32 and 2.50 in its nuclear magnetic resonance (nmr) spectrum taken in $CDCl_3$ corresponding to the four methylene protons at C-4 and C-6. Reaction of **9** with hexamethyldisilazane in dry chloroform gave the 2-

aminoacetyldimedone (**10**). Replacement of the enol by an enamine had occurred exclusively on the 2-acetyl side chain. Its structure was confirmed by having a singlet at δ 2.34 (4 protons) corresponding to two chemically equivalent methylene groups at



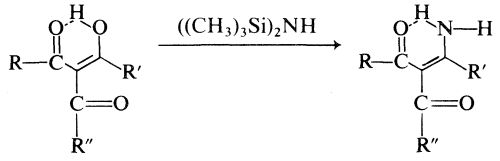
9



10

C-4 and C-6 in its nmr spectrum. A broad singlet at δ 11.57 shows the presence of one of the amino protons hydrogen bonded with the keto group. The other non-hydrogen bonded amino proton shows a broad singlet at δ 7.65. It possesses a correct molecular ion, *m/e*, at 181 in its mass spectrum. Further confirmation of its structure was obtained by synthesizing **10** by the use of ammonium acetate. The product synthesized by both procedures was identical in all respects.

The amination of β-triketones to their corresponding enaminodiketones by the use of hexamethyldisilazane (Scheme 3) appears to be general for enolizable β-triketones. It is an efficient, simple, and high yield reaction and seems to be superior to the ammonium acetate aminating pro-



SCHEME 3

cedure. We have successfully applied this procedure to several β-triketones and the results are illustrated in Table 2.

Using 2-acetyldimedone as an example, a possible mechanism for this reaction is illustrated in Scheme 4.

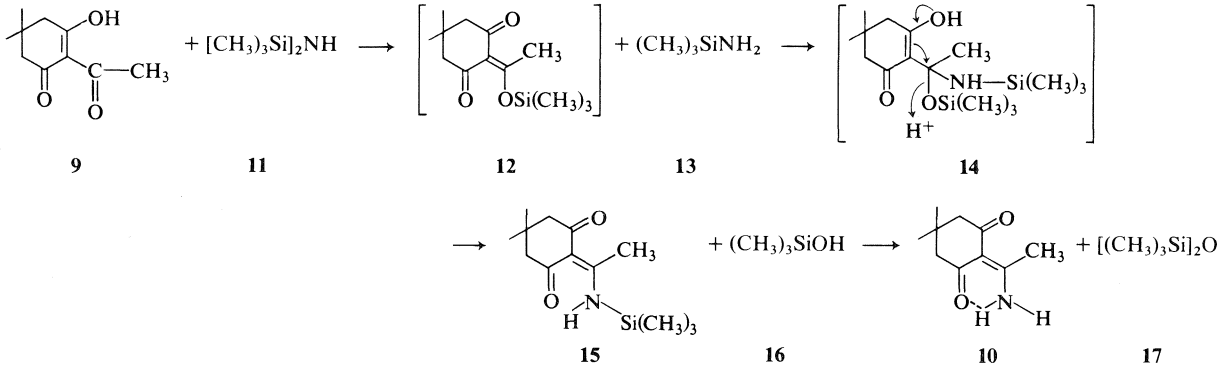
2-Acetyldimedone (**9**) was first silylated by hexamethyldisilazane (**11**) to give the unstable enol silyl ether (**12**) by a process parallel to the silylation of β-diketones. The trimethylsilazane (**13**) formed during the reaction underwent a Michael addition to the highly reactive double bond because it is doubly activated by two carbonyl groups at C-1 and C-3 to give the intermediate (**14**). This compound was then stabilized by elimination of the trimethylsilanol (**16**) by a retrograde Michael reaction to yield compound **15**. Nucleophilic attack on **15** by the trimethylsilanol (**16**) gave the 2-aminoacetyldimedone (**10**). As the proposed by-product, hexamethyldisiloxane (**17**) has a boiling point of 100–101°C (15), it was not isolated by our work-up procedure.

An alternative mechanism may involve compound **12** as an initial product which is subsequently aminated by ammonia derived from hydrolysis of trimethylsilazane (**13**) to give **10**. Since all experiments were performed under absolute dry conditions, it seems unlikely that the transformation involves this alternative mechanism.

Experimental

The ir spectra were recorded on a Perkin-Elmer Model 710A infrared spectrophotometer. The nmr spectra were recorded on a Varian Associates A-60 spectrometer in deuterated solvents; resonance positions are given on the δ scale (ppm) relative to internal tetramethylsilane. The nmr peaks were designated as follows: s, singlet; d, doublet; t, triplet; q, quartet; m, multiple; b, broad. The high resolution mass spectra were determined on an Associated Electrical Industries MS-902 Double Focussing mass spectrometer and were processed on an IBM 1800 computer. Melting points were determined on a Fisher-Johns melting point apparatus and are uncorrected. The ^{13}C nmr spectra were recorded on a Varian Associates XL-100-15/TT-100 spectrometer system in DMSO; resonance positions are given in ppm relative to internal tetramethylsilane. Parameters used were pulse width (30°) 3.5 μs, pulse delay 0.5–1.0 s, and sweep width 6K and 8K data table.

Since the ir absorption spectra of various derivatives reported here have a β-amino-, β-unsaturated carbonyl function which would have similar absorption to the β-triketone system, very

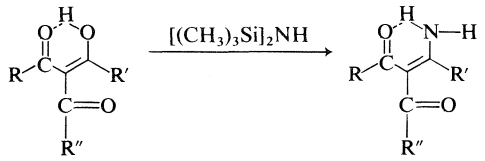


9 **11** **12** **13** **14**

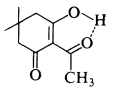
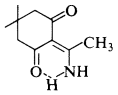
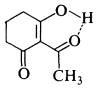
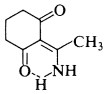
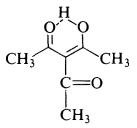
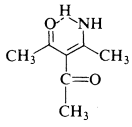
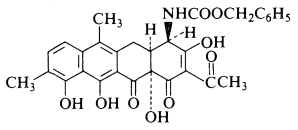
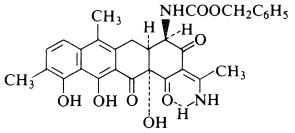
15 **16** **10** **17**

SCHEME 4

TABLE 2. Amination of β-triketones



(*a*) Reaction conditions

Entry	β-Triketone	Product	Reaction time, 20°C	Yield (%)
1			14 h	98
2			18 h	99
3			48 h	80
4			2 h[a]	80

(*b*) Physical data of product

Entry	Melting point (°C)	Nuclear magnetic resonance value ($CDCl_3$)	Analysis	Mass spectrum (M^+)	^{13}C nmr
1	127–128.5	1.03 (s, 6H), 2.34 (s, 4H) 2.53 (s, 3H), 7.65 (sb, 1H), 11.57 (sb, 1H).	Calcd. for $C_{10}H_{15}NO_2$: C 66.27, H 8.34, N 7.73, O 18.17; found: C 66.47, H 8.61, N 7.69, O 18.17	181	C-1 196.5 C-3 196.5 C-2 106.5 C-2′ 173.2 C-2′CH_3 24 C-4 52.3 C-6 52.3 C-5 29.5 2-C_5CH_3 27.8
2	78.5–8.0	1.90 (m, 2H), 2.43 (m, 4H), 2.53 (s, 3H), 7.20 (s, 1H), 11.52 (sb, 1H).	Calcd. for $C_8H_{11}NO_2$: C 62.75, H 7.19, N 9.15, O 20.92; found: C 62.38, H 7.36, N 9.08, O 21.33	151	—
3	65–67	2.12 (s, 3H), 2.31 (s, 6H), 6.19 (sb, 1H), 10.62 (sb, 1H).	Calcd. for $C_7H_{11}NO_2$: C 59.74, H 7.80, N 9.93, O 22.70; found: C 59.57, H 8.07, N 9.83, O 23.02	141	—
4	—	—	Calcd. for $C_{30}H_{28}N_2O_8$: C 66.18, H 5.15, N 5.15; found: C 65.82, H 5.00, N 5.02	544	C-1 190.0[b] C-3 192.1 C-2 105.0 C-2′ 174.7 C-2′CH_3 23.8

[a]Work-up procedure differs from others (see Experimental).
[b]Only A ring in ^{13}C nmr data is reported here for comparison.

little change in the carbonyl absorption region (1580–1680 cm^{-1}) was observed. Hence their absorption bands are not reported.

Silylation of β-Diketones

Other than reaction time (see Table 1), the conditions used for the silylation of the three β-diketones to their corresponding trimethylsilyl enol ethers were identical to those illustrated below with dimedone (**4**). Physical data and yields of all the products are compiled in Table 1.

Hexamethyldisilazane (1.5 g, 9.44 mmol) was added to a solution of dimedone (**4**) (1 g, 7.14 mmol) in dry dichloromethane (20 mL) under a nitrogen atmosphere. After stirring at room temperature (20°C) for 1½ h, the excess hexamethyldisilazane and by-products were evaporated at 10 Torr at room temperature. The residue solidified after standing overnight under dry nitrogen atmosphere yielding 1.49 g (98%) of pure **5**.

Amination of β-Triketones

Other than reaction time (see Table 2), the conditions used for the amination of the four β-triketones studied to their corresponding enaminodiketones were identical to those illustrated below with 2-acetyldimedone (**9**). Since there was a difference in work-up procedure for 2′-amino-*N*-carbobenzoxychelocardin (**8**), its experimental procedure is also reported. Physical data and yields of all products are compiled in Table 2.

Hexamethyldisilazane (600 mg, 3.72 mmol) was added to a solution of 2-acetyldimedone (500 mg, 2.75 mmol) in dry chloroform (10 mL) and the resulting solution was stirred under a nitrogen atmosphere at room temperature (20°C) for 14 h. It was evaporated to dryness under reduced pressure. Nuclear magnetic resonance spectra of the crude product showed the absence of enolsilyl or silylamino groups. It was then redissolved in chloroform (50 mL) and washed with water. The organic layer was dried over magnesium sulfate. Evaporation to dryness yielded 485 mg (**10**) (98%), mp 127.5–128.5°C.

*Preparation of 2-Aminoacetyldimedone (**10**) by the use of Ammonium Acetate*

Ammonium acetate (500 mg, 6.33 mmol) was added to a solution of 2-acetyldimedone (300 mg, 1.65 mmol) in tetrahydrofuran (20 mL) and the resulting mixture was stirred at room temperature (20°C) for 16 h. It was filtered and evaporated under reduced pressure to dryness. It was taken up in chloroform (50 mL) and washed with water. The crude product obtained was chromatographed on silica gel column to give 230 mg pure product (**10**) identical to the one prepared above. The yield was 76%.

*2′-Amino-N-carbobenzoxychelocardin (**8**)*

Hexamethyldisilazane (380 mg, 2.37 mmol) was added to a solution of *N*-carbobenzoxychelocardin (**7**) (450 mg, 0.83 mmol) in dry chloroform (20 mL) and the resulting solution was stirred under nitrogen atmosphere at room temperature for 2 h. It was evaporated under reduced pressure to dryness. The residue was refluxed in 0.01 *M* methanolic hydrogen chloride solution (25 mL) for 1 h. After concentrating to small volume, a precipitate appeared. It was filtered and washed with cold methanol yielding 365 mg **8**.

Acknowledgements

We thank G. Nettleship for recording nmr spectra and Sandra L. Mueller and her associates and Ruth S. Stanaszek of Abbott Laboratories, North Chicago, for recording the mass spectra and ^{13}C nmr spectra, respectively, and the staff of the microanalytical department of Abbot Laboratories for the elemental analyses. We also thank David L. Garmaise for his interest and encouragement throughout the course of this work.

1. Daniel T. W. Chu, D. L. Garmaise, and E. Bernstein. Can. J. Chem. **53**, 1434 (1975).
2. Daniel T. W. Chu, E. Bernstein, and S. N. Huckin. Can. J. Chem. **56**, 1059 (1978).
3. R. West. J. Am. Chem. Soc. **80**, 3246 (1958).
4. H. O. House, L. J. Czuba, M. Gall, and H. D. Olmstend. J. Org. Chem. **34**, 2324 (1969).
5. J. F. Klebe, H. Finkbeiner, and D. M. White. J. Am. Chem. Soc. **88**, 3390 (1966).
6. I. Ojima and Y. Nagai. J. Organomet. Chem. **57**, C42 (1973).
7. G. Simchen and W. Kober. Synthesis, 259 (1976).
8. E. Nakamura, T. Murotushi, M. Shimizu, and I. Kuwajima. J. Am. Chem. Soc. **98**, 2346 (1976).
9. S. Torkelson and C. Ainsworth. Synthesis, 722 (1976).
10. T. J. Oliver, J. F. Prokop, R. R. Bower, and R. H. Otto. Antimicrob. Agents Chemother. 583 (1962); A. C. Sinclair, J. R. Schenck, G. C. Post, E. V. Cardinal, S. Burkas, and H. H. Fricke. Antimicrob. Agents Chemother. 592 (1962).
11. L. A. Mitscher, W. Rosenbrook, Jr., W. W. Andres, R. S. Egan, J. Schenck, and J. V. Juvarkar. Antimicrob. Agents Chemother. 38 (1970); L. A. Mitscher, J. V. Juvarkar, W. Rosenbrook, Jr., W. W. Andres, J. Schenck, and R. S. Egan. J. Am. Chem. Soc. **92**, 6070 (1970).
12. Daniel T. W. Chu, Stuart N. Huckin, and Edith Bernstein. Can. J. Chem. **55**, 3341 (1977).
13. Daniel T. W. Chu, Stuart N. Huckin, Edith Bernstein, David L. Garmaise, R. S. Egan, and Ruth S. Stanaszek. In preparation.
14. W. Dieckmann and R. Stein. Ber. **37**, 3370 (1904).
15. Robert O. Sauer. J. Am. Chem. Soc. **66**, 1707 (1944).

The reaction of $R_2PC{=}CCl(CF_2)_n$ with iron carbonyls. Unusual complexes formed by ligand cleavage reactions

WILLIAM R. CULLEN AND MANGAYARKARASY WILLIAMS

Chemistry Department, University of British Columbia, Vancouver, B.C., Canada V6T 1W5

Received June 19, 1979

WILLIAM R. CULLEN and MANGAYARKARASY WILLIAMS. Can. J. Chem. **58**, 143 (1980).

The phosphines $R_2PC{=}CCl(CF_2)_n$ and arsine $(CH_3)_2AsC{=}CCl(CF_2)_3$ (L; R = C_6H_5 or C_6H_{11}; n = 2, 3, 4) react with iron carbonyls to afford a range of products. Simple substitution yields (L)Fe(CO)$_4$ and $L_2Fe(CO)_3$. Loss of chlorine from the ligands, symbolized (L − Cl), gives coupled complexes of formula $[(L - Cl)Fe(CO)_4]_2$ and loss of chlorine and fluorine gives the η^3-allyl bridged derivatives (L − Cl − F)$Fe_2(CO)_6$. Only substitution products are obtained from the cyclobutenes.

WILLIAM R. CULLEN et MANGAYARKARASY WILLIAMS. Can. J. Chem. **58**, 143 (1980).

Les phosphines $R_2PC{=}CCl(CF_2)_n$ et l'arsine $(CH_3)_2AsC{=}CCl(CF_2)_3$ (L; R = C_6H_5 ou C_6H_{11}; n = 2, 3, 4) réagissent avec les carbonyles de fer pour conduire à une variété de produits. La substitution simple donne (L)Fe(CO)$_4$ et $L_2Fe(CO_3)$. La perte de chlore à partir des ligands symbolisés (L − Cl) donne des complexes couplés de formule $[(L - Cl)Fe(CO)_4]_2$ et la perte de chlore et de fluor donne les dérivées ayant un groupement η^3-allyle en position de pont (L − Cl − F)$Fe_2(CO)_6$. A partir des cyclobutènes, on obtient seulement des produits de substitution.

[Traduit par le journal]

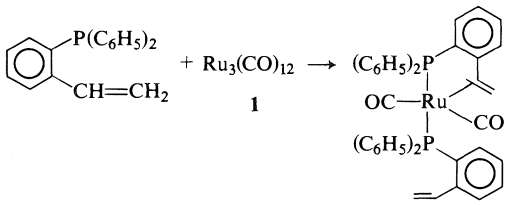
There is considerable current interest in the reactions of tertiary phosphines and arsines of the type R_2ER' (E = P, As; R′ = unsaturated hydrocarbon group) with transition metal complexes (1–18). The general thrust of these studies has been to establish what can happen to the unsaturated group held in close proximity to a transition metal by a bond formed between the metal and the Group V donor. Many types of behaviour have been observed which can be described as follows (only typical examples are given):

(*1*) Coordination by E with R′ being unaffected (1, 3), e.g.

$(C_6H_5)_2PC{=}CCl(CF_2)_3Mo(CO)_5$

and **1**.

(*2*) Coordination of both E and R′ to give a chelate derivative (3, 4), e.g. **1**.

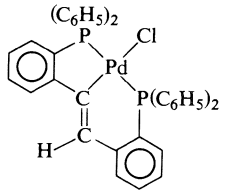


1

(*3*) Coordination of both E and R′ to different metal atoms (5–8), e.g.,

$(CO)_3FeP(C_6H_5)_2C{\equiv}C_6H_5 \quad (CO)_3FeP(C_6H_5)_2C{\equiv}C_6H_5$

(*4*) Modification of R′ to an η^1-bonding species by cleavage of an appropriate group such that (*a*) E and modified R′ are bonded to the same metal (9), e.g., **2** (by loss of H), (*b*) E and modified R′ are



2

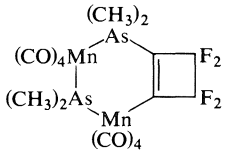
bonded to different metal atoms (10), e.g., **3** from

$(CH_3)_2AsC{=}CAs(CH_3)_2(CF_2)_2$

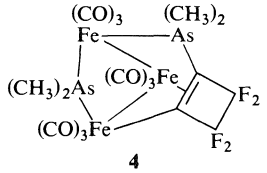
and (*c*) E is bonded to one metal, and the modified R′ is η^1-bonded to one metal and η^2-bonded to a third resulting in a cluster (11), e.g., **4** from

$(CH_3)_2AsC{=}CAs(CH_3)_2(CF_2)_2$

(*5*) Modification of R′ to an η^n-bonding species, $n > 2$, by cleavage of the appropriate groups with



3



4

concomitant formation of a cluster (2, 12), e.g., **5** from

$(C_6H_{11})_2PC{=}CCl(CF_2)_3$

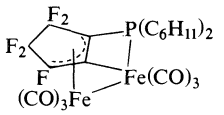
(this is also an example of class 4(*a*)).

(*6*) Coupling of ligands through R′ to give a new ligand which coordinates to the metal using the Group V donors and two σ-bonds from the newly formed bridging group (3, 13), e.g., **6**.

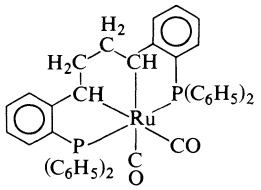
0008-4042/80/020143-08$01.00/0

©1980 National Research Council of Canada/Conseil national de recherches du Canada

Can. J. Chem. Downloaded from www.nrcresearchpress.com by 210.87.254.42 on 09/05/12
For personal use only.



5

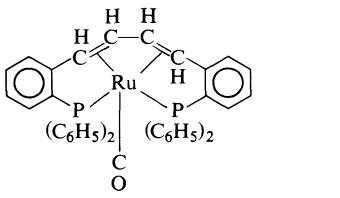


6

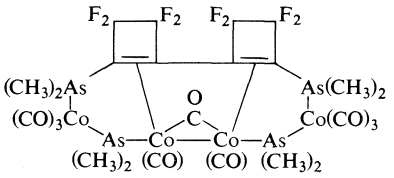
(*7*) Coupling of the ligand through R′ with cleavage of groups to give a new unsaturated ligand which bonds to (*a*) one metal (3, 13) using E and the bridging group, e.g., **7** and (*b*) two or more metal centres using E and the bridging group producing a cluster (14, 15), e.g., **8** from

$(CH_3)_3AsC{=}CAs(CH_3)_2(CF_2)_2$

(*8*) Cleavage of R′ from E associated with coupling reaction of the fragment with R_2PR' to yield clusters in which E and the new unsaturated systems bind (16, 17), e.g., **9** from



7



8

$(C_6H_5)_2PC{\equiv}CCF_3$

(*9*) Others (18), e.g.,

$(C_6H_5)_2PCH_2C(CF_3){=}CHP(C_6H_5)_2PtCl_2$

from $(C_6H_5)_2PC{\equiv}CCF_3$.

In this paper we describe the reaction of the unsaturated ligands

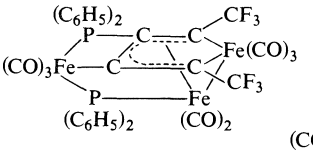
$R_2EC{=}CCl(CF_2)_n$

with $Fe(CO)_5$. In particular we describe the preparation and properties of a number of compounds related to **5**, however, other compounds belonging to class 1 are identified. We also report examples **10** of compounds which belong to a new subsection of class 7 (7*c*): **10** is formed by coupling the ligand through R′ with cleavage of groups to give a new unsaturated ligand which bonds to metal centres using the E donors alone.

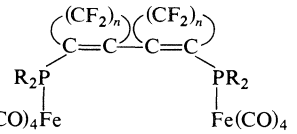
This work arose because it was recognized (1, 2) that unusual reactivity seems to be associated with ligands with the structure

$R_2EC{=}CX$

where X is a potential leaving group.



9



10

Experimental

Reactions with iron carbonyls were carried out in sealed Carius tubes. A standard vacuum system was used for the manipulation of volatile reactants. Involatile phosphines were handled in a nitrogen-filled glove bag.

Infrared spectra were recorded using a Perkin-Elmer 457 spectrophotometer. The KBr cell had a path length of 0.1 mm and the solvent was cyclohexane. Only selected bands are quoted in the text. Nuclear magnetic resonance spectra were run ($CDCl_3$ solution) on Varian T-60 and XL-100 instruments; chemical shifts are given in ppm downfield from internal TMS (^1H spectra), upfield from internal $CFCl_3$ (^{19}F spectra), and upfield from external 85% H_3PO_4 (^{31}P spectra, ^1H decoupled).[1] Mass spectra were obtained using an AEI MS-9 spectrometer. Microanalyses were performed by Mr. Peter Borda of the Chemistry Department, University of British Columbia.

Fluorocarbons and phosphine starting materials were obtained from Peninsular Chem Research Inc. and Strem Chemical Co. respectively. Pentacarbonyl iron also came from Strem. The ligands

$R_2EC{=}CCl(CF_2)_n$

were prepared as previously described (1, 19).

Reaction of the Tertiary Phosphines $R_2EC{=}CCl(CF_2)_n L$, with Iron Carbonyls

The following general procedure was used for all reactions of the phosphines with iron pentacarbonyl and triiron dodecacarbonyl. The details applying to specific complexes are listed in Table 1.

A benzene solution containing a 1:10 mole ratio of ligand-to-pentacarbonyliron (or 1:2 ratio when $Fe_3(CO)_{12}$ was used) was heated at the indicated temperature for 3–52 h. At the end of the reaction period the solvent was removed at reduced pressure. The residue was dissolved in petroleum ether (bp 40–60°C) and chromatographed on a Florisil column. The colored bands were eluted with mixtures of diethyl ether – petroleum ether. The eluate was evaporated leaving the crude products which were recrystallized from hexane.

Table 2 shows the percentage yield of various compounds

[1]The nmr data are listed in Table 5 which is available, at a nominal charge, from the Depository of Unpublished Data, CISTI, National Research Council of Canada, Ottawa, Ont., Canada K1A 0S2.

Can. J. Chem. Downloaded from www.nrcresearchpress.com by 210.87.254.42 on 09/05/12
For personal use only.

Can. J. Chem. Downloaded from www.nrcresearchpress.com by 210.87.254.42 on 09/05/12
For personal use only.

TABLE 1. Preparative data for iron carbonyl complexes obtained from $R_2EC{=}CCl(CF_2)_nL$

R_2E, n	Iron carbonyl	Reaction temp. (°C)	Reaction time (h)	Product[a]	Yield
$(C_6H_{11})_2P$, 2 0.39 g 1.11 mmol	$Fe(CO)_5$ 2.3 g 11.7 mmol	140	48	$(L)Fe(CO)_4$[b]	15.0
$(C_6H_5)_2P$, 2 0.32 g 0.93 mmol	$Fe(CO)_5$ 1.8 g 9.18 mmol	140	48	$(L)Fe(CO)_4$[c]	23.0
$(C_6H_{11})_2P$, 3 0.38 g 0.94 mmol	$Fe(CO)_5$ 1.84 g 9.4 mmol	150	48	$[(L-Cl)Fe(CO)_4]_2$[d] $(L-Cl-F)Fe_2(CO)_6$[c]	3.1 48.0
$(C_6H_{11})_2P$, 3 0.33 g 0.80 mmol	$Fe_3(CO)_{12}$ 0.80 g 1.58 mmol	150	4.5	$[(L-Cl)Fe(CO)_4]_2$[d] $(L)Fe(CO)_4$[d] $(L-Cl-F)Fe_2(CO)_6$[c]	19.0 4.6 40.0
$(C_6H_5)_2P$, 3 0.36 g 0.90 mmol	$Fe(CO)_5$ 1.92 g 9.8 mmol	150	48	$(L)Fe(CO)_4$[d] $(L-Cl-F)Fe_2(CO)_6$[c]	14.0 40.0
$(C_6H_5)_2P$, 3 0.312 g 0.79 mmol	$Fe(CO)_5$ 1.8 g 9.18 mmol	150	3	$(L)Fe(CO)_4$[d] $(L-Cl-F)Fe_2(CO)_6$[c] $(L)_2Fe(CO)_3$[c,e]	34.0 Trace 2.2
$(C_6H_5)_2P$, 3 0.22 g 5.6 mmol	$Fe(CO)_5$ 1.0 g 5.1 mmol	20[f]	48	$(L)Fe(CO)_4$[d] $(L-Cl-F)Fe_2(CO)_6$[d]	38.0 14.5
$(CH_3)_2As$, 3 0.70 g 2.1 mmol	$Fe(CO)_5$ 4.2 g 21.4 mmol	140	45.5	$(L)Fe(CO)_4$[c,e] $(L-Cl-F)Fe_2(CO)_6$[c,e]	28.0 6.6
$(C_6H_{11})_2P$, 4 0.3 g 0.65 mmol	$Fe(CO)_5$ 1.28 g 6.53 mmol	150	48	$(L)Fe(CO)_4$[d] $(L-Cl-F)Fe_2(CO)_6$[c]	5.4 44.0
$(C_6H_5)_2P$, 4 0.358 g 0.80 mmol	$Fe(CO)_5$ 1.6 g 8.0 mmol	150	52	$[(L-Cl)Fe(CO)_4]_2$[d] $(L-Cl-F)Fe_2(CO)_6$[c]	1.6 26.0

[a]In this table and elsewhere (L − Cl) is the symbol for the ligand L which has lost one Cl atom per formula unit likewise (L − Cl − F) is used when the ligand has lost one Cl and one F atom.
[b]Eluted with 5% diethyl ether – 95% petroleum ether.
[c]Eluted with 1% diethyl ether – 99% petroleum ether.
[d]Eluted with petroleum ether.
[e]Solids separated by fractional recrystallization.
[f]Irradiated with ultraviolet light, a Hanovia model 654-A36 200 W lamp was situated 20 cm from the reaction tube which was continuously shaken and cooled by an air stream.

isolated from the reaction of

$(C_6H_5)_2PC{=}CCl(CF_2)_3$

with $Fe(CO)_5$ after different time intervals.

Reaction of $(C_6H_5)_2PC{=}CCl(CF_2)_3Fe(CO)_4$ with the Iron Pentacarbonyl

Iron pentacarbonyl (2.1 g, 10.7 mmol) and the iron complex (0.6 g, 1.06 mmol) in benzene (8 mL) were heated at 150°C for 48 h. The procedure for working up the products was similar to that described above. Chromatography on a Florisil column gave a yellow band when eluted with petroleum ether. This was identified as unreacted complex $(L)Fe(CO)_4$ (0.21 g, 33% recovery). A 1% diethyl ether – 99% petroleum ether mixture eluted an orange band. Evaporation of solvent and recrystallization from hexane afforded orange-red crystals of the $(L-Cl-F)Fe_2(CO)_6$ derivative of known spectroscopic properties (0.22 g, 33%).[2]

[2]See footnote to Table 1.

Pyrolysis of $(C_6H_5)_2PC{=}CCl(CF_2)_3Fe(CO)_4$

When a solution of the iron complex (0.213 g, 0.38 mmol) in benzene (8 mL) was heated at 150°C for 48 h the solution turned orange. The tube contents were treated as described above. Chromatography on a Florisil column gave $(L)Fe(CO)_4$ (0.08 g, 37% recovery) as the only product.

Reaction of $(C_6H_5)_2PC{=}CCl(CF_2)_3W(CO)_5$ with Iron Pentacarbonyl

Iron pentacarbonyl (0.54 g, 2.75 mmol) and the tungsten complex (1) (0.2 g, 0.28 mmol) in benzene (10 mL) were heated at 150°C for 46 h. At the end of the reaction period the solution was orange with white solid particles. The usual procedure followed by chromatography on a Florisil column gave a yellow band which was eluted with petroleum ether. This was identified as

$(C_6H_5)_2PC{=}CCl(CF_2)_3Fe(CO)_4$

(0.015 g, 9.6%) of known spectroscopic properties. A 1% diethyl

TABLE 2. The reaction of $(C_6H_5)_2PC{=}CCl(CF_2)_3$, L, with $Fe(CO)_5$

L (mmol)	$Fe(CO)_5$ (mmol)	Reaction time (h)[a]	Products (%) $(L)Fe(CO)_4$	$(L - Cl - F)Fe_2(CO)_6$	$(L)_2Fe(CO)_3$
0.254	3.06	1	70.2	Trace	1.1
0.254	3.04	3	75.9	Trace	2.4
0.254	3.02	7.5	68.2	6	2.2
0.254	3.09	17	50	16.5	1.1
0.254	3.02	24	38	29.2	Trace
0.254	3.04	48	21	40.4	Trace

[a]All reactions were carried out at 150°C.

ether – 99% petroleum ether mixture eluted an orange band. This was identified as the corresponding $(L - Cl - F)Fe_2(CO)_6$ species (0.011 g, 6.3%) of known spectroscopic properties.

Results and Discussion

The simplest possible products anticipated from the reaction of a ligand

$R_2EC{=}CCl(CF_2)_n$

L, with an iron carbonyl are the mono-substituted derivatives

$R_2EC{=}CCl(CF_2)_nFe(CO)_4$

$(L)Fe(CO)_4$, where the group V donor has displaced one CO group from the parent carbonyl $Fe(CO)_5$.[3] As can be seen from Tables 1 and 2 both cyclobutene derivatives

$R_2PC{=}CCl(CF_2)_2$

($R = C_6H_5$ or C_6H_{11}) afford only these derivatives when reacted with $Fe(CO)_5$ at 140°C. At higher temperatures charring occurs.

This type of mono-substituted product is the one isolated when those ligands are reacted with the group VI hexacarbonyls (1). However,

$(C_6H_{11})_2PC{=}CCl(CF_2)_3$

reacts with iron pentacarbonyl to afford two novel products one of formula $(L - Cl - F)Fe_2(CO)_6$ (see footnote *a*, Table 1) and the other $(L - Cl)_2Fe_2(CO)_8$. The tetracarbonyl derivative $(L)Fe(CO)_4$ in this case is isolated from the reaction of L with $Fe_3(CO)_{12}$: the other two complexes are also produced.

The analogous diphenylphosphine complexes $(L - Cl - F)Fe_2(CO)_6$ and $(L)Fe(CO)_4$ (but not $(L - Cl)_2Fe_2(CO)_8$) are produced in the reaction of

$(C_6H_5)_2PC{=}CCl(CF_2)_3$

with $Fe(CO)_5$ at 150°C for 48 h. A shorter reaction time (3 h) affords a greater yield of the $(L)Fe(CO)_4$ complex and a disubstituted derivative $L_2Fe(CO)_3$ can also be isolated. The $(L)Fe(CO)_4$ and $(L - Cl - F)Fe_2(CO)_6$ complexes are also formed on ultraviolet irradiation of a benzene solution of the ligand and $Fe(CO)_5$.

In a similar manner

$(C_6H_5)_2PC{=}CCl(CF_2)_4$

affords a coupled $(L - Cl)_2Fe_2(CO)_8$ derivative and a cluster $(L - Cl - F)Fe_2(CO)_6$ (but no simple $(L)Fe(CO)_4$ derivative). The dicyclohexylphosphino analogue

$(C_6H_{11})_2PC{=}CCl(CF_2)_4$

yields the $(L)Fe(CO)_4$ and $(L - Cl - F)Fe_2(CO)_6$ complexes but not the coupled $(L - Cl)_2Fe_2(CO)_8$. Arsenic compounds apparently behave in a similar manner since

$(CH_3)_2AsC{=}CCl(CF_2)_3$

reacts with $Fe(CO)_5$ to give the $(L)Fe(CO)_4$ and $(L - Cl - F)Fe_2(CO)_6$ derivatives.

Characterization of the New Complexes

Analytical data are given in Table 3.

(L)Fe(CO)$_4$

$L = R_2PC{=}CCl(CF_2)_n$ ($R = C_6H_5$ or C_6H_{11}, $n = 2, 3, 4$) except

$(C_6H_5)_2PC{=}CCl(CF_2)_4$ and $(CH_3)_2AsC{=}CCl(CF_2)_3$

The mass spectra of these complexes show a parent ion followed by peaks corresponding to the loss of four carbonyl groups. The infrared spectra outside the ν(CO) region are similar to those of the free ligand and ν(C—F), ν(C=C), and ν(C—Cl) are essentially unshifted indicating that only the phosphorus (or arsenic) atom is involved in the bonding of L to the $Fe(CO)_4$ fragment. The ^{19}F nmr spectra are consistent with this interpretation.[1] In the ν(CO) region of the infrared spectra the $(L)Fe(CO)_4$ complexes show four bands one of which appears as a shoulder. This is to be expected if $(L)Fe(CO)_4$ is an axially substituted trigonal bipyramid and L is an asymmetric ligand (20). As can be seen from Table 4, the frequency of the ν(CO) bands for the

[3]These $(L)Fe(CO)_4$ complexes belong to class 1 described above.

Can. J. Chem. Downloaded from www.nrcresearchpress.com by 210.87.254.42 on 09/05/12
For personal use only.

TABLE 3. Analytical data for new iron carbonyl derivatives

Compound	Colour	Melting point (°C)	Analyses % C Calcd	C Found	H Calcd	H Found
$(C_6H_{11})_2PC{=}CCl(CF_2)_2Fe(CO)_4$	Orange	120	45.8	45.6	4.23	4.11
$(C_6H_5)_2PC{=}CCl(CF_2)_2Fe(CO)_4$	Orange	99	46.8	47.0	1.96	2.05
$[(C_6H_{11})_2C{=}C(CF_2)_3Fe(CO)_4]_2$	Pale yellow	131	46.7	46.4	4.11	4.29
$(C_6H_{11})_2PC{=}CCl(CF_2)_3Fe(CO)_4$	Yellow	118	43.9	43.9	3.86	3.80
$(C_6H_{11})_2PC{=}C{=}CF(CF_2)_2Fe_2(CO)_6$	Orange-red	78	43.6	43.6	3.50	3.55
$(C_6H_5)_2PC{=}CCl(CF_2)_3Fe(CO)_4$	Yellow-orange	110	44.8	44.8	1.80	1.87
$(C_6H_5)_2PC{=}C{=}CF(CF_2)_2Fe_2(CO)_6$	Orange-red	162	44.5	44.8	1.62	1.70
$((C_6H_5)_2PC{=}CCl(CF_2)_3)_2Fe(CO)_3$	Red	143	47.8	47.6	2.17	2.11
$(CH_3)_2AsC{=}CCl(CF_2)_3Fe(CO)_4$	Yellow	56	27.4	27.8	1.25	1.20
$(CH_3)_2AsC{=}C{=}CF(CF_2)_2Fe_2(CO)_6$	Red	152	28.9	28.6	1.12	1.10
$(C_6H_{11})_2PC{=}CCl(CF_2)_4Fe(CO)_4$	Yellow-orange	158	42.3	42.5	3.50	3.42
$(C_6H_{11})_2PC{=}C{=}CF(CF_2)_3Fe_2(CO)_6$	Orange	172	44.7[a]	44.3	3.89[a]	3.55
$[(C_6H_5)_2PC{=}C(CF_2)_4Fe(CO)_4]_2$	Yellow	75	45.7	45.7	1.74	2.00
$(C_6H_5)_2PC{=}C{=}CF(CF_2)_3Fe_2(CO)_6$	Orange	166	43.0	42.9	1.50	1.70

[a]Calculated for $C_{24}H_{22}F_7Fe_2O_6P.\ 0.5\ C_6H_{14}$.

diphenylphosphino derivatives are slightly higher than those of the dicyclohexylphosphino analogues. This feature is also observed for the $(L)M(CO)_5$ complexes (M = Cr, Mo, W) (1) and indicates that the diphenylphosphino complexes are the better π-acceptors (or σ-donors).

$(L)_2Fe(CO)_3$

L = $(C_6H_5)_2PC{=}CCl(CF_2)_3$. The mass spectrum confirms the formula and the nmr spectra indicate that the ligand is bound only through the phosphorus. The two ν(CO) bands suggest that the structure of $(L)_2Fe(CO)_3$ is a diaxially substituted trigonal bipyramid.

$(L - Cl)_2Fe_2(CO)_8$

L = $(C_6H_5)_2PC{=}CCl(CF_2)_4$, $(C_6H_{11})_2PC{=}CCl(CF_2)_3$. The infrared spectra of these complexes show no ν(C—Cl) bands and only weak ν(C=C) bands. The ν(CO) region shows four bands and the pattern is very similar to that of the $(L)Fe(CO)_4$ compounds described above. The absence of Cl is seen in both mass spectra. A peak corresponding to the molecular ion is present in the case of the diphenylphosphino derivative however the most intense peak corresponds to the ion $(L - Cl)Fe(CO)_4^+$ from which loss of four CO groups takes place. In the case of the dicyclohexylphosphino analogue, the parent ion is not seen in the mass spectrum and only peaks associated with $(L - Cl)Fe(CO)_4$ are observed. These data suggest that two complexes have the structure **10** (R = C_6H_5, n = 4; R = C_6H_{11}, n = 3) which is consistent with their ^{19}F nmr spectra.[1]

$(L - Cl - F)Fe_2(CO)_6$

L = $R_2PC{=}CCl(CF_2)_n$ R = C_6H_{11}, n = 3, 4; R = C_6H_5, n = 3, 4; and $(CH_3)_2AsC{=}CCl(CF_2)_3$.

It is easiest to describe this group of compounds in terms of the known structure of

$(C_6H_{11})_2PC{=}C{=}CF(CF_2)_2Fe_2(CO)_6$

5 even though the X-ray determination confirmed the structure deduced on the basis of the spectroscopic properties. Thus the infrared spectrum of **5** shows the absence of ν(C=C) and ν(C—Cl) and has a very different ν(C—F) pattern from the parent ligand. The ν(CO) region has six bands with a pattern similar to that reported for (L—L)-$Fe_2(CO)_6$ (6) (L—L =

$(CH_3)_2AsC{=}CAs(CH_3)_2(CF_2)_2$

and similar ligands) which have a similar structure. The Mössbauer spectrum shows the presence of two inequivalent iron atoms. The ^{19}F nmr (Fig. 1

Can. J. Chem. Downloaded from www.nrcresearchpress.com by 210.87.254.42 on 09/05/12
For personal use only.

TABLE 4. Infrared spectroscopic data for new iron carbonyl derivatives

Compound	ν(CO) cm^{-1}					
$(C_6H_{11})_2PC{=}CCl(CF_2)_2Fe(CO)_4$			2058(vs)	1985(s)	1970(sh)	1958(vs)
$(C_6H_5)_2PC{=}CCl(CF_2)_2Fe(CO)_4$			2060(vs)	1985(s)	1969(sh)	1960(vs)
$[(C_6H_{11})_2PC{=}C(CF_2)_3Fe(CO)_4]_2$			2058(s)	1983(s)	1950(sh)	1940(vs)
$(C_6H_{11})_2PC{=}CCl(CF_2)_3Fe(CO)_4$			2059(s)	1984(s)	1948(sh)	1945(vs)
$(C_6H_{11})_2PC{=}C{=}CF(CF_2)_2Fe_2(CO)_6$	2080(s)	2046(vs)	2020(s)	2012(s,sh)	1986(m)	1970(w)
$(C_6H_5)_2PC{=}CCl(CF_2)_3Fe(CO)_4$			2060(s)	1985(s)	1960(sh)	1952(vs)
$(C_6H_5)_2PC{=}C{=}CF(CF_2)_2Fe_2(CO)_6$	2080(s)	2050(vs)	2021(s)	2018(s,sh)	1998(m)	1985(w)
$((C_6H_5)_2PC{=}CCl(CF_2)_3)_2Fe(CO)_3$					1910(s)	1918(s)
$(CH_3)_2AsC{=}CCl(CF_2)_3Fe(CO)_4$			2056(s)	1982(s)	1958(sh)	1950(vs)
$(CH_3)_2AsC{=}C{=}CF(CF_2)_2Fe_2(CO)_6$	2084(s)	2050(vs)	2022(s)	2017(s,sh)	1998(m)	1975(w)
$(C_6H_{11})_2PC{=}CCl(CF_2)_4Fe(CO)_4$			2058(s)	1985(s)	1956(sh)	1950(vs)
$(C_6H_{11})_2PC{=}C{=}CF(CF_2)_3Fe_2(CO)_6$	2084(s)	2050(vs)	2025(s)	2018(s,sh)	1990(m)	1978(w)
$[(C_6H_5)_2PC{=}C(CF_2)_4Fe(CO)_4]_2$			2058(s)	1985(s)	1960(sh)	1950(vs)
$(C_6H_5)_2PC{=}C{=}CF(CF_2)_3Fe_2(CO)_6$	2090(s)	2055(vs)	2022(s)	2010(s,sh)	2022(m)	1990(w)

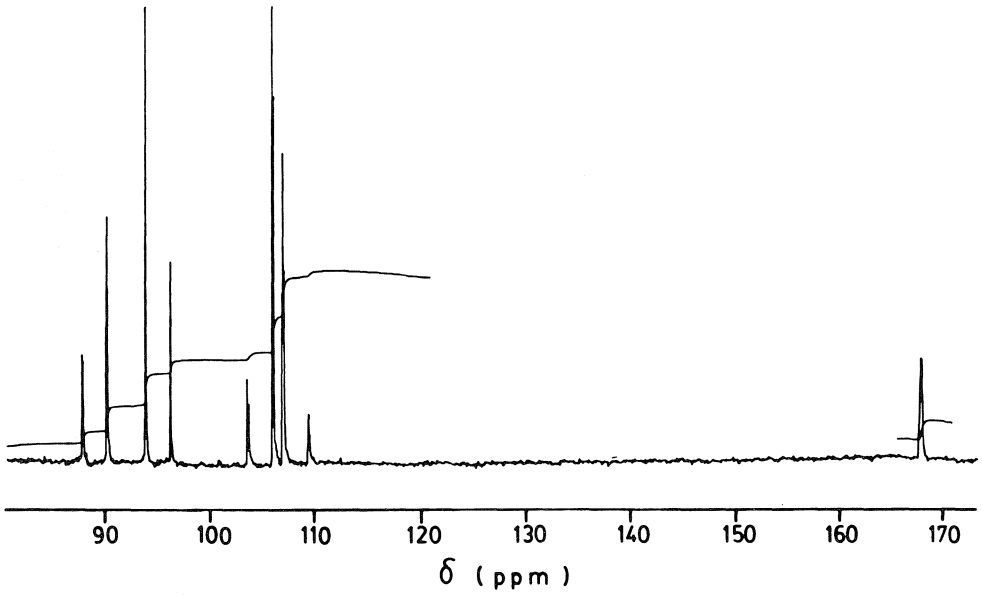


FIG. 1. The ^{19}F nmr spectrum of $(C_6H_{11})_2PC{=}C{=}CF(CF_2)_2Fe_2(CO)_6$.

and Table 5[1]) shows two "AB quartets" centred at 106.6 (J(F,F) = 224.7 Hz) and 92.06 ppm (J(F,F) = 224.9 Hz) and one up-field multiplet. The up-field shift of the single fluorine atom is probably due to a shielding effect of the allyl linkage (21, 22). The quartet with fewer additional couplings at 92.06 ppm can be assigned to the CF_2 group nearest the phosphorus atom. The ^{31}P nmr spectrum of **5** consists of a single multiplet (due to P–F coupling) but the down-field shift on complexing (Table 5) is much less than in the related $(L)Fe(CO)_4$ and $[(L-Cl)Fe(CO)_4]_2$ complexes indicating that the loss of electrons from the phosphorus atoms, because of donation to the metal, must be partly compensated by cluster formation.

The spectroscopic properties of the other complexes of formula $(L - Cl - F)Fe_2(CO)_6$ are very similar to those of **5** and they all undoubtedly have

Can. J. Chem. Downloaded from www.nrcresearchpress.com by 210.87.254.42 on 09/05/12
For personal use only.

Can. J. Chem. Downloaded from www.nrcresearchpress.com by 210.87.254.42 on 09/05/12
For personal use only.

the same basic skeleton. In the case of the cyclohexenyl derivative the ^{19}F nmr spectra show three sets of "AB quartets" but these cannot be assigned with any certainty to a particular CF_2 group.[1]

Coupling reactions of halocarbons in the presence of $Fe(CO)_5$ are well known, e.g. eq. [1] (23). The interesting feature of the reactions

[1] $(C_6H_5)_2CCl_2 + Fe(CO)_5 \rightarrow (C_6H_5)_2C{=}C(C_6H_5)_2$

which give rise to the two derivatives **10** is that the basic ligands

$$R_2\overline{PC{=}C(CF_2)_n}\,\overline{C{=}CPR_2(CF_2)_n}$$

have not been reported previously. Attempts to prepare them by reacting the appropriate phosphine R_2PH with

$$Cl\overline{C{=}C(CF_2)_n}\,\overline{C{=}CCl(CF_2)_n}$$

give disubstitution only when $n = 2$ (24). Related coupling reactions to give **8** and **7** have already been described in the Introduction. In these cases coupling occurs by loss of $-As(CH_3)_2$ and H respectively from the ligands, and the unsaturated bridging groups are coordinated to a metal center or metal centers. In **10** the newly formed unsaturated bridge is not involved in further bonding.

A compound of structure **10** $R = C_6H_5$, $n = 2$ is produced in low yield from the reaction of the free ligand with $Fe(CO)_5$ although in this case the main products are isomers of formula $(L)Fe_2(CO)_6$ in which the ligand has undergone considerable rearrangement (25).

There are numerous known η^3-allyl complexes of iron (26) including some which are partly fluorocarbon. However, only one example was previously known in which the allyl group is a fluorocarbon moiety (27), this is the (η^3-nonafluorocyclohexenyl)tricarbonyliron anion obtained from (η^4-octafluorocyclohexa-1,3-diene)tricarbonyliron by fluoride ion addition. The compounds of structure **5** (and **4**) are also very unusual in that they contain a ligand which is η^n-bonded with respect to one metal and η^1-bonded to another.

In an attempt to gain some insight into the mechanism of formation of these $(L - Cl - F)Fe_2(CO)_6$ complexes some studies were conducted with

$$(C_6H_5)_2P\overline{C{=}CCl(CF_2)_3}$$

In the presence of $Fe(CO)_5$ reaction occurs (Table 2) with the first formed product being $(L)Fe(CO)_4$. As the reaction time increases the first formed $(L)Fe(CO)_4$ appears to react with the excess $Fe(CO)_5$ to give $(L - Cl - F)Fe_2(CO)_6$. This is confirmed by a separate experiment. Thus heating $(L)Fe(CO)_4$ and $Fe(CO)_5$ at 150°C gives a 33% yield of $(L - Cl - F)Fe_2(CO)_6$. Because of these results, we hoped that a mixed metal derivative might be formed by reacting (150°C)

$$(C_6H_5)_2P\overline{C{=}CCl(CF_2)_3}W(CO)_5$$

with $Fe(CO)_5$. Only low yields of the appropriate $LFe(CO)_4$ and $(L - Cl - F)Fe_2(CO)_6$ were obtained. The reaction probably proceeds by ligand exchange followed by further reaction of the $(L)Fe(CO)_4$ with $Fe(CO)_5$.

The properties of complexes of structure **5** are of interest since potential sites of activation are the Fe—Fe bond the CO groups and the η^3-allyl group. A preliminary study has shown that the diphenylphosphino analogue of **5** is an efficient catalyst for the photochemical isomerization of olefins, though not their photochemical hydrogenation (28).

In conclusion it should be pointed out that it is difficult to explain why the derivatives of the cyclobutenes

$$R_2P\overline{C{=}CCl(CF_2)_2}Fe(CO)_4$$

do not react further to give the $Fe_2(CO)_6$ derivatives since there are numerous examples known of η^3-allyl groups derived from 4-carbon rings (26).

Acknowledgments

The authors are grateful to Natural Sciences and Engineering Council of Canada for financial support of this work. M.W. wishes to thank the Canadian Commonwealth Scholarship and Fellowship Committee for an award.

1. W. R. Cullen and M. Williams. J. Fluorine Chem. **14**, 273 (1979).
2. W. R. Cullen, M. Williams, F. W. B. Einstein, and A. C. Willis. J. Organomet. Chem. **155**, 259 (1978).
3. M. A. Bennett, R. N. Johnson, and I. B. Tomkins. J. Am. Chem. Soc. **96**, 61 (1974).
4. K. D. Tau, D. W. Meek, and T. Sorrell. Inorg. Chem. **17**, 3454 (1978).
5. H. N. Paik, A. J. Carty, K. Dymock, and G. J. Palenik. J. Organomet. Chem. **70**, C17 (1974).
6. W. R. Cullen, D. A. Harborne, B. V. Liengme, and J. R. Sams. Inorg. Chem. **8**, 95 (1969).
7. W. R. Cullen and D. A. Harbourne. Inorg. Chem. **9**, 1839 (1970).
8. J. P. Crow and W. R. Cullen. Inorg. Chem. **10**, 1529 (1971).
9. M. A. Bennett, P. W. Clark, G. B. Robertson, and P. O. Whimp. J. Organomet. Chem. **63**, C15 (1973).
10. J. P. Crow, W. R. Cullen, F. L. Hou, L. Y. Y. Chan, and F. W. B. Einstein. J. Chem. Soc. Chem. Commun. 1229 (1971).
11. W. R. Cullen, D. A. Harbourne, B. V. Liengme, and J. R. Sams. Inorg. Chem. **9**, 702 (1970).
12. W. R. Cullen, L. M. Mihichuk, F. W. B. Einstein, and J. F. Field. J. Organomet. Chem. **73**, C53 (1974).
13. M. A. Bennett, R. N. Johnson, and I. B. Tomkins. Inorg. Chem. **14**, 1908 (1975).

14. J. P. CROW and W. R. CULLEN. Inorg. Chem. **10**, 2156 (1971).
15. F. W. B. EINSTEIN and R. D. G. JONES. J. Chem. Soc. Dalton Trans. 2568 (1972).
16. T. O'CONNOR, A. J. CARTY, M. MATHEW, and G. J. PALENIK. J. Organomet. Chem. **38**, C15 (1972).
17. M. MATHEW, G. J. PALENIK, A. J. CARTY, and H. N. PAIK. J. Chem. Soc. Chem. Commun. 25 (1974).
18. A. J. CARTY, S. E. JACOBSON, R. T. SIMPSON, and N. J. TAYLOR. J. Am. Chem. Soc. **97**, 7254 (1975).
19. W. R. CULLEN, M. WILLIAMS, F. W. B. EINSTEIN, and C. H. HUANG. J. Fluorine Chem. **11**, 338 (1978).
20. W. R. CULLEN, D. A. HARBOURNE, B. V. LIENGME, and J. R. SAMS. Inorg. Chem. **8**, 1464 (1964).
21. R. D. CHAMBERS, A. PARKIN, and R. S. MATHEWS. J. Chem. Soc. Perkin Trans. 2107 (1976).
22. R. D. CHAMBERS, R. S. MATHEWS, and A. PARKIN. J. Chem. Soc. Chem. Commun. 509 (1973).
23. C. E. COFFEY. J. Am. Chem. Soc. **83**, 1623 (1961).
24. W. R. CULLEN, A. W. WU, A. R. DAVIS, F. W. B. EINSTEIN, and J. D. HAZLETT. Can. J. Chem. **54**, 2871 (1976).
25. R. E. COBBLEDICK, W. R. CULLEN, F. W. B. EINSTEIN, and M. WILLIAMS. Unpublished work.
26. R. B. KING. *In* The organic chemistry of iron. Vol. 1. *Edited by* F. A. Koerner von Gustorf, F. W. Grevels, and I. Fischler. Academic Press, London. 1978. p. 463.
27. G. W. PARSHALL and G. WILKINSON. J. Chem. Soc. 1132 (1962).
28. W. R. CULLEN and M. WILLIAMS. J. Fluorine Chem. In press.

Can. J. Chem. Downloaded from www.nrcresearchpress.com by 210.87.254.42 on 09/05/12
For personal use only.

3,5-Dimethylpyrazolylphosphine molybdenum(0) and tungsten(0) carbonyl complexes

HARRY B. DAVIS, JAMES K. HOYANO, PING YUEN LEUNG,
LOUIS K. PETERSON, AND BRIAN WOLSTENHOLME
Department of Chemistry, Simon Fraser University, Burnaby, B.C., Canada V5A 1S6

Received July 9, 1979

HARRY B. DAVIS, JAMES K. HOYANO, PING YUEN LEUNG, LOUIS K. PETERSON, and BRIAN WOLSTENHOLME. Can. J. Chem. **58**, 151 (1980).

Complexes with the general formula $[L_nM(CO)_m]$, where $L = \phi_xP(Me_2pz)_{3-x}$, $x = 0$–2, $n = 1$ or 2, M = Mo(0) or W(0), $m = 3$ or 4, were prepared by thermal or photolytic methods by the reaction of the appropriate 3,5-dimethylpyrazolyl phosphine ligand with $M(CO)_6$, norbornadienemetaltetracarbonyl $[C_7H_8M(CO)_4]$, cycloheptatrienylmetaltricarbonyl $[C_7H_8M(CO)_3]$, $[(Me_2N(CH_2)_3NMe_2)M(CO)_4]$, $[(CH_3CN)_2M(CO)_4]$, or $[CH_3CN)_3M(CO)_3]$. Structural evidence indicates octahedral geometry about the metal atom centre, and several modes of coordination for the ligands in those complexes isolated and characterized. For $x = 2$, the ligand $\phi_2P(Me_2pz)$ was monodentate, via phosphorus in $[(\phi_2P(Me_2pz))_2M(CO)_4]$ (**I**, **II**), and bidentate in $[\phi_2P(Me_2pz)M(CO)_4]$ (**III**, **IV**) where coordination by P and the 2N site of the pyrazolyl ring yielded four-membered $\overline{MPNN}$ metallocycles. For $x = 1$, the $\phi P(Me_2pz)_2$ ligand was bidentate, via the phosphorus atom and one of the 2N sites of one of the pyrazolyl substituents, thus giving the four-membered $\overline{MNNP}$ metallocycle in $[\phi P(Me_2pz)_2W(CO)_4]$ (**V**), and tridentate in $[\phi P(Me_2pz)_2M(CO)_3]$ (**VI**, **VII**) where three *facial* CO's, two 2N atoms of the pyrazolyl rings, and a part of the phenyl ring occupy the six coordination sites. For $x = 0$, the $P(Me_2pz)_3$ ligand was tridentate via the 2N atoms of all three pyrazolyl rings, thus giving tricyclic systems $[P(Me_2pz)_3M(CO)_3]$ (**VIII**, **IX**).

HARRY B. DAVIS, JAMES K. HOYANO, PING YUEN LEUNG, LOUIS K. PETERSON et BRIAN WOLSTENHOLME. Can. J. Chem. **58**, 151 (1980).

Les complexes de formule générale $[L_nM(CO)_m]$ où $L = \phi_xP(Me_2pz)_{3-x}$, $x = 0$–2, $n = 1$ ou 2, M = Mo(0) ou W(0), $m = 3$ ou 4 sont préparés au moyen de méthodes thermiques ou photolytiques par la réaction du ligand approprié: diméthyl-3,5 pyrazolyle phosphine avec $M(CO)_6$, norbornadiènemétaltétracarbonyle $[C_7H_8M(CO)_4]$ cycloheptatrièmylmétaltricarbonyle $[C_7H_8M(CO)_3]$, $[(Me_2N(CH_2)_3NMe_2)M(CO)_4]$, $[(CH_3CN)_2M(CO)_4]$ ou $[(CH_3CN)_3M(CO)_3]$. Les données structurales indiquent qu'il existe une géométrie octaèdrique autour de l'atome de métal central et plusieurs modes de coordination des ligands dans les complexes isolés et caractérisés. Pour $x = 2$, le ligand $\phi_2P(Me_2pz)$ est monodentate par l'intermédiaire du phosphore dans $[\phi_2P(Me_2pz))_2M(CO)_4]$ (**I**, **II**) et bidentate dans $[\phi_2P(Me_2pz)M(CO)_4]$ (**III**, **IV**) où la coordination par le phosphore et l'azote 2 du cycle pyrazolyle donne les métallocycles à 4 chaînons $\overline{MPNN}$. Pour $x = 1$ le ligand $\phi P(Me_2pz)_2$ est bidentate par l'intermédiaire de l'atome de phosphore et un des deux azote des substituants pyrazolyles donnant ainsi un métallocycle à 4 chaînons $\overline{MNNP}$ dans le complexe $[\phi P(Me_2pz)_2W(CO)_4]$ (**V**). Le ligand $\phi P(Me_2pz)_2$ est tridentate dans le complexe $[\phi P(Me_2pz)_2M(CO)_3]$ (**VI**, **VII**) où les trois CO en position faciale, deux atomes d'azote 2 des cycles pyrazolyles et une partie du cycle phényle occupent les six sites de coordination. Pour $x = 0$ le ligand $P(Me_2pz)_3$ est tridentate par l'intermédiaire des atomes d'azote 2 des trois cycles pyrazolyles donnant ainsi des systèmes tricycliques $[P(Me_2pz)_3M(CO)_3]$ (**VIII**, **IX**).

[Traduit par le journal]

Introduction

There is currently an interest in the chemistry of transition metal complexes formed by polydentate ligands containing different donor atoms, including various structural combinations of phosphine and amine type centres (1). The potential of such systems to exhibit subtle variations in properties, with possible applications in homogeneous catalytic processes, has stimulated much interest and research effort in this field. We have previously described the syntheses of pyrrolyl- (2) and pyrazolyl-phosphine (3) ligand systems, and the formation of complexes of the latter with manganese(I) and rhenium(I) (4).

We report here our investigations of 3,5-dimethylpyrazolylphosphine complexes of molybdenum(0) and tungsten(0).

Discussion

In general, the reactions of the dimethylpyrazolylphosphine ligands $\phi_xP(Me_2pz)_{3-x}$ ($x = 0$–2) with the substituted metal carbonyls $[C_7H_8M(CO)_4]$, $[(Me_2NCH_2CH_2CH_2NMe_2)M(CO)_4]$, $[(CH_3CN)_2M(CO)_4]$, $[C_7H_8M(CO)_3]$, and $[(CH_3CN)_3M(CO)_3]$ (M = Mo or W) proceed under relatively mild conditions, and the derivatives of molybdenum react more readily than those of tungsten. When hexacarbonyl $M(CO)_6$ was used, more vigorous reaction conditions were required. Preliminary studies showed that prolonged heating (> 12 h) of the pyrazolylphosphine ligands $\phi_xP(H_2pz)_{3-x}$ with $Mo(CO)_6$ in refluxing benzene gave highly insoluble products, with analyses and ir data (ν_{CO} region) consistent for tricarbonyl formulations $[LM(CO)_3]$, possibly with polymeric structures.[1] Prolonged heating of $[\phi_2P(Me_2pz)Mo(CO)_4]$ (**III**) under similar conditions also gave insoluble products.

[1]S. Fischer and L. K. Peterson, unpublished observations.

0008-4042/80/020151-08$01.00/0
©1980 National Research Council of Canada/Conseil national de recherches du Canada

Can. J. Chem. Downloaded from www.nrcresearchpress.com by 210.87.254.6 on 09/05/12
For personal use only.

Can. J. Chem. Downloaded from www.nrcresearchpress.com by 210.87.254.6 on 09/05/12
For personal use only.

TABLE 1. Carbonyl stretching frequencies (cm^{-1}) of 3,5-dimethylpyrazolylphosphine complexes of Mo(0) of W(0)*

(*a*) *trans*-Metaltetracarbonyl structures

Compound	Remark	Colour	E_u
$(\phi_2P(Me_2pz))_2Mo(CO)_4$	**I**	White	1900
$(\phi_3P)_2Mo(CO)_4$	Ref. 8		1902
$(\phi_2P(Me_2pz))_2W(CO)_4$	**II**	White	1895
$(\phi_3P)_2W(CO)_4$	Ref. 9		1894

(*b*) *cis*-Metaltetracarbonyl structures

Compound	Remark	Colour	Frequency			
			$A_1^{(2)}$	$A_1^{(1)}$	B_1	B_2
$\phi_2P(Me_2pz)Mo(CO)_4$†	**III**	Golden yellow	2012	1923	1915	1890
$(\phi_2PC_2H_4P\phi_2)Mo(CO)_4$	Ref. 21		2020	1919	1907	1881
$(Pyridine)_2Mo(CO)_4$	Ref. 24		2025	1907	1881	1839
$(dipy)Mo(CO)_4$	Ref. 24		2017	1909	1878	1829
$\phi_2P(Me_2pz)W(CO)_4$	**IV**	Yellow	2020	1910	1885	1850
$\phi_2P(Me_2pz)_2W(CO)_4$	**V**	Yellow	2020	1915	1895	1860
$(\phi_2PC_2H_4P\phi_2)W(CO)_4$	Ref. 21		2016	1912	1901	1876
$(Pyridine)_2W(CO)_4$	Ref. 24		2012	1888	1869	1828
$dipyl)W(CO)_4$	Ref. 24		2010	1899	1873	1826

(*c*) *fac*-Metaltricarbonyl structures

Compound	Remark	Colour	Frequency	
			A_1	E
$\phi P(Me_2pz)_2Mo(CO)_3$	**VI**	Orange	1920	1805
$\phi P(Me_2pz)_2W(CO)_3$	**VII**	Red	1920	1805
$P(Me_2pz)_3Mo(CO)_3$‡	**VIII**	Yellow	1905	1770
$P(Me_2pz)_3W(CO)_3$‡	**IX**	Yellow	1885	1755
$(Pyridine)_3Mo(CO)_3$	Ref. 31		1885	1755
$(4\text{-mpdpa})Mo(CO)_3$	Ref. 32		1898	1776
$MeC(CH_2P\phi_2)_3Mo(CO)_3$	Ref. 21		1930	1834
$MeC(CH_2P\phi_2)_3W(CO)_3$	Ref. 21		1930	1834

*Spectra were run in chloroform, unless noted otherwise.
†In hexane.
‡In Nujol.

The products **I**–**IX** were characterized according to elemental analyses, mass, infrared (Table 1), ^1H (Table 2), and ^{31}P (Table 3) nmr spectroscopic data. The pure complexes are moderately air-stable crystalline solids, whereas the free ligands are readily oxidized and hydrolysed in air (3).

Complexes of Diphenyl(3,5-dimethylpyrazolyl)-phosphine, $\phi_2P(Me_2pz)$

Six isomeric octahedral structures are possible for the $[L_2M(CO)_4]$ complexes $[(\phi_2P(Me_2pz))_2M(CO)_4]$ (M = Mo, **I**; W, **II**) where the pyrazolylphosphine ligands may coordinate via phosphorus or via nitrogen in *cis*- or *trans*-configurations. The ^{31}P spectra of **I** and **II** (Table 3) indicated equivalent phosphorus nuclei, and the coordination shifts (−66 and −44 ppm, respectively) suggest direct phosphorus–metal bonding. This conclusion is corroborated by evidence of a doublet satellite resonance in the ^{31}P spectrum of **II**, arising from coupling between phosphorus and the ^{183}W nucleus ($I = \frac{1}{2}$, natural abundance, 14.3%, giving a 7:86:7 triplet (5)). The coupling constant ($J_{^{31}P-^{183}W}$ = 320 Hz) is of a magnitude comparable to literature values for phosphine–tungsten complexes (5–7). Also, ^1H nmr evidence indicated equivalent 3,5-dimethylpyrazolyl rings in **I** and in **II**. The ir spectra of **I** and **II** show only one strong ν(CO) band, indicative of a *trans*-octahedral D_{4h} structure, and with essentially the same energy as the E_u mode of *trans*-$[(\phi_3P)_2M(CO)_4]$ complexes (M = Mo (8), W (9)). Similarly, the pyrrolylphosphine com-

TABLE 2. ^{1}H nmr data for 3,5-dimethylpyrazolylphosphine complexes of Mo(0) and W(0)*

Compound	Remark	Chemical shifts† 3-Me	5-Me	4-H
trans-$(\phi_2P(Me_2pz))_2Mo(CO)_4$	**I**	7.80	8.35	4.10(b)
trans-$(\phi_2P(Me_2pz))_2W(CO)_4$	**II**	7.76	8.57	4.08(b)
cis-$\phi_2P(Me_2pz)Mo(CO)_4$	**III**	7.82	8.10	4.03(b)
cis-$\phi_2P(Me_2pz)W(CO)_4$	**IV**	8.08	8.56	4.50(vb)
cis-$\phi P(Me_2pz)_2W(CO)_4$	**V**	7.62 7.82	7.68 8.27	3.92(b) 4.27(vb)
$\phi P(Me_2pz)_2Mo(CO)_3$	**VI**	7.44	7.48	3.95d‡
$\phi P(Me_2pz)_2W(CO)_3$	**VII**	7.41	7.45	3.97d§
$\phi_2P(Me_2pz)$	Ref. 4	7.57	7.78	4.10(b)
$\phi P(Me_2pz)_2$	Ref. 4	7.65	7.72	4.08(b)

*Spectra were measured in $CDCl_3$ solution, and data are given in τ values (ppm), relative to internal TMS.
†Resonances are singlets, unless specified otherwise. Phenyl resonances were observed at τ 2.5–2.8; b = broad, vb = very broad.
‡Doublet, J_{P-H} = 2.80 Hz.
§Doublet, J_{P-H} = 3.00 Hz.

TABLE 3. ^{31}P nmr data for 3,6-dimethylpyrazolylphosphine complexes of Mo(0) and W(0)*

Compound	Remark	Chemical shifts† $\delta^{31}P$	$\Delta^{31}P$‡
trans-$(\phi_2P(Me_2pz))_2Mo(CO)_4$	**I**	−104	−66
trans-$(\phi_2P(Me_2pz))_2W(CO)_4$	**II**	−88§	−44
cis-$\phi_2P(Me_2pz)Mo(CO)_4$	**III**	−96	−59
cis-$\phi_2P(Me_2pz)W(CO)_4$	**IV**	−91‖	−52
$\phi P(Me_2pz)_2W(CO_4$	**V**	−102¶	−45
$\phi P(Me_2pz)_2Mo(CO)_3$	**VI**	−44	+17
$\phi P(Me_2pz)_2W(CO)_3$	**VII**	−42	+19
$\phi_2P(Me_2pz)$	Ref. 4	−39	—
$\phi P(Me_2pz)_2$	Ref. 4	−61	—

*Measured with the Varian XL-100 instrument, operating in the FT mode under conditions of broad band proton decoupling. Solvents were toluene for Mo complexes and $CDCl_3$ for W complexes.
†In ppm, downfield relative to 85% H_3PO_4.
‡$\Delta^{31}P$ = coordination chemical shift = ($\delta^{31}P$(free ligand) − $\delta^{31}P$(complex)).
§$J_{^{31}P-^{183}W}$ = 320 Hz.
‖$J_{^{31}P-^{183}W}$ = 267 Hz.
¶$J_{^{31}P-^{183}W}$ = 314 Hz.

plexes $[(\phi_2P(R_2py))_2Mo(CO)_4]$ (R = H, pyrrolyl; R = Me, 2,5-dimethylpyrrolyl) prefer a *trans* rather than a *cis*-configuration.[2]

The complexes of $[\phi_2P(Me_2pz)M(CO)_4]$ (M = Mo, **III**; W, **IV**) showed mononuclear parent ions and loss of four CO groups in their mass spectra, and four ir bands were observed in the carbonyl stretching region (Table 1). In both cases the ^{31}P coordination shifts were appreciably downfield (Table 3) and, for **IV**, direct phosphorus–tungsten coupling ($J_{^{31}P-^{183}W}$ = 267 Hz) was observed. These data indicate a mononuclear, *cis*-tetracarbonyl pseudo-C_{2v} structure (10–12) for **III** and **IV**, containing coordinated phosphorus (5–7) in a four-membered $\overline{MPNN}$ metallocycle. Structurally similar $\overline{MPNN}$ and $\overline{MPCC}$ metallo-rings are found in $[\phi_2P(Me_2pz)Mn(CO)_3Cl]$ (13) and in *ortho*-metallated insertion products of the type $(CH_3C_6H_4)_2\overline{PC_6H_3(CH_3)Mn}(CO)_4]$ (14), respectively.

Whereas the phosphorus bonded *trans*-$[(\phi_2P(Me_2pz))_2M(CO)_4]$ (**I** and **II**) derivatives were readily obtained by employing excess ligand in solution, corresponding attempts to prepare bis-ligand manganese and rhenium analogs yielded only $[\phi_2P(Me_2pz)M(CO)_3X]$ (M = Mn, Re; X = Cl, Br). The latter compounds are also resistant to nucleophilic attack by excess $\phi_2P(Me_2pz)$, ϕ_3P, and CO (4).

Complexes of bis(3,5-Dimethylpyrazolyl)phenylphosphine, $\phi P(Me_2pz)_2$

The reaction of $\phi P(Me_2pz)_2$ with [(nbd)Mo(CO)$_4$],[3] $[(CH_3CN)_3Mo(CO)_3]$, or [(cht)Mo(CO)$_3$][4]

[2]L. K. Peterson and B. Gour, unpublished observations.

[3]nbd = norbornadiene.

[4]cht = cycloheptatriene.

Can. J. Chem. Downloaded from www.nrcresearchpress.com by 210.87.254.6 on 09/05/12
For personal use only.

Can. J. Chem. Downloaded from www.nrcresearchpress.com by 210.87.254.6 on 09/05/12
For personal use only.

gave the same complex $[\phi P(Me_2pz)_2Mo(CO)_3]$ (**VI**, orange-red). The reaction of $\phi P(Me_2pz)_2$ with $[(CH_3CN)_3W(CO)_3]$ gave $[\phi P(Me_2pz)_2W(CO)_3]$ (**VII**, dark red).

A crystal structure determination of **VII** (15) shows a monomeric species, with an octahedral tungsten centre coordinated by three facial carbonyl groups, by two 2N centres of the pyrazolyl rings, and by a portion of the phenyl group. The latter appears to function in a novel fashion as a "2-electron donor" in this structure, presumably in order to achieve an 18-electron configuration.

In the complexes $[H_2B(Me_2pz)_2Mo(CO)_2(C_7H_7)]$ (16) and $[(C_2H_5)_2B(pz)_2Mo(CO)_2(\eta^2\text{-allyl})]$ (17, 18), Cotton *et al.* have found that 16-electron configurations are avoided by virtue of B---H---Mo or αC---H---Mo three centre-two electron bridge bonding, respectively. The seemingly three-coordinate cation $[(\phi_3P)_3Rh]^+$ is apparently stabilized in a similar fashion, by interactions between Rh and two proximal carbon atoms and one *ortho* hydrogen of a phenyl ring (19). Interestingly, the steric requirements about four-coordinate boron in $[(C_6H_5)_2B(pz)_2(CO)_2(2\text{-methylallyl})Mo]$ (20) preclude a Mo---H---C interaction, thus leaving the metal with a 16-electron valence shell configuration. Three-coordinate phosphorus in our compound $[\phi P(Me_2pz)_2W(CO)_3]$ (**VII**) is less sterically demanding, allowing the phenyl ring to orient itself so as to interact with the metal centre.

On the basis of spectroscopic evidence, compounds **VI** and **VII** have essentially similar structures. Both species exhibit mononuclear parent ions and loss of three CO groups in their mass spectra. Their solution ir spectra show two strong bands in the carbonyl stretching region, indicative of pseudo C_{3v} structures. The relatively low frequencies of the ir bands, as compared to $[MeC(CH_2P\phi_2)_3M(CO)_3]$ (21) complexes (Table 1), suggest coordination by weak π-accepting centres (viz., the 2N's of the pyrazolyl rings and either the phenyl ring or a solvent molecule occupying the sixth coordination site). ^1H nmr spectra show that the pyrazolyl rings are equivalent at ambient temperature, and compounds **VI** and **VII** exhibit singlet ^{31}P resonances with positive coordination shifts (+17 and +19 ppm respectively). This latter effect may be attributed to changes in bond angles about phosphorus (7, 22, 23).

The compounds $[\phi P(Me_2pz)_2M(CO)_3]$ (**VI** and **VII**) slowly react with chloroform, but are stable under nitrogen in benzene, toluene, and tetrahydrofuran. Freshly prepared solutions of **VI** and **VII** react readily with carbon monoxide, as shown by a change in colour, from orange-red to yellow, and by the appearance of new ^{31}P nmr signals. The reactions of **VI** and **VII** with donor molecules will be reported later.

The reaction of $\phi P(Me_2pz)_2$ with $[(CH_3CN)_2W(CO)_4]$ yielded $[\phi P(Me_2pz)_2W(CO)_4]$ (**V**, yellow). Four ir bands were observed in the carbonyl stretching region, indicating a *cis*-tetracarbonyl pseudo C_{2v} configuration (10–12). Structures based on a six-membered $P(N—N)_2W$ metallocycle (Fig. 1) or on a four-membered $\overline{PNNW}$ metallocycle (Fig. 2) are possible. The ^1H nmr spectrum of **V** (Table 2) showed four equal intensity methyl and two equal intensity 4-H resonances, indicative of non-equivalent pyrazolyl rings. The ^{31}P spectrum consisted of a downfield singlet resonance, with tungsten satellites, indicating direct phosphorus-to-metal bonding (5–7). These data are consistent for a *cis*-tetracarbonyl, four-membered metallocycle, containing one coordinated and one free pyrazolyl moiety (Fig. 2). The alternative six-membered metallocycle arrangement (Fig. 1) is precluded.

The molybdenum analog $[\phi P(Me_2pz)_2Mo(CO)_4]$ of **V** is readily formed by the reaction of CO with a solution of $[\phi P(Me_2pz)_2Mo(CO)_3]$ (**VI**) in toluene, but has not yet been isolated pure. Its infrared, ^1H and ^{31}P nmr spectra indicate a structure analogous to that of $[\phi P(Me_2pz)_2W(CO)_4]$ (**V**). In fact, the ir spectra (ν_{CO} region) of the tetracarbonyl complexes $[\phi_2P(Me_2pz)M(CO)_4]$, $[\phi P(Me_2pz)_2M(CO)_4]$, and $[(\phi_2PC_2H_4P\phi_2)M(CO)_4]$ (21) are quite similar, but differ significantly from the spectra of *cis*-$[(pyridine)_2M(CO)_4]$ (24) and $[(dipyridyl)M(CO)_4]$ (24), in which two *cis* coordination sites are occupied by weakly π-bonding ligands that are similar to pyrazolyl moieties. Thus the ligands $\phi_2P(Me_2pz)$ and $\phi P(Me_2pz)_2$ closely resemble $\phi_2PC_2H_4P\phi_2$, in terms of σ donor and π acceptor behaviour, in molybdenum and tungsten tetracarbonyl complexes.

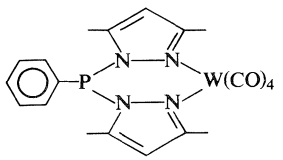


FIG. 1. Six-membered $P(N—N)_2W$ metallocycle.

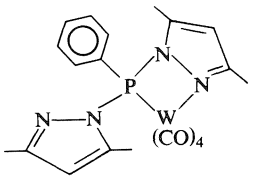


FIG. 2. Four-membered $\overline{PNNW}$ metallocycle.

Can. J. Chem. Downloaded from www.nrcresearchpress.com by 210.87.254.6 on 09/05/12
For personal use only.

Interestingly, the d^6 rhenium(I) complex $[\phi P(Me_2pz)_2Re(CO)_3Br]$ is structurally different from **V**. The former adopts a six-membered $P(N—N)_2Re$ boat metallocyclic form (15), a structure common among complexes of pyrazolylborate (25, 26) and pyrazolylgallate (27, 28) ligands, whereas **V** contains a four-membered metallocycle (Fig. 2). Using CPK Atomic Models,[5] we constructed molecular structures based on Figs. 1 and 2. Two boat configurations are possible for Fig. 1. One structure, with the phosphorus lone pair and a carbonyl group (say group "A") in "*endo*" positions, shows severe steric interaction between the phenyl ring and the two 5-methyl groups of the pyrazolyl rings. The second structure, with the phenyl ring and carbonyl group "B" ("B" being *trans* to "A") in "*endo*" positions, shows steric interference between the phenyl ring and group "B", and neatly accounts for the formation of the tricarbonyl derivatives $[\phi P(Me_2Pz)_2M(CO)_3]$ (**VI** and **VII**), via a sterically assisted elimination of CO. Note that in the analogous structure for $[\phi P(Me_2pz)_2Re(CO)_3Br]$ group "B" is CO, rather than Br, for steric reasons, and, being *trans* to the bromide ligand (corresponding to group "A"), is not as readily displaced as in the molybdenum- and tungsten-tetracarbonyl cases.

A study of the models also shows that the steric congestion of the boat forms of Fig. 1 is released when the four-membered metallocyclic structure (Fig. 2) is formed. This occurs because one of the 3,5-dimethylpyrazolyl rings is free to rotate. It also appears that an analogous metallocyclic structure would be accessible to $[\phi P(Me_2pz)_2Re(CO)_3Br]$, but would require the bromide ligand to orient *cis*, rather than *trans*, to a carbonyl group. The resulting structure would have an energy disadvantage associated with two *trans* carbonyl groups, and is presumably less stable than the all *cis* arrangement actually observed in the $P(N—N)_2Re$ boat form (15).

Complexes of tris-(3,4-Dimethylpyrazolyl) phosphine, $P(Me_2pz)_3$

The ligand $P(Me_2pz)_3$ was found to react with tetracarbonyl and with tricarbonyl derivatives of molybdenum and tungsten to yield highly insoluble products formulated as $[P(Me_2pz)_3M(CO)_3]$ (M = Mo, **VIII**; M = W, **IX**).

The complexes **VIII** and **IX** exhibit two strong ν(CO) bands in their ir spectra, and the pyrazolyl rings were found to be equivalent according to ^1H nmr spectra. Mass spectra showed mononuclear parent ions, and species corresponding to the consecutive loss of three CO groups. Hence, a C_{3v} tricyclic structure is indicated, with three *facial* CO groups, and the $P(Me_2pz)_3$ ligand coordinated symmetrically via the 2N atoms of all three pyrazolyl rings. Similar tridentate chelating character has also been reported for pyrazolylborate (25, 26, 29) and pyrazolylgallate (30) ligands.

The relatively low ν_{CO} stretching frequencies for **VIII** and **IX** (~1750–1770 and 1880–1900 cm^{-1}, Table 1) are consistent with the weak π-accepting character of the pyrazolyl ligands. Likewise, two low energy bands are observed for *fac*-$[(pyridine)_3Mo(CO)_3]$ (31) and for tri-(2-pyridyl)-aminemolybdenumtricarbonyl complexes (32), in which the pyridine ligands have coordination properties similar to those of pyrazolyl moieties (24). By contrast, the phosphorus bonded C_{3v} tricyclic structures $[MeC(CH_2P\phi_2)_3M(CO)_3]$ (M = Mo, W (21)) exhibit substantially higher ν_{CO} stretching frequencies.

Nuclear Magnetic Resonance Spectra

The ^1H nmr spectra of the ligands $\phi_2P(Me_2pz)$ and $\phi P(Me_2pz)_2$, and of the complexes **I–IV**, **VI**, and **VII** (Table 2) consisted of a phenyl multiplet (τ 2.5–2.8), a 4-H resonance (τ ~ 4), and two methyl resonances (τ 7.4–8.6). Complex **V** showed four equally intense methyl and two equally intense 4-H resonances, arising from the non-equivalence of the two 3,5-dimethylpyrazolyl groups (already discussed). The relative intensities of the bands corroborate the given formulations of the listed complexes.

The methyl resonances of $\phi_2P(Me_2pz)$ and $\phi P(Me_2pz)_2$ are quite sensitive to complexation. For the ligands themselves, the higher field resonance is assigned to the 5-Me group, on the basis of relatively greater paramagnetic shielding by the phenyl rings (33, 34).

The factors affecting the methyl ^1H chemical shifts in the complexes **I–VII** (Table 2) include (*a*) changes in C—H δ electron density, transmitted inductively as a result of coordination of phosphorus alone (**I**, **II**), or of phosphorus and one 2N site (**III–V**), or of two 2N sites and a portion of the phenyl ring (**VI**, **VII**); (*b*) changes in the π and/or π* electron density of the aromatic phenyl ring(s), the pseudo-aromatic pyrazolyl ring(s) and the carbonyl groups; (*c*) changes in the ring currents, and hence the anisotropic shielding effects (33, 34) associated with (*b*) above; and (*d*) paramagnetic shielding effects attributable to the *d* electrons of the Mo or W metal atom. While the individual shielding contributions of the above factors are

[5]CPK Atomic Models, Ealing Scientific Limited, 23 Leman Street, London, E.1., England.

Can. J. Chem. Downloaded from www.nrcresearchpress.com by 210.87.254.6 on 09/05/12
For personal use only.

difficult to assess, a study of CPK molecular models suggests the following: (*i*) in the *trans* complexes **I** and **II**, the Me_2pz ring is free to rotate about the P—N bond (Fig. 3). During rotation, the 5-methyl group encounters a steric interaction with carbonyl groups that are *cis* to the ligand, and the interaction with the phenyl ring is increased. These effects result in enhanced paramagnetic shielding, as observed. The much smaller shielding of the 3-methyl group, relative to free ligand, is attributable to a long range effect of the carbonyl groups that are *cis* to the ligands. (*ii*) In the metallocyclic systems **III** and **IV**, the 5-methyl group is "locked" in place, in close proximity to two phenyl rings (Fig. 4), and may again be assigned the higher field resonance. The 3-methyl group is similarly "locked" adjacent to a carbonyl group, and again experiences a small shielding effect. The 3- and 5-methyl resonances of $[\phi_2P(Me_2pz)M(CO)_4]$ are effected to a much greater extent in the tungsten complex (**IV**) than in its molybdenum analog (**III**). (*iii*) In $[\phi P(Me_2pz)_2W(CO)_4]$ (**V**) there is one free and one coordinated Me_2pz ring. The four methyl resonances can be paired to correspond closely with resonances of the free ligand (the two lower field signals), and to resonances typical of the Me_2pz ring in PNNM metallocyclic structures (**III**, **IV**) (the two higher field resonances). (*iv*) In the tricarbonyl complexes $[\phi P(Me_2pz)_2M(CO)_3]$ (**VI**, **VII**), the metal---phenyl interaction has three significant effects: first, it causes a deepening of the $P(N—N)_2W$ boat metallocycle; second, the steric interaction between the 5-methyl and the phenyl moieties is decreased; and third, the 3-methyl group is moved away from the carbonyl groups. These structural changes are consistent with the observed deshielding of the 3- and 5-Me protons,

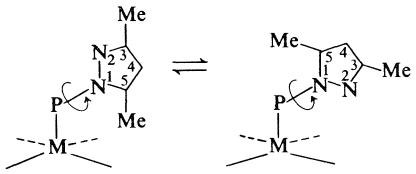


FIG. 3. Rotation about P—N bond.

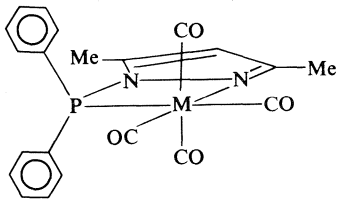


FIG. 4. Metallocycle systems **III** and **IV**.

but since the chemical shifts are now very similar (within ~0.04 ppm), the assignment of the resonances cannot be made with confidence.

In the free ligands $\phi_2P(Me_2pz)$ and $\phi P(Me_2pz)_2$, and in most of the complexes **I**–**VII**, the 4-H chemical shift variation is small, and the resonance is broad due to unresolved ^{31}P–H coupling. In two cases (**VI** and **VII**), however, the resonance was resolved into a doublet ($J_{^{31}P-H}$ = ~3 Hz). Similar couplings were reported for $[\phi P(Me_2pz)_2Re(CO)_3Br]$ and $[P(Me_2pz)_3Re(CO)_3Br]$ (4). Factors affecting long range phosphorus–hydrogen coupling have been discussed (7, 35, 36). Also in two cases an appreciable shielding of the 4-H proton is observed, in $[\phi_2P(Me_2pz)W(CO)_4]$ (**IV**) and for the coordinated Me_2pz ring in $[\phi P(Me_2pz)_2W(CO)_4]$ (**V**); these two 4-H resonances are further broadened, suggestive of both long range ^{183}W–H and ^{31}P–H unresolved coupling. The main factor affecting the 4-H resonance is probably attributable to changes in the shielding effects of the Me_2pz ring π electrons (37, 38).

The proton decoupled ^{31}P nmr spectra of complexes **I**–**VII** are listed in Table 3. The effects which influence the chemical shift of phosphorus include: (*a*) a local diamagnetic term, (*b*) a paramagnetic term, (*c*) neighbour anisotropy effects, and (*d*) interatomic currents (39, 40). Grim *et al.* (40) consider (*c*) and (*d*) to be the most important factors, at least in tertiary phosphine complexes of group VI metal carbonyls.

The phosphorus coordination shifts ($\Delta^{31}P$) for various *trans*-$L_2M(CO)_4$ complexes (41, 42) are listed in Table 4, for comparison with our compounds **I** and **II**. The ^{31}P values for $[(\phi_2P(Me_2pz))_2M(CO)_4]$ (**I**, **II**) are consistent with trends reported in the literature (41, 42), in that the greater numerical value is found in the molybdenum complexes.

For bis-phosphine chelate complexes $[\phi P(R)(CH_2)_nP(R)\phi M(CO)_4]$ (M = Mo, W), the ^{31}P coordination shift is small for four-membered chelate rings (6), but is unusually large for five-membered rings (43–45), the molybdenum complexes having the larger numerical values (typically −67 ppm for Mo and −52 ppm for W). By contrast, the $\Delta^{31}P$ values for our four-membered chelate systems are relatively large ($[\phi_2P(Me_2pz)Mo(CO)_4]$ (**III**), −58 ppm; $[\phi_2P(Me_2pz)W(CO)_4]$ (**IV**), −52 ppm; $[\phi P(Me_2pz)_2W(CO)_4]$ (**V**), −45 ppm) and differences between Mo and W are much less marked than in bidentate phosphine complexes.

Variable temperature nmr studies of the above complexes will be reported in a subsequent paper.

TABLE 4. Phosphorus coordination shifts ($\Delta^{31}P$) for bis-phosphine complexes of Mo(0) and W(0)

Compound	$\Delta^{31}P$(Mo)	$\Delta^{31}P$(W)	Remark
$(\phi_2P(Me_2pz))_2Mo(CO)_4$	−66	−55	This work
$(Me_3P)_2M(CO)_4$	−54	−28.5	Ref. 41
$(MeO)_3P)_2M(CO)_4$	−33	−6	Ref. 41
$(\phi_xBu_{3-x}P)_2M(CO)_4$	−55 – −56	−30 – −31.5	Ref. 42

Experimental

All experimental operations were carried out under anhydrous and oxygen-free conditions using high vacuum or inert atmosphere systems. In preparations where carbon monoxide evolution was monitored, heavy-walled Pyrex or quartz Teflon-valved reaction tubes were used, and reaction mixtures were initially outgassed in a series of three freeze–pump–thaw cycles. Evolved carbon monoxide was measured intermittently, or on completion of reaction, by means of a Sprengel pump (46). A water-jacketed Hanovia lamp was utilized in photochemical synthesis.

Solvents were dried by standard methods, distilled, and deaerated prior to use. Common reagents were purchased from commercial suppliers.

The pyrazolylphosphine ligands (2, 3) and the following transition metal complexes were prepared according to published procedures: [(nbd)Mo(CO)$_4$] (ref. 47, pp. 124, 125), [(cht)Mo(CO)$_3$] (ref. 47, pp. 125, 126), [(tmpda)W(CO)$_4$] (48), [(nbd)W(CO)$_4$] (49), [$(CH_3CN)_2$W(CO)$_4$] (50), [$(CH_3CN)_3$W(CO)$_3$] (51), and [(cht)W(CO)$_3$] (49) (nbd = norbornadiene, cht = cycloheptatriene, tmpda = *N*,*N*,*N*′,*N*′-tetramethylpropylene-1,3-diamine).

Elemental analyses for C, H, and N were performed by the University analyst, Simon Fraser University. ^1H and ^{31}P nuclear magnetic resonance spectra were obtained using Varian A56/50 and XL100 instruments, the latter having Fourier transform and nuclear decoupling facilities. Infrared spectra were recorded with a Perkin-Elmer 457 spectrophotometer and were calibrated against standard polystyrene film. Mass spectra were determined with the double-focussing Hitachi-Perkin-Elmer RMU-6E instrument.

*(a) Preparation of [$(\phi_2P(Me_2pz))_2Mo(CO)_4$] (**I**)*

A solution of [(nbd)Mo(CO)$_4$] (0.65 mmol) and $\phi_2P(Me_2pz)$ (1.80 mmol) in benzene (20 mL) was heated at 60°C for 15 h. The solution was evaporated to dryness and the residue recrystallized twice from chloroform–hexane to yield white crystals of [$(\phi_2P(Me_2pz))_2$Mo(CO)$_4$] (**I**). Yield 40%. *Anal.* calcd. for $C_{38}H_{34}N_4MoO_4P_2$: C 59.4, H 4.46, N 7.29; found: C 60.0, H 4.60, N 7.50.

*(b) Preparation of [$(\phi_2P(Me_2pz))_2W(CO)_4$] (**II**)*

A solution of [(tmpda)W(CO)$_4$] (0.82 mmol) and $\phi_2P(Me_2pz)$ (1.80 mmol) in 15 mL of benzene was heated at 80°C for 18 h. The evolved carbon monoxide (0.12 mmol) was collected, the reaction mixture was evaporated to dryness under vacuum, and the residue was crystallized from chloroform–hexane to yield white crystals of [$(\phi_2P(Me_2pz))_2$W(CO)$_4$] (**II**). Yield 50%. *Anal.* calcd. for $C_{38}H_{34}N_4O_4P_2W$: C 54.1, H 3.72, N 5.46; found: C 54.5, H 4.72, N 6.35.

*(c) Preparation of [$\phi_2P(Me_2pz)Mo(CO)_4$] (**III**)*

A solution of [(nbd)Mo(CO)$_4$] (0.50 mmol) and $\phi_2P(Me_2pz)$ (0.50 mmol) in benzene (10 mL) was stirred at room temperature for 3 h. The yellow solution was evaporated to dryness under reduced pressure, yielding a residue which was crystallized from benzene–hexane and identified as [$\phi_2P(Me_2pz)$Mo(CO)$_4$] (**III**) golden-yellow crystals, mp 90°C (dec.). Yield 80%. *Anal.* calcd. for $C_{21}H_{17}MoN_2O_4P$: C 51.7, H 3.51, N 5.74; found: C 51.9, H 3.64, N 5.80.

*(d) Preparation of [$\phi_2P(Me_2pz)W(CO)_4$] (**IV**)*

A mixture of [$(CH_3CN)_2$W(CO)$_4$] (1.5 mmol) and $\phi_2P(Me_2pz)$ in 20 mL of benzene was stirred under nitrogen at room temperature for 60 h. The solvent was removed under reduced pressure, and the light brown residue was chromotographed, under nitrogen, on a florisil column, using benzene/ether as eluant. The appropriate fraction of eluant was collected, the solvent was removed under vacuum, and the product was recrystallized from benzene/hexane, and identified as [$\phi_2P(Me_2pz)$W(CO)$_4$] (**IV**). Yellow crystals; mp 109°C (dec.). Yield 40–50%. *Anal.* calcd. for $C_{21}H_{17}N_2O_4PW$: C 43.8, H 2.97, N 4.86; found: C 44.0, H 3.10, N 4.97.

*(e) Preparation of [$\phi P(Me_2pz)_2W(CO)_4$] (**V**)*

A mixture of [$(CH_3CN)_2$W(CO)$_4$] (1.3 mmol) and $\phi P(Me_2pz)_2$ (1.3 mmol) in benzene was stirred under nitrogen at room temperature for 20 h. During this time, the yellow crystals of [$(CH_3CN)_2$W(CO)$_4$] gradually disappeared and the solution became brownish yellow. The solvent was removed under reduced pressure and the residue was chromatographed under nitrogen on a florisil column (80–100 mesh), using diethyl ether as eluant. The appropriate fraction of eluant was collected, the solvent was removed under vacuum, the product was recrystallized from Et_2O/hexane and identified as [$\phi P(Me_2pz)_2$W(CO)$_4$] (**V**). Yellow crystals. Yield ~40%. *Anal.* calcd. for $C_{20}H_{19}N_4O_4PW$: C 40.4, H 3.22, N 9.43; found: C 41.0, H 3.50, N 9.80.

*(f) Preparation of [$\phi P(Me_2pz)_2Mo(CO)_3$] (**VI**)*

A solution of [(nbd)Mo(CO)$_4$] (0.50 mmol) and $\phi P(Me_2pz)_2$ (0.50 mmol) in 15 mL of benzene was stirred for 2 h at room temperature, giving a clear orange solution. Hexane (30 mL) was added carefully on top and allowed to diffuse slowly into the benzene layer (overnight). The orange solid precipitate was collected and recrystallized from benzene–hexane to yield orange crystals identified as [$\phi P(Me_2pz)_2$Mo(CO)$_3$] (**VI**). Yield 60%. *Anal.* calcd. for $C_{19}H_{19}MoN_4O_3P$: C 47.7, H 4.00, N 11.7; found: C 48.1, H 4.10, N 12.0. The mass spectrum showed the molecular ion and the loss of 3 carbonyl groups.

*(g) Preparation of [$\phi P(Me_2pz)_2W(CO)_3$] (**VII**)*

A mixture of [$(CH_3CN)_3$W(CO)$_3$] (1.7 mmol) and $\phi P(Me_2pz)_2$ (1.7 mmol) in 20 mL of benzene was stirred under nitrogen at 75°C for 30 min. The deep red solution was filtered, the filtrate was concentrated to about 5 mL under vacuum, yielding orange-red crystals that were collected and recrystallized from benzene/hexane. The product was identified as [$\phi P(Me_2pz)_2$-W(CO)$_3$] (**VII**); yield, 45%. *Anal.* calcd. for $C_{19}H_{19}N_4O_3PW$: C 40.3, H 3.38, N 9.90; found: C 39.8, H 4.01, N 9.32. The mass spectrum showed the molecular ion and the loss of 3 carbonyl groups.

Can. J. Chem. Downloaded from www.nrcresearchpress.com by 210.87.254.6 on 09/05/12
For personal use only.

*(h) Preparation of [P(Me$_2$pz)$_3$Mo(CO)$_3$] (**VIII**)*

Solutions of P(Me$_2$pz)$_3$ (0.50 mmol) in benzene (10 mL) and of (nbd)Mo(CO)$_4$ (0.50 mmol) in benzene (5 mL) were mixed together and stirred at room temperature for 20 h. The yellow precipitate was collected, dried under vacuum, and identified as [P(Me$_2$pz)$_3$Mo(CO)$_3$] (**VIII**). Yield 80%. *Anal.* calcd. for $C_{18}H_{21}MoN_6O_3P$: C 43.6, H 4.26, N 16.9; found: C 43.9, H 4.50, N 16.9.

The identical product was obtained by reaction of [(cht)Mo(CO)$_3$] with P(Me$_2$pz)$_3$ in benzene at room temperature.

*(i) Preparation of [P(Me$_2$pz)$_3$W(CO)$_3$] (**IX**)*

A mixture of [(CH$_3$CN)$_3$W(CO)$_3$] (0.51 mmol) and P(Me$_2$pz)$_3$ (0.51 mmol) in 10 mL of benzene was stirred at room temperature for 18 h. The yellow precipitate was collected, washed with benzene (10 mL) and with tetrahydrofuran (10 mL), dried under vacuum, and identified as [P(Me$_2$pz)$_3$W(CO)$_3$] (**IX**). Yield 80%. *Anal.* calcd. for $C_{18}H_{21}N_6O_3PW$: C 37.0, H 3.62, N 14.4; found: C 37.6, H 3.91, N 13.9.

Heating equimolar amounts of [(tmpda)W(CO)$_4$] and P(Me$_2$pz)$_3$ in benzene solution at 60–70°C for 80 h gave **IX** in 95% yield.

Acknowledgements

The authors gratefully acknowledge the financial support of the Natural Sciences and Engineering Research Council of Canada, and a gift of molybdenum hexacarbonyl from Climax Molybdenum Company.

1. C. A. McAuliffe. Transition metal complexes of phosphorus, arsenic and antimony ligands. Wiley. 1973, and cited references.
2. (*a*) S. Fischer, L. K. Peterson, and J. F. Nixon. Can. J. Chem. **52**, 3981 (1974); (*b*) S. Fischer, J. K. Hoyano, I. Johnson, and L. K. Peterson. Can. J. Chem. **54**, 2708 (1976).
3. S. Fischer, J. K. Hoyano, and L. K. Peterson. Can. J. Chem. **54**, 2710 (1976).
4. J. K. Hoyano and L. K. Peterson. Can. J. Chem. **54**, 2697 (1976).
5. S. O. Grim, W. McFarlane, and D. A. Wheatland. Inorg. Nucl. Chem. Lett. **2**, 49 (1966).
6. S. O. Grim, W. L. Briggs, R. C. Barth, C. A. Tolman, and J. P. Jesson. Inorg. Chem. **13**, 1095 (1974).
7. J. F. Nixon and A. Pidcock. Ann. Rev. NMR Spectrosc. **2**, 345 (1969).
8. F. A. Cotton. Inorg. Chem. **3**, 702 (1964).
9. W. Hieber and J. Peterhans. Z. Naturforsch. **14**b, 462 (1959).
10. L. E. Orgel. Inorg. Chem. **1**, 25 (1962).
11. F. A. Cotton and C. S. Kraihanzel. J. Am. Chem. Soc. **84**, 4432 (1962).
12. M. A. Bennett, L. V. Interrante, and R. S. Nyholm. Z. Naturforsch. **20**b, 633 (1965).
13. R. E. Cobbledick and F. W. B. Einstein. Acta Crystallogr. B**33**, 2020 (1977).
14. R. J. McKinney, C. B. Knobler, B. T. Huie, and H. D. Kaesz. J. Am. Chem. Soc. **99**, 2988 (1977).
15. R. E. Cobbledick, L. R. J. Dowdell, F. W. B. Einstein, J. K. Hoyano, and L. K. Peterson. Can. J. Chem. **57**, 2285 (1979).
16. J. L. Calderon, F. A. Cotton, and A. Shaver. J. Organomet. Chem. **42**, 419 (1972).
17. F. A. Cotton, T. LaCour, and A. G. Stanislowski. J. Am. Chem. Soc. **96**, 754 (1974).
18. F. A. Cotton and A. G. Stanislowski. J. Am. Chem. Soc. **96**, 5074 (1974).
19. Y. W. Yared, S. L. Miles, R. Bau, and C. A. Reed. J. Am. Chem. Soc. **99**, 7076 (1977).
20. F. A. Cotton, B. A. Frenz, and C. A. Murillo. J. Am. Chem. Soc. **97**, 2118 (1975).
21. J. Chatt and H. R. Watson. J. Chem. Soc. 4980 (1961).
22. J. Emsley and D. Hall. *In* The chemistry of phosphorus. J. Wiley and Sons, Inc., New York. 1976.
23. V. Mark and J. R. Van Wazer. J. Org. Chem. **32**, 1187 (1967).
24. C. S. Kraihanzel and F. A. Cotton. Inorg. Chem. **2**, 533 (1963).
25. S. Trofimenko. Adv. Chem. Ser. **150**, 289 (1976).
26. S. Trofimenko. Chem. Rev. **72**, 497 (1972).
27. K. R. Breakell, D. J. Patmore, and A. Storr. J. Chem. Soc. Dalton, 749 (1975).
28. D. J. Patmore, D. F. Rendle, A. Storr, and J. Trotter. J. Chem. Soc. Dalton, **176**, 718 (1975).
29. S. Trofimenko. J. Am. Chem. Soc. **91**, 588 (1969).
30. K. R. Breakell, S. J. Rettig, D. L. Singheil, A. Storr, and J. Trotter. Can. J. Chem. **56**, 2099 (1978).
31. E. W. Abel, M. A. Bennett, and G. Wilkinson. J. Chem. Soc. 2325 (1959).
32. J. C. Lancaster and W. R. McWhinnie. J. Chem. Soc. C, 2435 (1970).
33. J. A. Pople, W. G. Schneider, and H. J. Bernstein. *In* High resolution nuclear magnetic resonance. McGraw-Hill Book Company, Inc., New York. 1954.
34. J. W. Emsley, J. Feeney, and L. H. Sutcliffe. *In* High resolution nuclear magnetic resonance spectroscopy. Vol. 1. Pergamon Press, Oxford. 1965.
35. G. Mavel. *In* Progress in nuclear magnetic resonance spectroscopy. Vol. 1. Pergamon Press, London. 1966. Chapt. 4.
36. J. G. Verkade, R. W. King, and C. W. Heitsch. Inorg. Chem. **3**, 884 (1964).
37. M. A. Bennett, R. S. Nyholm, and J. D. Saxby. J. Org. Chem. **10**, 301 (1967).
38. M. A. Bennett, L. Pratt, and G. Wilkinson. J. Chem. Soc. 2037 (1961).
39. K. J. Packer. J. Chem. Soc. 960 (1963).
40. S. O. Grim, D. A. Wheatland, and W. McFarlane. J. Am. Chem. Soc. **89**, 5573 (1967).
41. R. Mathieu, M. Lenzi, and R. Poilblanc. Inorg. Chem. **9**, 2032 (1970).
42. S. O. Grim and D. A. Wheatland. Inorg. Chem. **8**, 1716 (1969).
43. S. O. Grim, J. D. Gaudio, R. P. Molenda, C. A. Tolman, and J. P. Jesson. J. Am. Chem. Soc. **96**, 3416 (1974).
44. L. S. Meriwether and J. R. Leto. J. Am. Chem. Soc. **83**, 3192 (1961).
45. J. A. Connor, J. J. Day, E. M. Jones, and G. K. McEwen. J. Chem. Soc. Dalton Trans. 347 (1973).
46. B. Bartocha, W. A. G. Graham, and F. G. A. Stone. J. Inorg. Nucl. Chem. **6**, 119 (1958).
47. R. B. King. *In* Organometallic synthesis. Vol. 1. Academic Press. 1965.
48. G. R. Dobson and G. C. Faber. Inorg. Chim. Acta, **4**, 87 (1970).
49. R. B. King and A. Fronzaglia. Inorg. Chem. **5**, 1937 (1966).
50. R. H. Bleiger and K. Vrieze. Inorg. Chim. Acta, **19**, 195 (1976).
51. D. P. Tate, W. R. Knipple, and J. M. Augl. Inorg. Chem. **1**, 433 (1972).

Can. J. Chem. Downloaded from www.nrcresearchpress.com by 210.87.254.6 on 09/05/12
For personal use only.

A kinetic study of the oxidation of N(III) by ClO_2^- in aqueous acidic media

SAMIR S. EMEISH[1] AND KEITH E. HOWLETT
Department of Chemistry, Bedford College, London NW1 4NS, U.K.

Received July 5, 1979

SAMIR S. EMEISH and KEITH E. HOWLETT. Can. J. Chem. **58**, 159 (1980).

Kinetics of the reaction between nitrous acid and chlorite have been studied spectrophotometrically. The rate equation involves terms $[HNO_2]^{1.5}$ and $[ClO_2^-]^{0.5}$, and both an uncatalysed and a chloride ion-catalysed path have been identified. A mechanism involving peroxonitrite and hypochlorous acid as intermediates is shown to be consistent with the observations.

SAMIR S. EMEISH et KEITH E. HOWLETT. Can. J. Chem. **58**, 159 (1980).

On a étudié par spectrophotométrie la cinétique des réactions entre l'acide nitreux et l'ion chlorite. L'équation de vitesse fait intervenir les terms $[HNO_2]^{1.5}$ et $[ClO_2^-]^{0.5}$ et on a identifié deux types de réaction: l'une non catalysée et l'autre catalysée par l'ion chlorite. Ces observations sont compatibles avec un mécanisme impliquant un peroxynitrite et l'acide hypochloreux comme intermédiaires.

[Traduit par le journal]

Can. J. Chem. Downloaded from www.nrcresearchpress.com by 210.87.254.105 on 09/05/12
For personal use only.

Introduction

Although the kinetics of the redox reactions involving N(III) and halate anions have been reported before, and the reactivities of the various species and the mechanistic steps have been reviewed (1–3) further work on these systems is necessary. As a corollary to that work we now report a first study of the reaction between N(III) and Cl(III), a possible intermediate step in the N(III)/Cl(V) reaction.

Experimental

Preliminary work indicated no technical difficulties which would hinder a spectrophotometric study of this reaction.

When possible, Analar grade chemicals were used without further purification. Sodium chlorite was recrystallised from warm, slightly alkaline solution, the crystals being dried at 120°C for 2 h. The purity was checked iodometrically. Stock solutions of sodium nitrite and of sodium chlorite were stabilised by traces of NaOH (4) (and were discarded after a week).

Reaction was initiated in thermostatted solutions by thoroughly mixing first N(III) with Cl(III) and finally by adding buffer. Samples were withdrawn at intervals and analysed for [N(III)] by the Shinn method (5), here further modified from its use by Kershaw and Chamberlin (6). In the present instance, experimental samples (typically 2 cm^3) were quenched in ~80 cm^3 of 0.0025 mol dm^{-3} HCl containing 0.03 g sulphanilamide. After 5 min, 2 cm^3 of 3 mol dm^{-3} HCl was added to complete the diazotisation, and after a further 2 min, 1 cm^3 of 0.1% *N*(-1-naphthyl)-ethylenediamine dihydrochloride was added, the solution made up to 100 cm^3 and its absorbance determined at 538 nm between 10 and 60 min later.

Results

The reaction is immeasurably slow at 25°C and pH ≈ 7, but has a convenient speed at pH ≈ 4.5 (maintained in our work by either potassium hydrogen phthalate or acetate buffers) with [N(III)] ≈ [Cl(III)] ≈ 10^{-4} mol dm^{-3}. Minor observed irregularities in rates were removed by the presence of 10^{-3} mol dm^{-3} Na_2EDTA (see later) in all runs used to deduce kinetic parameters.

That N(III) and Cl(III) react in the molar ratio 2:1 to produce exclusively nitrate and chloride was variously confirmed. Firstly, the molar reacting ratio was determined by measuring the N(III) remaining after complete reaction, starting with excess N(III); the mean result was 1.99:1. Secondly, near 47 000 cm^{-1}, chlorite, hypochlorous acid, chloride, and nitrous acid are transparent or weakly absorbing whereas nitrate is more strongly absorbing. Reaction mixtures, acidified with HCl were allowed to react to completion and shown to have absorption spectra identical with corresponding solutions of $NaNO_3$ + HCl over the whole range 40 000 – 50 000 cm^{-1}. Thirdly, Cl^- in normal reaction products was determined by potentiometric titration, and it was shown that Cl^- was produced mole for mole from chlorite in its reaction with nitrite.

Cations such as Na^+ or K^+ have no specific effect upon the rate of reaction, even when present in 500-fold excess compared with the reactants, although there is a general decelerating effect of ionic strength *I* (see later). Distinct from this, the deliberate addition of ions such as Ni^{2+}, Cr^{3+}, Cu^{2+}, Co^{2+} at concentrations comparable with those of the reactants (4×10^{-4} mol dm^{-3}) produced a noticeable increase in rate of 10% or more. These catalytic effects are partially removed by 10^{-3} mol dm^{-3} Na_2EDTA. Similar additions of Fe^{2+} introduce a completely different, fast reaction path. It therefore seems probable that the consistent results observed in the presence of EDTA correspond to

[1]Present address: P.O. Box 2385, Amman, H. K. Jordan.

0008-4042/80/020159-05$01.00/0
©1980 National Research Council of Canada/Conseil national de recherches du Canada

Can. J. Chem. Downloaded from www.nrcresearchpress.com by 210.87.254.105 on 09/05/12
For personal use only.

TABLE 1. Illustration of the method of calculation and the applicability of rate equation. Results at $I = 0.016$ mol dm^{-3}, $T = 25$°C, and $[H^+] = 8.62 \times 10^{-5}$ mol dm^{-3}

t (min)	$10^4[NaNO_2]$ (mol dm^{-3}) (measured)	$10^4[NaClO_2]$ (mol dm^{-3}) (calcd)	$([NaClO_2]/[NaNO_2])^{0.5}$
0	(7.296)	(2.298)	0.561
1	7.130	2.215	0.557
5	6.506	1.903	0.541
10	5.847	1.573	0.519
15	5.326	1.313	0.496
20	4.897	1.098	0.473
25	4.575	0.937	0.452
35	4.077	0.688	0.411
45	3.755	0.527	0.375

TABLE 2. Some rate constants obtained at 25°C and $I = 0.016$ mol dm^{-3}

$10^4[NaNO_2]$ (mol dm^{-3})	$10^4[NaClO_2]$ (mol dm^{-3})	$10^5[H^+]$ (mol dm^{-3})	$10^{-6}k$ (dm$^{7.5}$ mol$^{-2.5}$ s^{-1})
3.37	0.988	8.65	1.29
6.74	2.47	17.2	1.36
6.74	2.47	2.75	1.27
1.348	2.47	17.2	1.39
3.37	4.94	17.2	1.30
3.37	0.988	17.2	1.37
3.37	0.980	4.38	1.41
3.37	2.47	50.9	1.39
7.30	2.30	8.62	1.34
4.77	2.13	9.91*	1.35
6.78	3.56	5.19*	1.41

*Acetate buffer, all others phthalate.

reactions uncatalysed by adventitious traces of transitional or polyvalent ions.

Preliminary experiments showed that the rate of reaction is uninfluenced by variation of intensity of illumination, surface/volume ratio, or oxygen-content of the solution.

Since the kinetics of the main reaction are not of a simple order, elucidation was begun by use of initial rates. At constant T, I, and $[H^+]$ these indicated

$$-\mathrm{d}[N(III)]/\mathrm{d}t = k_2[NO_2^-]^{1.5}[ClO_2^-]^{0.5}$$

which may be integrated to

$$k_2 t = \{2/([ClO_2^-]_0 - 0.5[NO_2^-]_0)\} \times \{([ClO_2^-]_t/[NO_2^-]_t)^{1/2} - ([ClO_2^-]_0/[NO_2^-]_0)^{1/2}\}$$

from which the rate constant, k_2, for an individual experiment may be derived from the variation of $([ClO_2^-]_t/[NO_2^-]_t)^{1/2}$ with t. This test showed that individual runs followed these kinetics to beyond 75% consumption of either reactant, as is illustrated by the results of Table 1.

Variation of $[H^+]$ alone showed that the order with respect to H^+ is 1.5. Values of $[H^+]$ were calculated from measurements of pH, e.g. at 25°C via

$$-\log H^+ = \mathrm{pH} - 0.509\{I^{1/2}/(1 + I^{1/2}) - 0.25I\}$$

Table 2 shows a selection of kinetic runs and the values of the 3.5 order rate constant, obtained at 25°C, $I = 0.016$ mol dm^{-3}, using two different buffer systems.

The effect of variation in I upon rate constant was investigated using additions of KNO_3 (deliberate additions of NO_3^- and of Cl^- in concentrations comparable with the reactants have no detectable effect). Table 3 lists one set of experimental results.

These results correspond closely to the equation

$$\log k(298) = 6.27 - 1.4_0 F(I)$$

where

$$F(I) = I^{1/2}/(1 + I^{1/2}) - 0.25I$$

and

$$k = k_2/[H^+]^{1.5}$$

When the temperature was varied, at constant I, the results given in Table 4 were obtained.

These results correspond to an activation energy of 42 kJ mol^{-1} for the N(III)/Cl(III) reaction.

The presence of one simple ion, namely chloride, has a specific catalytic effect upon the reaction when present in relatively large concentration. Table 5 records results obtained at 25°C when Cl^- is

Can. J. Chem. Downloaded from www.nrcresearchpress.com by 210.87.254.105 on 09/05/12
For personal use only.

TABLE 3. Effect of ionic strength on rate constants at 25°C using the initial concentrations, $[NaNO_2] = 7.30 \times 10^{-4}$ mol dm^{-3} and $[NaClO_2] = 2.30 \times 10^{-4}$ mol dm^{-3}

I (mol dm^{-3})	$10^4[H^+]$ (mol dm^{-3})	$10^{-6}k$ (dm$^{7.5}$ mol$^{-2.5}$ s^{-1})
0.0167	0.862	1.30
0.0367	1.05	1.15
0.0881	1.27	0.97
0.154	1.46	0.88
0.188	1.58	0.82
0.222	1.64	0.78
0.257	1.73	0.78

TABLE 4. Effect of temperature on rate constant at $I = 0.016$ mol dm^{-3} using the initial concentrations, $[NaNO_2] = 3.38 \times 10^{-4}$ mol dm^{-3}, $[NaClO_2] = 2.47 \times 10^{-4}$ mol dm^{-3}, and $[H^+] = 8.65 \times 10^{-5}$ mol dm^{-3}

T (°C)	$10^{-6}k$ (dm$^{7.5}$ mol$^{-2.5}$ s^{-1})
10.0	0.50
15.0	0.68
20.0	0.87
25.0	1.31
30.0	1.65
35.0	2.14
40.0	2.75

added as NaCl, I being maintained constant with $NaNO_3$.

Added chloride ion produces a first order catalytic effect which is maintained throughout a reaction (chloride produced in the reaction is present at concentrations 100-fold less than the deliberate additions and is insignificant in this respect). Since the order of reaction throughout each Cl^--catalysed experiment remains 1.5, 0.5, and 1.5 in NO_2^-, ClO_2^-, and H^+ respectively, the total rate equation becomes

$$\text{Rate} = k[NO_2^-]^{1.5}[ClO_2^-]^{0.5}[H^+]^{1.5} + k'[NO_2^-]^{1.5}[ClO_2^-]^{0.5}[H^+]^{1.5}[Cl^-]$$

Values of k and k' at 25°C are given in Table 5.

The results of variation of k' with temperature for the Cl^--catalysed process are given in Table 6.

These results correspond to an activation energy of 38 kJ mol^{-1}.

Discussion

The reactants are mixed as nitrite and chlorite but these two ions do not react together. At least one must be protonated before reaction. The acid ionisation constant for $HClO_2$ is about 20 times that of HNO_2 so that at our working pH, HNO_2 is a more important species than $HClO_2$. Since rate is directly proportional to $[NO_2^-]^{1.5}$, $[H^+]^{1.5}$, and $[ClO_2^-]^{0.5}$ the rate determining step must therefore involve species which are stoichiometrically related to $[HNO_2]$ in the ratio 1.5:1 and to $[ClO_2^-]$ in the ratio 0.5:1.

The two acid species, other than H^+, in the two buffer systems used, are present in very different concentrations, both well in excess of $[H^+]$. Since rates are unaffected by a change of buffer, the N(III)/Cl(III) reaction is specifically catalysed by H^+, not by acids in general.

The kinetic form thus puts definite restrictions upon the mechanism for which we propose:

$$HNO_2 + H_2O \rightleftharpoons H_3O^+ + NO_2^-$$

Step *1* $HNO_2 + ClO_2^- \rightleftharpoons ONOO^- + HOCl$

Step *2* $ONOO^- \rightarrow NO_3^-$

Step *3* $HOCl + HNO_2 \rightarrow NO_3^- + 2H^+ + Cl^-$

together with steps *4* and *5* in the presence of excess Cl^-

Step *4* $HOCl + Cl^- \rightleftharpoons HOCl_2^-$

Step *5* $HOCl_2^- + HNO_2 \rightarrow NO_3^- + 2H^+ + 2Cl^-$

(with appropriately numbered rate and equilibrium constants).

The proposed oxygen-transfer step *1* is essentially the means whereby the kinetic results can be understood. We assume that this equilibrium is relatively rapidly established with the position of equilibrium well to the left. In a steady state the species $ONOO^-$ and HOCl are produced and lost at equal rates, and since their initial concentrations are zero, their concentrations will always be either the same or in a constant ratio. Thus ignoring this ratio factor,

$$[HOCl] = [ONOO^-] = (K_1[HNO_2][ClO_2^-])^{0.5}$$

whence for the overall uncatalysed rate

$$d[NO_3^-]/dt = 2k_3K_1^{0.5}[HNO_2]^{1.5}[ClO_2^-]^{0.5}$$

and for the Cl^--catalysed component of the rate

$$d[NO_3^-]/dt = 2k_5K_4K_1^{0.5}[HNO_2]^{1.5} \times [ClO_2^-]^{0.5}[Cl^-]$$

Combining these equations with K_a, viz.

[1] $K_a = [H^+][NO_2^-]\gamma_{H^+}\gamma_{NO_2^-}/[HNO_2]\gamma_{HNO_2}$

where γ_A is the activity coefficient of A, and assuming that γ for an uncharged species is unity and further that those for singly charged species, γ_1, are all equal at constant I, we have

[2] $\text{Uncatalysed rate} = k[NO_2^-]^{1.5} \times [H^+]^{1.5}[ClO_2^-]^{0.5}$

where

[3] $k = 2k_3K_1^{0.5}K_a^{-1.5}\gamma_1^3$

TABLE 5. Variation of initial rate with $[Cl^-]$ at $I = 0.215$ mol dm^{-3} and 25°C, using initial concentrations, $[NaNO_2] = 6.71 \times 10^{-4}$ mol dm^{-3}, $[NaClO_2] = 2.45 \times 10^{-4}$ mol dm^{-3}, and $[H^+] = 8.80 \times 10^{-5}$ mol dm^{-3}, k and k' refer to eqs. [2] and [4]

$[Cl^-]$ (mol dm^{-3})	$10^7 \times$ init. rate (mol dm^{-3})	$10^{-6}k$ (dm$^{7.5}$ mol$^{-2.5}$ s^{-1})	$10^{-6}k'$ (dm$^{10.5}$ mol$^{-3.5}$ s^{-1})
0	1.75	0.78	—
0.0429	3.12	(0.78)	14.2
0.0714	4.05	(0.78)	14.4
0.100	4.96	(0.78)	14.3
0.143	6.37	(0.78)	14.4
0.200	8.21	(0.78)	14.4

TABLE 6. Effect of temperature on the rate constant of Cl^--catalysed reaction at $I = 0.232$, using the initial concentrations $[NaNO_2] = 3.66 \times 10^{-4}$ mol dm^{-3}, $[NaClO_2] = 2.29 \times 10^{-4}$ mol dm^{-3}, $[Cl^-] = 0.154$ mol dm^{-3}, and $[H^+] = 8.51 \times 10^{-5}$ mol dm^{-3}

T (°C)	$10^{-6}k'$ (dm$^{10.5}$ mol$^{-3.5}$ s^{-1})
15	8.07
20	10.75
25	14.27
30	18.08
35	22.67
40	28.58

and

[4] Catalysed rate component

$$= k'[NO_2^-]^{1.5}[H^+]^{1.5}[ClO_2^-]^{0.5}[Cl^-]$$

where

$$k' = 2k_5K_1^{0.5}K_4K_a^{-1.5}\gamma_1^3$$

We must note that the concentrations in eqs. [2] and [4] refer to equilibrium values whereas the experimental equation refers to "made up" concentrations. The experimental observations are of rates of loss of total [N(III)]. At pH 4–5

$$\text{Total [N(III)]} = [NO_2^-] + [HNO_2]$$

thus substituting for $[NO_2^-]$ in eq. [1] inserts the following extra term,

$$(1 + [H^+]\gamma_1^2/K_a)^{-1.5}$$

into both eqs. [2] and [4], and converts $[NO_2^-]$ into the measured quantity [N(III)]. Since $K_a \approx 10^{-3}$ mol dm^{-3}, this extra term varies by only some 10% over the range of experimental conditions of acidity. Thus the proposed mechanism is consistent with the experimental observations, and this consistency extends to the effect of variation of ionic strength. The activity coefficient terms of eqs. [2] and [3] imply that the theoretically expected variation of rate with I is

$$\log k = \log k_0 - 1.53F(I)$$

Returning to a consideration of the proposed mechanism, step *2* could involve participation of HNO_2. This would not affect the kinetics but the idea has been rejected. It is reported (7) that the probability of XOO species to undergo substitution varies directly with the negative inductive effect of X^- and that the nucleophilic strength for displacement at oxygen (8) in XOO decreases in the order $Br^- > NO_2^-$. Hence if HNO_2 were reacting with $ONOO^-$, Br^- would be expected to affect the rate of reaction. We have found that Br^-, present in 4-fold excess over N(III), has no effect upon rates. Further, Halfpenny and Robinson (9) observed that Br^- is oxidised by $ONOO^-$ but not by its isomerisation products. Thus $ONOO^-$ does not last very long in the present system otherwise Br_2 and HOBr would have been produced and these would have further oxidised N(III) at our acidities (10).

Peroxonitrite has long been recognised as a yellow species, although there is still debate about the mechanism of its isomerisation and about pK_a for peroxonitrous acid (9, 11–18). If our mechanism is correct, it seems to support a value for pK_a for HOONO smaller than 4 in order to keep the substance mainly in the anionic form under our working conditions. If this were not so the N(III)/Cl(III) reaction would have an order with respect to H^+ different from that observed.

Confirmation that peroxonitrite is a probable intermediate has been obtained by carrying out a rapid reaction between N(III) and Cl(III) at pH ≈ 1, when a transient orange-yellow colour characteristic of peroxonitrite was observed. Further, potentially useful information about peroxonitrite was obtained by reacting N(III) and Cl(III) together with a half life of about 3 min, and passing the reacting mixture through the cavity cell of a Varian E4 esr spectrometer. Although a wide range band (~5000 G, X band) was explored, no signals were detected. This apparent absence of radicals applies to all

Can. J. Chem. Downloaded from www.nrcresearchpress.com by 210.87.254.105 on 09/05/12
For personal use only.

steps of the N(III)/Cl(III) reaction including the isomerisation of peroxonitrite. This latter would therefore seem to be heterolytic in nature.

The species $HOCl_2^-$ postulated in the Cl^--catalysed process is one of a type of intermediates put forward frequently by others (19–21) in the reactions of chlorine oxyacids. The present kinetic form requires that the intervention of Cl^- occurs mechanistically after steps which determine the other kinetic orders.

Acknowledgements

We thank Dr. R. Bolton for many helpful discussions, and the British Council for an OSFAS Award to one of us (S.S.E.).

1. E. Abel. J. Chim. Phys. **48**, 23 (1951).
2. J. O. Edwards. Chem. Rev. **50**, 455 (1952).
3. M. T. Beck, L. Dozsa, and I. Szilassy. J. Indian Chem. Soc. **51**, 6 (1974).
4. M. C. Taylor, J. F. White, G. P. Vincent, and G. L. Cunningham. Ind. Eng. Chem. **32**, 899 (1940).
5. M. B. Shinn. Ind. Eng. Chem. Anal. Ed. **13**, 33 (1941).
6. N. F. Kershaw and N. S. Chamberlin. Ind. Eng. Chem. **14**, 312 (1942).
7. M. Anbar. J. Am. Chem. Soc. **83**, 2031 (1961).
8. J. O. Edwards and J. J. Muller. Inorg. Chem. **1**, 696 (1962).
9. E. Halfpenny and P. L. Robinson. J. Chem. Soc. 928 (1952).
10. J. N. Pendlebury and R. H. Smith. Aust. J. Chem. **26**, 1857 (1973).
11. M. N. Hughes and H. G. Nicklin. J. Chem. Soc. A, 450 (1968).
12. D. J. Benton and P. Moore. J. Chem. Soc. 3179 (1970).
13. G. Yagil and M. Anbar. J. Inorg. Nucl. Chem. **26**, 453 (1964).
14. H. M. Papee' and G. L. Petriconi. Nature, **204**, 142 (1964).
15. E. A. Shilov and Z. S. Stepanova. Zh. Fiz. Khim. **24**, 820 (1950).
16. W. G. Keith and R. E. Powell. J. Chem. Soc. A, 90 (1969).
17. L. R. Mahoney. J. Am. Chem. Soc. **92**, 5262 (1970).
18. J. D. Ray. J. Inorg. Nucl. Chem. **24**, 1159 (1962).
19. H. Taube and H. Dodgen. J. Am. Chem. Soc. **71**, 3330 (1949).
20. R. G. Kieffer and G. Gordon. Inorg. Chem. **7**, 239 (1968).
21. M. Anbar and H. Taube. J. Am. Chem. Soc. **80**, 1073 (1958).

Can. J. Chem. Downloaded from www.nrcresearchpress.com by 210.87.254.105 on 09/05/12
For personal use only.

S_N2 iodide displacement on unsymmetrical cyclic dioxenium salts. A stereoelectronically controlled reaction

NORMAND BEAULIEU[1] AND PIERRE DESLONGCHAMPS

Laboratoire de Synthèse Organique, Département de Chimie, Faculté des Sciences, Université de Sherbrooke, Sherbrooke (Qué.), Canada J1K 2R1

Received August 28, 1979

NORMAND BEAULIEU AND PIERRE DESLONGCHAMPS. Can. J. Chem. **58**, 164 (1980).

Iodide ion reacts with the cyclic dioxenium salts **1–6** to yield mixtures of iodoester and lactone plus alkyl iodide (Table 1). The formation of iodoester competing with the formation of lactone appears to be an unexpected result. It can, however, be explained by a stereoelectronic effect, similar to the anomeric effect in acetals, which is also responsible for the greater stability of the *Z* over the *E* form in dioxenium salts and in esters.

NORMAND BEAULIEU et PIERRE DESLONGCHAMPS. Can. J. Chem. **58**, 164 (1980).

Les sels cycliques dioxeniums **1–6** réagissent avec l'ion iodure pour donner un mélange d'iodoester, de lactone et d'iodure d'alkyle (Tableau 1). La formation d'iodoester en compétition avec celle de la lactone est un résultat inattendu. Ce résultat peut cependant être expliqué par un effet stéréoélectronique semblable à l'effet anomère que l'on retrouve dans les acétals. Cet effet stéréoélectronique serait aussi responsable de la plus grande stabilité des formes *Z* par rapport aux formes *E* dans les sels dioxeniums et les esters.

Our recent studies on the oxidative cleavage of conformationally rigid vinyl orthoesters[2] have provided evidence that when a tetrahedral intermediate (hemiorthoester) can break down with primary stereoelectronic control to give either a *Z* or an *E* ester, it yields preferentially the *Z* ester (Scheme 1).

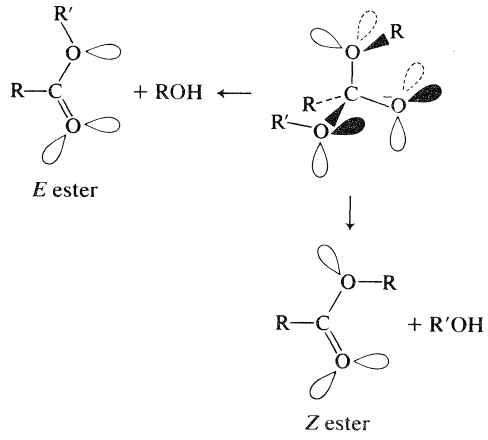
This preference was explained by a secondary electronic effect which lowers specifically the energy of the transition state leading to the *Z* ester. This secondary electronic effect in hemiorthoesters is equivalent to the classic anomeric effect observed in acetals (2).

The above analysis has led us also to realize that (*a*) this secondary electronic effect (or anomeric effect) exists in the ester function itself and (*b*) it is the major electronic parameter which stabilizes the *Z* form in preference to the *E* form in esters (3).

In order to provide evidence to show the importance of this electronic effect in esters, we have studied the S_N2 displacement reaction, by iodide ion, on a series of cyclic dioxenium salts. We wish to report this study.

Experimental Results

The cyclic dioxenium salts **1–6** (Table 1) were prepared by the reaction of trimethyl or triethyloxonium tetrafluoroborate salt with the appropriate lactone (4, 5). The products expected by the reaction of iodide ion on these dioxenium salts are the corresponding lactone plus methyl or ethyl iodide, and/or the corresponding iodoethyl or iodomethyl ester.[3] An instantaneous reaction was observed when the salts **1–6** dissolved in dichloromethane were treated with a solution of sodium iodide in acetonitrile at room temperature. A mixture of lactone, alkyl iodide, and iodoester was obtained in all cases. The iodoesters were found to be stable under the reaction conditions. The results are summarized in Table 1.



SCHEME 1

Discussion

The experimental results show clearly that the formation of iodoester (process A) can compete effectively with the formation of lactone and alkyl

[1]Holder of a Natural Sciences and Engineering Research Council of Canada (NSERC) Postgraduate Scholarship.

[2]This work has been described in a review article, see pp. 1290–1306 in ref. 1.

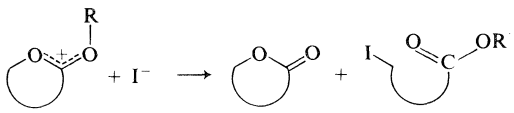
[3]Substitution reactions on cyclic dioxenium salts are known reactions, see ref. 6.

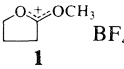
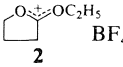
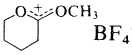
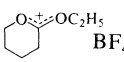
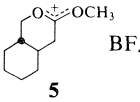
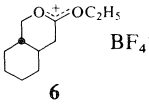
0008-4042/80/020164-04$01.00/0

©1980 National Research Council of Canada/Conseil national de recherches du Canada

Can. J. Chem. Downloaded from www.nrcresearchpress.com by 210.87.254.42 on 09/05/12
For personal use only.

TABLE 1. Reaction of iodide ion on dioxenium salts



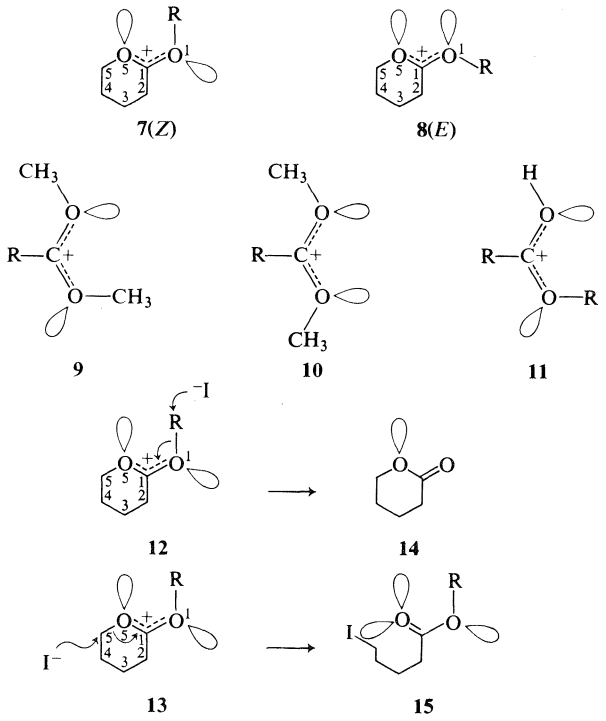
Salt	Lactone, %	Iodoesters, %
 **1**	76	24[a]
 **2**	32	68[a]
 **3**	29	71[a]
 **4**	18	82[a]
 **5**	95	5[b]
 **6**	90	10[b]

[a]Average of four experiments.
[b]Average of two experiments.

iodide (process B). We considered that this is a very unusual result because, if all the classic parameters are considered in both processes, we would have predicted that only process B would have taken place. In process B, two molecules are formed and the ring is not broken while in process A, only one molecule is formed and the ring is cleaved. Process A should therefore require more energy than process B. Furthermore, in the dioxenium salts having a methoxy group, iodide displacement on the primary methyl group should be favored over that on the secondary methylene group of the dioxenium ring. This factor favors again the formation of lactone and methyl iodide, yet important quantities of iodoester are observed (cf. **3**).

Thus, in resumé, good arguments can be found which favor process B and none for process A, yet process A remains competitive. It is also reasonable to assume that the combination of the factors discussed above should lower the energy of the transition state of process B to the point (≃3 kcal/mol) where process A would not be observed. It is therefore clear that there must be a new parameter which operates in process A only, lowering the energy of its transition state, so that it can compete with process B.

There is indeed an electronic effect which can



SCHEME 2

lower specifically the energy barrier of process A. We will see that this electronic effect is of the same nature as the anomeric effect (2) observed in acetals.

There is good evidence (X-ray supported by calculation) that dioxenium salts are planar (7, 8). The cyclic dioxenium salts **1–6** can exist theoretically in the *Z* form **7** or the *E* form **8** (Scheme 2). There is, however, good evidence that these salts exist in the *Z* form only.[4] It is known (by nmr, ref. 9) that dimethyl dioxenium salts exist in the *Z* (**9**) rather than the *E* form (**10**), and that protonation of esters in super acid medium yields the ion **11** (10). Similar results were obtained with carboxylic acids (11).

We therefore assume that the salts **1–6** exist in the *Z* form **7** with which iodine will react to give either the iodoester or the lactone plus alkyl iodide.

Structures **12** and **13** represent the two transition states (yielding **14** and **15** respectively). It can be seen that in **12** the bond to be broken (R—O1) is antiperiplanar to the non polar C1—C2 bond whereas in **13**, the bond to be broken (C5—O5) is antiperiplanar to the C1—O1 polar bond. In other words, in **13** the electron pair of the C5—O5 bond can be delocalized by an interaction with the an-

[4]The greater stability of the *Z* form over the *E* form in these compounds is also due to an electronic effect (*vide infra*).

Can. J. Chem. Downloaded from www.nrcresearchpress.com by 210.87.254.42 on 09/05/12
For personal use only.

Can. J. Chem. Downloaded from www.nrcresearchpress.com by 210.87.254.42 on 09/05/12
For personal use only.

tibonding orbital (σ^*) of the polar C1—O1 bond (12), whereas in **12**, the electron pair of the R—O1 bond cannot be delocalized into an antibonding orbital of a polar bond. Consequently, there is an electronic factor which can lower the energy barrier for the formation of the iodoester only.[5]

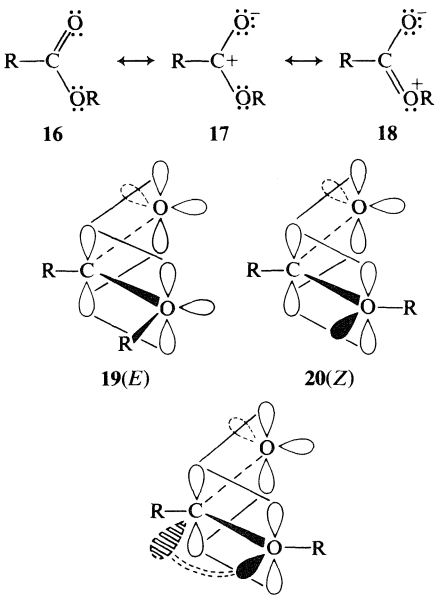
We believe that it is this electronic effect which makes iodoester formation competitive with the otherwise favored formation of lactone and alkyl iodide.

This electronic effect is similar to the anomeric effect in acetals (2). It only differs by the fact that the carbon C1 is trigonal (sp^2 hybridized) in dioxenium salts and tetrahedral (sp^3 hybridized) in acetals. We also believe that it is this kind of electronic effect which renders the *Z* form more stable than the *E* form in dioxenium salts as well as in esters (3).

In the *E* form of dioxenium salts **8**, the non-bonded electron pairs of O5 and O1 are not oriented antiperiplanar to a polar C—O bond whereas in the *Z* form **7**, the non-bonded electron pair of O1 is antiperiplanar to the polar C1—O5 bond. The electron pair on O1 in **7** can therefore be delocalized into the antibonding orbital of the sigma C1—O5 bond, lowering the energy content of this form.

It is also well known that esters are planar and that the *Z* form is much more stable than the *E* form (3). The *E* form is of course observed in small ring lactones but as soon as the size of the lactone ring allows the *Z* form, the *E* form is no longer observed (13). Even in the case of *tert*-butyl formate, the *Z* form predominates (≃90%) over the *E* form (14). Again, in the *Z* form of an ester, the ether oxygen has an electron pair properly oriented so that it can be delocalized into the antibonding orbital (σ^*) of the C—O sigma bond of the carbonyl group. This is not the case in the *E* form. We think that this electronic factor is the driving force which makes the *Z* form more stable.

Thus, as we have previously discussed (1), there are two different types of stereoelectronic effects in esters, a primary and a secondary one. In the primary electronic effect, one electron pair of the ether oxygen is delocalized with the π orbital of the C=O bond. This electron pair (*p* orbital) is therefore parallel to the π C=O bond. This primary electronic delocalization is usually expressed by the resonance structures **16**, **17**, and **18** (Scheme 3).



16 **17** **18**

19(*E*) **20**(*Z*)

21

SCHEME 3

This electronic delocalization conveys an sp^2 character on the two oxygens as well as the central carbon of the ester function. It is therefore responsible for the two geometrical forms *E* and *Z* of an ester function which can be represented respectively by structures **19** and **20**. In the *Z* form, there is an extra electronic delocalization which can occur between the other electron pair (sp^2 hybridized) of the ether oxygen and the antibonding orbital of the sigma bond of the carbonyl group as shown in **21**.[6,7]

The larger proportion of iodoester in the case of salts **2**, **4**, and **6** as compared with salts **1**, **3**, and **5** respectively can be readily explained because it is more difficult for iodine to attack an ethyl rather than a methyl group. Comparison of ring-size, **1** (or **2**) with **3** (or **4**), indicates that it takes more energy to break a five than a six-membered ring. Finally, the lower percentage of iodoester in the case of the bicyclic dioxenium salts **5** and **6** as compared with **3** and **4** respectively, can be explained by the presence of the second ring in **5** and **6** which causes

[5]Transition state **13** leads to an iodoester **15** having the stable *Z* conformation, whereas transition state **12** leads to a lactone **14** having the less stable *E* conformation. Consequently, the above results can be rationalized in this manner. However, we then arrive at the same conclusion, because *Z* esters are more stable than *E* esters for the same electronic reason (*vide infra*).

[6]This stabilizing electronic effect might be larger (≳3 kcal/mol) than the one (≃1.2 kcal/mol (2, 15)) observed in acetals, the reason being that the carbonyl C=O bond in esters is a more polarized bond than the C—OR bond in acetals. The very large difference in stability between *Z* and *E* esters could therefore be understood on that basis.

[7]If this electronic effect exists, it means that the CO—OR bond should be shorter in aliphatic esters (*Z* ester) than in lactones (*E* ester). X-ray analysis however, shows no difference (J. D. Dunitz, Eidgenossiche Technische Hochschule, personal communication).

Can. J. Chem. Downloaded from www.nrcresearchpress.com by 210.87.254.42 on 09/05/12
For personal use only.

extra steric hindrance to the attack by iodine on the methylene group of the dioxenium ring.

Experimental

Vapor-phase chromatographic (vpc) analyses and separations were carried out on a Varian aerograph instrument model 2800 with thermal conductivity detector (SE-30-5%; 5 ft × ¼ in.; Chromosorb W 100—120 mesh). The ir spectra were taken on a Perkin-Elmer 257 spectrophotometer. Proton nmr spectra were recorded on a Varian A-60 or a Bruker WP-60 instrument. Chemical shifts are reported in δ values relative to tetramethylsilane as internal standard. Mass spectral assays were obtained using a Hitachi-Perkin-Elmer RMU-6-A instrument at 70 eV.

Syntheses of the Dioxenium Salts

The dioxenium salts **2**, **4**, **5**, and **6** are known compounds; they were prepared by following the published procedure (4). The dioxenium salts **1** and **3** were prepared by the same method.

γ-Butyrolactone (0.5 mmol), or δ-valerolactone, and trimethyloxonium tetrafluoroborate (0.8 mmol) were mixed in anhydrous dichloromethane (5 mL) and left at room temperature for 15 h. Excess trimethyloxonium tetrafluoroborate salt was removed by filtration and the solution was evaporated. Nuclear magnetic resonance analyses indicated the presence of the expected dioxenium salt **1** or **3** only, the corresponding lactones were not detected. These salts were used without further purification.

Methyl Dioxenium Salt 1: nmr (CD_2Cl_2) δ: 2.5–3.0 (2H, multiplet), 3.3–3.6 (2H, triplet, J = 9 Hz), 4.4 (3H, singlet, CH_3O), and 5.4–5.7 (2H, triplet, J = 8 Hz, CH_2O).

Methyl Dioxenium Salt 3: nmr (CD_2Cl_2) δ: 2.0–2.4 (4H, multiplet), 2.9–3.3 (2H, multiplet), 4.45 (3H, singlet, CH_3O), and 5.1–5.4 (2H, broad triplet, CH_2O).

Reaction of Iodide Ion on the Dioxenium Salts

The dioxenium salts **1–6** (≈0.5 mmol) were dissolved in anhydrous dichloromethane (5 mL) and sodium iodide (≈1 mmol) dissolved in anhydrous acetonitrile (5 mL) was added. An instantaneous reaction was observed, the reaction mixture was filtered, concentrated, and analyzed by ^1H nmr spectroscopy, and by vpc (Table 1). In the case of dioxenium salts **1**, **2**, **3**, **4**, and **6**, the mixtures of the corresponding lactone and iodoester were separated by vpc. The lactones were properly identified with authentic samples and the iodoesters were characterized by spectroscopic methods (infrared, ^1H nmr, and ms). In the case of the dioxenium salt **5**, the corresponding iodoester and lactone were identified by vpc and ^1H nmr but were not isolated.

Methyl 4-Iodobutyrate: vpc (retention time) 18 min (100°C); ir ν_{max} ($CHCl_3$): 1740 cm^{-1}; nmr ($CDCl_3$) δ: 2.0–2.8 (4H, multiplet), 3.35 (2H, triplet, J = 8 Hz, CH_2I), and 3.9 (3H, singlet, CH_3O); ms m/e: 228 (M^+, absent), 197 ($M^+ - OCH_3$), 169 ($M^+ - CO_2CH_3$), and 101 ($M^+ - I$).

Ethyl 4-Iodobutyrate: vpc (retention time) 11.8 min (110°C); ir ν_{max} ($CHCl_3$): 1735 cm^{-1}; nmr ($CDCl_3$) δ: 1.33 (3H, triplet, J = 7 Hz, CH_3), 2.0–2.8 (4H, multiplet), 3.4 (2H, triplet, J = 8 Hz, CH_2I), and 4.3 (2H, quadruplet, J = 7 Hz, CH_2O); ms m/e: 242 (M^+, absent), 197 ($M^+ - OC_2H_5$), 169 ($M^+ - CO_2C_2H_5$), and 115 ($M^+ - I$).

Methyl 5-Iodopentanoate: vpc (retention time) 12.5 min (120°C); ir ν_{max} ($CHCl_3$): 1740 cm^{-1}; nmr ($CDCl_3$) δ: 1.8–2.8 (6H, multiplet), 3.4 (2H, triplet, J = 9 Hz, CH_2I), and 3.95 (3H, singlet, CH_3O); ms m/e: 242 (M^+, absent), 211 ($M^+ - OCH_3$), 183 ($M^+ - CO_2CH_3$), and 115 ($M^+ - I$).

Ethyl 5-Iodopentanoate: vpc (retention time) 18.8 min (110°C); ir ν_{max} ($CHCl_3$): 1740 cm^{-1}; nmr ($CDCl_3$) δ: 1.3 (3H, triplet, J = 7 Hz, CH_3), 1.6–2.7 (6H, multiplet), 3.35 (2H, triplet, J = 8 Hz, CH_2I), and 4.35 (2H, quadruplet, J = 7 Hz, CH_2O); ms m/e: 256 (M^+, absent), 211 ($M^+ - OC_2H_5$), 183 ($M^+ - CO_2C_2H_5$), and 129 ($M^+ - I$).

Ethyl trans *2-Iodomethylcyclohexane Acetate*: vpc (retention time) 13.7 min (170°C); ir ν_{max} ($CHCl_3$): 1735 cm^{-1}; nmr ($CDCl_3$) δ: 0.7–2.8 (12 H), 1.15 (3H, triplet, J = 7 Hz, CH_3), 3.2 (2H, multiplet, CH_2I), and 4.05 (2H, quadruplet, J = 7 Hz, CH_2O); ms m/e: 310 (M^+, absent), 265 ($M^+ - OC_2H_5$), 237 ($M^+ - CO_2C_2H_5$), and 183 ($M^+ - I$).

Methyl trans *2-Iodomethylcyclohexane Acetate*; vpc (retention time) 15 min (155°C); nmr ($CDCl_3$) δ: 3.7 (3H, singlet, CH_3O).

Acknowledgements

This research was supported by the Natural Sciences and Engineering Research Council of Canada and by the Ministère de l'Education of Québec.

1. P. Deslongchamps. Heterocycles, **7**, 1271 (1977).
2. R. U. Lemieux and S. Koto. Tetrahedron, **30**, 1933 (1974) and references quoted therein.
3. G. I. L. Jones and N. L. Owen. J. Mol. Struct. **18**, 1 (1973).
4. P. Deslongchamps, R. Chênevert, R. J. Taillefer, C. Moreau, and J. K. Saunders. Can. J. Chem. **53**, 1601 (1975).
5. H. Meerwein, P. Borner, O. Fucks, H. J. Sasse, H. Schrodt, and J. Spille. Chem. Ber. **89**, 2060 (1956).
6. H. Meerwein, K. Bodenbenner, P. Borner, F. Kunert, and K. Wunderlich. Justus Liebigs Ann. Chem. **632**, 38 (1960); K. Wunderlich. Ph.D. Thesis. University of Marburg, 1957.
7. H. Paulsen. Pure Appl. Chem. **49**, 1329 (1975).
8. H. Paulsen and R. Dammeyer. Chem. Ber. **109**, 1837 (1976).
9. B. G. Ramsey and R. W. Taft. J. Am. Chem. Soc. **88**, 3058 (1966).
10. G. A. Olah, D. H. O'Brien, and A. M. White. J. Am. Chem. Soc. **89**, 5694 (1967).
11. H. Hageven, A. F. Bickel, C. W. Hibbers, E. L. Mackor, and C. Macbean. Chem. Commun. 898 (1966); Recl. Trav. Chim. Pays-Bas, **86**, 687 (1967); M. Brookhart, G. C. Levy, and S. Winstein. J. Am. Chem. Soc. **89**, 1735 (1967); G. A. Olah and A. M. White. J. Am. Chem. Soc. **89**, 3591 (1967); H. Hageven. Recl. Trav. Chim. Pays-Bas, **87**, 1312 (1968).
12. C. Altona. Ph.D. Thesis. University of Leiden, 1964; C. Romers, C. Altona, H. R. Buys, and E. Havinga. Topics in stereochemistry. Vol. 4. *Edited by* E. L. Eliel and N. L. Allinger. Wiley-Interscience, New York, NY. 1969. p. 39.
13. R. Huisgen and H. Ott. Tetrahedron, **6**, 253 (1959).
14. M. Oki and H. Nakanishi. Bull. Chem. Soc. Jpn. **43**, 2558 (1970); H. Nakanishi, H. Fujita, and O. Yamamoto. Bull. Chem. Soc. Jpn. **51**, 214 (1978).
15. G. Descotes, M. Lissac, J. Delmau, and J. Duplan. C.R. Acad. Sci. Paris, **267**, 1240 (1968).

Raman spectroscopic studies of structural properties of solid and molten states of the magnesium chloride – alkali metal chloride system

M. H. BROOKER AND C.-H. HUANG[1]

Department of Chemistry, Memorial University of Newfoundland, St. John's, Nfld., Canada A1B 3X7

Received May 22, 1979

M. H. BROOKER and C.-H. HUANG. Can. J. Chem. **58**, 168 (1980).

Raman spectra have been recorded for solids and melts of composition $MgCl_2 + nACl$ (n = 0–4 and A = Cs, Rb, K, Na, Li). Characteristic spectra have been observed for each of the solids predicted from phase diagram studies and an additional two compounds formulated as Rb_3MgCl_5 and K_3MgCl_5 were detected. The compounds Cs_2MgCl_4, Cs_3MgCl_5, and Rb_3MgCl_5 contain the discrete $MgCl_4^{2-}$ tetrahedral ion which has been characterized by its Raman spectrum. These compounds melt with retention of the $MgCl_4^{2-}$ ion. Most other solids appear to contain distorted network octahedra with face-, edge-, or corner-shared chlorides. These solids melt to give the more stable tetrahedral $MgCl_4^{2-}$ ion. In melts of high $MgCl_2$ concentration a new peak was detected which appears to be characteristic of the dimeric $Mg_2Cl_7^{3-}$ ion which exists in equilibrium with the $MgCl_4^{2-}$ ion. The results are compared to similar studies on the better characterized $CsCl–AlCl_3$ system.

M. H. BROOKER et C.-H. HUANG. Can. J. Chem. **58**, 168 (1980).

On a enregistré les spectres Raman des sels à l'état solide et à l'état fondu ayant la composition suivante: $MgCl_2 + nACl$ (n = 0–4 et A = Cs, Rb, K, Na, Li). On a observé des spectres caractéristiques pour chacun des solides prédits à partir d'études de diagramme de phase et on a décelé deux composés additionnels identifiés comme étant: Rb_3MgCl_5 et K_3MgCl_5. Les composés Cs_2MgCl_4, Cs_3MgCl_5 et $RbMgCl_5$ contiennent un ion tétraédrique discret $MgCl_4^{2-}$ qu'on a identifié par son spectre Raman. Ces composés fondent avec rétention de l'ion $MgCl_4^{2-}$. La plupart des autres solides semblent contenir un système octaédrique déformé portant des ions chlorures sur la face, l'arête ou le coin. Les solides fondent en donnant l'ion tétraédrique $MgCl_4^{2-}$ le plus stable. Dans les sels fondus à forte concentration de $MgCl_2$, on a décelé un nouveau pic qui semble être caractéristique de l'ion dimère $Mg_2Cl_7^{3-}$ qui existe en équilibre avec l'ion $MgCl_4^{2-}$. On a comparé les résultats à des études similaires faites sur le système le mieux caractérisé $CsCl–AlCl_3$.

[Traduit par le journal]

Introduction

The concept of complex ion formation in molten salts has been the subject of considerable controversy. Evidence for MX_4^{2-} anions from phase diagram calculations was first noted by Flood and Urnes (1) for the $MgCl_2$ – alkali metal chloride system. Lumsden (2) has shown that solutions of up to about 30 mol% of MCl_2 (M = Mg, Mn, Fe, Zn) in KCl can be treated as ideal Temkin solutions of K^+ cations and the anions Cl^- and MCl_4^{2-}. Lumsden has argued that phase diagram calculations did not imply real $MgCl_4^{2-}$ entities but only a statistical order of ions. Failure of the calculations to extend into the MCl_2-rich region of the phase diagram has also been used as an argument against complex entities in the melt.

A number of species and polymeric structures have been proposed (3) but our recent Raman studies of the K_2MgCl_4 and Cs_2MgCl_4 as oriented single crystals and in the molten state were strongly in favour of the tetrahedral $MgCl_4^{2-}$ ion proposed by Maroni and co-workers (4, 5) for magnesium halide melts. Additional studies (6) on molten $MgCl_2$ suggested the presence of discrete polyatomic species, including $MgCl_4^{2-}$, and did not favour the residual ionic lattice model proposed by Capwell (7). The present study represents a continuation of our work to include the solids and molten salts of composition $MgCl_2 + nACl$, for n = 0 to 4, A = Cs, Rb, K, Na, Li. An attempt has been made to use Raman spectroscopy to identify and characterize the solids predicted by the phase diagram studies and to determine if information from the solids can be used to deduce structural properties of the melts. Generally it was found that the structure of species present in the melts was not related to the structure present in the solid but three compounds Rb_3MgCl_5, Cs_2MgCl_4, and Cs_3MgCl_5 did melt with retention of the tetrahedral $MgCl_4^{2-}$ coordination. The network lattice structures with distorted octahedral coordination of magnesium gave way to the smaller, melt-stabilized tetrahedral coordination on fusion.

Experimental

Anhydrous $MgCl_2$(Alpha) was dried under vacuum at 30°C for 24 h then the temperature was raised slowly (over 8 h) to 180°C where the solid was further dried under vacuum for 24 h. Reagent grade alkali metal chlorides were dried under vacuum at 180°C for 24 h before use. The salts and salt mixtures are somewhat hygroscopic so all manipulations were performed in a glove bag under dry N_2 or under vacuum. Appropriate quantities of the salts were placed in 6 mm id quartz tubes, further heated at

[1]Present address: Department of Geology, University of Windsor, Windsor, Ont., Canada.

0008-4042/80/020168-12$01.00/0

©1980 National Research Council of Canada/Conseil national de recherches du Canada

Can. J. Chem. Downloaded from www.nrcresearchpress.com by 210.87.254.42 on 09/05/12
For personal use only.

Can. J. Chem. Downloaded from www.nrcresearchpress.com by 210.87.254.42 on 09/05/12
For personal use only.

about 200°C under vacuum for 2 h, then the temperature was slowly raised until the sample melted. At this stage the melts were clear-colorless quiet liquids and showed no evidence of any impurities, in particular, MgO, the most likely impurity in $MgCl_2$. The samples were slowly cooled to room temperature and sealed under vacuum. Some of the tubes containing the sodium salts had a tendency to fracture on cooling. Attempts were made to grow single crystals of the salt mixtures by slowly passing the samples through a temperature gradient (vertical Bridgeman method). This technique also served to zone refine the materials.

Raman spectra of the solids and melts were obtained directly from these tubes. Results presented in the present study are for melts and unoriented polycrystalline samples (no depolarization properties were observed). Results for several oriented single crystals have been presented elsewhere (8). Raman spectra were measured with a Coderg PHO spectrometer after excitation with the 488.0 nm line of a Control Laser model 553A argon ion laser operating on the light control mode with about 1 W of power at the sample. Plasma lines were removed with a narrow-band-pass interference filter. Peak positions were calibrated against laser plasma lines. Polarization of the incident beam was controlled by a half-wave plate and the 90° scattered light was analyzed with a polaroid film placed before the monochromator slit. Depolarization measurements for the melts were made by analyzing the scattered light parallel ($I_{||}$) and perpendicular ($I_{\perp}$) to the incident laser beam. The large diameter (6 mm id) sample tubes helped to reduce the stray light and were employed even though they did not fit in the constant temperature furnace available. Stray-light and ghosts were reduced to a satisfactory low levels by employing a solution of 0.5 *M* $Pr(EDTA)^-$ complex as a post sample filter and by carefully adjusting the focus to ensure that a minimum of reflected laser light fell on the entrance slit of the monochrometer. These methods allowed distortion-free spectra to be recorded to within 20 cm^{-1} of the exciting line for these highly reflecting samples. Spectra recorded with and without these precautions showed no difference in peak positions or relative intensities but a much improved background was possible with the post-sample filter. Studies of KNO_3 and $CsNO_3$ with and without the post sample filter showed no appreciable alterations in the shapes or relative intensities of low frequency modes above 40 cm^{-1}. Generally 2 cm^{-1} slits were employed for the solids and 4 cm^{-1} slits for the melts.

Spectra of the melts were obtained in a simple nichrome heating coil with temperatures monitored with a chromel–alumel thermocouple on the sample container. Subsequent temperature variation studies revealed that the spectra were insensitive to sample temperature so that the ±15° uncertainty in the temperature actually in the laser beam would have little influence on the measured peak positions and halfwidths of the melts. Changes in cation and concentration caused the most significant spectral changes for the melts for the temperature range employed (600–700°C). Spectra of the solids were recorded at 25°C and no attempt was made to investigate possible phase transitions. Spectra of the solids and melts were recorded on two different occasions to establish the consistency of the band shapes and frequencies. Raman envelopes for the melts were manually digitallized, base-line corrected with a polynomial function, and the envelopes curve resolved into Gaussian components with a least-squares refinement. The number of components was kept to the minimum number that could be justified on the basis of visual inspection of the spectra. The primary concern of the curve resolving procedures was to obtain the ratio of the intensity of the peak at about 250 cm^{-1} (due to tetrahedral $MgCl_4^{2-}$) to that of the low frequency mode about 225 cm^{-1}. In this way one could obtain the ratio, $I = I_{225}/I_{250}$, or the fraction of the total intensity of the 160–260 cm^{-1} region which comes from the I_{250} peak, $f = I_{250}/I_{total}$. If one makes the approximation that the different intensities in the ν_1 portion are directly related to different polyatomic species concentrations then f represents the fraction of the total species concentration which comes from $MgCl_4^{2-}$. Serious band overlap and base-line uncertainties limit the accuracy of the ratio to about 15%. The computer resolved results were consistant with and probably not much better than results obtained by manual graphical methods. Although more precise data collection and treatment would be desirable one would still be faced with the lack of information on molar scattering efficiencies of the two species and species concentrations would remain uncertain.

Results and Discussion

Raman spectra for the solids of the $MgCl_2$–ACl systems are shown (Figs. 1–5) with peak frequencies, halfwidths, relative intensities, and assignments collected in Tables 1–5. Except for our recent work (3, 8) on single crystals the spectra of the solid compounds have not been reported previously. The results are in excellent agreement with

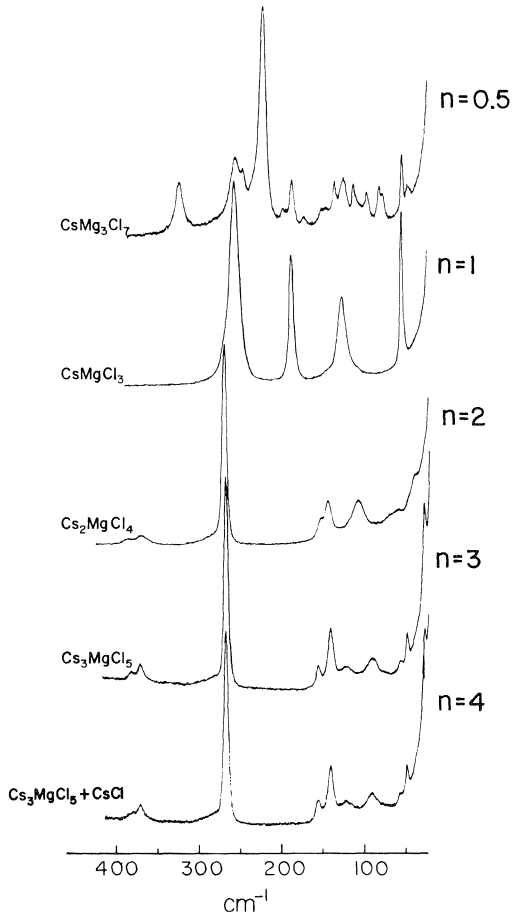


FIG. 1. Raman spectra of solids formed from the CsCl–$MgCl_2$ system.

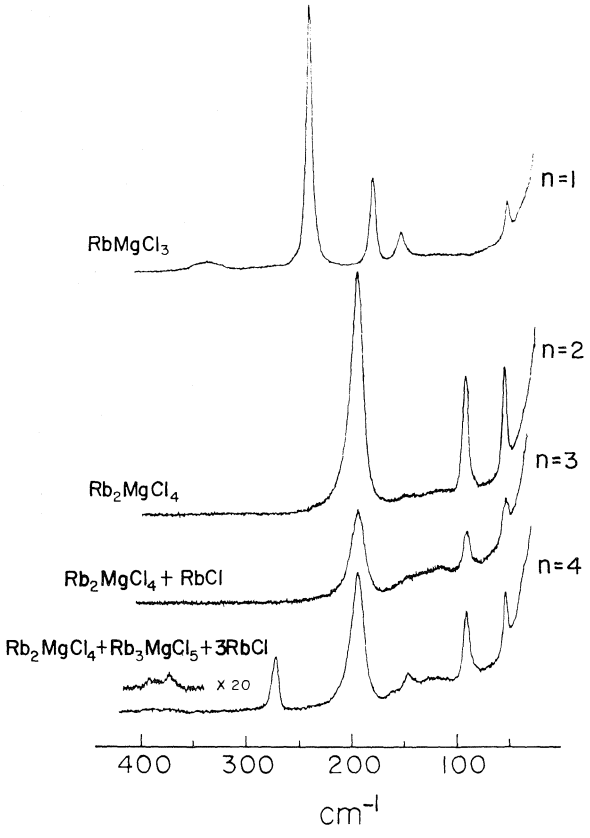


FIG. 2. Raman spectra of solids formed from the RbCl–$MgCl_2$ system.

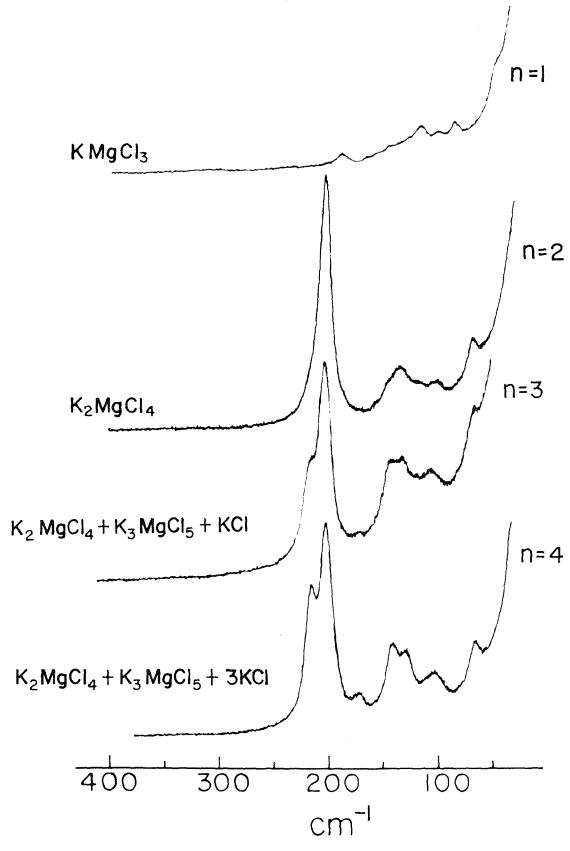


FIG. 3. Raman spectra of solids formed from the KCl–$MgCl_2$ system.

phase separation studies and characteristic peak frequencies have been assigned to each of the predicted double salts. Additional new compounds or solid solutions have been identified in the alkali metal-rich region of the RbCl–$MgCl_2$ and KCl–$MgCl_2$ systems. Previous studies (3–5, 8) have shown that the $MgCl_4^{2-}$ ion can be characterized by the typical spectrum of a tetrahedral molecule with T_d point-group symmetry, similar to CCl_4 but with peak frequencies: $\nu_1(A_1)$, 250 cm^{-1}; $\nu_2(E)$, 110 cm^{-1}; $\nu_3(F_2)$, 360 cm^{-1}; $\nu_4(F_2)$, 145 cm^{-1}. This ion has been identified in the Cs_2MgCl_4, Cs_3MgCl_5 salts and in the new salt of rubidium which has the probable formula Rb_3MgCl_5. Raman spectra of the other salts suggest that extended lattice structures with the Mg^{2+} in a distorted octahedral site with shared corners, faces, or edges are most probable. A discussion of the results for the pure-component starting materials and the solid mixtures follows.

Pure Components

First-order Raman scattering is not allowed for either the NaCl or CsCl forms of the alkali metal chlorides (9, 10). Weak second order scattering can occur (9, 11) but in the Raman spectra of the polycrystalline samples employed in the present study it appeared as a weak–broad structureless feature from 100 to 200 cm^{-1} with intensity an order of magnitude less than the processes reported (11). Magnesium chloride does have a first order Raman spectrum. On the basis of the crystal structure: space group, $R\,\bar{3}m$ (D_{3d}^5), $z = 1$ (12), two Raman active peaks are predicted, A_{1g} and E_g. These have been assigned to sharp peaks at 240 and 155 cm^{-1} respectively (6, 7). The assignment is consistent with partial polarization measurements (7) and analogous studies of isomorphous MCl_2 structures (13). The crystal has layers of chlorine ions which are nearly cubic close packed with magnesium ions between the layers with distorted octahedral coordination (D_{3d} sites). The A_{1g} mode at 240 cm^{-1} corresponds to the in-plane symmetric stretching motion of the chlorides while the E_g mode corresponds to the in-plane anti-symmetric stretch. Temperature variation studies from 77 to 973 K indicated that the peak positions decreased with increased temperature but no phase change was

Can. J. Chem. Downloaded from www.nrcresearchpress.com by
For personal use only.

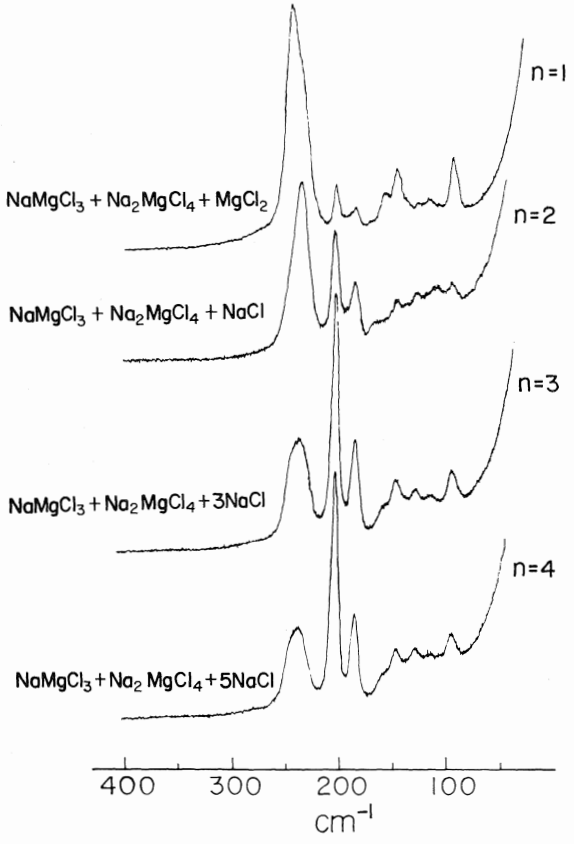


FIG. 4. Raman spectra of solids formed from the NaCl–$MgCl_2$ system.

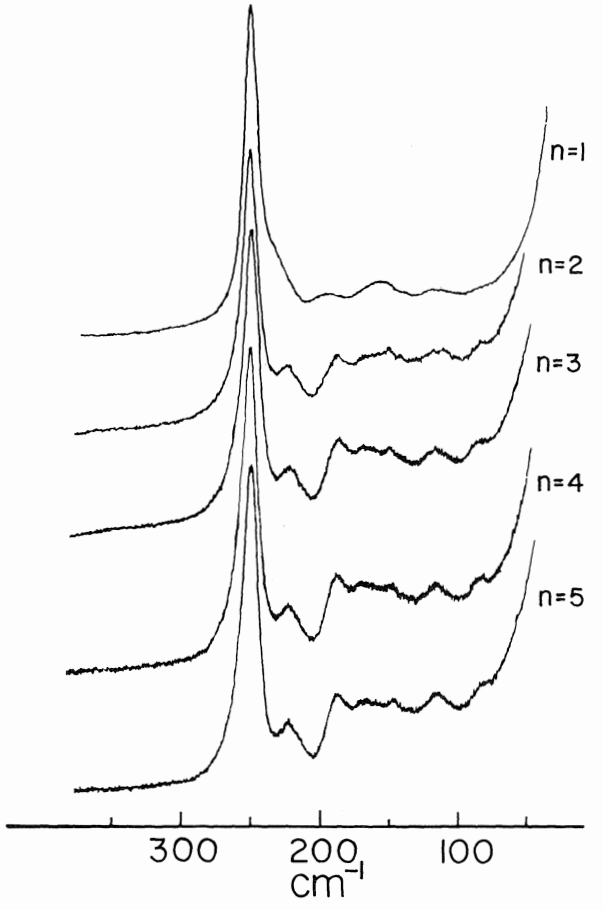


FIG. 5. Raman spectra of solids formed from the LiCl–$MgCl_2$ system.

detected (6, 7). In the $MgCl_2$–ACl systems we were unable to detect peaks which could clearly be assigned to $MgCl_2$ solid but in the results which follow it is possible that intensity in the 240 and 150 cm^{-1} region for the $MgCl_2$-rich solids could be due to pure $MgCl_2$.

CsCl–$MgCl_2$ System

The phase diagram of the CsCl–$MgCl_2$ system (14, 15) indicates the presence of four double salts, the incongruent melting $CsMg_3Cl_7$, stable below 565°C, and three congruent melting compounds; $CsMgCl_3$, mp 610°C; Cs_2MgCl_4, mp 545°C; and Cs_3MgCl_5, mp 527°C. All four compounds have been detected and characterized by their Raman spectra (Fig. 1, Table 1). The solid of composition $MgCl_2$ + 4CsCl can be seen to be a mixture of the Cs_3MgCl_5 salt and CsCl while the incongruent melting $CsMg_3Cl_7$ also contains some of the $CsMgCl_3$ salt.

$CsMgCl_3$ crystallizes with hexagonal symmetry, space group $P6_3/mmc$ (D_{6h}^4); $a = b = 7.269$ Å, $c = 6.187$ Å; 2 formula units per unit cell (16). There are no discrete molecular ions but a basic feature is the linear array of $MgCl_6$ octahedra sharing faces directed along the hexagonal c axis. Five Raman-active modes are predicted from the factor-group analysis: A_{1g}, E_{1g}, and $3E_{2g}$ modes. Four Raman peaks are clearly visible (Fig. 1) and depolarization measurements (8) indicate that the peak at 126 cm^{-1} has both E_{1g} and E_{2g} symmetry. The peak at 254 cm^{-1} of A_g symmetry corresponds to the symmetric stretching motion of the Cl^- ions in the σ_h (ab) plane of the crystal. A more complete discussion of the Raman results has been given elsewhere (8).

Cs_2MgCl_4 is orthorhombic; space group $Pnma$ (D_{2h}^{16}); $a = 9.777$, $b = 7.514$, $c = 13.234$ Å; 4 formula units per unit cell (17). Magnesium is tetrahedrally coordinated with distinct $MgCl_4^{2-}$ ions present in the lattice. The structure is isomorphous with Cs_2SO_4. Raman results for oriented single crystals have been presented in detail in a previous publication (3). Not all of the peaks reported previously have been observed in the present work (Table 1,

Can. J. Chem. Downloaded from www.nrcresearchpress.com by 210.87.254.42 on 09/05/12
For personal use only.

TABLE 1. Raman peak positions, halfwidths, and relative intensities for solids from $MgCl_2 + n$CsCl mixtures

$n = 0.5$ $CsMg_3Cl_7$ I	$n = 1$ $CsMgCl_3$ II	$n = 2$ Cs_2MgCl_4 III	$n = 3$ Cs_3MgCl_5 IV	$n = 4$ $Cs_3MgCl_5 + CsCl$ IV	Assignments[a]
			29[b] (4.0, 1.1)[c]	29 (4.0, 0.5)	IV (E_g)
		40 (10, 0.4)			III ($B_{1g} + B_{2g} + B_{3g}$)
47 (7.0, 0.4)					I
			50.3 (4.0, 0.6)	50.3 (4.0, 0.6)	IV (B_{2g})
54 (4.0, 0.8)	54 (4.3, 2.4)				II (E_{2g})
			58.2 (4.0, 0.2)	58.2 (4.0, 0.1)	IV (A_{1g})
		60 (12, 0.4)			III (B_{2g})
		70 (12, 0.3)			III (A_g)
76 (6.0, 0.6)					I
			76 (6.0, 0.2)	76 (6.0, 0.2)	IV (E_g)
81 (6.0, 0.7)					I
			92 (16, 2.1)	92 (16, 2.0)	IV (B_{2g})
95.8 (7.0, 0.8)					I
		108 (18, 3.8)			III $\nu_2(A_g + B_{1g} + B_{2g} + B_{3g})$
111 (7.0, 1.6)					I
123.5 (10, 1.8)	124.6 (12.0, 3.7)				II ($E_{1g} + E_{2g}$)
			124 (13, 1.4)	124 (13, 1.3)	IV $\nu_2(A_{1g})$
134 (8.0, 1.3)					I
			142 (8.0, 3.2)	142 (8.2, 3.1)	IV $\nu_4(E_g)$
		144 (10, 2.5)			III $\nu_4(A_g + 2B_{1g} + B_{2g} + B_{3g})$
150 (10, 0.6)					I
		153 (11, 1.4)			III $\nu_4(A_g)$
			157 (8.0, 1.1)	157 (9.0, 1.3)	IV $\nu_4(B_{2g})$
171 (8.0, 0.2)					I
185.5 (7.0, 1.3)	186.0 (6.8, 3.2)				II (E_{2g})
195.5 (10, 0.7)					I
219.5 (10, 10)					I
244 (10, 2.4)					I[d]
253 (12, 3.5)	253.8 (13.0, 10)				II (A_{1g})
			266.5 (6.4, 10)	266.5 (6.8, 10)	IV $\nu_1(A_{1g})$
		267.6 (6.8, 10)			III $\nu_1(A_g)$
280 (15, 0.5)					I
			285 (12, 0.5)	285 (14, 0.5)	IV $2\nu_4$
		288 (10, 0.4)			III $2\nu_4$
320 (11, 2.4)					I
		367 (18, 1.1)			III $\nu_3(A_g + B_{1g})$
			369 (10, 1.0)	369 (10, 1.1)	IV $\nu_3(E_g)$
			380 (12, 0.5)	380 (10, 0.4)	IV $\nu_3(B_{2g})$
		383 (16, 0.6)			III $\nu_3(A_g + B_{1g} + B_{2g} + B_{3g})$

[a]Assignments for compounds III and IV are based on the tetrahedral $MgCl_4^{2-}$ unit in these solids. Assignments for compound II are based on the factor group (D_{6h}^4) analysis of this extended lattice structure. More complete assignments have been given elsewhere (8).
[b]Peak frequency in cm^{-1}.
[c]Halfwidths and relative intensities based on the most intense peak given a value of 10 are listed in parentheses.
[d]Pure $MgCl_2$ has peaks at 155 and 240 cm^{-1} and may contribute in this region.

Fig. 1), but this is due to the fact that the previous work was done on oriented crystals at 77 K. Nevertheless, the typical four line spectrum of the $MgCl_4^{2-}$ species can be identified and the assignments (Table 1) are based on the oriented single crystal data.

The complete structure of Cs_3MgCl_5 has not been reported but Couch and Smith (18) deduced from X-ray powder patterns that the structure was isomorphous with Cs_3CoCl_5; space group $I4/mcm$ (D_{4h}^{18}); $a = b = 9.23$ Å, $c = 14.88$ Å; 2 formula units per primitive unit cell. Discrete $MgCl_4^{2-}$ tetrahedral are predicted and the Raman results are in excellent agreement with this prediction. Results of a full factor group analysis and depolarization measurements have been presented (8). The ν_3 mode (380, 369 cm^{-1}) and the ν_4 mode (142, 157 cm^{-1}) of the tetrahedral ion have been split by crystal field effects (Fig. 1, Table 1).

The crystal structure of $CsMg_3Cl_7$ is not known. Indeed it will be difficult to obtain structural information on this incongruent melting compound. A large number of Raman peaks have been detected with the intense peaks at 219.5 and 320 cm^{-1} the most prominent (Table 1, Fig. 1). Our samples also contained peaks due to $CsMgCl_3$ (Fig. 1) and a

Can. J. Chem. Downloaded from www.nrcresearchpress.com by 210.87.254.42 on 09/05/12
For personal use only.

TABLE 2. Raman peak positions, halfwidths, and relative intensities for solids from $MgCl_2$ + nRbCl mixtures

$n = 1$ $RbMgCl_3$ I	$n = 2$ Rb_2MgCl_4 II	$n = 3$ Rb_2MgCl_4 + RbCl II	$n = 4$ Rb_2MgCl_4 + Rb_3MgCl_5 + 3RbCl II	III	Assignments[a]
53.8[b] (5.7, 1.0)[c]					I (E_{2g})
	56.0 (4.6, 1.4)	56.0 (6.0, 1.3)		56.0 (5.0, 1.4)	II (E_g)
	92.6 (6.5, 2.4)	92.6 (8.0, 2.3)		92.6 (6.8, 2.3)	II (A_{1g})
				147.0 (10.0, 1.0)	III $\nu_4(MgCl_4^{2-})$
152.9 (9.2, 1.7)					I[d] ($E_{1g} + E_{2g}$)
179.0 (7.0, 3.7)					I (E_{2g})
	194.2 (13.5, 10)	194.2 (15.0, 10)		194.2 (14.0, 10)	II (E_g)
239.0 (6.3, 10)					I[d] (A_{1g})
				261.8 (8.0, 2.3)	III $\nu_1(MgCl_4^{2-})$
	320 (w, br)				
335 (32, 1.6)					I (153 + 179)
				374 (12, 0.3)	III } $\nu_3(MgCl_4^{2-})$
				390 (18, 0.3)	III }

[a]Assignment of peaks for I have been made by analogy with $CsMgCl_3$ (Table 1). Assignment of peaks for II has been made by analogy with the K_2MgCl_4 salt (Table 3).
[b]Peak frequency in cm^{-1}.
[c]Halfwidths, and relative intensities based on the most intense peak given a value of 10 are listed in parentheses.
[d]Pure $MgCl_2$ has peaks at 155 and 240 cm^{-1} and may contribute in this region.

TABLE 3. Peak frequencies, halfwidths, and relative intensities for solids from $MgCl_2$ + nKCl mixtures

$n = 1$ $KMgCl_3$ I	$n = 2$ K_2MgCl_4 II	$n = 3$ K_2MgCl_4 + K_3MgCl_5 + KCl II	III	$n = 4$ K_2MgCl_4 + K_3MgCl_5 + 3KCl II	III	Assignments[a]
51[b] (4.0, 1.0)[c]						I
	70 (9.0, 0.8)	69 (10, 1.2)		70 (10, 1.2)		II (E_g)
88 (9.0, 5.4)						I
103 (10, 2.4)	103 (10, 0.3)					I + II
		108 (15, 1.7)		107 (15, 1.5)		III
119 (14, 10)	119 (10, 0.2)					I
		134 (12, 3.0)		133 (12, 2.5)		III
	136 (22, 2.2)					II
		146 (13, 3.8)		146 (13, 3.2)		III
		175 (15, 0.6)		176 (18, 1.1)		III
190 (11, 5.2)						I
	205 (13, 10)	205 (12, 10)		205 (12, 10)		II (E_g)
		219 (15, 5.8)		219 (15, 8.2)		III
308 (24, 2.9)						I

[a]Assignment of I should be based on the D_{2h}^{16} space group but data are too scarce. Assignment of II is based on the D_{4h}^{17} structure. Intensity in the 100–200 cm^{-1} region may have a large second order component (3).
[b]Peak frequency in cm^{-1}.
[c]Halfwidths, and relative intensities based on the most intense peak given a value of 10 are listed in parentheses.

weak peak at 244 cm^{-1} may be due to $MgCl_2$. It seems doubtful that the structure contains a discrete species, such as $MgCl_4^{2-}$ or $MgCl_6^{4-}$ since the characteristic peaks are absent. Further speculation on the structure is not warranted.

RbCl–$MgCl_2$ System

The phase diagram of the RbCl–$MgCl_2$ system is characterized by two congruent melting compounds $RbMgCl_3$ and Rb_2MgCl_4 (15, 19). Full crystal structure data are not available but it has been suggested that the $RbMgCl_3$ salt is isostructural with $CsMgCl_3$ (20, 21) while the Rb_2MgCl_4 salt may have a tetragonal structure similar to K_2MgCl_4 (20). Raman results for $RbMgCl_3$ are consistent with the $CsMgCl_3$ structure and it can be seen (Figs. 1 and 2) that the spectra are quite similar. The assignments for $RbMgCl_3$ (Table 2) have been made by analogy with the cesium salt. The origin of the weak peak at 335 cm^{-1} is uncertain although it has been assigned to a combination mode. The lowest frequency mode in $CsMgCl_3$ (54 cm^{-1}) has been assigned to the Cs^+ sublattice (8) which would suggest that the mode at 54 cm^{-1} in the $RbMgCl_3$ should be due to the Rb^+ sublattice but this is not in keeping with mass differences. Possibly the modes at 152.8 and 124.6 cm^{-1} in the rubidium and cesium salts are due to the alkali metal sublattice mode.

The Rb_2MgCl_4 spectrum resembles the K_2MgCl_4

Can. J. Chem. Downloaded from www.nrcresearchpress.com by 210.87.254.42 on 09/05/12
For personal use only.

Can. J. Chem. Downloaded from www.nrcresearchpress.com by 210.87.254.42 on 09/05/12
For personal use only.

TABLE 4. Raman peak positions, halfwidths, and relative intensities for solids from the $MgCl_2 + n$NaCl mixtures

$n = 1$	$n = 2$		$n = 3$		$n = 4$		
$MgCl_2 + NaMgCl_3 + Na_2MgCl_4$ I	$MgCl_2 + NaMgCl_3 + Na_2MgCl_4 + NaCl$ II	$NaMgCl_3 + Na_2MgCl_4 + NaCl$ I	$NaMgCl_3 + Na_2MgCl_4 + 3NaCl$ II	$NaMgCl_3 + Na_2MgCl_4 + 5NaCl$ I	$NaMgCl_3 + Na_2MgCl_4 + 5NaCl$ II	Assignment[a]
94[b] (6.0, 0.5)[c]						I
98 (8.0, 1.3)	98 (12, 1.0)		98 (11, 1.6)		98 (10, 1.3)	I
	112 (16, 1.7)					
119 (10, 0.4)			118 (14, 0.8)		117 (15, 1.1)	
129 (10, 0.3)	130 (12, 1.3)		131 (12, 1.1)		131 (12, 1.5)	
140 (12, 0.4)						I
149 (10, 1.4)	149 (10, 1.1)		149 (10, 1.7)		149 (10, 1.5)	I
160 (13, 1.0)						I[d]
	165 (20, 1.1)		162 (16, 1.1)		162 (16, 1.0)	II + I
	187 (10, 2.4)		187 (8.0, 3.6)		187 (8.0, 3.0)	II
187 (10, 0.5)	206 (10, 4.4)		206 (8.0, 10)		206 (8.0, 10)	II
205 (8.0, 0.9)	237 (15, 10)		237 (16, 6.9)		237 (14, 4.4)	II[d]
237[e] (15, 5.0)	247[e] (16, 3.0)		247 (16, 6.9)		247 (14, 4.4)	I
247 (14, 10)						

[a]Mode assignments cannot be made since the structures of these compounds are not known and the spectra are not similar to other compounds of similar stoichiometry.
[b]Peak frequency in cm^{-1}.
[c]Halfwidths, and relative intensities based on the most intense peak given a value of 10 are listed in parentheses.
[d]Pure $MgCl_2$ has peaks at 155 and 240 cm^{-1} and may contribute in this region.
[e]Shoulder.

TABLE 5. Peak frequencies, halfwidths, and relative intensities for solid solutions from the $MgCl_2 + n$LiCl mixtures

$MgCl_2 \cdot 3LiCl$[a]	Assignment
85[b] (10, 0.2)[c]	
116 (24, 1.0)	
148 (15, 1.1)	
167 (16, 1.4)	
187 (16, 2.0)	
222 (24, 1.8)	
250 (14, 10)	ν_1 of $MgCl_4^{2-}$ unit?
345 (25, 0.02)	ν_3 of $MgCl_4^{2-}$ unit?

[a]Only the data for one solid solution have been given since the other spectra were essentially identical.
[b]Peak frequency in cm^{-1}.
[c]Halfwidths, and relative intensities based on the most intense peak given a value of 10 are listed in parentheses.

spectrum (Figs. 2, 3) insofar as the most intense peak at 194 cm^{-1} is close to the value of 205 cm^{-1} observed for K_2MgCl_4. The peaks at 56.0 and 92.6 cm^{-1} are much sharper than possible corresponding peaks at 70 and 103 cm^{-1} in the K_2MgCl_4 spectrum. Sharpening of peaks is to be expected on going to larger cations since environmental broadening is expected to be less. The peak at 92.6 cm^{-1} may be due to an A_{1g} mode predicted but not observed for the potassium salt. Assignments (Table 2) are based on the uncertain analogy with the K_2MgCl_4 salt which has been studied in more detail (3).

The spectrum of the solid of composition $n = 3$ resembles that of the Rb_2MgCl_4 salt which indicates that this solid is really $Rb_2MgCl_4 + RbCl$. However, the solid formed from the melt composition $n = 4$ shows several new features in addition to the Rb_2MgCl_4 peaks. The peaks at 147, 261.8, 374, and 390 cm^{-1} are similar in peak position and relative intensity to the ν_4, ν_1, and ν_3 (split by lattice forces) of the tetrahedral $MgCl_4^{2-}$ species as observed for Cs_2MgCl_4 and Cs_3MgCl_5 (Tables 1, 2). Markov and Panchenko (19) noted the peculiar behaviour of the line of crystallization extending up to 29 mol% $MgCl_2$ but their cooling curves indicated only one eutectic. Raman results suggest the presence of a new incongruent melting compound Rb_3MgCl_5. Presence of a solid solution cannot be ruled out but the clarity of the Rb_2MgCl_4 part of the spectrum suggests that this is not the case.

KCl–$MgCl_2$ System

Two congruent melting compounds have been reported from phase diagram studies of the KCl–$MgCl_2$ system (22). X-ray diffraction data are available for both salts and neither contains the $MgCl_4^{2-}$ ion. Brynestad *et al.* (23) reported that $KMgCl_3$ has an orthorhombically distorted

Can. J. Chem. Downloaded from www.nrcresearchpress.com by 210.87.254.42 on 09/05/12
For personal use only.

perovskite structure at room temperature which transforms to a cubic perovskite-type structure at 448 K. The room temperature structure has space group *Pbnm* (D_{2h}^{16}); $a = 6.954$ Å, $b = 6.971$ Å, $c = 9.922$ Å; 4 formula units per unit cell. Magnesium has approximately octahedral symmetry with face-shared chloride ions. Factor group analysis predicts the following mode distribution:

$$\Gamma_{total} = 7A_{1g} + 7B_{1g} + 5B_{2g} + 5B_{3g} + 8A_u + 8B_{1u} + 10B_{2u} + 10B_{3u}$$

$$\Gamma_{acoustic} = B_{1u} + B_{2u} + B_{3u}$$

Twenty-four Raman active modes are predicted and since no discrete structural units exist, the assignment of Raman peaks must await oriented single crystal studies. Raman scattering from this sample was weak and the peaks were broad and poorly defined (Fig. 3, Table 3). The spectrum does not resemble either $CsMgCl_3$ or $RbMgCl_3$ and is clearly distinguishable from the K_2MgCl_4 spectrum. There was no evidence of any $MgCl_2$ or K_2MgCl_4 in the sample.

K_2MgCl_4 has a tetragonal structure: space group I_4/mmm (D_{4h}^{17}); $a = b = 4.94$ Å, $c = 15.58$ Å; one formula unit per primitive unit cell (17). Magnesium is in a distorted octahedral site in a network structure with neighbouring octahedra sharing corners. Previous Raman results for oriented single crystals were in good agreement with the factor-group analysis based on this structure. Assignments (Table 3) are based on the previous study (3). The strong peak at 205 cm^{-1} is due to the out-of-plane rotatory motion of the Cl^- sublattice while the peak at 73 cm^{-1} has been assigned to a similar mode of the K^+ sublattice. Predicted A_{1g} modes were not observed but moderately strong second-order scattering was present between 100 and 160 cm^{-1} (Fig. 3).

Spectra of solids obtained from melts in the high KCl region of the phase diagram indicate the presence of an additional compound tentatively formulated K_3MgCl_5 (Fig. 3, Table 3). The most intense of the new peaks occurs at 219 cm^{-1} which is too low to be due to a $MgCl_4^{2-}$ species. It seems most likely that the new compound also contains a network octahedral coordination for the magnesium. The fact that the spectrum of K_2MgCl_4 persists into the solids of composition $n = 3$ and $n = 4$ suggests that the new compound melts incongruently. Presence of a solid solution cannot be ruled out.

NaCl–$MgCl_2$ System

Two incongruent melting compounds, $NaMgCl_3$ and Na_2MgCl_4 are proposed by phase diagram studies (22). No diffraction data are available for either salt. Characteristic Raman spectra have been assigned for each salt (Fig. 4, Table 4) but, as expected, for incongruent melting compounds it is difficult to obtain pure compounds. The spectrum of $NaMgCl_3$ seems to be less intense than that of Na_2MgCl_4 and may contain intensity due to $MgCl_2$ which is expected from phase diagram information. Raman spectra do suggest a network octahedral coordination for magnesium.

LiCl–$MgCl_2$ System

The LiCl–$MgCl_2$ system has been reported to form a solid solution over the whole composition range (24). Raman results (Table 5, Fig. 5) are in excellent agreement with this proposal. Spectra of the solids obtained for each composition were essentially identical (Fig. 5). There was no evidence for sharp peaks due to $MgCl_2$ which would have suggested that the solid had separated into a mixture of crystalline $MgCl_2$ and LiCl. In fact, the broad nature of all of the peaks is consistent with solid solution formation over the entire concentration range. It is difficult to assess possible local structure from the spectra but the presence of the strong peak at 250 cm^{-1} could be due to the presence of a local $MgCl_4^{2-}$ environment. A weak peak at 345 cm^{-1} was also observed which could be due to the ν_3 mode of the T_d species. The presence of the 250 cm^{-1} peak even in the solid of composition $LiMgCl_3$ would only seem possible if the tetrahedral geometry about magnesium was a network array with shared Cl^- ions over a lattice that included the Li^+ ions.

Melts

Raman spectra for melts of composition $MgCl_2 + n$ACl are shown (Figs. 6–10) while data for the $n = 4$ and $n = 1$ compositions are collected in Table 6. Peak positions were relatively constant over the concentration range studied as were the halfwidths except for the halfwidths of the peaks in the 200–250 cm^{-1} region which increased with increased $MgCl_2$ concentration. Peaks at about 110, 145, and 350 cm^{-1} were depolarized, whereas the peaks in the 200–250 cm^{-1} region were strongly polarized with depolarization ratios less than 0.02. For melts of low $MgCl_2$ concentration ($n = 4$), a four line spectrum was observed and there seems little doubt about the assignment of these peaks to the four lines expected for the tetrahedral $MgCl_4^{2-}$ ion (Table 6) (3–5). The similarity of the spectrum to that of CCl_4 has been noted (3). A marked cation dependence on the ν_1 mode can be seen by com-

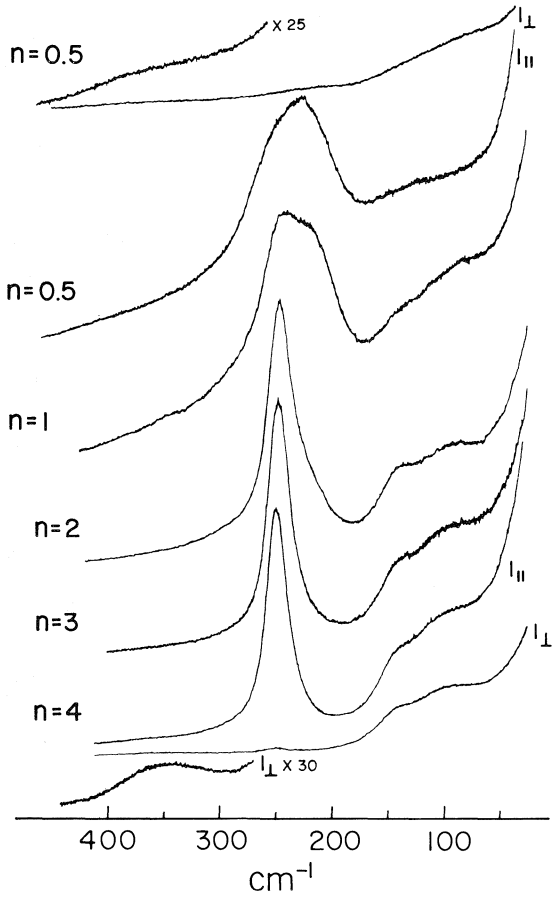


FIG. 6. Raman spectra of melts of the $CsCl–MgCl_2$ system. Depolarized spectra are shown for the highest and lowest $MgCl_2$ concentrations with the ν_3 region of $MgCl_4^{2-}$ considerably scale expanded.

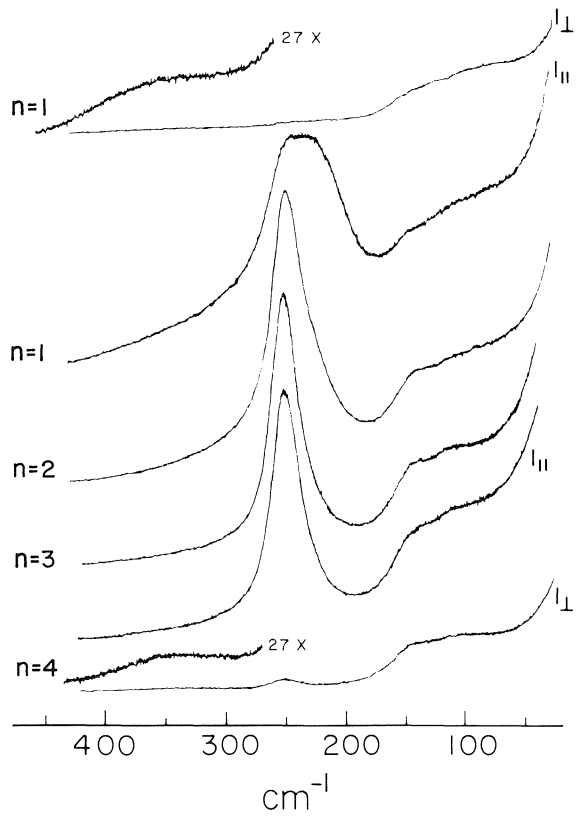


FIG. 7. Raman spectra of melts of the $RbCl–MgCl_2$ system (see Fig. 6).

parison of the melts of low $MgCl_2$ concentration. The peak maximum shifts to slightly lower frequencies while the halfwidth of the band increases considerably over the cation series Cs^+ to Li^+. This is not unexpected since the small Li^+ ion can compete quite favourably for the chloride ion which will weaken the Mg—Cl force constant and lower the frequency. Halfwidth variations of the ν_1 mode at about 250 cm^{-1} are probably due to vibrational relaxation caused by environmental broadening. The symmetric stretching mode of $MgCl_4^{2-}$ will occur in a greater range of environmental conditions in the neighborhood of the smaller, lighter Li^+ and Na^+ ions than for the larger Rb^+ and Cs^+ and this could explain the larger halfwidth for the lithium melt. Exchange broadening may also be a factor since the expected lifetime of the Cl^- ions in $MgCl_4^{2-}$ would be 10^{-10} to 10^{-12} s which is the correct range for these effects (25). The lifetime of the Cl^- in $MgCl_4^{2-}$ in the cesium melt is expected to be considerably longer than for the lithium melt.

An increase in the $MgCl_2$ concentration results in additional Raman scattering about 225 cm^{-1}. A second component at ~225 cm^{-1} is *clearly resolved* for the Cs, Rb, and K salts (Figs. 6–8) and there can be little doubt that there are two peaks in this region, i.e., the change in the envelope is not just simple broadening of the ν_1 mode. The formation of a new equilibrium species in the melts of high $MgCl_2$ concentration is suggested. It should be noted that the peaks due to the $MgCl_4^{2-}$ tetrahedron persist for all of the melts and can be detected in melts of high $MgCl_2$ concentration and even the pure $MgCl_2$ melts (Figs. 6–10, Table 6) (6). This is particularly obvious in the $I_\perp$ spectrum where the depolarized intensity remains in the 350, 145, and 110 cm^{-1} regions due to the ν_3, ν_4, and ν_2 modes. Relative intensities of these modes remained constant within experimental error over the concentration range studied. The ν_3 mode has been detected in the spectrum of molten $MgCl_2$ (6). If one makes the crude assumption that the molar scattering efficiencies of the ν_1 mode of $MgCl_4^{2-}$ at 250 cm^{-1} is equal to the molar scattering efficiency of the mode of the new species at 225 cm^{-1} then the intensity of the ν_1 mode divided by the total inten-

Can. J. Chem. Downloaded from www.nrcresearchpress.com by 210.87.254.42 on 09/05/12
For personal use only.

Can. J. Chem. Downloaded from www.nrcresearchpress.com by 210.87.254.42 on 09/05/12
For personal use only.

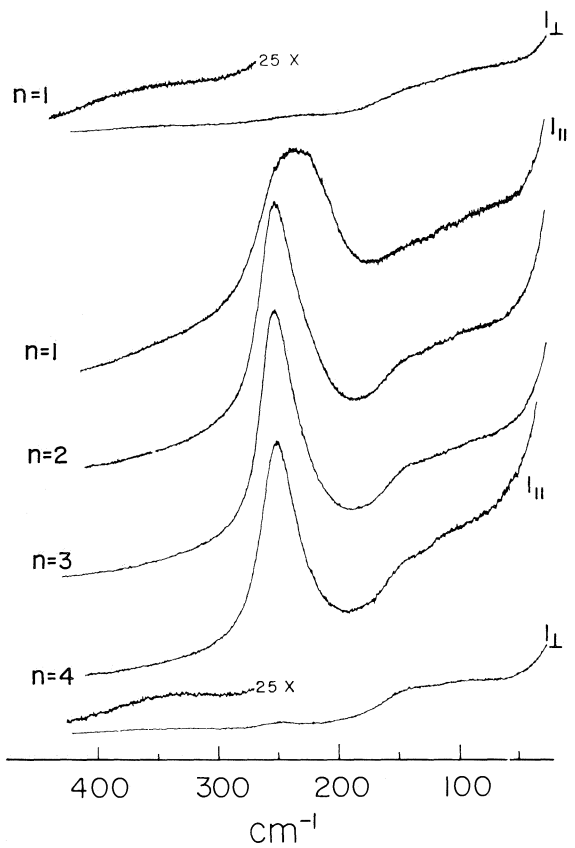


FIG. 8. Raman spectra of melts of the KCl–$MgCl_2$ system (see Fig. 6).

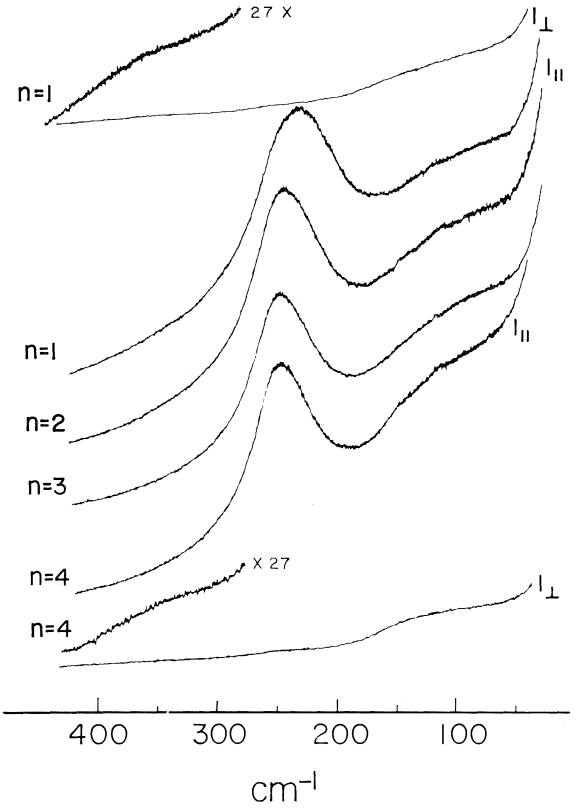


FIG. 9. Raman spectra of melts of the NaCl–$MgCl_2$ system (see Fig. 6).

sity in the 160–250 cm^{-1} region corresponds to the fraction of $MgCl_4^{2-}$ present in the melt. On this basis one finds that only $MgCl_4^{2-}$ is present at low $MgCl_2$ concentrations but this decreases slowly with increasing $MgCl_2$ concentration until only about 30% is left in pure $MgCl_2$ (Fig. 11). Possibly a third species exists in pure $MgCl_2$ since an additional polarized peak has been resolved at 130 cm^{-1} (6). The failure of simple mixture models to account for the phase diagrams of the $MgCl_2$–ACl systems would appear to be due to the presence of a new species in the high $MgCl_2$ region.

It is difficult to identify the species which gives rise to the polarized peak at 225 cm^{-1} since no other peaks have been detected. However, the present studies are quite analogous to those for the more stable, low melting CsCl–$AlCl_3$ system where two clearly resolved peaks at 350 and 312 cm^{-1} have been assigned to the $AlCl_4^-$ and $Al_2Cl_7^-$ ions on the basis of concentration studies and normal coordinate analysis. The $Al_2Cl_7^-$ ion is composed of two corner-shared tetrahedrons with probable D_{3d} symmetry (26, 27). It seems quite possible that in the present study the peak at 225 cm^{-1} is due to the $Mg_2Cl_7^{3-}$ ion since this would allow the magnesium to retain its tetrahedral coordination through corner-sharing with other magnesium centered tetrahedrons. An edge-shared $Mg_2Cl_6^{2-}$ would also be consistent with the results. $Mg_2Cl_6^{2-}$ ions, which we have preposed previously (3, 6), would be favoured by the lower charge but formation of $Mg_2Cl_7^{3-}$ would be statistically more favourable. A melt of composition $CsMgCl_3$ could possibly be described by the simplistic equilibrium although many others could be written.

$$8CsMgCl_{3(s)} \rightleftharpoons 8Cs^+ + 2Mg^{2+} + 6MgCl_4^{2-} \rightleftharpoons 3Mg_2Cl_7^{3-} + 3Cl^-$$

In the short time period of the Raman process smaller aggregates probably occur but with low concentration and/or with low intensity. It appears as if the tetrahedral coordination of Mg is highly favoured. Aggregates with 3Mg ions would be possible and have been proposed for molten $MgCl_2$ (6) but larger aggregates would probably have lifetimes shorter than Cl^- diffusion times. The presence of the $Al_2Cl_7^-$ ion was not predicted by phase diagram studies (28) and although the presence of the $CsMg_3Cl_7$ solid may suggest the presence of a dis-

TABLE 6. Raman data for melts[a] of composition $MgCl_2 + nACl$

n	Raman data					Assignment
	Li	Na	K	Rb	Cs	
4	100[b] (0.24[c], 60[d])	105 (0.20, 54)	110 (0.16, 40)	114 (0.18, 35)	106 (0.28, 45)	ν_2 (E)
	149 (0.20, 50)	145 (0.20, 60)	145 (0.11, 30)	145 (0.14, 25)	145 (0.18, 30)	ν_4 (F_2)
	237 (1.0, 58)	248 (1.0, 50)	251 (1.0, 34)	251 (1.0, 27)	250 (1.0, 23)	ν_1 (A_1)
	350 (0.005, 80)	350 (0.004, 70)	350 (0.005, 70)	350 (0.006, 70)	355 (0.010, 70)	ν_3 (F_2)
1	100 (0.18, 50)	105 (0.19, 50)	105 (0.19, 50)	114 (0.18, 40)	109 (0.26, 45)	ν_2 (E)
	149 (0.23, 50)	145 (0.15, 60)	145 (0.24, 50)	145 (0.15, 30)	144 (0.17, 30)	ν_4 (F_2)
	200 (0.55, 50)	210 (0.60, 45)	227 (0.75, 45)	227 (0.75, 45)	225 (0.70, 40)	ν_1 ($Mg_2Cl_7^{3-}$)
	237 (1.0, 55)	246 (1.0, 50)	248 (1.0, 40)	249 (1.0, 40)	250 (1.0, 35)	ν_1 (A_1)
	350 (0.01, 80)	350 (0.01, 70)	350 (0.01, 70)	350 (0.01, 70)	335 (0.01, 70)	ν_3 (F_2)

[a]Measured at approximately 650°C.
[b]Peak maximum in cm^{-1}.
[c]Intensity relative to the $\nu_1(A_1)$ mode taken as 1.0.
[d]Full width at half height.

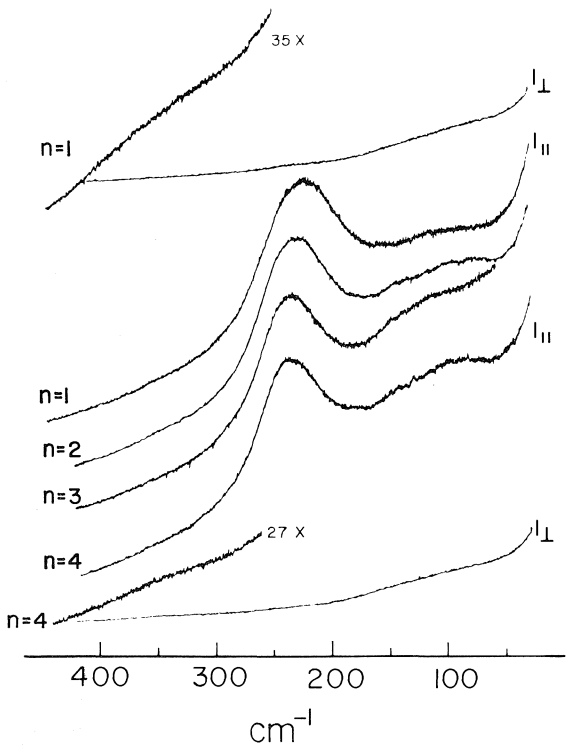


FIG. 10. Raman spectra of melts of the LiCl–$MgCl_2$ system (see Fig. 6).

crete dimeric or trimeric ion it appears that the $Al_2Cl_7^-$ and $Mg_2Cl_7^{3-}$ ions are melt stabilized. Spectroscopic studies of the $MnCl_2$–ACl and $ZnCl_2$–ACl systems indicate that tetrahedral coordination of the divalent metal cation is maintained over the whole concentration range and similar polynuclear tetrahedral species have been proposed for the concentrated melts (29, 30).

It does not seem likely that octahedral coordination occurs. A discrete $MgCl_6^{4-}$ ion seems extremely unlikely since even in the solids the octahedral coordination could only be stabilized by sharing of chlorides in a network lattice. Dimeric species with octahedral coordination and shared chlorides would require unrealistically large species charges and a discontinuous change in coordination when formed from the $MgCl_4^{2-}$ ion. There is no evidence to suggest the presence of $MgCl_3^-$ which would be expected to have a symmetric stretching mode at higher frequencies than ν_1 of $MgCl_4^{2-}$. An Mg_2Cl_4 molecule would require either improbable Mg–Mg contact or unfilled coordination sites.

An increase in $MgCl_2$ concentration appears to cause an increase in the halfwidths of both the 250 and 225 cm^{-1} components. The explanation of this effect is probably similar to that given above for the cation effect at fixed $MgCl_2$ concentration ($n = 4$), i.e., inhomogeneous broadening or lifetime broadening caused by the greater symmetry of the attraction of Cl^- ions between two magnesium ions than between a magnesium and cesium ion.

In summary the present results present a reasonably clear picture of the coordination behaviour of magnesium in the alkali metal chloride – magnesium chloride solids and melts. In solids the discrete tetrahedral $MgCl_4^{2-}$ species can only be stabilized by large cations such as Cs^+ or Rb^+ and then only when there is sufficient chloride. Edge-, face-, and corner-shared octahedral appear more often in the solid state structures. Nevertheless the fusion of the salts inevitably leads to stabilization of the $MgCl_4^{2-}$ ion which can probably coexist in equilibrium with an ionic dimer $Mg_2Cl_7^{3-}$. There is generally no reason to expect the species present in the melt to persist into the solid state although this does appear to be the case for Cs_2MgCl_4, Cs_3MgCl_5, and Rb_3MgCl_5. From a vibrational spectroscopic point of view there is little doubt that the presence of discrete equilibrium ionic species dominates the melt structure. Lattice-like structural models are not supported by this work. The

Can. J. Chem. Downloaded from www.nrcresearchpress.com by 210.87.254.42 on 09/05/12
For personal use only.

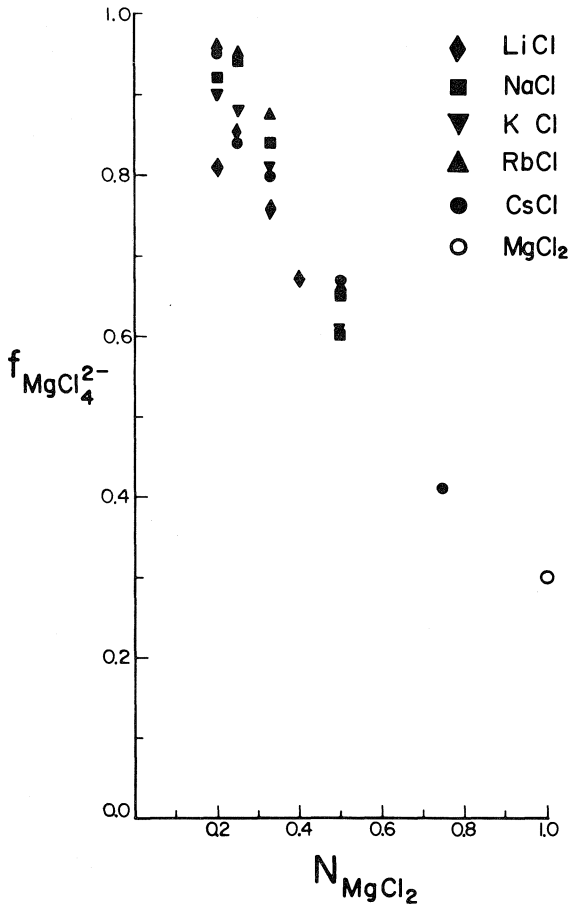


FIG. 11. Fraction of magnesium in the $MgCl_4^{2-}$ ion form obtained from the ratio of the intensity of the ν_1 mode at about 250 cm^{-1} to the total polarized intensity in the region.

moderately high conductivity of pure $MgCl_2$ (31) is consistent with the presence of the ions proposed above (the equivalent conductance for molten $MgCl_2$ at 1060 K is 33.2 ohm^{-1}). Improved data collection and treatment of the ionic melts over the critical concentration range ($n = 2$ to $n = 0$) would help to improve the determination of the relative species concentrations but lack of information on the relative scattering efficiencies would still need to be overcome. The halfwidths of the ν_1 peaks for the different melts suggest that the $MgCl_4^{2-}$ and $Mg_2Cl_7^{3-}$ ions have kinetic stability relative to chloride diffusion. The species lifetimes are considerably larger in the CsCl–$MgCl_2$ melts (probably 10^{-10} to 10^{-11} s) but decrease with increasing $MgCl_2$ concentration and with decreasing size of alkali metal cation.

Acknowledgements

This work was supported by the National Research Council of Canada. One of the authors (M.H.B.) is grateful to Professor Lascombe (University Bordeaux) for his generous hospitality while the author was on sabbatical leave.

1. H. FLOOD and S. URNES. Z. Elektrochem. **59**, 834 (1955).
2. J. LUMSDEN. Thermodynamics of molten salt mixtures. Academic Press, New York, NY. 1966.
3. M. H. BROOKER. J. Chem. Phys. **63**, 3054 (1975); and references therein.
4. V. A. MARONI, E. J. HATHAWAY, and E. J. CAIRNS. J. Phys. Chem. **75**, 155 (1971).
5. V. A. MARONI. J. Chem. Phys. **55**, 4789 (1971).
6. C.-H. HUANG and M. H. BROOKER. Chem. Phys. Lett. **43**, 180 (1976).
7. R. J. CAPWELL. Chem. Phys. Lett. **12**, 443 (1972).
8. M. H. BROOKER and C.-H. HUANG. Mat. Res. Bull. In press.
9. B. S. AGRAWAL, R. D. KIRBY, and J. R. HARDY. Phys. Rev. **B11**, 5153 (1975).
10. G. R. WILKINSON. *In* The Raman effect. Vol. 2. *Edited by* A. Anderson. Marcel Dekker, New York. 1973. Chapt. 1.
11. C.-H. HUANG and M. H. BROOKER. Unpublished work.
12. R. W. G. WYCKOFF. Crystal structures. Vol. 1. Interscience, New York. 1964.
13. D. J. LOCKWOOD. J. Opt. Soc. Am. **63**, 374 (1973).
14. B. F. MARKOV and I. D. PANCHENKO. Zh. Obshch. Khim. **25**, 2042 (1955).
15. E. M. LEVIN, C. R. ROBBINS, and H. F. MCMURDIE. Phase diagrams for ceramists. American Ceramic Society, Columbus, OH. 1964.
16. G. L. MCPHERSON, T. J. KISTENMACHER, and G. D. STUCKY. J. Chem. Phys. **52**, 815 (1970).
17. C. S. GIBBONS, V. C. REINSBOROUGH, and W. A. WHITLA. Can. J. Chem. **53**, 114 (1975).
18. T. W. COUCH and G. P. SMITH. J. Chem. Phys. **53**, 1336 (1970).
19. B. F. MARKOV and I. D. PANCHENKO. Zh. Obshch. Khim. **25**, 2039 (1955); Ukr. Khim. Zh. **20**, 620 (1954).
20. G. SVEDAHL. M.Sc. thesis, Institute of Inorganic Chem., Univ. of Trondheim, Norway, Dec. 1969. Quoted in J. L. Holm, B. J. Holm, B. Rinnan, and F. Grønvold, J. Chem. Thermodyn. **5**, 97 (1973).
21. J. FERNÁNDEZ, M. J. TELLO, and M. A. ARRIANDIAGA. Mat. Res. Bull. **13**, 477 (1978).
22. K. GRJOTHEIM, J. L. HOLM, and M. ROTNES. Acta Chem. Scand. **26**, 3802 (1972).
23. J. BRYNESTAD, H. L. YAKEL, and G. P. SMITH. J. Chem. Phys. **45**, 4652 (1966).
24. S. D. GROMAKOV. Zh. Fiz. Khim. **24**, 641 (1950).
25. M. M. KREEVOY and C. A. MEAD. J. Am. Chem. Soc. **84**, 4596 (1962).
26. G. TOSI, G. MAMANTOV, and G. M. BEGUN. Inorg. Nucl. Chem. Lett. **6**, 553 (1970).
27. H. A. ØYE, E. RYTTER, P. KLAEBOE, and S. J. CYVIN. Acta Chem. Scand. **25**, 559 (1971).
28. I. S. MOROZOV and A. T. SIMONICH. Zh. Neorg. Khim. **2**, 1908 (1957).
29. W. BUES, L. EL-SAYED, and H. A. ØYE. Acta Chem. Scand. **A31**, 461 (1977).
30. C. A. ANGELL, G. H. WEGDAM, and J. VAN DER ELSKEN. Spectrochim. Acta, **30A**, 665 (1974).
31. G. JANZ, F. W. DAMPIER, G. R. LAKSHMINARAYANAN, P. K. LORENZ, and R. P. T. TOMKINS. Natl. Stand. Ref. Data Ser. Natl. Bur. Stand. 15. Molten salts. Vol. 1. Electrical conductance, density and viscosity data. 1968.

Can. J. Chem. Downloaded from www.nrcresearchpress.com by 210.87.254.42 on 09/05/12
For personal use only.

A ^{31}P nuclear magnetic resonance spectroscopic study of complexes of cadmium(II) with some phosphine oxides, sulfides, and selenides[1,2]

PHILIP A. W. DEAN[3] AND MARY K. HUGHES

Department of Chemistry, University of Western Ontario, London, Ont., Canada N6A 5B7

Received June 18, 1979

PHILIP A. W. DEAN and MARY K. HUGHES. Can. J. Chem. **58**, 180 (1980).

Complexation between $Cd(SbF_6)_2$ and the ligands Ph_3PE (E = S or Se), $Ph_2P(E)(CH_2)_nP(E)Ph_2$ (n = 1 or 2, E = O, S or Se; n = 3, E = Se), $[Ph_2P(E)CH_2]_3CMe$ (E = S or Se) and $Ph_2P(E)(CH_2)_2PPh(E)(CH_2)_2P(E)Ph_2$ (E = O, S, or Se) in liquid SO_2 has been studied, mainly by low-temperature ^{31}P nmr spectroscopy. With the sulfides and selenides the maximum donor atom/Cd ratio observed is four, as shown by the limiting low temperature spectra of $(Ph_3PE)_4Cd^{2+}$ (E = S or Se), $[CH_2(PPh_2(Se))_2]_2Cd^{2+}$, and $[Ph_2P(E)CH_2CMe(CH_2PPh_2(E))_2]_2Cd^{2+}$ (E = S or Se). The last two complexes both contain a potentially tridentate ligand behaving in a bidentate manner and their spectra are unexpectedly complicated due, perhaps, to conformational effects. Slow exchange spectra of $[Ph_2P(E)(CH_2)_2PPh(E)(CH_2)_2PPh_2(E)]Cd^{2+}$ (E = S or Se) show that in each complex the ligand behaves in a tridentate manner. For the preceding complexes, two-bond $^{111/113}Cd$–^{31}P coupling is observed at the donor sites, and for the selenides a reduction in $|{}^1J(^{31}P—^{77}Se)|$ on complexation further identifies the bound —PSe groups.

The maximum coordination number appears to be six in the complexes of the phosphine oxides. Both 2:1 and 3:1 L:Cd complexes exist for both of the bidentate ligands $Ph_2P(O)(CH_2)_nP(O)Ph_2$ (n = 1 or 2) whereas in the system $Ph_2P(O)(CH_2)_2P(O)Ph(CH_2)_2P(O)Ph_2$–$Cd^{2+}$ the species identified is the presumably six-coordinate 2:1 complex. For comparison, the six-coordinate complex $[\{CH_2(PPh_2(O))_2\}_3Hg]^{2+}$ has been identified in solution also.

Competition studies between the dioxides, disulfides, and diselenides of the diphosphines show that the disulfides and diselenides cannot compete with the dioxides for cadmium, but that the diselenides can compete with the disulfides to a limited extent.

PHILIP A. W. DEAN et MARY K. HUGHES. Can. J. Chem. **58**, 180 (1980).

On a étudié la complexation entre $Cd(SbF_6)_2$ et les ligands: Ph_3PE (E = S ou Se), $Ph_2P(E)(CH_2)_nP(E)Ph_2$ (n = 1 ou 2, E = O, S ou Se; n = 3, E = Se), $[Ph_2P(E)CH_2]_3CMe$ (E = S ou Se) et $Ph_2P(E)(CH_2)_2PPh(E)(CH_2)_2P(E)Ph_2$ (E = O, S ou Se) dans le SO_2 liquide en utilisant principalement la rmn du ^{31}P à basse température. Avec les sulfures et les sélénures le rapport maximum atome–donneur Cd observé est 4 tel que montré par les spectres à basse température du $(Ph_3PE)_4CD^{2+}$ (E = S ou Se), du $[CH_2(PPh_2(Se))_2]_2Cd^{2+}$ et du $[Ph_2P(E)CH_2CMe(CH_2PPh_2(E))_2]_2Cd^{2+}$ (E = S ou Se). Les deux derniers complexes contiennent un ligand potentiellement tridentate se comportant de manière bidendate et leurs spectres sont compliqués de manière inattendue probablement à cause d'effets conformationnels. Les spectres d'échange lents du $[Ph_2P(E)(CH_2)_2PPh(E)(CH_2)_2PPh_2(E)]Cd^{2+}$ (E = S ou Se) montrent que dans chaque complexe le ligand se comporte de manière tridentate. Pour les complexes précédents on observe au niveau des sites donneurs un couplage à travers deux liaisons $^{111/113}Cd$–^{31}P et pour les sélénures la réduction de $|{}^1J(^{31}P–^{77}Se)|$ dans la complexation identifie d'avantage les groupes —^{2}PSe liés.

Le nombre maximum de coordination semble être 6 dans les complexes de phosphine oxydes. Les deux complexes 2:1 et 3:1 L:Cd existent pour les deux ligands bidentates $Ph_2P(O)(CH_2)_nP(O)Ph_2$ (n = 1 ou 2) alors que dans le système $Ph_2P(O)(CH_2)_2P(O)Ph(CH_2)_2P(O)Ph_2$–$Cd^{2+}$ l'espèce identifiée est probablement le complexe hexacoordonné 2:1. On a identifié en solution également pour fins de comparaison le complexe hexacoordonné $[\{CH_2(PPh_2(O))_2\}_3Hg]^{2+}$.

Les études de compétition entre les dioxydes, les disulfures et les disélénures des diphosphines montrent que les disulfures et les disélénures ne peuvent entrer en compétition avec les dioxydes dans le cas du cadmium mais que les disélénures peuvent jusqu'à une certaine limite entrer en compétition avec les disulfures.

[Traduit par le journal]

Introduction

The potential of Fourier Transform ^{113}Cd nmr for the study of cadmium complexes in solution has already been amply demonstrated (1–16). There is general agreement, however, that a lack of good "fingerprint" data on well-defined species is holding back development in this area (7, 13–15). As part of a project aimed towards identification of the regions where cadmium resonance of complexes with various numbers and types of Group VIA donor atoms should occur, we have used ^{31}P nmr to characterize, in solution, cadmium complexes with a range of phosphine oxides, sulfides, and selenides as model Group VIA donors. To try and reduce coordination by the anion or solvent, which may lead to undesired mixed-ligand complexes, we have used a strong acid salt, $Cd(SbF_6)_2$, in a weak-donor solvent, SO_2.

One previous room temperature ^{31}P nmr study involved the complexes $[Ph_2P(O)CH_2P(O)Ph_2]CdX_2$ (X = Cl, Br, or I) (17) and another complex $[Ph_2P(O)CHPr^nPPh_2]CdBr_2$ (18). (The related $[Ph_2P(O)CH_2PPh_2]CdBr_2$ was not soluble enough for study.) In both cases deshielding of the phosphoryl phosphorus occurred on complexation and in both cases rapid intermolecular ligand exchange

[1]Presented, in part, at the 62nd Annual Conference of the Chemical Institute of Canada, Vancouver, B.C., June 1979.

[2]No reprints available.

[3]To whom all correspondence should be addressed.

0008-4042/80/020180-11$01.00/0

©1980 National Research Council of Canada/Conseil national de recherches du Canada

Can. J. Chem. Downloaded from www.nrcresearchpress.com by 210.87.254.40 on 09/05/12
For personal use only.

Can. J. Chem. Downloaded from www.nrcresearchpress.com by 210.87.254.40 on 09/05/12
For personal use only.

TABLE 1. ^{31}P nmr spectral parameters of $EPPh_3$ (E = S or Se), $Ph_2P(Se)(CH_2)_nP(Se)Ph_2$ (n = 1, 2, or 3) and their complexes with Cd^{2+} in SO_2

Ligand	L/M	T (K)	δ_P[a] (ppm)	$\lvert^2J(PECd)\rvert$[b] (Hz)	$\lvert^1J(PSe)\rvert$[b] (Hz)	$\lvert^2J(PP)\rvert$[c] (Hz)
$SPPh_3$	—	209	41.0			
	4	209	40.6	37		
$SePPh_3$	—	209	33.1		655	
	4	209	30.7	48	585	
$Ph_2P(Se)(CH_2)P(Se)Ph_2$	—	220	22.6		694	9.8
	2	220	27.9	45	585	7.7
$Ph_2P(Se)(CH_2)_2P(Se)Ph_2$	—[d]	308	34.6		696	66.2
	2[e]	308	~42.6	Not obs.	~596	~40
$Ph_2P(Se)(CH_2)_3P(Se)Ph_2$	—	220	32.5		649	
	2	205	33.1_5	~38[f]	573 ± 3[g,h]	
			33.8_8	51	572 ± 3[g]	

[a]Relative to external $OP(OMe)_3$ in $(CD_3)_2CO$; shifts to increasing frequency are taken as positive; $\delta_{OP(OMe)_3}(ext) = \delta_{H_3PO_4}(ext) - 1.72$ ppm.
[b]Estimated error ± 1 Hz except where noted.
[c]Estimated error ± 0.3 Hz except where noted.
[d]Data for free ligand from ref. 23.
[e]This 2:1 complex gave very broad lines at low temperatures. The spectral parameters at 308 K were determined by extrapolation from the exchange-averaged spectra of samples with L/Cd > 2.
[f]Signal overlap prevents accurate determination of satellite splitting.
[g]At 308 K, the exchange-averaged spectrum yields $\lvert^1J(PSe)\rvert \approx 570$ Hz for the complex.
[h]Broadening of the satellites, but not the centre band, suggests $\lvert^5J(PSe)\rvert \approx 5$ Hz.

was thought to be occurring: no ^{31}P–$^{111/113}Cd$ coupling was evident. Complexation of the phosphoryl group to cadmium also occurs in $(Ph_3PO)_2CdX_2$ (X = Cl or Br) (19) and in the 1:1 complex of Ph_3PO with bis(thenoyltrifluoroacetonato)cadmium (20). To our knowledge the only phosphine chalcogenide complexes of cadmium reported are $(Et_3PSe)_2CdI_2$ (21) and $[(Ph_3PE)CdX_2]_n$ (E = S, X = I; E = Se, X = Br or I) (22). These are non-conductors in MeCN, but the Ph_3PE complexes, at least, dissociate in solution (22).

Results and Discussion

The Systems $Cd(SbF_6)_2$–Ph_3PE–SO_2 (E = O, S, or Se)

Key ^{31}P nmr spectral parameters for the complexes identified in these systems are given in Table 1.

In the 209 K spectra of solutions in which Ph_3PSe:Cd(II) > 4, separate signals from free and bound ligand are observed, as shown in Fig. 1. Integral analysis shows that the latter is present in a 4:1 complex. The signals from the complex are comprised of a centre band containing ca. 65% of the total bound ligand intensity, flanked by one pair of satellites with ca. 25% of the total intensity and a second more widely spaced pair of satellites with ca. 10% of the total intensity. The amplitude of the more closely spaced satellites make it clear that these are a superimposition of ^{111}Cd and ^{113}Cd satellites (^{111}Cd and ^{113}Cd have $I = \frac{1}{2}$, natural abundances of 12.75 and 12.26% and magnetic moments of −0.5922 and −0.6195 nuclear magnetons, close enough that overlap of signals will occur at small satellite splittings). The more widely spaced satellites are from molecules containing ^{77}Se. (^{77}Se:7.58% natural abundance, $I = \frac{1}{2}$). $^2J(^{31}P—^{111/113}Cd)$ in the 4:1 complex is more than an order of magnitude smaller than known values of $^1J(^{31}P—^{111/113}Cd)$ (24) (e.g. $^1J(^{31}P—^{113}Cd)$ = 1124–1308 Hz in a series of bis(phosphine) complexes of CdI_2 in CH_2Cl_2 at 183 K). This is good evidence for two-bond coupling in the $SePPh_3$ species. In addition, $\lvert^1J(^{31}P—^{77}Se)\rvert$ in the complex is reduced from the free ligand value, and such

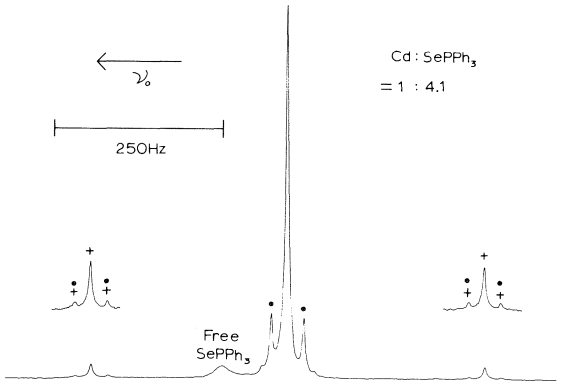
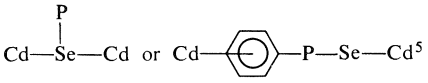


FIG. 1. The 209 K 40.5 MHz ^{31}P nmr spectrum of an SO_2 solution in which $Cd(SbF_6)_2$:$SePPh_3$ = 1:4.1. Filled circles indicate $^{111/113}Cd$ satellites, and crosses ^{77}Se satellites.

Can. J. Chem. Downloaded from www.nrcresearchpress.com by 210.87.254.40 on 09/05/12
For personal use only.

a change is known to accompany coordination of phosphine selenides through the selenium atom (23, 25). Hence the spectrum is consistent with the formation of $Cd(SePPh_3)_4^{2+}$ with a regular, presumably tetrahedral (at least on a time average), $CdSe_4$ core.

At ambient probe temperature,[4] or at 209 K in metal-rich mixtures, an intermolecular-exchange averaged spectrum is observed showing coupling to ^{77}Se but not to $^{111/113}Cd$. In the ligand-deficient mixtures $|^1J(^{31}P—^{77}Se)|$ is less than found in $Cd(SePPh_3)_4^{2+}$ (e.g. at 209 K $|^1J(^{31}P—^{77}Se)| = 528$ Hz in a mixture containing Ph_3PSe:Cd = 2.5:1), so that additional species, perhaps of lower coordination number are formed. In the metal-rich mixtures, the rapid intermolecular exchange may occur through formation of either



bridges, or both.

The Ph_3PS-containing system behaves in a manner identical to the selenide analog. The ^{31}P nmr spectral parameters of $Cd(SPPh_3)_4^{2+}$ are given in Table 1.

In contrast to the preceding, poorly-soluble products are formed in the system $Cd(SbF_6)_2$–$OPPh_3$–SO_2, and these could not be studied in detail by ^{31}P nmr. However, the 220 K spectrum of a saturated solution in which Cd:$OPPh_3$ = 1:3.8 shows a weak line deshielded by 6.8 ppm from the free ligand signal ($\delta_{OP(OMe)_3} = 31.8$ ppm), and in the corresponding spectrum of a saturated solution wherein Cd:$OPPh_3$ = 1:8.5, exchange is evidently occurring at an intermediate rate between free ligand and a species deshielded by ca. 2.7 ppm from it. By analogy with our findings for the diphosphine dioxides (see below) we tentatively suggest that the more deshielded signal might be due to $Cd(OPPh_3)_4^{2+}$ and the less deshielded to $Cd(OPPh_3)_6^{2+}$.

The Systems $Cd(SbF_6)_2$–$Ph_2P(E)(CH_2)_nP(E)Ph_2$–SO_2 (n = 1 or 2, E = O, S, or Se; n = 3, E = Se) and $Hg(SbF_6)_2$–$Ph_2P(O)(CH_2)_nP(O)Ph_2$ (n = 1 or 2)

The ^{31}P nmr spectral parameters for the species identified in solutions containing the diselenides are included in Table 1, while the data for the complexes of the diphosphine dioxides are given in Table 2.

At 220 K the behaviour of the system $Cd(SbF_6)_2$–$Ph_2P(Se)CH_2P(Se)Ph_2$–SO_2 is similar to that of the Ph_3PSe system at reduced temperature (see above) except that intermolecular exchange is slow only when L:Cd $\approx$ 2:1. At or near this ratio a $^{111/113}Cd$ satellite splitting of 45 Hz is observed, similar in magnitude to that found in $Cd(SePPh_3)_4^{2+}$ (see Table 1). Thus it is evident that a four-coordinate (in selenium atoms) bis(chelate) complex, $Cd[(SePPh_2)_2CH_2]_2^{2+}$, is formed. When L:Cd > 2:1, the spectrum is the weighted average of the spectra of the free ligand and the 2:1 complex: there is no significant formation of stable complexes with more than two ligands. When L:Cd < 2 the magnitude of $^1J(P—Se)$ is less than that of the 2:1 complex (e.g., at 220 K, $J \approx 550$ Hz when L:Cd = 1:1.26) and it is clear that other species are being formed. However, the rapid exchange-averaging prevents study of these. At ambient probe temperatures rapid exchange-averaging occurs at all L:Cd ratios.

Like samples containing $Ph_2P(Se)CH_2P(Se)Ph_2$, samples containing $Ph_2P(Se)(CH_2)_2P(Se)Ph_2$ exhibit fast-exchange spectra at ambient probe temperature for all L:Cd ratios. These spectra are consistent with $Cd[(SePPh_2(CH_2))_2]_2^{2+}$ being the species of highest coordination number formed. (The observation of the characteristic yellow colour of the free ligand in SO_2 only when L:Cd > 2 supports this conclusion.) However, in contrast to the behaviour of the system with the shorter-chain diselenide, intermediate-, not slow-, exchange spectra are observed at 220 K for samples with L:Cd $\approx$ 2. For example, a sample with L:Cd $\approx$ 2.1:1 exhibits two approximately equally intense lines, both with $w_{1/2} \approx 60$ Hz, and with $\delta_{OP(OMe)_3} \approx 41.1$ and 42.7 ppm together with a third, broader line ($w_{1/2} \approx 160$ Hz), at $\delta_{OP(OMe)_3} \approx 37.4$ ppm. The higher field signal is not greatly shifted from the free ligand resonance ($\delta_{OP(OMe)_3} = 35.4$ ppm). This spectrum is best interpreted in terms of either exchange between free ligand and two other species, or, more likely, exchange between free ligand and a second species with two inequivalent sites. The second interpretation receives considerable support from behaviour of complexes containing chelating unsubstituted or substituted

rings (see below). For samples containing the unsubstituted propylene ligand, as for the other diselenides, rapid exchange occurs at ambient probe temperature and at low temperatures when

[4]All the phosphine selenide – Cd^{2+} mixtures are unstable at room temperature: over a period of hours red selenium begins to form.

[5]Cadmium(II)–arene complexes are known to be formed in liquid SO_2 (16).

TABLE 2. ^{31}P nmr spectra of $(O)Ph_2P(CH_2)_nPPh_2(O)$ ($n = 1$ or 2) and their complexes with Cd^{2+} and Hg^{2+} and of $(O)PhP(CH_2CH_2PPh_2(O))_2$ and its complex with Cd^{2+}

Ligand	Metal cation	L/M	T (K)	δ_P[a] (ppm)	Comment
$Ph_2P(O)(CH_2)P(O)Ph_2$	—	—	220	27.2	
	Cd^{2+}	2	220	36.8	^2J(CdOP) is not observed. At 313 K, ligand exchange is fast in mixtures of the 1:2 and 1:3 complexes, but not in mixtures of the 1:3 complex and excess free ligand.
	Cd^{2+}	3	220	35.4	
	Hg^{2+}	2	220	~39.5	^2J(HgOP) is not observed; $w_{1/2} > 30$ Hz. Ligand exchange between 3:1 and large amounts of the 2:1 complex occurs at an intermediate rate at 210 K and rapidly at 313 K. Exchange between the 3:1 and excess free ligand is slow at 220 K but rapid at 313 K.
		3	220	37.0	$\lvert^2J(HgOP)\rvert = 46 \pm 1$ Hz
$Ph_2P(O)(CH_2)_2P(O)Ph_2$	—	—	220	36.7	
	Cd^{2+}	2	200	4.15	^2J(CdOP) is not observed. At 313 K, ligand exchange is fast both in mixtures of the 1:2 and 1:3 complexes and mixtures of the 1:3 complex with excess free ligand.
	Cd^{2+}	3	200	39.4	
	Hg^{2+}	2	205	~49.2	^2J(HgOP) is not observed; $w_{1/2}$ ~50 Hz
		3	205	40.8	$\lvert^2J(HgOP)\rvert$ ~30 Hz
$(O)PPh(CH_2CH_2P(O)Ph_2)_2$	—	—	313	42.9(A)[b] 33.4(B_2)[c]	$\lvert J(AB)\rvert = 53.0 \pm 0.3$ Hz
			220	46.4(A)[b] 37.2(B_2)[c]	$\lvert J(AB)\rvert$ ~53.2 Hz
	Cd^{2+}	2	313	46.4(A)[b] 37.8(B_2)[c]	No P–P coupling resolved. Slow exchange with excess free ligand
	Cd^{2+}	2	220	46.3(A)[b] 38.0(B)[c] 37.6(C)[c]	$\lvert J(AB)\rvert$ ~5.2 Hz $\lvert J(AC)\rvert$ ~2.4 Hz J(BC) not observed. Slow exchange with excess free ligand

[a]Relative to external $OP(OMe)_3$ in $(CD_3)_2CO$; shifts to increasing frequency are taken as positive; $\delta_{OP(OMe)_3}(ext) = \delta_{H_3PO_3}(ext) - 1.72$ ppm.
[b]Non-terminal phosphorus atom.
[c]Terminal phosphorus atoms.

L:Cd exceeds 2:1. When L:Cd ≈ 2, however, a slow-exchange spectrum can be observed at 205 K. This consists of two equally intense lines,[6] both with both $^{111/113}Cd$ and ^{77}Se satellites (see Table 3). The most plausible interpretation of this spectrum is in terms of a bis(chelate) complex, $Cd[(SePPh_2)_2(CH_2)_3]_2^{2+}$, in which the conformation of each eight-membered chelate ring is rigid at this low temperature and is such that C_2 symmetry exists about the cadmium.[7]

Downfield ^{31}P complexation shifts and blanching of pale yellow diphosphine disulfide – SO_2 solutions by $Cd(SbF_6)_2$[8] provide good evidence for complexation of cadmium by $Ph_2P(S)(CH_2)_nP(S)Ph_2$ ($n = 1$ or 2) but the exact nature of the complexes could not be established with certainty. With the shorter-chain ligand, intermolecular exchange was rapid for all L:Cd ratios both at ambient probe and reduced temperatures. Unfortunately the maximum downfield complexation shift (ca. 5.3 ppm from the free ligand signal ($\delta_{OP(OMe)_3}$ = 33.0 ppm at 220 K)) was too small to allow accurate determination of the stoichiometry of the complex(es) formed from the exchange-averaged shifts. With the ligand $Ph_2P(S)(CH_2)_2P(S)Ph_2$, intermolecular ligand exchange could be slowed, but incompletely and only in the absence of excess ligand. Thus the 220 K spectrum of a solution in which L:Cd = 2.0:1 showed two partially-coalesced, approximately equally intense, broad ($\omega_{1/2} \approx 30$ Hz) lines deshielded by 3.4 and 5.2 ppm from the free ligand resonance ($\delta_{OP(OMe)_3}$ = 43.7 ppm). A tentative explanation of this spectrum is in terms of the formation of a four-coordinate bis(chelate) complex of C_2 symmetry (see above)

[6]In most spectra an unassigned line of variable intensity was observed at $\delta_{OP(OMe)_3} \approx 32.1$ ppm.

[7]We note that in the tetrahedral complexes $[CHR(CH_2PPh_2)_2]_2Pt$ (R = H or $—CH_2PPh_2$), the puckered chelate rings give rise to two inequivalent pairs of phosphorus atoms, at reduced temperature when R = H, and at room temperature when R = $—CH_2PPh_2$ (26, 27).

[8]The $Ph_2P(S)(CH_2)_nP(S)Ph_2 - Cd(SbF_6)_2 - SO_2$ solutions were initially clear but on standing at room temperature became cloudy in about 1 h.

Can. J. Chem. Downloaded from www.nrcresearchpress.com by 210.87.254.40 on 09/05/12
For personal use only.

TABLE 3. ^{31}P nmr spectral parameters of (E)PPh($CH_2CH_2PPH_2$(E))$_2$ (E = S or Se) and their 1:1 complexes with Cd^{2+} in SO_2 at 220 K

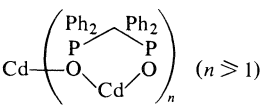
Compound	Phosphorus[a]	δ_P[b] (ppm)	$\lvert^2J$(PECd)$\rvert$[c] (Hz)	$\lvert^1J$(PSe)$\rvert$[c] (Hz)	$\lvert^3J$(PP)$\rvert$[c] (Hz)
(S)PPh($CH_2CH_2PPh_2$(S))$_2$ (TriphosS$_3$)	A	49.9	—		62
	B_2	42.9	—		
Cd[TriphosS$_3$]$^{2+}$	A	62.2	38		J(AB) = 45
	B	50.3	45		J(AC) = 66
	C	45.8	46		
(Se)PPh($CH_2CH_2PPh_2$(Se))$_2$ (TriphosSe$_3$)	A	43.0	—	685	67
	B_2	35.2	—	672	
Cd[TriphosSe$_3$]$^{2+}$	A	53.8	52	567	J(AB) = 52
	B	43.1	62	513	J(AC) = 65
	C	33.8	60	548	

[a]A = non-terminal phosphorus atom; B/C = terminal phosphorus atoms; see text for further discussion of these assignments.
[b]Relative to external $OP(OMe)_3$ in $(CD_3)_2CO$; shifts to increasing frequency are taken as positive; $\delta_{OP(OMe)_3}(ext) = \delta_{H_3PO_4}(ext) - 1.72$ ppm.
[c]Estimated error ± 1 Hz.

in which there occurs either conformational "flipping" or ligand exchange (or both) at an intermediate rate.

Two sharp single lines can be seen in the 200 K spectra of samples in which $Ph_2P(O)(CH_2)_2P(O)Ph_2$:Cd > 3:1. That at higher field is due to the free ligand and the other, deshielded by 2.7 ppm, is, by integral analysis, from the complex $Cd[(OPPh_2(CH_2))_2]_3^{2+}$ with, presumably, a CdO_6 octahedral core. The free ligand signal disappears when L:Cd = 3:1, and as the molar ratio is decreased further, there appears a second sharp line a further 2.1 ppm downfield, which becomes dominant at L:Cd = 2:1. Evidently a second, 2:1, complex, probably with tetrahedral coordination, is formed in this system. At still lower L:Cd ratios, very complicated multi-line spectra occur, and incompletely soluble species are eventually formed.

In the region $2{:}1 \gtrsim$ L:Cd $\gtrsim 1$, one or more poorly soluble species are formed, but otherwise the behaviour of the system $Cd(SbF_6)_2$–$Ph_2P(O)CH_2P(O)Ph_2$–SO_2 is very similar to that just described, and evidently both 3:1 and 2:1 species occur here too. These are characterized by the chemical shifts given in Table 2. In extremely cadmium-rich solutions (L:Cd < 1:1) a soluble species is formed which gives rise to two equally intense doublets deshielded by 13.6 and 29.3 ppm from the free ligand and with a common 14 Hz coupling. The more shielded doublet occurs in the same regions as the signals of the 3:1 and 2:1 complexes (Table 2). However the less shielded must represent a more severely perturbed phosphoryl group. Possibly a species of the type

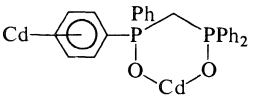


$(n \geqslant 1)$

is being formed in this region.[9]

Surprisingly,[10] no two-bond cadmium–phosphorus coupling is observed in the spectra of the complexes of the chelating diphosphine dioxides even under slow exchange conditions.[11] To determine whether ^2J(M—O—P) is generally very small, we have examined complexation of mercury(II) with $Ph_2P(O)(CH_2)_nP(O)Ph_2$ (n = 1 or 2), anticipating that in slow-exchange spectra coupling to ^{199}Hg might be visible (^{199}Hg; 16.84% natural abundance, $I = \frac{1}{2}$). This expectation was realized for the complex $Hg[(OPPh_2)_2CH_2]_3^{2+}$ (see Table 2) which, at 220 K in the presence of excess ligand, gives a

[9]No chemical change in the ligand occurs: the 313 K spectrum shows a single line with $\delta_{OP(OMe)_3} = 46.2$ ppm. It is unlikely that the observed low temperature spectrum is due to formation of an arene complex such as



as cadmium arene complexes are labile (16) so that both ends of the chelate would be equivalent on a time-average.

[10]Two-bond cadmium–phosphorus coupling is thought to occur in some complexes of CdX_2 with R_3PO (28).

[11]Downfield ^{31}P complexation shifts but not cadmium satellites were observed in the systems CdX_2–$Ph_2P(O)CH_2P(O)Ph_2$–DMSO (17). The absence of satellites was attributed to either rapid ligand exchange or a small value of ^2J(Cd—O—P) with a preference for the former. Rapid ligand exchange probably does occur in these systems, but our results show that ^2J(Cd—O—P) may well be small also.

Can. J. Chem. Downloaded from www.nrcresearchpress.com by 210.87.254.40 on 09/05/12
For personal use only.

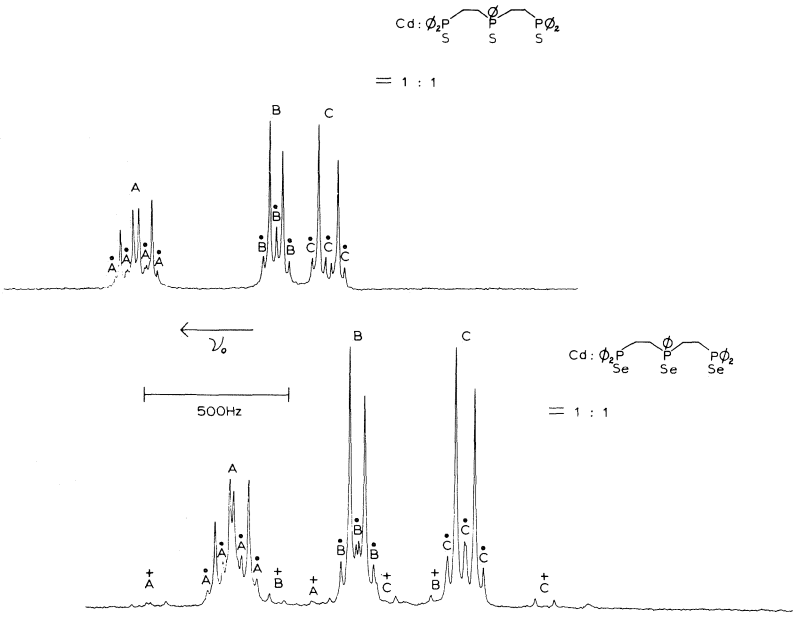


FIG. 2. The 220 K 40.5 MHz ^{31}P nmr spectra of SO_2 solutions containing (top) $Cd(SbF_6)_2$:triphosS_3 = 1:1 and (bottom) $Cd(SbF_6)_2$:triphosS_3 = 1:1. Satellites are indicated as in Fig. 1.

sharp line with ^{199}Hg satellites. On a time average, at least, this complex probably contains the comparatively rare (29) octahedral HgO_6 core. With a slight deficiency of ligand below the 3:1 ratio (e.g. L:Hg = 2.8:1) sharp signals from both the 3:1 and a second, presumably 2:1, complex can be seen. A greater deficiency of ligand leads to more rapid exchange, with much broader, though still separate, lines for the two complexes. At L:Hg $\approx$ 2:1 it is clear that an appreciable amount of the 3:1 complex occurs: this must be the preferred complex in the system. At ambient probe temperature rapid intermolecular exchange occurs for all ratios of $Ph_2P(O)CH_2P(O)Ph_2$:Hg.

The behaviour of the system $Hg(SbF_6)_2$–$Ph_2P(O)(CH_2)_2P(O)Ph_2$–SO_2 is similar: rapid intermolecular exchange occurs at ambient probe temperature but in the 205 K spectra, by variation of the L:Hg ratio it was possible to observe well-separated signals attributable to 3:1 and 2:1 complexes (see Table 2). Shoulders on the signal from the 3:1 complex suggest that ^2J(HgOP) is ca. 30 Hz. As with the preceding diphosphoryl ligand, the 2:1 complex is incompletely formed at L/Hg = 2:1, e.g. a weak signal from the 3:1 complex is evident in the spectrum of a solution with L:Hg = 1.74:1. Where 2:1 and 3:1 complexes coexist, the former gives a broader signal, suggesting it is the more labile species. The presence of trace amounts of the labile 2:1 complex might account for our observation that in ligand-rich samples at 205 K, the free ligand signal is considerably broader than the signal of the 3:1 complex.

The Systems $Cd(SbF_6)_2$–$Ph_2P(E)(CH_2)_2P(E)Ph$-$(CH_2)_2P(E)Ph_2$–SO_2 (E = O(triphosO_3), S(triphosS_3), or Se(triphosSe_3))

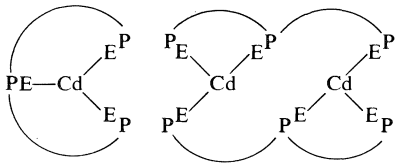
Pertinent ^{31}P spectra data for the trioxide containing system are included in Table 2. The corresponding data for the trichalcogenide-containing systems are given in Table 3.

The behaviour of the system containing triphosS_3 is straightforward. At ambient probe temperature, rapid intermolecular exchange occurs regardless of L:M ratio. Exchange is also rapid at 220 K if L:Cd > 1:1. However, when triphosS_3:Cd = 1:1, the spectrum shown in Fig. 2 (top) is obtained. In contrast to the AB_2 spectrum of the free ligand (Table 3), the spectrum of the 1:1 complex shows three regions of resonance, each of equal intensity. By analogy with the spectrum of the corresponding free triselenide the value of ^6J(PP) should be near zero (23). Therefore the double-doublet A must be due to the central $\geq$PS group and the doublets B and C must be signals from chemically-inequivalent terminal —P(S)Ph_2 groups. A, B, and C each exhibit $^{111/113}Cd$ satellites showing that all the sulfur atoms are bound to cadmium and that intermolecular exchange involving the 1:1 species is slow at this temperature. The

Can. J. Chem. Downloaded from www.nrcresearchpress.com by 210.87.254.40 on 09/05/12
For personal use only.

Can. J. Chem. Downloaded from www.nrcresearchpress.com by 210.87.254.40 on 09/05/12
For personal use only.

spectrum can be accounted for in terms of the formation of a mononuclear species **I**, provided, as seems probable, that conformational equilibration in the relatively rigid bicyclic system is slow at 220 K. Alternatively the ligand could be behaving in a bridging manner to give **II**, in which the terminal groups are clearly chemically inequivalent. Our prejudice is for the first of these species since conformational rigidity evidently occurs in the 2:1 complexes of $Ph_2P(Se)(CH_2)_3P(Se)Ph_2$ (see above) and $triphosO_3$ and $(Ph_2P(E)CH_2)_3CMe$ (E = S or Se) (see below) also. Both **I** and **II** involve coordination of three sulfur atoms to cadmium, but this does not necessarily mean that the total coordination number of the metal is three: the solvent or anion could be coordinated also. Work is presently underway to determine which ligands, if any, can coordinate to $Cd(triphosS_3)^{2+}$ and its $triphosSe_3$ analog (see below). With $triphosS_3$ itself, significant coordination beyond 1:1 does not occur: the exchange-averaged spectra observed when L:Cd > 1:1 are just the weighted average of the 1:1 complex and free ligand. Further, the 1:1 complex persists in the presence of excess cadmium.



I **II**

The behaviour of the system $Cd(SbF_6)_2$–$triphosSe_3$–SO_2 is similar to, but more complicated than, the preceding. The best-characterized species is a 1:1 complex giving the spectrum shown in Fig. 2 (bottom). This spectrum shows not only $^{111/113}Cd$ satellites but also the expected ^{77}Se satellites. Consistent with coordination of all three selenium atoms (see above), the values of $|{}^1J(^{31}P—^{77}Se)|$ are reduced from the free ligand values; significantly the values of $^1J(^{31}P_B—^{77}Se)$ and $^1J(^{31}P_C—^{77}Se)$ are not greatly different, suggesting no great distinction in the way the inequivalent PSe groups bind to the metal(s). Again this spectrum can be interpreted in terms of **I** or **II**.

At ambient probe temperature, a 1:1 $triphosSe_3$:Cd^{2+} mixture gives a spectrum in which the non-terminal PSe group gives rise to a sharp triplet but in which the terminal PSe groups give rise to a considerably broader doublet. As the signal of non-terminal PSe group is shifted further by complexation than those of the terminal PSe groups (Table 3), it is improbable that the former could be sharpened by intermolecular exchange while the latter are not. A more logical interpretation is in terms of fast exchange between traces of free ligand and an incompletely conformationally-averaged structure **I**.

When excess $triphosSe_3$ is present, intermolecular exchange is rapid even at 220 K and the exchange-averaged spectrum confirms that further coordination of $triphosSe_3$ beyond 1:1 does not occur. In the presence of excess cadmium, intermolecular exchange is rapid at ambient temperature, but at reduced temperatures quite complicated behaviour occurs. For example, a solution containing $triphosSe_3$:Cd = 1:2.0 has a spectrum which, at 220 K, consists of a sharp triplet with $\delta_{OP(OMe)_3} = 52.1$ ppm, close to the shift of resonance A of the 1:1 complex, and ^1J(P—P) and $^1J(^{31}P—^{77}Se)$ of 58 and ca. 556 Hz, respectively, and a broad doublet centred at $\delta_{OP(OMe)_3} \approx 38.6$ ppm, roughly the average position of resonances B and C of the 1:1 complex. On further lowering the temperature, to 200 K, the triplet broadens without shifting, while the doublet does not broaden significantly but splits into a strong central doublet and two weaker flanking doublets at $\delta_{OP(OMe)_3} \approx$ 34.3 and 43.4 ppm approximately the positions of B and C. Possibly the 1:1 complex and a further unidentified metal-rich species coexist in this solution and above 200 K undergo rapid intermolecular exchange of metal.

Both ambient probe and reduced temperature spectra provided evidence for the formation of the complex $Cd(triphosO_3)_2^{2+}$ in solutions in which triphos O_3:Cd $\geq$ 2. Even at ambient probe temperature, exchange with excess free ligand is slow and in ligand-rich solutions separate spectra of the bound and free trioxide can be seen as shown in Fig. 3. As B and C coalesce at the higher temperature these resonances must arise from the terminal PO groups of the bound $triphosO_3$, and A is therefore a signal from the non-terminal PO group; these assignments are consistent with the spectrum of the free ligand. At low temperatures B and C are doublets and A shows the incompletely-resolved fine structure of, presumably, a double-doublet (Fig. 3, bottom). At ambient probe temperature B and C coalesce and no A–B or A–C spin coupling is evident (Fig. 3, top). On complexation of the ligand then, there is not only the expected complexation shift, but also a marked reduction in ^3J(P—P) (Table 2 and Fig. 3). We have found such reductions to occur in both $triphosO_3$ and the parent triphosphine on *fac* coordination (30) and therefore we suggest that if, as expected, $Cd(triphosO_3)_2^{2+}$ is an octahedral complex, the tridentate ligand coordinates facially. Thus both *s*- and *u-fac* structure (as opposed to the *mer* structure) are possibilities.

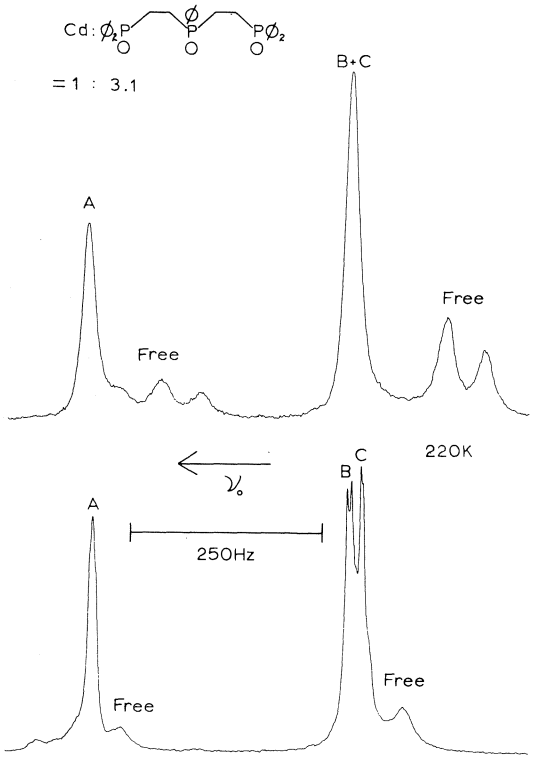


FIG. 3. The 40.5 MHz ^{31}P nmr spectra of an SO_2 solution containing $Cd(SbF_6)_2$:triphosO_3 = 1:3.1 at (top) 308 K and (bottom) 220 K.

Both the *fac* structures can account for the magnetic inequivalence of the terminal PO groups which is observed in the low temperature spectrum (Table 2 and Fig. 3). In the *s-fac* structure the two groups occupy chemically equivalent sites, and their inequivalence must arise from a rigid conformation of the bicyclic metal-chelate system, whereas in the *u-fac* structure, the groups occupy chemically inequivalent sites. At ambient probe temperature the signals from the terminal groups coalesce (Fig. 3, top). In the *s-fac* structure the coalescence of B and C which occurs at room temperature would be a natural consequence of fast conformational equilibration and for this reason we favour the symmetrical structure. However, a rapid partial ligand dissociation[12] – intramolecular rearrangement – recoordination process in the *u-fac* structure might also account for the observed room temperature equivalence of the terminal groups.

When triphosO_3:Cd < 2:1, many lines are observed in the low temperature spectra and no analysis was attempted. The spectra at ambient probe temperature are consistent with an intermediate rate of exchange between various triphosO_3-containing species.

The Systems $Cd(SbF_6)_2$–$(Ph_2P(E)CH_2)_3CMe$–SO_2 (E = S(tripodS_3) or Se(tripodSe_3))[13]

The 220 K spectra of samples containing tripodSe_3:Cd > 2:1 show a signal from the free ligand, as exemplified in Fig. 4 (bottom). Thus a 2:1 complex is the most highly ligated species formed in this system. The 220 K spectrum of the 2:1 complex has three regions of resonance, A, B, and C, each equally intense. The singlet A has a ^{77}Se satellite splitting of *larger* magnitude than that of the free ligand. This fact, and the absence of observable $^{111/113}Cd$ satellites about A, make it clear that A must be the resonance of an *unbound* PSe group. In contrast, the doublets B and C both have both observable $^{111/113}Cd$ satellites and ^{31}P—^{77}Se spin–spin coupling *smaller* in magnitude than in the free ligand. They must therefore be signals from bound PSe groups. Thus in the complex Cd(tripodSe_3)$_2^{2+}$ the potentially tridentate ligands are behaving in a bidentate manner and have one arm "dangling": the complex possesses a $CdSe_4$ core.

Each chelate ring in Cd(tripodSe_3)$_2^{2+}$ is 8-membered. By analogy with Cd[$(SePPh_2)_2(CH_2)_3]_2^{2+}$ (see above) we might then expect the signals from the bound PSe groups to be *singlets*, chemically shifted by their dissimilar orientations relative to the puckered chelate rings. In fact, as seen in Fig. 4 (bottom), B and C are *doublets*, though not, apparently, because of spin-coupling. It seems likely that with the $—CH_2P(Se)Ph_2$ substituent on the propylene backbone of the ligand a small distortion from C_2 symmetry occurs, leading to inequivalence of all four bound PSe groups in the presumably approximately tetrahedral coordinated complex.

In samples containing tripodSe_3:Cd < 2:1, the feature most noticeable in the 220 K spectra is the large relative broadening of resonance A. This is consistent with the expectation that the dangling PSe group will be involved in coordination in metal-rich mixtures. In these samples, as well as ligand-rich samples, the spectra at ambient probe temperature exhibit broad lines indicating exchange at an intermediate rate.

The tripodS_3 system behaves very like the tripodSe_3 system except that excess free ligand is only poorly soluble in SO_2. Close to the 2:1 tripodS_3:Cd ratio the 220 K spectrum (Fig. 4, top) shows features which, by analogy with the Cd(tri-

[12]Complete dissociation is ruled out by the absence of bound-free ligand exchange.

[13]TripodO_3 decomposes in the solid state on standing at room temperature and because of this instability was not used as a ligand.

Can. J. Chem. Downloaded from www.nrcresearchpress.com by 210.87.254.40 on 09/05/12
For personal use only.

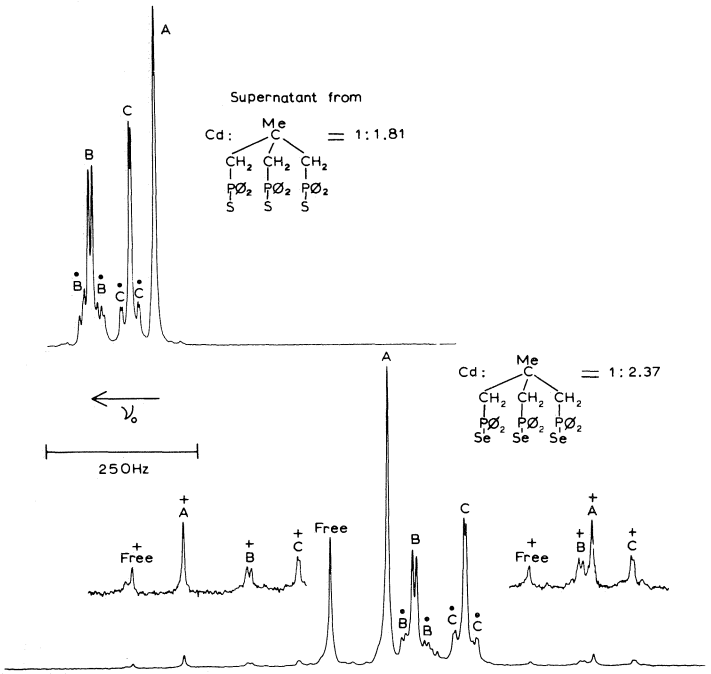


FIG. 4. The 220 K 40.5 MHz ^{31}P nmr spectra of (top) the supernatant liquor in an SO_2 solution containing $Cd(SbF_6)_2$:tripodS_3 = 1:1.81 and (bottom) an SO_2 solution containing $Cd(SbF_6)_2$:tripodSe_3 = 1:2.37. Satellites are indicated as in Fig. 1.

Can. J. Chem. Downloaded from www.nrcresearchpress.com by 210.87.254.40 on 09/05/12
For personal use only.

podSe$_3$)$_2^{2+}$ spectrum, can be interpreted in terms of a low-symmetry, but approximately tetrahedral, complex Cd(tripodS$_3$)$_2^{2+}$ in which the ligands behave in a bidentate manner.

The ^{31}P spectral parameters of Cd(tripodS$_3$)$_2^{2+}$ and Cd(tripodSe$_3$)$_2^{2+}$ are listed in Table 4.

Competition between Binary Mixtures of Diphosphine Dioxide, Disphosphine Disulfide, and Diphosphine Diselenide for Coordination to Cadmium(II)

As we (this work and ref. 30) and others (17, 31) have shown, complexation of phosphine oxides often leads to quite large ^{31}P complexation shifts. Thus if the chemical shift of a phosphine oxide complex is known and exchange-averaging with excess ligand occurs, the percentage complexation of the ligand in the presence of the acceptor can be assessed. Although the ^{31}P complexation shifts of phosphine selenides are usually smaller than those of phosphine oxides, a large change in $|^1J(^{31}P—^{77}Se)|$ accompanies complexation (this work and refs. 23, 25) and so, if the complexed value is known or can be estimated, the exchange-averaged value of this coupling constant allows determination of the extent of complexation of a phosphine selenide.

Using the preceding two indicators we have made semiquantitative measurements of the extent to which the two ligands compete in the ternary mixtures $Cd(SbF_6)_2$–$Ph_2P(E)(CH_2)_nP(E)Ph_2$–$Ph_2P(E')(CH_2)_nP(E')Ph_2$ (n = 1 or 2; E and E′ are O and S, or O and Se, or S and Se). The data and a brief summary of the conclusions are given in Table 5. In the interpretation of the results our principal assumption is that bound diphosphine diselenides, even in mixed ligand complexes, will have approximately the same value of $^1J(^{31}P—^{77}Se)$ as in the bis(diphosphine diselenide) complexes. From our study we conclude that neither diphosphine disulfides nor diphosphine diselenides can compete with homologous diphosphine dioxides for coordination to cadmium, but that diphosphine diselenides compete appreciably with diphosphine disulfides. This latter result is interesting since selenium compounds are antagonists for cadmium poisoning (32) and in biological systems cadmium is usually found bound to sulfur ligands (33).

Experimental

Materials

1,3-Bis(diphenylphosphino)propane, 1,1,1-tris(diphenylphosphinomethyl)ethane, and bis(2-diphenylphosphinoethyl)phenylphosphine (all from Strem Chemicals Inc.) showed no significant impurities by ^{31}P nmr and were used as received. Triphenylphosphine (Eastman Kodak Co.) was recrystallized from ethanol. Bis(diphenylphosphino)methane and 1,2-bis(diphenylphosphino)ethane were synthesized by the literature method (34).

Antimony pentafluoride (PCR) was distilled twice under dry nitrogen. Anhydrous cadmium fluoride (Alfa "Ultrapure") and anhydrous mercuric fluoride (Alfa) were used as received to prepare $Cd(SbF_6)_2$ (16) and $Hg(SbF_6)_2$ (35).

TABLE 4. ^{31}P nmr spectral parameters of $((E)(Ph_2PCH_2)_3CMe$ (E = S or Se), and their 2:1 complexes with Cd^{2+} at 220 K

Species	Phosphorus[a]	δ_P[b] (ppm)	$\lvert^2J(PECd)\rvert$[c] (Hz)	$\lvert^1J(PSe)\rvert$[c] (Hz)
$((S)Ph_2PCH_2)_3CMe$		33.5		
Me $Cd[((S)Ph_2PCH_2)_2C\ CH_2PPh_2(S)]_2^{2+}$	A[d]	30.7		
	B	33.2_7	29	
		33.4_1	29	
	C	31.6_9	30	
		31.7_6	30	
$((Se)Ph_2PCH_2)_3CMe$		22.0		655
Me $Cd[((Se)Ph_2PCH_2)_2C\ CH_2PPh_2(Se)]_2^{2+}$	A[d]	19.7		676
	B	18.5_2	38	549
		18.6_9	38	549
	C	16.5_0	37	552
		16.5_8	37	552

[a]See text for discussion of these assignments.
[b]Relative to external $OP(OMe)_3$ in $(CD_3)_2CO$; shifts to increasing frequency are taken as positive; $\delta_{OP(OMe)_3}(ext) = \delta_{H_3PO_4}(ext) - 1.72$ ppm.
[c]± 1 Hz except where noted.
[d]Unbound $-Ph_2P(E)$ group.

TABLE 5. Competition between some ditertiary phosphine dioxides, disulfides, and diselenides for Cd^{2+} at 313 K in SO_2

n in $\phi_{2E}^{P}(CH_2)_n{}_E^{P}\phi_2$	Mixture	δ_{PO}[a] (ppm)	δ_{PS}[a] (ppm)	δ_{PSe}[a] (ppm)	$\lvert^1J(PSe)\rvert$ (Hz)	Comment
1	P_2O_2 only	25.0				
1	P_2S_2 only		33.2			
1	P_2Se_2 only			23.0	719	
1	$P_2O_2:P_2S_2:Cd = 3.6:3.5:1$	34.5[b,d] 26.4[c,d]	33.1			No P_2S_2 complexed
1	$P_2O_2:P_2S_2:Cd = 3.4:3.5:1$	34.3[b]		22.8	719[e]	No P_2Se_2 complexed
1	$P_2S_2:P_2Se_2:Cd = 3.7:3.9:1$		33.0	23.6	700[e]	~15% P_2Se_2 complexed
2	P_2O_2 only	33.7				
2	P_2S_2 only		43.0			
2	Se_2 only			34.6	696	
2	$P_2O_2:P_2S_2:Cd = 3.7:4.2:1$	37.5[f,g]	43.0			No P_2S_2 complexed
2	$P_2O_2:P_2Se_2:Cd = 3.5:3.5:1$	37.3[f,h]		34.7[i]	698[i]	No P_2Se_2 complexed
2	$P_2S_2:P_2Se_2:Cd = 3.1:3.2:1$		43.3	38.6[i]	639[i]	~50% P_2Se_2 complexed

[a]Relative to external $OP(OMe)_3$ in $(CD_3)_2CO$; shifts to increasing frequency are taken as positive; $\delta_{OP(OMe)_3}(ext) = \delta_{H_3PO_4}(ext) - 1.72$ ppm.
[b]$\delta_P = 34.3$ ppm for $Cd(P_2O_2)_3^{2+}$ in the system $Cd(SbF_6)_2$ – excess P_2O_2 – SO_2 at 313 K.
[c]Uncomplexed ligand.
[d]Integral analysis gives free:complexed ligand $\approx$ 1:5.5.
[e]From the exchange-averaged spectrum of the system $Cd(SbF_6)_2$ – excess P_2Se_2 – SO_2 at 313 K, $\lvert^1J(PSe)\rvert \sim 598$ Hz in $Cd(P_2Se_2)_2^{2+}$.
[f]From the exchange-averaged spectrum of the system $Cd(SbF_6)_2$ – excess P_2O_2 – SO_2 at 313 K, $\delta_P = 37.8$ ppm for $Cd(P_2O_2)_3^{2+}$.
[g]For complexation by P_2O_2 only, $\delta_{PO}(calcd) \sim 37.0$ ppm.
[h]For complexation by P_2O_2 only, $\delta_{PO}(calcd) \sim 37.2$ ppm.
[i]$\lvert^1J(PSe)\rvert \sim 596$ Hz and $\delta_{PSe} \sim 42.6$ ppm for $Cd(P_2Se_2)^{2+}$ at 313 K (see Table 1).

The phosphine oxides were prepared by I_2/OH^- treatment of the phosphines (36). The phosphine sulfides resulted from the reflux of a slight excess of the phosphine with sulfur in benzene solution (37–39) (excess sulfur proves difficult to remove); the phosphine selenides were prepared in an earlier study (23) by an analogous procedure using an excess of selenium shot. The purity of the ligands was checked by mp and by ^{31}P nmr.

Sulfur dioxide (Matheson Anhydrous Grade) was dried by standing in the gas phase over 3A molecular sieves for 12–24 h.

Preparation of Nuclear Magnetic Resonance Samples

In a dry-nitrogen filled glove box, appropriate amounts of ligand and $Cd(SbF_6)_2$ were transferred to previously-described (16, 23) baked-out (140°C) 10 mm od nmr tubes made from standard-wall 10 mm tubing having attached a section of 9 mm special wall tubing. The tubes were capped for removal from the inert atmosphere. For addition of solvent, the cap was quickly removed, the tube attached to a standard glass/Teflon vacuum line via a $\frac{3}{8}$ in. "Ultratorr" fitting and evacuated, SO_2 (ca. 2 mL) condensed in from a storage tube, and a flame-seal made at the 9 mm tubing. The samples were stored at −196°C until run.

$^{31}P\{^1H\}$ Nuclear Magnetic Resonance Spectra

All nmr spectra were obtained using a Varian XL-100-12 spectrometer system operating at 40.54 MHz. The use of the $(CD_3)_2CO$–$OP(OMe)_3$ external lock-reference sample and the method of temperature measurement were described in a preceding publication (23).

Can. J. Chem. Downloaded from www.nrcresearchpress.com by 210.87.254.40 on 09/05/12
For personal use only.

NOTE ADDED IN PROOF

In more recent studies (40) both 1:4 and 1:3 Cd:EPR_3 (E = S or Se) complexes have been characterized by ^{31}P for a variety of groups R, including R = Ph. For R = *o*-tolyl apparent 1:2 complexes have also been identified.

Acknowledgements

This research was supported by both the Academic Development Fund of the University of Western Ontario and the Natural Sciences and Engineering Research Council of Canada.

1. G. E. MACIEL and M. BORZO. Chem. Commun. 394 (1973).
2. A. D. CARDIN, P. D. ELLIS, J. D. ODOM, and J. W. HOWARD, JR. J. Am. Chem. Soc. **97**, 1672 (1975).
3. R. A. HABERKORN, L. QUE, JR., W. O. GILLUM, R. H. HOLM, C. S. LUI, and R. C. LORD. Inorg. Chem. **15**, 2408 (1976).
4. J. F. CHLEBOWSKI, I. M. ARMITAGE, and J. E. COLEMAN. J. Biol. Chem. **252**, 7053 (1977).
5. I. M. ARMITAGE, A. J. M. SCHOOT-UITERKAMP, J. F. CHLEBOWSKI, and J. E. COLEMAN. Abstr. VIIth Int. Conf. Magn. Reson. Biol. Sys. St. Jovite, Quebec, Sept. 1976, Abstr. WP15; J. Magn. Reson. **29**, 375 (1978).
6. P. D. ELLIS. Abstr. VIIth Int. Conf. Magn. Reson. Biol. Sys. St. Jovite, Quebec, Sept. 1976, Abstr. TH-L5.
7. B. BIRGERSSON, R. E. CARTER, and T. DRAKENBERG. J. Magn. Reson. **28**, 299 (1977).
8. J. L. SUDMEIER and S. J. BELL. J. Am. Chem. Soc. **99**, 4500 (1977).
9. J. D. OTVOS and I. M. ARMITAGE. Abstr. Symp. on Metallothioneins and Other Low Molecular Weight Metal-Binding Proteins, Zurich, Switzerland, July, 1978.
10. D. B. BAILEY, P. D. ELLIS, A. D. CARDIN, and W. D. BEHNKE. J. Am. Chem. Soc. **100**, 5236 (1978).
11. P. J. SADLER, A. BAKKA, and P. J. BEYNON. FEBS Lett. **94**, 315 (1978).
12. K. T. SUZUKI and T. MAITANI. Experientia, **34**, 1449 (1978).
13. T. DRAKENBERG, N-O. BJÖRK, and R. PORTANOVA. J. Phys. Chem. **82**, 2423 (1978).
14. J. J. H. ACKERMAN, T. V. ORR, V. J. BARTUSKA, and G. E. MACIEL. J. Am. Chem. Soc. **101**, 341 (1979).
15. I. M. ARMITAGE, J. D. OTVOS, J. F. CHLEBOWSKI, and J. E. COLEMAN. Abstr. 20th Exptl. Nmr Conf., Asilomar, CA, Feb. 1979.
16. L. C. DAMUDE and P. A. W. DEAN. J. Organomet. Chem. **168**, 123 (1979).
17. S. O. GRIM and L. C. SATEK. J. Coord. Chem. **6**, 39 (1976).
18. S. O. GRIM, L. C. SATEK, C. A. TOLMAN, and J. P. JESSON. Inorg. Chem. **14**, 656 (1975).
19. M. J. FRAZER, W. GERRARD, and R. TWAITS. J. Inorg. Nucl. Chem. **25**, 637 (1966).
20. G. N. RAO and N. C. LI. J. Inorg. Nucl. Chem. **28**, 2931 (1966).
21. P. NIPCON and D. W. MEEK. Chem. Commun. 398 (1966).
22. G. EASTLAND, JR. Inorg. Nucl. Chem. Lett. **11**, 373 (1975).
23. P. A. W. DEAN. Can. J. Chem. **57**, 754 (1979).
24. B. E. MANN. Inorg. Nucl. Chem. Lett. **7**, 595 (1971).
25. S. O. GRIM, E. D. WALTON, and L. C. SATEK. Inorg. Chim. Acta, **27**, L115 (1978).
26. F. C. MARCH, R. MASON, D. W. MEEK, and G. R. SCOLLARY. Inorg. Chim. Acta, **19**, L25 (1976).
27. F. C. MARCH, R. MASON, and G. R. SCOLLARY. Aust. J. Chem. **30**, 2407 (1977).
28. R. G. GOEL. Personal communication.
29. D. L. KEPERT, D. TAYLOR, and A. H. WHITE. J. Chem. Soc. Dalton Trans. 670 (1973).
30. P. A. W. DEAN, D. D. PHILLIPS, and L. POLENSEK. Unpublished work.
31. M. ZELDIN, P. MEHTA, and W. D. VERNON. Inorg. Chem. **18**, 463 (1979).
32. E. J. UNDERWOOD. Trace elements in human and animal nutrition. 4th ed. Academic Press, New York. 1977. Chapts. 12 and 14 and reference therein.
33. M. G. CHERIAN and R. A. GOYER. Life Sci. **23**, 1 (1978).
34. W. HEWERTSON and H. R. WATSON. J. Chem. Soc. 1490 (1962).
35. L. C. DAMUDE and P. A. W. DEAN. J. Organomet. Chem. **181**, 1 (1979).
36. F. CANZIANI, F. ZINGALES, and U. SARTORELLI. Gazz. Chim. Ital. **94**, 848 (1964).
37. L. MAIER. Organic phosphorus compounds. Vol. 4. *Edited by* G. M. Kosolapoff and L. Maier. John Wiley, New York. 1972. Chapt. 7.
38. J. C. CLOYD, JR. and D. W. MEEK. Inorg. Chim. Acta, **6**, 607 (1972).
39. E. LINDNER and H. BEER. Chem. Ber. **105**, 3261 (1972).
40. P. A. W. DEAN and L. POLENSEK. To be published.

Can. J. Chem. Downloaded from www.nrcresearchpress.com by 210.87.254.40 on 09/05/12
For personal use only.

Crystal structure of *E*-1-(2,4,6-trimethylphenyl)ethanone oxime. The aryl–oxime rotational barrier problem and $^{13}C—^{15}N$ nmr coupling constant calculations[1,2]

SUZANNE FORTIER AND GEORGE I. BIRNBAUM[3]

Division of Biological Sciences, National Research Council of Canada, Ottawa, Ont., Canada K1A 0R6

AND

GERALD W. BUCHANAN AND BRIAN A. DAWSON

Department of Chemistry, Carleton University, Ottawa, Ont., Canada K1S 5B6

Received June 22, 1979

Can. J. Chem. Downloaded from www.nrcresearchpress.com by 210.87.254.42 on 09/05/12
For personal use only.

SUZANNE FORTIER, GEORGE I. BIRNBAUM, GERALD W. BUCHANAN, and BRIAN A. DAWSON. Can. J. Chem. **58**, 191 (1980).

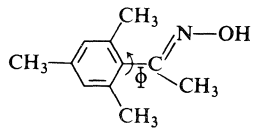
From an X-ray analysis of the title compound it is found that the dihedral angle between the plane of the aromatic ring and the oxime plane is 70.8°. This large angle precludes a significant π electron overlap between the oxime function and the benzene ring. The distortions of the internal ring angles attributable to the four substituents are examined in detail, and parameters are derived for the oxime group. The aryl–oxime C—C bond length (1.491 Å) is the longest yet reported for an aromatic oxime. Using the X-ray derived geometry as input for the calculation of $^{13}C—^{15}N$ coupling constants, one obtains markedly better agreement between calculated and observed couplings than was the case when a force-field calculated molecular geometry was employed. The barrier to rotation about the aryl–oxime bond is estimated to be about 5.8 kcal/mol.

SUZANNE FORTIER, GEORGE I. BIRNBAUM, GERALD W. BUCHANAN et BRIAN A. DAWSON. Can. J. Chem. **58**, 191 (1980).

Une analyse de diffraction aux rayons-X du composé de la présente étude montre que l'angle dièdre entre le plan de l'anneau aromatique et le plan du groupement oxime est de 70.8°. La dimension de cet angle empêche un recouvrement significatif des électrons-π entre la fonction oxime et l'anneau de benzène. Les déformations des angles, à l'intérieur de l'anneau, attribuables aux quatre substituants, sont examinées en détail et les paramètres de déformation du groupement oxime sont dérivés. La longueur de la liaison C—C entre les groupements aryle et oxime (1.491 Å) est la plus grande observée jusqu'à présent pour un oxime aromatique. L'accord entre les valeurs expérimentales et théoriques des constantes de couplage $^{13}C—^{15}N$ est sensiblement amélioré par l'utilisation de la géometrie moléculaire dérivée de l'étude aux rayons-X, comparativement au cas où la géometrie employée était calculée à partir des champs de force. La barrière de rotation autour du lien aryle–oxime est estimée à 5.8 kcal/mol.

Introduction

A recent publication from one of these laboratories (1) reported calculations of $^{13}C—^{15}N$ nmr coupling constants for aromatic oximes. Input for the coupling constant program were geometries as calculated from a force-field approach. In general, the agreement between observed and calculated couplings was rather poor, and therefore more accurate structural information was deemed desirable. Accordingly, we have obtained the X-ray crystal structure of *E*-1-(2,4,6-trimethylphenyl)ethanone oxime **1**, a compound for which the dihedral angle Φ between the plane of the aromatic ring and the oxime function is of particular interest.



1

The X-ray derived geometry, when used as input for the coupling constant program, results in markedly improved agreement between the experimental and calculated $^{13}C—^{15}N$ couplings. Also some conclusions, not previously available, regarding the magnitude of the rotational barrier about the aryl–oxime bond can be drawn.

Experimental

The title compound was prepared as described before (1) and crystallized from *n*-hexane to give colorless prisms, mp 98–99°C. Precession photographs indicated monoclinic symmetry and the following systematic absences: *h0l* for odd *h* and *0k0* for odd *k*. The space group was thus uniquely determined to be $P2_1/a$. A crystal fragment measuring 0.25 × 0.25 × 0.30 mm was mounted along the unique (*b*) axis on a card-controlled Picker four-circle diffractometer and the following crystal data were obtained.

$C_{11}H_{15}NO$ mw = 177.24
Monoclinic, a = 15.516(4), b = 8.702(2), c = 7.852(2) Å, β = 94.04(2)°; V = 1057.54 Å^3, D_m = 1.107 g cm^{-3}, Z = 4, D_c = 1.113 g cm^{-3} (21°C; CuKα$_1$, λ = 1.54051 Å, CuKα$_2$, λ = 1.54433 Å), F(000) = 384, μ(CuKα) = 5.3 cm^{-1}.

The moving-crystal – moving-counter method (θ–2θ scan) was used to measure the intensity data. Monochromatization was achieved by the use of a nickel filter and a pulse height analyzer. Two standard reflections were monitored at regular intervals; their intensities decreased by 15% during the data collection. A net count of 80 or 8% of the background,

[1]Taken, in part, from the Ph.D. thesis of B. A. Dawson, Carleton University, 1979.
[2]NRCC No. 17874.
[3]To whom all correspondence should be addressed.

0008-4042/80/020191-06$01.00/0
©1980 National Research Council of Canada/Conseil national de recherches du Canada

TABLE 1. Final fractional coordinates and thermal parameters (Å²)

(*a*) Nonhydrogen atoms[a]

Atom	*x*	*y*	*z*	U_{11}	U_{22}	U_{33}	U_{23}	U_{13}	U_{12}
C (1)	4363 (1)	3416 (2)	2482 (2)	568 (8)	470 (8)	474 (8)	113 (7)	35 (7)	−15 (7)
C (2)	3467 (1)	3172 (2)	2385 (2)	575 (10)	496 (9)	700 (11)	94 (8)	13 (8)	−48 (8)
C (3)	2925 (1)	4421 (2)	2567 (3)	561 (10)	616 (11)	868 (13)	114 (10)	51 (9)	29 (9)
C (4)	3238 (1)	5895 (2)	2830 (3)	751 (12)	519 (10)	715 (11)	123 (9)	130 (9)	87 (9)
C (5)	4119 (1)	6109 (2)	2910 (2)	854 (12)	442 (9)	550 (9)	76 (7)	127 (9)	−85 (9)
C (6)	4695 (1)	4908 (2)	2726 (2)	632 (10)	528 (9)	456 (8)	130 (7)	57 (7)	−88 (8)
C (7)	4961 (1)	2091 (2)	2322 (2)	552 (8)	520 (9)	499 (8)	112 (7)	52 (7)	−28 (8)
C (8)	5432 (2)	1917 (3)	730 (3)	900 (15)	742 (13)	626 (11)	167 (10)	224 (10)	136 (11)
C (9)	3083 (1)	1591 (3)	2079 (4)	633 (12)	608 (12)	1338 (21)	1 (13)	−25 (13)	−121 (10)
C (10)	2629 (2)	7226 (3)	3031 (4)	1064 (18)	650 (14)	1361 (24)	90 (15)	318 (17)	226 (13)
C (11)	5647 (1)	5230 (3)	2802 (3)	678 (12)	744 (13)	736 (12)	108 (10)	58 (10)	−199 (10)
N (1)	5010 (1)	1150 (2)	3563 (2)	589 (8)	470 (7)	558 (7)	96 (6)	86 (6)	69 (6)
O (1)	5568 (1)	−101 (2)	3327 (2)	801 (8)	616 (8)	701 (8)	188 (6)	207 (7)	242 (7)

[a]All parameters were multiplied by 10^4. The thermal parameters are expressed as exp $[-2\pi^2(U_{11}h^2a^{*2} + \ldots + 2U_{23}klb^*c^* + \ldots)]$.

(*b*) Hydrogen atoms[a]

Atom	*x*	*y*	*z*	*U*	Atom	*x*	*y*	*z*	*U*
H (1)	550 (2)	−64 (3)	425 (4)	95 (7)	H (93)	320 (3)	90 (5)	315 (5)	155 (13)
H (31)	232 (2)	423 (3)	253 (3)	87 (7)	H (101)	205 (4)	687 (7)	298 (7)	213 (20)
H (51)	435 (1)	712 (3)	307 (3)	68 (5)	H (102)	272 (3)	793 (5)	213 (6)	159 (13)
H (81)	502 (2)	170 (4)	−11 (4)	121 (10)	H (103)	286 (3)	788 (6)	380 (6)	179 (16)
H (82)	579 (2)	109 (3)	76 (4)	101 (7)	H (111)	598 (2)	448 (3)	326 (3)	82 (6)
H (83)	561 (2)	292 (4)	34 (4)	116 (10)	H (112)	580 (2)	615 (4)	354 (4)	106 (8)
H (91)	342 (2)	96 (4)	141 (5)	132 (11)	H (113)	584 (2)	538 (3)	167 (3)	86 (7)
H (92)	248 (2)	160 (4)	174 (4)	124 (10)					

[a]All parameters were multiplied by 10^3.

whichever was higher, was determined as threshold intensity below which reflections were considered unobserved. There were 1796 unique reflections accessible to the diffractometer ($2\theta \leq 130°$) of which 1522 (84%) had intensities above threshold values. The intensities were corrected for Lorentz and polarization factors; absorption corrections were considered unnecessary in view of the low value of μ.

The structure was determined by direct methods and the atomic parameters were refined by block-diagonal least-squares. All scattering factors were taken from the International tables for X-ray crystallography (2). The hydrogen atoms were located on difference Fourier maps and their parameters were refined isotropically. Throughout the refinement the function $\sum w(|F_o| - |F_c|)^2$ was minimized and the following weighting scheme was used during the final stages: $w = w_1w_2$, where $w_1 = 1$ for $|F_o| \leq 8.0$, $w_1 = 8.0/|F_o|$ for $|F_o| > 8.0$; $w_2 = \sin^2\theta/0.4$ for $\sin^2\theta < 0.4$, $w_2 = 1$ for $\sin^2\theta \geq 0.4$. Three strong, low-order reflections suffered severely from extinction effects and they were given zero weights. After the final cycle the average parameter shift equalled 0.05σ and the largest one 0.61σ. The conventional residual index R ($\sum|\Delta F|/\sum|F_o|$) is 0.049 and the weighted index R' ($\sum w\Delta F^2/\sum wF_o^2$) is 0.058 for 1545 reflections, including 26 unobserved ones for which $|F_o| < |F_c|$. A final difference Fourier map was featureless.

The final coordinates and temperature parameters, as well as their estimated standard deviations, are listed in Table 1. Table 2 lists the observed and calculated structure factors.[4] Bond lengths and bond angles are shown in Fig. 1.

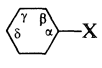
[4]Table 2 may be obtained, at a nominal charge, from the Depository of Unpublished Data, CISTI, National Research Council of Canada, Ottawa, Ont., Canada K1A 0S2.

Results and Discussion

(*a*) *X-ray Results*

A stereoscopic view of the molecule is shown in Fig. 2. Contrary to our previous estimate (1), the dihedral angle between the aromatic ring and the oxime plane is 70.8°. The ring itself is almost completely planar (Table 3), but its substituents are significantly displaced from the mean plane.

Bond lengths and angles in the mesityl moiety show excellent agreement with the expected C_{2v} symmetry, the substituents having distorted the original D_{6h} symmetry of the benzene ring. The angular distortions in benzene rings caused by various substituents have been studied extensively by Domenicano and co-workers (3–6) and by Norrestam and Schepper (7–9). These distortions affect the angles $\alpha, \beta, \gamma, \delta$, and they depend, in most cases, on the electronegativity of the substituent X.



A least-squares refinement of data obtained from five accurately determined crystal structures yielded the following values for the methyl substituent (7): $\Delta\alpha = -1.9(1)$, $\Delta\beta = 1.0(1)$, $\Delta\gamma = 0.3(1)$, $\Delta\delta = -0.7(1)°$. These values are in very good

Can. J. Chem. Downloaded from www.nrcresearchpress.com by 210.87.254.42 on 09/05/12
For personal use only.

Can. J. Chem. Downloaded from www.nrcresearchpress.com by 210.87.254.42 on 09/05/12
For personal use only.

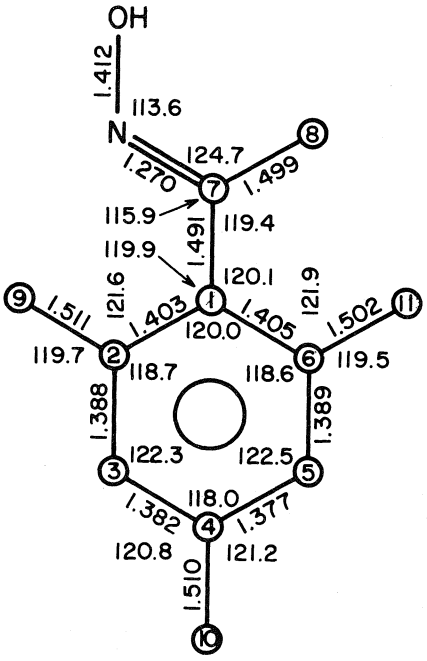
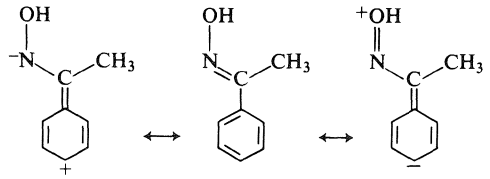


FIG. 1. Bond lengths (Å) and bond angles (deg); their esd are 0.002–0.003 Å and 0.14–0.21°, respectively.

agreement with those derived by Domenicano and Murray-Rust (6). Since the deformations have been shown to be additive (7), one can calculate that in a mesityl group the deviations from 120° would be ±1.3°, with smaller angles at the substituted and larger angles at the unsubstituted ring atoms. Consequently, the angles which we found in the present structure analysis enable us to derive the following distortions attributable to the oxime substituent: $\Delta\alpha = -1.3$, $\Delta\beta = 0$, $\Delta\gamma = 1.1$, $\Delta\delta = -0.7°$.

In the case of $-NO_2$ and —COOH substituents different parameters were found, depending on whether these groups were roughly coplanar with the benzene ring or highly twisted and thus unable to withdraw electrons from the ring (9). Therefore, in considering whether and how the deformation parameters which we obtained for the oxime group would change if that group was coplanar, we must determine whether this group donates or withdraws electrons from the ring. Although one can envisage three general types of resonance forms for acetophenone oxime, it is unlikely that the charged forms contribute much to the ground state. This



view is supported by ^{13}C nmr chemical shift evidence. In *E*-acetophenone oxime the *para*-carbon chemical shift is essentially identical to that of benzene itself (10). This indicates that, in the case of a nearly planar compound, there is no net electron withdrawal or release by the oxime function bonded to the benzene ring. Consequently, the distortion parameters for the oxime group are not likely to be affected by the dihedral angle between that group and the aromatic ring.

A methyl substituent also causes changes of the bond lengths in the benzene ring (3). However, the symmetrical substitution by the three methyl groups in our structure cancels out these changes. On the other hand, the inductive effect of the oxime group causes a polarization of the ring electrons. As a result, the aromatic bonds are longest near this substituent, C(1)—C(2) and C(1)—C(6), and shortest on the opposite side of the ring, C(3)—C(4) and C(4)—C(5). The absence of π electrons in the C(1)—C(7) bond accounts for the fact that this bond is longer in our structure than in any other aromatic oxime. Furthermore, while there is no interaction between N and the C(9) methyl group, one of the hydrogens attached to C(8) makes short contacts with N (2.58 Å) and with O (2.31 Å). This may explain the unusually low value of the N=C(7)—C(1) angle which is 8.8° smaller than the N=C(7)—C(8) angle. The C=N—O angles in oximes have been observed to be as small as 108.4° (11) and as large as 125.2° (12), therefore our value of 113.6° is not unusual.

There is an intermolecular hydrogen bond formed by a donation of the hydroxyl proton to the nitrogen atom of the molecule related by a center of symmetry. The geometry of this hydrogen bond is as follows: O···N 2.813(2), H···N 1.98(3), H···N_{corr}

TABLE 3. Least-squares planes and deviations of atoms from them[a]

Plane 1[b]		Plane 2[b]	
Atom	Δ, Å[c]	Atom	Δ, Å[c]
C (1)	−0.006	C (1)	0.009
C (2)	0.003	C (7)	−0.013
C (3)	0.001	C (8)	0.003
C (4)	−0.002	N (1)	−0.004
C (5)	−0.003	O (1)	0.006
C (6)	0.007		
C (7)*	−0.028		
C (9)*	0.024		
C (10)*	−0.011		
C (11)*	0.026		

[a]Atoms marked with an asterisk were not included in the calculation of the plane.
[b]Plane 1: $0.0245X + 0.1469Y - 0.9888Z + 1.3169 = 0$. Plane 2: $0.7321X + 0.5284Y + 0.4300Z - 7.2708 = 0$.
[c]Esd 0.0014–0.0024 Å.

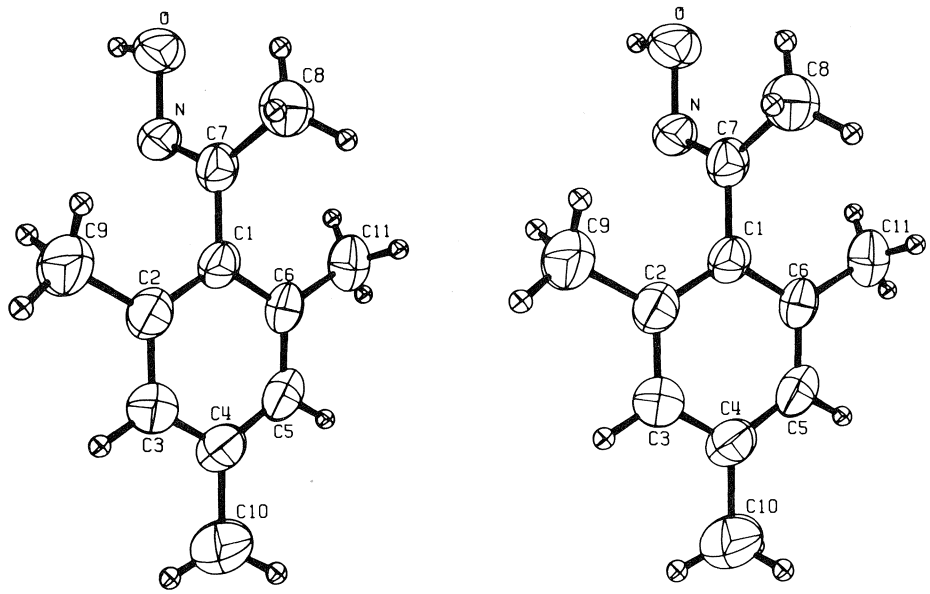


FIG. 2. Stereoscopic view of the molecule; the ellipsoids include 50% probability.

1.89 Å (9), O—H···N 156, H—O···N 17°. Apart from this there are no intermolecular distances shorter than van der Waals contacts.

(b) Rotational Barrier Problem

No experimental measurement of the rotational barrier about the aryl–oxime bond is presently available. Our attempts to "freeze out" this rotation on the nmr time scale to −100°C in both ^1H and ^{13}C spectra were unsuccessful. Input for the GEMO (14) program requires some estimate of this barrier, which essentially represents the conjugation energy between the aromatic ring and the oxime group. Using ketone results as an analogy (15), we estimated this barrier at 9.0 kcal/mol for **1**, and found the calculated dihedral angle to be 35.5° (1) with standard geometries as input (16). This angle is considerably lower than that found in the X-ray crystal structure, which suggests that our estimate of the rotational barrier may have been too high. A lower estimate of the conjugation energy between the oxime group and the aromatic ring would permit more facile deformation of the dihedral angle toward 90°, since it is known that the conjugation energy for two unsaturated networks varies in general as the square of the cosine of the dihedral angle between the networks (17).

In order to determine the dependence of the calculated dihedral angle on the barrier height for **1**, some further calculations were performed using GEMO. Input for GEMO in this approach was the X-ray derived bond lengths and angles, with only the dihedral angle Φ not being specified. The program then calculated the dihedral angle Φ for a series of barriers ranging from 0.0 to 9.0 kcal/mol. The results are presented in Fig. 3 in graphical form.

Interestingly, for a dihedral angle similar to that found in the X-ray analysis (i.e. 70°), the rotational barrier is about 5.8 kcal/mol. This low value is certainly consistent with our inability to freeze out the rotational process on the nmr time scale at −100°C. A very crude estimate of the barrier can also be obtained from electronegativity considerations. One might expect that the rotational barrier for an oxime function bonded to a benzene ring should lie in the range between 9.0 kcal/mol (observed for acetophenone) (15) and that calculated for styrene of 2.0 kcal/mol (18). Such indeed appears to be the case for **1**, although strict comparison of compounds is not valid due to the presence of the *ortho* methyl substituents in **1**.

(c) Coupling Constants

The Fermi contact contributions to the $^{13}C—^{15}N$ couplings, as calculated via the INDO MO approach (19), are presented in Table 4. Values obtained previously using standard geometries as input are included in parentheses for comparison. In three cases out of four, there is markedly better agreement between observed and calculated values using the X-ray geometry as input. For the other case, of geminal coupling to the C position, only slightly poorer agreement is found using the revised geometries.

The only instance for which sign determinations

Can. J. Chem. Downloaded from www.nrcresearchpress.com by 210.87.254.42 on 09/05/12
For personal use only.

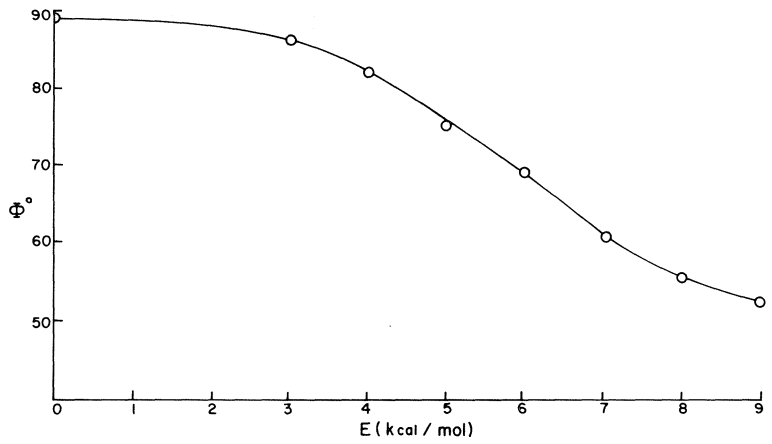
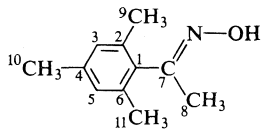


FIG. 3. Plot of the calculated dihedral angle (Φ) vs. conjugation energy (*E*) for **1**.

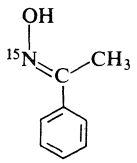
TABLE 4. Experimental and calculated $J_{^{13}C^{15}N}$



$^1J_{CN}$		$^2J_{NCC}$			$^3J_{NCCC}$		
Obsd	Calcd	Path	Obsd	Calcd	Path	Obsd	Calcd
|3.3|	+5.0[a] (−8.7)[b]	N—C_7—C_1	|8.0|	−5.4[a] (+7.4)[b]	N—C_7—C_1—$C_{2,6}$	|1.2|	−3.3[a] (−7.3)[b]
		N—C_7—C_8	|<0.6|	+1.1[a] (+6.5)[b]			

[a]This work.
[b]Parenthesized values are results of previous calculations (1).

are available for these couplings is for the system shown below,



$^2J_{N—C—CH_3} = +1.0$ Hz

where the sign of $^2J_{N—C—CH_3}$ was found to be positive (20), and the magnitude is small, i.e. 1.0 Hz. Interestingly for **1**, the calculated $^2J_{N—C—CH_3}$ is +1.1 Hz, while the observed value is also small, being less than 0.6 Hz.

The reasonably good agreement between calculated and observed $^{13}C—^{15}N$ couplings using this approach suggests an important contribution from the Fermi contact mechanism in one, two, and three bond couplings involving ^{13}C and ^{15}N.

Acknowledgments

G.W.B. and S.F. thank the National Research Council of Canada for financial assistance and for a Research Associateship, respectively. Figure 2 was drawn with the help of the ORTEP program by C. K. Johnson (21). All other crystallographic computations were performed with programs written by Ahmed *et al.* (22).

1. G. W. BUCHANAN and B. A. DAWSON. Can. J. Chem. **56**, 2200 (1978).
2. J. A. IBERS and W. C. HAMILTON (*Editors*). International tables for X-ray crystallography. Vol. 4. Kynoch Press, Birmingham. 1974.
3. A. DOMENICANO, A. VACIAGO, and C. A. COULSON. Acta Crystallogr. Sect. B, **31**, 221 (1975).
4. A. DOMENICANO, P. MAZZEO, and A. VACIAGO. Tetrahedron Lett. 1029 (1976).
5. A. DOMENICANO and A. VACIAGO. Acta Crystallogr. Sect. B, **35**, 1382 (1979).
6. A. DOMENICANO and P. MURRAY-RUST. Tetrahedron Lett. 2283 (1979).
7. R. NORRESTAM and L. SCHEPPER. Acta Chem. Scand. Sect. A, **32**, 889 (1978).
8. R. NORRESTAM and L. SCHEPPER. Acta Crystallogr. Sect. A, **34**, S111 (1978).
9. R. NORRESTAM and L. SCHEPPER. Fifth European Crystallographic Meeting, Copenhagen, Abstracts. 1979. p. 122.

Can. J. Chem. Downloaded from www.nrcresearchpress.com by 210.87.254.42 on 09/05/12
For personal use only.

10. G. W. BUCHANAN and B. A. DAWSON. Can. J. Chem. **54**, 790 (1976).
11. D. SHUGAR, C. P. HUBER, and G. I. BIRNBAUM. Biochim. Biophys. Acta, **447**, 274 (1976).
12. K. FOLTING, W. N. LIPSCOMB, and B. JERSLEV. Acta Crystallogr. **17**, 1263 (1964).
13. G. A. JEFFREY and S. TAKAGI. Acta Crystallogr. Sect. B, **33**, 738 (1977).
14. N. C. COHEN. Tetrahedron, **27**, 789 (1971).
15. H. KESSLER and K. O. KALINOWSKI. *In* Topics in stereochemistry. Vol. 7. *Edited by* N. L. Allinger and E. L. Eliel. Intersciences, New York, NY. 1972.
16. J. A. POPLE and D. L. BEVERIDGE. Approximate molecular orbital theory. McGraw-Hill Book Co., New York, NY. 1970. pp. 111, 112.
17. R. HOFFMANN and J. R. SEVENSEN. J. Phys. Chem. **74**, 415 (1970).
18. W. J. HEHRE, L. RADOM, and J. A. POPLE. J. Am. Chem. Soc. **94**, 1496 (1972).
19. J. A. POPLE, J. W. MCIVER, JR., and N. S. OSTLUND. J. Chem. Phys. **49**, 2960 (1968); **49**, 2965 (1968).
20. G. W. BUCHANAN and B. A. DAWSON. Can. J. Chem. **55**, 1437 (1977).
21. C. K. JOHNSON. ORTEP Report ORNL-3794 (2nd revision), Oak Ridge National Laboratory, Oak Ridge, TN. 1970.
22. F. R. AHMED, S. R. HALL, M. E. PIPPY, and C. P. HUBER. J. Appl. Crystallogr. **6**, 309 (1973).

Can. J. Chem. Downloaded from www.nrcresearchpress.com by 210.87.254.42 on 09/05/12
For personal use only.

Addendum: The effect of the variation of potential on progressive three-dimensional nucleation and growth

(Ref.: Can. J. Chem. **56**, 606 (1978))

Galvanostatic transients and crystallization overvoltage

(Ref.: Can. J. Chem. **56**, 908 (1978))

The fine structure of the Kolmogoroff–Avrami theorem

(Ref.: Can. J. Chem. **57**, 1304 (1979))

ARTHUR SMITH
Department of Mathematics, Carleton University, Ottawa, Ont., Canada K1S 5B6
AND
STEPHEN FLETCHER
Department of Chemistry, Carleton University, Ottawa, Ont., Canada K1S 5B6

Received September 13, 1979

One of us (Stephen Fletcher) wishes to acknowledge the generous financial support from the National Research Council of Canada and the Natural Sciences and Engineering Research Council of Canada grants of Dr. R. G. Barradas, Department of Chemistry, Carleton University. We both appreciate the time and resources given to produce these joint papers.

Can. J. Chem. Downloaded from www.nrcresearchpress.com by 210.87.254.40 on 09/05/12
For personal use only.

COMMUNICATION

Long-range phosphorus hyperfine coupling in a persistent nitroxide radical

P. LIVANT[1]

Department of Chemistry, Auburn University, Auburn, AL 36830, U.S.A.

AND

R. L. DUDLEY

Guelph–Waterloo Centre for Graduate Work in Chemistry, University of Guelph, Guelph, Ont., Canada N1G 2W1

Received October 12, 1979

P. LIVANT and R. L. DUDLEY. Can. J. Chem. **58**, 197 (1980).

An unusually large long-range hyperfine coupling to γ-phosphorus has been observed in nitroxide **2**. The magnitude of the coupling is ascribed to the rigidity of the ring system and the consequent importance of conformations like **7**. The radical forms upon lengthy exposure of **1** to air. It may also be prepared by standard methods, and is stable over a period of months at 0°C. Transient and as yet unidentified radicals are observed during the oxidation of **1** to **2** with aryl peracids.

P. LIVANT et R. L. DUDLEY. Can. J. Chem. **58**, 197 (1980).

On a observé dans le nitroxyde **2** un grand couplage hyperfin peu usuel à longue distance avec le phosphore en position γ. On a attribué l'importance de ce couplage à la rigidité du système cyclique et à l'importance résultante de la conformation du composé **7**. Le radical se forme après une longue exposition du produit **1** à l'air. On peut également le préparer par des méthodes classiques et il est stable pendant plusieurs mois à 0°C. On observe des radicaux transients (non encore identifiés) lors de l'oxydation du composé **1** par les peracides acycliques qui conduit au composé **2**.

[Traduit par le journal]

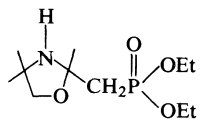
A number of studies have reported the spectra of phosphorus-containing nitroxides. The magnitude of the phosphorus hyperfine splitting constant (P-hfsc) was found to vary considerably as a function of the position of the phosphorus atom with respect to nitroxyl function, viz. α-position (—N(—O·)—P), 1.73–13.2 G(1–7); β-position (—N(—O·)—C—P), 0.0–41.8 G for acyclic cases (6–11), 29.6–54.7 G for cyclic cases (12); γ-position (—N(—O·)—C—C—P), 0.0–1.75 G (8).[2]

Phosphorus-containing iminoxyl radicals (13, 14) and aci-anions (8, 9) exhibit similar magnitudes of P-hfsc's as a function of position of phosphorus relative to the radical center.

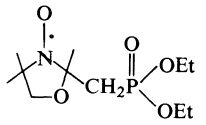
Though not stated explicitly, these nitroxides appear to be relatively short lived. Rassat and coworkers (4) have described a nitroxide that should be relatively persistent, but because of low yields in the preparation of this nitroxide, isolation of the pure material was not possible.

We would like to report the synthesis of diethyl 2,4,4-trimethyl-1,3-oxazolidin-2-ylmethylphosphonate *N*-oxyl. **2**. To our knowledge, this persistent radical shows the largest γ-P-hfsc yet reported for an aliphatic nitroxide.

Oxazolidine **1** was prepared from diethyl-β-



1



2

keto-propylphosphonate and 2-amino-2-methyl-1-propanol by the method of Keana *et al.* (15). This colorless liquid gave a satisfactory elemental analysis and nmr for the structure assigned.[3]

After three months exposure to air, compound **1** turned pale yellow. A benzene solution of the yellow material gave a six-line esr spectrum which is ascribed to **2**.[4] The splitting pattern consists of a triplet of doublets, with a N-hfsc of 14.06 G, typical for nitroxides. The doublet splitting of 1.81 G is consistent with the splitting for a γ-phosphorus. In more polar solvents **2** gave additional splitting due to three γ-hydrogens. These probably arise from one of the methyl groups on the oxazolidine ring.

[1]Author to whom correspondence should be addressed.

[2]Although further examples of coupling to remote phosphorus have been reported (K. Torssell. Tetrahedron, **33**, 2287 (1977)), these involve aromatic nitroxides and are therefore not directly comparable to the aliphatic systems under discussion here.

[3]For **1**: *Anal.* calcd.: C 49.07, H 10.40, N 5.20; found: C 49.47, H 10.24, N 5.12. P- and H-nmr agree with previously published data (P. Livant and M. Cocivera. J. Org. Chem. **43**, 3011 (1978)).

[4]Electron spin resonance spectra were obtained on a Varian E 104 esr spectrometer.

0008-4042/80/020197-03$01.00/0

©1980 National Research Council of Canada/Conseil national de recherches du Canada

TABLE 1. Electron spin resonance parameters for **2**[a]

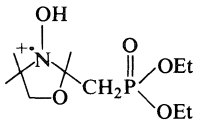
Solvent	a^N	a_γ^P	a_γ^H
C_6H_6	14.06	1.81	—
CH_2Cl_2	14.96	1.87	0.39(3H)
H_2O or D_2O	15.87	3.22	0.39(3H)

[a]In gauss.

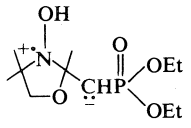
The esr findings are summarized in Table 1. The increase in the nitrogen and γ-phosphorus splittings in polar solvents is due to a solvent polarity effect (16, 17).

Conceivably, the doublet splitting in the esr spectrum of **2** might have been assigned to a H-hfsc in the protonated nitroxide **3**, or the zwitterionic radical **4** (18). This possibility was ruled out since both the hydroxyl proton and nitrogen hyperfine splitting should be significantly larger in such a radical (21). Either protonated radical should undergo deuterium exchange in D_2O, but identical spectra were obtained in both H_2O and D_2O solvent.

Why is the γ-P-hfsc in **2** so large? The only reported nitroxide with γ-P-hfsc nearly as large as that of **2** is **5** (γ-P-hfsc = 1.75 G). Radicals similar to **5**, however, lacking the α-phenyl substituent, have much lower γ-P-hfsc's (8). In **5**, rotation about the N—C_α bond is probably somewhat hindered, due to the bulky *tert*-butyl and phenyl groups, with the result that phosphorus spends more time in conformations such as **6**. The analogous rotation about the N—C_α bond in **2** is eliminated by the incorporation of the bond into the oxazolidine ring. Thus we have for **2** a large population of conformation **7**, resulting in a large γ-P-hfsc.



3

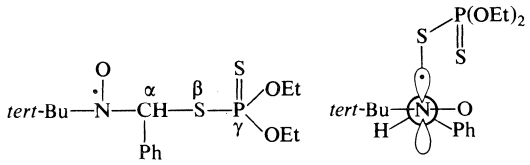


4

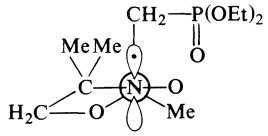
The air oxidation of aliphatic secondary amines to persistent nitroxides appears to be an uncommon reaction. The air oxidation of diaryl amines to nitroxides has been observed more widely (19).

In addition to air oxidation, **1** may be converted to **2** by oxidation with Na_2WO_4/H_2O_2 (20) followed by chromatography on silica gel with chloroform eluant. The orange oil obtained in this way gives an esr spectrum identical to that assigned to **2**, and is stable for months at 0°C.

Oxidation of **1** with either *m*-chloroperbenzoic acid or *m*-nitroperbenzoic acid in CH_2Cl_2 also gave **2**, and in addition two new radicals were observed



5 **6**



7

during the oxidation. For the first: $a^N = 15.87$ G and $a_\beta^H = 12.77$ G (3H). These coupling constants are similar to those of *N*-*t*-butyl-*N*-methyl nitroxide (21) and, therefore, the radical is probably of similar structure. For the second: $a^N = 15.48$ G, $a_\beta^H = 21.54$ G, and $a_\gamma^H = 0.39$ G (3H). The doublet splitting of 21.54 G is assigned to a hydrogen coupling since it is too large for an α-phosphorus splitting and too small for a cyclic β-phosphorus splitting. Since $a^N < a_\beta^H$, this radical is probably a cyclic nitroxide (22). The two radicals observed in addition to **2** in the aryl peracid oxidations are short-lived; at the end of the reaction only **2** ($a^N = 14.96$ G, $a_\gamma^P = 1.87$ G, $a_\gamma^H = 0.39$ G (3H)) is in evidence.

Akhrem *et al.* (23) found no esr signal during or after the reaction of perbenzoic or peracetic acid with piperidine, and proposed a non-radical route. The identity of the transient radicals observed in the present system and the mechanism operative here are under investigation.

Acknowledgments

Our thanks to Dr. V. Malatesta for illuminating discussions, and to Drs. M. Cocivera and E. Janzen for encouragement.

1. Y. G. SHERMOLOVICH, A. V. MISYURA, O. M. POLUMBRIK, and L. N. MARKOVSKII. Zh. Obshch. Khim. **49**, 232 (1979).
2. A. SH. MUKHTAROV, A. V. IL'YASOV, YA. A. LEVIN, and M. S. SKOROBOGATOVA. Izv. Akad. Nauk SSSR, Ser. Khim. 2816 (1976).
3. D. GRILLER and B. P. ROBERTS. J. Chem. Soc. Perkin Trans. II, 1416 (1973).
4. D. GAGNAIRE, A. RASSAT, J. B. ROBERT, and P. RUELLE. Tetrahedron Lett. 4449 (1972).
5. (*a*) H. KARLSSON and C. LAGERCRANTZ. Acta Chem. Scand. **24**, 3411 (1970); (*b*) G. ADEVIK and C. LAGERCRANTZ. Acta Chem. Scand. **24**, 2253 (1970).
6. (*a*) G. BOEKENSTEIN, W. G. VONCKEN, E. H. J. M. JANSEN, and H. M. BUCK. Recl. Trav. Chim. Pays-bas, **93**, 69 (1974); (*b*) G. BOEKENSTEIN and H. M. BUCK. Recl. Trav. Chim. Pays-bas, **92**, 1095 (1973).
7. M. ZANGER and R. POUPKO. Spectrosc. Lett. **10**, 737 (1977).

Can. J. Chem. Downloaded from www.nrcresearchpress.com by 210.87.254.40 on 09/05/12
For personal use only.

8. G. BRUNTON, B. C. GILBERT, and R. J. MAWBY. J. Chem. Soc. Perkin Trans. II, 650 (1976).
9. B. C. GILBERT, J. P. LARKIN, R. O. C. NORMAN, and P. M. STOREY. J. Chem. Soc. Perkin Trans. II, 1508 (1972).
10. A. V. IL'YASOV, YA. A. LEVIN, A. SH. MUKHTAROV, and M. S. SKOROBOGATOVA. Teor. Eksp. Khim. **11**, 612 (1975).
11. A. SH. MUKHTAROV, A. V. IL'YASOV, YA. A. LEVIN, I. P. GOZMAN, M. S. SKOROBOGATOVA, and E. I. ZOROATSKAYA. Teor. Eksp. Khim. **12**, 831 (1976).
12. P. TORDO, M. BOYER, A. FRIEDMANN, O. SANTERO, and L. PUJOL. J. Phys. Chem. **82**, 1742 (1978).
13. A. V. IL'YASOV, YA. A. LEVIN, A. SH. MUKHTAROV, and M. S. SKOROBOGATOVA. Izv. Akad. Nauk SSSR, Ser. Khim. 1654 (1975).
14. A. V. IL'YASOV, B. G. LIORBER, A. A. BARLEV, A. SH. MUKHTAROV, M. P. SOKOLOV, V. A. PAVLOV, and A. I. RAZUMOV. Teor. Eksp. Khim. **13**, 693 (1977).
15. J. F. W. KEANA, S. B. KEANA, and D. BEETHAM. J. Am. Chem. Soc. **89**, 3055 (1967).
16. B. R. KNAUER and J. J. NAPIER. J. Am. Chem. Soc. **98**, 4395 (1976).
17. A. V. GAGUA, G. G. MALENKOV, and V. P. TIMOFEER. Chem. Phys. Lett. **56**, 470 (1978).
18. V. MALATESTA and K. U. INGOLD. J. Am. Chem. Soc. **95**, 6400 (1973).
19. R. H. HOSKINS. J. Chem. Phys. **25**, 788 (1956); J. R. THOMAS. J. Am. Chem. Soc. **82**, 5955 (1960); K. ADAMIC, M. DUNN, and K. U. INGOLD. Can. J. Chem. **47**, 287 (1969); A. B. SHAPIRO, A. V. OSIPOVA, L. A. SKRIPKO, S. D. RAZUMOVSKII, and E. G. ROZANTSEV. Izv. Akad. Nauk SSSR, Ser. Khim. 1086 (1971).
20. E. G. ROZANTSEV. Free nitroxyl radicals. Plenum Press, New York. 1970. pp. 67–73.
21. J. Q. ADAMS, S. W. NICKSIC, and J. R. THOMAS. J. Chem. Phys. **45**, 654 (1966).
22. (*a*) M. B. NEIMAN and E. G. ROZANTSEV. Izv. Akad. Nauk SSSR, Ser. Khim. 1178 (1964); (*b*) M. S. KHLOPLYANKING, A. C. BACHACHENKO, M. B. NEIMAN, and H. C. VASILEVA. Kinet. Katal. **6**, 394 (1965); (*c*) Y. L. YASINA, V. B. MILLER, YU. H. SHLYAPNIKEV, and L. A. SKRIPTIC. Izv. Akad. Nauk SSSR, Ser. Khim. 1481 (1965).
23. (*a*) A. A. AKHREM, S. M. BEL'SKII, and D. I. METELITSA. Kinet. Katal. **17**, 887 (1976); (*b*) L. G. MELIK-OGANDZHANYAN, N. M. BEILERYAN, and O. A. CHALTYKYAN. Kinet. Katal. **15**, 569 (1974).

Can. J. Chem. Downloaded from www.nrcresearchpress.com by 210.87.254.40 on 09/05/12
For personal use only.

Canadian Journal of Chemistry
Published by
THE NATIONAL RESEARCH COUNCIL OF CANADA

Journal canadien de chimie
Publié par
LE CONSEIL NATIONAL DE RECHERCHES DU CANADA

Volume 58 Number 3 February 1, 1980

Volume 58 numéro 3 1 février 1980

Can. J. Chem. Downloaded from www.nrcresearchpress.com by 210.87.254.6 on 09/05/12
For personal use only.

On Ruhemann's Purple

DONALD C. WIGFIELD, GERALD W. BUCHANAN, AND STEPHEN M. CROTEAU
Department of Chemistry, E.W.R. Steacie Laboratories, Carleton University, Ottawa, Ont., Canada K1S 5B7

Received May 24, 1979

DONALD C. WIGFIELD, GERALD W. BUCHANAN, and STEPHEN M. CROTEAU. Can. J. Chem. **58**, 201 (1980).

The ^1H nmr spectrum previously reported for Ruhemann's Purple is shown to be inconsistent with the accepted structure of this material. The discrepancy with the reported ^1H nmr spectrum is shown to be due to the presence of a major impurity, identified as hydrindantin. Spectra (^1H nmr, ^{13}C nmr, ir, uv–visible) of Ruhemann's Purple, its protonated analogue DYDA, and other ninhydrin relatives are reported, and structural conclusions are based on these spectral data.

DONALD C. WIGFIELD, GERALD W. BUCHANAN et STEPHEN M. CROTEAU. Can. J. Chem. **58**, 201 (1980).

On montre que le spectre rmn du ^1H attribué antérieurement au pourpre de Ruhemann ne correspond pas à la structure proposée pour ce produit. On démontre que la différence par rapport au spectre rmn du ^1H est due à la présence de l'hydrindantine identifiée comme impureté principale. On a rapporté les spectres (rmn du ^1H et du ^{13}C, ir, uv–visible) du pourpre de Ruhemann, de ses analogues protonés DYDA et d'autres ninhydrines apparentées et les conclusions structurales décrites sont basées sur ces données spectrales.

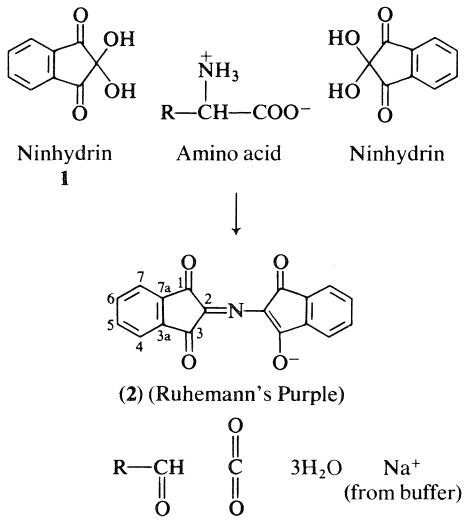
[Traduit par le journal]

The reaction of amino acids with ninhydrin is one that has been known for a long time (1), and which for thirty years has been used for the quantitative determination of amino acids (2). The reaction is shown in Scheme 1. Various inconsistencies in the literature, and, in particular, the reported ^1H nmr spectrum for Ruhemann's Purple (3), have led to our own investigations in this area.

Results and Discussion

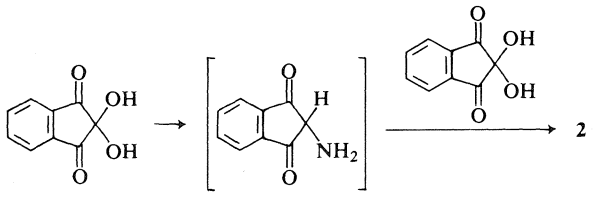
Evaluation of Previous Data

Extensive effort has been expended to elucidate the mechanism of formation of Ruhemann's Purple (4–8). Despite this, a recent review has pointed out that major texts are still at variance with each other regarding this mechanism of formation (9). In contrast to this concern with mechanism, the actual structure of Ruhemann's Purple appears to have received unquestioned acceptance. Ruhemann, in his extensive studies in this area in the early 1900's, discovered ninhydrin (**1**) (1), and uncovered the fact that it gave a purple colour with skin (1), and with amino acids (10). Based on analogy with the structure for purpuric acid (11, 12) (which had six years earlier been revised from Beilstein's 1858 suggestion involving an aziridine ring (13)), Ruhemann in 1911 proposed the structure **2** for the purple substance formed from ninhydrin (14). Ruhemann also converted ninhydrin to the unstable 1,3-diketohydrindamine (**3**), (15) from which he



SCHEME 1. Reaction of ninhydrin with amino acids to yield Ruhemann's Purple.

0008-4042/80/030201-05$01.00/0
©1980 National Research Council of Canada/Conseil national de recherches du Canada



SCHEME 2. Ruhemann's synthetic route to **2**.

subsequently also produced a purple substance by reaction with ninhydrin (14) (see Scheme 2). However, there was apparently no experimental evidence that this purple substance and the purple material produced by the ninhydrin – amino acid reaction were indeed one and the same thing. Nearly forty years later, elemental analysis confirmed the empirical formula corresponding to that of **2** (2), and later still the ir spectrum revealed a peak at 1670 cm^{-1} (16), consistent with the delocalized carbonyl system. Because of volatility problems, no mass spectrum has been reported.

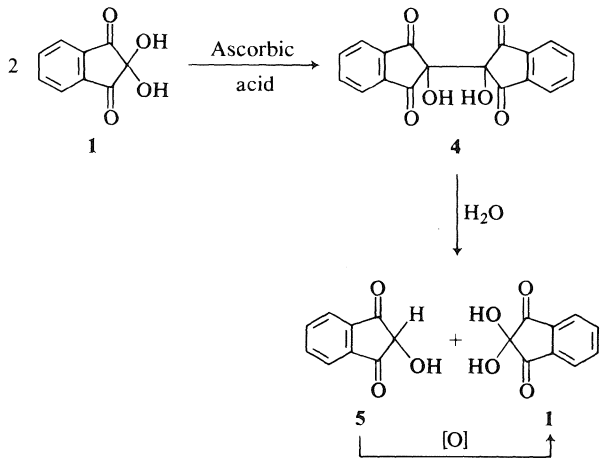
The proton nmr spectrum of Ruhemann's Purple in dimethyl sulfoxide-d_6 has been reported to consist of "two peaks of equal intensity which originate in the aromatic protons of the two nonequivalent indanedione rings" (3). Despite the fact that, in the structure **2** as written, the two benzene rings are different, this difference is completely eliminated by resonance delocalization of the negative charge. An alternative explanation of two peaks of equal intensity would be differentiation of the protons *ortho* and *meta* to the five-membered ring (i.e., C-4H vs. C-5H, etc.), but all ninhydrin derivatives appear to have accidental chemical shift equivalence of these two sets of protons (see Experimental). Because of this unsatisfactory situation regarding the interpretation of the reported nmr spectrum, we were led to consider that either (*a*) the spectrum reported was not that of Ruhemann's Purple, or (*b*) the structure long accepted for Ruhemann's Purple was incorrect.

Spectra of Ruhemann's Purple

Multiple reactions of ninhydrin with glycine under standard conditions (2) were performed, the purple precipitates collected, and the ^1H nmr spectra recorded. In contrast to the report of Friedman (3), that the spectrum consists of two peaks (δ 7.65 and 8.00) of equal intensity, we observe the following. (*1*) Spectra are not reproducible from one reaction to another. Some spectra have the two peaks (δ 7.65 and 8.00) of equal intensity, others have the δ 7.65 peak considerably more intense; in some spectra the peak at δ 8.00 is entirely absent. (*2*) There is an additional peak at δ 6.5. This peak has an intensity 25% that of the δ 8.00 peak. (*3*) The peaks at δ 6.5 and 8.00 slowly decrease with time and are replaced by peaks at δ 8.07 and 7.5, respectively. (*4*) The peaks at δ 6.5 and 7.5 disappear upon addition of D_2O.

These observations are most easily rationalized in the following way. Ruhemann's Purple gives rise to the single peak at δ 7.65. As previously discussed, a single-peak spectrum is consistent with structure **2**. The other two peaks (δ 6.5 and 8.00) are due to hydrindantin, **4**, a compound that has figured prominently in discussions of the mechanism of the ninhydrin reaction (9). Authentic samples of hydrindantin, **4**, prepared by reduction of ninhydrin with ascorbic acid (17), give these same two peaks. The decay of these peaks (δ 8.00 and 6.5) and their replacement by peaks at δ 8.07 and 7.5 is consistent with the known chemistry of hydrindantin (7) – retroaldol cleavage to give **5** and **1** (see Scheme 3), followed by rapid air oxidation (15) of hydroxydiketohydrindene **5** to ninhydrin, **1**. The final product is therefore ninhydrin, an authentic sample of which gives the same two spectral peaks at δ 8.07 and 7.5.

The ^{13}C nmr spectrum of Ruhemann's Purple should lead to a simple 5-line spectrum if structure **2** is correct. This is, in fact, observed, although one of the peaks (138.4 ppm) is extremely weak.[1] This signal was eventually detected by running the spectrum in non-deuterated dimethyl sulfoxide solvent (82 000 scans). Of the five peaks, two, 120.7 and 132.8 ppm, are immediately assignable to the aromatic C—H groups *ortho* and *meta* to the ring



SCHEME 3. Deliberate reduction of ninhydrin to hydrindantin and its spontaneous conversion back to ninhydrin.

[1]In connection with this problem, we also prepared indantrione (18), (dehydrated ninhydrin). This compound also exhibits very weak carbonyl ^{13}C signals.

Can. J. Chem. Downloaded from www.nrcresearchpress.com by 210.87.254.6 on 09/05/12
For personal use only.

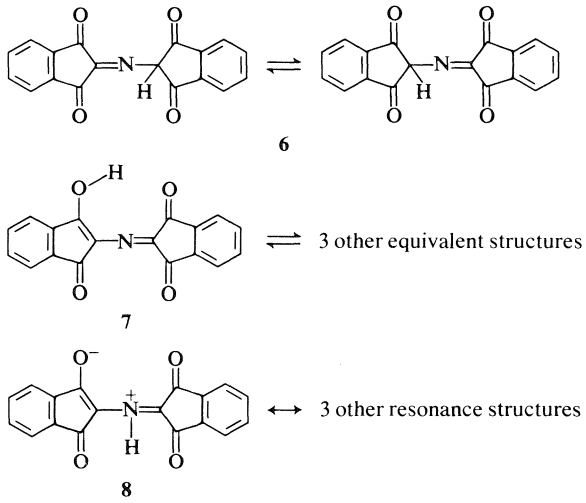
Can. J. Chem. Downloaded from www.nrcresearchpress.com by 210.87.254.6 on 09/05/12
For personal use only.

junction, respectively, on the basis of their high intensity, their multiplicity in off-resonance decoupled spectra, and the analogy to other, rigorously assigned, ring structures (19). A third peak (134.0 ppm) is assignable to C-2 (C—N) of the indanedione ring. The final two peaks (138.4 and 139.9 ppm) correspond to the ring junction carbon and the carbonyl carbons, the latter occurring at higher field than usual due to the resonance delocalization of the negative charge. A firm distinction between the two does not seem possible without further experimentation. The intensity of the peak at 138.4 ppm is very dependent on experimental conditions, being more intense than the 139.9 ppm peak for spectra taken in non-deuterated dimethyl sulfoxide, and essentially non-detectable for spectra taken in DMSO-d_6. On this basis, it seems probable that the peak at 138.4 ppm is due to the carbonyl carbons, and that at 139.9 ppm is due to the ring junction carbons. Either position is acceptably close to chemical shifts for the ring junction carbons in the other ninhydrin derivatives. The low intensity of the C=O resonance of **2** recorded in DMSO-d_6 solution is probably due to the absence of spatially proximate H's available for relaxation of this carbon, since there are no nearby H's in the same molecule and none available in the solvent. This problem is overcome when a protonated solvent is used, since intermolecular dipole – dipole relaxation of the C=O carbon can now occur via the solvent protons giving rise to a positive nuclear Overhauser effect and a shortened T_1 for the C=O resonance. Both these factors result in increased peak intensity in the Fourier transform ^{13}C spectrum (20). Although it is difficult quantitatively to predict the chemical shift of the C—O, due to lack of appropriate model compounds, one can suggest that the shift to higher field, relative to normal carbonyl resonances, results from averaging of keto and enol environments.

In summary, the spectral evidence on Ruhemann's Purple is consistent with the long-accepted structure **2**. The previously reported ^1H nmr spectrum (3) appears to have been obtained on a sample containing an equal amount of hydrindantin impurity, giving rise to the spurious peak at δ 8.00.

Spectra of DYDA

In addition to Ruhemann's Purple, **2**, spectra were also obtained on its unstable parent acid (diketohydrindylidenediketohydrindamine, DYDA), that arises from protonation of **2**, by subjecting **2** to mildly acidic solution. These spectra are recorded in the Experimental and we comment here only on the significant points.



SCHEME 4. Possible structures for DYDA.

Since the mass spectrum of Ruhemann's Purple is unavailable, the mass spectrum of DYDA is especially valuable. As expected, this shows peaks at *m/e* 303 (molecular ion), 275, 247 (successive losses of CO) and also *m/e* 132, 104, 76 (successive loss of CO from *m/e* 132) which also occur in the mass spectrum of ninhydrin. Metastable ions corresponding to all four steps involving loss of CO mentioned above were apparent, occurring at *m/e* 55.6 (104 → 76), 82.0 (132 → 104), 222.1 (275 → 247), and 250.0 (303 → 275). These data are clearly consistent with a species corresponding to a protonated **2**.

Three possible structures **6**, **7**, and **8**,[2] for DYDA are indicated in Scheme 4, depending on whether there is C, O, or N protonation, respectively. The ^{13}C nmr spectrum consists only of 5 signals, showing equivalence about the central nitrogen; this can be accommodated in structures **6** and **7** by rapid equilibration between equivalent structures, and is demanded by resonance in structure **8**. The δ_c value of the carbonyl carbons, 181.7, is consistent only with the tetracarbonyl structure **6**. For structures **7** and **8**, the 25% enol content for any one carbon would be expected to provide a substantial upfield shift, as in the case of Ruhemann's Purple itself (138.4). As a model for structure **6** it is noteworthy that the δ_c shift of the corresponding carbons of the structurally unambiguous indantrione (183.4) is very similar to those of DYDA.

There is further evidence against structures **7** and

[2]A referee urged us to consider this structure.

Can. J. Chem. Downloaded from www.nrcresearchpress.com by 210.87.254.6 on 09/05/12
For personal use only.

8. No evidence of an O—H or a $\overset{+}{N}$—H stretch in the ir spectrum is evident and there is not a strong M − 1 peak in the mass spectrum. Furthermore, in the case of **8**, the carbonyl absorption frequency would be expected to be low, due to the delocalized system (1655 cm^{-1} in the case of Ruhemann's Purple); in fact the absorption is at 1680 cm^{-1}, consistent with the unsaturated carbonyl system present in **6**. Finally, DYDA is soluble in organic solvents and does not exhibit zwitterionic behaviour expected of **8**.

In summary, the spectral data appear to be substantially in favour of the tetracarbonyl structure **6**. Initially we felt that the non-aromatic proton in the ^1H nmr spectrum (δ 5.0) was at low field for the C—H. However, the corresponding shift in a β-diketone is about δ 3.6, to which must be added as much as 1.7 ppm for the carbon–nitrogen substitution.[3] Wherever the proton is attached, it is highly acidic, and possibly hydrogen-bonded, and thus the variation in chemical shift is unremarkable.

Mechanistic Aspects

Two mechanistic aspects should briefly be mentioned.

The interconversion of hydroxydiketohydrindene (**5**) and the corresponding amine (**3**) figures prominently in various mechanistic proposals, particularly in relation to hydrindantin formation. (See ref. 9 and references therein.) It does not seem to have been mentioned previously that such a step is rarely encountered in organic chemistry. If and how this step occurs is an intriguing question.

A second point regarding mechanism of Ruhemann's Purple formation is a definition of the reaction itself. If current mechanistic thought is correct (9), it follows that the formation of a molecule of hydrindantin is tied to the formation of one *less* molecule of Ruhemann's Purple. Thus one would expect the use of Ruhemann's Purple as a quantitative measure of amino acid content to be highly irreproducible, paralleling the irreproducible quantities of hydrindantin we have observed. Biochemically, this has, in fact, been recognized to be the case for a long time, and is circumvented, in automatic amino acid analyzers, by addition of excess stannous chloride, as reducing agent (21). Mechanistic studies on the reaction, however, have not employed this experimental modification, and we wish to emphasize the unfortunate situation that conclusions on mechanism are, for the most part, based on experimental conditions significantly different from those used in actual biochemical practice.

[3]We are very grateful to another referee for pointing this out.

Experimental

General

Infrared spectra were recorded on a Perkin-Elmer 237B grating infrared spectrophotometer using a polystyrene film as a reference. Ultraviolet and visible spectra were recorded on a Beckman Model 25 spectrophotometer. Nuclear magnetic resonance spectra were obtained, using dimethyl sulfoxide-d_6 as solvent, unless otherwise noted, and TMS as internal standard, on a Varian Model T-60 instrument for proton spectra and on a Varian Model XL-100-12 instrument equipped with a Nicolet Technology Corporation Fourier transform data system for ^{13}C spectra. Sweep widths were routinely 6000 Hz, with 8192 data points being employed. Pulse angles were normally 45° and a pulse delay of 2 s was used. The number of spectral accumulations varied from 35 000 to 80 000. Mass spectra were obtained on an AEI MS-12 mass spectrometer at Trent University, Peterborough, Ont. Melting points were taken on a Fisher-Johns melting point apparatus and are uncorrected.

Ninhydrin (1)

This compound, obtained from Bio-Rad Laboratories, was recrystallized from water before use. Glycine, reagent grade (Fisher Scientific Co.), was used without further purification.

Ruhemann's Purple (2)

The reaction between glycine (75 mg, 1.0 mmol) and ninhydrin (700 mg, 3.93 mmol) was conducted in citrate buffer under the conditions of Moore and Stein (2). The product (150 to 290 mg), obtained on a medium mesh sintered glass funnel and dried *in vacuo* over sulfuric acid, was a brownish solid having superficial metallic lustre, λ_{max}(EtOH): 253 (ε, 44 000), 409 (ε, 21 400), and 575 (ε, 19 000) nm; ν_{max}(KBr): 1655 (delocalized carbonyl) cm^{-1}; ^1H nmr δ: 7.65 (s); ^{13}C nmr (in non-deuterated DMSO) δ: 120.7 (C-4, C-7), 132.8 (C-5, C-6), 134.0 (C-2), 138.4, 139.9 (C-1, C-3, and C-3a, C-7a).

Diketohydrindylidenediketohydrindamine (DYDA) (6)

Ruhemann's Purple (100 mg) in water (40 mL) was acidified with 4–5 drops of concentrated hydrochloric acid. The reddish precipitate was collected on a medium mesh sintered glass funnel and dried *in vacuo* over sulfuric acid, $\lambda_{max}(CHCl_3)$: 485 (ε, 16 000) nm; $\nu_{max}(CHCl_3)$: 1680 (C=O) cm^{-1}; ^1H nmr ($CDCl_3$) δ: 5.0 (1H, s, position concentration dependent, non-aromatic hydrogen), and 7.9 (8H, m, aromatic H's); ^{13}C nmr ($CDCl_3$) δ: 124.0 (C-4, C-7), 136.1 (C-5, C-6), 137.4 (C-2), 140.7 (C-3a, C-7a), and 181.7 (C-1, C-3); *m/e*: 303 (M^+), 275, 247, 132, 104, 76, with metastable transitions at 250.0 (303 → 275), 222.1 (275 → 247), 82.0 (132 → 104), and 55.6 (104 → 76).

Hydrindantin (4)

Ninhydrin (4.00 g, 2.24×10^{-2} mol) was reduced by ascorbic acid (2.00 g, 1.14×10^{-2} mol) in 0.5 *N* acetic acid solution following the conditions of Connell *et al.* (17). The product was collected on a coarse mesh sintered glass funnel, washed with water, and dried *in vacuo* over sulfuric acid yielding 3.08 g (1.91×10^{-2} mol, 85%) of crystalline material, λ_{max}(EtOH): 229 (ε, 80 000) and 246 (ε, 20 000) nm; ^1H nmr δ: 6.5 (2H, s, OH), and 8.00 (8H, s, aromatic H); ^{13}C nmr δ: 79.4 (C-2), 122.3 (C-4, C-7), 136.1 (C-5, C-6), 141.2 (C-3a, C-7a), and 196.3 (C-1, C-3).

Indantrione

Ninhydrin was dehydrated by overnight exposure to 125°C in a drying oven to produce the magenta-coloured crystals of indantrione (which rapidly reverted to ninhydrin upon exposure to moist air), mp 255–257°C (lit. (18) mp 254–256°C), ^1H nmr δ: 8.10 (s); ^{13}C nmr δ: 123.8 (C-4, C-7), 136.6 (C-5, C-6), 140.1 (C-3a, C-7a), 183.4 (C-1, C-3), and 187.0 (C-2).

1. S. RUHEMANN. J. Chem. Soc. **97**, 1438 (1910).
2. S. MOORE and W. H. STEIN. J. Biol. Chem. **176**, 367 (1948).
3. M. FRIEDMAN. Can. J. Chem. **45**, 2271 (1967).
4. D. J. MCCALDIN. Chem. Rev. **60**, 39 (1960).
5. M. FRIEDMAN and C. W. SIGEL. Biochemistry, **5**, 478 (1966).
6. P. J. LAMOTHE and P. G. MCCORMICK. Anal. Chem. **44**, 821 (1972).
7. P. J. LAMOTHE and P. G. MCCORMICK. Anal. Chem. **45**, 1906 (1973).
8. M. FRIEDMAN and L. D. WILLIAMS. Bioorg. Chem. **3**, 267 (1974).
9. C. B. BOTTOM, S. S. HANNA, and D. J. SIEHR. Biochem. Educ. **6**, 4 (1978).
10. S. RUHEMANN. J. Chem. Soc. **97**, 2025 (1910).
11. M. SLIMMER and J. STIEGLITZ. Am. Chem. J. **31**, 661 (1904).
12. O. PILOTY. Ann. **333**, 68 (1904).
13. F. BEILSTEIN. Ann. **107**, 176 (1858).
14. S. RUHEMANN. J. Chem. Soc. **99**, 1486 (1911).
15. S. RUHEMANN. J. Chem. Soc. **99**, 1306 (1911).
16. N. TOMINAGA. Bull. Chem. Soc. Jpn. **35**, 851 (1962).
17. G. E. CONNELL, G. H. DIXON, and C. S. HANES. Can. J. Biochem. Physiol. **33**, 416 (1955).
18. M. REGITZ and H. G. ADOLPH. Z. Naturforsch. B, **23**, 1269 (1968).
19. L. F. JOHNSON and W. C. JANKOWSKI. Carbon-13 nmr spectra. John Wiley and Sons, Inc., New York. 1972. Spectra 281, 417, 368.
20. K. F. KUHLMANN, D. M. GRANT, and R. K. HARRIS. J. Chem. Phys. **52**, 3439 (1970).
21. D. H. SPACKMAN, W. H. STEIN, and S. MOORE. Anal. Chem. **30**, 1190 (1958).

Can. J. Chem. Downloaded from www.nrcresearchpress.com by 210.87.254.6 on 09/05/12
For personal use only.

The reaction of *cis*-$Ru(CO)_4(SiCl_3)_2$ with bidentate ligands

R. K. POMEROY AND K. S. WIJESEKERA
Department of Chemistry, Simon Fraser University, Burnaby, B.C., Canada V5A 1S6

Received September 7, 1979

R. K. POMEROY and K. S. WIJESEKERA. Can. J. Chem. **58**, 206 (1980).

The substitution of the equatorial carbonyl groups in *cis*-$Ru(CO)_4(SiCl_3)_2$ by a variety of bidentate ligands (L—L) to give compounds of the type $Ru(L—L)(CO)_2(SiCl_3)_2$ is described. With $Ph_2E(CH_2)_2EPh_2$ (E = P, As) it was also possible to isolate the bridging derivatives, $(Cl_3Si)_2(OC)_3Ru(L—L)Ru(CO)_3(SiCl_3)_2$. The ^{31}P nmr spectra (of the phosphorus compounds) are discussed.

R. K. POMEROY et K. S. WIJESEKERA. Can. J. Chem. **58**, 206 (1980).

On décrit la substitution des groupes carbonyles équatoriaux du $Ru(CO)_4(SiCl_3)_2$ *cis* par une variété de ligands bidendates (L—L) conduisant aux composés de type $Ru(L—L)(CO)_2(SiCl_3)_2$. Avec le $Ph_2E(CH_2)_2EPh_2$ (E = P, As) on peut aussi isoler les dérivés pontés $(Cl_3Si)_2(OC)_3Ru(L—L)Ru(CO)_3(SiCl_3)_2$. On discute des spectres rmn du ^{31}P des composés du phosphore.

[Traduit par le journal]

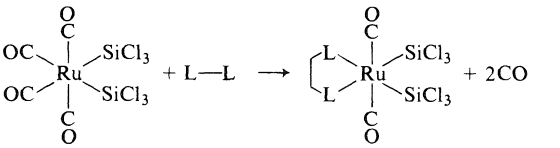
Introduction

The compound *cis*-$Ru(CO)_4(SiCl_3)_2$ is unusual in metal carbonyl chemistry in that the carbonyl ligands *trans* to the $SiCl_3$ groups undergo facile exchange with ^{13}CO at room temperature (1). The kinetics of the exchange was consistent with the reaction proceeding by a dissociative mechanism. It was expected that this compound would react with donor ligands to give the corresponding equatorially substituted derivatives. A preliminary investigation with monodentate ligands has indicated this to be the case (2). Herein we report the reaction of *cis*-$Ru(CO)_4(SiCl_3)_2$ with a variety of bidentate ligands (L—L) to give compounds of the type $Ru(L—L)(CO)_2(SiCl_3)_2$. In some cases it has also been possible to isolate the bridging derivatives, $(Cl_3Si)_2(OC)_3Ru(L—L)Ru(CO)_3(SiCl_3)_2$.

Results and Discussion

Sulfur Derivatives

The reaction of *cis*-$Ru(CO)_4(SiCl_3)_2$ with the sulfur chelates $CH_3S(CH_2)_2SCH_3$ and $R_2P(S)P(S)R_2$ (R = CH_3, C_2H_5) proceeds smoothly in solution at room temperature to give $Ru(L—L)(CO)_2(SiCl_3)_2$ derivatives (L—L = chelate ligand). These compounds, and the other $Ru(L—L)(CO)_2(SiCl_3)_2$ derivatives reported here, are white, moderately air-stable, crystalline solids which exhibit one absorption in the infrared carbonyl stretching region. The single carbonyl absorption is consistent with a *trans* arrangement of the carbonyl groups. This in turn agrees with the ^{13}CO exchange studies which indicated that only the carbonyl groups *trans* to the $SiCl_3$ ligands are labile (1). The synthesis of these derivatives may therefore be summarized in the following equation:



Although not measured accurately, the rate of substitution (except for dienes) appeared the same as that found for the CO exchange.

Substitution in metal carbonyl derivatives usually occurs *cis* to the non-carbonyl substituent (3). The unusual *trans* substitution which occurs in *cis*-$Ru(CO)_4(SiCl_3)_2$ may be attributed to the strong π-acceptor properties of the $SiCl_3$ group (1).[1]

Phosphorus Derivatives

The compounds $Ru(Ph_2P(CH_2)_nPPh_2)(CO)_2(SiCl_3)_2$ (n = 1, 2) were prepared in a similar manner to the sulfur chelates. However, unlike the sulfur compounds there was infrared evidence for the monodentate intermediates $Ru(L—L)(CO)_3(SiCl_3)_2$. These compounds could not be isolated due to their rapid conversion to $Ru(L—L)(CO)_2(SiCl_3)_2$. The intermediates (not unexpectedly) had identical carbonyl stretching frequencies to the corresponding bridged compounds $(L—L)[Ru(CO)_3(SiCl_3)_2]_2$ (*vide infra*). They were not compounds of this type, however, since the bridged derivatives do not give $Ru(L—L)(CO)_2(SiCl_3)_2$ under the same conditions.

For the case of L—L = $Ph_2P(CH_2)_2PPh_2$ it was verified that the same $Ru(L—L)(CO)_2(SiCl_3)_2$ derivative could be prepared by heating *trans*-$Ru(CO)_4(SiCl_3)_2$ with L—L in solution at 80°C. It has been found previously that *trans*-$Ru(CO)_4(SiCl_3)_2$

[1]See also ref. 3, footnote 36.

0008-4042/80/030206-04$01.00/0
©1980 National Research Council of Canada/Conseil national de recherches du Canada

Can. J. Chem. Downloaded from www.nrcresearchpress.com by 210.87.254.5 on 09/05/12
For personal use only.

TABLE 1. Analytical and infrared data for $Ru(CO)_2(L—L)(SiCl_3)_2$ compounds

L—L	Melting point (°C)	%C		%H		ν(CO), CH_2Cl_2 soln. (cm^{-1})
		Calcd.	Found	Calcd.	Found	
$(CH_3)_2P(S)P(S)(CH_3)_2$	183	11.77	12.06	1.97	2.04	2008
$(C_2H_5)_2P(S)P(S)(C_2H_5)_2$	165	17.97	18.17	3.02	2.98	2005
$CH_3S(CH_2)_2SCH_3$	204	13.14	13.45	1.84	1.86	2019
$(C_6H_5)_2P(CH_2)_2P(C_6H_5)_2$	245	40.80	40.62	2.93	3.13	2010
$(C_6H_5)_2PCH_2P(C_6H_5)_2$	243	40.02	38.70	2.74	3.01	2010
o-$C_6H_4[As(CH_3)_2]_2$	dec. > 200	20.24	20.61	2.26	2.23	2015
$(C_6H_5)_2As(CH_2)_2As(C_6H_5)_2$	dec. > 240	36.86	36.95	2.65	2.60	2008
C_7H_8[a]	160	20.86	21.30	1.57	1.61	2039
C_8H_{12}[a]	182	22.49	22.90	2.26	2.29	2030
C_8H_8[a]	150 dec.	22.66	23.20	1.52	1.50	2042
$C_{10}H_8N_2$[b]	205	24.75	25.30	1.39	1.39	2017

[a]Parent ion observed in mass spectrum.
[b]%N calcd. 4.81, found 4.85.

isomerizes to the *cis* isomer (to give an equilibrium mixture of the two forms) at 80°C (4). It is also known that the *trans* isomer does not exchange with ^{13}CO under normal conditions (1).

The dinuclear derivatives $(Cl_3Si)_2(OC)_3RuPh_2P(CH_2)_nPPh_2Ru(CO)_3(SiCl_3)_2$ (n = 1, 2) containing the phosphorus ligand in a bridging position were prepared by slowly adding a solution of the ligand dropwise to a solution containing excess *cis*-$Ru(CO)_4(SiCl_3)_2$. The identity of these compounds was established by infrared spectroscopy (which was typical of compounds of the type $RuL(CO)_3(SiCl_3)_2$ (5)), carbon and hydrogen analysis, and by the fact that they exhibit only one ^{31}P nmr resonance. The other reasonable possibility, $Ru(L—L)(CO)_3(SiCl_3)_2$, can be rejected from the analytical data and the fact that such compounds would exhibit two ^{31}P nmr resonances.

It is surprising that the reaction to form the chelate derivative:

$$Ru(L—L)(CO)_3(SiCl_3)_2 \rightarrow Ru(L—L)(CO)_2(SiCl_3)_2$$

does not occur, even though this process is known to be reasonably fast in CH_2Cl_2 solution. The formation of the bridged complex is presumed to involve combination of $Ru(L—L)(CO)_3(SiCl_3)_2$ with the five-coordinate intermediate $Ru(CO)_3(SiCl_3)_2$:

$$Ru(CO)_3(SiCl_3)_2 + (L—L)Ru(CO)_3(SiCl_3)_2 \rightarrow (L—L)[Ru(CO)_3(SiCl_3)_2]_2$$

A second order reaction between $Ru(L—L)(CO)_3(SiCl_3)_2$ and $Ru(CO)_4(SiCl_3)_2$ is thought unlikely since it would involve a seven-coordinate, 20-electron, transition species. It may be that in hexane the intermediate $Ru(L—L)(CO)_3(SiCl_3)_2$ initially precipitates from solution[2] such that its effective concentration is less than that of $Ru(CO)_3(SiCl_3)_2$ which is relatively high due to the large excess of $Ru(CO)_4(SiCl_3)_2$ employed. Under these conditions the formation of the bridged derivative would be the preferred reaction. Some support for this explanation is the observation that the bridged compound could not be prepared in CH_2Cl_2 solution in which the compounds are more soluble.

The ^{31}P nmr spectral data of these and the other phosphorus-containing derivatives are reported in Table 3. It has been observed previously that there is a large downfield shift of the ^{31}P signal on forming a chelate ring (6). This is also observed in the present molecules. From a comparison of the bridged with the chelate derivatives it is possible to say that in these compounds approximately half the downfield shift may be accounted for as due to coordination of the phosphorus to the transition metal and the other half of the shift as due to formation of the chelate ring.

Arsenic Derivatives

The preparation (in excellent yield) of $Ru(C_6H_4[As(CH_3)_2]_2)(CO)_2(SiCl_3)_2$ was similar to the preparation of the sulfur chelate derivatives. There was infrared evidence for the intermediate $Ru(C_6H_4[As(CH_3)_2]_2)(CO)_3(SiCl_3)_2$, but it could not be isolated. However, the reaction at room temperature (in CH_2Cl_2) of $Ph_2As(CH_2)_2AsPh_2$(As—As) with *cis*-$Ru(CO)_4(SiCl_3)_2$ in a 1:1 mole ratio gave approximately a 1:1 mixture of $Ru(As—As)(CO)_2(SiCl_3)_2$ and the bridged derivative $(Cl_3Si)_2(OC)_3Ru(As—As)Ru(CO)_3(SiCl_3)_2$. This mixture remained almost unchanged on stirring for a further four days. The pure mononuclear compound could be obtained at 80°C whereas the pure dinuclear compound could be prepared by reacting the arsine ligand

[2]Compounds such as $Ru(PPh_2Me)(CO)_3(SiCl_3)_2$ are insoluble in hexane (5).

Can. J. Chem. Downloaded from www.nrcresearchpress.com by 210.87.254.5 on 09/05/12
For personal use only.

TABLE 2. Analytical and infrared data for (L—L)[$Ru(CO)_3(SiCl_3)_2]_2$ compounds

L—L	%C Calcd.	%C Found	%H Calcd.	%H Found	ν(CO), CH_2Cl_2 soln. (cm^{-1})
$(C_6H_5)_2P(CH_2)_2P(C_6H_5)_2$	29.42	29.90	1.85	1.93	2117 m, 2075 s, 2049 vs
$(C_6H_5)_2PCH_2P(C_6H_5)_2$	28.81	29.13	1.72	2.25	2116 m, 2075 s, 2049 vs
$(C_6H_5)_2As(CH_2)_2As(C_6H_5)_2$	27.56	28.22	1.74	1.68	2117 m, 2072 s, 2049 vs

with a large excess of *cis*-$Ru(CO)_4(SiCl_3)_2$ in solution at room temperature.

Diene Derivatives

The reaction of the dienes, norbornadiene and cyclooctadiene, with *cis*-$Ru(CO)_4(SiCl_3)_2$ to give Ru(diene)$(CO)_2(SiCl_3)_2$ takes up to four days to go to completion even when the diene is used as a solvent. This is considerably longer than the preparation of the other derivatives reported here. There is no evidence for a monosubstituted derivative during the reaction which suggests that it is the initial attack on the presumed intermediate, $Ru(CO)_3(SiCl_3)_2$, which is the rate-determining step. It is probable that there is competition for the intermediate by the diene and the carbon monoxide produced from the reaction. In support of this suggestion is the fact that the reaction proceeds at the normal rate when the carbon monoxide is removed by continuously passing a slow stream of nitrogen over the stirred reaction solution.

Diene could not be displaced from Ru(diene)$(CO)_2(SiCl_3)_2$ by passing carbon monoxide through a solution of the appropriate compound. In contrast cyclooctatetraene (COT) was displaced from Ru(COT)$(CO)_2(SiCl_3)_2$ on treatment (in solution) with carbon monoxide. The much lower yield of the cyclooctatetraene derivative suggests it is less stable than the diene derivatives.

In the solid state the compounds are reasonably air-stable crystals which can be sublimed under vacuum at elevated temperatures. The mass spectra of these molecules exhibit a weak parent ion and a stronger set of peaks due to $[P—Cl]^+$. This behaviour is frequently observed in this type of compound (7). Similar to other molecules reported here the diene derivatives exhibit one strong carbonyl stretch in the infrared spectrum. However, Ru(norbornadiene)$(CO)_2(SiCl_3)_2$ did show (in hexane solution) two additional, very weak absorptions to higher frequency of the main CO stretching peak. These bands remained unchanged on recrystallization and sublimation. It is possible that these minor peaks are due to trace amounts of the isomer having one of the alkene linkages coordinated in the axial position.

TABLE 3. Phosphorus nuclear magnetic resonance data for new complexes

Compound	δ (ppm)	Δ_{cs} (ppm)[a]
$Ru(Ph_2P(CH_2)_2PPh_2)(CO)_2(SiCl_3)_2$	−48.1	−60.95
$Ru(Ph_2PCH_2PPh_2)(CO)_2(SiCl_3)_2$	−48.4	−61.5
$Ph_2P(CH_2)_2PPh_2[Ru(CO)_3(SiCl_3)_2]_2$	−15.3	−28.15
$Ph_2PCH_2PPh_2[Ru(CO)_3(SiCl_3)_2]_2$	−15.4	−28.7
$Ru[(C_2H_5)_2P(S)P(S)(C_2H_5)_2](CO)_2(SiCl_3)_2$[b]	−67.2	−16.3

[a]Δ_{cs} is the coordination chemical shift defined as (δ complex − δ ligand), where δ complex and δ ligand are the chemical shifts of the complexed and free ligand, respectively.
[b]Coordination of the ligand is through sulfur.

Experimental

Unless otherwise stated reactions were carried out under a nitrogen atmosphere. As a further precaution some of the reactions were carried out in a dry box (Vacuum Atmospheres). Solvents were meticulously dried and stored under nitrogen before use. Melting points were measured in sealed capillaries using a Gallenkamp apparatus; they are uncorrected. Infrared spectra were recorded on a Perkin-Elmer 237 spectrometer fitted with an external recorder. The spectra were calibrated using carbon monoxide. Proton nuclear magnetic resonance spectra were obtained on a Varian A56/60 or XL100 spectrometer using $CDCl_3$ as solvent and TMS as internal standard (δ = 0) unless otherwise stated. Phosphorus nmr spectra were obtained on the latter instrument (operating in the Fourier transform mode) using CH_2Cl_2 as solvent and H_3PO_4 (85%) as an external reference (δ = 0, downfield negative). Mass spectra were obtained on a Hitachi/Perkin-Elmer RMU-6E double focusing mass spectrometer using an ionization voltage of 80 eV. Microanalyses were performed by M. K Yang of the microanalytical laboratory of Simon Fraser University. Dodecacarbonyltriruthenium was prepared according to the literature (8). Ligands were commercially available and were used without further purification.

Preparation of cis-*Ru(CO)$_4$(SiCl$_3$)$_2$*

A quartz tube (30 cm × 3 cm, fitted with a Teflon valve) containing $Ru_3(CO)_{12}$ (0.64 g, 1.0 mmol) and Cl_3SiH (3 mL, 30 mmol) in hexane (20 mL) was evacuated and pressurized with carbon monoxide (2 atm). The stirred solution was irradiated for 3 days at a distance of 3 cm by a 200 W mercury arc lamp (contained in a quartz, water-cooled jacket). The colorless solution was then transferred to a Schlenk tube and cooled for 2 h at −78°C. The hexane and excess Cl_3SiH were then removed from the white, crystalline *cis*-$Ru(CO)_4(SiCl_3)_2$ (1.37 g, 95%) which was dried on the vacuum line. The compound at this stage is sufficiently pure for most purposes, however it may be further purified by sublimation at 40°C, 0.02 Torr onto a probe cooled to −78°C.

Preparation of Ru(CH$_3$S(CH$_2$)$_2$SCH$_3$)(CO)$_2$(SiCl$_3$)$_2$ and Related Derivatives

A solution of *cis*-$Ru(CO)_4(SiCl_3)_2$ (0.24 g, 0.5 mmol) and

Can. J. Chem. Downloaded from www.nrcresearchpress.com by 210.87.254.5 on 09/05/12
For personal use only.

Can. J. Chem. Downloaded from www.nrcresearchpress.com by 210.87.254.5 on 09/05/12
For personal use only.

dithiahexane (0.07 g, 0.6 mmol) in *n*-hexane (15 mL) was stirred at room temperature for 6 h. The solvent was then removed from the white solid which was washed (hexane) and dried under vacuum. The product $Ru(CH_3SCH_2CH_2SCH_3)(CO)_2(SiCl_3)_2$ (0.22 g, 80%) was analytically pure as obtained. Proton nmr δ: 2.60 (CH_2), 2.90 (CH_3) ppm. The corresponding $R_2P(S)P(S)R_2$ (R = CH_3, C_2H_5) derivatives were similarly prepared (85% and 90% yields, respectively). There was no spectroscopic evidence for the monocoordinated intermediate during these reactions.

Preparation of $Ru(Ph_2PCH_2CH_2PPh_2)(CO)_2(SiCl_3)_2$

A solution of *cis*-$Ru(CO)_4(SiCl_3)_2$ (0.273 g, 0.566 mmol) and $Ph_2PCH_2CH_2PPh_2$ (0.225 g, 0.565 mmol) in benzene (15 mL) was stirred overnight at 50°C. Hexane (15 mL) was then added and the solution placed in the refrigerator to complete precipitation. Solvent was removed from the white product which was further washed with *n*-hexane and dried on the vacuum line. The yield of $Ru(Ph_2PCH_2CH_2PPh_2)(CO)_2(SiCl_3)_2$ (0.460 g) was essentially quantitative. The analytical sample was obtained as fine white needles by recrystallization from benzene. The compound $Ru(Ph_2PCH_2PPh_2)(CO)_2(SiCl_3)_2$ was similarly prepared.

It was subsequently found that these reactions could be conveniently carried out at room temperature with reaction times of approximately 8 h. In these reactions there was infrared evidence for the monosubstituted derivatives $Ru(L—L)(CO)_3(SiCl_3)_2$ but the bands thought to be due to these compounds were never very intense and as the reaction progressed they weakened with a corresponding increase in the intensity of the band due to the dicarbonyl derivative.

It was also found that $Ru(Ph_2P(CH_2)_2PPh_2)(CO)_2(SiCl_3)_2$ could be prepared by heating molar proportions of $Ph_2P(CH_2)_2PPh_2$ and *trans*-$Ru(CO)_4(SiCl_3)_2$ (1) in heptane solution at 80°C. The reaction was complete after 6 h and was essentially quantitative.

Preparation of $Ph_2P(CH_2)_2PPh_2[Ru(CO)_3(SiCl_3)_2]_2$

To a stirred solution of *cis*-$Ru(CO)_4(SiCl_3)_2$ (0.70 g, 1.45 mmol) in *n*-hexane (30 mL), was added dropwise over 8 h $Ph_2P(CH_2)_2PPh_2$ (0.25 g, 0.63 mmol) in *n*-hexane (200 mL). After the addition was complete the solution was stirred for a further two hours. The supernatant liquid was then removed from the white solid of product, $Ph_2P(CH_2)_2PPh_2[Ru(CO)_3(SiCl_3)_2]_2$, which was washed with four 10 mL portions of *n*-hexane and dried under vacuum. The yield was essentially quantitative (based on $Ph_2P(CH_2)_2PPh_2$); the compound was analytically pure as prepared. The $Ph_2PCH_2PPh_2$ analogue was prepared similarly.

Preparation of $Ru[(CH_3)_2AsC_6H_4As(CH_3)_2](CO)_2(SiCl_3)_2$

A solution of *cis*-$Ru(CO)_4(SiCl_3)_2$ (0.24 g, 0.50 mmol) and *ortho*-$(CH_3)_2AsC_6H_4As(CH_3)_2$ (0.14 g, 0.70 mmol) in CH_2Cl_2 (15 mL) was stirred at room temperature for 24 h. The solution was then filtered, *n*-hexane added (15 mL), and cooled at −78°C. The solvent was removed from the product which was washed and dried as before. The white crystals so obtained were analytically pure. The ^1H nmr spectrum showed resonances at δ 7.2–8.2 (CH) and 2.05 (CH_3) ppm.

Preparation of $Ru(Ph_2AsCH_2CH_2AsPh_2)(CO)_2(SiCl_3)_2$

A solution of *cis*-$Ru(CO)_4(SiCl_3)_2$ (0.482 g, 1 mmol) and $Ph_2AsCH_2CH_2AsPh_2$ (0.486 g, 1 mmol) in benzene was heated at 75–80°C in an evacuated sealed tube (fitted with a Teflon valve). Approximately every 12 h the tube was cooled and reevacuated. After four days the tube was cooled and worked up in a similar manner to the derivatives of the phosphorus chelates. The yield was essentially quantitative.

When the reaction was carried out in CH_2Cl_2 solution at room temperature an infrared spectrum after 18 h showed approximately equal amounts of $Ru(Ph_2AsCH_2CH_2AsPh_2)(CO)_2(SiCl_3)_2$ and $(Ph_2AsCH_2CH_2AsPh_2)[Ru(CO)_3(SiCl_3)_2]_2$. A spectrum of the solution after it had been stirred for a further three days was virtually unchanged.

Preparation of $Ph_2As(CH_2)_2AsPh_2[Ru(CO)_3(SiCl_3)_2]_2$

A solution containing *cis*-$Ru(CO)_4(SiCl_3)_2$ (0.150 g, 0.31 mmol) and $Ph_2As(CH_2)_2AsPh_2$ (0.050 g, 0.10 mmol) in *n*-hexane (15 mL) was stirred overnight. The white precipitate of $Ph_2As(CH_2)_2AsPh_2[Ru(CO)_3(SiCl_3)_2]_2$ (0.12 g, 85%) was separated from the mother liquor, washed with *n*-hexane (five 10 mL portions), and dried on the vacuum line. The analytical sample was obtained by recrystallization from CH_2Cl_2/*n*-hexane.

Preparation of $Ru(C_8H_{12})(CO)_2(SiCl_3)_2$

A solution of *cis*-$Ru(CO)_4(SiCl_3)_2$ (0.482 g, 1 mmol) in cyclooctadiene (5 mL) was stirred at room temperature for four days. After this time *n*-hexane (10 mL) was added and the resulting solution stored in the refrigerator to complete precipitation. Excess diene and *n*-hexane was removed from the white crystalline product which was washed with further *n*-hexane and dried on the vacuum line. The yield of $Ru(C_8H_{12})(CO)_2(SiCl_3)_2$ was 80%, and appeared pure by infrared spectrum. The analytical sample was obtained by recrystallization from CH_2Cl_2/*n*-hexane; ^1H nmr δ: 2.55 and 5.35 ppm (ratio 2:1). The norbornadiene analogue was prepared similarly (75% yield) as was the cyclooctatetraene derivative $(Ru(C_8H_8)(CO)_2(SiCl_3)_2)$. However, in the latter case the initial compound was brown and was purified by stirring with decolorizing charcoal. The ^1H nmr of this compound showed two singlets at 6.05 and 6.50 ppm.

The compounds appeared stable in air for short periods, the norbornadiene derivative sublimes at 110°C (0.02 Torr). When carbon monoxide was bubbled through a solution of $Ru(C_8H_8)(CO)_2(SiCl_3)_2$ in CH_2Cl_2 it reverted to *cis*-$Ru(CO)_4(SiCl_3)_2$ over 18 h.

Preparation of $Ru[2,2'\text{-}(C_5H_4N)_2](CO)_2(SiCl_3)_2$

The preparation of this compound was essentially that given for the dithiahexane derivative. The compound was very air sensitive and decomposed rapidly in solution, preventing adequate study.

Acknowledgements

We wish to thank the following for financial support: the President's Research Fund (Simon Fraser University), Research Corporation (New York), and the Natural Sciences and Engineering Research Council of Canada.

1. R. K. POMEROY, R. S. GAY, G. O. EVANS, and W. A. G. GRAHAM. J. Am. Chem. Soc. **94**, 272 (1972).
2. R. K. POMEROY. J. Organometal. Chem. **177**, C27 (1979).
3. J. D. ATWOOD and T. L. BROWN. J. Am. Chem. Soc. **98**, 3160 (1976).
4. R. K. POMEROY and W. A. G. GRAHAM. J. Am. Chem. Soc. **94**, 274 (1972).
5. R. K. POMEROY and K. WIJESEKERA. Inorg. Chem. Submitted for publication.
6. J. A. CONNOR, J. P. DAY, E. M. JONES, and G. K. MCEWEN. J. Chem. Soc. Dalton Trans. 347 (1973); S. O. GRIM, J. DELGAUDIO, R. P. MOLENDA, C. A. TOLMAN, and J. P. JESSON. J. Am. Chem. Soc. **96**, 3416 (1974); S. O. GRIM, W. L. BRIGGS, R. C. BARTH, C. A. TOLMAN, and J. P. JESSON. Inorg. Chem. **13**, 1095 (1974).
7. R. K. POMEROY and W. A. G. GRAHAM. Can. J. Chem. **53**, 2985 (1975).
8. A. MANTOVANI and S. CENINI. Inorg. Synth. **16**, 47 (1976).

Thermal rearrangement of 5,6,6-triphenylbicyclo[3.1.0]hex-2-ene to 6,7-benzo-1,5-diphenyltricyclo[3.2.1.$0^{2,8}$]octane

STEFAN WEIGL[1] AND JOHN WARKENTIN[2]

Department of Chemistry, McMaster University, Hamilton, Ont., Canada L8S 4M1

Received September 13, 1979

STEFAN WEIGL and JOHN WARKENTIN. Can. J. Chem. **58**, 210 (1980).

The triphenyl vinylcyclopropane system, 5,6,6-triphenylbicyclo[3.1.0]hex-2-ene, **1**, undergoes clean thermal rearrangement, at 210°C, to 6,7-benzo-1,4-diphenyltricyclo[3.2.1.$0^{2,8}$]octane, **9**. This result indicates that **1** behaves like a phenylcyclopropane and not like a vinylcyclopropane in the thermal ring opening. The proposed mechanism involves initial formation of a 1,3-diradical, one site of which is benzyl as well as homoallyl and the other site of which is both benzhydryl and homoallyl. Subsequent steps involve coupling of the radical sites through one of the phenyl groups and a suprafacial 1,5-hydrogen shift concerted with generation of a new cyclopropane ring.

The ^{1}Hmr and ^{13}Cmr spectra of **9** are reported and discussed in terms of the shielding properties of cyclopropane and benzene rings.

STEFAN WEIGL et JOHN WARKENTIN. Can. J. Chem. **58**, 210 (1980).

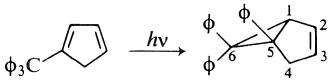
Le système triphényle vinylcyclopropane, triphényl-5,6,6 bicyclo[3.1.0]hexène-2 (**1**), se transpose thermiquement de façon très nette à 210°C en benzo-6,7 diphényl-1,4 bicyclo[3.2.1.$0^{2,8}$]octane (**9**). Ce résultat indique que ce système lors de l'ouverture thermique du cycle se comporte comme un phénylcyclopropane et non comme un vinylcyclopropane. Le mécanisme proposé fait intervenir la formation initiale d'un diradical-1,3 dont un site comporte le groupe benzyle aussi bien que le groupe homoallyle et dont l'autre contient les deux groupes benzhydryle et homoallyle. Les étapes subséquentes impliquent le couplage des sites du radical à travers l'un des groupes phényle et une transposition 1,5 suprafaciale concertée d'hydrogène avec formation d'un nouveau cycle cyclopropane.

On rapporte des spectres rmn du ^{1}H et du ^{13}C et on les discute en fonction des propriétés de blindage des cycles cyclopropane et benzène.

[Traduit par le journal]

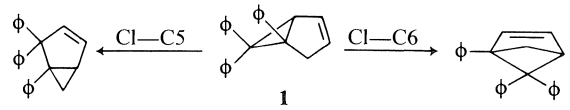
Introduction

Recently we reported (1) a convenient synthesis of 5,6,6-triphenylbicyclo[3.1.0]hex-2-ene, **1**, based on the photochemical di-π-methane rearrangement of 1-triphenylmethylcyclopentadiene (eq. [1]).

[1] 

1

That product has several structural features which were expected to make it thermally unstable. First, as a vinylcyclopropane system, it has the potential to rearrange in the vinylcyclopropane-to-cyclopentene sense.[3] In the present case the possible products would include a bicyclo[2.1.1]hexene from C1—C6 bond breaking and a new bicyclo[3.1.0]hex-2-ene (eq. [2]), from C1—C5 bond breaking. In addition to rearrangements from the vinylcyclopropane moiety, **1** might also be expected to undergo the thermolysis chemistry of phenylated cyclopropanes.[3] Thus, homolytic breaking of the C5—C6 bond of **1** would relieve ring strain and non-bonded interactions while leading to a relatively stabilized benzyl and benzhydryl diradical. Both of the radical sites of the latter would also be homoallylic.

[2] 

1

For each of the three ways of opening the cyclopropane ring one can envision a number of subsequent steps, including phenyl migration, aromatic substitution, and reclosure to new ring systems such as those of eq. [2]. The doubly homoallylic diradical referred to above is also capable, in principle at least, of rearrangement through cyclopropylcarbinyl radical intermediates (16).

In this paper we report the thermal rearrangement of **1** to **9**. The ^{1}Hmr and ^{13}Cmr spectra of **9** are reported and some unusual features of the former are discussed.[4,5]

[1]Present address: R & D Division, 3M Canada Ltd., P.O. Box 5757, London, Ont. N6A 4T1.

[2]Author to whom correspondence should be addressed.

[3]Thermal reactions involving ring opening of cyclopropane and substituted cyclopropanes (vinyl and aryl substituents in particular) have been studied extensively as well as intensively and it is not appropriate to review the subject here. Recent reviews and selected recent papers can be found in refs. 2–7 and 8–15 respectively.

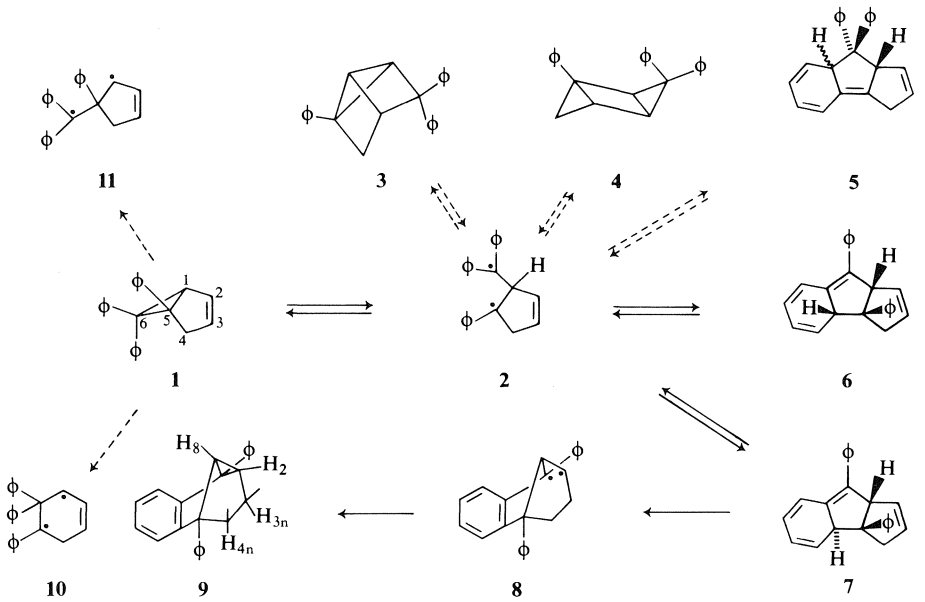
[4]The structure of **9** was determined by X-ray crystallography and the nmr spectra were assigned on the basis of that structure.

[5]R. Faggiani, P. Boldrini, and J. Warkentin. Manuscript in preparation.

0008-4042/80/030210-04$01.00/0

©1980 National Research Council of Canada/Conseil national de recherches du Canada

Can. J. Chem. Downloaded from www.nrcresearchpress.com by 210.87.254.5 on 09/05/12
For personal use only.



SCHEME 1

Discussion

In view of the large number of precedented thermal rearrangement pathways available to **1** (see above) it was surprising to find that only one product, **9**, is actually obtained. In the following paragraphs a mechanism for the formation of **9** is proposed and possible reasons for the failure of reasonable alternative pathways are discussed briefly.

A rationale for the rearrangement of **1** to **9** is depicted in Scheme 1, where full arrows are used to designate reactions that are part of the proposed mechanism and where dashed arrows show intermediates and products from potential competitive processes that were not realized. We discuss the main features (full arrows) of the scheme first and return later to examine its peripheral features.

The first step in the proposed mechanism is to cleave the C5—C6 bond of **1**, converting it to diradical **2** in which both free radical sites are delocalized. Of the options available to the latter, intramolecular radical coupling to the geometric isomers **6** and **7** is favoured. This coupling involves bond formation between the benzyl carbon and an *ortho* carbon of a phenyl ring of the benzhydryl group. Isomer **7** is geometrically suited for a suprafacial 1,5 hydrogen transfer, concerted with ring formation,[6] leading to the observed product, **9**, in which H3n was originally an *ortho* benzenoid hydrogen. Structure **8** is included only to aid with visualization of the **7**–**9** rearrangement; it would be an intermediate if H-migration were a discrete step preceding formation of the C1—C2 bond of **9**.

Compound **6** is the wrong stereoisomer for a concerted process analogous to that leading from **7** to **9**. To accommodate the clean formation of **9** we must either postulate that **6** is formed in trace amounts only or that it too finds a path to **9**. There is no good reason to expect a highly preferred sense of ring closure (**7** favoured greatly over **6**) from a radical coupling reaction, which must have a small activation energy. Therefore we suggest the alternative explanation, that **6** is formed and that it reverts to **2** under the conditions of the reaction.

Turning now to the alternative pathways leading from **1**, it is clear that the thermochemically most favoured intermediate, other than **2**, is diradical **11**. The main difference between **2** and **11** is the difference between benzyl and allyl radical stabilization. Its magnitude can be estimated from the C—H bond dissociation energies of toluene and propene (17) and works out to about 4 kcal mol^{-1}; the bond in toluene being the weaker. The uncertainty of that number (ca. ± 2 kcal mol^{-1}) together with the knowledge that only a part of it would be manifest at the transition states leading to **2** and **11**, made prediction of the direction of the ring opening quite risky. Although we had expected products from **11**, such as the diene resulting from phenyl migration, none were found. This result suggests that **11** was

[6]The rearrangement of **7** to **9** may also be viewed as a retro-"ene" reaction.

Can. J. Chem. Downloaded from www.nrcresearchpress.com by 210.87.254.5 on 09/05/12
For personal use only.

Can. J. Chem. Downloaded from www.nrcresearchpress.com by 210.87.254.5 on 09/05/12
For personal use only.

not formed, possibly because there really is a significant thermochemical advantage from benzylic, rather than allylic, resonance (see above) and/or because there is greater relief of non-bonded interactions among phenyl groups at the transition state leading to **2**.

Ring opening of **1** to form **10** has precedents from both vinylcyclopropane and phenylcyclopropane chemistry.[3] In the present case it could be excluded from serious consideration, however, because **1** is also a *gem* diphenylcyclopropane. It would have been surprising if benzhydryl radical stabilization had been insufficient to make either C5—C6 or C1—C6 bond homolysis the pathway of lowest activation energy.

There are at least five alternative pathways that **2** might follow instead of the proposed closures to **6** and **7**. Those routes (Scheme 1) lead to **3**, **4** (two isomers), and **5** (two isomers). Compounds **3** and **4** may be viewed as products derived, formally, from initial homoallyl-to-cyclopropylcarbinyl rearrangement of the benzyl site of **2**. Since that site is homoallylic in two senses, the rearrangement could involve either end of the double bond. The diradicals resulting from those formal rearrangements might then ring close to **3** and **4**.[7] In the present case there is no evidence for those processes, possibly because of the adverse thermochemistry associated with making both cyclobutane and cyclopropane rings. We point out the potential for forming **3** and **4** because it may be feasible to prepare those ring systems from starting materials of type **1**, possibly by blocking aromatic substitution with *ortho* substituents or by favouring homoallyl–cyclopropylcarbinyl rearrangement with other substituent changes.[8]

Compounds **5** would result from coupling of the benzhydryl radical site with an *ortho* carbon of the benzyl radical site. One isomer of **5** should be capable of the type of rearrangement shown by **7**. Since **9** was the only product detected, it seems reasonable to assume that **2** does not cyclize to either of the isomers **5** rather than that the expected 1,5 hydrogen shift fails for some unknown reason. Although cyclization to **5**, like the corresponding paths to **6** and **7**, is a radical coupling reaction, there are two features of **5** which suggest that there ought to be a significantly higher barrier to it than to **6** or **7**. First, **5** is a conjugated triene without further conjugation whereas **6** and **7** are phenyl-conjugated trienes. Second, **5** is a more crowded species than either **6** or **7**. If these features together contribute to an enhancement of E_a for formation of **5**,[9] amounting to only 3 kcal mol^{-1}, then about 4% of **2** would leak into **5** and as much as half of that might return to **2** by virtue of being the wrong isomer for sigmatropic rearrangement. Thus, the absence of readily detectable amounts of products from **5** can be accounted for, since barriers to ring closure of diradicals can vary by more than 5 kcal mol^{-1} with changes in substituents.[10]

TABLE 1. Nuclear magnetic resonance spectra of **9**[a–d]

Nucleus	Chemical shift (δ)	Coupling constants (Hz)
H3n	1.27	$J_{3n,3x} = -13.2$; $J_{3n,4x} = 11.2$
H3x	2.09	$J_{3x,2} = 7.1$; $J_{3x,4n} = 0.0$
H4n	2.12	$J_{4n,4x} = -9.5$; $J_{4n,3n} = 6.0$
H2	2.55	$J_{2,3n} = 2.0$
H4x	2.67	$J_{4x,3x} = 10.4$
H8	3.01	$J_{8,2} = 7.4$
C3	23.47	
C2	35.01	
C4	47.53	
C1	47.98	
C8	52.63	
C5	62.87	

[a] ^{1}Hmr spectrum at 220 MHz; ^{13}Cmr spectrum at 90 MHz; both with $CDCl_3$ and TMS reference.
[b] Spectral simulation of the ^{1}Hmr spectrum using the above chemical shifts and coupling constants gave an RMS error of < 0.5 Hz.
[c] Assignment of the ^{13}Cmr spectrum is based on the chemical shifts (see text) and on the degree of substitution inferred from the multiplicity of signals in a spectrum taken with partial decoupling ^{13}C from ^{1}H.
[d] The benzenoid carbon resonances have not been assigned but they are listed below. The first 10 signals are for H-bearing carbons and signals followed by (2) indicate two equivalent carbons. The last 4 signals are those of fully-substituted sp^2 carbons. ^{13}Cmr(aromatic): 122.76, 123.89, 126.20, 126.30, 126.66, 126.75, 127.73(2), 128.31(2), 128.51(2), 129.94(2), 141.70, 144.70, 145.15, 151.40.

In summary, the above analysis suggests that some of the potential reactions of **1**, and also **2**, may be nearly isoenergetic. Thus the rearrangement **1** → **9** is not only of interest for itself but also for the potential use of suitably substituted bicyclo[3.1.0]-hex-2-enes as precursors of other polycyclic compounds. Moreover, it seems likely that intermediates like **6** and **7** could be trapped with some dienophiles.

The ^{1}Hmr and ^{13}Cmr spectra of **9** (Table 1) deserve brief comment. The most striking feature of the ^{1}Hmr spectrum is the chemical shift of cyclopropyl hydrogen H8 (3.01 δ). Cyclopropane itself absorbs at 0.22 δ (18) and tertiary cyclopropyl hydrogens do not normally give signals below 1.0 δ in the absence of an electron-withdrawing α-substituent. Examination of a model of **9** suggests that the two phenyl groups have to avoid coplanarity (approximate) with the benzo function. Con-

[7] This description is intended as an aid to visualization of the relationships between **2** and **3** or **4** rather than as a description of a likely mechanism.

[8] A milder method (e.g., photochemical) for generating intermediates of type **2** might also be necessary, in order to preserve products like **3** and **4**.

[9] Relative to the E_a value for formation of **7**. This calculation involves the reasonable assumption that the pre-exponential factors for closure of **2** to **5** and **7** are not significantly different.

[10] For 1,3-diradicals (5).

formations that minimize non-bonded interactions between the benzo group and the phenyl ring at C1 leave H8 and H2 in the deshielding zone of that ring. Similarly, the phenyl ring at C5 deshields H8 also, as well as H4x. Thus, H8 is twice deshielded as a result of steric hindrance to rotation of the phenyl groups. On the other hand, H3n is shielded because it lies over the π-system of the benzo ring and the signal from it appears at the highest field in spite of a small deshielding effect exerted on it by the cyclopropane ring.[11]

The ^{13}Cmr shifts for the nonbenzenoid carbons of **9** show features analogous to those in the ^{1}Hmr spectrum. Thus, of the two secondary carbons, C3 is upfield from C4 and, of the two tertiary carbons, C8 is downfield from C2. The signals from the two quaternary carbons were assigned on the basis of the shielding shown by cyclopropane carbons (C1 > C5) (20).

Experimental

A solution of 5,6,6-triphenylbicyclo[3.1.0]hex-2-ene (**1**, 140.2 mg, 4.55×10^{-4} mol, mp 108–109°C) in 13 mL of spectro-quality cyclohexane was degassed and sealed into a thick-walled glass tube. The latter was heated at 210 ± 10°C in a steel pressure bomb for 46 h. The tube was cooled and opened, and the cyclohexane was evaporated with a rotary evaporator. A ^{1}Hmr spectrum (high gain) of the solid residue was indistinguishable from the corresponding spectrum of **9** that was subsequently recrystallized from benzene; yield estimated on the basis of nmr detection limit ≥ 95%.

Recrystallized **9** had mp 170°C; uv (cyclohexane) λ_{max} (log ε_{max}): 230 plateau (4.29), 259 (3.00), 262 (3.01), 264 (3.01), 269 (2.97), 280 (2.87); ir (μ, CCl_4, strong and medium bands listed): 3.24 m, 3.27 s, 3.30 s, 3.40 s, 3.42 s, 3.45 m, 3.49 m, 3.51 m, 6.27 m, 6.71 m, 6.80 m, 6.89 m, 6.93 s, 9.74 m, 9.86 m, 11.74 m, 12.84 m, 13.40 s, 13.87 m, 14.49 s, 14.81 m; ms *m/e*: 308; *Mol.Wt.* calcd. for $C_{24}H_{20}$: 308; found (osmometric): 307. *Anal.* calcd. for $C_{24}H_{20}$: C 93.46, H 6.54; found: C 93.53, H 6.67.

The ^{1}Hmr and ^{13}Cmr spectra of **9** are listed in Table 1.

[11] *cis*-Cyclopropylcarbinyl hydrogens in bicyclo[3.1.0]hexanes are deshielded by about 0.11 δ whereas corresponding *trans*-hydrogens are slightly shielded (0.07 δ) (19).

Acknowledgements

This work was supported by the National Research Council of Canada. We are grateful to Dr. Arthur Grey for the 220 MHz spectrum of **9** and to Mr. Brian Sayer for the simulation of that spectrum.

1. S. WEIGL and J. WARKENTIN. Can. J. Chem. **55**, 29 (1977).
2. H. M. FREY. Adv. Phys. Org. Chem. **4**, 147 (1966).
3. M. R. WILCOTT, R. L. CARGILL, and A. B. SEARS. Prog. Phys. Org. Chem. **4**, 147 (1966).
4. H. M. FREY and R. WALSH. Chem. Rev. **69**, 103 (1969).
5. R. G. BERGMAN. *In* Free radicals. Vol. 1. *Edited by* J. K. Kochi. Wiley, New York, NY. 1973. Chapt. 5.
6. B. HALTON. Alicyclic Chem. **5**, 60 (1976).
7. B. HALTON. Alicyclic Chem. **6**, 58 (1978).
8. J. E. BALDWIN and A. H. ANDRIST. Chem. Commun. 1561 (1970).
9. (*a*) J. E. BALDWIN and A. H. ANDRIST. J. Am. Chem. Soc. **93**, 3289 (1971); (*b*) J. Am. Chem. Soc. **93**, 4055 (1971).
10. (*a*) J. E. BALDWIN and C. ULLENIUS. J. Am. Chem. Soc. **96**, 1542 (1974); (*b*) J. E. BALDWIN and M. W. GRAYSTON. J. Am. Chem. Soc. **96**, 1629 (1974).
11. J. A. BERSON and L. D. PEDERSEN. J. Am. Chem. Soc. **97**, 238 (1975).
12. J. A. BERSON, L. D. PEDERSEN, and B. K. CARPENTER. J. Am. Chem. Soc. **97**, 240 (1975).
13. J. A. BERSON, L. PEDERSEN, and B. K. CARPENTER. J. Am. Chem. Soc. **98**, 122 (1976).
14. (*a*) G. D. ANDREWS and J. E. BALDWIN. J. Am. Chem. Soc. **98**, 6705 (1976); (*b*) J. E. BALDWIN and K. E. GILBERT. J. Am. Chem. Soc. **98**, 8283 (1976).
15. L. U. MEYER and A. DE MEIJERE. Chem. Ber. **110**, 2545 (1977).
16. A. L. J. BECKWITH and K. U. INGOLD. *In* Rearrangements in ground and excited states. *Edited by* P. de Mayo. Academic. In press.
17. H. E. O'NEAL and S. W. BENSON. *In* Free radicals. Vol. 2. *Edited by* J. K. Kochi. Wiley, New York, NY. 1973. Chapt. 17.
18. K. B. WIBERG and B. J. NIST. J. Am. Chem. Soc. **83**, 1226 (1961).
19. C. D. POULTER, R. S. BOIKESS, J. I. BRAUMAN, and S. WINSTEIN. J. Am. Chem. Soc. **94**, 2291 (1972).
20. J. J. BURKE and P. C. LAUTERBUR. J. Am. Chem. Soc. **86**, 1870 (1964).

Can. J. Chem. Downloaded from www.nrcresearchpress.com by 210.87.254.5 on 09/05/12
For personal use only.

Cell surface carbohydrates for targeting studies[1]

M. M. PONPIPOM,[2] R. L. BUGIANESI, AND T. Y. SHEN
Merck Sharp & Dohme Research Laboratories, Rahway, NJ 07065 U.S.A.

Received June 14, 1979

M. M. PONPIPOM, R. L. BUGIANESI, and T. Y. SHEN. Can. J. Chem. **58**, 214 (1980).

Syntheses of a series of glycolipids with 6-(5-cholesten-3β-yloxy)-1-thiohexane as the aglycon and the following carbohydrates as surface determinants are described: D-glucose, D-mannose, D-galactose, 2-acetamido-2-deoxy-D-glucose, 2-acetamido-2-deoxy-D-galactose, L-fucose, L-arabinose, D-xylose, *N*-acetyl-D-neuraminic acid, lactose, and cellobiose. These 6-(5-cholesten-3β-yloxy)hexyl 1-thioglycopyranosides have been incorporated into phospholipid vesicles for *in vivo* tissue distribution studies.

M. M. PONPIPOM, R. L. BUGIANESI et T. Y. SHEN. Can. J. Chem. **58**, 214 (1980).

On décrit la synthèse d'une série de glycolipides comportant le (cholesten-5 yloxy-3β)-6 thio-1 hexane comme aglycone et les carbohydrates suivants comme déterminant de surface: D-glucose, D-mannose, D-galactose, acétamido-2 déoxy-2 D-glucose, acétamido-2 déoxy-2 D-galactose, L-fucose, L-arabinose, D-xylose, acide *N*-acétyl-D-neuraminique, lactose et cellobiose. On a incorporé ces thio-1 glycopyrannosides de (cholesten-5 yloxy-3β)-6 hexyle dans les vésicules de phospholipides en vue d'en étudier *in vivo* la distribution dans les tissus.

[Traduit par le journal]

Liposomes have been used as carriers to introduce biologically active materials into cells (1–4). These lipid vesicles are formed when mixtures of phospholipid, cholesterol, and a charged amphiphile in varying molecular ratios are agitated or sonicated in an aqueous solution. Water-soluble and lipid-soluble chemotherapeutic agents can be accommodated in aqueous and lipid phases of liposomes, respectively. A wide variety of materials, e.g. enzymes (5, 6), antigens (7, 8), antibiotics (9), chelating agents (10, 11), small molecules, ions, etc., have been encapsulated in liposomes. The tissue distribution and clearance kinetics of drugs entrapped in liposomes are known to be affected by the liposome composition, particle size, and surface charge (12). Natural ligands such as aggregated immunoglobulins coated onto liposomes (4) have been used with partial success to direct vesicles to specific target organs and tissues. Saccharide determinants, such as glycolipids and glycoproteins present at the cell surface, are known to participate in intercellular recognition process. Alveolar macrophages have been shown to bind glycoproteins and synthetic glycoconjugates that have D-mannose, 2-acetamido-2-deoxy-D-glucose, or D-glucose in the exposed, nonreducing position (13). Mammalian hepatic receptors are specific for terminal D-galactose of desialylated serum glycoproteins, whereas in avian liver, the receptors recognize terminal 2-acetamido-2-deoxy-D-glucose (14). Neuraminidase-treated erythrocytes which have D-galactose as the terminal sugar are shown to be susceptible to rapid elimination and are sequestered in the liver and spleen (15). The specific binding of macrophages to MIF (migration inhibitory factor) involves the recognition of L-fucose (16). The uptake of some lysosomal enzymes by fibroblasts in culture involves recognition of D-mannose phosphate on the enzyme molecules (17). Following these and other examples, it would seem that synthetic glycolipids incorporated in liposomes may well change the *in vivo* tissue distribution and clearance kinetics of drugs. To extend a previous communication (18) from these laboratories, we report the syntheses of a series of glycolipids with 6-(5-cholesten-3β-yloxy)-1-thiohexane as the aglycon and the following carbohydrates which occur naturally in membrane oligosaccharides (19) as surface determinants: D-glucose, D-mannose (18), D-galactose (18), 2-acetamido-2-deoxy-D-glucose, 2-acetamido-2-deoxy-D-galactose, L-fucose, L-arabinose, D-xylose, and *N*-acetyl-D-neuraminic acid. Glycolipids with lactose and cellobiose as the surface determinants were also prepared for this study.

Initially, cholesteryl and stigmasteryl α-D-mannopyranosides (**3** and **5** respectively) were prepared for comparisons with 6-(5-cholesten-3β-yloxy)-hexyl 1-thio-α-D-mannopyranoside (**1**) (18) as synthetic ingredients for liposomes. In contrast to **1**, compounds **3** and **5** could not be incorporated at a concentration of 15–18% (by weight) into 1,2-dipalmitoyl-*sn*-glycero-3-phosphocholine (DPPC) liposomes by probe sonication of lipid mixtures in aqueous 0.1 *M* KCl and 10 m*M* Tris buffer at pH 8.0. This may be due to the more rigid structures of **3** and **5**. Therefore, 6-(5-cholesten-3β-yloxy)-1-thiohexane was chosen as a lipid tail for our

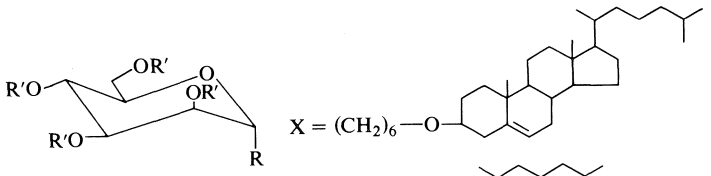
[1]Presented in part at the 178th Meeting of the American Chemical Society, Washington, D.C., September 9–14, 1979.

[2]Author to whom correspondence may be addressed.

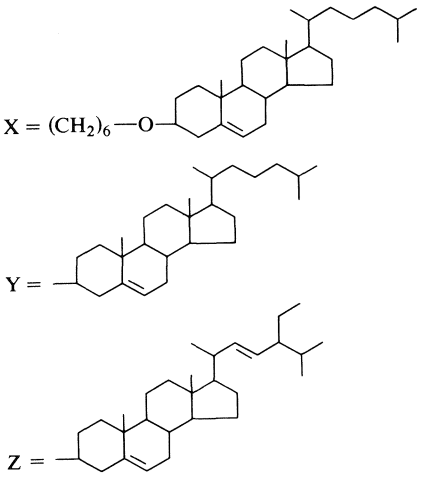
0008-4042/80/030214-07$01.00/0

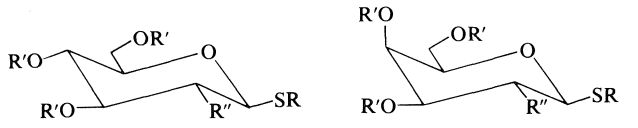
©1980 National Research Council of Canada/Conseil national de recherches du Canada

Can. J. Chem. Downloaded from www.nrcresearchpress.com by 210.87.254.105 on 09/05/12
For personal use only.



1 R = SX, R′ = H
2 R = OY, R′ = Ac
3 R = OY, R′ = H
4 R = OZ, R′ = Ac
5 R = OZ, R′ = H





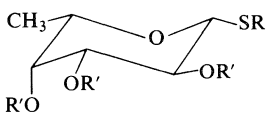
6 R = H, R′ = Ac, R″ = OAc
7 R = X, R′ = Ac, R″ = OAc
8 R = X, R′ = H, R″ = OH
9 R = H, R′ = Ac, R″ = NHAc
10 R = X, R′ = Ac, R″ = NHAc
11 R = X, R′ = H, R″ = NHAc
12 R = X, R′ = H, R″ = OH
13 R = H, R′ = Ac, R″ = NHAc
14 R = X, R′ = Ac, R″ = NHAc
15 R = X, R′ = H, R″ = NHAc

systematic studies on the effects of external carbohydrate determinants on liposome distribution. Thioglycosidic linkage was used because it is more stable towards acid and enzymatic hydrolysis than *O*-glycosides (20, 21). These thioglycosides were prepared from 6-(5-cholesten-3β-yloxy)hexyl iodide (**32**) (18) and per-*O*-acetyl-1-thioglycopyranoses in dichloromethane containing triethylamine (18) or better in tetrahydrofuran using 1,5-diazabicyclo[5.4.0]undec-5-ene (DBU) as a base. The coupling reactions were more rapid in the presence of DBU and usually completed within 0.5–3 h.[3] The per-*O*-acetylated analogs **7**, **10**, **14**, **17**, **20**, **23**, **37**, and **40** were synthesized by the above procedures in high yields. Trace amounts of the 1,2-*cis* isomers were also isolated in some cases. The α and β anomers can be determined in most cases, from their nmr spectra. For example, the H-1 signal of 6-(5-cholesten-3β-yloxy)hexyl 2,3,4-tri-*O*-acetyl-1-thio-α-L-arabinopyranoside (**23**) appears as a doublet at δ 4.52 ($J_{1,2}$ = 8.5 Hz) whereas in the β-L-anomer, it resonates at δ 5.64 ($J_{1,2}$ = 5.0 Hz). The chemical shifts and coupling constants of other protons are all in agreement with the assigned structures (see Experimental).

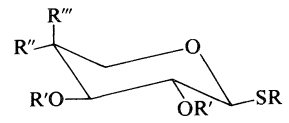
The synthesis of 5-acetamido-2-*S*-[6-(5-cholesten-3β-yloxy)hexyl]-3,5-dideoxy-2-thio-β-D-*glycero*-D-*galacto*-2-nonulopyranosonic acid (**29**) was more elusive. Difficulties were encountered in the preparation of the intermediates **26** and **27**. The reported R_f 0.58 (chloroform–methanol 92:8) for the thiouronium salt **26** was rather high in comparison with the mobility of its precursor **25** (R_f 0.67) (22). Because of our difficulties and the fact that the intermediates **26** and **27** were not well characterized (22), we decided instead to couple **25** with 6-(5-cholesten-3β-yloxy)-1-thiohexane (**34**) under various conditions (23, 24). Unfortunately, only methyl 5-acetamido-4,7,8,9-tetra-*O*-acetyl-2,3-dehydro-2,3,5-trideoxy-D-*glycero*-D-*galacto*-2-nonulopyranosonate was isolated as a major product. Recently, Ferrier and Furneaux (25) used boron trifluoride etherate to catalyse the condensation of carbohydrate peresters and thiols to provide a convenient synthesis of thioglycosides. When methyl 5-acetamido-2,4,7,8,9-penta-*O*-acetyl-3,5-dideoxy-D-*glycero*-D-*galacto*-2-nonulopyranosonate (26) and **34** were reacted in the presence of

[3]Private communication with Dr. J. V. Heck of these laboratories, who devised this procedure in connection with another study.

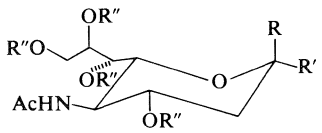
Can. J. Chem. Downloaded from www.nrcresearchpress.com by 210.87.254.105 on 09/05/12
For personal use only.



16 R = H, R′ = Ac
17 R = X, R′ = Ac
18 R = X, R′ = H



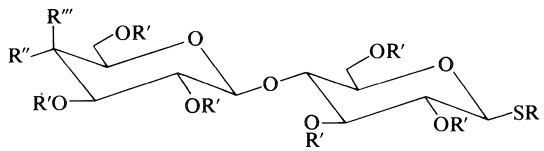
19 R = R‴ = H, R′ = Ac, R″ = OAc
20 R = X, R′ = Ac, R″ = OAc, R‴ = H
21 R = X, R′ = R‴ = H, R″ = OH
22 R = R″ = H, R′ = Ac, R‴ = OAc
23 R = X, R′ = Ac, R″ = H, R‴ = OAc
24 R = X, R′ = R″ = H, R‴ = OH



25 R = Cl, R′ = $COOCH_3$, R″ = Ac
26 R = $SC(=NH)NH_2 \cdot HCl$, R′ = $COOCH_3$, R″ = Ac
27 R = SH, R′ = $COOCH_3$, R″ = Ac
28 R = SX, R′ = $COOCH_3$, R″ = Ac
29 R = SX, R′ = COOH, R″ = H
30 R = OCH_3, R′ = $COOCH_3$, R″ = Ac
31 R = $COOCH_3$, R′ = OCH_3, R″ = Ac

R – X

32 R = I
33 R = $SC(=NH)NH_2 \cdot HI$
34 R = SH
35 R = SAc



36 R = R″ = H, R′ = Ac, R‴ = OAc
37 R = X, R′ = Ac, R″ = H, R‴ = OAc
38 R = X, R′ = R″ = H, R‴ = OH
39 R = R‴ = H, R′ = Ac, R″ = OAc
40 R = X, R′ = Ac, R″ = OAc, R‴ = H
41 R = X, R′ = R‴ = H, R″ = OH

boron trifluoride etherate, a major product was isolated and the structure was tentatively assigned as **28**. The nmr spectrum of this material has many features in common with that of methyl 5-acetamido-4,7,8,9-tetra-*O*-acetyl-3,5-dideoxy-2-*O*-methyl-β-D-*glycero*-D-*galacto*-2-nonulopyranosonate (**30**) which is quite different from the spectrum of **31** (see Tables 1 and 2). The anomeric configurations of *N*-acetyl-D-neuraminic acid analogs can generally be established from the chemical shifts of H-3e which resonate at a lower field in α anomers when compared with the corresponding β anomers (27), e.g., the H-3e of **31** is at δ 2.58 whereas that of **30** is at δ 2.45 (see Table 1). In the synthesis of **28**, a minor amount of the α anomer was also isolated as a mixture with **28** (see Experimental). The assignment of these products was verified by the chemical shifts of H-3e, i.e., δ 2.54 for **28** and δ 2.73 for the corresponding α anomer. It is noteworthy that the coupling constants ($J_{7,8}$) for **28**, **30**, and **31** are reflected by the anomeric configuration and possibly by the size of the aglycon (see Table 2). For example, $J_{7,8}$ for **31** is large (9.0 Hz) as expected for *N*-acetyl-α-D-neuraminic acid analogs (27) whereas $J_{7,8}$ for **30** and **28** are only 4.0 and 2.5 Hz, respectively. Although *N*-acetyl-D-neuraminic acid occurs almost exclusively as the α anomer in glycoproteins, glycolipids, and polysaccharides, we thought it would still be of interest to use the β-thioglycoside **29** (isolated as a major product) for our biological studies.

The deblocked 6-(5-cholesten-3β-yloxy)hexyl 1-thioglycosides have been incorporated into egg lecithin, dioleyl-(DOPC), dipalmitoyl-, and distearoylphosphatidylcholine vesicles (18, 28). Up to concentrations of 50 mol% of these synthetic glycolipids have been incorporated in DOPC multilamellar liposomes. For sonicated vesicles, the glycolipids have been incorporated up to 15 mol% in phosphatidylcholine. The average size of DOPC/glycolipid vesicles is not significantly changed by the nature of the carbohydrate deter-

Can. J. Chem. Downloaded from www.nrcresearchpress.com by 210.87.254.105 on 09/05/12
For personal use only.

TABLE 1. Proton chemical shifts for the *N*-acetyl-D-neuraminic acid analogs*

Compound	H-3e	H-4	H-5	H-6	H-7	H-8	H-9′	H-9
28	2.54	5.27	4.10	4.34	5.44	5.12	4.82	4.18
30	2.45	5.27	4.14	3.93	5.42	5.21	4.82	4.14
31	2.58	4.88	4.08	4.14	5.35	5.46	4.32	4.12

*The nmr spectra were measured at 300 MHz in $CDCl_3$ using a Varian SC300 spectrometer. Chemical shifts were expressed in ppm downfield from internal TMS. H-3e of the α anomer of **28** absorbed at 2.73 ppm.

TABLE 2. Coupling constants of the *N*-acetyl-D-neuraminic acid analogs (in Hz)

Compound	$J_{3e,4}$	$J_{4,5}$	$J_{5,6}$	$J_{6,7}$	$J_{7,8}$	$J_{8,9'}$	$J_{8,9}$	$J_{9,9'}$
28	5.0	10.5	10.5	2.5	2.5	2.5	8.0	12.5
30	5.0	10.5	10.0	2.0	4.0	2.5	7.0	12.5
31	4.5	9.5	9.5	2.0	9.0	3.0	5.5	12.5

minants. Similar observations were recently reported with other synthetic mannose-containing glycolipids (29).

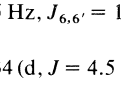
The *in vivo* tissue distribution studies of liposomes containing these synthetic glycolipids have been examined.[4] Some recognition of the carbohydrate determinants by specific organs and tissues was demonstrated. For example, liver took up injected liposomes much more readily if they contained the lactosyllipid **38** than if they contained the galactosyl analog **12** or no glycolipid, suggesting that the glucosyl moiety of the disaccharide **38** allowed better interaction of the terminal galactose with the putative cell-surface receptor. The importance of disaccharides was also demonstrated in the study of the influence of cerebrosides on the interaction of liposomes with HeLa cells (30). On the other hand, liposomes containing the sialyllipid **29** reduced the uptake of liposomes by liver. Similar observations were also reported on the tissue distribution of EDTA encapsulated within liposomes containing glycolipids (31). Details will be published elsewhere.

Experimental

Melting points were determined with a Thomas-Hoover "Unimelt" apparatus and are uncorrected. Optical rotations were measured with a Perkin-Elmer Model 241 polarimeter. Thin-layer chromatography (tlc) was performed on silica gel GF_{254} (Analtech) plates, and the spots were detected by a ceric sulfate (1%) – sulfuric acid (10%) spray. Column chromatography was conducted on silica gel 60 (70–230 mesh ASTM). Nuclear magnetic resonance spectra were recorded for solutions in chloroform-*d* (unless stated otherwise) at 60 or 300 MHz, with tetramethylsilane as the internal standard. Conventional processing consisted in drying organic solutions with anhydrous sodium sulfate, filtration, and evaporation of the filtrate under diminished pressure.

The following per-*O*-acetyl-1-thioglycopyranoses were prepared via 2-*S*-(per-*O*-acetylglycopyranosyl)-2-thiopseudourea hydrobromides according to known procedures: 2,3,4,6-Tetra-*O*-acetyl-1-thio-β-D-glucopyranose (**6**) (32); 2-acetamido-3,4,6-tri-*O*-acetyl-2-deoxy-1-thio-β-D-glucopyranose (**9**) (33, 34); 2-acetamido-3,4,6-tri-*O*-acetyl-2-deoxy-1-thio-β-D-galactopyranose (**13**), mp 188–189°C, $[\alpha]_D^{27}$ −2.5° (*c* 1.2, chloroform) (*Anal.* calcd. for $C_{14}H_{21}NSO_8$: C 46.27, H 5.83, N 3.38, S 8.83; found: C 46.55, H 5.86, N 3.68, S 8.73); 2,3,4-tri-*O*-acetyl-1-thio-β-L-fucopyranose (**16**) (35); 2,3,4-tri-*O*-acetyl-1-thio-β-D-xylopyranose (**19**) (36); 2,3,4-tri-*O*-acetyl-1-thio-α-L-arabinopyranose (**22**) (37, 38); 2,3,6-tri-*O*-acetyl-4-*O*-(2,3,4,6-tetra-*O*-acetyl-β-D-galactopyranosyl)-1-thio-β-D-glucopyranose (**36**) (39); and 2,3,6-tri-*O*-acetyl-4-*O*-(2,3,4,6-tetra-*O*-acetyl-β-D-glucopyranosyl)-1-thio-β-D-glucopyranose (**39**) (40, 41).

*Stigmasteryl 2,3,4,6-Tetra-O-acetyl-α-D-mannopyranoside (**4**)*

A solution of 2,3,4,6-tetra-*O*-acetyl-α-D-mannopyranosyl bromide (1.0 g) in dry benzene (7.5 mL) was added to a solution of stigmasterol (1.1 g) in benzene (65 mL) and nitromethane (65 mL) containing mercuric cyanide (0.7 g) and calcium sulfate (0.7 g). The mixture was stirred for 4 h at room temperature. Another batch of 2,3,4,6-tetra-*O*-acetyl-α-D-mannopyranosyl bromide (1.0 g) was added and the mixture was stirred for another 4 h. The solid was filtered and the filtrate was concentrated to a residue which was taken up in chloroform and washed successively with water, aqueous sodium hydrogencarbonate, and water. The dried solution was evaporated to an oil which was triturated with methanol to give crystals (1.85 g, two spots). The crude material was put on a column of silica gel and eluted with 3% 2-propanol in chloroform. The desired fractions were pooled and evaporated *in vacuo* to give **4** (1.3 g, 60%), mp 80–82°C, $[\alpha]_D^{27}$ +19° (*c* 1.5, chloroform); nmr (chloroform-*d*) δ: 4.95 (d, $J_{1,2}$ = 1.5 Hz, H-1), 5.19 (d, d, $J_{2,3}$ = 3.5 Hz, H-2), 5.38 (d, d, $J_{3,4}$ = 10.0 Hz, H-3), 5.25 (t, $J_{4,5}$ = 10.0 Hz, H-4), 4.24 (d, d, $J_{6,5}$ = 5.5 Hz, $J_{6,6'}$ = 12.0 Hz, H-6), 1.97, 2.02, 2.06, and 2.12 (4 OAc), 5.34 (d, *J* = 4.5 Hz, olefinic), 3.47 (m, ), 0.82 (d, *J* = 6.0 Hz, CH_3-21), 0.76, 0.78 (CH_3-26 and CH_3-27), and 0.67 (s, CH_3-18). *Anal.* calcd. for $C_{43}H_{66}O_{10}$: C 69.51, H 8.95; found: C 69.51, H 9.10.

*Stigmasteryl α-D-Mannopyranoside (**5**)*

A suspension of **4** (500 mg) in methanol was warmed until dissolution. Sodium methoxide (25 mg) was added and the solution was kept at room temperature overnight. The product

[4]With M. S. Wu and J. C. Robbins.

Can. J. Chem. Downloaded from www.nrcresearchpress.com by 210.87.254.105 on 09/05/12
For personal use only.

Can. J. Chem. Downloaded from www.nrcresearchpress.com by 210.87.254.105 on 09/05/12
For personal use only.

crystallized from the medium and was collected by filtration and washed successively with methanol, water, and ethyl ether to give **5** (300 mg), mp 220°C (dec.), $[\alpha]_D^{27}$ +26° (*c* 1.0, pyridine); nmr (dimethylsulfoxide-d_6) δ: 4.76 (H-1), 5.30 (H-6 olefinic), 4.99–5.20 (m, H-22 and H-23 olefinic), 0.99 (d, J = 6.0 Hz, CH_3-21), 0.95 (s, CH_3-19), 0.81, 0.83 (CH_3-26 and CH_3-27), 0.77 (CH_2—CH_3), 0.67 (s, CH_3-18). This material is insoluble in most organic solvents. *Anal.* calcd. for $C_{35}H_{58}O_6$: C 73.13, H 10.17; found: C 72.72, H 10.08.

Cholesteryl α-D-*Mannopyranoside* (*3*)

Cholesteryl 2,3,4,6-tetra-*O*-acetyl-α-D-mannopyranoside (**2**), mp 89–92°C, $[\alpha]_D^{27}$ +25° (*c* 1.0, chloroform) was prepared in a similar manner to **4**. Deblocking of **2** afforded **3** in a near quantitative yield, mp 213–216°C, $[\alpha]_D^{27}$ +31° (*c* 0.8, pyridine); nmr (dimethylsulfoxide-d_6) δ: 4.76 (H-1), 5.31 (olefinic), 0.94 (s, CH_3-19), 0.89 (d, J = 6.0 Hz, CH_3-21), 0.82, 0.84 (CH_3-26 and CH_3-27), 0.64 (s, CH_3-18). *Anal.* calcd. for $C_{33}H_{56}O_6$: C 72.22, H 10.29; found: C 72.24, H 10.18.

*6-(5-Cholesten-3*β*-yloxy)hexyl 1-Thioglycopyranosides*

Per-*O*-acetyl-1-thioglycopyranose (10 mmol) was reacted with **32** (18) (10 mmol) in dichloromethane (30 ml) containing triethylamine (10 mmol) under nitrogen for 1–3 days at room temperature. If DBU was used as a base in tetrahydrofuran, the condensation was usually complete within 0.5–3 h. Tetrahydrofuran was removed *in vacuo* and the residue was partitioned between dichloromethane and water. The organic layer was dried and concentrated to a syrup which was put on a column of silica gel and eluted with chloroform followed by 1–2% ethanol in chloroform. The desired fractions were combined and evaporated to give 6-(5-cholesten-3β-yloxy)hexyl per-*O*-acetyl-1-thioglycopyranoside which was deblocked either by Bio-Rad AG 1-x2 (OH) ion exchange resin in ethanol–tetrahydrofuran or by sodium methoxide in methanol. 6-(5-Cholesten-3β-yloxy)hexyl 1-thioglycopyranosides were usually isolated as crystalline materials.

*6-(5-Cholesten-3*β*-yloxy)hexyl 2,3,4-Tri-*O*-acetyl-1-thio-*α*-L-arabinopyranoside* (***23***)

This compound was prepared in 64% yield, $[\alpha]_D^{27}$ −22° (*c* 1.88, chloroform); nmr (chloroform-*d*) δ: 4.52 (d, $J_{1,2}$ = 8.5 Hz, H-1), 5.24 (t, $J_{2,3}$ = 8.5 Hz, H-2), 5.09 (d, d, $J_{3,4}$ = 3.5 Hz, H-3), 5.13 (b, H-4), 4.12 (q, $J_{5,5'}$ = 13.0 Hz, $J_{5,4}$ = 3.5 Hz, H-5), 3.68 (q, $J_{5',4}$ = 1.0 Hz, H-5′), 2.05, 2.09, and 2.14 (3 OAc), 5.36 (d, J = 4.5 Hz, olefinic), 3.46 (t, J = 6.5 Hz, C—CH_2—O— ), 3.14 (m, —O— ), 2.70 (m, —S—CH_2—C), 0.99 (s, CH_3-19), 0.91 (d, J = 6.0 Hz, CH_3-21), 0.84, 0.87 (CH_3-26 and CH_3-27), and 0.66 (s, CH_3-18). *Anal.* calcd. for $C_{44}H_{72}SO_8$: C 69.44, H 9.54, S 4.21, found: C 69.62, H 9.80, S 4.50.

A minor amount of the α anomer of **23** (higher R_f) was also isolated, nmr (chloroform-*d*) δ: 5.64 (d, $J_{1,2}$ = 5.0 Hz, H-1), 5.31 (q, $J_{2,3}$ = 10.0 Hz, H-2), and 5.22 (q, $J_{3,4}$ = 3.5 Hz, H-3). *Anal.* calcd. for $C_{44}H_{72}SO_8$: C 69.44, H 9.54, S 4.21; found: C 69.53, H 9.84, S 4.50.

*6-(5-Cholesten-3*β*-yloxy)hexyl 1-Thio-*α*-L-arabinopyranoside* (***24***)

This compound was obtained in 83% yield, $[\alpha]_D^{27}$ −18° (*c* 2.0, chloroform); nmr ($CDCl_3$ with D_2O spike) δ: 5.36 (d, J = 4.5 Hz, olefinic), 4.25 (d, $J_{1,2}$ = 8.5 Hz, H-1), 4.10 (q, $J_{3,2}$ = 12.5 Hz, $J_{3,4}$ = 2.0 Hz, H-3), 3.99 (b, H-4), 3.68 (q, H-2). *Anal.* calcd. for $C_{38}H_{66}SO_5$: C 71.88, H 10.48, S 5.05; found: C 71.85, H 10.70, S 5.12.

*6-(5-Cholesten-3*β*-yloxy)hexyl 2,3,4-Tri-O-acetyl-1-thio-*β*-D-xylopyranoside* (***20***)

Compound **20** was prepared in 65% yield, mp 106–108°C (methanol), $[\alpha]_D^{27}$ −56° (*c* 1.55, chloroform); nmr (chloroform-*d*) δ: 4.51 (d, $J_{1,2}$ = 9.0 Hz, H-1), 4.97 (t, $J_{2,3}$ = 8.5 Hz, H-2), 5.19 (t, $J_{3,4}$ = 8.5 Hz, H-3), 4.23 (d, d, $J_{5e,4}$ = 5.0 Hz, $J_{5e,5a}$ = 12.0 Hz, H-5e), 3.38 (d, d, $J_{5a,4}$ = 9.0 Hz, H-5a), 4.97 (H-4), 2.04 and 2.06 (3 OAc), 5.35 (d, J = 4.5 Hz, olefinic), 3.45 (t, J = 6.5 Hz, C—CH_2—O— ), 3.13 (m, —O— ), 2.66 (m, —S—CH_2—C), 0.98 (s, CH_3-19), 0.90 (d, CH_3-21), 0.85 and 0.87 (d, d, CH_3-26 and CH_3-27), and 0.67 (s, CH_3-18). *Anal.* calcd. for $C_{44}H_{72}SO_8$: C 69.44, H 9.54, S 4.21; found: C 69.35, H 9.82, S 4.25.

*6-(5-Cholesten-3*β*-yloxy)hexyl 1-Thio-*β*-D-xylopyranoside* (***21***)

Compound **21** was obtained as a crystalline material, mp 115°C (methanol), $[\alpha]_D^{27}$−45° (*c* 1.47, chloroform); nmr ($CDCl_3$ with D_2O spike) δ: 4.29 (d, $J_{1,2}$ = 9.5 Hz, H-1), 3.35 (t, $J_{2,3}$ = 9.0 Hz, H-2), 3.50 (t, $J_{3,4}$ = 9.0 Hz, H-3), 5.37 (d, J = 4.5 Hz, olefinic). *Anal.* calcd. for $C_{38}H_{66}SO_5$: C 71.88, H 10.48, S 5.05; found: C 71.77, H 10.26, S 5.09.

*6-(5-Cholesten-3*β*-yloxy)hexyl 2,3,4-Tri-*O*-acetyl-1-thio-*β*-L-fucopyranoside* (***17***)

This compound was prepared in 81% yield, $[\alpha]_D^{27}$ −4° (*c* 1.5, chloroform); nmr (chloroform-*d*) δ: 4.46 (d, $J_{1,2}$ = 10.0 Hz, H-1), 5.25 (t, $J_{2,3}$ = 10.0 Hz, H-2), 5.07 (d, d, $J_{3,4}$ = 3.5 Hz, H-3), 5.30 (d, H-4), 3.84 (q, J = 6.0 Hz, H-5), 1.22 (d, CH_3-5), 2.0, 2.08, and 2.19 (3 OAc), 5.37 (d, J = 4.5 Hz, olefinic), 3.48 (t, J = 6.5 Hz, C—CH_2—O— ), 3.15 (m, —O— ), 2.72 (m, —S—CH_2—C), 1.0 (s, CH_3-19), 0.91 (d, CH_3-21), 0.85 and 0.87 (d, d, CH_3-26 and CH_3-27), 0.67 (s, CH_3-18). *Anal.* calcd. for $C_{45}H_{74}SO_8$: C 69.73, H 9.62, S 4.14; found: C 69.62, H 9.68, S 4.09.

*6-(5-Cholesten-3*β*-yloxy)hexyl 1-Thio-*β*-L-fucopyranoside* (***18***)

This compound was obtained as needles in 80% yield, mp 110–112°C (EtOAc), $[\alpha]_D^{27}$ −11° (*c* 1.43, chloroform); nmr ($CDCl_3$ with D_2O spike) δ: 5.36 (d, J = 4.5 Hz, olefinic), 4.27 (H-1 and H-2), 3.78 (b, H-4), 3.68 (q, J = 6.5 Hz, H-5), 3.60 (H-3). *Anal.* calcd. for $C_{39}H_{68}SO_5 \cdot 0.5\ CH_3COOCH_2CH_3$: C 71.05, H 10.47, S 4.63; found: C 70.84, H 10.68, S 5.00.

*6-(5-Cholesten-3*β*-yloxy)hexyl 2,3,4,6-Tetra-*O*-acetyl-*β*-D-glucopyranoside* (***7***)

Compound **7** was prepared in 86% yield, mp 101–102.5°C (methanol), $[\alpha]_D^{27}$ −36° (*c* 1.59, chloroform). *Anal.* calcd. for $C_{47}H_{76}SO_{10}$: C 67.75, H 9.19, S 3.85; found: C 67.72, H 9.44, S 3.71.

*6-(5-Cholesten-3*β*-yloxy)hexyl 1-Thio-*β*-D-glucopyranoside* (***8***)

Compound **8** was obtained as a crystalline material, mp 110°C (aqueous isopropanol), $[\alpha]_D^{27}$ −41° (*c* 1.07, chloroform), R_f 0.27 (chloroform–methanol, 9:1); nmr ($CDCl_3$, with D_2O spike) δ: 5.34 (d, J = 4.5 Hz, olefinic), 4.43 (d, $J_{1,2}$ = 9.5 Hz, H-1). *Anal.* calcd. for $C_{39}H_{68}SO_6$: C 70.44, H 10.31, S 4.82; found: C 70.43, H 10.36, S 4.63.

*6-(5-Cholesten-3*β*-yloxy)hexyl 2-Acetamido-3,4,6-tri-*O*-acetyl-2-deoxy-1-thio-*β*-D-glucopyranoside* (***10***)

This compound was prepared in 85% yield, mp 176–179°C,

Can. J. Chem. Downloaded from www.nrcresearchpress.com by 210.87.254.105 on 09/05/12
For personal use only.

$[\alpha]_D^{27}$ −43° (*c* 1.5, chloroform). *Anal.* calcd. for $C_{47}H_{77}NSO_9$: C 67.83, H 9.33, N 1.68, S 3.85; found: C 67.54, H 9.78, N 1.80, S 3.90.

*6-(5-Cholesten-3β-yloxy)hexyl 2-Acetamido-2-deoxy-1-thio-β-D-glucopyranoside (**11**)*

Compound **11** was obtained in 77% yield, mp 183–187°C (dec.) (methanol), $[\alpha]_D^{27}$ −36° (*c* 1.5, dimethylsulfoxide), R_f 0.48 (chloroform–methanol–water, 80:20:2). *Anal.* calcd. for $C_{41}H_{71}NSO_6$: C 69.74, H 10.14, N 1.98, S 4.54; found: C 69.57, H 10.27, N 1.86, S 4.66.

*6-(5-Cholesten-3β-yloxy)hexyl 2-Acetamido-3,4,6-tri-O-acetyl-2-deoxy-1-thio-β-D-galactopyranoside (**14**)*

This compound was isolated as a crystalline material in 63% yield, mp 130–133°C (ethanol), $[\alpha]_D^{27}$ −37° (*c* 1.5, chloroform). *Anal.* calcd. for $C_{47}H_{77}NSO_9$: C 67.83, H 9.33, N 1.68, S 3.85; found: C 67.69, H 9.37, N 1.67, S 4.02.

*6-(5-Cholesten-3β-yloxy)hexyl 2-Acetamido-2-deoxy-1-thio-β-D-galactopyranoside (**15**)*

Compound **15** was obtained in 85% yield, mp 241–243°C, $[\alpha]_D^{27}$ −35° (*c* 1.5, *N*,*N*-dimethylformamide). *Anal.* calcd. for $C_{41}H_{71}NSO_6$: C 69.74, H 10.14, N 1.98, S 4.54; found: C 69.57, H 10.44, N 2.20, S 4.90.

*6-(5-Cholesten-3β-yloxy)hexyl 2,3,6-Tri-O-acetyl-4-O-(2,3,4,6-tetra-O-acetyl-βD-galactopyranosyl)-1-thio-β-D-glucopyranoside (**37**)*

This compound was prepared in 60% yield, $[\alpha]_D^{27}$ −22° (*c* 1.55, chloroform). *Anal.* calcd. for $C_{59}H_{92}SO_{18}$: C 63.19, H 8.27, S 2.86; found: C 63.27, H 8.46, S 2.88.

*6-(5-Cholesten-3β-yloxy)hexyl 4-O-(β-D-Galactopyranosyl)-1-thio-β-D-glucopyranoside (**38**)*

Compound **38** was obtained as a crystalline material, mp 189–192°C (aqueous isopropanol), $[\alpha]_D^{27}$ −21° (*c* 1.63, dimethylsulfoxide), R_f 0.26 (chloroform–methanol–water, 80:20:2). *Anal.* calcd. for $C_{45}H_{78}SO_{11}$: C 65.34, H 9.51, S 3.88; found: C 65.42, H 9.51, S 4.11.

*6-(5-Cholesten-3β-yloxy)hexyl 2,3,6-Tri-O-acetyl-4-O-(2,3,4,6-tetra-O-acetyl-β-D-glucopyranosyl)-1-thio-β-D-glucopyranoside (**40**)*

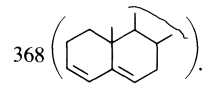
This compound was prepared in 76% yield, mp 178–180°C (ethyl ether – 95% ethanol), $[\alpha]_D^{27}$ −27.5° (*c* 1.0, chloroform). *Anal.* calcd. for $C_{59}H_{92}SO_{18}$: C 63.19, H 8.27, S 2.86; found: C 63.15, H 8.50, S 2.91.

*6-(5-Cholesten-3β-yloxy)hexyl 4-O-(β-D-Glucopyranosyl)-1-thio-β-D-glucopyranoside (**41**)*

This compound was obtained as a crystalline material, mp 197–201°C (aqueous isopropanol), $[\alpha]_D^{27}$ −32° (*c* 1.0, dimethylsulfoxide). *Anal.* calcd. for $C_{45}H_{78}SO_{11}\cdot H_2O$: C 63.95, H 9.54, S 3.79; found: C 63.87, H 9.86, S 3.91.

*6-(5-Cholesten-3β-yloxy)-1-thiohexane (**34**)*

Thiourea (7.5 g) was added to a solution of **32** (15 g, 25.3 mmol) in tetrahydrofuran (200 mL), and the mixture was heated under reflux with vigorous stirring for 6 h. The solution was concentrated to a residue which was triturated with anhydrous ethyl ether. The solid was filtered and dissolved in chloroform (100 mL), and the solution was added to a solution of potassium metabisulfite (15 g) in water (100 mL). The mixture was refluxed under nitrogen for 20 min. The cooled solution was separated and the organic layer was dried and evaporated *in vacuo* to a crude material which was put on a column of silica gel and eluted with 5% ethyl ether in petroleum ether. The desired fractions were pooled and evaporated to give **34** (11 g, 86%), mp 89–90°C; ms *m/e*: 502 ($M^{+\cdot}$), 487 ($M^{+\cdot}-CH_3$),



Anal. calcd. for $C_{33}H_{58}SO$: C 78.82, H 11.63, S 6.38; found: C 78.91, H 11.64, S 6.25.

A portion of **34** was acetylated with acetic anhydride in pyridine to give **35**, mp 81–81.5°C. *Anal.* calcd. for $C_{35}H_{60}SO_2$: C 77.14, H 11.10, S 5.89; found: C 77.20, H 11.23, S 6.13.

*Methyl 5-Acetamido-4,7,8,9-tetra-O-acetyl-2-S-[6-(5-cholesten-3β-yloxy)hexyl]-3,5-dideoxy-2-thio-β-D-glycero-D-galacto-2-nonulopyranosonate (**28**)*

Boron trifluoride etherate (0.7 mL, 5.5 mmol) was added to a solution of **34** (0.98 g, 1.96 mmol) and methyl 5-acetamido-2,4,7,8,9-penta-*O*-acetyl-3,5-dideoxy-β-D-*glycero*-D-*galacto*-2-nonulopyranosonate (**25**) (1.01 g, 1.96 mmol) in dry chloroform (5 mL). The mixture was stirred under nitrogen for 5 h at room temperature. Chloroform (25 mL) was added to the reaction mixture and the solution was washed with aqueous sodium hydrogencarbonate (20 mL) and water (20 mL). The dried solution was concentrated to a residue which was put on a column of silica gel and eluted with chloroform – ethyl ether – methanol (30:10:1). The desired fractions were pooled and evaporated to give **28** as a foam (400 mg), $[\alpha]_D^{27}$ −38.5° (*c* 1.5, chloroform); nmr (chloroform-*d*) δ: 5.44 (t, $J_{7,6} = J_{7,8} = 2.5$ Hz, H-7), 5.35 (d, $J = 4.5$ Hz, olefinic), 5.27 (o, $J_{4,5} = 10.5$ Hz, $J_{4,3a} = 12.0$ Hz, $J_{4,3e} = 5.0$ Hz, H-4), 5.28 (d, $J_{NH,5} = 10.5$ Hz, N—H), 5.12 (t, t, $J_{8,9} = 8.0$ Hz, $J_{8,9'} = 2.5$ Hz, H-8), 4.82 (d, d, $J_{9,9'} = 12.5$ Hz, H-9′), 4.34 (d, d, $J_{6,5} = 10.5$ Hz, H-6), 4.18 (d, d, H-9), 4.10 (q, H-5), 3.80 (s, $COOCH_3$), 3.44 (t, $J = 6.5$ Hz, C—CH_2—O— ), 3.13 (m, —O— ), 2.54 (H-3e), 2.13, 2.07, 2.04, 2.02, and 1.88 (5s, 4 OAc and NAc), 0.98 (s, CH_3-19), 0.91 (d, $J = 6.0$ Hz, CH_3-21), 0.84 and 0.86 (CH_3-26 and CH_3-27), 0.66 (s, CH_3-18). *Anal.* calcd. for $C_{53}H_{85}SNO_{13}$: C 65.20, H 8.78, N 1.44, S 3.28; found: C 65.20, H 9.03, N 1.97, S 3.68.

The overlapping fractions were combined and concentrated to give a mixture (60 mg) of **38** and the corresponding α anomer; nmr (chloroform-*d*) δ: 2.54 (H-3e of **28**), 2.73 (d, d, $J_{3e,4} = 4.5$ Hz, $J_{3e,3a} = 13.0$ Hz, H-3e of the α anomer of **28**).

*5-Acetamido-2-S-[6-(5-cholesten-3β-yloxy)hexyl]-3,5-dideoxy-2-thio-β-D-glycero-D-galacto-2-nonulopyranosonic acid (**29**)*

A solution of **28** (46 mg) in dry methanol (8 mL) containing sodium methoxide (3 mg) was kept for 3 h at room temperature. The solution was then adjusted to pH 9.0 by gradual addition of 2.5 *N* sodium hydroxide (~10 drops). The suspension was stirred for 16 h, and tetrahydrofuran (20 mL) was added to dissolve the precipitate. The solution was stirred with Bio-Rad AG50W-X2 (H^+) ion exchange resin, filtered, and the filtrate was concentrated to a residue which was triturated with ethyl ether – petroleum ether to give **29** as a sodium salt (30 mg, 80%), $[\alpha]_D^{27}$ −73° (*c* 1.0, dimethylsulfoxide; ms *m/e*: 816 ($M^{+\cdot}$ + Na). *Anal.* calcd. for $C_{44}H_{74}NSO_9Na\cdot H_2O$: C 63.35, H 9.18, N 1.67, S 3.84; found: C 63.45, H 9.19, N 1.72, S 4.00.

Acknowledgements

The authors thank Dr. J. V. Heck for samples of methyl 5-acetamido-4,7,8,9-tetra-*O*-acetyl-3,5-

dideoxy-2-*O*-methyl-α, and β-D-glycero-D-galacto-2-nonulopyranosonates, Dr. B. H. Arison and Mr. H. Flynn for recording 300 MHz spectra, and Mr. J. P. Gilbert and his associates for microanalyses.

1. G. Poste, D. Papahadjopoulos, and W. J. Vail. *In* Methods in cell biology. Vol. XIV. *Edited by* D. M. Prescott. Academic Press, New York. 1976. p. 33.
2. D. A. Tyrrell, T. D. Heath, C. M. Colley, and B. E. Ryman. Biochim. Biophys. Acta, **457**, 259 (1976).
3. G. Gregoriadis. N. Engl. J. Med. **295**, 704 (1976); **295**, 765 (1976); Nature, **265**, 407 (1977).
4. M. Finkelstein and G. Weissman. J. Lipid Res. **19**, 289 (1978).
5. G. Weissman, C. Cohen, and S. Hoffstein. Trans. Assoc. Am. Physicians, **89**, 171 (1977).
6. C. M. Colley and B. E. Ryman. Biochim. Biophys. Acta, **451**, 417 (1976).
7. T. Yasuda, G. F. Dancey, and S. C. Kinsky. Proc. Natl. Acad. Sci. USA. **74**, 1234 (1977).
8. A. C. Allison and G. Gregoriadis. Nature, **252**, 252 (1974).
9. E. Arakawa, Y. Imai, H. Kobayashi, K. Okumura, and H. Sezaki. Chem. Pharm. Bull. **23**, 2218 (1975).
10. M. M. Jonah, E. A. Cerny, and Y. E. Rahman. Biochim. Biophys. Acta, **401**, 336 (1975).
11. Y. E. Rahman and B. J. Wright. J. Cell. Biol. **65**, 112 (1975).
12. R. L. Juliano and D. Stamp. Biochim. Biophys. Res. Commun. **63**, 651 (1975).
13. P. D. Stahl, J. S. Rodman, M. J. Miller, and P. H. Schlesinger. Proc. Natl. Acad. Sci. USA. **75**, 1399 (1978).
14. J. Lunney and G. Ashwell. Proc. Natl. Acad. Sci. USA, **73**, 41 (1976).
15. D. Aminoff, W. F. Vorder Bruegge, W. C. Bell, K. Sarpolis, and R. Williams. Proc. Natl. Acad. Sci. USA, **74**, 1521 (1977).
16. H. G. Remold. J. Exp. Med. **138**, 1065 (1973).
17. A. Kaplan, D. T. Achord, and W. S. Sly. Proc. Natl. Acad. Sci. USA, **74**, 2026 (1977).
18. J. C. Chabala and T. Y. Shen. Carbohydr. Res. **67**, 55 (1978).
19. S. Roseman. *In* Cell membranes, biochemistry, cell biology and pathology. *Edited by* G. Weissman and R. Claiborne. HP Publishing Co., New York. 1975. p. 55.
20. C. Bamford, B. Capon, and W. G. Overend. J. Chem. Soc. 5138 (1962).
21. M. D. Saunders and T. E. Timell. Carbohydr. Res. **6**, 121 (1968).
22. M. Privalova and A. Ya. Khorlin. Izv. Akad. Nauk SSSR, Ser. Khim. 2785 (1969).
23. D. Horton and D. H. Hutson. Adv. Carbohydr. Chem. **18**, 123 (1963).
24. W. G. Overend. *In* The carbohydrates. Vol. 1A. *Edited by* W. Pigman and D. Horton. Academic Press, New York. 1972. p. 341.
25. R. J. Ferrier and R. H. Furneaux. Carbohydr. Res. **52**, 63 (1976).
26. R. Kuhn, P. Lutz, and D. L. MacDonald. Chem. Ber. **99**, 611 (1966).
27. P. Lutz, W. Lochinger, and G. Taigel. Chem. Ber. **101**, 1089 (1968).
28. M. R. Mauk and R. C. Gamble. Proc. Natl. Acad. Sci. USA, **76**, 765 (1979).
29. G. A. Orr, R. R. Rando, and F. W. Bangerter. J. Biol. Chem. **254**, 4721 (1979).
30. R. W. Bussian and J. C. Wriston, Jr. Biochim. Biophys. Acta, **471**, 336 (1977).
31. M. M. Jonah, E. A. Cerney, and Y. E. Rahman. Biochim. Biophys. Acta, **541**, 321 (1978).
32. M. Černý, J. Vrkoč, and J. Staněk. Collect. Czech. Chem. Commun. **24**, 64 (1959).
33. K. L. Matta, E. A. Z. Johnson, R. N. Girotra, and J. J. Barlow. Carbohydr. Res. **30**, 414 (1973).
34. W. Meyer Zu Reckendorf and W. A. Bonner. J. Org. Chem. **26**, 4596 (1961).
35. K. L. Matta, R. N. Girotra, and J. J. Barlow. Carbohydr. Res. **43**, 101 (1975).
36. J. Staněk, M. Šindlerová, and M. Černeý. Collect. Czech. Chem. Commun. **30**, 297 (1965).
37. C. V. Holland, D. Horton, and M. J. Miller. J. Org. Chem. **32**, 3077 (1967).
38. M. Géhrke and W. Kohle. Ber. **64**, 2696 (1931).
39. J. Staněk, M. Šindlerová, and M. Černeý. Collect. Czech. Chem. Commun. **30**, 297 (1965).
40. F. Wrede and O. Hettche. Z. Physiol. Chem. **172**, 169 (1927).
41. P. L. Durette and T. Y. Shen. Carbohydr. Res. **67**, 484 (1978).

Can. J. Chem. Downloaded from www.nrcresearchpress.com by 210.87.254.105 on 09/05/12
For personal use only.

Binuclear and mononuclear nickel(II) and zinc(II) complexes of the tetradentate ligand 1,4-di(2′-pyridyl)aminophthalazine

JAMES ALFRED DOULL AND LAURENCE KENNETH THOMPSON[1]

Department of Chemistry, Memorial University of Newfoundland, St. John's, Nfld., Canada A1B 3X7

Received February 5, 1979

JAMES ALFRED DOULL and LAURENCE KENNETH THOMPSON. Can. J. Chem. **58**, 221 (1980).

Previous studies with the title ligand, PAP, have shown a predominance of binuclear complexes with cobalt and copper in which the ligand-to-metal ratio is 1:2. The nickel complexes produced are more varied in composition; e.g., 1:2 binuclear systems $[PAPNi_2X(OH)(H_2O)_4]X_2$ (X = Cl, Br); 1:1 binuclear systems $[PAP_2Ni_2(H_2O)_4]X_4$ (X = Cl, Br), $[PAP_2Ni_2(NCS)_3]NCS$, $[PAP_2Ni_2(OH)I_2]I\cdot 2H_2O$, $[PAP_2Ni_2(OH)(H_2O)_2]X_3$ (X = ClO_4, BF_4, I); and 2:1 mononuclear systems $[(PAPH)_2Ni(H_2O)_2]X_4$ (X = I, BF_4). Zinc forms both mononuclear, $[PAPZnX_2]\cdot H_2O$ (X = Br, I), and a 1:1 binuclear system, $[PAP_2Zn_2Cl_4]$. Triple bridges are suggested between the nickel atoms in all binuclear systems involving bridging hydroxy groups. Weak antiferromagnetic exchange is observed ($-J < 10\ cm^{-1}$) in two binuclear nickel complexes, which is enhanced in the presence of a hydroxy bridge. Spin–spin coupling is assumed to occur via a superexchange mechanism. In all cases nickel appears to be six-coordinate while for the zinc complexes both four- and six-coordination are observed.

JAMES ALFRED DOULL et LAURENCE KENNETH THOMPSON. Can. J. Chem. **58**, 221 (1980).

Les études antérieures sur le ligand PAP ont révélé la formation prépondérante de complexes binucléaires avec le cobalt et le cuivre, dans lesquels le rapport ligand/métal est 1:2. On a préparé des complexes de nickel qui ont une composition plus variée i.e. des systèmes binucléaires 1:2 $[PAPNi_2X(OH)(H_2O)_4]X_2$ (X = Cl, Br), des systèmes binucléaires 1:1 $[PAP_2Ni_2(H_2O)_4]X_4$ (X = Cl, Br), $[PAP_2Ni_2(NCS)_3]NCS$, $[PAP_2Ni_2(OH)I_2]I\cdot 2H_2O$, $[PAP_2Ni_2(OH)(H_2O)_2]X_3$ (X = ClO_4, BF_4, I) et des systèmes mononucléaires 2:1 $[(PAPH)_2Ni(H_2O)_2]X_4$ (X = I, BF_4). Le zinc forme deux types de complexes: l'un mononucléaire $[PAPZnX_2]\cdot H_2O$ (X = Br, I) et l'autre binucléaire 1:1 $[PAP_2Zn_2Cl_4]$. On suggère un triple pont entre l'atome de nickel et tous les systèmes binucléaires faisant intervenir un groupe hydroxyle en position de pont. On observe un faible échange antiferromagnétique ($-J < 10\ cm^{-1}$) entre des complexes binucléaires du nickel. Cet échange est favorisé par la présence d'un groupe hydroxyle en position de pont. On pense que le couplage de spin se produit par l'intermédiaire d'un mécanisme de superéchange. Dans tous les cas le nickel semble être hexacoordonné alors que dans le cas des complexes de zinc on observe des composés tétra ainsi que hexacoordonnés.

[Traduit par le journal]

Introduction

Potentially binucleating ligands are important in model studies of metalloproteins containing two metal ions in close proximity, e.g., Type III copper systems, hemocyanin, and hemerythrin. Binuclear complexes, in which two metals are brought into close proximity, require bridging groups that generally involve one or two donor atoms. The binucleating ligand 2-pyridinealdazine (PAA), investigated by Stratton and Busch (1), was an early example of a system involving a two atom azine bridge. More recent examples of binuclear complexes involving azine type ligands include disubstituted pyrazole, pyridazine, and phthalazine systems (2–7). Binuclear Schiff base complexes involving single atom oxygen bridges have also been reported (8).

In previous papers (9, 10) we described some binuclear copper and cobalt complexes of the ligand 1,4-di(2′-pyridyl)aminophthalazine (Fig. 1, ligand abbreviated PAP). In all cases binuclear species were obtained with double or triple bridging units connecting the two metal centres. Strong antiferromagnetic exchange was observed for the complex $[PAPCu_2(OH)(H_2O)_4](IO_3)_3$ ($-J$ = 167 cm^{-1}) and much weaker exchange for the cobalt complexes $[PAPCo_2X_3]$ (X = Cl, Br, I), $[PAPCo_2(OH)(NCS)_2]\cdot H_2O$ ($-J$ = 3.3–5.5 cm^{-1}). We report here a series of binuclear 1:1 nickel and zinc derivatives of PAP, in which two metals are bound simultaneously to two adjacent ligands, 1:2 binuclear derivatives and also some mononuclear derivatives. For the binuclear complexes, bridging groups include just the phthalazine framework in some cases, while in others additional bridging groups, e.g., hydroxide and halide are proposed. Preliminary variable temperature magnetic susceptibility studies indicate weak antiferromagnetic exchange for two binuclear nickel complexes.

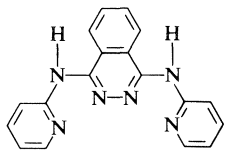


FIG. 1. 1,4-Di(2′-pyridyl)aminophthalazine.

Experimental

Electronic spectra were recorded with a Cary 17 spectrometer and infrared spectra with a Perkin-Elmer model 283 spectrometer. Magnetic susceptibilities were obtained at room tem-

[1]To whom all correspondence should be addressed.

0008-4042/80/030221-08$01.00/0

©1980 National Research Council of Canada/Conseil national de recherches du Canada

Can. J. Chem. Downloaded from www.nrcresearchpress.com by 210.87.254.40 on 09/05/12
For personal use only.

TABLE 1. Analytical and other data

Compound	Colour	Found				Calcd.			
		C	H	N	M	C	H	N	M
I, $[PAP_2Ni_2(H_2O)_4]Cl_4 \cdot 3H_2O$	Purple	42.7	3.84	16.6	12.0	42.6	4.14	16.6	11.6
II, $[PAP_2Ni_2(H_2O)_2Cl_2]Cl_2$	Green	46.5	3.53	18.1	12.7	46.7	3.46	18.2	12.7
III, $[PAP_2Ni_2(H_2O)_4]Br_4$	Purple	37.7	2.98	14.7	10.6	38.0	3.19	14.8	10.4
IV, $[PAP_2Ni_2(H_2O)_3Br]Br_3$	Green	38.7	2.66	15.1	10.7	38.6	3.06	15.0	10.5
V, $[PAP_2Ni_2(OH)I_2]I \cdot 2H_2O$	Green	36.3	2.55	13.9	9.7	36.6	2.79	14.2	10.0
VI, $[PAP_2Ni_2(NCS)_3]NCS$	Green	49.2	2.54	22.6	11.9	49.1	2.86	22.9	12.1
VII, $[PAP_2Ni_2(OH)(H_2O)_2](ClO_4)_3$	Green	39.4	3.13	15.3	10.9	39.4	3.01	15.3	10.7
VIII, $[PAP_2Ni_2(OH)(H_2O)_2](BF_4)_3$	Turquoise–green	40.5	3.13	15.9	10.8	40.7	3.11	15.8	11.1
IX, $[PAP_2Ni_2(OH)(H_2O)_2]I_3 \cdot 3H_2O$	Khaki–green	34.9	2.91	13.7	9.40	35.2	3.16	13.6	9.56
X, $[PAPNi_2Cl(OH)(H_2O)_4]Cl_2$	Bright green	34.5	3.22	13.3	18.1	34.5	3.67	13.4	18.8
XI, $[PAPNi_2Br(OH)(H_2O)_4]Br_2$	Pale green	28.5	2.67	11.0	15.2	28.4	3.02	11.0	15.5
XII, $[(PAPH)_2Ni(H_2O)_2](BF_4)_4$	Grey–green	40.3	3.27	15.7	5.20	40.3	3.17	15.7	5.50
XIII, $[(PAPH)_2Ni(H_2O)_2]I_4$	Yellow–green	35.1	2.63	13.5	4.50	35.0	2.75	13.6	4.78
XIV, $[PAP_2Zn_2Cl_4]$	Pale yellow	48.6	3.09	18.4	14.4	48.2	3.12	18.7	14.5
XV, $[PAPZnBr_2] \cdot H_2O$	Pale yellow	37.6	2.48	14.6	11.5	37.6	3.15	14.6	11.4
XVI, $[PAPZnI_2] \cdot H_2O$	Pale yellow	33.5	2.22	12.8	10.3	33.2	2.47	12.9	10.0

perature by the Faraday method using a Cahn model #7600 Faraday Magnetic Susceptibility system, coupled to a Cahn gram electrobalance. Variable temperature magnetic susceptibilities were measured in the Chemistry Department, University of British Columbia, by the Gouy method on equipment previously described (11). The molar susceptibilities, χ_{Ni}, were corrected for the diamagnetism of all atoms and temperature independent paramagnetism. Conductance data were obtained with a General Radio Company bridge with impedance comparator and a constant temperature bath adjusted to 25°C.

Microanalyses were carried out in part in the Chemistry Department at Memorial University using a Perkin-Elmer model #240 Elemental Analyzer and by Atlantic Microlab, Inc., Atlanta, GA. Metal analyses were determined by atomic absorption with a Varian Techtron AA-5, after digestion of the samples in concentrated HNO_3 or aqua regia.

Nickel Complexes of PAP

The ligand, 1,4-di(2′-pyridyl)aminophthalazine was prepared as described previously (9).

*$[PAP_2Ni_2(H_2O)_4]Cl_4 \cdot 3H_2O$ (**I**)*

PAP (1.50 g, 4.77 mmol) was added to a solution of $NiCl_2 \cdot 6H_2O$ (1.13 g, 4.77 mmol) in water (50 mL) and the mixture heated with stirring until all the ligand dissolved. The resulting purple solution was filtered and reduced in volume. A mixture of purple and green crystals was obtained on standing. On drying both crystalline forms at 80°C under vacuum for 1 h, green powders were obtained which were shown to be the same compound according to electronic and infrared spectral data. Recrystallization was effected from water giving a crystalline mixture as before. The two crystalline forms appear to be different hydrated species of the same basic structure. Controlled dehydration by heating under vacuum was difficult and various hydrates can be obtained, according to analytical data, depending on the temperature and the drying time. The air-dried purple complex (**I**) contained seven water molecules, whereas on drying under vacuum (0.05 mm Hg) at 80°C for 3 h a green complex (**II**) containing two water molecules (see Table 1) was obtained. The purple bromide salt (**III**) was prepared similarly and again differing hydrated species were obtained.

*$[PAP_2Ni_2(OH)I_2]I \cdot 2H_2O$ (**V**)*

PAP (1.00 g, 3.18 mmol) was added to a solution of NiI_2 (1.0 g, 3.19 mmol) in methanol (175 mL) and the mixture refluxed until a clear green solution was obtained. On filtering the solution and allowing it to stand for a week green crystals were obtained. The product was filtered, washed with methanol/ether (50/50), and dried under vacuum at 80°C for 2 h.

*$[PAP_2Ni_2(NCS)_3]NCS$ (**VI**)*

PAP (1.00 g, 3.18 mmol) was dissolved in a minimum volume of refluxing ethanol and $Ni(NCS)_2$ (1.20 g, 6.86 mmol) dissolved in ethanol containing a small amount of water. The solutions were mixed and refluxed until a pale green precipitate formed. The reaction mixture was allowed to stand overnight and the green powdery product filtered, washed with ethanol, and air dried. Recrystallization was effected from methanol and the product dried under vacuum at 80°C for 3 h.

*$[PAP_2Ni_2(OH)(H_2O)_2](ClO_4)_3$ (**VII**)*

PAP (1.50 g, 4.77 mmol) was added to a solution of $Ni(ClO_4)_2 \cdot 6H_2O$ (1.80 g, 4.92 mmol) in water (600 mL) and the mixture refluxed until a pale green solution was obtained. The solution was filtered and reduced in volume until green crystals formed. The product was recrystallized from water and dried under vacuum at 80°C for 3 h.

*$[PAP_2Ni_2(OH)(H_2O)_2](BF_4)_3$ (**VIII**), $[(PAPH)_2Ni(H_2O)_2](BF_4)_4$ (**XII**)*

PAP (0.750 g, 2.39 mmol) was added to $Ni(BF_4)_2 \cdot 6H_2O$ (0.850 g, 2.49 mmol) in water (75 mL) and the mixture refluxed for 2 h. The green solution was filtered and reduced in volume until a greyish green crystalline solid formed (**XII**). This product was filtered, washed with water, and dried under vacuum at room temperature for 1 h. The purple–blue mother liquor was reduced further in volume and allowed to stand at room temperature. Turquoise–green crystals (**VIII**) were obtained, and were filtered, washed with water, and dried under vacuum at room temperature. The binuclear derivative (**VIII**) was obtained as the sole product by adjusting the pH of the nickel tetrafluoroborate solution to 5.5 by addition of fluoride (see Discussion).

*$[PAP_2Ni_2(OH)(H_2O)_2]I_3 \cdot 3H_2O$ (**IX**), $[(PAPH)_2Ni(H_2O)_2]I_4$ (**XIII**)*

PAP (1.00 g, 3.18 mmol) was added to a solution of NiI_2 (1.00 g, 3.19 mmol) in water (100 mL) and the mixture refluxed until a purple–blue solution was formed. The solution was filtered and allowed to stand until yellow–green crystals formed

Can. J. Chem. Downloaded from www.nrcresearchpress.com by 210.87.254.40 on 09/05/12
For personal use only.

TABLE 2. Electronic spectra (cm^{-1})[a]

Compound	O_h[b]	$^3T_{2g} \leftarrow {}^3A_{2g}(\nu_1)$		$^1E_g \leftarrow {}^3A_{2g}$	$^3T_{1g}(F) \leftarrow {}^3A_{2g}(\nu_2)$	$\pi-\pi^*$ (log ε)
I, $[PAP_2Ni_2(H_2O)_4]Cl_4 \cdot 3H_2O$[c]	A		11 500	[15 400]	18 000	
	B		11 500(14)	[15 400](4)	18 000(17)	28 700(4.6)
II, $[PAP_2Ni_2(H_2O)_2Cl_2]Cl_2$[d]	A		11 400		17 700	
III, $[PAP_2Ni_2(H_2O)_4]Br_4$[c]	A		11 400	[15 400]	18 000	
	B	10 300(13)	[11 600](12)	[15 400](5)	17 900(12)	28 700(4.6)
IV, $[PAP_2Ni_2(H_2O)_3Br]Br_3$[d]	A		10 200		17 500	
V, $[PAP_2Ni_2(OH)I_2]I \cdot 2H_2O$	A	8 800	10 600		16 800	27 800
	B		11 600		18 500	28 600
VI, $[PAP_2Ni_2(NCS)_3]NCS$	A		10 500		17 400	27 800
VII, $[PAP_2Ni_2(OH)(H_2O)_2](ClO_4)_3$	A		11 400	[16 100]	17 900	
	B		11 400(15)		17 900(12)	28 600(4.3)
VIII, $[PAP_2Ni_2(OH)(H_2O)_2](BF_4)_3$	A		11 200		17 500	
	B		11 400(19)		17 700(15)	28 700(4.2)
IX, $[PAP_2Ni_2(OH)(H_2O)_2]I_3 \cdot 3H_2O$	A		11 000		18 000	
X, $[PAPNi_2Cl(OH)(H_2O)_4]Cl_2$	A	8 300	9 700		14 900	28 000
XI, $[PAPNi_2Br(OH)(H_2O)_4]Br_2$	A	7 500	9 700		14 500	27 800
XII, $[(PAPH)_2Ni(H_2O)_2](BF_4)_4$	A		11 400		17 900	
	B		11 600(12)		17 700(9)	28 700(4.2)
XIII, $[(PAPH)_2Ni(H_2O)_2]I_4$	A		11 300		18 000	28 000

[a][ ] shoulder; ( ) molar extinction coefficient.
[b]A, Solid state mull transmittance spectrum; B, aqueous solution.
[c]Purple.
[d]Green.

(**XIII**). The product was filtered, washed with water, and dried under vacuum at 80°C for 2 h. The mother liquor was reduced in volume on a steam bath until more product (**XIII**) formed. The mixture was cooled and treated as before. At this stage a total of about 0.4 g of material had been collected. Further reduction in volume produced a khaki–green crystalline material (**IX**) (0.8 g) which was filtered, washed with water, and dried under vacuum at 60°C for 2 h.

*[PAPNi$_2$Cl(OH)(H$_2$O)$_4$]Cl$_2$ (**X**)*

PAP (1.00 g, 3.18 mmol) was added to a solution of $NiCl_2 \cdot 6H_2O$ (1.55 g, 6.51 mmol) in 80% acetic acid (12 mL) and the mixture refluxed for 1 h. A pale green solid formed which was filtered, washed with ethanol and ether, and dried under vacuum at room temperature for 3 h.

The analogous bromide complex (**XI**) was prepared similarly as a green solid. On drying under vacuum at 80°C for 6 h the bromide complex was obtained as a buff–yellow solid while the chloride derivative changed to a yellow–green solid. On exposure to air both compounds reverted to their original green forms.

*[PAP$_2$Zn$_2$Cl$_4$] (**XIV**)*

PAP (1.00 g, 3.18 mmol) was dissolved in hot ethanol (100 mL) and added to a hot solution of anhydrous zinc chloride (1.00 g, 7.33 mmol) in ethanol (60 mL). A pale yellow precipitate formed in the hot solution. The product was purified by soxhlet extraction in methanol and dried under vacuum at 80°C for 2 h.

The other zinc complexes were prepared similarly from methanol using anhydrous zinc salts.

Results and Discussion

Characterization of the Complexes

Nickel Complexes

PAP preferentially binds two metal ions and mononuclear complexes are not common. Previously reported binuclear complexes of PAP with cobalt and copper include just systems in which the ligand-to-metal ratio is 1:2 (9, 10). The nickel complexes, however, are different in that 1:1 binuclear systems involving two ligands bridging two metals are most common. In these binuclear systems PAP behaves as a tetradentate ligand coordinating through two phthalazine and two pyridine nitrogen atoms and the nickel ions adopt pseudo-octahedral stereochemistries. 1:2 Binuclear derivatives can also be produced but are hydrolytically unstable. A 2:1 pseudo-octahedral mononuclear complex cation is formed in the reaction between PAP and both nickel tetrafluoroborate and nickel iodide in water. This system involves the coordination of two protonated bidentate ligands in which one phthalazine and an adjacent pyridine nitrogen are involved in bonding to the metal.

Electronic Spectra and Structure

Two major absorptions are observed in the solid state mull transmittance spectra of all the 1:1 binuclear nickel complexes corresponding to the ν_1 and ν_2 transitions for pseudo-octahedral nickel(II) (Table 2). The ν_3 transition, which should occur above 25 000 cm^{-1} for predominantly nitrogen bound systems, is obscured in all cases by charge transfer absorption associated with the ligand itself. In addition a shoulder is observed in some cases on the low energy side of ν_2, which is assigned to a spin-forbidden transition. No splitting of ν_2 is observed in these systems and only in the case of the iodide complex (**V**) is there any splitting of ν_1. This is perhaps surprising, since the symmetry of the crystal field around the nickel ion in these systems will be lower than octahedral. Other 1:1

Can. J. Chem. Downloaded from www.nrcresearchpress.com by 210.87.254.40 on 09/05/12
For personal use only.

Can. J. Chem. Downloaded from www.nrcresearchpress.com by 210.87.254.40 on 09/05/12
For personal use only.

binuclear nickel complexes involving similar ligands, e.g., 1,4-dihydrazinophthalazine and 3,6-di(2′-pyridyl) pyridazine (4) exhibit electronic spectra in which large splittings of ν_1 (1500–5900 cm^{-1}) and ν_2 (900–5100 cm^{-1}) are observed. These spectra are interpreted in terms of a tetragonal crystal field. The absence of splitting of ν_1 or ν_2 is perhaps indicative of *cis*- rather than *trans*-NiN_4X_2 chromophores (12). A splitting of ν_1 of 1800 cm^{-1} is observed for the iodide complex (**V**) which suggests a possible *trans* structure.

The binuclear 1:1 perchlorate (**VII**), tetrafluoroborate (**VIII**), and iodide (**IX**) complexes are assigned *cis*-NiN_4O_2 structures involving bridging phthalazines and bridging hydroxy groups, the sixth coordination site at each metal being occupied by water (Fig. 2). The solid state spectra of the purple 1:1 binuclear chloride (**I**) and bromide (**III**) complexes are identical, and since the aqueous solution spectrum of the chloride complex is the same as its solid state spectrum, *cis*-NiN_4O_2 solid state structures are proposed in which water molecules occupy the fifth and sixth coordination sites at each nickel centre.

In the case of the green chloride complex **II** obtained by heating **I** under vacuum, a slight lowering in energy of the ν_1 and ν_2 bands is observed in keeping with a system containing some coordinated halide. A more pronounced lowering of ν_1 is observed for the corresponding bromide complex (**IV**), while ν_2 decreases by only 200 cm^{-1}. It is clear that water is again displaced by halogen in the metal coordination sphere. Heating the purple hydrated chloride and bromide complexes under vacuum gives various lower hydrates. When the number of water molecules per nickel atom is less than two, green or khaki–green coloured complexes are obtained. However, determining just how many coordinated halide groups exist in these dried complexes and whether or not bridging halides are to be found is difficult. Far infrared spectra have not been useful and conductivity studies are of no use since solvated species are produced in solution.

The 1:2 binuclear chloride and bromide complexes (**X**, **XI**) have solid state spectra in which there is a significant splitting of ν_1 (Table 2) and the band positions are shifted to lower energy compared with the 1:1 systems. In a six-coordinate 1:2 binuclear species only two coordination sites per metal would be occupied by ligand nitrogen atoms and the remaining sites could be occupied by water, hydroxide, and possibly halide, in keeping with the lower energy absorptions. Analytical and infrared data indicate the presence of a hydroxy group in these compounds and binuclear structures involving both bridging phthalazine and hydroxy groups are suggested. An X-ray study on the complex $[PAPCu_2Cl_3(OH)]\cdot H_2O$ has shown the presence of a triple bridge between square pyramidal copper atoms, involving bridging phthalazine, hydroxy, and chloro groups (9, 13). Molecular models indicate that such a structure would be possible for the 1:2 nickel halide complexes and that including a sixth ligand (i.e. water) at each pseudo-octahedral metal centre would present no steric problems. Both ν_1 and ν_2 for the bromide complex occur at lower energy than corresponding bands for the chloride complex suggesting the presence of a halide bridge in both systems (Fig. 3) (see also discussion on infrared data). Prolonged drying of the complexes, by heating under vacuum, produced colour changes (Cl, yellow–green; Br, buff–yellow) which suggested a change in the metal coordination sphere. This was reflected in their electronic spectra in which shifts to lower energy were observed on drying, suggesting the presence of coordinated terminal halide groups. On exposure to air again the original spectra were obtained indicating that water had displaced halogen in the coordination sphere.

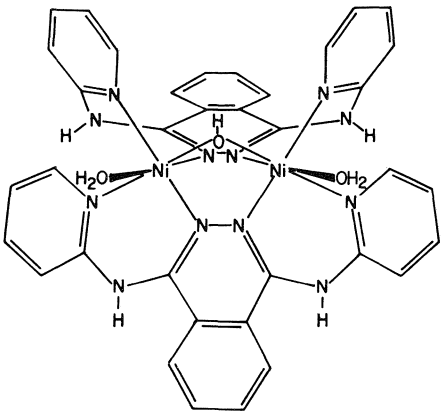


FIG. 2. A proposed structure for the cation in the complex $[PAP_2Ni_2(OH)(H_2O)_2](ClO_4)_3$.

Addition of the 1:2 binuclear derivatives to water produced an insoluble pale green precipitate, identified as nickel hydroxide, and purple solu-

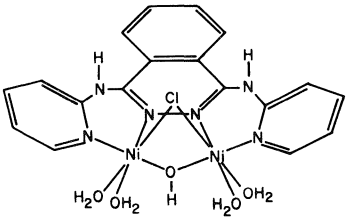


FIG. 3. A proposed structure for the cation in the complex $[PAPNi_2Cl(OH)(H_2O)_4]Cl_2$.

Can. J. Chem. Downloaded from www.nrcresearchpress.com by 210.87.254.40 on 09/05/12
For personal use only.

tions. Electronic spectra of these solutions exhibited bands due to $[PAP_2Ni_2(H_2O)_4]^{4+}$ and also an additional band around 9000 cm^{-1} assigned to ν_1 for $[Ni(H_2O)_6]^{2+}$. It appears therefore that the 1:2 binuclear complexes disproportionate in aqueous solution, possibly as follows:

$$2[PAPNi_2X(OH)(H_2O)_4]X_2 \rightarrow [PAP_2Ni_2(H_2O)_4]X_4 + NiX_{2\,(aq)} + Ni(OH)_{2\,(s)} + 4H_2O$$

The 1:1 binuclear complexes are clearly more stable in aqueous solutions. In concentrated acetic acid the minimal water present is sufficient to provide a source of ligands, but not to destroy the 1:2 system.

The 1:1 binuclear iodide complex (**V**) exhibits a splitting of ν_1 of 1800 cm^{-1}, suggesting the possibility of a *trans* structure involving four equatorial nitrogen donors. The lower energy absorptions indicate coordinated iodine and since PAP appears to be neutral (9) a hydroxide bridge is also proposed. The structure of this complex would thus be the *trans* equivalent of that proposed for **VII**, **VIII**, and **IX** (Fig. 2), but would have at least one axial site occupied by iodine. A *trans* structure is appropriate in this case in view of the bulk of the iodine atom. In aqueous solution ν_1 and ν_2 are observed at higher energy, consistent with an aquated species.

No splitting is observed for ν_1 or ν_2 in the case of the 1:1 binuclear thiocyanate complex (**VI**). ν_2 occurs at approximately the same energy as it does in the 1:1 halide complexes involving *cis*-NiN_4O_2 chromophores. However, ν_1 is reduced by 900 cm^{-1}, suggesting a somewhat weaker crystal field at the nickel centre.

The mononuclear 2:1 derivatives (**XII**, **XIII**) exhibit no splitting of ν_1 or ν_2 and the band energies are consistent with a Ni–N_4O_2 chromophore. The absence of splitting may be indicative of a *cis* rather than a *trans* structure. However, the tetrafluoroborate complex (**XII**) has an almost identical infrared spectrum to an analogous copper complex, $[(PAPH)_2Cu(H_2O)_2](BF_4)_4$, which has a tetragonal structure involving bidentate ligands coordinating via one pyridine and one nitrogen atom (the other pyridine nitrogen appears to be protonated) according to recent X-ray studies (14). It seems likely therefore that the nickel systems have a similar *trans* Ni—N_4O_2 structure.

In aqueous solution the nickel complexes exhibit an intense charge transfer absorption in the range 28 600–28 900 cm^{-1} (Table 2). In some cases this band can be observed in the solid state spectrum, but at slightly lower energies. This absorption is assigned to a π–π^* transition and has been used previously (9) to assess the charged state of the ligand. In a series of copper complexes, in which a neutral ligand species was involved, this band was found in the range 27 400–29 600 cm^{-1}. It is thus apparent, in keeping with other data, that PAP is a neutral species in all the nickel complexes.

The solution spectrum of the purple 1:1 chloride complex (**I**) is the same as its solid state spectrum, indicating a system involving two coordinated water molecules per nickel in both states. However, in the case of the purple bromide complex (**III**) the solution spectrum differs somewhat from its solid state spectrum. ν_1 occurs as a broad single band at 11 400 cm^{-1} in the solid state but in solution is replaced by a peak at 10 300 cm^{-1} and a shoulder of comparable intensity at 11 600 cm^{-1}. The component of ν_1 at 11 600 cm^{-1} corresponds almost exactly with ν_1 for the purple tetraaquo complex (**III**), while that at 10 300 cm^{-1} is close to ν_1 for the green bromo complex (**IV**). The bromide complex (**III**) may exist as a mixture of the tetraaquo complex and a bromo derivative in aqueous solution. The same spectrum is obtained by dissolving the green bromide complex (**IV**) in water.

Infrared Data

In a previous paper we assigned an absorption at 989 cm^{-1} in PAP to a ring breathing mode associated with the pyridine residues (9). A shift of this band above 1000 cm^{-1} indicated a coordinated pyridine ring. In most of the binuclear complexes this band is observed above 1000 cm^{-1} (Table 3) with no residual band associated with uncoordinated pyridine. In the case of the binuclear tetrafluoroborate complex (**VIII**) the ν_3 absorption associated with the tetrafluoroborate ion masked the coordinated pyridine band. However no absorption due to free pyridine was observed.

Rather broad absorptions are observed for the 1:1 binuclear halide complexes (**I**, **III**) in the range 3600–3200 cm^{-1}. However, a band at 3550 cm^{-1} in the bromide complex is assigned to coordinated water. The general similarity of the spectra of these species, especially in the far infrared region, suggests the same solid state cations involving coordinated water rather than halide. In the case of the 1:1 binuclear tetrafluoroborate complex (**VIII**) peaks at 3625 and 3550 cm^{-1} are assigned to coordinated water and bridging hydroxide, although distinction between the two may not be possible. The analogous perchlorate complex (**VII**) exhibits a broad shoulder in this region and assignments due to coordinated water and bridging hydroxide could not be made. Peaks at 3370 cm^{-1} (BF_4^-) and 3360 cm^{-1} (ClO_4^-) are assigned to NH stretch and absorptions associated with the tetrafluoroborate and per-

TABLE 3. Infrared spectra (cm^{-1})

Compound	Pyridine ring breathing mode	νOH	νNH	νM—X
I, $[PAP_2Ni_2(H_2O)_4]Cl_4 \cdot 3H_2O$	1012			
III, $[PAP_2Ni_2(H_2O)_4]Br_4$	1012	3550		
V, $[PAP_2Ni_2(OH)I_2]I \cdot 2H_2O$	1011		3270	
VI, $[PAP_2Ni_2(NCS)_3]NCS$[a]	1007		3300	269
VII, $[PAP_2Ni_2(OH)(H_2O)_2](ClO_4)_3$[b]	1014		3360	
VIII, $[PAP_2Ni_2(OH)(H_2O)_2](BF_4)_3$[b]	—	3625, 3550	3370	
IX, $[PAP_2Ni_2(OH)(H_2O)_2]I_3 \cdot 3H_2O$	1011	3550	3380	
X, $[PAPNi_2Cl(OH)(H_2O)_4]Cl_2$	1018	3530	3370	320, 308(N), 242(OH)
XI, $[PAPNi_2Br(OH)(H_2O)_4]Br_2$	1019	3530	3360	328, 312(N), 245(OH)
XII, $[(PAPH)_2Ni(H_2O)_2](BF_4)_4$	—	3480, 3520	3380	
XIII, $[(PAPH)_2Ni(H_2O)_2]I_4$	1015, 1008, 998			
XIV, $[PAP_2Zn_2Cl_4]$	1010		3360	330, 305(Cl)
XV, $[PAPZnBr_2] \cdot H_2O$	1018, 990		3365	238, 210(Br)
XVI, $[PAPZnI_2] \cdot H_2O$	1015, 990		3365	

[a]νCN(NCS) 2098, 2048, 2002; νCS(NCS) 463, 475 cm^{-1}.
[b]ClO_4^- ν_3 1100(br) cm^{-1}; BF_4^- ν_3 1050(br) cm^{-1}.

chlorate groups themselves indicate that these anions are uncoordinated.

The 1:1 binuclear iodide complexes (**V**, **IX**) have very similar infrared spectra and both bear a close resemblance to the spectra of the binuclear hydroxo bridged derivatives **VII** and **VIII**. $[PAP_2Ni_2(OH)(H_2O)_2]I_3 \cdot 3H_2O$ (**IX**) exhibits an OH stretching absorption at 3550 cm^{-1} and an absorption at 3380 cm^{-1} due to NH stretching. These peaks are close to those observed for **VII** and **VIII** and support a hydroxy bridged structure involving two coordinated water molecules. The iodide complex (**V**), prepared in methanol, exhibits only a broad absorption in this region with a peak at 3270 cm^{-1}, which can be associated with NH stretch. No peak due to OH stretch could be discerned. The differences in the range 3200–3600 cm^{-1} could be associated with a system having the same basic structure as **IX** but involving coordinated iodine rather than water.

The 1:2 binuclear halide complexes (**X**, **XI**) exhibit a sharp absorption at 3530 cm^{-1}, which is assigned to OH stretching associated with a bridging hydroxy group, while a broad absorption around 3360–3370 cm^{-1} is assigned to NH stretch. In the far infrared a comparison of the spectra of the hydrated complexes (**X**, **XI**) with their dried counterparts allowed certain assignments to be made. Bands in the range 308–328 cm^{-1}, common to all four species, are assigned to Ni—N stretch. Absorptions at 275, 282 cm^{-1} (Cl) and 231 cm^{-1} (Br) in the dried compounds disappear on exposure to air and are assigned to terminal nickel–halogen stretch, and a strong absorption around 242–246 cm^{-1}, common to all species, may be associated with nickel–oxygen stretch in the bridging hydroxy group. The absence of terminal nickel halogen stretching vibrations in **X**, **XI** suggests the coordination of two water molecules at each nickel centre.

The thiocyanate complex (**VI**) exhibits a most unusual infrared spectral region due to CN(NCS) stretching. Strong absorptions at 2098 and 2048 cm^{-1} are assigned to nitrogen bound and ionic thiocyanate respectively while a strong, low energy absorption at 2002 cm^{-1} cannot be assigned to a normal thiocyanate group. The complex is clearly a 1:1 binuclear derivative involving six-coordinate nickel which leaves four coordination sites available for thiocyanate coordination. Assuming the presence of one ionic thiocyanate a reasonable way for the other three groups to be accommodated would involve two isothiocyanates and a thiocyanate bridge. Molecular models and other data suggest that a three atom bridge between the two metal centres would be unlikely, but a single atom bridge would, of course, be possible. The low energy thiocyanate absorption could therefore be associated with a single atom nitrogen bridged thiocyanate in which the CN bond order is somewhat lower than usual. Further studies, including an X-ray structural determination, are necessary to confirm this.

NOTE ADDED IN PROOF: A recent X-ray structure of the complex $(n\text{-}Bu_4N)_3[Re_2(NCS)_{10}]$ reveals the presence of two solely N-bonded bridging thiocyanate groups (17). Infrared absorptions at 1920 and 1885 cm^{-1} are assigned to CN stretching in these bridging groups.

In the protonated mononuclear complexes (**XII**, **XIII**) PAP coordinates as a bidentate ligand via one phthalazine and one pyridine nitrogen atom. The ν_3

Can. J. Chem. Downloaded from www.nrcresearchpress.com by 210.87.254.40 on 09/05/12
For personal use only.

Can. J. Chem. Downloaded from www.nrcresearchpress.com by 210.87.254.40 on 09/05/12
For personal use only.

vibration associated with the tetrafluoroborate anion masks the pyridine ring breathing vibrations in **XII**, but three bands (Table 3) are observed in this region for the iodide complex. Bands at 1015 and 1008 cm^{-1} can be associated with coordinated pyridine moieties while the band at 998 cm^{-1} is consistent with a protonated pyridine ring (a hydrochloride salt of PAP in which both pyridine rings appear to be protonated has just one absorption in this region at 1003 cm^{-1}).

Magnetism and Conductance

The binuclear perchlorate (**VII**), tetrafluoroborate (**VIII**), and iodide (**V**) complexes have room temperature magnetic moments close to the spin only value, which are comparable with those observed for 1:1 binuclear complexes of 1,4-dihydrazinophthalazine (4) for which $-J$ values fall in the range 20–24 cm^{-1}. Variable temperature susceptibility studies have been carried out on the chloride (**I**) and perchlorate (**VII**) complexes in the temperature range 80–300 K and preliminary results using the conventional model for two interacting $S = 1$ states (4) (Table 4) indicate smaller J values ($-J$ less than 10 cm^{-1}) than were found for other disubstituted diazine systems (4). This difference may be due to the fact that in the PAP complexes six-membered chelate rings are formed, as opposed to five in the other diazine systems, with the result that orbital overlap between the metal centres and the π-molecular orbital system of the phthalazine bridge will be reduced because of the non-planarity of the ligand. Direct orbital overlap between the metal centres seems unlikely and a superexchange mechanism is suggested via the bridging groups. It is significant that a larger exchange is observed for the perchlorate complex which is assumed to have a hydroxy bridge in addition to the phthalazine bridge. Further studies on the spin–spin exchange in these systems are planned down to liquid helium rather than liquid nitrogen temperatures.

Conductance data (Table 4) were obtained for some systems in aqueous solution as a function of concentration and the slopes of Kohlrausch plots for the chloride (**I**) and perchlorate (**VII**) complexes indicate 1:4 and 1:3 electrolytes respectively (15). An anomalously large slope was observed for the mononuclear tetrafluoroborate complex (**XII**) indicating the presence of more ions in solution than expected. The tetrafluoroborate ion hydrolyses in aqueous solution are as follows (16):

$$BF_4^- + H_2O \rightleftharpoons BF_3(OH)^- + HF \qquad K = 2.3 \times 10^{-3}$$

Subsequent dissociation of HF and possible dissociation of protonated PAP could be responsible for the high conductance of this system. The pH of an approximately 0.1 mol dm^{-3} solution of nickel tetrafluoroborate was found to be 2.5 (calculated pH 2.3). It is thus no surprise that a protonated mononuclear complex is obtained from the reaction of PAP with $Ni(BF_4)_2$ in water. Adjustment of the pH of nickel tetrafluoroborate solution can be achieved by controlled addition of fluoride ion. Reaction of PAP with an aqueous solution of nickel tetrafluoroborate (pH adjusted to 5.5 by addition of fluoride) gave only the 1:1 binuclear derivative (**VIII**).

A similar mixture of compounds was obtained from the reaction between nickel iodide and PAP in water. In this case the formation of a protonated complex is somewhat surprising, since the aqueous nickel iodide used in our studies was only slightly acidic (approximately 0.1 mol dm^{-3}, pH = 6.0). However, if the hydroxy bridged species is the most thermodynamically favoured binuclear system, protons would be present in solution, which would be responsible for the formation of the protonated complex. That such a species is not observed for the perchlorate system may simply be a reflection on its solubility. In the case of the tetrafluoroborate system the hydrolysis of BF_4^- just enhances the acidity.

TABLE 4. Magnetic moment and conductance data

Compound	μ (BM) (room temperature)	B^a
I, $[PAP_2Ni_2(H_2O)_4]Cl_4 \cdot 3H_2O$	3.3[b]	527
III, $[PAP_2Ni_2(H_2O)_4]Br_4$	3.3	
V, $[PAP_2Ni_2(OH)I_2]I \cdot 2H_2O$	2.8	
VI, $[PAP_2Ni_2(NCS)_3]NCS$	3.1	
VII, $[PAP_2Ni_2(OH)(H_2O)_2](ClO_4)_3$	2.7[c]	325
VIII, $[PAP_2Ni_2(OH)(H_2O)_2](BF_4)_3$	2.9	
IX, $[PAP_2Ni_2(OH)(H_2O)_2]I_3 \cdot 3H_2O$	3.1	
X, $[PAPNi_2Cl(OH)(H_2O)_4]Cl_2$	3.1	
XI, $[PAPNi_2Br(OH)(H_2O)_4]Br_2$	3.0	
XII, $[(PAPH)_2Ni(H_2O)_2](BF_4)_4$	3.2	925
XIII, $[(PAPH)_2Ni(H_2O)_2]I_4$	3.1	

[a]Slope of Kohlrausch plot ($\Lambda_0 - \Lambda_e$ vs. $\sqrt{c_e}$) for aqueous solutions in the range 10^{-3}–10^{-5} M at 25°C.
[b]$-J = 3.2$ cm^{-1}, $g = 2.20$.
[c]$-J = 7.3$ cm^{-1}, $g = 1.93$.

Zinc Complexes

The zinc complexes of PAP were obtained as fairly insoluble yellow or pale yellow solids from ethanol or methanol. Elemental analyses indicate that in all the complexes the ligand-to-metal ratio is 1:1.

Infrared data (Table 3) indicate that in the chloro complex (**XIV**) PAP is acting as a tetradentate

ligand and so a 1:1 binuclear structure is proposed. Two sharp bands are observed in the far infrared spectrum of the chloro complex, which are assigned to Zn—Cl stretch, suggesting that each zinc ion is in a six-coordinate *cis*-N_4Cl_2 environment.

The other zinc complexes exhibit two pyridine ring breathing mode absorptions, which indicate that PAP coordinates as a bidentate ligand through one phthalazine and one pyridine nitrogen. Absorptions in the far infrared at 238, 210 cm^{-1} for the bromo-complex (**XV**) suggest a tetrahedral ZnN_2Br_2 chromophore, with water bound in the lattice. The similarity between the infrared spectrum of this system and that of the iodo-complex (**XVI**) suggests a tetrahedral ZnN_2I_2 structure for the iodide complex.

Acknowledgements

We are indebted to the Natural Sciences and Engineering Research Council of Canada for financial support for this study. We thank the Chemistry Department at the University of British Columbia for the use of the magnetic balance and Dr. R. C. Thompson for helpful discussions. Also we wish to thank Dr. P. D. Golding for computing assistance.

1. W. J. Stratton and D. H. Busch. J. Am. Chem. Soc. **82**, 4834 (1960).
2. J. E. Andrew, P. W. Ball, and A. B. Blake. Chem. Commun. 143 (1969).
3. J. E. Andrew and A. B. Blake. J. Chem. Soc. A, 1408 (1969).
4. P. W. Ball and A. B. Blake. J. Chem. Soc. A, 1415 (1969).
5. P. W. Ball and A. B. Blake. J. Chem. Soc. Dalton, 852 (1974).
6. D. A. Sullivan and G. J. Palenik. Inorg. Chem. **16**, 1127 (1977).
7. H. Alper. J. Organomet. Chem. **50**, 209 (1973), and references therein.
8. H. Okawa, S. Kida, Y. Muto, and T. Tokii. Bull. Chem. Soc. Jpn. **45**, 2480 (1972).
9. L. K. Thompson, V. T. Chacko, J. A. Elvidge, A. B. P. Lever, and R. V. Parish. Can. J. Chem. **47**, 4141 (1969).
10. A. B. P. Lever, L. K. Thompson, and W. M. Reiff. Inorg. Chem. **11**, 104 (1972).
11. H. C. Clark and R. J. O'Brien. Can. J. Chem. **39**, 1030 (1961).
12. A. B. P. Lever. Inorganic electronic spectroscopy. Elsevier, Amsterdam. 1968.
13. E. C. Lingafelter and G. Marongiu. To be published.
14. J. C. Dewan and L. K. Thompson. To be published.
15. R. D. Feltham and R. G. Hayter. J. Chem. Soc. 4587 (1964).
16. F. A. Cotton and G. Wilkinson. Advanced inorganic chemistry. 3rd ed. Wiley, Interscience, New York. 1972.
17. F. A. Cotton, A. Davison, W. H. Ilsley, and H. S. Trop. Inorg. Chem. **18**, 2719 (1979).

Can. J. Chem. Downloaded from www.nrcresearchpress.com by 210.87.254.40 on 09/05/12
For personal use only.

Excess volumes of toluene mixtures with some alcohols at 303.15 K

GOOLLA NARAYANA SWAMY, GOLLA DHARMARAJU, AND GURAJALA KODANDA RAMAN
Department of Chemistry, College of Engineering, Sri Venkateswara University, Tirupati 517 502, India

Received July 30, 1979

GOOLLA NARAYANA SWAMY, GOLLA DHARMARAJU, and GURAJALA KODANDA RAMAN. Can. J. Chem. **58**, 229 (1980).

Excess volumes for binary mixtures of toluene with 1-propanol, 2-propanol, 1-butanol, 2-methyl-1-propanol, 1-pentanol, 1-hexanol, 1-heptanol, and cyclohexanol have been measured as a function of composition at 303.15 K by a dilatometric method. The excess volume curves for 1-propanol and 1-butanol are sigmoid. For other alcohols V^E values are positive over the entire composition range.

GOOLLA NARAYANA SWAMY, GOLLA DHARMARAJU et GURAJALA KODANDA RAMAN. Can. J. Chem. **58**, 229 (1980).

On a mesuré les volumes d'excès des mélanges binaires du toluène avec les alcools suivants: propanol-1, propanol-2, butanol-1, méthyl-2 propanol-1, pentanol-1, hexanol-1, heptanol-1 et le cyclohexanol en fonction de la composition à 303.15 K en utilisant une méthode dilatométrique. Les courbes de volume d'excès du propanol-1 et du butanol-1 sont sigmoides. Dans le cas des autres alcools, les valeurs de V^E sont positives pour toutes les échelles de composition.

[Traduit par le journal]

Can. J. Chem. Downloaded from www.nrcresearchpress.com by 210.87.254.6 on 09/05/12
For personal use only.

Introduction

Alcohols are strongly self-associated (1) and for binary solutions rich in alcohol a three dimensional network of hydrogen bonded alcohol molecules is believed to be present (2, 3). A good deal of work has been reported by Washburn and Lightbody (4) on the excess volumes of mixtures of methanol, ethanol, and 2-propanol with toluene and benzene as common components. The purpose of the present investigation is to study the effect of a non-polar solvent like toluene on excess volumes of some alcohols. The alcohols selected were 1-propanol, 2-propanol, 1-butanol, 2-methyl-1-propanol, 1-pentanol, 1-hexanol, 1-heptanol, and cyclohexanol.

Experimental

Materials

Analytical grade toluene was purified in accordance with the procedure suggested in literature (5). All alcohols except 1-heptanol were dried by refluxing with fused calcium oxide and distilling from it. Heptanol (Koch-Light Laboratories Ltd., England) was used without further purification. The purities of the liquids were checked by comparing measured densities with those reported in the literature (6). Excess volumes as a function of composition were determined dilatometrically by the method described by Rao and Naidu (7). The experimental method was previously checked (8) against cyclohexane + benzene at 303.15 K, and the results obtained showed a standard deviation of ± 0.003 cm^3 mol^{-1}.

Results

The results[1] at 303.15 K are graphically represented in Fig. 1. The experimental values of V^E may

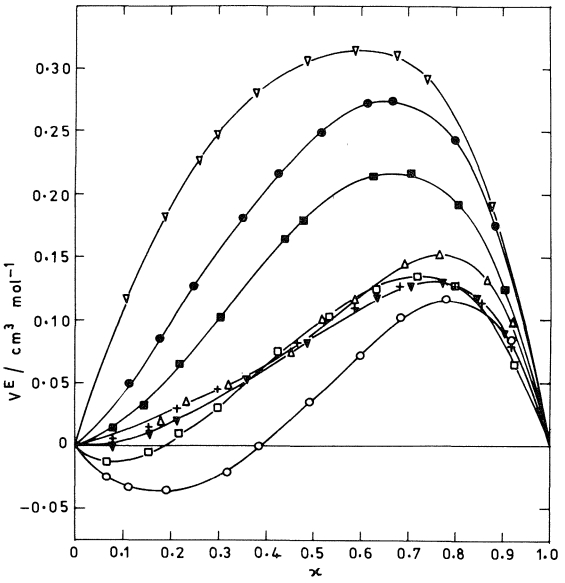


FIG. 1. Excess volumes V^E plotted against mole fraction x of toluene at 303.15 K for the mixtures of toluene with alcohols: ○, 1-propanol; ●, 2-propanol; □, 1-butanol; ■, 2-methyl-1-propanol; △, 1-pentanol; ▼, 1-hexanol; +, 1-heptanol; ▽, cyclohexanol.

be represented by an empirical equation

$$[1] \quad V^E/\text{cm}^3\,\text{mol}^{-1} = x(1-x)[a_0 + a_1(2x-1) + a_2(2x-1)^2]$$

where x is the mole fraction of toluene. The values of the parameters a_0, a_1, and a_2 evaluated by the method of least-squares are given in Table 1 along with standard deviation $\sigma(V^E)$.

Discussion

The curves for mixtures of toluene with 1-

[1]Complete set of the actual experimental data is available, at a nominal charge, from the Depository of Unpublished Data, CISTI, National Research Council of Canada, Ottawa, Ont., Canada K1A 0S2.

0008-4042/80/030229-02$01.00/0
©1980 National Research Council of Canada/Conseil national de recherches du Canada

TABLE 1. Standard deviation $\sigma(V^E)$ and values of the parameters in eq. [1]

Mixture	a_0	a_1	a_2	$\sigma(V^E)$ / cm^3 mol^{-1}
Toluene + 1-propanol	0.142	0.849	0.349	0.005
Toluene + 1-butanol	0.387	0.646	0.016	0.003
Toluene + 2-propanol	0.985	0.780	0.237	0.004
Toluene + 2-methyl-1-propanol	0.738	0.754	0.145	0.004
Toluene + 1-pentanol	0.359	0.645	0.577	0.002
Toluene + 1-hexanol	0.348	0.590	0.280	0.003
Toluene + 1-heptanol	0.367	0.573	0.306	0.004
Toluene + cyclohexanol	1.229	0.368	0.486	0.001

propanol and 1-butanol are sigmoid. The excess volumes for mixtures of toluene with 1-propanol and 1-butanol are negative at lower mole fractions of toluene and positive at higher mole fractions. For other mixtures the values of V^E are positive over the entire concentration range. V^E values for 2-propanol, 2-methyl-1-propanol, and cyclohexanol are larger than normal alcohols. For equimolar mixtures V^E values fall in the order 1-propanol < 1-butanol ≈ 1-pentanol ≈ 1-hexanol ≈ 1-heptanol < 2-methyl-1-propanol < 2-propanol < cyclohexanol.

Numerous studies (9–11) indicate that alcohols are associated through hydrogen-bonded linear chains (with restricted rotation about hydrogen bonds) into variable degrees of polymerisation. According to Treszczanowicz and Benson (12) the observed V^E data may be explained qualitatively by postulating that V^E is the resultant of opposing effects. The positive V^E values arise due to the breaking of hydrogen bonds in self-associated alcohols and physical dipole–dipole interactions between alcohol monomers and multimers. Negative contributions arise from changes of "free volume" in the real mixture and the presence of π-electrons in toluene resulting in the formation of weak intermolecular complexes. The results show that the negative contributions decrease with increase in chain length. But the positive values of V^E for 1-butanol, 1-pentanol, 1-hexanol, and 1-heptanol which are almost equal suggest that the positive V^E values are insensitive to the chain length. Negative contributions get more and more sterically hindered when the alkyl group in the alcohol becomes more and more branched, which is observed in the behaviour of mixtures with 2-propanol and 2-methyl-1-propanol. Washburn and Lightbody (4) have reported excess volumes of toluene + 2-propanol at 298.15 K using density measurements which also show similar trend. The maximum value of V^E for cyclohexanol may be due to less self-association than other alcohols.

1. F. FRANKS and D. J. G. IVES. Q. Rev. **20**, 1 (1966).
2. J. S. ROWLINSON. Liquid and liquid mixtures. 2nd ed. Butterworths, London. 1969. p. 159.
3. I. PRIGOGINE and R. DEFAY. Chemical thermodynamics. *Translated by* D. H. Everett. Longman Green and Co., London. 1953. p. 470.
4. E. R. WASHBURN and A. LIGHTBODY. J. Phys. Chem. **34**, 2701 (1930).
5. A. I. VOGEL. Practical organic chemistry. Longman Green, London. 1956. p. 172.
6. J. TIMMERMANS. Physico-chemical constants of pure organic compounds. Elsevier Publishing Co., Amsterdam. 1950.
7. M. V. P. RAO and P. R. NAIDU. Can. J. Chem. **52**, 788 (1974).
8. R. H. STOKES, B. J. LEVIEN, and K. N. MARSH. J. Chem. Thermodyn. **2**, 43 (1970).
9. R. K. NIGAM and P. P. SINGH. Trans. Faraday Soc. **65**, 950 (1969).
10. W. H. ZACHARIASEN. J. Chem. Phys. **3**, 158 (1935).
11. R. MECKE. Dişcuss. Faraday Soc. **9**, 161 (1950).
12. A. J. TRESZCZANOWICZ and G. C. BENSON. J. Chem. Thermodyn. **10**, 967 (1978).

Can. J. Chem. Downloaded from www.nrcresearchpress.com by 210.87.254.6 on 09/05/12
For personal use only.

Ion mobilities and collision frequencies in gaseous CH_3Cl, HCl, HBr, H_2S, NO, and SF_6: effects of polarity of the gas molecules

ERIC S. SENNHAUSER AND DAVID A. ARMSTRONG

Department of Chemistry, University of Calgary, Calgary, Alta., Canada T2N 1N4

Received August 13, 1979

ERIC S. SENNHAUSER and DAVID A. ARMSTRONG. Can. J. Chem. **58**, 231 (1980).

Mobilities of positive and negative ions at 296 K have been measured at pressures in the range 50 to 1200 Torr. Least-mean-squares analysis of the pressure dependences gave the following mobilities normalized to a density of 2.69×10^{19} molecules cm^{-3}: CH_3Cl $\mu_+ = 0.39$, $\mu_- = 0.37$; HCl 0.64, 0.59; HBr 0.48, 0.49; H_2S 0.59, 0.60; NO 0.97, 1.53; SF_6 $\mu_- = 0.49$ $cm^2 V^{-1} s^{-1}$. Except in one instance the ions exhibited a close to inverse dependence of mobility on gas density. The identities of the ions are discussed in the light of high pressure mass spectrometric data from the literature. The dependence of the collision frequencies of the ions on $\mu_D/\alpha^{1/2}$, the ratio of dipole moment to (polarizability)$^{1/2}$ for the neutral gas molecules, was very similar to that observed previously by the ion cyclotron resonance technique at much lower pressures. The magnitudes of the collision frequencies at unit concentration are in reasonable agreement with predictions based on the ion–molecule collision rate theory of Barker and Ridge, but the dependence on $\mu_D/\alpha^{1/2}$ is lower and closer to that predicted by ADO theory.

ERIC S. SENNHAUSER et DAVID A. ARMSTRONG. Can. J. Chem. **58**, 231 (1980).

On a mesuré les mobilités des ions positifs et négatifs à 296 K et à des pressions allant de 50 à 1200 Torr. Une analyse, par la méthode des moindres carrés, de l'effet de la pression conduit aux valeurs suivantes des mobilités normalisées à une densité de 2.69×10^{19} molécules cm^{-3}: CH_3Cl $\mu_+ = 0.39$, $\mu_- = 0.37$; HCl 0.64, 0.59; HBr 0.48, 0.49; H_2S 0.59, 0.60; NO 0.97, 1.53; SF_6 $\mu_- = 0.49$ $cm^2 V^{-1} s^{-1}$. A l'exception d'un seul cas, les ions montrent une tendance à inverser l'effet de la pression sur la mobilité dans le cas de la densité des gaz. On discute de l'identité des ions à la lumière des données sur la spectrométrie de masse à haute pression recueillies dans la littérature. L'effet de la fréquence des collisions sur $\mu_D/\alpha^{1/2}$, le rapport du moment dipolaire à une (polarisabilité)$^{1/2}$ pour les molécules de gaz neutre, ressemble beaucoup à celui observé antérieurement par la technique de résonance du cyclotron à des pressions plus faibles. L'ampleur de la fréquence des collisions à concentrations unitaires est raisonnablement en accord avec les prédictions basées sur la théorie de Barker et Ridge concernant la vitesse de collision ion–molécule, mais l'effet sur $\mu_D/\alpha^{1/2}$ est plus faible et plus près de celui prédit par la théorie "ADO".

[Traduit par le journal]

Introduction

The study of ion mobilities in gases leads to information on ion–neutral interaction potentials, and is also of importance for an understanding of ion transport and recombination mechanisms (1). A recent publication (2) from this laboratory described an ionization chamber-drift tube, which could be used at pressures in the range 50 to 1200 Torr. Mobilities for ions in ammonia vapor were reported, and compared to those calculated from ion–molecule collision rate theories (3, 4). This paper presents results for SF_6, H_2S, CH_3Cl, HBr, HCl, and NO. As well as being of interest in radiation chemistry, these gases possess dipole moments which cover a wide range. Therefore more extensive comparisons with ion–molecule rate theory predictions can be made. With the exception of CH_3Cl (5) all of the gases react rapidly with thermal electrons to form heavy negative ions.

Experimental

Materials

Sample preparation and material purification were performed in a mercury-free vacuum line. All gases were obtained from the Matheson Co. and subjected to several freeze–pump–thaw cycles to remove noncondensibles. In addition the NO (research grade), HCl (electronic grade, 99.99% minimum purity), and HBr (anhydrous, 99.8% minimum purity) were distilled several times from an alcohol slurry at 160 K; retaining only the first fractions. The H_2S (C.P., 99.5% minimum purity) was passed through a Linde molecular sieve (type 3A) at 0°C to remove traces of water. Mobility–current profiles were normally rerun after at least one repurification to make sure that no changes in the profile due to further removal of impurities occurred. Only with H_2S was any effect observed. The purified samples were stored at 77 K. Carbon tetrachloride was obtained from Baker Chemicals (spectrophotometric quality). A small quantity was stored in a tube after several freeze–pump–thaw cycles.

Apparatus

A diagram of the ionization chamber-drift tube is shown in Fig. 1. Details of its construction and of the associated electrical components were given in ref. 2. L_1 and L_2 are plane parallel electrodes, while G_1 and G_2 are nickel mesh grids. The radiation compartment of length d_1 (= 1.0 cm) is defined by L_1 and G_1 while the space between G_2 and L_2 of length d_3 (= 1.3 cm) is the collection compartment. The drift space between G_1 and G_2 has a length d_2 of 4.0 cm. The cell was pumped down to $\sim 10^{-6}$ Torr between fillings, and when a change to a new gas was made it was evacuated for several hours, while heated with a hot air blower.

During an experiment a constant intensity collimated 4 mm beam of 40 kV peak X-rays from a Müller MG 150 unit was centered in the radiation compartment. A constant potential, V_{dc}, was applied to G_2. Periodically a high voltage pulse (repetition frequency ~ 8 s^{-1}, rise time ~ 10 μs) of the same polarity as V_{dc} was applied to L_1 to produce fields E_r and E_d in the radiation and drift compartments. These fields could be varied by changing the magnitude of the high voltage pulse, or of R_1, R_2 and V_{dc}.

0008-4042/80/030231-07$01.00/0

©1980 National Research Council of Canada/Conseil national de recherches du Canada

Can. J. Chem. Downloaded from www.nrcresearchpress.com by 210.87.254.105 on 09/05/12
For personal use only.

Can. J. Chem. Downloaded from www.nrcresearchpress.com by 210.87.254.105 on 09/05/12
For personal use only.

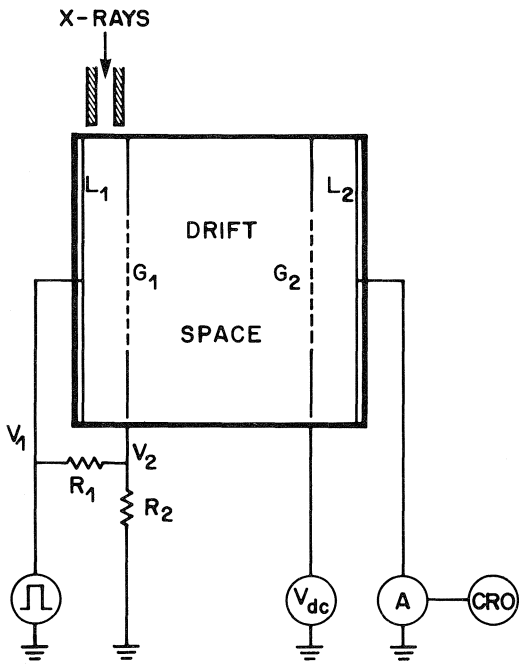


FIG. 1. Ionization chamber-drift tube. V_1 and V_2, pulsed high voltage applied to electrode L_1 and grid G_1; V_{dc}, steady potential applied to grid G_2; L_2, collecting electrode, A, amplifier.

The duration of the pulse was variable, and ions which crossed the 4.0 cm drift compartment before it ended were collected. Those which did not were returned to the irradiation compartment (or to grid G_1) by the potential on G_2. The "time off" of the high voltage was always long enough to allow steady state conditions to be reached in the radiation compartment.

In place of the Victoreen 475 A electrometer used in ref. 2 the output from electrode L_2 was fed into an Analog Device 46 J amplifier A. This has a high input impendance (10^{11} ohm) and high slew rate. It was connected as an inverting current amplifier with a current to voltage gain of $\sim 10^6$. The frequency response begins to drop at 20 kHz, but this was not a problem in following the present transients. The output from the amplifier was displayed on one beam of a Tektronix type 502 A dual beam oscilloscope. The second beam followed the profile of the square wave high voltage pulse, and provided a time base. When desired either trace from a single pulse could be recorded with a Model 8100 Biomation transient recorder and then reproduced on an X-Y recorder.

Data Analysis

In part (*c*) of Fig. 2 a typical trace of a current profile from the biomation recorder has been presented. The high voltage profile has been depicted by the solid line which crosses it and falls to zero just short of 20 ms, where the current profile also ends. As the duration of the high voltage pulse set by the time device (2) was shortened, the current profile was truncated correspondingly. In many experiments the time to peak maximum t_p was determined by shortening the voltage pulse until the "time off" coincided with it. Alternatively it could be measured from the abscissa of the oscilloscope or biomation traces.

In part (*a*) of Fig. 2 a representative detector signal of the type obtained with the electrometer used earlier (2) has been shown. This instrument measured the integrated charge per unit volume of the radiation compartment η/d_1, which reached the collection

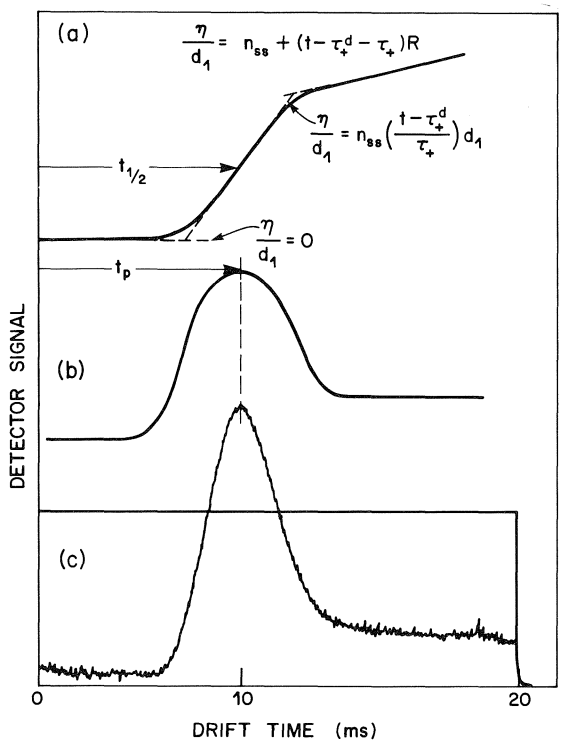


FIG. 2. Illustrations of detector signals. (*a*) Integrated charge reaching collecting electrode as a function of drift time or time on of the high voltage. (See text for explanation of dashed lines and equations.) (*b*) Differentiation of smooth curve in (*a*). (*c*) Smooth line, high voltage profile; line with noise, current–time profile for positive ions in HBr at 296 K and 191 Torr.

compartment as a function of drift time t. The charge–time profiles were analyzed in terms of the three straight lines shown. The equations for these lines, shown also in Fig. 2, were developed in ref. 2 on the assumption of no diffusional or space charge broadening of the ion cloud during drift. The smooth curve shows the effect of these processes.

The relation of the present detection method to the earlier one has been illustrated in part (*b*), which is a schematic differentiation of the smooth curve in (*a*). The time scale in (*a*) and (*b*) was somewhat expanded. The average ion drift time is now measured as t_p, rather than as $t_{1/2}$ in part (*a*) of Fig. 2. This was the time that an ion, starting its drift in the center of the irradiation compartment, would spend on average before detection. Therefore t_p is related to the ion mobility by eq. [1]:

$$[1] \quad t_p^{\pm} = \frac{1}{\mu_{\pm}}\left(\frac{d_1}{2E_r} + \frac{d_2}{E_d} + \frac{x}{E_c}\right)$$

Here, E_r, E_d, and E_c are the field strengths in the radiation, drift, and collection compartments and x is the distance into the collection compartment at which the ions are detected.

Results

The current profile in Fig. 2(*c*) was for the positive ions in 191 Torr of HBr at 296 K. The voltages at L_1 and G_1 were 1800 V and 1500 V respectively when the high voltage pulse was on and zero otherwise. The grid G_2 was kept at 400 V. This arrange-

Can. J. Chem. Downloaded from www.nrcresearchpress.com by 210.87.254.105 on 09/05/12
For personal use only.

ment gave rise to electric fields: $E_r = 300$, $E_d = 275$, and $E_c = 308$ V cm^{-1}.

For each ion and each pressure E_r and E_d were varied from about 110 to 400 V cm^{-1} with E_r being always somewhat larger. E_c was varied independently of E_r and E_d from ~120 to ~400 V cm^{-1}. To avoid any uncertainty in the parameter x eq. [1] was rearranged to:

$$[2] \quad t_p{}^{\pm}E_c = \frac{1}{\mu_{\pm}} E_c\left(\frac{0.5}{E_r} + \frac{4.0}{E_d}\right) + \frac{x}{\mu_{\pm}}$$

The ion mobility was then obtained from the reciprocal of the least-mean-squares slope of t_pE_c plotted against $E_c(0.5/E_r + 4.0/E_d)$. A typical plot of this has been shown in Fig. 3. It was for negative ions in HBr at 191 Torr. No systematic dependence of $\mu_{\pm}$ on field strength was observed for any of the conditions used. The E/P values ranged from 0.1 to 8 V cm^{-1} Torr^{-1} (E/N from 0.45 to 2.5 × 10^{-16}).

Values of the experimental mobilities are plotted against the neutral density in Fig. 4. Each point was derived from a least-mean-squares analysis of 10 to 20 points plotted as in Fig. 3. Except in NO, the mobilities of the positive and negative ions were similar. Table 1 summarizes the slopes of the solid lines in Fig. 4. They were obtained by the least-squares method. The reduced mobilities ($\mu_0 = \mu$ at $N = 2.69 \times 10^{19}$ cm^{-3}) are also given. With the exception of the positive ion in CH_3Cl the slopes all lay between −0.95 and −1.03.

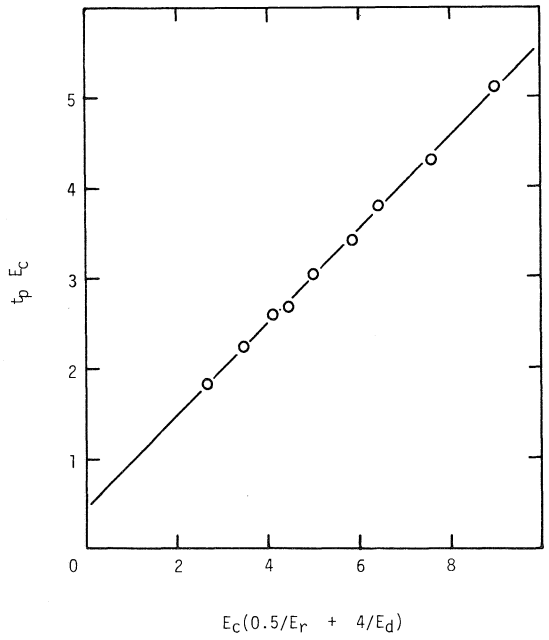


FIG. 3. Plot of t_pE_c against $E_c(0.5/E_r + 4.0/E_d)$ for negative ions in HBr at 191 Torr and 296 K.

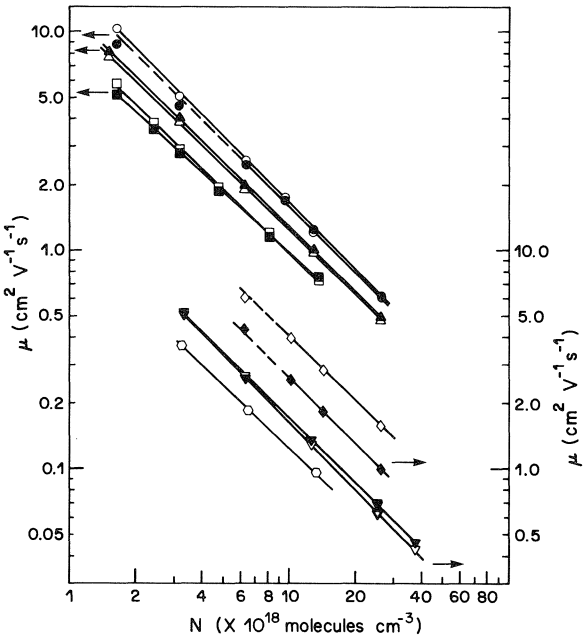


FIG. 4. Experimental mobilities plotted against gas densities. Filled symbols, positive ions; open symbols, negative ions: ○, H_2S; △, HBr; □, CH_3Cl; ◇, NO; ▽, HCl, ⬡, SF_6.

For H_2S, HCl, HBr, and CH_3Cl at one pressure, measurements were also made with a sample where a small amount (~1 Torr) of CCl_4 had been added. Within the experimental uncertainty positive and negative ion mobilities for samples with and without the e^- scavenger were the same. This molecule has a very large cross section for electron capture (6) and under the conditions used should have converted electrons to Cl^-:

$$[3] \quad CCl_4 + e \rightarrow \cdot CCl_3 + Cl^-$$

Thus the original negative ion would be replaced initially by Cl^-.

Discussion

The high pressures employed here would have caused a greater tendency for clustering of the ions than in the usual mobility studies carried out at or near 1 Torr. The Chapman–Enskog kinetic theory mobility equation (14), eq. [4]

$$[4] \quad \mu = \frac{3}{16}\left(\frac{1}{m} + \frac{1}{M}\right)^{1/2}\left(\frac{2\pi}{kT}\right)^{1/2}\frac{e}{N\omega}$$

shows the relation between μ, the masses m and M of the ion and neutral molecule, the ion charge e, and the averaged diffusion cross section ω. The dependence of μ on ion size (and clustering) arises from m and the contribution of hard sphere repulsive terms in ω. For large cluster sizes, as are likely

TABLE 1. Reduced mobility at 296 K and related data

Gas	Ion (sign)	μ_0[a] ($cm^2\ V^{-1}\ s^{-1}$)	y[a]	Related data: μ_D[e] (D)	Related data: $10^{24} \times \alpha$[e] (cm^3)	Related data: $10^{40} \times I_{min}$[f] (g cm^3)
CH_3Cl	+	0.39	0.919	1.87	5.43	5.49
	−	0.37	0.969			
HCl	+	0.64	0.981	1.03	3.09	
	−	0.59	1.024			
HBr	+	0.48	0.977	0.78	3.61	
	−	0.49	0.966			
H_2S	+	0.59	1.001	0.95	3.61	2.69
	−	0.60	1.008			
NO	+	0.97	0.995	0.16	1.78	
	−	1.53	0.977			
SF_6	−	0.49	0.956	0.0	6.23	
NH_3	+	0.72[b]	1.02	1.47	2.26	2.82
	−	0.75[b]	1.03			
H_2O	+	0.705[c]	1.0	1.85	1.49	1.02
	−	0.67[d]	1.0			

[a] Based on the formula: $\mu = \mu_0(2.69 \times 10^{19}/N)^y$; N = molecules cm^{-3}. All values μ_0 reported here are subject to an error of 7%.
[b] From refs. 2 and 7 for $NH_4^+ \cdot nNH_3$ and $Cl^- \cdot mNH_3$ ions. The positive ion value is a mean of the values from refs. 2 and 7.
[c] From ref. 8 for $K^+ \cdot nH_2O$ (see text).
[d] From ref. 9 for $OH^- \cdot nH_2O$ (see text) at 293 K. Identity based on mass identification in ref. 10.
[e] Taken from refs. 11 and 12.
[f] Taken from ref. 13.

here, $(1/m + 1/M)^{1/2}$ would approach the limit $(1/M)^{1/2}$. Also from typical rate constant data (15) it is reasonable to assume that clusters would reach equilibrium distributions, which would be maintained during drift. When this condition holds only one mobility peak will be observed (8). This was the case for all ions reported. There was some evidence for two non-equilibrated positive species in SF_6, which may stem from different primary ions (16). These will be discussed elsewhere.

Our values of μ_0 for negative ions in SF_6 were: 0.45, 0.46, and 0.48 $cm^2\ V^{-1}\ s^{-1}$ at 100, 200, and 408 Torr respectively. The significance of the slight increase with pressure, if real, is not understood. The value of 0.45 ± 0.03 $cm^2\ V^{-1}\ s^{-1}$ at 100 Torr compares very favorably with 0.47 (17) and 0.54 (18) for $SF_6^-(SF_6)$ and 0.42 (17) and 0.47 (18) for $SF_6^-(SF_6)_2$ previously obtained at low pressures. Given that increasing m from the mass of the trimer to infinity in eq. [4] would only decrease μ_0 by 5%, it would appear that any effect on ω is also small for the cluster sizes occurring under our conditions. We assume that they are at least trimeric and maybe even larger.

Nitric oxide was the only gas in which the negative and positive ion mobilities differed widely, indicating very different ion masses and/or ω values. Mass analysis of ions in discharged NO showed $(NO)_2^+$ and NO_2^- to be the major species at pressures near 1 Torr (19), but the masses of these would only cause a 10% lower mobility of the positive ion. Therefore the results suggest that the positive ion is clustered much more strongly than the negative one or that some other factor is responsible.

Another effect of high pressure not mentioned above is the increased absolute concentration of trace impurities in the drift cell. If polar molecules like H_2O are present they may preferentially cluster the ions, when gases of lesser polarity are being studied. In the case of H_2S the positive ion current profile exhibited a doublet before the gas was completely purified. After purification the faster ion had disappeared, but it returned on the addition of a small trace of H_2O. This behavior is consistent with the observed displacement of H_2S from ion clusters by H_2O (15, 20). The presence of traces of H_2O in the NO could cause strong clustering of the positive ion (21), but we found no behavior like that for H_2S, which would support this suggestion.

The remaining gases used here are themselves so polar that the above effect should be unimportant. Indeed for H_2S, HCl, HBr, and CH_3Cl ion clustering is sufficiently strong that equilibria have been studied for either the positive or the negative ions, and species of the following formulae have been identified by mass analysis: $H_3S^+ \cdot nH_2S$ (15, 20), $Cl^- \cdot mHCl$ (22), $Br^- \cdot mHBr$ (23), and $CH_3ClCH_3^+ \cdot nCH_3Cl$ (24). In addition H_2Cl^+ and H_2Br^+ are formed from the parent ions (25), and should be clustered at the pressures used here. Reactions of electrons and ions occurring in the

Can. J. Chem. Downloaded from www.nrcresearchpress.com by 210.87.254.105 on 09/05/12
For personal use only.

Can. J. Chem. Downloaded from www.nrcresearchpress.com by 210.87.254.105 on 09/05/12
For personal use only.

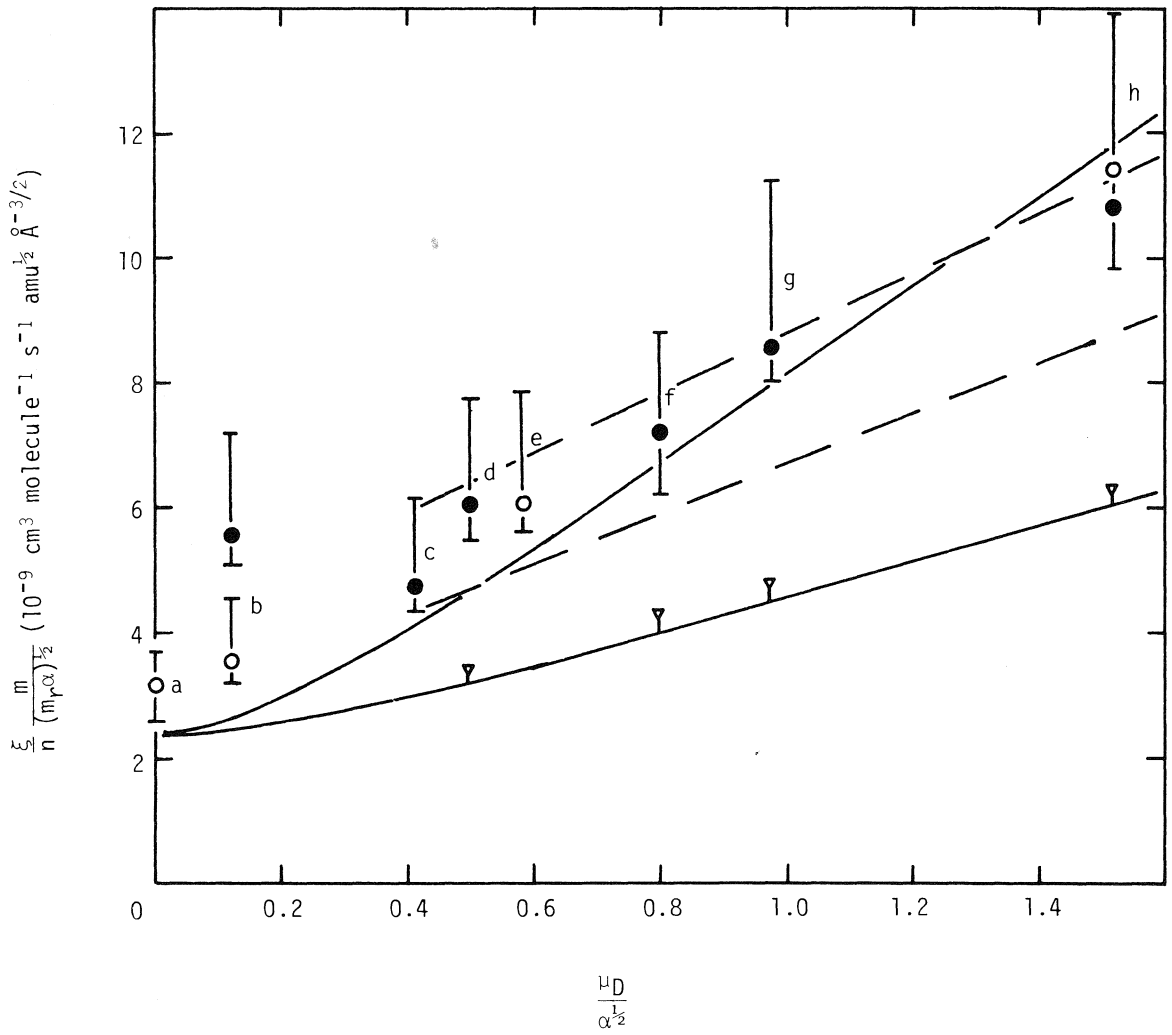


FIG. 5. Normalized collision density versus ratio of dipole moment to square root of polarizability. Experimental points for ions in different gases shown by: open symbols, negative ions; filled symbols, positive ions; *a*, SF_6; *b*, NO; *c*, HBr; *d*, H_2S; *e*, HCl; *f*, MeCl; *g*, NH_3 from refs. 2 and 7; *h*, H_2O from refs. 8–10. Dashed lines indicate region in which experimental data from ref. 4 for low pressure experiments fall. Upper solid line calculation of Barker and Ridge, ref. 4. Lower solid line calculated from equations and *C* values in ref. 31; inverted triangles show effect of *A* term in eq. [6].

hydrogen halides and H_2S under irradiation have been reviewed (26, 27). There is uncertainty about the negative ion species in H_2S (27, 28) and CH_3Cl. However, the low negative ion mobilities in these systems and the absence of any significant change on adding CCl_4 to capture electrons indicates that heavy ions were always present and some kind of electron capture process must operate. In the case of H_2S this agrees with the conclusions of others (27, 28).

A relatively simple relation exists between ion mobility and ξ, the collision frequency for momentum transfer between the ion and neutral molecules, viz.: $\xi = e/(m\mu)$ (4, 29). Therefore it is of interest to compare the present results with collision frequencies for other ion – polar molecule systems. For reasons which will become apparent we normalize ξ and μ to unit molecule concentration and compare the quantities $(\xi/N)(m/(M_r\alpha)^{1/2})$ and $e/\mu N(M_r\alpha)^{1/2}$, with M_r = reduced mass.

The points in Fig. 5 are values of $e/\{\mu N(M_r a)^{1/2}\}$ calculated from mobilities in Table 1 and plotted against $\mu_D/\alpha^{1/2}$, where μ_D is the dipole moment and α the polarizability of the neutral gas molecule. Values of these properties are given in Table 1. For the gases studied in this laboratory we chose to

Can. J. Chem. Downloaded from www.nrcresearchpress.com by 210.87.254.105 on 09/05/12
For personal use only.

calculate $e/\mu N(M_r\alpha)^{1/2}$ for the ion of each system, for which the average cluster size could be estimated at 200 Torr from the mass spectrometric – thermodynamic data in the references noted above. Mobilities at 200 Torr were evaluated from μ_0 and y in Table 1. The mobilities for NH_3 systems are from refs. 2 and 7. The average ion cluster sizes were: $Cl^-\cdot 4HCl$, $NH_4^+\cdot 4NH_3$, $H_3S^+\cdot 4H_2S$, $CH_3ClCH_3^+\cdot 2CH_3Cl$, and $SF_6^-\cdot 2SF_6$. For HBr and NO there is not enough information for realistic estimates and we arbitrarily used cluster sizes of four. The bars about each point show the extreme values taking $m = M$ and $m = \infty$. Uncertainties in ion mass are seen not to affect the arguments below.

The mobility for $K^+\cdot 6H_2O$ in water vapor at a few Torr is taken from a compilation by Smirnov (8) and the ion identity based on data in ref. 30. Lowke and Rees' negative ion mobility of 0.67 in water vapor below saturation at a few Torr (9) was assumed to be $OH^-\cdot 4H_2O$, as identified in ref. 10 (see Fig. 10, ref. 10).

The dashed lines in Fig. 5 enclose the area covered by a total of eighteen points in a similar plot presented by Barker and Ridge (4), and based on collision frequencies determined by ion cyclotron resonance. The high pressure mobility results obtained here and the data for H_2O vapor are seen to follow the same approximately linear dependence on $\mu_D/\alpha^{1/2}$ and to agree quantitatively with the low pressure data.

The calculation of ion collision frequencies at unit concentration has been considered by Barker and Ridge (4). From their work it appears that eq. [5] should be a good approximation (within ~10%) for ion–neutral hard sphere radii less than 10 Å.

$$[5]\quad \xi = N\left(\frac{M}{m+M}\right)k_c$$

Here k_c is the "orbiting collision" frequency of ion–molecule reaction rate theory, which is given by eq. [6] (3, 4):

$$[6]\quad k_c = \frac{2\pi e}{M_r^{1/2}}\left\{\alpha^{1/2} + C\mu_D\left(\frac{2}{\pi kT}\right)^{1/2} + A\right\}$$

C is a function of $\mu_D/\alpha^{1/2}$, which allows for the ion–dipole interaction and is obtained from theory, and A is a relatively new term defined in ref. 31 and added to take account of the requirement for angular momentum conservation. Substituting [6] into [5] and multiplying by $m/(M_r\alpha)^{1/2}$ one obtains:

$$[7]\quad \frac{\xi}{N}\frac{m}{(M_r\alpha)^{1/2}} = 2\pi e\left\{1 + \frac{\mu_D}{\alpha^{1/2}}C\left(\frac{2}{\pi kT}\right)^{1/2} + \frac{A}{\alpha^{1/2}}\right\}$$

Su and Bowers (3) and Barker and Ridge (4) have developed different methods for averaging the ion–dipole interaction, which is contained in the second term in the braces. The upper solid line in Fig. 4 is based on Barker and Ridge's prediction of k_c from ref. 4. The lowest line is a calculation of $\xi m/N(M_r\alpha)^{1/2}$ based on revised values of C (31) for the ADO theory. Also for some specific molecules the A term has been included. The experimental points all fall well above the ADO line. Su *et al.* (31) claim that the reason for this may lie predominantly in the omission of repulsive potentials rather than in the ADO evaluation of the dipole–ion interaction, which they believe to be correct. On the other hand it is evident that the original Barker–Ridge calculation gives better agreement with experimental collision frequencies. However, although the data at present are somewhat limited and exhibit scatter, there appears to be a tendency for the Barker–Ridge theory to underestimate the collision frequency at low $\mu_D/\alpha^{1/2}$ and to overestimate it at high $\mu_D/\alpha^{1/2}$. A part of this may be due to the approximation $\sigma_d \simeq \sigma_0$ made in obtaining [5] (see ref. 4, Fig. 2). It would appear that this problem and the not unrelated question of short range repulsive interactions require attention before either theory can provide an accurate representation of experimental collision frequencies.

Acknowledgements

This research was supported by Natural Sciences and Engineering Research Council of Canada grant A 3571. Helpful discussions with A. J. Elliot and R. Yamdagni, and technical assistance from R. Fair, F. Jarvis, and D. Lindsay are gratefully acknowledged.

1. E. W. McDaniel. Collision phenomena in ionized gases. Wiley, New York. 1964.
2. E. S. Sennhauser and D. A. Armstrong. Can. J. Chem. **56**, 2337 (1978).
3. T. Su and M. T. Bowers. J. Chem. Phys. **58**, 2037 (1973).
4. R. A. Barker and D. P. Ridge. J. Chem. Phys. **64**, 4411 (1976).
5. K. M. Bansal and R. W. Fessenden. Chem. Phys. Lett. **15**, 21 (1972).
6. F. J. Davis, R. N. Compton, and D. R. Nelson. J. Chem. Phys. **59**, 2324 (1973).
7. E. S. Sennhauser and D. A. Armstrong. J. Phys. Chem. In press.
8. B. M. Smirnov. Usp. Fiz. Nauk, **92**, 75 (1967). (Soviet Phys. Usp. **10**, 313 (1967)).

9. J. J. LOWKE and J. A. REES. Aust. J. Phys. **16**, 447 (1963).
10. J. F. WILSON, F. J. DAVIS, D. R. NELSON, R. N. COMPTON, and O. H. CRAWFORD. J. Chem. Phys. **62**, 4204 (1975).
11. LANDOLT-BÖRNSTEIN. Zahlenwerte und Funktionen. Vol. 1. Pt. 3; H. STUART. Elektrische und optische Polarisierbarheit von Molekeln.
12. J. O. HIRSCHFELDER, C. F. CURTIS, and R. B. BIRD. Molecular theory of gases and liquids. Wiley, New York. 1967.
13. G. HERZBERG. Molecular spectra and molecular structure. Van Nostrand, Princeton, NJ. 1949.
14. E. W. MCDANIEL and E. A. MASON. The mobility and diffusion of ions in gases. Wiley, New York. 1973.
15. M. MEOT-NER and F. H. FIELD. J. Am. Chem. Soc. **99**, 998 (1977).
16. A. GIARDINI-GUIDONI, R. TIRIBELLI, and F. ZOCCKI. Rend. Accad. Sci. Fis. Mat., Naples, **47**, 283 (1969).
17. P. L. PATTERSON. J. Chem. Phys. **53**, 696 (1970).
18. I. A. FLEEMING and J. A. REES. J. Phys. B**2**, 777 (1969).
19. C. S. WELLER and M. A. BIONDI. Phys. Rev. **172**, 198 (1968).
20. K. HIROAKA and P. KEBARLE. Can. J. Chem. **55**, 24 (1977).
21. W. C. LINEBERGER and L. J. PUCKETT. Phys. Rev. **187**, 296 (1969).
22. R. YAMDAGNI and P. KEBARLE. Can. J. Chem. **52**, 2449 (1974).
23. R. YAMDAGNI and P. KEBARLE. J. Am. Chem. Soc. **93**, 7139 (1971).
24. Z. XUCZYNSKI, W. MALICKI, and H. WINCEL. Int. J. Mass Spectrom. Ion Phys. **15**, 321 (1974).
25. C. W. POLLY and B. MUNSON. Int. J. Mass Spectrom. Ion Phys. **26**, 49 (1978); and references cited therein.
26. D. E. WILSON and D. A. ARMSTRONG. Radiat. Res. Rev. **2**, 297 (1970).
27. C. WILLIS, A. W. BOYD, and O. A. MILLER. Can. J. Chem. **51**, 1228 (1973).
28. M. FORYS. Radiat. Eff. **25**, 111 (1975).
29. D. P. RIDGE and J. L. BEAUCHAMP. J. Chem. Phys. **64**, 2735 (1976).
30. I. DŽIDIĆ and P. KEBARLE. J. Phys. Chem. **74**, 1466 (1970).
31. T. SU, E. C. F. SU, and M. T. BOWERS. J. Chem. Phys. **69**, 2243 (1978).

Can. J. Chem. Downloaded from www.nrcresearchpress.com by 210.87.254.105 on 09/05/12
For personal use only.

Evidence for anion coordination in hexafluorophosphate and hexafluoroarsenate complexes of nickel(II)

RAYMOND M. MORRISON, ROBERT C. THOMPSON, AND JAMES TROTTER

Department of Chemistry, The University of British Columbia, Vancouver, B.C., Canada V6T 1W5

Received August 20, 1979

RAYMOND M. MORRISON, ROBERT C. THOMPSON, and JAMES TROTTER. Can. J. Chem. **58**, 238 (1980).

Yellow crystals of tetrakis(4-methylpyridine)nickel(II)hexafluorophosphate, $C_{24}H_{28}F_{12}N_4NiP_2$, are monoclinic, $a = 19.709(5)$, $b = 9.866(2)$, $c = 16.515(9)$ Å, $\beta = 101.54(4)°$, $Z = 4$, space group $C2/c$. The structure was solved by Patterson methods and refined by full-matrix least-squares methods to $R = 0.071$ for 1002 observed reflections. The structure consists of a square-planar array of 4-methylpyridine ligands about nickel with hexafluorophosphate groups above and below the plane. The Ni—N distances are 1.916(9) and 1.919(10) Å with the pitch of the rings 102.06° and 97.32°. The shortest Ni—F distances are 3.031(8) Å. The structure shows that the anions are not fully coordinated to nickel but are nonetheless held in axial positions by weak, essentially ionic, interactions.

Tetrakis(pyridine)nickel(II)hexafluoroarsenate has been found to undergo a reversible structure change over the temperature range 180 to 200 K. Electronic and vibrational spectra and magnetic susceptibility studies suggest that the compound has a structure similar to that of $Ni(4\text{-mepy})_4(PF_6)_2$ with the anions only weakly interacting with cations in the high temperature form and fully coordinated in the low temperature form.

RAYMOND M. MORRISON, ROBERT C. THOMPSON et JAMES TROTTER. Can. J. Chem. **58**, 238 (1980).

Les cristaux jaunes de tétrakis(méthyl-4 pyridine) hexafluorophosphate de nickel(II) $C_{24}H_{28}F_{12}N_4NiP_2$ sont monocliniques $a = 19.709(5)$, $b = 9.866(2)$, $c = 16.515(9)$ Å, $\beta = 101.54(4)°$, $Z = 4$, groupe d'espace $C2/c$. On a résolu la structure par les méthodes de Patterson et on l'a affinée par la méthode des moindres carrés (matrice complète) jusqu'à une valeur de R 0.071 pour 1002 réflexions observées. La structure consiste en une rangée de ligands de méthyl-4 pyridine carré plan autour du nickel avec les groupes hexafluorophosphate au dessus et au dessous du plan. Les distances Ni—N sont de 1.916(9) et 1.919(10) Å alors que les cycles dévient du plan par 102.06° et 97.32°. Les distances Ni—F les plus faibles sont 3.031(8) Å. La structure montre que les anions ne sont pas complètement coordonnées au nickel, mais sont toutefois maintenus dans une position axiale par des interactions faibles essentiellement ioniques.

On a trouvé que le tétrakis(pyridine) hexafluoroarsenate de nickel(II) subit un changement reversible de structure sur une échelle de température allant de 180 à 200 K. L'étude des spectres de vibration, des spectres électroniques et de la susceptibilité magnétique suggère que le composé a une structure semblable à celle de $Ni(mepy\text{-}4)_4(PF_6)_2$. Cette structure se présente sous deux formes: l'une à haute température où les anions sont seulement en interaction faible avec les cations, l'autre à basse température où les anions sont complètement coordonnées.

[Traduit par le journal]

Introduction

The hexafluorophosphate and hexafluoroarsenate ions are commonly used as non-coordinating counter anions in coordination chemistry (1, 2). Examples of complexes in which there is evidence for PF_6^- and AsF_6^- coordination are scarce, consisting of a few unsolvated compounds, $CuAsF_6$ (3), $FeF(AsF_6)$ (4), and $Ni(AsF_6)_2$ (5) where there must be some anion—cation interaction and the pyridine complex, $Cu(py)_4(PF_6)_2$ (1, 6) where some spectral evidence for a form of anion coordination, termed semi-coordination, has been presented.

We previously described the 4-methylpyridine complexes, $Ni(4\text{-mepy})_4(PF_6)_2$ and $Ni(4\text{-mepy})_4(AsF_6)_2$, as consisting of square-planar $[Ni(4\text{-mepy})_4]^{2+}$ cations and non-coordinated or weakly semi-coordinated anions (2). This conclusion was based on electronic spectral and magnetic studies which indicated a spin-singlet electronic ground state and on infrared studies which indicated some lowering of anion symmetry possibly due to cation–anion interaction. More information on the nature of this interaction in $Ni(4\text{-mepy})_4(PF_6)_2$ is provided by the single-crystal X-ray diffraction study described in the present paper.

The original claim that the pyridine complex, $Ni(py)_4(PF_6)_2$, has anomalous magnetic properties (6) consistent with a singlet–triplet equilibrium and arising from anion coordination was later refuted (2). Further studies on this compound are reported here and we also describe the synthesis and characterization of the hexafluoroarsenate analogue, $Ni(py)_4(AsF_6)_2$. This latter compound is particularly interesting in that it has been found to undergo a reversible structure change over the temperature range 180 to 200 K. The strength of the anion-to-metal coordination in the low temperature form is significantly greater than in the room temperature form or in any other NiL_4A_2 hexafluoroarsenate or hexafluorophosphate complex.

Experimental

Preparations

Tetrakis(4-methylpyridine)nickel(II)hexafluorophosphate, $Ni(4\text{-mepy})_4(PF_6)_2$, was prepared as described previously (2) and crystals suitable for X-ray diffraction studies were obtained by slow evaporation (1 to 2 weeks in a nitrogen atmosphere

0008-4042/80/030238-07$01.00/0

©1980 National Research Council of Canada/Conseil national de recherches du Canada

Can. J. Chem. Downloaded from www.nrcresearchpress.com by 210.87.254.40 on 09/05/12
For personal use only.

Can. J. Chem. Downloaded from www.nrcresearchpress.com by 210.87.254.40 on 09/05/12
For personal use only.

dry-box) of a saturated solution of the compound in an equal volume mixture of dichloromethane and chloroform.

Tetrakis(pyridine)nickel(II)hexafluorophosphate and -arsenate were prepared in a dry-box as follows. A sample of the appropriate hexakis(pyridine) derivative, $Ni(py)_6A_2$, prepared by published methods (6), was placed in a flask with a large excess of dichloromethane. Upon stirring the suspended solids changed from blue–green to orange–yellow in colour and the dichloromethane became faint blue–green in colour. The solid material was filtered and washed with dichloromethane until the washings were colourless. The product was then dried under vacuum for 24 h. As previously noted (2), thermal preparative methods involving heating the hexakis(pyridine) precursors were avoided as these lead to products containing variable amounts of paramagnetic impurities.

Anal. calcd. for $NiC_{20}H_{20}N_4P_2F_{12}$: C 36.16, H 3.03, N 8.43; found: C 36.12, H 2.99, N 8.49. *Anal.* calcd. for $NiC_{20}H_{20}N_4As_2F_{12}$: C 31.90, H 2.68, N 7.44; found: C 31.70, H 2.74, N 7.31.

Elemental analyses were done by P. Borda of the Department of Chemistry, The University of British Columbia.

Spectroscopic and Magnetic Measurements

Magnetic susceptibility measurements were made as described previously (2). Electronic spectra at room and liquid nitrogen temperatures were obtained on finely ground powders between silica glass plates using a Cary model 14 spectrophotometer. Infrared spectra were also obtained on powders pressed between KRS-5 (Harshaw Chemical Co.) plates using a Perkin-Elmer Model 225 spectrophotometer. The low temperature cell has been described elsewhere (7). It was outfitted with silica glass plates for the electronic spectra and BaF_2 windows for the infrared studies. The low temperature Raman spectrum was obtained using a Spex Ramalog 5 instrument equipped with a 514.5 nm argon ion laser and a low temperature cell designed by Lee and Aubke (8). The room temperature Raman spectrum was obtained using a Cary Model 81 spectrometer equipped with a He–Ne laser ($\lambda = 632.8$ nm).

X-ray Diffraction Experiment

Crystals of $Ni(4\text{-mepy})_4(PF_6)_2$ were hygroscopic and were sealed in 0.3 mm diameter Lindemann capillaries for study. Preliminary Weisenberg and precession photographs indicated a monoclinic space group. The crystal was mounted in a random orientation on an Enraf-Nonius CAD4 diffractometer. The unit cell parameters were determined by least-squares fit of 25 reflections. The crystal data are

$C_{24}H_{28}F_{12}N_4NiP_2$ fw = 721.15

Monoclinic, space group $C2/c$ (C_{2h}^6, No. 15) from absences and structure analysis, $a = 19.709(5)$, $b = 9.866(2)$, $c = 16.515(9)$ Å, $\beta = 101.54(4)°$, $V = 3146$ Å^3, $Z = 4$, $\rho_c = 1.523$ g cm^{-3}, $\mu = 8.2$ cm^{-1}.

Intensity data were measured in the range $2° \leq 2\theta \leq 45°$ with monochromatic Mo Kα ($\lambda = 0.71073$ Å) radiation with an ω scan. The scan angle was $(0.90 + 0.45 \tan\theta)°$, extended 25% on each side for background count, with a horizontal aperture of $(2.75 + \tan\theta)$ mm. Three intensity control reflections were checked every 5000 s of X-ray exposure and three orientation controls were measured every 150 reflections. In the data reduction, Lorentz-polarization (LP) corrections were applied and an estimated standard deviation was assigned by $\sigma^2(I) = S + 4(B_1 + B_2) + (0.05I)^2$ where S = scan count and B_1 and B_2 = background counts. During the data collection, the mean scale factor of the intensity controls varied randomly (±3%). Of the 2058 reflection data collected, 1002 (49%) had $I > 3\sigma(I)$ and were considered observed.

Structure Determination

The structure was determined by Patterson and Fourier methods, and corresponded to space group $C2/c$. With anisotropic thermal parameters for all of the atoms, inclusion of the anomalous scattering of nickel and phosphorus (9), and use of a weighting scheme ($F_o \leq F_{avg}$, $\omega = 1$, $F_o > F_{avg}$, $\omega = F_{avg}/F_o$; F_{avg} = averaged observed structure factor), full-matrix least-squares refinement led to R and R_ω of 0.071 and 0.096. Extinction and absorption corrections were not made, nor were hydrogen positions determined. A subsequent cycle of full-matrix least-squares refinement showed no shifts greater than 0.25σ for the parameters determined. The observed and calculated structure factors have been placed in the Depository of Unpublished Data.[1] The final positional and thermal parameters are given in Tables 1 and 2.

Results and Discussion

The Crystal Structure of Ni(4-mepy)$_4$(PF$_6$)$_2$

The structure consists of nickel atoms on inversion centres with two pairs of crystallographically different 4-methylpyridine ligands defining a square-planar array around nickel. The hexafluorophosphate groups are crystallographically identical and situated above and below the square plane. Figure 1 shows a stereoview of the formula unit. The bond lengths and angles within the 4-methylpyridine rings (Table 3) are similar to those observed previously for coordinated 4-methylpyridine (10, 11). The rings are planar within experimental error. The PF_6 groups appear as somewhat distorted octahedra. The P—F distances vary from 1.466 to 1.593 Å, in the range normally observed (12) when uncorrected for thermal motion. The F—P—F angles range from 86.2 to 92.3° for adjacent fluorines and 175.7 to 177.8° for opposite fluorines. These apparent distortions and large thermal parameters which indicate a small amount of disorder are commonly observed in hexafluorophosphates (ref. 11 and references therein).

Clearly the hexafluorophosphate ions are not fully coordinated in this complex as evidenced by the fact that the Ni—F distance of 3.031 Å is only marginally less than the estimated sum of the van der Waals radii, 3.1 to 3.2 Å, and considerably greater than the sum of the covalent radii, 1.87 Å (13). This is consistent with the previously reported electronic properties of the molecule (2). On the other hand, we note that there is anion–cation interaction in the $Ni(4\text{-mepy})_4(PF_6)_2$ unit sufficiently strong to produce noticeable effects on the molecular structure. The anions occupy definite positions on the tetragonal axis, there is no evidence that they are rotating and, in addition, the

[1]Complete set of data is available, at a nominal charge, from the Depository of Unpublished Data, CISTI, National Research Council of Canada, Ottawa, Ont., Canada K1A 0S2.

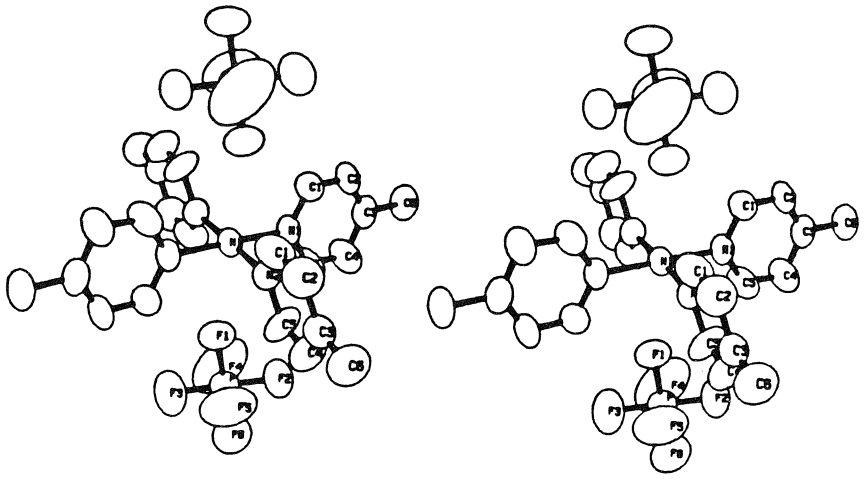


FIG. 1. Stereoview of $Ni(4\text{-mepy})_4(PF_6)_2$. All atoms drawn for 50% probability.

TABLE 1. Final positional parameters (fractional × 10^4) with estimated standard deviations in parentheses

Atom	*x*	*y*	*z*
Ni	5000	5000	5000
P	6395 (2)	1410 (4)	5992 (3)
N1	5712 (5)	5803 (10)	4522 (6)
C1-1	6351 (6)	5274 (13)	4664 (7)
C2-1	6376 (6)	5867 (15)	4361 (8)
C3-1	6765 (7)	7037 (16)	3916 (8)
C4-1	6105 (8)	7586 (17)	3743 (11)
C5-1	5601 (8)	6955 (18)	4084 (12)
C6-1	7353 (7)	7766 (17)	3586 (8)
N2	4615 (5)	4076 (12)	3987 (6)
C1-2	4696 (7)	2759 (16)	3898 (10)
C2-2	4395 (8)	2046 (15)	3186 (12)
C3-2	3960 (7)	2720 (18)	2547 (9)
C4-2	3874 (10)	4065 (20)	2653 (10)
C5-2	4194 (10)	4748 (18)	3358 (10)
C6-2	3583 (8)	1897 (18)	1788 (9)
F1	5922 (4)	2545 (9)	5474 (5)
F2	5930 (5)	1407 (11)	6648 (6)
F3	6880 (7)	1495 (16)	5352 (8)
F4	5991 (10)	319 (12)	5516 (8)
F5	6829 (6)	2631 (15)	6477 (8)
F6	6386 (7)	395 (14)	6534 (7)

fluorine atoms closest to the nickel have the smallest thermal parameters. This interaction is weaker even than the anion–cation interaction in bis(tetrafluoroborato)bis(ethylenediamine)copper(II) for which the term semi-coordination was given (14); nonetheless, it no doubt causes the lowering in anion symmetry, the effects of which were observed previously in the infrared spectrum (2).

It is instructive to compare the bond parameters obtained here with those of related perchlorate complexes. The Ni—O distance in $Ni(4\text{-mepy})_4(ClO_4)_2$ and the analogous 3,4-dimethylpyridine derivative where the anions are considered to be non-coordinated (15, 16) are 3.290 and 3.343 Å respectively (compared to 3.10 Å for the sum of the van der Waals radii (13)); whereas, when the perchlorate is fully coordinated as in the 3,5-dimethylpyridine derivative (17) this distance is shortened to 2.187 Å. The anion–metal contact of 3.031 Å in $Ni(4\text{-mepy})_4(PF_6)_2$ is slightly less than that in the complexes with non-coordinated perchlorates. The Ni—N distances in the perchlorate complexes are affected by anion coordination; the distances increase from 1.90 Å to 2.05–2.15 Å on going from non-coordinated to coordinated anions. The short Ni—N distances (~1.92 Å) observed in the hexafluorophosphate derivative are again closest to those observed in perchlorate complexes with non-coordinated anions. Consistent too is the observed pitch of the 4-methylpyridine rings. The angles between the NiN_4 plane and the planes of the ligand rings in the perchlorate complexes are near 90° for non-coordinated anions and 45° for coordinated anions. The angles observed in $Ni(4\text{-mepy})(PF_6)_2$ (102.1 and 97.3°) are considerably greater than the 45° expected for fully coordinated anions. Overall this bond parameter comparison is consistent only with the hexafluorophosphate complex having non-interacting or, as is thought to be the case, having very weakly interacting anions.

Spectral and Magnetic Studies on $Ni(py)_4(AsF_6)_2$

The magnetic properties of $Ni(py)_4(AsF_6)_2$ and, for comparison, $Ni(py)_4(PF_6)_2$ are given in Fig. 2. The hexafluorophosphate derivative shows only very weak paramagnetism over the temperature range 80 to 300 K; whereas, the hexafluoroarsenate analogue shows a reversible change from what is only very weak paramagnetism above 200 K to strong paramagnetism (corresponding to approxi-

Can. J. Chem. Downloaded from www.nrcresearchpress.com by 210.87.254.40 on 09/05/12
For personal use only.

Can. J. Chem. Downloaded from www.nrcresearchpress.com by 210.87.254.40 on 09/05/12
For personal use only.

TABLE 2. Final thermal parameters and their estimated standard deviations. Anisotropic thermal parameters ($U_{ij} \times 10^3$ Å^2)*

Atom	U_{11}	U_{22}	U_{33}	U_{12}	U_{13}	U_{23}
Ni	64(1)	67(1)	69(1)	12(1)	31(1)	14(1)
P	83(3)	91(3)	87(3)	29(3)	24(2)	28(3)
N1	76(7)	53(6)	66(6)	9(6)	36(5)	5(6)
C1-1	62(7)	69(10)	75(8)	2(8)	18(7)	−2(7)
C2-1	57(8)	92(10)	73(9)	−4(8)	33(7)	−8(9)
C3-1	85(10)	88(11)	61(8)	−11(9)	29(7)	0(8)
C4-1	99(12)	115(14)	160(15)	38(11)	75(11)	65(13)
C5-1	88(11)	119(13)	189(17)	43(10)	77(12)	96(14)
C6-1	76(9)	134(13)	93(10)	−28(9)	39(8)	17(10)
N2	68(7)	73(8)	64(7)	5(6)	21(6)	10(6)
C1-2	75(9)	59(10)	131(14)	1(8)	26(9)	8(10)
C2-2	93(11)	61(9)	117(13)	−24(9)	20(10)	−4(10)
C3-2	64(8)	101(12)	90(11)	7(9)	32(8)	39(11)
C4-2	150(16)	110(14)	69(11)	41(13)	21(10)	15(11)
C5-2	159(15)	114(14)	53(9)	59(13)	17(10)	27(11)
C6-2	108(12)	127(14)	79(10)	−6(11)	−2(9)	−27(10)
F1	94(5)	101(6)	109(6)	19(5)	9(5)	37(5)
F2	144(8)	159(9)	127(7)	60(7)	78(6)	47(7)
F3	203(12)	255(16)	204(12)	129(12)	135(10)	124(12)
F4	375(22)	110(10)	140(10)	−61(11)	−5(12)	−28(8)
F5	145(9)	211(14)	185(11)	−58(10)	−49(9)	41(11)
F6	213(12)	231(14)	157(9)	170(11)	74(9)	97(10)

*The anisotropic thermal parameters employed in the refinement are U_{ij} in the expression: $f = f^0 \exp(-2\pi^2 \Sigma_i \Sigma_j U_{ij} h_i h_j a_i^* a_j^*)$.

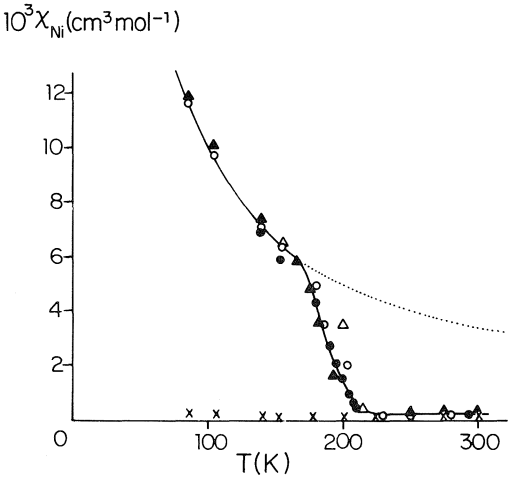


FIG. 2. Magnetic susceptibilities. ▲, ●, △, ○ are data points for $Ni(py)_4(AsF_6)_2$. Different symbols represent independent experiments. The solid line shows the trend of the data. The low temperature section which follows the Curie law is extended (dotted line) into the high temperature region for comparison with measured susceptibilities. × are data points for $Ni(py)_4(PF_6)_2$.

mately two unpaired electrons) at temperature below 180 K. Clearly the electronic ground state in $Ni(py)_4(AsF_6)_2$ changes from a spin-singlet to a spin-triplet at temperatures below the transition range. These magnetic properties show that, in the low temperature form, $Ni(py)_4(AsF_6)_2$ has fully coordinated AsF_6^- ions. This is confirmed by electronic spectral studies.

At room temperature the electronic spectrum of $Ni(py)_4(AsF_6)_2$ consists of a single band with a maximum at 450 nm consistent with a singlet ground state (18). At 80 K the spectrum changes (Fig. 3) to one which can be assigned as a superposition of two spectra: the original one-band spectrum plus a new one consisting of five bands assignable (Table 4) to the triplet–triplet transitions of a six-coordinate nickel(II) species with D_{4h} local symmetry. That this new species which forms at low temperatures has a structure involving *trans*-coordinated AsF_6^- is confirmed by comparison of the ligand field parameters calculated (including configuration interaction) for $Ni(py)_4(AsF_6)_2$, Dq = 1300, B = 887, Ds = 1588, and Dt = 568 (all in cm^{-1}), with those obtained for the known tetragonally distorted octahedral complexes $Ni(py)_4(BF_4)_2$ and $Ni(py)_4(ClO_4)_2$ (19). The parameters are comparable in magnitude with some differences (notably in Dt which is 540 cm^{-1} for the tetrafluoroborate and 500 cm^{-1} for the perchlorate derivative) which indicate a slightly higher degree of tetragonal distortion in the hexafluoroarsenate complex. The presence of a band at 450 nm shows that the conversion from the ground state singlet species to the ground state triplet species is not complete and this is borne out also by the magnetic studies. Six-coordinate nickel(II) complexes with triplet ground states normally have magnetic moments of the order of 3.1–3.2 BM. The observed values of ~2.85 BM suggests ~85% conversion to the triplet

Can. J. Chem. Downloaded from www.nrcresearchpress.com by 210.87.254.40 on 09/05/12
For personal use only.

TABLE 3

(*a*) Bond lengths (estimated standard deviations in parentheses)

Bond	Distance (Å)
Ni—N1	1.916 (9)
Ni—N2	1.919 (10)
P—F1	1.588 (8)
P—F2	1.556 (9)
P—F3	1.567 (11)
P—F4	1.466 (12)
P—F5	1.593 (13)
P—F6	1.543 (9)
Ni—F1	3.031 (8)

	Distance (Å)	
Bond	Ring 1	Ring 2
N—C1	1.337 (14)	1.322 (17)
C1—C2	1.368 (16)	1.393 (19)
C2—C3	1.362 (18)	1.385 (19)
C3—C4	1.383 (18)	1.353 (19)
C4—C5	1.386 (18)	1.380 (22)
C5—N	1.340 (16)	1.360 (16)
C3—C6	1.554 (17)	1.548 (20)

(*b*) Bond angles (with estimated standard deviations in parentheses)

Bonds	Angle (deg)
F1—P—F2	90.7 (5)
F1—P—F3	88.3 (5)
F1—P—F4	92.0 (7)
F1—P—F5	86.2 (6)
F1—P—F6	175.7 (7)
F2—P—F3	176.7 (9)
F2—P—F4	92.2 (9)
F2—P—F5	89.1 (8)
F2—P—F6	89.1 (6)
F3—P—F4	91.0 (10)
F3—P—F5	87.7 (9)
F3—P—F6	91.7 (6)
F4—P—F5	177.8 (7)
F4—P—F6	92.3 (9)
F5—P—F6	89.6 (8)
N1—Ni—N2	91.6 (4)
N1—Ni—F1	89.2 (4)
N2—Ni—F1	92.6 (4)

	Angle (deg)	
Bonds	Ring 1	Ring 2
C5—N—C1	117.8 (11)	117.6 (13)
N1—C1—C2	121.6 (12)	123.4 (14)
C1—C2—C3	120.7 (12)	119.3 (14)
C2—C3—C4	118.8 (12)	116.5 (16)
C3—C4—C5	117.5 (14)	122.7 (16)
C4—C5—N	123.3 (13)	120.5 (14)
C2—C3—C6	122.3 (13)	119.0 (16)
C4—C3—C6	118.8 (14)	124.5 (15)

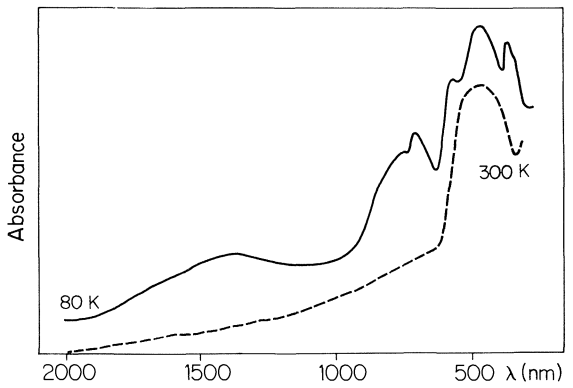


FIG. 3. Electronic absorption spectrum of $Ni(py)_4(AsF_6)_2$.

TABLE 4. Electronic spectrum of $Ni(py)_4(AsF_6)_2$

Band energies (kK)[a]	Assignment[b]
6.92	$^3B_{1g} \rightarrow {}^3E_g(^3F)$
13.0	$\rightarrow {}^3B_{2g}(^3F)$
14.3	$\rightarrow {}^3A_{2g}(^3F)$
17.5	$\rightarrow {}^3E_g(^3F)$
22.2	[c]
28.2	$\rightarrow \begin{cases} {}^3A_{2g}(^3P) \\ {}^3E_g(^3P) \end{cases}$

[a] Powdered sample at 80 K.
[b] Assignments from ref. 20.
[c] See text for assignment.

form. The hexafluorophosphate analogue, $Ni(py)_4(PF_6)_2$, does not undergo a similar transformation at low temperatures. This is indicated by the magnetic studies and confirmed by the electronic spectrum of the complex which remains a single band spectrum with a maximum at 450 nm from room temperature to 80 K.

While the evidence for full anion coordination in the low temperature form of $Ni(py)_4(AsF_6)_2$ is clear the question remains as to whether the anions are weakly associated with the metal in the high temperature form of this complex and in the hexafluorophosphate derivative. The room temperature infrared spectra of both complexes (Table 5) show very broad ν_3 absorptions and medium intensity infrared-forbidden bands (ν_1 in the case of the hexafluorophosphate and ν_2 in the case of the hexafluoroarsenate). These results indicate some distortion of the anions below O_h symmetry resulting possibly from weak anion–cation interaction as discussed previously (2).

The effect of the structural change in $Ni(py)_4(AsF_6)_2$ on its vibrational spectrum is interesting to note (Table 5). The spectrum shows that as the anions become more strongly coordinated at 80 K,

TABLE 5. Vibrational spectra

Infrared frequencies (cm^{-1})[a]				Raman frequencies (cm^{-1})[b]		
$Ni(py)_4(PF_6)_2$		$Ni(py)_4(AsF_6)_2$		$Ni(py)_4(AsF_6)_2$		
300 K	80 K	300 K	80 K	300 K	80 K	Assignments
						Anion[c]
735m	735m	[e]	[e]	680(3.2)	703(1.2) 678(1.4)	$\nu_1(A_{1g})$
			562w			
[f]	[f]	566m	533m	[g]	[g]	$\nu_2(E_g)$
			705sh			
835vs, br	835vs, br	695vs, br	685vs, br 660sh			$\nu_3(F_{1u})$
552s	553s	398vs	390vs			$\nu_4(F_{1u})$
				370(2.3)	367(0.8)	$\nu_5(F_{2g})$
						Pyridine[d]
1213m	1214m	1218m	1212m			9*a*
1158, 1150 m	1160m	1155m	1145m			15
1065m	1072, 1067 m	1068m	1060m	1030(10)	1023(10)	18*a*
1010m	1018, 1012 m					1
758, 752 s	760, 750 s	762s	755s			4
690s	690s					11
		[e]	632m	654(2.6)	653(1.4)	6*a*
			465w			
464w	468, 462 w	471m	432m			16*b*

[a] s = strong, m = medium, w = weak, v = very, br = broad.
[b] Numbers in parentheses give relative Raman intensities.
[c] Assignments (O_h symmetry) from ref. 21.
[d] Assignments from ref. 22.
[e] Not observed, possibly obscured by ν_3.
[f] Not observed, possibly obscured by ν_4.
[g] Expected but not observed, possibly too weak.

ν_3 broadens and becomes more structured and ν_2 shifts to a lower frequency. The weak band at 562 cm^{-1} in the 80 K spectrum is due probably to the small amount of "room temperature" isomer which remains at this temperature. The pyridine bands show little change except, as would be expected, for the stereochemically sensitive 6*a* and 16*b* bands. As the anion coordination increases, 16*b* decreases from 471 to 432 cm^{-1} (a weak band at 465 cm^{-1} in the 80 K spectrum due to incomplete isomerization is again observed) and the 6*a* band is observed at 632 cm^{-1}. This band is probably at higher frequencies in the room-temperature species and no doubt hidden in the broad ν_3 absorption in the 300 K spectrum.

Attempts to obtain Raman spectra on these coloured complexes were not particularly successful; nonetheless, the bands which were observed for the hexafluoroarsenate complex and their tentative assignments are given in Table 5. In view of the fact that only a few bands (most of very low intensity) were observed, no attempt was made to analyze the changes in the Raman spectrum on cooling as was done for the infrared spectra.

Of all the complexes of the type NiL_4A_2, where L is pyridine or substituted pyridine and A is an anion such as Cl^-, Br^-, ClO_4^-, BF_4^-, PF_6^-, or AsF_6^-, only the complex reported here, $Ni(py)_4(AsF_6)_2$, has been found to exist in two isomeric forms. We are unable to explain why the particular combination of ligand and anion sizes and coordinating abilities gives rise to this phenomenon. At room temperature $Ni(py)_4(AsF_6)_2$ probably has a structure very similar to that of $Ni(4\text{-mepy})_4(PF_6)_2$ with

Can. J. Chem. Downloaded from www.nrcresearchpress.com by 210.87.254.40 on 09/05/12
For personal use only.

anions occupying positions above and below a square-planar $Ni(py)_4$ entity, Ni—F distances of the order of 3 Å and pyridine rings aligned with their planes at angles of ~90° with respect to the NiN_4 plane. On cooling the anions likely move to positions closer to the nickel atoms with a concomitant change of the pitch of the ligand rings to a value closer to 45°. It would be interesting to confirm this with X-ray crystallographic studies; unfortunately we have not been able to obtain large enough crystals of the complex for such studies.

Acknowledgements

Financial assistance from the National Research Council of Canada and from the Natural, Applied and Health Sciences Grants Committee of U.B.C. is acknowledged. R.M.M. thanks the University Awards Committee for a MacMillan Family Fellowship.

1. S. A. Bell, J. C. Lancaster, and W. R. McWhinnie. Inorg. Nucl. Chem. Lett. **7**, 405 (1971).
2. R. M. Morrison and R. C. Thompson. Can. J. Chem. **56**, 985 (1978).
3. C. D. Desjardins and J. Passmore. J. Fluorine Chem. **6**, 379 (1975).
4. P. A. W. Dean. J. Fluorine Chem. **5**, 499 (1975).
5. J. P. Guertin, K. O. Christie, and A. E. Pavalath. Inorg. Chem. **5**, 1921 (1966).
6. H. G. Mayfield, Jr. and W. E. Bull. J. Chem. Soc. A, 2279 (1971).
7. W. W. Wilson, J. M. Winfield, and F. Aubke. J. Fluorine Chem. **7**, 245 (1976).
8. K. C. Lee and F. Aubke. Can. J. Chem. **57**, 2058 (1979).
9. International tables for X-ray crystallography. Vol. IV. Kynoch Press, Birmingham. 1974.
10. G. Allegra, E. Benedetti, C. Pedone, and S. L. Holt. Inorg. Chem. **10**, 667 (1971).
11. R. M. Morrison, R. C. Thompson, and J. Trotter. Can. J. Chem. **57**, 135 (1979).
12. F. C. March and G. Ferguson. Can. J. Chem. **49**, 3590 (1971).
13. J. E. Huheey. Inorganic chemistry principles of structure and reactivity. Harper and Row, New York. 1978.
14. D. S. Brown, J. D. Lee, B. G. A. Melsom, B. J. Hathaway, I. M. Procter, and A. A. G. Tomlinson. Chem. Commun. 369 (1967).
15. N. Bose and H. Lynton. Can. J. Chem. **51**, 1952 (1973).
16. F. Madaule-Aubry, W. R. Busing, and G. M. Brown. Acta Crystallogr. B**24**, 754 (1968).
17. F. Madaule-Aubry and G. M. Brown. Acta Crystallogr. B**24**, 745 (1968).
18. A. B. P. Lever. Inorganic electronic spectroscopy. Elsevier, Amsterdam. 1968.
19. D. A. Rowley and R. S. Drago. Inorg. Chem. **7**, 795 (1968).
20. J. Peeters. Bull. Soc. Chim. Belg. **81**, 333 (1972).
21. G. M. Begun and A. C. Rutenberg. Inorg. Chem. **6**, 2212 (1967).
22. N. S. Gill, R. H. Nuttall, D. E. Scarfe, and D. W. A. Sharpe. J. Inorg. Nucl. Chem. **18**, 79 (1961).

Can. J. Chem. Downloaded from www.nrcresearchpress.com by 210.87.254.40 on 09/05/12
For personal use only.

The mechanism of hydrogenation of activated olefins, including prochiral ones, using *trans*-chlorohydridobis(diop)ruthenium(II)

BRIAN R. JAMES AND DANIEL K. W. WANG

Department of Chemistry, University of British Columbia, Vancouver, B.C., Canada V6T 1W5

Received May 24, 1979

BRIAN R. JAMES and DANIEL K. W. WANG. Can. J. Chem. **58**, 245 (1980).

Solutions of the title complex *trans*-$HRuCl(diop)_2$, where diop is an optically active chelating ditertiary, hydrogenate under mild conditions activated olefinic substrates, including prochiral ones in high optical yields. Kinetic and spectroscopic studies on hydrogenation of acrylamide and α-phenylacrylic acid indicate an "unsaturate" mechanism involving rapid coordination of the substrate to give an alkyl intermediate, that subsequently reacts with H_2 in a rate-determining step to yield the saturated product and the starting monohydride complex. A diop ligand dissociates to provide necessary coordination sites at the metal. The α-phenylacrylic acid coordinates more strongly than acrylamide, but hydrogenates more slowly.

BRIAN R. JAMES et DANIEL K. W. WANG. Can. J. Chem. **58**, 245 (1980).

Les solutions du complexe $HRuCl(diop)_2$ *trans*, où diop est un agent chélatant optiquement actif, provoquent l'hydrogénation, dans des conditions douces, de substrats oléfiniques activés, incluant ceux qui sont prochiraux avec de bons rendements optiques. Les études cinétiques et spectroscopiques faites sur l'hydrogénation de l'acrylamide et de l'acide α-phénylacrylique indiquent un mécanisme "insaturé" faisant intervenir une rapide coordination du substrat pour conduire à un intermédiaire alkyle. Ce dernier réagit ensuite avec H_2 dans l'étape déterminante pour donner le produit saturé et le monohydrure complexe de départ. Un ligand diop se dissocie pour fournir les sites de coordination nécessaires au métal. L'acide α-phénylacrylique se coordonne plus fortement que l'acrylamide, mais il s'hydrogène plus lentement.

[Traduit par le journal]

Can. J. Chem. Downloaded from www.nrcresearchpress.com by 210.87.254.5 on 09/05/12
For personal use only.

Introduction

There is currently a great deal of interest in the use of transition metal complexes with chiral ligands for catalytic asymmetric synthesis (1, 2). Rhodium complexes with chiral phosphine ligands have been used principally for hydrogenation (2, 3), and indeed some prochiral α,β-unsaturated carboxylic acid substrates have been hydrogenated catalytically to products with essentially 100% optical purity (4). Based on the known (5) high catalytic hydrogenating activity of the ruthenium(II) complex $HRuCl(PPh_3)_3$, we studied corresponding systems with chiral phosphine ligands and found that a dimeric $Ru_2Cl_4(diop)_3$ containing a bridging diop ligand (**I**) was effective for catalytic asymmetric hydrogenation (6). The dimer reacts with H_2 at ambient conditions to yield the isolable active hydride species $HRuCl(diop)_2$, **II** (reaction [1]), and based on ^1H and proton-decoupled ^{31}P nmr data, which showed inequivalent phosphines, the complex was considered (7) to have a *cis* configuration of hydrogen and chlorine (**III**), and we had attributed catalytic activity to labilization of a phosphorus atom *trans* to the hydride. We were thus surprised when a recent crystal structure determination (Fig. 1) revealed a distorted octahedral structure with a *trans* H—Ru—Cl arrangement, the inequivalence of the phosphorus atoms arising from a bending of P(2) and P(2)′ toward the H, and a bending of P(1) and P(1)′ toward the Cl. The dioxolane ring of the diop ligand fixes the configuration of the 7-membered ruthenium-containing chelate ring and the geometry appears to distort to minimize phenyl–phenyl interactions (8).

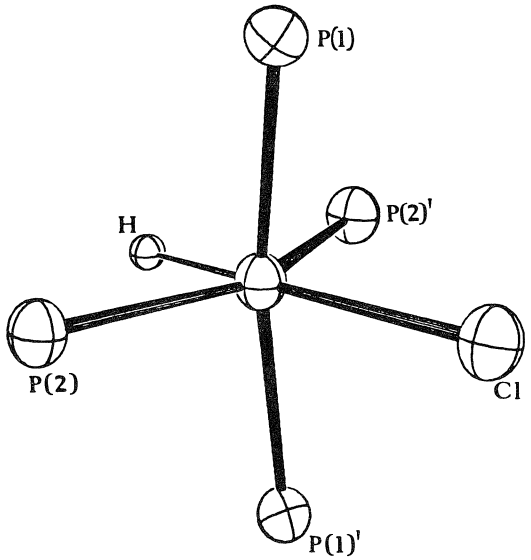
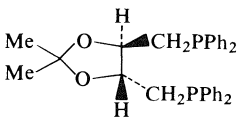


FIG. 1. The coordination geometry of the $HRuCl(diop)_2$ complex. Bond lengths (Å) and bond angles (deg) are: Ru—P(1), 2.393(1); Ru—P(2), 2.356(1); Ru—Cl, 2.548(2); and Ru—H, 1.65; ∠P(1)—Ru—P(1)′, 168.58(6); ∠P(2)—Ru—P(2)′, 149.52(7); and ∠P(2)—Ru—Cl, 105.24(3). P(1) and P(2) are part of the same diop molecule. A prime, e.g. P(1) and P(1)′, indicates atoms related by the 2-fold axis (8).

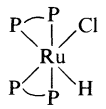
0008-4042/80/030245-06$01.00/0

©1980 National Research Council of Canada/Conseil national de recherches du Canada

Can. J. Chem. Downloaded from www.nrcresearchpress.com by 210.87.254.5 on 09/05/12
For personal use only.



(I) 4*R*,5*R*-(−)diop



(III)

[1] $Ru_2Cl_4(diop)_3 + H_2 \rightarrow HRuCl(diop)_2 + \frac{1}{2}[RuCl_2(diop)]_2 + HCl$

(II)

This paper describes kinetic and spectroscopic studies on the $HRuCl(diop)_2$-catalyzed hydrogenation of acrylamide (acryl), and the prochiral α-phenylacrylic acid in *N*,*N*-dimethylacetamide (DMA) solution in attempts to elucidate reaction mechanisms, particularly since other *trans*-$HRuCl(diphosphine)_2$ complexes are inactive catalysts (7).

Experimental

Synthesis of **II**, materials used, the hydrogenation procedures in a constant pressure apparatus, H_2 solubility data, the work-up of products for determining optical yields, and the spectroscopic instrumentation used, have been reported elsewhere (7).

Results

Catalytic Hydrogenation of Acrylamide

Hydrogen uptake plots at 60°C are illustrated in Fig. 2, and the rates in the initial substantial linear regions were measured to yield kinetic data over the following concentration ranges (*M*): Ru (1.0–5.0) × 10^{-3}, acryl (1.0–6.0) × 10^{-1}, H_2 (0.8–2.2) × 10^{-3}, and added diop (0.0–6.0) × 10^{-3}. The kinetic data are summarized in Figs. 3–6.

The dependence on catalyst goes from first-order to about half-order with increasing concentration; with added diop, the dependence remains first-order (Fig. 3*A*, *B*). The dependence on acrylamide concentration shows very similar behaviour (Fig. 4*A*, *B*), while the rate is strictly first-order in H_2 (Fig. 4*C*). The inverse diop dependence (Fig. 5*A*) may be replotted as $(rate)^{-1}$ vs. added diop to yield a straight line passing through, or close to, the origin (Fig. 5*B*).

The total H_2 uptake could be followed to complete reduction of acrylamide to propionamide, which was readily identified.

Yellow DMA solutions of the $HRuCl(diop)_2$ complex **II** (λ_{max} 380 nm, $\varepsilon = 3150\ M^{-1}\ cm^{-1}$) were unreactive toward 1 atm H_2 at 60°C. Addition of acrylamide to a DMA solution of **II** under argon gave immediate changes in the 350–500 nm region, the absorption below 425 nm decreasing with loss of the absorption maximum, and that above 435 nm increasing somewhat. The solution remained yel-

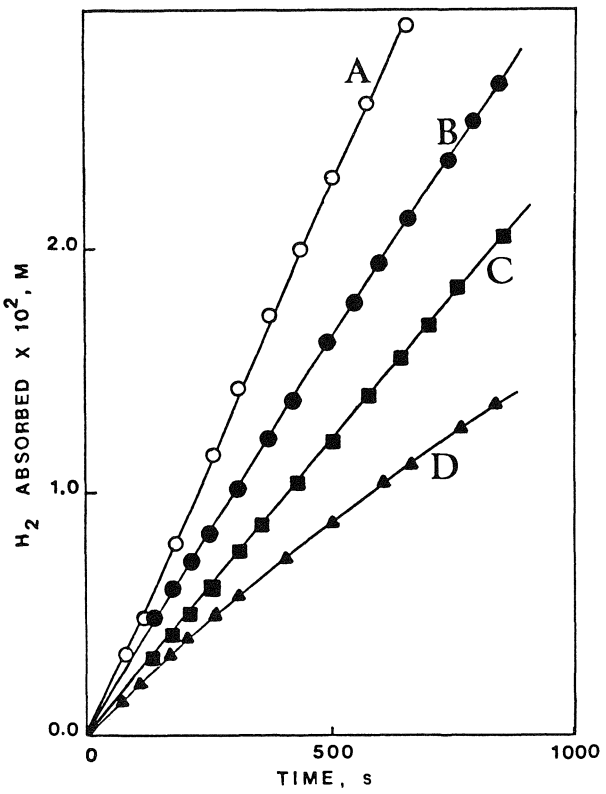


FIG. 2. Hydrogenation of acrylamide, DMA, 60°C; 0.2 *M* acryl, 2 × 10^{-3} *M* Ru. Pressure in Torr: *A*, 760; *B*, 600; *C*, 450; *D*, 300.

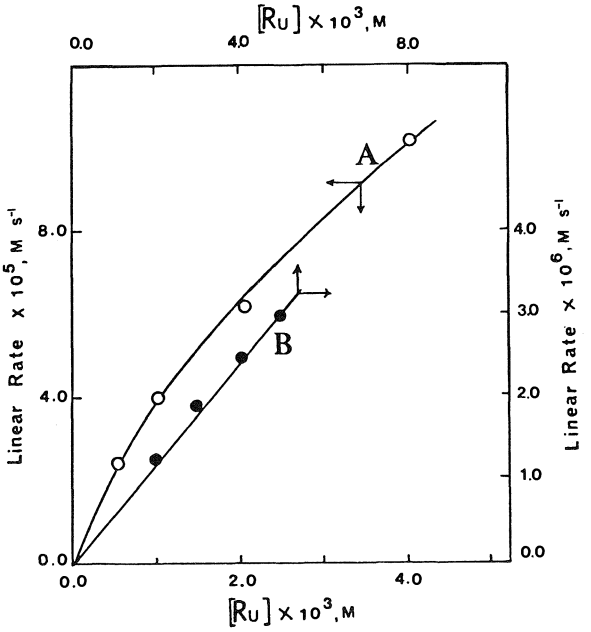


FIG. 3. Hydrogenation of acrylamide, DMA, 60°C. Curve *A*: 0.4 *M* acryl, 760 mm pressure. Curve *B*: 0.2 *M* acryl, 760 mm pressure, 6 × 10^{-3} *M* diop.

Can. J. Chem. Downloaded from www.nrcresearchpress.com by 210.87.254.5 on 09/05/12
For personal use only.

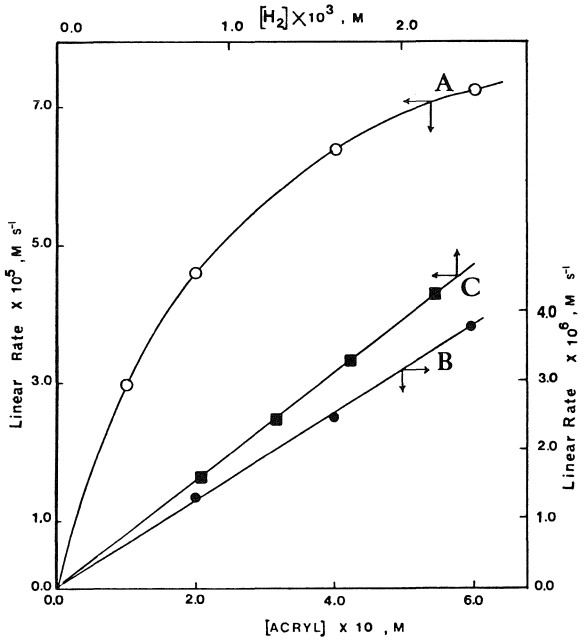


FIG. 4. Hydrogenation of acrylamide, DMA, 60°C. Curve *A*: 2 × 10^{-3} *M* Ru, 760 mm pressure. Curve *B*: 2 × 10^{-3} *M* Ru, 760 mm pressure, 6 × 10^{-3} *M* diop. Curve *C*: 0.2 *M* acryl, 2 × 10^{-3} *M* Ru.

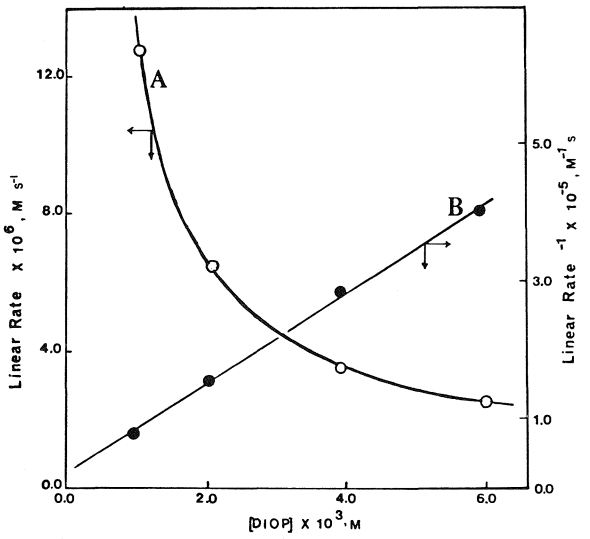


FIG. 5. Hydrogenation of acrylamide, DMA, 60°C. Curve *A*: 0.4 *M* acryl, 2 × 10^{-3} *M* Ru, 760 mm pressure. Curve *B*: curve *A* replotted as $(\text{rate})^{-1}$ vs. [diop] added.

low. A spectrophotometric titration yielded a set of spectra with a clean isosbestic point at 430 nm, and the data analyzed for the 1:1 equilibrium shown in reaction [2] with $K_1 = 3.8 \times 10^{-4}$:

[2] $\text{HRuCl(diop)}_2 + \text{acryl} \overset{K_1}{\rightleftharpoons} \text{complex} + \text{diop}$

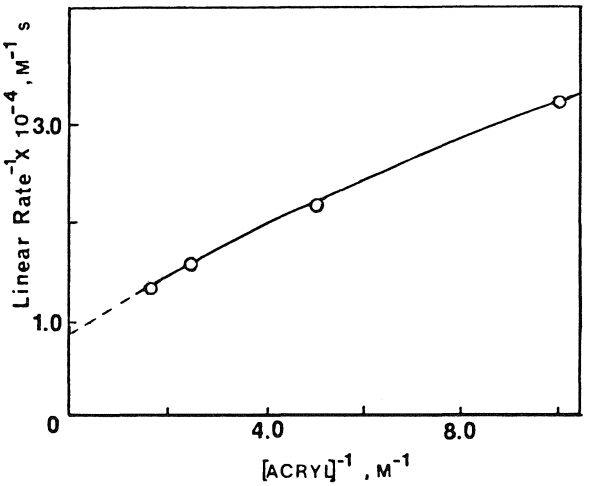


FIG. 6. Curve *A* of Fig. 4 replotted as $(\text{rate})^{-1}$ vs. $[\text{acryl}]^{-1}$.

The septet high-field ^{1}H resonance of **II** in $CDCl_3$ or DMA due to the coordinated hydride (7) disappears on the addition of acrylamide, and thus the complex formed in reaction [2] is considered to be an alkyl, although we have not been able to detect this by ^{1}H nmr in the amide solvent.

Catalytic Hydrogenation of α*-Phenylacrylic Acid*

The prochiral substrate α-phenylacrylic acid is readily hydrogenated catalytically to 2-phenylpropionic acid in 40% enantiomeric excess; use of the catalyst with (−)-diop yields the *S*(+) isomer, while the (+)-diop system gives the *R*(−) isomer (7).

[3] $\text{CH}_2{=}\text{C(C}_6\text{H}_5\text{)CO}_2\text{H} \rightarrow \text{CH}_3\text{CH(C}_6\text{H}_5\text{)CO}_2\text{H}$

The uptake plots resemble those for acrylamide but the rates are somewhat slower. The kinetics were determined as described above, and show a first-order dependence both on H_2 (Fig. 7*A*) and catalyst (Fig. 7*B*), a slight inverse dependence on added diop (Fig. 8*A*), and a first to zero-order in substrate (Fig. 8*B*).

The spectroscopic changes are similar to those for the acrylamide system, but K_1 is much larger (0.1).

Discussion

Acrylamide System

The kinetic and spectroscopic data are readily accommodated by the catalytic cycle outlined in reactions [4] to [6].

[4] $\text{HRuCl(diop)}_2 + \text{acryl} \overset{K_1}{\rightleftharpoons} \text{RuCl(alkyl)(diop)} + \text{diop}$

[5] $\text{HRuCl(alkyl)(diop)} + \text{H}_2 \xrightarrow{k} [\text{H}_2\text{RuCl(alkyl)(diop)}] \downarrow \text{HRuCl(diop)} + \text{propionamide}$

[6] $\text{HRuCl(diop)} + \text{diop} \xrightarrow{\text{fast}} \text{HRuCl(diop)}_2$

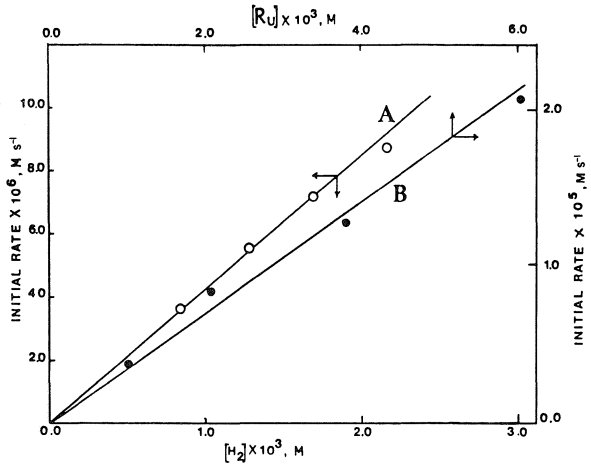


FIG. 7. Hydrogenation of α-phenylacrylic acid, DMA, 60°C. Curve *A*: 0.2 *M* phenylacrylic acid, 2×10^{-3} *M* Ru. Curve *B*: 0.4 *M* phenylacrylic acid, 760 mm pressure.

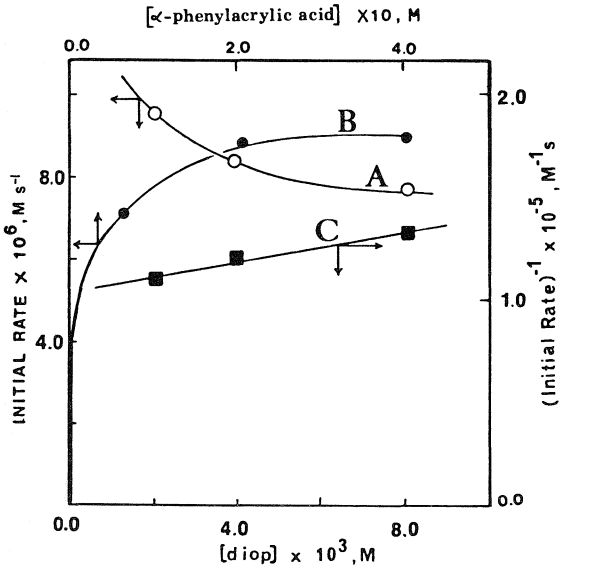


FIG. 8. Hydrogenation of α-phenylacrylic acid, DMA, 60°C. Curve *A*: 0.2 *M* phenylacrylic acid, 2×10^{-3} *M* Ru, 760 mm pressure. Curve *B*: 2×10^{-3} *M* Ru, 760 mm pressure. Curve *C*: curve *A* replotted as $(\text{rate})^{-1}$ vs. [diop] added.

The rapid alkyl formation is probably followed by a rate-determining oxidative addition of H_2 to give an octahedral ruthenium(IV) complex which then reductively eliminates the saturated product (see below). The dissociated diop may or may not reassociate to the HRuCl(diop) intermediate (which would be present as a solvated, likely 6-coordinate species) prior to commencement of the second catalytic cycle by further coordination of acrylamide.

The mechanism shown leads to the rate-law given in eq. [7], where a subscript "T" refers to the *total* concentration of species, e.g. $[\text{acryl}]_T$ refers to the free plus coordinated substrate.

$$[7] \quad \text{Rate} = \frac{-d[H_2]}{dt} = \frac{kK_1[\text{Ru}]_T[H_2][\text{acryl}]_T}{K_1[\text{acryl}]_T + [\text{diop}] + K_1[\text{Ru}]_T}$$

The rate law shows the experimentally determined first-order dependence on $[H_2]$, between first- and zero-order in acrylamide, and between first- and zero-order in ruthenium. This catalyst dependence pertains even when $[\text{acryl}]_T \gg [\text{Ru}]_T$ (denominator of eq. [7]), since the [diop] term increases as $[\text{Ru}]_T$ increases (reaction [4]).

Although rate expression [7], or its inverse form (eq. [8]), is complex, some limiting forms that exist for some of the experimental conditions used are simple, and the data can be analyzed accordingly.

$$[8] \quad \frac{1}{\text{Rate}} = \frac{1}{k[H_2]}\left(\frac{1}{[\text{Ru}]_T} + \frac{1}{[\text{acryl}]_T}\right) + \frac{[\text{diop}]}{kK_1[\text{Ru}]_T[H_2][\text{acryl}]_T}$$

For example, at constant $[H_2]$, $[\text{Ru}]_T$, and $[\text{acryl}]_T$, the plot of $(\text{rate})^{-1}$ vs. added [diop] yields a straight line (Fig. 5*B*) whose slope yields a kK_1 value of $8.9 \times 10^{-3}\ M^{-1}\ s^{-1}$ (eq. [8]), although the intercept is too small to give a reliable k value.

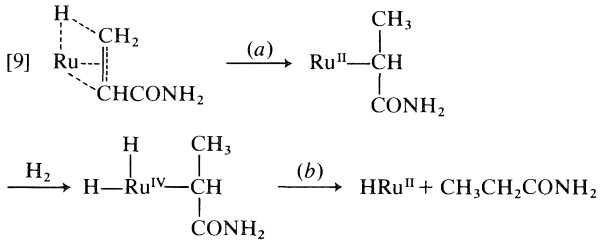
The intercept of the plot drawn of $(\text{rate})^{-1}$ vs. $[\text{acryl}]^{-1}$ (Fig. 6) yields (eq. [8]) a k value of $\sim 27\ M^{-1}\ s^{-1}$. Use of the determined kK_1 value yields $K_1 = 3.3 \times 10^{-4}$ which is in good agreement with the spectroscopically determined value of 3.8×10^{-4}. For reactions with excess diop at constant $[\text{acryl}]_T$ and $[H_2]$, when $[\text{diop}] \gg K_1[\text{acryl}]_T + K_1[\text{Ru}]_T$, the plot of the rate vs. $[\text{Ru}]_T$ gives a straight line passing through the origin (eq. [7], Fig. 3*B*), the slope giving $kK_1 = 8.6 \times 10^{-3}\ M^{-1}\ s^{-1}$. Similarly, for conditions with excess diop, the slope of Fig. 4*B* yields a kK_1 value of $9.0 \times 10^{-3}\ M^{-1}\ s^{-1}$. The slope of Fig. 4*C* at the conditions used, close to first-order in acrylamide, is given by the expression $kK_1[\text{Ru}]_T[\text{acryl}]_T/[\text{diop}]$; rewriting [diop] in terms of equilibrium [4] gives for the slope the expression $kK_1^{1/2}[\text{Ru}]^{1/2}{}_T[\text{acryl}]^{1/2}{}_T$. The measured slope yields $kK_1^{1/2} \approx 1.0\ s^{-1}$, in comparison to a value of about $0.5\ s^{-1}$ determined from the other kinetic dependences; the agreement is considered reasonable.

In summary, all the kinetic data are internally consistent yielding at 60°C, $k = 27\ M^{-1}\ s^{-1}$ and $K_1 = (3.2 \pm 0.1) \times 10^{-4}$, and the latter value agrees

Can. J. Chem. Downloaded from www.nrcresearchpress.com by 210.87.254.5 on 09/05/12
For personal use only.

well with a spectroscopic K_1 value determined independently.

The mechanism closely resembles that of the $HRuCl(PPh_3)_3$-catalyzed systems, where a phosphine ligand dissociates to provide a coordination site for the unsaturated substrate (2). The $HRuCl(diop)_2$ complex alone does not detectably dissociate a diop ligand (7), while substrate coordination does cause loss of this ligand. Dissociation of one end of the chelating diphosphine could in principle allow for acrylamide coordination, and indeed monodentate diop ligand complexes are known (7); however, steric problems may force complete dissociation of a diop during formation of a *cis* hydrido-olefin intermediate. Subsequent hydride transfer is considered to proceed through a four-centre transition state (9); the direction of hydrometallation is uncertain but on electronic grounds it would be expected to proceed as shown in reaction [9] (other Cl, and diop ligand omitted):



In principle the rate-determining step could then be either the oxidative-addition of H_2 or the subsequent hydrogen transfer steps; the former is usually preferred since hydrido-alkyl species are relatively rare (2), although a greater difficulty in hydride transfer to coordinated alkyl in this case due to the conformational rigidity of the diop ligand cannot be ruled out.

The hydrogenation rates are about 1/50 as large as those using $HRuCl(PPh_3)_3$ under corresponding conditions (10), but are still reasonably efficient with a turnover number of about 100 h^{-1} at 1 atm H_2 at 60°C. The higher rates for the PPh_3 system result from more effective binding of substrates, i.e. higher K_1 values (10). More heavily substituted substrates, such as α- and β-methylcinnamic and methylfumaric acids (which are prochiral), are not hydrogenated at all by the diop catalyst likely because of steric problems in their coordination.

Of interest, the complexes $HRuCl[Ph_2P(CH_2)_nPPh_2]_2$, with n = 1–4, the n = 4 system being analogous to the diop system, are probably undistorted *trans* structures with C_{4v} symmetry, the P atoms all being equivalent at 30°C (11). None of these are effective for catalytic hydrogenation of olefins under mild conditions. The distortions imposed by the dioxolane ring of the diop ligands presumably make them more readily displaced by the substrate (higher K_1 values).

The nonlinearity of the H_2-uptake at lower pressure during hydrogenation of even 5–10% of the acrylamide (Fig. 2*D*) suggests the presence of some reaction that competes with step [5] under these conditions. Utilization of hydrogen from the phenyl rings of the phosphine is one possibility (12).

α-Phenylacrylic Acid System

The system parallels that of acrylamide after allowance is made for the much stronger binding by this acidic substrate. This results in a zero-order dependence on substrate even at 0.2 *M* (Fig. 8*B*); this means that the $K_1[\text{substrate}]_T$ term in the denominator of rate-law [7] then dominates, and the rate-law becomes simply $k[H_2][Ru]_T$ due to complete formation of the alkyl (reaction [4]). The average value of k determined from the slopes of Fig. 7*A*, *B* is 2.08 M^{-1} s^{-1}. The inverse dependence on diop is small (Fig. 8*A*) due to the relatively large K_1 value, but the limited inverse plot shown in Fig. 8*C* (eq. [8]) yields k = 2.2 M^{-1} s^{-1} from the intercept and a kK_1 value of 0.36 M^{-1} s^{-1} from the slope; these numbers give K_1 = 0.16 in reasonable agreement with the spectrophotometric data.

The much higher binding constant of the phenylacrylic acid compared to acrylamide could be due to differences in the electron-withdrawing properties of the substituent groups (C_6H_5, CO_2H vs. H, $CONH_2$), but coordination via the carboxylic acid or even the phenyl group is feasible (2). Binding of styrene to a solvated $Rh[Ph_2P(CH_2)_2PPh_2]^+$ species occurs primarily via the phenyl ring (13). The slower hydrogenation (k) step of the phenylacrylic acid system could be attributed to a less favourable oxidative addition of H_2 due to lower electron density at the metal centre and/or greater difficulty in a hydride transfer step (eq. [9]) due to steric reasons.

The overall catalytic addition of H_2 to olefins is nearly always *cis* (ref. 5, p. 407), and to the olefinic face coordinated to the metal. The hydrometallation step (reaction [9], step (*a*)) is necessarily *cis* and this is thought to determine the chirality of the final product since the reductive elimination step (reaction [9], step (*b*)) occurs with retention of configuration at the metal-bonded carbon (14). Thus, preferential coordination of one olefinic face of the substrate is required for asymmetric hydrogenation. These mono(diop) systems probably achieve preferred coordination of one olefinic face due to an alternating edge-face arrangement of the four phenyl groups (2, 15).

A tentative correlation between the extent of

Can. J. Chem. Downloaded from www.nrcresearchpress.com by 210.87.254.5 on 09/05/12
For personal use only.

asymmetric induction and binding constants of prochiral olefinic substrates has been suggested for some Rh(diop)(solvent)$_2^+$ systems (16). The mechanism established in this work for the HRuCl(diop)$_2$ system should allow for a further testing of this hypothesis, studies that are in progress in this laboratory.

Acknowledgments

We thank the Natural Sciences and Engineering Research Council of Canada for financial support, and Johnson Matthey Ltd. for the loan of $RuCl_3 \cdot 3H_2O$.

1. J. W. SCOTT and D. VALENTINE, JR. Science, **184**, 943 (1974).
2. B. R. JAMES. Adv. Organomet. Chem. **17**, 319 (1979).
3. J. D. MORRISON, W. F. MASLER, and M. K. NEUBERG. Adv. Catal. **25**, 81 (1976).
4. M. D. FRYZUK and B. BOSNICH. J. Am. Chem. Soc. **99**, 6262 (1977).
5. B. R. JAMES. Homogeneous hydrogenation. Wiley, New York. 1973. p. 83.
6. B. R. JAMES, D. K. W. WANG, and R. F. VOIGT. J. Chem. Soc. Chem. Commun. 574 (1975).
7. B. R. JAMES, R. S. MCMILLAN, R. H. MORRIS, and D. K. W. WANG. Adv. Chem. Ser. **167**, 122 (1978), and references therein.
8. R. C. BALL, B. R. JAMES, J. TROTTER, D. K. W. WANG, and K. R. DIXON. J. Chem. Soc. Chem. Commun. 460 (1979).
9. J. HALPERN. Adv. Chem. Ser. **70**, 1 (1968).
10. L. D. MARKHAM. Ph.D. Dissertation, University of British Columbia, Vancouver, B.C. 1973.
11. B. R. JAMES and D. K. W. WANG. Inorg. Chim. Acta, **19**, L17 (1976).
12. B. R. JAMES, L. D. MARKHAM, and D. K. W. WANG. J. Chem. Soc. Chem. Commun. 439 (1974).
13. J. HALPERN, D. P. RILEY, A. S. C. CHAN, and J. J. PLUTH. J. Am. Chem. Soc. **99**, 8055 (1977).
14. A. NAKAMURA and S. OTSUKA. J. Am. Chem. Soc. **95**, 7262 (1973).
15. B. D. VINEYARD, W. S. KNOWLES, M. J. SABACKY, G. L. BACKMAN, and D. J. WEINKAUFT. J. Am. Chem. Soc. **99**, 5946 (1977).
16. J. HALPERN. Proc. Symp. Rhodium in Homogeneous Catal., Veszprém, Hungary. 1978. p. 30.

Can. J. Chem. Downloaded from www.nrcresearchpress.com by 210.87.254.5 on 09/05/12
For personal use only.

On the formation of cyclopentenium cations from all $C_6H_{10}^{+\cdot}$ molecular ion structures[1]

PEDER WOLKOFF AND JOHN L. HOLMES
Chemistry Department, University of Ottawa, Ottawa, Ont., Canada K1N 9B4
AND
F. P. LOSSING
Division of Chemistry, National Research Council of Canada, Ottawa, Ont., Canada K1A 0R6

Received August 31, 1979

PEDER WOLKOFF, JOHN L. HOLMES, and F. P. LOSSING. Can. J. Chem. **58**, 251 (1980).

The structures of $[C_5H_7]^+$ ions produced by methyl loss from thirty isomeric C_6H_{10} molecular ions have been assessed from measurements of ionic heats of formation and the kinetic energy release associated with the fragmentation. It is proposed that the thermodynamically most stable $[C_5H_7]^+$ ions [cyclopentenium]$^+$ are formed at the dissociation threshold irrespective of the initial molecular ion structure. Mechanistic aspects of the fragmentations were studied by mean of deuterium labelling.

Observations of metastable peak shapes for labelled compounds permitted the identification of reaction pathways having different energy requirements. The lowest energy routes involved little or no positional mixing of H and D prior to fragmentation. It is proposed that the molecular ions with sufficient energy to fragment on the μs time scale undergo successive (and reversible) isomerization by allylic 1,3-hydrogen shifts to their isomeric isolated diene molecular ions which, by an allylic 1,2-hydrogen shift, may isomerize to a methylcyclopentene molecular ion prior to loss of methyl. The sequence of isomerization of the molecular ions is alkyne → allene → conjugated diene → isolated diene. The de-conjugation step has an activation energy of ca. 10 kcal mol^{-1}. We suggest, however, that allene molecular ions rearrange directly to isolated diene molecular ions.

PEDER WOLKOFF, JOHN L. HOLMES et F. P. LOSSING. Can. J. Chem. **58**, 251 (1980).

On a déterminé la structure des ions $[C_5H_7]^+$ provenant de la perte d'un méthyle par trente ions moléculaires isomères C_6H_{10}, à partir des mesures de chaleur ionique de formation et de l'énergie cinétique associées à la fragmentation. On propose que les ions [cyclopentènium]$^+$ $[C_5H_7]^+$ les plus stables thermodynamiquement, sont formés au début de la dissociation quelle que soit la structure de l'ion moléculaire initial. On a étudié le mécanisme de ces fragmentations par marquage isotopique au deutérium.

L'observation de la forme des pics métastables des composés marqués a permis d'identifier des mécanismes réactionnels requérant des énergies différentes. La voie exigeant la plus faible énergie implique peu ou pas de mélange de position de l'hydrogène ou du deutérium avant la fragmentation. On propose également que les ions moléculaires ayant suffisamment d'énergie pour se fragmenter dans des temps de l'ordre de la μs subissent des isomérisations successives, (et reversibles) par transpositions 1,3 d'hydrogènes allyliques conduisant à leurs ions moléculaires isomères comportant des dienes non conjugués, qui par une transposition allylique-1,2 peuvent s'isomériser en un ion moléculaire méthylcyclopentène avant la perte d'un méthyle. Les ions moléculaires s'isomérisent suivant la séquence: alcyne → allène → diène conjugué → diène non conjugué. L'étape de déconjugaison a une énergie d'activation de l'ordre de 10 kcal mol^{-1}. Nous suggérons cependant que l'ion moléculaire allénique se transpose en ion moléculaire comportant un diène non conjugué.

[Traduit par le journal]

Introduction

Our understanding of the unimolecular decompositions of ionised unsaturated aliphatic hydrocarbons has improved only slowly during the last decade.

Although the development of new techniques (1) has made possible observations within well defined time frames, a fundamental and general understanding of the decomposition processes of alkenes has been rendered especially difficult by the extensive rearrangements which precede fragmentation. Levsen and Heimbrecht have examined non-decomposing molecular ions of alkenes by collisional activation mass spectrometry and they concluded that the isomerization of alkene molecular ions becomes less pronounced with increasing molecular size (2). Using metastable ion characteristics and thermochemical arguments Bowen and Williams have suggested (3) that up to a limiting chain length of six carbon atoms, complete interconversion takes place among isomeric monoalkene molecular ions prior to decomposition in the μs time frame.

Isotopic labelling studies have shown that the complete loss of positional identity of H and/or C atoms takes place prior to fragmentation in a wide variety of molecular ions of unsaturated hydrocarbons; examples have recently been reviewed (4). Incomplete atom randomization prior to fragmentation on the μs time scale only becomes prevalent in ions containing six or more C atoms, e.g., in dimethylpentenes (5), heptenes (6, 7), C_7H_{10} isomers (8), and octenes (9).

The structural integrity of ions which have insufficient internal energy to fragment in the μs time frame can be investigated by collisional activation

[1]NRCC No. 17982.

0008-4042/80/030251-07$01.00/0
©1980 National Research Council of Canada/Conseil national de recherches du Canada

Can. J. Chem. Downloaded from www.nrcresearchpress.com by 210.87.254.42 on 09/05/12
For personal use only.

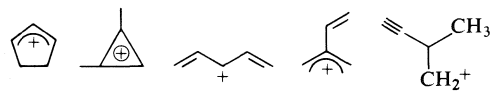
Can. J. Chem. Downloaded from www.nrcresearchpress.com by 210.87.254.42 on 09/05/12
For personal use only.

techniques. Varying degrees of isomerization have thus been identified among molecular ions of C_4H_8 (2), C_5H_{10} (10), C_6H_{10} (11), C_6H_{12} (10), C_7H_{14} (2), and C_8H_{16} (9). From the above it is evident that the relative rates of isomerization and fragmentation reactions are a complex function of internal energy and molecular size.

It has been shown recently (12) that isomeric cyclic C_6H_{10} molecular ions decompose by methyl loss via a methylcyclopentene molecular ion, producing cyclopentenium ions at their thermochemical threshold; the latter is the most stable $[C_5H_7]^+$ ion species, having a heat of formation (ΔH_f) of 199 kcal mol^{-1} (13).

In this paper, we describe methyl loss from *all* acyclic isomeric C_6H_{10} molecular ions; (*m/z* 67) is the base peak in the reported normal mass spectra of these compounds (14). The purpose of this investigation was to try to answer the following questions: What is the structure of the $[C_5H_7]^+$ ions and how are they formed? What influence has the position of unsaturation on the energetics and mechanism of $[C_5H_7]^+$ formation? How does loss of positional identity among H and D atoms come about?

Possible structures for $[C_5H_7]^+$ daughter ions whose thermochemistry has been investigated (13) are shown below, together with their heats of formation in kcal mol^{-1}. Methylcyclopentene



199 217 (est) 220 233 (est) 234

molecular ions with internal energy less than ca. 1 eV above the threshold for [cyclopentenium]$^+$ generation fragment (μs time scale) by a simple bond cleavage and there is no atom mixing (12). Ions having a greater internal energy and decomposing on the same time scale lose methyl containing randomly selected H atoms and the reaction is believed to proceed via a ring-opened species (12). We have measured ionization and appearance energies (AE) for *m/z* 67 using energy selected electrons (15) (molecular ion lifetime ~30 μs) and metastable peak shapes for $[C_5H_7]^+$ ion production. AE values afford $\Delta H_f(C_5H_7^+)$. The width of the metastable peak is directly related to the release of excess internal energy (which is made up of the non-fixed energy of the activated complex and any reverse activation energy (16)) into kinetic energy (T).

Results and Discussion

Thermochemistry

The heats of formation of the neutral C_6H_{10} molecules, molecular ions, and their $[C_5H_7]^+$ daughter ions are presented in Table 1, together with the kinetic energy releases evaluated from the half-height widths of the metastable peaks for $CH_3^\bullet$ loss. For convenience of presentation, Table 1 is subdivided according to the number and type of multiple bonds in the isomers.

(i) Molecular Ion Stability

The $\Delta H_f(C_6H_{10}^{+\bullet})$ values show that the relative stability of molecular ions having one unsaturated bond in a terminal position follows the order alkyne < allene < unconjugated diene < conjugated diene < cycloalkene. Stabilization by methyl substitution at a terminal unsaturated site is most significant for alkynes; thus the molecular ions of 2-hexyne and 3-hexyne have a $\Delta H_f(M^{+\bullet})$ 18 kcal mol^{-1} lower than that of 1-hexyne. This effect is smaller for conjugated and cumulated dienes; for example, $\Delta H_f(M^{+\bullet})$ of 2,3-hexadiene is 9 kcal mol^{-1} less than that of its 1,2-isomer.

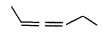
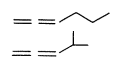
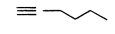
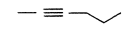
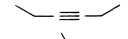
The IE values of all terminal alkynes, 1,2- and 1,5-hexadiene, and 2-methyl-1,4-pentadiene are close to or above the calculated thresholds for the generation of $CH_3^\bullet$ and the most stable $[C_5H_7]^+$ daughter ion, [cyclopentenium]$^+$, e.g., for 1-hexyne, AE calculated for [cyclopentenium]$^+$ + $CH_3^\bullet$ = (199 + 34 − 29.6)/23.06 = 8.82 eV, IE = 9.95 eV; AE $[C_5H_7]^+$ = 10.04 eV. It is noteworthy that these molecular ions require less than 0.2 eV of internal energy (above their IE) for this fragmentation to be observed on the 30–50 μs time scale. Such ions then are all "hot" with respect to the above dissociation at their ionization thresholds.

(ii) Heats of Formation of $[C_5H_7]^+$ Daughter Ions

These, as can be seen from Table 1, fall into three general groups. Those with apparent heats of formation in the range 200 → 206 kcal mol^{-1} must have the [cyclopentenium]$^+$ structure and need not be further discussed. The excess energies of up to 5 kcal mol^{-1} may be ascribed to a kinetic shift effect (17). A second group have ΔH_f in the range 211 ± 3 kcal mol^{-1}. It is formally possible that these values relate to the formation of an isomeric $[C_5H_7]^+$ daughter ion with a ΔH_f about 12 kcal mol^{-1} above that of [cyclopentenium]$^+$. In view of the uncertainty of ΔH_f[dimethylcyclopropenium]$^+$ (13), this ion is a candidate. However, the energy release values for this group of compounds, the majority of which are conjugated dienes, all are significantly greater than those for the isolated dienes (and cycloalkenes (12)) which produce [cyclopentenium]$^+$ at or near to threshold. Thus these ΔH_f values may arise from the presence of an energy barrier for a common rearrangement (e.g., de-

Can. J. Chem. Downloaded from www.nrcresearchpress.com by 210.87.254.42 on 09/05/12
For personal use only.

TABLE 1. Heats of formation of $[C_6H_{10}]^{+\cdot}$ and $[C_5H_7]^+$ ions and the kinetic energy release (T) of the reaction $[C_6H_{10}]^{+\cdot} \rightarrow [C_5H_7]^+ + CH_3^\cdot$

Compound	$\Delta H_f[M]$[a]	$\Delta H_f(M^{+\cdot})$ (±1.0 kcal/mol)	$\Delta H_f(C_5H_7^+)$ (±1.0 kcal/mol)	$T_{0.5}$ (meV)	IE (±0.05 eV)	AE (±0.05 eV)
	17.6	225	205	27.9	8.98	9.60
	18.6	227	206	27.4	9.04	9.61
	20.1	234	202[c]	21.6[b]	9.29	9.35
	18.6	235	204	25.9	9.40	9.54
	17.1	228	200[c]	18.1[d]	9.16	9.40
	22.0	222	200	21.9[b]	8.66	9.18
	10.6	201	210	33.9[b]	8.26	10.14
	11.6	202	211	35.5	8.24	10.10
	*cis*/*trans* 14.6/13.6	212	*205*[c]	29.8	8.54	9.74
	10.3	207	212[c]	36.9[d]	8.45	10.23
	11.0	201	212	40.9	8.26	10.18
	11.3	203	209	31.7[b]	8.37	10.06
	10.3	205	211	31.2	8.46	10.16
	10.1	210	212	33.9[b]	8.66	10.22
	13.3	216	212[c]	29.0	8.81	10.08
	31.6	242	213	25.3	9.12	9.34
	20.6	221	214	30.9	8.70	9.88
	41.4	239	210	29.4	8.58	8.78
	26.3	228	208	30.7[b]	8.76	9.38
	29.1	237	205	28.5[b]	9.00	9.12
	27.0	236	218	37.0	9.06	9.78
	25.7	227	209	33.1	8.74	9.44
	22.9	222	209	34.3	8.64	9.55
	29.6	259	227	45.6	9.95	10.04
	25.3	241	220	35.5	9.37	≤9.93
	25.5	241	219	37.1	9.34	9.88
	27.7	254	225	46.0	9.83	10.03
	27.7	254	223	38.6[b]	9.79	9.93
	23.1	238	212	32.6[b]	9.31	9.67
	25.4	251	220	37.3	9.80	9.90

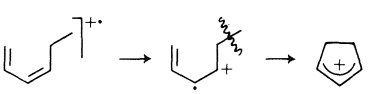
[a] Heats of formation of all neutral compounds were, for consistency, calculated by additivity (36). ±3%.
[b] ±6%.
[c] Reference 13.
[d] Reference 12.

Can. J. Chem. Downloaded from www.nrcresearchpress.com by 210.87.254.42 on 09/05/12
For personal use only.

conjugation of the double bonds) which precedes fragmentation to produce the most stable daughter ion; the larger $T_{0.5}$ values would thus reflect the higher internal energies of such ions (18). Indeed, the $[C_5H_7]^+$ daughter ion produced from 1,2,2-trimethylcyclopropene has a ΔH_f value too low for it to be [dimethylcyclopropenium]$^+$ and thus even this molecular ion undergoes rearrangement before fragmentation.

The alkynes form a third group. The terminal alkynes are "hot" ions (as discussed above) and the $T_{0.5}$ values are the largest for all compounds investigated. Although in principal two other daughter ions are thermochemically feasible, we suggest that again [cyclopentenium]$^+$ is being generated. The molecular ions of the non-terminal alkynes have significantly lower heats of formation and $CH_3^\bullet$ loss has an activation energy of 0.4–0.5 eV. The $T_{0.5}$ values and $\Delta H_f[C_5H_7]^+$ are also lower than for the terminal alkynes.

Two noteworthy exceptions to the above groupings should be discussed. 1,3-Hexadiene is the sole conjugated diene which has a low $\Delta H_f[C_5H_7]^+$ value. This is the only conjugated diene molecular ion which can formally lose a $CH_3^\bullet$ group by a favorable (19) allylic cleavage without the need of prior rearrangement.



1,2-Hexadiene also yields the same low $\Delta H_f[C_5H_7]^+$; this observation may be explained by proposing that the molecular ion may rapidly isomerize to that of 1,3-hexadiene with no appreciable energy barrier, because of the close similarity between their $\Delta H_f[C_5H_7]^+$ and energy release ($T_{0.5}$)values.

(iii) Kinetic Energy Releases

In previous work on cyclic $[C_6H_{10}]^{+\bullet}$, the difference in activation energies between two competing reactions leading to $[C_5H_7]^+$ could satisfactorily be related to the difference in their average released energies ($\Delta\langle T\rangle$) by use of Haney and Franklin's empirical equation (20), $\langle E\rangle^* = \Delta\langle T\rangle \times 0.44\ (3n - 6)$, where n is the number of atoms in the fragmenting ion.

Although the released kinetic energies ($T_{0.5}$) (Table 1) roughly follow the same trend as $\Delta H_f[C_5H_7]^+$, no simple relationship exists between them. For example, $\Delta H_f[C_5H_7]^+$ for the majority of the conjugated dienes is 211 ± 3 kcal mol^{-1}, while $T_{0.5}$ ranges from 25–41 meV. These observations could result from the fragmentations taking place over more than one potential surface, i.e., that the metastable peaks consist of two (or more) superimposed gaussian-type peaks having different energy releases and being present in different relative abundances. Second components can clearly be seen in the distributions of released energies (21) for the fragmentations of 2-methyl-1,4-pentadiene, 2,3-dimethyl butadiene, 1-hexyne, and 3,3-dimethylbut-1-yne. These are shown in Fig. 1.

Fragmentation Mechanisms

(i) Isolated Dienes

For these isomers, $[C_5H_7]^+$ is produced at energies close to that for [cyclopentenium]$^+$. It is noteworthy that although the molecular ion of 3-methyl-1,4-pentadiene has a structure appropriate for the generation of the 1,4-pentadien-3-yl cation (ΔH_f = 220 kcal mol^{-1}) (13) by a simple allylic bond cleavage, nevertheless [cyclopentenium]$^+$ ions are generated. [Cyclopentenium]$^+$ formation (possibly via a methylcyclopentene molecular ion) from these isomers may be accomplished by *one* 1,2-hydrogen shift, followed by ring closure; the itinerant H atom is secondary (or tertiary) and allylic. (There is indeed experimental precedent for 1,2-H shifts in molecular ions of hydrocarbons (22, 23).) Two principles are thus required: (*a*) that the charge is preferentially located at the most highly substituted carbon atom and the odd electron at the least substituted carbon atom; (*b*) that the driving force for the H-shift is to achieve allylic stabilization of the charge (see Scheme 1). These principles do not apply to the 1,5-hexadiene molecular ion; isomerization to its 1,3- or 1,4-isomer is unlikely because of the low $\Delta H_f[C_5H_7]^+$ value. Further-

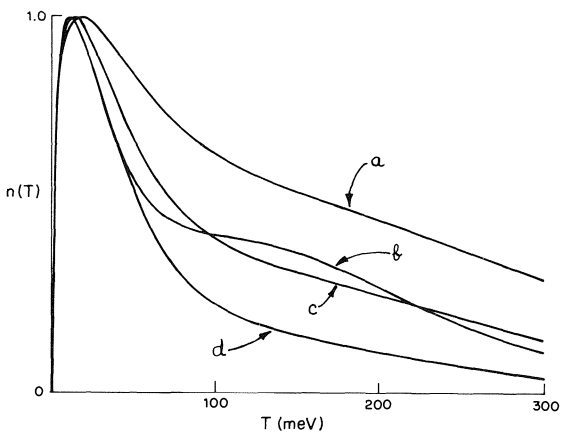
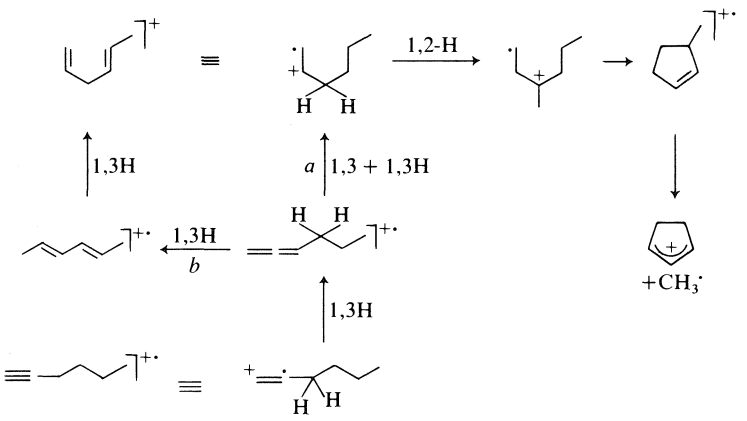
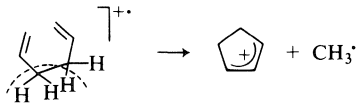


FIG. 1. Distributions of released energies ($n(T)$ represents the fraction of the energy released) derived from metastable peaks (21) for the fragmentation $C_6H_{10}^{+\bullet} \rightarrow C_5H_7^+ + CH_3^\bullet$ for (*a*) 1-hexyne, (*b*) 3,3-dimethylbut-1-yne, (*c*) 2,3-dimethyl-1,3-butadiene, and (*d*) 2-methyl-1,4-pentadiene.



SCHEME 1

more, this molecular ion has been shown to be stable with respect to isomerization at low internal energies (24). We propose that methyl is lost via the extrusion of a methylene group (C-3 or C-4) together with a neighboring secondary, allylic hydrogen atom leading to [cyclopentenium]$^+$ formation in a concerted manner (viz. internal methyl loss from alkane molecular ions (23) and the Cope rearrangement (see, for example, ref. 25)). The low $\Delta H_f[C_5H_7]^+$ value in the case of 2-propenylcyclopropane indicates that the ring opening has little or no activation energy, in keeping with recent studies of cycloalkanes (26).



(ii) Conjugated Dienes

With the exception of 1,3-hexadiene (discussed above) [cyclopentenium]$^+$ formation from the molecular ions of this group requires *two* H atom shifts if the above same two principles are applied. Isomerization of a 1,3-diene to its 1,4-isomer requires a 1,3-H shift, where the itinerant hydrogen atom is allylic and primary (cf., 1,3-H allylic shifts (27)), an additional 1,2-H shift then affords the methylcyclopentene molecular ion (see Scheme 1). The significantly higher $\Delta H_f[C_5H_7]^+$ values for the 1,3-dienes may arise from an activation energy for the deconjugation step, because the activation energy for a 1,3-allylic H-shift is negligible (12). $\Delta H_f[C_5H_7]^+$ for 2-ethyl-1,3-butadiene can be similarly explained even though two 1,3-allylic H-shifts are required for deconjugation. There are, however, (intuitively) alternative rationalizations for [cyclopentenium]$^+$ formation, e.g., a 1,4-H shift would afford the methylcyclopentene molecular ion directly from that of 2-methyl-1,3-pentadiene; indeed, the metastable peak was found to be composite from analysis of the peak shape (21), and thus indicative of competing fragmentation routes. The molecular ions of 2,3-dimethyl-1,3-butadiene and bicyclopropyl may rearrange via [2-propenylcyclopropane]$^{+\cdot}$ by a 1,2-H shift.

(iii) Allenes

$[C_5H_7]^+$ formations from allene molecular ions have ΔH_f and $T_{0.5}$ values lower than those of their conjugated isomers and so isomerization to the latter is unlikely (*b* in Scheme 1). Direct isomerization to a 1,4-isomer by two concerted 1,3-H shifts (*a* in Scheme 1) is a possible route.

(iv) Alkynes

We propose that these molecular ions first rearrange to an isomeric allene by a 1,3-H shift, a process for which there is a large thermodynamic driving force (see Table 1). This has been demonstrated for the [propyne]$^{+\cdot}$ → [allene]$^{+\cdot}$ system (28) and such a rearrangement has also been proposed for substituted acetylenes (29). However, the high $\Delta H_f[C_5H_7]^+$ values for 2- and 3-hexyne require either a substantial kinetic shift or an activation energy for the [alkyne]$^{+\cdot}$ → [allene]$^{+\cdot}$ step. (Note that the 1-ynes are "hot" ions as discussed earlier.) Only 3-methyl-2-pentyne produces $[C_5H_7]^+$ with a ΔH_f comparable to those from the allenes; this, however, is the *only* alkyne having a *tertiary* H-atom available for a 1,3-shift (to produce trimethylallene in this case); this may well have a lower energy requirement. The only deuterium-labelled alkyne studied in this work was 1-$^2H_1$-1-hexyne. The relative abundances of the metastable peaks for loss of $CH_3^\cdot$ and $CH_2D^\cdot$ were very close to the random statistical ratio (Table 2), in agreement with earlier work on ions of low internal energy content (30). Complete loss of positional identity among H atoms for $[C_6H_{10}]^{+\cdot}$ ions of such

Can. J. Chem. Downloaded from www.nrcresearchpress.com by 210.87.254.42 on 09/05/12
For personal use only.

TABLE 2. Metastable peak abundance ratios (peak areas)[a] and kinetic energy release values[b] ($T_{0.5}$ meV ±3% except where stated) for $CH_xD_{3-x}^{\cdot}$ loss from ^{2}H-labelled C_6H_{10} molecular ions

Compound	$CH_3^{\cdot}$ lost	$T_{0.5}$	$CH_2D^{\cdot}$ lost	$T_{0.5}$	$CHD_2^{\cdot}$ lost	$T_{0.5}$	$CD_3^{\cdot}$ lost	$T_{0.5}$
$CD_2{=}C(CH_3)CH_2CH{=}CH_2$	15.6(7.00)	17.7	6.6(7.00)	31.3	1.0(1.00)	28.3		
$CH_3CH{=}CD{-}CD{=}CHCH_3$	19.4(7.00)	30.9	10.0(7.00)	34.1[c]	1.0(1.00)	42.8[c]		
$CD_3CH{=}CH{-}CH{=}CHCH_3$	3.6(35.2)	34.1	3.5(63.2)	37.1	1.9(2.1)	34.8	1.0(1.00)	26.0
$HDC{=}C{=}CHCH_2CH_2CH_3$	1.00(2.33)	32.3	1.00(1.00)	25.8				
$DC{\equiv}C{-}CH_2CH_2CH_2CH_3$	2.53(2.33)	46.4[c]	1.00(1.00)	46.7[c]				

[a] Values in parentheses correspond to random distributions of H and D.
[b] From ref. 12, reevaluated.
[c] Values ±6%.

high internal energy content is to be expected from our earlier investigations (12).

Deuterium Labelling

(i) 2-Methyl-1,4-pentadiene-1,1-$^2H_2$

Results for this compound have been reported earlier (12), but they have been revised and are presented here (as metastable peak areas) in Table 2. The observations were interpreted as arising from a random statistical loss of labelled methyl which requires an activation energy in excess of the threshold for [cyclopentenium]$^+$ generation, plus a threshold methyl loss which involves *mainly*, but not exclusively, $CH_3^{\cdot}$ loss prior to, or in concert with ring closure. The latter conclusion follows from the observation that the daughter ions *m/z* 67, 68, and 69 had the same AE as the unlabelled compound. Note that the $T_{0.5}$ value for $CH_3^{\cdot}$ loss (17.7 meV) is significantly higher than that for the specific loss of $CH_3^{\cdot}$ from methylcyclopentenes (15.5 meV) (12), but these results are compatible with a weighted summation of T values of 15.5 and 31 meV (12). Similarly, $T_{0.5}$ ($CH_2D^{\cdot}$) > $T_{0.5}$ ($CHD_2^{\cdot}$), an observation which is in keeping with the proposal that for this molecule, the threshold reaction involves partial mixing of H and D, i.e., the rates of H/D positional exchange processes are similar to or less than the rate of fragmentation. Loss of $CH_2D^{\cdot}$ represents a more mixed state than loss of $CHD_2^{\cdot}$; for example, H/D mixing resulting from successive 1,3-H shifts.

(ii) 2,4-Hexadiene-3,4-$^2H_2$ and 1,1,1-$^2H_3$

The relative abundances of the metastable peaks for these compounds are not in the random statistical ratio (see Table 2). There is, however, no major isotope effect operating here because the weighted $T_{0.5}$ values for the labelled compounds, 32.3 and 34.2 meV respectively, lie close to that for the unlabelled molecule, 34 ± 1 meV. The largest $T_{0.5}$ values are for the fragmentations corresponding to the greatest degree of label mixing and vice versa. The loss of $CD_3^{\cdot}$ from the 1,1,1-$^2H_3$ compound must represent the mechanistically least complex reaction because the statistical contribution to such a process is the smallest (see Table 2). Thus, the loss of terminal methyl group makes up ca. 20% of the overall fragmentation; it has the lowest $T_{0.5}$ value and corresponds to the minimum energy pathway, $\Delta H_f[C_5H_7]^+ = 212$ kcal mol^{-1}. If [cyclopentenium]$^+$ were the daughter ion, then the excess internal energy (13 kcal mol^{-1}) plus that required to achieve the rate constant for fragmentation is available for partitioning into translational energy. In our earlier work (12) average excess energies were estimated using the empirical relationship of Haney and Franklin (see above). In this case $\langle \varepsilon^* \rangle = 0.44 \times 42\ (0.078 - 0.046) = 0.59$ eV = 13.6 kcal mol^{-1}, in excellent agreement with the observed excess energy.

(iii) 1,2-Hexadiene-1-$^2H_1$

The metastable characteristics of this compound show the same trends as for those just described (Table 2), with substantial H/D mixing prior to methyl loss (cf. ref. 29*b*). $T_{0.5}$ ($CH_2D^{\cdot}$) possibly contains some contribution from high $T_{0.5}$ values from high randomization processes. At low electron energies the ratio $[M - CH_3^{\cdot}]^+/[M - CH_2D^{\cdot}]^+$ decreases; at nominal 12 eV it is 1:3.3 in the normal spectrum (1:1 at 20 eV) showing that methyl loss involving the terminal methylene group is the lower energy process.

Conclusions

We propose that irrespective of the structure of a $[C_6H_{10}]^{+\cdot}$ precursor molecular ion, the fragment ion $[C_5H_7]^+$, generated in the μs time frame, will have the [cyclopentenium]$^+$ structure. No evidence was found for the formation of $[C_5H_7]^+$ ions of any other structure. We further suggest that [cyclopentenium]$^+$ is the $[C_5H_7]^+$ ion generated at the dissociation threshold from isomeric $C_7H_{12}^{+\cdot}$, $C_8H_{14}^{+\cdot}$ and some higher homologous ions (14), in whose mass spectra *m/z* 67 is base, or second largest peak.

Can. J. Chem. Downloaded from www.nrcresearchpress.com by 210.87.254.42 on 09/05/12
For personal use only.

Can. J. Chem. Downloaded from www.nrcresearchpress.com by 210.87.254.42 on 09/05/12
For personal use only.

Experimental Section

Metastable peak shapes were measured at a fixed electric sector voltage on a Kratos AEI MS 902S mass spectrometer by sweeping the acceleration voltage using good energy resolution as described previously (31). For the labelled compounds each metastable peak was measured at the same acceleration potential to avoid errors arising from the sampling of slightly different ion lifetimes. Sample pressure was $3–5 \times 10^{-7}$ Torr. Kinetic energy release (T) was calculated in the usual way (16), correcting for main beam width and overlapping processes arising from natural isotopic abundances. Ionization and appearance energies were obtained as described previously using monoenergetic electrons, and a mini-computer for data accumulation and analysis (13, 15).

Unlabelled compounds were purchased from Chem. Samples Co. and Fluka, isomeric purity 98–99%. 1,2-Hexadiene was prepared as described (32) and purified by GC; 1,2-hexadiene-1-$^2H_1$ was made using $LiAlD_4$ ($^2H_1 \sim 98\%$). 2,3-Hexadiene (33) and 4-methyl-1,2-pentadiene (33) were gifts from Dr. D. G. Garratt. 1,2,2-Trimethylcyclopropene was prepared as described by Closs *et al.* (34). 2,4-Hexadiene-1,1,1-$^2H_3$ ($^2H_3 \sim 90\%$) and 2,4-hexadiene-3,4$^2H_2$ ($^2H_2 \sim 98\%$) were prepared according to Claesson (35) but the isolation procedure was slightly modified; the diene was distilled from the hydrolysis mixture and the fraction boiling from 45–95°C was collected; the organic layer was dried and 2,4-hexadiene (consisting of a mixture of all three geometric isomers) was collected by PGLC. 1-Hexyne-$^2H_1$ ($^2H_1 \sim 90\%$) was from Chem. Samples Co.

Acknowledgements

This work was supported by the Natural Sciences and Engineering Research Council of Canada. P.W. thanks the Danish Natural Science Research Council for two travel grants and financial support which greatly helped the successful completion of this work. We wish to thank Dr. D. G. Garratt for the donation of two allenes, and Dr. J. Krause for assistance with the metastable peak shape measurements.

1. M. L. Gross (*Editor*). High performance mass spectrometry. Am. Chem. Soc. Symposium Series 70, American Chemical Society, Washington, DC. 1978; A. Maccoll (*Editor*). Mass spectrometry. Physical Chemistry Series Two, Vol. 5. Butterworths, London. 1975. Chapts. 1, 5, 6.
2. K. Levsen and J. Heimbrecht. Org. Mass Spectrom. **12**, 131 (1977).
3. R. Bowen and D. H. Williams. Org. Mass Spectrom. **12**, 453 (1977).
4. K. Levsen. Fundamental aspects of organic mass spectrometry. Progress in mass spectrometry. Vol. 4. *Edited by* H. Budzikiewicz. Chapt. 5.
5. S. Stefani. Org. Mass Spectrom. **7**, 17 (1973).
6. A. M. Falick and T. Gäumann. Helv. Chim. Acta, **59**, 987 (1976).
7. A. M. Falick, P. Tecon, and T. Gäumann. Org. Mass Spectrom. **11**, 409 (1976).
8. J. L. Holmes and D. McGillivray. Org. Mass Spectrom. **5**, 1349 (1971).
9. F. Borchers, K. Levsen, H. Schwarz, C. Wesdemiotis, and H. Winkler. J. Am. Chem. Soc. **99**, 6359 (1977).
10. T. Nishishita, F. M. Bockhoff, and F. W. McLafferty. Org. Mass. Spectrom. **12**, 16 (1977).
11. K. Levsen and E. Hilt. Liebigs Ann. Chem. 257 (1976).
12. P. Wolkoff and J. L. Holmes. Can. J. Chem. **57**, 348 (1979).
13. F. P. Lossing and J. C. Traeger. Int. J. Mass Spectrom. Ion Phys. **19**, 9 (1976).
14. A. Cornu and R. Massot. Compilation of mass spectral data. Vol. 1. 2nd ed. Heyden, London. 1975.
15. K. Maeda, G. P. Semeluk, and F. P. Lossing. Int. J. Mass Spectrom. Ion Phys. **1**, 395 (1968).
16. R. G. Cooks, J. H. Beynon, R. M. Caprioli, and G. R. Lester. Metastable ions. Elsevier, Amsterdam. 1973.
17. W. A. Chupka. J. Chem. Phys. **30**, 191 (1959).
18. G. Hvistendahl and D. H. Williams. J. Am. Chem. Soc. **97**, 3097 (1975).
19. F. W. McLafferty. Interpretation of mass spectra. 2nd ed. Benjamin, Reading. 1973.
20. M. A. Haney and J. L. Franklin. J. Chem. Phys. **48**, 4093 (1968).
21. J. L. Holmes and A. D. Osborne. Int. J. Mass Spectrom. Ion Phys. **23**, 189 (1977).
22. I. Howe. Org. Mass Spectrom. **10**, 767 (1975).
23. P. Wolkoff and J. L. Holmes. J. Am. Chem. Soc. **100**, 7346 (1978); J. L. Holmes, P. Wolkoff, and R. T. B. Rye. Chem. Commun. 544 (1979).
24. R. C. Benz and R. C. Dunbar. 27th Annual Conference on Mass Spectrometry and Allied Topics, Seattle. 1979.
25. H. M. Frey and R. Walsh. Chem. Rev. **69**, 103 (1969).
26. F. Borchers, K. Levsen, H. Schwarz, C. Wesdemiotis, and R. Wolfshutz. J. Am. Chem. Soc. **99**, 1716 (1977).
27. P. J. Derrick, A. M. Falick, and A. L. Burlingame. J. Am. Chem. Soc. **94**, 6494 (1972).
28. A. C. Parr, A. J. Jason, R. Stockbauer, and K. E. McCulloh. Int. J. Mass Spectrom. Ion Phys. **30**, 319 (1979).
29. (*a*) S. Arseniyadis, J. Gore, and M. L. Roumestant. Org. Mass Spectrom. **13**, 54 (1978); (*b*) Tetrahedron, **35**, 353 (1979).
30. Z. Dolejsek, V. Hanus, and K. Vokac. Adv. Mass Spectrom. **3**, 503 (1966).
31. J. L. Holmes and J. K. Terlouw. Can. J. Chem. **53**, 2076 (1975).
32. J. K. Crandall, D. J. Keyten, and J. Kohne. J. Org. Chem. **33**, 3655 (1968).
33. W. von E. Doering and P. M. Laflamme. Tetrahedron, **2**, 75 (1969); L. Skattebøl. Acta Chem. Scand. **17**, 1683 (1963); W. R. Moore and H. R. Wood. J. Org. Chem. **27**, 4179 (1962).
34. G. L. Closs, L. E. Closs, and W. A. Böll. J. Am. Chem. Soc. **85**, 3796 (1963).
35. A. Claesson. Acta Chem. Scand. Ser. B. **29**, 609 (1975).
36. S. W. Benson. Thermochemical kinetics. 2nd ed. Wiley, Interscience, New York. 1976.

An INDO-MO study of the spectral properties and transannular interaction in [6]-helicene

B. M. Deb and Geetharani Kavu

Department of Chemistry, Indian Institute of Technology, Bombay-400 076, India

Received December 22, 1978[1]

B. M. Deb and Geetharani Kavu. Can. J. Chem. **58**, 258 (1980).

The INDO-MO calculations on [6]-helicene reported here enable one to classify the four HOMO's as predominantly π, in contrast to other occupied MO's. A linear adjustment of these four HOMO's correlates well with the experimental photoelectron and optical spectra. Viewed through Mulliken's overlap population between overlapping rings, the transannular interaction in [6]-helicene appears to be unfavourable and therefore minimised. The use of a skeleton representation of the molecule is considered and found inadvisable.

B. M. Deb et Geetharani Kavu. Can. J. Chem. **58**, 258 (1980).

Les calculs des orbitales moléculaires INDO de l'hélicène-[6] que l'on rapporte ici permettent de confirmer que les 4 orbitales moléculaires HO sont d'une façon prédominante de type π, ce qui est à l'opposé des autres orbitales moléculaires occupées. Un ajustement linéaire de ces 4 orbitales moléculaires s'harmonise bien avec les spectres photoélectronique et optique expérimentaux. En se basant sur la population de recouvrement de Mulliken entre les deux cycles qui chevauchent, l'interaction transannulaire dans l'hélicène-[6] semble être défavorisé et de ce fait est minimisée. On a envisagé l'emploi d'un modèle pour représenter la molécule mais l'expérience montre que c'est à déconseiller.

[Traduit par le journal]

Can. J. Chem. Downloaded from www.nrcresearchpress.com by 210.87.254.6 on 09/05/12
For personal use only.

Introduction

In recent years, a number of experimental and theoretical studies have been reported on [5]- to [14]-helicenes (1–3). The main objectives of the present INDO-MO calculations (4) are the following: (*1*) to examine the INDO-MO energy levels of [6]-helicene (X-ray geometry (5)) in relation to its experimental photoelectron (PE) and optical spectra; (*2*) to compare the agreement between INDO and PE and optical spectra of [6]-helicene with that for its constituent unit benzene (experimental geometry (6)); (*3*) to obtain a semi-quantitative account of transannular interaction (TI), i.e., secondary π delocalisation, between overlapping rings in the molecule; (*4*) to study the consequences of employing a skeleton model upon PE and optical spectra, σ–π mixing and TI in the molecule (see Fig. 1). The broad conclusions reached here might remain valid for higher members of the helicene series.

Results and Discussion

(1) Energy Levels of Benzene and [6]-Helicene (X-ray Geometry)

A comparison (Table 1) of INDO-MO energy levels of benzene with those from *ab initio* (7) and PE (8) spectral data[2] shows that the INDO ordering of the $a_{2u}\pi$ level (π_{11} in Table 1) is incorrect. Since the σ and π AO's do not mix in any benzene MO, Fig. 2 clearly indicates two separate dependences of the σ and π MO's instead of a collective dependence (9). The four π levels show a least-squares linear fit (in eV),

$$[1] \quad -(\mathrm{IP})_i = 0.276\varepsilon_i - 5.72$$

with an rms error of 0.07 eV (Fig. 2). The π–π* transition energies, calculated from INDO-MO levels adjusted by eq. [1], compare well with the corresponding experimental (10) results (Table 1).

The INDO lowering, $|\varepsilon_{\mathrm{INDO}}| - \mathrm{IP}$, of the HOMO (π) energy for benzene is quite high, 4.02 eV (Table 1). The calculated occupied π levels of benzene clearly reflect an exaggerated delocalisation energy which seems to be an artefact of INDO calculations on such planar systems. In contrast, the INDO lowering of the HOMO energy in [6]-helicene is 1.98 eV (Table 2), since extensive σ–π mixing[3] in this non-planar molecule raises the π orbitals in energy; in other words, non-planarity causes a loss in delocalisation energy. One therefore concludes that in planar aromatics where no mixing of σ and π AO's occurs, with increasing delocalisation the INDO method is likely to provide increasingly exaggerated delocalisation energies, whereas for non-planar molecules where extensive σ–π mixing occurs the INDO method would provide a more realistic description.

(2) Nature of the MO's in [6]-Helicene

In spite of extensive σ–π mixing it is possible to study the MO's of [6]-helicene in a manner which

[1]Revision received July 3, 1979.

[2]Used in conjunction with the Koopmans theorem, viz. $-(\mathrm{IP})_i = \varepsilon_i$, where $(\mathrm{IP})_i$ and ε_i are experimental ionisation potential and energy, respectively, of the *i*th MO.

[3]σ and π refer separately to each ring in [6]-helicene, and not to the whole molecule.

0008-4042/80/030258-05$01.00/0

©1980 National Research Council of Canada/Conseil national de recherches du Canada

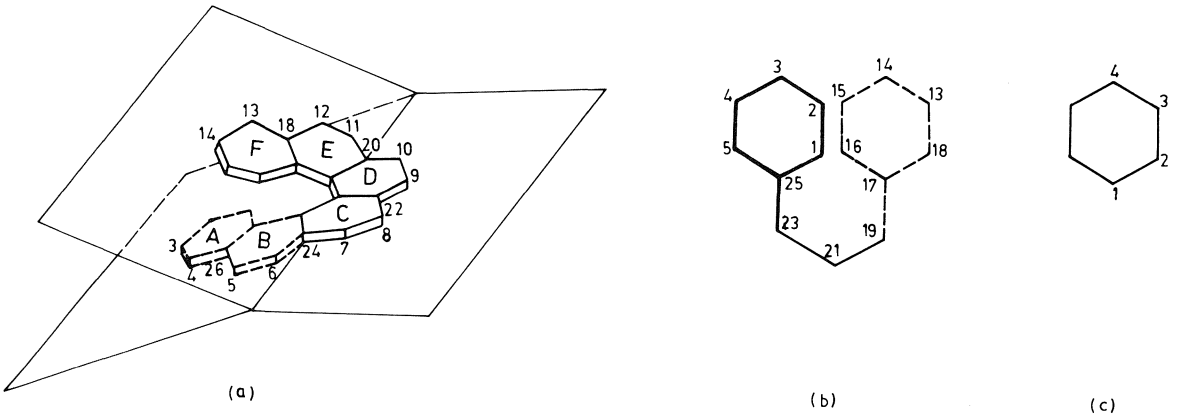


FIG. 1. (*a*) [6]-Helicence, (*b*) skeleton model of [6]-helicene, and (*c*) benzene. The same atom numbering is used for both (*a*) and (*b*) and hence some of those in (*b*) are not repeated in (*a*) for clarity. The H-atom numbering is the same as that of the C atom to which H is bonded. (*a*) is drawn after ref. 5. (*b*) is of C_2 symmetry with the two phenyl fragments, thick and dotted, respectively, above and below the plane of paper by 29.25°. In (*b*), the C—C and C—H bond lengths are taken as arithmetic means of the corresponding values in X-ray geometry, viz., 1.41 and 1.08 Å respectively, while all CCC angles are taken as 120°.

TABLE 1. INDO-MO and *ab initio* (7) MO energies compared with experimental ionisation potentials (8) of benzene. The "virtual orbital IP's" are *calculated* from PE and optical spectra (Koopmans theorem). The calculated and experimental (10) transition energies are given only for the first three bands. All values are in eV

MO type	INDO energy	*Ab initio* energy	−(IP)	α, *p*, β transition energies in ascending order	
				Calcd.	Expt.
π_{18}^*	9.71	—	−3.16	4.88	4.80
π_{16}^*, π_{17}^*	4.55	—	−4.56	6.29	6.14
π_{14}, π_{15}	−13.32	−9.25	−9.30	7.47	6.75
σ_{12}, σ_{13}	−13.63	−13.41	−11.40		
π_{11}	−22.81	−13.74	−12.1		
σ_9, σ_{10}	−18.63	−16.10	−13.8		
σ_8	−19.58	−16.95	−14.7		
σ_7	−20.80	−17.46	−15.4		
σ_6	−28.60	−19.48	−16.9		
σ_4, σ_5	−30.10	−22.50	−19.2		
σ_2, σ_3	−38.20	−27.79	−22.5		
σ_1	−51.60	−31.56	−25.9		

permits one to characterise the four HOMO's of the molecule as predominantly π, as follows. The orientation of the resultant *p* AO on a carbon atom with respect to the *X*-axis which is approximately perpendicular to the planes of the rings C, D (Fig. 1), together with an idea of the torsional angle of the planes[4] of A, B and E, F makes it possible to classify the resultant *p* AO in an MO as predominantly σ, π, or just σ–π. This permits classification of the four HOMO's as predominantly π, *in contrast to* the other occupied MO's whose σ character increases as one goes to higher binding energy. It may be noted that Obenland and Schmidt (3) empirically assign the π levels to be above 10 eV in the PE spectrum, thereby designating the first eight PE bands as π.

Although the nine HOMO's of [6]-helicene, for which PE spectral bands have been reported, apparently show a fairly good linear correlation (Fig. 3), such a correlation yields transition energies which are three to four times the corresponding experimental values. In accordance with the above observations on the π MO's of benzene and [6]-helicene, the four HOMO's and two LUMO's (Table 2) of the latter have been gathered into a

[4]It should be noted, however, that no two rings in the molecule are strictly coplanar.

Can. J. Chem. Downloaded from www.nrcresearchpress.com by 210.87.254.6 on 09/05/12
For personal use only.

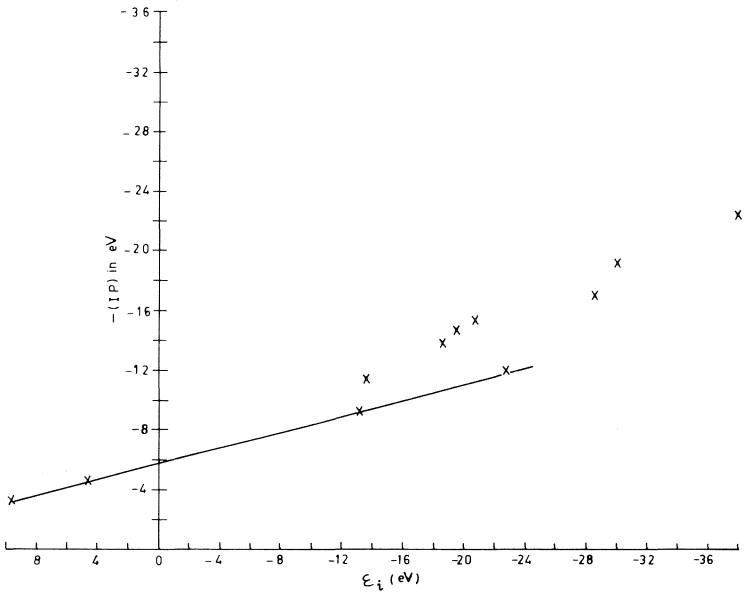


FIG. 2. Plot of experimental ionisation potentials $(IP)_i$ vs. INDO-MO energies (ε_i) of benzene. The "virtual orbital IP's" are calculated from observed PE and optical spectra (Koopmans theorem).

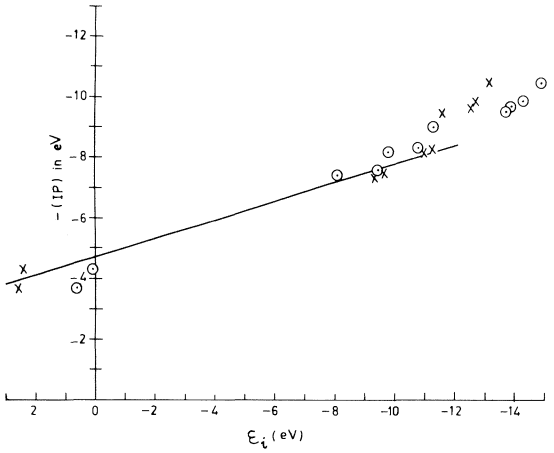


FIG. 3. Plot of experimental ionisation potentials $(IP)_i$ vs. INDO-MO energies (ε_i) of [6]-helicene in X-ray geometry (×) and skeleton model (○). The "virtual orbital IP's" are calculated from observed PE and optical spectra (Koopmans theorem).

least-squares linear (Fig. 3) expression,

$$[2] \quad -(IP)_i = 0.300\varepsilon_i - 4.74$$

with a slightly high rms error of 0.22 eV; this is due to a lack of perfect correlation between the MO's because of their differing π character, unlike benzene where the four MO levels are purely π. The close similarity between the slopes in eqs. [1] and [2] is quite significant, indicating that our characterisation of the four HOMO's as predominantly π is justified and a similar slope ($\sim$0.3) is likely to be encountered in INDO calculations on other helicenes. Since the agreement between the experimental and calculated (after adjustment according to eq. [2]) electronic transition energies is fairly good (Table 2), the identification of the α, p, and β bands as π–π^* transitions (2, 3, 11) is adequate.[5] In view of these observations, the skepticism (3) regarding INDO calculations on such molecules seems unjustified.

TABLE 2. Several INDO-MO energies, experimental (3) ionisation potentials and the first three transition energies of [6]-helicene. The "virtual orbital IP's" are *calculated* from PE and optical spectra (Koopmans theorem). All values are in eV and values in parentheses refer to the skeleton model

		α, p, β transition energies in ascending order	
INDO energy	−(IP)	Calcd.	Expt.
2.62(0.66)	−3.69	3.53 (3.18)	3.04
2.42(0.21)	−4.33		
−9.35(−8.11)	−7.37	3.59 (3.36)	3.68
−9.64(−9.53)	−7.50	3.62 (3.72)	
−11.02(−9.81)	−8.18		
−11.31(−10.84)	−8.30	3.68 (3.90)	3.93
−11.43(−11.41)	−8.97		
−11.55(−13.71)	−9.53		
−12.57(−13.94)	−9.74		
−12.65(−14.26)	−9.94		
−13.19(−14.87)	−10.50		

[5]This prescription (12) is somewhat arbitrary. Negative bond orders occur inevitably in such MO calculations irrespective of which axial system is employed (see, e.g., ref. 13).

Can. J. Chem. Downloaded from www.nrcresearchpress.com by 210.87.254.6 on 09/05/12
For personal use only.

TABLE 3. $n(r,s)$, $d(r,s)$, and $d'(r,s)$ values in au calculated for a few non-bonded pairs of atoms in [6]-helicene, whose interatomic distances are relatively small (Fig. 1)

Distance between atoms (Å)	Non-bonded pair	$n(r,s)$	$d(r,s)$	$d'(r,s)$
3.09	$C_{16}C_{25}$	0.0006	0.0673	−0.0431
3.10	$C_{16}C_{23}$	0.0004	0.0765	−0.0073
3.15	$C_{17}C_{23}$	−0.0024	0.2476	−0.0506
3.22	C_1C_{16}	0.0008	0.0656	0.0082
3.22	C_1H_{16}	−0.0002	0.0183	0.0021
3.28	$C_{17}C_{25}$	0.0001	0.0449	0.0323
3.40	H_1H_{16}	0.0000	0.0008	0.0008

TABLE 4. Mulliken overlap populations, $n(r,s) \times 10^4$, in au between certain non-bonded atom pairs in [6]-helicene (Fig. 1). Values in parentheses refer to the skeleton model and are listed only where they differ from the X-ray geometry

Atom	C_1	C_2	C_3	C_4	C_{23}	C_{25}	C_{26}
C_{14}	0	0	0	0	0	0	0
C_{15}	−1	0	0	0	0	0	0
C_{16}	8(−4)	0(−1)	0	0	4(−13)	6(54)	0(−1)
C_{17}	0	0	0	0	−24(−65)	1(14)	0

(3) Transannular Interaction

By virtue of their greater flexibility the helicenes can minimise TI which would otherwise increase their total energy, if the interaction is of the Möbius-type (3). An indication of the electron density between overlapping rings in [6]-helicene would help to assess the nature and extent of this interaction. It was found that of the three quantities given below, the Mulliken overlap population (MOP) is the most suitable index of overall electron distribution between a pair of bonded or non-bonded atoms (14). These quantities are:

$$[3] \quad d'(r,s) = \sum_{\mu\varepsilon r} \sum_{\nu\varepsilon s} P_{\mu\nu}$$

$$[4] \quad d(r,s) = \sum_{\mu\varepsilon r} \sum_{\nu\varepsilon s} |P_{\mu\nu}| \quad \text{(ref. 12)}^5$$

$$[5a] \quad n(r,s) = \sum_{i} \sum_{\mu\varepsilon r} \sum_{\nu\varepsilon s} n(i,\mu,\nu)$$

$$[5b] \quad n(i,\mu,\nu) = 2N_i C_\mu(i) C_\nu(i) S_{\mu\nu}$$

where $P_{\mu\nu}$ is a density matrix element of INDO calculations with the AO's μ and ν centred on the atoms r and s respectively; N_i is the occupation number of the ith MO; $C_\mu(i)$ is the LCAO coefficient of the μth AO of atom r in the ith MO and $S_{\mu\nu}$ is the overlap integral. Table 3 shows that there is no correspondence between $n(r,s)$ and either $d(r,s)$ or $d'(r,s)$, and Table 5 shows that, for benzene, $n(r,s)$ is the most reliable index of electron distribution. Tables 3 and 4 list the MOP values for a few atom pairs from overlapping rings in [6]-helicene. The sign of MOP indicates the favourable (positive sign) or unfavourable (negative sign) nature of TI while its magnitude is a measure of the strength of this interaction.

Table 3 indicates that the secondary π delocalisation between overlapping rings depends more sensitively on the relative orientations of the π orbitals concerned than on the interatomic distances. The values listed in Table 4 are quite small and confirm the earlier suggestion (3) that TI in [6]-helicene is unfavourable and therefore minimised. This is specifically reflected by the fact that the largest value of $n(r,s)$, viz., −0.0024, for the pair C_{17}, C_{23} is nearly equal in magnitude to the value of 0.0023 for C_1, H_3 in benzene.

(4) Effects of using a Skeleton Model for [6]-Helicene

Since the MO's of the skeleton model $C_{15}H_{10}$ (Fig. 1) show an overall linear correlation (Fig. 3), none of the occupied MO's can be classified as predominantly σ or π, in contrast to benzene or the X-ray geometry. Further, such a linear correlation embracing all the points does not reproduce the optical spectrum, although the five HOMO's of $C_{15}H_{10}$ have higher energies than the corresponding MO's of X-ray geometry because of an in-

TABLE 5. $n(r,s)$, $d(r,s)$, and $d'(r,s)$ values in au, calculated for non-bonded pairs of atoms in benzene (Fig. 1)

Interaction between	$n(r,s)$	$d(r,s)$	$d'(r,s)$
C_1C_4	−0.0115	0.4726	−0.3966
C_1H_1	0.6767	1.3461	−0.3067
C_1H_2	−0.0069	0.0605	−0.0605
C_1H_3	0.0023	0.1867	0.1867
C_1H_4	0.0001	0.0302	0.0302

Can. J. Chem. Downloaded from www.nrcresearchpress.com by 210.87.254.6 on 09/05/12
For personal use only.

creased $\sigma-\pi$ mixing in the former. Therefore, as with the X-ray geometry, a linear relationship was tested for only four HOMO's and two LUMO's, viz.

$$[6] \quad -(IP)_i = 0.382\varepsilon_i - 4.17$$

where the slope is considerably different from that in benzene or the X-ray geometry. Although eq. [6] well reproduces optical spectral results, such an agreement is superficial since there is no reason to differentiate the four HOMO's from other occupied MO's as far as $\sigma-\pi$ mixing is concerned. Furthermore, taken together, the skeleton energy levels show a worse agreement with experimental IP's and transition energies as compared with the unadjusted levels of X-ray geometry (Table 2).

The skeleton model also displays a different pattern of TI (Table 4) because of different orientations of the $p\pi$ AO's, as compared with the X-ray geometry. Except for two of the non-vanishing $n(r,s)$ values, the rest are negative, apparently indicating an unfavourable interaction. However, since the two largest $n(r,s)$ values, 0.0054 and -0.0065 for the atom pairs C_{16}, C_{25} and C_{17}, C_{23} respectively, are comparable in magnitude, one cannot conclude (*i*) whether TI in the skeleton is unfavourable or not, and (*ii*) if unfavourable, whether TI is minimised.

Thus we conclude that information and interpretations obtained from the skeleton model are not only quite different from those of the X-ray geometry, they are by and large unrealistic, although five skeleton HOMO's superficially show a "better" agreement with IP values (Table 2). Therefore in making semi-empirical MO calculations on large molecules, it is not always physically meaningful to replace the real molecules with certain skeleton ones.

Conclusion

The present INDO-MO calculations identify four HOMO's of [6]-helicene as predominantly π, in contrast to other occupied MO's. In a plot of $-(IP)_i$ of helicene against the corresponding ε_i(INDO), those MO's which are linearly correlated by a slope of ~ 0.3 should be predominantly π. Such a classification for [6]-helicene well reproduces its PE and optical spectra. The transannular interaction between overlapping rings in the molecule is examined by means of Mulliken overlap population. This confirms an earlier suggestion (3) that the TI in [6]-helicene is unfavourable and therefore minimised. The use of a skeleton model as a substitute for the real molecule was found to lead to unrealistic information and interpretation regarding $\sigma-\pi$ mixing, PE and optical spectra, and TI in the molecule. Therefore, one should be very careful in making such substitutions in semi-empirical calculations on large molecules.

Acknowledgements

The authors would like to thank the CSIR, New Delhi, and the IIT, Bombay, for financial support to each of them.

1. R. H. MARTIN. Angew. Chem. Int. Ed. Engl. **13**, 649 (1974).
2. (*a*) A. BROWN, C. M. KEMP, and S. F. MASON. J. Chem. Soc. A, 751 (1971); (*b*) W. S. BRICKELL, A. BROWN, C. M. KEMP, and S. F. MASON. J. Chem. Soc. A, 765 (1971).
3. S. OBENLAND and W. SCHMIDT. J. Am. Chem. Soc. **97**, 6633 (1975).
4. J. A. POPLE and D. L. BEVERIDGE. Approximate molecular orbital theory. McGraw-Hill. 1970.
5. C. DE RANGO, G. TSOUCARIS, J. P. DECLERQ, G. GERMAIN, and J. P. PUTZERS. Cryst. Struct. Commun. **2**, 189 (1973).
6. L. SUTTON. Interatomic distances and configurations in molecules and ions. Chemical Society Special Publication. No. 11, 1958; No. 18, 1965.
7. P. J. HAY and I. SHAVITT. J. Chem. Phys. **60**, 2865 (1974).
8. L. ASBRINK, T. O. EDQVIST, E. LINDHOLM, and L. E. SELIN. Chem. Phys. Lett. **5**, 192 (1970).
9. R. W. BIGELOW. J. Chem. Phys. **66**, 4241 (1977).
10. J. B. BIRKS. Photophysics of aromatic molecules. John Wiley. 1970. p. 70.
11. W. RHODES and M. F. A. EL-SAYED. J. Mol. Spectrosc. **9**, 42 (1962).
12. A. G. TURNER. Methods in molecular orbital theory. Prentice-Hall. 1974. pp. 67, 176.
13. (*a*) C. A. COULSON and M. D. NEWTON. Mol. Phys. **15**, 305 (1968); (*b*) C. A. COULSON. Mol. Phys. **15**, 317 (1968).
14. R. S. MULLIKEN. J. Chem. Phys. **23**, 1833 (1955); **23**, 1841 (1955).

Can. J. Chem. Downloaded from www.nrcresearchpress.com by 210.87.254.6 on 09/05/12
For personal use only.

Physico-chemical studies on areno-tropilidenes and tropones. I. The polarographic behaviour and electron affinities of thiophenotropone derivatives in buffer solutions of varying pH values and in DMF

SAFAA H. ETAIW[1]
Department of Chemistry, Faculty of Science, University of Tanta, Tanta, Egypt
MOHAMED I. ISMAIL
Department of Chemistry, Faculty of Science, University of Ain Shams, Egypt
AND
MOHAMED EL-BORAI
Department of Chemistry, Faculty of Science, University of Tanta, Tanta, Egypt
Received May 29, 1979

SAFAA H. ETAIW, MOHAMED I. ISMAIL, and MOHAMED EL-BORAI. Can. J. Chem. **58**, 263 (1980).

The polarographic behaviour of some thiophenotropone derivatives were studied in DMF and in Thiel buffer solutions of varying pH values and μ of 0.1 at 25 ± 0.1°C. It was found that the carbonyl group is the active centre towards reduction. In strong acid media, the reduction proceeds via one reversible electron forming a free radical which dimerises to produce pinacol. In solutions of pH values from 4 to 9, the polarograms consist of two reduction waves of equal heights each corresponding to 1 F. In strong alkaline media, one wave is observed; in most cases, depending on the molecular structure, the wave corresponds to the uptake of two electrons. The first step involves the direct reduction of the basic form to the anion radical which undergoes a further reduction forming the corresponding thiophenotropolone. At pH values > 13, the height of the limiting current decreases until it attains the height corresponding to 1 F indicating that the anion radical is stable in such media. Also, the electron affinities of these compounds were calculated.

SAFAA H. ETAIW, MOHAMED I. ISMAIL et MOHAMED EL-BORAI. Can. J. Chem. **58**, 263 (1980).

On a étudié le comportement polarographique de quelques thiophénotropones dans le DMF et dans des solutions tampons de Thiel ayant différents pH et μ = 0.1 à 25 ± 0.1°C. On a trouvé que le groupe carbonyle est le centre actif lors de la réduction. En milieu acide fort, la réduction se produit par l'intermédiaire d'un électron réversible en formant un radical libre qui se dimérise pour donner un pinacol. Dans les solutions où le pH varie de 4 à 9, le polarogramme consiste en deux ondes de réduction d'égale hauteur correspondant chacune à 1 F. En milieu fortement basique on observe une onde. Dans la plupart des cas, dépendant de la structure moléculaire, l'onde correspond à la fixation de deux électrons. La première étape implique la réduction directe de la forme basique en un anion radicalaire qui, par réduction plus poussée, conduit à la thiophénotropolone correspondante. Pour des valeurs du pH > 13 la hauteur du courant de saturation décroît jusqu'à ce qu'elle atteigne celle correspondant à 1 F indiquant ainsi que l'anion radicalaire est stable dans un tel milieu. On a également calculé les affinités électroniques de ces composés.

[Traduit par le journal]

Introduction

The polarographic studies on the carbonyl compounds were the subject of many investigations (1–6). On the other hand, the quinonoid compounds of fused aromatic systems as well as those of fused heterocyclic systems were extensively studied in organic solvents or in media of different pH values (7–13). The reduction mechanism and the number of electrons involved in reduction process were found to depend on the nature of the compound and on the medium used. However, the electro-reduction of arenotropones has not been studied so far except the polarographic work done by Guilard *et al.* (14) to elucidate the structure of arenotropones and their metal tricarbonyl complexes. They claimed that the polarograms of arenotropones consist of two reduction waves (pH = 6.7) each corresponds to 1 F producing the corresponding arenotropolones. In the course of our research, a detailed study of the reduction of thiophenotropone derivatives (**I** and **II**) is performed in Thiel buffer solutions of varying pH values and in DMF.

Experimental

The thiophenotropones were prepared according to the recommended procedure described by Guilard and Fournari (15). The solids were purified by recrystallization from the appropriate solvents and their purity and individuality were checked by mp determination, pmr, elemental analysis, and thin-layer chromatography. The polarograms were recorded by Radiometer PO_4 type recording polarograph using a dropping electrode with $m = 2.45$ mg s^{-1} and $t = 3.6$ s at a height h of 52 cm Hg and a kalousek polarographic cell with a thermostating jacket. The temperature was maintained with an ultrathermostat at 25 ± 0.1°C. Buffers used were boric acid, sodium sulphate, succinic acid, and borax solutions (Thiel buffer). After pH 12 a concentrated solution of NaOH was used to raise the pH of the

[1]To whom all correspondence should be addressed.

0008-4042/80/030263-07$01.00/0
©1980 National Research Council of Canada/Conseil national de recherches du Canada

Can. J. Chem. Downloaded from www.nrcresearchpress.com by 210.87.254.5 on 09/05/12
For personal use only.

Can. J. Chem. Downloaded from www.nrcresearchpress.com by 210.87.254.5 on 09/05/12
For personal use only.

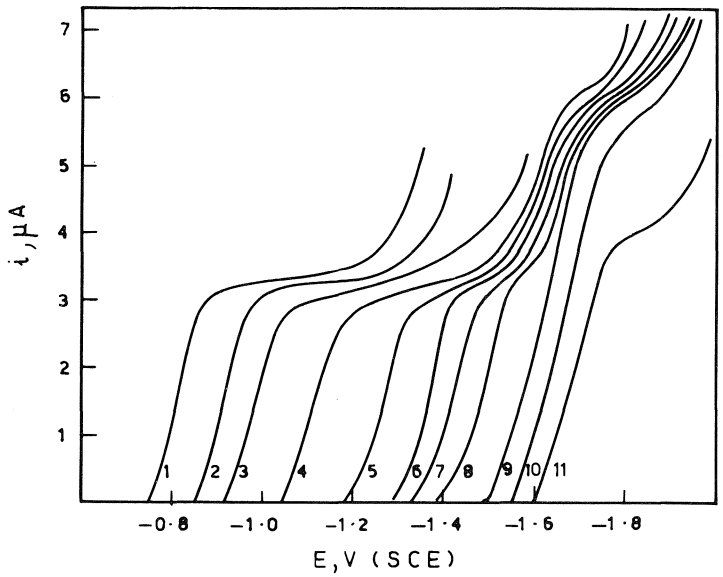
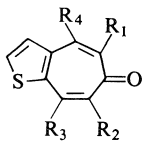
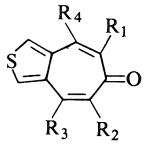


FIG. 1. Polarograms of 1 m*M* **I***a* in Thiel buffer solutions at 25 + 0.1°C. Run and pH: (*1*) 2.3; (*2*) 4.3; (*3*) 5.9; (*4*) 7.4; (*5*) 8.4; (*6*) 9.35; (*7*) 10.01; (*8*) 10.52; (*9*) 11.21; (*10*) 12.20; (*11*) 13.60.



I



II

Compound	R_1	R_2	R_3	R_4
I*a*	H	H	H	H
b	CH_3	H	H	H
c	OCH_3	H	H	H
d	H	OCH_3	H	H
e	CH_3	CH_3	H	H
f	C_6H_5	C_6H_5	H	H
g	CH_3	CH_3	CH_3	H
II*a*	H	H	H	H
b	H	OCH_3	H	H
c	CH_3	CH_3	H	H
d	C_6H_5	C_6H_5	H	H

medium. The thiophenotropones were dissolved in 20 vol% ethanol – water mixture. The polarograms in DMF were carried out using 0.1 mL^{-1} of *N*-tetrabutyl ammonium perchlorate as supporting electrolyte. Depolariser concentrations studied were 1×10^{-3} *M* at a μ of 0.1 (NaCl). A saturated calomel electrode (sce) was used as reference electrode. A Radiometer pH meter type 63 fitted with a combined glass electrode type GK 2301 C was employed for determination of pH. The instrument was accurate to ±0.01 pH unit. The electrolysis at controlled potential was made using a potentiostat TACUSSEL of type ASA 4/60. The electrolysis cell used was the same as that described by Peltier (16).

Results and Discussion

1. The Electro-reduction of Thiophenotropones

The polarograms of 1×10^{-3} *M* of **I***f* and **II***d* in Thiel buffer solutions of pH values 2.3–12.2 consist of one reduction wave corresponding to 2 F. The polarograms shift to more negative potentials and the limiting current decreases as the pH value of the medium increases. However, the polarograms of 1×10^{-3} *M* of the remaining compounds show a different behaviour depending on the molecular structure and the pH of the medium. In acid media, pH ≤ 5.9, the polarograms of **I***a*, *b* consist of one reduction wave *A* corresponds to 1 F while the remaining compounds show this behaviour at pH <4.0. Above these pH values, a new wave *B* is observed and the polarograms consist of two waves of equal heights. The total height of the two waves corresponds to 2 F. As the pH increases, wave *A* suffers a strong shift to more negative potentials than that of wave *B* until the two waves merge and appear as one wave (*C*) at pH ≥ 9.0. At pH > 12.5 the limiting current decreases until it attains the value corresponding to 1 F at pH ≃ 13.6 (wave *D*, Fig. 1). On the other hand, the polarograms of compounds **I***b*, *c* and **II***a*, *b* do not show this behaviour and they still consist of two reduction waves even in strong alkaline media. However, the polarograms of compounds **I***b*, *c* exhibit one reduction wave at pH ≃ 13.5 corresponding to 1 F while compounds **II***a*, *b* do not show this behaviour at all. These results are quite similar to those ob-

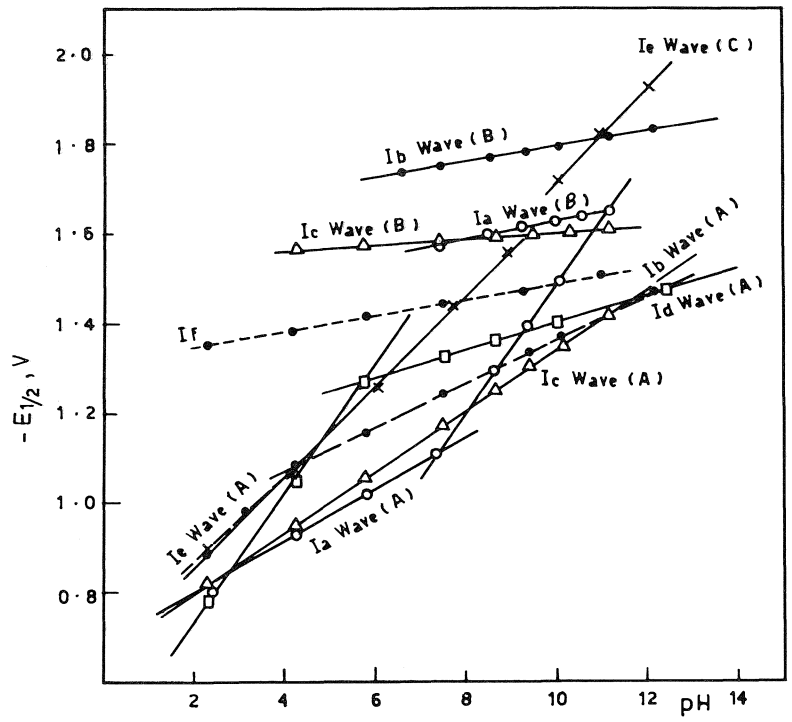


FIG. 2. Plot of $E_{1/2}$ vs. pH for **I**.

tained for the reduction of the carbonyl compounds (1). The values of n were determined coulometrically and using the Ilkovic equation (9). The diffusion coefficient (D_0) of the depolarizer has been experimentally determined (17) at pH values 2.3, 7.5, and 11.2 in Thiel buffer solutions. These pH values are particularly chosen so that well defined diffusion-controlled waves with least of other complications are obtained, as results obtained from the correlations between the pressure head of mercury and the limiting current (18) (Table 1) support this hypothesis.

In this case, Ilkovic equation could be applied for calculation of n using the mean values of D_0. Each of the waves (A, B, and D) corresponds to one electron while wave C exhibits two electrons. On the other hand, the reduction of **I***f* and **II***d* involves the uptake of 2 electrons while wave D corresponds to the uptake of one electron. These data are further supported by coulometry under controlled potential (19).

2. Reversibility of the Waves

Analysis of the waves was carried out by applying the fundamental equation for polarographic data (20). The correlations of E with log $[i/(i_1 - i)]$ are straight lines with somewhat varying slopes. Using the values of slope (Table 1), the values of the transfer coefficient α can be calculated. Wave A proceeds reversibly since the α values attain the unity. On the other hand, for waves B, C, and D and for compounds **I***f*, **II***d*, the α values equal to 0.31–0.77 (a quasi reversible reduction wave when α is more than 0.5; when α is less than 0.5, the reduction process proceeds irreversibly (21)).

3. Effect of pH on the Half-wave Potentials and the Limiting Current

The $E_{1/2}$ of the reduction waves shifts to more negative potentials as the pH of the medium increases, indicating that H^+ ions are involved in the electrode process. The correlation of $E_{1/2}$ with pH is straight lines for wave A of **I***c*, *e*, *f*, *g*, **II***c*, *d* while it is broken lines for compounds **I***a*, *b*, *d* and **II***a*, *b* (Figs. 2, 3). The plots of wave B in all compounds and wave C in compounds **I***e*, *g* are straight lines. The number of protons involved in the reduction process for each wave can be determined using the relation [1].

$$[1] \quad \Delta E_{1/2}/\Delta \mathrm{pH} = (0.059/\alpha n_a) Z(\mathrm{H}^+)$$

The values of H^+ ion indicate that one proton is consumed per electron for waves A and B, while the reduction process of **I***f* and **II***d* includes the uptake of two protons (Table 1).

The total limiting current decreases as the pH of the medium increases, the plots of i_1 vs. pH yield straight or curved lines. The reduction current of

Can. J. Chem. Downloaded from www.nrcresearchpress.com by 210.87.254.5 on 09/05/12
For personal use only.

TABLE 1. Polarographic results for **I** and **II**

Compound	pH	X^a	$-E_{1/2}$ (V)	i_l (μA)	$D \times 10^6$ (cm^2 s^{-1})	Slope of $\frac{\log i/(i_l - i)}{E^b}$	αn_a	n_a	α	$E_{1/2}$/pH^b	$Z(H^+)$
I*a*	2.30	0.50	0.83	3.50		16.80	0.99	1	0.99		0.96
	4.30	0.50	0.93	3.30		15.70	0.93	1	0.93	0.057[c]	0.90
	7.40	0.51[c]	1.12	3.00	14.566	16.20	0.96	1	0.96	0.15[d]	2.44
		0.53[d]	1.58	3.30		10.80	0.64	1	0.64	0.02[e]	0.22
	11.21	0.55	1.65	6.2		11.12	0.66	2	0.33		1.70
	13.6	0.51	1.70	4.00		10.81	0.64	1	0.64		
I*b*	2.30	0.53	0.88	3.21		16.60	0.98	1	0.98	0.08[b]	1.30
	7.50	0.53[c]	1.24	3.10		15.84	0.93	1	0.93	0.066[c]	1.04
		0.50[d]	1.75	3.40	9.20	9.63	0.59	1	0.59	0.019[d]	0.19
	11.21	0.52[c]	1.43	3.30		15.31	0.90	1	0.90		1.01
		0.54[d]	1.82	3.70		9.80	0.58	1	0.58		0.19
	13.60	0.52	1.53	4.10		10.42	0.61	1	0.61		
I*c*	2.30	0.52	0.82	2.6		16.70	0.98	1	0.98		1.25
	4.30	0.52[c]	0.95	2.2		15.80	0.93	1	0.93	0.075[c]	1.18
		0.53[d]	1.57	2.5	7.183	10.20	0.60	1	0.60	0.022[d]	0.22
	11.21	0.50[c]	1.43	1.95		15.10	0.89	1	0.89		1.13
		0.51[d]	1.61	2.45		9.30	0.55	1	0.55		0.21
	13.50	0.53	1.63	3.60		11.1	0.65	1	0.65		
I*d*	2.30	0.52	0.81	3.00		16.50	0.97	1	0.97	0.08[c]	1.32
	4.30	0.52[c]	1.04	2.80		16.40	0.96	1	0.96	0.045[c]	1.30
		0.35[d]	1.50	2.60		11.8	0.69	1	0.69	0.008[d]	0.09
	10.20	0.51[c]	1.38	3.30	8.725	15.60	0.92	1	0.92		0.70
		0.50[d]	1.58	2.60		10.70	0.63	1	0.63		0.08
	12.80	0.52	1.55	4.80		10.50	0.62	2	0.31		—
	13.60	0.52	1.53	3.80		10.40	0.61	1	0.61		—
I*e*	2.3	0.54	0.90	3.20		16.10	0.95	1	0.95		1.11
	4.3	0.53[c]	1.05	3.00	16.872	16.32	0.96	1	0.96	0.069[c]	1.12
		0.51[d]	1.35	2.80		10.80	0.64	1	0.64	0.018[d]	0.19
	9.35	0.48	1.70	5.76		12.80	0.76	2	0.38	0.078[e]	1.05
	13.60	0.52	1.91	3.62		8.42	0.49	1	0.49	—	—
I*f*	4.30	0.52	1.38	5.40		20.87	1.23	2	0.61		0.44
	7.50	0.50	1.44	4.80		17.31	1.02	2	0.51		0.36
	11.21	0.51	1.51	4.30	11.80	15.92	0.94	2	0.47	0.021	0.33
	13.80	0.53	1.54	3.10		11.10	0.65	1	0.65		
I*g*	2.30	0.53	1.03	2.80		15.81	0.93	1	0.93		0.95
	7.50	0.50[c]	1.34	2.65		15.62	0.92	1	0.92	0.06[c]	0.94
		0.52[d]	1.48	2.50	12.35	13.10	0.77	1	0.77	0.02[d]	0.26
	10.20	0.51	1.52	5.10		15.20	0.89	2	0.44	0.05[e]	0.76
	13.80	0.52	1.56	3.00		14.31	0.84	1	0.84		
II*a*	2.30	0.51	0.62	2.50		17.41	1.03	1	1.03		1.37
	4.30	0.49[c]	0.83	2.40		16.81	0.99	1	0.99		1.32
		0.52[d]	1.51	3.00		11.12	0.66	1	0.66	0.079[c]	0.16
	7.50	0.50[e]	0.96	2.30	6.531	14.12	0.83	1	0.83	0.041[c]	0.58
		0.53[d]	1.54	2.90		10.35	0.61	1	0.61	0.014[d]	0.14
	13.50	0.52	1.20	2.35		12.56	0.74	1	0.74		0.51
			1.58	2.45		10.81	0.64	1	0.64		0.15
II*b*	2.30	0.52	0.68	2.60		16.40	0.96	1	0.96	0.084[c]	1.36
	4.30	0.51[c]	0.88	2.30		15.43	0.91	1	0.91	0.04[c]	1.29
		0.50[d]	1.45	3.10		10.51	0.62	1	0.62	0.01[d]	0.11
	7.50	0.51[c]	1.00	2.20	5.72	15.20	0.89	1	0.89		0.61
		0.51[d]	1.47	3.10		10.39	0.61	1	0.61		0.10
	13.50	0.53[c]	1.24	2.30		14.28	0.84	1	0.84		0.57
		0.52[d]	1.50	3.00		10.20	0.60	1	0.60		0.10

Can. J. Chem. Downloaded from www.nrcresearchpress.com by 210.87.254.5 on 09/05/12
For personal use only.

TABLE 1. (*Concluded*)

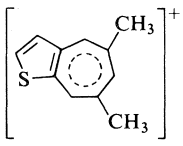
Compound	pH	X^a	$-E_{1/2}$ (V)	i_l (μA)	$D \times 10^6$ (cm^2 s^{-1})	Slope of $\frac{\log i/(i_l - i)}{E}^b$	αn_a	n_a	α	$E_{1/2}$/pH^b	$Z(H^+)$
II*c*	2.30	0.54	0.80	2.80		15.80	0.93	1	0.93	0.075[c]	1.18
	4.30	0.51[c]	0.95	2.70		15.90	0.94	1	0.94	0.04[d]	1.19
		0.53[d]	1.40	2.20	14.00	11.83	0.70	1	0.70	0.055[e]	0.47
	9.35	0.50	1.46	5.80		14.00	0.83	2	0.42		0.77
	13.80	0.52	1.64	2.62		9.32	0.55	1	0.55		
II*d*	4.30	0.49	1.24	4.90		19.35	1.14	2	0.57		0.58
	7.50	0.51	1.30	4.50	11.65	16.92	0.99	2	0.49	0.03	0.51
	11.21	0.53	1.39	4.10		15.82	0.93	2	0.46		0.47
	13.80	0.51	1.43	2.82		10.21	0.60	1	0.60		

[a] $i_l = Kh^X$.
[b] The slopes are calculated by the method of least-squares.
[c] Wave *A*.
[d] Wave *B*.
[e] Wave *C*.

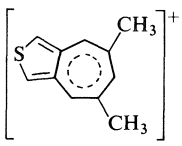
wave *A* is more or less constant in most cases, however, in a few cases it suffers a slight decrease as the pH of the medium increases.

4. Reduction Mechanism

Thiophenotropones may have two centres of reduction, the tropilidene ring and the carbonyl group. However, the reduction behaviour of these compounds resembles that of the carbonyl compounds (1). Firstly, we wish to investigate the reduction of tropilidene ring. For this purpose perchlorate salts of the type **III** or **IV** can be examined, but the unstability of these salts even in strong acidic media renders it difficult to carry out complete study on such salts. However, the salt **III**, $[(C_{11}H_{11}S)^+ClO_4^-]$, dissolved in 20 vol% ethanol – water mixture was studied in Thiel buffer solutions of varying pH values, since it is more stable than



III



IV

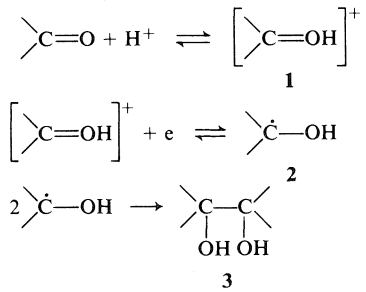
IV. In solutions of pH < 4, the polarograms consist of one reduction wave corresponding to 1 F. Within the pH range 4–7, a second wave appears which almost has equal height as that of the first wave. At pH > 7, the polarograms suffer deformation since the compound is hydrolysed. The polarographic characteristics are represented in Fig. 4. These results are in accordance with those obtained by Khopin and Zhdanov (22), who studied the electro-reduction of tropylium perchlorate salt. The first wave can be attributed to the formation of a free radical which undergoes dimerisation. At pH > 4, the new wave corresponds to the formation of thiophenotropilidene since the reduction process involves the uptake of two electrons and one proton.

$$(C_{11}H_{11}S)^+ + e \rightleftharpoons (C_{11}H_{11}S)^\cdot$$
$$2(C_{11}H_{11}S)^\cdot \rightarrow (C_{11}H_{11}S)_2 \quad \Big\} \text{ first wave, pH} < 4$$

$$(C_{11}H_{11}S)^+ + 2e \rightleftharpoons (C_{11}H_{11}S)^-$$
$$(C_{11}H_{11}S)^- + H^+ \rightarrow C_{11}H_{12}S \quad \Big\} \text{ pH} > 4$$

At pH > 4, the final product of reduction is the thiophenotropilidene itself as was supported by electrolysis at controlled potential (16). The electrolysis was carried out in aqueous solution at pH = 6 and at −1.38 V. After the extraction of the product of electrolysis, it was analysed by vapour phase chromatography. The electrochemical reduction was quantitative and the three isomers of **III** were separated in the proportions of 5:75:20%. These proportions are in agreement with those obtained chemically by Guilard and Fournari (15). Thus the tropilidene ring is inactive towards reduction at DME under these experimental conditions.

Wave *A* corresponds to the reduction of cation **1** and then forms the free radical **2** which dimerises to form pinacol **3**.



Wave *B* expresses the transformation of the radical **2** to the alcohol **4** as follows:

Can. J. Chem. Downloaded from www.nrcresearchpress.com by 210.87.254.5 on 09/05/12
For personal use only.

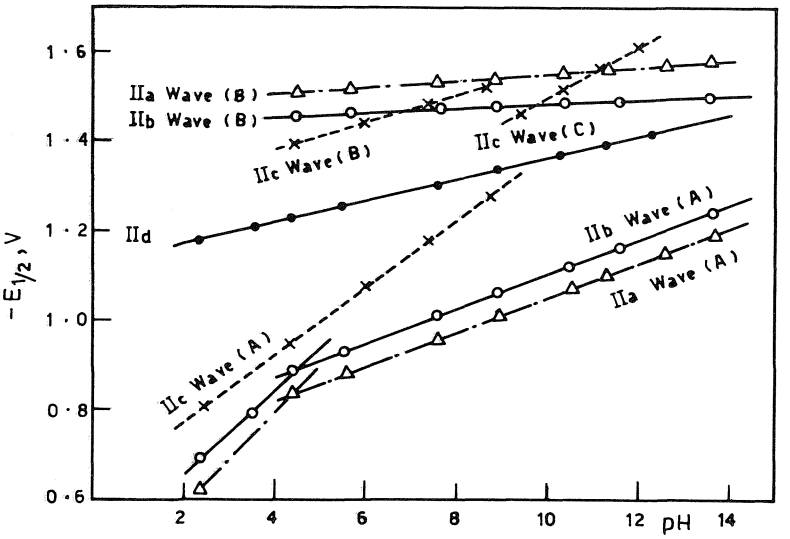
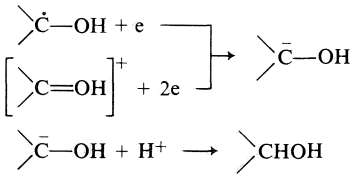
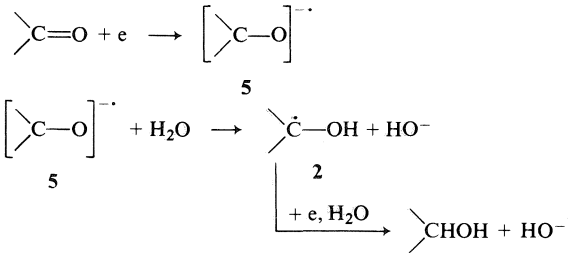


FIG. 3. Plot of $E_{1/2}$ vs. pH for **II**.



4

In strong alkaline media, pH > 10, as well as the reduction of **I***f* and **II***d* at different pH values, the first step involves the direct reduction of the basic form to the anion radical **5** which reacts with one molecule of water to reproduce **2**. The radical **2** can be reduced as follows:



5 **5** **2**

At pH > 12.5 and by increasing the pH of the solution, the anion **5** is predominant in solution and undergoes further reduction. This behaviour is not observed for compounds **II***a*, *b*.

5. The $E_{1/2}$*–Structure Correlation*

The $E_{1/2}$ values of thiophenotropone derivatives **I**, at one and the same pH value, are at more negative potentials than those of the corresponding thiophenotropones **II**. $\Delta E_{1/2}$ values equal 0.05–0.4 V depending on the nature of the wave, the molecular structure, and the pH value of the medium. Also, within one and the same series, the displacement in $E_{1/2}$ to less negative potentials goes in the order of decreasing donor character of the substituents. The increase of donor character of the substituent R or the increased delocalisation of π-electrons within the thiophenotropones **I** enhance the polarisation of the carbonyl group leading to easier formation of the anion **5**. This is the case which is substantiated by the direct formation of the anion **5** during the reduction of **I***f* and **II***d* even in strong acid media and by the appearance of two reduction waves for the polarograms of **I***b*, *c* and **II***a*, *b* in strong alkaline solutions. The last behaviour can be attributed to the decrease of the electron density of the tropilidene ring while it increases on the thiophene nucleus. This is the case which leads to localise the π-electrons of the carbonyl group.

6. The Correlation of Half Reduction Potentials ($E_{1/2}$) *with Absolute Electron Affinities (E.A.).*

The potential determining step in the polarographic reduction of a compound has been assumed to be the reversible addition of an electron to the molecule so that the half-wave reduction potential is a measure of the electron affinity of the compound according to eq. [2]

$$[2] \quad -E_{1/2} = \text{E.A.} - \Delta G_{sol} - \text{constant}$$

The constant term depends upon the reference electrode and is 5.07 eV for the saturated calomel electrode (23). The difference in solvation energies for the negative ion and the neutral, ΔG_{sol}, was determined by Briegleb (24) to have the value of −3.66 eV. Farragher and Page (25) assumed eq. [2] to be valid and calculated an average value of −2.37 eV for ΔG_{sol} for some charge transfer acceptors using the magnetron results for the absolute E.A. values of these compounds. Recently Chen (23, 26) proposed an average value for ΔG_{sol} to be

Can. J. Chem. Downloaded from www.nrcresearchpress.com by 210.87.254.5 on 09/05/12
For personal use only.

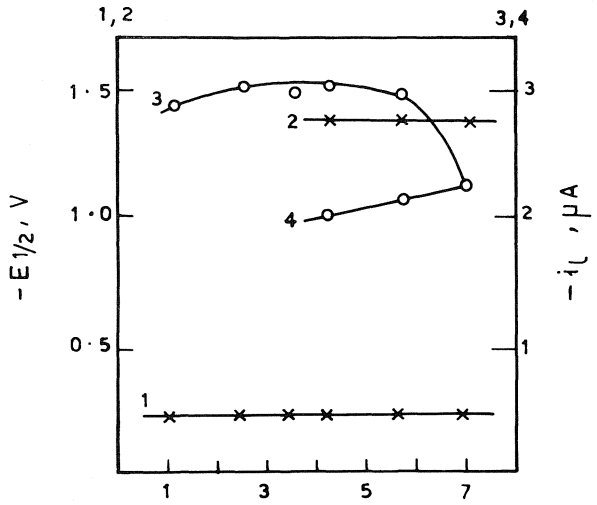


FIG. 4. Plot of $E_{1/2}$ and i_l vs. pH for **III** (0.5 m*M*).

equal to -2.58 ± 0.26 eV. Thus, the following equation can be used to calculate E.A. values from half-wave reduction potentials vs. the saturated calomel electrode (27–32).

[3] $\text{E.A.} = -E_{1/2} + 2.49 \pm 0.26$ eV

$E_{1/2}$ vs. sce, aprotic solvents

TABLE 2. Electron affinity values and $E_{1/2}$ of **I** and **II** measured in DMF

Compound	$-E_{1/2}$ (V)	E.A. (eV)
I*a*	1.60	0.89
b	1.62	0.87
c	1.55	0.94
d	1.65	0.84
e	1.76	0.73
f	1.93	0.56
g	1.85	0.64
II*a*	1.44, 1.86	1.05
b	1.50, 1.90	0.99
c	1.70	0.79
d	1.80	0.69

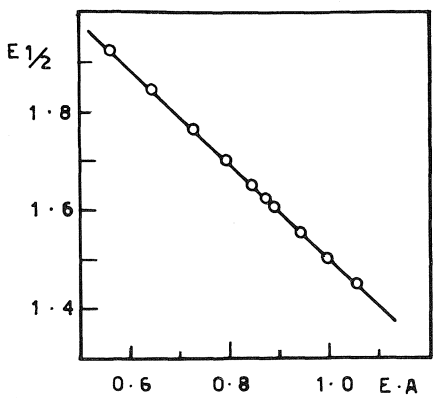


FIG. 5. Correlation of $E_{1/2}$ with E.A.

For this purpose, the polarograms of **I** and **II** are recorded in DMF and they consist of one or two reduction waves (Table 2). The electron affinities of **I** and **II** are tabulated in Table 2, and correlation of the $E_{1/2}$ values with the absolute E.A. values is shown in Fig. 5.

1. L. HOLLECK and H. MERSEN. Z. Elektrochem. **57**, 944 (1953).
2. R. JONES and T. MEL. Aust. J. Chem. **15**, 492 (1962).
3. H. SHIGEO and S. NORIKO. Bull. Chem. Soc. Jpn. **43**, 2083 (1970).
4. E. MUELLER and W. DILGER. Chem. Ber. **106**, 1643 (1973).
5. Y. ASAHI, K. SHINO ZAKI, M. MITANI, and H. OHTSUKA. Chem. Pharm. Bull. **22**, 254 (1974).
6. B. SHASHI and N. R. BANNERJEE. Indian J. Chem. **15A**, 777 (1977).
7. A. I. FODIMAA and E. S. LOVIN. Zav. Lab. **34**, 141 (1968).
8. A. D. BROADBEND and E. F. SOMMERWANN. J. Chem. Soc. **4**, 376 (1967).
9. J. M. ABDEL-KADER, A. M. SHAMS-ELDIN, B. KASTENING, and L. HOLLECK. J. Electroanalyt. Chem. **26**, 41 (1970).
10. I. M. ISSA, S. H. ETAIW, R. M. ISSA, and A. K. ABD-ELKADER. Ann. Chim. **67**, 211 (1977).
11. J. C. VIRE and Q. J. POTRIACHE. Analusis, **6**, 155 (1978).
12. S. H. ETAIW. Ann. Chim. **68**, 57 (1968).
13. A. M. KUTNEVICH, A. P. RUDENKO, L. L. RODINA, and F. PRAGST. Zh. Org. Khim. **14**, 1343 (1978).
14. R. GUILARD and P. FOURNARI. C.R. Acad. Sci. Paris, **273**, 160 (1971).
15. R. GUILARD and P. FOURNARI. Bull. Soc. Chim. Fr. **4**, 1437 (1971).
16. D. PELTIER, M. LE GUYADER, and J. TACUSSEL. Bull. Soc. Chim. 2609 (1963).
17. R. A. ROBINSON and R. H. STOKES. Electrolyte solutions. Butterworths, London. 1970. p. 256.
18. S. K. JHA and S. N. SRIVASTAVA. Acta Chim. Budapest, **80**, 375 (1974).
19. R. W. MURRAY, W. R. HEINEMAN, and G. W. O'DOM. Anal. Chem. **39**, 1668 (1967).
20. L. MEITES. Polarographic techniques. 2nd ed. Interscience Publishers, New York, London, Sydney. 1965.
21. R. GOTO and I. TACHI. Proc. Inten. Polarography Congr., Prague. Vol. 1. Hriodovedecke vydavatelstvi, Prague. 1951. p. 69.
22. A. M. KHOPIN and S. I. ZHDANOV. Electrokhimiya, **4**, 228 (1968).
23. R. S. BECKER and E. C. M. CHEN. J. Chem. Phys. **45**, 2403 (1966).
24. G. BRIEGLEB. Angew. Chem. Int. Ed. Engl. **3**, 617 (1964).
25. A. L. FARRAGHER and F. M. PAGE. Trans. Faraday Soc. **63**, 2369 (1967).
26. E. C. M. CHEN. Ph.D. dissertation, University of Houston. 1966.
27. F. M. PAGE and G. C. GOODE. Negative ions and the magnetron. Wiley Interscience, New York. 1969.
28. M. E. PEOVER. Trans. Faraday Soc. **58**, 1656 (1964); **58**, 2370 (1962); **60**, 417 (1964); **60**, 479 (1964).
29. M. E. PEOVER. Nature London, **191**, 702 (1961); **193**, 475 (1962).
30. M. E. PEOVER. J. Chem. Soc. 2540 (1962).
31. K. M. C. DAVIS, P. R. HAMMOND, and M. E. PEOVER. Trans. Faraday Soc. **61**, 1516 (1965).
32. A. H. MAKI and D. H. GESKE. J. Am. Chem. Soc. **83**, 1852 (1961).

Can. J. Chem. Downloaded from www.nrcresearchpress.com by 210.87.254.5 on 09/05/12
For personal use only.

Infrared spectra of the ammonium ion in crystals. Part VII. Existence of symmetrically trifurcated hydrogen bond in ammonium halides[1,2]

OSVALD KNOP AND WOLFGANG J. WESTERHAUS
Department of Chemistry, Dalhousie University, Halifax, N.S., Canada B3H 4J3
AND
MICHAEL FALK
Atlantic Regional Laboratory, National Research Council of Canada, Halifax, N.S., Canada B3H 3Z1

Received August 29, 1979

OSVALD KNOP, WOLFGANG J. WESTERHAUS, and MICHAEL FALK. Can. J. Chem. **58**, 270 (1980).

This investigation deals with the effect of temperature, between 10 and 293 K, on the ir spectrum of the NH_3D^+ probe ion in polycrystalline NH_4SnF_3, NH_4CuSO_3, cubic $(NH_4)_2SiF_6$, and $(NH_4)_2SnCl_6$. The results lead to the following conclusions. At 10 K these crystals contain symmetrically trifurcated N—H···3X bonds, i.e. bonds in which the N—H orientation of maximum probability is on the threefold axis. With increasing temperature these bonds lose progressively their symmetrically-trifurcated character to become highly bent, highly dynamic N—H···X bonds, and the strength of the hydrogen-bonding interaction increases. This is reflected in the decrease of the ND stretching frequency of the probe ion with increasing temperature, which is the opposite of the behaviour observed with normal (i.e. essentially straight) N—H···X bonds.

Re-determination of the room-temperature crystal structure of NH_4CuSO_3 has confirmed the correctness of the structure reported previously by Nyberg and Kierkegaard.

OSVALD KNOP, WOLFGANG J. WESTERHAUS et MICHAEL FALK. Can. J. Chem. **58**, 270 (1980).

Ce mémoire traite de l'effet de la température, entre 10 et 293 K, sur le spectre infrarouge de l'ion sonde NH_3D^+ dispersé dans les composés polycristallins NH_4SnF_3, NH_4CuSO_3, $(NH_4)_2SiF_6$ (phase cubique) ainsi que $(NH_4)_2SnCl_6$. Les résultats mènent aux conclusions suivantes. A 10 K ces cristaux contiennent des liaisons N—H···3X trifurquées symétriques, c'est-à-dire des liaisons dans lesquelles l'orientation la plus probable du vecteur N—H coïncide avec l'axe ternaire. Au fur et à mesure que la température augmente, ces liaisons perdent leur caractère trifurqué symétrique pour devenir des liaisons N—H···X dynamiques fortement coudées et l'interaction H···X devient plus forte. Conformément à ces changements, la fréquence de la vibration de valence ND de l'ion sonde diminue quand la température augmente, ce qui est à l'opposé du comportement des liaisons N—H···X normales, à savoir essentiellement droites.

La redétermination de la structure cristalline du NH_4CuSO_3 à la température de la pièce confirme la justesse de la structure rapportée antérieurement par Nyberg et Kierkegaard.

Can. J. Chem. Downloaded from www.nrcresearchpress.com by 210.87.254.105 on 09/05/12
For personal use only.

In Part VI (1) we pointed out that, in a crystal containing an NH_4^+ ion surrounded by potential hydrogen-bond acceptors X, a coordination geometry intuitively favourable to the formation of a symmetrically trifurcated N—H···3X bond does not guarantee the actual existence of such a bond, i.e. one in which the N—H orientation of maximum probability is demonstrably in a threefold axis. The distributions of proton density obtained in the only two neutron-diffraction studies bearing on the problem, those of cubic $(NH_4)_2SiF_6$ (2) and *fcc* $NH_4I(III)$ (3), both at room temperature, do not support the existence of symmetrically trifurcated N—H···3X bonds defined this way. However, they do indicate the presence of hydrogen-bonding interaction of pronounced dynamic character, associated with librational (and possibly also bending) motions of large amplitude ("fluxional" hydrogen bonds), and one may reasonably suppose that symmetrically trifurcated hydrogen *bonds* may exist in cubic $(NH_4)_2SiF_6$ at low temperatures.[3] At the time of writing Part VI the existence of such bonds was yet to be demonstrated.

We also called attention to the advantage which a variable-temperature study of the ir spectrum of the ammonium ion in NH_4SnF_3 would offer for an understanding of hydrogen bonding in trifurcated coordination geometries. Such a study of NH_4SnF_3 and of the companion compound NH_4CuSO_3 has now been carried out and the results are compared in the following to those, equally new, on cubic $(NH_4)_2SiF_6$ and $(NH_4)_2SnCl_6$ between 10 K and room temperature. We have again employed the NH_3D^+ ion at low concentration as a probe (cf. refs. 1 and 4). To assess the accuracy of the crystal-structure determination of NH_4CuSO_3 by photographic methods (5) we have also redetermined the room-temperature structure of the sulfite by X-ray diffractometry.

NH_4SnF_3

According to the determination of the room-tem-

[1]For Part VI, see ref. 1.
[2]NRCC No. 17898.

[3]$NH_4I(III)$ transforms on cooling to $NH_4I(II)$, in which the C.N. of the ammonium ion is 8 and the N—H···I bonds are normal.

0008-4042/80/030270-13$01.00/0
©1980 National Research Council of Canada/Conseil national de recherches du Canada

Can. J. Chem. Downloaded from www.nrcresearchpress.com by 210.87.254.105 on 09/05/12
For personal use only.

perature crystal structure of NH_4SnF_3 from X-ray diffractometer data (6) the N atom in this crystal is at a site of symmetry C_3 and is coordinated by three F atoms (belonging to three different SnF_3^- ions) at 2.75 Å and another three F atoms (belonging to the same SnF_3^- ion) at 3.00 Å; the F atoms in each set are related by the threefold axis. The FNF angle of 108.2° corresponding to the shorter N···F distances is very close to tetrahedral, whereas that corresponding to the longer N···F distances, 54.4°, is almost exactly half the tetrahedral angle. This geometry (Fig. 1) implies that the three nonaxial hydrogen atoms H_n of the ammonium ion are strongly bonded to the first set of F atoms by normal, practically straight N—H···F bonds.[4] This portion of the N environment thus resembles the tetrahedral hydrogen-bonding network in NH_4F. The axial N—H_a vector, on the other hand, is constrained by symmetry to point, in its mean position, at the centre of the equilateral triangle formed by the F atoms at 3.00 Å from the N atom, the NH_aF angle being 134°. The N—H_a bond thus not only finds itself in a trifurcated *geometrical* situation, but in view of the strong constraint imposed by the three N—H_n···F bonds may be expected to constitute a true symmetrically trifurcated hydrogen *bond*, possibly different in its spectroscopic properties from the "fluxional" bonds in, for example, $(NH_4)_2SiF_6$ (cf. ref. 1). An indication that such a difference might exist is observed in Fig. 9 of ref. 1, in which the $\nu_{4bc}(a)$ frequency of the NH_3D^+ probe ion is plotted against the NHX* angle that would be required by symmetric trifurcation: the point for NH_4SnF_3 falls far off the regression line appropriate to cubic and trigonal $(NH_4)_2MX_6$ (X = F, Cl, Br, I), in which compounds the C.N. of the ammonium ion is 12 and the ammonium ions are not engaged in normal N—H···X bonds. It is one of the aims of the present study to determine whether such a difference in fact exists.

NH_4CuSO_3

A similar hydrogen-bonding geometry is found in NH_4CuSO_3 (Fig. 1), for which a crystal-structure determination by photographic methods has been reported (5). In this crystal ($R\bar{3}m$, No. 166, $Z = 2$) the N atom is located on a threefold axis, like in NH_4SnF_3,[5] but the coordination of the ammonium

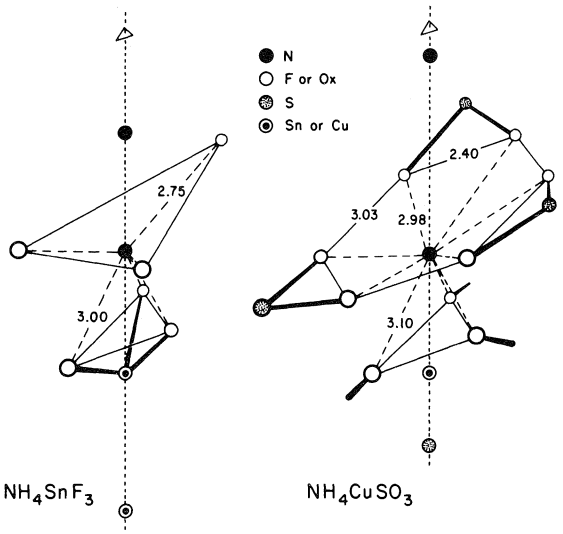


FIG. 1. Environments of the ammonium ion in NH_4SnF_3 and NH_4CuSO_3. Both drawings are on the same scale.

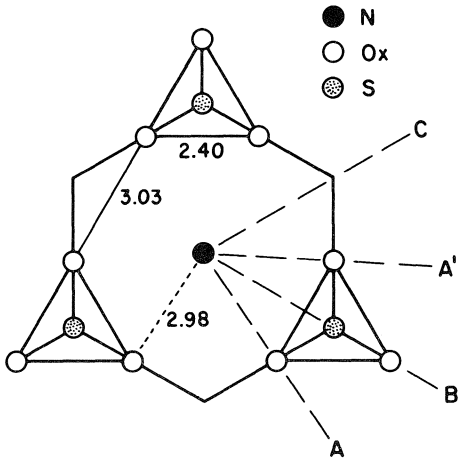


FIG. 2. Possible symmetric orientations of the ammonium ion in NH_4CuSO_3 about the threefold axis.

ion differs from that in the fluoride in the number of acceptor atoms available for the formation of strong hydrogen bonds. To the set of three F atoms at 2.75 Å from N there corresponds in NH_4CuSO_3 a set of six coplanar oxygens at 2.97(1) Å from the N atom. The six oxygens are arranged in three pairs, each pair belonging to an SO_3^{2-} ion (Fig. 2). The three O atoms constituting the trifurcated situation, at d(N···O) = 3.11(2) Å, each belong to a different sulfite ion. The NH_aO angle, 132°, is practically the same as the NH_aF angle in the fluoride, which suggests that the trifurcated hydrogen bonds in the two compounds may be expected to show similar behaviour. The mean positions of the hydrogen atoms H_n participating in the *strong* N—H_n···O bonds cannot, however, be surmised from the lo-

[4]In ref. 1 the orientation of the ammonium ion was erroneously stated to be the opposite of that proposed in ref. 6. See erratum (7) to ref. 1.

[5]The site symmetry of the N atom in NH_4CuSO_3 is C_{3v} but C_3 in NH_4SnF_3. Since *any* hexagonal or trigonal site symmetry produces the same number of component bands of $\nu_1(NH_3D^+)$ and $\nu_{4bc}(NH_3D^+)$ (4), no special mention of this difference will be required.

Can. J. Chem. Downloaded from www.nrcresearchpress.com by 210.87.254.105 on 09/05/12
For personal use only.

cation of the six coplanar O atoms. Inspection of Fig. 2 shows that a rigid $-NH_3$ triplet can in principle assume four orientations that might correspond to local energy minima: two symmetry-equivalent, A and A′, corresponding to normal N—H···O bonds, and two nonequivalent and bifurcated, B and C. Position B involves oxygens of the same sulfite ion; position C involves O atoms belonging to different SO_3^{2-} ions. A hydrogen bond corresponding to A would be somewhat bent, with an NH_nO angle of about 169°. It seems *a priori* probable that the ammonium ion in the crystal undergoes rapid reorientations about the threefold axis and that any one of the four orientations will be populated for some fraction of time, with the A and A′ orientations dominant.

$(NH_4)_2SiF_6$ and $(NH_4)_2SnCl_6$

The environment of the NH_4^+ ion in these two cubic, isostructural crystals is illustrated in Fig. 1 of ref. 8. The N atom is surrounded by 12 equivalent halogen atoms X arranged at the corners of a coordination cuboctahedron of symmetry T_d. The tetrahedral distortion of the cuboctahedron from O_h symmetry is smaller in the chlorostannate. The N—H vectors point to alternate triangular faces of the cuboctahedron, away from the Si and Sn atoms (2). Spectra of the NH_3D^+ probe ion in the two compounds recorded previously (9) between 10 K and room temperature contained no indication of transitions.

Combination bands involving the librational mode $\nu_6(NH_4^+)$ are present in the ir spectra of the fluorosilicate even at room temperature, but in the spectra of the chlorostannate they emerge only on cooling below 80 K (1). This indicates that hydrogen bonding is considerably stronger in the fluorosilicate.

Experimental

Preparation

NH_4SnF_3 was prepared by dissolving SnF_2 and a slight excess of NH_4F in a minimum quantity of hot water, filtering, and allowing the filtrate to cool. The crystalline product was filtered off, washed with a minimum volume of cold water, and dried *in vacuo* (10). The SnF_2 was obtained by dissolving freshly precipitated Sn(II) hydroxide in aqueous HF. Deuterated NH_4SnF_3 was obtained by recrystallization from aqueous HF of the appropriate D content.

NH_4CuSO_3 was prepared as in ref. 11. Because of the insolubility of the sulfite in water deuterium had to be incorporated at the outset using a weakly deuterated solution of cupric sulfate.

The two hexahalometallates(IV) were prepared by recrystallization of commercial material from acidified aqueous solutions and were deuterated by crystallization from aqueous solutions of the appropriate D_2O content.

The authenticity of the preparations was checked by X-ray powder diffraction and by comparing their ir spectra with spectra reported previously (1, 12).

Infrared Spectra

Spectra were recorded on a Perkin-Elmer model 180 spectrophotometer fitted with a closed-cycle He refrigerator (Displex model 202, Air Products and Chemicals Co.). Suitable samples were obtained by mulling finely ground crystals with hydrocarbon oil (for spectra in the 1330–400 cm^{-1} range) or fluorocarbon oil (4000–1330 cm^{-1}). The mulls were sandwiched between CaF_2 or KBr plates. Survey spectra of undeuterated NH_4SnF_3 and NH_4CuSO_3 are presented in Fig. 3.

For the study of ND bands specimens deuterated to 1–3% were used. Spectra of the 3% D material, especially at low temperatures, contained small side bands originating in the secondary isotopic species $NH_2D_2^+$ and in the coupling of ND vibrations of neighbouring NH_3D^+ ions in the crystal (Figs. 4 and 5). Although the relative intensity of these side bands (which increases with the square of the D content) is much reduced at 1% D, the reduction is at the cost of diminished intensity of *all* ND absorptions and a relatively high noise level, especially at sample temperatures approaching room temperature, when the ND bands become broader and less intense. The band parameters reported in Tables 2 and 4 were obtained by extrapolation to 0% D of values measured in spectra of samples of different D contents.

The very pronounced Christiansen effect (13) present, especially at low sample temperatures, in the spectra of $(NH_4)_2SiF_6$ and $(NH_4)_2SnCl_6$ is responsible for the increased uncertainty in the values of peak positions and band halfwidths (cf. Table 4). The present values of the ND stretching frequencies 2416 cm^{-1} for NH_4SnF_3 and 2439 cm^{-1} for $(NH_4)_2SiF_6$ at liquid-nitrogen temperature differ somewhat from the values reported earlier (1), 2408 and 2432 cm^{-1}, respectively. This discrepancy is likely to originate in the greater uncertainty in the sample temperature in the previous study.

Re-determination of the Crystal Structure of NH_4CuSO_3

To re-determine the room-temperature structure of the sulfite, intensities were collected on an Enraf-Nonius CAD-4 automatic diffractometer (Mo Kα radiation) from a crystal approximately 0.4 × 0.4 × 0.1 mm^3 in size. They were reduced to a standard scale by a routine procedure and were corrected for Lorentz and polarization factors but not for absorption. 177 independent reflections with $I > 3\sigma(I)$ were used in the calculation. The atomic scattering factors were taken from ref. 14 and were corrected for the real part of anomalous dispersion.

The Cu and S positions were established from a Patterson function. A subsequent Fourier synthesis revealed all S and O locations. Comparison of the positional parameters with those of ref. 5 produced no significant differences. A full-matrix least-squares refinement (using programs of ref. 15) with anisotropic temperature factors gave $R = 0.048$, $R_w = 0.043$ ($w = \sigma^2|F_o| + 0.005|F_o|^2$, σ = individual esd calculated from the diffractometer counting statistics). A difference Fourier map computed at this stage for the region around the N atom showed a maximum on the threefold axis pointing to the centre of a triangle of O atoms, and a torus-shaped maximum containing three weak peaks in the region between the N and the six nearest O atoms. The latter feature is compatible with a distribution of the orientations represented in Fig. 2, the three weak peaks corresponding to orientation B. Fixing the H atoms in these positions resulted in $R = 0.044$, $R_w = 0.041$. Refinement of the H positions starting with the values obtained from the difference Fourier map gave almost identical R values and large esd values for the H parameters. The refined positional parameters of the H atoms are considered too uncertain to be reported here. A low-temperature structure determination is planned.

The bond distances shown in Figs. 1 and 2 were calculated from the final values of the positional parameters (Table 1) using

Can. J. Chem. Downloaded from www.nrcresearchpress.com by 210.87.254.105 on 09/05/12
For personal use only.

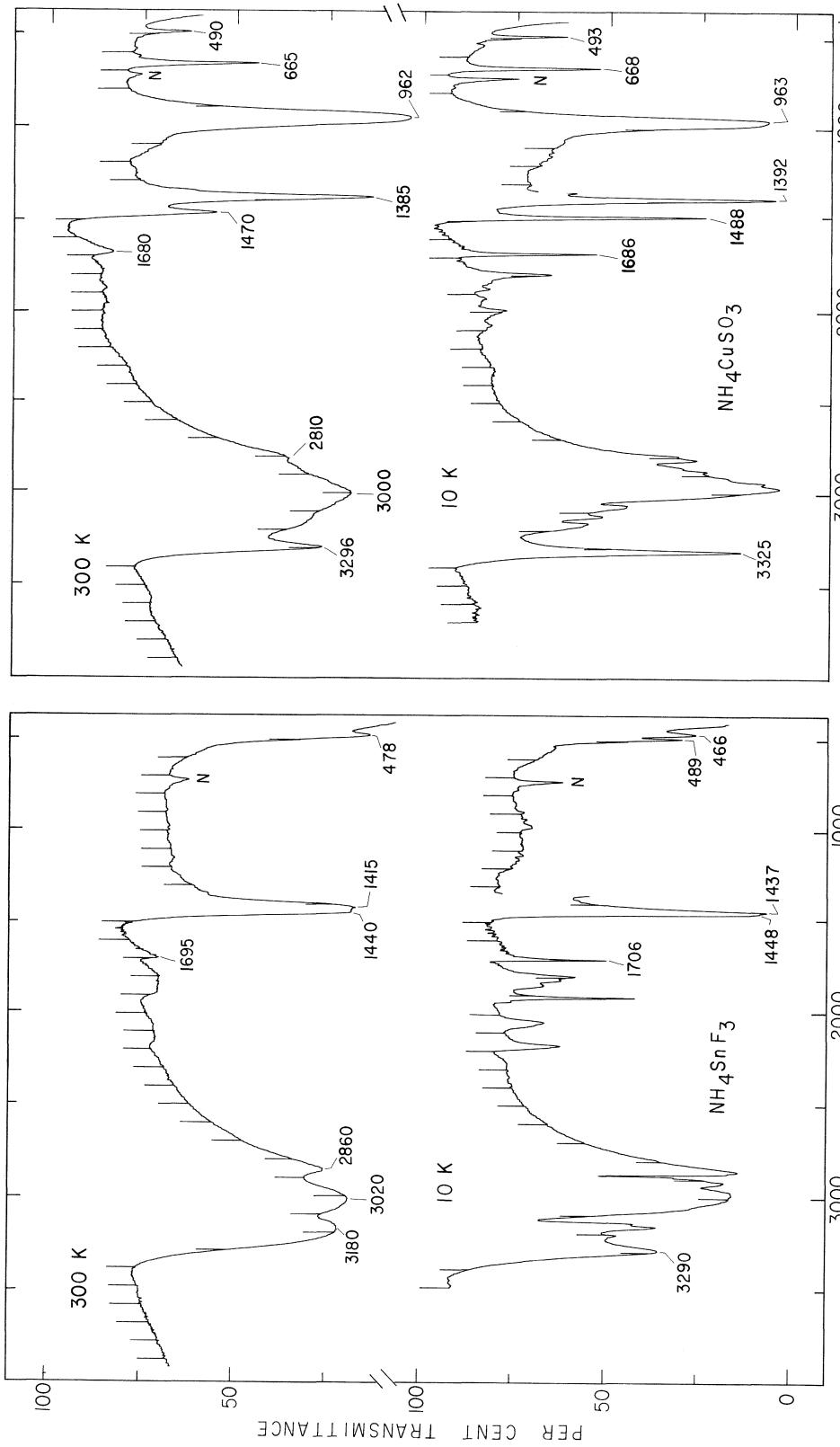


FIG. 3. Survey spectra of undeuterated NH_4SnF_3 and NH_4CuSO_3 (above 1330 cm^{-1}, fluorocarbon oil mulls; below 1330 cm^{-1}, hydrocarbon oil mulls). Features originating in the mulling oil are marked N. The 10 K spectra were recorded with much thinner mulls than the room-temperature spectra.

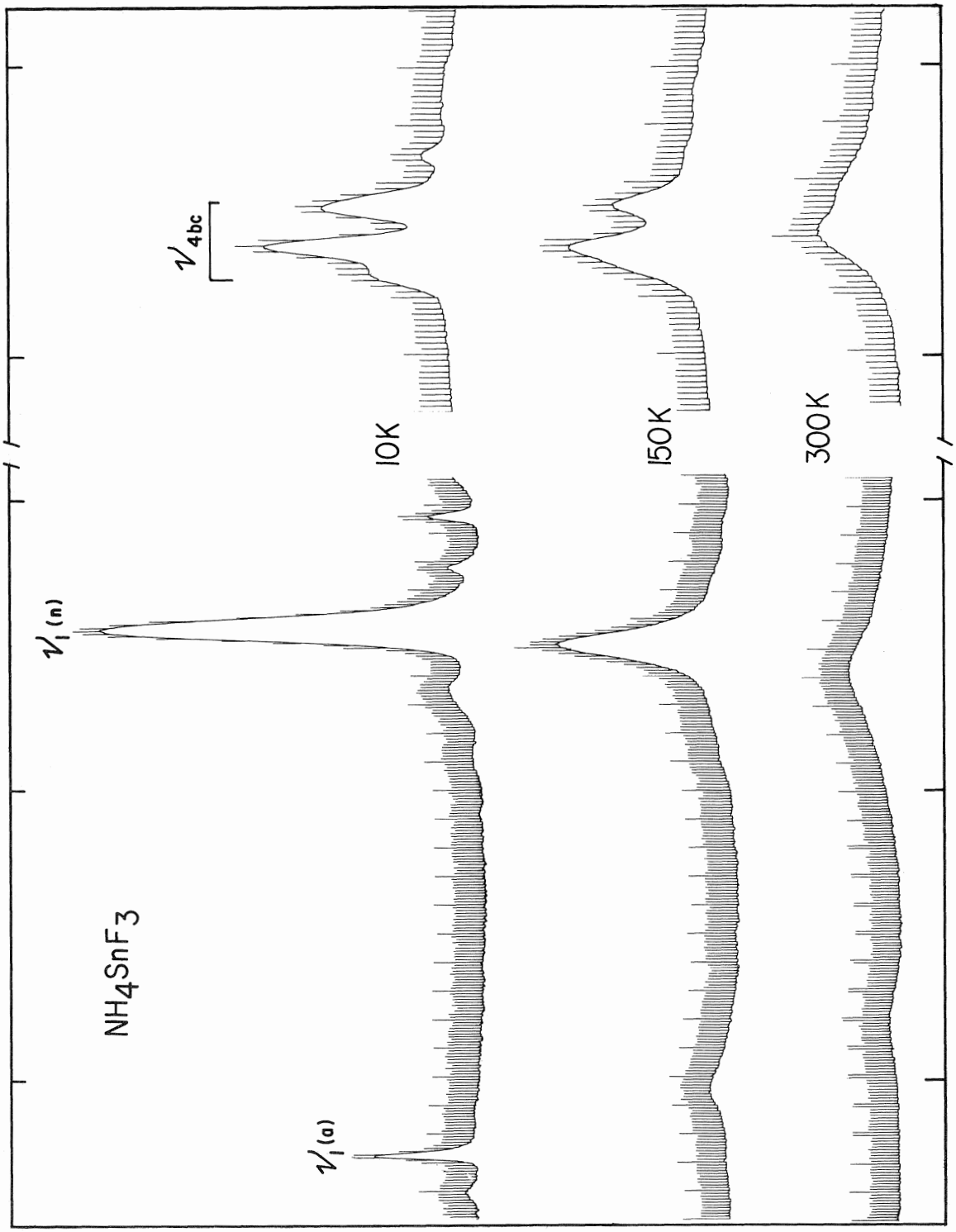


FIG. 4. The ND stretching and bending regions of the spectrum of NH_4SnF_3 (1.5% D) at different temperatures. Features other than those identified as components of the ν_1 and ν_{4bc} fundamentals of NH_3D^+ originate in the secondary isotopic species $NH_2D_2^+$ or in the coupling of vibrations of neighbouring NH_3D^+ ions in the crystal.

Can. J. Chem. Downloaded from www.nrcresearchpress.com by 210.87.254.105 on 09/05/12
For personal use only.

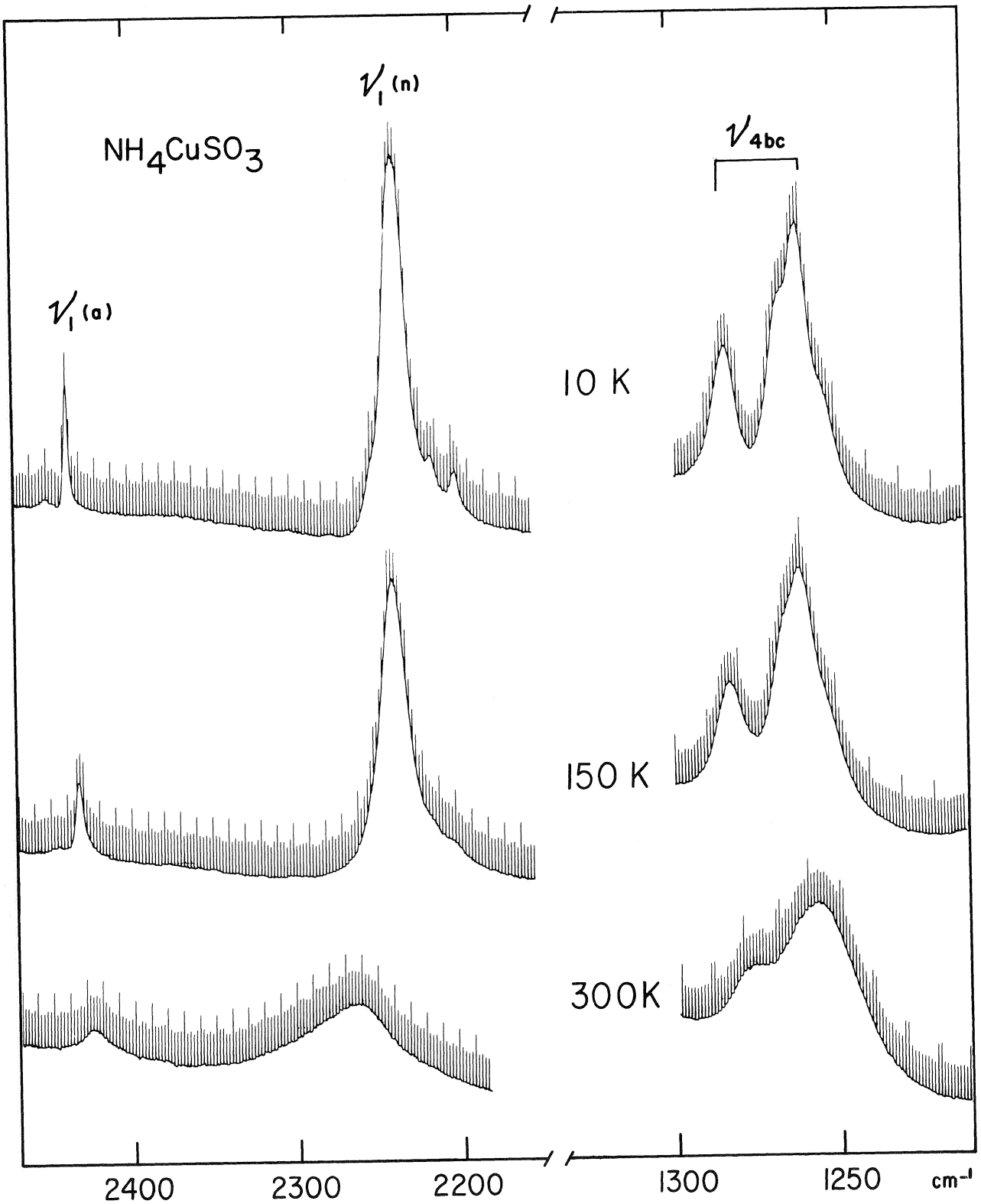


FIG. 5. The ND stretching and bending regions of the spectrum of NH_4CuSO_3 (3% D) at different temperatures. See caption of Fig. 4.

Can. J. Chem. Downloaded from www.nrcresearchpress.com by 210.87.254.105 on 09/05/12
For personal use only.

TABLE 1. Positional and thermal parameters for NH_4CuSO_3 at room temperature*

Atom	x	y	z	u_{11}	u_{33}	u_{12}	u_{13}	u_{23}
Cu	0	0	0.1999(1)	14(1)	13(1)	7(1)	0	0
S	0	0	0.1071(1)	4(1)	12(1)	2(1)	0	0
N	0	0	0.3621(4)	10(2)	27(4)	5(1)	0	0
O	0.8523(4)	0.1477(4)	0.0813(2)	26(2)	17(2)	24(2)	−1(1)	1(1)

*The anisotropic temperature factor is defined as $T = u_{11}a^{*2}h^2 + 2u_{12}a^*b^*hk + \ldots$; $u_{11} = u_{22}$. The u_{ij} values in the table have been multiplied by 10^3.

TABLE 2. Frequencies (cm^{-1}) of the NH_3D^+ probe ion absorptions in NH_4SnF_3 and NH_4CuSO_3

	Frequency			
	NH_4SnF_3		NH_4CuSO_3	
Assignment	10 K	293 K	10 K	293 K
ν_1(a)	2427(1)	2381(3)	2437(1)	2415(3)
ν_1(n)	2243(1)	2258(2)	2235(1)	2253(3)
ν_{4bc}(a)	1296(1)		1283(1)	1276(3)
ν_{4bc}(n)	1291(1)	1289(1)	1266(1)	
	1284(1)	1282(2)	1261(1)	1256(3)

the unit-cell dimensions given in ref. 5. They differ only slightly from those reported by Nyberg and Kierkegaard and quoted in the Introduction.

Results

For brevity, the $\nu_1(NH_3D^+)$ (essentially ND stretching) and $\nu_{4bc}(NH_3D^+)$ (essentially ND bending) absorptions will be referred to as ν_1 and ν_{4bc} throughout.

NH_4SnF_3 and NH_4CuSO_3: General Features of the Spectra

As required (4) by the trigonal site symmetry of the ammonium ion, a 1:3 doublet was observed in the ND stretching region of the spectra of both compounds (Figs. 4 and 5). The weaker, higher-frequency component ν_1(a) corresponds clearly to the axial and the more intense, lower-frequency component ν_1(n) to the nonaxial N—D bond. The two ν_1 components, whose separation is of the order of 150–200 cm^{-1} (see below), are present at all temperatures between 10 and 293 K. The composite absorption observed in the ν_{4bc} region is incompletely resolved (Figs. 4 and 5) but is consistent with the 2:3:3 triplet expected for trigonal site symmetry. The assignments of the three components of the observed triplet to the two bending fundamentals of the nonaxial N—D and to the one doubly degenerate bending fundamental of the axial N—D given in Table 2 are tentative and no structural conclusions will be drawn from them. There was no indication of a transition in the NH_3D^+ spectra of either compound in the temperature range studied.

In the spectra of *undeuterated* samples (Fig. 3, Table 3) the absorption in the NH stretching region extends from 3200 to 2200 cm^{-1}. Most of it appears to arise from the nonaxial hydrogens which are strongly bonded to the F or O atoms. The large breadth, relatively high ir intensity, and rich fine structure at low temperatures are characteristic of strong hydrogen bonds (16). A part of the structure arises from the dynamic coupling of the vibrations of different NH_4^+ ions in the crystal, but some of it is a consequence of Fermi resonance with overtone and combination modes of NH_4^+. In particular, we note the occurrence of one or perhaps two sharp absorption minima in the 10 K spectrum of NH_4SnF_3. These are the so-called "Evans holes", a common Fermi-resonance phenomenon (17, 18) hitherto not reported in the spectra of solid ammonium compounds. The highest-frequency peaks in the 10 K spectra (NH_4SnF_3, 3290 cm^{-1}; NH_4CuSO_3, 3325 cm^{-1}) can be assigned to the stretching of the axial N—H bond, by analogy with ν_1(a). This assignment is supported both by the similarity of the effect of temperature on the frequency of this band in the NH and ND spectra and by the NH/ND frequency ratios, which approach the ideal ratio of 1.369 for diatomic harmonic NH and ND oscillators: 3290/2427 = 1.356, 3325/2437 = 1.364. Apparently the exceptionally large difference between the hydrogen-bonding strengths of H_a and H_n in these crystals is sufficient to decouple their stretching motions.

The *combination bands* $\nu_2 + \nu_6$ and $\nu_4 + \nu_6$ involving one of the bending modes, ν_2 or ν_4, and the librational mode ν_6 of the NH_4^+ ion, are seen as a series of intense, sharp bands in the spectra of both compounds at low temperatures. They are clearly observable even at room temperature, which reflects the presence of significant hydrogen bonding (cf. ref. 1). The $\nu_2(NH_4^+)$ fundamental, which is ir-inactive under cubic site symmetry but would be expected to appear when the symmetry is lowered, is in fact observed as a small band in the spectra of both compounds at room temperature (at 1695 cm^{-1} in NH_4SnF_3 and at 1680 cm^{-1} in NH_4CuSO_3) and sharpens considerably at low temperatures (Fig. 3).

In the spectrum of NH_4CuSO_3 three out of the four vibrational fundamentals of the sulfite ion are observed. They are assigned by analogy with the

Can. J. Chem. Downloaded from www.nrcresearchpress.com by 210.87.254.105 on 09/05/12
For personal use only.

TABLE 3. Frequencies (cm^{-1}) and assignments of the main absorption bands in the ir spectra of undeuterated NH_4SnF_3 and NH_4CuSO_3

Assignment	Frequency			
	NH_4SnF_3		NH_4CuSO_3	
	10 K	293 K	10 K	293 K
	NH_4^+ ion			
Axial NH stretching	3290(2)	[3230]*	3325(1)	3296(2)
Nonaxial NH stretching	3207(2)	3180(5)	3160(2)	3140(20)
	3162(2)		3120(2)	
	3125(2)†		3070(2)	
	2980(20)	3020(5)	2972(1)	3000(5)
	2918(3)		2940(2)	
	2880(1)‡		2880(2)	
	2855(2)	2860(5)	2815(2)	2810(5)
Combination modes $\nu_2 + \nu_6$	2168(2)	2150(15)		
	2042(3)	2070(15)	2077(2)	
	1913(1)§		1993(1)§	
Combination modes $\nu_4 + \nu_6$	1845(3)	1880(15)	1927(2)	1940(15)
	1817(3)		1875(2)	1870(10)
	1796(2)	1800(10)	1799(1)	1780(10)
NH bending, ν_2	1706(1)	1695(3)	1686(1)	1680(2)
NH bending, ν_4	1448(3)	1440(3)	1488(1)	1470(1)
	1437(1)	1415(3)	1392(1)	1385(1)
	SnF_3^- and SO_3^{2-} ions			
$\nu_3(E)$	489(1)	478(3)	963(3)	962(3)
	466(2)			
$\nu_2(A_1)$			668(1)	665(1)
$\nu_4(E)$			493(1)	490(1)

*Estimated value; band obscured by nonaxial NH stretching.
†Minimum probably corresponding to an "Evans hole".
‡"Evans hole".
§The assignment of the 1913 and 1993 cm^{-1} bands to $\nu_2 + \nu_6$ is tentative.

TABLE 4. Peak frequencies and halfwidths (cm^{-1}) of the NH_3D^+ probe ion in $(NH_4)_2SiF_6$ and $(NH_4)_2SnCl_6$ at different temperatures

T (K)	$(NH_4)_2SiF_6$				$(NH_4)_2SnCl_6$			
	ν_1	$\Delta\nu_{1/2}$	ν_{4bc}	$\Delta\nu_{1/2}$	ν_1	$\Delta\nu_{1/2}$	ν_{4bc}	$\Delta\nu_{1/2}$
10	2443(2)	3(1)	1261(1)	4(1)	2376(3)	4(2)	1244(2)	9(2)
75	2439(1)	5(1)	1263(1)	5(1)	2375(1)	5(1)	1245(2)	9(2)
150	2434(1)	7(1)	1265(1)	6(1)	2374(1)	8(1)	1245(1)	10(1)
225	2430(1)	12(1)	1266(1)	10(1)	2373(2)	14(2)	1245(1)	13(1)
293	2427(2)	25(2)	1267(1)	14(2)	2373(3)	19(3)	1246(1)	16(2)

spectra of other solid sulfites (cf. Table 6.32 of ref. 19). The remaining fundamental, the symmetric stretching vibration $\nu_1(A_1)$, is only weakly ir-active in a flat pyramidal SO_3^{2-} ion; the corresponding absorption band is probably obscured by the broad and intense band due to the degenerate stretching vibration $\nu_3(E)$.

NH_4SnF_3 and NH_4CuSO_3: Effect of Temperature on Frequencies

The ν_{4bc} component frequencies vary only slightly over the range of temperatures investigated: in NH_4SnF_3 they decrease by 2 cm^{-1} and in NH_4CuSO_3 by 5–7 cm^{-1} when the temperature is raised from 10 to 293 K. By contrast, the variation of the ν_1 frequencies in both compounds is not only pronounced (Figs. 4–6) but the ν_1(a) and ν_1(n) frequencies vary in *opposite directions*. As the temperature increases, ν_1(a) shifts to lower and ν_1(n) to higher frequencies. The decrease of the ν_1(a) frequency is roughly three times as great as the increase of the ν_1(n) frequency, so that the mean frequency (weighted in the 1:3 ratio of the axial to nonaxial hydrogens) remains nearly stationary with

Can. J. Chem. Downloaded from www.nrcresearchpress.com by 210.87.254.105 on 09/05/12
For personal use only.

Can. J. Chem. Downloaded from www.nrcresearchpress.com by 210.87.254.105 on 09/05/12
For personal use only.

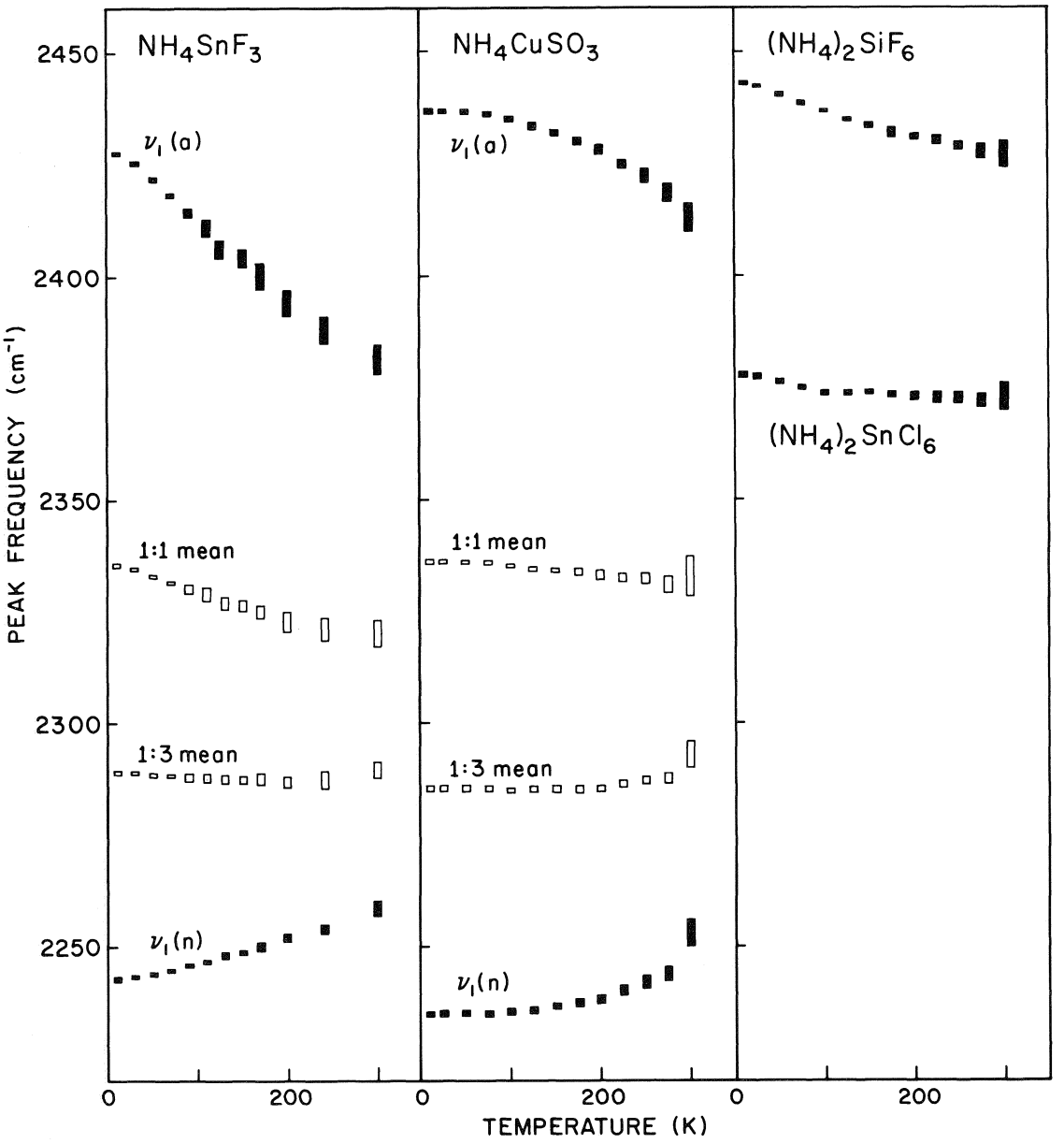


FIG. 6. Temperature variation of the ν_1(a) and ν_1(n) frequencies in NH_4SnF_3 and NH_4CuSO_3, compared with that of ν_1 in $(NH_4)_2SiF_6$ and $(NH_4)_2SnCl_6$.

temperature (Fig. 6). The range of variation of the ν_1(a) frequency in the fluoride in the 10–293 K range interval is 46 cm^{-1}, i.e. about 20% of the total ν_1 frequency range for ammonium halides (cf. ref. 1), and approximately twice as large as the corresponding range of variation in the sulfite. Furthermore, the decrease of the ν_1(a) frequency in NH_4SnF_3 begins to be appreciable at a much lower temperature than in NH_4CuSO_3.

Parallel shifts of frequency with temperature are observed for the NH stretching bands in the spectra of the undeuterated compounds. In the fluoride, cooling in fact shifts the axial frequency sufficiently away from the nonaxial frequency region to cause the axial vibration to uncouple from the nonaxial NH vibrations and the corresponding absorption band to become resolved (Fig. 3).

NH_4SnF_3 and NH_4CuSO_3: Effect of Temperature on Bandwidths

The halfwidths of the ν_1(n) absorptions in both compounds and of ν_1(a) in the sulfite remain nearly

Can. J. Chem. Downloaded from www.nrcresearchpress.com by 210.87.254.105 on 09/05/12
For personal use only.

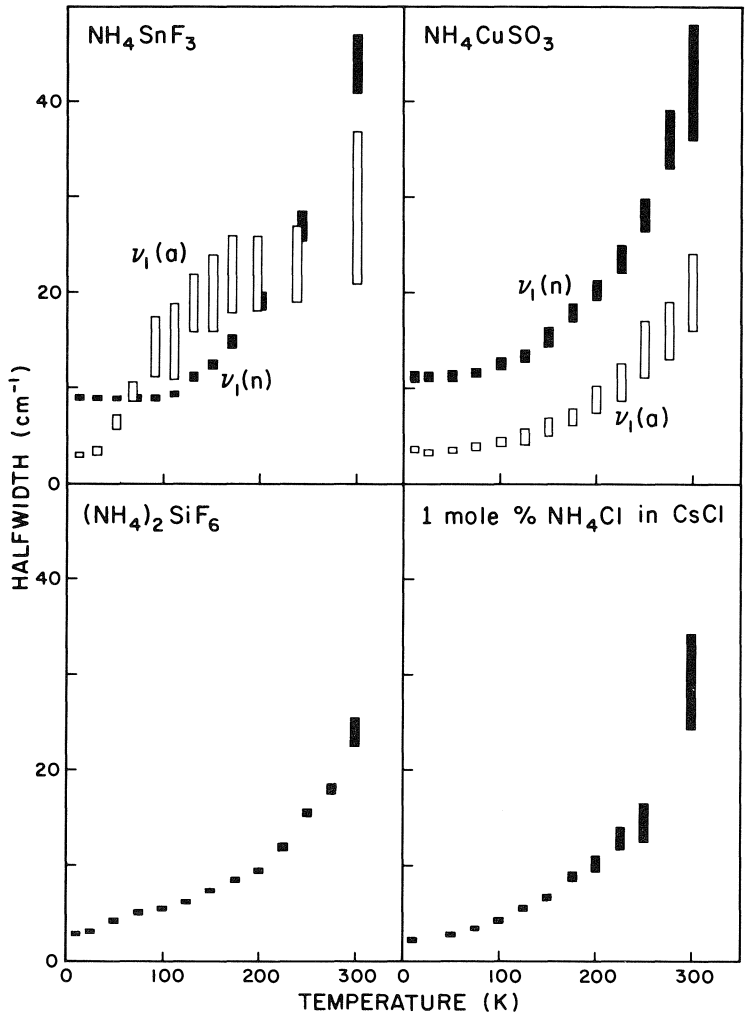


FIG. 7. Temperature variation of the halfwidths of the ν_1(a) and ν_1(n) absorption bands in NH_4SnF_3 and NH_4CuSO_3, compared with that of the halfwidth of the ν_1 absorption in $(NH_4)_2SiF_6$ and in a solid solution of NH_4Cl in CsCl.

constant up to about 100 K, after which they begin to increase at a progressively higher rate (Fig. 7). In this they resemble the ν_1 halfwidths in crystals containing NH_4^+ ions with four equivalent, normal (i.e. straight) N—H···X bonds and free from low-temperature transitions, such as NH_4F and solid solutions of NH_4Cl in CsCl at low ammonium concentrations (included in Fig. 7 for comparison).[6] However, the ν_1(a) halfwidth of NH_4SnF_3 follows an unusual pattern, with a steep initial increase at very low temperatures (about 30 K) and slowing down above 150 K. In both compounds the halfwidth of ν_1(n) at 10 K (the "residual" halfwidth) is greater than that of ν_1(a), the latter not exceeding 3 cm^{-1}.

[6]A detailed account of our study of NH_4F and of the "double-dilution" experiments on NH_4^+ dispersed in alkali halide matrices is scheduled to appear later in this series.

$(NH_4)_2SiF_6$ and $(NH_4)_2SnCl_6$

The N atoms in both compounds are at sites of symmetry T_d over the entire temperature range of our study, hence a single ν_1 and a single ν_{4bc} absorption bands are expected and observed. The peak frequencies and halfwidths of these bands are recorded in Table 4 and their variation with temperature is compared with that of NH_4SnF_3 and NH_4CuSO_3 in Figs. 6 and 7.

The ν_1 frequency in $(NH_4)_2SnCl_6$ is appreciably lower than in $(NH_4)_2SiF_6$. This is a consequence of the volume effect (1) and not an indication of a strengthening of the hydrogen-bonding interaction. On the contrary, as pointed out above, the temperature dependence of the intensity of combination bands involving the librational fundamental $\nu_6(NH_4^+)$ shows that hydrogen bonding is much weaker in the chlorostannate.

Can. J. Chem. Downloaded from www.nrcresearchpress.com by 210.87.254.105 on 09/05/12
For personal use only.

Discussion

The surprising feature of the ν_1 absorption in NH_4SnF_3 and NH_4CuSO_3 is not that it is a doublet, for this is expected from the trigonal site symmetry of the ammonium ion, but the magnitude of the splitting, the difference between the $\nu_1(a)$ and $\nu_1(n)$ frequencies at 10 K being 202 cm^{-1} for the sulfite and 184 cm^{-1} for the fluoride. When these frequency differences, which are the largest on record for ammonium compounds, are compared to the ν_1 (80 K) frequencies observed in a variety of ammonium halides (1), it is found that they amount to 70–80% of the total ν_1 range bounded by the ν_1 values in NH_4F and NH_4BF_4. The magnitude of the splitting clearly indicates that the hydrogen-bonding interactions involving the three H_n are much stronger than that involving H_a, i.e. the hydrogen atom in trifurcated acceptor geometry.

However, even more remarkable is the temperature variation of the $\nu_1(a)$ and $\nu_1(n)$ frequencies, which is both pronounced and in opposite directions (Fig. 6). This is unlike in any ammonium compounds for which a detailed temperature study has been reported to date. The increase in the ν_1 frequency of normal N—H···X bonds, in the absence of phase transitions, may be as low as 2 cm^{-1} from 10 to 293 K, as exemplified by the ammonium ion dispersed at low concentrations in CsCl and CsBr matrices[6] (cf. also ref. 1). By contrast, the corresponding shift, to *lower* frequencies, of $\nu_1(a)$ with increasing temperature is 46 cm^{-1} in NH_4SnF_3 and 22 cm^{-1} in NH_4CuSO_3. For $\nu_1(n)$ the shifts, to *higher* frequencies, are less dramatic but at least comparable with those encountered for other straight N—H···X bonds (9) and several times the value in CsCl and CsBr matrices.

These observations make it difficult to avoid the conclusion that the effect of increased temperature is to *weaken* the strong N—H_n···X bonds (the normal expectation) and simultaneously to *strengthen* the weak hydrogen-bonding interactions involving the axial hydrogen. The near constancy of the $\nu_1(a)$, $\nu_1(n)$ mean (Fig. 6) implies that the *overall* hydrogen-bonding strength of the ion changes little with temperature and in this resembles the behaviour of the ion in the matrices.

The strengthening of the interaction of H_a with the three equidistant acceptor atoms can be explained, qualitatively, by an increase in the amplitude of the motions of the ammonium ion with temperature. The motions likely to be involved would be largely low-frequency, librational motions; internal (bending) motion may participate. As the amplitude increases, H_a is brought closer to its acceptor neighbours, the NH_aX angle increases, and the N—H_a···X geometry begins to assume increasingly the character of a straight hydrogen bond. The larger the amplitude, the greater the anharmonicity of the motion of H_a as a result of the correspondingly reduced H_a ···X distance. Conversely, at very low temperatures H_a will remain on or close to the threefold axis, and in such circumstances the N—H_a bond must be viewed as forming a true *symmetrically trifurcated* hydrogen bond.

A similar situation is obtained in $(NH_4)_2SiF_6$, with the difference that in this crystal none of the four equivalent hydrogens of the ammonium ion engages in a normal hydrogen bond. The decrease in the frequency of the unique ν_1 absorption is 16 cm^{-1} from 10 to 293 K, i.e. only about one third of the decrease in $\nu_1(a)$ in NH_4SnF_3. There is little doubt that the frequency decrease in the hexafluorosilicate is attributable to the same cause as the decrease in $\nu_1(a)$ in NH_4SnF_3 and NH_4CuSO_3.

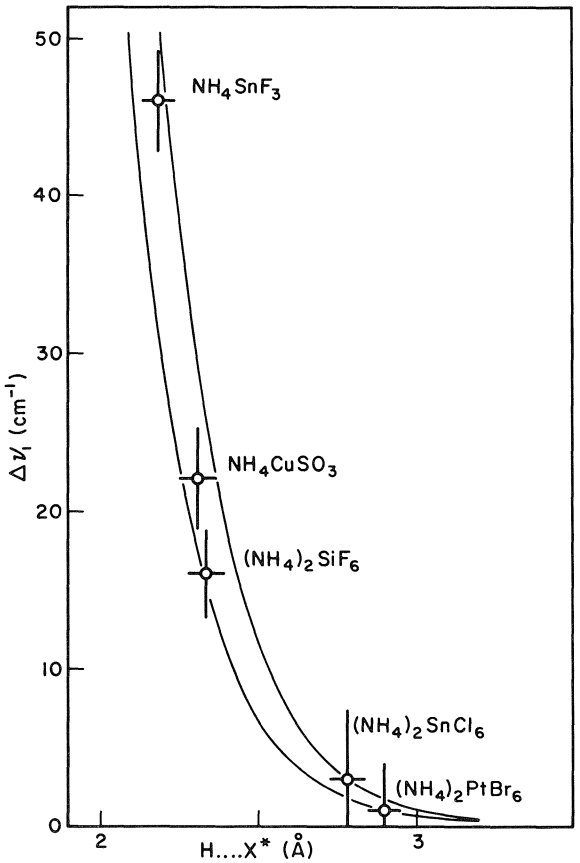


FIG. 8. Variation of $\Delta\nu_1 = \nu_1(10\text{ K}) - \nu_1(293\text{ K})$ with the H···X* distance corresponding to symmetric trifurcation. For NH_4SnF_3 and NH_4CuSO_3, $\nu_1 = \nu_1(a)$. The $\pm 1\sigma$ limits of the regression are shown.

Can. J. Chem. Downloaded from www.nrcresearchpress.com by 210.87.254.105 on 09/05/12
For personal use only.

However, in $(NH_4)_2SiF_6$ the ammonium ion is not anchored by strong normal hydrogen bonds. This and the cubic site symmetry must impart a different character to the thermal behaviour of the motions responsible for bringing the H atom closer to the F acceptors.

Although the structural situations in $(NH_4)_2SiF_6$ and $(NH_4)_2SnCl_6$ are completely analogous, the ν_1 frequency in the chloride decreases much less with increasing temperature than does the corresponding frequency in the fluoride; moreover, in the isostructural $(NH_4)_2PtBr_6$ it is known (9) to vary by only 1 cm^{-1} or less over the entire 10–293 K range. This supports the model proposed above for the response of a trifurcated hydrogen bond to temperature variation and shows the importance of the acceptor strength of the halogen atoms in the three compounds.[7] Raising the temperature of the three crystals by the same amount will, roughly speaking, cause the N—H bond to pivot about N by a comparable angle (and in any event by an angle which is not smaller in the chloride than in the fluoride), but as Cl is a weaker acceptor than F, the effect on ν_1 of the closer approach of the H atom to X will be considerably less in the chloride and even smaller in the bromide. Since the acceptor strength of X cannot be divorced from the effective size of X (and thus from the H···X* distance),[8] this means that decreasing the H···X distance by a certain amount produces a larger decrease in ν_1 when H···X is short than when it is long. When the $\Delta\nu_1 = \nu_1(10\text{ K}) - \nu_1(293\text{ K})$ values for the five compounds are regressed logarithmically on H···X* (Fig. 8), ln $\Delta\nu_1$ is found to be highly correlated with H···X*:

$$\ln \Delta\nu_1 = 14.41 - 4.89(\text{H}\cdots\text{X}^*)$$
$$r^2 = 0.98, \sigma = 0.27$$

i.e. $\Delta\nu_1$ can be approximated by a simple exponential function of the structural parameter H···X*. This is remarkable when one keeps in mind the various uncertainties involved and the structural dissimilarities, and considering the arbitrary choice of the temperature difference. It is possible that $\nu_1(10\text{ K})$ and $\nu_1(293\text{ K})$ in fact approximate, respectively, the "low-temperature" and the "high-temperature" limits of ν_1 and that the regression has a deeper meaning. The correlation is not very different when NH_4CuSO_3 is left out. Perhaps the reason that the sulfite is satisfactorily accommodated by the regression is the similarity of the formal charge on the oxygen of SO_3^{2-} and the fluorine of SnF_3^-.

We feel unable to discuss at present why the details of the temperature dependence of ν_1(a) and ν_1(n) are different in NH_4SnF_3 and NH_4CuSO_3. Apart from the obvious difference in the number of acceptors involved in the N—H_n···X bonds the structural situation is very similar in the two compounds.

The bandwidths at 10 K of the ν_1 absorptions corresponding to the trifurcated hydrogen bonds are comparable in all four compounds, not exceeding about 3 cm^{-1} (Fig. 7). The ν_1(n) absorptions in both NH_4SnF_3 and NH_4CuSO_3, however, have 10 K halfwidths about three times those of the respective ν_1(a) absorptions. The reason for this is not clear. On one hand we have the observation that the stronger the hydrogen-bonding interaction, the greater the halfwidth (as in ascorbic acid, ref. 16). On the other hand, the very strong hydrogen bonds in NH_4F have ν_1 halfwidths that at 10 K do not exceed 5 cm^{-1}.[6]

With the exception of ν_1(a) of NH_4SnF_3 the halfwidths of the ν_1 absorptions in all four compounds increase with temperature in a similar manner. The temperature dependence of these bandwidths cannot be very sensitive to the structure and chemistry of the individual crystal, as NH_4F and solid solutions of NH_4Cl in CsCl (Fig. 7) and of NH_4Br in CsBr behave in much the same way,[6] although the coordination of the ammonium ion and the hydrogen-bond strengths differ widely in these various cases. In view of this insensitivity the complex shape of the temperature dependence of the ν_1(a) halfwidth in NH_4SnF_3 is the more puzzling.

Conclusions

The most important conclusion from the present study of NH_4SnF_3, NH_4CuSO_3, cubic $(NH_4)_2SiF_6$, and $(NH_4)_2SnCl_6$ can be formulated as follows:

Where the geometry of the crystal structure of an ammonium compound provides an opportunity for the existence of a symmetrically trifurcated N—H···3X hydrogen bond, such a bond is likely to occur if the temperature is sufficiently low. With increasing temperature the strength of this bond will *increase*, but at the same time the bond will lose its symmetric trifurcation, the H atom will become progressively more associated with *one* acceptor

[7]The difference in the atomic mass of X undoubtedly plays a role in the lattice dynamics of the three crystals and may provide an additional contribution toward a strengthening of the H···X interaction in the fluoride.

[8]The H···X* distance is that between the H atom at rest on the C_3 axis and the acceptor atom X, i.e. corresponding to a symmetrically trifurcated bond. It depends on the metric properties of the crystal structure and varies from compound to compound. It should not be confused with the instantaneous H···X distance in a *particular* compound which varies with the amplitude of thermal motion of the axial hydrogen and hence with temperature.

atom at a time, and the hydrogen bond will acquire a more pronounced dynamic character.

Evidence for this conclusion is found in the decreasing frequency of the appropriate component of the ND stretching absorption ν_1 of the NH_3D^+ probe ion in the ir spectra of the four compounds as the temperature is raised from 10 to 293 K; in favourable circumstances the corresponding NH absorption in the spectrum of an undeuterated compound is resolved and a parallel frequency decrease is observable. In this respect the behaviour of the four compounds is quite similar, the main difference being in the magnitude of the frequency decrease. The magnitude appears to correlate with H···X*, the H···X distance for H in the symmetrically trifurcated position: the difference $\nu_1(10\ K) - \nu_1(293\ K)$ increases quasi-exponentially with decreasing H···X*. In contrast, the frequency of the ND stretching absorption corresponding to a *normal* N—H···X bond increases with temperature. The direction of the temperature variation, i.e. the sign of $d\nu_1/dT$, thus provides a diagnostic criterion for distinguishing between symmetrically trifurcated and normal N—H···X bonds.

Acknowledgments

We wish to thank Dr. T. S. Cameron for advice and assistance with the execution of the crystallographic study. This work was supported by a research grant from the National Research Council of Canada to one of us (O.K.).

1. O. KNOP, I. A. OXTON, and M. FALK. Can. J. Chem. **57**, 404 (1979).
2. E. O. SCHLEMPER, W. C. HAMILTON, and J. J. RUSH. J. Chem. Phys. **44**, 2499 (1966).
3. R. S. SEYMOUR and A. W. PRYOR. Acta Crystallogr. B**26**, 1487 (1970).
4. I. A. OXTON, O. KNOP, and M. FALK. J. Phys. Chem. **80**, 1212 (1976).
5. B. NYBERG and P. KIERKEGAARD. Acta Chem. Scand. **22**, 581 (1968).
6. G. BERGERHOFF and H. NAMGUNG. Acta Crystallogr. B**34**, 699 (1978).
7. O. KNOP, I. A. OXTON, and M. FALK. Can. J. Chem. **57**, 2003 (1979).
8. I. A. OXTON, O. KNOP, and M. FALK. Can. J. Chem. **53**, 2675 (1975).
9. O. KNOP, I. A. OXTON, W. J. WESTERHAUS, and M. FALK. To be published.
10. J. D. DONALDSON and J. D. O'DONOGHUE. J. Chem. Soc. 271 (1964).
11. L. RAMBERG. Z. Phys. Chem. **69**, 512 (1909).
12. R. A. NYQUIST and R. O. KAGEL. Infrared spectra of inorganic compounds. Academic Press, New York and London. 1971.
13. R. PROST. Clays Clay Miner. **21**, 363 (1973).
14. D. T. CROMER and J. B. MANN. Acta Crystallogr. A**24**, 321 (1968).
15. G. SHELDRICK. X-ray system report. University Chemical Laboratory, Lensfield Road, Cambridge, England. 1976.
16. M. FALK and M. WÓJCIK. Spectrochim. Acta, **35A**, 1117 (1979).
17. J. C. EVANS. Spectrochim. Acta, **16**, 994 (1960); **18**, 507 (1962).
18. D. A. OTHEN, O. KNOP, and M. FALK. Can. J. Chem. **53**, 3837 (1975).
19. S. D. Ross. Inorganic infrared and Raman spectra. McGraw-Hill, London. 1972.

Can. J. Chem. Downloaded from www.nrcresearchpress.com by 210.87.254.105 on 09/05/12
For personal use only.

The trifluoroacetic acid solvent system. Part VI. Density measurements

JOHN B. MILNE

Department of Chemistry, University of Ottawa, Ottawa, Ont., Canada K1N 9B4

Received July 25, 1979

JOHN B. MILNE. Can. J. Chem. **58**, 283 (1980).

The densities of solutions of several 1:1 trifluoroacetate electrolytes have been measured in 100% trifluoroacetic acid (HOTFA) and apparent molar volumes for their ion pairs have been determined. The density measurements coupled with limiting equivalent conductivities and dissociation constants, calculated by means of the Fuoss–Hsia equation, permit a more precise treatment of the conductivities of solutions at concentrations where the equivalent conductivity minimum occurs. The existence of triple ions in this solvent is not required to account for the conductivity minimum.

JOHN B. MILNE. Can. J. Chem. **58**, 283 (1980).

On a mesuré les densités de différents électrolytes de type trifluoroacétate 1:1 en solution dans l'acide trifluoroacétique pur (ATFA) et on a déterminé les volumes molaires apparents de leurs paires d'ions. Les mesures de densité utilisées conjointement avec les conductivités équivalentes limites et les constantes de dissociation, calculées au moyen de l'équation de Fuoss-Hsia permettent un traitement plus précis des conductivités des solutions à des concentrations où on atteint la conductivité minimum.

Il n'est pas nécessaire de faire appel à l'existence d'ions triples dans ce solvant, pour expliquer la conductivité minimum.

[Traduit par le journal]

Can. J. Chem. Downloaded from www.nrcresearchpress.com by 210.87.254.5 on 09/05/12
For personal use only.

Introduction

For many solvents with dielectric constant less than 20, a plot of equivalent conductivity against concentration exhibits a minimum and this behaviour has been attributed to the formation of triple ions (1). Trifluoroacetic acid, with a dielectric constant of 8.4, shows this type of plot. This behaviour was explained originally in terms of triple ions (2). However, in view of cryoscopic results, this interpretation was later shown to be doubtful (3). A thorough reconsideration of the electrical conductivity work in the light of this finding required the measurement of the densities of the electrolyte solutions, since the solutions in the original work (3, 4) were made up in molal terms and converted to molar concentrations, using the density of the pure acid. This work concerns the measurement of the density of electrolyte solutions in trifluoroacetic acid, their use in improving the electrical conductivity results reported, and some discussion of the solvation properties of the solvent.

Experimental

Trifluoroacetic acid (Halocarbon) was purified and handled as described earlier (4) but without the addition of small amounts of trifluoroacetic anhydride. Similarily, the alkali metal and ammonium trifluoroacetates were prepared as described in ref. 4. Silver trifluoroacetate was crystallized from an equimolar mixture of silver carbonate (Fisher) and aqueous trifluoroacetic acid. The solution was protected from light during preparation. The tetramethyl- and tetraethylammonium trifluoroacetates were prepared by neutralization of an aqueous quaternary ammonium hydroxide solution (Eastman) with trifluoroacetic acid. The tetra-*n*-propyl- and tetra-*n*-butylammonium trifluoroacetates were made by a metathetic reaction of the quaternary ammonium bromide (Eastman) and silver trifluoroacetate in aqueous solution. The crude quaternary ammonium trifluoroacetates were recrystallized from ethanol (Me_4NOTFA), 3:1 benzene/ethanol (Et_4NOTFA), and propanol (n-Pr_4NOTFA and n-Bu_4NOTFA). Compositions were confirmed by C and H analysis as determined by Chemalytics Inc.

Densities were determined using an Anton Paar Digital Density Meter, Model DMA 40, calibrated with air and distilled water. A glove bag was attached to the inlet port of the meter and all transfers were made under dry conditions. Temperature was controlled at 25.00 ± 0.01°C. As a check on the accuracy of the density meter, the densities of pure acetonitrile and carbon tetrachloride were measured and found to be 0.7767 and 1.5844 g cm^{-3} respectively. Literature values for these solvents are 0.7766 and 1.58439 g cm^{-3} respectively (5). The precision of the DMA 40 Digital Density Meter is stated by the manufacturer to be 1×10^{-4} g cm^{-3} (6). The error given for the densities reported here is the average deviation and is based upon reproducibility for separate runs on the same compound.

Results and Discussion

Densities

The density of pure HOTFA at 25°C was 1.4774 ± 0.0001 g cm^{-3} and that at 0.00°C was 1.5353 ± 0.0001 g cm^{-3}. The density of pure acid at 25°C has been reported, ranging from 1.477 to 1.4885 g cm^{-3} (7). The densities of HOTFA solutions of lithium, sodium, potassium, cesium, silver, ammonium, and quaternary ammonium (R = Me, Et, n-Pr, and n-Bu) trifluoroacetates, each over the concentration range 0.015 to 0.200 molal at an average of 5 concentrations were measured at 25.00°C. The densities of lithium and ammonium trifluoroacetates were measured at 0.00°C also.[1] Apparent

[1]A complete set of these data is available, at a nominal charge, from the Depository of Unpublished Data, CISTI, National Research Council of Canada, Ottawa, Ont., Canada K1A 0S2.

0008-4042/80/030283-04$01.00/0

©1980 National Research Council of Canada/Conseil national de recherches du Canada

TABLE 1. Apparent molar volumes of 1:1 ionic trifluoroacetates

Solute	Temperature (°C)	ϕ_v ($cm^3\ mol^{-1}$)	No. of measurements	$10^3\ \alpha$ at 0.05 *M*
LiOTFA	25	54±1	6	—
NaOTFA	25	54±1	5	0.0051
KOTFA	25	49±1	5	0.0082
CsOTFA	25	87±1	5	0.0117
AgOTFA	25	70	2	—
NH_4OTFA	25	52	5	0.0093
Me_4NOTFA	25	101±2	8	0.0346
Et_4NOTFA	25	161±4	6	0.0462
n-Pr_4NOTFA	25	239±1	5	0.0560
n-Bu_4NOTFA	25	313±3	5	0.0633
LiOTFA	0	56	5	—
NH_4OTFA	0	65	6	—

molar volumes, ϕ_v, were calculated in the usual way (8) for each concentration. The average values of ϕ_v for each electrolyte, the average deviation, and the number of measurements are listed in Table 1. The ϕ_v showed little variation with concentration as indicated by the average deviations and the variation was essentially random although the deviations in ϕ_v appeared to be negative for the small, and positive for the large cations. The solutes studied exist predominantly as ion pairs in the concentration range studied as indicated by the degree of dissociation, α, at 0.05 *M* listed in Table 1. The α were calculated from ion pair dissociation constants, given below, except in the case of the quaternary ammonium trifluoroacetates, where K_d was estimated, using the Fuoss equation (9), from the sum of cation radii, as determined from ionic volumes for these cations in water (10), and the average trifluoroacetate anion contact radius (r = 3.48 Å) as estimated from the distance of closest approach for alkali metal trifluoroacetates, a_0, and the Pauling ionic radius of the alkali metal cation.

The ion pair apparent molar volumes listed in Table 1 provide evidence for electrostriction of solvent in as much as HOTFA itself has a molar volume of 77.2 cm^3 while the volumes of LiOTFA, NaOTFA, and KOTFA are less than this. Another interesting result is the equivalent volumes for LiOTFA and NaOTFA followed by a monotonic increase up to *n*-Bu_4NOTFA. Similar behaviour is also observed in the case of individual ionic volumes measured in H_2O, MeOH, and EtOH (10). The near constancy of the ϕ_v for LiOTFA and NaOTFA in HOTFA may be due to the formation of a solvent cage determined principally by intersolvent molecule contacts. The increase in ϕ_v with increasing cation size, except for KOTFA, is apparently determined by increased bare cation size and decreased electrostriction. In the case of ϕ_v for ion pairs, three influences must be considered, (*a*) that of the cation, (*b*) that of the anion, and (*c*) that of each ion in the ion pair on its counter ion. Interionic effects may be the cause of the small values of ϕ_v for KOTFA and NH_4OTFA. The intensity of the positive charge in LiOTFA and NaOTFA may favour the simple cation – trifluoroacetate anion pair but where the positive field strength is less intense, as with KOTFA, NH_4OTFA, and the heavier homologues, the hydrogen bis(trifluoroacetate), $H(OTFA)_2^-$, may take part in the ion pair. The additional decrease in anion size due to hydrogen bonding to the solvent could account for the smaller ϕ_v values relative to those of LiOTFA and NaOTFA. Solids containing the $H(OTFA)_2^-$ anion are well documented (7). Further evidence that the nature of the anion changes as the cation is varied is found in the alteration of the least distance in the ion pair discussed below.

Electrical Conductivity

The limiting equivalent conductivities, Λ_0, and dissociation constants, K_d, for the alkali metal and ammonium trifluoroacetates were recalculated, using molar concentrations calculated from the molalities by means of the measured densities, instead of the density of pure acid (4). The results were not significantly different from those originally reported. The extrapolation was also carried out using the Fuoss–Hsia equation (11), which should yield better values for Λ_0 and K_d for use with the electrical conductivities in the so-called "triple ion" region of concentration (2–4). These values of Λ_0 and K_d are listed in Table 2. Although these values differ slightly from those reported earlier (the K_d are ca. 20% larger and the Λ_0, ca. 10% smaller than the previously reported results), the basic conclusions of the original work remain unaffected. It should, however, be noted that either solvation or solvent relaxation plays an important role, since the combined mobility of cation and

Can. J. Chem. Downloaded from www.nrcresearchpress.com by 210.87.254.5 on 09/05/12
For personal use only.

TABLE 2. Limiting equivalent conductivities and dissociation constants[a]

Compound	Λ_0[b] (ohm^{-1} equiv^{-1} cm^2)	r_{M^+}(Å) (crystal)	λ_0^+ (crystal) (ohm^{-1} equiv^{-1} cm^2)	$10^5 K_d$ (mol L^{-1})	a_0 (Å)[c]	Anion radius[d] (Å)
NaOTFA	62.8±0.1	0.95	107	0.053	4.12	3.17
KOTFA	55.3±0.4	1.33	76	0.290	4.74	3.41
RbOTFA	52.7±0.4	1.48	69	0.526	5.02	3.54
CsOTFA	47.8±0.3	1.69	60	1.22	5.47	3.78
NH_4OTFA	49.5±0.6	1.45	70	0.560	5.05	3.60

[a]Calculated by extrapolation of the Fuoss–Hsia equation (9).
[b]The error is the average deviation of the experimental points from the least-mean-squares fit to the data.
[c]Calculated from the Fuoss equation (6).
[d]$a_0 - r_{M^+}$.

trifluoroacetate anion (Λ_0) is smaller than that predicted for the cation alone from crystal ionic radii using Stokes' Law (λ_0^+) as shown in Table 2.

The variation in K_d with cation size is that expected for contact ion pairs (4) and the ion pair contact distances calculated by the Fuoss equation (9) approximate the sum of the ionic radii. Subtraction of the crystal radius of the cation from the contact distance should give the radius of the counter anion of the ion pair and this is listed for each solute in Table 2. Assuming that the $OTFA^-$ ion is the same size as the HOTFA molecule in the solvent (77.2 cm^3), $r(OTFA^-)$ is found to be 3.13 Å, while calculation of this radius from the density of NH_4OTFA (12) gives $r(OTFA^-) = 2.97$ Å. Estimation of $r(H(OTFA)_2^-)$, assuming the volume to be double that of HOTFA, gives 3.94 Å; calculation from the density of $K(H(OTFA)_2)$ (13) yields 3.59 Å. These estimates are close to the values for the anion radius calculated for the ion pairs and support the theory that the anion in the ion pair in the case of NaOTFA is the $OTFA^-$ anion but in the case of the larger cations, is the $H(OTFA)_2^-$ anion. This approach assumes, of course, that the anion is freely rotating in the ion pair, which may not be exactly true. Another possible explanation of the increase in anion radius with increasing cation size in the ion pair is the decrease in electrostatic compression on the anion as the positive field strength decreases. However, these effects are much smaller than the changes listed in Table 2, judging from the change in the size of the $H(OTFA)_2^-$ anion in the series $M(H(OTFA)_2)$ (M = K, Rb, and Cs) (13) and allowing for the Madelung effect in the crystalline solids. The $H(OTFA)_2^-$ anion radius increases from 3.59 to 3.70 Å on going from $K(H(OTFA)_2$ to $Cs(H(OTFA)_2)$ as calculated from molar volume of the crystal and cation size.

The limiting equivalent conductivities and dissociation constants were used in conjunction with the Fuoss–Hsia equation and an expression for the molar activity coefficient to explore the behaviour of Λ at higher concentrations ("triple ion region"). The degree of dissociation, α, was determined at each concentration by an iterative procedure from the equations:

$$K_d = c\, y_\pm^2\, \alpha^2/(1-\alpha)$$

$$y_\pm = (d_0/d)10^{-A\sqrt{c\alpha}/(1+Ba_0\sqrt{c\alpha})}$$

where c is molarity; $y_\pm$, the molar activity coefficient; d_0, the density of pure acid; d, the density of solution; a_0, the distance of closest approach calculated from K_d by the Fuoss expression (9); and A and B, constants defined in ref. 1, p. 230. The actual equivalent conductivity was then determined by

$$\Lambda = \alpha\Lambda'$$

where Λ', the equivalent conductivity corrected for ionic strength effects, was determined by the Fuoss–Hsia equation (11). A plot of the theoretical Λ vs. c is given in Fig. 1 along with the experimental points for NaOTFA, KOTFA, NH_4OTFA, and CsOTFA. It was found that the use of the more sophisticated expression for $y_\pm$ developed by Robinson and Stokes (ref. 1, p. 238), allowing for the effect of solvation on the activity coefficient, made virtually no change in the calculated values.

It may be seen from Fig. 1 that a minimum in Λ is expected from the theory without introducing triple ion equilibria (2). Cryoscopic results show that triple ions do not occur in the case of NaOTFA, KOTFA, and CsOTFA (3). The agreement between theory and experiment is quite good in the case of CsOTFA but becomes progressively poorer as the cation decreases in size. However, both the magnitude of Λ and the concentration at the minimum change as predicted by theory for the series of trifluoroacetates studied. It is interesting that LiOTFA has been shown to form triple ions and higher ion aggregates in propylene carbonate (14) and acetonitrile (15), both solvents of medium dielectric constant. The large discrepancy between

Can. J. Chem. Downloaded from www.nrcresearchpress.com by 210.87.254.5 on 09/05/12
For personal use only.

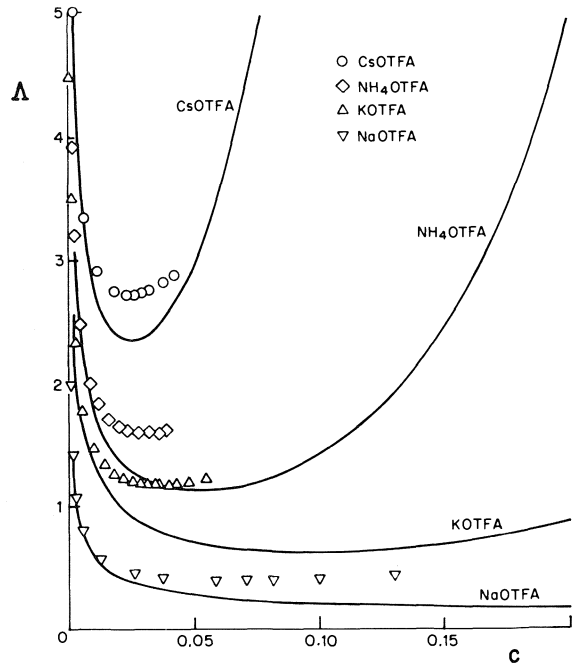


FIG. 1. Equivalent conductivity vs. molar concentration. The solid lines are calculated from theory; the points are experimental.

the minimum calculated for NaOTFA in HOTFA from theory (>0.25 *M*) and that observed (0.071 *M*) may be accounted for by the formation of triple ions.

The use of the measured densities in the calculation of freezing point depressions carried out in the cryoscopic study (3) has little effect on the conclusions of that work. The agreement of the calculation for the ion pair – simple ion model with the observed values is virtually unaffected while the agreement of the ion pair – simple and triple ions model with the measured values is worse.

Acknowledgement

The author thanks the National Research Council of Canada for financial support.

1. R. A. ROBINSON and R. H. STOKES. Electrolyte solutions. Butterworths, London. 1959. p. 402.
2. J. B. MILNE and M. G. HARRISS. Can. J. Chem. **50**, 3789 (1972).
3. J. B. MILNE and M. G. HARRISS. Can. J. Chem. **54**, 3031 (1976); **55**, 1592 (1977).
4. J. B. MILNE and M. G. HARRISS. Can. J. Chem. **49**, 1888 (1971).
5. J. A. RIDDICK and W. B. BUNGER. Organic solvents. *In* Techniques of chemistry. Vol. II. Wiley-Interscience, New York. 1970.
6. 'DMA-Digital Precision Density Meters', Anton Paar K. G., Graz, Austria.
7. J. B. MILNE. Trifluoroacetic acid. *In* The chemistry of non-aqueous solvents. Vol. VB. *Edited by* J. J. Lagowski. Academic Press, New York. 1978.
8. B. E. CONWAY, R. E. VERRALL, and J. E. DESNOYERS. Trans. Faraday Soc. **62**, 2738 (1966).
9. R. M. FUOSS. J. Am. Chem. Soc. **80**, 5059 (1958).
10. B. E. CONWAY. J. Solution Chem. **7**, 721 (1978) and references therein.
11. J. H. ROBERTS. Conductivity in non-aqueous solvents. *In* The chemistry of non-aqueous solvents. Vol. IV. *Edited by* J. J. Lagowski. Academic Press, New York. 1976. p. 9.
12. D. W. S. CRUICKSHANK, D. W. JONES, and G. WALKER. J. Chem. Soc. 1303 (1964).
13. L. GOLIC and J. C. SPEAKMAN. J. Chem. Soc. 2530 (1965).
14. M. L. JANSEN and H. L. YEAGER. J. Phys. Chem. **78**, 1380 (1974).
15. A. REGIS and J. CORSET. Chem. Phys. Lett. **32**, 462 (1975).

Can. J. Chem. Downloaded from www.nrcresearchpress.com by 210.87.254.5 on 09/05/12
For personal use only.

The solid phase synthesis of tertiary hydroxyesters from symmetrical diacid chlorides using organomanganese reagents[1,2]

CLIFFORD C. LEZNOFF AND VARDA YEDIDIA

Department of Chemistry, York University, Downsview, Ont., Canada M3J 1P3

Received July 30, 1979

CLIFFORD C. LEZNOFF and VARDA YEDIDIA. Can. J. Chem. **58**, 287 (1980).

A 1% crosslinked divinylbenzene–styrene copolymer, incorporating benzyl alcohol groups, was used to monoblock the symmetrical diacid chlorides, $ClOC(CH_2)_nCOCl$ (where $n = 4$ and 8). Further reaction of the polymer-bound monoester monoacid chloride with phenylmanganese iodide or butylmanganese iodide gave their respective polymer-bound tertiary hydroxyesters. Subsequent base cleavage and esterification yielded methyl 6-hydroxy-6,6-diphenylhexanoate, methyl 10-hydroxy-10,10-diphenyldecanoate, methyl 6-butyl-6-hydroxydecanoate, and methyl 10-butyl-10-hydroxytetradecanoate and some recovered dimethyl alkanoates. The reactions of some polymer-bound monoester monoacid chlorides with phenylcadmium chloride were also studied.

CLIFFORD C. LEZNOFF et VARDA YEDIDIA. Can. J. Chem. **58**, 287 (1980).

On a utilisé un copolymère styrène–divinylbenzène reticulé à 1% et contenant des groupes alcool benzylique pour bloquer une des fonctions des dichlorures de diacides symétriques $ClOC(CH_2)_nCOCl$ (où $n = 4$ et 8). La réaction de l'ester ainsi obtenu avec l'iodure de phénylmanganèse ou l'iodure de butylmanganèse conduit à leurs hydroxy-esters tertiaires respectifs fixés sur la résine. Le clivage subséquent par une base suivi d'une estérification conduit aux composés: hydroxy-6 diphényl-6,6 hexanoate de méthyle, hydroxy-10 diphényl-10,10 décanoate de méthyle, butyl-6 hydroxy-6 décanoate de méthyle et le butyl-10 hydroxy-10 tétradécanoate de méthyle et également à la récupération de quelques alkanoates de méthyle. On a également étudié les réactions de quelques monochlorures d'acides fixés sur la résine par une liaison ester avec le chlorure de phénylcadmium.

[Traduit par le journal]

Introduction

Tertiary hydroxyesters have been prepared before but in low yields and in multiple step reactions. Thus diethyl succinate reacted with benzophenone in a Stobbe condensation to give, after several further reactions, 4,4-diphenyl-γ-butyrolactone (5) useful against pathogenic viruses (6). Alternatively, reaction of succinic anhydride with phenylmagnesium bromide gave a mixture of products, one of which was 4-hydroxy-4,4-diphenylbutanoic acid (7).

It has been previously shown in our laboratory that insoluble polymer supports (8) can be used to monoprotect symmetrical diacid chlorides as the monoester monoacid chloride and several monoamide monoesters and primary hydroxyesters were prepared via solid phases (9, 10). In this paper we describe a general synthesis of hydroxyesters, disubstituted at the hydroxy position, from polymer-bound monoester monoacid chlorides.

Results and Discussion

The previously described (10) polymer-bound monoester monoacid chlorides (**1**) and (**2**), derived from adipyl and sebacyl chloride respectively, were treated in benzene at 0°C with an excess of phenylmanganese iodide (**3**) (11, 12) or butylmanganese iodide (**4**) (11, 12) in ether to give the polymer-bound tertiary hydroxyesters (**5–8**) respectively as shown in Scheme 1.

The infrared spectra of **5–8** exhibited strong absorptions at 1740 cm^{-1} and broad absorptions between 3200–3600 cm^{-1} indicative of ester and alcohol groups respectively. Cleavage of **5–8** with K_2CO_3 in methanol followed by esterification with diazomethane as previously described (10) yielded methyl 6,6-diphenyl-6-hydroxyhexanoate (**9**) (13), methyl 10,10-diphenyl-10-hydroxydecanoate (**10**), methyl 6-butyl-6-hydroxydecanoate (**11**), and methyl 10-butyl-10-hydroxytetradecanoate (**12**) respectively in good yield (Table 1). In addition, some dimethyl adipate (**13**) and dimethyl sebacate (**14**) were recovered from the reactions involving **1** and **2** respectively and separated from the products by preparative thin layer chromatography (tlc). The recovery of **13** and **14** is likely due to incomplete reaction of **1** and **2** with the organomanganese iodide reagents since our previous work (10) showed that most of the symmetrical diacid chlorides were monobound to the polymer although some double-binding of the diacid chlorides cannot be completely dismissed at this time (8, 14). The polymer itself was recovered as polymer-bound benzyl alcohol (**15**) and is recyclable by simple standard washing procedures as the organo-

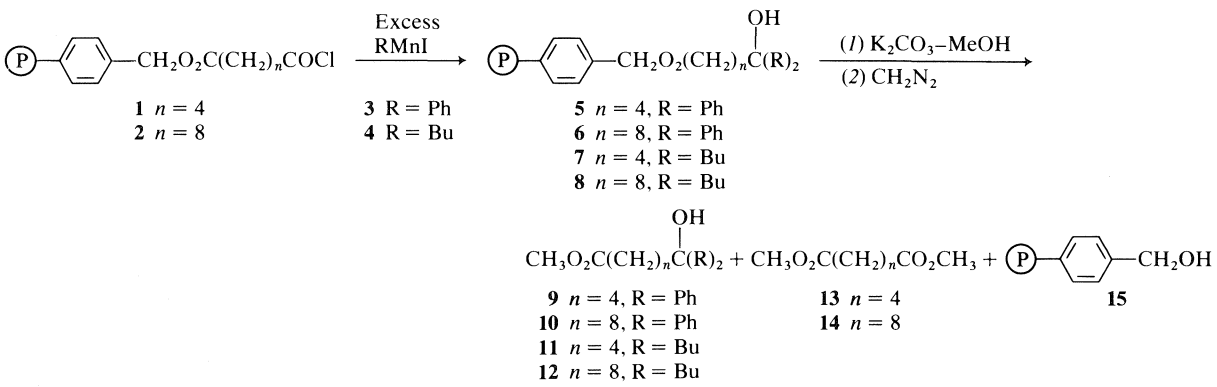
[1]The use of polymer supports in organic synthesis. Part XXI. For parts XX, XIX, XVIII, and XVII, see refs. 1–4 respectively.

[2]Presented, in part, at the 61st Annual Conference of the Chemical Institute of Canada, Winnipeg, Man., Canada, June 1978.

0008-4042/80/030287-04$01.00/0

©1980 National Research Council of Canada/Conseil national de recherches du Canada

Can. J. Chem. Downloaded from www.nrcresearchpress.com by 210.87.254.105 on 09/05/12
For personal use only.



SCHEME 1

TABLE 1. Yields of tertiary hydroxyesters **9–12** recovered from cleavage of polymers **5–8**

Tertiary hydroxy-ester	Loading capacity of **15** quantity of **13** and **14** per gram of **15**[a]		Recovered products quantity of **9–12** per gram of **15**[b]		Recovered diester quantity of **13** and **14** per gram of **15**[c]		Overall yield[d] (%)	Conversion[e] (%)
	(mg/g)	(mmol/g)	(mg/g)	(mmol/g)	(mg/g)	(mmol/g)		
9	72.0	0.41	104	0.35	7.0	0.04	85	94
10	126.5	0.55	69.7	0.27	21.7	0.09	49	59
11	73.1	0.42	69.3	0.27	18.3	0.105	64	84
12	121.9	0.53	77.3	0.26	27.3	0.12	49	63

[a]Obtained from cleavage of polymer-bound corresponding monoester monoacids.
[b]Obtained from cleavage of **5–8** respectively.
[c]Yields of dimethylesters recovered from the reaction mixture after cleavage of polymer-bound tertiary hydroxyesters.
[d]Yield of tertiary hydroxyesters compared to acid chloride initially bound to polymer.
[e]Yield of tertiary hydroxyester if the recovered dimethylester is recycled.

manganese and organocadmium reagents leave no insoluble impurities. The loading capacities of **1** and **2** were determined as previously described (10) and are given in Table 1. The spectroscopic and physical data of **9–12** are entirely consistent with the assigned structures and are given in the Experimental.

It should be noted that organomanganese iodide reagents were initially introduced as reacting selectively with acid chlorides to give ketones (11). It was later shown, however, that organomanganese iodide reagents do react with ketones albeit more slowly, but not at all with esters (12). Thus the syntheses of **5–8** utilized this selectivity for the first time so that the free acid chloride in the presence of an ester can react with two equivalents of **3** or **4** to give exclusively the tertiary hydroxyesters. The previously reported (13) synthesis of **5**, for example, was accomplished in 5 steps in ~20% overall yield from dimethyl adipate, compared to our 4-step synthesis in 85% yield (Table 1).

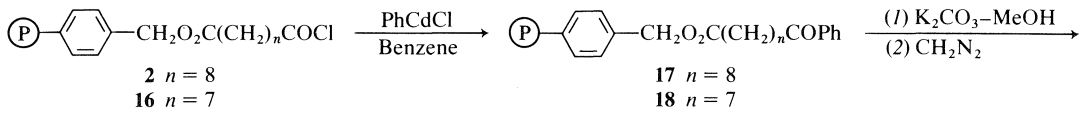
The possibility of preparing tertiary hydroxyesters with different substituents on the tertiary hydroxy carbon atom was then explored. Treatment of a polymer-bound monoester monoacid chloride (**16**) derived from azeloyl chloride with phenyl cadmium chloride (15) in benzene at 0°C yielded the polymer-bound keto esters **17** and **18** as shown in Scheme 2.

Cleavage and esterification of **17** and **18** as above gave methyl 10-oxo-10-phenyldecanoate (**19**) and methyl 9-oxo-9-phenylnonanoate (**20**) respectively. Unfortunately, **19** was contaminated with **13**, and **20** with dimethyl azelate (**21**), and in these cases the keto esters could not be readily separated from their respective diester precursors even by preparative tlc. The yields of **19** and **20** in the mixture obtained from the phenyl cadmium chloride reaction were estimated from the nmr spectrum of the fraction containing **19** and **13**, and **20** and **21**, respectively. Although a few attempts were made to synthesize unsymmetrical tertiary hydroxyesters by reaction of **18** with butylmanganese iodide, inseparable mixtures of products were obtained.

Conclusions

Hydroxyesters, symmetrically disubstituted at the carbon atom bearing the alcohol group, have been selectively prepared in good yield in a single key step from polymer-bound monoester monoacid chlorides. We have confirmed that the recently

Can. J. Chem. Downloaded from www.nrcresearchpress.com by 210.87.254.105 on 09/05/12
For personal use only.



2 $n = 8$
16 $n = 7$

17 $n = 8$
18 $n = 7$

$CH_3O_2C(CH_2)_nCOPh + CH_3O_2C(CH_2)_nCO_2CH_3$ + **15**

19 $n = 8$ **14** $n = 8$
20 $n = 7$ **21** $n = 7$

SCHEME 2

described organomanganese iodide and organocadmium chloride reagents are easy to prepare, easy to use, give no sludges during or on completion of the reaction and should find wide use in synthetic organic chemistry. Since these reagents leave no residues as can occur with some organocopper reagents (16), they are particularly useful in conjunction with organic syntheses on solid phases.

Experimental

A chloromethylated 1% divinylbenzene (DVB)–styrene copolymer, containing 1.09 mequiv. Cl/g of resin, obtained from Sigma Chemical Company was used as the starting resin in all resin transformations. Filtration was done under vacuum using sintered glass Büchner funnels. Suspensions and solutions were stirred using magnetic stirrers. Matheson high purity argon was used to maintain inert atmosphere conditions. Infrared (ir) spectra were recorded on a Pye Unicam SP1000 infrared spectrophotometer using KBr discs for solids or as neat films between NaCl discs. Nuclear magnetic resonance (nmr) spectra were recorded on a Varian LM 360 spectrometer using deuterochloroform as solvent and tetramethylsilane as the internal standard. The positions of the signals are reported in δ units. (The splittings of the signals are described as singlets (s), doublets (d), triplets (t), quartets (q), or multiplets (m).) Mass spectra (ms) were recorded at 70 eV on a Hitachi–Perkin-Elmer RMU 6E mass spectrometer. The number in parentheses after the indicated ion shows the percentage of the base peak represented by that ion. Melting points (mp) were determined using a Kofler hot stage melting point apparatus and are uncorrected. Thin-layer chromatography (tlc) was performed using silica gel G as the adsorbent. Microanalyses were done by G. Gygli of Toronto. Spectral and analytical data are given for all new compounds and for known compounds where data are unreported.

*Preparation of Polymer-bound Acid Chlorides **1**, **2**, and **16***

A suspension of a 1% crosslinked divinylbenzene (DVB)–styrene copolymer containing benzyl alcohol groups (**15**) (17) in THF was treated with the corresponding diacid chlorides by a method previously described (10) to give the polymer-bound acid chlorides **1**, **2**, and **16**.

The quantities of the corresponding diacid chlorides bound to polymer **1** were determined by hydrolysis of **1**, **2**, or **16** as before (10) to give their respective polymer-bound monoester monoacids. They were then cleaved with K_2CO_3 in methanol and esterified to yield the respective dimethylesters (10) from which the loading capacities of **1**, **2**, and **16** were calculated and given in Table 1.

*Preparation of Polymer-bound Tertiary Hydroxyesters **5–8***

To a suspension of 2 g of polymer **1** or **2** in 50 mL of dry benzene at 0°C under an argon atmosphere was added 15 mmol of phenylmanganese iodide (**3**) or butylmanganese iodide (**4**) in 10 mL at Et_2O (11). After the addition the reaction mixture was allowed to warm to room temperature and was stirred for 12 h. The excess organomanganese iodide was decomposed with 50 mL of a saturated solution of ammonium chloride. The polymer was filtered and washed with water (twice), methanol (twice), THF (twice), and Et_2O (3 times), and air dried to give the polymer-bound tertiary hydroxyesters **5–8**; ir (KBr): 3200–3600 (broad, O—H) and 1740 (CO_2R) cm^{-1}.

*Preparation of the Tertiary Hydroxyesters **9–12***

A suspension of 2 g of polymer **5** was cleaved with K_2CO_3 in methanol (10) and the product was esterified with CH_2N_2. The reaction mixture (250 mg) was purified by preparative tlc using hexane–acetone (4:1) to give 208 mg of methyl 6,6-diphenyl-6-hydroxyhexanoate (**9**) as a solid. The solid was recrystallized from hexane to give pure **9**, mp 81–82°C (lit (13) mp 82–83°C); ir (KBr): 3450 (OH), 1715 (CO_2Me), and 1600 (phenyl) cm^{-1}; nmr δ: 7.1–7.6 (m, 10, aromatic H), 3.55 (s, 3, CH_3O), 2.2–2.5 (m, 4, CH_2CO and $CH_2\overset{\overset{OH}{|}}{C}Ph_2$), 2.17 (s, 1, OH), and 1.1–1.9 (m, 4, CH_2); ms *m/e*: 280 (40) ($M^+ - H_2O$), 206 (100), 115 (68), 91 (83).

Similarly **6** gave methyl 10,10-diphenyl-10-hydroxydecanoate (**10**), mp 47–48°C; ir (KBr): 3500 (O—H), 1710 (CO_2R), and 1600 (phenyl) cm^{-1}; nmr δ: 7.2–7.6 (m, 10, aromatic *H*), 3.7 (s, 3, OCH_3), 2.1–2.5 (m, 4, $CH_2C{=}O$ and CH_2COPh_2), 2.14 (s, 1, O—*H*), 1.1–1.6 (m, 12, CH_2); ms *m/e*: 336 (40) ($M^+ - H_2O$), 193 (100), 115 (88), 91 (55). *Anal.* calcd. for $C_{23}H_{30}O_3$: C 77.93, H 8.53; found: C 77.89, H 8.67.

Similarly **7** yielded methyl 6-butyl-6-hydroxydecanoate (**11**) as an oil after purification on preparative tlc using methanol–chloroform (1:99) as eluant; ir (neat): 3300–3600 (b, OH), and 1740 (CO_2CH_3) cm^{-1}; nmr δ: 3.65 (s, 3, OCH_3), 2.3 (t, J = 6 Hz, 2, $CH_2C{=}O$), 1.6 (s, 1, O—*H*), 1.1–1.5 (m, 19, CH_2), 0.9 (t, J = 6 Hz, CH_3); ms *m/e*: 230 (6) ($M^+ - H_2O$), 85 (100), 55 (79). *Anal.* calcd. for $C_{15}H_{30}O_3$: C 69.72, H 11.70; found: C 69.73, H 11.86.

Similarly **8** gave methyl 10-butyl-10-hydroxytetradecanoate (**12**) as an oil; ir (neat): 3350–3550 (O—H), and 1730–1750 (CO_2R) cm^{-1}; nmr δ: 3.67 (s, 3, O—CH_3), 2.32 (t, J = 7 Hz, 2, $CH_2C{=}O$), 1.3–1.4 (m, 27, —CH_2— and O*H*), 0.9 (t, J = 6 Hz, CH_3); ms *m/e*: 298 (9) ($M^+ - H_2O$), 55 (100), 41 (86). *Anal.* calcd. for $C_{19}H_{38}O_3$: C 72.55, H 12.18; found: C 72.14, H 12.19.

In the separation of the products the corresponding dimethyl esters were detected and separated from the monoester monotertiary alcohols by preparative tlc. The quantities of recovered dimethyl esters and the yields of monoester monotertiary alcohols are reported in Table 1.

*Preparation of Polymer-bound Ketoesters **17** and **18***

To a suspension of 2 g of polymer **2** or **16** in 40 mL of dry benzene at 0°C under an argon atmosphere was added 7 mmol of phenyl cadmium chloride (15) in 15 mL of dry benzene. The

Can. J. Chem. Downloaded from www.nrcresearchpress.com by 210.87.254.105 on 09/05/12
For personal use only.

reaction mixture was allowed to warm to room temperature and was stirred for 24 h, after which 50 mL of 2% sulfuric acid was added and stirred for 10 min. The polymer was filtered and washed with benzene (twice), water (twice), methanol (twice), benzene (once), and ether (3 times), and air dried to give the polymer-bound ketoesters **17** or **18**; ir (KBr): 1735 (CO_2R) and 1690 (PhC=O) cm^{-1}.

*Preparation of Impure Ketoesters **19** and **20***

A suspension of 3 g of polymer **17** was cleaved with K_2CO_3 in methanol (10) and the product was esterified with CH_2N_2 to yield 400 mg of a mixture of 46% methyl 10-oxo-10-phenyldecanoate (**19**) (18) and 54% dimethyl sebacate (**14**) which was not further purified. Although the products **19** and **14** were inseparable by preparative tlc, the ratio of **19** to **14** could be readily determined from the nmr spectrum of the mixture using the nmr spectrum of pure **14** as a comparison. The ir (neat) spectrum of the mixture exhibited a strong absorbance at 1750–1730 (CO_2R), 1695 (PhCO), 1600 and 1590 (phenyl), and 1100 (C—O) cm^{-1}; nmr δ: 8.0 (m, *ortho* aromatic 2*H*), 7.4 (m, aromatic 3*H*), 3.7 (s, OCH_3), 3.0 (t, J = 7 Hz, CH_2COPh), 2.32 (t, J = 7.5 Hz, CH_2CO_2), and 1.1–1.9 (m, CH_2).

Similarly **18** yielded a mixture containing 54% methyl 9-oxo-9-phenylnonanoate (**20**) and 46% dimethyl azeloate (**21**), ir (neat): 1750–1730 (CO_2R), 1695 (PhCO), 1600 and 1590 (phenyl) cm^{-1}; nmr δ: 7.9 (m, *ortho* aromatic 2*H*), 7.4 (m, aromatic 3*H*), 3.7 (s, OCH_3), 2.98 (t, J = 7 Hz, CH_2COPh), 2.31 (t, J = 7 Hz, CH_2CO_2), and 1.2–1.8 (m, CH_2).

Acknowledgement

We are grateful for the financial assistance of the Natural Sciences and Engineering Research Council of Canada for support of this research.

1. P. M. Worster, C. R. McArthur, and C. C. Leznoff. Angew. Chem. Int. Ed. Engl. **18**, 221 (1979).
2. P. I. Svirskaya and C. C. Leznoff. J. Chem. Eng. Data, **24**, 152 (1979).
3. C. C. Leznoff and P. I. Svirskaya. Angew. Chem. Int. Ed. Engl. **17**, 947 (1978).
4. D. M. Dixit and C. C. Leznoff. Isr. J. Chem. **17**, 248 (1978).
5. W. S. Johnson, J. W. Peterson, and W. P. Schneider. J. Am. Chem. Soc. **69**, 74 (1947).
6. T. Veda, S. Kato, S. Toyoshima, and J. Takada. Chem. Abstr. **59**, 2726b (1963).
7. F. G. Baddar, L. S. El-Assal, and A. Habashi. J. Chem. Soc. 456 (1955).
8. C. C. Leznoff. Acc. Chem. Res. **11**, 327 (1978).
9. C. C. Leznoff and J. M. Goldwasser. Tetrahedron Lett. 1875 (1977).
10. J. M. Goldwasser and C. C. Leznoff. Can. J. Chem. **56**, 1562 (1978).
11. G. Cahiez, A. Masuda, D. Bernard, and J. F. Normant. Tetrahedron Lett. 3155 (1976); G. Cahiez, D. Bernard, and J. F. Normant. Synthesis, 130 (1977).
12. G. Cahiez and J. F. Normant. Tetrahedron Lett. 3383 (1977).
13. G. Cauquil, J. Rouzard, R. E. Lyle, H. L. Fielding, and G. G. Lyle. Bull. Chim. Soc. Fr. 513 (1955).
14. J. I. Crowley and H. Rapoport. Acc. Chem. Res. **9**, 135 (1976).
15. K. M. Patel, H. J. Pownall, J. D. Morrisett, and J. T. Sparrow. Tetrahedron Lett. 4015 (1976).
16. G. M. Whitesides, W. F. Fisher Jr., J. San Filippo Jr., R. W. Bashe, and H. O. House. J. Am. Chem. Soc. **91**, 4871 (1969).
17. J. M. Stewart and J. D. Young. Solid phase peptide synthesis. W. H. Freeman Ltd., San Francisco, CA. 1969. pp. 27–28.
18. M. D. Soffer, N. S. Strauss, M. D. Trail, and K. W. Sherk. J. Am. Chem. Soc. **69**, 1684 (1947).

Can. J. Chem. Downloaded from www.nrcresearchpress.com by 210.87.254.105 on 09/05/12
For personal use only.

Influence de la taille du cycle sur la substitution électrophile des cycloalkyltriméthylsilanes. Synthèse de cycloalkyldiméthylfluorosilanes

M. GRIGNON-DUBOIS, J. DUNOGUÈS ET R. CALAS[1]

Laboratoire de Chimie Organique et Laboratoire de Chimie des Composés Organiques du Silicium et de l'Etain associé au C.N.R.S. (No. 35), Université de Bordeaux I, 351, Cours de la Libération, 33405 Talence Cédex, France

Reçu le 20 juin 1979

Can. J. Chem. Downloaded from www.nrcresearchpress.com by 210.87.254.40 on 09/05/12
For personal use only.

M. GRIGNON-DUBOIS, J. DUNOGUÈS et R. CALAS. Can. J. Chem. **58**, 291 (1980).

A l'exception du dérivé cyclopropanique, les cycloalkyltriméthylsilanes réagissent sur les électrophiles avec scission de la liaison Si—Me. Cette propriété peut être mise à profit pour la fonctionnalisation au niveau du silicium ce qui nous a conduits à une synthèse nouvelle des cycloalkyldiméthylfluoro (ou chloro-) silanes. L'acétylation par $MeCOCl/AlCl_3$ donne, dans le cas des cycles en C_5 et C_6, des résultats qui s'interprétent par l'arrachement initial d'un ion hydrure au substrat silicié.

M. GRIGNON-DUBOIS, J. DUNOGUÈS, and R. CALAS. Can. J. Chem. **58**, 291 (1980).

Cycloalkyltrimethylsilanes, excepting cyclopropyl-, react with electrophiles by Si—Me bond splitting. Consequently silicon can be functionalized by this route. We also propose a new synthesis of cycloalkyldimethylfluoro (or chloro-)silanes. In the case of five or six member ring derivatives, the observed results are interpreted by a mechanism involving initial abstraction of hydride ion from the silicon substrate.

Introduction

Au cours de travaux antérieurs nous avons étudié la réactivité du cyclopropyltriméthylsilane vis-à-vis d'électrophiles et proposé la première synthèse de l'acide cyclopropane sulfonique (**1**) ainsi qu'une voie d'accès simple et pratique aux cyclopropylcétones (2). Par ailleurs nous avons montré que la sulfonation du cyclohexyltriméthylsilane avait lieu non par rupture de la liaison Si—$C_{alicyclique}$ mais au contraire par scission univoque d'une liaison Si—Me. Afin de déterminer d'une manière plus approfondie la réactivité de la liaison Me_3Si—$C_{alicyclique}$ en la comparant à celle de la liaison Si—Me, en vue d'éventuelles applications en synthèse, nous avons étudié le comportement de $(CH_2)_nCH$—$SiMe_3$ (n = 2, 3, 4, 5) vis-à-vis de quelques électrophiles. En particulier on pouvait se demander si, en série cyclobutanique, la fonctionnalisation serait possible comme en série cyclopropanique, par scission de la liaison Si—$C_{cyclobutanique}$ grâce à la tension du cycle à 4 chaînons. Cette étude nous a conduits à revoir la synthèse des substrats siliciés de départ pour n = 4 et 5 et à préparer le cyclobutyltriméthylsilane qui n'avait pas été décrit.

Nous rapportons ici les résultats que nous avons obtenus dans ce domaine.

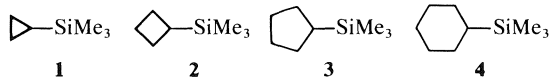
[1]Avec la collaboration technique de B. Rezzonico.

Résultats et discussion

Synthèse de $(CH_2)_nCH$—$SiMe_3$ (n = 2–5)

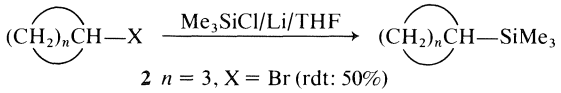
L'étude de **1** ne sera reprise qu'à titre comparatif puisque déjà publiée (1, 2).

Les composés **2**, **3** et **4** ont été synthétisés par silylation de $(CH_2)_nCH$—X (X = halogène) au



1 **2** **3** **4**

moyen du système $Me_3SiCl/Li/THF$ connu comme un excellent agent de silylation (3):



2 n = 3, X = Br (rdt: 50%)
3 n = 4, X = Br (rdt: 50%)
4 n = 5, X = Cl (rdt: 80%)

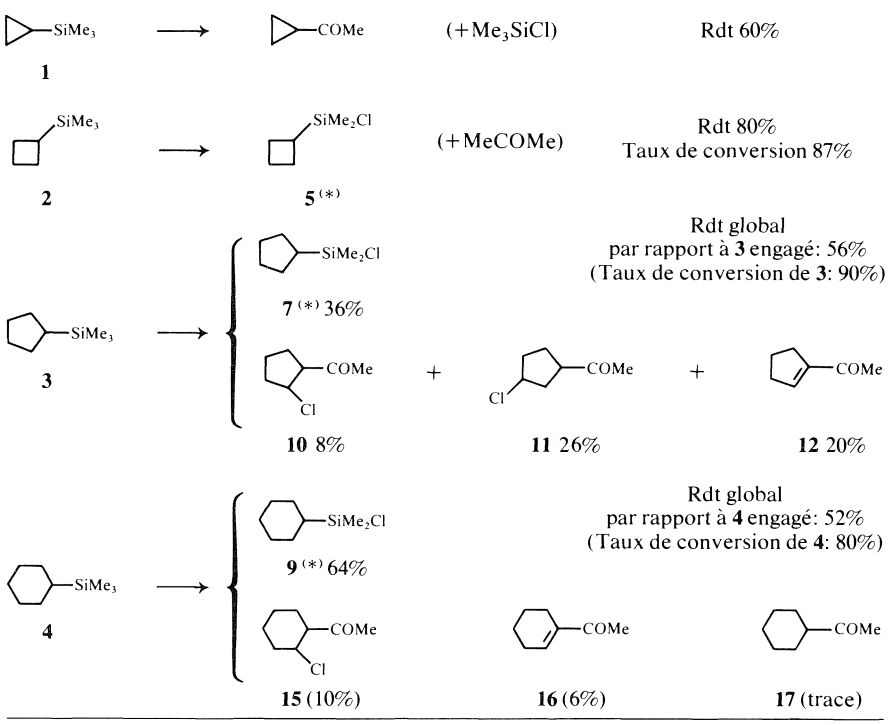
Acétylation avec $MeCOCl/AlCl_3$

Les résultats obtenus avec un équivalent de $MeCOCl/AlCl_3$ sont résumés dans le tableau 1.

Ce tableau appelle les commentaires suivants. (*a*) Seul le cyclopropyltriméthylsilane subit une scission univoque au niveau de la liaison Si—$C_{alicyclique}$. Le cyclobutyltriméthylsilane, au contraire ne réagit pas du tout à ce niveau et ne peut donc pas être comparé au dérivé cyclopropanique. (*b*) Avec les cycles en C_4, C_5 et C_6 le bilan réactionnel concernant les pourcentages relatifs de scission

0008-4042/80/030291-05$01.00/0
©1980 National Research Council of Canada/Conseil national de recherches du Canada

TABLEAU 1. Acétylation des cycloalkyltriméthylsilanes par 1 équivalent de $MeCOCl/AlCl_3$



*L'hydrolyse des chlorosilanes conduit aux disiloxanes (**6** $n = 3$; **7** $n = 4$; **9** $n = 5$) selon:

$$(CH_2)_n\overset{\frown}{CH}—SiMe_2Cl \xrightarrow{H_2O} (CH_2)_n\overset{\frown}{CH}—SiMe_2OH \rightarrow [(CH_2)_n\overset{\frown}{CH}—Si—Me_2]_2O$$

Avec $n = 5$ le silanol résultant de l'hydrolyse de **9** est relativement stable et a été isolé même dans nos conditions. En présence de Me_3SiCl, on obtient en outre les dérivés mixtes $(CH_2)_n\overset{\frown}{CH}—SiMe_2OSiMe_3$.

des liaisons Si—Me et Si—$C_{alicyclique}$ peut être schématisé comme suit:

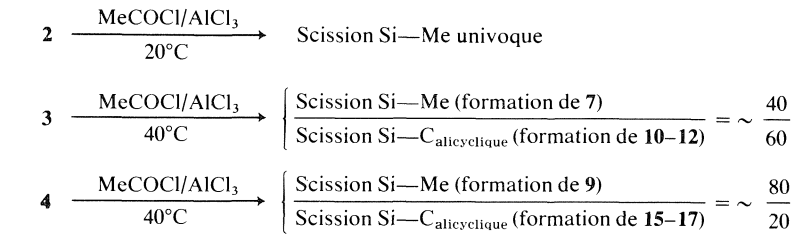


SCHÉMA 1. Bilan des scissions respectives Si—Me et Si—$C_{alicyclique}$ lors de l'acétylation de **2–4** par un équivalent de $MeCOCl/AlCl_3$.

Ce bilan fait ressortir que **3** ne se situe pas entre **2** et **4** comme on aurait pu l'imaginer.

L'acétylcyclopentane est absent du mélange réactionnel et son homologue cyclohexanique n'est présent qu'à l'état de traces. Par contre, on trouve dans les deux cas des chlorocétones en quantité abondante. Elles se décomposent partiellement dans le milieu par perte d'HCl pour conduire respectivement à l'acétylcyclopentène et à l'acétylcyclohexène.

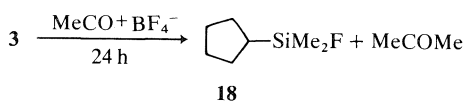
Nous avons vérifié que ces dérivés chlorés ne provenaient pas de la dégradation des méthylcycloalkylcétones dans le milieu, sous l'effet d'$AlCl_3$: l'acétylcyclopentane et l'acétylcyclohexane sont stables dans nos conditions opératoires. La formation des produits obtenus ne peut donc pas s'interpréter par une simple rupture de la liaison Si—$C_{alicyclique}$.

Ceci peut s'expliquer par l'intervention du chlorure d'aluminium . En effet l'acétylation de **3** par

Can. J. Chem. Downloaded from www.nrcresearchpress.com by 210.87.254.40 on 09/05/12
For personal use only.

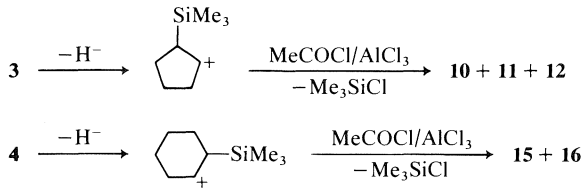
Can. J. Chem. Downloaded from www.nrcresearchpress.com by 210.87.254.40 on 09/05/12
For personal use only.

$MeCO^+BF_4^-$ a lieu par scission univoque d'une liaison Si—Me:



18

(ce qui constitue par ailleurs une voie d'accès pratique à **18**). Ceci suggère que les cétones formées lors de l'acétylation de **3** et **4** ne sont pas les produits primaires de la réaction. En fait nous pensons que $MeCOCl/AlCl_3$ produit un arrachement d'ion hydrure bien connu (4, 5) conduisant respectivement au cyclopentène et au cyclohexène dont l'acétylation peut expliquer la plupart des produits formés (6):



L'hypothèse de l'arrachement d'ion hydrure entraîne qu'une partie du chlorure d'acide engagé conduise à de l'éthanal puisqu'aucun dégagement gazeux (H_2 ou Me_3SiH) n'a été observé; celui-ci se polymériserait dans le milieu entraînant la formation de produits lourds dont nous avons noté la présence. En conséquence nous avons repris l'acétylation avec deux équivalents de complexe $MeCOCl/AlCl_3$. Les résultats observés sont rapportés dans le Tableau 2.

Il ressort de ces résultats que (*1*) le silane de départ réagit complètement; (*2*) le rendement global de l'acétylation augmente; (*3*) le rapport (scission Si—$C_{alicyclique}$/scission Si—Me) et le rendement en acétyl-1 chloro-3 cycloalcane augmentent. En effet, on sait que l'acétyl-1 chloro-3 cyclopentane se forme à partir de l'acétyl-1 chloro-2 cyclopentane par migration d'ion hydrure.

Avec 2 équivalents de complexe, on favorise donc la formation de cyclènes, ce qui est en accord avec l'interprétation proposée.

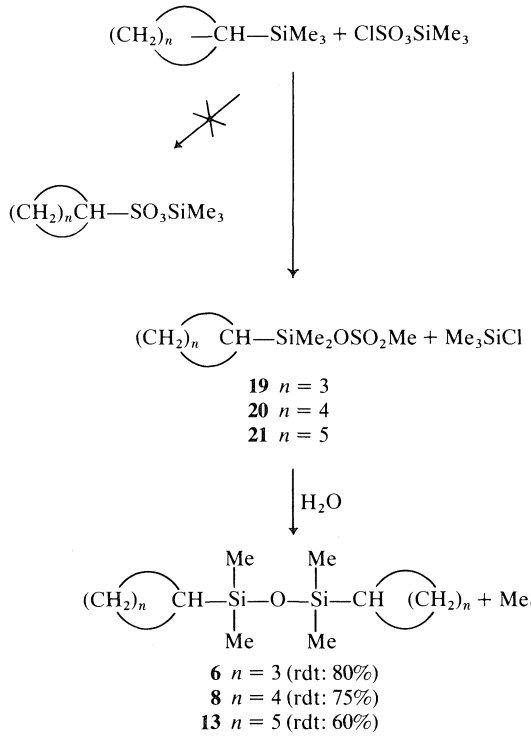
La formation de cyclène est moins importante pour le cycle en C_6 que pour celui en C_5. L'arrachement d'ion hydrure serait donc favorisé en série cyclopentanique. Il est bien connu que les réactions d'addition au carbonyle de la cyclohexanone transformant un carbone sp^2 en carbone sp^3 sont favorisées par rapport à celles de la cyclopentanone (7, 8), puisque la tension du cycle du cyclohexane est pratiquement nulle, ce qui n'est pas le cas du cyclopentane (6.5 kcal/mol) (9).

De ce fait on peut donc admettre que le passage d'un carbone sp^3 à un carbone sp^2 est plus facile en série cyclopentanique ce qui est corroboré par l'énergie de déstabilisation plus faible quand on passe du cyclopentane au cyclopentène (0.4 kcal/mol) que dans le cas du passage du cyclohexane au cyclohexène (2.6 kcal/mol) (9).

Ces considérations expliquent donc l'anomalie apparente du comportement du dérivé **3**, qui disparaît pour les réactions de substitution électrophile en l'absence de chlorure d'aluminium.

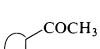
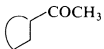
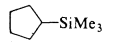
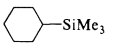
Sulfonation

La sulfonation, effectuée avec $ClSO_3SiMe_3$ (10), agent de sulfonation à la fois doux et efficace (11), a conduit à une scission de la liaison Si—Me, comme observé au cours d'essais préliminaires avec le cyclohexyltriméthylsilane (12). Ceci contraste avec les résultats que nous avons précédemment obtenus en série cyclopropanique (1):



Ceci confirme le caractère univoque de la scission Si—Me avec $n = 3$, 4 et 5 et donc que le cycle à 4 chaînons ne peut être comparé à celui à 3 chaînons, malgré son caractère π (13). Ce résultat est à rapprocher de ceux obtenus au Laboratoire par Bourgeois *et al.* (14) lors de la sulfonation de Bu-$SiMe_3$ qui s'effectue uniquement par scission de la liaison Si—Me. Les raisons stériques invoquées

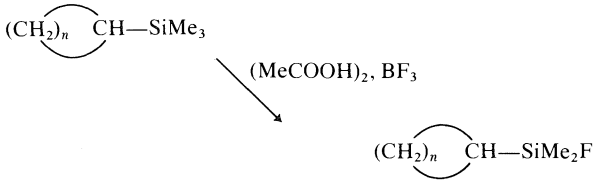
TABLEAU 2. Influence de la quantité de complexe sur l'acétylation de **3** et **4**

		Produits obtenus (Rdt %)						
$CH_3COCl/AlCl_3$ (équivalent)								Scission $\frac{Si—Me}{Si—C_{cycle}}$
	1	10	22	—	19	8	7	~40/60
	2	—	15	—	26	38	—	~20/80
	1	20	25	15	6	—	4	~80/20
	2	—	28	6	20	traces	15	~50/50

alors pour expliquer cette régiosélectivité sont applicables à notre cas.

Scission par $(MeCOOH)_2$, BF_3

Les conclusions des études précédentes permettaient de penser qu'avec les cycles en C_4, C_5 et C_6 la scission univoque de la liaison Si—Me permettait la fonctionnalisation au niveau du silicium. Nous avons donc appliqué cette réaction à la synthèse de cycloalkyldiméthylfluorosilanes en utilisant $(MeCOOH)_2$, BF_3 comme électrophile:



22 $n = 3$ (rdt: 50%)
18 $n = 4$ (rdt: 65%)
23 $n = 5$ (rdt: 70%)

Les rendements élevés confèrent à cette méthode une valeur synthétique pour accéder à des dérivés qui, à notre connaissance, n'avaient pas été décrits.

Conclusion

A l'exception du cyclopropyltriméthylsilane, les triméthylsilylcycloalcanes ne peuvent être utilisés comme précurseurs des dérivés alicycliques fonctionnels. En effet, dans les réactions de substitution électrophile, ce n'est pas le groupe silyle qui s'élimine mais seulement un groupe méthyle lié au silicium. Cette réactivité des liaisons Si—Me déjà mise en évidence au Laboratoire (14, 15) et généralisée aux liaisons silicium – groupe alkyle (16), peut être mise à profit pour transformer un groupe $—SiMe_3$ en $—SiMe_2X$, ce que nous avons illustré par la synthèse de cycloalkyldiméthylfluorosilanes.

En outre, nous avons proposé une interprétation cohérente de tous nos résultats, la réaction complexe observée entre **3** ou **4** et $MeCOCl/AlCl_3$ s'interprétant de façon satisfaisante par l'arrachement initial d'ion hydrure à ces deux substrats siliciés.

Partie expérimentale

Préparation du bromure de cyclobutyle

Nous l'avons obtenu à partir du cyclobutane carboxylate d'argent selon la méthode de Cason et Way (17) légèrement modifiée comme suit:

A une suspension refroidie à −25°C du sel d'argent dans le tétrachlorure de carbone (0.5 mol dans 500 cm^3) et vigoureusement agitée, on additionne, goutte à goutte, 0.5 mol de brome (séché sur P_2O_5). Il en résulte un important dégagement de CO_2. Lorsque le dégagement a cessé, on laisse remonter la température en maintenant l'agitation pendant 12 h. Le mélange réactionnel est alors filtré, le bromure d'argent lavé au tétrachlorure de carbone, puis l'ensemble des phases organiques est traité avec une solution saturée de thiosulfate de sodium et séché sur $MgSO_4$. Le solvant est distillé sous pression réduite (180 Torr) à l'aide d'une colonne à bande tournante, type Cadiot. Le rendement en bromocyclobutane (pé 63°C/180 Torr) est de 60%.

Silylation des halogénoalcanes

A une suspension de 0.2 at.g de lithium dans un mélange de 150 cm^3 de THF et 0.13 mol de Me_3SiCl, on additionne, goutte à goutte, 0.1 mol de dérivé halogéné, la température étant maintenue à −20°C. Les réactifs sont laissés en contact pendant 20 h. Le mélange réactionnel est alors filtré, les produits légers sont évaporés. Puis la phase organique est reprise deux fois au pentane afin d'éliminer toute trace de LiCl. Après élimination du solvant on obtient le dérivé silicié presque propre. Une filtration sur SiO_2 (2 cm de silice sur un verre fritté) permet d'isoler le produit pur; rdt: 50% à partir du bromocyclobutane et du bromocyclopentane, 80% à partir du chlorocyclohexane. La réaction donne de meilleurs résultats avec le dérivé chloré qu'avec les dérivés bromés; avec ces derniers, il se forme des produits lourds (séparés sur SiO_2).

Réactions d'acétylation

Elles ont été effectuées sous argon. A une suspension de 0.033 *M* de $AlCl_3$ dans 30 cm^3 de CH_2Cl_2 refroidie à 0°C, on additionne avec agitation 0.033 *M* de CH_3COCl. Après avoir maintenu pendant une heure cette température on ajoute, goutte à goutte, 0.03 mol de dérivé silicié en solution dans 10 cm^3 de CH_2Cl_2. Le milieu est maintenu à 0°C pendant une heure puis on laisse revenir à température ambiante avant de porter le mélange au reflux. Après 24 h de chauffage Me_3SiCl et le solvant sont éliminés sous vide (trompe à eau). Le résidu est versé sur un mélange glace–sel (−10°C) en présence de pentane, agité vigoureusement, puis extrait au pentane, lavé à l'eau jusqu'à neutralité et séché sur sulfate de magnésium.

Le mélange réactionnel est étudié en cpv, couplé à un spectrographe de masse (colonne S.E. 30, 10%, 3 m).

Can. J. Chem. Downloaded from www.nrcresearchpress.com by 210.87.254.40 on 09/05/12
For personal use only.

Can. J. Chem. Downloaded from www.nrcresearchpress.com by 210.87.254.40 on 09/05/12
For personal use only.

Une filtration rapide sur SiO_2 (éluant pentane) permet de séparer le produit de départ n'ayant pas réagi et les disiloxanes, des dérivés carbonylés. Le mélange de ces derniers est chromatographié sur colonne de silice afin d'isoler les différents constituants. Les essais effectués avec deux équivalents de $CH_3COCl/AlCl_3$ sont conduits de la même manière.

Réactions de sulfonation

Le triméthylsilylcycloalcane (0.05 mol) et $ClSO_3SiMe_3$ (0.05 mol) sont chauffés pendant une heure à 100°C. L'ester sulfonique est séparé par distillation.

L'hydrolyse est effectuée comme suit: 5 g de sulfonate de silyle sont versés dans 10 mL d'eau. L'addition est exothermique et il apparaît deux phases. La phase supérieure est constituée du disiloxane, la phase inférieure étant une solution aqueuse et $MeSO_3H$.

Scission par $(CH_3COOH)_2BF_3$

Un mélange de 0.05 mol de triméthylsilylcycloalcane et 0.05 mol du complexe $(CH_3COOH)_2BF_3$ sont chauffés à 100°C pendant 40 h. Le mélange est alors hydrolysé par une solution saturée de carbonate de sodium, extrait au pentane et séché sur $MgSO_4$. Après élimination du solvant on isole les fluorosilanes par distillation.

Description des produits obtenus

Les spectres de rmn (^1H) ont été enregistrés sur un appareil fonctionnant à 60 MHz (Perkin-Elmer R 24) (δ_{ppm}, solvant CCl_4, réf. int. $CHCl_3$ à 7.27).

En ir tous les composés triméthylsiliciés présentent les bandes d'absorption caractéristiques du groupe $SiMe_3$ à 1250, 840 et 755 cm^{-1} et les disiloxanes possèdent une absorption ν(Si—OSi) vers 1060 cm^{-1}.

Tous les produits nouveaux en particulier **2**, **6**, **18**, **19**, **20**, **21**, **22** et **23** ont des microanalyses C, H, Si en accord avec les formules proposées.

Bromure de cyclobutyle

Spectre de résonance magnétique nucléaire δ: 1.7 à 2.7 (massif complexe, 6 H); 4.4 (q élargi, 1 H); pé 63°C/170 Torr.

*Cyclobutyltriméthylsilane **2***

Point d'ébullition 84°C/270 Torr; rmn δ: 0 (1s, 9H); 1.7 à 2.5 (massif large, 7H).

*Dicycloalkyl tétraméthyl disiloxanes **6**, **8** et **13***

Point d'ébullition (**8**) 90°C/2 Torr; (**13**) 120°C/1 Torr. Ils présentent tous des spectres de rmn comparables, δ: 0.1 (1s, 12H, $SiMe_2$); entre 1 et 1.8 (1 massif, H du cycle).

*Acétyl-1 chloro-2 cyclopentane **10***

Infrarouge ν: 1710 (C═O), 760 (C—Cl) cm^{-1}; rmn δ: 1.6 à 2.1 (1 massif, 6H); 2 (1s, 3H); 2 à 2.8 (1m, 1H); 4 (1m, 1H); sm: pics moléculaires $M^+ = 146$ (^{35}Cl), $(M+2)^+ = 148$ (^{37}Cl) rapport 3/1; pic de base: $m/e = 43$ $(CH_3CO)^+$; **10** se décompose spontanément à température ambiante en **12** et HCl.

*Acétyl-1 chloro-3 cyclopentane **11***

Infrarouge ν: 1700 (C═O),760 (C—Cl) cm^{-1}; rmn δ: 1.5 à 1.9 (1 massif, 6H); 2 (1s, 3H); 3 (1m, 1H); 4.1 (1m, 1H); sm: pics moléculaires $M^+ = 146$ (^{35}Cl), $(M+2)^+ = 148$ (^{37}Cl) rapport 3/1; pic de base: $m/e = 43$ $(CH_3CO)^+$. Contrairement à **10**, **11** est stable à température ambiante.

*Acétylcyclopentène **12***

Infrarouge ν: 1680 (C═O), 1620 (C═C) cm^{-1}; rmn δ: 2 (1m, 2H); 2.2 (1s, 3H); 2.4 (1m, 4H); 6.6 (1 signal large, 1H); $M^+ = 110$.

*Acétyl 1-chloro-1 cyclohexane **15***

Infrarouge ν: 1710 (C═O), 750 (C—Cl) cm^{-1}; rmn δ: 1 à 1.8 (1 massif, 8H); 2 (1s, 3H), 2.2 à 2.8 (1 massif, 1H); 4 (1m, 1H); $M^+ = 160$.

*Acétyl cyclohexène **16***

Infrarouge ν: 1680 (C═O), 1650 (C═C) cm^{-1}; rmn δ: 1.2 à 2.2 (massif, 8H); 2.2 (1s, 3H); 6.8 (1 signal large, 1H); $M^+ = 124$.

*Esters sulfoniques **19**, **20** et **21***

Résonance magnétique nucléaire δ: 0.4 (1s, 6H); 1 à 2 (1 massif, CH du cycle); 3 (1s, 3H); pé (**20**) 90°C/1 Torr; (**21**) 100°C/0.4 Torr.

*Fluorosilanes **18**, **22**, **23***

En rmn du proton, outre les signaux dûs aux hydrogènes du cycle, ils se caractérisent par un doublet ($J \simeq 6$ Hz) dû au groupe $SiMe_2F$.

Remerciements

Nous remercions un des rapporteurs pour les suggestions qu'il a formulées.

1. M. Grignon-Dubois, J. Dunoguès et R. Calas. Tetrahedron Lett. 1197 (1976).
2. M. Grignon-Dubois, J. Dunoguès et R. Calas. Synthesis, 737 (1976).
3. R. Calas et J. Dunoguès. J. Organometal. Chem. Library 2, 277 (1976).
4. I. Tabushi, K. Fujita et R. Oda. Tetrahedron Lett. 4247 (1968).
5. C. D. Nenitzescu et I. Gavat. Ann. **519**, 260 (1935).
6. (*a*) F. Kögl et A. J. Ultée, Jr. Recl. Trav. Chim. Pays-Bas, **69**, 1976 (1950); (*b*) G. Baddeley, H. T. Taylor et W. Pickles. J. Chem. Soc. 124 (1953).
7. D. T. Mowry. Chem. Rev. **42**, 233 (1948).
8. J. D. Roberts et M. C. Caserio. Basic principles of organic chemistry. 2nd ed. W. A. Benjamin, Inc., London. 1977. p. 612.
9. J. F. Liebman et A. Greenberg. Chem. Rev. **76**, 311 (1976).
10. (*a*) M. Schmidt et H. Schmidbaur. Angew. Chem. **70**, 469 (1958); (*b*) N. Duffaut, R. Calas et J. Dunoguès. Bull. Soc. Chim. Fr. 512 (1963).
11. (*a*) P. Bourgeois et R. Calas. J. Organometal. Chem. **22**, 89 (1970); (*b*) P. Bourgeois et G. Mérault. C.R. Acad. Sci. Sér. C, **273**, 714 (1971).
12. M. Grignon-Dubois, J-P. Pillot, J. Dunoguès, N. Duffaut, R. Calas et B. Henner. J. Organometal. Chem. **124**, 135 (1977).
13. A. Y. Meyer et R. Pasternak. Theor. Chim. Acta, **45**, 45 (1977).
14. (*a*) P. Bourgeois. Thèse d'Etat, Bordeaux, 1970; (*b*) R. Calas, P. Bourgeois et N. Duffaut. C.R. Acad. Sci. Sér. C, **263**, 843 (1966).
15. (*a*) E. Frainnet, R. Calas et P. Gerval. C.R. Acad. Sci. Sér. C, **261**, 1329 (1965); (*b*) M. Birot, J. Dunoguès, N. Duffaut, R. Calas et M. Lefort. Bull. Soc. Chim. Fr. I, 442 (1978).
16. G. A. Olah. Synthesis, 677 (1977); L. H. Sommer, R. P. Pioch, N. S. Marans, G. M. Goldberg, J. Pockett et J. Kerlin. J. Am. Chem. Soc. **75**, 2932 (1953).
17. J. Cason et R. L. Way. J. Org. Chem. **14**, 31 (1949).

Viscosity of binary solutions of polar liquids[1]

ROBERT A. STAIRS
Department of Chemistry, Trent University, Peterborough, Ont., Canada K9J 7B8

Received June 4, 1979

ROBERT A. STAIRS. Can. J. Chem. **58**, 296 (1980).

The viscosity of mixtures of water with a number of organic liquids and of some mixtures of two organics has been analysed in terms of its deviation from "ideality", expressed as $\ln H = \ln \eta - (x_1 \ln \eta_1 + x_2 \ln \eta_2)$. For most of the systems the quantity $\ln H$ is a single-valued and linear, or nearly linear, function of the product $y_1 y_2$, where

$$y_1 = [1 + (V_2/V_1)^{\kappa}(x_1^{-1} - 1)]^{-1} \text{ and } y_2 = 1 - y_1$$

representing mole fractions (with $\kappa = 0$), or volume fractions ($\kappa = 1$), or various compromises ($0 < \kappa < 1$). Neither extreme, nor any single compromise, expresses the behaviour of all the systems. A linear relation between $1/H$ and the relative excess volume, suggested on the basis of the free-volume theory of fluidity, is shown to represent approximately the behaviour of the mixtures of two organic liquids. It fails with the water–organic mixtures.

ROBERT A. STAIRS. Can. J. Chem. **58**, 296 (1980).

La viscosité des mélanges de l'eau avec divers liquides organiques et des mélanges de deux produits organiques a été prise en compte afin d'étudier sa déviation par rapport à "l'idéalité" exprimée par la grandeur H, definie par: $\ln H = \ln \eta - (x_1 \ln \eta_1 + x_2 \ln \eta_2)$. Pour la plupart des systèmes $\ln H$ est une fonction à valeur unique, linéaire ou quasi-linéaire, du produit $y_1 y_2$, où

$$y_1 = [1 + (V_2/V_1)^{\kappa}(x_1^{-1} - 1)]^{-1} \text{ et } y_2 = 1 - y_1$$

représentant les fractions molaires pour $\kappa = 0$ ou les fractions volumiques pour $\kappa = 1$, ou des compromis divers pour $0 < \kappa < 1$. Cependant, ni l'un, ni l'autre des cas extrèmes, ni aucun des compromis n'exprime le comportement de tous les systèmes. Un parallèle entre $1/H$ et le volume d'excès relatif, suggéré à partir de la theorie du volume libre de la fluidité, représente approximativement le comportement des mélanges de deux liquides organiques. Il échoue avec les mélanges eau–organique.

Discussion of the viscosity behaviour of binary liquid solutions commonly starts from the concept of an "ideal" solution, with a view to considering particular systems as departing more or less from the ideal law. It is not clear, however, whether the ideal law should take the form of the (weighted) arithmetic, geometric, or harmonic mean of the viscosities of the pure components. The absolute rate theory, by focussing attention on excess thermodynamic functions of activation, most naturally works through the assumption that, in an ideal solution, the free enthalpy of activation, for instance, should be additive on a mole fraction basis

$$[1] \quad \Delta G^{\ddagger} = \Delta G_1^{\ddagger} x_1 + \Delta G_2^{\ddagger} x_2$$

where the subscripts refer to the two components, x is mole fraction, and the $\Delta G^{\ddagger}$ are standard free enthalpies of activation for flow. This implies the geometric mean law:

$$[2] \quad \ln \eta_g = x_1 \ln \eta_1 + x_2 \ln \eta_2$$

The free volume approach, as used, for example, by Hildebrand (1) leads naturally to a different choice. He writes, for the variation of both viscosity and density with temperature (following Batschinski (2) with modifications)

$$[3] \quad \eta^{-1} = a\rho^{-1} - b = B(V - V_0)/V_0$$

i.e. the fluidity η^{-1} is proportional to the "relative free volume". The constant B is an insensitive function of molecular size and shape, and V_0 is the intrinsic volume per mole.

An ideal solution, in the usual sense, shows no volume change on mixing. The assumption that there is also no free volume change on mixing leads to the expectation that, if the two kinds of molecules are similar in size and shape, as they must be if they are to form an ideal solution, the fluidities should be additive:

$$[4] \quad \eta_h^{-1} = \eta_1^{-1} x_1 + \eta_2^{-1} x_2$$

(The subscript h indicates the harmonic mean.)

There is no currently-favoured theory that leads naturally to the arithmetic mean:

$$[5] \quad \eta_a = \eta_1 x_1 + \eta_2 x_2$$

but a number of pairs of substances that might be expected to be nearly ideal most closely conform to this law, e.g. acetone and methylethylketone: Toropov's data (3) for the viscosity of mixtures of these at 20°C yield values of the quantity:

$$[6] \quad s = \left(\frac{\sum (\eta_{obs} - \eta_{theor})^2 / x_1 x_2)}{n - 2} \right)^{1/2}$$

[1]Presented in part at the 58th Canadian Chemical Conference, Toronto, May 1975.

0008-4042/80/030296-06$01.00/0
©1980 National Research Council of Canada/Conseil national de recherches du Canada

Can. J. Chem. Downloaded from www.nrcresearchpress.com by 210.87.254.42 on 09/05/12
For personal use only.

Can. J. Chem. Downloaded from www.nrcresearchpress.com by 210.87.254.42 on 09/05/12
For personal use only.

equal to 0.071 with $\eta_{theor} = \eta_h$, 0.040 with η_g, and 0.007 with η_a.

Except where the two components differ very much in viscosity, there is in fact not a great deal of difference between these three means. It may readily be shown that they differ most when $x_1 = x_2 = 0.5$. If the ratio of the viscosities of the pure liquids $\eta_2/\eta_1 = a$, it may also be shown that the ratios of the means to each other are then:

$$[7] \quad \eta_a/\eta_g = \eta_g/\eta_h = \tfrac{1}{2}(1/\sqrt{a} + \sqrt{a})$$

For the pair water–methanol, $a = 0.626$ and each of the outer measures, η_a and η_h, differs from η_g by only 3%. The real viscosity in this system passes through a maximum that differs from any of the assumed "ideal" values by a factor of about 2, and it makes little difference which is chosen. Accordingly, we have followed the *aurea mediocritas* and chosen the geometric mean η_g, as our defined "ideal" viscosity, η_i, and have discussed deviations from the ideal law in terms of the quantity:

$$[8] \quad H = \eta/\eta_g = \eta/\eta_i$$

From the point of view of the free volume approach it is not surprising that those systems that show large positive viscosity deviations tend also to show large negative deviations from volume additivity. If it is true that free volume is necessary for flow, then shrinkage on mixing, which would appear to reduce the free volume, should be associated with an increase in viscosity. One would like to know, at each composition, the fractional change in the free volume, which should be related to our quantity H. The free volume per mole of the real solution must be obtained from the Hildebrand–Batschinski relation, eq. [3], through which V_0, the intrinsic volume, may be obtained from a graph of η^{-1} versus the molar volume V which, if the relation holds for a solution at constant composition,[2] should yield a straight line with volume-intercept V_0. Then the actual free volume at a particular temperature is $v = V - V_0$, and the "ideal" free volume, i.e. the free volume that would have existed had there been no shrinkage, will be $v_i = v - V^E$ (recall that V^E, the excess volume, is here negative). If eq. [3] is applied to both the real and the ideal viscosities, eq. [8] becomes

$$[9a] \quad H = (B_i v_i/V_{0i})/(Bv/V_0)$$

or, with the further assumptions that $B_i = B$ and $V_{0i} = V_0$, i.e. that all the non-ideality appears in the free volume,

$$[9b] \quad H = v_i/v = v_i/(v_i + V^E)$$

Correct use of this argument requires data for all the solutions over a range of temperatures, which are not available at present. For now we are using the relative excess volume, defined (as percentage) by:

$$[10] \quad V_r^E = 100\left(\frac{V - V_1x_1 - V_2x_2}{V_1x_1 + V_2x_2}\right) = 100\left(\frac{(x_2^{-1} - 1)M_1/M_2 + 1}{\rho(x_2^{-1} - 1)M_1/M_2\rho_1 + 1/\rho_2} - 1\right)$$

where V is the molar volume, ρ, M, and x are density, molecular weight, and mole fraction, and the subscripts 1 and 2 refer to the two components. Values of the (negative) excess volume are approximately proportional to the product of the mole fractions, x_1x_2, as suggested by Biron (6) or to the product of the volume fractions, $\phi_1\phi_2$, as suggested by Hildebrand and Scott (7). From eq. [9*b*], one would expect a linear dependence of the reciprocal of H on V^E, and hence a linear dependence of H^{-1} on x_1x_2 or on $\phi_1\phi_2$.

Figure 1 shows the result of plotting H^{-1} vs. x_1x_2 for water–methanol mixtures (outer, full curve) and vs. $\phi_1\phi_2$ (inner, dashed curve). The arrows represent the direction of increasing proportion of methanol. Neither abscissa gives a good fit. The change from mole fraction to volume fraction over-corrects.

We now define a pair of variables y_1 and y_2 by

$$[11] \quad y_1 = [1 + (V_2/V_1)^\kappa(x_1^{-1} - 1)]^{-1}$$
$$y_2 = 1 - y_1$$

Here V_1 and V_2 are the molar volumes of the pure liquids 1 and 2, and κ is an adjustable parameter. If $\kappa = 1$, y_1 and y_2 represent volume fractions; if $\kappa = 0$, they are mole fractions. Intermediate values of κ represent various compromises, of which two have particular significance. If $\kappa = \frac{1}{3}$, y_1 represents the "line fraction" of component 1 in the mixture, that is, the fraction of an arbitrary line in the mixture that is occupied by molecules of component 1. If $\kappa = \frac{2}{3}$, y_1 is the corresponding "area fraction". Since viscosity involves the transfer of momentum across surfaces within the fluid, this particular value of κ, if found to be favoured by the data, would have been pleasing. Alas, it was not to be, in spite of some early results which were suggestive. Figure 2 contains a plot of H^{-1} vs. y_1y_2 for water–methanol, with $\kappa = 0.82$. The data now fall on a single curve, but it is not very linear.

[2]Lutschinsky (4) and Kottler (5) each report that Batschinski's formula holds for solutions.

Can. J. Chem. Downloaded from www.nrcresearchpress.com by 210.87.254.42 on 09/05/12
For personal use only.

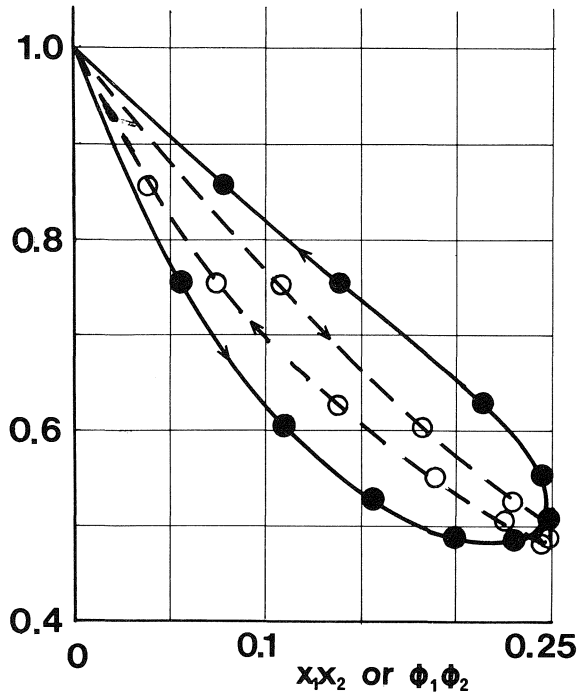


FIG. 1. Deviation of the viscosity of water–methanol mixtures from ideality, expressed as $H = \eta/\eta_i$ (where η_i is defined by log $\eta_i = x_1 \log \eta_1 + x_2 \log \eta_2$), plotted as H^{-1} against x_1x_2 (mole fractions, filled circles) and against $\phi_1\phi_2$ (volume fractions, open circles). The arrows indicate the direction of increasing proportion of methanol.

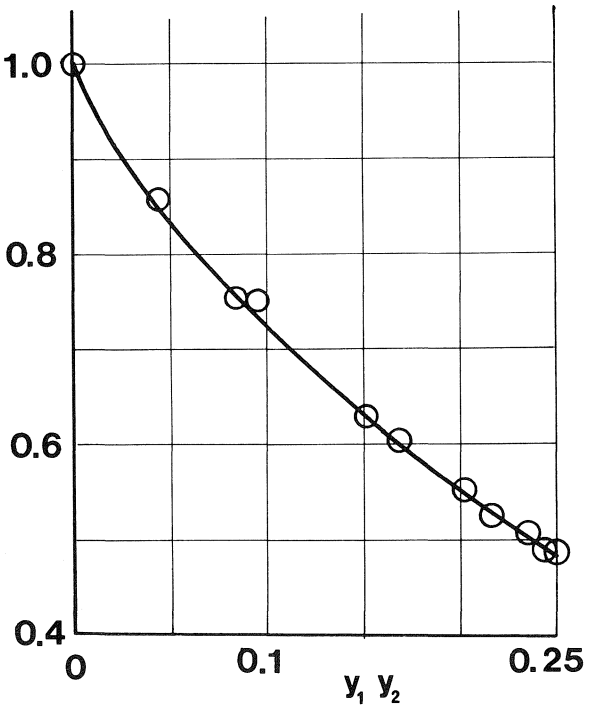


FIG. 2. H^{-1} (defined in Fig. 1) for water–methanol mixtures plotted against y_1y_2 (defined in text).

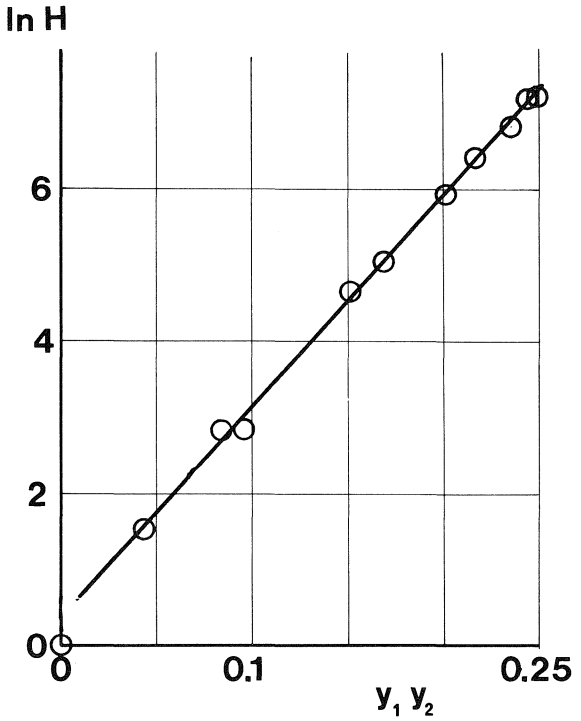


FIG. 3. Same data as in Fig. 2, plotted as ln H against y_1y_2.

An argument from the absolute rate theory has been used (8, 9) to predict a dependence of H on mole fraction of the form:

$$[12] \quad \ln H = -(W/RT)x_1x_2$$

where W is an interspecific interaction energy. This suggests trying a plot of ln H versus y_1y_2. This is shown, for the same data, in Fig. 3, and appears to yield a more nearly linear result. Not quite, however, for the best straight line fails to pass through the origin.[3] For practical purposes it seems the best.

Table 1 contains the results of applying similar treatments to data for a number of liquid pairs. The data are from a number of sources. Some are from our own laboratory (refs. 10, 11 and unpublished results), but most are from available tabulations (12–14). The fit obtained varies from satisfactory to poor, judged by the ability of the fitted equation to reproduce the original data as expressed by the relative standard error of estimate of viscosity,

$$[13] \quad S_{\ln\eta} = \{\sum (\ln \eta_i/\eta_{\text{calcd}})^2/(n-3)\}^{1/2}$$

Most of the published viscosity data are stated to three significant figures, which implies a relative precision of about 1%, i.e. $S_{\ln\eta} = 0.01$, though

[3]The best fit was obtained with an expression of the form ln $H = a(y_1y_2)^{1/2} + by_1y_2$. There seems to be no theoretical reason to expect this.

TABLE 1. Excess viscosity of liquid mixtures. Maximum values of $H = \eta/\eta_1^{x_1}\eta_2^{x_2}$, attained at $y_1y_2 = 0.25$ (where $y_2 = 1 - y_1 = [1 + k(x_2^{-1} - 1)]^{-1}$ and $k = (V_1/V_2)^{\kappa}$) with the maximum relative excess volume, V_r^E(max), for comparison, and the interaction parameter, $W = 4RT \ln H_{max}$

Components		t		$-V_r^E$(max)		κ	W
1	2	(°C)	$H_{(max)}$	(%)	V_1/V_2	(or k)*	(kJ mol^{-1})
Water	MeOH	25	2.12	3.50	0.44	0.73	7.4
Water	EtOH	25	2.55	3.40	0.309	0.69	9.3
Water	*n*-PrOH	25	2.53	2.02	0.241	0.98	9.2
Water	*i*-PrOH	25	2.85	2.09	0.240	1.09	10.4
Water	*t*-BuOH	25	3.55	2.67	0.190	0.82	12.6
Water	Formic acid	25	1.99	1.99	0.475	0.24	6.8
Water	Acetic acid	25	2.35	3.23	0.314	0.11	8.5
Water	Propionic acid	20	2.79	2.86	0.241	0.19	10.8
Water	*i*-Butyric acid	25	2.93	2.24	0.195	0.49	10.7
Water	Acetone	25	1.76	4.11	0.244	1.005	5.6
Water	DMF	25	2.76	2.77	0.233	0.72	10.1
Acetone	MeOH	25	0.84	0.74	1.816	0.40	—
Acetone	EtOH	25	0.75	0.16	1.265	(1.75)	—
Acetone	*i*-PrOH	25	0.63	−0.33	0.960	(1.69)	—
Acetone	BuOH	25	0.70	0.05	0.807	(1.55)	—
Acetone	MEK	25	1.01	0.02	0.820	(0.6)	0.1
Acetone	Formic acid	25	0.84	0.60	1.925	0.15	—
MEK	Formic acid	25	0.84	0.21	2.375	(1.42)	—
Acetone	Acetic acid	25	1.06	0.76	1.290	(3.98)	0.6
MEK	Acetic acid	25	0.98	0.59	1.568	—	—
Acetone	Propionic acid	25	1.16	1.18	0.989	(1.31)	1.5
Acetone	Butyric acid	25	1.15	0.99	0.800	(1.23)	1.4
Formic acid	Acetic acid	25	1.14	0.49	0.662	(0.49)	1.3
MeOH	PrOH	25	1.00	0.07	0.542	—	—
EtOH	PrOH	25	1.00	0.13	0.782	—	—
PrOH	BuOH	25	1.00	0.05	0.817	—	—
i-PrOH	BuOH	25	1.00	0.06	0.837	—	—
i-PrOH	*i*-BuOH	20	0.97	0.06	0.828	—	—
BuOH	*i*-BuOH	25	0.93	0.02	0.990	—	—

*Values in parentheses are k, entered for those cases where either scatter of the data or proximity of H or V_2/V_1 to unity rendered calculated values of κ meaningless. In those cases k replaces $(V_2/V_1)^{\kappa}$ in eq. [11].

some show more scatter than this. Fit was considered "poor" if the data were not reproduced to 3%. Aside from scatter, the main cause of poor fit appeared to be non-linearity of the graph of ln H versus y_1y_2. The largest deviations occur in mixtures of water with the non-hydroxylic liquids acetone and *N*,*N*-dimethylformamide and with the two propanols and *t*-butanol, the least "water-like" on the list. A closer look at the data for acetone revealed that with this non-donor (in the hydrogen-bonding sense) solvent, the viscosity was essentially ideal in all mixtures with acetone content greater than $x_2 = 0.8$, i.e. where the acetone-to-water ratio is greater than 4. Four acetone molecules are apparently enough to isolate each water molecule sufficiently to prevent formation of hydrogen-bonded chains. Below this ratio, a rather sudden rise occurs. This is most apparent when H is plotted against mole fraction of acetone, as in Fig. 4.

Leaving these anomalous cases aside, the remainder are reasonably well fitted, with values of κ ranging rather widely. Neither mole fraction nor volume fraction, nor any single compromise, best describes the data for all systems. Further, when a similar fit of excess-volume data to an analogous expression was tried for a few systems, it was found that the values of κ required differed from the best value for the viscosity (i.e. the maxima in H and V_r^E occur at different compositions).

Nevertheless, to pursue the suggested connection between the excess viscosity and the (negative) excess volume, the maximum value of H and the maximum value of V_r^E were computed, and the results for the liquid pairs in this study are plotted as $H_{(max)}^{-1}$ vs. V_r^E(max) in Fig. 5. There appears to be a correlation, especially for the mixtures of two organic liquids (omitting the nearly ideal mixtures of two alcohols and two ketones), where an approximate fit is possible with the linear expression

$$[14] \quad H_{(max)}^{-1} = 0.570 + 1.035 V_r^E(\text{max})$$

The mixtures of two alcohols appear to be essentially ideal both in their volume of mixing and in

Can. J. Chem. Downloaded from www.nrcresearchpress.com by 210.87.254.42 on 09/05/12
For personal use only.

Can. J. Chem. Downloaded from www.nrcresearchpress.com by 210.87.254.42 on 09/05/12
For personal use only.

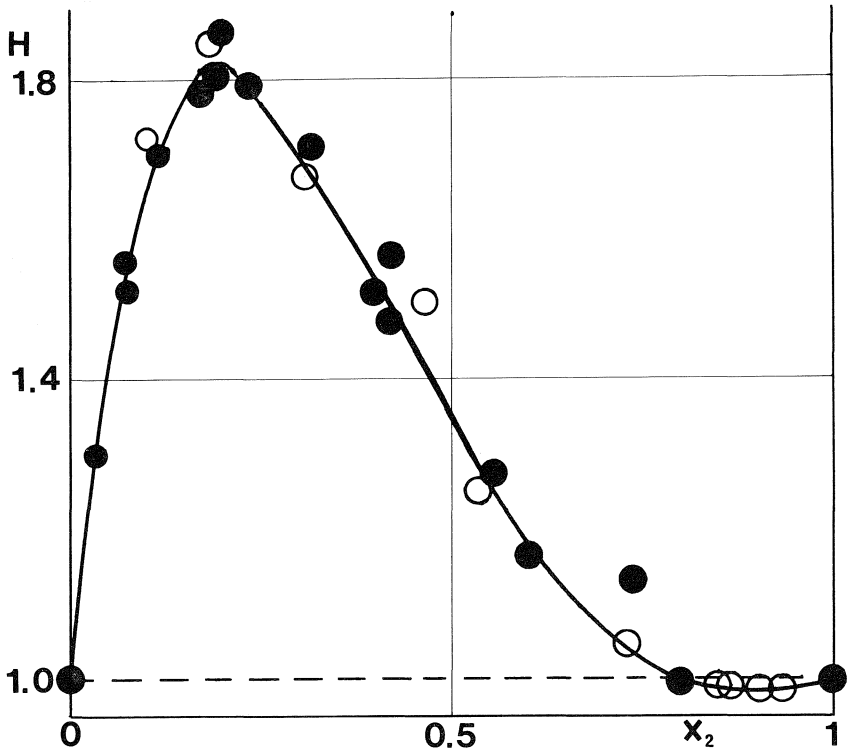


FIG. 4. Non-ideality H (defined in Fig. 1) for water–acetone mixtures, plotted vs. x_2, the mole fraction of acetone. Filled circles, ref. 13; open circles, this work.

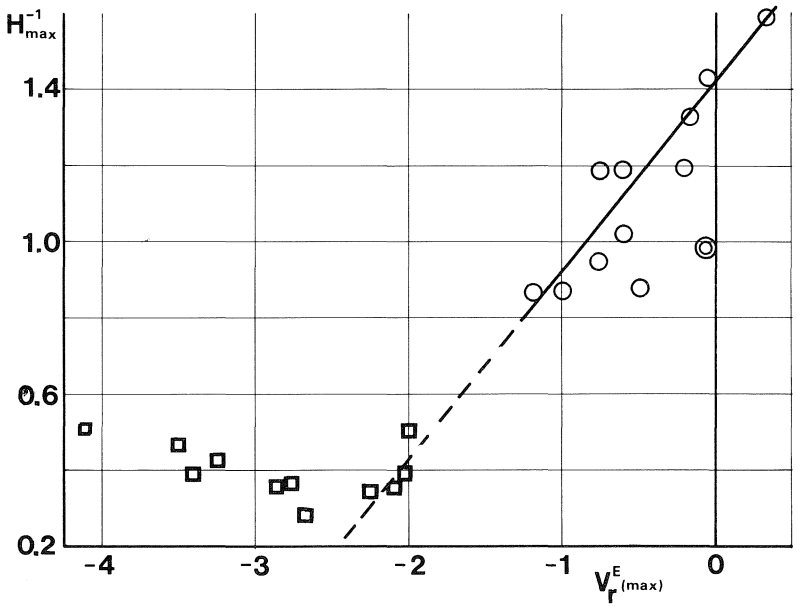


FIG. 5. Maximum value of H plotted as $H_{(max)}{}^{-1}$ against maximum relative excess volume V_r^E(max), percent, for a number of binary liquid mixtures. Data from Table 1. Squares, water–organic pairs; circles, two organics; double circles, average of seven systems, six of two alcohols, and one of two ketones, all close to ideal.

their viscosity. The aqueous–organic mixtures show the largest deviations in both properties, but do not conform to eq. [14].

Acknowledgement

The author wishes to acknowledge the assistance of A. Young with measurements and calculations.

1. J. H. HILDEBRAND. Science, **174**, 490 (1971).
2. A. J. BATSCHINSKI. Z. Phys. Chem. **84**, 643 (1913).
3. A. P. TOROPOV. Zh. Obshch. Khim. **26**, 1285 (1956).
4. G. P. LUTSCHINSKI. Z. Phys. Chem. A, **169**, 269 (1934).
5. F. KOTTLER. J. Phys. Chem. **48**, 76 (1944).
6. E. BIRON. J. Russ. Phys. Chem. Soc. **44**, 1264 (1912).
7. J. H. HILDEBRAND and R. L. SCOTT. Regular solutions. Prentice-Hall, Englewood Cliffs, NJ. 1962. pp. 102, 114.
8. L. GRUNBERG and A. H. NISSAN. Nature, **164**, 799 (1949).
9. P. K. KATTI and M. M. CHAUDHRI. J. Chem. Eng. Data, **9**, 442 (1964).
10. R. A. STAIRS. Adv. Chem. Ser. **155**, 332 (1976).
11. R. A. STAIRS. Adv. Chem. Ser. **177**, 167 (1979).
12. LANDOLT-BÖRNSTEIN. II 5a, Springer-Verlag. Berlin. 1969.
13. J. TIMMERMANS. The physico-chemical constants of binary systems. Interscience, New York. 1960.
14. International critical tables. Vol. III. McGraw-Hill, New York. 1928.

Can. J. Chem. Downloaded from www.nrcresearchpress.com by 210.87.254.42 on 09/05/12
For personal use only.

An analysis of the factors contributing to the regioselectivity observed in the opening of oxiranes

MARGARET M. KAYSER AND PETER MORAND

Department of Chemistry, University of Ottawa, Ottawa, Ont., Canada K1N 9B4

Received August 23, 1979

MARGARET M. KAYSER and PETER MORAND. Can. J. Chem. **58**, 302 (1980).

The regioselectivity of epoxide ring opening can be analyzed in terms of hard–soft acid–base (HSAB) theory. The coordination of the hard acid with the oxygen atom of the oxirane ring produces a "pulling effect" which determines the direction of the ring opening. In the absence of a strong "pulling effect" the "pushing effect" of the approaching base is examined and the consequences of relative softness or hardness of the nucleophile on the regioselectivity of the ring opening are discussed.

MARGARET M. KAYSER et PETER MORAND. Can. J. Chem. **58**, 302 (1980).

La régiosélectivité de l'ouverture du cycle époxyde peut être analysé en fonction de la théorie acide–base dur–mou (ABDM). La coordination de l'acide dur avec l'atome d'oxygène du cycle oxiranne produit un "effet de traction" qui détermine la direction de l'ouverture du cycle. En l'absence d'un "effet de traction" assez fort, on évalue l'effet "repoussement" de la base qui s'approche. On discute des conséquences de la nature relative molle ou dure du nucléophile sur la régiosélectivité de l'ouverture du cycle.

[Traduit par le journal]

Can. J. Chem. Downloaded from www.nrcresearchpress.com by 210.87.254.5 on 09/05/12
For personal use only.

Unsymmetrical epoxides have two possible sites at which nucleophilic substitution may occur. It has been generalized (1) that "nucleophiles attack at the less highly substituted carbon atom of the epoxide ring in neutral or basic media, as would be anticipated for a normal S_N2 process".

In the course of our work involving the preparation of β-substituted γ-butyrolactones, regioselective opening of the intermediate epoxide was of prime importance. The condensation of styrene oxide **1** with ethyl malonate under basic conditions according to the method described by DePuy, Breitbeil, and Eilers (2) yielded a mixture of two lactones. The major product was lactone **3** resulting from nucleophilic attack at the secondary carbon atom of the epoxide ring. In *para*-substituted styrenes **1***a* and **1***b*, the substituent exerted a significant effect on the direction of ring opening (Scheme 1). In the presence of the same counter ion (Na^+) and the same nucleophile (malonate anion), the electron-releasing methoxy group promoted nucleophilic attack at the secondary (more highly substituted) carbon atom, while the *p*-nitro substituent favoured reaction at the terminal carbon atom.

Similar substituent effects on the direction of ring opening in styrene oxides were observed for the reaction with sodium phenoxide in excess phenol (3). The percentage of product resulting from attack at the secondary carbon atom increased in the order $NO_2 < H < OCH_3$. These results contrast with the assumption (4, 5) that the effect of an electron-donating substituent on the direction of S_N2 ring opening in epoxides is to favour attack at the primary carbon atom (more disposed to accommodate a negative charge), while an electron-withdrawing group should promote attack at the secondary carbon atom. Also, the regioselectivity of these reactions cannot be attributed to steric factors (6) since the steric requirements of *p*-nitro- and *p*-methoxystyrene oxides resemble each other.

Regioselectivity of the Oxirane Ring Opening

By contrast with the results discussed above, the regioselectivity of $LiAlH_4$ reduction of substituted styrene oxides is much less sensitive to the influence of electron-releasing or electron-withdrawing groups (Table 1).

A search of the literature confirms that vastly different selectivities may be expected for the direction of ring opening in a series of substituted epoxides by different nucleophiles. A representative sample is included in Table 1. On the whole, the variations in regioselectivity of nucleophilic attack are particularly evident in the case of aromatic epoxides. Aliphatic epoxides (7, 8) conform better to the generalization stating that nucleophilic attack in basic media occurs at the least substituted carbon atom.

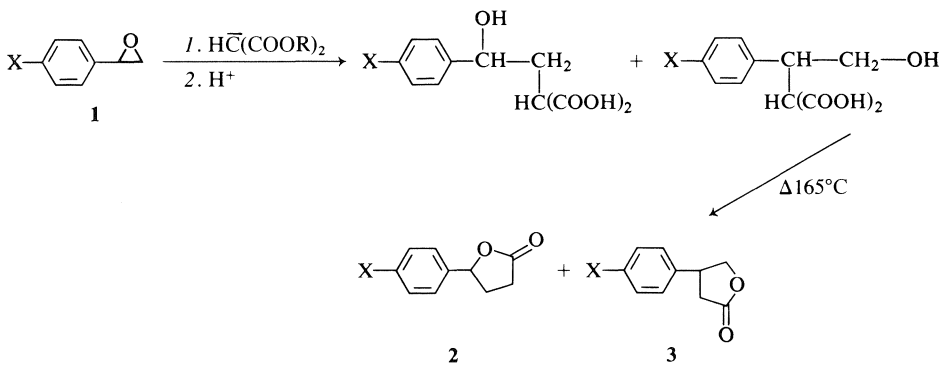
Since the commonly evoked electronic and steric effects do not adequately explain the observed results, the regioselectivity of epoxide ring opening should be reexamined in the light of more recent theories on molecular interactions.

Theoretical Considerations Applicable to Epoxide Ring Opening

CNDO/2 MO calculations (9) showed that in aromatic and conjugated epoxides the distribution of electric charges is very fluid (compared to aliphatic epoxides). This suggests that the direction

0008-4042/80/030302-05$01.00/0

©1980 National Research Council of Canada/Conseil national de recherches du Canada



1 2 3

Epoxide	X	Total yield %	Ratio 2 : 3
1	H	70	40 60
1*a*	CH_3O	66	— 100
1*b*	NO_2	60	100 —

SCHEME 1

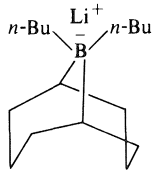
TABLE 1. Comparison of observed regioselectivity in the reduction of a series of structurally related oxiranes

Epoxide	Reagent	Over-all yield (%)	Attack at primary C atom	Attack at secondary C atom	Reference
Styrene oxide	$LiAlH_4$	94	100	—	7
Styrene oxide	$LiAlH_4(AlCl_3$ excess)	87	2–10	90–98	7
Styrene oxide	$LiBH_4$	100	74	26	5
Styrene oxide	**4***	100	1	99	8
p-Methoxystyrene oxide	$LiAlH_4$	90	80	20	
o-Methoxystyrene oxide	$LiAlH_4$	85	100	—	
o-Chlorostyrene oxide	$LiAlH_4$	95	100	—	
p-Methoxystyrene oxide	$LiBH_4$	70	5	95	5
p-Nitrostyrene oxide	$LiBH_4$	64	38	62	5
p-Bromostyrene oxide	$LiBH_4$	60	84	16	5
1,1-Diphenylethylene oxide	$LiAlH_4$	97	100	—	7
1,1-Diphenylethylene oxide	**4***	94	17	83	8

*Lithium 9,9-di-*n*-butyl-9-borabicyclo[3.3.1]nonate **4**.

of ring opening may be understood better in terms of Klopman's (10) application of perturbation theory to the hard–soft acid–base (HSAB) principle (11).

Briefly, according to HSAB principle a reaction occurs most readily between a hard acid and a hard base or between a soft acid and a soft base. The hard–soft combination binds reluctantly. The reaction between a hard acid and a hard base is charge controlled. Here, the energy difference of the frontier orbitals (HOMO of the nucleophile and LUMO of the electrophile) is large and as a result little charge transfer occurs in the transition state. On the other hand, when the energies of HOMO and LUMO of the reacting species are similar there is significant electron transfer in the transition state. This type of interaction (under frontier orbital control) is associated with soft acid – soft base reactions (10).



4

The Effect of the Coordination of the Oxygen Atom with an Electrophile

Acid-catalyzed hydrolysis of the oxirane presupposes initial protonation of the oxygen atom[1] (hard acid – hard base interaction). This assump-

[1]Although acid-catalyzed epoxide ring opening is frequently assumed to be an S_N1 type reaction (while base-catalyzed ring opening is considered to be S_N2), it is not always the case. The opening of ethylene oxide with HCl or HBr has been found to exhibit third-order rate law. Moreover, a number of acid-catalyzed ring openings proceed with almost complete inversion of configuration (12).

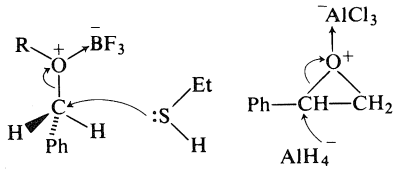
Can. J. Chem. Downloaded from www.nrcresearchpress.com by 210.87.254.5 on 09/05/12
For personal use only.

Can. J. Chem. Downloaded from www.nrcresearchpress.com by 210.87.254.5 on 09/05/12
For personal use only.

tion is supported by an *ab initio* SCF (Gaussian 70) calculation (13) which shows that the association of the oxygen atom with an electrophile (H^+) weakens the C—O bond and changes the charge on the C-atom from negative to positive. But even under basic conditions the epoxide ring is subject to initial coordination with the counter ion (14), followed by nucleophilic attack by the anion. Evidently, the "harder" the electrophile present, the more important is its effect on the direction of ring opening. This can be illustrated by the results obtained in the reduction of substituted epoxides by $LiAlH_4$ with or without $AlCl_3$. Under the usual reaction conditions ($LiAlH_4$ in diethylether or THF) attack by the nucleophile (AlH_4^-) occurs exclusively or preferentially at the least substituted carbon atom of the oxirane ring (Table 1). However, in the presence of $AlCl_3$ (hard acid) the regioselectivity of the reaction is reversed (7).

"Pulling" and "Pushing" Effects

A somewhat similar effect of the association with a hard acid has been observed (15) in the cleavage of the benzyl protecting group. The mixture of the hard acid (BF_3) and soft nucleophile (thiol) proved to be a particularly successful combination for the recovery of parent alcohols in excellent yields. The authors showed (15) that the coordination of a hard acid with the oxygen atom, the "pulling" effect, was a determining factor in these reactions. In fact the "pulling" factor appeared to be more important than the subsequent attack by a soft nucleophile on the carbon atom (the "pushing" effect, Scheme 2).



SCHEME 2

A similar sequence of events may be envisaged in the case of oxirane ring opening. In the presence of a hard acid (such as $AlCl_3$) the association of the oxygen atom with the Lewis acid results in the "pulling" effect, which significantly increases the positive charge at the carbon atom. In unsymmetrically substituted epoxides the positive charge develops at the carbon atom best suited to accommodate it. Thus the site of nucleophilic addition is predetermined.[2]

[2]Also, since $LiAlH_4$-$AlCl_3$ combination yields hard aluminum hydrides AlH_xCl_{3-x} (16) which participate in hard–hard (more ionic in nature) interactions, the site of attack will coincide with the site of the developing positive charge on the secondary carbon atom of the styrene oxide ring.

Epoxide Ring Opening in the Absence of an Effective Hard Acid

In reactions where "hard acid" is not available the softness of an anion and of the two sites on the epoxide ring controls regioselectivity of nucleophilic addition.

Li^+ is a hard acid (17). It is "harder" than Na^+, yet both ions are less effective (as "pulling" agents) than BF_3 or $AlCl_3$. In ether solvents (such as diethylether or THF commonly used in reduction reactions) the counter ions are highly solvated. Consequently the solvent molecule has to be removed before an ion can approach and coordinate with the oxygen atom of the epoxide ring. The association with the oxygen atom of the epoxide ring is not particularly more favourable than coordination with the oxygen atoms of the solvent. As a result Li^+ and Na^+ are ineffectual "pulling" agents.[3] Consequently, the reduction with $LiAlH_4$ and the condensation with malonate anion of substituted styrene oxides represent cases where an effective "pulling" factor is absent.

Reaction with a Soft Nucleophile

All organic bases in which the donor atom is carbon are relatively "soft". Thus, the condensation of substituted styrene oxide with malonate anion represents a soft–soft interaction. In this type of interaction the frontier orbitals of the donor HOMO and the acceptor LUMO are of similar energy. A new orbital differs in energy and form from either of the original ones. Thus, even a subtle difference in energy between the two LUMO's (on the two carbon atoms of epoxide ring) will affect the selectivity of the reaction (Fig. 1).

In the *p*-methoxystyrene oxide the carbon atom α to the benzene ring is the "softer" of the two and as a result nucleophilic addition occurs there. In *p*-nitrostyrene oxide, the situation is reversed (Scheme 3).

Reaction with Complex Metal Hydrides

While malonate anion is a soft base, metal hydride ions form a scale of more borderline cases. In general, the more covalent the M—H bond, the softer is the hydride ion. Thus, BH_4^- is softer than AlH_4^- which in turn is softer than $AlH(OR)_3^-$

[3]Dimethoxyethane (DME) appears to trap Li^+ even more effectively than THF or diethylether; this may explain why lithium trimethylsilyl acetonitrile in DME attacks selectively the primary carbon atom of styrene oxide (18) in contrast to the relative lack of selectivity exhibited by malonate anion (Na/ethanol) (Scheme 1). It should be also pointed out that in more polar solvents the "pulling" effect and thus charge redistribution are favoured.

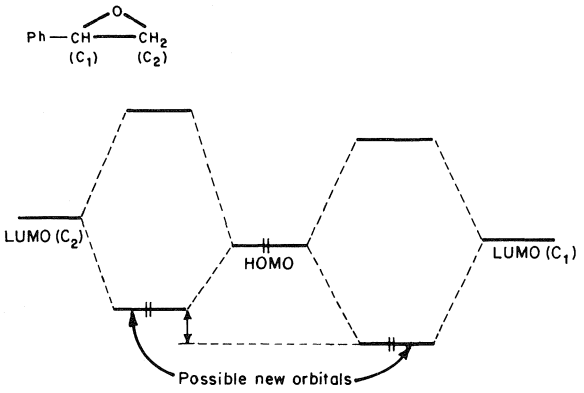


FIG. 1. Since the stabilization energy in the soft–soft interaction is large, even a small difference between LUMO (C1) and LUMO (C2) is significant.

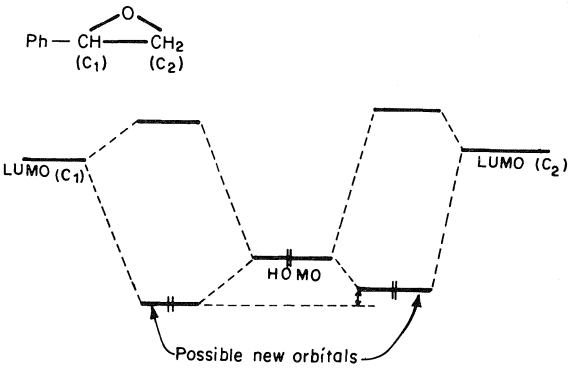
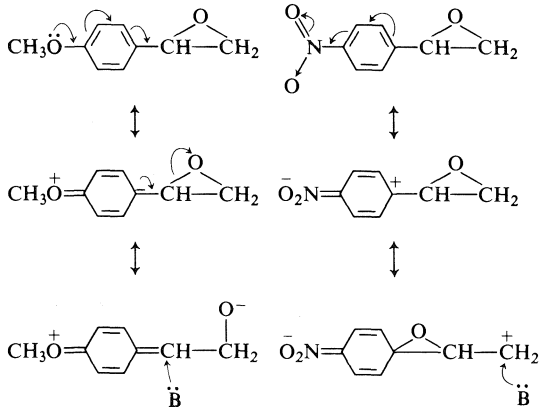


FIG. 2. The difference in stabilization energy between the two possible cases is small. It is therefore not an important driving force in this type of reaction.



SCHEME 3

where some of the soft hydride ions have been replaced by hard alkoxy groups (19).[4]

In effect AlH_4^- (a nucleophile harder than malonate anion or BH_4^-) is less sensitive to the nature of the substituents on the epoxide ring. Here, the energy difference between the frontier orbitals of the donor and acceptor is considerably larger. The new bonding orbital formed when the two species interact resembles that of the donor and the stabilization energy is small. The subtle difference in softness between the two carbon atoms of the epoxide ring does not have an important effect (Fig. 2). As a result, AlH_4^- is more sensitive to steric congestion than to a small difference in energy between the carbon atoms of the epoxide ring and the reaction takes place at the more accessible site.

Reductions with $LiBH_4$ (5) show quite a different order of selectivity (compared to $LiAlH_4$, see Table 1) principally due to the fact that BH_4^- is a softer nucleophile than AlH_4^- (18). The influence of the substituent on the phenyl ring is manifested in the ratios of products observed. The directive effect of the *p*-methoxy group is similar to that observed in reaction with malonate anion (i.e., the principal attack by nucleophile occurs at the secondary carbon atom). The distribution of isomers in the reduction of styrene oxide and *p*-bromostyrene oxide is also within the expected bounds. Quite unforeseen and intriguing, however, is the result of the reduction of *p*-nitrostyrene oxide. Here, one would have expected a higher percentage of the reaction taking place at the primary carbon atom.

The observed isomer distribution may be rationalized in the following manner. The powerful electron-withdrawing effect of the nitro group creates a diffuse positive charge in the epoxide ring. The LUMO energy levels on both carbon atoms are lowered considerably, thus promoting bond making over bond breaking in the transition state. BH_4^-, sterically less bulky and somewhat harder than malonate anion, shows preference for the secondary carbon atom which is slightly favoured towards bond making. The softer malonate anion forms the more thermodynamically stable bond.

A dramatic change in selectivity can be observed when reductions by $LiAlH_4$ are compared with reductions by lithium 9,9-di-*n*-butyl-9-borabicyclo-[3,3,1]nonate **4**. The latter provides H^-, a very soft nucleophile, as reducing agent. In reaction with styrene oxides, hydride addition occurs regiospecifically at the secondary carbon atom (Table 1).

Conclusions

Perturbation–HSAB theory correlates well the observed results and, although it can serve only as a rough guide, it is useful for a qualitative understanding of epoxide ring opening reactions.

The principal features of these reactions are (*1*) the importance of coordination with a hard acid and

[4] $LiAlH(SR)_3$ on the other hand is considerably softer due to softening of the reagent by the thio substituents.

Can. J. Chem. Downloaded from www.nrcresearchpress.com by 210.87.254.5 on 09/05/12
For personal use only.

the consequences of the "pulling" effect; (*2*) selectivity for the "softer" of the two carbon centres in reactions with soft nucleophiles; (*3*) preference for the sterically more accessible carbon atom in reactions with harder nucleophiles.

Experimental

Melting points were determined on a Thomas-Hoover capillary melting point apparatus and are uncorrected. Infrared spectra were obtained on a Beckman IR-20 spectrophotometer and proton nmr spectra in $CDCl_3$, with TMS as internal standard on a Varian HA-100 instrument.

Preparation of *p*-nitrostyrene oxide illustrates the general procedure for expoxide synthesis. *p*-Nitrobenzaldehyde (0.10 mol), trimethyl sulfonium chloride (0.15 mol), and triethylbenzyl ammonium chloride (TEBA chloride, phase transfer catalyst) were dissolved in methylene chloride (100 mL). The solution was placed in a 250 mL Erlenmeyer flask equipped with an efficient stirrer and cooled to 0°C. 50% Sodium hydroxide solution (60 g) was slowly added and the reaction mixture was stirred vigorously for 2 h. After dilution with distilled water, the layers were separated. The aqueous layer was extracted repeatedly with diethylether. The organic layers were washed separately with water, dried over anhydrous magnesium sulfate, and evaporated to dryness. The solid was recrystallized from ether to give orange crystalline *p*-nitrostyrene oxide (60%), mp 84–85°C. The nmr and ir spectra were consistent with the assigned structure.

Condensation of the substituted styrene oxides with ethyl malonate (Na, anhydrous ethanol) was performed according to the method described by Depuy *et al.* (2).

p-Methoxystyrene oxide, upon reaction with malonate ion, gave lactonic product in 66% yield. Only one structural isomer **3***a* was detected. Unequivocal proof of structure for the lactone was obtained by comparison of **3***a* with β-methoxyphenyl-γ-butyrolactone obtained from the $NaBH_4$ reduction of *p*-methoxyphenylsuccinic acid.

p-Nitrostyrene oxide treated with diethylmalonate gave γ-*p*-nitrophenyl-γ-butyrolactone **2***b*. This compound was identical with lactone obtained by nitration of γ-phenyl-γ-butyrolactone **2** (6).

The general procedure for $LiAlH_4$ reductions of styrene oxides is as follows. Epoxide (6.5 mmol) dissolved in dry THF (25 mL) was added slowly to a solution of $LiAlH_4$ (5.2 mmol) in THF (25 mL). The reaction mixture was stirred at ice-bath temperature and then allowed to warm to room temperature over a period of 3½ h. The reaction was cooled in an ice bath, quenched with 3 *N* HCl and stirred overnight. The layers were separated and the aqueous layer extracted with diethyl ether. Organic layers were combined, dried over anhydrous magnesium sulfate, and the solvents were evaporated. The products were analyzed by 100 Hz nmr.

Acknowledgement

We are grateful to the Natural Sciences and Engineering Research Council of Canada for financial support.

1. H. O. House. Modern synthetic reactions. 2nd ed. W. A. Benjamin, Reading, MA. 1972. p. 302.
2. C. H. DePuy, F. W. Breitbeil, and K. L. Eilers. J. Org. Chem. **29**, 2810 (1964).
3. C. O. Guss. J. Am. Chem. Soc. **74**, 2561 (1952); **71**, 3460 (1949).
4. D. N. Kirk. Chem. Ind. 103 (1973).
5. R. Fuchs and C. A. Vanderwerf. J. Am. Chem. Soc. **76**, 1631 (1954).
6. S. J. Cristol and R. F. Helmreich. J. Am. Chem. Soc. **74**, 4083 (1952).
7. E. L. Eliel and D. W. Delmonte. J. Am. Chem. Soc. **78**, 3226 (1956).
8. Y. Yamamoto, H. Toi, A. Sonodo, and S. Murahashi. J. Chem. Soc. Chem. Commun. 672 (1976).
9. E. G. Furman and A. P. Maleshevich. Teor. Eksp. Khim. **14**, 107 (1978).
10. G. Klopman. J. Am. Chem. Soc. **90**, 223 (1968).
11. R. G. Pearson. J. Am. Chem. Soc. **85**, 3533 (1963); Chem. Br. **3**, 103 (1962); J. Chem. Educ. **45**, 581 (1968).
12. E. S. Gould. Mechanism and structure in organic chemistry. Holt, Rinehardt, and Winston, New York. 1966.
13. P. Politzer, K. C. Daiker, V. M. Estes, and M. Baughaman. Int. J. Quantum Chem. Quantum Biol. Symp. **5**, 291 (1978).
14. J. L. Pierre, H. Handel, and R. Perraud. Tetrahedron, **31**, 2795 (1975).
15. K. Fuji, K. Ichikawa, M. Node, and E. Fujita. J. Org. Chem. **44**, 1661 (1979).
16. Tse-Lok Ho. Hard and soft acids and bases principle in organic chemistry. Academic Press, New York, NY. 1977. p. 159.
17. Tse-Lok Ho. Chem. Rev. **75**, 1 (1975).
18. T. Matsuda, S. Murata, and Y. Ishii. J. Chem. Soc. Perkin Trans. I, 26 (1979).
19. Tse-Lok Ho. J. Chem. Educ. **55**, 355 (1978).

Can. J. Chem. Downloaded from www.nrcresearchpress.com by 210.87.254.5 on 09/05/12
For personal use only.

Can. J. Chem. Downloaded from www.nrcresearchpress.com by 210.87.254.42 on 09/05/12
For personal use only.

COMMUNICATION

Hydrogen bond assisted reactions of carboxylic acids with alkyl halides in the gas phase by ion cyclotron resonance spectroscopy

R. L. CLAIR AND T. B. MCMAHON

Department of Chemistry, University of New Brunswick, P.O. Box 4400, Fredericton, N.B., Canada E3B 5A3

Received November 23, 1979

R. L. CLAIR and T. B. MCMAHON. Can. J. Chem. **58**, 307 (1980).

The reactions of the strongly hydrogen bonded anions, $CH_3CO_2HF^-$ and $(CH_3CO_2)_2H^-$, with alkyl halides have been studied in the gas phase by ion cyclotron resonance spectroscopy. A novel reaction of nucleophilic attack by $(CH_3CO_2)_2H^-$ with alkyl chlorides to produce $CH_3CO_2HCl^-$ and alkyl acetates is reported. Parallels are drawn to synthetically important analogous reactions in glacial acetic acid solutions of alkali metal fluorides.

R. L. CLAIR et T. B. MCMAHON. Can. J. Chem. **58**, 307 (1980).

On a étudié les réactions des anions fortement liés par des liaisons hydrogènes tels que $CH_3CO_2HF^-$ et $(CH_3CO_2)_2H^-$ avec les halogénures d'alkyles en phase gazeuse, en utilisant la spectroscopie à trajectoire cycloidale résonante. On rapporte une nouvelle réaction qui consiste en une attaque nucléophile de $(CH_3CO_2)_2H^-$ sur les chlorures d'alkyles et conduisant à $CH_3CO_2HCl^-$ et à des acétates d'alkyles. On l'a comparé aux réactions analogues importantes en synthèse qui mettent en jeu les fluorures de métaux alcalins en solution dans l'acide acétique glacial.

[Traduit par le journal]

Solutions of alkali metal fluorides in carboxylic acids have recently been demonstrated to be extremely efficient carboxylating agents and, as a result, are of considerable synthetic utility (1–4). In the present communication we wish to report an investigation of analogous reactions of fluoride – carboxylic acid systems *in the gas phase* by ion cyclotron resonance spectroscopy (ICR), with the aim of providing mechanistic details of the solution phase reaction.[1]

The reaction of *n*-heptylchloride with glacial acetic acid is observed to proceed in 85% yield to *n*-heptylacetate after 10 h under reflux in the presence of stoichiometric amounts of KF, reaction [1] (7).

[1] $$nC_7H_{15}Cl + CH_3CO_2H \xrightarrow{KF} CH_3CO_2{\cdot}nC_7H_{15} + KHF_2 + KCl$$

In the absence of KF no reaction occurs, even after prolonged heating at elevated temperatures. The driving force for this reaction has been postulated to be the increased nucleophilic character of the hydroxyl oxygen of acetic acid resulting from formation of a fluoride ion – acetic acid adduct, reaction [2],

[2] $$CH_3CO_2H + F^- \rightarrow CH_3CO_2HF^-$$

which strongly localizes negative charge on the hydroxyl oxygen. This conjecture is supported by ir and nmr detection of such an adduct (8, 9) and *ab initio* calculations on HCO_2HF^- and $CH_3CO_2HF^-$ which demonstrate that the hydroxyl oxygen of these adducts has a greater electron density than either the corresponding carboxylic acid *or carboxylate anion* (10).

We have previously demonstrated that the fluoride – acetic acid adduct may be facilely generated in the gas phase by fluoride transfer from trifluoromethoxide ion, CF_3O^-, reaction [3] (11).

[3] $$CF_3O^- + CH_3CO_2H \rightarrow CH_3CO_2HF^- + F_2CO$$

In order to examine the acetoxylating ability of the $CH_3CO_2HF^-$ ion in the gas phase, mixtures of CF_3OF, CH_3CO_2H, and a wide variety of alkyl halides were examined. A typical example for results obtained with alkyl chlorides is shown in Fig. 1 for a 4:1.5:1 mixture of C_2H_5Cl, CH_3CO_2H, and CF_3OF at a total pressure of 5×10^{-6} Torr. The reactions found to occur, verified by double resonance experiments, are summarized by reactions [4] and [5].

[4] $$CH_3CO_2HF^- + CH_3CO_2H \rightarrow (CH_3CO_2)_2H^- + HF$$

[5] $$(CH_3CO_2)_2H^- + C_2H_5Cl \rightarrow CH_3CO_2HCl^- + CH_3CO_2C_2H_5$$

Reaction analogous to reaction [5] was also observed for methyl, *i*-propyl, and *t*-butyl chlorides. No direct nucleophilic displacement reactions were

[1]All ICR techniques used were identical to those described previously (5). Previous comparisons of solution and gas phase ionic reactions by ICR may be found in ref. 6.

0008-4042/80/030307-03$01.00/0

©1980 National Research Council of Canada/Conseil national de recherches du Canada

observed, however, for either $CH_3CO_2HF^-$ or $(CH_3CO_2)_2H^-$ with any of the alkyl chlorides, reactions [6] and [7]

[6] $CH_3CO_2HF^- + RCl \nrightarrow Cl^- + HF + CH_3CO_2R$

[7] $(CH_3CO_2)_2H^- + RCl \nrightarrow Cl^- + CH_3CO_2H + CH_3CO_2R$

On the basis of results of the solution phase studies it is these reactions which might initially be expected to occur. Solutions of alkali metal acetates in glacial acetic acid also lead to production of alkyl acetates in reactions with alkyl halides (1, 7). However, these reactions are generally observed to be much slower than those involving alkali metal fluorides and it therefore seems unlikely that the solution phase reaction proceeds via the sequence of reactions, [4] and [5], found in the gas phase.

Reactions of $CH_3CO_2HF^-$ with alkyl fluorides, bromides, and iodides were also investigated. Both $CH_3CO_2HF^-$ and $(CH_3CO_2)_2H^-$ were observed to be completely unreactive toward all alkyl fluorides examined. With both alkyl bromides and iodides, $CH_3CO_2HF^-$ was found to undergo nucleophilic displacement to produce the corresponding halide ion and alkyl acetate, reactions [8] and [9].

[8] $CH_3CO_2HF^- + RBr \rightarrow Br^- + HF + CH_3CO_2R$

[9] $CH_3CO_2HF^- + RI \rightarrow I^- + HF + CH_3CO_2R$

However, the biacetate ion, $(CH_3CO_2)_2H^-$, was found to be unreactive toward all bromides and iodides studied.

These apparently ambiguous results for the gas phase reactions of fluoride acetic acid systems with various halides may be more clearly understood from an examination of the thermochemistry for representative reactions outlined in Table 1. In order for a gas phase ion–molecule reaction to be observed the reaction must be exothermic and involve little or no activation energy. Since all possible reaction channels for alkyl fluorides are endothermic no reaction is observed. For alkyl chlorides the possible nucleophilic displacement reactions, reactions [6] and [7], are also endothermic and as a result cannot occur. However, alternative exothermic reaction channels do exist, resulting in either $FHCl^-$ or $CH_3CO_2HCl^-$ and the desired ester. The reaction producing $ClHF^-$ does not occur, likely because the proton in the $CH_3CO_2HF^-$ is displaced strongly toward the fluorine with D(O—HF) calculated to be 1.40 Å (10). In the biacetate ion the O—H distance is much shorter (1.17 Å (7)) and the geometry of the ion–molecule intermediate is thus more favorable for reaction, resulting in facile $CH_3CO_2HCl^-$ production (reaction [5]). For alkyl bromides and iodides nucleophilic displacement by $CH_3CO_2HF^-$ is exothermic and this reaction is observed. Conversely, nucleophilic displacement by $(CH_3CO_2)_2H^-$ remains endothermic and this species is observed to be unreactive, as expected. Failure to observe formation of $CH_3CO_2HBr^-$ and $CH_3CO_2HI^-$ via reaction analogous to reaction [5] is likely, due to the increased steric requirements of the bulkier halogens which prevent reorientation of the methyl halide in the ion–molecule intermediate to a geometry favorable for elimination of these species.

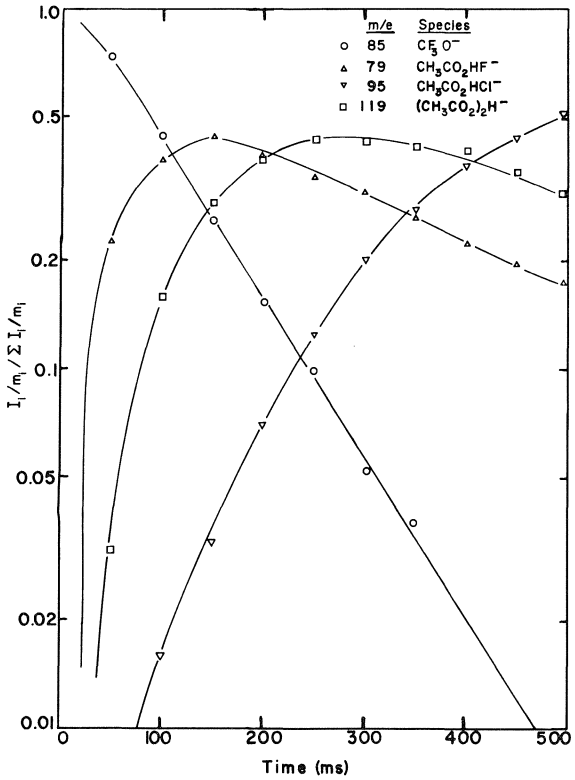


FIG. 1. Variation of relative ionic abundances with reaction time for a 4:1.5:1 mixture of C_2H_5Cl, CH_3CO_2H, and CF_3OF, following an 8 ms, 70 eV electron beam pulse. CF_3O^- is generated by dissociative electron attachment to CF_3OF.

In summary it appears that under the conditions where the esterification reactions have been examined in solution, the mechanism is exclusively direct nucleophilic displacement. The thermochemical data in Table 1 explain the decreasing time and temperature requirements for nucleophilic displacement as the size of the halogen increases (2, 3). It would be of interest, however, to examine solution phase reactions of alkali metal acetates in glacial acetic acid with alkyl chlorides at

Can. J. Chem. Downloaded from www.nrcresearchpress.com by 210.87.254.42 on 09/05/12
For personal use only.

TABLE 1. Enthalpy changes[a] for reactions of $CH_3CO_2HX^-$ with methyl halides, CH_3Y

$$CH_3CO_2HX^- + CH_3Y \xrightarrow{a} Y^- + HX + CH_3CO_2CH_3$$
$$CH_3CO_2HX^- + CH_3Y \xrightarrow{b} YHX^- + CH_3CO_2CH_3$$

		Enthalpy change	
$CH_3CO_2HX^-$	CH_3Y[b]	Channel *a*	Channel *b*
$CH_3CO_2HF^-$	CH_3F	38	3[c]
$(CH_3CO_2)_2H^-$	CH_3F	48	5
$CH_3CO_2HF^-$	CH_3Cl	9	−5
$(CH_3CO_2)_2H^-$	CH_3Cl	18	−3
$CH_3CO_2HF^-$	CH_3Br	−1	−13
$(CH_3CO_2)_2H^-$	CH_3Br	9	−6
$CH_3CO_2HF^-$	CH_3I	−7	−18
$(CH_3CO_2)_2H^-$	CH_3I	3	−8

[a] All reaction enthalpy changes in kcal/mol. Unless otherwise indicated $\Delta H_f^0(CH_3CO_2X^-)$ have been obtained from Yamdagni and Kebarle, ref. 16, or interpolated from gas phase acidity data as suggested by these authors. $\Delta H_f^0(CH_3CO_2HF^-)$ and $\Delta H_f^0((CH_3CO_2)_2H^-)$ are obtained in this fashion as outlined in ref. 11.

[b] Methylhalides are taken as representative of enthalpy changes for all alkyl halides studied. Available thermochemical data indicate that reaction enthalpies do not vary significantly with changes in alkyl group.

[c] $\Delta H_f^0(FHF^-)$ was calculated using $D(F^-—HF) = 35$ kcal/mol, obtained by interpolation from gas phase acidity data (see ref. 11). Recent studies of fluoride transfer reactions in our laboratory support a value of $D(F^-—HF) \leq 38$ kcal/mol.

relatively low temperatures to investigate the possibility of occurence of reaction analogous to [5] found in the gas phase. This possibility might be tested by monitoring such solutions by ir or nmr for presence of $CH_3CO_2HCl^-$.

More recent investigations have shown that fluoride ion is capable of enhancing nucleophilicity of a wide range of compounds with acidic hydrogens (12–15). We are currently extending our ICR studies to species such as fluoride bound to carbon acids and phenols to examine further parallels between reactivity in the gas phase and solution.

Acknowledgements

The financial support of the Natural Sciences and Engineering Research Council Canada is gratefully acknowledged. R. L. Clair acknowledges the financial support of the O'Brien Foundation.

1. J. H. CLARK and J. EMSLEY. J. Chem. Soc. Dalton. Trans. 2129 (1975).
2. J. H. CLARK and J. M. MILLER. J. Am. Chem. Soc. **99**, 498 (1977).
3. J. H. CLARK, J. EMSLEY, and O. P. A. HOYTE. J. Chem. Soc. Perkin Trans. I, 1091 (1977).
4. J. H. CLARK and J. M. MILLER. Tetrahedron Lett. 599 (1977).
5. C. E. DOIRON, F. GREIN, T. B. MCMAHON, and K. VASUDEVAN. Can. J. Chem. **57**, 1751 (1979).
6. (*a*) J. L. BEAUCHAMP. *In* Interactions between ions and molecules. *Edited by* P. Ausloos. Plenum, New York. 1975; (*b*) T. A. LEHMAN and M. M. BURSEY. Ion cyclotron resonance spectrometry. J. Wiley and Sons. New York. 1976; (*c*) M. COMISAROW. Can. J. Chem. **55**, 171 (1977).
7. J. EMSLEY, O. P. A. HOYTE, and R. E. OVERILL. J. Am. Chem. Soc. **100**, 3303 (1978).
8. J. H. CLARK and J. EMSLEY. J. Chem. Soc. Dalton Trans. 2154 (1973).
9. J. H. CLARK and J. EMSLEY. J. Chem. Soc. Dalton Trans. 1125 (1974).
10. J. EMSLEY and O. P. A. HOYTE. J. Chem. Soc. Perkin Trans. II, 2079 (1977).
11. R. L. CLAIR and T. B. MCMAHON. Can. J. Chem. **57**, 473 (1979).
12. J. H. CLARK and J. M. MILLER. J. Chem. Soc. Chem. Commun. 229 (1976).
13. J. H. CLARK and J. M. MILLER. J. Chem. Soc. Perkin Trans. I, 2063 (1977).
14. J. M. MILLER, K. H. SO, and J. H. CLARK. J. Chem. Soc. Chem. Commun. 466 (1978).
15. J. M. MILLER, K. H. SO, and J. H. CLARK. Can. J. Chem. **57**, 1887 (1979).
16. R. YAMDAGNI and P. KEBARLE. J. Am. Chem. Soc. **93**, 7139 (1971).

Can. J. Chem. Downloaded from www.nrcresearchpress.com by 210.87.254.42 on 09/05/12
For personal use only.

Canadian Journal of Chemistry
Published by
THE NATIONAL RESEARCH COUNCIL OF CANADA

Journal canadien de chimie
Publié par
LE CONSEIL NATIONAL DE RECHERCHES DU CANADA

Volume 58 Number 4 February 15, 1980 Volume 58 numéro 4 15 février 1980

Can. J. Chem. Downloaded from www.nrcresearchpress.com by 210.87.254.105 on 09/05/12
For personal use only.

Easily polarizable hydrogen bonds and solvate structure in aqueous solutions of acids with $pK_a < 1$

MARTIN LEUCHS AND GEORG ZUNDEL
Physikalisch-Chemisches Institut der Universität München, Theresienstraße 41, D-8000 München 2, West Germany

Received August 2, 1979

MARTIN LEUCHS and GEORG ZUNDEL. Can. J. Chem. **58**, 311 (1980).

Aqueous solutions of 15 acids with $pK_a < 1$ were studied by ir spectroscopy. The ir bands of the acid molecules demonstrate that the proton acceptor strength of the anions increases in the series $CF_3SO_3^-$, HSO_4^-, ClO_4^-, $HSeO_4^-$, $C_6H_5SO_3^-$, NO_3^-. At very high concentrations (number of H_2O/acid molecules, $n < 1$) easily polarizable

$$\underset{\mathbf{I}}{AH\cdots OH_2} \rightleftharpoons \underset{\mathbf{II}}{A^-\cdots H^+OH_2}$$

hydrogen bonds are formed causing continuous absorption in the ir spectra. The deeper well of the double minimum energy surface of these hydrogen bonds at the beginning of the above series is present at the water molecule, and at the end of the series at the anion. The H_3O^+ character of the vibrations of the H^+OH_2 groups increases with increasing n. For $n > 1$ the weight of proton limiting structure **II** increases and more and more protons transfer from the acid–water into the water–water hydrogen bonds, i.e., they are present in $H_5O_2^+$ groupings which are embedded in the whole hydrate structure network. H_3O^+ vibrations are no longer found. The easily polarizable hydrogen bond in these groupings causes continuous absorption and the water molecules of these groupings cause broad bands. Of all acids studied, this group is the only cause of continuum in the more diluted solutions. The absorbance of the continuum per $H_5O_2^+$ group at $n = 2$ increases in the series $HClO_4$, CF_3SO_3H, H_2SO_4, H_2SeO_4, $C_6H_5SO_3H$. This is because of the increasing polarity of the environment of the $H_5O_2^+$ in this series of acids. The position of the water bands in solutions with $n = 6$ can be used to characterize the hydrogen bond acceptor strength of the anions. The H_2O scissor vibration shows that it increases in the series $AuCl_4^-$, $PtBr_6^{2-}$, $PtCl_6^{2-}$, ClO_4^-, BF_4^-, $CF_3SO_3^-$, J^-, HSO_4^-, $HSeO_4^-$, $C_6H_5SO_3^-$, $C_7H_7SO_3^-$, Cl^-. Finally molecular quantities which determine the pK_a values of the acids (proton acceptor strength, hydrogen bond acceptor strength, and special interaction properties of the anions) are discussed.

MARTIN LEUCHS et GEORG ZUNDEL. Can. J. Chem. **58**, 311 (1980).

On a étudié, par spectroscopie ir, les solutions aqueuses de 15 acides ayant un $pK_a < 1$. Les bandes ir des molécules d'acide démontrent que la force des anions accepteurs de proton augmente dans les séries: $CF_3SO_3^-$, HSO_4^-, ClO_4^-, $HSeO_4^-$, $C_6H_5SO_3^-$, NO_3^-. A de fortes concentrations (nombre de molécules H_2O/par nombre de molécules d'acides, $n < 1$), il y a formation de liaisons hydrogènes

$$\underset{\mathbf{I}}{AH\cdots OH_2} \rightleftharpoons \underset{\mathbf{II}}{A^-\cdots H^+OH_2}$$

facilement polarisables qui provoquent une absorption continue dans les spectres ir. Dans la surface à double minimum d'énergie de ces liaisons hydrogènes, le point le plus bas au début de la série ci-dessus est présent au niveau de la molécule d'eau et à la fin de la série il se situe au niveau de l'anion. Le caractère H_3O^+ des vibrations des groupes H^+OH_2 augmente avec n. Pour les valeurs de $n > 1$, le poids de la structure limite **II** du proton augmente et de plus en plus de protons passent des liaisons hydrogènes acide–eau aux liaisons hydrogènes eau–eau, i.e. ils sont présents dans les groupement $H_5O_2^+$ qui sont noyés dans toute la structure réticulaire de l'hydrate. On ne trouve plus les vibrations dues à H_3O^+. La liaisons hydrogène facilement polarisable de ces groupes provoque une absorption continue et les molécules d'eau de ces combinaisons donnent de larges bandes. Parmi tous les acides étudiés, ce groupe est la seule cause du continuum dans les solutions plus diluées. L'absorption du continuum par le groupe $H_5O_2^+$ pour $n = 2$ augmente dans la séries: $HClO_4$, CF_3SO_3H, H_2SO_4, H_2SeO_4, $C_6H_5SO_3H$. L'augmentation de la polarité de l'environnement de $H_5O_2^+$ dans cette série d'acide est responsable de cette observation. La position des bandes de l'eau dans les solutions où $n = 6$ peut être utilisée pour caractériser la force des anions en tant qu'accepteurs de liaison hydrogène. La vibration de cisaillement du H_2O montre qu'elle augmente dans la série $AuCl_4^-$, $PtBr_6^{2-}$, $PtCl_6^{2-}$, ClO_4^-, BF_4^-, $CF_3SO_3^-$, J^-, HSO_4^-, $HSeO_4^-$, $C_6H_5SO_3^-$, $C_7H_7SO_3^-$, Cl^-. Finalement on discute des quantités moléculaires qui déterminent les valeurs du pK_a des acides (capacité d'accepter des protons, capacité d'accepter des liaisons hydrogène et les propriétés spéciales d'interaction des anions).

[Traduit par le journal]

0008-4042/80/040311-12$01.00/0
©1980 National Research Council of Canada/Conseil national de recherches du Canada

Can. J. Chem. Downloaded from www.nrcresearchpress.com by 210.87.254.105 on 09/05/12
For personal use only.

Introduction

Molecular properties of strong acids in aqueous solutions were studied by ir (1–7) and Raman (8–14) spectroscopy. The degree of dissociation can be determined from bands of acid molecules and anions in the ir (1–7) and Raman spectra (11–14*a*). Infrared continuous absorption indicates the formation of easily polarizable hydrogen bonds (1, 15–20). Hydrogen bonds are easily polarizable when they have double minimum energy surfaces or energy surfaces with very broad flat wells, as shown by analytical (17) and SCF treatments (17–19). The continuous absorption can be directly calculated from the SCF transition moments (20, 21).

Due to their large polarizabilities and dipole moments these hydrogen bonds interact strongly with their environment (16). Thus, as discussed in ref. 16, pp. 731*ff*, the main cause of these continua is the large polarizability of hydrogen bonds which causes the following interaction effects: (*1*) The local electrical fields in solutions polarize these hydrogen bonds and shift the energy levels (induced dipole interaction). These local fields show a broad distribution and therefore a broad distribution of energy level differences occurs (see Fig. 6 in ref. 19). With these shifts resonances occurring between the various transitions are of particular significance. (*2*) Due to the large polarizability, transitions in the hydrogen bond couple with transitions in their environment, whereby the coupling with low wave number transitions is probably of particular importance. Furthermore, in liquid systems the equilibrium bond length shows more or less broad distributions (22), causing an additional distribution of the energy levels.

Interaction effect *1* (deformation of the energy surface by the local fields) and the length distribution of the hydrogen bonds were taken into account with our calculations of the continua (20, 21). With regard to interaction effect *2* only the coupling with the OO vibration was taken into account in our calculations of the continua.

Recently, Sokolov and co-workers (23*a*) calculated continua on the basis of coupling of transitions in charged hydrogen bonds and phonons in their environment. There is, however, strong experimental evidence that not the charge (as assumed by Sokolov and co-workers) but the symmetry of the proton potential is the essential feature for the appearance of the continua (23*a*). Thus a different interpretation of the coupling constant *S* in Sokolov's theory, mainly based on the high polarizability of largely symmetrical hydrogen bonds, seems more appropriate (23*b*). With this reinterpretation this theory describes very well interaction effect *2* and may explain some observations as discussed below.

Infrared continua are observed with structurally symmetrical charged hydrogen bonds of the types (16)

$$B^+H\cdots B \rightleftharpoons B\cdots H^+B$$

or

$$B^-\cdots HB \rightleftharpoons BH\cdots {}^-B$$

or with largely symmetrical non-charged proton transfer hydrogen bonds

$$B_1H\cdots B_2 \rightleftharpoons B_1{}^-\cdots H^+B_2$$

With aqueous solutions of acids and with acidic polyelectrolytes ir continua were already studied by various authors (for a summary see ref. 16). Recently, Librovich and co-workers (6, 7, 25–27) investigated the ir continua of aqueous acid solutions with the ATR technique which is particularly suitable when the absorbance of the acids is very strong.

Aqueous solutions of $HClO_4$, CF_3SO_3H (28), and HNO_3 (29) were already investigated in detail. In this paper these studies were extended to aqueous solutions of 15 strong acids. The results obtained are discussed in terms of the strength of the respective acids.

Material and Methods

The acids were purchased from Merck in Darmstadt, Germany, Riedl-de-Haen in Seelze, Germany and Fluka in Buchs, Switzerland (see Table 1). The purity was analytical grade except CF_3SO_3H, HBF_4, H_2SeO_4, $C_6H_5SO_3H$ (synthetic grade), and $HAuCl_4$ (Lab).

Pure perchloric acid was obtained by vacuum distillation (50 Torr) of a 2.5:1 volume mixture of H_2SO_4 (97%) and $HClO_4$ (70%). Pure sulfuric acid was prepared by mixing H_2SO_4 and oleum; H_2SeO_4 (97%) was dried with P_2O_5. The other acids could be obtained free of water. For all acids the highest concentration measured is given in Table 1.

The cell used for the liquid acid solutions had silicon windows and a wedge-shaped layer; the latter in order to avoid an interference pattern superimposed on the spectra caused by the high reflectivity of silicon.

The absorbance had to be corrected, since with the wedge-shaped layer Lambert–Beer's law is no longer valid. The true absorbance is obtained as described in ref. 2*a*. The absorbance of the continuum is determined as described in ref. 31, taking the background absorbance of water into account. The absorbance of the continuum is referred to the same background absorbance at 4700 cm^{-1}.

The degree of dissociation was determined in the following way: The absorbance of a characteristic band of the non-dissociated acid molecules was plotted against the acid molarity. The intensity of this band in the spectrum of the water-free acid yields the molar absorbance of this band. With this molar absorbance, the concentration of non-dissociated acid molecules in each solution could be determined, and thus the degree of dissociation.

Can. J. Chem. Downloaded from www.nrcresearchpress.com by 210.87.254.105 on 09/05/12
For personal use only.

Results and Discussion

Aqueous solutions of 15 acids (Table 1) with $pK_a < 1$ were studied by ir spectroscopy as a function of concentration. Selected examples of spectra are shown in Fig. 1. With all these acids, a strong continuum arises with increasing concentration. This continuum begins at the band of the H_2O stretching vibration and extends towards smaller wave numbers. For acids which can be studied up to very high concentrations, the intensity of this continuum reaches a maximum after which it decreases with increasing concentration. This is illustrated with selenic acid in Fig. 1*c*. The absorbance of this continuum is listed in Table 1 for 1*M* and 5 *M* solutions.

A large number of these acids could be studied over the whole concentration range up to the pure acid. The results obtained with these acids at very high concentrations are summarized in Table 2.

Degree of Dissociation

The degree of dissociation can be determined from the ir bands of the acid molecules. Figure 2 shows the bands demonstrating the removal of the proton from the anion. With CF_3SO_3H, ν(S—O) at 930 cm^{-1} vanishes in the spectrum of the solution and with $n = 1.6$ this band no longer occurs, indicating complete dissociation. Analogously complete dissociation is indicated by the disappearance of the following bands: H_2SO_4 (first dissociation step), $\nu_{as}(S—(OH)_2)$ at 960 cm^{-1} and $\nu_{as}(SO_2)$ at 1360 cm^{-1}; $HClO_4$, ν(Cl—O) at 740 cm^{-1}; H_2SeO_4 (first dissociation step), $\nu_{as}(SeO_2)$ at 975 cm^{-1}; $C_6H_5SO_3H$, ν(S—O) at 900 cm^{-1}; HNO_3, γ HNO_3 at 765 cm^{-1}. To obtain exact n values for complete dissociation in Fig. 3, the degree of dissociation is plotted as a function of n, the number of water molecules per acid molecule. With sulfuric acid, the bands in the ir spectra taken by the usual method do not allow quantitative evaluation in the whole range, therefore the Raman data of Young (11) are used. These results agree very well, however, with those obtained by Maiorov and Librovich (6) who studied aqueous sulfuric acid solutions using the ATR technique. With selenic acid, a quantitative evaluation in the whole range is also not possible due to the strong overlapping of the bands in the ir as well as in the Raman spectra (32), in the following therefore the n value for complete dissociation taken directly from the spectra is used. The following n values for complete removal of the protons from the anion are obtained: trifluoromethane – sulfonic acid, $n = 1.6$ (9.3 *M*); sulfuric acid (first step), $n = 1.6$ (13.6 *M*); perchloric acid, $n = 1.8$ (12.9 *M*); selenic acid (first step), $n \approx 2.0$; benzene sulfonic acid, $n = 5$ (4.9 *M*); and nitric acid, $n = 12$ (4.0 *M*). Hence in this series more and more water molecules are required for the removal of the protons from the anions.

With these spectroscopically determined degrees of dissociation one must keep in mind that the acid molecules observed as dissociated are not only those the protons of which are removed from the anion and present in $H_5O_2^+$, but also those with which the proton is present in proton-limiting structure **II** in the acid–water hydrogen bond (see following section).

Water–Acid Ratio Less Than One

Let us consider first the case of less than one water molecule per acid molecule ($n < 1$). With all these acids the absorbance of the continuum increases in proportion to the molarity of water, as shown by Fig. 4*a*. Simultaneously the OH stretching vibration (Table 2, column 1) of the acid, observed in the pure acids, vanishes. All these results taken together demonstrate the formation of easily polarizable acid–water hydrogen bonds, as represented by the two proton-limiting structures

$$\underset{\mathbf{I}}{AH\cdots OH_2} \rightleftharpoons \underset{\mathbf{II}}{A^-\cdots H^+OH_2}$$

In Fig. 4*b* the concentrations of protons removed from the anion (M_{H^+}) are plotted as a function of the molarity of water. From these results (as described in ref. 28) the weights of the proton-limiting structures at $n = 1$ were calculated and given in Table 2. For all acids under these conditions the proton can be present in both limiting positions. Thus in these acids acid–water hydrogen bonds with double minimum energy surfaces occur, as expected from the observed continuum.

In the series F_3CSO_2OH, H_2SO_4, $HClO_4$, C_6H_5-SO_2OH, HNO_3, the weight of proton-limiting structure **II** decreases and the weight of proton-limiting structure **I** increases. Thus in this series of acids, when one water molecule is present per acid molecule, the deeper well of the energy surface in the acid–water hydrogen bonds at the beginning of the series is present at the water molecule, and at the end of the series at the anion.

Let us now consider the bands of the water molecules in the acid–water groupings. The OH stretching vibration is observed as a very broad band with maximum in the region 3000–2600 cm^{-1}. Here and in the following, nitric acid will be considered separately. The maximum of the OH bending vibration is listed in Table 2, columns 7 and 8. With $HClO_4$ this vibration is observed at about 1700 cm^{-1}, largely independent of n, whereas with the other acids this band is found for $n \approx 0.5$ in the

Can. J. Chem. Downloaded from www.nrcresearchpress.com by 210.87.254.105 on 09/05/12
For personal use only.

TABLE 1. Experimental data of the acids

Acid	Source*	Smallest n value measured	Absorbance of the continuum at 1900 cm^{-1} 1 M	5 M	$\delta(OH)(H_2O)$ cm^{-1} at $n \approx 6$	pK_a
$HAuCl_4$	(a)	6.9	0.125	0.49	1620†	
H_2PtCl_6	(c)	15.4	0.125	0.53	1620‡	
H_2PtBr_6	(b)	9.6	0.125	0.53	1622‡	
$HClO_4$	(a)	0.0	0.135	0.55	1631	−7
HBF_4	(b)	4.0	0.135	0.50	1634	
CF_3SO_3H	(a)	0.0	0.13	0.57	1635	
HJ	(b)	3.2	0.14	0.58	1633	−9.5
H_2SO_4	(a)	0.0	0.14§	0.50§	1638	−3
H_2SeO_4	(a)	0.0	0.14§	0.50§	1639	−3
$C_6H_5SO_3H$	(a)	0.0	0.14	0.58	1640	0.7
$C_7H_7SO_3H$	(a)	4.4	0.14	0.59	1640	0.9
HCl	(a)	3.4	0.14	0.60	1643	−6
HNO_3	(a)	0.0	0.14	0.53	—	−1.4
CF_3COOH	(a)	0.0	0.13	0.50	—	0.2
HJO_3	(b)	4.9	0.095	0.32	—	0.77

*(*a*) Merck, Darmstadt, Germany; (*b*) Riedl-de-Haen, Seelze, Germany; (*c*) Fluka, Buchs, Switzerland.
†At $n = 6.9$.
‡In these cases n not H_2O per acid molecule but per proton, with H_2PtCl_6 at $n = 7.2$.
§The continuum of a $NaHSO_4$ and $NaHSeO_4$ solution of equal molarity was subtracted.

TABLE 2. Continuous absorption, hydration, and dissociation

Acid	$\nu(OH)$(acid) cm^{-1} at $n = 0$	Complete dissociation at $n =$	Weight of proton-limiting structures I	II	Absorbance of the continuum/M_{H^+} (at $n = 2$)	$\delta(OH)(cm^{-1})$ $n = 0.5$	$n = 1.2$
CF_3SO_3H	3040	1.6	0.15	0.85	0.07	1650	1715
H_2SO_4	3000	1.6	0.15	0.85	0.085	1670	1705
$HClO_4$	3380	1.8	0.25	0.75	0.05	1705	1705
H_2SeO_4	3000	2				1660	1700
$C_6H_5SO_3H$	3000	5	0.45	0.55	0.11	1685	1708
HNO_3	3350	12	0.90	0.10	—	—	

region 1640–1685 cm^{-1}, from $n = 0.5$ to $n = 1.2$ this band shifts to about 1710 cm^{-1}. Thus, with the exception of $HClO_4$, the OH bending vibration is observed, at $n = 0.5$, in the position of the scissor vibration of water molecules, whereby the shift from 1640 to 1685 cm^{-1} indicates that these water molecules in this series form increasingly stronger hydrogen bonds. As already discussed in ref. 28, the relatively high constant position of the OH bending vibration with $HClO_4$ is due to the strong influence of the proton on the H_2O molecule. This vibration shows H_3O^+ character. As discussed in detail in ref. 28, the H_3O^+ character of the vibrations increases with decreasing asymmetry of the environment of the H^+OH_2 grouping in the

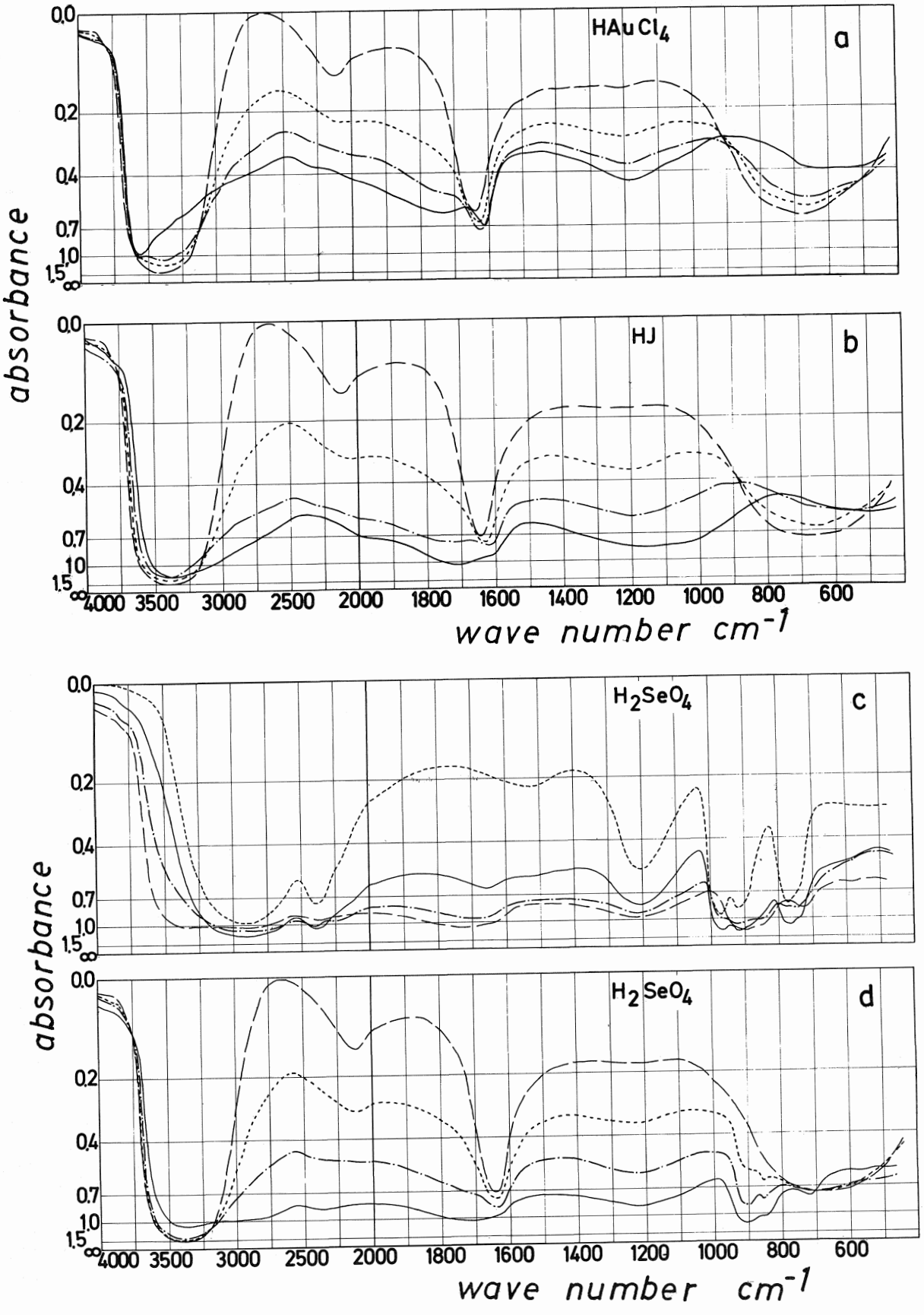
$$AH\cdots OH_2 \rightleftharpoons A^-\cdots H^+OH_2$$

hydrogen bonds. This explains the shift of the OH bending vibration. From $n = 0.5$ to $n = 1.2$, this band shifts towards larger wave numbers, because of the fact that the acceptors of these water molecules now change from O atoms of non-dissociated acid molecules to O atoms of anions. Therefore, the environment of the H^+OH_2 grouping in proton limiting structure **II** becomes more symmetrical and thus the vibrations gain H_3O^+ character.

In the case of nitric acid (29), the H_2O stretching vibration is observed at 3580 cm^{-1} and the scissor vibration at 1615 cm^{-1}, i.e., the water molecules in the acid–water groupings form only very weak hydrogen bonds. This can be explained by the fact that nitric acid is only weakly dissociated for $n < 1$. Hence the acceptors of these hydrogen bonds are preferentially O atoms of non-dissociated acid molecules, which are less strong acceptors than O atoms of anions.

FIG. 1. Infrared spectra of aqueous solutions: (*a*) $HAuCl_4$: — 5.3 M ($n = 6.9$), ····· 3.0 M ($n = 14.3$), --- 1.5 M ($n = 31$), – – – H_2O; (*b*) HJ: — 10.9 M ($n = 3.2$), ····· 6.3 M ($n = 6.9$), --- 2.0 M ($n = 26$), – – – H_2O; (*c*) H_2SeO_4: --- 20.7 M ($n = 0.0$), — 17.3 M ($n = 0.66$); ····· 14.5 M ($n = 1.3$), – – – 9.6 M ($n = 3.1$); (*d*) H_2SeO_4: — 8.5 M ($n = 4.0$), ····· 2.8 M ($n = 17.4$); --- 0.9 M ($n = 61$), – – – H_2O.

Can. J. Chem. Downloaded from www.nrcresearchpress.com by 210.87.254.105 on 09/05/12
For personal use only.



Can. J. Chem. Downloaded from www.nrcresearchpress.com by 210.87.254.105 on 09/05/12
For personal use only.

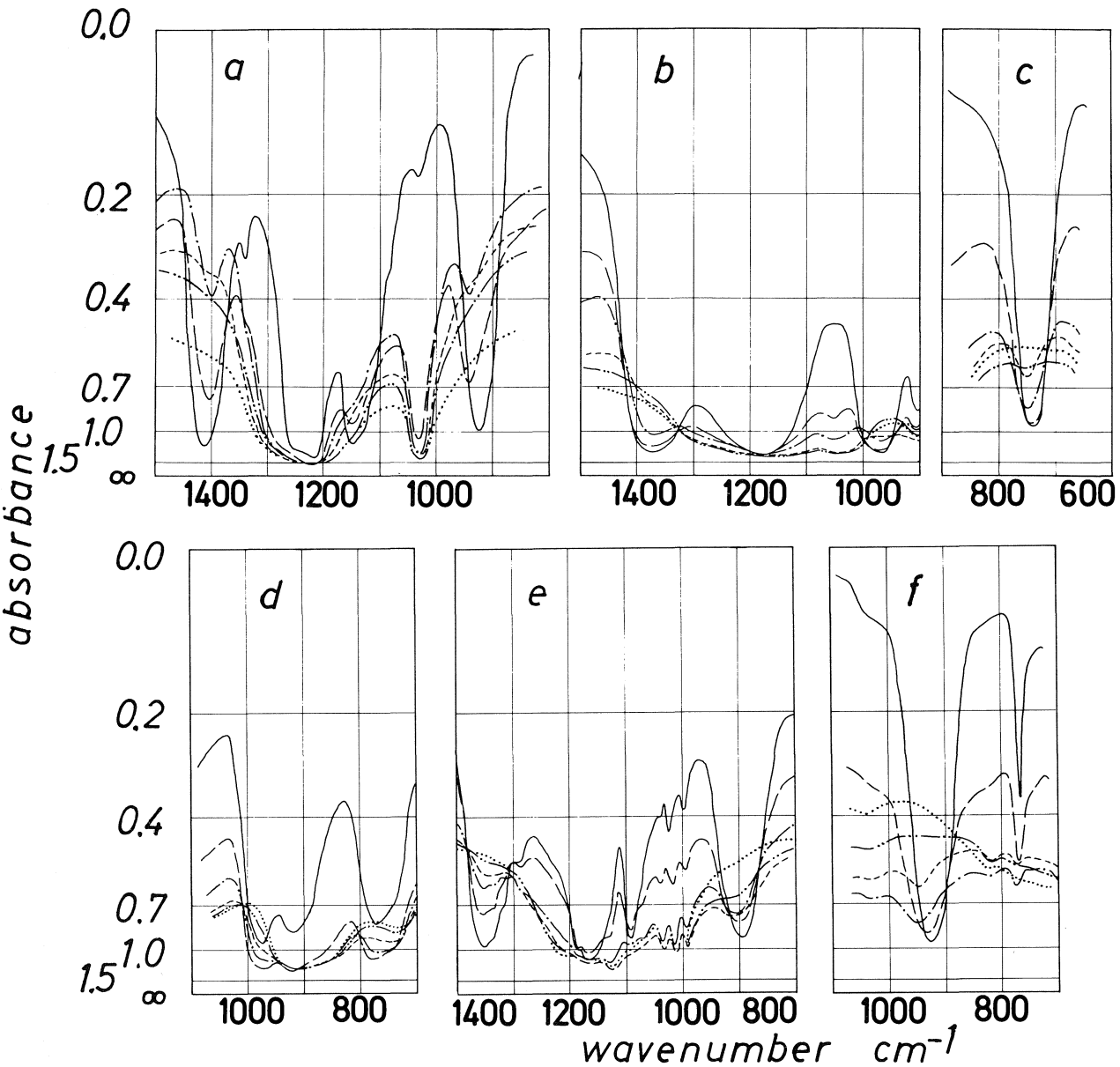


FIG. 2. Characteristic bands of non-dissociated acid molecules and their disappearance with increasing $n = M_{H_2O}/M_{acid}$. (*a*) CF_3SO_3H: — $n = 0.0$, – – – $n = 0.56$, ····· $n = 0.95$, --- $n = 1.28$, ····· $n = 1.55$, ··· $n = 1.87$; (*b*) H_2SO_4: — $n = 0.0$, – – – $n = 0.16$, ····· $n = 0.45$, --- $n = 1.04$, ····· $n = 1.61$, ··· $n = 2.0$; (*c*) $HClO_4$: — $n = 0.0$, – – – $n = 0.24$, ····· $n = 0.63$, --- $n = 1.27$, ····· $n = 1.46$, ··· $n = 2.0$; (*d*) H_2SeO_4: — $n = 0.0$, – – – $n = 0.40$, ····· $n = 1.05$, --- $n = 1.63$, ····· $n = 2.46$, ··· $n = 3.10$; (*e*) $C_6H_5SO_3H$: — $n = 0.0$, – – – $n = 0.3$, ····· $n = 0.9$, --- $n = 1.8$, ····· $n = 2.3$, ··· $n = 3.0$; (*f*) HNO_3: — $n = 0.0$, – – – $n = 0.53$, ····· $n = 2.1$, --- $n = 3.7$, ····· $n = 8.7$, ··· $n = 15.2$.

Water–Acid Ratio Greater Than One

With increasing n the degree of dissociation increases (Fig. 3). The addition of water molecules increases the weight of the polar proton limiting structure $A^- \cdots H^+OH_2$, an effect well known from other systems (2, 4). This increase of the weight of proton-limiting structure **II** is indicated by an increase of the intensity of the broad band of the OH stretching vibration in the region 3000–2600 cm^{-1}. With very strong acids, which are completely dissociated for $n = 2$, this band shows a maximum at about $n = 1.2$ (Fig. 7 in ref. 28).

With benzene sulfonic acid, i.e., an acid for which more water molecules must be present for

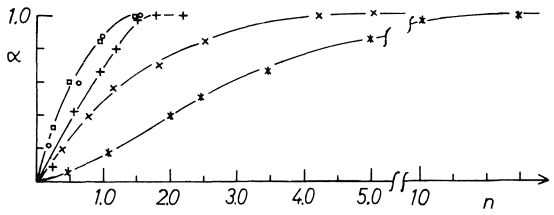


FIG. 3. Degree of dissociation of $HClO_4$: +; H_2SO_4: ○, CF_3SO_3H: □; $C_6H_5SO_3H$: ×; HNO_3: * depending on the mole ratio nH_2O/acid.

complete removal of the protons from the anions, this band has maximum intensity for $n = 2.0$. Finally, for nitric acid, this band is not observed as a pronounced band since at $n = 1$, the weight of proton limiting structure **II** is only 0.13. This weight of structure **II** increases slowly with increasing n. The presence of structure **II**, however, favours the transfer of the proton into the network of the hydrogen-bonded water molecules, i.e., the formation of $H_5O_2^+$. Thus, with nitric acid the concentration of proton-limiting structure **II** remains low.

The $H_5O_2^+$ Groupings

With the stronger acids, the ν(OH) band in the region 3000–2600 cm^{-1} is quite pronounced, but decreases for $n > 1.2$ and disappears with increasing n (Fig. 7 in ref. 28). This result indicates that in this case the protons transfer from the acid–water hydrogen bonds into hydrogen bonds between water molecules. As demonstrated earlier with acidic polyelectrolytes (1, 33) and aqueous solutions of strong acids (refs. 16, 26, see also ref. 23), the excess proton is present in $H_5O_2^+$ groupings which are embedded in the hydrate structure network.

The band observed with the strong acids for $n = 1$, with a maximum at about 1700 cm^{-1} caused by H^+OH_2 groupings of the proton limiting structure **II**, increases a little and shifts toward larger wave numbers. This band is found for $n = 2$ with a maximum at about 1740 cm^{-1}, caused by the bending vibration of the water molecules in $H_5O_2^+$ groupings. When more water molecules are added, i.e., with increasing n, the intensity of this band decreases, due to dilution of the acid solutions.

With all these acids, at $n = 2$, only one broad band of a H_2O scissor vibration is observed (Figs. 1*d* and 1*f* and in ref. 28 Figs. 1*a* and 1*b*). This clearly demonstrates, as discussed earlier (28, 34), that in $H_5O_2^+$, the proton is distributed between both water molecules, since otherwise, not only one but two bands ($\delta_{as}(H_3O^+)$ and $\delta(H_2O)$ of $H_3O^+H_2O$ grouping) should be observed. An additional OH bending vibration is only observed, however, with $n > 2$ (see following section). Thus, in aqueous solutions, in contrast to other statements (35–38), the H_3O^+ groups do not vibrate as an entity, when sufficient water molecules are present to form $H_5O_2^+$ groupings. The same conclusion was reached by Librovich, Maiorov, and Savalev comparing ir and Raman data (26).

In the liquid state, H_3O^+ vibrations (as mentioned above) may only be found when less than two water molecules per excess proton are present. In crystals, such vibrations are found when the excess proton is present at one water molecule (39). Finally, such vibrations can be observed when H_3O^+ is present in the gas phase (40).

The absorbance of the continuum at 1900 cm^{-1} is given for 1 *M* and 5 *M* solutions in Table 1, columns 1 and 2. Where pK_a values are known, the absorbance of these continua is plotted as a function of the pK_a values of the acids in Fig. 5.

The results in Table 1 and Fig. 5 demonstrate the following: for all acids completely dissociated at

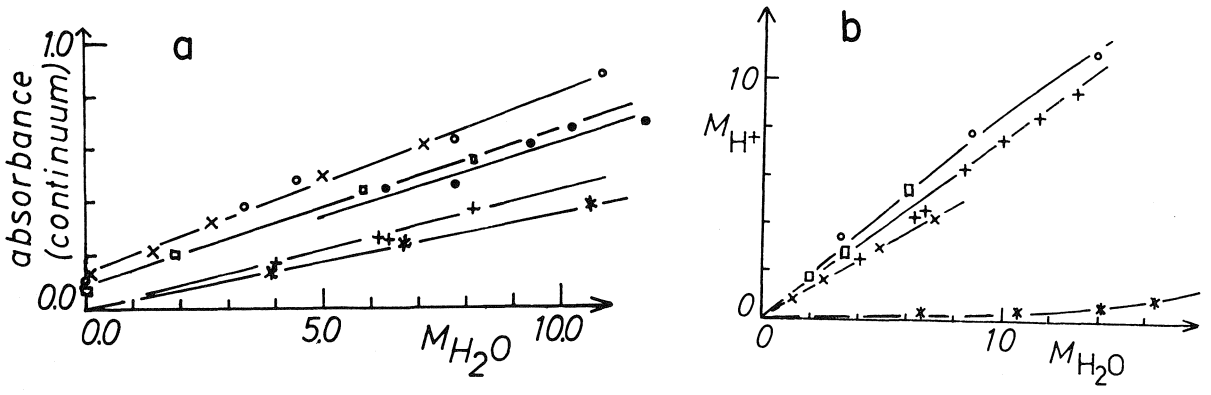


FIG. 4. (*a*) Absorbance of the continuum depending on the molarity of water. (*b*) Molarity of dissociated protons depending on the molarity of water $HClO_4$: +; H_2SO_4: ○; CF_3SO_3H: □; H_2SeO_4: ●; $C_6H_5SO_3H$: ×; HNO_3: *.

Can. J. Chem. Downloaded from www.nrcresearchpress.com by 210.87.254.105 on 09/05/12
For personal use only.

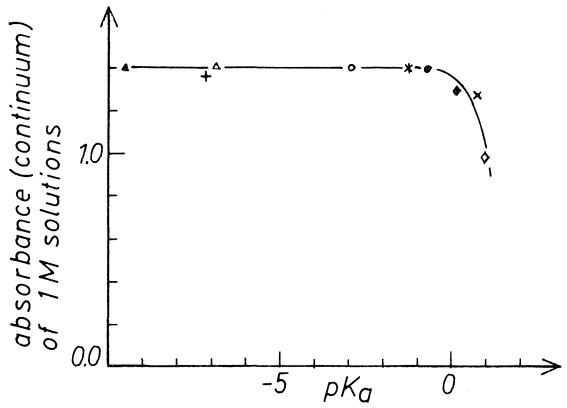


FIG. 5. Continuous absorption of 1 *M* solutions for HJ: ▲; HCl: △; $HClO_4$: +; H_2SO_4: ○; HNO_3: *; H_2SeO_4: ●; CF_3COOH: ◆; $H_2C_5O_4$: ×; HJO_3: ◇.

these concentrations, the absorbance of the continuum is the same, within experimental error. With increasing pK_a of the acids, the intensity of the continuum decreases since the acids are no longer completely dissociated. The fact that the strength of the absorbance of the continuum becomes independent of pK_a of the respective acid, for acids with $pK_a < 0$, suggests that in this pK_a region, with all acids at these concentrations, the same easily polarizable hydrogen bond causes the continuum. As discussed above and facts from the literature (1, 16, 20, 33), this polarizable hydrogen bond is the bond in $H_5O_2^+$ groupings.

The absorbance of these groupings, however, is equal, only if their interaction with the environment is the same. This will be demonstrated as follows. In Fig. 6, for $n > 2$, the absorbance of the continuum per proton removed from the anion is plotted as a function of n. As shown above, under these conditions, most of the protons of the strong acids are already present in easily polarizable hydrogen bonds of $H_5O_2^+$ groupings. Hence Fig. 6 shows the following: Result (*1*) For $n = 2$ to $n = 4$, the absorbance of the continuum per polarizable hydrogen bond increases in the series from perchloric acid to benzenesulfonic acid. Result (*2*) With increasing n in the region $n = 2$ to $n = 4$, the absorbance of the continuum per polarizable hydrogen bond increases. This increase is stronger the smaller the absorbance of the continuum per polarizable hydrogen bond at $n = 2$. Result (*3*) For larger n, the absorbance of the continuum per polarizable hydrogen bond becomes the same for all acids.

Theoretical calculations have shown that the interaction of the $H_5O_2^+$ groupings with their environment changes the intensity of the absorbance of the continuum per $H_5O_2^+$ grouping. These intensity

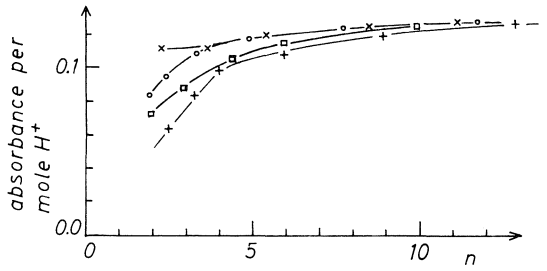


FIG. 6. Continuous absorption per mol of dissociated protons depending on the H_2O/acid mole ratio n. $HClO_4$: +; H_2SO_4: ○; CF_3SO_3H: □; $C_6H_5SO_3H$: ×.

changes have the following causes: firstly, when the $H_5O_2^+$ groupings are bound to stronger hydrogen bond acceptors, the OO distance in these groupings is stretched, and the barrier in the energy surfaces increased. From theory it is well known that many more transitions occur in the region 2500–1000 cm^{-1}, contributing to the continuum, when the mean OO distance of $H_5O_2^+$ is increased. This is shown by Fig. 6 in ref. 19 and demonstrated especially clearly by the calculated continua in ref. 20 (see Fig. 5 of ref. 20). Secondly, when the environment of $H_5O_2^+$ becomes more polar, transitions in the polarizable hydrogen bond may couple more strongly with low wave number vibrations in their environment. Thus, these vibrations may contribute and increase the intensity of the continuum. This intensity increase due to coupling with intermolecular vibrations can probably be described very well by the theory of Librovich, Sakun, and Sokolov (23).

These theoretical results explain the observed experimental findings: result *1*, the absorbance of the continuum per $H_5O_2^+$ in the series form $HClO_4$ to benzene sulfonic acid increases because the hydrogen bond acceptor strength of the anions and hence also the polarity of the environment of the $H_5O_2^+$ groupings increases in this series. Result *2*, the increase of the absorbance of the continuum per $H_5O_2^+$ with increasing n is analogously explained since the lone electron pairs of water molecules are much stronger acceptors than the O atoms of ClO_4^- ions. Therefore, when water molecules are added to $H_5O_2^+$ groupings the latter become more strongly bound to their environments and these environments become much more polar than when only the ClO_4^- ions are present. Thus, the absorbance of the continuum per polarizable hydrogen bond in $H_5O_2^+$ increases. This increase becomes less pronounced when the O atoms of the anions are stronger hydrogen bond acceptors, and vanishes when the acceptor strength becomes comparable to that of the lone pairs of the water molecules. At

Can. J. Chem. Downloaded from www.nrcresearchpress.com by 210.87.254.105 on 09/05/12
For personal use only.

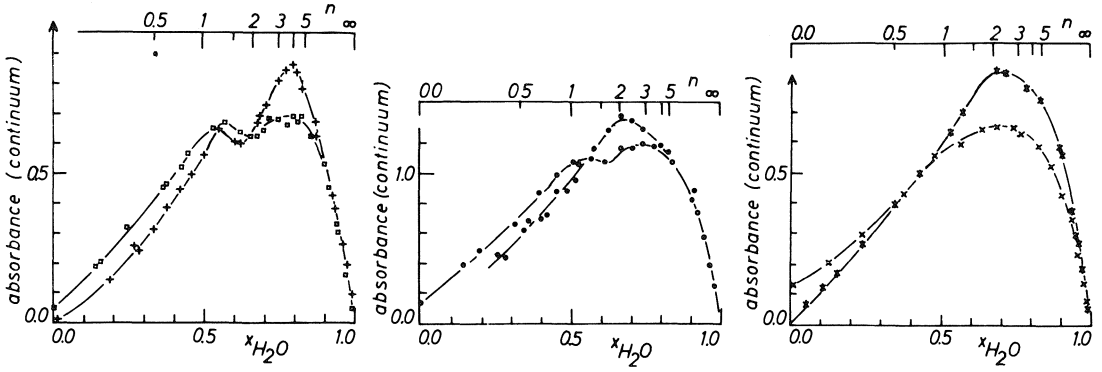


FIG. 7. Continuous absorption depending on the mole fraction of water x_{H_2O} and the water/acid mole ratio n: (*a*) $HClO_4$: +; CF_3SO_3H: □; (*b*) H_2SO_4: ○; H_2SeO_4: ●; (*c*) $C_6H_5SO_3H$: ×; HNO_3: *.

larger n, the absorbance of the continuum per proton becomes the same with all these acids (result *3*), since (as discussed above) $H_5O_2^+$ is then present, which is embedded in the network of hydrogen bonds formed by other water molecules.

In Fig. 7 the absorbance of the continuum at 1900 cm^{-1} is plotted as a function of mole fraction of water, X_{H_2O} and of n. In the case of acids with small pK_a a maximum of the absorbance is observed at $n = 1.2$, as already discussed in detail for $HClO_4$ and CF_3SO_3H in ref. 28. This maximum is caused by the slope of the broad band observed in the region 3000–2600 cm^{-1}. With these acids, a second maximum of the absorbance of the continuum is observed at larger n values, with $HClO_4$ at $n = 4.0$, with CF_3SO_3H at $n = 3.7$, and with H_2SO_4[1] at $n = 3.0$. The other acids show only one maximum, which is observed with H_2SeO_4 at $n = 2$, with $C_6H_5SO_3H$ at $n = 2.3$, and with HNO_3 at 2.3. This absorbance maximum is explained as follows: the increase of the absorbance is caused by the formation of $H_5O_2^+$ groupings. In the case of the acids with small pK_a, an additional increase of the absorbance is due to the above discussed increase of the absorbance per $H_5O_2^+$, caused by the addition of water molecules. The decrease of the absorbance of the continuum with increasing n is caused by decreasing concentration of $H_5O_2^+$ due to increasing dilution. Hence the shift of the maximum from $n = 4$ ($HClO_4$) to $n = 2$ (H_2SeO_4) is caused by the fact that the absorbance per $H_5O_2^+$ increases from $n = 2$ to $n = 4$ for $HClO_4$, whereas with H_2SeO_4 the absorbance per $H_5O_2^+$ is nearly the same for $n = 4$ and $n = 2$ (Fig. 6). The maximum of the absorbance with $C_6H_5SO_3H$ and HNO_3 is shifted towards larger n, since with these acids $H_5O_2^+$ groupings are still formed for $n > 2$.

Hydrogen Bond Acceptor Strength of the Anions

With increasing n at the low wave number slope of the band of the scissor vibration of the water molecules in the $H_5O_2^+$ grouping, the scissor vibration of the additional water molecules occurs. Some selected examples are shown in Fig. 8. This additional band is found in the region 1650–1615 cm^{-1}. The corresponding stretching vibration of these H_2O molecules is observed in the region 3580–3360 cm^{-1}. These water molecules are bound with their lone electron pairs to the OH groups of $H_5O_2^+$ and with their OH groups preferentially to acceptor groups of the anions. When these acceptors are very weak (as, for instance, it is the case with $AuCl_4^-$), the H_2O scissor vibration for $n = 6.9$ is observed at 1620 cm^{-1} and the stretching vibration at 3570 cm^{-1} (see Fig. 1*a*). The low position of the scissor vibration and the high position of the stretching vibration indicate that these water molecules are only very weakly bound to anions. In contrast to this result, with benzene sulfonic acid these bands are observed at 1640 and 3400 cm^{-1}, indicating that in this case the water molecules are bound to the anions via much stronger hydrogen bonds. In the following we consider the position of the scissor vibration, since the stretching vibration is very broad and in some cases superimposed on the OH stretching vibration of second OH groups of acid molecules. The position of the scissor vibration for $n = 6$ is given in Table 1, column 4. These band positions indicate the increase of the hydrogen bond acceptor strength in this series of anions from $AuCl_4^-$ to Cl^-.

The nitric acid solution is an exception since as long as the nitric acid is not completely dissociated, O atoms of non-dissociated acid molecules are acceptors for the OH groups of the water molecules.

[1]With previous measurements of aqueous H_2SO_4 solutions (34), the maxima of the intensity of the continuum at 1.2 and 3.0 could not be separated since the layer thickness of the samples was too great and the absorbance therefore too intense.

Can. J. Chem. Downloaded from www.nrcresearchpress.com by 210.87.254.105 on 09/05/12
For personal use only.

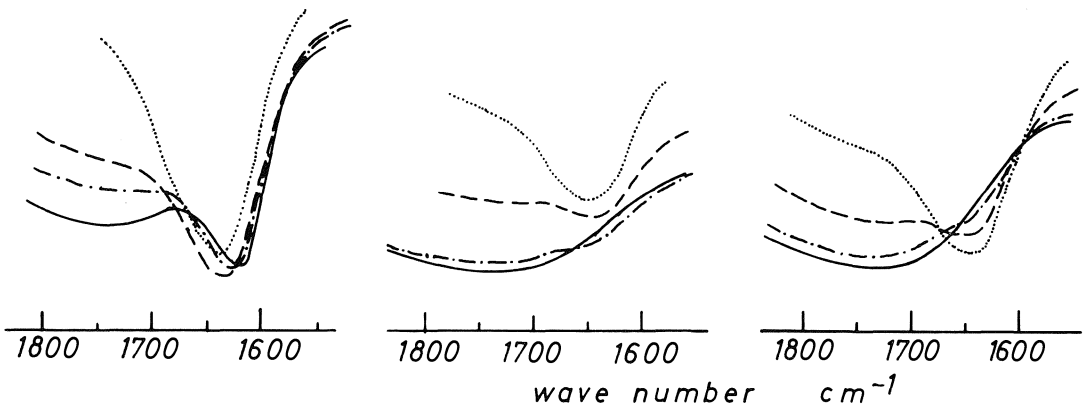


FIG. 8. (*a*) $HAuCl_4$: — $n = 6.9$; ····· $n = 9.9$; --- $n = 14.3$; ··· $n = 31.4$; (*b*) H_2SO_4: — $n = 2.4$; ····· $n = 4.9$; --- $n = 11.2$; ··· $n = 25.9$; (*c*) $C_6H_5SO_3H$: — $n = 2.2$; ····· $n = 3.5$; --- $n = 7.0$; ··· $n = 16.2$.

These O atoms are, however, much weaker acceptors than those of NO_3^- anions, and therefore the OH stretching vibration is observed at larger wave numbers, as already discussed in ref. 29.

With increasing n, for all these acids, the vibrations of the water molecules shift to the position in which these vibrations are observed in pure water, since more and more water–water hydrogen bonds are present in the solutions.

Conclusions

With acids ($pK_a < 1$), which are soluble up to concentrations at which one or less than one water molecule is present, the acid water hydrogen bonds formed under these conditions are easily polarizable proton transfer bonds

$$\underset{\mathbf{I}}{AH\cdots OH_2} \rightleftharpoons \underset{\mathbf{II}}{A^-\cdots H^+OH_2}$$

In the series CF_3SO_3H, H_2SO_4, $HClO_4$, H_2SeO_4, $C_6H_5SO_3H$, HNO_3, the weight of proton-limiting structure **I** increases and the weight of structure **II** decreases. The energy surfaces in these bonds are double minima, whereby with the stronger acids in the above series the deeper well is present at the water molecule and with the less strong acids at the anion.

Complete dissociation is reached with CF_3SO_3H at $n = 1.6$, H_2SO_4 (first step) at $n = 1.6$, $HClO_4$ at $n = 1.8$, H_2SeO_4 (first step) at $n \approx 2$, $C_6H_5SO_3H$ at $n = 5$, and HNO_3 at $n = 12$. Hence the acceptor strength of the anions for the proton in this series of acids increases.

The molecular processes associated with the removal of the proton from the anion are as follows: for $n = 0$ to $n = 1$, easily polarizable acid–water hydrogen bonds are formed. For $n > 1$, the weight of proton-limiting structure **II** increases due to the influence of the additional water molecules. The vibrations of the water molecules in the

$$AH\cdots OH_2 \rightleftharpoons A^-\cdots H^+OH_2$$

groupings gain more and more H_3O^+ character. Thereafter, the protons transfer from these acid—water hydrogen bonds into hydrogen bonds between water molecules, i.e., $H_5O_2^+$ groupings are formed. The excess proton in these groupings is distributed between both water molecules. H_3O^+ no longer vibrates as an entity. The easily polarizable hydrogen bond in $H_5O_2^+$ groupings causes strong ir continuous absorption, whereas the water molecules cause strong bands.

At $n = 2$, the continuous absorbance per $H_5O_2^+$ strongly depends on the acceptor strength of the O atoms of the anions, i.e. on the polarity of the environment. It increases with increasing acceptor strength in the series ClO_4^-, $CF_3SO_3^-$, HSO_4^-, $HSeO_4^-$, $C_6H_5SO_3^-$. In the case of acids with anions which are only weak hydrogen bond acceptors, the intensity of the continuum per $H_5O_2^+$ increases strongly with addition of water in the range $n = 2$ to $n = 4$, due to increasing interaction of the polarizable hydrogen bond in $H_5O_2^+$ with its environment.

With all acids studied, the hydrogen bond acceptor strength of the anions can be determined by considering the position of the bands of the water molecules. High wave number values of ν(OH) and low of δ(OH) indicate weak acceptor strength. From the positions of the H_2O scissor vibration at $n = 6$ (Table 1 column 6), the following series for increasing hydrogen bond acceptor strength of the anions is obtained: $AuCl_4^-$, $PtBr_6^{2-}$, ClO_4^-, BF_4^-, $CF_3SO_3^-$, I^-, HSO_4^-, $HSeO_4^-$, $C_6H_5SO_3^-$, $C_7H_7SO_3^-$, Cl^-.

The acceptor atoms of the non-dissociated acid molecules are much weaker hydrogen acceptors

Can. J. Chem. Downloaded from www.nrcresearchpress.com by 210.87.254.105 on 09/05/12
For personal use only.

Can. J. Chem. Downloaded from www.nrcresearchpress.com by 210.87.254.105 on 09/05/12
For personal use only.

than those of the anions. This is especially well demonstrated by nitric acid (29).

This series of the hydrogen bond acceptor strength of the anions of the respective acids does not agree with the series of the proton acceptor strength of the anions obtained as discussed above from the data in Table 2, columns 3–5. Complete dissociation occurs, for instance, with CF_3SO_3H and H_2SO_4 (first step) at smaller n values than with $HClO_4$, whereas the hydrogen bond acceptor strength of the O atoms of $CF_3SO_3^-$ and HSO_4^- is greater than that of ClO_4^-. As will be discussed in the following, both quantities determine the pK_a values of the acids.

The pK_a values are determined by measuring activities with potentiometric, indicator, or other classical methods. The aim of these methods is to obtain the number of dissolved particles. The macroscopic quantities measured with these procedures are determined, however, not only by the proton acceptor strength of the anions but also by the interactions of these ions with their environment, i.e., with the water molecules. Therefore, not only the proton acceptor strength of the anions but also the number and strength of the hydrogen bond acceptor sites of the anions, which are the decisive quantities for their hydration, determine the measured pK_a values.

In the case of $HClO_4$, a pK_a value smaller than that of H_2SO_4 is given in the literature (41–43) although the acceptor strength of ClO_4^- for the proton is greater than for HSO_4^-. The reason for the smaller pK_a value of $HClO_4$ is that ClO_4^- binds water molecules less strongly than HSO_4^-, due to the weaker hydrogen bond acceptor strength of the O atoms of ClO_4^- ions. In addition, the OH group of HSO_4^- also contributes to the interaction of HSO_4^- with the environment. Thus, the apparent particle number is smaller because of the stronger interaction of the water molecules with sulfuric acid. Hence a larger pK_a is measured with sulfuric acid than with $HClO_4$, although the proton acceptor strength of HSO_4^- is smaller than that of ClO_4^-.

The pK_a is smaller with HNO_3 ($pK_a = -1.4$ (43)) than with the sulfonic acids ($C_6H_5SO_3H$ ($pK_a = 1.5$ (42), 0.7 (44)), $C_7H_7SO_3H$ ($pK_a = 1.7$ (42), 0.9 (44))), whereas the ir spectroscopic results show that the proton acceptor strength is much stronger for nitric acid than for sulfonic acids. The latter is true not only for the sulfonic acids mentioned above but also for methane sulfonic acid as shown by Raman spectroscopy (12) and for polystyrene sulfonic acid as shown by ir (1), Raman (45), and nmr (46) studies. These discrepancies are caused by different interaction of the anions with their environment. NO_3^- is hydrophilic. In contrast to this property all mentioned sulfonic acids have hydrophobic groups besides the hydrophilic $—SO_3^-$ group. Because of these hydrophobic groups, the anions interact with one another, reducing the measured apparent particle number. Therefore the electrochemically observed pK_a is greater, although the removal of the proton from the anion, i.e., the spectroscopically observed dissociation is larger with the sulfonic acids than with nitric acid.

Thus the pK_a values are determined by various molecular quantities: *1*, the acceptor strength of the anions for the proton; *2*, the hydrogen bond acceptor strength of the anions, which determines the interaction of these anions with the water molecules; *3*, interactions due to hydrophobic groups causing association of the anions.

Acknowledgements

Our thanks are due to the Deutsche Forschungsgemeinschaft and to the Fond der Chemischen Industrie for providing the facilities for this work.

1. G. ZUNDEL. Hydration and intermolecular interaction. Academic Press, New York. 1969. p. 116*ff*; Mir Moscov 1972.
2. R. LINDEMANN and G. ZUNDEL. (*a*) J. Chem. Soc. Faraday II, **73**, 788 (1977); (*b*) Biopolymers, **16**, 2407 (1977); (*c*) Biopolymers, **17**, 1285 (1978).
3. M. MATTHIES and G. ZUNDEL. Biochem. Biophys. Res. Commun. **74**, 831 (1977).
4. A. NAGYREVI and G. ZUNDEL. J. Phys. Chem. **82**, 687 (1978).
5. K. STOPERKA. Z. Anorg. Allg. Chem. **344**, 263 (1966).
6. V. D. MAIOROV and N. B. LIBROVICH. Russ. J. Phys. Chem. **47**, 1295 (1973).
7. V. D. MAIOROV and N. B. LIBROVICH. Russ. J. Phys. Chem. **49**, 1661 (1975).
8. W. R. BUSING and D. F. HORNIG. J. Phys. Chem. **65**, 284 (1961).
9. T. F. YOUNG and G. E. WALRAFEN. Trans. Faraday Soc. **57**, 34 (1961).
10. G. E. WALRAFEN. J. Chem. Phys. **39**, 1479 (1963).
11. T. F. YOUNG, L. F. MERANVILLE, and H. M. SMITH. *In* The structure of electrolytic solutions. *Edited by* W. Hamer. Wiley, New York. 1959.
12. J. H. R. CLARKE and C. A. WOODWARD. Trans. Faraday Soc. **62**, 2226 (1966); **62**, 3022 (1966).
13. A. K. COVINGTON, J. G. FREEMAN, and TH. LILEY. J. Phys. Chem. **74**, 3773 (1970).
14. (*a*) H. CHEN and D. E. IRISH. J. Phys. Chem. **75**, 2672 (1971); (*b*) M. H. HERZOG-CANCE, J. POTIER, A. POTIER, P. DHAMELINCOURT, B. SOMBRET, and F. WALLART. J. Raman Spectrosc. **7**, 303 (1978).
15. G. ZUNDEL. Allgem. Prakt. Chem. Wien, **21**, 329 (1970).
16. G. ZUNDEL. *In* The hydrogen bond—recent developments in theory and experiments. Vol. II. *Edited by* P. Schuster, G. Zundel, and C. Sandorfy. North Holland Publ. Co., Amsterdam. 1976.

17. E. G. WEIDEMANN and G. ZUNDEL. Z. Naturforsch. **25**a, 627 (1970).
18. R. JANOSCHEK, E. G. WEIDEMANN, H. PFEIFFER, and G. ZUNDEL. J. Am. Chem. Soc. **94**, 2387 (1972).
19. R. JANOSCHEK, E. G. WEIDEMANN, and G. ZUNDEL. J. Chem. Soc. Faraday II, **69**, 505 (1973).
20. A. HAYD, E. G. WEIDEMANN, and G. ZUNDEL. J. Chem. Phys. **70**, 86 (1979).
21. R. JANOSCHEK, A. HAYD, E. G. WEIDEMANN, M. LEUCHS, and G. ZUNDEL. J. Chem. Soc. Faraday Trans. II, **74**, 1238 (1978).
22. A. H. NARTEN. *In* Proceedings of the International Symposium on Structure of Water and Aqueous Solutions. Marburg, Germany. 1973. *Edited by* W. A. P. Luck. Verlag Chemie, Weinheim, Germany. 1974.
23. (*a*) N. B. LIBROVICH, V. P. SAKUN, and N. D. SOKOLOV. Chem. Phys. **29**, 351 (1979); (*b*) G. ZUNDEL and E. G. WEIDEMANN. Chem. Phys. In press.
24. M. ROSPENK, A. KOLL, and L. SOBCZYK. Adv. Mol. Relaxation Processes, **11**, 129 (1977).
25. N. B. LIBROVICH, V. D. MAIOROV, and M. I. VINNIK. Zh. Strukt. Khim. **14**, 17 (1973).
26. N. B. LIBROVICH, V. D. MAIOROV, and V. A. SAVEL'EV. Dokl. Akad. Nauk SSSR, **225**, 1358 (1975).
27. V. D. MAIOROV and N. B. LIBROVICH. Russ. J. Phys. Chem. **51**, 141 (1977).
28. M. LEUCHS and G. ZUNDEL. J. Chem. Soc. Faraday II, **74**, 2256 (1978).
29. M. LEUCHS and G. ZUNDEL. J. Phys. Chem. **82**, 1632 (1978).
30. H. PFEIFFER, G. ZUNDEL, and E. G. WEIDEMANN. J. Phys. Chem. **83**, 2544 (1979).
31. D. SCHIÖBERG and G. ZUNDEL. Can. J. Chem. **54**, 2193 (1976).
32. R. PETZOLD and M. AMOULONG. Z. Anorg. Allg. Chem. **317**, 288 (1962).
33. G. ZUNDEL and H. METZGER. Z. Phys. Chem. Frankfurt, **58**, 225 (1968).
34. D. SCHIÖBERG and G. ZUNDEL. Z. Phys. Chem. Frankfurt, **102**, 169 (1976).
35. M. FALK and P. GIGUÈRE. Can. J. Chem. **35**, 1195 (1957).
36. P. GIGUÈRE and S. TURELL. Can. J. Chem. **54**, 3777 (1976).
37. H. D. DOWNING and D. WILLIAMS. J. Phys. Chem. **80**, 1640 (1976).
38. M. D. NEWTON. J. Chem. Phys. **67**, 5535 (1977).
39. J. M. WILLIAMS. *In* The hydrogen bond—recent developments in theory and experiment. Vol. II. *Edited by* P. Schuster, G. Zundel, and C. Sandorfy. North Holland Publ. Co., Amsterdam. 1976.
40. H. A. SCHWARZ. J. Chem. Phys. **67**, 5525 (1977).
41. G. C. HOOD and C. A. REILLY. J. Chem. Phys. **32**, 127 (1960).
42. A. ALBERT and E. P. SERJANT. Ionization constants of acids and bases. Wiley, New York. 1962.
43. E. HÖGFELDT. Acta Chem. Scand. **17**, 785 (1963).
44. R. C. WEAST (*Editor*). Handbook of chemistry and physics. 49th ed. Chemical Rubber Co., Cleveland, OH. 1968.
45. S. LAPANJE and S. A. RICE. J. Am. Chem. Soc. **83**, 496 (1961).
46. L. KOTIN and M. NAGASAWA. J. Am. Chem. Soc. **83**, 1026 (1961).

Can. J. Chem. Downloaded from www.nrcresearchpress.com by 210.87.254.105 on 09/05/12
For personal use only.

Thermodynamics of ionization of *trans*-crotonic and adipic acids in water; the silver – silver adipate electrode

UPENDRA NATH DASH AND UTTAM KUMAR NAYAK

Department of Chemistry, Gangadhar Meher College, Sambalpur (Orissa), India

Received June 18, 1979

UPENDRA NATH DASH and UTTAM KUMAR NAYAK. Can. J. Chem. **58**, 323 (1980).

The ionization constant, K, of *trans*-crotonic acid, and the first and second ionization constants, K_1 and K_2, of adipic acid have been determined in water at seven different temperatures ranging from 15 to 45°C with the help of the cells without liquid junction using silver – silver chloride and quinhydrone electrodes. The variations of pK, pK_1, and pK_2 with temperature have been expressed by the equations

$$pK = 105.54/T + 4.47 - 2.26 \times 10^{-2}T$$

$$pK_1 = 65.04/T + 4.65 - 1.52 \times 10^{-3}T$$

and

$$pK_2 = 4776.61/T - 27.98 + 6.01 \times 10^{-2}T$$

From the temperature coefficient of the ionization constants, the standard enthalpy, entropy, Gibbs energy, and heat capacity changes of the corresponding dissociation processes have been calculated. Using the values of ionization constants of adipic acid, the standard potential of the $Ag(s)/Ag_2Ad(s)/Ad^{2-}$ electrode, and the related standard thermodynamic quantities for the electrode process

$$Ag_2Ad(s) + 2e \rightleftharpoons 2Ag(s) + Ad^{2-}(solvated)$$

have been calculated in water at those temperatures.

UPENDRA NATH DASH et UTTAM KUMAR NAYAK. Can. J. Chem. **58**, 323 (1980).

On a déterminé la constante d'ionisation K de l'acide crotonique *trans* ainsi que les constantes de première et de deuxième ionisation K_1 et K_2 de l'acide adipique en solution aqueuse et à 7 températures différentes allant de 15 à 45°C. On a fait ces déterminations au moyen de cellules sans pont de jonction liquide et en utilisant des électrodes d'argent – chlorure d'argent et de quinhydrone. Les variations de pK, pK_1 et pK_2 en fonction de la température sont représentées par les équations suivantes:

$$pK = 105.54/T + 4.47 - 2.26 \times 10^{-2}T$$

$$pK_1 = 65.04/T + 4.65 - 1.52 \times 10^{-3}T$$

$$pK_2 = 4776.61/T - 27.98 + 6.01 \times 10^{-2}T$$

A partir du coefficient de température et des constantes d'ionisation, on a calculé, l'enthalpie normale, l'entropie, l'énergie de Gibbs et les variations de la capacité calorifique des réactions de dissociation correspondantes. En utilisant les valeurs des constantes d'ionisation de l'acide adipique, on a déterminé en solution dans l'eau et dans le même intervalle de température: le potentiel normal de l'électrode $Ag(s)/Ag_2Ad(s)/Ad^{2-}$ et les quantités thermodynamiques relatives à la réaction de l'électrode

$$Ag_2Ad(s) + 2e \rightleftharpoons 2Ag(s) + Ad^{2-}(solvaté)$$

[Traduit par le journal]

Introduction

Until quite recently, no work seems to have been done on the determination of ionization constants of *trans*-crotonic and adipic acids in aqueous medium over a range of temperature. A survey of the literature (1–3*a*, 4), however, shows that the pK values of these acids have been reported in water at 25°C, and the values of ΔH^0 and ΔS^0 are available (2, 5) at this temperature. The present work has been undertaken as a part of our programme of determining the ionization constants and the related thermodynamic quantities of organic acids in aqueous and mixed solvent media.

Electromotive force measurements of cells of the type

[A] $Ag,AgCl(s)/KCl(m_3),KA(m_2),HA(m_1),QH_2\text{–}Q/Pt$

[B] $Ag,AgCl(s)/KCl(m_3),KHAd(m_2),H_2Ad(m_1),QH_2\text{–}Q/Pt$

and

[C] $Ag,AgCl(s)/KCl(m_3),K_2Ad(m_2),KHAd(m_1),QH_2\text{–}Q/Pt$

where A stands for *trans*-crotonate ion, and Ad for adipate ion, were made in water at seven temperatures ranging from 15 to 45°C for determining the ionization constant of *trans*-crotonic and the first and second ionization constants of adipic acid, respectively.

Although the electrodes of the type, $Ag/Ag_2X(s)/X^{2-}$, where X^{2-} stands for oxalate, malonate, succinate, or chromate ion, have been studied by the authors (6–9) in aqueous, non-aqueous, and mixed media, the behaviour of the silver – silver adipate

0008-4042/80/040323-05$01.00/0

©1980 National Research Council of Canada/Conseil national de recherches du Canada

Can. J. Chem. Downloaded from www.nrcresearchpress.com by 210.87.254.40 on 09/05/12
For personal use only.

Can. J. Chem. Downloaded from www.nrcresearchpress.com by 210.87.254.40 on 09/05/12
For personal use only.

electrode has not yet been studied in aqueous medium. The present work, therefore, aims at determining the standard potential of this electrode in water at different temperatures. The cell of the type

[D] Pt/QH_2–$Q,H_2Ad(m)/Ag_2Ad(s)/Ag$

was used for this purpose.

Experimental

trans-Crotonic acid (Fluka AG, Buchs SG 574253) was crystallised from boiling conductivity water, dried at 60°C for 2 h, and kept in a vacuum desiccator over anhydrous calcium chloride. Adipic acid (G.R., Proanalysis) was used without further purification. Potassium salts of *trans*-crotonic and adipic acids were prepared by the method similar to that described elsewhere (10, 11). The salts were dried at 110–120°C and stored in vacuum desiccator over anhydrous calcium chloride. Potassium chloride (BDH, AnalaR) was dried above 100°C and stored *in vacuo*. Quinhydrone and silver – silver chloride electrodes were prepared by the method similar to that described earlier (12, 13).

Silver adipate was prepared by adding silver nitrate (BDH, AnalaR) solution (0.2 mol dm^{-3}) slowly to equal volume of potassium adipate solution (0.11 mol dm^{-3}). The precipitate formed was carefully washed by decantation with conductivity water and stored in an amber-coloured glass-stoppered bottle for subsequent use.

Silver oxide was prepared by the method described elsewhere (14).

Silver – silver adipate electrode was prepared by the method similar to that of the silver – silver oxalate electrode (6). After preparation, the electrodes were stored in a 0.05 mol dm^{-3} aqueous solution of adipic acid for about 24 h and then rinsed with the cell solution containing adipic acid before use. Only those electrodes showing a potential difference of 0.1 mV or less when mutually compared with each other were used.

The cell vessels were of the type recommended by Harned and Wright (15).

Solutions for emf measurements were prepared in conductivity water. The cell measurements were carried out with electrodes set up as described earlier (6, 12, 16).

Results and Discussion

The method of calculation of the ionization constants of mono- and di-basic acids has been adequately described (6, 10, 11, 16).

The ionization constant, K, of *trans*-crotonic acid, or the first ionization constant, K_1, of adipic acid, corresponding to the equilibrium

$$H_xA + \text{solvent} \rightleftharpoons H^+(\text{solvated}) + H_{x-1}A^-(\text{solvated})$$

where A is the *trans*-crotonate ion when $x = 1$, and adipate ion when $x = 2$, is defined as

$$[1] \quad K \text{ or } K_1 = \frac{m_{H^+} m_{H_{x-1}A^-}}{m_{H_xA}} \frac{\gamma_{H^+}\gamma_{H_{x-1}A^-}}{\gamma_{H_xA}}$$

where m and γ are the molality and activity coefficient, respectively.

The "apparent" hydrogen ion molality, m_{H^+}' is related to the emf E of the cell [A] or [B] through the relation (16),

$$[2] \quad -\log m_{H^+}' = \frac{(E - E^0)F}{2.3026RT} + \log m_{Cl^-} - \frac{2A(Id_0)^{1/2}}{1 + a^0B(Id_0)^{1/2}}$$

where I and d_0 are the ionic strength of the solution and density of the solvent, respectively, and a^0 is the ion-size parameter. As a first approximation I was taken to be equal to $m_2 + m_3$ but subsequently an accurate value was obtained by successive approximation and refinement to a constant value of I ($\simeq m_2 + m_3 + m_{H^+}'$). The "apparent" ionization constant K' (for *trans*-crotonic acid) or K_1' (for the first ionization step of adipic acid) was calculated from the expression

$$[3] \quad \log K' \text{ or } \log K_1' = -\frac{2A(Id_0)^{1/2}}{1 + a^0B(Id_0)^{1/2}} + \log \frac{m_{H^+}'(m_2 + m_{H^+}')}{(m_1 - m_{H^+}')}$$

The true ionization constants, K and K_1, were obtained from the intercepts of the log K' vs. I, and log K_1' vs. I plots, respectively.

The second ionization constant, K_2, of adipic acid corresponding to the equilibrium

$$HAd^- + \text{solvent} \rightleftharpoons H^+(\text{solvated}) + Ad^{2-}(\text{solvated})$$

is given by

$$[4] \quad K_2 = \frac{m_{H^+} m_{Ad^{2-}}}{m_{HAd^-}} \frac{\gamma_{H^+}\gamma_{Ad^{2-}}}{\gamma_{HAd^-}}$$

and the "apparent" second ionization constant, K_2', was calculated from the expression

$$[5] \quad -\log K_2' = \frac{(E - E^0)F}{2.3026RT} + \log\left(\frac{m_1 m_3}{m_2}\right) + \frac{2A(Id_0)^{1/2}}{1 + a^0B(Id_0)^{1/2}}$$

where m_1 is the molality of HAd^-, m_2 is the molality of Ad^{2-}, and m_3 is the molality of Cl^- used in the cell [C], E is the observed emf of the cell, and I is the ionic strength of the solution given by

$$[6] \quad I = m_1 + 3m_2 + m_3$$

The second ionization constant was obtained by linear extrapolation to zero ionic strength ($I = 0$) of the function, $-\log K_2'$.

The values of E^0(Ag,AgCl), $E^0(QH_2$–$Q)$, the Debye–Hückel constants, and density, d_0, of the solvent needed for the calculation of log K', log

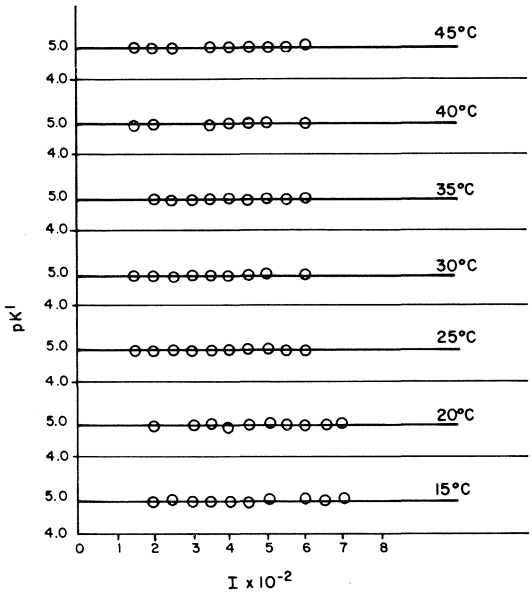


FIG. 1. Plot of $-\log K'$ versus ionic strength for *trans*-crotonic acid at different temperatures.

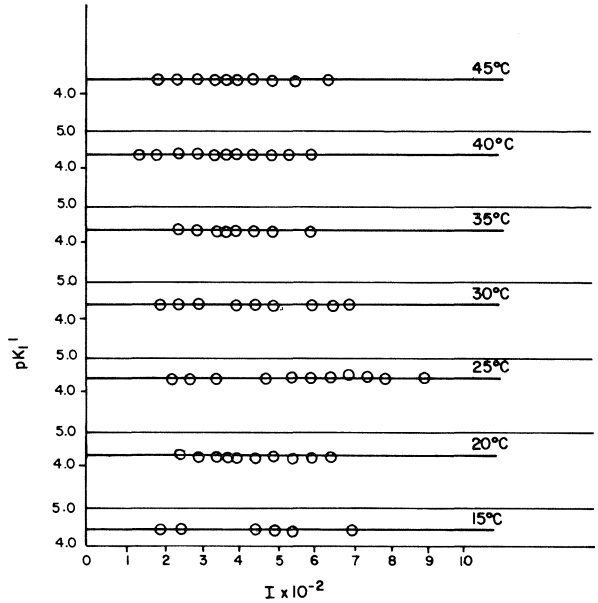


FIG. 2. Plot of $-\log K_1'$ versus ionic strength for the first step ionization process of adipic acid at different temperatures.

K_1', or $\log K_2'$ at different temperatures were obtained from the literature (17, 18). The values of the ion-size parameter a^0 were obtained by the method described earlier (16), and taken to be 0.6 and 0.55 nm for *trans*-crotonic and adipic acid, respectively.

The values of $\log K'$, $\log K_1'$, and $\log K_2'$ thus calculated were found to vary linearly with I (Figs. 1–3) for different temperatures and the linear extrapolation to $I = 0$ of values of $\log K'$, $\log K_1'$, or $\log K_2'$ yielded $\log K$, $\log K_1$, or $\log K_2$, respectively, for *trans*-crotonic and adipic acids. These values are presented in Table 1. The standard deviations calculated by the least-squares method are also shown in Table 1.

The standard molal potential, E_m^0 of silver – silver adipate electrode was obtained by the method of extrapolating (6, 8) the auxiliary function, $E^{0\prime}$, given by

$$[7] \quad E^{0\prime} = E + \left(\frac{2.3026RT}{2F}\right)\left(\frac{-6A(Id_0)^{1/2}}{1 + a^0B(Id_0)^{1/2}}\right) + \left(\frac{2.3026RT}{2F}\right)[2\log\{m\alpha(1+\beta)\} + \log(m\alpha\beta)]$$

to ionic strength, $I = 0$, where E is the observed emf of cell [D], m is the molality of adipic acid solution, and α and β are the degrees of first and second ionization constants of adipic acid, respectively, defined by the expressions

$$[8] \quad \alpha = \frac{[-K_1 + (K_1^2 + 4mK_1)^{1/2}]}{2m}$$

and

$$[9] \quad \beta = \frac{\{-(m\alpha + K_2) + [(m\alpha + K_2)^2 + 4m\alpha K_2]^{1/2}\}}{2m\alpha}$$

and the ionic strength I is given by

$$[10] \quad I = m\alpha(1 + 2\beta)$$

Using the K_1 and K_2 values of adipic acid obtained at different temperatures from emf measurements just described, the degrees of ionization α and β of adipic acid at the corresponding temperature were computed following a reiteration procedure. The values of E_m^0 are also included in Table 1 along with their standard deviations obtained by the least-squares method.

The variation of pK of *trans*-crotonic acid, pK_1 and pK_2 of adipic acid, and E_m^0 of the silver – silver adipate electrode with temperature has been expressed by the equations

$$[11] \quad \text{p}K = 105.54/T + 4.47 - 2.26 \times 10^{-2}T$$

$$[12] \quad \text{p}K_1 = 65.04/T + 4.65 - 1.52 \times 10^{-3}T$$

Can. J. Chem. Downloaded from www.nrcresearchpress.com by 210.87.254.40 on 09/05/12
For personal use only.

Can. J. Chem. Downloaded from www.nrcresearchpress.com by 210.87.254.40 on 09/05/12
For personal use only.

TABLE 1. Values of pK of *trans*-crotonic acid, pK_1 and pK_2 of adipic acid, and E_m^0 of the silver – silver adipate electrode in water at different temperatures

T (°C)	pK	pK_1	pK_2	E_m^0
15	4.829±0.022	4.444±0.042	5.914±0.051	0.4801±0.0003
20	4.819±0.015	4.421±0.057	5.937±0.053	0.4713±0.0002
25	4.817±0.012	4.419±0.039	5.974±0.052	0.4623±0.0003
30	4.808±0.014	4.404±0.028	6.016±0.047	0.4512±0.0003
35	4.805±0.014	4.393±0.021	6.030±0.033	0.4432±0.0002
40	4.798±0.018	4.391±0.022	6.079±0.044	0.4315±0.0003
45	4.792±0.020	4.368±0.009	6.174±0.026	0.4194±0.0004

TABLE 2. Values of ΔG^0, ΔH^0, ΔS^0, and ΔC_p^0 for the ionization processes of *trans*-crotonic and adipic acid and the electrode process of the silver – silver adipate electrode in water at 25°C

Process	ΔG^0 (kJ mol^{-1})	ΔH^0 (kJ mol^{-1})	ΔS^0 (J deg^{-1} mol^{-1})	ΔC_p^0 (J deg^{-1} mol^{-1})
$HA \rightleftharpoons H^+ + A^-$	10.90	40.43	172.23	257.77
$H_2Ad \rightleftharpoons H^+ + HAd^-$	25.20	3.83	−71.72	17.34
$HAd^- \rightleftharpoons H^+ + Ad^{2-}$	34.03	−10.78	−150.36	−686.11
$Ag_2Ad(s) + 2e \rightleftharpoons 2Ag(s) + Ad^{2-}$	44.61	55.26	35.75	—

[13] $pK_2 = 4776.61/T - 27.98 + 6.01 \times 10^{-2}T$

and

[14] $E_m^0 = 0.4626 - 1.92 \times 10^{-3}(t - 25) - 1.42 \times 10^{-5}(t - 25)^2$

respectively, where T and t are the temperatures in K and °C, respectively.

The values obtained for the standard thermodynamic quantities, ΔG^0, ΔH^0, ΔS^0, and ΔC_p^0 associated with the reactions investigated are listed in Table 2.

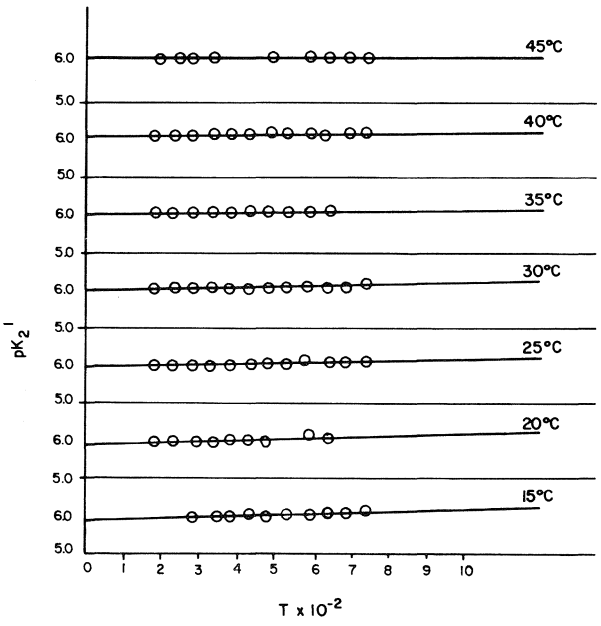


FIG. 3. Plot of − log K_2' versus ionic strength for the second step ionization process of adipic acid at different temperatures.

Since this work constitutes the first attempt to measure thermodynamic ionization constants for *trans*-crotonic and adipic acids in aqueous medium over a range of temperature using galvanic cells, a direct comparison with the results of other works is not possible. However, different values of dissociation constants for *trans*-crotonic and adipic acids are reported by various workers at 25°C. The values that have been reported earlier for *trans*-crotonic acid, pK = 4.698(1) and 4.686(4), and adipic acid, pK_1 = 4.418(5), 4.43(5), and 4.42(4), and pK_2 = 5.412(5), 5.42(5), and 5.277(3) at 25°C were determined from the studies of calorimetric and conductometric measurements. The different values of pK for *trans*-crotonic acid and pK_1 for adipic acid are in reasonably good agreement with each other, but the value pK_2 = 5.277 for adipic acid is found to be widely discrepant from the other values. The constants reported in Table 1 are somewhat higher than the constants reported earlier at 25°C excepting the pK_1 value for adipic acid. This discrepancy might be due to the use of ion-size parameter, a^0, in the calculation of pK values in the present work which was not considered in the previously reported values of pK of the investigated acids, since according to eq. [3] the pK is dependent on the ion-size parameter, and the pK values are expected to be higher than that calculated without considering the ion-size parameter (*3b*). Since the cells of the type [A], [B], and [C] have been employed satisfactorily for determination of pK values of a number of weak acids (19) and

the ion-size parameter was ascertained by following the method of Roy, Robinson, and Bates (20), it is believed that the present set of data is more trustworthy.

1. (*a*) W. L. GERMAN, G. H. JEFFERY, and A. I. VOGEL. J. Chem. Soc. 1604 (1937); (*b*) B. SAXTON and G. W. WATERS. J. Am. Chem. Soc. **59**, 1048 (1937).
2. J. J. CHRISTENSEN, R. M. IZATT, and L. D. HANSEN. J. Am. Chem. Soc. **89**, 213 (1967).
3. R. A. ROBINSON and R. H. STOKES. Electrolyte solutions. Butterworths. 1968. (*a*) p. 527; (*b*) p. 341.
4. A. E. MARTELL and D. E. SMITH. Critical stability constants. John Wiley and Sons, London. 1977.
5. J. J. CHRISTENSEN, L. D. HANSEN, and R. M. IZATT. Handbook of proton ionization heats and related thermodynamic quantities. John Wiley and Sons, New York. 1976.
6. U. N. DASH and B. NAYAK. Aust. J. Chem. **28**, 1373 (1975).
7. U. N. DASH and P. C. RATH. Thermochim. Acta, **13**, 250 (1975).
8. U. N. DASH. Thermochim. Acta, **16**, 177 (1976).
9. R. C. DAS, U. N. DASH, and K. N. PANDA. Electrochim. Acta, **24**, 99 (1979).
10. U. N. DASH and B. NAYAK. Aust. J. Chem. **25**, 941 (1972).
11. (*a*) U. N. DASH and B. NAYAK. Aust. J. Chem. **28**, 1377 (1975); (*b*) B. NAYAK and U. N. DASH. Aust. J. Chem. **26**, 115 (1973).
12. B. NAYAK and U. N. DASH. Aust. J. Chem. **26**, 111 (1973).
13. G. C. PAL and M. SENGUPTA. J. Indian Chem. Soc. **45**, 179 (1968).
14. B. NAYAK and U. N. DASH. J. Electroanal. Chem. **41**, 323 (1973).
15. H. S. HARNED and D. D. WRIGHT. J. Am. Chem. Soc. **55**, 4849 (1933).
16. R. C. DAS, U. N. DASH, and K. N. PANDA. Can. J. Chem. **54**, 1916 (1976).
17. H. S. HARNED and B. B. OWEN. The physical chemistry of electrolytic solutions. Reinhold. 1967.
18. R. G. BATES. Electrometric pH determination. Wiley, New York. 1954.
19. (*a*) U. N. DASH. Thermochim. Acta, **27**, 379 (1978); **30**, 73 (1979); (*b*) U. N. DASH. J. Electronanal. Chem. **98**, 297 (1979); (*c*) K. N. PANDA. Ph.D. Thesis, Sambalpur University, Orissa. 1979.
20. R. N. ROY, R. A. ROBINSON, and R. G. BATES. J. Am. Chem. Soc. **95**, 8231 (1973).

Can. J. Chem. Downloaded from www.nrcresearchpress.com by 210.87.254.40 on 09/05/12
For personal use only.

Constituents from *Salmalia malabaricum*

J. S. CHAUHAN, M. SULTAN, AND S. K. SRIVASTAVA
Chemical Laboratories, University of Allahabad, Allahabad, India

Received January 18, 1979

J. S. CHAUHAN, M. SULTAN, and S. K. SRIVASTAVA. Can. J. Chem. **58**, 328 (1980).

The phytochemical investigation of the root of *Salmalia malabaricum* has resulted in the isolation and identification of *n*-triacontanol, β-sitosterol, and a new glycoside which was characterized as 5,7,3′,4′-tetrahydroxy-6-methoxyflavan-3-*O*-β-D-glucopyranosyl-α-D-xylopyranoside on the basis of spectral and degradative studies.

J. S. CHAUHAN, M. SULTAN et S. K. SRIVASTAVA. Can. J. Chem. **58**, 328 (1980).

La recherche phytochimique entreprise sur la racine du "*Salmalia malabaricum*" a permis d'isoler et d'identifier le *n*-triacontanol, le β-sistostérol et un nouveau glycoside que l'on a caractérisé comme étant l'α-D-xylopyrannoside du tétrahydroxy-5,7,3′,4′ méthoxy-6 flavan-3-*O*-β-D-glucopyranoxyle. Cette caractérisation est basée sur les études de dégradation et sur l'analyse spectrale.
[Traduit par le journal]

Introduction

Salmalia malabaricum (syn. *Salmalia malabarica*; Bombacaceae) is a member of a genus of highly medicinal plants (1, 2), especially in the indigenous system of medicine. The root of this plant has been found to contain proteins, fatty matter, tannins, sugars, starch, and a monogalactan (3). The products isolated from its stem bark include lupeol and β-sitosterol (4).

The ethanolic extract of the root of this plant afforded three compounds, compound A, mp 70–72°C, compound B, mp 185°C (dec.), and compound C, mp 135–136°C.

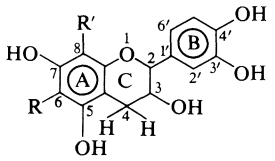
Results and Discussion

The alcoholic extract of the plant material on concentration afforded a white deposit (compound A) mp 80–82°C. It was characterized as *n*-triacontanol by its mp, ir, ^{1}H nmr, ms, oxidative degradation studies, and also by co-thin layer chromatography and superimposable ir spectra with an authentic sample.

The water-soluble portion of the alcoholic extract on extraction with ethyl acetate gave a compound B, $C_{27}H_{34}O_{16}$. This gave reactions characteristic of a catechin glycoside. The acid hydrolysis of the glycoside resulted in the isolation of one mol each of xylose and glucose and a flavan aglycone.

The aglycone, $C_{16}H_{16}O_7$, mp 176–177°C was found to contain five hydroxyl groups (penta-acetate; ir (KBr): 3340) and one methoxyl group (Zeisel; ir (KBr): 2832–2815 and 1190). The oxidative degradation of the aglycone with $KMnO_4$ yielded protocatechuic acid as one of the products, thereby confirming the presence of two hydroxyl groups at 3′ and 4′ positions in the ring B. The aglycone on alkaline degradation with 50% KOH gave two products which were identified as methoxyphloroglucinol and protocatechuic acid. The formation of these products in the degradation reactions could be explained by either of two possible structures of the aglycone.

Out of these two possibilities, the structure **1** was assigned to the aglycone on the basis of alkaline degradation of the completely methylated aglycone when antiarol (3,4,5-trimethoxyphenol) and veratric acid were obtained as the products of degradation. Only the structure **1** could furnish antiarol.



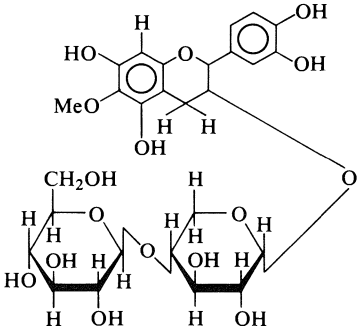
1 R = OCH_3, R′ = H
2 R = H, R′ = OCH_3

The periodate oxidation results showed the consumption of 3.1 mol of periodate with the liberation of 1.2 mol of formic acid per mole of the glycoside, thereby suggesting the presence of a disaccharide unit in pyranose form with either 1 → 4 or 1 → 2 linkage. The acid hydrolysis of the completely methylated glycoside gave 2-3-di-*O*-methyl xylose and 2,3,4,6-tetra-*O*-methyl glucose, indicating the sugars to be in pyranose form and that the disaccharide is glucopyranosyl xylose, C1 of glucose being linked to C4 of xylose. The glycoside on emulsin hydrolysis gave only glucose in the hydrolysate suggesting it to be terminal and β-linked with the other sugar moiety. The subsequent ready hydrolysis of this product with enzyme diastase to yield xylose confirmed the presence of an α-linkage between the aglycone and the xylose. The aqueous

0008-4042/80/040328-03$01.00/0
© 1980 National Research Council of Canada/Conseil national de recherches du Canada

Can. J. Chem. Downloaded from www.nrcresearchpress.com by 210.87.254.42 on 09/05/12
For personal use only.

hydrolysate from partial hydrolysis of the glycoside with 1% HCl showed first the appearance of glucose, further suggesting its position to be terminal in the disaccharide unit. The location of the linkage of the sugar moiety in the glycoside was deduced to be at 3 in ring C from the study of the colour reactions (6–10), and further supported by the alkaline degradation of the completely methylated glycoside when antiarol and veratric acid were obtained. Thus keeping all the facts in view, the compound B has been assigned 5,7,3′,4′-tetrahydroxy-6-methoxyflavan-3-*O*-β-D-glucopyranosyl-α-D-xylopyranoside structure (**3**).



3

The water-insoluble fraction of the alcoholic extract on extraction with petroleum ether (40–60°C) gave a compound C which was characterized as β-sitosterol by ir, ^{1}H nmr, ms, acetyl and benzoyl derivatives, superimposable ir spectra, and co-thin layer chromatography with an authentic specimen.

Experimental

Melting points are uncorrected. Column, thin-layer, and paper chromatographic analyses were performed at room temperature. Sugars were characterized spectrophotometrically by PhOH–H_2SO_4 method (11, 12) using a Klett-Summerson photoelectric colorimeter and also by Whatmann filter paper No. 1, descending paper chromatography using butanol – acetic acid – water (4:1:5 v/v) as a developing solvent and aniline hydrogen phthalate for revealing the spots.

Plant Material

The root of *Salmalia malabaricum* was obtained from the local city, Allahabad, and was identified by the Botanical Survey of India, Allahabad.

Isolation Procedures

The air-dried and powdered root (2 kg) of *S. malabaricum* was extracted with EtOH under reflux for 20 days. The extract on refrigeration gave a white deposit (compound A) which was filtered and the filtrate concentrated in a Rotavapour to 100 mL. It was then poured into excess of distilled water (500 mL). The water-insoluble material was filtered off and the residue was extracted with a number of increasingly polar organic solvents. The petroleum ether fraction gave the compound C in a workable yield. The filtrate on extraction with EtOAc gave compound B.

Structural Determination

Compound A

The white deposit obtained by concentrating the alcoholic extract on column chromatography over neutral alumina and elution with petroleum ether – benzene (1:1 v/v) gave a solid which on crystallization ($CHCl_3$–MeOH, 1:3 v/v), furnished *n*-triacontanol, mp 80–82°C (lit. (5*e*) mp 86.5°C), acetate (Ac_2O/Pyridine) mp 66°C (lit. (5*e*) mp 69°C); ir (KBr): 3333, 2920, 2850, 1460, 1430, 1378, 1064 and 1124, 735, 724; ^{1}H nmr ($CDCl_3$) δ: 0.95 (1-CH_3), 1.25 (28-CH_2), 1.6 (—CH_2OH), and 4.24 (1-H, OH); ms *m/e*: 438 (M^+), 420, 393, 56, 55, 43, 41, 29, etc. The compound on oxidation with HNO_3 gave an acid, mp 92–93°C (lit. (5*e*) mp 93.5–94°C), which was identified as *n*-triacontanoic acid by co-paper chromatography and neutralization equivalent (13). Thus from the above data, the compound A was identified as *n*-triacontanol and confirmed by co-thin layer chromatography and superimposable ir spectra.

Compound B

The ethyl acetate extract of the water-soluble portion was purified over a column of silica gel and was crystallized as yellow needles from petroleum ether – EtOAc, mp 185°C (dec.). The homogeneity of the compound was checked by thin-layer as well as paper chromatography in different solvent systems. *Anal.* calcd. for $C_{27}H_{34}O_{16}$: C 52.77, H 5.58; found: C 52.66, H 5.47. The compound B gave positive Molische test but it neither reduced Fehlings solution nor gave colouration with aniline hydrogen phthalate reagent, thereby indicating its glycosidic nature. The colour reactions exhibited by the compound B, viz. yellow colouration with NaOH, dark red colouration with concentrated H_2SO_4, formation of a brown product soluble in isoamyl alcohol with concentrated HCl, yellow spot with *p*-toluene sulphonic acid, together with an absorption peak at λ_{max} 280 nm in the uv region, suggested the possibility of the compound being a catechin glycoside. The infrared spectrum of the sample (KBr) showed peaks at 3333, 2900, 2850, 1613, 1536, 1450, 1282, 1120, 825, and 769 cm^{-1}.

Acid Hydrolysis

The glycoside (500 mg) was hydrolysed with boiling 7% ethanolic H_2SO_4 (50 mL) for 6 h. After cooling, the contents were diluted to 50% with H_2O. The precipitated aglycone was separated by filtration. The aqueous solution was neutralized ($BaCO_3$), filtered, and evaporated under reduced pressure to a syrup which was found to contain xylose and glucose by paper co-chromatography with authentic samples. These were separated by column chromatography on cellulose in *n*-butanol – isopropanol – H_2O (11:6:3) (14) and characterized: xylose; osazone and *p*-nitrophenylhydrazone, mp and mixture mp, 158 and 156°C respectively; glucose; osazone and *p*-nitrophenylhydrazone, mp and mixed mp 204–205 and 184–186°C respectively. Quantitative analyses (15) revealed the presence of 1 mol of each sugar.

Methylation

The glycoside (600 mg) was methylated according to Kuhn's procedure with CH_3I and Ag_2O in dimethylformamide giving a semisolid. Methanolysis (16) followed by hydrolysis with 5% aqueous HCl at 100°C for 6 h gave the 2,3-di-*O*-methyl derivative of xylose and 2,3,4,6-tetra-*O*-methyl derivative of glucose in 1:1 molar ratio indicating 1 → 4 linkage of xylose to glucose. The aglycone obtained on hydrolysis, was subjected to alkaline degradation when antiarol, mp 145–147°C (lit. (5*b*) mp 148°C) and veratric acid, mp 178–179°C (lit. (5*c*) mp 181°C) were isolated as the products. The formation of antiarol is ample proof for the location of the —OCH_3 group at position 6 in the aglycone of the compound B.

Can. J. Chem. Downloaded from www.nrcresearchpress.com by 210.87.254.42 on 09/05/12
For personal use only.

Can. J. Chem. Downloaded from www.nrcresearchpress.com by 210.87.254.42 on 09/05/12
For personal use only.

Periodate Oxidation

The glycoside (30 mg) was oxidized by $NaIO_4$ at room temperature in 20 mL of 90% EtOH. A blank was run similarly. Results after 60 h showed the consumption of 3.1 mol of periodate with the liberation of 1.20 mol of formic acid per mol of the glycoside.

Enzymatic Hydrolyses

About 150 mg of the glycoside was suspended in an almond emulsin solution (20 mL) and kept at 45°C for 18 h. The sugar (50 mg) was separated from hydrolysate by preparative partition chromatography and was found to be only glucose (1 mol) as determined by colorimetry (12). Appearance of only glucose in this hydrolysate indicated it to be terminal and β-linked with xylose. Hydrolysis of the glycoside (100 mg) with diastase gave a disaccharide. This disaccharide when hydrolysed with acids or emulsion afforded two sugars characterized as xylose and glucose. This indicated that the disaccharide consisting of glucose and xylose is linked with the aglycone through an α-linkage.

Partial Hydrolysis

The glycoside (15 mg) was dissolved in dioxane (5 mL) containing HCl (1%) and allowed to stand at room temperature. Aliquots were taken at different intervals and examined by paper chromatography. The results indicated that glucose was liberated after 72 h while xylose appeared after 120 h.

Characterization of the Aglycone

The aglycone was purified by paper chromatography and crystallized from EtOAc – petroleum ether mixture as brown-yellow needles, mp 176–177°C. The homogeneity was checked by tlc and paper chromatography in different organic solvents; ir (KBr): 3350, 2900, 2870, 1615, 1460, 1280, 1125, and 770 cm^{-1}. *Anal.* calcd. for $C_{16}H_{16}O_7$: C 60.00, H 5.04; found: C 59.96, H 5.05.

Acetylation and Acetyl Percentage Determination

A sample of 50 mg of the aglycone was acetylated using Ac_2O (2 mL) and pyridine (5 mL) by the usual method. The acetyl derivative was crystallized from methanol, mp 120°C. The percentage of the acetyl groups in the acetylated product was determined by the method of Wiesenberger (17) as described by Belcher and Godbert (18). *Anal.* calcd. for $C_{26}H_{26}O_{12}$: C 58.87, H 4.94, acetyl 40.52; found: C 58.79, H 4.85, 5 × acetyl 40.56.

Methoxyl Percentage Determination

The percentage of methoxyl group in the aglycone (20 mg) was determined by Zeisel's method as described by Belcher *et al.* (19). *Anal.* calcd. for $C_{15}H_{13}O_6$: —OMe 9.40; found: —OMe 9.38.

$KMnO_4$ Oxidation

The aglycone (20 mg) was dissolved in acetone and oxidized with 10% $KMnO_4$ solution (30 mL) on a water bath for 4 h. The reaction mixture was cooled, sodium bisulphite added, and shaken with ether. The ethereal layer was then shaken with aqueous $NaHCO_3$. The bicarbonate solution was acidified with HCl and finally shaken with ether. The ethereal solution gave a product which was identified as protocatechuic acid, mp 196–197°C (lit. (5*a*) mp 199°C) and mixed mp.

KOH Degradation

A solution of aglycone (200 mg) in ethanolic KOH (50%, 10 mL) was refluxed for 10 h following the method of Briggs and Locker (20). The reaction mixture on cooling gave a precipitate (P) which was filtered. CO_2 was bubbled through the filtrate and the mixture again filtered. This filtrate was acidified with dilute HCl and extracted with ether to give a residue which on crystallization yielded protocatechuic acid, mp and mixed mp 196–197°C. The precipitate (P) in H_2O on acidification with dilute HCl and extraction with ether gave a crystalline solid which was identified as methoxyphloroglucinol (Iretol), mp 182–183°C (lit. (5*f*) mp 186°C) and by mixed mp and co-chromatography.

Compound C

The petroleum ether extract of the water-insoluble portion, on column chromatography over neutral alumina and elution with benzene–chloroform (3:1 v/v), gave an amorphous compound which on crystallization (benzene–chloroform, 3:2 v/v) gave white needles, mp. 135–136°C (lit. (5*d*) mp 136–137°C). It showed bluish-violet colouration with Liebermann-Burchardt reagent (21); ir (KBr): 3440 and 1649; ms *m/e*: 414 (M^+), 396, 273, and 255. It formed an acetate, mp 128°C (lit. (5*d*) mp 134°C), and benzoate, mp 142°C (lit. (5*d*) mp 145.5°C). The identity of the compound as β-sitosterol (22) was established by mixed mp, co-thinlayer chromatography, and co-ir with an authentic specimen of β-sitosterol.

Acknowledgements

The authors express their gratitude to the Director, CIBA Geigy Research Centre, Bombay (India) for spectra and microanalyses, to the State Council of Science and Technology, U.P., India for financial assistance to M.S., and to the University Grants Commission, New Delhi, India for assistance to S.K.S.

1. K. R. KIRTIKAR and B. D. BASU. Indian medicinal plants. Vol. 1. 2nd ed. Lalit Mohan Basu Publication, Allahabad, India. 1935. pp. 354–357.
2. R. N. CHOPRA, S. L. NAYAR, and I. C. CHOPRA. Glossary of Indian medicinal plants. CSIR Publication, Delhi, India. 1956. pp. 218–219.
3. T. P. GHOSE. Indian For. **61**, 93 (1935).
4. J. MUKERJEE and B. ROY. J. Indian Chem. Soc. **48**, 769 (1971).
5. (*a*) I. HEILBRON and H. M. BUNBURY. Dictionary of organic compounds. Eyre and Spottiswoode, London. **4**, 260 (1953); (*b*) **1**, 196 (1953); (*c*) **4**, 662 (1953); (*d*) **4**, 361 (1953); (*e*) **4**, 538 (1953); (*f*) **3**, 52 (1953).
6. T. A. GEISSMAN. Modern methods of plant analysis. Vol. 3. *Edited by* K. Peach and M. V. Tracey. Springer Verlag, Berlin. 1955. p. 468.
7. K. VENKATARAMAN. Chemistry of flavonoid compounds. *Edited by* T. A. Geissman. Pergamon Press, Oxford. 1962. p. 72.
8. E. C. BATE-SMITH. Biochem. J. **58**, 122 (1954).
9. T. SWAIN and E. C. BATE-SMITH. Chemistry of vegetable tannins. Society of Leather Trade Chemists. 1956. p. 109.
10. D. G. ROUX. Nature, **180**, 972 (1957).
11. S. A. I. RIZVI, P. C. GUPTA, and R. K. KAUL. Planta Med. **20**, 24 (1971).
12. M. DUBOIS, K. A. GILLES, J. K. HAMILTON, P. A. REBERS, and F. SMITH. Anal. Chem. **28**, 350 (1956).
13. R. D. TIWARI, K. C. SRIVASTAVA, and J. P. SHARMA. Z. Anal. Chem. **187**, 161 (1962).
14. S. A. I. RIZVI. D. Phil. Thesis, Allahabad University, Allahabad, India. 1968.
15. P. ANDREWS, L. HOUGH, and J. K. N. JONES. J. Chem. Soc. 2744 (1952).
16. E. L. HIRST, L. HOUGH, and J. K. N. JONES. J. Chem. Soc. 928 (1949).
17. E. WIESENBERGER. Mikrochemie, **33**, 51 (1948).
18. R. BELCHER and A. L. GODBERT. Semimicro quantitative organic chemistry. Longman, New York. 1936. p. 168.
19. R. BELCHER, J. E. FILDES, and A. J. NUTTEN. Anal. Chim. Acta, **13**, 16 (1955).
20. L. H. BRIGGS and R. H. LOCKER. J. Chem. Soc. 2157 (1949).
21. C. LIEBERMANN. Ber. Dtsch. Chem. Ges. 1804 (1885).
22. J. S. CHAUHAN, S. K. SRIVASTAVA, and M. SULTAN. Vijnana Parishad Anushandhan Patrika, **20**, 153 (1977).

Sulfonyl radicals, sulfinic acid, and related species: an *ab initio* molecular orbital study

RUSSELL J. BOYD,[1] ABHA GUPTA, RICHARD F. LANGLER,[2] STEPHEN P. LOWNIE, AND JAMES A. PINCOCK
Department of Chemistry, Dalhousie University, Halifax, N.S., Canada B3H 4J3

Received August 15, 1979

RUSSELL J. BOYD, ABHA GUPTA, RICHARD F. LANGLER, STEPHEN P. LOWNIE, and JAMES A. PINCOCK. Can. J. Chem. **58**, 331 (1980).

Extensive *ab initio* molecular orbital calculations on six sulfonyl radicals (XSO_2 where X = H, CH_3, NH_2, OH, F, and Cl), the simplest sulfinic acid HSO_2H[3] and its isomeric sulfone H_2SO_2, the HSO_2^- anion of sulfinic acid, the isomeric anion SO_2H^-, and for completeness, the SO_2H radical are presented. By use of the STO-3G* basis set, which includes *d*-type polarization functions on second-row atoms, all geometrical parameters are varied until the total energy is minimized, subject only to certain symmetry restrictions specified for each system. The inclusion of *d* orbitals on S is observed to affect the S—O bond lengths by as much as 0.45 Å. The calculations suggest that the radical site in sulfonyl radicals is significantly delocalized over the entire functional group and that the geometrical parameters of the SO_2 functional group in sulfonyl radicals are nearly independent of the substituent (r(S—O) = 1.47 ± 0.01 Å, < OSO = 123 ± 2°). Estimates of the X—S bond energy in CH_3SO_2, NH_2SO_2, and $OHSO_2$ are consistent with the chemistry of alkylsulfonyl and aminosulfonyl radicals and lead to an interesting prediction for alkoxylsulfonyl radicals. Furthermore the calculations yield lower total energies for HSO_2H, HSO_2^-, and SO_2H than for the respective isomeric forms H_2SO_2, SO_2H^-, and HSO_2.

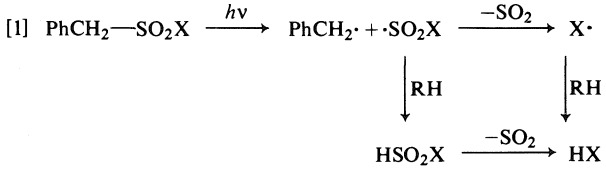
RUSSELL J. BOYD, ABHA GUPTA, RICHARD F. LANGLER, STEPHEN P. LOWNIE et JAMES A. PINCOCK. Can. J. Chem. **58**, 331 (1980).

On présente les calculs *ab initio* approfondis d'orbitales moléculaires de six radicaux sulfonyles (XSO_2 où X = H, CH_3, NH_2, OH, F et Cl) de l'acide sulfonique le plus simple HSO_2H,[3] de sa sulfone isomère H_2SO_2, de l'anion HSO_2^- de l'acide sulfinique, de l'anion isomère SO_2H^- et pour compléter du radical SO_2H. Par l'utilisation de l'ensemble de base STO-3G* qui inclut les fonctions de polarisation de type *d* des atomes de la deuxième rangée, on a fait varier tous les paramètres géométriques jusqu'à ce que la quantité totale d'énergie soit minimale, tout en étant assujetie seulement à certaines restrictions de symétrie spécifiées pour chaque système. On observe que l'inclusion des orbitales *d* du soufre affecte les longueurs de liaison S—O d'environ 0.45 Å. Les calculs suggèrent que les sites des radicaux sulfonyles sont délocalisés de façon significative sur tout le groupe fonctionnel et que les paramètres géométriques du groupe fonctionnel SO_2 des radicaux sulfonyles sont presqu'indépendants des substituants (r(S—O) = 1.47 ± 0.01 Å, ∠OSO = 123 ± 2°). Les évaluations de l'énergie de liaison X—S dans CH_3SO_2, NH_2SO_2 et $OHSO_2$ sont en corrélation avec la chimie des radicaux alkylsulfonyles et aminosulfonyles et conduisent à des prédictions intéressantes au sujet des radicaux alkylsulfonyles. De plus, dans le cas de HSO_2H, HSO_2^- et SO_2H les calculs conduisent à des énergies totales plus faibles que celles obtenues pour les formes isomères H_2SO_2, SO_2H^- et HSO_2.

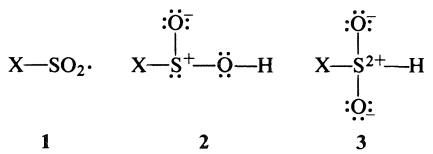
[Traduit par le journal]

Introduction

The photochemistry of benzylsulfonyl systems is characterized by homolytic cleavage of the C—S bond to benzyl and sulfonyl radicals (1). This is apparently general. However the products are variable because the fate of the sulfonyl radical depends on the nature of X and the H-atom donating ability of the solvent. If the sulfonyl radical readily loses SO_2, then hydrogen abstraction leads to HX. On the other hand if SO_2 is not readily lost, hydrogen abstraction leads to the corresponding sulfinic acid. Clearly the relative amounts of the two products are determined by the ease of loss of SO_2 from the sulfonyl radical and the relative stability of the sulfinic acid to desulfonylation.



In this paper we report the results of *ab initio* MO calculations on some simple models of the radicals and molecules shown in eq. [1]. In particular, extensive calculations on the sulfonyl radical **1**, the sulfinic acid **2**, and the sulfone **3** where X = H have been completed.



The calculations have been extended to include the bond strength of the X—S bond in **1** where X = H, CH_3, NH_2, OH, F, and Cl. For completeness several species derived from **2** are included.

[1]Author to whom correspondence may be addressed.

[2]Present address: Department of Chemistry, Mount Allison University, Sackville, N.B., Canada E0A 3C0.

[3]By convention, an H bonded to sulfur is written before the S and an H bonded to oxygen is written after the O.

0008-4042/80/040331-08$01.00/0
©1980 National Research Council of Canada/Conseil national de recherches du Canada

Can. J. Chem. Downloaded from www.nrcresearchpress.com by 210.87.254.40 on 09/05/12
For personal use only.

Can. J. Chem. Downloaded from www.nrcresearchpress.com by 210.87.254.40 on 09/05/12
For personal use only.

Method

Standard single determinant *ab initio* molecular orbital theory was used in this work. Singlet states were treated by the closed-shell, spin-restricted Hartree–Fock (RHF) procedure (2) and the doublet ground states of radicals were treated by use of the spin-unrestricted (UHF) procedure (3).

The STO-3G* basis set (4) was used for all species containing second-row elements. In this basis set, a manifold of five *d*-type functions, consisting of one second-order Gaussian each, is added to the minimal STO-3G basis for second-row atoms only. For hydrogen and first-row elements, a minimal basis having one Slater-type orbital (STO), approximated by three Gaussian functions (5), for each canonical atomic orbital completes the STO-3G* basis. For species which do not contain one or more second-row elements the minimal STO-3G basis (5) was used. Although very much better basis sets, such as the 6-31G** (6), are available for some of the cases of interest in this study, the same basis set is used for a given atom throughout. Thus the energy change for the process shown in eq. [2] is estimated by use of the STO-3G* basis

[2] $CH_3SO_2\cdot \rightarrow CH_3\cdot + SO_2$

set for $CH_3SO_2\cdot$ and SO_2 and the STO-3G basis set for $CH_3\cdot$. Clearly, the methyl radical would be expected to be described more accurately by an extended basis set but this would require an identical extension of the basis set for $CH_3SO_2\cdot$ and lead to a prohibitive increase in the computations.

All the results reported in this paper were obtained by use of the GAUSSIAN 76 program (7). Some preliminary results on **1**, **2**, and **3** where X = H were obtained by use of PHANTOM (8), a CDC-oriented version of POLYATOM.

A full geometry optimization, subject to assumed symmetry constraints,[4] was carried out for each structure. This involves variation of all bond lengths and angles until variations of the order of 0.001 Å and 0.1° lead to no further lowering of the total energy. In a few cases the possibility of a lower symmetry was ruled out by appropriate calculations.

Before discussing the results, one important point should be made in connection with the choice of the basis set. Initially we intended to use the STO-3G basis set to minimize the total energy with respect to all geometrical parameters and then to use the final STO-3G geometry to carry out single calculations with a larger basis set to obtain the final energies. This approach has been used extensively in many applications by Pople and his co-workers (9). However our first few calculations showed that the S—O bonds are very sensitive to the inclusion of *d* orbitals on S. Indeed omission of the *d* functions leads to S—O bonds as much as 0.45 Å longer than the values reported in this paper. Such differences between STO-3G and STO-3G* geometries are very much greater than in the molecules treated by Pople and co-workers (4). Where comparison with experimental geometries is possible the inclusion of *d* orbitals on sulfur improves the agreement and, therefore, we have reported only the STO-3G* geometries in this paper.

Results and Discussion

Sulfonyl Radicals

The calculated equilibrium geometries of six sulfonyl radicals are illustrated in Fig. 1. Despite the variety of substituents the structural parameters of the SO_2 functional group remain essentially constant: r(S—O) = 1.47 ± 0.01 Å, ∠OSO = 123 ± 2° and a nonplanar arrangement about the sulfur atom. Unfortunately the geometries of sulfonyl radicals are not available from experiment, but it is worth noting that the STO-3G* calculated geometry (4) of SO_2 (r(S—O) = 1.446 Å, ∠OSO = 119.9°) agrees very well with the spectroscopic (10) results (r(S—O) = 1.431, ∠OSO = 119.3°). Relative to SO_2, our MO calculations at the STO-3G* level predict a substantial lengthening of the S—O bond and a small opening of the ∠OSO angle. This reflects the loss of the substantial amount of multiple bonding in SO_2. Even so, the sulfonyl radical bond lengths are substantially shorter than the S—O standard bond length of 1.54 Å and longer than the S=O value of 1.43 Å proposed by Hehre *et al.* (11).

Table 1 reveals the strong preference of the HSO_2 radical for the nonplanar conformation and suggests the possibility of a chiral thiosulfonyl radical in which one of the oxygens of **1** is replaced by a sulfur atom. Inversion not only changes the geometrical parameters but leads to substantial changes in the electronic structure. The fluoro- and chlorosulfonyl radicals also possess a high barrier to inversion.

In order to determine the preferred conformations of **1***b*, **1***c*, and **1***d*, model geometries based on assumed X—S bond lengths and structural parameters from the calculated geometries of HSO_2, CH_3, NH_2, and OH were used to complete a

[4]The point group and number of geometrical parameters optimized for each species are as follows: HSO_2 (**1***a*), C_s (4); CH_3SO_2 (**1***b*), C_s (7, all ∠HCS angles were optimized simultaneously); NH_2SO_2 (**1***c*), C_s (7); $OHSO_2$ (**1***d*), C_1 (9); FSO_2 (**1***e*), C_s (4); $ClSO_2$ (**1***f*), C_s (4); HSO_2H (**2**), C_1 (9); H_2SO_2 (**3**), C_{2v} (4); SO_2H (4), C_1 (6); HSO_2^- (**5**), C_s (4); SO_2H^- (**6**), C_1 (6).

Can. J. Chem. Downloaded from www.nrcresearchpress.com by 210.87.254.40 on 09/05/12
For personal use only.

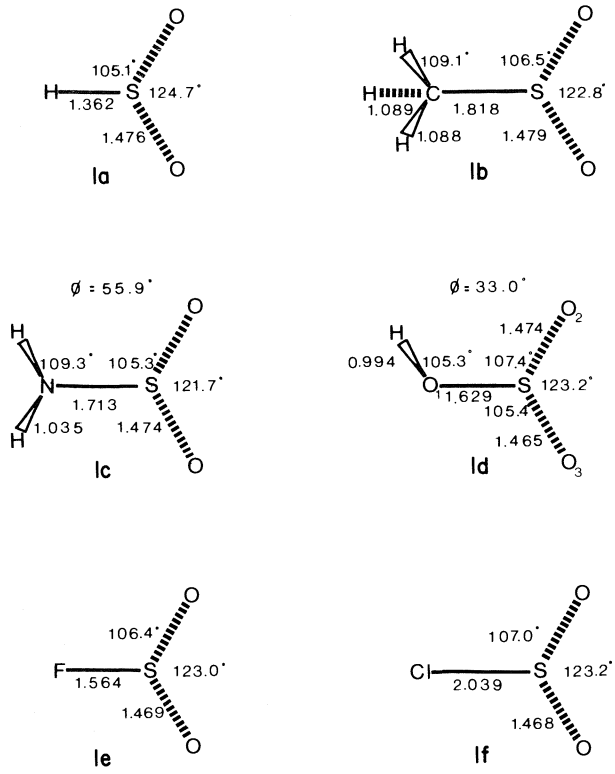


FIG. 1. Calculated geometries of sulfonyl radicals (bond lengths in Å, angles in degrees). ϕ refers to the HNSO dihedral angle in **1***c* and to the HO_1SO_2 dihedral angle in **1***d*.

TABLE 1. Comparison of nonplanar and planar forms of HSO_2

		Nonplanar	Planar
Relative energies		0	100.4 kJ/mol
Geometries	*r*(S—O)	1.476 Å	1.483 Å
	r(S—H)	1.362 Å	1.336 Å
	∠OSO	124.7°	133.2°
	∠HSO	105.1°	113.4°
Net atomic charges			
	S	0.331	0.261
	O	−0.208	−0.200
	H	0.085	0.140
Atomic spin densities			
	S	0.228	0.620
	O	0.421	0.388
	H	0.097	−0.062
Fermi contact analysis (au)			
	S	0.215	0.214
	O	0.009	0.058
	H	0.039	−0.027

limited potential surface scan for rigid rotation about the X—S bond. The results are shown in Fig. 2. For the methyl- and aminosulfonyl radicals the staggered (C_s) conformations are preferred, while the hydroxylsulfonyl radical prefers an asymmetrical (C_1) conformation to either of the two possible symmetrical (C_s) conformations. Geometry optimization of the preferred conformations leads to the calculated structures shown in Fig. 1. The barriers shown in Fig. 2 refer to rigid rotation only. Optimization of the geometrical parameters at each value of the rotational angle would lower the barriers but would not destroy the qualitative features.

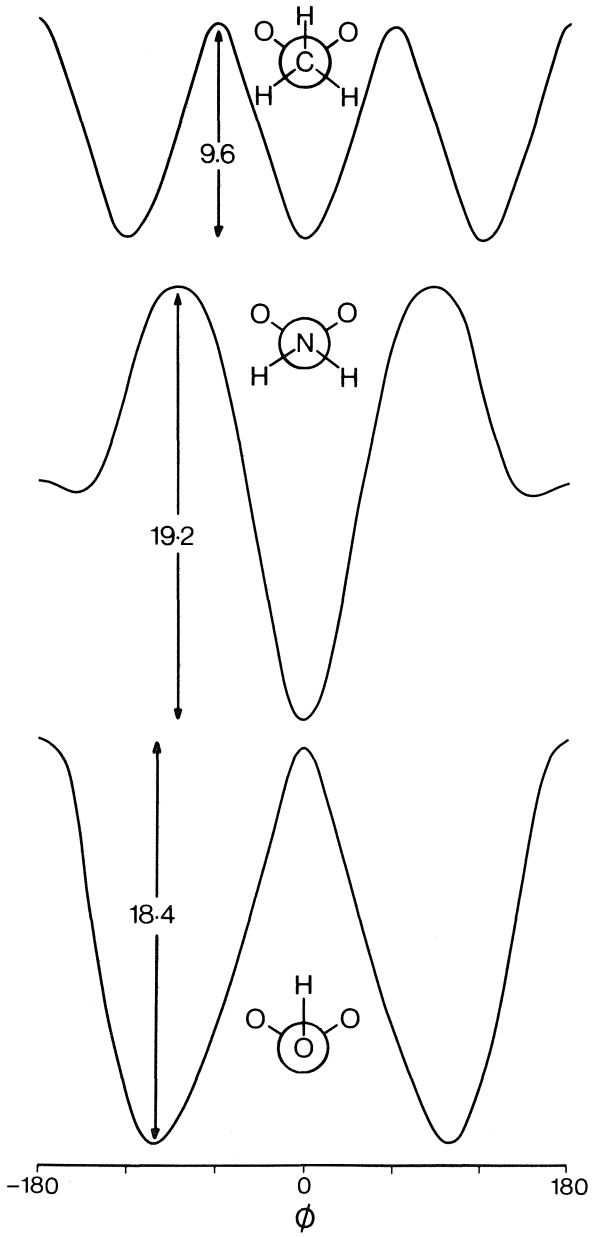


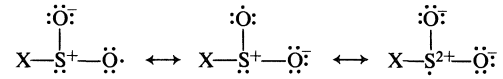
FIG. 2. One-dimensional cross-section of the conformational energy hypersurface of sulfonyl radicals. For each radical the origin of the rotational angle is defined by the conformation illustrated. Rotational barriers are in kJ/mol.

TABLE 2. Total energies and X—S bond properties of sulfonyl radicals

	Radical	Total energy (au)	Bond energy (kJ/mol)	Bond length (Å)	Force constant (mdyn/Å)
1*a*	HSO_2	−541.43082	142.1	1.362	5.3
1*b*	CH_3SO_2	−580.02986	112.2	1.818	4.4
1*c*	NH_2SO_2	−595.77788	74.7	1.713	5.5
1*d*	$OHSO_2$	−615.31484	104.6	1.629	6.7
1*e*	FSO_2	−638.95014	140.5	1.564	8.7
1*f*	$ClSO_2$	−995.49015	88.7	2.039	3.7

The conformations of **1***c* and **1***d* may be discussed in terms of the *gauche* effect (12). Analysis of *ab initio* calculations (13) on FCH_2OH has shown that the *gauche* effect in this molecule is dominated by the interactions between adjacent polar bonds (C—F and O—H) and not by the interactions between a polar bond (C—F) and the two adjacent lone pairs on the O atom. Apparently polar bonds play a similar role in the conformations of sulfonyl radicals. In **1***c* our results indicate a preferred conformation with the N lone pair *gauche* to the two O atoms, while the results for **1***d* correspond to the conformation with the maximum number of *gauche* interactions between the lone pairs of the hydroxyl O and the O atoms of the SO_2 functional group. Here it should be mentioned that the *gauche* effect has been studied in the case of a carbanion adjacent to SO_2 (14).

Before discussing the bond and electronic properties, we wish to comment further on the structure of sulfonyl radicals. In the literature, sulfonyl radicals are often (15) written simply as $RSO_2\cdot$ where the sulfur atom is understood to be bonded to two oxygens as well as substituent R. Evidently a more detailed description has not been proposed. Accordingly we have considered the results of a Mulliken population analysis (16) of the UHF wave functions for the sulfonyl radicals. Some relevant data are shown in Table 1 for the simplest sulfonyl radical. Although population analysis procedures are inherently arbitrary (17), we note that the net atomic charges of +0.33 and −0.21 on S and O, respectively, suggest a substantial polarization of the S—O bonds. Not surprisingly a positive charge is associated with the H atom. In order to comment on the radical site we now consider the spin densities. Bearing in mind that a positive spin density implies an excess of electrons of α spin, we observe significant net spin densities on all atoms, with the radical site appearing to be primarily on the O atoms. However, for the highest occupied MO we find a greater portion of the spin density on S. The difference between the two sets of spin densities is due to the use of an unrestricted wave function. We conclude[5] that the radical site is not on one particular atom but rather it extends over all three atoms of the SO_2 group. In terms of resonance forms, the sulfonyl radical may be represented by three principal contributors:



In view of the lone pair on S in the two equivalent resonance forms, the nonplanar arrangement about S in the sulfonyl radicals is not surprising. Also the formal charges are consistent with the polarity of the S—O bonds (see Table 1). Here it should be emphasized that our conclusion on the radical site is not entirely consistent with an esr study (18) according to which the radical site appears to be mainly centered on sulfur. Nevertheless our conclusion represents a combination of the practice whereby some authors (19) favour a S-centered radical and others (20) an O-centered radical.

The total energies and bond energies, defined by the dissociation process shown in eq. [2], are listed in Table 2 for the sulfonyl radicals included in this work. Although the STO-3G* values for bond energies are not expected to be as accurate as the calculated equilibrium geometries (4, 21, 22), the calculated bond energy of the methyl sulfonyl radical **1***b* agrees fairly well with the experimental value of 97.5 ± 7.5 kJ/mol reported by Busfield *et al.* (23). More recent work (24, 25) favours 84 ± 8 kJ/mol. It is interesting to note that the overestimation by theory in this case parallels a known regularity (22) in the six successive C—H dissociations of ethane to C2: STO-3G, and 4-31G calculations give too small a value for dissociations of a singlet molecule to a radical plus hydrogen atom, whereas the calculations give too large a value for dissociation of a radical. Insufficient thermochemical data prevents a similar analysis for sulfonyl radicals.

Photolysis of benzyl sulfonamides yields aminosulfonyl radicals which lose SO_2 to produce amines

[5]A RHF calculation yields a similar distribution for the unpaired electron.

Can. J. Chem. Downloaded from www.nrcresearchpress.com by 210.87.254.40 on 09/05/12
For personal use only.

Can. J. Chem. Downloaded from www.nrcresearchpress.com by 210.87.254.40 on 09/05/12
For personal use only.

(26) whereas alkylsulfonyl radicals generated by the photolysis of benzylic sulfones (1) abstract hydrogen to form sulfinic acids **2**. Evidently the C—S bond is stronger than the N—S bond in sulfonyl radicals. This conclusion is supported by the calculations reported in this paper. Here it is interesting to note that the hydroxylsulfonyl radical is predicted to be much more stable with respect to the loss of SO_2 than the aminosulfonyl radical and therefore derivatives of **1***d* would not be expected to produce alcohols as would be the case if the reaction proceeded by analogy with aminosulfonyl radicals which yield amines (26). This prediction regarding the chemistry of alkoxylsulfonyl radicals has not been tested experimentally.

To complete the series of isoelectronic first-row sulfonyl radicals we have included the fluorosulfonyl radical **1***e*. The results in Table 2 indicate that at the STO-3G* level, CH_3SO_2 may be regarded as the special case and not NH_2SO_2 as might be suspected in the absence of the calculations for **1***e*. In agreement with the general trends for sulfur–halogen bonds (27, 28), the bond energy of the chlorosulfonyl radical is predicted to be lower than the FSO_2 value. While direct comparison with experimental S—X bond energies is not possible for all the bonds considered in this work, it is interesting to note that the qualitative trend predicted in Table 2 is reflected by the available data for other series (28). For C—X bonds, the energies are 368, 305, 358, 485, and 327 kJ/mol for C, N, O, F, and Cl, respectively. The H—X bond energies are 411, 386, 459, 565, and 428 kJ/mol for C, N, O, F, and Cl, respectively. Thus in both series the nitrogen value is lower than the carbon and oxygen values.

Table 2 also includes the calculated bond lengths and force constants for X—S bonds. The bond lengths lie within the range of observed values (29, 30) and are surprisingly close to the standard bond lengths proposed by Hehre *et al.* (11). The largest discrepancies occur for N—S where the typical values (29) lie in the range 1.50 to 1.67 Å and O—S where a standard single bond length of 1.54 Å has been proposed (11).

Several electronic properties of sulfonyl radicals are reported in Table 3. The spin density on the oxygen atoms remains close to +0.4 and the net atomic charge at about −0.2. For the latter the largest departure from the mean occurs in $ClSO_2$ and is due to the inclusion of polarization functions on Cl. This anomaly would likely vanish at the Hartree–Fock limit. Even the S atom shows only a little more variation than O. Naturally the substituents show larger variations in electronic properties paralleling the substantial structural differences illustrated in Figs. 1 and 2. On the other hand the SO_2 functional group displays characteristic electronic and structural properties.

TABLE 3. Calculated electronic properties of sulfonyl radicals

Radical	S	O	A	H
		Net atomic charges		
HSO_2	0.33	−0.21		0.08
CH_3SO_2	0.36	−0.22	−0.20	0.09
NH_2SO_2	0.42	−0.21	−0.37	0.19
$OHSO_2$	0.42	−0.21[a]	−0.24	0.23
FSO_2	0.45	−0.19	−0.07	
$ClSO_2$	0.52	−0.16	−0.20	
		Atomic spin densities		
HSO_2	0.23	0.42		0.10
CH_3SO_2	0.23	0.41	0.12	±0.01[b]
NH_2SO_2	0.20	0.39	0.18	−0.01
$OHSO_2$	0.25	0.38[c]	0.14	−0.01
FSO_2	0.23	0.39	0.10	
$ClSO_2$	0.23	0.38	0.19	
		Fermi contact analysis		
HSO_2	0.21	0.01		0.04
CH_3SO_2	0.21	0.01	0.05	<0.01
NH_2SO_2	0.23	−0.01	0.02	<0.01
$OHSO_2$	0.29	−0.01	0.02	<0.01
FSO_2	0.23	−0.01	0.01	
$ClSO_2$	0.32	−0.01	0.02	

[a]This is the average of −0.209 for O2 and −0.203 for O3.
[b]Negative sign applies to the two stereochemically equivalent hydrogens.
[c]This is the average of 0.407 for O2 and 0.353 for O3.

Sulfinic Acid, Sulfone, and Related Species

The STO-3G* calculated geometries of the simplest sulfinic acid, HSO_2H, (**2**), the sulfone, H_2SO_2, (**3**), the SO_2H (**4**) isomer of **1***a*, and the two possible anions, HSO_2^- (**5**) and SO_2H^- (**6**), formed in the dissociative ionization of **2** are summarized in Fig. 3. The corresponding point groups are listed in footnote 4. As in the structure of **1***d*, the S—O bonds of **2**, **4**, and **6** are significantly longer for hydroxyl groups than for terminal oxygen atoms. With the exception of anion **6**, the former are remarkably constant at 1.63 Å while the latter are observed to deviate substantially from the sulfonyl radical values (1.47 ± 0.01 Å). Again there is a paucity of experimental data with which to compare the theoretical structures. Sulfone **3** is not known but several sulfones have been studied by electron diffraction and microwave spectroscopy (30). In particular electron diffraction studies on sulfuryl fluoride (31), SO_2F_2, sulfuryl chloride (32), and dimethyl sulfone (33) have yielded 124.0, 123.5, and 119.7°, respectively, for the ∠OSO angle and 1.405, 1.404, and 1.435 Å, respectively, for the S—O bond length. Although further comparisons with experiment are not possible at present it is

TABLE 4. Total energies and net atomic charges of sulfinic acid and related species

Species[a]	Total energy (au)	Net atomic charges[b]
HSO_2H (**2**)	−542.03847[c]	+0.34 (S), −0.28 (O1), −0.31 (O2), +0.04 (H1), +0.21 (H2)
H_2SO_2 (**3**)	−542.00088	+0.33 (S), −0.25 (O), +0.08 (H)
SO_2H (**4**)	−541.49560	+0.22 (S), −0.28 (O1), −0.14 (O2), +0.20 (H)
HSO_2^- (**5**)	−541.31759	+0.08 (S), −0.47 (O), −0.13 (H)
SO_2H^- (**6**)	−541.29343	−0.19 (S), −0.37 (O1), −0.52 (O2), +0.08 (H)

[a]See Fig. 3 for structures.
[b]Atoms correspond to those identified by the subscripts in Fig. 3.
[c]1 au = 627.5095 kcal/mol = 2625.502 kJ/mol.

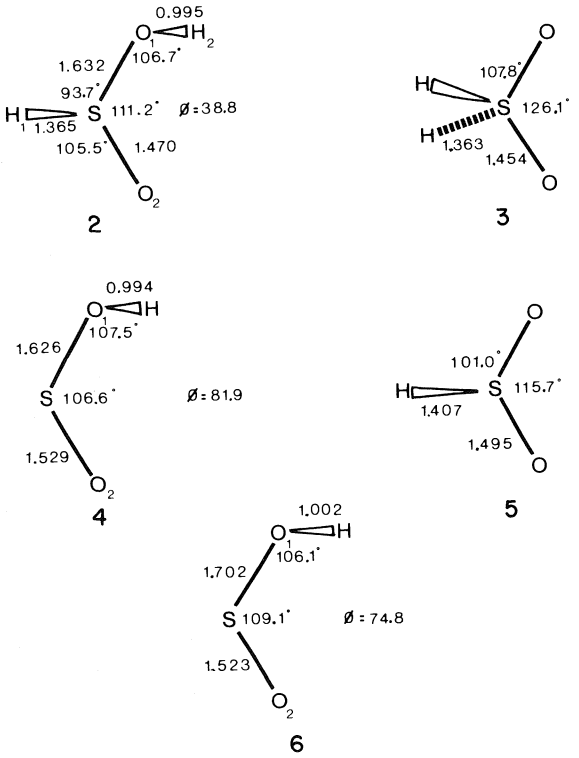


FIG. 3. Calculated geometries of sulfinic acid **2** and related species (bond lengths in Å, angles in degrees). ϕ refers to the $H_2O_1SO_2$ dihedral angle in **2** and to the HO_1SO_2 dihedral angle in **4** and **6**.

interesting to note some trends for the calculated structures. Removal of a hydrogen atom from sulphone **3** does not lead to a large geometry relaxation at S in the sulfonyl radical **1***a*. For the removal of H1 from **2** the only geometrical change is a lengthening of the S—O2 bond in radical **4**. And finally we note that **2**, **4**, and **6** adopt "staggered" conformations in which the dihedral angle differs considerably from the "ideal" 60° angle in ethane. These departures from ideality, which are also evident for the sulfonyl radicals shown in Fig. 1, are due to the low symmetry of the species included in this paper.

One of the objectives of our calculations was to compare the relative stabilities of the simplest sulfinic acid and its isomeric sulfone. From Table 4 it is clear that at the STO-3G* level the sulfinic acid **2** is predicted to be more stable by about 98.7 kJ/mol. Of course, our MO calculations pertain to the gas phase whereas sulfones and sulfinic acids are prepared in solution (1) where the solvent may have a major effect on the relative stabilities of the species of interest. Also the calculations do not account for kinetic factors.

The relatively high positive charge (see Table 4) on H2 of sulfinic acid **2** is consistent with the observed acidity. Loss of a proton at H2 leads to anion **5**. For comparison we have included the isomeric anion **6** formed by the dissociative ionization of the H—S bond in **2**. The much greater stability (~63 kJ/mol) of **5** is consistent with the charge distribution of **2** and the well-known chemistry of the oxy acids of sulfur (34). The net atomic charges listed in Table 4 suggest that sulfone **3** should not be appreciably acidic and that the negative charge on anions **5** and **6** resides primarily on the O atoms.

For completeness we have included the SO_2H radical **4**, which is isomeric with the sulfonyl radical **1***a*. Comparison of the respective total energies shown in Tables 2 and 4 indicates that **4** is more stable by about 0.065 au or 170 kJ/mol. Separation of the total energies into components yields 114.71488 au and 109.01803 au for the nuclear repulsion energy in **1***a* and **4**, respectively. The electronic energies are −656.14569 au and −650.51363 au, respectively. Thus the 5.63206 au difference in electronic energies is more than offset by the 5.69685 au difference in nuclear repulsion energies. Similar large differences occur in anions **5** and **6**: 113.79654 au and 106.68339 au, respectively, for the nuclear repulsion energies and −655.11413 au and −647.97681 au, respectively, for the electronic energies. However in the case of the anions the nuclear repulsion energy difference is insufficient to offset the lower electronic energy of **5**.

The large effect of *d*-type functions in the basis set for sulfur has been discussed in the previous

Can. J. Chem. Downloaded from www.nrcresearchpress.com by 210.87.254.40 on 09/05/12
For personal use only.

Can. J. Chem. Downloaded from www.nrcresearchpress.com by 210.87.254.40 on 09/05/12
For personal use only.

section. Here we note that it would be interesting to study the effect of further improvements in the basis set. Clearly a split-valence basis set would lead to lower total energies for all species (4). Further flexibility could be built in by including polarization functions on all atoms and not on S alone as in this paper. Here it should be mentioned that *ab initio* calculations on **3** have been reported by Van Wazer and Absar (35). With a larger basis and an assumed geometry a very much lower energy was obtained. No geometry optimizations were carried out. The inclusion of *d* orbitals on S lowered the energy by about 0.33 au and led to a large shift of electron density toward S. The resulting charge distribution (0.33 on S, −0.28 on O, and 0.11 on H) is very similar to the one listed for H_2SO_2 in Table 4. *Ab initio* calculations have not been reported for any of the other species included in this paper.

Conclusions

On the basis of the calculations reported in this paper, the following conclusions regarding sulfonyl radicals and related species may be drawn.

1. In agreement with previous studies (4, 36) on hypervalent molecules containing second-row atoms, *d* functions on sulfur are important for the prediction of S—O bond lengths. The STO-3G basis set yields values for S—O bonds which are as much as 0.45 Å longer than the STO-3G* basis set results which generally lead to better agreement with experiment.

2. The geometry of the SO_2 functional group in sulfonyl radicals XSO_2 is essentially independent of the nature of X: r(S—O) = 1.47 ± 0.01 Å, ∠OSO = 123 ± 2° and a nonplanar arrangement about the sulfur atom. The pyramidal geometry at S in sulfonyl radicals is consistent with recent electron spin resonance studies (37).

3. The radical site in sulfonyl radicals is significantly delocalized over the entire SO_2 functional group. This may be represented by three principal resonance contributors. Also the SO_2 functional group in sulfonyl radicals displays characteristic electronic properties which do not show a marked dependence on the choice of substituent.

4. The calculated X—S bond energy of CH_3SO_2 is ~38 kJ/mol greater than that of NH_2SO_2. This large difference is consistent with the chemistry of alkyl and aminosulfonyl radicals (1, 26). The corresponding bond energy in $OHSO_2$ is predicted to be ~30 kJ/mol greater than in NH_2SO_2. This suggests that alkoxylsulfonyl radicals might not react by analogy with the aminosulfonyl radicals.

5. At the STO-3G* level, sulfinic acid HSO_2H is predicted to be more stable than the simple sulfone H_2SO_2 by about 99 kJ/mol. Of the two possible anions formed by the dissociative ionization of sulfinic acid, HSO_2^- is predicted to be more stable than SO_2H^- by about 63 kJ/mol.

6. The SO_2H radical is predicted to be more stable than the isomeric sulfonyl radical HSO_2 by about 170 kJ/mol. As noted in the previous conclusion, the reverse situation is observed for the corresponding anions.

Acknowledgements

We are grateful to the Computer Centre at Dalhousie University for generous amounts of computing time and to the Natural Sciences and Engineering Research Council of Canada for financial assistance.

1. R. F. Langler, Z. A. Marini, and J. A. Pincock. Can. J. Chem. **56**, 903 (1978).
2. C. C. J. Roothaan. Rev. Mod. Phys. **23**, 69 (1951).
3. J. A. Pople and R. K. Nesbet. J. Chem. Phys. **22**, 571 (1954).
4. J. B. Collins, P. von R. Schleyer, J. S. Binkley, and J. A. Pople. J. Chem. Phys. **64**, 5142 (1976).
5. W. J. Hehre, R. F. Stewart, and J. A. Pople. J. Chem. Phys. **51**, 2657 (1969).
6. P. C. Hariharan and J. A. Pople. Theor. Chim. Acta, **28**, 213 (1973).
7. J. S. Binkley, R. A. Whitehead, P. C. Hariharan, R. Seeger, and J. A. Pople. QCPE, **11**, 368 (1978).
8. D. Goutier. R. Macaulay, and A. J. Duke. QCPE, **11**, 241 (1974).
9. (*a*) W. J. Hehre and J. A. Pople. J. Am. Chem. Soc. **97**, 6941 (1975); (*b*) W. J. Hehre, J. A. Pople, W. A. Latham, L. Radom, E. Wasserman, and Z. R. Wasserman. J. Am. Chem. Soc. **98**, 4378 (1976).
10. Y. Morino, Y. Kikuchi, S. Saito, and E. Hirota. J. Mol. Spectrosc. **13**, 95 (1964).
11. W. J. Hehre, R. Ditchfield, R. F. Stewart, and J. A. Pople. J. Chem. Phys. **52**, 2769 (1970).
12. S. Wolfe. Acc. Chem. Res. **5**, 102 (1972).
13. S. Wolfe, A. Rauk, L. M. Tel, and I. G. Csizmadia. J. Chem. Soc. B, 136 (1971).
14. S. Wolfe, A. Rauk, and I. G. Csizmadia. J. Am. Chem. Soc. **91**, 1567 (1969).
15. (*a*) B. C. Gilbert, H. A. H. Laue, R. O. C. Norman, and R. C. Sealy. J. Chem. Soc. Perkin Trans. II, 1040 (1976); (*b*) Y. Takahara, M. Iino, and M. Matsuda. Bull. Chem. Soc. Jpn. **49**, 2268 (1976).
16. R. S. Mulliken. J. Chem. Phys. **23**, 1833 (1955); **23**, 1841 (1955).
17. R. S. Mulliken. J. Chem. Phys. **36**, 3428 (1962); E. R. Davidson. J. Chem. Phys. **46**, 3320 (1967); M. L. Unland, J. H. Letcher, I. Absar, and J. R. Van Waser. J. Chem. Soc. A, 1328 (1971).
18. M. McMillan and W. A. Waters. J. Chem. Soc. B, 422 (1966).
19. (*a*) R. F. Hudson and K. A. F. Record. J. Chem. Soc. Chem. Commun. 831 (1976); (*b*) A. G. Davies, B. P. Roberts, and B. R. Sanderson. J. Chem. Soc. Perkin Trans. II, 627 (1973).

20. T. DURST, J. C. HUANG, N. K. SHARMA, and D. J. H. SMITH. Can. J. Chem. **56**, 512 (1978).
21. W. A. LATHAN, W. J. HEHRE, and J. A. POPLE. Chem. Phys. Lett. **3**, 579 (1969).
22. W. A. LATHAN, W. J. HEHRE, and J. A. POPLE. J. Am. Chem. Soc. **93**, 808 (1971).
23. W. K. BUSFIELD, K. J. IVIN, H. MACKLE, and P. A. G. O'HARE. Trans. Faraday Soc. **57**, 1064 (1961).
24. A. GOOD and J. C. J. THYNNE. Trans. Faraday Soc. **63**, 2708 (1967).
25. S. W. BENSON. Chem. Rev. **78**, 23 (1978).
26. J. A. PINCOCK and A. JURGENS. Tetrahedron Lett. 1029 (1979).
27. J. D. COX and G. PILCHER. Thermochemistry of organic and organometallic compounds. Academic Press, London. 1970. See also ref. 21.
28. J. E. HUHEEY. Inorganic chemistry: principles of structure and reactivity. 2nd ed. Harper and Row, New York. 1978.
29. Tables of interatomic distances and configurations in molecules and ions. Chem. Soc. London, Spec. Publ. No. 12, 1958 and No. 18, 1965.
30. I. HARTGITTAI. Sulphone molecular structures. Lecture notes in chemistry. No. 6. Springer-Verlag. 1978.
31. D. R. LIDE, D. E. MANN, and R. M. FRISTROM. J. Chem. Phys. **26**, 734 (1957).
32. I. HARGITTAI. Acta Chim. Budapest, **60**, 231 (1969).
33. M. HARGITTAI and I. HARGITTAI. J. Mol. Struct. **20**, 283 (1974).
34. F. A. COTTON and G. WILKINSON. Advanced inorganic chemistry. Interscience, New York, NY. 1972.
35. J. R. VAN WAZER and I. ABSAR. Advances in chemistry. No. 110. Sulfur research trends. American Chemical Society, Washington, DC. 1972. p. 20.
36. (*a*) H. B. SCHLEGEL, S. WOLFE, and K. MISLOW. J. Chem. Soc. Chem. Commun. 246 (1975); (*b*) I. H. HILLIER and V. R. SAUNDERS. Mol. Phys. **22**, 193 (1971); (*c*) M. F. GUEST, M. B. HALL, and I. H. HILLIER. J. Chem. Soc. Faraday Trans. II, **69**, 1829 (1973); (*d*) L. J. AARONS. I. H. HILLIER, and M. F. GUEST. J. Chem. Soc. Faraday Trans. II, **70**, 167 (1974).
37. (*a*) C. CHATGILIALOGLU, B. C. GILBERT, C. M. KIRK, and R. O. C. NORMAN. J. Chem. Soc. Perkin Trans. II, 1084 (1979); (*b*) C. CHATGILIALOGLU, B. C. GILBERT, and R. O. C. NORMAN. J. Chem. Soc. Perkin Trans. II, 770 (1979); (*c*) A. G. DAVIES, B. P. ROBERTS, and B. R. SANDERSON. J. Chem. Soc. Perkin Trans. II, 626 (1973).

Can. J. Chem. Downloaded from www.nrcresearchpress.com by 210.87.254.40 on 09/05/12
For personal use only.

The structure of Schiff reagent aldehyde adducts and the mechanism of the Schiff reaction as determined by nuclear magnetic resonance spectroscopy

J. H. ROBINS, G. D. ABRAMS, AND J. A. PINCOCK[1]

Department of Chemistry, Dalhousie University, Halifax, N.S., Canada B3H 4J3

Received July 5, 1979

J. H. ROBINS, G. D. ABRAMS, and J. A. PINCOCK. Can. J. Chem. **58**, 339 (1980).

An nmr study of compounds isolated from the Schiff aldehyde reaction between pararosaniline hydrochloride, sulfur dioxide, and acetaldehyde has demonstrated that these adducts are α-anilinoalkylsulfonic acids. The evidence is incompatible with the other structures most often accepted in the literature, *N*-phenyl alkylsulfonamides. In combination with nmr spectra obtained from solutions of the Schiff reagent and the Schiff reaction and with literature spectrophotometric data, this result leads to a reasonable proposal for the mechanism of the colour development. The effects of the concentrations of the dye, acetaldehyde, and in particular, sulfur dioxide are explained and suggest that the dominant coloured species is a 2:1 acetaldehyde–dye adduct. The nmr results also reveal a kinetic/thermodynamic competition for acetaldehyde between the aniline of the dye and the aldehyde carbonyl leading to bisulfite addition. The relation of the Schiff test with acetaldehyde and the Feulgen test for aldehydes in biological samples is also discussed.

J. H. ROBINS, G. D. ABRAMS et J. A. PINCOCK. Can. J. Chem. **58**, 339 (1980).

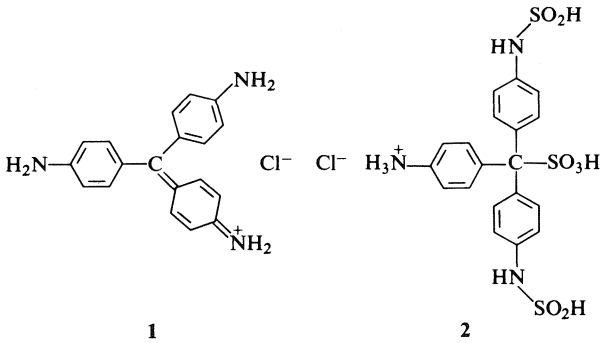
Une étude par rmn des composés isolés de la réaction de l'aldéhyde de Schiff entre le chlorohydrate de pararosaniline, le bioxyde de soufre et l'acétaldéhyde a démontré que ces adduits sont les acides α-anilinoalkylsulfoniques. Cette démonstration est compatible avec les autres structures le plus souvent acceptées dans la littérature, *N*-phényl-alkylsulfonamides. Ce résultat, combiné aux spectres rmn des solutions du réactif de Schiff et de la réaction de Schiff et également aux données spectrophotométriques de la littérature, conduit à suggérer un mécanisme raisonnable pour le développement de la couleur. On a expliqué l'effet de la concentration du colorant, de l'acétaldéhyde et en particulier du bioxyde de soufre et on a suggéré que l'espèce colorée-dominant est l'adduit 2:1 acétaldéhyde–colorant. Les résultats de la rmn révèlent également une compétition cinétique/dynamique de l'acétaldéhyde entre l'aniline du colorant et le carbonyle de l'aldéhyde, conduisant ainsi à une addition de bisulfite. On discute également de la relation du test de Schiff avec l'acétaldéhyde et du test de Feulgen pour les aldéhydes dans les échantillons biologiques.

[Traduit par le journal]

Introduction

The use of the Schiff reagent as a test for aldehydes in biological samples was first suggested by Feulgen and Rossenbeck (1) and, in standard references on staining procedures (2, 3), is referred to as the Feulgen reagent. The full histochemical test is usually a combination of the Schiff reagent plus other reagents that produce aldehydes from naturally occurring molecules; for instance, acid hydrolysis of nucleic acids to remove the purine or pyrimidine bases and free the ribose sugar, or periodic acid oxidation of polysaccharides (4). Despite the fact that the complexity of the chemistry has often been recognized, many attempts have been made to make the staining quantitative (2). This work has often been successful particularly when relative values have been obtained using carefully standardized Schiff reagents and conditions. Our interest in the chemistry of the reagent began when one of us (J.R.) measured by Feulgen microspectrophotometry (2) the DNA content of a marine invertebrate.

Organic chemists have, of course, used Schiff's reagent for many years as a qualitative test for the presence of aldehydes. A positive test is indicated by a change from pale yellow (colourless) to deep red-violet upon addition of the aldehyde to the reagent. Although a recent review lists some sixty different methods of preparing the reagent (4), most rely on converting a red solution of pararosaniline hydrochloride, **1**, to colourless by addition of sulfurous acid from some source of S^{IV} (sulfur dioxide, sodium bisulfite, sodium sulfite, thionyl chloride, etc.). The review (4) also gives an extensive list of aldehydes that give positive tests and contains considerable discussion of the effect of variables such as pH, sulfurous acid, and aldehyde concentration on the intensity and stability of the colour formed.



1 **2**

[1]To whom correspondence may be addressed.

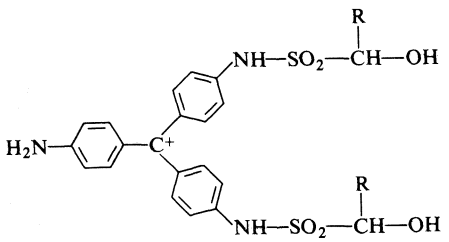
0008-4042/80/040339-09$01.00/0

©1980 National Research Council of Canada/Conseil national de recherches du Canada

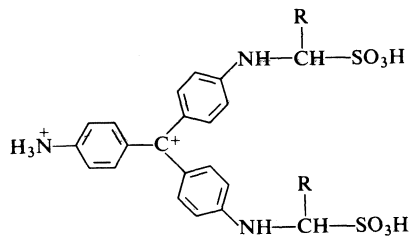
Can. J. Chem. Downloaded from www.nrcresearchpress.com by 210.87.254.5 on 09/05/12
For personal use only.

This evidence demonstrates that the chemistry involved is neither simple nor clearly understood. Because such colour tests are now of less importance to organic chemists, the reaction is seldom discussed in modern texts.

In older references (5, 6) the leuco derivative of the dye is usually shown as **2** and the coloured adduct as **3**. The formulation **3** ignores the question of whether —NH—SO_2—CHR—OH is an α-hydroxyalkyl sulfonamide (—NH—$\overset{\overset{O}{\|}}{\underset{\underset{O}{\|}}{S}}$—CHR—OH) or a sulfite ester (—NH—$\overset{\overset{O}{\|}}{\underset{\underset{\cdot\cdot}{}}{S}}$—O—$\overset{\overset{R}{|}}{CH}$—OH). Both



3



4

have been proposed in the literature. The structures **2** and **3** are based mainly on the early work of Wieland and Scheuing (7). Although there is no doubt that the colour change results from conversion of the saturated central carbon of the triarylmethane system to a highly delocalized cation, the other features are less certain. The amino sulfinic acids in **2** are suggested because no colour results either from a reagent prepared using equimolar quantities of sulfur dioxide and pararosaniline hydrochloride (**1**) or by reaction of aldehyde bisulfite addition compounds with **1**. Therefore the reasonable pathway to a coloured species like **3** is via preformed amino sulfinic acid moieties. Other evidence for **3** is that the stoichiometry of the adduct is 2:1 aldehyde–pararosaniline, at least for acetaldehyde. As discussed by Kasten (4) and Puchtler *et al.* (8), the literature before 1920 contains other proposals, including Schiff's imine (Schiff base) formulation, which are not compatible with more recent findings.

On the basis of extensive spectrophotometric and kinetic work, Hörmann *et al.* (9) have proposed that the coloured Schiff adduct is an aminoalkyl sulfonic acid dication as in **4**. This suggestion was originally advanced by Rumpf (10) and has been adopted by others more recently (11). Again spectral evidence suggests a 2:1 adduct for acetaldehyde and formaldehyde. Others have proposed, for formaldehyde, ratios ranging from 3:1 (11) to 6:1 (12, 13, 14) usually without comment on actual structures. Regardless of stoichiometry, adducts like **4** cannot be formed directly from **2**.

In view of the interest in the use of the Schiff reagent in biological staining and the confusion about the chemistry (in particular stoichiometry), a more thorough study of the test using spectral methods (ir, ^{1}Hmr, ^{13}Cmr) seemed necessary. Wieland and Scheuing (7) isolated and characterized compounds from acetaldehyde pararosaniline reactions. In the present work, spectra were taken of three compounds prepared according to their methods. These spectra were then compared with those obtained from solutions of the Schiff test. The results give a much clearer picture of the chemistry involved and, as will become apparent, explain many of the ambiguities previously observed and, as well, reveal some intriguing kinetic phenomena.

Results and Discussion

Researchers have frequently used basic fuchsin when studying the Schiff reaction (7, 9, 10). This dye is often a mixture of several triarylmethane derivatives and the proportions may vary among commercial samples (1). Pararosaniline hydrochloride **1** was used throughout this study. ^{1}Hmr[2] spectra of the crude commercial dye gave a broad featureless signal from δ 6.2–7.2; simple recrystallization from water gave material of a single spot on tlc that showed the expected AB type doublet of doublets in the aromatic region. The known carbinol base **5**, obtained by adding hydroxide to **1**, was also prepared. The dye pararosaniline hydrochloride, **1**, the carbinol **5**, 4-methylaniline, and 4-methylanilinium cation serve as useful models for interpreting the spectra of the less well-understood pararosaniline derivatives. Two different effects are relevant to this study. The first can be illustrated by comparing the spectra of the simpler systems 4-methylaniline and the 4-methylanilinium cation, and concerns the effect of a protonated

[2]All ^{1}Hmr and ^{13}Cmr spectra are in DMSO-d_6 with δ values relative to internal TMS unless otherwise stated.

Can. J. Chem. Downloaded from www.nrcresearchpress.com by 210.87.254.5 on 09/05/12
For personal use only.

Can. J. Chem. Downloaded from www.nrcresearchpress.com by 210.87.254.5 on 09/05/12
For personal use only.

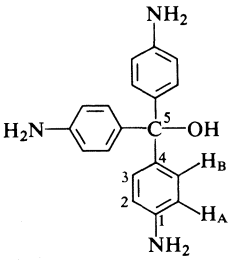
amino substituent on the chemical shifts of the aromatic hydrogens. The second effect, that of the influence on the aromatic proton shifts by the delocalized positive charge of the tris(4-aminophenyl)methyl cation, can be evaluated by comparison of the spectra of pararosaniline carbinol base (**5**) with pararosaniline hydrochloride (**1**). In the discussion that follows the δ values reported for *para*-substituted aromatic AB type systems are the centers of the doublets and are therefore not true chemical shifts.

Pararosaniline Carbinol Base (5)

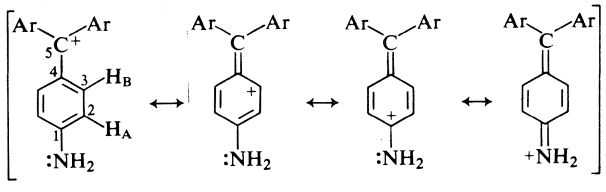
Since the central carbon is quaternary the substituent effect of the amino group should be similar to that in 4-methylaniline (MA). The ^{1}Hmr spectrum of **5**: δ 4.82 (NH_2; δ 4.70 in MA), 6.40 (H_A, J = 8 Hz; 6.48 in MA), and 6.78 (H_B, J = 8 Hz; 6.81 in MA) confirms this assertion. The chemical shifts also agree well with those expected on the basis of substituent additivity in aromatic rings (15). The ^{13}Cmr assignments are also straightforward; δ: 79.9 (C5), 112.6 (C2), 128.5 (C3), 137.0 (C4), and 146.1 (C1). Resonance delocalization from nitrogen puts negative charge on C2 and C4. Therefore of the quaternary pair C1/C4, C4 is at higher field and of the tertiary pair C2/C3, C2 is at higher field.

Pararosaniline Hydrochloride (1–6)

As shown in the resonance delocalized diagram of **6**, positive charge density is on C5, C3, C1, and NH_2. The ^{1}Hmr assignments of **6**: δ 6.84 (H_A, J = 9 Hz), 7.18 (H_B, J = 9 Hz), and 7.53 (NH_2) are then made on the basis that H_A is more shielded than H_B. Note as well the large downfield shift of the amino protons relative to those of the carbinol **5**. The ^{13}Cmr assignments for triarylmethyl cations have been made previously (16) according to parallel



5



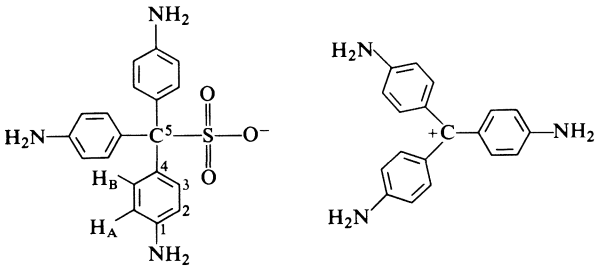
6

arguments: δ: 114.5 (C2), 126.0 (C4), 140.1 (C3), 157.5 (C1), and 177.8 (C5). The conversion from the carbinol **5** to the cation **6** obviously gives the largest change in shift for C5 (sp^3 becoming sp^2 (+)).

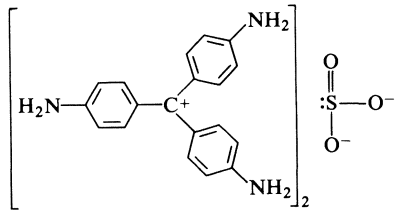
At this point it is worth mentioning that the ^{1}Hmr spectrum of an anilinium cation shows quite different behaviour for the aromatic protons. Electron donation by the resonance effect of the amino group is now removed and only an inductive electron-withdrawing effect remains. The signals of the aromatic protons coalesce to a singlet at δ 7.27 as can be observed in a spectrum of 1:1 molar ratio of 4-methylaniline – *p*-toluenesulfonic acid.

Pararosaniline Dye Salt, 7

This compound was originally prepared by Wieland and Scheuing (7) according to a procedure reported earlier (17). There has been some dispute about its structure with two of the favoured choices being **7** (the salt of a sulfonic acid) and **8** (a salt of sulfite anion). Although these two formulations are obviously very similar, the nmr evidence favours **7**. The ^{1}Hmr spectrum shows two AB sets of aromatic



7



8

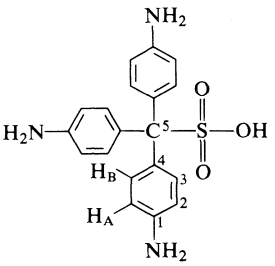
protons, one clearly from the cation: δ 6.78 (H_A), 7.18 (H_B), and 7.35 (NH_2), and one from the anion which has the central carbon quaternary in the triarylmethane system: δ 4.73 (NH_2), 6.34 (H_A), and 7.02 (H_B). The only significant change in the spectrum of the sulfonate anion from that of the carbinol **5** is the chemical shift of H_B, the proton nearest to the quaternary center. The two types of amino protons in the salt are different because of the slow exchange in DMSO. The ^{13}Cmr spectrum shows the same pair of ions. The cation spectrum is identical to that of **6** and the anion line positions are similar to those of **5**: δ 77.2 (C5), 112.2 (C2), 131.0

Can. J. Chem. Downloaded from www.nrcresearchpress.com by 210.87.254.5 on 09/05/12
For personal use only.

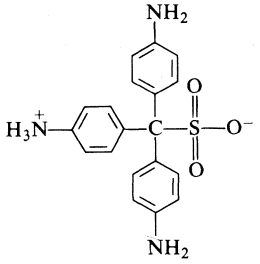
(C3), 133.7 (C4), and 145.7 (C1). There has been some discussion in the literature whether the attachment of the sulfur to the central carbon of these pararosaniline derivatives is a sulfonate (C—SO_2—O) or a sulfite ester (C—O—SO—O) (4). For this dye salt a choice can be made by consideration of the ir spectrum (KBr) which shows bands for sulfate, 1165 cm^{-1} and 1040 cm^{-1}, different from those expected for sulfite derivatives (18, 19). As well, Wieland and Scheuing (7) have demonstrated that the dye salt **7** is not oxidizable with iodine in agreement with the sulfonate formation. The ^{13}Cmr spectrum of **7** gives a resonance for C5 (δ 77.2) very similar to that for C5 (δ 79.9) of the carbinol base as expected from known chemical shifts of sulfonyl derivatives (20).

*Pararosaniline Leucosulfonic Acid (**9**)*

Several related compounds of this type have been prepared but they apparently only differ in the amount of water of crystallization (7, 17). Some difficulty was experienced obtaining nmr spectra for **9** since it was unstable in solution due to loss of sulfur dioxide. This is a well-known phenomenon since for solutions of pararosaniline hydrochloride there is an equilibrium between the coloured cation **1** and the colourless leuco derivative **9** which can be controlled by the sulfurous acid concentration. In fact, loss of SO_2 is the major problem in the stability of Schiff reagents (4). For **9**, spectra in DMSO could be obtained if run quickly but they were always those of mixtures of **9** and **1**. After several hours only **1** was present. This loss of sulfur dioxide could be slowed by adding D_2O to the DMSO solution. The ^{1}Hmr spectrum of **9** (δ 3.2–4.9 (—NH_2, H_2O of crystallization), 6.40 (H_A, J = 8 Hz), and 7.06 (H_B, J = 8 Hz)) gives values that are very similar to those of the anion portion of the dye salt **7**. The same relationship between **9** and **7** was observed in the ^{13}Cmr spectrum as well as the change of **9** to **1** with time. The pK_a of sulfonic acids, −2 to −3 (21), and anilinium ions, 4.6 (21), imply that **9** should exist predominantly as the zwitterion **10** in water. Even in DMSO where some changes in acidity from those in water might be expected, the very large difference in pK_a should favour **10**. A good model for **10** can be obtained from a solution consisting of a 3:1 molar ratio of 4-methylaniline – *p*-toluenesulfonic acid. The ^{1}Hmr spectrum of the aniline aromatic hydrogens, δ 6.76 (H_A, J = 8 Hz) and 6.95 (H_B, J = 8 Hz), is as expected for a 1:2 mixture of the protonated/unprotonated form with rapid exchange giving an average spectrum of the anilinium ion (δ 7.27, H_A and H_B) and the free amine (δ 6.48 (H_A) and 6.81 (H_B)). The ^{1}Hmr spectrum of



9



10

the leuco sulfonic acid is then consistent with the structure of the zwitterion **10**, the AB system at slightly lower field than in the carbinol, **5**. Finally, the ir (KBr) of **9**:**10** show the sulfonate pattern of bands at 1035 and 1170 cm^{-1}.

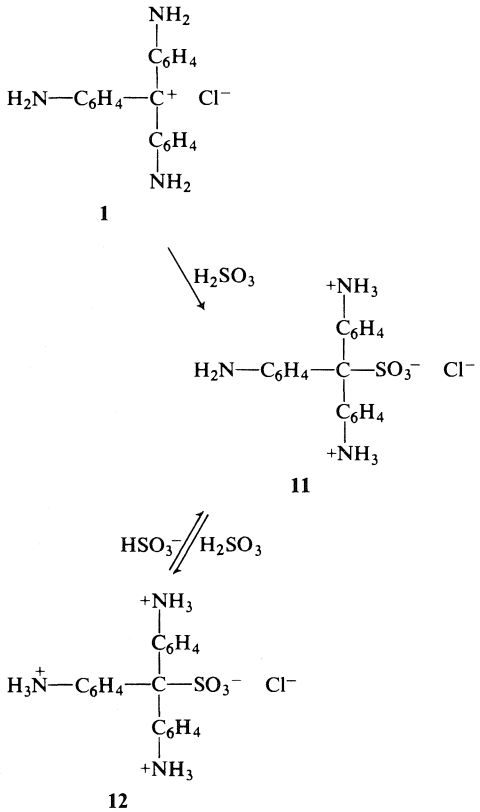
Schiff Reagent

The spectra of the previously described isolated compounds can now be compared to those of the Schiff reagent in D_2O. Peak positions for these spectra were assigned relative to δ HDO = 0. From the above discussion of the spectra in DMSO, it is the changes in chemical shift that are important. A solution (10 mg/mL) of pararosaniline hydrochloride **1** in D_2O shows the expected doublet of doublets in the ^{1}Hmr spectrum δ 2.08 (H_A, J = 9 Hz) and 2.50 (H_B, J = 9 Hz). The separation of the two doublets in D_2O (0.42 ppm) is similar to that observed in DMSO (0.34 ppm). In agreement with detailed experiments of triarylcarbinol pK_R values (23), there is no observable conversion of pararosaniline to its carbinol at pH = 7. On conversion to Schiff reagent by bubbling sulfur dioxide into the D_2O solution of **1** until the red colour just disappeared, the spectrum changed to a very close AB type system with the intense inner peaks at δ 2.70 and 2.74. Clearly that is not what is expected for formation of the leucosulfonic acid (**10**) where the separation of the doublets is 0.66 ppm and both H_A and H_B move to higher field. However, the change is compatible with saturation of the central carbon and more extensive protonation of the amino groups than in the zwitterion **10**.

It has been well established that excess sulfur dioxide or strong mineral acids (i.e., low pH) make the Schiff reagent inactive (4). This has always been a problem in the elaboration of a mechanism for the reagent's activity since more than one equivalent of sulfur dioxide is required for positive results and yet excess leads to no colour development on addition of the aldehyde. These facts can be explained by recognizing that extensive protonation of the amino groups will lower the effective concentration of nucleophilic nitrogens. Clearly any strong acid, including sulfurous acid, pK_1 =

Can. J. Chem. Downloaded from www.nrcresearchpress.com by 210.87.254.5 on 09/05/12
For personal use only.

1.9, $pK_2 = 7.4$ (24, 25), will cause this behaviour; in contrast, weak acids such as acetic acid ($pK = 4.8$) do not have sufficiently low pK_a values to fully protonate all three nitrogens and therefore are not effective (4) in decreasing the sensitivity of the reagent. That pararosaniline derivatives can be triply protonated is evident from the behaviour of **1** itself which is converted to a yellow salt with a chromophore similar to that of the unsubstituted triphenylmethyl cation at pH = 0 (26). For a solution of pararosaniline hydrochloride at the usual concentration ($\sim 4 \times 10^{-4}$ *M*) and two equivalents of sulfur dioxide the pH $\simeq$ 2 (9). Therefore the solution is not acidic enough to convert **11** completely to **12** (26). The ^{1}Hmr spectrum in D_2O where exchange is rapid should be an average of **11** and **12** and should show the aromatic ring protons to be in an environment similar to the 4-methylanilinium ion. Wieland and Scheuing formulated the Schiff reagent with the excess sulfurous acid bound to nitrogen as in **2** (*N*-sulfinic acids) (7). However, compounds of this type are known to be unstable in water (27, 28) and there is no uv spectral evidence for this formation (11). The main reasons for their continued consideration in the literature are the assumption that the complex of aldehydes with Schiff's reagent is an alkyl sulfonamide **3** and the observation that Schiff's reagent does not give a colour test with preformed aldehyde bisulfite addition compound (7).



1 **11** **12**

Schiff Reagent Acetaldehyde Addition Product

Wieland and Scheuing prepared a solid 1:1:1 addition product of pararosaniline hydrochloride – sulfurous acid – acetaldehyde to which they assigned the structure **13** (7). The ^{1}Hmr spectrum in DMSO-d_6 of material prepared by this method, however, indicates that the correct structure is **14**: δ 1.50 (CH_3, doublet, $J = 6$ Hz), 4.53 (—CH, complex multiplet), 6.80 (H_A, H_A', doublet, $J = 9$ Hz), 7.12 (H_B, H_B' doublet, $J = 9$ Hz), 7.36 (broad singlet, NH_2), 8.16 (broad doublet, NH). Decoupling experiments clearly showed the —NH—CH—CH_3 group. The position of the aromatic doublet of doublets is characteristic of the delocalized triphenylmethyl cation, and the single hydrogen on the substituted nitrogen is at different chemical shift than the other NH_2 hydrogens. Although 2:1 aldehyde–pararosaniline adducts are usually suggested (7, 9), this isolated material is a 1:1 adduct as shown by integration of the signal intensities. The ir (KBr) is also compatible with a sulfonic acid derivative, exhibiting the bands expected at 1075 cm^{-1} and 1150 cm^{-1} (18, 19). The ^{13}Cmr spectrum for **14** has the advantage that the better resolution shows that there are two types of aromatic rings: δ 17.4 (CH_3), 64.1 (CH), 114.5 (C2, C2′), 126.0 (C4′), 126.3 (C4), 139.4 (C3′), 140.0 (C3), 155.6 (C1), 157.3 (C1′), and 177.3 (C5). Both sets of aromatic carbon line positions are consistent in chemical shift with a delocalized cation structure. Assignments of the primed and unprimed carbons are based on relative intensities.

The spectral evidence leaves no doubt that this complex is a 1:1 adduct of structure **14** in agreement with more recent formulations of the coloured Schiff product as an α-aminosulfonic acid (9, 11). However, Wieland and Scheuing state that the actual dye is a 2:1 (aldehyde–pararosaniline) adduct (7) and Hörmann *et al.* have found that the colour developed is proportional to the square of the acetaldehyde concentration (9). For the usual 4.5×10^{-3} *M* pararosaniline hydrochloride concentration and acetaldehyde at 4×10^{-4} *M* the statistical distribution of products (assuming all three amino groups are equally reactive) would be 91.4% unsubstituted, 8.4% monosubstituted, 0.26% disubstituted, and negligible trisubstituted. If only disubstituted products form coloured species efficiently and the extinction coefficient is $\sim 10^5$, as expected

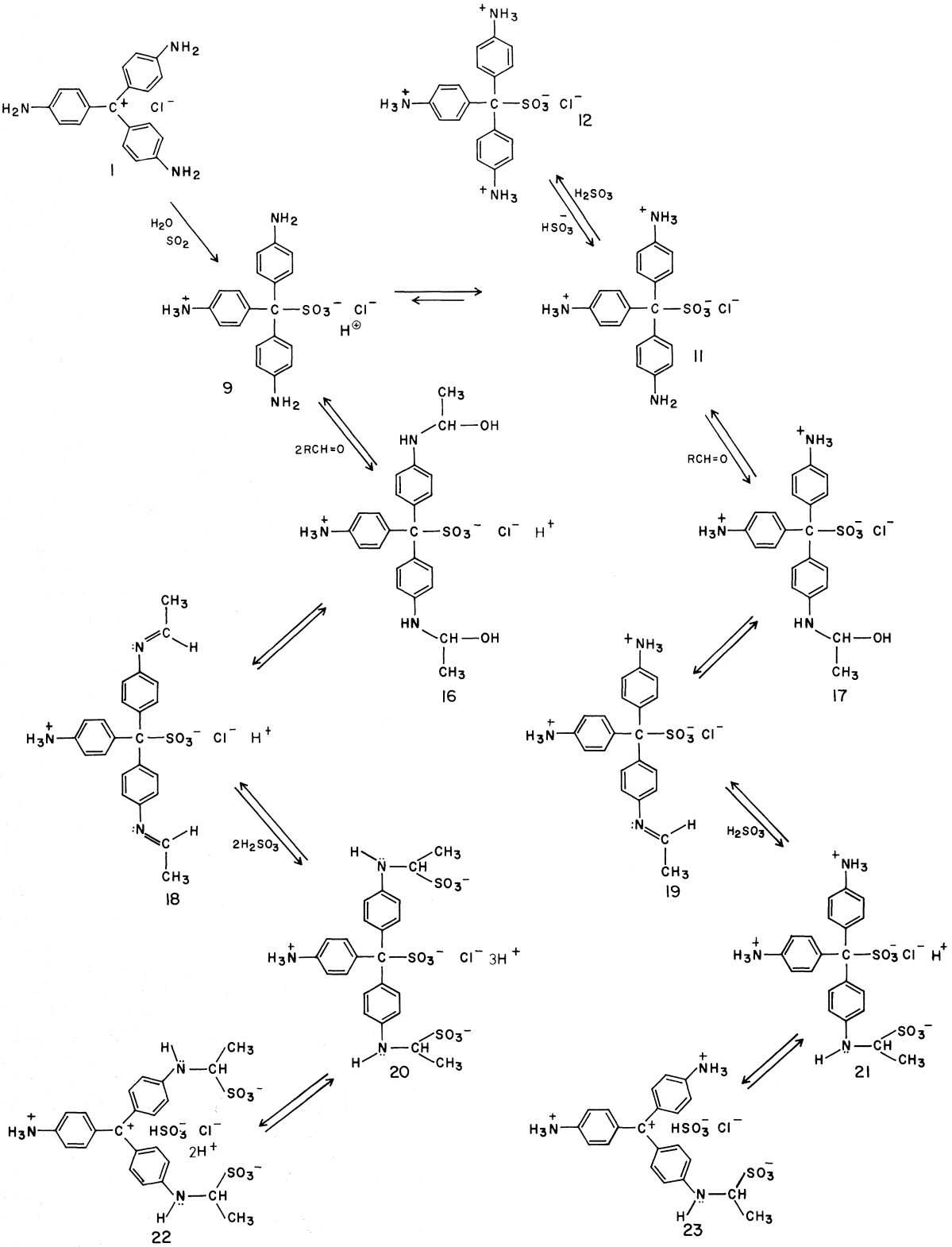
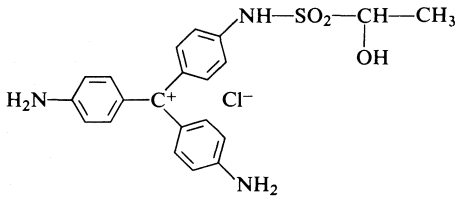
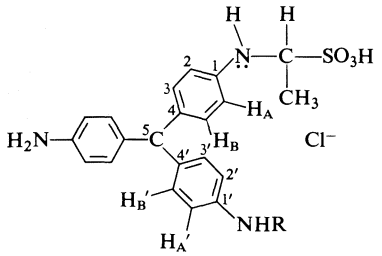


FIG. 1. Mechanism of the Schiff reaction.

Can. J. Chem. Downloaded from www.nrcresearchpress.com by 210.87.254.5 on 09/05/12
For personal use only.



13

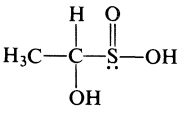


14 R = H
15 R = —CH(CH$_3$)SO$_3$H

for the pararosaniline derivative (23), the absorbance would be $4.5 \times 10^{-3} \times 2.6 \times 10^{-3} \times 10^5 \simeq 1.2\ cm^{-1}$ which is in reasonable agreement with, but about 60–70% of, the values observed by Hörmann *et al.* (9). Many workers have pointed out that there are probably at least two chromophores contributing to the total absorbance (4, 29, 30) and the simplest suggestion is that they are the cation of **14** and its disubstituted analogue **15**.

The complete mechanism for the Schiff reaction in water can then be written as in Fig. 1. Steps **9** → **16** → **18** and **11** → **17** → **19** are the well-known Schiff base or imine formation via a carbinolamine intermediate. The mechanism for these transformations has been studied extensively (31, 32) and the equilibrium constant for formation of imines from aromatic amines in water is known to be small (33, 34). The excess sulfurous acid is then required to shift the equilibria towards **20** and **21**. This, of course, lowers the sulfurous acid concentration of the solution and allows the final equilibria to be favorable i.e., **20** → **22** and **21** → **23**.[3] This explains the rather critical effect of sulfurous acid since more than one equivalent is required, but too high a concentration makes the final equilibria unfavorable (as well as increasing acidity to convert the pararosaniline to a fully protonated and unreactive derivative **12**). The discussion above on the stoichiometry of the complex suggests that loss of sulfur from the central carbon is much more favourable for **20** than **21**. This is reasonable because the pK_a of the amino group of α-aminosulfonic acids is lower by about 4 pK units than normal amines (35) and therefore will probably not be completely protonated under the reaction conditions. Therefore **22** has better resonance stabilization than **23**.

Finally, the observation that the Schiff reagent with acetaldehyde gives a positive test but that the colour slowly disappears with time should be explained (9). Again the ^{1}Hmr spectrum in D_2O is instructive since on adding acetaldehyde to the reagent the signals for the leuco sulfonic acid derivative **11**:**12** disappear immediately and signals for the new complex appear. After approximately two hours the signals for the leucosulfonic acid appear again and the aldehyde has been converted completely to the bisulfite addition compound **24**: δ − 0.32 (CH, quartet, J = 6 Hz) and −3.42 (CH_3, doublet, J = 6 Hz) (chemical shifts relative to HDO). This same spectrum can be duplicated with just acetaldehyde and sulfurous acid. If excess acetaldehyde is added, the sulfurous acid in solution is slowly converted entirely to **24** and the leucosulfonic acid is converted to pararosaniline hydrochloride. The colour of the solution is now stable but is the red (λ_{max}, 538 nm) of pararosaniline



24

hydrochloride rather than the red-violet (λ_{max}, 560 nm) of the Schiff aldehyde adduct. Clearly for qualitative tests this would still be considered positive.

These kinetic phenomena raise an interesting point. The amino groups of the dye react in kinetic preference with the aldehyde to give unstable carbinolamine or imine adducts whereas the thermodynamically favoured product is the bisulfite addition compound. The equilibrium constants for the first process are in the range 3–30 M^{-1} (36) whereas for bisulfite addition they are much higher, 10^4–10^5 M^{-1} (31, 34). As Young and Jencks (36) have demonstrated, the reactive species in bisulfite formation is the sulfite dianion and at pH ≃ 2 of the Schiff test, its concentration is 10^{-7} of the total concentration of S^{IV} species (24). The free amine concentration is given by the equilibria between **9**, **11**, and **12** in Fig. 1. The equilibrium between **11** ⇌ **19** can be estimated from the pK_a ≃ 2.0 for crystal violet (37) and therefore at the pH ≃ 2.0 the free amine concentration will be about half the total concentration of the dye. Therefore, in order for bisulfite to compete with the amine kinetically, the ratio of the second order rate constants, k_s/k_A, for reaction of bisulfite with acetaldehyde (k_s) and

[3]Note that **22** and **23** are the conjugate acids of **14** and **15** respectively and are the expected coloured species at the normal pH of 2 used for Schiff tests.

Can. J. Chem. Downloaded from www.nrcresearchpress.com by 210.87.254.5 on 09/05/12
For personal use only.

amine with acetaldehyde (k_A), must exceed 10^7. Estimates of this rate ratio can be made from literature data using aniline as the amine, although not for acetaldehyde as the aldehyde. For instance, for formaldehyde: $k_s \simeq 5 \times 10^6\ M^{-1}\ s^{-1}$ (38), $k_A \simeq 2.75\ M^{-1}\ s^{-1}$ (34), $k_s/k_A \simeq 1.8 \times 10^5$; for 4-methoxybenzaldehyde: $k_s \simeq 10^3\ M^{-1}\ s^{-1}$ (38), $k_A \simeq 4.5 \times 10^{-3}\ M^{-1}\ s^{-1}$ (39), $k_s/k_A \simeq 2.2 \times 10^5$. Therefore the formation of **22** (or **23**) occurs in kinetic preference and the initially formed adducts are slowly converted to the bisulfite addition complex **24** by reversal of the equilibria to **9** (or **11**).

Summary

The coloured species formed in the Schiff reaction of acetaldehyde have been shown to be α-aminosulfonic acids which are unstable in solution due to loss of the aldehyde bisulfite addition compound. These Schiff complexes may be of 1:1 or 2:1 stoichiometry for acetaldehyde – pararosaniline hydrochloride if the relative concentration of the aldehyde is low. As Hörmann *et al.* (9) have stated, colour development for simple aldehydes will depend in a complex way on the concentrations of each of the dye, sulfur dioxide, and aldehyde and therefore for quantitative results careful calibration is required (9).

The staining of histological samples may be quite different since in this case disubstitution on the dye by aldehydes is less likely because of the rigid nature of the tissue samples. Moreover excess dye and sulfurous acid are always removed by water washing so that the equilibrium between the corresponding analogues of **21** and **23** will be shifted entirely to **23**. In fact, Hörmann *et al.* (9) have shown that for the PAS test (periodic acid, Schiff) a simple linear dependence between absorbance and starch concentration is observed (9) which can be used for relative but not absolute values. As well, the colour of the stained dried tissue samples might be stable since loss of aldehyde bisulfite compound is not likely outside of the aqueous acid test solutions.

Experimental

Proton magnetic resonance spectra were run on either a Varian T-60, Varian HA-100, or Varian CFT-20 spectrometer. Carbon spectra were from the CFT-20. The samples were run in either DMSO-d_6 with internal TMS or D_2O using the HDO signal as standard. Infrared spectra were recorded on a Perkin Elmer 237 or 521 spectrometer using KBr discs. Spectra are reported in the text.

Pararosaniline Hydrochloride

Commercial (J. T. Baker, C.I. 42500, lot number 310911) material was purified by recrystallization from water and showed only one spot with slight tailing on tlc (silica gel; 4:1:5 butanol – acetic acid – water).

Pararosaniline Carbinol Base

The method is similar to that of Jennings (40). A stirred suspension of 3.24 g (10 mmol) of pararosaniline hydrochloride in 500 mL of water was brought to boil. A boiling solution of 625 mL of 0.2 *N* sodium hydroxide (125 mmol) was added and the mixture boiled for 30 min and then filtered hot. After standing at room temperature overnight the solid was collected, washed with cold water, then ethanol–ether (1:10), and finally ether (28% yield); mp 208–210°C as a red liquid.

Pararosaniline Dye Salt

The method is similar to that of Dürrschnabel and Weil (17). Sulfur dioxide was bubbled through a solution of pararosaniline hydrochloride (10 g) in 40 mL of water until the colour changed from dark red to yellow. The solution was gravity filtered and then heated until it became red again. After cooling to room temperature, the crystals were collected, washed with ethanol–ether (1:10) and then ether, and finally dried *in vacuo* over sulphuric acid for two hours (53% yield).

Schiff Reagent Acetaldehyde Addition Product

The method used is that of Wieland and Scheuing (7). Pararosaniline hydrochloride, 0.326 g (1 mmol), was dissolved in 500 mL of 0.006 *N* (3 mmol) hydrochloric acid and the solution was filtered. Then 1.0 mL of an aqueous solution (0.044 g/mL, 1 mmol) of acetaldehyde and 10 mL of 0.1 *M* (1 mmol) sulfurous acid was added with stirring. The mixture was left at room temperature overnight. The precipitate was collected, washed with water, ethanol–ether (1:10), and ether, and dried for two hours *in vacuo* over concentrated sulfuric acid (61% yield).

Acknowledgments

We wish to thank L. C. Vining, Biology Department, Dalhousie University, for advice throughout this study, J. Van Ingen of the Atlantic Regional Laboratory of the National Research Council of Canada for running the 100 MHz proton nmr spectra, and D. L. Hooper, Department of Chemistry, Dalhousie University, for running carbon and proton spectra. This research was supported in part by a National Research Council of Canada grant to I. A. McLaren of the Biology Department, Dalhousie University.

1. R. Feulgen and H. Rossenbeck. Z. Physiol. Chem. **135**, 203 (1924).
2. C. Leuchtenberger. *In* General cytochemical methods. Vol. 1. *Edited by* J. F. Danelli. Academic Press, New York. 1958. p. 220.
3. R. D. Lillie. *In* Biological stains. 9th ed. *Edited by* H. J. Conn. Williams and Wilkins, Baltimore. 1977.
4. F. H. Kasten. Int. Rev. Cytol. **10**, 1 (1960).
5. C. R. Noller. *In* Organic chemistry. 2nd ed. W. B. Saunders Co., Philadelphia. 1958. p. 490.
6. R. L. Shriner, R. C. Fuson, and D. Y. Curtin. *In* The systematic identification of organic compounds. 5th ed. J. Wiley & Sons, Inc., New York. 1964. p. 129.
7. H. Wieland and G. Scheuing. Ber. **54**, 2527 (1921).
8. H. Puchtler, S. N. Meloan, and B. R. Brewton. Histochemistry, **41**, 185 (1975).
9. H. Hörmann, W. Grassmann, and G. Fries. Justus Liebigs Ann. Chem. **616**, 125 (1958).
10. P. Rumpf. Ann. Chim. Paris, **3**, 327 (1935).
11. R. V. Nauman, P. West, and F. Tron. Anal. Chem. **32**, 1307 (1960).

Can. J. Chem. Downloaded from www.nrcresearchpress.com by 210.87.254.5 on 09/05/12
For personal use only.

12. H. PUCHTLER, S. N. MELOAN, and B. R. BREWTON. Histochemistry, **40**, 291 (1974).
13. T. BARKA and L. ORNSTEIN. Cytochem. **8**, 208 (1960).
14. T. HIRAOKA. J. Biophys. Biochem. Cytol. **8**, 286 (1960).
15. D. H. WILLIAMS and I. FLEMING. *In* Spectroscopic methods in organic chemistry. 2nd ed. McGraw Hill, London. 1973. p. 135.
16. J. B. STOTHERS. *In* Carbon-13 NMR spectroscopy. Academic Press, New York. 1972. p. 221.
17. K. DÜRRSCHNABEL and H. WEIL. Ber. **38**, 3492 (1905).
18. V. M. PARIKH. *In* Absorption spectroscopy of organic molecules. Addison-Wesley, Mass. 1974.
19. A. WOJCICKI. *In* Advances in organometallic chemistry. Vol. 12. *Edited by* F. G. A. Stone and R. West. Academic Press, New York. 1974. p. 31.
20. J. S. GROSSERT, M. M. BHARADWAJ, R. F. LANGLER, T. S. CAMERON, and R. E. CORDES. Can. J. Chem. **56**, 1183 (1978).
21. J. P. GUTHRIE. Can. J. Chem. **56**, 2342 (1978).
22. N. L. ALLINGER, M. P. CAVA, D. C. DE JONGH, C. R. JOHNSON, N. A. LEBEL, and C. L. STEVENS. *In* Organic chemistry. 2nd ed. Worth Publishers, Inc., New York. 1976. p. 260.
23. N. C. DENO, J. J. JARUZELSKI, and A. SCHRIESHEIM. J. Org. Chem. **19**, 155 (1954).
24. J. P. GUTHRIE. Can. J. Chem. **57**, 454 (1979).
25. T. D. STEWART and L. H. DONNALLY. J. Am. Chem. Soc. **54**, 3559 (1932).
26. H. PUCHTLER, S. N. MELOAN, and B. R. BREWTON. Histochemistry, **45**, 255 (1975).
27. G. KRESZE. Angew. Chem. Int. Ed. Engl. **1**, 89 (1962).
28. G. KRESZE and W. WUCHERPFENNING. Angew. Chem. Int. Ed. Engl. **6**, 149 (1967).
29. W. A. L. DUIJNDAM, J. HERMANS, and P. VAN DUIJN. J. Histochem. Cytochem. **21**, 729 (1973).
30. H. ELFTMAN. J. Histochem. Cytochem. **7**, 93 (1959).
31. W. P. JENCKS. *In* Progress in physical organic chemistry. Vol. 2. *Edited by* S. G. Cohen, A. Streitweiser, and R. W. Taft. Interscience, J. Wiley & Sons, New York. 1964. p. 63.
32. W. P. JENCKS. *In* Catalysis in chemistry and enzymology. McGraw-Hill, New York. 1969.
33. E. H. CORDES and W. P. JENCKS. J. Am. Chem. Soc. **84**, 826 (1962).
34. W. R. ABRAMS and R. G. KALLEN. J. Am. Chem. Soc. **98**, 7777 (1976).
35. R. G. LACOSTE and A. E. MARTELL. J. Am. Chem. Soc. **77**, 5512 (1955).
36. P. R. YOUNG and W. P. JENCKS. J. Am. Chem. Soc. **100**, 1228 (1978).
37. V. W. BROSER. Z. Naturforsch. Teil A, **10**, 350 (1955).
38. P. R. YOUNG and W. P. JENCKS. J. Am. Chem. Soc. **99**, 8238 (1977).
39. J. J. CHASETTE and E. DE HOFFMANN. J. Org. Chem. **44**, 2256 (1979).
40. W. L. JENNINGS. Ber. **36**, 4022 (1903).

Can. J. Chem. Downloaded from www.nrcresearchpress.com by 210.87.254.5 on 09/05/12
For personal use only.

A homopropargyl radical rearrangement. Kinetics of the rearrangement of the 2,2,5,5,-tetramethyl-3-hexyn-1-yl radical[1]

KEITH U. INGOLD

Division of Chemistry, National Research Council of Canada, Ottawa, Ont., Canada K1A 0R6

AND

JOHN WARKENTIN[2]

Department of Chemistry, McMaster University, Hamilton, Ont., Canada L8S 4M1

Received August 7, 1979

KEITH U. INGOLD and JOHN WARKENTIN. Can. J. Chem. **58**, 348 (1980).

The rate constants for rearrangement of the 2,2,5,5-tetramethyl-3-hexyn-l-yl radical to the 2,6,6-trimethyl-4-heptyn-2-yl radical have been measured from 45 to 88°C by kinetic epr spectroscopy. The temperature dependence can be represented by

$$\log(k^{C\equiv C}/s^{-1}) = (12.4 \pm 1.5) - (14.6 \pm 2.4)/\theta$$

where $\theta = 2.3RT$ kcal mol^{-1}. This rearrangement, which must involve an intermediate vinyl radical of the methylenecyclopropane type, is much slower than analogous rearrangement of homoallyl radicals but comparable in rate to rearrangement of homobenzyl (neophyl) radicals.

KEITH U. INGOLD et JOHN WARKENTIN. Can. J. Chem. **58**, 348 (1980).

On a mesuré, les constantes de vitesse de la transposition du radical tétraméthyl-2,2,5,5 hexyne-3 yle en radical triméthyl-2,6,6-heptyne-4 yle-2, à des températures allant de 45 à 85°C en utilisant la spectroscopie de rpe cinétique. L'effet de la température peut être représenté par l'équation:

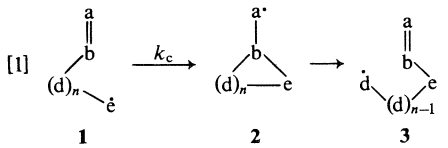
$$\log(k^{C\equiv C}/s^{-1}) = (12.4 \pm 1.5) - (14.6 \pm 2.4)/\theta$$

où $\theta = 2.3RT$ kcal mol^{-1}. Cette transposition, qui doit impliquer un radical vinylique du type méthylène-cyclopropane comme intermédiaire est beaucoup plus lent que la transposition analogue des radicaux homoallyliques, mais elle est comparable du point de vue vitesse à la transposition des radicaux homobenzyliques (néophyles).

[Traduit par le journal]

Introduction

The most common radical rearrangements are those involving intramolecular addition of the radical centre to a multiple bond situated β,γ, or further away, relative to the radical site (α).[3] In some cases this ring forming step completes the rearrangement of the initial radical **1** and the new radical **2** is a cyclic structural isomer, eq. [1]. In other cases the



1 **2** **3**

ring reopens in another sense, yielding an acyclic rearranged radical **3** from its acyclic progenitor **1**. A number of systems have been studied to date, including combinations of: (b=a) = aryl, C=C, C≡C, C=N, C≡N; n = 1, 3, 4, 5; d = carbon, heteroatoms; and e = carbon, nitrogen, oxygen, sulfur, silicon (1). Such rearrangements are not only potential steps in synthetic sequences but their rates can serve as reference points for measuring the rates of other radical processes (10,11).

Although rate constants for C5- and C6-ring closure (n = 4, 5; eq. [1]) of primary radical sites onto C≡C bonds (12)[4] and of C5-ring closure involving the C≡N bond (9) had been reported, there was no estimate of the rate constant for corresponding C3-ring closures involving triple bonds. The latter processes are of considerable interest because of the expected strain in the intermediate methylenecyclopropane system (e.g., **5**). It was not known, for example, whether that strain would provide a barrier to ring closure high enough to suppress completely the rearrangement of a homopropargyl radical relative to competing processes.

In this paper we report a study by kinetic epr spectroscopy of the homopropargyl radical 2,2,5,5-tetramethyl-3-hexyn-1-yl, **4**. This radical has been found to rearrange to 2,6,6-trimethyl-4-

[1]NRCC No. 17936.

[2]Author to whom correspondence should be addressed.

[3]For reviews of free radical ring closures and rearrangements, and for recent papers see refs. 1–9.

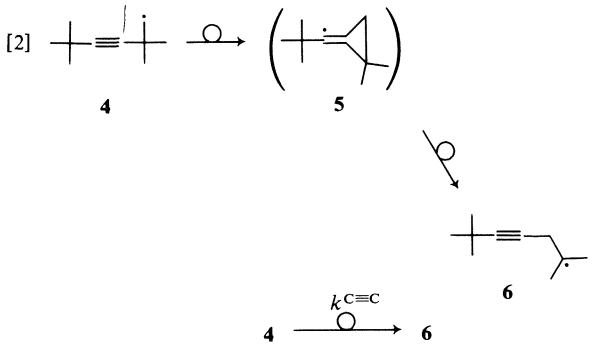
[4]The rate constant for C5-ring closure was estimated by A. L. J. Beckwith and A. G. Lawrence who communicated it personally. See footnote 7 of ref. 9.

0008-4042/80/040348-05$01.00/0

©1980 National Research Council of Canada/Conseil national de recherches du Canada

Can. J. Chem. Downloaded from www.nrcresearchpress.com by 210.87.254.42 on 09/05/12
For personal use only.

heptyn-2-yl, **6**. The rate constants $k^{C\equiv C}$, and Arrhenius parameters for the overall rearrangement of **4** to **6** have been determined.



Experimental

The steady state and kinetic epr techniques applicable to the study of radical isomerizations have been described (13–15). Radicals **4** and **6** (eq. [2]) were generated by photolysis of di-*tert*-butyl peroxide (BOOB) in 2,2,5,5-tetramethyl-3-hexyne (v:v = 1:6) and, less successfully, by bromine abstraction from 1-bromo-2,2,5,5-tetramethyl-3-hexyne. Both tri-*n*-butyltin radicals, from photolysis of hexa-*n*-butylditin, and trimethylsilyl radicals, from photolysis of BOOB in the presence of trimethylsilane, were tried as bromine abstracting species.

2,2,5,5-Tetramethyl-3-hexyne (Farchan or Chemical Samples Co.) was purified by preparative glpc with an OV-1 column (20 ft × ⅜ in., 100°C) to remove an impurity (0.5% or more, batch dependent) which was eluted just after the alkyne. Analysis of collected alkyne with analytical glpc columns did not reveal any remaining impurity.

1-Bromo-2,2,5,5-tetramethyl-3-hexyne was prepared by photolysis of *tert*-butyl hypobromite (16) in the parent alkyne, followed by washing with bicarbonate solution and with water, drying, and vacuum distillation. The bromide distilled after unreacted alkyne at oil bath temperature 80–90°C (0.25 Torr); ^{1}Hmr (CCl_4) δ: 1.20 (s, 9H), 1.30 (s, 6H), 3.49 (s, 2H). *Mol. Wt.* calcd.: 218.0494, 216.0514; found (ms): 218.0497, 216.0528.

The kinetic epr technique was used, with BOOB and alkyne, to determine the rate constant for bimolecular self termination of **4**, $2k_t(\mathbf{4})$, at 15°C (Table 2). On the same day, with the same lamp and optical configuration, photolysis of di-*tert*-butyl ketone in hexadecane, at 26°C, gave $2k_t(t\text{-Bu}^\cdot) = 3.0 \times 10^9\ M^{-1}\ s^{-1}$, (lit. (17), $2k_t(t\text{-Bu}^\cdot) = 2.9 \times 10^9\ M^{-1}\ s^{-1}$), for the same conditions. This excellent agreement serves to confirm that the light was uniformly distributed across the sample in our epr cavity.

Results and Discussion

The epr signals from **4** and **6** (eq. [2]) were quite weak even under optimum conditions (carefully purified alkyne; see Experimental) and were swamped by other signals if crude alkyne was used directly. Use of the bromide and either tri-*n*-butyltin or trimethylsilyl radicals (Experimental) did not lead to improvement in the signal-to-noise ratio. Those conditions gave very weak spectra of the radicals of interest together with strong spectra from unidentified, persistent radicals.

Radicals **4** and **6** have proton coupling constants typical of hydrocarbon radicals. Thus **4** has $a^{H\alpha}$ (2H) = 23.7 and $a^{H\gamma}$ (6H) = 0.85 G while **6** has $a^{H\beta}$ (6H) = 22.5 and $a^{H\beta}$ (2H) = 21.6 G.

The ratio of the rate constant for the overall rearrangement to that for the bimolecular self-reaction of **6** can be calculated from the absolute concentrations of **4** and **6** according to the equation (13–15)

$$k^{C\equiv C}/2k_t(\mathbf{6}) = [\mathbf{6}]^2/[\mathbf{4}] + [\mathbf{6}]$$

The data used to derive $k^{C\equiv C}/2k_t(\mathbf{6})$ are listed in Table 1. Measurements were made as quickly as possible to minimize effects from buildup of long-lived free radicals and non-radical products. Reused samples gave results which were consistent with the results obtained with new samples, indi-

TABLE 1. Rearrangement of **4** to **6** in 2,2,5,5-tetramethyl-3-hexyne

T^a (°C)	[4] × 10^8(M)	[6] × 10^8(M)	$k^{C\equiv C}/2k_t(\mathbf{6}) \times 10^7$($M$)
88	4.5	6.0	1.39
77	4.5	5.3	1.15
77	0.7	3.8	2.42
74	4.7	7.0	1.72
74	1.1	4.9	2.62
67	3.6	6.6	1.82
67	1.9	2.4	0.52
65	5.6	6.2	1.27
65	1.0	4.4	2.24
56.5	6.9	3.3	0.48
56.5	2.8	3.5	0.77
55	7.6	4.0	0.60
55	3.3	3.1	0.57
45	11.2	2.0	0.23
45	4.6	1.7	0.22

[a]Two sets of data for the same temperature are for the same tube run first with full lamp intensity and again at 29% of full intensity.

TABLE 2. Bimolecular rate constant for decay of **4** in 2,2,5,5-tetramethyl-3-hexyne[a]

T (°C)	$2k_t(\mathbf{4}) \times 10^{-9}$ ($M^{-1}\ s^{-1}$)
88	11.8
77	10.7
74	10.4
67	9.6
65	9.3
56.5	8.4
55	8.3
45	7.4
15	5.2

[a]The value at 15°C was measured in this work and the rest were calculated, as described in the text, from the temperature dependence of $2k_t$ for *tert*-butyl radicals.

Can. J. Chem. Downloaded from www.nrcresearchpress.com by 210.87.254.42 on 09/05/12
For personal use only.

Can. J. Chem. Downloaded from www.nrcresearchpress.com by 210.87.254.42 on 09/05/12
For personal use only.

cating that accumulation of interfering species was negligible during the short illumination periods. To some, the results in this table may appear rather irreproducible. They are, nevertheless, the best that can be obtained using present day kinetic epr procedures. The scatter of the data serves as a reminder of the errors inherent in this type of measurement when, even at full light intensity, the signal-to-noise ratio is rather poor.

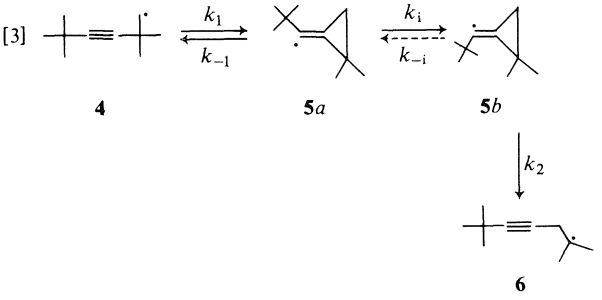
Table 2 lists the rate constants for the bimolecular self-reaction of **4**, $2k_t(\mathbf{4})$. These numbers were obtained as follows. The kinetic epr method was used to measure $2k_t(\mathbf{4})$ at 15°C, where its rate of rearrangement is very low. The resulting value, $5.2 \times 10^9\ M^{-1}\ s^{-1}$, indicates that **4** decays at the diffusion-controlled limit, as would be expected for this sterically unhindered radical. The value of $2k_t(\mathbf{4})$ at 15°C was then placed on the graph by Schuh and Fischer (17), of $2k_t$ against $1/T$ for *tert*-butyl radicals in various solvents. A line was drawn through that point and parallel to their line for *n*-decane solvent. Values of $2k_t(\mathbf{4})$, in the experimental temperature range for study of its rearrangement (Table 1), were then read from the ordinate of the graph. This procedure involves the reasonable assumption that the temperature (viscosity) dependence of $2k_t(\mathbf{4})$ in 2,2,5,5-tetramethyl-3-hexyne parallels that of $2k_t(t\text{-Bu}^\cdot)$ in *n*-decane. In view of the fact that the latter dependence is not very solvent sensitive (17) any error introduced through the above assumption is likely to be much smaller than other errors inherent in the kinetic epr method.

Since **6**, like **4**, is a sterically unhindered radical it also will undergo a bimolecular self-reaction at the diffusion-controlled limit. Because **6** and **4** are of equal molecular weight it is fairly safe to assume that $2k_t(\mathbf{6})$ and $2k_t(\mathbf{4})$ will be equal. The values of $2k_t(\mathbf{4})$ listed in Table 2 can therefore be combined with the data in Table 1 to obtain $k^{C\equiv C}$. A least-squares treatment leads to the Arrhenius equation

$$\log(k^{C\equiv C}/s^{-1}) = (12.40 \pm 1.5) - (14.6 \pm 2.4)/\theta$$

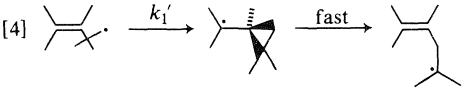
where the errors are standard deviations and $\theta = 2.3RT$ kcal mol^{-1}. These parameters give $k^{C\equiv C}$ (25°C) = 49 s^{-1}, which is nearly the same as the value for neophyl rearrangement (59 s^{-1} at 25°C) (15*e*).

The question now arises as to whether the measured rate constants for **4** and for neophyl have similar meanings, since the rearrangement of homopropargyl radicals is potentially complicated by a factor not present in the rearrangement of homoallyl or homobenzyl systems. This complication arises out of the known preference for *trans* addition to acetylenes via radical intermediates (18). Thus, the intramolecular addition step in the overall rearrangement of **4** is expected to lead to radical **5***a* in preference to **5***b*,[5] eq. [3].

[3] 

It follows from the principle of microscopic reversibility that the stereoelectronically preferred ring opening pathway for **5***a* is that leading back to **4** rather than directly forward to **6**. *In order to reach* **6** *by the pathway of lowest activation energy, it is presumably necessary to invert* **5**a *to* **5**b.

A possible consequence of the expected stereoelectronic preference is significant return of **5***a* to **4**; that is, inversion of **5***a* might not be much faster than its reopening to starting radical. In that case the experimental rate constant, $k^{C\equiv C}$, would not be the k_1 of [3] but instead, $k^{C\equiv C} = k_1k_i/(k_i + k_{-1})$. Detailed comparison of $k^{C\equiv C}$ for the present homopropargyl radical rearrangement with rate constants for homoallyl and homobenzyl radical rearrangements could then be misleading since the latter have no stereoelectronic constraint against direct ring opening of the cyclic radical intermediate in the thermodynamically favoured direction. That is, for rearrangements such as that shown in eq. [4] it is probably safe to assume that the experimentally measured rate constant is equal to k_1'.

[4] 

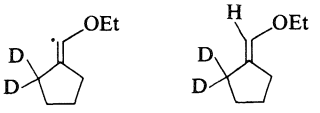
Very little is known about inversion rates of vinyl radicals. Fessenden and Schuler (19*a*) concluded that the parent radical inverts with a barrier of ca. 2 kcal mol^{-1} and with rate constant between 3×10^7 and 3×10^9 s^{-1} at −133°C. The 2-propenyl radical also inverts readily although somewhat more slowly (19*a*)[6] than the vinyl radical. Other qualitative evidence for facile inversion of vinyl radicals includes the requirement for highly efficient traps in

[5]Vinyl radicals with H or alkyl substituents are known to be bent σ-radicals (19) even in the face of steric hindrance (20).

[6]The rate constant was not reported.

Can. J. Chem. Downloaded from www.nrcresearchpress.com by 210.87.254.42 on 09/05/12
For personal use only.

order to capture vinyl radicals with retention of configuration (18*a*, 18*b*, 21). An α-alkoxy substituent, on the other hand, greatly reduces the inversion rate constant of a vinyl radical. Even at 60°C, **7** is reduced cleanly to **8** (96%) in the presence of 0.065 *M* (initial) Bu_3SnH (18*a*, 18*b*).



7 8

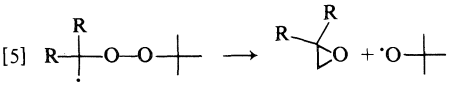
In the present case, the substituents are not likely to have a large effect on inversion rates. Although steric hindrance must be greater in **5***b* than in **5***a*, the difference is expected to be much smaller than it would be in the corresponding alkenes because vinyl radicals have a C—C—R bond angle[7] of at least 151°. Consequently, the steric factor is not likely to reduce k_1 or to increase k_{-i} and k_2 greatly, relative to corresponding rate constants for less hindered vinyls. Moreover, the last step is expected to be fast and irreversible because **5***b* will probably feel some of the driving force of strain relief and of the vinyl-to-tertiary alkyl radical isomerization at the transition state. Consequently, we suggest that k_1 is largely or entirely rate-determining in the rearrangement of **4** and that $k^{C\equiv C}$ either equals k_1 or sets a lower limit not different from k_1 by more than an order of magnitude.

In theory, the assumption that ring closure is rate-determining can be checked by calculating a minimum activation energy, E_a, for this reaction using thermochemical data and additivity principles (22). We calculate ΔH_f^0 (**4**) = 43 kcal mol^{-1} and ΔH_f^0 (**5***a*) = 61 kcal mol^{-1} by taking the methylenecyclopropane strain energy as 41.7 kcal mol^{-1} (23) and ignoring small corrections for steric hindrance. These estimated heats of formation suggest that cyclization is endothermic by some 18 kcal mol^{-1} and that E_a (k_1 step) > 18 kcal mol^{-1}. Thus, the observed rate constant appears[8] to be much too high; not too low as would be predicted if $k^{C\equiv C} = k_1k_i/(k_i + k_{-1})$, with substantial attenuation from the factor multiplying k_1. Although this result is qualitatively the one required to support the above assumption, it cannot be regarded as strong support because of problems with the quantitative aspects of such thermochemical estimates (see below).

It is interesting to examine measured activation energies and thermochemically estimated minimum activation energies for other radical cyclizations to form three-membered rings. For cyclization of the neophyl radical, ΔH_r has been estimated at 16 kcal mol^{-1}, using thermochemical data and assuming that the cyclohexadienyl stabilization energy is 22 kcal mol^{-1} and that there is no spiro strain in the intermediate.[9] Since the experimental E_a for the overall rearrangement is only 13.6 kcal mol^{-1} (15*e*), the calculated endothermicity is also too high, as it is for the present homopropargyl case. For rearrangement of the β-phenylethyl radical the agreement is better since the estimated[9] ΔH_r is 17 kcal mol^{-1} and the experimental E_a (> 19 kcal mol^{-1})[10] at least exceeds the endothermicity, as it should.

Similarly, cyclization of the 2,2,5,5-tetramethyl-3-hexen-l-yl and the 3-buten-l-yl radicals has a calculated endothermicity of about 7 kcal mol^{-1} whereas the corresponding experimental E_a values[10,11] are ca. 7 and 9 kcal mol^{-1}. Again the rate of ring closure for the system with *gem* dimethyl substitution is higher than one would predict on the basis of the estimated endothermicity while the rate for the corresponding unsubstituted system is in qualitative agreement with the thermochemical estimate.

Finally, in the exothermic oxirane-forming cyclization shown in eq. [5], there is a similar accelerating effect of methyl groups (R = CH_3 compared to R = H) which amounts to a rate factor of 350 at

[5] 

25°C, or to a reduction of E_a by 3.5 kcal mol^{-1} (24).

It is fairly clear that the relief of steric compression which accompanies formation of a *gem* disubstituted, small ring (Thorpe–Ingold effect) (25), causes significant rate enhancement[12] in radical processes. Reaction enthalpies should be affected even more strongly than activation energies by such steric factors. Since calculated enthalpies, based on group equivalents and additivity (22), do not reflect such steric factors adequately,[13] it appears that thermochemical kinetics can not be used, even for "order of magnitude" estimates of absolute rates, in systems where the Thorpe–In-

[7]The CCH bond angle of vinyl radical is about 151° (19*a*).

[8]The error in thermochemical estimates of this sort could be several kcal mol^{-1}.

[9]Personal communication from Professor R. Walsh to K.U.I.

[10]D. Griller, unpublished results.

[11]J. Warkentin, unpublished results.

[12]By factors of 10^2–10^4.

[13]Another example illustrating this point comes from calculation of the heats of formation of neopentane and 1,1-dimethylcyclopropane. Both calculated values, based on group increments and ring strain but without any allowance for the different methyl–methyl group interactions in the two compounds, come close to the experimental values.

Can. J. Chem. Downloaded from www.nrcresearchpress.com by 210.87.254.42 on 09/05/12
For personal use only.

gold effect operates. On the other hand, thermochemical estimates can be used effectively to rank reactivities of systems of the same type; i.e., systems all of which are (or are not) *gem* disubstituted.

For the homoallyl rearrangement corresponding to the homopropargyl rearrangement (**4** → **6**) we estimate $\Delta H_r = 7$ kcal mol^{-1}. In spite of the uncertainty surrounding the use of such numbers, in isolation, to estimate the minimum value of E_a, it is clear from comparison with corresponding values for the homopropargyl and neophyl systems that the homoallyl rearrangement ought to be very fast indeed. Although a rate constant has not been measured, preliminary experiments suggest that it exceeds 10^3 s^{-1} at -100°C.[11] It is reasonable to attribute the slowness of the homopropargyl and neophyl radical rearrangements primarily to the strain energy of a methylenecyclopropane and to the loss of aromaticity, respectively, involved in attaining the appropriate transition states.

The large difference between homoallyl and homopropargyl radical rearrangement rates has practical consequences pertinent to synthetic procedures. To capture homoallyl radicals efficiently before they rearrange it is necessary to use very reactive reagents at relatively high concentration. Homopropargyl radicals, on the other hand, are more easily intercepted. The difference was demonstrated qualitatively with *tert*-butyl hypobromite as capturing reagent. Whereas 2,2,5,5-tetramethyl-3-hexyne gave unrearranged bromide quite cleanly (Experimental), *trans*-2,2,5,5-tetramethyl-3-hexene, under similar conditions, gave unrearranged bromide and 2,6,6-trimethyl-2,4-heptadiene.[11] The latter most likely came from dehydrohalogenation of rearranged, tertiary bromide.

Acknowledgements

This work was carried out at the National Research Council of Canada. J.W. acknowledges the assistance of McMaster University in the form of a sabbatical leave and support from the National Research Council of Canada, which provided for an appointment as Visiting Scientist. He particularly appreciated the facilities and the stimulating atmosphere provided by Ted Edwards, David Griller, Keith Ingold, and their co-workers.

1. A. L. J. Beckwith and K. U. Ingold. *In* Rearrangements in ground and excited states. *Edited by* P. de Mayo. Academic Press Inc. In press.
2. J. W. Wilt. *In* Free radicals. Vol. 1. *Edited by* J. K. Kochi. Wiley, New York. 1973. Chapt. 8.
3. R. Kh. Freidlina. Adv. Free-Radical Chem. **1**, 211 (1965).
4. C. Walling. *In* Molecular rearrangements. Part 1. *Edited by* P. de Mayo. Interscience, New York. 1963. Chapt. 7.
5. M. Julia. Pure Appl. Chem. **40**, 553 (1974).
6. M. Julia. Acc. Chem. Res. **4**, 386 (1971).
7. A. L. J. Beckwith. Essays in free radical chemistry. Chem. Soc. Spec. Publ. No. 24. London. 1970. p. 239.
8. (*a*) R. Sustmann and F. Lübbe. Chem. Ber. **112**, 42 (1979); (*b*) F. Lübbe and R. Sustmann. Chem. Ber. **112**, 57 (1979).
9. D. Griller, P. Schmid, and K. U. Ingold. Can. J. Chem. **57**, 831 (1979).
10. P. Schmid and K. U. Ingold. J. Am. Chem. Soc. **100**, 2493 (1978).
11. (*a*) P. J. Wagner and K. C. Liu. J. Am. Chem. Soc. **96**, 5952 (1974); (*b*) J. F. Garst and F. E. Barton II. J. Am. Chem. Soc. **96**, 523 (1974); (*c*) J. F. Garst and C. D. Smith. J. Am. Chem. Soc. **98**, 1520 (1976).
12. (*a*) J. K. Crandall and D. J. Keyton. Tetrahedron Lett. 1653 (1969); (*b*) S. A. Dodson and R. D. Stipanovic. J. Chem. Soc. Perkin Trans. I, 410 (1975).
13. D. Lal, D. Griller, S. Husband, and K. U. Ingold. J. Am. Chem. Soc. **96**, 6355 (1974).
14. P. Schmid, D. Griller, and K. U. Ingold. Int. J. Chem. Kinet. **11**, 333 (1979).
15. (*a*) D. Griller and B. P. Roberts. Chem. Commun. 1035 (1971); (*b*) D. Griller and B. P. Roberts. J. Chem. Soc. Perkin Trans. II, 747 (1972); (*c*) A. G. Davies, D. Griller, and B. P. Roberts. J. Chem. Soc. Perkin Trans. II, 993 (1972); (*d*) G. B. Watts, D. Griller, and K. U. Ingold. J. Am. Chem. Soc. **94**, 8784 (1972); (*e*) B. Maillard and K. U. Ingold. J. Am. Chem. Soc. **98**, 1224 (1976); (*f*) B. Maillard, D. Forrest, and K. U. Ingold. J. Am. Chem. Soc. **98**, 7024 (1976).
16. C. Walling and A. Padwa. J. Org. Chem. **27**, 2976 (1962).
17. H. Schuh and H. Fischer. Helv. Chim. Acta, **61**, 2130 (1978).
18. (*a*) T. Ohnuki, M. Yoshida, and O. Simamura. Chem. Lett. 797 (1972); (*b*) T. Ohnuki, M. Yoshida, O. Simamura, and M. Fukuyama. Chem. Lett. 999 (1972); (*c*) M. S. Liu, S. Soloway, D. K. Wedegaertner, and J. A. Kampmeier. J. Am. Chem. Soc. **93**, 3809 (1971); (*d*) D. K. Wedegaertner, R. M. Kopchik, and J. A. Kampmeier. J. Am. Chem. Soc. **93**, 6890 (1971); (*e*) P. S. Skell and R. G. Allen. J. Am. Chem. Soc. **86**, 1559 (1964); (*f*) P. S. Skell and R. G. Allen. J. Am. Chem. Soc. **80**, 5997 (1958).
19. (*a*) R. W. Fessenden and R. H. Schuler. J. Chem. Phys. **39**, 2147 (1963); (*b*) E. L. Cochran, F. J. Adrian, and V. A. Bowers. J. Chem. Phys. **40**, 213 (1964); (*c*) F. J. Adrian and M. Karplus. J. Chem. Phys. **41**, 56 (1964); (*d*) R. W. Fessenden. J. Phys. Chem. **71**, 74 (1967); (*e*) P. H. Kasai and E. B. Whipple. J. Am. Chem. Soc. **89**, 1033 (1967); (*f*) S. Nagai, S. Ohnishi, and I. Nitta. Chem. Phys. Lett. **13**, 379 (1972).
20. D. Griller, J. W. Cooper, and K. U. Ingold. J. Am. Chem. Soc. **97**, 4269 (1975).
21. (*a*) G. D. Sargent and M. W. Browne. J. Am. Chem. Soc. **89**, 2788 (1967); (*b*) J. A. Kampmeier and G. Chen. J. Am. Chem. Soc. **87**, 2608 (1965).
22. (*a*) S. W. Benson. Thermochemical kinetics. 2nd ed. Wiley-Interscience, New York. 1976; (*b*) S. W. Benson, F. R. Cruickshank, D. M. Golden, S. R. Haugen, H. E. O'Neil, A. S. Rodgers, R. Shaw, and R. Walsh. Chem. Rev. **69**, 279 (1969).
23. P. v. R. Schleyer, J. E. Williams, and K. R. Blanchard. J. Am. Chem. Soc. **92**, 2377 (1970).
24. A. J. Bloodworth, A. G. Davies, I. M. Griffin, B. Muggleton, and B. P. Roberts. J. Am. Chem. Soc. **96**, 7599 (1974).
25. E. L. Eliel. Stereochemistry of carbon compounds. McGraw-Hill, New York. 1962. pp. 196–202.

Factor analysis as a complement to infrared band resolution. VII. The temperature dependence of the self association of phenol in carbon tetrachloride solution

B. U. PETELENZ[1] AND H. F. SHURVELL

Department of Chemistry, Queen's University, Kingston, Ont., Canada K7L 3N6

Received August 20, 1979

B. U. PETELENZ and H. F. SHURVELL. Can. J. Chem. **58**, 353 (1980).

Infrared absorption bands in the OH stretching region of phenol in carbon tetrachloride solution have been recorded for various concentrations and at several temperatures between 25 and 60°C. Factor analysis of the digitized spectra was carried out and the presence of three absorbing components in the OH stretching band was indicated at all temperatures in the range of 25–60°C. The three components are assigned to monomer, linear dimer, and a polymeric species. It is suggested that the polymeric species is a cyclic trimer.

Band contour resolution was carried out to obtain areas of the component bands. The variation of the monomer and dimer band areas with temperature was used to obtain a value for the enthalpy of dimerization of -15.8 ± 0.6 kJ mol^{-1}.

B. U. PETELENZ et H. F. SHURVELL. Can. J. Chem. **58**, 353 (1980).

On a enregistré les bandes d'absorption, dans la région d'élongation du OH, du phénol en solution dans le tétrachlorure de carbone à différentes concentrations et à des températures variant de 25 à 60°C. On a effectué une analyse factorielle des spectres numériques et on a mis en évidence la présence des trois constituants qui absorbent dans la bande d'élongation du OH à toutes les températures comprises dans l'intervalle 25–60°C. Les trois constituants sont identifiés comme étant le monomère, le dimère linéaire et les espèces polymérisées. On suggère que les espèces polymérisées sont des trimères cycliques.

On a effectué la résolution des pics dans le but d'obtenir les surfaces des bandes des constituants. On a utilisé la variation des surfaces des pics du monomère et du dimère en fonction de la température afin d'obtenir une valeur de l'enthalpie de dimérisation de -15.8 ± 0.6 kJ mol^{-1}.

[Traduit par le journal]

Introduction

Factor analysis (principal component analysis) together with infrared band contour resolution has been used previously in various studies of equilibria in CCl_4 solution (1–5).

The application of factor analysis to digitized infrared spectra leads to the determination of the number of absorbing components (NC) in a complex band (1). Subsequent resolution of the spectra into NC components yields band areas, from which molar absorption coefficients and concentrations of the species present at equilibrium can be calculated using a non-linear least-squares method. Finally equilibrium constants can be calculated from the concentrations of the species.

In our previous studies (1–5) a constant temperature was maintained and spectra of solutions of various concentrations were recorded and analyzed. The only thermodynamic quantity available from this type of study is the equilibrium constant. On the other hand, the temperature dependence of the areas of component bands can lead to the determination of the enthalpy of reaction.

The thermodynamics of self association of phenol in inert solvents has been the subject of numerous studies employing various experimental techniques (4, 6–17) and the earlier work has been reviewed recently (7). There has been considerable controversy over the interpretation of experimental results. Several models have been proposed involving phenol monomer in equilibrium with various associated species, and the structure of these species has been discussed. The problem of end-group OH absorption has also received attention. It was felt that the methods of factor analysis and band resolution might resolve some of the problems encountered in studies of self association of phenol in CCl_4 solution.

In our own previous study on phenol in CCl_4 (4), the equilibrium constant K_d for the monomer–dimer equilibrium at 34°C was found to be 0.76 ± 0.05 L^{-1} mol. We report here an extension to this work, in which spectra have been recorded at various temperatures between 25 and 60°C for various concentrations of phenol in CCl_4. The spectra have been digitized and subjected to factor analysis and band contour resolution in order to obtain a value for the enthalpy of dimerization. End-group absorption has been taken into account in our calculations and the nature and structure of the most likely polymeric species are discussed here.

[1]Present address: Institute of Nuclear Physics, Radzikowskiego 152, 31–342 Krakow, Poland.

0008-4042/80/040353-08$01.00/0

©1980 National Research Council of Canada/Conseil national de recherches du Canada

Can. J. Chem. Downloaded from www.nrcresearchpress.com by 210.87.254.105 on 09/05/12
For personal use only.

Can. J. Chem. Downloaded from www.nrcresearchpress.com by 210.87.254.105 on 09/05/12
For personal use only.

Experimental

Fisher Scientific Company spectroanalyzed carbon tetrachloride was dried over molecular sieve. Dryness was checked by monitoring water bands at 3709 and 3618 cm^{-1} in the infrared spectrum. Analytical reagent grade phenol was supplied by Mallinckrodt Chemical Company. Attempts were made to remove traces of moisture from the sample by refluxing a solution in benzene over molecular sieve. After distilling off the benzene–water azeotrope, the phenol was sublimed under reduced pressure and stored over P_2O_5. The effectiveness of the above treatment was checked by comparing the ir spectra of untreated and purified phenol in CCl_4 solution. Since there was no detectable difference in the spectra, it was concluded that the original sample probably contained less than 0.5% water.

All operations except weighing were performed in a dry-box in which the relative humidity was less than 20%. New solutions were prepared for each series of spectra. Details of solutions, pathlengths, and temperature ranges in which spectra were recorded are listed in Table 1.

Temperatures were precisely controlled with an RFL Industries Model 70 proportional controller. This device controls the electrical power supplied to a Beckman-R.I.I.C. model J3 heating jacket which surrounds a model FH-01 variable temperature NaCl cell supplied by the same company. The temperature was monitored by means of an iron–constantan thermocouple. The emf of the thermocouple was recorded on a Honeywell Electronik 194 recorder. The thermocouple was calibrated using standard thermometers made and calibrated to A.S.T.M. specifications.

Spectra were recorded on a Perkin-Elmer model 180 spectrometer without compensation in the reference beam. The spectral slit width was 2 cm^{-1} and a scanning rate of 15 cm^{-1}/min was used. Intensities were recorded as absorbance and the spectra were digitized manually at 2 cm^{-1} intervals.

Computational Methods

Factor Analysis

Factor analysis (principal component analysis) is a multivariate statistical technique, which can be used to determine the number of independent components contributing to an experimentally observed quantity, such as an infrared absorption band. Details of the method and its application to analysis of infrared and Raman spectra recorded for a series of solutions at a single temperature have been given in a recent review article (18). The present application to spectra recorded for a single solution at a series of temperatures differs only in notation.

If the number of temperatures at which spectra are recorded for a solution of fixed total phenol concentration is NT and if the number of wavenumber points at which intensity readings are taken is NW, then the absorbance matrix **A** (normalized to unit path length) will have NT rows and NW columns.

For the case where the temperature is fixed and spectra are recorded for NS solutions of various total phenol concentrations, a similar absorbance matrix is obtained with NS rows.

The method of factor analysis involves finding the rank of the absorbance matrix. Under the conditions of our experiments (NW > NT > NC), the rank of **A** may be interpreted as being equal to the number of absorbing components NC. To find the rank of **A**, the matrix $\mathbf{A}^T\mathbf{A}$ is formed, where $\mathbf{A}^T$ is the transpose of **A**. This matrix has the same rank as **A**, but has the advantage of being a square matrix with much smaller dimensions than **A** (NT × NT). The rank of **A** is given by the number of non-zero eigenvalues of $\mathbf{A}^T\mathbf{A}$. These can be determined using statistical tests (19–21).

Band Resolution

The computer programs for band contour resolution were written by Jones *et al.* (22). A Cauchy–Gauss product function was used to describe each component band in the envelope.

When the number of absorbing components NC is known, the fitting procedure consists of varying the peak position, height, and width parameters for all components until a satisfactory fit is obtained between the observed and computed contour. The quantity NC is obviously essential for this procedure and factor analysis provides this number.

TABLE 1. Concentrations, temperature ranges, and pathlengths for solutions of phenol in CCl_4

Total phenol concentration (*M*) at 20°C	Temperature range (K)	Cell pathlength (mm)
1.108	302–333	0.108
0.4542	298–323	0.188
0.4274	302–322	0.188
0.1147	298–323	0.52

Results and Discussion

The temperature dependence of the spectra of three solutions of phenol in CCl_4 in the OH stretching region is shown in Figs. 1–3. The sharp monomer peak at 3612 cm^{-1} increases in intensity relative to the broad dimer and polymer peaks as the temperature is increased. It is also evident in Fig. 2 that the dimer band at 3480 cm^{-1} gains intensity at the expense of the lower frequency polymer band centred near 3350 cm^{-1} as the temperature is increased.

Structures of Associated Species

In the subsequent paragraphs we will refer to dimer and higher polymers of phenol. Therefore some discussion of the structures of these species is necessary in order to justify our choice of the most likely self-associated species present in CCl_4 solutions.

It has been pointed out earlier (23) that the bent

Can. J. Chem. Downloaded from www.nrcresearchpress.com by 210.87.254.105 on 09/05/12
For personal use only.

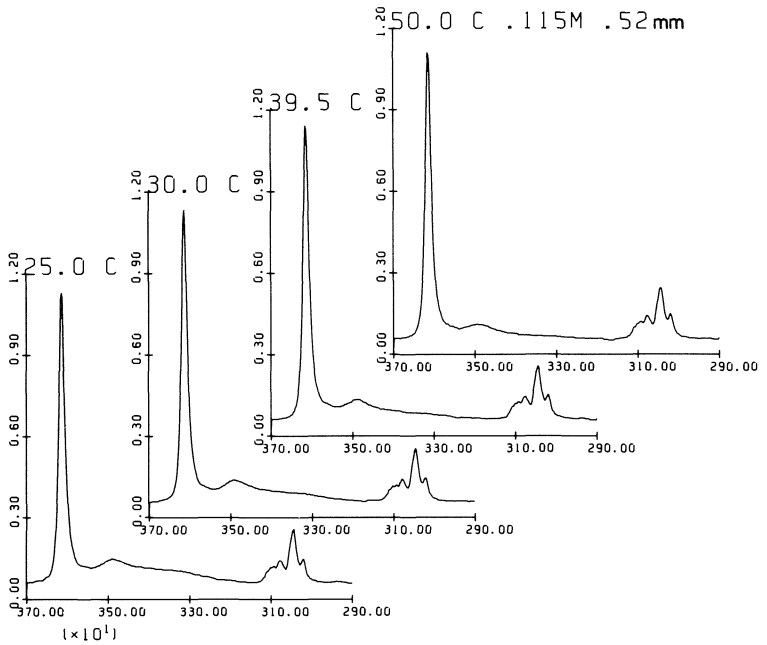


FIG. 1. The temperature dependence of the infrared spectrum of a 0.115 *M* solution of phenol in CCl_4.

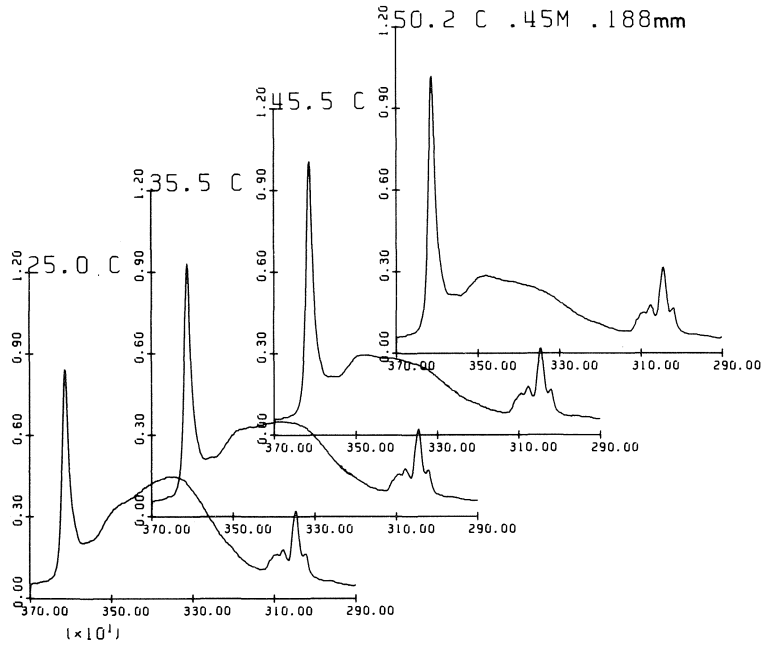


FIG. 2. The temperature dependence of the infrared spectrum of a 0.454 *M* solution of phenol in CCl_4.

hydrogen bonds in a cyclic dimer of phenol would be very weak and therefore the open-chain form is the most likely structure of the dimer.

Sterically the most favoured polymeric species appears to be the cyclic trimer, which has a planar strain-free six membered hydrogen bonded ring formed by the three OH groups. This structure is essentially the same as that found in the unit cell of crystalline phenol (24). The attack of a further phenol molecule to form a tetramer is sterically hindered and moreover, the formation of a tetramer would require ring opening which is energetically unfavoured. In solutions of low concentration in CCl_4 the formation of higher polymers is unlikely

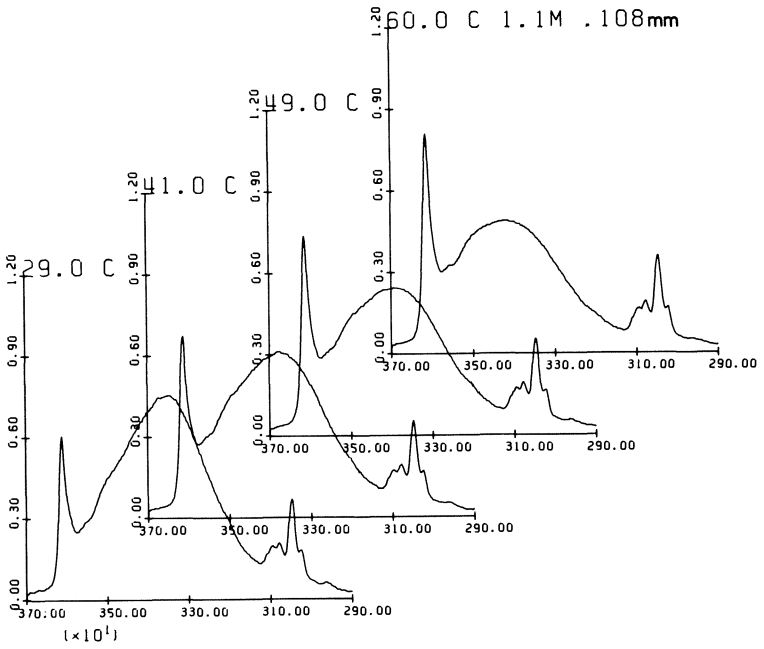


FIG. 3. The temperature dependence of the infrared spectrum of a 1.11 *M* solution of phenol in CCl_4.

and we assume that the species of phenol present under the experimental conditions used in this work are monomer, linear dimer, and cyclic trimer. This assumption appears to be in agreement with the results of factor analysis discussed below.

Factor Analysis Results

Spectra were recorded for several concentrations of phenol in CCl_4 at a series of temperatures. Factor analysis was carried out for each series of spectra. Table 2 lists the eigenvalues, and residual standard deviations (r.s.d.) (20) in the eigenvalues of $\mathbf{A}^T\mathbf{A}$ for a typical series of spectra recorded from a 1.108 *M* solution at six temperatures. Table 3 lists the eigenvalues of $\mathbf{A}^T\mathbf{A}$ and the corresponding standard errors (19) for a 0.4542 *M* solution of phenol for spectra recorded at seven temperatures.

In Table 3 it can be seen that the first three eigenvalues are larger than their standard errors. This indicates that three components are present. In Table 2 it is seen that the first three r.s.d. values are larger than the experimental standard deviation of 0.0015, while the fourth r.s.d. is close to this error estimate. However, examination of the eigenvalues reveals that there is a factor of 20 between the third and fourth eigenvalues, whereas there is only a factor of three between the fourth and subsequent eigenvalues. This surely indicates that only the first three eigenvalues are really non-zero.

Table 4 shows the distribution of misfit between

TABLE 2. Eigenvalues of $\mathbf{A}^T\mathbf{A}$ and their residual standard deviations for 1.108 *M* solution of phenol in CCl_4 at six different temperatures

Eigenvalue	Residual standard deviation[a]
44.359314	0.036823
0.521293	0.007269
0.019190	0.002181
0.000966	0.001528
0.000355	0.001201
0.000306	0.000820

[a]Estimated experimental s.d. = 0.0015.

TABLE 3. Eigenvalues of $\mathbf{A}^T\mathbf{A}$ and the corresponding standard errors for 0.4542 *M* solution of phenol in CCl_4 at seven different temperatures

Eigenvalue	Standard error[a]
310.515195	0.104326
3.649053	0.107945
0.134331	0.108219
0.006760	0.100388
0.002487	0.114042
0.002141	0.111665
0.001859	0.110999

[a]For an experimental absorbance error of 0.1%.

Can. J. Chem. Downloaded from www.nrcresearchpress.com by 210.87.254.105 on 09/05/12
For personal use only.

TABLE 4. Distribution of misfit between observed and regenerated absorbance matrix and the χ^2 criterion for 0.4542 *M* solution of phenol in CCl_4 at seven different temperatures

Number of eigenvectors	Ranges of standard deviations[a] 0–1	1–3	3+	χ^2	Expectation value of χ^2
1	1028	946	833	37 966.3214	2400
2	2371	463	0	1 475.7892	1995
3	2807	0	0	132.4748	1592
4	2807	0	0	64.8715	1191
5	2807	0	0	39.9984	792
6	2807	0	0	18.5913	395
7	2807	0	0	0.0	0

[a]For an experimental absorbance error of 0.1.

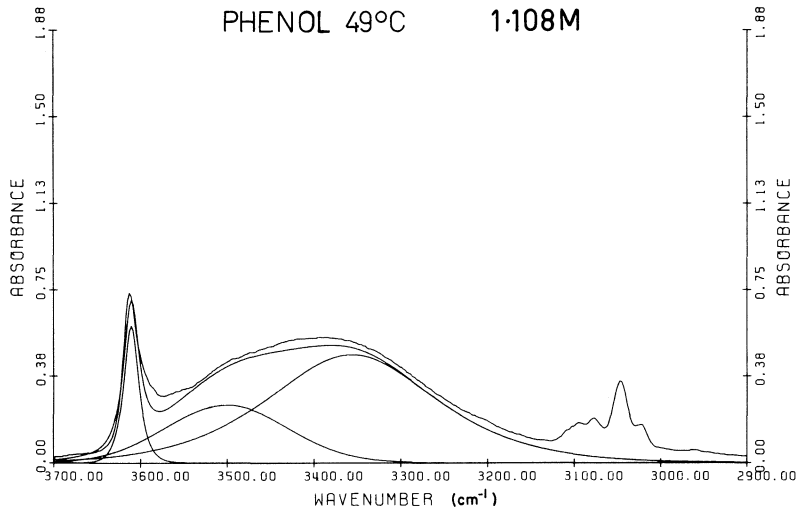


FIG. 4. A typical three-band fit to the spectrum of a 1.11 *M* solution of phenol in CCl_4 at 49°C.

observed and regenerated absorbance matrix (19) using from one to seven eigenvectors. The last two columns list the computed values of χ^2 (19) and the expectation values calculated from the formula $(NW - m)(NT - m)$ (21), where NW is the number of points in a digitized spectrum (401 in the present case) and NT is the number of temperatures at which spectra were recorded. From Table 4 it can be seen that using two eigenvectors leaves 463 points with up to three standard deviations from the experimental values. Addition of a third eigenvalue brings all calculated points to within one standard deviation of the experimental values. Again, this indicates that the number of absorbing components is three. The χ^2 criterion is ambiguous in that it indicates two components. This can be seen from the comparison of the calculated values with the expectation values in columns 5 and 6 of Table 4.

The analysis was carried out for each solution of Table 1 with similar results. Spectra of the four solutions of Table 1 were also analyzed at a single fixed temperature (50°C) and again three components were indicated by all except the χ^2 test. At present we are unable to explain the failure of this criterion to indicate three components.

Band Contour Resolution

As suggested by factor analysis, we carried out band resolution using three Cauchy–Gauss product functions in the hydroxyl stretching region. Plots of typical resolved spectra are shown in Fig. 4, where it is seen that (after baseline removal) the fit between the observed and calculated spectra is quite good. Four band fits were also tried, to take end-group OH absorption into account. An example of a four band fit, with baseline removed, is shown in Fig. 5. End-group absorption is undoubtedly present, but does not appear as a separate component in the factor analysis. This is because there is a linear relationship between the intensity of bonded and free OH stretching absorption of the open chain dimer. For reasons discussed above, it is believed

Can. J. Chem. Downloaded from www.nrcresearchpress.com by 210.87.254.105 on 09/05/12
For personal use only.

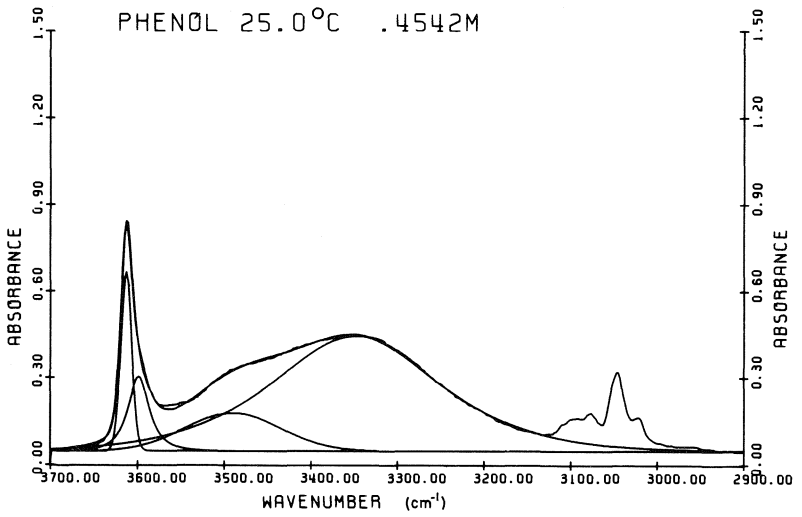


FIG. 5. A typical four-band fit to the spectrum of a 0.454 *M* solution on phenol in CCl_4 at 25°C. The baseline correction has not been subtracted from the experimental spectrum.

that a cyclic trimer is the most likely higher polymeric species. This trimer has no free OH end group. Open chain trimers and higher polymers would be expected to contribute to OH end-group absorption, but the concentration of these species is likely to be quite small.

Calculation of ΔH*(dimerization)*

Assuming that the activity coefficients of monomer and dimer are unity the equilibrium constant for the dimerization reaction is simply $K_d = C_2/C_1^2$ where C_1 and C_2 are the concentrations of monomer and dimer respectively. According to the Beer–Lambert law, the concentrations C_1 and C_2 are proportional to the absorbances of the corresponding resolved component bands and thus to the band areas A_1 and A_2.

If the dimerization constant is determined at several temperatures one can use the van't Hoff equation

$$[1] \quad d(\ln K_d)/d(1/T) = -\Delta H^0/R$$

But

$$[2] \quad \ln K_d = \ln (A_2/A_1^2) + \text{constant}$$

Thus, by plotting $\ln (A_2/A_1^2)$ versus inverse temperature one obtains the enthalpy of dimerization from the slope. The results obtained from four different total phenol concentrations are given in Table 5. It is assumed that neither ΔH^0 nor the molar absorption coefficients (ε_1 and ε_2) of monomer and dimer are temperature dependent in the small temperature range covered in the present study.

TABLE 5. Enthalpies of dimerization of phenol obtained for four different total concentrations of phenol in CCl_4

Total phenol concentration (*M*) at 20°C	$-\Delta H^0$(dimerization) (kJ mol^{-1})	
	Three-component fit	Four-component fit
1.108	16.489	13.200
0.4542	15.338	11.589
0.4274	16.146	16.334
0.1147	15.242	29.480
	Ave. 15.804	

End-group Absorption

The effect of end-group OH absorption is difficult to assess. It does not appear as a separate absorbing component in the factor analysis. However, in the band fitting program the intensity of the fourth component must be somehow distributed by the computational procedure between the monomer and the dimer band. An estimate can be made of the effect of neglect of end-group absorption on the final results.

It may be assumed that the molar absorption coefficient of the end-group band is equal to that of the monomer (ε_1), since this is a similar type of vibration. The areas of the monomer and dimer bands obtained from the three-band fit each contain some contribution from the end-group absorption.

Suppose the contribution from the end-group absorption is x to the monomer absorbance and $(1 - x)$ to the dimer absorbance. Using the Beer–Lambert law the corrected normalized absorbances can be expressed as follows:

Can. J. Chem. Downloaded from www.nrcresearchpress.com by 210.87.254.105 on 09/05/12
For personal use only.

Can. J. Chem. Downloaded from www.nrcresearchpress.com by 210.87.254.105 on 09/05/12
For personal use only.

Monomer:

[3] $A_1' = \varepsilon_1 C_1 + x\varepsilon_1 C_2$

Dimer:

[4] $A_2' = \varepsilon_2 C_2 + (1 - x)\varepsilon_1 C_2$

It is assumed here that the dimers are linear, i.e. the concentration of the end-group absorbing species is equal to the concentration of the dimer. Both the contribution of higher polymers to the end-group absorbance and the negative correction for the presence of cyclic dimers are neglected.

Thus, the dimerization constant becomes

$$[5] \quad K_d' = \frac{\varepsilon_1^2[\varepsilon_2 + (1 - x)\varepsilon_1]A_2'}{\{[\varepsilon_2 + (1 - x)\varepsilon_1]A_1' - x\varepsilon_1 A_2'\}^2}$$

Making use of eq. [5], it is found that calculated K_d values will be too high for low total concentration of phenol and too low in other cases. Consequently, there will be an error $\delta(\Delta H^0)$ in the calculated values of enthalpy of dimerization given by $-RT\delta K/K_d'$ where $\delta K = K_d' - K_d$.

If it is assumed that the intensity of the end-group band contributes equally to monomer and dimer intensities in the three-component fit, then $x = 1/2$. Three special cases will be considered: (*1*) an intermediate total concentration when $\mathbf{A}_1 = \mathbf{A}_2$; (*2*) a higher concentration when $\mathbf{A}_2 = 2\mathbf{A}_1$; (*3*) a low total concentration when $\mathbf{A}_2 = \mathbf{A}_1/2$.

The calculations were performed using the molar absorption coefficients determined in ref. 4 for monomer and dimer absorption bands. The results are presented in Table 6. Of course, due to the various assumptions made in the calculations, the results in Table 6 have a qualitative meaning only. Nevertheless, they seem to explain the concentration trend in the ΔH^0 values reported in Table 5.

Summary and Conclusions

Factor analysis (principal component analysis) has been used for the first time to study the temperature dependence of an infrared absorption band. The results for the OH stretching band in the infrared spectra of solutions of phenol in CCl_4 indicate the presence of three independent components in the spectra which are assigned to monomer, linear dimer, and one or more polymeric species. This conclusion is consistent with an earlier interpretation of the concentration dependence of the infrared spectra of phenol in CCl_4 solutions at a constant temperature (4).

It is possible to obtain a reasonable three-component fit to the observed spectra (Fig. 4). From the temperature dependence of the areas of the monomer and dimer components we have obtained an average value of $-15.8\,\text{kJ mol}^{-1}$ for the enthalpy of dimerization for four different concentrations of phenol in CCl_4 solution.

End-group absorption by the linear dimer, or higher linear polymers, contributes to the intensity of both monomer and dimer bands. The addition of a fourth component, due to end-group absorption, to the fitting procedure results in an improved fit between observed and computed band envelopes (Fig. 5). However, in this case the temperature dependence of the areas of the monomer and dimer component bands does not lead to consistent values of ΔH^0(dimerization) for solutions of different total phenol concentration. A slight trend with concentration might be noted in our reported values of ΔH^0(dimerization). This trend can be accounted for qualitatively by taking end-group absorption into account. It is not possible to assign definite structures to the polymeric species present in solutions of phenol in CCl_4, but we suggest that the predominant species is a cyclic trimer.

TABLE 6. Estimated error in ΔH^0 determined from the three-band fit

Case	Total phenol concentration	Error in ΔH^0 (kJ mol^{-1})
$\mathbf{A}_2 = 2\mathbf{A}_1$	High	−2.04
$\mathbf{A}_2 = \mathbf{A}_1$	Intermediate	−0.14
$\mathbf{A}_2 = \mathbf{A}_1/2$	Low	+0.05

Acknowledgements

This work has been supported by grants from the National Research Council of Canada. One of us (B.U.P.) thanks Queen's University for financial support in the form of graduate student scholarships.

1. J. T. BULMER and H. F. SHURVELL. J. Phys. Chem. **77**, 256 (1973).
2. J. T. BULMER and H. F. SHURVELL. J. Phys. Chem. **77**, 2085 (1973).
3. J. T. BULMER and H. F. SHURVELL. Can. J. Chem. **53**, 1251 (1975).
4. H. F. SHURVELL, K. CHITUMBO, A. DUNHAM, and L. CHAPPELL. Can. J. Spectrosc. **21**, 53 (1976).
5. J. KORPPI-TOMMOLA and H. F. SHURVELL. Can. J. Chem. **56**, 2959 (1978).
6. K. B. WHETSEL and J. H. LADY. *In* Spectrometry of fuels. *Edited by* R. A. Friedel. Plenum, New York. 1970. p. 259.
7. J. DOS SANTOS, F. CRUEGE, and P. PINEAU. J. Chim. Phys. **67**, 826 (1970).
8. D. L. POWELL and R. WEST. Spectrochim. Acta, **20**, 983 (1964).
9. M. M. MAGUIRE and R. WEST. Spectrochim. Acta, **17**, 369 (1961).

10. R. M. BADGER and R. C. GREENOUGH. J. Phys. Chem. **65**, 2088 (1961).
11. D. BONO. Thesis, Paris. 1956.
12. N. D. COGGESHALL and E. L. SAIER. J. Am. Chem. Soc. **73**, 5414 (1951).
13. R. MECKE. Discuss. Faraday Soc. **9**, 161 (1950).
14. H. KEMPTER and R. MECKE. Z. Phys. Chem. **46B**, 229 (1940).
15. M. MARTIN. J. Chim. Phys. **59**, 736 (1962).
16. M. SAUNDERS and J. B. HYNE. J. Chem. Phys. **29**, 1319 (1958).
17. J. R. JOHNSON, S. D. CRISTIAN, and H. F. AFFSPRUNG. J. Chem. Soc. 1 (1965).
18. H. F. SHURVELL and J. T. BULMER. *In* Vibrational spectra and structure. Vol. 6. *Edited by* J. R. Durig. Elsevier, Amsterdam. 1977. Chapt. 2. p. 91.
19. Z. Z. HUGUS, JR. and A. A. EL-AWADY. J. Phys. Chem. **75**, 2954 (1971).
20. J. J. KANKARE. Anal. Chem. **42**, 1322 (1970).
21. Z. Z. HUGUS, JR. Private communication.
22. R. N. JONES (*Editor*). Computer programs for infrared spectrophotometry. National Research Council of Canada, Ottawa. 1978.
23. L. J. BELLAMY and R. J. PACE. Spectrochim. Acta, **22**, 525 (1966).
24. R. W. G. WYCKOFF. Crystal structures. Vol. 6. Interscience, New York. 1963.

Can. J. Chem. Downloaded from www.nrcresearchpress.com by 210.87.254.105 on 09/05/12
For personal use only.

Carbon-13 nuclear magnetic resonance spectra of *E*-silyl-alkenes

CONSTANTINOS A. TSIPIS[1]

Laboratory of Inorganic Chemistry, University of Thessaloniki, Thessaloniki, Greece

AND

CONSTANTINOS A. TSOLERIDIS

Laboratory of Organic Chemistry, University of Thessaloniki, Thessaloniki, Greece

Received July 23, 1979

Can. J. Chem. Downloaded from www.nrcresearchpress.com by 210.87.254.40 on 09/05/12
For personal use only.

CONSTANTINOS A. TSIPIS and CONSTANTINOS A. TSOLERIDIS. Can. J. Chem. **58**, 361 (1980).

Carbon-13 nmr chemical shifts of a number of *E*-silyl-alkenes containing the silyl substituent at an sp^2 carbon atom are presented. Assignments of the chemical shifts have been made by noting systematic variations in the spectra with changes in substituents and by comparison of the chemical shifts to those of the corresponding unsubstituted alkenes. The substituent effects observed were explained on the basis of the π-acceptor ability of the silyl substituents and the structure of the molecules. Comparing the ^{13}C nmr spectra of the *E*-silyl-alkenes and those of the corresponding unsubstituted alkenes, differential chemical shifts have been obtained which can be used as empirical substituent parameters for the prediction of the ^{13}C nmr spectra of other *E*-silyl-alkenes not yet studied. It was also demonstrated that ^{13}C nmr spectroscopy can be used without resorting to special techniques (gated decoupling and the addition of paramagnetics) as an alternative method to the ^1H nmr for the quantitative analysis of mixtures of regio-isomer *E*-silyl-alkenes.

CONSTANTINOS A. TSIPIS et CONSTANTINOS A. TSOLERIDIS. Can. J. Chem. **58**, 361 (1980).

On présente les déplacements chimiques en rmn du ^{13}C d'un certain nombre d'alcènes silylés-*E* portant le groupe silyle sur un atome de carbone sp^2. On a identifié le déplacements chimiques en notant les variations systématiques des spectres résultant des changements de substituants, et en les comparant à ceux des alcènes non substitués correspondants. On explique les effets des substituants en se basant sur la propriété π des substituants silylés et sur la structure des molécules. En comparant les spectres rmn du ^{13}C des alcènes silylés-*E* à ceux des alcènes non substitués correspondants, on a obtenu des déplacements chimiques différentiels qui peuvent être utilisés comme des paramètres additifs empiriques pour prédire les spectres rmn du ^{13}C d'autres alcènes silylés-*E* qui n'ont pas encore été étudiés. On a également démontré que la spectroscopie rmn du ^{13}C peut être utilisée, sans recourir à des techniques spéciales (découplage ou addition de substances paramagnétiques) comme une alternative pour la rmn du ^1H pour l'analyse quantitative des mélanges des régioisomères des alcènes silylés-*E*.

[Traduit par le journal]

Introduction

The number of publications dealing with ^{13}C nmr spectra of some model systems has grown in the past ten years. Thus, systematic studies on the ^{13}C nmr spectra of alkanes (1), alkenes (2–5), alkynes (6, 7), as well as some of their substituted derivatives (8–10) and other classes of organic compounds (11, 12) have been reported. However, as far as we know, the systematic studies of ^{13}C nmr spectra of model systems in organosilicon chemistry are rather limited.

Recently, a few papers dealing with ^{13}C nmr spectra of a variety of organosilanes including phenylsilanes (13, 14), benzylsilanes (15, 16), methylsilanes (17), alkoxysilanes (18), siloxanes (19), and siloxyethers (20–23) have been published. In most of them ^{13}C nmr spectroscopy was used to study the interaction between silicon and a substituent capable of p_π–d_π bonding, such as phenyl, oxygen, vinyl, etc. Also, in some cases, some empirical substituent – chemical shift (SCS) parameters were determined and correlated with observed chemical shifts (13–15).

Conspicuously absent from the growing volume of the ^{13}C nmr data on organosilanes is a systematic study of silyl-alkenes containing the silyl substituent in an sp^2 carbon atom. In the present paper we report our ^{13}C nmr measurements on a number of *E*-silyl-alkenes, either terminal or internal, and some hydroxy-derivatives. The aim of the paper is to fill this gap giving the ^{13}C nmr spectra of some model *E*-silyl-alkenes and to study the influence of the silyl substituent on the ^{13}C nmr signals of the alkene moiety.

Results and Discussion

In Table 1 are listed the chemical shifts (δ, ppm), the relative intensities, and the assignments of the ^{13}C nmr signals of some *E*-1-silyl-1-alkenes and hydroxyderivatives.

Chemical shift assignments were made using previously noted (2–5, 8, 10) ranges of resonances for analogous compounds, as well as by noting systematic variations in the spectra with changes in substituents.

The ^{13}C resonances of the two sp^2 carbon atoms (C1 and C2) of the *E*-1-silyl-1-alkenes appear, as one would expect, in the region of 120–160 ppm down-

[1]Author to whom all correspondence should be addressed.

0008-4042/80/040361-08$01.00/0

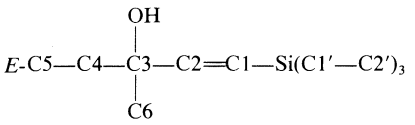
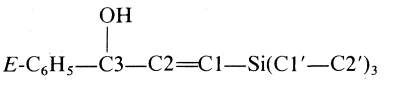
©1980 National Research Council of Canada/Conseil national de recherches du Canada

Can. J. Chem. Downloaded from www.nrcresearchpress.com by 210.87.254.40 on 09/05/12
For personal use only.

TABLE 1. ^{13}C chemical shifts (δ, ppm downfield from TMS) and assignments for some *E*-1-silyl-1-alkenes and a few hydroxyderivatives

Compound	Chemical shift
E-C5—C4—C3—C2=C1—$SiCl_3$	C1 = 122.09(58)*; C2 = 157.05(68); C3 = 37.80(95); C4 = 20.96(100); C5 = 13.51(69)
E-C5—C4—C3—C2=C1—$SiCl_2$(C1′)	C1′ = 5.46(73); C1 = 123.92(80); C2 = 154.04(76); C3 = 38.04(78); C4 = 21.18(100); C5 = 13.52(87)
E-C5—C4—C3—C2=C1—$Si(C1'—C2')_3$	C1′ = 3.69(52); C2′ = 7.33(100); C1 = 125.88(31); C2 = 148.54(26); C3 = 39.26(45); C4 = 21.55(44); C5 = 13.55(17)
E-C6—C5—C4—C3—C2=C1—$SiCl_3$	C1 = 121.90(55); C2 = 157.31(71); C3 = 35.54(91); C4 = 29.87(93); C5 = 22.21(100); C6 = 13.81(91)
E-C6—C5—C4—C3—C2=C1—$SiCl_2$(C1′)	C1′ = 5.46(72); C1 = 123.67(83); C2 = 154.29(80); C3 = 35.67(100); C4 = 30.12(95); C5 = 22.18(92); C6 = 13.82(96)
E-C6—C5—C4—C3—C2=C1—$Si(C1'—C2')_3$	C1′ = 3.88(62); C2′ = 7.32(100); C1 = 125.60(29); C2 = 148.88(17); C3 = 36.88(22); C4 = 31.22(31); C5 = 22.33(33); C6 = 13.88(25)
E-C7—C6—C5—C4—C3—C2=C1—$SiCl_3$	C1 = 121.98(52); C2 = 157.23(58); C3 = 35.89(92); C4 = 31.35(93); C5 = 27.49(100); C6 = 22.51(84); C7 = 14.03(86)
E-C7—C6—C5—C4—C3—C2=C1—$SiCl_2$(C1′)	C1′ = 5.44(52); C1 = 123.64(67); C2 = 154.40(63); C3 = 36.01(85); C4 = 31.32(91); C5 = 27.64(100); C6 = 22.43(91); C7 = 13.92(84)
E-C7—C6—C5—C4—C3—C2=C1—$Si(C1'—C2')_3$	C1′ = 3.59(100); C2′ = 7.30(76); C1 = 125.56(24); C2 = 148.83(22); C3 = 37.05(37); C4 = 31.41(34); C5 = 28.57(32); C6 = 22.54(31); C7 = 13.99(27)
E-(C5—C4—C5—C4)C3—C2=C1—$SiCl_3$	C1 = 119.77(39); C2 = 161.46(33); C3 = 46.30(46); C4 = 32.28(100); C5 = 25.46(79)
E-(C5—C4—C5—C4)C3—C2=C1—$SiCl_2$(C1′)	C1′ = 5.49(45); C1 = 121.32(48); C2 = 158.42(38); C3 = 46.26(34); C4 = 32.16(100); C5 = 25.22(95)
E-(C5—C4—C5—C4)C3—C2=C1—$Si(C1'—C2')_3$	C1′ = 3.66(44); C2′ = 6.51(100); C1 = 122.81(11); C2 = 153.09(5); C3 = 47.23(9); C4 = 32.78(20); C5 = 25.26(15)
E-C4(OH)—C3—C2=C1—$Si(C1'—C2')_3$ (C4)	C1′ = 3.35(87); C2′ = 7.10(62); C1 = 120.20(19); C2 = 154.93(19); C3 = 71.90(11); C4 = 29.07(100)

TABLE 1 (*Concluded*)

Compound	Chemical shift
	C1′ = 3.46(100); C2′ = 7.20(57); C1 = 121.52(28); C2 = 153.72(24); C3 = 74.35(16); C4 = 34.71(58); C5 = 8.06(32); C6 = 27.23(53)
	C1′ = 3.28(100); C2′ = 7.10(44); C1 = 125.54(37); C2 = 148.69(44); C3 = 76.61(41); *i*-C† = 142.72(9); *o*-C = 126.32(51); *m*-C = 127.30(55); *p*-C = 128.20(45)

*Figures in parentheses are the relative intensities of the signals.
†The abbreviations *i*-C, *o*-C, *m*-C, and *p*-C are used for the *ipso*-, *ortho*-, *meta*-, and *para*- carbon atoms of the phenyl group, respectively.

TABLE 2. Differential chemical shifts ($\Delta\delta_C$, ppm)* between the ^{13}C resonances of the *E*-1-silyl-1-alkenes and those of the corresponding unsubstituted 1-alkenes

Compound	$\Delta\delta_{C1}$	$\Delta\delta_{C2}$	$\Delta\delta_{C3}$	$\Delta\delta_{C4}$	$\Delta\delta_{C5}$	$\Delta\delta_{C6}$	$\Delta\delta_{C7}$
E-C5—C4—C3—C2=C1—$SiCl_3$	+7.63	+18.03	+1.56	−1.46	−0.12	—	—
E-C6—C5—C4—C3—C2=C1—$SiCl_3$	+7.66	+18.11	+1.76	−1.66	−0.24	−0.15	—
E-C7—C6—C5—C4—C3—C2=C1—$SiCl_3$	+7.78	+17.99	+1.86	−1.47	−0.33	−0.27	−0.03
E-C5—C4—C3—C2=C1—$SiMeCl_2$	+9.46	+15.02	+1.80	−1.24	−0.11	—	—
E-C6—C5—C4—C3—C2=C1—$SiMeCl_2$	+9.43	+15.09	+1.89	−1.41	−0.27	−0.14	—
E-C7—C6—C5—C4—C3—C2=C1—$SiMeCl_2$	+9.44	+15.16	+1.98	−1.32	−0.36	−0.35	−0.14
E-C5—C4—C3—C2=C1—$SiEt_3$	+11.42	+9.52	+3.02	−0.87	−0.08	—	—
E-C6—C5—C4—C3—C2=C1—$SiEt_3$	+11.36	+9.68	+3.10	−0.31	−0.12	−0.08	—
E-C7—C6—C5—C4—C3—C2=C1—$SiEt_3$	+11.36	+9.59	+3.02	−0.27	−0.39	−0.24	−0.07

*The comparison has been done between the ^{13}C nmr spectra, which were obtained in the same solvent ($CDCl_3$).

field from TMS. Comparing the chemical shifts of the sp^2 carbon atoms of the *E*-1-trichlorosilyl-1-alkenes under consideration with those of the vinyltrichlorosilane (8), which is the simplest 1-trichlorosilyl-1-alkene, we can make unambiguous assignments for the ^{13}C resonances of the two sp^2 carbon atoms. Thus, the signal at ca. 120 ppm is assigned unambiguously to the C1 and the signal at ca. 150 ppm to the C2 carbon atom. In order to support the above assignments of the ^{13}C resonances of the sp^2 carbon atoms of the *E*-1-silyl-1-alkenes, we also examined the ^{13}C nmr spectra of some internal *E*-silyl-alkenes. In the last case, it is clear from the comparison of the relative intensities of the ^{13}C nmr signals of the two sp^2 carbon atoms that the signal at higher field corresponds to the sp^2 carbon atom bearing the silyl group and that at lower field to the sp^2 carbon atom bearing the hydrogen. The signal at lower field has higher relative intensity than that at higher field because of the nuclear Overhauser enhancement effect (24). Details on the ^{13}C nmr spectra of the internal *E*-silyl-alkenes will be discussed later.

Assignments of the ^{13}C resonances of the saturated carbon atoms were made by comparison of their chemical shifts to those of the corresponding unsubstituted alkenes (2, 3, 5). It ought to be noted that it is possible to do this comparison, because, as it is known, the presence of a substituent causes small, usually, constant shifts of the resonances of the unsubstituted derivative, which can be expanded up to the fourth carbon atom relative to the carbon atom bearing the substituent (5).

Comparing the ^{13}C nmr spectra of the *E*-1-silyl-1-alkenes to those of the corresponding unsubstituted alkenes we noticed some remarkable trends concerning the sensitivity of the ^{13}C resonances of the alkene moiety to the organosilyl substituent.

In Table 2 are shown the differences ($\Delta\delta_C$) between the chemical shifts of the ^{13}C resonances of the *E*-1-silyl-1-alkenes and those of the corresponding unsubstituted 1-alkenes. In fact, the results reveal some patterns of chemical shift variations depending upon the nature of the silyl substituent.

Consideration of the substituent effects on the

Can. J. Chem. Downloaded from www.nrcresearchpress.com by 210.87.254.40 on 09/05/12
For personal use only.

TABLE 3. ^{1}H nmr parameters for the second order spectra of the olefinic protons of the *E*-1-silyl-1-alkenes*

Compound	(a − d)† (Hz)	(b − c)† (Hz)	$\nu_0\delta_{AB}$ (Hz)	$\nu_0\delta_A$ (Hz)	$\nu_0\delta_B$ (Hz)	J_{AB} (Hz)
E-(*n*-C_3H_7)CH=CHSiCl_3	75.0	37.5	53.0	349.1	402.1	19.0
E-(*n*-C_3H_7)CH=CHSiMeCl_2	67.5	30.0	45.0	346.3	391.3	19.0
E-(*n*-C_3H_7)CH=CHSiEt_3	54.5	16.5	30.0	334.5	364.5	19.0
E-(*n*-$_4H_9$)CH=CHSiCl_3	75.0	38.0	53.4	348.0	401.4	19.0
E-(*n*-C_4H_9)CH=CHSiMeCl_2	67.5	30.0	45.0	344.9	389.9	18.5
E-(*n*-C_4H_9)CH=CHSiEt_3	54.5	16.3	29.8	332.5	362.3	19.0
E-(*n*-C_5H_{11})CH=CHSiCl_3	75.0	38.0	53.4	348.8	402.2	18.5
E-(*n*-C_5H_{11})CH=CHSiMeCl_2	67.5	30.0	45.0	344.1	389.1	18.5
E-(*n*-C_5H_{11})CH=CHSiEt_3	55.0	16.5	30.0	334.0	364.0	19.0
E-$(CH_2)_4$CHCH=CHSiCl_3	76.0	40.0	55.1	346.5	401.6	18.5
E-$(CH_2)_4$CHCH=CHSiMeCl_2	67.5	30.0	45.0	341.9	386.9	19.0
E-$(CH_2)_4$CHCH=CHSiEt_3	55.5	17.5	31.2	332.2	363.4	19.0
E-Me_2C(OH)CH=CHSiEt_3	52.2	13.9	26.9	340.1	367.0	19.2
E-MeEtC(OH)CH=CHSiEt_3	47.0	8.9	20.4	341.6	362.0	19.0

*The ^{1}H nmr spectra were obtained in $CDCl_3$ or CCl_4 solutions using TMS as an internal standard.
†Values (a − d) and (b − c) are the differences between the resonance frequencies of the two outer and the two internal peaks of the quartet respectively.

chemical shifts of the sp^2 carbon atoms reveals that the silyl group introduces a downfield shift of the signals of both the sp^2 carbon atoms. These shifts for the three silyl substituents under consideration, e.g., $SiCl_3$, $SiMeCl_2$, and $SiEt_3$, are +7.69, +9.44, and +11.38 ppm for the C1 and +18.04, +15.09, and +9.60 ppm for the C2 carbon atoms respectively.

In the case of the trichlorosilyl and methyldichlorosilyl substituents the deshielding of the C2 is greater than that of the C1. In contrast, the triethylsilyl substituent introduces more deshielding on the C1 than on the C2.

Generally, as the number of chlorine atoms in the silyl substituent increases, the deshielding of the C2 increases, while just the opposite is true for the deshielding of the C1. This observation could be readily explained by considering the π-acceptor ability of the silyl substituents. Thus, as the number of chlorine atoms in the silyl substituent increases, its π-acceptor ability also increases, because of the −I inductive effect of the halogen. This, of course, has as a result the accumulation of more π-electron density on the C1 than on the C2 in the system C2⋯C1⋯SiX_3. In the case of the triethylsilyl substituent, although the +I inductive effect of the ethyl groups weakens its π-acceptor ability, there is still a net π-withdrawal registered at the C1 and C2. Therefore, in the three silyl substituents used the resonance effect predominates over the inductive effect. Of course, we cannot exclude the operation of other effects such as the "neighbor anisotropy" effect (25, 26) or the σ–π hyperconjugative effect, which has been postulated in many organosilicon compounds (14, 16, 27). These effects also contribute to the charge distribution on C1 and C2 and consequently to the observed ^{13}C resonances.

It ought to be specified that the same holds for the ^{1}H nmr spectra of the *E*-1-silyl-1-alkenes. The ^{1}H nmr parameters for the second order spectra of the olefinic protons of the compounds studied are listed in Table 3. As we can see from the data given in Table 3, the ^{1}H nmr parameters of the olefinic protons are independent of the nature of the alkyl chain of the alkene moiety but depend on the nature of the silyl group. The resonance frequency of the proton attached to the C1 (H_A proton) is lower than that of the proton attached to the C2 carbon atom (H_B proton). However, the resonance frequencies of both kinds of protons increase as the number of chlorine atoms in the silyl substituent increases. Also, it was observed that increasing the number of chlorine atoms in the silyl substituent increases the difference ($\nu_0\delta_{AB}$) between the resonance frequencies of the H_A and H_B protons. This is again in accordance with the π-acceptor ability of the silyl groups under consideration.

The effect of replacing H attached to the C1 with the silyl group on the ^{13}C nmr spectra of 1-alkenes is also a downfield shift at the C3 and an upfield shift at the C4 carbon atom. The carbon atoms C5, C6, and C7 which are further removed from the carbon bearing the silyl substituent are only slightly affected by the presence of the silyl group.

The magnitude of the deshielding of the C3 (1.5–3.0 ppm) depends on the nature of the silyl substituent and is proportional to the deshielding of the C1 and inversely proportional to the deshielding of the C2 carbon atom. The shielding of the C4, which also depends upon the nature of the silyl

Can. J. Chem. Downloaded from www.nrcresearchpress.com by 210.87.254.40 on 09/05/12
For personal use only.

Can. J. Chem. Downloaded from www.nrcresearchpress.com by 210.87.254.40 on 09/05/12
For personal use only.

group and the alkene moiety, is the well known γ-effect, which is due to the non-bonded steric interactions.

The effects of substitution on the ^{13}C resonances of the alkene moiety presented here can be very useful in the analysis of ^{13}C nmr spectra. Reasonable predictions of ^{13}C nmr spectra for compounds not yet studied can be made. This could be achieved using the differential chemical shifts listed in Table 2 as empirical substituent parameters. On the basis of these parameters in correlation with the Lindeman–Adams rule (1) and the additivity parameters for alkenes (11) we can calculate the chemical shifts of other *E*-1-silyl-1-alkenes not yet studied. Thus, for *E*-1-silyl-2-cyclopentyl-ethylene the calculated values (δ, ppm) are, for $SiCl_3$: C1 = 119.80, C2 = 161.04; for $SiMeCl_2$: C1 = 121.55, C2 = 158.09; for $SiEt_3$: C1 = 123.49, C2 = 152.60. The calculated values are in good agreement with the experimental values shown in Table 2.

As a next step, it would be worth applying the empirical substituent parameters in order to predict the ^{13}C chemical shifts of internal *E*-silyl-alkenes containing the silyl substituent at an sp^2 carbon atom and to examine if it is necessary to introduce some corrective parameters.

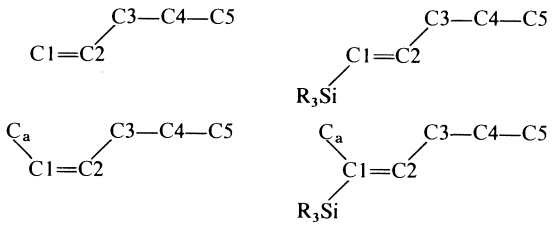
In Table 4 are presented the chemical shifts, the relative intensities, and the assignments of the ^{13}C nmr signals of some internal *E*-silyl-alkenes and a few hydroxy derivatives. Included are the ^{13}C nmr spectra of some mixtures of regio-isomer internal *E*-silyl-alkenes. Also, in Table 4 are shown in parentheses the calculated chemical shifts on the basis of the empirical substituent parameters given in Table 2 and the known ^{13}C resonances of the corresponding unsubstituted *Z*-alkenes (2–5).

There is thus a satisfying agreement between the experimental and the calculated chemical shifts of the ^{13}C resonances of the internal *E*-silyl-alkenes under study, particularly in the case of the *E*-2-silyl-2-alkenes. There exists, however, a slight difference of the order of ~2 ppm between the experimental and the calculated chemical shift of the carbon atom bearing the silyl group, especially in the case of the $SiCl_3$ and $SiMeCl_2$ substituents. In the case of the *E*-3-silyl-3-alkenes and the *E*-3-silyl-2-alkenes the differences between the experimental and the calculated chemical shifts of the sp^2 carbon atoms tend to be larger for all three silyl groups under consideration. These differences become clearer from the comparison of the differential chemical shifts shown in Table 3 and those obtained for each subgroup of the internal *E*-silyl-alkenes studied (Table 5).

Supposing that the substituent effect on the ^{13}C resonances of either the terminal or the internal *E*-silyl-alkenes operates through the same mechanism, the observed differences between the experimental and the calculated chemical shifts of the sp^2 carbon atoms may be due to non-bonded steric interactions between geminal substituents or between substituents possessing *Z*-position. Therefore, the differential chemical shifts, which are valid for each subgroup of the internal *E*-silyl-alkenes (Table 5), also comprise a factor which expresses the extent of the non-bonded steric interactions. It must be noted that this factor depends upon the position of the double bond and the nature of the silyl substituent as well.

Comparing the differential chemical shifts given in Tables 3 and 5 it is observed that except for the sp^2 carbon atoms, where those vary, for the rest of the carbon atoms of the alkene moiety the shifts are very close. Thus, although differences between the experimental and the calculated chemical shifts of the sp^2 carbon atoms of the internal *E*-silyl-alkenes do exist, the differential chemical shifts discussed previously are proved to be rather useful for the correct assignment of the ^{13}C resonances for a great number of *E*-silyl-alkenes (either internal or terminal).

In order to justify the correctness of the assignments of the ^{13}C resonances that were made by the use of the aforementioned differential chemical shifts, the comparison of the shifts caused by the introduction of a methyl group at the C1 of a 1-alkene and the corresponding *E*-1-silyl-1-alkene was also used. The results of the comparison are shown schematically below:



$R_3Si = Cl_3SiCl_2MeSiEt_3Si$

ΔC1 = +9.49	ΔC1 = +7.18	+7.38	+9.89
ΔC2 = −8.23	ΔC2 = −7.85	−8.15	−7.38
ΔC3 = −7.02	ΔC3 = −6.92	−7.38	−7.18
ΔC4 = +0.61	ΔC4 = +0.77	+0.70	+1.25
ΔC5 = +0.22	ΔC5 = +0.23	+0.19	+0.27

The introduction of the methyl group causes a downfield shift at the C1, C4, and C5 and an upfield shift at the C2 and C3. The observed shifts in both cases are in good agreement, although some small differences appear again for the shifts of the carbon atom bearing the silyl substituent.

TABLE 4. ^{13}C chemical shifts (δ, ppm downfield from TMS) and assignments of the ^{13}C resonances of some internal *E*-silyl-alkenes

Compound	Chemical shift
E-C1—C2—C3=C4—C5—C6 | $SiCl_3$	C1 = 14.42(—)* {45}†; C2 = 21.15(—){100}; C3 = 135.11(138.94){15}; C4 = 151.22(149.29){56}; C5 = 22.22(22.26){68}; C6 = 13.23(12.95){42}
E-C1—C2—C3=C4—C5—C6 | Cl_2Si—C1′	C1′ = 4.97(—){47}; C1 = 14.55(—){69}; C2 = 21.23(—){100}; C3 = 137.30(140.69){8}; C4 = 148.09(146.34){51}; C5 = 21.90(22.50){45}; C6 = 13.41(13.17){56}
E-C1—C2—C3=C4—C5—C6 | $Si(C1'—C2')_3$	C1′ = 3.38(—){100}; C2′ = 7.57(—){89}; C1 = 14.90(—){40}; C2 = 21.74(—){27}; C3 = 138.43(142.63){7}; C4 = 143.41(140.85){24}; C5 = 22.81(23.72){36}; C6 = 14.41(13.54){28}
E-C1—C2(OH)—C3=C4—C5(OH)$(C6)_2$ | | C1 $Si(C1'—C2')_3$	C1′ = 4.95{78}; C2′ = 7.52{55}; C1 = 31.74{100}; C2 = 72.27{31}; C3 = 141.53{17}; C4 = 147.36{43}; C5 = 74.60{31}; C6 = 31.74{100}
E-C1—C2(OH)—C3=C4—C5(OH)$(C6)_2$ | | C1 $Si(C1')_2(C_6H_5)$	C1′ = 0.15{51}; C1 = 31.60{84}; C2 = 72.22{34}; C3 = 143.67{17}; C4 = 148.67{52}; C5 = 74.75{29}; C6 = 32.03{78}; *i*-C = 139.74{21}; *o*-C = 127.70{98}; *m*-C = 133.82{100}; *p*-C = 128.77{44}
E-C1—C2=C3—C4—C5 | $SiCl_3$	C1 = 13.69(—){34}; C2 = 128.43(130.53){11}; C3 = 150.55(150.47){70}; C4 = 22.08(21.89){75}; C5 = 12.66(12.16){100}
E-C1—C2=C3—C4—C5 | $SiCl_3$	C1 = 14.41(13.57){17}; C2 = 144.05(140.88){22}; C3 = 136.54(140.12){3}; C4 = 20.68(—){32}; C5 = 12.45(—){41}
E-C1—C2=C3—C4—C5 | Cl_2Si—C1′	C1′ = 3.80(—){83}; C1 = 13.78(—){60}; C2 = 130.39(132.28){15}; C3 = 147.30(147.52){72}; C4 = 21.76(22.09){81}; C5 = 12.82(11.96){100}
E-C1—C2=C3—C4—C5 | Cl_2Si—C1′	C1′ = 4.73(—){46}; C1 = 14.09(13.77){41}; C2 = 140.58(137.93){43}; C3 = 138.46(141.87){8}; C4 = 20.74(—){45}; C5 = 12.52(—){57}
E-C1—C2=C3—C4—C5 | $Si(C1'—C2')_3$	C1′ = 3.27(—){60}; C2 = 7.47(—){100}; C1 = 14.20(—){22}; C2 = 135.22(135.48){9}; C3 = 142.92(142.80){16}; C4 = 22.51(23.35){24}; C5 = 13.93(13.31){19}
E-C1—C2=C3—C4—C5 | $Si(C1'—C2')_3$	C1′ = 2.88(—){31}; C2′ = 7.47(—){100}; C1 = 13.83(—){11}; C2 = 132.07(132.44){3}; C3 = 140.47(143.81){1}; C4 = 21.73(—){13}; C5 = 14.81(—){10}
E-C1—C2=C3—C4—C5—C6 | $SiCl_3$	C1 = 13.87(—){37}; C2 = 129.27(131.64){21}; C3 = 149.20(148.83){75}; C4 = 30.88(30.78){100}; C5 = 21.73(21.57){82}; C6 = 13.74(13.73){87}
E-C1—C2=C3—C4—C5—C6 | $SiCl_3$	C1 = 14.71(14.33){16}; C2 = 144.75(141.99){34}; C3 = 134.92(138.48){4}; C4 = 29.63(—){43}; C5 = 22.45(—){34}; C6 = 12.77(—){38}
E-C1—C2=C3—C4—C5—C6 | Cl_2Si—C1′	C1′ = 4.02(—){72}; C1 = 14.12(—){60}; C2 = 131.30(133.41){11}; C3 = 145.89(145.81){71}; C4 = 30.66(31.02){96}; C5 = 21.88(21.79){100}; C6 = 13.71(13.74){87}
E-C1—C2=C3—C4—C5—C6 | Cl_2Si—C1′	C1′ = 5.04(—){28}; C1 = 14.62(14.63){21}; C2 = 141.31(139.04){46}; C3 = 136.90(140.23){5}; C4 = 30.05(—){35}; C5 = 22.76(—){37}; C6 = 12.90(—){33}
E-C1—C2=C3—C4—C5—C6 | $Si(C1'—C2')_3$	C1′ = 2.88(—){100}; C2 = 7.47(—){93}; C1 = 13.82(13.77){17}; C2 = 135.77(135.33){11}; C3 = 141.16(140.39){22}; C4 = 32.08(32.24){33}; C5 = 22.80(22.72){29}; C6 = 14.30(—){14}

Can. J. Chem. Downloaded from www.nrcresearchpress.com by 210.87.254.40 on 09/05/12
For personal use only.

TABLE 4 (*Concluded*)

Compound	Chemical shift
E-C1—C2═C3(Si(C1′—C2′)$_3$)—C4—C5—C6	C1′ = 3.23(—){38}; C2 = 7.47(—){93}; C1 = 14.86(15.87){12}; C2 = 132.96(133.55){5}; C3 = 138.69(142.17){2}; C4 = 30.61(—){23}; C5 = 23.19(—){23}; C6 = 14.58(—){10}

*Figures in parentheses are the calculated chemical shifts.
†Figures in brackets are the relative intensities of the signals.

TABLE 5. Differential chemical shifts ($\Delta\delta_C$, ppm)* between the ^{13}C resonances of internal *E*-silyl-alkenes and those of the corresponding unsubstituted *Z*-alkenes

Compound	$\Delta\delta_{C1}$	$\Delta\delta_{C2}$	$\Delta\delta_{C3}$	$\Delta\delta_{C4}$	$\Delta\delta_{C5}$	$\Delta\delta_{C6}$
E-C1—C2—C3($SiCl_3$)═C4—C5—C6	—	+0.45	+3.86	+19.97	+1.52	−1.18
E-C1—C2—C3($SiMeCl_2$)═C4—C5—C6	+0.14	+0.53	+6.05	+16.84	+1.20	−1.00
E-C1—C2—C3($SiEt_3$)═C4—C5—C6	+0.49	+1.04	+7.18	+12.16	+2.11	—
E-C1—C2($SiCl_3$)═C3—C4—C5	+1.68	+5.59	+18.12	+1.75	−0.96	—
E-C1—C2($SiCl_3$)═C3—C4—C5—C6	+1.10	+5.32	+18.41	+1.66	−1.30	−0.11
E-C1—C2($SiMeCl_2$)═C3—C4—C5	+1.77	+7.55	+14.87	+1.43	−0.80	—
E-C1—C2($SiMeCl_2$)═C3—C4—C5—C6	+1.35	+7.35	+15.10	+1.44	−1.15	−0.14
E-C1—C2($SiEt_3$)═C3—C4—C5	+1.80	+11.92	+10.12	+1.91	−0.17	—
E-C1—C2($SiEt_3$)═C3—C4—C5—C6	+1.05	+11.82	+10.37	+2.86	−0.23	+0.45
E-C1—C2═C3($SiCl_3$)—C4—C5	+2.40	+21.21	+4.11	+0.35	−1.17	—
E-C1—C2═C3($SiCl_3$)—C4—C5—C6	+1.94	+20.80	+4.13	+0.41	−0.58	−1.08
E-C1—C2═($SiMeCl_2$)—C4—C5	+2.08	+17.74	+6.03	+0.41	−1.10	—
E-C1—C2═C3($SiMeCl_2$)—C4—C5—C6	+1.85	+17.36	+6.11	+0.83	−0.27	−0.95
E-C1—C2═↕↓↻⇒⁄↑↘*D*)—C4—C5	+1.82	+9.23	+8.04	+1.40	+1.05	—
E-C1—C2═C3($SiEt_3$)—C4—C5—C6	+2.09	+9.01	+7.90	+1.39	+0.16	+0.73

*The comparison has been done between the ^{13}C nmr spectra obtained in the same solvent ($CDCl_3$).

The trends of the substituent effect observed in the case of the internal *E*-silyl-alkenes are in accordance with those discussed previously for the terminal *E*-silyl-alkenes.

Considering the ^{13}C nmr spectra of the mixtures of the regio-isomer *E*-silyl-alkenes we found that it would be possible to quantify the mixtures using the peak heights of the ^{13}C resonances of certain of their carbon nuclei, without resorting to special techniques, such as gated decoupling (28) and the addition of paramagnetics (29). As is known, ^{13}C nmr spectroscopy has so far been little exploited for quantitative analysis because the signal areas rarely reflect carbon concentration. This is due to three factors which contribute to perturbing signal intensities. These factors are the differential relaxations, the nuclear Overhauser effect which does not always reach its theoretical maximum, and the failure to obtain sufficient pulse power to give a uniform excitation throughout the spectral region (12). However, in the case of the regio-isomers studied, there are carbon nuclei in each isomer with analogous chemical environments which also give ^{13}C resonances with very close chemical shifts. Such carbon atoms in the molecules of the regio-isomer *E*-silyl-alkenes are the C4, C5, and C6. For these carbon nuclei, it is reasonable to consider that the three factors contributing to the perturbation of the signal intensities are likely to be very similar and consequently the peak heights might reflect the concentration of each isomer in the mixture.

The results of the quantitative analysis of the mixtures studied, using the peak heights of the C4, C5, and C6 ^{13}C resonances of each isomer, are summarised in Table 6. Also, in Table 6 are shown the results obtained from the analysis of the mixtures by ^1H nmr spectroscopy. In fact, the results obtained by the two methods show a large measure of agreement. For some mixtures ^{13}C nmr spectroscopy gives better results than ^1H nmr spectroscopy because the separation of the ^1H signals of the two isomers is insufficient. Also, it can be noted that the analysis of the mixtures by glc, especially in the case of the chlorinated products, was unsuccessful. These products are very sensitive to the moisture and cause injection problems. Of course, we can get around these problems by converting the chlorinated products to the alkylated ones, via the Grignard reagents, but this method involves a chemical step which is destructive and takes some time.

Experimental

The silyl-alkenes studied were prepared by hydrosilylation of alkynes using *trans*-di-μ-hydrido-bis(tricyclohexylphosphine) bis(silyl)diplatinum complexes as catalysts, according to the method described elsewhere (30, 31).

Can. J. Chem. Downloaded from www.nrcresearchpress.com by 210.87.254.40 on 09/05/12
For personal use only.

TABLE 6. Percentage ratio of the regio-isomer *E*-silyl-alkenes determined by ^{13}C nmr and ^{1}H nmr spectroscopy

Mixture	^{13}C nmr*			^{1}H nmr
	C4	C5	C6	
E-C1—C2($SiCl_3$)=C3—C4—C5	70.1	70.9	—	70
E-C1—C2=C3($SiCl_3$)—C4—C5	29.9	29.1	—	30
E-C1—C2($SiMeCl_2$)=C3—C4—C5	64.3	63.7	—	65
E-C1—C2=C3($SiMeCl_2$)—C4—C5	35.7	36.3	—	35
E-C1—C2($SiEt_3$)=C3—C4—C5	64.9	65.5	—	65
E-C1—C2=C3($SiEt_3$)—C4—C5	35.1	34.5	—	35
E-C1—C2($SiCl_3$)=C3—C4—C5—C6	69.9	70.7	69.6	68
E-C1—C2=C3($SiCl_3$)—C4—C5—C6	30.1	29.3	30.4	32
E-C1—C2($SiMeCl_2$)=C3—C4—C5—C6	73.3	73.0	72.5	72
E-C1—C2=C3($SiMeCl_2$)—C4—C5—C6	26.7	27.0	27.5	28
E-C1—C2($SiEt_3$)=C3—C4—C5—C6	58.9	55.8	58.3	60
E-C1—C2=C3($SiEt_3$)—C4—C5—C6	41.1	44.2	41.7	40

*The calculation has been made using the peak heights of the ^{13}C resonances.

^{13}C nmr spectra were recorded on a Varian CFT-20 spectrometer operating in the Fourier transform mode at 20 MHz using 10 mm diameter sample tubes. An internal deuterium lock ($CDCl_3$) was employed with broad-band proton noise decoupling. The main parameters were: acquisition time 1.024 s; pulse delay 0 s; flip-angle 35° (7μs); noise bandwidth 1000 kHz; temperature 40°C. Samples were prepared as 20–40% v/v solutions in $CDCl_3$ containing 5–10% $CHCl_3$ with or without 1% TMS as an internal reference. In most cases, accumulation of 2000–3000 transient responses was sufficient to obtain adequate signals for all carbon atoms. Chemical shifts which were recorded with respect to internal $CHCl_3$ were converted to the TMS scale using the relationship $\delta_{(CHCl_3)} = +77.20$ ppm downfield from TMS. Positive shifts are reported downfield from TMS.

^{1}H nmr spectra were obtained with a Varian A 60A (60 MHz) spectrometer in CCl_4 or $CDCl_3$ solutions using TMS as an internal standard.

1. L. P. LINDEMAN and J. Q. ADAMS. Anal. Chem. **43**, 1245 (1971).
2. D. E. DORMAN, M. JAUTELAT, and J. D. ROBERTS. J. Org. Chem. **36**, 2757 (1971).
3. J. W. DE HAAN and L. J. M. VAN DEN VEN. Org. Magn. Reson. **5**, 147 (1973).
4. J. W. DE HAAN, L. J. M. VAN DEN VEN, A. R. N. WILSON, A. E. VAN DER HOUTLODDER, C. ALTONA, and D. H. FABER. Org. Magn. Reson. **8**, 477 (1976).
5. P. A. COUPERUS, A. D. H. GLAGUE, and J. P. C. M. VAN DONGEN. Org. Magn. Reson. **8**, 426 (1976).
6. D. E. DORMAN, M. JAUTELAT, and J. D. ROBERTS. J. Org. Chem. **38**, 1026 (1973).
7. J. E. DUBOIS and J. P. DOUCET. Org. Magn. Reson. **11**, 87 (1978).
8. G. MIYAJIMA, K. TAKAHASHI, and K. NISHIMOTO. Org. Magn. Reson. **6**, 413 (1974).
9. G. MIYAJIMA and K. NISHIMOTO. Org. Magn. Reson. **6**, 313 (1974).
10. E. C. CHUKOVSKAYA, V. I. DOSTOVALOVA, T. T. VASILÉNA, and R. KH. FREIDLINA. Org. Magn. Reson. **8**, 229 (1976).
11. G. J. MARTIN, M. L. MARTIN, and S. ODIOT. Org. Magn. Reson. **7**, 2 (1975).
12. F. W. WEHRLI and T. WIRTHLIN. Interpretation of carbon-13 nmr spectra. Heyden, London. 1976.
13. P. E. RAKITA, J. P. SREBRO, and L. S. WORSHAM. J. Organomet. Chem. **104**, 27 (1976).
14. C. D. SCHAEFFER, JR., J. J. ZUCKERMAN, and C. H. YODER. J. Organomet. Chem. **80**, 29 (1974).
15. P. E. RAKITA and L. S. WORSHAM. J. Organomet. Chem. **137**, 145 (1977).
16. S. Q. A. RIZVI, B. D. GUPTA, W. ADCOCK, D. DODDRELL, and W. KITCHING. J. Organomet. Chem. **63**, 67 (1973).
17. P. E. RAKITA and L. S. WORSHAM. Inorg. Nucl. Chem. Lett. **13**, 547 (1977).
18. P. E. RAKITA, L. S. WORSHAM, and J. P. SREBRO. Org. Magn. Reson. **8**, 310 (1976).
19. G. ENGLEHARDT, H. JANCKE, M. MÄGI, T. PEHK, and E. LIPPMAA. J. Organomet. Chem. **28**, 293 (1971).
20. R. K. HARRIS and B. J. KIMBER. Org. Magn. Reson. **7**, 460 (1975).
21. J. SCHRAML, NGUYEN-DUC-CHUY, and V. CHVALOVSKÝ. Org. Magn. Reson. **7**, 379 (1975).
22. J. SCHRAML, V. CHVALOVSKÝ, M. MÄGI, and E. LIPPMAA. Collect. Czech. Chem. Commun. **40**, 879 (1975).
23. J. POLA, Z. PAPOUSKOVA, and V. CHVALOVSKÝ. Collect. Czech. Chem. Commun. **41**, 239 (1976).
24. J. H. NOGGLE and R. E. SCHIRMER. The nuclear Overhauser effect. Academic Press, New York. 1971.
25. H. SPIESECKE and W. G. SCHNEIDER. J. Chem. Phys. **35**, 722 (1961).
26. H. SPIESECKE and W. G. SCHNEIDER. J. Chem. Phys. **35**, 731 (1961).
27. C. G. PITT. J. Organomet. Chem. **61**, 49 (1973).
28. R. FREEMAN, H. D. W. HILL, and R. KAPTEIN. J. Magn. Reson. **7**, 327 (1972).
29. J. H. SHOOLERY and W. C. JANKOWSKI. Applications Note, No 4. Varian Assoc., Palo Alto, CA. 1973.
30. M. GREEN, J. L. SPENCER, F. G. A. STONE, and C. A. TSIPIS. J. Chem. Soc. Dalton Trans. 1525 (1977).
31. C. A. TSIPIS. J. Organomet. Chem. In press.

Can. J. Chem. Downloaded from www.nrcresearchpress.com by 210.87.254.40 on 09/05/12
For personal use only.

Photochemical rearrangements of 2-azido-4-thiochromanone 1-oxide and 1,1-dioxide: formation of 2*H*-benzo[f]-1,2-thiazepine derivatives

IAN W. J. STILL AND TOONG S. LEONG

Department of Chemistry, University of Toronto, Toronto, Ont., Canada M5S 1A1

Received August 27, 1979

IAN W. J. STILL and TOONG S. LEONG. Can. J. Chem. **58**, 369 (1980).

Photolysis of 2-azido-4-thiochromanone 1,1-dioxide in benzene or dichloromethane leads to the formation of 2*H*-benzo[f]-1,2-thiazepin-5-one 1,1-dioxide, in very good yield. In contrast, the photolysis of the analogous sulfoxide was much more complex and no ring-expansion product could be isolated, although a small amount of a compound believed to be 2-aminothiochromone 1-oxide was formed. Several attempts to prepare the α-azidosulfide analogue, to compare its photochemical behavior, were unsuccessful and a rationale is proposed for the apparent instability of this member of the series.

IAN W. J. STILL et TOONG S. LEONG. Can. J. Chem. **58**, 369 (1980).

La photolyse du dioxyde-1,1 de l'azido-2 thio-4 chromanone en solution dans le benzène ou le dichlorométhane conduit à la formation du dioxyde-1,1 du 2*H* benzo[f] thiazépine-1,2 one-5 avec de bons rendements. Dans le cas de l'analogue sulfoxydé la photolyse est au contraire plus complexe et on n'a pas pu isoler de produits résultant d'une expansion de cycle, en dépit du fait que l'on croit à la formation de petites quantités d'oxyde-1 d'amino-2 thiochromone. Plusieurs tentatives de préparation de l'α-azidosulfure apparenté, dans le but de faire une étude comparative de son comportement photochimique, se sont révélées inefficaces. On propose une explication de l'instabilité apparente de ce composé.

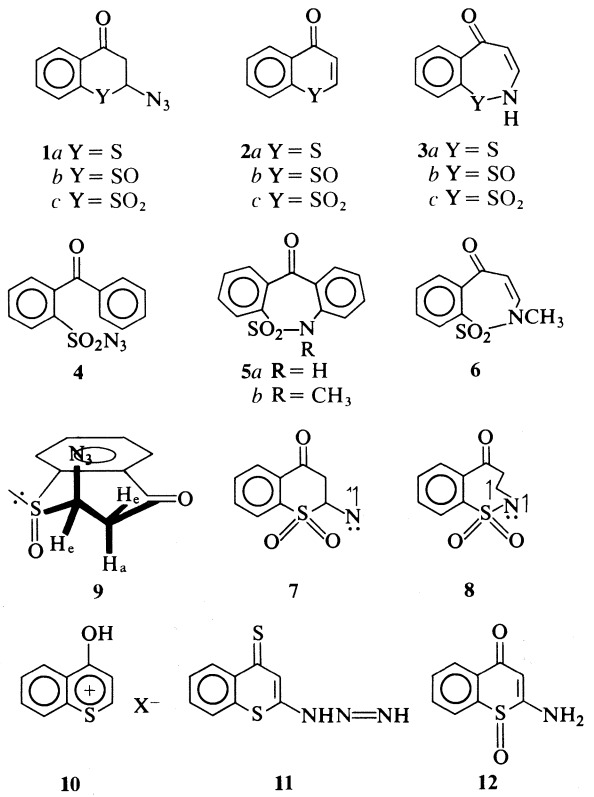
[Traduit par le journal]

Introduction

In an earlier investigation (1) we reported the preparation of 2-azido-4-thiochromanone 1,1-dioxide **1***c* by the addition of hydrazoic acid to thiochromone 1,1-dioxide **2***c*. Representatives of the α-azidosulfone class of compounds have rarely been reported in the literature, although Böhme and Ziegler recently reported another example (2). The combination of functional groups represented by **1***a–c* therefore seemed to warrant a more detailed chemical investigation.

In particular, it appeared to us that the photochemical or thermal decomposition of the α-azidosulfone **1***c* might provide a convenient synthetic route to the 1,2-thiazepine **3***c*. Despite fairly intensive research interest in the 1,3- and 1,4-thiazepine series of heterocycles, stemming in part from their relatively easy synthetic availability and in part from the interesting medicinal properties of certain members of these series of compounds, virtually no work at all on the chemistry of 1,2-thiazepines had appeared until recently (2–5). In contrast to the isomeric thiazepines, 1,2-thiazepines of course are distinguished by being cyclic sulfenamides, sulfinamides, or sulfonamides respectively, depending on the oxidation state of the sulfur atom.

Very recently, Abramovitch *et al.* (6) described an interesting study of the thermal decomposition of a series of substituted arylsulfonyl azides. In particular, it was found that 2-azidosulfonylbenzophenone **4** underwent intramolecular aromatic substitution to produce the dibenzothiazepine derivative **5***a*. Under a variety of experimental conditions, however, the yields obtained did not exceed 7% and the sultam was invariably accompanied by



0008-4042/80/040369-07$01.00/0

©1980 National Research Council of Canada/Conseil national de recherches du Canada

Can. J. Chem. Downloaded from www.nrcresearchpress.com by 210.87.254.105 on 09/05/12
For personal use only.

Can. J. Chem. Downloaded from www.nrcresearchpress.com by 210.87.254.105 on 09/05/12
For personal use only.

other products. Our expectation that the α-azidosulfone **1***c* should provide a convenient route to the 1,2-thiazepine system has been realized by an alternative photochemical rearrangement. We now present an account of our findings and also of the results of our attempts to extend this potentially useful reaction to the analogous conversions of the α-azidosulfoxide **1***b* and the α-azidosulfide **1***a* respectively.

Results and Discussion

The α-azidosulfone **1***c* first reported by us (1) was the first member of the series studied.[1] Photolysis of **1***c* in benzene ($\lambda_{irr} > 300$ nm) led to the isolation of 2*H*-benzo[f]-1,2-thiazepin-5-one 1,1-dioxide **3***c* in 39% yield. Surprisingly, after 10 h, starting material (33%) was also recovered but the only other product from the reaction appeared to be polymeric in nature. Lengthening the time of irradiation did not improve the yield of **3***c*, but led instead to increased formation of the polymeric product, so that after 35 h, for example, the yield of **3***c* had fallen to 2–3%, indicating that the product itself is photolabile. Irradiation of the azidosulfone in acetonitrile, or irradiation with light of shorter wavelength, failed to give any of the ring-expansion product.

The structure of the 1,2-thiazepine was established by spectroscopic methods, including ^{13}C nmr. The compound shows a molecular ion in the mass spectrum at $m/e = 209$ and its infrared spectrum (solid state) indicates the presence of the tautomeric form (**3***c*), shown by a broad peak centred at 3100 (NH) cm^{-1}.[2] In addition, the ^1H nmr spectrum revealed a characteristic pair of vinylic hydrogens, with $J = 10$ Hz. Further confirmation that this representation, rather than the alternative O—H (or C—H) tautomeric forms, is correct, was provided as a result of methylation of **3***c* with diazomethane in ether. A single product ($m/e = 223$) was obtained, in 62% yield, with a uv spectrum virtually indistinguishable from that of **3***c*. The ^1H nmr spectrum revealed a new signal at $\delta = 3.40$, attributed to the N—CH_3 group. The analogous N-methyl derivative **5***b* prepared by Abramovitch *et al.* (6), the structure of which was confirmed by an unambiguous synthesis, shows a value of $\delta = 3.36$ for the N-methyl group and, in other relevant respects, the two series of 1,2-thiazepines show the expected similarity in spectral characteristics. Thus we feel that the structures of both our N-methyl derivative **6** and its precursor **3***c* are secure.

In an attempt to establish the nature of the excited state responsible for this photochemical ring expansion, we conducted the irradiation of **1***c* in acetophenone as the solvent, a method used previously to establish reaction pathways in other azide photolyses (8). After the same length of time a much higher yield (81%) of **3***c* was obtained in this experiment, with no evidence for recovered starting material, unlike the direct irradiation in benzene. This suggests a triplet mechanism for the formation of **3***c*. The triplet nitrene species **7** first formed must undergo ring expansion by preferential migration of the $ArSO_2$ residue to afford **8**.[3] Spin inversion, followed by prototropy, then leads to **3***c*.

An attempt to show that a singlet species could not be involved by using the so-called singlet-sensitization conditions employed by Suschitzky and his co-workers (8), i.e., irradiation in dichloromethane containing pyrene, gave only traces of photoproduct and essentially 100% recovery of starting material. However, this result was found to be attributable to essentially complete absorption of the light by the pyrene at the wavelengths employed in the irradiation. One side benefit to arise from this experiment, however, was the finding that when the irradiation of **1***c* was conducted in dichloromethane alone, a much cleaner reaction resulted than in the benzene irradiation. A comparable amount of starting material (38%) was recovered after 10 h but the isolated yield of the 1,2-thiazepine **3***c* rose from 39 to 81% (based on starting material actually consumed).

Attempts to carry out the ring expansion of the α-azidosulfone by ground-state decomposition pathways have also been investigated. Refluxing in aromatic solvents such as toluene, bromobenzene, and chlorobenzene, as well as heating the α-azidosulfone alone in the same temperature range (110–150°C) led to slow decomposition but gave no useful products. Likewise, attempts to carry out the acid-catalyzed decomposition of **3***c* by treatment with sulfuric acid at 0°C, or with trifluoroacetic acid at 25–65°C, did not lead to any of the 1,2-thiazepine ring-expansion product.

[1]It should be pointed out that the experimental conditions for the preparation of **1***c* from thiochromone 1,1-dioxide were incorrectly reported in reference (1) (see also Experimental).

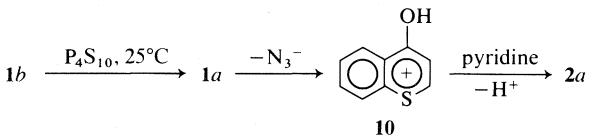
[2]This remarkably low value for the NH stretch, observed in the solid state, is observed in other secondary sulfonamides, e.g., $C_6H_5SO_2NHSO_2C_6H_5$ (7), where the NH group is flanked by two electron-withdrawing groups, as is the case for **3***c*. We thank one of the referees for drawing our attention to this point.

[3]Although the possibility of direct conversion of the triplet azide to product, with rearrangement accompanying concerted loss of N_2, cannot be absolutely ruled out, the most frequently encountered pathway in azide photolyses is via the nitrene intermediate.

Can. J. Chem. Downloaded from www.nrcresearchpress.com by 210.87.254.105 on 09/05/12
For personal use only.

Since the preparation of thiochromone 1-oxide **2***b* had earlier been described by us (9), we decided to synthesize the analogous 2-azido-4-thiochromanone 1-oxide **1***b* and to examine its photochemical behavior. Acid-catalyzed addition of hydrazoic acid to **2***b* did in fact afford the expected α-azidosulfoxide **1***b*, in 50% yield. This compound was much more difficult to purify than the analogous α-azidosulfone, and is particularly susceptible to acid-catalyzed decomposition, for example, during chromatography. Nevertheless, a single pure isomer could be isolated, which showed an ABX pattern in the ^{1}H nmr spectrum characteristic of a *trans*-diaxial arrangement of the strongly polar sulfoxide and azide groups, as shown in structure **9**. The assignments of the two C-3 protons follow from both the magnitude of their respective vicinal coupling constants with H_e at C-2 and also from the fact that the H_a proton at C-3 should be the more strongly deshielded by the antiperiplanar electronegative N_3-substituent at C-2 (10). Interestingly, each of the three protons in the non-aromatic ring in **9** has a strongly electronegative substituent in an antiperiplanar relationship and hence we have assumed that the ^3J coupling reducing effects predicted by Booth (11) in such situations will be mutually cancelling. Had the individual coupling constants not been evident by a first-order analysis of the ^{1}H nmr spectrum, the line-width of the C-2 proton signal alone would have established the equatorial location for this proton (10). The 1,2-diaxial relationship of the sulfoxide and azide functional groups not only minimizes repulsive interactions but is also in accord with the well-known axial preference for S=O bonds in six-membered heterocyclic rings (12).

Photolysis of the α-azidosulfoxide **1***b* in benzene under similar conditions to those used in the photolysis of **1***c* appeared to lead, as expected, to a mixture of the ring-expanded 1,2-thiazepine **3***b* and the starting azide. Once again, a characteristic vinylic doublet pattern (J = 10 Hz) was evident in the ^{1}H nmr spectrum but the previously mentioned instability of the starting α-azidosulfoxide rendered the separation and purification of **3***b* by chromatographic means impossible.[4] Attempts to isolate the *N*-methyl derivative of **3***b* by treatment of the crude photolysate with diazomethane were likewise unsuccessful. Instead, we decided to treat the crude photolysate (containing about a 4:1 ratio of starting material – **3***b*) with phosphorus pentasulfide in pyridine. We had earlier observed that **1***b* could be converted almost quantitatively into thiochromone **2***a* by this reagent, and it was our expectation that this would allow us to effect a relatively easy separation (by chromatography) of **3***b*, although it was conceivable that **3***b* itself could be reduced under the reaction conditions to its cyclic sulfenamide counterpart **3***a*. Our earlier studies (13) have clearly demonstrated the effectiveness of phosphorus pentasulfide as a reagent for reducing sulfoxides to sulfides but the concomitant loss of the elements of HN_3 from 2-azido-4-thiochromanone 1-oxide on treatment with P_4S_{10}-pyridine was at first sight surprising, especially since our usual conditions for achieving deoxygenation of sulfoxides (P_4S_{10}–CH_2Cl_2, 25°C) left **1***b* quite unchanged. We believe that the conversion of **1***b* to **2***a* proceeds by initial deoxygenation of the azidosulfoxide to produce the highly unstable α-azidosulfide **1***a* (see later discussion). Ionization of **1***a*, possibly via a small percentage of the enol form present at equilibrium, would produce the 4-hydroxybenzothiopyrylium (azide) salt **10**, which in turn is rapidly deprotonated by the excess of pyridine present, producing thiochromone **2***a*. In support of this suggestion, **1***b* was found to be unaffected by treatment with pyridine alone under similar conditions.



10

In the event, our hope of being able to isolate **3***b* by this procedure was not realized because, although thiochromone **2***a* was indeed isolated, presumably from the reaction of starting **1***b* as outlined above, the 1,2-thiazepine product did not survive the treatment with phosphorus pentasulfide – pyridine. However, careful chromatography and recrystallization from acetone–hexane did produce a new yellow solid, mp 157–159°C, albeit in very low yield. This compound had the same molecular mass (m/e = 221) as the starting α-azidosulfoxide, although lacking any azide band in the infrared, and high resolution mass measurement on this ion and the elemental analysis confirmed the molecular formula, $C_9H_7N_3S_2$. The only reasonable structure for the new product which satisfies this formula, as well as the ir and ^{1}H nmr spectral characteristics, is that of the triazene, **11**, or one of its tautomers. (It was, for example, observed that only one proton was exchanged even after several hours exposure to D_2O; this would likely be the proton on the nitrogen next to the ring.) Although simple mono-

[4]Sudden decomposition of the starting azide invariably occurred at some point during the passage of the mixture down the column. The resulting rapid release of N_2 caused much cracking and bubbling within the column.

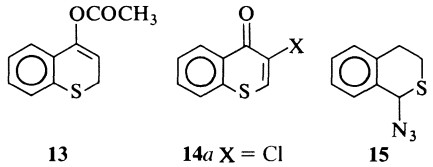
Can. J. Chem. Downloaded from www.nrcresearchpress.com by 210.87.254.105 on 09/05/12
For personal use only.

substituted triazenes are very uncommon, it does appear that the presence of an electron-withdrawing unit, as in **11**, significantly enhances the stability of this system (14). This product is not considered to be a photoproduct but a minor artifact of the procedure above, whereby phosphorus pentasulfide first deoxygenates the α-azidosulfoxide **1***b* and then subsequent thionation of the carbonyl group and pyridine-catalyzed prototropy (but not necessarily in that order) lead eventually to **11**.

Given the lack of success with the above photolysis, it was decided to repeat the photolysis of the α-azidosulfoxide in dichloromethane, since this solvent had been the solvent of choice for the α-azidosulfone photolysis. After 10 h, a reaction mixture resulted which looked (by ^{1}H nmr) generally similar to the one obtained in benzene, with the same ratio of starting material to product. It was found that the starting material could be removed by thick-layer chromatography, without the concomitant destruction of the products which occurred on column chromatography. Nevertheless, the reaction mixture was so complex that only one product could be isolated after extensive purification. A yellow solid, mp 172–174°C, was obtained in 13% yield, after repeated chromatography and fractional crystallization. This compound showed an apparent molecular ion at $m/e = 177$, but the elemental analysis indicated the formula $C_9H_7NO_2S$ and confirmation of this was obtained by high resolution mass measurement on the fragment at $m/e = 177$. Once again, NH (or OH) absorption was present in the ir spectrum, along with apparent carbonyl and sulfoxide bands at 1642 and 1070 cm^{-1}, respectively. All protons present were in the region from 7.1–8.1 ppm and thus D_2O exchange results were not meaningful. The ^{13}C nmr spectrum confirmed the presence of a carbonyl group at 184 ppm and the presence of four quaternary carbons. The structure which best accommodates these data, although it cannot be regarded as rigorously established, is that of 2-aminothiochromone 1-oxide **12**. The possibility that **12** exists as a mixture with the O—H and C—H tautomers of the corresponding imine is recognized, but the spectroscopic evidence, as well as analogy with related compounds, strongly favours this form. The formation of **12** can be accounted for by a well-precedented 1,2-hydrogen shift in the putative nitrene intermediate (most likely the singlet in this case) analogous to **7** (15). The ^{1}H nmr evidence cited earlier indicates that ring-expansion may also occur under these reaction conditions but clearly, if this is so, the 1,2-thiazepine 1-oxide (**3***b*) so formed must be more labile, photochemically as well as chemically, than **3***c*.

An additional photolysis of 2-azido-4-thiochromanone 1-oxide was conducted in acetophenone as solvent. Although this solvent had been successful in greatly improving the efficiency of the conversion of the analogous azidosulfone to **3***c*, in this instance a complex reaction mixture, similar in appearance (^{1}H nmr) to those from the direct irradiations, was obtained, with the single difference that there was no evidence for any recovered starting compound.

As the final representative of this series of 2-azido-4-thiochromanone derivatives, the α-azidosulfide **1***a* might be expected to lead by our photochemical route to the parent 2*H*-benzo[f]-1,2-thiazepin-5-one, **3***a*. The obvious route to **1***a* involving the conjugate addition of hydrazoic acid to thiochromone **3***a*, is not available in this instance, since the strong acid catalyst customarily required simply produces the unreactive thiopyrylium species **10** (1), which has proved to be inert towards nucleophilic substitution. Likewise, for the reasons discussed earlier, we were unable to convert the 2-azidosulfoxide **1***b* into **1***a* by simple deoxygenation, using either phosphorus pentasulfide (13) or thiophosphoryl bromide (16), thiochromone **2***a* being the only product obtained, in yields of 80–100%. The recent results of Chen *et al.* (17) indicated that it would be fruitless to attempt the direct chlorination of 4-thiochromanone with *N*-bromosuccinimide or *N*-chlorosuccinimide, but the treatment of 4-thiochromanone enol acetate **13** (18) with these reagents again led mainly to thiochromone (60–85%), although smaller amounts of the 3-halo derivatives **14***a*, *b* were also found.



13 **14***a* X = Cl, *b* X = Br **15**

We are forced to the conclusion that the presence of an effective leaving group at C-2 in the thiochromanone system is intrinsically destabilizing. Although Böhme and Ziegler (2) reported no difficulty in isolating and purifying the α-azidosulfide **15** derived from isothiochroman, this compound lacks the carbonyl group which is present in **1***a*. It is the apparent ease with which **1***a* is converted to the very stable aromatic 4-hydroxybenzothiopyrylium system (see earlier discussion), rather than any inherent instability associated with

Can. J. Chem. Downloaded from www.nrcresearchpress.com by 210.87.254.105 on 09/05/12
For personal use only.

the α-azidosulfide functionality, which in our view accounts for the inability to isolate **1***a*.

Experimental

General

The infrared spectra were recorded on a Perkin-Elmer 337 grating spectrophotometer and the ultraviolet spectra on a Unicam SP-800A spectrometer. Low resolution mass spectra were obtained on a Bell and Howell 21-490 instrument. ^{1}H nuclear magnetic resonance spectra were recorded on a Varian T-60 spectrometer with TMS as internal standard. Natural abundance ^{13}C nmr spectra were obtained on a Varian XL-100-15 instrument at 25.16 MHz in the pulsed Fourier transform mode, operating at 32 ± 3°C. Acquisition times of 0.666 s and pulse widths of 12 μs were employed. (A 90° "flip" angle is equivalent to ca. 55 μs.) Partially coupled spectra, as well as proton decoupled spectra, were recorded in all cases.

Elemental analyses were performed by the Scandinavian Microanalytical Laboratory, Box 25, DK2730 Herlev, Denmark or by A. B. Gygli, 329 St. George Street, Toronto, Ontario. Column chromatography and thin-layer chromatography (analytical and preparative) were conducted on silica gel using Fisher A.C.S. grade solvents. Melting points were recorded on an Electrothermal Mark II apparatus and are uncorrected.

*2-Azido-4-thiochromanone 1,1-Dioxide (**1**c)*

The preparation of **1***c* was adapted from the procedure previously reported by us (1). It was found, however, that the presence of a small quantity of a strong acid was essential for the reaction to proceed at a measurable rate, in contrast to the earlier report. A solution of thiochromone 1,1-dioxide (9.00 g, 46 mmol) in chloroform (120 mL) was mixed with a solution of hydrazoic acid in chloroform (140 mL, approx. 0.4 *M*) and concentrated H_2SO_4 (1.5 mL) was added to the resulting mixture. After stirring for 7 days at 25°C, the unsaturated C=O band (1667 cm^{-1}) in the ir spectrum of the starting sulfone had disappeared completely. The chloroform solution was washed with water and dried (Na_2SO_4). Evaporation of solvent afforded **1***c* as a pale yellow solid (10.10 g, 92%), mp 110–112°C (lit. (1) mp 110–111°C). The compound could be obtained as colorless needles by percolating through silica gel, followed by recrystallization from dichloromethane–hexane; uv (MeOH) λ_{max} (log ε): 247 (3.95), 287 (3.32), 295 (3.25) nm.

*Photolysis of 2-Azido-4-thiochromanone 1,1-Dioxide (**1**c) in Benzene*

A degassed solution of **1***c* (0.64 g, 2.71 mmol) in benzene (90 mL, freshly distilled from sodium) was irradiated through Pyrex with a 115 W medium pressure mercury arc lamp, in an immersion-well type of apparatus, under nitrogen for 10 h. The solvent was evaporated and the residual product was chromatographed on silica gel. Elution with dichloromethane gave **1***c* (0.21 g, 33%). Elution with 1–5% acetone in dichloromethane yielded a reddish-yellow product which was repeatedly washed with small amounts of acetone to give 2*H*-benzo[f]-1,2-thiazepin-5-one 1,1-dioxide (**3***c*) (150 mg, 39%), as a pale yellow solid.

The solid was decolorized with charcoal in acetone and recrystallized from acetone–hexane to give a colorless solid, mp 203–204°C (dec.). The compound could also be sublimed at 150–160°C/0.005 Torr; ir (KBr) ν_{max}: 3100 (broad, NH), 1618 (C=O), 1348, 1312, and 1178 (SO_2) cm^{-1}; uv (MeOH) λ_{max} (log ε): 298 (3.90) nm; ^{1}H nmr (acetone-d_6) δ: 5.73 (1H, d, J = 10 Hz, H-4), 7.05 (1H, d, J = 10 Hz, H-3), 7.77–8.10 (4H, m, aromatic, no signal observed for NH proton); ^{13}C nmr (acetone-d_6) δ: 191.5 (CO), 138.0, 136.1, 135.1, 134.8, 133.4, 131.1 (aromatic carbons), 124.3 (C-3), 112.8 (C-4); ms *m/e*: 209 (M^+). *Anal.* calcd. for $C_9H_7NO_3S$: C 51.66, H 3.38, N 6.70, S 15.32; found: C 52.30, H 3.70, N 6.27, S 15.18.

Further elution with higher percentages of acetone in dichloromethane afforded only polymeric material. The photolysis has been performed for various reaction times. The results are tabulated in Table 1.

*Photolysis of **1**c in Acetophenone*

A degassed solution of **1***c* (0.42 g, 1.76 mmol) in acetophenone (freshly distilled from K_2CO_3, bp 199–200°C, 80 mL) was irradiated under N_2 through Pyrex for 10 h. A pale yellow solution resulted. Acetophenone was removed (bp ~ 45°C/1 Torr, at bath temperature 80–85°C) to give a residue which was rather insoluble in chloroform and dichloromethane but soluble in acetone. The acetophenone-contaminated residue was triturated with chloroform and the $CHCl_3$ solution showed essentially only acetophenone absorptions in the ir. A yellowish solid (0.28 g, 75%) was filtered off and washed with chloroform. This product was shown to be identical with the photoproduct **3***c* obtained in benzene. Evaporation of the chloroform filtrate and elution from a preparative tlc plate with 30% acetone–CH_2Cl_2 afforded further **3***c* (22.1 mg, 6%).

*Photolysis of **1**c in Dichloromethane, in Presence of Pyrene*

A degassed solution of **1***c* (0.43 g, 1.79 mmol) and 1.28 g (6.30 mmol) pyrene (percolated through silica gel with pentane and recrystallized from ethanol, mp 154–155°C) in dry dichloromethane (80 mL) was irradiated under N_2 through Pyrex for 10 h. A brownish-yellow solution resulted. Evaporation of the solvent afforded a residue which consisted mainly of **1***c* and pyrene (identified by tlc). The residue was charged onto a column of silica gel (60 g). Elution with dichloromethane gave pyrene (1.25 g, 98%), followed by **1***c* (0.50 g, 95%). Elution with 5–30% acetone in dichloromethane afforded small amounts (14.8 mg) of a brownish-yellow residue which showed at least 3 spots on tlc examination. The R_f value of one of these spots matched that of the photoproduct **3***c*.

*Photolysis of **1**c in Dichloromethane*

A degassed solution of **1***c* (0.40 g, 1.70 mmol) in dry dichloromethane (80 mL) was irradiated under N_2 through Pyrex for 10 h. A yellow liquid together with a small amount of precipitate resulted. Evaporation of the solvent afforded a yellow residue which was charged onto a column of silica gel (60 g). Elution with dichloromethane gave **1***c* (0.16 g, 38%). Elution with 10–25% acetone in dichloromethane afforded **3***c* (0.18 g, 81%).

*2-Methyl-2H-benzo[f]-1,2-thiazepin-5-one 1,1-Dioxide (**6**)*

Compound **3***c* (116.2 mg, 0.56 mmol) was dissolved in absolute ethanol (50 mL) and the solution was cooled to 0–5°C. An ethereal solution of diazomethane was added dropwise until the yellow color persisted. The temperature of the solution was kept below 10°C during the addition. Thin-layer chromatography showed only a single product. Evaporation of the solvent gave a brownish-yellow oil. The oily residue was purified by preparative tlc. Elution with dichloromethane afforded **6** as a yellowish solid (76.2 mg, 62%), mp 46–48°C (pentane); ir ($CHCl_3$) ν_{max} 1624 (C=O), 1356, 1314, and 1133 (SO_2) cm^{-1}; uv (MeOH) λ_{max} (log ε): 306 (3.83) nm; ^{1}H nmr ($CDCl_3$) δ: 3.40 (3H, s, NCH_3),

TABLE 1. Effect of reaction time on photolysis of **1***c*

Reaction time (h)	Recovered **1***c* (%)	**3***c*[a]
10	33	26
12	33	21
35	8	2

[a]Percentage conversion.

Can. J. Chem. Downloaded from www.nrcresearchpress.com by 210.87.254.105 on 09/05/12
For personal use only.

5.80 (1H, d, J = 10 Hz, H-4), 6.70 (1H, d, J = 10 Hz, H-3), 7.60–8.10 (4H, m, aromatic); ^{13}C nmr (acetone-d_6) δ: 191.0 (CO), 139.9, 137.8, 136.7, 135.1, 133.5, 130.8 (aromatic carbons), 125.2 (C-3), 113.6 (C-4), 38.4 (NCH_3); ms *m/e*: 223 (M^+). *Anal.* calcd. for $C_{10}H_9NO_3S\cdot\frac{1}{2}H_2O$: C 51.71, H 4.34, N 6.03, S 13.81; found: C 51.65, H 4.41, N 5.90, S 13.68.

*(*trans*)-2-Azido-4-thiochromanone 1-Oxide (**1**b)*

A solution of HN_3 in $CHCl_3$ (prepared from 2.5 g, 0.04 mol NaN_3) was added dropwise to a solution of thiochromone 1-oxide **2***b* (9) (3.10 g, 0.01 mol) in $CHCl_3$ (30 mL). After the addition was complete, the solution was stirred at 25°C for 16 h. Evaporation of the solvent afforded a dark brown residue (3.81 g, 99%). This residue was repeatedly washed with small amounts of acetone to give **1***b* (1.92 g, 50%) as a pale yellow solid, mp 116–118°C; ir ($CHCl_3$) ν_{max}: 2122, 2095 (N_3), 1691 (C=O), 1060 (SO) cm^{-1}; uv (MeOH) λ_{max} (log ε): 243.5 (3.99), 297.5 (3.44) nm; ^{1}H nmr ($CDCl_3$) δ: 2.94 (1H, dd, J = 17 Hz, 3 Hz, H-3e), 3.37 (1H, dd, J = 17 Hz, 6 Hz, H-3a), 5.18 (1H, dd, J = 6 Hz, 3Hz, H-2e), 7.43–8.17 (4H, m, aromatic); ms *m/e*: 193($M^+ - N_2$). *Anal.* calcd. for $C_9H_7N_3O_2S$: C 48.87, H 3.19, N 19.00, S 14.47; found: C 49.14, H 3.25, N 18.91, S 14.55.

*Photolysis of (*trans*)-2-Azido-4-thiochromanone 1-Oxide (**1**b)*

A degassed solution of **1***b* (1.53 g, 6.89 mmol) in dry benzene (210 mL) was irradiated through Pyrex, using a 115 W medium pressure mercury arc lamp, for 6 h under nitrogen. A bright yellow solution together with traces of a yellow precipitate resulted. The filtrate was evaporated to dryness to give a brownish-yellow residue (1.55 g), which contained the starting material **1***b* and the photo-products, which had lower R_f values than **1***b* (10% acetone–CH_2Cl_2). ^{1}H nuclear magnetic resonance ($CDCl_3$) revealed the presence of two vinylic protons at δ 5.68 (d, J = 10 Hz) and 6.58 (d, J = 10 Hz), in the ratio 1:1. The ratio of vinylic to methylene protons (of **1***b*) was 1:4. An attempt to separate the crude products from the starting material by chromatography on silica gel resulted in the rapid decomposition of **1***b* and destruction of the column.

Attempted N*-Methylation of Above Photolysate*

An ethereal solution of CH_2N_2 was added dropwise to an ice-cooled solution of the crude product above (0.25 g) in EtOH (50 mL). After the addition was complete, the solvent was evaporated to give a brownish-yellow residue which did not show the nmr spectrum expected for the product. However, a singlet at δ 3.27 (possibly NCH_3) indicated that some *N*-methylated material may have been present.

*Treatment of the Crude Photolysate from **1**b with P_4S_{10}–Pyridine*

The crude photolysate (0.90 g, 4.06 mmol, based on **1***b*) from the photolysis of **1***b* in benzene was dissolved in pyridine (20 mL). To this solution was added phosphorus pentasulfide (0.90 g, 2.03 mmol). The mixture was stirred under N_2 at 25°C for 4 h. Most of the solvent was removed under vacuum. The dark brown residue was treated with dichloromethane (450 mL) and water (400 mL). Saturated sodium chloride solution (100 mL) was added to facilitate the separation. The organic layer (dark brown) was separated and the aqueous layer (yellow) was further extracted with dichloromethane (2 × 100 mL). The dichloromethane extracts were combined and washed with water (3 × 100 mL) and dried ($MgSO_4$). Evaporation of the solvent afforded a dark brown residue. The presence of thiochromone was strongly indicated by nmr.

The residue was chromatographed on silica gel. Elution with dichloromethane and 10% acetone in dichloromethane afforded sulfur (0.11 g), thiochromone (0.34 g, 2.10 mmol), and an unknown compound (0.17 g), as well as some pyridine. Further elution with 20–30% acetone in dichloromethane gave some deep red polymeric material. The crude unknown compound was then treated with charcoal in acetone. Recrystallization from acetone–hexane afforded some yellow solid (25 mg) **11**, mp 157–159°C; ir (KBr) ν_{max}: 3150, 3128 (NH), 1455, 1415 (N=N), 1125 (C=S) cm^{-1}; uv (MeOH) λ_{max} (log ε): 240 sh (3.65), 283 (2.91), 360–420 plateau (2.30) nm; ^{1}H nmr ($CDCl_3$) δ: 6.23 (1H, s), 7.12–7.49 (5H, m), 7.62 (1H, s); ms *m/e*: 221. *Anal.* calcd. for $C_9H_7N_3S_2$: C 48.86, H 3.19, N 19.00, S 14.49; found: C 49.14, H 3.25, N 18.91, S 14.55; calcd. for $C_9H_7N_3S_2$: 221.0081; found: 221.0081.

*Irradiation of (*trans*)-2-Azido-4-thiochromanone 1-Oxide **1**b in Dichloromethane*

Irradiation of a degassed solution of **1***b* (0.50 g, 2.67 mmol) in dichloromethane (100 mL) for 10 h led to the formation of a brownish-yellow solution. Evaporation of the solvent afforded a brownish-yellow residue consisting of **1***b* and a mixture of products. The acetone-insoluble material (19 mg) was filtered off. the ^{1}H nmr (acetone-d_6) of the acetone-soluble material revealed vinylic protons identical to those observed in the photolysis of **1***b* in benzene. (The ratio of the vinylic compound to **1***b* was approximately 1:4.) The acetone-soluble material was chromatographed on two preparative tlc plates and eluted with 30% acetone in dichloromethane to give a mixture of products. This material was reapplied on a preparative tlc plate and eluted with 30% acetone in dichloromethane. The major band on extraction with 40% acetone in dichloromethane gave a brownish-yellow residue (0.18 g) which was treated with charcoal in acetone. Filtration and evaporation afforded a yellow residue (0.12 g). The ^{1}H nmr (acetone-d_6) spectrum of this residue showed vinylic protons identical to those mentioned previously. The residue gave a yellow solid (14 mg, mp 172–174°C) upon precipitation with chloroform. Additional amounts (41 mg) of this yellow solid were obtained by extensive chromatography and fractional crystallization. The pure compound **12**[5] had the following characteristics:[6] ir: ($CHCl_3$) ν_{max}: 3492 (OH/NH), 1642 (C=O), 1070(S=O) cm^{-1}; uv (MeOH) λ_{max} (log ε): 308 (3.99), 415 (3.96) nm; ^{1}H nmr (DMSO-d_6) δ: 7.10–8.07 (m); ^{13}C nmr (DMSO-d_6) (21): 184.0 (CO), 150.1 (C-2), 145.0 (C-3), 142.9, 134.1, 132.5, 125.0, 124.4, 124.2 (aromatic); ms *m/e*: 177 (M^+ − 16). *Anal.* calcd. for $C_9H_7NO_2S$: C 55.96, H 3.65, N 7.25, S 16.57; found: C 55.64, H 3.84, N 7.16, S 16.26; calcd. for C_9H_7NOS (*m/e* = 177 fragment ion): 177.0248; found: 177.0250.

*Attempts to Prepare 2-Azido-4-thiochromanone, **1**a*

*(Non-catalyzed) Addition of Azide to Thiochromone (**2**a)*

Sodium azide (0.6 g, 9.31 mmol) was added in one portion to a solution of thiochromone (0.9 g, 5.6 mmol) in a 1:1 mixture of methanol–acetonitrile (6 mL). The reaction mixture was refluxed for 7 days. The solid (NaN_3) was filtered off and washed with dichloromethane. The washings and the filtrate were combined and evaporated to dryness. The residue was dissolved in ether and washed with water. Drying ($MgSO_4$) and evaporation of the solvent afforded only thiochromone (0.7 g, 78%).

*4-Thiochromanone Enol Acetate (**13**) and* N*-Chlorosuccinimide (NCS)*

A mixture of **13** (0.1 g, 0.5 mmol) and NCS (0.07 g, 0.5 mmol) in carbon tetrachloride (2 mL) was stirred at 25°C for 19 h. The floating material (succinimide) was filtered off and the residue

[5]Russian workers (19) recently reported the characterization of the analogous sulfide, 2-aminothiochromone. The two compounds show the expected spectral similarities.

[6]The vinylic compound could no longer be detected (^{1}H nmr in acetone-d_6) after this extensive chromatography and precipitation.

Can. J. Chem. Downloaded from www.nrcresearchpress.com by 210.87.254.105 on 09/05/12
For personal use only.

(0.09 g) obtained on evaporation of the filtrate was purified by preparative tlc, eluting with dichloromethane. Two major bands were observed. These were extracted with acetone to give (*i*) 3-chlorothiochromone (**14***a*) (10.4 mg, 11%) as yellowish needles, mp 148–149°C (lit. (20) mp 149°C); ir ($CHCl_3$) ν_{max}: 1625 (CO) cm^{-1}; ^1H nmr ($CDCl_3$) δ: 7.45–7.63 (3H, m), 8.01 (1H, s), 8.37–8.60 (1H, m); ms *m/e*: 198, 196 (M^+, ratio = 1:3). (*ii*) thiochromone (**2***a*) (68.1 mg, 85%).

Reaction of 4-Hydroxybenzothiopyrylium Perchlorate with Sodium Azide

A solution of the crude 4-hydroxybenzothiopyrylium perchlorate (21) (2.4 g, 9.4 mmol) in DMF (25 mL) was added to a solution of sodium azide (0.6 g, 9.2 mmol) in a minimum amount (250 mL) of DMF. The bright yellow mixture was stirred at 25°C for 18 h. It was then heated at 60–65°C for 6 h followed by a further period of heating at 95–100°C for 22 h. The DMF was evaporated *in vacuo* and the residue treated with ether–water mixture. The ether layer was separated and the aqueous layer re-extracted with ether. The ether extracts were combined and dried ($MgSO_4$). Evaporation gave thiochromone (1.1 g, 74%).

Reaction of 4-Acetoxybenzothiopyrylium Perchlorate with Sodium Azide

A mixture of 4-thiochromanone enol acetate **13** (0.5 g, 2.43 mmol) and triphenylmethyl perchlorate (1) (0.83 g, 2.42 mmol) in acetic acid (5 mL) was heated under reflux for 15 min. After cooling to 25°C the mixture was cooled in ice. The perchlorate salt (0.57 g, 77%) was filtered off and washed thoroughly with ether.

Sodium azide (0.12 g, 1.88 mmol) was added to a solution of the 4-acetoxybenzothiopyrylium perchlorate (0.57 g, 1.88 mmol) so prepared, in acetonitrile (5 mL). The reaction mixture was stirred at 25°C for 3 h. Sodium azide (0.12 g, 1.88 mmol) was again added. The mixture was stirred at 25°C for 3 h and an additional amount of sodium azide (0.24 g, 3.76 mmol) was added. The mixture was stirred at 25°C for 10 h and was then heated under reflux for 37 h. (Additional acetonitrile was added to maintain the liquid level.) The solid material was filtered off and washed with chloroform. The washings and the filtrate were combined and evaporated, affording only thiochromone (0.26 g, 87%).

Reaction of (trans)*-2-Azido-4-thiochromanone 1-Oxide* **1***b with Thiophosphoryl Bromide: Formation of Thiochromone* **2***a*

Thiophosphoryl bromide (0.024 mL, 0.23 mmol) was added dropwise (with a syringe) to a solution of **1***b* (50 mg, 0.23 mmol) in dry dichloromethane (2 mL) in a pre-dried two-neck flask equipped with magnetic stirrer, drying tube, and septum-cap inlet. The reaction mixture was stirred under N_2 at 25°C for 2 h. Some yellow precipitate (sulfur) was removed and the filtrate evaporated to afford a dark brown residue.

The residual material was stirred in a mixture of dichloromethane (50 mL) and 5% sodium carbonate (10 mL) for 0.5 h. The aqueous layer was discarded. The organic layer was extracted with 5% Na_2CO_3 (3 × 10 mL). Drying ($MgSO_4$) and evaporation afforded a yellowish residue (30.4 mg, 87%). The nmr ($CDCl_3$) and ir ($CHCl_3$) spectra indicated the residue consisted almost entirely of thiochromone **2***a*. The reaction was not further investigated.

Reactions of **1***b with Phosphorus Pentasulfide*

Phosphorus pentasulfide (40 mg, 0.09 mmol) was added in portions to a solution of **1***b* (40 mg, 0.18 mmol) in dry pyridine (2 mL). The reaction mixture was stirred under N_2 at 25°C for 4 h. The mixture was stirred briefly with water (10 mL) and dichloromethane (30 mL). The aqueous layer was discarded. The organic layer was repeatedly washed with water until the aqueous layer was colorless. Drying ($MgSO_4$) and evaporation afforded a yellowish residue (29.9 mg). Both nmr ($CDCl_3$) and ir ($CHCl_3$) indicated that this was mainly thiochromone in essentially quantitative yield.

Phosphorus pentasulfide (40 mg, 0.09 mmol) was added in portions to a solution of **1***b* (40 mg, 0.18 mmol) in dry dichloromethane (2 mL). The mixture was stirred under N_2 at 25°C for 4 h and diluted to 75 mL with dichloromethane. Water (25 mL) was added and the organic layer separated and washed with water (2 × 25 mL). Drying ($MgSO_4$) and evaporation of the solvent afforded a yellowish residue (39.4 mg, 98%). Nuclear magnetic resonance indicated that it was mainly the starting material, **1***b*.

Acknowledgements

Partial support of this work by the National Research Council of Canada is gratefully acknowledged. We thank Professor M. A. Winnik of this department for valuable discussions on photochemical aspects of the investigations.

1. I. W. J. Still, M. T. Thomas, and A. M. Clish. Can. J. Chem. **53**, 276 (1975).
2. H. Böhme and F. Ziegler. Justus Liebigs Ann. Chem. 734 (1974).
3. P. Catsoulacos and C. Camoutsis. J. Heterocycl. Chem. **13**, 1309 (1976).
4. R. A. Abramovitch, K. M. More, I. Shinkai, and P. C. Srinivasan. Heterocycles, **5**, 95 (1976).
5. H. Zenno and T. Mizutani. Jpn. Patent No. 70 04990 (August, 1966); Jpn. Patent No. 70 04991 (February, 1970); Chem. Abstr. **72**, 111525f (1970); 111527h (1970).
6. R. A. Abramovitch, C. I. Azogu, I. T. McMaster, and D. P. Vanderpool. J. Org. Chem. **43**, 1218 (1978).
7. C. J. Pouchert. Aldrich Library of Infrared Spectra. 2nd ed. Aldrich Chemical Co., Inc., Milwaukee, WI. 1975. Spectrum No. 10 192–10 193.
8. J. M. Lindley, I. M. McRobbie, O. Meth-Cohn, and H. Suschitzky. J. Chem. Soc. Perkin Trans. I, 2194 (1977).
9. I. W. J. Still, P. C. Arora, and S. N. Sokolowsky. Org. Prep. Proced. Int. **7**, 159 (1975).
10. L. M. Jackman and S. Sternhell. Applications of nuclear magnetic resonance spectroscopy in organic chemistry. 2nd ed. Pergamon Press, Oxford, England. 1969. p. 288.
11. H. Booth. Tetrahedron Lett. 411 (1965).
12. K. Bergensen, B. M. Carden, and M. J. Cook. J. Chem. Soc. Perkin Trans. II, 1001 (1978), and references therein.
13. I. W. J. Still, S. K. Hasan, and K. Turnbull. Can. J. Chem. **56**, 1423 (1978).
14. P. A. S. Smith. The chemistry of open-chain organic nitrogen compounds. Vol. II. W. A. Benjamin, Inc., New York, NY. 1966. pp. 336–340.
15. N. J. Turro. Modern molecular photochemistry. The Benjamin/Cummings Publishing Co., Inc., Menlo Park, CA. 1978. p. 551 *et seq*.
16. I. W. J. Still, J. N. Reed, and K. Turnbull. Tetrahedron Lett. 1481 (1979).
17. C. H. Chen, G. A. Reynolds, and J. A. Van Allan. J. Org. Chem. **42**, 2777 (1977).
18. I. W. J. Still and T. S. Leong. Tetrahedron Lett. 3613 (1979).
19. L. A. Zhurenko, O. M. Glozman, and V. A. Zagorevskii. Khim. Geterotsikl. Soedin. 182 (1978).
20. G. Hawthorne and W. N. Porter. Aust. J. Chem. **19**, 1751 (1966).
21. M. S. Chauhan and I. W. J. Still. Can. J. Chem. **53**, 2880 (1975).

Ion–molecule reactions in dimethylsulfoxide by high pressure photoionization mass spectrometry

JOHN A. STONE AND MARGARET S. LIN

Chemistry Department, Queen's University, Kingston, Ont., Canada K7L 3N6

Received August 14, 1979

JOHN A. STONE and MARGARET S. LIN. Can. J. Chem. **58**, 376 (1980).

Dimethylsulfoxide (DMSO) has been photoionized at 10.0 and 11.7 eV over the pressure range 0.3–210 mTorr. The rate constant for the disappearance of $DMSO^+$ is 1.0×10^{-9} cm^3 molecule^{-1} s^{-1}, independent of photon energy. The major products at low pressure are $CH_3SO(CH_3SO)CH_3^+$ and $CH_3SOHCH_3^+$ while at high pressure the ion series $(DMSO)_nH^+$ predominates with $n \leq 5$. In experiments with mixtures of DMSO and water or methanol very little mixed solvation of the proton was observed although isotopic D/H exchange between D_2O and $(DMSO)_2H^+$ is facile.

JOHN A. STONE et MARGARET S. LIN. Can. J. Chem. **58**, 376 (1980).

On a photoionisé le diméthylsulfoxyde (DMSO) à 10.0 et 11.7 eV sur une échelle de pression allant de 0.3 à 210 mTorr. La constante de vitesse de la disparition de l'ion $DMSO^+$ est de 1.0×10^{-9} cm^3 molécule^{-1} s^{-1} et est indépendante de l'énergie du photon. Les produits principaux à basse pression sont: $CH_3SO(CH_3SO)CH_3^+$ et $CH_3SOHCH_3^+$ tandis qu'à haute pression les ions de la série $(DMSO)_nH^+$ prédominent avec $n \leq 5$. On a observé, dans des expériences conduites avec des mélanges de DMSO avec de l'eau ou du méthanol, très peu de solvatation mixte du proton quoique l'échange isotopique D/H entre D_2O et $(DMSO)_2H^+$ soit facile.

[Traduit par le journal]

Introduction

The ion chemistry of dimethylsulfoxide (DMSO) received little attention for many years. Blais *et al.* (1, 2) studied both positive and negative ion reactions with a magnetic sector instrument at pressures around 10^{-4} Torr and first observed the products of positive ion reactions with *m/e* values greater than that of the molecular ion. It is now apparent that some of these *m/e* values were wrongly assigned so that the product designations are in error. Peers and Muller (3) obtained rate constants for the disappearance of the molecular ion and some primary ions formed by electron impact at pressures around 10^{-3} Torr. For the molecular ion, $k = 1.9 \times 10^{-9}$ cm^3 molecule^{-1} s^{-1} at ionizing electron energies of 11.0 and 16.0 eV. Reaction products were not identified.

Two ion cyclotron resonance (ICR) studies have recently helped identify some of the product ions and their precursors. McAllister (4) identified the major products originating from the reaction of the molecular ion (M^+) with the neutral molecule as the protonated molecule $(M+1)^+$ (reaction [1]), the proton bound dimer $(2M + 1)^+$ (reaction [2]), and a product obtained by transfer of CH_3SO^+ or CH_3SO (*m/e* 141) (reaction[3]).

[1] $CH_3SOCH_3^+ + CH_3SOCH_3 \rightarrow CH_3SOHCH_3^+ + CH_3SOCH_2^{\cdot}$

[2] $CH_3SOHCH_3^+ + CH_3SOCH_3 \rightarrow (CH_3SOCH_3)_2H^+$

[3] $CH_3SOCH_3^+ + CH_3SOCH_3 \rightarrow CH_3SO(SOCH_3)CH_3^+ + {}^{\cdot}CH_3$

Contemporaneously Nixon *et al.* (5) obtained qualitative results in general agreement with those of McAllister (4) and in addition obtained some rate constants and relative product yields. Their rate constant for the disappearance of M^+ (2.14×10^{-10} cm^3 molecule^{-1} s^{-1}) is an order of magnitude less than the value reported by Peers and Muller (3). M^+ disappeared to give mainly $(M+1)^+$ (95%), together with a small yield of the methylsulfinylated product arising from reaction [3]. Production of $(2M+1)^+$ from $(M+1)^+$ was found to be inefficient and further solvation of the proton was not observed. This slowness of reaction in the DMSO system was attributed to steric hindrance.

A quadrupole ion store (Quistor) was employed by Fulford *et al.* (6) in their study of DMSO. The major products obtained from M^+, $(M+1)^+$, and $(2M+1)^+$ were the same as those found by previous workers. However, other products were obtained which were either not reported by other workers or were present in yields far different from those reported previously.

The study of the reactions of the DMSO molecular ion is complicated to some extent by the reactions of fragment ions present in the initial spectrum. These latter ions do in most cases lead to the generation of the molecular ion (4). The present study was made using a photoionization source so that the reaction of the molecular ion alone could be examined, in the expectation that some of the inconsistencies of previous studies might be resolved.

0008-4042/80/040376-05$01.00/0

©1980 National Research Council of Canada/Conseil national de recherches du Canada

Can. J. Chem. Downloaded from www.nrcresearchpress.com by 210.87.254.105 on 09/05/12
For personal use only.

Can. J. Chem. Downloaded from www.nrcresearchpress.com by 210.87.254.105 on 09/05/12
For personal use only.

Experimental

A photoionization source similar to the one described previously (7) was employed. It was machined from a stainless steel bar and had appropriate apertures for LiF windows, a Baratron pressure gauge, and a gas inlet. Cartridge heaters fitted into wells in the block. At very low pressures (~0.3 to 3 mTorr) the ions emerged through a circular aperture 1 mm diameter in a thin stainless steel plate. At higher pressures a slit was employed which was fabricated from razor blades and had dimensions 1.5 × 0.045 mm^2. The source was operated in the field free mode at ground potential. A conventional electron impact source facilitated accurate mass assignment. An ion counting system and a signal averager were used for data collection. The resolution of the quadrupole filter was adjusted so that there was little mass discrimination up to *m/e* 180 and above that value a correction was applied using factors obtained by comparisons with standard spectra of perfluorinated compounds. These corrections were not required for rate constant determinations.

Photoionization was by resonance radiation from either a krypton or argon low pressure, microwave-powered lamp. The former lamp supplies photons of energy 10.03 eV with a small contribution from those of energy 10.64 eV while the latter gives photons of energies 11.83 eV and 11.62 eV (8). Henceforth radiation from these lamps will be described as 10 eV and 11.7 eV, respectively.

The "Baker Analyzed" Reagent grade DMSO was dried by standing over 3 Å molecular sieve and was passed into the ion source from a heated reservoir via a heated Granville Phillips variable leak valve.

Results and Discussion

The vapour pressure of DMSO is ~0.6 Torr at 25°C so that in order to prevent condensation within the ion source the maximum pressure employed was less than half this value. Except where noted the ion source temperature was 298 ± 2 K.

(a) The Disappearance of the Molecular Ion (M^+)

Figure 1 shows that at 10 eV and low pressure there is a linear decrease in log fractional yield of M^+ with increasing pressure. The line extrapolates to unity at zero pressure which signifies that M^+ is the only significant initial ion. At 11.7 eV (Fig. 2) the curve extrapolates to 0.81, the ions observed, which account for the rest of the primary ionization, being *m/e* 61 ($C_2H_5S^+$), *m/e* 63 (CH_3SO^+), and *m/e* 62 ($C_2H_6S^+$ and CH_2SO^+) which has an extremely small yield. This is consistent with the determinations of Blais *et al.* (1) who give

$$IP(CH_3SOCH_3^+) = 9.9 \pm 0.1 \text{ eV}$$

$$AP(C_2H_5S^+) = 11.1 \pm 0.1 \text{ eV}$$

$$AP(CH_3SO^+) = 11.8 \pm 0.1 \text{ eV}$$

$$AP(C_2H_6S^+) = 11.6 \pm 0.1 \text{ eV}$$

and

$$AP(CH_2SO^+) = 11.8 \pm 0.1 \text{ eV}$$

Rate constants may be obtained from the slopes

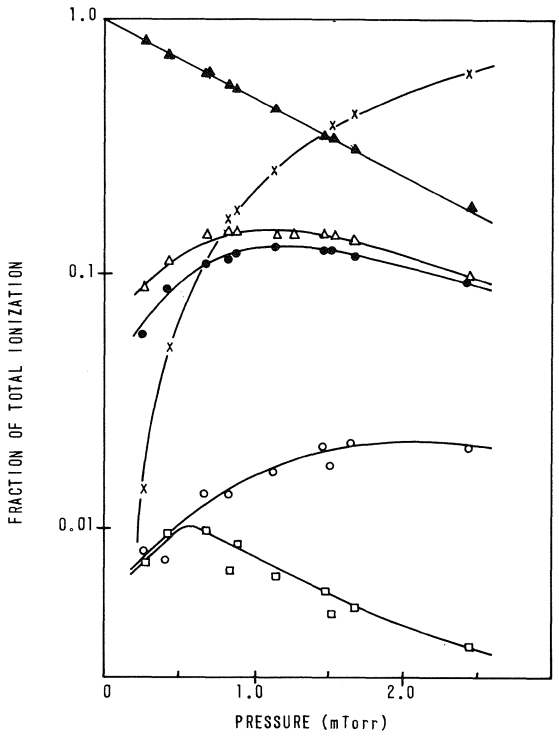


FIG. 1. Variation of the logarithm of the normalized ion abundances in DMSO with pressure at 298 K and 10 eV; ▲ $CH_3SOCH_3^+$ (*m/e* 78), △ $CH_3SO(CH_3SO)CH_3^+$ (*m/e* 141), ● $CH_3SOHCH_3^+$ (*m/e* 79), ○ $CH_3SO(CH_3)CH_3^+$ *m/e* 93, □ CH_3SO^+ (*m/e* 63) + $C_2H_5S^+$ (*m/e* 61), × $(CH_3SOCH_3)_2H^+$ (*m/e* 157).

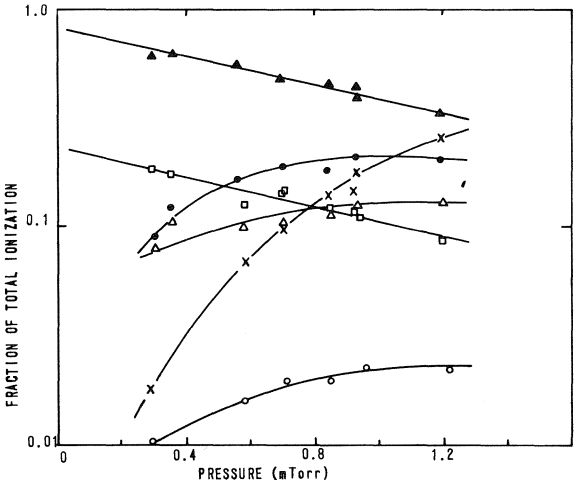


FIG. 2. Variation of the logarithm of the normalized ion abundances in DMSO with pressure at 298 K and 11.7 eV; ▲ $CH_3SOCH_3^+$ (*m/e* 78), ● $CH_3SOHCH_3^+$ (*m/e* 79), △ $CH_3SO(CH_3SO)CH_3^+$ (*m/e* 141), □ CH_3SO^+ (*m/e* 63) + $C_2H_5S^+$ (*m/e* 61), × $(CH_3SOCH_3)_2H^+$ (*m/e* 157), ○ CH_3SO-$(CH_3)CH_3$ (*m/e* 93).

Can. J. Chem. Downloaded from www.nrcresearchpress.com by 210.87.254.105 on 09/05/12
For personal use only.

of the lines for M^+ in Figs. 1 and 2 using the expression

$$\log I_{M^+}/\sum_i I_i = -kP\tau_{M^+}$$

where $I_{M^+}/\Sigma_i I_i$ is the fractional yield of the M^+ ions at a pressure P and τ_{M^+} is the average residence time of the M^+ ions in the source. Since the ion paths in the source are not well defined the value of τ_{M^+} was obtained by reference to a reaction with known rate constant. The disappearance of the molecular ion in propylene was measured and k was taken as 0.84×10^{-9} cm^3 molecule^{-1} s^{-1} at 10 eV and 0.68×10^{-9} cm^3 molecule^{-1} s^{-1} at 11.7 eV (9). $\tau_{M^+} = 1.36\tau_{C_3H_6^+}$, the correction factor being the square root of the ratio of molecular weights of DMSO and propylene.

The rate constant for the disappearance of the DMSO molecular ion is $1.0 \pm 0.1 \times 10^{-9}$ cm^3 molecule^{-1} s^{-1} (four determinations) at 10 eV and $0.9 \pm 0.1 \times 10^{-9}$ cm^3 molecule^{-1} s^{-1} (three determinations) at 11.7 eV. The error limits give the spread of the results. The non-dependence on ionizing energy is in agreement with the results of Peers and Muller (3) but their rate constant is higher by a factor of two (1.9×10^{-9} cm^3 molecule^{-1} s^{-1}). Such a large factor cannot be readily explained. Peers and Muller did not use a field-free source, the ions having a terminal kinetic energy of 0.71 eV, but it is expected that the rate constant will increase with decreasing ion kinetic energy for an exothermic reaction. The ICR value obtained by Nixon *et al.* (5) with 30 eV electrons, 2.14×10^{-10} cm^3 molecule^{-1} s^{-1}, appears to be too low. It is to be noted that on the graph showing typical kinetic data (Fig. 3 of ref. 5) the molecular ion constitutes less than 10% of total ionization at the shortest trapping time and the plot of log fractional yield of M^+ vs. time is decidedly non-linear.

The calculated ADO collision rate constant for M^+ is 2.5×10^{-9} cm^3 molecule^{-1} s^{-1} ($\alpha = 7.97 \times 10^{-24}$ cm^3 and $\mu_D = 4.11$ D). Our rate constant values show that reaction occurs with ~40% efficiency and therefore steric hindrance may play only a small role, if any, in the reaction.

A single experiment at 398 K using 11.7 eV photons yielded the same rate constant for the disappearance of M^+. The nature and yields of product ions were also not significantly changed.

(b) Product Ions at Low Pressure (0.3–3 mTorr)

The two major product ions at the lowest employable pressure are *m/e* 79, $CH_3SOHCH_3^+$ ($(M + 1)^+$) and *m/e* 141, $CH_3SO{\cdot}CH_3SOCH_3$ ($(2M - 15)^+$). Although the overall rate constant for the disappearance of M^+ appears independent of electronic excitation the relative yields of $(M + 1)^+$ and $(2M - 15)^+$ change with change of photon energy. The yield of $(2M - 15)^+$ decreases by roughly the same absolute amount that the initial yield of the molecular ion decreases in passing from 10 eV to 11.7 eV ionization energy. At the same time the yield of $(M + 1)^+$ increases. This behaviour suggests that none of the primary fragment ions produced at 11.7 eV leads to significant formation of $(2M - 15)^+$ and that electronic excitation of M^+ favours $(M+1)^+$ formation. This is consistent with the much higher relative yield of $(M + 1)^+$ observed when ionization is by electron impact with 30 eV electrons (5).

Nixon *et al.* (5) examined reaction [3] to determine whether the $(2M - 15)^+$ ion is formed in sufficiently large yield to serve as a methylsulfinium ion donor for analytical purposes, analogous to acetyl donation in acetone or 2,3-butanedione. They found that only 5% of the reactive collisons of M^+ lead to $(2M - 15)^+$. However, Fig. 1 shows that under present conditions, at the lowest pressure we employ, the methylsulfinylated product comprises 40% of total product, comparable with the 50% for self-acylation of 2,3-butanedione (10). With increasing pressure $(2M - 15)^+$ reacts further, by reaction [4] (5).

$$[4] \quad CH_3SO(CH_3SO)CH_3^+ + CH_3SOCH_3 \rightarrow (CH_3SOCH_3)_2H^+ + CH_2SO^{\cdot}$$

Since Nixon *et al.* (5) made observations only at times when most of M^+ had disappeared and since they were using 30 eV electrons for ionization, the small fraction of methylsulfinylated product observed by them is not surprising. We do still, however, concur with their conclusion that the utility of this ion as a chemical ionization reagent is severely limited, but this, under our conditions, is due to its rapid reaction with DMSO and not its low initial yield.

The failure to detect $(2M - 15)^+$ in the Quistor experiment cannot be, as suggested (6), that reaction [4] producing the proton bound dimer is endothermic for thermal ions since Figs. 1 and 2 clearly show that this reaction occurs. A more plausible explanation might be that the branching ratio for reactions [1] and [3] is dependent on ion kinetic energy as well as electronic excitation with [1] being favoured by the higher kinetic energies prevailing in the Quistor.

Very minor secondary ions at 10 eV are *m/e* 61 and 63. The yields are very low and only their sum is shown in Fig. 1. At 11.7 eV these ions are also primary fragment ions which are formed together with *m/e* 62. Measured as a composite peak they

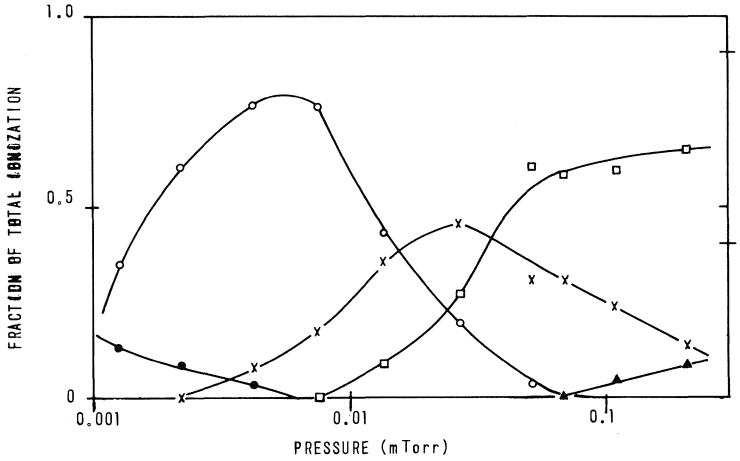


FIG. 3. Variation of the normalized ion abundances for the series $(CH_3SOCH_3)_nH^+$ at 10 eV and 298 K; values of n are ●*1*, ○*2*, × *3*, □*4*, and ▲*5*.

disappear with a rate constant very similar to that for the disappearance of the molecular ion (Fig. 2). The relative proportions of 61, 62, and 63 are 6/1/3, with a slight change in favour of *m/e* 63 at the highest pressures shown in Fig. 2.

The $(M+15)^+$ ion is present at both 10 and 11.7 eV and arises from the reaction of the molecular ion (4).

[5] $CH_3SOCH_3^+ + CH_3SOCH_3 \rightarrow CH_3SO(CH_3)CH_3^+ + CH_3SO^{\cdot}$

Its yield shows little dependence on photoionization energy.

(c) Product Ions at Higher Pressures (3–210 mTorr)

The major product ions in this pressure range belong to the series $(nM+1)^+$ with n = 2–5 which constitutes the progressive solvation of the proton. Figure 3 shows the relative yields of these ions at pressures up to 210 mTorr. Steric hindrance does not appear to be a factor in inhibiting solvation beyond $n = 2$ as has beeen suggested (5). It is probable that in the ICR experiments the pressure was not sufficient to observe the three body stabilization reactions for $n > 2$. The high yield of $(2M + 1)^+$ at low pressure shows that this ion is particularly stable. $(5M + 1)^+$ occurs at the limit of the mass range of the mass filter and its yield, although obviously small, is not accurately known. This ion, together with the $(4M + 1)^+$ ion, is completely absent at 210 mTorr when the temperature is raised to 398 K.

Two other ion series are present, corresponding to solvation of $(2M - 15)^+$ and $(M + 15)^+$. The maximum yield of any member of either series is less than 4% of total ionization. Most of the $(2M - 15)^+$ ions disappear via reaction [4] and are not solvated.

(d) Mixtures of DMSO with Water and Methanol

A separate inlet line was used to introduce a second gas into the ion chamber. With SF_6 (IP = 15.3 eV) the only effect observed with increasing total pressure up to 100 mTorr for a fixed small pressure of DMSO (< 2 mTorr) is a change in the yields of the product ions to those appropriate to a higher pressure of DMSO. No new ions are observed and the change in mass spectrum is due to an increase in ion reaction time.

Neither water nor methanol is ionized at 10 eV. Water behaves qualitatively in the same manner as SF_6. The only new product is $(CH_3SOCH_3 \cdot H_2O)^+$ which is in very low yield (< 0.5% total ionization). With D_2O the behaviour is very similar, there being a small $(CH_3SOCH_3 \cdot D_2O)^+$ peak and in addition an even smaller peak due to $(CH_3SOCH_3 \cdot H \cdot D_2O)^+$. At high D_2O pressures (> 50 mTorr) the $(M+1)^+$ and $(2M+1)^+$ peaks gradually change to $(M+2)^+$ and $(2M+2)^+$ as D replaces H. It is interesting that although this exchange occurs, essentially no mixed solvation is observed, even with water/DMSO ratios of 50:1. With methanol a prominent $(CH_3SOCH_3 \cdot H \cdot CH_3OH)^+$ peak constitutes 30% of total ionization in a mixture containing 0.3 mTorr DMSO and 60 mTorr methanol. With increasing DMSO pressure this fraction decreases and the yield constitutes only 2% of the total ionization at 2.1 mTorr DMSO.

The proton affinity of DMSO is 208.2 kcal mol^{-1} (11) so that proton transfer to water (PA 169 kcal mol^{-1}) or methanol (PA 182 kcal mol^{-1}) will not occur from $CH_3SOHCH_3^+$, which is formed only

Can. J. Chem. Downloaded from www.nrcresearchpress.com by 210.87.254.105 on 09/05/12
For personal use only.

via reaction [1]. The very limited mixed solvation of the $(2M + 1)^+$ ions is consistent with the relationship found between the hydrogen bond energies in $BH^+\cdots B_0$ and the proton affinity difference PA(B) − PA(B_0) where B and B_0 are gas phase bases (12). The maximum stabilization occurs when the difference in proton affinities is zero, in the present case when the second base is DMSO. Methanol, consistent with this thermodynamic argument, gives a greater yield of the mixed dimer than does water.

Acknowledgement

The authors thank the National Research Council of Canada for Financial Assistance.

1. J. C. Blais, M. Cottin, and B. Gitton. J. Chim. Phys. Physiochim. Biol. **67**, 1475 (1970).
2. J. C. Blais, M. Cottin, and B. Gitton. J. Chim. Phys. Physiochim. Biol. **68**, 737 (1971).
3. A. Mackenzie Peers and J. C. Muller. Int. J. Mass Spectrom. Ion Phys. **16**, 321 (1975).
4. T. McAllister. Int. J. Mass Spectrom. Ion Phys. **25**, 353 (1977).
5. W. B. Nixon, W. S. Woodward, M. M. Bursey, and J. D. Henion. Int. J. Mass. Spectrom. Ion Phys. **26**, 115 (1978).
6. J. E. Fulford, J. W. Dupuis, and R. E. March. Can. J. Chem. **56**, 2324 (1978).
7. J. E. Kronberg and J. A. Stone. Int. J. Mass Spectrom. Ion Phys. **24**, 373 (1977).
8. R. Gordon, Jr., R. E. Rebbert, and P. Ausloos. Natl. Bur. Stand. (U.S.) Tech. Note 496 (1969).
9. L. W. Sieck and P. Ausloos. J. Res. Natl. Bur. Stand. **76A**, 253 (1972).
10. J. R. Hass, W. B. Nixon, and M. M. Bursey. Anal. Chem. **49**, 1071 (1977).
11. P. Kebarle. Ann. Rev. Phys. Chem. **28**, 445 (1977).
12. W. R. Davidson, J. Sunner, and P. Kebarle. J. Am. Chem. Soc. **101**, 1675 (1979).

Can. J. Chem. Downloaded from www.nrcresearchpress.com by 210.87.254.105 on 09/05/12
For personal use only.

Binding sites between palladium(II) and nucleosides or nucleotides and crystal structure of [Pd(diethylenetriamine)(guanosine)]$(ClO_4)_2$

F. D. ROCHON, P. C. KONG, B. COULOMBE, AND R. MELANSON

Département de chimie, Université du Québec à Montréal, C.P. 8888, Montréal (Qué.), Canada H3C 3P8

Received August 23, 1979

F. D. ROCHON, P. C. KONG, B. COULOMBE, and R. MELANSON. Can. J. Chem. **58**, 381 (1980).

The interactions between [Pd(dien)Cl]Cl and some nucleosides and nucleotides were studied by nmr. The binding site of guanosine, guanosinemonophosphoric acid, xanthosine, and inosine is N(7). Cytidine is coordinated to palladium through N(3). Adenosinemonophosphate acts as a bidentate, binding two different palladium atoms at N(1) and N(7).

The crystal structure of [Pd(dien)(guanosine)]$(ClO_4)_2$ has been determined by X-ray diffraction. The crystals are orthorhombic, space group $P2_12_12_1$, with $a = 13.422$, $b = 14.587$, $c = 12.432$, and $Z = 4$. The structure was refined by block-diagonal least-squares analysis to a conventional R factor of 0.047 and a weighted $R_w = 0.043$. The coordination around the palladium atom is square planar. Guanosine is bonded to palladium through N(7). The planar purine ring makes an angle of 63.4° with the palladium coordination plane. The structure is stabilized by hydrogen bonding.

F. D. ROCHON, P. C. KONG, B. COULOMBE et R. MELANSON. Can. J. Chem. **58**, 381 (1980).

La réaction entre [Pd(dien)Cl]Cl et plusieurs nucléosides et nucléotides a été étudiée par rmn. Guanosine, l'acide guanosinemonophosphorique, xanthosine et inosine sont liés au palladium par N(7). Cytidine est coordinée au palladium par N(3). L'adénosinemonophosphate agit comme un bidentate, se liant à deux atomes de palladium différents par N(1) et N(7).

La structure cristalline de [Pd(dien)(guanosine)]$(ClO_4)_2$ a été déterminée par diffraction des rayons-X. Les cristaux appartiennent au groupe d'espace orthorhombique $P2_12_12_1$, avec $a = 13.422$, $b = 14.587$, $c = 12.432$ et $Z = 4$. Les coordonnées atomiques et les facteurs thermiques anisotropes ont été affinés par moindres-carrés (matrice diagonale) jusqu'à $R = 0.047$ et $R_w = 0.043$. La coordination autour de l'atome de palladium est plane. La guanosine est liée au palladium par N(7). Le plan du groupement purine fait un angle de 63.4° avec le plan de coordination du palladium. La structure cristalline est stabilisée par des ponts hydrogènes.

Can. J. Chem. Downloaded from www.nrcresearchpress.com by 210.87.254.42 on 09/05/12
For personal use only.

Introduction

The interaction of metals with nucleosides and nucleotides is of great biological importance. Recently, our work has been centered around platinum complexes because of their antitumour activity. The present work with palladium was undertaken in order to see if Pd(II) reacts in a way similar to Pt(II) with nucleosides and nucleotides. It is well known that Pd(II) complexes undergo ligand-exchange reactions much faster that Pt(II) complexes (1).

The interactions between [Pd(dien)Cl]Cl (dien = diethylenetriamine) and guanosine, guanosinemonophosphoric acid, xanthosine, inosine, cytidine, and adenosinemonophosphate were studied by nmr and compared to the results obtained with other palladium and platinum complexes (2–6). The reactions of the platinum and palladium complexes were found identical except for the faster rates of the palladium compounds.

A crystal structure determination was performed on one of the products. Since the chloro derivative did not give suitable crystals, the perchlorate complex was analysed by X-ray diffraction. Therefore in the second part of the publication we report the molecular and crystal structure of [Pd(dien)(guanosine)]$(ClO_4)_2$.

PART A

Experimental

[Pd(dien)Cl]Cl was synthesized according to the method described by Basolo, Gray, and Pearson (1).

The nucleosides and nucleotides were purchased from Raylo Chemicals Ltd.

The nmr spectra were measured on a Perkin-Elmer R-12 spectrometer at 27°C with DSS used as internal reference. All the solutions were stable since the spectra did not change with time.

Results and Discussion

The nmr spectra of the solutions formed from the interaction of [Pd(dien)Cl]Cl with different nucleosides and nucleotides are shown on Table 1. The interpretation of the spectra was based on several papers published on the nmr spectra of platinum and palladium nucleoside and nucleotide complexes (2–6).

Guanosine is insoluble in water but it reacts slowly with [Pd(dien)Cl] in D_2O to give a soluble compound [Pd(dien)(guanosine)]Cl. The downfield nmr spectrum consists of a doublet caused by H(1′) and a singlet caused by H(8). The signal of H(8) in $[Pd(dien)(guanosine)]^{2+}$ is more shifted downfield than H(1′) indicating that H(8) is close to Pd. Therefore we can conclude that the binding site of guanosine is N(7). This conclusion was confirmed later by an X-ray structure determina-

0008-4042/80/040381-06$01.00/0
©1980 National Research Council of Canada/Conseil national de recherches du Canada

TABLE 1. Nuclear magnetic resonance spectra of the ligands and palladium complexes. The values are in δ(ppm) with DDS used as internal standard

Compound	Solvent	δ				
		H(2)	H(5)	H(6)	H(8)	H(1′)
Guo	DMSO				8.06	5.80
$[Pd(dien)(Guo)]Cl_2$	D_2O				8.42	5.97
Guo MPA	D_2O				8.85	6.05
$[Pd(dien)(Guo\ MPA)]Cl_2$	D_2O				8.46	6.00
Xao	DMSO				8.02	5.85
$[Pd(dien)(Xao)]Cl_2$	D_2O				8.37	5.93
Ino	D_2O	8.26			8.38	6.11
$[Pd(dien)(Ino)]Cl_2$	D_2O	8.42			8.87	6.18
Cyt	D_2O		6.10	7.93		5.95
$[Pd(dien)(Cyt)]Cl_2$	D_2O		6.15	7.98		5.98
Ado MPD	D_2O	8.19			8.67	6.17
[Pd(dien)Cl]Cl + Ado MPD (1:1)	D_2O	8.39, 8.69, 8.86			9.35 (wide)	6.24 (wide)
(1:2)	D_2O	8.38, 8.75, 8.88			9.40 (wide)	6.22 (wide)
(1:3)	D_2O	8.92			9.41	6.23
Ado MPD (d_8)	D_2O	8.14				6.08
[Pd(dien)Cl]Cl + Ado MPD (d_8) (1:1)	D_2O	8.35, 8.71, 8.85				6.18 (wide)
(1:2)	D_2O	8.89 (wide)				6.22 (wide)
(1:3)	D_2O	8.91				6.23

tion of [Pd(dien)(guanosine)]$(ClO_4)_2$ (Part B of this publication). The experiment was repeated with guanosine 5′-monophosphoric acid (GuaMPA). Again the signal of H(1′) for the nucleotide and the complexed nucleotide is at about the same position, while the signal of H(8) is approximately at the same position as H(8) of $[Pd(dien)(guanosine)]^{2+}$ indicating that the binding site is N(7). But contrary to guanosine, this shift is upfield, since in the free ligand GuaMPA, the hydrogen ions interact with the nitrogen atoms of the base, causing a H(8) shift. This shift is pH-dependent as shown by Lim and Martin (4).

Since xanthosine is insoluble in D_2O, its reaction with [Pd(dien)Cl]Cl is slow. The nmr spectrum shows a reaction similar to guanosine. The signal of H(1′) is shifted downfield by 0.1 ppm while the signal of H(8) is shifted by 0.4 ppm indicating that N(7) is the binding site of xanthosine in [Pd(dien)(xanthosine)]Cl_2.

Inosine is soluble in D_2O. Its reaction with [Pd(dien)Cl]Cl is rapid. Table 1 shows that the signal of H(1′) is shifted by 0.07 ppm, the signal of H(2) by 0.17 ppm and H(8) by 0.51 ppm. Therefore the binding site of inosine in [Pd(dien)(inosine)]Cl_2 is again N(7).

Cytidine is slightly soluble in D_2O and reacts with [Pd(dien)Cl]Cl to give [Pd(dien)(cytidine)]Cl_2. The nmr spectrum of cytidine has already been published in DMSO (7). The signal of H(5) is a doublet close to the signal of H(1′) while the signal of H(6) is also a doublet at about 7.93 ppm. The signals of the three protons in [Pd(dien)(cytidine)]Cl_2 are shifted downfield by 0.03–0.05 ppm indicating that the binding site is far from H(1′), H(5), and H(6). N(3) was found to be the binding site in several platinum and palladium compounds (2, 6, 8). Therefore we can assume that N(3) is also the binding site of cytidine in [Pd(dien)(cytidine)]Cl_2.

Adenosine is not very soluble in D_2O. Therefore the reaction was studied with adenosine 5′ monophosphate disodium salt (AdoMPD). The reaction between AdoMPD and [Pd(dien)Cl]Cl was studied in 1:1, 1:2, and 1:3 proportions. In order to assign the signals of H(2) and H(8), AdoMPD was deuterated at H(8), and its reaction with [Pd(dien)(Cl)] was also studied by nmr. The nmr spectra are shown in Table 1. In 1:1 and 1:2 proportions the signals of H(1′), H(2), and H(8) were large, showing many peaks. When the proportion of Pd/ligand was 3:1, the signals were normal, that is a doublet for H(1′) and two singlets for H(2) and H(8). The shift of H(1′) in the complexed ligand is 0.06 ppm, while H(2) is shifted by 0.73 ppm and H(8) by 0.74 ppm. From these observations, we can conclude that AdoMPD acts as a bidentate, binding

Can. J. Chem. Downloaded from www.nrcresearchpress.com by 210.87.254.42 on 09/05/12
For personal use only.

Can. J. Chem. Downloaded from www.nrcresearchpress.com by 210.87.254.42 on 09/05/12
For personal use only.

two different atoms of palladium at N(1) and at N(7). The same conclusion was reached for the platinum analogue (2).

PART B

Experimental

[Pd(dien)(guanosine)]$(ClO_4)_2$ was prepared by the method already described for the platinum analogue (9).

A set of precession photographs indicated the $P2_12_12_1$ space group. The cell parameters were calculated by least-squares refinement of the setting angles of 15 independent peaks centered on a Syntex P$\bar{1}$ diffractometer using graphite monochromatized MoKA radiation.

Crystal Data

$PdCl_2C_{14}H_{26}N_8O_{13}$ mw = 691.71

Orthorhombic $P2_12_12_1$, a = 13.422(13), b = 14.587(7), c = 12.432(11) Å, Z = 4, V = 2434(4) Å^3, D_m = 1.89(2) g cm^{-3} (flotation), D_x = 1.887 g cm^{-3}, λMoKα = 0.71069 Å, μMoKα = 10.54 cm^{-1}, and T = 22°C.

Collection and Reduction of Intensity Data

The intensity data were collected from a crystal measuring about 0.3 × 0.3 × 0.2 mm and having approximately 15 faces. A total of 4043 MoKα independent reflections were measured up to a 2θ value of 60°. During the data collection, three standard reflections were measured after every 47 reflections as a test on crystal and instrument stability. No systematic changes were observed and the intensity fluctuations were within ±2%. The reflections (3234) for which the intensity was greater than 2.5σ(I) were considered as observed. The standard deviation σ(I) was calculated as already described (10). The data were corrected for the Lorentz and polarization effects. The scattering factors of Cromer and Waber (11) were used for palladium chlorine, oxygen, nitrogen, and carbon, those of Stewart *et al.* (12) were used for hydrogen. The anomalous dispersion terms (13) of palladium and chlorine were included in the calculations.

Structure Determination

The position of the palladium atom was easily located from the three-dimensional Patterson map. The positions of all the other atoms, except the hydrogen atoms, were obtained by structure factor and Fourier map calculations. The refinement of the parameters were carried out by block-diagonal least-squares methods. In the early stages of refinement, unit weight was assigned to all observed reflections. Later individual weights $1/w = a + bF_o + cF_o^2$ were calculated. The constants of the equation were adjusted to make the distribution of $w|\Delta F|^2$ almost constant with respect to $|F_o|$ and sin θ/λ (a = 12.30, b = −0.182, and c = 0.00095). The hydrogen atoms in the diethylenetriamine ligand and on the carbon atoms and on N(1) in the guanosine moiety were fixed at their calculated position[1] (C—H distance = 0.95 Å and N—H distance = 0.85 Å) and assigned isotropic thermal parameters of 6.0 Å^2. The refinement of the scale factor, the coordinates, and anisotropic temperature factors of all the non-hydrogen atoms converged to $R = \sum ||F_o| - |F_c|| / \sum |F_o| = 0.047$ and $R_w = [\sum w(|F_o| - |F_c|)^2 / \sum w|F_o|^2]^{1/2} = 0.043$. The final difference Fourier map did not show peaks higher than ±0.4 e Å^{-3}. Attempts to find on the final difference Fourier map the hydrogen atoms that could not be calculated were not successful. The torsion angles within the ribose segment confirmed the expected D-configuration of the molecule. The R factor for the other enantiomorphic structure was higher (0.050) indicating that the coordinates of Table 2 correspond to the absolute structure.

The calculations were carried out with a Cyber 73 computer and the programs used have already been described (10). A table of observed and calculated structure factors is available.[1]

TABLE 2. Final structure parameters (× 10^4). The estimated standard deviations are given in parentheses

Atom	x	y	z
Pd	−1866.8(3)	−1189.4(3)	−1369.3(4)
Cl(1)	−925(1)	−1263(1)	1430(2)
Cl(2)	−9(1)	−4136(1)	−1650(1)
O(1)	−1082(6)	−2143(5)	970(7)
O(2)	−443(5)	−1372(5)	2437(5)
O(3)	−317(6)	−777(5)	724(6)
O(4)	−1844(5)	−829(6)	1556(6)
O(5)	−318(5)	−4138(4)	−2745(5)
O(6)	−1994(3)	−2119(3)	−3853(4)
O(7)	934(5)	−4443(8)	−1557(6)
O(8)	−596(8)	−4755(8)	−1101(7)
O(9)	−139(10)	−3305(5)	−1191(8)
O(1′)	2323(3)	−942(3)	−1354(4)
O(2′)	2958(3)	−1732(4)	−3982(4)
O(3′)	4424(3)	−1412(3)	−2568(4)
O(5′)	2514(5)	907(4)	−2152(6)
N(1)	−588(4)	−2541(4)	−4738(4)
N(2)	782(4)	−3042(5)	−5728(5)
N(3)	1054(4)	−2291(4)	−4114(4)
N(4)	−1849(5)	201(4)	−1346(5)
N(5)	−3183(4)	−1045(4)	−655(4)
N(6)	−2217(4)	−2535(4)	−1347(6)
N(7)	−549(4)	−1400(3)	−2102(4)
N(9)	1068(4)	−1531(3)	−2409(4)
C(1)	−2732(7)	533(6)	−772(7)
C(2)	425(5)	−2608(5)	−4839(6)
C(3)	−3545(6)	−127(6)	−951(8)
C(4)	597(4)	−1910(4)	−3276(5)
C(5)	−403(4)	−1823(4)	−3096(5)
C(6)	−1085(4)	−2139(4)	−3875(5)
C(7)	−3771(5)	−1859(7)	−924(7)
C(8)	342(4)	−1244(5)	−1738(5)
C(9)	−3156(7)	−2660(6)	−770(7)
C(1′)	2146(4)	−1508(4)	−2236(5)
C(2′)	2723(4)	−1107(5)	−3163(5)
C(3′)	3655(4)	−748(4)	−2604(5)
C(4′)	3274(4)	−483(4)	−1492(5)
C(5′)	3121(7)	516(5)	−1337(7)

Results and Discussion

The refined atomic parameters are listed in Table 2. A list of the anisotropic temperature factors is available.[1] A labelled diagram of the ion [Pd(dien)(guanosine)]$^{2+}$ is shown on Fig. 1. (The size of the ellipsoids corresponds to a 50% probability.) The bond lengths within the ion are shown on Fig. 2, and the bond angles on Fig. 3.

As expected, guanosine is bonded to palladium through N(7). The coordination around the palladium atom is square planar. The deviations of the

[1]Lists of structure factors, calculated hydrogen positions, and anisotropic thermal parameters are available, at a nominal charge, from the Depository of Unpublished Data, CISTI, National Research Council of Canada, Ottawa, Ont., Canada K1A 0S2.

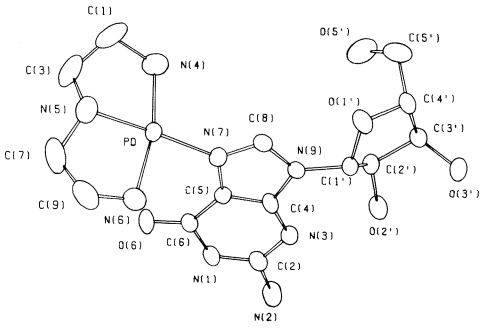


FIG. 1. Labelled diagram of the $[Pd(dien)(guanosine)]^{2+}$ ion.

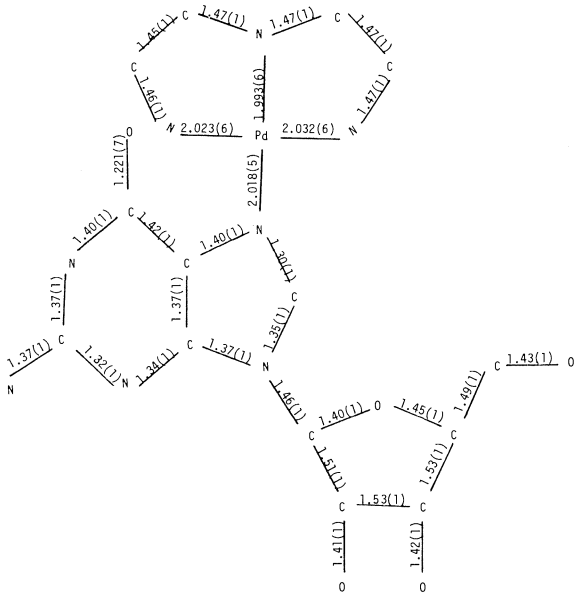


FIG. 2. Bond lengths within the $[Pd(dien)(guanosine)]^{2+}$ ion.

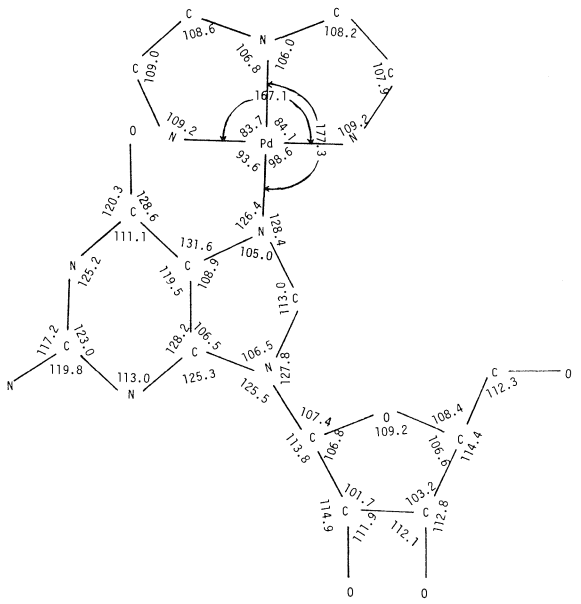


FIG. 3. Bond angles within the $[Pd(dien)(guanosine)]^{2+}$ ion.

TABLE 3. Torsion angles in the ribose group*

Atoms	Angle (deg)	Assignment
O(1′)—C(1′)—N(9)—C(8)	−13	ϕ_{CN} (*anti*)
O(1′)—C(1′)—N(9)—C(4)	171	
O(1′)—C(4′)—C(5′)—O(5′)	−66	ϕ_{OO} (*gauche*)
C(3′)—C(4′)—C(5′)—O(5′)	52	ϕ_{OC} (*gauche*)
C(2′)—C(1′)—O(1′)—C(4′)	−26	τ_0
C(3′)—C(2′)—C(1′)—O(1′)	36	τ_1
C(4′)—C(3′)—C(2′)—C(1′)	−31	τ_2
O(1′)—C(4′)—C(3′)—C(2′)	17	τ_3
C(1′)—O(1′)—C(4′)—C(3′)	5	τ_4
O(2′)—C(2′)—C(3′)—O(3′)	−33	

*The conventions suggested by Sundaralingam (19) and Trueblood and co-workers (20, 21) have been used.

five atoms from the weighted best plane are: Pd, −0.0009; N(5), 0.002; N(4), 0.071; N(6), 0.080, and N(7), 0.011 Å. The angles around palladium are close to the expected 90 and 180° but there are some distortions due to a slight strain caused by the tridentate ligand. The N(6)—Pd—N(5) and N(5)—Pd—N(4) angles (83.7 and 84.1°) are smaller than the N(6)—Pd—N(7) and N(7)—Pd—N(4) angles (93.6 and 98.6°). The N(4)—Pd—N(6) angle (167.1°) is also smaller than expected. The Pd—N bond lengths (1.99–2.03 Å) are normal and agree well with the published data (14, 15).

The purine ring is planar. The weighted best plane was calculated through the nine atoms. The deviations from this plane are: N(7), −0.015; N(1), −0.002; N(3), −0.005; N(9), 0.013; C(2), −0.016; C(4), 0.007; C(5), 0.001; C(6), 0.023; and C(8), −0.005 Å. The deviations of the substituents on the ring are as follows: N(2), −0.070; O(6), 0.022, and C(1′), −0.038 Å (esd = 0.005 to 0.008 Å). Since N(2) plays an important role in the hydrogen bonding system of the crystal, it might explain the slight deviation of N(2) from the purine plane. The latter plane makes an angle of 63.4° with the palladium coordination plane.

The bond lengths in the purine ring vary from 1.30 to 1.42 Å. They are similar to those found in guanosine rings mentioned in a review by Voet and Rich (16). They are identical to those found in guanosine dihydrate (17) and in [Pt(dien)-(guanosine)]$(ClO_4)_2$ (9). The bond angles also agree well with the published results mentioned above. The bond angles within the five member ring vary from 105 to 113°. In the six-membered ring, the range is from 111 to 128°. As pointed out by Singh (18) the internal ring angle at N(1) (125°) is greater than at N(3) (113°), the latter having no extra-annular attachment.

The glycosyl bond (1.46 Å) is normal (9, 16, 17).

Can. J. Chem. Downloaded from www.nrcresearchpress.com by 210.87.254.42 on 09/05/12
For personal use only.

Can. J. Chem. Downloaded from www.nrcresearchpress.com by 210.87.254.42 on 09/05/12
For personal use only.

TABLE 4. Bond distances and bond angles in ClO_4^-

Bond	Distance (Å)	Bond	Distance (Å)
Cl(1)—O(1)	1.423(8)	Cl(2)—O(5)	1.432(6)
Cl(1)—O(2)	1.425(7)	Cl(2)—O(7)	1.348(8)
Cl(1)—O(3)	1.398(8)	Cl(2)—O(8)	1.384(8)
Cl(1)—O(4)	1.398(8)	Cl(2)—O(9)	1.355(8)
Bonds	**Angle (deg)**	**Bonds**	**Angle (deg)**
O(1)—Cl(1)—O(2)	109.0(4)	O(5)—Cl(2)—O(7)	110.8(5)
O(1)—Cl(1)—O(3)	106.9(5)	O(5)—Cl(2)—O(8)	108.0(5)
O(1)—Cl(1)—O(4)	108.9(5)	O(5)—Cl(2)—O(9)	111.7(5)
O(2)—Cl(1)—O(3)	110.5(4)	O(7)—Cl(2)—O(8)	106.0(6)
O(2)—Cl(1)—O(4)	110.6(4)	O(7)—Cl(2)—O(9)	112.5(6)
O(3)—Cl(1)—O(4)	110.9(5)	O(8)—Cl(2)—O(9)	107.5(6)

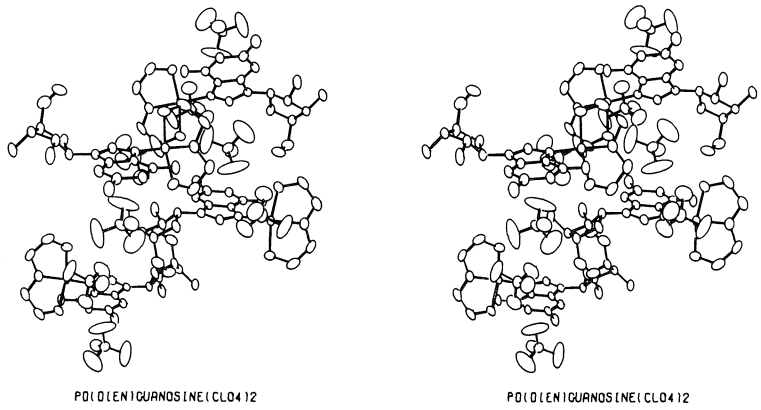


FIG. 4. Stereoscopic diagram of the packing in the [Pd(dien)(guanosine)]$(ClO_4)_2$ crystal.

TABLE 5. Distances and angles involved in hydrogen bonds

Atoms	Transformation (on third atom)	Distance (Å)	Atoms	Angle (deg)
O(2′)—H...N(3)	x, y, z	2.687(7)	C(2′)—O(2′)...N(3)	91.6(4)
O(3′)—H...O(1)	$x+\frac{1}{2}, -y-\frac{1}{2}, -z$	2.988(9)	C(3′)—O(3′)...O(1)	109.9(4)
N(2)—H...O(3′)	$x-1, -y-\frac{1}{2}, -z-1$	2.917(8)	C(2)—N(2)...O(3′)	120.1(5)
N(2)—H...O(6)	$x+\frac{1}{2}, -y-\frac{1}{2}, -z-1$	3.041(7)	C(2)—N(2)...O(6)	116.6(5)
N(1)—H...O(2′)	$x-1, -y-\frac{1}{2}, -z-1$	2.740(7)	C(6)—N(1)...O(2′)	105.9(4)
			C(2)—N(1)...O(2′)	128.7(4)
O(5′)—H...O(5)	$-x, \frac{1}{2}+y, -z-\frac{1}{2}$	2.952(9)	C(5′)—O(5′)...O(5)	126.4(5)
Possible hydrogen bonds involving the dien ligand				
N(4)—H...O(7)	$-x, \frac{1}{2}+y, -z-\frac{1}{2}$	2.946(10)	Pd—N(4)...O(7)	99.7(3)
			C(1)—N(4)...O(7)	135.6(5)
N(6)—H...O(5′)	$-x, y-\frac{1}{2}, -z-\frac{1}{2}$	2.978(9)	Pd—N(6)...O(5′)	140.0(3)
			C(9)—N(6)...O(5′)	95.8(5)
N(6)—H...O(9)	x, y, z	3.016(14)	Pd—N(6)...O(9)	98.5(3)
			C(9)—N(6)...O(9)	135.9(5)

The angles in the ribose ring are close to the tetrahedral values. O(1′), C(1′), C(3′), and C(4′) are coplanar and C(2′) is 0.54 Å distant from that plane, on the same side as C(5′) and N(9). This corresponds to the C(2′) *endo* conformation. The dihedral angle between the purine and the ribose planes is 30.4°. The torsion angles within the ribose group are listed in Table 3. The conventions suggested by Sundaralingam (19) and Trueblood and co-workers (20, 21) have been used. The torsion angle O(1′)C(1′)N(9)C(8), ϕ_{CN}, is −13° and defines an *anti* conformation about the glycosidic bond. The

C(5′)—O(5′) is in a *gauche–gauche* conformation relative to the ribose group: $\phi_{OO} = -66°$ and $\phi_{OC} = 52°$.

The bond lengths and the bond angles in the perchlorate ions are shown in Table 4. The distances vary from 1.35 to 1.43 Å. The bond angles are close to the tetrahedral values (107–112°).

A stereoscopic packing diagram is shown on Fig. 4. Base stacking plays an important role in most nucleoside crystal structures. In this structure, as in [Pt(dien)(guanosine)]$(ClO_4)_2$ (9), base stacking is not an important packing factor since the perchlorate ions are located between the bases. Hydrogen bonding is probably the predominant packing effect in this structure. The most important hydrogen bonds are listed in Table 5. All the hydrogen atoms attached to oxygen and nitrogen atoms in the guanosine group are involved in the hydrogen bonding system. O(2′)—H of each ribose group is intramolecularly hydrogen bonded to N(3). The other two hydroxyl groups O(3′)—H and O(5′)—H are involved in hydrogen bonds with the perchlorate ions. N(1) and N(2) form intermolecular hydrogen bonds, N(1)—H with O(2′) and N(2)$\begin{matrix}\diagup\\\diagdown\end{matrix}$N with both O(3′) and O(6). The role of the dien ligand in the hydrogen bonding system is doubtful. The most probable hydrogen bonds are shown on Table 5. The longer distances and the less favourable angles seem to suggest that these bonds are weaker.

Acknowledgments

The authors are grateful to the Natural Sciences and Engineering Research Council of Canada and to the Cancer Research Society Inc. for financial support, and to Matthey Bishop, Inc. for the loan of potassium chloroplatinite.

1. F. Basolo, H. B. Gray, and R. G. Pearson. J. Am. Chem. Soc. **82**, 4200 (1960).
2. P. C. Kong and T. Theophanides. Inorg. Chem. **13**, 1981 (1974).
3. P. C. Kong and F. D. Rochon. J. Chem. Soc. Chem. Commun. 599 (1975).
4. M. C. Lim and R. B. Martin. J. Inorg. Nucl. Chem. **38**, 1915 (1976).
5. P. C. Kong and T. Theophanides. Inorg. Chem. **13**, 1167 (1974).
6. G. Pneumatikakis, N. Hadjiliadis, and T. Theophanides. Inorg. Chem. **17**, 915 (1978).
7. L. S. Kan and N. C. Li. J. Am. Chem. Soc. **92**, 4823 (1970).
8. R. Melanson and F. D. Rochon. Inorg. Chem. **17**, 679 (1978).
9. R. Melanson and F. D. Rochon. Can. J. Chem. **57**, 57 (1979).
10. R. Melanson and F. D. Rochon. Can. J. Chem. **53**, 1139 (1975).
11. D. T. Cromer and J. T. Waber. Acta Crystallogr. **18**, 104 (1965).
12. R. T. Stewart, E. R. Davidson, and W. T. Simpson. J. Chem. Phys. **42**, 3175 (1965).
13. D. T. Cromer. Acta Crystallogr. **18**, 17 (1965).
14. N. B. Pahor, M. Calligaris, and L. Randaccio. J. Chem. Soc. Dalton Trans. 725 (1976).
15. G. M. Intille, C. E. Pfluger, and W. A. Baker, Jr. J. Cryst. Mol. Struct. **3**, 47 (1973); Cryst. Struct. Commun. **2**, 217 (1973).
16. D. Voet and A. Rich. Prog. Nucl. Acid Res. Mol. Biol. **10**, 183 (1970).
17. V. Thewalt, C. E. Bugg, and R. E. Marsh. Acta Crystallogr. B, **26**, 1089 (1970).
18. C. Singh. Acta Crystallogr. **19**, 861 (1965).
19. M. Sundaralingam. Biopolymers, **7**, 821 (1969).
20. J. Donohue and K. N. Trueblood. J. Mol. Biol. **2**, 363 (1960).
21. E. Shefter and K. N. Trueblood. Acta Crystallogr. **18**, 1067 (1965).

Can. J. Chem. Downloaded from www.nrcresearchpress.com by 210.87.254.42 on 09/05/12
For personal use only.

Asymmetric reduction of α,β-unsaturated iminium salts with 1,4-dihydronicotinamide sugar pyranosides

NAOMICHI BABA, TAKETOSHI MAKINO, JUN'ICHI ODA, AND YUZO INOUYE

Institute for Chemical Research, Kyoto University, Uji, Kyoto 611, Japan

Received August 31, 1979

NAOMICHI BABA, TAKETOSHI MAKINO, JUN'ICHI ODA, and YUZO INOUYE. Can. J. Chem. **58**. 387 (1980).

3;3,5-Trimethyl-2-cyclohexylidene iminium salts were reduced with 1,4-dihydronicotinamide sugar pyranosides to give optically active 3,3,5-trimethylcyclohexanone in enantiomeric excess ranging over 3–31%. The product stereochemistry changed sensitively with structural variation (including anomers, epimers, and deacetylation) of sugar residues. The reduction by more simplified chiral models, N^1-(1′*S*,2′*S*)-2′-hydroxy- or acetoxycyclohexyl-1,4-dihydronicotinamide revealed that operation of the functional groups on the sugar moiety is not merely steric in nature for induction of chirality in the product.

NAOMICHI BABA, TAKETOSHI MAKINO, JUN'ICHI ODA et YUZO INOUYE. Can. J. Chem. **58**, 387 (1980).

Les sels triméthyl-3,3,5 cyclohexylidène-2 iminium sont réduits par les pyrannosides du dihydro-1,4 nicotinamide pour donner la triméthyl-3,3,5 cyclohexanone optiquement active comportant un excès énantiomère allant de 3 à 31%. La stéréochimie du produit change d'une façon sensible avec les variations de structure (incluant les anomères les épimères et la déacétylation) des sucres. La réduction par des modèles chiraux plus simples N^1-(1′*S*,2′*S*)hydroxy-2′ ou acétoxycyclohexyldihydro-1,4 nicotinamides révèle que l'action des groupements fonctionnels sur les sucres n'est pas simplement de nature stérique lors de l'induction de la chiralité dans le produit.

[Traduit par le journal]

Can. J. Chem. Downloaded from www.nrcresearchpress.com by 210.87.254.5 on 09/05/12
For personal use only.

Introduction

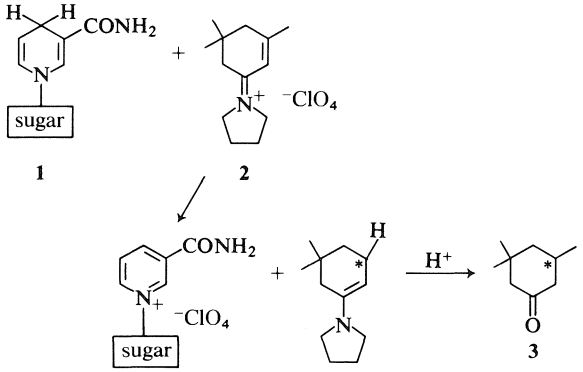
In recent work directed toward co-enzyme models for NADH dependent dehydrogenase reductions, simulation of their salient stereospecificity by the use of simplified chiral NADH models (1) and chiral environment (2) has become one of the major interests for delving into a new method for asymmetric synthesis as well as studying the origin of stereospecificity of enzyme reactions. Pandit *et al.* (3) found that iminium salts could be potential substrates or direct hydrogen acceptors in non-enzymic NADH model reactions. We noticed that a similar reduction of iminium salt derived from prochiral α,β-unsaturated carbonyl compounds was effected by the use of simple chiral NADH models to give an optically active ketone bearing the chiral center at the β-position. This approach is worthy of note since there has been so far scanty precedent for asymmetric synthesis of optically active ketones with the chiral center at the β-position. Such compounds have been obtained conventionally by resolution (4). From this view, even partial asymmetric synthesis thus attained will greatly facilitate the first crystallization in resolution processes which sometimes impose difficulties.

In the present paper, we describe the reduction of prochiral iminium salt **2** with 1,4-dihydronicotinamide sugar pyranosides **1** as NADH models to afford an optically active ketone, 3,3,5-trimethylcyclohexanone **3**. The factors governing the stereochemistry of the product are discussed with respect to structural changes in the model compounds and substrate. Direct hydrogen transfer from **1** to **2** was established by the use of *N*-benzyl-4,4-dideuterionicotinamide and the reduction constitutes a sort of nucleophilic 1,4-addition reaction (formally a hydride attack in the present case).

Results and Discussion

Substrate Modification

Results on the reduction of substrate **2** with 1,4-dihydronicotinamide α- and β-D-glucopyranosides were reported in our previous communication (1*d*) and the data are in part reproduced in Table 2 for convenience. The pyrrolidine moiety and perchlorate anion of substrate **2** can easily be replaced by other amines and anions. To examine the dependence of product stereochemistry on substrate



SCHEME 1

0008-4042/80/040387-06$01.00/0

©1980 National Research Council of Canada/Conseil national de recherches du Canada

TABLE 1. Enantiomeric excess and configuration of the ketone **3** in the reduction of **4–9**

Run	Substrate	Pyranoside	$[\alpha]_D^{25}$/°(*c*, *n*-Hexane)	e.e.[a] (%)	Configuration
1	**4**	**10**-OAc	−0.29 ± 0.04 (4.54)	3	*R*
2	**4**	**10**-OH	+0.75 ± 0.06 (3.19)	7	*S*
3	**5**	**10**-OAc	+0.29 ± 0.08 (2.45)	3	*S*
4	**5**	**10**-OH	+0.80 ± 0.08 (2.51)	8	*S*
5	**6**	**10**-OH	+2.60 ± 0.14 (1.35)	25	*S*
6	**7**	**10**-OH	+2.47 ± 0.16 (1.22)	24	*S*
7	**8**	**10**-OH	+2.83 ± 0.09 (2.26)	28	*S*
8	**9**	**10**-OAc	0	0	—
9	**9**	**10**-OH	−1.21 ± 0.13 (1.49[b])	9[c]	*S*

[a]Based on the reported maximum rotation (16) of 3,3,5-trimethylcyclohexanone, $[\alpha]_D^{25}$ 10.3° (*n*-hexane).
[b]Chloroform was used as solvent.
[c]Based on the reported maximum rotation (15) of 3-methylcyclohexanone, $[\alpha]_D^{25}$ 14.2° (chloroform).

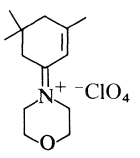
TABLE 2. Enantiomeric excess and configuration of the ketone **3** from the reduction with **10–22**

Run	1,4-Dihydronicotinamide	$[\alpha]_D^{25}$/°(*c*, *n*-Hexane)	e.e.[a] (%)	Configuration
1	**10**-OAc	+1.45 ± 0.18 (1.10)	14	*S*
2	**10**-OH	+2.82 ± 0.12 (1.63)	27	*S*
3	**11**-OAc	−1.23 ± 0.14 (1.38)	15	*R*
4	**11**-OH	+1.46 ± 0.11 (1.72)	14	*S*
5	**12**-OAc	+3.42 ± 0.13 (1.51)	31	*S*
6	**12**-OH	−0.34 ± 0.11 (1.74)	3	*R*
7	**13**-OAc	+1.23 ± 0.14 (1.39)	12	*S*
8	**13**-OH	+2.22 ± 0.10 (2.03)	21	*S*
9	**14**-OAc	−2.77 ± 0.28 (0.69)	27	*R*
10	**14**-OH	+1.00 ± 0.13 (1.55)	11	*S*
11	**15**-OAc	+0.87 ± 0.06 (3.35)	18[b]	*S*
12	**15**-OH	−0.31 ± 0.15 (1.31)	6[b]	*R*
13	**22**-OAc	+1.13 ± 0.14 (1.42)	11	*S*
14	**22**-OH	+1.25 ± 0.08 (2.56)	12	*S*

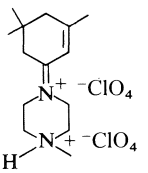
[a]Based on the reported maximum rotation (16) of 3,3,5-trimethylcyclohexanone, $[\alpha]_D^{25}$ 10.3° (*n*-hexane).
[b]Corrected for the optical purity of **11**-OAc and **11**-OH used.

structure, modified substrates **4–9** were prepared and subjected to reduction with 1,4-dihydronicotinamide β-D-glucopyranosides. The results are summarized in Table 1. Substrates **4** and **5** were investigated in the expectation that hydrogen bonding and electrostatic attraction of oxygen in the former and additional positive charge on the nitrogen in the latter may possibly interact with hydroxyl groups of the glucose residue. Product ketones from the reduction with 1,4-dihydronicotinamide β-D-glucopyranoside under the same conditions showed rather inferior enantiomeric excess (e.e.) as compared with that found for the simple iminium salt **2**, which suggested the absence of substantial attractive interaction as expected above.

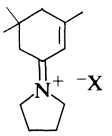
With **6–8**, a similar stereochemistry emerged, neither electronic nor steric participation of counter anions having been operative in the steric course as indicated by runs 5–7 in Table 1.



4



5

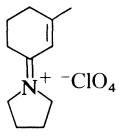


6 X = ^-OOC⟨⟩NO_2

7 X = ^-OOC⟨⟩OCH_3

8 X = $^-O_3SCH_2$





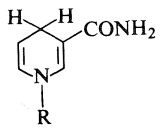
9

On the other hand, with the substrate **9**, which lacks the geminal dimethyl in the cyclohexenylidene moiety, (runs 8 and 9 in Table 1), the e.e. of the reduction product ketone was by far inferior to that with substrate **2** (runs 1 and 2 in Table 2). It then follows that structural change in proximity to the reaction center is important in the stereochemical process of hydrogen transfer in the present system.

Thus, practically, functionalization of the ketone with pyrrolidine was found to be the best method for the present system. Accordingly, **2** was chosen as a target substrate for the following study.

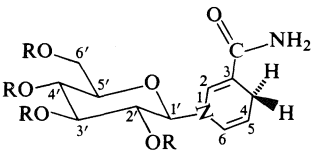
Structural Variation in Dihydronicotinamide Sugar Pyranosides

In Table 2 are listed the stereochemical results found for the reduction of substrate **2** with 1,4-dihydronicotinamide sugar pyranosides and their acetylated derivatives, **10–14**. Enantiomeric excess and configuration of the product were remarkably affected by structural difference in the sugar moiety despite the fact that the reaction center at



10–OAc R = β-D-tetraacetylglucopyranosyl
10–OH β-D-glucopyranosyl
11–OAc α-D-tetraacetylglucopyranosyl
11–OH α-D-glucopyranosyl
12–OAc D-tetraacetylmannopyranosyl
12–OH D-mannopyranosyl
13–OAc β-D-tetraacetylgalactopyranosyl
13–OH β-D-galactopyranosyl
14–OAc β-D-triacetylxylopyranosyl
14–OH β-D-xylopyranosyl

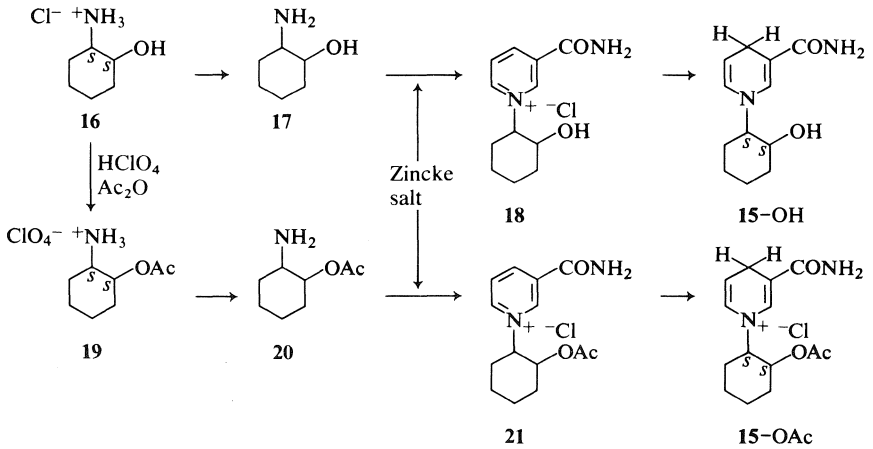
Can. J. Chem. Downloaded from www.nrcresearchpress.com by 210.87.254.5 on 09/05/12
For personal use only.



the 4-position of the dihydronicotinamide is apparently far removed from asymmetric carbons of the sugar moiety. The sole difference between β-D-glucopyranosides **10** and β-D-xylopyranosides **14** is that the latter lacks hydroxymethyl or acetoxymethyl groups at 5′-position of the pyranose ring. The reduction with acetyl-D-glucopyranoside, **10**-OAc, afforded the product ketone with preponderance of the *S*-enantiomer (run 1 in Table 2), whereas with acetyl-β-D-xylopyranoside, **14**-OAc, the *R*-counterpart was found in excess (run 9), so that the acetoxymethyl group at 5′-position of the pyranose ring functions to promote the *S*-chirality in the product. In contrast, both the OH-forms (runs 2 and 10) gave rise to the same *S*-product with higher e.e. in the former than in the latter case. As was also the case with OAc-forms, hydroxymethyl groups at 5′-position also favor the *S*-product. β-D-Galactopyranosides **13** are different from β-D-glucopyranosides **10** in that the configurations of the 4′-positions are opposite to each other. As can be seen from runs 1 and 7 in Table 2 for OAc-forms and runs 2 and 8 for OH-forms, this configurational difference did not cause substantial change in e.e. with the same *S*-product in preponderance. On the other hand, the configurational change from α to β at the anomeric carbons of OAc-forms of glucopyranosides resulted in a reversal of product configuration from *S* to *R*. With OH-forms, the α-anomer afforded a significantly higher e.e. of the product than the β-counterpart. Although the reduction data with D-mannopyranosides cannot be referred to with reasonable reliance because of the ambiguity in configurational integrity at the anomeric carbon, it is of interest to note that the OAc-form afforded much higher e.e. than the OH-form with reversal of configuration of the product. This change in product stereochemistry also suggests the importance of configuration at the epimeric 2′-carbon of the pyranose ring. Thus, the stereochemistry of reduction is greatly dependent on the structure of the sugar moiety as well as on whether or not the hydroxyl groups are acetylated. In addition, asymmetric centers adjacent to the nitrogen atom of the nicotinamide nucleus seem to exert more influence.

Hydroxyl groups at the 2′-position in nucleosides and nucleotides have been well documented to participate in determining their conformation through hydrogen bonding between the group and their base moiety (5), and also participate in enhancing the reactivity of dihydronicotinamide nucleoside by unidentified interaction between the group and dihydropyridine moiety (6). In this connection, we were particularly interested in the substituent at 2′-position of sugar pyranosides and prepared cyclohexanol derivatives of dihydronicotinamides **15**-OH and **15**-OAc as more simplified models for sugar pyranosides. Nicotinamide was incorporated in optically active amines **17** and **20** by the action of Zincke salt (7).

The stereochemical outcome (Table 2) revealed that the reduction of **2** with **15**-OH and **15**-OAc afforded the *R*-enantiomer with 6.3% e.e. and the *S*-counterpart with 17.7% e.e., respectively. Thus, OH and OAc groups at the 2′-position shifted the stereochemical course of the reduction in opposite directions despite the identical (1′*S*,2′*S*)-configuration in both reductants. This fact clearly shows that participation of these groups is not only steric but also electronic in nature. Molecular models revealed that the OH and OAc groups dispose spa-



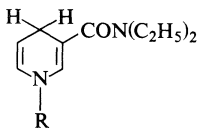
SCHEME 2

Can. J. Chem. Downloaded from www.nrcresearchpress.com by 210.87.254.5 on 09/05/12
For personal use only.

Can. J. Chem. Downloaded from www.nrcresearchpress.com by 210.87.254.5 on 09/05/12
For personal use only.

tially within the range of hydrogen bonding with pyridine nitrogen. The same must hold for 1,4-dihydronicotinamide sugar pyranosides.

When the carbamoyl group was modified by *N*,*N*-diethylation, both the OH and OAc forms of β-D-glucopyranosides, **22**-OH and **22**-OAc, produced the same *S*-product in predominance to a comparable extent, which is in contrast to the reduction with the parent model compound **10**. This implies that the carbamoyl group is appreciably responsible for the difference in stereoselectivity observed in the reduction with **10**-OH and **10**-OAc, and that the mode of participation of the carbamoyl group as well as the modified *N*,*N*-diethylcarbamoyl group is not simply steric. Consistently, the ^{1}Hmr signal of the two carbamoyl protons is shifted to higher magnetic field with rising temperature (Fig. 1), clearly indicating the existence of hydrogen bonding between carbamoyl and sugar hydroxyls and/or solvent (9).



22-OH R = β-D-glucopyranosyl
22-OAc R = β-D-tetraacetylglucopyranosyl

When the substrate **2** was reduced with an achiral NADH model, 1-benzyl-1,4-dihydronicotinamide, in the presence of an equimolar amount of β-D-glucose, no asymmetric induction was obtained in the product ketone **3**. Accordingly, dihydronicotinamide should at least be connected with β-D-glucose through a covalent linkage for the asymmetric bias to be produced in the product ketone. This shows that, since solvation of β-D-glucose by *N*,*N*-dimethylformamide (solvent used for the present reaction system) may isolate the molecule from 1-benzyl-1,4-dihydronicotinamide and the substrate molecules in this instance, the asymmetric induction should be preceded by proximity of the chiral part to the reaction site prior to any non-covalent interactions responsible for enantiotopic recognition at the substrate.

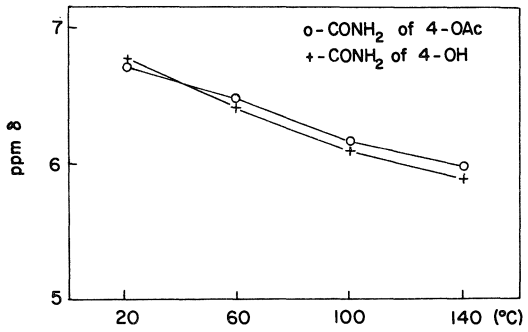


FIG. 1. Dependence of chemical shift of amide protons of 4-OAc and 4-OH on temperature (JEOL JNM-FX100 was used for the ^{1}Hmr spectra).

Finally, in view of the present data, the stereochemistry was very sensitive (including reversal of the stereochemistry) to structural variation in the sugar residue as well as the carbamoyl group, while the modification of substrate structure depressed the asymmetric bias equally with OAc- and OH-forms and the stereochemistry is virtually insensitive to the changes of the counter anions and external conditions (Table 3).

The present NADH model system is regarded as an example of asymmetric reaction in which the resulting stereochemistry cannot be understood without taking into account electronic factors, and the proximity effect of chiral source to reaction site is primarily important for the asymmetric induction. We prefer to leave the transition state topology open to speculation since insufficient stereochemical data is available at present. However, the information obtained here concerning the relationship between structure of NADH model compounds and stereochemistry of the reduction product ketone may help control and/or improve asymmetric syntheses in similar systems. The present system constitutes the first example of NADH model reaction by the use of sugars as chiral source to give optically active ketones with chirality at the β-position, and is applicable to other chiral α,β-unsaturated iminium salts as well.

Experimental

Infrared spectra were recorded with a Hitachi 215 spectrometer, ^{1}Hmr spectra with a Varian EM-360 spectrometer with tetramethylsilane as internal standard, and uv spectra were measured on a Hitachi EPS-3 spectrophotometer. Optical rotations were measured with a Perkin-Elmer 241 polarimeter and preparative vpc was performed on Varian Aerograph Model 920 with aluminum column (3 m) packed with 15% Apiezone at 170°C. Qualitative vpc was on a Shimadzu gas chromatograph GC-4CM with glass column (3 m) packed with 15% polyethylene glycol succinate at 170°C. The sugar pyranosides **10–14** were prepared according to the procedure of Haynes and Todd (10). Iminium salt **2** was prepared according to the method of Firrell and Hickmott (11). Counter anion analogues of **2**, *p*-nitro-, *p*-methoxybenzoate, and *d*-10-camphorsulfonate, **6–8**, were prepared (12) by exchange of the perchlorate anion with the carboxylate anions, stoichiometric quantity of potassium perchlorate having been separated out from a dry methanol solution of the corresponding potassium benzoates and **2**.

3,3,5-Trimethylcyclohexenylidenemorpholinium Perchlorate **4**

This salt was prepared by the same procedure as for **2** from a dienamine (from morpholine and isophorone, bp 80–90°C/0.35 Torr, 17.5 g, 84.4 mmol). Yield 17.1 g (65.8%). This salt was recrystallized from acetonitrile–ethanol–ether; mp 202–203°C; ^{1}Hmr (CF_3COOD) δ: 1.15 (6H, s, geminal CH_3), 2.3 (3H, s, CH_3 on vinyl group), 2.45 (2H, s), 2.75 (2H, s), 4.2 (8H, s.

TABLE 3. Results in reduction of **2** with **10**-OH under other specified conditions

Temperature (°C)	Reaction period (h)	Solvent	$[\alpha]_D^{25}$/°(*c*, *n*-Hexane)	e.e.[a] (%)	Configuration
140	1	DMF + TCE[a] (3:2)	+2.36 ± 0.35 (0.55)	23	*S*
180	0.5	No solvent	+2.31 ± 0.19 (1.04)	22	*S*
100	21	DMF	+2.93 ± 0.04 (5.35)	29	*S*

[a]TCE: 1,1,2,2-tetrachloroethane (dielectric constant = 8.20). Dielectric constant of solvent was lowered to 12.9 by an addition of TCE to DMF (dielectric constant = 37.6) according to the method described in ref. 17.

Can. J. Chem. Downloaded from www.nrcresearchpress.com by 210.87.254.5 on 09/05/12
For personal use only.

protons on morpholine ring), 8.7 (1H, s, vinyl proton). *Anal.* calcd. for $C_{13}H_{22}ClNO_5$: C 50.73, H 7.21, N 4.55; found: C 50.57, H 7.25, N 4.30.

3,3,5-Trimethylcyclohexenylidene-N-*methylpiperazinium Perchlorate* ***5***

This salt was prepared similarly by the quarternization of a dienamine (from isophorone and *N*-methylpiperazine, bp 86–87°C/0.15 Torr, 5.3 g, 24 mmol) with 70% perchloric acid. Yield 6.8 g (67%). The salt was recrystallized from acetonitrile – dry ether; mp 265–266°C; ^{1}Hmr (CF_3COOD) δ: 1.1 (3H, s, geminal CH_3), 1.2 (3H, s. another geminal CH_3), 2.3 (3H, s, CH_3 on vinyl group), 2.53 (2H, s), 2.84 (2H, s), 3.25 (3H, s, N—CH_3), 3.5–5.2 (8H, m, protons on piperazine ring), 6.85 (1H, s). *Anal.* calcd. for $C_{14}H_{26}Cl_2N_2O_8$: C 39.92, H 6.22, N 6.65; found: C 39.84, H 6.23, N 6.67.

3-Methylcyclohexenylidenepyrrolidinium Perchlorate ***9***

This salt was prepared by the same procedure as for **2** from a dienamine (from 3-methylcyclohexenone and pyrrolidine, bp 150–170°C/0.1 Torr, 10 g, 61 mmol). Yield 6.2 g (39%). The salt was recrystallized from methanol–ether; mp 84–86°C; ^{1}Hmr (CF_3COOD) δ: 1.15 (3H, s, CH_3), 1.3–2.8 (6H, m, methylene protons on cyclohexanone moiety), 2.8–4.4 (8H, m, methylene protons on pyrrolidine moiety). *Anal.* calcd. for $C_{12}H_{18}ClNO_4$: C 50.10, H 6.88, N 5.31; found: C 49.97, H 6.89, N 5.16.

N^1-β-D-*Triacetylxylopyranosyl-1,4-dihydronicotinamide* ***14***-*OAc*

The dihydro-form was obtained by sodium hydrosulfite reduction of its oxidized form which was prepared according to the method of Iff and Viscontini (13). Yield 5.4 g (59.3%); mp 175–177°C; $[\alpha]_D^{25}$, −29.3° (*c* 1.1, chloroform); uv (methanol) λ_{max}: 329 nm (ε 5 500). *Anal.* calcd. for $C_{17}H_{28}N_2O_8$: C 53.43, H 5.75, N 7.32; found: C 53.26, H 5.80, N 7.54.

N^1-β-D-*Xylopyranosyl-1,4-dihydronicotinamide* ***14***-*OH*

Deacetylation of **14**-OAc in methanol by ammonia (10) gave the OH-form. Melting point 177–178°C; $[\alpha]_D^{25}$ −18.8 ± 0.14° (*c* 1.12, water); uv (methanol) λ_{max}: 335 nm (ε 5 900). *Anal.* calcd. for $C_{11}H_{16}O_5N_2$: C 51.56, H 6.29, N 10.3; found: C 51.36, H 6.44, N 11.2.

N^1-*(1'S,2'S)-2'-Hydroxycyclohexylnicotinamide Chloride* ***18***

A solution of (*S*,*S*)-aminocyclohexanol (0.6 g, 5.2 mmol, 47.5% optical purity) in methanol (30 mL) was added dropwise to a solution of the Zincke salt (1.57 g, 4.4 mmol) in methanol (25 mL) with stirring. After the deep red color faded out, an excess of ether was added and the nicotinamide chloride separated from the solution was filtered, washed with ether, and dried over phosphorus pentoxide *in vacuo*. Yield 0.95 g (84%); mp 253–254°C; $[\alpha]_D^{25}$ 10.2 ± 0.15° (*c* 1.20, methanol); ^{1}Hmr (CF_3COOD) δ: 1.1–2.7 (8H, m, methylene protons on cyclohexane ring), 4.0–5.2 (2H, m, methyl protons on cyclohexane ring), 8.2 (1H, d of d, *J* = 8 Hz), 9.07 (1H, d, *J* = 8 Hz), 9.5 (1H, s). *Anal.* calcd. for $C_{12}H_{17}ClN_2O_2$: C 56.14, H 6.67, N 10.91; found: C 56.04, H 6.67, N 10.64.

N^1-*(1'S,2'S)-2'-Hydroxycyclohexyl-1,4-dihydronicotinamide* ***15***-*OH*

A solution of the chloride **18** (0.95 g, 3.7 mmol) in 5 mL of water was added dropwise to a solution of sodium hydrosulfite (1.31 g, 7.5 mmol) and sodium carbonate (1.55 g, 14.6 mmol) in water (8 mL) with stirring under ice-cooling in nitrogen atmosphere. After 30 min light yellow crystalline dihydronicotinamide separated from the reaction mixture, was filtered, washed with cold water, and dried over phosphorus pentoxide *in vacuo*. Yield 0.60 g (72.7%); mp 130–133°C (dec.); $[\alpha]_D^{25}$ 76.0 ± 0.03° (*c* 0.36, methanol); uv (methanol λ_{max}: 354 nm (ε 6 326); ^{1}Hmr (CD_3OD) δ: 0.9–2.3 (8H, m, methylene protons on cyclohexane ring), 3.1 (2H, d of d, *J* = 2 and 4 Hz, protons at 4-position), 5.85 (1H, d of d, *J* = 2 and 8 Hz, a proton at 6-position), 7.0 (1H, d, *J* = 2 Hz, a proton at 2-position). *Anal.* calcd. for $C_{12}H_{18}N_2O_2$: C 64.84, H 8.16, N 12.60; found: C 64.47, H 8.28, N 12.60.

(1S,2S)-2-Acetoxycyclohexylammonium Perchlorate ***19***

To the suspension of (1*S*,2*S*)-2-hydroxycyclohexylammonium chloride **16** (1.3 g, 8.6 mmol) in acetic anhydride (10 mL) was added 25 drops of 70% perchloric acid and the temperature was kept below 50°C by ice-cooling. The reaction mixture was stirred at room temperature overnight. Crystalline perchlorate **19** was separated from the solution by addition of ether. The perchlorate was recrystallized from acetonitrile–ether. Yield, 1.6 g (72%); mp 146–148°C. $[\alpha]_D^{25}$ 17.5 ± 0.14° (*c* 1.09, methanol). *Anal.* calcd. for $C_8H_{16}ClNO_6$: C 37.29, H 6.27, N 5.44; found: C 37.49, H 6.30, N 5.62.

N^1-*(1'S,2'S)-2'-Acetoxycyclohexyl-1,4-dihydronicotinamide* ***15***-*OAc*

A solution of the salt **19** (0.863 g, 3.37 mmol) in dry methanol (16.2 mL) was chilled in ice and added to 13.4 mL of 0.25 *N* methanolic potassium hydroxide. After a few min, a solution of Zincke salt (1.007 g, 2.82 mmol) in 16.2 mL of dry methanol was added dropwise and stirred gently at room temperature for 2 h. The reaction mixture was poured dropwise into about 2 L of ether with stirring and set aside until the ether phase became transparent. The bulk solvent was decanted, leaving very hygroscopic salt **21** which was dried over phosphorus pentoxide *in vacuo*. The crude yield was nearly quantitative; $[\alpha]_D^{25}$ 2.6 ± 0.15° (*c* 1.305, water); ^{1}Hmr (CD_3OD) δ: 1.8 (3H, s, acetyl protons), 1.1–2.6 (8H, m, methylene protons on cyclohexane ring), 5.2 (2H, amide protons), 8.0–9.4 (3H, m, protons at 4-, 5-, and 6-positions on pyridine ring), 9.5 (1H, s, protons at 2-position on pyridine ring). The salt **21** was dissolved in water (34 mL) and chilled in ice. This solution was added dropwise to a solution of sodium carbonate (1.042 g, 9.8 mmol) and sodium hydrosulfite (0.903 g, 5.2 mmol) in water (10 mL) under nitrogen atmosphere and stirred for 2 h at 0°C, followed by stirring for 1 h at room temperature. After this period, the organic phase was

Can. J. Chem. Downloaded from www.nrcresearchpress.com by 210.87.254.5 on 09/05/12
For personal use only.

extracted with chloroform (20 mL × 3) and the extract was dried over anhydrous sodium sulfate. The solvent was removed completely under reduced pressure at room temperature leaving the nicotinamide **15**-OAc as light yellow oil. This product could not be purified to an analytical grade because of its instability but the integrity was confirmed by the following data and tlc analysis (silica gel, methanol–chloroform 10:1, $R_f = 0.5$, fluorescence). $[\alpha]_D^{25}$ 13.2 ± 0.04° (*c* 3.80, chloroform); ir ν_{max}: 1690 (amide carbonyl), 1740 (ester carbonyl) cm^{-1}; uv (ethanol) λ_{max}: 348 nm (ε 6 944); ^{1}Hmr ($CDCl_3$) δ: 1.0–2.7 (8H, m, methylene protons on cyclohexane ring), 2.0 (3H, s, protons of acetyl), 3.0 (2H, d of d, J = 2 and 4 Hz, protons at 4-position), 4.3 (1H, m, proton at 5-position), 5.55 (2H, amide protons), 5.75 (1H, d of d, J = 2 and 8 Hz, a proton at 6-position), 6.98 (1H, d, J = 2 Hz, a proton at 2-position).

N^1-β-D-*Tetraacetylglucopyranosyl*-N,N-*diethyl-1,4-dihydronicotinamide* ***22-OAc***

According to the method of Haynes and Todd (10), the oxidized form was prepared from *N,N*-diethylnicotinamide (4.4 g, 24.7 mmol) and acetobromoglucose (9 g, 21.9 mmol), and this glucopyranoside was confirmed as the β-anomer from the coupling constant (J = 8 Hz) of 1′H with 2′H (14). The noncrystalline bromide was reduced as such by sodium hydrosulfite to give **22**-OAc as white powder, yield 5.2 g (46%). This product was recrystallized from ethanol; mp 138–140°C (dec.); $[\alpha]_D^{25}$ 30.3 ± 0.08° (*c* 1.48, methanol); uv (methanol) λ_{max}: 307 nm (ε 2 800); ^{1}Hmr ($CDCl_3$) δ: 1.15 (6H, t, J = 8 Hz, CH_3 at ethyl groups), 2.0–2.1 (12H, s, $COCH_3$ × 4), 3.1 (2H, m, protons at 4-position), 3.4 (4H, q, J = 8 Hz, CH_2 at ethyl groups), 5.86 (1H, m, a proton at 6-position). *Anal.* calcd. for $C_{24}H_{34}N_2O_{10}$: C 56.46, H 6.71, N 5.49; found: C 56.09, H 6.71, N 5.12.

N^1-β-D-*Glucopyranosyl*-N,N-*diethyl-1,4-dihydronicotinamide* ***22-OH***

Compound **22**-OAc (1.8 g, 3.51 mmol) was deacetylated as described above and acetamide was removed by extraction with a mixture of chloroform and benzene (1: 10). After removal of the acetamide, the residue, **22**-OH, was used immediately for the reduction of substrate because of its instability and hygroscopic nature at ambient temperature. Purification was not feasible with this compound, but the integrity was confirmed by the following data and tlc analysis (silica gel, methanol–chloroform 10:2, R_f = 0.6, fluorescence). $[\alpha]_D^{25}$ 3.9 ± 0.15° (*c* 1.27, chloroform); uv (chloroform) λ_{max}: 310 nm (ε 2 500); ^{1}Hmr ($CDCl_3$) δ: 1.15 (6H, t, J = 8 Hz, CH_3 in ethyl groups), 3.1 (2H, m, protons at 4-position), 6.0 (1H, m, a proton at 6-position, 6.38 (1H, a proton at 2-position).

General Procedure for Asymmetric Reductions

Dihydronicotinamide (NADH model, 2.5 mmol) and substrate (2.5 mmol) in 10 mL of dry *N,N*-dimethylformamide was heated at 140°C for 1 h under nitrogen with stirring. The reaction mixture was cooled to room temperature and the enamine formed was hydrolyzed with 3 *N* hydrochloric acid (10 mL). Cyclohexanone thus liberated was extracted with *n*-pentane (20 mL × 4). The pentane solution was dried over anhydrous sodium sulfate and concentrated to about 1 mL. Quantitative determination of the ketone was done by vpc (15% polyethyleneglycol succinate, 170°C, 3 m). The ketone was isolated by preparative vpc (15% Apiezone L, 190°C, 3 m). After the identification and purity of the ketone were checked by ^{1}Hmr and vpc, the optical rotation was measured in *n*-hexane.

1. (*a*) R. J. KILL and D. A. WIDDOWSON. Bioorganic chemistry. Vol. IV. *Edited by* E. E. van Tamelen. Academic Press, London. 1978. p. 239; (*b*) Y. OHNISHI, M. KAGAMI, and A. OHNO. J. Am. Chem. Soc. **97**, 4766 (1975); (*c*) K. NISHIYAMA, N. BABA, J. ODA, and Y. INOUYE. J. Chem. Soc. Chem. Commun. 101 (1976); (*d*) T. MAKINO, N. BABA, J. ODA, and Y. INOUYE. Chem. Ind. 277 (1977); (*e*) N. BABA, K. NISHIYAMA, J. ODA, and Y. INOUYE. Agric. Biol. Chem. **40**, 1441 (1976); (*f*) A. OHNO, T. KIMURA, S. G. KIM, H. YAMAMOTO, and S. OKA. Bioorg. Chem. **6**, 21 (1977); (*g*) T. ENDO, Y. HAYASHI, and M. OKAWARA. Chem. Lett. 391 (1977); (*h*) H. A. OHNO, M. IKEGUCHI, T. KIMURA, and S. OKA. J. Chem. Soc. Chem. Commun. 328 (1978); (*i*) J. J. VAN RAMESDONK, J. W. VERHOEVEN, U. K. PANDIT, and TH. J. DE BOER. Recl. Trav. Chim. Pays-Bas, **97**, 195 (1978); (*j*) T. MAKINO, T. NUNOZAWA, N. BABA, J. ODA, and Y. INOUYE. Tetrahedron Lett. 1683 (1979); (*k*) T. MAKINO, T. NUNOZAWA, N. BABA, J. ODA, and Y. INOUYE. J. Chem. Soc. Perkin Trans. I, (1979). In press; (*l*) J. G. DE VRIES and R. M. KELLOGG. J. Am. Chem. Soc. **101**, 2759 (1979).
2. N. BABA, Y. MATSUMURA, and T. SUGIMOTO. Tetrahedron Lett. 4281 (1978).
3. U. K. PANDIT, F. R. MAS CABRE, R. A. GASE, and M. J. DE NIE-SARINK. J. Chem. Soc. Chem. Commun. 627 (1974); 211 (1975).
4. P. H. BOYLE. Q. Rev. **25**, 323 (1971).
5. A. M. MICHELSON. Annu. Rev. Biochem. **30**, 133 (1961).
6. J. HAJDU and D. S. SIGMAN. Biochemistry, **16**, 2841 (1977).
7. H. LETTRÉ, W. HAEDE, and E. RUHBAUM. Justus Liebigs Ann. Chem. **579**, 123 (1953).
8. C. FODOR and J. KISS. J. Am. Chem. Soc. **72**, 3495 (1950).
9. L. M. JACKMAN and S. STERNHELL. Applications of nuclear magnetic resonance spectroscopy in organic chemistry. 2nd ed. Pergamon Press, London. 1969. p. 103.
10. L. J. HAYNES and A. R. TODD. J. Chem. Soc. 303 (1950).
11. N. F. FIRRELL and P. W. HICKMOTT. J. Chem. Soc. 293 (1969).
12. W. R. ADAMS, O. L. CHAPMAN, J. B. SIEJA, and W. J. WELSTEAD, JR. J. Am. Chem. Soc. **88**, 162 (1966).
13. R. IFF and M. VISCONTINI. Helv. Chim. Acta, **59**, 2892 (1976).
14. R. U. LEMIEUX and J. W. LOWN. Can. J. Chem. **41**, 889 (1963).
15. C. F. WANG, E. AUER, and R. T. LALONCLE. J. Org. Chem. **35**, 515 (1970).
16. M. SANZ-BURATA, J. IRRURE-PEREZ, and S. JULIA-ARECHAGA. Afinidad, **27**, 705 (1970).
17. Y. INOUYE, S. INAMASU, M. HORIIKE, M. OHNO, and H. M. WALBORSKY. Tetrahedron, **24**, 2907 (1968).

Oxygen exchange in methanol in acid solutions. Transition state activity coefficients

ROBERT A. MCCLELLAND

Department of Chemistry, Scarborough College, West Hill, Ont., Canada M1C 1A4

Received August 10, 1979

ROBERT A. MCCLELLAND. Can. J. Chem. **58**, 393 (1980).

Rate constants for oxygen exchange of methanol in sulfuric acid and perchloric acid solutions are reported, along with activity coefficients of methanol in sulfuric acid. Transition state activity coefficients ($f_{\neq}$*) for methanol exchange and *tert*-butanol exchange have been calculated. Values of $f_{\neq}$* for the latter behave very similarly to those for *tert*-butyl acetate hydrolysis, consistent with a carbonium ion-like transition state. Values for methanol exchange show considerably more salting-out, consistent with an oxonium ion-like transition state. A significant difference with the $A_{Ac}2$ hydrolyses of esters and amides is noted. For the latter the transition state is salted-out relative to its protonated precursor, whereas for methanol exchange, there is little difference between the activity coefficient of the protonated alcohol and the transition state, with the latter actually being somewhat salted-in. It is pointed out that the transition state activity coefficient approach can be rigorously applied even in the absence of protonation data.

ROBERT A. MCCLELLAND. Can. J. Chem. **58**, 393 (1980).

On rapporte les constantes de vitesse de la réaction d'échange d'oxygène du méthanol dans des solutions d'acides sulfurique et perchlorique, ainsi que les coefficients d'activité du méthanol dans l'acide sulfurique. On a calculé les coefficients d'activité de l'état de transition ($f_{\neq}$*) lors de la réaction d'échange du méthanol et du *tert*-butanol. Les valeurs de $f_{\neq}$* obtenues pour le *tert*-butanol se comportent comme celles relatives à l'hydrolyse de l'acétate de *tert*-butyle et sont en accord avec un état de transition impliquant un carbocation. Les valeurs dans le cas de l'échange de l'oxygène du méthanol montrent une diminution plus considérable qui est en accord avec un état de transition mettant en jeu un ion oxonium. On note une différence importe par rapport aux hydrolyses $A_{ac}2$ d'esters et d'amides. Dans ce dernier cas l'état de transition est relargué par rapport à son précurseur protoné alors que dans le cas de l'échange du méthanol il y a très peu de différence entre le coefficient d'activité de l'alcool protoné et l'état de transition, ce dernier étant actuellement quelque peu renforcé. On a mis en évidence le fait que l'approche du coefficient d'activité de l'état de transition peut être rigoureusement appliqué même en l'absence des données relatives à la protonation.

[Traduit par le journal]

We report here rate constants for the oxygen exchange reaction of methanol in aqueous sulfuric acid and perchloric acid solutions. Alcohol oxygen exchange reactions have been studied in the past (1), although no kinetic data appear to have been reported for methanol. With the exception of *tert*-butanol oxygen exchange, there also appears (1) to have been no kinetic study over a range of acidity sufficiently great to rigorously test the applicability of the various treatments now available for acid-catalyzed reactions (2–7). We in particular wished to test a new approach, the transition state activity coefficient method (7), on different types of reaction of known mechanism. For methanol exchange, there can be little mechanistic uncertainty; it is difficult to visualize a mechanism other than that involving an S_N2 displacement on the protonated alcohol by a solvent water molecule, proceeding through a symmetrical transition state.

[1] $CH_3—OH + H^+ \rightleftharpoons CH_3—{}^+OH_2 \rightleftharpoons$
$H_2O^{\delta+}\cdots CH_3\cdots{}^{\delta+}OH_2 \rightleftharpoons H_2O^+—CH_3 \rightleftharpoons HO—CH_3 + H^+$

Experimental

Sulfuric acid solutions and perchloric acid solutions were prepared and standardized as previously described (8, 9). [^{18}O]methanol (12.3% excess ^{18}O) was prepared from $H_2{}^{18}O$ (Miles Research) using the procedure of Sawyer (10).

Methanol exchange kinetics were initiated by dissolving [^{18}O]methanol (0.1 g) in the appropriate acid (10 mL) and placing this solution in a sealed tube in an oil bath thermostatted at 67.2°C. After an appropriate time interval the sealed tube was removed and immersed in an ice bath to quench the exchange. In the case of concentrated acids, a small quantity of water was also added. The solution was transferred to a small distillation apparatus, which was evacuated to 0.05 Torr. Volatile components were collected in a liquid nitrogen trap, until approximately 1–2 g of material had accumulated. Pyridine (50 mL) was added, followed by *p*-nitrobenzoyl chloride (20 g). This was stirred at 50–60°C for 10 min, at which point 5 mL of water was added to react with any excess acid chloride. After an additional 10 min stirring, the mixture was evaporated on a rotary evaporator. Ether (250 mL) and water were added, and the ether layer was washed with dilute aqueous hydrochloric acid, and three times with saturated sodium carbonate. Magnesium sulfate was added, and after filtration, the ether removed on a rotary evaporator. The remaining pale yellow solid was recrystallized from chloroform – petroleum ether. Based on its nmr spectrum this product is pure methyl *p*-nitrobenzoate, containing less than 5% *p*-nitrobenzoic acid. Between 20 and 50% of the methanol originally added can be accounted for in this product.

The methyl *p*-nitrobenzoate was analyzed for ^{18}O content directly on an AEI mass spectrometer, equipped with a Vacuumetrics Ratiometer. This use of this apparatus has been previously described (11). Methyl *p*-nitrobenzoate has a strong molecular ion peak in its mass spectrum, and this was chosen for analysis, the relative intensity of the two peaks at *m/e* 183 and *m/e* 181 being measured. The ester contains natural abundance ^{18}O in all oxygen atoms except, perhaps, the oxygen atom attached to the methyl group, that is, the oxygen derived from the methanol. The ^{18}O content in this oxygen was calculated from the formula

$$\%\ ^{18}O = 99.8\left(\frac{R - R_0}{1.002 + R - R_0}\right) + 0.2$$

where R = the 183/181 ratio in the sample in question, and R_0 =

0008-4042/80/040393-06$01.00/0

©1980 National Research Council of Canada/Conseil national de recherches du Canada

Can. J. Chem. Downloaded from www.nrcresearchpress.com by 210.87.254.42 on 09/05/12
For personal use only.

TABLE 1. Mass spectrometric data

A control experiment			Exchange run (60.5% H_2SO_4, 67.2°C)		
% $Me^{18}OH$[a]	$(183:181)_{obsd}$	$(183:181)^b_{calcd}$	Time (h)	183:181	% ^{18}O
100	0.1491	(0.1491)	0	0.1485	11.98
76.4	0.1190	0.1175	46.7	0.1286	10.33
52.6	0.0850	0.0855	94.5	0.1110	8.90
30.1	0.0563	0.0554	166.5	0.0888	7.02
0	0.015[c]	(0.015)	215	0.0769	5.98
			2000	0.016	

[a]Mol percent of enriched methanol in mixture of enriched methanol and natural abundance methanol.
[b]$(183:181)_{calcd} = (\%Me^{18}OH/100)(0.1491 - 0.015) + 0.015$.
[c]The same value is obtained for a sample of methyl *p*-nitrobenzoate containing only natural abundance ^{18}O atoms. The calculated 183/181 ratio for $C_8H_7NO_4$ is 0.012 (J. H. Beynon and A. E. Williams (18)).

the 183/181 ratio in a sample of methyl *p*-nitrobenzoate containing only natural abundance ^{18}O atoms. As a check on the analysis, enriched methanol was accurately mixed with natural abundance methanol, dissolved in 30% H_2SO_4, and immediately subjected to the experimental procedure for isolation as the *p*-nitrobenzoate. Excellent agreement was found between the observed value of the 183/181 ratio, and the value calculated on the basis of the amount of enriched methanol actually present (Table 1). First order rate constants for methanol oxygen exchange were evaluated as the slopes of plots in ln (% ^{18}O − 0.2) vs. time. A typical set of data is provided in Table 1. The first-order kinetic plots were all excellently linear over one to two half-lives of exchange. In the case of the more concentrated acids, we checked for the possibility of decomposition of the methanol under the experimental conditions by taking the nmr spectra of the solutions. With the exception of solutions above about 80% H_2SO_4, there is no change in the spectra over a time period corresponding to one to two half-lives of exchange.

Distribution coefficients for methanol in carbon tetrachloride/aqueous H_2SO_4 mixtures were obtained in the following way. A standard solution in carbon tetrachloride containing known amounts of methanol and toluene was prepared, and the relative intensity of the two methyl peaks in the nmr spectrum obtained. A known amount of this solution was shaken with a known amount of aqueous solution for 15 min in a thermostatted water bath (25°C), and, after separation, the relative intensity of the two methyl peaks in the nmr spectrum of the carbon tetrachloride layer obtained. The difference before and after shaking was used to calculate the concentration of methanol remaining in the CCl_4, while the difference between this and the starting concentration was set equal to the concentration in the aqueous phase. This experiment requires that the toluene remains in the organic phase, an assumption which is probably valid, on the basis of distribution coefficients obtained previously (8, 12). Methanol has a strong preference for the aqueous phase. Conditions were arranged such that the concentrations of methanol in the carbon tetrachloride phase after distribution were of the order 0.005–0.01 *M*, meaning that concentrations in the aqueous phase were of the order of 1–3 *M*. Distribution coefficients with water were measured using several different concentrations of methanol and were found to be, within experimental error, the same.

Results and Discussion

Activity Coefficients

For the equilibrium partitioning of methanol between carbon tetrachloride and various aqueous sulfuric acid solutions, we have obtained distribution coefficients equal to the ratio of the concentration of methanol in the aqueous phase to the concentration in carbon tetrachloride. Activity coefficients (Table 2) were then calculated in the normal manner as $f_s = D^0/D$ (12), where D^0 and D are the distribution coefficients involving water/CCl_4 and acid/CCl_4, respectively. These values of f_s do not necessarily represent the activity coefficient of the neutral molecule, since the concentration of methanol in the aqueous phase refers to the total methanol present, and in the more concentrated acids a significant amount of this must be in the protonated form (13). The activity coefficient of the neutral molecule, f_{MeOH}, is related to f_s via eq. [2] where

$$[2] \quad f_{MeOH} = f_s[MeOH]_{tot}/[MeOH]$$

$[MeOH]/[MeOH]_{tot} \equiv$ fraction of methanol in the unprotonated form. Values of f_{MeOH} based on literature protonation data (13) are also listed in Table 2.

Figure 1 compares the activity coefficient behavior of methanol with that of other small organic molecules, including two other alcohols. We have chosen to compare f_s values in this figure, since all of the molecules are probably partially protonated in the more concentrated acids, and no correction for this fact has been made in their determination (12). As can be seen in Table 2, the activity coefficients based on the neutral molecule may be different from the measured activity coefficients, but the form of the $\log f_s$ vs. % H_2SO_4 curve remains unchanged. Figure 1 shows that methanol is not

TABLE 2. Activity coefficients of methanol in sulfuric acid solutions (25°C)

% H_2SO_4	$\log f_s$	$\log f_{MeOH}$
0	0	
20.1	−0.01	0.01
30.0	−0.05	−0.02
40.5	−0.10	−0.06
51.0	−0.27	−0.20
60.9	−0.36	−0.25
65.3	−0.47	−0.32

Can. J. Chem. Downloaded from www.nrcresearchpress.com by 210.87.254.42 on 09/05/12
For personal use only.

Can. J. Chem. Downloaded from www.nrcresearchpress.com by 210.87.254.42 on 09/05/12
For personal use only.

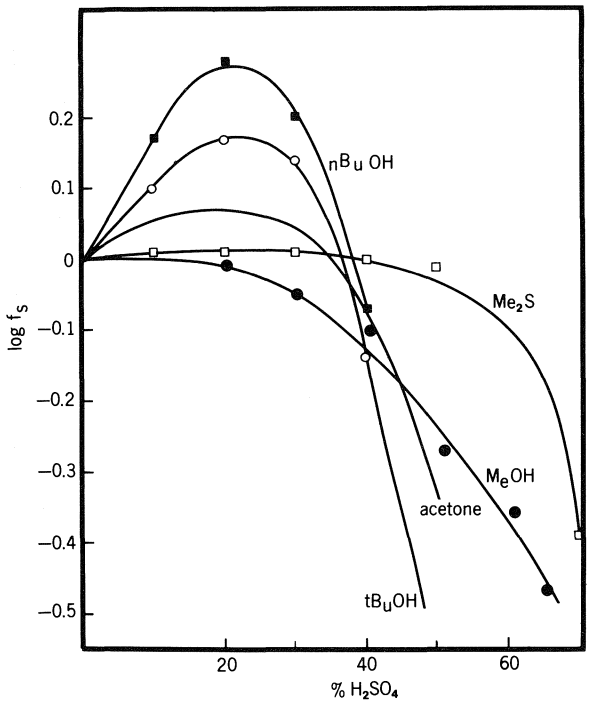


FIG. 1. Activity coefficients in sulfuric acid solutions. (Data taken from ref. 12, except for MeOH.)

unusual in its activity coefficient behavior. Neutral organic molecules generally show a small salting-out (positive log f_s) in dilute acids, followed by a pronounced salting-in in concentrated acids (12). This is also seen with methanol, with the minor difference that there is only little change in log f_s in dilute acids.

Kinetics of Oxygen Exchange

The oxygen exchange of methanol was studied by preparing an ^{18}O-labelled sample of the alcohol, and allowing this to exchange in natural abundance aqueous acids. The alcohol was separated and analyzed for ^{18}O content as its *p*-nitrobenzoate derivative. Observed first-order rate constants for exchange at 67.2°C are listed in Table 3, and plotted as a function of acid concentration in Fig. 2, along with literature data for *tert*-butanol exchange (14) and methyl acetate hydrolysis (4). One of the features of the methanol data is that unlike that of most A2 reactions (4, 15) the rate constants increase monotonically with increasing acid concentration and show no indication of reaching a maximum value. It is conceivable that in the more concentrated sulfuric acid solutions the rate increase could be due to the growing importance of a bisulfate ion catalyzed reaction, bisulfate displacing water from the protonated methanol, and then in turn being itself displaced by a solvent water molecule.[1] However the rate profile in perchloric acid solutions is very similar to that in sulfuric acid, and a similar reaction involving the less nucleophilic perchlorate ion is less likely. We presume therefore that at least up to 60–70% acid, the exchange occurs via the mechanism of eq. [1], with a solvent water molecule reacting with the protonated methanol.

TABLE 3. Rate constants for oxygen exchange in methanol at 67.2°C

% H_2SO_4	$10^7 k_{obsd}(s^{-1})$	% $HClO_4$	$10^7 k_{obsd}(s^{-1})$
20.1	0.17	26.3	0.38
30.0	0.56	42.1	2.0
40.5	1.4	50.5	5.6
51.0	3.9	59.9	18.8
60.9	9.2		
69.3	19.7		

Transition State Activity Coefficients

Before proceeding further, we wish to point out a feature of the transition state activity coefficient approach which has not been recognized in its earlier applications (7, 16) and which permits an even wider range of applicability for this method. Taking the methanol exchange reaction to illustrate the point,

$$H^+ + MeOH \overset{1/K_a}{\rightleftharpoons} \overset{+}{MeOH_2}$$

$$\overset{+}{MeOH_2} (+ H_2O) \xrightarrow{k_2^0} \neq$$

the following expression can be obtained:

$$[3] \quad \log f_{\neq}^* + \log (K_a/k_2^0) = \log a_{H^+}^* + \log f_{MeOH} - \log k_{obsd} + \log [MeOH]/[MeOH]_{tot}$$

where $f_{\neq}^*$ is the activity coefficient of the transition state relative to the tetraethylammonium ion,[2] $a_{H^+}^*$ is the activity of the proton relative to the same ion, K_a is the dissociation constant of $MeOH_2$, k_2^0 is the rate constant for the second step, k_{obsd} is the observed first-order rate constant for exchange, and other terms are as described previously. As before (7), the water molecule which is present in the second step is not explicitly included in this expression, but is considered as part of $f_{\neq}^*$. The procedure to determine log $f_{\neq}^*$ is to plot the quantity on the right hand side of eq. [3] as a function of acidity, and extrapolate to zero acid concentration where log $f_{\neq}^* = 0$ to determine the constant log (K_a/k_2^0).

[1]We did in fact notice that in solutions more concentrated than 80% H_2SO_4 a second signal appears in the nmr spectrum of methanol, attributable to methyl hydrogen sulfate.

[2]Single ion activity coefficients cannot be measured directly. In the case of acid solutions the standard practice has been to refer these to the same standard ion, the tetraethylammonium ion (12), so that for various cationic species values are *relatively* correct.

Can. J. Chem. Downloaded from www.nrcresearchpress.com by 210.87.254.42 on 09/05/12
For personal use only.

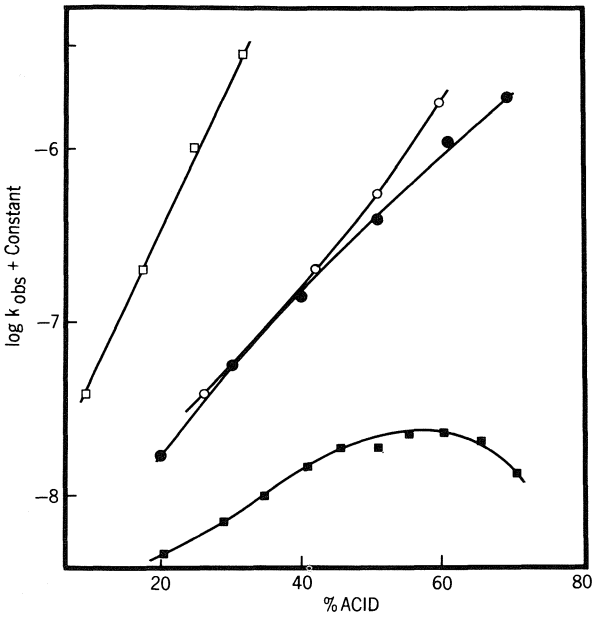


FIG. 2. Observed first-order rate constants in acid solutions. (○) MeOH exchange in perchloric acid at 67.2°C. (●) MeOH exchange in sulfuric acid at 67.2°C. (□) *t*-BuOH exchange in H_2SO_4 at 25°C (14); constant equals −2. (■) Methyl acetate hydrolysis in H_2SO_4 at 25°C (4); constant equals −5.

The final term in eq. [3] is important when the substrate is partially protonated, and in effect corrects k_{obsd} for that fact. What we would like to point out is that it is not necessary to apply this correction. From eq. [2]

$$\log f_{MeOH} = \log f_s - \log [MeOH]/[MeOH]_{tot}$$

so that substituting in eq. [3] the protonation corrections cancel, giving

$$[4] \quad \log f_{\neq}^* + \log (K_a/k_2^0) = \log a_{H^+}^* + \log f_s - \log k_{obsd}$$

It is therefore equally as valid to use the measured f_s values based on total substrate concentration in the acid solution, and k_{obsd} values, with no correction in either for partial protonation. In fact the actual extent of protonation is irrelevant, and knowledge of this is not necessary to determine $\log f_{\neq}^*$.

Values of $\log f_{\neq}^*$ for methanol oxygen exchange based on eq. [4] and rate constants and activity coefficients determined in this work are plotted as a function of acid concentration in Fig. 3. Also plotted in this figure are activity coefficients for some related cations and transition states, including values of $\log f_{\neq}^*$ for *tert*-butanol oxygen exchange which we have calculated using literature rate (k_{obsd}) (14) and activity coefficient (f_s) (12) data.

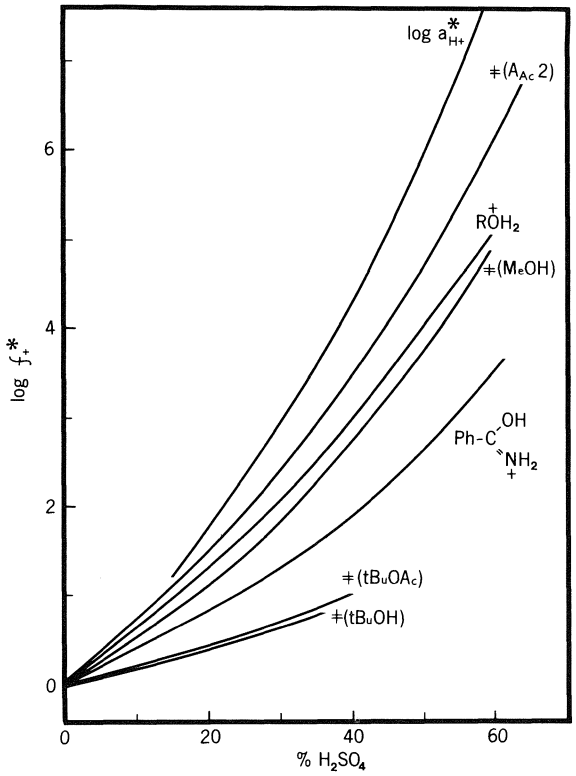
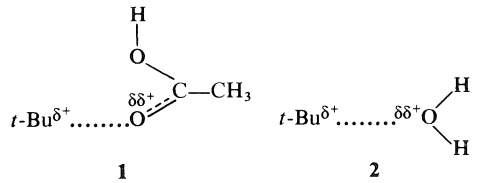


FIG. 3. Activity coefficients relative to the tetraethylammonium ion for cationic molecules and transition states. Values of log $a_{H^+}^*$ from ref. 17; ≠(A_{Ac}2), (7, 16*a*); ROH_2^+, (7); $PhC(OH)NH_2^+$, (12); ≠ (*t*-BuOAc), (7).

Values of ≠(A_{Ac}2) represent the normal bimolecular acid-catalyzed hydrolysis reactions of both esters and amides, for which there appears to be little difference in the behavior of $f_{\neq}^*$ (16*a*).

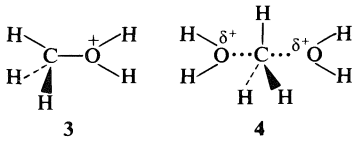
Values for ≠(*t*BuOAc) represent an $A_{Al}1$ hydrolysis reaction proceeding via the *tert*-butyl cation (7). One can note the very close similarity in the $f_{\neq}^*$ values for this latter reaction with the $f_{\neq}^*$ values for *tert*-butanol exchange. This exchange reaction has also been proposed to proceed via a *tert*-butyl carbonium ion (1), and its transition state is therefore very similar to that of the *t*-BuOAc hydrolysis (see **1** and **2**).



1 **2**

The transition state for methanol exchange is considerably more salted-out, in line with a change to a bimolecular reaction, and the transition state **4**.

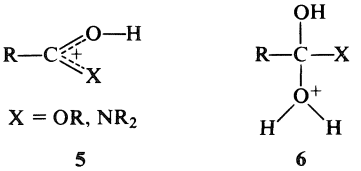
Can. J. Chem. Downloaded from www.nrcresearchpress.com by 210.87.254.42 on 09/05/12
For personal use only.



3 4

This oxonium ion-like transition state with its $O^{\delta+}$—H bonds has a much greater requirement for water of solvation than the carbonium ion-like transition states and is therefore more destabilized by the increase in acidity and concomitant lower water activity. An interesting comparison involves the $f_{\neq}$* values for the methanol exchange reaction with the activity coefficients of the protonated alcohol itself. These show a similar variation, with the transition state being slightly less salted-out by increased acidity. The protonated alcohol has a highly localized charge and two hydrogens of the type O^{+}—H capable of strong hydrogen bonding to solvent water molecules. The transition state has four such hydrogens, but the positive charge is now more dispersed, being shared by two oxygen atoms. We propose therefore, and the activity coefficients support this, that the protonated methanol molecule with a full positive charge on one oxygen is more solvated by water molecules than the transition state with two partially charged oxygen atoms (although the difference is not very great).

This behavior can be contrasted with that of the $A_{Ac}2$ hydrolysis reactions, where a large increase in the value of f* is observed as the protonated substrate proceeds to the transition state. The characteristic large salting-out of the $A_{Ac}2$ transition state has been commented on previously (7), being explained in terms of an oxonium ion-like transition state **6** closely resembling the tetrahedral intermediate, with charge localized on an electron deficient oxygen atom which contains two strongly acidic protons which require solvent hydrogen bonding stabilization. The protonated ester or amide **5** has its positive charge delocalized over



X = OR, NR_2

5 6

several atoms, and is salted-out considerably less. The greater salting-out of the $A_{Ac}2$ transition state as compared to the exchange transition state is in fact one reason why rate constants for the exchange increase more rapidly with increasing acidity when compared to rate constants for the hydrolysis (Fig. 2).

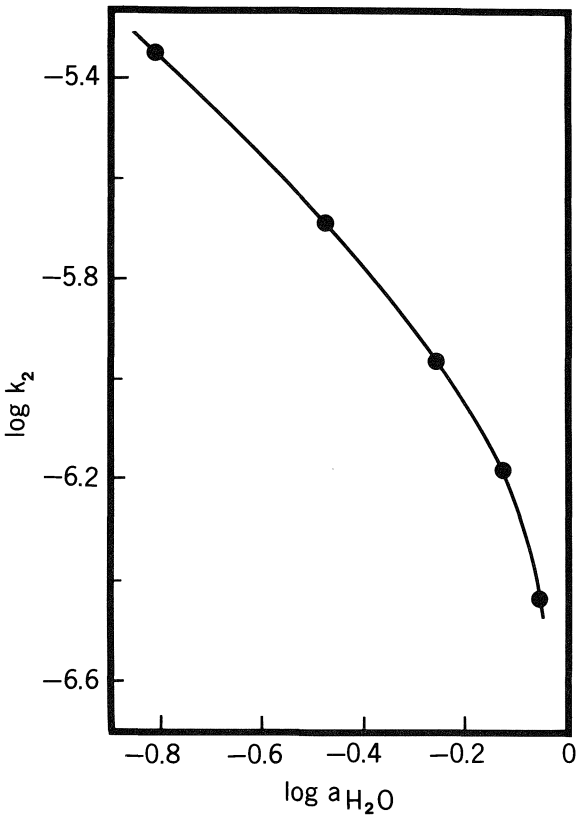


FIG. 4. "r" Hydration plot for methanol exchange in sulfuric acid solutions. Log k_2 = log k_{obsd} − log ($h_0^m/h_0^m + K'_{SH^+}{}^m$) where m = 0.22 and p$K'_{SH^+}$ = −6.88 (13).

The difference in the two types of reactions also shows up in a comparison of "r" hydration plots (4). This treatment plots log k_2 = log k_{obsd} − log {[SH^+]/([S] + [SH^+])} vs. log a_{H_2O}, and predicts that the slope of this plot (r) is equal to the number of water molecules in the transition state. For both ester and amide $A_{Ac}2$ hydrolysis, such plots produce positive "r" values, consistent with the presence of water molecules in the reaction with the protonated ester. The "r" plot (Fig. 4) for the methanol exchange reaction, using the literature protonation data (13), is significantly curved, *but* has a negative slope throughout. This is a somewhat surprising result since it implies that the methanol exchange reaction proceeds without the involvement of water. The explanation lies in the realization that what the "r" treatment actually represents is the variation in the difference in log $f_{\neq}$* and log f_{SH^+}* as a function of water activity. For most A2 reactions, such as the $A_{Ac}2$ hydrolyses,

this difference is positive and therefore the "r" value is positive. However for methanol exchange the difference is negative, and the apparently negative "r" value therefore results. In other words, the "r" value does not measure the number of water molecules, but rather a difference in activity coefficients.

Acknowledgement

Continued financial support of the Natural Sciences and Engineering Research Council of Canada is gratefully acknowledged.

1. D. SAMUEL and B. L. SILVER. Adv. Phys. Org. Chem. **3**, 123 (1965).
2. L. ZUCKER and L. P. HAMMETT. J. Am. Chem. Soc. **61**, 2791 (1939); F. A. LONG and M. A. PAUL. Chem. Rev. **57**, 935 (1957).
3. J. F. BUNNETT. J. Am. Chem. Soc. **83**, 4956 (1961); **83**, 4968 (1961); **83**, 4973 (1961); **83**, 4978 (1961).
4. K. YATES and R. A. MCCLELLAND. J. Am. Chem. Soc. **89**, 2686 (1967); K. YATES. Acc. Chem. Res. **4**, 136 (1971).
5. J. F. BUNNETT and F. P. OLSEN. Can. J. Chem. **44**, 1917 (1966).
6. G. SCORRANO. Acc. Chem. Res. **6**, 132 (1973).
7. R. A. MCCLELLAND, T. A. MODRO, M. F. GOLDMAN, and K. YATES. J. Am. Chem. Soc. **97**, 5223 (1975); K. YATES and T. A. MODRO. Acc. Chem. Res. **11**, 190 (1978).
8. K. YATES and R. A. MCCLELLAND. Can. J. Chem. **52**, 1098 (1974).
9. K. YATES, H. WAI, G. WELCH, and R. A. MCCLELLAND. J. Am. Chem. Soc. **95**, 418 (1973).
10. C. B. SAWYER. J. Org. Chem. **37**, 4225 (1972).
11. R. A. MCCLELLAND and M. AHMAD. J. Am. Chem. Soc. **99**, 5356 (1977).
12. K. YATES and R. A. MCCLELLAND. Prog. Phys. Org. Chem. **11**, 323 (1974).
13. P. BONVICINI, A. LEVI, V. LUCCHINI, G. MODENA, and G. SCORRANO. J. Am. Chem. Soc. **95**, 5960 (1973).
14. R. H. BOYD, R. W. TAFT, A. P. WOLF, and D. R. CHRISTMAN. J. Am. Chem. Soc. **82**, 4729 (1960).
15. C. R. SMITH and K. YATES. J. Am. Chem. Soc. **93**, 6578 (1971).
16. (*a*) T. A. MODRO, K. YATES, and F. BEAUFAYS. Can. J. Chem. **55**, 3050 (1977); (*b*) T. A. MODRO and K. YATES. J. Am. Chem. Soc. **98**, 4247 (1976).
17. T. A. MODRO, K. YATES, and J. JANATA. J. Am. Chem. Soc. **97**, 1492 (1975).
18. J. H. BEYNON and A. E. WILLIAMS. *In* Mass and abundance tables for use in mass spectrometry. Elsevier, Amsterdam. 1963.

Can. J. Chem. Downloaded from www.nrcresearchpress.com by 210.87.254.42 on 09/05/12
For personal use only.

Sulfur-bonded sulfoxide complexes of rhodium(III) and rhodium(I)

BRIAN R. JAMES AND ROBERT H. MORRIS

Department of Chemistry, University of British Columbia, Vancouver, B.C., Canada V6T 1W5

Received September 25, 1979

BRIAN R. JAMES and ROBERT H. MORRIS. Can. J. Chem. **58**, 399 (1980).

Aqueous 2-propanol solutions of $RhCl_3 \cdot 3H_2O$ on treatment with sulfoxides yield *mer*-$RhCl_3L_3$ complexes, the sulfoxide L being dimethyl (DMSO), tetramethylene (TMSO), methyl phenyl (MPSO), or (*R*)-methyl-*p*-tolyl (MPTSO); with diphenyl sulfoxide (DPSO), a $[RhCl(DPSO)_2]_2$ complex with S-bonded sulfoxide is obtained via the propanol reduction of a Rh(III) intermediate. The *mer*-rhodium(III) complexes in solution contain two sulfur-bonded sulfoxides (R_2SO), and one oxygen-bonded sulfoxide (R_2SO) that is *trans* to a (R_2SO) ligand. The DMS*O* ligand in *mer*-$RhCl_3(DMSO)_2(DMSO)$ is displaced by amides, amine oxides, and phosphine oxides; the DM*SO cis* to the oxygen-bonded ligands is identified in nmr by using the ring current shielding effects of $OPPh_2Me$. Salts of $[RhCl_4(R_2SO)_2]^-$ have been obtained with *n*-propyl sulfoxide and DMSO using several cations, including the symmetrically hydrogen-bridged species, $[R_2SO—H—OSR_2]^+$. The cyclooctene precursor $[RhCl(C_8H_{14})_2]_2$ has been used to synthesize $[RhCl(DPSO)(C_8H_{14})]_2$, $[RhCl(DMSO)_2]_2$, and $[RhCl(DIOS)_2]_2$, where DIOS is (2*R*,3*R*)-2,3-isopropylidene-2,3-dihydroxy-1,4-bis(methylsulfinyl)butane. The nature of rhodium–sulfur bonding is discussed, especially in terms of a contribution of metal–sulfur π-backbonding.

BRIAN R. JAMES et ROBERT H. MORRIS. Can. J. Chem. **58**, 399 (1980).

Lorsqu'on traite des solutions de $RhCl_3 \cdot 3H_2O$ avec des sulfoxydes dans le propanol-2 aqueux on obtient des complexes du type *mer*-$RhCl_3L_3$ où le groupe L est le sulfoxyde dérivant des radicaux suivants: diméthyle (DMSO), tétraméthylène (TMSO), méthylphényle (MPSO) ou (*R*)-méthyl-*p*-tolyle (MPTSO). On obtient avec le diphénylsulfoxyde (DPSO) un complexe $[RhCl(DPSO)_2]_2$ où le sulfoxyde est lié par le soufre, et qui résulte de la réduction par le propanol d'un intermédiaire Rh(III). Les complexes *mer*-rhodium(III) en solution contiennent deux sulfoxydes liés par l'atome de soufre (R_2SO) et un autre lié par l'atome d'oxygène (R_2SO) qui est en position *trans* par rapport au ligand (R_2SO). Les amides, les oxydes d'amines et les oxydes de phosphines déplacent le ligand DMS*O* du complexe *mer*-$RhCl_3(DMSO)_2$ (DM*SO*). On a identifié par la rmn le DM*SO* en position *cis* par rapport aux ligands liés par l'oxygène en utilisant les effets de blindage du courant de cycle du $OPPh_2Me$. On a obtenu les sels du type $[RhCl_4(R_2SO)_2]_2^-$ dérivés du *n*-propylsulfoxyde et du DMSO en utilisant plusieurs cations incluant les espèces liés symétriquement par un pont hydrogène: $[R_2SO—H—OSR_2]^+$. On a utilisé un précurseur cyclooctène $[RhCl(C_8H_{14})_2]_2$ pour synthétiser les complexes suivants: $[RhCl(DPSO)(C_8H_{14})]_2$, $[RhCl(DMSO)_2]_2$ et $[RhCl(DIOS)_2]_2$ où le groupe DIOS représente: (2*R*,3*R*) isopropylidène-2,3 dihydroxy-2,3 bis(méthylsulfinyl)-1,4 butane. On discute de la nature de la liaison Rh—S spécialement en fonction d'une contribution de retour π de la liaison métal–soufre.

[Traduit par le journal]

Introduction

Studies reported from this laboratory have described the successful use of ruthenium(II) complexes containing chiral sulfoxide ligands (L) as homogeneous catalysts for the asymmetric hydrogenation of some olefins (1–3). Some rhodium(I) complexes of the type Rh(diene)-$(PPh_3)(L)^+$, in which the chiral sulfoxide was oxygen-bonded (4), were found to be ineffective because of the relatively labile nature of the sulfoxide ligand in solution (1, 5). Anticipating that sulfur-bonded sulfoxides would be less labile (6), especially if metal $d_\pi \rightarrow$ sulfur d_π backbonding were significant (7, 8), we have synthesized several chlororhodium complexes containing such sulfoxides. We report here on an improved route to $RhCl_3(sulfoxide)_3$ complexes (9, 10), as well as on the preparation and characterization of other new Rh(III) and Rh(I) sulfoxide complexes.

Experimental

Synthetic procedures and solution measurements involving Rh(I) complexes were conducted under an argon atmosphere. All the Rh(I)–DMSO adducts were mulled in a glove bag under dry Ar. 2-Propanol with 0.1% water was used as supplied by Fisher Chem. Co. The phosphine oxides ($OPPh_2Me$, $OPPhMe_2$, $OPPhEt_2$) were prepared by oxidizing the phosphines in a slight excess of hot, dilute H_2O_2, and then extracting the product into $CHCl_3$, drying over $MgSO_4$, removing the solvent, and recrystallizing from EtOH. The sources of the sulfoxide ligands have been noted elsewhere (1, 4). Rhodium(III) trichloride trihydrate was obtained from Johnson Matthey Limited. The rhodium(I) complexes $[RhCl(cyclooctene)_2]_2$ and $[RhCl(C_2H_4)_2]_2$ were prepared according to literature procedures (11, 12).

Infrared data refer to Nujol mulls unless otherwise stated. Proton nmr data given to 3 decimals were acquired on a University-made 270 MHz spectrometer consisting of an Oxford Instruments superconducting magnet interfaced to a Nicolet 1080 computer. Other instruments used have been described previously (4). Microanalyses were performed by Mr. P. Borda of this department.

Preparation of the Complexes

$RhCl_3L_3$; L = DMSO, DMSO-d_6, TMSO, MPSO, R-*MPTSO*[1]

$RhCl_3 \cdot 3H_2O$ (0.2 g, 0.76 mmol) was dissolved and stirred for

[1]Sulfoxide abbreviations used are DMSO = dimethyl-, TMSO = tetramethylene-, MPSO = methyl phenyl(racemic)-, *R*-MPTSO = (*R*)-methyl *p*-tolyl-, DPSO = diphenyl-, NPSO = di-*n*-propyl-, DMSO and DMS*O*, for example, imply S- and O-bonded ligands, respectively. DIOS = (2*R*,3*R*)-2,3-*O*-isopropylidene-2,3-dihydroxy-1,4-bis)methyl sulfinyl)butane monohydrate (see ref. 2).

0008-4042/80/040399-10$01.00/0

©1980 National Research Council of Canada/Conseil national de recherches du Canada

Can. J. Chem. Downloaded from www.nrcresearchpress.com by 210.87.254.5 on 09/05/12
For personal use only.

Can. J. Chem. Downloaded from www.nrcresearchpress.com by 210.87.254.5 on 09/05/12
For personal use only.

TABLE 1. Infrared data (cm^{-1}) for rhodium sulfoxide complexes in degassed CH_2Cl_2

Complex	ν(SO)	$\rho_r(CH_3)$	Δν(SO)[a]
Rh(III)			
$RhCl_3(DMSO)_2(DMSO)$[b]	1142, 929	1021s, 981s, 940m	87, −126
$RhCl_3(TMSO)_2(TMSO)$	1139, 928		117, −94
$RhCl_3(MPSO)_2(MPSO)$[b]	1147, 932	968m, 957s	102, −113
$RhCl_3(MPTSO)_2(MPTSO)$	1154, 926	969m, 959s	109, −119
$RhCl_3(DPSO)_2(^iPrOH)$[b]	1145, 930		100, −109
$[(DMSO)_2H][RhCl_4(DMSO)_2]$	1127[c]		
$[NEt_4][RhCl_4(DMSO)_2]$	1138	1018s, 1000m, 976m	83
$[PS \cdot H][RhCl_4(DMSO)_2]$	1138	1027s, 1017m	83
$[(NPSO)_2H][RhCl_4(NPSO)_2]$[d]	1127, 1017[e]		110
	933		−84
Rh(I)	*ν(SO), under Ar*	*ν(SO) under air*	*Δν(SO)*[a]
$[RhCl(DMSO)_2]_2$	1100, 1055[e]	—	45
$[RhCl(DMSO\text{-}d_6)_2]_2$	1100, 1053[e]	1140, 1053[e]	45
$[RhCl(DPSO)_2]_2$	1125	1045[e]	80
$[RhCl(DPSO)(C_8H_{14})]_2$	1105	—	60

[a]Defined as ν(SO), coordinated sulfoxide − ν(SO), free sulfoxide; data under Ar is used for the Rh(I) systems.
[b]Mixture of isomers (see text).
[c]Measured in Nujol since complex insoluble in CH_2Cl_2.
[d]In CH_2Cl_2 rearrangement to $RhCl_3(NPSO)_2(NPSO)$ occurs (see text).
[e]ν(SO) of free sulfoxide.

30 min in 3 mL 2-propanol and 0.6 mL H_2O. On addition of L (2.3 mmol), the solution turned from red to yellow within 1 h. Brown suspensions sometimes formed intitially, but with stirring these were converted to suspensions of yellow product. Solutions for the L = DMSO, DMSO-d_6, and TMSO systems, sometimes remained clear, and deposited orange crystals (yield, 80–95%) on standing overnight. The L = MPSO and MPTSO systems yielded fine yellow powders on stirring for 18 h (90% yield). The products were filtered, washed with 2-propanol and ether, and dried *in vacuo*. All the complexes can be recrystallized from CH_2Cl_2 by addition of ether; the *R*-MPTSO adduct is obtained as feathery yellow crystals incorporating 0.5 mol CH_2Cl_2. The $RhCl_3(DMSO)_3$ compound can also be prepared by heating 0.2 g of $RhCl_3 \cdot 3H_2O$ in 1.0 mL DMSO at 70°C for 4 h, and then adding 100% EtOH until the microcrystalline solid precipitates. Table 1 lists some solution ir data for the compounds.

L = DMSO. Anal. calcd. for $RhC_6H_{18}Cl_3O_3S_3$: C 16.24, H 4.09; found: C 16.30, H 4.03. Nmr($CDCl_3$): Table 2, Fig. 1*a*. Nmr(CD_2Cl_2): δ 3.53 (s, 5, *S*—CH_3), 3.43 (s, 3, impurity of $RhCl_3(DMSO)_3$? See text), 3.35 (s, 5, *S*—CH_3), 2.80 (s, 5, *O*—S—CH_3). Ir: ν (SO) 1150s, 1135s, 935s; $\rho_r(CH_3)$ 1032s, 996s, 977s; ν(Rh—Cl) 355s, 340m, 297m.

L = TMSO. Anal. calcd. for $RhC_{12}H_{24}Cl_3O_3S_3$: C 27.62, H 4.63; found: C 27.61, H 4.82. Nmr($CDCl_3$): δ 4.37 (m, 2.6, *S*—C—H), 3.91 (m, 2.0, *S*—C—H), 3.53 (m, 6, *S*—C—H + *O*—S—C—H), 3.03 (m, 1.3, O—S—C—H), 2.29 (m, 12, S—C—CH_2—). Ir: ν(SO) 1150s, 1133s, 907s; ν(ring) 1095m, 1075s, 1035m, 955m, 890s, 880s; ν(Rh—Cl) 345s, 318s.

L = MPSO. Anal. calcd. for $RhC_{21}H_{24}Cl_3O_3S_3$: C 40.04, H 3.84; found: C 39.65, H 3.72. Nmr($CDCl_3$): δ 8.1–7.4 (m, 15, phenyl); resonances of *S*—CH_3: 4.03 (s, 1.2), 3.96 (s, 0.8), 3.91 (s, 0.5), 3.84 (s, 1.2), 3.76 (s, 1.1), 3.68 (s, 1.1); resonances of *O*—S—CH_3: 2.86 (s, 0.4), 2.80 (s, 0.3), 2.72 (s, 1.8), 2.52 (s, 0.2). Ir: ν(SO) 1150s, 1140s, 930s; $\rho_r(CH_3)$ 987s, 972s, 957s; ν(Rh—Cl) 352s, 317s.

L = R-MPTSO. Anal. calcd. for $RhC_{24}H_{30}Cl_3O_3S_3 \cdot 0.5\ CH_2Cl_2$: C 41.18, H 4.34; found: C 40.43, H 4.28. Nmr($CDCl_3$): δ 8.0–7.2 (m, 12, phenyl); 5.2 (s, 1, CH_2Cl_2); 3.86 (s, 3, *S*—CH_3), 3.58 (s, 3, *S*—CH_3), 2.80 (s, 3, *O*—S—CH_3); 2.38 (s, 3, C—CH_3). Ir: ν(SO) 1156s, 933s; $\rho_r(CH_3)$ 960s; ν(Rh—Cl) 354s, 310m.

$RhCl_3(DMSO)_2(O{=}L)$; (O=L) = Dimethylformamide (DMF), N-Formylpiperidine (F·pip), and Pyridine-N-oxide

$RhCl_3(DMSO)_3$ (0.15 g, 0.34 mmol) was dissolved and stirred for 4 h at 50°C in a stoppered tube containing 4 mL 1,2-dichloroethane and 15 mmol O=L. After reducing the volume to 2 mL under vacuum, ether was slowly added to obtain orange crystals (50% yield).

DMF Complex. Anal. calcd. for $RhC_7H_{19}Cl_3O_3S_2N$: C 19.16, H 4.36, N 3.19; found: C 19.27, H 4.47, N 3.27. Nmr($CDCl_3$): δ 8.27 (s, 1, O—C—H), 3.646 (s, 6, *S*—CH_3), 3.447 (s, 6, *S*—CH_3), 3.11 (s, 3, N—CH_3), 3.08 (s, 3, N—CH_3). Ir: ν(CO) 1635s; ν(SO) 1148s, 1135m; ν(Rh—Cl) 354s, 338m, 295m.

F·pip Complex. Anal. calcd. for $RhC_{10}H_{23}Cl_3O_3S_2N$: C 25.09, H 4.84, N 2.92; found: C 25.35, H 4.84, N 2.93. Nmr($CDCl_3$): 8.30 (s, 1, O—C—H), 3.647 (s, 6, *S*—CH_3), 3.437 (s, 6, *S*—CH_3). Ir: ν(CO) 1620s; ν(SO) 1145s, 1132s; ν(Rh—Cl) 355s, 333m.

C_5H_5NO Complex. Anal. calcd. for $RhC_9H_{17}Cl_3O_3S_2N$: C 23.46, H 3.69, N 3.04; found: C 23.60, H 3.80, N 3.00. Nmr($CDCl_3$): 9.00 (m, 2, *ortho*), 7.85–7.50 (m, 3, *meta*, *para*), 3.57 (s, 6, *S*—CH_3), 3.51 (s, 6, *S*—CH_3).

$RhCl_3(DPSO)_2(^iPrOH)$

$RhCl_3 \cdot 3H_2O$ (0.050 g, 0.19 mmol) was dissolved and stirred in 1 mL dried 2-propanol for 30 min. The brown–orange product precipitated soon after the addition of 0.14 g (0.57 mmol) of DPSO. The suspension was stirred for 4 h, filtered, washed with 2-propanol and ether, and dried *in vacuo* (70%). *Anal.* calcd. for $RhC_{27}H_{28}Cl_3O_3S_2$: C 48.12, H 2.99; found: C 47.99, H 3.26. Nmr($CDCl_3$): δ 8.2–7.4 (m, 20, phenyl); 4.05 (m, 0.5, methine), 2.3–1.9 (broad singlet, 3, CH_3), 1.22 (d, 3, CH_3). Ir: ν(OH) 3400w; ν(SO) 1147m, 936s; ν(Rh—Cl) 350s.

$[(NPSO)_2H][RhCl_4(NPSO)_2]$

(*a*) $RhCl_3 \cdot 3H_2O$ (0.16 g, 0.72 mmol) was dissolved and stirred in 2 mL degassed 2-propanol for 30 min. The solution lightened to red–orange when 0.29 mL NPSO (2.5 mmol) was added. After 1 day the volume was reduced to 1 mL under vacuum; addition of 3 mL degassed hexane precipitated an orange microcrystalline solid that was filtered, washed with hexane, and dried *in vacuo*. Use of $CHCl_3$/hexane allowed recrystallization. Yield, 40%. *Anal.* calcd. for $RhC_{24}H_{57}Cl_4O_4S_4$: C 36.82, H 7.28; found: C 36.67, H 7.24. Nmr($CDCl_3$): δ 4.3–3.3 (m, 8,

Can. J. Chem. Downloaded from www.nrcresearchpress.com by 210.87.254.5 on 09/05/12
For personal use only.

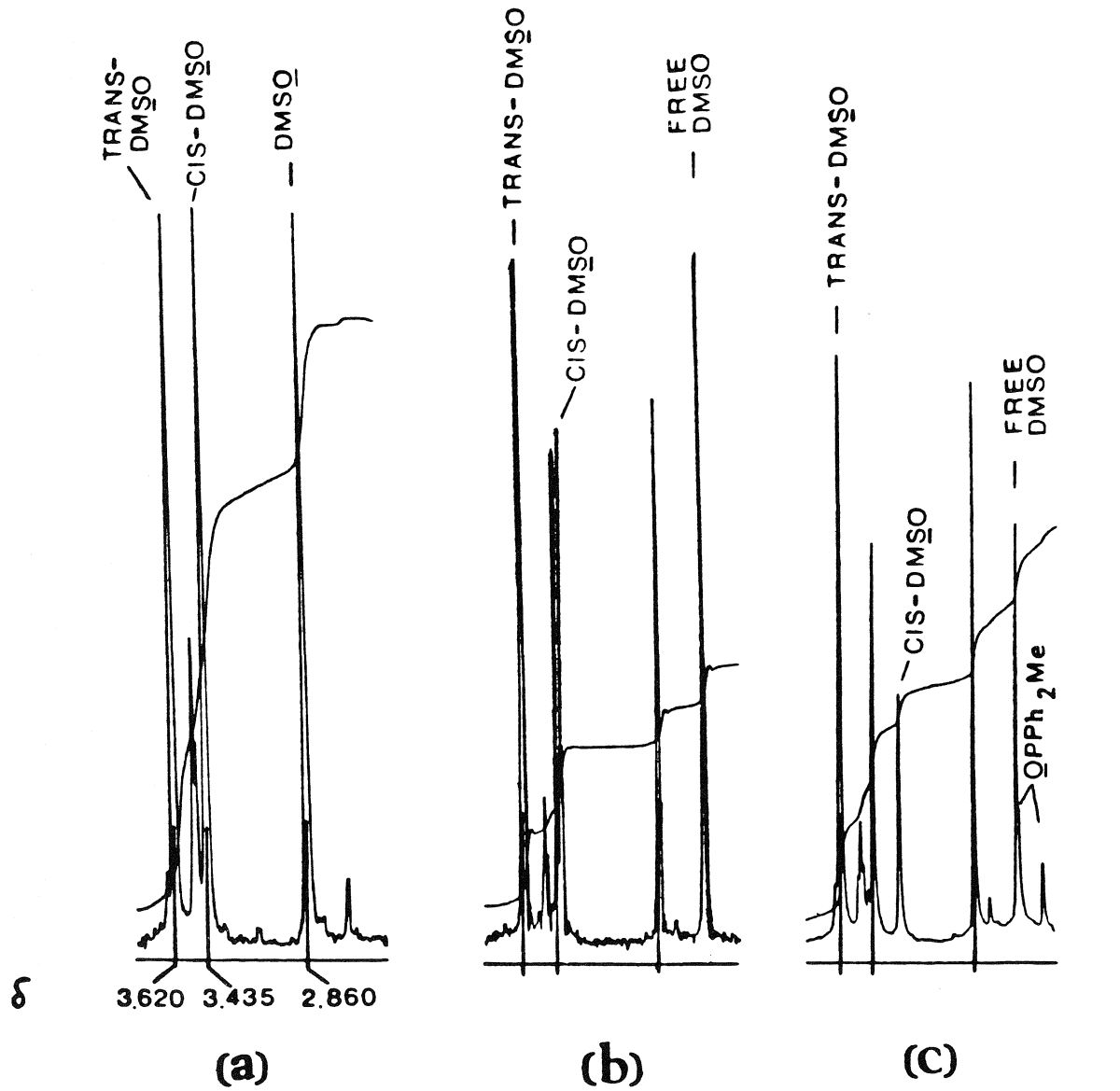


FIG. 1. 100 MHz ^{1}H nmr (δ 3.8–2.3 region) in $CDCl_3$ at 20°C of (*a*) $RhCl_3(DMSO)_3$, (*b*) $RhCl_3(DMSO)_3$ + 2 $OPPhMe_2$, and (*c*) $RhCl_3(DMSO)_3$ + 4.5 $OPPh_2Me$. The scale markings correspond to the peaks of $RhCl_3(DMSO)_2(DMSO)$ at δ 3.620, 3.435, and 2.860. The DMSO *cis* to O=L in the $RhCl_3(DMSO)_2(O{=}L)$ complexes in (*b*) and (*c*) (reaction [1]) are magnetically shielded by the phenyls of O=L.

S—C—H), 3.1–3.0 (m, 8, *O*—S—C—H + free O—S—C—H), 1.88 (m, 16, S—C—C—H), 1.1 (m, 24, S—C—C—C—H). Ir: ν(SO) 1122s; ν(S—O—H—O—S) 1600–1100 mb, 880–600 sb; ν(Rh—Cl) 350 m, 337s.

(*b*) A solution of $RhCl_3 \cdot 3H_2O$ (0.1 g, 0.38 mmol) in 0.15 mL concentrated HCl at 70°C was cooled to 25°C before 0.75 mL (5 mmol) of NPSO were added. The orange crystals that formed over 5 h were filtered, washed with a little 2-propanol, air-dried, and recrystallized as above. Yield, 65%. Spectral data agree with those given above in (*a*).

[H(DMSO)$_2$][RhCl$_4$(DMSO)$_2$]

A literature method (13) was used to prepare the compound as orange-red crystals. Nmr(D_2O): δ 3.56 (s, 4.2, *trans*-[$RhCl_4$(DMSO)(D_2O)]$^-$), 3.50 (s, 4.0, *trans*-[$RhCl_4(DMSO)_2]^-$), 2.70 (s, broad, 16, free DMSO). Ir: ν(SO) 1125; ν(S—O—H—O—S) 1600–1100 mb, 900–600 sb; $\rho_r(CH_3)$ 1020s, 972m; ν(Rh—Cl) 350s, 336s.

[NEt$_4$][RhCl$_4$(DMSO)$_2$]

After $RhCl_3(DMSO)_3$ (0.067 g, 0.15 mmol) and NEt_4Cl (0.025 g, 0.15 mmol) were warmed at 40°C for 30 min in CH_2Cl_2, solvent was pumped off until an orange precipitate formed. The mixture was cooled to 0°C and then filtered. Recrystallization from hot CH_2Cl_2/ether yielded a microcrystalline solid. Yield, 70%. *Anal.* calcd. for $RhC_{12}H_{32}Cl_4NO_2S_2$: C 27.13, H 6.07, N

Can. J. Chem. Downloaded from www.nrcresearchpress.com by 210.87.254.5 on 09/05/12
For personal use only.

TABLE 2. Proton nmr data[a] for reaction [1]

O=L	DMSO *trans* to O=L	DMSO *cis* to O=L	Peaks of coordinated OL	K_1[b]
DMSO	δ3.620	δ3.435	δ2.860	
DMA	3.67(+0.05)	3.49(+0.055)	3.17, 3.08(s, N—CH_3) 1.68(s, C—CH_3)	0.01
F-pip	3.647(+0.027)	3.437(0.0)	3.5(m, N—CH_2), 1.7(m, CH_2) 8.30(s, H—C=O)	0.2
DMF	3.646(+0.026)	3.447 (+0.012)	3.11, 3.08(s, N—CH_3) 8.27(s, H—C=O)	0.8
$OPPhMe_2$	3.63(+0.01)	3.41(−0.025)	2.11, J_{P-H} = 14(d, P—CH_3) 7.5–7.9(m, phenyl)	0.3
$OPPhEt_2$	3.63(+0.01)	3.43(0.0)	2.2–1.7(m, CH_2) 1.14, J = 8(t, CH_3), 7.5–7.9(m, phenyl)	1
$OPPh_2Me$	3.62(0.0)	3.29(−0.145)	2.54, J_{P-H} = 14(d, CH_3) 7.5–7.9(m, phenyl)	0.05
$OP(^nBu)_3$	3.58(−0.04)	3.37(−0.065)	2.0–1.5(m, CH_2) 0.9, J = 7(t, CH_3)	0.6
NPSO	3.62(0.0)	3.43(0.0)	3.1–2.5(m, S—CH_2) 2.0–1.8(m, —C—CH_2—), 1.07, J = 7(t, CH_3)	0.9
C_5H_5NO	3.57(−0.05)	3.51(+0.075)	9.0(m, *ortho*) 7.85, 7.50(m, *meta*, *para*)	100

[a]In $CDCl_3$ at 20°C using the peaks of $RhCl_3(DMSO)_3$ as an internal standard. Frequency shifts from these peaks to corresponding peaks of $RhCl_3(DMSO)_2(OL)$ are given in parentheses. All spectra contain "impurity" peaks at δ 3.503 and 3.492, possibly due to *mer*-$RhCl_3(DMSO)_3$ (see Fig. 1).
[b]K_1 is calculated from one spectrum and is accurate to ±50%.

2.63; found: C 27.25, H 6.0, N 2.50. Nmr(D_2O): δ 3.54 (s, 6, *S*—CH_3); 2.67 (s, 6, free DMSO); 3.19 (q, 8, N—CH), 1.25 (t, 12, N—C—CH). Nmr(CD_2Cl_2): 3.43 (s, 12, *S*—CH_3); 3.26 (q, 8, N—CH), 1.31 (t, 12, N—C—CH). Ir: ν(SO) 1140s; $\rho_r(CH_3)$ 1017m, 979m, 935m; ν(Rh—Cl) 345m, 335s.

[PS·H][$RhCl_4$(DMSO)$_2$]; PS = "Proton Sponge", 1,8-Bis(dimethylamino)naphthalene

[$H(DMSO)_2$][$RhCl_4(DMSO)_2$] (29 mg) was dissolved in 5 mL CH_2Cl_2 by adding 11 mg proton sponge. The orange–pink precipitate that formed when the solvent was gradually removed *in vacuo* was filtered, washed with ether, and air-dried. *Anal.* calcd. for $RhC_{18}H_{31}Cl_4N_2O_2S_2$: C 35.07, H 5.07, N 4.54; found: C 35.13, H 4.96, N 4.52. Nmr(D_2O): δ 7.9 (m, 6, aromatic H); 3.14 (s, 12, N—CH_3); 3.57 (s, 6, *S*—CH_3), 2.70 (s, 6, free DMSO). Nmr(CD_2Cl_2): 8.0–7.5 (m, 6, aromatic H); 3.29 (d, J = 2 Hz, 12, N—CH_3); 3.47 (s, 12, *S*—CH_3).

[RhCl(DPSO)$_2$]$_2$

To the red solution, obtained by stirring $RhCl_3 \cdot 3H_2O$ (0.1 g, 0.38 mmol) in degassed 2-propanol (1.5 mL) and H_2O (0.4 mL) for 30 min, was added DPSO (0.27 g, 1.3 mmol). The resulting solution deposited red crystals after standing from 8 to 24 h. The product was filtered under Ar, washed with degassed 2-propanol, and dried *in vacuo*. Yield, 65%. An attempt at recrystallization from degassed CH_2Cl_2/ether yielded brown, partially oxidized product. *Anal.* calcd. for $RhC_{24}H_{20}ClO_2S_2$: C 53.09, H 3.71, Cl 6.53; found: C 52.98, H 3.83, Cl 7.32. Ir: ν(SO) 1101s; ν(phenyl) 1068s; ν(Rh—Cl) < 250.

[RhCl(DPSO)(cyclooctene)]$_2$

(*a*) [RhCl(cyclooctene)$_2$]$_2$ (0.1 g, 0.14 mmol) was added to a degassed solution of DPSO (1.2 g, 6 mmol) in 3 mL CH_2Cl_2. After 8 mL of dry EtOH were added, the solution was warmed to 35°C, and concentrated by evacuation until a yellow powder formed. The air-sensitive microcrystalline solid obtained by cooling the mixture at −10°C was filtered under Ar, washed with dry EtOH, and dried *in vacuo*. *Anal.* calcd. for $RhC_{20}H_{24}ClOS$: C 53.28, H 5.26; found: C 52.97, H 5.26. Nmr($CDCl_3$): δ 7.8–7.2 (m, 20, phenyl); 3.9 (m, 4, olefinic H), 2.00 (m, 8, C=C—CH), 1.40 (m, 16, C=C—C—CH). Ir: ν(SO) 1109s; ν(phenyl) 1062s; ν(C_8H_{14}) 1180m, 1137m, 1128m, 960m, 922m, and others; ν(Rh—Cl) < 250.

(*b*) [RhCl(DPSO)$_2$]$_2$ (57 mg) was added to 14 μL *cis*-cyclooctene in 0.5 mL degassed CH_2Cl_2. Degassed EtOH (0.8 mL) was added and procedure (*a*) was followed. An orange oil first formed but soon crystallized yielding [RhCl(DPSO)-(C_8H_{14})]$_2$.

Other Olefin/Sulfoxide Complexes

The complex [RhCl(TMSO)(C_8H_{14})]$_2$ was likely prepared via procedure (*a*) above, but was too air-sensitive to obtain a good analysis. Ir: ν(SO) 1118s; ν(C_8H_{14}) 1175m, 1135m, etc.

Procedure (*a*), but using [RhCl(C_2H_4)$_2$]$_2$ and DPSO, gave an air-sensitive compound containing coordinated C_2H_4 (ir: 1217s, 997s) and DPSO (ν(SO) 1113s), but a good analysis was not obtained.

[RhCl(DMSO)$_2$]$_2$ and the Deuterated Derivative

To a degassed solution of excess sulfoxide (1.5 mL) in 5 mL of CH_2Cl_2 was added 0.25 g [RhCl(cyclooctene)$_2$]$_2$. After filtration under Ar, the solution was concentrated to 1.5 mL; 10 mL dry EtOH was added followed by 4 mL dry ether, and the resulting degassed solution was cooled to −10°C. The very hygroscopic and air-sensitive orange crystals were filtered and washed with dry ether under Ar; the nondeuterated complex is obtained with a solvate DMSO molecule, ν(SO) 1020s. *Anal.* calcd. for $RhC_4H_{12}ClO_2S_2 \cdot C_2H_6SO$: C 17.98, H 4.49; found: C 18.04, H 4.44. Nmr($CDCl_3$): δ 2.8 (s, broad, DMSO). Ir: ν(SO) 1101s; $\rho_r(CH_3)$ 1020s, 1007s, 972s, 937w; ν(Rh—Cl) < 250.

[RhCl(DMSO-d_6)$_2$]$_2$ was prepared similarly using DMSO-d_6. *Anal.* calcd. for $RhC_4D_{12}ClO_2S_2$: C 15.67, D 3.91; found: C 15.34, D 4.00. Ir: ν(SO) 1109s, 1099s, 1089s; $\delta_s(CD_3)$ 1022m,

Can. J. Chem. Downloaded from www.nrcresearchpress.com by 210.87.254.5 on 09/05/12
For personal use only.

1008m; $\rho_r(CD_3)$ 820s, 767m; ν(Rh—Cl) <250 (the yellow mull turned black within 3 min on exposure to air).

[RhCl(DIOS)$_2$]$_2$

A degassed solution of DIOS (0.25 g, 0.92 mmol) in 5 mL CH_2Cl_2 was added to [RhCl(cyclooctene)$_2$]$_2$ (0.1 g, 0.14 mmol) under Ar. Solvent was removed under vacuum to yield a red–brown oil. After being washed with degassed ether (3 × 10 mL), the resulting light brown powder was taken up in 1 mL CH_2Cl_2 and reprecipitated by slowly adding ether. The product was filtered, and dried *in vacuo*. Yield, 90%. *Anal.* calcd. for $RhC_{18}H_{36}ClO_8S_4 \cdot H_2O$: C 31.63, H 5.85; found: C 31.76, H 5.70. Nmr($CDCl_3$): δ 4.6–4.0 (m, 4, methine); 3.9–3.2 (m, 6, *S*—CH_3 + *S*—CH_2); 3.0 (s, broad, 6, free S—CH_2); 2.65 (s, broad, 8, free S—CH_3); 1.45 (s, 12, O—C—CH_3). Ir: ν(OH) 3600–3200 mb; ν(*S*O), ν(SO), + $\rho_r(CH_3)$ 1150–1000 sb; $\rho_r(CH_3)$ 980–950sb, 890m; ν(Rh—Cl) <250.

Results and Discussion

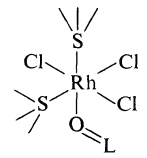
Infrared and ^{1}H nmr spectroscopy have been widely used to distinguish between oxygen- and sulfur-bonded sulfoxide ligands (4 and references therein). On comparison with the free ligand, donation via oxygen causes a shift of ν(SO) to a lower range (1000–900 cm^{-1}), while S-bonding generally causes an increase of ν(SO) to above 1100 cm^{-1}; however, assignments of ν(SO) for O-bonded sulfoxides with α-methyl groups (DMSO and MPTSO in the present studies) are complicated by methyl rocking vibrations which appear at similar energies, and comparison with a deuterated analogue is often helpful. Downfield nmr shifts of protons in O-bonded complexes are usually small and close to the free values, while with S-bonded systems the α-protons are closer to the metal and experience shifts of up to 1 ppm.

All the complexes reported in this paper contain some S-bonded sulfoxides.

Neutral Rh(III) Complexes

A convenient preparation of $RhCl_3L_3$ complexes (L = DMSO, DMSO-d_6, TMSO, MPSO, and *R*–MPTSO) was discovered during attempts to generate Rh(I) complexes from $RhCl_3 \cdot 3H_2O$ and sulfoxides by using 2-propanol as the solvent and reductant (see below). The Rh(III) complexes are obtained in high yields (80–95%) simply by collecting after 1 day the yellow precipitate resulting from the addition of 3 equivalents of sulfoxide to one of $RhCl_3 \cdot 3H_2O$, predissolved for at least 15 min in 2-propanol containing 20% V/V water. The brown compounds that sometimes precipitated initially were found by ir to contain water or 2-propanol, but on stirring over several hours these intermediates were converted to $RhCl_3L_3$. Crystalline samples for L = DMSO, DMSO-d_6, and TMSO, were sometimes deposited on leaving the systems to stand.

The $RhCl_3L_3$ complexes (L = DMSO, DMSO-d_6, TMSO, and diethylsulfoxide) have been prepared previously from hot aqueous solutions of $Na_3[RhCl_6]$ (9). For L = DMSO, crystallographic (10) and ir analysis (14) show that in the solid state the isomer present is *mer*-$RhCl_3(DMSO)_2(DMSO)$ (see **1**), but solution spectra were not examined. When crystals of $RhCl_3(DMSO)_3$, prepared from 2-propanol, water, or DMSO media, are dissolved in $CHCl_3$ or CH_2Cl_2, the ir spectra show a broad ν(*S*O) band and a ν(S*O*) band (Table 1). The nmr spectrum (Table 2; Fig. 1*a*), however, displays more than the two DM*S*O methyl resonances expected for a *mer*-$RhCl_3(DMSO)_2(DMSO)$ species. Selective replacement of the O-bonded DMSO ligand by other oxygen donors (O = L) in solution occurs with the retention of *mer* stereochemistry in all cases (**1**, see below) and allows the assignment of the prominent nmr peaks of $RhCl_3(DMSO)_3$ in $CDCl_3$. The δ 3.620 resonance is attributed to DM*S*O *trans* to DMS*O*, the 3.435 signal to DM*S*O *trans* to Cl, and the 2.860 signal to DMS*O* (Table 2). A 5% impurity of *mer*-



1

$RhCl_3(DMSO)_3$ could explain the smaller methyl resonances at δ 3.503 and 3.492 (intensity 2:1) observed in $CDCl_3$, and the corresponding degenerate single peak at δ 3.43 in CD_2Cl_2. This could also account for the observed DM*S*O/DMS*O* integration ratio of greater than 2:1, that is expected for *mer*-$RhCl_3(DMSO)_2(DMSO)$. The proportion of this "impurity" in solution increases slowly at 25°C over several days, along with a new species containing DMS*O* that resonates at δ 2.72. Attempts at separating the isomers by repeated recrystallizations from CH_2Cl_2/ether, or by thin layer chromatography on silica gel, failed. Analytical data, and the fact that added DMSO has no effect on the spectra, argue against the presence of chloride-bridged species. Since planes of symmetry of the molecule make the methyls of each DMSO equivalent, methyl inequivalence cannot account for the extra DM*S*O peaks (15). Autoionization to $[RhCl_2(DMSO)_4]^+[RhCl_4(DMSO)_2]^-$, similar to that observed for the analogous dimethyl sulfide complex (16), is also not consistent with the nmr data. A recent paper (17) that appeared after completion of the present work reports ^{1}H nmr and ^{1}H-{^{103}Rh} INDOR data on $[RhCl_{6-n}(DMSO)_n]^{n-3}$

Can. J. Chem. Downloaded from www.nrcresearchpress.com by 210.87.254.5 on 09/05/12
For personal use only.

species and also concludes that with $n = 3$, the major species in CH_2Cl_2 solution is *mer*-$RhCl_3(DMSO)_2(DMSO)$ with small amounts of *mer*-$RhCl_3(DMSO)_3$, interconversion being slow.

Table 2 presents nmr data for reaction [1] in $CDCl_3$ and rough estimates for the associated equilibria constants, K_1. All equilibria were shown to be established by warming the solutions at 40°C for 30 min. Addition of O=L has little influence on the peaks assigned to the *mer*-$RhCl_3(DMSO)_3$ impurity (see Fig. 1).

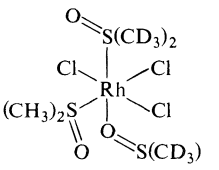
[1] *mer*-$RhCl_3(DMSO)_2(DMSO)$ + O=L

$$\overset{K_1}{\rightleftharpoons} \textit{mer}\text{-}RhCl_3(DMSO)_2(O{=}L) + DMSO$$

The nmr spectra of the isolated compounds, *mer*-$RhCl_3(DMSO)_2(O{=}L)$, where O=L is DMF, F·pip, and C_5H_5NO, show only the expected two equally intense, DMSO methyl resonances. A 30-fold excess of each of the weaker donors, DMA and $OPPh_2Me$, refluxed with $RhCl_3(DMSO)_3$ in 1,2-$C_2H_4Cl_2$ yields mixtures of the tris-DMSO and the desired bis-DMSO complexes. No reaction was observed with large excesses of $OPPh_3$, O_2SMe_2, and $OP(OEt)_3$. In all the studies of reaction [1], the ratio of methyl peak integrations for the S-bonded DMSO to the O-bonded DMSO plus free DMSO was 2.0. Strong donors such as PPh_3, pyridine, piperidine, and NEt_3, as well as greater than 1:1 excesses with respect to Rh of $OP(^nBu)_3$, C_5H_5NO, and NPSO, displace some DMSO as well as DMSO from $RhCl_3(DMSO)_3$.

In general, the O=L ligands cause greater shifts in the *cis*-DMSO resonances than in the *trans*. The diamagnetic shielding of the *cis*-DMSO methyl group by the phenyls of coordinated $OPPh_2Me$ is great enough to allow the unambiguous assignment of the upfield methyl peak to the *cis*-DMSO in the *mer*-$RhCl_3(DMSO)_2(O{=}L)$ complexes. The chemical shifts of the DMSO methyls *trans* to O=L might be explained by a *trans*-directed shielding of these methyl protons by the O=L ligand. Indeed the amount of shielding of these methyl protons, as judged by δ, correlates roughly with the oxygen donor strength of O=L (18–20): DMA < DMF < $OPPhMe_2$ ~ $OPPhEt_2$ ~ DMSO < $OPPh_2Me$ ~ NPSO < $OP(^nBu)_3$ < C_5H_5NO (see Table 2). By analogy, the downfield DMSO methyl peak of $IrCl_3(DMSO)_2(DMSO)$ (21) at δ 3.66 likely corresponds to DMSO *trans* to DMSO, and the other at 3.56, to DMSO *trans* to Cl. A similar technique, involving selective replacement of DMSO in the complex *trans*-$RuCl_2(DMSO)_3(DMSO)$ (22) by some O=L ligands, has been used (5) to explain the complex ^1H nmr spectrum of the tetrakis(dimethylsulfoxide) complex (15).

We have confirmed by nmr studies the earlier observation that the S-bonded ligands of $RhCl_3(DMSO)_3$ exchange at different rates (15), and can now state that it is the DMSO *trans* to DMSO that exchanges faster than the DMSO *trans* to Cl. Thus, after a solution of $RhCl_3(DMSO)_3$ (0.04 *M*) and DMSO-d_6 (0.4 *M*) in $CHCl_3$ is reacted at 35°C for 80 min, the yellow powder obtained on addition of ether contains 75% DMSO-d_6 *trans* to DMSO, <5% DMSO-d_6 *trans* to Cl, and 85% DMSO-d_6 (**2** shows the main product). Such labelled complexes could be useful in nmr studies of substitution reactions.



2

The ir (Table 1) and nmr data (see Experimental section) of the $RhCl_3L_3$ complexes with L = TMSO, MPSO, and *R*–MPTSO, are also consistent with two S- and one O-bonded ligands. The MPTSO complex shows just the two *S*-CH_3 ^1H nmr resonances expected for the *mer*-$RhCl_3(S$–MPTSO$)_2(R$–MPTSO$)$ structure.[2] The complex set of methyl peaks observed with the racemic MPSO ligand system must result from a mixture of "multistereoisomers", e.g. $RhCl_3(R$–MPSO$)_2(R$–MPSO$)$, $RhCl_3(S$–MPSO$)(R$–MPSO$)$-$(R$–MPSO$)$, etc. The detection of only two ν(Rh—Cl) for the L = TMSO, MPSO, and *R*-MPTSO complexes, is more consistent with a *fac* configuration, but in view of the nmr data for the *R*-MPTSO species, the *mer* formulation is favoured. The three metal–chloride bands are detected for the DMSO complex. Attempts at isolating $RhCl_3L_3$ complexes, or Rh(I) species (see below), with (*R*)-*t*-butyl-*p*-tolyl sulfoxide and (*S*)-*o*-tolyl-*p*-tolyl sulfoxide were unsuccessful, presumably because of steric problems, noted previously with Pt(II) centers (24). The $RhCl_3$-(sulfoxide)$_3$ complexes are useful starting materials for other complexes, for example, $RhCl_3$-$(DMSO)(py)_2$ which has anti-tumour properties (25).

Diphenylsulfoxide Complexes

On adding DPSO to $RhCl_3 \cdot 3H_2O$, predissolved in

[2] *R*–MPTSO becomes *S*–MPTSO when S-bonded to a metal.

Can. J. Chem. Downloaded from www.nrcresearchpress.com by 210.87.254.5 on 09/05/12
For personal use only.

wet 2-propanol (sulfoxide: Rh ~ 3), fairly air-stable, red crystals are deposited after 8–24 h, and these are formulated $[RhCl(DPSO)_2]_2$, ν(SO) indicating S-bonded sulfoxides (Table 1). The dimer formulation is consistent with the lack of a terminal ν(Rh—Cl), normally expected at >250 cm^{-1} (26), and the analytical data, since 3-coordinate Rh(I) is rare (27). The air-sensitivity of solutions of the complex (Table 1), and a stoichiometric reaction with cyclooctene in CH_2Cl_2 to give $[RhCl(DPSO)(C_8H_{14})]_2$ (see below), are consistent with a Rh(I) formulation. A brown product that precipitates out of an air-oxidized CH_2Cl_2 solution of the complex shows no ν(C—H) and is presumably some chlorooxide of Rh(III); free DPSO remains in solution.

Formation of $[RhCl(DPSO)_2]_2$ likely occurs according to reaction [2], as established for the cyclooctene dimer (11):

$$[2]\quad RhCl_3\cdot 3H_2O + 2L + (CH_3)_2CHOH \rightarrow \tfrac{1}{2}[RhClL]_2 + 3H_2O + 2HCl + (CH_3)_2CO$$

On using dry 2-propanol as solvent, we isolated a product analyzing correctly for $RhCl_3(DPSO)_2$(2-propanol), the ir (Table 1) showing the presence of both DP*S*O and DPS*O* (there could be one of each, or the compound could be a mixture of isomers). A broadening of the isopropyl methyl peaks in the nmr ($CDCl_3$) indicates exchange processes involving coordinated alcohol. The complex is likely an intermediate in reaction [2], since on suspension in 2-propanol/water under Ar, red crystals of $[RhCl(DPSO)_2]_2$ are deposited. The dehydrogenation of the alcohol is thought (28) to proceed via alkoxide formation and β-hydride elimination (reaction [3]):

$$[3]\quad Rh^{III}(^iPrOH) \xrightarrow[(a)]{-H^+} [Rh^{III}—O—\overset{\diagup}{C}H\overset{\diagdown}{}] \xrightarrow{-(CH_3)_2CO} HRh^{III} \xrightarrow[(b)]{-HCl} Rh^{I}$$

Water likely enhances elimination of H^+ (and Cl^-) in step (*a*) and the reductive elimination of HCl in step (*b*). Traces of a similar alcohol adduct containing only O-bonded sulfoxide were obtained using (*S*)-*o*-tolyl-*p*-tolyl sulfoxide, but the corresponding Rh(I) complex could not be isolated.

The milder conditions required for synthesis of the $RhCl_3L_3$ complexes in 2-propanol rather than water (9) may well result from a trace of Rh(I), generated by reaction [3], that is known to promote formation of Rh(III) species via a redox-catalyzed substitution process (29, 30).

Anionic Rhodium(III) Complexes

The $RhCl_3\cdot 3H_2O$/sulfoxide/wet 2-propanol reaction precipitated no neutral $RhCl_3L_3$ complex with L = NPSO, possibly because of solubilization by the alkyl chains. Addition of hexane, however, precipitated $[(NPSO)_2H][RhCl_4(NPSO)_2]$ in 40% yield. It is possible that some of the rhodium is converted by the alcohol to the univalent state, this reduction process (reaction [2]) furnishing the chloride required for the tetrachlororhodate(III) species. The complex is prepared in better yield in concentrated HCl media as initially described by Henbest and Trocha-Grimshaw (13) for the analogous $[(DMSO)_2H][RhCl_4(DMSO)_2]$ complex, although no spectral data were reported.

Both the NPSO and DMSO tetrachlororhodate(III) complexes have surprisingly intense and broad ir bands in the solid state at 1600–1100 and 900–600 cm^{-1} that are not due to the anion, as evidenced by the spectrum of the corresponding NEt_4^+ salt. Such bands can result from cations comprised of hydrogen-bonded bases (31), and a recent X-ray crystal structure of *trans*-$[(DMSO)_2H][RhCl_4(DMSO)_2]$ (32) has confirmed the existence of a proton bridge between the oxygen atoms of DMSO molecules in the cation $[(CH_3)_2SO—H—OS(CH_3)_2]^+$. The structure also confirms the S-bonded sulfoxides in the anion, as indicated by the nmr and ir (Experimental, Table 1, and ref. 17).

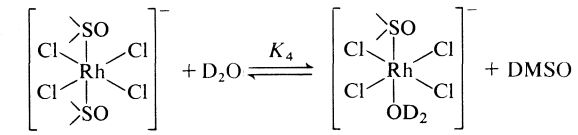
An approximate structure of the anion, as the sodium salt, has been reported by Sokol *et al.* (33). The *trans*-$RhCl_4L_2^-$ anions are readily formed via the $RhCl_3L_3$ complexes (L = DMSO, TMSO, MPSO) by treatment with NaCl in H_2O (14), or $[NEt_4]Cl$ in CH_2Cl_2 or H_2O. Other salts of the anions can be prepared from the $(R_2SO)_2H^+$ derivatives by adding strong bases, as reported previously (21) for $[(DMSO)_2H]$ $[IrCl_4(DMSO)_2]$, and we isolated in this way the protonated proton sponge[3] derivatives $[PS\cdot H][RhCl_4(R_2SO)_2]$ with DMSO (see Experimental section) and NPSO.

Spectroscopic observation of $(NPSO)_2H^+$ in CH_2Cl_2 or of $(DMSO)_2H^+$ in D_2O is not possible. The solution ir of the former suggests that HCl is eliminated when the tetrachlororhodate(III) salt is dissolved, since $RhCl_3(NPSO)_2(NPSO)$ appears to form (Table 1). The $(DMSO)_2H^+$ salt is insoluble in CH_2Cl_2, and in D_2O the DMSO of the cation appears in the nmr at the chemical shift for free DMSO.

[3]Proton sponge was chosen since we use this base to promote heterolytic cleavage of H_2 by Rh(III) complexes (to be published). For example, see ref. 23.

Can. J. Chem. Downloaded from www.nrcresearchpress.com by 210.87.254.5 on 09/05/12
For personal use only.

Dissolution of the NEt_4^+ or PS·H^+ salts of $RhCl_4(DMSO)_2^-$ in D_2O at 35°C gives complete formation of $RhCl_4(DMSO)(D_2O)^-$ within 30 s as evidenced by nmr (Experimental)

[4] 

δ3.50 δ3.56

Addition of DMSO moves equilibrium [4] to the left, and indeed when $[(DMSO)_2H][RhCl_4(DMSO)_2]$ is added to D_2O, both rhodate(III) species are detected due to the DMSO contributed by the cation. An nmr titration in the presence of added known amounts of DMSO yielded a K_4 value of $0.5 \pm 0.2\ M$ at 35°C. Reaction [4] illustrates the high kinetic *trans* effect of S-bonded sulfoxides (34). The monoaquated species is stable for weeks in aqueous solution at 20°C. The corresponding *trans*-$[IrCl_4(DMSO)_2]^-$ anions undergo aquation at a slower rate, $t_{1/2}$ being several minutes at 65°C (5).

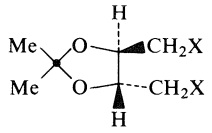
Rhodium(I) Complexes from $[RhCl(olefin)_2]_2$ Precursors

The displacement of labile *cis*-cyclooctene or ethylene from the title Rh(I) dimers in CH_2Cl_2 by donor ligands provides convenient routes to $[RhClL_2]_2$ and $RhClL_3$ complexes, when L is a phosphine, arsine, etc., added at the required 2:1 or 3:1 ligand:metal ratios (35). However, even with a ten-fold excess of DPSO or TMSO per rhodium, only $[RhCl(C_8H_{14})L]_2$ complexes were isolated, L being the S-bonded ligand. Similar mixed olefin – chiral sulfoxide complexes of Pt(II) have been used to study the extent to which a Pt – chiral S moiety distinguishes between the prochiral faces of a coordinated olefin, which is important, for example, in considering catalytic asymmetric hydrogenation of the olefin (36). The $[RhCl(C_8H_{14})_2]_2$ precursor can be used to give complexes of the type $[RhCl(MPSO)(PPh_3)]_2$ (5).

Use of a large excess of sulfoxide with $[RhCl(C_8H_{14})_2]_2$ did lead to isolation of $[RhCl(DMSO)_2]_2$ and the DMSO-d_6 analogue. The complexes are extremely hygroscopic and air-sensitive in the solid state; on exposure to O_2, the ν(SO) at ~1100 cm^{-1} is rapidly replaced by one at 1140 cm^{-1} which must pertain to a higher oxidation state, Rh(II) or Rh(III). Formation of sulfone, $(CH_3)_2SO_2$, was not detected. In degassed water, the complexes rapidly disproportionate to Rh metal and a green filtrate likely containing Rh(II) (37, 38). Lack of a terminal ν(Rh—Cl) and the analytical data are again the criteria used for dimer formulation of the Rh(I) complexes.

The solution ir of $[RhCl(DMSO)_2]_2$ (Table 1) consists of peaks for S-bonded and free DMSO, but not O-bonded DMSO. The nmr spectrum in $CDCl_3$ is a single broad peak at δ2.80, a chemical shift intermediate between that of free and S-bonded ligand, showing that dissociation of DMSO is occurring rapidly on the nmr time scale. Such labile behaviour, not observed for *trans*-$PdCl_2(DMSO)_2$ (39), would in part account for the reactivity of the Rh(I) complex.

A complex, best formulated as $[RhCl(DIOS)_2]_2 \cdot 2H_2O$, was also prepared from the cyclooctene dimer. The ir and nmr data show S-bonded ligands are present, although they are clearly labile on the nmr time-scale. There is no good evidence for a O-bonded DIOS ligand, ν(SO) ~ 930 cm^{-1} (2) and the nmr shifts at δ 3.0, 2.65 are those of free ligand (either as such, or of a monodentate, "dangling" type). The lack of a terminal ν(Rh—Cl) indicates a chloride-bridged dimer, and we tentatively favour two monodentate S-bonded DIOS ligands completing the four-coordination. Such monodentate coordination has been realized with the analogous DIOP ligand (1).



X = $SOCH_3$ gives DIOS
X = PPh_2 gives DIOP

The Nature of Rhodium–Sulfur Bonding in Sulfoxide Complexes

Table 3 lists some spectroscopic and structural data for some S-bonded DMSO complexes. Considering the range of bonding modes illustrated in **I–III**, the S—O bond order likely increases from about 2 (that of free sulfoxide) in the Fe(II) and Ru(II) pentammine complexes to probably almost 3 for the Au(III) complex (7, 49); this seems reasonable in that in the low-spin d^6 systems metal $d_\pi \rightarrow$ sulfur d_π backbonding is optimized and competes successfully with backbonding from oxygen p_π (**I**), while the highly electronegative Au(III) has poor backbonding capacity (**III**). The other complexes listed, including those of Rh, lie in the intermediate range, presumably mainly of type **II** bonding with little metal–sulfur backbonding, although the two Rh(I) complexes have relatively small Δν(SO) values implying perhaps some type **I** contribution. The

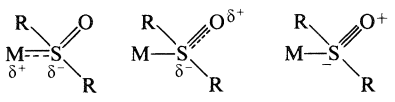


TABLE 3. Spectroscopic and crystal structure data for some sulfur-bonded DMSO complexes

Complex	$\Delta\nu$(SO)[a]	$\bar{r}$(S—O)[b]	$\bar{r}$(M—S)[c]	Reference
Free DMSO	0	1.531		40
$[Fe(CN)_5(DMSO)]^{3-}$	15			8
$[Ru(NH_3)_5(DMSO)]^{2+}$	0	1.53	2.19	7
fac-$[RuCl_3(DMSO)_3]^-$	45	1.49	2.26	41
cis-$RuCl_2(DMSO)_3(DMSO)$	35, 65	1.48	2.27	22
$[RhCl(DMSO)_2]_2$	46			This work
$RhCl(CO)(DMSO)_2$	52, 62			42
$[Rh(OAc)_2(DMSO)]_2$	31			43
trans-$[RhCl_4(DMSO)_2]^-$	65–85	1.47	2.29	10, 17, 32, this work
mer-$RhCl_3(DMSO)_2(DMSO)$	80–95	1.43	2.24	9, 17, this work
$[RhCl(DMSO)_5]^{2+}$	92–108			17, 44
trans-$PdCl_2(DMSO)_2$	61	1.47	2.29	45
cis-$Pd(NO_3)_2(DMSO)_2$	81, 102	1.46	2.24	46
cis-$[Pd(DMSO)_2(DMSO)_2]^{2+}$	85, 95			6, 39
cis-$[IrCl_4(DMSO)_2]^-$	45, 85			5, 21
trans-$[IrCl_4(DMSO)_2]^-$	70			5, 21
mer-$IrCl_3(DMSO)_2(DMSO)$	85			21
$IrCl_3(DMSO)_3$	95			21
$Ir(C_{15}H_{13}O)Cl_2(DMSO)_2$[d]	72	1.45	2.235	5, 47
cis-$PtCl_2(DMSO)_2$	80, 105	1.46	2.235	48
cis-$[Pt(DMSO)_2(DMSO)_2]^+$	88, 99			6
$AuCl_3(DMSO)$	143			49

[a] $\Delta\nu(SO) = \nu(SO) - 1055$ (free DMSO) in cm^{-1}. Data refer to Nujol mulls.
[b] The averaged S—O bond distance for DMSO in the molecule (Å).
[c] The average metal–sulfur distance in Å.
[d] $C_{15}H_{13}O$ is benzylacetophenone chelated to Ir by oxygen and benzyl carbon.

neutral Rh(III) complexes show $\nu(SO)$ at 20–40 cm^{-1} higher than similar Rh(I) adducts (and the same is true for DPSO and TMSO systems, see Table 1 and Experimental), and this could be rationalized in terms of either a small contribution of **I** in the Rh(I) systems or of **III** in the Rh(III) systems. *Ignoring metal–sulfur backbonding*, it is generally expected that a larger $\Delta\nu(SO)$ pertains to a stronger metal–S bond. There are insufficient structural data, but based on $\Delta\nu(SO)$, the metal–S bond strengths for the neutral d^8 systems decrease in the order Au(III) > Pt(II) ≈ Pd(II) > Rh(I), which would imply a relatively hard sulfur donor of sulfoxides (50). It is clearly difficult to estimate by spectroscopy the extent of metal–sulfur backbonding in the Rh(I) complexes. Chemical studies are likely to be more profitable: a greater resistance of $[RhCl(DPSO)_2]_2$ to disproportionate to metal (compared to $[RhCl(DMSO)_2]_2$) is strongly indicative of such backbonding, at least in the DPSO complex.

The relatively low $\Delta\nu(SO)$ value for the Rh(II) acetate complex probably results from the high *trans* influence of the metal–metal bond (51). Decreasing $\Delta\nu(SO)$ values on going from $RhClL_5^+$ (92–108 cm^{-1}), to $RhCl_3L_3$ (80–95 cm^{-1}) and $RhCl_4L_2^-$ (65–85 cm^{-1}) seem consistent with changes in the charges of the complexes.

Acknowledgements

We thank the Natural Sciences and Engineering Research Council of Canada for financial support in terms of a research grant and a postgraduate scholarship (R.H.M.), and Johnson Matthey Ltd. for the loan of $RhCl_3 \cdot 3H_2O$. One of us (B.R.J.) wishes to thank Professor F. Calderazzo of the Instituto di Chimica Generale, Università di Pisa, for discussions and for the facilities and cooperation of the Institute during the writing of the paper.

1. B. R. JAMES, R. S. MCMILLAN, R. H. MORRIS, and D. K. W. WANG. Adv. Chem. Ser. **167**, 122 (1978).
2. B. R. JAMES and R. S. MCMILLAN. Can. J. Chem. **55**, 3927 (1977).
3. R. S. MCMILLAN. Ph.D. Dissertation, University of British Columbia, Vancouver, B.C. 1976.
4. B. R. JAMES, R. H. MORRIS, and K. J. REIMER. Can. J. Chem. **55**, 2353 (1977).
5. R. H. MORRIS. Ph.D. Dissertation, University of British Columbia, Vancouver, B.C. 1978.
6. J. H. PRICE, A. N. WILLIAMSON, R. F. SCHRAMM, and B. B. WAYLAND. Inorg. Chem. **11**, 1280 (1972).
7. (*a*) C. V. SENOFF, E. MASLOWSKY, and R. G. GOEL. Can. J. Chem. **49**, 3585 (1971); (*b*) F. C. MARCH and G. FERGUSON. Can. J. Chem. **49**, 3590 (1971).
8. H. E. TOMA, J. M. MALIN, and E. GIESBRECHT. Inorg. Chem. **12**, 2084 (1973).
9. E. F. STRIZHEV, K. A. KHOKHRYAKOV, Y. N. KUKUSHKIN, and A. V. GORDIEVSKII. Russ. J. Inorg. Chem. **20**, 1685 (1975).
10. V. I. SOKOL and M. A. PORAI-KOSHITS. Koord. Khim. **1**, 577 (1975).
11. A. VAN DER ENT and A. L. ONDERDELINDEN. Inorg. Synth. **14**, 92 (1973).
12. R. CRAMER. Inorg. Chem. **1**, 722 (1962).
13. H. B. HENBEST and J. TROCHA-GRIMSHAW. J. Chem. Soc. Perkin I, 607 (1974).

Can. J. Chem. Downloaded from www.nrcresearchpress.com by 210.87.254.5 on 09/05/12
For personal use only.

14. Y. V. FADEEV, Y. N. KUKUSHKIN, and K. A. KHOKHRYAKOV. Russ. J. Inorg. Chem. **20**, 1519 (1975).
15. I. P. EVANS, A. SPENCER, and G. WILKINSON. J. Chem. Soc. Dalton Trans. 204 (1973).
16. V. I. SOKOL, V. N. NIKOLAEV, M. A. PORAI-KOSHITS, A. P. KOCHETKOVA, and L. B. SVESKNIKOVA. Koord. Khim. **1**, 675 (1975).
17. J. R. BARNES, P. L. GOGGIN, and R. J. GOODFELLOW. J. Chem. Res. (M), 1610 (1979).
18. E. M. ARNETT, E. J. MITCHELL, and T. S. S. R. MURTY. J. Am. Chem. Soc. **96**, 3875 (1974).
19. J. REEDIJK, P. W. N. M. VAN LEEUWEN, and W. L. GROENEVELD. Recl. Trav. Chim. **87**, 1073 (1968).
20. R. S. DRAGO, G. C. VOGEL, and T. E. NEEDHAM. J. Am. Chem. Soc. **93**, 6014 (1971).
21. Y. M. Y. HADDAD, H. B. HENBEST, and J. TROCHA-GRIMSHAW. J. Chem. Soc. Perkin I, 592 (1974).
22. A. MERCER and J. TROTTER. J. Chem. Soc. Dalton Trans. 2480 (1975).
23. B. R. JAMES, A. D. RATTRAY, and D. K. W. WANG. J. Chem. Soc. Chem. Commun. 792 (1976).
24. H. BOUCHER and B. BOSNICH. Inorg. Chem. **16**, 717 (1977).
25. P. COLAMARINO and P. ORIOLI. J. Chem. Soc. Dalton Trans. 845 (1976).
26. M. A. BENNETT, R. J. H. CLARK, and D. L. MILNER. Inorg. Chem. **6**, 1647 (1967).
27. Y. W. YARED, S. L. MILES, R. BAU, and C. R. REED. J. Am. Chem. Soc. **99**, 7076 (1977).
28. B. R. JAMES. Adv. Organomet. Chem. **17**, 319 (1979).
29. B. R. JAMES and G. L. REMPEL. J. Chem. Soc. A, 78 (1969).
30. A. W. ADDISON, R. D. GILLARD, P. S. SHERIDAN, and L. R. H. TIPPING. J. Chem. Soc. Dalton. Trans. 709 (1974).
31. D. HADŽI and S. BRATOS. *In* The hydrogen bond. Vol. 2. *Edited by* P. Schuster, G. Zundal, and C. Sandorfy. North-Holland, New York. 1976. p. 567.
32. B. R. JAMES, R. H. MORRIS, F. W. B. EINSTEIN, and A. WILLIS. J. Chem. Soc. Chem. Commun. In press.
33. V. I. SOKOL, N. D. RUBTSOVA, and A. Y. GRIBENYUK. Zh. Strukt. Chim. **15**, 318 (1974).
34. Y. N. KUKUSHKIN. Inorg. Chim. Acta, **9**, 117 (1974).
35. W. PARTENHEIMER and E. F. HOY. J. Am. Chem. Soc. **95**, 2840 (1973), and references therein.
36. H. BOUCHER and B. BOSNICH. J. Am. Chem. Soc. **99**, 6253 (1977).
37. K. THOMAS, J. A. OSBORN, A. R. POWELL, and G. WILKINSON. J. Chem. Soc. A, 1801 (1968).
38. B. R. JAMES and G. ROSENBERG. Coord. Chem. Rev. **16**, 153 (1975).
39. B. B. WAYLAND and R. F. SCHRAMM. Inorg. Chem. **8**, 971 (1969).
40. R. THOMAS, C. B. SHOEMAKER, and K. ERIKS. Acta Crystallogr. **21**, 12 (1966); M. A. VISWAMITARU and K. K. KANNAN. Nature, **209**, 1016 (1966).
41. R. S. MCMILLAN, A. MERCER, B. R. JAMES, and J. TROTTER. J. Chem. Soc. Dalton Trans. 1006 (1975).
42. D. N. LAWSON and G. WILKINSON. J. Chem. Soc. 1900 (1965).
43. S. A. JOHNSON, H. R. HUNT, and H. M. NEUMANN. Inorg. Chem. **2**, 960 (1963).
44. Y. N. KUKUSHKIN, N. D. RUBTSOVA, and N. V. IVANNIKOVA. Russ. J. Inorg. Chem. **15**, 1032 (1970).
45. M. J. BENNETT, F. A. COTTON, D. L. WEAVER, R. J. WILLIAMS, and G. H. WATSON. Acta Crystallogr. **23**, 788 (1967).
46. D. A. LANGS, C. R. HARE, and R. G. LITTLE. J. Chem. Soc. Chem. Commun. 1080 (1967).
47. M. MCPARTLIN and R. MASON. J. Chem. Soc. A, 2206 (1970).
48. R. MELANSON and F. D. ROCHON. Can. J. Chem. **53**, 2371 (1975).
49. R. A. POTTS. J. Inorg. Nucl. Chem. **34**, 1749 (1972).
50. R. G. PEARSON. J. Am. Chem. Soc. **85**, 3533 (1963).
51. J. G. NORMAN, JR. and H. J. KOLARI. J. Am. Chem. Soc. **100**, 791 (1978).

Can. J. Chem. Downloaded from www.nrcresearchpress.com by 210.87.254.5 on 09/05/12
For personal use only.

Pyrrole chemistry. XXI. Synthetic approaches to cyanopyrroles

GRAHAM H. BARNETT, HUGH J. ANDERSON, AND CHARLES E. LOADER

Department of Chemistry, Memorial University of Newfoundland, St. John's, Nfld., Canada A1B 3X7

Received October 2, 1979

GRAHAM H. BARNETT, HUGH J. ANDERSON, and CHARLES E. LOADER. Can. J. Chem. **58**, 409 (1980).

The Vilsmeier–Haack reaction with pyrrole and 1-methylpyrrole has been modified to provide a direct synthesis of the corresponding 2-nitriles. Chlorosulfonyl isocyanate may be used to prepare the same compounds, but less satisfactorily. The latter reagent does enable the synthesis of pyrrole-2,4-dicarbonitrile in one step. This dinitrile may be reduced to pyrrole-2,4-dicarboxaldehyde.

GRAHAM H. BARNETT, HUGH J. ANDERSON et CHARLES E. LOADER. Can. J. Chem. **58**, 409 (1980).

On a modifié la réaction de Vilsmeier–Haack appliquée aux pyrroles et le méthyl-1 pyrrole dans le but d'obtenir la synthèse directe des nitriles-2 correspondants. On peut utiliser l'isocyanate de chlorure de sulfonyle pour préparer les mêmes composés mais cette méthode donne de moins bons résultats. Le dernier réactif permet de réaliser la synthèse du pyrrole dicarbonitrile-2,4 en une seule étape. Ce dinitrile peut être réduit en pyrrole dicarboxaldéhyde-2,4.

[Traduit par le journal]

Recently we reported some further reactions of simple 2-cyanopyrroles (1). The synthetic usefulness of these compounds has caused us to investigate improved methods for the preparation of pyrrole-2-carbonitrile and its 1-methyl derivative. At present no direct synthesis from pyrrole gives the 2-nitrile in better than 50–60% yield (2) and, until recently, methods starting from the 2-aldehyde or 2-amide were no better (2*a*). The procedure of Streith *et al.* (3) appears to be the best conversion of 2-aldehyde to 2-nitrile reported so far. Taken together with the usual synthesis of the 2-aldehyde (4) it should give close to 70% of the 2-nitrile in two steps from pyrrole. The sequence from 2-aminopyridine used by Abramovitch and Cue (5) also gave good yields for each of several steps, but overall did not greatly improve the routine preparation of the 2-nitrile.

The recent use of chlorosulfonyl isocyanate (CSI) for the direct introduction of a cyano group onto activated aromatics (6, 7) prompted us to examine its use in the pyrrole series. However, although crude (2-pyrrolylcarbonyl)-sulfamoyl chloride could be obtained in excellent yield, and subsequent hydrolysis (8) gave a very good yield of pyrrole-2-carboxamide, the best preparation of the 2-nitrile was no better than 40%. There was a modest improvement in the yield in preparations of the 2-nitriles from 1-methyl- and 1-carbomethoxypyrroles. However, the overall results were not encouraging for an improved preparation of simple 2-cyanopyrroles. A number of modifications of the procedure using bases other than dimethylformamide (7*a*) were explored with no real success.

The use of 2.25 molar equivalents of CSI on pyrrole gave isolated yields of 53% 2,4- and 2.5% 2,5-dicyanopyrrole on quite a large scale. The availability of the 2,4-isomer in one step from pyrrole caused us to examine methods of selective reduction of this substance with a view to preparing 4-cyanopyrrole-2-carboxaldehyde. This should lead to an easy preparation of 3-cyanopyrrole through decarbonylation (1). Selectivity was not easily achieved, however. A mild reagent such as lithium triethoxyaluminohydride gave only starting material, while lithium aluminum hydride under a variety of conditions led to overreduction. The best isolated yields approached 50%. The use of the dissolving Raney nickel alloy method (1) was no more selective, but it was possible to prepare the 2,4-dialdehyde by this latter method in 55% yield on a moderate scale, although the reduction was much more successful on a small scale. Part of the difficulty lies with the low solubility of these compounds, all possessing electron-withdrawing groups in both 2- and 4-positions, making it time consuming to separate partially reduced mixtures of product and starting material.

A different approach to the synthesis of pyrrole-2-carbonitrile was suggested by the report of Liebscher and Hartmann (9). They used hydroxylammonium chloride in refluxing dimethylformamide (DMF) to convert aromatic aldehydes to nitriles in excellent yield, and were also successful in a reaction of the type:

$$\underset{\mathbf{1}}{Ar{-}CH{=}\overset{+}{N}(CH_3)_2ClO_4^-} \xrightarrow[DMF/\Delta]{NH_2OH\cdot HCl} Ar{-}CN$$

As these authors point out, immonium salts such as **1** are intermediates in the Vilsmeier–Haack formylation and may be isolated from that reaction (10).

We felt that, since the Vilsmeier aldehyde syn-

0008-4042/80/040409-03$01.00/0

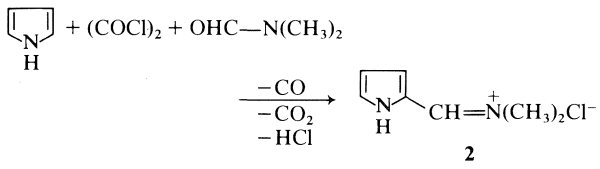
©1980 National Research Council of Canada/Conseil national de recherches du Canada

Can. J. Chem. Downloaded from www.nrcresearchpress.com by 210.87.254.40 on 09/05/12
For personal use only.

Can. J. Chem. Downloaded from www.nrcresearchpress.com by 210.87.254.40 on 09/05/12
For personal use only.

thesis is so successful with pyrrole (4), it should be possible to adapt that reaction to a direct nitrile synthesis using the above method. When we prepared the Vilsmeier complex in 1,2-dichloroethane solution using phosphorus oxychloride and DMF, the nuclear magnetic resonance (nmr) spectrum revealed a clean conversion to a 2-substituted pyrrole salt, corresponding to **1**. Thus, there seemed to be no real reason to isolate the perchlorate salt before proceeding. Hydroxylammonium chloride dissolved in warm excess DMF was added and the temperature raised to distil out the dichloroethane. When the boiling point of DMF was reached, the solution was refluxed and worked up according to Liebscher and Hartmann (9). There was a small yield of both 2-nitrile and 2-aldehyde and much destruction to a black tarry solid.

After several variations of the technique produced no real improvement, we decided to simplify the nature of the Vilsmeier intermediate in solution through the use of oxalyl chloride instead of phosphorus oxychloride. This avoided the possible complication of the presence of the phosphorus-containing by-product. We then obtained a solution of **2** in dichloroethane which showed a clean nmr spectrum.



2

As reflux with hydroxylammonium chloride in excess DMF still gave considerable destruction to tarry material, a molar equivalent of pyridine was added to the hydroxylammonium chloride solution in DMF. After addition of this mixture to the immonium salt, the solution was refluxed at the boiling point of dichloroethane. We were able to use nmr spectra to follow the conversion of the immonium salt, **2**, to the 2-nitrile over the course of about ten hours. On working up, there was much less tarry material and a yield of 64% of pyrrole-2-carbonitrile was obtained. The same procedure gave 67% of the 1-methyl analog from 1-methylpyrrole. Thus we have a "one-pot" synthesis of these two useful starting materials using simple reagents applicable on a large scale which gives satisfactory results.

Experimental

Melting points are uncorrected. Elemental analyses were by Atlantic Microlabs, GA, U.S.A. The ir spectra were recorded on a Perkin-Elmer 273B grating spectrophotometer. The ^{1}Hmr spectra were determined using a Varian EM360 instrument. Values are given on the δ scale using tetramethylsilane as internal reference. Mass spectra were recorded on a Hitachi-Perkin-Elmer RMU-6E spectrometer using a direct inlet system.

Reactions of Pyrrole and Chlorosulfonyl Isocyanate

Pyrrole-2-carboxamide

Chlorosulfonyl isocyanate (18.75 g, 132 mmol) in dichloromethane (35 mL) was added dropwise over 1 h to a stirred solution of pyrrole (6.7 g, 100 mmol) in dichloromethane (200 mL) kept about −24°C under dry nitrogen. Stirring was continued for a further 2 h while the bath temperature was allowed to rise slowly to ambient. The cream-colored powdery product was collected, washed with cold carbon tetrachloride, and dried in a vacuum desiccator. It was very sensitive to moisture. The crude product, (2-pyrrolylcarbonyl)-sulfamoyl chloride (17.9 g, 85%), had an nmr spectrum (acetone-d_6) δ: 7.25 (m, 2H), 6.30 (m, 1H).

The crude (2-pyrrolylcarbonyl)-sulfamoyl chloride was dissolved in ice water and filtered. The filtrate was warmed to ~80°C at which it turned red and precipitated some black solid. After a second filtration the solution was taken to pH 7 with saturated aqueous sodium hydrogen carbonate. The product, a white solid, then precipitated and was filtered off. More of the product was obtained by concentration of the filtrate. The crude product was easily sublimed to give pyrrole-2-carboxamide (8.12 g, 74% from pyrrole), mp 172–173.5°C (lit. (11) mp 172.5–174°C).

Pyrrole-2-carbonitrile

The adduct from CSI (53 mmol) and pyrrole (35 mmol) in 35 mL dichloromethane was prepared as above. To the stirred solution at −15 to −10°C was added DMF (5.7 mL, 73.5 mmol) over a period of 30 min. After 1 h further stirring, the reaction mixture was poured onto ice and, eventually, extracted with dichloromethane. The extract was washed successively with water and aqueous NaCl, dried (Na_2SO_4), and then evaporated to give a brown oil. Vacuum distillation of the oil gave pyrrole-2-carbonitrile (1.3 g, 40%), bp 118–120°C/14 Torr.

When acetonitrile was used as solvent and triethylamine as the base (*7a*) on a sample of (2-pyrrolylcarbonyl)-sulfamoyl chloride, the usual work-up gave 25% of 2-pyrrolecarbonitrile.

Pyrrole-2,4-dicarbonitrile and Pyrrole-2,5-dicarbonitrile

While the temperature was maintained at −24°C, a solution of CSI (318.4 g, 2.25 mol) in anhydrous ether (600 mL) was added over a period of 2 h to pyrrole (67 g, 1 mol) in anhydrous ether (400 mL) under an atmosphere of dry nitrogen. Over the following 2½ h the temperature was allowed to rise to ambient. DMF (320 mL, 4.14 mol) was then added over 1 h, keeping the temperature at about −12°C. After a further 1 h at room temperature, the reaction mixture was poured into ice-cold hydrochloric acid (3 *M*, 500 mL), and stirred for 20 min. This solution was extracted repeatedly with ethyl ether and finally with ethyl acetate. The combined layers were washed with dilute aqueous hydrochloric acid, aqueous sodium hydrogen carbonate, and with saturated aqueous NaCl, then dried ($MgSO_4$). After removal of the solvent the crude solid was extracted into toluene using a Soxhlet and, after crystallization from toluene, gave pyrrole-2,4-dicarbonitrile[1] (61.6 g, 53%), mp 181–183°C; ir ν: 2225 (CN) cm^{-1}; nmr (acetone-d_6) δ: 7.81 (1H, d), 7.28 (1H, d); *m/e*: 117. *Anal.* calcd. for $C_6H_3N_3$: C 61.54, H 2.58; found: C 61.55, H 2.61.

Evaporation of the toluene extract and residues from crystallization of the pyrrole-2,4-dicarbonitrile gave a crude solid which was recrystallized from ethyl ether – petroleum (bp 35–50°C), pyrrole-2,5-dicarbonitrile[1] (2.8 g, 2.5%), mp 148.5–149.5°C; ir ν: 2230, 2245 cm^{-1}; nmr ($CDCl_3$) δ: 6.93; *m/e*: 117. *Anal.* calcd. for $C_6H_3N_3$: C 61.54, H 2.58; found: C 61.46, H 2.59.

[1]Compound is referred to in ref. 12. No physical constants are given in that publication.

Can. J. Chem. Downloaded from www.nrcresearchpress.com by 210.87.254.40 on 09/05/12
For personal use only.

Reaction of 1-Methylpyrrole and Chlorosulfonyl Isocyanate

A solution of 1-methylpyrrole (11.34 g, 140 mmol) in dichloromethane (80 mL) was treated with CSI (24.80 g, 175 mmol) in dichloromethane (120 mL), followed 2 h later with DMF (22.7 mL, 29 mmol) as for pyrrole (above). The reaction product was poured into ice-cold 4 *M* HCl and worked up to give a yellow oil together with some white solid. Vacuum distillation then gave 1-methylpyrrole-2-carbonitrile (8.6 g, 58%) bp 82–87°C/10 Torr. The solid residue was chromatographed on EM Reagents neutral alumina Grade II using dry ethyl ether as eluant. The two products were recrystallized from ethyl ether – petroleum (bp 35–50°C): (*a*) 1-methylpyrrole-2,5-dicarbonitrile (0.46 g, 2.5%), mp 102–103°C; nmr ($CDCl_3$) δ: 6.82 (2H, s), 3.91 (3H, s); *m/e*: 131. *Anal.* calcd. for $C_7H_5N_3$: C 64.11, H 3.84; found: C 64.10, H 3.84; (*b*) 1-methylpyrrole-2,4-dicarbonitrile (0.51, 2.8%); mp 109–109.5°C; nmr ($CDCl_3$) δ: 7.35 (1H, d), 7.07 (1H, d), 3.96 (3H, s); *m/e*: 131. *Anal.* calcd. for $C_7H_5N_3$: C 64.11, H 3.84; found: C 64.11, H 3.87.

Reaction of Ethyl Pyrrole-1-carboxylate with Chlorosulfonyl Isocyanate

Following the procedure for pyrrole (above), ethyl pyrrole-1-carboxylate (4.17 g, 30 mmol), CSI (4.66 g, 33 mmol), and DMF (6.96 mL, 60 mmol) gave, upon working up, a purple oil which partly solidified on refrigeration. Vacuum distillation afforded ethyl 2-cyanopyrrole-1-carboxylate (2.9 g, 58%), bp 131–133°C/11 Torr; ir ν: 2220 (C≡N), 1760 (C=O) cm^{-1}; nmr ($CDCl_3$) δ: 7.35 (1H, m), 6.87 (1H, m), 6.19 (1H, m), 4.43 (2H, q), 1.46 (3H, t); *m/e*: 164. *Anal.* calcd. for $C_8H_8N_2O_2$: C 58.53, H 4.91, N 17.06; found: C 58.32, H 4.97, N 16.99.

Reductions of Pyrrole-2,4-dicarbonitrile

A solution of pyrrole-2,4-dicarbonitrile (0.117 g, 1 mmol) in tetrahydrofuran (2 mL, distilled from $LiAlH_4$) was added to a stirred suspension of $LiAlH_4$ (0.040 g, 1.06 mmol) in THF (5 mL) at 0°C under dry N_2. After 2½ h at 0°C the mixture was hydrolyzed with 2.5 *M* H_2SO_4 (6 mL). Extraction with ethyl ether was followed by washing with brine and drying ($MgSO_4$). Evaporation gave a cream-colored solid. This crude material was recrystallized from ethyl ether – petroleum (bp 35–50°C) affording 4-cyanopyrrole-2-carboxaldehyde (56 mg, 45%), mp 175–177°C (lit (13) mp 177–177.5°C).

When twice the amount of $LiAlH_4$ was used, the isolated product was about 80% 4-cyano-2-pyrrolecarboxyaldehyde, with the rest starting material, plus a trace of pyrrole-2,4-dicarboxaldehyde. Over half of the starting material was not accounted for.

Pyrrole-2,4-dicarbonitrile (2.0 g, 17.1 mmol) was added to a gently refluxing mixture of Raney nickel alloy (0.6 g) in formic acid (18 mL, 50% aqueous) which was evolving H_2 gas. Stirring and heating was continued for 1½ h. The hot solution was then continuously extracted with toluene. After drying ($MgSO_4$) and vacuum removal of solvent, the yellow solid was sublimed to give pyrrole-2,4-dicarboxaldehyde (1.18 g, 56%), mp 149–152°C (lit. (14) mp 151.5–152°C). The melting point of a mixture with authentic material was not depressed.

Modified Vilsmeier–Haack Synthesis for Pyrrolecarbonitriles

(a) Pyrrole-2-carbonitrile

A solution of dimethylformamide (20.1 g, 0.275 mol) in 1,2-dichloroethane (60 mL) in a 3-necked flask was cooled in an ice-salt bath. To the stirred and cooled solution was added a solution of oxalyl chloride (34.9 g, 0.275 mol) in 1,2-dichloroethane (40 mL) over a period of 20 min. The suspension of white solid was then allowed to stir at room temperature for 15 min. The suspension was cooled in ice and a solution of pyrrole (16.8 g, 0.25 mol) in 1,2-dichloroethane (50 mL) was added over 20 min. The light orange solution obtained was allowed to stir 15 min at room temperature.

Hydroxylammonium chloride (18.9 g, 0.275 mol) was dissolved in warm dimethylformamide (50 mL) and pyridine (21.7 g, 0.275 mol) was then added. This solution was added rapidly to the Vilsmeier complex prepared above. The reaction mixture, heated by an oil bath, was refluxed for 10 h. After cooling, about 500 mL saturated $NaHCO_3$ solution was added. The dark brown solution was extracted with ethyl ether. The ether extracts were washed with saturated aqueous NaCl and then with 1 *M* hydrochloric acid. The dark colored mixture was filtered through a thick pad of Celite. After several further washings with 1 *M* HCl, the ether layer was washed with saturated aqueous NaCl, several portions of 5% aqueous $NaHCO_3$, and with water. The ether layer was dried (K_2CO_3) and the solvent removed. Vacuum distillation gave pyrrole-2-carbonitrile (14.7 g, 64%), bp 74–76°C/1 Torr.

(b) 1-Methylpyrrole-2-carbonitrile

Following the procedure of (*a*) above using 1-methylpyrrole (20.3 g, 0.25 mol), vacuum distillation of the crude product gave 1-methyl-2-pyrrolecarbonitrile (17.7 g, 67%), bp 72–75°C/9 Torr.

Acknowledgements

The authors gratefully acknowledge the continued financial support of the National Research Council of Canada and the Memorial University of Newfoundland. They also thank Mr. Aidan Foster for assistance in scaling up the modified Vilsmeier–Haack synthesis.

1. H. J. ANDERSON, C. R. RICHE, T. G. COSTELLO, C. E. LOADER, and G. H. BARNETT. Can. J. Chem. **56**, 654 (1978).
2. (*a*) A. GOSSAUER. Die chemie der pyrrole. Springer Verlag, Berlin, Heidelberg, New York. 1974. p. 320; (*b*) Y. TAMURA, T. KAWASAKI, M. ADACHI, M. TANIO, and Y. KITA. Tetrahedron Lett. 4417 (1977); (*c*) K. YOSHIDA. J. Am. Chem. Soc. **99**, 6111 (1977).
3. J. STREITH, C. FIZET, and H. FRITZ. Helv. Chim. Acta, **59**, 2786 (1976).
4. R. M. SILVERSTEIN, E. E. RYSKIEWICZ, and C. WILLARD. Org. Synth. **36**, 74, (1956).
5. R. A. ABRAMOVITCH and B. W. CUE, JR. J. Am. Chem. Soc. **98**, 1478 (1976).
6. G. LOHAUS. Chem. Ber. **100**, 2719 (1967); Org. Synth. **50**, 52 (1970).
7. (*a*) H. VORBRÜGGEN. Tetrahedron Lett. 1631 (1968); (*b*) G. MEHTA and D. N. DHAR. Synthesis, 374 (1978).
8. R. GRAF. Justus Liebigs Ann. Chem. **661**, 111 (1963).
9. J. LIEBSCHER and H. HARTMANN. Z. Chem. **15**, 302 (1975).
10. S. SESHADRI. J. Sci. Ind. Res. **32**, 128 (1973).
11. W. A. ROELFSMA and H. J. DEN HERTOG. Tetrahedron Lett. 5089 (1967).
12. R. HARDER and C. WENTRUP. J. Am. Chem. Soc. **98**, 1259 (1976).
13. P. E. SONNET. J. Heterocycl. Chem. **10**, 113 (1973).
14. C. E. LOADER and H. J. ANDERSON. Tetrahedron, **25**, 3879 (1969).

Experimental and theoretical investigation of the unusual substituent effect of the vinyl group

W. F. REYNOLDS AND T. A. MODRO
Department of Chemistry, University of Toronto, Toronto, Ont., Canada M5S 1A1
P. G. MEZEY
Department of Chemistry, University of Saskatchewan, Saskatoon, Sask., Canada S7N 0W0
AND
E. SKORUPOWA AND A. MARON
Institute of Chemistry, University of Gdansk, Gdansk, Poland

Received June 28, 1979

W. F. REYNOLDS, T. A. MODRO, P. G. MEZEY, E. SKORUPOWA, and A. MARON. Can. J. Chem. **58**, 412 (1980).

σ^+ Substituent constants for the *ortho*- and *para*-vinyl group have been determined by the application of the linear free-energy relationship to the nitration of the β-substituted styrene derivatives.

Energy changes (relative to benzene system) for the proton and hydride ion transfer to individual positions in the styrene molecule have been calculated. Both approaches indicate that the vinyl group is capable of stabilizing both positively and negatively charged transition states. The interactions of the vinyl group with other substituents in the phenyl ring are also determined. Again, stabilizing effects with respect to both π-donor and π-acceptor substituents have been demonstrated for the vinyl group.

W. F. REYNOLDS, T. A. MODRO, P. G. MEZEY, E. SKORUPOWA et A. MARON. Can. J. Chem. **58**, 412 (1980).

On a déterminé les constantes de substituant σ^+ du groupe vinyle en position *ortho* et *para* en appliquant la relation linéaire d'énergie libre à la nitration des dérivés du styrène substitués en position β. On a calculé les variations d'énergie (par rapport au système benzénique) résultant du transfert du proton et de l'ion hydrure à des positions individuelles dans la molécule de styrène. Les deux approches indiquent que le groupe vinyle peut stabiliser de façon à la fois positive et négative les états de transition chargés. On a également déterminé les interactions du groupe vinyle avec les autres substituants du phényle. On a encore démontré l'effet stabilisateur du groupe vinyle par rapport aux substituants donneur π et accepteur π.

[Traduit par le journal]

Introduction

Most substituent groups attached to organic molecules can be classified as either electron donor or electron acceptor groups. Electron donor groups accelerate rates of reactions in which positive charge is developed in the transition state and slow down reactions involving development of negative charge, while electron withdrawing groups have the opposite effect. In the context of aromatic reactivity, substituent effects on a group X in a system RX can be predicted by the Hammett equation (1)

$$[1] \quad \log (k_X/k_H) = \rho\sigma_x$$

The substituent constant, σ_x, is respectively negative and positive for donor and acceptor groups while ρ is respectively negative and positive for reactions involving development of positive and negative charge in the transition state. A large number of σ constant scales have been proposed (2), including σ^+ (3) and σ^- (4) scales which are respectively intended for systems in which there is a large degree of positive or negative charge development in the transition state. Nevertheless, for most substituents σ^+ and σ^- have the same sign, characteristic of the donor or acceptor nature of the group.

However, there are a number of exceptions. For example, the halogens and most oxygen-bonded substituents have opposing field/inductive and resonance effects (e.g., $\sigma_I = +0.27, \sigma_R^0 = -0.45$ for OCH_3 and $\sigma_I = +0.50, \sigma_R^0 = -0.34$ for F according to Taft's dual substituent parameter scale (5)). Thus the net effect of the substituent depends upon the relative magnitudes of the two effects and may change sign for different positions of substituents (e.g., $\sigma_{meta} = +0.12, \sigma_{para} = -0.27$ for OCH_3 (6)) or for different types of reaction sites (e.g., $\sigma_p^- = +0.06, \sigma_p^+ = -0.07$ for F(6)).

Another more unusual class of exceptional substituents are those which have intrinsically small substituent effects in neutral systems but which are capable of stabilizing both negatively and positively charged species. For example, alkyl groups are both acid-strengthening and base-strengthening in gas phase proton transfer reactions, apparently due to the polarizability of these groups (7). However, for aromatic reactions in solution, this effect must be relatively unimportant since alkyl groups act as weak electron donors in this case (e.g., $\sigma_p^+ =$

0008-4042/80/040412-06$01.00/0
©1980 National Research Council of Canada/Conseil national de recherches du Canada

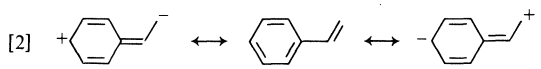
Can. J. Chem. Downloaded from www.nrcresearchpress.com by 210.87.254.42 on 09/05/12
For personal use only.

TABLE 1. Nitration of β-substituted styrenes in TFA/H_2SO_4, 25°C

X in Ph—CH=CH—X	σ_X^+ [a]	k_2 ($s^{-1} M^{-1}$)	Orientation (%)		k_2 ($s^{-1} M^{-1}$)	
			Para	*Ortho*	*Para*	*Ortho*
Br	0.15	1.69 ± 0.19	43	57	0.726 ± 0.080	0.963 ± 0.106
CO_2H	0.42[b]	0.256 ± 0.029[c]	46	54	0.118 ± 0.013	0.138 ± 0.015
CO_2Et	0.48	0.147 ± 0.014	49	51	0.0720 ± 0.0072	0.0750 ± 0.0075
CN	0.66	0.0427 ± 0.0061	59	41	0.0252 ± 0.0035	0.0175 ± 0.0024
NO_2	0.79	0.0202 ± 0.0018	58	42	0.0117 ± 0.0010	0.00848 ± 0.00075
PO_3H_2	—	0.413 ± 0.058	26	74	0.107 ± 0.015	0.306 ± 0.043

[a]Reference 6.
[b]Reference 14.
[c]This value gives the relative rate of nitration of cinnamic acid (relative to benzene), $k_{rel} = 0.31$. Early value (16) estimated in acetic anhydride gives for cinnamic acid $k_{rel} = 0.11$.

-0.31, $\sigma_p^- = -0.17$ for CH_3 (6)). Two other substituents which should fall into this category even in solution are the phenyl and vinyl groups. In fact σ_p^+ ($= -0.20$ (6)) and σ_p^- ($\simeq \sigma_I + \sigma_R^- = +0.14$ (6)) constants for the phenyl group confirm that it will have a rate-accelerating effect on reactions involving the development of either positive or negative charge in the transition state. This presumably reflects the ability of the phenyl group to act as either a π-donor or a π-acceptor. Similarly, the vinyl group has a very small substituent effect in neutral systems (e.g., $\sigma_I = +(0.01\text{–}0.05)$, $\sigma_R^0 = -0.03$ (8)) but can act as a π-donor or π-acceptor, on demand:

[2] 

Thus one might expect opposite signs for σ_p^+ and σ_p^- for the vinyl group. The evidence on this point is contradictory. $\sigma_p^- = +0.14$ for the vinyl group (9). However, values of $\sigma_p^+ = -0.16$ and $+0.10$ have been reported for this substituent, based respectively on rates of solvolysis of cumyl chlorides (10) and ^{13}C chemical shifts of mono-substituted benzenes (11). Consequently, we decided to redetermine σ_p^+ for the vinyl group, based upon rates of nitration (12). One cannot investigate the nitration of styrene directly since the favoured site for electrophilic attack is the vinyl group. However, one can determine rates of nitration for *trans*-β-substituted styrenes, $C_6H_5CH{=}CHX$ where X is an electron withdrawing group. One can then plot rate of nitration vs. σ_X^+ and extrapolate to $\sigma^+ = 0.0$, i.e., X = H, using a Hammett plot.

It was also decided to carry out a theoretical investigation of the stabilizing effect of a vinyl group in aromatic systems, both for comparison with the experimental results and to check whether there was any relationship between induced charge densities and stabilization energies, such as has been recently noted in other systems (13).

Results of these investigations are reported below.

Results and Discussion

Experimental Data

Data for nitration of C_6H_5—CH=CH—X derivatives are summarized in Table 1. Rates of substitution at positions *para* and *ortho* correlate well with the values of σ^+ for the groups X:

$$\log k_p = -2.80\sigma_X^+ + 0.253 \; (r = 0.998)$$

$$\log k_o = -3.28\sigma_X^+ + 0.477 \; (r = 0.998)$$

(see Fig. 1.)[1] The plot yields $k_p = 1.79\ s^{-1} M^{-1}$ for nitration of the *para* position of styrene. Similarly $k_o = 3.00\ s^{-1}M^{-1}$ for nitration of the *ortho* position ($1.50\ s^{-1}M^{-1}$ for nitration at each carbon). By comparison, the determined value of k_2 for benzene = $0.832\ s^{-1}M^{-1}$ ($0.139\ s^{-1}M^{-1}$ at each carbon atom); ρ^+ for the nitration of benzene derivatives = -6.0 (14). Therefore,

[3] $$\log (k(\text{styrene})/k(1\text{H, benzene})) = -6.0\,\sigma_{(CH=CH_2)}^+$$

Using this equation the values of $\sigma_p^+ = -0.18$[2] and $\sigma_o^+ = -0.17$ are obtained for the vinyl group. The data also allow one to set a limit on the value of σ_m^+.

[1]Table 1 also includes nitration data obtained for the β-styrylphosphonic acid. From these data, together with Fig. 1, the (previously unreported) σ^+ value for the phosphonic group could be evaluated. It follows that $\sigma_{PO_3H_2}^+ = 0.44$, similar to that for the carboxylic group ($\sigma_{CO_2H}^+ = 0.42$ (14)). Close similarity of substituted effects of groups CO_2H and PO_3H_2 has been demonstrated before (15). The excellent correlations in Fig. 1 justify the use of σ_p^+ values for side-chain substituent groups.

[2]The different value estimated by Levy and co-workers (11) presumably is in error because *para* ^{13}C chemical shifts are not, in fact, related to σ_p^+ but rather must be correlated with σ_I and σ_R^0 (5).

Can. J. Chem. Downloaded from www.nrcresearchpress.com by 210.87.254.42 on 09/05/12
For personal use only.

Can. J. Chem. Downloaded from www.nrcresearchpress.com by 210.87.254.42 on 09/05/12
For personal use only.

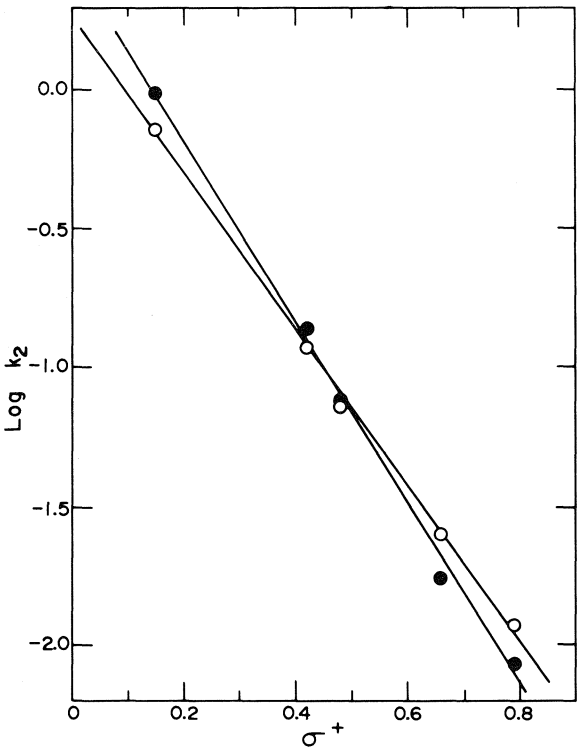


FIG. 1. Log k_2 for nitration of Ph—CH=CH—X vs. σ_x^+, TFA/H_2SO_4, 25°C. (○) *para* nitration; (●) *ortho* nitration.

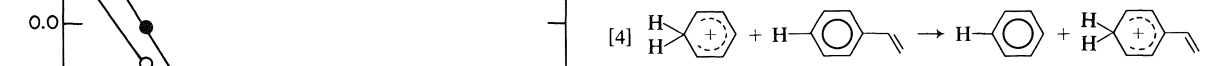
The maximum concentration of *meta*-nitro product is 2% (see Experimental). Thus, the rate constant for *ortho*-nitration is at least 30 times as great as for *meta*-nitration. This corresponds to $\sigma_m^+ > +0.06$.

The σ_p^+ and σ_m^+ values are close to those estimated from the solvolysis of *p*- and *m*-vinylcumyl chloride ($\sigma_p^+ = -0.16$, $\sigma_m^+ = +0.11$ (1)). Thus, σ_p^+ is in fact negative for the vinyl group. Comparison with σ_p^- (+0.14 (9)) confirms that, as suggested in the Introduction, the vinyl group can act as both a donor (to positively charged groups) and an acceptor (from negatively charged groups). In fact, the vinyl group appears to be almost equally effective at stabilizing positively and negatively charged transition states in solution, judging from the similar magnitudes of σ_p^+ and σ_p^-.

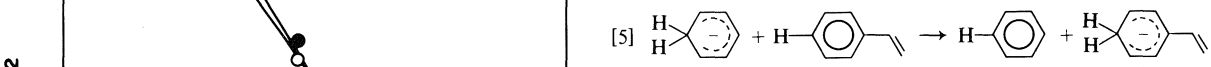
As shown in Table 1, the extent of *para* substitution increases with increasing polarity of X in C_6H_5—CH=CHX derivatives. This is consistent with the expected through-space field effect of X which should disfavour approach of an electrophile to the *ortho* position (17).

Theoretical (ab initio) *Calculations*

The effect of a vinyl group on electrophilic aromatic substitution can be estimated from the energy change for the isodesmic proton transfer reaction (18):

[4] 

and the similar reactions involving *ortho*- and *meta*-protonated styrenes. Similarly, the effect of a vinyl group on nucleophilic aromatic substitution can be estimated from the corresponding hydride transfer reactions:

[5] 

Results for these calculations are summarized in Table 2.

The calculations clearly demonstrate the ability of the vinyl group to stabilize positively and negatively charged transition states to a similar degree. They also show that this results from π charge transfer between the vinyl and phenyl groups. In fact, there is a close parallel between ΔE and $|q_\pi|$, the magnitude of π charge transfer. The calculations also indicate that the vinyl group stabilized the *para*-protonated intermediate slightly more than the *ortho*-protonated intermediate, consistent with the experimental σ_p^+ (−0.18) and σ_o^+ (−0.17) values. However, the calculations differ from the experimental results in predicting a slight stabilization of electrophilic substitution at the *meta* position. This may reflect a difference between gas phase and solution reactivity.

In view of the effect of a vinyl group on charged systems, it is also interesting to consider the effect of the vinyl group in neutral aromatic species. The calculated π charge distribution in styrene is shown in Fig. 2. It is seen that the group is essentially neutral (with only 0.0001 π electron transferred to the phenyl group, compared to almost ±0.2 π electron transfer between the vinyl group and charged

TABLE 2. Energy changes (in kcal/mol) for isodesmic proton transfer reaction[a] and hydride reaction[b] and extent of π charge transfer, Δq_π, to or from vinyl group

Species	ΔE (kcal/mol)	Δq_π[d]
p-H^+-styrene[c]	−13.46	+0.148
p-H^--styrene	−15.02	−0.182
m-H^+-styrene	−1.47	+0.028
m-H^--styrene	−2.84	−0.035
ϕ-H^+-styrene	−9.68	+0.136
ϕ-H^--styrene	−10.79	−0.163

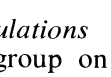
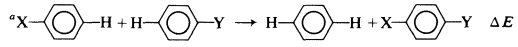
[a]Equation [4].
[b]Equation [5].
[c]*p*-H^+-styrene ≡  etc.
[d]Total change in π charge density for the vinyl group, relative to styrene. Positive sign corresponds to decreased electron density, i.e., π electron transfer to ring.

TABLE 3. Energy changes (in kcal/mol) for isodesmic reaction[a] measuring the energy of interaction between a variable substituent X and a fixed substituent Y in a *para*-disubstituted benzene XC_6H_4Y

	ΔE			
X	Y = CH=CH_2	Y = CH_3	Y = CO_2H	Y = CO_2^-
CO_2^-	−0.99	+0.74	—	—
NH_2(pl)	−0.12	+0.56	−1.56	+3.58
NH_2(py)	−0.08	+0.43	−1.13	+1.97
OH	−0.08	+0.24	−0.71	−0.11
F	−0.06	+0.14	−0.25	−1.77
CH_3	−0.01	+0.10	−0.35	+0.74
CH=CH_2	—	−0.01	−0.27	−0.99
C(=O)H	−0.26	−0.30	+0.41	−4.12
CF_3	−0.27	−0.30	+0.60	−4.66
CO_2H	−0.27	−0.35	—	—
CN	−0.38	−0.61	+0.95	−8.91
NO_2	−0.47	−0.75	+1.44	−12.10

[a]  ΔE

phenyl groups, see Table 2). However, there is significant π charge redistribution within the phenyl and vinyl groups. Within the orbital approximation, charge redistribution schemes may be modelled in terms of orbital interactions. It has previously been suggested in the case of halobenzenes and alkylbenzenes that repulsion between a filled orbital on the substituent and the phenyl π system will lead to an increase in π electron density at the *ortho* and *para* carbons (19). However, in these cases, it is difficult to separate this orbital repulsion effect from the electron donating resonance effects of these groups. With no net π electron transfer, the vinyl group provides very clear evidence for the existence of an orbital repulsion effect. This may account for the σ values of the vinyl group in neutral systems ($\sigma_m = +0.08$, $\sigma_p = -0.08$ (6)).

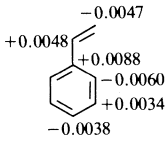
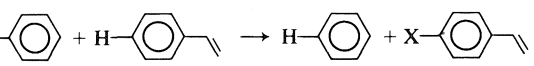


FIG. 2. Calculated π charge distribution in styrene.

It is also informative to consider the interaction of the vinyl substituent with other groups. This can be determined from the energy change for the isodesmic reaction:

[6] 

Results are summarized in Table 3. The interaction of the vinyl group with both electron donor groups (e.g., NH_2) and electron acceptor groups (e.g., NO_2) is stabilizing, although weak in the case of electron donor groups. The latter weak interaction may reflect a partial cancellation of the stabilizing π acceptor ability of the vinyl group by its orbital repulsion effect. The ability of the vinyl group to have stabilizing interactions with both donor and acceptor groups is most unusual. This can be seen by comparing with three other substituent groups with differing properties: a weak donor group, CH_3 ($\sigma_p^0 = -0.15$); a moderately strong acceptor group, CO_2H ($\sigma_p^0 = +0.44$); and a charged group CO_2^-. These data are shown in Table 3. The interactions of the methyl group with acceptor groups and donor groups are respectively stabilizing and destabilizing (as expected from the same signs for σ^+ and σ^-, see above). The CO_2H group shows the exact opposite pattern of stabilizing and destabilizing interactions, as expected from its opposite substituent effect. Finally, interactions of CO_2^- with acceptor and donor groups are respectively stabilizing and destabilizing. Interactions with highly polar groups (e.g., NO_2) are particularly strong. This presumably reflects the strong (through-space) field interaction between a polar and a charged group (20). This is also reflected in the apparently anomalous interactions with OH and F. These two groups have opposing field and resonance interactions (see Introduction). The former must dominate in the interaction with a

Can. J. Chem. Downloaded from www.nrcresearchpress.com by 210.87.254.42 on 09/05/12
For personal use only.

Can. J. Chem. Downloaded from www.nrcresearchpress.com by 210.87.254.42 on 09/05/12
For personal use only.

charged group while the latter dominates in the interaction with neutral groups (where field effects should be less important (20)). Finally, it is noteworthy that, of the various X groups, only vinyl shows stabilizing interactions with all three CH_3, CO_2H, and CO_2^-.

Summary and Conclusions

Experimental and theoretical investigations of the substituent effect of the vinyl group indicate that this group is capable of stabilizing both positively and negatively charged transition states by acting as either a π donor or a π acceptor, depending upon the demand of the system. A close parallel is noted between the stabilization energy and the extent of π charge transfer.

The vinyl group appears to have an intrinsically small substituent effect in neutral systems; mainly a weak orbital repulsion effect. However, the interaction of the vinyl group with both π donor and π acceptor substituents in *p*-disubstituted benzenes is a stabilizing interaction.

Experimental

Solvents were purified by conventional methods. AnalaR nitric acid (d. 1.42) was distilled from an equal volume of concentrated H_2SO_4 immediately before use. Trifluoroacetic acid was distilled from trifluoroacetic anhydride immediately before use. Ultraviolet spectra were determined with a Perkin-Elmer 402 spectrophotometer. ^1H nuclear magnetic resonance spectra were obtained with a Tesla BS-487 (80 MHz.) spectrometer. Gas chromatography was performed using a Pye Unicam, series 104 instrument.

Substrates

Benzene (**1**), β-bromostyrene (**2**), cinnamic acid (**3**), ethyl cinnamate (**4**), cinnamic nitrile (**5**), and β-nitrostyrene (**6**) were obtained commercially and were purified by distillation or crystallization until chromatographically pure (glc). β-Styrylphosphonic acid (**7**) was prepared according to Bergmann and Bondi (21); mp (from H_2O) 149–150°C (lit. (21), mp 146°C).

Product Determination

Substrate (ca. 10^{-2} *M*) was dissolved in TFA containing concentrated H_2SO_4 in the amount equimolar to that of the aromatic compound. The solution of nitric acid (slight excess) in TFA was added slowly at 0°C with stirring. The mixture was then left at room temperature until tlc showed that the reaction was complete. The product was then isolated by evaporation of TFA and extraction; in all cases the yield was practically quantitative and the elemental analysis (nitrogen) of the product agreed with the composition of a mononitro derivative. The nitration product was examined by tlc to determine the number of isomers formed and then oxidized with alkaline permanganate (22) to a mixture of nitrobenzoic acids (in all cases only *ortho* and *para* isomers were observed). The proportion of isomers was determined by quantitative separation of individual compounds and by comparison of the uv spectrum of the oxidation product with the spectra of model mixtures of known composition.

The oxidation product was also examined by nmr spectroscopy and the proportion of *ortho*- and *para*-nitrobenzoic acids was determined from the integrated signals of the aromatic protons of the *ortho* (δ 7.50–7.80) and *para* (δ 7.95–8.25) isomers. All determinations gave good internal agreement. Control experiments showed that the amount of *meta*-nitro product should not exceed 2%.

Rates of Nitration

A solution of HNO_3 in TFA was added to a stirred solution of an equimolar amount of substrate in TFA containing one equivalent of concentrated H_2SO_4 at 25.0°C, and aliquot portions were withdrawn at suitable times. For substrates **1**, **2**, **3**, **4**, **5**, and **7** aliquots were quenched in water and the concentration of nitro compounds in the reaction mixture was determined spectrophotometrically (uv) in the usual way. The following wavelengths and extinction coefficients of substrate (ε_s) and product (ε_p) were used: **1**, $\lambda = 258$ nm; $\varepsilon_s = 150$, $\varepsilon_p = 8500$; **2**, $\lambda = 265$ nm, $\varepsilon_s = 17000$, $\varepsilon_p = 4500$; **3**, $\lambda = 273$ nm, $\varepsilon_s = 21500$, $\varepsilon_p = 10800$; **4**, $\lambda = 275$ nm, $\varepsilon_s = 22000$, $\varepsilon_p = 11200$; **5**, $\lambda = 271$ nm, $\varepsilon_s = 22600$, $\varepsilon_p = 13100$; **7**, $\lambda = 258$ nm, $\varepsilon_s = 18700$, $\varepsilon_p = 11500$. For β-nitrostyrene (**5**) aliquots were extracted with *n*-hexane, extracts were evaporated under reduced pressure, and the residue was dissolved in *n*-hexane containing a known amount of 4-bromodiphenyl as a standard. The mixture was then separated by gas chromatography (column: 3% OV-225 on a Chromosorb W (AW-DMCS) 60/80 mesh, 1 m; temperature 115°C; flow rate (argon) 25 cm^3/min) and concentrations of individual nitro products were determined by the planimetric estimation of the peak areas.

Kinetic runs were followed to ca. 80% of conversion. Good second-order kinetics were obtained in all cases. Values of k_2 for nitration of benzene and substrates listed in Table 1 represent the average of 4–6 independent runs. Individual rate constants are reproducible to within ±5–15%.

Details of Calculations

A STO-3G basis set as contracted to a minimal basis set (23) was used for the *ab initio* molecular orbital calculations. Calculations were performed on an IBM 370/16S computer using a version of the Gaussian 70 program (24). Standard geometries were assumed for phenyl and vinyl groups (25) while the geometry of the protonated phenyl group was that given by McKelvey *et al.* (26). Other substituent geometries were identical to those previously reported (20).

Acknowledgements

The financial assistance of the National Research Council of Canada and of the Polish Academy of Sciences is gratefully acknowledged.

1. L. P. HAMMETT. J. Am. Chem. Soc. **59**, 96 (1937).
2. C. G. SWAIN and E. C. LUPTON. J. Am. Chem. Soc. **90**, 4328 (1968).
3. H. C. BROWN and Y. OKAMOTO. J. Am. Chem. Soc. **80**, 4979 (1958).
4. R. W. TAFT. J. Am. Chem. Soc. **79**, 1045 (1957).
5. E. EHRENSON, R. T. C. BROWNLEE, and R. W. TAFT. Prog. Phys. Org. Chem. **10**, 1 (1973) and references therein.
6. C. D. JOHNSON. The Hammett equation. Cambridge University Press, London. 1973.
7. J. I. BRAUMAN and L. K. BLAIR. J. Am. Chem. Soc. **90**, 5636 (1968); **90**, 6501 (1968).
8. P. R. WELLS, S. EHRENSON, and R. W. TAFT. Prog. Phys. Org. Chem. **6**, 147 (1968).
9. T. MILLER. Aromatic nucleophilic substitution. Elsevier, Amsterdam. 1968. Chapts. 4, 5, and 6.
10. E. N. PETER. J. Polym. Sci. Polym. Lett. Ed. **13**, 479 (1975).
11. G. L. NELSON, G. C. LEVY, and J. D. CARGIOLI. J. Am. Chem. Soc. **94**, 3089 (1972).

12. J. G. HOGGETT, R. B. MOODIE, J. R. PENSON, and R. SCHOFIELD. Nitration and aromatic reactivity. Cambridge University Press, London. 1971. Chapts. 3 and 7.
13. W. F. REYNOLDS, P. G. MEZEY, W. J. HEHRE, R. D. TOPSOM, and R. W. TAFT. J. Am. Chem. Soc. **99**, 5821 (1977).
14. L. M. STOCK and H. C. BROWN. Adv. Phys. Org. Chem. **1**, 35 (1963).
15. T. A. MODRO, W. F. REYNOLDS, and E. SKORUPOWA. J. Chem. Soc. Perkin Trans. II, 1479 (1977).
16. F. G. BORDWELL and K. ROHDE. J. Am. Chem. Soc. **70**, 1191 (1948).
17. D. M. BISHOP and D. P. CRAIG. Mol. Phys. **6**, 139 (1963).
18. W. J. HEHRE, R. DITCHFIELD, L. RADOM, and J. A. POPLE. J. Am. Chem. Soc. **92**, 4796 (1970).
19. D. T. CLARK, J. N. MURRELL, and J. M. TEDDER. J. Chem. Soc. 1250 (1963).
20. P. G. MEZEY and W. F. REYNOLDS. Can. J. Chem. **55**, 1567 (1977).
21. E. BERGMANN and A. BONDI. Ber. **63**, 1158 (1930).
22. W. E. TRUCE and J. A. SIMMS. J. Org. Chem. **22**, 762 (1957).
23. W. J. HEHRE, R. F. STEWART, and J. A. POPLE. J. Chem. Phys. **51**, 2657 (1969).
24. Gaussian 70. Quantum chemistry program exchange. Indiana University, Bloomington, IN.
25. J. A. POPLE and M. GORDON. J. Am. Chem. Soc. **89**, 4253 (1967).
26. J. M. MCKELVEY, S. ALEXANDRATOS, A. STREITWIESER, J-L. M. ABBOUD, and W. J. HEHRE. J. Am. Chem. Soc. **98**, 244 (1976).

Can. J. Chem. Downloaded from www.nrcresearchpress.com by 210.87.254.42 on 09/05/12
For personal use only.

Canadian Journal of Chemistry
Published by
THE NATIONAL RESEARCH COUNCIL OF CANADA

Journal canadien de chimie
Publié par
LE CONSEIL NATIONAL DE RECHERCHES DU CANADA

Volume 58 Number 5 March 1, 1980

Volume 58 numéro 5 1 mars 1980

Can. J. Chem. Downloaded from www.nrcresearchpress.com by 210.87.254.42 on 09/05/12
For personal use only.

A systematic investigation of the reaction of SiF_2 with ethylene and six methyl-substituted ethylenes. I. Product yields and mechanistic conclusions[1]

WILLIAM F. REYNOLDS, JAMES C. THOMPSON,[2] and A. P. GERALD WRIGHT
Department of Chemistry, University of Toronto, Toronto, Ont., Canada M5S 1A1

Received July 19, 1979

WILLIAM F. REYNOLDS, JAMES C. THOMPSON, and A. P. GERALD WRIGHT. Can. J. Chem. **58**, 419 (1980).

SiF_2 produced by the quartz tube reaction has been reacted with ethylene and six methyl-substituted ethylenes. All major products (polymers, disilacyclobutanes, disilacyclohexanes, and open chain compounds) have been characterized by a combination of ^{19}F, ^{1}H, ^{13}C, and ^{29}Si nmr spectroscopy. While polymer is always formed in highest yield, the relative proportions of other products vary significantly from alkene to alkene.

Key observations concerning structures and stereochemistries and product yields are summarized. Consideration of this evidence leads to a mechanism involving attack of SiF_2 on the olefin to form an excited silirane which either ring opens or relaxes to its ground state, followed in either case by further reaction.

WILLIAM F. REYNOLDS, JAMES C. THOMPSON et A. P. GERALD WRIGHT. Can. J. Chem. **58**, 419 (1980).

On a fait réagir le SiF_2, obtenu par la réaction du tube de quartz, avec de l'éthylène et six composés éthyléniques portant un substituant méthyle. On a identifié les produits principaux (polymères, disilacyclobutanes, disilacyclohexanes et des composés à chaîne linéaire) en utilisant les données de la rmn du ^{19}F, ^{1}H, ^{13}C et ^{29}Si. Tandis que le polymère se forme toujours avec de très bons rendements, les proportions relatives des autres produits varient de façon importante d'un alcène à l'autre.

On résume les observations fondamentales relatives aux structures et à la stéréochimie des produits obtenus. En tenant compte des preuves obtenues, on aboutit à un mécanisme qui fait intervenir une attaque de l'oléfine par du SiF_2 conduisant à la formation d'un siliranne excité dont le cycle s'ouvre ou revient à l'état fondamental; dans un cas comme dans l'autre une réaction subséquente se produit.

[Traduit par le journal]

Introduction

Since the initial report that SiF_2 could be generated in good yield by the reaction of SiF_4 with Si in a high temperature furnace (1), there have been numerous investigations of the reactions of SiF_2 with unsaturated organic compounds. These reactions yield a bizarre variety of compounds (e.g. see refs. 2–4). This has led to considerable speculation concerning the mechanism of these reactions (5–7). However, the mechanistic proposals were all based on incomplete information since the major polymeric products of these reactions had never been characterized.

Consequently, it was decided to carry out a systematic investigation of the reaction of SiF_2 with a series of methyl-substituted ethylenes, characterizing the products as completely as possible. It was hoped that this would provide a better understanding of this obviously complex reaction.

We have already published a preliminary account of the characterization of the polymeric products by ^{13}C and ^{29}Si nmr spectroscopy (8). This paper discusses product yields and stabilities, summarizes the key observations concerning structure, and presents a comprehensive mechanism which accounts for the structures and stereochemistry of the products as well as the product yields. Two subsequent papers (9, 10) will describe in detail the spectroscopic characterization of the products.

Experimental

SiF_2 was prepared in a greaseless vacuum line by the standard quartz tube method (1). In a typical reaction, 0.147 mol SiF_4 were converted to SiF_2 and co-condensed at −196°C with 0.139 mol *trans*-butene, using flow rates of about 170 mmol/h for each

[1]Taken in part from the Ph.D. Thesis of A. P. G. Wright, University of Toronto, Toronto, 1979.

[2]To whom all correspondence should be addressed.

0008-4042/80/050419-06$01.00/0
©1980 National Research Council of Canada/Conseil national de recherches du Canada

TABLE 1. Fraction of olefin reacting with SiF_2 and relative product yields (% alkene) of isolated products

Olefin	Reacted olefin (%)	Relative product yields: 		Chain isomer	Fragments	Polymer
ET	44	1	9	0	0	90
PR	62	2	12[b]	12	0	74
CB	51	2[a]	10[c]	0	10[e]	78
TB	54	37	0	0	0	63
IB	61	2	32	32	0	34
MB	51	2	14[b]	14	0	70
DB	28	Trace	2	25[d]	0	73

[a]Two isomers in 9:1 ratio. Minor component corresponded to TB four-membered ring.
[b]Two isomers in comparable yields.
[c]Two major isomers plus traces of other isomers.
[d]Two products in 4:1 ratio.
[e]At least two products.

reactant. The resultant condensate was allowed to warm to room temperature. Unreacted SiF_4, olefin, and volatile products were pumped to U traps or to a low temperature distillation column (11) for separation. The polymers, which varied in viscosity with olefin, were weighed and scraped into storage bottles in a glove bag. Some of the volatile products polymerized readily at room temperature. Any unstable product was condensed directly into an nmr tube glass-blown to the bottom of a U tube. The nmr tube was then sealed and stored in liquid nitrogen until use.

SiF_2 was reacted with ethylene (ET), propene (PR), *cis*-2-butene (CB), *trans*-2-butene (TB), isobutylene (2-methylpropene) (IB), 2-methyl-2-butene (MB), and 2,3-dimethyl-2-butene (DB). All olefins were of commercial purity. CB contained 0.2–0.5% of the *trans* isomer. Each reaction was repeated at least twice. Product yields were reproducible in all cases.

Elemental analyses could not be obtained since the products were thermally unstable and air sensitive (see below). In addition, complete separation of products was rarely possible. However, reaction products could be fully characterized by a combination of ^1H, ^{19}F, ^{13}C, and ^{29}Si nmr spectroscopy. ^1H spectra were obtained on Varian A56/60D, HA-100, and XL-100 spectrometers respectively operating at 60.0, 100.0, and 100.06 MHz. ^{19}F spectra were obtained on the A56/60D and XL-100 spectrometers operating at 56.4 and 94.16 MHz, respectively. The XL-100 was also used to obtain ^1H-decoupled ^{19}F spectra and ^{19}F-decoupled ^1H spectra. ^{13}C spectra were obtained on Varian XL-100 and CFT-20 spectrometers at 25.16 and 20.00 MHz while ^{29}Si spectra were obtained on a Bruker WP-80 spectrometer operating at 15.89 MHz. ^1H and ^{19}F spectra were generally obtained in continuous wave mode while other spectra were obtained in pulsed Fourier transform mode.

Results and Discussion

(a) Product Yields

In general, four types of products were observed in the olefin–SiF_2 reactions. In addition to polymeric products, 1,2-disilacyclobutanes and disilacyclohexanes were normally found as well as open chain products which usually were isomers of the disilacyclohexanes. However, a different open chain product was observed in the CB reaction. The disilacyclobutane and disilacyclohexane products produced from the reaction of ET with SiF_2 have been reported and characterized by mass spectrometry and ^1H and ^{19}F nmr spectroscopy (2). No chain isomer was found in that reaction but this type of product has been noted in other reactions of SiF_2 with unsaturated compounds (3, 12).

The overall and relative product yields for the various olefin–SiF_2 reactions are summarized in Table 1. Typically ca. 50% of olefin reacted while polymer usually constituted 60–90% (by weight) of isolated product. While there are some patterns to the overall product distribution, there are also a number of unusual results. For example, TB gave a high yield of disilacyclobutane but no disilacyclohexane or chain isomer. On the other hand, IB produced an unusually high yield of the latter two products but a low polymer yield while DB produced an unusually high yield of chain compound relative to disilacyclohexane. It is also noteworthy that several of the disilacyclohexanes were formed in two isomeric forms and that two different chain derivatives were found for the DB reaction. Finally, only one disilacyclobutane was formed in the TB reaction. However, two disilacyclobutane isomers were formed in the CB reaction, with the product of the TB reaction representing 10% of the yield and a new isomer (referred to as CB isomer) representing 90% of the yield. Since the yield of disilacyclobutane from the TB reaction is ca. 20 times as great as from the CB (see Table 1), the 10% TB isomer from the CB reaction probably comes from traces of TB in the starting CB (see Experimental). Thus the formation of disilacyclobutanes is essentially 100% stereospecific. Evidence is presented elsewhere that these derivatives are formed with retention of alkyl stereochemistry (9).

Can. J. Chem. Downloaded from www.nrcresearchpress.com by 210.87.254.42 on 09/05/12
For personal use only.

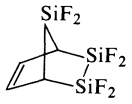
Can. J. Chem. Downloaded from www.nrcresearchpress.com by 210.87.254.42 on 09/05/12
For personal use only.

(b) Product Stabilities and Physical Properties

All products were air- and moisture-sensitive and were handled in vacuum. The polymers were yellow–white amorphous solids and were thermally stable at room temperature. All volatile products were clear liquids. The disilacyclohexanes were least volatile and were thermally stable at room temperature. Chain isomers were often sufficiently more volatile to allow partial column separation. A number of these compounds were thermally unstable. All of the disilacyclobutanes were unstable at room temperature, yielding clear polymeric products. The approximate order of the rate of polymerization was PR > IB > MB > ET > CB > TB with half-lives ranging from minutes to hours.

(c) Mechanism of Reaction of SiF_2 with Olefins

The main form of $(SiF_2)_n$ produced by the quartz tube method (11) is monomeric SiF_2 in its singlet state (13). However, Margrave and Perry suggested that the main reactive $(SiF_2)_n$ species in reactions with olefins and other unsaturated organic compounds is $F_2\dot{S}i—\dot{S}iF_2$, possibly produced via intermediate formation of $F_2Si{=}SiF_2$ (5). The main basis for this suggestion was the observation that most addition products from reaction of SiF_2 with unsaturated compounds contain Si_2F_4 units (2, 3), although insertion of SiF_2 into SiF and CF bonds is well established (6, 13). 2,2,3,3,7,7-Hexafluoro-2,3,7-trisilanorborn-5-ene (**V**) is the only well characterized compound with an isolated SiF_2 group (3, 14), resulting from reaction of SiF_2 with an unsaturated organic compound.



V

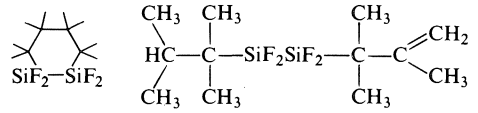
According to this suggestion, 1,2-disilacyclobutanes and 1,2-disilacyclohexanes are produced by the reaction of $F_2\dot{S}i—\dot{S}iF_2$ with 1 and 2 mol of olefin, respectively (5). If this mechanism is correct, then the reaction polymers should also contain mainly Si_2F_4 units.

Very recently, Seyferth and Duncan synthesized a difluorosilirane, **VI** (7)



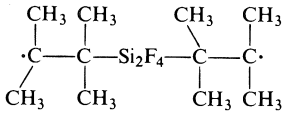
VI

They observed that thermolysis of this product yielded two products (7) corresponding to those which have been observed from the reaction of SiF_2 with olefins (2, 3, 12).



VII **VIII**

This led them to suggest that the mechanism of the reaction of SiF_2 with olefins involved the initial formation of a silirane, followed by either ring opening or further reaction with SiF_2 (7). For example, ring opening of **VI** followed by dimerization should yield a biradical



which gives **VII** by ring closure and **VIII** by hydride transfer. Disilacyclobutanes could be formed by the reaction of SiF_2 with a silirane, by analogy with a similar reaction of dimethylsilyene (15).

This investigation has provided a significant amount of new information which can be used to test and modify these mechanistic proposals. Among the key points are: (*1*) the reaction polymers, which typically form 60–70% of isolated product, mainly contain isolated SiF_2 units (8, 9); (*2*) CB and TB produce 1,2-disilacyclobutanes with complete retention of configuration (9); (*3*) unsymmetric alkenes yield disilacyclohexanes with greater alkyl substitution at C(2) (10). More than one isomer is formed, whenever possible. For example, the disilacyclohexane from CB produces two major isomers, one with all-*cis* and the other with all-*trans* CH_3 groups (10); (*4*) the IB reaction gives a much smaller yield of polymer (34%) than other reactions plus a higher than normal yield of disilacyclohexane (32%) and its chain isomer (32%) (Table 1); (*5*) TB provides a much higher than normal yield of disilacyclobutane (37%) but no detectable amount of disilacyclohexane or chain isomer (Table 1). However, a mixed reaction of TB and PR with SiF_2 produces as one product a disilacyclohexane containing one TB and one PR unit (10); (*6*) TB (and to a lesser extent CB) yields a polymer with a significant proportion of Si_2F_4 units (8, 9). The polymerization reaction involves isomerization of the alkene linkages (9); (*7*) several alkenes yield open chain compounds which are isomers of 1,2-disilacyclohexanes while DB also yields a chain compound with an $(SiF_2)_3$ linkage (9); (*8*) a matrix isolation study of the reaction of SiF_2 with olefins has shown that when SiF_2 is co-

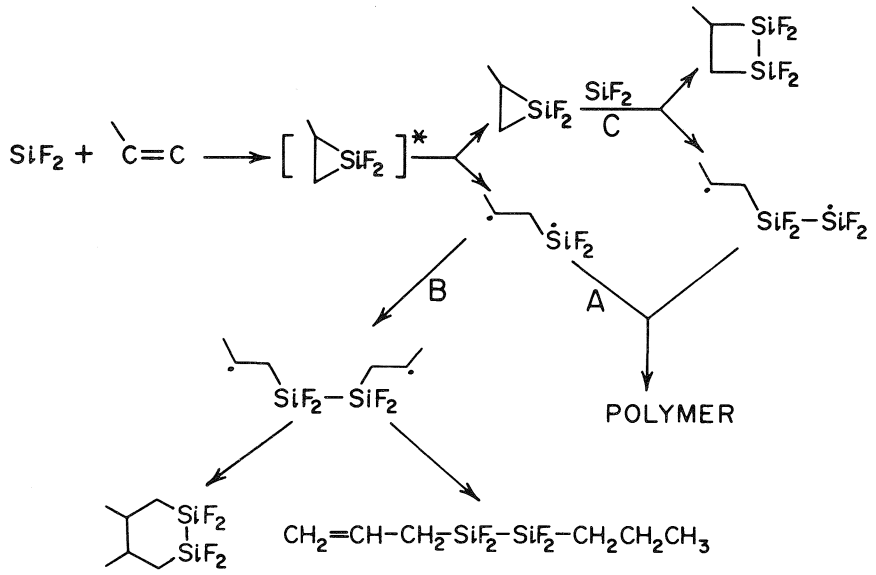


FIG. 1. Proposed mechanism to account for the reaction of SiF_2 with alkenes. Note that pathways *A* and *B* involve reaction of one of the biradicals with a silirane.

condensed with TB, a different esr signal is observed than for the $(SiF_2)_n$ polymer (16), suggesting the formation of radical intermediates in the SiF_2/olefin reaction.

Point *1* clearly demonstrates that SiF_2 is the major reactive $(SiF_2)_n$ species in this reaction series, in direct contradiction with the main assumption of the mechanism of Margrave and Perry (5). Point *2* also appears to be inconsistent with this mechanism since addition of $\dot{S}iF_2$—$\dot{S}iF_2$ to an olefin should either lead to scrambling of configuration if the reaction is stepwise or inversion of configuration if concerted (17).

However, points *1–4* as well as point *8* all appear to be consistent with the suggestion of Seyferth and Duncan that the reaction involves initial attack of singlet SiF_2 on the olefin. The one problem with the suggestion of Seyferth and Duncan concerns the observed stability of siliranes. **II** has a half-life in tetrahydrofuran solution of 1.75 h at 60°C (7), corresponding to a free energy of activation (presumably via ring opening) of 25 kcal/mol. The reactions under consideration here take place at −196°C in a frozen matrix. While some reaction may occur during subsequent warm-up, ring-opening of a ground state silirane appears improbable under these reaction conditions.

However, it appears possible to account for all of the observations for the unsymmetric alkenes by a minor modification of the mechanism of Seyferth and Duncan (7), shown in Fig. 1 for propene. The reaction of SiF_2 with alkenes should be strongly exothermic, leading to the formation of a vibrationally highly excited silirane. In a solid matrix, where normal mechanisms of energy relaxation such as collisional deactivation should be inefficient, some of the excited siliranes may open ring before they can drop down to the ground state. The probability of ring opening should be greatest for the reaction of unsymmetric alkenes since one of the Si—C bonds in the silirane should be weaker, corresponding to the carbon center which forms the more stable radical. There is direct evidence for the formation of an excited state product under identical experimental conditions for the analogous reaction of SiF_2 with C_6F_6 (18). In this case, chemiluminescence from excited $C_6F_5SiF_3$ can be observed visually as flashes of light in the solid matrix (18). There is also an analogy with the gaseous reaction of singlet CH_2 with alkenes. In this case, a "hot" cyclopropane is formed which partially isomerizes (19), presumably by ring opening. By contrast, the same reaction in solution, where collisional deactivation should be effective, yields unisomerized product (19).

The ring-opened silirane can attack a normal silirane, either initiating polymerization by carbon–silicon bond formation (path *A*) or forming a dimer by Si—Si bond formation (path *B*). Path *A* should normally be favoured due to the greater strength of C—Si bonds. However, in the IB reaction, path *B* must be the major reactive pathway (64% products derived from dimer as opposed to 34% polymer), probably because the dimer con-

Can. J. Chem. Downloaded from www.nrcresearchpress.com by 210.87.254.42 on 09/05/12
For personal use only.

Can. J. Chem. Downloaded from www.nrcresearchpress.com by 210.87.254.42 on 09/05/12
For personal use only.

tains two relatively stable tertiary carbon radical centers. The dimer from an unsymmetric alkene will yield disilacyclohexane with greater methyl substitution at C(2) and methyl isomerization at C(2) can occur by rotation about the C(1)—C(2) bond in the dimer.

Reaction of the silirane with a second mole of SiF_2 provides another reactive pathway (path *C*). Again one might obtain either a disilacyclobutane (formed with retention of configuration by SiF_2 bond insertion) or a ring-opened isomer. The latter could be incorporated into the polymer, accounting for the minor proportion of Si_2F_4 units.

In most reactions, no more than about 5% of the isolated products can be attributed to path *C*. The one major exception is TB where no products are observed corresponding to path *B* while disilacyclobutane is formed in 37% yield. Furthermore the polymer (63% yield) contains ca. 1/3 Si_2F_4 units which likely are due to path *C*. Thus in this case, it appears that the reaction proceeds by paths *A* and *C* in about a 40:60 ratio. The most likely explanation is that the TB silirane is particularly stable and a negligible amount of the ring-opened isomer is formed. The TB silirane might reasonably be expected to be the most stable silirane since the corresponding TB disilacyclobutane is the thermally most stable disilacyclobutane. However, formation of ring-opened disilacyclobutane is not unreasonable since all of the disilacyclobutanes are significantly less stable than **VI**. The ring-opened disilacyclobutane must have the structure shown since the alternative $\dot{S}iF_2$—C—C—$\dot{S}iF_2$ structure could not account for the observed isomerizations of alkene linkages in the TB reaction polymer. Kinetic factors may determine the structure of the ring-opened biradical. Polymerization presumably is initiated by the attack of a biradical on a silirane, yielding a polymer with both SiF_2 and Si_2F_4 units.

Other symmetric alkenes such as CB and DB appear to have reaction pathways intermediate between TB and the unsymmetric alkenes. It is significant that DB yields a relatively high yield of a chain isomer with Si_3F_6 units. This is most likely formed by attack of $(CH_3)_2\dot{C}$ — $C(CH_3)_2$ — SiF_2 — $\dot{S}iF_2$ on **VI** and is again favoured by the fact that the resultant biradical involves two tertiary carbon centers. CB reaction polymer contains about 10% Si_2F_4 units, suggesting a significant contribution from path *C* in this reaction. The only products whose origin cannot reasonably be attributed to this proposed mechanism are the fragments observed in the CB reaction. Basically the same mechanism can also account for the products of the acetylene/SiF_2 (5) and vinyl chloride/SiF_2 reactions (20), albeit with a different mode of hydride transfer to form the chain derivatives in the latter two cases.

Summary and Conclusions

The reaction of SiF_2 with olefins in a frozen matrix at −196°C produces four main types of products, with the relative yields varying significantly depending upon the olefin. The structures and stereochemistries of all of the observed disilacyclobutanes, disilacyclohexanes, chain isomers and polymers and the relative product yields can be accounted for by a mechanism in which the reaction of singlet SiF_2 with an alkene produces an activated silirane which can either open ring or relax to the ground state, followed in either case by subsequent reaction. While one cannot rule out the possibility of some involvement of $F_2\dot{S}i$—$\dot{S}iF_2$ in the reaction (5), we agree with the conclusion of Seyferth and Duncan that it is unnecessary to invoke this intermediate to account for the products (7).

The one obvious difficulty with this mechanism is the fact that no silirane has been directly detected in the reaction of SiF_2 with olefins (although small amounts of a compound of empirical formula $C_2H_4SiF_2$ was detected in the mass spectrum of the products of the reaction of SiF_2 with ET (2)). In view of the relative stability of ground state siliranes in solution (7), the failure to detect silirane might seem surprising. However, siliranes are also likely to be highly reactive (7). Since the reaction mixture likely contains SiF_2, ring-opened biradical isomers of the silirane and free radical polymer chains, all of which should be very reactive towards siliranes, the failure to observe siliranes as products is probably not surprising. It would appear that the best chance to detect silirane would be to condense SiF_2 into an excess of liquid olefin, where collisional deactivation may allow the silirane to relax rapidly to the ground state. This possibility is currently being investigated.

Acknowledgements

Financial support from the Natural Sciences and Engineering Research Council of Canada and the Department of Chemistry of the University of Toronto is gratefully acknowledged.

1. P. L. Timms, R. A. Kent, T. C. Ehlert, and J. L. Margrave. J. Am. Chem. Soc. **87**, 2824 (1965).
2. J. C. Thompson, J. L. Margrave, and P. L. Timms. Chem. Commun. 566 (1966).
3. C. S. Liu, J. L. Margrave, J. C. Thompson, and P. L. Timms. Can. J. Chem. **50**, 459 (1972).
4. D. L. Perry and J. L. Margrave. J. Chem. Educ. **53**, 696 (1976).

5. J. L. MARGRAVE and D. L. PERRY. Inorg. Chem. **16**, 1820 (1977).
6. C. S. LIU and T. L. HWANG. J. Am. Chem. Soc. **100**, 2577 (1978).
7. D. SEYFERTH and D. P. DUNCAN. J. Am. Chem. Soc. **100**, 7734 (1978).
8. J. C. THOMPSON, A. P. G. WRIGHT, and W. F. REYNOLDS. J. Am. Chem. Soc. **101**, 2236 (1979).
9. W. F. REYNOLDS, J. C. THOMPSON, and A. P. G. WRIGHT. Can. J. Chem. **58**, 425 (1980).
10. W. F. REYNOLDS, J. C. THOMPSON, and A. P. G. WRIGHT. Can. J. Chem. **58**, 436 (1980).
11. J. DOBSON and R. SCHAEFFER. Inorg. Chem. **9**, 2183 (1970).
12. C. S. LIU. Ph.D. Thesis. University of Toronto, Toronto, Ont. 1971.
13. D. L. PERRY and J. L. MARGRAVE. J. Chem. Educ. **53**, 696 (1976).
14. C. S. LIU, J. C. THOMPSON, J. T. SZYMÁNSKI, and J. L. MARGRAVE. J. Chem. Soc. A, 1129 (1972).
15. D. SEYFERTH and S. C. VICK. J. Organomet. Chem. **125**, C11 (1977).
16. A. P. G. WRIGHT. Ph.D. Thesis. University of Toronto, Toronto, Ont. 1979.
17. C. S. LIU and J. C. THOMPSON. Tetrahedron Lett. 1581 (1973).
18. P. L. TIMMS, D. D. STUMP, R. A. KENT, and J. L. MARGRAVE. J. Am. Chem. Soc. **88**, 940 (1966).
19. W. KIRMSE. Carbene chemistry. Academic Press, New York. 1971.
20. C. S. LIU and T. L. HWANG. J. Am. Chem. Soc. **101**, 2996 (1979).

Can. J. Chem. Downloaded from www.nrcresearchpress.com by 210.87.254.42 on 09/05/12
For personal use only.

A systematic investigation of the reaction of SiF_2 with ethylene and six methyl-substituted ethylenes. II. Characterization of polymeric products, open chain organosilicon derivatives, and 1,2-disilacyclobutanes[1]

WILLIAM F. REYNOLDS, JAMES C. THOMPSON,[2] AND A. P. GERALD WRIGHT
Department of Chemistry, University of Toronto, Toronto, Ont., Canada M5S 1A1

Received July 19, 1979

WILLIAM F. REYNOLDS, JAMES C. THOMPSON, and A. P. GERALD WRIGHT. Can. J. Chem. **58**, 425 (1980).

Polymers produced by the reaction of SiF_2 with olefins have been characterized by ^{13}C and ^{29}Si nmr spectroscopy and have been found to have a regular head-to-tail structure with isolated SiF_2 groups between olefin units. Only minor proportions of Si_2F_4 units are formed. The open chain organosilicon derivatives formed in the reaction are, with one exception, isomers of 1,2-disilacyclohexanes. The 1,2-disilacyclobutanes are formed stereospecifically with retention of alkyl stereochemistry. ^{19}F chemical shifts can be predicted by additive chemical shift parameters for the effect of alkyl substitution.

WILLIAM F. REYNOLDS, JAMES C. THOMPSON et A. P. GERALD WRIGHT. Can. J. Chem. **58**, 425 (1980).

La spectroscopie rmn du ^{13}C et du ^{29}Si a permis d'identifier les polymères issus de la réaction du SiF_2 avec les oléfines; on a trouvé qu'ils possèdent une structure régulière tête-queue avec des groupes SiF_2 isolés entre des unités oléfiniques. On rencontre de faibles proportions de groupes Si_2F_4. Les chaînes ouvertes de silanes formées au cours de la réaction sont, à une exception près, les isomères des disila-1,2 cyclohexanes. Les disila-1,2 cyclobutanes sont formés stéréospécifiquement avec rétention de la stéréochimie du groupe alkyle. Les déplacements chimiques du ^{19}F peuvent être prévus à l'aide des paramètres additifs de déplacement chimique relatif à l'effet des substituants alkyles.

[Traduit par le journal]

Can. J. Chem. Downloaded from www.nrcresearchpress.com by 210.87.254.6 on 09/05/12
For personal use only.

Introduction

In the previous paper in this series, we have reported the product yields for the reaction of SiF_2 with a series of olefins (1). The evidence provided by both the product yields and the structures of the products was used to postulate a mechanism for this complex reaction (1). In this paper, we discuss the details of the spectroscopic characterization of three types of products: 1,2-disilacyclobutanes, open chain compounds, and polymers. These products were characterized by a combination of ^{19}F, ^{13}C, and ^{29}Si nmr spectroscopy.

The formation of disilacyclobutanes in the SiF_2–olefin reaction has been known for some time (2). Subsequently, reactions of SiF_2 with *cis*-2-butene (CB) and *trans*-2-butene (TB) were shown to be highly stereospecific with respect to alkyl configuration, although it was not known whether this involved retention or inversion of alkyl stereochemistry (3). This investigation has demonstrated that the reaction is 100% stereospecific (1). It is important to determine the absolute stereochemistry since it has been predicted that the reaction should involve inversion of configuration if it occurred by concerted addition of $\dot{S}iF_2$—$\dot{S}iF_2$ to the olefin (3).

The formation of open chain compounds has been observed in the reaction of SiF_2 with both alkenes (4) and alkynes (5), although the former have not been well characterized. Similarly, although polymers are usually the major products of the reaction of SiF_2 with unsaturated organic compounds (2, 4) (typically 60–70% for the olefin reaction (1)), these polymers have not been characterized. Rather, speculation concerning the mechanism of the reaction of SiF_2 with unsaturated organic compounds has been based upon the structures of the volatile products (6–8) which are in fact only minor products in these reactions. The structures of the polymers are obviously the key to answering the primary question of whether SiF_2 (8) or Si_2F_4 (6) is the major attacking species in this reaction. The answers to these structural questions are provided below.

Experimental

All experimental details are given in ref. 1.

Results and Discussion

(a) Nomenclature

The olefin used in the reaction is identified by capital letters, as shown above. Four-membered rings (1,2-disilacyclobutanes) and six-membered rings (1,2-disilacyclohexanes) are designated -c4 and -c6 respectively. Thus a disilacyclobutane from the reaction of SiF_2 with *cis*-2-butene is shown as CB-c4. Possible stereochemical variations of such compounds are discussed in the text.

[1]Taken in part from the Ph.D. Thesis of A. P. G. Wright, University of Toronto, Toront, Ont., Canada, 1979.

[2]To whom all correspondence should be addressed.

0008-4042/80/050425-11$01.00/0

©1980 National Research Council of Canada/Conseil national de recherches du Canada

Can. J. Chem. Downloaded from www.nrcresearchpress.com by 210.87.254.6 on 09/05/12
For personal use only.

(b) Structures of Polymers[3]

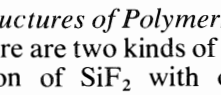
There are two kinds of polymers produced in the reaction of SiF_2 with olefins. The first is the polymer which is produced directly in the reaction. This in each case was an amorphous yellow solid or highly viscous liquid. The polymers produced from propene (PR), *cis*-2-butene (CB), *trans*-2-butene (TB), and 2-methyl-2-butene (MB) reactions were all soluble in $CDCl_3$ while the isobutylene (2-methylpropene) (IB) polymer was sparingly soluble. The polymers from ethylene (ET) and 2,3-dimethyl-2-butene (DB) were insoluble in non-polar solvents and reacted with polar solvents.

In addition to the reaction polymers, the disilacyclobutanes also thermally polymerize (1). In a number of the cases, the initial yield of disilacyclobutane was so small that there was insufficient polymer to characterize. However, the polymers produced from the CB and TB disilacyclobutane derivatives (henceforth designated CB-c4 and TB-c4) were characterized. Since the ratio of alkene to SiF_2 is known (1:2) in these compounds, these compounds proved to be particularly useful in characterizing the CB and TB reaction polymers.

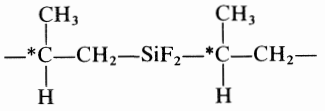
^1H and ^{19}F spectra of the polymers were generally uninformative with broad, poorly resolved peaks (the exception to this was the ^{19}F spectrum of the PR polymer, see below). However, ^{13}C and particularly ^{29}Si spectra proved to be very useful for polymer characterization. These spectra demonstrated that PR, IB, and MB reaction polymers all have surprisingly simple and regular structures. The PR polymer will be discussed in detail since it is typical. ^{29}Si and ^{13}C spectra for this polymer are shown in Fig. 1. The ^{29}Si spectrum is a 1:2:1 triplet with a 314 Hz coupling constant, typical of a one bond ^{29}Si–^{19}F coupling constant in organosilicon fluorides (10). No splitting is observed due to two-bond ^{29}Si–Si–^{19}F coupling. Consequently, the polymer must contain isolated SiF_2 units between alkene units. The ^{13}C spectrum is also simple, showing a singlet at δ15.3 assigned to methyl groups and two triplets ($J_{^{13}C-^{19}F}$ = 15 Hz) at δ11.3 and δ10.4, assigned to CH_2 and CH groups adjacent to SiF_2 units. This simple spectrum plus the fact that the ^{29}Si spectrum showed only one type of silicon demonstrates that the polymer has a regular



structure. More than one ^{29}Si signal and more than one ^{13}C methyl signal would be expected if the polymer contained a mixture of head-to-head and head-to-tail units or if it contained blocks of



and $-(SiF_2)_n-$ units. The ^{19}F spectrum of the PR polymer showed two AB quartets, indicative of two types of diastereotopic SiF_2 units (10). Since the propene linkage contains a chiral center, two types of SiF_2 units are possible, depending upon whether the SiF_2 is between two alkene linkages with the same or opposite stereochemistry (respectively labelled isotactic and syndiotactic diads (11))



The two AB quartets had essentially equal areas indicating that the polymer had an atactic (i.e. random) structure with respect to the stereochemistry of the alkene linkages (10).[4]

IB and MB reaction polymers show similar simple ^{29}Si and ^{13}C spectra (see Table 1 for ^{29}Si data) (9). However, the TB and CB reaction polymers have a more complicated structure. The TB polymer ^{29}Si spectrum shows not only the normal triplet spectrum but a significant additional component which is a triplet of triplets (Fig. 2*a*). This additional component exactly corresponds to the ^{29}Si spectrum of the polymer from the thermal polymerization of TB-c4 (Fig. 2*b*). Thus it can be attributed to Si_2F_4 units. Allowing for the fact that the spectrum due to Si_2F_4 units should be twice as intense, the ratio of SiF_2:Si_2F_4 is about 1:0.5 in the TB reaction polymer. The CB reaction polymer also has Si_2F_4 units but only in the ratio SiF_2:Si_2F_4 = 1:0.2 (Table 1). The other polymers contain only trace amounts (ca. 1–2%) of Si_2F_4 units (e.g. see Fig. 1).

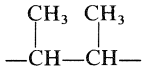
The ^{13}C spectra of the CB and TB reaction polymers are complex (Fig. 3). Both polymers show four methyl peaks at δ13.6, 11.6, 10.0, and 8.9. By contrast, the polymers produced by polymerization of TB-c4 and CB-c4 each show a single methyl peak, respectively at δ8.9 and δ11.6 (precisely corresponding to two of the peaks in the reaction polymer spectra). The single peak methyl spectra indicated that TB-c4 and CB-c4 both polymerize with retention of configuration, as expected if the polymerization involves breaking of the weak Si—Si bond. Assuming that the polymer chains prefer to adopt an *anti* conformation, the CB methyl groups should be in *anti* conformation while the methyl groups are in a *gauche* conformation for

[3]A preliminary account of part of this work has appeared elsewhere (9).

[4]Liu has reached identical conclusions concerning the structure of these polymers based on their ^{19}F spectra (12).

the TB-c4 polymer. The methyl ^{13}C chemical shifts are consistent with this assumption since the methyl groups in the TB-c4 polymer show the expected high field shift due to a *gauche* γ interaction (13).

The methyl peaks in the CB and TB reaction polymers can be assigned by assuming that two types of



linkages are present with the same stereochemistries as the linkages in CB-c4 and TB-c4 polymers (respectively referred to as CB and TB linkages). In addition, different chemical shifts should be noted for CH_3 groups adjacent to SiF_2 and Si_2F_4 linkages, leading to four peaks. Methyl groups in CB and TB linkages and adjacent to Si_2F_4 units are assumed to have the same chemical shifts as methyl groups in CB-c4 and TB-c4 polymers (respectively δ11.6 and δ8.9). The remaining two peaks are assigned to CH_3 groups adjacent to SiF_2 units with the peak in a TB linkage again assumed to be at high field to the methyl group in a CB linkage. With this assignment, it is seen that the TB reaction polymer again contains a higher proportion of Si_2F_4 than the CB reaction polymer (see Fig. 3). However, it also indicates that both reaction polymers contain about the same ratio of CB linkages:TB linkages of about 2:1. This suggests that isomerization of the alkene linkages occurs during polymerization, apparently leading to a thermodynamic product distribution (the CB linkages should be more stable since there is a *gauche* methyl steric interaction in the TB linkage (see above)).

To summarize this section, PR, IB, and MB polymers show a regular structure with isolated SiF_2 units between alkene units oriented in a head-to-tail fashion. CB and particularly TB reaction polymers also contain Si_2F_4 units although SiF_2 units still predominate (SiF_2:Si_2F_4 = 1:0.5 for TB and 1:0.2 for CB). The polymerization involves isomerization of alkene linkages, yielding an apparent thermodynamic distribution with a ratio of CB linkages:TB linkages of about 2:1.

(c) Structure of Open Chain Organosilicon Derivatives

PR, IB, MB, and DB all give open chain organosilicon derivatives while ET and TB give no compounds of this type and CB yields different fragment compounds (1). The open chain organosilicon compounds all give complex ^1H spectra for the alkyl region, compounded by the fact that these

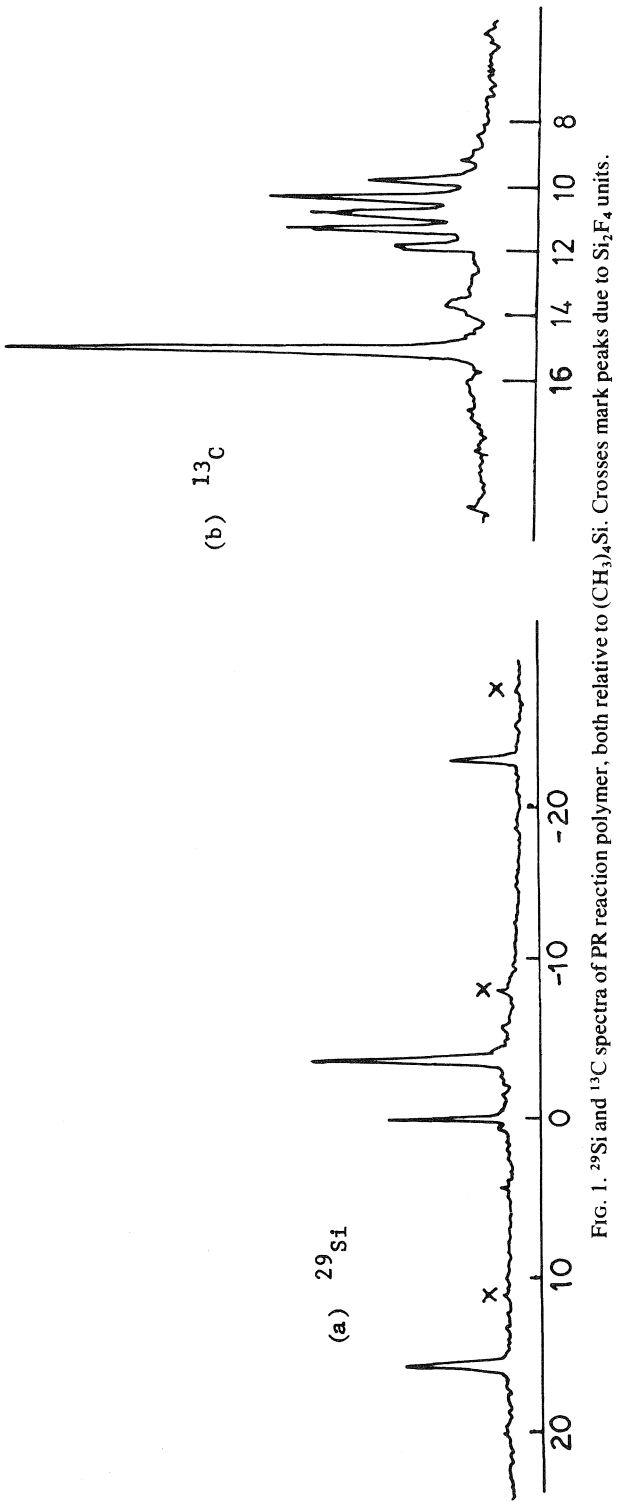


FIG. 1. ^{29}Si and ^{13}C spectra of PR reaction polymer, both relative to $(CH_3)_4Si$. Crosses mark peaks due to Si_2F_4 units.

Can. J. Chem. Downloaded from www.nrcresearchpress.com by 210.87.254.6 on 09/05/12
For personal use only.

TABLE 1. ^{29}Si nmr data from the polymers

Polymer	SiF_2 (monomer) δSi[a]	SiF_2 (monomer) $^1J_{SiF}$[b]	Si_2F_4 (dimer) δSi	Si_2F_4 (dimer) $^1J_{SiF}$	Si_2F_4 (dimer) $^2J_{SiF}$	Ratio $SiF_2:Si_2F_3$
ET reaction[c]						
PR reaction	−3.8	314.0	−8.3	314.0	[d]	1:0.03
CB reaction	−4.9	324.5	−7.5	353.2	48.2	1:0.2
TB reaction	−4.9	324.5	−7.6	354.9	48.5	1:0.4
IB reaction	−4.4	323.7				
MB reaction	−5.5	332.9				
DB reaction[c]						
CB-c4 polymer			−7.7	355.0	47.8	
TB-c4 polymer			−7.7	355.0	47.8	

[a]In ppm relative to internal $(CH_3)_4Si$. High field shift is negative.
[b]^{29}Si–^{19}F coupling constant in Hz.
[c]Not observed due to insoluble nature of polymer.
[d]Peaks not observed due to low concentration of Si_2F_4 units.

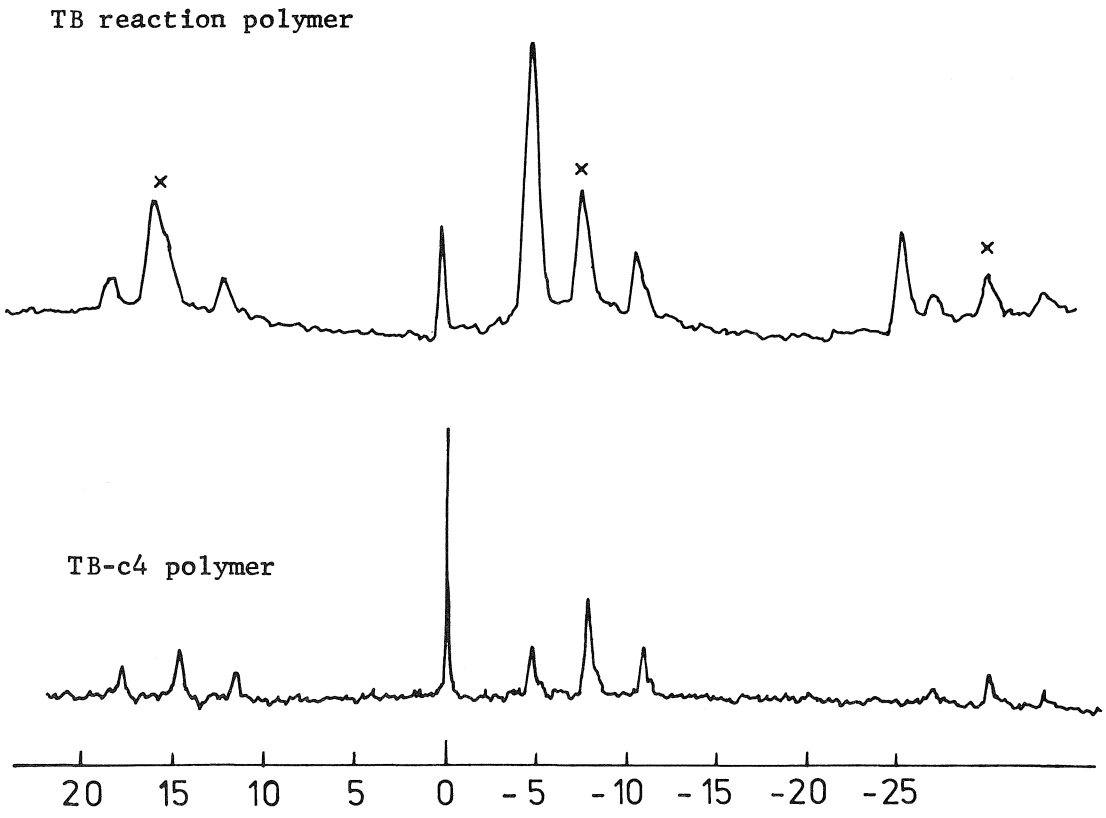
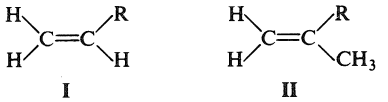


FIG. 2. (*a*) ^{29}Si spectrum of TB reaction polymer; (*b*) ^{29}Si spectrum of polymer from TB-c4. Peak at δ = 0 is $(CH_3)_4Si$.

derivatives cannot be completely separated from the disilacyclohexane products. However, the ^1H spectra of the alkene region as well as ^{19}F and sometimes ^{13}C spectra all yield useful structural information (see Table 2). The chain derivative from PR clearly contains a terminal vinyl group **I**, while IB and MB chains have terminal vinylidene groups **II** (as indicated by the absence of large vicinal ^1H couplings):



I **II**

DB gives two isomers in a 4:1 ratio, each con-

Can. J. Chem. Downloaded from www.nrcresearchpress.com by 210.87.254.6 on 09/05/12
For personal use only.

Can. J. Chem. Downloaded from www.nrcresearchpress.com by 210.87.254.6 on 09/05/12
For personal use only.

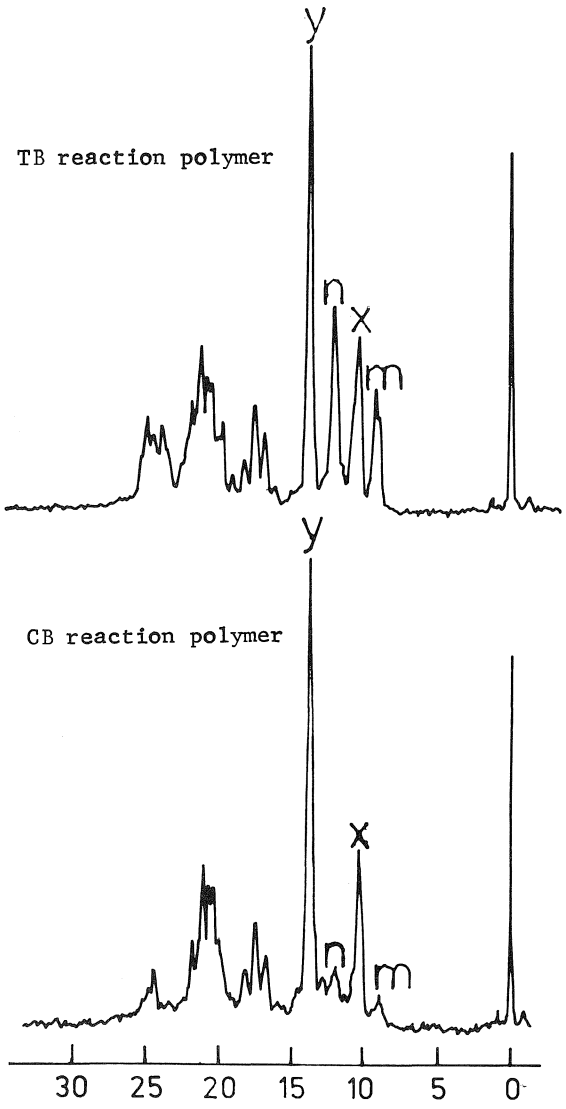


FIG. 3. ^{13}C spectra of TB and CB reaction polymers. Peaks m and n are CH_3 signals identical to those observed for the corresponding polymers from TB-c4 and CB-c4 while peaks x and y are CH_3 signals adjacent to SiF_2 units and with the same respective stereochemistry for the —CH(CH$_3$)—CH(CH$_3$)— linkage as in TB-c4 and CB-c4 (see text).

taining a vinylidene group. PR and IB chains give two SiF_2 signals in their ^{19}F spectra while DB gives two compounds with unsymmetric SiF_2SiF_2 and $(SiF_2)_3$ units in a 1:4 ratio. MB also gives a compound with an SiF_2—SiF_2 linkage but with four non-equivalent fluorines, indicating the presence of at least one chiral center in the molecule. Finally, the ^{13}C spectra of the PR chain shows two olefinic carbons and four saturated carbons, two with significant ^{13}C–^{19}F coupling (the olefinic carbons show no significant coupling).

Structures for the chain derivatives which are consistent with all the spectral information are shown in Table 2. With the exception of the $(SiF_2)_3$ derivative from DB, all of these compounds are isomers of the corresponding disilacyclohexanes (14), suggesting a common intermediate (8). The proposed structure of the $(SiF_2)_2$ derivative of DB is identical to one of the products observed by thermolysis of a tetramethylsilirane (8). One other interesting observation is that the alkene group in each chain isomer is apparently formed between a carbon β to silicon plus a γ carbon which was an alkyl group in the starting alkene. This is apparently essential in this system since ET gives no chain isomer (1, 2). This contrasts with the reactions of acetylene (5) and vinyl chloride (15) with SiF_2 since these yield chain compounds with respective structures **III** and **IV**:

$HC{\equiv}C{-}Si_2F_4{-}CH{=}CH_2$ **III** $ClCH{=}CH{-}Si_2F_4{-}CH_2CH_2Cl$ **IV**

Apparently relatively subtle electronic effects determine the preference for formation of an unsaturated α,β or β,γ bond in these chain derivatives.

CB gives no chain derivatives similar to those shown in Table 1. Instead, a small amount of two other compounds are formed which cannot be completely separated and have not been fully characterized. However, one compound appears to contain a terminal vinyl group but no SiF_2 units. It is of too low volatility to be a butene isomer (10). The other compound contains apparent SiF_2H and SiF_3 units and saturated carbons but no vinyl groups (10). The origins of these derivatives are unknown.

(d) Characterization of Disilacyclobutane Derivatives, Including Stereochemistry

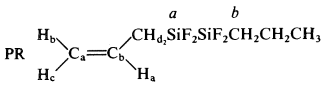
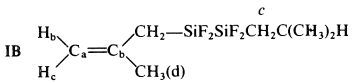
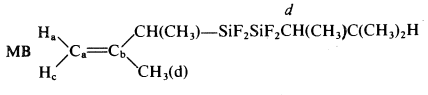
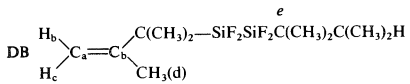
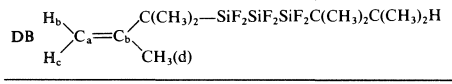
(i) Establishment of Basic Structure

All compounds showed extensive ^{19}F–^{19}F coupling (see below), indicative of the presence of an SiF_2—SiF_2 unit and thus ruling out a 1,3-disilacyclobutane structure. The empirical formula of the ET derivative has already been established as $C_2H_4Si_2F_4$ by mass spectrometry (2). The ^{13}C spectrum of this derivative shows a single peak in the aliphatic region (δ8.9), ruling out a possible open chain structure such as $CH_2{=}CH{-}SiF_2{-}SiF_2H$. Thus it is clear that these products are 1,2-disilacyclobutanes.

Many cyclobutanes undergo rapid interconver-

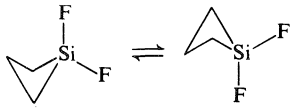
Can. J. Chem. Downloaded from www.nrcresearchpress.com by 210.87.254.6 on 09/05/12
For personal use only.

TABLE 2. Available ^{19}F, ^{1}H, ^{13}C, and ^{29}Si data on chain derivatives

Compound	δH_a[f]	δH_b	δH_c	J_{ab}[g]	J_{ac}	J_{ad}	J_{bc}	J_{bc}	J_{cd}	δF Low field	δF High field	δC_a	δC_b
PR 	5.72	5.12	5.12	17.5	10.0	7.5	1.5	1.5	<1	135.4	136.2	119.0	126.9
IB 		4.95	5.03				1.5		1.5	129.7	131.6	113.4	136.5
MB 		4.62	4.95				1.5		1.5	133.6	135.2	111.9	142.0
DB 		4.79	4.94				≈1.5		≈1.5	134.5 138.8	136.3 139.9		
DB 		4.85	5.02			≈1.5		≈1.5		Middle SiF_2 135.4		113.7	147.0

[a] ^{29}Si spectra of PR CHAIN one Si δ3.0, $^{1}J_{SiF}$ 341.8, $^{2}J_{SiF}$ 49.3, 2nd Si δ11.3, $^{1}J_{SiF}$ 349.1, $^{2}J_{SiF}$ 49.3.
[b] ^{13}C spectra PR CHAIN δ23.1(m), δ18.8(m), δ17.2, δ14.2.
[c] ^{13}C spectra IB CHAIN δ27.5(m), δ27.1(m), δ25.7, δ25.0, δ24.3, δ23.1.
[d] ^{13}C spectra MB CHAIN δ28.0, δ28.7, δ23.6, δ22.1, δ11.2, δ8.5-some peaks obscured by MB spectrum.
[e] ^{13}C spectra DB CHAIN-complicated spectrum of mixture-major peaks δ68.3, δ48.1, δ39.9, δ34.1, δ21.7, δ20.4, δ18.4, δ15.1, δ12.1.
[f] In ppm relative to $(CH_3)_4Si$.
[g] Magnitude of coupling constant (in Hz).

sion between non-planar forms (e.g. E_A = 1.3 kcal/mol for ring flipping in difluorosilacyclobutane (16)).



On the other hand, a recent X-ray crystal structure determination for a 1,2-disilacyclobutane has shown a planar ring (17). We have measured the ^{19}F spectra of disilacyclobutanes down to −113°C without seeing any evidence of "freezing out" of a conformational process. Since, in practical terms, it is impossible to distinguish between a planar ring and a rapidly interconverting non-planar structure, we will discuss these products as if they were planar.

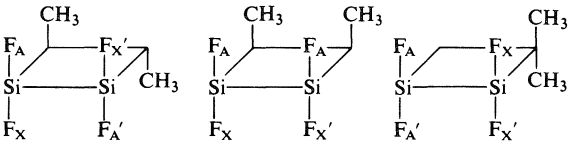
(ii) Stereochemistry of Formation of Disilacyclobutanes

As noted above, the formation of a 1,2-disilacyclobutane from an alkene is a highly stereospecific reaction. This is very important from a mechanistic viewpoint since, if one assumes that $F_2\dot{S}i—\dot{S}iF_2$ is the attacking species in the formation of disilacyclobutane (6), orbital symmetry arguments predict inversion of configuration for a concerted thermal cycloaddition reaction (3). Thus it is important to establish the stereochemistry of the reaction.

^{19}F spectra proved most useful for determining the specific structures of disilacyclobutanes. All spectra were recorded at −40°C to minimize thermal polymerization. The disilacyclobutane from ethylene (thereforth designated ET-c4) gave an $A_4{}^{19}F$ spectrum but the ^{29}Si satellite peaks (due to ET-c4 containing one ^{29}Si atom) showed an AA′XX′ pattern. The products of propene (PR-c4) and methylbutene (MB-c4) reactions showed four non-equivalent ^{19}F peaks in essentially first order (AKRX) spectra. IB-c4 and TB-c4 gave AA′XX′ spectra while CB-c4 gave an AA′BB′ spectrum due to the smaller ^{19}F chemical shift difference in this compound (1.6 ppm).

The spectra were complicated by significant ^1H–^{19}F coupling. However, the ^1H-decoupled spectra showed simple splitting patterns (see Fig. 4). Although there are, in principle, two *gauche*, two *trans*-vicinal, and two *cis*-vicinal ^{19}F–^{19}F coupling constants in compounds such as PR-c4, pairs of coupling constants were similar in magnitude. PR-c4 showed three splittings of ca. 41 Hz, 15 Hz, and 2 Hz while MB-c4 showed splittings of ca. 44 Hz, 16 Hz, and 2 Hz. Similar splittings were observed in the ^{29}Si satellite spectra of CB-c4 and TB-c4 (the satellites give AKRX spectra due to the four non-equivalent fluorines in a singly-labelled compound). Thus ^{19}F–^{19}F coupling constants in disilacyclobutanes are relatively insensitive to methyl substitution and the observed splittings of ca. 42 Hz, 16 Hz, and 2 Hz can be assigned as geminal, *trans*-vicinal, and *cis*-vicinal couplings although not necessarily in that order.

TB-c4 must have either structure **VI** (retention of alkyl configuration) or **VII** (inversion of configuration) while CB-c4 has the other structure of this pair (IB-c4 must have structure **VIII**):



VI **VII** **VIII**

Note that the coupling between equivalent fluorines $J_{AA'}$ (and $J_{XX'}$) respectively corresponds to *trans*-vicinal, *cis*-vicinal, and geminal coupling constants in **VI**, **VII**, and **VIII**. $J_{AA'}$ for TB-c4, CB-c4, and IB-c4 can be determined by spectral analysis. Consequently, if the relative magnitudes of the *trans*- and *cis*-vicinal coupling constants are known, then it should be possible to assign unambiguously the structures of TB-c4 and CB-c4. Unfortunately, ^{19}F–^{19}F couplings in analogous carbon compounds provide no help in making this assignment since they vary in an extremely complex way with substitution and are of little value in assigning stereochemistry (18). However 2,2,3,3,7,7- heptafluoro-2,3,7-trisilanorborn-5-ene (5) (see Fig. 5) contains an Si_2F_4 unit in which *trans*- and *cis*-vicinal coupling constants can be assigned with confidence since the *cis*-vicinal coupling must be between equivalent fluorines. Detailed analysis of the AA′XX′ spectrum for the Si_2F_4 unit of this compound (including the use of ^{29}Si satellites) has shown that $|J_{trans\text{-vicinal}}| = 15$ Hz while $J_{cis\text{-vicinal}} = 0 \pm 0.5$ Hz (10). The geminal coupling has a magnitude of 33 Hz while the bridgehead SiF_2 shows a geminal coupling of 61 Hz. These are sufficiently close to the observed splittings of ca. 42 Hz, 15 Hz, and 2 Hz in disilacyclobutanes that the latter can be assigned with reasonable confidence as respectively geminal, *trans*-vicinal, and *cis*-vicinal coupling constants.

These splittings can be used to generate sample AA′XX′ spectra for comparison with the experimental AA′XX′ (or AA′BB′) spectra for IB-c4, CB-c4, and TB-c4. One problem is that it is not normally possible to determine relative signs of coupling constants by analysis of AA′XX′ spectra since different solutions are possible, corresponding to different signs and magnitudes of the cou-

Can. J. Chem. Downloaded from www.nrcresearchpress.com by 210.87.254.6 on 09/05/12
For personal use only.

Can. J. Chem. Downloaded from www.nrcresearchpress.com by 210.87.254.6 on 09/05/12
For personal use only.

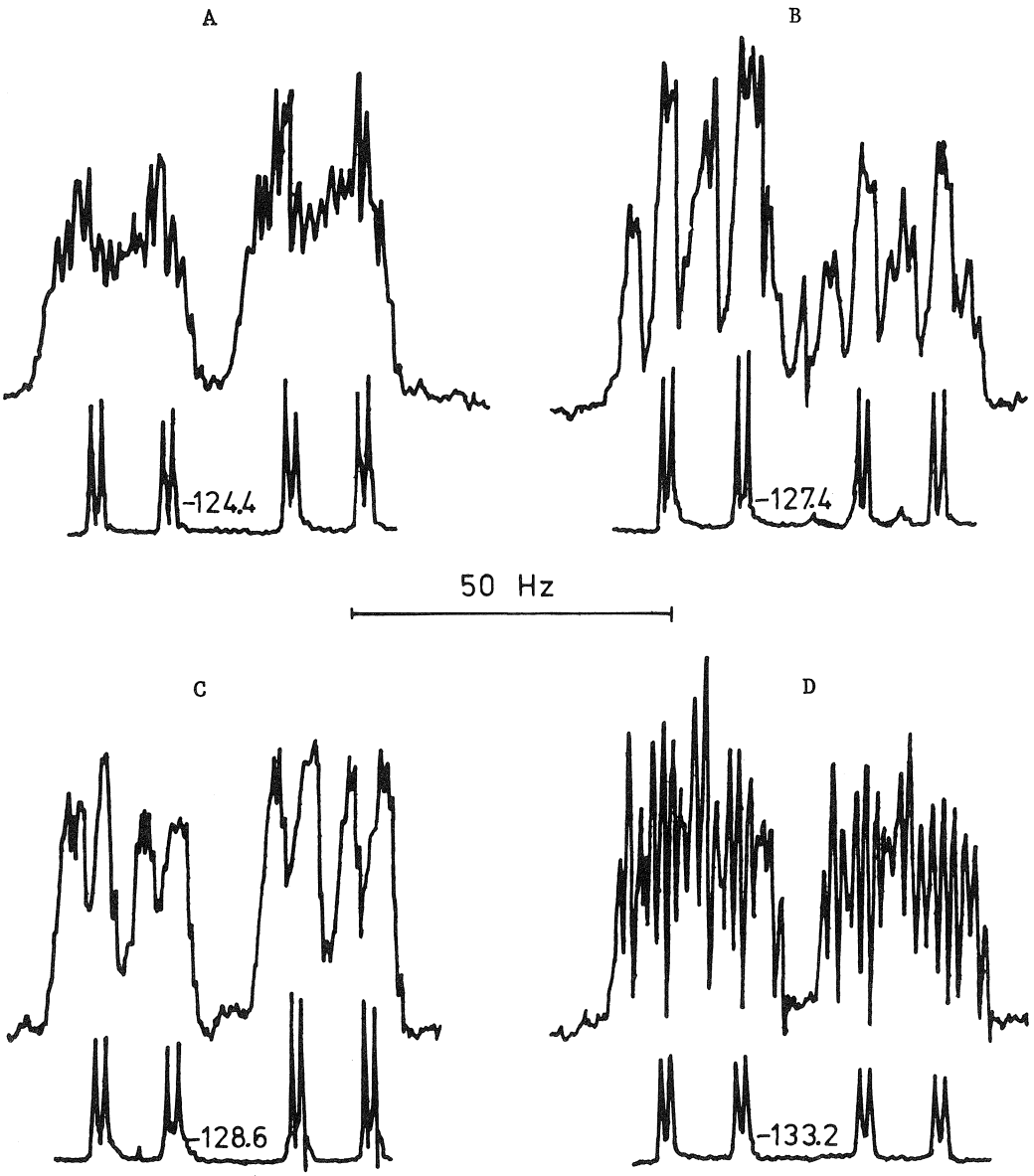


FIG. 4. ^{19}F peaks for four non-equivalent fluorines in PR-c4. The lower spectrum in each case is ^{19}F decoupled.

pling constants (19). However, in this case, it is possible to determine the relative signs of all three coupling constants because the magnitudes of the couplings are known and because three compounds of different symmetry are available for comparison. The sample spectra showed that the only combination which provided a good fit for all three experimental spectra was one in which the geminal coupling constant had the opposite sign to the two vicinal coupling constants (10). Since $J_{^{19}F-C-^{19}F}$ is typically ca. +200 Hz (18), it is likely that the geminal ^{19}F–Si–^{19}F coupling is also positive and that the vicinal coupling constants are negative.

More importantly, the TB-c4 spectrum could only be fitted if the coupling between equivalent fluorines was 15 Hz, corresponding to a *trans*-vicinal coupling constant. Consequently TB-c4 has structure **VI** and must be formed from TB with *retention of stereochemistry*. Similarly, the CB-c4 spectrum was only fitted with $|J_{AA'}| = 2$ Hz, i.e. a *cis*-vicinal coupling, indicating that CB-c4 had structure **VII**.

The above-mentioned signs and magnitudes of the three coupling constants were used as initial input parameters for an interative spectral analysis, using the computer program LAOCN3 (20). This

Can. J. Chem. Downloaded from www.nrcresearchpress.com by 210.87.254.6 on 09/05/12
For personal use only.

TABLE 3. Best values of ^{19}F chemical shifts and coupling constants for disilacyclobutanes from computer output

Ring + fluorine	Chemical shift[a]	$^2J_{FF}$ (gem)[b]		$^3J_{FF}$ (*cis*)		$^3J_{FF}$ (*trans*)	
ET-c4[c]	−125.6			−3.0		−13.15	
		AB	CD	AD	BC	AC	BD
PR-c4 A	−124.4	±41.08	+41.88	−1.95	−2.10	−15.32	−15.83
B	−127.4						
C	−128.6						
D	−133.2						
CB-c4 B	−130.2	+42.78		−2.30[d,e]		−15.11	
C	−132.7						
TB-c4 A	−125.0	+41.70		−2.08		−15.23[d,e]	
D	−137.0						
		AA	DD				
IB-c4 A[f]	−126.1	+37.0[d,e]	+37.0[d,e]	−3.7		−13.8	
D	−134.2						
		AC	BD	AD	BC	AB	CD
MB-c4 A	−125.2	+43.97	+45.05	−2.30	−2.22	−14.56	−14.50
B	−131.4						
C	−135.6						
D	−139.0						
Average		+42.7		−2.4		−14.9	

[a]In ppm relative to internal $CFCl_3$ (high field shifts negative).
[b]Coupling assumed positive by analogy with $^2J_{^{19}F-C-^{19}F}$ (see text).
[c]The ^{29}Si satellites of ET-c4 resembled the IB-c4 spectrum and allowed determination of only the *cis*-vicinal and *trans*-vicinal coupling.
[d]Iterative analysis gave identical values for this pair of coupling constants even though they could in principle be non-equivalent.
[e]Coupling between equivalent fluorines ($J_{AA'}$, $J_{XX'}$).
[f]The geminal couplings have a relatively larger uncertainty (ca. 5 Hz) since the spectrum is relatively insensitive to the magnitude of this coupling.

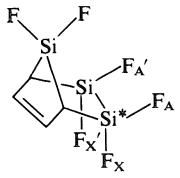


FIG. 5. Structure of trisilanobornene which was used to assign vicinal and geminal $^{19}F-^{19}F$ coupling constants. Note that when the molecule contains one ^{29}Si in the Si_2F_4 unit, all four fluorines in this unit are non-equivalent.

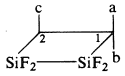
gave more precise values for the various coupling constants. The results are summarized in Table 3. It is particularly noteworthy that the vicinal coupling constants show little effect of alkyl substitution, lending further confidence to their use in stereochemical assignments. Similarly the geminal couplings fall in the range +41 ± 4 Hz.

Further support for the assigned structures of TB-c4 and CB-c4 is obtained from the ^{13}C chemical shift data for the disilacyclobutanes (see Table 4). The key point concerns the ^{13}C chemical shifts for the methyl groups of CB-c4 and TB-c4. The methyl peak for the former compound (δ7.5) is more than 5 ppm to high field to the methyl peak for the latter (δ12.6). It is well established that two methyl groups in a γ orientation are more shielded when they are spatially proximate (13). Thus the compound with *cis* methyl groups should give a methyl signal to high field of that with *trans* methyl groups. Thus the ^{13}C chemical shift data also indicate that CB-c4 and TB-c4 are formed with retention of alkyl stereochemistry.

TABLE 4. ^{13}C chemical shifts of 1,2-disilacyclobutanes[a]

	δ[b]				
	Ring carbon[c]		Methyl carbon[c]		
Compound	1	2	a	b	c
ET-c4	8.92	8.92	—	—	—
PR-c4	20.99	18.00	14.50	—	—
CB-c4	23.93	23.93	7.50	—	7.50
TB-c4	29.01	29.01	—	12.50	12.50

[a]Chemical shifts were not assigned for IB-c4 and MB-c4 due to low concentrations and because ^{13}C peaks were partially obscured by peaks from chain and disilacyclohexane derivatives.
[b]In ppm from internal $(CH_3)_4Si$. Low field shifts positive.
[c]Carbon labelled



This is also indicated by consideration of the ^{19}F chemical shifts. The ^{19}F chemical shift difference for TB-c4 (12.0 ppm) is much larger than for CB-c4 (1.6 ppm) while the four non-equivalent fluorines in PR-c4 give signals over an 8.8 ppm range. The relatively large effect of a methyl group upon individual

TABLE 5. Comparison of observed and predicted ^{19}F chemical shifts for disilacyclobutanes

Compound		Predicted and observed chemicals shifts (δ)[a]			
		A	B	C	D
CB-c4	Observed		−130.2	−132.7	
	Predicted		−130.4	−132.0	
TB-c4	Observed	−125.0			−137.0
	Predicted	−127.4			−135.0
IB-c4	Observed	−126.1			−134.2
	Predicted	−126.2			−136.2
MB-c4	Observed	−125.2	−131.4	−135.6	−139.0
	Predicted	−129.2[b](−129.1)[c]	−135.0 (−133.0)	−133.8 (−133.7)	−138.0 (−136.0)
DB-c4	Observed				(134)[d]
	Predicted				−136.8 (−134.4)

[a]Relative to internal $CFCl_3$ in ppm. High field (low frequency) shifts are negative. Solutions contained ca. 10% compound in $CFCl_3$ with 10% $(CD_3)_4Si$ added to provide the internal lock signal.
[b]Predicted using additivity parameters from PR-c4 (see Fig. 3).
[c]Predicted using additivity parameters from PR-c4 for the effect of a $CHCH_3$ group and parameters for IB-c4 for the effect of $C(CH_3)_2$ (see Fig. 3).
[d]A minor peak was noted at this frequency which may be due to DB-c4 which is produced in a very low yield.

^{19}F chemical shifts in PR-c4 suggests the possibility of deriving additive chemical shift parameters to predict ^{19}F chemical shifts in **VI** and **VII** for comparison with CB-c4 and TB-c4. The average chemical shifts for ET-c4 (δ − 125.6), PR-c4 (δ − 128.4), CB-c4 (δ − 131.4), and TB-c4 (δ − 131.0) indicate that this procedure should be valid since they show an incremental shift of δ − 2.8 ± 0.2 for addition of each methyl group.

In order to derive an additivity scheme, one must first assign the individual ^{19}F resonances in PR-c4. There are sufficient differences in the two geminal couplings to allow one to conclude that fluorines A (δ − 124.4) and B (δ − 137.4) are on one silicon while fluorines C (δ − 128.6) and D (δ − 133.2) are on the other silicon (this was confirmed by homonuclear decoupling). A more complete assignment can be arrived at by making use of the ^1H–^{19}F coupling which is clearly visible in Fig. 4. Selective hydrogen decoupling plus consideration of the magnitudes of the individual ^1H–^{19}F coupling constants leads to the assignment shown in Fig. 6 (10). This assignment allows the derivation of parameters for the effect of CH_3 on individual ^{19}F chemical shifts. The chemical shift parameters in Fig. 6 indicate an upfield ^{19}F shift due to a proximate γ methyl and a downfield shift due to a proximate δ methyl. Similar effects were noted in disilacyclohexanes (14). Interestingly, ^{13}C spectra also show upfield γ

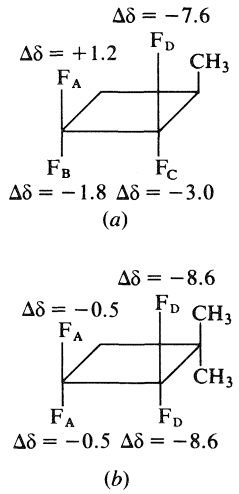


FIG. 6. Additive chemical shift parameters indicating the effect of (*a*) a single methyl group and (*b*) a $(CH_3)_2C$ group on the ^{19}F chemical shifts of 1,2-disilacyclobutanes.

Can. J. Chem. Downloaded from www.nrcresearchpress.com by 210.87.254.6 on 09/05/12
For personal use only.

Can. J. Chem. Downloaded from www.nrcresearchpress.com by 210.87.254.6 on 09/05/12
For personal use only.

(13) and downfield δ (21) shifts due to methyl–methyl steric interactions.

The parameters for Fig. 6 can be used to predict the chemical shifts of other disilacyclobutanes (Table 5). These predictions again indicate that CB-c4 and TB-c4 have respectively *cis* and *trans* methyl groups, i.e. they are formed with retention of stereochemistry. The additivity parameters are not as good at predicting MB-c4 ^{19}F chemical shifts. Additivity apparently breaks down when two methyls are substituted on the same carbon since the incremental contribution to the average chemical shifts is only -1.6 ± 0.2 ppm in this case (e.g. PR-c4 (δ − 128.4) → IB-c4 (δ − 130.1), CB-c4 (δ − 131.4) or TB-c4 (δ − 131.0) → MB-c4 (δ − 132.8)), compared to -2.8 ± 0.2 ppm for addition of a methyl group to an unsubstituted carbon. This may reflect either a saturation of substitutent effects or an alteration of the conformational equilibrium between different non-planar forms of the disilacyclobutane ring (see above). One way around this problem is to use IB-c4 shifts as a measure of the effects of a $(CH_3)_2C$ grouping (Fig. 6). When this is done, the agreement for MB-c4 is improved. In addition, the predicted ^{19}F chemical shift for DB-c4 is much closer to that observed for a minor peak tentatively assigned to this compound.

Summary and Conclusions

The polymers produced by the reaction of SiF_2 with olefins generally have a regular structure with isolated SiF_2 units between olefin linkages, with the olefin linkages in a regular head-to-tail fashion. This demonstrates that monomeric SiF_2 is the major reactive $(SiF_2)_n$ species in this reaction. The polymers from TB and, to a lesser extent, from CB also contain Si_2F_4 units. Polymerization occurs via a mechanism which allows scrambling of the alkene configuration.

Open chain derivatives have the general formula $R—(SiF_2)_n—R'$ where R is an alkyl group and R′ contains a terminal olefin function. With one exception, they contain Si_2F_4 units and are isomers of the corresponding 1,2-disilacyclohexane. DB also yields a derivative with an $(SiF_2)_3$ unit.

1,2-Disilacyclobutanes are formed with complete retention of stereochemistry of the alkyl groups in the starting olefin. This is clearly apparent from a consideration of ^{19}F–^{19}F coupling constants and ^{13}C and ^{19}F chemical shifts.

This information, along with further data concerning product yields (1) and structure of 1,2-disilacyclohexanes (14) are used to develop a detailed mechanism of the SiF_2–olefin reaction (1).

1. W. F. Reynolds, J. C. Thompson, and A. P. G. Wright. Can. J. Chem. **58**, 419 (1980).
2. J. C. Thompson, J. L. Margrave, and P. L. Timms. Chem. Commun. 566 (1966).
3. C. S. Liu and J. C. Thompson. Tetrahedron Lett. 1581 (1973).
4. C. S. Liu. Ph.D. Thesis. University of Toronto, Toronto, Ont. 1971.
5. C. S. Liu, J. L. Margrave, J. C. Thompson, and P. L. Timms. Can. J. Chem. **50**, 459 (1972).
6. J. L. Margrave and D. L. Perry. Inorg. Chem. **16**, 1820 (1977).
7. C. S. Liu and T. L. Hwang. J. Am. Chem. Soc. **100**, 2577 (1978).
8. D. Seyferth and D. P. Duncan. J. Am. Chem. Soc. **100**, 7734 (1978).
9. J. C. Thompson, W. F. Reynolds, and A. P. G. Wright. J. Am. Chem. Soc. **101**, 2236 (1979).
10. A. P. G. Wright. Ph.D. Thesis. University of Toronto, Toronto, Ont. 1979.
11. J. C. Randall. Polymer sequence determination: C13 NMR Method. Academic Press, New York. 1977.
12. C. S. Liu. Private communication.
13. J. B. Stothers. Carbon 13 NMR spectroscopy. Academic Press, New York. 1972.
14. W. F. Reynolds, J. C. Thompson, and A. P. G. Wright. Can. J. Chem. **58**, 436 (1980).
15. C. S. Liu and T. L. Hwang. J. Am. Chem. Soc. **101**, 2996 (1979).
16. R. M. Irvin, J. M. Cooke, and J. Laane. J. Am. Chem. Soc. **99**, 3273 (1977).
17. A. G. Brook and S. C. Nyburg. Private communication.
18. J. W. Emsley, L. Phillips, and V. Wray. Fluorine coupling constants. Pergamon Press, Oxford. 1977.
19. R. J. Abraham. Analysis of high resolution N.M.R. spectra. Elsevier, Amsterdam. 1971.
20. A. A. Bothner-By and S. Castellano. J. Chem. Phys. **41**, 3863 (1964).
21. G. Mann, E. Kleinpeter, and G. Werner. Org. Magn. Reson. **11**, 561 (1978).

A systematic investigation of the reaction of SiF_2 with ethylene and six methyl-substituted ethylenes. III. Structures and conformational behaviour of 1,2-disilacyclohexane products[1]

WILLIAM F. REYNOLDS, JAMES C. THOMPSON,[2] AND A. P. GERALD WRIGHT

Department of Chemistry, University of Toronto, Toronto, Ont., Canada M5S 1A1

Received July 19, 1979

WILLIAM F. REYNOLDS, JAMES C. THOMPSON, and A. P. GERALD WRIGHT. Can. J. Chem. **58**, 436 (1980).

1,2-Disilacyclohexanes are generally formed as products in the reaction of SiF_2 with alkenes. Unsymmetric methyl-substituted alkenes yield disilacyclohexanes with greater methyl substitution at C(2). Often two (or more isomeric) products are formed, and the reaction proceeds by a mechanism which allows isomerization of the methyl configurations. The disilacyclohexanes exist in distorted chair conformations and the chair-to-chair interconversion can be observed at low temperature in many cases. Consideration of the variable temperature ^{19}F spectra and the effect of methyl groups on average and individual ^{19}F chemical shifts allows assignment of configurations and preferred conformations of all disilacyclohexane derivatives.

WILLIAM F. REYNOLDS, JAMES C. THOMPSON et A. P. GERALD WRIGHT. Can. J. Chem. **58**, 436 (1980).

La réaction du SiF_2 avec les alcènes conduit généralement aux disila-1,2 cyclohexanes. Les alcènes non symétriques portant un substituant méthyle conduisent à des disilacyclohexanes dans lesquels le groupe méthyle est porté de préférence par le carbone en position 2. Il se forme souvent deux (ou plusieurs) produits isomères et la réaction a lieu selon un mécanisme qui permet une isomérisation de la configuration des méthyles. Les disilacyclohexanes existent sous la forme chaise déformée, et dans plusieurs cas, on peut observer des interconversions chaise–chaise à basse température. On peut attribuer les configurations et les conformations préférentielles de tous les dérivés disilacyclohexanes en tenant compte des spectres du ^{19}F à des températures variables et de l'effet des substituants méthyles sur les déplacements chimiques moyens et individuelles du ^{19}F.

[Traduit par le journal]

Can. J. Chem. Downloaded from www.nrcresearchpress.com by 210.87.254.40 on 09/05/12
For personal use only.

Introduction

Disilacyclohexanes are often formed in significant yield in the reaction of SiF_2 with alkenes (1–3). In our systematic investigation of the reaction of SiF_2 with ethylene and six methyl-substituted ethylenes, disilacyclohexane products were found in six of the seven reactions (3). In a number of cases, two or more isomeric disilacyclohexanes were formed (3). Furthermore, when a mixture of ethylene (ET) and propene (PR) was reacted with SiF_2, one of the major products was a mixed disilacyclohexane containing 1 mol ET and 1 mol PR (4). A similar mixed disilacyclohexane (in two isomeric forms) was obtained from the reaction of SiF_2 with a mixture of PR and *trans*-2-butene (TB) (4).

There are a number of possible structures for these derivatives. In addition, they would be expected to exist in chair conformations, with the possibility of observing the chair-to-chair interconversions from low temperature nmr spectra, just as in the case of cyclohexane (5).[3] Thus it is an interesting spectroscopic problem to determine the structures of these products and to investigate their conformational behavior. In addition the structures provide relevant information about the mechanism of the SiF_2–olefin reaction (6, 7). Fortunately it has proved possible to identify all of the major disilacyclohexane products and to determine their preferred conformations, using ^{13}C and variable temperature ^{19}F nmr spectroscopy, in conjunction with additive ^{19}F chemical shift parameters (4). These results are discussed below.

Experimental

Experimental details are given in ref. 3.

Results and Discussion

(a) Nomenclature

The olefin used in the reaction is identified by capital letters, as shown above. Four-membered rings (1,2-disilacyclobutanes) and six-membered rings (1,2-disilacyclohexanes) are designated -c4 and -c6 respectively. Thus, a disilacyclohexane resulting from the reaction of SiF_2 with a mixture of *trans*-2-butene and propene is shown as TBPR-c6. Further stereochemical differences between such compounds are shown in the tables and discussed in the text.

(b) Basic Structures of Disilacyclohexanes

The reaction of PR with SiF_2 is typical of alkene–SiF_2 reactions. The room temperature ^{19}F

[1]Taken in part from the Ph.D. Thesis of A. P. G. Wright, University of Toronto, Toronto, Ont. 1979.

[2]To whom all correspondence should be addressed.

[3]After completion of this investigation, Liu and Hwang reported the observation of chair-to-chair interconversion in a disilacyclohexane produced from the reaction of SiF_2 with vinyl chloride (2).

0008-4042/80/050436-11$01.00/0

©1980 National Research Council of Canada/Conseil national de recherches du Canada

Can. J. Chem. Downloaded from www.nrcresearchpress.com by 210.87.254.40 on 09/05/12
For personal use only.

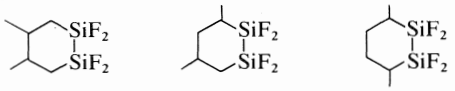
spectrum of the disilacyclohexane (henceforth designated as PR-c6) shows that two isomers were formed, each with two ^{19}F signals (see Fig. 1). Either 1,2 (**I**) or 1,4 (**II**) isomers could be formed:



I **II**

However, the spectrum shows large $^{19}F-^{19}F$ coupling for both isomers. Thus they both must have ring structure **I** since the 1,4 isomer would be expected to show very small (5-bond) $^{19}F-^{19}F$ coupling (8). In fact, all of the disilacyclohexanes detected in this investigation had the 1,2 structure. This is an interesting observation since the reaction of $SiCl_2$ with ethylene yields 1,4-disilacyclohexane (9).

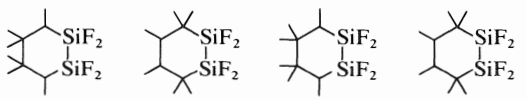
There are three possible substitution patterns for the 1,2 PR-c6 isomers:



III **IV** **V**

In addition, there are two possible configurational isomers for each positional isomer: a *cis* (up,up or U,U) isomer, where both methyl groups are attached to the same face of the ring and a *trans* (up,down or U,D) isomer, where the two methyl groups are on opposite faces. Structure **IV** can be ruled out since each configurational isomer should show four non-equivalent fluorine peaks, rather than two. A choice can be made between structures **III** and **V** on the basis of ^{13}C spectral data. Each isomer gives three peaks. In each case, it is possible to assign C(1) (the carbon adjacent to Si) since it shows significant $^{13}C-^{19}F$ coupling. Off-resonance ^{1}H decoupling showed a complex multiplet for this peak while the remaining two peaks for each isomer appeared as a doublet and a quartet. The latter must be the methyl group while the former must be C(2). C(2) must be a tertiary carbon to account for the doublet splitting, indicating methyl substitution at C(2), i.e. structure **III**. Thus the two PR-c6 isomers must be the *cis* and *trans* isomers of **III**.

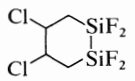
The 1,2-disilacyclohexanes produced from isobutylene (IB-c6) and 2-methyl-2-butene (MB-c6) also have two different possible structures (the ^{19}F spectra again ruled out unsymmetrically substituted isomers);



IB-c6 (**A**) IB-c6 (**B**) MB-c6 (**A**) MB-c6 (**B**)

Again, off-resonance decoupling indicated greater methyl substitution at C(2) in each case (structure **A**) (4).

Preferred methyl substitution at C(2) is also indicated by the ^{13}C chemical shift data. All of the disilacyclohexanes gave methyl peaks in the range δ17–29 (see Table 1) comparable with the methyl ^{13}C chemical shift in methylcyclohexane (δ23.8 (10)). However, the *cis*-2-butene derivative (CB-c6, MB-c6) and the mixed *trans*-2-butene-propene derivative (TBPR-c6) each gave an additional CH_3 signal in the range δ7–12, similar to the methyl chemical shifts in 1,2-disilacyclobutanes (3). In each case, the peak showed ^{19}F coupling. Thus the additional peak in the δ7–12 range can logically be assigned as a C(1) methyl while the peak at δ17–29 is a C(2) methyl signal. MB-c6 and TBPR-c6 gave C(2) and C(1) methyl peaks in a 2:1 ratio, again indicating greater methyl substitution at C(2). Thus, one can state, as a general rule that unsymmetric methyl-substituted alkenes give 1,2-disilacyclohexanes with greater methyl substitution at C(2). This may also apply to other substituents since vinyl chloride yields a disilacyclohexane with structure **VI** (2):



VI

(c) Variable Temperature ^{19}F Spectra and Identification of Configurational Isomers

As noted above, two isomers of PR-c6 were formed. These can be distinguished by their variable temperature ^{19}F nmr spectra (Fig. 2). The spectrum for one isomer remains essentially unchanged on cooling while the other changes from a two peak to a four peak spectrum (with each peak of equal area) on cooling. The *cis* (U,U) isomer should exist as two forms which are conformational enantiomers (each with one axial, a, and one equatorial, e, methyl group; see Fig. 3). At room temperature these will be rapidly interconverting, yielding an average spectrum with two peaks, equivalent to that for a planar ring. However, if cooling slows the chair-to-chair interconversion sufficiently, then one will see the spectrum of either mirror image chair in which there are four fluorine peaks of equal area. By contrast, the *trans* (U,D) isomer exists as two conformational diastereomers (with a,a and e,e methyl groups). The averaged spectrum will again show two peaks. However, on cooling, one should observe two unequal sets of two peaks (corresponding to a,a and e,e conforma-

Can. J. Chem. Downloaded from www.nrcresearchpress.com by 210.87.254.40 on 09/05/12
For personal use only.

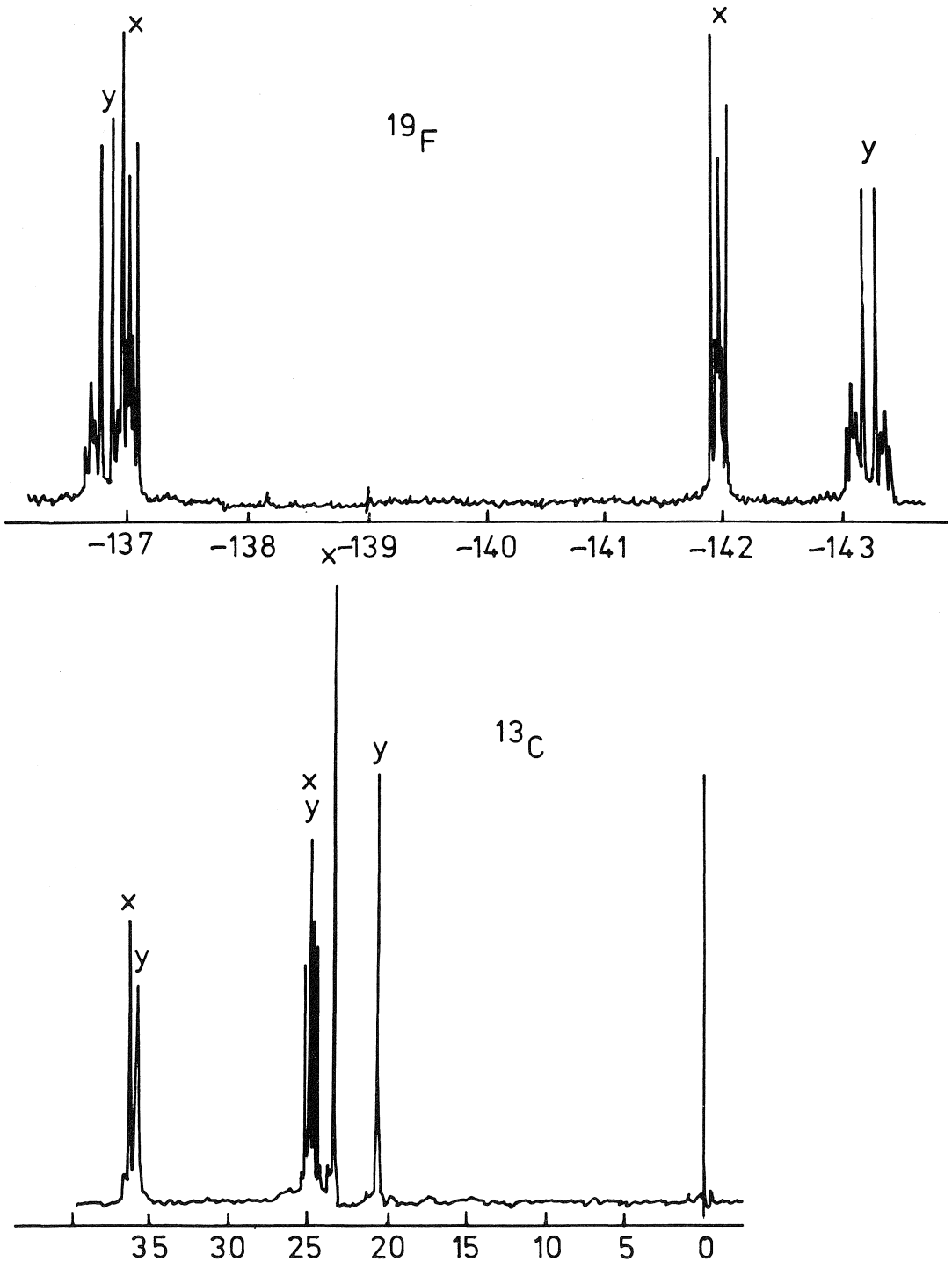
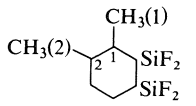


FIG. 1. ^{19}F and ^{13}C spectra of PR-c6 at 31°C (both spectra ^{1}H-decoupled): x = *trans*-PR-c6, y = *cis*-PR-c6.

tions, Fig. 3). Alternatively, if one conformation is strongly favoured and/or if the barrier to interconversion is low, one might observe a low temperature spectrum with only two peaks. Thus the compound which splits from two to four ^{19}F peaks on cooling can be assigned to the *cis* isomer while the compound whose spectrum remains unchanged on cooling can be assigned as the *trans* isomer.

Can. J. Chem. Downloaded from www.nrcresearchpress.com by 210.87.254.40 on 09/05/12
For personal use only.

TABLE 1. ^{13}C chemical shifts of 1,2-disilacyclohexanes[a,b]



c6-Compound	Chemical shift C(1)	C(2)	$CH_3(1)$	$CH_3(2)$
ET	19.97	24.17		
PR-a,a[c,d]	24.31	35.97		23.18
PR-a,e[c,d]	24.55	35.47		20.34
CB-e,e,e,e[e]	27.22	38.89	11.20	19.33
CB-a,e,a,e	27.22	38.89	10.62	17.48
IB-(a,e)(a,e)	31.44	39.18		28.64 26.04
MB-a(a,e)(a,e)e[e]	33.59	42.57	8.93	25.17
MB-e(a,e)(a,e)e	30.46	42.16	7.62	21.23 23.38
DB	[f]	[f]	[f]	[f]
PRET-e	[g]	32.40 32.30	[g]	[g]
TBPR-e,e,e	30.25 26.60	43.88 36.16	12.21	20.14 24.94

[a]In ppm relative to internal $(CH_3)_4Si$. Low field shifts positive.
[b]See text concerning assignments.
[c]Axial (a) and equatorial (e) conformations of methyl groups as determined in subsequent tables.
[d]Resonances assigned in this order since low temperature behaviour showed peak at δ20.34 split into a doublet $\Delta\delta = 10.4$ (257 Hz). Also PR-c6 ae has *gauche* methyls to high field.
[e]Assignment made on basis of variable temperature behaviour.
[f]Concentration too small relative to chain derivatives to make unambiguous assignment.
[g]Not observed due to overlap with other peaks in spectrum.

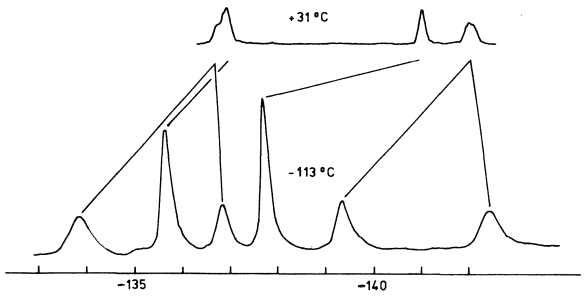


FIG. 2. Proton coupled ^{19}F spectra of PR-c6 at 31°C and −113°C.

Identical arguments have very recently been used to assign *cis* and *trans* isomers of **VI** (2). The ^{13}C spectra of the two PR-c6 isomers also showed similar variable temperature nmr behaviour, thus aiding in the assignment of the ^{13}C signals of these isomers (4).

Variable temperature ^{19}F spectra allowed assignment of the isomers of several of the other disilacyclohexane derivatives while in other cases the number of possible structures can be limited by symmetry considerations (see Table 2). Thus variable temperature ^{19}F spectra in conjunction with symmetry arguments provide a very useful method for assigning these isomers.

Free energies of activation, $\Delta G^{\ddagger}$, for chair-to-chair interconversion can be estimated from the coalescence temperatures of the ^{19}F spectra (Table 3). The values of $\Delta G^{\ddagger}$ show a rough trend with the number of possible eclipsing methyl–methyl steric interactions in the transition state (which can be estimated from the number of 1,2 eclipsing interactions in the planar form). $\Delta G^{\ddagger}$ for *cis*-PR-c6 (8.2 kcal/mol) is smaller than $\Delta G^{\ddagger}$ for the *cis* isomer of **VI** (11.2 kcal/mol (2)). This is reasonable since there should be additional electrostatic repulsion between the chlorines in the transition state of the latter compound. The failure to freeze out the chair-to-chair interconversions of ET-c6 and *trans*-PR-c6 is consistent with the lack of eclipsing CH_3–CH_3 interactions in those derivatives. The estimated axial–equatorial ^{19}F chemical shift difference for ET-c6 (see below) allows one to set a limit of $\Delta G^{\ddagger} < 6$ kcal/mol for this compound (4). This is considerably lower than $\Delta G^{\ddagger}$ for cyclohexane (10.3 kcal/mol (11)), indicating that the long Si—Si bonds significantly destabilize the ground state of 1,2-disilacyclohexane by ring distortion.

(d) Average ^{19}F Chemical Shifts and Assignment for Preferred Methyl Conformations

While many of the disilacyclohexane isomers have been assigned by variable temperature ^{19}F spectra, not all compounds could be assigned. In addition, the variable temperature behaviour provides no direct information about preferred methyl conformations (a or e). However, low temperature ^{19}F chemical shifts provide useful information about both configuration and conformation through the use of additive ^{19}F chemical shift parameters similar to those derived for 1,2-disilacyclobutanes (3). Average chemical shifts will be considered first (Table 4).

Comparison of ET-c6 and PRET-c6 indicates that a single methyl group at C(2) causes a very small change in average chemical shift ($\Delta\delta = -0.3$ ppm). By analogy with methylcyclohexane (12), the methyl group is very likely equatorial. By contrast, *cis*-c6, which has a,e methyl groups, shows a significant low field shift relative to ET-c6 ($\Delta\delta = +2.0$ ppm) which must reflect the effect of the axial methyl group. Thus, the large low field shift for *trans*-PR-c6 ($\Delta\delta = +3.3$ ppm) indicates that the methyl groups are a,a rather than e,e even though the latter conformation is favoured in *trans*-1,2-dimethylcyclohexane (12). Molecular models indicate that chair distortion by the long Si—Si bond decreases the dihedral angle between C(2) equatorial bonds to ca. 20°, introducing severe steric interactions in e,e-*trans*-PR-c6 which are not present in the cyclohexane analogue (Fig. 4). Mod-

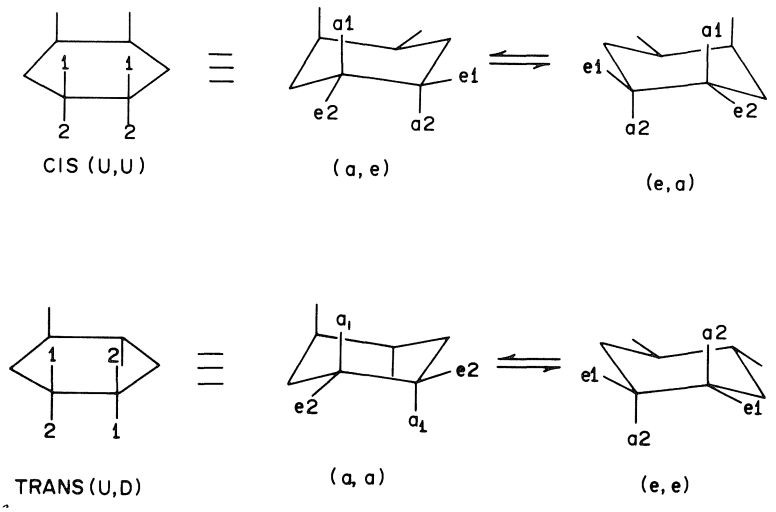


FIG. 3. Chair conformations of *cis*- and *trans*-PR-c6 isomers. Note that with rapid chair-to-chair interconversion, each isomer gives a spectrum similar to that expected for a planar ring.

Can. J. Chem. Downloaded from www.nrcresearchpress.com by 210.87.254.40 on 09/05/12
For personal use only.

els also indicate that there is an even larger 1,3-diaxial CH_3–CH_3 steric interaction. Thus in TBPR-c6 and CB-c6, where there are isomers with either all e or all a methyl groups, the former should be favoured to avoid 1,3-diaxial interactions, even though this involves 1,2-diequatorial interactions. Also the isomer of MB-c6, which can have either an e(ae)(ea)e or an a(ae)(ae)a conformation, should favour the former conformation.

These ideas can be checked, using additive chemical shift parameters. $\Delta\delta = +3.3$ ppm for *trans*-PR-c6, indicating that the effect of a single axial methyl group at C(2), $\Delta\delta_{2a} = +1.7$ ppm (assuming an a,a conformation for *trans*-PR-c6). Similarly, $\Delta\delta$(*cis*-PR-c6) $= +2.0$ ppm $= \Delta\delta_{2a} + \Delta\delta_{2e}$ (where $\Delta\delta_{2e}$ is the effect of an equatorial methyl group at C(2)). Therefore $\Delta\delta_{2e} = 2.0 - \Delta\delta_{2a} = +0.3$ ppm. Alternatively $\Delta\delta_{2e} = \Delta\delta$(PRET-c6) $= -0.3$ ppm. On average, $\Delta\delta_{2e} = (+0.3 - 0.3)/2 = 0.0$. Similar calculations yield $\Delta\delta_{1e} = -3.3$ ppm and $\delta_{1a} = -1.4$ ppm for the effects of equatorial and axial C(1) methyl groups, with uncertainties comparable to that for δ_{2e} (4). Thus the average ^{19}F chemical shifts at -113°C can be estimated, assuming $\Delta\delta_{2e} = 0.0$, $\Delta\delta_{2a} = +1.7$ ppm, $\Delta\delta_{1e} = -3.3$ ppm, and $\Delta\delta_{1a} = -1.4$ ppm. Results of these calculations are summarized in Table 4. There is generally good agreement for 1,2-disilacyclohexanes with four or fewer CH_3 groups and in these cases all compounds can be assigned except for one TBPR-c6 and one CB-c6 isomer. The agreement is not as good for derivatives with six or eight CH_3 groups, possibly because the additivity of substituent effects begins to break down in these highly substituted derivatives (3).

Alternative conformations could be assigned. For example, *trans*-PR-c6 could have a preferred e,e conformation. However, in that case, the observed chemical shifts for PRET-c6, *cis*-PR-c6, and IB-c6 could only be rationalized by assuming an axial conformation of the methyl group in PRET-c6 and that $\Delta\delta_{2e} > \Delta\delta_{2a}$. However, this would lead to illogical results for the effects of CH_3 groups on individual ^{19}F chemical shifts (see below).

As noted above, several disilacyclohexanes which form conformational diastereomers give ^{19}F nmr spectra which do not "freeze out" on cooling. This could indicate either a low interconversion barrier or a predominance of one conformation (or both factors). This can be checked using additive chemical shift parameters. The majority of disilacyclohexanes show a change in average chemical shift of -1.0 ± 0.4 ppm on going from -113°C to $+31$°C (Table 4). However, three compounds give chemical shift changes which lie outside this range (the compounds assigned as a,aPR-c6, e,e,eTBPR-c6, and e,e,e,eCB-c6). In each case, calculations of the expected chemical shift for the two possible conformations indicate that the anomalous shift can be attributed to a small fraction of the less favoured conformation at higher temperature. Thus it is likely the failure to observe "frozen out" forms of these derivatives reflects both a low $\Delta G^{\ddagger}$ value (since all three derivatives have no CH_3–CH_3 eclipsing interactions in their transition states) and a predominance of one form at low temperature.

(e) Effects of Methyl Groups on Individual ^{19}F Chemical Shifts

More complete understanding of the origins of the additive chemical shift parameters as well as

Can. J. Chem. Downloaded from www.nrcresearchpress.com by 210.87.254.40 on 09/05/12
For personal use only.

TABLE 2. Assignment of configurational isomers of 1,2-disilacyclohexanes based on variable temperature ^{19}F spectra

c6-Compound	Structure	Methyl configurations 1	2	2′	1′	Predicted No. of ^{19}F peaks: Room temp.	Low temp.	Observed No. of ^{19}F peaks: Room temp.[a]	Low temp.[b]	Methyl conformations
ET		—	—	—	—	1	2[c]	1	1	—
PRET		—	U	—	—	4	4 + 4[d]	4	4	a ⇌ e
PR		—	U	U	—	2	4	2	4	a,e ⇌ e,a[e]
		—	U	D	—	2	2 + 2[d]	2	2	a,a ⇌ e,e
TBPR		U	U	U	—	4	4 + 4	4	4[f]	e,a,e ⇌ a,e,a
		D	U	U	—	4	4 + 4			a,a,e ⇌ e,e,a
		U	D	U	—	4	4 + 4	4	4[f]	e,e,e ⇌ a,a,a
		U	U	D	—	4	4 + 4			e,a,a ⇌ a,e,e
IB		—	(U,D)	(U,D)	—	1	2	1	2	(a,e)(a,e) ⇌ (e,a)(e,a)[e]
CB		U	U	U	U	2	4	2	4[g]	a,e,a,e ⇌ e,a,e,a[e]
		U	D	D	U	2	4			a,a,e,e ⇌ e,e,a,a[e]
		U	D	U	D	2	2 + 2	2	2[g]	a,a,a,a ⇌ e,e,e,e
		U	U	D	D	2	2 + 2			a,e,e,a ⇌ e,a,a,e
MB		U	(UD)	(UD)	U	2	4	2	4	a(a,e)(a,e)e ⇌ e(e,a)(e,a)a[e]
		U	(UD)	(UD)	D	2	2 + 2	2	2	a(a,e)(a,e)a ⇌ e(e,a)(e,a)e
DB		(UD)	(UD)	(UD)	(UD)	1	2	2[h]	2	(a,e)(a,e)(a,e)(a,e) ⇌ (e,a)(e,a)(e,a)(e,a)[e]

[a] 31°C.
[b] −113°C.
[c] Two peaks of equal area.
[d] Two sets of peaks of unequal area.
[e] Conformational enantiomers.
[f] Compound could have one of four possible configurations.
[g] Compound could have one of two possible configurations.
[h] Spectrum coalesces to single peak above 60°C.

Can. J. Chem. Downloaded from www.nrcresearchpress.com by 210.87.254.40 on 09/05/12
For personal use only.

TABLE 3. Coalescence temperatures and free energies of activation for chair-to-chair interconversion in 1,2-disilacyclohexanes

c6-Compound	Methyl configuration	Δν (Hz)[a]	Coalescence temp. (K)	k^b (s^{-1})	$\Delta G^{\ddagger c}$ (kcal/mol)	CH_3–CH_3 interactions[d]
PR	U,U	273	189	607	8.2	1
		283	189	626	8.2	
IB	(U,D)(U,D)	238	245	529	10.9	2
CB	U,U,U,U[e]	485	258	1078	11.5	3
		885	275	1967	11.5	
MB	U(U,D)(U,D)U	158	216	372	9.7	4
		887	248	1971	10.1	
DB	(U,D)(U,D)(U,D)(U,D)	724	333	1609	14.2	6

[a] ^{19}F peak separation at low temperature (160 K) for peaks which coalesce on warming. If two values are given, molecule showed four peaks at low temperature, coalescing to two on warming.
[b] Rate constant for chain-to-chain interconversion estimated from coalescence temperature (17).
[c] Free energy of activation estimated from Eyring equation (18).
[d] Number of possible 1,2 CH_3–CH_3 eclipsing interactions in transition state.
[e] Configuration established in Table 5.

TABLE 4. Calculated and observed average ^{19}F chemical shifts for 1,2-disilacyclohexanes (in ppm relative to internal $CFCl_3$)

c6-Compound	Methyl conformation 1	2	2	1[a]	δ_{calcd} (−113°C)[b]	δ_{obs} (−113°C)	δ_{obs} (31°C)	Δδ[c]	Δδ[d] major → minor
ET	—	—	—	—	−140.0	−140.0	−141.5	−1.5	—
PRET	—	e	—	—	−140.0[e]	−140.3	+141.6	−1.5	
	—	a	—	—	−138.0				
PR	—	a	a	—	−136.6[e]	−136.7	−139.0	−2.3	−3.4
	—	e	e	—	−140.0[f]				
PR	—	a	e	—	−138.3	−138.0	−139.4	−1.4	
TBPR	e	e	e	—	−143.3[e]	−143.3	−143.1	+0.2	+5.3
	a	a	a	—	−138.0[f]				
TBPR	a	a	e	—	−139.7[g]				
	a	e	a	—	−138.7	−138.8	[h]	—	—
	e	a	a	—	−139.9				
	a	e	e	—	−141.4				
	e	a	e	—	−141.6				
	e	e	a	—	−141.6				
IB	—	(a,e)	(a,e)	—	−136.6	−137.2	−138.4	−1.2	—
CB	e	e	e	e	−146.6[e]	−145.8	−145.5	+0.3	+7.2
	a	a	a	a	−139.4[f]				
	a	e	e	a	−142.8				
	e	a	a	e	−143.2				
CB	a	e	a	e	−143.0[i]	−142.5	−143.4	−0.9	
	a	a	e	e	−143.0				
MB	e	(ae)	(ae)	e	−143.2[e]	−144.9	−145.7	−0.8	
	a	(ae)	(ae)	e	−139.4				
MB	a	(ae)	(ae)	e	−141.3	−142.1	−143.0	−0.8	
DB	(ae)	(ae)	(ae)	(ae)	−146.0	−143.3	−144.1	−0.8	

[a] Conformation of methyl attached to carbon 1 or 2 a = axial, e = equatorial.
[b] Calculated using additivity parameters derived in text.
[c] Chemical shift change on going from −113°C to +31°C.
[d] Predicted chemical shift change on going from major to minor component.
[e] Probable conformation at −113°C.
[f] This conformation likely present as minor component at 31°C (see text).
[g] Three possible conformations.
[h] Signals at +31°C obscured by other more intense peaks.
[i] Two possible conformations.

TABLE 5. Geminal and vicinal $^{19}F-^{19}F$ coupling constants and $^{29}Si-^{19}F$ coupling constants and ^{29}Si chemical shifts for 1,2-disilacyclohexanes

c6-Compound	$^2J_{F-F}(gem)$[a]	$^3J_{F-F}(cis)$[a]	$^3J_{F-F}(trans)$[a] a,a[d]	$^3J_{F-F}(trans)$[a] e,e[d]	$^1J_{SiF}$[b]	$^2J_{SiF}$[b]	δ_{Si}[c]
ET	+6.8	+2.2	⟨−14.6⟩[e]		±348	±39.4	−4.9
PRET	+6, +7	+2, +2	−18	−11	[f]	[f]	[f]
a,a-PR	+7.0	+3.0	−14.5	−11.0	±347	±37.4	−4.4
a,e-PR	⟨+6.4⟩[e]	+3.4, +2.9	−13.8[c]		⟨±348⟩	±36.6	−2.8
e,e,e-TBPR	+10, +6	+2, +2	−15	−11	[f]	[f]	[f]
a,a,e-TBPR	+8, +7	~0	−18	−8	[f]	[f]	[f]
e,e,e,e-CB	+8	+2.5	−14.0	−12.4	±351	±35	−6.8
a,e,a,e-CB	+10, +3	~0	−17	−10	[f]	[f]	[f]
e(a,e)(a,e)e-MB	+4.0	+4.0	−14.0	−8.5	±350[g]		
a(a,e)(a,e)e-MB	+10, +6	+4, +4	−14	−10	[f]	[f]	[f]
DB	+10.0	−3.5	−17.0	−8.6	±353[g]		

[a]F–F coupling constants for chair conformation at −80°C or lower.
[b]Si–F coupling constants obtained at 31°C from spectra corresponding to rapid chair-to-chair conversion.
[c]Chemical shifts relative to $^{29}Si(CH_3)_4$. Low field shifts positive.
[d]a,a refers to diaxial fluorine pairs while e,e refers to diequatorial fluorines (see VIII).
[e]Averaged value at 31°C. Chair-to-chair conversion was still rapid at −95°C.
[f]^{29}Si peaks obscured by peaks due to other compounds.
[g]Determined from ^{29}Si satellites in ^{19}F spectra.

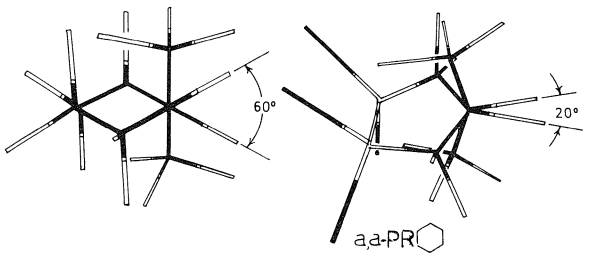


FIG. 4. Comparison of diequatorial dihedral angle in a,a-1,2-dimethylcyclohexane and a,a,-PR-c6.

confirmation of the assignment of the individual isomers can be obtained from a consideration of the effect of CH_3 groups on individual ^{19}F chemical shifts. To accomplish this one must first assign individual ^{19}F resonances to axial or equatorial fluorines. The low temperature spectra must be used for this purpose since, in many of the high temperature spectra, axial and equatorial peaks are averaged due to chair-to-chair interconversion (see above).

One major aid in the assignment is the empirical observation that axial ^{19}F peaks in ^1H coupled spectra are always broader than equatorial peaks (4) (e.g. see Fig. 2). Two factors appear to contribute to this. First, detailed analysis of ^1H-decoupled ^{19}F spectra shows that $^{19}F-^{19}F$ coupling between the vicinal diaxial fluorines has a value of about −16 Hz while the corresponding diequatorial coupling is only −10 Hz (see Table 5). Second, there should be a large $^3J_{HF}$ coupling between an axial fluorine and an axial C(1) hydrogen while the corresponding $^3J_{HF}$ couplings involving an equatorial fluorines show much smaller splittings. Indiple, the axial fluorines in PRET-c6 show an 18 Hz splitting due to $^1H-^{19}F$ coupling while the equatorial fluorines show much smaller splittings. Individual axial and equatorial resonances can be assigned (4) using a combination of symmetry arguments (e.g. in *cis*-PR-c6 each pair of peaks in the low temperature spectrum which coalesce at high temperature must be due to an axial fluorine on one silicon and an equatorial fluorine on the second silicon, see Fig. 3), homonuclear $^{19}F-^{19}F$ decoupling and considerations of the effect of CH_3 groups on individual ^{19}F chemical shifts (see below). Assignments are given in Table 6.

The next problem is to assign ^{19}F chemical shifts for axial and equatorial fluorines in the absence of methyl substitution. Unfortunately, this cannot be determined directly since ET-c6 does not freeze out on cooling. However, reasonable assignments of δ_{axial} and $\delta_{equatorial}$ can be made from the data in Table 5, noting that $(\delta_{axial}+\delta_{equatorial})/2 = -140.00$, the average shift for ET-c6. The key observation is that for all four compounds with only C(2) methyl groups (PRET-c6, *cis*- and *trans*-PR-c6, and IB-c6), all eight equatorial fluorine signals come in the region $\delta - 138.0 \pm 1.2$. Thus it seems logical to assign $\delta_{equatorial} = -138$. Therefore, $\delta_{axial} = -142 \pm 1$. In fact three of the axial ^{19}F signals for the four compounds fall in this range (including both axial fluorines in PRET-c6). Thus this assignment also seems reasonable.

Having made this assignment, it is now possible to consider effects of individual methyl groups on ^{19}F chemical shifts. The following notation will be

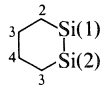
Can. J. Chem. Downloaded from www.nrcresearchpress.com by 210.87.254.40 on 09/05/12
For personal use only.

TABLE 6. Observed and (in parentheses) predicted ^{19}F chemical shifts for equatorial and axial fluorines of 1,2-disilacyclohexanes at −113°C[a]

	Methyl conformation[b]				Observed and (predicted)[c] ^{19}F chemical shifts			
c6-Compound	1	2	2′	1′	a(1)[d]	e(1)	e(2)	a(2)
ET						⟨−140.0⟩		
					(−142)	(−138)	(−138)	(—142)
PRET					−143.0	−139.2	−137.0	−142.0
	—	e	—	—	(−142)	(−138)	(−138)	(−142)
PR					−135.7	−137.7	−137.7	−135.7
	—	a	a	—	(−135)	(−138)	(−138)	(−135)
					−133.9	−139.2	−136.8	−142.2
	—	a	e	—	(−135)	(−138)	(−138)	(−142)
TBPR					−150.5	−141.5	−136.4	−144.2
	e	e	e	—	(−150)	(−142)	(−138)	(−142)
TBPR					−139.8	−144.2	−136.2	−135.0
	a	a	e	—[e]	(−139)	(−146)	(−138)	(−135)
	e	a	a	—[f]	(−143)	(−142)	(−138)	(−135)
	a	e	a	—	(−146)	(−146)	(−138)	(−128)
IB					−135.9	−138.4	−138.4	−135.9
	—	(a,e)	(a,e)	—	(−135)	(−138)	(−138)	(−135)
CB					−151.7	−139.9	−139.9	−151.7
	e	e	e	e	(−150)	(−142)	(−142)	(−150)
					−147.6	−144.6	−142.5	−135.2
	a	e	a	e[g]	(−146)	(−146)	(−142)	(−135)
	a	a	e	e	(−139)	(−136)	(−142)	(−143)
MB					−146.1	−143.7	−143.7	−146.1
	e	(a,e)	(a,e)	e	(−143)	(−142)	(−142)	(−142)
					−144.7	−144.9	−143.4	−135.5
	a	(a,e)	(a,e)	e	(−139)	(−146)	(−142)	(−136)
DB					−136.8	−149.7	−149.7	−136.8
	(a,e)	(a,e)	(a,e)	(a,e)	(−140)	(−150)	(−150)	(−140)

[a]In ppm relative to $CFCl_3$ (high field shifts negative).
[b]Conformation for which chemical shifts is calculated. Numbers refer to carbon to which methyl group is attached. Cl is adjacent to Si(l), Cl′ adjacent to Si(2).
[c]Predicted using parameters given in text.
[d]Axial fluorine attached to Si(l), etc.
[e]Probable conformation.
[f]Possible conformation.
[g]Assigned conformation.

used: the numbers 1,n (n = 2–4) will be used to designate the silicon and the carbon to which a particular fluorine and methyl are attached where n = 2 for the carbon next to silicon, etc. (see **VII**).



VII

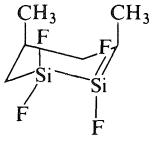
(Note that there are two possible 1,3 interactions involving Si—C—C and Si—Si—C paths.) The symbols a and e will indicate axial or equatorial orientation and M and F refer to methyl and fluorine. Thus $\Delta\delta_{1,2aMaF}$ refers to the chemical shift change of an axial fluorine due to an axial methyl on the adjacent carbon.

In view of the complexity of the problem, we will only attempt to identify substituent effects which are greater in magnitude than 2 ppm. To begin, it is unlikely that any of the $\Delta\delta_{1,4}$ terms will exceed this magnitude since they involve fluorines and methyl groups which are far removed. Considering the compounds with only C(2) methyl groups, the fact that the equatorial fluorine shifts bunch so closely about −138 ppm suggests that $\Delta\delta_{1,3aMeF}$ and $\Delta\delta_{1,3eMeF}$ are both essentially zero. Considering axial fluorines, both signals in e-PRET-c6 come at δ − (142–143) ppm. In a,e-*cis*-PR-c6 one peak comes at δ − 142 while the other axial signal in this compound plus both axial fluorines in a,a-*trans*-PR-c6 and (a,e),(a,e)-IB-c6 comes in the range δ − 135 ± 1. Thus the logical assignments are $\Delta\delta_{1,3eMaF} \approx 0$ and $\Delta\delta_{1,3aMaF} \approx +7$ ppm, i.e. the only significant effect of a C(2) methyl is in the case of a 1,3 diaxial

Can. J. Chem. Downloaded from www.nrcresearchpress.com by 210.87.254.40 on 09/05/12
For personal use only.

Can. J. Chem. Downloaded from www.nrcresearchpress.com by 210.87.254.40 on 09/05/12
For personal use only.

interaction. This is logical since the methyl group and fluorine are much closer in this case than in any of the other combinations (see **VIII**).



VIII

A C(1) methyl also has 1,3 interactions with the fluorines on one Si (see **VIII**), in addition to 1,2 interactions with the other SiF_2 unit. The former are assumed to have the same magnitude as 1,3 interactions of a C(2) methyl group. Detailed consideration of the ^{19}F chemical shifts for C(1)-methyl substituted derivatives indicates that $\Delta\delta_{1,2aMeF} \approx \Delta\delta_{1,2eMaF} \approx -8$ ppm (average $\Delta\delta = -8.0 \pm 1.1$ ppm (4)) and $\Delta\delta_{1,2aMaF} \approx \Delta\delta_{1,2eMeF} \approx -4$ ppm (average $\Delta\delta = -3.9 \pm 2.3$ ppm (4)). Molecular models provide a rationalization for the fact that these parameters occur in pairs. The ring flattens about the silicons so that an axial fluorine and an equatorial methyl group or an equatorial fluorine and an axial methyl group are spatially proximate while diaxial and diequatorial pairs are more remote. Electron diffraction studies of other silacyclohexanes confirm flattening of the ring around silicon (13).[4]

Thus, the ^{19}F chemical shifts for silacyclohexanes can be accounted for by only three methyl substituent effects: a large low field shift due to 1,3 diaxial interactions ($\Delta\delta_{1,3aMaF} = +7$ ppm), a large high field shift due to spatially proximate 1,2 interactions ($\Delta\delta_{1,2aMeF} \approx \Delta\delta_{1,2eMaF} \approx -8$ ppm) and a smaller high field shift due to other 1,2 interactions (≈ -4 ppm). These values can be used to derive parameters for the effect of methyl groups on average chemical shifts ($\Delta\delta_{2e} = 0$, $\Delta\delta_{2a} = +1.75$, $\Delta\delta_{1e} = -3.0$, $\Delta\delta_{1a} = -1.25$) which are very similar to those developed above. The $\Delta\delta_{1,2}$ and $\Delta\delta_{1,3}$ parameters also show surprisingly close parallel with the corresponding ^{13}C chemical shift parameters for CH_3–CH_3 interactions in cyclohexane derivatives. In the latter case, $\Delta\delta_{1,2}(\gamma)$ parameters show maximum shielding (ca. -5 ppm (10)) for proximate methyl groups while 1,3 diaxial interactions cause low field shifts (+4.5 ppm (15)).

Calculated and observed ^{19}F chemical shifts are compared in Table 6. *All* of the equatorial shifts are predicted within 2 ppm along with the axial shifts for all derivatives with four or fewer methyl groups. The close agreement for the derivatives with four or less methyl groups allows one to conclude that the previously unidentified TBPR-c6 isomer probably has an a,a,e conformation while very clearly indicating that the CB-c6 isomer which freezes out on cooling is a,e,a,e rather than a,a,e,e. In this regard, it is interesting to note that the two main CB isomers respectively have all-*cis* (a,e,a,e or U,U,U,U) and all-*trans* (e,e,e,e or U,D,U,D) methyl groups, indicating that the mechanism of formation of disilacyclohexanes allows isomerization of alkene linkages. This contrasts with the disilacyclobutanes which are formed with complete retention of configuration (3).

It is surprising that the chemical shifts for these complex derivatives can be predicted with only three additive chemical shift parameters. Nevertheless, the very close agreement for derivatives with four or fewer methyl groups plus the close parallels with the ^{13}C additive parameters lends a great deal of confidence to the conformational and configurational assignments given in the previous sections. All other possible assignments seem less logical. For example, if *trans*-PR-c6 was assigned to e,e conformation (along with a for PRET-c6), then it would follow that $\delta_{1,3eMaF} \approx +7$ ppm and $\delta_{1,3eMaF} \approx 0$ ppm. This would be inconsistent with the corresponding additive ^{13}C chemical shift parameters and also with the CH_3—F distances in the two cases.

(f) ^{19}F–^{19}F and ^{29}Si–^{29}Si Coupling Constants in 1,2-Disilacyclohexanes

These coupling constants are summarized in Table 5. They are discussed elsewhere as part of a general discussion of trends in F–F and Si–F coupling constants (16).

Summary and Conclusions

Unsymmetric alkenes react with SiF_2 to form disilacyclohexanes with greater methyl substitution at C(2). The reaction of an alkene with SiF_2 often gives more than one disilacyclohexane derivative and the reaction proceeds by a pathway which allows isomerization of the alkene. These observations have been incorporated in a proposed comprehensive mechanism for the SiF_2–olefin reaction (3).

The disilacyclohexanes exist in distorted chair conformations. In a number of cases the chair-to-chair interconversion is sufficiently slow at low temperatures to observe the individual chair forms by ^{19}F nmr spectroscopy. The number of ^{19}F peaks in the low temperature spectra allows assignment of individual configurational isomers in several

[4]This is also indicated by an X-ray structure determination for **VI** (14).

cases. In addition, consideration of the effect of CH_3 groups on averaged ^{19}F chemical shifts allows further assignment of configurational isomers and determination of conformational preference. Individual ^{19}F chemical shifts can be predicted accurately using only three parameters to describe effects of 1,2 and 1,3 CH_3–F interactions. These parameters allow final assignment of all configurations and conformations of eleven 1,2 disilacyclohexane derivatives.

Acknowledgements

Financial support from the Natural Sciences and Engineering Research Council of Canada and the Department of Chemistry of the University of Toronto is gratefully acknowledged. We also thank Professor C. S. Liu for communicating results prior to publications.

1. J. C. THOMPSON, J. L. MARGRAVE, and P. L. TIMMS. Chem. Commun. 566 (1966).
2. C. S. LIU and T. L. HWANG. J. Am. Chem. Soc. **101**, 2996 (1979).
3. W. F. REYNOLDS, J. C. THOMPSON, and A. P. G. WRIGHT. Can. J. Chem. **58**, 419 (1980).
4. A. P. G. WRIGHT. Ph.D. Thesis, University of Toronto, Toronto, Ont. 1979.
5. F. R. JENSEN, D. S. NOYCE, C. H. SEDERHOLM, and A. J. BERLIN. J. Am. Chem. Soc. **82**, 1256 (1960).
6. J. L. MARGRAVE and D. L. PERRY. Inorg. Chem. **16**, 1820 (1977).
7. D. SEYFERTH and D. P. DUNCAN. J. Am. Chem. Soc. **100**, 7734 (1978).
8. J. W. EMSLEY, L. PHILLIPS, and V. WRAY. Fluorine coupling constants. Pergamon Press, Oxford. 1977.
9. D. L. SMITH. Ph.D. Thesis, University of Bristol, Bristol, England. 1973.
10. J. B. STOTHERS. Carbon 13 NMR spectroscopy. Academic Press, New York. 1972. Chapt. 3.
11. H. BOOTH and J. R. EVERETT. J. Chem. Soc. Chem. Commun. 278 (1976).
12. E. L. ELIEL. Stereochemistry of carbon compounds. McGraw-Hill, New York. 1962. Chapt. 8.
13. L. VAN DEN ENDEN, H. J. GEISE, R. CARLEER, and F. C. MIJLHOFF. J. Mol. Struct. **50**, 345 (1978).
14. S. C. LIU. Private communication.
15. G. MANN, E. KLEINPETER, and H. WERNER. Org. Magn. Reson. **11**, 561 (1978).
16. W. F. REYNOLDS, J. C. THOMPSON, and A. P. G. WRIGHT. To be submitted.
17. J. A. POPLE, W. G. SCHNEIDER, and H. J. BERNSTEIN. High resolution nuclear magnetic resonance. McGraw-Hill, New York. 1959. p. 223.
18. H. EYRING. Chem. Rev. **17**, 65 (1935).

Can. J. Chem. Downloaded from www.nrcresearchpress.com by 210.87.254.40 on 09/05/12
For personal use only.

Carbocyclization in natural products. III.[1] Brominative cyclization of dehydrosaussurea lactone and costunolide[2,3]

TIKAM C. JAIN[4] AND CALVIN M. BANKS[5]

Department of Chemistry, University of Victoria, Victoria, B.C., Canada V8W 2Y2

Received June 21, 1979

TIKAM C. JAIN and CALVIN M. BANKS. Can. J. Chem. **58**, 447 (1980).

Treatment of dehydrosaussurea lactone **4** and costunolide **1** with *N*-bromosuccinimide (NBS) in aqueous acetone at room temperature furnished bromolactones **6**, **7**, and **8**. Structural evidence for these bromolactones rests upon spectral data and transformation to the hydrogenated bromolactones **9**, **10**, and **11**. The latter were found identical with the corresponding products obtained by the brominative cyclization of dihydrocostunolide **2**.

TIKAM C. JAIN et CALVIN M. BANKS. Can. J. Chem. **58**, 447 (1980).

Le traitement de la dehydrosaussurea lactone **4** et de la costunolide **1** avec le *N*-bromosuccinimide dans acétone aqueux à la température ambiente a fourni les bromolactones **6**, **7** et **8**. L'évidence structurelle pour ces bromolactones reste sur des résultats spectraux et des transformations aux bromolactones hydrogénées **9**, **10** et **11**. Les derniers sont identiques aux produits correspondants obtenus par le cyclization brominatif de dihydrocostunolide **2**.

The anomalous ultraviolet absorption of costunolide **1** and other germacranolides has been attributed to the transannular interaction of the double bonds in the medium ring (3, 4). In contrast, dehydrosaussurea lactone **4** and saussurea lactone **3** differ from **1** in that there is freedom of rotation about the bonds that carry the olefinic linkages. Yet the ultraviolet spectra of these two compounds demonstrated an interaction of the double bonds (Table 1). Having compared the ultraviolet maximum of dehydrosaussurea lactone with that of saussurea lactone it was immediately apparent that the position of the maximum was not altered by the unsaturation in the lactone ring; however the extinction coefficient was increased. Thus the interactions of the double bonds in dehydrosaussurea lactone **4** indicated the strong possibility of cyclization in this molecule.[6]

Treatment of dehydrosaussurea lactone **4** with *N*-bromosuccinimide (NBS) furnished a crude semi-crystalline product which showed three spots on silica gel tlc plates in several solvent systems (2). Chromatography over a silica gel column gave the bromohydrin **6** and the bromolactones **7** and **8** in 43, 15, and 15% yields respectively.

TABLE 1. Ultraviolet data in EtOH

Substrate	Absorption maximum (nm)	Extinction coefficient ε
Costunolide **1**	214.5	11 841
Dihydrocostunolide **2**	214	6 166
Saussurea lactone **3**	209	741
Dehydrosaussurea lactone **4**	211.5	8 630
Tetrahydrodehydro-saussurea lactone **5**	213	6 300

The reaction was applied to costunolide **1** which when treated with NBS in aqueous acetone furnished the bromohydrin **6** and the bromolactones **7** and **8** in 50, 18, and 23% yields respectively. The three bromolactones derived from costunolide **1** were found identical to those made from dehydrosaussurea lactone **4** (ir, nmr, mixed melting point). For the hydrogenation experiments (*vide infra*) the compounds employed were those that were prepared from substrate **1**.

The bromohydrin **6**, mp 186–188°C, was analyzed for $C_{15}H_{21}O_3Br$ and further confirmed by high resolution mass spectrometry (Table 2). The major structural features were deduced by infrared and nmr spectroscopy. (For details, see Experimental.) The relative configuration of the molecule was established in a relatively simple manner. Catalytic hydrogenation in glacial acetic acid (PtO_2) of the bromohydrin **6** yielded the bromohydrin **9**, a compound of known stereochemistry (1, 6) prepared from dihydrocostunolide **2**. Mixed melting point and spectral comparison (ir and nmr) proved them to be identical.

[1]For Part II in this series see ref. 1.

[2]For a preliminary communication on this work see ref. 2.

[3]Abstracted, in part, from the Ph.D. Dissertation of Calvin M. Banks, University of Victoria, 1970.

[4]Present address: Smith, Kline & French Laboratories, 1500 Spring Garden Street, Philadelphia, PA 19101, U.S.A. Inquiries about this paper should be addressed to T. C. Jain at Philadelphia.

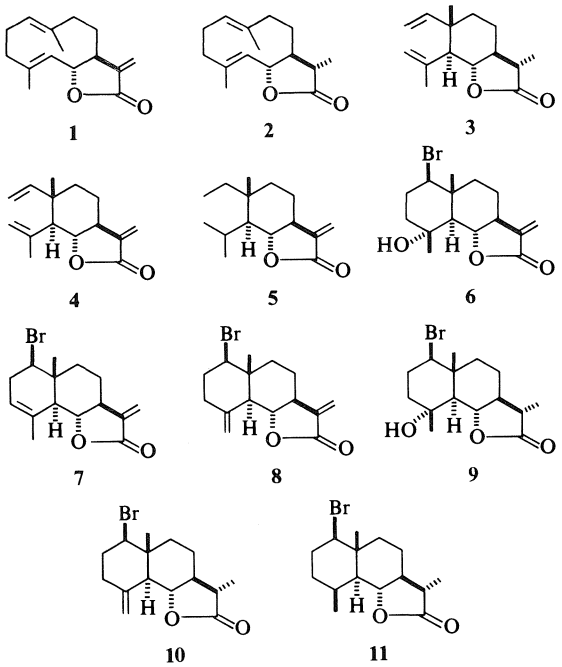
[5]Holder of a University of Victoria Bursary, 1967–68; an N.R.C.C. Postgraduate Scholarship, 1968–71.

[6]For a comprehensive review on the cyclization of medium ring 1,5-dienes and related compounds such as **1** and **4** see ref. 5.

0008-4042/80/050447-03$01.00/0

©1980 National Research Council of Canada/Conseil national de recherches du Canada

Can. J. Chem. Downloaded from www.nrcresearchpress.com by 210.87.254.40 on 09/05/12
For personal use only.



SCHEME 1

The bromolactones **7** and **8** were analyzed for $C_{15}H_{19}O_2Br$, this being supported by high resolution mass measurement (Table 2). The spectroscopic data given in the Experimental were fully in accord with their structures portrayed as **7** and **8**. Final proof of the structures of the isomeric bromolactones **7** and **8** was secured through catalytic hydrogenation in ethanol (PtO_2) which provided the bromolactones **11** and **10** respectively.

Novelty of Cyclization

To the best of our knowledge, neither naturally occurring, nor synthetic, sesquiterpene lactones based on the elemane framework have hitherto been converted to bicyclic sesquiterpene lactones (2). The biogenetic significance of the facile carbocyclization in this class of compounds will be reported in due course.

Experimental[7]

N-*Bromosuccinimide (NBS) Cyclization of Dehydrosaussurea Lactone* ***4***

To a solution of dehydrosaussurea lactone **4** (1.0 g) in 5% acetone/H_2O (120 mL) an equimolar amount of *N*-bromosuccinimide (460 mg) was added and the solution was stirred magnetically for 42 h. Distillation of the solvent under reduced pressure furnished a crystalline product which was extracted with ether and washed with water (5 × 20 mL). The ethereal layer was dried over Na_2SO_4 and concentrated *in vacuo* to yield a semi-crystalline product (1.55 g) showing three spots on tlc plates. Silica gel chromatography of the crude reaction mixture followed by crystallization of the relevant fractions yielded three crystalline products **6**, **7**, and **8** described below.

Bromohydrin ***6***

The compound was recrystallized from ethyl acetate to yield flakes of **6**, mp 186–188°C; λ_{max} 206, ε 14 800; $[\alpha]_{589}$ +12.7°, $[\alpha]_{578}$ +13.0°, $[\alpha]_{546}$ +14.9°, $[\alpha]_{436}$ +25.0°, $[\alpha]_{365}$ +34.2° (*c* 1.01 at 25°C); ir: 3535 (hydroxyl) cm^{-1}, 1764, 1670, and 888 (α,β-unsaturated γ-lactone) cm^{-1}; nmr τ: 3.85, 4.50 (d, *J* = 3.0 Hz, 2H, —C=CH_2), 5.90 (m, 2H, HC—Br, HC—O—C=O), 8.62 (s, 3H, HO—C—CH_3), 8.88 (s, 3H, —C—CH_3). ms *m/e*: 313 (M^+ − CH_3, $\%\sum_{27}$ 1.73). *Anal.* calcd. for $C_{15}H_{21}O_3Br$: C 54.71, H 6.42; found: C 54.83, H 6.37.

Bromolactones ***7*** *and* ***8***

The mixture containing the bromolactones was rechromatographed on a silica gel column and the relatively nonpolar fractions were combined and crystallized from methanol to give bromolactone **7** (15% yield), mp 116–118°C; λ_{max} 206, ε 17 800; $[\alpha]_{589}$ +49.9°, $[\alpha]_{578}$ +52.7°, $[\alpha]_{546}$ +60.0°, $[\alpha]_{436}$ +104.0°, $[\alpha]_{365}$ +164.7° (*c* 1.12 at 25°C); ir: 1765, 1679, and 882 (α,β-unsaturated γ-lactone) cm^{-1}, 1624, 844, and 810 (trisubstituted double bond) cm^{-1}; nmr τ: 3.90, 4.57 (d, *J* = 3.0 Hz, 2H, —C=CH_2), 4.71 (s, broad, 1H, —C=CH), 5.90 (m, 2H, HC—Br, HC—O—C=O), 8.16 (t, broad, *J* = 1.0 Hz, 3H, HC=C—CH_3), 9.01 (s, 3H, —C—CH_3); ms *m/e*: 310 (M^+, $\%\sum_{27}$ 1.25). *Anal.* calcd. for $C_{15}H_{19}O_2Br$: C 57.88, H 6.15; found: C 57.94, H 6.17. The polar fractions were combined and crystallized from methanol to give bromolactone **8** (15% yield), mp 137–138°C; λ_{max} 206 nm, ε 18 400; $[\alpha]_{589}$ +106.2°, $[\alpha]_{578}$ +111.3°, $[\alpha]_{546}$ +126.9°, $[\alpha]_{436}$ +214.5°, $[\alpha]_{365}$ +331.8° (*c* 0.97 at 25°C); ir: 1771 (γ-lactone) cm^{-1}, 1673, 1650, and 920 (exocyclic methylene) cm^{-1}; nmr τ: 3.89, 4.55 (d, *J* = 3.0 Hz, 2H, —C=CH_2), 4.97, 5.09 (s, 2H, —C=CH_2), 5.98 (m, 2H, HC—Br and HC—O—C=O), 9.03 (s, 3H, —C—CH_3); ms *m/e*: 310 (M^+, $\%\sum_{27}$ 0.27). *Anal.* calcd. for $C_{15}H_{19}O_2Br$: C 57.88, H 6.15; found: C 57.82, H 6.20.

NBS Cyclization of Costunolide ***1***

Costunolide **1** (4.5 g) was dissolved in 5% acetone/H_2O (900 mL) and reacted with NBS (3.44 g) for 16.5 h. Removal of solvent at a reduced pressure produced a viscous gum which was taken up in ether and extracted with water (6 × 10 mL). The aqueous layer was back extracted and the combined ethereal solution was dried over Na_2SO_4 and the solvent was removed *in vacuo* yielding a crude gum (5.85 g). Thin layer chromatography (silica gel) in the following solvent systems, benzene, 5% methanol/benzene, and chloroform, revealed the presence of three compounds. The reaction mixture was expeditiously resolved into its three components **6**, **7**, and **8** by a simple silica gel column chromatography.

Bromohydrin ***6***

The bromohydrin **6** was crystallized from ethyl acetate, mp 186–188°C (undepressed upon mixing with the sample prepared from dehydrosaussurea lactone **4**), λ_{max} 208 nm, ε 15 600, their infrared spectra were superimposable; $[\alpha]_{589}$ +12.9°, $[\alpha]_{578}$ +13.4°, $[\alpha]_{546}$ +15.3°, $[\alpha]_{436}$ +25.8°, $[\alpha]_{365}$ +35.4° (*c* 1.58 at 30°C). *Anal.* calcd. for $C_{15}H_{21}O_3Br$: C 54.71, H 6.42, Br 24.27; found: C 55.08, H 6.47, Br 23.98.

Saturated Bromohydrin ***9***

The bromohydrin **6** (128 mg) was hydrogenated (12 h) with PtO_2 (50 mg) in ethanol (50 mL) to yield fully saturated bromohydrin **9**, mp 160–165°C (undepressed upon admixture with an authentic sample); the infrared spectrum was superimposable with that of authentic **9**; $[\alpha]_{589}$ −18.4°, $[\alpha]_{578}$ −19.9°, $[\alpha]_{546}$ −22.6°, $[\alpha]_{436}$ −40.4°, $[\alpha]_{365}$ −68.1° (*c* 1.14 at 28°C).

[7]For general experimental details see ref. 7.

Can. J. Chem. Downloaded from www.nrcresearchpress.com by 210.87.254.40 on 09/05/12
For personal use only.

TABLE 2. Accurate mass measurements and composition of ions

Lactone	Obsd. mass	Calcd. mass	Composition	Fragment
6	313.0440	313.0440	$C_{14}H_{18}O_3{}^{79}Br$	$M^+ - CH_3$
	231.1385	231.1385	$C_{15}H_{19}O_2$	$M^+ - Br - H_2O$
7	310.0573	310.0569	$C_{15}H_{19}O_2{}^{79}Br$	M^+
	295.0334	295.0334	$C_{14}H_{16}O_2{}^{79}Br$	$M^+ - CH_3$
	231.1385	231.1385	$C_{15}H_{19}O_2$	$M^+ - Br$
8	310.0573	310.0569	$C_{15}H_{19}O_2{}^{79}Br$	M^+
	231.1385	231.1385	$C_{15}H_{19}O_2$	$M^+ - Br$

Bromolactone 7

Crystallization of the appropriate fractions of the column furnished the bromolactone **7**, (18% yield), mp 116–118°C (undepressed with the sample prepared from **4**), the infrared spectrum was coincident with that of **7** obtained from dehydrosaussurea lactone **4**; $[\alpha]_{589}$ +48.9°, $[\alpha]_{578}$ +51.1°, $[\alpha]_{546}$ +58.4°, $[\alpha]_{436}$ +101.0°, $[\alpha]_{365}$ +159.0° (*c* 1.19 at 29°C). *Anal.* calcd. for $C_{15}H_{19}O_2Br$: C 57.88, H 6.15; found: C 57.90, H 6.59.

The bromolactone **7** (100 mg) was hydrogenated (2 h) with PtO_2 (1 mg) in ethanol (12 mL) to yield, after filtration and removal of solvent *in vacuo*, 1-bromosantanolide "c" **11**; crystallization from ethyl acetate produced needles, mp 198–200°C (undepressed upon admixture with an authentic sample), the infrared spectrum was superimposable with that of authentic bromolactone **11**; $[\alpha]_{589}$ +11.0°, $[\alpha]_{578}$ +11.8°, $[\alpha]_{546}$ +13.9°, $[\alpha]_{436}$ +24.0°, $[\alpha]_{365}$ +39.6°, (*c* 0.60 at 32°C). *Anal.* calcd. for $C_{15}H_{23}O_2Br$: C 57.14, H 7.35; found: C 57.18, H 7.34.

Bromolactone 8

The compound was obtained as needles of bromolactone **8** (23% yield) after crystallization from methanol, mp 136–138°C (undepressed upon admixture with an authentic sample), the infrared spectrum was superimposable with that of bromolactone **8** prepared from dehydrosaussurea lactone **4**; $[\alpha]_{589}$ +106.5°, $[\alpha]_{578}$ +111.1°, $[\alpha]_{546}$ +126.4°, $[\alpha]_{436}$ +214.2°, $[\alpha]_{365}$ +331.9° (*c* 1.60 at 32°C). *Anal.* calcd. for $C_{15}H_{19}O_2Br$: C 57.88, H 6.15; found: C 57.90, H 6.24.

The bromolactone **8** (100 mg) was hydrogenated (1 h) with PtO_2 (1 mg) in ethanol (12 mL) giving partially saturated bromolactone **10**; crystallization from ethyl acetate gave needles, mp 167–169°C (undepressed upon admixture with an authentic sample). The infrared spectrum was superimposable with that of authentic bromolactone **10**; $[\alpha]_{589}$ +85.7°, $[\alpha]_{578}$ +89.4°, $[\alpha]_{546}$ +101.9°, $[\alpha]_{436}$ +175.3°, $[\alpha]_{365}$ +282.8° (*c* 1.10 at 32°C). *Anal.* calcd. for $C_{15}H_{21}O_2Br$: C 57.51, H 6.75; found: C 58.09, H 6.61.

Acknowledgement

The authors wish to thank the National Research Council of Canada for financial support.

1. T. C. JAIN, C. M. BANKS, and J. E. MCCLOSKEY. Tetrahedron, **35**, 885 (1979).
2. T. C. JAIN, C. M. BANKS, and J. E. MCCLOSKEY. Tetrahedron Lett. 2387 (1970).
3. R. V. A. JONES and M. D. SUTHERLAND. Aust. J. Chem. **21**, 2255 (1968).
4. J. PALDUS and J. KOUTECKY. Collect. Czech. Chem. Commun. **27**, 2139 (1962).
5. J. K. SUTHERLAND. Tetrahedron, **30**, 1651 (1974).
6. T. C. JAIN, C. M. BANKS, and J. E. MCCLOSKEY. Experientia, **25**, 906 (1969) and references cited therein.
7. T. C. JAIN, C. M. BANKS, and J. E. MCCLOSKEY. Tetrahedron, **32**, 765 (1976).

Can. J. Chem. Downloaded from www.nrcresearchpress.com by 210.87.254.40 on 09/05/12
For personal use only.

Studies on allylic peroxides. II.[1] Allyl-*t*-butyl peroxide

R. HIATT AND V. G. K. NAIR

Department of Chemistry, Brock University, St. Catharines, Ont., Canada L2S 3A1

Received August 21, 1979

R. HIATT and V. G. K. NAIR. Can. J. Chem. **58**, 450 (1980).

Allyl-*tert*-butyl peroxide decomposes thermally in toluene with $k_d = 10^{13.8} \exp(-33200/\theta)$ (s^{-1}). Product studies show the reaction to be a mixture of homolysis and radical-induced decomposition, the latter involving both radical addition to C=C and allyl hydrogen abstraction by alkoxy radicals. Computer modelling of the system gives good agreement with the experimental results and suggests that the overall decomposition is about 50% homolysis.

R. HIATT et V. G. K. NAIR. Can. J. Chem. **58**, 450 (1980).

Le peroxyde d'allyle et de *tert*-butyle se décompose thermiquement dans le toluène avec un $k_d = 10^{13.8} \exp(-33200/\theta)$ (s^{-1}). L'étude des produits obtenus montre que la réaction consiste en une homolyse et en une décomposition induite de façon radicalaire. Cette dernière implique à la fois l'addition du radical benzyle sur la double liaison carbone–carbone et l'enlèvement d'un hydrogène allylique par les radicaux alkoxy. Le modèle du système réalisé par ordinateur est en accord avec les résultats expérimentaux et suggère que la décomposition dans son ensemble est à 50% une homolyse.

[Traduit par le journal]

Introduction

Studies on the decomposition of 2,3-dimethyl-3-butenyl-2-hydroperoxide, (TMEH), have suggested a new mode of free radical initiation peculiar to allylic hydroperoxides (1). A follow-up investigation using allyl hydroperoxide was planned, but initial results with that substance proved extremely complicated. Allyl-*tert*-butyl peroxide seemed somewhat better behaved, and a useful vehicle for sorting out some of the peculiarities of allylic peroxide decompositions.

Experimental

Decompositions of the peroxide were carried out in evacuated, sealed pyrex ampoules, as previously (1). Residual peroxide and the volatile products were determined by glc, using known compounds as standards. Non-volatile residues were subjected to ir and nmr analysis.

Allyl-*tert*-butyl peroxide was prepared by the reaction of *t*-BuO_2H with allyl bromide in methanolic KOH at −5°C. *Tert*-BuO_2H (22.5 g, 0.250 mol) and allyl bromide (30.25 g, 0.250 mol) were mixed with 30 mL of methanol and the solution cooled in an ice-salt bath. A solution of 14 g of KOH in 100 mL of methanol was added dropwise over 20 min. The mixture was stirred for 5 h; 4.5 g (0.05 mol) of *t*-BuO_2H was added and stirring continued for 10 h. Extraction with pentane followed by distillation (55–56°C/75 Torr) gave 95% pure peroxide which was further purified by preparative glc (20% isodecyl phthalate on Chromosorb W). Yields averaged 16%.

Infrared: 815 (C—O—O), 1365 and 1385 (CMe_3), 1650 (C=C) cm^{-1}; nmr δ: 1.1 (s, 9H), 4.2 (d, 2H), 4.8–6.3 (m, 3H); ms *m/e*: 130 (M^+), 59 (Me_2COH^+?), 57 (CMe_3^+), 41 ($CH_2CHCH_2^+$), 28 ($CH_2CH_2^+$).

Results and Discussion

Rate constants for thermal decomposition of allyl *tert*-butyl peroxide, (*P*), in toluene are shown in Table 1. Although the first-order plots were linear, and the rate constants insensitive to initial concentration, the decompositions were relatively fast and the activation energy was ~5 kcal too low for simple homolysis (cf. *t*-Bu_2O_2, $k_{150°} = 1.9 \times 10^{-4}$ s^{-1} and $E_a = 37.8$ kcal (2)). Thus there appears to be a substantial amount of radical-induced decomposition.

Repeating the decompositions in the presence of 1.0 *M* α-methylstyrene gave only slightly different rate constants (Table 1). The Arrhenius parameters appear somewhat closer to normal for unimolecular homolysis but are not convincingly different from those obtained in pure toluene. The success of this

TABLE 1. Rates of decomposition of allyl-*tert*-butyl peroxide in toluene

T(°C)	P_0[a,b]	$10^5 k_1(s^{-1})$[c]
130	0.05	6.58
	0.10	6.61
	0.10[b]	5.76[b]
	0.20	6.90
140	0.10	19.19
	0.10[b]	17.85[b]
	0.20	20.04
150	0.10	49.35
	0.10[b]	48.00[b]
	0.20	48.25
160	0.10	115.20
	0.10[b]	127.00[b]
	0.20	121.50

[a] Initial peroxide concentration in mol/L.
[b] With added 1 mol/L α-methylstyrene.
[c] For toluene above, $\log k_1 = 13.47 - 32.5/\theta$, with added α-methylstyrene, $\log k_2 = 13.84 - 33.2/\theta$; ($\theta = 2.303 RT$).

[1] Paper I in this series is ref. 1.

0008-4042/80/050450-04$01.00/0

©1980 National Research Council of Canada/Conseil national de recherches du Canada

Can. J. Chem. Downloaded from www.nrcresearchpress.com by 210.87.254.6 on 09/05/12
For personal use only.

TABLE 2. Products from 0.2 *M* allyl-*tert*-butyl peroxide in PhMe at 150°C

Product	Mol/mol of decomposed peroxide	
	Experimental	Computer model
t-BuOH	0.73	0.725
Acetone	0.27	0.274
Acrolein	0	0.053
Allyl OH	0.295	0.248
$PhCH_2CH_2\underset{\diagdown O \diagup}{CH}—CH_2$	0.08	0.083
$(PhCH_2—)_2$	0.15	0.168
Residue	54[a]	0.250
CO	0.21	—
CH_4	0.25	—

[a] Gram/mol dec., contains all the bibenzyl, but none of the other listed products.

attempt to suppress induced decomposition is questionable.

At 60°C in toluene the peroxide is stable but subject to attack by *tert*-butoxy radicals. After 2 h, a solution originally 0.166 *M* in peroxide and 0.332 *M* in DBPO (di-*tert*-butyl peroxyoxalate) contained no DBPO and 0.124 *M* peroxide, a 25% reduction. The yield of *t*-BuOH was nearly quantitative showing that attack of *t*-BuO· on the peroxide proceeded via abstraction rather than addition.

The products from thermolysis of the peroxide in toluene at 150°C (Table 2) are remarkable in several respects. All *t*-BuO· is found as either *t*-BuOH or acetone and the *t*-BuOH – acetone ratio, (2.7), is more than twice as large as found from *t*-Bu_2O_2 under the same conditions (3). Thus addition of *t*-BuO· to C=C is not significant, and more than half of the H-abstractions by *t*-BuO· are from species other than toluene. Some abstraction from the peroxide itself seems probable, but attack on

[1] $t\text{-BuO}\cdot + CH_2{=}CH{-}CH_2O_2t\text{-}Bu \longrightarrow t\text{-BuOH} + CH_2{=}CH{-}\dot{C}HO_2t\text{-Bu} \xrightarrow{O_2} CH_2{=}CH{-}CHO + t\text{-BuO}\cdot$

products, allyl alcohol, acrolein, and acrolein polymer must be considered as well. Cage disproportionation of *t*-BuO· and allyloxy radicals would also tend to increase *t*-BuOH yields.

[2] $t\text{-BuO}\cdot + CH_2{=}CH{-}CH_2OH \longrightarrow t\text{-BuOH} + CH_2{=}CH{-}\dot{C}HOH$

[3] $t\text{-BuO}\cdot + \underset{\|}{\overset{O}{C}}{-}H \longrightarrow t\text{-BuOH} + \underset{\|}{\overset{O}{C}}\cdot$

[4] $[CH_2{=}CH{-}CH_2{-}O\cdots O\text{-}t\text{-Bu}] \downarrow CH_2{=}CH{-}CHO + t\text{-BuOH}$

Evidence for benzyl radical attack on the peroxide is found in the 8% yield of 4-phenyl-1,2-epoxybutane. Benzyl radicals are also found as

[5] $PhCH_2\cdot + CH_2{=}CH{-}CH_2O_2t\text{-Bu} \longrightarrow Ph(CH_2)_2\dot{C}H{-}CH_2O_2t\text{-Bu} \xrightarrow{O_2} Ph(CH_2)_2\underset{\diagdown O \diagup}{CH}{-}CH_2 + t\text{-BuO}\cdot$

dimer and in the non-volatile residue (see below). Methyl radicals apparently do not add to the peroxide since no epoxypentane was found, and the methane yield is the same as acetone within experimental error.

Of the allyloxy portion of the peroxide, 30% is accounted for as allyl alcohol and 8% as epoxide. The remainder is presumably incorporated in the non-volatile residue. Infrared spectra of the latter revealed strong O—H and C=O absorptions, while nmr showed benzyl hydrogens superimposed on a broad, unresolved aliphatic absorption in a ratio of 1:5.2, but no vinyl C—*H*, nor any absorption due to *t*-Bu. Samples of residue taken after only 50% decomposition of peroxide showed a small amount of $\underset{\|}{\overset{O}{C}}{-}H$, but no aldehyde groups remained in material isolated after complete decomposition.

We surmise that the residue is a mixture of telomers, originally $PhCH_2(CH_2{-}\underset{|}{\overset{X}{C}}H)_nCH_2Ph$, where *n* is small and X is CH_2OH or CHO. Subsequent radical attack on —CHO yields $\underset{\|}{\overset{O}{C}}\cdot$ which may or may not decarbonylate prior to adding a few more monomer units and/or terminating. The possibility that "X" might be *t*-$BuCH_2O_2$ was worrisome since this would have biased the rate measurements. But while the peroxide itself is certainly a suitable monomer for the copolymerization, its absence from the polymer can be rationalized. The S_Hi to give epoxide + *t*-BuO· is probably much faster, under the circumstances, than addition of another monomer unit.

At this point, the general outlines of the thermal decomposition of allyl-*tert*-butyl peroxide in toluene are fairly clear. It is a mix of homolysis and radical-induced decomposition. At minimum, homolysis accounts for 15% (based on bibenzyl yield alone) or 22–23% if all the benzyl radicals found in the residue are counted. A maximum is impossible to assess, depending, as it does, both on

Can. J. Chem. Downloaded from www.nrcresearchpress.com by 210.87.254.6 on 09/05/12
For personal use only.

TABLE 3. Model for allyl-*tert*-butyl peroxide decomposition

	Reaction	Rate constant
R1	$P^a \rightarrow CH_2CHCH_2O\cdot + t\text{-}BuO\cdot$	2.4 E − 4
R2	$P^a \rightarrow CH_2CHCHO + t\text{-}BuOH$	2 E − 5
R3	$t\text{-}BuO\cdot + PhCH_3 \rightarrow PhCH_2\cdot + t\text{-}BuOH$	6 E + 4
R4	$t\text{-}BuO\cdot \rightarrow AcMe + PhCH_2\cdot$	4.3 E + 4
R5	$CH_2CHCH_2O\cdot + PhCH_3 \rightarrow CH_2CHCH_2OH + PhCH_2\cdot$	6 E + 4
R6	$CH_2CHCH_2O\cdot + CH^b \rightarrow PL^c + CH_2CHCH_2OH$	1 E + 6
R7	$PhCH_2\cdot + P^a \rightarrow OX^d + t\text{-}BuO\cdot$	7 E + 2
R8	$PhCH_2\cdot + CH_2CHCHO \rightarrow PL^c + CH^b$	1 E + 4
R9	$PhCH_2\cdot + PhCH_2\cdot \rightarrow PhCH_2CH_2Ph$	2 E + 9
R10	$t\text{-}BuO\cdot + P^a \rightarrow CH_2CHCHO + t\text{-}BuOH + t\text{-}BuO\cdot$	4.4 E + 6
R11	$PL^c + CH_2CHCHO \rightarrow PL^c + CH^b$	2 E + 4
R12	$PL^c + PL \rightarrow POL^e$	8 E + 9
R13	$CH_2CHCH_2O\cdot + PhCH_2\cdot \rightarrow CH_2CHCHO + PhCH_3$	5 E + 9
R14	$CH_2CHCH_2O\cdot + P^e \rightarrow CH_2CHCHO + CH_2CHCH_2OH + CH_2CHCH_2O\cdot$	4.4 E + 6
R15	$PL^c + PhCH_2\cdot \rightarrow POL^e$	8 E + 9
R16	$t\text{-}BuO\cdot + CH_2CHCHO \rightarrow PL^c + t\text{-}BuOH$	1 E + 6
R17	$t\text{-}BuO\cdot + CH^b \rightarrow PL + t\text{-}BuOH$	1 E + 6
R18	$PhCH_2\cdot + CH_2CHCH_2OH \rightarrow PL^c + CH^b$	2 E + 2
R19	$PL^c + CH_2CHCH_2OH \rightarrow PL^c + CH$	2 E + 2
R20	$CH_2CHCH_2O\cdot + CH_2CHCHO \rightarrow PL^c + CH_2CHCH_2OH$	1 E + 6

[a] Allyl O_2t-Bu.
[b] Polymer side chain, either CH_2OH or CHO.
[c] Polymer radical.
[d] 4-Phenyl-1,2-epoxybutane.
[e] Dead polymer.

acrolein yield, and the apportioning of the several routes for its production, neither of which can be assessed from the data.

Two kinds of radical-induced decomposition are evident, addition to C=C by alkyl radicals and allyl H-abstraction by alkoxy radicals. S_H2 displacement by alkyl radicals on the O—O bond is a third possibility but there is no evidence for it.

The foregoing conclusions, while instructive, seemed to underutilize the data at hand. The modelling exercise which follows suffers, however, from too little hard data, particularly in respect of residue structure. The basis set of reactions was chosen, after some experimentation, as the minimum number that with some stylization could match the significant products and the overall rate (Table 3).[2]

All polymer radicals were assumed to have the same free radical activity. Side chain reactivity was encompassed by an artificial device (CH, Table 3) used to indicate —CHO or CH_2OH in the polymer or polymer radical, and given an independent concentration.

Methyl radicals were included initially, but as this increased the number of equations by 6 or 7 and considerably enhanced the stiffness[3] of the set, all CH_3's were required to abstract from toluene (R4). This seemed fairly reasonable chemically, and did no violence to the fit. Prediction of CO yields was also deemed too complicated for similar reasons.

Toluene was taken to be constant at 9.4 *M* and its concentration incorporated into the rate constants where appropriate. Other conditions matched those of the experimental product studies; P_0 = 0.22 *M* and T = 150°C. Rate constants for H-abstractions and radical–radical combinations were assigned by reference to reviews by Hendry and co-workers (4, 5), and Ingold (6), respectively, while methyl acrylate (7) seemed to be the best available model for acrolein polymerization. Other rate constants were considered adjustable within reasonable limits. (In fact, all rate constants apart from free radical combinations could be so regarded since assignments for 150°C involved a substantial extrapolation from temperature ranges of the original data.)

Computations were carried out on a UNIX system, using Gear-type numerical integration, and were typically carried to 80–85% decomposition for comparison of predictions with the experimen-

[2] Table 3 and textual references to it are purposely stylized in order to make a clear distinction between chemistry and computational simulation. Adopting ordinary computer notation for the latter seems a readily comprehensible way of emphasizing the difference; Thus "E" for 10 to a power and *K* instead of *k* for rate constants.

[3] "Stiffness" is used in the mathematical sense, as a quality of differential equations that manifests itself in difficulty of numerical integration. Either the routine or the precision of the computer may be the limiting factor in the degree of stiffness that can be handled. In our case it was the computer, which had to be coaxed to solve even the 20 equations set.

Can. J. Chem. Downloaded from www.nrcresearchpress.com by 210.87.254.6 on 09/05/12
For personal use only.

Can. J. Chem. Downloaded from www.nrcresearchpress.com by 210.87.254.6 on 09/05/12
For personal use only.

tal results. Analytical minimization was not employed because the UNIX system proved incapable of handling both a minimization routine and Gear at the same time, and because minimization results for a scheme of this complexity have little credibility in any case. Instead a combination of intuition and hands-on experimental adjustment was used to produce a reasonable fit. The rate constants juxtaposed to the reactions (Table 3) produced the predicted product yields of Table 2 and an overall rate constant of 4.9×10^{-4} s^{-1} (cf. Table 1).

The predicted yields do approximate the experimental guide closely, the only serious inconsistencies being in the yields of acrolein (too high) and allyl alcohol (too low).[4] The model proved fairly rigid; attempts to improve the predictions for these products worsened the fit in other areas, and we suspect another reaction, perhaps a Diels–Alder, to be partly responsible for acrolein consumption.

Increasing the allyl alcohol yield is a more severe problem since it is generated only via the unimolecular homolysis and some of its is incorporated in the polymer. A partial solution to both difficulties would be to eliminate the cage disproportionation of t-BuO· with CH_2CHCH_2O· (R2), which was included with a rate constant arbitrarily set to equal 10% of all homolysis. It's difficult to see *why* cage disportionation should not be a factor, particularly as the t-BuO· + alkyl radical reaction is well documented (8), but perhaps it is not. Some years ago (9) we found that the thermal decomposition of $(MeEtCDO)_2$ in toluene yielded no MeEtCDOD. We were not wholly convinced at the time, nor are we now, but merely state our findings, to which as yet there has been no direct contradiction.

Generally speaking, the model lends support to the qualitative judgments about the course of the decomposition. The rate constants have little validity as yet, of course, but the important ones can be considered in the light of other data. A $K1$ of 2.4×10^{-4} s^{-1} is entirely believable. A value for $K10$ (and $K14$), abstraction of allyl-H from peroxide by alkoxy radicals, can be estimated for 60°C from the DBPO experiment. The relative concentrations of toluene and (average) peroxide, the efficiency of t-BuO· attack and k for t-BuO· + $PhCH_3$ (5)[5] give $K10_{60} = 1.28 \times 10^6$ M^{-1} s^{-1}. Comparing this to the model value of 4.4×10^6 M^{-1} s^{-1} at 150°C gives $K10 = 10^{8.62} \exp(-3840/RT)$, a value snugly between t-BuO· abstraction from a secondary alkene ($10^{8.2} \exp(-3350/RT)$) and from a secondary ether ($10^{8.7} \exp(-3910/RT)$) (5). The benzyl addition to peroxide is more difficult to gauge since good values for benzyl addition seem non-extant. A not unreasonable comparison can be made to RO_2· addition to 1-butene, however, which extrapolates to 157 M^{-1} s^{-1} at 150°C (5). The $K7$ value of 700 M^{-1} s^{-1} thus does not seem out of line.

In any case, we look forward to a forthcoming validity test when the numbers will be used in modelling a study of allyl hydroperoxide.

Acknowledgements

We are grateful to Professor T. G. Traylor and the Department of Chemistry of the University of California, San Diego for providing facilities for the computational part of this work, to International Mathematical and Statistical Library, Inc. for permission to use the Gear routine, DVOGER, and to Drs. T. Mill and D. Hendry for a preprint of their chapter on absolute rate constants. The experimental part of the work was supported by a grant from the National Research Council of Canada.

1. R. HIATT and T. MCCARRICK. J. Am. Chem. Soc. **97**, 5234 (1975).
2. L. BATT and S. W. BENSON. J. Chem. Phys. **36**, 895 (1962).
3. J. T. H. BROOK. Trans. Faraday Soc. **53**, 327 (1957).
4. D. G. HENDRY, T. MILL, L. PISZKIEWICZ, J. A. HOWARD, and H. K. EIGENMAN. J. Phys. Chem. Ref. Data, **3**, 937 (1974).
5. T. MILL and D. HENDRY. Comprehensive chemical kinetics. In press.
6. K. U. INGOLD. Free radicals. Vol. 1. *Edited by* J. K. Kochi. J. Wiley & Sons, New York. 1977.
7. M. S. MATHESON, E. E. AUER, E. B. BEVILAQUA, and E. J. HORT. J. Am. Chem. Soc. **73**, 1700 (1951).
8. J. P. LORAND. J. Am. Chem. Soc. **96**, 2867 (1974).
9. R. HIATT and S. SZILAGYI. Can. J. Chem. **48**, 615 (1970).
10. R. D. SMALL, JR. and J. C. SCAIANO. J. Am. Chem. Soc. **100**, 296 (1978).

[4]Note that a comparison of polymer yields is not possible since the model doesn't assign a structure and permits initiation by radicals other than benzyl.

[5]We are not unaware of a more recent value of k for t-BuO· + $PhCH_3$ (10). However, (*a*) this value was not yet published when our computations were done, and (*b*) the new value does not have an associated activation energy; thus the necessary extrapolations to higher temperatures would be dubious. Since our conclusions are admittedly unprecise, it seems hardly worth jumping from one uncertainty to another just because the latter is newer.

Excitation spectrum of the near-ultraviolet bands of CS_2[1]

R. VASUDEV AND J. C. D. BRAND

Department of Chemistry, The Photochemistry Unit,[2] University of Western Ontario, London, Ont., Canada N6A 5B7

Received September 5, 1979

R. VASUDEV and J. C. D. BRAND. Can. J. Chem. **58**, 454 (1980).

An excitation spectrum of the triplet–singlet band system of CS_2 vapor has been measured in the range 365–378 nm using a tunable laser source. Overall intensity is relatively insensitive to pressure in the range (150 mTorr – 340 Torr) tested in these observations. The results indicate that collisions with ground state molecules of CS_2 are efficient in promoting intersystem crossing to the ground state, and that the spontaneous emission observed is primarily resonance emission from the state populated by the radiation.

R. VASUDEV et J. C. D. BRAND. Can. J. Chem. **58**, 454 (1980).

On a mesuré le spectre d'excitation du système de bandes triplet–singulet du CS_2 gazeux entre 365 et 378 nm en utilisant une source réglable de laser. Entre 150 mTorr et 340 Torr la pression n'a relativement aucune influence sur l'intensité globale. Les résultats indiquent que les collisions avec les molécules de CS_2 dans l'état fondamental sont efficaces en ce sens qu'elles provoquent le passage d'un système à un autre vers l'état fondamental et que l'émission spontanée observée est essentiellement une émission de résonance à partir de l'état peuplé par la radiation.

[Traduit par le journal]

Can. J. Chem. Downloaded from www.nrcresearchpress.com by 210.87.254.40 on 09/05/12
For personal use only.

Introduction

The near-ultraviolet $\tilde{a}$–$\tilde{X}$ band system (Kleman's R-system) of CS_2 in absorption is described in many papers. In the first comprehensive study, Kleman (1) established the vibration–rotation analysis and demonstrated that the $\tilde{a}$ state has a wide-angled equilibrium structure, $\theta \approx 136°$, with a low barrier, ~ 0.4 eV, to linearity. Zeeman measurements showed that the levels that combine radiatively with the ground state belong to the $B_2(\Sigma = 0)$ substate of a $^3A_2$ state split by case c coupling into $B_2(\Sigma = 0)$ and $A_1 + B_1(\Sigma = \pm 1)$ components (2–4). The electric dipole moment of the excited state is small, < 0.5 D, as expected from the wide-angle structure (5). Weak transitions to the $A_1 + B_1$ substates have been observed in the low-temperature crystal spectrum (6) but are apparently too weak to distinguish from the background of other transitions in the vapor absorption. As first suggested by Mulliken (7), $^3A_2$ is the lower-energy component of the $^3\Delta_u$ state of linear CS_2, split by Renner–Teller coupling into $^3B_2 + {}^3A_2$ (4, 6). No excited state of CS_2 has been found below $^3A_2$ in optical absorption or electron-impact studies (8–10).

In contrast to the absorption, emission from the $\tilde{a}$ state has hardly been studied at all. Hochstrasser and Wiersma (6) reported structureless emission from CS_2 in argon matrices, and similar unstructured emission results from thermal, shock-wave excitation of the vapor (11, 12). To the present, no report has appeared of optically-excited emission from the $\tilde{a}$ state of the vapor. This paper describes a laser-excitation vapor spectrum obtained by scanning the absorption in the region 365–378 nm with a pulsed laser. The results, though qualitative, indicate that rapid self-quenching by collision competes strongly with radiative emission from the $\tilde{a}$ state.

Experimental and Results

CS_2 emission was excited by an N_2-laser pumped tunable dye laser operated in the range 365–380 nm with PBD dye in toluene–ethanol mixtures as the lasing medium. The excitation spectrum (Fig. 1) was recorded with CS_2 vapor in a cell fitted with light baffles, using an EMI 9558 photomultiplier protected from residual scattered light by Corning 3-74 filters ($\lambda > 415$ nm), the PMT output being processed with a PAR boxcar averager. Peak power at the sample was 7–10 kW. Observation windows of different diameters were used to confirm that diffusion of molecules from the excitation region did not influence the results. A wavelength calibration (± 0.1 Å) was established by tuning a 0.5 m monochromator to a standard line in the Fe/Ne hollow cathode emission, then tuning the laser into coincidence.

The CS_2 sample was purified by freeze–pump–thaw cycles and the excitation spectrum (ES) recorded at pressures between 150 mTorr and 340 Torr. The high- and low-pressure ES show qualitatively similar though not identical intensity distribution, while the overall intensity was essentially independent of pressure (< 2-fold variation within the above range). Table 1 gives relative in-

[1]Work supported by the Natural Sciences and Engineering Research Council of Canada.

[2]Publication No. 214 from the Photochemistry Unit.

0008-4042/80/050454-04$01.00/0

©1980 National Research Council of Canada/Conseil national de recherches du Canada

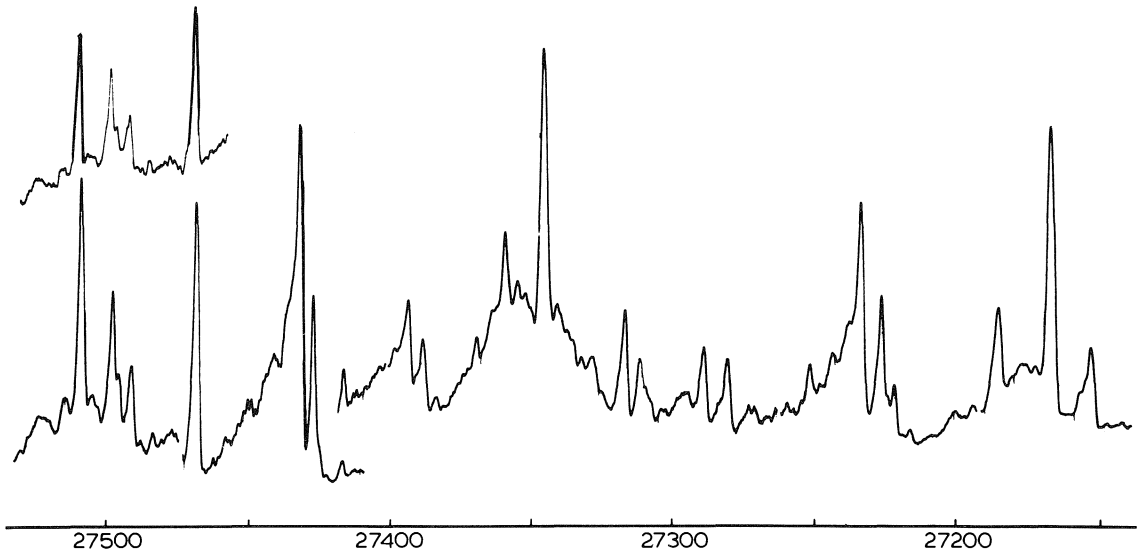


FIG. 1. Excitation spectrum, 27100–27550 cm^{-1} (360–368 nm). Full curve, 340 Torr pressure; inset, partial spectrum at 150 mTorr.

TABLE 1. Excitation spectrum of CS_2, 365–378 nm

$v_1'v_2'$	$\delta v_1 v_2^{l_2}$	ν, cm^{-1}	I_{es}[c]	I_{ab}[a]	$v_1'v_2'$	$\delta v_1 v_2^{l_2}$	ν, cm^{-1}	I_{es}	I_{ab}[a]
14	04^4	26 594[b]	2		S	04^0	27 078	6	
16	05^1	26 606	2		08	04^4	27 083	9	
04	02^2	26 634[b]	2.5	9	S	04^2	27 111[b]	8	7
07	04^0	26 649[b]	5	7	08	12^2	27 131	6	
S	05^1	26 672	2.5				27 136	8	9
07	04^2	26 688[b]	6	7	07	03^3	27 152[b]	12	17
18	06^2	26 703	2		15	03^1	27 166[b]	43	23
15	04^0	26 745[b]	10	5	06	02^0	27 184[b]	13	26
15	04^2	26 780[b]	14		S	04^4	27 220	4	
06	03^1	26 788[b]	7	21	06	02^2	27 225[b]	18	36
07	04^4	26 810[b]	3		15	03^3	27 232[b]	30	14
S	13^1	26 857	3		S	12^0	27 250	5	
06	03^3	26 865[b]	6	13	14	02^0	27 279[b]	11	13
15	04^4	26 873[b]	2		17	04^2	27 287	11	
14	03^1	26 882[b]	5	11	05	01^1	27 309[b]	8	24
05	02^0	26 895[b]	3	17	14	02^2	27 314[b]	14	21
		26 924[d]	4		08	03^1	27 343[b]	35	22
		26 927	3		17	04^4	27 353	3	
05	02^2	26 933[b]	4	19			27 357	11	11
14	03^3	26 949[b]	6		S + 1	04^2	27 386[b]	9	7
08	04^2	26 956[b]	7				27 391	13	
17	05^5	26 987	4				27 415	4	
04	01^1	27 013[b]	8	13	08	03^3	27 425[b]	47	26
17	13^1	27 035	3		16	03^1	27 430[b]	90	13
16	04^2	27 040[b]	14		07	02^0	27 467[b]	67	32
07	03^1	27 070[b]	18	21	16	03^3	27 491[b]	22	
					S	03^1	27 497[b]	42	23
					07	02^2	27 508[b]	76	42

[a] $I_{ab} = 100(I^0 - I)/I^0$ (eq. [1]).
[b] Band reported and assigned by Kleman (1).
[c] Intensity, $\lambda > 415$ nm, corrected for laser power variation with incident λ.
[d] Assigned by Kleman to the $05–02^2$ transition of $CS^{34}S$. This assignment is not compatible with the relative intensity in ES.

Can. J. Chem. Downloaded from www.nrcresearchpress.com by 210.87.254.40 on 09/05/12
For personal use only.

Can. J. Chem. Downloaded from www.nrcresearchpress.com by 210.87.254.40 on 09/05/12
For personal use only.

tensities I_{es} in ES recorded through the $\lambda > 415$ nm blocking filters, corrected for the variation of laser power with excitation wavelength. The columns headed I_{ab} in Table 1 give relative numbers of photons absorbed from the exciting radiation,

$$[1] \quad I_{ab} = 100(I^0 - I)/I^0 = 100(1 - 10^{-d})$$

where $d = \log_{10} I^0/I$ is the optical density of the sample determined from separate measurements of the absorption spectrum recorded with the same bandpass used in ES experiments. In the case when the vibronic state pumped by the laser radiation relaxes first to a Boltzmann population in the electronic $\tilde{a}$ state, followed by spontaneous emission or collision-induced intersystem crossing to the ground state, the ratio I_{es}/I_{ab} is proportional to the quantum yield of emission. However, it is shown in the next section that vibrational relaxation of excited CS_2 does not precede emission; hence I_{es}/I_{ab} responds to changes in the Franck–Condon profile of emission as well as in quantum yield.

Errors due to overlapping bands are troublesome in both ES and absorption (see, e.g., re. 5), but the optical density data for Σ bands are in fair agreement with the intensity measurements of Barrow and Dixon (4). Peak frequencies in the ES correlate well with bandheads in absorption though a number of weak bands in absorption are relatively prominent in ES. The limits of the ES were determined by low absorbance of CS_2 on the long-wavelength side and by the gain profile of PBD at short wavelengths.

Although attempts to disperse the CS_2 emission were unsuccessful the frequency range in the emission was explored crudely by filters. Using a 580 nm cut-off filter the emission intensity for certain bands is reduced 50% (see Table 2); therefore, since the S-20 response of the photomultiplier drops sharply at $\lambda > 575$ nm, an important fraction of the total emission must occur in the red spectral region. However, not all bands are affected equally by the long-wavelength cut-off filter, and comparisons offer some insight to the relaxation of excited CS_2 as discussed in the following section.

Table 1 offers a number of new assignments in the band system. Since the resolution in ES, $\sim 0.7\ cm^{-1}$, is not sufficient to determine the value of the rotational quantum number K, these assignments are based on frequency considerations only and should be regarded as tentative.

Discussion

Table 2 summarizes relative intensity measurements in ES using 415 and 580 nm cut-off filters for a selected group of strong bands. The ratio $I(415)/I(575)$ shows a definite upward trend with

TABLE 2. Comparison of ES intensities with different blocking filters, and of ES with absorption

$v_1'v_2'$	$\delta v_1 v_2^{l_2}$	Term value (cm^{-1})	$I_{es}(415)/I_{es}(575)$	$I_{es}(415)/I_{ab}$ (arbitrary scale)
08	03^3	28 613	3.2	1.8
08	03^1	28 550	3.2	1.6
07	02^2	28 300	2.1	1.8
07	02^0	28 270	1.9	2.1
06	02^2	28 017	1.8	0.5
06	02^0	27 986	1.9	0.5
05	02^2	27 725	—	0.2
05	02^0	27 698	—	0.2
04	02^2	27 402	—	0.3
04	01^1	27 410	—	0.6
16	03^1	28 637	3.8	7
15	03^3	28 420	2.8	2.1
15	03^1	28 374	2.9	1.9
14	02^2	28 106	1.8	0.7
14	02^0	28 082	2.0	0.8

increasing values of v_2' in the emitting state. To the extent that a shift in this ratio indicates a shift in the center of gravity of the Franck–Condon distribution in emission, it follows that the frequency characteristics of the emission depend on the quantum numbers of the state populated by the radiation. This is surprising because, especially at 340 Torr pressure, one might expect that collisions would lead to a Boltzmann population of upper state levels. This cannot be the case however; instead, the excited state must be quenched rapidly by collisions so that an important fraction of spontaneous emission occurs from the state excited by the laser. We do not claim that the emission is exclusively resonance emission, though it appears that it is predominantly so. Taking into account the striking pressure-insensitivity of overall ES intensity (see above) the kinetic scheme, in lowest order, becomes:

$$[2] \quad CS_2 + h\nu = CS_2^* \qquad k_1$$

$$[3] \quad CS_2^* + M = CS_2 + M \qquad k_2$$

$$[4] \quad CS_2^* = CS_2 + h\nu \qquad k_3$$

where CS_2^* is a single vibronic state populated by the radiation, and $k_2(M) \gg k_3$ for $M = CS_2$. At high pressure the likelihood that a unimolecular radiationless decay channel will compete effectively with the collision-induced intersystem crossing [3] is remote, and this possibility is not considered in the scheme above.

Our explanation of the intensity shift between different cut-off filters can be outlined by reference to the potential energy section in Fig. 2. The ground state potential curve is based on the force field given by Suzuki (13); this curve is extrapolated far beyond its fitted range and should be considered

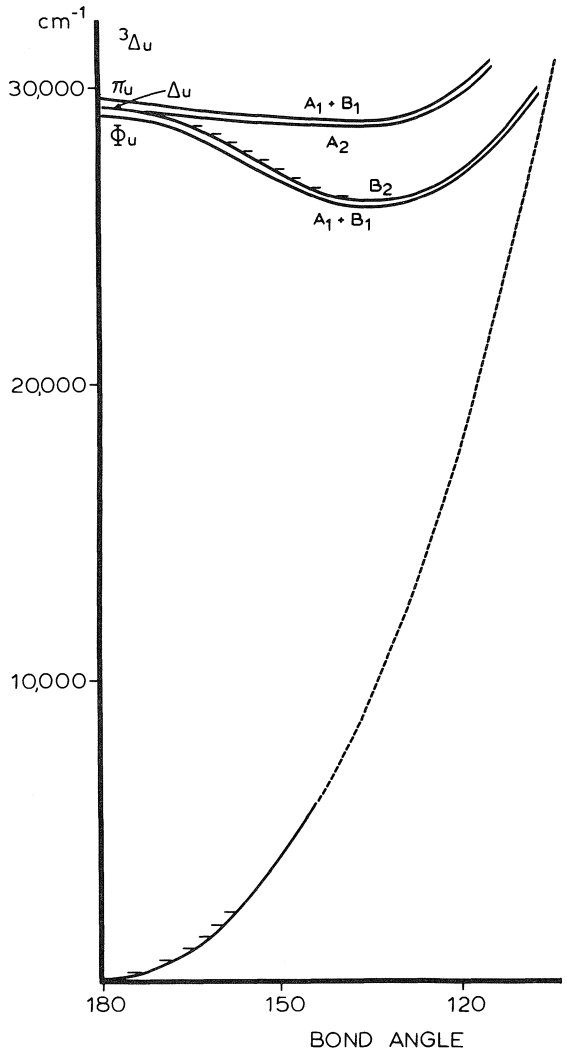


FIG. 2. Potential energy section in the plane of the bending coordinate. Spin splittings in the excited state (see refs. 3, 4, 6) are expanded to avoid congestion. Energy levels of the bending vibration are indicated in both states of the transition.

schematic at energies much above 5000 cm^{-1}. For the sake of argument, we also assume that emission from a given upper state with quantum number v_2' is concentrated in vertical transitions from the inner and outer turning points of the vibration, though this may not be a good quantitative description. Unless v_2' is small, the vertical transition from the outer turning point of the upper state potential occurs at an infrared frequency, whereas that from the inner turning point falls in the near-ultraviolet region; further, intensity will be distributed unequally since the ν^3 factor in the expression for spontaneous emission favors the higher-frequency transition. If we now relax the condition that the emission is concentrated into vertical transitions, it is reasonable to expect that the center of gravity of its Franck–Condon envelope will shift progressively towards higher frequencies with increasing v_2', which is also the direction of increasing phototube response. Consequently, in monitoring the total emission from different upper-states vibrational levels, the contribution of red wavelengths (transmitted by the $\lambda > 575$ nm filter) should fall as v_2' increases, which accords with the results in column 3 of Table 2.

Finally, the last column of Table 2 shows the variation of ES intensity relative to the absorption parameter I_{ab} defined in eq. [1]. This ratio changes considerably from one band to another, corresponding to the fact that the ES profile for CS_2 is by no means superimposable on the absorption spectrum. As mentioned earlier, I_{es}/I_{ab} is proportional to quantum yield *provided* the emission is preceded by vibrational relaxation in the upper electronic state, so that the large variation observed supports the conclusion that the self-quenching rate-constant is greater than that for vibrational energy transfer within the excited state. Since the ratios I_{es}/I_{ab} in Table 2 are un-normalized, the absolute values have no meaning; but trends are expected to be significant. Thus, the tendency for I_{es}/I_{ab} to increase with increasing v_2' is almost certainly due in part to the factors discussed in the previous paragraph, i.e., to the response of the detection system to the changing Franck–Condon envelope of the emission. However, we doubt if this is a complete explanation for two reasons: (*i*) the vibrational dependence is sharper than expected, and (*ii*) there is a suggestion that I_{es}/I_{ab} reaches a minimum in the $v_1' = 0$ series near $v_2' = 5$, which is not predicted from Franck–Condon arguments. At present, there is no clear indication of the reason for these anomalies and more experiments are needed.

1. B. KLEMAN. Can. J. Phys. **41**, 2034 (1963).
2. A. E. DOUGLAS and E. R. V. MILTON. J. Chem. Phys. **41**, 357 (1964).
3. J. T. HOUGEN. J. Chem. Phys. **41**, 363 (1964).
4. T. BARROW and R. N. DIXON. Mol. Phys. **25**, 137 (1973).
5. M. LARZILLIÈRE and D. A. RAMSAY. Can. J. Phys. **53**, 1579 (1975).
6. R. M. HOCHSTRASSER and D. A. WIERSMA. J. Chem. Phys. **54**, 4165 (1971).
7. R. S. MULLIKEN. Can. J. Chem. **36**, 10 (1958).
8. M. J. HUBSIN-FRANSKIN and J. E. COLLIN. J. Electron Spectrosc. **7**, 139 (1975).
9. D. F. DANCE, G. A. KEENAN, and I. C. WALKER. J. Chem. Soc. Faraday Soc. Trans. II, **74**, 440 (1978).
10. W. M. FLICKER, O. A. MOSHER, and A. KUPPERMANN. J. Chem. Phys. **69**, 3910 (1978).
11. S. J. ARNOLD and G. H. KIMBALL. J. Phys. Chem. **73**, 3751 (1969).
12. S. J. ARNOLD and G. H. KIMBALL. Can. J. Chem. **49**, 3075 (1971).
13. I. SUZUKI. Bull. Jpn. Chem. Soc. **48**, 1685 (1975).

Can. J. Chem. Downloaded from www.nrcresearchpress.com by 210.87.254.40 on 09/05/12
For personal use only.

Photoreactions of α-sulfonyloxyketones

JAMES LESLIE CHARLTON,[1] HOI KIONG LAI, AND GERALD NICHOLAS LYPKA
Department of Chemistry, University of Manitoba, Winnipeg, Man., Canada R3T 2N2

Received September 18, 1979

JAMES LESLIE CHARLTON, HOI KIONG LAI, and GERALD NICHOLAS LYPKA. Can. J. Chem. **58**, 458 (1980).

Earlier work on the photochemistry of α-sulfonyloxyketones uncovered their propensity to form the corresponding α-keto carbonium ions on photolysis. Typical reactions such as intramolecular cyclizations, carbonium ion rearrangements, and solvent trapping were found. This paper describes an attempt to extend this reaction to a general synthetic technique for polyene cyclizations. During the course of this work two other major reaction pathways were found. The first is an α-keto carbonium ion to acylium ion rearrangement and the second is a photoreduction–elimination process that leads to an α-keto radical rather than the corresponding cation.

JAMES LESLIE CHARLTON, HOI KIONG LAI et GERALD NICHOLAS LYPKA. Can. J. Chem. **58**, 458 (1980).

Des travaux antérieurs sur la photochimie des α-sulfonyloxycétones ont permis de mettre en évidence leur tendance à former les ions α-céto carbonium par photolyse. On a trouvé des réactions typiques telles que des cyclisation intramoléculaires, des transpositions de l'ion carbonium et sa capture par le solvant. Cette publication décrit une tentative d'étendre cette réaction à une technique générale de synthèse pour la cyclisation des polyènes. On a trouvé au cours de ce travail deux autres voies principales pour la réaction. La première est une transposition d'un ion α-céto carbonium en un ion acylium et la deuxième un procédé de photoréduction–élimination qui conduit au radical α-cétonique plutôt qu'au cation correspondant.

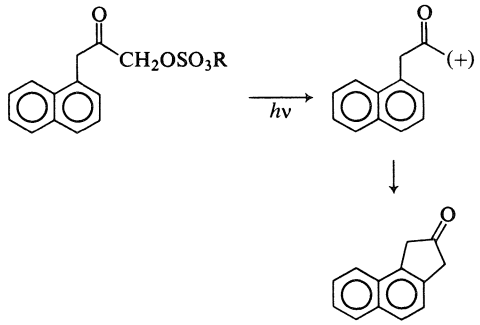
[Traduit par le journal]

Introduction

Concurrent with the discovery in 1966 that squalene oxide was enzymatically converted to lanosterol (1), several groups, notably those of Stork (2), Eschenmoser (3), Johnson (4), and van Tamelen (5) attempted to extend the scope of such reactions to provide a general nonenzymatic method for cyclization of polyenes. Most of the work has involved the intermediacy of cations (for example, see ref. 6) although both Breslow (7) and Julia (8) have demonstrated that free radical intermediates can also be used in initiating such polyene cyclizations.

Although the cationic or free radical intermediates of these reactions are usually generated by chemical and/or thermal catalysis, photochemical initiation has the advantage that the temperature can be kept low and no secondary chemical catalyst need be added. Witkop and co-workers have exploited this photochemical approach in their study of the cyclization reactions of *N*-chloroacetyl compounds (9). Schaffner and co-workers have also found that the photolysis of α-sulfonyloxyketones leads to cyclization, presumably via an α-keto carbonium ion as illustrated below (10).

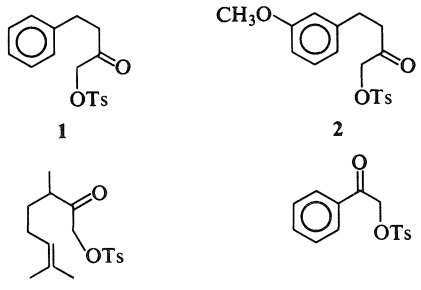
This paper describes our attempt to extend the scope of the cyclization reactions of α-sulfonyloxyketones. In the course of this work we have encountered two major photochemical reaction pathways for these systems in addition to that described above.



Syntheses and Photolyses

In order to determine the scope of the photocyclization reaction of α-sulfonyloxyketones we have synthesized and photolysed the α-tosyloxyketones **1**, **2**, and **3** shown below. α-Tosyloxyketone **4** was synthesized and photolysed to investigate the competing side reactions.

The sequence shown in Scheme 1, wherein an acid chloride is converted to a diazoketone and thence to the α-tosyloxyketone, was found to be the

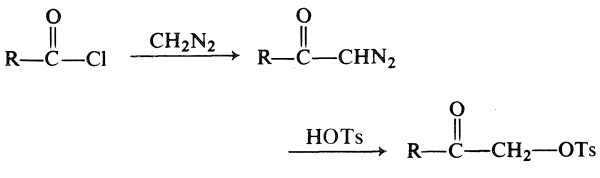


1 **2** **3** **4**

[1]Author to whom correspondence may be addressed.

0008-4042/80/050458-05$01.00/0
©1980 National Research Council of Canada/Conseil national de recherches du Canada

Can. J. Chem. Downloaded from www.nrcresearchpress.com by 210.87.254.105 on 09/05/12
For personal use only.

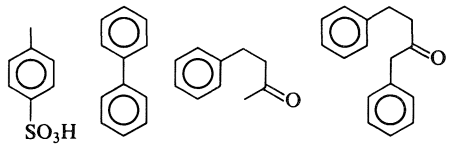


SCHEME 1

best generally applicable synthetic method for these compounds. The synthesis of the acid chlorides leading to the tosylates **1**, **2**, and **3** was accomplished using standard methods as described in the Experimental. Tosylate **4** was synthesized from benzoyl chloride.

1-Tosyloxy-4-phenyl-2-butanone 1

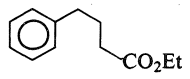
α-Tosyloxyketone **1** was irradiated in benzene, diethyl ether, ethanol, and acetonitrile. Compounds **7**, **8**, **9**, and **10**, shown below, were isolated after irradiation in benzene.



7 74% **8** 13% **9** 7% **10** 10%

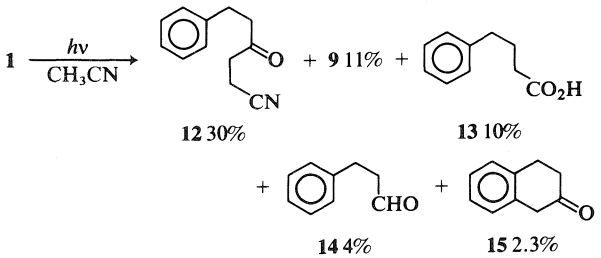
All products were identified by comparison (gas chromatography and/or mass spectrometry) with authentic samples. The yield of toluenesulfonic acid was estimated from titration of total acid, while the yields of **8**, **9**, and **10** were determined by gas chromatography.

In ether solution, the yield of toluenesulfonic acid was 88% and the yield of methyl ketone **9** was 32%. Many minor components were also observed but not identified. In ethanol–acetonitrile the major products were the methyl ketone **9** (28%) and ethyl 4-phenylbutanoate **11** (10%, isolated yield).



11

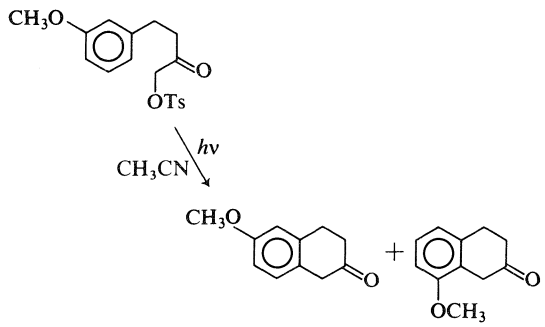
In dry acetonitrile, the major product had spectral data most consistent with the acetonitrile adduct **12**. This adduct was not identified by comparison with an authentic sample and hence its structural assignment is tentative. The remaining products were all identified unambiguously.



12 30% **13** 10% **14** 4% **15** 2.3%

1-Tosyloxy-4-(3-methoxyphenyl)-2-butanone

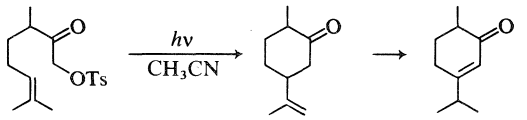
The irradiation of tosyloxyketone **2** was carried out in acetonitrile and benzene. The major products from irradiation in acetonitrile were the β-tetralones **16** and **17**, both identified by comparison with authentic samples. Photolysis in benzene and analysis of the volatile components by gas chromatography indicated that the product mixture was qualitatively similar to that obtained in acetonitrile.



16 24% **17** 23%

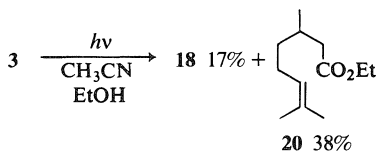
1-Tosyloxy-3,7-dimethyl-6-octene-3-one

Tosylate **3** was irradiated in acetonitrile in the presence of anhydrous potassium carbonate added to stop a slow, acid-catalysed decomposition of the tosylate. Gas chromatograph – mass spectrograph analysis showed the major product to be dihydrocarvone **18**, which isomerized very readily to 2-carvenone **19**.



dihydrocarvone **18** 2-carvenone **19**

Irradiation in acetonitrile containing ethanol gave dihydrocarvone **18** and ethyl 3,7-dimethyl-6-octenoate **20**.



20 38%

α-Tosyloxyketone 4

Photolysis of tosylate **4** in ethanol–acetonitrile gave increasing amounts of acetophenone and decreasing amounts of ethyl phenylacetate as the ethanol concentration was increased (Table 1).

Can. J. Chem. Downloaded from www.nrcresearchpress.com by 210.87.254.105 on 09/05/12
For personal use only.

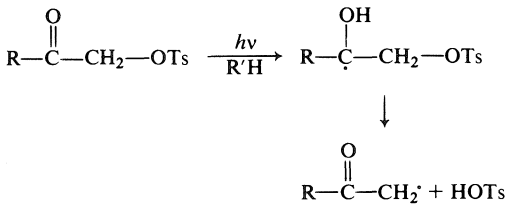
TABLE 1. Yields of acetophenone and ethyl phenylacetate

% Ethanol	% Acetophenone	% Ethyl phenylacetate
2	7.6	19
20	28	11
50	47	2.2

The products were found to be unstable under the reaction conditions. Maximum yields were obtained at less than full conversion of the tosylate and are not corrected for unreacted tosylate. The rate of photolysis was considerably increased at the higher ethanol concentration.

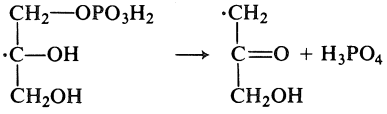
Discussion

From the first three tosyloxyketones studied, it appears that photocyclization yields are too variable to make this reaction a general synthetic method, but some conclusions regarding the general photoreactivity of these systems can be made. There seem to be two main reaction pathways, the first being a reduction–elimination route to the α-keto radical (Scheme 2).



SCHEME 2

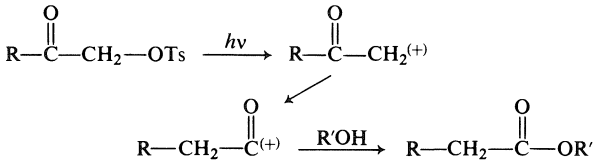
This mechanism was first proposed by Szarek and Dmytraczenko (11) and is analogous to the elimination of phosphate from radical **23**, as reported by Schulte-Frohlinde and co-workers (12) and Samuni and Neta (13).



23

The results obtained from the photolysis of tosylate **4** in mixed acetonitrile–ethanol solvents are also consistent with the proposed mechanism. Ethanol, being a better hydrogen atom donor, increases the amount of photoreduction as its concentration is increased. Methyl ketone **9**, adducts **11** and **12**, and dihydrocarvone **18** (7) may all arise from the α-keto radical formed in the photoreduction–elimination reaction.

The second main reaction pathway for α-tosyloxyketones, as previously described by Schaffner and co-workers (10), is the heterolysis to the α-keto carbonium ion. However, we find that the major process following the formation of this ion is rearrangement to the acylium ion as shown in Scheme 3.



SCHEME 3

Thus from tosylates **1**, **3**, and **4** we obtain the butanoate ester **11**, the octenoate ester **20**, and ethyl phenylacetate, respectively. The rearrangement appears to compete effectively with cyclization reactions as the yield of tetralone from tosylate **1** is less than 3 percent under the best conditions. Only for compound **2** is cyclization the major process. Whether the cyclization process is free radical or ionic is unknown but it does appear that a very reactive center, such as the methoxyphenyl group, is necessary before cyclization is dominant.

Experimental

Mass spectra were recorded on a Finnegan 1015 mass spectrometer and only molecular ions and major fragments are reported. Nuclear magnetic resonance (nmr) spectra were obtained on a Varian EM360 or A-56/60 spectrometer using tetramethylsilane as internal standard. Camag Kieselgel DSF-5 and Davidson Chemical, grade H silica gel (60–200 mesh) were used for thin layer and column chromatography. Gas chromatographic analyses were performed on a Hewlett-Packard 700 instrument. Elemental analyses were performed by Chemalytics Inc., Tempe, AZ.

Hydrocinnamoyl and 3-Methoxyphenylhydrocinnamoyl Chloride

trans-Cinnamic acid (Eastman Kodak) and 3-methoxyphenyl cinnamic acid (Aldrich) were hydrogenated in ethanol over platinum to yield 83% and 95% of the hydro derivatives respectively. The acids were converted to the acid chlorides by refluxing in a mixture of thionyl chloride and benzene.

4-Phenyl-1-diazobutan-2-one

The 4-phenylbutanoyl chloride (hydrocinnamoyl chloride) was added to 3 equivalents of diazomethane in ether and followed by one equivalent of triethyl amine. The solution was stirred at room temperature for one hour, evaporated to dryness *in vacuo*, and chromatographed on silica gel using benzene–ether as eluant. The diazo ketone was obtained in 80% yield as a yellow oil; ir (neat): 2115 ($COCHN_2$), 1740 (C=O) cm^{-1}; nmr (CCl_4) δ: 7.1 (s, 5H), 4.93 (s, 1H), 2.40–2.85 (m, 4H); ms *m/e*: 174.

1-Tosyloxy-4-phenyl-2-butanone ***1***

p-Toluenesulfonic acid monohydrate (6.34 g, 0.033 mol) was added at room temperature to a solution of 4-phenyl-1-diazobutan-2-one (5.74 g, 0.033 mol) in anhydrous ether (50 mL). After 0.5 h the solution was washed with water, dried ($MgSO_4$), and evaporated to give crystals which recrystallized from benzene–pentane to yield 6.9 g (66%); mp 69–70°C; ir

Can. J. Chem. Downloaded from www.nrcresearchpress.com by 210.87.254.105 on 09/05/12
For personal use only.

Can. J. Chem. Downloaded from www.nrcresearchpress.com by 210.87.254.105 on 09/05/12
For personal use only.

(Nujol): 1730 (C=O) cm^{-1}; nmr δ: 7.1–7.7 (q, 4H), 7.05 (s, 5H), 4.25 (s, 2H), 2.78 (s, 4H), 2.45 (s, 3H); ms *m/e*: 318, 155, 146, 133, 105, 91, 77; *Anal.* calcd. for $C_{17}H_{18}O_4S$: C 64.15, H 5.66, S 10.06; found: C 64.40, H 5.76, S 10.15.

4-(3-Methoxyphenyl)-1-diazobutan-2-one

The procedure was identical to that found for the 4-phenyl derivative. The yield was 88% of yellow oil; ir (neat): 2125 ($COCHN_2$), 1730 (C=O) cm^{-1}; nmr (CCl_4) δ: 6.35–7.1 (m, 4H); ms *m/e*: 204.

1-Tosyloxy-4-(3-methoxyphenyl)butan-2-one

4-(3-Methoxyphenyl)-1-diazobutan-2-one (3.52 g, 0.017 mol) was reacted with *p*-toluenesulfonic acid monohydrate (3.61 g, 0.019 mol) as described above. After chromatography on silica gel (eluant benzene) 3.5 g (59%) of oil was obtained; ir (neat): 1740 cm^{-1}; nmr (CCl_4) δ: 7.2–7.66 (q, 4), 6.4–7.1 (m, 4), 4.25 (s, 2, $—COCH_2O—$), 3.6 (s, $—OCH_3$), 2.67 (broad s, 4, $—CH_2CH_2$), 2.3 (s, 3H, CH_3); ms *m/e*: 348, 194, 163, 155, 135, 121; *Anal.* calcd. for $C_{18}H_{20}O_5S$: C 62.07, H 5.75, S 9.20; found: C 62.51, H 5.86, S 9.43.

6-Methyl-5-hepten-2-ol

6-Methyl-5-hepten-2-one (12.6 g, 0.1 mol, Aldrich) was reduced in ether with $LiAlH_4$ (1.33 g, 0.035 mol) to give a quantitative yield of the alcohol; nmr (CCl_4) δ: 4.9 (broad t, 1H), 4.0 (broad s, 1H), 3.5 (m, 1H), 1.6–2.18 (m, 4H), 1.53 (s, 3H), 1.52 (s, 3H), 1.0 (d, 3H); ms *m/e*: 128, 110, 95.

2-Bromo-6-methyl-5-heptene

The alcohol above (4.65 g, 0.036 mol) was treated with pyridine (1.58 g) and PBr_3 (3.06 g, 0.018 mol) in ether. Work up and distillation yielded 2.9 g (42%) of colourless oil; nmr (CCl_4) δ: 4.9 (broad t, 1H), 4.1–4.4 (m, 1H), 1.75–2.3 (m, 4H), 1.54 (broad s, 6H), 1.2 (d, 3H).

2-Cyano-6-methyl-5-heptene

The 2-bromo-6-methyl-5-heptene was converted to the 2-cyano derivative using the method of Smiley and Arnold (14). Thus, the bromo compound (9.13 g, 0.048 mol) was reacted with NaCN (3.35 g) in DMSO (40 mL) to give the nitrile (3.91 g, 60%); nmr (CCl_4) δ: 4.8 (broad t, 1H), 2.1–2.3 (m, 1H), 1.4–1.9 (m, 4H), 1.3 (broad s, 6H), 0.9 (d, 3H); ms *m/e*: 137, 110, 95.

2,6-Dimethyl-5-heptenoic Acid

The nitrile from above (0.85 g, 6.2 mmol) in ethanol (2 mL) was added to a solution of KOH (3.36 g) in ethylene glycol (10 mL) and water (2 mL). After 18 h at reflux, the usual workup yielded the acid (0.65 g, 67%) with nmr and ir consistent with those reported in the literature (15).

2,6-Dimethyl-5-heptenoic Acid Chloride

A mixture of 2,6-dimethyl-5-heptenoic acid (0.16 g) and dry pyridine (3 drops) in dry benzene (25 mL) was treated at 0.5°C with freshly distilled oxalyl chloride (1.26 g) and then warmed to room temperature and left for 2 h. Filtration and evaporation gave the acid chloride 0.15 g (86%) (15).

1-Diaza-3,7-dimethyl-6-octene-2-one

The diazoketone was prepared by the method described for 4-phenyl-1-diazobutan-2-one in 76% yield. (See also ref. 15.)

1-Tosyloxy-3,7-dimethyl-6-octene-2-one

The diazoketone was converted to the tosyloxy derivative by treatment with ethereal *p*-toluenesulfonic acid (1.1 equivalents) in 82% yield; ir (neat): 1740, 1380, 1190, 780, 820 cm^{-1}; nmr (CCl_4) δ: 7.19–7.76 (q, 4H), 4.95 (bt, 1H), 4.46 (2H, s), 2.4 (s, 3H), 1.52 (s, 3H), 0.95 (d, 3H); ms *m/e*: 170, 155, 152, 139, 110, 95.

α-Tosyloxyacetophenone **4**

α-Diazoacetophenone was prepared according to the method described above (16) and converted to the α-tosyloxyacetophenone (17) with ethereal toluenesulfonic acid. The overall yield from benzoyl chloride was 51%.

Photolyses

All irradiations were carried out in water cooled quartz or Vycor vessels at 2537 Å (UV Products PCQX1 or Rayonet photochemical reactor).

Photolysis of 1-Tosyloxy-4-phenyl-2-butanone **1**

A solution of **1** (10 mg) in dry thiophene-free benzene (6 mL) was irradiated for 1 h, the solution washed with water, and the water evaporated. The residue, identified as *p*-toluenesulfonic acid by mass spectroscopy, was titrated with standard base and required 2.31×10^{-5} equivalents (73.5%). The organic layer was evaporated and analysed by a tandem gas chromatograph – mass spectrograph (gc–ms) (gc: 10% Se30 on Chromosorb W, 6 ft × 1/8 in., programmed from 100 to 220°C). The identity of products was confirmed by comparison with authentic samples (see below) and yields were determined by gc using 2-phenylacetophenone as internal calibrant. In order of gc retention times the products identified were: (*1*) 4-phenyl-2-butanone (7%); an authentic sample was prepared by hydrogenation of benzalacetone (18) in absolute ethanol in the presence of PtO_2 (100%); (*2*) 4-phenyltoluene (12%), identical to a commercial sample (Aldrich Chemicals); and (*3*) 1,4-diphenyl-2-butanone (10% yield). The authentic sample was prepared by reacting the Grignard of benzylchloride with hydrocinnamaldehyde in the usual way, giving the alcohol (24%) which was subsequently oxidized in ether to the ketone (88%) using 10% CrO_3 in 5% aqueous H_2SO_4 (19).

Irradiation of tosyloxyketone **1** (100 mg) in absolute ethanol (25 mL) led to a complex mixture of at least 6 volatile components. From among these, only two major components were identified by gc–ms as 4-phenyl-2-butanone and ethyl 4-phenylbutanoate. (The authentic ester was prepared from 4-phenylbutanoic acid and ethanol in the usual manner.) A solution of **1** (500 mg) in acetonitrile–ethanol (4:1, 100 mL) in the presence of anhydrous potassium carbonate (50 mg) was similarly irradiated and gc analysis indicated a higher yield of the ketone and ester. The solution was filtered, evaporated, the residue dissolved in ether, and this extracted with dilute aqueous bicarbonate. The ether layer after drying ($MgSO_4$) and evaporation yielded 190 mg which was chromatographed on tlc (benzene) to yield 4-phenyl-2-butanone (65 mg, 28%) and ethyl 4-phenyl-1-butanoate (32 mg, 10%).

Compound **1** (1.013 g), in dry acetonitrile (100 mL) with anhydrous potassium carbonate (500 mg), was irradiated under nitrogen for 18 h in a Rayonet photochemical reactor. The mixture was filtered, evaporated, and then dissolved in ether – aqueous bicarbonate. The aqueous layer was separated, acidified, and extracted with ether to yield 4-phenylbutanoic acid (50 mg, 10%), identified by comparison to a commercial sample (Aldrich). The ether layer was dried ($MgSO_4$), evaporated, and chromatographed on silica gel (benzene–ether, Camag DSF-5) to yield: (*1*) hydrocinnamaldehyde (14.5 mg, 3.7%), compared to commercial sample (Aldrich); (*2*) 4-phenyl-2-butanone (48 mg, 11%); (*3*) β-tetralone (9 mg, 2%) identified by comparison to commercial sample (Aldrich); (*4*) unreacted tosyloxyketone **1** (74 mg); and (*5*) a crystalline compound (168 mg, 30% as $C_{12}H_{13}NO$); nmr ($CHCl_3$) δ: 7.06 (s, 5H), 2.8 (s, 2H) 2.3–2.78 (m, 3H), 2.27 (s, 3H); ms *m/e*: 187, 164, 146, 104, 91.

Photolysis of 1-Tosyloxy-4-(3-methoxyphenyl)-2-butanone **2**

A mixture of tosyloxyketone **2** (395 mg), anhydrous potas-

Can. J. Chem. Downloaded from www.nrcresearchpress.com by 210.87.254.105 on 09/05/12
For personal use only.

sium carbonate (400 mg), and acetonitrile (45 mL) was irradiated under nitrogen for 8 h in a Rayonet photochemical reactor. The mixture was filtered, evaporated (at room temperature), dissolved in ether – aqueous bicarbonate, the ether dried ($MgSO_4$), evaporated, and the residue chromatographed on tlc (ethyl acetate – benzene) to yield: (*1*) 6-methoxy-2-tetralone (44.3 mg, 24%), identified by comparison of gc retention time (10% Carbowax 20 m on Chromosorb W, 6 ft × 1/8 in., 180°C) and mass spectrum to a commercial sample (Aldrich), and (*2*) 8-methoxy-2-tetralone (42 mg, 23%), identical to a sample synthesized by the method of Robins and Walker (20).

Irradiation of tosyloxyketone **2** (10 mg) in benzene (6 mL) under nitrogen and analysis by gc (as above) indicated that the products were qualitatively similar to the results obtained in acetonitrile.

Photolysis of 1-Tosyloxy-3,7-dimethyl-6-octen-2-one ***3***

Tosyloxyketone **3** (410 mg) and anhydrous sodium carbonate (400 mg) were irradiated in acetonitrile (60 mL) under nitrogen for 2 h. The solution was then filtered, evaporated, and worked up by ether–water extraction. The crude product (160 mg) analyzed by gc–ms (10% Apiezon – 1% DEGS on Chromosorb W, 8 ft × 1/4 in., 160°C) showed the presence of both dihydrocarvone and 2-carvenone, synthesized as described by Wallach (21) and Buchi and Erickson (22). The 2-carvenone was subsequently shown to arise from isomerization on the gc column. The total yield of dihydrocarvone and 2-carvenone, isolated by gc, was 42 mg (22%).

Irradiation of **3** (2.91 g) in acetonitrile and ethanol (100 mL, 99:1) with potassium carbonate (3.0 g) under nitrogen, followed by the usual workup (see above) and chromatography on silica gel (Camag DSF-5, benzene–pentane) gave ethyl 3,7-dimethyl-6-octenoate (200 mg, 17% based on 65% conversion), dihydrocarvone (150 mg, 17% based on 65% conversion), starting tosyloxyketone **3** (1.0 g), and a mixed fraction (500 mg), eluted with ether, that still contained the tosyl group (nmr). This later fraction was not investigated further. An authentic sample of ethyl 3,7-dimethyl-6-octenoate was synthesized from citronellal (Chemical Service) by oxidation (23) and esterification with absolute ethanol.

A similar irradiation in acetonitrile–ethanol (4:1) yielded 38% of the ester.

Photolysis of α-Tosyloxyacetophenone ***4***

A mixture of the tosylate (300 mg), anhydrous potassium carbonate (500 mg), absolute ethanol, and purified acetonitrile (50 ml) was irradiated under nitrogen in a Vycor vessel using a low pressure mercury lamp (2537 Å). Yields of acetophenone and ethyl phenylacetate were obtained from gas chromatography (10% Se-30 on Chromosorb P, 10 ft × 1/8 in., 145°C) using diphenylmethane as an internal standard, and were determined at peak product concentrations. They were not corrected for any unreacted starting material. Yields are recorded in Table 1.

Acknowledgement

The financial assistance of the Natural Sciences and Engineering Research Council of Canada is gratefully acknowledged.

1. (*a*) E. J. Corey, W. E. Russey, and P. R. Oritz de Montellano. J. Am. Chem. Soc. **88**, 4750 (1966); (*b*) E. E. van Tamelen, J. D. Willett, R. B. Clayton, and K. E. Lord. J. Am. Chem. Soc. **88**, 4752 (1966).
2. G. Stork and A. W. Burgstahler. J. Am. Chem. Soc. **77**, 5068 (1955).
3. A. Eschenmoser, L. Ruzicka, O. Jeger, and D. Arigoni. Helv. Chim. Acta, **38**, 1890 (1955).
4. W. S. Johnson. Bioorg. Chem. **5**, 51 (1977).
5. E. E. van Tamelen. Acc. Chem. Res. **8**, 152 (1974).
6. W. S. Johnson, N. P. Jensen, and J. P. Hooz. J. Am. Chem. Soc. **88**, 3859 (1966).
7. R. Breslow, E. Barrett, and E. Mohassi. Tetrahedron Lett. 1207 (1962); R. Breslow, J. T. Groves, and S. Olin. Tetrahedron Lett. 4717 (1966); R. Breslow, S. S. Olin, and J. T. Groves. Tetrahedron Lett. 1837 (1968).
8. M. Julia. Pure Appl. Chem. **40**, 553 (1974) and references cited.
9. O. Yonemitsu, P. Cerntii, and B. Witkop. J. Am. Chem. Soc. **88**, 3941 (1966).
10. A. Tuinman, S. Iwasaki, K. Schaffner, and O. Jeger. Helv. Chim. Acta, **51**, 1778 (1968); S. Iwasaki and K. Schaffner. Helv. Chim. Acta, **51**, 557 (1968); G. Huppi, G. Eggart, S. Iwasaki, H. Wehrli, K. Schaffner, and O. Jeger. Helv. Chim. Acta, **49**, 1986 (1966).
11. W. A. Szarek and A. Dmytraczenko. Synthesis, **6**, 579 (1974).
12. S. Steeken, G. Behren, and D. Schulte-Frohlinde. Int. J. Radiat. Biol. **25**, 205 (1974).
13. A. Samuni and P. Neta. J. Phys. Chem. **77**, 2425 (1973).
14. R. A. Smiley and C. Arnold. J. Org. Chem. **25**, 257 (1960).
15. K. Mori and M. Matsui. Tetrahedron, **25**, 5013 (1969).
16. W. Bradley and R. Robinson. J. Chem. Soc. 1310 (1928).
17. L. Prajer-Janczewska. Rocz. Chem. **36**, 549 (1962).
18. A. I. Vogel. A text-book of practical organic chemistry. 3rd ed. Longmans, Green and Co. Ltd., London. 1956. p. 738.
19. H. C. Brown, C. P. Garg, and K.-T. Liu. J. Org. Chem. **36**, 387 (1971).
20. P. A. Robins and J. Walker. J. Chem. Soc. 409 (1958).
21. O. Wallach. Ann. **306**, 237 (1899).
22. G. Buchi and R. E. Erickson. J. Am. Chem. Soc. **76**, 3403 (1954).
23. E. Campaigne and W. M. LeSeur. Org. Synth. Coll. Vol. **IV**, 919 (1963).

A comparison of the stereochemistry and kinetics of thermolysis of *R*-(+)-laurolenic acid, *R*-(+)-laurolenal, and *R*-(+)-laurolenol

ROBERT J. CRAWFORD AND HIROKAZU TOKUNAGA

Department of Chemistry, The University of Alberta, Edmonton, Alta., Canada T6G 2G2

Received September 12, 1979

ROBERT J. CRAWFORD and HIROKAZU TOKUNAGA. Can. J. Chem. **58**, 463 (1980).

The thermolysis of *R*-(+)-laurolenal (**1**) produces *R*-(+)-1,2,3-trimethylcyclopentene in high optical purity. The alcohol **3**, at 297°C, similarly produces the alkene *R*-(+)-**4**, but with mechanistic complications in that the formaldehyde produced oxidizes the alcohol **3** to the corresponding aldehyde **1**. The alcohol **3**-d_2 was used to show the extent of aldehyde conversion by virtue of the formation of **4**-d_1. Comparison of the decarboxylation of the acid, decarbonylation of the aldehyde, and demethanalation of the alcohol gives relative rates of 9:2:1 at 297°C.

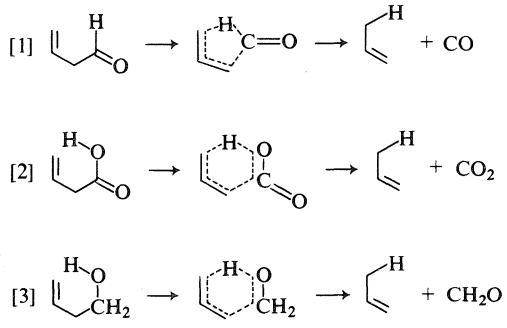
ROBERT J. CRAWFORD et HIROKAZU TOKUNAGA. Can. J. Chem. **58**, 463 (1980).

La thermolyse du *R*-(+) laurolenal (**1**) produit le *R*-(+) triméthyl-1,2,3 cyclopentène avec une grande pureté optique. De la même manière l'alcool **3** chauffé à 297°C produit l'alcène *R*-(+)-**4** mais selon un mécanisme compliqué car il implique que le formaldéhyde produit oxyde l'alcool **3** en l'aldéhyde correspondant **1**. On a utilisé l'alcool **3**-d_2 pour mettre en évidence l'importance de la transformation en aldéhyde au moyen de la formation de **4**-d_1. En comparant la cinétique de la thermolyse de l'acide, de l'aldéhyde et de l'alcool on obtient des vitesses relatives de 9:2:1 à 297°C.

[Traduit par le journal]

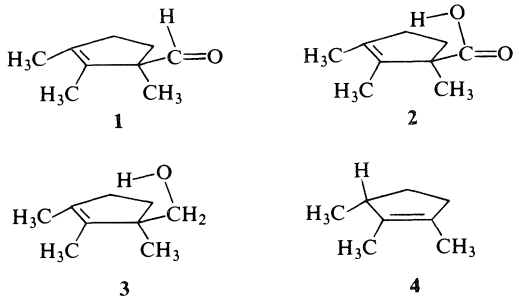
Introduction

Earlier we presented kinetic and isotope effect evidence that supported a cyclic transition state (as in eq. [1]) for the decarbonylation of β,γ-unsaturated aldehydes (**1**). We now wish to report that the implied stereochemistry for this process has been verified by using *R*-(+)-laurolenal (**1**). While examining the stereochemical implications of the aldehyde decarbonylation, we undertook a comparison of this process with the analogous decarboxylation of the β,γ-unsaturated acid (eq. [2]) and the thermolysis of γ,δ-unsaturated alcohols.



The kinetics of decarboxylation of β,γ-unsaturated acids have been examined in detail by Bigley and May, and by Smith and Blau (2) as have the kinetics for the γ,δ-alcohol thermolysis (3). A comparison of the stereochemistry and the ease of the reactions is made for the substrates **1**, **2**, and **3**.

The aldehyde (**1**), acid (**2**), and alcohol (**3**) can be prepared optically pure from (−) α-bromocamphoric anhydride (5) by the procedures of Meyer *et al.* (4) and Baggiolini *et al.* (6).



1 **2** **3** **4**

Results and Discussion

Samples of *R*-(+)-laurolenal (**1**), upon thermolysis in a static system at 297°C, gave rise to carbon monoxide and (*R*)-(+)-1,2,3-trimethylcyclopentene (**4**). Kinetically, the reaction is first order, the rate constant k_1 being (2.14 ± 0.04) × 10^{-5} s^{-1} at 297°C. The olefin **4** produced from **1**, $[\alpha]_D^{25}$ +630.7° (*c* 1.57, $CHCl_3$), lit. (5) value for optically pure aldehyde $[\alpha]_D^{23}$ +624.2 ± 4.7° (*c* 1.50, $CHCl_3$), was dextrorotatory implying the *R* configuration on the basis of the absolute configuration assigned by Baggiolini *et al.* (6). The magnitude of the olefin's rotation, $[\alpha]_D^{25}$ +64.5° (*c* 4.47, $CHCl_3$), lit. value $[\alpha]_D^{23}$ +63.4° (neat), allows one to conclude that the reaction is stereospecific and that the aldehydic hydrogen is delivered to the γ carbon on the same face as the carbon monoxide is expelled. Samples of the unreacted aldehyde recovered after one half-life showed no indication of any racemization and similarly samples of olefin taken at 50, 75, and 90% completion gave, within experimental error, the same rotational values.

0008-4042/80/050463-03$01.00/0

©1980 National Research Council of Canada/Conseil national de recherches du Canada

Can. J. Chem. Downloaded from www.nrcresearchpress.com by 210.87.254.40 on 09/05/12
For personal use only.

Can. J. Chem. Downloaded from www.nrcresearchpress.com by 210.87.254.40 on 09/05/12
For personal use only.

The aldehyde **1** has been shown to undergo photolysis to give *S*(−)**4**, and thus can be used as a source of either enantiomer.

The acid **2** decarboxylates readily at 297°C, $k_2 = (9.37 \pm 0.30) \times 10^{-5}\ s^{-1}$, to give cleanly the alkene **4**, $[\alpha]_D^{25}$ +65.5°. Studies at 1, 3, and 5 half-lives indicated that neither the reactant nor the product was undergoing any racemization.

The alcohol **3** was slower in thermolysis than **1** or **2**, and gave poor kinetic results, rate plots indicating that the reaction was going faster at higher conversion. A carefully degassed sample of **3** which had been purified by gas–liquid chromatography gave, after 20 h, 67% of **4**, 26% of **3**, and 7% of **1** along with methanol, formaldehyde, and carbon monoxide. Figure 1 shows the concentrations of **1**, **3**, and **4** at various times during the thermolysis of thoroughly degassed samples of **3**. In order to verify that a significant portion of the thermolysis of **3** was first undergoing oxidation to the aldehyde a sample of **3**-d_2 was studied. Table 1 gives the percentage of alkene containing deuterium upon thermolysis of **3**-d_2 under a variety of conditions. While 14% of the alkene contained deuterium when **3**-d_2 underwent thermolysis to 90% completion, the percentage alkene-d_1 rose to 51% when formaldehyde was added at the outset, demonstrating that formaldehyde acts as an oxidizing agent to transform the alcohol **3** into the aldehyde **1**. This also explains the appearance of carbon monoxide and methanol as thermolysis products.

We suggest that the thermolysis of **3**, and of **3**-d_2, occurs by two paths.

Initially the thermolysis of **3** is about half the rate of **1**, but as the concentration of formaldehyde builds up the rate of formation of **4** increases and detectable amounts of aldehyde **1**-d_1 are found to be present.

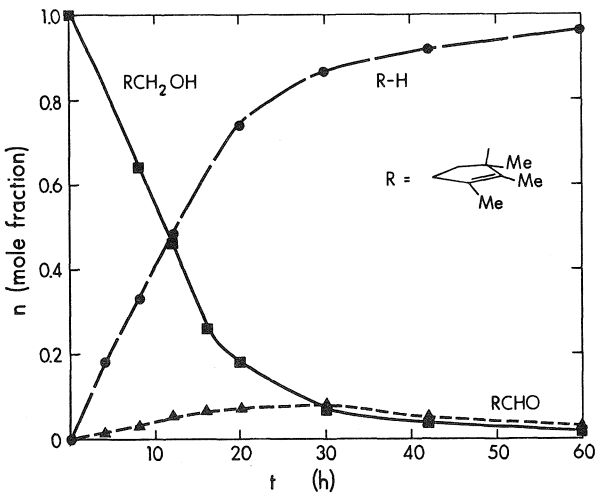


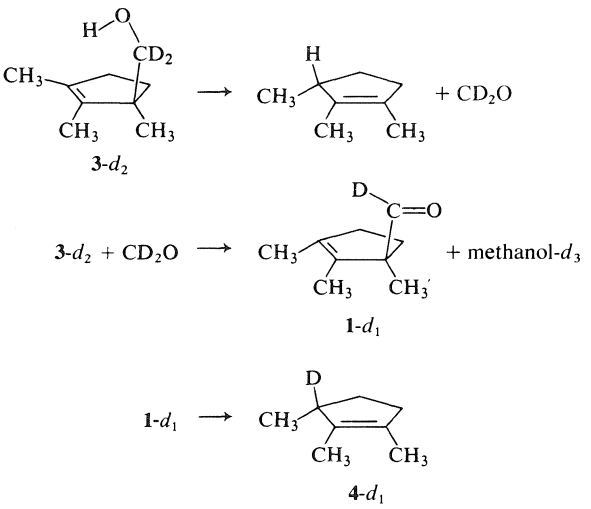
FIG. 1. Product composition for the thermolysis of laurolenol at 297°C.

TABLE 1. Percentage **4**-d_1 produced by the thermolysis of **3**-d_2 in the presence of formaldehyde, methanol, and carbon monoxide. Analysis by mass spectrometry

Conditions	Pressure (atm)*	(RD/RH + RD)100 at 25% conversion	75% conversion	90% conversion
3-d_2	3.2	3.4	11.4	26.5
	1.5	1.4	6.2	21.2
3-d_2 + CH_2O(11-fold)	3.2	13	40	51
3-d_2 + CH_3OH + (11-fold)	3.2	1.3	4.2	7.1

*Calculated pressure of **4**-d_2 at 297°C.

The presence of methanol suppresses the amount of deuterium incorporated, suggesting that the oxidation of **3**-d_2 by formaldehyde is reversible.



Conclusions

The thermolyses of **1**, **2**, and **3** all occur by the transfer of a hydrogen across the face of the cyclopentenyl ring to give **4** in high optical purity. The thermolysis of **2** is slightly faster than that of **1** and the thermolysis of **3** is complicated in that the formaldehyde produced acts as an oxidizing agent to convert some **3** into **1**, but this does not perturb the stereochemistry of the product.

Experimental

All boiling points are uncorrected. Samples were first purified by preparative gc using a Nester Faust model 350 "Prepkromatic". The rotations were measured on a Perkin Elmer Model 121 polarimeter. Mass spectral data were obtained on a Vickers MS-2 and an AEI-MS-50. The ^{1}Hmr spectra were obtained using a Varian A-56/60 spectrometer. The kinetic procedures were the same as those reported previously (1).

(R)-(+)-Laurolenic Acid (2)

The procedure used was essentially that of Meyer *et al.* (4)

starting from (−) α-bromocamphoric anhydride (5), $[\alpha]_{589}^{25}$ +172°, $[\alpha]_{365}^{25}$ +733° (*c* 2.70, $CHCl_3$) (lit. (6) $[\alpha]_D^{23}$ +155° (*c* 2.20, $CHCl_3$)).

(R)-(+)-Laurolenol (3)

The procedure used was that of Baggiolini *et al.* (6) and the sample was purified by gc using a 20 ft SF-96 column at 120°C; $[\alpha]_{589}^{25}$ +15.5°, $[\alpha]_{365}^{25}$ +52.7° (*c* 3.01, $CHCl_3$) (lit. (6) $[\alpha]_D^{23}$ +16° (*c* 3.2, $CHCl_3$)).

(R)-(+)-Laurolenol-d_2 *(3-*d_2*)*

The deuterated alcohol was prepared by reducing the acid **2** with $LiAlD_4$ by the aforementioned procedure (6). Mass spectrum $d_2 > 99\%$.

(R)-(+)-Laurolenal (1)

The procedure of Doering *et al.* (7) involving the use of sulfur trioxide – pyridine complex in dimethyl sulfoxide was used to oxidize the alcohol to the corresponding aldehyde. The aldehyde was purified by preparative gc using a 20 ft SF96 column at 120°C; $[\alpha]_{589}^{25}$ +630°, $[\alpha]_{365}^{25}$ +4960° (*c* 1.57, $CHCl_3$) (lit. (6) $[\alpha]_D^{23}$ +624° (*c* 1.5, $CHCl_3$)).

Acknowledgements

The authors wish to thank the Natural Sciences and Engineering Research Council of Canada for a grant in aid, and Dr. A. M. Hogg for the mass spectrometric analysis.

1. R. J. Crawford, S. Lutenar, and H. Tokunaga. Can. J. Chem. **55**, 3951 (1977).
2. D. B. Bigley and R. W. May. J. Chem. Soc. B, 557 (1967); G. G. Smith and S. E. Blau. J. Phys. Chem. **68**, 1231 (1964).
3. G. G. Smith and B. L. Yates. J. Chem. Soc. 7242 (1965).
4. W. L. Meyer, A. P. Lobo, and E. J. Marquis. J. Org. Chem. **30**, 181 (1965).
5. O. Aschan. Ber. **27**, 2112 (1894); **27**, 3504 (1894); Ann. **290**, 185 (1896).
6. E. Baggiolini, H. P. Hamlow, and K. Schäffner. J. Am. Chem. Soc. **92**, 4906 (1970).
7. J. R. Parikh and W. v. E. Doering. J. Am. Chem. Soc. **89**, 5505 (1967).

Can. J. Chem. Downloaded from www.nrcresearchpress.com by 210.87.254.40 on 09/05/12
For personal use only.

Etude par rmn du proton et du carbone-13 de pyrimidines substituées. IV.[1] Empêchement de rotation dans des *N*,*N*-diméthylamino-4 pyrimidines à l'état monoprotoné

JACQUES RIAND,[2] MARIE-THÉRÈSE CHENON ET NICOLE LUMBROSO-BADER

Université Paris VI, Laboratoire de Spectrochimie, Centre National de la Recherche Scientifique, 2, rue Henri Dunant, 94320 Thiais, France

Reçu le 6 septembre 1979

JACQUES RIAND, MARIE-THÉRÈSE CHENON et NICOLE LUMBROSO-BADER. Can. J. Chem. **58**, 466 (1980).

L'enthalpie libre d'activation pour le processus de rotation autour de la liaison C—N exocyclique dans divers chlorures de *N*,*N*-diméthylaminopyrimidinium a été déterminée par analyse de la forme des bandes observées en rmn du proton et du carbone-13.

La monoprotonation des *N*,*N*-diméthylaminopyrimidines entraîne une augmentation importante (de 14 à 24 kJ mol^{-1}) de l'enthalpie libre d'activation relative au groupe diméthylamino. Du fait de la prédominance de la forme monoprotonée (N-1 H) cet accroissement est plus grand quand le groupement diméthylamino est en position 4 que lorsqu'il est en position 2. Il en résulte que la différence de conjugaison des groupes diméthylamino en position 4 et 2 avec le cycle pyrimidique se trouve accentuée par la monoprotonation de ces composés.

JACQUES RIAND, MARIE-THÉRÈSE CHENON, and NICOLE LUMBROSO-BADER. Can. J. Chem. **58**, 466 (1980).

The free energy of activation for hindered rotation about the C—N exocyclic bond in some *N*,*N*-dimethylaminopyrimidine hydrochlorides has been determined by ^1H and ^{13}C nmr line-shape analysis.

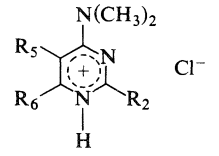
Monoprotonation of *N*,*N*-dimethylaminopyrimidines induces a large increase of the free energy of activation (from 14 to 24 kJ mol^{-1}). This increase is larger for the 4-dimethylamino group than for the 2-dimethylamino group due to the predominance of the monoprotonated (N-1 H) form. Consequently, the difference of conjugation of the 4- and 2-dimethylamino groups with the pyrimidine ring is more pronounced in the monoprotonated species.

Introduction

Dans un précédent travail nous avions étudié par rmn le problème de la conjugaison du groupement diméthylamino avec le cycle pyrimidique dans une série de *N*,*N*-diméthylamino-4 pyrimidines (1). Nous avons poursuivi ce travail en examinant de façon quantitative l'influence de la protonation sur la conjugaison dans ces mêmes molécules. Cette étude devait permettre en outre une comparaison intéressante avec les résultats de calculs théoriques déjà effectués sur des composés voisins (2, 3).

Les enthalpies libres d'activation $\Delta G^{\neq}$ des groupes diméthylamino dans les processus de rotation empêchée autour de la liaison C—N exocyclique ont été déterminées par rmn du proton et du carbone-13.

Les composés étudiés sont le chlorure de *N*,*N*-diméthylaminopyrimidinium **1** et quelques uns de ses dérivés chlorés **2** et **4**, méthylé **3** et diméthylaminé **5**.



1 $R_2 = R_5 = R_6 = H$
2 $R_2 = Cl, R_5 = R_6 = H$
3 $R_2 = R_6 = CH_3, R_5 = H$
4 $R_2 = Cl, R_5 = CH_3, R_6 = H$
5 $R_2 = N(CH_3)_2, R_5 = R_6 = H$

Résultats

La méthode de détermination des paramètres thermodynamiques d'activation a déjà été décrite dans une précédente publication (1). L'analyse complète par forme de bande a été faite en rmn du carbone-13 pour les composés **1** à **5**. Elle permet d'obtenir les paramètres thermodynamiques $\Delta H^{\neq}$, $\Delta S^{\neq}$ et $\Delta G^{\neq}$ relatifs au processus de rotation. A titre de confirmation, l'enthalpie libre d'activation $\Delta G^{\neq}$ a été déterminée à la température de coalescence, pour l'ensemble des composés, en rmn du proton. Dans ce cas la constante de vitesse k_c a été calculée à l'aide de la relation (4) $k_c = \pi\Delta\nu_\infty/\sqrt{2}$ et l'équation d'Eyring (5) permet alors de déterminer $\Delta G^{\neq}$.

En ce qui concerne le choix du solvant, le méthanol ayant été utilisé pour les pyrimidines à l'état neutre (1), nous avons repris ce même solvant pour faciliter les comparaisons. Il était toutefois fondamental de vérifier que celui-ci n'entraînait pas de déprotonation des sels étudiés. Or le méthanol étant un peu plus acide que l'eau (6), les pK_a dans ce solvant sont voisins ou légèrement supérieurs à ceux obtenus dans l'eau. Ainsi la méthyl-4 pyridine a un pK_a de 6.02 ± 0.02 dans l'eau et de 6.09 ± 0.01 dans le méthanol (7). En ce qui concerne la *N*,*N*-diméthylamino-4 pyrimidine, **1**, son pK_a dans l'eau étant de 6.35 (8), on a calculé qu'aucune déprotonation n'intervient dans l'eau et

[1]Pour la partie III, voir réf. 1.

[2]Auteur à qui toute correspondance doit être adressée.

0008-4042/80/050466-06$01.00/0

©1980 National Research Council of Canada/Conseil national de recherches du Canada

Can. J. Chem. Downloaded from www.nrcresearchpress.com by 210.87.254.6 on 09/05/12
For personal use only.

Can. J. Chem. Downloaded from www.nrcresearchpress.com by 210.87.254.6 on 09/05/12
For personal use only.

donc *a fortiori* dans le méthanol. Il en est de même pour les dérivés **3** et **5**, la substitution du noyau pyrimidique par un groupement méthyle ou diméthylamino ayant pour effet d'augmenter le pK_a. Le seul problème est relatif aux molécules substituées en position 2 par un chlore, c'est-à-dire les pyrimidines **2** et **4**. Ce substituant a pour effet de diminuer notablement leur basicité en raison de son caractère électroattracteur; ainsi la chloro-2 *N*-méthylamino-4 pyrimidine a un pK_a de 2.83 (9). Un groupe méthyle sur l'atome d'azote exocyclique a par contre pour effet d'augmenter la basicité de la pyrimidine; la différence de pK_a entre la *N*,*N*-diméthylamino-4 pyrimidine et l'amino-4 pyrimidine est en effet de 0.64 (8, 10). Le pK_a dans l'eau de la chloro-2 *N*,*N*-diméthylamino-4 pyrimidine peut, dans ces conditions, être évalué à environ 3.15. Il sera un peu plus élevé pour la chloro-2 *N*,*N*-diméthylamino-4 méthyl-5 pyrimidine du fait de la présence du groupe méthyle en position 5. En conséquence la déprotonation que pourrait éventuellement subir les chlorures **2** et **4** dans le méthanol n'excéderait pas 3.5%; elle peut être considérée comme négligeable.

Nous avons néanmoins tenu à corroborer les valeurs des enthalpies libres d'activation obtenues dans le méthanol avec celles obtenues dans un autre solvant. Nous avons choisi l'alcool benzylique dont l'acidité est sensiblement la même que celle du méthanol (11). Or il a été montré que, pour des solvants d'acidité voisine, le pK_a d'un soluté donné serait inversement proportionnel à la constante diélectrique du solvant (12, 13). Dans l'alcool benzylique ($\varepsilon = 13.1$) la déprotonation des chlorures étudiés serait donc encore plus faible que dans le méthanol ($\varepsilon = 32.6$).

Les paramètres thermodynamiques d'activation et certaines données relatifs à la rotation empêchée autour de la liaison C—N exocyclique dans les pyrimidines protonées sont donnés dans le tableau 1.

Les diagrammes d'Eyring $\log_{10} k/T$ en fonction de $1/T$ pour les pyrimidines **1** à **5** sont donnés sur la fig. 1.

Discussion

Nous discuterons nos résultats en considérant les valeurs de $\Delta G^{\neq}$ de préférence à celles de $\Delta H^{\neq}$, compte tenu de la meilleure précision obtenue sur la détermination de $\Delta G^{\neq}$ (14) et du fait que l'entropie d'activation $\Delta S^{\neq}$ doit être voisine de zéro dans les processus de rotation.

Effets de solvant

Bien que des travaux antérieurs aient montré une augmentation de la valeur de l'enthalpie libre d'activation $\Delta G^{\neq}$ avec la constante diélectrique du solvant (15, 16), nous avons observé ici un effet contraire en comparant les résultats obtenus dans le méthanol ($\varepsilon = 32.6$) et dans l'alcool benzylique ($\varepsilon = 13.1$). Or il ne peut s'agir d'une déprotonation des sels dans ces solvants, l'écart entre les valeurs de $\Delta G^{\neq}$ déterminées dans le méthanol et l'alcool benzylique étant le même (1.5 kJ mol^{-1}) pour les pyrimidines **1** et **2**, de pK_a très différents (voir plus haut).

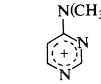
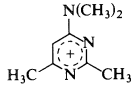
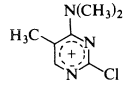
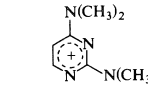
L'augmentation (de 1.5 à 3.3 kJ mol^{-1}) de l'enthalpie libre d'activation déterminée dans l'alcool benzylique pourrait alors s'interpréter par l'existence d'interactions spécifiques entre le noyau pyrimidique et le solvant benzénique. Des interactions de ce type ont d'ailleurs déjà été mises en évidence pour de tels systèmes (17). La proximité des deux noyaux aromatiques entraînerait une gêne stérique pour le processus de rotation, ce qui conduirait à une élévation de la hauteur de la barrière de rotation. Pour confirmer cette hypothèse, nous avons étudié le chlorure de pyrimidinium **3** dans l'alcool butylique; le pK_a de la pyrimidine correspondante est suffisamment élevé pour qu'aucune déprotonation ne puisse intervenir. Aucun effet de solvant n'a été observé sur les valeurs des $\Delta G^{\neq}$ obtenues dans les deux solvants non aromatiques, alcool butylique ($\varepsilon = 17.1$) et méthanol ($\varepsilon = 32.6$). Aucune variation notable des valeurs de $\Delta G^{\neq}$ n'avait d'ailleurs été observée dans le cas des pyrimidines à l'état neutre (1) étudiées dans des solvants non aromatiques.

Effets de substituant

En ce qui concerne l'influence de la nature des substituants en position 2 sur la barrière de rotation du groupe diméthylamino en position 4, on ne retrouve pas une augmentation des valeurs de $\Delta G^{\neq}$ avec le caractère électroattracteur de ces substituants comme nous l'avions observé sur les molécules neutres. Une corrélation du même type avait cependant été obtenue pour des sels de *N*,*N*-diméthylaminopyrylium (18). Dans le cas des chlorures de pyrimidinium, la présence d'un proton très acide peut favoriser des interactions de type liaison hydrogène avec le milieu, interactions dont l'importance pourrait être liée non seulement à l'acidité du chlorure considéré mais encore à l'encombrement des substituants en position 2. Compte tenu de la gamme relativement restreinte des valeurs de $\Delta G^{\neq}$, ces phénomènes secondaires pourraient justifier l'absence de corrélation entre les enthalpies libres d'activation et les pouvoirs

Can. J. Chem. Downloaded from www.nrcresearchpress.com by 210.87.254.6 on 09/05/12
For personal use only.

TABLEAU 1. Paramètres thermodynamiques[a] relatifs à l'empêchement de rotation du groupe diméthylamino dans les chlorures de *N*,*N*-diméthylaminopyrimidinium

Composé	Solvant	Noyau	MHz	ΔT^b (K)	$\Delta\nu_\infty(T_c)^c$ (Hz)	T_c (K)	$\Delta H^\ddagger$ (kJ mol^{-1})	$\Delta S^\ddagger$ (J mol^{-1} K^{-1})	$\Delta G^\ddagger(T_c)^d$ (kJ mol^{-1})
 1	CD_3OD	^{13}C	20	287.6–332.2	13.2	317.2 ± 0.5	62 ± 1	−21 ± 4	69.0
		^{1}H	100		8.2	308.9 ± 0.5			68.1
	$C_6H_5CH_2OH$	^{13}C	20		9.7	317.2 ± 0.5			70.2
		^{1}H	100		28.0	330.8 ± 0.5			70.0
 2	CD_3OD	^{13}C	20	306.5–334.7	12.4	327.8 ± 0.5	69 ± 4	−8 ± 12	72.3
		^{1}H	100		6.4	323 ± 0.5			71.9
	$C_6H_5CH_2OH$	^{1}H	100		12.7	338 ± 0.5			73.6
	CD_3OD	^{1}H	100		11.0	335 ± 1			73.2
 3	$C_6H_5CH_2OH$	^{13}C	20	332.2–357.7	13.1	337 ± 1	70 ± 4	−13 ± 16	74.4
		^{1}H	100		22.5	356.5 ± 0.5			76.1
	$CH_3(CH_2)_3OH$	^{1}H	100		8.5	329.6 ± 0.5			72.7
 4	CD_3OD	^{13}C	20	193.2–220.2	18.4	204.2 ± 0.5	37 ± 1	−21 ± 4	41.8
 5	CD_3OD	^{13}C	20	293 –335.5	14.0	338 ± 1	72 ± 1	−5 ± 4	73.6[e]
				251 –308	7.3	260 ± 1	57 ± 1	−2 ± 4	57.7[f]
	$C_6H_5CH_2OH$	^{13}C	20		12.8	348 ± 1			76.5[e]
		^{1}H	100		11.3	353 ± 0.5			77.3[e]

[a]Les erreurs indiquées sont les erreurs standard déterminées à partir du graphe d'Eyring.
[b]Gamme de température considérée pour la détermination des paramètres d'activation.
[c]Difference de déplacements chimiques entre les deux groupes méthyles à la température de coalescence, extrapolée à partir des résultats obtenus en l'absence d'échange.
[d]Enthalpie libre d'activation à la température de coalescence.
[e]Paramètres relatifs au groupement diméthylamino en position 4.
[f]Paramètres relatifs au groupement diméthylamino en position 2.

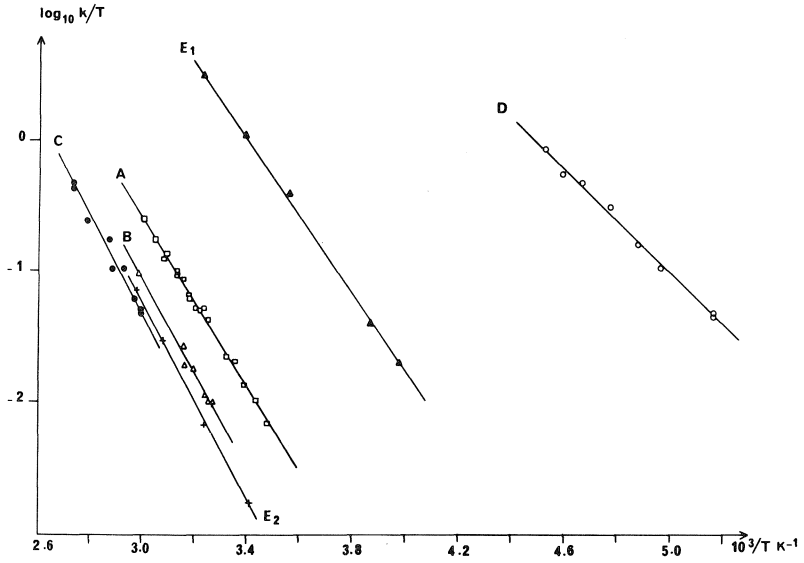


FIG. 1. Diagrammes d'Eyring relatifs à la rotation empêchée du groupement diméthylamino dans les chlorures de *N*,*N*-diméthylaminopyrimidinium (^{13}C rmn): (A) pyrimidine **1** en solution dans CD_3OD (R = 0.998) (R est le coefficient de corrélation); (B) pyrimidine **2** en solution dans CD_3OD (R = 0.990); (C) pyrimidine **3** en solution dans $C_6H_5CH_2OH$ (R = 0.985); (D) pyrimidine **4** en solution dans CD_3OD (R = 0.997); (E) pyrimidine **5** en solution dans CD_3OD (1) diméthylamino en position 2 (R = 0.9994) (2) diméthylamino en position 4 (R = 0.9996).

électroattracteurs des substituants considérés. Par contre, la corrélation entre ces pouvoirs électroattracteurs et les constantes de couplage $^1J(NMe_2\text{-}4)$ relatives au groupement diméthylamino en position 4 subsiste pour les molécules protonées.

La comparaison des résultats obtenus sur les composés **2** et **4** montre que l'introduction d'un groupement méthyle en position 5 abaisse, par effet stérique, la barrière de rotation d'environ 30 kJ mol^{-1}. Un résultat analogue avait été obtenu sur les mêmes molécules à l'état neutre (1).

Influence de la monoprotonation

Nos résultats montrent que la monoprotonation des *N*,*N*-diméthylaminopyrimidines entraîne une augmentation importante $\Delta(\Delta G^{\neq})$ de l'enthalpie libre d'activation relative à la rotation empêchée du groupe diméthylamino (voir tableau 2).

Cet accroissement de $\Delta G^{\neq}$ peut s'expliquer par la prédominance, parmi les formes de résonance, des structures limites quinoïdes favorisées par l'augmentation de la charge positive de l'atome d'azote exocyclique dans le cas des cations.

Des calculs sur l'amino-4 pyridine ont en effet montré que la contribution de telles formes limites est plus importante à l'état monoprotoné qu'à l'état neutre (3). Par ailleurs des travaux théoriques portant sur l'amino-4 diméthyl-2,5 pyrimidine (19) et sur des *N*,*N*-diméthylaminopyridines (2) indiquent une augmentation de l'indice de liaison pour la liaison C—N exocyclique lors de la protonation, augmentation en bon accord avec les résultats de notre étude.

Ces travaux théoriques prévoient également que l'accroissement de cet indice de liaison est plus

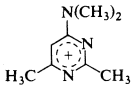
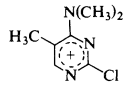
TABLEAU 2. Enthalpies libres d'activation relatives à l'empêchement de rotation du groupe diméthylamino dans les *N*,*N*-diméthylaminopyrimidines à l'état neutre[a] et à l'état monoprotoné

Composé		Solvant	$\Delta G^{\neq}(T_c)$[b] kJ mol^{-1}	$\Delta(\Delta G^{\neq})$ kJ mol^{-1}
1	N[c]	CD_3OD	53.7	15
	P[c]	CD_3OD	68.5	
2	N	CD_3OD	58.6	13.5
	P	CD_3OD	72.1	
3	N	CD_3OD	51.4	22
	P	CD_3OD	73.2	
4	N	$CDCl_3$–CH_2Cl_2 (2:1)	< 32	> 10
	P	CD_3OD	41.8	
5	N	CD_3OD	49.4[d] 43.5[e]	24[d] 14[e]
	P	CD_3OD	73.6[d] 57.7[e]	

[a]Voir réf. 1. Dans le cas de la pyrimidine **5**, les valeurs déterminées à la température de coalescence (cf. réf. 1) ont été confirmées par une analyse de forme de bandes (voir partie expérimentale).
[b]$\Delta G^{\neq}$ à la température de coalescence.
[c]N et P: composé à l'état neutre et à l'état monoprotoné respectivement.
[d]Paramètre relatif au groupement diméthylamino en position 4.
[e]Paramètre relatif au groupement diméthylamino en position 2.

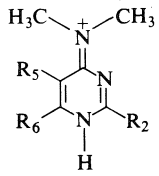
Can. J. Chem. Downloaded from www.nrcresearchpress.com by 210.87.254.6 on 09/05/12
For personal use only.

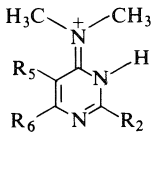
TABLEAU 3. Données expérimentales relatives aux chlorures de *N,N*-diméthylaminopyrimidinium

Composé	Solvant	Concentration mol L^{-1}	Rmn du carbone-13[a]	Rmn du proton[a]
 1	CD_3OD	0.55	$\Delta\nu_\infty = 13.70 - 0.011\,t$ $\Delta W_{diox}^{N(CH_3)_2} = 0.36 - 0.001\,t$	$\Delta\nu_\infty = 8.22 - 0.0005\,t$
	$C_6H_5CH_2OH$	0.28	$\Delta\nu_\infty = 11.10 - 0.031\,t$ $\Delta W_{diox}^{N(CH_3)_2} = 0.17\ (t = 7°C)^b$	$\Delta\nu_\infty = 2.80\ (t = 35°C)^c$
 2	CD_3OD	0.62	$\Delta\nu_\infty = 12.99 - 0.011\,t$ $\Delta W_{diox}^{N(CH_3)_2} = 0.30 - 0.006\,t$	$\Delta\nu_\infty = 6.51 - 0.004\,t$
	$C_6H_5CH_2OH$	0.6	—	$\Delta\nu_\infty = 11.55 + 0.023\,t$
 3	CD_3OD	0.44	$\Delta\nu_\infty = 14.90 - 0.018\,t$	$\Delta\nu_\infty = 11.0\ (t = 35°C)^b$
	$C_6H_5CH_2OH$	0.70	$\Delta\nu_\infty = 13.86 - 0.012\,t$ $\Delta W_{diox}^{N(CH_3)_2} = 0.58 - 0.003\,t$	$\Delta\nu_\infty = 22.5\ (t = 35°C)^b$
 4	CD_3OD	0.57	$\Delta\nu_\infty = 16.20 - 0.032\,t$ $\Delta W_{diox}^{N(CH_3)_2} = 0.27 - 0.013\,t$	—
 5	CD_3OD	1.7	$\Delta\nu_\infty(2) = 6.68 - 0.046\,t$ $\Delta\nu_\infty(4) = 16.04 - 0.031\,t$ $\Delta W_{diox}^{N(CH_3)_2(4)} = 0.5\ (t = 7 \text{ et } 20°C)^b$	—
	$C_6H_5CH_2OH$	1.0	$\Delta\nu_\infty(4) = 15.00 - 0.03\,t$ $\Delta W_{diox}^{N(CH_3)_2(4)} = 1.7 - 0.02\,t$	$\Delta\nu_\infty(4) = 7.55 + 0.065\,t$

[a]Les valeurs de $\Delta\nu_\infty$ et ΔW sont données en Hz et les températures en degré Celsius. Les chiffres entre parenthèses indiquent la position des groupements diméthylamino dans le composé **5**.
[b]Les valeurs de ΔW et $\Delta\nu_\infty$ déterminées aux températures indiquées ont été considérées constantes dans la gamme de température étudiée.

important lorsque le proton se fixe sur l'atome d'azote en *para* du groupement diméthylamino (2, 19). Or, notre étude de la monoprotonation des


Forme (N-1 H)


Forme (N-3 H)

amino-4 pyrimidines (20, 21) a montré que la forme prédominante est bien la forme (N-1 H). Dans ces conditions, on s'attend, pour ces composés, à un effet de la protonation sur la valeur de $\Delta G^{\neq}$ supérieur à celui observé lors de la protonation de l'adénine, par exemple, pour laquelle le site préférentiel de protonation est l'atome d'azote en *ortho* du groupe amino (22). C'est bien ce qui est observé, si l'on compare la valeur $\Delta(\Delta G^{\neq})$ pour la *N,N*-diméthylamino-4 pyrimidine (15 kJ mol^{-1}) à la valeur obtenue pour la *N,N*-diméthyladénine (9.7 kJ mol^{-1}) (23, 24). De même dans le cas de la bis *N,N*-diméthylamino-2,4 pyrimidine, l'augmentation de $\Delta G^{\neq}$ est de 24 kJ mol^{-1} pour le groupement diméthylamino en position 4 alors qu'elle n'est que de 14 kJ mol^{-1} lorsque ce groupement est en position 2 (cf. tableau 2). La différence entre les valeurs de $\Delta G^{\neq}$ pour ces deux groupements en position 4 et 2 est de 5.9 kJ mol^{-1} pour la molécule neutre alors qu'elle est de 15.9 kJ mol^{-1} pour la molécule protonée. La différence de conjugaison des groupes diméthylamino en position 4 et 2 avec le cycle pyrimidique se trouve donc accentuée par la monoprotonation du composé.

Conclusion

Cette étude a permis de montrer que la monoprotonation des *N,N*-diméthylaminopyrimidines entraîne une augmentation importante de l'enthalpie libre d'activation du groupe diméthylamino. Du fait de la prédominance de la forme monoprotonée (N-1 H), cet accroissement de $\Delta G^{\neq}$ est plus grand quand le groupement diméthylamino est en position 4 que lorsqu'il se trouve en position 2. Ceci met en évidence le fait que la différence de conjugaison des groupes diméthylamino en position 4 et 2 avec le cycle pyrimidique se trouve accentuée par la monoprotonation de ces composés.

Partie expérimentale

Les chlorures de pyrimidinium **1** à **5** ont été préparés par action de HCl sur les pyrimidines correspondantes et purifiés par sublimation sous vide poussé.

Les spectres rmn du proton et du carbone-13 ont été réalisés sur les appareils et selon les conditions opératoires déjà décrits dans la précédente étude (1). Il a été nécessaire d'utiliser un thermomètre à mercure pour les mesures des températures dans les expériences en rmn du carbone-13. Le mercure subissant un échauffement lié à la haute fréquence, les mesures ont été effectuées sans découplage des protons, une correction de température due à l'utilisation du découpleur étant faite ensuite.

Can. J. Chem. Downloaded from www.nrcresearchpress.com by 210.87.254.6 on 09/05/12
For personal use only.

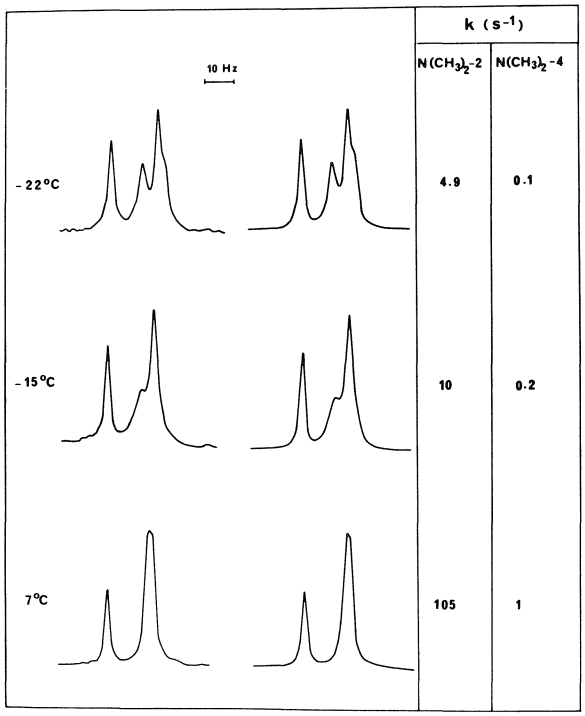


FIG. 2. Spectres rmn du carbone-13 relatifs aux groupements diméthylamino dans le chlorure de bis *N*,*N*-diméthylamino-2,4 pyrimidinium en solution dans CD_3OD. Spectres expérimentaux (à gauche) et simulés (à droite) à différentes températures.

Attribution des spectres rmn du carbone-13

Les déplacements chimiques des carbones et les constantes de couplage $J(^{13}C—^{1}H)$ ont été déterminés[3] pour les chlorures de *N*,*N*-diméthylaminopyrimidinium **1** à **5**. L'attribution des spectres résulte de la détermination de ces constantes de couplage et de l'application des différentes règles caractérisant ces constantes dans le noyau pyrimidique (25). Dans le cas du composé **5**, l'attribution des signaux relatifs aux deux groupements diméthylamino en position 2 et 4 a été établie sans équivoque. Elle résulte de l'attribution obtenue pour la molécule neutre (1) et de l'évolution des déplacements chimiques de ces groupes pour des mélanges de molécules neutre et monoprotonée en proportions variables.

Analyse de la forme des bandes

En absence d'échange, la largeur du signal relatif au groupe diméthylamino $W_{N(CH_3)_2}$ ainsi que la différence $\Delta\nu_\infty$ des déplacements chimiques entre les deux sites ont été déterminées par les mêmes méthodes que celles utilisées dans l'étude précédente (1). Les résultats concernant ce dernier paramètre $\Delta\nu_\infty$ ainsi que la différence ΔW entre les largeurs des raies relatives au groupe diméthylamino et à la référence utilisée (dioxanne) sont donnés dans le tableau 3 pour l'ensemble des produits étudiés par analyse de forme de bandes. Ces paramètres $\Delta\nu_\infty$ et ΔW varient peu avec la température mais il est cependant nécessaire de tenir compte de ces faibles variations dans le calcul pour affiner les résultats. On remarque que $\Delta\nu_\infty$ augmente en rmn du proton alors que ce paramètre diminue en rmn du carbone-13 quand le solvant utilisé est $C_6H_5CH_2OH$ au lieu de CD_3OD.

L'analyse totale par forme de bandes a été effectuée à l'aide du programme DNMR que nous avons modifié pour tenir compte du recouvrement des bandes relatives aux deux groupements diméthylamino en position 2 et 4 dans le cas du composé **5** à l'état neutre et à l'état monoprotoné (cf. fig. 2).

[3]Dépôt de données; on peut obtenir ces données supplementaires à un prix nominal en s'adressant au Dépôt de données non publiées, ICIST, Conseil national de recherches du Canada, Ottawa, Canada K1A 0S2.

1. J. RIAND, M. TH. CHENON et N. LUMBROSO-BADER. J. Chem. Soc. Perkin Trans. II, 1248 (1979).
2. G. BARBIERI, R. BENASSI, R. GRANDI, U. M. PAGNONI et F. TADDEI. J. Chem. Soc. Perkin Trans. II, 330 (1979).
3. C. U. PITTMAN, O. M. ATTALLAH et L. D. KISPERT. J. Chem. Soc. Perkin Trans. II, 1776 (1975).
4. H. S. GUTOWSKY et C. H. HOLM. J. Chem. Phys. **25**, 1228 (1956).
5. S. GLASSTONE, K. J. KLAIDER et H. EYRING. Theory of rate processes. McGraw-Hill, New York. 1941. p. 195.
6. C. MOREAU. Bull. Soc. Chim. Fr. 31 (1968).
7. C. D. RITCHIE et P. D. HEFFLEY. J. Am. Chem. Soc. **87**, 5402 (1965).
8. D. J. BROWN et L. N. SHORT. J. Chem. Soc. 331 (1953).
9. D. J. BROWN et N. N. JACOBSEN. J. Chem. Soc. 3172 (1962).
10. A. ALBERT, R. GOLDACRE et J. PHILLIPS. J. Chem. Soc. 2240 (1948).
11. J. HINE et M. HINE. J. Am. Chem. Soc. **74**, 5266 (1952).
12. R. P. BELL. The proton chemistry. Methuen, London. 1959. p. 51.
13. E. J. KING. *Dans* The international encyclopedia of physical chemistry and chemical physics. Vol. 4. *Edité par* R. A. Robinson. Pergamon Press, Oxford. 1965. p. 284.
14. C. PICCINNI-LEOPARDI, O. FABRE, D. ZIMMERMANN, J. REISSE, F. CORNEA et C. FULEA. Can. J. Chem. **55**, 2649 (1977).
15. R. C. NEUMAN et V. JONAS. J. Org. Chem. **39**, 929 (1974).
16. L. M. JACKMAN, T. E. KAVANAGH et R. C. HADDON. Org. Magn. Reson. **1**, 109 (1969).
17. W. W. PAUDLER et S. A. HUMPHREY. Org. Magn. Reson. **3**, 217 (1971).
18. M. TH. CHENON, S. SIB et M. SIMALTY. Org. Magn. Reson. **12**, 71 (1979).
19. J. FOURNIER, E. J. VINCENT, A. M. CHAUVET et A. CREVAT. Org. Magn. Reson. **5**, 573 (1973).
20. J. RIAND, M. TH. CHENON et N. LUMBROSO-BADER. J. Am. Chem. Soc. **99**, 6838 (1977).
21. J. RIAND, M. TH. CHENON et N. LUMBROSO-BADER. Sixième symposium international sur la résonance magnétique. Résumés. Banff, Alta., Canada. 1977. p. 190.
22. V. MARKOWSKI, G. R. SULLIVAN et J. D. ROBERTS. J. Am. Chem. Soc. **99**, 714 (1977).
23. T. P. PITNER et J. D. GLICKSON. Biochemistry, **14**, 3083 (1975).
24. T. P. PITNER, H. STERNGLANZ, C. E. BRUGG et J. D. GLICKSON. J. Am. Chem. Soc. **97**, 885 (1975).
25. J. RIAND et M. TH. CHENON. À paraitre.

Can. J. Chem. Downloaded from www.nrcresearchpress.com by 210.87.254.6 on 09/05/12
For personal use only.

A ^{13}Cmr study of 2′-deoxynucleotides in the *syn* and *anti* conformation

WALTER P. NIEMCZURA[1] AND FRANK E. HRUSKA

Department of Chemistry, University of Manitoba, Winnipeg, Man., Canada R3T 2N2

Received August 29, 1979

WALTER P. NIEMCZURA and FRANK E. HRUSKA. Can. J. Chem. **58**, 472 (1980).

The geminal and vicinal ^{13}C—^{31}P coupling constants for the 3′- and 5′-monophosphates and 3′,5′-diphosphates of thymidine and its isomer 6-methyl-2′-deoxyuridine have been obtained for aqueous solutions at various pH values. Since the thymine base is *anti* and the 6-methyluracil base is *syn*, the data provide information about the influence of the orientation about the *N*-glycosyl linkage on the conformation about the C(5′)—O(5′)(ϕ) and C(3′)—O(3′)(ϕ′) bonds. The ^3J(C4′—P5′) couplings reveal a preference for the t(ϕ) conformer of the 5′-nucleotidyl units, in agreement with previous measurements of ^{1}H—^{31}P coupling constants. The ^3J(C4′—P3′) and ^3J(C2′—P3′) couplings are consistent with a preference for the t(ϕ′) conformer for both the *syn* and *anti* 3′-nucleotidyl units. The response of these couplings to secondary ionization of the phosphate is different for the thymine and 6-methyluracil derivatives and suggests a phosphate–phosphate interaction for the *syn*, but not the *anti*, 3′,5′-diphosphates. A correlation between the sugar-pucker and the ϕ′ orientation is revealed. The ^2J(C5′—P5′) and ^2J(C3′—P3′) are relatively insensitive to the ionization state of the phosphate as well as to other structural features of the deoxyribose phosphate backbone.

WALTER P. NIEMCZURA et FRANK E. HRUSKA. Can. J. Chem. **58**, 472 (1980).

On a obtenu les constantes de couplage géminal et vicinal du ^{13}C et du ^{31}P des monophosphates 3′ et 5′ et des diphosphates-3′-5′ de la thymidine et de son isomère méthyl-6 déoxy-2′ uridine en solutions aqueuses et à différents pH. Puisque la base thymine est *anti* et la base méthyl-6 uracile est *syn* les données fournissent des informations au sujet de l'influence de l'orientation autour du lien *N*-glycosyle sur la conformation autour des liaisons C(5′)—O(5′) (ϕ) et C(3′)—O(3′) (ϕ′). Les couplages ^3J(C4′—P5′) révèlent une préférence pour le conformère t(ϕ) du nucléotidyle-5′ en accord avec les mesures antérieures des constantes de couplage ^{1}H—^{31}P. Les couplages ^3J(C4′—P3′) et ^3J(C2′—P3′) sont conformes avec une préférence pour le conformère t(ϕ′) dans le cas des deux nucléotidyles-3′ *syn* et *anti*. La reponse de ces couplages à une ionisation secondaire du phosphate est différente pour les dérivés de la thymine et de la méthyl-6 uracyle, et suggère une interaction phosphate–phosphate dans les dérivés *syn*. Cette interaction n'existe pas dans les diphosphates-3′,5′ *anti*. On révèle une corrélation entre la molécule fléchie de sucre et l'orientation ϕ′. Les couplages ^2J(C5′—P5′) et ^2J(C3′—P3′) sont relativement indépendants de l'état d'ionisation du phosphate et des autres particularités structurales du squelette de déoxyribose phosphate.

[Traduit par le journal]

Introduction

An important conformational feature of nucleosides is the sugar-base torsion angle (χ) which defines the relative orientation of the base and sugar moieties (Fig. 1). Useful model compounds for evaluating the consequences (1) of the presence of a *syn* pyrimidine base are nucleosides possessing a 6-methyl substituent since it is certain that molecules so substituted are *syn* (2–6).[2] It has been demonstrated that ^{13}C nmr can provide for nucleotides structural information complementary to that derived from ^{1}H nmr (7–11).[3] In this work we report our determination of the pH dependence of the ^{13}C—^{31}P coupling constants of the 3′-, 5′-, and 3′,5′-phosphate derivatives of dT and dT* in aqueous solution. The data provide information about the influence of *syn* and *anti* bases on the orientation about the C(5′)—O(5′)(ϕ) and C(3′)—O(3′)(ϕ′) bonds.

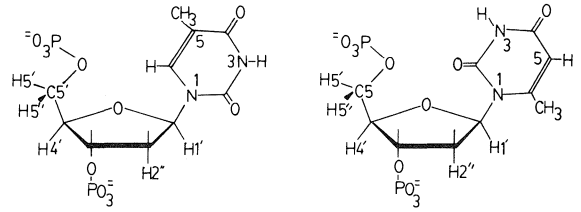


FIG. 1. Structural formulae of d(pTp) (left, *anti* conformation) and d(pT*p) (right, *syn* conformation), the 3′,5′-diphosphates of 2′-deoxythymidine (dT) and 6-methyl-2′-deoxyuridine (dT*).

Experimental

Materials

The dT, 3′dTMP, and 5′dTMP were purchased from the Sigma Chemical Co. The dT* was synthesized according to the Holy procedure (12). The 3′dT*MP and 5′dT*MP were prepared by direct phosphorylation of the appropriately blocked (5′-O-trityl or 3′-O-benzyl) derivative of dT*, according to published procedures (6). The 3′,5′-diphosphates were made by direct phosphorylation of unprotected dT and dT* using condi-

[1]Holder of a University of Manitoba Fellowship. This work represents for W. P. N. partial fulfillment of a doctoral degree.

[2]Dr. G. I. Birnbaum has informed us that crystalline dT* is *syn*.

[3]Abbreviations used: nmr, nuclear magnetic resonance. For convenience T and T* will represent the thymine (5-methyluracil) base and 6-methyluracil base, respectively; dT and dT*, the 2′-deoxynucleosides; 3′dTMP, 3′dT*MP, 5′dTMP, and 5′dT*MP, the 3′- or 5′-monophosphate derivatives; d(pTp) and d(pT*p), the 3′,5′-diphosphates. A, adenosine; U, uridine; 3′UMP etc., uridine-3′-monophosphate, etc.

0008-4042/80/050472-07$01.00/0

©1980 National Research Council of Canada/Conseil national de recherches du Canada

Can. J. Chem. Downloaded from www.nrcresearchpress.com by 210.87.254.6 on 09/05/12
For personal use only.

Can. J. Chem. Downloaded from www.nrcresearchpress.com by 210.87.254.6 on 09/05/12
For personal use only.

tions identical to those used to generate the monophosphates. Details of all syntheses may be found in the doctoral thesis of W. P. N.

Spectra

^{13}C spectra were obtained in the Fourier transform mode on a Bruker WH-90DS spectrometer (22.63 MHz), equipped with a Nicolet-1180 computer, the NTC-FT-1180 software package and quadrature phase detection. Spectral widths were typically 3800 Hz acquired into 16 K data points and zero-filled to 32 K. To apodize the free-induction decay (FID), exponential multiplication using a line broadening equal to the digital resolution (ca. 0.2 Hz) was applied. Normally spectra were recorded with complete proton noise decoupling, though some proton-coupled spectra were obtained to facilitate peak assignments.

All samples were examined in 10 mm outer diameter tubes, at concentrations of 80–100 mg/mL in D_2O, containing 1% dioxane as internal reference.[4] The probe temperature was regulated to 297 ± 1 K. Paramagnetic ions were removed by chromatography on Chelex-100 (Bio-Rad Laboratories) and treatment with dithizone (J. T. Baker Chemical Co.) in CCl_4, as suggested by Cozzone and Jardetzky (13). The 3′,5′-diphosphate solutions contained small amounts (~2 m*M*) of EDTA. The pH was adjusted by the addition of dilute NaOD or DCl and is given as the pH meter reading. (In Figs. 2, 4, and 5 (see below) 0.4 units should be added to this reading to correct for the deuterium isotope effect (14).)

Results and Discussion

Spectral Assignment

The assignment of the base and sugar carbon atoms was carried out by comparison of our ^{13}C spectra with published data (7–11, 15–18). The presence of splittings (1–8 Hz) attributable to ^{13}C—^{31}P couplings facilitated location of the C(2′), C(3′), and C(4′) atoms of the 3′-nucleotides and of the C(4′) and C(5′) atoms of the 5′-nucleotides. The influence of phosphorylation and phosphate ionization on the sugar carbon shifts also proved useful. Several proton-coupled spectra were also obtained for assigment purposes.

Geminal ^{13}C—^{31}P Coupling Constants

The following comments can be made about the geminal coupling constants, ^2J(C3′—P3′) and ^2J(C5′—P5′), of the 3′-, 5′-, and 3′,5′-phosphates of dT and dT* (see pH titration curves in Fig. 2). The magnitudes of ^2J(C3′—P3′) and ^2J(C5′—P5′) lie in the ranges 4.1–5.1 Hz and 4.2–5.3 Hz, respectively, and show little variation over the entire pH range. They are similar to the ^2J(C,P) couplings reported (9) as a function of pH, for 3′UMP, 3′AMP, 5′UMP, and 5′AMP (4.3–5.0 Hz). They are also similar to the ^2J(C,P) values of (*a*) the 2′-, 3′-, and 5′-AMP fragments of the ribodinucleoside monophosphates, 3′, 5′ApA, and 2′,5′ApA, (10), (*b*) the dTMP and dT*MP fragments of the 2′-deoxydinucleoside monophosphates d(TpT), d(T*pT), d(TpT*), and d(T*pT*),[5] and (*c*) the UMP fragments of the ribopolynucleotide, poly U (7). Thus, the ^2J(C,P) couplings appear to be relatively intensive to structural changes. It should be stressed, however, that certain modifications can lead to large changes in ^2J(C,P) couplings. Thus, in the strained 3′,5′-cyclic nucleotides ^2J(C5′—P5′) can be as large as 7.0 Hz (8, 19), reflecting perhaps changes in the P—O—C bond angle (20) and P—O torsion angle (20, 21).

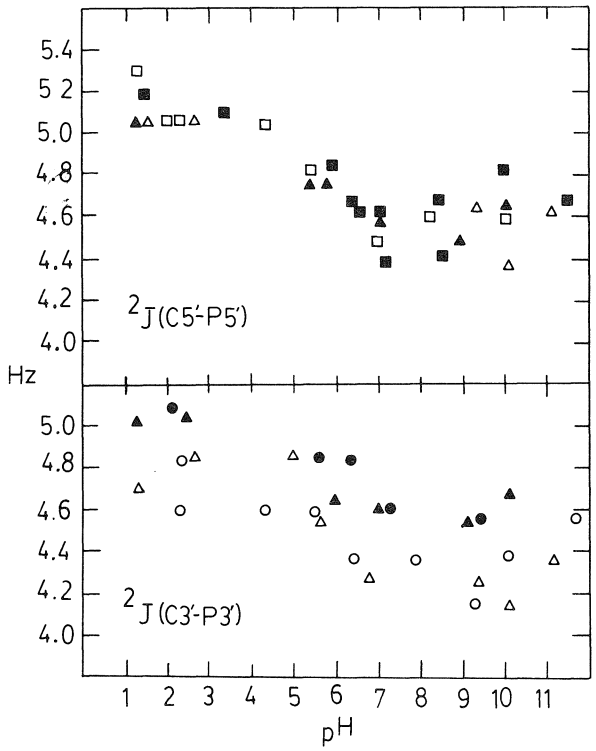


FIG. 2. Geminal ^2J(C3′—P3′) (*a*) and ^2J(C5′—P5′) (*b*) coupling constants in Hz versus pH of the solution (uncorrected for deuterium isotope effect). Solid symbols, T derivatives; open symbols, T* derivatives (see footnote 2). 3′dTMP (●), 3′dT*MP (○), 5′dTMP (■), 5′dT*MP (□), dpTp (▲), dpT*p (△).

Though the ^2J(C,P) couplings vary little, a weak, sigmoidal trend can be discerned in the pH titration curves (Fig. 2). For both couplings, decreases of a few tenths of a Hz occur for the T and T* derivatives in the pH range 5–7, due presumably to the phosphate ionization. The plots are in reasonable agreement with the pK_a values (~6.3) reported for secondary phosphate ionization of 3′- and 5′-nucleotides in the 2′-deoxyribose series (13, 22).

[4]No concentration dependence of the *J* values of 3′dT*MP was noted in the 30–100 mg/mL range.

[5]Unpublished data of the authors.

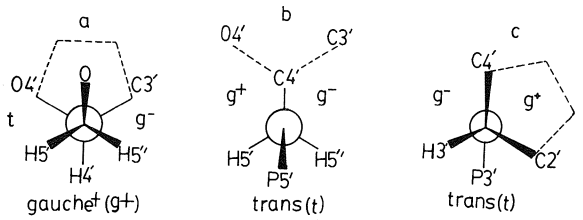


FIG. 3. Newman projections viewed along (*a*) C4′—C5′(ψ), (*b*) C5′—O5′(ϕ), and (*c*) C3′—O3′(ϕ′); g^+, t, and g^- refer respectively to the conformational domain containing the 60°, 180°, (−180°), and 300° (−60°) conformer defined according to ref. 24. (*a*) $g^+(\psi)$ conformer shown; t, g^- give location of O5′ in t(ψ) and $g^-(\psi)$ respectively. (*b*) t(ϕ) conformer shown; g^+, g^- give location of P5′ in $g^+(\phi)$ and $g^-(\phi)$ respectively. (*c*) t(ϕ′) conformer shown; g^+, g^- give location of P3′ in $g^+(\phi')$ and $g^-(\phi')$, respectively.

Conformation about the C(5′)—O(5′)(ϕ) Bond

The work of Mantsch and Smith on 5′-nucleotides (7) first showed that ^3J(C4′—P5′) coupling constants provide information about the ϕ bond orientation (Fig. 3). This vicinal coupling should, according to Govil and Smith (11), be large (~10 Hz) for the t(ϕ) conformer and small (~2 Hz) for the $g^+(\phi)$ and $g^-(\phi)$ conformers. Then, it is simple to derive:

$$[1] \quad n(t\phi) \approx [^3J(C4'—P5') - 2]/8$$

where $n(t\phi)$ is the fractional contribution from t(ϕ) to the conformer blend.[6]

The effect of pH on the vicinal ^3J(C4′—P5′) couplings of 5′dTMP, dpTp, 5′dT*MP, and d(pT*p) is shown in Fig. 4. The Alderfer–Ts'o data (9) for the ribose derivatives, 5′UMP and 5′AMP, are included. (Note that the ordinate of Fig. 4 is given in Hz and in %t(ϕ) obtained from eq. [1].) Overall, the ^3J(C,P) values span a range from 7.8–8.9 Hz. Weak sigmoidal behaviour can be discerned in the 5′dTMP data, with ^3J(C,P) at pH > 8, on the average, 0.3 Hz less than at pH < 6.0. (This behaviour cannot be discerned in the data for d(pTp), 5′UMP, and 5′AMP.) Similarly, the data for the T* derivatives define a sigmoidal curve, but here an increase of ~0.3 Hz is seen in ^3J(C,P) as the solution becomes basic. If the ionization of the phosphate exerted only a direct (through-bond) effect on ^3J(C,P), this difference in behaviour for the T and T* derivatives would not be expected. Therefore, it is reasonable to conclude that these variations in

[6]Also, $n(t\phi)$ has been related (6) to $\sum'(=^3J(H5'—P5') + ^3J(H5''—P5'))$ via $n(t\phi) \approx (25 - \sum')/20.8$ which provides an *independent* means of determining the population of t(ϕ) and the combined weighting of $g^+(\phi)$ and $g^-(\phi)$. This expression may be combined with eq. [1] to yield $^3J(C4'—P5') \approx 11.6 - 0.38\sum'$ which describes the expected correlation between the $^{13}C—^{31}P$ and $^1H—^{31}P$ coupling data. Similar, simple expressions have proven to be useful in correlating nmr data for nucleotides (23).

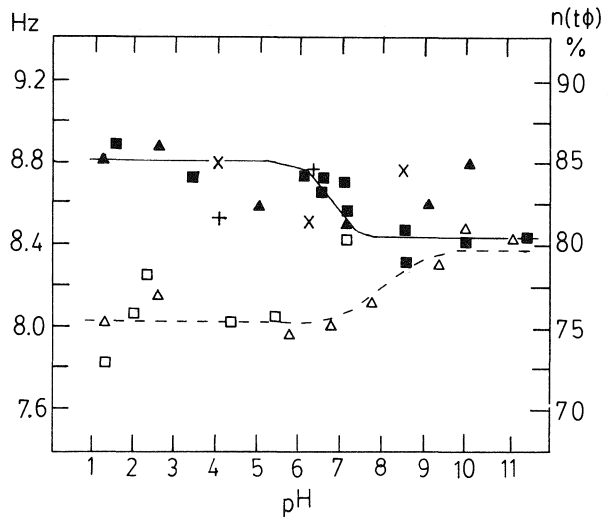


FIG. 4. Vicinal ^3J(C4′—P5′) coupling constants in Hz versus pH of the solution (uncorrected for deuterium isotope effect). Solid symbols, T derivatives; open symbols, T* derivatives. 5′dTMP (■), 5′dT*MP (□). dpTp (▲), dpT* (△), Alderfer–Ts'o data (9) for 5′UMP (×) and 5′AMP (+).

^3J(C,P), are in part due to the conformational effects.

In conformational terms, our ^3J(C,P) data (Fig. 4) are in general agreement with previous ^1H nmr and X-ray diffraction studies. Thus, a distinct preference for t(ϕ) is indicated, with $n(t\phi) > 71\%$ in all instances. In the crystal state all known 5′-nucleotidyl fragments are t(ϕ) (24). Furthermore, for 5′dTMP, d(pTp), 5′UMP, and 5′AMP, the ^3J(C4′—P5′) values are identical at all pH values to within 0.5 Hz, with $n(t\phi)$ in the range 78–87%. Thus, for this collection of molecules, neither the nature of the base (purine or pyrimidine) nor of the sugar (ribose or deoxyribose), nor the presence of a 3′-phosphate influences $n(t\phi)$, in agreement with the ^1H nmr work of Davies and Danyluk (25).

At acid pH the ^3J(C4′—P5′) values for the T* molecules are on the average 0.7 Hz smaller than those for the T derivatives. This apparent decrease in $n(t\phi)$ for the dT*MP and d(pT*p), relative to their T counterparts, is in line with previous findings, based on ^1H nmr (6), that *syn* pyrimidine bases lead to decreases in the population of the $g^+(\psi)$ conformer about the C(4′)—C(5′) bond, a consequence of which is a decrease in the t(ϕ) population for C(5′)—O(5′). This interdependence of the ϕ and ψ conformers has been discussed in detail (ref. 6 and references therein).

At basic pH, however, little difference is noted in the ^3J(C4′—P5′) values for the T and T* molecules. Apparently ionization of the phosphate has led to some ϕ bond changes in, particularly, the T* molecules.

Can. J. Chem. Downloaded from www.nrcresearchpress.com by 210.87.254.6 on 09/05/12
For personal use only.

ERRATA * and the t(φ') domain (centered at 180°)

Can. J. Chem. Downloaded from www.nrcresearchpress.com by 210.87.254.6 on 09/05/12
For personal use only.

Conformation about the C(3')—O(3') (φ') Bond

In principle three staggered conformers, $g^+(\phi')$, $t(\phi')$, and $g^-(\phi')$, are accessible to the C(3')—O(3') bond of a 3'-nucleotide (Fig. 3). However, steric considerations and energy calculations (26–28) have indicated that the $g^+(\phi')$ conformer can be excluded in any evaluation of the φ' conformer weightings. Thus, nmr spectroscopists have been led to interpreting their $^{13}C—^{31}P$ and $^1H—^{31}P$ coupling constant data in terms of a two-state $t(\phi') \rightleftarrows g^-)\phi')$ model (9, 25, 29, 30). However, because of a recent survey by Sundaralingam and co-workers[7] of the crystal structures of 3'-ribonucleotides, the appropriateness of the two-state model for interpretation of solution coupling data must itself remain open to question. They have found that, for these ribose derivatives (eight in total), the φ' values define a *single* broad range from −91.5° to −164.9°. This range comprises adjoining segments of the $g^-(\phi')$ domain (centered at −60°). In one instance, 3'AMP·2H_2O, φ' is −123°, which means that the H(3') and P(3') are but 3° from the eclipsed situation. Thus, it seems that this eclipsed conformer does not present a particularly large barrier to interconversion between $t(\phi')$ and $g^-(\phi')$. Energy calculations (31,32) also point to the absence of a major barrier to rotation about the C(3')—O(3') bond. Given these studies by Sundaralingam and co-workers, translation of nmr data into $t(\phi')$ and $g^-(\phi')$ populations in a two-state model may be unjustified since the coupling constants could equally well be a reflection of averaging within a single broad range of conformer angles approximating that observed in the crystal state.[8]

Because of this uncertainty, we shall interpret our coupling constants in a qualitative manner which does not imply a choice between a two-state or broad "single-state" model. We shall assume simply that the vicinal $^{13}C—^{31}P$ couplings in the C(2') or C(4')—C(3')—O(3')—P(3') fragments vary in a Karplus manner with the φ' torsion angle. Thus, ^3J(C2'—P3') and ^3J(C4'—P3') should be relatively large in the $g^-(\phi')$ and $t(\phi')$ *domains*, respectively, and relatively small in the $t(\phi')$ and $g^-(\phi')$ *domains* respectively (Fig. 3). If, in the future, evidence is provided for a two-state situation, then separate populations for $t(\phi')$ and $g^-(\phi')$ could be obtained quite simply from our data.

Figure 5 shows the pH dependence of the vicinal ^3J(C2'—P3') and ^3J(C4'—P3') couplings for 3'dTMP, d(pTp), 3'dT*MP, and d(pT*p); also included are the data for 3'UMP (indicated by ×) taken from Alderfer and Ts'o (9). For our 2'-deoxyribose derivatives, as well as for 3'UMP, the ^3J(C2'—P3') and ^3J(C4'—P3') couplings are confined to the ranges 0.5–3.9 Hz and 5.9–8.5 Hz, respectively. Thus, in all cases a preference is indicated for the $t(\phi')$ domain in which P(3') is *trans* to C(4') and *gauche* to C(2'). There are, however, some important differences in the trends for the T and T* molecules.

The ^3J(C2'—P3') couplings on the one hand and ^3J(C4'—P3') couplings on the other are similar for 3'dTMP and d(pTp) over the entire pH range. Thus, the presence of a 5'-phosphate, in either the monoanionic form (pH < 6.0) or dianionic form (pH

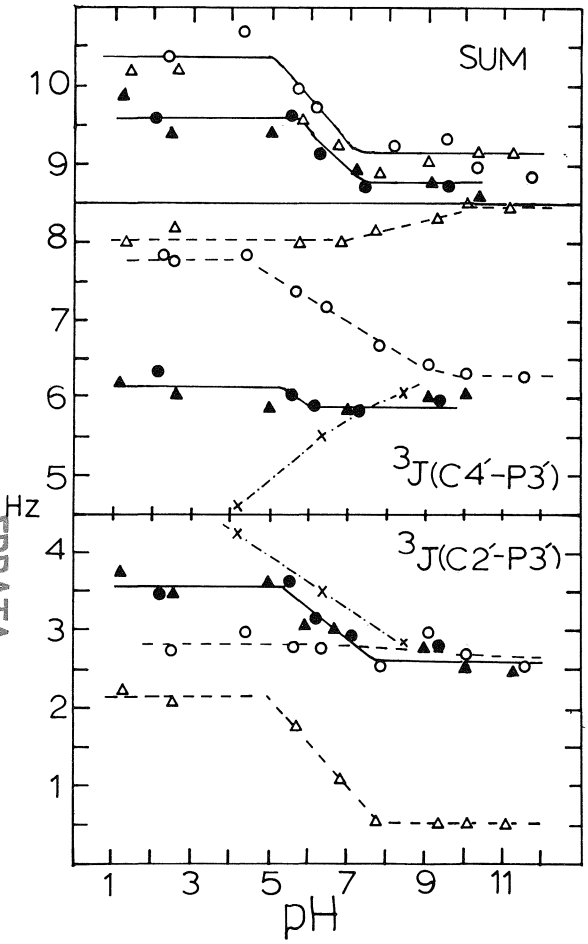


FIG. 5. Vicinal ^3J(C2'—P3') and ^3J(C4'—P3') coupling constants and the sum, ^3J(C2'—P3') + ^3J(C4'—P3'), for a 3'-nucleotidyl unit versus pH of the solution (uncorrected for the deuterium isotope effect). Solid symbols, T derivatives; open symbols, T* derivatives. 3'dTMP (●), 3'dT*MP (○), 5'dTMP(■), 5T*MP (□), d(pTp)(▲), d(pT*p) (△). 3'UMP (×) from Alderfer and Ts'o (9). The 0.5 Hz ^3J(C2'—P3') couplings for d(pT*p) in basic solution were estimated from the line width of the C(2') resonance since no splitting was observed.

[7]Private communication from M. Sundaralingam.

[8]More meaningful here would be a survey of crystal φ' data for 2'-*deoxy*-3'-nucleotides. Unfortunately, only the value for the internal C(3')—O(3') bond of d(pTpT) is available (33): φ' = −108°, 12° from the H(3')—P(3') eclipsed conformer.

FOR ERRATA SEE
V.58 #16 19..80 AUG ...P.1678

Can. J. Chem. Downloaded from www.nrcresearchpress.com by 210.87.254.6 on 09/05/12
For personal use only.

> 8.0), appears to have little influence on the preferred orientation of the ϕ' bond. The ^3J(C4′—P3′) couplings are to within experimental error invariant over the pH range, while the ^3J(C2′—P3′) couplings decrease by about 0.5 Hz in basic solution, reflecting presumably the secondary ionization of the 3′-phosphate. It would, however, be difficult to disentangle the contributions of the through-bond and the conformational effects of this ionization, but overall it seems that ϕ' for the T derivatives is not affected by the changes in charge on the 3′- and 5′-phosphates.

It is interesting to note that in *basic* solution the corresponding couplings of 3′UMP and 3′dTMP are identical. In acid solution, however, ^3J(C4′—P3′) in 3′UMP is about 1.5 Hz smaller than its counterpart in 3′dTMP. Thus, in basic solution the 2′-hydroxyl has no influence on the ϕ' orientation which is apparent in the ^{13}C, ^{31}P couplings. However, in acid solution, when the phosphate groups are monoanionic, the 2′-hydroxyl appears to destabilize slightly the t(ϕ') domain. The near equality of the ^3J(C2′—P3′) (4.2 Hz) and ^3J(C4′—P3′) (4.6 Hz) couplings of 3′UMP in acid solution would indicate a near balance in time spent in the t(ϕ') and g$^-$(ϕ') domains.

For 3′dT*MP and d(pT*p) at *acid* pH the ^3J(C4′—P3′) couplings are about 1.5–2.0 Hz larger than those for the T molecules. On the other hand, the ^3J(C2′—P3′) couplings are smaller for the T* molecules, by ~0.5 Hz for 3′dT*MP and by ~1.5 for d(pT*p). Thus, the t(ϕ') domain appears to be stabilized by the *syn* T* base, the effect being noticeably larger at the 3′,5′-diphosphate level. This apparent dependence of the ϕ' orientation upon the conformation about the *N*-glycosyl link (χ) cannot be due to a direct effect since the base and 3′-phosphate lie on opposite sides of the sugar ring. It is more likely that this dependence of ϕ' on χ is mediated by the changes in the sugar ring conformation elicted by the *syn* base (see below).

Some interesting changes (Fig. 5) are seen in the T* data as the solution enters the *basic* range in which the phosphates bear two negative charges. Thus, while ^3J(C4′—P3′) for 3′dT*MP shows a decrease from ~7.8 Hz to 6.3 Hz, ^3J(C2′—P3′) shows little dependence on pH. In basic solution the couplings of 3′dT*MP are to within experimental error identical to their counterparts in 3′dTMP. This indicates that the *syn* base does not have large effects on the ϕ' torsion angle distribution of a 3′-nucleotide in basic solution.

More dramatic pH effects are noted for the 3′,5′diphosphate of T*. Thus, in basic solution ^3J(C2′—P3′) decreases by 1.5 Hz to 0.5 Hz[9] while ^3J(C4′—P3′) increases by ~0.5 Hz to 8.5 Hz. For 3′dT*MP and d(pT*p), the magnitudes of the corresponding couplings diverge as the phosphates undergo secondary ionization. And, in basic solution large differences (2 Hz) are evident in the couplings for the pair of T* derivatives. (In acid solution these differences are much smaller, about 0.7 Hz for ^3J(C2′—P3′) and 0.2 Hz for ^3J(C4′—P3′).) These 2 Hz differences indicate that, for a T* unit, the 5′-phosphate influences the conformation about the C(3′)—O(3′) bond, particularly when the 3′- and 5′-phosphates bear two negative charges. This contrasts with the situation for 3′dTMP and d(pTp) where no difference in the corresponding couplings is noted at any pH, no 5′-phosphate influence thus being apparent. The magnitudes of the couplings for d(pT*p) in basic solution, 0.5 Hz for ^3J(C2′—P3′) and ~8.5 Hz for ^3J(C4′—P3′), indicate a very strong preference for the t(ϕ') conformer. The diminutive value of ^3J(C2′—P3′) suggests further a strong tendency towards a 90° Karplus angle between the C(2′)—C(3′) and O(3′)—P(3′) bonds. The Govil–Smith equation (11) for ^{13}C, ^{31}P couplings predicts a 0.5 Hz coupling for an 86° Karplus angle. This Karplus angle corresponds to a ϕ' value of −154° which falls near to the t(ϕ') extreme of the broad range defined by the ϕ' values of crystalline 3′-ribonucleotides (see above).

Also, given the diminutive value of ^3J(C2′—P3′) (0.5 Hz) in d(pT*p) in basic solution, we may consider the magnitude of ^3J(C4′—P3′) (8.5 Hz) as a lower-limit estimate for a *trans* (180° Karplus angle) ^3J(C,P) coupling for the C(4′)—C(3′)—O(3′)—P(3′) and C(2′)—C(3′)—O(3′)—P(3′) fragments in basic solution.

Requiring some explanation are (*a*) the apparent stabilization of the t(ϕ') conformer by the *syn* T* base and (*b*) the apparent influence of the 5′-phosphate on the ϕ' orientation in the T*, but not the T, derivatives, and the strong, if not overwhelming, preference for t(ϕ') in d(pT*p). The apparent dependence of the ϕ' orientation upon the conformation about the *N*-glycosyl linkage cannot be due to a direct interaction since the base and the 3′-phosphate lie on opposite sides of the sugar ring. The results of X-ray crystallographic and theoretical studies (discussed below) suggest that this dependence of ϕ' on χ is mediated by changes in the sugar ring pucker elicited by the change from the *anti* T base to the *syn* T* base. More explicitly, this

[9]The 0.5 Hz couplings were estimated from the C(2′) bandwidth (0.7 Hz). No splitting was detected.

Can. J. Chem. Downloaded from www.nrcresearchpress.com by 210.87.254.6 on 09/05/12
For personal use only.

ϕ', χ dependence is probably a further manifestation of a sugar pucker – ϕ' correlation apparent for the nucleotide units of yeast tRNA(phe) (34) and 3′-nucleotides in solution (35), and predicted by energy calculations (36). The correlation is such that $g^-(\phi')$ is likely only for 2′ *endo* sugars and is destabilized by the 3′ *endo* pucker. This suggested correlation is consistent with the crystalline structure of d(pTpT) (33) and the 3′-ribonucleotide structures surveyed by Sundaralingam and coworkers (see above).

The trends in the ^3J(C,P) data of the T and T* derivatives can, for the most part, be understood in terms of this pucker – ϕ' correlation. Thus, 2′-deoxyribosides are known to favor the 2′*endo* pucker in solution and in the crystal state (23,24). However, the presence of the *syn* T* base leads to a partial shift towards the 3′*endo* conformation (4, 6). (In addition, the *syn* base leads to a flattening [10] of the sugar ring in solution (6) as well as the crystal state.[11]) The general shift towards $t(\phi')$ for the T* derivatives is reasonable now if the $g^-(\phi')$ conformer is in fact unstable in a 3′ *endo* unit. Furthermore, the pronounced shift towards $t(\phi')$ in d(pT*p) upon secondary phosphate ionization suggests that the destabilization of the 3′ *endo* – $g^-(\phi')$ combination is, at least in part, due to an electrostatic repulsion between the 3′- and 5′-phosphates. This repulsion would be particularly severe when the C(4′)—C(5′) bond is $g^-(\psi)$ and less important for the $g^+(\psi)$ and $t(\psi)$ conformers (Fig. 3).

Clearly then, rotation into $t(\phi')$ seems to be a mechanism to reduce the repulsion of the negatively charged phosphates. Apparently, when the 3′- and 5′-phosphates bear two negative charges (pH > 8.0) a preponderance of $t(\phi')$ obtains. However, no phosphate–phosphate interactions are apparent in d(pTp) since the $^{13}C,^{31}P$ couplings are identical, at all pH values, to the corresponding couplings in 5′dTMP. This suggests that phosphate–phosphate interactions are important only in 3′ *endo* sugars.

The Sum $^3J(C4'—P3') + {}^3J(C2'—P3')$

A useful quantity to consider is the sum ^3J(C4′—P3′) + ^3J(C2′—P3′). These sums for the 3′-, 5′-, and 3′,5′-phosphates of dT and dT* are plotted versus pH in Fig. 5. The sums lie for the most part within the broad range from 8.3 Hz to 10.5 Hz. The data for the T and T* derivatives show a sigmoidal pH dependence, with the sums decreasing by ~1 Hz as the solution becomes basic. That the inflection points occur in the pH 6–7 range suggests a dependence upon the ionization state of the phosphates. In both the acid and basic range the T* sums are typically larger than those of the T derivatives by, on the average, 0.5 Hz. The sum values are smaller for the ribose derivatives 3′UMP (8.8–9.0 Hz) and 3′AMP (8.3–9.0 Hz) (9).

The sums in Fig. 5 may serve to caution proponents of a two-state model who estimate $t(\phi')$ and $g^-(\phi')$ conformer populations from ^3J(C,P) couplings. In a two-state model with interconversion between "fixed" $t(\phi')$ and $g^-(\phi')$ conformers the sum values are expected to be constant (9). However, it is clear from Fig. 5 that the structure changes in the sugar and the phosphate ionization state have led to a spread of about 20% in the sum values. This variation may be due in part to alterations in the angular characteristics of the "fixed" conformers and, in the case of phosphate ionization, to direct effects on the individual ^3J(C,P) coupling. Some care must be taken then in comparisons of the measured data and calculated ϕ' populations.

Conclusions

The pH dependence of the $^{13}C—^{31}P$ couplings of the 3′-, 5′-, and 3′,5′-phosphates of the *syn* dT* and *anti* dT nucleosides has been provided. The ^2J(C,P) couplings are relatively insensitive to pH changes for the entire series of molecules, though a weak sigmoidal behavior was discerned. A preference for the $t(\phi)$ conformer is indicated by the ^3J(C4′—P5′) data, in line with previous $^1H—^{31}P$ data. A high degree of flexibility in the ϕ' bond is apparent in the ^3J(C4′—P3′) and ^3J(C2′—P3′) couplings. The preference for the $t(\phi')$ domain noted for the 3′-nucleotidyl units in the T series is enhanced upon replacement with the *syn* T* base. This indicates that the orientation of a pyrimidine base about the *N*-glycosyl linkage is reflected in the ϕ' orientation. The trends suggest a correlation between the 3′ *endo* pucker and the $t(\phi')$ conformation.

Acknowledgements

Special thanks to Dr. K. Sadana for his expert help with the synthetic aspects of this work. This work was supported by an operating grant from the National Research Council of Canada. We acknowledge also the Faculty of Graduate Studies and the Department of Chemistry of the University

[10]Flattening means a reduction in the amplitude of pucker (τ_m) of a sugar ring (37). It has been loosely referred to (6) as a reduction in the extent of eclipsing of the substituents on the C(2′)—C(3′) fragment i.e., a reduction in the time-averaged τ_2 value (37), which can result from a reduction in τ_m and/or a shift *towards* the *O*endo pucker on the pseudorotational cycle (37).

[11]G. I. Birnbaum. Private communication.

of Manitoba for the funds used to purchase the Bruker WH-90 spectrometer. We thank Drs. J. L. Markley and J. Dallas of the Biochemical Magnetic Resonance Laboratory, Purdue University, Lafayette, IN. for the use of the NT-360 spectrometer used to acquire the ^{1}H nmr data referred to. (The BMRL is supported by an NIH Grant RR-01077.) We thank Dr. G. I. Birnbaum (Biological Sciences, National Research Council of Canada, Ottawa) and Dr. M. Sundaralingam (Madison) for useful discussions and for communicating crystallographic data prior to publication. W. N. is grateful to the University of Manitoba for a Manitoba Fellowship. Discussions with the members of the NMR group in Winnipeg are gratefully acknowledged. We thank Dr. P. C. Loewen for the use of his laboratory facilities.

1. C. CHACHATY, T. YOKONO, S. TRAN-DINH, and W. GUSCHLBAUER. Biophys. Chem. **6**, 151 (1977), and references therein.
2. D. W. MILES, M. J. ROBINS, R. K. ROBINS, M. W. WINKLEY, and J. EYRING. J. Am. Chem. Soc. **91**, 831 (1969).
3. M. P. SCHWEIZER, E. B. BANTA, J. T. WITKOWSKI, and R. K. ROBINS. J. Am. Chem. Soc. **95**, 3770 (1973).
4. J. CADET, R. DUCOLOMB, and C. TAIEB. Tetrahedron Lett. 3455 (1975).
5. D. SUCK, W. SAENGER, and H. VORBRUGGEN. Nature, **235**, 333 (1972).
6. A. L. GEORGE, F. E. HRUSKA, K. K. OGILVIE, and A. HOLY. Can. J. Chem. **56**, 1170 (1978).
7. H. H. MANTSCH and I. C. P. SMITH. Biochem. Biophys. Res. Commun. **46**, 808 (1972).
8. F. HAYASHI, K. AKASAKA, and H. HATANO. Nucl. Acids Res. Special Publication No. 2, s53 (1975).
9. J. L. ALDERFER and P. O. P. Ts'O. Biochemistry, **16**, 2410 (1976).
10. T. SCHLEICH, B. P. CROSS, and I. C. P. SMITH. Nucl. Acids Res. **3**, 355 (1976).
11. G. GOVIL and I. C. P. SMITH. Biopolymers, **12**, 2589 (1973).
12. A. HOLY. Tetrahedron Lett. 1147 (1973).
13. P. J. COZZONE and O. JARDETZKY. Biochemistry, **15**, 4853 (1976).
14. P. K. GLASCOE and F. A. LONG. J. Phys. Chem. **64**, 188 (1960).
15. D. E. DORMAN and J. D. ROBERTS. Proc. Natl. Acad. Sci. U.S.A. **65**, 19 (1970).
16. A. J. JONES, D. M. GRANT, M. W. WINKLEY, and R. K. ROBINS. J. Phys. Chem. **74**, 2684 (1970).
17. D. B. DAVIES. Stud. Biophys. Berlin, **55**, 29 (1976).
18. C. M. NOTTOLI, J. B. LAMBERT, amd R. L. LETSINGER. Org. Magn. Reson. **9**, 500 (1977).
19. R. D. LAPPER, H. H. MANTSCH, and I. C. P. SMITH. J. Am. Chem. Soc. **95**, 2878 (1973).
20. A. K. CHWANG and M. SUNDARALINGAM. Acta Crystallogr. Sect. B, **30**, 1233 (1974).
21. C. GIESSNER-PRETTRE and B. PULLMAN. J. Theor. Biol. **48**, 425 (1974).
22. R. PHILIPS, S. J., P. EISENBERG, P. GEORGE, and R. J. RUTMAN. J. Biol. Chem. 240 (1965).
23. D. B. DAVIES. Prog. Nucl. Magn. Reson. Spectrosc. **12**, 135 (1978).
24. M. SUNDARALINGAM. *In* Proceedings international symposium on the conformation of biological molecules and polymers, symposia on quantum chemistry and biochemistry. *Edited by* B. Pullman and E. D. Bergmann. Academic Press, Jerusalem. 1973. p. 417.
25. D. B. DAVIES and S. S. DANYLUK. Biochemistry, **14**, 543 (1975).
26. B. PULLMAN, D. PERAHIA, and A. SARAN. Biochim. Biophys. Acta, **269**, 1 (1972).
27. W. K. OLSON and P. J. FLORY. Biopolymers, **11**, 1 (1972); **11**, 25 (1972); **11**, 57 (1972).
28. N. YATHINDRA and M. SUNDARALINGAM. Proc. Natl. Acad. Sci. U.S.A. **71**, 3325 (1974).
29. D. J. WOOD, F. E. HRUSKA, and K. K. OGILVIE. Can. J. Chem. **52**, 3353 (1974).
30. D. M. CHENG and R. H. SARMA. J. Am. Chem. Soc. **99**, 7333 (1977).
31. P. PRUSINER, N. YATHINDRA, and M. SUNDARALINGAM. Biochim. Biophys. Acta, **366**, 115 (1974).
32. N. YATHINDRA and M. SUNDARALINGAM. Biochim. Biophys. Acta, **308**, 17 (1973).
33. N. CAMERMAN, J. K. FAWCETT, and A. CAMERMAN. Science, **182**, 1142 (1973).
34. A. JACK, J. E. LADNER, and A. KLUG. J. Mol. Biol. **108**. 619 (1976).
35. C. H. LEE, F. S. EZRA, N. S. KONDO, R. H. SARMA, and S. S. DANYLUK. Biochemistry, **15**, 3627 (1976).
36. B. K. SATHYANARAYANA and V. SASISEKHARAN. *In* Structure and conformation of nucleic acids and protein – nucleic acid interactions. *Edited by* M. Sundaralingam and S. R. Rao. University Park Press, Baltimore, MD. 1975. p. 677.
37. C. ALTONA and M. SUNDARALINGAM. J. Am. Chem. Soc. **95**, 2333 (1973).

Can. J. Chem. Downloaded from www.nrcresearchpress.com by 210.87.254.6 on 09/05/12
For personal use only.

Hydrodesulphurization mechanism of thiophene and tetrahydrothiophene on a cobalt molybdenum catalyst

JOSÉ M. PAZOS AND PAULINO ANDRÉU

Centro de Petróleo y Química, Instituto Venezolano de Investigaciones Científicas, Caracas, Venezuela[1]

Received June 6, 1979

JOSÉ M. PAZOS and PAULINO ANDRÉU. Can. J. Chem. **58**, 479 (1980).

The hydrodesulphurization mechanism of thiophene and tetrahydrothiophene has been developed at high pressures and over a broad range of temperature and contact time on a commercial $CoMo-Al_2O_3$ catalyst. The influence of the pretreatment on the catalyst activity and stability was also studied. The pretreatment with a mixture of H_2 and H_2S was found to be the most convenient. It was found that the sulphur uptake of the fresh catalyst increases with temperature and that an excess of sulphur in the catalyst leads to an initial higher activity.

The thiophene reaction seems to occur simultaneously by two pathways: one consists of ring opening, and the second is yielding tetrahydrothiophene. The latter is the slowest step. The tetrahydrothiophene reacts faster than the thiophene and its reaction mechanism involves mainly the rupture of the C—S bond. However, thiophene was detected in small concentrations, showing the contribution of a second route for the tetrahydrothiophene hydrodesulphurization. Experiments carried out with benzene seem to indicate the existence of three different kinds of active sites in the catalyst: desulphurization, aromatics hydrogenation, and olefin saturation sites.

JOSÉ M. PAZOS et PAULINO ANDRÉU. Can. J. Chem. **58**, 479 (1980).

On a élaboré le mécanisme d'hydrodésulfurisation du thiophène et du tétrahydrothiophène à haute pression et sur une large échelle de température et de temps de contact avec une catalyseur commercial mixte: $CoMo-Al_2O_3$. On a également étudié la stabilité ainsi que l'influence d'un traitement préalable sur l'activité du catalyseur. On a trouvé que le traitement préalable, par un mélange de H_2 et de H_2S, est celui qui convient le mieux. On a constaté que la fixation de soufre sur le catalyseur frais augmente avec la température et que l'excès de soufre sur le catalyseur conduit à une activité initiale plus forte.

La réaction du thiophène semble se produire suivant deux voies: l'une consiste en une ouverture du cycle, et l'autre conduit au tétrahydrothiophène. La dernière voie est l'étape la plus lente. Le tétrahydrothiophène réagit plus vite que le thiophène et le mécanisme de sa réaction implique principalement la rupture de la liaison C—S. Cependant on a décelé de faibles concentrations de thiophène indiquant par là l'existence d'une deuxième façon d'hydrodésulfuriser le tétrahydrothiophène. Les expériences conduites dans le benzène semblent indiquer l'existence de trois différentes sortes de sites actifs sur le catalyseur: un site de désulfurisation un d'hydrogénation aromatique et un de saturation des oléfines.

[Traduit par le journal]

Introduction

Numerous sulphur compounds have been used to study different aspects of the hydrodesulphurization of crude oil distillates. As the greater part of the sulphur in the crude is held in stable ring structures of the thiophene type, thiophene has often been chosen as a model compound. Since the pioneering work of Pease and Keighton (1), several papers have been published dealing mainly with the mechanism of thiophene hydrodesulphurization. The most accepted reaction models imply two separated mechanisms. Either the C—S bond is ruptured, a condition leading to such intermediates as mercaptanes and butadiene (2–4), or ring saturation occurs, which forms tetrahydrothiophene (5–7). In both proposed models, the final products are always a mixture of butanes, butenes, and hydrogen sulphide.

The authors consider that the thiophene reaction is worth a further study because there is no general consensus about its reaction mechanism. On the other hand, the mechanisms proposed are generally valid only at conditions far from those used industrially. Therefore, in this work we studied the mechanism of thiophene hydrodesulphurization over a wide range of pressures, temperatures, and contact times. The reaction of the intermediate tetrahydrothiophene and the influence of different pretreatments on the catalyst stability and activity were also studied in detail.

Experimental

Apparatus and Procedure

The experiments were carried out in a bench scale unit using a flow microreactor with a fixed bed of catalyst. The whole system was made of stainless steel. The reactor was 21 cm long and 1 cm id. The catalyst bed was always 3 cm^3 placed at the centre of the reactor. The top and the bottom of the reactor were filled with an inert ceramic material.

The reactant, thiophene or tetrahydrothiophene, was diluted in heptane and mixed with an excess of hydrogen (H_2/solvent = 2 mol/mol), just before the reactor. A gas-chromatograph was connected in series with the reactor, so that the reactor effluents could be analysed continuously. The extent of the reaction was followed by the weight conversion of the reactant.

Materials

A typical commercial $CoMo-Al_2O_3$ was used in all the ex-

[1]Correspondence address: Instituto Tecnológico Venezolano del Petróleo (INTEVEP), Apdo. 76343, Caracas, Venezuela.

0008-4042/80/050479-06$01.00/0

©1980 National Research Council of Canada/Conseil national de recherches du Canada

Can. J. Chem. Downloaded from www.nrcresearchpress.com by 210.87.254.40 on 09/05/12
For personal use only.

Can. J. Chem. Downloaded from www.nrcresearchpress.com by 210.87.254.40 on 09/05/12
For personal use only.

periments. It was supplied by Akzo Chemie (Ketjenfine 124 – 1.5 E) as 1.5 mm diameter extrudates. The catalyst was used as particles of an equivalent diameter equal to 0.75 mm. The catalyst characteristics are 4% CoO, 12%, MoO_3, surface area = 250 $m^2 g^{-1}$, pore volume = 0.52 mL g^{-1}.

The chemicals used were hydrogen (99% purity), thiophene from Aldrich (99% purity), tetrahydrothiophene from Eastman Kodak, heptane from Fluka (99% purity), and benzene from Merck (99% purity).

Analysis

The reaction products were analysed as they left the reactor by a gas-chromatograph provided with a flame ionization detector. The chromatographic column was SE-30 over Varaport (400 × 0.318 cm od), which was used to obtain a preliminary group separation of C_4 gases, thiophene, tetrahydrothiophene, and heptane. The C_4 gases were resolved by using a 16% bis-2-methoxiethyladipate (730 × 0.318 cm od) plus 30% DC-200 (100 × 0.318 cm od) over Chromosorb column.

The products detected in the thiophene reaction were C_4 gases, tetrahydrothiophene, and unreacted thiophene. A typical gas distribution obtained at 290°C and 28 atm was isobutane (ca. 50 wt%), 1-butene (ca. 30 wt%), and *trans*-2-butene (ca. 20 wt%). A more exhaustive analysis of the liquid products was carried out by using a GC-MS system. In addition to tetrahydrothiophene, small amounts of 2-methyl-2-propanethiol and traces of di-*n*-butylsulphide, 2-*n*-butylthiophene, and 2-*n*-butyltetrahydrothiophene were also detected.

The products observed in the tetrahydrothiophene reaction were C_4 hydrocarbons, thiophene, and unreacted tetrahydrothiophene. The distribution of gases and liquids was found to be similar to that of thiophene, but no trace of 2-*n*-butyl thiophene and 2-*n*-butyl- tetrahydrothiophene was detected.

Results

Pretreatment of the Catalyst

A study of the influence of different pretreatments on the catalyst stability and activity was carried out initially. Fresh samples (A, B, C) of the same catalyst were submitted to different pretreatments in the reactor. Sample A was exposed directly to the feedstock at reaction conditions; sample B was initially reduced with hydrogen at 300°C for 1 h and finally 2 h at 350°C, and sample C was presulphided with a mixture of $H_2 + H_2S$ (3.5% volume of H_2S) for 1 h at 300°C and 2 h at 350°C. Figure 1 shows the activity of the three catalyst samples as a function of the hours on stream (HOS). It can be observed that catalyst A exibits the lowest initial activity due to the fact that it was present as an oxide. As HOS increases, the catalyst becomes sulphided with the H_2S formed under reaction conditions. It took about 20 h for the catalyst to become stable. The prereduced catalyst B shows a higher initial activity than catalyst A and required only 6 h to be sulphided. Finally it reaches the same level of activity of catalyst A. Catalyst C, previously sulphided, shows the highest initial activity, and thus indicating the importance of the sulphided form for the catalyst activity.

It follows from Fig. 1 that catalyst C shows also the highest activity, ca. 90%, while A and B give

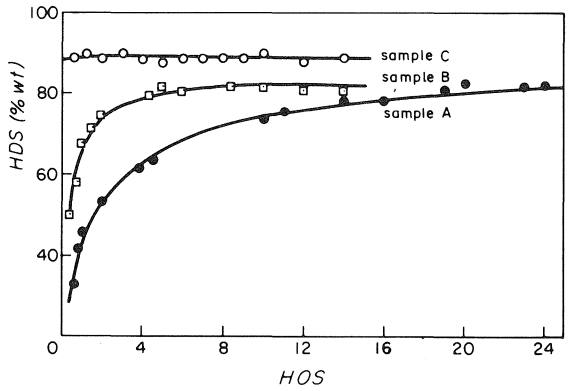


FIG. 1. Influence of the pretreatment in the catalyst activity and stability. Reaction conditions: P = 42 atm, T = 310°C, θ = 0.97 h, $p_H{}^0$ = 26.3 atm, $p_T{}^0$ = 2.5 atm. Sample A, catalyst without pretreatment. Sample B, catalyst prereduced with H_2. Sample C, catalyst presulphided with $H_2 + H_2S$.

80%. This is due to a higher sulphur content of catalyst C. The reasons for this higher sulphur concentration may be explained as follows: (*a*) The higher H_2S concentration in the reactor, since catalyst C was presulphided with $H_2 + H_2S$. (*b*) The higher sulphiding temperature of catalyst C. The dependence of sulphur uptake with temperature has been previously reported (8). (*c*) The reduction of catalysts A and B before their sulphidation. The reduced catalysts are more refractory to sulphidation than the corresponding oxides (9). Therefore, their sulphiding should be lower.

A used catalyst was regenerated by heating it up

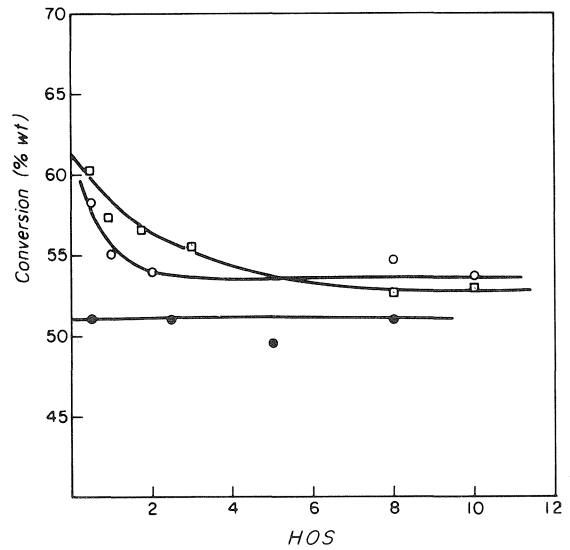


FIG. 2. Presulphiding effect on catalyst activity. Reaction conditions: P = 28 atm, T = 290°C, θ = 0.56 h, $p_H{}^0$ = 17.6 atm, $p_T{}^0$ = 1.66 atm. ●, fresh catalyst presulphided for 3 h; □, catalyst sulphided for 7 h; ○, regenerated catalyst presulphided for 3 h.

Can. J. Chem. Downloaded from www.nrcresearchpress.com by 210.87.254.40 on 09/05/12
For personal use only.

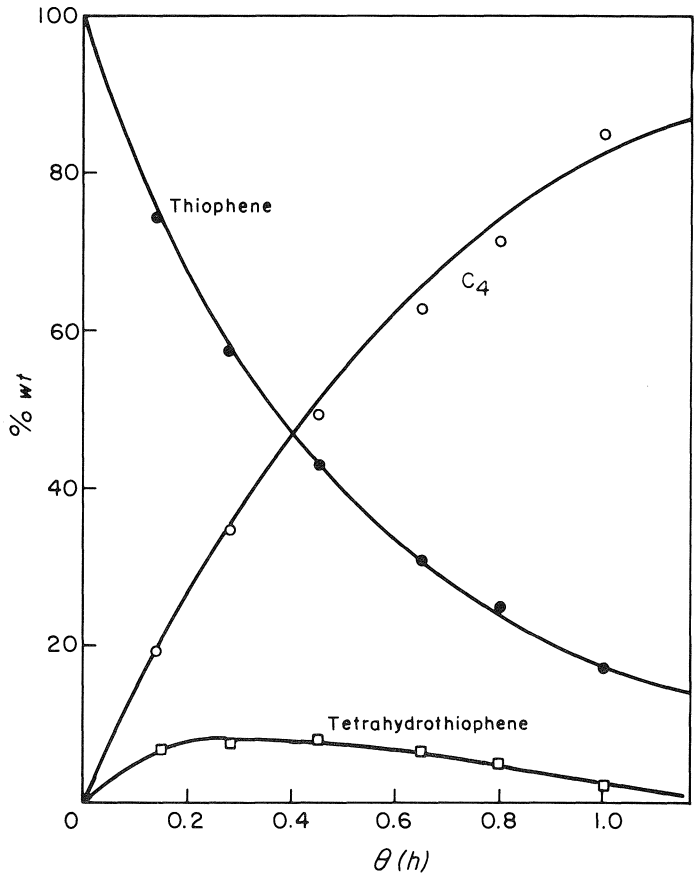


FIG. 3. Thiophene product distribution as a function of the contact time, θ. Reaction conditions: P = 28 atm, T = 290°C, p_H^0 = 17.6 atm, p_T^0 = 1.66 atm.

in air for 10 h and subsequently presulphided again under the same conditions with H_2 + H_2S (3.5% volume H_2S) for 1 h at 300°C and 2 h at 350°C. Its initial activity was surprisingly higher than that of the fresh catalyst, as can be observed in Fig. 2. We reasoned that the regenerated catalyst still had some remaining sulphur and consequently, it showed after sulphiding an excess of sulphur concentration, which is responsible for the initial higher activity. In order to confirm this, the fresh catalyst, already presulphided, was sulphided for 4 h more at 350°C with H_2 + H_2S (3.5% volume H_2S). This catalyst showed a behaviour similar to the regenerated catalyst, as can be observed in Fig. 2. This fact indicates again that the initial higher activity is probably due to an excess of sulphur in the catalyst.

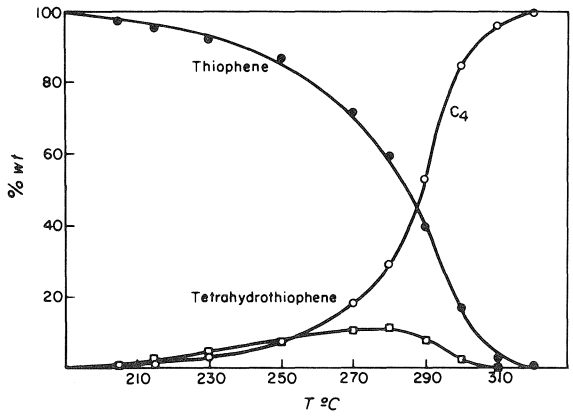


FIG. 4. Thiophene product distribution as a function of the temperature. Reaction conditions: P = 28 atm, θ = 0.56 h, p_H^0 = 17.6 atm, p_T^0 = 1.66 atm.

Product Distribution of Thiophene Hydrodesulphurization

The product distribution obtained in the thiophene reaction was studied over wide conversion ranges as a function of the contact time (θ) and temperature (Figs. 3 and 4, respectively). It can be observed in both figures that tetrahydrothiophene is the main intermediate detected. The low tetrahydrothiophene concentration, as shown in Fig. 3, indicates that the thiophene reaction occurs by a

Can. J. Chem. Downloaded from www.nrcresearchpress.com by 210.87.254.40 on 09/05/12
For personal use only.

consecutive reaction, where the first step is the hydrogenation of the thiophenic ring to form tetrahydrothiophene. However, a deeper analysis of Fig. 3 shows that the thiophene hydrodesulphurization also takes place by rupturing of the C—S bond: the yield curve of the C_4 hydrocarbons formed do not exhibit the typical induction period characteristic of the consecutive reactions. These two facts clearly support that the thiophene hydrodesulphurization occurs by parallel reactions.

The thiophene product distribution as a function of the temperature, Fig. 4, indicates that at $T <$ 250°C, the conversion of thiophene is very small (less than 10 wt%) and that the predominant reaction is the hydrogenation of thiophene to tetrahydrothiophene. At $T >$ 250°C, the tetrahydrothiophene formation goes through a maximum and then decreases because the tetrahydrothiophene reacts very fast to give C_4 hydrocarbons. On the other hand, at $T >$ 250°C the contribution of the ring opening of the thiophene to give directly C_4 gases increases markedly.

The thiophene conversion data are consistent with the pseudo-first order reaction rate as can be observed in Fig. 5.

Product Distribution of Tetrahydrothiophene Hydrodesulphurization

For a better understanding of the thiophene hydrodesulphurization mechanism, a further study of the tetrahydrothiophene hydrodesulphurization has been carried out under similar experimental conditions. Figures 6 and 7 show the product distribution as a function of contact time and temperature respectively. These figures indicate the following facts: (*a*) Thiophene, product of the dehydrogenation of tetrahydrothiophene, is the main intermediate, although its concentration is very small (generally under 5 wt%). The presence of thiophene has been observed by other workers (10, 11). (*b*) Tetrahydrothiophene reacts faster than thiophene at similar operating conditions. This is in agreement with the fact that the hydrogenated compounds are more reactive than the corresponding aromatic compounds (12). (*c*) The mechanism of tetrahydrothiophene hydrodesulphurization is similar to the thiophene reaction and can be expressed by parallel reactions. One reaction yields thiophene, and the other one is the rupture of the C—S bond of the tetrahydrothiophene. This second reaction is the predominant one.

The tetrahydrothiophene reaction can be adjusted by the pseudo-first order kinetic equation as is shown in Fig. 5.

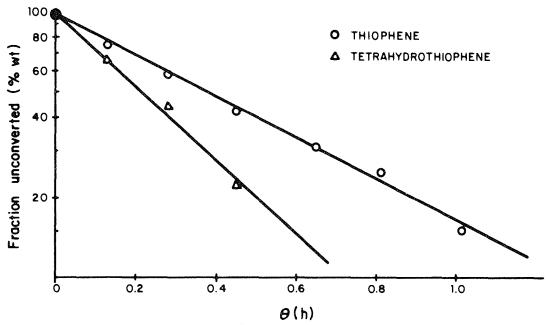


FIG. 5. Pseudo first-order kinetic equation for thiophene and tetrahydrothiophene conversion. Reaction conditions: P = 28 atm, T = 290°C, p_H^0 = 17.6 atm, p_s^0 = 1.66 atm (S is thiophene and tetrahydrothiophene, respectively).

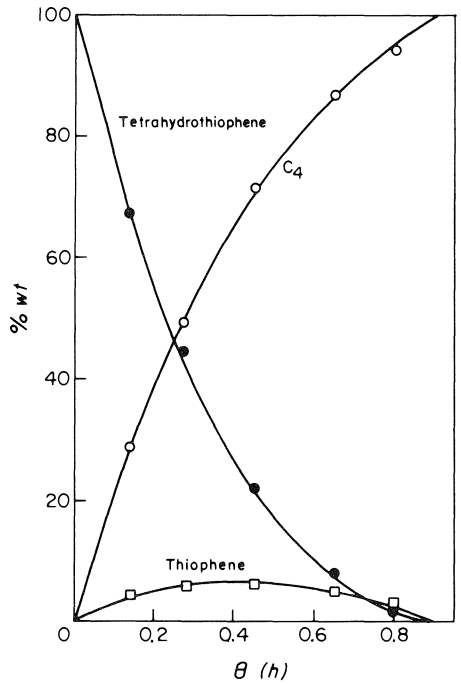
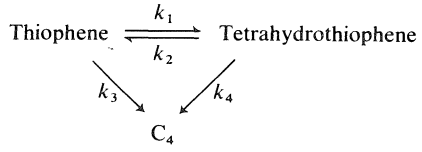


FIG. 6. Tetrahydrothiophene product distribution as a function of the contact time. Reaction conditions: P = 28 atm, T = 290°C, p_H^0 = 17.6 atm, p_{Th}^0 = 1.66 atm.

Discussion

The former results show that the thiophene hydrodesulphurization is a complex reaction, which can be expressed as follows:



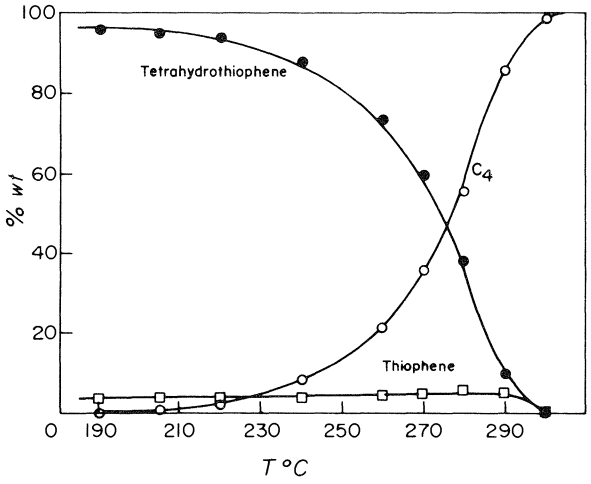


FIG. 7. Tetrahydrothiophene product distribution as a function of the temperature. Reaction conditions: P = 28 atm, θ = 0.56 h, p_H^0 = 17.6 atm, p_{Th}^0 = 1.66 atm.

Thus the thiophene reaction occurs simultaneously by hydrogenation to tetrahydrothiophene and by a straight ring opening, which involves the rupture of the C—S bond.

The concentration of thiophene (T), tetrahydrothiophene (Th), and C_4 hydrocarbons can be expressed by the following equations:

$$[1]\quad T(\theta) = A_1 \exp(\alpha_1\theta) + A_2 \exp(\alpha_2\theta)$$

$$[2]\quad Th(\theta) = A_1\alpha_3 \exp(\alpha_1\theta) + A_2\alpha_4 \exp(\alpha_2\theta)$$

$$[3]\quad C_4(\theta) = A_3 + A_1\alpha_5 \exp(\alpha_1\theta) + A_2\alpha_6 \exp(\alpha_2\theta)$$

where A_i (wt%) and α_i (h^{-1}) are empirical constants and θ is the contact time (h). These equations are the solutions of the rate expressions for the thiophene network. Each reaction was assumed to be first order.

To evaluate the contribution of the different reactions to the thiophene network, the individual rate constants k_i were estimated. Several methods are available to determine kinetic coefficients for complex reaction models (13). In the present work, the coefficients A_i and α_i were determined from the experimental points of Fig. 3 with a non-linear least-squares program. From α_i, the individual rate constants were estimated. The following values were obtained:

$$k_1 = 2.06 \times 10^{-4}\ s^{-1}$$

$$k_2 = 4.94 \times 10^{-4}\ s^{-1}$$

$$k_3 = 3.69 \times 10^{-4}\ s^{-1}$$

$$k_4 = 9.58 \times 10^{-4}\ s^{-1}$$

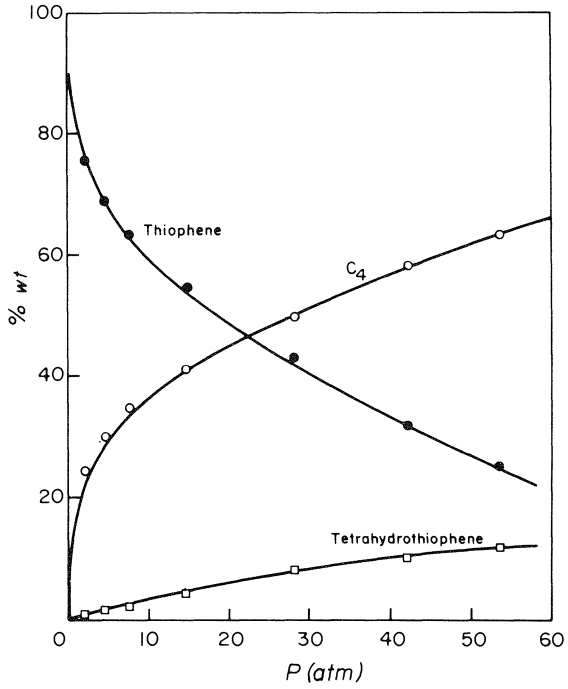


FIG. 8. Thiophene product distribution as a function of the total pressure. Reaction conditions: T = 290°C, θ = 0.45 h.

The lines of Fig. 3 show the concentration profile of thiophene, tetrahydrothiophene, and C_4 predicted by eqs. [1], [2], and [3]. There is a close agreement between these curves and the experimental points.

The values of the rate constants obtained indicate that the thiophene reaction occurs mainly through the rupture of the C—S bond. On the other hand, it is shown that tetrahydrothiophene has higher desulphurization activity than thiophene.

This mechanism has been proved to be valid over a broad range of pressures, as shown in Fig. 8. It can be observed that the tetrahydrothiophene concentration increases with the total pressure. This can be an explanation of why tetrahydrothiophene has not been proposed as an intermediate by several authors who usually worked at atmospheric pressure (2–4).

In Fig. 9, we present a more complete picture of the mechanism of the thiophene reaction, based on the products observed by mass spectrometry at typical reaction conditions. Not only tetrahydrothiophene and butenes, but also mercaptanes and sulphides have been detected as intermediates, which show the complexity of this reaction. However, they were found in small concentrations.

Finally, some experiments were carried out by substituting the solvent heptane by benzene in

Can. J. Chem. Downloaded from www.nrcresearchpress.com by 210.87.254.40 on 09/05/12
For personal use only.

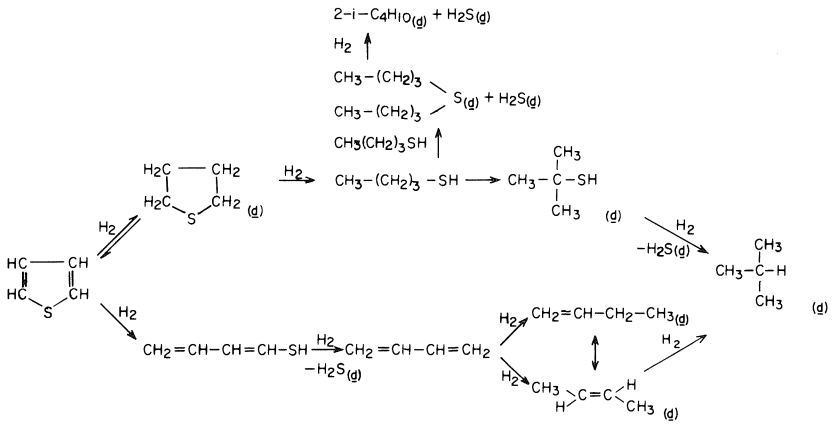


FIG. 9. Mechanism of thiophene HDS.

order to ellucidate the type of sites involved in the thiophene reaction. The effect of changing the solvent from pure heptane to pure benzene through various ratios was to decrease the C_4 from 5.7% to 4.5% and the tetrahydrothiophene from 6.6% to 5.4%, but the ratio tetrahydrothiophene/C_4 remained constant at 1.2. The benzene should adsorb on hydrogenation sites affecting the tetrahydrothiophene concentration but it should not be affected to the same extent as the C_4 concentration. The results obtained seem to indicate that benzene is adsorbed on both aromatic hydrogenation and desulphurization sites; therefore, it competes for the same adsorption sites of thiophene. Though there is need for further evidence, we could suggest the existence of three different types of active sites involved in hydrodesulphurization reactions: aromatics hydrogenation, olefines saturation, and desulphurization sites.

Acknowledgments

The authors acknowledge the contribution of A. V. Sapre and B. C. Gates to the kinetic model; they also wish to thank the contribution of F. González to the mathematical calculations.

1. R. N. PEASE and W. B. KEIGHTON. Ind. Eng. Chem. **25**, 1012 (1933).
2. V. I. KOMAREWSKY and E. A. KNAGGS. Ind. Eng. Chem. **43**, 1414 (1951).
3. P. J. OWENS and C. H. AMBERG. Adv. Chem. Ser. **33**, 182 (1961).
4. J. M. J. C. LIPSCH and G. C. A. SCHUIT. J. Catal. **15**, 179 (1969).
5. C. M. CAWLEY and C. C. HALL. J. Soc. Chem. Ind. **62**, 116 (1943).
6. C. G. BERTIL HAMMAR. *In* Proceedings of the Third World Petroleum Congress, Sect. IV. The Hague. 1951. p. 295.
7. J. KRAUS and M. ZDRAZIL. React. Kinet. Catal. Lett. **6**(4), 475 (1977).
8. F. E. MASSOTH. J. Catal. **36**, 164 (1975).
9. Q. A. NPRA. Oil Gas J. **76**(24), 74 (1978).
10. P. DESIKAN and C. H. AMBERG. Can. J. Chem. **42**, 483 (1964).
11. P. KIERAN and C. KEMBALL. J. Catal. **4**, 394 (1965).
12. D. R. KILANOWSKI, H. TEENWEN, V. H. J. DE BEER, B. C. GATES, G. C. A. SCHUIT, and H. KWART. J. Catal. **55**, 129 (1978).
13. D. M. HIMMELBLAN, C. R. JONES, and K. B. BISCHOFF. Ind. Eng. Chem. Fundam. **6**, 539 (1967).

Can. J. Chem. Downloaded from www.nrcresearchpress.com by 210.87.254.40 on 09/05/12
For personal use only.

Studies on the rearrangement of (trichloromethyl)carbinols to α-chloroacetic acids[1]

WILKINS REEVE, JAMES R. MCKEE, ROBERT BROWN,
SITARAMA LAKSHMANAN, AND GERTRUDE A. MCKEE
Chemistry Department, University of Maryland, College Park, MD 20742, U.S.A.

Received July 3, 1979

WILKINS REEVE, JAMES R. MCKEE, ROBERT BROWN, SITARAMA LAKSHMANAN, and GERTRUDE A. MCKEE. Can. J. Chem. **58**, 485 (1980).

Phenyl(trichloromethyl)carbinol undergoes an unimolecular, predominantly intramolecular conversion into potassium α-chlorophenylacetate on stirring with 10% aqueous potassium hydroxide at 0°C for several days. Besides providing an interesting example of a 1–2 chlorine shift, the reaction is of potential importance for the synthesis of α-chloro acids. The study of a variety of (trichloromethyl)carbinols shows the reaction is general for secondary (trichloromethyl)carbinols as well as trichloroethanol. The mechanism of the reaction involves the preliminary formation of an epoxide. Several mechanisms are considered for the conversion of the epoxide to the α-chloroacetate anion, but none accounts for all of the experimental facts. Tertiary carbinols break down at the epoxide stage into a ketone and carbon monoxide.

WILKINS REEVE, JAMES R. MCKEE, ROBERT BROWN, SITARAMA LAKSHMANAN et GERTRUDE A. MCKEE. Can. J. Chem. **58**, 485 (1980).

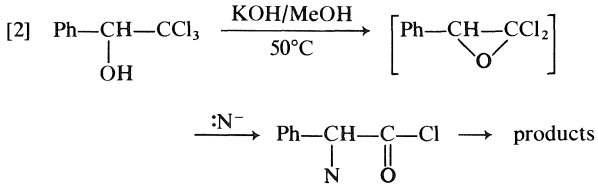
Le phényl(trichlorométhyl)carbinol subit une transformation unimoléculaire (intramoléculaire de façon prédominante) en α-chlorophénylacétate de potassium par agitation avec de l'hydroxyde de potassium en solution 10% aqueuse à 0°C pendant plusieurs jours. En plus de fournir un exemple intéressant de glissement 2–1 du chlore, la réaction est d'une grande importance pour la synthèse des acides α-chlorés. L'étude de plusieurs types de (trichlorométhyl)carbinols montre que la réaction est générale pour les (trichlorométhyl)carbinols aussi bien que pour le trichloréthanol. Le mécanisme de cette réaction implique la formation préliminaire d'un époxyde. On a considéré plusieurs mécanismes dans le cas du passage de l'époxyde à l'anion α-chloroacétate mais aucun d'eux explique les faits expérimentaux. Les carbinols tertiaires au stade de l'époxyde se dégradent en cétone et en monoxyde de carbone.
[Traduit par le journal]

Can. J. Chem. Downloaded from www.nrcresearchpress.com by 210.87.254.40 on 09/05/12
For personal use only.

Phenyl(trichloromethyl)carbinol was reported by Jocic in 1897 to react with ice-cold aqueous potassium hydroxide solution over a two or three day period to form α-chlorophenylacetic acid in 27% yield (1). This is a reaction without precedent and raises questions about the mechanism by which the new carbon–chlorine bond is formed. There has been no subsequent use of the reaction, and its scope and usefulness have never been studied.

[1] $\mathrm{Ph{-}CHOH{-}CCl_3} \xrightarrow[0°C]{\mathrm{KOH}} \mathrm{Ph{-}CHCl{-}COOH}$

Phenyl(trichloromethyl)carbinol reacts with a wide variety of nucleophiles in methanolic potassium hydroxide at 50°C to form α-substituted phenylacetic acids, or if structural features allow ring closure, heterocyclic compounds are formed (2). These reactions involve the preliminary formation *in situ* of a dichloro epoxide which undergoes ring opening by S_N2 attack of the nucleophile (3). Other reactions of phenyl(trichloromethyl)carbinol have also been studied (4).

[2] 

Unlike the reaction of (trichloromethyl)carbinols with nucleophiles, the reaction described by Jocic (1) is best carried out by stirring a suspension of phenyl(trichloromethyl)carbinol at 0°C for a few days in four equivalents of aqueous 10% potassium hydroxide solution. Our work shows that it is predominately an intramolecular, unimolecular reaction which differs from the bimolecular reaction in mechanism, optimum reaction conditions, and structural requirements of the carbinol.[2]

Scope of Reaction

The reaction works well with phenyl(trichloromethyl)carbinol, so this compound was chosen to

[1]Taken in part from the doctoral theses of J. R. McKee (1974) and R. Brown (1968).

[2]In our laboratories we refer to this intramolecular transformation carried out in a heterogeneous, aqueous reaction mixture at 0°C as the Jocic reaction to distinguish it from the bimolecular reactions with various nucleophiles carried out in alcoholic potassium hydroxide solution at 50°C. Ж. Іоцича (1870–1914) was a student of A. E. Favorskii at the University of St. Petersburg. His name has been transliterated into German as Jozitsch and Jocicz and into French as Iotsitch. Chemical Abstracts (J. T. Dickman) suggests Z. Jocic as the preferred Anglicized form.

0008-4042/80/050485-09$01.00/0
©1980 National Research Council of Canada/Conseil national de recherches du Canada

Can. J. Chem. Downloaded from www.nrcresearchpress.com by 210.87.254.40 on 09/05/12
For personal use only.

determine the optimum reaction conditions. The optimum temperature is 0°C; at −5°C the reaction occurs too slowly with no gain in yield, and at 5°C the formation of mandelic acid becomes more important as a side reaction. Ten percent aqueous potassium hydroxide is the best reaction medium; 5% and 20% solutions give somewhat lower yields of products. With 10% sodium hydroxide solution a gel formed; the reaction occurred more slowly, and lower yields of product were obtained. Four molar equivalents of base are used. Surprisingly, the addition of methanol or other oganic solvents caused a drastic decrease in the rate of reaction; the use of 80% ethanol – 20% water slows down the reaction rate about 35-fold. Solvation of the leaving chloride ion may be important in the rate-determining step; as the media becomes more non-aqueous, this driving force decreases. The reaction in 10% aqueous potassium hydroxide is heterogeneous, and vigorous mechanical stirring speeds up the reaction. The use of oleic acid (5% of the weight of the carbinol) as a dispersing agent helps if less vigorous stirring is used (such as with the use of a magnetic stirring bar), but is without effect if a motor-driven paddle stirrer is used. The half life of the reaction is variable due to the heterogeneous nature of the reaction, but can be as low as 15 h with vigorous stirring. In a typical experiment of one half life duration at 0°C, the reaction mixture consisted of about 15% benzaldehyde, 51% unreacted phenyl(trichloromethyl)carbinol, and 30% α-chlorophenylacetic acid. After three half lives, 60–70% of α-chlorophenylacetic acid was formed.

The reaction is successful with a wide variety of secondary carbinols as is shown in Table 1.

No measurable reaction occurs with 2,2,2-trichloroethanol at 0°C, but the reaction does occur slowly at 25°C. Tertiary (trichloromethyl)carbinols do not form α-chloro acids except in small amounts; these are presumably formed by the competing, slow bimolecular reaction (eq. [2]). Thus dimethyl(trichloromethyl)carbinol gives 3% of α-chloroisobutyric acid (5). The major products formed from the tertiary (trichloromethyl)carbinols are carbon monoxide and the ketone from which the starting carbinol could be prepared by the addition of chloroform.

Molecularity of Reaction

With phenyl(trichloromethyl)carbinol, the reaction was found to be 83% intramolecular by adding radioactive chloride ion to the initial aqueous potassium hydroxide solution and determining how much was incorporated into the final isolated chloro acid. In a similar manner, a displacement reaction by which chloride ion in solution might replace part of the covalently bound chlorine of the chloro acid was demonstrated to be too slow to account for more than 0.6% of the chlorine in the final chloro acid. Accordingly, approximately 17% of the chlorine in the final chloro acid is due to a mechanism in which chloride ion in solution is captured by some reactive intermediate, and 83% of the chlorine in the chloro acid comes from an intramolecular rearrangement.

A kinetic study of the reaction using phenyl(trichloromethyl)carbinol shows the reaction to be first order in carbinol and zero order in base (because the hydroxyl group is largely in the alkoxide form) with a half life of 15 to 30 h depending on how efficiently the mixture is stirred. It is difficult to draw mechanistic conclusions from the data because of the heterogeneous nature of the mixture. Fortunately, two (trichloromethyl)carbinols were found which are soluble under the reaction conditions. One is *p*-chlorophenyl(trichloromethyl)carbinol; this is somewhat more acidic than the parent phenyl(trichloromethyl)carbinol and dissolves in excess 10% potassium hydroxide solution.

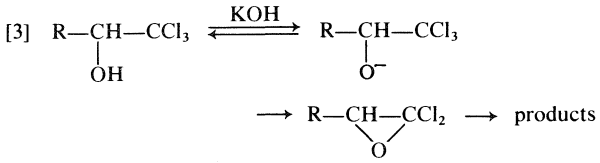
Concerning the acidity of the carbinols, we could not determine the pK_a of the neutral (trichloromethyl)carbinols by electrometric titration since excess base had to be present before they would dissolve, but the potassium salt of *p*-carboxyphenyl(trichloromethyl) carbinol was soluble, and titration with aqueous potassium hydroxide indicated the pK_a of the carbinol function to be approximately 11.3. Trichloroethanol is known to have a pK_a in the 11.8 to 12.2 range (6), and presumably most of the (trichloromethyl)carbinols have similar pK_a values. *p*-Methoxyphenyl (trichloromethyl)carbinol should be a weaker acid due to the electron releasing *p*-methoxy group, and this probably accounts for the unreactivity of this carbinol.

The kinetics of the reaction of *p*-chlorophenyl(trichloromethyl)carbinol with 10% aqueous potassium hydroxide at 0°C was followed by titrating aliquots of the reaction mixture for unreacted base, and the reaction was found to follow first order kinetics to at least 50–70% of completion. An experiment in which the carbinol concentration was halved demonstrated the reaction was first order in carbinol. Another experiment at twice the concentration of base showed the reaction rate to be independent of increases in base concentration.

Similar kinetic data at 30°C were obtained with 2,2,2-trichloroethanol which is also soluble in 10% potassium hydroxide solution. Carbon monoxide

Can. J. Chem. Downloaded from www.nrcresearchpress.com by 210.87.254.40 on 09/05/12
For personal use only.

was evolved during the course of the reaction. Its evolution also followed first order kinetics and the moles evolved were about 5% of the moles of starting alcohol. The major product of the reaction was chloroacetic acid, formed in 23% yield, but under the basic reaction conditions, some of the chloroacetate reacts with the trichloroethanol to form trichloroethoxyacetate in 15% yield, so the product isolated consisted of a mixture of these two acids.



The kinetic experiments clearly establish the rate determining step to be the formation of the intermediate dichloro epoxide. The rapid equilibration established between the carbinol and its anion cannot be rate determining, and a slow step subsequent to dichloro epoxide formation would involve a relatively rapid consumption of the first third of the base followed by a slower consumption of the remainder. No such behavior is observed and no evidence has been obtained for a build-up of the dichloro epoxide. Experimentally, the disappearance of total base was measured rather than the disappearance of alkoxide alone, but if a large fraction of the carbinol is in the alkoxide form, the two are proportional to each other.

Under the same experimental conditions, both the *p*-chloro ($t_{\frac{1}{2}}$ = 27 h) and the *p*-methyl ($t_{\frac{1}{2}}$ = 45 h) analogs react more slowly than phenyl(trichloromethyl)carbinol ($t_{\frac{1}{2}}$ = 16 h) but this is of limited mechanistic significance as far as the chlorine migration step is concerned since the rate controlling step is in the initial formation of epoxide.

Stereochemistry

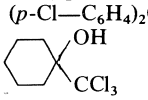
The reaction of (*R*)-(−)-phenyl (trichloromethyl) carbinol with 10% aqueous potassium hydroxide at 0°C for eight hours gave α-chlorophenylacetic acid which was 91% racemized and 9% inverted. Control experiment with (*S*)-(+)-α- chlorophenylacetic acid showed 70% was racemized in eight hours under the same reaction conditions. This corresponds to 45% racemization during the four hour period that the average α-chlorophenylacetate molecule was exposed to the base in the initial reaction. Racemization occurs about eight times faster than the substitution of the chlorine by hydroxyl. Racemization involves the formation of an enolate anion whereas substitution proceeds unimolecularly via an α-lactone (3, 8). The relatively easy racemization of the α-chloroacetate anion makes it difficult to tell how much racemization occurs during the intramolecular migration of the chlorine. Seventeen percent of the reaction is intermolecular, and chloro acid formation by attack of chloride ion on an intermediate such as the epoxide shown in reaction sequence [2] should involve inversion. Accordingly, the observed results are consistent with complete racemization during the intramolecular chlorine migration to form chloro acetate, with the observed 9% of inverted chloro acid arising from the 17% of product not formed by the intramolecular pathway. It has previously been shown that the optical activity of the starting phenyl(trichloromethyl)carbinol is unchanged by treatment with methanolic potassium hydroxide at 40°C for 90 min (3).

Control experiments with (*R*)-(−)-α-chloro phenylacetyl chloride (71% optically pure) showed the reaction time for 50% reaction with excess 1 *M* potassium hydroxide solution at 0°C to be a maximum of seven minutes under heterogeneous reaction conditions. After eighty minutes, the potassium (*R*)-(−)-α-chlorophenylacetate formed was converted to the acid; no racemization could be detected.

By-products

The major by-products of the reaction, aside from unreacted starting carbinol, are carbon monoxide and a carbonyl compound. The (trichloromethyl)carbinols can be made by the base catalyzed condensation of chloroform with aldehydes and ketones, and Jocic postulated that the carbonyl by-product was formed by the reverse of this condensation reaction (1). With phenyl(trichloromethyl)carbinol, the benzaldehyde and the carbon monoxide are 10 to 20% of theory, and this is typical of the behavior of the secondary carbinols. With the tertiary (trichloromethyl)carbinols, the reaction proceeds almost exclusively to give the ketone and carbon monoxide, and little chloro acid is formed. With phenyl(trichloromethyl)carbinol the formation of carbon monoxide is first order in carbinol. That the source of the carbon monoxide is not chloroform (and therefore not trichloromethide anion (7)) is shown by: (*a*) chloroform is absent in the alkaline reaction mixture at the end of the reaction; (*b*) (trichloromethyl)carbanion, generated from 1,1,1-trichloropropanone, gives chloroform and little or no carbon monoxide under the reaction conditions; (*c*) extra chloroform added at the beginning of an otherwise normal reaction between phenyl(trichloromethyl)carbinol and aqueous potassium hydroxide solu-

TABLE 1. Reactions of substituted (trichloromethyl)carbinols with 10% potassium hydroxide solution at 0°C

Carbinol	Major product (% yield)
$CCl_3—CH_2OH$ (at 30°C)	$ClCH_2COOH$ (23) $CCl_3CH_2OCH_2COOH$ (15)
$(CH_3)_3C—CHOH—CCl_3$	$(CH_3)_3CCHClCOOH$ (78)[b]
$C_2H_5—CHOH—CCl_3$	$C_2H_5CHClCOOH$ (23)[a]
$CH_2=CH—CHOH—CCl_3$	*Z*-$CH_3CH=CClCOOH$ (24)[a]
$Ph—CHOH—CCl_3$	PhCHClCOOH (60)
p-$Cl—C_6H_4—CHOH—CCl_3$	*p*-$Cl—C_6H_4CHClCOOH$ (63)[c]
p-$Br—C_6H_4—CHOH—CCl_3$	*p*-$Br—C_6H_4CHClCOOH$ (93)[c]
o-$Allyl—C_6H_4—CHOH—CCl_3$	*o*-$C_3H_5—C_6H_4CHClCOOH$ (46)[c]
p-$CH_3—C_6H_4—CHOH—CCl_3$	*p*-Tolyl—CHOHCOOH (69)[c]
p-$CH_3O—C_6H_4—CHOH—CCl_3$	No reaction
$(CH_3)_2COH—CCl_3$	Acetone[a]
(*p*-$Cl—C_6H_4)_2COH—CCl_3$	(*p*-$Cl—C_6H_4)_2C=O$ (100)
	Cyclohexanone (63)
	$(CH_2)_5CCl—COOH$ (ca. 8)

[a] Data from ref. 5.
[b] The composition of methyl ester mixture after treatment of acid fraction with diazomethane.
[c] Allowing for recovered unreacted carbinol.

tion at 0°C survives the reaction and can be measured by glc of a xylene extract of the reaction mixture. Since the formation of carbon monoxide involves fragmentation of the molecule and chloroform is not an intermediate, the most likely source is the dichloro epoxide slowly breaking down to the carbonyl component and dichlorocarbene which hydrolyzes to carbon monoxide.

Another side reaction that occurs is the hydrolysis of the chloro acid to the hydroxy acid under the alkaline reaction conditions. As shown in Table 1, all of the chloro acid is hydrolyzed when starting with *p*-tolyl(trichloromethyl)carbinol, but virtually no hydrolysis occurs with *p*-chlorophenyl(trichloromethyl) carbinol. This behavior is in accord with the σ values of the two *para* substituents. If one uses the ρ value of -2.66 found for the hydrolysis of α-bromophenylacetate anion (8), the Hammett equation predicts the α-chloro-*p*-tolylacetate anion would hydrolyze 10 or 13 times more rapidly than the α,*p*-dichlorophenylacetate anion, depending on whether the comparison is based on σ or σ^+ (used by Kemp and Metzger) substituent values respectively.

Reaction in Deuterium Oxide

Phenyl(trichloromethyl)carbinol, and its *p*-chloro and *p*-methyl analogues, were allowed to react with potassium hydroxide in deuterium oxide under the usual conditions; the unreacted carbinol was separated by ether extraction, and the reaction mixture was then acidified with aqueous hydrochloric acid to give the product acid. This was examined by ^{1}Hmr to determine the deuterium uptake.

The recovered phenyl(trichloromethyl)carbinol showed a phenyl to α-hydrogen ratio of 5:1; no deuterium exchange occurred prior to the reaction. The chloro acids produced showed considerable deuterium incorporation in the α-position but no more than was observed in control experiments in which the chloro acids were equilibrated with deuterium oxide under approximately the same reaction conditions. Accordingly, it appears the chloro acid with a proton in the α-position is initially formed and deuterium incorporation occurs subsequent to this. The results are in Table 2.

Mechanism of Reaction

The reaction occurs under conditions which suggest there are no radical intermediates. We have considered a number of ionic mechanisms; none is in complete accord with all the known facts. McDonald *et al.* have studied the rearrangement of 1-chloro-4-methylcyclohexene oxide to 2-chloro-4- methylcyclohexanone both thermally and catalyzed by zinc chloride, and postulated an α-ketocarbonium ion – chloride ion pair intermediate (9). Similar results were obtained with 2-chloronorbornene *exo*-oxide (10), and with 2-chlorobicyclo[2.2.2]oct-2-ene oxide (11). 2-Chloronorbornene *exo*-oxide on treatment with lithium diethylamide in refluxing bezene–ether forms mostly tricyclo[2.2.1.$O^{2,6}$] heptan-3-one, presumably by α-elimination, chloride ion loss, and transannular insertion of the α-keto carbene (12). McDonald has reviewed the literature covering reactions of this type (13). Unfortunately, these reactions in non-protic solvents seem to bear little relationship to the reaction we have studied in cold,

Can. J. Chem. Downloaded from www.nrcresearchpress.com by 210.87.254.40 on 09/05/12
For personal use only.

TABLE 2. Percent incorporation of deuterium in the Jocic reaction

Starting carbinol	Product acid (% D)	% Deuterium in control acid
Ph—CHOH—CCl_3	Ph—CHCl—COOH (47)	45
p-Cl—C_6H_4—CHOH—CCl_3	*p*-Cl—C_6H_4—CHCl—COOH (72)	82
p-Me—C_6H_4—CHOH—CCl_3	*p*-Me—C_6H_4—CHOH—COOH (12)	7

aqueous, basic solution. As stated before, the presence of organic solvent causes a drastic decrease in the rate of the Jocic reaction.

The experimental observations that a mechanism should account for include the following. (*a*) The apparent structural requirement for a proton on the α-carbon of the carbinol. (*b*) The intramolecular nature of the chlorine migration. (*c*) The requirement for aqueous, basic reaction conditions. 1,1,3,3,3-Pentachloropropylene oxide is a known stable dichloro expoxide (14) which undergoes no reaction with water or with potassium chloride solution, but in the presence of cold dilute base undergoes both chlorine and hydrogen migration; trichloroacrylic acid is the product formed by chlorine migration (15). (*d*) Extensive or complete racemization. (*e*) The failure of the α-hydrogen of the chloro acid to be replaced by deuterium during the conversion of the dichloro epoxide to the initially formed α-chloro acetate when the reaction is carried out in deuterium oxide.

Carbonium Ion Mechanism

A carbocation is formed either by chloride ionization, or by epoxide ring opening, or by a concerted mechanism involving both processes perhaps with an intermediate chloronium ion. These mechanisms fail to explain why base is necessary (see *c* preceding paragraph), how a neopentyl group can go through the reaction unrearranged, and why the reaction should fail with tertiary (trichloromethyl)carbinols.

Carbene Mechanism

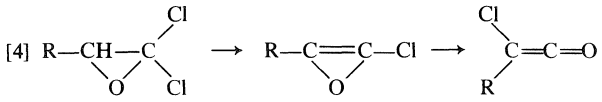
The base removes a proton from the dichloro epoxide and the ring opens forming a carbene which abstracts the neighboring chlorine to form a carbanion of the chloro acid. This mechanism requires that the α-hydrogen of the chloro acid be replaced by deuterium if the reaction is carried out in deuterium oxide, and this did not occur. Otherwise, it is consistent with all the known facts.

Enol Hypochlorite Mechanism

The chlorine is assumed to migrate from carbon to oxygen to form an enol hypochlorite which then chlorinates the α-carbon via a quasi four-membered ring. This mechanism fails to explain why the reaction fails with tertiary (trichloromethyl)carbinols. The predicted intermediate hypochlorite should be capable of being trapped by a wide variety of general reducing agents whereas the following reducing agents were without effect: potassium stannite, potassium iodide, potassium arsenite, hydroquinone, and β-naphthol. Two reducing agents, potassium dithionite and sodium formaldehydesulfoxylate, did cause phenylacetic acid to be formed in 42 and 19% yields, respectively, from phenyl(trichloromethyl)carbinol. These are unusual reducing agents, and the mechanism by which they participate in the reaction is not clear.

Chlorooxirene Mechanism

Oxirenes have been postulated as intermediates in the oxidation of acetylenes (16, 17). They may have a transient existence in the Wolff rearrangement by photolysis (18, 19). They are highly strained unstable compounds, and chlorooxirenes are unknown. The strain energy of oxirene has been estimated to be 40 kcal/mol vs. 13 kcal/mol for oxirane (16).



The mechanism requires the α-hydrogen to be completely replaced by deuterium in a reaction carried out in deuterium oxide, and this did not occur. Unpublished evidence obtained by Tsuk (20) against the chlorooxirene mechanism follows. (Dibromochloromethyl)phenylcarbinol under the Jocic conditions yields mostly α-bromophenylacetic acid. If the oxirene mechanism were operating, the two bromines would be eliminated in the first two steps giving a chlorooxirene, and this would yield a chloro acid.

Of the above four mechanisms, the one involving a carbene (or carbenoid) accounts for all of the experimental evidence except the lack of deuterium exchange. The lack of exchange may be rationalized by assuming a carbenoid transition state. The α-proton is not completely abstracted by the base, the epoxide ring opens, and predominately intramolecular migration of the neighboring chlorine then occurs concurrent with the reformation of the carbon–hydrogen bond. This is speculation, and perhaps it is best to say that the true

Can. J. Chem. Downloaded from www.nrcresearchpress.com by 210.87.254.40 on 09/05/12
For personal use only.

mechanism by which the reaction occurs is still not established.

Experimental

Melting points and boiling points are corrected. The infrared spectra were recorded on a Perkin-Elmer Model 337 infrared grating spectrophotometer and the nmr spectra on either a Varian A-60D or a Perkin-Elmer R-12 spectrometer. Chemical shift values are expressed as δ values (ppm) downfield from tetramethylsilane as internal standard. Rotations were measured on a Franz, Schmidt, and Haensch (Berlin S) polarimeter with a sodium lamp as a light source. Polarimeter tubes of 2-dm length were used; concentration terms are grams of solute per 100 mL of solution. Elemental microanalyses were performed by Dr. Franz J. Kasler and Mrs. Shelesa L. A. Brew. Mass spectra were obtained by Dr. Martha Gay on a Du Pont mass spectrometer. Gas–liquid chromatographic analyses were performed on a Hewlett Packard 5750B research chromatograph. "Isooctane" used in recrystallization was 2,2,4-trimethylpentane.

Phenyl(trichloromethyl)carbinol

This is best prepared from benzene (30 mol), commercial anhydrous chloral (3 mol), and anhydrous aluminum chloride (0.75 mol) following the procedure of Dinesmann (21). The optimum amount of aluminum chloride was determined in a preliminary run. Too little caused incomplete reaction and too much causes large amounts of α,β,β,β- tetrachloroethylbenzene and high boiling materials to be formed. The reaction mixture was washed twice with 5% sodium carbonate solution to destroy chloral and chloral polymers. The carbinol, 500 g (63% of theory after allowing for 15% of α,β,β,β- tetrachloroethylbenzene impurity), was distilled rapidly to minimize decomposition and collected at 120–140°C (1 Torr). The completion of the distillation is marked by a sharp rise (ca. 40°C) in the temperature as 2,2-diphenyl-1,1,1-trichloroethane begins to distill. The composition of the distilled carbinol can be determined from its ^{1}Hmr spectrum: the α-hydrogens of the carbinol, the tetrachloroethylbenzene, and the diphenyltrichloroethane occur at δ 5.17, 5.37, and 5.0 respectively (CCl_4).

We have found that the best way to purify the distilled carbinol is to crystallize 500 g from 300 mL of "isooctane". After seeding the solution and cooling to 10°C for 30 min, 210 g of the pure crystalline carbinol was filtered off. An equal amount could be obtained by a similar treatment of the concentrated mother liquors. An equilibrium melting point obtained by immersing a thermometer in several grams of the material in a test tube was 32–34°C, and 34–35°C after a final recrystallization from ethanol. The capillary mp was 37°C (lit. (21) mp 37°C); ^{1}Hmr ($DCCl_3$) δ: 7.42 (broad s, 5, Ph), 5.12 (s, 1, CH), and 3.52 (s, 1, OH); in CCl_4, δ: 7.56 (m, 2, Ph), 7.3 (m, 3, Ph), 5.13 (s, 1, CH), and 4.67 (s, 1, OH).

The carbinol was converted to α-chlorophenylacetic acid by the general procedure given below. From 22.4 g of the carbinol there was obtained 11.6 g of α-chlorophenylacetic acid, mp 74–76°C (lit. (22) mp 78°C) after crystallization from hexane.

Conversion of p-*Chlorophenyl(trichloromethyl)carbinol to* p-*Chlorophenyl-α-chloroacetic Acid*

This illustrates the general procedure for the "Jocic reaction" (see footnote 2); this procedure was used with all of the (trichloromethyl)carbinols. The starting material was prepared as above from chlorobenzene and chloral and purified by conversion to the acetate by refluxing overnight with acetic anhydride and acetyl chloride. After recrystallization from ethanol, the acetate melted at 122–123°C (lit. (23) mp 120–121°C); ^{1}Hmr (CCl_4) δ: 7.86 (d, 2, J = 9 Hz, Ph), 7.63 (d, 2, J = 9 Hz, Ph), 6.53 (s, 1, CH), and 2.29 (s, 3, CH_3). The acetate was converted back to the carbinol by refluxing overnight with a solution composed of ten volumes each of isopropyl alcohol, concentrated hydrochloric acid, and water. The carbinol was recrystallized from "iso-octane" to give crystals (19% overall yield), mp 47–48°C (lit. (24) mp 47°C); ^{1}Hmr (CCl_4) δ: 7.90 (d, 2, J = 9 Hz, Ph), 7.61 (d, 2, J = 9 Hz, Ph), 5.33 (s, 1, CH), and 3.33 (s, 1, OH).

In a 250-mL, round-bottomed flask equipped with a magnetic stirrer and thermometer were placed 13 g (0.05 mol) of *p*-chlorophenyl(trichloromethyl)carbinol and 11.2 g (0.2 mol) of potassium hydroxide in 100 mL of water, all at 0°C. The solution was stirred for three days at 0°C. During this time a number of 2-mL aliquots were titrated with standard hydrochloric acid to obtain kinetic data. The alkaline reaction mixture was extracted with ether to obtain the neutral fraction (4.0 g), and the aqueous solution on acidification and extraction with ether yielded 4.5 g (44% of theory, 63% allowing for unreacted carbinol) of *p*-chlorophenyl-α-chloroacetic acid which had the following properties after recrystallization from "isooctane"; mp 75–77°C (lit. (25) mp 75–76°C); ir (KBr): 3300–2400, 1725, 1600, 1475, 1420, 1410, 1290, 1270, 1215, 1190, 1170, 1095, 1080, 1005, 960, 890, 855, 820, 790, 745, 660, 605, and 505 cm^{-1}; ^{1}Hmr ($CDCl_3$) δ: 11.43 (s, 1, COOH), 7.51 (s, 4, Ph), and 5.40 (s, 1, CH).

The neutral fraction was shown by ^{1}Hmr to consist of 78% *p*-chlorophenyl (trichloromethyl)carbinol and 22% of *p*-chlorobenzaldehyde.

Radiochemistry

Ten grams of phenyl(trichloromethyl)carbinol (0.045 mol) was stirred for 69 h at 0°C with 105 mL of 1.5 *N* aqueous potassium hydroxide (0.158 mol), and 10 μCi of chloride-36 ion (1.02×10^7 counts/min measured with a methane-flow proportional counter with a counting efficiency of 46%). The concentration of ionic chloride in the reaction mixture varied from near zero initially to 0.9 *M* after 69 h, determined by titration. The 3.64 g of α-chlorophenylacetic acid (47% yield) obtained gave 196 counts/(mg min). Accordingly, 6.9% of the radioactive chloride and therefore a maximum of 6.9% of the chloride in solution was incorporated into the α-chlorophenylacetate. Since the average amount of chloride ion present during the reaction was 50 mequiv., 3.5 mequiv. of chloride ion is the maximum that could be incorporated into the 21.3 mequiv. of final α-chlorophenylacetic acid. From this it follows that at least 83% of the chlorine in the α-chlorophenylacetate comes from the original phenyl(trichloromethyl)carbinol by an intramolecular migration.

Unreacted carbinol recovered from the above reaction mixture had no radioactivity.

A possible S_N2 displacement reaction between radioactive ionic chloride and the α-chlorophenylacetate was shown to be too slow to have appreciable effect on the above results. Twenty milliequivalents of potassium α-chlorophenylacetate, 80 mequiv. of potassium chloride, 100 mequiv. of potassium hydroxide, and 20 μCi (2.04×10^7 counts/min) of chloride-36 ion were stirred in 100 mL of water at 0°C for 68 h as in the above experiment. α-Chlorophenylacetic acid was isolated quantitatively and found to have only 8 counts/(mg min). Accordingly less than 0.2% of the available radioactive chloride ion was incorporated into the α-chlorophenylacetate.

Kinetic Data

Seven 2-mL aliquots of the *p*-chlorophenyl(trichloromethyl)-carbinol reaction mixture were titrated with 0.1 *N* hydrochloric acid to a phenolphthalein end point. From the amount of base consumed, the percent of carbinol converted to the chloro acid was calculated. Plotting the log of the percent of carbinol reacted against the reaction time at 0°C gave a straight line with a first order rate constant of 4.2×10^{-4} min^{-1}. A second experiment identical to the first, except the amount of carbinol was halved, likewise followed first order kinetics with $k_1 = 4.2 \times 10^{-4}$ min^{-1}.

Can. J. Chem. Downloaded from www.nrcresearchpress.com by 210.87.254.40 on 09/05/12
For personal use only.

Can. J. Chem. Downloaded from www.nrcresearchpress.com by 210.87.254.40 on 09/05/12
For personal use only.

A third experiment identical to the first, but with the potassium hydroxide doubled, likewise gave the same first order reaction rate constant. The calculation of the percent of carbinol converted to chloro acid from the base consumption is somewhat in error due to the by-product dichlorocarbene which also consumes base. Accordingly, the value of the above kinetic experiments is limited to establishing that the reaction is first order in *p*-chlorophenyl (trichloromethyl)carbinol and zero order with respect to base under these experimental conditions. No reaction occurs in the absence of base.

A similar study was carried out starting with trichloroethanol at 30°C, and the reaction was found to be first order in the trichloroethanol.

Kinetic data on trichloroethanol reaction

[Trichloroethanol] (mol/L)	[Base] (mol/L)	Calcd. k_1 ($min^{-1} \times 10^3$)
0.2	1.12	2.3
0.67	1.12	2.3
1.91	1.12	2.2
0.67	0.536	3
0.67	5.36	4.6

Stereochemistry

R-(−)-Phenyl(trichloromethyl)carbinol (1.1 g, 0.05 mol, $[\alpha]_D^{25}$ −15.8° (*c* 11.7, EtOH) (42% optically pure)) (3), 1.25 g (0.02 mol) of potassium hydroxide, 1 mL of 10% potassium oleate solution, and sufficient water to make 10 mL of final solution were stirred together for 8 h at 0°C. The crude acid fraction was sublimed (40–60°C for 1 week) and recrystallized from "isooctane" to give 0.044 g of *S*-(+)-α-chlorophenylacetic acid, $[\alpha]_D^{27}$ +7.3° (*c* 1.295, benzene) (3.8% optically pure). The literature $[\alpha]_D^{12}$ of *R*-(−)-α-chlorophenylacetic acid is −191° (*c* 3.35, benzene) (26).

For a control experiment, 1.15 g of *S*-(+)-α-chlorophenylacetic acid, $[\alpha]_D^{28}$ +53.2° (*c* 3.1, EtOH) was dissolved in 100 mL of 1.11 *N* potassium hydroxide and allowed to stand at 0°C for 8 h. The reaction mixture was poured into ice and dilute sulfuric acid, and extracted with ether. The *S*-(+)-α- chlorophenylacetic acid had a rotation of $[\alpha]_D^{25}$ +15.9° (*c* 31, benzene).

Deuterium Exchange

Phenyl(trichloromethyl)carbinol (2.2 g, 0.01 mol) and 2.5 g (0.045 mol) of potassium hydroxide, dissolved in sufficient deuterium oxide (99.8% pure) to make 20 mL of solution, were stirred at 0°C for 22 h. Aliquots were periodically withdrawn and titrated and the time for 50% reaction calculated to be 21 h. The reaction mixture was extracted with ether to recover the neutral fraction (0.8 g). This was washed with a saturated bisulfite solution to remove benzaldehyde and the residual oil shown to be unreacted phenyl(trichloromethyl)carbinol from its ^{1}Hmr spectra. The phenyl to α-hydrogen ratio was 5:1 showing that no deuterium exchange had occurred prior to the rearrangement to the chloro acid.

After removing the neutral fraction, the reaction mixture was acidified with ice and hydrochloric acid and the acid fraction extracted with ether to give 0.48 g of α-chlorophenylacetic acid, mp 76–79°C after crystallization from hexane. Its ^{1}Hmr spectra (CCl_4) showed a phenyl to α-hydrogen ratio of 5:0.53, showing that 47% deuterium incorporation occurred at the α-position. The results obtained with two other carbinols in similar experiments are given in Table 2.

Control experiments were carried out by dissolving the product acids in alkaline dueterium oxide under the same reaction conditions as above but for one-half the time of the main reaction. The results are in Table 2.

o-*Allylphenyl(trichloromethyl)carbinol Reactions*

o-Iodoallylbenzene was prepared in 18% yield from *o*-allylaniline (from zinc chloride catalyzed rearrangement of *N*-allylaniline at 140°C (27), by diazotization and reaction with potassium iodide, bp 131–137°C (40 Torr); ir (film): 3100, 3080, 3010, 2990, 2910, 1645, 1600, 1580, 1460, 1440, 1020, 990, 920, and 750 cm^{-1}; ^{1}Hmr (CCl_4) δ: 7.87 (m, 1, Ph), 7.21 (m, 2, Ph), 6.91 (m, 1, Ph), 6.0 (d of d of t, 1, J = 19, 11, and 6 Hz, —CH═), 5.16 (d of d, 1, J = 11 and 1.5 Hz, ═CH_2), 5.1 (d of d, 1, J = 19 and 1.5 Hz, ═CH_2), and 3.5 (d, 2, J = 6 Hz, —CH_2—). *Anal.* calcd. for C_9H_9I: 44.29, H 3.72, I 51.99; found: C 44.34, H 3.65, I 51.80.

The *o*-iodoallylbenzene was converted into its Grignard reagent and this was poured into an ether solution containing 90% of the theoretical amount of anhydrous chloral. Distillation gave a 48% yield of *o*-allylphenyl(trichloromethyl)carbinol, bp 124–135°C (0.4 Torr); ir (film): 3600–3300, 3100–2900, 1640, 1450, 1390, 1290, 1175, 1050, 990, 920, 820, 770, 730, 640, and 600 cm^{-1}; ^{1}Hmr (CCl_4) δ: 7.83 (m, 1, Ph), 7.3 (m, 3, Ph), 6.0 (m, 1, —CH═), 5.53 (s, 1, —C*H*OH—), 5.00 (m, 2, ═CH_2), 3.63 (d of d, 2, J = 6 and 8 Hz, —CH_2—), and 3.07 (s, 1, —OH). *Anal.* calcd. for $C_{11}H_{11}Cl_3O$: C 49.75, H 4.17, Cl 40.05; found: C 49.52, H 4.22, Cl 39.80.

A mixture of 9.3 g of the above carbinol and 7.9 g of potassium hydroxide in sufficient water to make 70 mL was stirred at 0°C for 72 h. The crude acid fraction (2.0 g) was converted to methyl *o*-allylphenyl-α-chloroacetate containing an estimated 15% methyl *o*-allylmandelate based on elemental analyses and the presence of a weak absorption peak at 3500 cm^{-1} in the ir spectrum. The distilled material had the following properties: bp 148–154°C (7 Torr); ir (film): 1760 (C═O); ^{1}Hmr (CCl_4) δ: 7.2 (m, 4, Ph), 6.25–5.5 (m, 1, allyl), 5.58 (s, 1, —CHCl—), 5.1 (s, 1, allyl), 5.0 (m, 1, allyl), 3.67 (s, 3, OCH_3), and 3.5 (m, 2, CH_2); high-resolution (ms) obsd./calcd. *Exact Mass* for $C_{12}H_{13}ClO_2$: 224.0604/224.0651. *Anal.* calcd. for $C_{12}H_{13}ClO_2$: C 64.29, H 5.79, Cl 15.8; found: C 65.20, H 5.88, Cl 12.80.

The neutral fraction amounted to 6.2 g and was shown (^{1}Hmr) to consist of 1.5 g of *o*-allylbenzyaldehyde and 4.7 g unreacted carbinol. The two were separated by column chromatography on neutral Brockman alumina using benzene and methanol successively as eluents.

p-*Bromophenyl(trichloromethyl)carbinol Reactions*

The crude carbinol was prepared as above from bromobenzene and chloral, purified by conversion to the acetate, mp 145–147°C; ir (KBr): 1750, 1230, 1065, 1045, 1020, 940, 880, 830, 780, 720, 675, 615, and 530 cm^{-1}. The acetate was hydrolyzed to the carbinol by the same procedure used with the *p*-chloro analog. The crystals were recrystallized from "isooctane", mp 55°C; ir (KBr): 3600–3400, 2940, 1600, 1500, 1400, 1320, 1285, 1240, 1185, 1110, 1065, 1005, 870, 825–810, 770, 710, 660, 630, and 615 cm^{-1}; ^{1}Hmr (CCl_4) δ: 7.42 (broad s, 4, Ph), 5.04 (s, 1, CH), and 3.3 (s, 1, OH).

A mixture of 15.2 g of the above carbinol and 11.2 g of potassium hydroxide in sufficient water to make 100 mL was stirred at 0°C for 48 h. The crude *p*-bromophenyl-α-chloroacetic acid (6.1 g) was recrystallized from "isooctane" and melted at 82–84°C (lit. (28) mp 82–83°C). The neutral fraction consisted of *p*-bromobenzaldehyde (0.34 g) and unreacted carbinol (7.5 g), bp 159–162°C (2 Torr).

tert-*Butyl(trichloromethyl)carbinol Reactions*

The carbinol was prepared in 17% yield from trichloromethylmagnesium chloride (29) (from *n*-butylmagnesium chloride and chloroform in THF at −78°C) and 2,2-dimethylpropanal at−70°C; bp 102–108°C (45 Torr), mp 47–48°C (lit. (30) mp 49°C); ir (film): 3500, 3000–2850, 1480, 1380, 1060, 1020, 810, 780, 710, and 630 cm^{-1}.

Can. J. Chem. Downloaded from www.nrcresearchpress.com by 210.87.254.40 on 09/05/12
For personal use only.

A mixture of 4.1 g of the above carbinol and 4.5 g of potassium hydroxide in sufficient water to make 40 mL was stirred at 0°C for 24 h. The crude acid fraction amounted to 0.35 g; it was methylated with diazomethane. The ester mixture consisted (glc with a silicon gum rubber column at 100°C) of 22% methyl trimethyllactate (8 min retention time) and 78% methyl 2-chloro-3,3-dimethylbutyrate (10 min retention time). The methyl trimethyllactate was identified by comparison with an authentic sample (31, 32). The methyl 2-chloro-3,3-dimethylbutyrate was characterized as follows: ir (film): 2950, 1760, 1280, and 1160 cm^{-1}; ^{1}Hmr (CCl_4) δ: 4.14 (s, 1, —CHCl—), 3.85 (s, 3, —OCH_3), and 1.17 (s, 9, CH_3). *Anal.* calcd. for $C_7H_{13}ClO_2$: C 51.07, H 7.96, Cl 21.54; found: C 50.86, H 8.21, Cl 21.25.

Trichloroethanol Reactions

From 14.9 g of trichloroethanol and 22.4 g of potassium hydroxide in 200 mL of water at 30°C for 6 h there was obtained 3.7 g of a crude acid mixture consisting (^{1}Hmr analysis) of 2.1 g of chloroacetic acid and 1.6 g of trichloroethoxyacetic acid. One liter of carbon monoxide was evolved during the first 203 min of reaction. The gas was dried and characterized by the 2160 and 2110 cm^{-1} bands in its ir spectrum (33). The evolution was first order in trichloroethanol with $k_1 = 1.07 \times 10^{-4}$ min^{-1}. Chloroacetic acid was isolated by distillation and identified by its mp of 55–57°C, and its ir and ^{1}Hmr spectra. The residue was identified as trichloroethoxyacetic acid by its mp of 70°C (lit. (34) mp 69.5°C) and its ^{1}Hmr spectrum.

p-*Tolyl(trichloromethyl)carbinol Reactions*

The crude carbinol, bp 128–150°C (2 Torr), containing 25% of the *ortho* isomer and 8% tetrachlorotolylethanes (^{1}Hmr analysis) was prepared from toluene and chloral (21), and converted to the acetate by refluxing with a six-fold excess of acetic anhydride and acetyl chloride (2 to 1 ratio) for 8 h. Properties of *p*-tolyl(trichloromethyl)carbinol acetate after two recrystallizations from ethanol: mp 106–108°C (lit. (21) mp 107–108°C); ir (KBr): 3500–3300, 1620, 1510, 1400, 1330, 1300, 1250, 1200, 1180, 1065, 865, 825–780, 740, 720, 650, 620, and 510 cm^{-1}; ^{1}Hmr (CCl_4) δ: 7.04 (d, 2, J = 9 Hz, Ph), 6.74 (d, 2, J = 9 Hz, Ph), 5.88 (s, 1, —C*H*OH), 2.08 (s, 3, CH_3—), and 2.05 (s, 3, CH_3).

The above carbinol acetate was hydrolyzed to the carbinol by the same procedure used for the chloro analog. The crystals were recrystallized from "isooctane": mp 63–64°C (lit. (21) mp 63–64°C), ir (KBr): 3020–2900, 1730, 1360, 1220, 1170, 1050–1030, 925, 870, 785, 740, 710, 670, 615, 595, 550, and 510 cm^{-1}; ^{1}Hmr (CCl_4) δ: 7.38 (d, 2, J = 8.5 Hz, Ph), 6.71 (d, 2, J = 8.5 Hz, Ph), 4.93 (s, 1, CH), 3.43 (s, 1, OH), 2.32 (s, 3, CH_3).

A mixture of 11.9 g of the above carbinol and 11.2 g of potassium hydroxide in sufficient water to make 100 mL was stirred at 0°C for 48 h. The neutral fraction (8.9 g) consisted (^{1}Hmr analysis) of 0.7 g of *p*-tolualdehyde and 7.6 g of *p*-tolyl(trichloromethyl)carbinol. The compounds were separated by glc (silicon gum rubber at 200°C), and identified by comparison with authentic samples. The acid fraction (2.1 g) was *p*-tolylglycollic acid and was recrystallized from benzene: mp 145–147°C (lit. (35) mp 145–146°C); ir (KBr): 3450, 3350, 3100–2500, 1700, 1290, 1180, 1060, 935, 880, 820, 730, 705, and 580 cm^{-1}; ^{1}Hmr (DMSO-d_6) δ: 7.14 (d, 2, J = 8 Hz, Ph), 6.97 (d, 2, J = 8 Hz, Ph), 4.9 (s, 1, CH), and 2.2 (s, 3, CH_3).

A reference sample of *p*-tolylglycollic acid was prepared by the method outlined in Organic Syntheses (36).

1-(Trichloromethyl)-1-cyclohexanol Reactions

The carbinol, mp 57–59°C, was prepared from cyclohexanone and chloroform (37). A mixture of 10.6 g of the carbinol, 11.2 g of potassium hydroxide, and 90 mL of water was stirred at 0°C for 10 h. The neutral fraction (3.0 g) was cyclohexanone, identified by its ir and the mp of its dinitrophenylhydrazone. The acid fraction (0.85 g) could not be thoroughly characterized. Its ^{1}Hmr spectrum suggested that it was mostly 1-chlorocyclohexanecarboxylic acid with around 25% 1-cyclohexenecarboxylic acid. This corresponds to an 8% yield of the chloro acid.

*Di(*p*-Chlorophenyl)(trichloromethyl)carbinol Reactions*

A mixture of 18.5 g of di(*p*-chlorophenyl) (trichloromethyl) carbinol[3] and 12.5 g of potassium hydroxide in sufficient water to make 100 mL was stirred at 0°C for three days. The acid fraction was negligible. The crude neutral fraction appeared by nmr analysis to be substantially pure 4,4′-dichlorobenzophenone together with its isomeric impurity. After one recrystallization from 95% ethanol, it melted at 144–148°C (lit. (38) mp 145°C), and its ir spectrum was identical with that of an authentic sample.

Acknowledgement

The work with deuterium oxide was carried out at South Dakota State University, Brookings, SD by J. R. M. and G. A. M.

1. Z. Jocic. Zh. Russ. Fiz. Khim. Ova. **29**, 97 (1897).
2. W. Reeve. Synthesis, 131 (1971).
3. W. Reeve, R. J. Bianchi, and J. R. McKee. J. Org. Chem. **40**, 339 (1975).
4. J. H. T. Ledrut and G. Combes. Ind. Chim. Belge, **19**, 120 (1954); **19**, 635 (1962).
5. T. F. Steckel. Ph.D. Dissertation, University of Maryland. 1970.
6. F. A. Long and P. Ballinger. *In* Electrolytes. *Edited by* B. Pesce. Pergamon Press, New York. 1962. p. 152; R. N. Haszeldine. J. Chem. Soc. 1757 (1953).
7. J. Hine, R. C. Peek, and B. D. Oakes. J. Am. Chem. Soc. **76**, 827 (1954).
8. K. C. Kemp and D. Metzger. J. Org. Chem. **33**, 4165 (1968).
9. R. N. MacDonald and T. E. Tabor. J. Am. Chem. Soc. **89**, 6573 (1967).
10. R. N. McDonald and R. N. Steppel. J. Am. Chem. Soc. **91**, 782 (1969).
11. R. N. McDonald and R. N. Steppel. J. Org. Chem. **35**, 1250 (1970).
12. R. N. McDonald, R. N. Steppel, and R. C. Cousins. J. Org. Chem. **40**, 1694 (1975).
13. R. N. McDonald. *In* Mechanisms of molecular migrations. *Edited by* B. S. Thyagarajan. Wiley Interscience, New York, NY. 1971. pp. 67–107.
14. O. Neunhoeffer and A. Spange. Justus Liebigs Ann. Chem. **632**, 22 (1960).
15. R. Brown. Ph.D. Dissertation, University of Maryland. 1968.
16. R. N. McDonald and P. A. Schwab. J. Am. Chem. Soc. **86**, 4866 (1964).
17. J. K. Stille and D. D. Whitehurst. J. Am. Chem. Soc. **86**, 4871 (1964).
18. J. Fenwick, G. Frater, K. Ogi, and O. P. Strausz. J. Am. Chem. Soc. **95**, 124 (1973).
19. O. P. Strausz, R. K. Gosavi, A. S. Denes, and I. G. Csizmadia. J. Am. Chem. Soc. **98**, 4784 (1976).
20. R. Tsuk. M.S. Dissertation, University of Maryland. 1972.

[3]We are indebted to Dr. Richard S. Cook of the Rohm & Haas Company for a generous gift of "Kelthane". This is about 65% di(*p*-chlorophenyl)(trichloromethyl)carbinol, 20% (*o*-chlorophenyl) (*p*′-chlorophenyl)(trichloromethyl)carbinol and 15% other impurities. The material was used as received.

21. A. DINESMANN. C. R. Acad. Sci. **141**, 201 (1905).
22. B. RADZISZEWSKI. Ber. **2**, 207 (1869).
23. J. W. HOWARD. J. Am. Chem. Soc. **57**, 2317 (1935).
24. G. T. BARRY and R. BOYER. Can. J. Res. Sect. B, **26**, 511 (1948).
25. H. L. HALLER *et al.* J. Am. Chem. Soc. **67**, 1601 (1945).
26. A. MCKENZIE and G. W. CLOUGH. J. Chem. Soc. **93**, 818 (1908).
27. C. D. HURD and W. W. JENKINS. J. Org. Chem. **22**, 1418 (1957).
28. H. GOTTHARDT. Chem. Ber. **105**, 188 (1972).
29. J. VILLIERAS. Bull. Soc. Chim. France, 1520 (1967).
30. D. SEYFERTH, J. E. HALLGREN, and P. L. K. HUNG. J. Organomet. Chem. **50**, 265 (1973).
31. A. H. RICHARD and P. LANGLAIS. Bull. Soc. Chim. France, **7**, 466 (1910).
32. A. RICHARD. Ann. Chim. Phys. **21**, 398 (1910).
33. Sadtler standard spectra catalogue. Sadtler Research Laboratory, Philadelphia, PA. Spectrum No. 1142.
34. K. GARZAROLLI-THURNLACKH. Justus Liebigs Ann. Chem. **210**, 72 (1881).
35. J. L. RIEBSOMER, J. IRVINE, and R. ANDREWS. J. Am. Chem. Soc. **60**, 1015 (1938).
36. J. J. KLINGENBERG. Organic syntheses. Coll. Vol. IV. John Wiley and Sons, Inc., New York, NY. 1963. p. 110.
37. D. G. KUNDIGER, E. A. IKENBERRY, E. B. W. OVIST, J. G. PETERSON, and C. R. DEEK. J. Am. Chem. Soc. **82**, 2953 (1960).
38. F. BODROUX. C. R. Acad. Sci. **137**, 710 (1903).

Can. J. Chem. Downloaded from www.nrcresearchpress.com by 210.87.254.40 on 09/05/12
For personal use only.

Reaction of pyrylium salts with hydrazine and methylhydrazine. Concerning the scope of the 1,2(4*H*)-diazepine synthesis[1,2]

D. J. HARRIS,[3] G.Y.-P. KAN, T. TSCHAMBER,[4] and V. SNIECKUS[5]

Guelph–Waterloo Centre for Graduate Work in Chemistry, University of Waterloo, Waterloo, Ont., Canada N2L 3G1

Received October 10, 1979

D. J. HARRIS, G.Y.-P. KAN, T. TSCHAMBER, and V. SNIECKUS. Can. J. Chem. **58**, 494 (1980).

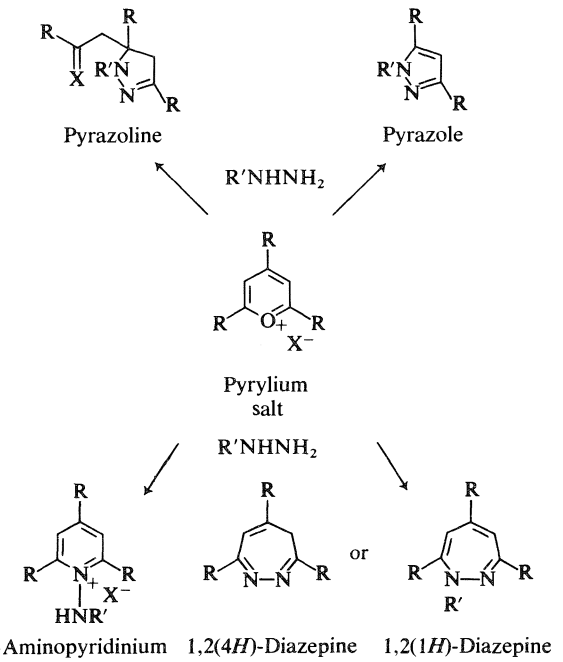
The reaction of pyrylium salts **1***a*–e with methylhydrazine gives pyrazolines (**2**), pyrazoles (**3**), pyridines (**4**), 1,2-diazepine (**5**), and *N*-methylaminopyridinium salts (**6**). Product composition has been studied as a function of pyrylium salt counter anion, concentration of methylhydrazine, and conditions of the reaction (Table 1). Pyridines (**4**) and 1,2-diazepines (**5**) are minor components, the major products being the pyrazolines (**2**) and pyrazoles (**3**). The reactions of more unusual pyrylium salts (**1***f*–i, **8***a*, **9***a*, **9***c*, and **11***a*) with hydrazine have been shown to provide 1,2(4*H*)-diazepines (**10**, **12**–**15**) and *N*-aminopyridinium salts (**8***b*, **9***b*) (Table 2), the nature of the product apparently depending on the absence or presence of 2-methyl substitution respectively in the starting pyrylium salts.

D. J. HARRIS, G.Y.-P. KAN, T. TSCHAMBER et V. SNIECKUS. Can. J. Chem. **58**, 494 (1980).

La réaction des sels de pyrylium **1***a*–*e* avec la méthylhydrazine conduit aux pyrazolines (**2**), aux pyrazoles (**3**), aux pyridines (**4**), à la diazépine-1,2 (**5**) et aux sels de *N*-méthylaminopyridinium (**6**). On a étudié la composition des produits en fonction de l'anion des sels de pyrylium, de la concentration de la méthylhydrazine et des conditions de la réaction (Tableau 1). Les pyridines (**4**) et les diazépines-1,2 (**5**) sont des produits secondaires, les produits principaux de la réaciton étant les pyrazolines (**2**) et les pyrazoles (**3**). On a montré que les réactions des sels de pyrylium les moins usuels (**1***f*–*i*, **8***a*, **9***a*, **9***c* et **11***a*) avec l'hydrazine conduisent aux (4*H*)-diazépines-1,2 (**10**, **12**–**15**) et aux sels de *N*-aminopyridinium (**8***b*, **9***b*) (Tableau 2). La nature des produits dépend apparemment de l'absence ou de la présence d'un substituant méthyle en position 2 dans les sels de pyrylium de départ.

[Traduit par le journal]

Pyrylium salts undergo reaction with a host of nucleophiles to give a variety of heterocyclic, benzenoid, and open chain products (2–6). We initiated work on the reaction of highly, invariably aryl, substituted pyrylium and thiapyrylium salts with hydrazines in connection with our interest to prepare new 1,2-diazepine derivatives (1, 7). This reaction, first briefly described by Schneider and Seebach (8), well documented (5), and extensively studied more recently by several groups (7, 9–12), leads to pyrazolines (9), pyrazoles (10), *N*-aminopyridinium salts (9*a*, 9*c*, 10, 11), or 1,2-diazepines (9*e*, 9*f*, 9*g*, 12) (Scheme 1). The products obtained are dependent on the structures of the pyrylium salts and hydrazine derivatives and the reaction conditions. Balaban has isolated intermediates in some of these reactions (9*g*–*h*) and we have studied the interrelationships of these substances by thermal and acid-catalyzed reactions (13). Subsequent to our preliminary communication (1), we have studied the reaction of a number of diverse pyrylium salts with hydrazine in attempts to extend the scope and define the limitations of the 1,2-diazepine synthesis (12). The details of both studies (1, 6) constitute the current report.



SCHEME 1

[1]Part of this study has appeared in preliminary form (1).

[2]Abstracted from the Ph.D. theses of D.J.H. (1976) and G.Y.-P.K. (1970), University of Waterloo.

[3]National Research Council of Canada Postgraduate Scholar, 1973–1976.

[4]Present address: Ecole Nationale Supérieure de Chimie de Mulhouse, Université de Haute Alsace, 68093 Mulhouse, France.

[5]Author to whom correspondence may be addressed.

0008-4042/80/050494-07$01.00/0

©1980 National Research Council of Canada/Conseil national de recherches du Canada

Can. J. Chem. Downloaded from www.nrcresearchpress.com by 210.87.254.40 on 09/05/12
For personal use only.

TABLE 1. Reaction of 2,4,6-triphenylpyrylium salts 1*a–e* with methylhydrazine

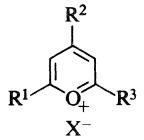
Compound	Ratio 1:$MeNHNH_2$	Reaction conditions	Products (% yield)[a]			
1*a*	1:2	PhH, 0°C → room temperature, 6 h		3*a*(50–68)	4*a*(5)	
1*a*	1:4	PhH, room temperature, 2 h	2*a*(33)	3*a*(38)	4*a*(1)	
1*a*	1:2	Et_2O, room temperature, 4 h		3*a*(64)	4*a*(5)	5(13)
1*a*	1:2.5	EtOH, room temperature, 4 h		3*a*(87)		
1*a*	1:60	Neat, room temperature, 5 h		3*a*(90)		5(1)
1*b*	1:2.5	EtOH, room temperature, 4 h		3*a*(81)		
1*c*	1:60	Neat, 0°C, 7 h		3*a*(92)		
1*d*	1:2.5	PhH, room temperature, 9 h	2*b*(15)	3*a*(8)		6(57)
1*e*	1:2.5	EtOH, room temperature, 4 h	2*b*(2)	3*a*(80)		
1*e*	1:60	Neat, 0°C, 16 h	2*b*(40)	3*a*(42)		

[a] 10–40% of acetophenone was isolated from all of the reactions listed.

Reaction of Pyrylium Salts 1a–e *with Methylhydrazine*

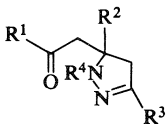
The results from the reaction of pyrylium salts 1*a–c* with methylhydrazine are summarized in Table 1. In the non-polar solvents benzene and ether as well as with neat methylhydrazine, the pyrylium iodide 1*a* gave the pyrazole 3*a* as the major product with minor amounts of pyrazoline (2*a*), pyridine (4*a*), and diazepine (5) derivatives. In addition, acetophenone was always detected by nmr in the crude reaction mixtures from 1*a* as well as from 1*b* and 1*c*. The yield of the diazepine 5 is not a maximum limit since it was shown that this compound partially decomposed in solution or on chromatography over silica gel into 2,4,6-triphenylpyridine (4*a*) and 1-methyl-3,5-diphenylpyrazole (3*a*) (see Experimental). Change of counter anion from iodide (1*a*) to fluoroborate (1*b*) or perchlorate (1*c*) had little effect on the distribution of products (compare 1*a* and 1*b* to EtOH, 1*a* and 1*c* in neat methylhydrazine). In contrast to the same reaction with the corresponding thiapyrylium salts which provided good yields of the diazepine 5 (7), the pyrylium salts 1*a–c* gave trace or minor amounts of this product (e.g., in Et_2O as solvent). Pyrazolines 2*a* and 2*b* were identified by their characteristic nmr spectra (7, 9*g*, 14) and their quantitative thermal fragmentation to the pyrazoles 3*a* and 3*b* and acetophenone. The structures of the other products 4*a* and 5 were confirmed by comparison with authentic samples.

Attempts to obtain diazepine products from the 2-methyl-4,6-diphenylpyrylium salts 1*d* and 1*e* were totally unsuccessful (Table 1). However, in comparison to the reaction of 1*a*, the product composition in benzene at room temperature changes to yield, besides minor amounts of the pyrazoline 2*b* and the pyrazole 3*a*, the *N*-aminopyridinium salt 6. Although 6 was first isolated in 1921 by Schneider and Seebach (8), its structure was not firmly established (15) but this is clear from its spectral and analytical data and its hydrogenolysis into 2-methyl-4,6-diphenylpyridine (4*b*) (see Experimental). The contrast in the reaction of 1*a* and 1*d* with methylhydrazine in benzene may be attributed to steric hindrance in cyclization of the respective open-chain methylhydrazone intermediates 7*a* and



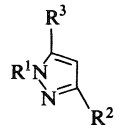
1

a $R^1 = R^2 = R^3 = Ph$, X = I
b $R^1 = R^2 = R^3 = Ph$, X = BF_4
c $R^1 = R^2 = R^3 = Ph$, X = ClO_4
d $R^1 = R^2 = Ph$, $R^3 = Me$, X = I
e $R^1 = R^2 = Ph$, $R^3 = Me$, X = BF_4
f $R^1 = R^2 = Ph$, $R^3 = C_6H_4$—*p*-OMe, X = ClO_4
g $R^1 = R^2 = Ph$, $R^3 = CH{=}CHPh$, X = ClO_4
h $R^1 = R^3 = Ph$, $R^2 = H$, X = ClO_4
i $R^1 = R^2 = R^3 = t$-Bu, X = ClO_4



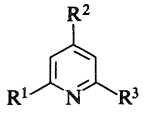
2

a $R^1 = R^2 = R^3 = Ph$, $R^4 = Me$
b $R^1 = R^2 = Ph$, $R^3 = R^4 = Me$
c $R^1 = R^2 = R^3 = R^4 = Ph$
d $R^1 = R^3 = Ph$, $R^2 = R^4 = H$



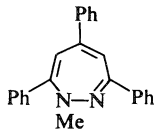
3

a $R^1 = Me$, $R^2 = R^3 = Ph$
b $R^1 = R^2 = Me$, $R^3 = Ph$
c $R^1 = R^3 = H$, $R^2 = Ph$

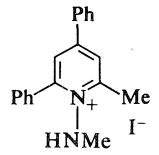


4

a $R^1 = R^2 = R^3 = Ph$
b $R^1 = R^2 = Ph$, $R^3 = Me$

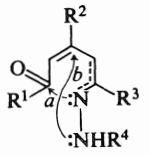


5



6

Can. J. Chem. Downloaded from www.nrcresearchpress.com by 210.87.254.40 on 09/05/12
For personal use only.



7
a $R^1 = R^2 = R^3 = Ph, R^4 = Me$
b $R^1 = R^2 = Ph, R^3 = R^4 = Me$
c $R^1 = R^2 = R^3 = R^4 = Ph$

7*b* (7, 9*g–h*). In the case of **1***a*, cyclization of **7***a* to *N*-methylamino-2,4,6-triphenylpyridinium hydroiodide (path *a*) is presumably prevented by the steric congestion of the contiguous *N*-methylamino and 2,6-diphenyl substituents which would result upon final dehydration. A less stringent steric requirement is presented by the Michael reaction of **7***a* (path *b*), leading to the pyrazoline **2***a*. In fact, an open-chain hydrazone (**7***c*) may be isolated from the reaction of **1***a* with phenylhydrazine which requires forcing conditions (refluxing EtOH) for conversion into the corresponding pyrazoline **2***c* (9*h*). The duality of *N*-aminopyridinium salt or pyrazole formation from 2,6-dimethyl substituted pyrylium salts has been previously observed (10*b–d*). The production of similar amounts of **2***b* and **3***a* from the reaction of the unsymmetrical pyrylium salt **1***d* in benzene or without solvent suggests the lack of steric discrimination in the initial attack of methylhydrazine at the 2- and 6-positions.

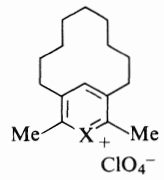
In marked contrast and contrary to expectation based on a steric argument, predominant formation of the pyrazole **3***a* results when the reaction is carried out in ethanol solution. Similar behaviour has been observed in the reaction of 2-methyl-4,6-diphenylpyrylium perchlorate with hydrazine (10*d*). On the other hand, Reissenweber and Sauer recently showed that 2-methyl-4,6-diphenylpyrylium salts with an additional methyl or phenyl substituent at the 3-position undergo reaction with hydrazine to give the corresponding 1,2(4*H*)-diazepines (12*a*). Undoubtedly complex equilibria are involved in these reactions, and a satisfactory mechanistic explanation is presently not available. However, we have observed similar behaviour in the reaction of unsymmetrical *N*-iminopyridinium ylides with peroxides (16).

Reactions of Pyrylium Salts **1**f–i, **8**a, **9**a, **9**c, *and* **11** *with Hydrazine*

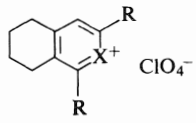
As an extension of the reaction of pyrylium salts with hydrazine (12) and in the hope of preparing new diazepine derivatives, we tested a diverse group of substrates. The results (Table 2) are a continuation of the previously observed trend (see above), i.e., 2,6-dialkylpyrylium salts (**8***a*, **9***a*), excluding the 2,6-di-*tert*-butyl case (**1***i*), yield *N*-aminopyridinium derivatives (**8***b*, **9***b*), whereas 2,6-diaryl systems (**1***f–g*, **9***c*, **11**) containing 4-substituents provide 1,2(4*H*)-diazepines (**13**, **14**, **10**, **12**).

Treatment of the (9)-pyrylophanium perchlorate **8***a* with hydrazine in ethanol at room temperature afforded the *N*-aminopyridinium salt **8***b* in 75% yield. The physical and spectral data are identical to those reported by Balaban for **8***b* subsequent to the completion of our work (9*c*). We also prepared the acetylated product **8***c* which is a potential intermediate for a photochemical synthesis of the (9)-diazepinophanium system. Under the conditions used for **8***a*, the dimethyltetrahydro-2-benzopyrylium salt **9***a* also gave an *N*-aminopyridinium derivative **9***b* (60% yield). These products (**8***b*, **8***c*, **9***b*) all showed mass spectra characteristic of *N*-aminopyridinium salts (major fragmentation by loss of $HClO_4$ and NH_2 or NHAc) (17).

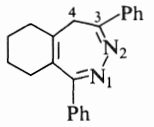
The effect of 2,6-dialkyl vs. -diaryl substituents may be gleaned from the comparison of the reaction of pyrylium salts **9***a* and **9***c* with hydrazine. Under identical conditions to those used for **9***a*, compound **9***c* gave the bicyclic 1,2(4*H*)-diazepine **10** in moder-



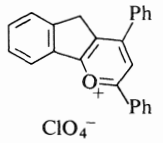
8
a X = O
b X = NNH_2
c X = NNHAc



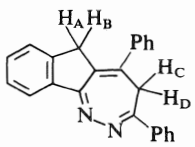
9
a R = Me, X = O
b R = Me, X = NNH_2
c R = Ph, X = O



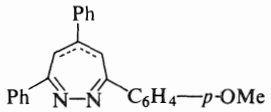
10



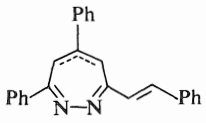
11



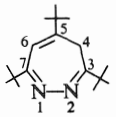
12



13



14



15

Can. J. Chem. Downloaded from www.nrcresearchpress.com by 210.87.254.40 on 09/05/12
For personal use only.

Can. J. Chem. Downloaded from www.nrcresearchpress.com by 210.87.254.40 on 09/05/12
For personal use only.

ate yield. The structure of **10** is fully consistent with the spectral data (see Experimental). An interesting feature of its nmr spectrum at ambient temperature is the sharp doublet at δ 3.45 (J = 12 Hz) assigned to half of the C-4 methylene AB pattern. This contrasts with simple 1,2(4*H*)-diazepines which show broadened AB systems near room temperature owing to the ring inversion phenomenon (6, 12*e*, 18). In **10**, such a process has a considerably higher activation energy as a result of the carbocyclic ring fusion. Evidence for this could not be obtained by temperature variable nmr studies due to decomposition of **10** above +50°C. Hungarian workers have recently shown that fully aromatic compounds corresponding to **9**, X = O, even with a 3-methyl substituent may be ring expanded to the 1,2(4*H*)-diazepines by reaction with hydrazine (12*d*). The ring-fused diphenylpyrylium salt **11** also furnished a diazepine derivative (**12**) in 85% yield. The nmr spectrum of compound **12** shows an interesting temperature dependence for the benzylic (H_A, H_B) and diazepine ring (H_C, H_D) protons. Envelope-like peaks are observed at δ 4.58 and 4.4 at ambient temperature which split into two AB spin systems at δ 4.85 (d, J = 20 Hz) and 4.46 (d, J = 20 Hz), and δ 5.33 (d, J = 12 Hz) and 3.51 (d, J = 12 Hz), respectively, at the lower temperature limit (−40°C). The latter AB pattern is characteristic both in the large chemical shift difference and coupling constant of the C-4 methylene absorptions of the 1,2(4*H*)-diazepine system (12*e*, 18) and can therefore be assigned to the H_C and H_D protons of **12**. The absorptions at δ 4.85 and 4.46 are thus assigned to the H_A and H_B protons. Since the low temperature limit spectrum shows no evidence for doubling of the two AB systems which would implicate four isomers, we conclude that the coalescence phenomenon is due to a single synchronous process involving five-membered ring and diazepine ring inversions. This is supported by the almost identical free energies of activation calculated for the H_A, H_B ($\Delta G_C^{\ddagger}$ = 13.1 kcal/mol, T_C = +2.5 ± 2°C) and the H_C, H_D ($\Delta G_C^{\ddagger}$ = 13.4 kcal/mol, T_C = +17 ± 2°C) systems at their respective coalescence temperatures. Compared to the 3,5,7-triaryl-1,2(4*H*)-diazepine ring system (Scheme 1), compound **12** is modified by a methylene bridge between C-6 and the *ortho* position of the C-7 phenyl group. The effect of this bridge is to pinch the diazepine at the C-6 to C-7 bond thereby inducing greater ring planarity which, in turn, is expected to facilitate the ring inversion process in **12** compared to the simple triaryl-1,2(4*H*)-diazepines. The higher activation energy observed for the latter systems, $\Delta G_C^{\ddagger}$ = 17–18 kcal/mol is in agreement with this view.

The unsymmetrical triaryl pyrylium perchlorate **1***f* and the 2-styrylpyrylium fluoroborate **1***g* afforded 1,2(4*H*)-diazepines **13** and **14** respectively in moderate yields. That **13** was a mixture of Δ^4- and Δ^5- double bond isomers was inferred from the nmr spectrum which showed two singlets for the methoxyl hydrogens at δ 3.9 and 3.75 in a ratio of 3:1 and a broadened ABX pattern for the methylene (δ 4.4, 2.65) and diazepine ring vinyl (δ 6.7) protons (12*e*, 18). That the appearance of two methoxyl singlets is not due to two diazepine conformational isomers undergoing slow ring inversion was established by variable temperature nmr studies (room temperature → 130°C) which showed the collapse of the methylene protons but no change in the methoxyl absorptions. Attempts to separate the two double bond isomers by thin-layer chromatography were not successful. Treatment of **13** with acid over a long period of time resulted only in equilibration to a 1:1 mixture (nmr analysis). The product **14**, on the other hand, appeared to be a single isomer on the basis of tlc and nmr spectral criteria. Aside from the ABX pattern for the methylene and vinyl hydrogens at δ 2.5, 4.2, and 6.22 respectively, the nmr spectrum showed a sharp singlet at δ 6.9 assigned to the coincidental absorption of the styryl hydrogens. The available evidence does not allow the definite assignment of the Δ^4- or Δ^5-isomer to product **14**.

Treatment of 2,6-diphenylpyrylium perchlorate **1***h* with hydrazine gave the unstable pyrazoline **2***d*. Its structure was supported by the characteristic nmr spectrum which could be compared with those of the previously obtained pyrazolines (**2***a–c*) (7, 9*g*, 14) (see Experimental) and by its thermal fragmentation into 3-phenylpyrazole (**3***d*) and acetophenone. From this and other (10*b*, 12*b–c*) observations, it appears that a 4-substituent in the pyrylium salt is essential for the formation of diazepine products.

Since methyl substituted pyrylium salts gave only *N*-aminopyridinium salts, pyrazoles, or pyrazolines, we wished to test the reaction of an alkyl substituted pyrylium salt lacking acidic hydrogens. Treatment of 2,4,6-tri-*tert*-butylpyrylium perchlorate **1***i* with hydrazine resulted in smooth conversion into the corresponding 1,2(4*H*)-diazepine **15** in 90% yield. The structure was consistent with the nmr spectrum which showed an ABX system at δ 2.25 (d, J = 13 Hz, C-4 H_A), δ 3.3 (d, J = 13 Hz, C-4 H_B), and δ 6.15 (br s, C-6 H) typical for the 3,5,7-triaryl-1,2(4*H*)-diazepines (12*e*, 18) but shifted to higher field on account of lack of the anisotropic effect of the aryl rings. Balaban has recently prepared the 5-methyl- and 5-

TABLE 2. Reaction of pyrylium salts **1***f–i*, **8***a*, **9***a*, **9***c*, and **11** with hydrazine

Pyrylium salt	Product[a] (yield %)	Melting point (°C) (solvent)	Nuclear magnetic resonance ($CDCl_3$) δ values	Mass spectra *m/e* (% relative intensity)
1*f*	**13** (58)	185–189 (EtOH)	2.7 (d, 1H, J = 13 Hz, C-4 H), 3.9, 3.85 (2s, 3:1 ratio, 3H, OMe), 4.4 (d, 1H, J = 13 Hz, C-4 H), 6.65 (br s, 1H, C-6 H), 7.0 (d, 2H, J = 9 Hz, *p*-$MeOC_6H_4$ *ortho* H), 7.3–8.2 (m, 12H, Ar H)	352(M^+, 68), 324(39), 249(100), 234(68), 115(82)
1*g*	**14** (54)	201–202 (EtOH)	2.2–2.7 (br s, 1H, C-4 H), 3.8–4.5 (br s, 1H, C-4 H), 6.58 (s, 1H, C-6 H), 6.92 (s, 2H, C*H*=C*H*), 7.13–7.65 and 7.8–8.17 (2m, 16H, Ar H)	348(M^+, 75), 347(100), 244(75), 219(75), 115(75)
1*h*	**2***d*[b] (59)	108.5–117.5 (dec.) (EtOH)	2.45–3.5 (m, 2H, J = 10 Hz, ring CH_2), 3.3 (d, 2H, J = 7 Hz, CH_2), 4.1–4.6 (m, 1H, C-5 H), 5.35 (br s, H, exch. D_2O, NH), 7.2–8.3 (m, 10H, Ar H)	264(M^+, 8) 144(100), 143(66), 105(50)
1*i*	**15** (90)	72 –75[c]	1.30 (s, 27H, *tert*-Bu H), 2.25 (d, 1H, J = 13 Hz, C-4 H), 3.3 (d, 1H, J = 13 Hz, C-4 H), 6.2 (s, 1H, C-6 H)	262(M^+, 25), 247(30), 220(45), 205(30), 164(100)
8*a*	**8***b* (75)	248 –250[d] (EtOH)	1.2 (br s, 10H, CH_2), 1.65–2.1 (br s, 4H, CH_2), 2.8–3.2 (m, 4H, β-pyridine CH_2), 2.9 (s, 6H, $2CH_3$), 8.15 (s, 1H, γ-pyridine H)[e]	247(16, $M^+ - ClO_4$), 231 (92), 134(67), 133 (100)
9*a*	**9***b* (60)	103–104 (EtOH)	1.65–2.2 (br, 4H, CH_2CH_2), 2.6–3.2 (br, 4H, CH_2CH_2), 2.75 (s, 6H, $2CH_3$), 5.6–6.6 (br s, 2H, exch D_2O, NH_2), 7.45 (s, 1H, pyridine β-H)	177(26, $M^+ - ClO_4$), 161(100), 160(80), 146(70)
9*c*	**10** (40)	104–106 (EtOH)	1.2–2.8 (m, 9H, cyclohexane CH_2, C-4 H), 3.3 (d, 1H, J = 13 Hz), C-4 H), 7.2–8.2 (m, 10H, Ar H)	300(M^+, 24), 197(24), 85(68), 83(100)
11	**12** (85)	202.5–203 (dec.) (EtOH)	3.15–3.95 (br, 2H, C-4 H_2), 3.7 (br s, 2H, benzylic CH_2), 7.2–7.85, 7.95–8.25 (m, 14H, Ar H)	335(M^+, 25), 334(100), 333(48), 231(70)

[a] *Anal.* calcd. (found): **13** ($C_{24}H_{20}N_2O$): C 81.79 (81.83), H 5.72 (5.77), N 7.95 (7.88); **14** ($C_{25}H_{20}N_2$): C 86.18 (86.33), H 5.79 (6.01), N 8.04 (8.08); **15** ($C_{17}H_{30}N_2$): C 77.80 (77.77), H 11.52 (11.40), N 10.67 (10.66); **9***b* ($C_{11}H_{17}N_2O_4Cl$): C 47.74 (47.49), H 6.14 (6.71), N 10.13 (10.17); **10** ($C_{21}H_{20}N_2$): C 84.00 (83.78), H 6.67 (6.64), N 9.33 (9.17); **12** ($C_{24}H_{18}N_2$): C 86.20 (86.01), H 5.43 (5.54), N 8.38 (8.29).
[b] The instability of this compound precluded determination of analytical data.
[c] Obtained on a sample sublimed at 70°C/1 Torr.
[d] Literature (9*c*) mp 249°C.
[e] Recorded in CF_3CO_2D.

trideuteromethyl-3,7-di-*tert*-butyl-1,2(4*H*)-diazepines from the corresponding pyrylium salts (12*c*) demonstrating that 4-alkyl substituents (bearing acidic hydrogens) are compatible with the formation of diazepine products.

In summary, we have shown that the reaction of pyrylium salts with hydrazine, previously demonstrated to give 1,2(4*H*)-diazepines (7, 12), can be extended to provide some new monocyclic (**13–15**) and more highly condensed (**10**, **12**) diazepine derivatives. In contrast, the reaction of 2-methyl substituted pyrylium salts (**8***a*, **9***a*) with hydrazine leads to *N*-aminopyridinium salts (**8***b*, **9***b*) whereas the reactions of simple salts **1***a–e* with methylhydrazine leads mainly to ring contracted products (**2**, **3**).

Experimental

General Methods

Melting points were determined on a Mel-Temp or Fisher-Johns apparatus and are uncorrected. Analyses were performed by A. B. Gygli, Toronto, Ont., Micro-Tech Lab Inc., Skokie, IL., Galbraith Laboratories, Inc., Knoxville, TN., Enviro Analytical Laboratory, Knoxville, TN., and Heterocyclic Chemical Corporation, Harrisonville, MO. The infrared spectra were recorded on Beckman IR-5A, IR-10, and PE-180 instruments. Nuclear magnetic resonance spectra were recorded on Varian T-60, HA-100, and Perkin-Elmer R-12B spectrometers in deuteriochloroform solution using TMS as internal standard unless otherwise stated. Mass spectra were determined on AEI-MS 30, double beam, double-focussing spectrometer with perfluorokerosene mass marker. Thin layer and preparative chromatography were carried out with Merck silica gel GF-254 and column chromatography was performed using silica gel (0.05–0.20 mm), both obtained from Brinkman (Canada). Benzene and ether were dried over sodium using benzophenone as

Can. J. Chem. Downloaded from www.nrcresearchpress.com by 210.87.254.40 on 09/05/12
For personal use only.

Can. J. Chem. Downloaded from www.nrcresearchpress.com by 210.87.254.40 on 09/05/12
For personal use only.

indicator. Ethanol was dried over magnesium activated with iodine followed by distillation. Hydrazine hydrate (99–100%) and methylhydrazine (bp 87–89°C) were used directly without purification.

Preparation of Pyrylium Salts

All pyrylium salts are known compounds and were prepared according to literature procedures or slight variations thereof.

*2,4,6-Triphenylpyrylium Iodide (**1**a):* mp 220–222°C (lit. (19) mp 221°C).

*2,4,6-Triphenylpyrylium Fluoroborate (**1**b):* mp 214–215°C (lit. (19) mp 214–215°C).

*2,4,6-Triphenylpyrylium Perchlorate (**1**c):* mp 287–288°C (lit. (19, 20) mp 290°C).

*2-Methyl-4,6-diphenylpyrylium Iodide (**1**d):* mp 218–220°C (lit. (19) mp 222°C).

*2-Methyl-4,6-diphenylpyrylium Fluoroborate (**1**e):* mp 242–246°C (lit. (21) mp 247–249°C).

*2-(p-Methoxyphenyl)-4,6-diphenylpyrylium Perchlorate (**1**f):* mp 238–239°C (lit. (21) mp 236°C).

*2-Styryl-4,6-diphenylpyrylium Perchlorate (**1**g):* mp 230–232°C (lit. (22) mp 235°C).

*2,6-Diphenylpyrylium Perchlorate (**1**h):* mp 230–231°C (lit. (19) mp 220–225°C).

*2,4,6-Tri-*tert*-butylpyrylium Perchlorate (**1**i):* mp 254–255°C (lit. (23) mp 254–255°C).

*11,13-Dimethyl[9](2,6)-pyrylophanium Perchlorate (**8**a):* mp 170–171°C (lit. (24) mp 170°C).

*1,3-Dimethyl-5,6,7,8-tetrahydro-2-benzopyrylium Perchlorate (**9**a):* mp 80–82°C (lit. (25) mp 79–80.5°C).

*1,3-Diphenyl-5,6,7,8-tetrahydro-2-benzopyrylium Perchlorate (**9**c):* mp 222–226°C (lit. (26) mp 215°C).

*2,4-Diphenyl-5H-indeno[1,2-b]pyrylium Perchlorate (**11**):* mp 267–268.5°C (lit. (27) mp 269–270°C).

*Reaction of Pyrylium Salts **1**a–e with Methylhydrazine (Table 1)*

The following experiments represent typical conditions and isolation procedures for the reactions summarized in Table 1. Pyrazole (**3**)–pyrazoline (**2**) product composition varied somewhat as a function of the chromatographic procedure (size of column, rate of elution).

*Reaction of **1**a in Benzene at 0°C*

Methylhydrazine (0.92 g, 20 mmol) was added to a stirred suspension of **1***a* (4.36 g, 10 mmol) in dry benzene (150 mL) at 0°C. The mixture was stirred for 6 h during which time it was allowed to warm to room temperature. The orange-red solution was carefully concentrated *in vacuo* at room temperature to give a gum which was dissolved in ethanol (1 mL) to deposit overnight 120 mg (5%) of red crystals of *1-methyl-3,5,7-triphenyl-1,2(1H)-diazepine* (**5**), mp 116°C (lit. (7) mp 116.5–118°C) shown to be identical by mixture mp and nmr spectral comparison with an authentic sample (7).

Chromatography (CH_2Cl_2 eluent) of the mother liquor gave in order of elution acetophenone (90 mg, 7.5%), *2,4,6-triphenylpyridine* (**4***a*) (160 mg, 5%), and *1-methyl-3,5-diphenylpyrazole* (**3***a*) (1.67 g, 68%). Acetophenone was characterized by comparison of its phenylhydrazone with an authentic sample. Compounds **4***a*, mp 137°C (lit. (19) mp 137–138°C) and **3***a*, mp 52°C (lit. (28) mp 59–60°C) were shown to be identical by mixture mp and nmr spectral comparison with authentic samples prepared by literature methods.

*Reaction of **1**a in Benzene at Room Temperature*

Methylhydrazine (1.06 mL, 20 mmol) was added dropwise to a rapidly stirred suspension of **1***a* (2.13 g, 5 mmol) in benzene (60 mL) and the mixture was stirred for 2 h. The reaction mixture was evaporated to dryness *in vacuo* and the residue was chromatographed. Elution with methylene chloride – hexane (7:3) gave *2,4,6-triphenylpyridine* (**4***a*) (14 mg, 1%) and acetophenone (115 mg, 19%) characterized as described above. Further elution with methylene chloride gave in order *1-methyl-3,5-diphenylpyrazole* (**3***a*) (475 mg, 38%), identified as given above, and *1-methyl-3,5-diphenyl-5-phenacylpyrazoline* (**2***a*) (624 mg, 33%) as a viscous unstable oil, nmr δ:2.63 (s, 3H, NCH_3), 3.30 and 3.98 (AB q, 2H, J = 16 Hz, ring CH_2), 3.48 (s, 2H, CH_2CO), 6.95–7.75 (m, 15H, Ar H).

Thermolysis of **2***a* under nitrogen at 135°C (oil bath temperature) for 1 h gave, after chromatography (silica gel, CH_2Cl_2–hexane (7:3), then CH_2Cl_2 elution), quantitative yields of acetophenone and the pyrazole **3***a* which were characterized as described above.

*Reaction of **1**d in Benzene*

The reaction was carried out in benzene as described for **1***a* using **1***d* (1.84 g, 5 mmol) and hydrazine (0.53 mL, 10 mmol). After a few minutes, a yellow precipitate appeared. After stirring for 9 h, the precipitate was collected and recrystallized ($CHCl_3$–EtOH) to give 1.06 g (53%) of *1-methylamino-2-methyl-4,6-diphenylpyridinium iodide* (**6**), mp 179–180°C (lit. (15) mp 180°C); nmr δ:2.7 (d, 3H, J = 6 Hz, $NHCH_3$), 3.3 (s, 3H, CH_3), 7.05 (q, 1H, J = 6 Hz, NH), 7.5–7.95 (m, 10H, Ar H), 7.8 and 8.4 (2d, 2H, J = 2.5 Hz, pyridine β-H).

Hydrogenation (Pd/C, EtOH) of **6** (200 mg) as described previously (13) afforded, after chromatography (CH_2Cl_2 eluent), *2-methyl-4,6-diphenylpyridine* (**4***b*), 109 mg, 88%, mp 217–218°C (lit. (29) mp 218°C), which was shown to be identical with an authentic sample by mp, mixture mp, and nmr spectral comparison.

The filtrate obtained after separation of **6** was concentrated *in vacuo* and the residue was chromatographed (CH_2Cl_2–Et_2O eluent) to give *1-methyl-3,5-diphenylpyrazole* (**3***a*) (94 mg, 8%) followed by *1,3-dimethyl-5-phenyl-5-phenacylpyrazoline* (**2***b*) (210 mg, 15%) as a viscous, unstable oil, nmr δ:1.91 (s, 3H, CH_3), 2.53 (s, 3H, NCH_3), 3.20 (s, 2H, CH_2CO), 3.33 and 3.92 (AB q, 2H, J = 16 Hz, ring CH_2), 7.09–7.58, 7.76–8.05 (m, 10H, Ar H).

Thermolysis of **2***b* under the conditions described for **2***a* above gave, after chromatography (CH_2Cl_2–hexane (7:3), then CH_2Cl_2 elution), acetophenone and *1,3-dimethyl-5-phenylpyrazole* (**3***b*) in quantitative yields. Compound **3***b*, oil, lit. (30*a*) mp 21°C; nmr δ:2.25 (s, 3H, CH_3), 3.60 (s, 3H, NCH_3), 6.0 (s, 1H, C-4 H), 7.10–7.30 (m, 5H, Ar H) was shown to be identical by tlc and nmr spectral comparison with an authentic sample prepared by a literature method (30*b*).

*Rearrangement of 1-Methyl-3,5,7-triphenyl-1,2(1H)-diazepine (**5**) in the Presence of Silica Gel*

Compound **5** (104 mg, 0.31 mmol) and silica gel (2 g) in benzene (30 mL) suspension were stirred at room temperature for 72 h. The mixture was evaporated to dryness and chromatographed to give 6 mg (7%) of *2,4,6-triphenylpyridine* (**4***a*) and 63 mg (86%) of *1-methyl-3,5-diphenylpyrazole* (**3***a*) both of which were characterized by mp, mixture mp, and uv and nmr spectral comparisons with authentic samples.

*Reaction of Pyrylium Salts **1**f–i, **8**a, **9**a, **9**c, and **11** with Hydrazine*

These reactions were carried out according to the representative example (**8***a*) given below. All products were purified by direct crystallization with the exception of **10** which was chromatographed (silica gel, PhH eluent). The yields and physical and spectral data are summarized in Table 2.

N-*Amino-11,13-dimethyl-[9](2,6)-pyridophanium Perchlorate* (**8**b)

Hydrazine (0.16 mL, 3.2 mmol) was added to a slurry of the pyrylium salt **8***a* (530 mg, 1.55 mmol) in ethanol (14 mL) and the reaction mixture was stirred at room temperature for 0.5 h. The resulting solid was collected and recrystallized from ethanol to give 780 mg (75%) of **8***b* whose spectral data were identical with those reported by Balaban (9*c*).

N-*Acetamido-11,13-dimethyl-[9](2,6)-pyridophanium Perchlorate* (**8**c)

Compound **8***c* was obtained in 95% yield according to a literature method (31), mp 198–199°C; ir (KBr): 3200, 1720, 1600 cm^{-1}; nmr δ:8.3 (s, 1H, pyridine γ-H), 3.2–2.8 (t, 4H, 2β-CH_2 to pyridine ring), 2.75 (s, 6H, $2CH_3$), 2.4 (s, 3H, CH_3CO), 2.0–1.55 (br s, 4H, $2CH_2$), 1.4–0.9 (br s, 10H, CH_2); ms *m/e* (% relative intensity): 388 (M^+, nil), 289(14, $M^+ - ClO_4$), 273(96), 231(82), 134(54), 133(68), 122(46), 120(36), 106(78). *Anal.* calcd. for $C_{18}H_{29}N_2O_5Cl$: C 55.60, H 7.46, N 7.21; found: C 55.78, H 7.30, N 7.15.

Thermolysis of 3-Phenyl-5-phenacyl-2-pyrazoline (**2**d)

Compound **2***d* (400 mg, 1.51 mmol) was heated neat at 120°C (oil bath temperature) for 3 h. Chromatography (silica gel, benzene eluent) gave 54 mg (30%) of acetophenone and 90 mg (41%) of *3(5)-phenylpyrazole* (**3***c*), mp 76–77°C (lit. (32) mp 78°C), which was shown to be identical by mp, mixture mp, and nmr spectral comparison with an authentic sample prepared by a literature method (33).

Acknowledgements

This work was supported by the Natural Sciences and Engineering Research Council of Canada and Bristol Laboratories. We also thank NATO for a Research Grant (No. 1542) which made the work of T. Tschamber possible. We are grateful to P. Lukasewich and H. Waterman for early exploratory work and to undergraduates N. Burnett and C. G. Evans for the preparation of starting materials. We thank Mr. B. Sayer (McMaster University) for the temperature variable nmr studies and Drs. G. A. Reynolds and J. A. Van Allen for a generous sample of compound **1***i*.

1. V. Snieckus and G. Kan. J. Chem. Soc. Chem. Commun. 1208 (1970).
2. A. T. Balaban, W. Schroth, and G. Fischer. Adv. Heterocycl. Chem. **10**, 241 (1969).
3. H. Perst. Oxonium ions in organic chemistry. Academic Press, New York, NY. 1971. p. 149.
4. O. P. Shvaika and V. N. Antemov. Russ. Chem. Rev. **41**, 833 (1972).
5. H. C. Van Der Plas. Ring transformations of heterocyclic compounds. Vol. 2. Academic Press, New York, NY. 1973. p. 1.
6. D. J. Harris. Ph.D. Thesis, University of Waterloo. 1976.
7. D. J. Harris, G. Y.-P. Kan, V. Snieckus, and E. Klingsberg. Can. J. Chem. **52**, 2798 (1974).
8. W. Schneider and F. Seebach. Chem. Ber. **54**, 2285 (1921).
9. (*a*) M. Lempert-Sreter and K. Lempert. Acta Chim. Acad. Sci. Hung. **88**, 189 (1976); (*b*) L. Jurd. Tetrahedron, **31**, 2884 (1975); (*c*) A. T. Balaban. Rev. Roum. Chim. **18**, 1609 (1973); (*d*) G. I. Zhungietu, E. A. Revenko, and F. N. Chukhrii. Khim. Geterotsikl. Soedin. 347 (1973); Chem. Abstr. **78**, 147927b (1973); (*e*) G. I. Zhungietu, I. V. Shantsevoi, and S. V. Krivun. Khim. Geterotsikl. Soedin. 45 (1973); Chem. Abstr. **78**, 111271u (1973); (*f*) I. V. Shantsevoi and G. I. Zhungietu. Khim. Geterotsikl. Soedin. 184 (1972); Chem. Abstr. **76**, 140638h (1972); (*g*) A. T. Balaban. Tetrahedron, **26**, 739 (1970); (*h*) A. T. Balaban. Tetrahedron, **24**, 5059 (1968).
10. (*a*) J. A. Van Allen and S. C. Chang. J. Heterocycl. Chem. **11**, 1065 (1974); (*b*) G. N. Dorofeenko, A. V. Kablick, B. A. Terlov, and T. I. Polyakova. Khim. Geterotsikl. Soedin. 1016 (1973); Chem. Abstr. **79**, 137012h (1973); (*c*) J. A. Van Allen, G. A. Reynolds, and C. C. Petropoulos. J. Heterocycl. Chem. **9**, 783 (1972); (*d*) G. N. Dorofeenko, A. N. Narkevich, and Y. A. Zhdanov. Khim. Geterotsikl. Soedin. 1130 (1968); Chem. Abstr. **69**, 67175 (1968).
11. A. R. Katritzky and J. W. Suwinski. Tetrahedron, **31**, 1549 (1975).
12. (*a*) G. Reissenweber and J. Sauer. Tetrahedron Lett. 4393 (1977); (*b*) V. V. Derbenev, V. A. Bren, A. N. Popova, and G. N. Dorofeenko. Khim. Geterotsikl. Soedin. 1025 (1976); Chem. Abstr. **84**, 4742s (1976); (*c*) A. T. Balaban. Rev. Roum. Chim. **21**, 241 (1976); (*d*) J. Korosi and T. Lang. Chem. Ber. **107**, 3883 (1974); (*e*) O. Buchardt, C. L. Petersen, U. Svanholm, A. M. Duffield, and A. T. Balaban. Acta Chem. Scand. **23**, 3125 (1969).
13. D. J. Harris, M. T. Thomas, V. Snieckus, and E. Klingsberg. Can. J. Chem. **52**, 2805 (1974).
14. A. T. Balaban and W. Silhan. Tetrahedron, **26**, 743 (1970).
15. W. Schneider. Ann. **438**, 115 (1924).
16. V. Snieckus and G. Kan. Tetrahedron Lett. 2267 (1970).
17. M. Ikeda, N. Tsujimoto, and Y. Tamura. Org. Mass Spectrom. **5**, 61 (1971).
18. U. Svanholm. Acta Chem. Scand. **25**, 640 (1971).
19. K. Dimroth and K. H. Wolf. Newer methods of preparative organic chemistry. Vol. III. *Edited by* W. Foerst. Academic Press, New York, NY. 1964. p. 357.
20. A. T. Balaban. C. R. Acad. Sci. Ser. C, **256**, 4239 (1963).
21. R. Wizinger, S. Losinger, and P. Ulrich. Helv. Chim. Acta, **39**, 5 (1956).
22. A. W. Dilthy and J. Fischer. Chem. Ber. **56**, 1012 (1923).
23. G. A. Reynolds and J. A. Van Allen. J. Heterocycl. Chem. **11**, 1075 (1974).
24. A. T. Balaban. Tetrahedron Lett. 4643 (1968).
25. G. N. Dorofeenko and V. I. Dulenko. Zhur. Obshch. Khim. **32**, 3445 (1962); Chem. Abstr. **58**, 9013e (1963).
26. G. N. Dorofeenko, G. P. Safarayan, and V. I. Dulenko. Zhur. Obshch. Khim. **36**, 811 (1966); Chem. Abstr. **65**, 12159d (1966); A. T. Balaban and C. D. Nenitzescu. J. Chem. Soc. 3561 (1961).
27. G. V. Boyd. J. Chem. Soc. 55 (1959).
28. R. Huisgen, H. Gotthardt, and R. Grashey. Chem. Ber. **101**, 536 (1968).
29. W. Zecher and F. Krohnke. Chem. Ber. **94**, 698 (1961).
30. (*a*) K. von Auwers and H. Stuhlmann. Chem. Ber. **59**, 1043 (1926); (*b*) K. von Auwers and R. Hugel. J. Prakt. Chem. **143**, 157 (1935).
31. T. Okamoto, M. Hirobe, and A. Ohsawa. Chem. Pharm. Bull. Jpn. **14**, 518 (1966).
32. K. Bowden and E. R. H. Jones. J. Chem. Soc. 953 (1946).
33. J. Elguero and R. Jacquier. Bull. Soc. Chim. Fr. 2832 (1966).

Can. J. Chem. Downloaded from www.nrcresearchpress.com by 210.87.254.40 on 09/05/12
For personal use only.

The chemistry of aurodox and related antibiotics

HUBERT MAEHR, MICHAEL LEACH, THOMAS H. WILLIAMS, AND JOHN F. BLOUNT
Chemical Research Department, Hoffmann–La Roche Inc., Nutley, NJ 07110, U.S.A.
Received September 17, 1979

HUBERT MAEHR, MICHAEL LEACH, THOMAS H. WILLIAMS, and JOHN F. BLOUNT. Can. J. Chem. **58**, 501 (1980).

The studies which led to the complete structure elucidation of the antibiotic aurodox, including the chiralities of all eleven asymmetric centers and the *cis–trans* isomerism of all seven exocyclic double bonds, are summarized. Aurodox was correlated stereochemically with mocimycin. Thus, aurodox can be described as *N*-[7-[5(*R*)-[7-[1,2-dihydro-4-hydroxy-1-methyl-2-oxo-3-pyridinyl]-6-methyl-7-oxo-1(*E*),3(*E*),5(*E*)-heptatrienyl]tetrahydro-3(*S*),4(*R*)-dihydroxyfuran-2(*S*)-yl]-6(*S*)-methoxy-5,7(*R*)-dimethyl-2(*E*),4(*E*)-heptadienyl]-α(*S*)-ethyl-5,5-dimethyltetrahydro-2(*R*),3(*R*),4(*R*)-trihydroxy-6(*S*)-[1(*E*),3(*Z*)-pentadienyl]-2*H*-pyran-2-acetamide. Mocimycin, probably identical with kirromycin, is the corresponding *N*-desmethyl homolog.

HUBERT MAEHR, MICHAEL LEACH, THOMAS H. WILLIAMS et JOHN F. BLOUNT. Can. J. Chem. **58**, 501 (1980).

On résume les études qui ont conduit à la résolution complète de la structure de l'antibiotique aurodoxe incluant la chiralité des onze centres asymétriques et l'isomérie *cis–trans* des sept doubles liaisons exocycliques. On a relié stéréochimiquement l'aurodoxe à la mocimycine. Alors, on peut décrire l'aurodoxe comme étant: *N*-[[[[dihydro-1,2 hydroxy-4 méthyl-1 oxo-2 pyridinyl-3]-7 méthyl-6 oxo-7 heptatriényl-1(*E*),3(*E*),5(*E*)]-5(*R*) tétrahydrodihydroxy-3(*S*),4(*R*)furannyl-2(*S*)]-7 méthoxy-6(*S*) diméthyl-5,7 heptadiène-2(*E*),4(*E*)yl] α(*S*)-éthyl diméthyl-5,5 tétrahydro trihydroxy-2(*R*),3(*R*),4(*R*) [pentadiène-1(*E*),3(*Z*)yl]-6(*S*) 2*H* pyranne acétamide-2. La mocimycine probablement identique à la kirromycine est l'homologue *N*-desméthyle correspondant.
[Traduit par le journal]

Introduction

Within the past few years a chemically novel group of narrow-spectrum antibiotics has emerged and already comprises six members. Aurodox[1] (**1***b*) (1–3) and its *N*-desmethyl analog mocimycin (**1***a*) (4–6) were the first members discovered. Kirromycin (7) is most likely identical with mocimycin (8). Efrotomycin (**1***c*) (9, 10) is a glycoside consisting of a disaccharide and aurodox as the aglycone. Dihydromocimycin (**1***e*) (11) and kirrothricin (**1***f*) (12, 13) each contain a 4-hydroxy-5,6-dihydro-2-pyridone ring. Kirrothricin deviates further from the general theme of the other members as it lacks both the central tetrahydrofuran ring and the hydroxy group at position 3 on the terminal tetrahydropyran arrangement. That same 3-deoxy function differentiates heneicomycin (**1***d*) (14) from aurodox. From a biosynthetic viewpoint, therefore, dihydro-**1***d* would have represented a more likely structure for kirrothricin than the proposed structure **1***f*. The structure of azdimycin (15) is as yet unknown.

In addition to great chemical similarity, these antibiotics are all primarily active against a limited number of Gram-positive bacteria, notably bacilli (3, 7, 16, 17), the narrow antibacterial spectrum being ascribed to inefficient uptakes.

The mechanism of action was studied most intensively with kirromycin (18–26) and was found to involve inhibition of protein synthesis. In prokaryotic cells interaction with the elongation factor Tu was demonstrated. A similar mode of action is probable for all antibiotics of this group and for this reason the cumulative term elfamycins was proposed to emphasize elongation-factor involvement (27). The subsequent observation that elfamycins with EF-Tu specificity include labilomycin (pulvomycin) (26) as a remote structural relative suggests caution in the use of a cumulative term based on mechanism of action alone.

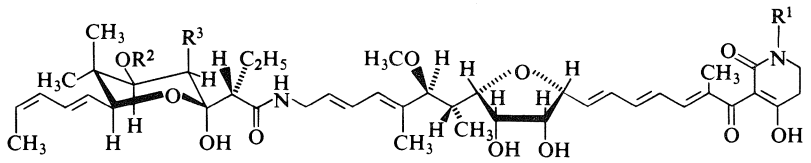
Aurodox (28, 29), mocimycin (30, 31), and efrotomycin (32, 33) are intended for veterinary use, especially as growth-promoting feed additives for farm animals and as chemotherapeutic agents in the control of dysentery caused by Treponema infections. Although mocimycin (**1***a*) and dihydromocimycin (**1***e*) have very similar chemical structures and antimicrobial *in vitro* spectra, only mocimycin promoted growth in animals (11, 34). However, both antibiotics were active against Treponema infections.

Production of these antibiotics appears to be afflicted by generally low fermentation yields; not surprisingly, therefore, aurodox biosynthesis was found to be regulated by feedback inhibition (35) so that production of the other members are likely to be subject to the same phenomenon. Increased yields of aurodox were achieved by aurodox-resistant mutants (36). In addition, a chemical conversion of mocimycin to aurodox was described (27).

[1]Aurodox is the designation of antibiotic X-5108 adopted by the USAN committee. The previously proposed name "goldinodox" has been withdrawn.

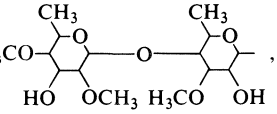
0008-4042/80/050501-26$01.00/0
©1980 National Research Council of Canada/Conseil national de recherches du Canada

Can. J. Chem. Downloaded from www.nrcresearchpress.com by 210.87.254.40 on 09/05/12
For personal use only.



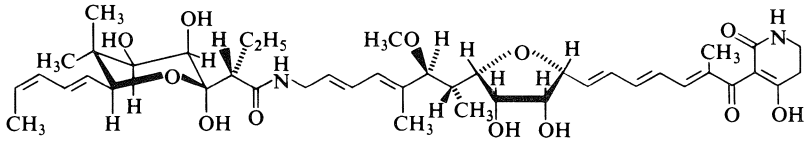
1*a*: $R^1 = R^2 = H$, $R^3 = OH$ (mocimycin, kirromycin)

1*b*: $R^1 = CH_3$, $R^2 = H$, $R^3 = OH$ (aurodox)

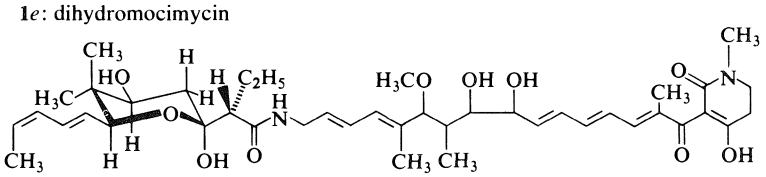


1*c*: $R^1 = CH_3$, $R^2 =$, $R^3 = OH$(efrotomycin)

1*d*: $R^1 = CH_3$, $R^2 = R^3 = H$ (antibiotic A21A, heneicomycin)



1*e*: dihydromocimycin



1*f*: kirrothricin

Aurodox was the first antibiotic of this group to receive a complete structural analysis. In view of the increasing interest in these antibiotics, both as potential commercial agents and biochemical tools, the chemical studies which led to the structure elucidation of aurodox and which were published only in part, are summarized in this paper.

Configuration of Aurodox

Aurodox was isolated from the fermentation broth of *Streptomyces goldiniensis* by extraction with organic solvents and was precipitated as the sodium salt (3). Although the antibiotic is a yellow, amorphous, monoprotic acid with $pK_a = 6.1$, salts of aurodox could be converted to the acid by extraction with an organic solvent such as dichloromethane even at pH 7. Further purification was achieved by Craig-distribution or chromatography (3).

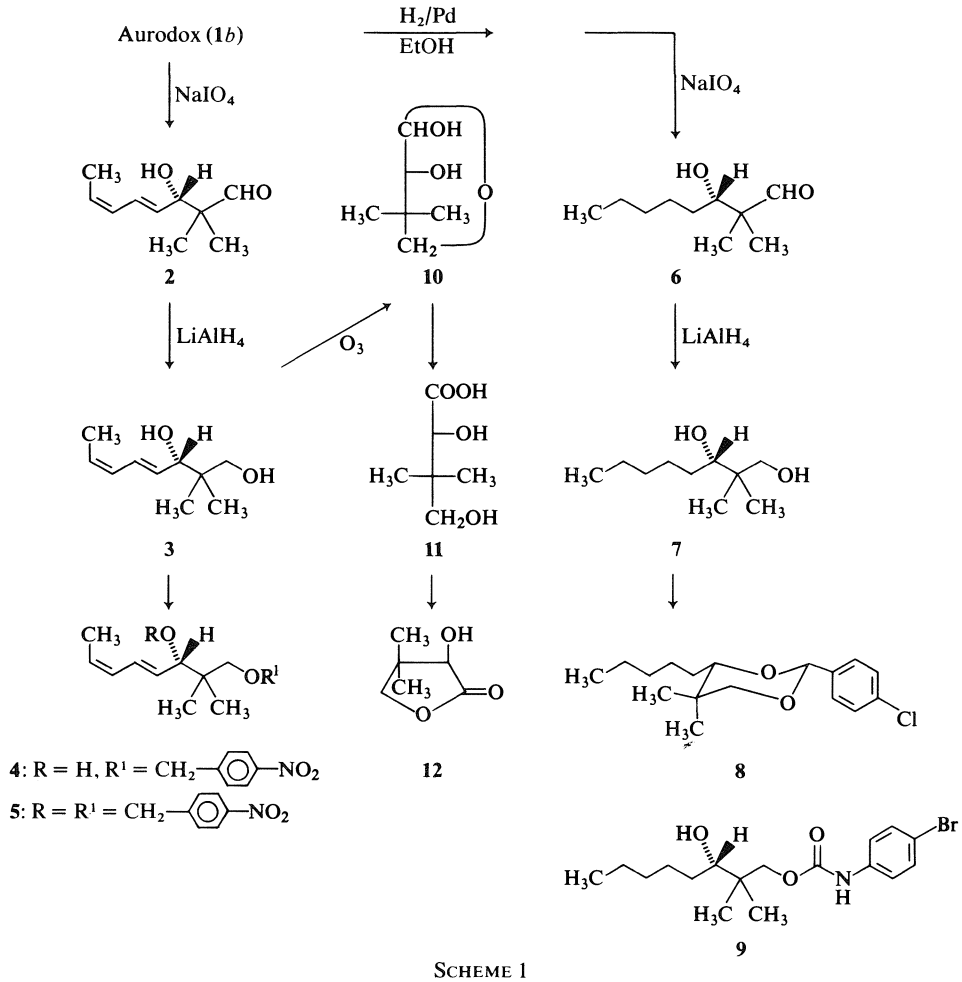
The acid is soluble in solvents such as ethanol, acetone, chloroform, and ethyl acetate, but is insoluble in water. Alkali salts dissolve in water, pyridine, methanol, and ethanol but are insoluble in acetone and chloroform. Prolonged exposure to light or standing in acidic or basic solutions reduces the antibacterial activity of the antibiotic. Whereas antibiotic titers of the free acid dropped significantly upon storage at room temperature for six months in solid form, no decrease was observed when the sodium salt was stored in the refrigerator for several years.

Elemental analyses of aurodox and alkali salts thereof suggested an empirical formula of $C_{44}H_{62}N_2O_{12} \cdot H_2O$ with $[\alpha]_D$ −82.8° (*c* 0.52, ethanol). Thermoosmotic molecular-weight determination in methanol supported the calculated value of 810. The empirical formula requires 15 units of unsaturation, 7–8 of which were accounted for by rapid hydrogen uptake upon catalytic hydrogenation in ethanol over palladium-on-charcoal.

Aurodox exhibited a characteristic and unique uv spectrum (3) and the ir spectrum indicated polyhydroxy nature. Moreover, aurodox was rapidly oxidized by periodate. Extraction of the oxidation mixture afforded β-hydroxyaldehyde **2** as impure syrup which was reduced with metal hydride and characterized as the resulting diol **3** and its mono- and di-(4-nitrobenzoic) esters **4** and **5** (Scheme 1). The uv maximum at 235 nm observed in **2** prevailed in **3** suggesting the presence of a diene not in conjugation with the aldehyde carbonyl group.

The structure of **2**, including the configuration of the diene, was primarily deduced from the ^1H nmr spectrum of **3** and confirmed by those of **4** and **5** (Fig. 1) (37). Coupling constants of 15 and 11 Hz permitted the assignment of the 4*E* and 6*Z* configurations, respectively, in **2** and the diastereotopic

Can. J. Chem. Downloaded from www.nrcresearchpress.com by 210.87.254.40 on 09/05/12
For personal use only.



SCHEME 1

nature of the protons on C1 was evident from the resulting AB pattern in the spectra of **3** and **4**. Coincidentally, however, these protons became isochronous in the corresponding spectrum of the di-nitrobenzoic ester **5** (Fig. 1).

As expected, **1***b* yielded 2,2-dimethyl-3-hydroxyoctanal (**6**) after catalytic hydrogenation and oxidation by periodate. Reduction of **6** with lithium aluminum hydride gave the crystalline diol **7**, which was further characterized as the 2-(4-chlorophenyl)-4-pentyl-5,5-dimethyl-1,3-dioxane (**8**), a colorless liquid obtained by short-path distillation at 3 Torr (bath temperature 145°C), and as the 2,2-dimethyl-1,3-octanediol-1-(4-bromophenyl)carbamate (**9**), obtained as colorless plates with mp 124°C, $[\alpha]_D$ −19.9° (*c* 0.5, dioxane). Ozonolysis of **3** gave D-glycero-3,3-di-*C*-methyltetrose (**10**) which was oxidized to the known D-pantoic acid (**11**) and isolated as D-(−)-pantolactone (**12**) (38, 39) with the same $[\alpha]_D$, and hence with the same chirality, as natural pantothenic acid, thus establishing the chiral center in **2** as 3*S*.

Whereas catalytic hydrogenation of aurodox in ethanol yielded a homogeneous product, a similar reduction in acetic acid caused fragmentation (Scheme 2). One of these degradation products was obtained in crystalline form and ultimately identified as [1*R*-(1β,3α,5α,6α,9α)]-9-ethyl-1,5-dihydroxy-4,4-dimethyl-3-pentyl-2,7-dioxabicyclo[4.3.0]nonan-8-one (**14**) by single-crystal Roentgen-diffraction analysis of its 4-bromobenzoate **15** (Fig. 2) (37). Consonant with the isolation of **14** from aurodox by catalytic hydrogenation in acetic acid, mild treatment of aurodox with acetic acid gave diene **13**, termed goldinono-1,4-lactone-3,7-hemiacetal, derived from the hypothetical parent goldinonic acid **16**[2] and

[2]Trivial names of degradation products were derived from the name of the aurodox-producing Streptomyces goldiniensis.

Can. J. Chem. Downloaded from www.nrcresearchpress.com by 210.87.254.40 on 09/05/12
For personal use only.

Can. J. Chem. Downloaded from www.nrcresearchpress.com by 210.87.254.40 on 09/05/12
For personal use only.

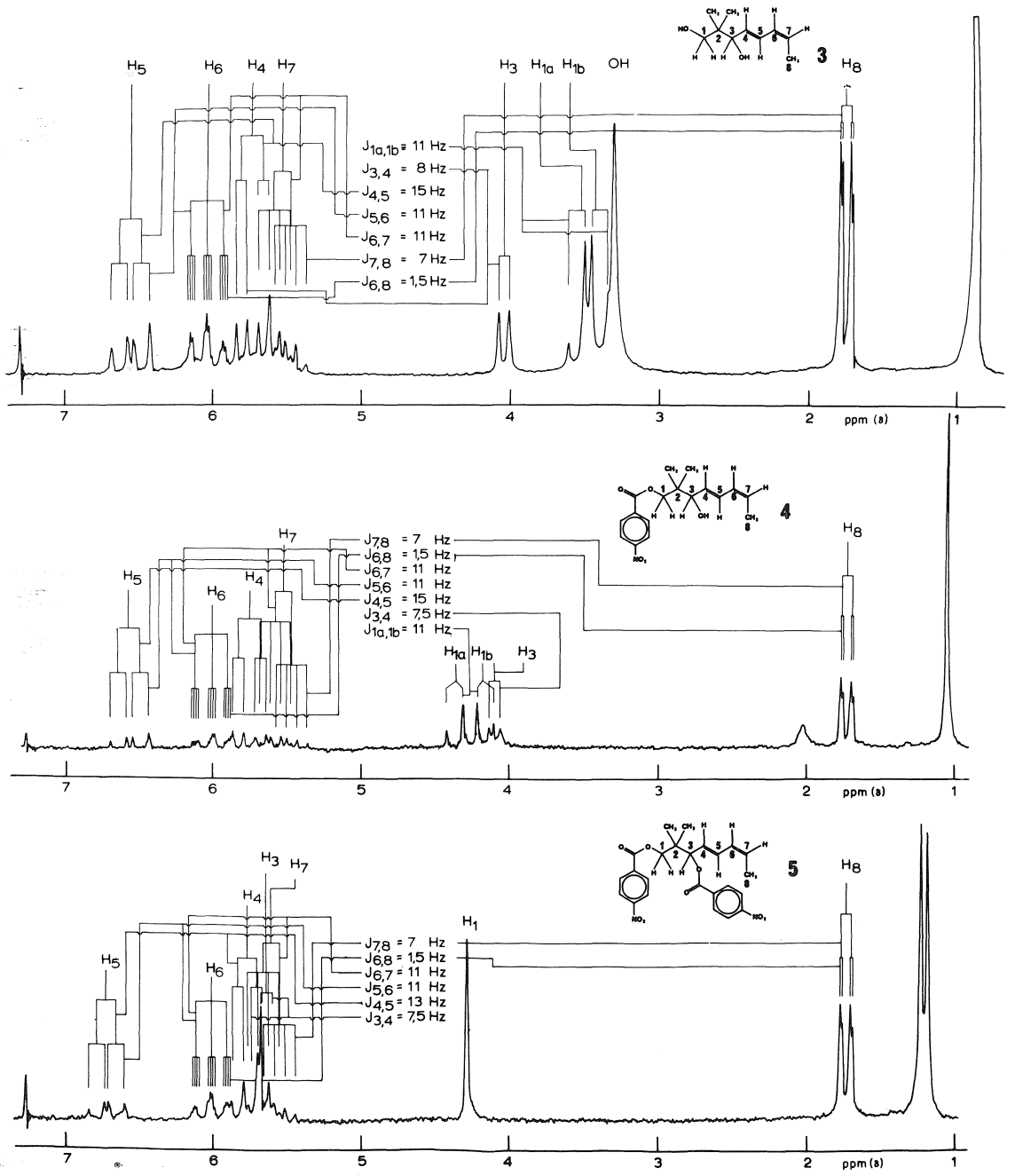
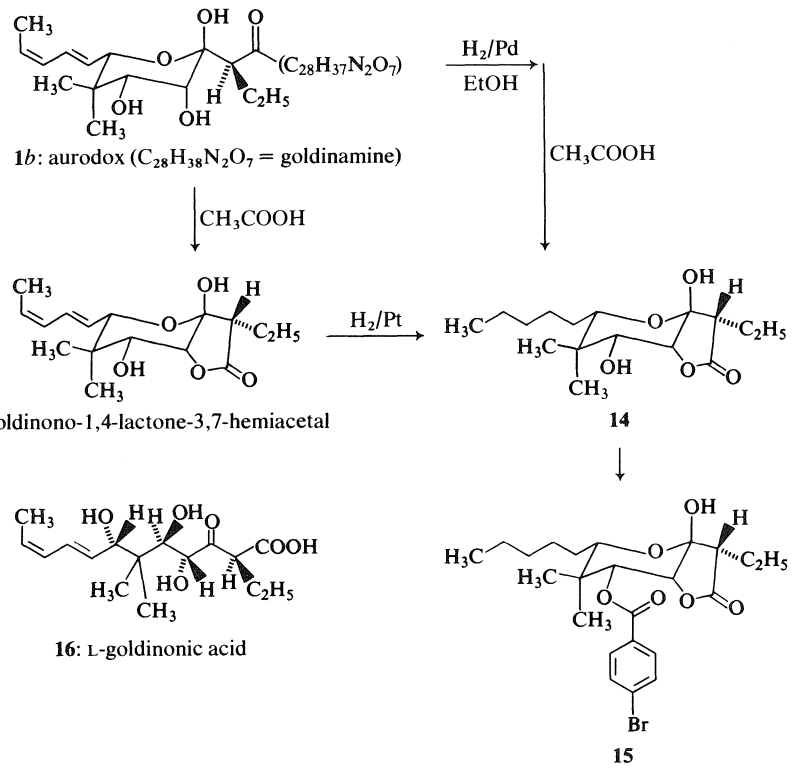


FIG. 1. ^{1}H nmr spectra of **3**, **4**, and **5**.

readily converted to the lactone **14** by catalytic hydrogenation.

Clearly, dienal **2**, obtained by oxidative fission of aurodox by periodate (Scheme 1), is derived from the goldinonic acid moiety, supplying evidence for the (1*E*,3*Z*)-configuration of the pentadienyl side chain in **13** and the presence of a vicinal diol function in aurodox shown in goldinonic acid **16** but absent in goldinono-1,4-lactone-3,7-hemiacetal **13** which is resistant to periodate. Further, the absence of carboxyl-, non-conjugated keto-, and δ-lactone-bands in the ir spectrum of aurodox suggested the goldinonic-acid portion to be arranged in aurodox as the goldinonyl-3,7-hemiacetal form shown in **1***b* (Scheme 2). The facile cleavage of the amide bond with concomitant formation of the δ-



SCHEME 2

lactone function in **13** is explained by anchimeric participation of the axial hydroxyl group of the tetrahydropyran ring resulting in lactone formation and expulsion of the remaining molecular portion $C_{28}H_{38}N_2O_7$.

As potential 1,3-dicarbonyl compounds, **1***b*, **13**, and **14** could conceivably be subject to racemization at the α-carbon center. The nearly quantitative isolation of **14** after hydrogenation and mild acetic acid treatment of **1***b*, however, was interpreted as a good indication that the α(*S*)-configuration is also present in **1***b*.

Catalytic hydrogenation of aurodox sodium salt over palladium-on-charcoal in ethanol followed by hydrolysis in hot water liberated 4-hydroxy-1-methyl-2(1*H*)-pyridone (**19**) (40), characterized as the formaldehyde condensation product **20** (Scheme 3), whereas unreduced aurodox was resistant to hydrolysis under the same conditions. With a pK_a of 6.67, **19** was suspected to be responsible for the acidic nature of the antibiotic and to be linked via C3 in the aurodox molecule, for the two protons at C5 and C6 in **19** were readily identified as a characteristic AB pattern in the ^1H nmr spectrum of **1***b*. Further, the liberation of **19** by hydrolysis after catalytic reduction of **1***b* suggested linkage to a carbonyl group; reduction of the carbonyl group generates an aldol-type arrangement severable by mild hydrolysis.

To exploit the mild fragmentation reaction by acetic acid, which had led to **13** as the only crystalline product together with numerous other components, aurodox sodium salt was reacted with 4-bromobenzyl bromide to yield aurodox(4-bromobenzyl) ether **18**. Subsequent acetic acid treatment of **18** and analysis of the reaction mixture were hoped to be facilitated by the bromobenzyl group providing ready recognizability, blockage of one reactive site, and a heavy atom for possible crystallographic analysis of **18** or appropriate fragments thereof. Aurodox derivative **18**, however, was an amorphous but homogeneous compound and the resulting reaction mixture with acetic acid fortunately contained only two major components, namely **13** and a new, larger fragment, termed goldinamine(4-bromobenzyl) ether (**22**), easily separated from each other by Craig-distribution or chromatography on silicic acid. Goldinamine(4-bromobenzyl) ether contained the uv-chromophore of aurodox with the characteristic maximum at 325 nm and proved to be an amorphous amine, generating salts with acids, a yellowish color with ninhydrin, and *N*-(2,4-dinitrophenyl) derivative **26** with 1-fluoro-2,4-dinitrobenzene.

Can. J. Chem. Downloaded from www.nrcresearchpress.com by 210.87.254.40 on 09/05/12
For personal use only.

Can. J. Chem. Downloaded from www.nrcresearchpress.com by 210.87.254.40 on 09/05/12
For personal use only.

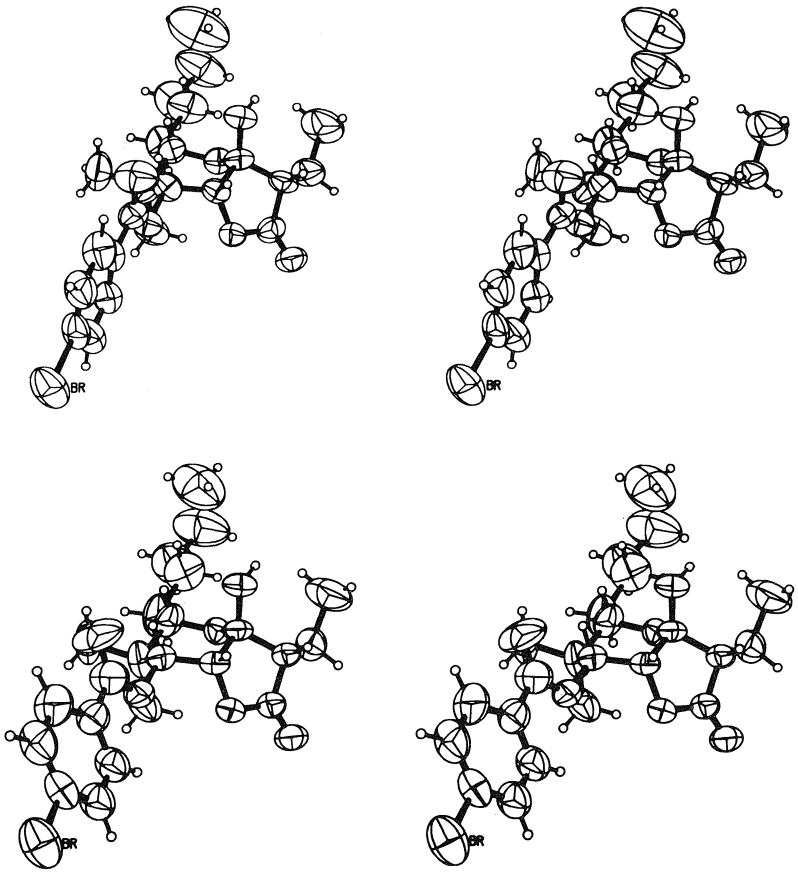


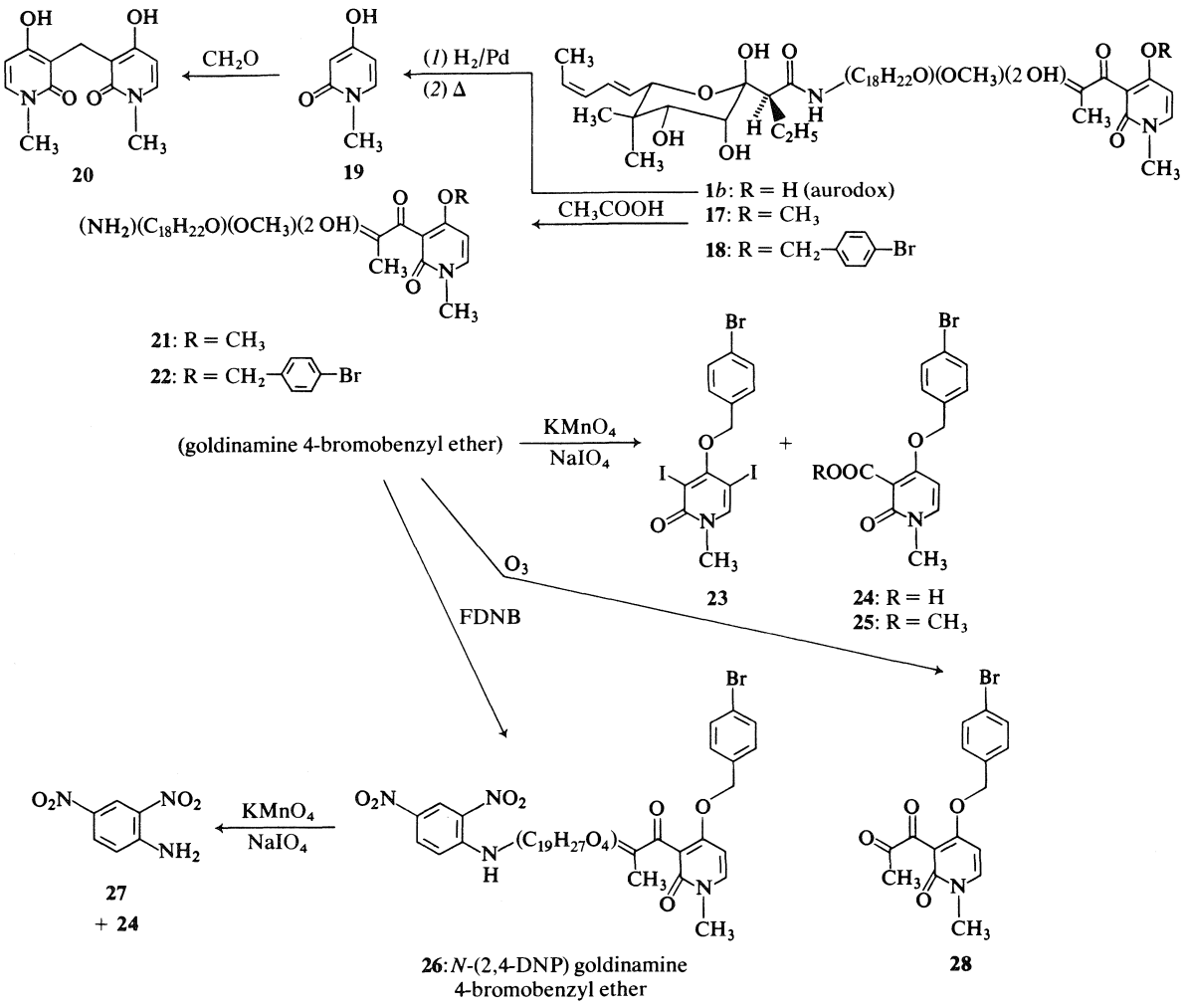
FIG. 2. Stereodrawing showing the absolute configuration of **15** (37) and the conformations of the two independent molecules found in the crystal. The thermal ellipsoids are scaled to the 50% probability level. The hydrogen atoms are shown as spheres of arbitrary size at their calculated positions; they were not included in the structure analysis.

The absence of an amino function in the intact antibiotic suggested goldinonic acid 3,7-hemiacetal to be linked to goldinamine through an amide bond as shown in Scheme 3.

The elemental composition of goldinamine, $C_{28}H_{38}N_2O_7$, was originally estimated by analyses of a number of salts and amino derivatives of **22**, none of which were obtainable in crystalline form.

Oxidation of **22** with a mixture of potassium permanganate and sodium metaperiodate gave crystalline 4-(4-bromobenzyloxy)-1-methyl-1,2-dihydro-2-oxopyridine-3-carboxylic acid (**24**), further characterized as methyl ester **25**, and slightly yellow needles of an artifact, identified as 4-(4-bromobenzyloxy)-3,5-diiodo-1-methyl-2(1*H*)-pyridone (**23**). Ozonolysis of **22** in methanol deposited crystalline 4-(4-bromobenzyloxy)-1-methyl-3-pyruvoyl-2(1*H*)-pyridone (**28**), whereas oxidation of goldinamine derivative **26** with potassium permanganate and sodium metaperiodate afforded **24** as well as 2,4-dinitrobenzeneamine (**27**).

N-Acetylgoldinamine(4-bromobenzyl) ether (*N*-acetyl-**22**) formed a di-*O*-acetyl derivative with acetic anhydride and pyridine, a cyclic carbonate with ethyl chloroformate, an *O*-isopropylidene derivative with acetone and a dialkoxyphenylborane with benzeneboronic acid indicating two vicinal non-tertiary hydroxyl groups. A methoxy group evident from the ^{1}H nmr spectra of **1***b* and **22** led to **1***b* (Scheme 3) as partial structure for aurodox. Indeed, **22** reacted rapidly with sodium metaperiodate liberating 8-[4-(4-bromobenzyloxy)-1,2-dihydro-1-methyl-2-oxo-3-pyridyl]-7-methyl-8-oxo-2,4,6-octatrienoic acid (**31**), obtained in crystalline form, syrupy 8-amino-3-methoxy-2,4-dimethyl-4,6-octadienal (**33**), and two equivalents of formic acid (Scheme 4) (41). Both trienoic acids **29** and **31**, the former accessible by an analogous oxidation of goldinamine methyl ether (**21**), contained the long-wave uv maximum of aurodox and of goldinamine derivatives **21** and **22**, and were readily converted to methyl esters **30** and **32** with diazo-



SCHEME 3

methane. Both **31** and **32** were degraded by ozonolysis to **28** previously obtained from **22**.

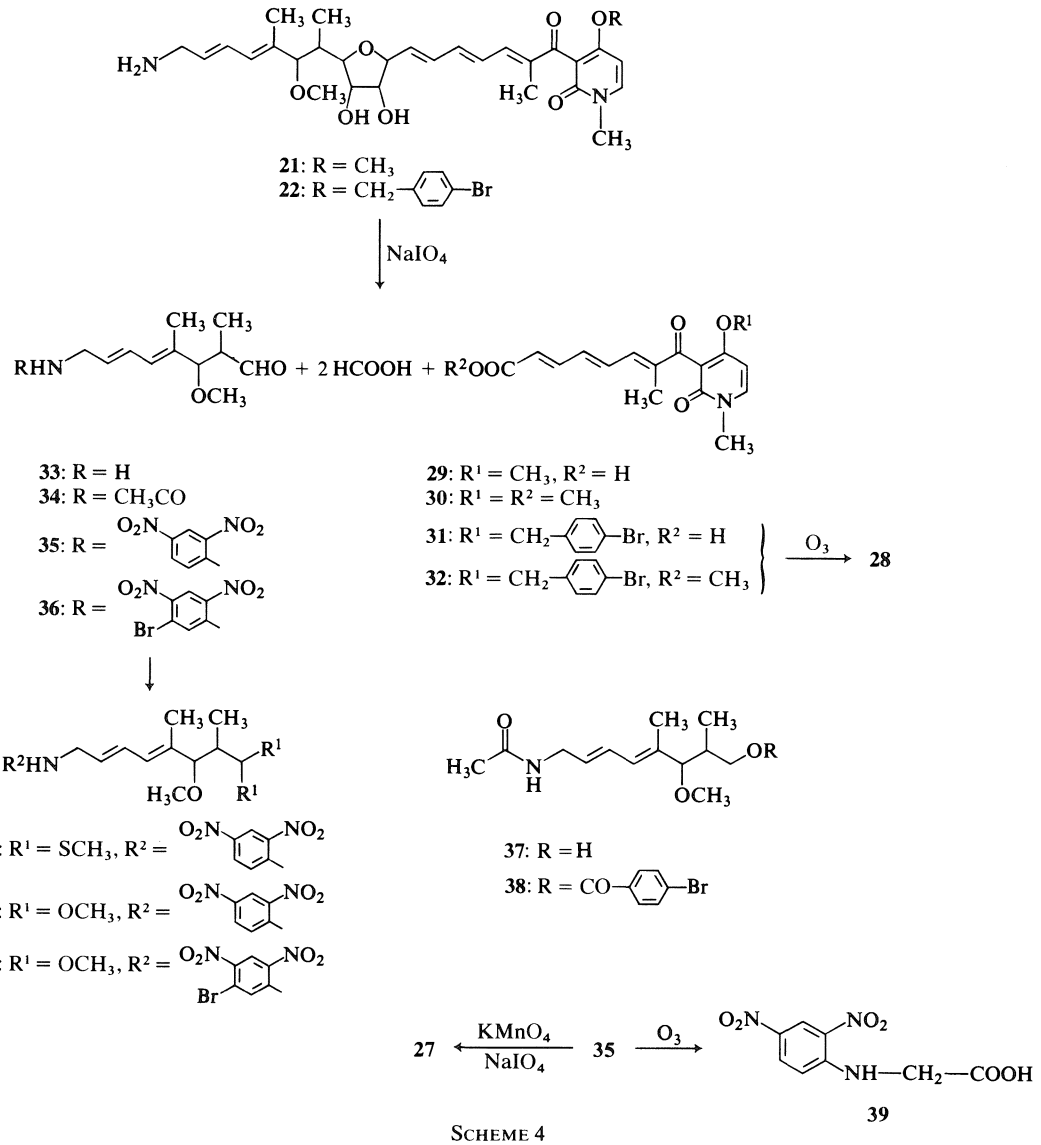
With the exception of the double bond at position 6, the configuration of trienoic acid **31** could be deduced from the ^1H nmr spectrum as shown in Fig. 3.

The olefin protons exhibited a five-spin system consisting of one doublet at δ 5.98 ($J_{2,3}$ = 15 Hz) attributed to H2, one doublet of quartets at δ 6.81 ($J_{5,6}$ = 11 and $J_{6,Me}$ = 1 Hz) attributed to H6, and three doublets of doublets. The doublet of doublets at lowest field at δ 7.32 was assigned to H3, since it possesses the same splitting ($J_{2,3}$ = 15 Hz) present in the H2 doublet. Both H4 and H5 exhibited doublets of doublets with identical coupling constants, but the doublet of doublets at δ 7.13 was assigned to H5 on the basis of the distortion of the H6 signal. Thus, it was possible to assign the (2*E*,4*E*)-configuration on the basis of the two large coupling constants $J_{2,3}$ and $J_{4,5}$.

The (6*E*)-configuration was established by single-crystal Roentgen-diffraction analysis (41) of **31**. The crystal was obtained as a 1:1 adduct with chloroform. As seen in Fig. 4, the *xy*-plane bisecting the π-orbital at carbonyl carbon C8 is not parallel with the corresponding plane bisecting the π-orbital of the pyridone ring and renders the molecule dissymmetric. The crystal is centrosymmetric with both enantiomeric conformations present.

The dienal **33** (Scheme 4) was isolated as the syrupy *N*-acetyl and *N*-(2,4-dinitrophenyl) derivatives **34** and **35**, respectively, and yielded the elemental composition of the parent substance **33** as $C_{11}H_{19}NO_2$ by mass spectrometry. Oxidation of **35** with potassium permanganate and sodium metaperiodate gave 2,4-dinitrobenzeneamine. With

Can. J. Chem. Downloaded from www.nrcresearchpress.com by 210.87.254.40 on 09/05/12
For personal use only.



SCHEME 4

ozone, followed by oxidative work-up, *N*-(2,4-dinitrophenyl)-glycine (**39**) was obtained from **35** and indicated the presence of an allylic amine in **33**. Sodium borohydride reduced **34** to the dienol **37** with the unaltered uv maximum at 240 nm, originally observed in both **33** and its *N*-acetyl derivative **34**, implying the presence of a 2,4-pentadienylamine in **33** without conjugation of the diene with the aldehyde group. The structure of **35** as shown in Fig. 5, with the exception of the double-bond configuration at C4, was readily derived from the ^{1}H nmr spectrum.

The *threo*-configuration in **33** was originally deduced from the intensity ratio of free vs. bonded hydroxyl stretching-absorptions in the ir spectrum of alcohol **37** (42). The observed value of 0.26 was in good agreement with the reported value of 0.15 for *threo*-3-ethoxy-2,4-dimethyl-4-hexenol (43), permitting hydrogen bonding in a stereochemically less crowded conformation as compared to the less stable hydrogen-bonded arrangement of the *erythro* isomer with a reported value of 1.4 (Fig. 6). Further, inspection of the rather diagnostic ^{1}H nmr chemical shift of the methyl group at C2 in **37** (δ 0.66) was also in good agreement with that of *threo*-3-ethoxy-2,4-dimethyl-4-hexenol (δ 0.60), whereas two synaxial interactions between a methyl group and an unshared electron pair on oxygen cause a significant paramagnetic shift of the methyl group in the *erythro* isomer (δ 0.90) (43).

Can. J. Chem. Downloaded from www.nrcresearchpress.com by 210.87.254.40 on 09/05/12
For personal use only.

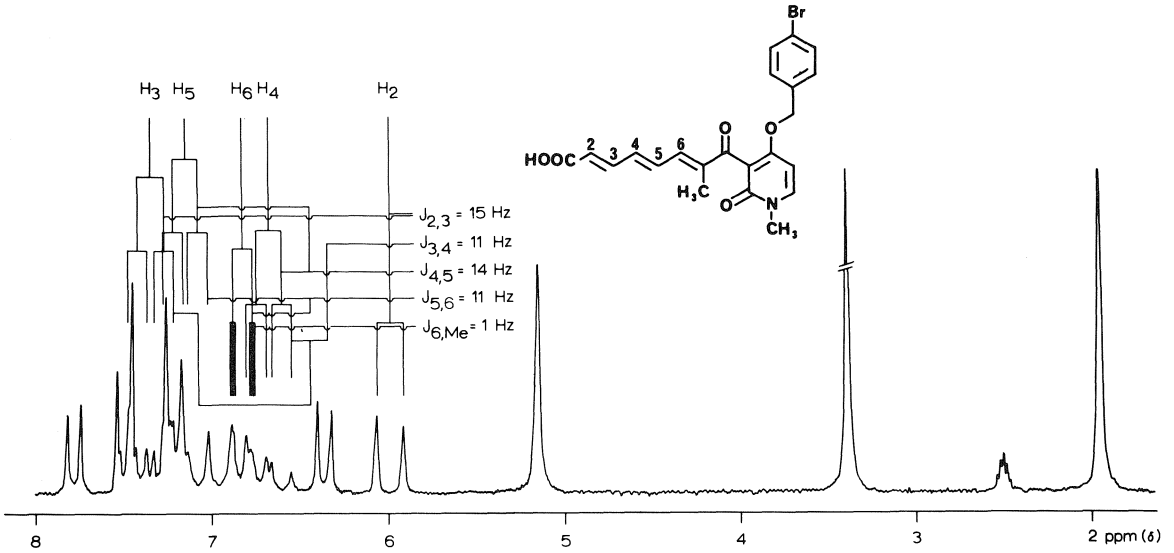


FIG. 3. ^{1}H nmr spectrum of **31**.

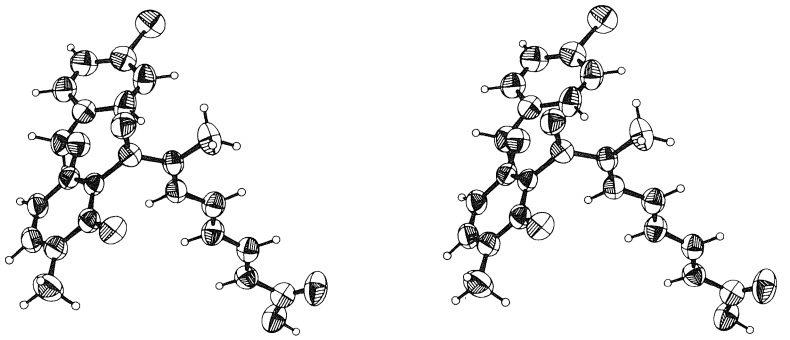


FIG. 4. Stereodrawing of one of the two enantiomeric conformations of **31** present in the crystal.

Attempts to crystallize **37** or esters such as **38** failed. Of a number of acetals prepared only **40** and **41** were crystalline. Of the two only **41** was suitable for a single-crystal Roentgen-diffraction analysis which confirmed the previously assigned *threo* configuration, established the all-*trans* isomerism, but, in the absence of a heavy atom, left the chirality undetermined. Introducing an anomalous scatterer while maintaining all other structural features of the one crystallographically suitable acetal **41** was accomplished with a new reagent, 1-bromo-5-fluoro-2,4-dinitrobenzene (42). Accordingly, [*threo*-(4*E*,6*E*)]-8-[(5-bromo-2,4-dinitrophenyl)-amino]-3-methoxy-2,4-dimethyl-4,6-octadienal (**36**) was prepared from **33** and converted to the crystalline acetal **42** which was indeed suitable for crystallographic analysis (42) establishing the absolute configuration shown in Fig. 7 (bottom). The crystal structure of **41** (41) is shown on top of Fig. 7 for comparison.

As illustrated in Scheme 4, periodate cleaves goldinamine derivatives **21** and **22** in the center, each liberating two moles of formic acid as well as dienal **33** and a trienoic acid as the two terminal fragments. The identification of this center as a 2,5-disubstituted 3,4-dihydroxytetrahydrofuran ring was first accomplished by analysis of the ^{1}H nmr spectra of goldinamine derivatives **26** and **43** (Fig. 8) (41). There were four methine protons, H2′–H5′, attached to sp^3-hybridized carbons in *N*-(2,4-dinitrophenyl) goldinamine (4-bromobenzyl) ether (**26**) which were not part of either degradation products **31** or **33**. Conversion of **26** to the di-*O*-acetyl derivative **43** shifted protons H2′–H5′ paramagnetically, rendering them recognizable as four dd sets and part of a multiple-spin system. Subjected to the more intensive paramagnetic shifts, protons H3′ and H4′ were assigned to carbons bearing acetoxy groups in vicinal relationship based on a common coupling constant

Can. J. Chem. Downloaded from www.nrcresearchpress.com by 210.87.254.40 on 09/05/12
For personal use only.

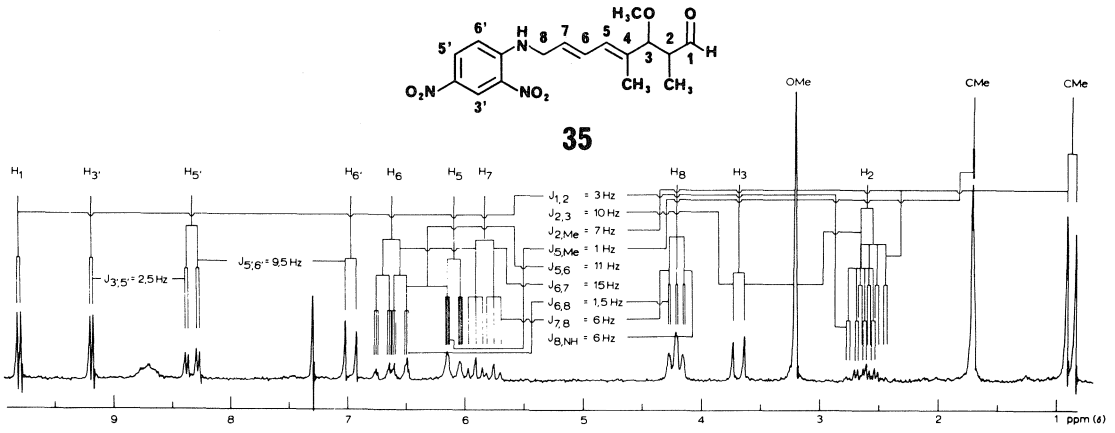


FIG. 5. ^{1}H nmr spectrum of **35**.

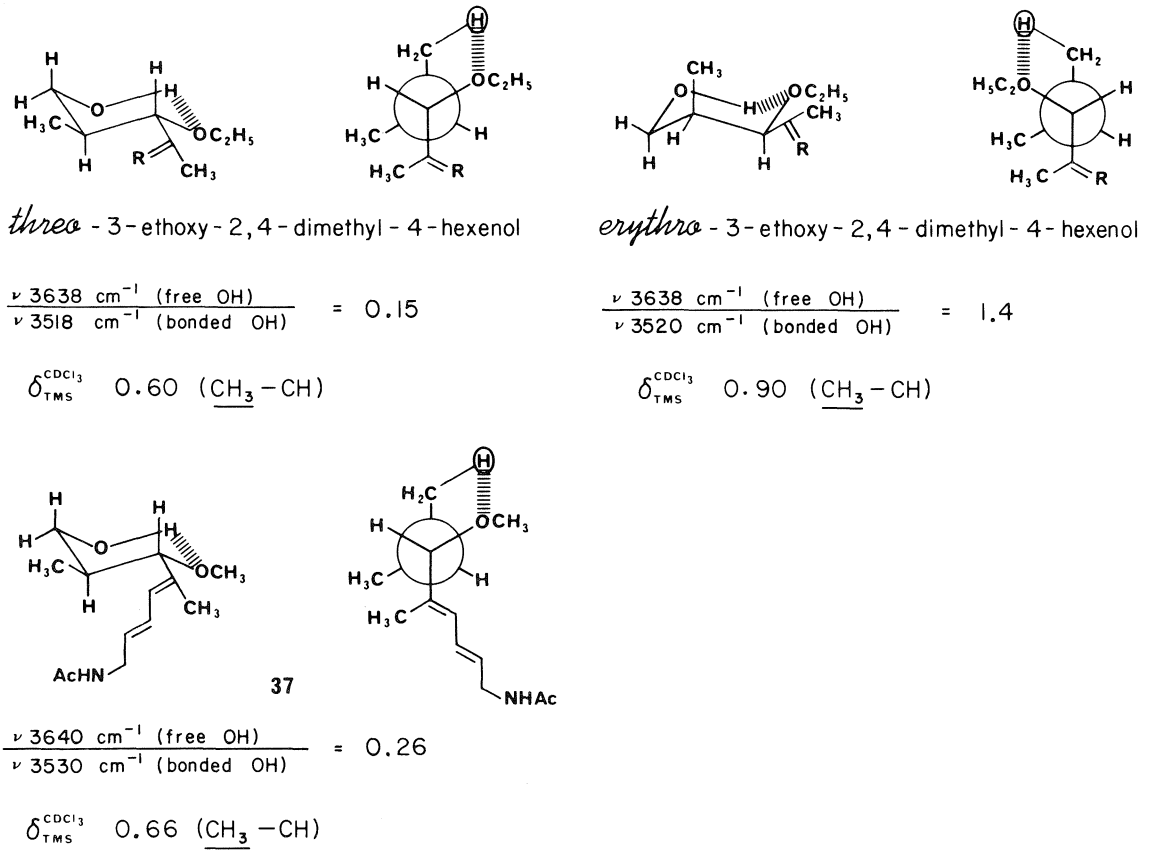


FIG. 6. Determination of the *threo* configuration in **37**.

of 5 Hz. Coupling constants $J_{2',3'} = 7$ and $J_{4',5'} = 4$ Hz established the connection C2′—C3′—C4′—C5′. Irradiations indicated by bold arrows (Fig. 9), at the proton frequencies of H1 and H2′ in **43**, resulted in the expected multiplicity changes as depicted; the surviving coupling constants are also shown. The resulting side-chain assignments to positions 2′ and 5′ in **43** could be confirmed by analysis of the ^{1}H nmr spectrum of the *O*-isopropylidene-*N*-(2,4-dinitrophenyl)-goldinamine(4-bromobenzyl) ether (**44**) exhibiting a new set of coupling constants; concordantly, irradiations at the proton frequencies of H4′ and H6′ in **44** led to the spectral simplifications illustrated in Fig. 9 (8).

To ascertain the exact elemental composition of

Can. J. Chem. Downloaded from www.nrcresearchpress.com by 210.87.254.40 on 09/05/12
For personal use only.

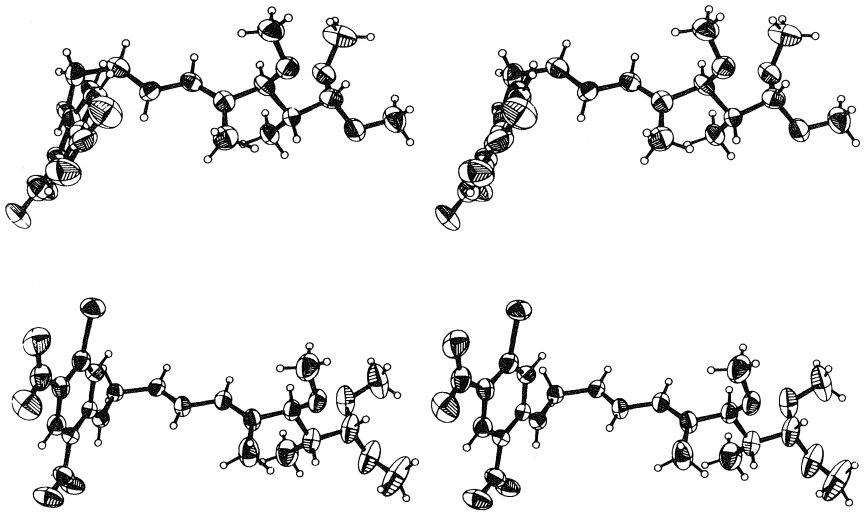


FIG. 7. Stereodrawings showing the conformation and absolute configuration of **41** (upper) and **42** (lower). The thermal ellipsoids are scaled to 50% probability level. The hydrogen atoms are shown as spheres of arbitrary size.

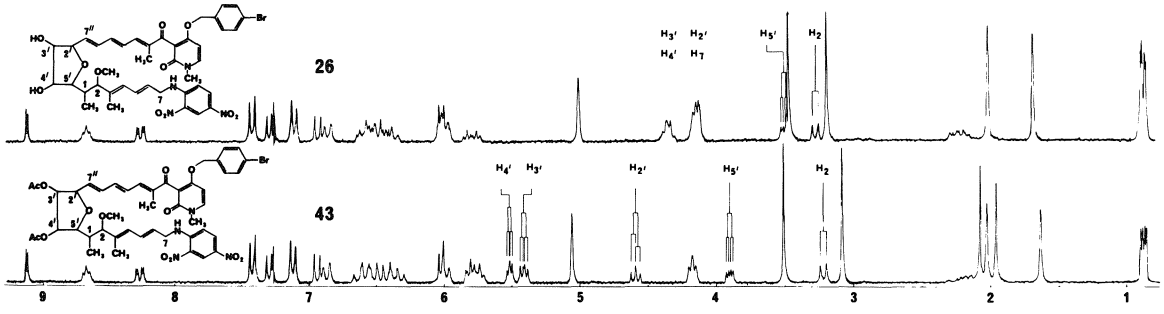


FIG. 8. 220 MHz nmr spectra of goldinamine derivatives **26** and **43**.

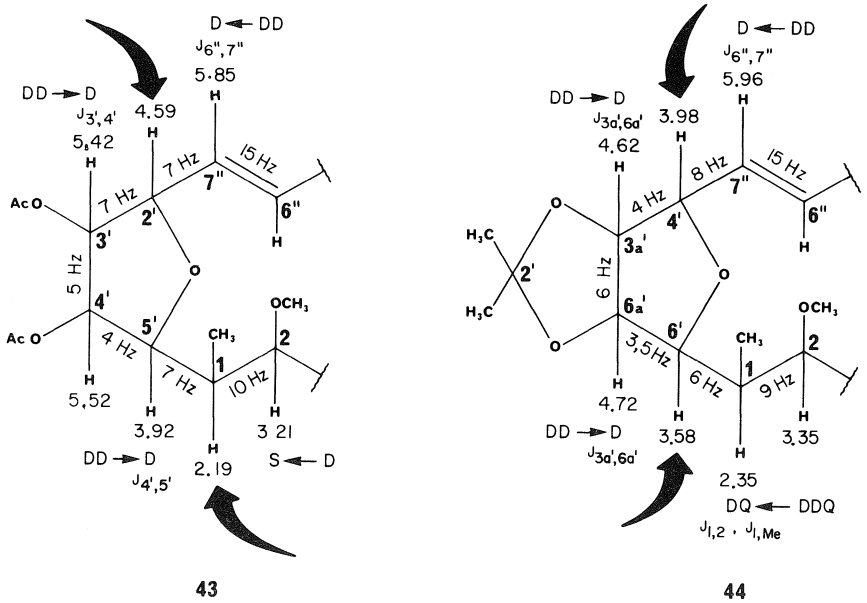
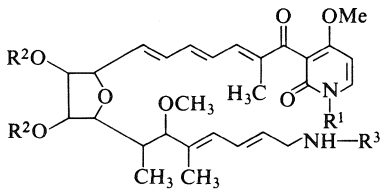


FIG. 9. 220 MHz nmr data characterizing the tetrahydrofuran moiety of goldinamine derivatives **43** and **44**.

Can. J. Chem. Downloaded from www.nrcresearchpress.com by 210.87.254.40 on 09/05/12
For personal use only.

Can. J. Chem. Downloaded from www.nrcresearchpress.com by 210.87.254.40 on 09/05/12
For personal use only.

goldinamine, various derivatives were investigated by electron-impact mass spectrometry, but useful spectra were only obtained after replacement of the 4-bromobenzyl group in **22** by a methyl substituent. The resulting **21** was readily prepared by acetic acid treatment of aurodox methyl ether (**17**) (Scheme 3) and converted to goldinamine derivatives **47–50** whose mass spectra exhibited molecular ions, with the exception of **48** which gave *m/e* 588 ($M - CO_2 - H_2O$) as the highest observable mass peak. Molecular formulas of **21** and **47–50**, and hence that of goldinamine itself, could be deduced unequivocally on the basis of the low-resolution mass spectra of **47–50** and the known chemistry of the periodate-oxidation products derived from **22** (Scheme 4), but were further confirmed by high-resolution mass spectra of **49** and **50**.



21: R^1 = Me, R^2 = R^3 = H	$C_{29}H_{40}N_2O_7$ (528)
45: R^1 = R^2 = R^3 = H	$C_{28}H_{38}N_2O_7$ (514)
46: R^1 = R^2 = H, R^3 = $COCF_3$	$C_{30}H_{37}F_3N_2O_8$ (610)
47: R^1 = Me, R^2 = H, R^3 = $COCF_3$	$C_{31}H_{39}F_3N_2O_8$ (624)
48: R^1 = Me, $2R^2$ = CO, R^3 = $COCF_3$	$C_{32}H_{37}F_3N_2O_8$ (650)
49: R^1 = Me, R^2 = H, R^3 = Ac	$C_{31}H_{42}N_2O_8$ (570)
50: R^1 = R^2 = Me, R^3 = Ac	$C_{33}H_{46}N_2O_8$ (598)

The tetrahydrofuran structure in goldinamine and aurodox does not remain unexplained by the surprising periodate-oxidation products shown in Scheme 4. Hesse and Mix had demonstrated that carbon–carbon double bonds are cleavable by periodate if at least one carbon is substituted by a free hydroxyl group and if the double bond is in conjugation with a carbonyl group (44). The oxidation of **22** by periodate could thus be postulated to proceed as depicted in Scheme 5 without intention to differentiate between homolytic and heterolytic processes or to show actual hydration states of the iodine compounds. After initial glycol cleavage one of the formyl groups enolizes to become part of a conjugated system; the new double bond conforms to the Hesse–Mix criteria of cleavability by periodate as it contains a hydroxyl group and is in conjugation with a carbonyl group, although only in a hexatrienylogous fashion. A molecule of periodate, it is now implied, adds across the enolic double bond, followed by decomposition of the resulting cyclic iodic ester to liberate formic acid, hypothetical iodous acid, and an ester which yields **31** as well as an α-hydroxyaldehyde upon hydrolysis, the latter being subject to further oxidation with periodate to afford a second mole of formic acid and dienal **33**. The possible intermediacy of iodous acid is supported by the transient appearance of free iodine by disproportionation (41).

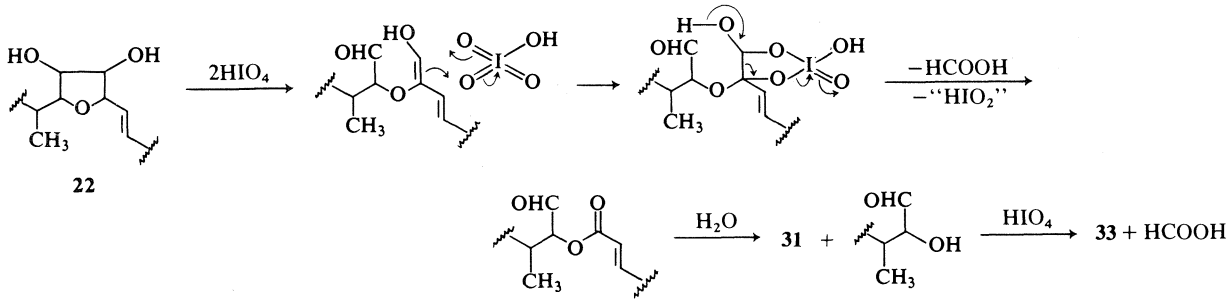
To determine the stereochemistry of the tetrasubstituted tetrahydrofuran ring in goldinamine, the relative configuration was investigated initially (45). Assuming a *cis* relationship between the two vicinal hydroxyl groups, as suggested by the ease of *O*-isopropylidenation and cyclic borate-ester formation, there are only four possible arrangements as depicted in Fig. 10 (**51–54**).

In view of the great variability of the dihedral angles in five-membered rings, and hence of the corresponding coupling constants (46–48), the problem of stereochemical assignments was thought to be resolvable by comparison of coupling constants after increasing conformational rigidity of goldinamine by introduction of a 1,3-dioxolane ring and by selecting model tetrahydrofurans with substituents closely approximating those of *O*-isopropylidene-*N*-(2,4-dinitrophenyl)goldinamine(4-bromobenzyl) ether (**44**). Thus, four model substances **55–58** (Fig. 10) were synthesized by standard reactions from D-mannose (**55** and **57**) and D-glucose (**56** and **58**). Coupling constants for vicinal hydrogens ranged from 3–6 Hz for *cis* and were less than 1 Hz for *trans* relationships. The observed values of 3.5, 6, and 4 Hz in **44** were in agreement with the corresponding coupling constants 3, 6, and 4 Hz in **55** and **57** (Figs. 9 and 10), consistent with an all-*cis* configuration of the tetrahydrofuran moiety in **44** and hence in goldinamine (45).

Chirality of the Tetrahydrofuran Moiety: Absolute Configuration of Aurodox

We had established the geometry of all double bonds, the absolute configuration of the five chiral centers of the goldinonic acid 3,7-hemiacetal portion, the two in the exocyclic part of goldinamine, and the relative configuration of the central tetrahydrofuran ring in goldinamine. There were, therefore, only two structural possibilities for aurodox remaining, differing with respect to enantiomeric tetrahydrofuran rings, but identical otherwise.

A distinction was thought possible by fusing a 6-membered ring onto the 4′–5′ face of the tetrahydrofuran ring in **22** (Scheme 6) containing the two known chiral centers C1 and C2 derived from the exocyclic diene-chain of goldinamine. This approach would lead to a conformationally fixed carbon–carbon bond between two chiral centers. De-



SCHEME 5

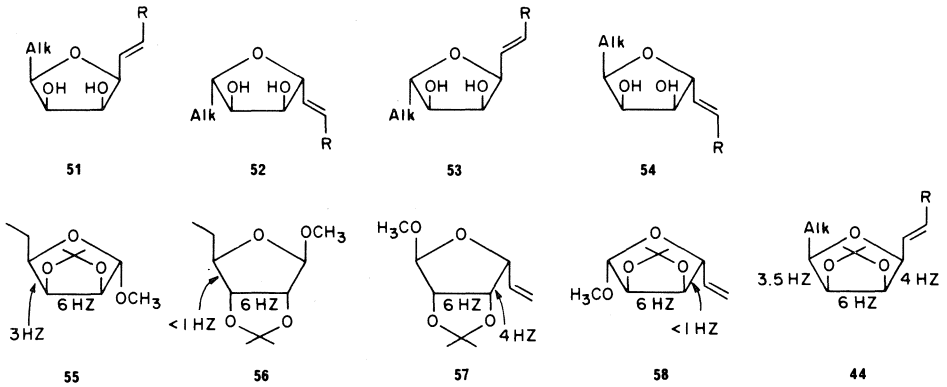


FIG. 10. Possible relative configurations of the tetrahydrofuran moiety in goldinamine (**51–54**) and selected model compounds (**55–58**).

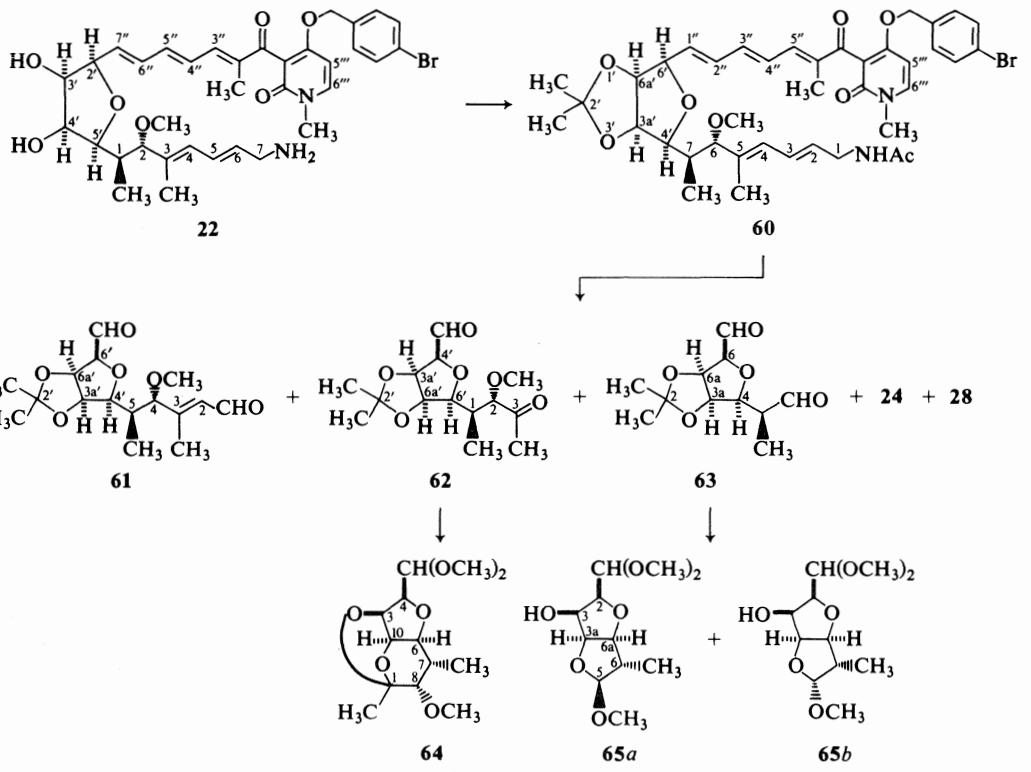
rived from the diene side-chain of goldinamine and designated C1, one of the two carbons possesses an established (*S*) configuration, the other being part of the tetrahydrofuran system. With the known relative configuration of the tetrahydrofuran ring, therefore, determination of the *threo*- or *erythro*-configuration of this bond, on the basis of its coupling constant, would obviously yield the chirality of C5′ in goldinamine and hence the absolute configuration of the entire tetrahydrofuran system. Thus, the *N*-acetyl derivative of **22** was converted to the *O*-isopropylidene compound **60** (Scheme 6)[3] and then oxidatively cleaved with osmium tetroxide and periodate yielding a mixture containing predominantly the α,β-unsaturated aldehyde **61**, smaller quantities of ketone **62** and other minor products, one of which presumably was the dialdehyde **63** as suggested by evidence presented later. The expected pyridones **24** and **28** were also isolated.

The most attractive starting material for the planned ring closure was the ketone **62**. Consequently, the oxidation mixture derived from **60** was chromatographed on a column of silica gel removing crystalline **24** and **28** and affording a fraction containing **61** as major and **62** as minor products but presumably still contaminated with small amounts of **63**. This mixture was treated with ozone, affording ketone **62** as major product, and subsequently with methanolic hydrogen chloride to effect acetalization of the aldehyde and transacetalization involving the 3-oxo position. This procedure led to a mixture of three products (Scheme 6). The major one was the expected (7*S*,8*S*) - 4 - (dimethoxymethyl) - 1,7 - dimethyl - 8-methoxy - 2,5,9 - trioxatricyclo [4.2.2.$0^{3,10}$] decane (**64**) derived from **62**, whereas the two minor components were identified as the two anomeric (6*S*)-hexahydro - 5 - methoxy - 2 - (dimethoxymethyl) - 6 - methylfuro[3,2-*b*]furan-3-ols (**65***a* and **65***b*) derived from **63**.

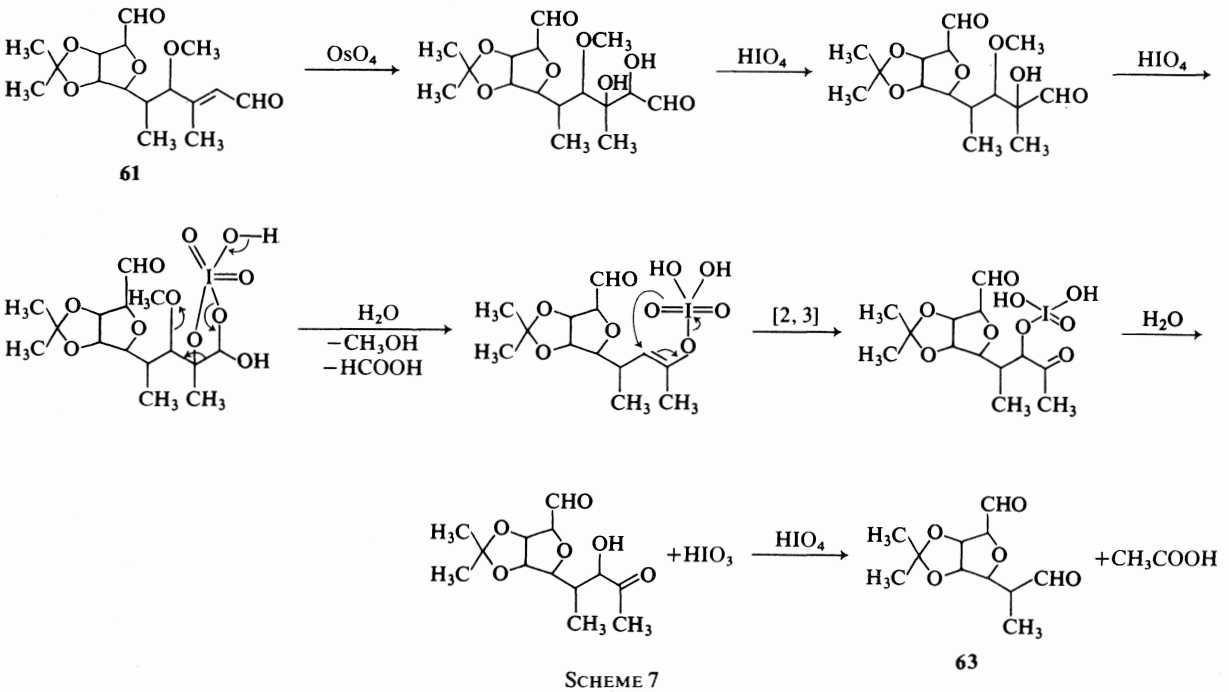
Both **62** and **63** contain a diastereotopic carbonyl group in their side chain and a protected chiral diol on their tetrahydrofuran rings. Involving these two groups, transacetalization of **62** occurs in stereorestricted fashion forming stereospecifically but one acetal **64**. Only one of the two potential hydroxyl groups in **63** participates in the transacetalization

[3]To differentiate graphically between relative and absolute configurations we chose bold (▼) and dashed (▽) wedges to indicate absolute stereochemistry, sets of bold lines (▮) and/or broken lines (≡) represent relative configuration.

Can. J. Chem. Downloaded from www.nrcresearchpress.com by 210.87.254.40 on 09/05/12
For personal use only.



SCHEME 6



SCHEME 7

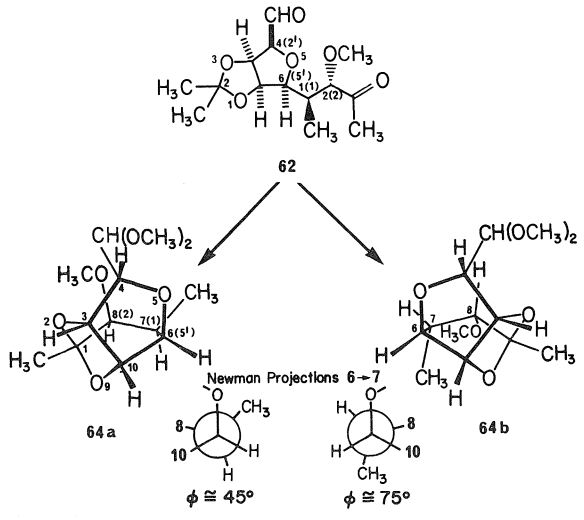
Can. J. Chem. Downloaded from www.nrcresearchpress.com by 210.87.254.40 on 09/05/12
For personal use only.

Can. J. Chem. Downloaded from www.nrcresearchpress.com by 210.87.254.40 on 09/05/12
For personal use only.

process; the second hydroxyl group is donated by the solvent affording two anomeric products **65***a* and **65***b*.

The generation of 2-[2,2-dimethyl-6-formyltetrahydrofuro[3,4-*d*]-1,3-dioxol-4-yl]-2-methylethanal (**63**) from **60** is entirely unexpected but could conceivably be explained as depicted in Scheme 7. Hydroxylation of dialdehyde **61** is followed by glycol cleavage to form a new dialdehyde which forms a cyclic periodic ester. This ester could either decompose to furnish oxoaldehyde **62**, which is actually observed, or the decomposition of the ester could occur with fragmentation as indicated. The resulting mono-coordinated periodic ester could then undergo a 2,3-sigmatropic rearrangement actually reoxygenating position 2 of the side chain and hence yielding an iodic ester which is hydrolyzable to a species cleavable by periodate to yield dialdehyde **63**.

Of the condensation products **64**, **65***a*, and **65***b* the tricyclic acetal **64** appeared most suitable for the ascertainment of chirality. Its existence confirmed the vicinal *cis*-orientation of 3′, 4′, and 5′ in goldinamine and since acetalization generated only one new chiral center in **64** there were only two diastereomeric alternatives **64***a* and **64***b* for consideration (Scheme 8). They are enantiomeric with respect to the acetal carbon 1, derived from the 3-oxo position of **62** and C3 of goldinamine, and the tetrahydrofuran ring, but are identical with respect to the chiral centers 7 and 8 derived from C1 and C2 of **62** and goldinamine. The bond C6—C7 in **64***a* is, therefore, of *threo*- and that in **64***b* of *erythro*-configuration with dihedral angles of ca. 45° and 75°,



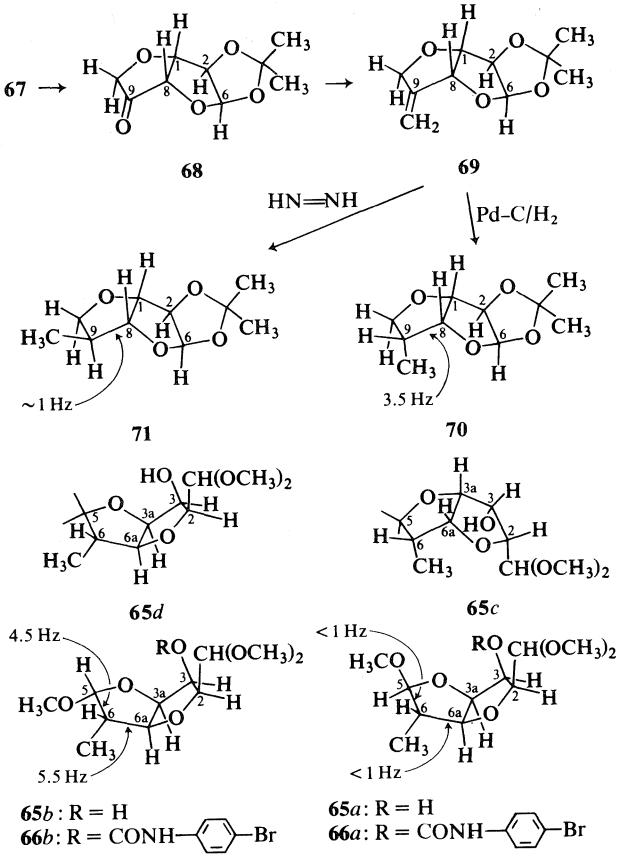
SCHEME 8. Possible configurations of **64**. The numbers shown in parentheses refer to carbon designations of the original goldinamine derivative **60**.

respectively (Scheme 8). Using a $J^{\circ} = 12$ Hz the Karplus equation led to a prediction of $J_{6,7} = 6$ Hz for the *threo* configuration (**64***a*) and $J_{6,7} = 0.5$ Hz for the *erythro* configuration (**64***b*). In view of the observed coupling constant $J_{6,7} = 2$ Hz the *erythro* configuration and hence structure **64***b* appeared somewhat more likely than **64***a*, but no unequivocal assignment was possible by this analysis (49).

The search for an alternative to determine the chirality of C5′ in goldinamine by analysis of the C1—C5′ bond led to the study of the minor methanolysis products **65***a* and **65***b* derived from **60** (Scheme 7). Mass spectrometry established **65***a* and **65***b* as closely related isomers with elemental compositions of $C_{11}H_{20}O_6$, ir spectra suggested the absence of carbonyl groups, and ^1H nmr spectra were compatible with (6*S*)-hexahydro-5-methoxy-2-(dimethoxymethyl)-6-methylfuro[3,2-*b*]furan-3-ols obviously derived from dialdehyde **63**. Concerning their configuration, the chirality of C6 had previously been established by single-crystal analysis of **42** and the relative configuration of the tetrahydrofuran ring, derived from goldinamine, was considered to possess vicinal all-*cis* substituents. Disregarding the configuration at C5, only the two structures **65***c* and **65***d* (Scheme 9) had to be assessed; both are identical with respect to the chirality at C6 but are related enantiomerically with respect to the tetrahydrofuran rings located on the right-hand side. The crucial problem consisted of the differentiation of the two possible bonds between carbons 6 and 6a; a *cis* configuration would establish structure **65***c* and a *trans* relationship structure **65***d*.

To aid analysis, 3,6-anhydro-1,2-*O*-isopropylidene-α-D-glucofuranose (**67**) (58) was oxidized with osmium tetroxide – periodate to [1*R*-(1β,2α,6α,8β]-4,4-dimethyl-3,5,7,11-tetraoxatricyclo[6.3.0.0^{2,6}]undecan-9-one (**68**) which served as substrate in a Wittig reaction with triphenylmethylphosphorane leading to olefin **69**. Catalytic hydrogenation of **69** gave the expected [1*S*-(1β,2α,6α,8β,9α)]-4,4,9-trimethyl-3,5,7,11-tetraoxatricyclo[6.3.0.0^{2,6}]undecane (**70**) as major (88%) and the 9β isomer **71** as minor product (12%) by preferential hydrogen addition to the double bond from the least hindered side.

Stereoselective hydrogenation with diimide involving hydrogen addition from the more hindered side has been demonstrated, *inter alia*, with 7-oxynorbornadienes via *exo–cis* addition (51). To prepare the 9β-epimer **71** stereoselective hydrogen addition from the more hindered side was required. Accordingly, hydrogenation of olefin **69** was attempted with diimide. This reduction indeed pro-



SCHEME 9

ceeded stereoselectively yielding **71** as major (64%) and **70** (36%) as minor product.

The two model compounds **70** and **71** thus obtained possess identical central tetrahydrofuran rings but differ in the chirality of C9. As a result, **70** exhibits a *cis* and **71** a *trans* configuration between carbons 8 and 9. $J_{8,9} = 1$ Hz allowed unequivocal assignment of structure **71** to the major diimide hydrogenation product; the isomer with $J_{8,9} = 3.5$ Hz, therefore, had to be represented by structure **70**.

The availability of **70** and **71** was thought to enable identification of the methanolysis products derived from **63**, both possessing the same basic moiety of either structure **65***c* or **65***d*. The configurations at centers 8 and 9 of the tetrahydrofuran rings in **70** and **71** resemble the C6—C6a face of **65***c* and **65***d*, respectively, so that $J_{6,6a} \leqq 1$ Hz would point to structure **65***d* and $J_{6,6a} \gg 1$ Hz would favor **65***c*.

Spectral analysis of the two methanolysis products revealed that one of them had two coupling constants $J_{5,6}$ and $J_{6,6a}$ of < 1 Hz each, signifying two vicinal *trans* relationships and hence establishing **65***a* as shown in Scheme 9. The other isomer was most likely the 5-epimer demanding configuration **65***b*.

In view of the close relationship between the configurations represented by **65***a* and **65***b*, the two greatly different coupling constants $J_{6,6a}$ of < 1 Hz (**65***a*) and 5.5 Hz (**65***b*) did not appear to support a *trans* configuration between carbons 6 and 6a in structure **65***b*, a conclusion supported by the *trans* coupling constant $J_{8,9} = 1$ Hz in **70**. Hence, doubt was cast upon the chiral integrity of C6. Racemization at C6 was unlikely, however, in view of the reaction conditions employed and because only two methanolysis products derived from **63** were observed, both of which exhibited virtually identical chemical shifts of the 6-CH_3 groups but differed markedly in the chemical shifts of H5. With two oxygen substituents on the same ring side, moreover, H5 of **65***b* would be expected to absorb at lower field than H5 of **65***a*, and it is indeed observed that H5 of **65***b* absorbs at a field 0.29 ppm lower than H5 of **65***a*. C5 in **65***b* was thus certainly of the *R*-configuration shown. One of the two coupling constants $J_{5,6} = 4.5$ and $J_{6,6a} = 5.5$ Hz in **65***b* therefore had to be assigned to a *trans* configuration since one vicinal *cis* and one *trans* configuration between carbons 5, 6, and 6a must be involved regardless of the chirality of C6.

These results could be summarized as follows. The *R*-configuration of **63** is most probably preserved in the methanolysis products **65***a* and **65***b*. Structure **65***a* (Scheme 9) could then be assigned to one of the methanolysis products in view of $J_{5,6} = J_{6,6a} < 1$ Hz. The C6—C6a bond in **65***a* and **65***b*, and the C1—C5′ bond in goldinamine are of *erythro* configuration so that **64***b* is indeed the structure of the methanolysis product of **63** and C5′ of goldinamine has the *S*-configuration.

A single-crystal Roentgen analysis of **64** subsequently established **64***b* as the correct structure (49). It was also possible to prepare and analyze the crystalline hexahydro-5-methoxy-2-(dimethoxymethyl)-6-methylfuro[3,2-*b*]furan-3-ol(4-bromophenyl)carbamic acid esters **66***a* and **66***b* (Fig. 11) confirming the structures **65***a* and **65***b* as the methanolysis products derived from **63**.

The crystal structure analyses of **64***b* and **66***b* yielded the absolute configurations which, in turn, were in agreement with the previously determined chiral centers of **42**. Thus, the previously assigned all-*cis* configuration of the tetra-substituted tetrahydrofuran ring in goldinamine, the *erythro* configurations of C6—C6a, the chiral integrities of C6, and the epimeric relationship in **65***a* and **65***b* were confirmed.

These studies and others (52) demonstrated that

Can. J. Chem. Downloaded from www.nrcresearchpress.com by 210.87.254.40 on 09/05/12
For personal use only.

Can. J. Chem. Downloaded from www.nrcresearchpress.com by 210.87.254.40 on 09/05/12
For personal use only.

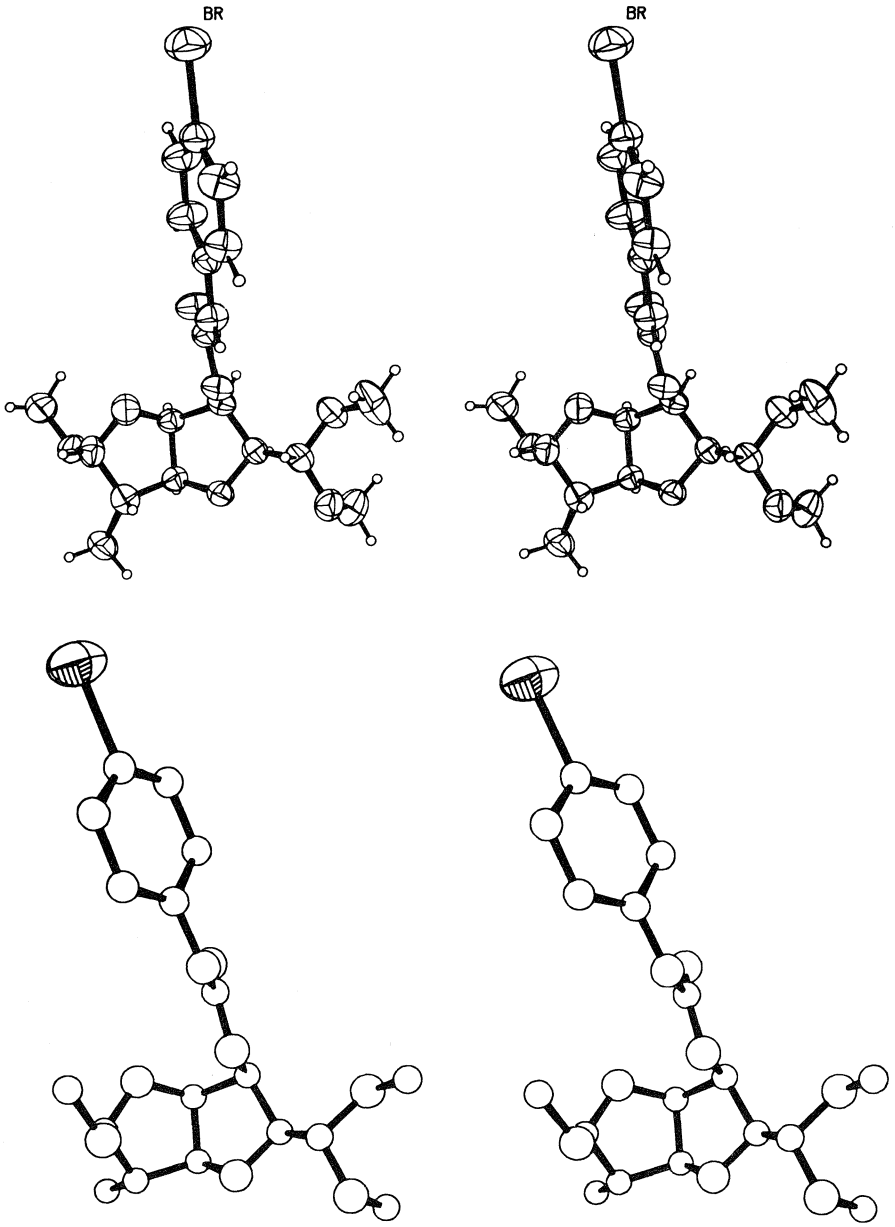


FIG. 11. Stereodrawings showing the conformations and absolute configurations of **66***b* (upper) and **66***a* (lower). The thermal ellipsoids of the anisotropic atoms are scaled to 50% probability level. The isotropic atoms are shown as spheres of arbitrary size.

vicinal coupling constants in the relatively rigid tetrahydrofuro[3,4-*d*]-1,3-dioxoles and tetrahydrofuro[2,3-*d*]-1,3-dioxoles can vary over a range of 0–6.5 Hz yielding very little configurational information. The only permissible conclusion appears to be based on $J \leqq 1$ Hz diagnostic for *trans* configurations. We seemed to have demonstrated convincingly the relative configuration of the tetrahydrofuran ring in goldinamine by ^{1}H nmr spectroscopy in conjunction with model compounds **55–58** and the resulting conclusions turned out to be correct. The study of the 5-epimers **65***a* and **65***b* as well as the 9-epimers **70** and **71** explicitly showed, however, that any extension of assignments due to coupling constants considerably larger than 1 Hz, although based on carefully chosen model systems, will remain problematic.

With the completed structure analyses of **64**, **65***a*,

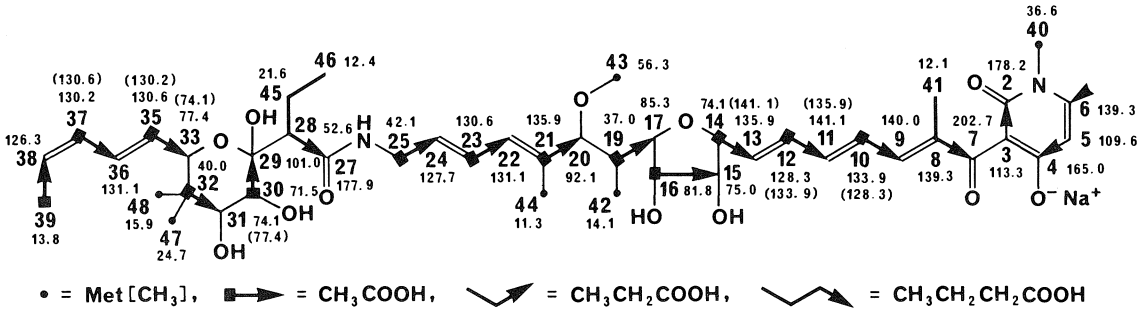


FIG. 12. Biosynthetic pattern and ^{13}C nmr chemical shifts of aurodox sodium salt.

and **65***b* the last stereochemical problems were resolved so that the structure of aurodox can be represented by **1***b*.

Configuration and Chirality of Mocimycin

Constitutional parity of des-*N*-methyl aurodox (**1***a*) with mocimycin (53, 54) was likely in view of very similar nmr spectra of aurodox (**1***b*) and mocimycin, differing only by the presence or absence, respectively, of an *N*-methyl signal. Proof for this assumption was furnished (8) by the demonstration that mocimycin gave mono- and dimethylated products identified as des-*N*-methyl **17** and **17**, the latter also prepared from **1***b* (Scheme 3). Both methylation products of **1***a*, upon treatment with acetic acid, yielded goldinono-1,4-lactone-3,7-hemiacetal (**13**) identical with authentic **13** as shown by spectral and chiroptical properties, and also afforded des-*N*-methyl **21** and **21**, respectively. The latter two goldinamine derivatives, both derived from mocimycin, were *N*-trifluoroacetylated furnishing **46** and **47**, respectively, whose elemental formulas were deduced by mass spectrometry. Further, **47** was also prepared from aurodox via **21** and exhibited a mass spectrometric fragmentation pattern identical to **47** from mocimycin (8). Configurational and chiral parity of the goldinamine moieties of mocimycin and goldinamine was conclusively demonstrated (8) by identical ord and cd spectra of **47** derived from **1***a* and **1***b*, by additional degradation and derivatization reactions of mocimycin yielding des-*N*-methyl-**29**, **29**, [4*E*, 6*E*, 2*R*, 3*S*]-8-acetylamino-3-methoxy-2,4-dimethyl-4,6-octadienal (**34**), and (1*R*,3*R*,4*S*,6*S*,7*S*,8*S*,10*R*)-4-(dimethoxymethyl)-1,7-dimethyl-8-methoxy-2,5,9-trioxatricyclo [4.2.2.$0^{3,10}$]decane (**64***b*), encompassing all remaining chiral centers.

Biosynthesis and ^{13}C nmr Spectrum of Aurodox

The availability of various degradation products of aurodox permitted the ^{13}C spectral assignments of aurodox with very few ambiguities remaining.[4] As expected, the 14 olefin methine carbons, especially C9–C13 of the trienone portion, posed problems in view of their similar chemical shifts. The incorporation of acetate, previously demonstrated (55, 56), was used to divide C9–C13 into two categories: C9, C11, and C13 derived from [1-^{13}C]-acetate, and C10 and C12 from [2-^{13}C]acetate. Assigning C9 by SFOR residual coupling led to the spectral results summarized in Fig. 12.

Biosynthetic studies with ^{14}C- and ^{13}C-labeled precursors (55, 56) showed the goldinonic acid portion derived from five acetate and one butyrate units with the geminal dimethyl group at C32 labeled by L-[Me-^{13}C]methionine. The goldinamine portion is derived from eight consecutive acetate units involving a sixteen-carbon polyketide chain methylated at C19 and C21, and a propionate unit. The origin of the pyridone moiety is somewhat obscure, in part due to general peak-broadness of C3 and C5 in [2-^{13}C]acetate labeled aurodox. The peak at 139.3, now assigned to C6, showed threefold enrichment in [1-^{13}C]acetate labeled aurodox while C2 and C4 were two and sevenfold enriched, respectively. It appears, therefore, that acetate is involved in the biosynthesis of the pyridone ring although a detailed proposal remains to be determined. The biosynthetic results are summarized in Fig. 12.

Experimental

All evaporations were carried out at reduced pressure. For chromatography we used silica gel (Woelm, <0.08 mm), silicic acid (Mallinckrodt, 100 mesh), and precoated tlc plates (Merck, silica gel F-254 for analytical and Merck, silica gel PF-254 for preparative plates). All solvent ratios are v/v. The following solvent systems were employed: chloroform–methanol – concentrated ammonium hydroxide, 40:10:1 (*A*); chloroform – ethyl acetate – methanol, 5:5:1, (*B*); chloroform – diethyl ether, 1:1 (*C*); chloroform – diethyl ether, 1:2 (*D*); chloroform – diethyl ether, 2:1 (*E*); chloroform–methanol, 4:1 (*F*); chloroform–methanol, 9:1 (*G*); cyclohexane – diethyl ether, 1:1 (*H*); cyclohexane–chloroform, 1:1 (*I*); and 1-butanol – acetic acid – water, 4:1:1 (*J*). Spots were visualized under uv light unless stated otherwise. Melting points were obtained on a hot stage (Reichert, Thermopan) and are uncorrected. ^1H and ^{13}C nmr spectra were obtained on a Varian XL-100 spectrometer in the

[4]Unpublished results.

Can. J. Chem. Downloaded from www.nrcresearchpress.com by 210.87.254.40 on 09/05/12
For personal use only.

Downloaded from www.rcsearchpress.com by 210.87.254.40 on 09/05/12
For personal use only.

continuous-wave mode and Fourier-transform mode, respectively.

(3S, 4E, 6Z)-3-Hydroxy-2,2-dimethyl-4,6-octadienal (2)

Aurodox sodium salt (4.2 g, 5 mmol) was dissolved in water (200 mL) containing sodium hydrogen carbonate (4 g). The solution was diluted with dioxane (400 mL), cooled in an ice bath, and further diluted with an ice-cold solution of sodium metaperiodate (10.7 g, 50 mmol) in water (400 mL). The reaction mixture was stirred at ca. 4°C for 20 h, immersed in an ice bath, quenched by the addition of ethylene glycol (5.6 mL), stirred for 2 h, and extracted with diethyl ether (4 × 400 mL). The combined extracts were washed with water (2 × 150 mL) and dried. Evaporation of the solvent gave crude **2** as oil (830 mg), R_f 0.60 (*B*). A small sample was purified by preparative tlc; uv (dioxane) λ_{max}: 235(ε 18770, diene) nm; *Mol. Wt.* calcd. for $C_{10}H_{16}O_2$: 168.24; found (ms) *m/e* (%): 168 (38), 97 (100).

(3S, 4E, 6Z)-2,2-Dimethyl-4,6-octadiene-1,3-diol (3)

A solution of crude **2** (820 mg) in diethyl ether (75 mL) was added dropwise over a 30 min period to a stirred mixture of lithium aluminum hydride (2 g) in diethyl ether (300 mL). After stirring for 4 h at 5°C excess hydride was destroyed by dropwise addition of saturated sodium sulfate solution. The ether layer was removed by decantation, the white precipitate was washed with ether, and the ethereal solutions were combined, dried, and concentrated to a syrup of crude **3** (810 mg). A solution of this material in chloroform was chromatographed on a column of silica gel (25 g) with chloroform (200 mL) and system *E* as mobile phase affording pure **3** as a syrup, R_f 0.55 (*B*), 0.28 (*E*); uv (2-propanol) λ_{max}: 233 (ε 24700) nm. The ^{1}H nmr spectrum is shown in Fig. 1. *Mol. Wt.* calcd. for $C_{10}H_{18}O_2$: 170.25; found (ms) *m/e* (%): 170 (6), 97 (100).

Aurodox (4-Bromobenzyl) Ether (18)

4-Bromobenzyl bromide (3 g, 12 mmol) was added to a solution of **1***b* sodium salt (8.33 g, 10 mmol) in dimethylformamide (125 mL). The solution was kept for 3 days at room temperature in the dark, transferred to a separatory funnel with ethyl acetate (1 L) and saturated sodium hydrogen carbonate solution (350 mL). The organic phase was washed once with sodium hydrogen carbonate solution (350 mL), three times with water (100 mL each), and dried ($MgSO_4$). Concentration gave a thin, yellow syrup which was dissolved in acetone (20 mL) and chromatographed on a column of Sephadex LH-20 (9 cm × 47 cm) with acetone as mobile phase. Fractions containing pure **18** were combined (tlc), concentrated to a volume of 50 mL, and slowly added to ether (500 mL) under vigorous stirring. After further addition of petroleum ether (500 mL) the precipitate was collected by filtration, washed with ether and petroleum ether, and dried under reduced pressure, R_f 0.72 (*A*), 0.20 (*B*). *Anal.* calcd. for $C_{51}H_{67}BrN_2O_{12}\cdot H_2O$ (998.03): C 61.38, H 6.97, N 2.81, Br 8.01; found: C 61.37, H 7.14, N 2.71, Br 8.18.

[1R-(1β,3α,5α,6β,9α,E,Z)]-9-Ethyl-1,5-dihydroxy-4,4-dimethyl-3-(1,3-pentadienyl)-2,7-dioxabicyclo-[4.3.0]nonan-8-one (Goldinono-1,4-lactone-3,7-hemiacetal, 13) and [2R,3R,4S,5S,1(R),2(S*)]-4-(4-Bromobenzyloxy)-1-methyl-3-[7-[5-[7-amino-2-methoxy-1,3-dimethyl-3(E),5(E)-heptadienyl]-3,4-dihydroxytetrahydro-2-furyl]-2-methyl-1-oxo-2(E),-4(E),6(E)-heptatrienyl]-2(1H)-pyridinone (Goldinamine (4-Bromobenzyl) Ether, 22)*

A solution of **18** (400 mg) in acetic acid (10 mL) was kept at room temperature for three days in the dark or was heated on the steam bath for 20 min. The acetic acid was removed by distillation and codistillation with toluene. The residue was dissolved in chloroform and chromatographed on a column containing silicic acid (35 g). Elution started with chloroform (fractions 1–6, 12 mL each) and was followed by chloroform–methanol, 20:1 (7–20), chloroform–methanol, 4:1 (21–40), and chloroform–methanol – acetic acid, 16:4:1 (41–86). Fractions 14–17 contained crude **13** (111 mg, R_f 0.24, (*A*)) which were purified by rechromatography or preparative tlc (0.48 (*B*)) to give white crystals of **13**, mp 110°C; $[\alpha]_D$ −23° (*c* 1.0, $CHCl_3$) (37). *Anal.* calcd. for $C_{16}H_{24}O_5$ (296.35): C 64.84, H 8.16; found: C 64.56, H 8.29. Fractions 54–77 were pooled and concentrated to a syrup, redissolved in water and freeze-dried to yield amorphous **22** acetic acid salt hemihydrate (116 mg), R_f 0.6 (*A*); nmr (CD_3OD)[5] δ: 0.82 (d, 3, $J_{1,Me}$ = 7 Hz, 1-Me), 1.71 (s, 3, 3-Me), 1.89 (s, 3, *Me*COO^-), 1.94 (s, 3, 2″Me), 2.20 (m, 1, $J_{1,Me}$ = 7 Hz, H1), 3.15 (s, 3, OMe), 3.37 (d, 1, $J_{1,2}$ = 10 Hz, H2), 3.47 (s, 3, NMe), 3.57 (d, 2, $J_{6,7}$ = 6 Hz, H7), 3.71 (dd, 1, $J_{1,5'}$ = 7 and $J_{4',5'}$ = 4 Hz, H5′), 4.19 (dd, 1, $J_{3'4'}$ = 5 and $J_{4'5'}$ = 4 Hz, H4′), 4.32 (m, 2, H2′ and H3′), 5.11 (s, 2, CH_2—C_6H_5), 5.75 (dt, 1, $J_{5,6}$ = 15 and $J_{6,7}$ = 7 Hz, H6), 6.03 (d, 1, $J_{4,5}$ = 10 Hz, H4), 6.08 (dd, 1, $J_{2',7''}$ = 7 and $J_{6'',7''}$ = 14 Hz, H7″), 6.41 (dd, 1, $J_{5'',6''}$ = 11 and $J_{6'',7''}$ = 14 Hz, H6″), 6.43 (d, 1, $J_{5''',6'''}$ = 7.5 Hz, H5‴), 6.48 (dd, 1, $J_{4''5''}$ = 14 and $J_{5''6''}$ = 11 Hz, H5″), 6.61 (dd, 1, $J_{4,5}$ = 10 and $J_{5,6}$ = 15 Hz, H5), 6.68 (dd, 1, $J_{3''4''}$ = 11 and $J_{4'',5''}$ = 14 Hz, H4″), 6.91 (d, $J_{3'',4''}$ = 11 Hz, H3″), 7.18, 7.43 (AA′BB′, 4, J_0 = 8.5 Hz, C_6H_4), and 7.70 (d, 1, $J_{5''',6'''}$ = 7.5 Hz, H6‴). *Anal.* calcd. for $C_{35}H_{43}BrN_2O_7\cdot CH_3COOH\cdot\frac{1}{2}H_2O$ (752.71): C 59.04, H 6.43, N 3.72, Br 10.62; found: C 59.01, H 6.33, N 3.77, Br 10.89.

The free base of **22** was prepared by dissolving **22** acetic acid salt (50 g) in water (5 mL) and adding 0.1 *N* sodium hydroxide solution to pH 9.2. The precipitate was collected, washed with water, and dried to yield a light tan, amorphous powder; nmr ($CDCl_3$) similar to **22** acetic acid salt but lacking a signal for acetate, and H7 shifted diamagnetically to δ 3.28.

[2S,3S,4R,5R,7(R),6(S*)]-N-[7-[5-[7-[(4-Bromobenzyloxy)-1,2-dihydro-1-methyl-2-oxo-3-pyridinyl]-6-methyl-7-oxo-1(E),3(E),5(E)-heptatrienyl]tetrahydro-3,4-dihydroxy-furan-2-yl]-6-methoxy-5,7-dimethyl-2(E),4(E)-heptadienyl]acetamide (N-Acetyl 22)*

Acetic anhydride (8 mL) was added to a solution of **22** acetic acid salt (2 g) in methanol (20 mL). After one hour the mixture was added dropwise to a rapidly stirred mixture of ether (700 mL) and petroleum ether (600 mL). The precipitate was collected, dried, redissolved in acetone (4 mL), and chromatographed on a column of Sephadex LH-20 (51 mm × 510 mm) with acetone as mobile phase. Pure fractions were pooled, evaporated, and redissolved in acetone. The resulting solution was added dropwise to rapidly stirred petroleum ether (400 mL). The precipitate was collected by filtration and dried to give an amorphous powder (1.65 g) (R_f 0.15 (*B*); 0.85 (*F*); 0.50 (*G*)); nmr (CD_3OD) similar to that of **22** acetic acid salt, but shows δ 1.94 (s, 3, N—Ac).

[2S,3R,4S,5R,7(R),6(S*)]-N-[7-[5-[7-[(4-Bromobenzyloxy)-1,2-dihydro-1-methyl-2-oxo-3-pyridinyl]-6-methyl-7-oxo-1(E),3(E),5(E)-heptatrienyl]tetrahydro-3,4-bis(acetyloxy)-furan-2-yl]-6-methoxy-5,7-dimethyl-2(E),4(E)-heptadienyl]acetamide (N,O,O-Triacetyl 22)*

A solution of **22** acetic acid salt (150 mg) was dissolved in anhydrous pyridine (4 mL) and acetic anhydride (2 mL) was added. The solution was kept in the dark overnight, evaporated to dryness, the residue dissolved in chloroform, and chromatographed on silica gel (8 g). With system *B* as mobile phase pure fractions were obtained which were pooled and evaporated. Dissolving the residue in chloroform and precipitating with petroleum ether gave amorphous *N,O,O*-triacetyl **22** (140 mg), R_f 0.25 (*B*); nmr (CD_3OD) δ: 0.85 (d, 3, $J_{7,Me}$ = 7 Hz, 7-Me), 1.63 (s, 3, 5-Me), 1.92, 1.95, 2.04 (3s, 9, CH_3CO), 1.98 (s, 3, 6″-Me), 2.21 (m, 1, H7), 3.03 (s, 3, CH_3O), 3.23 (d, 1, $J_{6,7}$ = 10 Hz, H6), 3.50 (s, 3, NMe), 3.86 (d, 2, $J_{1,2}$ = 6 Hz, H1), 3.92 (dd, 1, $J_{2',7'}$ = 7 and

[5]For proton designations see Scheme 6.

Can. J. Chem. Downloaded from www.nrcresearchpress.com by 210.87.254.40 on 09/05/12
For personal use only.

$J_{2',3'}$ = 3 Hz, H2'), 4.57 (dd, 1, $J_{4'5'}$ = 6 and $J_{1'',5'}$ = 7 Hz, H5'), 5.11 (s, 2, CH_2—C_6H_5), 5.41 (dd, 1, $J_{4',5'}$ = 6, $J_{3',4'}$ = 4.5 Hz, H4'), 5.46 (t, 1, $J_{3',4'} = J_{2',3'}$ = 4.5 Hz, H3'), 5.64 (dt, 1, $J_{2,3}$ = 15 and $J_{1,2}$ = 6 Hz, H2), 5.84 (dd, 1, $J_{1'',5'}$ = 7 and $J_{1'',2''}$ = 14.5 Hz, H1''), 5.94 (d, 1, $J_{4,5}$ = 11 Hz, H4), 6.38 (dd, 1, $J_{2'',3''}$ = 11 and $J_{1'',2''}$ = 14 Hz, H2''), 6.41 (d, 1, $J_{5''',6'''}$ = 7.5 Hz, H5'''), 6.45 (dd, 1, $J_{3'',4''}$ = 14 and $J_{2'',3''}$ = 11 Hz, H3''), 6.50 (dd, 1, $J_{4,5}$ = 11 and $J_{5,6}$ = 15 Hz, H3), 6.69 (dd, 1, $J_{4'',5''}$ = 11 and $J_{3'',4''}$ = 14 Hz, H4''), 6.87 (d, 1, $J_{4'',5''}$ = 11 Hz, H5''), 7.17, 7.41 (AA'BB', 4, J_0 = 8.5 Hz, C_6H_5), and 7.67 (d, 1, $J_{5''',6'''}$ = 7.5 Hz, H6''').

[2R,3R,4S,5S,1(R),2(S*)]-4-(4-Bromobenzyloxy)-1-methyl-3-[7-[5-[7-(2,4-dinitrophenylamino)-1,3-dimethyl-2-methoxy-3(E),5(E)-heptadienyl]-3,4-dihydroxytetrahydro-2-furyl]-2-methyl-1-oxo-2(E),4(E),6(E)-heptatrienyl]-2(1H)-pyridone (**26**)*

2,4-Dinitrofluorobenzene (0.35 mL) was added to a mixture of **22** acetic acid salt (0.5 g), potassium carbonate (1 g), and acetone (30 mL). After shaking for 20 h in the dark, the suspension was filtered, the filtrate evaporated, and the residue chromatographed on a column of Sephadex LH-20 (25 mm × 510 mm) with acetone as mobile phase to furnish **26** by precipitation with petroleum ether from concentrated solution (0.3 g), R_f 0.71 (*G*); nmr ($CDCl_3$)[6] δ: 0.87 (d, 3, $J_{1,Me}$ = 7 Hz, 1-Me), 1.70 (s, 3, 3-Me), 2.02 (s, 3, 2''-Me), 2.20 (m, 1, H1), 3.22 (s, 3, 2-OMe), 3.31 (d, 1, $J_{1,2}$ = 9.5 Hz, H2), 3.50 (s, 3, NMe), 3.56 (m, 1, H5'), 4.22 (m, 3, NCH_2 and H2'), 4.42 (m, 2, H3' and H4'), 5.03 (s, 2, OCH_2), 5.85 (dt, 1, $J_{5,6}$ = 15.5 and $J_{6,7}$ = 6 Hz, H6), 6.06 (d, 1, $J_{5''',6'''}$ = 7.5 Hz, H5'''), 6.06 (m, 2, H4 and H7''), 6.30–6.80 (m, 4, H4'', H5, H5'', H6''), 6.90 (d, 1, $J_{3'',4''}$ = 10 Hz, H3''), 6.99 (d, 1, $J_{5,6}$ = 9 Hz, H6 of DNP), 7.17, 7.48 (AA'BB', 4, J_0 = 8.5 Hz, C_6H_4), 7.35 (d, 1, $J_{5''',6'''}$ = 7.5 Hz, H6'''), 8.35 (dd, 1, $J_{3,5}$ = 3 and $J_{5,6}$ = 9 Hz, H3 of DNP), 8.72 (t, 1, $J_{7,NH}$ = 6 Hz, NH), 9.20 (d, 1, $J_{3,5}$ = 3 Hz, H5 of DNP). A 220 MHz spectrum is shown in Fig. 8.

[2R,3S,4R,5S,1(R),2(S*)]-4-(4-Bromobenzyloxy)-1-methyl-3-[7-[5-[7-(2,4-dinitrophenylamino)-2-methoxy-1,3-dimethyl-3(E),5(E)-heptadienyl]-3,4-bis(acetyloxy)tetrahydrofuran-2-yl]-2-methyl-1-oxo-2-methyl-2(E),4(E),6(E)-heptatrienyl]-2(1H)-pyridinone (**43**)*

A mixture of **26** (0.30 g), pyridine (3 mL), and acetic anhydride (1.5 mL) was stirred at 25°C for 26 h and then added dropwise to diethyl ether – petroleum ether (1:2, 200 mL). The resulting precipitate of crude **43** (0.29 g) was chromatographed on Sephadex LH-20 (acetone) yielding pure **43** (0.26 g), R_f 0.52 (*B*); nmr shown in Fig. 8.

[3aS,4R,6aR,6S,1(R),2(S*)]-4-(4-Bromobenzyloxy)-1-methyl-3-[7-[6-[7-(2,4-dinitrophenylamino)-2-methoxy-1,3-dimethyl-3(E),5(E)-heptadienyl]-tetrahydro-2,2-dimethyl-furo[3,4-d]-1,3-dioxol-4-yl]-2-methyl-1-oxo-2(E),4(E),6(E)-heptatrienyl]-2(1H)-pyridinone (**44**)*

2,2-Dimethoxypropane (0.5 mL) and bis(4-nitrophenyl) phosphate (75 mg) were added to a solution of **26** (100 mg) in acetone (5 mL). The mixture was neutralized with Dowex 1 (HCO_3^-) after 2 h, the resin filtrate and washings (methanol) were evaporated, and the residue chromatographed on Sephadex LH-20 (acetone) to yield pure **44** as yellow powder by precipitation with petroleum ether, R_f 0.52 (*B*); nmr ($CDCl_3$)[7] δ: 0.93 (d, 3, $J_{1,Me}$ = 6 Hz, 1-Me), 1.29, 1.43 (2s, 3 each, 2-Me_2), 1.70 (s, 3, 3-Me), 2.03 (s, 3, 2''-Me), 2.31 (m, 1, H1), 3.18 (s, 3, 2-OMe), 3.36 (d, 1, $J_{1,2}$ = 9.5 Hz, H2), 3.49 (s, 3, NMe), 3.57 (dd, 1, $J_{1',6}$ = 6 and $J_{6',6a'}$ = 3.5 Hz, H6'), 3.97 (dd, 1, $J_{3a',4'}$ = 4 and $J_{4',7''}$ = 8 Hz, H4'), 4.16 (t, 2, $J_{6,7} = J_{7,NH}$ = 6 Hz, NCH_2), 4.62 (dd, 1, $J_{3a',4'}$ = 4 and $J_{3a',6a'}$ = 6 Hz, H3a'), 4.71 (dd, 1, $J_{3a',6a'}$ = 6 Hz and $J_{6',6a'}$ = 3.5 Hz, H6a'), 5.03 (s, 2, OCH_2), 5.75 (dt, 1, $J_{5,6}$ = 15 and $J_{6,7}$ = 6 Hz, H6), 6.02 (d, 1, $J_{5''',6'''}$ = 7.5 Hz, H5'''), 6.03 (m, 2, H4 and H7''), 6.30–6.80 (m, 4, H4'', H5, H5'', H6), 6.88 (d, 1, $J_{3'',4''}$ = 10 Hz, H3''), 6.95 (d, 1, $J_{5,6}$ = 9 Hz, H6 of DNP), 7.13, 7.45 (AA'BB', 4, J_0 = 8.5 Hz, C_6H_4), 7.37 (d, 1, $J_{5''',6'''}$ = 7.5 Hz, H6'''), 8.28 (dd, 1, $J_{3,5}$ = 3 and $J_{5,6}$ = 9 Hz, H5 of DNP), 8.65 (t, 1, $J_{7,NH}$ = 6 Hz, NH), 9.15 (d, 1, $J_{3,5}$ = 3 Hz, H3 of DNP).

*[1R-(1β,3α,5α,6β,9α)]-9-Ethyl-1,5-dihydroxy-4,4-dimethyl-3-pentyl-2,7-dioxabicyclo[4.3.0]nonan-8-one (Tetrahydrogoldinono-1,4-lactone-3,7-hemiacetal, **14**)*

Crude **13** (2 g) in acetic acid (30 mL) was stirred with prehydrogenated platinum oxide (160 mg) for 8 h under hydrogen pressure of 2 atm. Removal of the catalyst and solvent gave a syrup which was dissolved in chloroform and chromatographed on alumina (40 g). Changing to chloroform – ethyl acetate (9:1) as the mobile phase eluted **14**. Final purification was achieved by chromatography on Sephadex LH-20 (50 mm × 570 mm) with acetone as mobile phase. Crystallization from ethanol–water gave white needles (1.2 g), R_f 0.60 (*B*) (37).

*4-Hydroxy-1-methyl-2(1H)-pyridone (**19**)*

A solution of **1***b* sodium salt (10 g) in ethanol (150 mL) was hydrogenated (3.5 atm) over 10% palladium-on-barium sulfate (2 g) for 6.5 h. The catalyst was filtered off, the filtrate was diluted with water (150 mL), refluxed for 5 h, and evaporated to dryness. The dry residue was extracted three times with chloroform, the remaining solids were dissolved in methanol–water, 2:1, and the solution passed through a column of Dowex 50 X-4 (200–400 mesh, H^+, 50 mL). The resin was rinsed with methanol–water (2:1, 100 mL) followed by methanol–water–pyridine (2:2:1) which eluted **19**. Pooling and concentration of the appropriate fractions gave a syrup which solidified on standing. Recrystallization from ethanol–diethyl ether gave large prisms of **19** (700 mg), R_f 0.19 (*A*), 0.25 (*B*); mp 168–170°C. *Anal.* calcd. for $C_6H_7NO_2$ (125.14): C 57.59, H 5.64, N 11.19; found: C 57.62, H 5.75, N 11.13; (40).

The acid was converted to the thallium salt with thallium ethoxide and recrystallized from methanol–ethanol–ether to afford colorless needles, mp 203–204°C. *Anal.* calcd. for $C_6H_6NO_2Tl$ (328.51): C 21.94, H 1.84, N 4.26; found: C 21.83, H 1.71, N 4.26.

*Methylenebis(4-hydroxy-1-methyl-2(1H)-pyridinone) (**20**)*

Formaldehyde solution (37%, 0.1 mL) and piperidine (one drop) were added to a solution of **19** (120 mg) in ethanol–water (1:1, 4 mL). The mixture was refluxed on the steam bath for 10 min and refrigerated. The precipitate was recrystallized from ethanol–chloroform (84 mg), R_f 0.80 (*A*); mp 300–305°C; uv λ_{max} (ε): 282 (11 580) in 0.1 *N* HCl, 281–282 (12 900) nm in 0.1 *N* KOH; nmr ($CDCl_3$) δ: 3.49 (s, 6, 2 NMe), 3.74 (s, 2, CH_2), 6.09 (d, 1, $J_{5,6}$ = 8 Hz, H5), 7.06 (d, 1, $J_{5,6}$ = 8 Hz, H6), and 13.01 (s, 2, 2 OH). *Anal.* calcd. for $C_{13}H_{14}N_2O_4$ (262.26): C 59.4, H 5.38, N 10.68; found: C 59.72, H 5.35, N 10.52.

*4-(4-Bromobenzyloxy)-1,2-dihydro-1-methyl-2-oxopyridine-3-carboxylic Acid (**24**)*

A solution of potassium carbonate (4.14 g), sodium metaperiodate (8.5 g), and potassium permanganate (63 mg) in water (400 mL) was added to a solution of **22** acetic acid salt (500 mg) in 90% *tert*-butanol (500 mL). The mixture was stirred overnight at room temperature in the dark, acidified (pH 1.5, 6 *N* sulfuric acid), and extracted with diethyl ether (500 mL). The dried extract was evaporated and the residue triturated repeatedly with chloroform. The remaining solids were then extracted with chloroform–methanol (9:1, 50 mL). This extract was evaporated and the residue allowed to crystallize from hot methanol. Recrystallization from methanol–ethanol–water gave colorless

[6]For proton designations see Fig. 8.

[7]For proton designations see Fig. 9.

Can. J. Chem. Downloaded from www.nrcresearchpress.com by 210.87.254.40 on 09/05/12
For personal use only.

prisms of **24**, R_f 0.10 (*A*); mp 224°C. *Anal.* calcd. for $C_{14}H_{12}BrNO_4$ (338.16): C 49.73, H 3.58, N 4.14; found: C 49.68, H 3.58, N 4.23 (40).

*4-(4-Bromobenzyloxy)-1,2-dihydro-1-methyl-2-oxopyridine-3-carboxylic Acid Methyl Ester (**25**)*

Diethyl ether (2 mL) containing an excess of diazomethane was added to a suspension of **24** (15 mg) in tetrahydrofuran (3 mL) and methanol (0.5 mL). After stirring for 45 min a clear solution resulted. The mixture was concentrated after 3 h and addition of ether and petroleum ether gave needles of **25**, R_f 0.45 (*B*), 0.88 (*F*); mp 180°C. *Anal.* calcd. for $C_{15}H_{14}BrNO_4$ (352.19): C 49.43, H 4.15, N 4.12; found: C 49.43, H 4.10, N 3.91.

*4-(4-Bromobenzyloxy)-3,5-diiodo-1-methyl-2(1H)-pyridone (**23**)*

The combined chloroform extracts of the residue, which were described in the preparation of **24** were concentrated and chromatographed on a column of silicic acid (8 g) with chloroform as mobile phase. Fractions containing the spot with R_f 0.45 (*C*) were pooled and evaporated. The residue was further purified by preparative tlc with the same solvent system. The silicic acid was extracted with system *G* and the product crystallized from diethyl ether – petroleum ether to give slightly yellow needles (29 mg), R_f 0.75 (*B*); mp 204–205°C; nmr ($CDCl_3$) δ: 3.58 (s, 3, NMe), 5.02 (s, 2, CH_2), 7.49, 7.53 (AA′BB′, 4, J_0 = 8.5 Hz, C_6H_4), and 7.65 (s, 1, H6). *Mol. Wt.* calcd. for $C_{13}H_{10}BrI_2NO_2$: 544.7989; found (ms) *m/e*: 544.8033.

*(6S,7R,2E,4E)-N-(7-Formyl-6-methoxy-5-methyl-2,4-octadienyl)acetamide (**34**)*

A solution of sodium metaperiodate (1.9 g) in water (160 mL) was added to a solution of **22** acetate (1 g) in a mixture of dioxane (140 mL) and methanol (20 mL). A transient wine-red color developed immediately indicating the liberation of iodine. The mixture was stirred in the dark for 2.5 h and centrifuged after addition of barium hydroxide to pH 8.3. Acetic anhydride (15 mL) was added to the stirred supernatant and, after one hour, the pH was adjusted to 8.4 with 19 *M* sodium hydroxide solution and extracted with ether (400, 200, and 200 mL). The combined and dried extracts were evaporated to a syrup (350 mg) of nearly pure **34**. Preparative tlc (*B*) gave a straw-colored syrup with R_f 0.55 (*B*) and 0.68 (*G*); cd (*c* 0.012 *M*, dioxane): $[\theta]_{318}$ 0, $[\theta]_{290}$ + 3750, $[\theta]_{248}$ 0, $[\theta]_{220}$ + 8750, $[\theta]_{204}$ 0; nmr ($CDCl_3$) δ: 0.85 (d, 3, $J_{2,8}$ = 7 Hz, H8), 1.69 (s, 3, 5-Me), 2.00 (s, 3, CH_3CO), 2.59 (ddq, 1, $J_{7,CHO}$ = 3, $J_{6,7}$ = 10, and $J_{7,8}$ = 7 Hz, H7), 3.17 (s, 3, OCH_3), 3.63 (d, 1, $J_{6,7}$ = 10 Hz, H6), 3.95 (t, 2, $J_{1,2}$ = $J_{1,NH}$ = 6 Hz, NCH_2), 5.67 (dt, 1, $J_{2,3}$ = 15 and $J_{1,2}$ = 6 Hz, H2), 6.00 (d, 1, $J_{3,4}$ = 10 Hz, H4), 6.06 (broad, 1, NH), 6.48 (dd, 1, $J_{3,4}$ = 10 and $J_{2,3}$ = 15 Hz, H3), and 9.75 (d, 1, $J_{7,CHO}$ = 3 Hz, 7-CHO).

*(2E,4E,6E)-8-[4-(4-Bromobenzyloxy)-1,2-dihydro-1-methyl-2-oxo-3-pyridyl]-7-methyl-8-oxo-2,4,6-octatrienoic Acid (**31**)*

The aqueous phase obtained after extraction of **34** in the above procedure was adjusted to pH 3.0 with 18 *N* sulfuric acid and the solution repeatedly extracted with dichloromethane. The dried extract was evaporated and the residue redissolved in chloroform. Upon standing the concentrated chloroform solution deposited a monochloroform solvate of **31** as yellow needles. Drying at 75°C and 0.5 Torr gave the chloroform-free product, R_f 0.15 (*A*) and 0.58 (*J*). *Anal.* calcd. for $C_{22}H_{20}BrNO_5$ (458.31): C 57.66, H 4.40, N 3.06, Br 17.43; found: C 57.71, H 4.36, N 3.18, Br 17.47 (40).

The ^1H nmr spectrum of **31** and a stereoscopic view of the crystal structure are shown in Figs. 3 and 4, respectively.

*(2E,4E,6E)-8-[4-(4-Bromobenzyloxy)-1,2-dihydro-1-methyl-2-oxo-3-pyridyl]-7-methyl-8-oxo-2,4,6-octatrienoic Acid Methyl Ester (**32**)*

A suspension of **31** (350 mg) in tetrahydrofuran (30 mL) and methanol (2 mL) was mixed with diethyl ether (30 mL) containing an excess of diazomethane and stirred overnight. The resulting clear solution was evaporated. Crystallization from methanol–water gave **32** as yellow needles, R_f 0.62 (*J*) and 0.75 (*F*); mp 164°C; nmr (DMSO-d_6) δ: 1.98 (s, 3, 7-Me), 3.43 (s, 3, NMe), 3.73 (s, 3, OMe), 5.19 (s, 2, CH_2), 6.11 (d, 1, $J_{2,3}$ = 15 Hz, H2), 6.41 (d, 1, $J_{5',6'}$ = 7.5 Hz, H5′), 6.74 (dd, 1, $J_{3,4}$ = 11 and $J_{4,5}$ = 14.5 Hz, H4), 6.86 (d, 1, $J_{5,6}$ = 11 Hz, H6), 7.25 (dd, 1, $J_{4,5}$ = 14.5 and $J_{5,6}$ = 11 Hz, H5), 7.26, 7.54 (AA′BB′, 4, J_0 = 8.5 Hz, C_6H_4), 7.47 (dd, 1, $J_{2,3}$ = 15 and $J_{3,4}$ = 11 Hz, H3), and 7.84 (d, 1, $J_{5',6'}$ = 7.5 Hz, H6′). *Anal.* calcd. for $C_{23}H_{22}BrNO_5$ (472.34): C 58.49, H 4.69, N 2.97; found: C 58.17, H 4.86, N 2.93.

*(6S,7S,2E,4E)-N-(8-Hydroxy-5,7-dimethyl-6-methoxy-2,4-octadienyl)acetamide (**37**)*

A solution of **34** (100 mg) in ethanol (10 mL) was cooled in an ice bath and treated with sodium borohydride (100 mg). After 20 min at 0°C water (20 mL) was added and the pH of the solution was adjusted to 3.1. The mixture was extracted with diethyl ether (3 × 25 mL). The dried extracts were evaporated and the residue purified by preparative tlc in system *B* to yield a colorless syrup of **37** (90 mg), R_f 0.48 (*B*) and 0.59 (*G*); uv (2-propanol) λ_{max}: 239 (ε 21 500) nm; nmr ($CDCl_3$) δ: 0.67 (d, 3, $J_{6,7}$, $J_{7,Me}$ = 6.5 Hz, 7-Me), 1.66 (s, 3, 5-Me), 1.94 (m, 1, H7), 1.98 (s, 3, CH_3CO), 3.16 (broad, 1, OH), 3.16 (s, 3, 6-OMe), 3.34 (d, 1, $J_{6,7}$ = 9 Hz, H6), 3.60 (d, 2, $J_{7,8}$ = 6 Hz, H8), 3.91 (t, 2, $J_{1,2}$ = $J_{1,NH}$ = 6 Hz, NCH_2), 5.67 (dt, 1, $J_{2,3}$ = 15 and $J_{1,2}$ = 6 Hz, H2), 5.96 (d, 1, $J_{3,4}$ = 11 Hz, H4), 6.37 (d, 1, $J_{1,NH}$ = 6 Hz, NH), and 6.42 (dd, 1, $J_{3,4}$ = 11 and $J_{2,3}$ = 15 Hz, H3).

*(2S,3S,4E,6E)-8-Acetylamino-3-methoxy-2,4-dimethyl-4,6-octadien-1-yl 4-Bromobenzoic Acid Ester (**38**)*

The ester was prepared with 4-bromobenzoyl chloride in pyridine in the usual fashion yielding **38** as a syrup, R_f 0.73 (2); nmr ($CDCl_3$) δ: 0.86 (d, 3, $J_{2,Me}$ = 7 Hz, 2-Me), 1.68 (s, 3, 4-Me), 2.00 (s, 3, CH_3CO), 2.09 (m, 1, H2), 3.14 (s, 3, 3-OMe), 3.31 (d, $J_{2,3}$ = 9 Hz, H3), 3.94 (t, 2, $J_{7,8}$ = $J_{8,NH}$ = 6 Hz), 4.30 (dd, 1, J_{gem} = 11 Hz, $J_{1a,2}$ = 6.5 Hz, H1a), 4.54 (dd, J_{gem} = 11 Hz, $J_{1b,2}$ = 4 Hz, H1b), 5.66 (dt, 1, $J_{6,7}$ = 15.5 and $J_{7,8}$ = 6 Hz, H7), 5.96 (d, 1, $J_{5,6}$ = 10.5 Hz, H5), 5.98 (broad, 1, NH), 6.44 (dd, 1, $J_{5,6}$ = 10.5 and $J_{6,7}$ = 15.5 Hz, H6), and 7.57, 7.92 (AA′BB′, 4, J_0 = 8.5 Hz, C_6H_4).

*(2R,3S,4E,6E)-8-[(2,4-Dinitrophenyl)amino]-3-methoxy-2,4-dimethyl-4,6-octadienal (**35**)*

A solution of sodium metaperiodate (1.5 g) in water (160 mL) was added to a solution of **22** acetic acid salt (1 g) in dioxane (140 mL) and methanol (20 mL). After standing in the dark for 5 h the pH was adjusted to 8.4 (barium hydroxide) and the suspension was centrifuged. Sodium hydrogen carbonate (1.5 g) was added to the supernatant, followed by 2,4-dinitrofluorobenzene (1 g) in methanol (5 mL). After stirring in the dark for 16 h, the mixture was extracted with diethyl ether and the extracts were combined, dried, and evaporated. A chloroform solution of the residue was chromatographed on silicic acid (75 g) with chloroform as mobile phase. The major yellow band was isolated and gave **35** as a yellow syrup (270 mg), R_f 0.67 (*D*); ^1H nmr shown in Fig. 5. *Mol. Wt.* calcd. for $C_{17}H_{21}N_3O_6$: 363.14, found (ms) *m/e* (%): 363 (6), 196 (100).

*(2R,3S,4E,6E)-8-[(2,4-Dinitrophenyl)amino]-3-methoxy-2,4-dimethyl-4,6-octadienal Dimethyl Acetal (**41**)*

To a solution of **35** (110 mg) in methanol (5 mL) and 2,2-

Can. J. Chem. Downloaded from www.nrcresearchpress.com by 210.87.254.40 on 09/05/12
For personal use only.

dimethoxypropane (1 mL) was added bis(4-nitrophenyl)phosphate (50 mg). After two h at room temperature, the solution was neutralized with Dowex 1 (HCO_3^-). The filtrate and resin washings (acetone) were concentrated, redissolved in chloroform, and chromatographed on a column of silicic acid (35 g) with chloroform as mobile phase. The major band was concentrated to a syrup which solidified on standing. Recrystallization from acetone–ethanol gave yellow prisms of **41**, R_f 0.78 (*D*); nmr ($CDCl_3$) δ: 0.71 (d, 3, $J_{2,Me}$ = 7 Hz, 2-Me), 1.68 (s, 3, 4-Me), 1.97 (m, 1, H2), 3.17 (s, 3, 3-OMe), 3.40 (d, $J_{2,3}$ = 9 Hz, H3), 3.43, 3.50 (2s, 3 each, 1-$(OMe)_2$), 4.17 (t, 2, $J_{7,8}$ = $J_{8,NH}$ = 6 Hz, NCH_2), 4.53 (d, 1, $J_{1,2}$ = 3 Hz, H1), 5.77 (dt, $J_{6,7}$ = 15 and $J_{7,8}$ = 6 Hz, H7), 6.04 (d, 1, $J_{5,6}$ = 10.5 Hz, H5), 6.60 (dd, 1, $J_{5,6}$ = 10.5 and $J_{6,7}$ = 15 Hz, H6), 6.95 (d, 1, $J_{5',6'}$ = 9.5 Hz, H6′), 8.30 (dd, 1, $J_{3',5'}$ = 2.5 and $J_{5',6'}$ = 9.5 Hz, H5′), 8.66 (broad, 1, NH), 9.16 (d, 1, $J_{3',5'}$ = 2.5 Hz, H3′).

*(2*R*,3*S*,4*E*,6*E*)-8-[(3-Bromo-4,6-dinitrophenyl)amino]-3-methoxy-2,4-dimethyl-4,6-octadienal Dimethyl Acetal (**42**)*

A solution of sodium metaperiodate (1.9 g) in water (70 mL) was added to a solution of **22** acetic acid salt (500 mg) in dioxane (70 mL) and methanol (10 mL). After standing for 4 h in the dark, the mixture was adjusted to pH 8.3 with barium hydroxide solution and centrifuged. Sodium hydrogen carbonate (1.5 g) and 1-bromo-5-fluoro-2,4-dinitrobenzene (42) (1 g) were added, the mixture stirred in the dark for 3 h and stored overnight at 4°C. The octadienal **36** was isolated and converted to the dimethyl acetal **42** as described (42), R_f 0.75 (*D*) and 0.24 (*H*); nmr ($CDCl_3$) δ: 0.71 (d, 3, $J_{2,Me}$ = 7 Hz), 1.68 (s, 3, 4-Me), 1.97 (m, 1, H2), 3.17 (s, 3, 3-OMe), 3.39 (d, 1, $J_{2,3}$ = 9 Hz, H3), 3.43, 3.49 (2s, 3 each, 1-$(OMe)_2$), 4.10 (t, 2, $J_{7,8}$ = $J_{8,NH}$ = 6 Hz, NCH_2), 4.50 (d, 1, $J_{1,2}$ = 3 Hz, H1), 5.71 (dt, $J_{6,7}$ = 15 and $J_{7,8}$ = 6 Hz, H7), 6.02 (d, 1, $J_{5,6}$ = 10.5 Hz, H5), 6.60 (dd, 1, $J_{5,6}$ = 10.5 and $J_{6,7}$ = 15 Hz, H6), 7.21 (s, 1, H2′), 8.43 (broad, 1, NH), and 8.98 (s, 1, H5′).

*[3a*R*,4*S*,6*R*,6a*S*,6(*S**),7(*R**)]-N[6-[7-[(4-Bromobenzyloxy)-1,2-dihydro-1-methyl-2-oxo-3-pyridinyl]-6-methyl-7-oxo-1(*E*),3(*E*),5(*E*)-heptatrienyl]tetrahydrofuro-[3,4-d]-2,2-dimethyl-1,3-dioxol-4-yl]-6-methoxy-5,7-dimethyl-2(*E*),4(*E*)-heptadienyl]acetamide (**60**)*

Bis(4-nitrophenyl)phosphate (0.5 g) was added to a solution of *N*-acetyl **22** (2 g) in acetone (40 mL) and 2,2-dimethoxypropane (15 mL). The solution was neutralized the next day with Dowex 1-X2 (HCO_3^-), filtered, and evaporated. The resulting syrup was chromatographed on a column of Sephadex LH-20 (51 mm × 510 mm) with acetone as mobile phase to yield homogeneous **60** as yellow powder upon concentration to dryness (1.47 g), R_f 0.35 (*B*) and 0.60 (*G*); nmr ($CDCl_3$)[5] δ: 0.90 (d, 3, $J_{7,Me}$ = 7 Hz, 7-Me), 1.28, 1.42 (2s, 3 each, 2′-Me_2), 1.66 (s, 3, 5-Me), 1.97 (s, 3, 6″-Me), 1.99 (s, 3, $COCH_3$), 2.29 (m, 1, H7), 3.13 (s, 3, 6-OMe), 3.29 (d, 1, $J_{6,7}$ = 9 Hz, H6), 3.45 (s, 3, NMe), 3.48 (broad, 1, H4′), 3.87 (t, 2, $J_{1,2}$ = $J_{1,NH}$ = 6 Hz, NCH_2), 3.90 (broad, 1, H6′), 4.62 (m, 2, H3a′ and H6a′), 5.04 (s, 1, OCH_2), 5.64 (dt, 1, $J_{2,3}$ = 15 and $J_{1,2}$ = 6 Hz, H2), 5.92 (m, 3, H4, H1″ and NH), 6.04 (d, 1, $J_{5''',6'''}$ = 7.5 Hz, H5‴), 6.49 (m, 4, H3, H2″, H3″, H4″), 6.87 (d, 1, $J_{4'',5''}$ = 10 Hz, H5″), 7.30 (d, 1, $J_{5''',6'''}$ = 7.5 Hz, H6‴), and 7.10, 7.43 (AA′BB′, 4, J_0 = 8.5 Hz, C_6H_4).

*[3a*R*,4*S*,6*S*,6a*R*,4(*S**),5(*R**)]-5-[6-Formyltetrahydro-2,2-dimethylfuro[3,4-d]-1,3-dioxol-4-yl]-4-methoxy-3,5-dimethyl-2-pentenal (**61**), [3a*R*,4*S*,6*S*,6a*R*,1(*R**),2(*S**)]-Tetrahydro-6-(2-methoxy-1-methyl-3-oxobutyl)furo[3,4-d]-1,3-dioxole-4-carboxaldehyde (**62**), and 4-(4-Bromobenzyloxy)-1-methyl-3-pyruvoyl-2(1*H*)-pyridone (**28**)*

A solution of osmium tetroxide (102 mg) in dioxane–water (1:1, 160 mL) was combined with a solution of **60** (6.3 g, 8 mmol) in dioxane (160 mL). Sodium metaperiodate (71 g, 0.33 mol) was added in portions to the stirred solution over a one hour period. After three additional hours of stirring in the dark the mixture was filtered and the filtrate extracted continuously with diethyl ether for six hours. The dried extract was evaporated to a syrup (6.2 g) which was chromatographed on silicic acid (350 g) taking fractions of 15 mL and using chloroform (fractions 1–120), chloroform – 2-propanol (99:1, fractions 121–240), and chloroform–methanol (9:1, fractions 241–360) as mobile phases.

Fractions 206–216 contained a mixture of **61** as major and **62** as minor component and was obtained as a colorless syrup (1.5 g).

Fractions 218–236 gave a crystalline residue, which was recrystallized from methanol as colorless needles of **28** (0.68 g), R_f 0.06 (*C*) and 0.72 (*G*, blue tetrazoleum) (40).

Fractions 260–300 furnished **24** as white needles from aqueous ethanol, R_f 0.10 (*A*).

The mixture of **61** and **62** was partially resolved by chromatography on silicic acid (85 g) with chloroform as mobile phase taking 15 mL fractions. Fractions 36–48 gave a mixture of **61** and **62** in a ratio of 3:1 (0.60 g) and fractions 49–75 afforded pure **61** (0.57 g) as a colorless syrup, R_f 0.32 (*C*) and 0.86 (*G*, blue tetrazoleum); nmr ($CDCl_3$) δ: 1.09 (d, 3, $J_{5,Me}$ = 7 Hz, 5-Me), 1.27, 1.43 (2s, 3 each, 2′-Me_2), 2.15 (d, 3, $J_{2,Me}$ = 1.5 Hz, 3-Me), 2.47 (sextet, $J_{4,5}$ = $J_{4',5}$ = $J_{5,Me}$ = 7 Hz, H5), 3.26 (s, 3, 4-OMe), 3.49 (d, 1, $J_{4,5}$ = 7 Hz, H4), 3.62 (dd, 1, $J_{3a',4'}$ = 3.5 and $J_{4',5}$ = 7 Hz, H4′), 3.87 (dd, 1, $J_{6',6a'}$ = 4 and $J_{6',CHO}$ = 1.5 Hz, H6′), 4.68 (dd, 1, $J_{3a',4'}$ = 3.5 and $J_{3a',6a'}$ = 6 Hz, H3a′), 4.96 (ddt, 1, $J_{3a',6a'}$ = 6 and $J_{6',6a'}$ = 4 Hz, H6a′), 6.03 (d, 1, $J_{1,2}$ = 8 Hz, H2), 9.62 (d, 1, $J_{6',CHO}$ = 1.5 Hz, 6′-CHO), 10.08 (d, 1, $J_{1,2}$ = 8 Hz, H1).

The mixture of **61** and **62** (0.60 g) was dissolved in methanol (15 mL) and ozonized at −78°C for 30 min although ozone-uptake required only 5 min. Excess ozone was removed with nitrogen and dimethyl sulfide was added at room temperature until potassium iodide was no longer oxidized. The solution was concentrated to yield crude **62** without any remaining **61**. For further purification the residue was chromatographed on silicic acid (35 g) with chloroform as mobile phase yielding **62** (0.40 g) as the major detectable component with blue tetrazoleum, R_f 0.43 (*C*) and 0.90 (*G*); nmr ($CDCl_3$) δ: 1.11 (d, 3, $J_{1,Me}$ = 7 Hz, 1-Me), 1.25, 1.39 (2s, 3 each, 2-Me_2), 2.16 (s, 3, 3-Me), 2.56 (ddq, 1, $J_{1,2}$ = 9, $J_{1,6}$ = 5, and $J_{1,Me}$ = 7 Hz, H1), 3.35 (s, 3, 2-OMe), 3.44 (d, 1, $J_{1,2}$ = 5 Hz, H2), 3.58 (dd, 1, $J_{1,6}$ = 5 and $J_{6,6a}$ = 9 Hz, H6), 3.86 (dd, 1, $J_{3a,4}$ = 4.5 and $J_{4,CHO}$ = 1.5 Hz, H4), 4.22 (dd, 1, $J_{3a,6a}$ = 6 and $J_{6,6a}$ = 3.5 Hz, H6a), 4.46 (dd, 1, $J_{3a,4}$ = 4.5 and $J_{3a,6a}$ = 6 Hz, H3a), and 9.57 (d, 1, $J_{4,CHO}$ = 1.5 Hz, 4-CHO).

*[1*R*,3*R*,4*S*,6*S*,7*S*,8*S*,10*R*]-4-(Dimethoxymethyl)-1,7-dimethyl-8-methoxy-2,5,9-trioxatricyclo[4.2.2.0^{3,10}]decane(**64***b*), [2*S*-(2β,3β,3aα,5β,6α,6aα)]-Hexahydro-5-methoxy-2-(dimethoxymethyl)-6-methylfuro[3,2-b]furan-3-ol (**65***a*), and [2*S*-(2β,3β,3aα,5α,6α,6aα)]-Hexahydro-5-methoxy-2-(dimethoxymethyl)-6-methylfuro[3,2-b]furan-3-ol(**65***b*)*

A solution of crude **62** (560 mg) in methanol (10 mL) was cooled to −78°C and acetyl chloride (1 mL) was added. The mixture was allowed to warm to 23°C, kept for 3 h at 23°C, and then refrigerated overnight. After the solution was neutralized with 2.25 *N* methanolic sodium methoxide (6.3 mL), cyclohexane (50 mL) and water (30 mL) were added. The aqueous phase was extracted twice more with cyclohexane. From the combined, water-washed cyclohexane extracts, **64***b* was obtained as colorless prisms and recrystallized from petroleum ether (80 mg), mp 98°C (49). Additional **64***b* could be obtained by chromatography of the mother liquors on silicic acid with system *I* as mobile phase, R_f 0.67 (*C*) (sulfuric acid spray); nmr ($CDCl_3$) δ: 0.94 (d, 3, $J_{7,Me}$ = 7.5 Hz, 7-Me), 1.49 (s, 3, 1-Me), 2.40 (d quintet, 1, $J_{6,7}$ = 2 and $J_{7,8}$ = $J_{7,Me}$ = 7.5 Hz, H7), 3.36, 3.43, 3.48 (3s, 3 each, 3-OMe), 3.40 (d, 1, $J_{7,8}$ = 7.5 Hz, H8), 3.75

Can. J. Chem. Downloaded from www.nrcresearchpress.com by 210.87.254.40 on 09/05/12
For personal use only.

(dd, 1, $J_{3,4}$ = 2 and $J_{4,CH}$ = 7.5 Hz, H4), 4.20 (dd, 1, $J_{6,7}$ = 2 and $J_{6,10}$ = 7.5 Hz, H6), 4.25 (dd, 1, $J_{3,4}$ = 2 and $J_{3,10}$ = 4 Hz, H3), 4.53 (d, 1, $J_{4,CH}$ = 7.5 Hz, 4-CH), 5.02 (dd, 1, $J_{3,10}$ = 4 and $J_{6,10}$ = 7.5 Hz, H10).

The aqueous phase remaining after the extraction with cyclohexane was extracted twice with chloroform to yield a residue which was chromatographed on silicic acid (10 g) collecting 10-mL fractions and using system *I* as mobile phase. Fractions 24–26 gave pure **65***b* as colorless syrup (30 mg), R_f 0.48 (*C*, sulfuric acid); nmr ($CDCl_3$) δ: 1.05 (d, 3, $J_{6,Me}$ = 7 Hz, 6-Me), 2.29 (ddq, $J_{5,6}$ = 4.5, $J_{6,6a}$ = 5.5 and $J_{6,Me}$ = 7 Hz, H6), 2.76 (broad, 1, OH), 3.35, 3.41, 3.47 (3s, 3 each, 3 OMe), 3.73 (dd, 1, $J_{2,3}$ = 3 and $J_{2,CH}$ = 7.5 Hz, H2), 4.10 (dd, 1, $J_{2,3}$ = 3 and $J_{3,3a}$ = 5.5 Hz, H3), 4.24 (dd, 1, $J_{3a,6a}$ = 6.5 and $J_{6,6a}$ = 5.5 Hz, H6a), 4.64 (d, $J_{2,CH}$ = 7.5 Hz, 2-CH), 4.64 (dd, 1, $J_{3,3a}$ = 5.5 and $J_{3a,6a}$ = 6.5 Hz, H3a), and 5.03 (d, $J_{5,6}$ = 4.5 Hz, H5).

Fractions 28–35 yielded pure **65***a* as colorless syrup (30 mg), R_f 0.43 (*C*, sulfuric acid); nmr ($CDCl_3$) δ: 1.03 (d, 3, $J_{6,Me}$ = 7.5 Hz, 6-Me), 2.48 (q, $J_{5,6}$ = $J_{6,6a}$ < 1 and $J_{6,Me}$ = 7.5 Hz, H6), 3.35 (m, 1, H2), 3.42, 3.46, 3.51 (3s, 3 each, 3 OMe, overlapping with OH), 4.06 (d, 1, $J_{3a,6a}$ = 6 Hz, H6a), 4.11 (dd, 1, $J_{2,3}$ = 3 and $J_{3,3a}$ = 6 Hz, H3), 4.66 (d, 1, $J_{2,CH}$ = $J_{2,CH}$ = 7.5 Hz, 2-CH), 4.77 (s, 1, H5), 4.92 (t, $J_{3a,5}$ = 6 Hz, H3a).

*[2S-(2β,3β,3aα,5β,6α,6aα)]-Hexahydro-5-methoxy-2-(dimethoxymethyl)-6-methylfuro[3,2-b]furan-3-ol 4-Bromophenylcarbamic Acid Ester (**66**a)*

A mixture of **65***a* (25 mg), pyridine (1.5 mL), benzene (1.5 mL), and 4-bromophenylisocyanate (35 mg) was allowed to react overnight, diluted with cyclohexane (3 mL), and filtered. The filtrate was evaporated and purified by preparative tlc, and the band with R_f 0.22 (*C*) was extracted with system *G* to afford a crystalline residue of **66***a* which was recrystallized from benzene–cyclohexane (21 mg), mp 165°C. $[\alpha]_D$ −50.5° (*c* 0.5, ethanol); nmr ($CDCl_3$) δ: 1.07 (d, 3, $J_{6,Me}$ = 7.5 Hz, 6-Me), 2.43 (tq, 1, $J_{5,6}$ = $J_{6,6a}$ = 3 and $J_{6,Me}$ = 7.5 Hz, H6), 3.28, 3.37, 3.43 (3s, 3 each, 3 OMe), 3.90 (dd, 1, $J_{2,3}$ = 4 and $J_{2,CH}$ = 7.5 Hz, H2), 4.17 (dd, 1, $J_{3a,6a}$ = 6 and $J_{6,6a}$ = 3 Hz, H6a), 4.66 (d, 1, $J_{2,CH}$ = 7.5 Hz, 2-CH), 4.72 (d, 1, $J_{5,6}$ = 3 Hz, H5), 4.88 (t, 1, $J_{3,3a}$ = 5.5 and $J_{3a,6a}$ = 6 Hz, H3a), 5.21 (dd, 1, $J_{2,3}$ = 4 and $J_{3,3a}$ = 5.5 Hz, H3), 6.89 (s, 1, NH), and 7.34, 7.40 (AA′BB′, 4, J_0 = 8.5 Hz, C_6H_4). *Anal.* calcd. for $C_{18}H_{24}BrNO_7$ (446.30): C 48.44, H 5.42, N 3.14; found: C 48.56, H 5.52, N 3.21.

A crystal of **66***a* with the dimensions of 0.01 mm × 0.08 mm × 0.35 mm served for crystallographic analysis. It was of space group $P2_1$ with unit-cell dimensions a = 5.245(6), b = 13.981(10), c = 13.980(20) Å, β = 94.85(8)° and d calcd. = 1.449 g/cm³ for Z = 2. Of the 1020 reflections examined (2θ < 96.5°) only 520 were considered significant due to the small size of the crystal. The structure was solved by Patterson and Fourier methods with final refinement by full-matrix least squares. Anisotropic thermal parameters were used for the bromine atom and isotropic temperature factors were used for the lighter atoms; the hydrogen atoms were not included. The final discrepancy index is R = 0.082 (Fig. 11). Attempts to determine the absolute configuration of **66***a* on the basis of the available crystallographic data gave inconclusive results.

*[2S,(2β,3β,3aα,5α,6α,6aα)]-Hexahydro-5-methoxy-2-(dimethoxymethyl)-6-methylfuro[3,2-b]furan-3-ol 4-Bromophenylcarbamic Acid Ester (**66**b)*

The alcohol **65***b* was converted to the urethane **66***b*, purified by preparative tlc (R_f 0.53, *C*) as described for the anomer, and obtained as colorless needles from benzene–cyclohexane, mp 156°C; $[\alpha]_D$ −129.9° (*c* 0.5, ethanol); nmr ($CDCl_3$) δ: 1.07 (d, 3, $J_{6,Me}$ = 7.5 Hz, 6-Me), 2.32 (tq, 1, $J_{5,6}$ = $J_{6,6a}$ = 4.5 and $J_{6,Me}$ = 7.5 Hz, H6), 3.32, 3.37, 3.42 (3s, 3 each, 3 OMe), 4.00 (dd, 1, $J_{2,3}$ = 4.5 and $J_{2,CH}$ = 7.5 Hz, H2), 4.31 (dd, 1, $J_{3a,6a}$ = 6.5 and $J_{6,6a}$ = 4.5 Hz, H6a), 4.64 (d, 1, $J_{2,CH}$ = 7.5 Hz, 2-CH), 4.79 (dd, 1, $J_{3,3a}$ = 6 and $J_{3a,6a}$ = 6.5 Hz, H3a), 4.95 (d, 1, $J_{5,6}$ = 4.5 Hz, H5), 5.28 (dd, 1, $J_{2,3}$ = 4.5 and $J_{3,3a}$ = 6 Hz, H3), 6.70 (s, 1, NH), and 7.33, 7.41 (AA′BB′, 4, J_0 = 8.5 Hz, C_6H_4). *Anal.* calcd. for $C_{18}H_{24}BrNO_7$ (446.30): C 48.44, H 5.42, N 3.14; found: C 48.52, H 5.53, N 2.98.

Diffraction data of **66***b* were collected from a crystal with the dimensions of 0.15 mm × 0.30 mm × 0.45 mm, space group $P2_1$, and unit-cell dimensions of a = 11.371(5), b = 8.965(5), c = 10.116(5) Å, β = 94.66(4)° and d calcd. = 1.441 g/cm³ for Z = 2. Of the 2286 accessible reflections with 2θ < 152°, 2011 were considered significant. The structure was solved by the heavy atom method. Four Fouriers, based on successively more complete trial structures, were required to locate all non-hydrogen atoms. During the preliminary refinement of the structures the imaginary part of the anomalous dispersion correction ($\Delta f''$) was set to zero. At the conclusion of this refinement, in which all atoms were anisotropic, the positions of the hydrogen atoms were calculated. The hydrogen atoms were included in all subsequent calculations but their parameters were not refined. The final refinement of the structure was carried out by full-matrix least squares. In order to establish the absolute configuration, two separate refinements were made. In one the correct value of the imaginary part of the dispersion correction was used and in the other the sign of $\Delta f''$ was reversed (equivalent to refining the antipode of **66***b*). The absolute configuration was taken as the one which had the lower weighted R-value (0.0529 and 0.0572). The configuration corresponding to the higher R-value could be rejected (as being the correct absolute configuration) at a significance level substantially better than 0.005, according to the test described by Hamilton (57). The final unweighted discrepancy index is R = 0.037 for the 2011 observed reflections (Fig. 11).

*Mocimycin Methyl Ether (N-Desmethyl-**17**) and Aurodox Methyl Ether (**17**)*

Methyl iodide (2 mL) was added to a solution of mocimycin sodium salt (3 g) in dimethylformamide (15 mL) and the mixture kept in the dark for 4 days. The mixture was then equilibrated with ethyl acetate (250 mL) and water (50 mL). The ethyl acetate phase was washed with water (2 × 50 mL), 0.5 *M* trisodium phosphate solution (6 × 50 mL), water (5 × 50 mL), dried, and evaporated to afford an amorphous, yellow powder (1.7 g) which proved to be a mixture of two major components. Upon chromatography of this mixture on a column of Sephadex LH-20 (55 mm × 720 mm) with acetone as mobile phase, **17** (8) was eluted first (R_f 0.76, *A*) and obtained as yellow powder upon evaporation of the pooled fraction (0.4 g), rechromatography (Sephadex LH-20, 2-butanone) and precipitation from acetone – petroleum ether.

Continued elution furnished *N*-desmethyl-**17** (8), obtained as yellow powder (0.6 g) after rechromatography (Sephadex LH-20, 2-butanone) and precipitation from acetone – petroleum ether. Additional *N*-desmethyl-**17** (0.3 g) was obtained from aqueous extracts of the combined trisodium phosphate phases after chromatographic purification.

Compound **17** could also be prepared directly from **1***b*. A solution of **1***b* sodium salt in dimethylformamide and methyl iodide (10 mL) was shaken for 4 days in the dark and poured into a separatory funnel containing ethyl acetate (75 mL) and 5% aqueous sodium hydrogen carbonate solution (25 mL).

The organic phase was washed twice with sodium hydrogen carbonate solution, three times with brine, dried, filtered, and evaporated yielding crude **17** (4.59 g). A portion (1.5 g) was chromatographed on a column of Sephadex LH-20 (51 mm × 510 mm) with acetone as mobile phase. Homogeneous fractions (tlc) were pooled and evaporated to afford **17** as yellow, amorphous powder (1.0 g) (8).

Can. J. Chem. Downloaded from www.nrcresearchpress.com by 210.87.254.40 on 09/05/12
For personal use only.

[2R,3R,4S,5S,1(R),2(S*)]-4-Methoxy-3-[7-[5-[7-amino-2-methoxy-1,3-dimethyl-3(E),5(E)-heptadienyl]-3,4-dihydroxytetrahydro-2-furyl]-2-methyl-1-oxo-2-(E),4(E),6(E)-heptatrienyl]-2(1H)-pyridinone Acetic Acid Salt (**45** Acetic Acid Salt)*

A solution of mocimycin methyl ether (*N*-desmethyl-**17**, 0.6 g) in acetic acid (6 mL) was heated on the steam bath for 30 min. After evaporation to dryness, the residue was chromatographed on a column of silicic acid (30 g) with chloroform (100 mL), chloroform – 2-propanol (19:1, 350 mL), and chloroform–methanol – acetic acid (15:4:1) as mobile phases. From the pooled and concentrated fractions *N*-desmethylgoldinamine methyl ether acetic acid salt was obtained as amorphous, yellow powder by freeze-drying (0.2 g), R_f 0.45 (*A*); nmr (CD_3OD)[8] δ: 0.82 (d, 3, $J_{1,Me}$ = 7 Hz, 1-Me), 1.73 (s, 3, 3-Me), 1.91 (s, 3, OAc), 1.97 (s, 3, 2″-Me), 2.16 (m, 1, H1), 3.17 (s, 3, 2-OMe), 3.38 (s, 1, $J_{1,2}$ = 9.5 Hz, H2), 3.66 (m, 3, NCH_2 and H5′), 3.84 (s, 3, 4‴-OMe), 4.19 (m, 1, H4′), 4.30 (m, 2, H2′ and H3′), 5.97 (m, 3, H4, H6, H7″), 6.45 (d, 1, $J_{5''',6'''}$ = 7.5 Hz, H5‴), 6.30–6.80 (m, 4, H4″, H5, H5″, H6″), 6.96 (d, 1, $J_{3'',4''}$ = 10 Hz, H3″), and 7.55 (d, 1, $J_{5''',6'''}$ = 7.5 Hz, H6‴).

[2S,3S,4R,5R,6(S),7(R*)]-N[7-[5-[7-(1,2-Dihydro-4-methoxy-2-oxo-3-pyridinyl)-6-methyl-7-oxo-1(E),3(E),5(E)-heptatrienyl]tetrahydro-3,4-dihydroxyfuran-2-yl]-6-methoxy-5,7-dimethyl-2(E),4(E)-heptadienyl]trifluoroacetamide (**46**)*

To a solution of **45** acetic acid salt (71 mg) in 1 mL of methanol containing triethylamine (0.1 mmol/mL) was added trifluoroethanethioic acid *S*-ethyl ester (25 μL). The mixture was concentrated after 18 h and purified by preparative tlc (R_f 0.25, acetone) to afford amorphous **46** as yellow powder; ord (*c* 0.35, dioxane): $[\phi]_{700}$ −257° (start), $[\phi]_{589}$ −426°, $[\phi]_{344}$ −14 190° (trough), $[\phi]_{328}$ 0° (intersects), $[\phi]_{308}$ +14 190° (peak), $[\phi]_{282}$ +9 310 (trough), $[\phi]_{252}$ +28 380° (peak), $[\phi]_{246}$ 0° (intersects), $[\phi]_{215}$ −31 930° (trough), $[\phi]_{212}$ −29 710° (last); cd (0.006 *M*, dioxane): $[\theta]_{380}$ 0 (start), $[\theta]_{329}$ −17 425, $[\theta]_{289}$ −2 010, $[\theta]_{265}$ −3 350, $[\theta]_{257}$ 0 (intersects), $[\theta]_{234}$ +29 320, $[\theta]_{210}$ 0 (last). *Mol. Wt.* calcd. for $C_{30}H_{37}F_3N_2O_8$: 610.63; found (ms) *m/e* (%): 610 (0.3), 152 (1,2-dihydro-4-methoxy-2-oxo-3-carbonyl cation, 100).

[2R,3R,4S,5S,1(R),2(S*)]-4-Methoxy-1-methyl-3-[7-[5-[7-amino-2-methoxy-1,3-dimethyl-3(E),5(E)-heptadienyl]-3,4-dihydroxytetrahydro-2-furyl]-2-methyl-1-oxo-2(E),4(E),6(E)-heptatrienyl]-2(1H)-pyridone Acetic Acid Salt (**21** Acetic Acid Salt)*

A solution of **17** (2.35 g) in acetic acid (20 mL) was either allowed to stand at room temperature in the dark for 4.5 days or was heated on the steam bath for 20 min, the solvent was evaporated, and the residue subjected to Craig distribution in chloroform–methanol – acetic acid – water (5:1:1:4). After 199 transfers, tubes 145–177, which contained a homogeneous solute, were pooled, concentrated, and freeze-dried, yielding goldinamine methyl ether acetic acid salt (**21** acetic acid salt) as amorphous, yellow powder (0.97 g), R_f 0.64 (*A*); nmr ($CDCl_3$) δ: 0.84 (d, 3, $J_{1,Me}$ = 7 Hz, 1-Me), 1.67 (s, 3, 3-Me), 2.00 (s, 6, OAc and 2″-Me), 2.17 (m, 1, H1), 3.17 (s, 3, 2-OMe), 3.25 (d, 1, $J_{1,2}$ = 9.5 Hz, H2), 3.49 (s, 3, NMe), 3.49 (broad, 3, NCH_2 and H5′), 3.76 (s, 3, 4″-OMe), 4.17 (m, 1, H2′), 4.34 (m, 2, H3′ and H4′), 5.97 (m, 3, H4, H6, H7″), 6.10 (d, 1, $J_{5''',6'''}$ = 7.5 Hz, H5‴), 6.49 (m, 4, H4″, H5, H5″, H6″), 6.86 (d, 1, $J_{3'',4''}$ = 10 Hz, H3″), 7.38 (d, 1, $J_{5''',6'''}$ = 7.5 Hz, H6‴).

[8]Proton designations are those used in **22** (Scheme 6).

[2S,3S,4R,5R,6(S),7(R*)]-N-[7-[5-[7-(1,2-Dihydro-4-methoxy-1-methyl-2-oxo-3-pyridinyl)-6-methyl-7-oxo-1(E),3(E),5(E)-heptatrienyl]tetrahydro-3,4-dihydroxyfuran-2-yl]-6-methoxy-5,7-dimethyl-2(E),4(E)-heptadienyl]trifluoroacetamide (**47**)*

Goldinamine methyl ether acetic acid salt (**21** acetic acid salt, 105 mg) was converted to the *N*-trifluoroacetamide as described above in the preparation of **46**. The evaporated reaction product was chromatographed on a column of Sephadex LH-20 (acetone) to yield **47** as yellow powder (87 mg), R_f 0.23 (*B*). *Mol. Wt.* calcd. for $C_{31}H_{39}F_3N_2O_8$: 624.66; found (ms) *m/e* (%): 624 (0.4), 166 (1,2-dihydro-4-methoxy-1-methyl-2-oxo-3-carbonyl cation, 100).

[2S,3S,4R,5R,6(S),7(R*)]-N-[7-[5-[7-(1,2-Dihydro-4-methoxy-1-methyl-2-oxo-3-pyridinyl)-6-methyl-7-oxo-1(E),3(E),5(E)-heptatrienyl]tetrahydro-3,4-dihydroxyfuran-2-yl]-6-methoxy-5,7-dimethyl-2(E),4(E)-heptadienyl]acetamide (**49**)*

A solution of **21** acetic acid salt (200 mg) in methanol (1.5 mL) and acetic anhydride (0.7 mL) was kept overnight at 25°C and added to a mixture of ether (55 mL) and petroleum ether. The precipitate was collected by centrifugation, washed repeatedly, and chromatographed on a column of Sephadex LH-20 with 2-butanone as mobile phase. The *N*-acetyl compound, **49**, was obtained as amorphous, yellow powder (152 mg), R_f 0.53 (*A*). *Mol. Wt.* calcd. for $C_{31}H_{42}N_2O_8$: 570; found (ms) *m/e*: 570, 552 (M − H_2O), 538 (M − MeOH), 520 (M − H_2O − MeOH), and 506 (M − 2MeOH) as highest mass peaks. Calculated: 552.2840 ($C_{31}H_{40}N_2O_7$), 538.2683 ($C_{30}H_{38}N_2O_7$), 520.2577 ($C_{30}H_{36}N_2O_6$), 506.2420 ($C_{29}H_{34}N_2O_6$); found: 552.2844, 538.2701, 520.2566, 506.2429.

[2S,3R,4S,5R,6(S),7(R*)]-N-[7-[5-[7-(1,2-Dihydro-4-methoxy-1-methyl-2-oxo-3-pyridinyl)-6-methyl-7-oxo-1(E),3(E),5(E)-heptatrienyl]tetrahydro-3,4-dimethoxyfuran-2-yl]-6-methoxy-5,7-dimethyl-2(E),4(E)-heptadienyl]acetamide (**50**)*

To a solution of **49** (100 mg) in dimethylformamide (1 mL) was added barium oxide (100 mg) and barium hydroxide octahydrate (100 mg) followed by dimethylsulfate (0.2 mL) (58). After stirring for 24 h additional barium oxide (100 mg) and dimethylsulfate (0.1 mL) were added. After a total reaction time of 40 h concentrated ammonium hydroxide solution (0.2 mL) was added and stirring continued for 10 min. Addition of chloroform (10 mL) to the stirred mixture was followed by centrifugation. The chloroform solution was decanted and the syrupy solids were washed repeatedly with chloroform. The combined chloroform extracts were washed with brine (3 × 10 mL) and water (10 mL) and evaporated. The resulting solution of **50** in *N,N*-dimethylformamide was diluted with acetone and chromatographed on a column of Sephadex LH-20 (acetone). Pure **50** (30 mg) was isolated as usual, R_f 0.10 (*B*). *Mol. Wt.* calcd. for $C_{33}H_{46}N_2O_8$: 598.74; found (ms) *m/e*: 598, 566 (M − MeOH), and 534 (M − 2MeOH) as highest mass peaks. Calculated: 598.3259 ($C_{33}H_{46}N_2O_8$), 566.2996 ($C_{32}H_{42}N_2O_7$), 534.2734 ($C_{31}H_{38}N_2O_6$); found: 598.3326 (extrapolated over 30 mass units), 566.2979, 534.2728.

*(2E,4E,6E)-8-[4-Methoxy-1,2-dihydro-1-methyl-2-oxo-3-pyridinyl]-7-methyl-8-oxo-2,4,6-octatrienoic Acid (**29**)*

To a solution of **21** acetic acid salt (200 mg) in methanol (4 mL) and dioxane (16 mL) was added sodium metaperiodate (0.5 g) in water (20 mL). The mixture was stirred for 4 h at 25°C in the dark, the pH was adjusted to 8.4 with barium hydroxide and the

Can. J. Chem. Downloaded from www.nrcresearchpress.com by 210.87.254.40 on 09/05/12
For personal use only.

resulting suspension centrifuged. Acetic anhydride (1.5 mL) was added to the supernatant under stirring, followed by another 0.5 mL 30 min later. After one hour the mixture was adjusted to pH 8.4 with sodium hydroxide and repeatedly extracted with diethyl ether. Drying and evaporation of the combined ether phase gave **34** (50 mg). The aqueous phase was adjusted to pH 3 (sulfuric acid) and extracted with dichloromethane (2 × 40 mL). Evaporation gave a residue which crystallized from methanol–chloroform–ether to yield **29** as yellow prisms, R_f 0.13 (*A*), 0.52 (*J*); mp 220–222°C; uv λ_{max} (ε): 208–209 (32 500), inflection 232–233 (5 500), inflection 295 (16 000), 331–332 (41 200), and inflection 340 (39 900) nm in 0.1 *N* HCl, 208–209 (33 000), inflection 232 (8 000), inflection 295 (16 000), and 333–340 (39 600) nm in buffer (pH = 7), inflection 232 (7 800), inflection 295 (16 500), and 332–340 (40 000) nm in 0.1 *N* KOH; nmr (Me_2SO-d_6) δ: 1.91 (s, 3, 7-Me), 3.37 (s, 3, OMe), 3.72 (s, 3, NMe), 5.95 (d, 1, $J_{2,3}$ = 15 Hz, H2), 6.31 (d, 1, $J_{5',6'}$ = 7.5 Hz, H5′), 6.70 (dd, 1, $J_{3,4}$ = 11 and $J_{4,5}$ = 14.5 Hz, H4), 6.81 (d, 1, $J_{5,6}$ = 11 Hz, H6), 7.12 (dd, 1, $J_{4,5}$ = 14.5 and $J_{5,6}$ = 11 Hz, H5), 7.30 (dd, 1, $J_{2,3}$ = 15 and $J_{3,4}$ = 11 Hz, H3), and 7.79 (d, 1, $J_{5',6'}$ = 7.5 Hz, H6′). *Mol. Wt.* calcd. for $C_{16}H_{17}NO_5$: 303.33; found (ms) *m/e (%)*: 303 (17), 166 (100).

*[1R-(1β,2α,6α,8β)]-4,4-Dimethyl-3,5,7,11-tetraoxatricyclo-[6.3.0.0^{2,6}]undecan-9-one (**68**)*

To a vigorously stirred solution of 3,6-anhydro-1,2-*O*-isopropylidine-α-D-glucofuranose (**67**, 1.70 g, 8.41 mmol) (50) (R_f 0.07 (*H*), greenish color with anisaldehyde – sulfuric acid spray) in dichloromethane (50 mL) was added dropwise ca. 0.2 *M* sodium metaperiodate solution while keeping the pH at 6–7 with intermittent addition of sodium hydrogen carbonate solution (59). Addition was complete after 30 min as indicated by a permanent color change from dark to greenish yellow. Stirring was continued for 3 h, 1-propanol (0.5 mL) was added, and the mixture was filtered 15 min later. The dichloromethane phase was decanted, combined with two further extracts, washed twice with a little water, dried, and evaporated to yield **68** as a syrup. Short-path distillation (bath temperature 105°C, 0.5 Torr) gave a colorless syrup (1.45 g, 7.24 mmol, 86%) which crystallized very slowly on standing, R_f 0.06 (*H*), reddish color with anisaldehyde; ir (neat) ν: 1778 (ketone) cm^{-1}; nmr ($CDCl_3$) δ: 1.33, 1.48 (2s, 3 each, 4-Me_2), 3.90, 4.24 (AB, 2, $J_{10a,10b}$ = 17 Hz, H10), 4.40 (d, 1, $J_{1,8}$ = 3 Hz, H1), 4.71 (d, 1, $J_{1,8}$ = 3 Hz, H8), 4.75 (d, 1, $J_{1,2}$ = 0 and $J_{2,6}$ = 3.5 Hz, H2), 6.02 (d, 1, $J_{2,6}$ = 3.5 Hz, H6).

*[1S-(1β,2α,6α,8β)]-4,4-Dimethyl-9-methylene-3,5,7,11-tetraoxatricyclo[6.3.0.0^{2,6}]undecane (**69**)*

A hexane solution of *n*-butyllithium (3.75 mL, 1.6 *M*) was added to diethyl ether (15 mL) under argon followed by methyltriphenylphosphonium bromide (2.14 g, 6 mmol) in one portion under stirring. A solution was gradually obtained and after 4 h of continued stirring a solution of **68** (1 g, 5 mmol) in diethyl ether (15 mL) was added. The resulting suspension was refluxed under stirring for 3 h and stirred overnight at room temperature. The ethereal supernatant was combined with three additional ether extracts, washed with water, dried, and evaporated to a syrup. Dissolving the syrup in a little chloroform and adding petroleum ether deposited crystalline triphenylphosphine oxide. Evaporation of the mother liquor gave a syrup containing mostly **69** purified by chromatography on a column of silica gel with system *I* as mobile phase to give **69** as colorless syrup (0.249 g, 1.26 mmol), R_f 0.53 (*H*), brownish color with anisaldehyde – sulfuric acid spray; nmr ($CDCl_3$) δ: 1.34, 1.52 (2s, 3 each, 4-Me_2), 4.30, 4.54 (tAB, 2, $J_{6,7}$ = 2 and $J_{10a,10b}$ = 13 Hz, H10), 4.43 (d, 1, $J_{1,2}$ = 0 and $J_{1,8}$ = 3.5 Hz, H1), 4.67 (d, 1, $J_{1,2}$ = 0 and $J_{1,8}$ = 4 Hz, H2), 5.00 (d, 1, $J_{1,8}$ = 3.5 Hz, H8), 5.15, 5.40 (2t, 1 each, $J_{6,7}$ = 2 Hz, =CH_2), 5.93 (d, 1, $J_{2,6}$ = 4 Hz, H6).

*[1S-(1β,2α,6α,8β,9α)]-4,4,9-Trimethyl-3,5,7,11-tetraoxatricyclo[6.3.0.0^{2,6}]undecane (**70**)*

Catalytic hydrogenation of **69** (50 mg) over palladium-on-charcoal (10%, 50 mg) in ethanol (2.5 mL) for 2 h at 3.5 atm gave a mixture of **70** (88%) and **71** (12%) both with R_f 0.53 (*H*), olive-green color with anisaldehyde – sulfuric acid spray.

Nuclear magnetic resonance of **70** ($CDCl_3$) δ: 1.08 (d, 3, $J_{9,Me}$ = 7 Hz, 9-Me), 1.31, 1.47 (2s, 3 each 4-Me_2), 2.23 (m, 1, $J_{8,9}$ = 3.5, $J_{9,10a}$ = 7, and $J_{9,10b}$ = 10.5 Hz, H9), 3.35 (dd, 1, $J_{9,10b}$ = 10.5 and $J_{10a,10b}$ = 7.5 Hz, H10b), 3.90 (t, 1, *J* = 7.5 Hz, H10a), 4.43 (d, 1, $J_{1,2}$ = 0 and $J_{1,8}$ = 3.5 Hz, H1), 4.50 (d, 1, $J_{1,2}$ = 0 and $J_{2,6}$ = 3.5 Hz, H2), 4.68 (t, 1, $J_{1,8}$ = $J_{8,9}$ = 3.5 Hz, H8), 5.86 (d, 1, $J_{2,6}$ = 3.5 Hz, H6).

*[1S-(1β,2α,6α,8β,9β)]-4,4,9-Trimethyl-3,5,7,11-tetraoxatricyclo[6.3.0.0^{2,6}]undecane (**71**)*

Potassium azodicarboxylate (971 mg, 5 mmol) was added to a solution of **68** (198 mg, 1 mmol) in methanol (5 mL) and a solution of 2 *N* acetic acid in methanol (5 mL) was added to the yellow suspension at a rate of 1 mL/6 min under vigorous stirring. Stirring was continued for 1 h. Diethyl ether (10 mL) was added to the colorless mixture, the salts were filtered off, and the filtrate evaporated. The resulting residue was extracted with hot cyclohexane affording a mixture of **69** (35.9%), **70** (21.5%), and **71** (42.6%) as determined by glpc (column 3 m × 4 mm; OV-225, 10%, on GCQ 100/200; column temperature 80→190°C, 2°/min, retention times 54, 51.0, and 51.6 min, respectively).

Nuclear magnetic resonance of **71** ($CDCl_3$: 0.97 (d, 3, $J_{9,Me}$ = 7 Hz, 9-Me), 1.31, 1.47 (2s, 3 each, 4-Me_2), 2.42 (ddq, 1, $J_{9,10b}$ = $J_{9,Me}$ = 7 Hz and $J_{8,9}$ = 1 Hz, H9), 3.51 (dd, 1, $J_{9,10a}$ = 1.5 and $J_{10a,10b}$ = 8 Hz, H10a), 3.94 (dd, 1, $J_{9,10b}$ = 5.5 and $J_{10a,10b}$ = 8 Hz, H10b), 4.43 (d, 1, $J_{1,2}$ = 0 and $J_{1,8}$ = 3.5 Hz, H1), 4.54 (d, 1, $J_{1,2}$ = 0 and $J_{2,6}$ = 3.5 Hz, H2), 4.58 (dd, 1, $J_{1,8}$ = 3.5 and $J_{8,9}$ = 1 Hz, H8), 5.86 (d, 1, $J_{2,6}$ = 3.5 Hz, H6).

1. J. Berger. Ger. Patent No. 2,140,322 (February 17, 1972).
2. J. Berger. U.S. Patent No. 3,657,421 (April 18, 1972).
3. J. Berger, H. H. Lehr, S. Teitel, H. Maehr, and E. Grunberg. J. Antibiot. **26**, 15 (1973).
4. C. Vos and J. den Admirant. Ger. Patent No. 2,140,674 (May 18, 1972).
5. C. Vos and J. den Admirant. U.S. Patent No. 3,923,981 (December 2, 1975).
6. C. Vos and J. den Admirant. U.S. Patent No. 3,927,211 (December 16, 1975).
7. H. Wolf and H. Zähner. Arch. Mikrobiol. **83**, 147 (1972).
8. H. Maehr, M. Leach, L. Yarmchuk, and A. Stempel. J. Am. Chem. Soc. **95**, 8449 (1973).
9. R. Wax, W. Maiese, R. Weston, and J. Birnbaum. J. Antibiot. **29**, 670 (1976).
10. W. Maiese and R. Wax. U.S. Patent No. 4,024,251 (February 12, 1976).
11. H. M. Jongsma, H. J. Kooreman, J.L. Os, and C. Vos. Ger. Patent No. 2,621,615 (November 25, 1976).
12. I. Hummel. Diplomarbeit, Göttingen. 1977.
13. I. Thein. Dissertation, Tübingen. 1977.
14. S. B. Zimmerman, J. H. Chalmers, Jr., R. S. Dewey, and E. O. Stapley. J. Antibiot. **32**, 665 (1979).
15. M. W. Nimeck, E. Meyers, and W.-C. Liu. U.S. Patent No. 3,898,327 (August 5, 1975).

16. B. M. FROST, M. E. VALIANT, B. WEISSBERGER, and E. L. DULANEY. J. Antibiot. **29**, 1083 (1976).
17. M. W. STUTZ, S. L. JOHNSON, and F. R. JUDITH. J. Anim. Sci. **43**, 260 (1976).
18. H. WOLF, G. CHINALI, and A. PARMEGGIANI. Proc. Natl. Acad. Sci. U.S.A. **71**, 4910 (1974).
19. S. BROWN and T. BLUMENTHAL. J. Biol. Chem. **251**, 2749 (1976).
20. G. CHINALI, H. WOLF, and A. PARMEGGIANI. Eur. J. Biochem. **75**, 55 (1977).
21. H. WOLF, G. CHINALI, and A. PARMEGGIANI. Eur. J. Biochem. **75**, 67 (1977).
22. T. BLUMENTHAL and J. DOUGLASS. Abstr. Annu. Meet. Am. Soc. Microbiol. **77**, 194 (1977).
23. E. FISCHER, H. WOLF, K. HANTKE, and A. PARMEGGIANI. Proc. Natl. Acad. Sci. U.S.A. **74**, 4341 (1977).
24. A. PARMEGGIANI, E. FISCHER, O. FASANO, J. B. CRECHET, and H. WOLF. Chem. Abstr. **89**, 71471c (1978).
25. I. SMITH and P. PARESS. J. Bacteriol. **135**, 1107 (1978).
26. H. WOLF, D. ASSMANN, and E. FISCHER. Proc. Natl. Acad. Sci. U.S.A. **75**, 5324 (1978).
27. H. MAEHR, M. LEACH, L. YARMCHUK, and M. MITROVIC. J. Antibiot. **32**, 361 (1979).
28. W. L. MARUSICH, E. F. OGRINZ, and M. MITROVIC. Poult. Sci. **52**, 2059 (1973).
29. W. L. MARUSICH, E. F. OGRINZ, and M. MITROVIC. Poult. Sci. **53**, 936 (1974).
30. R. BEUKERS, J. G. OOSTENDORP, and C. J. VAN EEKEN. Abstracts, Second World Congress on Animal Feeding, Madrid. October 23–28, 1972. p. 127.
31. T. VAN EEK and R. BEUKERS. Ger. Patent No. 2,406,164 (August 14, 1974).
32. A. G. FOSTER and D. L. HARRIS. J. Anim. Sci. **43**, 252 (1976).
33. M. W. STUTZ, S. L. JOHNSON, K. G. OTTO, and B. M. MILLER. J. Anim. Sci. **43**, 259 (1976).
34. T. VAN EEK and R. BEUKERS. U.S. Patent No. 3,928,573 (December 23, 1975).
35. C.-M. LIU, T. HERMANN, and P. A. MILLER. J. Antibiot. **30**, 244 (1977).
36. J. UNOWSKY and D. C. HOPPE. J. Antibiot. **31**, 662 (1978).
37. H. MAEHR, J. F. BLOUNT, R. H. EVANS, JR., M. LEACH, J. W. WESTLEY, T. H. WILLIAMS, A. STEMPEL, and G. BÜCHI. Helv. Chim. Acta, **55**, 3051 (1972).
38. R. KUHN and T. WIELAND. Chem. Ber. **73**, 971 (1940).
39. R. BEUTEL and M. TISHLER. J. Am. Chem. Soc. **68**, 1463 (1946).
40. H. MAEHR, J. F. BLOUNT, M. LEACH, A. STEMPEL, and G. BÜCHI. Helv. Chim. Acta, **55**, 3054 (1972).
41. H. MAEHR, M. LEACH, T. H. WILLIAMS, W. BENZ, J. F. BLOUNT, and A. STEMPEL. J. Am. Chem. Soc. **95**, 8448 (1973).
42. H. MAEHR, J. F. BLOUNT, M. LEACH, and A. STEMPEL. Helv. Chim. Acta, **57**, 936 (1974).
43. A. F. THOMAS. J. Am. Chem. Soc. **91**, 3281 (1969).
44. G. HESSE and K. MIX. Chem. Ber. **92**, 2427 (1959).
45. H. MAEHR, T. H. WILLIAMS, M. LEACH, and A. STEMPEL. Helv. Chim. Acta, **57**, 212 (1974).
46. K. S. PFITZER and W. E. DONATH. J. Am. Chem. Soc. **81**, 3213 (1959).
47. R. TOLMAN, R. K. ROBINS, and L. B. TOWNSEND. J. Heterocycl. Chem. **4**, 230 (1967).
48. J. D. STEVENS and H. G. FLETCHER, JR. J. Org. Chem. **33**, 1799 (1968).
49. H. MAEHR, M. LEACH, J. F. BLOUNT, and A. STEMPEL. J. Am. Chem. Soc. **96**, 4034 (1974).
50. B. A. LEWIS, F. SMITH, and A. M. STEPHEN. Methods Carbohydr. Chem. **2**, 182 (1963).
51. W. C. BAIRD, J. B. FRANZUS, and J. H. SHRRIDGE. J. Am. Chem. Soc. **89**, 410 (1967).
52. H. OHURI, H. J. GORDON, J. G. MOFFATT, M. L. MADDOX, A. T. CHRISTENSEN, and S. K. BYRAM. J. Am. Chem. Soc. **97**, 4602 (1975).
53. C. VOS and P. E. J. VERWIEL. Tetrahedron Lett. 2823 (1973).
54. C. VOS and P. E. J. VERWIEL. Tetrahedron Lett. 5173 (1973).
55. C.-M. LIU, H. MAEHR, M. LEACH, M. LIU, and P. A. MILLER. J. Antibiot. **30**, 416 (1977).
56. C.-M. LIU, T. H. WILLIAMS, and R. G. PITCHER. J. Antibiot. **32**, 414 (1979).
57. W. C. HAMILTON. Acta Crystallogr. **18**, 506 (1965).
58. R. KUHN and H. TRISCHMANN. Chem. Ber. **96**, 284 (1963).
59. V. M. PARIKH and J. K. N. JONES. Can. J. Chem. **43**, 3452 (1965).

Can. J. Chem. Downloaded from www.nrcresearchpress.com by 210.87.254.40 on 09/05/12
For personal use only.

Interaction of ruthenium(II) octaethylporphyrin with carbon monoxide on a fused-quartz surface

ALFIO CORSINI, HUSAIN MEHDI, AND ALLEN CHAN
Department of Chemistry, McMaster University, Hamilton, Ont., Canada L8S 4M1

Received September 7, 1979

ALFIO CORSINI, HUSAIN MEHDI, and ALLEN CHAN. Can. J. Chem. **58**, 527 (1980).

When carbon monoxide gas is interacted with a methanolic reagent solution of hydrazine and K[Ru(III)OEP(CN)$_2$] (OEP = octaethylporphyrin), a carbonylated complex of Ru(II)OEP is formed and excess carbon monoxide is strongly adsorbed on the walls of the fused-quartz reaction cell. The adsorbed carbon monoxide is very difficult to remove and unless appropriate measures are taken, it remains on the cell walls to interact with the reagent solution in subsequent experiments, thus leading to the possibility of erroneous interpretation. The amount of adsorbed carbon monoxide, while less than a complete monolayer, is significant.

ALFIO CORSINI, HUSAIN MEHDI et ALLEN CHAN. Can. J. Chem. **58**, 527 (1980).

Quand le monoxyde de carbone gazeux réagi avec une solution méthanolique de réactif d'hydrazine et de K[(Ru(III)OEP(CN)$_2$], il se forme un complexe carbonylé de Ru(III)OEP et l'excès de monoxyde est fortement adsorbé par les parois de la cellule de la réaction en quartz fondu. Le monoxyde carbone adsorbé est très difficile à enlever et bien que des précautions soient prises, il demeure dans les parois de la cellule et réagi par la suite avec le réactif en solution dans d'autres expériences conduisant ainsi à des interprétations erronées. La quantité de monoxyde de carbone absorbée est significative bien qu'elle soit moindre qu'une monocouche complète.

[Traduit par le journal]

Can. J. Chem. Downloaded from www.nrcresearchpress.com by 210.87.254.6 on 09/05/12
For personal use only.

There has been considerable interest in the study of dioxygen, dinitrogen, and carbonyl derivatives of synthetic metalloporphyrins with the view towards the development of simple models that mimic the behaviour of the more complex biological heme proteins (e.g., refs. 1–6).

Our interest in metalloporphyrins has been focused on their suitability as potential selective analytical reagents for the determination of carbon monoxide in polluted atmospheres. In an effort to improve upon the sensitivity of the Fe(II)TPP(pip)$_2$ system (TPP = *meso*-tetraphenylporphine, pip = piperidine) for CO (7), we have initiated a study of Ru(II) porphyrins as potential reagents. This study was stimulated by reports of the formation of stable carbonylated complexes of several Ru(II) porphyrins (6, 8–12).

We wish to report that in the course of investigations with the Ru(II)OEP complex (OEP = octaethylporphyrin), we found that the surface of the fused-quartz cells used in the work became grossly contaminated with strongly adsorbed CO, which subsequently interacted with the Ru(II)OEP reagent solution in later experiments. A purpose of this report is to caution other workers engaged in similar studies with metalloporphyrins to ensure that the surfaces of reaction vessels are free of adsorbed CO prior to experimentation.

Experimental

Spectrophotometric Measurements

Spectra of the ruthenium complexes of OEP in the visible range were recorded on a GCA McPherson double-beam spectrophotometer, Model EU-700, against methanol or distilled water references. Stoppered fused-quartz cells (1 cm) were used. Differential infrared measurements to identify CO adsorbed on the surface of a thin plate (1 mm) of fused quartz were made with a Nicolet 7199 FT-IR instrument. The quartz plate was clamped onto a cell holder and positioned in the same way each time a spectrum (100 scans) was taken.

Materials

All chemicals used were of sufficient purity for the purpose intended. CO gas was used directly from lecture bottles. $Ru_3(CO)_{12}$ and OEP were obtained from the Strem Chemical Co.

Syntheses

Ru(II)OEP(CO)(CH$_3$OH)

$Ru_3(CO)_{12}$ (250 mg) and OEP (250 mg) were refluxed in toluene (100 mL) for 24 h under nitrogen. Removal of unreacted solid and of the solvent yielded crude Ru(II)OEP(CO) which was chromatographed in benzene on Grade V alumina. The intense orange band was collected and the benzene removed to give the purified orange carbonyl complex (ν_{CO}^{KBr} = 1950 cm^{-1}). A dilute solution (~5×10^{-6} *M*) in methanol gave a spectrum in the visible range virtually identical to that for Ru(II)OEP(CO)-(C_2H_5OH) reported by Farrell *et al.* (6).

Ru(II)OEP(py)$_2$

The dipyridinate was prepared by modification of the procedure used by Hopf *et al.* (11). The solution of Ru(II)OEP(CO) (60 mg) in freshly distilled pyridine (10 mL) was placed in a thick-walled quartz tube and subjected to at least 5 freeze–pump–thaw cycles. The tube was sealed and irradiated at 300 nm (Rayonet apparatus) for 3 days. Ru(II)OEP(py)$_2$ formed as a dark precipitate. After removal of the excess pyridine, the solid was dissolved in benzene and chromatographed in 90% benzene – 10% pyridine on Grade 1 alumina. The major dark band was collected. If a band at 1950 cm^{-1} was observed in the infrared spectrum of the product, the latter was rechromatographed. The spectrum in the visible range has been previously reported (11).

K[Ru(III)OEP(CN)$_2$]

The procedure of Chow and Cohen (8) for K[Ru(III)-

0008-4042/80/050527-03$01.00/0
©1980 National Research Council of Canada/Conseil national de recherches du Canada

Can. J. Chem. Downloaded from www.nrcresearchpress.com by 210.87.254.6 on 09/05/12
For personal use only.

$TPP(CN)_2$] was followed except that 50 mg of $Ru(II)OEP(py)_2$, 50 mL of THF (freshly distilled), and 1 mL of a saturated aqueous solution of KCN (freshly recrystallized) were interacted under reflux (using a double-condenser system) for 4 days, with a stream of filtered air gently bubbling through the mixture. Any THF lost by evaporation was replaced. Progress of the reaction was followed by periodic removal of an aliquot for spectral testing. The spectrum of $K[Ru(III)OEP(CN)_2]$ is quite distinct from that of $Ru(II)OEP(py)_2$. After complete reaction, the solvent was removed and the residue treated with a small volume of water to dissolve excess solid KCN. The product was collected on a fine frit, washed with water, dried at 80°C in a vacuum desiccator for 2 days, and recrystallized from methanol. The visible spectrum is given in Fig. 1.

Reagent Solution and Reaction with CO

A 5.0×10^{-5} *M* stock solution of $K[Ru(III)OEP(CN)_2]$ in methanol was prepared. Exactly 1.000 mL of this solution was placed in a 10-mL volumetric flask by means of a Gilmont micropipette, followed by about 5 mL of methanol, 100 μL (Eppendorf pipet) of fresh hydrazine, and then sufficient methanol to the mark. The final solution was about 0.3 *M* in hydrazine. A 1.00-cm fused quartz cell was filled with this solution and CO gas from a lecture bottle was gently bubbled through it for 2 to 10 min. The spectrum was then recorded and compared to that of the reagent solution through which no CO gas was passed (Fig. 1). The cell was cleaned, normally by rinsing twice with methanol which is sufficient to remove $Ru(II)OEP(CO)(CH_3OH)$ from the quartz walls, and fresh reagent solution was then introduced for additional experiments.

Results and Discussion

The experiments described in this work were qualitative in nature; quantitative experiments relating to the analytical determination of CO in atmospheres will be reported later.

The spectrum of $K[Ru(III)OEP(CN)_2]$ (curve 1, Fig. 1) is characteristic of Ru(III) porphyrins (Soret band at 390 nm and broad, less intense absorption at about 480–560 nm) and is very similar to that reported for $K[Ru(III)TPP(CN)_2]$ (8) and the $Ru(III)(OEP)(CH_3CN)_2^+$ cation (6). The addition of hydrazine results in a spectrum (curve 2, Fig. 1) resembling those (6, 11, 12) of non-carbonylated Ru(II) porphyrins (a broadened, less intense Soret band at 394 nm than exhibited by carbonylated Ru(II) porphyrins and maxima at 498 and 526 nm). We believe the spectrum corresponds to the complex $Ru(II)OEP(N_2H_4)_2$ for which the hydrazine (in large excess at 0.3 *M*) serves not only to reduce Ru(III) to Ru(II) but also to ligate the metal ion. We have not been able to isolate the complex in purity because of its decomposition in solution. At analytical concentrations of 4.98×10^{-6} and 2.49×10^{-6} *M*, a pseudo first-order rate constant of $1.50 \pm 0.01 \times 10^{-4}$ s^{-1} was calculated for the decomposition.

When CO gas is passed through a freshly prepared reagent solution, a spectrum (curve 3, Fig. 1) typical of those (6, 11, 12) for carbonyl derivatives of 6-coordinate Ru(II) complexes is obtained, with

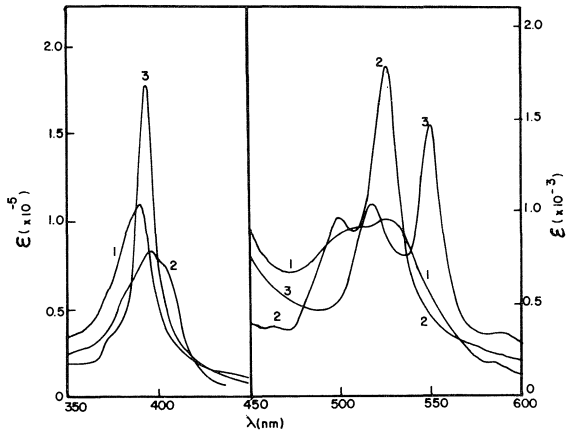


FIG. 1. Spectra of 5.0×10^{-6} *M* $K[Ru(III)OEP(CN)_2]$ in methanol, curve 1; with N_2H_4 (0.3 *M*) added, curve 2; and with CO gas subsequently passed through the solution for 2 min, curve 3.

a sharp intense Soret band at 394 nm ($\varepsilon = 1.75 \times 10^5$ M^{-1} cm^{-1}) and maxima at 518 nm ($\varepsilon = 10.3 \times 10^3$) and 550 nm ($\varepsilon = 14.8 \times 10^3$). Maximum absorbance was attained after 2 min of gentle bubbling. A FTIR spectrum (250 scans) in which the solvent absorption was subtracted showed the ν_{CO} bands at 1939 cm^{-1}, indicating the formation of a monocarbonyl rather than a dicarbonyl Ru(II) porphyrin, the latter being characterized by appreciably higher stretching frequencies (8, 10). Unlike the reagent solution, the CO complex is stable and is, presumably, $Ru(II)OEP(CO)(N_2H_4)$. As indirect evidence supporting this formulation, it was observed that the 391 and 548 nm bands of Ru(II)-OEP(CO)MeOH were shifted precisely to 394 and 550 nm on addition of N_2H_4 to a solution of the methanol complex. Also, the addition of N_2H_4 to a solution of Ru(II)OEP(CO) in CCl_4 caused shifts of the 395, 517, and 549 nm bands of the 5-coordinate complex to 398, 520, and 551 nm, respectively. In the infrared region, ν_{CO} shifted from 1955 to 1960 cm^{-1}. These shifts strongly indicate coordination of N_2H_4. (The NH_2 stretching frequencies in the region 3300–3100 cm^{-1} were due in part to excess N_2H_4.)

We noted that, curiously, when fresh reagent solution was placed and allowed to stand in a previously used fused-quartz cell cleansed in the normal manner, the characteristic maxima of the CO complex at 394, 518, and 550 nm "grew" into the spectrum with time. Typically, after 2.5 h, the absorbance of the Soret band at 394 nm was nearly 0.5 units. As the quartz cell was tightly sealed to eliminate the atmosphere as a source of CO, it was deemed that the CO was adsorbed on the inside surface of the cell from previous experiments. This

Can. J. Chem. Downloaded from www.nrcresearchpress.com by 210.87.254.6 on 09/05/12
For personal use only.

source was confirmed by the following observations: (*a*) when an identical cell not exposed to CO was used, the spectrum was that of the reagent with no appearance of the bands at 394, 518, and 550 nm, but when the interior surface of the cell was exposed beforehand to a stream of CO, the bands reappeared and grew with time; (*b*) a FTIR difference spectrum between two plates of a disassembled quartz cell, one exposed to CO and the other not, revealed a band at 2068 cm^{-1} due to adsorbed CO. This band was greatly diminished in intensity after the contaminated plate was submerged in reagent solution for several hours and the 394, 518, and 550 nm bands were clearly evident in the visible spectrum of the resulting solution.

The binding of CO to surfaces of silica, silicates, metal oxides, and transition metals to form an adsorbed phase is well documented (13–19). In fact, CO is one of the most strongly chemisorbed of the simple gases. Often, both vacuum pumping and baking are not sufficient to entirely remove the adsorbed CO from the surface. This observation was confirmed in the present study. Thus, when cells contaminated with CO were rinsed 6 times with methanol and subsequently either heated in a vacuum desiccator at 120°C for 0.5 h or soaked in an ammoniacal cuprous chloride solution for 1 day and then filled with the reagent solution, the bands of the CO complex were still observed, although with a reduction in intensity of about 75%. The most effective cleaning agent proved to be the reagent solution itself. The bands were not observed after the cells had been twice soaked in the reagent solution for 3.5 h and then refilled. This strong affinity of the Ru(II)OEP complex for CO is consistent with that observed for $Ru(II)TPP(aniline)_2$, which is reported to decarbonylate acetic anhydride (8). The tenacity with which the CO is bound to the fused-quartz surface suggests that it is chemisorbed rather than physically entrained.

From Beer's law and the volume of the cell, the amount of CO adsorbed on the cell walls was calculated to be 2.2×10^{-7} g. If the surface is assumed to be smooth, the number of CO molecules adsorbed per cm^2 is $\sim 10^{14}$; however, because the surface of fused quartz is very flawed and irregular, the actual value will be considerably lower and certainly much lower than that required for a complete monolayer ($\sim 10^{15}/cm^2$).

Our suspicions regarding surface contamination by CO were initially aroused in experiments to determine whether dinitrogen would bind to the Ru(II) porphyrin, as had been observed with Ru(II)mesoporphyrinIX(py) in monolayer assemblies (12) and, apparently, with $Ru(II)OEP(DMF)_2$ (6). The bubbling of N_2 gas through the reagent solution sometimes produced spectral changes (i.e., the growth of maxima at 394, 518, and 550 nm) and sometimes yielded only the spectrum of the decomposing reagent. These observations can now be understood in terms of CO contamination of some of the cells. (Under the solution conditions reported above and with clean cells, formation of the dinitrogen complex was not observed. Chow and Cohen (8) also observed no reaction between molecular nitrogen and Ru(II) porphyrins.) It is our hope that this report will provide a note of caution to other investigators involved in work related to the binding of gaseous species to metalloporphyrins.

Acknowledgements

We wish to thank the National Research Council of Canada for the support of this work. One of us (S.H.M.) is grateful to McMaster University for the award of a Teaching Postdoctoral Fellowship. We are also indebted to Professor P. Nicholson, Department of Ceramics Engineering, and Professor P. Dawson, Department of Chemistry, McMaster University, for their most helpful advice and suggestions.

1. R. D. JONES, D. A. SUMMERVILLE, and F. BASOLO. Chem. Rev. **79**, 139 (1979).
2. J. W. BUCHLER. Angew. Chem. Int. Ed. Engl. **17**, 407 (1978).
3. J. P. COLLMAN, J. I. BRAUMAN, T. R. HALBERT, and K. S. SUSLICK. Proc. Natl. Acad. Sci. USA, **73**, 3333 (1976).
4. C. K. CHANG and D. DOLPHIN. Proc. Natl. Acad. Sci. USA, **73**, 3338 (1976).
5. B. R. JAMES, K. J. REIMER, and T. C. T. WONG. J. Am. Chem. Soc. **99**, 4815 (1977).
6. N. FARRELL, D. H. DOLPHIN, and B. R. JAMES. J. Am. Chem. Soc. **100**, 324 (1978).
7. S. H. MEHDI and A. CORSINI. Talanta, **24**, 291 (1977).
8. B. C. CHOW and I. A. COHEN. Bioinorg. Chem. **1**, 57 (1971).
9. M. TSUTSUI, D. OSTFELD, and L. M. HOFFMAN. J. Am. Chem. Soc. **93**, 1820 (1971).
10. G. R. EATON and S. S. EATON. J. Am. Chem. Soc. **97**, 235 (1975).
11. F. R. HOPF, T. P. O'BRIEN, W. R. SCHEIDT, and D. G. WHITTEN. J. Am. Chem. Soc. **97**, 277 (1975).
12. F. R. HOPF and D. G. WHITTEN. J. Am. Chem. Soc. **98**, 7422 (1976).
13. M. L. HAIR. Infrared spectroscopy in surface chemistry. Marcel Dekker, Inc., New York. 1967.
14. R. R. FORD. Advan. Catal. **21**, 51 (1970).
15. D. J. C. YATES. J. Phys. Chem. **65**, 746 (1961).
16. S. MATSUSHITA and J. NAKATA. J. Chem. Phys. **36**, 665 (1962).
17. D. A. SEANOR and C. H. AMBERG. J. Chem. Phys. **42**, 2967 (1965).
18. J. H. SCHULMAN (*Editor*). Second international congress of surface activity. Vol. II. Solid-gas interface. Butterworths, London. 1957. pp. 252–259.
19. B. W. KRUPAY and R. R. ROSS. Can. J. Chem. **56**, 2447 (1978).

Carbocyclic phenylaminephosphonate stereochemistry as probed via ^{13}C nmr chemical shifts and nuclear spin couplings from ^{13}C to ^{31}P and ^{15}N

GERALD W. BUCHANAN AND FREDERICK G. MORIN

Department of Chemistry, Carleton University, Ottawa, Ont., Canada K1S 5B6

Received July 16, 1979

GERALD W. BUCHANAN and FREDERICK G. MORIN. Can. J. Chem. **58**, 530 (1980).

^{13}C nmr chemical shifts and ^{13}C—^{31}P couplings through one, two, and three bonds are reported for eleven carbocyclic phenylaminephosphonates with ring sizes from four to seven. On the basis of these data, inferences regarding preferred conformations are drawn. Low temperature spectra of the 4-methylcyclohexyl derivative show the existence of two conformers, populated in the ratio of approximately 2:1 at 183 K.

GERALD W. BUCHANAN et FREDERICK G. MORIN. Can. J. Chem. **58**, 530 (1980).

On rapporte les déplacements chimiques en rmn du ^{13}C et les constantes de couplage ^{13}C—^{31}P à travers un, deux et trois liens pour onze phenylaminophosphonates carbocycliques avec les grandeurs des cycles allant de quatre à sept chaînons. Sur la base de ces données, on tire des conclusions concernant les conformations privilegiées. Les spectres, obtenus à la basse temperature montrent l'existence de deux conformations peuplées dans la proportion approximative de 2:1 à 183 K, pour le dérivé 4-méthylcyclohéxyle.

Can. J. Chem. Downloaded from www.nrcresearchpress.com by 210.87.254.6 on 09/05/12
For personal use only.

Introduction

Recent publications from this laboratory (1, 2) have dealt with the application of ^{13}C nmr (chemical shifts and ^{13}C—^{31}P couplings) to the stereochemistry of carbocyclic hydroxyphosphono compounds. Some evidence for increased $^1J_{CP}$ and attenuated $^3J_{CP}$ values due to the presence of the electronegative OH function has been presented. We have now synthesized a series of carbocyclic phenylaminephosphonates to examine the influence of the less electronegative, but sterically more bulky NH—ϕ group on the nmr parameters. Some inferences regarding the preferred conformations of these molecules can be made, and the configurational effects on $^1J_{^{13}C^{31}P}$ and $^1J_{^{13}C^{15}N}$ are discussed.

Results and Discussion

The structures and numbering schemes for the materials examined are presented in Fig. 1. Table 1 contains the ^{13}C chemical shift data while Tables 2, 3, and 4 contain one, two, and three bond ^{13}C—^{31}P coupling constants respectively. Compounds **4** and **5** were also synthesized using ^{15}N enriched aniline and the ^{13}C—^{15}N couplings are recorded in Table 5.

Spectral Assignments

The carbon spectra were routinely recorded using complete ^1H noise decoupling. Subsequently the single frequency off-resonance decoupling method (SFORD) was employed to differentiate between CH_3, CH_2, CH, and quaternary carbons. Selective ^1H decoupling was used occasionally, and model compounds studied previously (1, 3) were valuable in many instances.

Conformational Implications

Before discussing the geometries of the

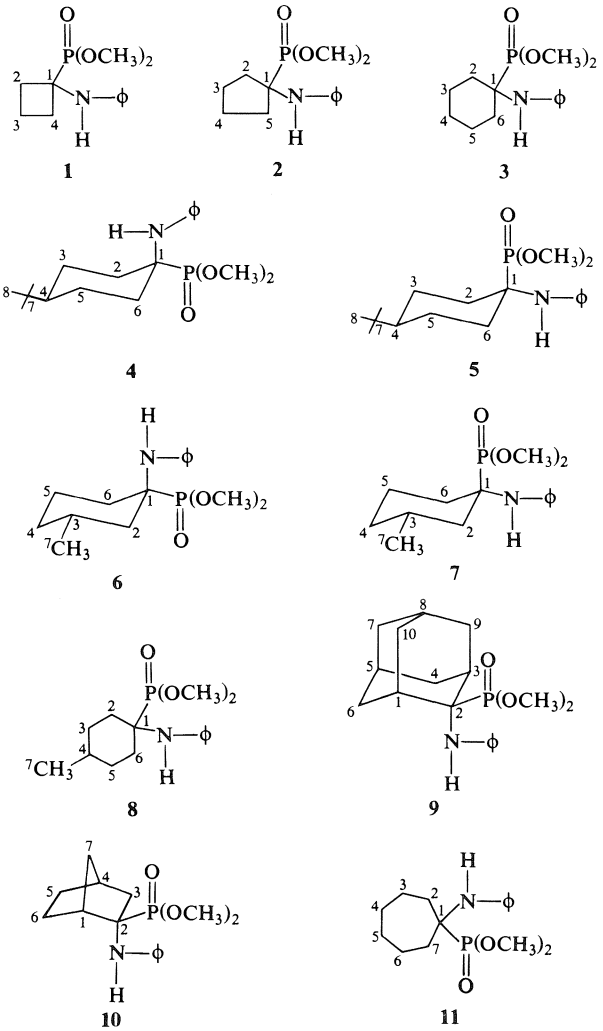


FIG. 1. Structures and numbering schemes for amine phosphonates.

0008-4042/80/050530-07$01.00/0

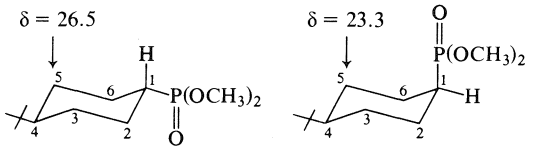
©1980 National Research Council of Canada/Conseil national de recherches du Canada

Can. J. Chem. Downloaded from www.nrcresearchpress.com by 210.87.254.6 on 09/05/12
For personal use only.

"mobile" systems **1–3**, it is instructive to look at data for the model compounds **4** and **5**. Generally, the ^{13}C shifts and vicinal CP couplings seem to be the most useful for obtaining insight into conformational preferences.

In **4**, the large $^3J_{CP}$ of 12.1 Hz to C-3,5 is indicative of an equatorial phosphorus atom with a dihedral angle of near 180° to C-3,5 (1, 2, 4). Compound **5** shows a non-resolvable $^3J_{CP}$ to C-3,5 indicative of an axial phosphorus atom (1, 2). It is important to note, however, that introduction of the axial phenylamino group in **4** causes a *reduction* of ca. 4 Hz in the $^3J_{CP}$ value to C-3,5, compared to compound **12**.

Another indicator of the configuration at C-1 in these materials is the chemical shift at C-3,5, and in this context it is useful to compare data for **4** and **5** with those reported earlier (3) for **12** and **13**.



12 $^3J_{3,5CCCP} = 16.2$ Hz

13 $^3J_{3,5CCCP} < 0.6$ Hz

The C-3,5 shift for **4** is 20.9 ppm, manifesting a *gauche*-"γ" (5) upfield steric shift of 5.6 ppm due to the introduction of the axial NH—ϕ group. By contrast the C-3,5 shift of **5** is essentially identical to that of **13** above, showing no chemical shift perturbation due to the equatorial phenylamino function.

Another interesting difference, although its origin is less clear, is the upfield "β" shift of 4.0 ppm found at C-2,6 of **4** vs. **5**.

With these data for "model" compounds in hand, we can now turn our attention to the conformationally less well-defined systems, starting with the cyclobutyl derivative **1**. In a puckered 1,1-disubstituted cyclobutane (6), one of the substituents will be axial and the other equatorial. The C-3 ring carbon experiences two *gauche*-butane type interactions with the axial substituent and should therefore experience an upfield shift at C-3 when an axial substituent is present at C-1. Our previous work (1, 3) demonstrated that an axial dimethylphosphono group induces an upfield shift of ca. 2.5 ppm at C-3,5 of a cyclohexane ring. The present results (above) for **4** vs. **12** indicate a much larger *gauche*-γ shielding (5.6 ppm) at C-3,5 due to an axial phenylamino function.

We now can consider the influence of introduc-

TABLE 1. ^{13}C chemical shifts for **1–11** (δ_c from TMS ± 0.1)*

Compound	C-1	C-2	C-3	C-4	C-5	C-6	C-7	C-8	C-9	C-10	C-1′	C-2′	C-3′	C-4′	OCH_3
1	56.3	30.6	15.6	30.6							145.0	114.9	128.9	118.0	52.8
2	64.0	35.8	24.3	24.3	35.8						145.5	117.5	128.7	119.1	53.0
3	57.7	30.5	20.1	25.5	20.1	30.5					145.9	118.7	128.8	119.6	52.9
4	57.3	31.0	20.9	47.4	20.9	31.0	32.5	27.6			145.9	118.8	128.6	119.7	52.9
5	58.8	35.0	23.3	47.2	23.3	35.0	32.6	27.7			145.7	122.1	129.7	121.7	53.2
6	58.3	38.9	26.1	34.3	20.2	30.0	22.3				145.8	118.4	128.8	119.6	53.0
7	59.0	42.4	28.1	33.8	21.8	33.8	22.6				144.7	121.1	128.6	120.7	52.9
8	57.9	28.2	27.4	28.3	27.4	28.2	19.1				145.5	120.1	128.8	119.6	53.0
9	33.4	64.9	33.4	32.7	(26.8)†	32.7	38.5	(27.2)†	33.3	33.3	146.4	118.5	128.9	116.7	52.7
10	44.6	63.8	44.2	36.5	29.0	24.2	39.0				147.9	119.0	129.6	116.4	53.2
11	61.1	34.9	22.3	29.4	29.4	22.3	34.9				145.8	119.7	128.7	119.1	52.9

*0.2 *M* solutions in $CDCl_3$.
†Parentheses denote uncertain assignments.

Can. J. Chem. Downloaded from www.nrcresearchpress.com by 210.87.254.6 on 09/05/12
For personal use only.

TABLE 2. One bond $^{13}C—^{31}P$ couplings (±0.2 Hz)*

Compound	^1J
1	158.7
2	163.5
3	159.9
4	161.1
5	151.4
6	159.6
7	150.4
8	156.2
9	150.2
10	151.4
11	151.7

*Sign assumed to be positive (18).

TABLE 3. Geminal $^{13}C—^{31}P$ couplings (±0.2 Hz)*

Compound	Path	^2J
1	$^{2,4}C—^1C—P$	N.R.†
2	$^{2,5}C—^1C—P$	6.6
3	$^{2,6}C—^1C—P$	1.1
4	$^{2,6}C—^1C—P$	1.2
5	$^{2,6}C—^1C—P$	4.5
6	$^2C—^1C—P$	N.R.
	$^6C—^1C—P$	N.R.
7	$^2C—^1C—P$	4.2
	$^6C—^1C—P$	4.2
8	$^{2,6}C—^1C—P$	2.9
9	$^{1,3}C—^2C—P$	N.R.
10	$^1C—^2C—P$	8.9
	$^3C—^2C—P$	N.R.
11	$^{2,7}C—^1C—P$	2.8

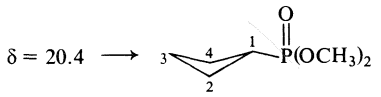
*$^{13}CH_3—O—^{31}P$ J's for **1–11** are all 7.4 ± 0.4 Hz and are not listed individually.
†N.R. = non-resolvable, i.e., < 0.6 Hz.

TABLE 4. Vicinal $^{13}C—^{31}P$ couplings (±0.2 Hz)

Compound	Path	^3J
1	$^3C—C—C—P$	6.1
2	$^{3,4}C—C—C—P$	10.6
3	$^{3,5}C—C—C—P$	11.0
4	$^{3,5}C—C—C—P$	12.1
5	$^{3,5}C—C—C—P$	N.R.*
	$^{1'}C—N—C—P$	3.8
6	$^3C—C—C—P$	11.1
	$^5C—C—C—P$	12.4
7	$^3C—C—C—P$	N.R.
	$^5C—C—C—P$	N.R.
	$^{1'}C—N—C—P$	3.5
8	$^{3,5}C—C—C—P$	6.9
9	$^{4,6}C—C—C—P$	11.1
	$^{9,10}C—C—C—P$	N.R.
10	$^4C—C—C—P$	3.6
	$^6C—C—C—P$	9.8
	$^7C—C—C—P$	N.R.
11	$^{3,6}C—C—C—P$	10.7

*N.R. = nonresolvable, i.e., less than 0.6 Hz.

tion of the NH—ϕ group at C-1 in **1**, relative to **14** below, in which the dimethylphosphono group is deemed to be almost exclusively equatorial (7). The C-3 shift of **1** is 4.8 ppm upfield from that of **14**,

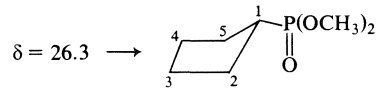


14

indicative of a preponderance of an axial phenylamino group. This finding is reasonable in view of the recent results (8) which show that $-\Delta G^0$ for the dimethylphosphono group is 2.0 kcal/mol in cyclohexane, while the $-\Delta G^0$ for the phenylamino group, although not known precisely, is likely to be somewhat smaller, ca. 1.0 kcal/mol (9) and *vide infra*.

The vicinal coupling from ^{31}P to C-3 of **1** is 6.1 Hz, nearly identical to that (6.5 Hz) of the corresponding hydroxyphosphonate (2), and much smaller than the 18.7 Hz value found in **14** (7). As was demonstrated in **4** vs. **12**, the introduction of the phenylamino group reduces $^3J_{CP}$ by ca. 4 Hz for a constant dihedral angle. Thus the further reduction observed relative to **14** must be due to changes in the average $^3C—C—C—P$ torsional angle to a value closer to 90°. A combination of ring flattening in **1** as well as some contribution from the conformer with an axial phosphorus is probably present.

For the cyclopentyl derivative **2**, the C-3,4 shift is upfield by 2.0 ppm relative to the model compound **15** (below), consistent with the presence of a sec-



15

$^3J_{3,4CCCP}$ = 12.6 Hz

ond substituent at C-1. The vicinal $^{13}C—^{31}P$ coupling of 10.6 Hz in **2** indicates a preference for the equatorial dimethylphosphono group. The axial phenylamino function of **2** induces a much smaller upfield "γ" shift at C-3,4 than in the 6-membered ring model **4**. This appears to be a general phenomenon in the ^{13}C spectra of cyclopentyl compounds (10) and has been attributed to a lesser amount of ring puckering in a cyclopentane than in a cyclohexane ring system.

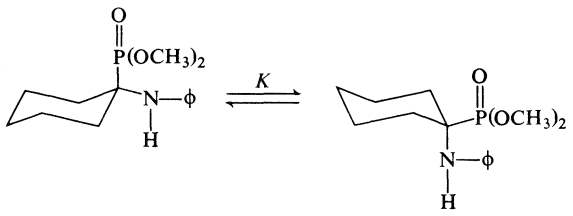
For the simple cyclohexyl derivative **3**, the nmr parameters indicate a strong preference for the conformer in which the dimethylphosphono group is equatorial. Using the isomeric 4-*tert*-butyl cyclo-

TABLE 5. $^{13}C—^{15}N$ couplings (±0.2 Hz)

Compound	^1J		^2J*	^3J*
	$^1C—N$	$^1'C—N$	$N—^1'C—^{2',6'}C$	$N—^1'C—^{2',6'}C—^{3',5'}C$
4	6.4	10.2	1.8	1.4
5	4.9	11.5	1.9	N.R.

*All two and three bond $^{13}C—^{15}N$ J's into the aliphatic ring were N.R. i.e., < 0.6 Hz.

hexyl compounds **4** and **5** as models, one can calculate an equilibrium constant K for the process:



from the Eliel equation below (11) and the values for $^1J_{CP}$, i.e.,

$$K = \frac{J_{ax} - J_{mix}}{J_{mix} - J_{eq}}$$

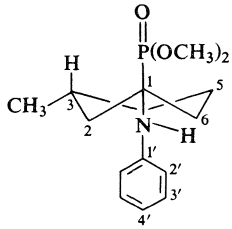
where J_{ax} is the $^1J_{CP}$ value for the model compound **5**, J_{eq} is the $^1J_{CP}$ value for **4**, and J_{mix} represents $^1J_{CP}$ for **3**.

On this basis K is found to be 7.0 at 303 K. Low temperature experiments on **3** verify the large value of K, since the amount of the conformer with an axial phosphorus atom is insufficient for detection at 183 K. The ^{13}C spectrum of **3** at 183 K shows a $^1J_{CP}$ value of 161.0 Hz and $^3J_{CCCP}$ of 12.0 Hz, indicating that **4** is indeed a reasonable "model" for the conformer with an equatorial dimethylphosphono group.

These results for **3** reflect the published value for the conformational free energy of the dimethylphosphono group (2.0 kcal/mol) (8) which is sterically much larger than the NH—ϕ function. No data for this latter group itself are available, but the value for the $NHCH_3$ group is 1.0 kcal/mol (9).

For the 3-CH_3 compound **6**, the large $^3J_{CP}$ values to C-3 and C-5 are consistent with the presence of an equatorial phosphorus atom. The slightly smaller ^3J to the C-3 position may be due to some minor ring flattening due to the presence of the methyl function. In the case of **7**, the non-resolvable vicinal $^{13}C—^{31}P$ coupling to C-3 and C-5 suggests axial phosphorus by analogy with **5**. It is interesting to note for **5** and **7**, which are the only materials having a purely equatorial phenylamino group, that a substantial ^3J is found between the C-1′ position of the aromatic ring and the phosphorus atom.

In the isomers **5** and **7**, which possess an equatorial phenylamino group, the conformation below in which the ^{31}P and the C-1′ carbon are *trans*-coplanar, is relatively free of repulsive van der Waals forces. By contrast, in isomers having an axial phenylamino function, a *trans*-coplanar disposition of the ^{31}P and the C-1′ carbon produces conformations in which severe van der Waals repulsion is present between the aryl ring and the axial cyclohexane hydrogens at C-3 and C-5. Since it is well-documented (1, 2, 4) that *trans*-coplanar geometries produce maximal $^3J_{CP}$ values, this argument satisfactorily accounts for the observation of substantial ^3J values only when the phenylamino moiety is equatorial.



Chemical shift trends in **6** vs. **7** support the assignment of stereochemistry based on the vicinal C—P coupling. For example in **6**, the axial NH—ϕ group induces upfield "β" shifts of ca. 4 ppm at C-2 and C-6 relative to **7**, consistent with the trend noted earlier for **4** vs. **5**. Also, the larger *gauche*-"γ" shielding effect arising from the axial NH—ϕ is manifest in the C-3,5 shifts of **6** vs. **7**. The methyl group appears to be predominantly equatorial in both **6** and **7**, since its shift in both isomers is near that (23.3) found in methylcyclohexane itself (12, 13) where the strong preference for the equatorial position is well known.

A further point of interest regarding the chemical shifts as a function of configuration, is that the aromatic *ortho* and *para* resonances are consistently deshielded in isomers having the phenylamine group equatorial, i.e., **5** and **7**, compared to their respective counterparts **4** and **6**.

For the 4-methyl cyclohexyl compound **8**, the $^1J_{CP}$ and $^3J_{CCCP}$ values lie nearly mid-way between those of the "model" compounds **4** and **5**. Also, the

Can. J. Chem. Downloaded from www.nrcresearchpress.com by 210.87.254.6 on 09/05/12
For personal use only.

Can. J. Chem. Downloaded from www.nrcresearchpress.com by 210.87.254.6 on 09/05/12
For personal use only.

rather highly shielded 4-methyl group (δ = 19.1) suggests an appreciable contribution from a conformation having an axial CH_3 (14).

Low temperature spectra of **8** (in CD_2Cl_2 at 183 K) indeed showed the presence of two conformers. Although the spectrum was complicated by peak overlap, the CH_3 resonance of **8**, occurring at 19.1 ppm at 303 K, split into two resonances below 203 K. At 183 K, which represents the slow exchange limit, the chemical shifts of the axial and equatorial 4-CH_3 group are 17.0 and 23.4 ppm respectively. This 6.4 ppm chemical shift difference is comparable to that found in methylcyclohexane itself at 163 K (13).

At 183 K, the aromatic carbon resonances of **8** also split into two, but the chemical shift differences are only ca. 0.3 ppm. Extensive overlap in the cyclohexyl carbon resonance region of the spectrum prevents extraction of the full details of the spectra of the separate conformers of **8**.

Nevertheless, one can discuss the conformations of **8** in terms of the two situations I and II depicted below.

From the low temperature spectra of **3** discussed earlier, we know that the steric size of the dimethylphosphono group must be considerably larger than that of the phenylamino function. Also, the conformational free energy of the CH_3 group is known to be ca. 1.7 kcal/mol (15). Thus, one can conclude that in scheme II above, conformer *A* would be expected to dominate to a very large extent over conformer *B*, and at low temperature, the spectrum would be essentially that of *A*.

By contrast, in scheme I, more equal populations of conformers *A* and *B* are expected. Examining the 4-CH_3 chemical shift of **8** at room temperature (δ = 19.1), in relation to the low temperature values (23.4 and 17.0), it is evident that the preferred conformation of **8** is in fact *B* of scheme I.

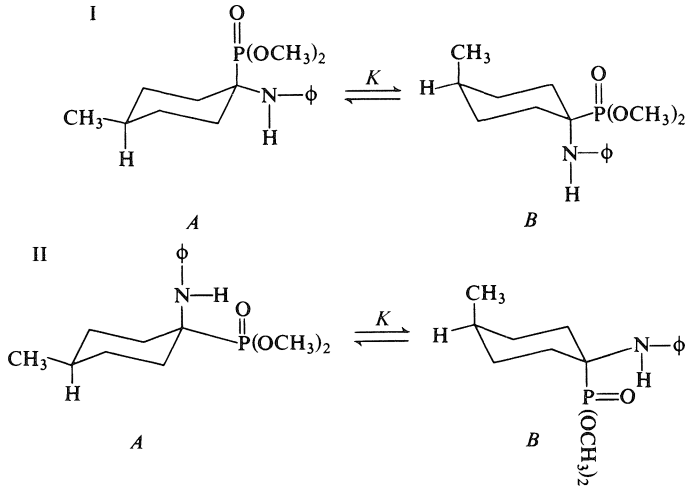
The equilibrium constant *K* calculated from the Eliel equation (11), is approximately 2.0, which translates into a free energy difference (at 183 K), of 0.25 ± 0.03 kcal/mol, between *A* and *B*, calculated from $-\Delta G^0 = RT \ln K$, using the chemical shift data of the preceding paragraph.

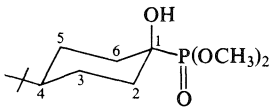
If one assumes additivity of conformational free energies, this result is surprising, in view of the published conformational free energy of the CH_3 group (1.7 kcal/mol) (15) and that for the dimethylphosphono group (2.0 kcal/mol) (8). It has been shown, however (16), that additivity of $-\Delta G^0$ values breaks down in 1,1-disubstituted cyclohexanes, especially when hydrogen bonding can occur between the substituents, as is the case in **8**.

Of course, it would have been preferable to obtain *K* for **8** directly from the peak areas at 183 K, but spectral overlap ruled out such an approach. Also, ^1J's and ^3J's for the separate conformers of **8** could not be extracted from the spectrum at 183 K due to spectral complexity. High field spectrometers could solve this problem.

For the adamantyl compound **9**, the vicinal $^{13}C—^{31}P$ couplings are nearly identical to those reported (1) for the corresponding hydroxyphosphonate. The same holds true for the stereochemically "anchored" systems **4** vs. **16** (below) (1) and **10** vs. **17** (below). It appears therefore, that the electronic effects of OH vs. NH—ϕ substitution on $^3J_{CP}$ are comparable.

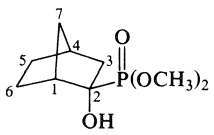
The cycloheptyl compound **11** shows a $^3J_{CP}$ value of 10.7 Hz, again nearly identical to that in the





16

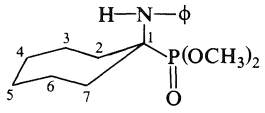
$^3J_{PCC^{3,5}C} = 12.6$



17

$^3J_{PCC^7C} < 0.6$
$^3J_{PCC^4C} = 4.7$
$^3J_{PCC^6C} = 9.1$

corresponding hydroxyphosphonate (2). This large value for ^3J precludes the dominance of a twist chair conformation with isoclinal substituents, as has been discussed by us in detail earlier (2) for the hydroxyphosphonate. Indeed, X-ray crystallography (17) of 1-dimethylphosphono-1-hydroxycycloheptane has shown the presence of a substantial amount of the chair conformation in the solid. In this conformation, the dihedral angles P—C1—C2—C3 and P—C1—C7—C6 are 168.7 and 173.0° respectively. We suggest therefore that **11** is predominantly in the chair form below, with an equatorial phosphorus atom, leading to the large observed $^3J_{CP}$.



11

One-bond Couplings

The sign of $^1J_{CP}$ in pentavalent organophosphorus compounds is likely to be positive (18). For $^{13}C—^{31}P$ coupling in phosphonates (3) and hydroxyphosphonates (2), it has been shown that $^1J_{CP}$ becomes less positive as the number of *gauche* interactions experienced by the C—P bond increases. This trend is again apparent in these phenylaminophosphonates for cyclohexyl derivatives (Table 2).

Comparing the isomeric pair **4** and **5**, $^1J_{CP}$ is 9.7 Hz smaller in **5**, having the axial C—P bond, than in **4**. In the simple cyclohexyl compound **3** which lacks the *tert*-butyl group, $^1J_{CP}$ lies between the values for the "models" **4** and **5**, but much closer to the value for **4**, as discussed earlier.

In the case of the isomeric 3-CH_3 compounds **6** and **7**, the $^1J_{CP}$ for **7**, having the axial C—P bond, is 9.2 Hz less than for **6**. In the adamantyl derivative **9**, $^1J_{CP}$ is very close in value to results for **5** and **7**, which is reasonable, since in **9**, the C—P bond experiences the same number of *gauche* interactions as does the C—P bond of **5** and **7**.

For the 4-CH_3 compound **8**, the $^1J_{CP}$ value is approximately mid-way between results for the "model" compounds **4** and **5**, indicating two appreciably populated conformers, a finding borne out by the low temperature spectra of **8** discussed previously.

With respect to the configurational dependence of the one-bond $^{13}C—^{15}N$ couplings (Table 5), it is important to note that the sign of this interaction is probably negative (19). Thus, a trend consistent with $^1J_{CP}$ is evident in **4** and **5**. Specifically, in **4**, where the $^1C—N$ bond has two more *gauche* interactions than in **5**, the one bond coupling again becomes less positive, *i.e.*, *more negative* in **4** than **5**.

Experimental

Spectra

^{13}C nmr spectra were obtained using techniques described previously (1–3) on a Varian XL-100-12 spectrometer equipped with a Nicolet TT-100 Fourier Transform data system. For measurement of $^{13}C—^{31}P$ and $^{13}C—^{15}N$ couplings, normal sweep widths were 500 Hz and 8K data points were employed.

Materials

The following general procedure (20) was used for synthesis of the amine phosphonates from the appropriate carbocyclic ketone.

A mixture of 1.0 mmol ketone, 1.0 mmol aniline, and 1.0 mmol dimethyl phosphite in 1.0 mL benzene was stirred with 0.4 g 5 Å molecular sieves in a stoppered flask for 3 days. A further 20.0 mL benzene was added and the sieves and undissolved solids were filtered by gravity. The solvent was removed by rotary-evaporator and the crude product recrystallized from hexanes or hexanes/ethyl acetate. No attempt was made to maximize yields which were generally 30–40%.

All compounds displayed a 6 proton $CH_3O—P$ doublet at 3.8 ppm in ^1H nmr and the ^1H spectra integrated correctly. Melting points were obtained on a Buchi SMP-20 melting range apparatus and are uncorrected.

The following compounds were obtained in this fashion.

1-Dimethylphosphono-1-phenylaminocyclobutane (**1**): mp 121–122°C. *Anal.* calcd.: C 56.47, H 7.11, N 5.49, P 12.13; found: C 56.47, H 7.00, N 5.35, P 12.16.

1-Dimethylphosphono-1-phenylaminocyclopentane (**2**): mp 120–121°C. *Anal.* calcd.: C 57.99, H 7.49, N 5.20, P 11.50; found: C 57.81, H 7.27, N 5.29, P 11.58.

1-Dimethylphosphono-1-phenylaminocyclohexane (**3**): mp 110–111°C (lit. (21) mp 110–112°C).

1-Dimethylphosphono-1-phenylamino-4-*tert*-butylcyclohexanes (**4** and **5**): a first crop from recrystallization gave the pure isomer with axial phosphorus group (**5**), mp 139–140°C. ^1H nuclear magnetic resonance shows one $CH_3O—P$ doublet at 3.8 ppm and one *tert*-butyl singlet at 0.85 ppm. *Anal.* calcd.: C 63.70, H 8.91, N 4.13, P 9.13; found: C 63.83, H 8.80, N 4.02, P 9.02. A second crop furnished a sample of approximately a 1:1 mixture of **4**:**5**, mp 123–125°C; ^1H nmr shows two $CH_3O—P$ doublets at 3.8 ppm and two *tert*-butyl singlets at 0.85 and 0.87 ppm. *Anal.* calcd.: C 63.70, H 8.91, N 4.13, P 9.13; found: C 63.60, H 8.80, N 4.03, P 8.99. The procedure was repeated using ^{15}N-enriched aniline (99%, Stohler Isotope Company) to provide ^{15}N-enriched samples of **4** and **5**.

1-Dimethylphosphono-1-phenylamino-3-methylcyclohexanes (**6** and **7**): mp 109–115°C obtained as two isomers ratio **6**:**7** = 1:5; ^1H nmr shows two $CH_3O—P$ doublets at 3.8 ppm

Can. J. Chem. Downloaded from www.nrcresearchpress.com by 210.87.254.6 on 09/05/12
For personal use only.

and two CH_3—CH doublets at 0.9 ppm. *Anal.* calcd.: C 60.59, H 8.14, N 4.71, P 10.42; found: C 59.71, H 7.90, N 4.76, P 10.14.

1-Dimethylphosphono-1-phenylamino-4-methylcyclohexane (**8**): mp 84–86°C. *Anal.* calcd.: C 60.59, H 8.14, N 4.71, P 10.42; found: C 60.64, H 8.15, N 4.83, P 10.33.

2-Dimethylphosphono-2-phenylaminoadamantane (**9**): mp 126–126.5°C. *Anal.* calcd.: C 64.45, H 7.81, N 4.18, P 9.24; found: C 64.42, H 7.68, N 4.25, P 9.34.

2-Dimethylphosphono-2-phenylaminobicyclo[2,2,1]heptane (**10**): mp 163.5–164.5°C. *Anal.* calcd.: C 61.43, H 6.87, N 4.78, P 10.56; found: C 61.31, H 7.00, N 4.64, P 10.45.

1-Dimethylphosphono-1-phenylaminocycloheptane (**11**): mp 105.5–106.5°C. *Anal.* calcd.: C 60.59, H 8.14, N 4.71, P 10.42; found: C 60.47, H 8.14, N 4.88, P 10.45.

Microanalyses were carried out by Spang Microanalytical Laboratory, Eagle Harbor, Michigan.

Acknowledgements

We thank the Natural Sciences and Engineering Research Council of Canada for generous financial support (A 6612 to G.W.B.).

1. G. W. Buchanan and C. Benezra. Can. J. Chem. **54**, 231 (1976).
2. G. W. Buchanan and F. G. Morin. Can. J. Chem. **55**, 2885 (1977).
3. G. W. Buchanan and J. H. Bowen. Can. J. Chem. **55**, 604 (1977).
4. L. Ernst. Org. Magn. Reson. **9**, 35 (1977).
5. J. B. Stothers. Carbon-13 nmr spectroscopy. Academic Press, New York, NY. 1972. p. 167.
6. R. M. Moriarty. Top. Stereochem. **8**, 273 (1974).
7. G. W. Buchanan and F. G. Morin. Can. J. Chem. **57**, 21 (1979).
8. J. Thiem, B. Meyer, and H. Paulsen. Chem. Ber. **111**, 3325 (1978).
9. H. Feltkamp, N. C. Franklin, K. D. Thomas, and W. Brugel. Ann. **683**, 64 (1965).
10. M. Christl, H. J. Reich, and J. D. Roberts. J. Am. Chem. Soc. **93**, 3463 (1971).
11. E. L. Eliel. Angew. Chem. Int. Ed. Engl. **4**, 461 (1965).
12. D. K. Dalling and D. M. Grant. J. Am. Chem. Soc. **89**, 6612 (1967).
13. F. A. L. Anet, C. H. Bradley, and G. W. Buchanan. J. Am. Chem. Soc. **93**, 258 (1971).
14. D. K. Dalling and D. M. Grant. J. Am. Chem. Soc. **94**, 5318 (1972).
15. J. A. Hirsch. Topics in stereochemistry. Vol. 2. *Edited by* E. L. Eliel and N. L. Allinger. Interscience, New York, NY. 1967. p. 215.
16. J. J. Uebel and H. W. Goodwin. J. Org. Chem. **33**, 3317 (1968).
17. G. I. Birnbaum, G. W. Buchanan, and F. G. Morin. J. Am. Chem. Soc. **99**, 6652 (1977).
18. W. McFarlane. Proc. R. Soc. London, Ser. A, **306**, 185 (1968).
19. G. W. Buchanan and B. A. Dawson. Org. Magn. Reson. In press.
20. N. S. Kozlov, V. D. Pak, and E. S. Elin. Vestsi Akad. Navuk B. SSR Ser. Khim. Navuk, (6), 78 (1969). Chem. Abstr. **72**, 100833 d (1971).
21. R. F. Hudson, R. J. G. Searle, and F. H. Devitt. J. Chem. Soc. B, 789 (1966).

Can. J. Chem. Downloaded from www.nrcresearchpress.com by 210.87.254.6 on 09/05/12
For personal use only.

Quantitative determination of tantalum in niobium by neutron activation analysis

DONALD R. SADOWAY[1] AND S. N. FLENGAS
Department of Metallurgy and Materials Science, University of Toronto, Toronto, Ont., Canada M5S 1A4
AND
R. G. V. HANCOCK
SLOWPOKE Nuclear Reactor Facility, University of Toronto, Toronto, Ont., Canada M5S 1A4

Received August 1, 1979

DONALD R. SADOWAY, S. N. FLENGAS, and R. G. V. HANCOCK. Can. J. Chem. **58**, 537 (1980).

A method was devised for the determination of Ta both in mixtures of $NbCl_5$–$TaCl_5$ and in mixtures of $ANbCl_6$–$ATaCl_6$, where A = Na, K, Rb, or Cs. The method involves neutron activation analysis of Nb_2O_5–Ta_2O_5 samples prepared by conversion of the chlorocompounds.

DONALD R. SADOWAY, S. N. FLENGAS et R. G. V. HANCOCK. Can. J. Chem. **58**, 537 (1980).

On a conçu une méthode de détermination du tantale dans les deux mélanges suivants: $NbCl_5$–$TaCl_5$ et $ANbCl_6$–$ATaCl_6$ où A = Na, K, Rb ou Cs. La méthode implique l'analyse pour l'activation de neutrons des échantillons du Nb_2O_5–Ta_2O_5 préparés par la transformation des composés chlorés.

[Traduit par le journal]

Can. J. Chem. Downloaded from www.nrcresearchpress.com by 210.87.254.40 on 09/05/12
For personal use only.

During the course of an investigation to test the proposition that it is possible to separate Ta from Nb by the reaction of vapour mixtures of $NbCl_5$–$TaCl_5$ with either solid or molten ACl, where A = Na, K, Rb, or Cs, it became necessary to devise a technique for determining the concentration of Ta both in mixtures of $NbCl_5$–$TaCl_5$ and in mixtures of $ANbCl_6$–$ATaCl_6$, where the Ta concentration ranged from 0.5 to 10 wt.% on a metal–metal basis with Nb (1). Quantitative analysis of tantalum–niobium systems is difficult by standard chemical methods. X-ray fluorescence has been used successfully under carefully controlled conditions (2–6). To avoid potential problems such as matrix effects and the high dependence on the method of sample preparation inherent in this technique neutron activation analysis was chosen for the present work.

Sample Preparation

Since the chlorocompounds of niobium and tantalum hydrolyse readily, it was necessary to convert them to a stable form, in this case their pentoxides, by adding the salt mixtures to water, boiling for 5 min, and then evaporating to dryness. The cake which formed was ground to a powder which was then added to water, boiled for 5 min, and evaporated to dryness. Prior to this second evaporation, in the analysis of $ANbCl_6$–$ATaCl_6$ mixtures only, filtration was performed to separate the alkali-metal chloride presumed to have dissolved in the water. The dried cake was ground to a powder, added to concentrated NH_4OH, and evaporated to dryness. After grinding, the product was ignited in a platinum crucible at 900°C.

X-ray powder diffraction patterns verified that the hydrolysis of the pentachlorides to the pentoxides was complete, i.e. that Nb_2O_5 and Ta_2O_5 were formed. Furthermore, to prove that the hydrolysis of $AMCl_6$ proceeded according to the reaction

$$[1] \quad 2AMCl_6 + 5H_2O \rightarrow M_2O_5 + 10HCl + 2ACl$$

the filtrate, which was assumed to contain dissolved ACl, was evaporated to dryness. The X-ray powder pattern of the dried filtrate was identified as that of ACl in each case.

A reliable procedure for sample preparation having been established, a set of standards spanning the range 0.1 < wt.% Ta < 10 was made. First, large quantities of $NbCl_5$ and $TaCl_5$ were hydrolysed separately to make Nb_2O_5 and Ta_2O_5. The materials were screened through a 200 mesh sieve, and the appropriate amounts were mixed by a novel technique. Campbell and Carl (3) and Mitchell (4) have reported that mixed Ta_2O_5–Nb_2O_5 samples can be prepared by co-precipitation from hydrofluoric acid solutions. In this laboratory the oxides were found to be extremely difficult to dissolve, an observation made also by Campbell and Carl (3). A different method was used to mix the oxides.

The two powders were put into a 600 mL beaker containing approximately 300 mL of water. The water was heated to a violent boil and for about 10 min was stirred with a glass rod. The water was evaporated, and the powder was passed again through a 200 mesh sieve. Samples of the same nominal composition, some having been prepared by co-precipitation and others "wet mixed", were compared by neutron activation analysis. Results were within limits of statistical error of one another. As well, several samples from the same batch of wet-mixed material were analyzed to determine if the particle distribution was random. Again, the results agreed within statistical limits of error.

Results

The powdered samples weighed approximately 300 mg and were contained in polyethylene vials. They were irradiated in the SLOWPOKE nuclear reactor at this university in a neutron flux of 1.0×10^{11} n/cm^2 s for 60 s. After a decay time of 60 s the irradiated samples were counted for 300 s. Thus, the total time to analyze a sample was 7 min. Mea-

[1]Present address: Department of Materials Science and Engineering, Massachusetts Institute of Technology, Cambridge, MA 02139, U.S.A.

0008-4042/80/050537-02$01.00/0
©1980 National Research Council of Canada/Conseil national de recherches du Canada

surements of γ-ray activities were made with a Canberra Ge(Li) detector coupled through a 452 Ortec spectroscopy amplifier to an 8100 series, 4096 channel Canberra analyzer. The detector has a nominal relative counting efficiency of 6.7% and a FWHM resolution of 1.9 keV for the 1332 keV γ-ray of ^{60}Co. γ-Ray peak intensities were evaluated by automatic analyzer integration of suitable manually selected spectral regions of interest at and near each peak.

Every time a set of samples was measured, the entire set of standards was also irradiated. While both Nb and Ta were counted, the Nb results were not found to be useful. Below about 3 wt.% Ta there was no discernible trend in the Nb results. Although self absorption effects in samples high in Ta give rise to curvature in the calibration curve, the measurements of the standards were best represented for our purposes by two least-squares lines, one for Ta concentrations less than 4 wt.% and one for Ta concentrations between 4 wt.% and 10 wt.%. The elemental Ta content of a sample was determined by comparison with the standard line recorded on the same day.

Typical results are the following. In the range, $0 < \text{wt.\% Ta} < 4$,

$$[2] \quad \text{wt.\% Ta} = -(0.20 \pm 0.07) + (117 \pm 3) \times 10^{-6} n$$

where n represents the number of counts $s^{-1}\,g^{-1}$ of oxide sample. The correlation coefficient[2] was $r = 0.9986$, and standard error of estimate was $\hat{S}_{y,x} = 0.08$. In the range $4 < \text{wt.\% Ta} < 10$,

$$[3] \quad \text{wt.\% Ta} = -1.07 \pm 0.24 + (142 \pm 4) \times 10^{-6} n$$

The correlation coefficient was $r = 0.9996$, and the standard error of estimate was $\hat{S}_{y,x} = 0.12$.

The corresponding amount of Ta_2O_5 present in the sample was then calculated, and the difference between this and the total mass of the sample was presumed to be the mass of Nb_2O_5. From the latter figure the mass of elemental Nb was calculated. Finally, the Ta concentration was reported as wt.% Ta in Ta–Nb metal. It has an absolute error of estimate of less than 0.1 wt.% over the range of interest. The lower limit of detection for this method using samples such as these described herein was determined to be 330 ppm Ta in Nb on a metal–metal basis (8).

This method is accurate provided that the sample consists of only Nb_2O_5–Ta_2O_5. As a precaution, then, the entire γ spectrum of each sample was scanned to detect the presence of any other metals. In samples prepared from the pentachloride mixtures of $NbCl_5$–$TaCl_5$ only Ta and Nb were found. However, samples prepared from $ANbCl_6$–$ATaCl_6$ mixtures contained small but measurable amounts of alkali metal representing less than 5% of the total mass of the sample. Since the chlorine content was below the lower limit of detection which was approximately 100 μg in those samples, it was concluded that the alkali metal was not present in the form of its chloride. So, it was assumed that the alkali metal was present as oxide or, more likely, niobate or tantalate, and the appropriate correction was made to the Ta concentration reported. Table 1 shows the isotope which was measured for each element. For tantalum both the tabulated γ-ray peaks were routinely counted. With the spectrometer employed, the 172 keV peak was approximately 25% greater than that at 147 keV, and the bremsstrahlung in the region of the former is approximately 30% weaker. Indeed, the results for the peak at 172 keV proved to be more reproducible and, thus, were favoured in the quantitative determination of tantalum.

TABLE 1. Nuclear data for sample analysis (7)

Element	Isotope measured	Half-life	γ-ray (keV)
Nb	^{94m}Nb	6.6 min	871.1
Ta	^{182m}Ta	16.2 min	146.7, 171.7
Na	^{24}Na	15 h	1368.4
K	^{42}K	12.52 h	1524.7
Rb	^{86m}Rb	1.02 min	555.8
Cs	^{131m}Cs	3.15 h	127.4
Cl	^{38}Cl	37.29 min	1642.0

Acknowledgement

The financial assistance to one of the authors (D.R.S.) by the National Research Council of Canada in the form of a Postgraduate Scholarship is gratefully acknowledged.

1. D. R. SADOWAY and S. N. FLENGAS. Met. Trans. B. In press.
2. L. S. BIRKS and E. J. BROOKS. Anal. Chem. **22**, 1017 (1950).
3. W. J. CAMPBELL and H. F. CARL. Anal. Chem. **28**, 960 (1956).
4. B. J. MITCHELL. Anal. Chem. **30**, 1895 (1958).
5. B. J. MITCHELL. Anal. Chem. **32**, 1652 (1960).
6. C. H. MUENDEL and R. A. ROWE. Purification of columbium pentachloride by distillation. *In* The design of metal producing processes. *Edited by* R. M. Kibby. AIME, New York. 1969. pp. 287, 288.
7. F. ADAMS and R. DAMS. J. Radioanal. Chem. **3**, 99 (1969).
8. R. JENKINS and J. L. DEVRIES. Practical X-ray spectrometry. Springer-Verlag, New York. 1967.

[2]Correlation coefficients are determined to the 67% confidence level.

Can. J. Chem. Downloaded from www.nrcresearchpress.com by 210.87.254.40 on 09/05/12
For personal use only.

The phase diagrams of the chlorides of the metals of Groups IIa and IIb with indium trichloride and water at 24°C

ELINOR M. KARTZMARK

Department of Chemistry, University of Manitoba, Winnipeg, Man., Canada R3T 2N2

Received September 12, 1979

ELINOR M. KARTZMARK. Can. J. Chem. **58**, 539 (1980).

The double salt formation between indium chloride and the chlorides of Groups IIa and IIb has been investigated, and a comparison is made with the double salts of the Group I chlorides and indium trichloride. Three double salts of formula $2BeCl_2 \cdot InCl_3 \cdot (4–5)H_2O$, $MgCl_2 \cdot InCl_3 \cdot (6–8)H_2O$, and $CaCl_2 \cdot InCl_3 \cdot 7H_2O$ were found. The phase diagrams of the chlorides of Groups IIa and IIb with indium trichloride and water prove that the double salts $MgCl_2 \cdot 2InCl_3 \cdot 10H_2O$, $2MgCl_2 \cdot InCl_3 \cdot 12H_2O$, $CaCl_2 \cdot 2InCl_3 \cdot 12H_2O$, $3CaCl_2 \cdot 4InCl_3 \cdot 30H_2O$, $SrCl_2 \cdot 2InCl_3 \cdot 8H_2O$, $SrCl_2 \cdot InCl_3 \cdot 8H_2O$, $ZnCl_2 \cdot 2InCl_3 \cdot 8H_2O$, and $2ZnCl_2 \cdot InCl_3 \cdot 5H_2O$ reported by Ensslin *et al.* (1) and recorded in Solubility of inorganic and metal organic compounds by Linke and Seidell (2) do not exist.

ELINOR M. KARTZMARK. Can. J. Chem. **58**, 539 (1980).

On a étudie la formation des sels doubles entre le chlorure d'indium et les chlorures des groupes IIa et IIb et on les a comparé aux chlorures doubles d'indium et des éléments du groupe I. On a trouvé trois sels doubles de formule $2BeCl_2 \cdot InCl_3 \cdot (4–5)H_2O$, $MgCl_2 \cdot InCl_3 \cdot (6–8)H_2O$ et $CaCl_2 \cdot InCl_3 \cdot 7H_2O$. Quant aux sels suivants $MgCl_2 \cdot 2InCl_3 \cdot 10H_2O$, $2MgCl_2 \cdot InCl_3 \cdot 12H_2O$, $CaCl_2 \cdot 2InCl_3 \cdot 12H_2O$, $3CaCl_2 \cdot 4InCl_3 \cdot 30H_2O$, $SrCl_2 \cdot 2InCl_3 \cdot 8H_2O$, $SrCl_2 \cdot InCl_3 \cdot 8H_2O$, $ZnCl_2 \cdot 2InCl_3 \cdot 8H_2O$ et $2ZnCl_2 \cdot InCl_3 \cdot 5H_2O$ rapportés par Ensslin *et al.* (1) et répertorés dans "Solubilité des composés inorganiques et organométalliques" de Linke et Seidell (2), les diagrammes de phase des chlorures doubles hydratés d'indium et des éléments du groupe IIa et IIB prouvent qu'ils n'existent pas.

[Traduit par le journal]

Introduction

In this paper the solubilities of indium trichloride together with the chlorides of the Group II metals in water were studied, with a view to determining the formulae of any double salts. In a previous paper (3) it was reported that all of the Group Ia metal chlorides, except sodium chloride, form one or more double salts with indium trichloride. Most of the studies in this area were done by Ensslin *et al.* (1) who reported many double salts with the general formula: $xMeCl_2 \cdot yInCl_3 \cdot zH_2O$ where x, y, z have values shown in Table 1.

The experimental technique of these studies was not such as would guarantee equilibrium; it was merely to analyse the wet residue, without reference to the solution, and did not ensure the nature of the solid phase. It seemed of interest to determine the complete phase diagrams and to compare double salt formation of the Group II chlorides with that of the chlorides of Group I. The phase diagram for the system hydrogen chloride – indium chloride – water, was also determined as completely as possible to round out the Group I series.

TABLE 1. Formulas of double salts of indium trichloride reported by Ensslin *et al.* (1) ($xMeCl_2 \cdot yInCl_3 \cdot zH_2O$)

Me	x	y	z	Me	x	y	z
Mg	1	2	10*	Sr	1	2	8*
	1	1	7		1	1	8*
	2	1	12*	Zn	1	2	8*
Ca	1	2	12*		2	1	5*
	3	4	30*				
	1	1	8				

*As shown in text, these double salts do not exist.

Experimental Method

All chemicals were of "Reagent" grade and were used without further purification. The closed solubility system was stirred for 2 or 3 days with a magnetic stirrer and separation of the solid phase was done with a centrifuge. (The saturated solutions in all of these systems were very viscous, making ordinary filtration impossible.) The saturated mother liquors and the wet solids were analysed and plotted. Ideally, tie-lines drawn through a series of such points intersect at a point corresponding to the pure solid phase. If, however, the wet solid has much mother liquor adhering its composition lies on the tie-line very close to the saturated solution end, and errors in extrapolation to the point of intersection result. For this reason, the wet residue was placed between pads of filter paper and subjected to hydraulic pressure (2000 psi) so as to remove as much mother liquor as possible without evaporation of water. The solids so obtained had compositions which plotted on tie-lines very close to the pure solid phase, thus minimizing error.

Methods of Analysis

The System $HCl–InCl_3–H_2O$

Anhydrous indium chloride was added to concentrated hydrochloric acid and the system stirred for 48 h. A white crystalline solid separated. To obtain a solution as high in hydrogen chloride as possible, dry hydrogen chloride gas was bubbled through the solution; the system was then closed and stirred overnight. The phases were separated by centrifuging and analysed gravimetrically for chloride as silver chloride and for indium as indium oxide, by precipitating with ammonia.

0008-4042/80/050539-07$01.00/0

©1980 National Research Council of Canada/Conseil national de recherches du Canada

Can. J. Chem. Downloaded from www.nrcresearchpress.com by 210.87.254.40 on 09/05/12
For personal use only.

Can. J. Chem. Downloaded from www.nrcresearchpress.com by 210.87.254.40 on 09/05/12
For personal use only.

The System $BeCl_2$–$InCl_3$–H_2O

Attempts to determine the solubility of beryllium chloride were complicated by its reactivity with water according to a reaction proposed by Sidgwick and Lewis (4):

$$BeCl_2 + H_2O \rightleftharpoons Be(OH)Cl + HCl$$

Because of the evolution of HCl, estimation of beryllium chloride by chloride determination gave a low result of 42.9%, which is comparable with that of Blidin (5), 41.72%. Precipitation of Be^{2+} as beryllium oxide gave a value of 51.7% but, since the solid with which the saturated solution was in equilibrium is undoubtedly a mixture of $BeCl_2 \cdot xH_2O$ and BeO, neither of these values can be considered to be the true solubility. The formula of the hydrate is undefined: Everest (6) states that evaporation of a saturated aqueous beryllium chloride solution gives a hygroscopic solid, usually formulated as the tetrahydrate but the actual composition approaches $BeCl_2 \cdot 4.5H_2O$. It is a complex structure of close-packed layers of dihydrate with interstitial water between the layers.

Because of these difficulties which persist in systems containing low concentrations of indium chloride it was decided to work with larger proportions of indium chloride with a view to obtaining double salts. The method of analysis consisted in determining total oxide, i.e. BeO + In_2O_3, by addition of ammonia. In^{3+} was estimated by precipitation as In_2S_3, using gaseous H_2S. The Be^{2+} was obtained by difference. A great many systems were prepared yielding intersecting tie-lines, which established the salt ratio in the double salt, and the hydration with an uncertainty of one water molecule.

The System $MgCl_2$–$InCl_3$–H_2O

In^{3+} was estimated as In_2O_3 (by addition of ammonia and ammonium chloride); under these conditions Mg^{2+} remains in solution. To remove adsorbed Mg^{2+}, the gelatinous $In(OH)_3$ was dissolved in hydrochloric acid, reprecipitated, filtered, washed, and ignited to In_2O_3. Chloride was estimated as silver chloride and Mg^{2+} was calculated by difference. The same method of analysis was followed in the systems $SrCl_2$–$InCl_3$–H_2O, $BaCl_2$–$InCl_3$–H_2O, and $ZnCl_2$–$InCl_3$–H_2O.

The System $CaCl_2$–$InCl_3$–H_2O

In an earlier paper (7), a double salt with salt ratio of 6:5 was reported. In view of the simple formula of all other double salts in Groups I and II, as given in Table 2, it seemed appropriate to examine this system again, specifically to subject the solid phase to pressure removal of mother liquor.

TABLE 2. Double salts of indium trichloride with the chlorides of Groups Ia, IIa, and IIb

Ion	Formula of double salt
H^+	$HCl \cdot InCl_3 \cdot 3H_2O$
NH_4^+	$2NH_4Cl \cdot InCl_3 \cdot H_2O$
Li^+	$3\,LiCl \cdot InCl_3 \cdot 8H_2O$
Na^+	—
K^+	$3\,KCl \cdot InCl_3 \cdot H_2O$ $2\,KCl \cdot InCl_3 \cdot H_2O$
Rb^+	$2\,RbCl \cdot InCl_3 \cdot H_2O$
Cs^+	$2\,CsCl \cdot InCl_3 \cdot H_2O$
Be^{2+}	$2\,BeCl_2 \cdot InCl_3 \cdot (4\text{ to }5)H_2O$
Mg^{2+}	$MgCl_2 \cdot InCl_3 \cdot (6\text{ to }8)H_2O$
Ca^{2+}	$CaCl_2 \cdot InCl_3 \cdot 7H_2O$
Sr^{2+}	—
Ba^{2+}	—
Zn^{2+}	—
Cd^{2+}	—
Hg^{2+}	—

The System $CdCl_2$–$InCl_3$–H_2O

The analysis of this system follows the method of Dennis and Bridgman (8), in which Cd^{2+} is held in solution by the presence of ammonium chloride and the maintenance of very high pH using 25% sodium hydroxide solution as precipitant of the In^{3+}.

The System $HgCl_2$–$InCl_3$–H_2O

Hg^{2+} was precipitated as mercuric sulphide in the presence of sulphuric acid. The solid was filtered through a sintered glass crucible, washed with water, and dried at low temperature. To remove sulphur, it was refluxed with freshly distilled carbon disulphide and dried at 120°C. The filtrate was analysed for chloride as silver chloride. Mercuric ion must be removed before the precipitation of silver chloride, because of complex formation, as is well known. In^{3+} was obtained by difference except in systems low in In^{3+}, where it was determined directly as In_2O_3.

Discussion

The phase diagrams resulting from the solubility data[1] and analyses of wet solids are given in Figs. 1 to 8. The compositions of wet solids have been plotted as open squares on the tie-lines and are found to lie very close to the compositions of the pure solid phase in most of the diagrams. Where they do not, there is some question as to the degree of hydration of the double salt (Figs. 2 and 3) and this has been indicated by a solid bar on the diagram.

In the system HCl–$InCl_3$–H_2O, only three solubility systems were studied but these were sufficient to prove the existence of the double salt, $HCl \cdot InCl_3 \cdot 3H_2O$, as shown in Fig. 1. The compositions of two of the wet solids are so close to that of the double salt that they do not show on the diagram. No attempt was made to obtain the invariant system with $InCl_3 \cdot 4H_2O$ and double salt as solid phases. The rest of the solubility curve of the double salt is unobtainable at ordinary pressures.

As with Fig. 1, Fig. 2 is a partial phase diagram for the system $BeCl_2$–$InCl_3$–H_2O, the beryllium chloride side being unattainable because of hydrolysis. The ternary solubility point with 42% beryllium chloride is probably in error for the same reason. The remaining five systems "intersect" the line joining H_2O to $2BeCl_2 \cdot InCl_3$, over a range of hydration corresponding to from 4 to 5 mol of water. The double salt, then, has formula $2BeCl_2 \cdot InCl_3 \cdot (4\text{ to }5)H_2O$.

Figure 3 shows a double salt in the system $MgCl_2$–$InCl_3$–H_2O with a 1:1 salt ratio and a range of hydration of from 6 to 8 mol of water. The wet solid point containing 34.3% $MgCl_2$ and 33.2% $InCl_3$ which is in equilibrium with the invariant

[1]Experimental data are available, at a nominal charge, from the Depository of Unpublished Data, CISTI, National Research Council of Canada, Ottawa, Ont., Canada K1A 0S2.

Can. J. Chem. Downloaded from www.nrcresearchpress.com by 210.87.254.40 on 09/05/12
For personal use only.

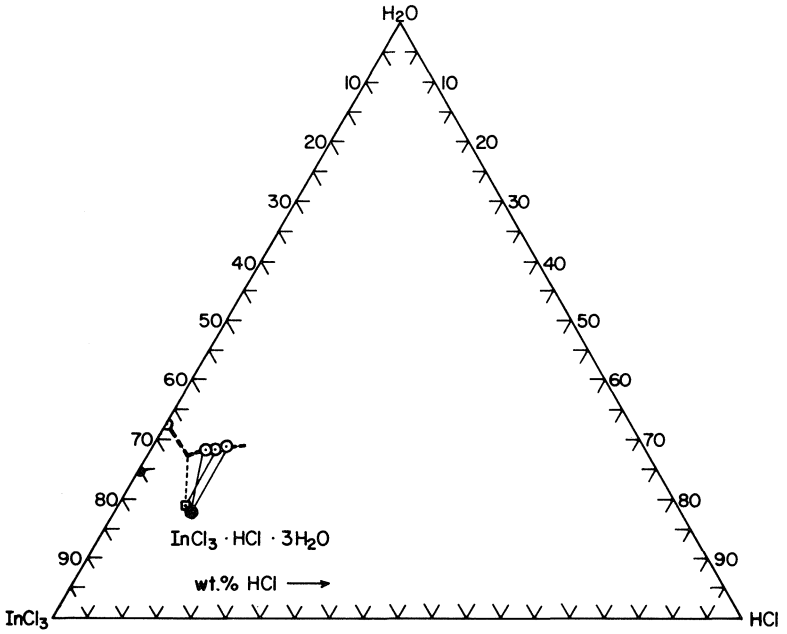


FIG. 1. The system $InCl_3$–H_2O at 24°C.

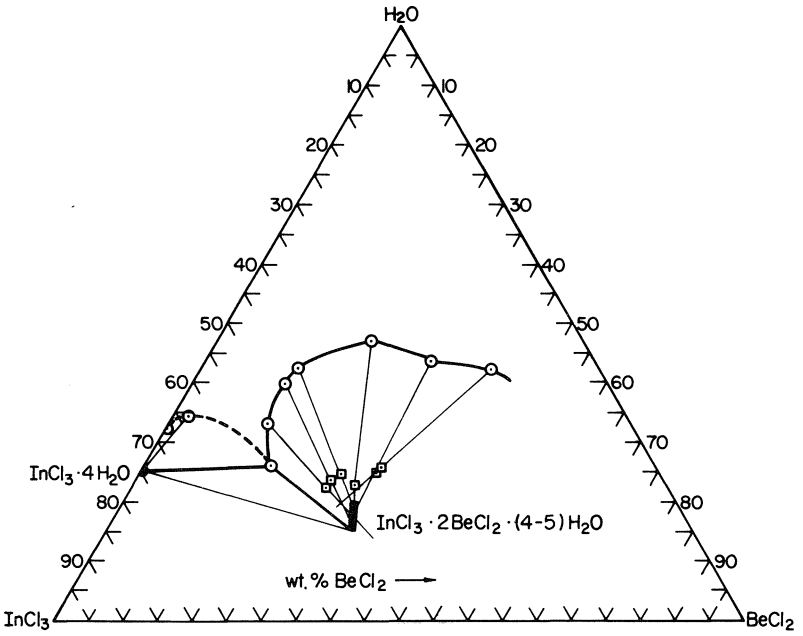


FIG. 2. The system $InCl_3$–$BeCl_2$–H_2O at 24°C.

solution 26.3% $MgCl_2$ and 28.8% $InCl_3$ lies outside of the invariant triangle for double salt and $MgCl_2 \cdot 6H_2O$ and is therefore in error: probably the result of loss of water.

The phase diagram for the system $CaCl_2$–$InCl_3$–H_2O has not been included in this paper; it is identical with that given in a former paper (7) except that the more accurate analysis of the wet solid yielded tie-lines intersecting at $CaCl_2 \cdot InCl_3 \cdot 7H_2O$.

There is no double salt in the system $SrCl_2$–$InCl_3$–H_2O, as shown in Fig. 4. The third field in the phase diagram results from the partial dehydration of $SrCl_2 \cdot 6H_2O$ to the dihydrate. This reaction occurs at 61.4°C in the absence of indium chloride, as reported in the $SrCl_2$–H_2O system by

Can. J. Chem. Downloaded from www.nrcresearchpress.com by 210.87.254.40 on 09/05/12
For personal use only.

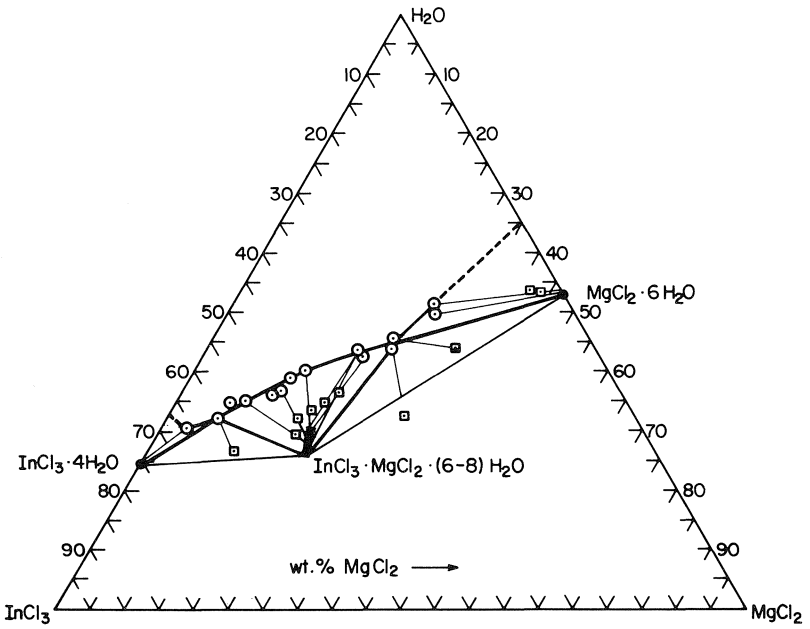


FIG. 3. The system $InCl_3$–$MgCl_2$–H_2O at 24°C.

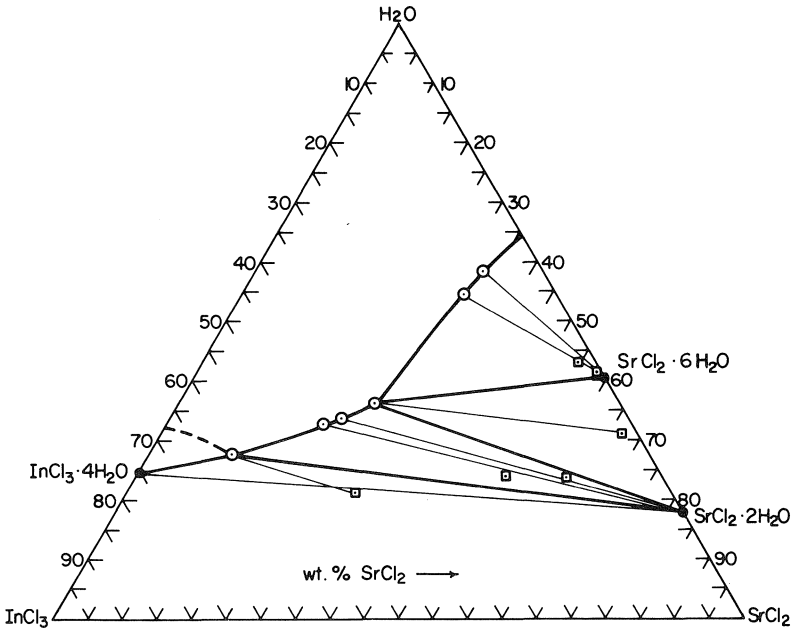


FIG. 4. The system $InCl_3$–$SrCl_2$–H_2O at 24°C.

Menzies (9). Further dehydration to the anhydrous salt occurs at a much higher temperature and thus does not take place at 24°C under the influence of indium trichloride.

In the phase diagram for the system $BaCl_2$–$InCl_3$–H_2O, shown in Fig. 5, it is proven that no double salt exists. The major field of the diagram is occupied by $BaCl_2 \cdot 2H_2O$, which is not dehydrated by indium chloride at 24°C.

The systems involving Group IIb metal chlorides do not produce double salts with indium trichloride, as is shown in Figs. 6, 7, and 8. The notable feature of the $ZnCl_2$–$InCl_3$–H_2O diagram, Fig. 6, is the fact that the invariant solution contains more than 50% zinc chloride. This is very unusual as is attested to by all of the other figures, where the invariant solution associated with $InCl_3 \cdot 4H_2O$ rarely contains more than 10% of the second com-

Can. J. Chem. Downloaded from www.nrcresearchpress.com by 210.87.254.40 on 09/05/12
For personal use only.

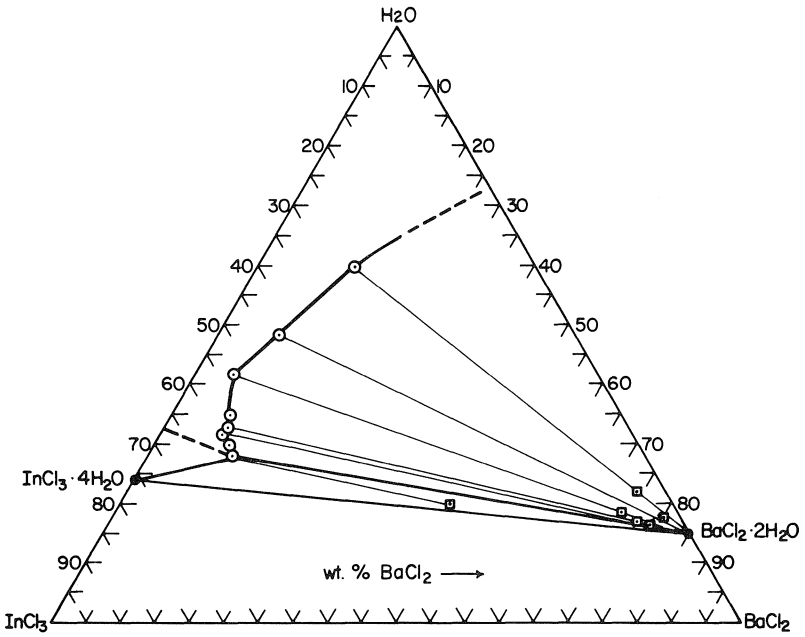


FIG. 5. The system $InCl_3$–$BaCl_2$–H_2O at 24°C.

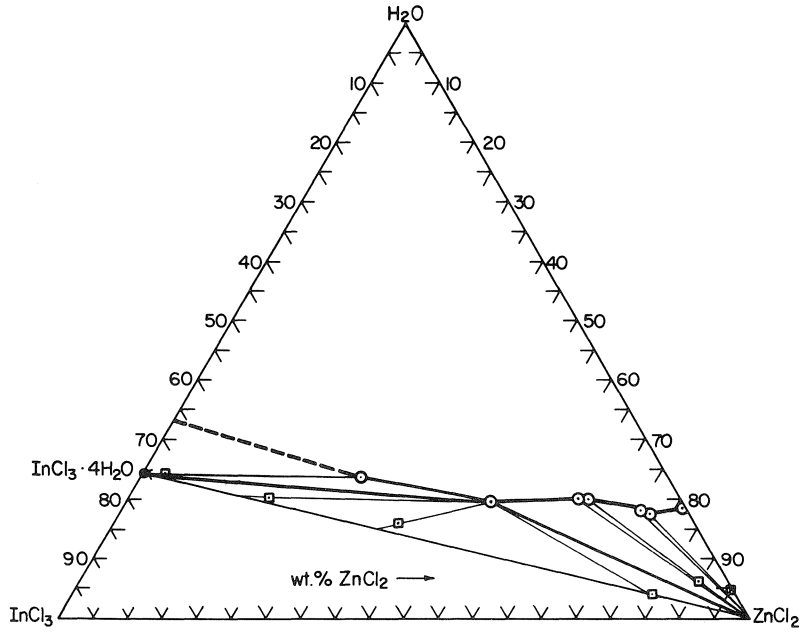


FIG. 6. The system $InCl_3$–$ZnCl_2$–H_2O at 24°C.

ponent. The behaviour in the $ZnCl_2$ system is possibly owing to the extremely high solubility of zinc chloride.

The solubility of cadmium chloride in water is reported in Linke's book Solubility of inorganic and metal organic compounds (2) as 54.65% at 25°C, the solid phase being $CdCl_2 \cdot 2\frac{1}{2}H_2O$. At 33.8°C the transition to the monohydrate occurs. The dehydration of $CdCl_2 \cdot 2\frac{1}{2}H_2O$ takes place at a lower temperature in the presence of indium trichloride; a large field of stability of the monohydrate occurs in the phase diagram at 24°C, as shown in Fig. 7. Finally, the system $HgCl_2$–$InCl_3$–H_2O, while it has no double salt, as proven in Fig. 8, is very interesting because it shows a sevenfold increase in the solubility of mercuric chloride, owing to the presence of 20% $InCl_3$. The $HgCl_2$ (s) field occupies the major portion of the diagram. This

Can. J. Chem. Downloaded from www.nrcresearchpress.com by 210.87.254.40 on 09/05/12
For personal use only.

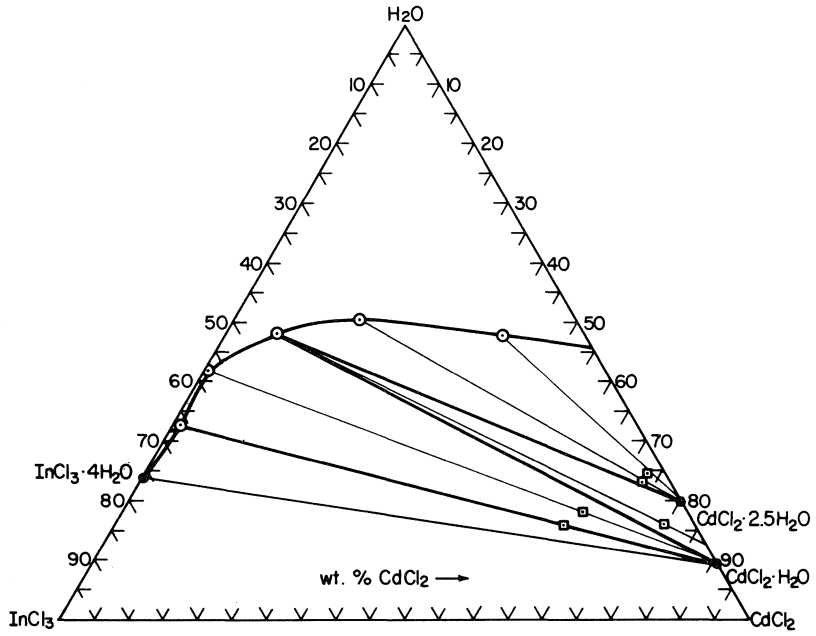


FIG. 7. The system $InCl_3$–$CdCl_2$–H_2O at 24°C.

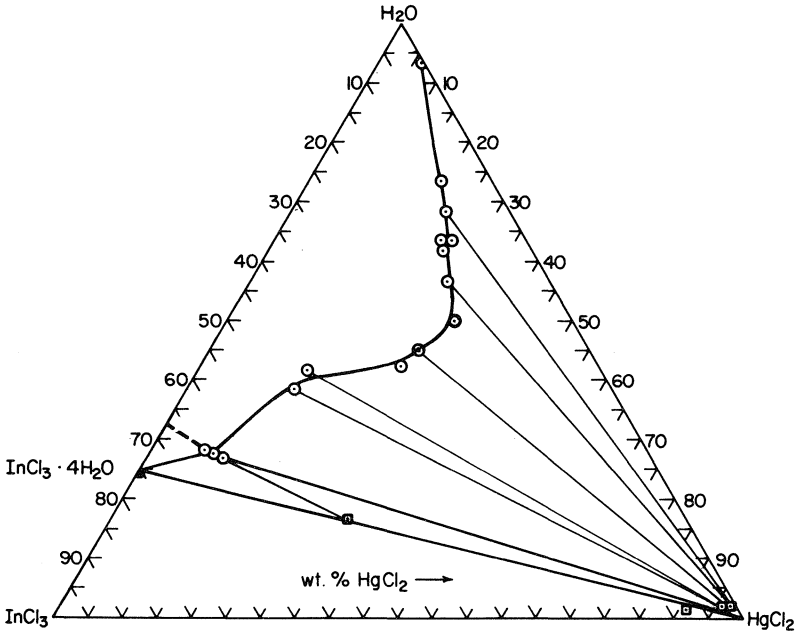


FIG. 8. The system $InCl_3$–$HgCl_2$–H_2O at 24°C.

increase in the solubility of mercuric chloride, which occurs also in the system HCl–$HgCl_2$–H_2O investigated by Thomas (10), may be due to complex ion formation in the solution. Nevertheless, the solid phase is anhydrous $HgCl_2$.

In conclusion, a summary of double salt formation between indium chloride and the chlorides of hydrogen, ammonium, and the metals of Groups Ia, IIa, and IIb are given in Table 2. All the double salts are congruently saturating.

The compositions of these ternary compounds have been reported in the usual way as double salts. Some, or all of them, may be salts containing the chloroindate anion. However, a phase rule study cannot decide this point.

Of immediate note in Table 2 is the absence of

eight double salts claimed by Ensslin *et al.* (2), viz. those marked * in Table 1. These systems are reported in Linke along with similar work on indium fluoride, indium iodide, and indium iodate, by the same author. It is questionable whether the several double salts reported in the latter systems have any validity either.

Among the chlorides of Group I, sodium chloride is the only one which does not form a double salt with indium trichloride. Indeed, sodium chloride forms few double salts with other chlorides. Exceptions reported in Linke are $Na_2PtCl_6 \cdot 5H_2O$ and $HgCl_2 \cdot NaCl \cdot 2H_2O$. Salt deposits formed by the evaporation of sea water (containing the ions Na^+, K^+, Mg^{2+}, Cl^-, and SO_4^{2-}) contain sodium chloride as the simple salt, while potassium chloride and magnesium chloride exist as double salts.

It is interesting to compare aluminum chloride, ferric chloride, and indium chloride with regard to double salt formation with other chlorides, as far as these are known. In the case of aluminum chloride, the only system reported by Linke is that with potassium chloride and in this case there is no double salt. On the other hand, however, ferric chloride shows a close correspondence with indium chloride, in that there is no double salt with sodium chloride, but one, and in the case of cesium chloride, two, double salts with the other Group I type ions.

The chlorides of Be, Mg, and Ca each form a double salt with indium trichloride. Strontium chloride and barium chloride do not form double salts with indium trichloride and neither do the chlorides of Group IIb. That mercuric chloride does not form a double salt with indium chloride is surprising, since it forms many double salts with the chlorides of Group I and Group II. Ferric chloride has not been studied as to its behaviour with the chlorides of Group II, so no comparison is possible.

1. F. Ensslin, B. Ziemeck, and L. de Schaepdryver. Z. Anorg. Chem. **254**, 293 (1947).
2. W. F. Linke and A. Seidell. Solubility of inorganic and metal organic compounds. Vol. 1. 4th ed. Am. Chem. Soc. Washington. 1958. p. 711.
3. E. M. Kartzmark. Can. J. Chem. **55**, 2792 (1977).
4. N. V. Sidgwick amd N. B. Lewis. J. Chem. Soc. 1296 (1926).
5. V. P. Blidin. Dokl. Akad. Nauk SSSR, **84**, 947 (1952).
6. D. A. Everest. Comprehensive inorganic chemistry. 1st ed. *Edited by* J. C. Bailar *et al.* Pergamon Press, New York. 1973. p. 552.
7. E. M. Kartzmark. Can. J. Chem. **52**, 3459 (1974).
8. L. M. Dennis and J. A. Bridgman. J. Am. Chem. Soc. **40**, 1556 (1918).
9. A. W. C. Menzies. J. Am. Chem. Soc. **58**, 934 (1936).
10. H. C. Thomas. J. Am. Chem. Soc. **61**, 1921 (1939).

Can. J. Chem. Downloaded from www.nrcresearchpress.com by 210.87.254.40 on 09/05/12
For personal use only.

Canadian Journal of Chemistry
Published by
THE NATIONAL RESEARCH COUNCIL OF CANADA

Journal canadien de chimie
Publié par
LE CONSEIL NATIONAL DE RECHERCHES DU CANADA

Volume 58 Number 6 March 15, 1980 Volume 58 numéro 6 15 mars 1980

Can. J. Chem. Downloaded from www.nrcresearchpress.com by 210.87.254.40 on 09/05/12
For personal use only.

Organocation speciation. I. A comparison of the interactions of methylene blue and paraquat with bentonite and humic acid

R. D. GUY,[1] D. R. NARINE, AND S. DESILVA
Trace Analysis Research Centre, Department of Chemistry, Dalhousie University, Halifax, N.S., Canada B3H 4J1

Received July 27, 1979

R. D. GUY, D. R. NARINE, and S. DESILVA. Can. J. Chem. **58**, 547 (1980).

A model system composed of bentonite, humic acid (HA), polystyrene sulphonic acid (PSSA), methylene blue (MB), and paraquat was used to characterize the possible interactions of organocations in natural waters. The adsorption and desorption studies with bentonite indicated that the clay had a strong preference for the organocations over alkali and alkaline earth cations. Paraquat saturated the bentonite up to the cation exchange capacity whereas methylene blue did not completely saturate the clay but did form methylene blue aggregates on the clay surface. The aggregates could be readily removed by washing with distilled water. The organocation interactions with the anionic polyelectrolytes were more susceptible to changes in pH or ionic strength. Paraquat could be completely desorbed from HA and PSSA by raising the solution ionic strength to 0.1. Methylene blue could not be completely removed from the humic acid but could be removed from PSSA by raising the ionic strength to 0.1. The studies indicate that a combination of dialysis separations, variation of ionic strength, and spectrophotometric analysis could be used to determine the free paraquat and the bound paraquat susceptible to changes in environmental levels of pH and ionic strength.

R. D. GUY, D. R. NARINE et S. DESILVA. Can. J. Chem. **58**, 547 (1980).

Nous avons utilisé un système composé de bentonite, d'acide humique (AH), d'acide polystyrène sulfonique (APSS), de bleu de méthylène (BM) et de paraquat afin de caractériser les interactions possibles des organocations dans les eaux naturelles. Les études d'adsorption et de désorption avec la bentonite indiquent que l'argile préfère de beaucoup les organocations aux cations des terres alcalines. Le paraquat sature la bentonite jusqu'à la capacité d'échange des cations alors que le bleu de méthylène ne le sature pas complètement mais forme des agrégats de bleu de méthylène à la surface de l'argile. Les agrégats peuvent être facilement enlevés par lavage à l'eau distillée. Les interactions entre les organocations et les polyélectrolytes anioniques sont plus susceptibles de varier selon la force ionique ou le pH. Le paraquat peut être complètement désorbé du AH ou du APSS en augmentant la force ionique de la solution à 0.1. Le bleu de méthylène ne peut être enlevé complètement de l'acide humique; dans le cas du APSS on peut toutefois l'enlever en augmentant la force ionique à 0.1. Les études indiquent qu'on peut utiliser une combinaison de séparation par dialyse, de variation de la force ionique et d'analyse spectrophotométrique, pour déterminer le paraquat sous forme libre ou combinée susceptible de changer dans des milieux de différents pH ou de force ionique.

[Traduit par le journal]

Introduction

The chemical interactions of organic compounds in the environment play an important role in the transport and persistence of the chemicals. The interactions also determine the ultimate biological activity of the toxic compounds. The concentration of a compound in an aquatic system will be determined by the rate of addition from the external environment, the rates of chemical, photochemical, and microbial decomposition, and the adsorption of the compound onto sedimentary and colloidal material. The partition of a chemical among soluble, colloidal, and particulate species plays a vital role in the toxicity of organic herbicides. Gillott *et al.* (1) have shown that the presence of sediment in test systems significantly reduces the toxicity of carbaryl and abate to algae. Guy and Narine (2) have shown that clay and colloidal humic substances reduce the toxicity of paraquat to algae. Other workers have indicated that herbicides in aquatic systems are associated with inorganic colloids (3), associated with dissolved and particulate humic substances (4), and dissolved in lipid coatings on particulates (5) and in biotic material. Since the role of adsorption reactions in environmental systems is so important it is necessary to develop

[1]Author to whom correspondence should be addressed.

0008-4042/80/060547-08$01.00/0
©1980 National Research Council of Canada/Conseil national de recherches du Canada

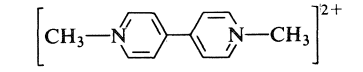
Can. J. Chem. Downloaded from www.nrcresearchpress.com by 210.87.254.40 on 09/05/12
For personal use only.

analytical methods for the speciation of organics in water systems.

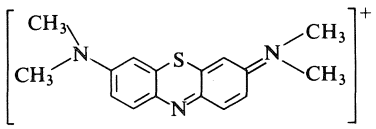
Most work reported in the literature (6–8) has been concerned with the speciation of metal ions. One problem illustrated by the metal speciation studies is that the interpretation of the analytical response is often difficult. To overcome this problem Guy *et al.* (9, 10) have proposed that metal speciation schemes be developed using a chemical model approach. The first step in a model study is to characterize the physicochemical properties of cations in clay and humic colloid systems. The second step in this approach is to use the model system to test methods of speciation and correlate the analytical response with the physicochemical properties of the system. The purpose of this paper is to describe a model system suitable for testing the speciation of organic cations in fresh and marine waters.

Model Background

A viable model system should include organocations, dissolved inorganic salts, particulate matter, and dissolved organic material. Two organic cations are included in the model: 1,1′-dimethyl-4,4′-bipyridinium dichloride (**1**) (methyl viologen or paraquat), and methylene blue (MB, **2**).



1



2

Paraquat is included in the model because of its use as a herbicide. Methylene blue is included in the model to illustrate the relationships between the interaction of the cation with particulates and the charge and hydrophobic character of the organocation. Other reasons for the inclusion of methylene blue in the study are the demonstrated toxicity of the dye to algae (2), the extensive use of the dye as a method of evaluating cation exchange capacities of clays (11), and the significant body of literature describing the dye interactions with anionic polyelectrolytes (12–14).

Bentonite and humic acid (HA) are included in the model to represent suspended particulates and dissolved organic matter, respectively. The literature available describing the interactions between paraquat and soil colloids is voluminous (15–23). The principal conclusions reported in the literature are:

(*i*) The paraquat interaction with clay is an ion exchange reaction. Montmorillonite has a strong preference for paraquat and little paraquat (< 10%) is desorbed in the presence of a 1000-fold excess of Ba^{2+} (18).

(*ii*) Paraquat interacts with humic colloids using an ion exchange reaction. Calderbank and Tomlinson (24) have shown that the amount of paraquat adsorbed is inversely proportional to the stability of the metal cation – humic acid complex in the presence of a number of metal cations. Khan (16) has suggested that charge transfer may also be involved in the interaction between paraquat and humic acid.

A number of workers (25–28) have studied the interactions of methylene blue with clays. The results of these studies can be summarized as follows: the adsorption consists of two interactions, an ion exchange reaction and a physical adsorption reaction (25), and the methylene blue can be readily exchanged using alkaline earth cations.

Little work has been published on the interactions of methylene blue with humic substances. A number of papers (12–14) have been published on the interactions between dyes and synthetic polyelectrolytes. These investigations indicate that the interactions are very dependent on ionic strength and at high coverages adsorbed dye – soluble dye interactions are present. Polystyrene sulphonic acid (PSSA) has been included in the model studies so that a comparison can be made between cation interactions with HA and a well-characterized polyelectrolyte.

This paper describes the characterization of the organocations, bentonite, and humic acid model system at different values of pH (varied from pH 1 to pH 9) and ionic strength (over the range 10^{-4} to 0.6). This characterization had to be repeated, despite the large body of literature, for a number of reasons. Paraquat is applied as an aquatic herbicide at levels of 0.8–2.0 μg/mL (29). Water samples collected near the surface typically contain suspended solid loads of 1 mg to 100 mg/mL and dissolved organic carbon levels of 0–10 μg/mL. The pH values of natural waters are most commonly in the range 5.0 to 8.0. The studies reported in the literature are for soil systems using clay levels of 1.25–25 g/L and humic acid levels of 0.50–50 mg/mL. Few, if any, studies report the pH of the clay systems, and the humic acid studies were usually done at pH 4.0 in unbuffered systems. The paraquat concentrations used in the literature (at equilibrium) were at the 1–10 m*M* level. This study reports adsorption and desorption experiments using systems containing paraquat at the μg/mL level and colloid levels of 10 μg/mL to better

Can. J. Chem. Downloaded from www.nrcresearchpress.com by 210.87.254.40 on 09/05/12
For personal use only.

reflect environmental levels. A second departure from previous studies is the use of dissolved humic acid (i.e., filterable through a 0.2 μm Nuclepore filter) instead of slurry techniques. The results reported in this study are closer to natural water systems than earlier reports.

Experimental

Chemicals

Bentonite (Fisher) was converted to the potassium form by an equilibration with 1 *M* KNO_3. The potassium form of the clay was placed in 300 mL of distilled water, blended at high speed for five minutes in a Waring blender, transferred to a one litre graduated cylinder, and made up to volume with distilled water. A 48 h settling period was used to remove the more dense particles and the upper 900 mL of the suspension was transferred into a second container. The clay content was determined by filtering through a 0.2 μm Nuclepore membrane filter. A typical suspension contained 3.21 ± 0.15 mg clay/mL. The cation exchange capacity was determined using both an ammonium acetate exchange method and a calcium exchange. The ammonium acetate method gave a cation exchange of 62 mmol K/100 g and the calcium uptake also gave a value of 62 mequiv./100 g (i.e., 31 mmol Ca/100 g).

Humic acid (Aldrich) was acid-washed with 3 *M* HNO_3 to remove heavy metals and to convert the humic acid to the fully protonated form. Solutions of humic acid were prepared by dissolving 300 mg of dried acid in one litre of distilled water to which five pellets of KOH were added. The concentration of humic acid was determined by allowing the undissolved entities to settle for seven days and filtering the solution. The undissolved matter was dried, weighed, and the concentration calculated by difference. A typical solution contained 187 μg HA/mL. The total acidity of the humic acid and the carboxyl content were found to be 6.7 mequiv./g and 2.4 mequiv./g, respectively.

Methylene blue was obtained as the hydrated chloride salt (Matheson). The dye content of the salt was obtained by drying under vacuum with anhydrone as the drying agent. The moisture content was found to be 19.0 ± 0.2%. All solutions were prepared using the dried solid. The purity of the methylene blue was checked by thin layer chromatography on a silica gel developed with 1:9 glacial acetic acid – methanol. A comparison of the developed chromatograms with possible contaminants (thionine, Azures, A, B, and C) indicated only methylene blue was present. Methyl viologen hydrate (Aldrich) was standardized by passing a 25.00 mL aliquot of the stock solution through a Rexyn 100 cation exchange resin in the hydrogen form. The protons released were titrated with standard base to a phenolpthalein endpoint.

Methods

The distribution of methylene blue and paraquat between solution and clay particulates was determined by two methods. The first was a bulk adsorption experiment in which known amounts of organocation were equilibrated with 40 mL of 5 ppm bentonite in polyethylene centrifuge tubes. After a 12 h equilibration the suspensions were centrifuged, decanted onto 0.20 μm Nuclepore membrane filters, and the residue washed with distilled water. Preliminary studies indicated that the adsorption of methylene blue and paraquat onto the bentonite was complete after 3 h. Controls indicated that no MB and paraquat were adsorbed onto the centrifuge tubes, filter, and associated glassware. The washings and the decantate were analyzed using visible spectrometry at 667 nm for MB. Paraquat was determined using the procedure of Calderbank and Yuen (30). The amount of cation adsorbed was determined by difference.

The second method for organocation–bentonite adsorption studies used a dialysis bag (Fisher, pore size 4.8 nm) to contain the clay suspension. The clay/dialysis bag was equilibrated with a solution containing known amounts of organocation. A 72 h equilibration was found to be sufficient. The suspension inside the dialysis bag was filtered and washed, as above, and the filtrate and outer solution analyzed for organocation. The amount of cation adsorbed by the dialysis bag was determined from controls (always less than 1% of the total) and the amount adsorbed onto the clay calculated by difference. The adsorption studies were done at different values of ionic strength (set by KNO_3) and pH.

Desorption experiments were done by equilibrating bentonite (saturated with organocation) and solutions containing monovalent, divalent, and trivalent cations at concentrations of 0.1 *M* and 0.5 *M* in centrifuge tubes. The amount of organocation released was determined at 24, 168, and 720 h. No difference was noted between the three measurements.

The distribution of MB and paraquat between solution and HA or PSSA was studied using the dialysis bag method. Solutions containing known amounts of organocation and HA or PSSA were shaken for 18 h with a dialysis bag containing distilled water. Preliminary studies indicated that dialysis equilibrium (organocation only) was attained in 3 h and in the presence of the polyelectrolytes within 6 h. An uv scan of the dialyzate of HA and PSSA indicated that no HA and PSSA diffused through the membrane or adsorbed onto the membrane. The concentration of organocation inside the dialysis bag was taken as the concentration of the free organocation. The amount adsorbed was calculated from the difference between total and free cation concentrations. Studies were done as a function of pH and ionic strength.

A study of the paraquat exchange reaction between solution and Dowex 50 × 8 (100–200 mesh) was initiated to determine the possibility of using a preconcentration step in a speciation procedure. One hundred millilitre aliquots of solutions containing paraquat, humic acid, and NaCl were passed through a column of 6 cm × 0.38 cm^2 of Dowex 50 × 8 in the H^+ form. The column was washed with 25 mL of 1 *M* NaCl and the paraquat eluted with 25 mL of saturated NH_4Cl. The paraquat concentrate was analyzed in the usual manner using an NH_4Cl (saturated) reference in the spectrophotometer.

Results and Discussion

Adsorption isotherms for paraquat and methylene blue onto clay are given in Fig. 1. The adsorption maxima for the two organocations at different values of ionic strength are given in Table 1. A preliminary set of experiments indicated that the same value of adsorption maxima was obtained whether the organocation was adsorbed onto the bentonite and then exposed to KNO_3 solutions (i.e., a desorption study) or the organocation was added to a KNO_3/bentonite suspension (i.e., adsorption experiment). The bulk adsorption and dialysis equilibration methods gave the same adsorption maxima. Table 2 presents the amount of organocation released from bentonite after equilibration with 0.1 *M* solutions of metal ions. Within experimental error the results indicate that the exchange reaction is reversible and little organocation is released in the presence of 10 000-fold excess of metal ion.

The results of the adsorption-desorption studies

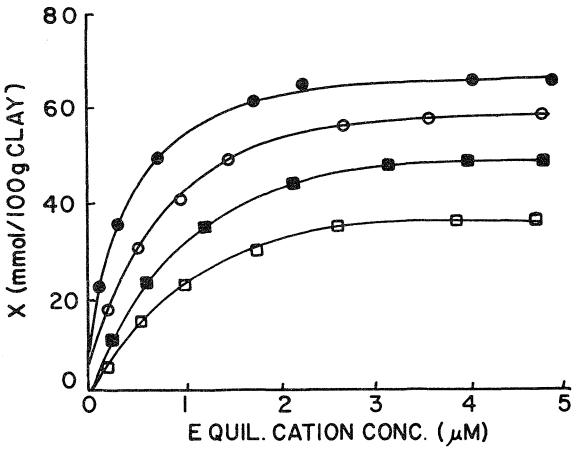


FIG. 1. Adsorption isotherms for paraquat and methylene blue onto bentonite. The solution pH was 6.1 and the free cation concentration was determined by dialysis. Point size reflects experimental uncertainty: ● MB, 0 *M* KNO_3; ○ MB, 0.1 *M* KNO_3; ■ paraquat, 0 *M* KNO_3; □ paraquat, 0.1 *M* KNO_3.

TABLE 1. Adsorption maxima* for bentonite–organocation systems

KNO_3 (*M*)	Paraquat (mequiv./100 g)	MB (mequiv./100 g)
0	90.2	64.0
0.01	80.2	61.0
0.05	76.6	59.2
0.10	74.0	57.0
0.50	66.2	52.0

*Experimental uncertainties in the adsorption maxima were ±3 mequiv./100 g.

TABLE 2. Desorption results* in the presence of 0.1 *M* cations

Cation	Paraquat released (%)	MB released (%)
Ca	9.4	0.6
Mg	8.0	0.7
Ba	9.4	0.7
Zn	8.7	—
Al	14.8	1.1
Li	4.1	0.4

*Organocation initially adsorbed at 0.01 *M* KNO_3 and then exposed to metal cation solutions. Uncertainties in amount released were ±1% for paraquat and ±0.2% for methylene blue.

indicate that the clay has a strong preference for methylene blue and paraquat over metal cations. The amount of methylene blue adsorbed was equal to the measured cation exchange capacity. Paraquat, however, was adsorbed in excess of the cation exchange capacity. This is in agreement with the work of Weber and Weed (18) done at higher clay and paraquat levels. Two possible reasons for the excess adsorption of paraquat are either a low measured cation exchange capacity or the presence of a second interaction other than cation exchange. A low cation exchange capacity can result when a clay suspension hydrolyzes and aluminum or iron replaces K^+ at the exchange sites. A sodium bentonite specially prepared to overcome hydrolysis[2] had a cation exchange capacity of 93.0 mequiv./100 g but when suspended in water the capacity decreased to 80 mequiv./100 g. An adsorption experiment found that the sodium bentonite adsorbed 93 mequiv./100 g of paraquat. This is strong evidence that the paraquat cation can displace adsorbed hydrolysis products. Methylene blue, however, could not displace the cations resulting from hydrolysis because of the lower charge of the dye cation and only 80 mequiv. MB/100 g were absorbed onto the sodium bentonite.

The bulk adsorption and dialysis equilibration methods used in this study included a washing of the filtered clay with distilled H_2O before analysis. Other workers who have used MB to determine the cation exchange capacity (CEC) of particulates centrifuge the equilibrated sample and determine the MB content of the centrifugate. A comparison of the two procedures indicated that high CEC results were obtained without washing. Methylene blue in solution at high concentrations can form dimers and tetramers (31) and Bergman and O'konski (25) noted that dimer formation on the clay surface occurred in the presence of montmorillonite.

[1] $MB^+ + K—Mont. \rightleftharpoons MB—Mont. + K^+$(ion exchange)

[2] $MB^+ + MB—Mont. \rightleftharpoons MB...MB—Mont.$ (aggregation)

Our studies showed that at MB/bentonite ratios below the clay CEC all of the MB was adsorbed and none could be removed by water washing. Above the CEC, however, the aggregated MB at the bentonite surface could be removed by washing with distilled water. Similar experiments with paraquat indicated no aggregation at the clay surface. The different aggregation behaviour of paraquat and methylene blue is probably a result of stronger repulsions between two divalent cations of paraquat whereas the lower, more delocalized, charge of a MB cation will tend to decrease the repulsions between ions.

Two exchange isotherms were done at pH 8 and 3 in 0.01 *M* KNO_3 to determine the competition between organocations and protons. The adsorption maxima at pH 8 were 65.0 ± 3 mequiv. MB/100 g and 88.0 ± 3 mequiv. paraquat/100 g whereas at pH 3 the values were 57.0 ± 3 mequiv. MB/100 g and 81.4 ± 3 mequiv. paraquat/100 g. The proton ap-

[2]Obtained from J. C. T. Kwak and L. L. Schramm, Department of Chemistry, Dalhousie University.

Can. J. Chem. Downloaded from www.nrcresearchpress.com by 210.87.254.40 on 09/05/12
For personal use only.

Can. J. Chem. Downloaded from www.nrcresearchpress.com by 210.87.254.40 on 09/05/12
For personal use only.

pears to compete more favourably with the organocations than the alkali earth cations.

The adsorption and desorption behaviour of methylene blue and paraquat in the presence of bentonite has a number of important consequences with respect to analytical speciation methods. If one wishes to estimate the application rate of paraquat to aquatic systems necessary to maintain a toxic dose of free paraquat, then a preliminary adsorption capacity of the particulates should be made. Some workers have suggested (11) that a CEC measurement with MB as the exchanger would be useful for both inorganic and organic ions. This work suggests, however, that the paraquat cation can displace hydrolysis products adsorbed on the bentonite particulates. The preliminary CEC measurement for paraquat should be made with paraquat and not extrapolated from regular CEC measurements using NH_4^+ or Ca^{2+} exchange. The strong adsorption of both methylene blue and paraquat onto the bentonite indicates that less than 10% of the bound cation is released under normal environmental conditions. In the environment a pH drop from 8 to 4 (caused by acid rain, for example) or an increase in ionic strength from 0.010 to 0.5 in the estuaries would cause only a slight shift in the adsorption equilibria from bentonite clays.

The dialysis of methylene blue and paraquat as a function of concentration in 0.01 *M* KNO_3 and 0.01 *M* KNO_3/7.8 μg HA/mL is shown in Fig. 2. It is evident that the interaction between organocation and humic acid is more favourable for MB than paraquat. Figures 3 and 4 present the adsorption isotherms at different values of ionic strength for paraquat and methylene blue, respectively. Both sets of isotherms fail to attain a plateau and the paraquat interaction is more susceptible to ionic strength variations. The isotherms for methylene blue and paraquat adsorption onto humic acid at different solution pH values are given in Figs. 5 and

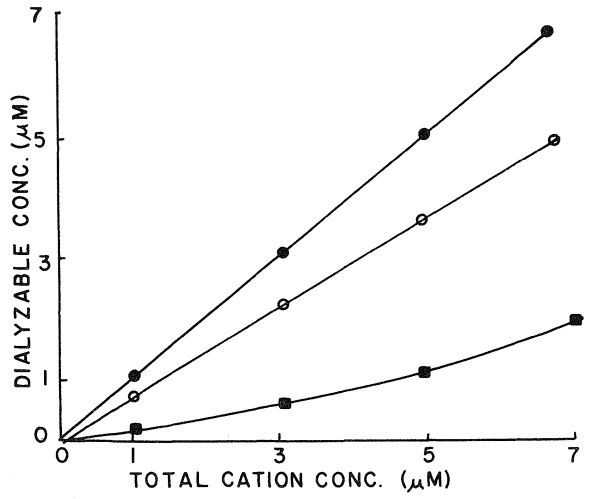


FIG. 2. A comparison of dialysis results for paraquat and methylene blue in the presence of humic acid. The separation was done at pH 6.5 and in 0.01 *M* KNO_3: ● MB, paraquat with no humic acid; ○ paraquat in 7.8 ppm HA; ■ MB in 7.8 ppm HA.

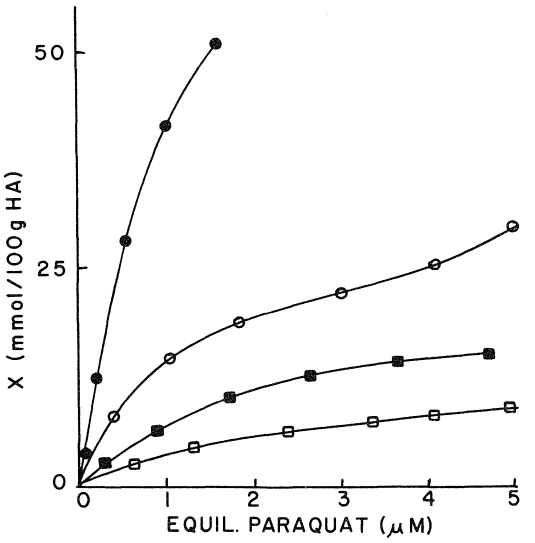


FIG. 3. Adsorption isotherms for paraquat and humic acid in the presence of KNO_3. All isotherms were done at pH 6 and the point size reflects the experimental uncertainty: ● 0 *M* KNO_3; ○ 0.01 *M* KNO_3; ■ 0.05 *M* KNO_3; □ 0.10 *M* KNO_3.

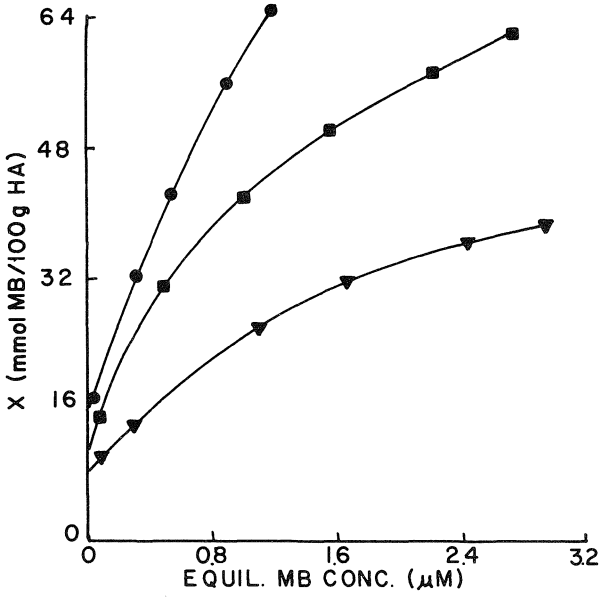


FIG. 4. Adsorption isotherms for methylene blue and humic acid in the presence of KNO_3. All isotherms were done at pH 6.0 and point size reflects experimental uncertainty: ● 0 *M* KNO_3; ■ 0.1 *M* KNO_3; ▼ 0.5 *M* KNO_3.

Can. J. Chem. Downloaded from www.nrcresearchpress.com by 210.87.254.40 on 09/05/12
For personal use only.

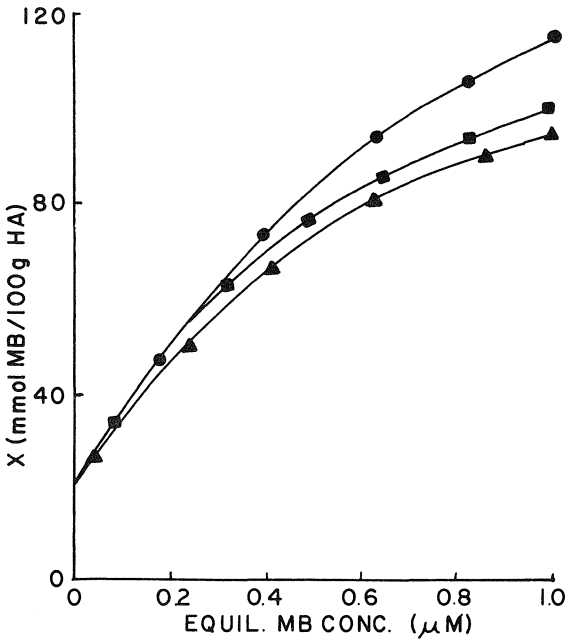


FIG. 5. Adsorption isotherms for methylene blue onto humic acid at different values of solution pH. All isotherms were done in the presence of 0.01 *M* KNO_3: ● pH 8.1; ■ pH 6.3; ▼ pH 1.0.

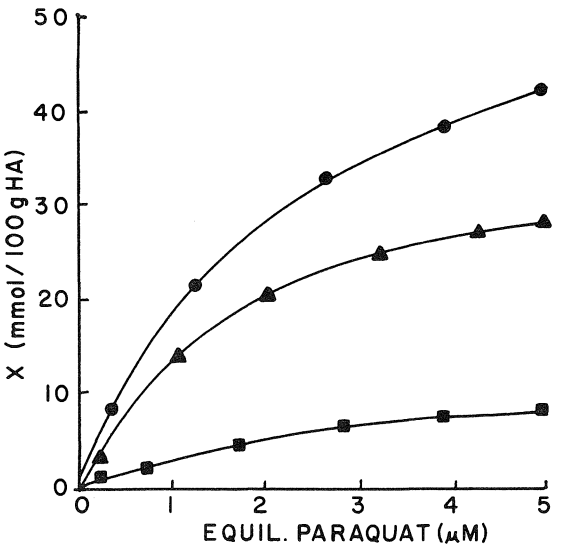
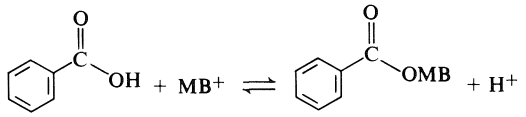


FIG. 6. Adsorption isotherms for paraquat and humic acid at different values of solution pH. All isotherms were done in the presence of 0.005*M* KNO_3: ● pH 8.2; ▼ pH 6.2; ■ pH 2.5.

6, respectively. Again, pH is more important for paraquat than MB. Desorption experiments indicate that 0.1 *M* KNO_3 and pH 1 solutions are capable of completely removing paraquat from humic acid. Similar experiments with methylene blue indicate that at pH 1 approximately 65% of the MB remains bound to humic acid and in 0.5 *M* KNO_3 50% of the MB remains bound to HA. Under similar conditions the copper – humic acid complex is completely dissociated at pH 1.0 (10).

The humic acid functional group responsible for exchange properties is a carboxylic acid:



The pH and ionic strength variations of paraquat indicate that the ion exchange reaction is the predominant interaction with humic acid. Methylene blue must have a secondary interaction with the humic colloid to account for the unusual pH dependence of the MB–HA system. It is possible that interactions between the more hydrophobic MB cation and aromatic backbone of humic acid may be present.

The isotherms for organocation interactions with HA can be compared to the interactions with PSSA shown in Fig. 7. The paraquat interacts with PSSA and HA in a similar fashion, that is, both isotherms are very dependent on ionic strength. The MB interaction with PSSA differs from the HA system in two respects. First the MB–PSSA system is very dependent on ionic strength. Secondly the MB–PSSA isotherm indicates that adsorbed molecules enhance the adsorption of additional molecules. Other workers (12–14) have interpreted this type of isotherm as indicative of dye–dye interactions on the polyelectrolyte.

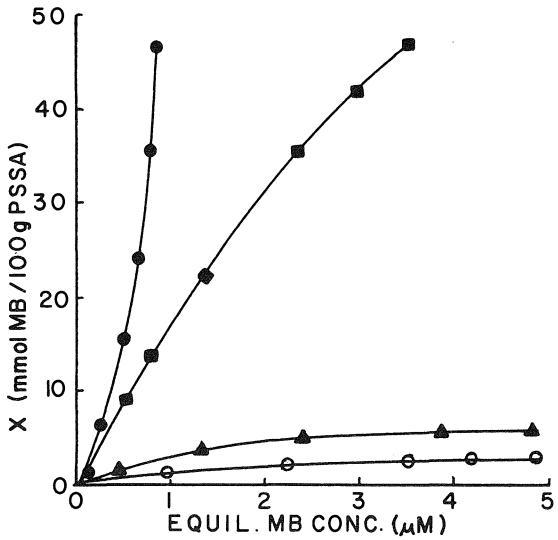


FIG. 7. Adsorption isotherms for methylene blue and paraquat onto PSSA. All isotherms were done at pH 6.0 and point size reflects experimental uncertainty of three samples: ● MB, 0 *M* KNO_3; ▼ paraquat, 0.01 *M* KNO_3; ■ MB, 0.05 *M* KNO_3; ○ paraquat, 0.1 *M* KNO_3.

Can. J. Chem. Downloaded from www.nrcresearchpress.com by 210.87.254.40 on 09/05/12
For personal use only.

The isotherms for the organocations with HA and PSSA have some importance with respect to speciation of aquatic systems. The paraquat–HA system is more susceptible to variations in pH and ionic strength than clay–paraquat systems. In transitions from fresh to salt water one can expect a significant release of paraquat from the humic substances; if the inorganic particulates are already saturated with paraquat then one can expect an increase in the concentration of free paraquat in the estuaries and in acidic waters. The interactions of MB with humic acid suggest that hydrophobic organic pollutants may be less susceptible to changes in pH and ionic strength.

The studies of bentonite/HA/organocation systems suggest the speciation scheme illustrated in Fig. 8. Table 3 presents the results obtained when the scheme is applied to a paraquat/bentonite/HA system and to paraquat/bentonite and paraquat/HA systems. The data summarized in Table 3 indicate that the humic acid and clay systems are additive. This probably is a result of the saturation of the clay with organocation and followed by a free paraquat/paraquat bound to humic acid equilibrium. As the ionic strength is increased the paraquat is completely released from the humic acid and partially released from the bentonite. Similar systems using humic acid at different levels indicate that the bentonite is always saturated before paraquat is bound to the humic acid.

The competition between clay and humic acid for paraquat suggests that an ion exchange resin should be able to remove bound paraquat from humic acid. Table 4 presents the results of column studies for humic acid and paraquat systems. The results indicate that a significant difference exists between dialyzable paraquat and total paraquat values but no significant difference between ion exchangeable and total paraquat results. This suggests that an ion exchange preconcentration step may be used to estimate the paraquat concentration in solutions after filtration to remove particulates.

The results of this study indicate that clay particulates will control the organocation concentration at levels of paraquat that do not exceed the clay cation exchange capacity. At paraquat levels above the exchange capacity of the clay humic acid will bind cations. The humic acid – paraquat interaction is very susceptible to changes in ionic strength and significant amounts will be released in the estuaries.

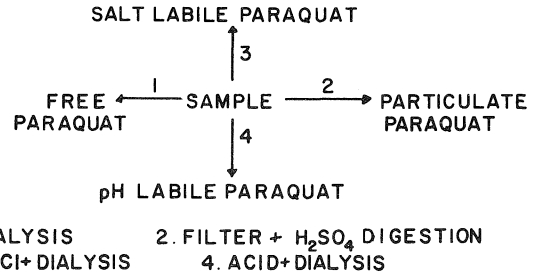


FIG. 8. Suggested speciation scheme for paraquat in natural waters.

TABLE 3. Paraquat* speciation in model systems

Added NaCl (*M*)	HA/clay	Free paraquat (μg/mL) Clay	HA
0	0	0.61	0.43
0.01	0.19	0.63	0.70
0.05	0.44	0.71	0.1
0.10	0.59	0.73	1.0
0.30	0.66	0.76	1.0
0.50	0.71	0.77	1.0
Organic bound paraquat	0.42	—	0.57

*Uncertainties in paraquat concentrations for runs done in triplicate were: HA/clay ±0.05 μg/mL; clay ±0.02 μg/mL; HA ±0.02 μg/mL. Initial concentration of paraquat was 1.0 ppm and clay and humic acid concentrations were 5 and 10 ppm, respectively. The organic bound paraquat was determined from: amt. bound (0 *M* NaCl) − amt. bound (0.1 *M* NaCl) − amt. released from clay.

TABLE 4. Ion exchange preconcentration recoveries*

Total paraquat (ppm)	HA (ppm)	NaCl (M)	Paraquat dialysis (ppm)	Paraquat (ppm) ion exchange
1.0	0	0	1.0	1.00
1.0	0	0.01	1.0	0.99
1.0	0	0.1	1.0	1.00
1.0	0	0.5	1.0	0.98
1.0	1	0	0.95	1.00
1.0	2	0	0.90	0.97
1.0	4	0	0.80	1.00
1.0	8	0	0.60	0.99
1.0	10	0	0.43	0.99
1.0	10	0.01	0.70	1.00
1.0	10	0.1	1.0	1.00
1.0	10	0.5	1.0	1.00

*All sets were done in triplicate. Uncertainties in dialysis results were ±0.02 μg/mL and in ion exchange recoveries ±0.03 μg/mL.

Acknowledgements

The authors wish to thank L. Schramm and J. C. T. Kwak for samples of specially prepared bentonite. The authors also wish to acknowledge the Natural Sciences and Engineering Research Council of Canada for financial support of this research.

1. M. A. GILLOTT, G. L. FLOYD, and D. V. WARD. Environ. Entomol. 4, 622 (1975).
2. R. D. GUY and D. R. NARINE. A model system for the investigation of methods of herbicide speciation. *In* Pro-

ceedings of hydrocarbons and halogenated hydrocarbons in the environment. Hamilton, Ont. 1978. In press.
3. R. HAQUE. Role of adsorption in studying the dynamics of pesticides in the soil environment. *In* Environmental dynamics of pesticides. *Edited by* R. Haque and V. H. Freed. Plenum, New York. 1975. p. 97.
4. G. W. BAILY and L. L. WHITE. Residue Rev. **32**, 29 (1970).
5. R. HARTUNG. Accumulation of chemicals in the hydrosphere. *In* Environmental dynamics of pesticides. *Edited by* R. Haque and V. H. Freed. Plenum, New York. 1975. p. 185.
6. J. C. VAN LOON, J. LICHWA, and B. RADZIUK. J. Chromatogr. **136**, 301 (1977).
7. P. BENES and E. STEINNES. Water Res. **8**, 947 (1974).
8. Y. K. CHAU and K. LUM-SHUE-CHAN. Water Res. **8**, 383 (1974).
9. R. D. GUY, C. L. CHAKRABARTI, and L. L. SCHRAMM. Can. J. Chem. **53**, 661 (1975).
10. R. D. GUY and C. L. CHAKRABARTI. Can. J. Chem. **54**, 2600 (1976).
11. P. T. HANG and G. W. BRINDLEY. Clays Clay Miner. **18**, 203 (1970).
12. M. K. PAL and M. CHAUDHURI. Makromol. Chem. **133**, 151 (1970).
13. M. SHIRAI, T. NAGATSUKA, and M. TANAKA. Makromol. Chem. **178**, 37 (1977).
14. M. SHIRAI, Y. MARAKAMI, and M. TANAKA. Makromol. Chem. **178**, 2142 (1977).
15. J. A. BEST, J. B. WEBER, and S. B. WEED. Soil Sci. **114**, 444 (1972).
16. S. U. KHAN. Residue Rev. **52**, 14 (1974).
17. I. G. BURNS and M. H. B. HAYES. Residue Rev. **52**, 116 (1974).
18. J. B. WEBER and S. B. WEED. Soil Sci. Soc. Am. Proc. **32**, 485 (1968).
19. M. DAMANAKIS, D. S. H. DRENNAN, J. W. FRYER, and K. HOLLY. Weed Res. **10**, 264 (1970).
20. B. A. G. KNIGHT and P. J. DENNY. Weed Res. **10**, 40 (1970).
21. I. G. BURNS, M. H. B. HAYES, and M. STACEY. Weed Res. **13**, 79 (1973).
22. S. B. WEED and J. B. WEBER. Soil Sci. Soc. Am. Proc. **33**, 379 (1969).
23. M. H. B. HAYES, M. E. PICK, and B. A. TOMS. J. Colloid Interface Sci. **65**, 254 (1978).
24. A. CALDERBANK and T. E. TOMLINSON. PANS, **15**, 446 (1969).
25. K. BERGMAN and C. T. O'KONSKI. J. Phys. Chem. **67**, 2169 (1963).
26. D. K. DE, J. L. D. KANUNGO, and S. K. CHAKRAVARTI. J. Indian Chem. Soc. **11**, 507 (1973).
27. D. K. DE, J. L. D. KANUNGO, and S. K. CHAKRAVARTI. J. Indian Chem. Soc. **12**, 1187 (1974).
28. D. K. DE, J. L. D. KANUNGO, and S. K. CHAKRAVARTI. J. Indian Soc. Soil Sci. **21**, 251 (1973).
29. A. A. AKHAVEIN and D. L. LINSCOTT. Residue Rev. **23**, 97 (1968).
30. A. CALDERBANK and S. H. YUEN. Analyst, **90**, 99 (1965).
31. E. BRASWELL. J. Phys. Chem. **72**, 2477 (1968).

Can. J. Chem. Downloaded from www.nrcresearchpress.com by 210.87.254.40 on 09/05/12
For personal use only.

Organocation speciation. II. Methylene blue photosensitization as a model for speciation and toxicity of herbicides

ROBERT D. GUY[1] AND DEORAJ R. NARINE

Trace Analysis Research Centre, Department of Chemistry, Dalhousie University, Halifax, N.S., Canada B3H 4J1

Received July 27, 1979

ROBERT D. GUY and DEORAJ R. NARINE. Can. J. Chem. **58**, 555 (1980).

A chemical model that employs the photosensitization properties of methylene blue to mimic herbicide toxicity is used to test size separation as a method of chemical speciation. A spectrophotometric study of the dye interactions with the humic colloid indicated that the dye – humic acid complex has a weaker absorption spectrum than the free dye. The absorption spectra suggested that the binding sites on the humic acid are sufficiently isolated to prevent dye–dye interactions on the colloid surface. The dye photosensitization of tryptophan degradation indicated that only the free methylene blue was active in the presence of humic acid, clay, and polystyrene sulphonic acid. The model suggests that if the pollutant must be in true solution to be biologically active then a size separation by dialysis would be a satisfactory speciation procedure.

ROBERT D. GUY et DEORAJ R. NARINE. Can. J. Chem. **58**, 555 (1980).

On a utilisé un modèle chimique qui fait appel aux propriétés photosensibilisatrices du bleu de méthylène dans la toxicité de l'herbicide mimique, pour vérifier la séparation dimensionnelle comme une méthode de détermination de l'espèces chimique. Une étude spectrophotométrique des interactions entre le colorant et le colloide humique indique que le complexe colorant – acide humique a un spectre d'absorption plus faible que le colorant à l'état libre. Les spectres d'absorption suggèrent que les sites de liaison dans l'acide humique sont suffisamment isolés pour prévenir les interactions colorant–colorant à la surface du colloide. La dégradation du tryptophane photosensibilisée par le colorant indique que seul le bleu de méthylène est actif en présence d'acide humique, d'argile et de l'acide polystyrène sulfonique. Le modèle suggère que si le polluant doit se trouver réellement en solution pour être biologiquement actif la séparation par dialyse peut être satisfaisante comme méthode de détermination de l'espèce.

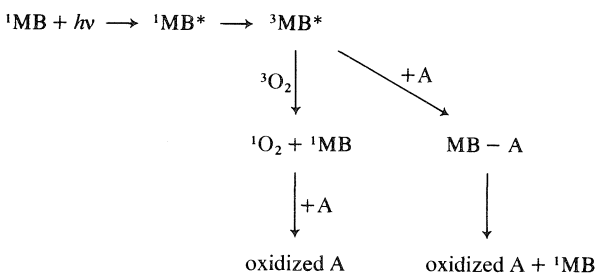
[Traduit par le journal]

Introduction

Chemical speciation of toxic substances in the aquatic environment plays an important role in biological toxicity. Previous studies (1) have shown that paraquat, a cationic herbicide, was less toxic to an unicellular alga in the presence of bentonite and humic acid. Two mechanisms of pollutant toxicity to algae have been reported in the literature. The first mechanism is an interaction between the cell wall and pollutant that changes the wall's permeability. Cupric and mercuric ions have been found (2, 3) to interact with cell walls and cause a leakage of potassium ions out of the cell. The second mechanism is an interaction between a pollutant and cellular components that interferes with metabolism. Methyl viologen (paraquat) acts as a herbicide because the cation interferes in the electron transport chain in photosynthesis (4). In photosystem I the excited chlorophyll complex reduces paraquat instead of ferredoxin. The paraquat radical is rapidly oxidized by O_2 to form H_2O_2 and paraquat. It is the H_2O_2 produced that is the toxic substance. Paraquat, therefore, can be thought of as a photochemical herbicide; the chlorophyll absorbs light and reduces the paraquat which acts as a catalyst in the production of the toxic substance, H_2O_2.

Methylene blue (MB), a cationic dye, was found (1) to be toxic to algae at the 10^{-8} *M* concentration level. A preliminary study indicated that light was a prerequisite for toxicity. If the algae were grown in the presence of methylene blue but with an outer filter designed to reduce the incident light level at 665 nm (λ_{max} for MB) to 0.1% of its initial level the effect of the dye was algistatic. Algal flasks surrounded by the filter were found to exhibit normal growth and flasks containing MB but no outer filter were algicidal. Heitz and Wilson (5) have found similar insecticidal activity for the xanthene dyes; when insects fed xanthene dyes were exposed to visible light the dye was toxic.

The prerequisite of light for the toxicity of the dye indicates that the toxic effect is probably the result of a photosensitization reaction. Methylene blue absorbs light at 665 nm to form a singlet excited state which can cross over to yield a triplet excited state:



[1]Author to whom correspondence should be addressed.

0008-4042/80/060555-04$01.00/0

©1980 National Research Council of Canada/Conseil national de recherches du Canada

Can. J. Chem. Downloaded from www.nrcresearchpress.com by 210.87.254.40 on 09/05/12
For personal use only.

Can. J. Chem. Downloaded from www.nrcresearchpress.com by 210.87.254.40 on 09/05/12
For personal use only.

The photosensitization reaction has been reported in the literature (6–8) for the decomposition of nucleotides, aminoacids, and enzymes. The result of the dye attack on algal cell components would be algal death.[2]

The similarity in toxic mechanisms, a photochemical step and a catalytic production of the toxic substance, for methylene blue and paraquat allows one to design a chemical model to study organocation speciation. If one uses methylene blue as the organocation then one can substitute an amino acid as the speciation monitor instead of an algae. The advantages of a chemical model over the biological model is the ability to vary ionic strength and pH over larger ranges in a chemical system. This paper describes a study of the degradation of tryptophan in methylene blue, humic acid, and bentonite model systems.

Experimental

The clay, humic acid, polystyrene sulphonic acid (PSSA), and methylene blue preparations were described in Part I of this series (9). The tryptophan (Eastman Kodak) was dissolved in NaOH and stored in the dark.

The degradation studies were done in a light box composed of four cool-white, 35 W fluorescent lamps (13 cm apart). The temperature inside the light box was 27°C, and a flow rate of 350 mL air per min through the flasks was maintained using aquarium pumps. Solutions or suspensions containing humic acid or bentonite, methylene blue, and tryptophan ($1.0 \times 10^{-4}M$) in 250 mL Erlenmeyer flasks were irradiated in the light box. Tryptophan was monitored using uv spectrometry at 280 nm, MB and humic acid were found not to interfere, and the bentonite was removed by centrifugation before analysis. Dialysis separations were used to determine the free concentration of methylene blue in the suspensions.

Results and Discussion

Figure 1 presents the tryptophan degradation as a function of time for different levels of methylene blue at pH 7.8 in $1 \times 10^{-3}M$ $NaHCO_3$. A similar set of curves was generated for methylene blue in the presence of 0.5 ppm humic acid (also at pH 7.8 and $1.0 \times 10^{-3}M$ $NaHCO_3$). Figure 2 shows the amount of tryptophan degraded after eight hours as a function of total methylene blue concentration. The presence of the humic acid (curve *B*) significantly reduces the amount of tryptophan degraded. When the degradation results are replotted as a function of dialyzable methylene blue, curves *A* and *B* coincide (the triangles in curve *A* are for the dialyzable methylene blue in the presence of humic acid). A similar study of tryptophan/bentonite/methylene blue and tryptophan/PSSA/methylene blue systems showed that only the free or dialyzable methylene blue was responsible for tryptophan degradation.

One of the principal conclusions of the model studies reported in Part I (9) was that as the ionic strength increases significant desorption would occur for MB/HA systems but no desorption for MB/bentonite systems. Figure 3 presents the re-

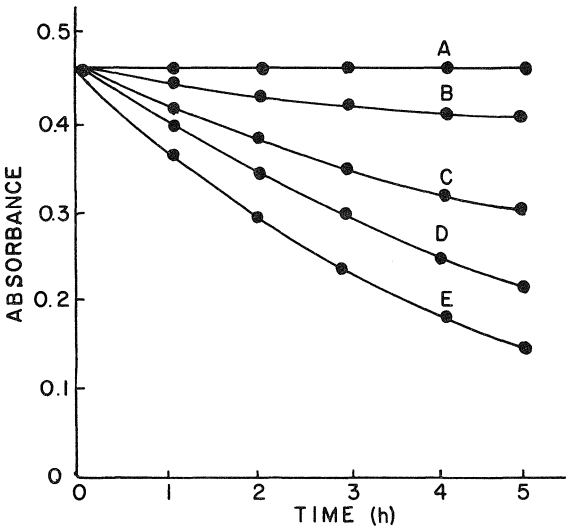


FIG. 1. Free methylene blue and tryptophan degradation in the presence of 100 ppb MB and 0.5 ppm humic acid at different NaCl concentrations. ● Free MB. ■ Tryptophan degradation.

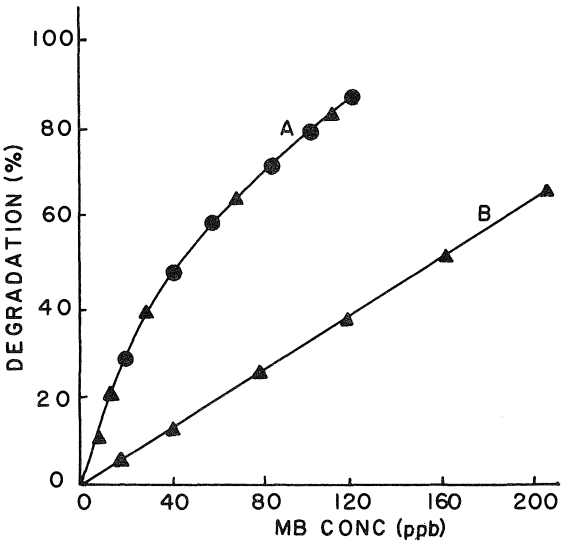


FIG. 2. Absorption spectra of MB and MB–HA solutions: (*A*). 2 ppm MB, (*B*). 2 ppm MB and 2 ppm HA, (*C*). 2 ppm MB and 4 ppm HA, (*D*). 2 ppm MB and 4 ppm HA (dialysate as reference).

[2]The algistatic effect observed in the flask surrounded by the filter is probably the result of the reduction of methylene blue by photosystem I. This will deprive the cell of a source of energy and over the long term will result in death. At the methylene blue levels used in these experiments, however, the principal short-term toxic effect is the photosensitization reaction.

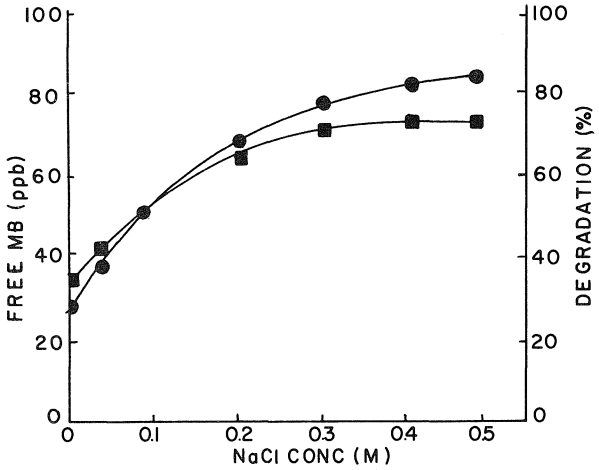


FIG. 3. Absorption spectra of MB and PSSA solutions: (*A*). MB control, (*B*). 5 ppm PSSA and 2 ppm MB, (*C*). 5 ppm PSSA and 1.2 ppm MB, (*D*). 5 ppm PSSA and 0.4 ppm MB. (*B*, *C*, and *D* are against the dialysate as reference.)

sults of a degradation study as a function of NaCl concentration. As the concentration of NaCl increases the dialyzable MB and the tryptophan degradation increase. For a 100 ppb MB/1 ppm bentonite system no release of MB and no degradation of tryptophan was observed over the same range of NaCl concentrations.

The results reported in Figures 1, 2, and 3 indicate that methylene blue in homogeneous solutions was a good photosensitizer for tryptophan degradation whereas in colloidal systems the degradation was proportional to the dialyzable methylene blue. Studies of methylene blue/colloid/algae systems (1) indicated that toxicity was related to the free MB. Within experimental error (±5%) there was no evidence that the bound dye was toxic to algae (1) or that the bound MB could act as a photosensitizer for tryptophan degradation. There are a number of possible reasons for the decrease in MB toxicity or the ability of MB to act as a photosensitizer. The colloidal polyelectrolytes (HA and PSSA) and bentonite may quench the $^1O_2$ produced by the bound MB. Silical gel, for example, quenches the production of $^1O_2$ in the silica gel/adsorbed MB systems (10). In algal systems the bound MB may be less toxic to algae because the MB is unavailable to the algae either for adsorption onto cell walls or for transfer across the cell membrane. In the MB/colloid/tryptophan systems, however, the tryptophan molecule should be able to interact either with $^1O_2$ or ^{3}MB at the colloid surface. A third possibility for the unreactive nature of bound MB is different light absorption and emission properties of MB bound to the colloid. A spectroscopic study of MB/HA and MB/PSSA systems was undertaken to investigate this possibility.

Figure 4 presents the visible absorption spectra of methylene blue in the presence of humic acid. Curves *A*, *B*, and *C* in Fig. 4 are for the total solutions against a water reference. The spectra are indistinguishable from the spectrum of free methylene blue. Curves *C* and *D* in Fig. 1 are for a solution of 2 ppm MB and 4 ppm humic acid. Spectrum *D* was recorded using the dialyzable methylene blue as a reference and hence is a difference spectrum representing the MB – humic acid complex (humic acid had no absorption in this region). A comparison of spectra for a constant humic acid concentration and varying methylene blue concentration indicated that the two new absorptions at 618 nm and 688 nm increased in height linearly as the concentration of MB increased. An increase in the MB – humic acid ratio did not cause a shift in absorption maxima (at 618 and 688 nm).

The solutions employed for spectra *C* and *D* in Fig. 4 contained 50% of the methylene blue in a dialyzable form. The decrease in absorption intensity of the bound methylene blue may result in a decrease in the number of MB molecules available for sensitization reactions. In solutions containing high humic acid to dye ratios, such that all of the methylene blue is bound to the colloid, no fluorescence below 800 nm is observed. It appears that the low photosensitization efficiency of bound methylene blue is a result either of poor light absorption properties or of quenching properties of the humic colloid.

Figure 5 presents the spectra of methylene blue in the presence of PSSA. Spectra *B*, *C*, and *D* were

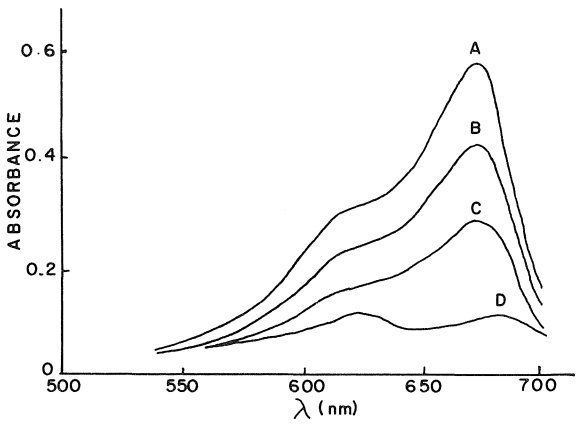


FIG. 4. Tryptophan degradation curves for a 1.0×10^{-3} *M* $NaHCO_3$ solution in the presence of methylene blue. The points are averages of three runs and experimental variation is within the size of the point: (*A*). no MB, (*B*). 10 ppb MB, (*C*). 40 ppb MB, (*D*). 80 ppb MB, (*E*). 120 ppb MB.

Can. J. Chem. Downloaded from www.nrcresearchpress.com by 210.87.254.40 on 09/05/12
For personal use only.

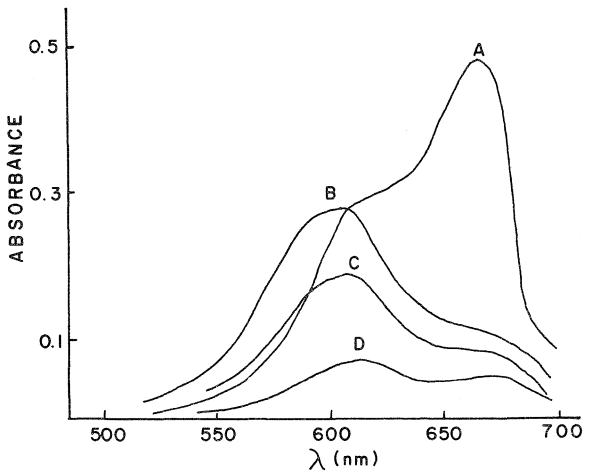


FIG. 5. Tryptophan degradation after 8 h in the presence of MB and humic acid in 1.0 m*M* $NaHCO_3$. The point size reflects the experimental variation of three runs. (*A*). Free MB: ● distilled water, ▲ dialyzable. (*B*). In the presence of 0.5 ppm humic acid.

recorded with the dialyzable methylene blue as the reference. As the dye–polyelectrolyte ratio increases the absorption maximum shifts to a lower wavelength. The difference in spectra between humic acid and PSSA can be interpreted as the sites in humic acid being farther apart than in PSSA. A number of workers (11–13) have suggested that the shift in absorption maxima is a result of the interaction of adjacent dye molecules when adsorbed onto polyelectrolytes. Bound methylene blue in the presence of PSSA does not fluoresce below 800 nm. It appears that the PSSA polyelectrolyte also quenches the bound methylene blue photosensitization reaction.

The model system described in this study indicates that only free methylene blue is capable of a photosensitization reaction. The dialysis separation procedure was able to determine the active methylene blue in clay and polyelectrolyte systems. This suggests that a dialysis separation could be used to determine the toxic components in natural waters if the toxic component had to be in a free form to interact with the algae cell.

Acknowledgements

The authors wish to acknowledge the support of the Natural Sciences and Engineering Research Council of Canada for this research.

1. R. D. GUY and D. R. NARINE. A model system for the investigation of methods of herbicide speciation. *In* Proc. Int. Conf. Hydrocarbons and Halogenated Hydrocarbons in the Environment, McMaster University, Hamilton, Ont. May, 1978. In press.
2. D. C. H. MACBRIEN and K. A. HASALL. Physiol. Plant. **18**, 1959 (1965).
3. L. KAMP-NIELSEN. Physiol. Plant. **24**, 556 (1971).
4. A. A. AKHAVEIN and D. L. LINSCOTT. Residue Rev. **23**, 97 (1968).
5. J. R. HEITZ and W. W. WILSON. Photodegradation of halogenated xanthene dyes. *In* Disposal and decontamination of pesticides. *Edited by* M. V. Kennedy. ACS Symposium Series No. 73. 1978.
6. I. SAITO, K. INOUE, and T. MATSAURO. Photochem. Photobiol. **21**, 27 (1975).
7. I. B. C. MATHESON, R. D. ETHERDIGE, N. R. KRATOWICH, and J. LEE. Photochem. Photobiol. **21**, 165 (1975).
8. A. KNOWLES. Photochem. Photobiol. **13**, 473 (1971).
9. R. D. GUY, D. R. NARINE, and S. DESILVA. Can. J. Chem. **58**, 547 (1980).
10. R. NILSSON and D. R. KEARNS. Photochem. Photobiol. **19**, 181 (1974).
11. E. RABINOWITCH and L. P. EPSTEIN. J. Am. Chem. Soc. **63**, 69 (1941).
12. B. SIMIONESCU and G. J. SMETS. Makromol. Chem. Suppl. **1**, 249 (1975).
13. G. J. SMETS and B. SIMIONESCU. Makromol. Chem. **178**, 2719 (1977).

Can. J. Chem. Downloaded from www.nrcresearchpress.com by 210.87.254.40 on 09/05/12
For personal use only.

A non-empirical SCF-MO study on the conformational properties and asymmetric deformations of dimethyl sulfoxide

PAUL G. MEZEY[1] AND ANIL KAPUR

Department of Chemistry and Chemical Engineering, University of Saskatchewan, Saskatoon, Sask., Canada S7N 0W0

Received August 21, 1979

PAUL G. MEZEY and ANIL KAPUR. Can. J. Chem. **58**, 559 (1980).

Conformational properties of dimethyl sulfoxide (DMSO) have been studied by *ab initio* molecular orbital method, using various gaussian basis sets. Polarization *d* functions are essential in reproducing the correct experimental geometry. Barriers to pyramidal inversion on sulfur and Me—S bond rotation have been calculated. The calculated asymmetric S—Me stretching potential indicates that minor intermolecular interactions may cause considerable geometric distortions in the DMSO molecule. These distortions are likely to contribute to the versatile biochemical effects of DMSO.

PAUL G. MEZEY et ANIL KAPUR. Can. J. Chem. **58**, 559 (1980).

On a étudié les propriétés conformationnelles du diméthylsulfoxyde (DMSO) par la méthode *ab initio* des orbitales moléculaires, en utilisant différents ensembles de base de gauss. Les fonctions de polarisation *d* sont essentielles pour reproduire la géométrie expérimentale convenable. On a calculé les barrières d'inversion pyramidale du soufre et de la rotation de la liaison Me—S. Le potentiel d'élongation asymétrique de la liaison S—Me calculé indique que des interactions intermoléculaires faibles peuvent causer des distorsions géométriques considérables dans la molécule de DMSO. Ces distorsions sont susceptibles de contribuer aux multiples effets biochimiques du DMSO.

[Traduit par le journal]

Introduction

A common feature appears to dominate the general conformational behaviour of most organosulfur compounds: along some internal coordinates the molecule shows very little resistance against deformations (1–10). By using a macroscopic analogy, along some coordinates these compounds show an "elasticity" similar to that of rubber, where, incidentally, sulfur bridges are largely responsible for the elastic properties. This "conformational elasticity" is by no means general for all internal coordinates. In fact, force constants for most normal modes of sulfur compounds fall in the usual range of stretching, bending etc. force constants of organic compounds. What appears characteristic, however, is the readiness of organosulfur molecules to undergo large deformations along one or some of the internal coordinates. The same trend is apparent for most organic molecules containing second row elements. However, the rich variety of organosulfur compounds, where this feature is present, suggests that sulfur moieties are particularly prone to deformations. The general "looseness" of the valence shell electron distribution in sulfur and also the near equivalence of carbon and sulfur electronegativities are factors that may facilitate such geometrical deformations.

The easy deformability of organosulfur compounds is unusual when compared to the deformability of molecules containing no second row elements. However, when comparing the relative ease of deformations for a given molecule along various internal coordinates, sulfur compounds appear even more peculiar. The deformability varies to a large extent from coordinate to coordinate for a given sulfur-containing molecule, and usually there is one coordinate direction along which the deformability far exceeds that in other coordinate directions.

Organic sulfur compounds frequently exhibit unusual conformational properties, that correspond to characteristic features on the conformational potential energy hypersurface of the molecule. Certain cross sections of the energy hypersurface are clearly distinguished by their flatness, giving rise to shallow minima or flat maxima. Earlier theoretical studies on various sulfilimines (7–10) indicated that potential curves corresponding to N—S bond rotations are extremely flat in rather wide angle intervals, although a complete 360° rotation is hindered. These studies indicated the presence of an unexpected low energy reaction path for the interconversion of enantiomeric forms (7, 8). Studies on the conformational energy hypersurface of the $H_2S{=}NH$ model molecule revealed segments along the S—N bond rotation coordinate, where the total energy E_t showed only negligible variations (10). The calculated transition states for various conformational processes were also unusual, showing very large variations of the curvature at the saddle point with the coordinate direction (Don Quixote type saddle surface (11, 12)).

[1]To whom all correspondence should be addressed.

0008-4042/80/060559-08$01.00/0

©1980 National Research Council of Canada/Conseil national de recherches du Canada

Can. J. Chem. Downloaded from www.nrcresearchpress.com by 210.87.254.5 on 09/05/12
For personal use only.

Can. J. Chem. Downloaded from www.nrcresearchpress.com by 210.87.254.5 on 09/05/12
For personal use only.

The presence of extensive flat regions is not restricted to ground state energy hypersurfaces; *ab initio* studies of the first triplet state hypersurfaces of various thiocarbonyls showed similar features (13–16).

Of particular interest are those domains along a flat conformational path of sulfur compounds, which do not lie in the immediate neighbourhood of any of the energy minima, and, hence, the harmonic potential approach is no longer applicable there. In such cases the evaluation of the potential function from spectroscopic information is not always a trivial task. Similarly, the harmonic potential approach is inadequate in those regions, usually around points of inflection about halfway between a minimum and a maximum, where the slope is approximately constant. The more extensive this domain is and the closer it lies to the minimum, the narrower is the interval where the harmonic approximation can be applied. In the case of a symmetric potential, the curve is V shaped with a narrow harmonic region at the rounded off bottom of the V. In the linear regions Hooke's law is clearly inapplicable since there the restoring force is independent of the displacement, and a given force may result in unusually large deformations.

Dimethyl sulfoxide (DMSO) is an excellent model for a study of the above conformational problems. DMSO forms a wide variety of molecular complexes and many of its biochemical effects are believed to be related to the formation of such complexes (17). Experimental evidence indicates that the formation of a molecular complex may be accompanied by extensive geometric distortions of the DMSO structure (6). Interactions between two or more DMSO molecules are also thought to cause large geometric deformations. An X-ray analysis of DMSO crystals at 5°C showed a puzzling asymmetry of the molecule: the two chemically equivalent S—C bonds were found to differ by 0.05 Å (1), and refinement of the structure determination resulted in an even slightly larger difference. Although the reported large extent of discrepancy between the two bond lengths could possibly be an artefact of data processing, the authors of the study found no straightforward explanation. At a much lower temperature (−60°C), however, an independent X-ray study showed only minor differences between the two S—C bonds (18). While the experimental information appears somewhat contradictory, it is likely that the two C—S bonds in DMSO may undergo large deformations due to crystal forces without a large increase in the molecular total energy.

Method

The above findings motivated our present *ab initio* study on the conformational properties and asymmetric deformations of DMSO. Several points in various domains and along various cross sections of the conformational energy hypersurface of DMSO were calculated using the Hartree–Fock–Roothaan LCAO-MO-SCF technique. In order to maintain comparability with the results of earlier *ab initio* studies on sulfilimines (10) most calculations were carried out employing a 4-31 G (44-31 G for sulfur) gaussian basis set (Basis III). For preliminary surface scanning and geometry optimization, however, minimum 3G basis sets (Basis I), and for correct reproduction of the S=O stretching potential, 3 G basis sets augmented with *d* polarization functions (Basis II) have also been employed (19–22).

Deformations along four internal coordinates, corresponding to four characteristic conformation or geometry changes of DMSO were considered in some detail: (*i*) the C—S bond rotation, $\alpha_{S—Me}$; (*ii*) out-of-plane bending angle of S=O bond (pyramidal inversion on sulfur), $\theta_{S=O}$; (*iii*) S=O bond stretching, $r_{S=O}$; (*iv*) asymmetric S—Me stretching, represented by stretching of *one* of the S—C bonds, $r_{S—Me}$. All geometric parameters were optimized for a large number of DMSO structures, including pyramidal and planar forms, in two cycles of sequential approximations, using the minimum 3G basis set (Basis I). Points along cross sections (*ii*)–(*iv*) were reoptimized using the 4-31 G (44-31 G) basis sets (Basis III). The lowest energy pyramidal and planar DMSO structures that were obtained in the 3 G basis (Basis I) calculations, as well as points along crossections (*ii*)–(*iv*), were also reoptimized using the basis sets including polarization *d* functions on sulfur (Basis II).

As pointed out in detailed studies by Collins, v. R. Schleyer, Binkley, and Pople, small constrained gaussian basis sets without polarization *d* functions on sulfur are inadequate to give even qualitatively correct S=O bond lengths (22). This finding is rather intriguing as the same authors have also found that in spite of this inadequacy all other geometrical parameters of a representative set of sulfur compounds are considerably better reproduced than the S=O bond length, with the same gaussian basis sets, which do not include polarization *d* functions (22). Using model potentials for the atomic cores in SO_2, and representing the valence region with gaussian functions, both with and without polarization *d* functions, a detailed study by Huzinaga and Yoshimine (23) has indicated a simi-

TABLE 1. Optimum geometrical parameters, nuclear repulsion energies, and total energies of DMSO models, calculated with various gaussian basis sets

Structure of DMSO	Parameter	Basis I		Basis II	Basis III		Experimental (ref. 24)
		A[a]	B[b]		A[a]	B[b]	
Pyramidal	r_{SO} (Å)	1.47	1.82	1.49	1.47	1.73	1.48
	r_{SC}	1.86	1.81	1.82	1.81	1.81	1.81
	r_{HC}	1.09	1.09	1.09	1.09	1.09	1.09
	θ_{SO} (deg)	64.6	70.6	62.7	70.6	69.7	64.5
	θ_{CSC}	94.6	97.9	94.4	97.9	97.9	96.4
	θ_{HCS}	109.9	109.9	109.9	109.9	109.9	107.5
	E_n (au)	182.43426	174.16313	183.64173	185.44409	176.49171	—
	E_t	−545.14572	−545.19190	−545.34942	−550.77636	−550.81065	—
Planar	r_{SO} (Å)		1.97	1.55	1.47	1.92	
	r_{SC}		1.80	1.78	1.80	1.80	
	r_{HC}		1.09	1.09	1.09	1.09	
	θ_{SO} (deg)		0.0	0.0	0.0	0.0	
	θ_{CSC}		102.7	106.5	102.7	102.7	
	θ_{HCS}		110.2	110.2	110.2	110.2	
	E_n (au)		166.98509	179.47587	181.81792	168.13812	
	E_t		−545.15934	−545.25509	−550.70496	−550.76323	

[a] The S=O bond length was kept fixed at the X-ray experimental value of 1.47 Å (1).
[b] Geometric parameters correspond to optimized S=O bond length.

lar discrepancy in reproducing geometric parameters. The exclusion of polarization *d* functions caused a much larger relative error in the calculated S=O bond length than in the O—S—O bond angle. Apparently, predictions on bond angles in these molecules are much less sensitive to the presence of polarization *d* functions in the basis set than are predictions on S=O bond lengths, in spite of the directional properties of *d* functions. Similarly, calculated S—C and S—H bond lengths are also less sensitive to the inclusion of sulfur *d* functions in the basis set. The above findings suggest that cross sections (*i*), (*ii*), and (*iv*) of the DMSO energy hypersurface are likely to be adequately represented by employing *s* and *p* type basis functions only. By contrast, for calculation of the S=O stretching potential (*iii*) of DMSO, *d* functions appeared to be essential. For comparison, however, all three crossections, (*ii*), (*iii*), and (*iv*), have been recalculated using the Basis II that includes polarization *d* functions.

Results and Discussion

The optimized values of various geometric parameters of pyramidal and planar DMSO structures, and also the corresponding values of nuclear repulsion energies E_n and total energies E_t, as calculated with basis sets I, II, and III, are listed in Table 1. Experimental geometry data, taken from a recent compilation (24), are also included in the table. Using Bases I and III, two separate sets of optimizations were carried out. The parameters listed in the columns marked with an A were obtained by keeping the r_{SO} bond length constant at 1.47 Å, the value taken from the X-ray study of ref. 1. In the columns marked with a B the optimized value of the S=O bond length and the reoptimized values of the rest of the parameters are listed.

It is remarkable that the optimized values of the S=O bond length, calculated with the three bases, are extremely sensitive to variations in the bases, particularly to the inclusion of polarization *d* functions. This sensitivity exceeds even those of the set of simple sulfur compounds studied in ref. 22, and for Basis I the error (as measured from the experimental S=O bond length value of 1.48 Å, ref. 24) was as large as 0.34 Å. The calculated 1.82 Å S=O bond length is much larger than the Schomaker–Stevenson S—O single bond length of 1.69 Å (25). In fact, in the first optimization cycle with Basis I the S=O bond distance appeared divergent indicating the possibility of dissociation, and several optimization cycles were required to locate a real minimum at 1.82 Å. In spite of the qualitatively correct result of a stable S=O bond, Basis I fails to give even a qualitatively correct S=O bond length. By contrast, it is remarkable that the optimized values for the rest of the geometric parameters are markedly more accurate, although the error for the out-of-plane angle θ_{SO} is also rather large (6°). When restricting the S=O bond length to 1.47 Å (X-ray result, ref. 1) the corresponding optimum value of θ_{SO} (given in column A, Basis I) improves markedly (64.6°, in error by only 0.1°). However,

Can. J. Chem. Downloaded from www.nrcresearchpress.com by 210.87.254.5 on 09/05/12
For personal use only.

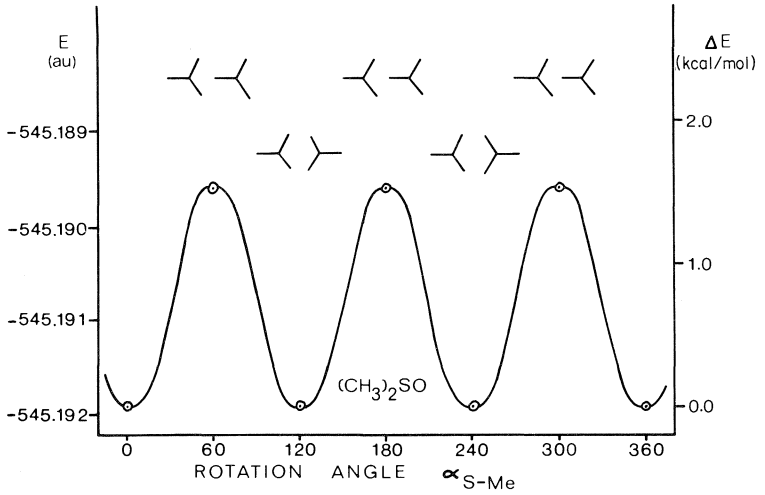


FIG. 1. Rotation potential curve along the α_{S-Me} coordinate of DMSO, calculated with basis I. Relative positions of the hydrogen atoms are shown above the extrema of the curve.

the optimized C—S bond length becomes much too long (1.86 Å as opposed to 1.81 Å). Nevertheless, the restriction on the S=O bond length brings about an overall improvement of the geometrical parameters.

Basis III gives a slightly better prediction for the S=O bond length, however, the 1.73 Å optimized value is still longer than the single bond value of 1.69 Å and much longer than the experimental value of 1.48 Å. The optimum out-of-plane angle 69.7° (θ_{SO} in column B) is somewhat better than the corresponding 70.6° result with Basis I (column B). In general, geometry predictions are reasonable for all but the SO bond length.

The inclusion of polarization *d* functions on sulfur (Basis II) gives rather accurate optimum values for all geometric parameters, in spite of the fact that in terms of total molecular energy this basis is inferior to Basis III. Bond lengths are accurate to 0.01 Å and bond angles to 2°. This finding is in excellent agreement with the results of Collins, Schleyer, Binkley and Pople on a set of simple sulfur compounds (22).

All three basis sets give consistently longer S=O bond predictions for planar DMSO than for the pyramidal optimum structure although both Bases I and III predict unreasonably long bond distances. By contrast, the 1.55 Å SO bond length predicted for the planar DMSO form by Basis II appears reasonable. The slight shortening of the S—C bonds may also be expected on a qualitative basis.

The periodic potential curve for the S—Me rotation (*i*), as calculated with Basis I is shown in Fig. 1. The relative positions of the hydrogen atoms in the two methyl groups are shown schematically above the extrema of the curve. This cross section does not show unusual flat regions or other unexpected features, and the calculated rotation barrier of 1.5 kcal/mol is close to the average value of barriers to Me group rotations.

In Fig. 2 the pyramidal inversion potentials (as a function of the out of plane angle θ_{SO}) are compared for basis sets I, II, and III. For Bases I and II the fully optimized total energy values are plotted, while for Basis III three different potential curves were calculated. Curve III A was obtained by constraining the S=O bond length to the X-ray experimental value of $r_{S=O}$ = 1.47 Å, curve III B was calculated with the S=O bond length reoptimized along the pyramidal inversion path (relaxed potential curve), while curve III C was obtained by recalculating the Basis II optimum structures with the larger Basis III. The calculated value for the inversion barrier is apparently very sensitive to the basis set, as well as to the constraints on the S=O bond length. Basis II predicts the largest inversion barrier, 59 kcal/mol, and the shortest optimum S=O bond length. For all other calculations, the shorter the S=O bond length, the larger the inversion barrier.

Polarization *d* functions appear to be essential in predicting correct geometry, particularly in predicting the correct value for the S=O bond length. For the calculation of the barrier height, however, the direct contribution of *d* functions to the calculated energy values appears to be less significant. Rather, the overall size of the basis set and the assumed geometry are of greater importance. The effect of geometry is clearly shown by the three curves III A, III B, and III C. Potential curve III A,

Can. J. Chem. Downloaded from www.nrcresearchpress.com by 210.87.254.5 on 09/05/12
For personal use only.

Can. J. Chem. Downloaded from www.nrcresearchpress.com by 210.87.254.5 on 09/05/12
For personal use only.

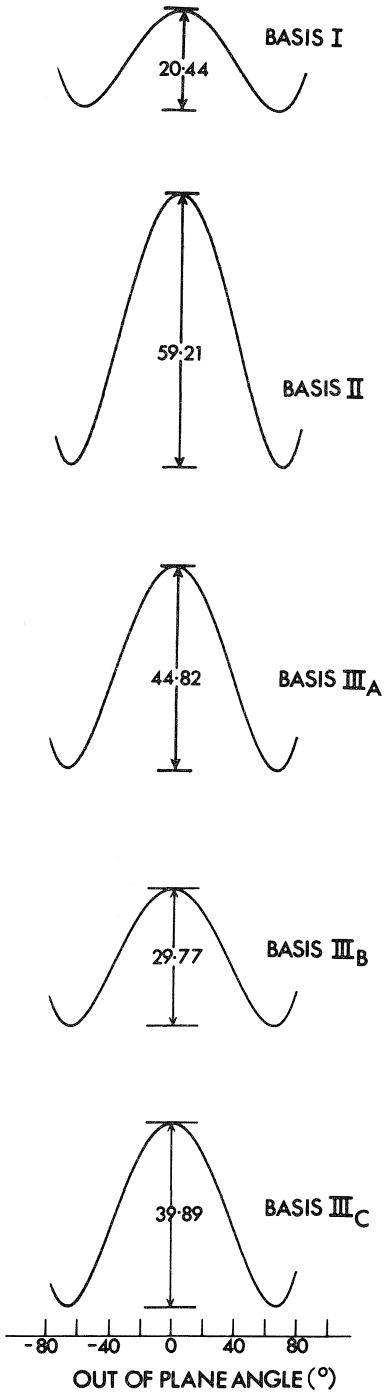


FIG. 2. Pyramidal inversion potentials and inversion barriers of DMSO as calculated with various gaussian basis sets. All barrier heights in kcal/mol.

calculated with a fixed $r_{S=O} = 1.47$ Å bond length, gives a barrier of 44.8 kcal/mol. This may be considered as an upper bound for the barrier of the true process that is likely to involve bond length variations. Curve III B, on the other hand, is likely to represent a lower bound (29.8 kcal/mol) for the true barrier, since the corresponding S=O bond lengths in the pyramidal and planar DMSO structures are far too large. The extreme case of infinite S=O bond length would certainly correspond to a lower bound for "pyramidal inversion", with no barrier at all. The 39.9 kcal/mol barrier of curve III C, that is, the energy difference between optimum pyramidal and planar Basis II structures recalculated with the large basis set III, falls in between these two bounds. This value is indeed a reasonable estimate for the inversion barrier on qualitative grounds (26). This barrier is about 16 kcal/mol higher than the calculated barrier to pyramidal inversion of the sulfilimine model $H_2S{=}NH$ (10), in qualitative agreement with available experimental information (26). The potential curve for the inversion process does not show unusual flat regions nor pathological V-type potentials.

In Fig. 3 the S=O stretching potentials are shown as calculated with basis sets I, II, and III. It is remarkable, that these curves are very different not only in terms of the position of their minima, but also in their shape. While curve II predicts the optimum S=O distance rather accurately, it shows

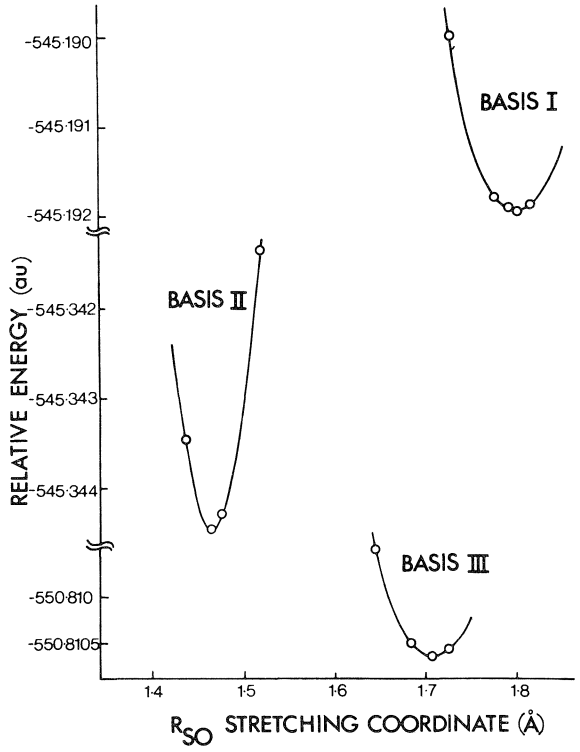


FIG. 3. Sulfur–oxygen bond stretching potentials of DMSO as calculated with various basis sets.

Can. J. Chem. Downloaded from www.nrcresearchpress.com by 210.87.254.5 on 09/05/12
For personal use only.

a much steeper potential than the other two curves. This feature is related to the shorter bond length and the implied steeper change in the nuclear repulsion energy, that, in general, is accompanied by a similarly steep change in the total electronic energy (12). While a perfectly parallel change in the slopes of the above two contributions would result in no net change in the slope of the total energy curve, the very fact that the slope of the total energy is the difference of two larger components, gives rise to a less-than-perfect cancellation, and leads to a steeper potential curve. The presence of diffuse polarization *d* functions for any *fixed* minimum position is likely to cause the potential curve to become shallower; thus the calculated steep potential is *not* a direct result of *d* function participation. The effect of *d* functions is indirect; they cause a shift of the calculated potential minimum from the unrealistic large values to the shorter $r_{S=O}$ = 1.49 Å value, accurate to 0.01 Å. The shorter bond length, in turn, gives rise to a steeper potential curve.

One of the characteristic features of the DMSO conformational hypersurface is the cross section along the plane defined by pyramidal inversion coordinate $\theta_{S=O}$ and asymmetric S—Me stretching coordinate $r_{S—Me}$. The energy surface associated with this cross section is shown in Fig. 4. It is remarkable, that in a 0.16 Å interval along the $r_{S—Me}$ coordinate, the calculated total energy E_t shows very small changes only, as compared to the variations along inversion coordinate $\theta_{S=O}$. In the two narrow valleys, along the $r_{S—Me}$ stretching coordinate containing the two symmetrically equivalent minima M_1 and M_2, the surface shows two extended flat regions. Bases I and II result in very similar flat regions, although the optimum stretching potentials along the bottom of the valley differ slightly, as it is shown in Fig. 5. The addition of polarization *d* functions to the basis set results in a more anharmonic stretching potential, that is, the curve becomes steeper for shorter bond lengths and less steep for longer distances. This result is in agreement with a general observation that polarization *d* functions lower the potential of distorted structures if the molecular distortion is associated with an increase in the atom–atom distances.

The calculated optimum S—C bond distances (1.81 Å and 1.82 Å with Bases I and II, respectively) fall in the range of the two asymmetric bond length values (1.775 and 1.821) found in the X-ray study of ref. 1. For such an asymmetric displacement of the two Me groups the calculated theoretical total energy increase is less than 0.4 kcal/mol. Consequently, our results indicate that as little as 0.4 kcal/mol may distort the DMSO ground state structure to the extent reported in the quoted X-ray study (1). Apparently, the looseness of the valence shell gaussian functions on sulfur and the relatively long equilibrium C—S bond length are responsible for the flatness of the stretching potential.

The $r_{S—Me}$ stretching potential is certainly flat in

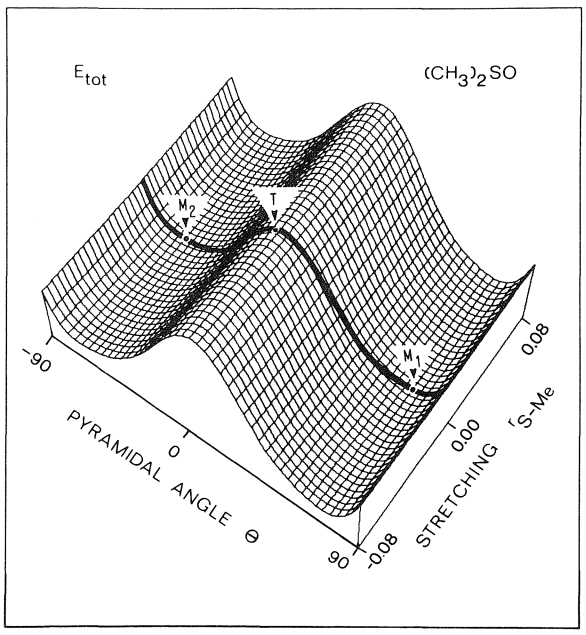


FIG. 4. Cross section of the DMSO conformational hypersurface along the plane of pyramidal inversion and S—Me asymmetric stretching coordinates.

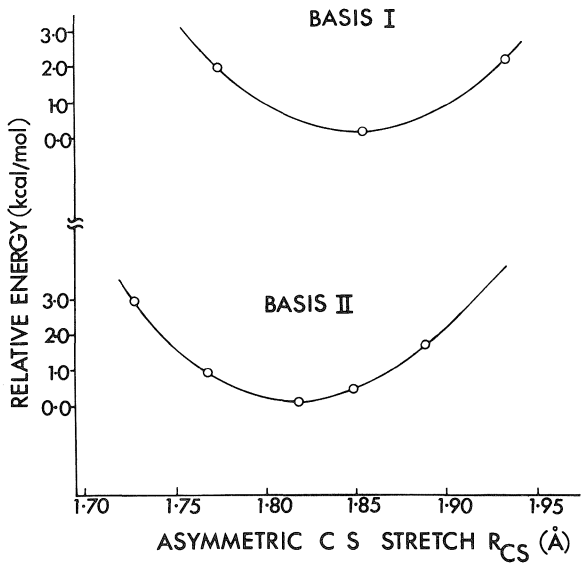


FIG. 5. Asymmetric S—Me stretching potentials of DMSO as calculated with Bases I and II.

Can. J. Chem. Downloaded from www.nrcresearchpress.com by 210.87.254.5 on 09/05/12
For personal use only.

an absolute sense: the variation of total energy is small in the given interval. The flatness of an energy surface, however, is also a relative characterization. A given cross section of the surface may appear flat as compared to another cross section, as is the case in our example for cross sections along coordinates $r_{S—Me}$ and $\theta_{S=O}$, respectively. Alternatively, one may consider a relative measure of variations of the total energy, relevant to the given molecule. Formally, one could assume that molecules composed from atoms of larger nuclear charge would show larger variations in total energy upon changes in geometry, simply as a result of larger variations in the nuclear repulsion terms. However, most often this is not the case: when comparing various conformational processes the total energy changes are not proportional to the accompanying changes in the nuclear repulsion terms. By generalizing this observation, one may consider the partitioning of the molecular total energy E_t into nuclear and electronic terms, E_n and E_e, respectively:

$$[1] \quad E_t = E_n + E_e$$

The repulsive nuclear term,

$$[2] \quad E_n = \sum_{i<j} Z_i Z_j / R_{ij}$$

certainly shows much larger variations in a given type of conformational process, if the nuclear charges Z_i are larger. It is the variation of E_n that must be compensated by opposite variations in the electronic term E_e, to approximately maintain the total energy of the molecular system. Consequently, a relative scale for the variations in total energy, E_t, relevant to a given molecular system may be obtained by comparing the variations of E_t to that of E_n, that is, ΔE_t to ΔE_n. The relative variation,

$$[3] \quad \Delta E_{rel} = \Delta E_t / \Delta E_n$$

is a relative measure of energy change along a potential curve. ΔE_{rel} is measured on an internal energy scale of the molecule, relative to ΔE_n, and is characteristic of the conformational change of the given molecule. As an example, one may consider molecules H_2 and F_2. While the force constants for these two molecules are of the same order of magnitude,[2] the nuclear repulsion term for F_2 is nearly two orders of magnitude larger than that of H_2. The similarity of the two force constants implies that a given elongation of the H—H and F—F bonds causes approximately equivalent ΔE_t changes in both molecules, in spite of the fact that the corresponding ΔE_n change in the nuclear repulsion term is nearly two orders of magnitude larger for F_2 than for H_2. This implies that in a relative sense the ΔE_n changes are far better compensated by opposite ΔE_e electronic energy changes in the case of F_2 than in the case of H_2. For F_2 the net energy change $\Delta E_t = \Delta E_n + \Delta E_e$ is a much smaller fraction of the underlying ΔE_n change than it is for H_2, and this difference is properly reflected in the corresponding relative variations, ΔE_{rel}.

The internal energy scale concept may be generalized to an entire conformational domain of an energy hypersurface; it is convenient to choose an internal energy scale on which the maximum variation of E_n (in the given domain) is unity. In the classical mechanical sense the flatness of a total energy surface, given in some absolute energy units, indicates the deformability of the molecular structure. The flatness of the scaled energy surface, on the other hand, is a relative measure of the degree of compensation between the ΔE_n and ΔE_e components.

Such a rescaling of the DMSO $E_t(r_{S—Me}, \theta_{SO})$ energy surface to the internal energy scale is shown in Fig. 6, together with component surfaces $E_n(r_{S—Me}, \theta_{SO})$ and $E_e(r_{S—Me}, \theta_{S=O})$. The two highest points in the given domain of the E_n surface ($r_{S—Me} = -0.08, \theta_{SO} = 90°$, and $r_{S—Me} = -0.08, \theta_{SO} = -90°$) correspond to 1.0 on the internal energy scale (equivalent to ~4.0 au on the absolute energy scale).

It is striking that the variations in E_t are almost unnoticeable on the internal energy scale, and the E_t surface appears almost perfectly flat. Apparently, the cancellation in the variations of E_n and E_e is close to 100%.

In most conformational processes there is a certain degree of cancellation between variations of E_n and E_e. By using the formal analogy of the le Chatelier principle, a partial cancellation between E_n and E_e may be interpreted as a tendency to approximately conserve the total energy E_t (12). A conformational change, that is, a rearrangement of the nuclei causes a change in the nuclear repulsion term E_n. This change may be regarded as a "perturbation" of the molecular system. Apparently, the electron distribution (and E_e) then readjusts in such a way as to counterbalance this perturbation by reducing the change in the molecular total energy, E_t. The loose valence orbitals of second row elements appear to facilitate this process. The appearance of flat regions on the E_t surface of DMSO, particularly, when represented on the internal energy scale, shows that this compensation process is extremely efficient for this molecule.

[2]The force constants are 5.2×10^{-5} and 4.5×10^{-5} dyn/cm for H_2 and F_2, respectively (27).

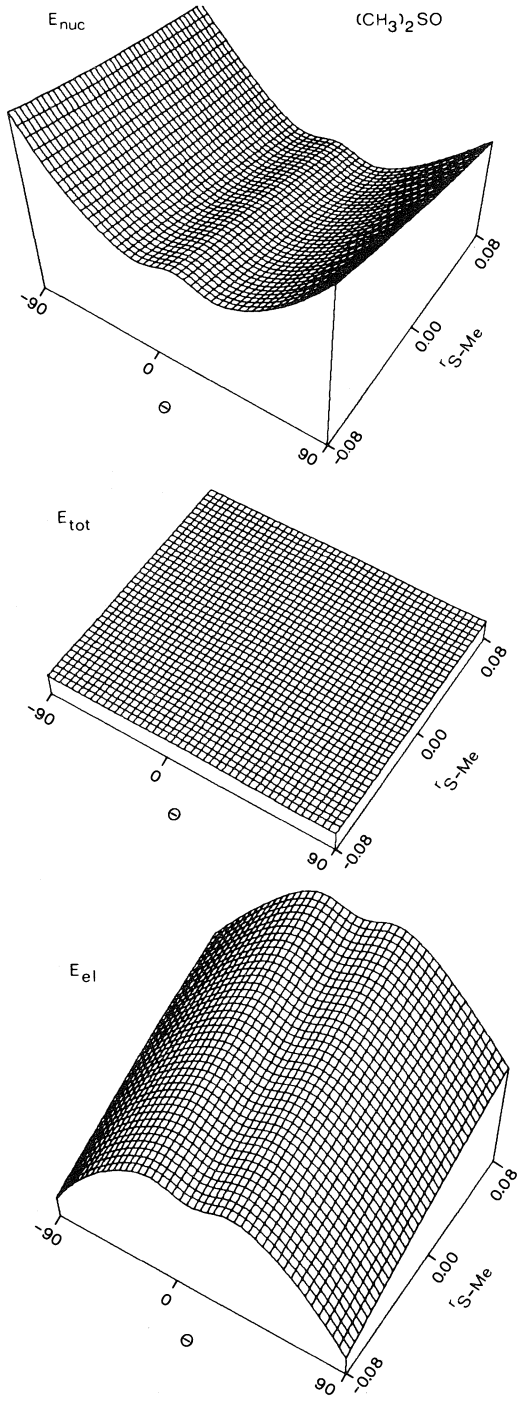


FIG. 6. Decomposition of the pyramidal inversion – asymmetric stretching total energy surface into nuclear and electronic components, as represented on the internal energy scale.

Acknowledgement

The financial support of the Natural Sciences and Engineering Research Council of Canada is gratefully acknowledged.

1. R. THOMAS, C. B. SHOEMAKER, and K. ERICS. Acta Crystallogr. **21**, 12 (1966).
2. L. VAN ACKER and M. ANTENUNIS. Tetrahedron Lett. 849 (1973).
3. D. N. HARPP and J. G. GLEASON. J. Org. Chem. **36**, 1314 (1971).
4. M. M. L. CHEN and R. HOFFMANN. J. Am. Chem. Soc. **98**, 1647 (1976).
5. J. P. SNYDER and L. CARLSEN. J. Am. Chem. Soc. **99**, 2931 (1977).
6. A. E. PEKARY. J. Phys. Chem. **78**, 1744 (1974).
7. P. G. MEZEY and A. KUCSMAN. J. Chem. Soc. Chem. Commun. 1448 (1971).
8. P. G. MEZEY and A. KUCSMAN. J. Chem. Soc. Faraday II, **68**, 2060 (1972).
9. K. ÖSAPAY, P. G. MEZEY, and A. KUCSMAN. Prog. Theor. Org. Chem. **2**, 34 (1977).
10. P. G. MEZEY, A. KUCSMAN, G. THEODORAKOPOULOS, and I. G. CSIZMADIA. Theor. Chim. Acta, **38**, 115 (1975).
11. P. G. MEZEY. Prog. Theor. Org. Chem. **2**, 127 (1977).
12. P. G. MEZEY. Chem. Phys. Lett. **47**, 70 (1977).
13. A. KAPUR, R. P. STEER, and P. G. MEZEY. J. Chem. Phys. **69**, 968 (1978).
14. P. G. MEZEY, R. P. STEER, and A. KAPUR. J. Photochem. **9**, 130 (1978).
15. A. KAPUR, R. P. STEER, and P. G. MEZEY. J. Chem. Phys. **70**, 745 (1979).
16. A. KAPUR, R. P. STEER, and P. G. MEZEY. J. Chem. Phys. **71**, 588 (1979).
17. C. D. LEAKE. Ann. N. Y. Acad. Sci. **141**, 1 (1967).
18. M. A. VISWAMITRA and K. K. KANNAN. Nature, London, **209**, 1016 (1966).
19. R. DITCHFIELD, W. J. HEHRE, and J. A. POPLE. J. Chem. Phys. **54**, 724 (1971).
20. W. J. HEHRE and W. A. LATHAN. J. Chem. Phys. **56**, 5255 (1972).
21. W. J. HEHRE, R. F. STEWART, and J. A. POPLE. J. Chem. Phys. **51**, 2657 (1969).
22. J. B. COLLINS, P. v. R. SCHLEYER, J. S. BINKLEY, and J. A. POPLE. J. Chem. Phys. **64**, 5142 (1976).
23. S. HUZINAGA and M. YOSHIMINE. J. Chem. Phys. **68**, 4486 (1978).
24. D. MARTIN and H. G. HAUTHAL. Dimethyl sulphoxide. Van Nostrand Reinhold Co. Ltd., Wokingham, England. 1975.
25. V. SCHOMAKER and D. P. STEVENSON. J. Am. Chem. Soc. **63**, 37 (1941).
26. S. OAE. Private communication; S. OAE (*Editor*). Organic chemistry of sulfur. Plenum Press, New York. 1977; C. C. PRICE and S. OAE. Sulfur bonding. Ronald Press Co. 1962.
27. G. M. BARROW. Introduction to molecular spectroscopy. McGraw Hill, 1962. p. 42.

Can. J. Chem. Downloaded from www.nrcresearchpress.com by 210.87.254.5 on 09/05/12
For personal use only.

Acid catalysed hydrolysis of orthoesters: mechanism of hydrolysis of 2,4,10-trioxaadamantanes substituted in position 3[1,2]

OTMANE BOUAB, GÉRARD LAMATY, CLAUDE MOREAU, AND ODILE POMARES

Laboratoire de Chimie Organique Physique, Université des Sciences et Techniques du Languedoc, 34060 Montpellier, France

AND

PIERRE DESLONGCHAMPS AND LUC RUEST

Laboratoire de Synthèse Organique, Département de Chimie, Faculté des Sciences, Université de Sherbrooke, Sherbrooke (Qué.), Canada J1K 2R1

Received August 2, 1979

OTMANE BOUAB, GÉRARD LAMATY, CLAUDE MOREAU, ODILE POMARES, PIERRE DESLONGCHAMPS, and LUC RUEST. Can. J. Chem. **58**, 567 (1980).

The rates of hydrolysis of orthoesters, 2,4,10-trioxaadamantanes, substituted in position 3 (R = H, CH_3, C_2H_5, C_6H_5) have been determined at 25 and 40°C in dioxane/water (60:40 by volume). Substitution of hydrogen by the groups CH_3, C_2H_5, and C_6H_5 shows clearly a decrease in rate: 0.018 (CH_3), 0.014 (C_2H_5), and 0.003 (C_6H_5). This decrease, in accord with substituent effects, plus the strongly negative entropies of activation observed, suggests that the rate-determining step is the addition of water to the carboxonium ion intermediate.

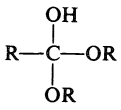
OTMANE BOUAB, GÉRARD LAMATY, CLAUDE MOREAU, ODILE POMARES, PIERRE DESLONGCHAMPS et LUC RUEST. Can. J.Chem. **58**, 567 (1980).

Les vitesses d'hydrolyse des orthoesters trioxa-2,4,10-adamantanes substitués en position 3 (R = H, CH_3, C_2H_5, C_6H_5) ont été déterminées à 25 et 40°C dans un mélange eau/dioxanne 40/60 en volume. La substitution de H par les groupes CH_3, C_2H_5 et C_6H_5 entraîne un très net ralentissement: 0.018 (CH_3), 0.014 (C_2H_5) et 0.003 (C_6H_5). Ce ralentissement, en accord avec les effets de substituants et les entropies d'activation fortement négatives observées, suggère que l'étape déterminant la vitesse de réaction est l'addition de l'eau sur l'ion carboxonium intermédiare.

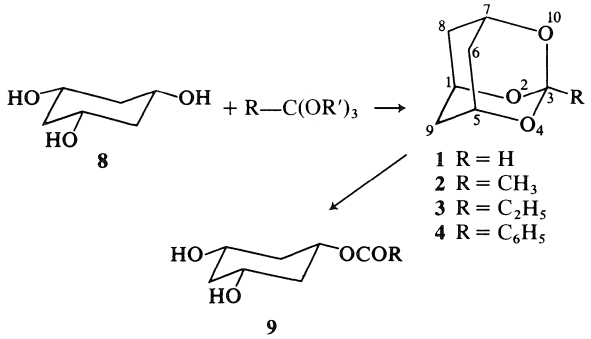
Introduction

In many hydrolysis reactions, a reactive intermediate is formed in which an atom of carbon is bonded to three electronegative atoms. The study of the reactivity of such intermediates is therefore a necessary and essential step in the elucidation of the mechanism of these reactions which have biological importance.

We believe that an important step has been realised lately by the work resulting in the elaboration of the stereoelectronic theory which demonstrates the significance of conformation in these intermediates, and in particular, intermediates of the type hemiorthoester which are formed in ester hydrolyses (2).



We wish to report on our study of the influence of the stereoelectronic effect on the hydrolysis rates of the system 2,4,10-trioxaadamantane substituted in position 3 (compounds **1**, **2**, **3**, and **4** in Scheme 1). These orthoesters possess the features of being rigid and favorable to stereoelectronic control as they contain two oxygen atoms (O_2 and O_4 each possessing a non-bonded electron pair antiperiplanar to the bond (C3—O10) susceptible to cleavage. The 2,4,10-trioxaadamantanes were prepared by the reaction of the appropriate aliphatic orthoester and *cis*-cyclohexane-1,3,5-triol (**8**) and on acid hydrolysis they yield the corresponding monoester **9** of *cis*-cyclohexane-1,3,5 triol (**8**).



SCHEME 1

Results

Hydrolysis of the 2,4,10-trioxaadamantanes was carried out in relatively strong concentrations (0.05

[1]Preliminary communication, see ref. 1.

[2]This work was carried out as part of the integrated France–Quebec project no. 01.05.13.

0008-4042/80/060567-07$01.00/0

©1980 National Research Council of Canada/Conseil national de recherches du Canada

Can. J. Chem. Downloaded from www.nrcresearchpress.com by 210.87.254.6 on 09/05/12
For personal use only.

Can. J. Chem. Downloaded from www.nrcresearchpress.com by 210.87.254.6 on 09/05/12
For personal use only.

to 2 *M*) of hydrochloric acid in order to obtain reasonable rates. The solvent dioxane/water 60:40 by volume was chosen for solubility reasons and also because comparison of the results could be made with literature values; the Hammett H_0 acidity functions are known for this medium (3). The experimental results are given in Table 1.

By plotting the observed rate constants k_{obs} against proton concentration $[H^+]$, there is a linear relationship up to acid concentrations of 0.5 *M*, which gives directly the catalytic constant k_{H^+}. Above 0.5 *M* , the relationship is no longer linear, nor is it when k_{obs} is plotted against H_0, the Hammett acidity function.

In Table 2 are the catalytic constants k_{H^+} obtained for the different products studied as well as activation energies calculated from k_{H^+}. These activation energies are identical within experimental error with those calculated from k_{obs} at different acid concentrations. The results of De Wolfe and Jensen (4) on the corresponding aliphatic orthoesters, ethylorthoformate (**5**), ethylorthoacetate (**6**), and ethylorthobenzoate (**7**) are given for comparison in Table 3.

TABLE 1. Hydrolysis rate constants of 2,4,10-trioxaadamantanes in dioxane/water (60:40)

(*a*) 2,4,10-Trioxaadamantane (**1**)

[HCl] *M*	$k_{obs} \times 10^2$ s^{-1} (25.2°C)	$k_{obs} \times 10^2$ s^{-1} (41.5°C)
0.05	0.144	0.503
0.105	0.326	0.965
0.26	0.858	2.41
0.53	1.72	—
1.00	5.03	—

(*b*) 3-Methyl-2,4,10-trioxaadamantane (**2**)

[HCl] *M*	$k_{obs} \times 10^3$ s^{-1} (25.2°C)	$k_{obs} \times 10^3$ s^{-1} (41.5°C)
0.26	0.124	0.609
0.53	0.291	1.34
1.00	0.754	3.30
2.06	2.38	9.70

(*c*) 3-Ethyl-2,4,10-trioxaadamantane (**3**)

[HCl] *M*	$k_{obs} \times 10^3$ s^{-1} (25.8°C)	$k_{obs} \times 10^3$ s^{-1} (40.2°C)
0.265	0.104	—
0.47	0.206	0.831
0.71	0.385	1.41
0.94	0.571	2.27
1.84	2.40	7.08

(*d*) 3-Phenyl-2,4,10-trioxaadamantane (**4**)

[HCl] *M*	$k_{obs} \times 10^4$ s^{-1} (25.0°C)	$k_{obs} \times 10^4$ s^{-1} (40.3°C)
0.265	0.191	—
0.47	0.442	2.32
0.71	0.777	3.86
0.94	1.17	5.93
1.84	4.20	18.5

TABLE 2. Hydrolysis of 2,4,10-trioxaadamantanes in dioxane/water (60:40) at 25.2°C

Orthoesters	k_{H^+} M^{-1} s^{-1}	k_{rel}	$\Delta H^{\neq}$ kcal/mol	$\Delta S^{\neq}$ eu
1 R = H	3.3×10^{-2}	350	11.5 ± 0.5	−27 ± 3
2 R = CH_3	6.2×10^{-3}	7	16.2 ± 0.5	−19 ± 2
3 R = C_2H_5	4.5×10^{-4}	5	17.3 ± 0.5	−16 ± 2
4 R = C_6H_5	9.4×10^{-5}	1	19.4 ± 0.5	−12 ± 2

TABLE 3. Hydrolysis of $RC(OC_2H_5)_3$ (R = H (**5**), R = CH_3 (**6**), and R = C_6H_5 (**7**)) in dioxane/water (60:40). Values are extrapolated to 25°C from the results of De Wolfe and Jensen (4)

Orthoesters	k_{H^+} M^{-1} s^{-1}	k_{rel}	$\Delta H^{\neq}$ kcal/mol	$\Delta S^{\neq}$ eu
5 R = H	4.2×10^3	2.6	15.5	8 ± 5
6 R = CH_3	2.1×10^5	130	13.0	7 ± 2
7 R = C_6H_5	1.6×10^3	1	14.6*	1.4 ± 1.1*

*20.5% dioxane.

Interpretation of Results

Comparison of our experimental results (Table 2) with those reported in the literature on the corresponding aliphatic orthoesters (Table 3) shows three fundamental differences. (*1*) The activation entropies are strongly negative for the 2,4,10-trioxaadamantanes, whereas they are slightly positive for the aliphatic orthoesters. (*2*) Substitution of H by CH_3, C_2H_5, or C_6H_5 decreases the hydrolysis rate in the trioxaadamantanes. Substitution of H by CH_3 in the aliphatic orthoesters augments the rate of hydrolysis. Substitution of H by C_6H_5 decreases the rate in the aliphatic orthoesters which is a particular case to be discussed later. (*3*) The rates of hydrolysis for the 2,4,10-trioxaadamantanes are considerably lower (10^{-6} to 10^{-9}) than those of the aliphatic orthoesters.

This behavior suggests that the mechanism of hydrolysis in the trioxaadamantanes is different from that in aliphatic orthoesters. A plot of $\Delta H^{\neq}$ against $\Delta S^{\neq}$ for the trioxaadamantanes shows a linear relationship (Fig. 1). The slope of the line β, isokinetic temperature, is 525 K which means that the hydrolysis of the 2,4,10-trioxaadamantanes is enthalpy controlled. The linear correlation also indicates that these products are all hydrolysed by the same mechanism (5).

The generally accepted mechanism for acid-catalysed hydrolysis of orthoesters involves 3 steps (6, 7), (*1*) formation of a carboxonium ion (eq. [1], Scheme 2), (*2*) formation of a hemiorthoester (eq. [2]), and (*3*) decomposition of hemiorthoester (eq. [3]). Hemiorthoester formation could equally result

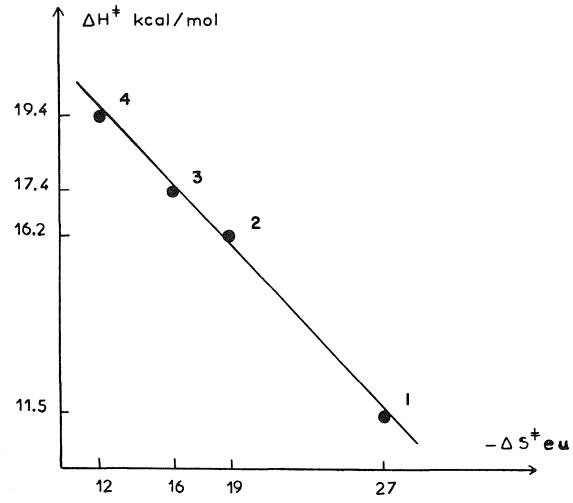
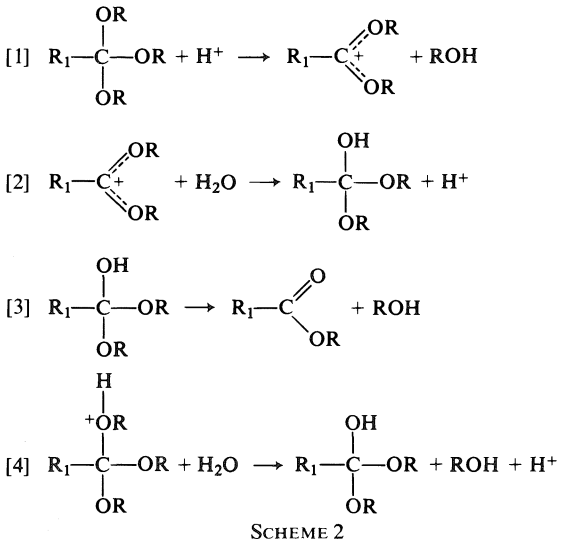


FIG. 1. Plot of $\Delta H^{\ddagger}$ against $\Delta S^{\ddagger}$ for the trioxaadamantanes ($\Delta H^{\ddagger} = -\beta\Delta S^{\ddagger}$).

from attack by water on the conjugate acid of the orthoester (eq. [4]).

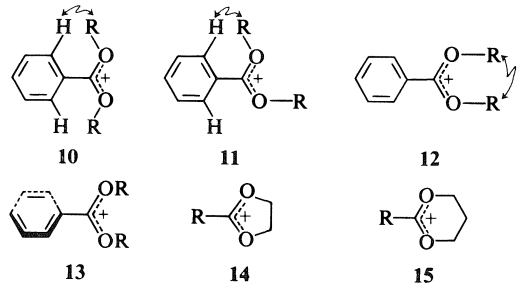
In most of the orthoester hydrolysis studied so far, the slow step is the carboxonium ion formation (eq. [1]); there is, however, a recent example implicating the decomposition of the hemiorthoester (eq. [3]) as being the critical process (8). A mechanism in which the rate-determining step is the carboxonium ion formation (eq. [1]) must be eliminated for the 2,4,10-trioxaadamantanes.

Examination of Table 3 (aliphatic orthoesters) gives the following conclusions: (*a*) the activation entropies of the processes for the catalytic constant k_{H^+} are low and positive (unimolecular reaction, mechanism A1); (*b*) the substituent effects go in the direction of increased resonance stabilisation of the



SCHEME 2

transition state when H is substituted by CH_3 and the rate is augmented in the substituted derivative. Following the same reasoning, substitution of H by C_6H_5 should further augment this stabilisation giving $k_{C_6H_5} > k_H$. In fact there is a rate decrease which could suggest a mechanistic change (9), but recent work serves to explain this rate decrease on the basis of steric factors (10). Four possible structures (**10**, **11**, **12**, and **13**) can be written for the carboxonium ion of ethylorthobenzoate (Scheme 3).



SCHEME 3

In the carboxonium ions **10**, **11**, and **12**, steric interactions (between the ortho hydrogens and the R groups in **10** and **11**, between the two R groups in **12**) make these structures unfavorable. In order to avoid these strong steric interactions, the benzene ring tends to lie perpendicular to the plane of the carboxonium ion (structure **13**), preventing at the same time conjugation between these two functions. It is therefore normal to observe a decrease in rate when H is substituted by C_6H_5. On the other hand, in the 1,3-dioxolenium ion **14** and in the 1,3-dioxenium ion **15**, (R = C_6H_5), conjugation is favored. Consequently, it is not surprising to observe an increase in rate when H is substituted by C_6H_5 in the hydrolysis of 2-methoxy-1,3-dioxolanes (10) and 2-methoxy-1,3-dioxanes (Table 4).[3]

Thus, whatever evidence is compared, activation entropies[4] or substituent effects, the reactivity of 2,4,10-trioxaadamantanes is incompatible with a mechanism involving carboxonium ion formation as the rate-determining step.

The decomposition of the hemiorthoester can equally be excluded as the rate-determining step as

[3]O. Pomares. Unpublished results.

[4]One referee has suggested that the negative entropy of activation could result from the fact that there could be a concerted process in eq. [1]. This is effectively what does occur when the hydrolysis of orthoesters is subjected to general acid catalysis: the $\Delta S^{\ddagger}$ values calculated from the catalytic constants of weak acids are strongly negative (−20 to −30 eu); however, the $\Delta S^{\ddagger}$ values calculated from the proton catalytic constants are near zero. In the present work, the discussion concerns only the rate constants k_{H^+}. The concerted process can therefore be safely eliminated from the $\Delta S^{\ddagger}$ values as well as from the substituent effects.

Can. J. Chem. Downloaded from www.nrcresearchpress.com by 210.87.254.6 on 09/05/12
For personal use only.

Can. J. Chem. Downloaded from www.nrcresearchpress.com by 210.87.254.6 on 09/05/12
For personal use only.

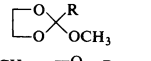
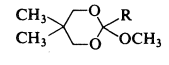
it is a unimolecular reaction which would give imperceptible or weakly positive activation entropies. There remains only the formation of the hemiorthoester to represent the rate-determining step in the hydrolysis of the 2,4,10-trioxaadamantanes.

The hemiorthoester can be formed in two ways: (*a*) by nucleophilic attack of water on the conjugate acid of the orthoester, an A2 mechanism (eq. [4]; (*b*) by addition of water to the carboxonium ion intermediate (eq. [2]). In both cases, water is implicated in the slow step which is in accord with the strongly negative activation entropies observed (5).

The A2 mechanism which involves the addition of water to the conjugate acid of the orthoester (Scheme 4, **16** → **17** must, however, be ruled out. By analogy with the S_N2 mechanism, the rate decrease on substituting H with CH_3 and C_2H_5 would be compatible with steric interactions but not when H is replaced by C_6H_5 as the resonance effect should give a rate increase ($k_{C_6H_5} > k_H$ (11)). Furthermore, if the hydrolysis of the 2,4,10-trioxaadamantanes involved an A2 mechanism, the 2,8,9-trioxabicyclo[3.3.1]nonane (**18**) which has a similar structure as well as electron pair orientation, should have a similar rate to **1**. However, it reacts much faster ($k_{18}/k_1 \simeq 4 \times 10^4$), at a rate comparable to that of the aliphatic orthoesters ($k_{18}/k_5 = 0.3$) (12) and probably according to the same mechanism. The addition of water to the conjugate acid of the orthoester as the slow step is therefore not the interpretation of the experimental results.

The addition of water to a carboxonium ion intermediate as the slow step in the hydrolysis of 2,4,6-trioxaadamantanes must therefore be examined. Table 2 indicates a rate decrease on substituting H by CH_3, C_2H_5, and C_6H_5. This can be interpreted on the basis of either steric and/or electronic factors. The steric interaction increases in the direction H, CH_3, C_2H_5, C_6H_5. It is therefore conceivable that the addition of water becomes more difficult in the same sense, which is in agreement with the experimental results. The carboxonium ion is increasingly stabilized on going from H to CH_3, C_2H_5, and C_6H_5. This stabilization of the ion increases the difficulty of water addition in the same sense, $k_H > k_{CH_3} > k_{C_2H_5} > k_{C_6H_5}$, which is again supported by the experimental results. Also, as the carboxonium ion becomes more highly stabilized, the charge on the reactive carbon will be increasingly dispersed; solvation would diminish, giving less and less negative activation entropies on going from H, CH_3, C_2H_5, and C_6H_5, which is in fact observed experimentally.[5]

TABLE 4. Relative rate constants (k_{H^+}) for the hydrolysis of aliphatic orthoesters, 1,3-dioxolanes, and 1,3-dioxanes

Orthoesters	k_{R^+} R = H	R = C_6H_5	References
R—$C(OC_2H_5)_3$	1	0.6	4
	1	40	8*b*, 10
	1	120	Footnote 3

The experimental results are therefore compatible with the addition of water to a carboxonium ion as the slow step. This is the first time that such a hypothesis is envisaged in the hydrolysis of orthoesters. A reaction sequence is proposed in accord with the above requirements.

Two hypotheses can be theoretically considered depending on whether the carboxonium ions are planar or non-planar.[6] It is well established (X-rays supported by calculation), that 1,3-dioxolenium and 1,3-dioxenium ions (**14** and **15**) are planar (13, 14).[7] Consequently, we will consider only the planar carboxonium ions.

In the hydrolysis of the 2,4,10-trioxaadamantanes, the conjugate acid **16** of the orthoester would first give, with stereoelectronic control, the planar carboxonium ion **21**.[8] However, in the ion **21**, the most likely reaction is the internal return (k_{-2}): the hydroxyl group is close to the charged carbon and stereoelectronic control favors the attack on the carboxonium ion (15). The stereoelectronically controlled addition of water on the ion **21** to give **20** is therefore not likely, the return reaction (internal nucleophilic addition) being favored. The addition of water without stereoelectronic control to give **19** is equally excluded for the same reason. Furthermore that last sequence is equivalent to the A2 mechanism **16** → **17** → **19** previously eliminated.

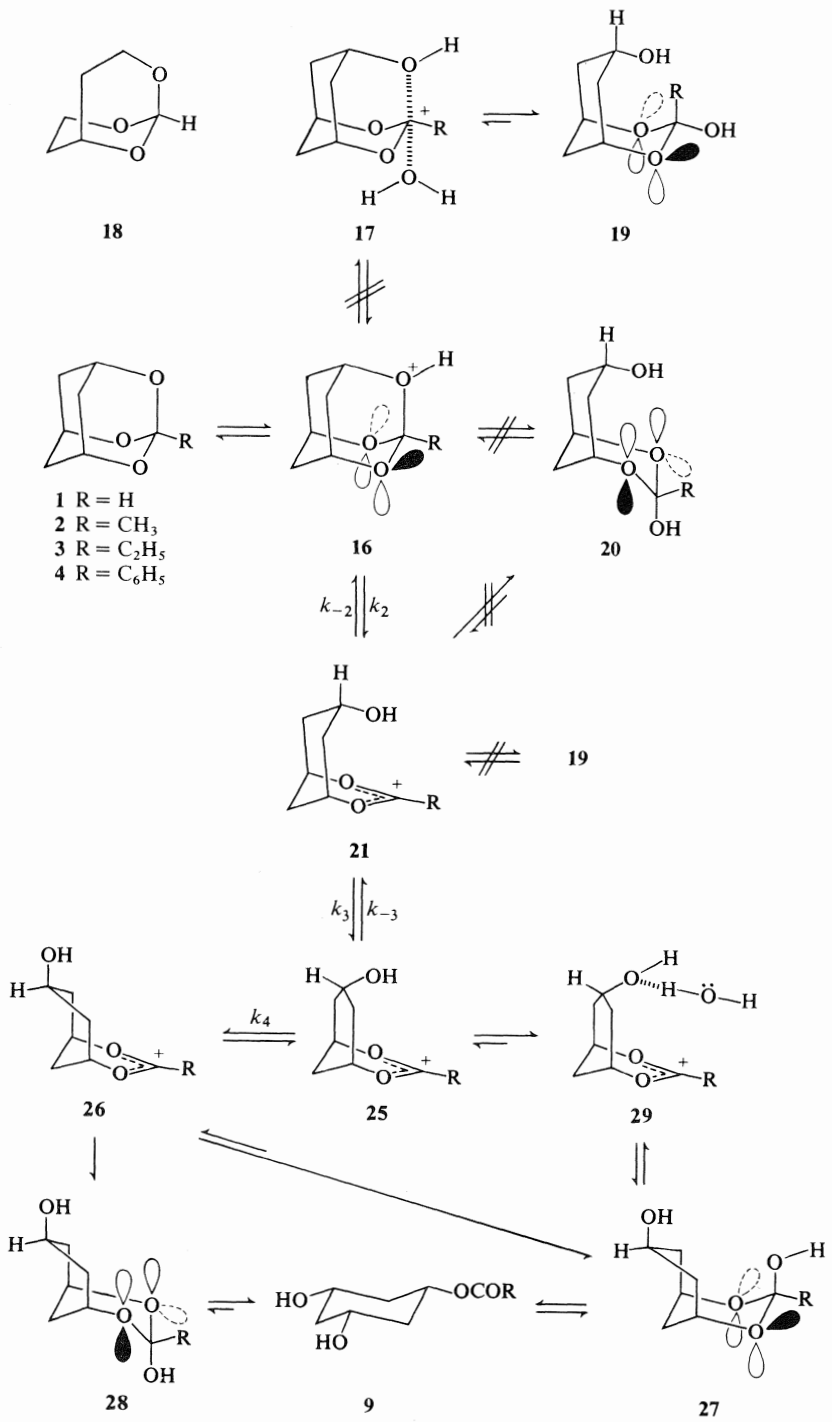
Conformational change on the ion **21** is therefore necessary prior to the addition of water to the carboxonium ion. Consequently, higher energy is needed, unlike the case of the aliphatic orthoesters where addition of water is rapid. This explains the much slower rate observed in the 2,4,10-trioxaadamantanes; a ring inversion is necessary

[5]Further work is in progress to determine if the electronic factors have the dominant influence.

[6] These two hypotheses were considered in the preliminary communication (1).

[7]Also H. Paulsen. Personal communication.

[8]The planar carboxonium ion implies that the atoms C1, O2, C3, O4, and C5 are in the same plane. The non-planar carboxonium ion would have the classical chair conformation.

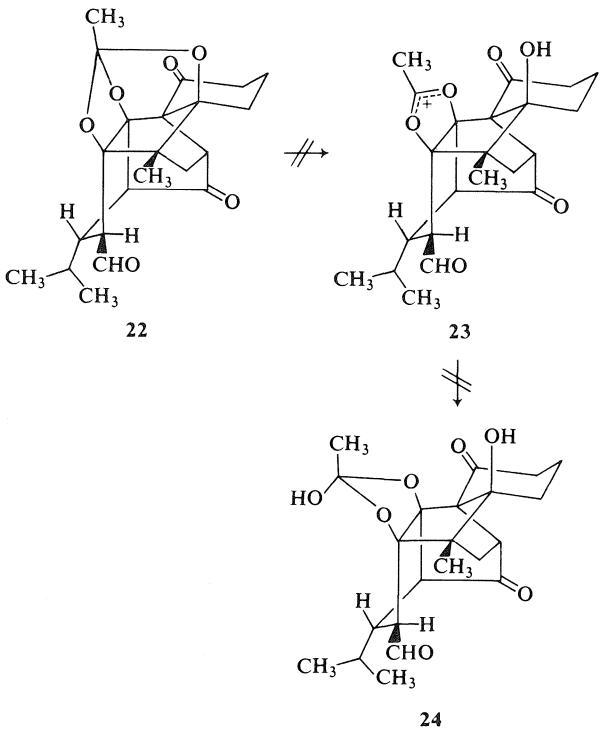


SCHEME 4

($\Delta G^{\ddagger}$ inversion $\simeq$ 10 kcal/mol) and there is loss of translational entropy of one water molecule (4 to 5 kcal/mol). The 2,4,10-trioxaadamantanes therefore need 10 to 15 kcal/mol more than the aliphatic orthoesters for hydrolysis. Experimentally, the energy differences between the aliphatic series and the trioxaadamantanes is between 7 and 12 kcal/mol ($\Delta G^{\ddagger}_1 - \Delta G^{\ddagger}_5 \simeq 7$ kcal/mol; $\Delta G^{\ddagger}_2 - \Delta G^{\ddagger}_6 \simeq 12$ kcal/mol; $\Delta G^{\ddagger}_4 - \Delta G^{\ddagger}_7 \simeq 10$ kcal/mol).

An experimental result obtained independently

Can. J. Chem. Downloaded from www.nrcresearchpress.com by 210.87.254.6 on 09/05/12
For personal use only.



SCHEME 5

from this work indicates that the ring containing the hydroxyl group must undergo conformational changes prior to the attack of water on the carboxonium ion. In the orthoester **22** which is an intermediate product in the synthesis of ryanodine (16) (Scheme 5), such conformational change is impossible and the product was found to be completely resistant to hydrolysis (HCl, 1 *N*, dioxane (1:4), 25°C, 8 days). This result also excludes the possibility of a non-planar carboxonium ion or a hemiorthoester intermediate containing a boat form dioxane ring. The carboxonium ion **23** does not appear to be able to hydrate to give the equivalent of the boat form dioxane, i.e., the envelope 1,3-dioxolane **24**.

The first conformational change that can take place in ion **21** is its transformation into ion **25**. This ion could then be further transformed into the boat form **26**. Hydration of **26** with stereoelectronic control could then take place from the top or the bottom face of the ion to give respectively the hemiorthoesters **27** and **28** which can then break down to the reaction product **9** with stereoelectronic control.

This sequence of events must, however, be eliminated because the hydration of ion **26**, which would be a fast process, would occur after the slow step, the conformational change **21** → **25** → **26**. The large negative entropy of activation which has been experimentally observed could not be accounted for. In fact, ion **25** should behave similarly to ion **21**, in the sense that the internal return (k_{-3}) must be a more favorable process than the boat formation (k_4) because there must be some electrostatic attraction between the OH group and the positively charged carbon in **25**.

Ion **25**, however, can attract a molecule of water to form a species such as **29**. Examination of molecular models indicates that there is indeed room for the association of a molecule of water to **25** to give **29**. The species **29** would then undergo a conformational change to the boat form which would be synchronous with the attack of the associated water molecule on the carboxonium ion to give the hemiorthoester **27** which would then break down to the reaction product **9**.

There is also the possibility of a stereoelectronically controlled hydration on the α face of ion **25**, being concerted with a conformational change to a boat form cyclohexane ring (→ **25** → **28**). This would lead however, to the high energy, double boat conformer, **28**. The process **21** → **25** → **28** might therefore be incapable of competing with the preceding sequence **21** → **25** → **29** → **27**.

Conclusion

Hydrolysis of the 2,4,10-trioxaadamantanes reveals a comportment peculiar to these orthoesters. The substituent effects, the activation entropies, and the slow rates of hydrolysis led to the proposal of synchronous water addition to the carboxonium ion and conformational change (→ **21** → **25** → **29** →) as being the rate determining step of these hydrolysis reactions.

Experimental

Products

The 2,4,10-trioxaadamantanes substituted in position 3 were prepared by the transesterification of the corresponding methyl or ethyl orthoesters and from *cis*-cyclohexane-1,3,5 triol (**8**) (17–19). The products obtained show physical properties in accord with literature values. The nmr spectra were recorded on a Varian EM 390 in deuterochloroform with tetramethylsilane as internal reference and agree with the structure of the products.

Compound 1

Nuclear magnetic resonance δ: 1.79 (3H, doublet, $J \simeq 14$ Hz, H6a, H8a, and H9a), 2.76 (3H, doublet, $J \simeq 14$ Hz, H6e, H8e, and H9e), 4.36 (3H, wide singlet, H1, H5, and H7), and 5.80 (1H, singlet, H3).

Compound 2

Nuclear magnetic resonance δ: 1.40 (3H, singlet, CH_3), 1.67 (3H, doublet, $J \simeq 14$ Hz, H6a, H8a, and H9a), 2.58 (3H, doublet, $J \simeq 14$ Hz, H6e, H8e, and H9e), and 4.36 (3H, wide singlet, H1, H5, and H7).

Compound 3

Nuclear magnetic resonance δ: 0.94 (3H, triplet, $J \simeq 7$ Hz,

Can. J. Chem. Downloaded from www.nrcresearchpress.com by 210.87.254.6 on 09/05/12
For personal use only.

CH_3), 1.65 (2H, quadruplet, $J = 7$ Hz, CH_2—CH_3), 1.69 (3H, doublet, $J \simeq 14$ Hz, H6a, H8a, and H9a), 2.60 (3H, doublet, $J \simeq 14$ Hz, H6e, H8e, and H9e), and 4.38 (3H, wide singlet, H1, H5, and H7).

Compound 4

Nuclear magnetic resonance δ: 1.78 (3H, doublet, $J \simeq 14$ Hz, H6a, H8a, and H9a), 2.78 (3H, doublet, $J \simeq 14$ Hz, H6e, H8e, and H9e), 4.53 (3H, wide singlet, H1, H5, and H7), and 7.2–7.9 (5H, two multiplets, C_6H_5).

Acidic Solutions

Acidic solutions were prepared from analytical material; the solvent dioxane/water 60:40 by volume includes the water in concentrated hydrochloric acid; dioxane from Merck Uvasol, spectrophotometric grade, was used. The acid concentrations were determined by pH measurements ($[H^+] = 10^{-pH}$) or by volumetric measurements.

Kinetics

The hydrolysis reactions were followed by uv spectrophotometry (Gilford 250 equipped with a thermostated compartment and automatic cell) measuring the increase in optical density due to appearance of products. The wavelengths used were 225 nm (**1**, **2**, **3**) and 239 nm (**4**). The quartz cells contained 2 mL of solution at the required temperature and a few μL of orthoester solution in pure dioxane were added (20 μL of 1 *M* solution (**1**, **2**, **3**); 5 μL of solution of 0.06 *M* (**4**)).

After shaking, the optical density was recorded as a function of time. Rate constants were obtained either on finding the exponential $D = D_\infty + (D_\infty - D_0)e^{-kt}$ by least squares (20) or by plotting ln $(D_\infty - D)$ with time. The orthoester concentrations were chosen for convenient variation of optical density of 0.3 to 0.4 (**1**, **2**, **3**), and 1.4 (**4**). Temperatures were read directly in the cells and the maximum error was ±0.05°C at 25°C and ±0.1°C at 40°C. Average reproducibility of rate constants was ±2%.

Product Analysis

After hydrolysis of a sample of orthoester under kinetic conditions, the solution was evaporated to dryness, and the hydrolysis product acetylated with pyridine and acetic anhydride. Nuclear magnetic resonance analysis confirmed the structures of the products.

In the hydrolysis of **4**, the nmr spectrum of the product obtained was found identical with that described in the literature (19). An indirect structural proof was obtained for the hydrolysis product of **2**. Acetylation of **8** gave *cis*-1,3,5-triacetatecyclohexane which was found identical to the product obtained from compound **2**.

Cis-*1,3,5-triacetoxycyclohexane*

Nuclear magnetic resonance (90 MHz) δ: 1.40 (3H, quadruplet, $J \simeq 12$ Hz, H2a, H4a, and H6a), 2.02 (9H, singlet, CH_3CO), 2.40 (3H, broad singlet, H2e, H4e, and H6e), and 4.83 (3H, multiplet, H1, H3, and H5).

Calculation of Activation Energies

The activation energies were calculated on the basis of the Arrhenius equation $k = A \exp(-E_a/RT)$ (21); error calculations were done by the method described in Wiberg (22).

1. O. Bouab, G. Lamaty, and C. Moreau. J. Chem. Soc. Chem. Commun. 678 (1978).
2. P. Deslongchamps. Heterocycles, **7**, 1271 (1977) and references therein.
3. F. Coussemant, M. Hellin, and B. Torck. Cours et documents de chimie. Vol. 3. Gordon and Breach Science Publishers, Inc., New York, NY. 1969. p. 33.
4. R. H. De Wolfe et J. L. Jensen. J. Am. Chem. Soc. **85**, 3264 (1963).
5. L. L. Schaleger and F. A. Long. Adv. Phys. Org. Chem. **1**, 23 (1963).
6. E. H. Cordes and H. G. Bull. Chem. Rev. **74**, 581 (1974).
7. T. H. Fife. Acc. Chem. Res. **5**, 264 (1972).
8. (*a*) M. Ahmad, R. G. Bergstrom, M. J. Cashen, A. J. Kresge, R. A. McClelland, and M. F. Powell. J. Am. Chem. Soc. **99**, 4827 (1977); (*b*) M. Ahmad, R. G. Bergstrom, M. J. Cashen, Y. Chiang, A. J. Kresge, R. A. McClelland, and M. F. Powell. J. Am. Chem. Soc. **101**, 2669 (1979).
9. H. Kwart and M. B. Price. J. Am. Chem. Soc. **82**, 5123 (1960).
10. Y. Chiang, A. J. Kresge, P. Salomaa, and C. I. Young. J. Am. Chem. Soc. **96**, 4494 (1974).
11. A. Streitwieser, Jr. Solvolytic displacement reactions. McGraw-Hill, New York, NY. 1962. p. 13.
12. H. K. Hall, Jr., F. De Blauwe, and T. Pyriadi. J. Am. Chem. Soc. **97**, 3854 (1975).
13. H. Paulsen and R. Dammeyer. Chem. Ber. **109**, 1837 (1976).
14. H. Paulsen. Pure Appl. Chem. **41**, 69 (1975).
15. G. Wipff. Tetrahedron Lett. 3269 (1978).
16. P. Deslongchamps. Pure Appl. Chem. **49**, 1329 (1977).
17. H. Stetter and K. H. Steinacker. Chem. Ber. **86**, 451 (1952).
18. H. Stetter and K. H. Steinacker. Chem. Ber. **86**, 790 (1953).
19. P. N. Strong and J. F. W. Keana. J. Org. Chem. **40**, 956 (1975).
20. W. E. Deming. Statistical adjustment of data. J. Wiley and Sons, New York, NY. 1958.
21. A. Streitwieser, Jr. Solvolytic displacement reactions. McGraw-Hill, New York, NY. 1962. p. 7.
22. K. B. Wiberg. Physical organic chemistry. J. Wiley and Son, New York, NY. 1964. p. 378.

Can. J. Chem. Downloaded from www.nrcresearchpress.com by 210.87.254.6 on 09/05/12
For personal use only.

Aspects of organocadmium chemistry. II.[1] Crystal and molecular structure of a complex between bis(trimethylsilylmethyl)cadmium and 2,2′-bipyridyl

GORDON W. BUSHNELL AND STEPHEN R. STOBART
Department of Chemistry, University of Victoria, Victoria, B.C., Canada V8W 2Y2

Received June 21, 1979

GORDON W. BUSHNELL and STEPHEN R. STOBART. Can. J. Chem. **58**, 574 (1980).

The crystal structure of bipyridylbis(trimethylsilylmethyl)cadmium(II) hemibipyridyl, $[Cd(C_{10}H_8N_2)((CH_3)_3SiCH_2)_2]\cdot\frac{1}{2}(C_{10}H_8N_2)$ has been solved and refined to an *R*-value of 0.140 using 1230 reflections. The space group is $P2_1/c$ and the cell dimensions are a = 887.4(4), b = 947.0(5), c = 3245.(1) pm, β = 92.01(4)°, with four Cd-containing molecules and two bipyridyl molecules of crystallisation per cell. The 4-coordinate geometry at cadmium is most closely related to that of a linear cadmium dialkyl since the angle C—Cd—C = 156(2)°, and the bipyridyl ligand is weakly bound (Cd—N = 252, 253 pm) in a symmetrical manner with the angle N—Cd—N = 65(1)°. The distortion from linearity is away from the bipyridyl. The trimethylsilyl groups are also bent back from the heterocyclic ligand and are slightly staggered. The line between the methylene carbon atoms is approximately perpendicular to the mean plane of the bipyridyl molecule.

GORDON W. BUSHNELL et STEPHEN R. STOBART. Can. J. Chem. **58**, 574 (1980).

On a résolu la structure du cristal de bipyridilbis(triméthylsilylméthyl)cadmium(II) hemibipyridyle $[(Cd(C_{10}H_8N_2)-((CH_3)_3SiCH_2)_2]\cdot\frac{1}{2}(C_{10}H_8N_2)$ et on l'a affinée jusqu'à une valeur conventionnelle R de 0.140 pour 1230 réflexions. Le groupe d'espace est $P2_1/c$ et les dimensions de la maille sont a = 887.4(4), b = 947.0(5), c = 3245.(1) pm, β = 92.01(4)° pour 4 molécules contenant du Cd et deux molécules bipyridyle de cristallisation par maille. La géométrie tétracoordonnée du cadmium est reliée de plus près à celle d'un cadmium dialkyle linéaire puisque l'angle C—Cd—C = 156(2)° et le ligand bipyridyle est faiblement lié (Cd—N 252, 253 pm) d'une manière symétrique à l'angle N—Cd—N = 65(1)°. La distorsion par rapport à la linéarité est à l'opposé du bipyridyle. Les groupes triméthylsilyles sont aussi courbés le ligand hétérocyclique et sont légèrement décalés. La ligne entre les atomes de carbone du méthylène est approximativement perpendiculaire au plan moyen de la molécule bipyridyle.

[Traduit par le journal]

Introduction

Structural data for organocadmium derivatives are extremely limited. Dimethylcadmium in the gas phase has a linear configuration with a Cd—C bond length of 211.2(4) pm, as shown by an analysis of the pure rotational lines of the high resolution Raman spectrum (1). Recently we encountered (2) formation of thermally stable crystalline adducts between bis(trimethylsilylmethyl) cadmium (**1**) and the chelating donor molecules 1,10-phenanthroline or 2,2′-bipyridyl. Such behaviour contrasts markedly with that of dimethylcadmium, corresponding adducts of which dissociate completely at ambient temperature (3). While the adduct (**2**) of **1** with bipyridyl is very volatile, subliming easily *in vacuo* at 20°C and suggesting dissociation in the vapour phase, it is stable as a solid in the absence of air over many months. Microanalytical results were consistent with the formulation $Cd(CH_2SiMe_3)_2\cdot 1.5bpy$ and the availability of crystals led us to investigate the nature of complex **2** using X-ray crystallography, with a view to rationalising the unusual stoichiometry as well as achieving structural characterisation of the dialkylcadmium residue. Substantial difficulties associated with the volatility, air-sensitivity, and instability of the material to X-rays led to several repetitions of the crystal growth experiment and the mounting of more than ten crystals for the diffractometer. The structure of complex **2** has been solved from measurements which were evidently limited in precision. We now report the results which, despite their low accuracy, help to fill a sizeable gap in the literature.

Experimental

Preparation of the compound has already been described (2). Clear yellow crystals were grown *in vacuo* by vapour diffusion across a small temperature gradient. The material was sensitive to air and moisture, tended to volatilise in the Lindemann tube, and decomposed under X-radiation to an ochre solid. The crystal data are as follows:

$C_{23}H_{34}CdN_3Si_2$ fw = 521.1
Monoclinic, space group $P2_1/c$ (No. 14), unit cell a = 887.4(4), b = 947.0(5), c = 3245(1) pm, β = 92.01(4)°, cell volume 2.725(2) nm^3, density 1.27 g cm^{-3} (calcd), Z = 4, T = 23°C, λ = 71.069 pm ($MoK_{\bar{\alpha}}$), μ = 8.96 cm^{-1}.

The crystals were mounted on the a axis. Weissenberg and precession photography using $CuK_{\bar{\alpha}}$ radiation gave the symmetry and approximate cell dimensions. Fifteen pairs of reflections were centered at $\pm 2\theta$ (range 17–39°) on a Picker 4-circle diffractometer controlled by a PDP-11/10 minicomputer. Zr filtered $MoK_{\bar{\alpha}}$ radiation was used. The cell and orientation matrix were refined by least squares. Intensity measurements were done with $\omega = 0$ in the bisecting position using 50 steps of 0.04° in 2θ, counting for 1 s per step, with a 10 s background count at each end of the scan. Standards 0,0,14 and 0,5,2 were measured after each batch of 50 reflections and used to correct for instrument instability and crystal decomposition. Reflections were

[1]Part I is ref. 2.

0008-4042/80/060574-05$01.00/0
©1980 National Research Council of Canada/Conseil national de recherches du Canada

Can. J. Chem. Downloaded from www.nrcresearchpress.com by 210.87.254.42 on 09/05/12
For personal use only.

Can. J. Chem. Downloaded from www.nrcresearchpress.com by 210.87.254.42 on 09/05/12
For personal use only.

scaled using the preceding set of standards. When the sum of the standards fell below 50% of its original value the crystal was replaced. Measurements were completed to $2\theta = 40°$, but were not punched unless $I > 3\sigma(I)$. Lorentz and polarisation factors were applied. Corrections for absorption were not possible since the shapes of the crystals, initially blocks elongated in the *a* direction, were soon ill defined.

Structure Determination

The Patterson function was used to solve the phase problem. The programs used were supplied by Penfold (4) and are based upon FORDAP, ORFLS, ORFFE, and ORTEP. The atomic scattering factors (5) were for unchanged atoms. The refinement was by minimisation of $\sum w(|F_o| - |F_c|)^2$ with the final weights derived from a weighting scheme: $w = 1/(A + Bx + Cx^2 + Dx^3)$ where $x = |F_o|$ and $A = 58.220$, $B = 0.29927$, $C = 1.4601 \times 10^{-2}$, $D = -0.31296 \times 10^{-4}$. Systematic variations in $w\Delta^2$ were thus largely eliminated. Only the cadmium and silicon atoms were given anisotropic vibration parameters. The final agreement factors were $R = 0.140$ and $R_w = 0.196$. The numbers of observations and variables are 1230 and 132 respectively. The final difference map had a maximum of 1.74×10^{-6} e pm^{-3} and a minimum of -1.05×10^{-6} e pm^{-3}. The hydrogen atoms were not located. The structure factor table, and atomic vibration parameters are available from the Depository of Unpublished Data.[2]

Results

Figure 1 shows the molecular structures and the atom labelling scheme. The fractional atomic coordinates are given in Table 1. Figure 2 gives the packing of the molecules in the unit cell. There are two uncoordinated bipyridyl molecules per cell. A crystallographic centre of symmetry is located in these molecules at the midpoint of the bond joining the two rings. The four cadmium-containing molecules and the two uncoordinated bipyridyl molecules account for the stoichiometry of the compound. The conformation of the free bipyridyl mole-

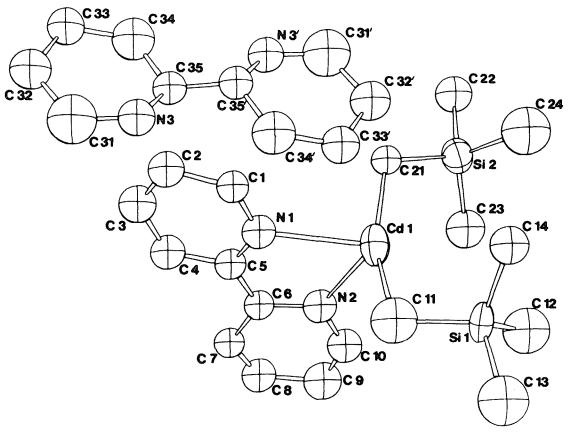


FIG. 1. Molecular structures and atom labelling.

[2]Copies may be obtained, at a nominal charge, from the Depository of Unpublished Data, CISTI, National Research Council of Canada, Ottawa, Ont., Canada K1A 0S2.

TABLE 1. Fractional atomic coordinates* ($\times 10^3$)

Atom	*x*	*y*	*z*
Cd	207.5(5)	61.3(4)	115.7(1)
Si (1)	−2.6(16)	259.9(16)	176.9(4)
Si (2)	467.6(17)	−113.2(17)	179.0(4)
C(11)	6(7)	191(7)	123(2)
C(12)	−3(8)	106(8)	212(2)
C(13)	−196(7)	360(8)	185(2)
C(14)	164(6)	375(6)	192(2)
C(21)	431(5)	−1(5)	127(1)
C(22)	653(6)	−222(6)	182(2)
C(23)	301(6)	−238(6)	188(2)
C(24)	507(8)	26(8)	221(2)
N (1)	238(4)	42(4)	39(1)
N (2)	81(4)	−149(4)	82(1)
C (1)	332(5)	135(5)	21(1)
C (2)	374(5)	121(5)	−23(1)
C (3)	306(6)	10(5)	−43(2)
C (4)	203(5)	−89(5)	−22(2)
C (5)	172(5)	−68(5)	20(1)
C (6)	83(4)	−170(4)	40(1)
C (7)	2(5)	−282(5)	20(1)
C (8)	−76(6)	−372(6)	42(2)
C (9)	−89(6)	−359(6)	87(2)
C(10)	−7(5)	−249(6)	101(1)
N (3)	402(4)	−95(4)	459(1)
C(31)	390(7)	−118(7)	420(2)
C(32)	514(6)	−67(6)	394(2)
C(33)	633(6)	6(6)	416(2)
C(34)	618(6)	48(6)	457(2)
C(35)	505(6)	−10(5)	480(1)

*Estimated standard deviations are given in parentheses.

TABLE 2. Bond lengths (pm)*

Bond	Length	Bond	Length
	(*a*) Cadmium coordination		
Cd—C(11)	219(6)	Cd—N(1)	253(3)
Cd—C(21)	209(5)	Cd—N(2)	252(4)
	(*b*) Trimethylsilylmethyl groups		
Si(1)—C(11)	187(6)	Si(2)—C(21)	202(5)
Si(1)—C(12)	185(7)	Si(2)—C(22)	193(5)
Si(1)—C(13)	198(7)	Si(2)—C(23)	192(6)
Si(1)—C(14)	188(6)	Si(2)—C(24)	192(7)
	(*c*) Coordinated bipyridyl		
N(1)—C(1)	136(5)	N(2)—C(10)	138(6)
C(1)—C(2)	149(6)	C(10)—C(9)	134(6)
C(2)—C(3)	135(6)	C(9)—C(8)	147(7)
C(3)—C(4)	149(6)	C(8)—C(7)	132(6)
C(4)—C(5)	143(6)	C(7)—C(6)	142(5)
C(5)—N(1)	132(5)	C(6)—N(2)	137(5)
C(5)—C(6)	142(5)		
	(*d*) Uncoordinated bipyridyl		
N(3)—C(31)	129(7)	N(3)—C(35)	138(5)
C(31)—C(32)	148(7)	C(35)—C(34)	137(6)
C(32)—C(33)	142(6)	C(34)—C(33)	142(7)
C(35)—C(35)′	135(8)		

*Estimated standard deviations are given in parentheses.

Can. J. Chem. Downloaded from www.nrcresearchpress.com by 210.87.254.42 on 09/05/12
For personal use only.

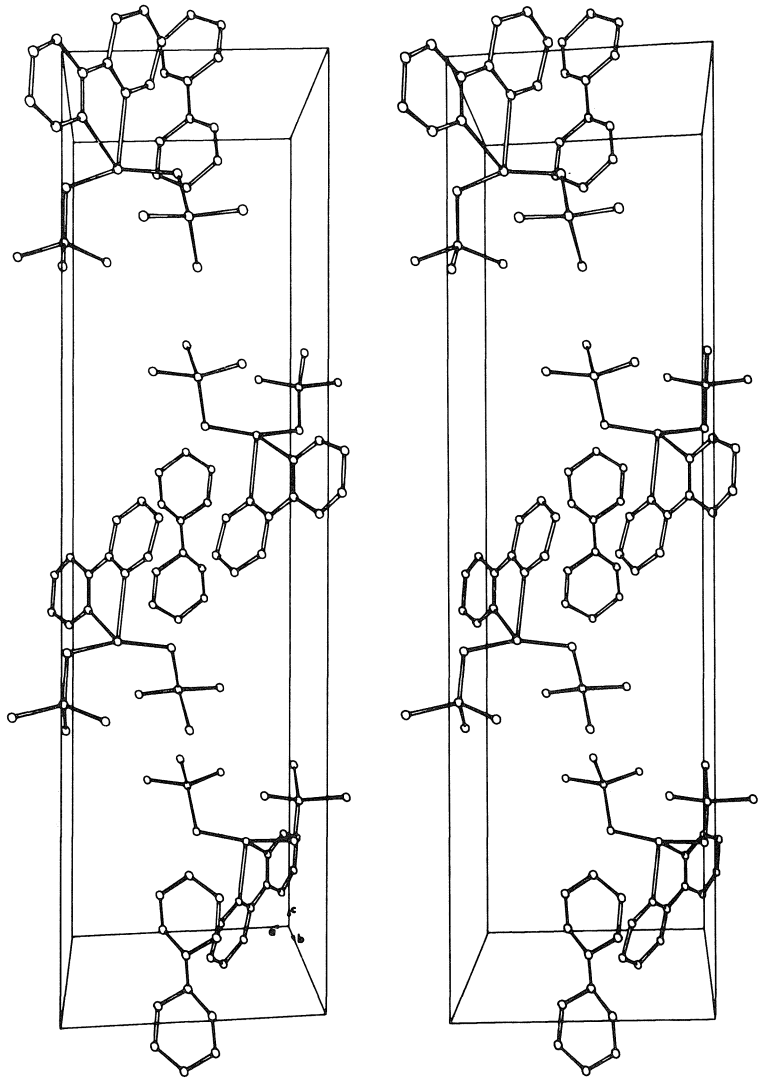


FIG. 2. Stereoscopic view of the unit cell.

cules in **2** is probably *trans*, as in bipyridyl itself (6), and opposite to the approximate *cis* conformation found in many complexes. However, a disordered structure with *cis* bipyridyl molecules cannot be excluded on the basis of the available measurements.

The bond lengths are given in Table 2. The Cd—C distances (mean 214 pm) agree with those determined for $CdMe_2$ in the gas phase (1). The Cd—N bond lengths (252, 253 pm) are considerably greater than the sum of the covalent radii (148 + 70 pm) indicating weak bonding. The Si—C lengths are normal, as are the bond lengths of the bipyridyl molecules, to the accuracy of the determination.

The bond angles are presented in Table 3. The coordinated bipyridyl molecule and the two alkyl groups complete the four coordination at the cadmium centre. The most striking feature of the latter is the very wide angle of 156(2)° made by the methylene groups at the metal. The bulky trimethylsilylmethyl groups are bent back from the coordinated base and staggered to minimise steric repulsions. This is clearly consistent with complexation of a linear dialkyl skeleton as was suggested (2) on the basis of vibrational spectroscopy. The three pyridyl rings are planar with $\chi^2 = 0.16, 0.58, 18.7$ respectively, where $\chi^2 = \sum P_i^2/\sigma^2(P_i)$ and P_i is the perpendicular distance of atom i from the mean plane. The angle between planes 1 and 2 is 9.3°.

Table 4 contains selected non-bonding interatomic distances and is complete to 380 pm. The first four entries are the intramolecular distances which may explain sterically the departure of the

TABLE 3. Bond angles (deg)*

Bonds	Angle	Bonds	Angle
		(*a*) Cadmium	
N(1)—Cd—N(2)	65(1)	C(11)—Cd—C(21)	156(2)
N(1)—Cd—C(11)	105(2)	N(1)—Cd—C(21)	91(2)
N(2)—Cd—C(11)	98(2)	N(2)—Cd—C(21)	105(2)
		(*b*) Trimethylsilylmethyl groups	
C(11)—Si(1)—C(12)	108(3)	C(21)—Si(2)—C(22)	116(2)
C(11)—Si(1)—C(13)	110(3)	C(21)—Si(2)—C(23)	110(2)
C(11)—Si(1)—C(14)	112(3)	C(21)—Si(2)—C(24)	105(3)
C(12)—Si(1)—C(13)	106(3)	C(22)—Si(2)—C(23)	109(3)
C(13)—Si(1)—C(14)	111(3)	C(23)—Si(2)—C(24)	116(3)
C(14)—Si(1)—C(12)	108(3)	C(24)—Si(2)—C(22)	101(3)
Cd—C(11)—Si(1)	111(3)	Cd—C(21)—Si(2)	114(2)
		(*c*) Coordinated bipyridyl	
N(1)—C(5)—C(4)	117(4)	N(2)—C(6)—C(7)	122(4)
C(1)—N(1)—C(5)	126(4)	C(10)—N(2)—C(6)	111(4)
C(2)—C(1)—N(1)	122(4)	C(9)—C(10)—N(2)	134(5)
C(3)—C(2)—C(1)	113(4)	C(8)—C(9)—C(10)	110(5)
C(4)—C(3)—C(2)	124(5)	C(7)—C(8)—C(9)	122(5)
C(5)—C(4)—C(3)	119(4)	C(6)—C(7)—C(8)	121(4)
C(4)—C(5)—C(6)	119(4)	C(7)—C(6)—C(5)	125(4)
N(1)—C(5)—C(6)	125(4)	N(2)—C(6)—C(5)	113(4)
		(*d*) Uncoordinated bipyridyl	
C(31)—C(32)—C(33)	117(5)	C(34)—C(35)—N(3)	118(4)
C(31)—N(3)—C(35)	128(5)	C(33)—C(34)—C(35)	119(5)
C(32)—C(33)—C(34)	120(5)	C(32)—C(31)—N(3)	117(6)
C(34)—C(35)—C(35)′	123(6)	N(3)—C(35)—C(35)′	120(6)

*Estimated standard deviations are given in parentheses. C(35)′ is related by inversion to C(35).

TABLE 4. Non-bonding interatomic distances (pm)

Atoms	Symmetry*	Distance	Atoms	Symmetry*	Distance
C(11)—N(1)	*1*	375	C(21)—N(1)	*1*	330
C(11)—N(2)	*1*	356	C(21)—N(2)	*1*	366
C(11)—C(4)	*2*	383	C(21)—C(3)	*3*	365
C(13)—C(32)	*4*	381	C(14)—C(23)	*5*	387
N(1)—C(7)	*2*	362	C(1)—C(2)	*3*	356
C(1)—C(3)	*3*	354	C(1)—C(7)	*2*	350
C(1)—C(8)	*2*	375	C(2)—C(2)	*3*	350
C(2)—C(3)	*3*	371	C(2)—C(7)	*2*	367
C(2)—C(8)	*2*	359	C(3)—C(6)	*2*	377
C(4)—C(5)	*2*	365	C(4)—C(6)	*2*	356
C(5)—C(5)	*2*	352	C(5)—C(6)	*2*	370
N(3)—C(1)	*6*	353	C(35)—C(1)	*6*	366
N(3)—C(4)	*7*	354	C(31)—C(4)	*7*	377
N(3)—C(8)	*4*	358	C(31)—C(9)	*4*	363
C(34)—C(6)	*8*	376	C(34)—C(7)	*8*	379
C(31)—C(13)	*9*	377			

*Symmetry positions of the second atom relative to Table 1 coordinates. *1*, x, y, z; *2*, $-x, -y, -z$; *3*, $1-x, -y, -z$; *4*, $-x, \frac{1}{2}+y, \frac{1}{2}-z$; *5*, $x, 1+y, z$; *6*, $1-x; y-\frac{1}{2}, \frac{1}{2}-z$; *7*, $x, -\frac{1}{2}-y, \frac{1}{2}+z$; *8*, $1-x, \frac{1}{2}+y, \frac{1}{2}-z$; *9*, $-x, y-\frac{1}{2}, \frac{1}{2}-z$.

cadmium dialkyl from linearity. The next four entries and the last in the table are for the methylene and methyl carbon atoms, and show that the more important contacts are intermolecular. The coordinated bipyridyl shows fourteen intermolecular distances in the range 350–380 pm. The remainder of the table is concerned with intermolecular distances for the uncoordinated bipyridyl.

The most suitable comparison in relation to nitrogen coordination is that with the structure (7) of 2,2-bipyridylbis[pentacarbonylmanganese] cadmium(II). However, in this complex the mean Cd—N bond length of 235 pm may be contracted by enhanced acceptor ability at the cadmium centre through π back donation to the manganese atoms. This multiple bond character is held to account for the significantly shortened metal–metal distance. In octahedral $[Cd(N_3)_2(py)_2]$ (8), all of the Cd—N

Can. J. Chem. Downloaded from www.nrcresearchpress.com by 210.87.254.42 on 09/05/12
For personal use only.

distances are 234–235 pm, but a longer bond (mean 246 pm) is present (9) in [$CdBr_2 \cdot N,N,N',N'$- tetramethylethylenediamine]. The present value (mean 253 pm) and the narrow angle of 65° for N—Cd—N are complementary to one another and suggest a rather weak bond resulting from steric interaction with the bulky alkyl substituents, or electronic effects. On the basis of the latter, however, it is not clear why complex **2** should be more stable than its dimethyl cadmium analogue since Me_3SiCH_2— is more electron releasing than Me— (10).

Acknowledgements

We thank the Natural Sciences and Engineering Research Council of Canada and the University of Victoria for operating grants, Mr. D. M. Heinekey for growing the crystals, Mrs. K. Beveridge for technical assistance, and Mr. Blaine Hawkins for the illustrative photography.

1. K. S. Rao, B. P. Stoicheff, and R. Turner. Can. J. Phys. **38**, 1516 (1960).
2. D. M. Heinekey and S. R. Stobart. Inorg. Chem. **17**, 1463 (1978).
3. G. E. Coates and S. I. E. Green. J. Chem. Soc. 3340 (1962).
4. B. R. Penfold. University of Canterbury Crystallographic programs. Christchurch, New Zealand.
5. D. T. Cromer and J. T. Waber. Acta Crystallogr. **18**, 104 (1965).
6. L. L. Merritt and E. D. Schroeder. Acta Crystallogr. **9**, 801 (1956).
7. W. Clegg and P. J. Wheatley. J. Chem. Soc. Dalton, 511 (1974).
8. I. Agrell. Acta Chem. Scand. **24**, 3575 (1970).
9. S. Htoon and M. F. C. Ladd. J. Cryst. Mol. Struct. **4**, 97 (1974).
10. H. Bock and H. Alt. J. Am. Chem. Soc. **92**, 1569 (1970); T. G. Traylor, W. Hanstein, H. J. Berwin, N. A. Clinton, and R. S. Brown. J. Am. Chem. Soc. **93**, 5715 (1971).

Can. J. Chem. Downloaded from www.nrcresearchpress.com by 210.87.254.42 on 09/05/12
For personal use only.

The configuration at C-28 of rapamycin is opposite to that depicted in structure **1** (*S* and not *R*). Reference 2 should read D. C. N. Swindells, P. S. White, and J. A. Findlay. Can. J. Chem. **56**, 2491 (1978).

ERRATA

On the chemistry and high field nuclear magnetic resonance spectroscopy of rapamycin

JOHN A. FINDLAY

Chemistry Department, University of New Brunswick, Fredericton, N.B., Canada E3B 5A3

AND

LAJOS RADICS

NMR Laboratory, Central Research Institute for Chemistry, P.O. Box 17, H-1525 Budapest, Hungary

Received October 9, 1979

This paper is dedicated to Prof. Karel Wiesner on the occasion of his 60th birthday

JOHN A. FINDLAY and LAJOS RADICS. Can. J. Chem. **58**, 579 (1980).

Base catalysed hydrolysis of rapamycin ($C_{51}H_{79}NO_{13}$) affords six neutral compounds identified by chemical and spectroscopic means as **2***a*, **3***b*, **3***d*, **5**, 2,4-dimethylphenol, and L(−)-piperidine-2-carboxylic acid **6**, and whose generation has been plausibly rationalized. These findings as well as detailed analyses of ^{13}C nmr and ^{1}H nmr spectra provide independent corroboration of the X-ray derived rapamycin crystal structure **1**. Structurally homogeneous in the solid state, rapamycin is found to occur in solutions as a mixture of two conformational isomers (approximately 4:1). Through nearly complete assignment of the high field ^{1}H (400 MHz) and ^{13}C (100.6 MHz) nmr spectra, the isomerism is shown to be associated with *trans–cis* rotation of an amidic bond within the 31-membered macrolide ring. The predominant form corresponds to the conformer portrayed by X-ray analysis.

JOHN A. FINDLAY et LAJOS RADICS. Can. J. Chem. **58**, 579 (1980).

L'hydrolyse basique de la rapamycine ($C_{51}H_{79}NO_{13}$) fournit six composés neutres que l'on a identifiés par des méthodes chimiques et spectroscopiques comme étant les composés **2***a*, **3***b*, **3***d*, **5** ainsi que le diméthyl-2,4 phénol et l'acide L-pipéridinecarboxylique-2 **6** dont on a expliqué l'origine de façon plausible. Ces résultats aussi bien que les analyses complètes obtenues par la rmn du ^{13}C et du ^{1}H corroborent indépendamment la structure cristalline obtenue par rayon-X. On a trouvé que la rapamycine qui du point de vue structural est homogène en phase solide devient en solution, un mélange de deux conformères (approx. 4:1). En se basant sur une identification presque complète à partir des spectres de rmn du ^{13}C (100.6 MHz) et du ^{1}H (400 MHz), on a trouvé que l'isomérie est associée à une rotation *trans–cis* du lien amide du cycle macrolide à 31 atomes. La forme prédominante correspond au conformère révélé par analyse aux rayons-X.

[Traduit par le journal]

Recently we initiated concerted efforts towards the elucidation of the structure of the antifungal antibiotic rapamycin, isolated from cultures of *Streptomyces hygroscopicus* and originally believed to be $C_{56}H_{89}NO_{14}$ (1). While at the outset crystals of rapamycin were prepared for X-ray diffraction work, we also began chemical and nuclear magnetic resonance studies with the expectation that the structural question could be solved by studying various less complex degradation fragments in the event that the direct X-ray analysis of rapamycin proved unmanageable.

As we have already reported (2) our successful X-ray study has revealed the complete structure and relative stereochemistry of crystalline rapamycin **1**. The solution of the X-ray problem was assisted by information on structural moieties gleaned by preliminary scrutiny of ^{13}C nmr data providing such important details as the number, hydridization, degree, and nature of substitution of carbon atoms in the molecule. In addition, as the X-ray structural picture began to develop, information obtained from the ongoing chemical and spectroscopic studies proved helpful in confirming certain skeletal carbon sequences and functional features prior to the ultimate refinements. Of particular importance was the finding that the analysis of ^{13}C nmr data (see Table 3) confirmed independently that rapamycin has only 51 carbons and not 56 as initially reported (1). Early (25.16 MHz) carbon-13 nmr spectra also revealed that in solutions of various organic solvents rapamycin, structurally homogeneous in the solid state, occurs as a mixture of two non-separable isomers. The isomeric ratio of approximately 4:1 was found to be practically independent of the solvent and temperature (between 30 to 70°C). Attempts to remove the minor component either by chromatography or repeated crystallizations proved unsuccessful. The occurrence of two forms of rapamycin in solutions raised the obvious question as to which, if any, of these isomeric forms corresponds to the X-ray portrayed structure and geometry of the macrolide molecule. To answer this question and to obtain a detailed insight into the structural and conformational features of rapamycin in solutions, we carried out a high-field ^{1}H and ^{13}C nmr study of the antibiotic. (The complexity of the molecular structure and the presence of two isomers have rendered the proton and carbon-13 nmr spectra

0008-4042/80/060579-12$01.00/0

©1980 National Research Council of Canada/Conseil national de recherches du Canada

FOR ERRATA SEE
V59#1 ... 81 ... 49

Can. J. Chem. Downloaded from www.nrcresearchpress.com by 210.87.254.6 on 09/05/12
For personal use only.

Can. J. Chem. Downloaded from www.nrcresearchpress.com by 210.87.254.6 on 09/05/12
For personal use only.

unmanageable for purposes of detailed spectral assignments when these were recorded at the frequencies of our iron magnet instrument.) As shown in the sequel, the results of the nmr analysis have afforded an independent and detailed corroboration for the X-ray derived molecular structure **1** and also disclosed that the two solution forms of rapamycin are interrelated by hindered rotation about a formal single bond within the 31-membered macrolide ring.

We now report details of these complementary chemical and spectroscopic studies.

Much of our chemical effort has been focussed on the base catalysed hydrolysis of rapamycin since this was known[1] to yield neutral and acidic fragments. Our attention was first devoted to the hydrolysis at room temperature using 1 *N* methanolic NaOH. While several neutral products could be noted by tlc they proved to be relatively unstable. Basic hydrolysis at reflux temperature gave, in ~ 20% yield, a mixture of five neutral products designated A, B, C. D, and E. The major acidic fraction proved to be a complex and intractable mixture and was not pursued.

Separation of the neutral compounds was achieved on silica gel columns. Compound A, the least abundant product, can be eluted with CH_2Cl_2, has a distinct phenolic odour, and is quite volatile. Spectroscopic data showed this compound to be 2,4-dimethylphenol and this was confirmed by comparison with an authentic sample.

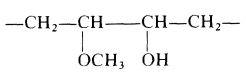
Compound C, the major neutral product, displays a base peak *m/e* 304 in its mass spectrum corresponding to $C_{19}H_{28}O_3$. Structure **2***a* is assigned to C on the basis of the following data. The diol nature was established by facile and reversible conversion to a diacetate **2***b* which displays in its 100 MHz ^{1}H nmr spectrum (see Table 1) a downfield multiplet at δ 4.71 assigned to a secondary acetate and two acetoxy methyl signals (δ 2.04 and δ 2.22). The presence of a double bond was confirmed by hydrogenation of C-diol, **2***a*, and C-diacetate, **2***b*, to the corresponding dihydroderivatives **3***a* and **3***b*, respectively. The additional hydrogen deficiencies in C-diol are accounted for by a 2,4,6-trisubstituted phenol moiety and a six-membered ring containing two secondary vicinal oxygen-substituted carbons for which ample support exists in the ^{1}H nmr and ^{13}C nmr spectra of C-diol and its derivatives (see Tables 1 and 2). In particular the *meta* relationship of the aromatic protons follows from their mutual coupling (J = 2.3 Hz) while their *meta* relationship to the phenolic group follows from the relatively small acetylation shifts observed for the aromatic protons in both C-diol, **2***a* (+ δ 0.04 and δ 0.17), and dihydro-C-diol, **3***a* (δ 0.10 for both). Anticipated acetylation shifts for *ortho* and *para* protons are + δ 0.25 to 0.40 (3).

That the double bond is conjugated follows from consideration of uv spectra of C-diol and dihydro-C-diol, while the placement of a trisubstituted double bond *ortho* to the phenolic group is confirmed by the facile conversion of C-diol to an isomeric ether **4** (1:1 mixture of C8 diastereomers) whose ^{1}H nmr spectrum features two downfield methyl singlets (δ 2.1 and δ 2.2), a 3H singlet at δ 1.4 assigned to the C8 methyl, and a 2H singlet at δ 2.95 assigned to the allylic C7 protons. All other spectral data are in accord with the assigned structure **4**.

Careful analysis of the 100 MHz ^{1}H nmr data of C-diol, **2***a*, and C-diacetate, **2***b*, reveals the existence of a mixture of isomers (~ 7:1) in each case, no doubt due to geometrical isomerism at the double bond. From ^{13}C nmr chemical shift information on these compounds and comparison with literature data (4), we conclude that the major component has the *Z* configuration in each case.

The major mass spectral fragments of C-diol are at *m/e* 161 (52%) and 175 (41%) corresponding to fission between C8/C9 and C9/C10, respectively, while the dihydro-C-diol **3***a* shows major fragments at *m/e* 121 (33%), 135 (94%), and 162 (16%) attesting to the C6 to C9 sequence in **3***a* (see Scheme 1).

The existence, substitution pattern, and stereochemistry of a cyclohexane ring in C-diol and related compounds was established by 100 MHz ^{1}H nmr studies. Thus the sequence



as a part of a six-membered ring in a highly preferred chair conformation was determined by standard decoupling techniques. Furthermore, the two oxygen substituents were found to be *trans* diequatorial since the respective C12H and C13H show the large coupling (J = 9.0–9.2 Hz) associated with α-diaxial protons in a cyclohexane chair conformation. It follows that the C10 substituent should also be equatorial in view of the high conformational preference.

C-diol, **2***a*, and its diacetate, **3***b*, fail to undergo elimination when treated with paratoluenesulfonic acid in boiling benzene indicating that the C13 oxygen substituent does not readily achieve an axial conformation favourable for 1,2-*trans* elimination in agreement with a 1,2,4-triequatorial configuration for the ring substituents.

[1]Private communications from Ayerst Research Laboratories, Montreal, P.Q.

Can. J. Chem. Downloaded from www.nrcresearchpress.com by 210.87.254.6 on 09/05/12
For personal use only.

TABLE 1. ^{1}H nuclear magnetic resonance parameters of rapamycin degradation products[a]

Proton	2*a*		2*b*		3*a*	3*b*
	Major isomer	Minor isomer	Major isomer	Minor isomer		
3-H	6.84 $J(3, 5) = 2.3$	6.84 $J(3, 5) = 2.3$	6.88[b] $J(3, 5) = 2.3$	6.8[b] $J(3,5) = 2.3$	6.72 $J(3, 5) = 2.3$	6.82 $J(3, 5) = 2.3$
5-H	6.71 $J(3, 5) = 2.3$ $J(5, 7) = 0.4$	6.65 $J(3, 5) = 2.3$ $J(5, 7) = 0.4$	6.88[b] $J(3, 5) = 2.3$ $J(5, 7) = 0.4$	6.8[b] $J(3, 5) = 2.3$ $J(5, 7) = 0.4$	6.78 $J(3, 5) = 2.3$	6.88 $J(3, 5) = 2.3$
7-H	6.13	6.17	6.03	6.09	—	—
11-H(CH_2)	2.05–2.2	2.05–2.2	1.9–2.2	1.9–2.2	Not measured	Not measured
12-H	3.02 $J(12, 13) = 9.0$ $J(12, 11eq) = 4.2$ $J(12, 11ax) = 11.0$		3.18 $J(12, 13) = 9.0$ $J(12, 11eq) = 4.2$ $J(12, 11ax) = 11.0$		2.92 $J(12, 13) = 9.0$ $J(12, 11eq) = 4.2$ $J(12, 11ax) = 11.0$	3.16 $J(12, 13) = 9.0$ $J(12, 11eq) = 4.2$ $J(12, 11ax) = 11.0$
13-H	3.42 $J(12, 13) = 9.0$ $J(13, 14eq) = 4.5$ $J(13, 14ax) = 11.0$		4.71 $J(12, 13) = 9.0$ $J(13, 14eq) = 4.5$ $J(13, 14ax) = 11.0$		3.38 $J(12, 13) = 9.0$ $J(13, 14eq) = 4.5$ $J(13, 14ax) = 11.0$	4.68 $J(12, 13) = 9.0$ $J(13, 14eq) = 4.5$ $J(13, 14ax) = 11.0$
14-H(CH_2)	2.05–2.2		1.9–2.2	1.9–2.2	Not measured	Not measured
16-H(OMe)	3.42	3.38	3.38	3.34	3.39	3.38
17-H(CH_3)	1.65 $J(7, 17) = 1.4$	1.92 $J(7, 17) = 1.4$	1.69 $J(7, 17) = 1.4$	1.83 $J(7, 17) = 1.4$	0.86 $J(8, 17) = 6.5$	0.84 $J(8, 17) = 6.5$
18-H(CH_3)	2.22	2.14	2.11	—	2.20	2.09
19-H(CH_3)	2.22	2.14	2.27	—	2.22	2.26
1(OH)	4.86	—	—	—	4.40	—
13(OH)	2.70	—	—	—	Not measured	—
1-OAcMe	—	—	2.20	2.20	—	2.267 + 2.274
13-OAcMe	—	—	2.04	2.02	—	2.03

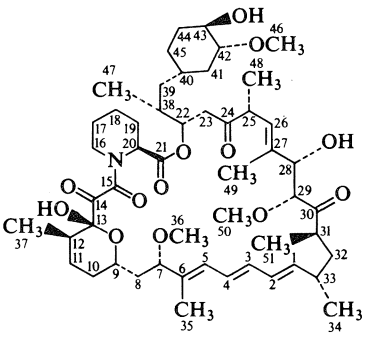
[a]In $CDCl_3$. Chemical shifts in ppm relative to internal TMS. Couplings in Hz as obtained from first-order approximation at 100 MHz.
[b]Couplings measured in C_6D_6 solution.

Can. J. Chem. Downloaded from www.nrcresearchpress.com by 210.87.254.6 on 09/05/12
For personal use only.

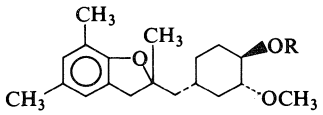
TABLE 2. Carbon-13 chemical shifts of rapamycin degradation products[a]

Carbon	2*a*	2*b*	3*a*	3*b*
C-1	148.85	145.27	149.91	146.01
C-2	123.61	129.96	122.88	129.96
C-3	127.63	128.73	129.21	129.25
C-4	123.81	131.08	126.70	132.70
C-5	130.32	129.96	129.45	129.57
C-6	128.63	134.89	129.09	135.08
C-7	121.03	121.77	38.22, 38.35	38.61, 38.79
C-8	141.29	138.42	30.90	30.90
C-9	47.02	47.09	44.44	44.37
C-10	34.13	33.93	33.64	33.25
C-11	35.06	36.44	34.72, 35.70	36.30, 37.40
C-12	84.69	81.28	84.83	81.19
C-13	73.94	76.12	74.15	76.43
C-14	31.44	29.95	31.32, 31.50	30.00
C-15	30.51	30.36	30.28, 30.84	30.00
C-16	56.47	57.33	56.34, 56.45	57.16
C-17	17.18	17.59	19.95	19.80
C-18	15.95	16.19	15.35	16.39
C-19	20.47	20.46	20.45	20.56
ArOCOMe	—	21.31	—	21.36
ROCOMe	—	20.87	—	20.80

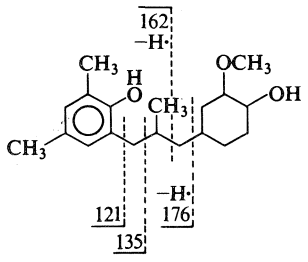
[a]In $CDCl_3$. Chemical shift values in ppm relative to internal TMS. Two values in a row indicate resonance doubling due to isomerism (isomeric ratio 1:1).



1



4



SCHEME 1. Mass spectral fragmentation of dihydro C-diol, **3***a*.

Compound D ($C_{19}H_{30}O_4$) is assigned structure **3***c* since its ^1H nmr spectrum shows a doublet for the C8 methyl at δ 0.8 (J = 7 Hz) and a doublet at δ 4.3 (J = 7 Hz) for the C7H. Compound D is quantitatively dehydrated to C-diol, **2***a* upon treatment with paratoluenesulfonic acid in benzene at room temperature. This assignment is fully supported by other spectroscopic data.

Compound B ($C_{19}H_{32}O_4$) proved to be a 1:1 diastereomeric mixture of methyl ethers, **3***d*, since the novel features of its ^1H nmr spectrum are a pair of methyl doublets at δ 0.95 (J = 6 Hz) and δ 0.7 (J

= 6 Hz) each integrating for ~ 1.5 H, and at δ 7.75 (0.5 H) and δ 7.8 (0.5 H), a pair of singlets assigned to the phenolic hydrogen of each isomer.

While the structures of compounds B, C, and D are fully supported by additional spectral data, chemical corroboration of their relationships comes from their individual conversions to the common product **4** by paratoluenesulfonic acid in refluxing benzene.

The neutral compound E ($C_{10}H_{18}O_2$) is assigned structure **5**. Its mass spectrum displays a strong molecular ion at *m/e* 186 (62%) and a base peak at *m/e* 129 ($M - CH_2COCH_3$) while less intense ions at *m/e* 111 and 97 correspond to 129 − H_2O and − CH_3OH, respectively. The infrared spectrum of E shows bands at 3450 cm^{-1} and 1700 cm^{-1} in accord with hydroxyl and ketone features. Assuming that E arises from the same moiety of rapamycin that affords B, C. and D, the stereochemistry should be as in structure **5**.

Thus the hydrolysis products A, B, C, D, and E all appear to be derived from the same portion of rapamycin. Since the latter was believed to feature a triene system but no aromatic moiety, we originally speculated that the aromatic ring might arise by condensation/cyclization of some suitably substituted trienone system. In support of this hypothesis was the observation that perhydrorapamycin, prepared by catalytic (Pt) hydrogenation, did not yield any A, B, C, or D. An equally attractive theory was that the neutral phenolic products are formed by condensation/cyclization/elimination of some suitably substituted 2,6-dicarbonyl system or equivalent.

The need to pursue these hypotheses further chemically was made unnecessary by the appearance of the preliminary and incomplete X-ray structural portrayals of rapamycin which featured a 1,2,4-trisubstituted six-membered ring remote from the triene system allowing us to abandon the trienone hypothesis. At this stage it was possible to confirm the sequence C22 to C30 (see structure **1**), establish the oxygen and methyl placements, and confirm the segment C38 to C47 and substituents in the developing rapamycin X-ray structural picture from our conclusions about compounds A, B, C, and D and their generation.

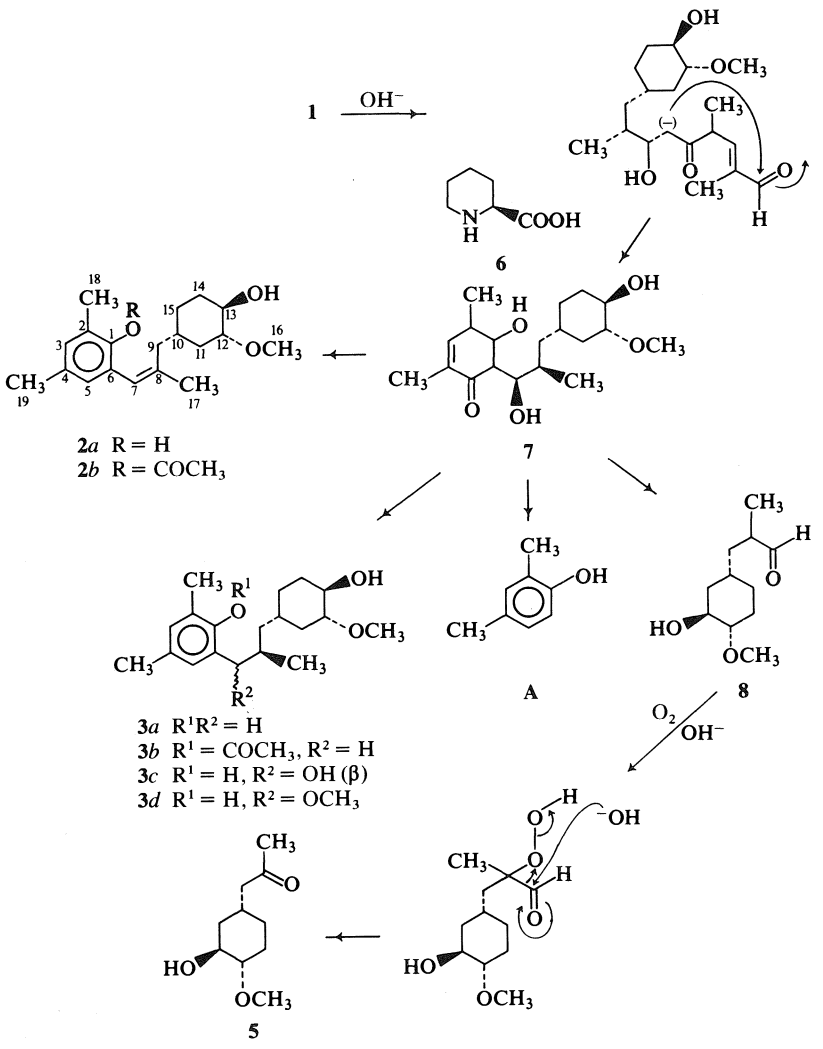
With the fully refined X-ray derived rapamycin structure **1** at hand (2), it is appropriate to account in detail for the formation of compounds A, B, C, D, and E. Plausible mechanistic rationalizations are given in Scheme 2 in which rapamycin **1** is first dissected via a β-hydroxyketone cleavage and a base catalysed ester hydrolysis. The resulting δ keto unsaturated aldehyde can then undergo self condensation and elimination of water to produce the aromatic fragments B, C, and D, while compound A is accounted for via a β-hydroxyketone cleavage of **7** which also supplies the aldehyde **8**. The latter is perceived as undergoing base catalysed oxidation at the position α to the aldehyde followed by oxidative decarboxylation to give compound E, **5**. It is worthy to note that the mass spectrum of rapamycin shows a remarkable similarity to those of compounds C, **2***a*, and D, **3***c*. Thus, the base peak of the rapamycin spectrum is at *m/e* 175 while the ion of next greatest intensity corresponds to the mass of C at *m/e* 304 (28%). Other prominent ions common to all three mass spectra are at *m/e* 161 and 135. Thus the major ion fragments from C and D at *m/e* 175 (C10/C9 cleavage), 161 (C9/C8), and 135 (C8/C7) are major features of the rapamycin mass spectrum indicating that electron impact on rapamycin results in cleavages leading to some fragments similar or identical to those obtained from the hydrolysis derived compounds C, **2***a*, and D, **3***c*.

Since D, unlike the oil B, is a sharp melting (63–65°C) crystalline compound, it is likely that its benzylic oxygen is derived directly from the rapamycin C22 ester ether by hydrolytic ester cleavage.

Not unexpectedly, we have isolated pipecolic acid **6** (piperidine-2-carboxylic acid) among the base catalysed hydrolysis products of rapamycin. This, together with the compounds cited above, accounts for the carbon sequence and substitution pattern C16 through C31 and constitutes an independent corroboration of more than half of the rapamycin structure as learned by X-ray.

More detailed information about the structural moieties and conformational features of rapamycin in solution is afforded by the analysis of the high-field ^1H and ^{13}C nmr spectra. Summarized in Tables 3 and 4, respectively, are the carbon-13 and proton nmr parameters of *both* isomeric species of the macrolide molecule as derived from the 100.6 MHz ^{13}C and 400 MHz ^1H nmr spectra of the $CDCl_3$ solution of rapamycin. The increased spectral dispersion, illustrated on Fig. 1, has made it possible to identify and, accordingly, characterize in terms of chemical shifts and ^1H — ^1H coupling constants 65 of the 79 protons and assign unambiguously *each* of the 51 carbon-13 resonances to the respective carbon atoms in both isomeric forms. Evaluation of the chemical shift differentials for the two isomers has led to elucidation of the nature and site of the isomerization. The differential shieldings of the carbon atoms in the two solution forms are also reported in Table 3.

Can. J. Chem. Downloaded from www.nrcresearchpress.com by 210.87.254.6 on 09/05/12
For personal use only.



SCHEME 2

The assignment of the resonances to the individual atoms in the molecule is based on standard FT nmr procedures. First, through a series of $^1H—\{^1H\}$ double resonance experiments, partial structures involving sequentially spin-coupled protons and terminated by proton-non-bearing carbon atoms were identified. Previous chemical information about the presence in rapamycin of a pipecolic acid unit and a trisubstituted cyclohexane moiety made it unnecessary to fully characterize five of the methylene groups (i.e., C-17, C-18, C-39, C-44, and C-45) giving rise to extensively coupled and strongly overlapping multiplets the analysis of which would have required a special experimental approach. Although their resonances were unambiguously located by simple double resonance methods, the pertinent ^1H nmr parameters, owing to the insufficient precision, are either omitted from Table 4 or reported indirectly through the couplings determined for contiguous protons. The partial structures thus derived are displayed in Fig. 2.

Subsequently, broad-band decoupled and a series of single frequency off-resonance decoupled $^{13}C—\{^1H\}$ spectra were recorded to yield off-resonance multiplicities, variable-frequency residual $^{13}C—^1H$ couplings, and off-resonance band shape informations which were then matched to the ^1H nmr-derived partial structures. Experimental verification of the assignments thus deduced was attained through an extensive series of single-frequency selective $^{13}C—\{^1H\}$ decoupling experiments. The assignment of resonances due to some of the methylene carbons with overlapping

Can. J. Chem. Downloaded from www.nrcresearchpress.com by 210.87.254.6 on 09/05/12
For personal use only.

TABLE 3. Carbon-13 chemical shifts[a] in rapamycin isomers

Carbon	Major isomer	Minor isomer	Δδ[b]	Carbon	Major isomer	Minor isomer	Δδ
1	126.72	126.87	−0.15	27	136.09	136.19[c]	−0.10
2	130.16	129.93	0.23	28	77.23	77.13	0.10
3	126.38	126.34	0.04	29	84.87	84.46	0.41
4	133.60	133.42	0.18	30	215.48	215.35	0.13
5	129.55	129.35	0.20	31	41.39	40.81	0.58
6	135.54	135.93[e]	−0.39	32	31.66	31.76	−0.10
7	84.35	86.40	−2.05	33	35.18	35.64	−0.46
8	38.87	38.55[d]	0.32	34	15.94	16.17	−0.23
9	67.16	67.83	−0.67	35	13.01	12.85	0.16
10	38.37	38.46[d]	−0.09	36	59.40	59.29	0.11
11	27.00	26.93	0.07	37	13.81	14.97	−1.16
12	33.15	32.93	0.22	38	33.74	34.06	−0.32
13	98.49	98.78	−0.29	39	40.21	38.92	1.29
14	192.51	196.48	−3.97	40	33.22	33.29	−0.07
15	166.76	165.61	1.15	41	34.22	34.22	0
16	44.17	40.99	3.18	42	84.41	84.41	0
17	25.25	24.24	1.01	43	73.90	73.87	0.03
18	20.59	20.51	0.08	44	31.27	31.27[e]	0
19	27.26	27.85	−0.59	45	31.27	31.15[e]	0.12
20	51.37	56.19	−4.82	46	55.81	55.86	−0.05
21	169.22	169.86	−0.64	47	16.20	16.26	−0.06
22	75.66	75.77	−0.11	48	21.52	21.71	−0.19
23	40.68	40.44	0.24	49	10.13	10.28	−0.15
24	208.10	207.65	0.45	50	56.54	56.51	0.03
25	46.53	46.08	0.45	51	15.89	15.79	0.10
26	140.14	140.79	−0.65				

[a]In $CDCl_3$ solution, relative to internal TMS.
[b]$\Delta\delta = \delta_{major} - \delta_{minor}$.
[c, d, e]Assignments may be interchanged in this isomer.

complex ^1H resonance pattern was aided by ^{13}C chemical shift information gleaned by preceding studies of base-catalysed hydrolysis products (see Table 2). Low-power selective irradiation of resonances due to the terminal proton(s) in the partial structures of Fig. 2 gave rise to signal enhancement of neighbouring quaternary carbon resonance, a method that was fully exploited in establishing the missing links between the ^1H nmr-based structural units. The only carbon-13 resonances where the above experimental approach failed to yield connectivity information were those due to the α,β-diketo fragment (C-14 and C-15). In principle, in the event of lack of X-ray structure determination, chemical shift arguments and the variations of the isomerization-induced chemical shift changes (*vide infra*) would have been sufficient to define the placement of the latter unit in the macrolide ring and establish thereby the chemical structure of rapamycin in a one-to-one correspondence with the X-ray analysis.

Thanks to the greatly enhanced spectral dispersion used (and duly appreciated) in the present study, the above experimental assignment techniques could be applied with practically no added difficulties for the resonances due to the minor component of the rapamycin solution as well. Carbon-13 nmr spectra recorded at 100.6 MHz disclosed that each resonance of the major component has its own exact counterpart in the spectrum of the minor isomer, a finding that strongly suggested the occurrence of conformational differences, rather than structural changes between the two forms. Another remarkable fact about the isomerism is that it causes sizable differential shieldings of carbon atoms and protons practically throughout the entire molecule (see Tables 3 and 4) which can only be expected to occur when the isomerism is associated with an alteration of the overall geometry of the macrolide system. In principle, two alternative explanations may be considered that can account for such effects, (*1*) epimerization of the hemiacetal carbon atom (C-13), or (*2*) *trans* to *cis* amide isomerization via hindered rotation about the pipecolic acid N—CO bond. Closer examination of the chemical shift data for two isomers in Tables 3 and 4, however, reveals that the first alternative must be discarded. The differential shieldings observed for the hemiacetal ring atoms are less than or equal to the values noted in the other part of the molecule not involved directly in the isomerism, whereas epimerization of C-13 should

Can. J. Chem. Downloaded from www.nrcresearchpress.com by 210.87.254.6 on 09/05/12
For personal use only.

TABLE 4. ^{1}H nuclear magnetic resonance parameters of rapamycin isomers[a]

Proton	Chemical shift: Major isomer	Chemical shift: Minor isomer	^{1}H—^{1}H coupling constants (both conformers)[d]
H-1	5.51	5.46	$J(1, 33) = 8.6$; $J(1, 2) = 15.0$
H-2	6.12	6.11	$J(1, 2) = 15.0$; $J(2, 3) = 10.0$; $J(2, 33) = 1.0$
H-3	6.36	6.37	$J(2, 3) = 10.0$; $J(3, 4) = 14.5$
H-4	6.28	6.21	$J(3, 4) = 14.5$; $J(4, 5) = 10.0$
H-5	5.94	5.87	$J(4, 5) = 10.0$; $J(5, 35) = 1.4$
H-7	3.64	3.57	$J(7, 8A) = 6.6$; $J(7, 8B) = 8.8$
H-8A, 8B	1.73	[b]	$J(7, 8A) = 6.6$; $J(7, 8B) = 8.8$
H-9ax	3.85	3.81	$J(9ax, 10ax) = 9.5$; $J(9ax, 10eq) = 2.0$; $J(9ax, 8A) = 7.0$; $J(9ax, 8B) = 4.5$
H-11ax	1.45	[b]	$J(11ax, 11eq) = 12.5$; $J(11ax, 12ax) = 9.5$
H-11eq	2.32	[b]	$J(11ax, 11eq) = 12.5$; $J(11eq, 12ax) = 5.0$; $J(11eq, 10ax) = 3.0$; $J(11eq, 10eq) = 2.5$
H-12ax	1.95	2.18	$J(11ax, 12ax) = 9.5$; $J(11eq, 12ax) = 5.0$; $J(12ax, 37) = 6.5$
H-16ax	3.40	[b]	$J(16ax, 16eq) = 13.0$; $J(16ax, 17ax) = 12.0$; $J(16ax, 17eq) = 3.0$
H-16eq	3.56	4.41	$J(16ax, 16eq) = 13.0$; $J(16eq, 17ax) = 3.0$; $J(16eq, 17eq) = 3.0$; $J(16eq, 20eq) = 1.5$
H-19ax	1.60	[b]	$J(19ax, 20eq) = 5.0$
H-19eq	1.92	[b]	$J(19eq, 20eq) = 2.0$
H-20eq	5.26	4.26	$J(19ax, 20eq) = 5.0$; $J(19eq, 20eq) = 2.0$; $J(16eq, 20eq) = 1.5$
H-22	5.15	5.08	$J(22, 38) = 4.0$; $J(22, 23A) = 6.2$; $J(22, 23B) = 6.0$[c]
H-23A	2.56	2.8	$J(23A, 23B) = 16.8$; $J(22, 23A) = 6.2$
H-23B	2.72	2.9	$J(23A, 23B) = 16.8$; $J(22, 23B) = 6.0$
H-25	3.30	3.30	$J(25, 26) = 9.5$; $J(25, 48) = 6.8$
H-26	5.38	5.46	$J(25, 26) = 9.5$; $J(26, 49) = 1.5$; $J(26, 28) = 1.5$
H-28	4.15	4.18	$J(28, 29) = 6.0$; $J(26, 28) = 1.5$
H-29	3.70	3.65	$J(28, 29) = 6.0$
H-31	2.72	2.72	$J(31, 51) = 6.3$; $J(31, 32A) = 5.0$; $J(31, 32B) = 9.0$
H-32A	1.68	[b]	$J(32A, 32B) = 13.5$; $J(31, 32A) = 5.0$; $J(32A, 33) = 3.0$
H-32B	1.83	1.83	$J(32A, 32B) = 13.5$; $J(32B, 33) = 7.0$; $J(31, 32B) = 9.0$
H-33	2.29	2.29	$J(1, 33) = 8.6$; $J(32A, 33) = 3.0$; $J(32B, 33) = 7.0$; $J(2, 33) = 1.0$; $J(33, 34) = 6.8$
H-34	1.02	1.01	$J(33, 34) = 6.8$
H-35	1.62	1.62	$J(5, 35) = 1.4$
H-36	3.32	3.37	—
H-37	0.92	0.80	$J(12ax, 37) = 6.5$
H-38	1.95	[b]	$J(22, 38) = 4.0$; $J(38, 47) = 6.8$
H-40ax	1.50	[b]	$J(40ax, 41ax) = 12.0$; $J(40ax, 41eq) = 3.0$
H-41ax	0.64	0.61	$J(41ax, 41eq) = 12.5$; $J(41ax, 42ax) = 11.0$; $J(40ax, 41ax) = 12.0$
H-41eq	2.08	2.08	$J(41ax, 41eq) = 12.5$; $J(40ax, 41eq) = 3.0$; $J(41eq, 42ax) = 4.5$
H-42ax	2.91	2.91	$J(41ax, 42ax) = 11.0$; $J(41eq, 42ax) = 4.5$; $J(42ax, 43ax) = 8.5$
H-43ax	3.35	[b]	$J(42ax, 43ax) = 8.5$; $J(43ax, 44ax) = 11.0$; $J(43ax, 44eq) = 4.2$
H-46	3.11	3.11	—
H-47	0.89	0.88	$J(38, 47) = 6.8$
H-48	1.06	1.12	$J(25, 48) = 6.8$
H-49	1.72	1.71	$J(26, 49) = 1.5$
H-50	3.39	3.37	—
H-51	0.96	1.03	$J(31, 51) = 6.3$
C13-OH	4.78	[b]	—

[a]Chemical shifts ($CDCl_3$) in ppm, relative to internal TMS, coupling constants in Hz. All parameter values were obtained by first-order approximation at 400 MHz.
[b]Near-coincidence with the lines of the major isomer.
[c]In the minor isomer: $J(22, 23A) + J(22, 23B) = 10$; $J(22, 38) = 6.5$.
[d]The identity (within experimental errors) of most of the ^{1}H—^{1}H coupling constants in the two conformers indicates that, presumably due to the size of the macro ring, the isomerism-induced changes in the overall molecular geometry (mirrored by the chemical shift differentials, see also Table 3) may occur without affecting significantly most of the H—C—C—H dihedral angles.

cause, through differences in the 1,3 steric interactions of the C-13 (OH) group and the C-13 (CO—CO..) side chain (3), considerable shielding variations at C-1 and C-11. The most significant isomerization shifts, both for protons and carbon atoms, are seen to appear in the immediate vicinity of the amide nitrogen, in particular, at C-16 and C-20. The alternating signs and the magnitude of these differential shieldings are fully consistent with the effects well known for hindered amide rotation (5, 3). If, on the other hand, it is assumed that the conjugation of the amide carbonyl with the C-14 oxo group does not reverse the sign of anisotropy and steric effects for the N—CO group, from the observed ^{1}H and ^{13}C shielding differentials it can be concluded that the configuration of the

Can. J. Chem. Downloaded from www.nrcresearchpress.com by 210.87.254.6 on 09/05/12
For personal use only.

Can. J. Chem. Downloaded from www.nrcresearchpress.com by 210.87.254.6 on 09/05/12
For personal use only.

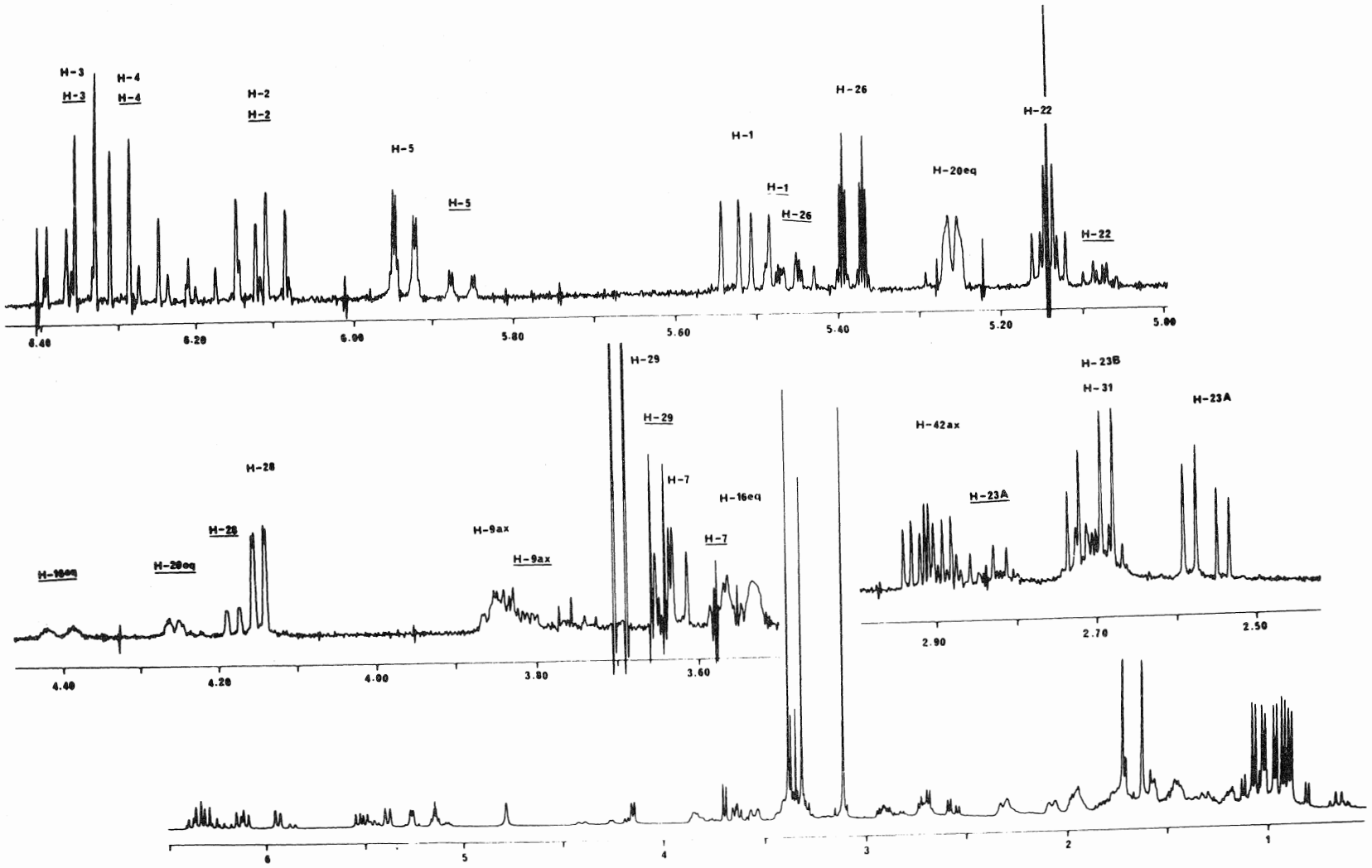


FIG. 1. 400 MHz ^{1}H nmr spectrum of rapamycin in $CDCl_3$. Underlined denotations refer to the minor isomer.

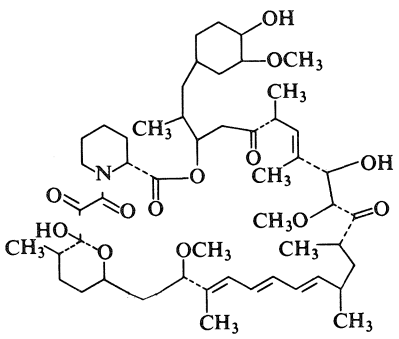


FIG. 2. Partial structures of rapamycin as obtained from the 400 MHz spectra. Dashed lines represent connections established by single frequency selective $^{13}C—\{^1H\}$ decouplings.

amide group (following the peptide denotation) is *trans* in the major isomer, i.e., identical with the X-ray portrayed stereochemistry, and *cis* in the minor component of rapamycin. Molecular models furthermore show that, in order to avoid excessive steric crowding, the *trans* to *cis* isomerization should cause the C-14 oxo group to change its orientation such that the two carbonyls maintain their *s-trans* arrangement. Support for this contention seems to be available from the observed significant downfield shift of the C-14 resonance in the minor isomer relative to this value in the major form and a simultaneous upfield shift of the C-37 methyl proton resonance.

Further important stereochemical details of the solution forms of rapamycin emerge from the analysis of the 400 MHz ^1H nmr data. The observed $^1H—^1H$ coupling constants afford a fairly comprehensive description of the relative steric orientations of substituent groups attached to the macrocycle in full agreement with the results of X-ray analysis and, in a similar way, confirm the all-*trans* geometry of the triene moiety. According to the X-ray structure, the side chain comprising the substituted cyclohexane is bent over the 31-membered macro ring such that the cyclohexane ring itself assumes a position above the sequence C-25, C-26, C-27 with its C-41 methylene group closer to the $\Delta^{26,27}$ double bond. As attested by the ^1H nmr observations, this particular conformational feature seems to be retained in the solution forms as well; due to the proximity of anisotropic environment, the *axial* C-41 methylene proton resonance appears at 0.64 ppm as the most shielded one in the entire molecule, while its *equatorial* partner resonates by 1.4 ppm to lower fields (at 2.08 ppm).

It has been assumed (6) that, by virtue of considerable intramolecular interactions characteristic of sterically crowded systems, the carbon-13 chemical shifts in macrolides may exhibit sizable deviations from the values generally encountered in "ordinary" molecules. This has been clearly borne out by the present study. Chemical shift calculations providing an accuracy of 2 to 3 ppm for open chain systems were found to be in error by typically 5 to 8 ppm in the rapamycin case. Most certainly, intramolecular interactions are to be invoked not only to explain the failure of empirical shift calculations in this and similar systems but also to account for the differential shieldings encountered with carbon atoms a great many bonds away from the site of the amide isomerization.

We have also ascertained that the absolute configuration of rapamycin is as portrayed in structure **1** by isolating L(−)-pipecolic acid **6** from its 6 *N* HCl hydrolysis products.

Experimental

Low field nmr spectra were recorded on Varian EM 360 (^1H, 60 MHz) and Varian XL-100-15 FT (^1H, 100.1 MHz and ^{13}C, 25.16 MHz) instruments. The high field nmr spectra were obtained with a Bruker WH 400E spectrometer operating at 400 MHz for protons and 100.62 MHz for carbon-13. Some of the $^1H—\{^1H\}$ double resonance experiments were carried out at 250 MHz using a Bruker WH 250 instrument, whereas many of the time consuming single frequency selective $^{13}C—\{^1H\}$ decouplings were made at 25.16 MHz using the large data table facilities of the Varian Disk FT accessory. The ir spectra were recorded with a Perkin-Elmer 247 spectrophotometer and uv spectra were measured with a Beckman Acta CIII instrument. Mass spectra were recorded with an Hitachi Perkin-Elmer RMU-6D instrument.

Basic Hydrolysis of Rapamycin

Rapamycin (2.15 g) in methanol (80 mL) was treated with aqueous NaOH (1 *N*, 80 mL) at reflux temperature for 1 h and then evaporated to remove the bulk of the methanol leaving a cloudy yellow-brown solution which was diluted to 700 mL and extracted continuously for 11 h. Evaporation of the ether extract after drying (anhydrous Na_2SO_4), gave a neutral oil (0.396 g). Acidification of the aqueous portion to pH 2 with HCl and continuous ether extraction afforded, after drying (anhydrous Na_2SO_4), an acidic oily mixture (1.46 g). A portion (64 mg) of neutral oil in ether (50 mL) was extracted twice with HCl (1 *N*, aqueous) washed with water, and evaporated, yielding a mixture indistinguishable from non acid extracted material on tlc basis. Neutralization of the aqueous HCl extract and extraction with ether afforded no basic product.

Chromatography of Neutral Hydrolysis Products

Neutral material (0.33 g) from the base hydrolysis of rapamycin was chromatographed on a column of silica gel (33 g). Eluting with $CHCl_3$ – ethyl acetate (9:1) gave compounds A (6 mg), B (4 mg), mixtures of B + C (195 mg), mixtures of C + E (71 mg), and compound D (28 mg). Rechromatography of the mixed fractions on silica gel (200 ×) using CH_2Cl_2 – ethyl acetate (100:15) gave further separation of B from C and with CH_2Cl_2 – ethyl acetate (7:3) C from E (C preceding). Fractions were examined by tlc using Merck silica gel 60F precoated plates (0.25 mm thick). Visualization was done with H_2SO_4/CH_2O spray followed by heating. The R_f factors were as follows: A (0.85), B (0.45), C and E (0.35), D (0.2). Initial coloration of B, C, and D was purple, while A was grey and all four were detectable by uv light prior to spraying. Compound E was not detectable by uv

Can. J. Chem. Downloaded from www.nrcresearchpress.com by 210.87.254.6 on 09/05/12
For personal use only.

Can. J. Chem. Downloaded from www.nrcresearchpress.com by 210.87.254.6 on 09/05/12
For personal use only.

and gave a yellow colour on spraying with H_2SO_4/CH_2O. All compounds except D were oils.

Compound A

The uv spectrum (95% ethanol) λ_{max} (ε): 232 (1320), 281 1830); 95% ethanol + OH^-) λ_{max} (ε): 244 (3170), 287 (2075), 297 (1585) (s). The ir spectrum (neat) ν_{max}: 3400 (hydroxyl), 1650–1605 (weak, aromatic) cm^{-1}. The mass spectrum *m/e*:122 (100, M^+), 121 (29, *M* – H), 107 (71, *M* – CH_3), 94 (24, *M* – CO), 78 (24).

Compound B, **3**d

The uv spectrum (95% ethanol) λ_{max} (ε) : 231 (2150), 281 (2350); (95% ethanol + OH^-) λ_{max} (ε) : 231 (2285), 245 (1545) (s), 281 (2350), 305 (670) (s). The ir spectrum (neat) ν_{max}: 3450 (hydroxyl), 1660–1610 (weak, aromatic) cm^{-1}. The ^1H nmr spectrum ($CDCl_3$) : δ_{TMS} : 0.7 (d, 1.5 H, *J* = 6 Hz, CH_3CH), 0.95 (d, 1.5 H, *J* = 6 Hz, CH_3CH), 1–2.1 (m, 11H), 2.2 (s, 6H, CH_3 aromatic), 2.5–3.2 (m, 2H, —CHO—), 3.3 (3H, s, CH_3O), 3.8 (m, 1H, benzylic $CHOCH_3$, 6.5 (s, 1H, $W_{1/2}$ = 4 Hz), 6.8 (s, 1H, $W_{1/2}$ = 4 Hz), 7.75 (s, 0.5 H, phenolic H), 7.8 (s, 0.5 H, phenolic H). *Exact Mass* calcd. for $C_{20}H_{32}O_4$: 336.2300; found (ms): 336.2299; ms (*m/e*): 306 (44, M^+), 304 (100, *M* – CH_3OH), 272 (16, *M* – CH_3OH – H_2O), 254 (16), 175 (66), 162 (44), 161 (88), 137 (50), 136 (95), 110 (44), 91 (44).

Compound C, **2**a

The uv spectrum (95% ethanol) λ_{max} (ε): 249 (5625), 293 (2675); (95% ethanol + OH^-) λ_{max} (ε): 243 (7905), 327 (3150). The ir spectrum (neat) λ_{max}: 3400 (hydroxyl), 1620, 1595 (aromatic) cm^{-1}. The mass spectrum *m/e*:304 (100, M^+), 272 (12, *M* – CH_3OH), 176 (11), 175 (41), 173 (12), 162 (16), 161 (52), 160 (16), 137 (12), 136 (12), 135 (24), 111 (12), 110 (32), 109 (12).

Compound D, **3**c

Melting point 63–65°C. The uv spectrum (95% ethanol) λ_{max} (ε): 230 (2265), 282 (2230); (95% ethanol + OH^-) λ_{max} (ε): 250 (3455), 302 (3380). The ir spectrum ($CHCl_3$) ν_{max}: 3450 (hydroxyl), 1650 – 1610 (aromatic) cm^{-1}. The ^1H nmr spectrum ($CDCl_3$) δ_{TMS}: 0.8 (d, 3H, *J* = 7 Hz, CH_3CH), 1 – 2 (complex m, 10H), 2.2 (s, 6H, aromatic CH_3), 2.3 – 2.6 (complex m, ~ 4H, O*H*, C*HOH*, $CHOCH_3$), 3.3 (s, 3H, CH_3O), 4.3 (d, 1H, *J* = 7 Hz, benzylic C*H*OH), 6.5 (bs, 1H, $W_{1/2}$ = 5 Hz, aromatic), 6.8 (bs, 1H, $W_{1/2}$ = 5 Hz, aromatic), 7.9 (bs, 1H, phenolic H). *Exact mass* calcd. for $C_{19}H_{30}O_4$: 322.2144; found: 322.2153. The mass spectrum *m/e*: 322 (10, M^+), 304 (38, *M* – H_2O), 175 (32), 161 (36), 151 (100), 135 (35), 123 (31), 110 (30), 97 (35).

Compound E, **5**

The ir spectrum (neat) ν_{max}:3450 (hydroxyl), 1700 (ketone) cm^{-1}. The ^1H nmr spectrum ($CDCl_3$) δ_{TMS} : 1 – 2.2 (m, 8H), 2.2 (s, 3H, CH_3CO), 2.4 (d, 2H, *J* = 6 Hz, $COCH_2$—CH), 2.7 – 3.5 (m, 2H, —CHO), 3.4 (s, 3H, CH_3O). Mass spectrum *m/e* : 186 (62, M^+), 129 (100, *M* – CH_3COCH_2), 110 (12, 129 – H_3O), 97 (12, 129 – CH_3OH), 32 (24, CH_3OH^+).

Dihydro-C-diol, **3**a

Compound C (12 mg) in ethanol (2 mL) was hydrogenated over prehydrogenated Adams' catalyst (10 mg) overnight at atmospheric pressure and room temperature. Filtration of the catalyst and evaporation of solvent gave oily dihydro-C-diol **3***a* (12 mg). The uv spectrum (95% ethanol) λ_{max} (ε): 230 (2860), 281 (2200); (95% ethanol + OH^-) λ_{max} (ε) : 230 (3165), 247 (s) (1585), 280 (2175), 304 (1265). The ir spectrum (neat) ν_{max} : 3400 (hydroxyl), 1650 – 1665 (aromatic) cm^{-1}. Mass spectrum *m/e* : 306 (45, M^+), 274 (48, *M* – CH_3OH), 256 (48), 176 (6), 175 (6), 162 (16), 136 (48), 135 (94), 122 (16), 121 (33), 120 (12).

C-diacetate, **2**b

Compound C (1.5 g) was treated with NaOAc (0.33 g) and Ac_2o (10 mL) at 90°C for 2 h after which time tlc indicated complete reaction. Water was added and extraction with CH_2Cl_2 was made. After washing the CH_2Cl_2 layer with dilute cold $NaHCO_3$ solution, drying (Na_2SO_4), and evaporating, an oil (1.76 g) was obtained. A partial purification was effected by chromatographing (1.6 g) on a silica gel (100 g) column using $CHCl_3$/EtOH (100:0.75). Rechromatography of the best fractions (0.25 g) on a silica gel column (75 g) using benzene/ether (19:1) gave the oily C-diacetate, **2***b* (0.198 g). The uv spectrum (95% ethanol) λ_{max} (ε) : 247 (5660); (95% ethanol + OH^-) λ_{max}: unchanged. The ir spectrum (neat) ν: 1760, 1740 (acetates), 1605 (aromatic) cm^{-1}. Mass spectrum *m/e*: 388 (40, M^+), 347 (21), 346 (80, *M* – CH_2CO), 286 (12), 272 (14), 255 (12), 254 (38), 176 (17), 175 (31), 161 (29), 111 (31), 110 (100).

Hydrolysis of C-diacetate, **2**b

C-diacetate (30 mg) in CH_3OH (4 mL) and NaOH solution (4 mL, 2 *N*) was stirred at room temperature for 12 h. (After 5 min tlc indicated complete hydrolysis.) Evaporation of CH_3OH and addition of H_2O and extraction with CH_2Cl_2 gave, after drying (Na_2SO_4), compound C, **2***a* (12 mg), clear oil.

Dihydro-C-diacetate, **3**b

C-diacetate (62 mg) in ethanol (3 mL) was hydrogenated over prehydrogenated Adams' catalyst (25 mg) for 23 h. Filtration and evaporation gave the oily dihydro-C-diacetate, **3***b* (60 mg). The uv spectrum (95% ethanol) λ_{max} (ε): 266 (14 700), 274 (s) (13 500); λ_{max} (OH^-): no change. The ir spectrum ν_{max}: 1750, 1730 (acetates), 1600 (aromatic) cm^{-1}. The mass spectrum *m/e*: 390 (13, M^+), 348 (28, *M* – CH_2CO), 316 (13), 288 (19), 274 (44), 256 (47), 136 (19), 135 (22), 122 (16), 121 (100).

Hydrolysis of Dihydro-C-diacetate, **3**b

Dihydro-C-diacetate (20 mg) in C_2H_5OH (2 mL) was treated with NaOH solution (1 *N*, 3 mL) at room temperature. After 15 min tlc showed complete hydrolysis. Evaporation and extraction with CH_2Cl_2 yielded an oil (12 mg) identical with dihydro-C-diol, **3***a*, obtained by catalytic reduction of C-diol, **2***a*.

Transformation of Compound D, **3**c, *to Compound C*, **2**a

Compound D (20 mg) in benzene (10 mL) was stirred with paratoluenesulfonic acid (5 mg) for 48 h at room temperature. Examination by tlc indicated conversion to compound C which was verified by extraction and purification giving an oil (11 mg) identical with C-diol, **2***a*.

Transformation of Compound C, **2**a, *to* **4**

Compound C (42 mg) in benzene (15 mL) was stirred with paratoluenesulfonic acid at room temperature for 3 days (tlc showed no change) and then heated at reflux for 8 h. After washing with water and evaporation, an oil (30 mg) was obtained which after chromatography on a silica gel (75 g) column eluted with $CH_2Cl_2/CH_3COOC_2H_5$ (7:3) gave **4**, an oil (20 mg), followed by recovered C (8 mg). The ir spectrum (neat) ν_{max}: 3430 (hydroxyl), 1600 (aromatic) cm^{-1}. The ^1H nmr spectrum ($CDCl_3$) δ_{TMS}: ~ 1–2 (m, 9H), 1.4 (s, 3H, CH_3C — O, (2.1 (s, 3H, CH_3), 2.2 (s, 3H, CH_3), 2.3–3.2 (m, 2H, —CH — O), 2.95 (s, 2H, benzylic), 3.3 (s, 1.5H, CH_3O), 3.35 (s, 1.5H, CH_3O), 6.75 (bs, 2H, aromatic) ppm. The mass spectrum of **4** *m/e*: 304 (100, M^+), 272 (11), 175 (50), 161 (81), 141 (16), 137 (22), 136 (24), 135 (36), 110 (36), 109 (20).

Transformation of Compound B, **3**d, *to* **4**

Compound B (60 mg) in benzene (20 mL) was treated with paratoluenesulfonic acid (20 mg) and stirred at room temperature for 3 days. Examination by tlc indicated no substantial change. After heating to reflux for ½ h, tlc revealed the presence of B, **3***d*, C, **2***a*, and **4**. After heating 5 h the mixture was worked up as above and yielded an oil (41 mg) identical with **4** obtained by dehydration of C, **2***a*, above.

Isolation of Piperidine-2-carboxylic Acid **6**

Rapamycin (1 g) in methanol (30 mL) was treated with 2 *N* NaOH (30 mL) under reflux for 1 h, then acidified to pH 2 and continuously extracted with ether for 48 h. Drying (anhydrous Na_2SO_4) and evaporation of the ether extract gave an oil (0.92 g) which was dissolved in $CHCl_3$ and extracted with water. Evap-

oration of the water afforded an oily product (55 mg) which when dissolved in 95% ethanol and applied to the several tlc systems below proved homogeneous and indistinguishable from an authentic sample of piperidine-2-carboxylic acid both in R_f and colour reactions. On cellulose plates (Merck 0.1 mm) (*a*) 2-propanol – 2-butanone – 1 *N* HCl (60:15:25 v/v), $R_f = 0.75$; (*b*) *n*-propanol – 25% NH_3 aqueous (7:3, v/v), $R_f = 0.70$. On silica gel plates (Merck 60F, 0.25 mm), *n*-propanol – 25% NH_3 aqueous (7:3, v/v), $R_f = 0.26$. Visualization employed ninhydrin in chloroform solution containing collidine applied by spraying. Subsequent heating (100°C, ~ 5 min) caused development of blue spot changing to reddish purple on exposure to air.

Rapamycin Mass Spectrum

Rapamycin (mp 183–185°C) was introduced via direct inlet system at 150–190°C and 70 ev. Mass spectrum *m/e*: 305 (8), 304 (28), 229 (5), 197 (8), 193 (5), 176 (15), 175 (100), 162 (5), 161 (6), 160 (7), 147 (13), 145 (8), 141 (5), 135 (11), 133 (7), 122 (6), 119 (8), 109 (9), 107 (6), 105 (11), 98 (7), 97 (7), 95 (8), 93 (7), 91 (12), 69 (10), 67 (9), 57 (8), 55 (18).

L(−)-Piperidine-2-carboxylic Acid (Pipecolic Acid) from Rapamycin

Rapamycin (5.0 g) in methanol (70 mL) was treated with 6 *N* HCl (200 mL) under reflux for 32 h. The reaction mixture was extracted with $CHCl_3$ and the aqueous layer was evaporated to dryness *in vacuo* yielding a yellow non-crystalline solid (0.33 g) which was purified by preparative tlc and proved to be identical with an authentic sample of pipecolic acid. Measurement of the ORD curve ($c = 0.1068$, 80% ethanol) showed it to be L(−)-piperidine-2-carboxylic acid by comparison with literature data (7).

Acknowledgements

Financial assistance from the Consiglio Nazionale delle Ricerche, Italy, the National Research Council of Canada, and the Department of External Affairs, Ottawa, is gratefully acknowledged. One of us (J.A.F.) is grateful to Professor G. B. Marini-Bettolo, Istituto di Chimica, Università Cattolica, Rome, for accommodation in his laboratory and for providing financial assistance during tenure of a Visiting Professorship. Thanks are due to Professor L. Boniforti, Laboratori di Chimica, Istituto Superiore di Sanità, Rome, for assistance in obtaining mass spectra. The authors are grateful to Ayerst Research Laboratories for providing a generous supply of rapamycin and for helpful discussions. The authors are indebted to Dr. H. Schneiders of Bruker-Physik AG, Karlsruhe, W. Germany, for making the company's high field nmr facilities available for the present study and to Dr. W. E. Hull for his assistance in recording the WH 400E spectra. Thanks are due to Dr. E. Baitz-Gács (Central Research Institute of Chemistry, Budapest) for her skillful assistance in the evaluation and compilation of the nmr data. Thanks are due to Johanne Rommens for assistance in isolating and identifying L(−)-pipecolic acid from rapamycin and to A. Taylor (Atlantic Regional Laboratory, Halifax) and J. A. Verpoorte (Department of Biochemistry, Dalhousie University) for providing its ORD curve.

1. C. VEZINA, A. KUDELSKI, and S. N. SEHGAL. J. Antibiot. **XXVIII**, 721 (1975); S. N. SEHGAL, H. BAKER, and C. VEZINA. J. Antibiot. **XXVIII**, 727 (1975).
2. P. S. WHITE, N. SWINDELLS, and J. A. FINDLAY. Can. J. Chem. **56**, 2491 (1978).
3. J. B. STOTHERS. Carbon-13 nuclear magnetic resonance spectroscopy. Academic Press, New York. 1972.
4. C. NISHINO and W. BOWERS. Tetrahedron, **32**, 2875 (1976).
5. L. M. JACKMAN and S. STERNHELL. Applications of nuclear magnetic resonance spectroscopy in organic chemistry. Pergamon Press, Oxford. 1969.
6. J. G. NOURSE and D. J. ROBERTS. J. Am. Chem. Soc. **97**, 4584 (1975).
7. J. CYMERMAN CRAIG and S. K. ROY. Tetrahedron, **21** (2), 391 (1965).

ERRATA

FOR ERRATA SEE V59 #1 10 81 p. 149

Can. J. Chem. Downloaded from www.nrcresearchpress.com by 210.87.254.6 on 09/05/12
For personal use only.

Photochemical reactions of fluoro-substituted ketones with amines, tetraphenylborates, and organometals: an electron spin resonance study

KUANG S. CHEN, TERRY FOSTER, AND JEFFREY K. S. WAN
Department of Chemistry, Queen's University, Kingston, Ont., Canada K7L 3N6

Received August 24, 1979

KUANG S. CHEN, TERRY FOSTER, and JEFFREY K. S. WAN. Can. J. Chem. **58**, 591 (1980).

Ammonium ion-pairs, solvent-separated alkali-metal ion-pairs, and Group IVB organometallic adducts of fluoro-substituted ketones were generated photochemically. The structure and the controlling factors for the formation of contact ammonium ion-pair were deduced from the effects of solvent, amine, and fluorine substitution. The effect of fluorine on the formation of the alkali-metal ion-pairs and organometallic adducts was discussed.

KUANG S. CHEN, TERRY FOSTER et JEFFREY K. S. WAN. Can. J. Chem. **58**, 591 (1980).

On a produit photochimiquement des paires d'ions ammonium, des paires d'ions de métaux alcalins séparés par un solvant et des adduits organométalliques du groupe IVB de fluorocétones. On a déduit la structure et les facteurs contrôlant la formation de la paire d'ions ammonium de contact, à partir des effets de solvant et de la substitution par une amine ou un fluor. On discute de l'effet du fluor sur la formation des paires d'ions de métaux alcalins et des adduits organométalliques.

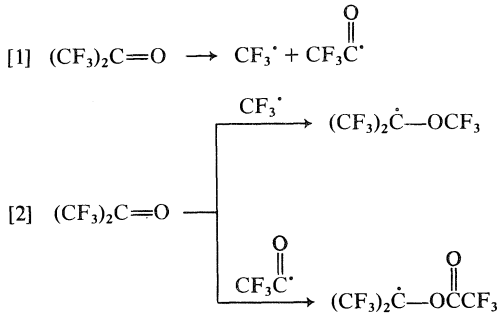
[Traduit par le journal]

Introduction

The primary process in the quenching of triplet state carbonyl compounds with amines has remained controversial (1–3). The extent of charge transfer in the triplet exciplex seems to depend on the chemical system involved. Laser photolysis (4–6), CIDEP (7, 8), and CIDNP (9) are currently employed to clarify these mechanisms. The CIDEP and CIDNP applications to photochemistry have been reviewed recently (10).

While the successful esr observations of contact ammonium ion-pairs in the ketone–amine photochemical systems will shed some light on the controversial mechanism (11), the understanding of the structures and the controlling factors for the formation of contact ion-pairs may provide further insight into the fate of the counter amine radical cation. The photochemical reactions of various fluoro-substituted ketones with different amines in a wide range of solvents were studied, and the results will be presented and discussed.

The formation of contact ion-pairs has been partially ascribed to the exceptionally electron-deficient carbonyl group in the fluoro-substituted ketones (11), and this feature also dominates the chemistry of these compounds (12–14). Previous esr studies (15) have surmised that photolysis of perfluoroketones is similar to that of their hydrocarbon analogs with several outstanding exceptions. Among them, the radical addition to perfluoroketone is a significantly more facile process than it is with alkyl ketones as evidenced by the observations of products of Norrish type 1 reactions, reactions [1] and [2], on photolysing hexafluoroacetone in an inert fluorocarbon solvent,



We will utilize this kind of electron-deficient carbonyl and various fluoro-substituted ketones to trap the Group 1VB organometallic-centered radicals. The effect of fluorine on the adduct formation will be discussed.

The failure of resolving esr signal by the reaction of hexafluoroacetone with alkali metal in tetrahydrofuran (16) prompts us to investigate the alternative, by photolysing the tetrahydrofuran solution of fluoroketones in the presence of alkali-metal tetraphenylborates. This method has been proved useful in the preparation of ion-pairs and triple-ions of various carbonyl compounds (17). The results together with the effect of crown ethers will be described.

Experimental

Hexafluoroacetone was prepared from the dehydration of hexafluoroacetone sesquihydrate (Aldrich) in the presence of phosphorus pentoxide and was vacuum distilled at low temperature prior to use. 1,1,1-Trifluoroacetone, α,α,α-trifluoroacetophenone and decafluorobenzophenone from Aldrich and organometals from Alfa were used as received. Amines and organic solvents were further purified by the appropriate method prior to use (18). The gaseous chemicals were used as

0008-4042/80/060591-08$01.00/0
©1980 National Research Council of Canada/Conseil national de recherches du Canada

Can. J. Chem. Downloaded from www.nrcresearchpress.com by 210.87.254.6 on 09/05/12
For personal use only.

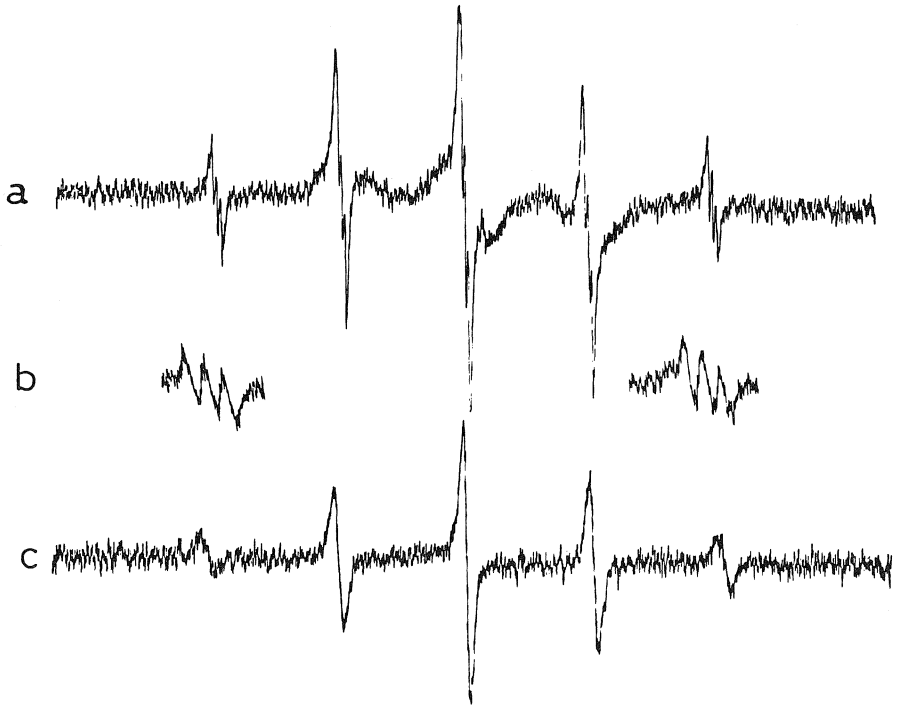


FIG. 1. Electron spin resonance spectra obtained at −78°C during the uv irradiation of hexafluoroacetone and triethylamine in (*a*) cyclopropane, (*b*) cyclopropane with an expanded scale (× 4), and (*c*) THF.

obtained from Matheson. Crown ethers and sodium tetraphenylborate were received from Aldrich. Other salts of tetraphenylboron were prepared by the method of Coplan and Fuoss (19).

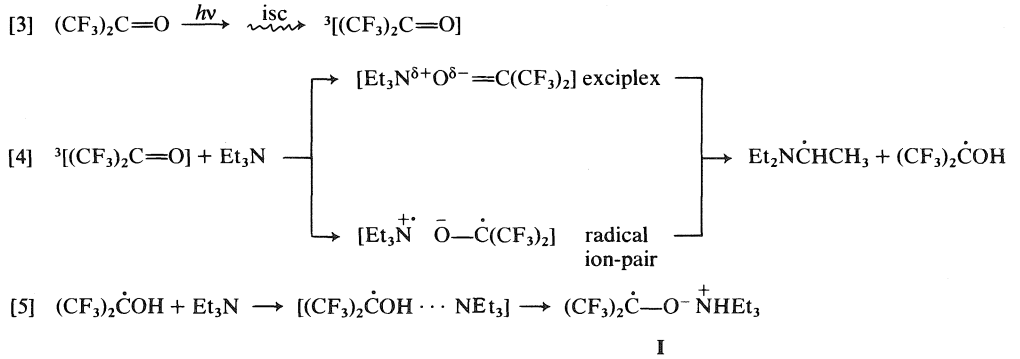
The preparations of samples and the measurements of electron spin resonance and CIDEP by rotating sector were accomplished according to the previously described procedures (17, 20).

Results and Discussion

Photolysis of Fluoroketone Solutions in the Presence of Amines

When a degassed cyclopropane solution of hexafluoroacetone (HFA) and triethylamine (Et_3N) was uv irradiated in cavity at −78°C, a well resolved esr spectrum shown in Fig. 1*a* was recorded. No decay of signal on rotating sector was observed (20). The septet splitting can be unambiguously assigned to the six fluorines, since the hexafluoroacetone ketyl generated electrochemically in acetonitrile (16) gives the comparable fluorine splittings (see Table 1). The inserts on an expanded scale in Fig. 1*b* show that the additional triplet splitting with the correct theoretical intensity ratio is due to a nitrogen nucleus (^{14}N, $I = 1$). The partially resolved second order hyperfine splittings from six equivalent fluorine nuclei are in accordance with Fessenden's prediction (21). The spectrum is therefore assigned to the contact ammonium ion-pair of HFA.

The contact ammonium ion-pair is probably produced via the following scheme:



I

Can. J. Chem. Downloaded from www.nrcresearchpress.com by 210.87.254.6 on 09/05/12
For personal use only.

Can. J. Chem. Downloaded from www.nrcresearchpress.com by 210.87.254.6 on 09/05/12
For personal use only.

TABLE 1. Electron spin resonance parameters of paramagnetic species derived from HFA and 1,1,1-trifluoroacetone

Species	Solvent	T (°C)	A_F^{β} (G)	A_x^{ox} (G)	$A_{^{13}C}^{\alpha}$ (G)	$A_{^{13}C}^{\beta}$ (G)	Other	Note
$(CF_3)_2\dot{C}$—OH	▽[a]	−78	24.88 ± 0.05	2.01(H)				
$(CF_3)_2\dot{C}$—$\overset{-}{O}\overset{+}{N}HEt_3$	▽	−78	30.54	1.08(N)				
$(CF_3)_2\dot{C}$—$O^-/\overset{+}{N}HEt_3$	THF	−78	31.65					
$(CF_3)_2\dot{C}$—O^-/M^+	THF	25	32.22					M = Li, Na, K, Bu^n_4N
$(CF_3)_2\dot{C}$—O^-	CH_3CN	25	34.7					Ref. 16
$(CF_3)_2\dot{C}$—OPh_3	▽	−94	24.70					
$(CF_3)_2\dot{C}$—OMe_3	▽	−90	22.30	7.9(^{13}C)	49.8	12.4		
$(CF_3)_2\dot{C}$—$OCH(CF_3)_2$	▽	−36	20.3				2.2(γ-6F)	Ref. 15
$(CF_3)_2\dot{C}$—OCF_3	CF_2Cl_2	−42	18.74					Ref. 15
$(CF_3)_2\dot{C}$—$OSiPh_3$	▽	−86	23.00	9.02(Si)	50 ± 2	11.7		
$(CF_3)_2\dot{C}$—$OSiHPh_2$	▽	−88	23.13	7.02(Si)		12.2	0.72(Si—H)	
$(CF_3)_2\dot{C}$—$OSiH_2Ph$	▽	−81	23.15				1.18(Si—H)	
$(CF_3)_2\dot{C}$—$OSiMe_3$	▽	−89	23.51	8.61(Si)	53.1	11.7		
$(CF_3)_2\dot{C}$—$OSiFMe_2$	▽	−85	22.72				0.86(Si—F)	
$(CF_3)_2\dot{C}$—$OGePh_3$	▽	−83	22.29					
$(CF_3)_2\dot{C}$—$OSnPh_3$	▽	−85	26.10					
$(CF_3)_2\dot{C}$—$OSnMe_3$	▽	−97	28.61	17.31(Sn)	57 ± 4	9.9		
$(CF_3)_2\dot{C}$—$OPbPh_3$	▽	−104	27.45					
$(CF_3)_2\dot{C}$—$OPbMe_3$	▽	−101	27.81					
$CF_3\dot{C}(CH_3)OH$	$CF_3(CH_3)CHOH$	−109	29.00				21.38(CH_3)	Ref. 15
$CF_3\dot{C}(CH_3)OSiPh_3$	▽	−91	28.57				21.89(CH_3)	
$CF_3\dot{C}(CH_3)OSiMe_3$	▽	−98	28.82				21.66(CH_3)	
$CF_3\dot{C}(CH_3)OSnMe_3$	▽	−95	33.65				20.05(CH_3)	

[a]▽ = cyclopropane.

Can. J. Chem. Downloaded from www.nrcresearchpress.com by 210.87.254.6 on 09/05/12
For personal use only.

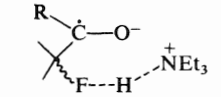
The structure of ion-pair **I** will be discussed later. The intermediate step in reaction [4] has remained controversial and seems to depend on the chemical systems studied (4–9). Reaction [5] has been postulated for other ketone–amine systems (7, 22). Although photoexcited HFA in its triplet state is a powerful hydrogen abstracting agent as evidenced by its photoreduction in the presence of even poor hydrogen donors such as cyclopropane (15), the efficient quenching of triethylamine on the excited state of HFA can neglect the contribution of $(CF_3)_2\dot{C}$—OH via reaction [6].

$$[6]\quad {}^3[(CF_3)_2C{=}O] \xrightarrow{c\text{-}C_3H_6} (CF_3)_2\dot{C}{-}OH$$

The ion-pair **I** can be either a contact ion-pair or solvent-separated ion-pair (23) depending on the solvent used. For example, while a contact ion-pair was observed in a non-polar solvent cyclopropane, a solvent-separated ion-pair resulted when THF was employed as the solvent (Fig. 1*c*). The modification of esr parameters from those of anion radical were used as the criteria to assign the formation of ion-pair since the additional hyperfine structure (hfs) from the counter cation is not resolved. This argument was used to propose the observation of ammonium ion-pairs of ninhydrin (24) even though the additional nitrogen hfs was not observed.

Surprisingly, no solvent-effect on the ammonium ion-pairs of α,α,α-trifluoroacetophenone (TFA) was noticed. A contact ion-pair was always observed when TFA and Et_3N were photolyzed in the following solvents, toluene, 2-propanol, tetrahydrofuran (THF), acetonitrile, and *N*,*N*-dimethylformamide (DMF). The esr parameters are given in Table 2. This result is in contrast with the usual observation in the alkali-metal ion-pairs of carbonyl compounds. For example, contact alkali-metal ion-pairs of xanthone were observed in THF but they would dissociate in a polar solvent such as DMF (25). On the other hand, the amine seems to play a very important role in determining the types of ion-pairs of TFA observed. While Et_3N, Bu_3N, and Am_3N gave the contact ion-pairs, NH_3, Me_3N, $(C_4F_9)_3N$, Et_2NH, $(Me_3Si)_2NH$, Me_3SiNMe_2, and Me_3SiNEt_2 produced the solvent-separated ion-pairs. It seems only tertiary amines will produce the contact ion-pairs but not all of the tertiary amines will work. The right basicity is a key factor too, the stronger Et_2NH or weaker Et_2NSiMe_3 than that of Et_3N only gave the solvent-separated ion-pairs. The effects of solvent and amine on the type of ion-pair formation clearly depend on the individual fluoroketone studied.

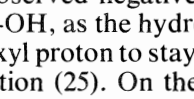
Furthermore, if a THF solution of the unsubstituted acetophenone, benzophenone, or 1,1,1-trifluoroacetone and Et_3N was irradiated, no esr signal or only protonated ketyl (22) was observed. However, when decafluorobenzophenone was employed, a contact ion-pair was observed (see Table 3). It appears that in order for the ketone to form a stable contact ammonium ion-pair as depicted in structure **II**, it is essential to have a fluoro-substituted alkyl group to serve as a powerful hydrogen-bonding source and an additional strong electron-withdrawing group to render the carbonyl exceptionally electron-deficient.



R = CF_3, C_6H_5, and C_6F_5

II

Evidence of fluorine hydrogen bonding was suggested by the observed negative hydroxyl proton hfs in $(CF_3)_2\dot{C}$—OH, as the hydrogen-bonding will cause the hydroxyl proton to stay more likely in the "in-plane" position (25). On the other hand, one can expect that without the influence of hydrogen-bonding, the hydroxyl proton hfs in the $(CH_3)_2\dot{C}$—OH radical would now be positive with the hydroxyl proton being in the most probable "out-of-plane" position. This is indeed the observed result (15).



III

Another possible structure, **III**, has been proposed in other ketone–amine systems (22). In the case of a contact ion-pair such as that found in our system, structure **III** should have led to the observation of the hfs from the proton in the ammonium cation. The hydrogen atom in the ammonium cation probably as an important "bridge" to bring the nitrogen closer to the fluoroketone radical anion, as represented in structure **II**. This can also account for the fact that a solvent-separated ion-pair was observed when tetra-*n*-butylammonium tetraphenylborate was used instead of tri-*n*-butylamine. The formation of solvent-separated ion-pairs in the photolyses of fluoroketones in THF in the presence of various tetraphenylborates will be described in the next section.

Photolysis of THF Solutions containing Fluoroketones and Tetraphenylborates

The standard alkali-metal reduction in an

Can. J. Chem. Downloaded from www.nrcresearchpress.com by 210.87.254.6 on 09/05/12
For personal use only.

TABLE 2. Electron spin resonance parameters of paramagnetic species derived from TFA and acetophenone

Species	Solvent	T (°C)	A_F^{β} (G)	A_x^{ox} (G)	A^o (G)	A^m (G)	A^p (G)	Note
$(CF_3)(C_6H_5)\dot{C}—OH$	IPA[a]	−40	24.79 ± 0.05	2.15(H)	3.31 5.73	1.52	5.01	
$(CF_3)(C_6H_5)\dot{C}—\bar{O}\overset{+}{N}HEt_3$	IPA	−40	26.13	1.20(N)	5.24	1.20	4.23	
	THF	−40	27.21	1.12(N)	5.01	1.12	3.98	
	DMF	−40	27.39	1.07(N)	4.83	1.07	4.03	
$(CF_3)(C_6H_5)\dot{C}—\bar{O}/\overset{+}{N}H_2Et_2$	IPA	−40	26.31		3.94	1.34	5.10	
	THF	−40	27.03		4.48	n.s.	4.48	
	DMF	−40	27.11		3.94	1.25	4.83	
$(CF_3)(C_6H_5)\dot{C}—\bar{O}/\overset{+}{N}HMe_3$	THF	−67	26.42		3.94	1.07	5.08	
$(CF_3)(C_6H_5)\dot{C}—\bar{O}/\overset{+}{N}HEt_2SiMe_3$	IPA	−40	26.31		4.48	1.34	4.74	
$(CF_3)(C_6H_5)\dot{C}—\bar{O}/\overset{+}{N}H_2(SiMe_3)_2$	IPA	−40	26.13		4.03	1.34	5.01	
$(CF_3)(C_6H_5)\dot{C}—\bar{O}K^+$ [b]	THF	−58	26.81		3.97	1.18	5.16	
$(CF_3)(C_6H_5)\dot{C}—\bar{O}/M^+$ [c]	THF	−72	26.49		3.79	1.16	5.08	M = Li, Na, K, Bu^n_4N
$(CF_3)(C_6H_5)\dot{C}—O^-$	DMF	25	24.2		3.3 3.9	1.2	4.8	Ref. 37
$(CF_3)(C_6H_5)\dot{C}—OH$	IPA	25	14.15(CH_3)	0.36(H)	4.70 4.97	1.57	5.94	Ref. 38
$(CF_3)(C_6H_5)\dot{C}—\bar{O}$	DME		6.96(CH_3)		3.76 4.31	0.91 1.13	6.55	Ref. 39
$(CF_3)(C_6H_5)\dot{C}—OSiPh_3$	Benzene	5	21.66		4.48	1.58	5.19	
$(CF_3)(C_6H_5)\dot{C}—OSnPh_3$	THF	−60	25.62		4.22	1.40	4.93	
$(CF_3)(C_6H_5)\dot{C}—OSnMe_3$	THF	−60	25.04		4.27	1.40	4.84	

[a] IPA = 2-propanol.
[b] 18-Crown-6 solvated potassium ion pair.
[c] Data were given as M = Bu^n_4N.

TABLE 3. Electron spin resonance parameters of paramagnetic species derived from decafluorobenzophenone

Species	Solvent	T (°C)	A_x^{ox} (G)	A^o (G)	A^m (G)	A^p (G)	Other
$(C_6F_5)_2\dot{C}$—OH	THF	−32	1.90(H)	4.40	1.90	8.32	
$(C_6F_5)_2\dot{C}$—$\bar{O}\overset{+}{N}HEt_3$	▽	−95	0.63(N)	4.22	1.97	8.44	
$(C_6F_5)_2\dot{C}$—$OSiPh_3$	Benzene	70		5.47	1.60	7.83	
$(C_6F_5)_2\dot{C}$—$OSiHPh_2$	Benzene	71		5.05	1.72	8.04	0.57(Si—H)
$(C_6F_5)_2\dot{C}$—$OSiH_2Ph$	Benzene	19		4.69	1.97	8.26	0.47(Si—H)
$(C_6F_5)_2\dot{C}$—$OSiMe_3$	Benzene	56		4.80	1.75	7.99	
$(C_6F_5)_2\dot{C}$—$OSiFMe_2$	Benzene	64		4.74	1.90	8.15	0.60(Si—F)
$(C_6F_5)_2\dot{C}$—$OSnPh_3$	Benzene	75		4.85	1.50	7.84	

ethereal solvent (26) has failed to produce the esr signal of ion-pair of HFA, TFA, or decafluorobenzophenone, but a solid precipitate, presumable salts of of pinacol (12*a*), was observed. However, when a THF solution of TFA and 18-crown-6 was brought to contact briefly with the potassium mirror, a well resolved esr signal of crown ether complexed potassium ion-pair of TFA was observed. The esr parameters are given in Table 2. This simple method of producing benzene radical anion (27) and sodium ion-pair of 2,6-di-*tert*-butylbenzoquinone (28) in non-polar solvent has been recently reported.

Another method, by irradiating a THF solution of carbonyl compounds in the presence of tetraphenylborates, has been successful in generating a variety of ion-pairs and triple-ions (17). We have employed this method to the following three fluoro-substituted ketones, HFA, TFA, and decafluorobenzophenone and the results are quite surprising.

When a THF solution of HFA and various tetraphenylborates was irradiated, an esr signal of two species was always observed. One of them can be generated in the absence of tetraphenylborate and was assigned as the protonated species. Although the counter solvent radical was not observed in THF or cyclopropane, they can be observed when propionic acid or 2-propanol was used as solvent. The other one has the similar esr parameters as those of solvent-separated ammonium ion-pair of HFA formed by photolysing a THF solution of HFA and Et_3N (see Table 1). It was assigned as solvent-separated ion-pairs of HFA. They were formed presumably via the following mechanism:

$$[7]\quad {}^3[(CF_3)_2C{=}O] \xrightarrow{\text{O-H}} (CF_3)_2\dot{C}{-}OH$$

$$[8]\quad (CF_3)_2\dot{C}{-}OH \rightleftharpoons (CF_3)_2\dot{C}{-}O^- + H^+$$

$$[9]\quad (CF_3)_2\dot{C}{-}O^- + M^+BPh_4^- \longrightarrow (CF_3)_2\dot{C}{-}O^-/M^+BPh_4^-$$

$$M = Li, Na, K, Bu_4^n \qquad \textbf{IV}$$

The photoreduction of the triplet HFA by a hydrogen donor has been described in the previous section. Reactions similar to [7] and [8] have been proposed in the photochemical generation of ion-pairs and triple ions (17). The solidus in **IV** was used to distinguish the solvent-separated ion-pair from the contact ion-pair.

Whether one can observe the protonated species or the ion-pair or both species depends on the dissociation process [8] as well as the driving force by the formation of ion-pairs, reaction [9]. When TFA was exposed to the similar condition, only solvent-separated ion-pairs were observed (Table 2). In the absence of tetraphenylborates, a weak esr signal of protonated species was detected. This signal can be enhanced by photolysis of a slowly flowing 2-propanol solution (0.5 mL/min). No counter solvent radical was observed in THF or 2-propanol. No polarization was detected for the protonated species. However, when a 2-propanol solution of TFA containing phenol with high concentration (>1 *M*) was irradiated, both protonated TFA and phenoxy radical were observed. Emissive CIDEP was observed in the phenoxy radical (20), again no polarization was observed in protonated TFA. If the phenol was replaced by hydroquinone or 2,6-di-*tert*-butylphenol, the emissive counter phenoxy radical was observed but no esr signal of protonated TFA was detected. The effect of fluorine anisotropic tensor on shortening the T_1 of protonated TFA is not clear yet. The short T_1 could be one of the possible reasons for not observing the polarization of protonated fluoroketones, although CIDNP has been observed in many fluoroketones (9).

The dissociation process, similar to reaction [8], must be very inefficient in the system of decafluorobenzophenone. The protonated species was the sole esr signal observed when THF solutions of decafluorobenzophenone and various tetraphenylborates, even in the presence of crown ethers, was irradiated. The esr parameters are given in Table 3. Reaction [8] also depends on the

Can. J. Chem. Downloaded from www.nrcresearchpress.com by 210.87.254.6 on 09/05/12
For personal use only.

Can. J. Chem. Downloaded from www.nrcresearchpress.com by 210.87.254.6 on 09/05/12
For personal use only.

solvent, when cyclopropane, instead of THF, was used, only the protonated species of HFA observed, no alkali-metal solvent-separated ion-pair was detected. This is inconsistent with the observations in ammonium ion-pairs, namely contact ion-pair was observed on cyclopropane while solvent-separated ion-pair was observed in THF.

A competitive reaction was also carried out by photolysing a THF solution of TFA in the presence of both Et_3N and tetraphenylborates. Only the contact ammonium ion-pair was observed. This indicates that the following exchange reaction is not important in this case,

[10] $TFA^{-\cdot}\overset{+}{N}HEt_3 + M^+BPh_4^- \xrightarrow{THF} TFA^{-\cdot}/M^+ + \overset{+}{Et_3N}HBPh_4^-$

Group IVB Organometallic Adducts of Fluoroketones

A complete series of Group IVB organometallic adducts of HFA was observed by photolysing cyclopropane solution of HFA in the presence of organometals and di-*tert*-butylperoxide. Under the similar conditions, 1,1,1-trifluoroacetone, TFA, decafluorobenzophenone, and benzophenone were studied. The observed esr parameters are given in Tables 1, 2, and 3, respectively.

The exceptionally electron-deficient carbonyl group of HFA results in several unusual features which merit further considerations. Although thioketones have trapped various carbon-centered radicals (29), benzil (30) and 2,6-di-*tert*-butylbenzoquinone (31) are the only two compounds that can utilize their "modified" carbonyl groups to trap alkyl radicals. HFA is the sole ketone, so far, that has successfully trapped carbon-centered radicals probably including triphenylmethyl radical. There are two reasons to believe that the observed esr signal during the photolysis of cyclopropane solution of HFA in the presence of triphenylmethane and di-*tert*-butylperoxide is due to the HFA adduct of triphenylmethyl radical: (*1*) There is no esr signal of triphenylmethyl radical which can always be observed under similar conditions except in the absence of HFA. (*2*) There is no additional hfs from hydroxyl proton of protonated species which can be resolved in the absence of triphenylmethane. TFA which can also form the contact ammonium ion-pair did not give any esr signal of alkyl radical adduct. This may imply that the exceptionally electron-deficient carbonyl group is not the only requirement for the formation of the adduct, some unknown fluorine effect may be involved. The weakness of lead–oxygen bond (32) may be the major reason for not observing esr signal of organolead adduct of acetone (33) or 1,1,1-trifluoroacetone. The observation of both trimethyl and triphenylplumbyl adducts of HFA may be partially ascribed to the two extremely electron-withdrawing CF_3 groups which tend to stabilize the negative charge on the organic molecule in the transition state through the polar effect.

[11] $(CF_3)_2C{=}O + {}^{\cdot}PbR_3 \rightarrow (CF_3)_2C{=}O{}^{\cdot}PbR_3 \longleftrightarrow (CF_3)_2\dot{C}{-}O{-}PbR_3 \rightarrow (CF_3)_2\dot{C}{-}\overset{-}{O}\overset{+}{P}bR_3$

The effect of fluorine on the stability of adducts also reflected in the reactions of benzophenone and perfluorobenzophenone with various phenylsilanes. Under similar conditions, while decafluorobenzophenone can give very good signals of all three triphenyl, diphenyl, and phenylsilyl adducts, benzophenone can only give a very good esr signal of triphenylsilyl adduct (34) and no signal of phenylsilyl adduct was observed.

The excellent esr signal of HFA adducts gives some hfs of carbon-13 and metals which may provide additional information on the structure of the adducts (35). For example, in the following three organosilyl adducts, the unusual small ^{29}Si splitting may be due to the highly pyramidal radical center or an expanded C_α—O—Si angle (15). The effect of β-fluorine on the radical configuration is minimum since the α-^{13}C splitting is not too far away from that of simple alkyl radicals (35). The big difference in α-^{13}C splittings between adducts **V** and **VI** is in accordance with an approximate molecular orbital theory calculation which predicted a decrease of more than 6 G in α-^{13}C splitting by going from ethyl to benzyl radicals (36). This in turn implies that the adduct **V** is planar at the radical site.

	Value (G)		
Parameter	$(CF_3)_2\dot{C}$—$OSi(C_6H_5)_3$ **V**	$(C_6H_5)_2\dot{C}$—$OSi(C_6H_5)_3$ **VI** (ref. 34)	$F_2\dot{C}$—$OSiEt_3$ **VII** (ref. 15)
$A_{^{29}Si}$	9.0	7.1	1.9
$A_{^{13}C}{}^{\alpha}$	50	25	

Acknowledgment

This research is supported by the Natural Sciences and Engineering Research Council of Canada.

1. S. G. COHEN, A. PAROLA, and G. H. PARSONS. Chem. Rev. **73**, 141 (1973).
2. A. J. DOBBS. Mol. Phys. **30**, 1073 (1975).
3. R. SEHEERER and M. GRÄTZEL. J. Am. Chem. Soc. **99**, 865 (1977).
4. S. ARIMITSU, H. MASUHARA, N. MATAGA, and H. TSUBOMURA. J. Phys. Chem. **79**, 1255 (1975).
5. H. KOBASHI, T. NAGUMO, and T. MORITA. Chem. Phys. Lett. **57**, 369 (1978).
6. V. A. KUZMIN, A. P. DARMANYAN, and P. P. LEVIN. Chem. Phys. Lett. **63**, 509 (1979).
7. K. A. MCLAUCHLAN and R. C. SEALY. Chem. Phys. Lett. **39**, 310 (1976).
8. S. K. WONG. J. Am. Chem. Soc. **100**, 5488 (1978).
9. H. D. ROTH. *In* Chemically reduced magnetic polarization. *Edited by* L. T. Muus, P. W. Atkins, K. A. McLauchlan, and J. B. Pedersen. Reidel Publishing Co., Holland. 1977. Chapt. IV.
10. J. K. S. WAN. Adv. Photochem. To be published.
11. K. S. CHEN, T. FOSTER, and J. K. S. WAN. Can. J. Chem. **57**, 600 (1979).
12. (*a*) C. G. KRESPAN and W. J. MIDDLETON. Fluorine Chem. Rev. **1**, 145 (1967); (*b*) H. P. BRAENDLIN and E. T. MCBEE. Adv. Fluorine Chem. **3**, 1 (1963); (*c*) J. HEICKLEN. Adv. Photochem. **7**, 57 (1969).
13. W. A. SHEPPARD and C. M. SHORTS. Organic fluorine chemistry. W. A. Benjamin, New York, NY. 1969. p. 437*ff*.
14. R. D. CHAMBERS. Fluorine in organic chemistry. John Wiley and Sons, New York, NY. 1973. p. 216*ff*.
15. P. J. KRUSIC, K. S. CHEN, P. MEAKIN, and J. K. KOCHI. J. Phys. Chem. **78**, 2036 (1974).
16. E. G. JANZEN and J. L. GERLOCK. J. Phys. Chem. **71**, 4577 (1967).
17. K. S. CHEN and J. K. S. WAN. J. Am. Chem. Soc. **100**, 6051 (1978).
18. A. WEISSBERGER (*Editor*). Technique of organic chemistry. Vols. III and VII. Wiley Interscience, New York, NY. 1955 and 1956.
19. M. A. COPLAN and R. M. FUOSS. J. Phys. Chem. **68**, 1177 (1964).
20. A. J. ELLIOT and J. K. S. WAN. J. Phys. Chem. **82**, 444 (1978).
21. R. W. FESSENDEN. J. Chem. Phys. **37**, 747 (1962).
22. (*a*) R. S. DAVIDSON and R. WILSON. J. Chem. Soc. B, 71 (1970); (*b*) R. S. DAVIDSON and M. SANTHANAM. J. Chem. Soc. Perkin II, 2355 (1972).
23. (*a*) N. HIROTA and R. KRELICK. J. Am. Chem. Soc. **88**, 614 (1966); (*b*) A. CROWLEY, N. HIROTA, and R. KRELICK. J. Chem. Phys. **46**, 4815 (1967).
24. G. R. STEVENSON and W. MARTIR. J. Phys. Chem. **82**, 1171 (1978).
25. K. S. CHEN, S. W. MAO, K. NAKAMURA, and N. HIROTA. J. Am. Chem. Soc. **93**, 6004 (1971).
26. (*a*) T. R. TUTTLE, JR., R. L. WARD, and S. I. WEISSMAN. J. Chem. Phys. **25**, 189 (1956); (*b*) A. CANINGTON, F. DRAVNIEKS, and M. C. R. SYMMONS. J. Chem. Soc. 947 (1959).
27. (*a*) B. KAEMPF, S. RAYNAL, A. COLLET, F. SCHUE, S. BOILEAU, and J. LEHN. Angew. Chem. Int. Ed. Engl. **13**, 611 (1974); (*b*) M. A. KOMARYNSKY and S. I. WEISSMAN. J. Am. Chem. Soc. **97**, 1589 (1975).
28. K. S. CHEN and J. K. S. WAN. Spectrosc. Lett. **12**, 647 (1979).
29. J. C. SCAIANE and K. U. INGOLD. J. Am. Chem. Soc. **98**, 4727 (1976), and refs. therein.
30. B. SCHROEDER, W. P. NEUMANN, and H. HILLGÄRTNER. Chem. Rev. **107**, 3494 (1974).
31. V. A. ROGONSKI and V. A. BELYAKOV. Dokl. Akad. Nauk SSSR, **237**, 1404 (1977).
32. R. A. JACKSON. Special publication No. 24. The Chemical Society. 1970. p. 295.
33. J. COOPER, A. HUDSON, and R. A. JACKSON. J. Chem. Soc. Perkin II, 1933 (1973).
34. A. R. MCINTOSH and J. K. S. WAN. Can. J. Chem. **49**, 812 (1971); Molec. Phys. **22**, 183 (1971).
35. H. FISCHER. *In* Free radicals. Vol. 2. *Edited by* J. K. Kochi. Wiley Interscience, New York, NY. 1973. Chapt. 19.
36. J. A. POPLE and D. L. BEVERIDGE. Approximate molecular orbital theory. McGraw-Hill, New York, NY. 1970.
37. C. P. ANDRIEUX and J. M. SAVEANT. Bull. Soc. Chim. Fr. Part 2, 2090 (1973).
38. R. WILSON. J. Chem. Soc. B, 1581 (1968).
39. N. STEINBERGER and G. K. FRAENKEL. J. Chem. Phys. **40**, 723 (1964).

Can. J. Chem. Downloaded from www.nrcresearchpress.com by 210.87.254.6 on 09/05/12
For personal use only.

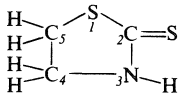
Part I. Conformational analysis of thiazolidine-2-thione

F. CHANON, M. RAJZMANN, M. CHANON, AND J. METZGER
Faculté des Sciences de Saint-Jérôme, 13397 Marseille, France
AND
G. POUZARD
Université de Provence, Saint-Jérôme, 13397 Marseille, France

Received August 1, 1978[1]

F. CHANON, M. RAJZMANN, M. CHANON, J. METZGER, and G. POUZARD. Can. J. Chem. **58**, 599 (1980).

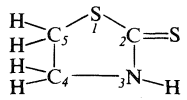
^{1}H nmr ($^3J_{HH}$ values) and ^{13}C nmr results (shielding effect of *vicinal* methyl ^{13}C signals in *cis*-4,5-dimethylthiazolidine-2-thione) allows an estimation of the puckering in the five-membered monounsaturated heterocycle, thiazolidine-2-thione:



Application of Lambert's *R*-value equation provides a value of 41° for the torsional angle between C4 and C5, in contrast to an upper limit value of 25°, deduced from consideration of ^{13}C γ-effects; this disparity is discussed and compared with finite perturbation treatment of $^3J_{HH}$ values.

F. CHANON, M. RAJZMANN, M. CHANON, J. METZGER et G. POUZARD. Can. J. Chem. **58**, 599 (1980).

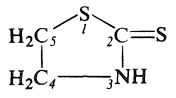
Les résultats fournis par la rmn du proton ($^3J_{HH}$) et par la rmn du carbone-13 (effets de masquage des ^{13}C des méthyles *vicinaux* dans la *cis*-diméthyl-4,5 thiazolidinethione-2) permettent d'évaluer le taux de plissement de l'hétérocycle pentagonal à une insaturation, la thiazolidinethione-2:



L'utilisation des valeurs *R* de Lambert fournit comme valeur du plissement 41°, alors que l'étude conduite à partir du masquage du carbone-13 des méthyles à partir de l'effet γ donne une limite supérieure de 25°. Cette différence d'évaluation est discutée et confrontée au calcul par les perturbations finies des $^3J_{HH}$.

Introduction

Conformational analysis of heterocyclic systems did not begin (1, 2) until well after the birth of classical conformational analysis (3). The uncertainty associated with the extension of well accepted tools of analysis for classical conformational systems, to unknown systems, is the main cause of this late development. For any new heterocyclic system under study, the obtained informations must be cross-checked by the use of different methods. The following reports illustrate this approach. The purpose of this paper is to define the conformational properties of the nonsymmetric monounsaturated heterocyclic system, namely thiazolidine-2-thione (TH-2-TH) **1**.



1

[1]Revision received November 12, 1979.

In this report, we will study the unsubstituted ring and in the next report (4), we will consider the effect of perturbations in this system due to the presence of substituents at positions 3, 4, and 5. This first paper tentatively answers the questions: is the heterocycle planar or puckered? If indeed the ring is puckered, to what extent is it, compared with its alicyclic homologs? Do the experimental results allow us to affirm that a pseudo-rotation process exists in this ring system?

Results and Discussion

Observation and Evaluation of the Degree of Puckering of the Thiazolidine-2-thione Ring

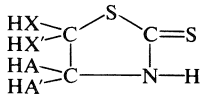
^{1}H Nuclear Magnetic Resonance — J_{vic} — Application of the Simplified Karplus Equation

The analysis of the ^{1}H nmr spectra (Table 1) gives nearly alike $^3J_{cis}$ and $^3J_{trans}$ values for the C4–C5 fragment in TH-2-TH. It had been pointed out (5) that similar J_{cis} and J_{trans} values in a five-membered ring suggest a highly flexible system. Following Karplus (6) $^3J_{HH}$ values can be described as functions of the

0008-4042/80/060599-05$01.00/0
©1980 National Research Council of Canada/Conseil national de recherches du Canada

Can. J. Chem. Downloaded from www.nrcresearchpress.com by 210.87.254.40 on 09/05/12
For personal use only.

TABLE 1. ^{1}H nmr parameters for thiazolidine-2-thione heterocyclic protons*



$\delta_A = \delta_{A'}$	$\delta_X = \delta_{X'}$	J_{AX}	$J_{AX'}$
4.01	3.58	8.75	7.35

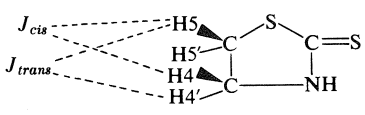
*Shifts in ppm; coupling constant in Hz; in ($^2H_6$)–acetone with TMS as internal reference; assignment of the heterocyclic proton signals deposited in the Journal archives.

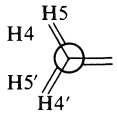
torsional angle φ between the two corresponding *vicinal* carbon atoms.

[1] $^3J_{HH} = J_{0°} \cos^2 \varphi \qquad 0° \leq \varphi \leq 90°$

[2] $^3J_{HH} = J_{180°} \cos^2 \varphi \qquad 90° \leq \varphi \leq 180°$

In the case of a planar ring in TH-2-TH:





[3] $J_{cis}^{exp} = J_{45} = J_{4'5'} = J_{0°} = 8.75$ Hz

[4] $J_{trans}^{exp} = J_{45'} = J_{4'5} = J_{120°} = 7.35$ Hz

$= J_{180°} \cos^2 120°$ according to [2]

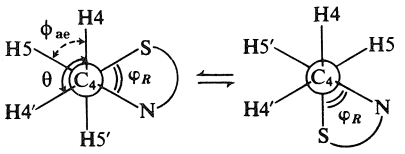
So

$J_{180°} = 29.4$ Hz with $J_{180°}/J_{0°} = 3.4$

The abnormally large value for 180° (6–8) rules out the possibility of a planar conformation for the TH-2-TH ring.

^1H Nuclear Magnetic Resonance — J_{vic} — The Use of Lambert's R*-value Method*

Assuming a puckered ring, thiazolidine-2-thione exists in a rapidly interconverting equilibrium mainly between two energetically equivalent conformations:



The N—C4—C5—S torsional angle φ_R can be evaluated (Lambert's *R*-value method (9)) using the ratio of the experimental *vicinal* coupling constant values in the CH_2—CH_2 fragment: i.e.

[5] $R = J_{trans}^{exp}/J_{cis}^{exp}$

and

[6] $\cos \varphi_R = [3/(2 + 4R)]^{1/2} \qquad$ for $\theta = 120°$

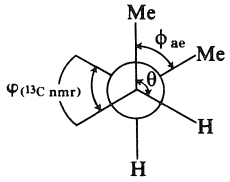
This type of calculation can be used for most of the six-membered rings and according to Lambert "there appears to be no theoretical reason to preclude applications to all common and medium rings" (9). In the TH-2-TH case, $R = 0.84$, i.e. $\varphi_R = 41°$; therefore Lambert's *R*-value implies a significant puckering of the ring as in the cyclopentane (10) and dioxolane cases (11).

^1H Nuclear Magnetic Resonance — $^2J_{H5H5'}$ and $^2J_{H4H4'}$ Values

In the series of 4- and 5-alkyl-substituted (Me, Et, *i*Pr, *t*Bu) TH-2-TH derivatives, the $^2J_{H4H4'}$ or $^2J_{H5H5'}$ values vary in a continuous and coherent way (4). However, substituent electronegativities vary only slightly along the series; thus the main factor which induces deviations in the J_{gem} values in the $\ddot{X} - CH_2$ fragment is the variation of the dihedral angle between the *C*—H bonds and the "lone-pairs orbitals" of the heteroatom Ẍ (12). The observed change in the J_{gem} values in the alkylated series was therefore assigned to conformational modifications of the ring (4): that establishes the mobility of the thiazolidine-2-thione ring.

^{13}C Nuclear Magnetic Resonance — $^{13}CH_3$ Signal in the cis*-Dimethylated Derivatives of TH-2-TH and in some* Vicinal *Dimethylated Models*

Stothers and co-workers (13, 14) showed the relationship between the spatial proximity and the observed shielding effects of the $^{13}CH_3$ signal in *vicinal* methyl groups. Inspections of the computed electron density distributions and details of the geometrical dependences lead to the suggestion that the mecanism of γ-effect may be considerably more complex than the commonly accepted C—H bond polarisation by nonbonded H · · · H interaction (15). However,[2] a graph of the shielding effect by a *vicinal* methyl group versus the estimated dihedral angle $\phi_{ae} = \varphi_{^{13}C\ nmr}$ in some model compounds



(14, 16–18) gives nearly a straight line (Fig. 1). To a large extent, this quasi-linearity agrees with the result of Seidman and Maciel (15); they performed a set of "computer experiments" using the modified-INDO finite perturbation theory of ^{13}C chemical shifts to explore the geometrical dependence of the shielding of methyl groups in systems presenting

[2]Recently Beierbeck and Saunders (19) have proposed a re-interpretation of the γ-effect. But they estimate that "their re-interpretation is of little consequence for the phenomenological use of ^{13}C chemical shifts as a tool in structure elucidation work" (private communication).

Can. J. Chem. Downloaded from www.nrcresearchpress.com by 210.87.254.40 on 09/05/12
For personal use only.

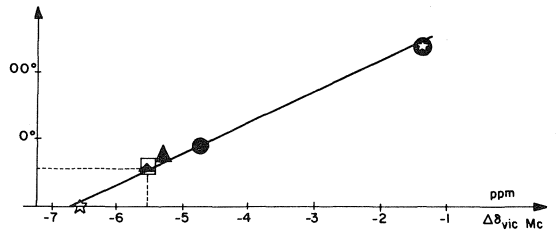


FIG. 1. ^{13}C nmr. Effects on $^{13}CH_3$ chemical shift by the introduction of a *vicinal* methyl ($\Delta\delta_{vic\ Me}$ in ppm). The dimethylated derivatives are: ✡, 2-*exo*-3-*exo*-dimethylnorbornane (14); ▲, *cis*-3,4-dimethylcyclopentanone (16); ●, *endo*-2-methylnorbornane (towards C6 γ-carbon) (14); ✪, 2-*endo*-3-*exo*-dimethylnorbornane (14); ○, *cis*-4,5-dimethylthiazolidine-2-thione (Table 2); □, *cis*-1,2-dimethylcyclopentane (18).

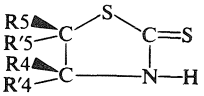
steric γ-effects. The γ-effects observed (Table 2) for the alkylthiazolidine-2-thiones suggest a Φ value of 25° (Fig. 1). This implies that the TH-2-TH ring can exist in a puckered conformation in solution. Moreover, in the case of the unsubstituted TH-2-TH, the torsional angle between C4 and C5 could even be smaller than 25°, when no steric interactions between adjacent methyls occur: i.e.

$$0° \leq \varphi_{(^{13}C\ nmr)} < 25°$$

Lambert's method gives a φ_R value of 41°. The same difference is observed in the cyclopentane case where $R = 0.80$ (10), indicating an average dihedral angle of 41° in contrast to the experimental value (10) or the calculated value (10*b*) of 27°. The $\Delta\delta_{vic\ Me}$ method in ^{13}C nmr gives a value of about 27° in *cis*-1,2-dimethylcyclopentane (18). Wilson and Bazzone (11*a*) found a φ_R value of 41° for dioxolane while $\varphi_{X\ ray}$ is found to be 21° (11*b*). These discrepancies can be explained in several ways. Fuchs (9*c*) had attributed them to appreciable deviation of θ from 120°. We took θ = 126° in eq. [7] (9*c*)

$$[7] \quad \varphi_R = \arccos\left[\frac{1 - \cos 2\theta}{2(R - \cos 2\theta)}\right]^{1/2}$$

TABLE 2. ^{13}C nmr. *Vicinal* methyl chemical shift in alkylthiazolidine-2-thiones



Substituents				Chemical shifts (ppm)		
R4	R'4	R5	R'5	$\delta_{^{13}CH_3-C4}$	$\delta_{^{13}CH_3-C5}$	$\Delta\delta_{vic\ Me}$ (γ-effect)
Me	H	Me	H	13.83	15.10	
Me	H	H	H	19.56		−6.73
H	H	Me	H		20.54	−5.44

and as Wilson and Bazzone (11*a*) we have noticed that this change in θ produces only a slight displacement of the rotational angle. On the other hand, Buys (20) has calculated that the rate of change of φ_R as a function of R is described by eq. [8]:

$$[8] \quad \partial\varphi_R/\partial R = 120 \cos^3 \varphi_R/\sin \varphi_R \qquad (\varphi_R \text{ in deg})$$

This rate is maximum near 45°. However, in this area, a change in R of 0.05 induces a variation of 1° in φ_R, and therefore the experimental error on R (0.03) cannot be the main cause of the elevated φ_R values. Furthermore, Lambert (9*a*) used the simplified Karplus equation [9]:

$$[9] \quad {}^3J_{HH} = A \cos^2 \varphi_R$$

neglecting the small second and third order terms B and C. Also, despite Lambert's assertion, one can wonder whether the presence of heteroatoms (nitrogen and sulfur) introduces errors that are not entirely compensated for in the R-value method. For example, the electronegativities of the S (χ_S) and N (χ_N) atoms linked to the CH_2—CH_2 fragment have additive influences on the ^3J values (6, 8); the influence of the difference in electronegativities ($\Delta\chi = \chi_X - \chi_H$ with X = S or N) may give rise to disparate contributions to J_{cis} and J_{trans}. Lambert's equation does not take this into account. In order to study the influence of this approximation on φ_R, we have treated the TH-2-TH ring within the finite perturbation approximation (21), using the CNDO-2 method. We obtain the values of the *cis* and *trans* coupling constants (21*a*). Table 3 lists these calculated ^3J values together with the corresponding $\varphi_{R(CNDO)}$ torsional angles of the C4—C5 bond, calculated by eq. [6] using R(CNDO) obtained from:

$$R\,(\text{CNDO}) = \langle J_{trans}{}^{calcd}\rangle / \langle J_{cis}{}^{calcd}\rangle$$

where $\langle J^{calcd}\rangle$ are CNDO-2 results.[3] Examination of Table 3 indicates that for the whole simulation, $\varphi_{R(CNDO)}$ is larger than $\varphi_{(geometry)}$, the real dihedral angle deduced from cartesian coordinates. This disparity could partly originate from an electronegativity effect. But, as the same type of discrepancy exists for dioxolane and cyclopentane rings, it seems that other factors could contribute to the overestimation of φ by the R-method.

Attempts to Determine the Existence of a Pseudorotational Process in the TH-2-TH Ring

In cyclopentane (22) the ring puckering rotates

[3]For a given geometry: $\langle J_{cis}{}^{calcd}\rangle = 1/2\ (J_{H4aH5e}{}^{calcd} + J_{H4eH5a}{}^{calcd})$, $\langle J_{trans}{}^{calcd}\rangle = 1/2\ (J_{H4aH5a}{}^{calcd} + J_{H4eH5e}{}^{calcd})$.

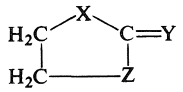
Can. J. Chem. Downloaded from www.nrcresearchpress.com by 210.87.254.40 on 09/05/12
For personal use only.

TABLE 3. Calculated coupling constants $^3J_{H4H5}$ in TH-2-TH (Hz) using CNDO-2 and the finite perturbations approximation*

Geometry	Calculated J_{cis}			Calculated J_{trans}			$R_{CNDO} = \frac{\langle J_{trans}\rangle}{\langle J_{cis}\rangle}$	$\varphi_{geometry}$†	$\varphi_{R(CNDO)}$‡
	J_{H4aH5e}	J_{H4eH5a}	$\langle J_{cis}\rangle$	J_{H4eH5e}	J_{H4aH5a}	$\langle J_{trans}\rangle$			
Plane	10.03		10.03	5.21		5.21	0.52	0	31
Envelope C4 out-of-plane No. 1§	10.32	10.73	10.52	4.54	7.24	5.89	0.56	16	33
Envelope C4 out-of-plane No. 2	8.74	11.095	9.92	5.95	8.26	7.11	0.72	21.5	38.5
Half-chair C4C5 out-of-plane No. 1	10.23	11.07	10.65	4.52	7.30	5.91	0.55	18	32
Half-chair C4C5 out-of-plane No. 2	10.38	11.59	10.98	4.39	5.42	4.91	0.45	24	27
Envelope C5 out-of-plane No. 1	10.03	10.93	10.48	4.68	6.86	5.77	0.55	14	32
Envelope C5 out-of-plane No. 2	9.155	11.69	10.42	4.45	5.75	5.10	0.49	22	29.5

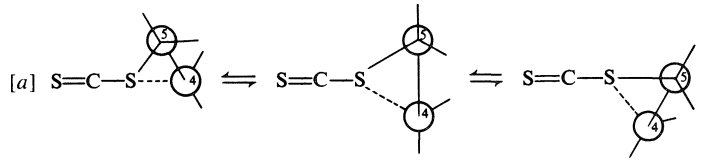
*The cartesian coordinates and CNDO-parameters are available in the Depository of Unpublished Data.
†Deduced from cartesian coordinates.
‡Calculated by Lambert's R value method from R(CNDO).
§No. 1 and No. 2 correspond respectively to weak and higher puckering (see $\varphi_{(geometry)}$).

around the carbocyclic skeleton without forcing the ring to pass over high potential energy barriers: this is pseudo-rotation. Among all the possible conformations for the cyclopentane ring, two possess elements of symmetry: the half-chair (C_2) and the envelope (C_s) arrangements. Calculations (22*a*, *c*, *d*) accounting for pseudo-rotation in cyclopentane, and accurate spectroscopic (10*a*, 22*h*, *i*) and thermodynamic (22*j*) evidences for such a phenomenon have been reported. Substitution of CH_2 groups in cyclopentane, by functions such as heteroatoms or sp_2 hybridized carbon atoms alters the course and the ability of the pseudo-rotation process (22). Significantly, X-ray analysis established (23) the planarity of the X—C (=Y)—Z portion in heterocycles of type **2**:



2

By analogy we can assume that the TH-2-TH ring is planar in the S—C(=S)—NH region. This reduces the number of degrees of freedom of the C4C5 fragment. That is to say, the low energy TH-2-TH conformations are those of equilibrium [*a*]:



a1 C5 out-of-plane envelope

a2 C4C5 out-of-plane half-chair

a3 C4 out-of-plane envelope

Interestingly, interactions due to Pitzer strain are weaker in methanethiol than in methylamine (24). For this reason, saturated heterocycles having at least two heteroatoms (of which one is sulfur (25)) preferentially adopt conformations in which the atom adjacent to the sulfur and the sulfur atom itself lie in the same plane. We deduce from this that the C5 atom in TH-2-TH would have a smaller tendency to leave the plane of the S—C (=S)—N fragment than the C4 atom. Such a discussion indicates that the order of the preferred conformations of TH-2-TH would be:

a3 > a2 > a1

However no experimental evidence exists for such an order of conformational stability. But the results of substituent effects introduced in 4- and 5-position agree with this order (4).

Conclusion

It would appear that, in solution, the TH-2-TH ring exists in a puckered form in which the C4—C5 dihedral angle is estimated to be smaller than 25°.

Discussion of the possible sources of error in Lambert's R value method indicates that results obtained by this approach for five-membered heterocycles must be treated with utmost caution. The results from nmr studies of 4-hydroxy-thiazolidine-2-thiones (4) confirm these suspicions. Although it is difficult to provide experimental evidence for a pseudo-rotation phenomenon in TH-2-TH, considerations of data on related heterocyclic systems

Can. J. Chem. Downloaded from www.nrcresearchpress.com by 210.87.254.40 on 09/05/12
For personal use only.

Can. J. Chem. Downloaded from www.nrcresearchpress.com by 210.87.254.40 on 09/05/12
For personal use only.

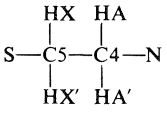
that it does occur and that the order of preference of the conformations of this molecule would be in the order:

C4 out-of-plane envelope > C4C5 out-of-plane half-chair > C5 out-of-plane envelope

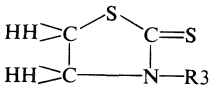
Experimental

^1H Nuclear Magnetic Resonance — Spectra Analysis

Spectra were recorded at ambient temperature on Varian A60 (60 MHz) and HA 100 (100 MHz) spectrometers as ca. 0.1 *M* solutions in acetone-d_6–TMS was used as internal reference. The spectra of protons at C4 and C5 in the system:



in compound such as



are interpreted in terms of a "deceptively simple" AA′XX′ spin-system (26, 27). Since the 60 MHz spectrum exhibits more "visible" lines than that of the 100 MHz spectrum, an interpretation of the former is first carried out from which we estimate an average value of -12 Hz for the $J_{AA'}$ and $J_{XX'}$ coupling constants (as a matter of fact, calculated spectra do not depend on $J_{AA'}$ and $J_{BB'}$ values). Then, the series of parameters which gives the most satisfactory calculated spectrum (MLACO program) is refined (LAOCON program). Using refined parameters obtained at 60 MHz, we calculate (MLACO) the 100 MHz spectrum and find a good agreement between calculated and experimental spectra. Results are listed in Table 1.

The assignment of the proton chemical shifts is available in the Depository of Unpublished Data.[4]

^{13}C Nuclear Magnetic Resonance Spectra

The apparatus and conditions are described in the following paper (4).

Acknowledgements

We thank Mlle J. Berger for recording the spectra and M. Llinas for allowing us to use the MLACO and LAOCON programs.

1. F. G. RIDDEL. Q. Rev. Chem. Soc. **21**, 364 (1967).
2. E. L. ELIEL. Acc. Chem. Res. **3**, 1 (1970).
3. D. H. R. BARTON. Experientia, **6**, 316 (1950).
4. F. CHANON, M. RAJZMAN, M. CHANON, J. METZGER, G. POUZARD, and T. DRAKENBERG. Can. J. Chem. **58**, 604 (1980).
5. F. ALDEWEIRELDT and M. ANTEUNIS. Bull. Soc. Chim. Belg. **74**, 488 (1965).
6. (*a*) M. KARPLUS. J. Chem. Phys. **30**, 11 (1959); (*b*) M. KARPLUS. J. Am. Chem. Soc. **85**, 2870 (1963).
7. M. BARFIELD and D. M. GRANT. Advances in magnetic resonance. *Edited by* J. S. Waugh. Academic Press, New York. 1965.
8. S. STERNHELL. Q. Rev. 236 (1969).
9. (*a*) J. B. LAMBERT. Acc. Chem. Res. **4**, 87 (1971); (*b*) J. B. LAMBERT. J. Am. Chem. Soc. **89**, 1836 (1967); (*c*) B. FUCHS. Topics in stereochemistry. Vol. 10. *Edited by* E. L. Eliel and N. L. Allinger. Interscience, New York. 1978.
10. (*a*) W. J. ADAMS, H. J. GEISE, and L. S. BARTELL. J. Am. Chem. Soc. **92**, 5013 (1970); (*b*) J. B. HENDRICKSON. J. Am. Chem. Soc. **83**, 4537 (1961) and erratum, **85**, 4509 (1963).
11. (*a*) G. E. WILSON, JR. and T. J. BAZZONE. J. Am. Chem. Soc. **96**, 1465 (1974); (*b*) S. FURBERG and D. HASSEL. Acta Chem. Scand. **4**, 1584 (1950).
12. R. CAHILL, R. C. COOKSON, and T. A. CRABB. Tetrahedron, (*a*) **25**, 4711 (1969); (*b*) **25**, 4681 (1969).
13. J. B. STOTHERS and C. T. TAN. Can. J. Chem. **52**, 308 (1974).
14. J. B. STOTHERS, C. T. TAN, and K. C. TEO. Can. J. Chem. **51**, 2893 (1973).
15. K. SEIDMAN and G. E. MACIEL. J. Am. Chem. Soc. **99**, 659 (1977).
16. C. SABLAYROLLES, R. GRANGER, and L. BARDET. J. Chim. Phys. **11-12**, 1000 (1976).
17. J. B. GRUTZNER, M. JAUTELAT, J. B. DENCE, R. A. SMITH, and J. D. ROBERTS. J. Am. Chem. Soc. **92**, 7107 (1970).
18. M. CHRISTL, H. J. REICH, and J. D. ROBERTS. J. Am. Chem. Soc. **93**, 3463 (1970).
19. H. BEIERBECK and J. K. SAUNDERS. Can. J. Chem. (*a*) **53**, 1307 (1975); (*b*) **54**, 2985 (1976).
20. H. R. BUYES. Recl. Trav. Chim. Pays-Bas, **88**, 1003 (1969).
21. (*a*) J. A. POPLE, J. W. MCIVER, and N. S. OSLUND. J. Chem. Phys. **49**, 2960 (1968); (*b*) G. POUZARD. Thèse Sciences, Marseille. 1972; (*c*) M. RAJZMANN. Thèse Sciences, Marseille. 1973; (*d*) G. POUZARD, M. RAJZMANN, H. BODOT, and L. PUJOL. Org. Magn. Reson. **5**, 209 (1973).
22. (*a*) K. S. PITZER. Sciences, **101**, 672 (1945); (*b*) C. G. LE FEVRE and R. J. LE FEVRE. J. Chem. Soc. 3549 (1956); (*c*) J. E. KILPATRICK and K. S. PITZER. J. Am. Chem. Soc. **69**, 2483 (1947); (*d*) R. PITZER and H. M. HUFFMAN. J. Am. Chem. Soc. **69**, 211 (1947); (*e*) J. P. MC. CULLOUGH. J. Chem. Phys. **29**, 966 (1958); (*f*) J. P. MC. CULLOUGH, R. E. PENNINGTON, J. C. SMITH, I. A. HOSSENLOPP, and G. WADDINGTON. J. Am. Chem. Soc. **81**, 5880 (1959); (*g*) J. A. GREENHOUSE and H. L. STRAUSS. J. Chem. Phys. **50**, 124 (1969); (*h*) R. DAVIDSON and P. A. WARSOP. J. Chem. Soc. Faraday Trans. II, **68**, 1875 (1972); (*i*) L. A. CARREIRA, G. J. TIANG, W. B. PERSON, and J. N. WILLIS. J. Chem. Phys. **56**, 1440 (1972); (*j*) K. PITZER and W. E. DONATH. J. Am. Chem. Soc. **81**, 3213 (1959).
23. (*a*) F. A. L. ANET. J. Am. Chem. Soc. **84**, 747 (1962); (*b*) C. J. BROWN. Acta Crystallogr. **7**, 92 (1954); (*c*) P. J. WHEATLEY. Acta Crystallogr. **6**, 369 (1953); (*d*) G. B. ANSELL, D. M. FORKEY, and D. W. MORE. Chem. Commun. 56 (1970).
24. R. W. KILB. J. Chem. Phys. **23**, 1736 (1955).
25. (*a*) J. L. LARICE. Thèse Sciences, Marseille. 1972. p. 110; (*b*) G. E. WILSON, M. G. HUANG, and F. A. BOVEY. J. Am. Chem. Soc. **92**, 5907 (1970); (*c*) D. J. PASTO, F. M. KLEIN, and T. W. DOYLE. J. Am. Chem. Soc. **89**, 4368 (1967); (*d*) G. E. WILSON. J. Am. Chem. Soc. **96**, 2426 (1974); (*e*) M. GIULIANO. Thèse Sciences, Marseille. 1977. p. 28.
26. R. J. ABRAHAM. Analysis of high resolution NMR spectra. Elsevier Publishing Co., Amsterdam, London, New York. 1971. pp. 91, 116.
27. J. A. POPLE, W. G. SCHNEIDER, and H. J. BERNSTEIN. (*a*) Can. J. Chem. **35**, 1060 (1957); (*b*) High resolution nuclear magnetic resonance. McGraw Hill, Book Co., Inc., New York. 1959.

[4]Complete set of data is available, at a nominal charge, from the Depository of Unpublished Data, CISTI, National Research Council of Canada, Ottawa, Ont., Canada K1A 0S2.

Part II. Conformational analysis of 4- and 5-substituted thiazolidine-2-thiones

F. CHANON, M. RAJZMANN, M. CHANON, AND J. METZGER
Faculté des Sciences de St.-Jérôme, 13397 Marseille, France
G. POUZARD
Université de Provence, Saint-Jérôme 13397, France
AND
T. DRAKENBERG
Kemi Centrum P.O.B. 740, Lund, Sweden

Received August 1, 1978[1]

F. CHANON, M. RAJZMANN, M. CHANON, J. METZGER, G. POUZARD, and T. DRAKENBERG. Can. J. Chem. **58**, 604 (1980).

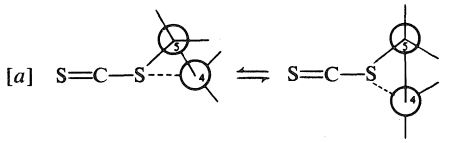
Variation of the conformational properties in a series of 4-R-thiazolidine-2-thiones (4-R = Me, Et, *i*Pr, *t*Bu, OH) and 5-R-thiazolidine-2-thiones (5-R = Me, Et, *i*Pr, *t*Bu) is deduced from ^{1}H nmr (Karplus ^3J, chemical shifts, $^2J_{44'}$, $^2J_{55'}$) ^{13}C nmr data and CNDO-2 calculations. In the absence of any transannular interaction, *vicinal* constraints and van der Waals requirements of the substituents control the conformational equilibrium. The pseudo-axial arrangement is favoured when 4-R = Me, while the substituent presents no preferential orientation when 5-R = Me. As the size of the 5-alkyl and the 4-alkyl substituent increases, its pseudo-equatorial orientation and the predominance of the C4C5 out-of-plane half-chair conformation are favoured. This does not lead to conformational exclusivity even when 4-R or 5-R is *t*Bu. When 4-R is hydroxy, there is a definite pseudo-axial conformation (anomeric effect) and the ring preference is of the C4 out-of-plane type.

F. CHANON, M. RAJZMANN, M. CHANON, J. METZGER, G. POUZARD et T. DRAKENBERG. Can. J. Chem. **58**, 604 (1980).

Les évolutions conformationnelles dans les R-4 thiazolidinethiones-2 (R-4 = Me, Et, *i*Pr, *t*Bu, OH) et les R-5 thiazolidinethiones-2 (R-5 = Me, Et, *i*Pr, *t*Bu) sont déduites de l'ensemble des résultats rmn ^{1}H (^3J-Karplus, δ_H, $^2J_{55'}$, $^2J_{44'}$), rmn ^{13}C et calculs CNDO-2. En l'absence d'interactions transannulaires, les contraintes *vicinales* et de van der Waals des substituants contrôlent l'équilibre conformationnel. Lorsque R-4 = Me, sa préférence est légèrement pseudo-axiale tandis que le substituant R-5 = Me n'a pas d'orientation spécifique. On observe, simultanément à une augmentation de la taille du substituant alkyle, une orientation de plus en plus équatoriale de ce dernier et une prédominance accrue de la conformation demi-chaise avec C4C5 hors plan. Ceci ne conduit pas toutefois à un blocage conformationnel même pour le *t*Bu. Pour R-4 = OH, une nette préférence pseudo-axiale se manifeste (effet d'anomérie) et le plissement du cycle est du type enveloppe avec C4 hors du plan du thiocarbonyle.

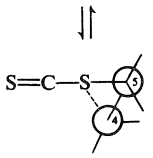
Introduction

In the preceding paper (1) we have shown for thiazolidine-2-thione (**1***a*) the existence of equilibrium [*a*]:



C5 out-of-plane envelope **a1**

C4C5 out-of-plane half-chair **a2**

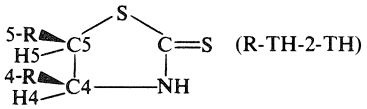


C4 out-of-plane envelope **a3**

The conformer stability increases from left to right and the C4C5 torsional angle was evaluated to be ca. 25°.

[1]Revision received November 12, 1979.

Having introduced substitution at C4 (**1***b*, **1***c*, **1***d*, **1***e*, **1***f*) and C5 (**2***b*, **2***c*, **2***d*, **2***e*), i.e.



(R-TH-2-TH)

1*a*: 4-R = H; 5-R = H
1*b*: 4-R = Me; 5-R = H
1*c*: 4-R = Et; 5-R = H
1*d*: 4-R = *i*Pr; 5-R = H
1*e*: 4-R = *t*Bu; 5-R = H
1*f*: 4-R = OH; 5-R = H

2*b*: 4-R = H; 5-R = Me
2*c*: 4-R = H; 5-R = Et
2*d*: 4-R = H; 5-R = *i*Pr
2*e*: 4-R = H; 5-R = *t*Bu

we must answer the following questions: (*1*) What are the orientations of the (4-R)—C4 and (5-R)—C5 bonds? (*2*) How is equilibrium [*a*] modified? (*3*) What are the conformations resulting from rotation around the C—C4 and C—C5 bonds? (*4*) What origin can have these conformational effects?

The starting point is the application of the method of ratios (ref. 2, ref. 31, Annexe V, p. 111) to ^3J

0008-4042/80/060604-13$01.00/0
©1980 National Research Council of Canada/Conseil national de recherches du Canada

Can. J. Chem. Downloaded from www.nrcresearchpress.com by 210.87.254.5 on 09/05/12
For personal use only.

values of the ethanic fragment using the Karplus equation. CNDO-2 simulation results are compared with those from ^{13}C (Table 2) and ^{1}H nmr experimental data (Table 1).

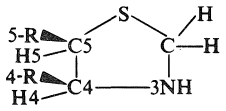
Part A. 4-Alkyl and 5-Alkylthiazolidine-2-thiones

Results and Discussion

Pseudo-axial or Pseudo-equatorial Substituent Orientation

The $^{3}J_{cis}^{exp}$ and $^{3}J_{trans}^{exp}$ values of the ethanic fragment are used in the calculations based on the Karplus equation to obtain the C4C5 torsional angle φ_{calcd} and the proportion of the pseudo-axial conformer x (ref. 2, ref. 31, Annexe V, p. 111). The results are listed in Table 3. They reveal a slight pseudo-equatorial preference exhibited by the 4-methyl derivative **1***b* and a slight pseudo-axial one for the 5-methyl derivative **2***b*. The orientation of R is increasingly equatorial with increasing substituent size, particularly so for 4-R or 5-R = Et and *i*Pr. A pseudo-equatorial preference close to 100% is not observed. The effective orientation of the methyl substituent is supported by substituent effects on ^{13}C chemical shifts due to the introduction of methyl group (Table 4). α- and β-effects are both deshielding. The α4- and β5-effects are produced by introducing a methyl group at C4, while the α5- and β4-effects are produced by introducing a methyl group at C5.

First, we notice that the α4- and β5-effects are of the same order of magnitude as in thiazolidine derivatives (R-TH) **3** (5).



3*a*: 4-R = H; 5-R = H
3*b*: 4-R = Me; 5-R = H
3*c*: 4-R = H; 5-R = Me

Whestheimer calculations (6) and ir–Raman study (7) have shown a pseudo-axial preference for the methyl group in 4-methyl thiazolidine **3***b*; this similarity may provide an axial orientation of methyl group in both 4-methyl-TH-2 (**1***b*) and 4-methyl-Th (**3***b*). This is confirmed by examining α′4- and β′5-effects when introducing a second methyl group at C4 in **1***b*. Usually, the introduction of a *gem* methyl group on $C—CH_3$ induces weaker α′- and β′-effects, particularly when the second methyl group is "introduced" in a pseudo-axial position as in cyclopentane series (3, 4, 8). The larger the $\Delta\alpha_{Me}$ ($\Delta\alpha_{Me} = \alpha - \alpha'$) and $\Delta\beta_{Me}$ ($\Delta\beta_{Me} = \beta - \beta'$) differences, the more important is the proportion of equatorial methyl group in the monosubstituted derivative and vice-versa. By comparing the cyclopentane series (8) ($\Delta\alpha_{Me} = +5$ ppm, $\Delta\beta_{Me} = +2.8$ ppm) and the 4-R-THTH-2 series ($\Delta\alpha 4_{Me} = +1.12$ ppm, $\Delta\beta 5_{Me} = +1.38$ ppm), it appears that the proportion of equatorial methyl group is larger in methyl cyclopentane than in 4-methyl-2-TH (**1***b*); this is consistent with the predominance of the pseudo-axial position of the 4-methyl group, as in 4-Me-TH (**3***b*). Then for 4-methyl-TH-2-TH **1***b* the equilibrium [*b*]

$$[b] \qquad \underset{\mathbf{b1}}{\text{axial R}} \rightleftharpoons \underset{\mathbf{b2}}{\text{equatorial R}}$$

is slightly shifted to the left.

This result differs somewhat from the one obtained by the method of ratios which gave a slight pseudo-equatorial preference. Many authors (9) have emphasized that it is dangerous to calculate torsional angles from *vicinal* coupling constants in 5-membered rings. The coupling constant must be integrated on the basis of a pseudo-rotational circuit rather than from an ideal situation with an equilibrium between two conformations only. Furthermore, in our calculations, the C4 and C5 carbons were considered as perfectly tetrahedral, which is not the case in a 5-membered heterocycle with a sp^2 carbon atom (10). The use of a 126° value (instead of 120°) for the H4C4C5H4′ dihedral angle in 4-Me-TH-2-TH **1***b* gives a 52% value for x showing a slight pseudo-axial preference for the 4-methyl group. The ratio method, therefore, underestimates the pseudo-axial preference in **1***b*.

With respect to 5-methyl-TH-2-TH **2***b*, we note the important α5-value (already observed on the chemical shifts of carbons next to the sulfur atoms (5, 11)). Qualitative considerations (11*b*) on the charge distribution in $R—C_{sp^3}—X$ (X = S, N, O) imply that α-effects would be larger for X = S, due to the presence of vacant 3*d* orbitals on the sulfur. Thus, it is unwise to employ here α5- and α′5-effects as indices of conformational variation. Moreover, in none of the compounds discussed in the literature (5, 11) is the deshielding effect as large as the α5-effect noted here. Its value (+12 ppm) suggests that the methyl group in **2***b* cannot exist in a pseudo-axial conformation (4). By contrast, it is possible to use the β4- and β′4-values (the deshielding effects on the $^{13}C4$ chemical shift by introducing successive methyl groups at C5 on TH-2-TH **1***a*) which have mostly a steric origin. We note that

$$[1] \quad \Delta\beta 5_{(\text{Me at C4 in TH-2-TH})} < \Delta\beta 4_{(\text{Me at C5 in TH-2-TH})} < \Delta\beta_{(\text{Me in cyclopentane})}$$

Can. J. Chem. Downloaded from www.nrcresearchpress.com by 210.87.254.5 on 09/05/12
For personal use only.

Can. J. Chem. Downloaded from www.nrcresearchpress.com by 210.87.254.5 on 09/05/12
For personal use only.

TABLE 1. ^{1}H nuclear magnetic resonance*

(*a*) 4-Alkylthiazolidine-2-thiones

		Heterocyclic protons								Protons on the substituent					
Compound	4-R	$\delta_{3\text{-R}}$	δ_{H5}	$\delta_{H5'}$	δ_{H4}	$J_{55'}$	J_{54}	$J_{5'4}$	J_{vic} H4H subst	δ_{CH_3}	δ_{CH_2}	δ_{CH}	J_{CH_3/CH_2}	$J_{CH_3/CH}$	$J_{gem\ CH_2}$
1*a*	H		3.58	3.58	4.01		8.75	7.35							
1*b*	Me	—	3.68	3.205	4.42	−11.04	7.77	7.12	6.35	1.36					
1*c*	Et	3.25	3.64	3.25	4.23	−11.18	7.88	7.15	5.97 7.1	0.985	1.705 1.845		7.55		13.7
1*d*	*i*Pr	2.82	3.57	3.33	4.13	−11.52	8.27	7.90	6.4	0.98 1.00		2.035		7.1 7	—
1*e*	*t*Bu	2.80	3.53	3.42	4.07	−11.63	8.78	7.95	—	1.03					
1*f*	Ambient	—	3.35	3.93	5.88	−12.6	6.25	1.85							
	OH −60°C	—	3.39	3.9	—	−12.6	6.4	1.6							

(*b*) 5-Alkylthiazolidine-2-thiones

		Heterocyclic protons								Protons on the substituent					
Compound	5-R	δ_{H-N}	δ_{H4}	$\delta_{H4'}$	δ_{H5}	$J_{44'}$	J_{45}	$J_{4'5}$	J_{vic} H5H subst	δ_{CH_3}	δ_{CH_2}	δ_{CH}	J_{CH_3/CH_2}	$J_{CH_3/CH}$	$^2J_{CH_2}$
2*b*	Me†‖	2.88	4.08	3.58	4.04	−11.5	7.56	5.85	6.38	1.4					
2*c*	Et‡‖	2.99	4.06	3.69	3.98	−11.78	7.59	5.90	7.5 6.4	0.953	1.74 1.82		7.4		−13.8
2*d*	*i*Pr§‖	2.86	4.03	3.70	3.96	−11.73	7.84	6.5	6.98	0.95 0.967		1.90		6.9	
2*e*	*t*Bu		3.87	3.75	3.92	−12.5	8.8	6.2		0.985					

*Spectra were recorded in acetone-d_6 with TMS as internal reference (δ in ppm; J in Hz).
†$J_{NH/H4}$ = 1.4 Hz.
‡$J_{NH/H4}$ = 1.3 Hz.
§$J_{NH/H4}$ = 1.2 Hz.
‖These couplings are suppressed with the addition of one drop of TFA.

TABLE 2. ^{13}C nuclear magnetic resonance chemical shifts (ppm) and coupling constants (Hz) of 4- and 5-alkylthiazolidine-2-thiones in $CDCl_3$ with TMS as internal reference

		Heterocyclic carbons					Carbons of the substituent				
4-R	5-R	$\delta_{^{13}C2}$	$\delta_{^{13}C4}$	$J_{^{13}C4H4}$	$\delta_{^{13}C5}$	$J_{^{13}C5H5}$	$\delta_{^{13}CH_3}$	$J_{^{13}CH_3}$	$\delta_{^{13}CH_2}$	$\delta_{^{13}CH}$	$\delta_{^{13}C}$
H	H	198.33	51.15	145.6	33.59	147.5					
H	Me	200.20	59.82	148.5	40.14	147	19.56	128			
H	Et	199.64	65.38		31.68		9.66		26.63		
H	*i*Pr	199.7	69.7		35.55		18.06			31.74	
H	*t*Bu	201.4	73.5		34.4		25.9				34.4
H	Me, Me	197.74	67.37		45.31		26.35				
Me	H	201.49	58.42		45.60		20.54				
Et	H	206.12	56.78		52.64		11.97		28.70		
*i*Pr	H	200.24	54.25		57.43		19.60			32.39	
*t*Bu	H	201.19	61.81		52.54		26.63				33.98
Me, Me	H	201.19	63.40		56.84		28.02				

TABLE 3. Determination of the C4C5 torsional angle (φ_{calcd}) and the molar ratio (x) of the pseudo-axial conformation with the help of the method of ratios for 4- and 5-alkylthiazolidine-2-thiones

4-R	5-R	Compound	J_{trans}^{exp} (Hz)	J_{cis}^{exp} (Hz)	$R_{exp} = \frac{J_{trans}}{J_{cis}}$	φ_{calcd} (deg)*	x (%)†
H	H	**1***a*	7.35	8.75	0.84	39	—
Me	H	**1***b*	7.12	7.77	0.91	42	47
Et	H	**1***c*	7.15	7.88	0.91	42	45
*i*Pr	H	**1***d*	7.90	8.27	0.95	36.5	38
*t*Bu	H	**1***e*	7.95	8.78	0.90	35.5	36
OH	H	Ambient temperature **1***f*	1.85	6.25	0.296	44.5	88
OH	H	−60°C **1***f*	1.6	6.4	0.25	44	90
H	Me	**2***b*	5.82	7.56	0.77	40.5	57
H	Et	**2***c*	5.90	7.59	0.77	40.5	57
H	*i*Pr	**2***d*	6.5	7.84	0.83	39.5	51
H	*t*Bu	**2***e*	6.2	8.8	0.70	35.5	49

*φ_{calcd} is such that $J_{\varphi_{calcd}} = 4.22 - 0.5 \cos \varphi_{calcd} + 4.5 \cos 2\varphi_{calcd}$ with $J_{\varphi_{calcd}} = J_{cis}^{exp}/1.83$ (2).
†$x = 100 \times (R_{exp} J_{\varphi_{calcd}} - J_{120°} + \varphi_{calcd})/(J_{120°} - \varphi_{calcd} - J_{120°} + \varphi_{calcd})$ (2).

This intermediate value for $\Delta\beta 4_{(Me\ at\ C5\ on\ TH—TH)}$ implies that the proportion of equatorial methyl in 5-methyl-TH-2-TH (**2***b*) is included between the one existing in methylcyclopentane (a bit more than 50%) and the one in 4-methyl-TH-2-TH (**1***b*) (a bit less than 50%); then the proportion of equatorial methyl in 5-methyl-TH-2-TH (**2***b*) should be about 50%, as in the 5-methyl-TH (**3***c*) case (6, 7). This result disagrees with the one previously found by the Karplus method ($x_{2b} = 57\%$). We have seen that x is underestimated by 5% (which gives $x_{2b} = 62\%$) if C4 and C5 are perfectly tetrahedral. The discrepancy between the two methods probably comes from the fact that we considered only two preferred conformations in the Karplus method.

Assuming the presence of equilibria [*a*] and [*b*], we would have to sum $^3J_{cis}$ and $^3J_{trans}$ over at least six conformational arrangements (3 × 2), where the concentrations of **a1**, **a2**, **a3** are not negligible.

In the 4-methyl **1***b* case, we gave evidence of **a3** predominance, with probably weak concentrations of **a1** and **a2**. Thus, the conformational equilibrium would limit itself to:

C4 (out-of-plane envelope with axial methyl)

$\leftrightharpoons$ C4 (out-of-plane envelope with equatorial methyl)

Thus the 4-Me-TH-2-TH **1***b* case is situated nearly within the domain of application of the ratio method and the results are in better agreement with those of the ^{13}C nmr data than in the 5-Me-TH-2-TH **2***b* case.

The H5,H4 chemical shift variations between **1***b* and **1***e*, **2***b* and **2***e* are reported in Table 5. In the absence of data for 5-membered rings, we chose the *cis*-6-alkyl-4-methyl dioxanes **4***b* and **4***e* (12), and the *trans*-6-alkyl-4-methyl dioxanes **5***b* and **5***e* (12) for comparison purposes. We notice that for both the dioxane and the TH-2-TH series, the chemical shift

Can. J. Chem. Downloaded from www.nrcresearchpress.com by 210.87.254.5 on 09/05/12
For personal use only.

Can. J. Chem. Downloaded from www.nrcresearchpress.com by 210.87.254.5 on 09/05/12
For personal use only.

TABLE 4. ^{13}C nuclear magnetic resonance (TMS in $CDCl_3$), substituent effects on the ^{13}C chemical shifts in 4- and 5-alkylthiazolidine-2-thiones (ppm; + is deshielding; − is shielding)

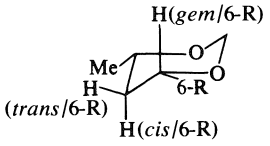
Introduction of a methyl group on *C*	α-effect on			β-effect on			γ-effect on			δ-effect on
	$^{13}C4$	$^{13}C5$	^{13}C—$C_{heterocyclic}$	$^{13}C4$	$^{13}C5$	$^{13}CH_3$—C—$C_{heterocyclic}$	$^{13}C4$	$^{13}C5$	$^{13}C2$	$^{13}C2$
*C*4 of TH-2-TH	+8.67				+6.55				+1.87	
*C*4 of TH	+8.0				+6.7					
*C*4 of 4-Me-TH-2-TH	+7.55				+5.17				−2.46	
CH_3 of 4-Me-TH-2-TH			+7.07	+5.48				−2.44		−0.56
CH_3—CH_2 of 4-Et-TH-2-TH			+5.11	+4.4		+8.42 +9		−2.15		−0.06
CH_3 \>CH of 4-*i*Pr-TH-2-TH CH_3			+2.66	+3.8		+7.82 +7.24		−1.15		+1.7
*C*5 of TH-2-TH		+12		+7.26					+3.16	
*C*5 of 5-Me-TH-2-TH		+11.24		+4.98					−0.30	
CH_3 of 5-Me-TH-2-TH			+8.24		+7.04		−1.64			+4.62
CH_3—CH_2 of 5-Et-TH-2-TH			+3.69		+5.79	+7.63	−2.53			−5.88
CH_3 \>CH of 5-*i*Pr-TH-2-TH CH_3			+1.59		+4.38	+7.03	−1.71			+0.95

TABLE 5. ^{1}H nuclear magnetic resonance: substituent effect on chemical shifts (ppm) and proton *geminal* coupling constants for the protons α to the substituent (Hz). (− and + are respectively shielding and deshielding effects)

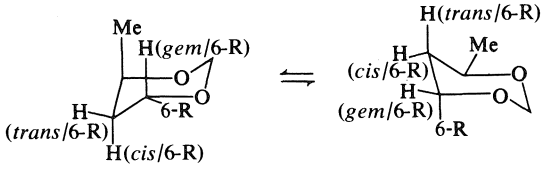
R from Me to *t*Bu	$\Delta\delta_{H_{gem/R}}$	$\Delta\delta_{H_{trans/R}}$	$\Delta\delta_{H_{cis/R}}$	ΔJ_{gem}
1, 4-R-thiazolidine-2-thiones*	−0.35	−0.15	+0.22	−0.59
2, 5-R-thiazolidine-2-thiones*	−0.12	−0.21	+0.17	−1
4, *cis*-6-R-4-methyl-1,3-dioxanes† (12)	−0.50	−0.1	+0.06	−0.2
5, *trans*-6-R-4-methyl-1,3-dioxanes† (12)	−0.67	−0.36	+0.36	−0.2

*In acetone-d_6.
†In CCl_4.

variations follow the same trend: a shielding effect on the *transoid* proton and a deshielding effect on the *cisoid* proton.



4
4*b*: 6-R = Me
4*e*: 6-R = *t*Bu



5
5*b*: 6-R = Me
5*e*: 6-R = *t*Bu

In series **4**, where both the methyl and 6-R substituents are equatorial (fixed ring geometry and substituent orientation), these effects are very small. In series **5**, assuming a constant ring geometry, the proportion of conformer with 6-R axial should decrease as the size of 6-R increases. Then, the observed variation of the chemical shift of the *transoid* and *cisoid* protons in compounds **1**, **2**, and **5** must have the same origin: the increasing tendency of the bulkier substituent to adopt a pseudo-equatorial orientation.

A circular dichroism study (ref. 31, p. 56) of **1***b*, **1***c*, and **1***d*, which are endowed with rotatory power, confirms the fact that a larger substituent shifts equilibrium [*b*] to the right.

Ring Geometry

Inspection of Table 3 shows that: (*i*) introduction of a methyl group at C4 or C5 in TH-2-TH brings in a slight increase of the dihedral angle φ_{calcd}, the effect being larger for the 4-position; (*ii*) an increase of the substituent size results in a decrease of φ_{calcd}, particularly so between 5-R = *i*Pr and *t*Bu, and 4-R = Et and *i*Pr.

The observed discontinuity in the variation of φ_{calcd} can originate either from two types of conformational change or from an artefact due to the method. In order to eliminate the possibility of such an artefact, we corroborated the φ_{calcd} variation by comparing the experimental proton chemical shifts and the $^2J_{55'}$ and $^2J_{44'}$ values with those calculated by the CNDO-2 method (14).

First, let us examine the variation of the experimental chemical shifts with substituents by comparing TH-2-TH **1**, **2**, and TH **3** series. As ^{13}C nmr conclusions, we have seen that equilibrium [*b*] is comparable in the 4-methyl derivatives **1***b* and **3***b* (light preference of axial methyl), and in the 5-methyl derivatives **2***b* and **3***c* (no preference of the substituent). We shall consider that H4 and H5 are far away from the anisotropic zone of thiocarbonyl group. As a second approximation, we shall admit that for the same H4 orientation, the anisotropic effect of the lone pair on the nitrogen is alike in TH-2-TH and in TH rings. An equatorial proton usually gives a signal at a lower field than an axial proton (16). Then, the difference in the intensity of the methyl substituent effects will originate from difference in the proton orientation, thus in ring geometries. First, the introduction of a methyl group at C4 or C5 deshields both the *geminal* and *transoid* protons while the *cisoid* proton is shielded (Table 6). In the 4-methyl derivatives **1***b* and **3***b*, the deshielding $\Delta\delta_{H4}$ effect is negligible in the case of thiazolidine **3***b*. It follows that H4 in **1***b* takes up a more equatorial orientation than in **3***b*, whose preferential ring conformation had been found (6, 7) as a half-chair geometry with C4N3 out-of-plane. Molecular models show that an equatorial H4 proton is closer to the ring plane, for a C4 out-of-plane envelope than for a C4N3 out-of-plane half-chair.

Therefore, the preferred ring geometry of **1***b* would be the C4 out-of-plane envelope **a3**. This corresponds to a shift of [*a*] to the right in going from **1***a* to **1***b*. Such a displacement would manifest itself in decreasing the C4C5 torsional value (17).

In the case of the 5-methyl derivatives **2***b* and **3***c*, the $\Delta\delta_{H5}$ deshielding value for the TH-2-TH ring **2***b* is smaller than for the TH ring **3***c*; it follows that H5 in **2***b* takes a more axial orientation than in **3***c*, where a C4 out-of-plane envelope and a C4N3 out-of-plane

Can. J. Chem. Downloaded from www.nrcresearchpress.com by 210.87.254.5 on 09/05/12
For personal use only.

Can. J. Chem. Downloaded from www.nrcresearchpress.com by 210.87.254.5 on 09/05/12
For personal use only.

TABLE 6. ^{1}H nuclear magnetic resonance: effects on the chemical shifts of heterocyclic protons by the introduction of a methyl group at position 4 and 5 of TH-2-TH and TH (ppm; + is deshielding; − is shielding)

Introduction of a methyl group in position	$\Delta\delta_{H4'}$	$\Delta\delta_{H4}$	$\Delta\delta_{H5}$	$\Delta\delta_{H5'}$
4 of TH-2-TH		+0.41 (*gem*)	+0.10 (*transoid*)	−0.38 (*cisoid*)
4 of TH (ref. 6, p. 62)		+0.02 (*gem*)	+0.18 (*transoid*)	−0.50 (*cisoid*)
5 of TH-2-TH	−0.43 (*cisoid*)	+0.07 (*transoid*)	+0.46 (*gem*)	
5 of TH (ref. 6, p. 110)	−0.50 (*cisoid*)	+0.02 (*transoid*)	+0.64 (*gem*)	

half-chair are found preferential (6, 7). In molecular models, it appears that H5 becomes more axial when C5 leaves the plane of the thiocarbonyl group. Thus the above weak $\Delta\delta_{H5}$ in **2***b* originates from an increase in the half-chair population **a2**: going from **1***a* to **2***b* displaces [*a*] to the left and brings about an increase of the C4C5 torsional angle (17).

Another conclusion can be drawn from Table 6. The large shielding effect on the H_{gem}/6-R proton (−0.50 ppm, Table 5) in the dioxanes **4**, in going from R = Me to R = *t*Bu, arises from spatial substituent interactions (12). The shielding effects, $\Delta\delta_{H_{gem}/R}$, in thiazolidine-2-thiones **1** and **2**, when R = Me to *t*Bu, being somewhat smaller (−0.35 ppm for **1** and −0.12 ppm for **2**, Table 5), something must exist which induces an incremental deshielding effect as H4 and H5 become more and more axial. If we neglect the anisotropic effect of the thiocarbonyl group, the deshielding increment can be assigned to a modification of the ring geometry in **1** and **2** as the substituent becomes larger. Simulation of such changes in 4-methyl-TH-2-TH and 5-methyl-TH-2-TH by the CNDO-2 method (Fig. 1) shows that:
(*i*) For **1***b*, the shift

[*c*] C4 out-of-plane envelope ⇋ C4C5 out-of-plane half-chair
(axial methyl) (equatorial methyl)

indeed results in the following simultaneous effects: deshielding of *cisoid* H5′ and particularly of H4; shielding of *transoid* H5.
(*ii*) For **2***b*, the change

[*d*] C5 out-of-plane envelope ⇋ C4C5 out-of-plane half-chair
(axial methyl) (equatorial methyl)

gives rise to the following simultaneous effects: deshielding of *cisoid* H′4 and, particularly, of H5; shielding of *transoid* H4.

The observed deshielding increment on H_{gem}/R, in going from R = Me to R = *t*Bu, can therefore originate from such conformational modifications

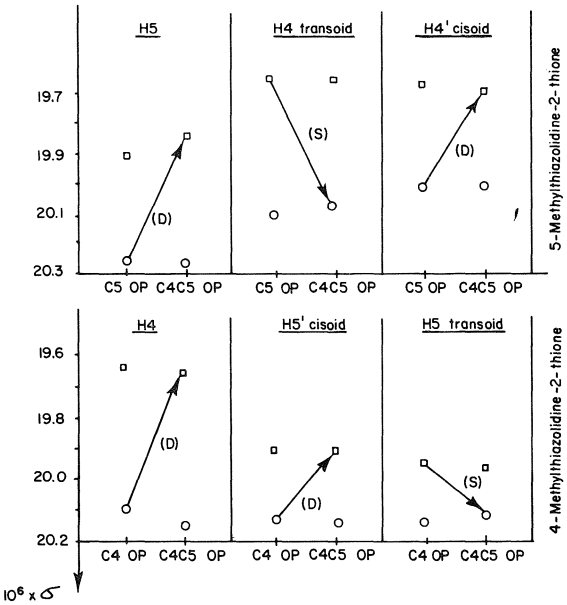


FIG. 1. ^{1}H nmr/CNDO-2 calculations. Screening constants of heterocyclic protons for two geometries of 4-methyl- and 5-methylthiazolidine-2-thiones. ○ = equatorial proton, □ = axial proton, C4 OP = C4 out-of-plane envelope, C5 OP = C5 out-of-plane envelope, C4C5 OP = C4C5 out-of-plane half-chair, (D) = deshielding, (S) = shielding.

which should correspond in fact to a shift in equilibria [*a*] and [*b*]:

Series	Shift: Equilibrium [*a*]	Shift: Equilibrium [*b*]
1	To the left	To the right
2	To the right	To the left

Such changes in ring geometry may influence the interaction between the heteroatom lone pair and the antibonding orbitals (18), which are the most important factors influencing J_{gem} values of a CH_2 β to

TABLE 7. CNDO-2 calculations: variation* in the $J_{55'}$ and $J_{44'}$ values as a function of the thiazolidine-2-thione conformation

Thiazolidine-2-thiones	$^2J_{55'}$ (Hz)	$^2J_{44'}$ (Hz)
Thiazolidine-2-thione†		
C4 out-of-plane No. 1 (envelope **a3**)	2.71	2.13
C4 out-of-plane No. 2	1.55	1.32
C4C5 out-of-plane No. 1 (half-chair **a2**)	2.59	1.67
C4C5 out-of-plane No. 2	1.43	0.98
C5 out-of-plane No. 1 (envelope **a1**)	3.10	2
C5 out-of-plane No. 2	1.67	1
Plane	5.08	4.5
4-Methylthiazolidine-2-thione		
C4 out-of-plane No. 1 pseudo-equatorial 4-Me	3.82	
C4 out-of-plane No. 1 pseudo-axial 4-Me	2.80	
C4C5 out-of-plane No. 1 pseudo-equatorial 4-Me	3.85	
C4C5 out-of-plane No. 1 pseudo-axial 4-Me	2.59	
Plane	3.78	
5-Methylthiazolidine-2-thione		
C4C5 out-of-plane No. 1 pseudo-equatorial Me		2.40
C4C5 out-of-plane No. 1 pseudo-axial Me		2.32
C5 out-of-plane No. 1 pseudo-equatorial Me		2.64
C5 out-of-plane No. 1 pseudo-axial Me		2.47
Plane		3.53

*One must not attach too much importance to the intrinsic value of an isolated result (ref. 13, ref. 31, Annexe 2, p. 36). Only the variation in a series of homologous compounds can have a real significance.
†No. 1 = slight puckering of the ring (1), No. 2 = important puckering of the ring (1) (see Table 2).

an heteroatom. An increase in χ or/and in orbital overlapping has positive contribution to ^2J (as ^2J is normally negative, a positive contribution implies a diminution of the absolute value). In series **1** and **2** we observe a diminution of $^2J_{55'}^{exp}$, and $^2J_{44'}^{exp}$ (Table 1, parts *a* and *b*), and particularly so between **1***c* and **1***d*, and **2***d* and **2***e*. Molecular orbital calculations performed by Bothner-By and Pople (19) for ^2J values account for most of the experimental trends. Accordingly, simulation by Pople and Santry CNDO-2 method (14*b*) (Table 7) shows that a diminution of $J_{55'}$ in 4-methyl-TH-2-TH **1***b* can have several conformational origins: (*i*) an increase in the proportion of axial conformer, the ring geometry remaining fixed; (*ii*) an increase of the half-chair (**a2**) proportion with 4-R being axial.

In this series (from **1***b* to **1***c*), we saw an increase of the proportion of the equatorial orientation of R. Then only factor (*ii*) can be considered responsible for the diminution of $J_{55'}^{exp}$.

In 5-methyl-TH-2-TH calculation, a diminution in $J_{44'}$ can be manifested in the following ring phenomena: (*i*) increase in ring puckering; (*ii*) increasing population of the axial conformation while the ring geometry remains fixed; (*iii*) passage from the **a3** to the **a1** conformation while the orientation of the substituent remains constant (5-R axial or equatorial); and (*iv*) increasing the population of the equatorial conformer with a passage from the **a3** to the **a2** conformation.

We previously demonstrated the increasing equatorial tendency of the substituent from **2***b* to **2***c* and no indication of an increase in the ring puckering has been experimentally noticed. Thus we can retain factor (*iv*), i.e., the diminution of $J_{44'}^{exp}$ value comes principally from the equilibria [*a*] and [*b*] being shifted to the right.

Spatial Orientation of the Substituents

The population of each rotamer about the C—C4 or C—C5 bonds follows from the application of the simplified Karplus equation (20) $J_\varphi = A^0 \cos^2 \varphi$ to the *vicinal* coupling constants in the

CH—C4 or CH—C5
| |
H H

fragment (see Experimental section).

For 4-R-TH-2-TH (4-R = Et, *i*Pr), the conformations with a methyl *gauche* to N are particularly energetic, while for 5-R-TH-2-TH (5-R = Et, *i*Pr) the conformations with a methyl group *gauche* to C4 are less stable. It then appears that the steric interactions are important: between a methyl group and N for the series **1***b* to **1***d*, between a methyl group and C4 for the series **2***b* to **2***d*.

Factors Influencing the Conformational Equilibria

We have summarized all the above conclusions, by schematically representing the observed conformational trends respectively in series **1** and **2** respectively in Tables 8 and 9.

Can. J. Chem. Downloaded from www.nrcresearchpress.com by 210.87.254.5 on 09/05/12
For personal use only.

TABLE 8. Conformational variations of the 4-alkylthiazolidine-2-thiones **1**

[*a*] C5 out-of-plane envelope ⇋ C4C5 out-of-plane half-chair ⇋ C4 out-of-plane envelope
a1 **a2** **a3**

[*b*] axial 4-R ⇋ equatorial 4-R
b1 ⇋ **b2**

4-R changes from	Substituent orientation Δx_{calcd} (%)	Ring geometry $\Delta J_{55'}^{exp}$ (Hz)	Ring geometry $\Delta\varphi_{calcd}$ (deg)	Conformational conclusions	Number of Me groups *gauche* to N in preferential rotamer
H to Me	—	—	+3	Variation of ring geometry: [*a*] is displaced to the right	0
Me to Et	−2	−0.14	0	[*a*] and [*b*] are only slightly displaced	0
Et to *i*Pr	−5	−0.34	−5.5	Variation in the ring geometry: [*a*] is displaced to the left Change in the orientation of the substituent: [*b*] is displaced to the right	1
*i*Pr to *t*Bu	−2	−0.11	−1	Small change in ring geometry: [*a*] is displaced to the left Small change in substituent orientation: [*b*] is displaced to the right	2

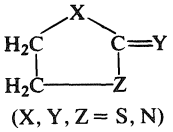
TABLE 9. Conformational evolutions of 5-alkylthiazolidine-2-thiones **2**

[*a*] C5 out-of-plane ⇋ C4C5 out-of-plane ⇋ C4 out-of-plane
(envelope) (half-chair) (envelope)

[*b*] axial 5-R ⇋ equatorial 5-R

5-R passes from	Substituent orientation Δx_{calcd} (%)	Ring geometry $\Delta J_{44'}^{exp}$ (Hz)	Ring geometry $\Delta\varphi_{calcd}$ (deg)	Conformational conclusions	Number of methyl groups *gauche* to C4 in preferential rotamer
H to Me	—	—	+1.5	Change in ring geometry: [*a*] is displaced to the left	—
Me to Et	0	−0.28	0	No change in conformational properties	0
Et to *i*Pr	−6	+0.05	−1	Change in the orientation of the substituent: [*b*] is displaced to the right Small change in ring geometry	1
*i*Pr to *t*Bu	−2	−0.77	−4	Change in substituent orientation and in ring geometry; both [*a*] and [*b*] are displaced towards the right	2

By analogy with molecules of the type



(X, Y, Z = S, N)

the S—C—NH fragment is considered as planar (21).

S

We noted that the TH-2-TH ring singularity lies in the absence of any transannular interaction (1). The minimization of angle and Pitzer strains controls the ring conformation with equilibrium

a1 ⇋ **a2** ⇋ **a3**

being shifted to the right.

We are going to examine successively the conformational effects related to the introduction of heavier substituent on C4 and C5.

Introducing a 4-methyl group involves CH_3/C5H and CH_3/NH van der Waals interactions. To minimize them, the C4 atom moves off the thiocarbonyl

Can. J. Chem. Downloaded from www.nrcresearchpress.com by 210.87.254.5 on 09/05/12
For personal use only.

Can. J. Chem. Downloaded from www.nrcresearchpress.com by 210.87.254.5 on 09/05/12
For personal use only.

plane, increasing the proportion of **a3** with a preferential axial substituent (Fig. 2). The steric origin of this last conformational change is corroborated in that it is accentuated by the presence of a *N*-methyl group (ref. 31, p. 124). Part of the effect could also lie in an attractive nonbonded interaction between the methyl carbon and the ring sulfur (23).

Introducing successive methyl groups on the *C*—C4 atom leads to a simultaneous introduction of other van der Waals interactions ($CH_3/C5H_2$ and CH_3/N), inducing the recorded modification (Table 8) in the conformational properties. Such changes are connected with the presence of a methyl group *gauche* to nitrogen. For the 4-ethyl substituent, we have seen that the methyl group lies preferentially *anti* to N; now the $CH_3/C5H_2$ interaction seems to be weak; so that 4-ethyl-TH-2-TH **1***c* has conformational properties comparable to that of the methyl derivative **1***b* (Fig. 3).

In 4-isopropyl-TH-2-TH **1***d*, the presence of a methyl group *gauche* to N results in a CH_3/N *gauche* interaction (Fig. 3) which is reduced in an equatorial substituent orientation. However, such an orientation corresponds to a maximum N—H/CH_3 *vicinal* interaction (Fig. 2), opening the H—N—C4—R4 dihedral angle, by forcing C4 back into the thiocarbonyl plane it results in a shift of equilibrium [*a*] to the left with an increasing proportion of **a2** (C4C5 out-of-plane half-chair form) and equilibrium [*b*] towards **b2** (pseudo-equatorial 4-R). The presence of an additional methyl group on the *C*—C4 atom in 4-*tert*-isobutyl-TH-2-TH (**1***e*), increases the former trends.

The 5-methyl group in 5-methyl-TH-2-TH **2***b* induces the C5 atom to leave the ring plane (24) due to an increase in C5—Me/C4—H Pitzer strain. This is necessarily accompanied by the re-entry of the C4 atom into the thiocarbonyl plane and an increase of the population of the half-chair **a2** form (displacement of the equilibrium [*a*] towards the left). Since the Pitzer interactions about a sulfur atom are weak, and in the absence of transannular interactions, no particular methyl orientation is preferred ($x = 50\%$).

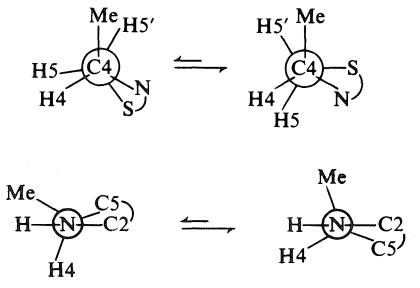


FIG. 2. *Vicinal* interactions in 4-methylthiazolidine **1***b*.

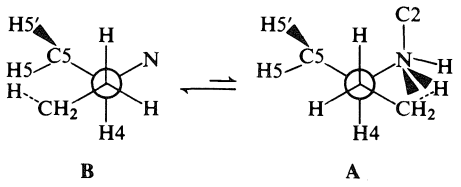


FIG. 3. Rotamers **B** and **A** for a pseudo-axial ethyl orientation in 5-ethylthiazolidine-2-thione **1***c*.

On introducing successive methyl groups on *C*—C5 (R5 = Et, *i*Pr, *t*Bu), there is a simultaneous setting up of van der Waals interactions, which explains the observed conformational changes (Table 9). These interactions are particularly important when a methyl group is *gauche* to C4. For the 5-ethyl derivative **2***c*, there is no such interaction in the preferred rotamer and the substituent orientation and ring geometry are comparable to those adopted by the 5-Me-Th-2-TH (**2***b*). By contrast with the 5-isopropyl derivative, **2***d*, one of the methyl groups is *gauche* to C4. The $CH_3/C4H_2$ interaction is minimized in an equatorial substituent orientation, which promotes a diminution in x without inducing a large change in ring geometry. In the 5-*t*Bu derivative **2***e*, two methyl groups are *gauche* to C4 (Fig. 4). The $CH_3(a)$/C4H′4 interaction forces the substituent to adopt an equatorial position which simultaneously gives rise to a $CH_3(b)$/C4H′4 repulsion. The latter is minimized by C4 going out of the thiocarbonyl plane: displacement of equilibrium [*a*] to the right.

Part B. 4-Hydroxy-thiazolidine-2-thione

The application of the method of ratios suggests (Table 3) a TH-2-TH ring modification by introducing an hydroxyl group on C4 (increase φ_{calcd}). The value of x for 4-hydroxy-TH-2-TH **1***f* is the same at ambient temperature and at −60°C (88–90%). Therefore, at ambient temperature **1***f* exists in a nearly totally biased equilibrium (x is underestimated as in the case of **1***b*).

The replacement of a methyl by an hydroxyl group exerts a negative effect on $^2J_{55'}{}^{exp}$ ($\Delta^2J_{55'}{}^{exp} = -1.56$ Hz). Such an effect is, however, reversed in the acyclic series (i.e. a positive effect ca. +2 Hz (24)). This behaviour is related to what has been observed

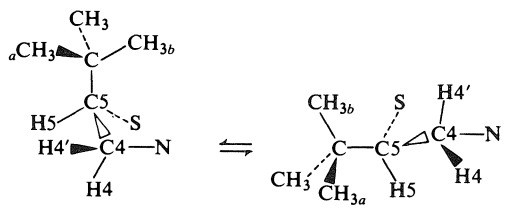


FIG. 4. Equilibrium [*b*] in 5-tertiobutylthiazolidine-2-thione **2***e*.

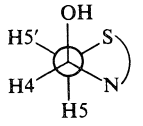
(25) in pyranose rings which exists in the forms **p1** and **p2**.



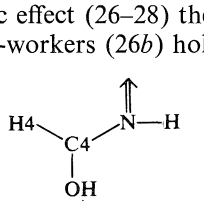
p1 **p2**

In agreement with the LCAO treatment described by Pople and Bothner-By (14*a*), the CH_2 protons occupying the *trans–gauche* position to an electronegative substituent as in **p1** have a smaller J_{gem} value (therefore a greater absolute value) than the *gauche–gauche* arrangement in **p2**.

Therefore the notable decrease in J_{gem}^{exp}, when a methyl group is replaced by an hydroxyl at C4 in TH-2-TH, is compatible with an orientation of **p1** type; thus the hydroxyl group occupies a pseudo-axial orientation.



Such an orientation of an electronegative atom bearing lone pairs is encountered in many heterocycles where the phenomenon is referred to as the anomeric effect (26). Among various factors invoked to account for the anomeric effect (26–28) the interpretation of Havinga and co-workers (26*b*) holds the attention:



the non-bonding N electrons (*p* orbital of a sp^2 atom) are delocalized into the conveniently oriented C4—O antibonding σ orbital. This satisfactorily explains the preferred pseudo-axial orientation of the C4—OH bond. The overlapping is thus maximum in a C4 out-of-plane envelope.

Experimental

Obtention of the Substituted Thiazolidine-2-thiones

The alkyl-TH-2-TH **1***a*, **1***b*, **1***c*, **2***b*, **2***c*, **2***d*, and **2***e* were obtained by reacting an aminoalkyl hydrogenosulfate with CS_2 in presence of NaOH (29, 30). The **1***d* and **1***e* compounds result from the action of CS_2 on appropriate aziridines (22, 29).

The 4-hydroxy-TH-2-TH **1***f* was obtained by the reaction of bromacetaldehyde with ammonium dithiocarbamate (15, 29).

(a) ^1H Nuclear Magnetic Resonance

The 60 MHz spectra were recorded on Varian A60 and HA100 Spectrometers. Approximatively 0.1 *M* solutions in acetone-d_6 were used with TMS as internal reference. The ^1H nmr spectra of the 5-alkyl-TH-2-TH (**2**) were considered to originate from ABC, ABCX, $ABCX_2$, $ABCX_3$ spin systems, while the 4-alkyl-TH-2-TH (**1**) one originates from ABX, ABXY, $ABXY_2$, and $ABXY_3$ spin systems. The methods of analysis has been reviewed (ref. 31, Annexe III, p. 69). The spectral parameters are given in Table 1.

(b) ^{13}C Nuclear Magnetic Resonance

The ^{13}C nmr spectra were recorded from natural abundance signals at a frequency of 25.16 MHz on a Fourier Transform Varian XL100/15 spectrometer. Solutions (1 *M* or 2 *M*) were used in chloroform-*d* which also served as internal reference. The spectral parameters are listed in Table 2.

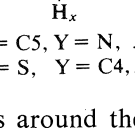
Spectra Interpretation

^1H Nuclear Magnetic Resonance — ^5J values in the Ethanic Fragment: an Application of the Karplus Equation to Calculate the C4C5 Torsional Angles and Conformer Populations

The two classical methods of conformational analysis (ratios and differences) based on Karplus equation have been compared (2*k*) using *cis* and *trans vicinal* coupling constants of the C4C5 fragment. We chose, as did Elguero and Fruchier (2*j*), the ratio method, which gave the most coherent results for the variously substituted TH-2-TH; these results are listed in Table 3. The values of J_φ, $J_{120°-\varphi}$, $J_{120°+\varphi}$, ΔJ_φ, $R(J_\varphi)$, ΔJ_K, and $R(J_K)$ for values of φ_{calcd} between 0° and 360° were kindly provided by Elguero.

Spatial Orientation of the Substituent. Calculations

(i) Methyl Derivatives **1**b *and* **2**b



1*b*: X = C5, Y = N, $x = 4$
2*b*: X = S, Y = C4, $x = 5$

The three rotamers around the C—H_x bond are energetically equivalent; if we suppose only one *gauche J* value, we can write (1):

[3] $J_{HH_x} = \frac{1}{3}(2J_{gauche} + J_{anti})$

Applying the simplified Karplus relationship (20)

[4] $J_\varphi = A^0 \cos^2 \varphi$

and supposing that $\varphi_{gauche} = 60°$ and $\varphi_{anti} = 180°$, we obtain

$$J_{gauche} = (A^0/4) \quad \text{and} \quad J_{anti} = A^0$$

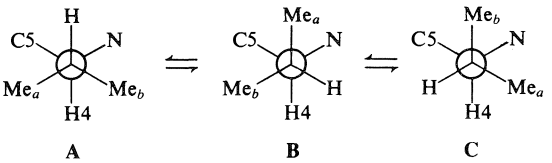
Therefore by applying [3] to the experimental value we obtain:

$$A^0_{(1b)} = 12.7 \text{ Hz} \quad \text{and} \quad A^0_{(2b)} = 12.76 \text{ Hz}$$

(ii) 4-Isopropyl-TH-2-TH **1**d

The **A**, **B**, and **C** conformations being not energetically equivalent, the corresponding populations

Can. J. Chem. Downloaded from www.nrcresearchpress.com by 210.87.254.5 on 09/05/12
For personal use only.



A B C

P_A, P_B, and P_C are such that

[5] $J_{HH4} = P_A J_A + (P_B + P_C)J_{gauche}$

We equate J_{HH4} with J_{exp} value to obtain

$J_{HH4} = 6.4$ Hz (Table 1)

It follows

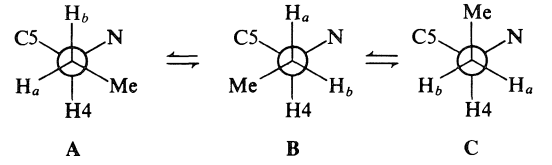
$P_A = 0.34$ and $(P_C + P_B) = 0.66$

In the absence of a third equation for resolving the system, a consideration of the ^{13}C nmr data (Table 4) is helpful. The successive introduction of methyl groups on the *C*—C4 atom of **1***b* induces γ5-, γ′5-, and γ″5-effects, respectively (Table 4). The weakest γ″5-effect is associated to the introduction of a methyl *anti* to C5. This implies that conformation **B** is favoured. Therefore

$P_B > (P_A = 0.34) > P_C$

(iii) 4-Ethyl-TH-2-TH **1**c

By analogy with the preceding paragraph we



A B C

write:

[6] $J_{H_aH4} = (P_A + P_C)J_{gauche} + P_B J_{anti}$

[7] $J_{H_bH4} = (P_B + P_C)J_{gauche} + P_A J_{anti}$

We identify these average values with the experimental values. There are two possibilities. The first estimation

[I] $J_{H_aH4} = 5.97$ Hz and $J_{H_bH4} = 7.1$ Hz

leads to the following result

[I′] $P_C = P_B = 0.29$, $P_A = 0.41$

The second estimation

[II] $J_{H_aH4} = 7.1$ Hz and $J_{H_bH4} = 5.97$ Hz

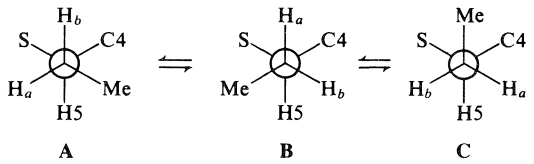
gives

$P_A = P_C = 0.29$, $P_B = 0.41$

The two methyl groups in **1***d* being *gauche* to C5 in the preferential conformation, the ethyl substituent must adopt a conformation presenting a methyl *gauche* to C5. **C** is sterically disfavoured; then **B** is the preferred arrangement. This corresponds to hypothesis [II]; the H_a and H_b chemical shifts (Table 1) confirm this choice, since in conformation **B**, H_a, *gauche* to both C5 and N, is more shielded than H_b *gauche* to N but *anti* to C5.

(iv) 5-Ethylthiazolidine-2-thione **2**c

By analogy with the 4-ethyl-TH-2-TH (**1***c*) case, the two experimental values ($J_1^{exp} = 7.5$ Hz and



A B C

$J_2^{exp} = 6.4$ Hz) lead to two solutions for the set of population:

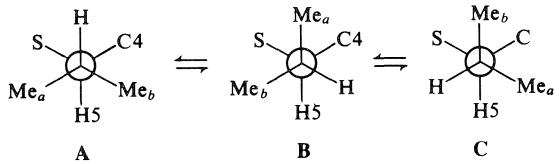
[i] $P_A = 0.33$; $P_B = 0.45$; $P_C = 0.22$

[ii] $P_A = 0.45$; $P_B = 0.33$; $P_C = 0.22$

Inspection of the ^{13}C nmr γ-effects (Table 4) helps for the choice of the correct solution. Let the γ4-, γ′4-, and γ″4-effects be experienced by the $^{13}C4$ chemical shift on introducing successive methyl groups on the *C*-C4 atom. The smallest γ4-effect must be assigned to the methyl group situated *anti* to C4. Therefore in **2***c*, the preferential rotamer has its methyl group *anti* to C4, i.e. rotamer **B** is favoured (solution *i*). This result is corroborated by ^1H nmr: proton H_a is more shielded ($\delta_{H_a} = 1.74$ ppm) than H_b ($\delta_{H_b} = 1.84$ ppm).

(v) 5-Isopropyl-TH-2-TH **2**d

The only values that can be evaluated are: $P_A = 0.40$ and $P_B + P_C = 0.60$. In **2***c* the methyl



A B C

group is preferentially *anti* to C4. Similarly in **2***d*, one of the methyl group must be *anti* to C4 (**C** is eliminated) while the other one must be *gauche* to C4 (γ′4 = −2.53 ppm). In our evaluation, we have seen that groups *gauche* to both endocyclic bonds are particularly disfavoured. This leads us to conclude

$P_A = 0.40 > P_B > 0.30 > P_C$

1. F. CHANON, M. RAJZMANN, M. CHANON, J. METZGER, and G. POUZARD. Can. J. Chem. **58**, 599 (1980).
2. (*a*) R. U. LEMIEUX, T. D. STEVENS, and R. R. FRASER. Can. J. Chem. **40**, 1955 (1962); (*b*) M. ANTEUNIS and F.

Can. J. Chem. Downloaded from www.nrcresearchpress.com by 210.87.254.5 on 09/05/12
For personal use only.

ALDERWEIRELDT. Bull. Soc. Chim. Belg. **73**, 889 (1964); (*c*) M. ANTEUNIS and F. ALDEWEIRELDT. Bull. Soc. Chim. Belg. **73**, 903 (1964); (*d*) F. ALDEWEIRELDT and M. ANTEUNIS. Bull. Soc. Chim. Belg. **74**, 488 (1965); (*e*) D. GAGNAIRE and J. B. ROBERTS. Bull. Soc. Chim. Fr. 3646 (1965); (*f*) J. B. LAMBERT. Acc. Chem. Res. **4**, 87 (1971); (*g*) T. A. CRABB and R. F. NEWTON. Chem. Ind. 339 (1966); (*h*) M. ANTEUNIS. Bull. Soc. Chim. Belg. **75**, 413 (1966); (*i*) J. L. AUBAGNAC, P. BOUCHET, J. ELGUERO, R. JACQUIER, and C. MARZIN. J. Chim. Phys. **64**, 1649 (1967); (*j*) J. ELGUERO and A. FRUCHIER. An. Quim. **70**, 141 (1974).

3. M. CHRISTL, H. J. REICH, and J. D. ROBERTS. J. Am. Chem. Soc. **93**, 3463 (1971).
4. J. B. STOTHERS and C. T. TAN. Can. J. Chem. **52**, 308 (1974).
5. R. FAURE, J. R. LLINAS, E. J. VINCENT, and J. L. LARICE. C.R. Acad. Sci. **279**C, 717 (1974).
6. J. L. LARICE. Thèse Sciences, Marseille. 1972.
7. M. GUILIANO. Thèse Sciences, Marseille. 1977. p. 116.
8. D. K. DALLING and D. M. GRANT. J. Am. Chem. Soc. **89**, 6612 (1967).
9. (*a*) V. TABACIK. Tetrahedron Lett. **5**, 555 (1968); **5**, 561 (1968); (*b*) W. E. WILLY, G. BINSCH, and E. L. ELIEL. J. Am. Chem. Soc. **92**, 5394 (1970).
10. P. LAZLO and P. J. STANG. Spectroscopie organique. Hermann, Paris. 1972. p. 60.
11. (*a*) W. J. STILL, N. PLAVAC, D. M. MCKINNON, and M. S. CHAUHAN. Can. J. Chem. **54**, 1660 (1976); (*b*) M. T. HEARN. Aust. J. Chem. **29**, 107 (1976); (*c*) T. F. PAGE, JR., T. ALGER, and D. M. GRANT. J. Am. Chem. Soc. **87**, 5333 (1965); (*d*) M. S. CHAUHAN and I. W. J. STILL. Can. J. Chem. **53**, 2880 (1975).
12. P. MARONI and J. P. GORRICHON. Bull. Soc. Chim. Fr. **2**, 786 (1972).
13. G. POUZARD, M. RAJZMANN, J. BODOT, and L. PUJOL. Org. Magn. Reson. **5**, 209 (1973).
14. (*a*) J. A. POPLE and A. A. BOTHNER-BY. J. Chem. Phys. **42**, 1339 (1965); (*b*) J. A. POPLE and D. P. SANTRY. Mol. Phys. **8**, 1 (1964).
15. M. CHANON and J. METZGER. Bull. Soc. Chim. Fr. 2863 (1968).
16. J. W. EMSLEY, J. FEENEY, and L. H. SUTCLIFFE. High resolution NMR spectroscopy. Vol. 2. Pergamon Press. 1966. p. 696.
17. K. S. PITZER and W. E. DONATH. J. Am. Chem. Soc. **81**, 3213 (1959).
18. (*a*) L. M. JACKMAN and S. STERNHELL. Applications of NMR spectroscopy in organic chemistry. Pergamon Press, Oxford. 1969. p. 281; (*b*) R. CAHILL, R. C. COOKSON, and T. A. CRABB. Tetrahedron, **25**, 4711 (1969); (*c*) R. CAHILL, R. C. COOKSON, and T. A. CRABB. Tetrahedron, **25**, 4681 (1969); (*d*) A. JAWORSKY, I. EKIEL, and D. SHUGAR. J. Am. Chem. Soc. **100**, 4357 (1978).
19. A. A. BOTHNER-BY. Advances in magnetic resonance. Vol. 1. *Edited by* J. S. Waugh. Academic Press, New York. 1965.
20. M. KARPLUS. (*a*) J. Am. Chem. Soc. **85**, 2870 (1963); (*b*) J. Chem. Phys. **30**, 11 (1959).
21. (*a*) F. A. ANET. J. Am. Chem. Soc. **84**, 747 (1962); (*b*) C. J. BROWN. Acta Crystallogr. **7**, 92 (1954); (*c*) P. J. WHEATLEY. Acta Crystallogr. **6**, 369 (1953).
22. (*a*) S. GABRIEL and R. STELZNER. Chem. Ber. **28**, 2929 (1895); (*b*) T. A. FOGLIA, L. M. GREGORY, G. MAERKER, and S. F. OSMAN. J. Org. Chem. **36**, 1068 (1971).
23. H. E. VAN MART, LL. SHIPMAN, and H. A. SCHERAGA. J. Phys. Chem. **79**, 1436 (1975).
24. S. STERNHELL. Q. Rev. 236 (1969).
25. R. U. LEMIEUX, E. FRAGA, and K. A. WATANABE. Can. J. Chem. **46**, 6 (1968).
26. (*a*) C. ALTONA, C. ROMERS, and E. HAVINGA. Tetrahedron Lett. **10**, 16 (1959); (*b*) C. ROMERS, C. ALTONA, H. R. BUYS, and E. HAVINGA. Topics in stereochemistry. Vol. 4. *Edited by* E. L. Eliel and H. L. Allinger. Wiley Interscience. 1969. p. 73.
27. (*a*) J. T. EDWARD. Chem. Ind. London, 1102 (1955); (*b*) E. L. ELIEL, N. M. ALLINGER, S. J. ANGYAL, and G. A. MORRISON. Conformational analysis. Interscience. 1965. p. 376.
28. (*a*) C. ALTONA. Thèse Leiden, 1964; (*b*) C. ALTONA and C. ROMERS. Acta Crystallogr. **16**, 1225 (1963); (*c*) C. ALTONA, C. KNOBLER, and C. ROMERS. Acta Crystallogr. **16**, 1217 (1963); (*d*) N. DE WOLF, C. ROMERS, and C. ALTONA. Acta Crystallogr. **22**, 715 (1967).
29. R. A. BAFFORD, F. CHANON, M. CHANON, and J. METZGER. Bull. Soc. Chim. Fr. **3**, 971 (1973).
30. (*a*) F. DICKEY, W. FICKET, and H. LUCAS. J. Am. Chem. Soc. **74**, 944 (1952); (*b*) S. GABRIEL and E. OHLE. Chem. Ber. **50**, 804 (1917); (*c*) C. S. DEWEY and R. A. BAFFORD. J. Org. Chem. **32**, 3108 (1967).
31. F. CHANON. Thèse Sciences, Marseille, France. 1977.

Can. J. Chem. Downloaded from www.nrcresearchpress.com by 210.87.254.5 on 09/05/12
For personal use only.

Synthesis and carbon-13 nuclear magnetic resonance spectra of monoethyl 4-nitro and 4-amino phthalates

KALKUNTE S. SESHADRI AND JOHN D. BACHA

Gulf Research & Development Company, P.O. Box 2038, Pittsburgh, PA 15230, U.S.A.

Received March 23, 1979[1]

KALKUNTE S. SESHADRI and JOHN D. BACHA. Can. J. Chem. **58**, 617 (1980).

Carbon-13 nmr has been found to be an effective spectroscopic method for measuring the ratio of isomeric monoethyl esters resulting from the esterification of 4-nitrophthalic acid, the alcoholysis of 4-nitrophthalic anhydride, and the catalytic reduction of monoethyl 4-nitrophthalates. Precise values of the ^{13}C chemical shifts for 1-ethyl and 2-ethyl 4-nitrophthalate and the corresponding 4-aminophthalates were determined; the shielding parameters are explained in terms of known structural effects. Details of the esterification, alcoholysis, reduction reactions, and the isolation of 1-ethyl 4-nitrophthalate are described.

KALKUNTE S. SESHADRI et JOHN D. BACHA. Can. J. Chem. **58**, 617 (1980).

On a trouvé que la spectroscopie de la rmn du ^{13}C est une méthode efficace de mesure du rapport des isomères des esters monoéthyliques provenant de l'estérification de l'acide nitro-4 phtalique, de l'alcoolyse de l'anhydride nitro-4 phtalique et de la réduction catalytique des nitro-4 phtalates d'éthyle. On a déterminé les valeurs exactes des déplacements chimiques du ^{13}C pour les nitro-4 phtalates d'éthyle-1 et d'éthyle-2 et les amino-4 phtalates correspondants. On explique les paramètres de blindage en fonction d'effets structuraux connus. On décrit en détail l'estérification, l'alcoolyse, les réactions de réduction et la séparation du nitro-4 phtalate d'éthyle.

[Traduit par le journal]

Introduction

Polyimide resins, for industrial high-temperature applications, are usually prepared by copolymerization of aromatic acid anhydrides or their monoalkyl esters and aromatic diamines. Thermally stable polyimides can also be prepared by homopolymerization of suitable multi-functional monomers, e.g., monoethyl 4-aminophthalates.

Monoethyl 4-aminophthalates can exist in two isomeric forms which are obtained by the catalytic reduction of the corresponding 4-nitrophthalates. The monoethyl 4-nitrophthalates are prepared by treating 4-nitrophthalic acid or its anhydride with excess ethanol. In both of these reactions, one of the monoesters might be formed at the exclusion of the other or a mixture of both isomers could be formed. ^{13}C nmr spectroscopy was selected as an analytical tool to determine the structure and the distribution of the products formed. This report describes the following: (*1*) the synthesis of 4-nitrophthalic anhydride (4NPAN) from 4-nitrophthalic acid (4NPAC), (*2*) esterification of 4NPAC, (*3*) alcoholysis of 4NPAN, (*4*) isolation of 1-ethyl 4-nitrophthalate, (*5*) the catalytic hydrogenation of monoethyl 4-nitrophthalates, and (*6*) the ^{13}C spectra of model compounds and reaction products.

Results and Discussion

The compounds pertinent to this work and their carbon-13 shielding data are presented in Fig. 1 and Table 1, respectively. The assignment of resonance positions in the carbon-13 spectra depends on several factors: (*1*) observation of proton-induced splitting patterns in the off-resonance decoupling experiments, (*2*) reduced nuclear Overhauser enhancement for quaternary centers, (*3*) available data on model compounds, and (*4*) empirical schemes for predicting the ^{13}C chemical shifts for a proposed structure.

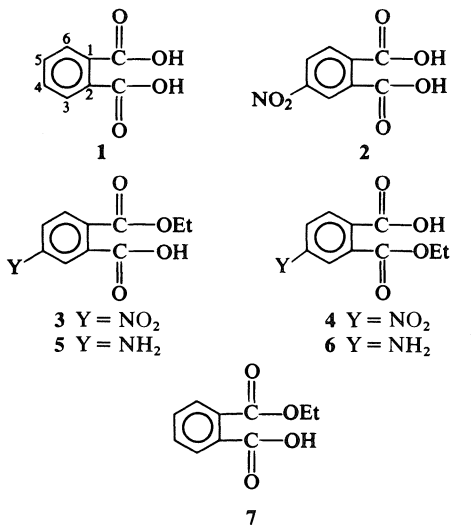


FIG. 1. Identification of compounds whose ^{13}C shieldings are given in Table 1.

The spectra of the esterification and the reduction reaction product mixtures are complex with closely spaced resonance positions. The fortuitous

[1]Revision received August 8, 1979.

0008-4042/80/060617-05$01.00/0

©1980 National Research Council of Canada/Conseil national de recherches du Canada

Can. J. Chem. Downloaded from www.nrcresearchpress.com by 210.87.254.105 on 09/05/12
For personal use only.

TABLE 1. ^{13}C shielding for **1–7** (δ_c ppm from TMS ± 0.1)*

Position	1	2	3	4	5	6	7
C-1	133.7	139.5	139.9	138.7	117.5	116.4	133.9
C-2	133.7	133.6	133.3	134.3	137.5	138.7	132.7
C-3	129.6	124.8	125.0	124.4	115.0	114.6	129.8
C-4	131.7	149.5	149.5	149.7	152.6	153.1	131.5
C-5	131.7	126.9	127.1	126.6	113.8	113.3	132.0
C-6	129.6	130.9	130.7	131.2	132.3	132.9	129.1
>C=O	169.3	168.1	166.0	166.1	170.1	171.1	169.3
		166.7	167.1	167.3	167.2	168.4	168.4
CH_2	—	—	62.7	62.7	61.1	61.6	61.4
CH_3	—	—	14.1	14.1	14.3	14.2	13.9

*Spectra of all samples were obtained in acetone – acetone-d_6 solution.

isolation of 1-ethyl 4-nitrophthalate, its complete reduction to the amino derivative, and the spectra of the nitro and the amino derivatives, however, greatly aided the spectral analysis.

The spectrum of **2** can be readily interpreted. Since the effect of the nitro group on the shielding of aromatic ring carbons is known (1), ring carbon shifts for **2** could be calculated from the data for phthalic acid. The calculated values are in good agreement with the experimental results. The doublet at the lowest field in the spectrum is assigned to the two carbonyl carbons.

Published chemical shift data for carbonyl compounds that are pertinent to the present work are the results on acetophenones (2), in which the shielding of carbonyl carbon is practically insensitive to the substituents in the *para* and *meta* positions. In general, our results concur with this observation. In the present case, however, the shielding of carbonyl carbons is shifted more, due to the nitro group, than in the *para* and the *meta* nitroacetophenones.

The assignments of a particular shielding to a specific ring nucleus in **3** is straightforward by comparison with 4NPAC. However, an interesting aspect of the spectrum is the near equality of the shieldings of carbonyl carbons in the acid and the ester function in acetone. This equality is probably due to the solute–solvent interactions. Normally, the shieldings of ester and acid carbonyl carbons are separated by about 7 ppm (3, 4). To understand this feature, we prepared (5) and examined the spectrum of monoethyl phthalate. This ethyl phthalate is soluble both in chloroform and acetone, whereas the nitro derivative is sparingly soluble in $CHCl_3$.

The carbon-13 spectrum of monoethyl phthalate in $CDCl_3$ has been reported (6) and the chemical shifts for the acid and the ester carbonyl carbons are 172.3 and 168.2 ppm, respectively. This is in agreement with our results. In acetone, the shielding of the acid carbonyl carbon is shifted upfield to 169.3 ppm; however, the carbonyl carbon of the ester group is practically unchanged. The shielding of the carbonyl carbon of an acid is shifted upfield as it is diluted in an aprotic or protic solvent. This is due to the disruption of the dimeric species of the acid by the rupture of hydrogen bonds. The upfield shift is substantial in an aprotic solvent and marginal in a protic solvent since, in the latter medium, the ruptured hydrogen bonds are replaced by weaker hydrogen bonds via interaction with the solvent molecules (7). Based on this analysis, it is expected that the shielding of the acid carbonyl carbon of ethyl nitrophthalate in acetone will be at a higher field than in hydrogen bonded acids. Therefore, the resonances of the acid and the ester carbonyl carbons are close to each other. The elimination of hydrogen bonding, in addition to the shielding effect, narrows the resonance absorption. Therefore, specific assignment of chemical shifts to individual carbonyl carbons has not been possible.

The partial ^{13}C spectrum of the reaction products of esterification of 4NPAC is shown in Fig. 2. The spectrum has extraneous peaks due to unconverted 4NPAC which are disregarded. The remaining spectrum suggests that the reaction product is a mixture of two structurally similar ethyl esters. Due to the strategic location of the nitro group, it is expected that the esterification should result in the two isomeric half-esters (8). This is substantiated by the ^{13}C spectrum. As a first step in the analysis of the spectrum, protonated ring carbon resonances of equal intensity were grouped together. By comparison with the spectrum of **3**, one group (peaks at 125.0, 127.1, and 130.7 ppm) is due to the presence of the 1-ethyl isomer. It is natural to expect that the other group (peaks at 124.4, 126.6, and 131.2) is due to the presence of the 2-ethyl isomer. The diester is a possibility. However, the sum of the integrated intensity of a peak from each group is equal to the integrated intensity of the methylene resonance at

Can. J. Chem. Downloaded from www.nrcresearchpress.com by 210.87.254.105 on 09/05/12
For personal use only.

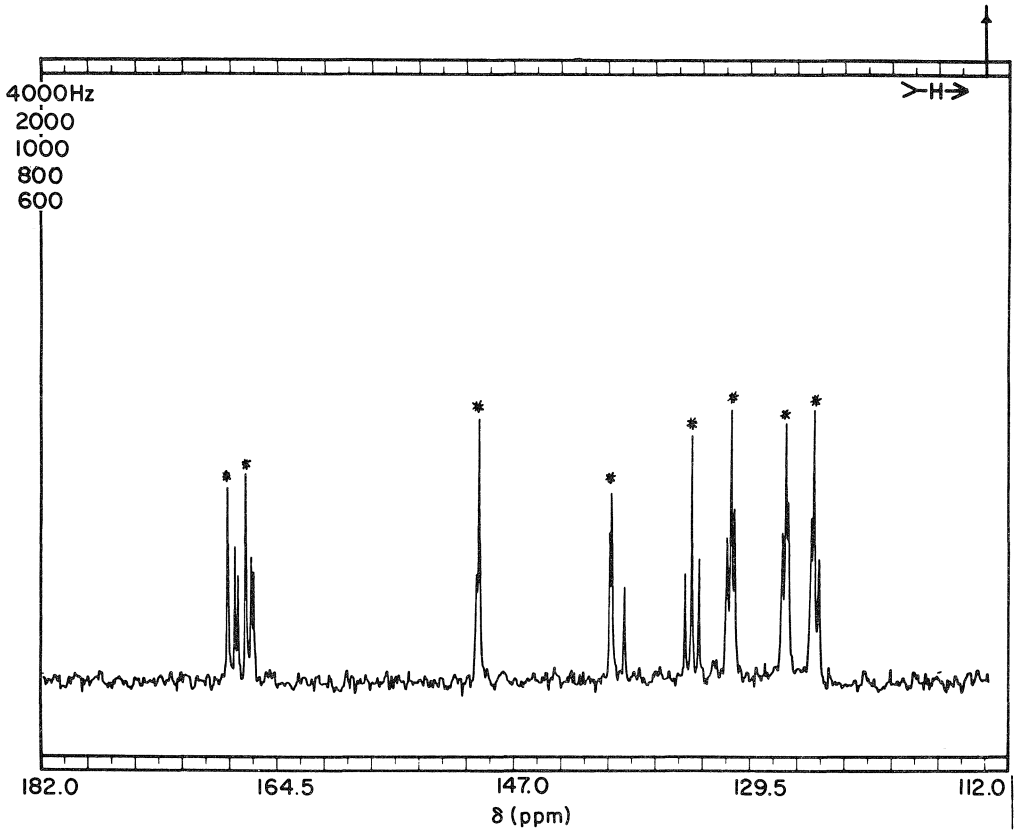


FIG. 2. Proton decoupled ^{13}C spectrum of reaction products of 4NPAC with EtOH. Asterisks indicate absorptions due to the unconverted 4NPAC.

62.7 ppm. Therefore, the reaction product is a mixture of 1-ethyl and 2-ethyl isomers. Their relative concentration is given in Table 2 (entry 2). The shielding of ring carbons in the two isomers differs enough to give well separated peaks, whereas the shielding of the methyl and methylene carbons are identical.

Regarding the quantification of results, all the spectra in this study were obtained with a tip angle of 42°, acquisition time of 1.024 s, and a pulse delay of 10 s. These conditions are adequate for quantitative analysis (9), provided the resonances due to the quaternary centers are neglected. The accuracy of intensity measurement is ±5.0%, with a precision within 1%.

TABLE 2. Percent composition of isomers

Method*	1-Ethyl isomer	2-Ethyl isomer
1	61.5	38.5
2	56.3	43.7
3	55.0	45.0
4	50.0	50.0
5	57.8	42.2

*(1) Alcoholysis of 4-nitrophthalic anhydride (reflux method), (2) esterification of 4-nitrophthalic acid, (3) alcoholysis of 4-nitrophthalic anhydride (room temperature method), (4) Pd/C catalyzed reduction of monoethyl 4-nitrophthalates, (5) Pt_2O catalyzed reduction of monoethyl 4-nitrophthalates.

The alcoholysis of 4NPAN at room temperature and at the boiling point of ethyl alcohol also results in a mixture of half-esters with a slight variation in the product distribution (cf. Table 2, entries 3 and 1).

The catalytic reduction of 4-nitrophthalic anhydride in ethanol could eventually result in the two isomers of monoethyl 4-aminophthalates. The carbon spectrum supports this thesis. The partial spectrum, with Pd/C as the catalyst, is shown in Fig. 3.

Three regions of the spectrum are relevant to the discussion. The resonances around 61 and 14 ppm prove that the esterification has taken place, while the absence of resonance absorptions between 124–127 ppm and the appearance of new signals at a higher field, 113–118 ppm, establishes that the reduction is complete. The reduction of a nitro group to an amino group results in the upfield shift of the three ring carbons, *ortho* and *para* to the amino group.

Can. J. Chem. Downloaded from www.nrcresearchpress.com by 210.87.254.105 on 09/05/12
For personal use only.

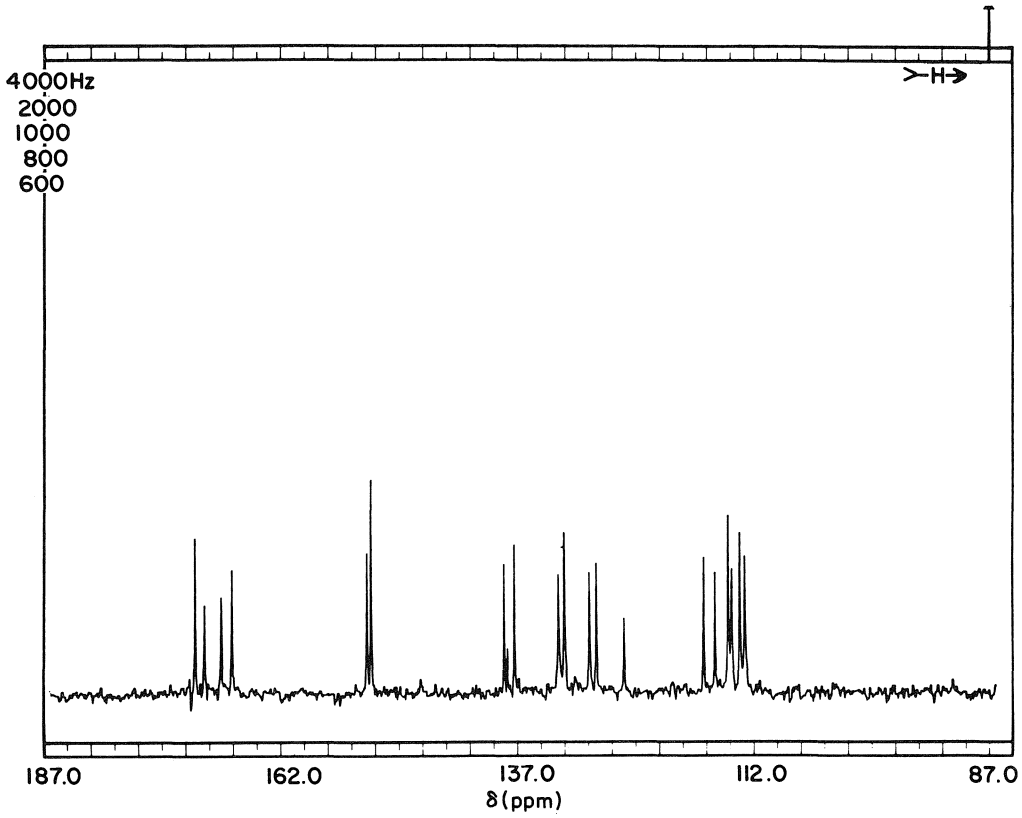


FIG. 3. Proton decoupled ^{13}C spectrum of products from reduction reaction: hydrogen reduction (Pd/C catalyst) of 4NPAN in EtOH.

The spectrum has ten pairs of closely spaced peaks, suggesting that the reaction product is a mixture of two similar compounds. The pair around 61 ppm is due to the methylene carbons. The pair at 132.3 and 132.9 ppm is due to a protonated ring carbon from each structure in the mixture. As before, the sum of the intensities of the pair at 61 ppm is equal to that of the pair around 132 ppm, proving that the two isomers of the half-esters are the products of reduction reaction. Here they are formed in equal amounts (Table 2, entry 4). Pt_2O also catalyses this reaction to give identical products. However, the isomers are formed in a different ratio (Table 2, entry 5).

To assign resonance positions in the spectrum of the reduction reaction product to individual isomers of the aminophthalate, we obtained the 1-ethyl isomer from 1-ethyl 4-nitrophthalate. The reduction of the nitro group to the amino group was accomplished by a process known as *catalytic transfer hydrogenation*, instead of by the conventional method in which hydrogen gas and a metal catalyst are used. Many commonly encountered functional groups, including the nitro group, can be reduced with cyclohexene as the hydrogen donor and Pd/C as the catalyst (10).[2] The spectrum of **5**, thus prepared, was obtained with the same instrumental parameters as the other spectra in this study. It has resonance positions in the expected positions and no extraneous signals are observed. Also, the signals due to the protonated ring carbons, the methylene, and the methyl carbons are of equal intensity. These observations clearly prove that the reduction has proceeded to completion without any side reactions. Since the shielding data are now available for **5**, the data for **6** were obtained from the spectrum of the reduction product mixture.

The unusual shieldings of C-1 and of carbonyl carbons in **5** and **6** prompt the following comments. The electron donating group shields the *para* carbon nuclei in an aromatic structure and the extent of the upfield shift varies with the *para* substituent. For example, in aniline (1), *p*-toluidine (11) and methyl *p*-dimethylaminobenzoate (12), the shifts in

[2]The catalytic transfer hydrogenation procedure described in the literature has been modified by Dr. D. M. Jewell of our laboratory and has been tested using several nitro compounds with complete success. We are extremely grateful to Dr. Jewell for preparing for us the amino isomer from the nitro isomer.

Can. J. Chem. Downloaded from www.nrcresearchpress.com by 210.87.254.105 on 09/05/12
For personal use only.

Can. J. Chem. Downloaded from www.nrcresearchpress.com by 210.87.254.105 on 09/05/12
For personal use only.

the shielding of *para* carbon by the NH_2 group are −10.3, −9.5, and −13.6, respectively. In **5** and **6** compared to **7** the shifts are −16.4 and −17.5, respectively. The larger shifts observed may be due to the electronic interaction of the carbonyl group bound to C-1 with the lone pair of electrons of the *para* NH_2. Such interaction is supported by the significant differences in the shielding of the two carbonyl carbons in **5** or **6** when compared with **3** or **4**.

Experimental

Isolation of 1-Ethyl Hydrogen 4-Nitrophthalate

Five grams of the mixture of isomeric monoethyl 4-nitrophthalates (mp 95–105°C), prepared from 4-nitrophthalic anhydride at room temperature, and water (100 mL), were heated with stirring in a 50°C water bath for 1 h. The resulting mixture was vacuum filtered without cooling to separate 3.45 g of insoluble material, mp 104–109°C (after vacuum oven drying at 50°C). Upon cooling to room temperature over 1 h, the filtrate yielded fine, needlelike crystals which were separated and dried. The melting point of the isolated crystals (0.3 g, 126–129°C) was in good agreement with the literature value (8) (127–128°C) for 1-ethyl 4-nitrophthalate. After standing for several days at room temperature, the filtrate yielded a second crop of less well-formed crystals which were separated and dried (0.4 g, mp 104–125°C). The 2-ethyl isomer has a melting point of 137°C (8), which further substantiates that this procedure isolates the 1-ethyl isomer.

Synthesis of 4-Nitrophthalic Anhydride

This compound was prepared from 4-nitrophthalic acid (Eastman Kodak Co., No. 3112) via azeotropic dehydration (13). The quality of the product, a very pale yellow powder, mp 118–119°C (lit. (14) mp 117–119°C), was established by titration with 0.10 *N* aqueous NaOH.

Esterification of 4-Nitrophthalic Acid

4-Nitrophthalic acid (21.1 g, 0.1 mol) and anhydrous ethanol were refluxed with stirring under nitrogen for 30 h. The solvent was then removed on a Rotavap and the solid yellow residue (22.7 g) dissolved in 10% aqueous sodium carbonate (100 mL). This solution was extracted with diethyl ether and then reacidified with 3 *N* aqueous HCl. This resulted in an insoluble oil which solidified upon chilling. The solid was then separated by vacuum filtration, washed with cold water, and dried in an unheated vacuum oven, giving 21.8 g of yellow solid, mp 144–149°C.

Alcoholysis of 4-Nitrophthalic Anhydride at Reflux

4-Nitrophthalic anhydride (19.3 g, 0.1 mol) and absolute ethanol (300 mL) were refluxed with stirring under nitrogen for 24 h. After evaporation on a Rotavap, a granular yellow solid (23.9 g) resulted. The solid was slurry washed twice with 100 mL portions of hexane and thoroughly evaporated in an unheated vacuum oven, giving 23.3 g (97.5%) of monoethyl 4-nitrophthalates, a very pale yellow powder, mp 95–110°C.

Alcoholysis of 4-Nitrophthalic Anhydride at Room Temperature

4-Nitrophthalic anhydride (19.3 g, 0.1 mol) was dissolved in absolute ethanol (300 mL) by stirring at room temperature for about 1 h. This solution was then evaporated on a Rotavap for several hours; the resulting crystalline residue was treated as above. This resulted in 22.8 g (95%) of monoethyl 4-nitrophthalate, mp 95–105°C. The material was characterized by titration (0.5 g sample dissolved in a mixture of water–ethanol: 100:50 mL) with 0.2 *N* aqueous NaOH (*Equiv. Wt.* calcd.: 239.2; found: 237.2).

Pd/C Catalyzed Reduction of Monoethyl 4-Nitrophthalates

4-Nitrophthalic anhydride (1.93 g, 0.1 mol) was dissolved in absolute ethanol (100 mL) in a 300 mL heavy walled glass vessel. 5% Pd/C (0.015 g) was added and hydrogen pressure (80 psig) was applied to the magnetically stirred mixture. After 0.5 h at 24–26°C, pressure had fallen to 50 psig. The system was repressured with hydrogen, and after 5 h the pressure had fallen to 70 psig. The system was again repressured and the reduction allowed to run overnight. During the 18 h period, an additional 8 psig of hydrogen was absorbed. The catalyst was separated by vacuum filtration, and the product solution stripped of solvent on a Rotavap. Ethanol was completely removed by slurrying the residue twice with toluene and reevaporating and then holding the final residue overnight in an unheated vacuum oven under a slight nitrogen stream. This resulted in 1.8 g (86% yield) of monoethyl 4-aminophthalates (yellow powder), mp 114–123°C.

PtO_2 Catalyzed Reduction of Monoethyl 4-Nitrophthalates

4-Nitrophthalic anhydride (2.42 g, 0.0125 mol) was dissolved in absolute ethanol (100 mL) in a 300 mL heavy walled glass vessel. Platinum oxide (0.2 g) was added and a hydrogen pressure (60 psig) applied to the magnetically stirred mixture. Hydrogen absorption was rapid. The temperature rose from 27 to 40°C despite air cooling of the reaction vessel. After about 3 min, pressure stabilized at 41 psig. The system was repressured with hydrogen. After about 4 h at 26°C, only 6 psig of additional hydrogen was absorbed.

The product mixture was worked up as in the previous example. This resulted in 2.3 g (88% yield) of monoethyl 4-aminophthalates (yellow powder), mp 107–120°C.

Spectra

Carbon-13 nuclear magnetic resonance spectra, were obtained by the pulsed Fourier transform technique at 20.0 MHz on a Varian CFT-20 spectrometer.

Samples were studied in acetone – acetone-d_6 solutions containing a few drops of TMS and all chemical shifts are expressed in ppm downfield from TMS.

1. H. Spiesecke and W. G. Schneider. J. Chem. Phys. **35**, 731 (1961).
2. K. S. Dhami and J. B. Stothers. Can. J. Chem. **43**, 479 (1965).
3. D. H. Marr and J. B. Stothers. Can. J. Chem. **45**, 225 (1967).
4. R. Hagen and J. D. Roberts. J. Am. Chem. Soc. **91**, 4504 (1969).
5. J. F. Goggans, Jr. and J. E. Copenhaver. J. Am. Chem. Soc. **61**, 2909 (1939).
6. Choo-Seng Giam, T. E. Goodwin, and T. K. Yano. J. Chem. Soc. Perkin Trans. II, 831 (1978).
7. G. E. Maciel and D. F. Traficante. J. Am. Chem. Soc. **88**, 220 (1966).
8. I. Heilborn (*Editor*). Dictionary of organic compounds. Vol. III. Oxford University Press, New York. 1953. pp. 772–774.
9. K. S. Seshadri, R. G. Ruberto, D. M. Jewell, and H. P. Malone. Fuel, **75**, 549 (1978).
10. G. Brieger and T. J. Nestrick. Chem. Rev. **74**, 567 (1974).
11. M. J. Shapiro. J. Org. Chem. **43**, 212 (1978).
12. K. S. Dhami and J. B. Stothers. Can. J. Chem. **45**, 233 (1967).
13. J. D. Bacha, J. G. D. Schulz, and A. Onopchenko. J. Org. Chem. **44**, 648 (1979).
14. J. Fernandex-Bolanos, W. G. Overend, A. Sykes, J. C. Tatlow, and E. H. Wiseman. J. Chem. Soc. 4003 (1960).

Photoelectron spectra of substituted acetophenones. Correlations with reactivity

E. J. McAlduff

Department of Chemistry, St. Francis Xavier University, Antigonish, N.S., Canada B2G 1C0

Received September 6, 1979

E. J. McAlduff. Can. J. Chem. **58**, 622 (1980).

Ultraviolet photoelectron spectra of 4-R-acetophenones (R = $N(CH_3)_2$, *t*-Bu, Cl) have been determined and the three lowest ionization potentials assigned. Combination of these data with literature data on other 4-R-acetophenone allows correlations of n_O IP with redox potentials, nmr chemical shifts of acetyl protons, and chemical reactivity data. Both Ph_S and n_O IP's correlate with Hammett σ_P constants of the substituent and Ph_S IP's are found to be linearly related to the first IP's of the analogous monosubstituted benzenes.

E. J. McAlduff. Can. J. Chem. **58**, 622 (1980).

On a déterminé les spectres photoélectroniques ultraviolets de R-4 acétophénones (R = $N(CH_3)_2$, *t*-Bu, Cl) et on a attribué les trois potentiels d'ionisation les plus faibles. Ces données combinées à celles de la littérature relatives à d'autres R-4 acétophénones permettent des corrélations de n_OPI avec les potentiels rédox, les déplacements chimiques en rmn des protons du groupe acétyle et avec les données de réactivité chimique. Il existe une corrélation entre les Ph_S ainsi que les PI_s avec les constantes σ_P de Hammett des substituants et on a trouvé qu'il existe une relation linéaire entre les Ph_S ainsi que les premiers PI's des benzènes monosubstitués analogues.

[Traduit par le journal]

Introduction

Ultraviolet photoelectron spectroscopy provides a method of monitoring the effects of substituents on valence orbital ionization potentials. One of the main empirical approaches to the problem of the effects of substituents on reactivity has been the use of linear free energy correlations. Since substituted benzene systems are prime examples of cases where linear free energy relationships are demonstrated, the photoelectron spectra of substituted benzenes have been extensively studied (1–8). The first ionization energy might be expected to correlate directly with reactivity when electron transfer is involved. Thus satisfactory correlations have been obtained using polarographic oxidation potentials and optical charge transfer absorption bands (9). Correlations have also been observed between rate and ionization potential for H–D exchange in hydrocarbons catalysed by Pt(π) chloro complexes (10).

The photochemical, electrochemical, and chemical reactivity of acetophenones has been thoroughly investigated. Consequently this class of disubstituted benzenes should be a fruitful area for correlations of PES data with chemical reactivity. The three highest occupied molecular orbitals of acetophenone are designated n_O, Ph_S, and Ph_A. n_O is the non-bonding oxygen lone pair orbital. Ph_S is the component of the doubly degnerate e_{1g} of benzene which has maximum electron density at the position of substitution and *para* to it. This orbital is the one whose IP should be most influenced by *para* substituents. The Ph_A orbital is the component of e_{1g} which has a node at the position of substitution and *para* to it and high electron density at the *ortho* and *meta* positions. In theory it should be possible to distinguish between acetophenone reactions occurring at the carbonyl oxygen and those occurring at the phenyl ring in that the former rates should correlate better with n_O IP and the latter with phenyl-type IP's.

The PE spectra of a wide variety of substituted acetophenones have been previously published (3–5). In this investigation the PE spectra of 4-dimethylamino-, 4-*t*-butyl, and 4-chloro acetophenone have been determined in order to complete the series of acetophenones and to make more extensive correlations possible.

Results and Discussion

The PE spectra are shown in Fig. 1 and the vertical IP's and assignments are listed in Table 1.

Electron releasing substituents interact conjugatively with the phenyl e_{1g} orbital via a high lying lone pair orbital to produce an antibonding combination (Ph_S) which is shifted to lower IP and a stabilized level (Ph) which results from the bonding combination of phenyl and lone pair orbital. Generally this Ph level is of sufficiently high IP that it is obscured by the σ bands. When a strong electron releasing group is substituted on benzene as in *N*,*N*-dimethylaniline, the lone pair is sufficiently high lying that the Ph level is well separated from the σ bands. The Ph level is also raised by interaction with a lower lying phenyl orbital (11.5 eV in benzene) and as a consequence the destabilization of Ph_S is not matched by the stabilization of Ph. Thus in *N*,*N*-dimethylaniline the Ph_S and Ph IP's

0008-4042/80/060622-05$01.00/0

©1980 National Research Council of Canada/Conseil national de recherches du Canada

Can. J. Chem. Downloaded from www.nrcresearchpress.com by 210.87.254.6 on 09/05/12
For personal use only.

Can. J. Chem. Downloaded from www.nrcresearchpress.com by 210.87.254.6 on 09/05/12
For personal use only.

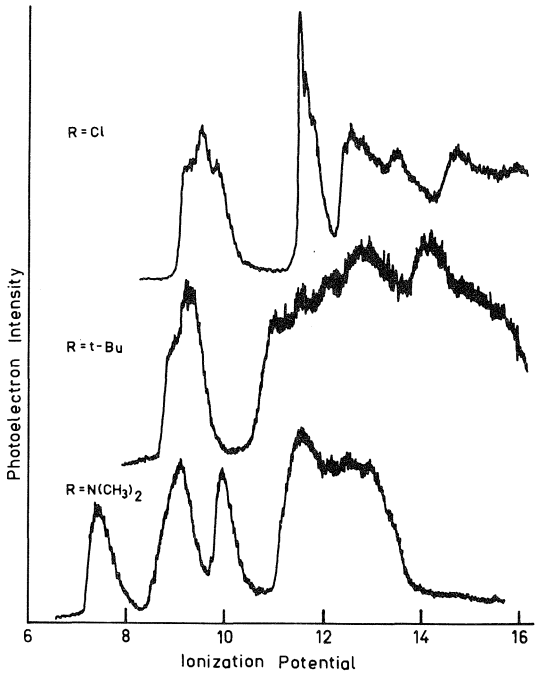


FIG. 1. Photoelectron spectra of 4-R-acetophenones.

TABLE 1. Substituted acetophenone IP's in eV (±0.05) and assignments

	Ph_S	Ph_A	n_O	Other
4-$N(Me)_2$	7.57	9.13	8.85	9.99 Ph
4-*t*-Bu	9.01	9.51	9.25	
4-Cl	9.60	9.90	9.38	11.52 *n*Cl

are located at 7.37 and 9.80 eV respectively (3). An analogous result is observed for 4-$N(Me)_2$-acetophenone in that Ph_S is observed at 7.57 eV and Ph at 9.99 eV which is clearly separated from the σ bands. The broad band at 9.13 eV in 4-$N(CH_3)_2$ acetophenone is assumed to contain ionizations from two levels. The main band at 9.13 eV is assigned to Ph_A which has been destabilized from 9.77 eV in acetophenone (3) whereas the shoulder at 8.85 eV is assigned to the n_O orbital which has decreased from 9.37 eV in acetophenone (3). The change in IP from acetophenone to 4-$N(Me)_2$-acetophenone of 0.64 eV for Ph_A and 0.42 eV for n_O is significantly less than that observed for Ph_S (1.98 eV).

The three bands are no longer resolved in 4-*t*-Bu-acetophenone and the result is a band at 9.25 eV with shoulders on both sides at 9.01 and 9.51 eV. The Ph IP is no longer identifiable since it is masked by the broad σ envelope which begins at 10.6 eV. The central band is assigned to ionization from the n_O orbital and the shoulders at 9.01 and 9.51 are assigned to Ph_S and Ph_A. All three IP's are about 0.1 eV lower than those observed for 4-Me acetophenone (3). This is analogous to the effect observed when the IP's of toluene (3) and *t*-butylbenzene are compared (6).

For 4-Cl acetophenone the PE spectrum shows a broad band centred at 9.60 eV with shoulders on both sides at 9.38 and 9.90 eV. If the previous order of energy levels were maintained in 4-Cl acetophenone the IP at 9.38 eV would be assigned to Ph_S and that at 9.60 eV to n_O. This assignment does not seem reasonable in that it predicts a change in n_O IP upon Cl substitution of acetophenone to be ~0.2 eV and essentially no change in Ph_S as a result of Cl substitution. In general one would expect Cl substitution on the phenyl ring to produce a larger change in Ph_S IP than in n_O. Furthermore, if this assignment is used, it predicts a destabilizing of Ph_S upon Cl substitution from 9.55 in acetophenone to 9.38 which is opposite to the Cl substituent effect observed from benzene to chlorobenzene (9.24 to 9.31 eV) (2). For these reasons a reversal in the order of energy levels is assumed for 4-Cl-acetophenone and the IP at 9.38 eV is assigned to n_O and the main band at 9.60 eV to Ph_S. This assignment is then consistent with the direction and magnitude of substituent effects anticipated if one considers 4-Cl-acetophenone to be formed either by Cl substitution of acetophenone or $COCH_3$ substitution of chlorobenzene. The IP at 9.90 eV in 4-Cl-acetophenone is assigned to Ph_A which represents a stabilization by ~0.2 eV from chlorobenzene or 0.1 eV from acetophenone.

The correlation diagram in Fig. 2 shows the three highest levels of 4-substituted acetophenones using literature data (3, 4) for those acetophenone IP's previously determined. The inversion of levels is assumed to occur at the parent acetophenone and is maintained for Cl and NO_2. If this assignment is correct, it would mean that Br and Cl produce opposite effects on the Ph_S IP of acetophenone with Br destabilizing Ph_S to 9.23 eV and Cl stabilizing Ph_S to 9.60 eV. This phenomenon is not confined to acetophenones, however, and is also present in substituted toluenes (6) where Br destabilizes the toluene IP from 8.85 to 8.71 eV and Cl stabilizes it to 8.90 eV. The correlation diagram in Fig. 2 also suggests that an error has been made in the assignment of 4-Br-acetophenone and the IP at 9.53 eV should be assigned to n_O and the one at 9.8 should be assigned to Ph_A rather than vice versa (4). This is

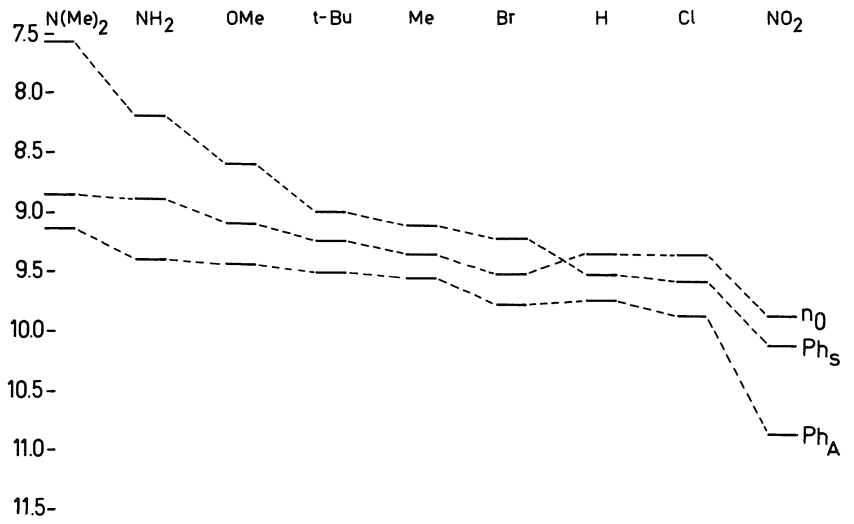


FIG. 2. Correlation diagram of three highest occupied molecular orbitals of 4-R-acetophenones. IP's for R = NH_2, OMe, Br, NO_2 from ref. 4, R = Me, H from ref. 3, R = $N(CH_3)_2$, *t*-Bu, Cl, this work.

the only change made from the literature data in Fig. 2.

Linear relationships, whose slopes are related to electron donor ability of the substituent, have been shown to exist between the first phenyl IP of disubstituted and monosubstituted benzenes (6, 7). A similar relationship, in basic agreement with that of Koenig *et al.* (11), has been shown to exist for substituted acetophenones. Least-squares analysis of this relationship results in the equation

$$IP(Ph_SX\text{-}C_6H_4\text{-}COCH_3) = -0.26 + 1.06\,IP(Ph_SX\text{-}C_6H_4)$$

with a correlation coefficient of 0.988.

Reactivity Correlations

Substituent Constants

Correlations of substituted benzene IP's with substituent constants have frequently been attempted (5, 7, 12). Figure 3 shows a correlation of Ph_S and n_O IP as a function of substituent constant σ_P. (For a comprehensive discussion of Hammett constants see Johnson (13).) σ_P contains a contribution from both inductive and resonance effects and thus should correlate with both Ph_S and n_O IP's. For both n_O and Ph_S, as the electron-withdrawing strength of the substituent increases, the IP increases. Least-squares analysis of the data in Fig. 3 yields the equations

$$Ph_S = 9.15 + 1.53\sigma_P$$

and

$$n_O = 9.36 + 0.65\sigma_P$$

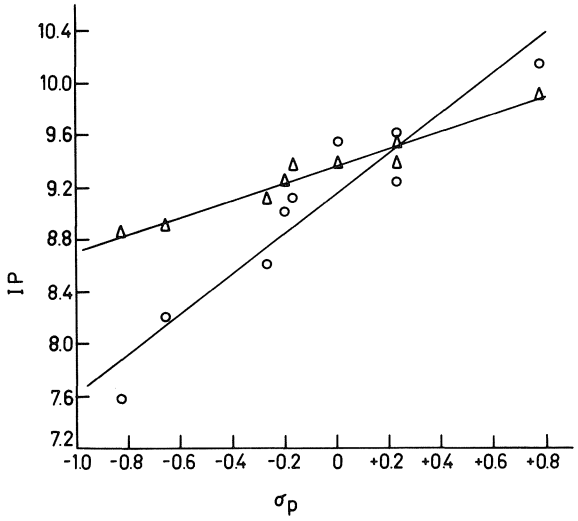


FIG. 3. IP vs. σ_P for 4-R-acetophenones ○ Ph_S, △ n_O.

with correlation coefficients of 0.95 and 0.975 respectively.

Correlations with Redox Potentials

The single configuration formulas for singlet and triplet excitation energies are given by the following equations

$$E_S = E_{HO} - E_{LU} - J_{12} + 2K_{12}$$

$$E_T = E_{HO} - E_{LU} - J_{12}$$

where E_{HO} and E_{LU} are the energies of the highest occupied and lowest vacant orbitals and J_{12} and K_{12} are Coulomb and exchange integrals (14). The lowest gas phase ionization potential gives a measure

Can. J. Chem. Downloaded from www.nrcresearchpress.com by 210.87.254.6 on 09/05/12
For personal use only.

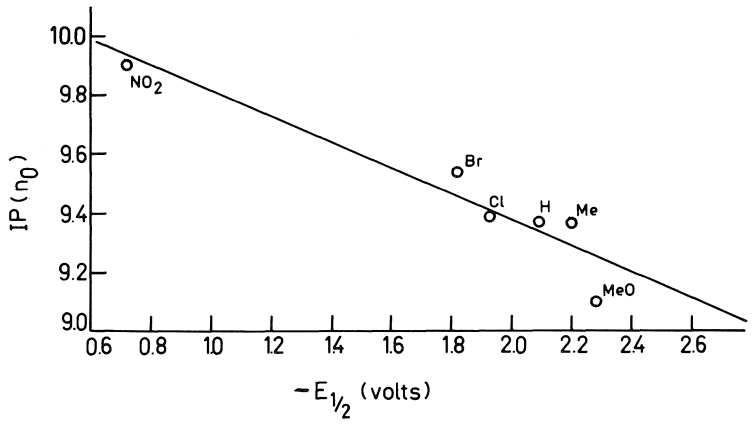


FIG. 4. IP(n_0) vs. $-E_{1/2}$ (reduction potential) for acetophenones.

of the HOMO energy whereas electron affinity data provide information on LUMO energies. In solution, polarographic half-wave reduction potentials ($E_{1/2}^{red}$) and oxidation potentials ($E_{1/2}^{oxid}$) are assumed to be linearly related to the LUMO and HOMO energies respectively. Loutfy and Loutfy (15–18) have obtained linear correlations between the $n \rightarrow \pi^*$ triplet energy and the reduction poential for a wide variety of aromatic ketones. An implicit assumption in these correlations was that the HOMO energy and the Coulomb integral, J_{12}, remained constant throughout the series. Figure 4 shows the results of a correlation between n_0 IP and the negative of the electroreduction potential (15) for a variety of acetophenones. Least-squares analysis of the results leads to the equation

$$IP(n_0) = 10.24 - 0.435(-E_{1/2})$$

with a correlation coefficient of 0.945. The result points out the fact that as the substituent changes both the n orbital energy and the π^* orbital energy, as indicated by the reduction potential, are changing. Thus the linear correlation between the $n \rightarrow \pi^*$ triplet energy and E_{LUMO} or reduction potential must result from changes in E_{HOMO} and J_{12} cancelling each other rather than from constancy in these parameters. The result also suggests that care must be exercised in correlating data from one medium or type of experiment to another since these correlations contain ambiguities which are difficult to quantify.

Chemical Reactivity

Young and Jencks have studied the reversible reaction of bisulfite with substituted acetophenones (19). In that investigation a modified Yukawa–Tsuno equation (20) was used to separate substituent effects into polar and resonance components. When the logarithms of the second order rate constant for attack of sulfite dianion on the carbonyl compound is plotted against the n_0(IP) a linear relationship is obtained for six acetophenones. Least-squares treatment of the data resulted in the equation

$$\log k = -20.96 + 2.45IP$$

with correlation coefficient of 0.96. The stronger electron-withdrawing substituents (high n_0 IP) are observed to produce a faster reaction rate with the anionic species which can be explained in terms of stabilization of the transition state by electron withdrawal.

Similar behavior is observed when one plots the logarithm of the detritiation rate constant (21) for substituted acetophenones vs. n_0(IP). Least-squares analysis of the log k vs. IP(n_0) data yields the equation

$$\log k = -17.60 + 1.64IP(n_0)$$

with a correlation coefficient of 0.95. In the interest of brevity the graphs of log k vs. IP for the rate correlations are not presented.

Correlations with Nuclear Magnetic Resonance Data

Correlations of photoelectron spectra with nmr data have been attempted previously for substituted benzamides (6). If the n_0(IP) of substituted acetophenones is plotted against the chemical shift of acetyl protons in CCl_4 (22) a linear relationship is observed. This is expected since the extent of chemical shift is proportional to the electron density in the region of the acetyl protons and the n_0(IP) is also a function of the acetyl group electron density. It is observed that substituents which act to remove electron density from the acetyl group

Can. J. Chem. Downloaded from www.nrcresearchpress.com by 210.87.254.6 on 09/05/12
For personal use only.

produce both a higher n_O(IP) and a larger acetyl proton chemical shift. Least-squares analysis of the correlation between n_O(IP) and chemical shift yields the equation

$$IP(n_O) = -2.45 + 4.71\delta$$

with a correlation coefficient of 0.97 for seven *para*-substituted acetophenones.

Experimental

Photoelectron spectra were determined on a Perkin-Elmer PS-18 photoelectron spectrometer with heated probe. Xenon and argon were used as internal calibrants and the resolution as measured on the 15.76 eV peak of Ar was 25–30 meV. Peak positions (band maxima) listed in Table 1 represent the average of at least five determinations. The acetophenones were commercial samples and were used without further purification.

Acknowledgments

Financial support by the Natural Sciences and Engineering Research Council of Canada and St. Francis Xavier University Council for Research is acknowledged. The cooperation and assistance of Professor K. N. Houk of Louisiana State University in whose laboratory the photoelectron spectra were determined is also gratefully acknowledged.

1. D. W. Turner, C. Baker, A. D. Baker, and C. R. Brundle. Molecular photoelectron spectroscopy. Wiley Interscience, New York. 1970. Chapts. 10, 11.
2. A. D. Baker, D. P. May, and D. W. Turner. J. Chem. Soc. B, 22 (1968).
3. T. Kobayashi and S. Nagakura. Bull. Chem. Soc. Jpn. **47**, 2563 (1974).
4. R. Egdell, J. C. Green, and C. N. R. Rao. Chem. Phys. Lett. **33**, 600 (1975).
5. C. N. R. Rao. Tetrahedron, **32**, 1561 (1976).
6. E. Nagy-Felsobuki and J. B. Peel. J. Electron Spectrosc. **16**, 397 (1979).
7. E. J. McAlduff, B. M. Lynch, and K. N. Houk. Can. J. Chem. **56**, 495 (1978).
8. E. J. McAlduff and T. Chan. Can. J. Chem. **56**, 2714 (1978).
9. A. Pullman and B. Pullman. Quantum biochemistry. Wiley, London. 1963.
10. R. J. Hodges, D. E. Webster, and P. B. Wells. J. Chem. Soc. Dalton, 2571 (1972); 2577 (1972).
11. T. Koenig, R. Wielosek, L. L. Miller, and Y-H. So. J. Am. Chem. Soc. **99**, 7061 (1977).
12. M. Thompson, P. A. Hewitt, and D. S. Wooliscroft. Handbook of X-ray and ultraviolet photoelectron spectroscopy. Heyden Press, London. 1977. Chapt. 10, p. 349.
13. C. D. Johnson. The Hammett equation. Cambridge University Press, London. 1973.
14. R. Ditchfield, J. E. Del Bene, and J. A. Pople. J. Am. Chem. Soc. **94**, 703 (1972).
15. R. O. Loutfy and R. O. Loutfy. Tetrahedron, **29**, 2251 (1973).
16. R. O. Loutfy and R. O. Loutfy. J. Phys. Chem. **76**, 1650 (1972).
17. R. O. Loutfy and R. O. Loutfy. J. Phys. Chem. **77**, 336 (1973).
18. R. O. Loutfy and R. O. Loutfy. Can. J. Chem. **50**, 4050 (1972).
19. P. R. Young and W. P. Jencks. J. Am. Chem. Soc. **101**, 3288 (1979).
20. Y. Yukawa and Y. Tsuno. Bull. Chem. Soc. Jpn. **32**, 965 (1959); **32**, 971 (1959).
21. D. W. Earls, J. R. Jones, and T. G. Rumney. J. Chem. Soc. Perkin II, 878 (1975).
22. G. A. Caplin. Org. Magn. Reson. **6**, 99 (1974).

Can. J. Chem. Downloaded from www.nrcresearchpress.com by 210.87.254.6 on 09/05/12
For personal use only.

Erratum: A reformulation of the theory of unimolecular reactions

Andrew W. Yau and Huw O. Pritchard
Centre for Research in Experimental Space Science, York University, Downsview, Ont., Canada M3J 1P3

Received January 10, 1980
(Ref: Can. J. Chem. **56**, 1389 (1978))

Five small but substantive errors in this paper have come to our attention:

(*i*) In [14], γ_i should read λ_i.

(*ii*) In eq. [26], κ_{rr} and κ_{ss} should be interchanged in the numerator.

(*iii*) In eq. [42], $\tilde{n}_j$ should read $\tilde{n}_i$.

(*iv*) In Table 2, the value of B_r for C_2H_5NC should be 33.26 cm^{-1}.

(*v*) Dr. J. M. Simmie (Galway) has found that the deposited algorithm yields slightly different answers on different computing machines: the trouble is caused by a ubiquitous mixed-mode FORTRAN operation in the 59th instruction of the program which should read NMAX(I) = 0.5E0*(1.E0/XE(I)−1.E0) + 1.E−4; adding 1×10^{-4} at this point causes all machines to give the correct answers, or subtracting 1×10^{-4} causes all machines to give the answers deposited as a test case with the algorithm.

Determination of oxalate by gas chromatographic measurement of carbon dioxide evolved from the photochemical decomposition of iron(III) oxalate

JEAN M. COOLEY[1] AND B. KRATOCHVIL[2]

Department of Chemistry, University of Alberta, Edmonton, Alta., Canada T6G 2G2

Received September 25, 1979

JEAN M. COOLEY and B. KRATOCHVIL. Can. J. Chem. **58**, 627 (1980).

Oxalate over the range of 0.4 *M* to 1×10^{-5} *M* can be determined with an accuracy of about 2% by injection of sample solutions into a photolytic cell containing an acidic solution of iron(III). Ultraviolet irradiation decomposes the iron(III) oxalate complex to iron(II) and carbon dioxide. The carbon dioxide then is purged from the cell in a stream of helium, dried, separated from other gases on a column of silica gel, and measured with a thermal conductivity detector. Interference from calcium, magnesium, thorium, aluminum, and several carboxylic acids is slight, while that from malonic, citric, formic, and tartaric acids is moderate. Strong ultraviolet absorbing species affect results by reducing the efficiency of photolysis.

JEAN M. COOLEY et B. KRATOCHVIL. Can. J. Chem. **58**, 627 (1980).

On peut déterminer l'oxalate sur une échelle de concentration allant de 0.4 *M* à 1×10^{-5} *M* avec une précision de 2% en injectant des échantillons de solution dans une cellule photolytique contenant une solution acide de fer(III). L'irradiation ultraviolette décompose le complexe oxalate de fer(III) en fer(II) et en bioxyde de carbone. Le bioxyde de carbone est retiré de la cellule en faisant passer un courant d'hélium, puis après séchage, on le sépare des autres gaz sur une colonne de silica gel et on en détermine la quantité à l'aide d'un détecteur à conductivité thermique. Le calcium, le magnésium, le thorium, l'aluminium et plusieurs acides carboxyliques interfèrent faiblement tandis que l'interférence due aux acides malonique, citrique, formique et tartrique est modérée. Les espèces absorbant fortement dans l'ultraviolet affectent les résultats en réduisant l'efficacité de la photolyse.

[Traduit par le journal]

Introduction

The photochemical oxidation–reduction reaction of the iron(III) monooxalate complex,

$$2FeC_2O_4^+ \xrightarrow{h\nu} 2Fe^{2+} + 2CO_2 + C_2O_4^{2-}$$

has been used for the determination of both iron(III) and oxalate. Rao and Aravamudan (1) applied it to the measurement of oxalate by titrating the resultant iron(II) with sodium vanadate. Later, Riggs and Bricker (2) measured the iron(II) by titration with sodium dichromate or, for smaller amounts of oxalate, by spectrophotometric determination with 1,10-phenanthroline. Cooley and Kratochvil (3) determined the carbon dioxide formed by using a CO_2 electrode in a continuous flow system. The advantage of analysis of carbon dioxide is that interferences from substances that reduce iron(III) but do not produce carbon dioxide are avoided. Although the CO_2 electrode has several merits, it is subject to interference from aromatic and low molecular weight carboxylic acids.

Accordingly, a gas chromatographic detector system for carbon dioxide similar to that employed by Swinnerton, Linnenbom, and Cheek (4) was investigated. In the procedure developed the iron(III) monooxalate complex is decomposed photochemically to carbon dioxide in a reaction cell. The carbon dioxide is purged from the cell with a stream of helium and separated from other volatiles on a column of silica gel prior to measurement with a thermal conductivity detector. The method is simple, more sensitive to small amounts of oxalate than the CO_2 electrode method, and relatively insensitive to the sample matrix.

Experimental

Apparatus

As shown in Fig. 1, helium carrier gas flowed through one side of the thermal conductivity cell (GOW-MAC Instrument Co., Model TR 11B), through a four-way stopcock, and into the 2.3- × 8-cm irradiation compartment via a 10- to 20-μm glass frit. For ease of disassembly, polypropylene fittings (Cheminert, Chromatronix, Inc.) were used on the capillary tubing that connected the compartment to the stopcock. A low pressure mercury lamp (Pen Ray, Model 11SC-1, Ultra Violet Products, Inc.) placed in a quartz finger (o.d. 1.5 cm) in the compartment lid provided the necessary ultraviolet radiation. An O-ring joint and No. 35 clamp held the finger assembly in place. In the assembled cell the bottom of the finger nearly touched the frit. In this way the sample solution occupied an annular space around the lamp and thereby was efficiently exposed to radiation. Reagent solutions and samples were introduced and removed with a syringe through a septum near the bottom of the compartment. During use the cell was wrapped in aluminum foil to shield the operator from ultraviolet radiation and to increase the efficiency of the irradiation step.

The gases purged from the cell after radiation passed through the stopcock via 1.6-mm (1/16-in.) stainless steel tubing to a 1- × 30-cm column of 8-mesh calcium sulfate desiccant (Drierite, W. A. Hammond Co.). (A ground-glass joint near one end of the column facilitated replacement of spent drying agent.) The gases were separated on a U-shaped 0.6- × 90-cm column of 40- to

[1]Present address: Syncrude Research, Syncrude Canada Ltd., P.O. Box 5790, Edmonton, Alta., Canada T6C 4G3.

[2]To whom all correspondence should be addressed.

0008-4042/80/060627-04$01.00/0

©1980 National Research Council of Canada/Conseil national de recherches du Canada

Can. J. Chem. Downloaded from www.nrcresearchpress.com by 210.87.254.40 on 09/05/12
For personal use only.

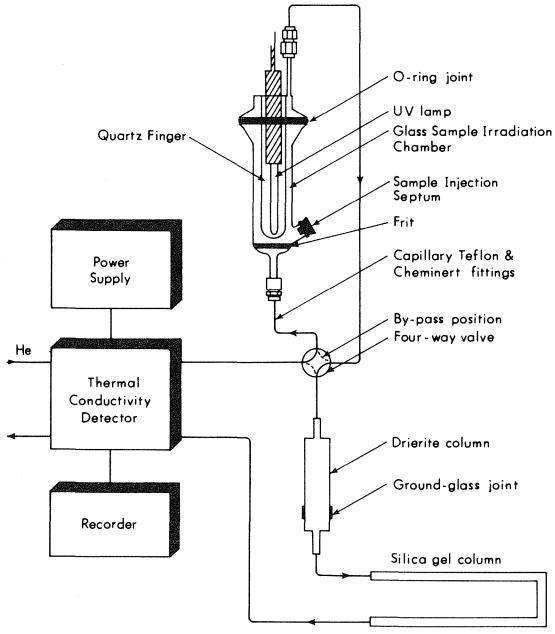


FIG. 1. Apparatus for the determination of oxalate by gas chromatographic measurement of carbon dioxide generated by photolytic decomposition of iron(III) oxalate.

60-mesh silica gel (Fisher) thermostated at 40°C. Connections were Swagelok fittings, 8-mm one-hole silicone rubber stoppers, or Kovar seals. The output of the thermal conductivity detector was monitored with a Hewlett Packard 7101 BM strip chart recorder.

Procedure

A 1-mL portion of a mixture of iron(III) in sulfuric or hydrochloric acid was injected into the assembled compartment. The optimum concentrations depend on the amount of oxalate in the sample (see later discussions). Next, a 5-mL portion of the oxalate sample was injected. A Chaney adaptor on the syringe aided in reproducing sample volumes. The stopcock was then turned so that a stream of helium passed through the frit and purged volatile components, particularly residual carbon dioxide, from the compartment. Purging was continued until the air peak appeared on the recorder. The compartment was then isolated from the helium flow and the sample exposed to ultraviolet light for 5 min; during this time a stream of air was directed over the surface of the uv lamp to provide cooling.

At the end of the irradiation period the stopcock was turned to purge the solution with helium. The gas was directed through the Drierite column, where water vapour was removed, and then through the silica gel column and the detector. Upon completion of each run the solution in the cell was removed through the septum using a needle attached to a length of tubing. Helium pressure from within forced the contents to waste.

Calibration curves were prepared by measurement of solutions of known oxalate concentration. As the peaks were very narrow, peak heights rather than areas were recorded.

Chemicals

Potassium oxalate solutions were prepared in a 0.5 M NaCl – 0.1 M H_2SO_4 matrix. Iron(III) solutions were prepared from sulfate or chloride salts in sulfuric or hydrochloric acid. All chemicals were reagent grade or better and were used as received.

Results and Discussion

Examination of a number of variables in the system was carried out to optimize operating conditions.

Stripping Efficiency

The efficiency of the helium purge for removal of carbon dioxide from the reaction cell was ascertained by comparison of the peak heights obtained from (*1*) injection of sodium bicarbonate solutions into sulfuric acid and (*2*) decomposition of sodium bicarbonate solutions by direct injection into an Aerograph heated inlet (220°C) ahead of the silica gel column. The two procedures gave similar results, showing the helium purge to be a suitable method for removal of carbon dioxide from solutions in the cell.

Helium Flow Rate

For the injection of 5 mL of 1.0×10^{-4} M potassium oxalate into 1 mL of 3.1×10^{-3} M iron(III) ammonium sulfate in 4 M H_2SO_4, the relative standard deviation for four determinations was 5.11% at a flow rate of 143 mL/min, 2.80% at 115 mL/min and 0.87% at 86 mL/min. Although slower flow rates gave improved precision, the time required per determination also increased. Carrier flow rates of about 100 mL/min were generally chosen, allowing a determination to be completed in about 15 min.

Irradiation Time

To determine the optimum irradiation time, a series of measurements was made in which 5-mL portions of a 1.0×10^{-4} M potassium oxalate solution were irradiated in the presence of 1 mL of 1.1×10^{-3} M iron(III) ammonium sulfate in 0.6 M HCl for varying times. Table 1 lists the extent of reaction, assuming a 20-min irradiation time gave 100% conversion of oxalate to carbon dioxide. Since the rate of carbon dioxide evolution is rapid initially, and

TABLE 1. Extent of reaction of iron(III)–oxalate complex as a function of time

Time, min	Extent of reaction, %[a]
0.5	62
1	76
2	83
3	88
6	95
10	98
15	99
20	100

[a]Based on assumption that a 20-min irradiation period gives 100% conversion of oxalate to carbon dioxide. Five mL of 1.0×10^{-4} M potassium oxalate and 1 mL of 1.1×10^{-3} M iron(III) ammonium sulfate in 0.6 M HCl taken for each run.

Can. J. Chem. Downloaded from www.nrcresearchpress.com by 210.87.254.40 on 09/05/12
For personal use only.

Can. J. Chem. Downloaded from www.nrcresearchpress.com by 210.87.254.40 on 09/05/12
For personal use only.

then falls off, 5 min was selected as a compromise between excessive time per determination and sufficient reaction to obtain satisfactory results. A disadvantage of lengthy irradiation is that expansion of the cell contents by warming from the lamp causes a small portion of the solution to be forced through the frit. This problem is minimized by keeping irradiation times short, cooling the lamp and compartment with a stream of air, keeping the volume below the frit to a minimum and placing the stopcock higher than the frit so that the connecting tubing slopes upward.

Effect of Wavelength of Irradiation

In previous work (3) the sample was irradiated by a medium pressure 140-W Hanovia lamp (λ_{max} 366 nm). To assess the effect of radiation wavelength on the reaction, investigation of different low pressure 5.5-W Pen Ray lamps was carried out. The Model 11SC-1 lamp emits most of its radiation at 254 nm, while the Model 11SC-1L contains a fluorescent sleeve and filter that converts the 254 nm radiation to a band peaking at 366 nm. Little difference was observed between the two. The Model 11SC-1 was used for subsequent work because of its greater availability.

Effect of Acid Concentration

The previous studies (3) with a continuous flow system showed that the extent of carbon dioxide production from oxalate increases with increasing pH. These results were confirmed with this system. Examples of the effect of two different concentrations of H_2SO_4 and HCl are shown in Fig. 2. A final acidity of 0.5 *M* or lower appears optimum.

Effect of Iron(III) Concentration

To measure the effect of varying iron(III) concentration, a set of seven solutions 0.6 *M* in HCl and ranging between 0.53 and 5.3×10^{-4} *M* in $FeCl_3$ was prepared. Acidified iron(III) chloride solution (1 mL) and 5 mL of 1.0×10^{-4} *M* potassium oxalate solution were injected into the compartment, and the carbon dioxide production was measured. The optimum ratio of iron(III) to oxalate was found to be between 2:1 and 20:1. A low (2:1) ratio is best for higher oxalate concentrations because high concentrations of iron(III)–chloro species block ultraviolet radiation from reaching the oxalate complex. These optimum iron to oxalate ratios are higher than those measured in the earlier system (3) because the initial purging removes oxygen and prevents in situ oxidation of iron(II) to iron(III).

Similar results were obtained when $FeNH_4(SO_4)_2$ and H_2SO_4 were substituted for the chloride species. The iron(III)–sulfate complexes absorb in the ultraviolet region as strongly as the corresponding iron(III)–chloride species.

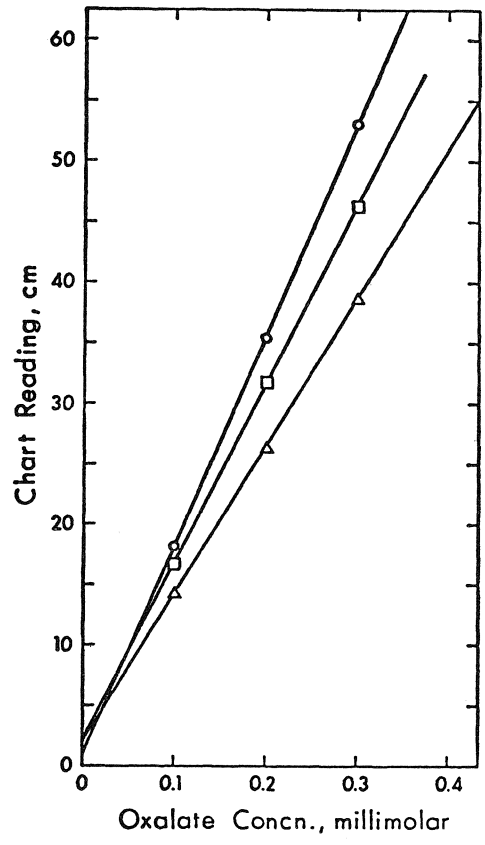


FIG. 2. Effect of concentration of hydrochloric and sulfuric acid on the iron(III)–oxalate reaction: ○, 0.10 *M* H_2SO_4 and HCl; □, 0.70 *M* HCl; △, 0.70 *M* H_2SO_4.

Effect of Metal Ions

A number of ions in addition to iron(III) react with oxalate. To evaluate the level of their interference, solutions of calcium chloride, magnesium chloride, thorium chloride, and potassium aluminum sulfate were added in varying amounts to oxalate samples. Table 2 shows that calcium and magnesium interfere little over the concentration range studied, whereas thorium and aluminum begin to interfere significantly only at concentrations 50 times that of oxalate. Addition of selected chelating agents to samples containing these metals would likely decrease this interference even further.

Effect of Other Carboxylic Acids

Since iron(III) forms complexes with a number of carboxylate anions, their effect on the determination was investigated, with the results shown in Table 3. In general, the absolute error was 10% or less when the ratio of interfering salt to oxalate was

Can. J. Chem. Downloaded from www.nrcresearchpress.com by 210.87.254.40 on 09/05/12
For personal use only.

TABLE 2. Effect of several cations on the determination of oxalate by oxidation with iron(III)

Metal ion	Ratio of metal ion to oxalate[a]	Absolute error, %
Ca^{2+}	0.4:1	< 1
	4:1	< 1
	40:1	< 1
Mg^{2+}	0.5:1	~ 1
	5:1	~ 1
	50:1	~ 1
Th^{4+}	0.5:1	~ 1
	5:1	~ 1
	50:1	9
Al^{3+}	0.5:1	< 1
	5:1	~ 1
	50:1	22

[a]Oxalate added in each run as 2.5 mL of 2.0×10^{-4} *M* potassium oxalate.

TABLE 3. Effect of carboxylate species on determination of oxalate

Carboxylate species added	Ratio of carboxylate species to oxalate[a]	Absolute error, %
Sodium acetate	1:1	0
	10:1	2
	100:1	7
Succinic acid	1:1	2
	10:1	1
	100:1	4
Sodium propionate	1:1	3
	10:1	5
	100:1	2
Malic acid	1:1	7
	10:1	8
	100:1	20
Malonic acid	1:1	2
	10:1	10
	100:1	86
Sodium citrate	1:1	5
	10:1	9
	100:1	60
Sodium formate	1:1	5
	10:1	37
	100:1	49
Potassium sodium tartrate	1:1	6
	10:1	10
	100:1	85

[a]Oxalate added as 2.5 mL of a 2.0×10^{-4} *M* potassium oxalate solution to a reagent solution of 1 mL of 2.1×10^{-3} *M* iron(III) ammonium sulfate in 0.6 *M* H_2SO_4. Each carboxylate species added in 2.5-mL volume.

10 or less. Malonate, citrate, formate, and tartrate interfered more seriously than the other acids. The amount of carbon dioxide produced can be related in a general way to the magnitude of the conditional formation constant between the carboxylic acid and iron(III) (3).

Applicability to the Determination of Oxalate in Urine

Preliminary experiments were performed to assess the possibility of applying the method to the determination of oxalate in urine. Because urine samples absorb strongly in the ultraviolet region, it was found necessary to increase the amount of iron(III) added. Aliquots of individual urine samples spiked with varying amounts of oxalate gave straight-line calibration plots, indicating that the method merits further study.

In summary, the photochemical oxidation of oxalate to carbon dioxide provides a useful method for the determination of oxalate. The system described here has several advantages over the continuous flow system using the CO_2 electrode. It is relatively rapid, does not require expensive equipment, and is subject to fewer interferences than most other methods. Replicate 5-mL portions of solutions containing from 1×10^{-4} *M* to 4×10^{-5} *M* oxalate were analyzed with an accuracy of about 2% and a relative standard deviation of about 0.9%. By use of appropriate concentrations of iron(III), linear calibration curves can be obtained for oxalate concentrations over the range of 0.4 *M* to 1×10^{-5} *M*.

Acknowledgments

Financial support from the National Research Council of Canada and the University of Alberta is gratefully acknowledged.

1. G. G. RAO and G. ARAVAMUDAN. Anal. Chim. Acta, **13**, 415 (1955).
2. W. M. RIGGS and C. E. BRICKER. Anal. Chem. **38**, 897 (1966).
3. J. M. COOLEY and B. KRATOCHVIL. Can. J. Chem. **56**, 2452 (1978).
4. J. W. SWINNERTON, V. J. LINNENBOM, and C. H. CHEEK. Anal. Chem. **34**, 483 (1962).

The conformations of oligosaccharides related to the ABH and Lewis human blood group determinants

R. U. LEMIEUX, K. BOCK,[1] L. T. J. DELBAERE,[2] S. KOTO,[3] AND V. S. RAO[4]

Department of Chemistry, University of Alberta, Edmonton, Alta., Canada T6G 2G2

Received May 25, 1979

R. U. LEMIEUX, K. BOCK, L. T. J. DELBAERE, S. KOTO, and V. S. RAO. Can. J. Chem. **58**, 631 (1980).

Nuclear magnetic resonance properties are shown to be in good accord with those that are expected for synthetic oligosaccharides in the conformations which are predicted by hard-sphere molecular modelling and taking into consideration the important contribution by the *exo*-anomeric effect. The studies involve first a comparison of the βDGal(1→3)βDGlcNAc (Type 1) and βDGal-(1→4)βDGlcNAc (Type 2) disaccharide structures based mainly on ^{13}Cmr and then an examination of the relationships between the calculated conformations and ^{1}Hmr and ^{13}Cmr parameters for human blood group determinants which are derived from the Type 1 core disaccharide. Among the structures examined are the di-, tri-, and tetrasaccharides for the ABH and Lewis antigenic determinants. Certain immunological–conformational relationships are noted.

R. U. LEMIEUX, K. BOCK, L. T. J. DELBAERE, S. KOTO et V. S. RAO. Can. J. Chem. **58**, 631 (1980).

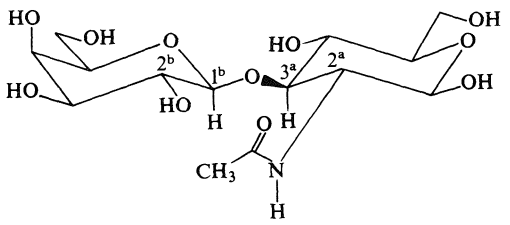
On montre que les propriétés de rmn sont en accord avec celles attendues pour les oligosaccharides synthétiques selon les conformations prévues par les modèles sphériques rigides et en tenant compte de la contribution importante de l'effet anomérique *exo*. Les études impliquent en premier lieu une comparaison des structures des disaccharides βDGal(1→3)βDGlcNAc (type 1) et βDGal(1→4)βDGlcNAc (type 2) basée principalement sur les données de la rmn du ^{13}C et en second lieu l'étude des relations existant entre les conformations calculées et les paramètres de la rmn du ^{1}H et du ^{13}C des déterminants du groupe sanguin humain qui dérivent du noyau disaccharide de type 1. Parmi les structures examinées on trouve le di, tri et tétrasaccharides pour le ABH et les déterminants antigéniques de Lewis. On note certaines relations immunologiques–conformationnelles.

[Traduit par le journal]

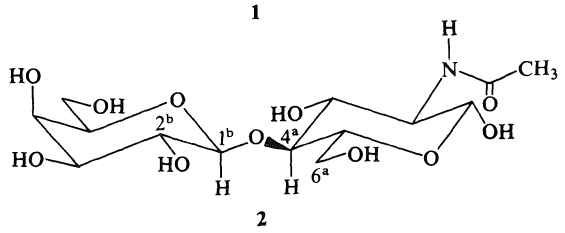
Introduction

Oligosaccharidic structures are present in a variety of natural products and are implicated in a wide range of biological phenomena. An appreciation of the conformational properties of these substances is basic to progress toward a proper understanding of their biological activities especially in terms of their interactions with a wide range of receptor sites. This paper first considers the conformational properties of two disaccharides which serve as building units of a variety of human blood group determinants found at cell surfaces and in body fluids either as glycosphingolipids (1) or blood-group specific glycoproteins (2). The further glycosidation of these structures yields more complete determinants related to the ABH and Lewis blood group systems and the conformational analyses of these structures is then considered.

The Lewis-a (Le^{a}) and -b (Le^{b}) antigenic determinants are derived from the disaccharide *N*-acetyllacto-*N*-biose I (βDGal(1→3)βDGlcNAc) (**1**). The human A and B blood group determinants are



1



2

derived from either this disaccharide or *N*-acetyllactosamine (βDGal(1→4)βDGlcNAc) (**2**). These structures are said to be of Type 1 and Type 2, respectively. The human O blood group is characterized by the H determinant (αLFuc(1→2)-βDGal(1→4)βDGlcNAc) which is the precursor to the Type 2 A and B determinants and which is bound by the lectin *Ulex europaeus* (3). The H (Type 1) determinant (αLFuc(1→2)βDGal(1→3)βDGlcNAc) was recently (4) associated with the Lewis-d activity and will be referred to herein as the Le^{d} determinant. This determinant is not bound by *Ulex europaeus* which agglutinates human H red

[1]Institute of Organic Chemistry, Technical University of Denmark, Building 201, 2800 Lyngby, Denmark.

[2]Department of Biochemistry, University of Alberta, Edmonton, Alta. T6G 2H7.

[3]University of Alberta Postdoctoral Fellow 1972–1974. Present address: School of Pharmaceutical Sciences, Kitasato University, Shirokane, Minato-ku, Tokyo 108, Japan.

[4]University of Alberta Postdoctoral Fellow 1976–1978.

0008-4042/80/060631-23$01.00/0

©1980 National Research Council of Canada/Conseil national de recherches du Canada

Can. J. Chem. Downloaded from www.nrcresearchpress.com by 210.87.254.5 on 09/05/12
For personal use only.

Can. J. Chem. Downloaded from www.nrcresearchpress.com by 210.87.254.5 on 09/05/12
For personal use only.

cells.[5] The Le^d determinant is the immediate biosynthetic precursor of the Le^b determinant. The ABH (Type 2) determinants are related to glycosphingolipids present at the surface of human red blood cells whereas the Type 1 antigens are basically related to epithelial cells but are transported by the serum to red cells (5).

It has become increasingly evident that the receptor sites of antibodies, lectins, and enzymes are not necessarily specific for that sugar unit of an oligosaccharide upon which these act but, instead, may require that structure as substrate which is provided by a substantially larger unit of the oligosaccharide. Paulson and co-workers (6) have recently detected interesting examples. Thus, although a β-D-galactopyranosidase efficiently catalyzed the hydrolysis of the terminal β-D-galactopyranosyl unit of βDGal(1→4)βDGlcNAc-(1→3)βDGal(1→4)βDGlc (lacto-*N*-neotetraose), the enzyme was ineffective for the hydrolysis of βDGal(1→3)-βDGlcNAc(1→3)βDGal(1→4)βDGlc (lacto-*N*-tetraose). Also, whereas the terminal galactosyl unit of lacto-*N*-neotetraose was sialylated by a βDGal-α-(2→6)-sialyl transferase, the isomer was inert. This is not surprising from a chemical structure point of view since the attachment of a glycosyl group to another sugar provides a structure with the atoms in substantially different environments than were present in the individual sugars. Even for a small receptor site, only the very terminal grouping atoms remain in a constant environment. Therefore, an understanding of antibody and enzyme specificities, for example, will require precise information on the preferred conformations for oligosaccharide chains. In general, the conformations of the pyranose rings in the sugar unit can be expected to be those preferred for the sugar as a simple glycoside and this can usually be readily ascertained by nuclear magnetic resonance spectroscopy. Therefore, the conformations of oligosaccharide chains are expected to depend mainly on conformational preferences involving the glycosidic bonds.

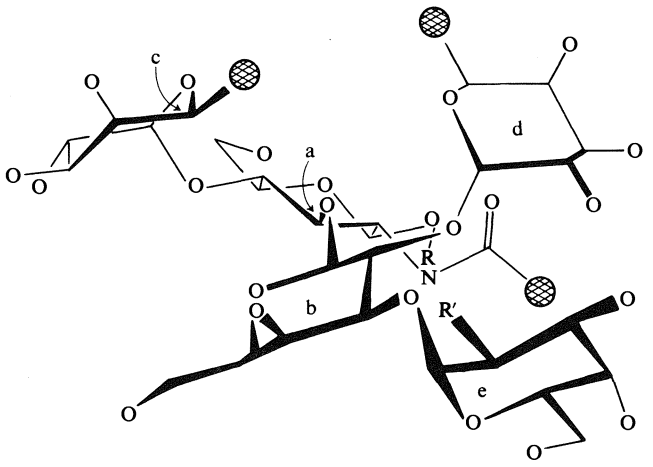
Lemieux and Koto (7) reviewed the earlier literature concerned with the conformational properties of glycosidic linkages including molecular modelling through hard-sphere calculations and the role of the *exo*-anomeric effect (8). At that time, there existed no basis for anticipating the magnitude of the dependence of the *exo*-anomeric effect on torsion angle. Therefore, it was assumed that the torsion angles defined by the aglyconic carbon and the anomeric hydrogen (termed the ϕ^H angle), because of the *exo*-anomeric effect, would be near ±55° and ±50° for α- and β-glycopyranosides (the sign depending on the absolute configuration of the glycoside and with the aglyconic carbon in *syn*-clinal orientation with both the anomeric hydrogen (H-1) and the ring-oxygen (O-5) of the glycosyl group). Their considerations of the preferred conformations for the cyclohexyl α- and β-D-glucopyranosides and derivatives of these compounds by way of substitutions at the 2 and 6 positions of the cyclohexyl ring appeared to substantiate this proposal (7). Furthermore, it became apparent that the "virtual" torsion angle defined by the anomeric and aglyconic hydrogen atoms (by projection through the anomeric and aglyconic carbons) would normally be less than |30°|. Therefore, oligosaccharide structures may be usefully represented by approximate conformational formulas such as those presented above for the βDGal(1→3)βDGlcNAcOR (**1**) and βDGal(1→4)βDGlcNAcOR (**2**) glycosides. Thus presented, the formulas imply that, whereas $O\text{-}2^b$ is in close proximity to $N\text{-}2^a$ in the Type-1 linkage of **1**, this atom ($O\text{-}2^b$) is remote from $N\text{-}2^a$ but near $C\text{-}6^a$ in the Type-2 structure (**2**). An appreciation of both the conformational preferences of such glycosidic linkages and how strongly these are held is the purpose of this communication. The approach in this regard which is used herein is first to estimate the preferred conformations by way of molecular model considerations and then to test the conclusions thereby reached by nuclear magnetic resonance studies. These studies were made possible by the chemical syntheses of the ABH and Lewis related compounds listed in Scheme 1. These syntheses were outlined in a preliminary communication (9) wherein some of the conclusions reached in this paper were briefly presented. The projection formulas in Scheme 1 display the general conclusions reached regarding the Type 1 determinants. The conclusions reached regarding the conformations of the A and B trisaccharides are expected to apply as well to the Type 2 determinants.

It is to be noted that throughout this presentation the various monosaccharide units are specified as units a to e as shown in the formula of Scheme 1. Furthermore, these ring designations will be used to specify φ and ψ torsion angles for the glycosidic bonds and, also, to specify atoms within each unit.

Discussion

The designations for the various torsion angles

[5]Since the submission of this manuscript, it was found (R. U. Lémieux, J. Le Pendu, and O. Hindsgaul. J. Antibiot. In press) that, as expected from considerations of structural analogies, the de-*N*-acetylated form of the Le^d determinant is strongly bound by this lectin.



SCHEME 1. Projected conformational formulas for Type 1 human blood-group related oligosaccharides (R = $(CH_2)_8COOCH_3$, $\phi^b = 50°$, $\psi^b = 20°$, $\phi^c = 55°$, $\psi^c = 25°$, $\phi^d = 40°$, $\psi^d = 20°$, $\phi^e = -70°$, $\psi^e = -60°$).

Structure	Residues
βDGal(1→3)βDGlcNAc (Type 1 core disaccharide, **1**)	a, b
αLFuc(1→4)βDGlcNAc (Le-disaccharide, **14**)	a, c
βDGal(1→3)[αLFuc(1→4)]βDGlcNAc (Le^a-trisaccharide, **15**)	a, b, c
αLFuc(1→2)βDGal(1→3)βDGlcNAc (Le^d-trisaccharide, **16**)	a, b, d
αLFuc(1→2)βDGal(1→3)[αLFuc(1→4)]βDGlcNAc (Le^b-tetrasaccharide, **17**)	a, b, c, d
αLFuc(1→2)βDGal (H-disaccharide, **18**)	b, d
αDGalNAc(1→3)βDGal (A-disaccharide, **19**)	b, e (R′ = NHAc)
αDGal(1→3)βDGal (B-disaccharide, **20**)	b, e (R′ = OH)
αLFuc(1→2)[αDGalNAc(1→3)]βDGal (A-trisaccharide, **21**)	b, d, e (R′ = NHAc)
αLFuc(1→2)[αDGal(1→3)]βDGal (B-trisaccharide, **22**)	b, d, e (R′ = OH
αLFuc(1→2)[αDGalNAc(1→3)]βDGal(1→3)βDGlcNAc (A-tetrasaccharide, **23**)	a, b, d, e (R′ = NHAc)
αLFuc(1→2)[αDGal(1→3)]βDGal(1→3)βDGlcNAc (B-tetrasaccharide, **24**)	a, b, d, e (R′ = OH)

defined by neighboring atoms about a glycosidic linkage in terms of ϕ and ψ angles used herein are those proposed by Lemieux and Koto (7), except that in this communication the use of ϕ and ψ will infer ϕ^H and ψ^H, respectively. Also, the same general procedure was used for the hardsphere calculations; namely, that recommended by Venkatachalam and Ramachandran (10).

In order to program the hard-sphere calculations, it was necessary to prepare the three-dimensional models for the individual sugar units by using atomic parameters provided by X-ray crystallographic structures. Since neither the crystal structure for compound **1** nor that for **2** was available, the parameters used were derived from those reported for 4-*N*-(2-acetamido-2-deoxy-β-D-glucopyranosyl)-L-aspargine trihydrate (11) and lactose hydrate (12). The coordinates for the β-D-galactopyranosyl group were taken from this latter structure rather than those reported for methyl 6-*O*-acetyl-β-D-galactopyranoside (13) because the group, as in structures **1** and **2**, is the non-reducing unit of a disaccharide and, also, the crystal structure was more highly resolved. In these and all other calculations involving the acetamido group, the group was placed in that orientation wherein the vicinal C═O and C—N bonds are eclipsed. As previously done by Rees and Skerrett (14), all the calculations reported herein were simplified by treating the hexose units as 6-deoxyhexose structures.

This paper also deals with a variety of structures related to the AB and Lewis human blood group determinants which contain αDGalNAc, αDGal, and αLFuc residues. The atomic parameters for these units were derived from those reported for 2-acetamido-2-deoxy-α-D-galactopyranose (15) and methyl α-D-galactopyranoside (16). The atomic parameters for the α-L-fucopyranoside units were synthesized by inversion of those reported for methyl α-D-galactopyranoside rather than using the less precise data reported for α-L-fucopyranose (17, 18).

It is expected that crystal field forces can

Can. J. Chem. Downloaded from www.nrcresearchpress.com by 210.87.254.5 on 09/05/12
For personal use only.

Can. J. Chem. Downloaded from www.nrcresearchpress.com by 210.87.254.5 on 09/05/12
For personal use only.

influence bond lengths and valence angles so that appreciable changes may occur when the compound leaves the crystal to enter into aqueous solution. Such effects are assumed to be negligible except for atoms which interact about the glycosidic bond. Bond lengths are expected to remain essentially constant except as influenced by changes in the ϕ angle as a consequence of the *exo*-anomeric effect (8, 19). Substantial changes in bond angles appeared more likely. Therefore, tests were made in an attempt to gauge the influence such changes have on the interaction energies provided by the hard-sphere calculations. The tests indicated that $\pm 2\%$ changes in bond lengths have negligible influence. However, $\pm 2\%$ changes in valence bond angles had appreciable effects on the calculated total interaction energy. In extreme cases the effect was up to near 0.8 kcal/mol. However, the influence on torsion angles appeared negligible within the range ($\pm 5°$) which was arbitrarily set for this study. As a consequence of these tests, it was decided to attach significance to energy calculations that differed by more than ± 0.5 kcal/mol. However, it must be stressed that these assumptions are made solely to provide a basis for the hard-sphere calculations that is sufficiently rigid to be tested for utility. The goal was to determine whether or not such analyses provided conformations in good general accord with assessments made by other physical methods, especially nuclear magnetic resonance spectroscopy. If so, then justification would be gained for using the method to anticipate conformational preferences for structures in aqueous solution when other methods of analysis are not applicable and thereby assist in studies of structure – biological activity relationships.

A choice of a general value for the valence angle defined by the atoms (C-1^b)—(O-1^b)—(C^a) of the glycosidic bond which is termed the τ angle was made, since this procedure greatly simplified the calculations while appearing to not adversely affect the conclusions reached. The effect of the value of this angle on energy content can be judged from the data plotted in Fig. 1. It is seen that, as previously noted by Sundaralingam (20), changes of τ in the range 113° to 119° with $\psi = 50°$ have little influence on the value of the ψ angle predicted for the lowest energy conformer. This was also the case at other values for ϕ. Since the net attractive interactions remain nearly constant, evidently, the net repulsive interactions diminish with increasing τ angle with the energy contents of more conformers becoming nearly equal. It is apparent from Fig. 1 that any τ value in the range 113° to 119° could serve our

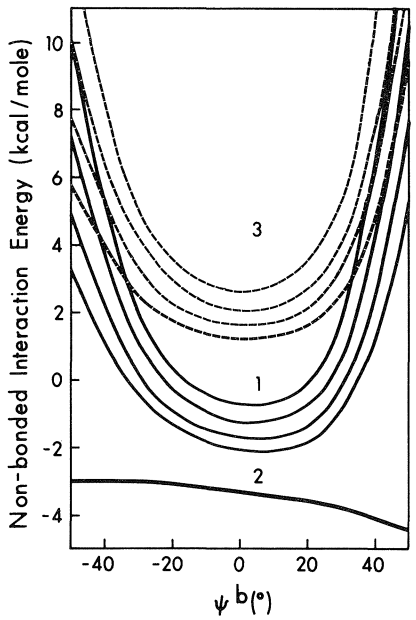


FIG. 1. Changes in non-bonded interaction energies which arise from rotation about the aglyconic bond (change in ψ^b torsion angle) of the βDGal(1→3)βDGlcNAc disaccharide (**1**) with the ϕ^b torsion angle set at 50°. The calculations are reported for τ valence angle values of 113°, 115°, 117°, and 119°. Plots 1 show that the non-bonded interaction energies decrease with increasing τ angle. Plot 2 is a composite curve and shows that the attractive interactions did not change with change in τ angle. Plots 3 display how the repulsive interactions decreased with increasing τ angle.

present purposes. Nevertheless, the specific value of 117° was adopted for all our calculations involving intersugar glycosidic bonds, primarily since this higher value would tend to minimize "hard" repulsive interactions. This is considered desirable since, in a real situation, a "hard" interaction could be effectively avoided by a slight change in the valence angle and the computer program used did not allow for such an adjustment. It may be noted in this regard that the τ values for both α- and β-linked disaccharides in the crystalline state are somewhat larger than 116° (19, 21).

The energy profiles for compounds **1** and **2** obtained by plotting the energy of the most stable conformer (that is, that with the most favorable ψ angle for the given ϕ angle) against the ϕ angle are presented in plots 2 of Fig. 2. It is seen that the minimum energy conformer in both cases is predicted to be that with a ϕ value near 50°. Since the conformations in the range $0 \leq \phi \leq 70°$ all differ in energy by less than one kcal/mol, this approach to the gaining of information on conformational preferences, on its own, would therefore predict a large range of energetically near-equivalent con-

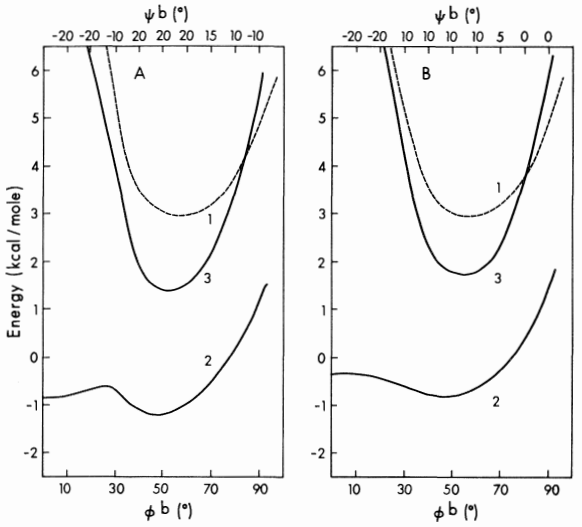


FIG. 2. The changes in energy estimated to occur with changes in the ϕ^b torsion angles; *A*: for the βDGal(1→3)βDGlcNAc disaccharide (**1**); *B*: the βDGal(1→4)βDGlcNAc disaccharide (**2**). Plots 1 display the change in bonding energy attributed to the *exo*-anomeric effect (Table 1). Plots 2 show the change in non-bonded interaction energy, and plots 3 provide the changes in energy content obtained by addition of plots 1 and 2. The ψ^b torsion angles calculated to be the energetically most favorable are provided at 10° intervals of the ϕ^b torsion angle.

formers; that is, conformationally highly flexible structures for these disaccharides. However, the range of energetically near-equivalent conformers was expected (7) to be very substantially restricted for reasons of the *exo*-anomeric effect.

Lemieux *et al.* (8) recently provided further experimental evidence in the support of the *exo*-anomeric effect having a strong influence on the conformational preference for a glycosidic linkage. Furthermore, Jeffrey *et al.* (21) have recently published the potential energy surfaces for internal rotation in dimethoxymethane as derived by *ab initio* molecular orbital calculations and thereby provided an estimate of the change in potential energy that should occur with change in the ϕ torsion angle. As previously expected on theoretical grounds (19), the most favorable value for ϕ is near 60° and the energy rises (because of weakening of the glycosidic bond) as this torsion angle is either increased or decreased from this favorable orientation for the *exo*-anomeric effect. Our procedure then is to add changes in energy expected to arise from changes in the *exo*-anomeric effect to the changes estimated by hard-sphere calculations. It must be stressed at this point that Jeffrey *et al.* (21) did not calculate the shapes for these curves but, instead, only presented possible trends. As presented, the trends provide little energy change in the

TABLE 1. Values for the *exo*-anomeric effect at different ϕ torsion angles[a]

	exo-Anomeric effect, kcal/mol	
ϕ	α-Anomers	β-Anomers
0	8.5	8.7
15	4.8	7.9
30	1.7	4.8
45	0.2	2.8
60	0	2.4
75	0.1	3.0
90	1.3	4.5

[a]Estimated from the plots presented by Jeffrey and co-workers (21).

range 60 ± 15° and, therefore, minimize the influence of the *exo*-anomeric effect in this important region. Nevertheless, we felt that there was no alternative, at this time, than to accept the plots as provided in order to construct our approach for estimating conformational preferences about glycosidic linkages by way of a combination of hard-sphere calculations and values for the *exo*-anomeric effect. These latter values are presented in Table 1 and are taken from the plots provided by Jeffrey *et al.* (21)[6].

For convenience, we propose to designate this approach for the calculation of conformational preferences about glycosidic linkages as the HSEA (hard-sphere, *exo*-anomeric) method.

As seen in Fig. 2, the coupling of the hard-sphere calculations with the *exo*-anomeric effect provides potential energy curves (plots 3) for the disaccharides **1** and **2** which indicate that the glycosidic linkages possess ϕ angles in the range 40° to 60°. We conclude, therefore, that the glycosidic linkages for these compounds in aqueous solution largely adopt conformations in this range and that the weighted average of this conformer population will be well represented by the mid-way conformer with ϕ = 50°. It must be noted in this regard that the procedure involves no effort to judge the influence of either dipole–dipole interactions or of the solvent water. Kitaygorodsky, whose expressions (22) for the calculation of the non-bonded interactions are used in the hard-sphere calculations, has recently reviewed (23) these limitations. We entertain the primitive approach used herein because, as will be seen, the procedure provided conformations for the

[6]A copy of the computer programs, both listings and writeups, used in the hard-sphere calculations is available, at a nominal charge, from the Depository of Unpublished Data, CISTI, National Research Council of Canada, Ottawa, Ont., Canada K1A 0S2.

Can. J. Chem. Downloaded from www.nrcresearchpress.com by 210.87.254.5 on 09/05/12
For personal use only.

Can. J. Chem. Downloaded from www.nrcresearchpress.com by 210.87.254.5 on 09/05/12
For personal use only.

structures examined in this investigation that proved well substantiated by their nuclear magnetic resonance properties. In other words, we expect that more sophisticated approaches such as force-field calculations (24) will be developed but that such developments will require theoretical insights on such matters as dipole–dipole interactions, possible intramolecular hydrogen bonding effects, and solvation which are not, to our knowledge, presently available. Under such circumstances, we see little alternative than to use the simplest possible approach and to be ready to adjust this approach as likely will be required by future experimental findings. The pertinent question at this point is to ask why do the simple HSEA calculations used herein appear to provide useful approximations to the conformational properties of these oligosaccharides in aqueous solution. That is, it may prove, in fact, that the *exo*-anomeric effect and non-bonded interactions about the glycosidic bond dominate over other possible effects on conformational preference to such an extent that other influences are, to a useful first approximation, negligible. As will be seen, the agreement between the calculated structures and those inferred by the nuclear magnetic resonance studies appear too good in too many circumstances to be merely fortuitous and the communication of these findings is the main purpose of this paper.

In the following discussions, the conformational preference for a glycosidic linkage is expressed in terms of a single conformer. It must be understood in this regard that the intention is simply to indicate what may comprise the most highly populated conformer within a range of conformers in the well of the potential energy surface. The nuclear magnetic resonance parameters reflect a weighted average of these conformers and it is this conformer which is expected to coincide with that anticipated by the HSEA method.

The most favorable ψ angles provided in Fig. 2 were obtained from ψ energy profiles such as those plotted in Fig. 3 for the $\phi = 50°$ conformers for **1** and **2**. It is seen that rather broad energy wells are obtained so considerable conformational flexibility may also be expressed by rotation about the aglyconic bonds. These curves, as was discussed above with regard to Fig. 1 can be somewhat "sharpened" by decreasing the τ angle in order to "harden" the interactions. However, this did not alter the conclusion reached that the "best" conformations for the disaccharides **1** and **2** appear to be those with $\phi = 50°, \psi = 20°$ and $\phi = 50°, \psi = 10°$, respectively. These conformations display that, although the constituent sugars are the same, the

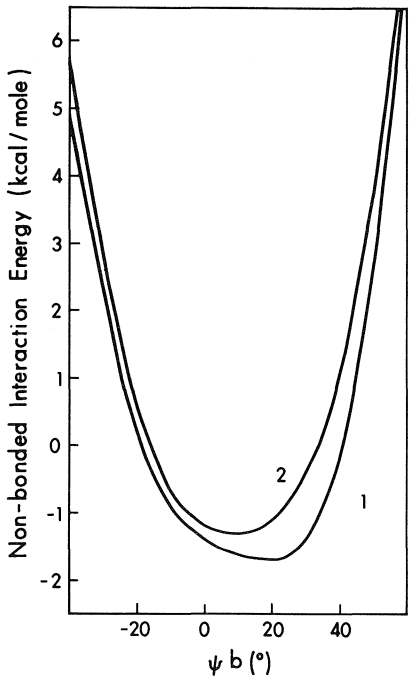


FIG. 3. Changes in non-bonded interaction energy which result from changes in the ψ^b torsion angles and keeping the ϕ^b torsion angles at the values (50° in each case; see Fig. 2) which are expected to be energetically most favorable. Plot 1 is for the βDGal(1→3)βDGlcNAc disaccharide (**1**) and plot 2 is for the βDGal(1→4)βDGlcNAc isomer (**2**).

two structures are stereochemically very different except in the immediate environment of C-4′ of the β-D-galactopyranosyl groups and, therefore, must be expected to possess significantly different immunological properties. Also, the near environments of the O-2′ atoms of the βDGal residues of **1** and **2** are sufficiently different that it seems improbable (9) that, as is commonly assumed, it is the same α-L-fucosyl transferase that converts **1** and **2** to the Le^d and H determinants, respectively. Furthermore, the αLFuc residues in these determinants are in such substantially different environments that anti-Le^d antibodies may react only very weakly if at all with the H-determinant and vice versa. As was noted above, the lectin *Ulex europaeus* combines with the H (Type 2) determinant, but is not appreciably bound by the Le^d (Type 1) determinant (3).

In order to gain experimental evidence for the conformations of the disaccharides **1** and **2** that are indicated by the plots 1 of Fig. 2, the ^1H- and ^{13}Cmr spectra of these compounds were examined as glycosides of 8-methoxycarbonyloctanol. All of the complex glycosides that were examined have this aglycon since the synthesis of such structures provides a linking arm for the preparation of artificial

TABLE 2. ^{13}Cmr chemical shifts[a] for the Type 1 (**1**) and Type 2 (**2**) disaccharides and related structures

Compound		1^b	Δ	2^b	3^b	Δ	1^a	Δ	2^a	3^a	Δ	4^a	Δ	5^a
βDGalOCH$_3$ (**9**)		104.6	—	71.6	73.7	—	—	—	—	—	—	—	—	
βDGlcNAcOR (**8**)							101.9	—	56.5	74.7	—	70.9	—	76.7
βDGal(1 → 3)βDGlcNAcOR (**1**)		104.3	—	71.6	73.4	—	101.7	—	55.5	83.4	8.7	69.7	—	76.2
βDGal(1 → 4)βDGlcNAcOR (**2**)		103.8	—	71.8	73.4	—	101.9	—	56.0	73.3	—	79.6	8.7	75.6
βDGlcNOR′ (**7**)	Base	—	—	—	—	—	104.3	4.9	57.0	76.5	4.3	70.2	—	76.0
	Salt	—	—	—	—	—	99.4		56.1	72.2		70.1	—	76.9
βDGal(1 → 3)βDGlcNOR′ (**6**)	Base	103.5	0.4	71.4	72.9	0.1	104.3	5.3	56.2	86.7	5.6	68.7	—	76.1
	Salt	103.1		71.2	72.8		99.0		55.1	81.1		68.8	—	76.4
βDGlcN(1 → 3)βDGlcNOR′ (*3a*)	Base	103.8	7.1	57.5	77.1	4.5	104.5	4.1	56.4	86.7	9.1	69.0	—	76.4
	Salt	96.7[b]		55.5	72.6		100.4		55.6	77.6		68.0	—	77.3
βDGlcN(1 → 4)βDGlcNOR′ (**4**)	Base	103.3	5.2	57.0	76.5	4.4	103.9	4.8	56.6	74.4	4.3	78.9	—	76.0
	Salt	98.1		56.3	72.1		99.1		55.9	70.1		77.1	—	76.3

[a]In D_2O at 300 K with 1% dioxane, δ = 67.4 ppm, as internal reference and measured at 67.89 MHz except for compounds **3**, **4**, **6**, and **7** which were measured as previously described (25). R = $(CH_2)_8COOCH_3$ and R′ = CH_2CCl_3. Further nmr parameters are provided for compounds **1**, **8**, and **9** in Tables 3 and 6. For **2**, the chemical shifts (in D_2O relative to 1% acetone, δ = 2.48, as internal reference) assigned to H-1, H-2, H-3, H-4, H-5, H-6, and H-6′, of the βDGlcNAc residue were *4.79*, *3.98*, *3.98*, *3.96*, *3.85*, 4.24, and 4.10 and the corresponding shifts for the βDGal group were assigned to 4.74, 3.82, 3.94, 4.20, *3.99*, 4.06–4.00 ppm. The proton chemical shifts in italics were assigned from the ^{13}Cmr spectra by selective proton irradiation and are considered accurate to ± 0.02 ppm. The other shifts are within ± 0.005 ppm. Using the same ordering of positions, the chemical shifts (± 0.02 ppm) assigned to the carbon atoms were 101.85, 56.02, 73.30, 79.59, 75.60, 61.05 and 103.78, 71.84, 73.44, 69.41, 76.19, 61.83 ppm.

[b]This signal was previously erroneously assigned (25). Contrary to the previous conclusion, both C-3[a] and C-1[b] are strongly shielded on protonation of the amino groups; nmr parameters for *3a* and the closely related compound *3b* (R′ = CH_3) are presented in Table 4.

TABLE 3. Coupling constants for reference glycopyranosides[a]

Compound	Coupling constant, Hz						
	$J_{1,2}$	$J_{2,3}$	$J_{3,4}$	$J_{4,5}$	$J_{5,6}$	$J_{5,6'}$	$J_{6,6'}$
Methyl 2-*N*-acetamido-2-deoxy-β-D-glucopyranoside	8.4	9.6	9.2	9.2	1.6	4.8	12.0
8-Methoxycarbonyloctyl 2-*N*-acetamido-2-deoxy-β-D-glucopyranoside (**8**)	8.0	10.0	—	—	1.6	—	12.0
Methyl β-D-galactopyranoside (**9**)	8.0	10.0	3.8	0.8	7.6	4.4	11.2
8-Methoxycarbonyloctyl β-D-galactopyranoside (**11**)	8.0	10.0	3.6	0.8	7.2	4.8	11.2
Methyl α-L-fucopyranoside (**10**)	2.8	—	—	1.0	6.3	—	—
Methyl 2-*N*-acetamido-2-deoxy-α-D-galactopyranoside (**12**)	3.6	10.8	3.2	0.8	6.0	6.0	—
Methyl α-D-galactopyranoside (**13**)	2.8	10.0	2.7	1.0	6.4	6.4	—

[a]Measured under the conditions reported for the ^{1}Hmr spectra in the Experimental and are expected to be within 0.1 Hz. The vicinal coupling constants observed for the oligosaccharides listed in Tables 6–10, when the chemical shift could be determined directly, were in good accord with those listed above for the corresponding glycosyl group.

antigens and immunoadsorbents (9). Inspection of the data presented and referred to in Tables 2 and 6 shows a close correspondence between the ^{13}C- and ^{1}H-chemical shifts found for the βDGal groups of the disaccharides **1** and **2**. Furthermore, these shifts differ little from those found for methyl β-D-galactopyranoside (**9**). The vicinal coupling constants listed in Table 3 require the $^4C_1$ conformation and it is concluded that this conformation is maintained in the oligosaccharides. Because of substitutional effects, the chemical shifts listed in Table 2 for the βDGlcNAc residues of **1** and **2** are not expected to correlate directly with those found for the simple βDGlcNAc glycoside **8**. However, the patterns of the shifts observed are in general accord with expectation and there can be no doubt that these residues are in the $^4C_1$ conformation.

It is seen that the introduction of the βDGal group at C-3 of **8** to form **1** caused an 8.7 ppm deshielding of this atom. This deshielding was also observed at C-4 in the formation of **2**. As will be seen later on, these deshielding effects appear highly sensitive to changes in the hybridization of the atoms about the glycosidic linkage. It is perhaps noteworthy in this regard that the energy calculations presented in Figs. 2 and 3 indicate that the preferred conformations for these two disaccharides possess about the same conformational energy minima and that no

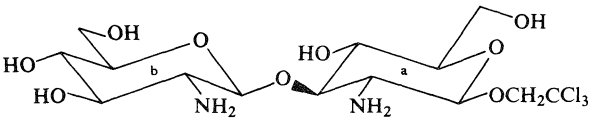
Can. J. Chem. Downloaded from www.nrcresearchpress.com by 210.87.254.5 on 09/05/12
For personal use only.

Can. J. Chem. Downloaded from www.nrcresearchpress.com by 210.87.254.5 on 09/05/12
For personal use only.

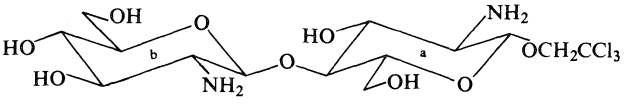
important non-bonded interactions are present in these conformations which could cause appreciable distortion of the glycoside valence angles. The close correspondence of the chemical shifts for H-1^b and C-1^b of the β-D-Gal residues of **1** and **2**, namely 4.69 and 104.33, and 4.74 and 103.78 ppm, respectively, lend support to this contention. These data do not provide evidence in support of the conformational preferences provided by the HSEA calculations. However, these calculations require conformations for **1** and **2** which bring the anomeric and aglyconic hydrogens in near van der Waals contact and, therefore, the selective irradiation of the signal for one of these hydrogens could be expected to cause nuclear Overhauser enhancement of the intensity of the signal for the other hydrogen. With the advent of FT high-field spectrometers, measurements of nuclear Overhauser enhancements can be detected with confidence to within ±2%. Indeed, meaningful enhancement of the signal for H-3^a by 14% was observed on irradiating H-1^b of **1**. Similarly the signal for H-4^a of **2** was enhanced by 12% on irradiation of H-1^b, therefore requiring that the "virtual" torsion angle for these hydrogen atoms be so small as to bring them into contact. On the basis of the HSEA calculations the H-1^b to H-3^a and H-1^b to H-4^a internuclear distances for **1** and **2** are expected to be 2.36 and 2.44 Å, respectively. The internuclear distances for *syn*-axial hydrogens on a β-galacto pyranose ring are 2.53 (H-1 to H-3) and 2.36 Å (H-1 to H-5) and their signals were enhanced by 12–15%.

It seemed possible that further evidence in support of the conformations assigned to **1** and **2** (Fig. 3) could be gained by an nmr study of the disaccharides **3***a* and **4**. That is, it was expected that changes in the substituents at C-2^a from acetamido to amine and at C-2^b from hydroxyl to amine would cause changes in conformational preference of little if any consequence to this work. Also, it was expected that the *gluco* configuration for the nonreducing sugar unit in **3***a* and **4** is conformationally equivalent to the *galacto* configuration present in **1** and **2**. These expectations were supported by hard-sphere calculations.

As would be anticipated, since the acetamido group of **2** is remote from the galactosyl group, hard-sphere calculations showed no influence on conformational preference to result from changing this substituent to an amino group. In the case of compound **1**, with φ set at 50°, the lowest energy conformer for the corresponding amine was estimated to have a ψ angle of 10° rather than the 20° calculated for **1**. Essentially the same results were found for compounds **3***a* and **4**. In this regard, it



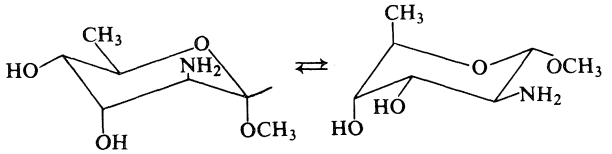
3*a*



4

may be noted that, whereas the β-shift (25) of C-1^b of **4** caused by di-*N*-acetylation was the same (1.4 ppm) as that found on *N*-acetylation of 2,2,2-trichloroethyl 2-amino-deoxy-β-D-glucopyranoside, the β-shift obtained on di-*N*-acetylation of **3***a* was slightly greater (1.0 ppm). As will be seen below, this difference is not necessarily related to more than a very slight change in conformation to result from changing the C-2^b substituent in **1** from $NHCOCH_3$ to NH_2.

Lemieux *et al.* (26) obtained direct evidence for a change in the steric requirement for a free amino group as compared to the protonated form. Thus, for example, whereas the equilibrium constant estimated for the $^4C_1$ (**5***a*) and $^1C_4$ (**5***b*) forms by



5*a* **5***b*

analysis of the ^{1}Hmr spectra of methyl 2-amino-2,6-dideoxy-α-D-altropyranoside was 0.33, in acid media, where the amino groups were protonated, the equilibrium favored the $^1C_4$ conformer (K_e = 4.00). This result can be attributed to the positively charged ammonium group which, because of stronger solvation by water, is more space-demanding than is the neutral amino group. These authors (26) also examined the effect of protonation of the amino groups in compounds **3***a* and **4** on the chemical shifts of the ^{13}C-atoms. As seen in Table 2, the β-shifts (25) observed for **4** are near the 4.5 ± 0.5 ppm values normally observed (27). However, for compound **3***a*, although the shifts observed for C-1^a and C-3^b are in the normal range, the shifts for C-3^a and C-1^b (those carbon atoms involved in the intersugar glycosidic bond) are exceptionally high. This effect must arise in part from the normal β shifts but also as a result of a conformational change. The conformation anticipated for **3***a* by hard-sphere calculation (φ = 50°, ψ = 10°, τ = 117°) has an internuclear distance for N-2^a and N-2^b of

Can. J. Chem. Downloaded from www.nrcresearchpress.com by 210.87.254.5 on 09/05/12
For personal use only.

3.80 Å. Since the N to N distance for solid ammonia is 3.38 Å, then the amino groups in **3***a* may be expected to be separated, on the average, by only about 0.4 Å. Consequently, should protonation of these groups lead to the more space-demanding ammonium groups, then some alteration in conformation should result both for this reason and because an electrostatic repulsion is created between the two positively charged ammonium groups. In these regards, it is to be noted that protonation of the free amino form of **6** (Table 2) caused substantially smaller upfield shifts for C-3^a and C-1^b than those observed for **3***a*. This is as expected since the O-2^b of **6** was not protonated as a result of the change in pH. The shift of 5.6 ppm observed for C-3^a in the case of **6** is large enough to be taken as an indication that the nitrogen atom is in close proximity to an atom (considered to be O-2) in the β-D-galactopyranosyl group. The situation is also seen in the shift of 5.2 ppm observed for C-1^b of the lactosamine analog **4**. In this case, the prognosis is that N-2^b is in close proximity to C-6^a. The chemical shifts for C-2^a, C-4^a, C-5^a, and C-2^b are included in Table 2 to indicate that the protonations did not cause substantial change in the conformations of the pyranose ring since, if so, these atoms would be expected (28), along with C-3^a and C-1^b, to show appreciable shift differences between the free amine and protonated form. This matter has an important bearing on the discussions that follow.

The interaction of the ammonium groups in the protonated form of **3***a* could effect a conformational change either by changes in the ϕ and ψ torsion angles and/or by a change in the τ angle. On the basis of the $\phi = 50°$, $\psi = 10°$, and $\tau = 117°$ model for compound **3***a*, the internuclear H-3^a to H-1^b distance is 2.31 Å. A change of the τ angle to 113° reduces this distance to 2.21 Å whereas a change to 121° increases the distance to 2.41 Å. These changes have, however, little effect on the N-2^a to N-2^b distance which remains within 3.80 ± 0.03 Å. Therefore, an alternate explanation for the abnormally high β-shifts for both C-3^a and C-1^b of **3***a* was sought. The calculations suggested that the energetically most favorable way to achieve a substantial change in the N-2^a and N-2^b distance was by increasing the ϕ angle from 50° to 70°. The changes in non-bonded interactions and the *exo*-anomeric effect that would result would involve a conformational energy gain estimated to be about 0.7 kcal/mol and provide H-3^a to H-1^b and N-2^a to N-2^b distances of 2.51 and 4.39 Å, respectively. Nuclear magnetic resonance evidence in support of this postulate was sought on the basis that accurate measurement of the relaxation contributions between individual protons via the intramolecular dipole–dipole mechanism can be made (29) and can be used to estimate interproton distances within ±0.1 Å.

The T_1-values that could be determined for the ^{1}H and ^{13}C atoms of **3***b* both as the diamine and as the dihydrochloride salt are listed in Table 4. It is seen that the T_1-values for hydrogen atoms at the extremities of the molecules, namely H-1^a, H-6^a, and H-6^b are, within experimental error, the same for the compound in both forms. Therefore it can be assumed that the transformation and the change in medium have not altered appreciably the rates at which the molecules tumble. The ^{13}C-data also support this conclusion. On the basis of the assumption that the *N*-deuteration has not altered the rates of tumbling, the rather considerable changes in T_1 values observed for the more internal H-1^b and H-3^a atoms can be assigned to a change in the conformational preference about the intersugar glycosidic bond. That is, since the measurements were made at high dilution (0.05 *M*) in deuterium oxide and the solutions were free of paramagnetic contributions to the relaxations, it can be expected that these changes are largely the result of changes in the distances of these hydrogen atoms to other hydrogens in the same molecule. In other words, the rate of relaxation ($1/T_1$) may be considered as directly proportional to the sum of the inverse ratios of the various distances between the given hydrogen and all the other hydrogen atoms in the molecule; that is,

$$1/T_1 = C \sum_{i \neq j} r_{ij}^{-6}$$

where *C* is a proportionality constant (30). Using appropriate X-ray crystallographic data to locate the positions of the various hydrogen atoms relative to both H-1^b and H-3^a in compound **3***b* in various conformations, values for these sums can be estimated. The O-6 atoms were placed in *anti*-periplanar orientation to the C-4 atoms in each of the sugar units since this orientation appears preferred in the case of glucopyranosyl groups (31, 32). The values for the sums calculated for H-1^b and H-3^a of compound **3***b* in the conformations $\phi = 50°$, $\psi = 10°$ and $\phi = 70°$, $\psi = 10°$ (the conformations expected for the compound as the free diamine and dihydrochloride salt, respectively) are presented in Table 5. This table also presents the values for the constant *C* that are inferred by these values and the T_1 values for these hydrogen atoms which are given in Table 4. The T_1 value for H-3^a of the diamine could not be measured with good precision and may be neglected for these purposes. However, the val-

TABLE 4. Nuclear magnetic resonance spectra[a] of methyl 3-*O*-(2-amino-2-deoxy-β-D-glucopyranosyl)-2-amino-2-deoxy-β-D-glucopyranoside (**3***b*)

	Free diamine					Dihydrochloride salt					
	^{1}Hmr			^{13}Cmr		^{1}Hmr			^{13}Cmr		
Position	δ	*J*	T_1	δ	T_1	δ	*J*	T_1	δ	Δ	T_1
a-Unit											
1	4.20	8.5	0.71	104.53	0.43	4.56	8.3	0.72	100.40	4.13	0.43
2	2.68	9.3	1.49	56.40	0.40	3.18	9.0	—	55.62	0.78	0.39
3	3.49	9.0	0.49[b]	86.71	0.42	4.06	10.0	0.69	77.60	9.11	0.42
4	3.40	9.0	0.82	69.02	0.43	3.70	9.5	—	67.96	1.06	0.42
5	3.38	1.5	0.83	76.41	0.42	3.48	2.0	—	77.29	−0.88	0.46
6	3.80	5.0	0.36	61.61	0.23	3.84	5.0	0.35	61.04	0.57	0.22
6′	3.63	12.0	0.39	—	—	3.69	12.5	—	—	—	—
b-Unit											
1	4.42	8.5	0.50	103.85	0.40	5.00	8.3	0.63	96.69	7.16	0.41
2	2.61	9.0	1.70	57.51	0.43	3.17	9.0	—	55.55	1.96	0.39
3	3.30	9.0	1.30	77.06	0.42	3.63	10.0	1.09	72.62	4.44	0.42
4	3.27	9.0	—	70.44	0.40	3.44	9.5	—	70.04	0.40	0.41
5	3.38	1.5	0.83	76.41	0.42	3.48	2.0	—	76.68	0.03	0.39
6	3.80	6.0	0.36	61.49	0.23	3.83	5.0	0.35	60.95	0.54	0.22
6′	3.61	12.0	0.39	—	—	3.69	12.5	—	—	—	—
OCH_3	3.46			58.16		3.49			58.37		

[a]The ^{1}Hmr data were obtained at 270 MHz, the ^{13}Cmr data 67.89 MHz and the ^{13}C-T_1 values at 22.63 MHz. The solutions for the ^{1}Hmr were 0.05 *M* in D_2O (1% dioxane as internal reference, δ = 3.64 ppm) and for the ^{13}Cmr 0.3 *M* in D_2O (5% dioxane as internal reference, δ = 67.40 ppm) and all the experiments were performed at 300 K. The assignments for H-6[a]; H-6′[a]; H-6[b], H-6′[b]; and C-6[a], C-6[b] may be reversed. Also, the assignments for C-2, C-2[b] and C-6[a], C-6[b] of the dihydrochloride.
[b]Determined from the zero crossover.

TABLE 5. The relationship between T_1 values for H-1[b] and H-3[a] of the disaccharide **3** and the intramolecular interproton distances

		$\sum_{i \neq j} r_{ij}^{-6} \times 10^3$ (Å^{-6})		T_1 (s)		*C*	
φ°	ψ°	H-1[b]	H-3[a]	H-1[b]	H-3[a]	H-1[b]	H-3[a]
50	10	17.2	17.3	0.495	0.491	117	118
70	10	14.6	14.7	0.631	0.687	109	99

ues for *C* obtained for the other three are seen to all be within 114 ± 5. This finding is considered to offer important circumstantial evidence in support of the general conclusions reached regarding the slight conformational change expected to result on the basis of HSEA calculations. That is, the method would have been expected to detect a major change in the distance between H-1[b] and H-3[a]. It may be noted in this regard that the protonation of **3***b* caused a change in molecular rotation of 31.4° which is near that observed on protonation of methyl 2-amino-2-deoxy-β-D-glucopyranoside; namely 25.8°. These observations can be taken as further indication that the protonation of **3***b* caused little change in the torsion angles about the inter-sugar glycosidic bond (7).

In view of the generally good agreement between the conformations expected for **3***b* on the basis of HSEA calculations and the physical properties expressed by **3***b*, the conformation φ = 50°, ψ = 20°, τ = 117° inferred for **1** by HSEA calculation is taken as well representative of its actual conformation. As will be seen below, the conformation for **1** found further support in terms of the conformation required for the Lewis-a trisaccharide (**15**). The conformation of the Type 2 disaccharide (**2**) predicted by HSEA calculation (Figs. 2 and 3); namely, φ = 50°, ψ = 10°, τ = 117°, places the C-6[a] to O-2[b] and H-4[a] to H-1[b] internuclear distances at 3.96 and 2.44 Å respectively. Rees and Skerrett (14) have proposed the conformation φ = 42°, ψ = −18° for cellobiose in aqueous solution. It may be expected that cellobiose would have conformational properties about the glycosidic bond which are closely similar to that proposed above for *N*-acetyllactosamine (**2**).

The above conclusion that the unexpectedly large chemical shifts for C-1[b] and C-3[a] which occur

Can. J. Chem. Downloaded from www.nrcresearchpress.com by 210.87.254.5 on 09/05/12
For personal use only.

Can. J. Chem. Downloaded from www.nrcresearchpress.com by 210.87.254.5 on 09/05/12
For personal use only.

on protonation of **3***b* are caused not by a substantial change in conformation but, instead, largely by changes in valence angle (because of a change in the *exo*-anomeric effect with the change in ϕ) appears confirmed by the changes in chemical shift observed for aglyconic carbons as the result of a glycosidation at a neighboring position.

Examination of the ^{1}Hmr data for the Lewis-a trisaccharide (**15**) and related structures, which are presented in Table 6, shows that the spectrum for **15** is closely approximated by the addition of the appropriate chemical shifts for the disaccharides **1** and **14**. The main apparent discrepancies are with H-3^a and H-5^c. Relative to the chemical shift of H-5 in methyl α-L-fucopyranoside (**10**), H-5^c is deshielded by 0.32 ppm in the case of the disaccharide **14** and by 0.83 ppm in the case of the trisaccharide **15**. Lemieux *et al.* (33) assigned these strong specific deshielding effects to electrostatic interaction of H-5^c with O-3^a and O-5^b in the case of **15**. This indication that the αLFuc residues of **14** and **15** are similarly oriented relative to the βDGlcNAc residue is further supported by the values for $\delta_{15} - (\delta_1 + \delta_{14})$ found for the other hydrogens in these αLFuc groups. Similarly, these values for the βDGal units of **1** and **15** require that the orientation of the βDGal group for **1** is only slightly altered by the introduction of the αLFuc group to form **15**. That is, it is concluded on the basis of this ^{1}Hmr data that the preferred conformations about the glycosidic bonds in the disaccharides **1** and **14** are closely maintained in the composite trisaccharide **15**. As will be seen later on with reference to Table 11, nuclear Overhauser enhancement measurements are in accord with this conclusion. On this basis, a consideration of the ^{13}Cmr data presented in Table 6 leads to the conclusion that the formation of **15** from either **1** or **14** must have caused changes in hybridization about the already formed glycosidic bonds without causing substantial change in overall conformation. This conclusion is indicated by the pronounced shielding of the intersugar aglyconic carbons of **1** and **14** on glycosidation of the neighboring position. As seen from Table 6, the galactosylation of **8** to form **1** caused a deshielding of C-3^a by 8.70 ppm and the fucosylation of **8** to form **14** caused a deshielding of C-4^a by 7.63 ppm. These effects are those normally found in linear oligosaccharide structures (34). However, the glycosidation of the position vicinal to the existing glycosidic linkage of either **1** or **14** to form **15** causes strong shielding of the neighboring aglyconic carbon; that is C-3^a of **1** is shielded by 6.36 ppm and C-4^a of **14** is shielded by 5.08 ppm. Furthermore, the deshielding of C-4^a of **1** on fucosylation to form **15** is 3.77 ppm and that of C-3^a of **14** on galactosylation to form **15** is 3.60 ppm, substitutional effects on chemical shifts that are only about half those normally observed. In view of the shielding effects discussed above in relation to the protonation of **3** and the conclusion that these arose as a consequence of changes in hybridization and, consequently, screening of the carbon atoms with only slight changes in the overall conformation of the molecule, it is proposed that the ^{13}C-shifts observed for C-3^a and C-4^a of **15** mainly arise from non-bonded interactions between the vicinal glycosyl groups which in turn lead to changes in the geometries of the glycosidic bonds, mainly in terms of valence angles, away from the less constrained situation and that these changes result in changes in the screening of the nuclei from the magnetic field while causing only a slight change in the overall conformation of the molecule. These effects on chemical shift would be in line with the conclusions reached by Gorenstein (28) on influence of valence angle change on ^{13}C-chemical shifts.

The hypothesis presented above for the rationalization of the ^{13}C-chemical shifts is supported by the data presented in Tables 7 and 8 for the A and B trisaccharide determinants. The fucosylation of the galactoside **11** to form **18** deshielded C-2^b by 5.72 ppm. Introduction of the αDGalNAc or αDGal group at C-3^b of **11** deshielded this carbon by 4.17 and 4.58 ppm, respectively. These latter substitutional effects are seen to be considerably smaller than those observed in the formation of the disaccharides **1**, **14**, and **18** and this matter will be considered later on in connection with HSEA calculations, nuclear Overhauser enhancements, and $^3J_{C,H}$ coupling constants. Completion of the trisaccharides **21** and **22** from **18** caused shieldings of C-2^b by 4.45 and 4.12 ppm, respectively. On the other hand, completion of **21** and **22** from **19** and **20**, respectively, caused shieldings of C-3^b by only 1.03 and 0.73 ppm, respectively. It is apparent that these glycosidations cannot strongly shield a vicinal carbon (C-3^b) which was already strongly shielded relative to other aglyconic carbons in disaccharide structures. Examination of the ^{1}Hmr data in Tables 7 and 8 as was done above for that in Table 6 again leads to the conclusion that the conformations of the glycosidic linkages in the disaccharide structures are well maintained in the composite trisaccharide. The only substantial differences in chemical shift are for H-2^b and H-3^b where, as for H-3^a and H-4^a of **15** (Table 6), appreciable (>0.2 ppm) shifts to lower field were observed between the actual spectrum

Can. J. Chem. Downloaded from www.nrcresearchpress.com by 210.87.254.5 on 09/05/12
For personal use only.

TABLE 6. Comparisons of the ^{1}Hmr and ^{13}Cmr chemical shifts found for the Lewis-a determinant (**15**) and related glycosides[a]

Residue (Scheme 1)		βDGlcNAc (a)							βDGal (b)							αLFuc (c)					
Position		1	2	3	4	5	6[b]		1	2	3	4	5	6[b]		1	2	3	4	5	6
^{1}Hmr Data																					
Reference glycosides	**8**	4.75	3.97	3.83	*3.68*	*3.68*	4.16 3.99	**9**	4.56	3.75	3.89	4.17	3.93	4.05 4.00	**10**	5.01	4.08	—	3.99	4.27	1.47
βDGal(1→3)βDGlcNAcOR	**1**	4.81	*4.05*	*4.05*	*3.74**	*3.74**	4.17* 4.02*		4.69	3.79	3.89	*4.15*	*3.96*	4.05 3.99							
$\delta_1 - \delta_8$		0.06	0.08	0.22	0.06	0.06	0.01 0.03	$\delta_1 - \delta_9$	0.13	0.04	0.00	−0.02	0.03	0.00 −0.01							
αLFuc(1→4)βDGlcNAcOR	**14**	4.76*	3.92*	*3.91**	*3.80*	*3.82*	4.23 4.10									5.22	4.02	*4.05*	*4.08*	4.59	1.42
$\delta_{14} - \delta_8$		0.01	−0.05	0.08	0.12	0.14	0.07 0.11								$\delta_{14} - \delta_{10}$	0.21	−0.06	—	0.09	0.32	−0.05
$\delta_1 + \delta_{14}$		4.81	4.05	4.05	3.80	3.82	4.23 4.10		4.69	3.79	3.89	4.15	3.96	4.05 3.99		5.22	4.02	4.05	4.08	4.59	1.42
βDGal(1→3)[αLFuc(1→4)]βDGlcNAcOR	**15**	4.79	*4.13*	4.35	*3.97*	*3.84*	4.21 4.10		4.73	3.76	3.87	4.16	*3.89*	4.03 3.99		5.27	*4.06*	*4.17*	*4.06*	5.10	1.46
$\delta_{15} - (\delta_1 + \delta_{14})$		−0.02	0.08	0.30	0.17	0.02	−0.02 0.00		0.04	−0.03	−0.02	0.01	−0.07	−0.02 0.00		0.05	0.04	0.12	−0.02	0.51	0.04
^{13}Cmr Data																					
Reference glycosides	**8**	101.94	56.50	74.72	70.87	76.70	61.68	**9**	104.62	71.59	73.65	69.54	75.88	61.87	**10**	100.49	68.96	70.62	72.83	67.47	16.33
βDGal(1→3)βDGlcNAcOR	**1**	101.69	55.48	83.42	69.65*	76.22*	61.70*		104.33	71.55	73.39	69.40	76.12	61.83							
$\delta_1 - \delta_8$		−0.25	−1.02	8.70	−1.22	−0.48	0.02	$\delta_1 - \delta_9$	−0.29	−0.04	−0.26	−0.14	0.24	−0.04							
αLFuc(1→4)βDGlcNAcOR	**14**	101.80*	56.94*	73.46*	78.50	76.05	61.00									100.43	68.91	70.28	72.72	67.85	16.07
$\delta_{14} - \delta_8$		−0.14	0.44	−1.26	7.63	−0.65	−0.68								$\delta_{14} - \delta_{10}$	−0.06	0.05	−0.34	−0.11	0.38	−0.26
$\delta_1 + \delta_{14}$		101.69	55.48	83.42	78.50	76.05	61.00		104.33	71.55	73.39	69.40	76.12	61.83		10.43	68.91	70.28	72.72	67.85	16.07
βDGal(1→3)[αLFuc(1→4)]βDGlcNAcOR	**15**	101.80	56.72	77.06	73.42	76.36	60.80		103.66	71.46	73.34	69.25	75.71	62.52		98.92	68.76	70.09	72.87	67.67	16.26
$\delta_{15} - (\delta_1 + \delta_{14})$		0.11	1.24	−6.36	−5.08	0.31	−0.20		−0.67	−0.09	−0.05	−0.15	−0.41	0.69		−1.51	−0.15	−0.19	0.15	−0.18	0.19

[a]Measured as described in Table 2 but at 310 K. The shifts used in the comparisons are not asterisked.
[b]The low field value given for a C-6 hydrogen atom corresponds to H-6 and the other to H-6′ except where a range is indicated by a bracket.

TABLE 7. Comparisons of the ^{1}Hmr and ^{13}Cmr chemical shifts found for the A determinant (**21**) and related glycosides[a]

		βDGal (b)							αLFuc (d)							αDGalNAc (e)					
Position		1	2	3	4	5	6[b]		1	2	3	4	5	6		1	2	3	4	5	6[b]
^{1}Hmr Data																					
Reference glycosides	**11**	4.62	3.75	3.89	4.18	3.93	4.03 4.00	**10**	5.01	4.03	—	3.99	4.27	1.47	**12**	5.03	4.41	4.11	4.27	4.15	4.03 3.98
αLFuc(1→2)βDGalOR	**18**	4.72	3.86	4.09*	4.16*	3.92*	4.04* 4.00*		5.52	4.05	*4.08*	*4.03*	4.59	1.47							
$\delta_{18} - \delta_{11}$		0.10	0.11	0.20	−0.02	−0.01	−0.01 0.00	$\delta_{18} - \delta_{10}$	0.51	−0.03	—	0.04	0.32	0.00							
αDGalNAc(1→3)βDGalOR	**19**	4.68*	3.86*	3.99	4.35	*3.87*	4.04 3.98									5.34	4.48	4.25	4.28	4.43	4.04 3.98
$\delta_{19} - \delta_{11}$		0.06	0.11	0.10	0.17	−0.06	0.01 0.02								$\delta_{19} - \delta_{12}$	0.31	0.07	0.14	0.01	0.28	0.01 0.00
$\delta_{18} + \delta_{19}$		4.72	3.86	3.99	4.35	3.87	4.04 3.98		5.52	4.05	4.08	4.03	4.59	1.47		5.34	4.48	4.25	4.28	4.43	4.04 3.98
αLFuc(1→2)[αDGalNAc(1→3)]βDGalOR	**21**	4.77	4.09	4.22	4.49	3.89	4.10 3.94		5.58	*4.03*	*4.11*	*3.99*	4.72	1.54		5.44	4.52	4.17	4.26	4.47	4.07 4.00
$\delta_{21} - (\delta_{18} + \delta_{19})$		0.05	0.23	0.23	0.14	0.02	0.06 −0.04		0.06	−0.02	0.03	−0.04	0.13	0.07		0.10	0.04	−0.08	−0.02	0.04	0.03 0.02
^{13}Cmr Data																					
Reference glycosides	**11**	103.65	71.64	73.75	69.52	75.89	61.74	**10**	100.49	68.96	70.62	72.83	67.47	16.33		99.05	50.77	68.71	69.40	71.59	62.11
αLFuc(1→2)βDGalOR	**18**	102.37	77.36	74.74*	69.86*	75.78*	61.75*		100.13	69.20	70.46	72.78	67.58	16.25	**12**						
$\delta_{18} - \delta_{11}$		−1.28	5.72	0.99	0.34	−0.11	−0.01	$\delta_{18} - \delta_{10}$	−0.36	0.24	−0.16	−0.05	0.11	−0.08							
αDGalNAc(1→3)βDGalOR	**19**	103.41*	70.16*	77.92	65.65	75.83	61.78									94.73	50.53	68.49	69.30	71.76	61.86
$\delta_{19} - \delta_{11}$		−0.24	−1.48	4.17	−3.87	−0.06	0.04								$\delta_{19} - \delta_{12}$	−4.32	−0.24	−0.22	−0.10	0.17	0.75
αLFuc(1→2)[αDGalNAc(1→3)]βDGalOR	**21**	102.28	72.91	76.89	63.95	75.95	61.77		99.20	68.66	70.63	72.86	67.57	16.19		92.31	50.33	68.75	69.37	71.96	62.15
$\delta_{21} - (\delta_{18} + \delta_{19})$		−0.09	−4.45	−1.03	−1.70	0.12	−0.01		−0.93	−0.54	0.17	0.08	−0.01	−0.06		−2.42	−0.20	0.26	0.07	0.20	0.29

[a, b]See Table 6.

Can. J. Chem. Downloaded from www.nrcresearchpress.com by 210.87.254.5 on 09/05/12
For personal use only.

and that anticipated by choosing appropriate signals from the spectra for the disaccharides. These deshielding effects are in all likelihood related to the shielding of the corresponding carbon atoms caused by the glycosidations and attributed to changes in hybridization to accommodate the neighboring glycosyl groups.

The basic objective of this investigation was to examine whether or not the conformations for oligosaccharides predicted by the simple HSEA calculations are in acceptable agreement with the nuclear magnetic resonance properties found for these compounds. If so, then sufficient confidence would be gained in the results of the HSEA calculations to warrant their consideration in studies of structure–activity relationships in, for example, antibody–antigenic determinant binding. The remainder of this presentation is concerned with the finding that the conformations implied by HSEA calculation do indeed allow acceptable rationalization of the ^{1}Hmr spectral data.

The disaccharide (**14**), 4-*O*-(α-L-fucopyranosyl)-2-acetamido-2-deoxy-β-D-glucopyranoside, is a building unit for the Lewis-a and -b antigenic determinants. Plot 2 of Fig. 4 shows that the changes in non-bonded interactions, which result from changes in the φ torsion angle of the glycosidic linkages and estimating the most favorable ψ torsion angle by hard-sphere calculations only, describe a broad and shallow trough within the range

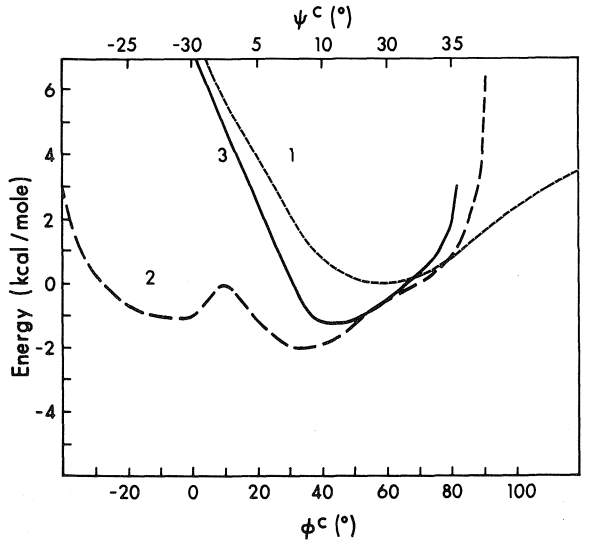


FIG. 4. Change in energy estimated to occur with changes in the ϕ^c and ψ^c torsion angles for the αLFuc(1→4)βDGlcNAc disaccharide (**14**). Plot 1 displays the change in bonding energy attributed to the *exo*-anomeric effect (Table 1), plot 2 shows the change in non-bonded interaction energy, and plot 3 indicates the change in energy content obtained by addition of plots 1 and 2. The ψ^c torsion angles calculated to be the energetically most favorable for the various ϕ^c angles are presented above.

TABLE 8. Comparisons of the ^{1}Hmr and ^{13}Cmr chemical shifts found for the B determinant (**22**) and related compounds[a]

		βDGal (b)						αLFuc (d)						αDGal (e)					
	Position	1	2	3	4	5	6[b]	1	2	3	4	5	6	1	2	3	4	5	6[b]
^{1}Hmr Data																			
Reference glycosides	**11**	4.62	3.75	3.89	4.18	3.93	4.03 4.00	**10**	5.01	4.08	—	3.99	4.27	1.47	**13** 5.08	4.07	4.05	4.21	4.14	4.01 3.96
αLFuc(1→2)βDGalOR	**18**	4.72	3.86	4.09*	4.16*	3.92*	4.00* 4.00*		5.52	4.05	*4.08*	*4.03*	4.59	1.47						
	$\delta_{18} - \delta_{11}$	0.10	0.09	0.20	−0.02	−0.01	0.01 0.00	$\delta_{18} - \delta_{10}$	0.51	−0.03	—	0.04	0.32	0.00						
αDGal(1→3)βDGalOR	**20**	4.70*	3.89*	*3.94*	4.43	3.89	4.02 3.94								5.41	4.12	4.21	4.28	4.44	3.98 3.90
	$\delta_{20} - \delta_{11}$	0.08	0.14	0.05	0.25	−0.04	−0.01 −0.06								$\delta_{20} - \delta_{13}$ 0.33	0.05	0.16	0.07	0.30	−0.03 −0.06
	$\delta_{18} + \delta_{20}$	4.72	3.86	3.94	4.43	3.89	4.02 3.94		5.52	4.05	4.08	4.03	4.59	1.47		4.12	4.21	4.28	4.44	3.98 3.90
αLFuc(1→2)[αDGal(1→3)]βDGlcOR	**22**	4.74	4.09	4.22	*4.50*	3.85	4.02 3.96		5.53	*3.95*	*4.02*	*3.98*	4.68	1.47		5.48	*4.09*	*4.09*	*4.20*	4.02 3.95
	$\delta_{22} - (\delta_{18} + \delta_{20})$	0.02	0.23	0.28	0.07	−0.04	0.00 0.02		0.01	−0.10	−0.06	−0.05	0.09	0.00		0.07	−0.03	−0.12	−0.08	0.04 0.05
^{13}Cmr Data																				
Reference glycosides	**11**	103.65	71.64	73.75	69.52	75.89	61.74	**10**	100.49	68.96	70.62	72.83	67.47	16.33	**13** 100.16	69.07	70.35	70.03	71.54	62.09
αLFuc(1→2)βDGalOR	**18**	102.37	77.36	74.74*	69.86*	75.78*	61.75*		100.13	69.20	70.46	72.78	67.58	16.25						
	$\delta_{18} - \delta_{11}$	−1.28	5.72	0.99	0.34	−0.11	0.01	$\delta_{18} - \delta_{10}$	−0.36	0.24	−0.16	−0.05	0.11	−0.08						
αDGal(1→3)βDGalOR	**20**	103.43*	70.17*	78.33	65.73	75.64	61.78								96.15	69.07	70.12	70.03	71.72	61.81
	$\delta_{20} - \delta_{11}$	−0.22	−1.47	4.58	−3.79	−0.25	0.04								$\delta_{20} - \delta_{13}$ −4.01	0.00	−0.23	0.00	0.18	−0.28
	$\delta_{18} + \delta_{20}$	102.37	77.36	78.33	65.73	75.64	61.78		100.13	69.20	70.46	72.78	67.58	16.25	96.15	69.07	70.12	70.03	71.72	61.81
αLFuc(1→2)[αDGal(1→3)]βDGalOR	**22**	102.37	73.24	77.60	64.39	75.31	61.69		99.42	68.72	70.41	72.92	67.47	16.30	94.11	68.96	70.74	70.16	72.04	62.15
	$\delta_{22} - (\delta_{18} + \delta_{20})$	0.00	−4.12	−0.73	−1.34	−0.33	−0.09		−0.71	−0.48	−0.05	0.14	−0.11	0.05	−2.04	−0.11	0.62	0.13	0.32	0.34

[a], [b]See Table 6.

Can. J. Chem. Downloaded from www.nrcresearchpress.com by 210.87.254.5 on 09/05/12
For personal use only.

(−40° to 120°) plotted. Within the *arbitrary* level of confidence of ± 0.5 kcal/mol which is placed on this method of calculation, plot 2 would allow conformations within very broad ranges for both the ϕ (−10° to 60°) and the ψ (−30° to 30°) torsion angles. However, addition of the contributions expected for the *exo*-anomeric effect (plot 1) provides plot 3 which strongly restricts the allowed conformations. Plot 3 indicates that the glycosidic linkage should tend to adopt ϕ angle values in the range 35° to 60° and ψ angle values in the range 5° to 30°. As seen in Table 6, H-5^c of the α-L-fucosyl group is deshielded by 0.32 ppm relative to the position of the signal for this hydrogen in methyl α-L-fucopyranoside. Inspection of a molecular model for the disaccharide shows that the above-mentioned range of ϕ and ψ torsion angles places H-5^c in close proximity to O-3^a (2.30 Å) and this interaction was expected to be the origin of the intramolecular deshielding of H-5^c.

As can be appreciated by consideration of molecular models, variation of the ϕ and ψ angles for this compound within the ranges 35° to 60° and 5° to 30°, respectively, should mainly influence the interactions between H-4^a and H-1^c and O-3^a and H-5^c. An examination of these changes showed that the changes in the H-4^a to H-1^c distances caused little change (<0.1 kcal/mol) in the non-bonded interactions between these atoms. However, the range of conformations involves a substantial change in the O-3^a to H-5^c interactions. These changes are plotted against the ϕ torsion angles in Fig. 5. It is seen that as the angle is increased, the internuclear distance decreases, and that, whereas the interaction is near zero for ϕ = 40°, ψ = 10°, the interaction increases to near 0.7 kcal/mol at ϕ = 55°, ψ = 25°. It is further seen in Fig. 5 that this increase in energy is paralleled by the total energy calculated (plot 2) for the molecule as ϕ is increased from 35° to 55°. As seen from Table 6, H-5^c is substantially (0.32 ppm) deshielded relative to the position of the signal for this atom in methyl α-L-fucopyranoside. This deshielding suggests considerable compression between H-5^c and O-3^a in this disaccharide and, consequently, a value of ϕ for the energetically most favorable conformer that is greater than 40°. The influence of the *exo*-anomeric effect is expected to be only 0.2 kcal/mol for a change in ϕ angle from 45° to 60°. That the orientation of the fucosyl group in this disaccharide (**14**) is nearly the same as in the Lewis-a trisaccharide (**15**) is inferred by the small difference (0.05 ppm) in the chemical shifts for H-1^c. It seems probable that the conformation of **14** is nearly the same as that for this unit in **15** both for this reason and, as will be considered below, the more pronounced deshielding of H-5^c in **15**.

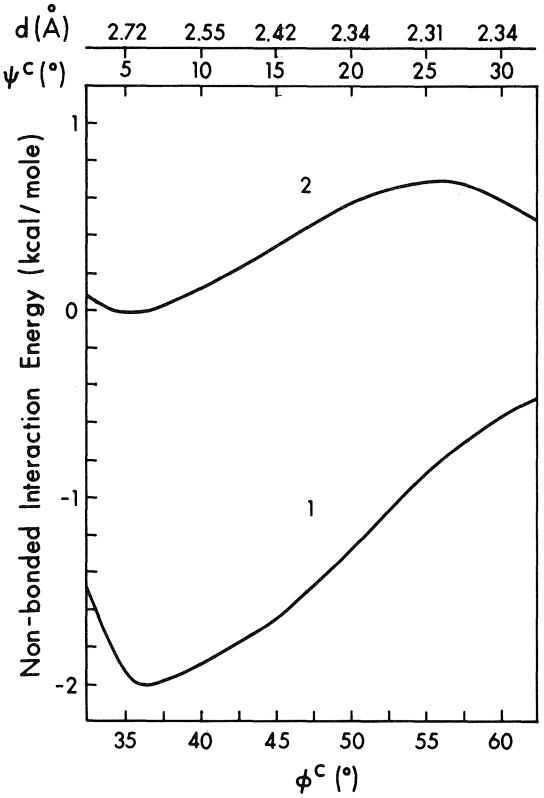


FIG. 5. Changes in non-bonded interaction energy with changes in the ϕ^c and ψ^c torsion angles for the αLFuc(1→4)-βDGlcNAc disaccharide (**14**). Plot 1 indicates the change in total non-bonded interaction energy and plot 2 shows the contribution to the total change in non-bonded interaction energy made by the interaction between O-3^a and H-5^c. The internuclear distances (d) between these atoms are presented above with the ψ^c torsion angles calculated to be the energetically most favorable at the various ϕ^c torsion angles.

In order to estimate by HSEA calculations which conformation appears most favorable for the Lewis-a trisaccharide (**15**), it was assumed that the fucosyl group would have an orientation within the above-set range for the disaccharide (**14**). The energetically most favorable conformation that was obtained had ϕ^b = 50°, ψ^b = 20° and ϕ^c = 55°, ψ^c = 25° (see Fig. 6). It seemed remarkable that the values for ϕ^b and ψ^b are those which appeared most favorable for the component βDGal(1→3)-βDGlcNAc disaccharide (**1**) (see Fig. 2).

Judging from Fig. 5, values of ϕ^c = 40°, ψ^c = 10° would be expected to be favorable for the trisaccharide (**15**) since these parameters seemed favorable for the parent disaccharide (**14**). However, on

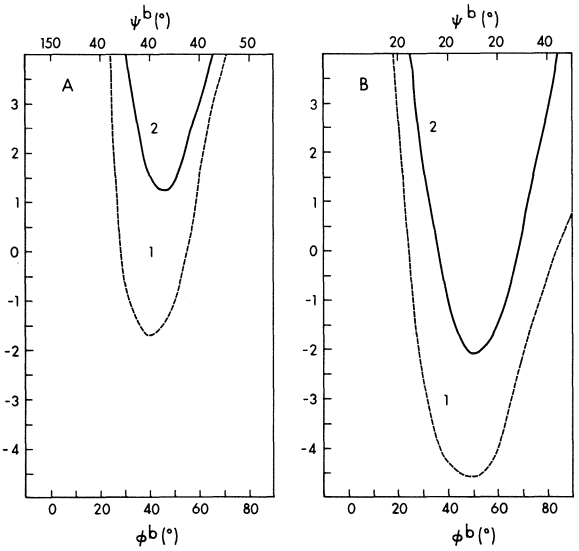


FIG. 6. Changes in energy with changes in ϕ^b and ψ^b torsion angle for the βDGal(1→3)[αLFuc(1→4)]βDGlcNAc (Lewis-a) trisaccharide (**15**) with ϕ^c and ψ^c set in *A* at 40° and 10° (*A*) and in *B* at 55° and 25°. Plots 1 indicate the calculated non-bonded interaction energies and plots 2 indicate the energy contents obtained by addition of the influence of the *exo*-anomeric effect (Table 1). The ψ^b values are those calculated to be the energetically most favorable at the various ϕ^b values.

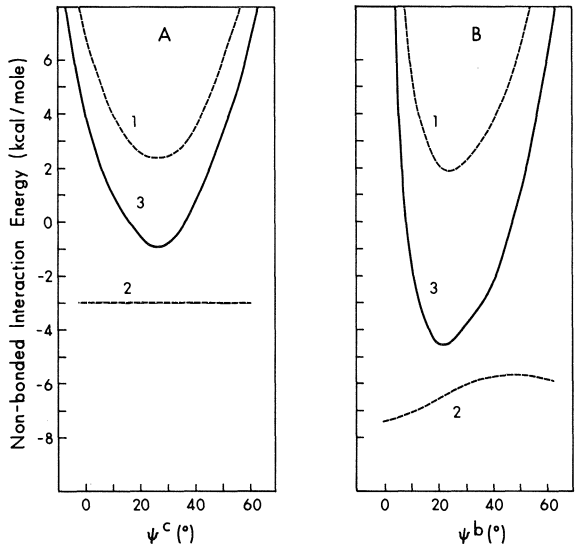


FIG. 7. Changes in non-bonded interaction energies; *A*: with changes in ψ^c for the αLFuc(1→4)βDGlcNAc disaccharide (**14**) with ϕ^c set at 55°, and *B*: with changes in ψ^b for the βDGal(1→3)[αLFuc(1→4)]βDGlcNAc (Lewis-a) trisaccharide (**15**) with ϕ^b, ϕ^c, and ψ^c set at 50°, 55°, and 25°, respectively. Plots 1 show the changes in repulsive interactions, plots 2 indicate the changes in attractive interactions, and plots 3 are the sums of plots 1 and 2.

using these values to calculate the most favorable conformation for **15**, the conformation (see Fig. 6*A*) with $\phi^b = 50°$ and $\psi^b = 40°$ has an energy content 3.5 kcal/mol greater than the above-mentioned $\phi^b = 50°$, $\psi^b = 20°$, $\phi^c = 55°$, $\psi^c = 25°$ conformer (see Fig. 6*B*). This significant difference in energy arose from a net decrease (0.5 kcal/mol) in attractive interactions and a net increase (3 kcal/mol) in repulsive interactions. These calculations form an interesting example of how the branching of an oligosaccharide chain from vicinal positions of the branching sugar unit can result in substantial interaction between the two branched sugar units and likely has a bearing, as mentioned above, on the chemical shifts of the aglyconic carbon atoms.

The plots in Fig. 7 provide an indication of how attractive forces can influence conformational preference. Plot 7*A* shows that for the disaccharide (**14**) with $\phi^c = 55°$, changes in the ψ^c angle had little influence on the attractive interactions. However, as seen in plot *B*, with ϕ^c, ψ^c, and ϕ^b set at 55°, 25°, and 50°, respectively, the branched trisaccharide **15** shows a change in net attractive forces of nearly 1 kcal/mol for a change in ψ^b from 20° to 40°. Thus, as will be seen below, although repulsive interactions between H-5^c and both O-3^a and O-5^b are expected to exist, adoption of the $\psi^b = 20°$ orientation appears to set up attractive interactions between the α-fucosyl and β-galactosyl residues that can effectively compensate for the additional repulsive interactions.

In view of the foregoing, the conformation $\phi^b = 50°$, $\psi^b = 20°$, $\phi^c = 55°$, $\psi^c = 25°$ (Fig. 7*B*) is taken as well representative of that most favorable for the Lewis-a trisaccharide (**15**). In this conformation, both O-3^a and O-5^b are expected to have internuclear distances with H-5^c calculated to be in the range 2.3 to 2.5 Å. The resulting interaction of H-5^c with the lone-pair electrons of O-3^a and O-5^b would be near one kcal/mol. This presumably accounts for the strong deshielding (0.83 ppm) observed for H-5^c relative to H-5 of methyl α-L-fucopyranoside (**10**) and why this atom is more deshielded than it is in the related disaccharide (**14**) where the chemical shift would be influenced intramolecularly by O-3^a only.

It is seen from Table 9 that the chemical shifts for H-1^c and H-5^c are, within experimental error, the same for the Lewis-a (**15**) and Lewis-b (**17**) determinants. Therefore, it could be concluded that the conformation of the Lewis-a trisaccharide is maintained in the Lewis-b determinant which contains an additional α-fucosyl group. It may be noted in this regard that the heterogeneous population of

Can. J. Chem. Downloaded from www.nrcresearchpress.com by 210.87.254.5 on 09/05/12
For personal use only.

Can. J. Chem. Downloaded from www.nrcresearchpress.com by 210.87.254.5 on 09/05/12
For personal use only.

antibodies raised against an artificial antigen formed from the Lewis-b tetrasaccharide determinant (3) cross-reacted extensively with the Lewis-a trisaccharide determinant. This observation requires similarities in the conformations of the Lewis-a and -b determinants as is indicated by the nmr data (Table 9).

Since the chemical shifts for H-1^c and H-5^c are very nearly the same for the Lewis-a (**15**) and Lewis-b (**17**) oligosaccharides (see Table 9) and $\phi^b = 50°, \psi^b = 20°, \phi^c = 55°, \psi^c = 25°$ were expected to well represent the conformation for the Lewis-a portion of **17**, the orientation of the second α-fucosyl group (ring d) in **17** was calculated using these conformational parameters. The results of these HSEA calculations are plotted in Fig. 8*A*. It is seen that the most favorable conformation is predicted to have $\phi^d = 40°$ and $\psi^d = 20°$. The plot shows that a ϕ^d torsion angle of 55° is strongly prohibited. As already discussed, the core disaccharide, βDGal(1→3)βDGlcNAc (**1**) has the acetamido group in very close proximity to O-2^b of the βDGal unit. Therefore, it was to be expected that the energy barrier in the range of φ angles of 40° to 60° in the case of the Lewis-b tetrasaccharide (**17**) arose mainly because of non-bonded interactions between the acetamido group and the α-L-fucosyl group which is attached to O-2^b. Indeed, as seen from Fig. 8*B*, this barrier was not present when HSEA calculations were made for the simple H-disaccharide (**18**). However, as for the Lewis-b tetrasaccharide, the most favorable value for ϕ^d remained in the region of 40°. This low value as compared to $\phi^c = 55°$ for the other α-L-fucosyl group in **17**, appears to arise because of interaction between H-1^d and O-3^b. That is, with $\phi^d = 40°$, the H-1^d to O-3^b interaction was calculated to be 0.3 kcal/mol as compared to 3 kcal/mol with $\phi^d = 55°$. It is noteworthy at this point that the orientation of this α-L-fucosyl group is influenced by interactions between both H-1^d and O-3^b and H-5^d and O-3^a. Movement to reduce the H-1^d to O-3^b interaction increases the other. Thus, the Le^d determinant (**16**) may be expected to have a particularly well defined conformation. As a consequence of these interactions with oxygen atoms, H-1^d and H-5^d would be expected to be deshielded. Certainly, as seen from Table 9, H-5^d in both the Lewis-d (**16**) and Lewis-b determinants (**17**) is significantly deshielded (0.3 ppm) as compared to the chemical shift of H-5 in methyl α-L-fucopyranoside (**10**). The occurrence in **17** of H-1^d at 5.39 ppm as compared to 5.25 ppm for H-1^c is more difficult to appreciate but is in line with extra deshielding of H-1^d by O-3^b. However, in this case, the difference in non-bonded interactions about the anomeric center is expected to be

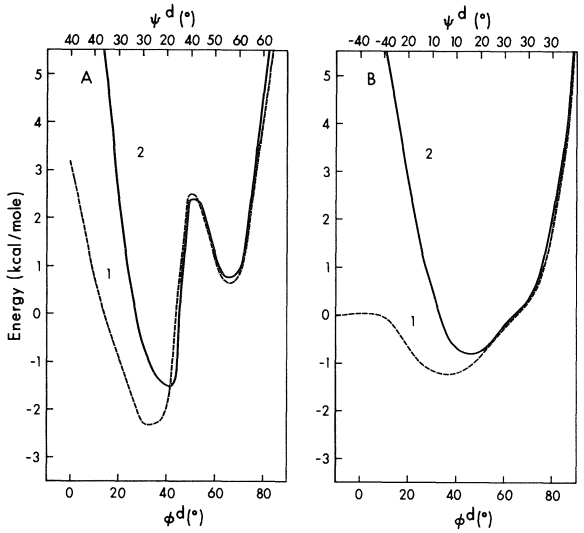


FIG. 8. Changes in energy with changes in ϕ^d and ψ^d; *A*: for the αLFuc(1→2)βDGal(1→3)[αLFuc(1→4)]βDGlcNAc (Lewis-b) tetrasaccharide (**17**) and setting ϕ^b, ψ^b, ϕ^c, and ψ^c at 50°, 20°, 55°, and 25°, respectively; and *B*: for the αLFuc(1→2)βDGal disaccharide (**18**). Plots 1 provide the changes in non-bonded interaction energy and plots 2 provide in each case the changes in energy obtained by adding the contribution expected to be made by the *exo*-anomeric effect (Table 1) to plots 1.

significant and may have an appreciable effect. It is remarkable in this regard that both C-1^d and H-1^d produce their signals at lower field than C-1^c and H-1^c, respectively.

In view of the above-noted expectation that the orientation of the αLFuc residue of the H-disaccharide (**18**) is well buttressed into position, it was of interest to compare the results of HSEA calculations for the Le^d-trisaccharide (**16**) obtained on setting $\phi^d = 40°$ and $\psi^d = 20°$ (the favorable orientation (Fig. 8) for the fucosyl group of **18**) with the results obtained on setting $\phi^b = 50°$ and $\psi^b = 20°$ (the favorable orientation (Fig. 2*A*) for the galactosyl group of **1**). The results of these calculations are presented in Fig. 9. A comparison of the plots shows that for $\phi^d = 40°, \psi^d = 20°$, the conformation with $\phi^b = 60°, \psi^b = 20°$ (see Fig. 9*B*) appears very considerably more favorable than that for $\phi^b = 50°, \psi^b = 20°$ (see Fig. 9*A*). Returning to Fig. 6*B*, it is seen that the choice of $\phi^b = 50°, \psi^b = 20°$ instead of $\phi^b = 60°, \psi^b = 20°$ as representing the most favorable conformation for the Lewis-a trisaccharide (**15**) rested on a difference of only about 0.5 kcal/mol. Since a difference of this magnitude in the present context must be considered as insignificant, there can be no basis for revising the conformation of the Lewis-a trisaccharide on this account. However, the influence of the values for ϕ^b and ψ^b on the Lewis-d trisaccharide (a matter of 2 kcal/mol, see Fig. 9*B*), made interesting a comparison of the total

Can. J. Chem. Downloaded from www.nrcresearchpress.com by 210.87.254.5 on 09/05/12
For personal use only.

TABLE 9. Relation of the ^{1}H- and ^{13}Cmr chemical shifts found for the Lewis-b (αLFuc(1→2)βDGal(1→3) [αLFuc(1→4)]βDGlcNAcOR, **17**) and those for the component trisaccharides (**15** and **16**)[a]

Position	1	2	3	4	5	6[b]	1	2	3	4	5	6[b]
^{1}Hmr Data												
Residue			βDGlcNAc (a)						βDGal (a)			
						4.18						4.04
16	4.65	*4.07*	*4.29*	*3.76*	*3.77*	4.01	4.87	3.85	*4.11*	4.15	*3.95*	4.00
						4.22						4.04
17	4.65	4.11	4.35	3.93	*3.76*	4.10	4.88	3.84	*4.05*	*4.11*	*3.80*	4.00
						4.21						4.04
$\delta_{15} + \delta_{16}$	4.79	4.13	4.34	3.97	3.84	4.10	4.87	3.85	4.11	4.15	3.95	4.00
						0.01						0.00
$\delta_{17} - (\delta_{15} + \delta_{16})$	−0.14	−0.02	0.01	−0.04	−0.08	0.00	0.01	−0.01	−0.06	−0.04	−0.15	0.00
Residue			αLFuc (c)						αLFuc (d)			
16	—	—	—	—	—	—	5.44	4.07	—	3.96	4.56	1.50
$\delta_{16} - \delta_{10}$	—	—	—	—	—	—	0.43	−0.01	—	−0.03	0.29	0.03
17	5.25	*4.10*	4.21	*4.13*	5.05	1.53	5.39	4.14	—	3.99	4.58	1.52
$\delta_{15} + \delta_{16}$	5.27	4.06	4.17	4.06	5.10	1.46	5.44	4.07	—	3.96	4.56	1.50
$\delta_{17} - (\delta_{15} + \delta_{16})$	−0.02	0.04	0.04	0.07	−0.05	0.07	−0.05	0.07	—	0.03	0.02	0.02
^{13}Cmr Data												
Residue			βDGlcNAc (a)						βDGal (b)			
16	102.67	55.67	78.37	69.62	76.32	61.72	101.03	77.50	74.39	70.00	75.94	61.96
17	102.70	56.43	75.59	73.05	76.24	60.60	101.42	77.36	74.53	69.00	75.59	62.40
$\delta_{15} + \delta_{16}$	101.80	56.72	77.06	73.42	76.36	60.80	101.03	77.50	74.39	70.00	75.94	61.96
$\delta_{17} - (\delta_{15} + \delta_{16})$	0.90	−0.29	−1.47	−0.37	−0.12	−0.20	0.39	−0.14	0.14	−1.00	−0.35	0.44
Residue			αLFuc (c)						αLFuc (d)			
16	—	—	—	—	—	—	100.33	68.96	70.33	72.67	67.33	16.06
$\delta_{16} - \delta_{10}$	—	—	—	—	—	—	−0.16	0.00	−0.29	−0.16	−0.14	−0.27
17	98.61	68.70	69.98	72.78	67.77	16.17	100.38	69.13	70.30	72.78	67.03	16.07
$\delta_{15} + \delta_{16}$	98.92	68.76	70.09	72.87	67.67	16.26	100.33	68.96	70.33	72.67	67.33	16.06
$\delta_{17} - (\delta_{15} + \delta_{16})$	−0.31	−0.06	−0.11	−0.09	0.10	−0.09	0.05	0.17	−0.03	0.11	−0.30	0.01

[a]The values given for $\delta_{15} + \delta_{16}$ are those for the βDGlcNAc and αLFuc residues of **15** with the remaining values being those for **16**. For experimental conditions see Tables 2 and 6.
[b]See Table 6.

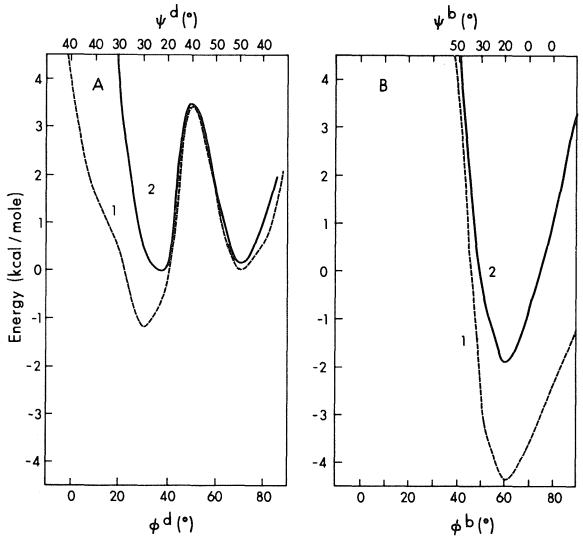


FIG. 9. Changes in energy with changes in values for ϕ^b, ψ^b, ϕ^d, and ψ^d for the αLFuc(1→2)βDGal(1→3)βDGlcNAc (H-Type 1 or Lewis-d) trisaccharide (**16**); *A*: for changes in ϕ^d and ψ^d with ϕ^b and ψ^b set at 50° and 20°, respectively; and *B*: for changes in ϕ^b and ψ^b with ϕ^d and ψ^d set at 40° and 20°, respectively. Plots 1 provide the changes in the non-bonded interaction energies and plots 2 provide the changes in energy obtained on adding to plots 1 the contribution expected to be made by the *exo*-anomeric effect (Table 1).

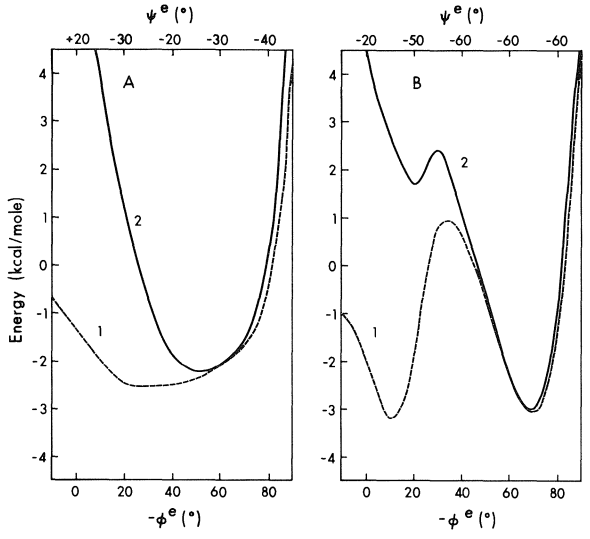


FIG. 10. Changes in energy with changes in values for ϕ^e while keeping ϕ^d = 40° and ψ^d = 20°; *A*: for the αDGalNAc(1→3)-βDGal (**19**) and αDGal(1→3)βDGal (**20**) disaccharides (the A(B) disaccharides); and *B*: for the αLFuc(1→2)[αDGalNAc-(1→3)]βDGal (**21**) and αLFuc(1→2)[αDGal(1→3)]βDGal (**22**) trisaccharides (the A(B) trisaccharides). Plots 1 and 2 are the results of the hard-sphere and HSEA calculations, respectively.

energy contents for the Lewis-b tetrasaccharide in the two conformations. These were found to be −8.6 kcal/mol for $\phi^b = 50°$, $\psi^b = 20°$, $\phi^c = 55°$, $\psi^c = 25°$, $\phi^d = 40°$, $\psi^d = 20°$, and −9.9 kcal/mol for $\phi^b = 60°$, $\psi^b = 20°$, $\phi^c = 55°$, $\psi^c = 25°$, $\phi^d = 40°$, $\psi^d = 20°$. This difference in energy could be traced to interactions between the α-L-fucosyl (d) group and the acetamido group of the a-unit, mainly interactions involving H-3^d. Since the orientation of the acetamido group was arbitrarily set, no significance is attached to this difference. The change of ϕ^b from 50° to 60° would provide an increase of the H-5^c to O-5^b distance by 0.17 Å. This matter was not investigated further since the difference in conformation is considered to be too slight to be of consequence to this present work.

The conformation of the Lewis-b tetrasaccharide is illustrated by the projection formula presented in Scheme 1 (units a, b, c, d). It is seen that the two fucosyl residues are expected both to extend above the β-sides of the βDGal(1 → 3)βDGlcNAc core chain and in near van der Waals contact since the internuclear distances between H_3C-6^c and H_3C-6^d and between H_3C-6^c and O-5^d are expected to be near 4.3 and 3.9 Å respectively. This latter interaction and that between H_3C-6^d and O-3^a (which are separated by nearly 4.1 Å) are likely responsible for the signals for C-6 methyl groups of the fucosyl groups in the Lewis-b tetrasaccharide (**17**) being slightly but significantly to lower field (see Table 9) than the signals for these groups in the Lewis-a (**15**) and Lewis-d (**16**) trisaccharides. Examination of the $\delta_{17} - (\delta_{15} - \delta_{16})$ values presented in Table 9 shows that the ^{1}Hmr spectrum for the Lewis-b tetrasaccharide (**17**) is in good accord with that which would be anticipated ($\delta_{15} + \delta_{16}$) from the spectra of the related trisaccharides. The agreement is not as good in the case of the ^{13}Cmr spectra. This is not surprising in view of the evidence presented above that these chemical shifts are highly sensitive to even slight changes in the valence angles.

The energies calculated for conformations for the A and B disaccharides with the same φ and ψ angles were essentially identical. This is understandable since, as can be appreciated from the conformational formulas shown in Scheme 1, all energetically plausible conformations have the 2-substituent (R′) of the α-D-*galacto* (e) residue directed away from the other sugar units. Therefore, to simplify the presentation, these structures will be considered together and termed the A(B) oligosaccharides.

As seen from Fig. 10*A*, hard-sphere calculation would allow a broad range of ϕ^e and ψ^e angles (plot 1) for the A(B) disaccharide. The range is reduced to −40 to −70° (plot 2) by introducing the *exo*-anomeric effect. Therefore, unless the *exo*-anomeric effect has a much stronger influence in the range 60° ± 15° than that provided in Table 1,

Can. J. Chem. Downloaded from www.nrcresearchpress.com by 210.87.254.5 on 09/05/12
For personal use only.

Can. J. Chem. Downloaded from www.nrcresearchpress.com by 210.87.254.5 on 09/05/12
For personal use only.

substantial conformational flexibility about the glycosidic linkage can be expected.

It was concluded above that the Le^d-trisaccharide (**16**) has the α-L-fucosyl group in the orientation $\phi^d = 40°$ and $\psi^d = 20°$. These values were used to calculate the ϕ^e energy profile plotted in Fig. 10*B* for the A(B) trisaccharides (**21** and **22**). Comparison of plots 1 in Fig. 10 shows that the introduction of the α-L-fucosyl group to form the trisaccharide introduced an important barrier to rotation with the maximum at near $\phi^e = -40°$. In the absence of an influence by the *exo*-anomeric effect, energy minima at both $\phi = -10°$ and $-70°$ would be expected. However, on completing the HSEA calculation to provide plot 2 of Fig. 10*B*, it is seen that the conformation $\phi^d = 40°$, $\psi^d = 20°$, $\phi^e = -70°$, $\psi^e = -60°$ is expected to be strongly favorable for the trisaccharides **21** and **22**. Fig. 10*B* is an interesting example of how the *exo*-anomeric effect can seriously influence a decision based on hard-sphere calculations only.

Furthermore, it appears useful (see Table 10) to compare the ^{1}Hmr parameters for the B-tetrasaccharide (**24**) with those of the two component trisaccharides; namely, the Le^d-trisaccharide (**16**) and the B-trisaccharide (**22**). It is at once seen that the spectrum for **24** can be anticipated quite well from those observed for **16** and **22**. As mentioned above with regard to the Le^b determinant (Table 9), ^{13}Cmr chemical shifts are not expected to be well anticipated by this procedure. Nevertheless, the agreement between the anticipated spectrum ($\delta_{16} + \delta_{22}$) and that found for **24** is noteworthy.

The results achieved in terms of nuclear Overhauser enhancements (nOe) and the coupling of ^{13}C to ^{1}H atoms over three bonds and involving the anomeric hydrogen of the α-linked residues c, d, and e of Scheme 1 lend strong support to the conclusions reached above regarding the conformation of the structures listed in Scheme 1. These experiments could be conducted since the H-1 signals are well separated from the other signals in the spectra and these equatorial hydrogens are essentially free of interactions with other intraunit hydrogens except for the neighboring H-2 atoms. Furthermore, the availability of FT high field nmr spectrometers renders routine the reliable detection of nOe's of as little as 2% of the normal intensity of the signal under the conditions of the measurement.

Measured nOe effects are highly sensitive to a number of experimental factors including concentration, the presence of paramagnetic substances, the complexity and nature of the molecule under investigation, and the measurement itself. Therefore, the absolute value of a nOe is not in itself significant except in the sense that a strong observed nOe requires a close proximity of the two hydrogen atoms. However, the relative values of nOe's for two or more hydrogens within the same molecule and obtained at the same time through the irradiation of a specific hydrogen atom are significant in the sense that hydrogen which has the greatest nOe must, on the average, be closer to the hydrogen that was irradiated. Thus, although the absolute value is only of qualitative value, the ratios of nOe's measured at the same time are of at least semiquantitative value.

As seen from Table 11, significant enhancements of the H-2 atoms were observed on irradiation of the neighboring H-1 atoms. This is in keeping with the fact that these two atoms are separated by only 2.36 Å. These enhancements therefore can serve as an internal standard for interpreting the nOe's observed for other hydrogens which showed enhancement. As seen from Table 11, the ratios of the nOe's observed for H-2^c and H-4^a (the hydrogen at the aglyconic carbon (termed H-A) of the αL-Fuc(c) units of the Lewis-related oligosaccharides, **14**, **15**, and **17**) are nearly the same as those found for H-3^a of **1**. These results require that these H-A hydrogen atoms are nearly the same distance from H-1 and, in view of the constancy of the chemical shifts observed for both H-1 and C-1 for these compounds, the indication is clear that the orientation of this unit (c) is the same for the Le-disaccharide (**14**), the Le^a trisaccharide (**15**), and the Le^b tetrasaccharide (**17**). Furthermore, the HSEA calculations place H-1^c and H-4^a at an internuclear distance of 2.68 Å in accord with the general trend of the relative nOe's. Also, the HSEA calculations place H-1^c at a distance of 2.69 Å from C-6^a, a distance which would require strong interaction between H-1^c and the H-6^a and H-$6'^a$ atoms. The observation of a readily measurable nOe for the H-$6'^a$ atom (that which is strongly coupled to H-5^a) supports this conclusion. Furthermore, the relaxation time of H-1^c is 0.41 s as compared to that (0.60 s) for H-1^d which requires a greater proton density about H-1^c, namely, the proximity of the H-6^a atoms. Finally, it was noted from the HSEA molecular model that H-5^c should be only 2.40 Å from H-2^b. Therefore, selective irradiation of H-5^c (which was readily possible because of its deshielding by O-3^a and O-5^b) could be expected to provide an nOe for H-2^b of nearly the same magnitude as that expected for the *syn*-clinal H-4^c which is separated from H-5^c by 2.45 Å. In fact, irradiation of H-5^c caused enhancements of 6% for H-2^b and 5% for H-4^c. The *syn*-axial H-3^c which is estimated to be 2.67 Å from H-5^c was enhanced by 4%.

The HSEA calculations indicate internuclear

Can. J. Chem. Downloaded from www.nrcresearchpress.com by 210.87.254.5 on 09/05/12
For personal use only.

TABLE 10. Relation of the ^{1}H- and ^{13}Cmr chemical shifts observed for the B determinant (Type 1) (αLFuc(1→2) αDGal(1→3)]βDGal(1→3)βDGlcNAcOR, **24**) and those expected[a] from the data for the component trisaccharides (**16** and **22**)

Position	1	2	3	4	5	6[b]	1	2	3	4	5	6[b]
^{1}Hmr Data												
Residue			βDGlcNAc (a)						βDGal (b)			
						4.22						4.06
24	4.64	4.05	*4.24*	*3.73*	3.77	4.14	4.96	4.09	*4.17*	4.52	*3.95*	4.02
						4.18						4.04
$\delta_{16} + \delta_{22}$	4.65	4.07	4.29	3.76	3.77	4.01	4.87	4.09	4.22	4.50	3.95	4.00
						0.04						0.02
$\delta_{24} - (\delta_{16} + \delta_{22})$	−0.01	−0.02	−0.05	−0.03	0.00	−0.13	0.09	0.00	−0.05	0.02	0.00	0.02
Residue			αLFuc (d)						αDGal (e)			
												4.03
24	5.48	4.04	*3.90*	*4.06*	4.62	1.48	5.49	4.18	4.13	4.23	4.50	3.97
												4.02
$\delta_{16} + \delta_{22}$	5.44	3.95	4.02	3.98	4.68	1.47	5.48	4.09	4.09	4.20	4.47	3.95
												0.01
$\delta_{24} - (\delta_{16} + \delta_{22})$	0.04	0.09	−0.12	0.08	−0.06	0.01	0.01	0.09	0.04	0.03	0.03	0.02
^{13}Cmr Data												
Residue			βDGlcNAc (a)						βDGal (b)			
24	102.70	55.57	78.40	69.68	76.25	61.66	100.86	74.52	77.13	64.42	75.44	61.97
$\delta_{16} + \delta_{22}$	102.67	55.67	78.37	69.62	76.32	61.72	101.03	73.24	77.60	64.39	75.31	61.69
$\delta_{24} - (\delta_{16} + \delta_{22})$	0.03	−0.10	0.03	0.06	−0.07	−0.06	−0.17	1.28	−0.47	0.03	0.13	0.28
Residue			αLFuc (d)						αDGal (e)			
24	99.95	68.55	70.55	72.69	67.40	15.99	94.05	68.95	70.24	70.17	71.97	62.13
$\delta_{16} + \delta_{22}$	99.42	68.72	70.41	72.92	67.47	16.30	94.11	68.96	70.74	70.16	72.04	62.15
$\delta_{24} - (\delta_{16} + \delta_{22})$	0.53	0.17	0.13	−0.23	−0.07	−0.31	−0.06	−0.01	−0.50	0.01	−0.07	−0.02

[a]The values given for $\delta_{16} + \delta_{22}$ are those for the βDGlcNAc residue and the anomeric center of the βDGal residue of **16** with the remaining values being those for **22**. For experimental details, see Tables 2 and 6.
[b]See Table 6.

TABLE 11. Nuclear Overhauser enhancements and $^3J_{C\text{-}1,H\text{-}A}$[a] coupling constants

Residue	αLFuc (c)			αLFuc (d)			αDGalNAc (e)			αDGal (e)		
	nOe %		^3J	nOe %		^3J	nOe %		^3J	nOe %		^3J
Compound	H-2	H-A	Hz	H-2	H-A	Hz	H-2	H-A	Hz	H-2	H-A	Hz
14	12	8	3.5									
15	11	8[b]	4									
16				14	16	4						
17	11	10	3.5	10	9	5						
18				14	18	4						
19							12	4(4)[c]	—[d]			
20										19	6(10)[c]	—[d]
21				11	7[e]	4	6	6(9)[c]	—[d]			
22				14	11	4				17	−(6)[c]	—[d]
24				4	4	4				5	3(4)[c]	—[d]

[a]The term H-A is used for the proton at the aglyconic carbon. The relevant interatomic distances estimated by HSEA calculations are provided in the text.
[b]Nuclear Overhauser enhancements of 2 and 5% were observed for H-6[a] and H-6'[a], respectively.
[c]Nuclear Overhauser enhancements presented in parentheses are those for H-4[b].
[d]Coupling was not detectable (< 1.5 Hz).
[e]An nOe of 4% was observed for H-3[e].

distances for H-1[d] and H-2[b] of 2.44 Å and, therefore, the nOe for H-2[b] would be expected to be about the same as that for H-2[d] on irradiation of H-1[d]. It is seen from Table 11 that this was indeed the case for all the compounds which contain the αLFuc(d) unit. Furthermore, the ψ^c angles for the αLFuc(c) units was estimated to be 25° and somewhat greater than the ψ^d torsion angle of 20° estimated for the compounds with αLFuc(d) units. Therefore, it could be expected (7, 8) that these latter compounds would possess somewhat greater values for the anomeric carbon to aglyconic hydrogen coupling constants than for the former αLFuc(c) units. It is seen from Table 11 that the general trend of coupling constants is in accord with this expectation.

The HSEA calculations predict the rather remarkable $\phi = -70°$, $\psi = -60°$ for the e-units (βDGalNAc or βDGal). On the basis of the general trends observed for $^3J_{C,H}$ coupling constants, the $^3J_{C\text{-}1^e,H\text{-}3^b}$ values would be expected to be small in comparison to either the $J_{C\text{-}1^c,H\text{-}4^a}$ or $J_{C\text{-}1^d,H\text{-}2^b}$ values. As seen from Table 11, this was the case. Furthermore, the ratios of the nOe's for the H-2[e] to H-3[b] atoms on irradiation of H-1[e] appear definitely greater than for the similar situations involving the αLFuc(d) units. This is in accord with the calculated greater separation of the H-1[e] to H-3[b] atoms (3.19 Å) than the H-1[d] to H-2[b] atoms (2.44 Å). Furthermore the HSEA molecular models place the H-1[e] atom 2.17 Å from the H-4[b] atom. Thus, the very significant nOe's observed for the H-4[b] atoms noted in Table 11 are in further accord with the calculated structure. Also, in the case of the A trisaccharide (**21**) a significant nOe of H-3[e] was observed on irradiation of H-1[d]. In accord with this, the molecular model predicts an internuclear distance of 2.47 Å for these two atoms. Finally, in this regard, it is of interest to examine the effects on the internuclear distances for the anomeric and aglyconic hydrogens of changing the ϕ and ψ torsion angles presented in Scheme 1 by ±5° since these torsion angles cannot be expected to have been estimated more accurately than within this range. For ϕ^c and ψ^c in the ranges 55 ± 5° and 25 ± 5°, the H-1[c] to H-4[a] distance is in the range 2.68 ± 0.11 Å. Similarly for the ϕ^d,ψ^d and ϕ^e,ψ^e torsion angles, variations of ±5° provided internuclear distances of 2.48 ± 0.10 Å and 3.19 ± 0.11 Å. These relative distances are in accord with the relative nOe's observed and these considerations stress that the torsion angles presented in Scheme 1 must be interpreted with considerable latitude.

In summary, the above-noted correlations based on ^{13}C- and ^1H-chemical shifts, $^3J_{H,H}$ and $^3J_{C,H}$ coupling constants, T_1 and nOe measurements appear to well justify the conformations for the various oligosaccharides presented in Scheme 1. Therefore, it is concluded that the simple HSEA approach to the anticipation of the preferred conformation of oligosaccharide structures may find a useful role in the conformational analyses of these biologically important structures. In contrast to the approaches based on *ab initio* force field calculations (24, 32), the computing costs are readily met. Also, the HSEA calculations are conceptually simple and manageable by most practising chemists and offer the important advantage of bringing to the experimentalist an appreciation in semiquantitative fashion of the specific non-bonded interactions which dominate the situation. Furthermore, once

Can. J. Chem. Downloaded from www.nrcresearchpress.com by 210.87.254.5 on 09/05/12
For personal use only.

the coordinates for the various atoms are placed in the computer memory, the approach provides a simple access to spatial characteristics of the model which may be of interest to structure – biological activity correlations which is much superior to consideration of space-filling molecular models only. On the other hand, it must be kept well in mind that the approach at this time is not rigorous in many regards and conclusions drawn from such calculations must be treated accordingly.

Experimental

^{1}Hmr spectra were obtained at 310 K in D_2O unless otherwise stated, on a Bruker HX-270 instrument operating at 270 MHz. The use of a spectral width of 3 kHz, with a data memory of 64 K gave a digital resolution of ±0.1 Hz. The pulse width used was 15μs (90°). Acetone 1% was used as internal reference (δ = 2.480). Assignments were done using (*a*) double resonance experiments in connection with partial relaxed spectra (35), (*b*) observing carbon spectra with selective proton irradiation (^{1}H chemical shifts determined by this method are given in italics), and (*c*) nuclear Overhauser enhancement experiments (36).

Relaxation data were obtained by the inversion recovery method using the initial slope approximation, and the T_1-values determined from a semilogarithmic fit and from an exponential fit to all the relaxation data using the expression given by Saas and Ziessow (37). The agreement between these two was in general within 5% which was also considered the experimental error. This indicates that it is reasonable to assign a single exponential behavior to the relaxation of a given proton.

^{13}Cmr spectra were obtained at 310 K in D_2O on the same instrument operating at 67.89 MHz. The use of a spectral width of 10 kHz with a memory of 32 K gave a digital resolution of ±0.6 Hz. The pulse width used was 12 μs (90°). Dioxane 1% was used as internal reference (67.40 ppm). Assignments were done using (*a*) selective proton irradiation, (*b*) coupled carbon spectra, and (*c*) isotope effects (38).

The T_1 values were obtained at 22.63 MHz on a Bruker WH-90 instrument using the inversion recovery method. This field was used in order to avoid heating of the ionic samples which occur at the high field (39).

*Methyl 2-Amino-2-deoxy-3-O-(2-amino-2-deoxy-β-D-glucopyranosyl)-β-D-glucopyranoside (***3b***)*

The compound was prepared following the procedure described (25) for the preparation of the corresponding 2,2,2-trichloroethyl glycoside (**3a**). The only appreciable difference was in the separation of the diphthalimido derivative of **3** from inorganic salts. Since this intermediate was soluble in water, the neutralized aqueous solution was taken to dryness and the diphthalimido compound was extracted from the residue using boiling acetone. The crude product resisted crystallization and was converted directly to **3** by treatment with hydrazine in the usual manner. Pure amorphous **3**, $[\alpha]_D^{25}$ −25.8° (water) as the diamine was obtained by chromatography on a column of Dowex 1 × 8 resin (hydroxide form). *Anal.* calcd. for $C_{13}H_{26}N_2O_9$: C 44.04, H 7.40, N 7.91; found: C 43.51, H 7.30, N 8.18.

The ^{13}Cmr spectrum (Tables 2 and 4) required a high state of purity. The ^{1}Hmr spectrum (Table 4) measured at 270 MHz was virtually first-order and in complete accord with the assigned structure.

In order to prepare the dihydrochloride salt of **3**, an aqueous solution was taken to pH 1 with hydrochloric acid and the resulting solution was freeze-dried to a highly deliquescent amorphous powder; $[\alpha]_D$ −16.9° (water).

Acknowledgements

The nmr studies reported herein were made possible by the availability of the required oligosaccharides by chemical syntheses. Dr. D. A. Baker, Dr. Y. Fouron, and Dr. Z. Abbas synthesized the B di- and trisaccharides. Dr. Z. Abbas and Dr. Y. Fouron accomplished the synthesis of the B-tetrasaccharide. Dr. R. M. Ratcliffe synthesized the A blood-group related structures as well as the derivative of lactosamine. The details of these fine synthetic accomplishments will be reported separately. Mr. P. Senn and Mr. K. Kong provided valuable assistance in terms of programming and computer services.

The authors are extremely grateful and wish to thank all of the above-mentioned colleagues for very special cooperation in these matters.

The financial support of the National Research Council of Canada (A172) and the Medical Research Council of Canada (SP-3) through grants to R. U. Lemieux and valuable cooperation provided by Chembiomed Ltd. are gratefully acknowledged.

The microanalyses and 100 MHz nmr spectra were carried out by the analytical and spectral service laboratories of this department.

The high field Bruker HX-270 NMR instrument was provided by the Danish Natural Science Research Council.

1. S. Hakamori and A. Kobata. *In* The antigens. Vol. II. *Edited by* M. Sela. Academic Press, New York. 1977. p. 79.
2. W. M. Watkins. *In* Glycoproteins: their composition, structure and function. *Edited by* A. Gottschalk. Elsevier, Amsterdam. 1972. p. 830.
3. R. U. Lemieux, D. A. Baker, C. Switzer, and W. M. Weinstein. Biochemistry. Submitted.
4. H. A. Graham, H. F. Hirsch, and D. M. Davies, Jr. *In* Human blood groups. 5th Intern. Convoc. Immunology, Buffalo, New York. Karger, Basel. 1977. p. 257.
5. D. M. Marcus and L. E. Cass. Science, **164**, 553 (1969).
6. J. C. Paulson, J.-P. Prieels, L. R. Glasgow, and R. L. Hill. J. Biol. Chem. **253**, 5617 (1978).
7. R. U. Lemieux and S. Koto. Tetrahedron, **30**, 1933 (1974).
8. R. U. Lemieux, S. Koto, and D. Voisin. *In* Anomeric effect, origin and consequences. *Edited by* W. A. Szarek and D. Horton. ACS Symposium Series, No. 87. 1979. p. 17.
9. R. U. Lemieux. Chem. Soc. Rev. **7**, 423 (1978).
10. C. M. Venkatachalam and G. N. Ramachandran. *In* Conformation of biopolymers. Vol. 1. *Edited by* G. M. Ramachandran. Academic Press, New York. 1967. p. 83.
11. L. T. J. Delbaere. Biochem. J. **143**, 197 (1974).
12. D. C. Fries, S. T. Rao, and M. Sundaralingam. Acta Crystallogr. Sect. B, **27**, 994 (1971).
13. K. B. Lindberg. Acta Crystallogr. Sect. B, **32**, 645 (1976).
14. D. A. Rees, and R. J. Skerrett. Carbohydr. Res. **7**, 334 (1968).
15. R. D. Gilardi and J. L. Flippen. Acta Crystallogr. Sect. B, **30**, 2931 (1974).
16. B. M. Gatehouse and B. J. Poppleton. Acta Crystallogr. Sect. B, **27**, 654 (1971).

Can. J. Chem. Downloaded from www.nrcresearchpress.com by 210.87.254.5 on 09/05/12
For personal use only.

17. P. F. LONGCHAMBON, J. OHANNESSIAN, D. AVENEL, and A. NEUMAN. Acta Crystallogr. Sect. B, **31**, 2623 (1975).
18. W. J. COOK and C. E. BAGG. Biochim. Biophys. Acta, **389**, 428 (1975).
19. G. A. JEFFREY, J. A. POPLE, and L. RADOM. Carbohydr. Res. **25**, 117 (1972).
20. M. SUNDARALINGAM. Biopolymers, **6**, 189 (1968).
21. G. A. JEFFREY, J. A. POPLE, J. S. BINKLEY, and S. VISHVESHWARA. J. Am. Chem. Soc. **100**, 373 (1978).
22. A. I. KITAYGORODSKY. Tetrahedron, **14**, 230 (1961).
23. A. I. KITAYGORODSKY. Chem. Soc. Rev. **7**, 133 (1978).
24. S. MELBERG and K. RASMUSSEN. Carbohydr. Res. **69**, 27 (1979).
25. R. U. LEMIEUX, T. TAKEDA, and B. Y. CHUNG. Am. Chem. Soc. Symp. Ser. No. 39. 1976. p. 90.
26. R. U. LEMIEUX, S. KOTO, and B. Y. CHUNG. 2nd Joint Conf. Chem. Inst. Can. and Am. Chem. Soc., Montreal. Abstracts of Papers, CARB 4. 1977.
27. R. U. LEMIEUX and S. KOTO. Abstracts of Papers, Am. Chem. Soc. **165**, Medi 022 (1973).
28. D. G. GORENSTEIN. J. Am. Chem. Soc. **99**, 2254 (1977).
29. K. BOCK, R. BURTON, and L. D. HALL. Can. J. Chem. **55**, 1045 (1977).
30. L. D. HALL, K. BOCK, C. PEDERSEN, and H. THOEGERSEN. To be published.
31. R. U. LEMIEUX and J. T. BREWER. Adv. Chem. Ser. **117**, 121 (1973).
32. K. KILDEBY, S. MELBERG, and K. RASMUSSEN. Acta Chem. Scand. Ser. A, **31**, 1 (1977).
33. R. U. LEMIEUX, D. R. BUNDLE, and D. A. BAKER. J. Am. Chem. Soc. **97**, 4076 (1975).
34. D. BASSIEUX, D. GAGNAIRE, and M. VIGNON. Carbohydr. Res. **56**, 19 (1977), and references therein.
35. K. BOCK, B. MEYER, and J. THIEM. Angew. Chem. Int. Ed. Engl. **17**, 447 (1978).
36. R. RICHARZ and K. WÜTHRICH. J. Magn. Reson. **30**, 147 (1978).
37. M. SAAS and D. ZIESSOW. J. Magn. Reson. **25**, 263 (1977).
38. P. E. PFEFFER, K. M. VALENTINE, and F. W. PARRISH. J. Am. Chem. Soc. **101**, 1265 (1979), and references therein.
39. J. J. LED and S. B. PETERSEN. J. Magn. Reson. **32**, 1 (1978).

Can. J. Chem. Downloaded from www.nrcresearchpress.com by 210.87.254.5 on 09/05/12
For personal use only.

Canadian Journal of Chemistry

Published by
THE NATIONAL RESEARCH COUNCIL OF CANADA

Journal canadien de chimie

Publié par
LE CONSEIL NATIONAL DE RECHERCHES DU CANADA

Volume 58 Number 7 April 1, 1980

Volume 58 numéro 7 1 avril 1980

^{13}C and ^{2}H spin–lattice relaxation in solid adamantane

RODERICK E. WASYLISHEN AND BRIAN A. PETTITT

Department of Chemistry, University of Winnipeg, Winnipeg, Man., Canada R3B 2E9

Received October 25, 1979

RODERICK E. WASYLISHEN and BRIAN A. PETTITT. Can. J. Chem. **58**, 655 (1980).

Spin–lattice relaxation times for the ^{13}C nuclei of adamantane and the ^{2}H nuclei of adamantane-d_{16} are reported for most of the temperature range of the solid I (plastic) phase, and for the solid II phase just below the transition point. Angular correlation times are shown to be in good agreement with those previously obtained from proton nmr data by Resing.

RODERICK E. WASYLISHEN et BRIAN A. PETTITT. Can. J. Chem. **58**, 655 (1980).

On rapporte les temps de relaxation spin–réseau du noyau ^{13}C de l'adamantane et du noyau ^{2}H de l'adamantane-d_{16} pour la plupart des intervalles de température de la phase solide I (plastique) et de la phase solide II juste en dessous du point de transition. On montre que les temps de corrélation angulaire sont en parfait accord avec ceux obtenus antérieurement par Resing à partir de données de la rmn du proton.

[Traduit par le journal]

Introduction

Adamantane (tricyclo[3,3,1,1,^{3,7}]decane, $C_{10}H_{16}$) figures centrally in the experimental and theoretical investigation of orientational disorder in crystals (1,2). The solid II → solid I phase transition at 208.6 K (ΔS = 1.95 R) (3) is complicated by hysteresis but can be grossly characterized as a tetragonal → face-centred cubic transformation accompanied by a 9% increase in volume and substantial thawing of rotational modes (4). The molecules in phase I are thought to be randomly distributed between two distinguishable orientations connected by rotations through $\pi/2$ about the cubic four-fold axes (Fig. 1), and a study of the neutron incoherent elastic structure factor (5) concluded that the dynamics of the disorder are probably dominated by jumps about these axes. A recent study of coherent inelastic neutron scattering from a single crystal of $C_{10}D_{16}$ at 293 K (6) revealed that heavily damped collective librations are also present on the scale of 25 times the jump frequency.

Rotational and translational jump times for phases I and II were measured by Resing (7) via a thorough investigation of proton nmr relaxation rates. In a previous article (8) on another disordered crystal (succinonitrile), we showed that the conventional proton-decoupled ^{13}C inversion–recovery experiment (and, to a lesser extent, ^{14}N linewidths) can be an efficacious means of determining jump times. In this article, we report correlation times for the solid I states of $C_{10}H_{16}$ and $C_{10}D_{16}$ determined by an investigation of the ^{13}C and ^{2}H resonances.

Experimental

Adamantane (99+%, Gold Label) was obtained from the Aldrich Chemical Company and adamantane-d_{16} (98 at% D) from Merck, Sharp, and Dohme.

^{13}C nmr spectra were measured at 20 MHz on a Varian CFT-20 spectrometer equipped with an 8 mm variable temperature probe, using polycrystalline samples and a coaxial tube for the acetone-d_6, D_2O, or methyl sulphoxide-d_6 deuterium lock material. Typically, 30 to 60 scans were accumulated using acquisition times of 0.5 s to 1.0 s, sweep widths of 2 kHz, and an rf decoupling field ($\gamma B_2/2\pi$) of about 4.5 kHz. ^{2}H spectra of adamantane-d_{16} were measured at 13.81 MHz on a Bruker SXP pulsed spectrometer. All T_1's were obtained by a nonlinear least squares analysis (9) of the standard inversion–recovery pulse sequence. The $\pi/2$ pulse was 16 μs for the ^{13}C measurements and 6 μs for the ^{2}H measurements. The temperature was maintained with an accuracy of ±2 K by a nitrogen gas flow.

Results and Discussion

The methine (CH) ^{13}C resonance is 184 Hz to high field of the methlyene (CH_2) ^{13}C at 20 MHz and proton-decoupling reduces the linewidths from

0008-4042/80/070655-03$01.00/0

©1980 National Research Council of Canada/Conseil national de recherches du Canada

Can. J. Chem. Downloaded from www.nrcresearchpress.com by 210.87.254.42 on 09/05/12
For personal use only.

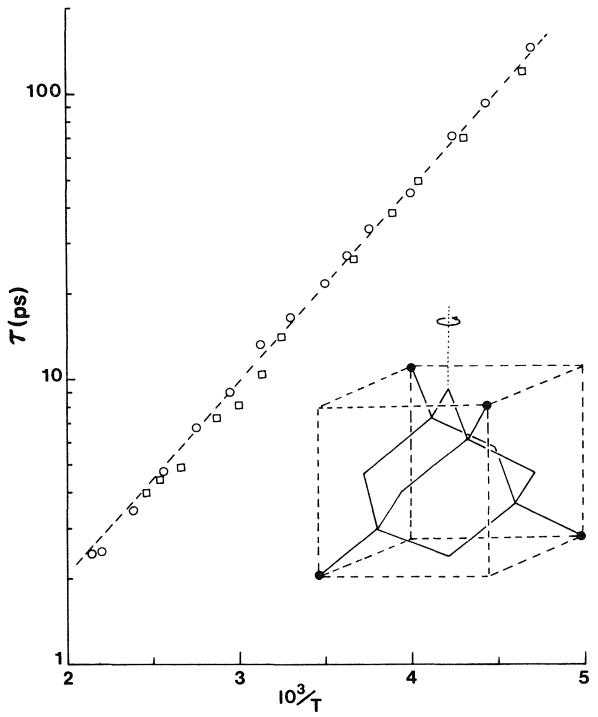


FIG. 1. Temperature dependence of angular correlation times in the solid I phase of adamantane: squares, ^{13}C data for $C_{10}H_{16}$; circles, ^{2}H data for $C_{10}D_{16}$; broken line, representation of the ^{1}H data of ref. 7. The inset shows one of the two distinguishable orientations of adamantane and one of the cubic four-fold axes.

1.1 kHz to approximately 40 Hz in the solid I phase, thus producing a well-resolved pair of lines throughout this phase. T_1's for the naturally abundant ^{13}C's of polycrystalline $C_{10}H_{16}$ are listed in Table 1 along with methine–methylene T_1 ratios and effective angular correlation times. The τ's were calculated from the $T_1(CH_2)$'s under the assumption that dipolar coupling with the bonded (1.09 Å) and nearest neighbour (2.16 Å) protons, modulated by isotropic rotation, dominates the relaxation (10), a procedure that is supported by an observation of full nuclear Overhauser enhancement factors (11) and satisfactory agreement between the average $T_1(CH)/T_1(CH_2)$ ratio (1.72) and the theoretical value (1.85). The temperature dependence of both T_1's is characterized by an activation energy, E_a, of 3.2 kcal/mol, and the τ's are shown in Fig. 1 to be in good agreement with those determined by proton nmr (7). The two values of τ for the solid II phase are also in agreement with the proton data, but at lower temperatures resolution of the lines is precluded by broadening characteristic of the "non-extreme narrowing" region.

Deuterium quadrupolar T_1's for the solid phase of $C_{10}D_{16}$ are listed in Table 2 along with angular correlation times derived from them assuming that the quadrupolar coupling constant, e^2qQ/h, is 174 kHz (the value in cyclohexane) and that the assymmetry parameter is negligible (10). Good agreement of these τ's with the ^{13}C and ^{1}H data is illustrated in Fig. 1. The τ's of $C_{10}D_{16}$ are systematically a little longer than those of $C_{10}H_{16}$, as the larger moment of inertia (24%) would lead one to expect, but the observed differences are within the uncertainties in the experimental data and e^2qQ/h.

It is worth noting that if the high symmetry of the adamantane system is broken by substituents, orientational disorder persists. Differential scanning calorimetry experiments (12) have indicated the existence of disordered phases in the 1-haloadamantanes and molecules with from one to four methyl groups. We have examined the ^{13}C nmr spectra of several 1-substituted adamantanes, showing that the 1-amino species is disordered at room temperature, and that 1-hydroxyadamantane

TABLE 1. ^{13}C spin–lattice relaxation times and angular correlation times in solid adamantane

T(K)	$T_1(CH_2)$(s)*	$T_1(CH)$(s)*	$T_1(CH)/T_1(CH_2)$	τ(ps)
406	5.96	9.95	1.67	3.97
395	5.31	9.76	1.84	4.46
375	4.86	9.20	1.89	4.87
349	3.26	5.61	1.72	7.27
334	2.95	4.96	1.68	8.03
318	2.29	3.66	1.60	10.4
303	1.72	3.00	1.75	13.8
292	1.51	2.50	1.66	15.6
272	0.898	1.42	1.58	26.3
257	0.624	1.21	1.88	37.9
247	0.484	0.952	1.76	48.9
232	0.344	0.576	1.67	68.8
215	0.201	0.313	1.56	118
198†	0.025	0.040	1.60	18 ns
190†	0.044	0.076	1.72	38 ns

*Estimated error ±10%.
†Solid II phase.

TABLE 2. ^{2}H spin–lattice relaxation times and angular correlation times in solid adamantane-d_{16}

T(K)	T_1(ms)*	τ(ps)	T(K)	T_1(ms)*	τ(ps)
467	923	2.42	276	83.4	26.8
455	907	2.46	266	66.8	33.4
421	643	3.47	251	50.3	44.4
390	472	4.73	241	38.1	58.6
364	331	6.74	236	31.4	71.0
339	245	9.12	225	24.1	92.6
321	169	13.2	213	15.5	144
303	136	16.4			
286	103	21.7	200†	0.79	14 ns

*Estimated error ±5%.
†Solid II phase.

Can. J. Chem. Downloaded from www.nrcresearchpress.com by 210.87.254.42 on 09/05/12
For personal use only.

undergoes an order ↔ disorder phase transition at 366 ± 2 K. ^{13}C relaxation times in the disordered phases of these molecules reflect a high degree of anisotropy, but we were unable to obtain a consistent account of the T_1 ratios in terms of Woessner's two-parameter rotational diffusion model (13). Perhaps anisotropic jump models along the lines of those used by Brot and co-workers (14) in the analysis of neutron scattering and nmr data for disordered quinuclidine, $HC(CH_2CH_2)_3N$, will prove to be useful in this regard, but many more experiments are needed.

Acknowledgements

We are grateful to M. Graham and J. S. Lewis for technical assistance, and to Professor E. Tomchuk for use of the Bruker SXP spectrometer. This research was supported by grants from the Natural Sciences and Engineering Research Council of Canada.

1. N. G. PARSONAGE and L. A. K. STAVELEY. Disorder in molecular crystals. Clarendon Press, Oxford. 1978.
2. J. N. SHERWOOD (*Editor*). The plastically crystalline state. John Wiley and Sons, New York. 1979.
3. S. CHANG and E. F. WESTRUM. J. Phys. Chem. **64**, 1547 (1960).
4. C. E. NORDMAN and D. L. SCHMITKONS. Acta Crystallogr. **18**, 764 (1965); D. W. MCCALL and D. C. DOUGLASS. J. Chem. Phys. **33**, 777 (1960).
5. R. E. LECHNER and A. HEIDEMANN. Commun. Phys. **1**, 213 (1976).
6. J. C. DAMIEN, J. LEFEBVRE, M. MORE, B. HENNION, R. CURRAT, and R. FOURET. J. Phys. C, **11**, 4323 (1978).
7. H. A. RESING. Mol. Cryst. Liq. Cryst. **9**, 101 (1969).
8. R. E. WASYLISHEN and B. A. PETTITT. Mol. Phys. **36**, 1459 (1978).
9. M. SASS and D. ZIESSOW. J. Magn. Reson. **25**, 263 (1977).
10. A. ABRAGAM. The principles of nuclear magnetism. Clarendon Press, Oxford. 1961.
11. D. A. TORCHIA. J. Magn. Reson. **30**, 613 (1978).
12. T. CLARK, T. MC. O. KNOX, H. MACKLE, and M. A. MCKERVEY. J. Chem. Soc. Faraday Trans. I, **73**, 1224 (1977).
13. D. E. WOESSNER. J. Chem. Phys. **37**, 647 (1962).
14. C. BROT, B. LASSIER-GOVERS, R. E. LECHNER, and F. VOLINO. J. Phys. Paris, **40**, 563 (1979); C. BROT and J. VIRLET. J. Phys. Paris, **40**, 573 (1979).

Can. J. Chem. Downloaded from www.nrcresearchpress.com by 210.87.254.42 on 09/05/12
For personal use only.

Conformations of bridged diphenyls. XV. Crystal structure of (4′-carbomethoxy-2′-nitrophenoxy)benzene and the effect of intramolecular interactions in nitro substituents

RAMANATHAN GOPAL, W. DAVID CHANDLER, AND BEVERLY E. ROBERTSON[1]

Department of Chemistry, University of Regina, Regina, Sask., Canada S4S 0A2

Received November 2, 1978[2]

RAMANATHAN GOPAL, W. DAVID CHANDLER, and BEVERLY E. ROBERTSON. Can. J. Chem. **58**, 658 (1980).

The structure of (4′-carbomethoxy-2′-nitrophenoxy)benzene, $C_{14}H_{11}NO_5$, has been determined by X-ray diffraction. The crystals are monoclinic, $a = 8.880(7)$, $b = 9.792(4)$, $c = 14.820(5)$, $\beta = 90.07(5)$, $P2_1/c$ with $Z = 4$. The integrated intensities of 2966 independent reflections were measured on a four-circle diffractometer, 2072 of which were used in the refinement to give a final least-squares weighted residual of 0.062 and a conventional R factor of 0.086. The absence of *ortho* substituents on one ring of the molecule allows it to adopt the twist-nitro-*distal* conformation. The lengths of the bonds from the unsubstituted ring and the substituted ring to the bridging oxygen atom are 1.409(3) and 1.353(3) Å respectively. The torsional angles about those bonds are 54.6° and 16.5°. The angle subtended at the bridging oxygen atom is 120.0(3)°.

The unusual thermal ellipsoids associated with one of the nitro oxygen atoms of this structure and with a nitro oxygen atom of three related structures occur when the nitro substituent is nearly coplanar with the phenyl ring on which it is substituted and also has a neighbouring substituent or bridging group. The unusual thermal ellipsoids then result from repulsive exchange forces.

RAMANATHAN GOPAL, W. DAVID CHANDLER et BEVERLY E. ROBERTSON. Can. J. Chem. **58**, 658 (1980).

On a déterminé par diffraction de rayons-X la structure du (carbométhoxy-4′ nitrophénoxy-2′) benzène $C_{14}H_{11}NO_5$. Les cristaux sont monocliniques $a = 8.880(7)$, $b = 9.792(4)$, $c = 14.820(5)$, $\beta = 90.07(5)$, $P2_1/c$ avec $Z = 4$. On a mesuré les intensités intégrées de 2966 réflexions indépendantes à l'aide d'un diffractomètre à 4 cycles. De ces réflexions 2072 sont affinées pour avoir une moyenne résiduelle finale des moindres carrés de 0.062 et une valeur conventionnelle R de 0.086. L'absence de substituants en position *ortho* sur un cycle de la molécule lui permet d'adopter une conformation croisée du groupe nitro le plus éloigné. Les longueurs de liaison entre les cycles substitué et non substitué et l'atome d'oxygène sont respectivement de 1.409(3) et 1.353(3) Å. Les angles de torsion autour de ces liaisons sont de 54.6° et 16.5°. L'angle sous tendu à l'atome d'oxygène en position de pont est de 120.0(3)°.

L'ellipsoide thermique peu usuel associé à l'un des atomes d'oxygène du groupe nitro de cette structure et à l'atome d'oxygène du groupe nitro de trois structures apparentées se produit quand le substituant nitro est quasi coplanaire avec le cycle phényle sur lequel il est substitué et qui a également un substituant voisin ou un groupe en position de pont. L'ellipsoide thermique peu usuel résulte alors des forces de répulsion.

[Traduit par le journal]

Introduction

We have established the important role of the *ortho* substituents of di-*ortho*-substituted phenyl rings of bridged diphenyl compounds in determining the conformation of such compounds (1–5). In particular, the steric requirements of the *ortho* substituents outweigh competing conjugative effects (6). In tri-*ortho*-substituted bridged diphenyls with bridging groups which contain more than one atom and which are strongly electronegative (SO, SO_2, CO) the conformation is twist with the mono-*ortho*-substituent *proximal*.[3] If the bridging group is weakly electron donating (CH_2) or less bulky (O and S) the conformation is skew with the mono-*ortho*-substituent *distal*. It has recently been demonstrated by Paulus that intramolecular hydrogen bonding involving the bridging group and *ortho* substituents can also fix the orientation of one of the rings (7).

In di- or tri-*ortho*-substituted bridged diphenyls which do not contain large electronegative bridging groups the main steric interactions are between *ortho* substituents on one ring and the *ortho* substituents or π-electrons on the other ring. These interactions do not necessarily exist in a mono-*ortho*-substituted bridged diphenyl and other effects such as conjugation and interaction between the single *ortho* substituent and the bridge become important. We have therefore chosen to determine the structure of the mono-*ortho*-substituted bridged diphenyl, (4′-carbomethoxy-2′-nitrophenoxy)benzene.

A number of bridged diphenyl compounds whose structure we have reported previously have contained a nitro substituent with one oxygen atom showing an unusual thermal ellipsoid. The phenomenon occurs again in (4′-carbomethoxy-2′-nitrophenoxy)benzene. We shall therefore attempt to shed some light on the origin of this phenomenon.

Experimental

(4′-Carbomethoxy-2′-nitrophenoxy)benzene was formed by

[1]To whom all correspondence should be addressed.

[2]Revision received September 7, 1979.

[3]The nomenclature used here has been defined in a previous paper (3).

0008-4042/80/070658-06$01.00/0

©1980 National Research Council of Canada/Conseil national de recherches du Canada

the reaction of phenol, NaOH, and methyl 4-chloro-3-nitrobenzoate. They were reacted for 20 h according to the method of Wright and Jorgenson (8) as generalized by Chandler *et al.* (9). The mp after four recrystallizations from absolute ethanol was 103.5–105.0°C. The crystals are translucent with a slight yellowish colour and have well defined faces. A sample with dimensions 0.65 mm on a side was used for data collection. The systematic absences ($h0l$, $l = 2n + 1$; $0k0$, $k = 2n + 1$) and the Laue symmetry gave the space group $P2_1/c$.

The integrated intensities of 2966 independent reflections with 2θ values between 2° and 55° were measured on a Picker FACS-1 automated diffractometer using MoKα radiation with a graphite monochromator. The θ–2θ scan mode was used with a scan rate of 2° min^{-1} and a minimum base width of 2.95° in 2θ. The background was counted for 40 s at each limit of the scan. The intensities of three standard reflections were monitored after the intensities of each 100 reflections were measured and were not observed to change significantly. The centered positions of 21 reflections with 2θ values between 40° and 45° (MoKα_1) were used to calculate the cell parameters by least-squares. The estimated standard deviations given below for the lattice constants were taken directly from the least-squares calculations.

Crystal data are as follows:

$C_{14}H_{11}NO_5$ fw = 273.6
Monoclinic, $P2_1/c$; $a = 8.880(7)$, $b = 9.792(4)$, $c = 14.820(5)$ Å, $\beta = 90.07(5)°$, $\rho_o = 1.40(1)$ g cm^{-3} (flotation)$_3$, $\rho_c = 1.408$ g cm^{-3}, $Z = 4$, $F(000) = 568$ e, λ(MoKα_1) = 0.70926 Å, μ(MoKα) = 1.13 cm^{-1}, $T = 22(1)$°C.

The intensity data were reduced to observed structure factors using standard procedures. No corrections were made for the effects of absorption or extinction. The scattering factors for the carbon, oxygen, and nitrogen atoms were taken from Cromer and Mann (10). The scattering factor for the hydrogen atoms was taken from Stewart *et al.* (11). The 374 reflections with $|E| > 1.40$ were used to solve the structure using the logical symbolic addition method.[4] An E-map calculated with the non-trivial solution with the highest figures of merit yielded all carbon, nitrogen, and oxygen atoms. The structure was refined anisotropically and the hydrogen atoms were found from a difference Fourier calculation. The structure was refined further treating the hydrogen atoms isotropically. The final cycles of refinement used the 2072 reflections for which $|F_o| > \sigma(F_o)$, where $\sigma(F_o) = 1.0 + 0.01(F_o) + \sigma'(F_o)$ and where $\sigma'(F_o)$ is an estimated standard deviation based entirely on counting statistics. At this point the final value of the weighted residual R_w and the conventional R factor were 0.067 and 0.086 respectively.

It was apparent that the thermal ellipsoid for the atom O(5) was elongated normal to the plane of the nitro group which is itself nearly coplanar with the phenyl ring to which it is bonded. It was decided that an attempt should be made to examine the electron density associated with this atom in more detail. The atom O(5) was removed from the refinement and a difference Fourier map was prepared. The electron density associated with the atom O(5) showed as a ridge of electron density with a saddle point slightly lower in electron density (~10%) than the two peaks at the end of the ridge.

The electron density associated with O(5) was then represented by two half atoms, O(51) and O(52), initially positioned at the two peaks in the ridge. Refinement was continued using isotropic temperature factors for these half atoms. The final values of R_w and R were 0.062 and 0.086 respectively. The final positional and thermal parameters are given in Table 1 with estimated standard deviations. The observed and calculated structure factors have been placed in the Depository of Unpublished Data.[5] The bond lengths and angles and the atomic numbering are given in Fig. 1.

Discussion

In the closely related compound 2-(4′-carbomethoxy-2′-nitrophenoxy)-1,3,5-trimethylbenzene, the mesityl ring deviates 11.0° from being orthogonal to the plane of the central C—O—C plane and the conformation is skew-nitro-*distal* (3). In the present compound, (4′-carbomethoxy-2′-nitrophenoxy)benzene, the absence of the di-*ortho* substituents allows the equivalent ring to rotate further and the conformation is twist-nitro-*distal*. The angles between the planes of the molecule, as labelled in Fig. 2 are given in Table 2. The torsional angles [C(4)—O(1)—C(7)—C(8)] and [C(7)—O(1)—C(4)—C(5)], which correspond to the dihedral angles *2,3* and *1,2*, are ±16.5° and ±54.6° respectively. The plus and minus signs refer to the two enantiomers which must be present because the space group of the structure is centrosymmetric.

The bonds to the bridging oxygen atom differ by 0.056(5) Å which compares with 0.053(3) Å in the similar trimethyl substituted compound (3). In a previous paper (2) we have discussed the relationship between these bond length differences and the electronic properties of the substituents on the rings.

The use of two half atoms to represent the electron density at the atom O(5) decreased R_w by 0.005. Similar anomalous thermal ellipsoids have been observed previously for nitro oxygen atoms in this series of structures; in the two independent molecules of 2-(3′-methyl-4′-nitrophenoxy)-1,3-diisopropylbenzene (1), in 2-(4′-carbomethoxy-2′-nitrothiophenyl)-1,3,5-trimethylbenzene (4), and in 2-(4′-carbomethoxy-2′-nitrobenzyl)-1,3,5-trimethylbenzene. In these four cases the refinement with half atoms replacing a single atom to represent the anomalous thermal ellipsoid was not attempted.

It has been observed previously that the O—N—O angle of *ortho*-nitro substituents in these compounds tends to increase as the dihedral angle between the NO_2 group and the phenyl ring to which it is bonded increases (16). Figure 3 shows

[4]The structure was solved using the Germain and Woolfson program LSAM (12). All Fourier calculations were carried out using the Zalkin program FORDAP (13). The Busing *et al.* program ORFLS (14) was used for least-squares refinement. Stereograms were prepared with the aid of the Johnson program ORTEP (15).

[5]Complete set of tabular data is available, at a nominal charge, from the Depository of Unpublished Data, CISTI, National Research Council of Canada, Ottawa, Ont., Canada K1A 0S2.

TABLE 1. Structural parameters of (4′-carbomethoxy-2′-nitrophenoxy)benzene (esd in parentheses)

(*a*) Fractional coordinates of atoms with anisotropic temperature factors (× 10^4)

Atom	*x*	*y*	*z*
C(1)	3945(4)	3785(4)	987(2)
C(2)	3225(5)	4992(4)	1137(2)
C(3)	2856(4)	5411(4)	2004(2)
C(4)	3248(4)	4572(3)	2707(2)
C(5)	3980(4)	3359(4)	2578(2)
C(6)	4323(4)	2960(4)	1706(2)
C(7)	2188(4)	4340(3)	4182(2)
C(8)	1273(4)	3253(3)	3956(2)
C(9)	470(4)	2547(3)	4599(2)
C(10)	552(3)	2924(3)	5503(2)
C(11)	1442(4)	4022(3)	5735(2)
C(12)	2247(3)	4716(3)	5092(2)
C(13)	−261(4)	2202(4)	6236(2)
C(14)	−1901(7)	384(6)	6615(3)
N(1)	3153(4)	5876(3)	5403(2)
O(1)	2976(3)	5090(2)	3578(1)
O(2)	−188(3)	2528(3)	7015(1)
O(3)	−1071(3)	1151(3)	5937(1)
O(4)	3035(4)	6237(3)	6154(2)

(*b*) Anisotropic thermal parameters (× 10^3) U_{ij} (esd in parentheses)

t.f. = $\exp\{-2\pi^2(a^{*2}h^2U_{11}+\cdots+2a^*b^*hkU_{12}\}$

Atom	U_{11}	U_{22}	U_{33}	U_{12}	U_{13}	U_{23}
C(1)	75(3)	81(3)	50(2)	−3(2)	8(2)	−5(2)
C(2)	89(3)	82(3)	51(2)	10(2)	0(2)	7(2)
C(3)	86(3)	61(2)	54(2)	7(2)	4(2)	1(2)
C(4)	67(2)	59(2)	45(2)	−10(2)	3(2)	−3(2)
C(5)	76(3)	65(2)	58(2)	−2(2)	−7(2)	7(2)
C(6)	68(3)	67(2)	71(2)	3(2)	4(2)	−8(2)
C(7)	73(2)	51(2)	42(2)	7(2)	−5(2)	1(1)
C(8)	80(3)	62(2)	38(2)	−2(2)	−6(2)	−7(2)
C(9)	64(2)	60(2)	45(2)	3(2)	−1(2)	−6(2)
C(10)	57(2)	61(2)	41(2)	11(2)	−3(1)	−2(1)
C(11)	60(2)	66(2)	38(2)	17(2)	−6(2)	−7(2)
C(12)	61(2)	52(2)	45(2)	5(2)	−8(2)	−8(2)
C(13)	64(2)	72(2)	49(2)	17(2)	0(2)	1(2)
C(14)	109(4)	96(4)	77(3)	−7(3)	32(3)	6(3)
N(1)	94(3)	75(2)	53(2)	−5(2)	−9(2)	−13(2)
O(1)	113(2)	61(1)	44(1)	−17(2)	7(1)	−5(1)
O(2)	94(2)	108(2)	40(1)	6(2)	4(1)	−1(1)
O(3)	95(2)	80(2)	54(1)	−9(2)	12(1)	−1(1)
O(4)	157(3)	181(3)	88(2)	−71(3)	11(2)	−65(2)

(*c*) Fractional coordinates (× 10^3) and isotropic temperature factors

Atom	*x*	*y*	*z*	*B*(Å^2)
H(1)	425(3)	349(3)	36(2)	6(1)
H(2)	303(4)	563(4)	64(2)	8(1)
H(3)	239(4)	628(3)	214(2)	7(1)
H(5)	418(4)	281(3)	307(2)	6(1)
H(6)	483(4)	212(3)	160(2)	7(1)
H(8)	121(3)	299(3)	336(2)	5(1)
H(9)	10(3)	675(3)	56(2)	5(1)
H(11)	144(3)	434(3)	636(2)	5(1)
H(14,1)	−254(6)	−29(5)	630(3)	12(2)
H(14,2)	−248(5)	101(4)	695(3)	9(1)
H(14,3)	−116(5)	−1(4)	707(3)	11(1)
O(51)	439.5(6)	616.4(5)	499.0(3)	6.3(1)
O(52)	339.0(7)	679.1(6)	488.0(4)	7.3(1)

TABLE 1 (*Concluded*)

the O—N—O angle plotted against the dihedral angle for all of the compounds reported in this series.[6] The correlation between O—N—O angle and dihedral angle seems to be followed for all cases where the nitro group is *ortho* to any substituent, including the bridging group of a bridged diphenyl compound. It is not followed when there are not restrictions to the nitro group being coplanar with the phenyl ring, as in the case of the *ortho*-nitro-substituents in the two independent molecules of 2-(2′-carbomethoxy-4′-nitrophenoxy)-1,3,5-trichlorobenzene and the *para*-nitro-substituent of 2-(2′,4′-dinitrophenoxy)-1,3,5-tri-*tert*-butylbenzene (2).

The anomalous thermal ellipsoids occur in these compounds when the nitro-substituents form lower dihedral angles with the phenyl ring in spite of the presence of a neighbouring substituent or bridging group. The apparent exception is the *ortho*-nitro substituent in 2-(2′,4′-dinitrophenoxy)-1,3,5-tri-*tert*-butylbenzene. In this substituent both oxygen atoms show highly anisotropic thermal ellipsoids extended normal to the plane of the nitro group, although not as severe as in the five cases where only one oxygen atom is unusual.

The appearance of the anomalous thermal ellipsoids only in those cases where steric effects decrease the O—N—O angle suggests that repulsive exchange forces arising from contact with neighbouring substituents or bridging groups are involved in the creation of the anomalous thermal ellipsoids. In terms of potential energy maps, these forces together with the effect of conjugation between the nitro group and the ring (which restricts the rotation of the substituent) lead to a potential well, which when traversed normal to the plane of the phenyl ring, shows a broad minimum or perhaps double minima. If the barrier between those minima are large with respect to kT, then the anomalous thermal ellipsoids would represent static disorder.

In other cases it is clearly possible for the nitro

[6]For the purpose of calculating the dihedral angle between the NO_2 group and the phenyl ring and the O—N—O angle in the case of the compound reported here, the position of the single atom of unit weight representing the electron density of O(5) was used.

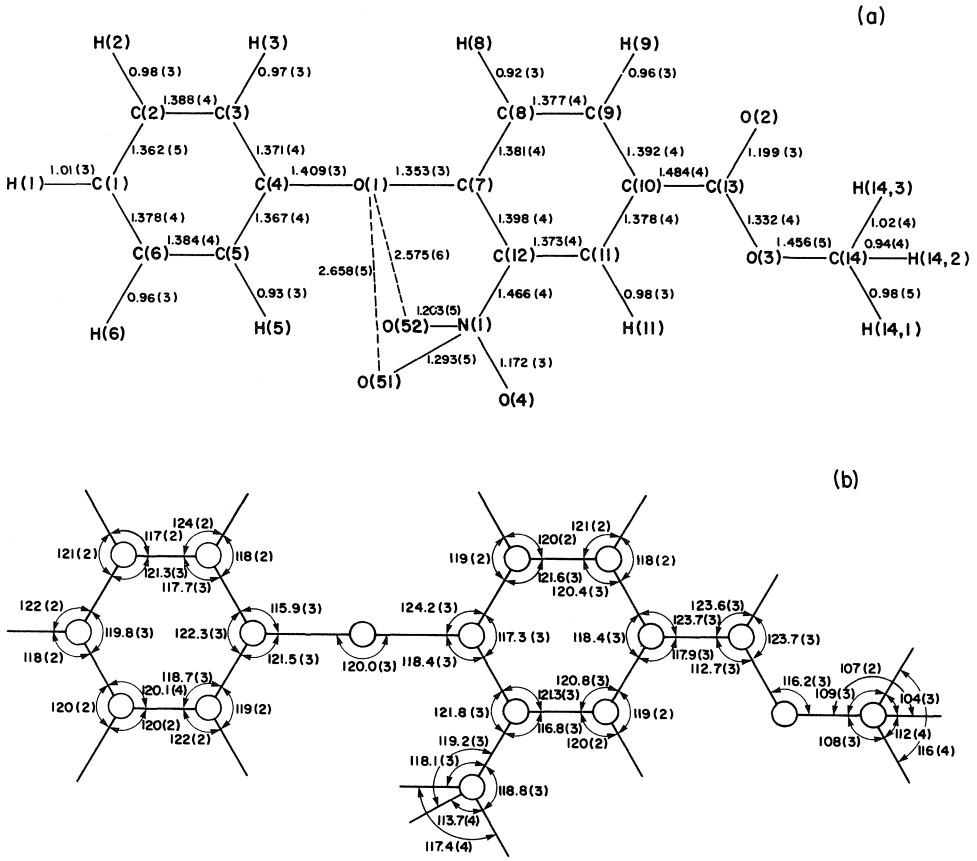


FIG. 1. (*a*) Bond lengths (Å) and atom numbering. (*b*) Bond angles (deg). The numbers in parentheses are the estimated standard deviations.

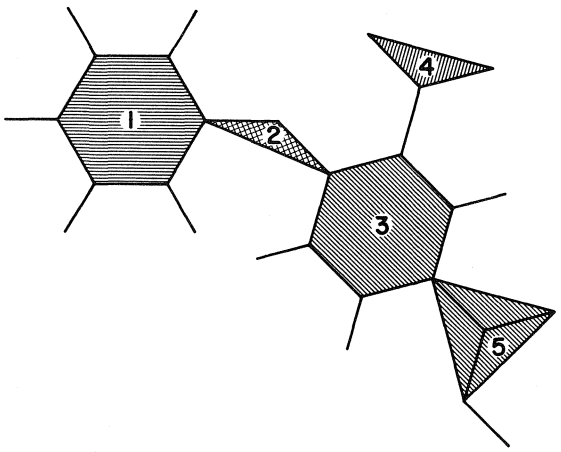


FIG. 2. Labeling of the least-squares planes.

TABLE 2. Least-squares planes

(*a*) Equations of planes $Ax + By + Cz = D$. Coordinates refer to the directions *a*, *b*, and c^*. The planes are defined in Fig. 2

Plane	*A*	*B*	*C*	*D*
1	−0.8817	−0.4659	−0.0739	−4.9225
2	−0.8496	0.4169	−0.3231	−1.8754
3	−0.7727	0.6204	−0.1346	0.3133
4	−0.7648	0.5895	−0.2598	−0.8214
5	−0.7856	0.6056	−0.1267	0.3245

(*b*) Dihedral angles

Planes	Angles (deg)
1,2	54.6
1,3	66.3
2,3	16.5
3,4	7.4
3,5	1.2

group to be rotated adequately out of the plane of the phenyl ring in order to avoid close contact with neighbouring groups, as, for instance, in bridged diphenyls with proximal conformations or in 2-(4′-carbomethoxy-2′-nitrophenoxy)-1,3,5-trimethylbenzene (3). Therefore, other factors must be present in those compounds in which the substituent is not rotated. The nature of the packing of the molecules might be expected to be an important factor in restricting the rotation of the substituent.

In the present structure, (4′-carbomethoxy-2′-

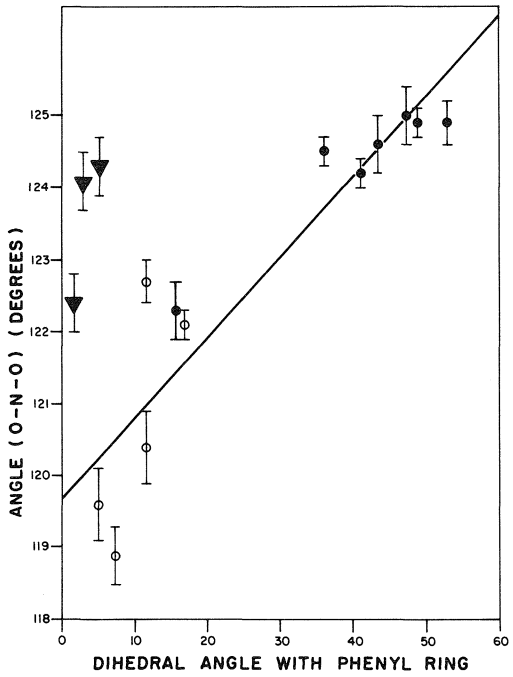


FIG. 3. O—N—O angle (deg) for nitro groups versus dihedral angle between the nitro substituent and the phenyl ring to which it is bonded. All circles represent nitro groups with neighbouring substituents or bridging groups. Open circles represent groups with an unusual thermal ellipsoid representing one of the oxygen atoms. The least-squares line is fitted to all circles. The triangles represent nitro groups with no neighbouring substituent or bridging group. The correlation coefficient is 0.92.

nitrophenoxy)benzene, the reason that the nitro group is constrained from rotation is apparent from the packing diagram as shown in Fig. 4. The nitro groups are sandwiched between the parts of two neighbouring molecules which are approximately coplanar with the nitro substituent and its phenyl ring. In other cases where the nitro substituent is nearly coplanar with its phenyl ring, in spite of the crowding from neighbouring groups, the reason is not clear. In the two independent molecules of 2-(3′-methyl-4′-nitrophenoxy)-1,3-diisopropylbenzene (1) and in 2-(4′-carbomethoxy-2′-nitrobenzyl)-1,3,5-trimethylbenzene (5) the oxygen atoms showing the anomalous thermal ellipsoids share the common feature that they face two hydrogen atoms of a neighbouring methyl group or bridging CH_2 group which straddle the plane of the phenyl ring on which the nitro group is substituted, and therefore also straddle the oxygen atom in question. It is our opinion that in all of these cases, adequate information is not available for us to predict the nature of the motion, or lack thereof, of the anomalous oxygen atom.

The possibility must be considered that the unusual behavior of the oxygen atom leads to an artificially low value for the O—N—O angle, and the true value of the angle, after corrections, is therefore relatively constant. However, in order to generate the single anomalous oxygen thermal ellipsoid, we must assume either a rotation of the NO_2 group about the N—O bond to the normal oxygen atom or a "riding motion" of the anomalous oxygen atom about the N atom which maintains a constant N—O distance to that atom (18). In both cases, the O—N—O angle is not artificially reduced by the thermal motion. In the event that the anomalous thermal ellipsoids represent static disorder, the O(51)—N(1)—O(4) and O(52)—N(1)—O(4) angles (117.4(4) and 113.7(4)° respectively) must be taken as a measure of the O—N—O angle in these circumstances, and they are lower than those used in Fig. 3, which are based on single atoms.[7]

In the compound reported here the nitro-substituents occur in pairs related by centers of symmetry. The O(5)···O(5) distance of 3.46 Å is shorter than the O···O distances involving any of the other oxygen atoms showing anomalous thermal ellipsoids, but it is greater than the van der Waals contact distance. However, the separation between the position of two symmetry-related O(51) half atoms is shorter than ver der Waals contacts at 2.52 Å. Therefore, the two O(51) positions cannot be occupied simultaneously. The two O(5) atoms related by the center of symmetry must either move concertedly or be disordered so as to violate the local center of symmetry between them.[8]

The reason for the existence of the anomalous thermal ellipsoids seems to be related to repulsive exchange forces. However, we would expect the entire nitro group to be affected, as in the case of the *ortho*-nitro-substituent in 2-(2′,4′-dinitrophenoxy)-1,3,5-tri-*tert*-butylbenzene (2) because of the rigidity of the NO_2 group. This implies a weakening (and thus a lengthening) of the bond to the anomalous oxygen atom, and a strengthening (and thus a shortening) of the bond to the normal oxygen atom.

[7]The errors quoted for bond lengths and angles were calculated with the program ORFFE (17). The true errors in the bond lengths and angles which involve the half atoms O(51) and O(52) representing the thermal ellipsoid of atom O(5) suffer from additional effects involving the inadequacies of the model and are, therefore, larger than those quoted, but by an indeterminate amount.

[8]If both atoms resided simultaneously in the position O(52), the temperature factor for O(52) should be smaller than that of O(51), which it is not.

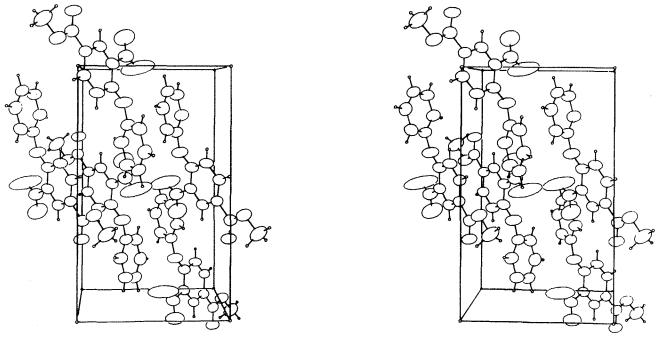


FIG. 4. Stereoscopic view of the molecular packing. The ***a*** axis points to the right, the ***b*** axis is into the paper, and the ***c*** axis points up.

In order to test this hypothesis it is necessary to use accurate bond lengths and therefore the effects of thermal motion on the bond lengths should be removed. It is difficult to make accurate corrections for thermal motion for all of the bonds involved because of the large values of the anisotropic temperature factors and because of the uncertainty as to what they really represent. The results obtained are not conclusive. Nevertheless, we suspect that the close contact between the nitro substituent and a neighbouring group cause additional changes within the molecule.

Acknowledgements

The authors thank the National Research Council of Canada for support in the form of Operating Grants, the Alexander von Humboldt Foundation of West Germany for the award of a Fellowship to B.E.R., the University of Regina for computer time, and Dr. S. Levine for valuable discussions.

1. E. A. H. GRIFFITH, W. D. CHANDLER, and B. E. ROBERTSON. Can. J. Chem. **50**, 2963 (1972).
2. E. A. H. GRIFFITH, W. D. CHANDLER, and B. E. ROBERTSON. Can. J. Chem. **50**, 2972 (1972); **50**, 2979 (1972); S. P. N. VAN DER HEIJDEN, W. D. CHANDLER, and B. E. ROBERTSON. Can. J. Chem. **53**, 2108 (1975); **53**, 2115 (1975); **53**, 2127 (1975); R. GOPAL, W. D. CHANDLER, and B. E. ROBERTSON. Can. J. Chem. **57**, 2767 (1979).
3. S. P. N. VAN DER HEIJDEN, E. A. H. GRIFFITH, W. D. CHANDLER, and B. E. ROBERTSON. Can. J. Chem. **53**, 2084 (1975).
4. S. P. N. VAN DER HEIJDEN, W. D. CHANDLER, and B. E. ROBERTSON. Can. J. Chem. **53**, 2102 (1975).
5. S. P. N. VAN DER HEIJDEN, W. D. CHANDLER, and B. E. ROBERTSON. Can. J. Chem. **53**, 2121 (1975).
6. K. GURTU, W. D. CHANDLER, and B. E. ROBERTSON. Can. J. Chem. **53**, 2093 (1975).
7. E. F. PAULUS. Private communication.
8. J. WRIGHT and E. C. JORGENSON. J. Org. Chem. **33**, 1245 (1968).
9. W. D. CHANDLER, J. J. BERGMAN, and G. H. HAAS. Can. J. Chem. **49**, 583 (1971).
10. D. T. CROMER and J. B. MANN. Acta Crystallogr. A**24**, 321 (1968).
11. R. F. STEWART, E. R. DAVIDSON, and W. T. SIMPSON. J. Chem. Phys. **42**, 3175 (1965).
12. G. GERMAIN and M. M. WOOLFSON. Acta Crystallogr. B**24**, 91 (1968).
13. A. ZALKIN. FORDAP, A. Fortran program for Fourier calculations. University of California, Berkeley, CA. 1965.
14. W. R. BUSING, K. O. MARTIN, and H. A. LEVY. ORFLS, Report ORNL-TM-305. Oak Ridge National Laboratory, Oak Ridge, TN. 1962.
15. C. K. JOHNSON. ORTEP, Report ORNL-3794. Oak Ridge National Laboratory, Oak Ridge, TN. 1965.
16. S. P. N. VAN DER HEIJDEN. Ph.D. Thesis, University of Regina, Regina, Sask. 1974.
17. W. R. BUSING AND H. A. LEVY. ORFFE. Report ORNL-TM-306. Oak Ridge National Laboratory, Oak Ridge, TN. 1965.
18. W. R. BUSING and H. A. LEVY. Acta. Crystallogr. **17**, 142 (1964).

The crystal structure of [Pt(tetraethyldiethylenetriamine)I]I

ROSEMARY C. E. DURLEY AND WILLIAM L. WALTZ

Department of Chemistry and Chemical Engineering, University of Saskatchewan, Saskatoon, Sask., Canada S7N 0W0

AND

BEVERLY E. ROBERTSON

Department of Physics and Astronomy, University of Regina, Regina, Sask., Canada S4S 0A2

Received September 14, 1979

ROSEMARY C. E. DURLEY, WILLIAM L. WALTZ, and BEVERLY E. ROBERTSON. Can. J. Chem. **58**, 664 (1980).

Crystals of [Pt(Et_4dien)I]I, where Et_4dien = $(C_2H_5)_2NC_2H_4NHC_2H_4N(C_2H_5)_2$, have been prepared. A three dimensional crystal structure analysis has been carried out in a monoclinic unit cell having $a = 12.565(8)$, $b = 7.576(6)$, $c = 21.040(15)$ Å, $\beta = 91.12(2)°$ and space group $P2_1/c$, $Z = 4$. Full-matrix least-squares using 1982 independent, observed reflections converged at $R = 0.067$. The platinum atom has square-planar co-ordination. The orientation of the four ethyl groups with respect to the plane of the ligand is similar to that observed in related molecules, in spite of a lack of similarity of the molecular packing. The iodide ion appears to be hydrogen bonded to the ligand.

ROSEMARY C. E. DURLEY, WILLIAM L. WALTZ et BEVERLY E. ROBERTSON. Can. J. Chem. **58**, 664 (1980).

On a préparé des cristaux de [Pt(Et_4dien)I]I où Et_4dien = $(C_2H_5)_2NC_2H_4NHC_2H_4N(C_2H_5)_2$. On a effectué une analyse tridimensionnelle de la structure du cristal pour une maille monoclinique ayant $a = 12.565(8)$, $b = 7.576(6)$, $c = 21.040(15)$ Å, $\beta = 91.12(2)°$ et un groupe d'espace $P2_1/c$, $Z = 4$. Une analyse par la méthode des moindres carrés (matrice complète) de 1982 réflexions indépendantes observées conduit à une valeur de $R = 0.067$. L'atome de platine a une coordination plan-carrée. L'orientation des 4 groupes éthyles par rapport au plan du ligand est semblable à celle observée dans les molécules apparentées en dépit d'un manque de similitude de l'entassement moléculaire. Les ions iodures semblent être liés au ligand au moyen de l'hydrogène.

[Traduit par le journal]

Introduction

Studies of the substitution reactions of palladium(II) and platinum(II) complex ions of the type $[M(dien)X]^+$ and $[M(Et_4dien)X]^+$, where dien and Et_4dien represent the tridentate ligands diethylenetriamine and *N,N,N′,N′*-tetraethyldiethylenetriamine respectively and X is a replacable ligand such as a halogen or pseudohalogen, have played a prominent role in the elucidation of the substitution mechanisms of square-planar metal complexes (1, 2). This prominence is due in part to the marked difference in kinetic behavior between these two types of systems. For the dien compounds, their substitutional processes involve an associative mechanism of the type commonly encountered with many square-planar complex ions containing palladium or platinum centers. In contrast, the Et_4dien species are remarkably less reactive and the mechanism now shows signs of having considerable dissociative character. The origin of these features has been attributed to the fact that the ethyl groups may severely limit access to the metal center owing to their possible occupancy of positions above and below the molecular plane (1). In a limiting sense, the Et_4dien ligand would then give rise to a *pseudo-octahedral* geometry about the metal center. In keeping with this view, molecular models suggest the possibility of considerable steric hindrance arising from the presence of the ethyl moieties. However, recent reports by Bresciani and co-workers (3) on the crystal structure analysis of $[Pd(Et_4dien)NO_2]^+$ and $[Pd(dien)N_3)^+$ indicate a more open structure. In order to discern if these structures may be representative of a more general situation, we have undertaken a crystal structure investigation of the Et_4dien compound, [Pt(Et_4dien)I]I, where the metal center is now platinum(II) and the X group is iodine. Crystals of this compound were found to be more suitable for X-ray studies than the analogous chlorine material. While this platinum–iodide compound exhibits a different space group and packing factors from those of the palladium systems, the relative positions of the ethyl groups are very similar in all three cases. Furthermore, our results suggest the possibility of hydrogen bonding between the complex cation and the iodide anion. The pattern of this interaction appears to differ from that reported for [Pt(dien)Br]Br (4).

Experimental

Preparation of [Pt(Et_4dien)I]I

[Pt(Et_4dien)I]I refers to iodo-*N,N,N′,N′*-tetraethyldiethylenetriamineplatinum(II) iodide. The compound was prepared by a procedure similar to that used by Watt and Cude to prepare iodo(diethylenetriamine)platinum(II) iodide (5). $PtI_2 \cdot H_2O$ was mixed with Et_4dien and baked to dryness. The solid was extracted with water at 90°C, and the unreacted $PtI_2 \cdot H_2O$ was separated by filtration. The latter was again treated with Et_4dien as before. The various filtrate fractions

0008-4042/80/070664-05$01.00/0

©1980 National Research Council of Canada/Conseil national de recherches du Canada

Can. J. Chem. Downloaded from www.nrcresearchpress.com by 210.87.254.42 on 09/05/12
For personal use only.

Can. J. Chem. Downloaded from www.nrcresearchpress.com by 210.87.254.42 on 09/05/12
For personal use only.

were combined and the pH was adjusted to ca. 6–7 by the addition of HI. The solution volume was reduced by use of a rotoevaporator until crystallization occurred. The crystals were collected, washed with ice-cold water, and then recrystallized from hot water (80°C). The solution was allowed to stand overnight in a refrigerator. After collection, the pale yellow crystals were washed with icy water and then dried under vacuum. The yield was 65% and aqueous solutions exhibited a peak at 313 nm ($\varepsilon = 54.7\,m^2/mol$). *Anal.* calcd. for [Pt(Et_4dien)I]I: Pt 29.37, C 21.70, H 4.40, I(total) 38.21; found: Pt 29.15 ± 0.8, C 21.87 ± 0.2, H 4.32 ± 0.2, I 38.35 ± 0.5.

Crystal Data

$PtI_2C_{12}H_{29}N_3$ fw = 664.26

Monoclinic $P2_1/c$, $a = 12.565(8)$, $b = 7.576(6)$, $c = 21.040(15)$ Å, $\beta = 91.12°(2)$, $V = 2002.5Å^3$, $\rho_c = 2.204\,g/cm^3$, $\rho_o = 2.26(4)\,g/cm^3$ (flotation), $Z = 4$, $\mu(MoK\alpha) = 104.8\,cm^{-1}$.

The pale yellow crystals were predominately plates and all were of relatively poor crystalline quality. Several crystals of this form were examined but all were found to be twinned. A needle shaped crystal was then selected (dimensions 0.12 × 0.08 × 0.40 mm³). Systematic absences ($h0l$, $l = 2n + 1$; $0k0$, $k = 2n + 1$) indicated the space group $P2_1/c$. The cell parameters were calculated by least-squares refinement of 27 manually centred reflections on a Picker four-circle diffractometer using MoKα radiation.

Crystal Structure Determination

Intensity data were collected on an automated Picker diffractometer in the θ/2θ scan mode using MoKα radiation. A scan rate of 1°/min was used with a minimum scan width of 2° and a 40 s background count at each limit of the scan. Three reflections were monitored after every 50 reflections and their intensities did not change significantly. The intensity of 2731 independent reflections was measured below $2\theta = 46°$. The quality of the crystal did not warrant any further data collection. Only the 1982 independent reflections with intensity greater than $1.75\sigma(I)$ were used in the least-squares refinement. Full anisotropic absorption corrections were applied and the data were corrected for Lorentz and polarization factors. The scattering factors were taken from Cromer and Mann (6).

A Patterson synthesis was computed and possible platinum and iodine positions were postulated and used to calculate phases for a Fourier analysis. Successive Fourier synthesis gave positions for all 18 non-hydrogen atoms in the asymmetric unit. Refinement was carried out by use of full-matrix least-squares. A difference synthesis suggested anisotropy in thermal parameters. For the latter cycles of least-squares the platinum, iodine, nitrogen, and ring carbon atoms were refined with anisotropic temperature factors. Refinement converged with R equal to 0.067. Hydrogen atoms were not observed in the difference Fourier synthesis and therefore were not included in any model of the structure. The largest peaks observed in the difference Fourier (1.8 e A^{-3}) were associated with the platinum atom. Final observed and calculated structure factors have been placed in the Depository of Unpublished Data.[1] The square root of the standard deviation of an observation of unit weight is 1.266. The weights were calculated from $w^{-1/2} = 3.93 + 0.270|F_o| + 0.000048|F_o|^2$. This function was found to give constant distribution of $w|\Delta F|^2$ with respect to $|F_o|$. The final weighted residual was 0.105. The large weighted residual reflects the fact that it was not possible to obtain good quality crystals of this compound and the weighting scheme emphasizes the contribution of the many weak reflections which were recorded. Final atomic positional parameters together with their estimated standard deviations are listed in Table 1.

[1]Complete set of tabular data is available, at a nominal charge, from the Depository of Unpublished Data, CISTI, National Research Council of Canada, Ottawa, Ont., Canada K1A 0S2.

Results and Discussions

The numbering scheme for [Pt(Et_4dien)I]I is shown in Fig. 1 together with co-ordination bond lengths. A stereoscopic view of the cation is shown in Fig. 2. Selected angles are given in Table 2.

Structure of Cation

The complex cation is found to have square-planar co-ordination with the platinum bonded to one iodine and three nitrogen atoms. A pseudo-mirror plane normal to the plane of the ligand is evident in Fig. 2. The differences in some of the bond lengths given in Fig. 1 and the bond angles in Table 2 for bonds and angles related by this local mirror plane exceed the sum of the related standard deviations. We suspect that this implies that the true standard deviations are larger than those given by the least squares.

The Pt atom is slightly removed from the plane of its four ligands and that plane shows some tetrahedral distortion. The following are the distances of the four ligands from least-squares plane parallel to the four ligands but which passes through the position of the Pt atom: I(1), 0.027; N(1), 0.073; N(2), 0.016; N(3), 0.074 Å. The angles around the Pt atom deviate from 90° reflecting the fact that the *bite* of the tridentate ligand is slightly smaller than ideal for bonding to a Pt atom. This is shown by the large N(1)—Pt—I(1) and N(3)—Pt—I(1) angles of 96° whereas the N(1)—Pt—N(2) and N(2)—Pt—N(3) angles are contracted to 85° and 83° respectively. The platinum bond lengths are all within the normal range (4, 7, 8). The central nitrogen bond length [Pt—N(2)] is 1.98(2) Å and is significantly shorter than the other two dentate bonds (2.10(2) and 2.09(2) Å). Such contractions of the central bond and angles were observed in [Pd(Et_4dien)X]$^+$ where X is NO_2 or N_3 (3). The complex ion, [Pt(dien)Br]$^+$, shows similar angular geometry but the central Pt—N bond is no longer the shortest co-ordination bond (4). The average bond distances in the [Pt(Et_4dien)I]$^+$ cation are [C—N], 1.49(3) Å and [C—C], 1.57(3) Å. These are within the expected range (3, 4, 9).

The orientation of the ethyl groups with respect to the ligand plane is shown in Fig. 2. The ethyl groups are spread away from the ligand plane although the extent of this differs above and below the plane. It is noteworthy that the conformation of the Et_4dien ligand, in particular the ethyl positions

Can. J. Chem. Downloaded from www.nrcresearchpress.com by 210.87.254.42 on 09/05/12
For personal use only.

TABLE 1. Structural parameters of [Pt(tetraethyldiethylenetriamine)I]I
(*a*) Fractional atomic coordinates (esd in parentheses) (× 10^3). Temperature factor of atoms refined isotropically are also included

Atom	*x*	*y*	*z*	*B*
Pt	222.44(8)	211.11(16)	119.61(5)	
I(1)	23.3(2)	111.8(4)	109.8(1)	
I(2)	441.2(2)	726.2(3)	129.6(1)	
N(1)	231(2)	214(3)	219(1)	
N(2)	374(2)	281(4)	124(1)	
N(3)	250(2)	205(4)	22(1)	
C(1)	39(3)	293(5)	236(1)	
C(2)	421(3)	221(5)	185(2)	
C(3)	430(3)	234(3)	72(2)	
C(4)	360(3)	287(5)	12(2)	
C(11)	223(3)	5(5)	240(2)	7.6(8)
C(12)	232(3)	0(6)	316(2)	10.3(1.1)
C(13)	150(4)	329(6)	250(2)	9.8(1.0)
C(14)	134(4)	495(8)	222(2)	12.5(1.4)
C(31)	248(2)	25(4)	2(2)	6.4(7)
C(32)	275(3)	−9(5)	−71(2)	8.5(9)
C(33)	170(3)	303(5)	−16(2)	8.3(9)
C(34)	157(4)	504(6)	9(2)	10.3(1.1)

(*b*) Thermal parameters (U_{ij}) for anisotropically refined atoms (× 10^2)

Atom	U_{11}	U_{22}	U_{33}	U_{12}	U_{13}	U_{23}
Pt	4.21(6)	5.88(7)	4.36(6)	−0.65(5)	0.10(4)	0.26(5)
I(1)	4.7(1)	14.8(3)	7.3(2)	−3.0(1)	0.0(1)	−0.2(2)
I(2)	7.2(1)	4.9(1)	7.5(1)	−0.9(1)	0.2(1)	−0.1(1)
N(1)	3(1)	4(1)	2(1)	0(1)	1(1)	−2(1)
N(2)	2(1)	11(2)	2(1)	3(2)	0(1)	1(1)
N(3)	2(1)	4(1)	3(1)	−2(1)	0(1)	2(1)
C(1)	8(2)	10(2)	8(2)	2(2)	−1(2)	−3(2)
C(2)	8(2)	9(2)	11(3)	−3(2)	0(2)	−1(2)
C(3)	8(2)	1(1)	22(4)	−1(1)	−3(2)	0(2)
C(4)	6(2)	13(3)	11(3)	−1(2)	1(2)	1(2)

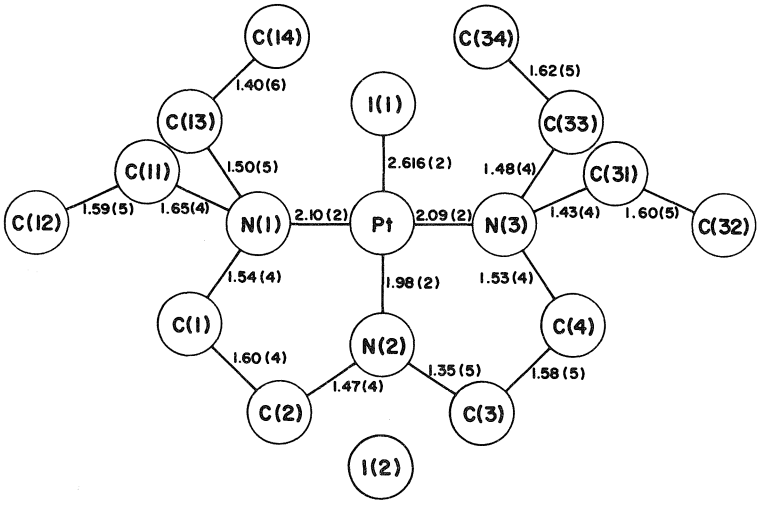


FIG. 1. Atom labelling and bond lengths with esd's in the cation.

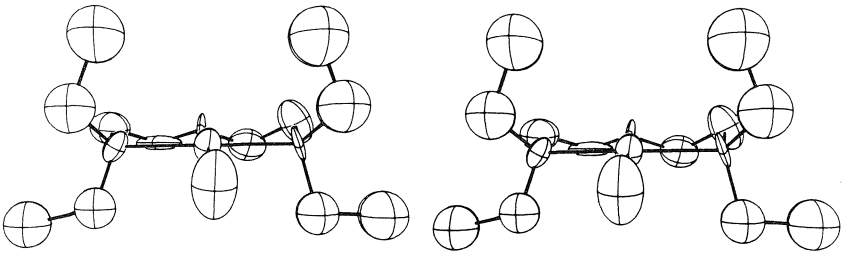


FIG. 2. Stereoscopic view of the cation showing the orientation of the ethyl groups with respect to the plane of the ligand and the pseudo-mirror plane.

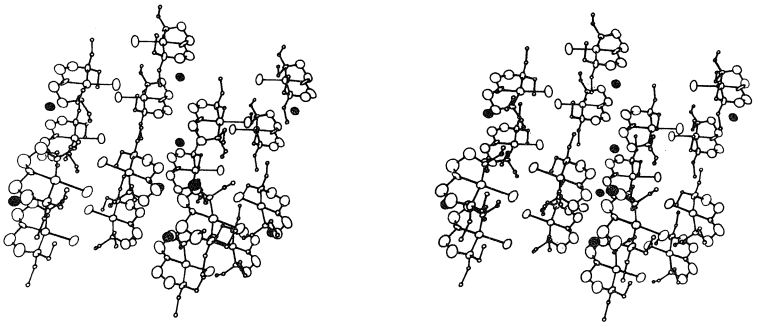


FIG. 3. Packing of the molecules and the environment of the iodide ion. The *a* axis points to the right, the *b* axis points down, and *c* is into the page.

and distribution of the metal–nitrogen bonds, are very similar in the palladium and platinum complexes in spite of the differing substituents (NO_2, N_3, I), differing space groups and different molecular packing. It appears that these structures have less congestion in the axial positions above and below the coordination plane than is implied by molecular models (1). Thus we would suggest that the conformation of the ethyl groups may reflect the inherent properties of the Et_4dien ligand system in a square-planar environment rather than constraints imposed by the X group or by packing factors such as hydrogen bonding.

TABLE 2. Bond angles in degrees with estimated standard deviations in parentheses

Bonds	Angle	Bonds	Angle
I(1)—Pt—N(1)	96(1)	I(1)—Pt—N(3)	96(1)
N(1)—Pt—N(2)	85(1)	N(3)—Pt—N(2)	83(1)
Pt—N(1)—C(1)	105(1)	Pt—N(3)—C(4)	107(2)
N(1)—C(1)—C(2)	107(2)	N(3)—C(4)—C(3)	106(3)
C(1)—C(2)—N(2)	103(3)	C(4)—C(3)—N(2)	107(2)
C(2)—N(2)—Pt	109(2)	C(3)—N(2)—Pt	114(2)
Pt—N(1)—C(11)	105(2)	Pt—N(3)—C(31)	107(2)
Pt—N(1)—C(13)	114(2)	Pt—N(3)—C(33)	113(2)
C(1)—N(1)—C(11)	112(2)	C(4)—N(3)—C(31)	111(3)
C(1)—N(1)—C(13)	107(2)	C(4)—N(3)—C(33)	110(2)
N(1)—C(11)—C(12)	107(3)	N(3)—C(31)—C(32)	116(3)
N(1)—C(13)—C(14)	115(4)	N(3)—C(33)—C(34)	111(3)
C(11)—N(1)—C(13)	113(2)	C(31)—N(3)—C(33)	108(2)
C(2)—N(2)—C(3)	114(3)		

Packing in the Crystal

Figure 3 illustrates the packing in the [Pt(Et_4-dien)I] crystal. Layers of cations alternate with iodide ions. Contacts of less than 4 Å were examined for possible hydrogen bonding. The iodide ion sits between the cation nitrogen atom N(2) of one molecule and the C(2) and C(3) atoms of a neighboring molecule. The close contacts and related angles are given in Table 3. The I(2)—N(2) distance of 3.48 Å is 0.17 Å smaller than the sum of the van der Waal's radii of the two elements (7). Since the angles about N(2) are also favourable (10), it may be postulated that there is hydrogen bonding between the iodide ion I(2) and the acidic proton attached to N(2). This hydrogen bonding would be consistent with the kinetic data (1); the effect of the hydroxyl ion in promoting substituents is believed to involve loss of a proton from this

TABLE 3. Close contacts to iodide ion and related angles

Bond	Distance (Å)	Bonds	Angle (deg)
N(2)—I(2)	3.48(2)	C(2)—N(2)—I(2)	99(2)
		C(3)—N(2)—I(2)	101(2)
		Pt—N(2)—I(2)	114(1)

Can. J. Chem. Downloaded from www.nrcresearchpress.com by 210.87.254.42 on 09/05/12
For personal use only.

central nitrogen atom. Hydrogen bonding of a less specific nature was postulated for the bromide ion in [Pt(dien)Br]Br (4). The different possible hydrogen bonding patterns of [Pt(dien)Br]Br and [Pt(Et_4dien)I]I may explain the differences observed between the Pt—N bond lengths of the two complexes as mentioned in the previous section.

Acknowledgements

We acknowledge the Natural Sciences and Engineering Research Council of Canada for financial support of this work. Our thanks go to C. Brierley for preparative work and to F. Basolo for sending a sample of his material which could be used for comparison. In Regina we are grateful to S. van der Heijden, R. Gopal, and K. Wolbaum for their help in computation.

1. F. Basolo and R. G. Pearson. Mechanisms of inorganic reactions. 2nd ed. John Wiley and Sons, NY. 1967. pp. 388, 414–417.
2. C. H. Langford and H. B. Gray. Ligand substitution processes. W. A. Benjamin, New York. 1965. Chapt. 2.
3. N. Bresciani Pahor, M. Calligaris, and L. Randaccio. J. Chem. Soc. Dalton, 725 (1976); N. Bresciani, M. Calligaris, L. Randaccio, V. Ricevuto, and U. Belluco. Inorg. Chim. Acta, **14**, L19 (1975).
4. R. Melanson, J. Hubert, and F. D. Rochon. Can. J. Chem. **53**, 1139 (1975).
5. G. W. Watt and W. A. Cude. Inorg. Chem. **7**, 335 (1968).
6. D. T. Cromer and J. B. Mann. Acta. Crystallogr. A**24**, 321 (1968).
7. L. Pauling. The nature of the chemical bond. 3rd ed. Cornell University Press, Ithaca. 1960. pp. 224, 260.
8. N. W. Alcock and P. G. Leviston. J. Chem. Soc. Dalton, 1834 (1974); W. A. Freeman. Inorg. Chem. **15**, 2235 (1976); R. R. Robinson, E. O. Schlemper, and R. K. Murmann. Inorg. Chem. **14**, 2035 (1975).
9. R. F. Ziolo, M. Allen, D. D. Titus, H. B. Grey, and Z. Dori. Inorg. Chem. **11**, 2045 (1972).
10. P. Schuster, G. Zundel, and C. Sandorfy. The hydrogen bond. Vol. II. North Holland, New York. 1976. pp. 395–456.

Can. J. Chem. Downloaded from www.nrcresearchpress.com by 210.87.254.42 on 09/05/12
For personal use only.

Autohydrolysis of aspen milled wood lignin

JAIRO H. LORA AND MORRIS WAYMAN

Department of Chemical Engineering and Applied Chemistry, University of Toronto, Toronto, Ont., Canada M5S 1A4

Received August 3, 1979

JAIRO H. LORA and MORRIS WAYMAN. Can. J. Chem. **58**, 669 (1980).

In order to obtain further understanding of the nature of lignin reactions during autocatalysed hydrolysis (autohydrolysis) of wood, milled wood lignin (MWL) was isolated from aspen (*Populus tremuloides*) and treated under autohydrolysis conditions. By this means reactions of the lignin itself could be distinguished from those taking place between lignin and the carbohydrate or other components of the wood. The material after the reaction was separated into a dioxane insoluble fraction (DI), a dioxane soluble but ether insoluble fraction (DSEI), and an ether soluble fraction (ES). Studies were carried out on the DI and DSEI fractions; no direct study was made of the small ES fraction.

The formation of DI material increased linearly during the first 7.5 min at 170°C and then levelled off. At the same time DSEI decreased and then levelled off. Gel permeation chromatography of the DSEI fraction suggested that during autohydrolysis there is an initial generation of low molecular weight fragments which recombine to form first a high molecular weight soluble fraction and from this the insoluble product. The DSEI fraction contained increased conjugated and unconjugated keto groups. Carboxylic acids were also detected; they have been attributed to the reincorporation of low molecular weight aromatic acids generated by the hydrolysis of the corresponding esters. The dioxane insoluble (DI) fraction had fewer unconjugated keto groups than the DSEI fraction, indicating that these groups participated in the condensation reactions leading to the formation of insoluble material. These probably involve position 6 of the aromatic ring.

JAIRO H. LORA et MORRIS WAYMAN. Can. J. Chem. **58**, 669 (1980).

Dans le but d'obtenir de plus amples informations sur la nature des réactions de la lignine lors de l'hydrolyse autocatalysée (autohydrolyse) du bois, on a isolé du peuplier (*Populus tremuloides*) la lignine de bois moulu (LBM) et on l'a soumise à une autohydrolyse. Par ces réactions de la lignine on peut distinguer celles qui ont lieu entre la lignine et les carbohydrates ou d'autres dérivés du bois. Les produits de la réaction sont séparés en fraction insoluble dans le dioxanne (ID), fraction soluble dans le dioxanne mais insoluble dans l'éther (SDIE) et en une fraction soluble dans l'éther (SE). On a étudié les fractions ID et SDIE mais on n'a pas fait d'études directes sur la petite fraction SE.

La formation de produits ID augmente linéairement durant les 7.5 premières minutes puis se stabilise. En même temps la fraction SDIE diminue puis se stabilise. La chromatographie sur gel de la fraction SDIE suggère que lors de l'autohydrolyse il y a formation initiale de fragments de faibles poids moléculaires qui se recombinent d'abord pour donner la fraction soluble de poids moléculaire élevé et à partir duquel se forme le produit insoluble. La fraction SDIE contient des groupes cétoniques conjugués et non conjugués. On a également décelé des acides carboxyliques et on les attribue à la réincorporation d'acides aromatiques de faibles poids moléculaires issus de l'hydrolyse d'esters correspondants. La fraction insoluble dans le dioxanne (ID) a moins de groupes cétoniques conjugués que la fraction SDIE. Ceci indique que ces groupes participent aux réactions de condensation qui conduisent à la formation de produits insolubles. Ces derniers font probablement intervenir la position 6 du cycle aromatique.

[Traduit par le journal]

Introduction

It has been reported by several authors (1–6) that by autocatalysed hydrolysis (autohydrolysis) of wood, the lignin is modified in such a way that it can be partially extracted in a second stage at low temperatures using certain organic solvents or dilute aqueous alkalies. Earlier work at this laboratory (7–10) has shown that at any given temperature there is a characteristic autohydrolysis time for maximum lignin extractability. This has been explained in simple terms as the result of reactions of two different types, in one of which extractable lignin is formed, while in the other, insoluble structures are generated.

Previous studies of the reactions affecting lignin during autohydrolysis (7–20) have used wood, and thereby the wood carbohydrates or their derivatives were present to react with the lignin. In order to avoid such reactions, it was decided to study the effects of autohydrolysis on isolated lignin. By this means, reactions of the lignin itself could be characterized and distinguished from those taking place between lignin and other wood components. The findings of these studies are presented and discussed here.

Aspen milled wood lignin (MWL) was used as a model for lignin and treated under conditions similar to those prevailing during autohydrolysis. After the treatment the products were separated into three fractions: (*i*) material insoluble in dioxane–water (9:1) (DI), (*ii*) material soluble in dioxane–water (9:1) but insoluble in ether (DSEI), and (*iii*) material soluble in ether (ES).

This paper discusses the yields and chemical structures of the DI and DSEI fractions, and the changes in molecular weight distribution of the DSEI material. The DI and DSEI fractions were characterized by elemental and methoxyl analysis, and by spectroscopic methods. The ES fraction, which contained low molecular weight aromatic

0008-4042/80/070669-08$01.00/0
©1980 National Research Council of Canada/Conseil national de recherches du Canada

Can. J. Chem. Downloaded from www.nrcresearchpress.com by 210.87.254.42 on 09/05/12
For personal use only.

compounds, and was a minor proportion of the total, was not studied further.

Results

Yields

Figure 1 shows the yields of DI and DSEI fractions as a function of autohydrolysis time at 170°C. After 2 min the formation of DI lignin began; between 2 and 7.5 min the amount of DI lignin increased linearly with a slope equal to 10.1% min^{-1} and then tended to level off. The DSEI fraction showed an opposite trend, decreasing initially very quickly, and then at a slower rate. An estimate of ES may be obtained as ES = 100 − (DI + DSEI). This amounted to about 10% during the first 5 min of heating, then fell rapidly to zero. Between 10 and 30 min ES was formed to about 5% of the total.

Molecular Weight Distribution of DSEI Fractions

Figure 2 presents gel permeation chromatograms (GPC) for representative DSEI samples as well as for the MWL used as starting material. Most chromatograms took the form of a bimodal curve. The first peak was eluted at the exclusion volume, determined by running blue dextran (mw ≃ 2×10^6) through the column, and may thus represent the accumulation of molecules of hydrodynamic volume greater than that separable by Sephadex G100 (21). The sequence of chromatograms is rather similar to that obtained with wood autohydrolysis lignin (10), except that the sharp peak of high molecular weight soluble lignin was obtained in 40 min at 195°C with wood, and in 2 min at 170°C with the isolated lignin. The high molecular weight peak almost disappeared by 30 min at 170°C with MWL, whereas its disappearance required 120 min at 195°C on autohydrolysis of wood. Each chromatogram was divided into two fractions: (*i*) a high molecular weight lignin (HML) including material eluted up to fraction number 30 (elution volume less than 77 mL), (*ii*) a low molecular weight lignin (LML) including material eluted after fraction number 30 (elution volume more than 77 mL).

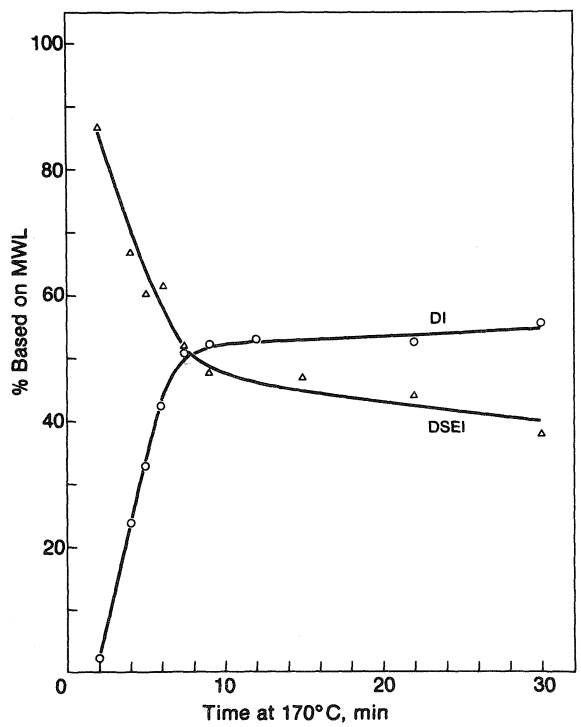


FIG. 1. Yield of DI and DSEI fractions after simulated autohydrolysis of aspen MWL at 170°C.

The relative amounts of HML and LML in the DSEI samples were estimated as the ratio between the area under either the HML or the LML fractions and the total area under the chromatograph. The figures obtained in this way should be taken only as approximations since the absorptivity at 280 nm (wavelength used in the detector of the gpc system) may be somewhat different for the HML and LML fractions due to chemical differences. With the information generated in this way, estimated yields of HML and LML were obtained (Fig. 3).

Figures 2 and 3 indicate that at the beginning of the treatment there was an increase in the yield of HML and a reduction in the yield of LML indicating that the former was being obtained from the latter. The yield of HML was highest for the sample obtained after 2 min of autohydrolysis, that is, when formation of DI material was just beginning (Fig. 1). As time progressed the yield of HML decreased due to the increasing formation of DI material and to depolymerization. The decrease in the yield of HML for times above 6 min (when little DI lignin was being formed) was mostly due to depolymerization resulting in the formation of LML. The linearity of the curve of log of yield of HML vs. time for times above 6 min (Fig. 3) suggests first order kinetics for the depolymerization reaction with a rate constant $k_1 = 0.084\,min^{-1}$, as a first approximation.

In the case of LML, after the initial very fast decrease, the yield levelled off. Thus, during the first minutes condensation of LML producing HML prevailed while in the latter stages of the reaction little HML formed and there was a balance between the depolymerization of HML with formation of LML and the depolymerization of LML with formation of ES materials.

Elemental Analysis

Table 1 presents the C, H, O, and OCH_3 content

Can. J. Chem. Downloaded from www.nrcresearchpress.com by 210.87.254.42 on 03/03/12
For personal use only.

Can. J. Chem. Downloaded from www.nrcresearchpress.com by 210.87.254.42 on 09/05/12
For personal use only.

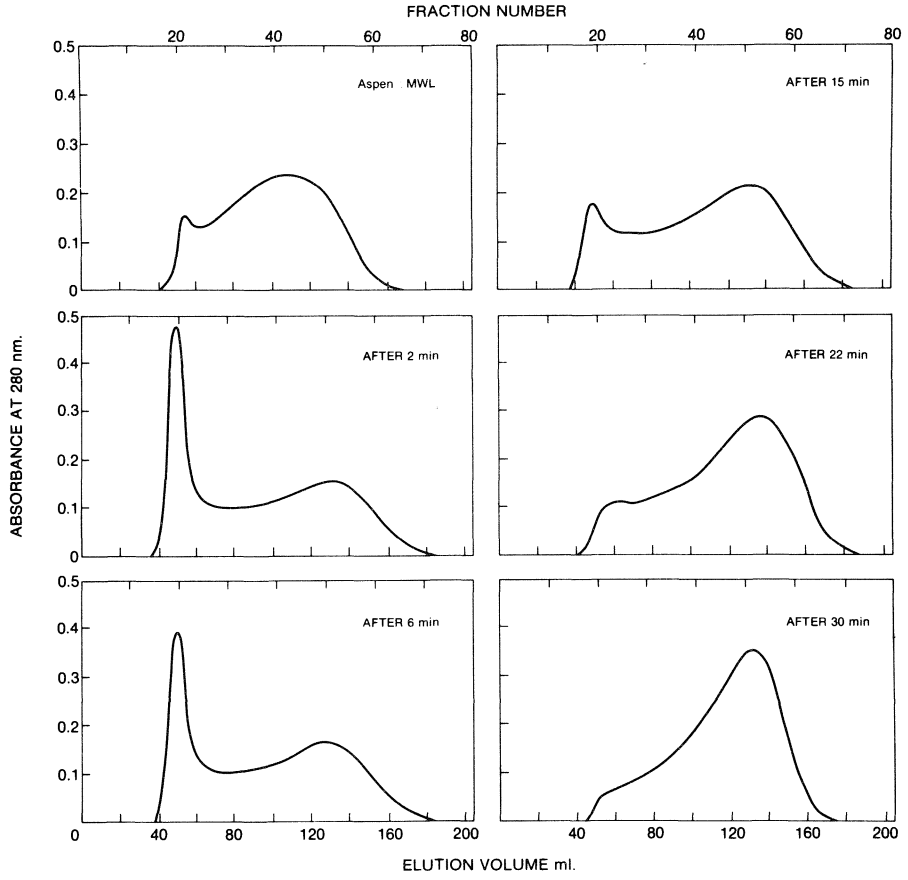


FIG. 2. Molecular weight distributions of DSEI samples obtained after simulated autohydrolysis of aspen MWL at 170°C.

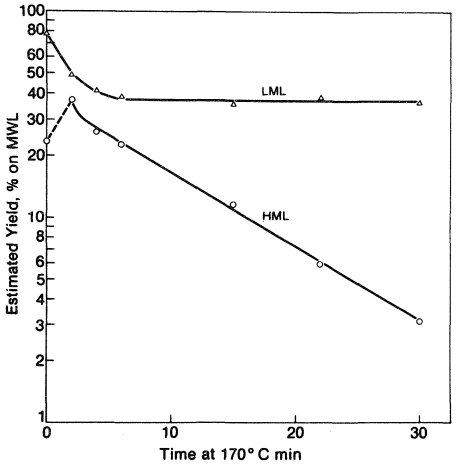


FIG. 3. Effect of time on the yield of LML and HML after simulated autohydrolysis of aspen MWL.

for aspen MWL and for the DSEI and DI samples obtained after autohydrolysis for 30 min at 170°C. Based on these data C_9 formulae were calculated and have been included in Table 1. The values obtained for MWL are within accepted ranges for hardwoods. A value of O/C_9 higher than 3 has been observed in other lignins of the genus *Populus* (22), and is consistent with the presence of aromatic esters, which has been shown by ir spectroscopy. As observed, the DI sample showed higher carbon content and lower oxygen content than MWL, while the DSEI material exhibited lower carbon and higher oxygen content than the starting material. Little variation was observed in methoxyl content, the DI sample exhibiting a slightly lower OCH_3/C_9 than MWL.

Infrared Spectroscopy

Figure 4 shows the infrared spectra obtained for aspen MWL and for representative DSEI and DI samples. The clearest differences occurred in the 1650–1800 cm^{-1} and the 700–930 cm^{-1} regions, the remainder being typical of aspen MWL and hardwood lignins in general. In the 1000–1400 cm^{-1} region, the absorption due to the aromatic methoxyl groups is strongly affected by the presence of carbonyl groups, rendering interpretation of changes difficult.

TABLE 1. Chemical analysis and C_9 formulae of lignins after autohydrolysis of aspen MWL at 170°C

Type of material	Time at 170°C (min)	Analysis (%) C	H	O	OCH_3	C_9 formula	Molcular weight C_9 unit
MWL		59.2	5.92	34.9	20.1	$C_9H_{8.27}O_{3.23}(OCH_3)_{1.36}$	210.20
		60.0	6.19	33.9	20.4	$C_9H_{8.65}O_{3.03}(OCH_3)_{1.37}$	207.53
DSEI	30	58.6	5.51	35.9	20.0	$C_9H_{7.50}O_{3.39}(OCH_3)_{1.37}$	212.13
DI	30	61.0	6.14	32.8	20.2	$C_9H_{8.41}O_{2.85}(OCH_3)_{1.32}$	202.86

The 1650–1800 cm^{-1} Region

In addition to the 1670 cm^{-1} band characteristic of conjugated carbonyl groups, MWL exhibited a shoulder at 1700–1720 cm^{-1} which disappeared upon saponification. Reduction of MWL with alkaline $NaBH_4$ caused a general decrease in the absorption between 1650 cm^{-1} and 1800 cm^{-1} and uncovered a broad maximum between 1700 and 1715 cm^{-1}. Based on the results of these tests and in agreement with other authors (23–25), the 1700–1720 cm^{-1} absorption was assigned to conjugated ester groups.

In the DSEI fractions the 1700–1720 cm^{-1} band was very prominent and increased with time of autohydrolysis. Reduction with $NaBH_4$ caused a partial decrease in the intensity of the band, which indicated the presence of unconjugated β-keto groups (26). Upon saponification it was not possible to reprecipitate the lignin at pH 6–7, which suggested the presence of carboxylic acids. A fraction precipitated at pH 4 showed also a lower absorption at 1700–1720 cm^{-1} interpreted as due to the presence of β-keto as well as carboxylic acid groups. For the DI samples the absorption at 1700–1720 cm^{-1} was comparatively small and diminished with increasing time.

The 700–930 cm^{-1} Region

Bands appearing in this region are attributed to aromatic C—H out-of-plane in-phase (umbrella) deformations which are strongly affected by proximity among hydrogen atoms. As a general rule, proximity to other hydrogens will decrease the frequency of the absorption. Thus, from the ir spectra in this region, the substitution pattern may be inferred (27).

As illustrated in Fig. 4, the DI samples exhibited clear signs of modification of the substitution pattern as evidenced by the lowering of intensity in the syringyl band at 922 cm^{-1} and by the appearance of a strong band at 872 cm^{-1} and a weaker one at 890 cm^{-1}. The bands at 872 and 890 cm^{-1} are attributed to isolated aromatic C—H vibrations, that is, they indicate condensation. On the basis of wide evidence from the literature (28–31), the 872 cm^{-1} band can be assigned to a 1,3,4,6 tetra substitution pattern (1,2,4,5, in IUPAC nomenclature[1]) or to penta substitution. Thus penta substitution (in the case of syringyl units) and 1,3,4,6 tetra substitution (in the case of guaiacyl units) appear to be the prevailing structures in the insoluble lignins. These results agree with the work of others (32–36), who have found that, under acid conditions, condensation preferentially occurs in position 6 through an electrophilic substitution reaction. Proof of structure would require a wet chemistry procedure such as neutral permanganate oxidation and identification of the carboxylic acids so produced.

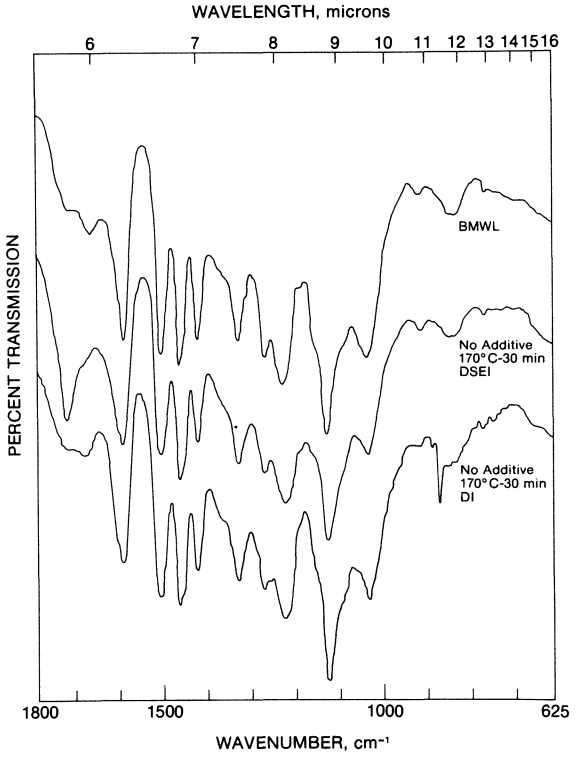


FIG. 4. Infrared spectrum of DSEI and DI lignins obtained after simulated autohydrolysis of aspen MWL at 170°C.

[1]IUPAC nomenclature names the phenolic position as 1, whereas in the lignin literature, position 1 is the point of attachment of the aliphatic side chain. In this paper we shall use the lignin nomenclature.

Can. J. Chem. Downloaded from www.nrcresearchpress.com by 210.87.254.42 on 09/05/12
For personal use only.

Can. J. Chem. Downloaded from www.nrcresearchpress.com by 210.87.254.42 on 09/05/12
For personal use only.

The DSEI samples showed the same bands as MWL but some differences in shape indicates that the substitution pattern had been modified. With increase in reaction time, the absorption above 860 cm^{-1} progressively increased, thus affecting the shape of the 830–860 cm^{-1} band; the absorption between 700 and 800 cm^{-1} decreased as indicated by the change of slope of the base line in that region. Since absorption above 860 cm^{-1} is characteristic of isolated aromatic C—H bands and absorption below 800 cm^{-1} is typical of more than one adjacent aromatic C—H bond, the trends observed here indicate increasing condensation, that is, a decrease in the number of adjacent aromatic C—H bonds and increase in the number of isolated aromatic C—H bonds. This modification of the substitution pattern, however, did not reach the same extent as in the DI samples.

Ultraviolet Spectroscopy

Two maxima (296 and 366 nm) appeared in the alkali–acid difference spectrum for a DSEI sample obtained after autohydrolysis at 170°C for 30 min. The absorption at 366 nm corresponds to ionized phenolic hydroxyl groups conjugated with carbonyl groups, carbon–carbon double bonds, or biphenyl groups; the 296 nm band corresponds to any other ionized phenolic hydroxyl groups (37). Sodium borohydride reduction caused a considerable decrease in the absorption at 366 nm and an increase in the intensity of the 296 nm band, suggesting that the higher wavelength absorption must be mainly due to the presence of conjugated carbonyl groups. The lack of significant absorption above 320 nm in the difference spectrum of the reduced sample indicated the absence of high amounts of stilbene and phenyl coumarone structures conjugated with ionized phenolic hydroxyl groups.

Discussion

The decrease in the yield of DSEI lignin, accompanied by the increase in the formation of DI materials, indicates that the latter are being obtained from the former. The initial linearity of the curve relating yield of DI lignin to autohydrolysis time suggests that the formation of insoluble material proceeds through a zero order reaction. This can be understood as a result of the reaction taking place in a medium in which lignin is not soluble and thereby the formation of DI material depends on the physical proximity of the sites involved, rather than on concentration. That proximity is largely predetermined by the structure of lignin.

From molecular weight distribution studies, a scheme for the depolymerization and repolymerization reactions can be postulated. MWL is a polydispersed material composed of high and low molecular weight fractions, HML and LML. By depolymerization HML produces low molecular weight DSEI materials similar to LML as well as a small amount of ES. By repolymerization, the LML produces high molecular weight DSEI materials similar to HML, as well as a small amount of ES. Insoluble DI is formed from the soluble HML as the reaction continues.

The postulated overall mechanism indicates that lignin repolymerization under autohydrolysis conditions does not necessarily result in the immediate formation of insoluble materials. It is only after condensation has proceeded to a certain extent that the molecule becomes insoluble. The findings reported here give support to the conclusion that the HML fraction reported by Chua and Wayman (10) in their study of lignins obtained by autohydrolysis of aspen wood, instead of being a relatively unchanged fragment of the original lignin of the wood, is the result of recondensation reactions involving the low molecular weight fragments generated at the onset of autohydrolysis. These reactions take place much more rapidly upon autohydrolysis of the isolated lignin than they do in the wood. While physical (diffusional) effects may account for part of this rate difference, the major rate-retarding effect in the wood may be attributable to the participation of hemicellulose degradation products in the reactions, which become incorporated into the products (10). However, from a molecular point of view, the course of the reaction appears to be much the same, that is, depolymerization to low molecular weight fragments followed by repolymerization to soluble higher molecular weight condensation products, which, as the condensation proceeds, become insoluble.

The presence of conjugated and unconjugated carbonyl groups in the products can be attributed to the splitting of ether linkages resulting in the formation of structures with side chains analogous to the side chains of Hibbert's ketones. This agrees with what has been reported for other acid degradation processes of lignin, such as acidolysis or ethanolysis (38–50). The increase of absorption with increasing time agrees with the predominance of lower molecular weight materials at longer times in agreement with the gpc studies. The carboxylic acid groups are attributed to the incorporation into the lignin of low molecular weight carboxylic acids generated by the hydrolysis of the corresponding esters; this has also been proposed in the studies of autohydrolysis wood lignins (18). These low

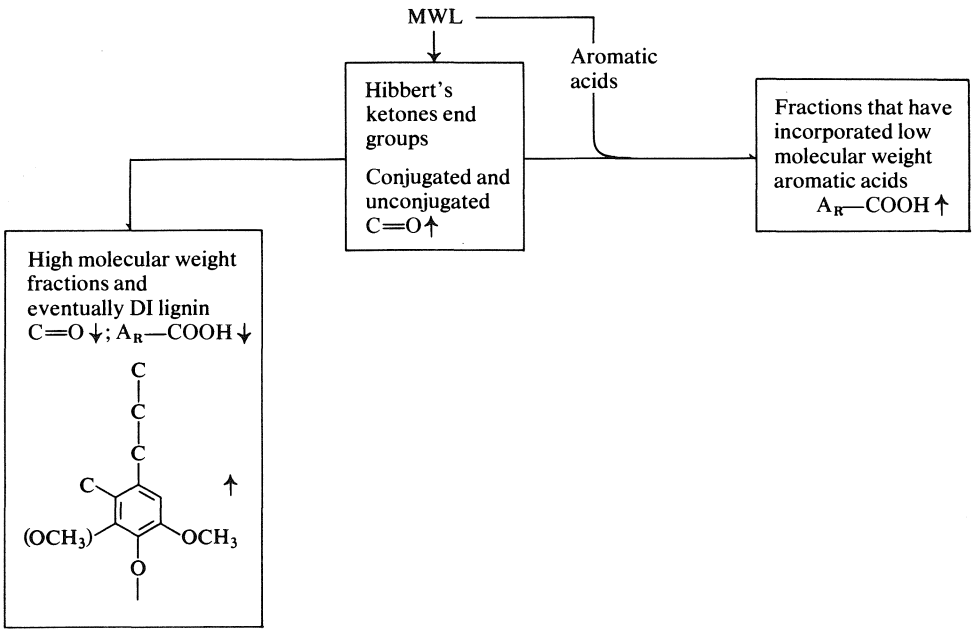


FIG. 5. Structural changes during simulated autohydrolysis of aspen MWL as revealed by spectral studies.

molecular weight compounds can act as blocking agents for lignin repolymerization, in the same way as the aromatic additives reported by Wayman and Lora (51).

The low absorption at 1700–1720 cm^{-1} shown by the DI samples suggests that the β-keto groups appearing in the DSEI fraction participated in condensation reactions leading to the formation of DI materials. The absence of keto groups in the DI samples agrees with the low values of O/C_9 exhibited by the insoluble materials. The participation of ketols in acid condensation reactions has been proposed by Marton (52). The weak absorption at these frequencies also indicates that the aromatic carboxylic acids are present only in relatively small amounts in the DI samples, in agreement with their proposed role as preventives of lignin repolymerization.

The appearance in the DI samples of a new bond at position 6 of the aromatic ring indicates its involvement in the condensation reactions leading to the formation of insoluble materials. In contrast, Wayman and Chua (20), in their ir studies of lignins unextractable after aspen wood autohydrolysis, did not observe substantial modifications of the substitution pattern of the ring. This suggests that in the case of wood the formation of insoluble lignin is mainly the result of condensation with the carbohydrates or their derivatives, rather than the result of lignin self-condensation. The incorporation into the lignin of non-lignin substances during wood autohydrolysis is also supported by the fact that the values for OCH_3/C_9 for the DSEI and DI samples obtained from aspen MWL are very similar to those of the starting material, and considerably higher than those reported for autohydrolysis lignins obtained from wood (10, 16, 20). The slightly lower value of OCH_3/C_9 for the DI sample reported here is attributed to the predominance of guaiacyl type lignin in the insoluble materials, in agreement with the findings of Wayman and Chua (19).

Figure 5 gives a summary of the structural changes occurring as a result of autohydrolysis of aspen MWL.

Experimental

*Preparation of Aspen MWL (*Populus tremuloides*)*

Extractive-free wood meal (prepared according to TAPPI Standard T12m59) (100 g) was ground in a ball mill under CO_2. After 18 days the material was extracted with dioxane–water (9:1) and the extract concentrated to dryness under vacuum and purified according to the method of Lundquist *et al.* (53).

Autohydrolysis of Aspen MWL

Aspen MWL (100 mg) was placed in a small glass beaker specially designed to fit 25-mL stainless steel pressure vessels. After the addition of 0.6 mL of water (pH 3.5, adjusted with acetic acid) the pressure vessel was put in a desiccator under vacuum in order to remove trapped air and then was closed in a glove box under a nitrogen atmosphere. The moisture was distributed by immersing in an oil bath at 105°C; after 10 min of immersion with constant shaking provided by a wrist action machine, the pressure vessel was taken out and immersed with

Can. J. Chem. Downloaded from www.nrcresearchpress.com by 210.87.254.42 on 09/05/12
For personal use only.

Can. J. Chem. Downloaded from www.nrcresearchpress.com by 210.87.254.42 on 09/05/12
For personal use only.

constant shaking in an oil bath at 170°C. It was found that after 2.5–3 min, the temperature inside the vessel was within 0.5°C of the bath temperature. After the reaction time was completed, the vessel was taken out of the oil bath and immersed in an ice water bath, opened, and the contents transferred quantitatively to 20-mL vials using dioxane and water in such amounts that at the end 15 mL of dioxane–water (9:1) was in the vial. Then, three 6-h extractions were carried out using 15 mL of dioxane–water (9:1), centrifuging after each extraction. The material remaining insoluble in the solvent, DI, was filtered into a preweighed C porosity sintered glass crucible, washed, first with dioxane, then with anhydrous ether, and finally with petroleum ether, dried under vacuum at room temperature, and weighed. The material soluble in dioxane–water (9:1) was concentrated to about 1 mL at 30°C under vacuum, dissolved in 1.5 mL of dichloroethane–ethanol (2:1) and precipitated into 45 mL of anhydrous ether. The material insoluble in ether but soluble in dioxane–water (9:1), DSEI, was washed 3 times with anhydrous ether and twice with petroleum ether; each washing was done by adding 15 mL of the corresponding solvent, shaking overnight with a wrist action machine and centrifuging. At the end, the DSEI product was transferred with petroleum ether to a preweighed M or F porosity sintered glass crucible, dried under vacuum, and weighed.

Molecular Weight Distributions

The procedure described by Chua and Wayman (10) was followed. The chromatograms in Fig. 2 were obtained on 2 mg samples.

Elemental Analysis

C, H, and methoxyl were determined by Schwarzkopf Microanalytical Laboratory, New York.

Infrared Spectroscopy

Pellets were prepared using 1 mg of sample and 300 mg of KBr; spectra referred to 300 mg pure KBr pellets obtained with a Beckman IR-9 spectrophotometer operated in a double beam mode.

Difference Ultraviolet Spectroscopy

Solution A was obtained by dissolving 5 mg of lignin in dioxane (9 mL), methanol (25 mL), and 1 *N* HCl (1 mL). The acid solution was prepared by mixing 5 mL of solution A with water (5 mL) and dioxane (2.5 mL). The alkali sample was prepared analogously but using 0.5 *N* NaOH instead of water. The difference spectrum was obtained by running the alkali solution against the acid solution in a Unicam SP 1700 spectrophotometer.

Derivatization

Borohydride reduced samples and saponified samples were prepared according to the procedure of Sarkanen *et al.* (23).

Acknowledgements

This work was supported in part by the Natural Sciences and Engineering Research Council of Canada. The authors also wish to thank Dr. Miranda G. S. Chua for helpful discussion of the results.

1. S. I. Aronowsky and R. A. Gortner. Ind. Eng. Chem. **22**(3), 264 (1930).
2. W. Overbeck and H. Muller. Sven. Papperstidn. **45**, 317 (1942); Ber. **75**, 547 (1942).
3. E. C. Jahn and C. V. Holmberg. Paper Trade J. **114**(17), 33 (1942).
4. P. Traynard and A. Eymery. Holzforschung, **9**, 172 (1955).
5. O. Goldschmid. Tappi, **38**(12), 728 (1955).
6. D. J. Brasch and K. W. Free. Tappi, **48**(4), 245 (1965).
7. J. H. Lora. M.A.Sc. Thesis. University of Toronto, Toronto, Ont. 1976.
8. J. H. Lora and M. Wayman. Tappi, **61**(6), 47 (1978).
9. J. H. Lora and M. Wayman. Report 27 in Poplar research, management and utilization in Canada. *Edited by* D. C. F. Fayle, L. Zsuffa, and H. W. Anderson. Ontario Ministry of Natural Resources. 1979.
10. M. G. S. Chua and M. Wayman. Can. J. Chem. **57**, 1141 (1979).
11. A. Sohn and P. Lenel. Das Papier, **3**(7/8), 109 (1942).
12. D. A. Stanek. Tappi, **41**(10), 601 (1958).
13. K. D. Sears, A. Beelik, R. L. Casebier, R. J. Engen, J. K. Hamilton, and H. L. Hergert. J. Polymer Sci. Part C, **36**, 425 (1971).
14. A. Klemola. Suom. Kemistil. A**41**, 166 (1968).
15. A. Klemola. Suom. Kemistil. B**41**, 83 (1968).
16. A. Klemola. Suom. Kemistil. B**40**, 329 (1967).
17. A. Klemola. Suom. Kemistil. B**41**, 99 (1968).
18. M. G. S. Chua and M. Wayman. Can. J. Chem. **57**, 2603 (1979).
19. M. Wayman and M. G. S. Chua. Can. J. Chem. **57**, 2599 (1979).
20. M. Wayman and M. G. S. Chua. Can. J. Chem. **57**, 2612 (1979).
21. H. I. Bolker, H. E. W. Rhodes, and K. S. Lee. J. Agric. Food Chem. **25**(4), 708 (1977).
22. K. V. Sarkanen, H. M. Chang, and G. G. Allan. Tappi, **50**(12), 587 (1967).
23. K. V. Sarkanen, H. M. Chang, and G. G. Allan. Tappi, **50**(12), 583 (1967).
24. D. C. C. Smith. J. Chem. Soc. 2347 (1955).
25. D. C. C. Smith. Nature, **176**, 267 (1955).
26. H. L. Hergert. *In* Lignins. *Edited by* K. V. Sarkanen and C. H. Ludwig. Wiley-Interscience, New York. 1971.
27. C. J. Pouchert. The Aldrich Library of IR Spectra. 2nd ed. Aldrich Chemical Co., Milwaukee. 1975.
28. H. W. Thompson and P. Torkington. Trans. Faraday Soc. **41**, 256 (1945).
29. C. G. Cannon and G. B. B. M. Sutherland. Spectrochim. Acta, **4**, 373 (1951).
30. L. J. Bellamy. The infrared spectra of complex molecules. Methuen, London. 1954.
31. G. Varsanyi. Vibrational spectra of benzene derivatives. Academic Press, New York. 1969.
32. J. C. Pew. J. Am. Chem. Soc. **74**, 2850 (1952).
33. B. O. Lindgren. Acta Chem. Scand. **17**, 2199 (1953).
34. J. M. Harkin. Adv. Chem. Ser. **59**, 65 (1966).
35. H. Richtzenhain. Acta Chem. Scand. **4**, 589 (1950).
36. B. Ericsson, B. Nist, and K. V. Sarkanen. Actes du symposium international de Grenoble, July 1964. pp. 59–71.
37. O. Goldschmid. *In* Lignins. *Edited by* K. V. Sarkanen and C. H. Ludwig. Wiley-Interscience, New York. 1971.
38. H. E. Fisher, M. Kulka, and H. Hibbert. J. Am. Chem. Soc. **66**, 602 (1944).
39. L. Mitchell and H. Hibbert. J. Am. Chem. Soc. **66**, 598 (1944).
40. H. E. Fisher and H. Hibbert. J. Am. Chem. Soc. **69**, 1208 (1947).

41. L. MITCHELL, T. H. EVANS, and H. HIBBERT. J. Am. Chem. Soc. **66**, 604 (1944).
42. E. ADLER and B. O. LINDGREN. Sven. Papperstidn. **55**, 563 (1952).
43. E. ADLER and S. YLLNER. Sven. Papperstidn. **55**, 238 (1952).
44. E. ADLER and S. YLLNER. Sven. Papperstidn. **57**, 78 (1954).
45. E. ADLER, B. O. LINDGREN, and U. SAEDEN. Sven. Papperstidn. **55**, 245 (1952).
46. E. ADLER, J. M. PEPPER, and E. ERIKSOO. Ind. Eng. Chem. **49**(9), 1391 (1957).
47. E. ADLER. Pap. Puu, **43**, 634 (1961).
48. E. ADLER. Actes du symposium international de Grenoble, July 1964. pp. 73–83.
49. K. LUNDQUIST and R. LUNDGREN. Acta Chem. Scand. **26**(5), 2005 (1972).
50. K. LUNDQUIST and K. HEDLUND. Acta Chem. Scand. **21**(7), 1750 (1967); **25**(6), 2199 (1971).
51. M. WAYMAN and J. H. LORA. Tappi, **61**(6), 55 (1978).
52. J. MARTON. Pap. Puu, **43**, 665 (1961).
53. K. LUNDQUIST, B. OHLSSON, and R. SIMONSON, Sven. Papperstidn. **80**(5), 143 (1977).

Can. J. Chem. Downloaded from www.nrcresearchpress.com by 210.87.254.42 on 09/05/12
For personal use only.

Absolute rate constants for hydrocarbon autoxidation. 28. A low temperature kinetic electron spin resonance study of the self-reactions of isopropylperoxy and related secondary alkylperoxy radicals in solution[1]

EDWARD FURIMSKY,[2] JAMES A. HOWARD, AND JENNIFER SELWYN[3]

Division of Chemistry, National Research Council of Canada, Ottawa, Ont., Canada K1A 0R9

Received November 7, 1979

EDWARD FURIMSKY, JAMES A. HOWARD, and JENNIFER SELWYN. Can. J. Chem. **58**, 677 (1980).

Isopropylperoxy radicals at low temperatures exist in equilibrium with di-isopropyl tetroxide. The thermodynamic parameters for this equilibrium are very similar to the values of ΔH^0 and ΔS^0 for the *tert*-butylperoxy radical – di-*tert*-butyl tetroxide equilibrium. Differences in second-order rate constants for mutual destruction of secondary and tertiary alkylperoxy radical appear to result from differences in rate constants for unimolecular decomposition of secondary and tertiary alkyl tetroxides.

Isopropylperoxy radicals have the same termination rate constant in the gas phase and in solution.

EDWARD FURIMSKY, JAMES A. HOWARD et JENNIFER SELWYN. Can. J. Chem. **58**, 677 (1980).

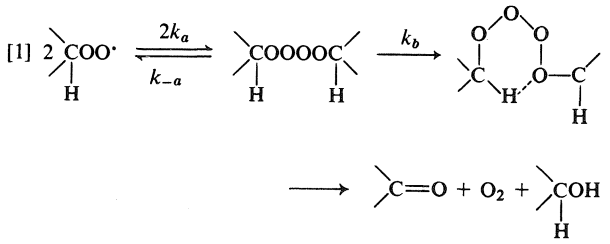
A basse température, les radicaux isopropylperoxy existent en équilibre avec le tétroxyde de di-isopropyle. Les paramètres thermodynamiques de cet équilibre ressemblent beaucoup aux valeurs de ΔH^0 et ΔS^0 de l'équilibre entre le radical *tert*-butylperoxy et le tétroxyde de di-*tert*-butyle. Les différences dans les constantes de vitesse d'ordre 2 pour la destruction mutuelle du radical alkylperoxy secondaire et tertiaire semblent résulter des différences entre les constantes de vitesse de la décomposition unimoléculaire des tétroxydes d'alkyles secondaires et tertiaires.

Les radicaux isopropylperoxy ont la même constante de vitesse de rupture en phase gazeuse et en solution.

[Traduit par le journal]

Introduction

The self-reaction of secondary alkylperoxy radicals at ambient temperatures and below in solution is generally believed to proceed through a cyclic transition state (the Russell mechanism) although kinetic and product studies are not entirely consistent with this mechanism.[4]



At temperatures above about 193 K irreversible decays of s-$RO_2^{\bullet}$ are second-order with respect to the radical concentration and activation energies fall in the range 1–5 kcal mol^{-1} and pre-exponential factors in the range 10^8–10^{10} M^{-1} s^{-1} (1).

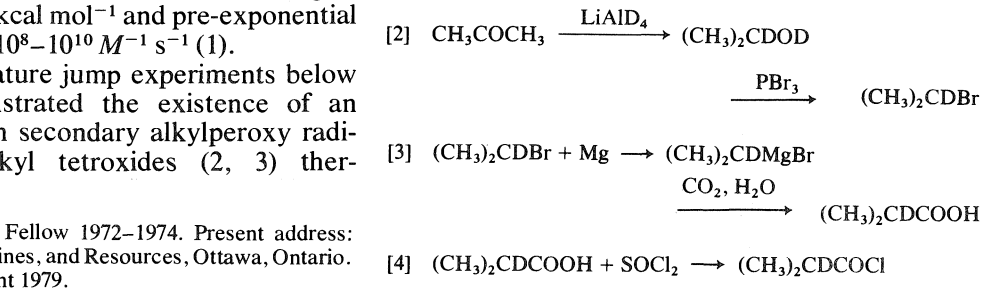
Although temperature jump experiments below 193 K have demonstrated the existence of an equilibrium between secondary alkylperoxy radicals and di-*sec*-alkyl tetroxides (2, 3) thermodynamic parameters for this equilibrium (ΔH_a^0 and ΔS_a^0) have not been determined because irreversible radical decays have been too fast.

In this article we present the results of a low temperature kinetic electron spin resonance spectroscopic study of the self-reaction of the isopropylperoxy radical which enables us to report the approximate values of ΔS_a^0 and ΔH_a^0 for this radical and also to demonstrate that some secondary alkylperoxy radicals can decay with first-order kinetics below 173 K.

Experimental

Materials

Acyl peroxides were synthesized from the appropriate acid chloride and sodium peroxide (4). Isobutyryl chloride (Eastman) and 2-methylbutyryl chloride (Eastman) were used without further purification. Cyclopentanecarbonyl chloride was prepared from cyclopentane carboxylic acid (Aldrich) by the method of Brown (5). Isobutyryl chloride-α-d_1 was synthesized by the reaction sequence,



Radical Production

The radicals were produced directly in the cavity of a Varian

[1] NRCC No. 18023.

[2] NRCC Postdoctorate Fellow 1972–1974. Present address: Department of Energy, Mines, and Resources, Ottawa, Ontario.

[3] NRCC Summer Student 1979.

[4] For a recent review of the self-reactions of alkylperoxy radicals in solution see ref. 1.

0008-4042/80/070677-04$01.00/0

©1980 National Research Council of Canada/Conseil national de recherches du Canada

Can. J. Chem. Downloaded from www.nrcresearchpress.com by 210.87.254.105 on 09/05/12
For personal use only.

E-4 EPR spectrometer equipped with a variable temperature accessory by photolysis of the alkylformyl peroxide in oxygen-saturated dichlorodifluoromethane.

$$[5]\quad \mathrm{RC(O)OC(O)R} \longrightarrow 2\mathrm{R}^{\cdot} + 2\mathrm{CO_2}$$

$$[6]\quad \mathrm{R}^{\cdot} + \mathrm{O_2} \longrightarrow \mathrm{RO_2}^{\cdot}$$

Radical concentrations were measured and decays followed by standard kinetic electron spin resonance spectroscopic techniques (2, 6).

Results and Discussion

Above 173 K isopropylperoxy, isopropyl-α-d_1-peroxy, cyclopentylperoxy, and *sec*-butylperoxy decayed with clean second-order kinetics, i.e., $-\mathrm{d}[s\text{-ROO}^{\cdot}]/\mathrm{d}t = 2k_t[s\text{-RO}_2^{\cdot}]^2$, where $2k_t$ is the second-order rate constant for mutual radical destruction. Values of $2k_t$ and Arrhenius parameters for these radicals are listed in Table 1. Included in this table are kinetic parameters for the s-$\mathrm{RO_2}^{\cdot}$ prepared by photolysis of di-*tert*-butyl peroxide in the oxygenated hydrocarbon (RH) (3). Agreement between kinetic data for secondary alkylperoxy radicals prepared by the two methods is satisfactory.

Below 173 K temperature jump experiments indicated that cyclopentylperoxy and *sec*-butylperoxy radicals exist in equilibrium with their tetroxide. Values of ΔH_a^0 and ΔS_a^0 could, however, not be estimated because irreversible radical decay was too fast.

The isopropylperoxy radical decays irreversibly more slowly than either cyclopentylperoxy or *sec*-butylperoxy and below 173 K the radical concentration could be reversibly increased and decreased by raising and lowering the temperature with no significant loss in radical concentration. Equilibrium constants for this process were estimated using the procedure of Scaiano and Ingold (7). Thus a sample of isobutyryl peroxide in oxygen-saturated CF_2Cl_2 was photolysed continuously at 143 K. The initial rate of production of i-$\mathrm{PrO_2}^{\cdot}$, $(\mathrm{d}[i\text{-PrO}_2^{\cdot}]/\mathrm{d}t)_0$, was measured and the steady-state radical concentration $[i\text{-PrO}_2^{\cdot}]_{ss}$ was determined at the end of the period of photolysis, t. If it is assumed that i-$\mathrm{PrO_2}^{\cdot}$ at low temperatures only disappear by combination to give tetroxide the total number of i-$\mathrm{PrO_2}^{\cdot}$ produced, $[i\text{-PrO}_2^{\cdot}]_{tot} = (\mathrm{d}[i\text{-PrO}_2^{\cdot}]/\mathrm{d}t)_0 t$ and the equilibrium constant can be calculated from

$$[7]\quad K_a = \frac{[i\text{-PrO}_2^{\cdot}]_{tot} - [i\text{-PrO}_2^{\cdot}]_{ss}}{2[i\text{-PrO}_2^{\cdot}]_{ss}^2}$$

Values of $[i\text{-PrO}_2^{\cdot}]_{ss}$ were measured at each temperature and K_a calculated from [7]. The plot of $\ln (K_a/M^{-1})$ against the reciprocal of the absolute temperature yielded the thermodynamic parameters $\Delta H_a^0 = -8.0$ kcal mol^{-1} and $\Delta S_a^0 = -25$ cal deg^{-1} mol^{-1}.

TABLE 1. Absolute rate constants and Arrhenius parameters for self-reaction of some *sec*-alkylperoxy radicals*

Temperature (K)	$10^{-5}[2k_t/(M^{-1}\,s^{-1})]$ Isopropylperoxy	Cyclopentylperoxy	*sec*-Butylperoxy
175	—	9(13)	4(4)
181	—	15.5(18)	5(5.5)
186	0.055(0.08)	22(23)	—
191	—	36(28)	7(8)
196	0.035	25(35)	—
200	—	48(41)	9(11)
206	0.26(0.26)	—	—
229	0.8(0.8)	—	—
$\log[A_t/(M^{-1}\,s^{-1})]$	—	9.6(10.0)	7.1(9.0)
E_p/(kcal mol^{-1})	—	2.6(3.1)	1.1(2.7)

*The data shown in parentheses are from ref. 3 for cyclopentylperoxy and *sec*-butylperoxy and ref. 14 for isopropylperoxy.

Isopropyl-α-d_1-peroxy radicals decay irreversibly somewhat more slowly than isopropylperoxy because of a lower rate constant for termination (8). Below 173 K this radical exists in equilibrium with its tetroxide and $\Delta H_a^0 = -8.0 \pm 0.4$ kcal mol^{-1} and $\Delta S_a^0 < -33 \pm 3$ cal deg^{-1} mol^{-1}.

The thermodynamic parameters for the equilibrium between i-$\mathrm{PrO_2}^{\cdot}$ and its tetroxide are very similar to the values of ΔH_a^0 and ΔS_a^0 for *tert*-butylperoxy and related tertiary alkylperoxy radicals (2, 6). We are, therefore, tempted to conclude that thermodynamic parameters for the alkylperoxy radical – tetroxide equilibrium are not influenced to any great extent by the nature of the alkyl moiety.

Mill and Stringham (9), a number of years ago, failed to prepare diisopropyl tetroxide by photolysis of 2,2′-azoisopropane in oxygenated $CFCl_3$–CF_2Cl_2 while Adamic, Howard, and Ingold (6) did not observe the esr spectrum of the isopropylperoxy radical in this system. Our success with isobutyryl peroxide as a source for the isopropylperoxy radical implies that acyl peroxides are better photochemical sources of alkyl radicals at low temperatures than azo compounds.

It has been reported that secondary alkylperoxy radicals prepared by photolysis of di-*tert*-butyl peroxide in oxygen-saturated alkane decay with second-order kinetics below 193 K (3). Rates of radical decay in this system would, however, appear to have been influenced by the presence of an unstable mixed *tert*-alkyl *sec*-alkyl trioxide (10).

We find that plots of $[s\text{-RO}_2^{\cdot}]^{-1}$ against time for radicals prepared from the acyl peroxide at temperatures around 173 K showed pronounced upward curvature and below this temperature decayed with

Can. J. Chem. Downloaded from www.nrcresearchpress.com by 210.87.254.105 on 09/05/12
For personal use only.

Can. J. Chem. Downloaded from www.nrcresearchpress.com by 210.87.254.105 on 09/05/12
For personal use only.

TABLE 2. Rate constants for first-order decay of some *sec*-alkylperoxy radicals

Temperature (K)	$10^3 k_{epr}^1/s^{-1}$		
	Isopropyl-peroxy	Cyclopentyl-peroxy	*sec*-Butyl-peroxy
148	—	2.6	—
152	—	6.7	4
157.5	0.6	21.5	—
163	—	80	24
167	5.3	100	—

"clean" first-order kinetics. In this respect secondary alkylperoxy radicals behave like other radicals which exist in equilibrium with an excess of a diamagnetic dimer (11).

Values of the first-order rate constant k_{epr}^1 for isopropylperoxy, cyclopentylperoxy, and *sec*-butylperoxy were measured (Table 2) and found to increase in the order isopropylperoxy < *sec*-butyl peroxy < cyclopentylperoxy, i.e., k_{epr}^1 depends on the nature of the secondary alkyl group attached to oxygen.

Unfortunately, k_{epr}^1 could not be measured over a wide temperature range because above 173 K radical decays were not first-order while below 143 K radical concentrations were very small because of the high ratio of tetroxide to free radical. A plot of log (k_{epr}^1/s^{-1}) against K^{-1} for cyclopentylperoxy did, however, yield log $(A_{epr}^1/s^{-1}) = 12 \pm 1$ and $E_{epr}^1 = 10 \pm 0.6$ kcal mol^{-1}.

If reaction [1] describes the overall self-reaction of *sec*-alkylperoxy radicals, the rate of radical decay is given by

$$\frac{-d[s\text{-}RO_2^{\cdot}]}{dt} = \frac{2k_bK_a[s\text{-}RO_2^{\cdot}]^2}{1 + 4K_a[s\text{-}RO_2^{\cdot}]}$$

where $K_a = k_a/k_{-a}$ and when $K_a[s\text{-}RO_2^{\cdot}] > 1$ radical decays will be first-order. If this is the case $k_{epr}^1 = 0.5k_b$, where k_b is the unimolecular rate constant for tetroxide decomposition. This suggests that for cyclopentylperoxy $k_b/s^{-1} \sim 2 \times 10^{12} \exp(-10$ kcal mol$^{-1})/RT$.

Analogous first-order decays at low temperatures have not been observed for tertiary alkylperoxy radicals because these radicals are very persistent in the presence of significant concentrations of tetroxide.

Activation parameters for unimolecular decomposition of tertiary alkyl tetroxides = 10^{15}–10^{17} s^{-1} and 16–18 kcal mol^{-1} have, however, been calculated from kinetic and thermodynamic parameters for irreversible and reversible decays at temperatures where $4K_a[t\text{-}RO_2^{\cdot}] < 1$ and $2k_t = 2k_bK_a$ (2, 6).

Calculation of the activation parameters for unimolecular decomposition of dicyclopentyl tetroxide by this method gives $A_b = 10^{15}$–$10^{15.5}$ s^{-1} and $E_b = 10.6$–11.1 kcal mol^{-1}. Clearly there is poor agreement between pre-exponential factors estimated from k_{epr}^1 and $2k_t/K_a$ while activation energies calculated by the two methods are in good agreement.

A similar situation also exists for di-*tert*-butyl tetroxide because Mill and Stringham (9) and Bartlett and Guaraldi (12) have estimated $A_b = 10^{9.3}$–10^{12} s^{-1} and $E_b = 11$–12 kcal mol^{-1} from rates of oxygen evolution from solutions containing the tetroxide.

It has been suggested by Bowman, Gillan, and Ingold (13) that an additional 14.4 cal deg^{-1} mol^{-1} of entropy are lost in the formation of a cyclic rather than a linear transition state from two peroxy radicals, i.e., $A_b(s\text{-}RO_2^{\cdot})$ should be $\sim 10^{-3}A_b(t\text{-}RO_2^{\cdot})$. The value of A_b for cyclopentylperoxy radicals determined from k_{esr}^1 is consistent with this proposal whereas the more accurate value of A_b estimated from $2k_t/K_a$ is not consistent with this proposal. Clearly kinetic data for tetroxide decompositions are not accurate enough to provide information regarding the geometry of the transition state.

It would, however, appear that $E_b(s\text{-}RO_2^{\cdot}) < E_b(t\text{-}RO_2^{\cdot})$ suggesting that $A_b(s\text{-}RO_2^{\cdot})$ is almost certainly $< A_b(t\text{-}RO_2^{\cdot})$.

Conclusions

Secondary alkylperoxy radicals exist in equilibrium with di-*sec*-alkyl tetroxides with thermodynamic parameters which appear to be similar to the corresponding parameters for tertiary alkylperoxy radicals. At temperatures below 173 K radical decays follow first-order kinetics which is consistent with the influence of a radical-diamagnetic dimer equilibrium on rates of radical decay. Bimolecular rate constants for self-reaction of *sec*-alkylperoxy radicals depend on the nature of the alkyl moiety almost certainly because of differences in the rates of irreversible tetroxide decomposition.

Kinetic and thermodynamic parameters for irreversible and reversible decay of these radicals are not entirely self consistent and cannot be used with any certainty as evidence for or against the Russell mechanism for self-reaction of secondary alkylperoxy radicals (1).

Values of $2k_t$ for isopropylperoxy at 229 K and below are in excellent agreement with rate constants calculated using the Arrhenius parameters reported by Kirsch, Parkes, Waddington, and Woolley (14) obtained at higher temperatures in the gas phase. The similarity between these two sets of

data substantiates the conclusion that an alkylperoxy radical has the same termination rate constant in the gas and liquid phases (14).

1. J. A. HOWARD. Am. Chem. Soc. Symp. Ser. **69**, 413 (1978).
2. J. E. BENNETT, D. M. BROWN, and B. MILE. Trans. Faraday Soc. **66**, 397 (1970).
3. J. A. HOWARD and J. E. BENNETT. Can. J. Chem. **50**, 2374 (1972).
4. H. HART and D. D. WYMAN. J. Am. Chem. Soc. **81**, 4891 (1959).
5. H. C. BROWN. J. Am. Chem. Soc. **60**, 1325 (1938).
6. K. ADAMIC, J. A. HOWARD, and K. U. INGOLD. Can. J. Chem. **47**, 3803 (1969).
7. J. C. SCAIANO and K. U. INGOLD. J. Am. Chem. Soc. **99**, 2079 (1977).
8. J. A. HOWARD and K. U. INGOLD. J. Am. Chem. Soc. **90**, 1058 (1968).
9. T. MILL and R. S. STRINGHAM. J. Am. Chem. Soc. **90**, 1062 (1968).
10. J. E. BENNETT and G. BRUNTON. Private communication.
11. K. U. INGOLD. Free radicals. Vol. 1. *Edited by* J. K. Kochi. Wiley, New York, NY. 1973. Chapt. 2.
12. P. D. BARTLETT and G. GUARALDI. J. Am. Chem. Soc. **89**, 4799 (1967).
13. D. E. BOWMAN, T. GILLAN, and K. U. INGOLD. J. Am. Chem. Soc. **93**, 6555 (1971).
14. L. J. KIRSCH, D. A. PARKES, D. J. WADDINGTON, and A. WOOLLEY. J. Chem. Soc. Faraday Trans. 1, **74**, 2293 (1978).

Can. J. Chem. Downloaded from www.nrcresearchpress.com by 210.87.254.105 on 09/05/12
For personal use only.

Trends in field desorption mass spectra of several series of alkali metal cryptates: thermodynamic rationale and analytical implications

GORDON WALTER WOOD,[1] MEI-KUEN AU, NING MAK, AND PUI-YAN LAU

Department of Chemistry, University of Windsor, Windsor, Ont., Canada N9B 3P4

Received September 11, 1979

GORDON WALTER WOOD, MEI-KUEN AU, NING MAK, and PUI-YAN LAU. Can. J. Chem. **58**, 681 (1980).

Field desorption mass spectra have been recorded for most of the 45 cryptates which may be formed from complexation of [2.2.2]-, [2.2.1]-, and [2.1.1]-cryptand with Li^+, Na^+, and K^+ ions in combination with the anions Cl^-, Br^-, I^-, OTs^-, and BPh_4^-. The cryptate cation predominated in almost all of the spectra. The stability of the complexes was found not to be simply related to goodness of fit of the cation in the cryptand cavity, but a significant trend in stability in the order $BPh_4 > I > Br > Cl$ was found. This order of complex stability was shown to be consistent with known thermodynamic parameters. These results are discussed briefly in terms of applications to analysis of alkali metal cations.

GORDON WALTER WOOD, MEI-KUEN AU, NING MAK et PUI-YAN LAU. Can. J. Chem. **58**, 681 (1980).

On a enregistré les spectres de masse à ionisation par désorption de champ pour la plupart des 45 cryptates qui peuvent se former par suite de la complexation des cryptands [2.2.2]-, [2.2.1]-, et [2.1.1] avec les ions Li^+, Na^+, K^+ dont les anions sont Cl^-, Br^-, I^-, OTs^- et BPh_4^-. Le cryptate de cation prédomine dans presque tous les spectres. On a trouvé que la stabilité des complexes n'est pas simplement reliée à la façon parfaite avec la quelle le cation se glisse dans la cavité du cryptand mais qu'il existe une tendance significative de stabilité dans l'ordre: $BPh_4 > I > Br > Cl$. On montre que cet ordre de stabilité du complexe est en accord avec des paramètres thermodynamiques connus. On discute brièvement des résultats en fonction des applications à l'analyse des cations de métaux alcalins.

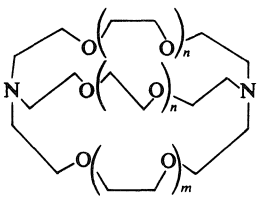
[Traduit par le journal]

Introduction

Although field desorption mass spectrometry (FDMS) has now become established among the standard methods for analysis and structure determination (1), the technique continues to be plagued by unwanted side-effects from the presence of alkali metal ions in samples. For those samples which contain these ions only as impurities, various clean-up procedures have been used with mixed results. In addition, a significant proportion of the non-volatile samples for which FDMS is in principle applicable are presented as salts with Na^+ or other cation as an integral part of the species. Examples of the latter are barbiturates, nucleotides, and carboxylates.

One of our early attempts to improve FD spectra of alkali metal containing samples involved the addition of macrocyclic ligands to complex the metal ion and thus remove its deleterious effect (2, 3). During that work we noted a number of interesting trends in behavior, particularly for the class of macrobicyclic ligands now called cryptands (4). The ready formation of alkali metal ion complexes with these ligands and the widespread study of their kinetic and thermodynamic properties in other connections (5–9) led us to examine an extended set of these complexes by FDMS. The results obtained provide some insights on management of alkali metal ion impurities in FDMS, on the potential of these complexes for analysis of metal ions, and on the nature of the FD process.

Spectra of complexes of cryptands **I–III** with a variety of Li^+, Na^+, K^+ salts are compared for ease of ionization, stability, and other features.



I, [2.2.2]-cryptand; $n = m = 1$
II, [2.2.1]-cryptand; $n = 1, m = 0$
III, [2.1.1]-cryptand; $n = 0, m = 1$

Results and Discussion

The complexes studied comprise a 3 × 3 × 5 matrix as follows. Cryptands **I–III** were combined with Li^+, Na^+, K^+ salts of the following anions: Cl^-, Br^-, I^-, OTs^-, BPh_4^-. Of the 45 potential complexes in this set, 39 were attempted; 3 failed to give a spectrum: **I**·LiCl, **I**·KCl, and **II**·KCl. Tables 1–3 report results on the 36 complexes successfully desorbed. Trials were not made of the remaining 6 combinations with ligand **III**.

Field desorption mass spectra of the 13 complexes with [2.2.2]-cryptand, **I**, are presented in Table 1. The base peak for these complexes is generally the cryptate cation ($L + C$). Considera-

[1]To whom all correspondence should be directed.

0008-4042/80/070681-05$01.00/0

©1980 National Research Council of Canada/Conseil national de recherches du Canada

Can. J. Chem. Downloaded from www.nrcresearchpress.com by 210.87.254.5 on 09/05/12
For personal use only.

TABLE 1. FD spectra of complexes of alkali metal salts with [2.2.2]-cryptand (**I**)[a]

Complex (mA)[b]	TI[c]	L	$L+1$	$L+C$ −2	$L+C$ −1	$L+C$ —	$L+C$ +1	$L+C$ +2	Others (%)
I·KBr(16)	<1	16		2	1	100	13	8	$L-2$(19)
I·KI(20)	2	4		1		100	16	9	
I·KOTs(19)	52			8	6	100	22	10	
I·$KBPh_4$(21)	38				2	100	21	10	
I·NaCl(12)	<1		1	5	4	100	15	2	
I·NaBr(16)	2	100	23		5	12	2		$L-2$(4)
I·NaI(18)	3	2		3	1	100	21	2	
I·NaOTs(14)	34		1	2	1	100	20	3	[d]
I·$NaBPh_4$(20)	13			2	1	100	22	4	
I·LiBr(16)	75	1			8	100	19	3	
I·LiI(18)	73			1	9	100	21	4	$L+2C^{2+}$(18)
I·LiOTs(14)	5	11	6		15	100	8	4	
I·$LiBPh_4$(17)	77				1	100	19	2	

[a]L = ligand, [2.2.2]-cryptand; C = metal cation.
[b]Anode heating current.
[c]TI = total ion intensity in arbitrary units.
[d]m/z 523 (1); assigned to $L + 2C$ + OTs − 70, where loss may be C_4H_6O.

TABLE 2. FD spectra of complexes of alkali metal salts with [2.2.1]-cryptand (**II**)[a]

Complex (mA)[b]	TI[c]	L −1	L —	L +1	$L+C$ −2	$L+C$ −1	$L+C$ —	$L+C$ +1	$L+C$ +2	Others (%)
II·KBr(16)	11		100	18			2			
II·KI(12–18)[d]	<1		100				100			
II·KOTs(13)	4	1	8	5		7	100	25	15	[e]
II·$KBPh_4$(12)	5	1					100	34	20	
II·NaCl(11)	2		24	1			100	17	1	
II·NaBr(17)	3		30	10			100	18	1	
II·NaI(18)	123				5	1	100	21	5	[f]
II·NaOTs(13)	65				1		100	25	5	[g]
II·$NaBPh_4$(19)	165				1		100	18	3	
II·LiCl(14)	2		15	9	2	23	100			
II·LiBr(13)	12				6	16	100	23	2	
II·LiI(22)	5				1	7	100	18		
II·LiOTs(7)	178	1		1	2	11	100	17	3	$L+1^{2+}$(11)
II·$LiBPh_4$(18)	118				1	3	100	19	2	

[a]L = ligand, [2.2.1]-cryptand; C = metal cation.
[b]Anode heating current.
[c]TI = total ion intensity in arbitrary units.
[d]Average of 5 scans.
[e]m/z 505(49), 506(8), 507(3); assigned to L + 2H + OTs. m/z 459(19); assigned to $3C$ + 2OTs. m/z 557(11); assigned to $2L + C$ − 146, where loss may be $2xC_4H_7O$. m/z 536(3); assigned to $L + 2C$ + OTs − 45, where loss may be C_2H_5O.
[f]m/z 837(6); not reproducible; assigned to $(2L + 2C + \mathbf{I})^+$.
[g]At 20 mA and above salt clusters Na_3OTs_2 and Na_2OTs dominate the spectrum.

tion of the exception, **I** · NaBr, along with the fact that **I** · KCl and **I** · LiCl failed to give a spectrum, is the first suggestion of an important anion effect that will be discussed later. Minor peaks are recorded at $L + C \pm 1$ and $L + C \pm 2$ for most of these complexes. Each of these may represent gain or loss of the corresponding number of H atoms from the complex, but allowance must first be made for the contribution to these peaks of isotopes. Thus, in addition to the usual contributions from ^{13}C and ^{18}O, we have ^{41}K and ^{6}Li in the appropriate complexes. With these corrections made, the only peak that remains with significant intensity is $L + C - 2$. Further support for apparent loss of 2H from the ligand is seen in the $L - 2$ peaks of two of the spectra.

Complexation of two Li^+ ions with the oversized ligand **I** was found only for **I** · LiI. This doubly charged ion appeared throughout the series of scans with appropriate isotope peaks at half-integral mass values, but was unexplainedly absent from complexes containing anions other than I^-.

The **I** · NaOTs complex shows a minor peak at m/z 523, apparently containing the anion. Stronger peaks of this kind are seen in Table 2.

Since FDMS is frequently limited in reproduci-

Can. J. Chem. Downloaded from www.nrcresearchpress.com by 210.87.254.5 on 09/05/12
For personal use only.

TABLE 3. FD spectra of complexes of alkali metal salts with [2.1.1]-cryptand (III)[a]

Complex (mA)[b]	TI[c]	L	$L+1$	$L+C$ −2	$L+C$ −1	$L+C$ —	$L+C$ +1	$L+C$ +2	Others (%)
III·$KBPh_4$(14)	4	12	3			100	14	6	$2L + C$(20)
III·NaCl(15)	6	1	8		1	100	11	3	
III·NaI(18)	<1	3				100	11	2	
III·$NaBPh_4$(19)	10	1				100	23	2	[d]
III·LiCl(17)	3	19	2		6	100	16	2	
III·LiBr(19)	8			4	12	100	14	1	
III·LiI(23)	20			3	9	100	16	2	
III·LiOTs(22)	3				8	100	18	2	
III·$LiBPh_4$(21)	39				3	100	16	2	

[a]L = ligand, [2.1.1]-cryptand; M = metal cation.
[b]Anode heating current.
[c]TI = total ion intensity in arbitrary units.
[d]Above 20 mA several ions corresponding to portions of the salt are found: $NaBPh_4^{+\cdot}$, $(Na_2BPh_4)^+$, $BPh_3^{+\cdot}$, BPh_2^+, $(NaBPh_3)^+$.

bility by ion statistics, we have reported for each of the spectra in this paper a measure of the total ion intensity, TI. The units of TI are arbitrary but previous experience indicates that on average each unit represents 10^2–10^3 ions at the detector. It is thus expected that scan-to-scan reproducibility will deteriorate rapidly for low values of TI (<1), and also where individual peak intensities fall below this threshold.

A number of features already discussed may be seen in the spectra of cryptates in Table 2. Once again, the complex with KCl failed to give a reproducible spectrum. Of the remaining 14 members of this set, only II·KBr and II·KI failed to give spectra in which $L + C$ was the dominant single peak. The apparent excess abundance of some isotope peaks may simply reflect poor ion statistics, but it appears that both II·KOTs and II·$KBPh_4$ may contain one extra H ($L + C + 1 = 25, 34, L + C + 2 = 15, 20$ respectively). Likewise, $L + C - 2$ is fairly consistent in Li complexes and the more intense spectra of Na complexes.

Both II·KOTs and II·LiOTs exhibit some unusual ions. The peaks in the former at m/z 505, 506, 507 are the most clear-cut example in this study of protonation of the macrobicyclic ligands, a reaction which is well-known in solution (8). The ions m/z 557, 536 from the same complex appear to reflect some decomposition of the ligand. The doubly-charged $L + 1$ ion from II·LiOTs may be rationalized as arising from protonation and ionization of the same ligand, presumably at the two nitrogens.

Results for cryptand III complexed with all 5 Li salts and representative Na and K examples are shown in Table 3. Although all spectra contain $L + C$ as base peak, only III·LiI, III·$LiBPh_4$, and perhaps III·$NaBPh_4$, III·LiBr give reasonably intense peaks for this dominant ion. As before, there is some loss of 2H ($L + C - 2$). Although the large K^+ ion is accommodated surprisingly well by this small ligand ($L + C = 100$), there is a significant ion corresponding to complexation of two ligands by one cation. This process may occur even where sizes are matched, as in I·KBr where $2L + C$ is found above 18 mA.

There is some judgement involved in the selection of one scan from a sequence at increasing anode temperatures, and thus an uncertainty in the "best" anode temperature. In spite of this fact, two generalizations seem to be fairly safe. First, the anode temperature reported for the "best fit" complex is higher than for the "misfits". Thus the average anode current for [$K^+ \subset$ 2.2.2] is 19 mA, compared to 16 mA for both Na^+ and Li^+ complexes with this cryptand. Desorption of [$Na^+ \subset$ 2.2.1] complexes was only 1–2 mA higher than for the other cations, but [$Li^+ \subset$ 2.1.1] complexes desorbed at 20 mA compared to 17 mA for [$Na^+ \subset$ 2.1.1] complexes and 14 mA for the one [$K^+ \subset$ 2.1.1].

The average anode temperature for the various halide salts also appeared to increase from Cl^- to Br^- to I^- (14 to 16 to 19 mA). This trend may be related to the lattice energy of the alkali metal halides as presented subsequently.

Perhaps the most striking general conclusion that can be drawn from these spectral data is the lack of correlation between apparent complex stability in FDMS and the well-known solution measurements of thermodynamic stability in which each cryptand complexes selectively with the alkali metal ion which most nearly fits its cavity. Thus [2.2.1]-cryptand accommodates Na^+ well (log K_s = 5.3 in H_2O); K^+ to a lesser extent (log K_s = 3.9); and even less, Li^+ (log K_s = 2.5). These stability constants reflect free energy changes upon exchange of the cation between cryptand cavity and the solvent.

Can. J. Chem. Downloaded from www.nrcresearchpress.com by 210.87.254.5 on 09/05/12
For personal use only.

Can. J. Chem. Downloaded from www.nrcresearchpress.com by 210.87.254.5 on 09/05/12
For personal use only.

TABLE 4. Enthalpy and entropy of ligation of alkali metal ions[a]

Cryptand	Transfer function	Alkali metal ion Li	Na	K
[2.2.2] (I)	H_l	—	113	97
	S_l	—	33	31
[2.2.1] (II)	H_l	132	111	93
	S_l	22	20	22
[2.1.1](III)	H_l	137	111	—
	S_l	25	29	—

[a]$M^+_{gas} + L_{aq} \rightarrow [M^+ \subset L]_{aq}$ as reported in ref. 7.

The most obvious difference between this process and decomposition of a cryptate complex on the FD anode is the lack of solvation for the cation released. As a first approximation to the FD situation, we may compare the free energies of transfer of the cations in question from a cryptand cavity to the gas phase (free energy of ligation, ΔG_l). Such numbers have recently been determined where the cryptand is in aqueous solution and further dissected into enthalpies and entropies of ligation, Table 4 (7).

Clearly, selectivity of cryptand for different cations cannot be found in the entropy of ligation terms, which are essentially constant for each ligand regardless of the cation. The enthalpy terms increase for the smaller cations *irrespective of the goodness of fit*. Thus transfer of Li^+ from [$Li^+ \subset$ 2.2.1] hydrate to the gas phase costs 20 kcal/mol more than the same change for Na^+, in spite of the log K_s difference of ca. 3 (5.3 − 2.5) in the other direction. Likewise, the enthalpy of the hydrated [$Na^+ \subset$ 2.2.2] is 16 kcal/mol more favorable with respect to the gas phase ion than is [$K^+ \subset$ 2.2.2], whereas stabilities of the cryptates in H_2O differ by 1.4 log units in the other sense.

This analysis allows one to attribute the usual selectivity of these cryptands to solvation of the uncomplexed cation (7) and thus justify the absence of selectivity in FD. However, some further rationale for the marked anion effect would be desirable. Among the several gross approximations[2] in equating the transfer process above with the FD situation is the assumption that the released cation enters the gas phase. Indeed, other experience indicates that at the moderate anode temperatures employed here, the cation will simply join the waiting external anion. If the free energy gain of that recombination may be approximated by

$$M^+_{gas} + X^-_{gas} \rightarrow MX_{solid}$$

a likely source of the large anion effect on stability in FDMS becomes evident. Thus for the alkali halides, X = Cl, Br, I; M = Li, Na, K; chlorides are ca. 9 kcal/mol more stable in terms of ionic lattice energy than bromides which in turn are ca. 11 kcal/mol more stable than iodides. Although the thermodynamic data for tetraphenylborates are less complete, combination of available experimental (10) and theoretical (11) values enables one to estimate the corresponding change from I to BPh_4 at 65 kcal/mol. According to this interpretation, the variation of cryptate stability as measured by FDMS abundance of the $L + C$ ion is at least partly a function of the ionic lattice energy of the ion pair formed when the cryptate cation is released. The general trend of increased stability I > Br > Cl may be seen in Tables 1–3 with a few apparent exceptions. The much smaller ionic interaction in tetraphenylborate salts is accompanied by an additional improvement in stability of cryptates of these compounds.

Several procedures for analysis of alkali metal ions by FDMS have been reported (12). For trace amounts of alkali metal ions, cryptate formation would no doubt improve sensitivity and reproducibility of desorption in FDMS. The present results suggest that a single cryptand large enough to accommodate the largest ion to be analyzed should be just as satisfactory as a series of ligands selected to match the size of each cation. Further, conversion of the analyte to BPh_4^- or other suitable low lattice energy form should give improved results.[3]

Experimental

Mass spectra were recorded on a Varian MAT CH5 DF mass spectrometer operating under the control of an INCOS 2000 data system as previously described (13).

Cryptates were prepared by the addition of an equimolar amount of salt to a solution of 50 mg of cryptand in 5 mL $CHCl_3$. The mixture was stirred at room temperature overnight, and the solvent evaporated. The residue was redissolved in 1 mL of $CHCl_3$ for FDMS analysis.

Acknowledgement

Support of this work by the Natural Sciences and Engineering Research Council of Canada is gratefully acknowledged.

1. H. D. BECKEY. Principles of field ionisation and field desorption mass spectrometry. Pergamon, Oxford. 1977.

[2]Among these is neglect of differences in hydration of the "full" and "empty" ligand, see ref. 4.

[3]An observation which we believe may be related to this point has been published (14). In that paper $LiBPh_4$ is advocated for cationization in FD, but no attention is drawn to the reason for anion choice.

2. G. W. WOOD, P.-Y. LAU, and N. MAK. Biomed. Mass Spectrom. **1**, 425 (1974).
3. N. MAK. M.Sc. Thesis, University of Windsor, Windsor, Ont. 1975.
4. J.-M. LEHN. Acc. Chem. Res. **11**, 49 (1978).
5. J.-M. LEHN. *In* Structure and bonding. Vol. 16. *Edited by* J. D. Dunitz *et al.* Springer-Verlag, New York. 1973.
6. J.-M. LEHN and J.-P. SAUVAGE. J. Am. Chem. Soc. **97**, 6700 (1975).
7. E. KAUFMANN, J.-M. LEHN, and J.-P. SAUVAGE. Helv. Chim. Acta, **59**, 1099 (1976).
8. K. HENCO, B. TÜMMLER, and G. MAASS. Angew. Chem. Int. Ed. **16**, 538 (1977).
9. B. G. COX, H. SCHNEIDER, and J. STROKA. J. Am. Chem. Soc. **100**, 4746 (1978).
10. Y.-C. WU and H. L. FRIEDMAN. J. Phys. Chem. **70**, 501 (1966).
11. M. SALOMON. J. Phys. Chem. **74**, 2519 (1970).
12. H.-R. SCHULTEN, U. BAHR, and W. D. LEHMANN. Mikrochim. Acta, 191 (1979) and references therein.
13. G. W. WOOD, E. J. OLDENBURG, P.-Y. LAU, and D. L. WADE. Can. J. Chem. **56**, 1372 (1978).
14. H. J. VEITH. Angew. Chem. Int. Ed. **15**, 696 (1976).

Can. J. Chem. Downloaded from www.nrcresearchpress.com by 210.87.254.5 on 09/05/12
For personal use only.

Reactions of some substituted phenols with chromyl and vanadyl chlorides

JOHN F. HARROD AND ASHA PATHAK
Chemistry Department, McGill University, 801 Sherbrooke Street West, Montreal, P.Q., Canada H3A 2K6

Received August 22, 1979

JOHN F. HARROD and ASHA PATHAK. Can. J. Chem. **58**, 686 (1980).

The oxidation of 2,4,6-tritertbutylphenol and several other alkyl and halophenols by CrO_2Cl_2 and $VOCl_3$ was studied. The products of CrO_2Cl_2 oxidation are mostly quinones and diphenoquinones, whilst those of $VOCL_3$ oxidation also include major amounts of dealkylated phenols and C—C coupled dimers. The product distributions are interpreted in terms of a mechanism involving phenoxyl radicals, ligand transfer from metal to radical, and either phenoxonium ions or metallate esters where there is sufficient electron withdrawal from the organic group for it to exhibit carbenium ion properties. The differences in behaviour between CrO_2Cl_2, $VOCl_3$, and $CuCl_2$ are attributed to different balances between the oxidation potential and Lewis acidity of the metal complexes. It is concluded that CrO_2Cl_2 is not a good model for proposed ferryl intermediate in heme oxidase systems since it induces 1 → 3 rather than 1 → 2 halogen shifts and an NIH shift that is best explained by carbenium ion-like intermediates.

JOHN F. HARROD et ASHA PATHAK. Can. J. Chem. **58**, 686 (1980).

On a étudié l'oxydation du tritert-butyl-2,4,6 phénol et de plusieurs autres phénols alkylés et halogénés par CrO_2Cl_2 et $VOCl_3$. Les produits de l'oxydation par CrO_2Cl_2 sont principalement des quinones et des diphénoquinones alors que ceux résultant de l'oxydation par $VOCl_3$ comprennent également des quantités appréciables de phénols désalkylés et des dimères liés par une liaison C—C. On interprète la répartition des produits en fonction d'un mécanisme qui fait intervenir des radicaux phénoxyles, des transferts de ligands du métal au radical et soit des ions phénoxonium ou des esters de type métallique dans lequel le groupe organique est suffisamment polarisé pour exhiber les propriétés d'un ion carbénium. On attribue les différences de comportement entre le CrO_2Cl_2, le $VOCl_3$ et le $CuCl_2$ aux différents équilibres entre les potentiels d'oxydation et l'acidité de Lewis des complexes métalliques. On a conclu que le CrO_2Cl_2 n'est pas un bon modèle pour l'intermédiaire ferryle proposé dans les systèmes hème oxydase puisqu'il induit un glissement 1→3 d'halogène plutôt que 1→2 et un glissement NIH qui s'explique mieux par un intermédiaire de type carbénium.

[Traduit par le journal]

Introduction

Oxochromium(VI) compounds have been cited as models for the reactive intermediates in oxygenases such as cytochromes P-450 (1, 2). Both the experimentally observed NIH shift in chromate oxidations of aromatic nuclei (1) and theoretical calculations on orbital populations in the chromate ion (2) have been adduced as evidence for a similarity between the oxygen transfer in Cr(VI) oxidations and in oxygenations catalysed by cytochrome P-450. As part of a wider investigation of the mechanisms whereby metal ions oxidize phenols (3), or catalyse their oxidation by dioxygen, we have studied the oxidation of tritertbutylphenol by chromyl chloride. The choice of this reaction was based on the usefulness of tritertbutylphenol in detecting radical, as opposed to other mechanistic pathways in phenol oxidation (3, 4). An earlier study of the oxidation of phenols by chromyl chloride showed the reaction to be quite selective for the production of 1,4-quinones (5).

The scope of the present investigation was broadened to include the reaction of tritertbutylphenol with vanadyl trichloride. Besides the chemical similarity of vanadyl chloride to chromyl chloride and to the supposed "ferryl" species that have been suggested as intermediates in the active cycles of a number of heme-containing oxidative enzymes (6), the reagent is of interest in view of its exceptional selectivity in certain phenol-coupling reactions (7).

Results

Reaction of 2,4,6-Tritertbutylphenol with Chromyl Chloride

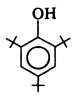
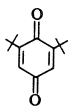
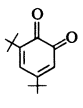
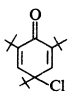
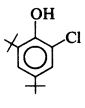
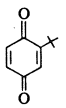
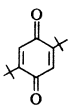
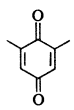
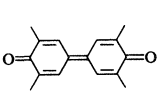
The title reaction occurred extremely rapidly in hexane at −65°C with the precipitation of a buff coloured, apparently amorphous solid. This solid was extremely moisture sensitive and all attempts to isolate products directly from it resulted in intractable, tarry material. Most of the organic material was bound up in this solid and could most easily be recovered by hydrolysis and extraction with organic solvents. Much of the organic material could also be released under anhydrous conditions by treatment of the solid with pyridine. Such treatment led to the formation of an insoluble, apparently polymeric, pyridine–chromium(III) compound and released most of the organic reaction products into solution.[1] This technique was less convenient to use than aqueous hydrolysis, but it served to show that most of the products released on hydrolysis did not depend on externally supplied water for their production. It should be stressed,

[1]Similar observations were made by Leigh and Strickson (5*c*).

0008-4042/80/070686-08$01.00/0
©1980 National Research Council of Canada/Conseil national de recherches du Canada

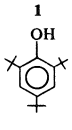
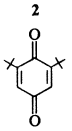
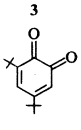
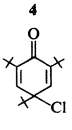
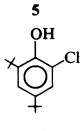
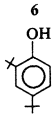
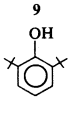
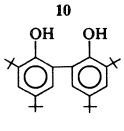
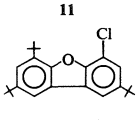
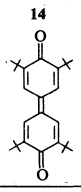
Can. J. Chem. Downloaded from www.nrcresearchpress.com by 210.87.254.5 on 09/05/12
For personal use only.

TABLE 1. Products of oxidation by CrO_2Cl_2

Reactant (ratio to CrO_2Cl_2)	Weight per cent of recovered product[a]								
	1 	2 	3 	4 	5 	7 	8 	16 	17 
1 (1:1)	31	28	6	28	4				
1 (1:2)		43	36	5					
6 (1:2)						70	20		
2,6-Xylenol (1:2)								55	28

[a]Total recovered product usually 90–100% based on reactant.

TABLE 2. Products of oxidation by $VOCl_3$

Reactant (ratio to $VOCl_3$)	Weight per cent of recovered product[a]										Temperature (°C)
	1 	2 	3 	4 	5 	6 	9 	10 	11 	14 	
1 (1:2)		14	3	15	18	26		17	7		−60
1 (1:2)		10	3	15	16	31		10	8		25
1 (1:2)	14	12	3		33	29		4			90
1 (1:4)		16	3	10	14	22		18	10		25
1 (1:8)		20	2	10	19	5		28	13		25
6 (1:2)		6	2			67		10	15		25
6 (1:4)		9	3		21	38		8	16		25
5 (1:2)		4	2	3	85	3					25
9 (1:2)		2				17	45			34	25
4 (1:2)		15	2	11	69						25

[a]Total recovered product generally 80–90% based on reactant.

however, that the infrared spectrum of the buff coloured precipitate, even when samples were prepared under scrupulously anhydrous conditions, was dominated by bands due to water. This water was probably a reaction product and most likely ligated to the Cr(III) in the product.

The major products from oxidation of 2,4,6-tritertbutylphenol **1** with CrO_2Cl_2 are shown in Table 1. The most significant difference between the cases with 1:1 and 2:1 mole ratio of oxidant to substrate was the production of a substantial amount of the 2-electron oxidation product **4** under oxidant-deficient conditions.

In order to establish whether or not the formation of the orthoquinone **3** involved prior dealkylation of **1** to 2,4-ditertbutylphenol, **6**, a reaction of the latter with excess CrO_2Cl_2 was studied. The results for this reaction are also shown in Table 1.

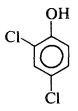
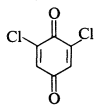
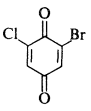
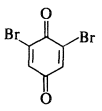
Reactions of 2,4,6-Tritertbutylphenol and Some of its Derivatives with $VOCl_3$

Addition of $VOCl_3$ to a solution of **1** in hexane resulted in the immediate formation of a dark blue precipitate and a dark blue supernatant liquor. Attempts to isolate a crystallizable product from the dark blue solid were not successful, probably because it was a fairly complicated mixture. These attempts to characterize the solid were complicated by its extremely deliquescent nature. It was therefore decided to use a hydrolytic workup similar to that used with the product of the chromyl chloride reaction.

From the results depicted in Table 2, it is evident that the $VOCl_3$ reaction is much more complicated than that of CrO_2Cl_2, at least in terms of the reaction products. The products of the $VOCl_3$ reaction may be classified in terms of their oxidation level,

Can. J. Chem. Downloaded from www.nrcresearchpress.com by 210.87.254.5 on 09/05/12
For personal use only.

TABLE 3. Products of halophenol oxidation by CrO_2Cl_2

Reactant phenol	Weight per cent of recovered product 			
2,4-Dichloro-	30	70		
2-Bromo-4,6-dichloro-		89	~1	
2,4,6-Tribromo-		59	17	9

namely, (*i*) dealkylated phenol (no oxidation), (*ii*) C—C coupled dimers (one-electron oxidation), (*iii*) chlorophenol and cyclohexadienones (two-electron oxidation), and (*iv*) quinones (four-electron oxidation). A particularly striking feature of the reactions listed in Table 2 is the apparent insensitivity of the total organic product oxidation level to reaction conditions. The average number of electrons lost per molecule of reactant **1** ranged from 1.3 to 1.9 even though the minimum available oxidizing equivalents (assuming V^V to be a one-electron oxidant) ranged from two to eight. Although little change occurred in the average oxidation level of the organic product, there was an appreciable increase in the amounts of C—C dimers and 1,4-quinone relative to other products.

The distribution of products was quite insensitive to temperature from ambient down to −60°C, but at higher temperature the chlorodealkylation product **5** increased at the expense of C—C coupled dimers.

A single test reaction was run using the tritertbutylphenoxyl radical instead of **1**. The product distribution obtained was essentially the same as that for **1** under the same conditions.

The reactions of the chlorocyclohexadienone **4**, and the phenols **5**, **6**, and 2,6-ditertbutylphenol, **9**, were studied to establish their possible roles as intermediates in the tritertbutylphenol reaction. Neither **5** nor **6** reacted rapidly enough to be implicated as essential intermediates, although **6** did give the same C—C coupled dimers and quinones as did **1**. The product of the latter reaction at a $VOCl_3$ to phenol ratio of two was notable for the absence of the chlorophenol **5**, even though the chlorodealkylated dimer, **11**, was the major product. At a $VOCl_3$ to phenol ratio of four, a considerable amount of **5** was produced but the yields of the C—C coupled dimers and quinones were not appreciably altered.

The products of the reaction of **9** with $VOCl_3$, in addition to excluding **9** as an intermediate in the tritertbutylphenol reaction, underline the curious regioselectivities which must be operative to give rise to the products observed in the reactions of **1**. Thus, **9** yields the diphenoquinone **14** as the major product and only a trace of the quinone **2**. Although a considerable amount of alkyl migration occurred, as indicated by the production of an appreciable amount of **6**, no *ortho*-coupled oxidation products were detected.

Oxidation of 2,6-Dimethyl-4-deuteriophenol by CrO_2Cl_2

Oxidation of the title phenol by chromyl chloride yielded 2,6-dimethylbenzo-1,4-quinone, **16**, (55% based on phenol) and 3,3′,5,5′-tetramethyldiphenoquinone, **17**, (30%), as expected from the results of Strickson and Leigh (*5b*). Mass spectrometric analysis showed that ca. 30% of **16** had retained a single deuterium and that ca. 10% of **2** contained a single deuterium.

Oxidation of the title phenol by ferricyanide gave **17** in almost quantitative yield, but with zero retention of deuterium.

Oxidation of Polyhalophenols by CrO_2Cl_2

Since the oxidation of 2,6-dichlorophenol, **18**, was known to give 2,6-dichloro-1,4-benzoquinone, **19**, quite selectively on oxidation with CrO_2Cl_2 (*5a*) (see Table 3), an attempt to synthesize the corresponding orthoquinone, **20**, by oxidation of 2,4-dichlorophenol was made. Instead of **20**, the product proved to be almost entirely **19** (Table 3). To determine whether **19** resulted from intramolecular halogen shift, or from oxidative dehalogenation accompanied by chlorination with CrO_2Cl_2, a number of oxidations of bromo- and chlorobromophenols by CrO_2Cl_2 were investigated. The results of some of these reactions are shown in Table 3.

Discussion

Reactions of Phenols with Chromyl Chloride

The general features of the chromyl chloride oxidation of alkyl and halophenols have been outlined in a series of papers by Strickson *et al.* (5). Contrary to the report of Leigh and Strickson (*5c*), who detected only the orthoquinone as a product of tritertbutylphenol oxidation, the ortho- and paraquinones **2** and **3** were isolated in roughly equal

Can. J. Chem. Downloaded from www.nrcresearchpress.com by 210.87.254.5 on 09/05/12
For personal use only.

Can. J. Chem. Downloaded from www.nrcresearchpress.com by 210.87.254.5 on 09/05/12
For personal use only.

amounts in the present study and accounted for 80% of the reacted phenol. The occurrence of large amounts of orthoquinone appears to be unique to this reaction. The reaction of 2,4-ditertbutylphenol, **6**, which might be expected to favour orthoquinone formation even more, gave the monotertbutylparaquinone as the major product, together with a significant amount of the tertbutyl-migrated product **8**. Since these two products account for 90% of reactant phenol, it cannot be assumed that orthoquinone was lost through secondary reactions. The fact that tertbutyl migration occurs on reaction of **6** but not of **1** suggests that there is an intermediate with considerable carbenium ion character prior to the loss of the tertbutyl group from a tritertbutyl moiety, but that migration cannot occur due to steric constraints. Following loss of a tertbutyl group on the way to formation of quinone, the system appears to be no longer susceptible to migration. In the case of **6**, the steric restraint to migration is absent on the side of the ring lacking an orthotertbutyl substituent and migration of the alkyl group can occur. It is presumably at the same stage of the reaction that the deuterium migration takes place when 2,6-dimethyl-4-deuteriophenol is oxidized.

There is no doubt that the formation of free radicals is an important step (probably the first) in this complicated reaction (*5c*). However, it also seems most likely that carbenium ions or analogous species are involved. The series of reactions [1]–[4] seems to explain all of the results obtained with alkyl phenols.

Since the exact oxidation and coordination states of the chromium species are unknown, those illustrated in [1] to [4] are only exemplary of the kinds of species that might be involved. Reactions [1*a*] and [1*b*] are generically similar in that either one, or both, fragments from homolytic cleavage of the phenolic O—H bond are captured by chromyl chloride. The products of [1*a*] and [1*b*] are designated to be in equilibrium to satisfy the requirement that the phenoxyl radical and a phenoxonium-like species be interchangeable for reasons to be enlarged upon below. The same applies to the reactants and products of reaction [2*b*].

The formation of esters **21** and **22** is expected to lead to the concentration of a great deal of positive charge on the carbocycle, if not to the formation of a free phenoxonium ion, and it is from such a species that dealkylation, or alkyl migration, will occur. Following loss of the alkyl group, rapid collapse of the hydroquinone ester intermediate **23/24** to the quinone will occur with facility.

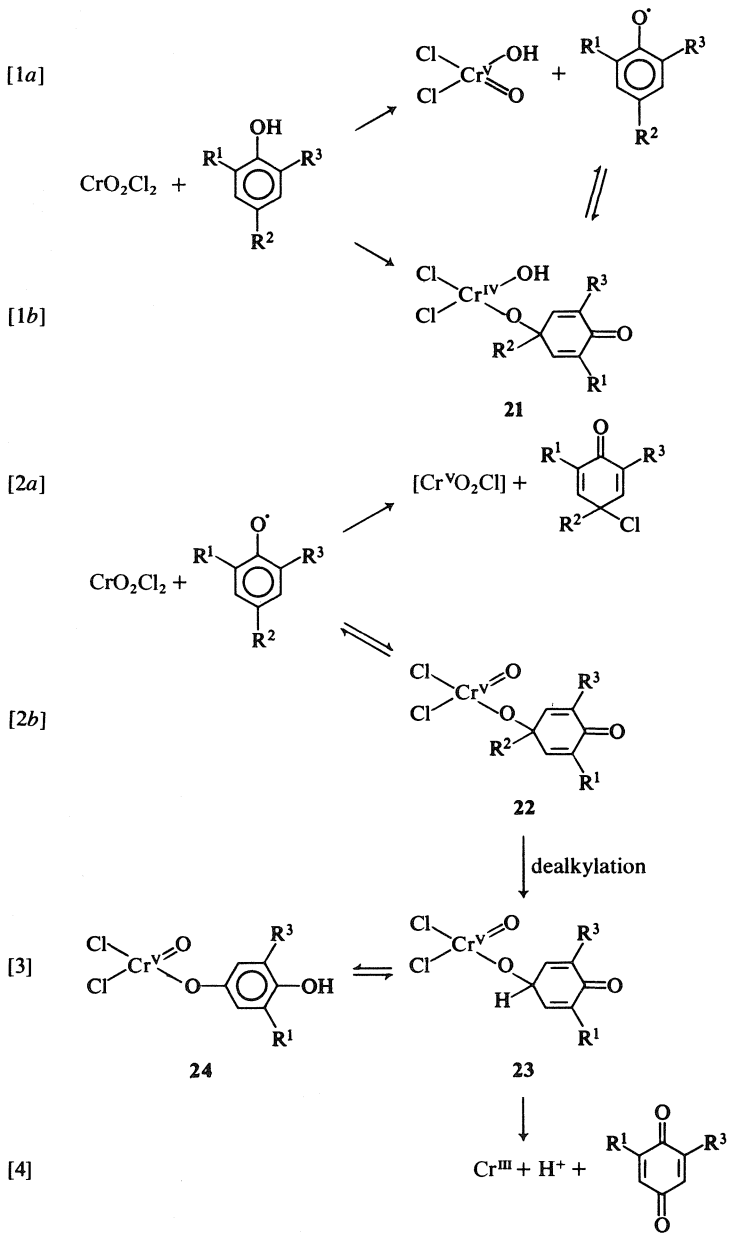
Reactions [2*a*] and [2*b*] are both ligand transfer reactions from Cr^{VI} to the phenoxyl radical. Under chromyl chloride deficient conditions the production of large amounts of **4** (see Table 1) indicates that [2*a*] competes kinetically very favourably with [2*b*]. However, the absence of **4** under conditions of excess chromyl chloride indicates that the oxygen attachment [2*b*], leading ultimately to quinone, is thermodynamically favoured. This reasoning also requires that **4** be somehow recycled back through species such as **21** or **22**. The production of **4** by ligand transfer has been observed previously in the oxidation of **1** by cupric chloride (3).

The observation of orthoquinone formation from **1**, but not from other phenols, is difficult to rationalize. If the carbocycle in **21** and **24** has a great deal of carbenium ion character, it might be presumed that attachment to the Cr—O moiety might be favoured for those carbons carrying an alkyl rather than a hydrogen substituent. The formation of a mixture of ortho- and paraquinone for the case where $R^1 = R^2 = R^3$ = tertbutyl does not therefore seem unreasonable. Similarly, the replacement of R^1 = tertbutyl by R^1 = hydrogen might be expected to diminish the tendency to produce orthoquinone, as observed. However, the expectation that replacement of R^2 = tertbutyl by R^2 = H would encourage production of orthoquinone is not realized and only the paraquinone is obtained on oxidation of 2,6-ditertbutylphenol (*5b*). It is likely in this case, however, that the anticipated monotertbutylorthoquinone product would not be stable against self-condensation like the orthoquinone **3**.

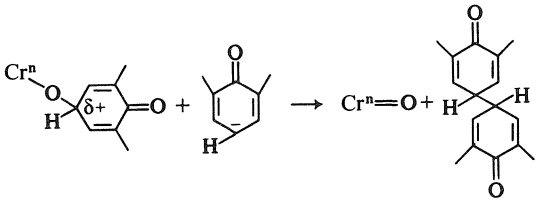
The observed NIH shift accompanying oxidation of 2,6-dimethyl-4-deuteriophenol to the paraquinone **16** is expected to occur in species such as **21** and **22**. Retention of deuterium in the diphenoquinone **17** was unexpected since this product is likely to result from simple coupling of phenoxyl radicals. It was confirmed in the present study that production of **17** by oxidation of xylenol-*d* with ferricyanide occurred with complete loss of deuterium. It is for this reason that equilibria between chromate esters **21** and **22** and the phenoxyl radical have been postulated in reactions [1] and [2*b*], thus allowing for the generation of some NIH-shifted radicals. An alternative but unlikely possibility is that some or all of the diphenoquinone results from the heterolytic displacement reaction [5].

The oxidations of chloro- and bromophenols presumably also occur by reactions analogous to [1] and [2]. The halogenation, or halogen exchange, reactions are explained by a rapid reaction [2*a*] followed by a reversion of the chlorocyclohexadie-

Can. J. Chem. Downloaded from www.nrcresearchpress.com by 210.87.254.5 on 09/05/12
For personal use only.



none back to a phenoxy species by a halogen abstraction process. The halogen may be removed in the form of an atom either by a phenoxyl radical or a metal complex species, depicted in [6], or as a halide ion by a Lewis acid to generate a phenoxonium ion. Such reactions are expected to occur



in both *ortho* and *para* positions. When the carbon atom which undergoes halogenation in reaction [2*a*] already bears a halogen atom, interchange can occur. If the carbon atom bears a hydrogen atom, enolization of the cyclohexadienone produces a chlorinated phenol.

As in the case of alkyl phenols, it seems that the halogenation and dehalogenation steps are kinetically favoured while the oxygenation process is thermodynamically favoured.

Reactions of Phenols with Vanadyl Chloride

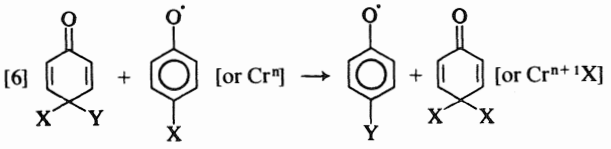
The reactivity patterns observed with $VOCl_3$ are quite different from those observed with CrO_2Cl_2

Can. J. Chem. Downloaded from www.nrcresearchpress.com by 210.87.254.5 on 09/05/12
For personal use only.

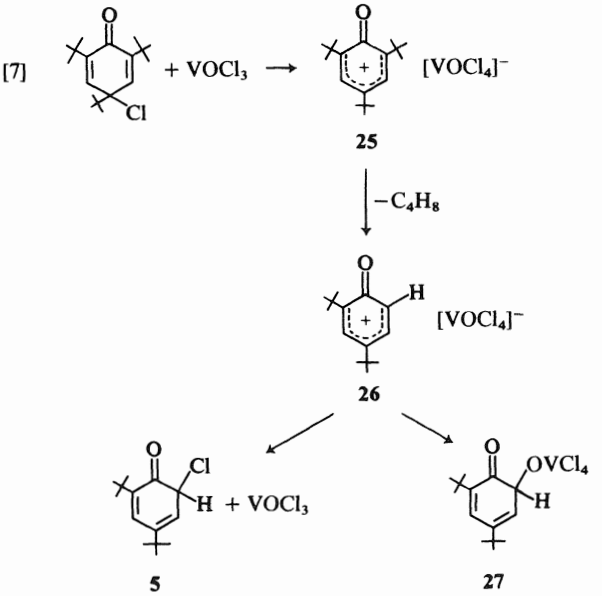
in a number of respects. The rather effective dealkylation of **1**, the production of modest yields of quinones and of chlorinated products are reminiscent of the CrO_2Cl_2 reaction, but the production of large amounts of orthodealkylated chlorophenol or C—C coupled dimers and the absence of the corresponding paradealkylated products (see Table 2) are peculiar to the $VOCl_3$ reaction. Since it is quite common for mild Lewis acids to selectively catalyze orthoalkylation (8), selective orthodealkylation catalyzed by $VOCl_3$, or some related species, is not too surprising. The relatively low reactivity of phenols with less than three alkyl substituents makes it unlikely that they are the intermediates responsible for the dealkylated products from oxidation of **1**. However, the similarities of product distributions are sufficiently strong to suggest common reactive intermediates in the cases of di- and tritertbutylphenols.

The differences in reactivity between trialkyl- and dialkylphenols are probably related to the marginal ability of $VOCl_3$ to generate phenoxyl radicals. It is well established that phenol itself and cresols form relatively stable trialkyl vanadate(V) esters with $VOCl_3$ (9), although monoalkylphenols can undergo oxidative coupling under certain conditions (7). The present results indicate that the phenols **5** and **6** react slowly with $VOCl_3$ under the conditions used but that, once brought into reaction, they produce some of the products also arising from the much more reactive **1**.

The ease with which **4** is transformed to **5** by $VOCl_3$ makes it very likely that **5** is produced by way of **4** and that the formation of **4** is a kinetically favoured reaction, as in the case of CrO_2Cl_2. The regiospecific deposition of the chlorine at the *para*-position in **4** and the *ortho*-position in **5** fits the pattern expected if **4** is formed by chlorine atom transfer from $VOCl_3$ to a tritertbutylphenoxyl radical (cf. the $CuCl_2$ reaction, ref. 3) and **5** is formed by way of a carbenium ion intermediate as, for example, in eq. [7]. Collapse of the ion pair **26** by chloride ion transfer will lead to the irreversible formation of **5**, whereas collapse by oxygen attachment will give **27**, a potential precursor to the C—C coupled products **10** and **11** and the orthoquinone, **3**.[2] The failure to produce C—C coupled products by reaction of **4** with $VOCl_3$ suggests that the presence of phenol, or phenoxide, is critical to the coupling reaction. Clearly, the production of quinone from **4**



by way of a species such as **27** (or the 4-dealkylated analogue) does not need the intervention of a phenoxyl moiety. The reason why the production of paraquinone is greatly favoured over that of orthoquinone whilst the reverse is true of chlorination remains obscure. A very interesting reversal of specificity between the CrO_2Cl_2 and $VOCl_3$ systems is observed in the oxidation of **9**. With CrO_2Cl_2 this compound gave the 1,4-quinone **2** in ca. 90% yield and no isolable diphenoquinone **14**. On the other hand, $VOCl_3$ gave a product containing diphenoquinone (and diphenol **15**) in twenty-fold excess over 1,4-quinone. These selectivities presumably reflect the relative rates of 4–4 homocoupling of the free phenoxy radical and of the attachment of radicals to oxygen to form metallate esters. The coupling reaction clearly dominates with the mildly oxidizing $VOCl_3$, whereas the oxygen attachment dominates in the case of CrO_2Cl_2. The fact that 2,6-dimethylphenol gives a substantial yield of the diphenoquinone **17**, in addition to the 1,4-quinone **16**, illustrates that the rates of the two alternative pathways are quite similar.



A Comparison of $CuCl_2$, $VOCl_3$, and CrO_2Cl_2

The differences between the three title oxidants in their behaviour towards tertbutylphenols is strongly related to the relationship between the oxidizing power of the metal ion and its acidity. In the case of copper, the oxidizing power is sufficient

[2]The mechanism whereby such a coupling takes place is not clear. Since some of the chlorine ligands of **27** are likely to have been replaced by phenoxide, the possibilities of both intramolecular and intermolecular coupling processes exist. The high specificity for 2,2′-coupling does suggest specific involvement of the vanadium.

Can. J. Chem. Downloaded from www.nrcresearchpress.com by 210.87.254.5 on 09/05/12
For personal use only.

to generate phenoxyl radicals and these radicals can easily abstract chlorine atoms from copper; they cannot, however, abstract oxygen as evidenced by the fact that the presence of water does not measurably impair the chlorine atom transfer (3). Thus, the only product obtained from $CuCl_2$ oxidation of **1** is the cyclohexadienone **4**. Although $VOCl_3$ is seemingly less able to oxidize phenols to the radical, the greater acidity of the highly charged ion[3] facilitates dealkylation and other reactions typical of carbenium ions, in addition to rendering the formation of the chlorocyclohexadienone, **4**, reversible. It is believed that this reversibility is the key to formation of quinones, since it allows transit beyond the kinetically favoured **4** to the thermodynamically favoured quinones and chlorophenols, and the failure of copper(II) to effect these reactions may be attributed to its low acidity. The very high effective charge of Cr^{VI} seems to render the transfer of oxygen ligand sufficiently fast to diminish considerably the leakage of radicals, or carbenium ions, into halogenation and C—C coupling reactions, and gives a much greater selectivity for the production of quinones than is obtained with $VOCl_3$.

Oxometal Complexes as Models for Heme-containing Oxidases

There has been considerable discussion of the possibility that the peroxidase I and II compounds (and analogous compounds of other heme proteins) and the active intermediate in functioning cytochrome P-450 may be "ferryl" species (6). Both chemical evidence and theoretical calculations have been put forward to support the claim that oxometal complexes such as CrO_2Cl_2 can mimic important characteristics of oxidase activity (1, 2), in particular the NIH proton shift and halogen shift (10). From the present investigation it is concluded that the similarity between the behaviour of CrO_2Cl_2 and heme proteins is superficial and of very limited use. The most evident failure of CrO_2Cl_2 to mimic cytochrome P-450 lies in the fact that it does not induce 1,2-halogen shifts, but does effect halogenation in the 3-position relative to the transferred oxygen. Because CrO_2Cl_2 does effect an NIH proton shift, it cannot be taken to indicate more than the fact that there is probably an intermediate with carbenium ion character whose genesis may result from a number of quite different reactions (e.g., halide ion abstraction, electron abstraction, opening of an epoxide). Given the observed and potential complexity of the $VOCl_3$ and CrO_2Cl_2 reactions described above, it would not be surprising if one of the reaction pathways bore more resemblance to that occurring in a functioning heme oxidase. Although the present results do not exclude the possibility of oxygen atom transfer from Cr^{VI} or V^V as a two-electron single-step ligand transfer process, they certainly do not require it and it is considered that the one-electron process of eq. [2*b*] is more likely. While Cr^V species in the past have been regarded as, at best, very unstable transients, a recent report indicates that oxochromium(V) compounds with simple organooxygen ligands can be produced as very stable entities by one-electron reduction of Cr^{VI} (11).

[3]The exact nature of the acidic species remains undetermined. The possible involvement of hydrolytically-produced HCl and oxidation levels other than those of V^V and Cr^{VI} cannot be excluded.

Experimental

Materials

Both CrO_2Cl_2 and $VOCl_3$ were prepared according to published procedures (12) and redistilled immediately prior to use. Hydrocarbon solvents were freshly distilled from sodium benzophenone before use. Phenols were obtained as reagent grade materials from Aldrich Chemical Co. and were subject to either a single recrystallization or distillation before use.

Analytical Procedure for Products of Tritertbutylphenol Oxidation

The reaction products were subject to gradient elution chromatography on silica gel. Tritertbutylphenol was rapidly eluted by hexane, other phenols moved rapidly with toluene. The cyclohexadienone **4** required chloroform or methylene chloride for an appreciable elution rate and the quinones required ethanol. A gradient elution based on this sequence of solvents gave a sufficiently good separation of all major reaction products to allow their subsequent purification and characterization. Following identification of the major products, a more exact analysis of the composition of the eluate fractions was carried out by ^1H nmr and a complete material balance deduced.

Under the above conditions the products eluted in the following order: 2,4,6-tritertbutylphenol, 2-chloro-4,6-ditertbutylphenol (13), 2,2′-dihydroxy-3,3′,5,5′-tetraterbutylbiphenyl (14), 1-chloro-3,6,8-tritertbutyldibenzofuran, 2,4-ditertbutylphenol,[4] 4-chloro-2,4,6-tritertbutylcyclohexadienone (15), 2,6-ditertbutylbenzo-1,4-quinone (16), 4,6-ditertbutylbenzo-1,2-quinone (17).

The only product not commonly available, or previously described in the literature, was the cross-coupled dibenzofuran, **11**, produced in the $VOCl_3$ oxidation reaction (see Table 2). The structure assignment of this compound was based on the previous observation of dibenzofuran formation in oxidative degradation of hindered phenols (14) and on the following physical evidence. The compound had a melting range of 105–106°C. Infrared spectrum: complete absence of bands due to OH or dienone carbonyl. ^1H nmr spectrum: three non-equivalent tertbutyl resonances (1.63, 1.57, and 1.43 τ in $CDCl_3$) each of relative intensity 9 and a complex multiplet (7.3–7.8 τ) due to aromatic protons of total relative intensity 4. Mass spectrum *m/e* (abundance): 370 (M^+, 8), 355 ($M - CH_3$, 15). Each of the cited peaks was accompanied by the appropriate ^{37}Cl satellite indicating the presence of a single chlorine. *Anal.* calcd. for

[4]Compared to authentic sample from Aldrich Chemical Co.

$C_{24}H_{31}OCl$: C 77.9, H 8.37, O 4.32, Cl 9.4; found: C 77.8, H 8.35, O 4.2, Cl 9.19.

Oxidation of Tritertbutylphenol by CrO_2Cl_2

The following is a description of a representative reaction. A solution of **1** (2.5 g) in hexane (50 mL) was cooled under nitrogen to −65°C with vigorous stirring. After temperature equilibration, a freshly distilled sample of CrO_2Cl_2 (1.5 g) was injected into the reaction vessel. Although the reaction appeared to be almost instantaneous, the dark green slurry was stirred for a further two hours before warming to room temperature. The solvent was removed under vacuum and the residual solid was shaken with water and extracted several times with diethyl ether. Following drying over anhydrous $MgSO_4$ and evaporation of the ether, the product was fractionated by column chromatography.

The oxidation of other phenols was carried out in essentially the same way.

Oxidations using $VOCl_3$

The procedure with $VOCl_3$ was essentially the same as that used with CrO_2Cl_2 except that most of the $VOCl_3$ reactions were carried out at room temperature. Heptane was employed for the reaction of **1** at 90°C. The reaction of $VOCl_3$ with the tritertbutylphenoxyl radical was effected by adding the $VOCl_3$ to a hexane solution of the radical prepared by standard procedures (15).

Synthesis and Oxidation of 2,6-Dimethyl-4-deuteriophenol

The title phenol was prepared by a method analogous to that used by Butte and Price (18). A solution of 2,6-dimethylphenol (1.22 g, 0.01 mol) and sodium methoxide (0.54 g, 0.01 mol) in D_2O (10 mL) was sealed in a thick-walled, pyrex tube and heated at 100°C for four days. Following neutralization with CO_2 and extraction with ether, the recovered xylenol was found to have undergone ca. 80% exchange at the 4-position by ^{13}C nmr and mass spectroscopy. This xylenol was subject to oxidation by CrO_2Cl_2 in hexane and the resulting quinone and diphenoquinone were easily separated on a silica column. The deuterium retention was measured by conventional mass spectroscopy.

Acknowledgement

Financial support from the Natural Sciences and Engineering Research Council of Canada is gratefully acknowledged.

1. K. B. Sharpless and T. C. Flood. J. Am. Chem. Soc. **93**, 2316 (1971).
2. L. M. Hjelmeland and G. H. Loew. J. Am. Chem. Soc. **99**, 3514 (1977).
3. J. F. Harrod and P. van Gheluwe. Can. J. Chem. **57**, 890 (1979), and references therein.
4. L. R. Mahoney and M. A. Daroge. J. Am. Chem. Soc. **97**, 4722 (1975).
5. (*a*) J. A. Strickson and C. A. Brooks. Tetrahedron, **23**, 2817 (1967); (*b*) J. A. Strickson and M. Leigh. Tetrahedron, **24**, 5145 (1968); (*c*) M. J. Leigh and J. A. Strickson. J. Chem. Soc. Perkin Trans. II, 1476 (1973).
6. G. A. Hamilton. *In* Molecular mechanisms of oxygen activation. *Edited by* O. Hayaishi. Academic Press, New York and London. 1974. p. 415.
7. M. A. Schwartz, B. F. Rose, R. A. Holton, S. W. Scott, and B. Vishnuvajjala. J. Am. Chem. Soc. **99**, 2571 (1977).
8. S. H. Patinkin and B. S. Friedman. *In* Friedel-Crafts and related reactions. Vol. 2, Part 1. *Edited by* G. Olah. Interscience, New York. 1964. p. 94.
9. W. J. Carrick, G. L. Karapinka, and G. T. Kwiatowski. J. Org. Chem. **34**, 2388 (1969).
10. G. Guroff, J. W. Daly, D. M. Jerina, J. Rensen, B. Witkop, and S. Udenfriend. Science, **157**, 1524 (1967).
11. M. Krumpolc and J. Roček. J. Am. Chem. Soc. **101**, 3206 (1979).
12. G. Braver (*Editor*). Handbook of preparative inorganic chemistry. Vol. 2. Academic Press, New York. 1965. pp. 1264 and 1384.
13. E. Müller and K. Ley. Chem. Ber. **91**, 2670 (1978).
14. E. Müller and K. Scheffler. Chem. Ber. **94**, 25 (1961).
15. E. Müller and K. Ley. Chem. Ber. **87**, 922 (1954).
16. E. Müller and K. Ley. Chem. Ztg. **80**, 618 (1956).
17. W. Flaig, T. Ploetz, and H. Biergans. Ann. **597**, 196 (1955).
18. W. A. Butte and C. C. Price. J. Am. Chem. Soc. **84**, 3567 (1962).

Can. J. Chem. Downloaded from www.nrcresearchpress.com by 210.87.254.5 on 09/05/12
For personal use only.

N_{1s} core binding energies for 2-, 3-, and 4-substituted pyridines determined by X-ray photoelectron spectroscopy. Correlations with theoretical models, substituent parameters, and gas phase basicities

R. S. BROWN AND A. TSE

Department of Chemistry, University of Alberta, Edmonton, Alta., Canada T6G 2G2

Received November 9, 1979

R. S. BROWN and A. TSE. Can. J. Chem. **58**, 694 (1980).

N_{1s} binding energies for 36 pyridines substituted at the 2-, 3-, and 4-positions have been determined by X-ray photoelectron spectroscopy. The differences in BE relative to pyridine are analysed in terms of existing theoretical approaches (electrostatic, ground potential, and relaxation potential models) and compared with $\Delta BE_{C_{1s}}$ values calculated for analogous monosubstituted benzenes. One finds good correlations of $\Delta BE_{N_{1s}}$ with solution determined σ-substituent values although some substituent values deviate from the correlation probably due to solution effects which are not present in the gas phase. Correlations between $\Delta BE_{N_{1s}}$ and ^{14}N nmr chemical shifts are poor, particularly for electron withdrawing substituents. The relationship between $BE_{N_{1s}}$ and gas phase basicity values (ΔG^0) is good, and it appears as if the $BE_{N_{1s}}$ is more sensitive to the substituent than ΔG^0. MINDO/3 calculations on the methoxypyridines and their conjugate acids employing full geometry optimizations are presented and analysed in order to determine the effect of geometric relaxation on the gas phase basicity.

R. S. BROWN et A. TSE. Can. J. Chem. **58**, 694 (1980).

On a déterminé les énergies de liaison N_{1s} de 36 pyridines substituées en positions 2, 3 et 4 par la spectroscopie photoélectronique de rayons-X. On a analysé la différence des EL relatives à la pyridine en fonction d'approches théoriques existantes (modèles électrostatique, de potentiel de l'état fondamental et de potentiel de relaxation) et on les a comparées aux valeurs de $\Delta EL_{C_{1s}}$ calculées pour les benzènes monosubstitués analogues. On trouve de bonnes corrélations entre les $\Delta EL_{N_{1s}}$ et les valeurs σ des substituants déterminées en solution bien que certaines valeurs de substituants dévient de la corrélation probablement par suite des effets de solution qui ne sont pas présents dans la phase gazeuse. Les corrélations entre les $\Delta EL_{N_{1s}}$ et les déplacements chimiques en rmn ^{14}N ne sont pas bonnes, particulièrement dans le cas des substituants électroattracteurs. La relation entre les $EL_{N_{1s}}$ et les valeurs de basicité de la phase gazeuse (ΔG^0) sont bonnes et il semble que les $EL_{N_{1s}}$ sont plus sensibles aux substituants qu'à ΔG^0. On présente des calculs MINDO/3 sur les méthoxypyridines et leurs acides conjugués en utilisant une optimisation maximale de la géométrie et on les analyse dans le but de déterminer l'effet de la relaxation géométrique sur la basicité de la phase gazeuse.

[Traduit par le journal]

I. Introduction

During the last decade, much attention has been devoted to the effect of a substituent on the binding energies (BE's) of a core 1*s* electron. Initial work in this area involved mechanisms by which a substituent X altered the C_{1s} BE in some substituted benzenes (1), and models were developed which explained the substituent effect in terms of ground state inductive and/or mesomeric effects (1), and excited state or relaxation effects (2) in which the entire molecule relaxes electronically accompanying core ionization. The work was gradually extended to recognise the formal similarity between loss of a core electron, and gain of a proton (3) which led to correlations between gas phase basicities and core BE's (3, 4).

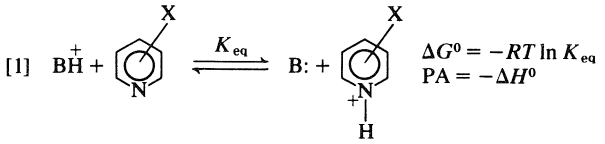
As part of a project designed to experimentally determine situations under which the correlations between gas phase basicities and core BE's fail, we required a large number of pyridine N_{1s} ionization energies. Considering the amount of work expended on the substituted benzenes, it seemed rather surprising that virtually no work (with the exception of that of Davis and Shirley (2*d*)) had been performed on the substituted pyridines. A regular series of 2-, 3-, and 4-substituted pyridines would offer considerable experimental benefits over the analogous benzenes for several reasons. Firstly in terms of C_{1s} BE's, the monosubstituted benzenes should in principle show four different ionizations, but in practise these are badly overlapped so that assignment of the BE belonging to a particular carbon is ambiguous. Since the pyridine N_{1s} ionization is far removed from others, there would be no difficulty in determining the effect of a remote substituent on the N_{1s} BE. Comparison of these shifts with those predicted from CNDO/2 calculations for the substituted benzenes (1*f*) would offer definitive experimental evidence to test the strength of the CNDO/2 model. Secondly these N_{1s} BE's would provide clear data to test the scope of both the ground potential model (GPM) and relaxation potential model (RPM) (2) as well as other more empirical substituent parameters (σ^+ or σ values) which had been derived from solution chemical processes only remotely related to the ionization process. Thirdly, since there is much available data (5) on gas phase basicities (ΔG^0) and

0008-4042/80/070694-10$01.00/0

©1980 National Research Council of Canada/Conseil national de recherches du Canada

Can. J. Chem. Downloaded from www.nrcresearchpress.com by 210.87.254.105 on 09/05/12
For personal use only.

proton affinities (PA or $-\Delta H^0$) for substituted pyridines determined by equilibrium studies according to eq. [1], these values could be correlated with the BE's for an extended series of pyridines.



In section II we present the BE's for 36 pyridines and discuss them in section III in terms of the above correlations. Section IV describes the experimental procedures.

II. Results

Core binding energies ($BE_{N_{1s}}$) for a series of 2-, 3-, and 4-X-pyridines (X = NO_2, CF_3, CN, F, Cl, Br, (H), CH_3, OH, OCH_3, $COCH_3$, NH_2, and $N(CH_3)_2$) are presented in Table 1 along with their gas phase basicities where available (5).[1] Additionally the ΔBE and $\delta\Delta G^0$ values representing the change in binding energy and gas phase basicity respectively relative to pyridine are included in the table. Each BE value is the average of at least three sequential cycles which alternatively scanned the N_{1s} region and the reference neon Auger (6) region and has a precision of ± 0.03 eV unless noted. Since the shifts are rather small, being at most ± 1 eV from pyridine, the precision is important for the correlations discussed in section III.

III. Discussion

A comparison of the BE for each substituted pyridine with that of pyridine allows one to establish the ΔBE or "chemical shift" provided by a certain substituent on the N_{1s} ionization. For the monosubstituted benzenes the experimental determination of ΔBE for the C_{1s} ionizations is not as simple since the bands are badly overlapped. For the latter cases, one approach (1*f*, *e*) has been to

$$[2]\quad \Delta BE_i = k_c q_i + \sum_{j \neq i} \frac{q_i}{R_{ij}}$$

estimate the relative chemical shift (ΔBE_i) of an atom *i* as being affected by the charge on that atom (q_i) and the charges on the adjacent atoms modified by their distance (R_{ij}) from the test atom where k_c is a constant which commonly has a value of ~22 eV/unit charge. This particular model (the electrostatic potential model) (1*e*) assumes therefore that the change in BE is simply related to the ground-state environment of the molecule and is often found to provide satisfactory agreement with experiment (1). Correlations with this model assume that differences in relaxation terms accom-

TABLE 1. Gas phase N_{1s} binding energies (BE) and basicities for some 2-, 3-, and 4-substituted pyridines[a,b]

Compound	BE (eV)	ΔBE[c] (kcal/mol)	δΔG⁰[d,e] (kcal/mol)
Pyridine	404.94	0.0	0.0
2-CH_3	404.63	7.15	−3.7
2-OH[f]	404.96	−0.46	—
2-NH_2	404.48	10.61	−3.44
2-OCH_3	404.68	5.60	−1.17
2-$N(CH_3)_2$	404.05	20.52	(−8.8)
2-Br	405.22	−6.46	6.82
2-Cl	405.23	−6.68	6.7
2-F	405.34	−9.22	10.35
2-CF_3	405.54	−13.84	9.70
2-CN	405.54	−13.84	13.34
2-NO_2	405.89	−21.91	—
2-$COCH_3$	405.12	−4.15	—
3-CH_3	404.75	4.38	−2.9
3-OH	404.97	−0.69	—
3-OCH_3	404.87	1.6	−3.2
3-NH_2	404.67	6.22	(−0.6)
3-$N(CH_3)_2$[g]	404.57	8.53	(−9.5)
3-Cl	405.20	−6.0	6.2
3-F	405.34	−9.22	7.0
3-CF_3	405.41	−10.84	8.6
3-CN	405.55	−14.07	12.1
3-NO_2	405.67	−16.83	—
3-$COCH_3$	405.11	−3.92	3.95
4-CH_3	404.68	6,.00	−4.3
4-OCH_3	404.49	10.38	−7.15
4-NH_2	404.26	15.68	(−9.4)
4-OH	404.95	−0.23	—
4-$N(CH_3)_2$	404.03	20.9	(−15.3)
4-Cl	405.08	−3.23	3.3
4-Br	405.18	−5.53	(2.5)
4-F	405.12	−4.15	4.2
4-CN	405.58	−14.76	11.2
4-NO_2	405.66	−16.60	12.7
4-$COCH_3$	404.98	−0.92	3.7
4-CF_3	405.44	−11.53	8.32

[a] $BE_{N_{1s}}$ values are reported as the average of at least 3 runs and have a precision $\geq \pm 0.03$ eV.
[b] Calibrated against an internal standard N_e Auger line (KE = 804.56 eV) (6).
[c] $\Delta BE_{N_{1s}} = BE_{N_{1s}}$ (pyridine) − $BE_{N_{1s}}$ (substituted pyridine); a positive value indicates the base is easier to ionize than pyridine. ΔEB (kcal/mol) = 23.06 (ΔEB (eV)).
[d] $\delta\Delta G^0 = \Delta G^0$ (pyridine) − ΔG^0 (substituted pyridine); a negative value for $\delta\Delta G^0$ indicates the base is stronger than pyridine.
[e] Values are from ref. 5*a* and from R. W. Taft, private communication; we thank Prof. Taft for generously informing us of his corrected basicities. Values in brackets are those from ref. 5*d* (see footnote 1).
[f] 2-Hydroxypyridine exists in the gas phase in equilibrium with 2-pyridone, and different N_{1s} BE's are seen for each. For assignment of the N_{1s}BE for 2-OH pyridine see ref. 4*h*.
[g] The N_{1s} ionization region for 3-$N(CH_3)_2$-pyridine shows a single broad peak (half-width = 1.9 eV) which was deconvoluted assuming two equal half-width ionizations. We assign the low binding energy peak to the pyridine N_{1s} in analogy to the 3- and 4-substituted systems: precision ±0.1 eV.

[1] Most ΔG^0 and ΔH^0 values for substituted pyridines are derived from a single laboratory and can be found in ref. 5. The values in ref. 5*d* were kindly supplied by Prof. D. H. Aue, Department of Chemistry, University of California, Santa Barbara, and can be found in D. H. Aue and M. T. Bowers. *In* Gas phase ion chemistry. *Edited by* M. T. Bowers. Academic Press, New York, NY. 1979.

Can. J. Chem. Downloaded from www.nrcresearchpress.com by 210.87.254.105 on 09/05/12
For personal use only.

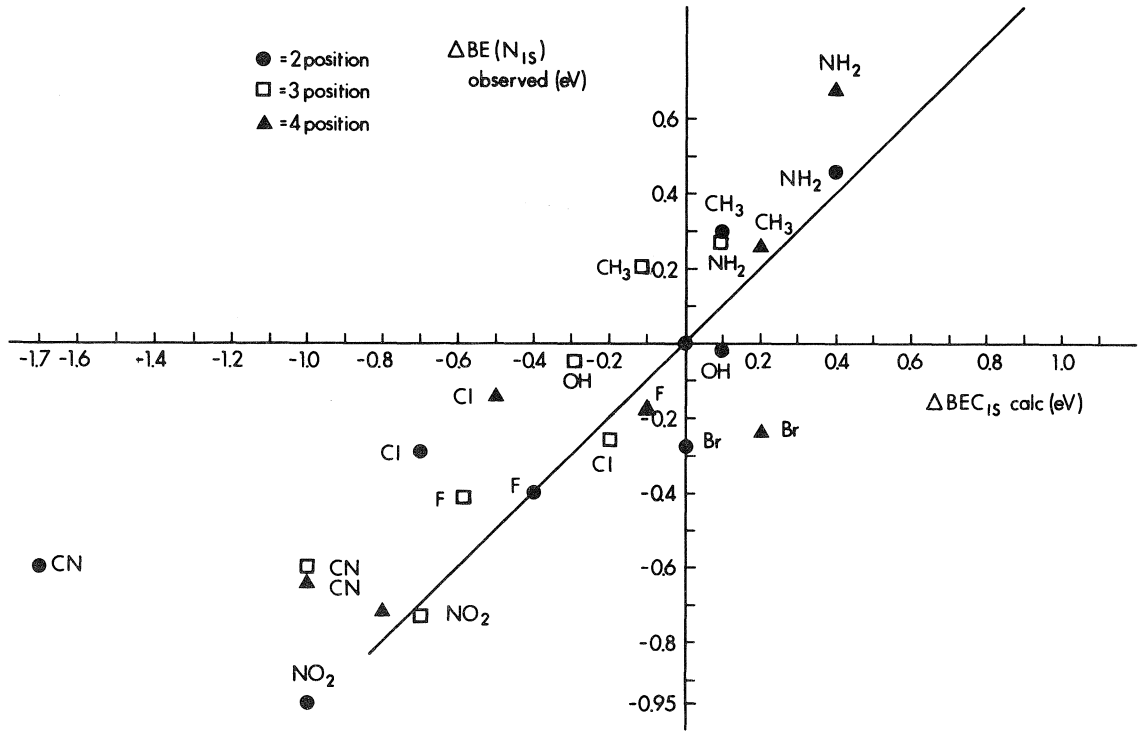


FIG. 1. A plot of $\Delta BE_{N_{1s}}$ against $\Delta BE_{C_{1s}}$ (calculated) for substituted pyridines and benzenes, respectively. Values for $\Delta BE_{C_{1s}}$ are from ref. 1*f*.

panying ionization within a series of molecules will cancel so that the dominant factors influencing chemical shifts are ground-state inductive and/or mesomeric effects. It is therefore instructive to compare the $\Delta BE_{N_{1s}}$ values for the substituted pyridines with the predicted $\Delta BE_{C_{1s}}$ values for various positions of substituted benzenes (1*f*) (Fig. 1).

In principle the slope of the graph in Fig. 1 should be unity if substituents influence C_{1s} and N_{1s} ionizations to the same extent, and the line should pass through the origin. A least squares analysis shows the slope to be near unity (1.14) but there is sufficient scatter in the points ($r = 0.82$) to indicate some shortcoming in the correlation. Notably the 3-CH_3, 4-Br, and 2-CN positions deviate badly. The probable source of the lack of correlation is related to deficiencies in the CNDO/2 parameterization (7), the inapplicability of applying a point charge electrostatic model to π-systems, or the inability of the electrostatic model to account for relaxation effects in the ions.

Correlations of Observed $\Delta BE_{N_{1s}}$ with CNDO/2 Calculations based on the Ground Potential (GPM) and Relaxation (RPM) Models

The GPM developed by Davis *et al.* (1*c*) calculates the electrostatic potential of an electron at a nucleus as being

$$e^2 < \sum_i 1/r_i > -e^2 \sum_j Z_j/R_{ij}$$

where r_i and R_{ij} refer to the distance between the parent nucleus and the i^{th} electron and j^{th} other nucleus respectively, and Z_j indicates the nuclear charge on the j^{th} nucleus. Based on CNDO wave functions, the shift in electrostatic potential (ΔV) at a given nucleus can be related to ΔBE as $\Delta BE = -\Delta V$. Figure 2 shows a correlation between the observed and calculated $\Delta BE_{N_{1s}}$ for the series of 2-, 3- and 4-pyridines based on this approach. Standard bond lengths and angles were assumed for the substituents (7*a*), and the geometry of the pyridine ring was taken to be that of pyridine itself as determined by gas phase electron diffraction (7*b*, *c*). Figure 2 shows a general agreement between experiment and theory that could be considered acceptable considering the crudeness of the model. Qualitatively, ionizations calculated to be larger or smaller respectively than pyridine are experimentally found to be as predicted but quantitatively the agreement is poor. Comparison of experimental and calculated shifts based on the GPM have been found to be more or less satisfactory in other systems (1*c*, *d*, 8). In the present case the best fit

Can. J. Chem. Downloaded from www.nrcresearchpress.com by 210.87.254.105 on 09/05/12
For personal use only.

Can. J. Chem. Downloaded from www.nrcresearchpress.com by 210.87.254.105 on 09/05/12
For personal use only.

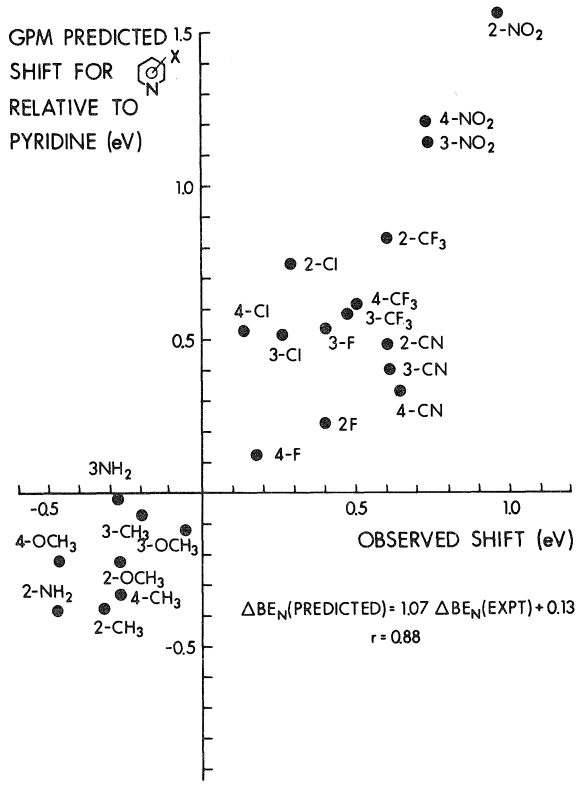


FIG. 2. A plot of $\Delta BE_{N_{1s}}$ (observed) against $\Delta BE_{N_{1s}}$ (calculated) on the basis of the ground potential model (GPM).

straight line has a near unit slope as predicted from the theory; $\Delta BE_{N_{1s}}$ (calcd) = 1.07 $\Delta BE_{N_{1s}}$ (obsd) + 0.13 (r = 0.88). the reason for the lack of quantitative agreement could be related to a number of shortcomings in the CNDO method (parameterizations) or incorrect geometries or more fundamental difficulties in treating delocalized π-systems with point charge models (1*c*).

Since the GPM approach is based solely on ground state factors and ignores electronic relaxation accompanying core ionization (which is expected to be substituent and position dependent), it might be expected that allowances made for the latter effect would improve the correlation. One such approach within the CNDO framework is the relaxation potential model (RPM) (2) in which for the purposes of calculating the nitrogen "hole state" an equivalent core approximation is used whereby the ionized atom (N) is replaced by the next highest element (O). Equations [3] and [4] outline the approach, where

$$[3] \quad \Delta BE = -\Delta V_n - \Delta V_R$$

$$[4] \quad V_R = \tfrac{1}{2}[V_n(Z+1) - V_n]$$

V_R is the relaxation potential, V_n is the potential experienced by an electron at nucleus n, and $Z + 1$ represents the equivalent core. The RPM approach has provided better agreement with experimental ΔBE's when molecular polarizability affects V_R markedly (2*e*, 3, 8).

A plot of the RPM against experimental $\Delta BE_{N_{1s}}$ is shown in Fig. 3. Visually the graph appears similar to that in Fig. 2 except that the calculated $\Delta BE_{N_{1s}}$ values are somewhat smaller particularly for the 2- and 4-substituents (i.e., the intercept of the graph is lowered from that in Fig. 2) and the best fit straight line is ΔBE (calcd) = 1.04 ΔBE (obsd) − 0.06 (r = 0.88). It would appear that inclusion of the relaxation terms in the model offers no improvement in correlation over that found for the GPM. However it is instructive to qualitatively assess the position dependence of including relaxation in the calculations. Table 2 lists the calculated differences in N_{1s}-BE ($\delta\Delta BE_{N_{1s}}$ (GPM − RPM)) which gives some measure of the importance of electronic relaxation of the substituents at various positions. One expects that, if relaxation is important, the $\delta\Delta BE_{N_{1s}}$ values in Table 2 would be large, and decrease when it is of lesser importance. In all cases it would appear that for a given substituent the order of importance of relaxation is 2 > 4 > 3. Hence for a given substituent, the inclusion of relaxation in the model is between two and three times as important for 2- and 4-substituents as for 3-substituents. This

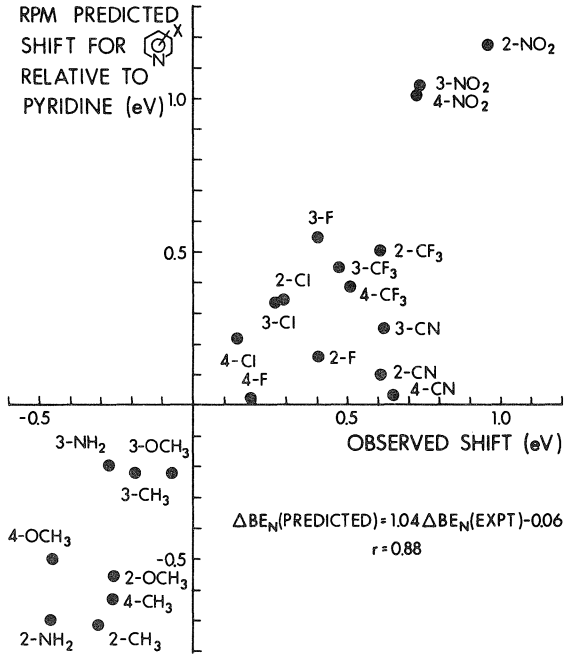


FIG. 3. A plot of $\Delta BE_{N_{1s}}$ (observed) against $\Delta BE_{N_{1s}}$ (calculated) on the basis of the relaxation potential model (RPM).

Can. J. Chem. Downloaded from www.nrcresearchpress.com by 210.87.254.105 on 09/05/12
For personal use only.

TABLE 2. Calculated differences in binding energy based upon GPM and RPM approaches[a,b]

	$\delta\Delta BE_{N_{1s}}$(GPM − RPM) (eV)		
Substituent	2	3	4
—F	0.07	−0.02	0.09
—Cl	0.39	0.18	0.20
—CF_3	0.32	0.13	0.22
—CH_3	0.33	0.14	0.29
—OCH_3	0.31	0.14	0.27
—CN	0.38	0.15	0.30
—NO_2	0.38	0.10	0.29
—NH_2	0.30	0.16	—

[a]Calculations based upon CNDO/2 methods in ref. 2.
[b]These values represent differences in the vertical axes for Figs. 2 and 3.

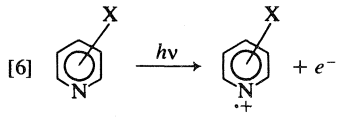
amounts simply to saying that 2- and 4-substituents can better respond to N_{1s} photoionization through electronic polarization than can 3-substituents.

Correlations between ΔBE and σ-Substituent Parameters

For chemical processes the substituent effects are described by σ-parameters derived according to eq. [5] where

[5] $y = \rho\sigma + b$

y is the change in reactivity of the system relative to a suitable reference and σ is the substituent parameter; ρ is the sensitivity factor. For N_{1s} ionization (eq. [6]) the process can also be correlated by existing substituent parameters (9).[2]

[6] 

A graph of $\Delta BE_{N_{1s}}$ vs. σ-values is given in Fig. 4, and the best fit straight line is $\Delta BE_{N_{1s}} = -1.07\sigma + 0.06$ eV ($r = 0.985$). Considering that the substituent values were determined in aqueous media for a chemical process only remotely related to N_{1s} photoionization the correlation is remarkably good. The fact that both 3- and 4-substituents lie on the same line (within the precision of the experiment) would tend to indicate that the mechanisms by which they interact with the N_{1s} core hole are not markedly different. While direct resonance interactions are *not* of significance in stabilizing the core hole (the resonance structures involve the valence electrons), one might have thought that the changes in nitrogen charge density accompanying core ionization might be influenced considerably more by good electron donors such as OR or NR_2 at the 4-position. This should have been observed as a significant upward deviation from the graph for 4-NH_2, $N(CH_3)_2$, and OCH_3, contrary to what is actually observed. These groups are better electron donors at the 4- than at the 3-position according to their σ values, but the graph would tend to indicate similar mechanisms by which the substituent interacts with charged species produced by either benzoic acid ionization or pyridine N_{1s} photoionization. Correlations of 1*s* BE values with σ-substituent values has been observed (9*b*) in a limited series of anilines. While the σ-values are not explicitly derived for photoionization processes, relaxation due to polarization in response to benzoic acid ionization *is* incorporated into the substituent σ-value by measuring the overall substituent effect at various positions. Hence for electron donors, the measured σ-values at the 4-position are more negative than at the 3-position. It is interesting to note that the *p*-OH group which is according to either σ or σ^+ values a good electron

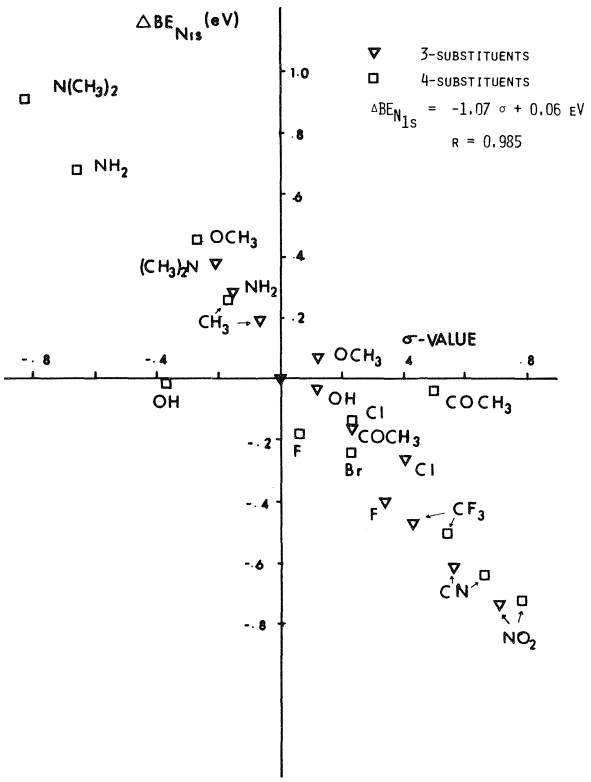


FIG. 4. A plot of $\Delta BE_{N_{1s}}$ (observed) against σ-substituent parameters from ref. 9.

[2]All of the present σ and σ^+ parameters have been abstracted from ref. 9. Correlation coefficients (r) were obtained from standard least-squares plots and are perhaps not in themselves particularly valuable in determining the precisions of structure–activity relations in that graphs which visually appear to have quite poor statistical fits still have large r-values. See ref. 10 for a discussion of this point.

Can. J. Chem. Downloaded from www.nrcresearchpress.com by 210.87.254.105 on 09/05/12
For personal use only.

donor, falls badly off the correlation in Fig. 4. This substituent is known (10, 11) to show marked H-bonding effects in solution. The present gas phase results which are free from solvent effects would indicate that the OH group at the 3- and 4-positions is not particularly different from H in terms of its overall substituent effect in this process. A similar conclusion might be drawn for 4-$COCH_3$ from Fig. 4. This substituent appears to be far too electron withdrawing from solution data to correlate well with the graph.

Correlations between $\Delta BE_{N_{1s}}$ Values with Pyridine ^{14}N nmr Chemical Shifts

The connection between binding energy and nmr chemical shifts was first discussed by Basch (12) and early correlations between $\Delta BE_{C_{1s}}$ and δ ^{13}C chemical shifts for a series of closely related halomethanes were presented (13). The correlations for an expanded set of substituted methanes and *p*-substituted fluorobenzene ^{19}F chemical shifts have been reviewed by Lindberg (14), who concluded that useful correlations between nmr and ESCA (electron spectroscopy for chemical analysis) shifts should be expected "provided that the objects for correlation are wisely chosen". A comparison of $\Delta BE_{N_{1s}}$ data from Table 1 with existing ^{14}N chemical shift values for a limited series of pyridines (Fig. 5) (15) shows a rather poor correlation ($r < 0.65$) in that large changes in ΔBE do not appear to lead to predictable ^{14}N shifts particularly for electron withdrawers. Gelius *et al.* (16) have questioned the overall applicability of comparisons between nmr and ESCA chemical shifts since the factors responsible for each shift depend upon different terms; the present data would appear to support this conclusion at least for pyridines.

Correlations between $\Delta BE_{N_{1s}}$ and Gas Phase Basicity ($\delta\Delta G^0$)

Much effort has been expended in determining correlations between ΔBE's and $\delta\Delta G^0$ relative to a suitable reference material according to eq. [1] (3, 4).

Figure 6 illustrates the correlation between $\Delta BE_{N_{1s}}$ for these substituted pyridines and their existing gas phase basicities relative to pyridine ($\delta\Delta G^0$). The best fit straight line including 24 bases substituted at the 2-, 3-, and 4-position is $\Delta BE_{N_{1s}} = -1.40\ (\delta\Delta G^0) + 2.0$ kcal/mol ($r = 0.980$).[3] It is

[3]The best fit straight line for (*a*) 2-X pyridines: $\Delta BE_{N_{1s}} = -1.5\ (\delta\Delta G^0) + 3.65$ kcal/mol ($r = 0.980$, 10 data); (*b*) 3-X pyridines: $\Delta BE_{N_{1s}} = -1.36\ (\delta\Delta G^0) + 1.55$ kcal/mol ($r = 0.988$, 7 data); (*c*) 4-X pyridines; $\Delta BE_{N_{1s}} = -1.34\ (\delta\Delta G^0) + 0.16$ kcal/mol ($r = 0.996$, 10 data).

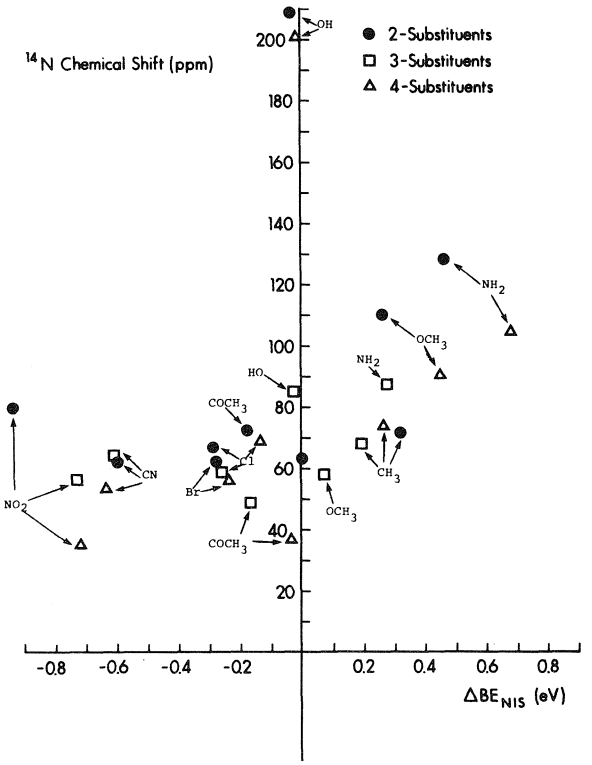


FIG. 5. A plot of $\Delta BE_{N_{1s}}$ (observed) against ^{14}N chemical shifts (in ppm relative to CH_3NO_2) abstracted from ref. 15. The NH_2, OH, and NO_2 values were determined in acetone, while the remainder were obtained from neat liquids.

important to note that the slope[3] of the line is somewhat greater than the theoretically modelled (−) unit slope (2*c*, 3) indicating the substituent influences ΔBE to a greater extent than $\delta\Delta G^0$. This has been observed in correlations with oxygenated molecules (4*a*, *d*) and phosphines (4*e*). However, it is in contrast to a (−) unit slope assumed for some aliphatic and aromatic amines (including pyridine) (4*f*), although the latter authors explicitly stated that the unit slope did not represent a best fit. Inspection of Fig. 6 shows the fit is generally quite good although there are some exceptions (*vide infra*). One could on the basis of the calculated best line for Fig. 6 predict some unknown basicities given the values in Table 1, and we anticipate the $\delta\Delta G^0$ values would be good to ±2.0 kcal/mol.

One should note an interesting *lack* of correlation in the methoxy pyridines whose order of basicity is 2< 3< 4, while the ΔBE values are 3< 2< 4. The reason for the lack of correlation is not clear and therefore MINDO/3 calculations were utilized to attempt to provide some insights.

MINDO/3 Calculations on Methoxy Pyridines

The photoionization process is a vertical one in

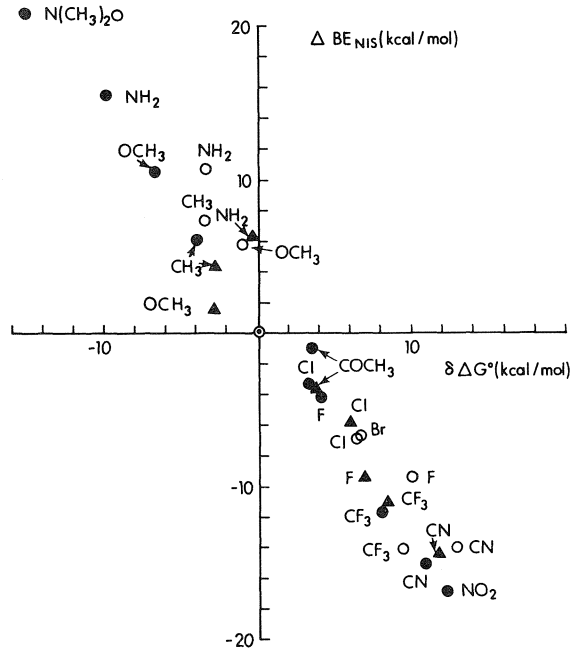


FIG. 6. A plot of $\Delta BE_{N_{1s}}$ (observed) against the differences in gas phase basicities ($\delta\Delta G^0$) for 2-, 3-, and 4-substituted pyridines. Open circles (○) are for 2-, while (▲) are for 3-, and closed circles (●) are for 4-substituents.

the Franck–Condon sense requiring that the geometry of the ground and ion states remain the same. Hence factors influencing the photoemission process are those related to electronic (inductive and mesomeric) effects on the ground and ion states.

On the other hand, basicity values may be considered adiabatic in the sense that the protonated bases are fully relaxed electronically as well as geometrically, as required by equilibrium conditions. Lack of correlation between ΔBE and $\delta\Delta G^0$ values can at least conceptually be considered to arise from either differences in the site of ionization and protonation (4*f*, *h*) or geometric relaxation of the protonated species which cannot be important in the ionization process (4*g*).

MINDO/3 calculations have been found to give reasonable heats of formation (ΔH_f) for a wide variety of compounds (17) and have been used to provide some insight into the protonation of some dihydropyridines (17*b*). It therefore appeared reasonable that the application of this method to the protonation of the methoxypyridines might provide some correlation with the experimental PA's.[4] For the purposes of comparison, standard free energies ($\delta\Delta G^0$) for eq. [1] have been converted to standard enthalpy changes (δPA) by a common small correction for the changes in the ratio of rotational symmetry numbers for the various B: and $\overset{+}{B}H$. The actual calculations were performed on each of the species in Scheme 1 as follows and the ΔH_f values obtained are listed in Table 3 along with those for various ring-protonated positions for 3-methoxypyridine.

The ΔH_f for the fully geometry-optimized methoxypyridines were calculated according to the MINDO/3 geometry optimization procedure (17). For all species, the plane of the methoxy group was found to be tilted very slightly downward from the plane of the ring, minimizing "ortho" buttressing but still keeping large interactions between the ring and oxygen "*p*" type lone pair. Then a proton was added to each species maintaining the same ground-state ring geometry and the ΔH_f for this so-called "vertical ion" calculated. In principle the calculated difference in ΔH_f for the vertical ion and ground state base should be influenced primarily by electronic relaxation. Finally, a full geometry optimization was performed to yield a ΔH_f for the "adiabatic" ion, which now incorporates geometric relaxation.

According to the calculation, addition of a proton to form the vertical ion is endothermic by 133.9 kcal/mol. Geometric relaxation here appears to involve reorientation of the OCH_3 group and releases some 2.4 kcal/mol so that the overall process of adding a "bare" proton to 3-methoxypyridine is endothermic by 131.5 kcal/mol. Absolute comparison of this value to the PA of 3-methoxypyridine (221 kcal/mol) (19)[5] is valid only if we consider the ΔH_f for H^+ however, differences in the calculated ΔH_f's for each reaction should provide relative PA's since the $\Delta H_f(H^+)$ cancels in the subtraction. The analogous values for the 2- and 4-isomers are 130.9 and 127.3 kcal/mol and according to the calculation the ordering of calculated proton affinity in 3-OCH_3 is less basic than 2-OCH_3 by 0.6 kcal/mol, and less basic than 4-OCH_3 by 4.2 kcal/mol. The experimental proton affinity ordering shows 2-OCH_3 to be less basic than 3-OCH_3 by 2 kcal/mol and less basic than 4-OCH_3 by 6 kcal/mol, contrary to the MINDO/3 result. While it is perhaps optimistic to expect this semi-empirical technique to provide accurate relative values, it does at least show the correct relative order for 2- and 4-methoxypyridine. Calculations performed on optimized ring-protonated 3-methoxypyridine (Table

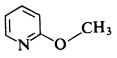
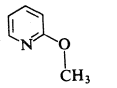
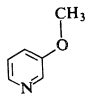
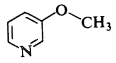
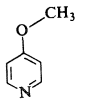
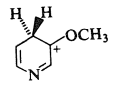
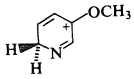
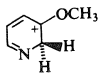
[4]Recently *ab initio* calculations at the STO-3G level (5*b*, 18) have been found to provide excellent correlations with experimental proton affinities of some substituted benzenes and some pyridines (5*b*).

[5]Based on a proton affinity of 202.3 kcal/mol for NH_3.

Can. J. Chem. Downloaded from www.nrcresearchpress.com by 210.87.254.105 on 09/05/12
For personal use only.

Can. J. Chem. Downloaded from www.nrcresearchpress.com by 210.87.254.105 on 09/05/12
For personal use only.

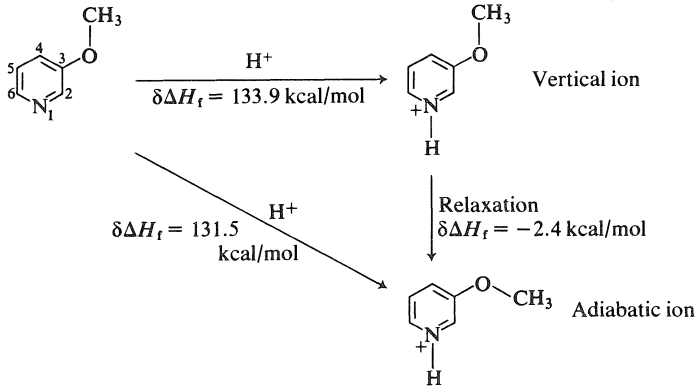
TABLE 3. MINDO/3 heats of formation for methoxy pyridines and methoxy pyridinium ions[a]

Species	ΔH_f (kcal/mol) B:	Vertical BH^+	Adiabatic BH^+
	−20.96	113.69	109.32
	−22.24	113.36	108.71
	−13.36	120.60	118.16
	−12.82	120.82	118.10
	−15.83	115.63	111.43
	—	—	148.08
	—	—	145.81
	—	—	147.78

[a]All structures optimized according to MINDO/3 procedure (17). Methoxy group is found to lie ~2° out of the plane of the pyridine ring in all structures.

3) indicate that it is energetically more unfavorable by some 25–30 kcal/mol to break the aromaticity, than to protonate on nitrogen.

It would appear from the calculation that geometric relaxation in passing from the "vertical" ion to the "adiabatic" ion releases more energy when the substituent is at the 2- and 4-positions (~4.5 and 4.2 kcal/mol respectively) than at the 3-position (2.5 kcal/mol), since the substituent is better able to interact with the positive charge in the former cases. Analysis of the calculated geometric changes in *all* cases shows that the primary geometric relaxation involves (using the numbering of Scheme 1) a compression of the N_1—C_4 distance by ~0.05 Å, lengthening of the C_2—C_6 distance by ~0.10 Å and shortening of the ring—O distance by



SCHEME 1

Can. J. Chem. Downloaded from www.nrcresearchpress.com by 210.87.254.105 on 09/05/12
For personal use only.

0.03–0.04 Å relative to the unprotonated free base. Differential charge analysis shows the (+) charge to be borne mostly by N_1, NH, the ring carbon to which the substituent is attached, and methyl hydrogens.

It would appear then that there are not large energetically favorable geometric changes accompanying pyridine protonation. Such changes are expected, however, when the protonated atom changes its hybridization (bond angles) significantly (4*g*).

IV. Experimental

Binding energies of gaseous samples were determined using a MacPherson 36 ESCA spectrometer with a MgKα X-ray source (1253.64 eV) and calibrated against an internal standard neon Auger line (804.56 eV kinetic energy) (6). The data were least-squares analysed (20) assuming Gaussian peaks, and the reported values are the averages of at least three runs which alternately scanned the reference line five times, and the nitrogen 1*s* line twenty or more times depending on the volatility. Since a number of the samples were found to be involatile they were introduced into the ionization region of the machine by a heated inlet assembly consisting of a 1/16 in id stainless steel tube bifilar wrapped with nichrome wire. The tube was affixed to an aluminium target chamber which was heated by four 30-Ω Hot Watt pencil heaters in series. The target chamber was affixed to the analyser by a machinable glass insulator which minimized heat conduction to the latter. A thermocouple inserted into the target chamber body allowed determination of the temperature at that point. Electrical feed-throughs allowed entry of the leads for the heating assembly and thermocouple. Determination of the BE's for standards with this assembly reproduced known values, indicating that no anomalous field-effects of the heaters were influencing the BE values. Utilizing this assembly, temperatures of 100–180°C could routinely be reached although in principle temperatures of > 250°C should be attainable.

The following pyridines were commercially available and purified by sublimation and/or distillation prior to use: 2,3,4-CH_3, 2-Br, 2,3-Cl, 2F, 2,3,4-NH_2, 2,4-$N(CH_3)_2$, 2,3,4-CN, 2,3,4-OH, 2,3,4,-$COCH_3$. Their purities were checked by either glpc or tlc.

The substituted pyridines 3-F (21), 2- and 4-NO_2 (22), 3-NO_2 (23), 4-OCH_3 (24), and 3-OCH_3[6] were prepared according to published procedure. 4-Chloropyridine was prepared from basification of the commercial hydrochloride salt with aqueous $NaHCO_3$. The mixture was extracted with methylene chloride, dried (Na_2SO_4), and stripped of solvent to give a red liquid which was distilled (67–69°C/35 Torr) to yield 4-chloropyridine as a colorless liquid. All glassware was treated with NH_4OH and oven dried prior to use. Omission of this step led to decomposition of the 4-halopyridines on distillation.

4-Bromopyridine was prepared analogously to 4-chloropyridine, and micro-distilled (80°C/20 Torr) to give a colorless liquid.

4-Fluoropyridine was prepared by a modified procedure of Lyle and Taft (25) and Desai (26). Four-aminopyridine (3.6 g, 0.038 mol) was dissolved in 16 mL of 48% fluoroboric acid, and cooled to 0°C. Diazotization was accomplished by the addition of 3 g (0.04 mol) $NaNO_2$ in small portions with stirring at such a rate as to keep the temperature < 10°C. After complete addition, the mixture was stirred at 0°C for 1 h and then decomposed by warming to 25°C. After the cessation of N_2 evolution, the solution was quickly cooled to 0°C and neutralized by the addition of solid $NaHCO_3$. Extraction of this mixture with 100 mL CH_2Cl_2, drying of the extracts (Na_2SO_4) and solvent removal gave 0.5 g (13.6%) of 4-fluoropyridine, bp 60–62°C/150 Torr, which was stored over a pellet of NaOH to prevent decomposition.

3-Dimethylaminopyridine was prepared in 47.5% yield overall by the procedure of Clarke *et al.* (27) and purified by micro-distillation (100°C/0.3 Torr) (lit. (28) bp 108–110°C/12 Torr).

The CF_3-substituted pyridines were generously provided by Drs. A. E. Feiring, W. A. Sheppard, and M. Raasch and Mr. E. Wonchoba of the Central Research and Development Department, E. I. DuPont de Nemours and Co., Wilmington, DE 19898.

[6]Prepared analogously to the procedure for 4-OCH_3 (24) and isolated by preparative glpc.

Acknowledgements

The authors gratefully acknowledge the financial support of the Natural Sciences and Engineering Research Council of Canada and of the University of Alberta. They are also indebted to Mr. E. Schartner and Ed Feschuk for construction of the heated inlet assembly and to Profs. R. W. Taft and D. H. Aue who supplied gas phase basicity data.

1. (*a*) D. T. Clark, D. Kilcast, and W. K. R. Musgrave. J. Chem. Soc. D, 516 (1971); (*b*) D. T. Clark, D. Kilcast, D. B. Adams, and W. K. R. Musgrave. J. Electron Spectrosc. **1**, 227 (1972/73); (*c*) D. W. Davis, D. A. Shirley, and T. D. Thomas. J. Am. Chem. Soc. **94**, 6565 (1972); (*d*) D. W. Davis, D. A. Shirley, and T. D. Thomas. J. Chem. Phys. **56**, 671 (1972); (*e*) K. Siegbahn *et al.* ESCA applied to free molecules. North-Holland Publishing Co., Amsterdam. 1969; (*f*) T. Ohta, T. Fujikawa, and H. Kuroda. Bull. Chem. Soc. Jpn. **48**, 2017 (1975); (*g*) B. C. Trudell and S. J. W. Price. Can. J. Chem. **55**, 1279 (1977); (*h*) B. C. Trudell and S. J. W. Price. Can. J. Chem. **56**, 538 (1978).
2. (*a*) D. A. Shirley. Chem. Phys. Lett. **16**, 220 (1972); (*b*) D. W. Davis and D. A. Shirley. Chem. Phys. Lett. **15**, 185 (1972); (*c*) D. W. Davis and J. W. Rabalais. J. Am. Chem. Soc. **96**, 5305 (1974); (*d*) D. W. Davis and D. A. Shirley. J. Am. Chem. Soc. **98**, 7898 (1976); (*e*) D. W. Davis and D. A. Shirley. J. Electron Spectrosc. **3**, 137 (1974).
3. R. L. Martin and D. A. Shirley. J. Am. Chem. Soc. **96**, 5299 (1974).
4. (*a*) S. R. Smith and T. D. Thomas. J. Am. Chem. Soc. **100**, 5459 (1978); (*b*) T. X. Carroll, S. R. Smith, and T. D. Thomas. J. Am. Chem. Soc. **97**, 659 (1975); (*c*) B. E. Mills, R. L. Martin, and D. A. Shirley. J. Am. Chem. Soc. **98**, 2380 (1976); (*d*) F. M. Benoit and A. G. Harrison. J. Am. Chem. Soc. **99**, 3980 (1977); (*e*) B. E. Mills, R. L. Martin, and D. A. Shirley. J. Am. Chem. Soc. **98**, 2380 (1976); (*f*) R. G. Cavell and D. A. Allison. J. Am. Chem. Soc. **99**, 4203 (1977); (*g*) A. J. Ashe, M. K. Bahl, K. D. Bomben, W.-T. Chan, J. K. Gimzewski, P. G. Sitton, and T. D. Thomas. J. Am. Chem. Soc. **101**, 1764 (1979); (*h*) R. S. Brown, A. Tse, and J. C. Vederas. J. Am. Chem. Soc. In press.
5. (*a*) M. Taagepera, W. G. Henderson, R. T. C. Brownlee, J. L. Holtz, and R. W. Taft. J. Am. Chem. Soc. **94**, 1369 (1972); (*b*) R. W. Taft. *In* Proton transfer reactions. *Edited by* E. Caldin and V. Gold. Chapman and Hall, London. 1975. p. 31; (*c*) E. M. Arnett. *In* Proton transfer reactions. *Edited by* E. Caldin and V. Gold. Chap-

man and Hall, London. 1975. p. 79; (*d*) D. H. AUE, H. M. WEBB, M. T. BOWERS, C. L. LIOTTA, C. J. ALEXANDER, and H. P. HOPKINS. J. Am. Chem. Soc. **98**, 854 (1976).
6. T. D. THOMAS and R. W. SHAW. J. Electron Spectrosc. **5**, 1081 (1974).
7. (*a*) J. A. POPLE and M. GORDON. J. Am. Chem. Soc. **89**, 4253 (1967); (*b*) B. BAK, L. H. NYGAARD, and J. R. ANDERSEN. J. Mol. Spectrosc. **2**, 361 (1958).
8. D. W. DAVIS and D. A. SHIRLEY. Chem. Phys. Lett. **15**, 185 (1972).
9. (*a*) C. D. RITCHIE and W. F. SAGER. Prog. Phys. Org. Chem. **2**, 323 (1964); (*b*) B. LINDBERG, S. SVENSSON, P. Å. MALMQUIST, E. BASILIER, U. GELIUS, and K. SIEGBAHN. Chem. Phys. Lett. **90**, 175 (1976).
10. S. EHRENSON, R. T. C. BROWNLEE, and R. W. TAFT. Prog. Phys. Org. Chem. **10**, 1 (1973).
11. (*a*) H. H. JAFFÉ. Chem. Rev. **53**, 191 (1953); (*b*) R. W. TAFT, E. PRICE, I. R. FOX, I. C. LEWIS, K. K. ANDERSEN, and G. T. DAVIS. J. Am. Chem. Soc. **85**, 709 (1963); **85**, 3146 (1963).
12. H. BASCH. Chem. Phys. Lett. **5**, 337 (1970).
13. (*a*) R. E. BLOCK. J. Magn. Reson. **5**, 155 (1971); (*b*) G. D. MATEESCU and J. L. RIEMENSCHNEEDER. *In* Electron spectroscopy. *Edited by* D. A. Shirley. North-Holland Publishing Co., Amsterdam. 1972. p. 661.
14. B. J. LINDBERG. J. Electron Spectrosc. **5**, 149 (1974), and references therein.
15. M. WITANOWSKI, T. SALUVERE, L. STEFANIAK, H. JANIUSZEWSKI, and G. A. WEBB. Mol. Phys. **23**, 1071 (1972).
16. U. GELIUS, G. JOHANSSON, H. SIEGBAHN, C. J. ALLAN, D. ALLISON, J. ALLISON, and K. SIEGBAHN. J. Electron Spectrosc. **1**, 285 (1972/73).
17. (*a*) R. C. BINGHAM, M. J. S. DEWAR, and D. H. LO. J. Am. Chem. Soc. **97**, 1285 (1975); **97**, 1294 (1975); **97**, 1302 (1975); **97**, 1306 (1975); **97**, 1311 (1975); (*b*) N. BODOR and R. PEARLMAN. J. Am. Chem. Soc. **100**, 4946 (1978).
18. (*a*) Y. K. LAU and P. KEBARLE. J. Am. Chem. Soc. **98**, 7452 (1976); (*b*) J. M. MCKELVEY, S. ALEXANDRATOS, A. STREITWEISER, J.-L. M. ABBOUD, and W. J. HEHRE. J. Am. Chem. Soc. **98**, 244 (1976).
19. P. KEBARLE. Annu. Rev. Phys. Chem. **28**, 445 (1977).
20. R. S. BROWN and D. A. ALLISON. J. Am. Chem. Soc. **99**, 3568 (1977).
21. A. ROE and G. F. HAWKINS. J. Am. Chem. Soc. **69**, 2443 (1947).
22. R. H. WILEY and J. H. HARTMAN. J. Am. Chem. Soc. **73**, 494 (1951).
23. A. FISCHER, W. J. GALLOWAY, and J. VAUGHAN. J. Chem. Soc. 3591 (1964).
24. A. ALBERT and J. N. PHILLIPS. J. Chem. Soc. 1294 (1956).
25. J. L. LYLE and R. W. TAFT. J. Heterocycl. Chem. **9**, 745 (1972).
26. P. B. DESAI. J. Chem. Soc. Perkin Trans. I, 1865 (1973).
27. H. T. CLARKE, H. B. GILLESPIE, and S. Z. WEISSHAUS. J. Am. Chem. Soc. **55**, 4571 (1933).
28. A. BINZ and O. VON SCHICKKH. Chem. Ber. **68**, 315 (1935).

Can. J. Chem. Downloaded from www.nrcresearchpress.com by 210.87.254.105 on 09/05/12
For personal use only.

Apparent molar heat capacities and volumes of unsaturated heterocyclic solutes in aqueous solution at 25°C[1]

OCTAVIAN ENEA
Laboratoire de Chimie I – Electrochimie et Interactions, Université de Poitiers, Poitiers, France
CARMEL JOLICOEUR
Département de chimie, Université de Sherbrooke, Sherbrooke (Qué.), Canada J1K 2R1
AND
LOREN G. HEPLER
Department of Chemistry, University of Lethbridge, Lethbridge, Alta., Canada T1K 3M4

Received November 23, 1979

OCTAVIAN ENEA, CARMEL JOLICOEUR, and LOREN G. HEPLER. Can. J. Chem. **58**, 704 (1980).

Measurements at 25°C with flow calorimeters and densimeters have led to heat capacities and densities of aqueous solutions of 15 unsaturated heterocyclic compounds containing nitrogen. From the results of these measurements we have obtained apparent molar heat capacities and volumes of the solutes. Extrapolations to infinite dilution have led to corresponding standard state apparent and partial molar heat capacities and volumes, which have been analyzed in terms of atomic and group additivity relationships.

OCTAVIAN ENEA, CARMEL JOLICOEUR et LOREN G. HEPLER. Can. J. Chem. **58**, 704 (1980).

On a déterminé les capacités calorifiques et les densités de 15 composés hétérocycliques non saturés contenant de l'azote en solution aqueuse en effectuant des mesures à 25°C à l'aide d'un calorimètre et d'un densimètre dynamiques. A partir des résultats de ces mesures, on a obtenu les capacités calorifiques molaires apparentes et les volumes molaires apparents des solutés. Par extrapolation à dilution infinie, on obtient les capacités calorifiques et les volumes molaires partiels et apparents dans l'état standard qui sont analysés en fonction des relations d'additivité atomique et de groupe.

[Traduit par le journal]

Introduction

Thermodynamic properties of aqueous solutions of nonelectrolytes have been of interest for a long time. Most early research in this area focussed on free energies (solubilities, activity coefficients, etc.), followed by increasing interest in the temperature dependences of free energies and thence the corresponding enthalpies. More recently, there has been substantial interest in such properties as volumes and heat capacities, which are first and second derivatives of free energies with respect to pressure and temperature, respectively. Reasons for these latter interests are generally of two kinds. (*i*) There is frequently interest in measuring thermal and volumetric properties of aqueous solutions so that the derived thermodynamic functions ($\bar{C}_p{}^0$ and $\bar{V}^0$ in this paper) can be used for thermodynamic calculations of properties of solutions at different temperatures and pressures. (*ii*) Thermodynamic properties, including partial molar heat capacities and volumes, are proving to be useful probes for investigating relationships between structures of solute molecules, solute–solvent interactions, and the "structures" of aqueous solutions.

Various atomic and group additivity schemes for both partial molar heat capacities and volumes have been proposed and used in connection with both (*i*) and (*ii*) above.

In this paper we report the results of our calorimetric and volumetric measurements at 25°C on aqueous solutions of 15 unsaturated nitrogen heterocyclic compounds. Results are given in forms that are appropriate to interests (*i*) and (*ii*) above and are also discussed briefly in relation to additivity schemes.

Experimental

All of our heat capacity measurements have been made with Picker flow calorimeters of the type that has been described in several publications (1–3) from the Université de Sherbrooke. Operation of the calorimeters has been checked as recently recommended (4). Densities of solutions were measured with flow densimeters that have been described previously (5). The results of all measurements refer to 25.0°C.

Compounds from Aldrich were purified by distillation (pyridazine and quinoline), by vacuum sublimation (2,2′-bipyridyl, 4,4′-bipyridyl, *sym*-triazine, quinazoline, imidazole, pyrimidine, and 4-phenylpyrimidine), or by repeated recrystallizations from appropriate solvents (quinoxaline, pyrazole, and benzimidazole). Aldrich gold label compounds (pyrazine, benzotriazole, and 1,10-phenanthroline) were used as received. Purities of all compounds were tested by melting point and by gas chromatography. In addition, water content of each sample was determined by Karl Fischer titration.

Most solutions were prepared from known masses of organic solute and freshly deionized and deaerated water. A few other solutions were prepared by dilution of these original solutions. Finally, the pH of each solution was measured to ensure that acid–base reactions between solute and water were negligible.

[1]Research reported here was done during 1978 when Octavian Enea was on leave in Sherbrooke and Lethbridge from the Université de Poitiers.

0008-4042/80/070704-04$01.00/0
©1980 National Research Council of Canada/Conseil national de recherches du Canada

Can. J. Chem. Downloaded from www.nrcresearchpress.com by 210.87.254.6 on 09/05/12
For personal use only.

Can. J. Chem. Downloaded from www.nrcresearchpress.com by 210.87.254.6 on 09/05/12
For personal use only.

Results

Results of measurements with the Picker flow calorimeter are heat capacities per unit volume of solution, which we express in terms of J K^{-1} cm^{-3}. Combinations of these heat capacities with the densities permits calculation of specific heat capacities expressed in terms of J K^{-1} (g of solution)$^{-1}$. These latter heat capacities are then used in obtaining the desired apparent molar heat capacities that we represent by ϕ_C and express in terms of J K^{-1} mol^{-1}. Similarly, densities lead to apparent molar volumes that we represent by ϕ_V and express in terms of cm^3 mol^{-1}. For these calculations of apparent molar properties we have used equations of the type

$$[1] \quad \phi_Y = [Y(\text{solution}) - n_1 Y_1^0]/n_2$$

in which the symbols have the following meaning: Y is the extensive property (heat capacity or volume here) of a specified quantity of solution, n_1 is the amount (moles) of solvent in this specified quantity of solution, Y_1^0 is the property (heat capacity or volume) of 1 mol of pure solvent, and n_2 is the amount (moles) of solute in the specified quantity of solution.

To obtain apparent molar heat capacities and apparent molar volumes at infinite dilution, where apparent molar properties become identical with the corresponding partial molar properties, we have fitted our experimental results[2] for dilute solutions to the equations

$$[2] \quad \phi_C = \phi_C^0 + B_C m$$

and

$$[3] \quad \phi_V = \phi_V^0 + B_V m$$

in which $\phi_C^0 = \bar{C}_p^0$ and $\phi_V^0 = \bar{V}^0$ are the desired properties at infinite dilution and B_C and B_V are adjustable parameters. Our derived ϕ_C^0, B_C, ϕ_V^0, and B_V values are listed in Table 1. We estimate that *total* uncertainties (chemicals, calorimetry, densities, extrapolations) in our ϕ_C^0 and ϕ_V^0 values are about ± 5 J K^{-1} mol^{-1} and ± 0.5 cm^3 mol^{-1} for most solutes; uncertainties for the less soluble compounds are a little larger. In Table 1 we also list values for the same quantities obtained previously (6) for aqueous pyridine.

[2]A complete set of the experimental results is available, at a nominal charge, from the Depository of Unpublished Data, CISTI, National Research Council of Canada, Ottawa, Ont., Canada K1A 0S2.

Discussion

Earlier investigators have proposed various additivity schemes for ϕ_C^0 (6–18) and ϕ_V^0 (6, 15–24). These additivity schemes, all useful in various ways, were developed in relation to the ϕ_C^0 and ϕ_V^0 values that were then available; hence these earlier schemes are not generally applicable to unsaturated heterocyclics of the sort under consideration here for the first time.

The ϕ_C^0 values listed in Table 1 for isomers show that atomic group additivity schemes that do not take into account the arrangements of these atoms or groups cannot account very accurately for the experimental results. For example, the ϕ_C^0 values for aqueous pyrazine, pyrimidine, and pyridazine should be the same on the basis of any simple atomic or group additivity scheme. But the experimental ϕ_C^0 values cover a range of 16 J K^{-1} mol^{-1}. Experimental ϕ_C^0 values for the isomeric imidazole and pyrazole differ by 28 J K^{-1} mol^{-1} while those for the isomeric 2,2′-bipyridyl, 4,4′-bipyridyl, and 4-phenylpyrimidine cover a range of 52 J K^{-1} mol^{-1}. Finally, the ϕ_C^0 values for the isomeric quinazoline and quinoxaline differ by 27 J K^{-1} mol^{-1}. All of these ranges and differences are larger than likely uncertainties (± 5 J K^{-1} mol^{-1}) in the ϕ_C^0 values.

We also consider the ϕ_C^0 values for isomers in another way, as follows. For the isomeric pyrazine, pyrimidine, and pyridazine we calculate the average $\phi_C^0 = 210.1$ J K^{-1} mol^{-1} and find that differences between experimental values and this average amount to 7.3, 1.2, and 8.6 J K^{-1} mol^{-1}. Similar calculations for other isomers lead to similar average values and thence to differences between experimental values and averages for sets of isomers. The average of all these 10 differences is 13.1 J K^{-1} mol^{-1}, which is more than twice the uncertainty assigned to most of our ϕ_C^0 values.

Similar considerations of ϕ_V^0 values lead to the following. The largest range of values for any set of isomers is 1.31 cm^3 mol^{-1} for the imidazole–pyrazole pair. The average of the various differences calculated from ϕ_V^0 values as described in the preceding paragraph amounts to 0.39 cm^3 mol^{-1}, which is less than the uncertainty (± 0.5 cm^3 mol^{-1}) assigned to most individual ϕ_V^0 values.

Our consideration in the three preceding paragraphs show that a simple additivity scheme for ϕ_V^0 values *might* fit the experimental results with an average accuracy comparable to the experimental accuracy, while a similar additivity scheme for ϕ_C^0 values cannot fit with an average accuracy better than about two or three times the uncertainty in the

Can. J. Chem. Downloaded from www.nrcresearchpress.com by 210.87.254.6 on 09/05/12
For personal use only.

TABLE 1. Parameters for eqs. [2] and [3]

Solute	ϕ_C^0 / J K^{-1} mol^{-1}	B_C / J K^{-1} mol^{-2} kg	ϕ_V^0 / cm^3 mol^{-1}	B_V / cm^3 mol^{-2} kg
Pyridine	305.7	−41.2	77.5	−1.4
Pyrazine	217.$_4$	−23	70.8$_2$	−0.0$_7$
Pyrimidine	211.$_3$	−17.1	70.3$_3$	0.11
Pyridazine	201.$_5$	−9.2	70.4$_2$	−0.16
sym-Triazine	13.$_9$	−113	54.7$_9$	0
Imidazole	182.$_1$	−12	59.9$_5$	0.1$_2$
Pyrazole	210.$_2$	−11.6	62.2$_6$	0.10
Benzimidazole	302.8	−23	98.53	0
Benzotriazole	314.8	192	94.49	−0.0$_3$
2,2′-Bipyridyl	498.3	−424	134.29	−5
4,4′-Bipyridyl	445.9	−621	133.21	6
4-Phenylpyrimidine	461.9	−1023	134.09	∼−28
Quinoline	419.6	−156	115.53	1.$_4$
Quinazoline	365.1	−26	108.48	−3.$_1$
Quinoxaline	391.7	−65	109.16	−2.$_7$
1,10-Phenanthroline	537.9	−1495	142.42	∼−12

individual values. Because the considerations described so far have not been concerned with relationships between ϕ_C^0 and ϕ_V^0 values for different sets of isomers or those compounds that are not isomeric with others listed in Table 1, we now turn to testing two specific additivity schemes.

We first consider atomic additivity schemes for ϕ_C^0 and ϕ_V^0 values according to which

$$[4] \quad \phi_Y^0 = n_C(C)_Y + n_H(H)_Y + n_N(N)_Y$$

Here n_C, n_H, and n_N represent the numbers of indicated atoms in the molecule of interest while $(C)_Y$, $(H)_Y$, and $(N)_Y$ represent the contributions of the indicated atoms to the molar ϕ_Y^0 values. We have chosen to apply eq. [4] in the form

$$[5] \quad \phi_Y^0/n_N = (N)_Y + (n_C/n_N)(C)_Y + (n_H/n_N)(H)_Y$$

which permits convenient multiple linear regression for the desired $(C)_Y$, $(H)_Y$, and $(N)_Y$ values.

Application of eq. [5] to ϕ_V^0 values leads to $(C)_V$, $(H)_V$, and $(N)_V$ equal to 4.86, 9.45, and 5.34 cm^3 mol^{-1}, respectively. We have used these values in eq. [4] to calculate ϕ_V^0 values for all solutes listed in Table 1 and then have found that the average magnitude of the difference between calculated and experimental values is 2.07 cm^3 mol^{-1}, which is

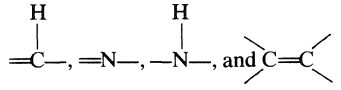
Can. J. Chem. Downloaded from www.nrcresearchpress.com by 210.87.254.6 on 09/05/12
For personal use only.

about four times the uncertainty assigned to most individual ϕ_V^0 values.

Similar application of eq. [5] to ϕ_C^0 values leads to $(C)_C$, $(H)_C$, and $(N)_C$ equal to 13.11, 48.71, and -21.13 J K^{-1} mol^{-1}, respectively. We have used these values in eq. [4] to calculate ϕ_C^0 values for all solutes listed in Table 1 and then have found that the average magnitude of the difference between calculated and experimental values is 27.41 J K^{-1} mol^{-1}, which is about five times the uncertainty assigned to most individual ϕ_C^0 values.

We thus see that this simple atomic additivity scheme works about as well (or badly) for ϕ_C^0 values as for ϕ_V^0 values for our unsaturated heterocyclic solutes, fitting both sets of results with an average accuracy corresponding to about five times the uncertainty assigned to most experimental values.

We also consider simple group additivity schemes as follows, based upon



groups that we henceforth represent by (CH), (N), (NH), and (CC), with subscripts Y, C, and V as used previously. Instead of applying multiple linear regression to all of the ϕ_Y^0 values in Table 1 to obtain "best" values of the four parameters $(CH)_Y$, $(N)_Y$, $(NH)_Y$, and (CC) simultaneously, we have applied the following stepwise procedure. Application of

$$[6] \quad \phi_Y^0/n_N = (N)_Y + (n_{CH}/n_N)(CH)_Y$$

to ϕ_Y^0 values for the first five compounds listed in Table 1 permits simple least squares evaluation of desired $(CH)_Y$ and $(N)_Y$ group values. Next, average $(NH)_Y$ values are obtained by application of

$$[7] \quad (NH)_Y = \phi_Y^0 - 3(CH)_Y - (N)_Y$$

to results listed in Table 1 for aqueous imidazole and pyrazole. Finally, average $(CC)_Y$ values are obtained from ϕ_Y^0 values for the last nine compounds listed in Table 1.

The procedure described in the paragraph above has led to $(CH)_C$, $(N)_C$, $(NH)_C$, and $(CC)_C$ values equal to 71.99, -47.69, 27.87, and 10.80 J K^{-1} mol^{-1}, respectively. We have used these group contribution values to calculate ϕ_C^0 values for all solutes listed in Table 1 and have then found that the average magnitude of the difference between calculated and experimental values is 31.56 J K^{-1} mol^{-1}, which is about six times the uncertainty assigned to most individual ϕ_C^0 values.

Application of a similar procedure for ϕ_V^0 values leads to $(CH)_V$, $(N)_V$, $(NH)_V$, and $(CC)_V$ values equal to 14.52, 5.45, 11.60, and 8.99 cm^3 mol^{-1}. The average magnitude of differences between resulting calculated and experimental ϕ_V^0 values is 1.87 cm^3 mol^{-1}, which is a little less than four times the uncertainty assigned to most individual ϕ_V^0 values.

This group additivity scheme fits the ϕ_V^0 and ϕ_C^0 results with an average accuracy of about four and six times the uncertainties of individual experiment results.

Acknowledgment

We all thank the Natural Sciences and Engineering Research Council of Canada for support of this research.

1. P. Picker, P.-A. Leduc, P. R. Philip, and J. E. Desnoyers. J. Chem. Thermodyn. **3**, 631 (1971).
2. J.-L. Fortier, P.-A. Leduc, and J. E. Desnoyers. J. Solution Chem. **3**, 323 (1974).
3. G. Perron, J.-L. Fortier, and J. E. Desnoyers. J. Chem. Thermodyn. **7**, 1177 (1975).
4. J. E. Desnoyers, C. de Visser, G. Perron, and P. Picker. J. Solution Chem. **5**, 605 (1976).
5. P. Picker, E. Tremblay, and C. Jolicoeur. J. Solution Chem. **3**, 377 (1974).
6. O. Enea, P. P. Singh, and L. G. Hepler. J. Solution Chem. **6**, 719 (1977).
7. S. Cabani, G. Conti, A. Martinelli, and E. Matteoli. J. Chem. Soc. Faraday Trans. I, **69**, 2112 (1973).
8. S. Cabani, G. Conti, and E. Matteoli. J. Solution Chem. **5**, 125 (1976).
9. S. J. Gill and I. Wadsö. Proc. Natl. Acad. Sci. USA, **73**, 2955 (1976).
10. N. Nichols and I. Wadsö. J. Chem. Thermodyn. **7**, 329 (1975).
11. S. J. Gill, N. F. Nichols, and I. Wadsö. J. Chem. Thermodyn. **8**, 445 (1976).
12. N. Nichols, R. Sköld, C. Spink, J. Suurkuusk, and I. Wadsö. J. Chem. Thermodyn. **8**, 1081 (1976).
13. J. P. Guthrie. Can. J. Chem. **55**, 3700 (1977).
14. S. Cabani, G. Conti, and E. Matteoli. J. Chem. Soc. Faraday Trans. I, **74**, 2408 (1978).
15. O. Kiyohara, G. Perron, and J. E. Desnoyers. Can. J. Chem. **53**, 2591 (1975).
16. C. Jolicoeur and G. Lacroix. Can. J. Chem. **54**, 624 (1976).
17. J. C. Ahluwalia, C. Ostiguy, G. Perron, and J. E. Desnoyers. Can. J. Chem. **55**, 3364 (1977).
18. G. Perron and J. E. Desnoyers. Fluid Phase Equil. **2**, 239 (1979).
19. S. Cabani, G. Conti, and L. Lepori. J. Phys. Chem. **78**, 1030 (1974).
20. J. T. Edward and P. G. Farrell. Can. J. Chem. **53**, 2965 (1975).
21. S. Terasawa, H. Itsuki, and S. Arakawa. J. Phys. Chem. **79**, 2345 (1975).
22. F. Shahidi, P. G. Farrell, and J. T. Edward. J. Solution Chem. **5**, 807 (1976).
23. F. J. Millero, A. Lo Surdo, and C. Shin. J. Phys. Chem. **82**, 784 (1978).
24. F. Shahidi and P. G. Farrell. J. Chem. Soc. Faraday Trans. I, **74**, 858 (1978); **74**, 1268 (1978).

A comparison of the crystal structures of Sb_2Tl_7, Cu_5Zn_8 (γ-brass), and Ir_3Ge_7

ERWIN HELLNER AND ELKE KOCH

Institut für Mineralogie, Petrologie und Kristallographie der Philipps-Universität, D-3550 Marburg/Lahn, Germany

Received October 3, 1979

ERWIN HELLNER and ELKE KOCH. Can. J. Chem. **58**, 708 (1980).

The crystal structures of Sb_2Tl_7, Cu_5Zn_8, and Ir_3Ge_7 are discussed with the aid of shortest distances of Dirichlet domains and of voids in their frameworks. It will be pointed out that all three frameworks must be regarded as different though relations between the atomic parameters are obvious. The Sb_2Tl_7 structure represents a superstructure of an *I* lattice. The frameworks of Sb_2Tl_7 and of Cu_5Zn_8 contain tetrahedral voids only, while in Ir_3Ge_7 voids with a larger coordination number also exist.

ERWIN HELLNER et ELKE KOCH. Can. J. Chem. **58**, 708 (1980).

Les structures cristallines des composés Sb_2Tl_7, Cu_5Zn_8 et Ir_3Ge_7 sont discutées par les distances les plus courtes des domaines Dirichlet et par les cavités contenus dans leurs enchaînements ("frameworks"). On va demontré que, tous les trois enchaînements sont à regarder en differentes, quoique les rélations évidents entres les paramètres atomiques sont données. La structure de composé Sb_2Tl_7 représente une superstructure d'une reséau *I*-centrée. Les enchaînements des structures de Sb_2Tl_7 et de Cu_5Zn_8 ne contiennent que des cavités tétraédriques, tandis que des cavités supplementaires avec une plus grande nombre de coordination existent dans la structure de Ir_3Ge_7.

Can. J. Chem. Downloaded from www.nrcresearchpress.com by 210.87.254.40 on 09/05/12
For personal use only.

In a recent paper Stokhuizen, Chieh, and Pearson (1) compared the crystal structures of Sb_2Tl_7, Cu_5Zn_8 (γ-brass), and Ir_3Ge_7 to each other. In the following, the common features and the differences of these three crystal-structure types shall be discussed in more detail. For this the approach of frameworks and sphere packings has been applied, using a symbolism which consists of capital letters representing invariant lattice complexes and numbers and small letters describing coordination polyhedra (2–5).

The parameters of the three crystal structures are listed in Table 1. The Sb_2Tl_7 structure is built up by four symmetrically different kinds of atoms. The crystal structure as a whole may be regarded as a slightly deformed *I* lattice, the translation period of which amounts to one third of the lattice constants of this structure. The idealized parameters for such an I_{333} lattice (for short I_3 in the cubic system) are also recapitulated in Table 1 (cf. ref. 1). In addition, for each of the four point positions those parameters referring to a sphere-packing condition are given (8, 9). The atomic parameters for Sb_2Tl_7 differ slightly as well from the idealized I_3 parameters as from the sphere-packing parameters. The Tl(1) position by itself forms an *I* lattice and therefore refers to a sphere packing. The shortest distance between Tl(1) atoms, however, is much longer than the shortest distance in the Sb_2Tl_7 structure. The Tl(2) position and the Sb position consist of arrangements of cubes (8*c*) and octahedra (6*o*), respectively, around the points of that *I* lattice. Therefore these configurations are symbolized by *I*(8*c*) and by *I*(6*o*). In both cases the distances between atoms of neighbouring polyhedra are shorter than the edges of the polyhedra themselves. On the contrary the Tl(3) arrangement is very closely related to a sphere packing consisting of tetrahedra with common vertices ($4t_c$), the centers of which form a point configuration of the cubic invariant lattice complex W^*. Therefore, the Tl(3) configuration may be symbolized by $W^*(4t_c)$.

In an ideal *I* lattice there exist for each point eight nearest neighbours (8*c*) and six further neighbours (6*o*) in the second coordination shell forming together a rhomb-dodecahedron (14*rd*). The differences between the distances from the center to these two kinds of neighbours are 15% only. The total coordination number, therefore, may be considered as 14. The Dirichlet domain (or Wirkungsbereich or Wigner-Seitz cell) for a point of a cubic *I* lattice is a cuboctahedron with 24 vertices and 14 faces the dual of the rhomb-dodecahedron. The hexagonal faces correspond to the eight nearest neighbours and the quadrangular faces to the six further ones.

In Table 2 the shortest distances between atoms in Sb_2Tl_7 are collected. For each of the four symmetrically different kinds of atoms fourteen distances are clearly shorter than the following ones, but it is impossible to separate them in eight plus six in a distinct way.

Stokhuizen, Chieh, and Pearson (1) designated the coordination number eight for Tl(1), Tl(3), and Sb and the coordination number ten for Tl(2). The table of distances on which these coordination numbers are based contains, however, an error and an inconsistency: (*1*) each Tl(2) atom possesses only one Tl(2) neighbour at a distance of 3.20 Å; (*2*) the distance 3.55 Å between a Tl(2) and a Tl(3) atom

0008-4042/80/070708-06$01.00/0

©1980 National Research Council of Canada/Conseil national de recherches du Canada

Can. J. Chem. Downloaded from www.nrcresearchpress.com by 210.87.254.40 on 09/05/12
For personal use only.

TABLE 1. The structural parameters of Sb_2Tl_7 (1), Cu_5Zn_8 (6), and Ir_3Ge_7 (7) compared with the parameters for an undistorted I_3 lattice with symmetry $Im3m$ and with those for related sphere packings. The symbols of the corresponding sphere-packing types (8, 9) are added in the last column

Sb_2Tl_7	Cu_5Zn_8	Ir_3Ge_7	Undistorted I_3	Sphere packing
$Im3m$ $a_0 = 11.618$ Å	$I\bar{4}3m$ $a_0 = 8.878$ Å	$Im3m$ $a_0 = 8.753$ Å	$Im3m$	$Im3m$
2(*a*) 000 Tl(1) *I*			2(*a*) 000 *I*	2(*a*) 000 8/4/*c*1
16(*f*) *xxx* Tl(2) $x = 0.1704$ *I*(8*c*)	8(*c*) *xxx* Zn(1) $x = 0.1089$ $I(4t^+)$	16(*f*) *xxx* Ge(2) $x = 0.156$ *I*(8*c*)	16(*f*) *xxx* $x = 0.1667$ *I*(8*c*)	16(*f*) *xxx* $x = 0.1585$ 4/4/*c*2
	8(*c*) *xxx* Cu(1) $x = -0.1720$ $I(4t^-)$			
12(*e*) *x*00 Sb $x = 0.3138$ *I*(6*o*)	12(*e*) *x*00 Cu(2) $x = 0.3558$ *I*(6*o*)	12(*e*) *x*00 Ir $x = 0.342$ *I*(6*o*)	12(*e*) *x*00 $x = 0.3333$ *I*(6*o*)	12(*e*) *x*00 $x = 0.2929$ $[5/3/c3]^2$
24(*h*) *xx*0 Tl(3) $x = 0.3497$	24(*g*) *xxz* Zn(2) $x = 0.3128$ $z = 0.0366$	12(*d*) $0\frac{1}{4}\frac{1}{4}$ Ge(1)	24(*h*) *xx*0 $x = 0.3333$	24(*h*) *xx*0 $x = 0.3536$
$W^*(4t_c)$	$W^*(4t_c)$	W^*	$W^*(4t_c)$	6/3/*c*6

TABLE 2. The shortest distances between atoms in the Sb_2Tl_7 structure, the enlargement referring to the shortest distance from the same central atom and the frequency

Atoms	Distance (Å)	Enlargement	Frequency
Tl(1)—Tl(2)	3.43		8×
—Sb	3.65	6%	6×
—Tl(3)	5.75	68%	12×
Tl(2)—Tl(2)	3.20		1×
—Sb	3.26	2%	3×
—Tl(1)	3.43	7%	1×
—Tl(3)	3.55	11%	3×
—Tl(3)	3.84	20%	3×
—Tl(2)	3.96	24%	3×
—Tl(3)	5.35	67%	6×
Sb—Tl(2)	3.26		4×
—Tl(3)	3.28	1%	4×
—Tl(1)	3.65	12%	1×
—Tl(3)	4.08	25%	4×
—Sb	4.33	33%	1×
—Sb	5.16	58%	4×
Tl(3)—Sb	3.28		2×
—Tl(3)	3.39	3%	4×
—Tl(3)	3.49	6%	2×
—Tl(2)	3.55	8%	2×
—Tl(2)	3.84	17%	2×
—Sb	4.08	24%	2×
—Tl(3)	4.94	50%	1×

is only reported in connection with Tl(2). Taking these facts into account the coordination number of Tl(2) becomes eight and that of Tl(3) becomes ten.

For each of the four different kinds of atoms in Sb_2Tl_7 the computation of Dirichlet domains yields cuboctahedra which are deformed in different ways. Figure 1 shows these differences. Their similarity with the Dirichlet domains of the points of an ideal *I* lattice, however, may be taken as a further argument for describing the Sb_2Tl_7 structure as superstructure of an *I* lattice.

On the other hand the Tl(3) atoms by themselves build up a three-dimensional framework $W^*(4t_c)$, with large voids around the points of an *I* configuration. Each of these voids is centered by a Tl(1) atom and filled up by a Tl(2) cube and an Sb octahedron. This framework $W^*(4t_c)$ has also been found in α-Mn, sodalite $Na_4Cl[AlSiO_4]_3$, and related structures.

In Cu_5Zn_8 the site analogous to Tl(1) in Sb_2Tl_7 is not occupied. Each Tl(2) cube corresponds to two tetrahedra with different size and orientation in Cu_5Zn_8. They are built up by Zn(1) and Cu(1) and may be symbolized by $I(4t^+)$ and $I(4t^-)$, respectively. The Cu(2) atoms, like the Sb atoms, are arranged in an *I*(6*o*) configuration with relatively larger octahedra. The arrangement of the Zn(2) atoms, like that of the Tl(3) atoms, may be regarded as a $W^*(4t_c)$ configuration, though the deviation from the sphere-packing parameters is larger than for Tl(3). The comparison between the atomic coordinates of Sb_2Tl_7 and of Cu_5Zn_8 indicates a similarity of both frameworks. Closer inspection of the neighbourhood for the four different kinds of atoms

Can. J. Chem. Downloaded from www.nrcresearchpress.com by 210.87.254.40 on 09/05/12
For personal use only.

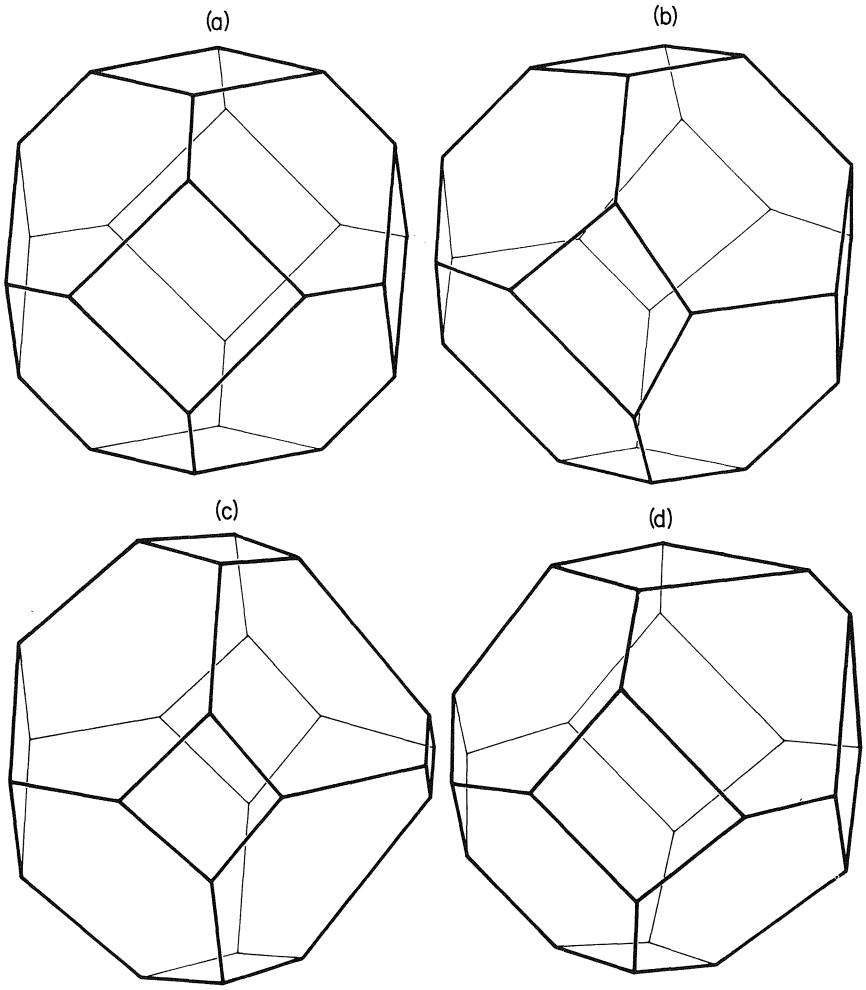


FIG. 1. Dirichlet domains for Sb_2Tl_7: (*a*) Tl(1), (*b*) Tl(2), (*c*) Sb, (*d*) Tl(3).

in Cu_5Zn_8, however, shows essential differences between both crystal structures (see Table 3).

If the Cu_5Zn_8 framework would be similarly connected as that of Sb_2Tl_7, except for the two omitted atoms per unit cell, the total coordination numbers should amount to 13 for Zn(1), Cu(1), and Cu(2) and 14 for Zn(2). Table 3 shows that, as far as distances are concerned, the coordination number is 11 for Zn(2), 12 for Zn(1) and Cu(1), and 13 for Cu(2). These numbers are in agreement with those stated by Pearson, Brandon, and Brizard (10). On the contrary Brandon, Chieh, Pearson, and Riley (11) used the coordination number 12 for all different kinds of atoms in Cu_5Zn_8. Such a delimitation of 12 nearest neighbours, however, is not possible in a reasonable way (cf. Table 3). The calculation of Dirichlet domains, always giving a "maximal" coordination number, yields polyhedra with 13 faces for Zn(1), Cu(1), and Cu(2) and 15 faces for Zn(2) (Fig. 2). Those three faces of the Zn(1) polyhedron which refer to the distance of 2.73 Å and those two faces of the Zn(2) polyhedron which refer to the distance of 3.47 Å, however, do not correspond to any face of the I_3 cuboctahedron. For this reason connections exist within the framework of Cu_5Zn_8 which do not correspond to any connection within the Sb_2Tl_7 framework and the two frameworks must be regarded as different.

This difference also manifests itself in the site and the number of polyhedral voids in both frameworks built up by all the atoms of the structures. Each polyhedral void in a framework corresponds to a vertex of the Dirichlet domain of a framework atom. This vertex may be regarded as the center of the void, because it is the point with equal distances to all the vertices of the polyhedron (cf. ref. 12). A space partition into voids of a framework constructed in this way is always unique.

Can. J. Chem. Downloaded from www.nrcresearchpress.com by 210.87.254.40 on 09/05/12
For personal use only.

TABLE 3. Shortest distances between atoms in the Cu_5Zn_8 structure, the enlargement referring to the shortest distance from the same central atom and the frequency. Distances not corresponding to one of the 14 shortest distances in Sb_2Tl_7 are marked by an *

Atoms	Distance (Å)	Enlargement	Frequency
Zn(1)—Cu(2)	2.58		3×
—Cu(1)	2.62	1%	3×
—Zn(2)	2.64	2%	3×
—Zn(1)	2.73*	6%	3×
—Cu(1)	3.37	30%	1×
—Zn(2)	3.92	52%	3×
Cu(1)—Zn(2)	2.56		3×
—Zn(2)	2.59	1%	3×
—Zn(1)	2.62	2%	3×
—Cu(2)	2.71	6%	3×
—Zn(1)	3.37	31%	1×
—Cu(2)	4.13	61%	3×
Cu(2)—Zn(2)	2.54		2×
—Cu(2)	2.56	1%	1×
—Zn(1)	2.58	2%	2×
—Cu(1)	2.71	7%	2×
—Zn(2)	2.82	11%	4×
—Zn(2)	2.85	12%	2×
—Zn(2)	4.06	60%	4×
Zn(2)—Cu(2)	2.54		1×
—Cu(1)	2.56	1%	1×
—Cu(1)	2.59	2%	1×
—Zn(1)	2.64	4%	1×
—Zn(2)	2.64	4%	4×
—Cu(2)	2.82	11%	2×
—Cu(2)	2.85	12%	1×
—Zn(2)	3.39	33%	2×
—Zn(2)	3.47*	37%	2×
—Zn(1)	3.92	55%	1×

In both frameworks under consideration no other than tetrahedral voids exist, that is 324 within the unit cell of Sb_2Tl_7 and 310 within the unit cell of Cu_5Zn_8. While in Sb_2Tl_7 all these voids correspond directly to the voids of an ideal I_3 lattice, in Cu_5Zn_8 this relation exists for a small part of the voids only. In Tables 4 and 5 the size and the coordinates of the centers are listed for all voids in the frameworks of Sb_2Tl_7 and of Cu_5Zn_8, respectively. It is possible to construct infinitely many other space partitions into tetrahedra for these structures. One of these possibilities has been used by Brandon *et al.* (11) for the purpose of calculating "average root-mean-square error parameters per tetrahedra" for a γ-brass structure. However, each space partition into tetrahedra differing from that deducible from Dirichlet domains has the following property: there must exist tetrahedra with distances between their centers and vertices which are longer than the shortest distances between the tetrahedra centers and the nearest neighbours out of the framework.

TABLE 4. Tetrahedral voids in the Tl_7Sb_2 framework: position of their centers, the volume, and the distance from the centers to the vertices of the tetrahedra

Centers of the voids			Volume (Å³)	Distance (Å)
12(*d*)	$0\ \frac{1}{2}\ \frac{1}{4}$		4.71	2.10
24(*g*)	$x\ 0\ \frac{1}{2}$	$x = 0.0350$	4.40	2.20
48(*i*)	$\frac{1}{4}, x, \frac{1}{2}-x$	$x = 0.1594$	5.09	2.19
48(*j*)	$0\ y\ z$	$y = 0.0987$ $z = 0.1569$	4.76	2.15
48(*j*)	$0\ y\ z$	$y = 0.1826$ $z = 0.2566$	5.01	2.22
48(*j*)	$0\ y\ z$	$y = 0.1687$ $z = 0.3921$	4.69	2.16
96(*l*)	$x\ y\ z$	$x = 0.0699$ $y = 0.1750$ $z = 0.3306$	4.87	2.20

TABLE 5. Tetrahedral voids in the Cu_5Zn_8 framework: position of their centers, the volume, and the distance from the centers to the vertices of the tetrahedra. Voids not corresponding to any void in the Sb_2Tl_7 framework are marked by an *

Centers of the voids			Volume (Å³)	Distance (Å)
* 2(*a*)	$0\ 0\ 0$		2.42	1.68
12(*d*)	$0\ \frac{1}{2}\ \frac{1}{4}$		2.14	1.78
* 8(*c*)	$x\ x\ x$	$x = -0.0652$	2.26	1.64
24(*f*)	$x\ 0\ \frac{1}{2}$	$x = 0.1352$	2.35	1.76
*24(*g*)	$x\ x\ z$	$x = 0.1883$ $z = 0.3392$	2.19	1.76
24(*g*)	$x\ x\ z$	$x = 0.1916$ $z = 0.2722$	1.95	1.78
*24(*g*)	$x\ x\ z$	$x = 0.1385$ $z = 0.3066$	2.48	1.79
*24(*g*)	$x\ x\ z$	$x = 0.1431$ $z = 0.3440$	2.56	1.80
*24(*g*)	$x\ x\ z$	$x = 0.0434$ $z = -0.1844$	2.16	1.62
48(*h*)	$x\ y\ z$	$x = -0.0062$ $y = 0.1474$ $z = 0.2467$	2.19	1.63
*48(*h*)	$x\ y\ z$	$x = 0.1762$ $y = 0.3344$ $z = 0.4295$	2.16	1.62
48(*h*)	$x\ y\ z$	$x = 0.0098$ $y = 0.1734$ $z = 0.4504$	2.38	1.76

The framework of Ir_3Ge_7 shows distinct differences to both frameworks discussed above. As in Cu_5Zn_8 the Tl(1) position is unoccupied in Ir_3Ge_7, but in contrast to Cu_5Zn_8, Ge(2) cubes exist analogous to the Tl(2) cubes in Sb_2Tl_7. Because of the missing atoms in their centers, the Ge(2) cubes are much smaller than the Tl(2) cubes. The coordinates of Ge(2) meet the sphere-packing condition (Table 1) in good approximation. The configuration of the Ir atoms is comparable to that of Cu(2). Instead of tetrahedra with common vertices around a *W** configuration, in Ir_3Ge_7 the *W** site itself is

Can. J. Chem. Downloaded from www.nrcresearchpress.com by 210.87.254.40 on 09/05/12
For personal use only.

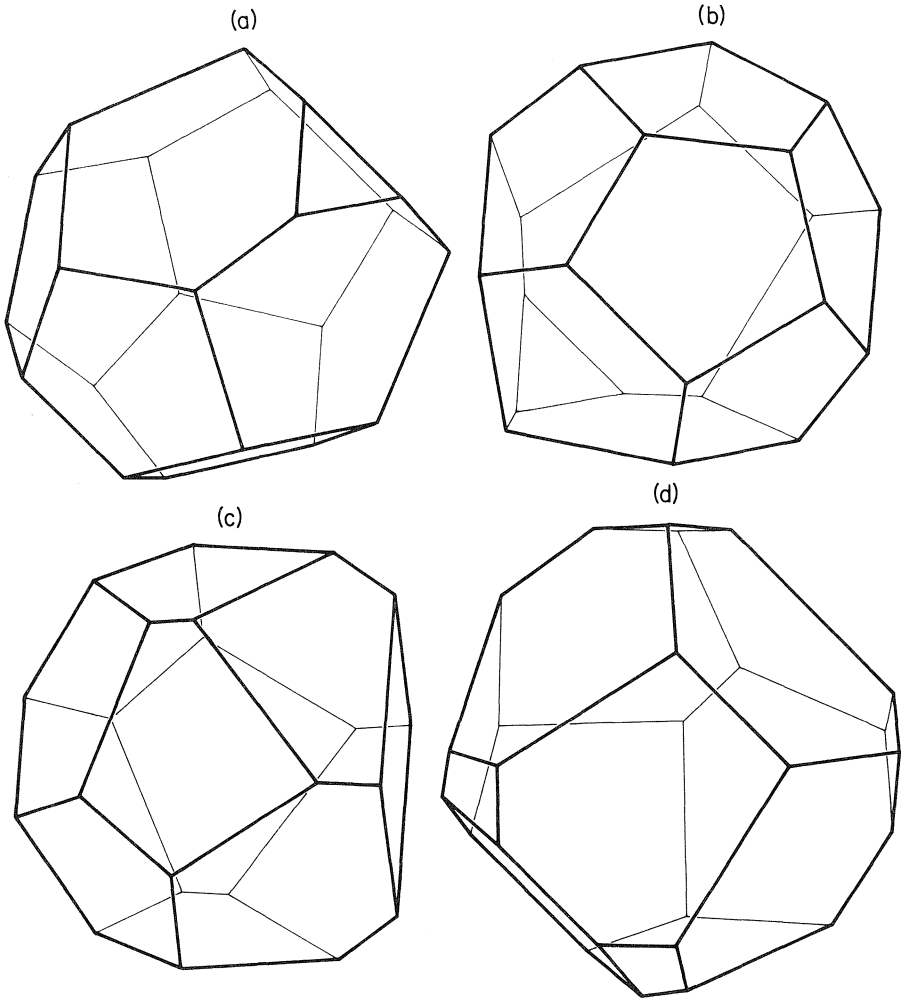


FIG. 2. Dirichlet domains for Cu_5Zn_8: (*a*) Zn(1), (*b*) Cu(1), (*c*) Cu(2), (*d*) Zn(2).

TABLE 6. Shortest distances between atoms in the Ir_3Ge_7 structure, the enlargement referring to the shortest distance from the same central atom and the frequency

Atoms	Distance (Å)	Frequency	Enlargement
Ge(2)—Ir	2.53		3×
—Ge(2)	2.73	8%	3×
—Ge(2)	2.85	13%	1×
—Ge(1)	3.41	35%	6×
—Ge(2)	3.86	53%	3×
Ir—Ge(2)	2.53		4×
—Ge(1)	2.59	2%	4×
—Ir	2.77	10%	1×
—Ir	4.23	68%	4×
Ge(1)—Ir	2.59		4×
—Ge(1)	3.09	20%	4×
—Ge(2)	3.41	32%	8×
—Ge(1)	4.38	69%	2×

occupied by the Ge(1) atoms. They build up a three-dimensional connected framework with only one kind of voids, i.e., cuboctahedra (24*co*), the centers of which form an *I* lattice. The distances within the framework of Ir_3Ge_7 are given in Table 6. The Dirichlet domains show nine faces for Ir, 16 faces for Ge(1), and 13 faces for Ge(2). Because of the replacement of the $W^*(4t_c)$ configuration by the W^* configuration no relationships to the I_3 cuboctahedra are recognizable. The structure of Ir_3Ge_7 may, however, be designated as homeotype of both the others (5, 13).

Ir_3Ge_7 may not be regarded as a tetrahedrally closed packed structure. In addition to tetrahedral voids it contains other kinds of voids with higher coordination numbers. The best way of looking at it seems to be the following: Ge(1) and Ge(2) together build up the heterogeneous framework [W^* +

$I(8c)$] with four kinds of voids: cubes ($8c$) around I, i.e. 1(a) 000, tetragonal antiprisms ($8a$) around $I(6o)$, i.e. 12(e) $x00$, $x = 0.3481$, and tetrahedra ($4t$) with centers in 24(h) $xx0$, $x = 0.2734$ and in 48(k), xxz, $x = 0.1843$, $z = 0.3813$. The tetragonal antiprismatic voids in the Ge framework are occupied by Ir atoms.

Acknowledgement

We are grateful to the Gesellshaft für Information und Dokumentation GmbH, Frankfurt, for financial support.

1. R. STOKHUIZEN, C. CHIEH, and W. B. PEARSON. Can. J. Chem. **55**, 1120 (1977).
2. C. HERMANN. Z. Kristallogr. **113**, 142 (1960).
3. J. D. H. DONNAY, E. HELLNER, and A. NIGGLI. Z. Kristallogr. **120**, 364 (1964).
4. J. D. H. DONNAY, E. HELLNER, and A. NIGGLI. Z. Kristallogr. **123**, 255 (1966).
5. E. HELLNER. Struct. Bonding, **37**, 61 (1979).
6. J. K. BRANDON, R. Y. BRIZARD, P. C. CHIEH, R. K. MCMILLAN, and W. B. PEARSON. Acta Crystallogr. B**30**, 1412 (1974).
7. Structure Reports, **13**, 111 (1950).
8. W. FISCHER. Z. Kristallogr. **138**, 129 (1973).
9. W. FISCHER and E. KOCH. Acta Crystallogr. A**32**, 225 (1976).
10. W. B. PEARSON, J. K. BRANDON, and R. Y. BRIZARD. Z. Kristallogr. **143**, 387 (1976).
11. J. K. BRANDON, P. C. CHIEH, W. B. PEARSON, and P. W. RILEY. Acta Crystallogr. A**31**, 236 (1975).
12. E. HELLNER, R. GERLICH, E. KOCH, and W. FISCHER. Physik Daten — Physics Data, **16**-1 (1979).
13. E. HELLNER. Acta Crystallogr. **19**, 703 (1965).

Can. J. Chem. Downloaded from www.nrcresearchpress.com by 210.87.254.40 on 09/05/12
For personal use only.

Synthesis of a protein modifying agent. A water-soluble stable free radical[1,2]

SANGRAM SISODIA, R. DEAN MARTZ, N. BOSWORTH, GARY LAMMERT, AND J. D. REINHEIMER[3]

Severance Chemistry Laboratories, The College of Wooster, Wooster, OH 44691, U.S.A.

Received August 31, 1979

SANGRAM SISODIA, R. DEAN MARTZ, N. BOSWORTH, GARY LAMMERT, and J. D. REINHEIMER. Can. J. Chem. **58**, 714 (1980).

Two synthetic routes to prepare a water-soluble stable free radical were investigated. The first product, sodium-2,4-dinitro-5-(4′-amino-2′,2′,6′,6′-tetramethylpiperidine-1-oxyl)benzene sulfonate, was water soluble but the sulfonate group was not readily replaceable with nucleophiles. The second synthetic route yielded *N*(4′-(2′,2′,6′,6′-tetramethylpiperidine-1-oxyl))-3,5-dinitro-4-sodium sulfonate benzamide, which was water soluble and its sulfonate group was readily replaced by nucleophiles.

SANGRAM SISODIA, R. DEAN MARTZ, N. BOSWORTH, GARY LAMMERT et J. D. REINHEIMER. Can. J. Chem. **58**, 714 (1980).

On a exploré deux méthodes de synthèse d'un radical libre stable soluble dans l'eau. La première méthode conduit au dinitro-2,4 (amino-4′ tétraméthyl-2′,2′,6′,6′ pipéridineoxyl-1)-5 benzène sulfonate de sodium soluble dans l'eau mais dont le groupe sulfonate ne peut être remplacé facilement par les nucléophiles. La deuxième méthode permet d'obtenir le composé *N*[(tétraméthyl-2′,2′,6′,6′ pipéridineoxy-1)-4′] dinitro-3,5 sulfonate-4 de sodium benzamide qui est soluble dans l'eau et dont le groupe peut être facilement remplacé par des nucléophiles.

[Traduit par le journal]

Introduction

Protein structure has been investigated by many "reporter groups" which are part of modifying agents. Reporter groups may be radioactive isotopes, elements which are not normally found in the native protein such as ^{19}F, stable free radicals such as the nitroxyl group, as well as chromophoric groups. The stable reporter groups are observed by means of magnetic resonance spectrometers (1–4) or uv and visible spectrometers. The purpose of this research was to synthesize a stable water-soluble free radical which could form a covalent bond to a protein.

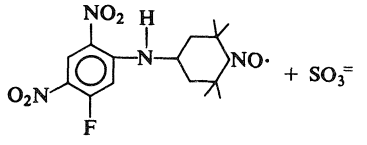
Covalent bonds between a modifying agent and a protein may be formed by an aromatic nucleophilic substitution reaction (5). If the reagent contains sulfonate as the replaceable group, the advantage of water solubility may be realized (6). Gerig *et al.* (7) prepared **1** from the commercially available stable free radical **4** and 4,6-dinitro-1,3-difluorobenzene. The relative ease of replacement of the first fluorine in 4,6-dinitro-1,3-difluorobenzene by amino groups, as well as the lessened reactivity of the second fluorine, was described by Zahn and Meienhoffer (9) and exploited by Cautrecasas and co-workers (8). The fluorine in **1** is still sufficiently reactive to be replaced by reactive amino groups in human serum albumin (7).

Replacement of the fluorine in **1** by $SO_3^=$, eq. [1], gave a water-soluble substance, **2**. This new substance was characterized by infrared and elemental analysis. The compound, **2**, was added to solution(s) of nucleophiles, but the SO_3^- group was not replaced.

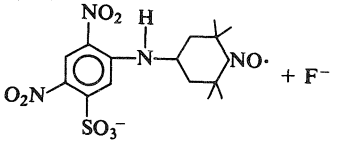
Equation [2] presents a synthesis from a different difunctional starting material. The more reactive acid chloride was readily replaced to form **5**, but the aromatic chlorine was still sufficiently reactive to be readily replaced in the subsequent step to form **6**. In contrast to **2**, the sulfonate group of **6** was replaced in aqueous solution. Compound **6** is recommended as a water-soluble reagent which contains the chromophore NO_2 and the stable nitroxyl radical as "reporter groups".

Non-radical analogs of **1**, **2**, **4**, **5**, and **6**, in which the oxygen of the radical was replaced by H, were used in preliminary experiments. These experiments were used as a guide to establish conditions for eqs. [1] and [2].

[1]



1



2

[1]Taken in part from the thesis of Sangram Sisodia, The College of Wooster, 1977.

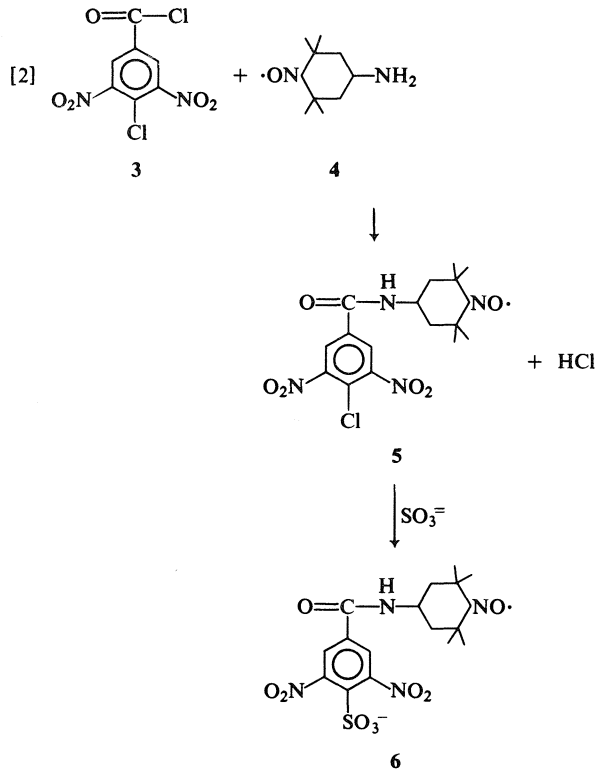
[2]Part of this work was supported by the URP program of NSF, Grant SMI 76-81996, 1977 (N. Bosworth, 1978, and G. Lammert, 1979).

[3]Author to whom correspondence should be addressed.

0008-4042/80/070714-02$01.00/0

©1980 National Research Council of Canada/Conseil national de recherches du Canada

Can. J. Chem. Downloaded from www.nrcresearchpress.com by 210.87.254.105 on 09/05/12
For personal use only.



Experimental

The ^{1}H nmr spectra were observed in DMSO-d_6 with a Varian T-60 spectrometer. The ir spectra were observed in KBr pellets with a Perkin Elmer 700 and later with a Perkin Elmer 283 spectrometer. The starting materials, 4,6-dinitro-1,3-difluorobenzene, **4**, and 4-amino-2,2,6,6,-tetramethylpiperidine were commercial chemicals from Aldrich Chemical Co. The other reagent, **3**, was prepared by literature methods (9, 10).

Compound **2**, sodium-2,4-dinitro-5-(4′-amino-2′,2′,6′,6′-tetramethylpiperidine-1-oxyl)benzene sulfonate, was prepared from **1** (7). A solution of **1**, 0.3 g in 50 mL of alcohol and 25 mL of water, was slowly added over a period of 25 min to a solution of sodium sulfite, 0.50 g in 25 mL of water. The temperature was maintained at 45°C during the addition. The alcohol was removed with a rotary evaporator and the product was salted out with NaCl. The product, **2**, was removed by filtration and recrystallized twice from HOH/NaCl; ir (KBr pellet) ν_{max}: 3300 (N—H), 1600 and 1375 (NO_2), 1350 (N—O) (11), 1210 and 1060 (sh)(SO_3^-).

Compound **5**, *N*(4′-(2′,2′,6′,6′-tetramethylpiperidine-1-oxyl))-3-5-dinitro-4-chlorobenzamide was prepared as follows. Anhydrous Na_2CO_3, 0.2 g, compound **3**, 0.20 g, and 2.5 mL chloroform were placed in a round-bottomed flask with a magnetic stirrer. Compound **4**, 0.2 g, was dissolved in 3.5 mL of chloroform and added (dropwise) to the reaction mixture over a period of 20 min. A precipitate appeared; the chloroform was removed by evaporation and the solid washed three times with 10 mL of water. The crude yield was 58–60%, mp 236–238°C (dec.) after 2 recrystallizations from alcohol/water; ir (KBr pellet) ν_{max}: 1670 (C=O), 1540 and 1450 (NO_2), 1330 (NO·).

To prepare compound **6**, *N*(4′(2′,2′,6′,6′-tetramethylpiperidine-1-oxyl))-3,5-dinitro-4-sodiumsulfonate benzamide, a solution of **5**, 0.050 g in 10 mL of ethanol and 5 mL of water, was added over a period of 25 min to 0.08 g of sodium sulfite dissolved in 5 mL of water. The temperature was maintained at 45°C. The ethanol was removed by means of a rotary evaporator, and the solution cooled in a refrigerator overnight. The product was removed by filtration and recrystallized from NaCl/HOH. The yield was 57–69% and the product did not melt below 400°C; ir (KBr pellet) ν_{max}: 1660 (C=O), 1550 and 1370 (NO_2), 1330 (NO·), 1250 and 1090 (SO_3^-). *Anal.* calcd. for $C_{16}H_{20}SO_9N_4Na$: C 41.13, H 4.28, N 11.99; found: C 40.93, H 4.50, N 11.80.

1. J. T. Gerig and J. D. Reinheimer. J. Am. Chem. Soc. **97**, 1680 (1975).
2. C. L. Hamilton and H. M. McConnell. *In* Structural chemistry and molecular biology. *Edited by* A. Rich and N. Davidson. W. H. Freeman & Co., San Francisco, CA. 1968. p. 115.
3. L. J. Berlinar. Spin labelling: theory and applications. Academic Press, New York, NY. 1976.
4. H. Dugas. Acc. Chem. Res. **10**, 47 (1977).
5. G. E. Means and R. E. Feeney. Chemical modification of proteins. Holden-Day, San Francisco, CA. 1971.
6. C. Jacobsen. Int. J. Pept. Protein Res. **7**, 159 (1975).
7. J. T. Gerig, J. D. Reinheimer, and R. H. Anderson. Biochim. Biophys. Acta, **579**, 409 (1979).
8. P. Cautrecasas, S. Fuchs, and C. B. Anfinsen. J. Biol. Chem. **244**, 406 (1969).
9. H. Zahn and J. Meienhofer. J. Makromol. Chem. **26**, 126 (1958).
10. Beilstein. Handbuch der organischen Chemie. 4th ed. Vol. IX. Springer Verlag, Berlin. p. 416.
11. E. G. Rozanstev and V. D. Scholle. Inst. Chem. Phys. Acad. Sci. USSR, 190 (1970).

Can. J. Chem. Downloaded from www.nrcresearchpress.com by 210.87.254.105 on 09/05/12
For personal use only.

Dianions of glyoxylic acid thioketals: convenient α-keto acid equivalents

GORDON S. BATES[1] AND S. RAMASWAMY

Department of Chemistry, University of British Columbia, Vancouver, B.C., Canada V6T 1Y6

Received October 15, 1979

GORDON S. BATES and S. RAMASWAMY. Can. J. Chem. **58**, 716 (1980).

By varying the solvent, reaction temperature, and bases (i.e., gegenions present), optimum conditions for the alkylation of the dianions of glyoxylic acid derivatives **8** and **9** were established. It was found that the easily prepared, thermally stable, tetrahydrofuran-soluble potassium dianion of bis(ethylthio)acetic acid was readily alkylated by alkyl halides, tosylates, epoxides, and *N*-tosyl aziridines. The latter alkylation is being used to develop a possible cytochalasin synthesis.

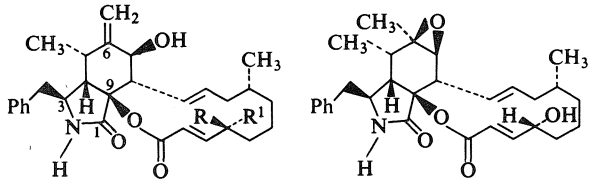
The alkylated products may be readily converted into the corresponding α-keto acids or methyl 2,2-bismethoxycarboxylates.

GORDON S. BATES et S. RAMASWAMY. Can. J. Chem. **58**, 716 (1980).

On a établi des conditions idéales d'alkylation des dianions de dérivés **8** et **9** de l'acide glyoxylique en faisant varier le solvant, la température et les bases (i.e., ions opposés). On a trouvé que le dianion de potassium de l'acide bis(éthylthio) acétique, soluble dans le tétrahydrofuranne que l'on peut préparer facilement et qui est thermiquement stable, peut être alkylé facilement par les halogénures d'alkyles, les tosylates, les époxydes et les *N*-tosyl-aziridines. On utilise la dernière alkylation pour développer une synthèse réalisable de la cytochalasine. Les produits alkylés peuvent être transformés facilement en acides α cétoniques correspondants ou en carboxylates de bisméthoxy-2,2 de méthyle.

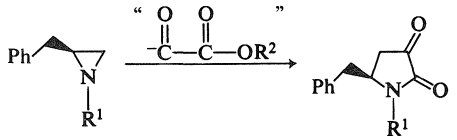
[Traduit par le journal]

In connection with a preliminary investigation directed at a synthesis of the microbial metabolites cytochalasins A, B, and F (1, 2)[2] we required a glyoxylic acid (ester) anion equivalent (3).[3] Our strategy involves alkylation of such an anion with an aziridine unit **1** which incorporates the chirality at C-3 of the cytochalasins, eventually followed by lactam formation to give compound **2**. This intermediate contains an oxygen function at what will eventually become the C-9 position of the target molecules, and thus overcomes a possible difficulty arising from attempted oxidation at this hindered position later in the synthesis (2*g*). Cleavage of the aziridine by a nucleophile will result in a developing negative charge on the nitrogen atom. To facilitate the opening of the aziridine, the group R^1 (attached to nitrogen) should thus be capable of stabilizing this negative charge, and in addition should not itself be very susceptible to nucleophilic attack. The *p*-toluenesulphonyl group appeared to fulfil the necessary criteria (4).[4] L-Phenylalanine was converted to the corresponding chiral amino alcohol (5), which was subsequently ditosylated and cyclized to the desired crystalline chiral aziridine derivative **1** (R^1 = *p*-$MeC_6H_4SO_2$—) which was used in our subsequent studies.



Cytochalasin A R = R^1 = O
Cytochalasin B R = H, R^1 = OH

Cytochalasin F



1 **2**

The glyoxylic acid (ester) anion equivalent should possess a number of characteristics: ready availability, ease of preparation, high reactivity, and thermal stability. In addition, alkylation of this synthon should proceed in high yield to give a product which is stable and easily purified and yet is readily convertible into the desired α-keto acid (ester). An investigation of the literature yielded several likely candidates for the required synthon. The monoanions of glyoxylic ester derivatives **3**–**7**

$(R^1O)_2CHCO_2R^2$	$(R^1S)_2CHCO_2R^2$
3 $R^1 = R^2 = Me$	**5** $R^1 = Et, R^2 = Me$
4 $R^1 = R^2 = Et$	**6** $R^1 = —[CH_2]_2—, R^2 = Et$
	7 $R^1 = —[CH_2]_3—, R^2 = Et$
	8 $R^1 = Et, R^2 = H$
	9 $R^1 = —[CH_2]_3—, R^2 = H$

(6) were investigated. However, when we attempted to open the aziridine **1** (R^1 = *p*-$MeC_6H_4SO_2$—)

[1]Author to whom correspondence should be addressed.

[2]For recent reviews of (*a*) the chemistry and (*b*) the biological activity of the cytochalasins see ref. 1. For synthetic approaches see ref. 2.

[3]For another approach to α-keto acid derivatives see ref. 3*b*.

[4]*N*-Tosyl aziridines have been successfully opened by Grignard reagents.

0008-4042/80/070716-07$01.00/0

©1980 National Research Council of Canada/Conseil national de recherches du Canada

Can. J. Chem. Downloaded from www.nrcresearchpress.com by 84.22.46.98 on 09/08/12
For personal use only.

Can. J. Chem. Downloaded from www.nrcresearchpress.com by 84.22.46.98 on 09/08/12
For personal use only.

with the anions of any of the above compounds, either starting material was recovered or an unidentifiable mixture was obtained. Assuming that the problem was the instability of the ester anions (loss of $^{-}OR^{2}$ produces a ketene derivative), we reasoned that the dianions of the corresponding carboxylic acids[5] should be much more stable, and in addition the dianion should be more reactive than the monoanion. Although the use of dianions of carboxylic acids containing α-thioalkyl (8), α-thioaryl (9), α-selenoaryl (10), α-alkoxy (11), and α-aryloxy (12) stabilizing groups have been reported, and although various thioketals (13) of glyoxylic acid are known, we found no reference to the dianions of the latter compounds (14).[6] We thus decided to study dianions derived from **8** and **9**. The former acid was conveniently prepared in quantitative yield either by cautious addition of dichloroacetic acid to a tetrahydrofuran (THF) suspension of 3 equiv. of sodium hydride, followed by addition of an excess of ethanethiol, or by thioketalization of glyoxylic acid monohydrate. Compound **9** was prepared by alkaline hydrolysis of the corresponding ethyl ester (6*e*, 13*c*) or by the thioketalization procedure (13*e*).

Optimum alkylation conditions were then established by varying the solvent, reaction temperature, and metallation reagents (i.e., gegenions present), etc. Initially, the soluble lithium dianions of carboxylic acids **8** and **9** were prepared by addition of 2 equiv. of *n*-BuLi to a THF solution of the free-flowing, stable, non-hygroscopic dicyclohexylammonium salts of the carboxylic acids.[7] However, it was later found that the *n*-BuLi could be added directly to a THF solution of **8** or **9** to yield a solution of the corresponding dianion with no apparent nucleophilic attack on the carboxylates. Our first alkylation experiments (see Table 1) were very encouraging. Iodomethane rapidly and quantitatively alkylated the lithium dianions of either **8** or **9** (entry 1). However, as can be seen in the table, it quickly became apparent that the dianion derived from **9** was much more reactive than that derived from **8**. This difference may be attributed to a directed anion at C-1 of the dithiane ring of the dianion (13*d*) of **9** or simply to steric reasons. Unfortunately, even the lithium dianion of **9** was only alkylated by very reactive alkylating agents and failed completely to react with the aziridine derivative **1** ($R^{1} = p\text{-}MeC_6H_4SO_2$—).

Although the use of dianions derived from **9** is recommended in cases of alkylating agents with low reactivity, we decided to optimize alkylation conditions for the more readily obtainable and less expensive **8**. Benzyl chloride was used as the alkylating agent in the optimization studies. The solvent and temperature variation studies are shown in Table 2. A good yield of alkylated product was obtained by carrying out the reaction in refluxing THF (entry 2), indicating that the lithium dianion is thermally stable. The use of cosolvents such as HMPA which can coordinate with the lithium cation, thus making the dianion more nucleophilic, resulted in moderate-to-good yields of alkylation product (entries 3–5). A report (15) that the rate of alkylation of the butyrophenone anion with bromoethane depends greatly on the cation present

TABLE 1. Alkylations of the lithium dianions of **8** and **9**[a]

$$(RS)_2CHCO_2H \xrightarrow{i,\,ii,\,iii} (RS)_2CR'CO_2H$$

i, 2 equiv. *n*-BuLi; *ii*, R′—X; *iii*, H_3O^{+}

	Yield, % (time, h)	
R′—X	R = Et	R = —$(CH_2)_3$—
1 MeI	100 (1)	100 (1)
2 $PhCH_2Cl$	0 (18)	100 (3)
3 EtI	0 (18)	100 (5)
4 $CH_3(CH_2)_3Br$	0 (18)	55 (18)
5 **1** $R^{1} = Ts$[b]	0 (18)	0 (18)

[a]All reactions 0.1 *M* in carboxylic acid in THF at 25°C; metallation carried out at 0°C; 1.1 equiv. alkylating agent used.
[b]Ts = *p*-MeC_6H_2—.

TABLE 2. Solvent and temperature variations[a]

$$(EtS)_2CHCO_2H \xrightarrow{i,\,ii,\,iii} (EtS)_2C(CH_2Ph)CO_2H$$

i, 2 equiv. *n*-BuLi; *ii*, $PhCH_2Cl$; *iii*, H_3O^{+}

Solvent[b]	Temperature (°C)	Yield (%)
1 THF	25	0
2 THF	65	70
3 THF–HMPA	25	65
4 THF–TMEDA	25	45
5 DME–HMPA	25	35

[a]All reactions 0.1 *M* in carboxylic acid for 18 h; metallation carried out at 0°C; 1.1 equiv. benzyl chloride used; 5 equiv. of chelating agents used where indicated.
[b]HMPA = hexamethylphosphoric triamide; TMEDA = *N,N,N′N′*-tetramethylethylenediamine; DME = 1,2-dimethoxyethane.

[5]For recent reviews of di- and poly-alkali metallated compounds see ref. 7.

[6]Recently, a report of the acylation of the lithium dianion of diphenoxyacetic acid has appeared (14*a*); see ref. 11*b* for alkylation of this anion, and ref. 14*b* for a recent report of the use of the dianion of **9**.

[7]Dicyclohexylamine (1.1 equiv.) was added to a solution of the acid (1.0 equiv.) in hexane. The mixture was stirred for 1 h at 25°C and the precipitate collected by filtration (yield ~90%). Such salts are a convenient precursor to carboxylic acid dianions in general. In addition, they may be recrystallized from a number of organic solvents, thus affording an excellent method of purification for carboxylic acids.

Can. J. Chem. Downloaded from www.nrcresearchpress.com by 84.22.46.98 on 09/08/12
For personal use only.

TABLE 3. Gegenion variation [a]

$$(EtS)_2CHCO_2H \xrightarrow{i,\,ii,\,iii} (EtS)_2C(CH_2Ph)CO_2H$$

i, bismetallation; *ii*, $PhCH_2Cl$; *iii*, H_3O^+

Metallation reagents[b]				
First equiv.	Second equiv.	Solvent	Time (h)	Yield (%)
1 *n*-BuLi	*n*-BuLi	THF	18	0
2 *n*-BuLi	*n*-BuLi	THF–HMPA	18	65
3 NaH	*n*-BuLi	THF	1	32
			18	80
4 NaH	*n*-BuLi	THF–HMPA	1	38
			18	75
5 KH	*n*-BuLi	THF	1	95
6 KOH[c]	*n*-BuLi	THF	1	35
7 *n*-BuLi(K)[d]	*n*-BuLi	THF	1	0
8 $KN(SiMe_3)_2$	$KN(SiMe_3)_2$	THF	1	100

[a] All reactions 0.1 *M* in carboxylic acid at 25°C; metallation carried out at 0°C; 1.1 equiv. benzyl chloride used; 5 equiv. HMPA used where indicated.
[b] The second equiv. of base was added, after 15 min, to the thick slurry of the monoanion. The mixture was stirred 30 min before the addition of benzyl chloride.
[c] Potassium salt was dried in vacuo over P_2O_5 for 24 h.
[d] 5% KH or freshly sublimed KO*t*Bu present in reaction.

(K > Na > Li) suggested the next modification. An increase in the ionic nature of the dianion of **8** should also be possible by using different gegenions. This change hopefully would result in increased reactivity without a significant decrease in the stability of the dianion reagent. Table 3 summarizes the results of varying the gegenions associated with the dianion. Since all of the monoanions of **8** (Li, Na, or K cation) are virtually insoluble in THF, it was necessary that the base used to accomplish the second deprotonation be soluble in THF. The soluble dianions were thus generated by reaction of 1 equiv. of *n*-BuLi with the appropriate monoanion. The use of a sodium–lithium pair of cations (entry 3) had the desired effect; now a good yield of alkylated product could be obtained by stirring the reaction overnight at room temperature. Even more dramatic was the use of the potassium–lithium cation pair (entry 5); a virtually quantitative alkylation occurred in 1 h. An attempt to deprotonate a sample of previously prepared potassium salt (entry 6) resulted in a poor yield of alkylated material. Apparently, the freshly precipitated monoanion is sufficiently soluble in THF to react readily with the *n*-BuLi, but if aggregation of the salt occurs the reactivity is greatly decreased (presumably due to difficulty in overcoming the lattice energy of the salt). Entry 7 suggests that metathesis, to yield a highly reactive dipotassium salt, is unlikely to be operating as a major pathway in the alkylation of the mixed cation reagent. A final improvement would be the use of a soluble potassium base which is strong enough to doubly deprotonate acid **8**. Potassium bis(trimethylsilyl)amide

TABLE 4. Alkylations of the potassium dianion of **8**[a]

$$(EtS)_2CHCO_2H \xrightarrow{i,\,ii,\,iii} (EtS)_2CRCO_2H$$

i, 2 equiv. $KN(SiMe_3)_2$; *ii*, R—X; *iii*, H_3O^+

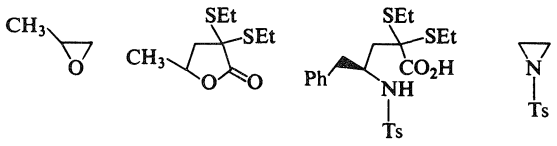
RX	Yield[b](%)	R—X	Yield[b](%)
1 MeI	100	8 *c*-$C_6H_{11}OTs$[c,d]	64
2 EtI	100	9 $Me(CH_2)_3Br$	100
3 EtBr	100	10 $CH_2{=}CHCH_2Br$	100
4 EtOTs[c]	100	11 $PhCH_2Cl$	100
5 *i*-PrI	50	12 **10**	95[e,f] as **11**
6 *i*-PrBr	50	13 **1** R^1=Ts	93[f] as **12**
7 *i*-PrOTs[c]	72	14 **13**	90[f] as **14**

[a] All reactions 0.1 *M* in carboxylic acid in THF for 2.5 h at 25°C.
[b] Purified, isolated material. All compounds had ^{1}Hmr, ir, elemental analysis, and exact parent mass spectrum measurements fully consistent with the proposed structures.
[c] Ts = *p*-$MeC_6H_4SO_2$—.
[d] *c*-C_6H_{11} = cyclohexyl.
[e] Pure by gas chromatography (OV-17; OV-101).
[f] Reaction time 18 h.

(16) was found to be ideal for this purpose.[8] Reaction of 2 equiv. of this base with **8** in THF at 0°C readily generated the *soluble* potassium dianionic species. Alkylations[9] were then carried out with a variety of substrates (Table 4). Although most reactions were complete in less than 1 h at 25°C, the mixtures were left for 2.5 h since their mixing efficiencies decreased with time owing to the precipitation of the *insoluble* potassium monoanion of the alkylated product. Of particular note are entries 4, 7, and 8 which show that tosylates (17) cleanly

[8] The pK_{BH^+} of this base has been estimated to be ~29 (ref. 16), thus establishing an upper limit for the pK_{BH^+} of the dianion of **8**.

[9] The potassium dianion of **9** also is readily alkylated in excellent yield by a wide variety of substrates.



10 11 12 13

Ts = p-$MeC_6H_4SO_2$—

alkylate the dianion in good yield, entry 12 which illustrates the site-specific opening of an epoxide, and most importantly, the almost quantitative cleavage of the aziridine ring (entries 13 and 14). This latter reaction yields the desired α-keto acid equivalent by a transformation which we were unable to achieve using existing methods. Compound **12** has been successfully transformed into pyrrolidinone **2** (R^1 = p-$MeC_6H_4SO_2$—) in high yield and investigations are currently underway to elaborate this compound into the cytochalasin nucleus.

The somewhat lower yields obtained with isopropyl derivatives (entries 5, 6, and 7) and with cyclohexyl tosylate (entry 8) are undoubtedly due to competing elimination reactions, although no attempt was made to isolate the resulting alkenes. However, the significant decrease in elimination with isopropyl tosylate (entry 7) is in agreement with the well-known greater reactivity of tosylates compared with halides in substitution reactions (18). The relatively good yield of substitution product with cyclohexyl tosylate was somewhat surprising in a ring system so extremely prone to elimination.

The reactions were rapid, high yielding, and simple to carry out. There was no need to remove the oil from the potassium hydride used to generate the bis(trimethylsilyl)amide base, since the work-up included an extraction to yield essentially pure carboxylic acid.

The 2,2-bis(ethylthio)carboxylic acids may be readily converted into the corresponding α-keto acids by *N*-bromosuccinimide hydrolysis (19) or directly into the corresponding methyl 2,2-bis-methoxycarboxylates by treatment with iodine–methanol (20). These latter compounds are useful starting materials for the synthesis of α-methyleneketals (21), α-cyclopropylideneketals (22), the monoketals of vicinal diketones (23), and the corresponding carbonyl compounds (20–22, 24). The hydrolysis and transketalisation–esterification procedures are illustrated in Scheme 1 for compound **14** which is a potential precursor for 4-amino-2-hydroxybutanoic acid, a chemical modifier of the aminoglycoside antibiotic kanamycin (25).

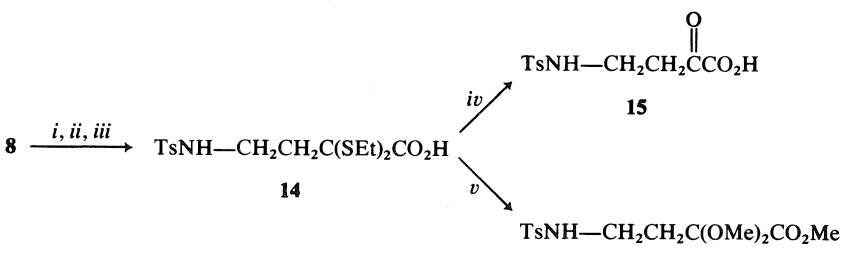
Experimental

General

All reactions were carried out under a nitrogen or argon atmosphere. Stirring was accomplished using Teflon-coated magnetic stirring bars. Tetrahydrofuran and dimethoxyethane were freshly distilled from sodium benzophenone ketyl under a nitrogen atmosphere. Hexamethylphosphoric triamide and *N,N,N′,N′*-tetramethylethylenediamine were distilled from calcium hydride and stored over Linde 4 Å molecular sieves. Sephadex LH-20 (25–100 μ) was purchased from Pharmacia Fine Chemicals. Potassium hydride was obtained as a 25% dispersion in mineral oil from Alpha Division, Ventron Corporation. All other reagents were obtained from the Aldrich Chemical Company, Inc. and were used without further purification. Ethyl, isopropyl, and cyclohexyl tosylates were prepared by reaction of an excess of the appropriate alcohol for 12 h at 0°C with *p*-toluenesulphonyl chloride in pyridine followed by a standard work-up. Full experimental details for the exploratory experiments summarized in Tables 1–3 are available from the authors upon request.

Melting points were taken on a Gallenkamp melting point apparatus and are corrected. Proton magnetic resonance spectra were obtained on Varian Associates T-60 and HA-100 spectrometers. Spectra were run in deuteriochloroform solution with tetramethylsilane as an internal reference. The multiplicity, integrated peak area, and coupling constants (Hz) (if observable) are indicated in parentheses after each signal. Infrared spectra were recorded in chloroform solution using a Perkin-Elmer 700 spectrometer, and were calibrated with the 1601 cm^{-1} band of polystyrene. High resolution mass spectra were obtained using an AEI MS-50 mass spectrometer. Specific rotations were determined using a Perkin-Elmer 241 MC polarimeter which was calibrated using a standardized sucrose solution. Elemental analyses were performed at the Microanalytical Laboratory, University of British Columbia.

The following abbreviations are used: THF = tetrahydrofuran, Bz = benzene, Et = C_2H_5, EtOAc = ethyl acetate, EtOH



i, 2 equiv. $KN(SiMe_3)_2$; *ii*, **13**; *iii*, H_3O^+; *iv*, NBS, MeCN, H_2O; *v*, I_2, MeOH

SCHEME 1

Can. J. Chem. Downloaded from www.nrcresearchpress.com by 84.22.46.98 on 09/08/12
For personal use only.

Can. J. Chem. Downloaded from www.nrcresearchpress.com by 84.22.46.98 on 09/08/12
For personal use only.

= ethanol, Et_2O = ethyl ether, py = pyridine, TsOH = *p*-toluenesulphonic acid monohydrate, TsCl = *p*-toluenesulphonyl chloride, b = broad, s = singlet, d = doublet, t = triplet, q = quartet, m = multiplet.

Bis(ethylthio)acetic Acid **8**

Procedure 1

At 0°C and with vigorous stirring, 1.29 g (10 mmol) of Cl_2CHCO_2H was added to a suspension of 1.9 g (40 mmol) of 50% NaH dispersion in 100 mL of THF. Then 1.86 g (30 mmol) of EtSH was added slowly to the suspension. The resulting thick reaction mixture was stirred overnight at 25°C. (Mechanical stirring is necessary on larger scale reactions.) Sufficient H_2O was added to the mixture to dissolve the salts, and the THF was removed under reduced pressure. The aqueous phase was extracted with 2 × 25 mL of hexanes, and was then acidified with aqueous 2 *N* HCl. The milky mixture was extracted with 4 × 50 mL EtOAc, the organic phase dried over anhydrous $MgSO_4$, and the solvent evaporated to give 1.6–1.8 g (90–100%) of **8** as a pale yellow liquid.

Procedure 2

A solution of 0.92 g (10 mmol) of glyoxylic acid monohydrate, 1.37 g (22 mmol) of EtSH, and 0.19 g (1 mmol) of TsOH in 25 mL of Bz was refluxed (pot temperature 45°C) for 3 h. The reaction mixture was diluted with 100 mL of Et_2O and washed with 2 × 20 mL H_2O and 1 × 20 mL aqueous saturated NaCl. The organic phase was dried over anhydrous $MgSO_4$, and the solvent evaporated to give 1.75 g (97%) of **8** as a pale yellow liquid.

The material from either preparation is of sufficient purity for most reactions but may be distilled (110°C, 0.02 Torr) if necessary. The reactions have been carried out on 250 mmol scales with equally good yields; ir: 3800–2300 and 1705 cm^{-1}; ^{1}Hmr δ: 1.25 (t, 6, J = 7), 2.72 (q, 4, J = 7), 4.35 (s, 1), 9.9 (s, 1). *Anal.* calcd. for $C_6H_{12}O_2S_2$ (180.29): C 39.97, H 6.71, S 35.57; found: C 39.63, H 6.91, S 35.33. *Mol. Wt.* calcd. for $C_6H_{12}O_2S_2$: 180.0279; found (high resolution ms): 180.0281.

1,3-Dithiane-2-carboxylic Acid **9**

Procedure 1

A solution of 1.92 g (10 mmol) of ethyl 1,3-dithiane-2-carboxylate (6*e*, 13*c*), prepared from ethyl diethoxyacetate (26) and 1,3-propanedithiol, in 10 mL of aqueous 1 *N* KOH and 10 mL *tert*-butyl alcohol was stirred overnight at 25°C. The alcohol was evaporated and the aqueous phase acidified with aqueous 2 *N* HCl. The mixture was extracted with 4 × 50 mL EtOAc, the organic phase dried over anhydrous $MgSO_4$, and the solvent evaporated to give 1.5 g of **9** as a pale yellow solid.

Procedure 2

A solution of 0.92 g (10 mmol) of glyoxylic acid monohydrate, 1.19 (11 mmol) of 1,3-propanedithiol, and 0.19 g (1 mmol) of TsOH in 25 mL Bz was refluxed for 1 h. The reaction was cooled to 25°C and the organic phase extracted with 3 × 10 mL aqueous saturated $NaHCO_3$. The aqueous phase was washed with 1 × 25 mL Et_2O, then cautiously acidified with aqueous 6 *N* HCl and finally extracted with 4 × 50 mL EtOAc. The organic phase was dried over anhydrous $MgSO_4$, and the solvent evaporated to give 1.4 g of **9** as a pale yellow solid, mp 115–116°C (pentane–Bz); ir: 3400–2500 and 1710 cm^{-1}; ^{1}Hmr δ: 2.1 (m, 2), 2.55 (m, 2), 3.4 (m, 2), 4.15 (s, 1), 10.3 (s, 1). *Anal.* calcd. for $C_5H_8O_2S_2$ (164.25): C 36.56, H 4.91, S 39.04; found: C 36.33, H 4.94, S 38.70. *Mol. Wt.* calcd. for $C_5H_8O_2S_2$: 163.9966; found (high resolution ms): 163.9967.

Standard Procedure for Alkylation of **8**

To a suspension of 3.2 g (20 mmol) of 25% KH in mineral oil in 100 mL of THF at 0°C was added 3.55 g (22 mmol) of $HN(SiMe_3)_2$. After 1 h at 25°C, the slightly turbid solution was cooled to 0°C, and a solution of 1.8 g (10 mmol) of **8** in 10 mL of THF was added dropwise over 10 min with stirring. Any precipitate that formed was allowed to dissolve before additional acid was added. After 15 min, 11 mmol of alkylating agent was added to the dianion solution and the reaction mixture was stirred at 25°C for 2.5 h (18 h for epoxides and *N*-tosyl aziridines). Sufficient H_2O was added to dissolve the thick precipitate which had formed and the THF was evaporated. The resulting mixture was transferred to a separatory funnel with the aid of a little H_2O, and the aqueous solution was washed with hexanes to remove the mineral oil (from the KH) and excess alkylating agent. The aqueous phase was acidified with aqueous 2 *N* HCl, and extracted several times with Et_2O. The organic extract was dried over anhydrous $MgSO_4$ and evaporated to yield the alkylated product. The trace of yellow-coloured material in the crude products could be conveniently removed by filtration of the product through a short column of LH-20 Sephadex using $CHCl_3$ as eluent. The coloured material moves rapidly off the column, followed shortly by the colourless acid. The material balance is quantitative.

N-(p-*Toluenesulphonyl)aziridine* **13**

A mixture of 6.1 g (100 mmol) of 2-aminoethanol and 38.1 g (200 mmol) TsCl in 50 mL py was allowed to react at 0°C for 18 h. The thick slurry was slowly poured into a stirred mixture of 50 g of ice, 250 mL of CH_2Cl_2, and 60 mL of aqueous concentrated HCl. The CH_2Cl_2 layer was separated and the aqueous phase was extracted with 3 × 75 mL of CH_2Cl_2. The combined organic phase was filtered through a cotton plug and the solvent was evaporated (27). Addition of 100 mL of Et_2O to the residue caused an immediate precipitation to occur. Filtration of the pale yellow solid gave 31.5 g (85%) of the desired ditosylate of sufficient purity for the next reaction. A pure sample was prepared by recrystallization from Et_2O, mp 84–85°C; ir: 3350, 1605, 1370, 1340, 1180, and 1160 cm^{-1}; ^{1}Hmr δ: 2.38 (s, 3), 2.41 (s, 3), 3.20 (q, 2, J = 6), 4.05 (t, 2, J = 6), 5.35 (t, 1, J = 6), 7.25 (m, 4), 7.72 (m, 4). *Anal.* calcd. for $C_{16}H_{19}NO_5S_2$ (369.46): C 52.02, H 5.18, N 3.79, S 17.36; found: C 51.85, H 5.21, N 3.85, S 17.19. *Mol. Wt.* calcd. for $C_{16}H_{19}NO_5S_2$: 369.0705; found (high resolution ms): 369.0732.

To a solution of 18.45 g (50 mmol) of the above ditosylate in 50 mL of THF was added 50 mL of aqueous 1 *N* KOH. The resulting solution was stirred at 25°C for 5 min and the THF was evaporated. The aqueous residue was extracted with 4 × 75 mL of CH_2Cl_2. The organic phase was filtered through a cotton plug and the solvent evaporated. Recrystallization from EtOH gave 9.5 g (97%) of **13**, mp 52–53°C; ir: 1605, 1330, 1165 and 920 cm^{-1}; ^{1}Hmr δ: 2.3 (s, 4), 2.4 (s, 3), 7.2 (d, 2, J = 8.5), 7.7 (d, 2, J = 8.5). *Anal.* calcd. for $C_9H_{11}NO_2S$ (197.26): C 54.80, H 5.62, N 7.10, S 16.25; found: C 54.66, H 5.58, N 7.07, S 16.08. *Mol. Wt.* calcd. for $C_9H_{11}NO_2S$: 197.0511; found: (high resolution ms): 197.0500.

N-(p-*Toluenesulphonyl)-2S-(benzyl)aziridine* **1**

L-Phenyl alanine ($[\alpha]_D^{25}$ −33.6° (*c* 1.54, H_2O) was converted into *S*-(−)-2-amino-3-phenylpropan-1-ol ($[\alpha]_D^{25}$ −24.6° (*c* 1.72, $CHCl_3$) according to the procedure of Seki *et al.* (5). Ditosylation of this aminoalcohol according to the procedure outlined above for 2-aminoethanol gave an 83% yield of the chiral ditosylate, mp 100–101.5°C (EtOAc–hexane); ir: 3600, 1600, 1370, 1170, 1150, 1090, 990, 940, and 800 cm^{-1}; ^{1}Hmr δ: 2.35 (s, 3), 2.40 (s, 3), 2.70 (m, 2), 3.55 (m, 1), 3.90 (m, 2), 5.25 (d, 1, J = 8), 6.8–7.8 (m, 13); $[\alpha]_D^{25}$ −47.7° (*c* 1.69, $CHCl_3$). *Anal.* calcd. for $C_{23}H_{25}NO_5S_2$ (459.59): C 60.11, H 5.48, N 3.05, S 13.95; found: C 59.97, H 5.30, N 3.00, S 13.76. *Mol. Wt.* calcd. for $C_{16}H_{18}NO_5S_2$ (M − 91): 368.0627; found (high resolution ms): 368.0631.

Can. J. Chem. Downloaded from www.nrcresearchpress.com by 84.22.46.98 on 09/08/12
For personal use only.

Treatment of this ditosylate with aqueous KOH in THF as described above yielded the chiral aziridine **1** in 92% yield, mp 91–91.5°C (EtOH); ir: 3050, 1610, 1330, 1318, 1170, 1100, 990, 950, 890, 870, 825, and 700 cm^{-1}; ^{1}Hmr δ: 2.1 (d, 1, J = 5), 2.36 (s, 3), 2.55–3.05 (m, 4), 6.9–7.3 (m, 7), 7.65 (d, 2, J = 9); $[\alpha]_D^{25}$ +16.6° (*c* 1.81, $CHCl_3$). *Anal.* calcd. for $C_{16}H_{17}NO_2S$ (287.38): C 66.87, H 5.96, N 4.87, S 11.16; found: C 66.9, H 6.0, N 4.90, S 11.20. *Mol. Wt.* calcd. for $C_{16}H_{17}NO_2S$: 287.0990; found (high resolution ms): 287.0985.

2,2-Bis(ethylthio)propanoic Acid

Infrared: 3600–2300 and 1705 cm^{-1}; ^{1}Hmr δ: 1.26 (t, 6, J = 7), 1.75 (s, 3), 2.75 (q, 4, J = 7), 9.6 (s, 1). *Anal.* calcd. for $C_7H_{14}O_2S_2$ (194.31): C 43.27, H 7.26, S 33.00; found: C 43.10, H 7.35, S 32.90. *Mol. Wt.* calcd. for $C_7H_{14}O_2S_2$: 194.0435; found (high resolution ms): 194.0439.

2,2-Bis(ethylthio)butanoic Acid

Infrared: 3600–2300 and 1700 cm^{-1}; ^{1}Hmr δ: 1.08 (t, 3, J = 7), 1.23 (t, 6, J = 7), 1.92 (q, 2, J = 7), 2.60 (q, 4, J = 7), 10.6 (s, 1). *Anal.* calcd. for $C_8H_{16}O_2S_2$ (208.34): C 46.12, H 7.74, S 30.78; found: C 45.94, H 7.78, S 30.55. *Mol. Wt.* calcd. for $C_8H_{16}O_2S_2$: 208.0592; found (high resolution ms): 208.0598.

2,2-Bis(ethylthio)-3-methylbutanoic Acid

Infrared: 3500–2400 and 1701 cm^{-1}; ^{1}Hmr δ: 1.14 (d, 6, J = 7), 1.20 (t, 6, J = 7), 2.35 (m, 1), 2.68 (q, 4, J = 7), 10.3 (s, 1). *Anal.* calcd. for $C_9H_{18}O_2S_2$ (222.36): C 48.61, H 8.16, S 28.84; found: C 48.55, H 8.32, S 28.59. *Mol. Wt.* calcd. for $C_9H_{18}O_2S_2$: 222.0749; found (high resolution ms): 222.0745.

2,2-Bis(ethylthio)-2-(cyclohexyl)acetic Acid

Infrared 3500–2300 and 1705 cm^{-1}; ^{1}Hmr δ: 1.22 (t, 6, J = 7), 1.1–2.2 (bm, 11), 2.72 (q, 4, J = 7), 9.3 (s, 1). *Anal.* calcd. for $C_{12}H_{22}O_2S_2$ (262.44): C 54.92, H 8.45, S 24.44; found: C 54.81, H 8.42, S 24.18. *Mol. Wt.* calcd. for $C_{12}H_{22}O_2S_2$: 262.1061; found (high resolution ms); 262.1066.

2,2-Bis(ethylthio)hexanoic Acid

Infrared: 3550–2400 and 1705 cm^{-1}; ^{1}Hmr δ: 0.95 (t, 3, J = 7), 1.25 (t, 6, J = 7), 1.15–1.7 (m, 4), 1.88 (m, 2), 2.65 (q, 4, J = 7), 10.6 (s, 1). *Anal.* calcd. for $C_{10}H_{20}O_2S_2$ (236.39): C 50.81, H 8.53, S 27.13; found: C 51.06, H 8.65, S 26.88. *Mol. Wt.* calcd. for $C_{10}H_{20}O_2S_2$: 236.0904; found (high resolution ms): 236.0907.

2,2-Bis(ethylthio)pent-4-enoic Acid

Infrared: 3600–2300, 1701, and 1650 cm^{-1}; ^{1}Hmr δ: 1.25 (t, 6, J = 7), 2.65 (q, 4, J = 7 and d, 2), 5.1 (m, 2), 5.8 (m, 1), 10.9 (s, 1). *Anal.* calcd. for $C_9H_{16}O_2S_2$ (220.35): C 49.06, H 7.32, S 29.10; found: C 49.10, H 7.36, S 28.80. *Mol. Wt.* calcd. for $C_9H_{16}O_2S_2$: 220.0590; found (high resolution ms): 220.0584.

2,2-Bis(ethylthio)-3-phenylpropanoic Acid

Melting point 66–67°C (hexanes); ir: 3600–2300, 1700, and 1620 cm^{-1}; ^{1}Hmr δ: 1.20 (t, 6, J = 7), 2.65 (q, 4, J = 7), 3.30 (s, 2), 7.25 (m, 5), 9.2 (s, 1). *Anal.* calcd. for $C_{13}H_{18}O_2S_2$ (270.41): C 57.74, H 6.71, S 23.71; found: C 57.38, H 6.76, S 23.60. *Mol. Wt.* calcd. for $C_{13}H_{18}O_2S_2$: 270.0748; found (high resolution ms): 270.0751.

2,2-Bis(ethylthio)-4-methyl-4-hydroxybutanoic Acid-γ-lactone ***11***

Infrared: 1775 cm^{-1}; ^{1}Hmr δ: 1.3 (m, 9), 2.2–3.0 (m, 6), 4.7 (m, 1). *Anal.* calcd. for $C_9H_{16}O_2S_2$ (220.35): C 49.06, H 7.32, S 29.10; found: C 48.79, H 7.02, S 29.30. *Mol. Wt.* calcd. for $C_9H_{16}O_2S_2$: 220.0592; found (high resolution ms) 220.0592.

2,2-Bis(ethylthio)-4S-(p-toluenesulphonamido)-5-phenylpentanoic Acid ***12***

Melting point 151–152°C (Et_2O–hexanes); ir: 3700–2400, 1705, 1610, 1175, and 1095 cm^{-1}; ^{1}Hmr δ: 0.95 (t, 3, J = 7), 1.13 (t, 3, J = 7), 1.77 (m, 2), 2.0–3.2 (m, 6), 2.35 (s, 3), 3.9 (m, 1), 5.9 (m, 1), 7.1 (m, 7), 7.8 (d, 2, J = 8.5), 9.3 (s, 1); $[\alpha]_D^{25}$ −27.9° (*c* 2.02, $CHCl_3$). *Anal.* calcd. for $C_{22}H_{29}NO_4S_3$ (467.67): C 56.50, H 6.25, N 3.00, S 20.57; found: C 56.48, H 6.24, N 3.06, S 20.38. *Mol. Wt.* calcd. for $C_{15}H_{22}NO_4S_3$ (M − 91): 376.0711; found (high resolution ms): 376.0694.

2,2-Bis(ethylthio)-4-(p-toluenesulphonamido)butanoic Acid ***14***

Infrared: 3700–2400 and 1705 cm^{-1}; ^{1}Hmr δ: 1.17 (t, 6, J = 7), 2.16 (t, 2, J = 7), 2.39 (s, 3), 2.60 (q, 4, J = 7), 3.12 (t, 2, J = 7), 7.25 (d, 2, J = 8.5), 7.75 (d, 2, J = 8.5), 9.6 (s, 1). *Anal.* calcd. for $C_{15}H_{23}NO_4S_3$ (377.55): C 47.72, H 6.14, N 3.73, S 25.48; found: C 47.59, H 6.25, N 3.62, S 25.22. *Mol. Wt.* calcd. for $C_{15}H_{23}NO_4S_3$: 377.0789; found (high resolution ms): 377.0777.

2-Oxo-4-(p-toluenesulphonamido)butanoic Acid ***15***

A solution of 1.88 g (5 mmol) of acid **14** in 10 mL of CH_3CN was added dropwise at 0°C to a stirred solution of 5.34 g (30 mmol) of *N*-bromosuccinimide in 100 mL of aqueous 10% CH_3CN. After 15 min solid Na_2SO_3 was added and the CH_3CN evaporated. The aqueous solution was adjusted to pH 4.5 by the addition of solid NaOAc and was continuously extracted overnight with Et_2O to remove the succinimide. The aqueous phase was then acidified to pH 1.0 with concentrated HCl and was continuously extracted with a fresh portion of Et_2O. The organic extract was dried over anhydrous $MgSO_4$ and evaporated. The residue was recrystallized from $CHCl_3$ to give 582 mg (43%) of the keto acid as a white solid, mp 135.5–136°C ($CHCl_3$); ir (Nujol): 3500–2500, 1770, 1725, 1600, and 1150 cm^{-1}; ^{1}Hmr (acetone-d_6) δ: 2.35 (s, 3), 3.1 (m, 4), 7.35 (d, 2, J = 8.5), 7.75 (d, 2, J = 8.5), 8.3 (s, 1). *Anal.* calcd. for $C_{11}H_{13}NO_5S$ (271.29): C 48.70, H 4.83, N 5.16, S 11.82; found: C 48.52, H 4.70, N 5.25, S 11.60. *Mol. Wt.* calcd. for $C_{11}H_{13}NO_5S$: 271.0515; found (high resolution ms): 271.0519.

Methyl 2,2-Bismethoxy-4-(p-toluenesulphonamido)butanoate ***16***

A solution of 1.88 g (5 mmol) of acid **14** and 1.33 g (5.25 mmol) of I_2 in 50 mL of CH_3OH was refluxed for 12 h. The brown solution was cooled to room temperature and a few mL aqueous dilute $Na_2S_2O_3$ was added to destroy the excess I_2. The solvent was evaporated and the residue was dissolved in EtOAc and the organic phase was washed with aqueous 2% $Na_2S_2O_3$, dried over anhydrous $MgSO_4$, and evaporated. The residue was recrystallized to yield 1.07 g (65%) of **16** as colourless needles, mp 121–122°C (Et_2O); ir: 1740, 1601, 1330 cm^{-1}; ^{1}Hmr δ: 2.10 (t, 2, J = 7), 2.42 (s, 3), 2.95 (q, 2, J = 7), 3.28 (s, 6), 3.75 (s, 3), 5.28 (bt, 1, J = 7), 7.32 (d, 2, J = 8.5), 7.78 (d, 2, J = 8.5). *Anal.* calcd. for $C_{14}H_{21}NO_6S$ (331.39): C 50.74, H 6.39, N 4.23, S 9.68; found: C 50.60, H 6.45, N 4.23, S 9.44. *Mol. Wt.* calcd. for $C_{13}H_{17}NO_5S$ (M − 32): 299.0810; found (high resolution ms): 299.0808.

Acknowledgments

This work was supported by the Natural Sciences and Engineering Research Council of Canada and in part by a Grant-in-Aid of Research from Sigma Xi, The Scientific Research Society of North America. The authors are grateful to Mr. M. A. Varelas for checking the preparation of **8** and **9**, and for the purification of several products.

1. (*a*) M. Binder and Ch. Tamm. Angew. Chem. Int. Ed. Engl. **12**, 370 (1973); (*b*) S. B. Carter. Endeavour, **113**, 77 (1972).
2. (*a*) G. Stork, Y. Nakahara, Y. Nakahara, and W. J.

GREENLEE. J. Am. Chem. Soc. **100**, 7775 (1978); (*b*) J. AUERBACH and S. M. WEINREB. J. Org. Chem. **40**, 3311 (1975); (*c*) R. BRETTLE and D. P. CUMMING. J. Chem. Soc. Perkin Trans. I, 2385 (1977); (*d*) S. MASAMUNE, Y. HAYASE, W. SCHILLING, W-K. CHAN, and G. S. BATES. J. Am. Chem. Soc. **99**, 6756 (1977); (*e*) E. VEDEJS and R. C. GADWOOD. J. Am. Chem. Soc. **100**, 376 (1978); (*f*) S. J. BAILEY, E. J. THOMAS, W. B. TURNER, and J. A. J. JARVIS. Chem. Commun. 474 (1978); (*g*) C. OWENS and R. A. RAPHAEL. J. Chem. Soc. Perkin Trans. I, 1504 (1978); (*h*) T. SCHMIDLIN and CH. TAMM. Helv. Chim. Acta, **61**, 2096 (1978); (*i*) M. Y. KIM and S. M. WEINREB. Tetrahedron Lett. 579 (1979); (*j*) D. A. CLARK and P. L. FUCHS. J. Am. Chem. Soc. **101**, 3567 (1979).

3. (*a*) G. S. BATES. Chem. Commun. 161 (1979); (*b*) K. OGURA, N. KATOH, I. YOSHIMURA, and G. TSUCHIHASHI. Tetrahedron Lett. 375 (1978).
4. W. OPPOLOZER and E. FLASKAMP. Helv. Chim. Acta, **60**, 204 (1977); A. P. KOZIKOWSKI, H. ISHIDA, and K. ISOBE. J. Org. Chem. **44**, 2788 (1979).
5. H. SEKI, K. KOGA, H. MATSUO, S. OHKI, I. MATSUO, and S. YAMADA. Chem. Pharm. Bull. Jpn. **13**, 995 (1965).
6. (*a*) G. NEEF and U. EDER. Tetrahedron Lett. 2825 (1977); F. HUET, M. PELLET, and J. M. CONIA. Synthesis, 33 (1979); (*b*) R. E. DAMON and R. H. SCHLESSINGER. Tetrahedron Lett. 4551 (1975); (*c*) R. J. CREGGE, J. L. HERRMANN, J. E. RICHMAN, R. F. ROMANET, and R. H. SCHLESSINGER. Tetrahedron Lett. 2595 (1973); J. L. HERRMANN, J. E. RICHMAN, and R. H. SCHLESSINGER. Tetrahedron Lett. 2599 (1973); L. M. LERNER. J. Org. Chem. **41**, 2228 (1976); (*d*) H. PAULSEN, W. KOEBERNICK, and H. KOEBERNICK. Tetrahedron Lett. 2297 (1976); (*e*) E. L. ELIEL and A. A. HARTMANN. J. Org. Chem. **37**, 505 (1972).
7. D. IVANOV, G. VASSILEV, and I. PANAYOTOV. Synthesis, 83 (1975); E. M. KAISER, J. D. PETTY, and P. L. A. KNUTSON. Synthesis, 509 (1977); A. P. KRAPCHO, D. S. KASHDAN, and E. G. E. JAHNGEN, JR. J. Org. Chem. **42**, 1189 (1977).
8. B. M. TROST and Y. TAMURA. Tetrahedron Lett. 3797 (1975); J. Am. Chem. Soc. **99**, 3101 (1977); B. M. TROST, M. J. CRIMMIN, and D. BUTLER. J. Org. Chem. **43**, 4549 (1978).
9. K. IWAI, M. KAWAI, H. KOSUGI, and H. UDA. Chem. Lett. 385 (1974); H. KOSUGI, H. UDA, and S. YAMAGIWA. Chem. Commun. 192 (1975); P. A. GRIECO and C-L. J. WANG. Chem. Commun. 714 (1975); K. IWAI, H. KOSUGI, H. UDA, and M. KAWAI. Bull. Chem. Soc. Jpn. **50**, 242 (1977); S. YAMAGIWA, N. HOSHI, H. KOSUGI, and H. UDA. J. Chem. Soc. Perkin Trans. I, 214 (1978).
10. N. PETRAGNANI and H. M. C. FERRAZ. Synthesis, 476 (1978).
11. (*a*) G. CARON and J. LESSARD. Can. J. Chem. **51**, 981 (1973); (*b*) W. ADAM, L. A. ENCARNACION, and H-H. FICK. Synthesis, 828 (1978); (*c*) W. ADAM and L. A. ENCARNACION. Synthesis, 388 (1979).
12. R. BONJOUKLIAN and B. GANEM. Tetrahedron Lett. 2835 (1977); W. ADAM and H-H. FICK. J. Org. Chem. **43**, 772 (1978); **43**, 4574 (1978); S. HARA, K. KISHIMURA, and A. SUZUKI. Tetrahedron Lett. 2891 (1978).
13. (*a*) G. M. OKSENGENDLER and Y. E. GERASIMENKO. Zh. Obshch. Khim. **29**, 919 (1959) (Chem. Abstr. **54**, 1389b (1960)); (*b*) W. TAGAKI, K. UEYAMA, I. MINAMIDA, Y. H. KIM, Y. IKEDA, and S. OAE. Bull. Chem. Soc. Jpn. **39**, 917 (1966); (*c*) I. MINAMIDA, Y. IKEOK, K. UNEYAMA, W. TAGAKI, and S. OAE. Tetrahedron, **24**, 2593 (1968); (*d*) E. L. ELIEL, A. A. HARTMANN, and A. G. ABATJOGLOU. J. Am. Chem. Soc. **96**, 1807 (1974); (*e*) E. COSSEMENT, R. BINAMÉ, and L. GHOSEZ. Tetrahedron Lett. 997 (1974); (*f*) D. SEEBACH and E. J. COREY. J. Org. Chem. **40**, 231 (1975); (*g*) M. SCHMIDT and E. WEISSFLOG. Z. Naturforsch. Teil B, **31**, 136 (1976) (Chem. Abstr. **84**, 121792c (1976)).
14. (*a*) W. ADAM and H-H. FICK. J. Org. Chem. **44**, 356 (1979); (*b*) K. C. NICOLAOU, S. P. SEITZ, W. J. SIPIO, and J. F. BLOUNT. J. Am. Chem. Soc. **101**, 3884 (1979).
15. H. D. ZOOK and W. L. GUMBY. J. Am. Chem. Soc. **82**, 1386 (1960).
16. C. A. BROWN. Synthesis, 427 (1974).
17. D. SEEBACH and E-M. WILKA. Synthesis, 476 (1976).
18. P. VEERAVAGU, R. T. ARNOLD, and E. W. EIGENMANN. J. Am. Chem. Soc. **86**, 3072 (1964); R. C. BINGHAM and P. v. R. SCHLEYER. J. Am. Chem. Soc. **93**, 3189 (1971).
19. E. J. COREY and B. W. ERICKSON. J. Org. Chem. **36**, 3553 (1971).
20. B. M. TROST and T. N. SALZMANN. J. Org. Chem. **40**, 148 (1975).
21. F. HUET, M. PELLET, and J. M. CONIA. Tetrahedron. Lett. 3505 (1977).
22. F. HUET, A. LECHEVALLIER, and J. M. CONIA. Tetrahedron Lett. 2521 (1977).
23. F. HUET, M. PELLET, and J. M. CONIA. Tetrahedron Lett. 3579 (1976).
24. F. HUET, A. LECHEVALLIER, M. PELLET, and J. M. CONIA. Synthesis, 63 (1978).
25. H. KAWAGUCHI, T. NAITO, S. NAKAGAWA, and F. FUJISAWA. J. Antibiot. **25**, 695 (1972).
26. N. RABJOHN (*Editor*). Organic Synthesis Coll. Vol. IV. John Wiley and Sons, New York, NY. 1963. p. 427.
27. E. LEWARS. Aldrichimica Acta, **8**, 38 (1975).

Can. J. Chem. Downloaded from www.nrcresearchpress.com by 84.22.46.98 on 09/08/12
For personal use only.

The reaction between 2,2-diphenyl-1-picrylhydrazyl and bromine

PATRICIA F. CURRIE, J. WILSON QUAIL, AND JOHN A. WEIL[1]

Department of Chemistry and Chemical Engineering, University of Saskatchewan, Saskatoon, Sask., Canada S7N 0W0

Received June 18, 1979

PATRICIA F. CURRIE, J. WILSON QUAIL, and JOHN A. WEIL. Can. J. Chem. **58**, 723 (1980).

The reaction between 2,2-diphenyl-1-picrylhydrazyl and bromine in solution has been studied at several temperatures. Despite the literature, reporting simple phenyl bromination products, a substantial yield of nitration products is observed. These have been identified by use of thin-layer chromatography, mass spectrometry, nuclear magnetic resonance, and elemental analysis. Among various products, 2-(*p*-nitrophenyl)-2-phenyl-1-picrylhydrazine is a major one at room temperature and above. It is thought that this compound is formed by reaction of DPPH with NO_2, displaced from *ortho* nitro groups in the picryl rings by bromine. Yields were found to vary, depending on experimental conditions, with the temperature and the rate of bromine addition as primary controlling factors.

PATRICIA F. CURRIE, J. WILSON QUAIL et JOHN A. WEIL. Can. J. Chem. **58**, 723 (1980).

On a étudié à différentes températures, la réaction entre la diphényl-2,2 picryl-1 hydrazyle et le brome en solution. Contrairement aux résultats rapportés dans la littérature où on ne mentionne que la formation des produits résultant de la bromation du groupe phényle, on a obtenu des produits nitrés avec des rendements importants. On les a identifiés par chromatographie sur couche mince, par spectrométrie de masse, par rmn et par l'analyse élémentaire. Parmi les différents produits, la (*p*-nitrophényl)-2 phényl-2 picryl-1 hydrazine est majoritaire à la température ambiante et au dessus. On pense que ce composé se forme par la réaction de la DPPH avec le NO_2 alors que le brome déplace le groupe nitro en position *ortho* sur le cycle picryle. On trouve que les rendements varient suivant les conditions expérimentales avec la température et la vitesse d'addition du brome qui seraient des facteurs primaires contrôlant la réaction.

[Traduit par le journal]

Introduction

In the course of preparing brominated hydrazyl free radicals, e.g., 2-(*p*-bromophenyl)-2-phenyl-1-picrylhydrazyl, for certain electron spin resonance studies, it was found that the literature preparation (1) failed to give satisfactory yields of the desired product. Instead, treatment of the starting material, 2,2-diphenyl-1-picrylhydrazyl, with bromine leads to substantial yields of 2-(*p*-nitrophenyl)-2-phenyl-1-picrylhydrazine. The results of a study of the reaction are presented herein.

Adopting a previously used notation (2), the compound 2,2-diphenyl-1-picrylhydrazyl is denoted as $DH_2\cdot$. More generally, the various corresponding *p*-substituted diphenylpicrylhydrazines are represented by DG_aG_b—H, and their hydrazyl radical forms as $DG_aG_b\cdot$. Here G represents any group attached at the phenyl sites *para* to nitrogen 2.

Because of its unusual stability, $DH_2\cdot$ has long been of special interest. Numerous mono- and di-*p*-phenyl substituted compounds have been prepared (2, 3) and their epr spectra studied (4). In particular, the reaction of NO_2 with $DH_2\cdot$ in organic solvents to form $DH(NO_2)$—H and $D(NO_2)_2$—H has been studied in some detail (2). The compound DHBr—H has been reported (*5a*, *b*) prepared by the method of Goldschmidt and Renn (1). This synthesis involves the addition of a $CHCl_3$ solution of Br_2 to a $CHCl_3$ solution of $DH_2\cdot$ with resulting formation of DHBr—H. Our attempts to prepare DHBr—H by this method resulted in the formation of $DH(NO_2)$—H in substantial yields. The effect of reaction conditions has now been investigated and methods of separation of the reaction products have been developed.

Experimental

The $DH_2\cdot$ was prepared by oxidation of 2,2-diphenyl-1-picrylhydrazine (DH_2—H) (Eastman 7365) with PbO_2 in benzene. Shiny black crystals ($DH_2\cdot$):C_6H_6, mp 129–134°C, were obtained (6). (For brevity, the solvated molecule will simply be referred to as $DH_2\cdot$.) Reagent grade Br_2 was used to prepare 3% by weight solutions in the solvent ($CHCl_3$ or C_6H_6). Hydrazyls $DHNO_2\cdot$ and $D(NO_2)_2\cdot$ were prepared according to the procedure in ref. 2.

A weighed quantity of $DH_2\cdot$, typically 1–3 g, was dissolved in the solvent of choice and maintained at the desired temperature. An amount of 3% Br_2 in the same solvent was added with stirring (molar ratio 2 $DH_2\cdot/Br_2$). Temperature ranges were ice temperature, IT = 0–2°C, room temperature, RT = 20–25°C, or elevated temperature, ET = 60–70°C. Two experiments were performed at each temperature range, varying the rate of Br_2 addition. Rapid addition of Br_2 was completed in ~1 min. Slow addition of Br_2 took 1.5 h. During rapid Br_2 addition the solution turned from its intense purple $DH_2\cdot$ color to orange–brown. Slow Br_2 addition resulted in intense purple–brown color; here the intense coloration and observable epr spectra indicated the presence of hydrazyl compounds. To simplify subsequent analysis, the product solutions were reduced to transform all hydrazyls to their corresponding hydrazines by shaking with sufficient sodium dithionite and ~5–10 mL of 3% hydrogen peroxide to cause the solution color to become orange–brown.

At IT, $CHCl_3$ was used as the solvent. At RT and ET, the usual solvent was C_6H_6; substitution of $CHCl_3$ at RT made no

[1]Author to whom correspondence should be addressed.

0008-4042/80/070723-04$01.00/0

©1980 National Research Council of Canada/Conseil national de recherches du Canada

Can. J. Chem. Downloaded from www.nrcresearchpress.com by 210.87.254.6 on 09/05/12
For personal use only.

Can. J. Chem. Downloaded from www.nrcresearchpress.com by 210.87.254.6 on 05/05/12
For personal use only.

difference to subsequent product analysis results. During reaction, no significant temperature change from ambient was observed.

In two experiments, the parent hydrazine DH_2—H was treated slowly in $CHCl_3$ (IT) and C_6H_6 (ET) with a 3% Br_2 solution. In both instances the color remained orange–red so that the reduction procedure was unnecessary. One slow addition experiment was performed with $DH(NO_2)\cdot$ at ET, and with $D(NO_2)_2\cdot$ at IT, RT, and ET.

Adsorption chromatography was utilized to separate reaction products. Columns of alumina (Alcoa F-20 or Brinkmann Aluminum Oxide 90 basic) proved to be satisfactory. These columns were eluted successively with benzene, chloroform, and ethanol, the general order of elution being (*a*) any (non-reduced) hydrazyls, (*b*) unreacted DH_2—H, (*c*) brominated products, and (*d*) nitrated products. The purity of the fractions was checked by thin-layer chromatography (tlc); where necessary these were rechromatographed to obtain uncontaminated products. Following evaporation of the eluant, recrystallization of the residue was carried out using a variety of solvents, including benzene – petroleum ether, chloroform – petroleum ether, anhydrous ether, acetic acid, and ethanol. Recrystallization tended to be difficult; the hydrazines show a strong tendency to precipitate in a "tarry" form containing solvent of crystallization, and heating isolated products *in vacuo* to remove solvent tended to result in decomposition of the hydrazine.

Thin-layer chromatography was employed not only as a rapid method for indicating the purity of isolated chromatographic fractions, but also as a rough guide to the nature of the fraction, since phenyl-nitrated and phenyl-brominated products have significantly different R_f values. Commercial plates (Brinkmann 5538 silica gel 60, 0.2 mm precoated tlc sheets) were used without further activation, with toluene as the developer. The compounds were observed as colored spots. The R_f values of unknowns were compared with those of authentic samples: $D(NO_2)_2$—H, 0.043; $DH(NO_2)$—H, 0.232; DH_2—H, 0.453; DHBr—H, 0.494; DBr_2—H, 0.523.

Combustion C,H,N analyses of the product hydrazines $DH(NO_2)$—H, DHBr—H, and DBr_2—H, as well as their respective versions in which an NO_2 group in the picryl ring has been replaced by Br, gave reasonable results. The respective melting temperatures (°C) of the compounds in this set were 110–115 (1:1 complex with acetic acid), 182–184, 158–162, 93–97, 148–154, 174–177°C. A summary of product yields is given in Table 1.

Mass spectra were recorded on an AEI MS-12 mass spectrometer at 70 eV with an ion source temperature of 150–220°C. Single bromine substitution in a molecule was readily identified by its characteristic isotope cluster. It was also observed that multiple (mainly dibromo) substitution occurred, but in minor amounts. The mass spectra of DH_2—H, $DH_2\cdot$, and $DH(NO_2)$—H have been reported by Filby and Kalus (7). Fragmentation of the parent molecular ion occurs via fission of the N—N bond and in some species is accompanied by hydrogen addition. The picrylamine portion of the molecule is observed as a prominent ion at *m/e* 228 in all three compounds. An intense peak at *m/e* 168 in DH_2—H and $DH_2\cdot$ indicates formation of a diphenylnitrene cation (or isomer thereof). In $DH(NO_2)$—H, the peak at *m/e* 214 is ascribed to the phenyl-*p*-nitrophenylamine cation radical. Presence of bromine in the diphenylnitrene portion of the molecule is expected to give a fragment of *m/e* 247 (and 249), whereas bromine substituted for NO_2 in the picrylamine portion would produce a fragment of *m/e* 261 (and 263). Both of these peaks have been observed in the spectra of purified products. Comparison spectra of DHBr—H, 2-bromo-4,6-dinitroaniline, and 4-bromo-2,6-dinitroaniline (8) do display prominent peaks at *m/e* 247 (249) and at 261 (263) for the latter two, respectively.

TABLE 1. Product yields after slow addition of Br_2 to $DH_2\cdot$ in solution

Compound	Percentage of total weight recovered[a]		
	IT[b]	RT[b]	ET[b]
$DH(NO)_2$—H	9–14	15–22	37–49
DHBr—H + DBr_2—H	76–81	53–62	0–20
"Picryl brominated"[c]	~5	~20	40–49
DH_2—H	~5	~3	0–2

[a]Calculated on the basis of the total weight of purified products recovered.
[b]IT = 0–2°C; RT = 20–25°C; ET = 60–70°C.
[c]Species in which Br has replaced NO_2.

Some of the products were examined qualitatively by epr, using a Bruker B-ER418S spectrometer. The spectral patterns of $DH_2\cdot$, DHBr·, and $DBr_2\cdot$ are very similar, while $DH(NO_2)\cdot$ and $D(NO_2)_2\cdot$ exhibit sufficiently different characteristic spectra (2) to be useful for product identification.

Proton magnetic resonance spectra were recorded on a Bruker WP-60 spectrometer. Samples of DH_2—H, $DH(NO_2)$—H, and DHBr—H from the reaction mixture were studied at 60 MHz in dichloromethane-d_2 over the range −100°C to +50°C. At +50°C the picryl protons were observed as a single line. Below room temperature the spectra of the picryl protons resolved in all cases into AB quartets, consistent with the results of Heidberg *et al.* (9) for DH_2—H.

The location of the substituted Br (for one NO_2 in the $DH_2\cdot$ picryl ring) was determined by proton nmr studies of the two relatively abundant picryl-brominated reaction products **1** and **2**, derivatives of $DH(NO_2)$—H and DHBr—H respectively, as follows.

The dinitrophenyl ring protons of compound **1** in dichloromethane-d_2 at 27.3°C gave an AB quartet (δ_1 = 8.60, δ_2 = 8.67, J = 2.5 Hz; chemical shifts measured relative to the proton in $CHDCl_2$, taken as δ = 5.25). The quartet did not change appreciably as the temperature was raised to +50°C, and a similar result was obtained in chloroform up to 70°C. This indicates that no dynamic averaging of proton parameters, such as is observed (9) for the picryl protons in DH_2—H, occurs. For the protons in a 4-bromo-2,6-dinitrophenyl group attached to nitrogen, one would expect such nmr coalescence to occur at a lower temperature than is observed for the corresponding picryl group, as indeed was observed with the *N*-methylaniline compounds.[2] Thus, the non-equivalence of the protons indicates that the Br atom has substituted for the 2-NO_2 group to yield 2-(*p*-nitrophenyl)-2-phenyl-1-(2-bromo-4,6-dinitrophenyl)hydrazine. In dichloromethane-d_2 at −63.5°C, two AB quartets with unequal intensities (ratio 1:0.51) were observed (δ_1 = 8.34, δ_2 = 8.54, J = 2.3 Hz, and δ_1' = 8.59, δ_2' = 9.04, J = 2.5 Hz).

Compound **2** in benzene-d_6 at +28°C gave an AB quartet (δ_1 = 7.78, δ_2 = 7.89 relative to C_6HD_5, J = 2.7 Hz). This quartet only sharpened somewhat as the temperature was raised to 50°C. Here too, the non-equivalence of the protons indicates that the Br has substituted for the 2-NO_2 group, to yield 2-(*p*-bromophenyl)-2-phenyl-1-(2-bromo-4,6-dinitrophenyl)hydrazine. In dichloromethane-d_2 at +28°C, **2** gave a single line at δ = 8.56, apparently due to accidental equivalence of the 3,5 protons. As the temperature of the nmr probe was reduced, the single line changed and evolved at −73°C into two AB quartets with rela-

[2]J. W. Quail, P. F. Currie, and J. A. Weil. Unpublished work, 1979.

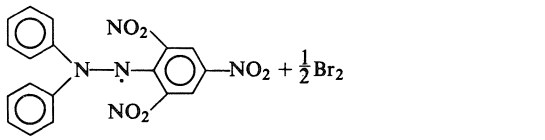
Can. J. Chem. Downloaded from www.nrcresearchpress.com by 210.87.254.6 on 09/05/12
For personal use only.

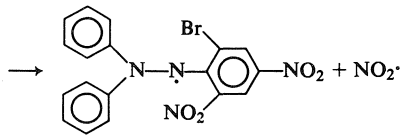
tive intensities 1:0.30 ($\delta_1 = 8.29$, $\delta_2 = 8.53$, $J = 2.5$ Hz, and $\delta_1' = 8.57$, $\delta_2' = 9.10$, $J = 2.4$ Hz).

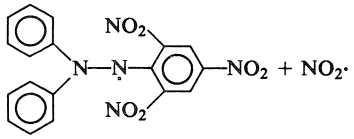
The temperature dependence of the nmr spectra of **1** and **2** in dichloromethane-d_2 is similar to that observed by Heidberg and Scheve (10) for *N*-acetyl-*N*-methyl (d_3)-2-chloro-4,6-dinitroaniline in toluene-d_8. The complexity of the nmr spectra of **1** and **2** at low temperature is attributed to the existence of *cis* and *trans* isomers of both **1** and **2**, resulting from partial double bonding between atoms N-1 of the hydrazine and C-1 of the attached phenyl group, induced primarily by the presence of the two nitro groups on the phenyl ring. Similar effects have been observed[2] in low-temperature nmr spectra of 2,2-di(*p*-bromophenyl)-1-(2-bromo-4,6-dinitrophenyl)hydrazine.

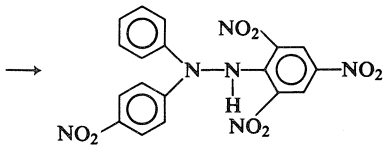
Results and Discussion

In all of the experiments involving both slow and rapid addition of bromine to $DH_2\cdot$, $DH(NO_2)$—H has been identified as a product. The proportion of $DH(NO_2)$—H isolated at various temperatures (Table 1) followed the order IT rapid < IT slow < RT rapid < RT slow < ET rapid < ET slow. The reaction scheme proposed to account for the formation of this product involves the replacement by bromine of one (or more) nitro groups of the picryl ring, freeing nitrogen dioxide, which can then attack $DH_2\cdot$:

[1] 



[2] 



Temporary formation of NO_2Br in reaction [1] is not excluded.

It is noteworthy that no 2,2-diphenyl-1-(2-bromo-4,6-dinitrophenyl)hydrazyl (or the corresponding hydrazine) was isolated as a reaction product. Apparently this hydrazyl reacts efficiently with bromine and/or nitrogen dioxide to form products substituted in the *p*-phenyl position. Traces of product $D(NO_2)_2$—H also were detected by tlc and mass spectrometry.

Indirect evidence for the presence of free nitrogen dioxide during the reaction was obtained as follows. Nitrogen gas was bubbled through the reaction mixture during the addition of bromine. The exiting gas was passed through the Griess–Ilovsay solution of sulfanilic acid and α-napthylamine (11). Red color development in the test solution indicated the presence of nitrogen dioxide. Intense color development occurred at elevated temperatures, and decreased with decreasing temperature. Blank runs excluding either $DH_2\cdot$ or bromine failed to give a positive color test.

The detailed mechanism of the nitration reaction is presently unknown. Attack of the picryl ring by a bromine atom seems indicated. Exposure of the reaction mixture to ultraviolet light (Hanovia Model 30620 quartz lamp with a Vycor filter) during addition of Br_2 at IT and ET significantly enhanced the yields of $DH(NO_2)$—H. A blank run at IT exposing only $DH_2\cdot$ in solution indicated formation of some nitrated product, but with a low yield.

Presumably, in our system, asymmetry caused by the steric effects of the diphenylamine group on the picryl ring causes one nitro group *ortho* to the amine linkage, by definition the 2-nitro group, to be further out of the ring plane than the 4- and 6-nitro groups, causing it to be the most reactive to free radical attack; such asymmetry has been reported for $DH_2\cdot$ in the solid state (12). We note that the Br atom is substantially less bulky than the NO_2 group. A free radical mechanism has been postulated to occur in the analogous reaction of $DH_2\cdot$ with 2,4,6-tri-*tert*-butylbenzenethiol (13*a*, *b*). However, the authors indicate that one of the reaction products is formed by displacement of a nitro group from the *para*- rather than the *ortho*-position of the picryl ring by a 2,4,6-tri-*tert*-butylphenylthiyl radical.

Phenyl bromination only at *para*-positions was found (by nmr) to occur when the parent compound DH_2—H was reacted with bromine at IT and ET. The products recovered were DHBr—H, unreacted DH_2—H, and a minor amount of DBr_2—H. There was no evidence of formation of nitrated product. To our knowledge there has been no previous report of direct bromination of the hydrazine DH_2—H. It has been noted (2) that $D(NO_2)_2$—H can also be obtained with DH_2—H as the starting material, using NO_2.

At ET, when $DH(NO_2)\cdot$ was reacted slowly with Br_2, mass spectral data indicated the formation of $D(NO_2)_2$—H, as well as derivative **1** (with bromine substitution in the picryl ring of $DH(NO_2)$—H).

However, the bulk of the material recovered was unreacted $DH(NO_2)$—H.

The hydrazyl $D(NO_2)_2\cdot$ was less reactive with Br_2 in solution than either $DH_2\cdot$ or $DH(NO_2)\cdot$. Mass spectra indicated no substitution of bromine occurred in the molecule. No rigorous identification of products was made; one of the products appeared to have lost one NO_2 from the picryl ring but most of the recovered material was the parent hydrazine $D(NO_2)_2$—H.

Acknowledgements

We acknowledge with thanks the financial support of the Natural Sciences and Engineering Research Council of Canada. The assistance of D. Bain and B. Teed in obtaining mass spectral and elemental analyses was greatly appreciated. We particularly wish to thank several student assistants (D. Hager, M. Hunter, J. Mehollin, and J. Vodvarka) at Argonne National Laboratory who participated in early stages of this project. We are grateful to P.J. Smith and J. M. Pepper for helpful discussions.

1. S. GOLDSCHMIDT and K. RENN. Ber. **55**, 628 (1922).
2. J. A. WEIL, K. V. SANE, and J. M. KINKADE, JR. J. Phys. Chem. **65**, 710 (1961).
3. M. M. CHEN, A. F. D'ADAMO, JR., and R. I. WALTER. J. Org. Chem. **26**, 2721 (1961).
4. M. M. CHEN, K. V. SANE, R. I. WALTER, and J. A. WEIL. J. Phys. Chem. **65**, 713 (1961).
5. (*a*) R. O. MATEVOSYAN, I. YA. POSTOVSKII, and A. K. CHIRKOV. J. Gen. Chem. USSR, **29**, 843 (1959); (*b*) B. M. KOZYREV, YU. V. YABLOKOV, R. P. MATEVOSYAN, M. A. IKRINA, A. V. ILYASOV, YU. M. RYZHMANOV, L. I. STASHKOV, and L. E. SHATRUKOV. Opt. Spectrosc. USSR, **15**, 340 (1963).
6. A. R. FORRESTER, J. M. HAY, and R. H. THOMSON. Organic chemistry of stable free radicals. Academic Press, New York, NY. 1968.
7. W. G. FILBY and W. H. KALUS. Z. Naturforsch. Teil B, **31**, 1372 (1976).
8. R. O. MATEVOSYAN and M. A. IKRINA. J. Gen. Chem. USSR, **33**, 491 (1963).
9. J. HEIDBERG, J. A. WEIL, G. A. JANUSONIS, and J. K. ANDERSON. J. Chem. Phys. **41**, 1033 (1964).
10. J. HEIDBERG and H. SCHEVE. Z. Phys. Chem. **92**, 295 (1974).
11. J. C. GAGE, N. STRAFFORD, and R. TRUHAUT. Methods for the determination of toxic substances in air. Butterworths, London. 1963.
12. C. TH. KIERS, J. L. DEBOER, R. OLTHOF, and A. L. SPEK. Acta Crystallogr. Sect. B, **32**, 2297 (1976).
13. (*a*) J. FLOOD, K. E. RUSSELL, and J. A. STONE. J. Chem. Soc. Chem. Commun. 482 (1972); (*b*) J. FLOOD and K. E. RUSSELL. Can. J. Chem. **53**, 1123 (1975).

Can. J. Chem. Downloaded from www.nrcresearchpress.com by 210.87.254.6 on 09/05/12
For personal use only.

Magnetic and spectroscopic studies on nickel(II) and copper(II) complexes of some neutral tridentate ONS ligands

M. Akbar Ali

Department of Chemistry, University of Chittagong, Chittagong, Bangladesh

Received August 21, 1979

Can. J. Chem. Downloaded from www.nrcresearchpress.com by 210.87.254.105 on 09/05/12
For personal use only.

M. Akbar Ali. Can. J. Chem. **58**, 727 (1980).

New Schiff base ligands formed from 2-methoxybenzaldehyde and 2,4-dimethoxybenzaldehyde with *N*-methyl-*S*-alkyldithiocarbazates and their nickel(II) and copper(II) complexes have been prepared and characterised by elemental analysis and magnetic and spectroscopic measurements. The Schiff bases behave as neutral tridentate chelating agents forming stable nickel(II) complexes of stoichiometry $NiLX_2 \cdot xC_2H_5OH$ (L = 2-methoxy- or 2,4-dimethoxybenzaldehyde Schiff bases of *N*-methyl-*S*-methyldithiocarbazate; X = I^-, SCN^-; x = 0, 1). Conductivity, magnetic, and spectral data support an octahedral structure for the nickel(II) complexes. The $CuLCl_2$ complexes were also isolated. Magnetic and spectral evidence are in accord with a chloro-bridged dimeric structure. The chloro-complex of copper(II) with the 2-methoxybenzaldehyde Schiff base displays a room-temperature magnetic moment of 1.81 BM, which remains virtually constant over the temperature range 343–123 K.

Hydrated copper(II) chloride promotes complete hydrolysis of the 2,4-dimethoxybenzaldehyde and 2-methoxybenzaldehyde Schiff bases of *N*-methyl-*S*-benzyldithiocarbazate with the concomitant formation of copper(II) complexes of the parent *N*-methyl-*S*-benzyldithiocarbazate of general formula, $Cu(N—SR)Cl_2$ (R = $C_6H_5CH_2$—).

M. Akbar Ali. Can. J. Chem. **58**, 727 (1980).

On a préparé des nouveaux ligands de bases de Schiff à partir de la réaction du méthoxy-2 et du diméthoxy-2,4 benzaldéhyde avec le *N*-méthyl-*S*-alkyldithiocarbazate et leurs complexes de Ni(II) et de Cu(II) et on les a caractérisés par l'analyse élémentaire et par des mesures magnétiques et spectroscopiques. Les bases de Schiff se comportent comme des agents chélatants tridentates neutres en formant des complexes stables de Ni(II) de formule $NiLX_2 \cdot xC_2H_5OH$ (L = méthoxy-2 ou diméthoxy-2,4 benzaldéhyde bases de Schiff du *N*-méthyl-*S*-alkyldithiocarbazate; X = I^-, SCN^-; x = 0, 1). La conductivité, les données magnétiques et les données spectrales sont en faveur d'une structure octaédrique des complexes de nickel. On a également isolé des complexes de type $CuLCl_2$. Les preuves magnétiques et spectrales sont en accord avec une structure de dimère ayant un chlore en position de pont. Le moment magnétique du complexe chloré de Cu(II) avec la base de Schiff dérivant du méthoxy-2 benzaldéhyde à la température ambiante, est 1.81 BM et il reste virtuellement constant sur une échelle de température de 343–123 K.

Le chlorure cuivrique hydraté favorise l'hydrolyse complète des bases de Schiff du diméthoxy-2,4 ainsi que du méthoxy-2 benzaldéhyde et de la *N*-méthyl-*S*-benzyldithiocarbazate avec la formation concomittante de complexes de Cu(II) du *N*-méthyl-*S*-benzyldithiocarbazate apparenté de formule générale $Cu(N—SR)Cl_2$ (R = $C_6H_5CH_2$—).

[Traduit par le journal]

Introduction

Metal complexes of tridentate chelating agents containing the ONS donor set have received considerable attention over the past few years (1–6), since some of these ligands have been shown to yield copper(II) complexes with anomalous magnetic properties. As part of a general investigation of metal complexes of ligands containing the ONS donor sequence, some nickel(II) and copper(II) complexes of Schiff bases formed from 2-methoxybenzaldehyde and 2,4-dimethoxybenzaldehyde with *N*-methyl-*S*-alkyldithiocarbazates are presented herein.

Experimental

All the physical measurements and analytical procedures employed in the present work have been described in detail previously (7).

Preparation of the Methoxybenzaldehyde Schiff Base of N-*Methyl*-S-*methyldithiocarbazate (ONS)*

N-Methyl-*S*-methyldithiocarbazate was prepared according to the method of Akbar Ali *et al.* (8). *O*-Methoxybenzaldehyde (6.8 g) was dissolved in 95% ethanol (50 mL) and the solution so obtained was mixed with a hot solution of *N*-methyl-*S*-methyldithiocarbazate (6.8 g) in the same solvent (50 mL). The mixture was heated on a steam bath for about 30 min and left standing for about 3 h, whereupon the crystals which had formed were filtered off: mp 145°C, yield 11.0 g. *Anal.* calcd. for $C_{11}H_{14}N_2OS_2$: C 51.94, H 5.55, N 11.01; found: C 52.21, H 5.52, N 11.21.

Preparation of the 2,4-Dimethoxybenzaldehyde Schiff Base of N-*Methyl*-S-*methyldithiocarbazate (MeONS)*

To a filtered solution of *N*-methyl-*S*-methyldithiocarbazate (6.8 g) in hot absolute ethanol (100 mL) was added a solution of 2,4-dimethoxybenzaldehyde (8.75 g) in the same solvent (50 mL). The mixture was heated on a steam bath for about 1 h and allowed to stand overnight. The compound was obtained as creamy white crystals: mp 149°C (yield, 8.0 g). *Anal.* calcd. for $C_{12}H_{16}N_2O_2S_2$: C 50.68, H 5.67, N 9.85; found: C 50.56, H 5.71, N 9.67.

Preparation of the O-*Methoxybenzaldehyde Schiff Base of* N-*Methyl*-S-*benzyldithiocarbazate (ONSBz)*

N-Methyl-*S*-benzyldithiocarbazate was prepared following the method of Akbar Ali and Teoh (8). The Schiff base was prepared by a method similar to that used for the ONS Schiff base except that *N*-methyl-*S*-benzyldithiocarbazate was used instead of *N*-methyl-*S*-methyldithiocarbazate: mp 203°C (yield, 10.0 g). *Anal.* calcd. for $C_{17}H_{18}N_2OS_2$: C 61.79, H 5.49, N 8.48; found: C 61.59, H 5.46, N 8.64.

0008-4042/80/070727-06$01.00/0

©1980 National Research Council of Canada/Conseil national de recherches du Canada

Can. J. Chem. Downloaded from www.nrcresearchpress.com by 210.87.254.105 on 09/05/12
For personal use only.

Preparation of the 2,4-Dimethoxybenzaldehyde Schiff Base of N-Methyl-S-benzyldithiocarbazate (MeONSBz)

This compound was prepared following the procedure of Bose (9) by using *N*-methyl-*S*-benzyldithiocarbazate and 2,4-dimethoxybenzaldehyde. *Anal.* calcd. for $C_{18}H_{20}N_2O_2S_2$: C 59.97, H 5.57, N 7.77; found: C 60.18, H 5.62, N 7.72.

Preparation of Metal Complexes

Unless otherwise stated all the complexes were dried *in vacuo* over P_4O_{10}.

Preparation of Ni(ONS)I_2

A solution of nickel iodide was first prepared by heating nickel nitrate hexahydrate (3.0 g) and sodium iodide (3.0 g) in absolute ethanol and filtering off the precipitated sodium nitrate. To this nickel iodide solution was added a solution of the Schiff base (1.5 g) in acetone (100 mL) and the mixture was heated at reflux for ca. 1 h. It was then allowed to cool down to room temperature and the reddish-brown crystals which had formed were filtered off and washed with a little acetone followed by benzene and ether. *Anal.* calcd. for $C_{14}H_{14}N_2OS_2$: C 23.31, H 2.49, Ni 10.36; found: 24.07, H 2.45, Ni 10.10.

Preparation of Ni(ONS)$(NCS)_2$

A solution of nickel(II) thiocyanate prepared by heating nickel(II) nitrate hexahydrate (3.0 g) and sodium thiocyanate (3.0 g) in absolute ethanol was mixed with solution of the Schiff base (1.5 g) in a mixture of butanol (20 mL) and 2,2-dimethoxypropane (10 mL). The mixture was heated under reflux for about 2 h and the solvents were then evaporated slowly on a steam bath whereby deep green crystals of the complex were obtained. These were filtered off and washed successively with methanol and acetone. *Anal.* calcd. for $C_{13}H_{14}N_4OS_4Ni$: C 36.39, H 3.29, Ni 13.69; found: C 36.29, H 3.19, Ni 13.50.

Preparation of Cu(ONS)Cl_2

A solution of copper(II) chloride dihydrate (1.7 g) in absolute ethanol (50 mL) was mixed with a solution of the Schiff base (2.5 g) in acetone (100 mL) and the resultant solution was heated on a steam bath until green crystals appeared.

The crystals were filtered off and washed several times with ethanol and acetone. *Anal.* calcd. for $C_{11}H_{14}N_2OS_2CuCl_2$: C 33.98, H 3.63, Cu 16.34, Cl 18.20; found: C 33.50, H 3.22, Cu 16.70, Cl 18.60.

Preparation of Cu(MeONS)Cl_2

The compound was prepared by a similar method as described for Cu(ONS)Cl_2. *Anal.* calcd. for $C_{12}H_{16}N_2O_2S_2CuCl_2$: C 34.41, H 3.85, Cu 15.17; found: C 34.20, H 3.76, Cu 15.30.

Preparation of Ni(MeONS)$I_2 \cdot C_2H_5OH$

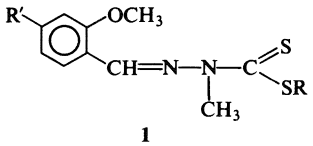
Butanol (30 mL) was added to a solution of nickel iodide (1.4 g) in absolute ethanol (50 mL) followed by the addition of ligand (1.42 g) in acetone (50 mL). The reaction mixture was heated under reflux for ca. 1 h and then allowed to evaporate on a steam bath with occasional addition of acetone. When the volume of the reaction mixture dropped to about 30 mL, some brown crystals began to settle down. At this stage 2,2-dimethoxypropane (10 mL) was added and the mixture further heated on a steambath whereupon the brown crystals formed were filtered off and washed with a few millilitres of acetone followed by benzene. *Anal.* calcd. for $C_{14}H_{22}N_2O_2S_2NiI_2$: C 26.15, H 3.45, Ni 9.13; found: C 26.17, H 2.73, Ni 9.40.

Reactions of ONSBz and MeONSBz with $CuCl_2 \cdot 2H_2O$

A solution of the appropriate Schiff Base (ca. 1.7 g) in benzene (50 mL) was mixed with a hot solution of $CuCl_2 \cdot 2H_2O$ (1.7 g) in methanol (50 mL) and the reaction mixture was heated under reflux for about 3 h whereupon the green crystals formed were filtered off and washed with benzene and methanol. *Anal.* calcd. for $C_9H_{12}N_2S_2CuCl_2$: C 31.17, H 3.50, Cu 18.32, Cl 20.10; found: C 31.44, H 3.45, Cu 18.40, Cl 20.55 (for the reaction of MeONSBz with $CuCl_2$). For the reaction of MeONSBz with $CuCl_2$, found: Cu 18.30, Cl 20.45.

Results and Discussion

The Schiff bases (**1**; R = CH_3 or $CH_2C_6H_5$; R′ = H or OCH_3) were obtained readily by condensation of appropriate aldehydes with *N*-methyl-*S*-alkyldithiocarbazates.



1

The metal complexes which were isolated in the present study are presented in Table 1 together with some of their properties. For steric considerations the present Schiff bases can act either as ONS tridentates, coordinating via the methoxyl group, the azomethine nitrogen and the thioketo sulphur atoms or as SS bidentates coordinating through the two sulphur atoms. However, previous studies by Akbar Ali *et al.* have shown that such ligands prefer ONS coordination to SS coordination (5, 6). Some important ir bands of the Schiff bases and their metal complexes are shown in Table 2. The assignments shown in the table are only tentative and based on comparisons of the ir spectra with those of similar compounds (6, 7, 10). Two strong peaks appear at ca. 1600 and 1592 cm^{-1} in the ir spectra of all the present Schiff bases. These are assigned to the C=N stretchings of the azomethine group (6). The shifts of these bands to lower frequencies by 10–15 cm^{-1} in the ir spectra of the complexes indicate that bond formation takes place through the azomethine nitrogen atom (11).

A strong band at about 1002 cm^{-1} in the ir spectra of the subject Schiff bases may be attributed to the $\nu_{(H_3C-O)}$ (12–14). This band is also shifted to lower frequencies (Table 2) in the spectra of the metal complexes suggesting that the methoxyl group is also involved in coordination to the metal ions. Further evidence in favour of methoxyl oxygen coordination comes from the presence of a medium to weak band at about 600 cm^{-1} in the spectra of the complexes. This band does not correspond to any ligand band in this region and consequently may be assigned to the metal–oxygen stretching frequency (13).

Bands at ca. 1235 and 942 cm^{-1} in the ir spectra of the Schiff bases may be assigned to the coupled modes of ν_{CS} and ν_{CN} (6, 7, 10). It has been observed in the case of metal complexes of thiocarbohydrazide (10), *S*-benzyldithiocarbazate (6) and

TABLE 1. Colour, conductivity, magnetic moments, and electronic spectral data on metal complexes of the Schiff bases

Compound	Colour	Λ^a (ohm^{-1} cm^2 mol^{-1})	μ_{eff}^c (BM)	Electronic spectral data (ν_{max} in kK)
$[Ni(ONS)(NCS)_2]$	Green	85.1	3.10	9.2, 11.2sh, 16.0
$[Ni(ONS)I_2]$	Reddish-brown	17.3[b]	3.10	7.8sh, 9.8, ca. 14.8
$[Ni(MeONS)I_2]\cdot C_2H_5OH$	Reddish-brown	6.4[b]	3.12	7.0 sh, 8.4, 12.3 sh
$[Cu(ONS)Cl_2]$	Green	23.6[b]	1.81	11.4sh, 13.6
$[Cu(MeONS)Cl_2]$	Dark green	13.2[b]	1.85	13.0br, 20.8
$[Cu(N—SBz)Cl_2]$[d]	Green	40.0	1.72	13.3, 24.7
$[Cu(N—SBz)Cl_2]$[e]	Green	48.0	1.73	13.3, 24.8

[a] Molar conductance of ca. 10^{-3}–5×10^{-4} *M* solutions in *N,N*-dimethylformamide.
[b] Molar conductance in nitromethane.
[c] $\mu_{eff} = 2.83(\chi_M^{corr} T)^{1/2}$ at 296 ± 2 K.
[d] Prepared by the reaction of $CuCl_2\cdot 2H_2O$ with ONSBz.
[e] Prepared by the reaction of $CuCl_2\cdot 2H_2O$ with MeONSBz; sh, shoulder; br, broad.

some of its derivatives (7) that these coupled ν_{CS} and ν_{CN} modes in the spectra of the ligands are raised to higher frequencies in the spectra of the complexes. This fact has been attributed to the coordination of the thioketo sulphur which causes an increase in the C—N bond order and nullifies any lowering of ν_{CS} upon coordination (6, 7, 10). In the present study, although the $\nu_{CN} + \nu_{CS}$ band does not show any appreciable raise in frequency in the spectra of the complexes compared to those in the ligands, the $\nu_{CS} + \nu_{CN}$ band is raised to higher frequencies (Table 2), indicating that the thioketo sulphur atom is involved in coordination.

The preceding ir evidence supports the fact that the subject Schiff bases are behaving as ONS tridentates and not as SS bidentates as has been found in the case of similar ligands studied by other workers (5, 6).

The Nickel(II) Complexes

Reaction of the Schiff bases with nickel(II) iodide and nickel(II) thiocyanate in a mixture of ethanol and 2,2-dimethoxypropane resulted in the formation of crystalline complexes of empirical formula, $NiLX_2\cdot nC_2H_5OH$ (where L = ONS, MeONS; X = I^- or NCS^-; n = 0 or 1). These compounds were found to be stable in a dry atmosphere, but slowly decomposed in the presence of moisture. Attempts to prepare similar iodo- and thiocyanato-complexes of nickel(II) with the Schiff bases containing the benzyl groups on one of the sulphurs were unsuccessful. In each case the unreacted ligands could be isolated almost quantitatively. Similarly all the ligands studied herein failed to yield any complex with nickel(II) chloride and nickel(II) bromide. The inability of the Schiff bases to produce any complex with nickel in the presence of hard donors such as the chloride and bromide ions seems to suggest that symbiosis phenomenon may be playing a very important role in the formation of the iodo- and thiocyanato-complexes. The nickel(II) ion has been termed as a fairly hard ion (15) and consequently, its coordination to soft donors present in the subject Schiff bases would be favoured only in the presence of soft anions such as the iodide and thiocyanate ions which most probably symbiotically motivate the nickel(II) to act as a soft acceptor.

The presence of ethanol in $Ni(MeONS)I_2\cdot C_2H_5OH$ is confirmed by the presence of a broad band at 3660 cm^{-1} in its ir spectrum. The O—H stretching frequency generally appears as a broad band at 3660 cm^{-1} in the ir spectrum of free ethanol (16) and this is observed at a lower frequency in coordinated ethanol (17). The presence of O—H stretch at 3660 cm^{-1} in the ir spectrum of the above iodo-complex is an indication that the ethanol molecule is present as ethanol of crystallization and not as a coordinated ethanol molecule. The conductivity data of all the complexes isolated in the present study are set aside in Table 1.

The nickel(II) complexes, although show some dissociation in nitromethane, have conductance values much lower than that expected for a uni-univalent electrolyte in this solvent. On the basis of these data the complexes may be formulated as $[NiLX_2]$. Support in favour of anion coordination also comes from the ir spectrum of the thiocyanato-complex. Because of its ambidentate nature, the NCS^- ion is known to coordinate in different

Can. J. Chem. Downloaded from www.nrcresearchpress.com by 210.87.254.105 on 09/05/12
For personal use only.

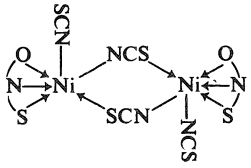
TABLE 2. Infrared absorption frequencies (cm^{-1}) of the Schiff bases and their metal complexes.

Compound	Assignments[a]				
	$\nu_{C=N}$	$\nu_{CN} + \nu_{CS}$	$\nu_{CS} + \nu_{CN}$	$\nu_{(H_3C-O)}$	$\nu_{(M-O)}$
ONS	1602s 1592m	1235s	942s	1002s	—
MeONS	1605s 1582s	1230s	920s	1002s	—
ONSBz	1602s 1590s	1250s	938m	1002s	
MeONSBz	1608s 1592s	1265s	938m	1025s	—
$[Ni(ONS)(NCS)_2]$	1592s 1565m	1235s	940s	970w	600w
$[Ni(ONS)I_2]$	1595 1570s	1230m	962s	985s	600s
$[Ni(MeONS)I_2] \cdot C_2H_5OH$	1592s 1575m	1255s	940s	972s	625s
$[Cu(ONS)Cl_2]$	1592s 1565s	1250s	948s	970s	595sh
$[Cu(MeONS)Cl_2]$	1600s 1585sh	1232s	940s	970s	602s

Compound[e]	Assignments			
	ν_{NH_2}	δ_{NH_2}	$\nu_{CN} + \nu_{CS}$	$\nu_{CS} + \nu_{CN}$
$[Cu(N—SBz)Cl_2]$[b]	3218w, 3042s 3150s	1612s	1280w	965w
$[Cu(N—SBz)Cl_2]$[c]	3218w, 3140s, 3040	1610s	1250sh	990w
$[Cu(N—SBz)Cl_2]$[d]	3210 3040sh, 3150s	1608s	1250sh	990s

[a] ν and δ denote stretching and bending modes respectively. Relative band intensities are denoted by s, m, w, sh, meaning strong, medium, weak, and shoulder respectively.
[b] Prepared from the reaction of $CuCl_2 \cdot 2H_2O$ with ONSBz.
[c] Prepared from the reaction of $CuCl_2 \cdot 2H_2O$ with MeONSBz.
[d] Band positions reported by Akbar Ali and Teoh (7).
[e] N—SBz denotes *N*-methyl-*S*-benzyldithiocarbazate.

modes (18) and ir spectroscopy has been very helpful in distinguishing between these modes (19). The C≡N stretching frequency has been observed in the range 2040–2080 cm^{-1} for *N*-bonded thiocyanate and in the range 2080–2120 cm^{-1} for *S*-bonded thiocyanate. A number of metal complexes are known where the C—N stretching frequencies are observed at 30–60 cm^{-1} higher than that in the terminal thiocyanate groups (20–27). This has been attributed to the presence of M—NCS—M bridges. Furthermore, it has been suggested that extensive splitting of the band corresponding to the antisymmetric stretch occurs in the ir spectra of complexes containing both terminal and bridging thiocyanato-groups (23, 27). The ir spectrum of $[Ni(ONS)(NCS)_2]$ exhibits two strong bands at 2090 and 2130 cm^{-1} with definite shoulders at 2100 and 2140 cm^{-1}. This is strong evidence that both terminal and bridging thiocyanato-groups are present. Since the ligand behaves as a tridentate and there are two thiocyanate ions per nickel(II) ion, a thiocyanate-bridged six-coordinate structure shown below would be in keeping with the observed ir and conductivity data.



The room-temperature magnetic moments of the nickel complexes (Table 1) are normal for a six-coordinate nickel(II) in an octahedral or pseudo-octahedral field (28). The solid reflectance elec-

Can. J. Chem. Downloaded from www.nrcresearchpress.com by 210.87.254.105 on 09/05/12
For personal use only.

Can. J. Chem. Downloaded from www.nrcresearchpress.com by 210.87.254.105 on 09/05/12
For personal use only.

tronic spectral data (Table 1) also support an octahedral structure for the present nickel(II) complexes. The spectra exhibit two bands at about 9.9 and 15.0 kK attributable to the transitions $^3A_{2g} \rightarrow {}^3T_{2g}(P)$ and $^3A_{2g} \rightarrow {}^3T_{1g}(F)$ respectively of octahedral nickel(II). The third expected band corresponding to the transition $^3A_{2g}(F) \rightarrow {}^3T_{1g}(P)$ is probably hidden beneath the charge-transfer band. The presence of donor atoms of unequal field strengths in the ligands is expected to cause some distortion from the regular O_h symmetry with the consequent broadening of the ν_1 and ν_2 bands. Although no such splittings have been observed in the present spectra, the ν_1 band has been found to be very broad with definite shoulders. This suggests that some distortion might have been present. On the basis of their stoichiometry, low solubility, electronic spectra, and magnetic moments, a dimeric or a polymeric structure involving the iodo- or thiocyanato-bridge is assigned to the present nickel(II) complexes. From a comparison of the electronic spectra of the two iodo-complexes, it appears that the ligand field strength of the *S*-methyl derivative is greater than that of the *S*-benzyl derivative.

The Copper(II) Complexes

The Schiff bases, ONS and MeONS, react with copper(II) chloride forming crystalline complexes of general formula, $CuLCl_2$, which behave as non-electrolytes in nitromethane. Reactions of these ligands with either copper(II) perchlorate or copper(II) nitrate under similar conditions did not yield any isolable products. The Schiff bases, however, reacted with copper(II) bromide yielding some orange products which were found to be diamagnetic in nature. Since these compounds could not be obtained in an analytically pure form, they are not characterized herein. However, from the diamagnetic nature of these complexes, it can be safely inferred that the subject ligands reduce copper(II) bromide to yield a copper(I) complex. As the Schiff bases behave as neutral ONS tridentates and there are two chloride ions per copper(II) ion in the coordination sphere, the $CuLCl_2$ complexes may be thought to possess either a monomeric five-coordinate structure or a dimeric or polymeric chlorine-bridged structure. The electronic spectra of these complexes (Table 1) display a broad band at ca. 13.5 kK, which do not resemble spectra of other known five-coordinate copper(II) species (29), but are close to the spectra of distorted octahedral copper(II) complexes (30). The room temperature magnetic moments of the $CuLCl_2$ complexes are about 1.81 BM which are quite normal for a $3d^9$ ion. The magnetic susceptibilities of the $Cu(ONS)Cl_2$ complex were measured over the temperature range 343–93 K. The compound obeys the Curie–Weiss law of the form shown below, where χ_M^{corr} is the molar susceptibility corrected for diamagnetism, $N\alpha = 60 \times 10^{-6}$ cgs units is the assumed value of the T.I.P., and all the other symbols have their usual meanings.

$$\chi_M^{corr} = Ng^2\beta^2/k(T - \theta) + N\alpha$$

A plot of $1/\chi_M^{corr} - N\alpha)$ vs. T gave a straight line from which the value of the Weiss constant θ was obtained. The small value of the Weiss constant ($\theta = +14$ K) indicates that the compound is a normal Curie–Weiss paramagnet and there is no appreciable magnetic interaction in the complex.

When the Schiff bases, ONSBz and MeONSBz, reacted with copper(II) chloride, instead of the expected Schiff base complexes, the complexes isolated were those of the parent *N*-methyl-*S*-alkyldithiocarbazates. The identities of these complexes were confirmed from the analytical data (Table 1) and from a comparison of their ir, magnetic, and electronic spectral data with those reported by Akbar Ali and Teoh (7). The ir spectra of these complexes do not display the $\nu_{C=N}$ band of the Schiff bases, but instead they show the ν_{NH_2} and δ_{NH_2} bands of the parent amines (Table 2). This shows that in the presence of copper(II) chloride the Schiff bases are hydrolysed with the concomitant formation of copper(II) complexes of the parent *N*-methyl-*S*-alkyldithiocarbazates. In a recent communication (9) it has been claimed that the MeONSBz ligand gives copper(II) chloride and bromide complexes. This author was unable to isolate the reported complexes by following the procedure reported in the literature (9). Each time the Schiff bases were found to be hydrolysed resulting in copper(II) complexes of the parent amines. Nickel(II) (31–34) and copper(II) (35) have been shown to catalyse the hydrolysis of the C=N bond of Schiff bases with the concomitant formation of a metal complex of parent amines. The activation of the azomethine group toward hydrolytic cleavage may be considered to be analogous to the activation of the azo group (36) in the cobalt(II) catalysed hydrolysis of the latter. The coordination of the azomethine nitrogen facilitates the electron cloud being drawn away from the C=N bond and thereby weakens it, so that it becomes more susceptible to hydrolytic cleavage. This mechanism is very similar to the interpretation provided by Kroll (37) of the catalytic hydrolysis of amino acid esters by heavy metal ions.

Acknowledgements

The author wishes to express his sincere thanks

to Professor S. E. Livingstone and Associate Professor H. A. Goodwin of the School of Chemistry, University of New South Wales, Sydney, Australia for their help in connection with some solid reflectance spectra. Thanks are also due to the School of Chemical Sciences, Universiti Sains Malaysia, Penang, Malaysia and the Department of Chemistry, University of Chittagong, Bangladesh for the provision of some facilities for this work.

1. M. Akbar Ali and S. E. Livingstone. Coord. Chem. Rev. **13**, 101 (1974).
2. M. Akbar Ali, S. E. Livingstone, and D. J. Phillips. Chem. Commun. Chem. Soc. London, 909 (1972).
3. M. Akbar Ali, S. E. Livingstone, and D. J. Phillips. Inorg. Chim. Acta, **7**, 179 (1973).
4. M. Akbar Ali, S. E. Livingstone, and D. J. Phillips. Inorg. Chim. Acta, **7**, 531 (1973).
5. M. Akbar Ali and R. Bose. J. Inorg. Nucl. Chem. **39**, 265 (1977).
6. M. Akbar Ali and S. G. Teoh. J. Inorg. Nucl. Chem. **40**, 2013 (1978).
7. M. Akbar Ali and S. G. Teoh. J. Inorg. Nucl. Chem. **40**, 451 (1978).
8. M. Akbar Ali, S. E. Livingstone, and D. J. Phillips. Inorg. Chim. Acta, **6**, 11 (1972).
9. R. N. Bose. Inorg. Nucl. Chem. Lett. **14**, 193 (1978).
10. G. R. Burns. Inorg. Chem. **7**, 277 (1968).
11. J. E. Kovacic. Spectrochim. Acta, **23A**, 183 (1967).
12. F. K. Batchew, W. Gerrard, E. F. Mooney, R. G. Rees, and H. A. Willis. Spectrochim. Acta, **20**, 51 (1964).
13. Y. Kawasaki and R. Okawara. J. Inorg. Nucl. Chem. **27**, 1168 (1965).
14. R. Okawara and M. Wada. J. Organomet. Chem. **1**, 81 (1965).
15. L. Sacconi. Trans. Met. Chem. **4**, 199 (1968).
16. G. M. Barrow. J. Chem. Phys. **20**, 1739 (1952).
17. R. C. Dickinson and G. J. Long. J. Inorg. Nucl. Chem. **36**, 1235 (1974).
18. R. A. Bailey, S. L. Kozak, T. W. Michelson, and M. N. Mills. Coord. Chem. Rev. **6**, 407 (1971).
19. K. Nakamoto. Infrared spectra of inorganic and coordination compounds. 2nd ed. Wiley-Interscience, New York. 1970.
20. W. J. Davis and J. Smith. J. Chem. Soc. A, 317 (1971).
21. G. Contreras and R. Schmidt. J. Inorg. Nucl. Chem. **32**, 127 (1970).
22. R. S. Tobias. Inorg. Chem. **9**, 2682 (1970).
23. A. R. Davis, C. J. Murphy, and R. A. Plane. Inorg. Chem. **9**, 423 (1970).
24. S. M. Nelson and A. Rodgers. Inorg. Chem. **6**, 1390 (1967).
25. L. Sacconi, I. Bertini, and F. Mani. Inorg. Chem. **6**, 262 (1967).
26. A. Sabatini and I. Bertini. Inorg. Chem. **4**, 959 (1965).
27. J. Chatt and L. A. Duncanson. Nature, **178**, 997 (1965).
28. C. J. Ballhausen. Introduction to ligand field theory. McGraw-Hill, New York. 1962.
29. M. Akbar Ali, S. E. Livingstone, and D. J. Phillips. Inorg. Chim. Acta, **6**, 39 (1972).
30. A. B. P. Lever. Inorganic electronic spectroscopy. Elsevier, Amsterdam. 1968.
31. G. L. Eichhorn and J. C. Bailar. J. Am. Chem. Soc. **75**, 2905 (1953).
32. R. K. Y. Ho and S. E. Livingstone. Aust. J. Chem. **18**, 659 (1965).
33. L. T. Taylor, F. L. Urbach, and D. H. Busch. J. Am. Chem. Soc. **91**, 1072 (1969).
34. M. Das and S. E. Livingstone. Inorg. Chim. Acta, **19**, 5 (1976).
35. C. M. Harris, S. L. Lenzer, and R. L. Martin. Aust. J. Chem. **14**, 420 (1961).
36. R. Price. J. Chem. Soc. A, 521 (1967).
37. H. Kroll. J. Am. Chem. Soc. **74**, 2036 (1952).

Can. J. Chem. Downloaded from www.nrcresearchpress.com by 210.87.254.105 on 09/05/12
For personal use only.

Ab initio MO predictions for the geometries and energies of the Σ and Π states of some conjugated free radicals

N. Colin Baird and Kathleen F. Taylor

Department of Chemistry, University of Western Ontario, London, Ont., Canada N6A 5B7

Received October 5, 1979

N. Colin Baird and Kathleen F. Taylor. Can. J. Chem. **58**, 733 (1980).

Ab initio MO calculations are reported for the lowest Σ and Π doublet states of the radicals **1**–**10**. Configuration interaction is included, using the restricted open-shell MO's as a base. The important geometric variables are optimized in calculations using the STO-3G basis set; in some cases energies and geometries are redetermined using the 4-31G basis. In most cases the energy separation between the Σ and Π doublet states is calculated to be small; the results are very dependent upon the basis set whenever the radical is localized upon a nitrogen atom. For radicals XYZ with different terminal groups, a valid prediction of the structure is obtained only if the basis set properly distinguishes between the π energies of X=Y and Y=Z bonds. Small basis sets appear to underestimate the π energy of carbonyl bonds, and thus are overbiased in favour of X=C—O· structures. Unsymmetrical structures are predicted for the Σ states of some radicals, even when the terminal groups are identical.

N. Colin Baird et Kathleen F. Taylor. Can. J. Chem. **58**, 733 (1980).

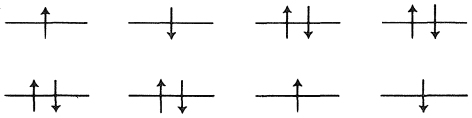
On rapporte des calculs *ab initio* des orbitales moléculaires (OM) des états doublets Σ et Π des radicaux **1** à **10**. On y inclut les interactions de configuration en utilisant comme base la couche incomplète restreinte des OM. Lors des calculs, on amplifie les variables géométriques importantes en utilisant l'ensemble STO-3G comme base; dans certains cas, on redétermine les énergies et les géométries en utilisant la base 4-31G. Dans la plupart des cas, on calcule que l'énergie de séparation entre les états doublets Σ et Π doit être faible. Si le radical est localisé sur l'atome d'azote, les résultats dépendent beaucoup de l'ensemble de base utilisé. Pour les radicaux XYZ avec des groupes terminaux différents, on n'obtient une prédiction satisfaisante de structure que si l'ensemble de base distingue clairement les énergies π des liaisons X=Y et Y=Z. Des petits ensembles de base semblent sous-évaluer l'énergie π des liaison des composés carbonylés et favorisent ainsi indûment les structures X=C—O·. On prédit des structures dissymétriques pour les états Σ de quelques radicaux, même quand les groupes terminaux sont identiques.

[Traduit par le journal]

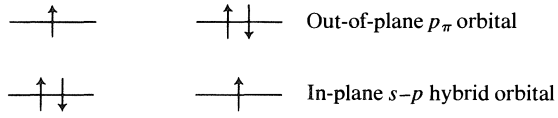
Introduction

Molecules which have very low-lying excited states are expected whenever the highest-occupied molecular orbital differs little in stability from one or more others *and* this collection of nearly-degenerate MO's is not completely filled with electrons.

In examples which involve free radicals, a singly-occupied orbital is of similar stability to one or more doubly-occupied (or empty) MO's. When only a pair of orbitals is involved, there are two states of interest, both doublets:



If the two MO's are degenerate, so are the two states (aside from a small splitting due to spin–orbit interaction). An example is the hydroxyl radical, OH, in which the orbitals of concern essentially are 2*p* atomic functions of the oxygen atom. Although the amino radical, NH_2, is isoelectronic with hydroxyl, the two comparable MO's are not degenerate if the molecule is bent, since one is a 2*p* orbital (that perpendicular to the plane) whereas the other primarily is a 2*s*, 2*p* hybrid of nitrogen. Since the hybrid orbital is substantially more stable than is the 2*p*, the energy splitting between the two doublet states in NH_2 is not small (~31 kcal mol^{-1} experimentally (1)). The states are usually designated Σ or Π, according to the type of MO which the unpaired electron occupies.



Energy splittings which are intermediate between those for OH and NH_2 should arise in radicals when the two MO's are not exactly degenerate but are more comparable in stability than are those of NH_2. In the present study, we undertook to explore free radicals which are isoelectronic with allyl and which possess one or more heteroatoms (nitrogen and/or oxygen) which bear lone pairs of electrons. For such species, the doublet states should be separated by only a small gap whenever the nonbonding MO of the π system is similar in stability to the nonbonding σ orbital which contains the lone pair.

0008-4042/80/070733-06$01.00/0

©1980 National Research Council of Canada/Conseil national de recherches du Canada

Can. J. Chem. Downloaded from www.nrcresearchpress.com by 210.87.254.40 on 09/05/12
For personal use only.

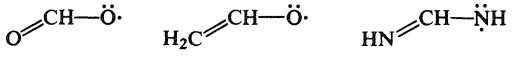
Can. J. Chem. Downloaded from www.nrcresearchpress.com by 210.87.254.40 on 09/05/12
For personal use only.

Method of Calculation

For each of the free radicals **1–10** (see Table 1) a geometry search was performed for the more important structural variables using the STO-3G basis set with standard molecular exponents (2). Configuration interaction was included between all $M_S = +\frac{1}{2}$ distributions (i.e. all single, double, and triple excitations) of the π electrons and the higher-lying σ nonbonding electrons,[1] as detailed in Table 1. At the optimum STO-3G + CI geometry, the energy was recalculated, often with a larger number of nonbonding MO's in the CI, and in many cases[2] also using the same number of configurations (typically 45) and the more extensive 4-31G basis set (3). Since all radicals were assumed to be planar, the lowest Σ and Π states are of different symmetry. The single-determinant wavefunctions were obtained using Roothaan's restricted open-shell SCF method (4). The final energies and geometries are listed in Table 1. In a few cases, the geometries were reoptimized at the 4-31G + CI level; these results are reported in the text.

Results and Discussion

In the Σ state of the free radicals considered herein, there are four π electrons — two bonding and two nonbonding — in the dominant electron configuration. Conjugated molecules XYZ which have a closed-shell of σ electrons and four π electrons usually are expected to have symmetrical structures; examples here are carbon dioxide, and the allyl anion for which our STO-3G + CI calculations predict both CC bond lengths to be 1.39 Å. In fact it is an unsymmetrical ("alternating") structure which is predicted by the calculations to be optimum for the lowest Σ state of the carbon-centered radicals (**7**, **8**, and **10**), see Table 1. The alternation of bond lengths is extreme in HCO_2·; the short bond is similar to that of 1.26 Å predicted by this method for the double bond in formaldehyde, and the longer bond is about that expected for a single CO linkage. The difference between the lengths of the two bonds is much less in the equivalent nitrogen radical **10**, although the unpaired spin density is 90% localized on the nitrogen Z whose bond is longer.[3] The free radical **9** has only one heteroatom, and thus the unpaired electron is localized at Z and a very unsymmetrical structure (compared to that for the Π state) results, see Table 1.



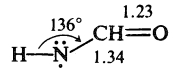
7 **9** **10**

For the formamido radical **8** the STO-3G calculations predict only a single potential minimum for the Σ state, with the unpaired σ electron and the π lone pair localized almost completely on the oxygen, i.e. a "Σ_O" structure:



8 "Σ_O" **8** "Σ_N"

In contrast, STO-3G calculations without CI included predict the existence of minima both for Σ_O, and for Σ_N structure in which the unpaired σ electron and π lone pair are localized on the nitrogen (6). To investigate further this discrepancy between the predictions, the geometry of the Σ_N form was optimized by 4-31G + CI calculations; a minimum of this type was again found, as illustrated in the results shown below.



The 4-31G + CI energy for this Σ_N minimum (−168.0318 au), however, is less stable than that predicted for the Σ_O form (even without any reoptimization of the latter), in agreement with the non-CI calculations reported previously. The difficulties in the calculations are that, to obtain a realistic prediction, the MO method which is used must be able to differentiate accurately (*a*) the relative energies of the two types of double bonds compared to the single bonds, and (*b*) the energy of addition of an electron to a singly-occupied p_π orbital of nitrogen compared to that for an s–p hybrid AO. Calculations for the NH_2 free radical (6) show that the STO-3G basis favours too strongly an s–p hybrid for the lone pair over a purely p orbital, whereas the 4-31G basis is better balanced. (Compared to the experimental advantage of ~31 kcal in favour of the Π state (1) the STO-3G splitting is

[1]For a few cases, optimized geometries for the Π state are available from our previous work, but with CI included only among different distributions of the π electrons (5); as indicated in Table 1, these have been used directly, as re-optimization with inclusion of the excitation of σ electron pairs should have little effect.

[2]Calculations with the 4-31G + CI method were not done for all the radicals, for reasons discussed in the text and because of memory limitations of our computer.

[3]The optimum bond angle about the nitrogen is a good indicator of the delocalization of unpaired spin density. A CNH angle of about 105° is obtained when the nonbonding atomic orbital on N is doubly-occupied, whereas it is 130° or more when the AO is singly-occupied. Thus the angles of 111° and 125° for **10** indicate a small amount of spin density at X and a much larger quantity at Z.

Can. J. Chem. Downloaded from www.nrcresearchpress.com by 210.87.254.40 on 09/05/12
For personal use only.

TABLE 1. Calculated geometries and energies for free radicals

	Radical XYZ	State	R_{YX}	R_{YZ}	∠XYZ	Other geometric variables[a]	Total energy (in au) by STO-3G	Total energy (in au) by 4-31G	ΔE (relative to Π) in kcal mol^{-1} by STO-3G	ΔE (relative to Π) in kcal mol^{-1} by 4-31G	No. of σ MO's included in CI for Geometry	No. of σ MO's included in CI for Final energy
1,	ONO	Π	1.36	1.36	107°		−201.3871	−203.7135	−10.0	−22.3	3	3
		Σ	1.28	1.28	126°		−201.4030	−203.7491			3	3
2,	HNNO	Π	1.36	1.38	107°	∠HNN = 103°	−181.8571	−183.9301	−7.9	−8.7	0	3
		Σ	1.32	1.38	110°	∠HNN = 103°	−181.8697	−183.9440			2	3
3,	H_2CNO	Π	1.34	1.40	110°		−166.1048		−3.8	—	2	2
		Σ	1.33	1.34	116°		−166.1108				2	2
4,	HNNNH	Π	1.39	1.39	107°	∠HNN = 102°	−162.3280	−164.1422	+16.0	−1.6	0	3
		Σ	1.32	1.32	126°	∠HNN = 107°	−162.3025	−164.1448			3	3
5,	H_2CNCH_2	Π	1.38	1.38	115°		−130.8250		+67.9	—	1	1
		Σ	1.34	1.34	154°		−130.7168				1	1
6,	H_2NNN	Σ	1.40	1.28	117°		−162.3558	−164.1937	—	—	3	3
7,	OCHO	Π	1.33	1.33	121°	RCH = 1.10	−185.6710	−187.8658	+2.8	+1.4	2	2
		Σ	1.41	1.25	121°	RCH = 1.10 ∠HCO = 126°	−185.6666	−187.8635			2	2
8,	HNCHO	Π	1.37	1.35	122°	∠HNC = 105° ∠NCH = 118°	−166.1320	−168.0553	+4.8	+6.7	0	2
		Σ	1.31	1.40	122°	∠HNC = 108° ∠NCH = 122°	−166.1243	−168.0447			2	2
9,	H_2CCHO	Π	1.40	1.34	(120°)[b]		−150.3698		+5.9	—	1	1
		Σ	1.34	1.41	(120°)[b]		−150.3604				1	1
10,	HNCHNH	Π	1.36	1.36	127°	∠CNH = 107°	−146.5903		+37.1	—	2	2
		Σ	1.37	1.33	122°	∠HN_1C = 125° ∠HN_2C = 111° ∠HCN_1 = 118°	−146.5312				2	2

[a]Except as indicated otherwise, all C—H and N—H distances were assumed to be 1.105 Å and 1.013 Å respectively, and all angles were assumed to be 120°.
[b]Assumed value.

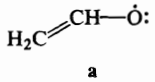
Can. J. Chem. Downloaded from www.nrcresearchpress.com by 210.87.254.40 on 09/05/12
For personal use only.

14 kcal too high, whereas that from 4-31G is 4 kcal mol^{-1} too low.) However, both basis sets predict that the π components of C=N and C=O bonds are almost equally strong, whereas from recent thermochemical data it is known that the carbonyl is substantially stronger. In particular, for the reaction

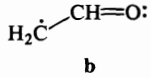
$$H_3C—NH^{\cdot} + H_2C=O \rightarrow H_2C=NH + H_3C—O^{\cdot}$$

the experimental enthalpy[4] is $+11 \pm 3$ kcal mol^{-1} whereas ΔE predicted for it with (without) CI in calculations using the STO-3G and 4-31G bases is $+0.7(-2.9)$ and $-1.9(-3.0)$ kcal mol^{-1} respectively.[5] Thus the calculations will favour too greatly the Σ_O structure for formamido over the Σ_N. (Indeed it is possible that with a properly-balanced basis set the Σ_O and Σ_N minima could be essentially degenerate). Semiempirical calculations could suffer from the same difficulties if they are not properly balanced.

A similar problem involving bond energies exists in the calculation of the geometry and resonance stabilization energy for the Π state of radical **9** (5). With the STO-3G + CI method, the calculated CC and CO bond lengths each are about midway between those expected for double and single bonds, due to significant resonance between the extreme forms **a** and **b**:



a

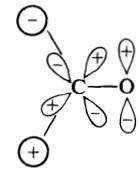


b

The resonance stabilization for the intermediate structure occurs because the calculations predict near-equal strengths for the π components of C=O and C=C bonds, i.e. that $\Delta E \sim 0$ for the reaction

$$H_3C—CH_2^{\cdot} + H_2C=O \rightarrow H_2C=CH_2 + H_3C—O^{\cdot}$$

A similar result is obtained at the 4-31G + CI level. In reality, the enthalpy for the reaction above is $+15.5$ kcal mol^{-1}, i.e. the π component of a C=O bond is much stronger than that of a C=C bond (5). Experimentation with various basis sets shows that the ingredients which are essential to predict this dominance are a double-ζ representation of the $2s$ orbital of oxygen, and a $3d_{yz}$ orbital on the carbonyl carbon atom. The function of the latter AO is to stabilize the nonbonding $2p_y$ lone pair of oxygen by the participation of bonding through to the hydrogens:



With CI, a double-ζ basis for $2s$ orbitals on oxygen, and a $3d_{yz}$ orbital on all carbon and oxygen atoms, the ΔE for the reaction above is calculated[6] to be $+9$ kcal mol^{-1}. (Presumably, further improvements in the basis set will further improve the agreement.)

Given the uncertainties in the structures and location of the unpaired electrons and lone pairs in radicals with nonidentical terminal groups, the energy gaps calculated for **8** and for **9** must be regarded as very tentative. Since comparable difficulties do not exist for $HCO_2^{\cdot}$, the prediction that its Σ and Π states lie very close energetically is probably realistic. (The unpaired and lone pair electrons are restricted to oxygen in both the symmetric and the alternating forms.) Semiempirical INDO calculations by Koenig *et al.* also predict a Π ground state for this species, although the geometry searches for the Σ states assumed equality in the CO distances (8).

Kikuchi has reported STO-3G calculations without CI for $HCO_2^{\cdot}$; the OCO angle was optimized but assumed values for the bond lengths were used (9). Both the Σ and Π states were found to prefer the unsymmetrical geometry, and the Σ state was predicted to be the more stable by a margin of 7 kcal mol^{-1}. As we have discussed elsewhere (5), the prediction for the Π state geometry is unreliable if CI is neglected, due to the doublet instability problem. Unrestricted SCF calculations do yield a symmetrical Π state (9).

For **10**, the preference of 37 kcal mol^{-1} in favour of the Π state over the Σ state is slightly lower than that computed for $NH_2^{\cdot}$; both are too high probably by about the same amount (~ 14 kcal mol^{-1}) due to the too-strong bias of the STO-3G basis in favour of s–p hybrids rather than p AO's for lone pairs on nitrogen.

Radicals **1** through **6** of Table 1 have nitrogen atoms as the central group. Thus for the Σ states there is the possibility that the unpaired electron is located mainly at the centre of the radical rather than at the terminal position(s). In such cases, a symmetrical structure is expected since the potential field experienced by the π electrons at X and Z

[4]Calculated from ΔH_f's of $+26.4 \pm 3.2$ kcal mol^{-1} for H_2C=NH (*7a*), +45 for H_3C—NH (*7b*), −26.0 for H_2CO (*7c*), and +3.5 for CH_3O (*7c*).

[5]Calculated using optimum STO-3G, non-CI geometries in all cases.

[6]In particular, the energies for C_2H_4, C_2H_5, CH_2O, and CH_3O are −77.1238, −77.6641, −112.4793, and −113.0052 au when the $3d$ exponents are 2.0, the oxygen $2s$ exponents are 1.66 and 2.67, and the geometries used are optimum STO-3G structures.

Can. J. Chem. Downloaded from www.nrcresearchpress.com by 210.87.254.40 on 09/05/12
For personal use only.

is comparable. This condition is met in radicals **1** (nitrogen dioxide), **4**, and **5**, and indeed the Σ state of each radical in this set is predicted to have equal XY and YZ bond lengths. In **1** and **4**, significant unpaired spin density is delocalized onto the terminal groups, with the result that the angles about the central nitrogen are smaller for them than for NH_2· and for **5**. The Σ state of NO_2 corresponds to the $^2A_1$ ground state, for which the NO length is known to be 1.19 Å and the ONO angle 134° (11). Recalculation of the structure with the 4-31G + CI basis gives 1.20 Å and 134° respectively, in much better agreement with the experimental result than is the minimal basis set result. The energy gap for NO_2 between the ground Σ state and the Π state (i.e. $^2A_2$) with the 4-31G + CI geometry is 28 kcal mol^{-1}, in fair agreement with that of 42 ± 7 kcal mol^{-1} determined in a definitive multi-configuration SCF calculation by Gillespie *et al.* (10). The minimal basis set value for the energy gap is some 18 kcal mol^{-1} lower, due again to the overestimated bias in favour of *s–p* hybrids of nitrogen. Similarly the minimal basis set predicts a Π ground state for HNNNH, but this is reversed to Σ at the 4-31G level (see Table 1). Based upon the experience with nitrogen dioxide, the latter result is the more reliable and the Σ state probably would be favoured even further by optimization of geometry with an extended basis set. Experimentally, for the dimethyl derivative of **4**, i.e. CH_3—NNN—CH_3, the esr spectrum indicates that most of the spin density is located on equivalent terminal groups, and from this it is concluded that it is a Π state which is detected (11). (An INDO calculation reported by the same authors predicts the Σ state to be more than the Π state by 5 kcal mol^{-1}.) The esr spectrum of the derivative of the trinitrogen chain which has alkyl and —SiR_3 groups indicates that both substituents probably are on the same nitrogen (12), i.e. that it is a derivative of **6** (see Table 1). Our calculations for the Σ state of H_2NNN predict that it is more stable than is **4**, and has an alternating structure of the $H_2\ddot{N}$—N=N· type.

For HNNO (**2**) and to a lesser extent for H_2CNO (**3**), the unpaired electron of the Σ state is predicted in STO-3G + CI calculations to be almost completely localized on the terminal oxygen atom, corresponding to the structures HN=N—Ö· and H_2C=N—Ö· respectively (see Table 1). Because in the Π states the unpaired electron is also present mainly on the oxygen atom and there is also a double bond from nitrogen to the other terminal atom, the calculated energy gap between the states is quite small. In both **2** and **3** it is the Σ state which is predicted to be the lower. Unfortunately the lack of reliable thermochemistry concerning the strengths of the π components of N=N and N=O bonds prevents us from determining any bias in the calculations in favour of O-centered radicals from that source. Experimentally, the esr spectra of iminoxyl radicals R_2CNO (where R is an alkyl or aryl group) have been interpreted in terms of a Σ_O structure (13) and similarly for the radicals Ar—N=N—O (14).

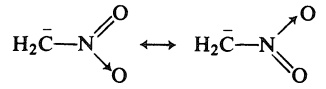
Conclusions

According to past experience, the geometry predicted by *ab initio* MO theory for a molecule usually agrees very well with its experimental structure. Our calculations for free radicals indicate that this generalization does not necessarily hold whenever two or more resonance structures with comparable energies, but with inequivalent assignments of π bonds and lone pairs, can be drawn; e.g.

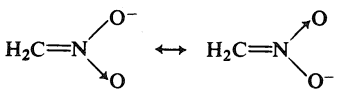
$$:X{=}Y{-}\ddot{Z}\cdot \leftrightarrow \cdot\ddot{X}{-}Y{=}Z:$$

To give an accurate prediction in such cases, the MO method must be able to distinguish accurately the π bond energies of X=Y and Y=Z linkages as well as the energies of the π and the in-plane nonbonding orbitals of the three atoms involved. Even when the differential error is small (~0.01 au compared to the total bonding energy (~1 au)), an incorrect structure could be predicted.

We believe that similar difficulties arise in calculations for closed-shell species as well as for radicals. Thus, using a minimal basis set, the optimum structure predicted for the nitromethyl anion is that of a carbanion with an NO double bond (15):



At the 4-31G level, however, the optimum structure has a CN double bond (16) with the negative charge of the π system located presumably at the oxygens:



In order to judge which is the more realistic prediction, it is necessary to know the relative abilities of the two basis sets in handling the (unknown) balance between the π bond energies of C=N and N=O bonds and the relative energies of a lone pair of π electrons on carbon and oxygen.

Acknowledgements

The authors are grateful to the National Re-

search Council of Canada for financial support of this research, to Mrs. Rashmi Gupta for assistance with some of the calculations, and to Professor J. P. Guthrie for helpful discussions.

1. C. F. BENDER and H. R. SCHAEFER III. J. Chem. Phys. **55**, 4798 (1971).
2. W. J. HEHRE, R. F. STEWART, and J. A. POPLE. J. Chem. Phys. **51**, 2657 (1969).
3. R. DITCHFIELD, W. J. HEHRE, and J. A. POPLE. J. Chem. Phys. **54**, 724 (1971).
4. C. C. J. ROOTHAAN. Rev. Mod. Phys. **32**, 179 (1960).
5. N. C. BAIRD, R. R. GUPTA, and K. F. TAYLOR. J. Am. Chem. Soc. **101**, 4531 (1979).
6. N. C. BAIRD and H. B. KATHPAL. J. Am. Chem. Soc. **98**, 7532 (1976).
7. (*a*) D. J. DE FREES and W. J. HEHRE. J. Phys. Chem. **82**, 391 (1978); (*b*) R. B. SHAW. *In* The chemistry of the hydrazo, azo and azoxy groups. Part 1. *Edited by* S. Patai. John Wiley and Sons, NY. 1975. p. 60; (*c*) S. W. BENSON. Thermochemical kinetics. 2nd ed. John Wiley and Sons, NY. 1976.
8. T. KOENIG, R. A. WIELESEK, and J. G. HUNTINGTON. Tetrahedron Lett. 2283 (1974).
9. O. KIKUCHI. Tetrahedron Lett. 2421 (1977) and references therein.
10. G. D. GILLESPIE, A. U. KHAN, A. C. WAHL, R. P. HOSTENY, and M. KRAUSS. J. Chem. Phys. **63**, 3425 (1975).
11. F. BERNARDI, M. GUERRA, L. LUNAZZI, G. PANCIERA, and G. PLACUCCI. J. Am. Chem. Soc. **100**, 1607 (1978).
12. J. W. COOPER, B. P. ROBERTS, and J. N. WINTER. J. Chem. Soc. Chem. Commun. 320 (1977).
13. J. L. BROCKENSHIRE, J. R. ROBERTS, and K. U. INGOLD. J. Am. Chem. Soc. **94**, 7040 (1972).
14. A. R. FORRESTER. *In* Free radical reactions. *Edited by* W. A. Waters. Butterworth, London. 1972. p. 151.
15. J. N. MURRELL, B. VIDAL, and M. F. GUEST. J. Chem. Soc. Faraday Trans. 2, **71**, 1577 (1975).
16. J. R. MURDOCH, A. STREITWIESER, JR., and S. GABRIEL. J. Am. Chem. Soc. **100**, 6338 (1978).

Can. J. Chem. Downloaded from www.nrcresearchpress.com by 210.87.254.40 on 09/05/12
For personal use only.

The $Fe_{1-x}S$–PbS–ZnS phase system

J. E. DUTRIZAC

Metallurgical Chemistry Section, Mineral Sciences Laboratories, CANMET, Department of Energy, Mines and Resources, Ottawa, Ont., Canada K1A 0G1

Received November 23, 1979

J. E. DUTRIZAC. Can. J. Chem. **58**, 739 (1980).

High temperature phase relationships have been determined for the binary systems FeS–PbS, $Fe_{0.92}S$–PbS, $Fe_{0.92}S$–ZnS, and PbS–ZnS, and for the ternary system $Fe_{0.92}S$–PbS–ZnS. All the systems were of the eutectic-type with eutectic points being noted at 53 mol% FeS – 47 mol% PbS and 850°C, 53 mol% $Fe_{0.92}S$ – 47 mol% PbS and 852°C, 90 mol% $Fe_{0.92}S$ – 10 mol% ZnS and 1178°C, 87 mol% PbS – 13 mol% ZnS and 1050°C, and at 46 mol% $Fe_{0.92}S$ – 41 mol% PbS – 13 mol% ZnS and 850°C, respectively. Solid solubilities were less than 1 mol% except for an appreciable solubility of $Fe_{1-x}S$ in ZnS.

J. E. DUTRIZAC. Can. J. Chem. **58**, 739 (1980).

On a déterminé les relations de phase à haute température des systèmes binaires suivants: FeS–PbS, $Fe_{0.92}S$–PbS, $Fe_{0.92}S$–ZnS et PbS–ZnS et du système ternaire $Fe_{0.92}S$–PbS–ZnS. Tous ces systèmes forment des eutectiques. On a déterminé les points eutectiques des systèmes ayant respectivement les compositions molaires suivantes: FeS–PbS 53–47%: 850°C; $Fe_{0.92}S$–PbS 53–47%: 852°C; $Fe_{0.92}S$–ZnS 90–10%; 1178°C; Pbs–ZnS 87–13%: 1050°C et $Fe_{0.92}S$–PbS–ZnS 46–13%: 850°C. Les solubilités des solides sont inférieures à 1 mol% à l'exception de la solubilité non négligeable de $Fe_{1-x}S$ dans ZnS.

[Traduit par le journal]

Introduction

The $Fe_{1-x}S$–PbS–ZnS phase system is of concern to pyrometallurgists treating either iron and zinc-rich lead concentrates or pyritic zinc–lead sulphide ores and concentrates of the type found, for example, in northeastern New Brunswick. Regardless of whether the iron sulphide mineral present in the ore is pyrrhotite (FeS–Fe_7S_8) or pyrite (FeS_2), an iron sulphide of approximate composition FeS will be formed on heating. Pyrite decomposes to pyrrhotite and sulphur vapour (1 atm) at about 740°C (1, 2) and the pyrrhotite itself evolves sulphur, approaching the stoichiometric compound at elevated temperatures. Although $Fe_{1.00}S$ melts incongruently, the composition $Fe_{0.92}S$ was found to melt congruently at about 1190°C (3).

The $Fe_{1-x}S$–ZnS binary has been investigated several times, but the melting relationships are still not fully resolved. Friedrich (4) observed a eutectic-type system with a eutectic at 5.5 mol% ZnS and 1170–1180°C; his experiments were carried out in open cells. The eutectic behaviour was confirmed by Kullerud (5), who reported a eutectic at 6 mol% ZnS and 1170°C, by Avetisyan and Gnatyshenko (6), who found the eutectic at 6 mol% ZnS and 1180°C and by Kerby (7), who noted the point at 6 mol% ZnS and 1135°C. All workers are in accord concerning the high solubility of FeS in ZnS and that the liquidus temperature rises sharply on the ZnS side of the eutectic.

The $Fe_{1-x}S$–PbS system was first investigated by Wiedmann (8), who reported a simple eutectic at 48 mol% FeS and 782°C. Later, Friedrich (9) using the same open cell technique observed the eutectic at 51 mol% FeS and 863°C. Kopylov (10) reported a eutectic at 52 mol% FeS and 860°C and Kerby (7) observed the point at 52 mol% FeS and 835°C.

The PbS–ZnS binary was studied by Friedrich (4) using open cells; he observed simple eutectic behaviour with the eutectic at 13 mol% ZnS and 1045°C. Kerby (7) remeasured this system with sealed cells and reported a eutectic at 22 mol% ZnS and 988°C.

The FeS–PbS–ZnS ternary has been studied only by Avetisyan and Gnatyshenko (6), who used open cells under a nitrogen atmosphere. They observed a single ternary eutectic at 49.8 mol% FeS, 37.5 mol% PbS, and 12.7 mol% ZnS and 820°C. The liquidus surface rose abruptly in the direction of ZnS once the eutectic valley had been passed.

Because of the importance of this system in pyrometallurgy, it was decided to re-evaluate the $Fe_{1-x}S$–PbS–ZnS phase diagram using sealed-cell DTA techniques. This was effected by measuring the bounding binaries and by determining several "cuts" across the ternary itself. The results were checked by quenching-petrographic methods and by X-ray diffraction and electron microprobe techniques.

Experimental

Lead sulphide (PbS) was obtained from Atomergic Chemetals Ltd. and was 99.999% pure with respect to metallic impurities; unlike some "pure" PbS materials examined, this was also low in sulphate, hydroxide, etc. Zinc sulphide (ZnS) was purchased from Electronic Space Products and was 99.9995% pure with respect to metallic impurities; it was received in the wurtzite

0008-4042/80/070739-05$01.00/0
©1980 National Research Council of Canada/Conseil national de recherches du Canada

Can. J. Chem. Downloaded from www.nrcresearchpress.com by 210.87.254.40 on 09/05/12
For personal use only.

TABLE 1. Analytical data for the pure sulphides

Compound	wt% Fe	wt% Pb	wt% Zn	wt% S	X-ray
Synthesized FeS	63.40	—	—	36.46	FeS (troilite structure)
FeS (theoretical)	63.53	—	—	36.46	—
Synthesized $Fe_{0.92}S$	61.60	—	—	38.31	—
$Fe_{0.92}S$ (theoretical)	61.65	—	—	38.35	—
Purchased PbS	—	87.03	—	13.64	PbS (galena) plus faint trace of unknown compound
PbS (theoretical)	—	86.60	—	13.39	
Purchased ZnS	—	—	66.81	33.35	ZnS (sphalerite) plus trace of ZnS (wurtzite)
ZnS (theoretical)	—	—	67.09	32.90	

modification which was converted to the sphalerite structure by heating in a vacuum sealed ampoule to 900°C for a few hours. The iron sulphides FeS and $Fe_{0.92}S$ were synthesized using established procedures (11). The various starting materials were analyzed chemically and by Guinier X-ray diffraction analysis, and the results are presented in Table 1. The X-ray data show the general absence of oxide lead compounds and the predominately sphalerite form of the ZnS. When the wurtzite modification was used, data interpretation was greatly complicated because in some experiments the wurtzite would, on heating, convert to sphalerite which would revert to wurtzite on further heating (>900°C) before the liquidus was reached. In other runs the wurtzite would "melt" before any wurtzite ⇄ sphalerite reactions occurred.

The sulphides were mixed in suitable proportions and were vacuum sealed in 4 mm id silica glass DTA tubes; the sulphides did not attack the silica glass although they seemed to promote devitrification at the highest temperatures employed. For the purpose of calculating mole percentages, the formula of the congruently melting iron sulphide was expressed as $Fe_{0.92}S$. The samples were run on a Stone DTA System equipped with a palladium holder and Pt–Pt:10%Rh thermocouples. The sulphides were heated against a calcined alumina reference, and the system was calibrated against the melting point of gold (1063°C). Programming rates of 5, 10, or 15°C/min were used depending on the system response, and data were recorded on both heating and cooling. Selected samples were analyzed microscopically and by X-ray diffraction analysis after they had been heated and cooled.

To estimate solid solubilities, suitable compositions were melted in vacuum-sealed silica glass ampoules (8 mm id) and then annealed for 2 to 3 days at a temperature just below the appropriate eutectic. Longer annealing times did not yield significantly different results and it was assumed that equilibrium was fairly quickly attained in the fine eutectic structures produced. The samples were then quenched in water and examined microscopically and by electron microprobe analysis to estimate the maximum extent of solid solubility.

Results and Discussion

(a) $Fe_{1-x}S$–PbS

The phase diagram for the FeS–PbS binary system is presented in Fig. 1 and the corresponding diagram for the $Fe_{0.92}S$–PbS system is given in Fig. 2. PbS melted at 1115°C in agreement with the reported value. FeS and $Fe_{0.92}S$ fused at 1165°C and 1190°C, respectively, and both these values are in accord with the published data (3). Aside from the different melting points for the iron sulphides,

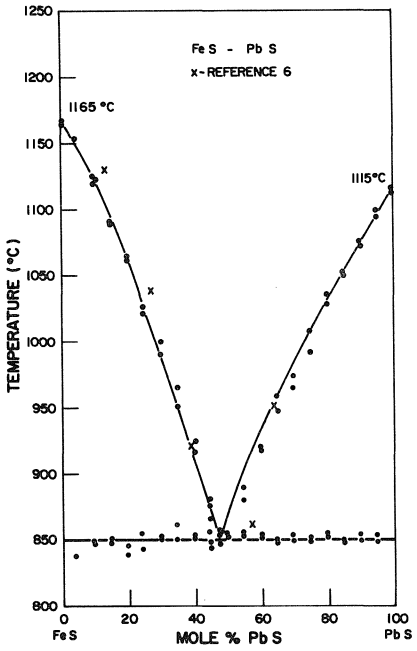


FIG. 1. High temperature portion of the FeS–PbS phase diagram; eutectic temperature is 850°C.

the two systems are very similar. Both are of the simple eutectic type with the eutectic composition being at 53 mol% $Fe_{1-x}S$ and 47 mol% PbS; the eutectic temperature was 850°C for FeS–PbS and 852°C for $Fe_{0.92}S$–PbS. The eutectic composition is in essential agreement with earlier work (7, 9, 10). The eutectic temperature is supported by the studies of Friedrich (9), 863°C, and Kopylov (10), 860°C, but is substantially higher than Kerby's value of 835°C; examination of his PbS suggested oxide contamination which may have caused his lower melting temperatures. The ×'s marked on the FeS–PbS binary are liquidus temperatures taken from the ternary data of Avetisyan and Gnatyshenko (6), and the agreement is acceptable.

The only phases identified by X-ray diffraction analysis of cooled samples were PbS (galena) and

Can. J. Chem. Downloaded from www.nrcresearchpress.com by 210.87.254.40 on 09/05/12
For personal use only.

Can. J. Chem. Downloaded from www.nrcresearchpress.com by 210.87.254.40 on 09/05/12
For personal use only.

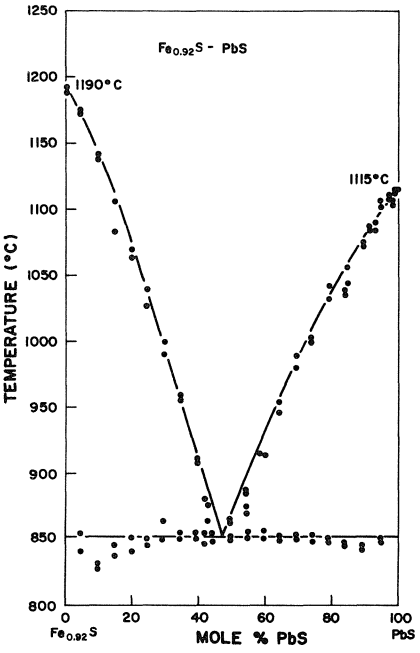


FIG. 2. High temperature portion of the $Fe_{0.92}S$–PbS phase diagram; eutectic temperature is 852°C.

iron sulphides of the type $Fe_{1-x}S$. Electron microprobe examination of various samples annealed at 840°C for 2–3 days and then quenched indicated less than 0.5 wt% Fe in the primary PbS and less than 0.5 wt% Pb in the primary $Fe_{1-x}S$. Microscopic examination likewise confirmed that solid solubilities were considerably less than 1 wt% in these binary systems.

(b) $Fe_{0.92}S$–ZnS

The determined phase diagram for the $Fe_{0.92}S$–ZnS binary system is presented in Fig. 3; because of the steep liquidus on the ZnS side of the eutectic, liquidus points were not usually detected by the DTA apparatus. The liquidus falls from the 1190°C melting point of $Fe_{0.92}S$ to the eutectic which occurs at 90 mol% $Fe_{0.92}S$ – 10 mol% ZnS and 1178°C, and then rises sharply. The eutectic temperature observed in this study is consistent with previous work (4–6) except that of Kerby (7), which appears low at 1135°C. The eutectic composition observed in the present study is slightly richer in zinc than was previously observed.

The only phases detected in this system were $Fe_{1-x}S$ and iron-rich sphalerite. Samples annealed at 1165°C for 2–3 days and quenched indicated that the iron sulphide contained less than 0.5 wt% Zn. Since very fine ZnS inclusions could be seen in the $Fe_{1-x}S$ phase, the amount of zinc actually in solution in $Fe_{1-x}S$ might be lower than this amount.

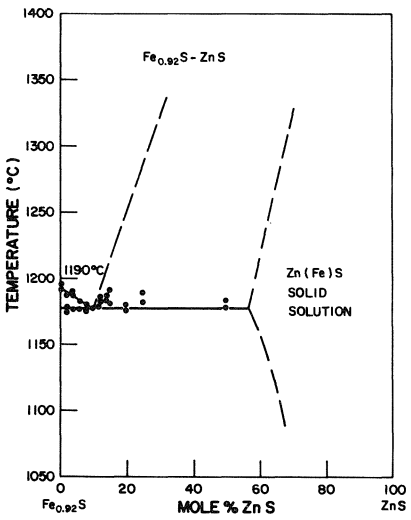


FIG. 3. The $Fe_{0.92}S$–ZnS phase diagram showing the approximate range of $Fe_{1-x}S$ solubility in ZnS; eutectic temperature is 1178°C.

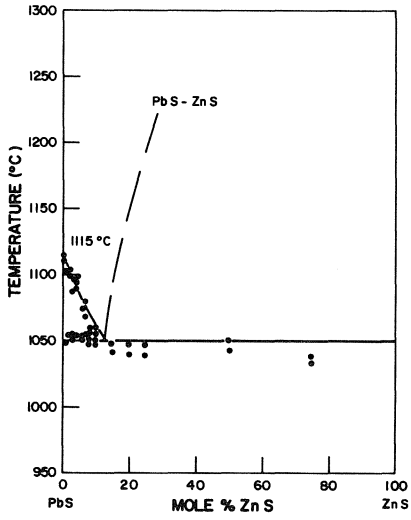


FIG. 4. The PbS–ZnS phase diagram; the eutectic temperature is 1050°C.

Barton and Toulmin (12) found the maximum Zn content of $Fe_{1-x}S$ to be less than 0.24 atom%. The ZnS phase dissolves considerable amounts of iron sulphide at 1165°C. Electron microprobe examination of the quenched samples indicated 26–27 wt% Fe and this corresponds to about 43 mol% FeS in the ZnS. The solubility of FeS in ZnS is somewhat variable because the sulphur fugacity of the system is not buffered. Kullerud (5) reported 45 mol% FeS solubility at 1190°C; Barton and Toulmin (12) observed a molar FeS solubility of 56% at 850°C and 52% at 580°C for (Zn,Fe)S in equilibrium with FeS and metallic iron; lower solubilities were noted

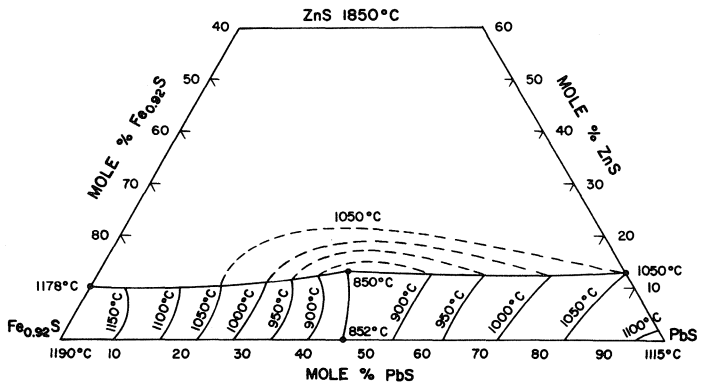


FIG. 5. The $Fe_{0.92}S$–PbS–ZnS ternary phase diagram.

when $Fe_{1-x}S$ was used. Neuhaus and Cemic (13) reported a value of 51 mol% FeS at 900°C and 5 kbars pressure.

(c) PbS–ZnS

Figure 4 illustrates the liquidus relationships in the PbS–ZnS binary system. The eutectic was observed at about 13 mol% ZnS and 1050°C, in general agreement with Friedrich (4) who reported a eutectic at 13 mol% ZnS and 1045°C. Neither study agrees with the recent work of Kerby (7), but it is felt that his purchased lead sulphide was badly oxidized. The slight curvature in the liquidus on the PbS side of the system was also noted by Friedrich (4). Microscopic examination of solidified melts in the vicinity of the eutectic composition indicated that the eutectic contained more than 12 mol% ZnS but less than 15 mol% of this component.

Electron microprobe study of samples annealed just below the eutectic temperature and then quenched suggested that solid solubilities were less than 0.5 mol% at either end of the phase diagram; the zinc sulphide contained 0.4 wt% Pb and the lead sulphide assayed 0.2 wt% Zn.

(d) $Fe_{0.92}S$–PbS–ZnS

Liquidus relationships in the $Fe_{0.92}S$–PbS–ZnS ternary were elucidated by measuring seven pseudobinary cuts across the system. In the interest of brevity, the seven pseudobinaries are not presented but are available from the author on demand. The various binary and pseudobinary systems were then used to construct the ternary phase diagram shown in Fig. 5. The ternary is of the simple eutectic type with the ternary eutectic point at 46 mol% $Fe_{0.92}S$ – 41 mol% PbS – 13 mol% ZnS and 850°C. The ternary eutectic composition is similar to that of Avetisyan and Gnatyshenko (6), 49.8 mol% FeS – 37.5 mol% PbS – 12.7 mol% ZnS, although those authors noted the ternary eutectic temperature at 820°C. The liquidus surfaces fall

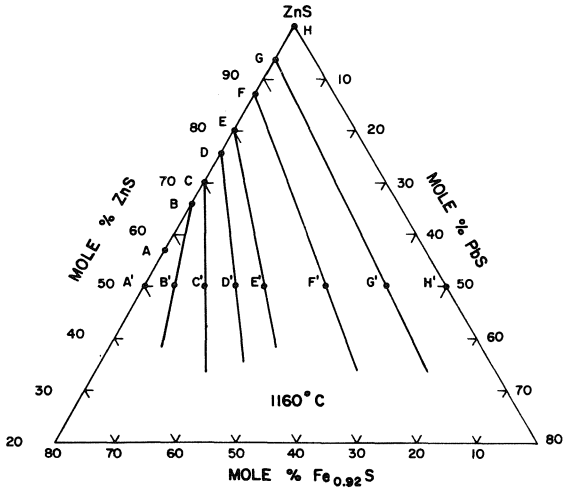


FIG. 6. The solubility of $Fe_{1-x}S$ in solid ZnS as a function of total composition in the $Fe_{0.92}S$–PbS–ZnS ternary system.

rather gradually from either $Fe_{0.92}S$ or PbS, but rise steeply on the ZnS-rich side of the figure. The steep ZnS liquidus combined with the location of the ternary eutectic close to the $Fe_{0.92}S$–PbS binary causes ZnS to be a difficult impurity in the processing of iron and/or lead mattes.

(e) Ternary Solid Solutions

Study of the bounding binary systems revealed that solid solubilities were low except for $Fe_{1-x}S$ in ZnS. To test for solid solubilities in the ternary system, nine ternary compositions were prepared and heated to 1200°C in vacuum sealed tubes for 2 to 4 h. The tubes were then cooled to 1040°C and held at that temperature for 2 to 3 days. After water quenching, the samples were examined microscopically and by the electron microprobe to evaluate the extent of solid solubility. Solubilities in $Fe_{0.92}S$ and PbS were always less than 1%, in agreement with the binary data. Extensive $Fe_{1-x}S$ solubility in ZnS as well as the possibility of trace PbS solid solubility was indicated.

Can. J. Chem. Downloaded from www.nrcresearchpress.com by 210.87.254.40 on 09/05/12
For personal use only.

A series of compositions consisting of 50 mol% ZnS and various amounts of $Fe_{0.92}S$ and PbS were prepared and annealed at 1160°C; i.e., just below the $Fe_{1-x}S$–ZnS binary eutectic temperature. These compositions are indicated (A′–H′) on Fig. 6, and the corresponding compositions of the solid zinc sulphide phases are given by A–H, respectively. The solubility of lead in the ZnS phase was always less than 1 wt%; at 1160°C and 5 mol% PbS in the charge, the ZnS phase assayed 0.25 wt% Pb; the corresponding value for a charge containing 40 mol% PbS was 0.76 wt% Pb. The iron concentration of the ZnS phase depends strongly on the activity of FeS in the associated melt. This value was 6 mol% FeS in ZnS when the charge contained 10 mol% FeS, and 43 mol% FeS along the $Fe_{0.92}S$–ZnS binary (Fig. 6).

Conclusions

High temperature phase relationships have been determined for the binary systems FeS–PbS, $Fe_{0.92}S$–PbS, $Fe_{0.92}S$–ZnS, and PbS–ZnS, and for the ternary system $Fe_{0.92}S$–PbS–ZnS. All the systems were of the eutectic-type with eutectic points being noted at 53 mol% FeS – 47 mol% PbS and 850°C, 53 mol% $Fe_{0.92}S$ – 47 mol% PbS and 852°C, 90 mol% $Fe_{0.92}S$ – 10 mol% ZnS and 1178°C, 87 mol% PbS – 13 mol% ZnS and 1050°C, and at 46 mol% $Fe_{0.92}S$ – 41 mol% PbS – 13 mol% ZnS and 850°C, respectively. Solid solubilities were less than 1 mol% except near the $Fe_{1-x}S$–ZnS binary where an appreciable solubility of $Fe_{1-x}S$ in ZnS was observed.

Acknowledgements

The assistance of O. Dinardo with the experimental program and D. R. Owens with the electron microprobe analyses is recognized.

1. P. Toulmin and P. B. Barton. Geochim. Cosmochim. Acta, **28**, 641 (1964).
2. R. G. Arnold. Econ. Geol. **57**, 72 (1962).
3. E. Jenson. Am. J. Sci. **240**, 695 (1942).
4. K. Friedrich. Metallurgie, **5**, 114 (1908).
5. G. Kullerud. Norsk. Geol. Tidsskr. **32**, 61 (1953).
6. K. K. Avetisyan and G. I. Gnatyshenko. Izv. Akad. Nauk Kaz. SSR, Ser. Gorn. Dela Met. Stroit. it Stroim. **6**, 11 (1956).
7. R. C. Kerby. Mines Branch Report IR 73–49, Department of Energy, Mines and Resources, Ottawa, Ont., Canada K1A 0G1.
8. H. Wiedmann. Metallurgie, **3**, 660 (1906).
9. K. Friedrich. Metallurgie, **4**, 479 (1907).
10. N. I. Kopylov. Russ. J. Inorg. Chem. **12**(10), 1494 (1967).
11. J. E. Dutrizac and R. J. C. MacDonald. Mater. Res. Bull. **8**(8), 961 (1973).
12. P. B. Barton and P. Toulmin. Econ. Geol. **61**(5), 815 (1966).
13. A. Neuhaus and L. Cemic. Naturwissenschaften, **57**(7), 354 (1970).

Can. J. Chem. Downloaded from www.nrcresearchpress.com by 210.87.254.40 on 09/05/12
For personal use only.

The preparation of polymeric siloxyphosphine rhodium(I) complexes

ZOFIA C. BRZEZIŃSKA AND WILLIAM R. CULLEN

Chemistry Department, University of British Columbia, Vancouver, B.C., Canada V6T 1W5

Received May 10, 1979

ZOFIA C. BRZEZIŃSKA and WILLIAM R. CULLEN. Can. J. Chem. **58**, 744 (1980).

Hydrolysis in dioxane/water (4:1 by volume) of performed rhodium(I) complexes of the phosphines $Cl_3Si(CH_2)_nP(C_6H_5)_2$ (n = 2, 8) either alone or in the presence of excess ligand or Cl_3SiCH_3 affords insoluble polymeric globules. Typical products have idealized formulae $\{[O_{3/2}Si(CH_2)_2P(C_6H_5)_2]_3RhCl\cdot(O_{3/2}SiCH_3)_{200}\}_x$, $\{[O_{3/2}Si(CH_2)_8P(C_6H_5)_2]_4Rh_2Cl_2\}_x$, and $\{[O_{3/2}Si(CH_2)_2P(C_6H_5)_2]_2Rh(CO)Cl\}_x$ and seem to contain only rhodium(I). Apart from the last example the polymers in toluene suspension react with H_2 and CO at 60°C. In the case of CO the uptake ranges from 0.27–1.30 mol of CO per atom of rhodium. The main products appear to be Rh(CO)Cl derivatives.

ZOFIA C. BRZEZIŃSKA et WILLIAM R. CULLEN. Can. J. Chem. **58**, 744 (1980).

Les complexes préformés de rhodium(I) et de phosphines $Cl_3Si(CH_2)_nP(C_6H_5)_2$ (n = 2, 8) seuls ou en présence d'un excès de ligand ou de Cl_3SiCH_3 fournissent par hydrolyse dans un mélange de dioxanne/eau (4:1) des globules de polymères insolubles. Les produits typiques ont la formule théorique suivante $\{[O_{3/2}Si(CH_2)_2P(C_6H_5)_2]_3RhCl\cdot(O_{3/2}SiCH_3)_{200}\}_x$, $\{[O_{3/2}Si(CH_2)_8P(C_6H_5)_2]_4Rh_2Cl_2\}_x$, et $\{[O_{3/2}Si(CH_2)_2P(C_6H_5)_2]_2Rh(CO)Cl\}_x$ et semblent contenir seulement du rhodium(I). A l'exception du dernier exemple, les polymères en suspension dans le toluène réagissent avec H_2 et CO a 60°C. Dans le cas du CO, la fixation se situe entre 0.27 et 1.30 mol de CO par atome de rhodium. Les produits principaux semblent être des dérivés du Rh(CO)Cl.

[Traduit par le journal]

Introduction

Most supported catalysts of the class known as heterogenized homogeneous catalysts use polystyrene or inorganic materials such as silica or glass as the support (1, 2). We are interested in preparing hydrogenation catalysts which have silicone backbones because of the possibility of easy chemical modification of the supporting material and in the hope that such catalysts might have significantly different properties from those based on other systems.

Our chosen method of synthesis, as outlined in reactions [1]–[3], depends on the hydrolysis of the preformed complexes **2**, **3**, and **4** either alone or in the presence of excess ligand, or excess CH_3SiCl_3.[1]

[1] $[Cl_3Si(CH_2)_nP(C_6H_5)_2]_3RhCl + mCH_3SiCl_3 \xrightarrow{H_2O} [O_{3/2}Si(CH_2)_nP(C_6H_5)_2]_3RhCl\cdot(O_{3/2}Si(CH)_3)_m$

2, 3 → **B**(n,m)

n = 2(**2**), 8(**3**); m = 0–200

[2] $[Cl_3Si(CH_2)_2P(C_6H_5)_2]_4Rh_2Cl_2 + mCH_3SiCl_3 \rightarrow [O_{3/2}Si(CH_2)_2P(C_6H_5)_2]_4Rh_2Cl_2\cdot(O_{3/2}Si(CH_3)_3)_m$

4 → **C**(2,m)

m = 0–200

[3] $[Cl_3Si(CH_2)_2P(C_6H_5)_2]_3RhCl + mCl_3Si(CH_2)_2P(C_6H_5)_2 \xrightarrow{H_2O} [O_{3/2}Si(CH_2)_2P(C_6H_5)_2]_3RhCl\cdot(O_{3/2}Si(CH_2)_2P(C_6H_5)_2)_m$

2 → **D**

m = 0.7

This method is formally analogous to the synthesis of more conventional organometallic macromolecular complexes by polymerization and copolymerization of vinylic moieties on a ligand attached to a metal centre (3, 4); for example, vinylcyclopentadienyl manganese tricarbonyl can be homopolymerized or copolymerized with styrene. This method of synthesizing polymer-supported metal centres has not been explored to its full potential.

The synthesis of the polymer precursors **2**, **3**, and **4** and the carbonyl monomer $[Cl_3Si(CH_2)_2P(C_6H_5)_2]$-Rh(CO)Cl, **1**, has been described elsewhere (5). We have also discussed (5) the model complexes L_3RhCl, $L_4Rh_2Cl_2$, and $L_2Rh(CO)Cl$ where L = $[(CH_3)_3SiO]_2(CH_3)Si(CH_2)_2P(C_6H_5)_2$ which were

[1]In the symbol (n,m) n is the number of CH_2 groups (either 2 or 8) between the phosphorus and silicon atoms in the original ligand and m is the number of moles of CH_3SiCl_3 co-polymerized with 1 mol of the ligand. In a homopolymer m is 0.

0008-4042/80/070744-06$01.00/0

©1980 National Research Council of Canada/Conseil national de recherches du Canada

Can. J. Chem. Downloaded from www.nrcresearchpress.com by 210.87.254.105 on 09/05/12
For personal use only.

Can. J. Chem. Downloaded from www.nrcresearchpress.com by 210.87.254.105 on 09/05/12
For personal use only.

especially prepared so that they would have similar properties to the anticipated macromolecules **A**–**D**,[1] yet would be soluble and hence allow facile study.

Experimental Section

The monomers $[Cl_3Si(CH_2)_2P(C_6H_5)_2]_2Rh(CO)Cl$, $[Cl_3Si(CH_2)_nP(C_6H_5)_2]_3RhCl$ (n = 2, 8), and $[Cl_3Si(CH_2)_2P(C_6H_5)_2]_4Rh_2Cl_2$ were prepared as previously described (5). All manipulations of air and moisture sensitive compounds were carried out in Schlenk apparatus under nitrogen.

A constant pressure and temperature apparatus was used for measurements of gas uptake.

Electron micrographs were obtained using an ETEC Autoscan microscope with ORTEC Multichannel X-ray analyzer model 6200. Samples were placed on an aluminum specimen stub coated with a dispersion of graphite in isopropyl alcohol. The stub was placed in a vacuum carbon evaporator where the surface was coated with a thin layer of graphite. Infrared spectra were recorded on Perkin-Elmer model 457 and 225 spectrophotometers.

Polymerization of $[Cl_3Si(CH_2)_2P(C_6H_5)_2]_2Rh(CO)Cl$

(*A*) A benzene solution (ca. 3.5 mL) of 5.93 g (6.89 mmol) of $[Cl_3Si(CH_2)_2P(C_6H_5)_2]_2Rh(CO)Cl$ prepared *in situ* was introduced dropwise into 5 mL of a vigorously stirred mixture of dioxane and water (4:1 v/v). The suspension of the resultant pale yellow precipitate was stirred for 2 h. A solution of 4 g of $NaHCO_3$ in ca. 50 mL of water was added to the suspension. The product was filtered off, washed with water, 10% aqueous $NaHCO_3$, water, dioxane, and benzene, and dried *in vacuo* for 24 h.

The solid product was extracted with refluxing dichloromethane in a Soxhlet extractor for 24 h. The insoluble polymer **A** was dried *in vacuo* for 24 h (3.92 g, 81.7% yield), dec. 255-265°C. *Anal.* calcd. for $C_{29}H_{28}ClO_4P_2RhSi_2$: C 50.0, H 4.3, Cl 5.1, Rh 14.8, P 8.9; found: C 50.0, H 3.8, Cl 12.3, Rh 14.8, P 9.1, ir(Nujol): ν(C≡O) 1965(s) cm^{-1}.

(*B*) A benzene solution (ca. 1.5 mL) of $[Cl_3Si(CH_2)_2P(C_6H_5)_2]_2Rh(CO)Cl$ (0.086 g, 0.1 mmol) prepared *in situ* was added dropwise into 1 mL of an aqueous solution of 0.1 g KOH. A pale yellow precipitate formed immediately. It was filtered off, washed with water, benzene, and then dried *in vacuo* for 24 h; ir(Nujol): ν(C≡O) 1965(s) cm^{-1}.

(*C*) Triethylamine (0.1 g, 1.0 mmol) was added to $[Cl_3Si(CH_2)_2P(C_6H_5)_2]_2Rh(CO)Cl$ (0.086 g, 0.1 mmol) which had been prepared *in situ* in 1.5 mL of benzene. The mixture was added dropwise to ca. 2 mL of water. A pale yellow precipitate formed immediately. It was filtered off, washed with water, benzene, and then dried *in vacuo* for 24 h; ir(Nujol): ν(C≡O) 1965(s) cm^{-1}.

Homopolymerization of $[Cl_3Si(CH_2)_2P(C_6H_5)_2]_3RhCl$ *in Dioxane/Water Mixture*

A benzene solution (1.5 mL) of 0.402 g (34.1 mmol) of $[Cl_3Si(CH_2)_2P(C_6H_5)_2]_3RhCl$ prepared *in situ* was introduced dropwise into 4 mL of a vigorously stirred mixture of dioxane and water (3:1 v/v). The suspension of the resulting pale yellow precipitate was stirred for an additional 2 h. The precipitate changed colour to orange upon addition of ca. 8 mL of an aqueous solution of 0.5 g of $NaHCO_3$. The product was filtered off, washed with water, 10% aqueous $NaHCO_3$, water, dioxane, and benzene, and then dried *in vacuo* for 24 h.

Copolymerization of $[Cl_3Si(CH_2)_2P(C_6H_5)_2]_3RhCl$ *with* Cl_3SiCH_3 *in Dioxane/Water Mixture*

Methyltrichlorosilane (4.030 g, 27.0 mmol) was added to 1.5 mL of a benzene solution of $[Cl_3Si(CH_2)_2P(C_6H_5)_2]_3RhCl$ (0.318 g, 0.27 mmol) prepared *in situ*. The mixture was polymerized by a procedure analogous to the homopolymerization described above (11.5 mL dioxane/water in 4:1 v/v ratio).

Analytical and Spectroscopic Data for Polymers and Copolymers of Different Rh(I) Phosphine Complexes

All the polymeric complexes used for any further reactions were prepared by hydrolysis with dioxane/water (4:1) as described above and were Soxhlet extracted with CH_2Cl_2 for 24 h and dried under vacuum for 24 h. All the homopolymers proved to be pyrophoric upon exposure to air.

$[O_{3/2}Si(CH_2)_2P(C_6H_5)_2]_3RhCl$, **B**(2,0): 85.3% yield, dec. 220–230°C. *Anal.* calcd. for $C_{42}H_{42}ClO_{9/2}P_3RhSi_3$: C 54.0, H 4.5, Cl 3.8, P 10.0, Rh 11.0, Si 9.0; found: C 50.8, H 4.5, Cl 6.2, P 9.5, Rh 10.5, Si 8.9. Ir(Nujol): ν(Rh—Cl) 285(w); 255(sh) cm^{-1}.

$[OSi(CH_3)(CH_2)_2P(C_6H_5)_2]_3RhCl$: not analyzed; the product was completely soluble in CH_2Cl_2.

$[O_{3/2}Si(CH_2)_8P(C_6H_5)_2]_3RhCl$, **B**(8,0): 84.1% yield, dec. 185–195°C. *Anal.* calcd. for $C_{60}H_{78}ClO_{9/2}P_3RhSi_3$: C 60.8, H 6.6, Cl 3.0, P 7.7, Rh 8.7, Si 7.1; found: C 59.2, H 6.3, Cl 4.6, P 7.6, Rh 8.4, Si 6.9. Ir(Nujol): ν(Rh—Cl) 285(w); 255(sh) cm^{-1}.

$[O_{3/2}Si(CH_2)_2P(C_6H_5)_2]_4Rh_2Cl_2$, **C**(2,0); 70.2% yield, dec. 220–230°C. *Anal.* calcd. for $C_{56}H_{56}Cl_2O_6P_4Rh_2Si_4$: C 50.3, H 4.2, Cl 5.3, P 9.3, Rh 15.4, Si 8.4; found: C 50.6, H 4.5, Cl 6.6, P 9.0, Rh 15.1, Si 8.3. Ir(Nujol): ν(Rh—Cl) 290(w); 265(sh) cm^{-1}.

$[O_{3/2}Si(CH_2)_2P(C_6H_5)_2]_{3.7}RhCl$, **D**: 78.9% yield, dec. 260–265°C. *Anal.* calcd. for $C_{51.8}H_{51.8}ClO_{5.55}P_{3.7}RhSi_{3.7}$: C 55.6, H 4.6, Cl 3.2, P 10.3, Rh 9.2, Si 9.3; found: C 50.3, H 4.8, Cl 6.6, P 10.2, Rh 9.1, Si 9.1.

$[O_{3/2}Si(CH_2)_2P(C_6H_5)_2]_3RhCl\cdot(O_{3/2}SiCH_3)_{75}$, **B**(2,75): 73.5% yield, dec. 255–265°C. *Anal.* calcd. for $C_{117}H_{269}ClO_{117}P_3RhSi_{78}$: C 23.6, H 4.5, Cl 0.6, P 1.6, Rh 1.7; found: C 23.6, H 5.3, Cl 1.4, P 1.5, Rh 1.7.

$[O_{3/2}Si(CH_2)_2P(C_6H_5)_2]_3RhCl\cdot(O_{3/2}SiCH_3)_{150}$, **B**(2,150): 78.2% yield, dec. 255–265°C. *Anal.* calcd. for $C_{192}H_{492}ClO_{229.5}P_3RhSi_{153}$: C 21.0, H 4.5; found: C 20.2, H 4.5.

$[O_{3/2}Si(CH_2)_2P(C_6H_5)_2]_3RhCl\cdot(O_{3/2}SiCH_3)_{200}$, **B**(2,200): 71.2% yield, dec. 255–265°C. *Anal.* calcd. for $C_{242}H_{642}ClO_{304.5}P_3RhSi_{203}$: C 20.3, H 4.5; found: C 20.2, H 4.3.

$[O_{3/2}Si(CH_2)_8P(C_6H_5)_2]_3RhCl\cdot(O_{3/2}SiCH_3)_{100}$, **B**(8,100): 86.8% yield, dec. 250–260°C. *Anal.* calcd. for $C_{160}H_{378}ClO_{154.5}P_3RhSi_{103}$: C 24.4, H 4.8; found: C 24.4, H 4.8.

$[O_{3/2}Si(CH_2)_2P(C_6H_5)_2]_4Rh_2Cl_2\cdot(O_{3/2}SiCH_3)_{200}$, **D**(2,200): 70.2% yield, dec. 270–280°C. *Anal.* calcd. for $C_{256}H_{656}Cl_2O_{306}P_4Rh_2Si_{204}$: C 20.9, H 4.5, Cl 0.5, P 0.8, Rh 1.4, Si 38.8; found: C 21.0, H 4.4, Cl 0.2, P 0.8, Rh 1.5, Si 38.6.

Polymerization of $Cl_3Si(CH_2)_2P(C_6H_5)_2$

The trichlorosilylphosphine, $Cl_3Si(CH_2)_2P(C_6H_5)_2$ (1.740 g, 5.0 mmol), in benzene solution (3 mL) was polymerized by a mixture (2.5 mL) of dioxane and water (4:1 v/v) by the usual procedure, yielding a white solid which was not extracted with CH_2Cl_2. *Anal.* calcd. for $O_{3/2}Si(CH_2)_2P(C_6H_5)_2$: Cl 0.0; and for $O(Cl)Si(CH_2)_2P(C_6H_5)_2$: Cl 12.1; found: Cl 9.2.

Reactions of the Polymers with CO

The homopolymeric complex (1.33×10^{-1} mmol) or the copolymeric complex (5.4×10^{-2} mmol) was suspended in

3 mL of toluene in the reaction flask of the gas uptake apparatus. The carbon monoxide pressure was 760 mm Hg and the temperature 60°C. The total gas uptake was measured for each complex after 3 days. The degree of conversion was calculated by comparison of the observed gas consumption and the expected carbon monoxide uptake value for one molecule of CO for each atom of rhodium. Each complex was filtered, washed with benzene, and dried *in vacuo*.

Reaction of B(2,75) and B(2,0) with H_2

The hydrogen uptake was monitored with **B**(2,0) (0.124 g) or **B**(2,75) (0.269 g) suspended in 3 mL of toluene at 60°C. The pressure was 690 mm. At the end of each reaction the suspensions were filtered and the solid dried in a stream of nitrogen (2 h).

Results and Discussion

Synthesis of the Polymeric Complexes

Since the range of physio-chemical analytical techniques which can be applied to obtain useful information about insoluble solids is very limited, preliminary studies were made on the hydrolysis of **1** $[Cl_3Si(CH_2)_2P(C_6H_5)_2]_2Rh(CO)Cl$ (reaction [4]) because of the presence of the CO group. This can act as a built-in probe since ν(CO) is very sensitive to changes in the environment of the metal

[4] $[Cl_3Si(CH_2)_2P(C_6H_5)_2]_2Rh(CO)Cl$

1

$$\xrightarrow[-HCl]{+H_2O} [O_{3/2}Si(CH_2)_2P(C_6H_5)_2]_2Rh(CO)Cl$$

A

It was found that when a benzene solution of **1** is added to dioxane/water (4:1 by volume) an insoluble solid precipitates in good yield. The solid product was extracted with refluxing dichloromethane (24 h) to give the polymer **A**. The ν(CO) frequency for **A** is 1965 cm^{-1}, which is close to that of **1** (1970 cm^{-1} (5)), indicating that the environment of the metal center is not greatly changed in the process of polymerization.

The microanalytical data for **A** agree well with the idealized formula except for the halogen content, which at 12.3% is more than twice that expected. Since the extra halogen is not on the rhodium (ν(CO) for a Rh(III) carbonyl would be considerably shifted (6)) it is possibly the result of incomplete hydrolysis. Polymerization of the ligand $Cl_3Si(CH_2)_2P(C_6H_5)_2$ alone under the same conditions yields a product which also has a high chlorine content (9.2%).

Although base hydrolysis (KOH or $(C_2H_5)_3N$) of **1** gives a polymer with the same ν(CO), when this technique is applied to the polymerization of **2**, $[Cl_3Si(CH_2)_2P(C_6H_5)_2]_3RhCl$, the products darken on exposure to H_2 (1 atm, 60°C, toluene suspension). In these cases the H_2 uptake is greater than 1 mol per rhodium atom; being in some experiments as much as 1.82 (7). The darkening and high hydrogen uptake are probably due to reduction to rhodium metal, as has been established in other systems using electron microscopy (8). Base catalyzed cohydrolysis of **2** with Cl_3SiCH_3 also gives products with similar undesirable properties (7) even when the ratio of **2** to Cl_3SiCH_3 is varied from 1:20 to 1:200.

Because of these results the hydrolysis and cohydrolysis of **2** (reaction [1]) was performed using the dioxane/water method developed for **1**.[2] Thus the polymers **B**(2,*m*)[1] were obtained.

The solids **B**(2,*m*) have satisfactory properties (Table 1) on exposure to hydrogen. Thus they do not darken and take up less than 1 mol of H_2 per mole of rhodium. However, the results are not very reproducible and, as can be seen in particular for **B**(2,100), Table 1, a number of preparations give differing uptake figures. Polymers which are satisfactory in all respects (although some homopolymers are pyrophoric), giving low and reproducible H_2 uptake without darkening, are obtained only when the initially precipitated solids are Soxhlet extracted with CH_2Cl_2 for 24 h. This procedure was used for all subsequent preparations.

It seems that the ease of hydrogen uptake is related to the "diluteness" of the rhodium centres. Possibly the addition of 1 mol of H_2 per rhodium atom represents the polymeric counterpart of the known oxidative addition reaction of H_2 to Wilkinson's complex (9) (reaction [5]).

[5] $[(C_6H_5)_3P]_3RhCl + H_2 \rightleftharpoons [(C_6H_5)_3P]_3Rh_2ClH$

Only in one case does the hydrolysis–extraction method fail to yield an insoluble polymer. This is the polymer produced from $[Cl_2(CH_3)Si(CH_2)_2P(C_6H_5)_2]_3RhCl$, which dissolves upon extraction with dichloromethane. The lower cross-linked structure of the polymer produced by hydrolysis of the $SiCl_2$ groups probably accounts for this solubility.

The microanalytical data obtained for the solids **B**, **C**, and **D** are occasionally not those expected for the idealized formulae. The Cl content found for all the homopolymers and for some copolymers, e.g., **B**(2,75), is higher than expected, again presumably due to incomplete hydrolysis. The Si content found is in good agreement with the calculated values for the polymers tested. So are the values for P and Rh found in the homopolymers and copolymers **B**(2,75) and **D**(2,200); for all the other copolymers the percentage of P, Rh, and Cl are too low for meaningful determination. The carbon content in all the copolymers and **C**(2,0) is found as predicted but it is low in all the other homopolymers in spite of the

[2]DMF/water mixture gives irreproducible results (9).

Can. J. Chem. Downloaded from www.nrcresearchpress.com by 210.87.254.105 on 09/05/12
For personal use only.

Can. J. Chem. Downloaded from www.nrcresearchpress.com by 210.87.254.105 on 09/05/12
For personal use only.

TABLE 1. Representative hydrogen uptake data for the polymers **B**(2,*m*)[a]

Polymer	Dioxane/water	H_2 uptake per Rh atom	Polymer colour after exposure[b]
B(2,0)	3/1	0.27	Yellow
B(2,50)	4/1	0.75	Yellow
B(2,100)	4/1	0.50–0.97	Yellow
B(2,200)	5/1	1.0	Yellow
B(2,0)[c]	4/1	0.12	Light orange
B(2,100)[c]	4/1	0.50	Light orange

[a]Toluene suspension (4.5×10^{-2} mmol of Rh atom; 3 mL), 60°C, and 1 atm H_2.
[b]All initially orange.
[c]Polymer was extracted with CH_2Cl_2.

use of an improved analytical method (10) which seems to prevent the formation of silicon carbide.

The infrared spectra of the polymers seem to indicate that few if any rhodium(III) centres, resulting from oxidative addition of HCl to rhodium(I), are present. Thus the homopolymeric complexes show weak broad bands in the ν(Rh—Cl) region at 285 cm^{-1} with a shoulder at 255 cm^{-1} (**B**(2,0) and **B**(8,0)) and at 290 cm^{-1} with a shoulder at 265 cm^{-1} (**C**(2,0)) but there is no band near 2100 cm^{-1} due to ν(Rh—H). The copolymers do not absorb in the ν(Rh—Cl) or ν(Rh—H) regions although it must be noted that absence of these bands could be due to dilution effects (by $O_{3/2}SiCH_3$) and the intrinsically low intensity of both these stretching bands.

An interesting trend in the values for the decomposition points of the polymers is seen in the data in Table 2. None of the polymers actually melt; they all decompose at disappointingly low temperatures over a range of about 10°C leaving either black or grey residues. All the homopolymers decompose at temperatures 30–50°C lower than the corresponding copolymers. For example **B**(2,0) decomposes at 220–230°C whereas **B**(2,75), **B**(2,150), and **B**(2,200) decompose at 255–265°C. The homopolymer **B**(8,0) with "8-carbon" ligands decomposes at the lowest temperature whereas the copolymer with an excess of the phosphine, **D**, is almost as stable as **C**(2,200), which has the highest decomposition temperature of all. All the other copolymers decompose at roughly the same temperature (ca. 260°C) regardless of their composition.

TABLE 2. Decomposition points of the polymeric complexes

Polymer	Decomposition point (°C)
B(2,0)	220–230
B(8,0)	185–195
D	260–265
C(2,0)	220–230
B(2,75)	255–265
B(2,150)	255–265
B(2,200)	255–265
B(8,100)	250–260
C(2,200)	270–280

The secondary image electron micrographs of the polymer **B**(2,75) are shown in Fig. 1 at a range of magnifications. The freshly prepared polymer consists of relatively smooth globules clustered together in bigger conglomerates. The rhodium is distributed evenly as revealed by X-ray EM micrographs and no clusters are observed at the magnification used.

In order to gain more knowledge of the nature of the polymers some were treated with CO and H_2 because of the known reactions of rhodium(I) centres with these reagents. Thus L'_3RhCl gives $L'_2Rh(CO)Cl$ and L'_3RhH_2Cl, and $L'_4Rh_2Cl_2$ gives $L'_2Rh(CO)Cl$ and $L'_4Rh_2H_2Cl_2$ ($L' = (C_6H_5)_3P$) (9, 11, 12).

The polymeric complexes **B**(2,0) and **B**(2,75) were exposed to H_2 both in a toluene suspension and in the solid state. Data in Fig. 2 show the amount of H_2 uptake vs. time for the reaction carried out in toluene. After 33 h the homopolymer takes up 11.5% and the copolymer 56% of the H_2 compared with the amounts calculated for 1:1 uptake (reaction [5]). However, the infrared spectra of all the hydrogenated products show no ν(Rh—H) peaks in the expected region, 2050–2150 cm^{-1}. This may be because of the generally low intensity of ν(Rh—H) although the possibility of instability of the hydrido species cannot be overlooked in spite of mull preparation in an argon atmosphere.

The model complexes L_3RhCl and $L_4Rh_2Cl_2$ react with H_2 to give L_3RhH_2Cl and $L_4Rh_2H_2Cl_2$, respectively (5). The reactions are reversible at 25°C.

Some results of the reactions of some polymeric complexes with CO are listed in Table 3. In toluene suspension the amount of uptake varies widely and seems to indicate that accessibility to the metal centres is greater in the copolymers which show high uptake values. The infrared spectra of the exposed polymers show ν(CO) bands at 1965 or 1968 cm^{-1}. The chlorine bridged homopolymer **C**(2,0) and the copolymer **B**(2,75) also show a weaker absorption at 2080 cm^{-1} and **B**(2,75) has a band at 1995 cm^{-1}. The absorptions at ~1965 cm^{-1} indicate that the CO reacts to give a polymer in which the metal centre has a similar environment to that found in the polymeric carbonyl complex **A** with *trans*-phosphines.

It is not unusual to find more than one ν(CO) band in polymers of this type, and one to four have been observed for $P_2Rh(CO)Cl$ derivatives derived from

Can. J. Chem. Downloaded from www.nrcresearchpress.com by 210.87.254.105 on 09/05/12
For personal use only.

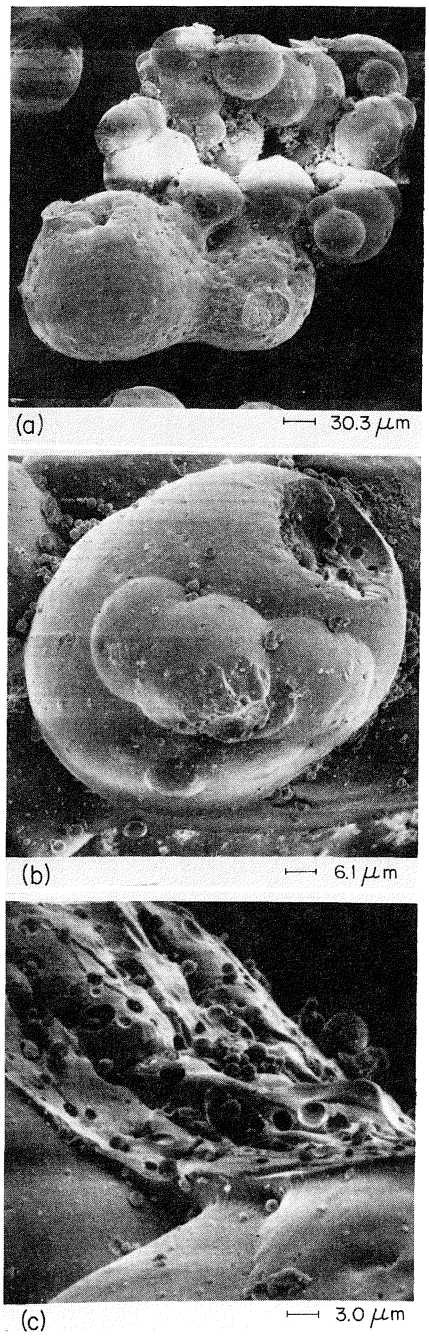


FIG. 1. Secondary image electron microscope micrographs of polymer **B**(2,75) at a beam power of 5 kV. The magnifications are (*a*) 220, (*b*) 1100, and (*c*) 2200.

the polyphosphinite derivative of poly(methallyl alcohol) (13).

The ν(CO) frequencies for *cis*-phosphine complexes of the type (chelate-P_2)Rh(CO)Cl (14–16) and the dicarbonyl *cis*-$(CO)_2$PRhCl (17–19), are higher than for *trans*-P_2Rh(CO)Cl. However, it is difficult

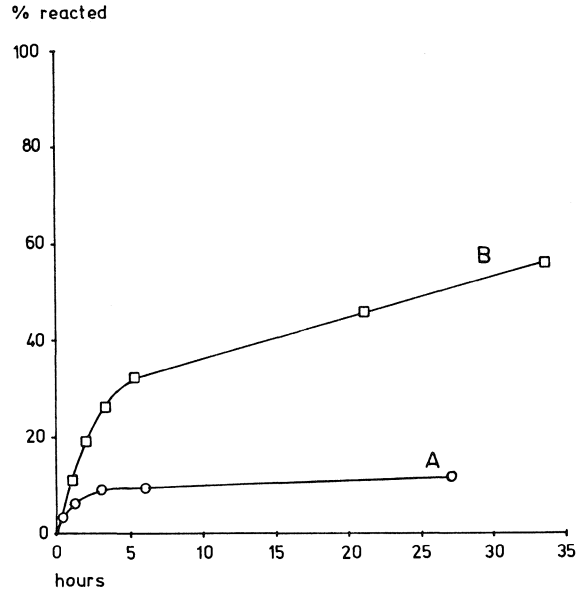


FIG. 2. Hydrogen uptake by **B**(2,0) and **B**(2,75). Curve *A* was obtained from 1.33×10^{-1} mmol of **B**(2,0); curve *B* from 4.5×10^{-2} mmol of **B**(2,75). Reaction conditions; temperature 60°C; P_{H_2}, 690 mm; toluene as solvent (3 mL).

TABLE 3. Reactions of polymeric complexes with carbon monoxide[a]

Starting complex	Conversion	ν(C≡O) (cm^{-1})
B(2,0)	0.36	1965(s)
B(8,0)	0.40	1965(s)
C(2,0)	0.43	1968(s), 2080(w)
B(2,75)	0.91	1968(s), 1995(s), 2080(m)
B(2,75)	1.00[b]	1965(s), 1995(s), 2080(m)
B(2,0)[c]	0.27[d]	1970(b, vs), 2080(m)
C(2,0)[c]	1.30[d]	1970(b,vs), 2080(m)

[a]In toluene suspension (3 days, 1 atm CO; 60°C) unless otherwise indicated.
[b]Reaction at 70°C.
[c]In the absence of solvent; 3 days; 25°C.
[d]After pumping for 24 h the 0.27% conversion changed to 0.25% and the 1.30% changed to 0.86%.

to assign the bands at 2080 and 1995 cm^{-1} (Table 3) to particular species.

The model complexes L_3RhCl and $L_4Rh_2Cl_2$ both give L_2Rh(CO)Cl quantitatively and irreversibly.

Exposure of the solid polymer **B**(2,0) to HCl(g) (1 atm) at 25°C results in an uptake of more than 2 mol of HCl per mole of rhodium (7). This absorption is not reversed by pumping at 25°C. The infrared spectrum of the solid polymer shows no band in the ν(Rh—H) region and no change in absorption in the ν(Rh—Cl) region so the HCl is probably strongly chemisorbed. There seems to be no HCl uptake by the polymers **B**(2,0) or **B**(2,75) in toluene suspension (60°C). Instead, it seems that the first effect of dropping the polymers into the toluene in an appara-

tus which has been pre-equilibrated with HCl(g) is the evolution of the chemisorbed HCl.

From the results presented above it seems that the polymers contain mainly rhodium(I) centres and that the accessibility of these centres is inversely related to their concentration. They also react with CO and H_2 much less readily than their soluble model compounds L_3RhCl and $L_4Rh_2Cl_2$. Thus it is to be anticipated that the homogeneous hydrogenation of, say, styrene would be catalyzed much more readily by the soluble complexes than by toluene suspensions of the polymeric analogues. This is found to be so and these results together with other related findings are presented in the following paper.

Acknowledgment

The authors wish to thank the Natural Sciences and Engineering Research Council of Canada for financial support.

1. R. H. GRUBBS. Chemtech. 512 (1977).
2. F. R. HARTLEY and P. N. VEZEY. Adv. Organomet. Chem. **15**, 189 (1977).
3. C. U. PITTMAN, JR. Macromolecules, **7**, 396 (1974).
4. C. U. PITTMAN, JR., G. V. MARLIN, and T. D. ROUNSEFELL. Macromolecules, **6**, 1 (1973).
5. W. R. CULLEN and Z. C. BRZEZIŃSKA. Inorg. Chem. **18**, 3132 (1979).
6. G. M. INTILLE. Inorg. Chem. **11**, 695 (1972).
7. Z. C. BRZEZIŃSKA. Ph.D. Thesis, University of British Columbia, Vancouver, B.C. 1978.
8. K. G. ALLUM, R. D. HANCOCK, I. V. HOWELL, T. E. LESTER, S. MCKENZIE, R. C. PITKETHLY, and P. J. ROBINSON. J. Organomet. Chem. **107**, 393 (1976).
9. J. A. OSBORN, F. M. JARDINE, J. F. YOUNG, and G. WILKINSON. J. Chem. Soc. A, 1711 (1966).
10. P. BORDA and Z. C. BRZEZIŃSKA. Unpublished results.
11. P. Z. MEAKIN, J. P. JESSON, and C. A. TOLMAN. J. Am. Chem. Soc. **94**, 3240 (1972).
12. C. A. TOLMAN, P. Z. MEAKIN, D. L. LINDNER, and J. P. JESSON. J. Am. Chem. Soc. **96**, 2762 (1974).
13. W. R. CULLEN, B. R. JAMES, A. D. JENKINS. G. STRUKUL, and Y. SUGI. Inorg. Nucl. Chem. Lett. **13**, 577 (1977).
14. A. R. SANGER. J. Chem. Soc. Dalton Trans. 120 (1977).
15. G. K. N. REDDY and E. G. LELLAMANI. Indian J. Chem. **4**, 540 (1966).
16. A. R. SANGER. J. Chem. Soc. Chem. Commun. 893 (1975).
17. K. G. ALLUM, R. D. HANCOCK, I. V. HOWELL, S. MCKENZIE, R. C. PITKETHLY, and P. J. ROBINSON. J. Organomet. Chem. **87**, 203 (1975).
18. L. D. ROLLMAN. Inorg. Chim. Acta, **6**, 137 (1972).
19. A. R. SANGER and L. R. SCHALLIG. J. Mol. Catal. **3**, 101 (1977/78).

Can. J. Chem. Downloaded from www.nrcresearchpress.com by 210.87.254.105 on 09/05/12
For personal use only.

Polymeric siloxyphosphine rhodium(I) complexes as hydrogenation catalysts

ZOFIA C. BRZEZIŃSKA, WILLIAM R. CULLEN, AND GIORGIO STRUKUL

Chemistry Department, University of British Columbia, Vancouver, B.C., Canada V6T 1W5

Received October 29, 1979

ZOFIA C. BRZEZIŃSKA, WILLIAM R. CULLEN, and GIORGIO STRUKUL. Can. J. Chem. **58**, 750 (1980).

Polymers of idealized formulae $[O_{3/2}Si(CH_2)_nP(C_6H_5)_2]_3RhCl\cdot(O_{3/2}SiCH_3)_m$, **B**(*n*,*m*), $[O_{3/2}Si(CH_2)_2P(C_6H_5)_2]_4Rh_2Cl_2\cdot(O_{3/2}SiCH_3)_m$, C(2,*m*), and $[O_{3/2}Si(CH_2)_2P(C_6H_5)_2]_3RhCl\cdot(O_{3/2}Si(CH_2)_2P(C_6H_5)_2)_{0.7}$, **D** are hydrogenation catalysts for olefins in benzene suspension at 25°C and 1 atm H_2. With respect to styrene, the activity order is **B** > **D** ~ **C**. All the catalysts lose activity on recycling but the copolymers retain their activity over a greater number of cycles with **D** being the best catalyst in this regard. Possible reasons for this behaviour are discussed.

ZOFIA C. BRZEZIŃSKA, WILLIAM R. CULLEN et GIORGIO STRUKUL. Can. J. Chem. **58**, 750 (1980).

Les polymères de formule théorique $[O_{3/2}Si(CH_2)_nP(C_6H_5)_2]_3RhCl\cdot(O_{3/2}SiCH_3)_m$, **B**(*n*,*m*), $[O_{3/2}Si(CH_2)_2P(C_6H_5)_2]_4Rh_2Cl_2\cdot(O_{3/2}SiCH_3)_m$, C(2,*m*), et $[O_{3/2}Si(CH_2)_2P(C_6H_5)_2]_3RhCl\cdot(O_{3/2}Si(CH_2)_2P(C_6H_5)_2)_{0.7}$ **D** catalysent l'hydrogénation des oléfines en suspension dans le benzène à 25°C et sous 1 atm de H_2. Par rapport au styrène, l'ordre d'activité est **B** > **D** ~ **C**. Tous les catalyseurs perdent leur activité lorsqu'on les recycle mais les copolymères retiennent leur activité pendant un grand nombre de cycles. Sous ce rapport, **D** est le meilleur catalyseur. On discute des raisons possibles de ce comportement.

[Traduit par le journal]

Introduction

When analogues of the well known homogeneous catalyst $[(C_6H_5)_3P]_3RhCl$ are supported on inert materials to give a "heterogenized homogeneous catalyst" (1–4) (polystyrene derivatives or silica are often used) olefin hydrogenation rates appear to be influenced by the same factors as are observed in homogeneous solution (5–10). However, the activity of the supported catalyst is almost invariably far inferior to its homogeneous counterpart (2, 3).

Silicones are well known polymers with a wide variety of uses (11) however, surprisingly, they have been little investigated as supports for "heterogenized homogeneous catalysts" (12–15). In these earlier studies the preformed silicone was functionalized to afford a polymeric phosphine which was subsequently used to prepare an appropriate metal derivative by ligand exchange. We have prepared silicone polymers by hydrolyzing preformed monomeric complexes of rhodium(I) (1) either alone or in the presence of CH_3SiCl_3 or $(C_6H_5)_2PCH_2CH_2SiCl_3$ to give a range of polymeric solids of the following idealized formulae:

$[O_{3/2}Si(CH_2)_nP(C_6H_5)_2]_3RhCl\cdot(O_{3/2}SiCH_3)_m$ **B**(*n*,*m*)

$[O_{3/2}Si(CH_2)_2P(C_6H_5)_2]_4Rh_2Cl_2\cdot(O_{3/2}SiCH_3)_m$ C(2,*m*)

$[O_{3/2}Si(CH_2)_2P(C_6H_5)_2]_3RhCl\cdot(O_{3/2}Si(CH_2)_2(PC_6H_5)_2)_{0.7}$ **D**

The present article describes their application as catalysts for the hydrogenation of olefins, in particular, styrene.

Experimental Section

Gas–liquid chromatography was done using an Aerograph A-90-P instrument. Saturated and unsaturated hydrocarbons were separated using 10% Carbowax 1500 on 60/80 mesh Chromosorb W-AW.

All liquid olefins were passed through an alumina column prior to use in reactions. A double manifold apparatus was used for hydrogenation reactions carried out at 1 atm. Usually a few reactions were carried out simultaneously in 25 mL round-bottomed flasks equipped with a Teflon-rubber septum plug and magnetic stirrer and connected to the apparatus via a water-cooled condenser (17). The temperature of the stirred glycerine bath in which the flasks were immersed was maintained constant (±0.1°C) by a thermoregulator and relay circuit which operated a 25 W elongated electric light bulb.

The catalyst prepared as previously described (1) was weighed out into the flask in a helium filled glove-box and the solvent and olefin were introduced into the flask using standard inert atmosphere techniques. Progress of the reaction was monitored by glc; samples being withdrawn periodically through the septum.

Results and Discussion

Hydrogenation of Olefins Using the Complex B(2,0)

Cyclohexene, styrene, 1-heptene, and 1-octene are hydrogenated at 25°C (1 atm H_2), using a suspension of **B**(2,0) in benzene (Table 1). The reduction of cyclohexene, following the general trend expected for internal olefins, proceeds at a slower rate. Isomerization *and* hydrogenation take place in the case of 1-heptene and 1-octene. Styrene affords only ethylbenzene.

These results parallel those obtained for other supported catalysts (7) although it has been reported that when ethanol is used as solvent the cyclohexene hydrogenation proceeds faster than that of styrene. In the case of **B**(2,0) the color of the polymer remains orange only when it is suspended in benzene or toluene. Addition of co-solvents such

0008-4042/80/070750-05$01.00/0

©1980 National Research Council of Canada/Conseil national de recherches du Canada

Can. J. Chem. Downloaded from www.nrcresearchpress.com by 210.87.254.105 on 09/05/12
For personal use only.

Can. J. Chem. Downloaded from www.nrcresearchpress.com by 210.87.254.105 on 09/05/12
For personal use only.

TABLE 1. Hydrogenation of olefins using **B**(2,75) as catalyst[a]

Olefin	Conversion (%)	Saturated product yield (%)	Isomerized product yield (%)
Cyclohexene	8.1	8.1	—
Styrene	88.5	88.5	—
1-Heptene	86.4	46.3	40.1
1-Octene	88.8	42.9	45.9

[a]The olefin (3 mmol) in benzene solution (3 mL) was hydrogenated (1 atm H_2) using the catalyst (1.33×10^{-2} mmol, based on the number of Rh(I) atoms) at 25°C. The reaction was stopped after 23 h.

as triethylamine and ethanol causes a color change to grey, and in pure ethanol the polymer turns black presumably because of rhodium metal formation (1). This solvent effect has not been noted before.

The rate of hydrogenation of styrene, as model substrate, increases by a factor of about two on changing the temperature from 35°C to 60°C. The rate also increases by increasing the concentration or the amount of catalyst (17). These results parallel those obtained in other systems (5, 6, 9).

In order to evaluate the effect of varying the polymeric catalyst, the hydrogenation of styrene was studied at constant concentration and constant solution volume. The weight of catalyst was chosen so as to have a constant "concentration" of rhodium atoms present in suspension.

The data presented in Fig. 1 show that the "P_3RhCl" polymers **B**(*n*,*m*) are generally considerably more active than their "$P_4Rh_2Cl_2$" analogues **C**(*n*,*m*). In homogeneous solution the catalytic activity of $[(C_6H_5)_3P]_3RhCl$ appears to be due (18) to the formation of a phosphine dissociated species, reaction [1], which in the presence of hydrogen forms an important catalytic species, $[(C_6H_5)_3P]_2RhH_2Cl$ (reaction [2]). Otherwise dimerization takes place, reaction [3], and this equilibrium lies far to the right.

[1] $[(C_6H_5)_3P]_3RhCl \rightleftharpoons [(C_6H_5)_3P]_2RhCl + (C_6H_5)_3P$

[2] $[(C_6H_5)_3P]_2RhCl + H_2 \rightarrow [(C_6H_5)_3P]_2RhH_2Cl$

[3] $2[(C_6H_5)_3P]_2RhCl \rightleftharpoons [(C_6H_5)_3P]_4Rh_2Cl_4$

The dimer itself is described as a good hydrogenation catalyst (19) but with little substantiation. We have shown that model complexes for the silicone polymers **B**, **C**, and **D**, L_3RhCl and $L_4Rh_2Cl_2$ (20) (L = $[(CH_3)_3SiO]_2Si(CH_3)CH_2CH_2P(C_6H_5)_2$) are *both* active catalysts for styrene hydrogenation with the dimer being less active. In this respect the heterogeneous reaction parallels the homogeneous one. However comparable hydrogenation rates are obtained using the polymeric analogues as catalysts only if the concentrations of both catalyst and olefin are increased by a factor of 10 (17). This loss of activity on heterogenization is a general phenomenon as mentioned in the Introduction.

In the set of first cycle hydrogenations shown in Fig. 1 there is not much difference between the behaviour of the homo- or copolymers of a given type with the exception of **B**(8,0) which is appreciably less active than **B**(8,100). This behaviour is changed little by preconditioning the polymer in benzene suspension under an atmosphere of hydrogen prior to the addition of styrene (Fig. 2). Figure 2 also shows that there is an increase in the

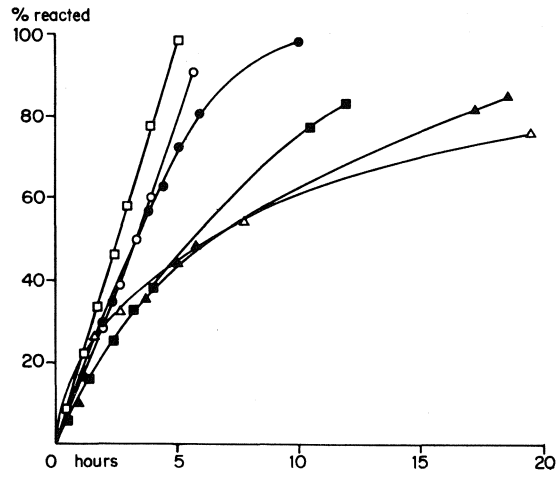


FIG. 1. First cycle of hydrogenation of styrene in benzene with different polymers as catalysts. Reaction conditions: temperature, 35°C; benzene solvent, 3 mL; styrene, 3.0 mmol; suspended catalyst, 3.0×10^{-2} mmol as Rh(I). □, **B**(8,100); ■, **B**(8,0); ○, **B**(2,75); ●, **B**(2,0); △, **C**(2,200); ▲, **C**(2,0).

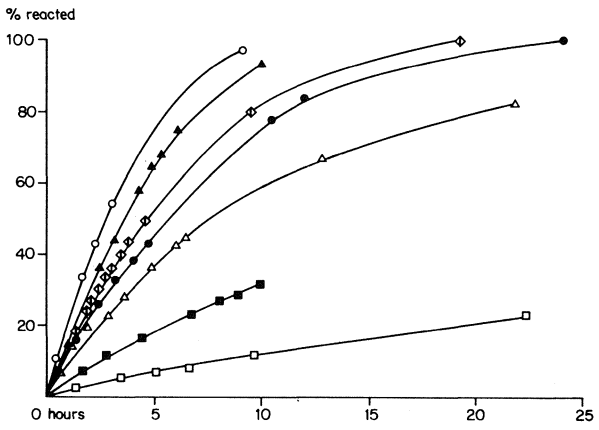


FIG. 2. Recycled **B**(8,0) as catalyst for styrene hydrogenation. Reaction conditions are as described in the caption to Fig. 1. Cycles: ●, 1st; ○, 2nd; ▲, 3rd; △, 4th; ■, 5th; □, 6th; ▨, 1st with catalyst stirred in benzene suspension for 24 h under H_2 (1 atm) prior to the injection of styrene.

Can. J. Chem. Downloaded from www.nrcresearchpress.com by 210.87.254.105 on 09/05/12
For personal use only.

activity of this catalyst in the second cycle and that the activity drops steadily on subsequent recycling. There is no appreciable loss of rhodium from the catalyst to the reaction solution as judged by its color before the fifth run (Table 2). Other workers have reported similar increases after the first cycle for silica (21) and polystyrene (22) supported catalysts.

A typical example of the more usual behaviour observed on recycling is seen in Fig. 3 where there is a gradual drop in activity of the catalyst **B**(2,0) until it reaches a negligible level in the fifth cycle. The polymer used as catalyst here is air sensitive (1) and when it is deliberately exposed to air between cycles the loss of activity is much more rapid than shown in Fig. 3.

The results obtained for a number of these recycling experiments are summarized in Table 2, and in the case of the "P_3RhCl" polymers copolymerization with CH_3SiCl_3 helps maintain activity but it has little effect on prolonging the already low activity of the "$P_4Rh_2Cl_2$" polymers. The most stable catalyst **D** contains excess ligand although its initial activity is low (Fig. 4). This is not unexpected since studies in homogeneous systems show that excess phosphine slows down reaction rates, presumably because of its effect on the reactions shown in reactions [1] to [3] and similar effects have been noted for other supported catalysts (12, 21, 23–25). This excess phosphine should stabilize the polymer by preventing rhodium elution (22, 25–28) as found in the present case. This should also result in a catalyst which maintains its activity over a greater number of cycles if dimer production is the cause of activity loss on recycling (reaction [3]). As the present results show the "$P_4Rh_2Cl_2$" polymers **C**(2,*m*) have a lower activity; and dimer formation has been observed on polystyrene based catalysts of the P_3RhX type (29).

TABLE 2. Effect of recycling catalysts for styrene hydrogenation[a]

Catalyst	Number of cycles required for activity to drop to zero[b]	Cycles in which rhodium loss is observed
B(2,0)	5	4 and 5 (4 < 5)
B(8,0)	6	5 and 6 (5 < 6)
C(2,0)	3	1
D	5[c]	—
B(2,75)	5[d]	3 and 5 (3 < 5)
B(2,150)	5[d]	3 and 5 (3 < 5)
B(2,200)	5[e]	—
B(8,100)	5	—
C(2,200)	3	—

[a]The conditions for all experiments were as described in the caption for Fig. 1.
[b]Zero is defined rather loosely. Recycling was stopped when the activity was approximately that shown in the fifth run in Fig. 2.
[c]Polymer had lost only half its activity (Fig. 4).
[d]There is little loss of activity in the first three cycles.
[e]There is little loss of activity in the first four cycles.

Inhibition of dimer formation could also partly account for the slower initial drop in activity found on recycling the copolymers (Table 2) since the rhodium centres will be further away from each other. Related to this is the observation that copolymerization of the dimeric complexes does not improve their activity or behaviour on recycling.

When the length of the spacer arm between the metal and the matrix is increased, the resulting catalysts **B**(8,*m*) maintain their activity over a greater number of cycles and, apart from the initial anomalous behaviour of **B**(8,0), their activity is always higher than **B**(2,*m*) in a given cycle. This is possibly also due to some inhibition of dimer for-

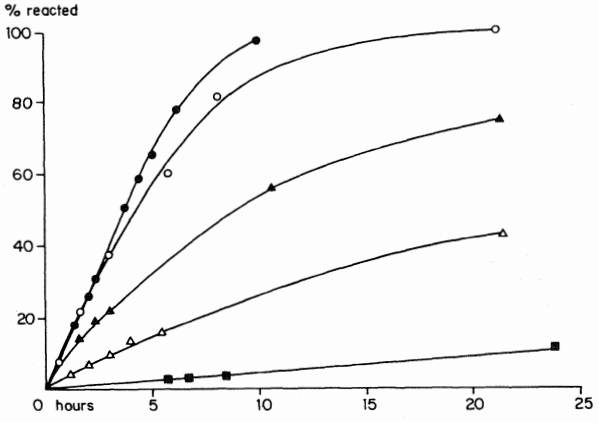


FIG. 3. Recycled **B**(2,0) as catalyst for styrene hydrogenation. Reaction conditions are as described in the caption to Fig. 1. Cycles: ●, 1st; ○, 2nd; ▲, 3rd; △, 4th; ■, 5th.

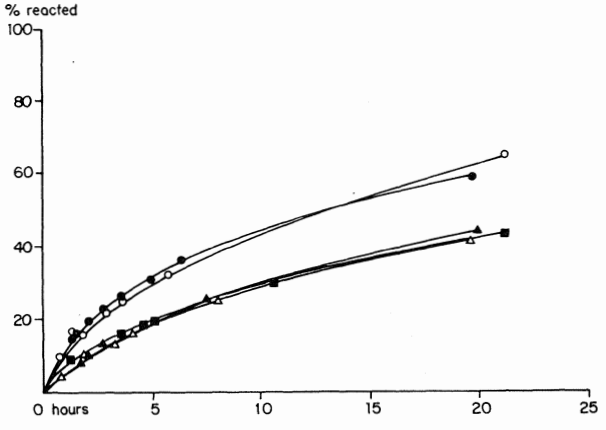


FIG. 4. Recycled **D** as catalyst for styrene hydrogenation. Reaction conditions are as described in the caption to Fig. 1. Cycles: ●, 1st; ○, 2nd; ▲, 3rd; △, 4th; ■, 5th.

Can. J. Chem. Downloaded from www.nrcresearchpress.com by 210.87.254.105 on 09/05/12
For personal use only.

mation. In addition, the long arms probably allow the active sites to behave much more like species in solution. In this connection epr studies of polysaccharide supported nitroxides (30, 31) show that longer spacer arms give more freedom of mobility to the anchored sites and the spectra become similar to those of the species in solution. The increase of the spacer arms beyond a length equivalent to a C_8 chain causes no further change (30, 31).

The above model accounts for most of the gross features observed in the catalytic hydrogenation of styrene. However, it is probably an oversimplification since, for example, some of the polymers are air sensitive (1) and in spite of careful handling they could become exposed to traces of air during cycling. The used catalyst could be particularly sensitive in this regard since it almost certainly contains some rhodium hydride species (reaction [2]).

Although the model complex L_3RhCl reacts with H_2 at 25°C to give L_3RhH_2Cl, and $L_4Rh_2Cl_2$ affords a mixture of compounds whose main constituent is $L_4Rh_2H_2Cl_2$ under the same conditions (both hydrogenations are reversible), the polymers **B**(2,0) and **B**(2,75) themselves take up hydrogen slowly in toluene suspension at 60°C (1). The amounts taken up are only 11.5% and 56% of the amount calculated for 1-to-1 uptake after 33 h. Furthermore, the catalytic activity of **B**(8,0) is little affected by preconditioning with H_2 (Fig. 2). Thus hydrides with compositions similar to L_3RhH_2Cl and $L_4Rh_2H_2Cl_2$ are probably not formed to a great extent during the styrene hydrogenation reactions.

Undoubtedly some loss of activity on recycling some catalysts is due to elution of metal (Table 2). This is generally assumed to be related to the dissociation equilibrium shown in reaction [1] (the right-to-left reaction is responsible for the stability of the polymer **D** as described above). Loss of rhodium from supported hydroformylation catalysts supported on silica and polystyrene has been related to oxygen exposure (25). Elution of rhodium also occurs from related polysiloxane supported hydroformylation catalysts (16) and in this case a mechanism involving initial loss of phosphine is advanced. Although there is no evidence for phosphine loss in the present study, it is always a possibility.

More extensive deactivation per cycle is observed when the polymer **B**(2,0) is used to hydrogenate cyclohexene under the same conditions used for styrene (17). In addition the degree of conversion to cyclohexane is less than to ethylbenzene in a given time in all cycles.

An unusual phenomenon is observed when the hydrogenation reactions are run in "solution volumes" different from the standard 3 mL usually used. Data plotted in Fig. 5 show that the degree of hydrogenation of styrene catalyzed by **B**(2,0) is smaller at a given time for larger volumes. On recycling the difference slowly disappears. Polymer **C**(2,200) shows this phenomenon to a lesser extent and polymer **D** hardly at all. When cyclohexene is the substrate and **B**(2,0) the catalyst, conversion is slightly *higher* in solutions of greater volume. These results are quite reproducible and are not due to variation of stirring speed. Rate effects on changing the speed of stirring have been observed by others (12).

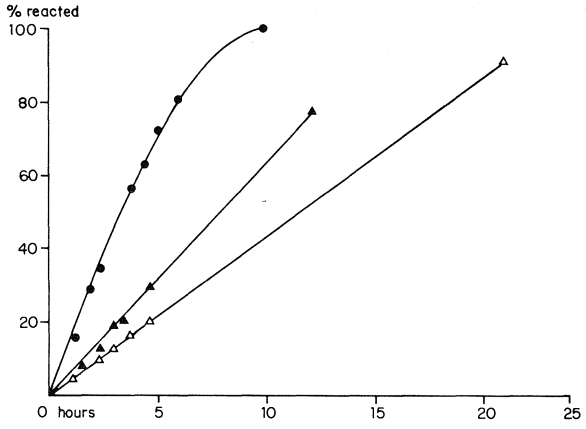


FIG. 5. Effect of solution volume on the hydrogenation of styrene catalyzed by **B**(2,0). Reaction conditions are as described in the caption to Fig. 1 and the amounts of styrene and catalyst are proportional to the solution volume. Solution volume; ●, 3 mL; ▲, 9 mL; △, 12 mL.

In summary, all the polymers **B**, **C**, **D** are effective catalysts for olefin hydrogenation but their activity decreases on recycling. This deactivation could be caused by (*a*) dimerization of the **B** polymers to form macromolecules related to **C**, (*b*) "poisoning" of the catalyst by traces of oxygen, (*c*) elution of rhodium from the catalyst perhaps also caused by exposure to oxygen. However, it is possible that loss of activity is partly due to physical changes in the polymeric matrix of the catalyst which occur either during the hydrogenation reaction or in the handling between cycles. Electron microscope studies reveal that the physical appearance of the polymeric beads is greatly changed once they have been used in a hydrogenation reaction (1, 17).

Acknowledgments

The authors are grateful to the Natural Sciences and Engineering Research Council of Canada for financial assistance. One of us (G.S.) wishes to

thank the Instituto di Chimica Generale, Universitá di Venezia, Italy for provision of study leave.

1. Z. C. BRZEZIŃSKA and W. R. CULLEN. Can. J. Chem. **58**, 744 (1980).
2. R. H. GRUBBS. Chemtech. 512 (1977).
3. F. R. HARTLEY and P. N. VEZEY. Adv. Organomet. Chem. **15**, 189 (1977).
4. J. C. BAILAR, JR. Cat. Rev-Sci. Eng. **10**, 17 (1974).
5. K. G. ALLUM, R. D. HANCOCK, I. V. HOWELL, T. E. LESTER, S. MCKENZIE, R. C. PITKETHLY, and P. J. ROBINSON. J. Organomet. Chem. **107**, 393 (1976).
6. R. H. GRUBBS, L. C. KROLL, and E. M. SWEET. J. Macromol. Sci. Chem. A7, 1047 (1973).
7. J. M. MORETO, J. ALBAIGES, and F. CAMPS. *In* Catalysis homogeneous and heterogeneous. *Edited by* B. Delmon and G. Jannes. Elsevier, Amsterdam. 1975. p. 339.
8. M. ČAPKA, P. SVOBODA, M. ČERNÝ, and J. HETFLEJŠ. Tetrahedron Lett. **50**, 4787 (1971).
9. J. A. OSBORNE, F. H. JARDINE, J. F. YOUNG, and G. WILKINSON. J. Chem. Soc. A, 1711 (1966).
10. S. MONTELATICI, A. VAN DER ENT, J. A. OSBORNE, and G. WILKINSON. J. Chem. Soc. A, 1054 (1968).
11. W. NOLL. Chemistry and technology of silicones. Academic Press, New York, NY. 1968.
12. J. CONAN, M. BARTHOLIN, and A. GUYOT. J. Mol. Catal. **1**, 375 (1975/1976).
13. M. BARTHOLIN, CH. GRAILLAT, A. GUYOT, G. COUDURIER, J. BANDIERA, and C. NACCACHE. J. Mol. Catal. **3**, 17 (1977/1978).
14. A. R. SANGER and L. R. SCHALLIG. J. Mol. Catal. **3**, 101 (1977/1978).
15. F. G. YOUNG. U.S. Pat. 3,987,009 Oct. 19, 1976.
16. M. O. FARRELL. Ph.D. Thesis. Carnegie-Mellon University. 1978.
17. Z. C. BRZEZIŃSKA. Ph.D. Thesis. University of British Columbia. 1978.
18. J. HALPERN. *In* Organotransition-metal chemistry. *Edited by* Y. Ishii and M. Tsutsui. Plenum Press, New York, NY. 1975. p. 109.
19. C. A. TOLMAN, P. Z. MEAKIN, D. L. LINDNER, and J. P. JESSON. J. Am. Chem. Soc. **96**, 2762 (1974).
20. W. R. CULLEN and Z. C. BRZEZIŃSKA. Inorg. Chem. **18**, 3132 (1979).
21. Z. M. MICHALSKA. J. Mol. Catal. **3**, 125 (1977/1978).
22. G. STRUKUL, P. D'OLIMPIO, M. BONIVENTO, F. PINA, and M. GRAZIANI. J. Mol. Catal. **2**, 179 (1977).
23. R. H. GRUBBS and E. M. SWEET. J. Mol. Catal. **3**, 259 (1977/1978).
24. R. H. GRUBBS, E. M. SWEET, and S. PHISANBUT. *In* Catalysis in organic syntheses 1976. *Edited by* P.N. Rylander and H. Greenfield. Academic Press, New York, NY. 1976. p. 153.
25. K. G. ALLUM, R. D. HANCOCK, I. V. HOWELL, R. C. PITKETHLY, and P. J. ROBINSON. J. Catal. **43**, 322 (1976).
26. G. STRUKUL, M. BONIVENTO, M. GRAZIANI, M. CERNIA, and N. PALLADINO. Inorg. Chim. Acta, **12**, 15 (1975).
27. S. L. DAVIDOVA and N. A. PLATE. Coord. Chem. Rev. **16**, 195 (1975).
28. W. R. CULLEN, B. R. JAMES, A. D. JENKINS, G. STRUKUL, and Y. SUGI. Inorg. Nucl. Chem. Lett. **13**, 577 (1977).
29. J. REED, P. EISENBERGER, B.-K. TEO, and B. M. KINCAID. J. Am. Chem. Soc. **100**, 2375 (1978).
30. J. D. APLIN and L. D. HALL. J. Am. Chem. Soc. **99**, 4162 (1977).
31. J. D. APLIN and L. D. HALL. J. Am. Chem. Soc. **100**, 1934 (1978).

Can. J. Chem. Downloaded from www.nrcresearchpress.com by 210.87.254.105 on 09/05/12
For personal use only.

Can. J. Chem. Downloaded from www.nrcresearchpress.com by 210.87.254.6 on 09/05/12
For personal use only.

COMMUNICATION

A total synthesis of (±)-stemarin, a diterpenoid with a unique bicyclic C/D ring system

RONALD B. KELLY, MARY LOU HARLEY, AND SANDRA J. ALWARD

Department of Chemistry, University of New Brunswick, P.O. Box 5050, Saint John, N.B., Canada E2L 4L5

Received January 7, 1980

This paper is dedicated to Professor Karel Wiesner on the occasion of his sixtieth birthday

RONALD B. KELLY, MARY LOU HARLEY, and SANDRA J. ALWARD. Can. J. Chem. **58**, 755 (1980).

A total synthesis of (±)-stemarin, a diterpenoid with a unique C/D ring system, is described. The synthesis features photoaddition of allene to an α,β-unsaturated ketone and two skeletal rearrangements. Application of the synthetic strategy described herein to a synthesis of stemodinol and aphidicolin is anticipated.

RONALD B. KELLY, MARY LOU HARLEY et SANDRA J. ALWARD. Can. J. Chem. **58**, 755 (1980).

On décrit une synthèse totale de la (±) stémarine, un diterpène ayant un système cyclique C/D particulier. La synthèse est caractérisée par l'addition photochimique d'un allène sur une cétone α,β non saturée et par deux transpositions moléculaires. On envisage d'appliquer la stratégie décrite à la synthèse du stémodinol et de l'aphidicoline.

[Traduit par le journal]

Because of their unique structures, the diterpenoids stemarin (**1**) (1), stemodinol (**2**), and their relatives (2, 3) are attractive candidates for total synthesis. While contemplating syntheses of these diterpenoids, it occurred to us that they might be obtained via rearrangement of epimeric intermediates such as **3***a* and **3***b* where migration of bond *a* would lead to the stemarin skeleton and migration of bond *b* to the stemodinol skeleton. Since bond migration would be controlled by the stereoalignment of the migrating bond relative to the leaving group (OTs), **3***a* should rearrange to the stemarin skeleton and its epimer (**3***b*) to the stemodinol skeleton. We now wish to describe a total synthesis of stemarin (**1**) by application of this strategy.[1]

The tosylate **3***a* was prepared from the totally synthetic (5) racemic ketone **4** along lines previously employed in these laboratories (6) involving photoaddition of allene to **4** and subsequent skeletal rearrangement. Thus, stereo- and regiospecific photoaddition of allene to **4** afforded, in 78% yield, the adduct **5** (mp 121°C; ir: 1662 and 900 (olefin) cm^{-1}; nmr δ: 4.90 (m, 2H, vinylic protons))[2] which, on treatment with methyl iodide in THF in the presence of LDA at −10°C, gave (74% yield) the ketone **6** (mp 124°C; nmr δ: 1.16 (d, J = 6.5 Hz, 3H, secondary methyl)). The ketone **6** was converted in the usual manner, in 90% yield, into the ketal **7** (mp 131°C; nmr δ: 3.64 (br s, 4H, ethylene of ketal)).

1

3*a* Y = H, Z = OTs
3*b* Y = OTs, Z = H

2

4

5 R = H
6 R = CH_3

7 Z = CH_2
8 Z = O
9 Z = H, OH

10 Z = O
11 Z = $S(CH_2)_2S$
12 Z = H, H

13

14

[1]A synthesis of aphidicolin (4) by a similar strategy can be envisaged; for syntheses of aphidicolin by a different approach, see refs. 4*b*, *c*.

[2]Throughout, the ir spectra (in Nujol unless specified) and the nmr spectra (in $CDCl_3$) are entirely consistent with assigned structures. Satisfactory elemental analyses were obtained for all crystalline compounds and correct molecular ions were found in the mass spectra of the remaining compounds.

0008-4042/80/070755-02$01.00/0
©1980 National Research Council of Canada/Conseil national de recherches du Canada

Can. J. Chem. Downloaded from www.nrcresearchpress.com by 210.87.254.6 on 09/05/12
For personal use only.

Oxidation of **7** with osmium tetroxide – periodate under conditions previously employed for the cleavage of exocyclic methylenes (*6a*) gave, in 77% yield, the cyclobutanone **8** (mp 155°C; ir: 1779 (cyclobutanone) cm^{-1}; nmr: devoid of signals for vinylic protons). Reduction of **8** with $NaBH_4$ afforded quantitatively the cyclobutanol **9** (mp 164°C; ir: 3450 (OH) cm^{-1}; nmr δ: 4.22 (m, 1H, H—C—OH)). The cyclobutanol **9** was subjected to the first of two skeletal rearrangements featured in this synthesis. This was accomplished by heating it with hydrochloric acid in aqueous THF, whereupon it underwent deketalization then retroaldalization and spontaneous aldol condensation to produce two epimeric keto alcohols, **10** and its C-12 epimer.[3]

The keto alcohols, after separation by chromatography on silica gel in ether–petroleum, were obtained in 98% yield in the ratio of 3:1. The minor epimer **10** (mp 197°C; ir: 3520 (OH) cm^{-1}; nmr δ: 3.63 (m, 1H, H—C—OH), no methyl doublet) was converted quantitatively into the thioketal **11** (mp 172°C; nmr δ: 3.22 (m, 4H, ethylene of ketal)). Reduction of **11** with Raney nickel afforded, in 94% yield, the alcohol **12** (mp 136°C; ir: 3460 (OH) and 1720 (ester) cm^{-1}; nmr δ: 3.54 (m, 1H, H—C—OH)). The alcohol **12** was converted into the tosylate *3a* which, being unstable, was used immediately it was obtained without purification. In *3a*, the configuration at C-12 follows from the subsequent rearrangement *3a* → **13**, requiring the alignment of the migrating bond *a* to be *anti* to the tosylate group as shown.

Heating of *3a* in DMSO at 60°C with methylsulfinyl carbanion (7) smoothly brought about the second rearrangement to produce, in 79% yield, the olefin **13** (oil; ir (film): 1730 (ester) and 898 (olefin) cm^{-1}; nmr δ: 1.58 (d, J = 2 Hz, 3H, vinylic methyl) and 4.90 (m, 1H, vinylic proton)). In the penultimate step, **13** was converted, with *m*-chloroperbenzoic acid, into the epoxide **14** (oil; nmr δ: 1.28 (s, 3H, methyl attached to oxirane ring)). The configuration assigned to the oxirane ring follows from the reduction of **14** to stemarin (**1**).

Finally, reduction of **14** with $LiAlH_4$ afforded racemic stemarin (**1**) (mp 178°C) in 63% yield. The synthetic diterpenoid was found to be identical with an authentic sample of stemarin by the following criteria: identical ir and nmr spectra; identical behavior on tlc in a variety of solvents.

[3]For precvious examples of this type of rearrangement accomplished in these laboratories and an explanation of the mechanism, see ref. 6.

Acknowledgments

We are grateful to Dr. P. S. Manchand, Hoffmann-LaRoche Inc., Nutley, NJ for a sample of stemarin and for spectra of this diterpenoid. Also, we thank the Natural Sciences and Engineering Research Council of Canada for a grant awarded to R.B.K. and for a Postgraduate Scholarship awarded to M.L.H.

1. P. S. Manchand and J. F. Blount. J. Chem. Soc. Chem. Commun. 894 (1975).
2. C. D. Hufford, R. O. Guerrero, and N. J. Doorenbos. J. Pharm. Sci. **65**, 778 (1976).
3. P. S. Manchand, J. D. White, H. Wright, and J. Clardy. J. Am. Chem. Soc. **95**, 2705 (1973).
4. (*a*) K. M. Brundret, W. Dalziel, B. Hesp, J. A. J. Jarvis, and S. Neidle. J. Chem. Soc. Chem. Commun. 1027 (1972); (*b*) B. M. Trost, Y. Nishimura, K. Yamamoto, and S. S. McElvain. J. Am. Chem. Soc. **101**, 1328 (1979); (*c*) J. E. McMurry, A. Andrus, G. M. Ksander, J. H. Musser, and M. A. Johnson. J. Am. Chem. Soc. **101**, 1330 (1979).
5. T. A. Spencer, T. D. Weaver, R. M. Villarica, R. J. Friary, J. Posler, and M. A. Schwartz. J. Org. Chem. **33**, 712 (1968).
6. (*a*) R. B. Kelly, J. Eber, and H. K. Hung. Can. J. Chem. **51**, 2534 (1973); (*b*) R. B. Kelly, J. Zamecnik, and B. A. Beckett. Can. J. Chem. **50**, 3455 (1972).
7. E. J. Corey and M. Chaykovsky. J. Am. Chem. Soc. **87**, 1345 (1965).

Canadian Journal of Chemistry

Published by
THE NATIONAL RESEARCH COUNCIL OF CANADA

Volume 58 Number 8 April 15, 1980

Journal canadien de chimie

Publié par
LE CONSEIL NATIONAL DE RECHERCHES DU CANADA

Volume 58 numéro 8 15 avril 1980

Complexation of Zn(II) to a native sequence tripeptide of human serum albumin studied by ^{13}C nuclear magnetic resonance

HELEN LAKUSTA, CHARLES M. DEBER, AND BIBUDHENDRA SARKAR

The Research Institute, The Hospital for Sick Children, Toronto, Ont., Canada M5G 1X8 and the Department of Biochemistry, University of Toronto, Toronto, Ont., Canada M5S 1A8

Received October 12, 1979

HELEN LAKUSTA, CHARLES M. DEBER, and BIBUDHENDRA SARKAR. Can. J. Chem. **58**, 757 (1980).

Serum albumins from several species, which specifically bind and transport several divalent metals in blood, contain an Asp-X-His or Glu-X-His amino acid triad as their NH_2-terminal sequence. We have synthesized a tripeptide, Asp-Ala-His-*N*-methylamide, corresponding to the native sequence of the human serum albumin *N*-terminus, and examined its interaction with Zn(II) ions in aqueous solution using carbon-13 nmr techniques. Variations in carbon chemical shifts and spin–lattice relaxation times (T_1's) as a function of pH and increments of added Zn(II) were used to delineate sites of Zn(II):peptide interactions. Trends in T_1 values indicated that local motions of several of the tripeptide carbons were restricted by an induced order accompanying metal binding. Analysis of spectral data suggested that Zn(II) is coordinated to the His imidazole nitrogen atom and the Asp β-carboxylate oxygen atom(s) in each peptide molecule. Similar experiments using a tripeptide analogue, Gly-Gly-His-*N*-methylamide, demonstrated that in the absence of a side chain carboxylate group, Zn(II) ions will complex the peptide through the His imidazole group and the *N*-terminal Gly α-amino group. These results support the possibility of a biologically functional role for the Asp-X-His triad as a liganding template for Zn(II)/protein binding.

HELEN LAKUSTA, CHARLES M. DEBER, et BIBUDHENDRA SARKAR. Can. J. Chem. **58**, 757 (1980).

Les sérums d'albumine provenant de différentes espèces, qui se lient spécifiquement et transportent plusieurs métaux bivalents dans le sang, contiennent des triades d'acides aminés Asp-X-His ou Glu-X-His comme séquence *N*-terminale. Nous avons synthétisé le tripeptide Asp-Ala-His-*N*-méthylamide correspondant à la séquence *N*-terminale naturelle du sérum d'albumine humain et on a étudié son interaction avec les ions Zn(II) en solution aqueuse en utilisant les techniques de la rmn du ^{13}C. Pour délimiter les sites des interactions Zn(II):peptide, on a utilisé les variations des déplacements chimiques du carbone, des temps de relaxation spin–réseau (T_1) en fonction du pH et des quantités de Zn(II) ajouté. La tendance observée pour les valeurs de T_1 indique que des mouvements localisés de plusieurs carbones du tripeptide sont restreints par un ordre induit accompagnant le mode de liaison du métal. L'analyse des données spectrales indiquent que le Zn(II) est coordonné à l'azote du noyau imidazole de l'histidine et à l'atome (atomes) d'oxygène de la fonction carboxylate en position β de l'acide aspartique de chaque molécule de peptide. Des expériences semblables utilisant le tripeptide analogue Gly-Gly-His-*N*-méthylamide démontrent qu'en l'absence d'une chaîne latérale ayant au groupement carboxylate les ions Zn(II) se complexeront au peptide au niveau du groupe imidazole de l'histidine et du groupe amine en α de la glycine *N*-terminale. Ces résultats suggèrent la possibilité d'un rôle fonctionnel biologique de la triade Asp-X-His comme modèle de ligand du mode de liaison Zn(II)/protéine.

[Traduit par le journal]

Serum albumin is a multifunctional plasma protein which has been shown to bind several divalent metal ions and has been implicated in the transport processes of both Cu(II) (1–3) and Zn(II) (4–6). Albumin-bound Zn(II) has been found to account for approximately 98% of the exchangeable fraction of Zn(II) in serum (7). This fraction is known to be associated with the transport process of Zn(II) (4, 6, 7).

The affinity of Zn(II) both for the imidazole side chain of histidyl residues, and for the carboxylate group of dicarboxylic acid residues, has been established by chemical modification studies and through X-ray crystallographic analysis. For example, Zn(II) binding to His or Glu, or both, residues occur in several metalloenzymes including carboxypeptidase A (8), thermolysin (9), carbonic anhydrase B (10), and carbonic anhydrase C (11). Studies of Zn(II):albumin coordination have also implicated a His imidazole side chain in the binding

0008-4042/80/080757-10$01.00/0
©1980 National Research Council of Canada/Conseil national de recherches du Canada

Can. J. Chem. Downloaded from www.nrcresearchpress.com by 210.87.254.42 on 09/05/12
For personal use only.

Can. J. Chem. Downloaded from www.nrcresearchpress.com by 210.87.254.42 on 09/05/12
For personal use only.

of Zn(II) (12, 13). Examination of the NH_2-terminal regions of serum albumins from species such as human (Asp-Ala-His-) (14), bovine (Asp-Thr-His-) (15), and rat (Glu-Ala-His-) (14), reveals the presence not only of a common His-3 residue, but also a second common feature: the occurrence of a carboxylic acid-containing residue (Glu or Asp) at position 1. In the binding of albumin to Cu(II), which is known to prefer nitrogen ligands (see, for example, ref. 16) the α-amino group of the NH_2-terminal residue participates in binding along with the His-3 imidazole nitrogen atom (in addition to the two intervening peptide nitrogens) (15, 17, 18). However, a compilation of binding sites in protein–metal ion complexes of 3*d* cations such as Zn(II) demonstrates the widespread occurrence and enhanced stability of mixed imidazole/oxygen coordination systems (19). In the present work, we sought to determine if a further functional role can be ascribed to the albumin Asp (or Glu) NH_2-terminal residue, namely, the utilization of the side chain carboxylate moiety in Zn(II) binding.

Macromolecules such as serum albumin (584 amino acids in the monomer) are sufficiently complex that it becomes advantageous to investigate metal binding to smaller molecules containing the functional groups representative of the protein metal-binding site (for examples of this approach, see ref. 20). In this context, we have synthesized two tripeptides: Asp-Ala-His-*N*-methylamide (AAHNMA) (see Fig. 1), which contains the native sequence of the three *N*-terminal residues of human serum albumin; and Gly-Gly-His-*N*-methylamide (GGHNMA), which also contains the combination of an α-amino group and a His residue separated by one amino acid, but lacks the side chain carboxyl group on the *N*-terminal residue. The *C*-terminal residues of these tripeptides are bound into amide linkages to simulate the peptide bond of the protein. Copper(II)-binding properties of AAHNMA (21) correspond closely to those observed for albumin–Cu(II) binding (17). Analytical potentiometric studies of the Zn(II):AAHNMA system have also demonstrated that the tripeptide forms stable complexes with Zn(II) (22); however, while this technique is extremely valuable for quantitative measurements of metal:peptide affinity constants and species stoichiometries (see, for example, ref. 23), it cannot provide direct information as to the actual site(s) of metal:peptide interaction.

Since Zn(II) ion has neither intrinsic color nor unpaired electrons, the range of spectroscopic techniques available for investigation of its binding properties is limited. However, Zn(II) is

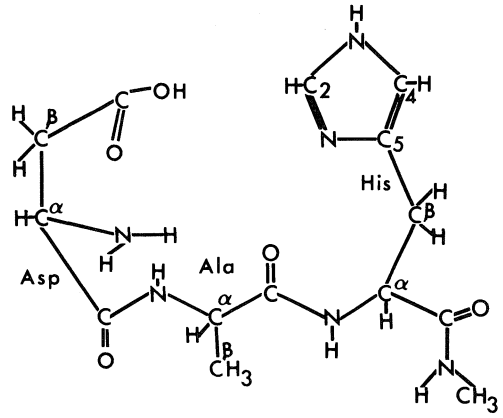


FIG. 1. Structure of Asp-Ala-His-*N*-methylamide, with component carbon atoms labelled as referred to in the text.

diamagnetic and does not cause the line broadening induced by paramagnetic ions; thus nuclear magnetic resonance spectra of Zn(II)/peptide complexes should be sharp and informative. In the present article, we have employed carbon-13 nuclear magnetic resonance to examine structural and dynamic properties of Zn(II):AAHNMA and Zn(II):GGHNMA complexes in aqueous solution.

Experimental

The tripeptides L-aspartyl-L-alanyl-L-histidine-*N*-methylamide (L-Asp-L-Ala-L-His-*N*-methylamide = AAHNMA) and glycyl-glycyl-L-histidine-*N*-methylamide (Gly-Gly-His-*N*-methylamide = GGHNMA) were prepared according to published procedures (21, 24).

Carbon-13 nmr spectra were recorded on a Varian XL-100 nmr spectrometer of field strength 23.5 kG (25.16 MHz for carbon-13) at a probe temperature of ca. 30°C. All chemical shifts were reported in ppm upfield from external carbon disulfide; these may be converted to ppm vs. external tetramethylsilane by subtracting chemical shifts given from 193.8 ppm.

Spin–lattice relaxation times (T_1's, reported in ms) were determined using the inversion–recovery method (25) employing a pulse sequence of $-(180°-t-90°-5T_1)-$. Values of T_1 were generally calculated by measuring peak intensity as a function of the variable time, t, and using a non-linear least-squares fitting procedure for the equation:

$$[1] \quad A = A_0(1 - 2\,e^{-t/T_1})$$

where A is the peak intensity at time t, and A_0 is the peak intensity at time $t = \infty$. Standard error in reported T_1's is approximately 10%. T_1 values (collected in Table 1) are reported as NT_1 values, where N is the number of protons directly bonded to any given carbon atom.

Spectra were recorded using natural abundance carbon-13, which necessitated sample concentrations of about 0.3 *M* to minimize spectra collection times. Samples were prepared in D_2O; values of pH (uncorrected for D_2O) were adjusted using either KOD or high purity concentrated HNO_3. Stock Zn(II) nitrate solutions (2 *M*) were prepared using "69 Grade" metallic zinc (see text) and high purity concentrated HNO_3. Solutions of Mn(II) and Cu(II) were prepared from reagent grade $MnCl_2 \cdot 4H_2O$ and $CuCl_2$, respectively.

Can. J. Chem. Downloaded from www.nrcresearchpress.com by 210.87.254.42 on 09/05/12
For personal use only.

Results

Carbon-13 Nuclear Magnetic Resonance Studies on L-*Asp*-L-*Ala*-L-*His*-N-*methylamide*

Assignments of resonances were made by comparisons with published chemical shifts of constituent amino acids (for a survey, see ref. 26); specific assignments within the peptide carbonyl regions of the spectra were obtained from the pH dependencies of their chemical shifts (*vide infra*). Through the range of pH 2–10, AAHNMA loses, in succession, protons from the Asp carboxyl side chain ($pK_a = 2.93$), the His imidazole ring ($pK_a = 6.32$), and the amino terminus ($pK_a = 7.73$) (24). In Fig. 2, the assigned His C=O reflects the titration of an imidazole moiety near neutral pH, and the assigned Asp C=O reflects the titration of an amino group between pH 7 and 10. The Asp side chain carboxylate carbon reflects both its own titration at acidic pH and the titration of the Asp amino group terminus at basic pH. The remaining carboxyl resonance shows essentially no change and is therefore assigned to the Ala residue. Chemical shifts of carbons adjacent to titratable groups also display corresponding behavior, notably the His C_2, C_5, and C_β resonances, and the Asp C_β resonance.

Titration of AAHNMA with Zn(II) nitrate (maintaining constant pH) also results in a series of significant chemical shift changes, presumably associated with Zn(II)–peptide binding. The largest chemical shift changes, as great as 4 ppm, are displayed by His imidazole resonances (shown in Fig. 3 at pH 7) in accord with the tendency of Zn(II) to bind imidazole nitrogens.

Titrations of AAHNMA with Zn(II) nitrate at pH 9 (Fig. 4) were limited to a lower range of Zn(II)–peptide ratios, due to the tendency toward precipitation with increasing additions of Zn(II). Further, as Zn(II) is added at pH 9, spectral lines begin to broaden, and spectra beyond a 1:2 Zn(II)–peptide ratio were virtually broadened into the baseline. This effect is illustrated in Fig. 5, where spectrum (*b*) differs from (*a*) only in that the pH is 9 rather than 7. Local rigidification of atoms specifically involved as bridging sites in aggregate or polymer formation at pH 9, such as His imidazole or pyrrole-type nitrogens (27–29), could produce the observed spectral effect of differentially broadened resonances.

Spin–Lattice Relaxation Times (T_1's) of Asp-Ala-His-N-*methylamide*

Systematic measurements of AAHNMA T_1's can, in principle, provide information regarding stoichiometry of complex(es) present, and restrictions to molecular motion along the peptide chain (for a discussion, see ref. 30). Table 1 summarizes the NT_1 values obtained for AAHNMA as a function of pH and of Zn(II)–peptide ratios. In general, pH had little or no effect on NT_1's of free peptide. However, at pH 7.0, where the most extensive data were collected, a large decrease in observed NT_1's of Zn(II)-bound vs. free AAHNMA was noted upon the addition of Zn(II). At a 1:4 Zn(II)–peptide ratio, most NT_1's have already dropped by about a factor of three (although NT_1's of the two methyl groups have decreased by lesser factors). This trend continues with NT_1's decreasing by a further factor of two when the ratio of Zn(II)–peptide was doubled to 1:2 (indicated as 2:4 in Table 1). Above this ratio, however, few significant changes in NT_1's occur.[1]

At pH 9.0, reliable NT_1 values could be obtained only on the free peptide and at a 1:4 ratio, where NT_1's largely parallel those for the 1:4 ratio at pH 7.

Carbon-13 Nuclear Magnetic Resonance Studies on Gly-Gly-His-N-*methylamide*

Results of pH titrations (in the range 2–10) with GGHNMA are given in Fig. 6. As with AAHNMA, resonance assignments were based upon empirical correlations with chemical shifts of constituent amino acids (26). The assignment of the appropriate carbonyl resonance to the *N*-terminal Gly peptide carbonyl carbon was made on the basis of its titration behavior (i.e., shift of 8 ppm downfield) reflecting the deprotonation of the *N*-terminal amino group ($pK_a = 7.87$). The NH_2-terminal Gly C_α resonance shows similar behavior, while the His C_2 and C_5 resonances reflect deprotonation of the imidazole moiety ($pK_a = 6.39$).

Additions of Zn(II) nitrate to GGHNMA at pH 7 resulted in the spectral changes presented in Fig. 7.

[1]The assay of trace paramagnetic metals in 69 Grade metallic zinc indicated that Cu(II) and Fe(III) might be present up to a total of ca. 0.1 ppm (about 10^{-7} *M* in a 1 *M* solution of $Zn(NO_3)_2$). Copper(II) is known to bind AAHNMA and related peptides specifically through the histidyl residue, the amino terminus, and the peptide nitrogens (21, 23, 32). Although addition of Cu(II) (as the chloride) to AAHNMA up to a maximum concentration of 10^{-5} *M* did result in a decrease of a few percent in the observed NT_1's (see ref. 31 for examples of paramagnetic ion effects on NT_1 values) — for example, Ala C_β decreases from 1350 to 1210 ms; His C_β from 400 to 370 ms — this clearly did not account for the drop in NT_1's accompanying the addition of Zn(II). In another experiment, the paramagnetic Mn(II) ion was added at pH 7 (as the chloride) to AAHNMA, to a maximum concentration of 3×10^{-5} *M*, a Mn(II) level high enough to have resulted in a decrease in peptide NT_1's, even via non-specific binding to AAHNMA (33). The resulting NT_1's (e.g., Ala C_β, 1120 ms; His C_β, 390 ms) paralleled those observed in the presence of Cu(II), indicating that Mn(II) did not have a significant effect on peptide relaxation times under these conditions.

TABLE 1. Spin–lattice relaxation values (NT_1's) (ms) measured for L-Asp-L-Ala-L-His-*N*-methylamide and its Zn(II) complexes*

pH	Ratio Zn(II)–peptide	Ala-CH_3	His *N*-methyl-amide	His C_β	Asp C_β	Ala C_α	Asp C_α	His C_α	His C_4	His C_2
4.0	0	1040	—	—	500	310	310	290	200	190
4.0	1:4	1300	—	—	410	290	310	280	160	120
4.0	1:1	1070	—	—	330	270	230	240	160	170
7.0	0	1350	2610	400	520	360	350	300	—	—
7.0	1:4	790	1230	140	180	130	150	130	44	120
7.0	2:4	660	1140	74	96	73	73	60	—	—
7.0	3:4	560	730	94	92	59	59	56	51	55
7.0	4:4	560	840	74	82	65	65	74	73	78
9.0	0	1410	2370	420	560	320	460	280	—	—
9.0	1:4	790	1220	130	180	120	140	130	64	76

*Spectra recorded at 25 MHz on solutions of 120–150 mg/mL peptide + added Zn(II) nitrate at the indicated Zn(II)–peptide ratios and values of pH (uncorrected for D_2O). Estimated uncertainty in NT_1's: ±10%. Values not given represent overlaps of resonances, or insufficient data for reliable determination. See Experimental section for further details of experimental parameters.

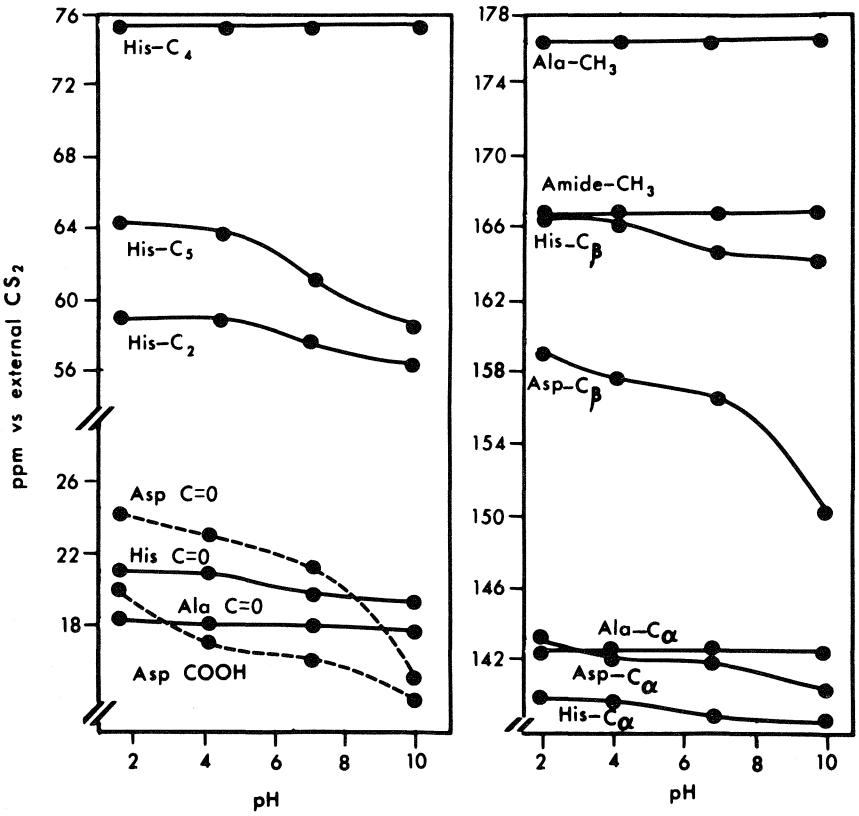


FIG. 2. Dependence of carbon-13 resonances of L-Asp-L-Ala-L-His-*N*-methylamide on pH over the range 2–10. Data were collected on samples containing 55 mg/mL peptide in D_2O solutions. Values of pH are uncorrected for D_2O. The pH was adjusted with KOD or HNO_3 as required.

As with AAHNMA (see Fig. 3), initial addition of Zn(II) produced immediate changes in His resonances, implicating the imidazole group in Zn(II) binding. However, in contrast to the carbonyl region of AAHNMA spectra, which remained relatively insensitive to initial portions of added Zn(II), the amino terminal Gly carbonyl resonance (ca. 24 ppm at pH 7, see also Fig. 6) displays clear titration behavior, moving downfield ca. 5.5 ppm over the range of 0 to 1:1 ratios of Zn(II)–GGHNMA. The Zn(II) had no appreciable effect on other GGHNMA carbonyl chemical shifts.

Can. J. Chem. Downloaded from www.nrcresearchpress.com by 210.87.254.42 on 09/05/12
For personal use only.

Can. J. Chem. Downloaded from www.nrcresearchpress.com by 210.87.254.42 on 09/05/12
For personal use only.

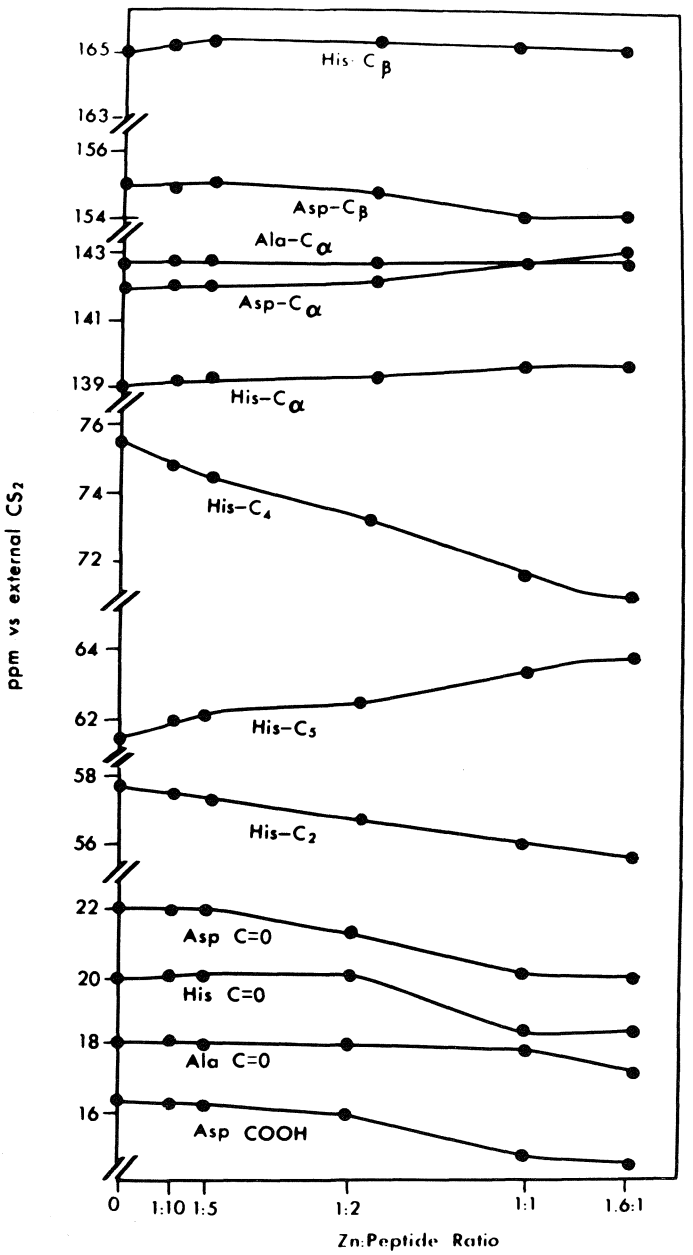


FIG. 3. Variations in chemical shifts of carbon atoms of L-Asp-L-Ala-L-His-*N*-methylamide as a function of added Zn(II) nitrate at pH = 7. Data were collected on samples containing 55 mg/mL peptide in D_2O solutions. Values of pH (uncorrected for D_2O) were adjusted as required after additions of $Zn(NO_3)_2$ with KOD. Chemical shifts of resonances due to Ala C_β (ca. 176.5 ppm) and His-*N*-methylamide (ca. 166.5 ppm) were essentially unchanged over this range of Zn(II) additions.

A preliminary set of NT_1 values for the Zn(II)–GGHNMA system was obtained on the same sample used to compile the spectra represented by Fig. 7. It was found that GGHNMA NT_1 values drop substantially upon additions of $Zn(NO_3)_2$, by at least a factor of two at 1:2 Zn(II)–peptide ratios (and for some resonances, by a factor of four at that ratio). For example, values of NT_1 were 2260 ms for His *N*-methylamide (free GGHNMA) vs. 1120 ms (1:2 Zn(II)–peptide). NT_1's did not appear to vary significantly upon additions of Zn(II) between 1:2 and 1:1.

Can. J. Chem. Downloaded from www.nrcresearchpress.com by 210.87.254.42 on 09/05/12
For personal use only.

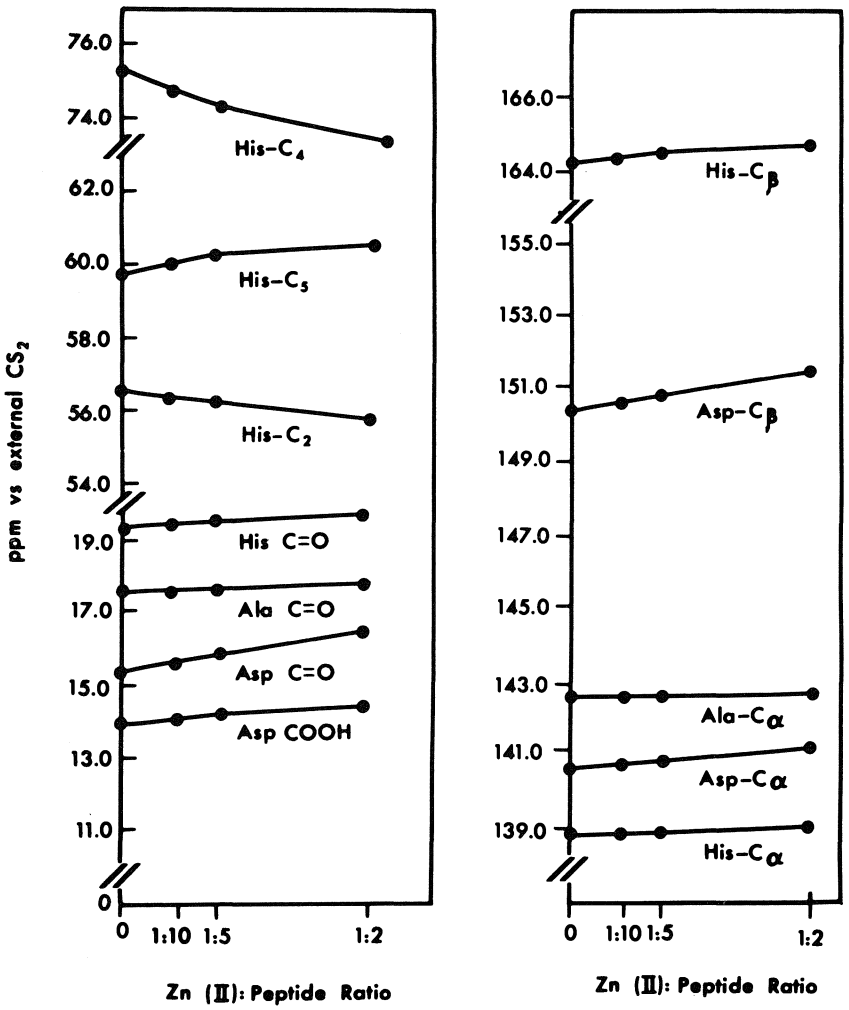


FIG. 4. Variations in chemical shifts of carbon atoms of L-Asp-L-Ala-L-His-*N*-methylamide as a function of added Zn(II) nitrate at pH = 9. Data were collected on samples containing 55 mg/mL peptide in D_2O solutions. Values of pH (uncorrected for D_2O) were adjusted as required after additions of $Zn(NO_3)_2$ with KOD. Chemical shifts of resonances due to Ala C_β (ca. 176.5 ppm) and His-*N*-methylamide (ca. 166.5 ppm) were essentially unchanged over this range of Zn(II) additions.

Discussion

Chemical shift data for AAHNMA at pH 7 (Fig. 3) demonstrate that His imidazole carbon resonances change positions over a wide range of Zn(II) additions (0 to 1:1), consistent with the suggestion that Zn(II) binding involves the histidyl side chain. The apparent lack of complex formation inferred from T_1 data at pH 4 (where the His imidazole ring is essentially protonated) supports this suggestion. Data on Gly-Gly-His-*N*-methylamide (as summarized in Figs. 6 and 7) indicate that Zn(II) also binds to this peptide, with His imidazole again a site of strong interaction.

One crucial difference between spectral effects noted with GGHNMA (vs. AAHNMA) is the downfield shift (ca. 6 ppm, Fig. 7) of the GGHNMA *N*-terminal Gly carbonyl resonance over the range of added Zn(II). (In the AAHNMA case, the Asp carbonyl shifts ca. 1 ppm downfield between 1:2 and 1:1 Zn(II)–peptide ratios.) Such an effect is likely the result of metal-assisted deprotonation of the GGHNMA Gly-*N*-terminal amino group at pH 7, and implicates the amino group as a site of direct Zn(II):GGHNMA interaction. These findings lead to the conclusion that *in AAHNMA it is the Asp carboxylate rather than the Asp amino terminal group which serves as a Zn(II) coordination site.*

The overall drop in NT_1's by factors of 5–6 (Table 1) in several AAHNMA carbons suggests that complexation results in a restriction of segmental motion throughout much of the peptide, most likely due to an induced order accompanying

Can. J. Chem. Downloaded from www.nrcresearchpress.com by 210.87.254.42 on 09/05/12
For personal use only.

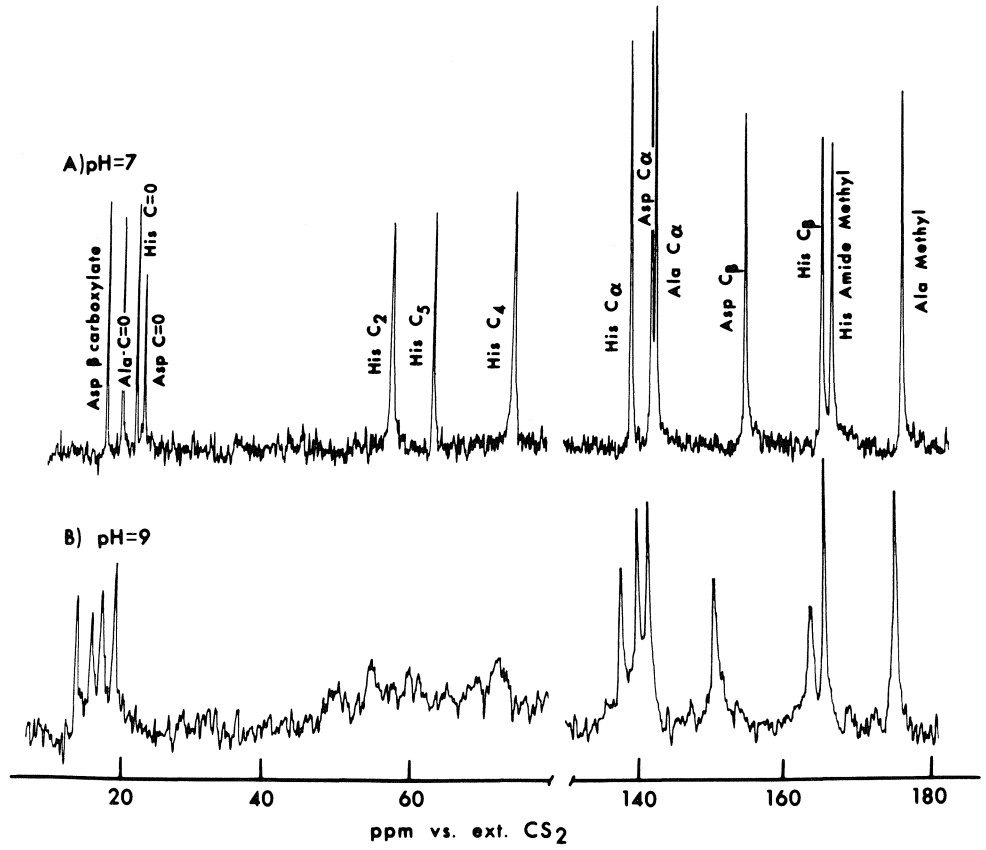


FIG. 5. Carbon-13 nmr spectra (25 MHz) of L-Asp-L-Ala-L-His-*N*-methylamide + Zn(II) nitrate (*a*) at pH = 7, and (*b*) at pH = 9. The ratio of Zn(II):peptide in both spectra is 1/2. Concentration: ca. 55 mg/mL in D_2O. See text for a further discussion of these spectra.

binding which tends to stabilize the peptide in its binding conformation. In fact, the NT_1 data suggest rigidification of a large portion of the tripeptide carbons, including the imidazole ring, His C_α, His C_β, Ala C_β, Asp C_α, and Asp C_β (see Fig. 1). In structural terms, these results suggest that in the Zn(II):AAHNMA complex, the Zn(II) binds the peptide at liganding sites located at opposite ends of the molecule (in effect, bridging them to form a closed loop). The fact that the Asp side chain C_β carbon experiences the same relative decreases in NT_1's as several of its neighboring carbons is consistent with the binding of Zn(II) to the Asp side chain carboxylate group. Since nitrogen-type coordination sites (34, 35) and oxygen-type sites (8, 9) both occur widely in Zn(II) chemistry, the preference for Zn(II) to bind the AAHNMA Asp carboxylate group rather than the Asp α-amino group may reflect a greater affinity at pH 7 of Zn(II) for the negatively-charged carboxylate group rather than the (still protonated) α-amino group.

Aspects of AAHNMA NT_1 data (Table 1) indicate that the predominant species at pH 7 may have a stoichiometry of one Zn(II):two peptides. Such a bis-complex is suggested from NT_1's which do not decrease significantly after a 1:2 Zn(II):peptide ratio is reached.[2] The NT_1's observed for the two AAHNMA methyl groups are in reasonable accord with those anticipated on stoichiometric grounds for bis-complex formation; note that these groups are external to the rigidified array of carbons which would be bridged by Zn(II) complexation. However, chemical shift data for the Zn(II):AAHNMA

[2]The necessity of recording T_1 data at relatively high peptide concentrations (ca. 100 to 150 mg/mL) probably gives rise to species of stoichiometry higher than might be the case for more dilute solutions or under physiological conditions. By comparison, analytical potentiometric analysis of the Zn(II):AAHNMA system, performed at concentrations of [Zn(II)] = 0.046 m*M* and [AAHNMA] = 0.44 m*M* (compared with [AAHNMA] = 300 m*M* in nmr experiments) over the pH range ca. 6–8, indicates that two predominant species are present: a 1:1 Zn(II):AAHNMA complex which accounts for 60% of bound Zn(II) at pH 7, and a 1:2 Zn(II):AAHNMA complex which accounts for 40% of bound Zn(II) at pH 8 (22).

Can. J. Chem. Downloaded from www.nrcresearchpress.com by 210.87.254.42 on 09/05/12
For personal use only.

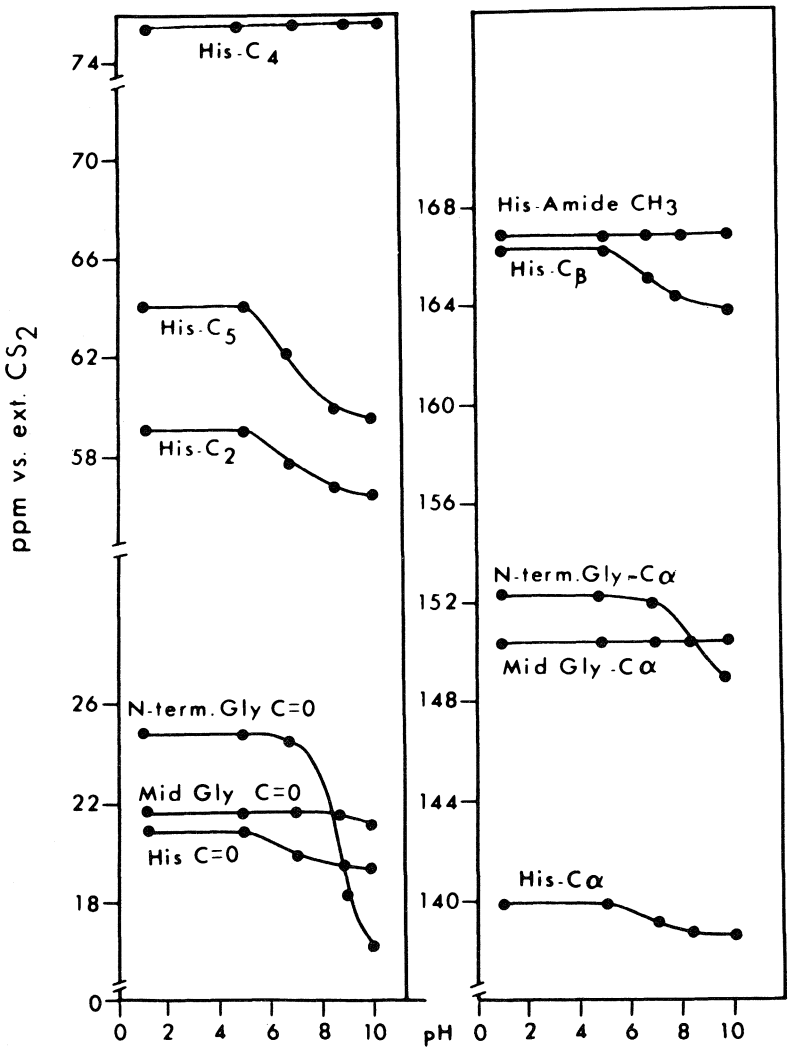


FIG. 6. Dependence of carbon-13 resonances of Gly-Gly-L-His-*N*-methylamide on pH over the range 2–10. Data were collected on samples containing 100 mg/mL peptide in D_2O solutions. Values of pH are uncorrected for D_2O.

system (Fig. 3) suggest that the peptide undergoes a "titration" process (chemical shifts change ca. 1 ppm) between 1:2 and 1:1 Zn(II):peptide ratios. This may be a spectral manifestation of the conversion of some bis-species to 1:1 Zn(II):AAHNMA species with increasing Zn(II) concentration, and/or the interaction of added Zn(II) atoms with the AAHNMA free α-amino group which would still be available as a ligating site.

From the overall chemical shift data, and model building studies, one may infer a possible structure for the Zn(II) complex with AAHNMA, in which Zn(II) is coordinated to each AAHNMA molecule at two sites: the imidazole nitrogen atom of the His residue and the carboxyl group of the Asp residue. Remaining coordination sites would be occupied by solvent molecules. If indeed the bis-complex is the predominant stoichiometric species in the present experimental system, carbon-13 spectra indicate that the two component peptide molecules are geometrically symmetric on the nmr time scale at probe temperature; the data do not provide direct information concerning the spatial relationship, or dihedral angles of individual peptide chains. In the bis-complex, models suggest octahedral coordination for the Zn(II) atom; the tetrahedral bis-complex was found to be sterically unwieldly with the above four (two His, two Asp) ligands coordinated. Sites of Zn(II):peptide coordination remain the same, regardless of whether the stoichiometry of the complex is one Zn(II):one peptide or one Zn(II):two peptides.

If the peptide binds Zn(II) through His imidazole and Asp carboxyl groups only, the chelate ring size

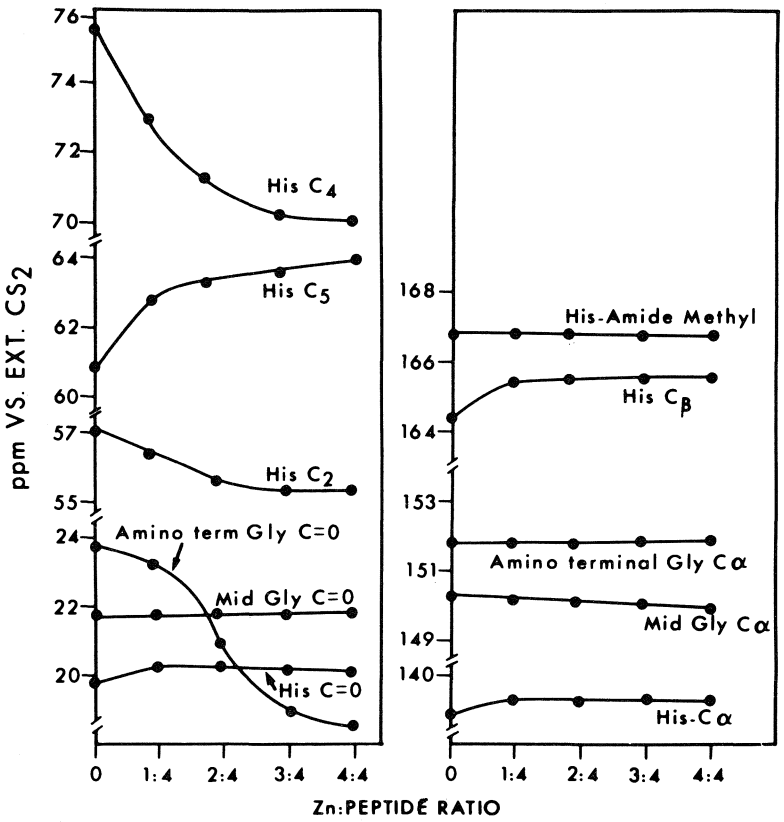


FIG. 7. Variations in chemical shifts of carbon atoms of Gly-Gly-L-His-*N*-methylamide as a function of added Zn(II) nitrate at pH = 7. Data were collected on samples containing 100 mg/mL peptide in D_2O solutions. Values of pH (uncorrected for D_2O) were adjusted as required after additions of $Zn(NO_3)_2$ with KOD.

is rather large (13-membered). Since the stability of a chelate complex generally decreases as the size of the chelate ring increases (36), it is possible that one (or more) of the intervening potential ligand atoms on the peptide may also stabilize the complex via Zn(II) binding (although no experimental manifestation of this possibility emerged from the nmr data). Alternatively, the free peptide itself, containing substituents with a variety of charge and bulk, may possess a narrow range of allowed conformations in solution. This could include a particular set of conformers where proximity of carboxylate and imidazole groups facilitates Zn(II) binding even though the resulting ring size may be large.

The sequence of 584 amino acids of human serum albumin (37, 38) contains 16 His residues and 100 carboxylic acid residues (39 Asp's; 61 Glu's). Although the globular nature of transport proteins obviously does not preclude the proximity of functional groups from sequentially-distant amino acids, only twice in the protein does the combination occur of a side chain carboxyl group and a His residue separated by one intervening amino acid: the *N*-terminus and in a Asp-Glu-His triad (residues 35–37) (or Glu-Asp-His (21)). Note that this triad can bind Zn(II) in the manner deduced herein for AAHNMA, whether it occurs at the N-terminus or at interior portions of the protein sequence. The contrasting results determined by ^{13}C nmr for Zn(II) binding with AAHNMA, vs. its binding with a peptide lacking the side chain carboxyl group, GGHNMA, support the possibility of involvement in Zn(II):serum albumin binding of the side chain carboxyl group of Glu or Asp residues when they occur in a 1–3 relationship with His residues.

Acknowledgement

The research was supported, in part, by grants to C.M.D. (No. 5810) and B.S. (No. 1800) from the Medical Research Council of Canada.

1. P. Z. NEUMANN and A. SASS-KORTSAK. J. Clin. Invest. **46**, 646 (1967).
2. A. G. BEARN and H. G. KUNKEL. Proc. Soc. Exp. Biol. Med. **85**, 44 (1954).
3. B. SARKAR and Y. WIGFIELD. Can. J. Biochem. **46**, 601 (1968).
4. E. L. GIROUX and R. I. HENKIN. Bioinorg. Chem. **2**, 125 (1972).

Can. J. Chem. Downloaded from www.nrcresearchpress.com by 210.87.254.42 on 09/05/12
For personal use only.

5. J. A. HALSTEAD, C. J. SMITH, JR., and M. I. IRWIN. Nutrition, **104**, 1974 (1974).
6. F. FRIEDBERG. FEBS Lett. **59**, 140 (1975).
7. E. L. GIROUX and R. I. HENKIN. Biochem. Biophys. Acta, **273**, 64 (1972).
8. W. N. LIPSCOMB, J. A. HARTSUCK, F. A. QUIOCHO, and G. N. REEKE, JR. Proc. Natl. Acad. Sci. U.S.A. **64**, 28 (1969).
9. B. W. MATTHEWS, J. N. JANSONIUS, P. M. COLMAN, B. P. SCHOENBORN, and D. DUPOURQUE. Nature, New Biol. **238**, 37 (1972).
10. A. LILJAS, K. K. KANNAN, P. C. BERGSTEN, I. WAARA, K. FRIDBORG, B. STRANDBERG, V. CARLBOM, L. JARUP, S. LOVGREN, and M. PETEF. Nature, New Biol. **235**, 131 (1972).
11. K. K. KANNAN, B. NOTSTRAND, K. FRIDBORG, S. LOVGREN, A. OHLSSON, and M. PETEF. Proc. Natl. Acad. Sci. U.S.A. **72**, 51 (1975).
12. F. R. N. GURD and D. S. GOODMAN. J. Am. Chem. Soc. **74**, 670 (1952).
13. M. S. N. RAO and H. LAL. J. Am. Chem. Soc. **80**, 3226 (1958).
14. R. A. BRADSHAW and T. PETERS, JR. J. Biol. Chem. **244**, 5582 (1969).
15. W. T. SHEARER, R. A. BRADSHAW, F. R. N. GURD, and T. PETERS, JR. J. Biol. Chem. **242**, 5451 (1967).
16. E. BRESLOW. *In* Inorganic biochemistry. Vol. 1. *Edited by* G. L. Eichhorn. Elsevier, New York. 1973.
17. T. PETERS, JR. and F. W. BLUMENSTOCK. J. Biol. Chem. **242**, 1574 (1967).
18. R. A. BRADSHAW, W. T. SHEARER, and F. R. N. GURD. J. Biol. Chem. **243**, 3817 (1968).
19. H. SIGEL, B. E. FISCHER, and B. PRIJS. J. Am. Chem. Soc. **99**, 4489 (1977).
20. P. Q. BEHRENS, A. M. SPIEKERMAN, and J. R. BROWN. Fed. Proc. **34**, 591 (1975).
21. K. S. N. IYER, S. LAU, S. H. LAURIE, and B. SARKAR. Biochem. J. **169**, 61 (1978).
22. H. LAKUSTA and B. SARKAR. J. Inorg. Biochem. **11**, 303 (1979).
23. B. SARKAR. Ind. J. Chem. Soc. **54**, 117 (1977).
24. T. P. A. KRUCK, S. LAU, and B. SARKAR. Can. J. Chem. **54**, 1300 (1976).
25. D. DODDRELL, V. GLUSHKO, and A. ALLERHAND. J. Chem. Phys. **56**, 3683 (1972).
26. O. W. HOWARTH and D. M. J. LILLEY. Prog. Nucl. Magn. Reson. Spectrosc. **12**, 1 (1978).
27. J. E. BAUMAN and J. C. WANG. Inorg. Chem. **3**, 368 (1968).
28. C. SANDMARK and C. J. BRANDEN. Acta Chem. Scand. **21**, 993 (1967).
29. D. W. APPLETON and B. SARKAR. Proc. Natl. Acad. Sci. U.S.A. **71**, 1686 (1974).
30. K. WUTHRICH. *In* NMR in biological research: peptides and proteins. North-Holland Publishing Co., Amsterdam. 1976.
31. R. E. WASYLISHEN and M. R. GRAHAM. Can. J. Chem. **54**, 617 (1976).
32. N. CAMERMAN, A. CAMERMAN, and B. SARKAR. Can. J. Chem. **54**, 1309 (1976).
33. R. A. DWEK. *In* NMR in biochemistry: applications to enzyme systems. Clarendon Press, Oxford. 1973.
34. H. C. FREEMAN. *In* Inorganic biochemistry. Vol. 1. *Edited by* G. I. Eichhorn. Elsevier, New York. 1973.
35. M. A. WELLS and T. C. BRUICE. J. Am. Chem. Soc. **99**, 5341 (1977).
36. F. J. C. ROSSOTI. *In* Modern coordination chemistry. *Edited by* J. Lewis and R. G. Wilkins. Interscience Publishers, New York. 1960.
37. B. MELOUN, L. MORAVEK, and V. KOSTKA. FEBS Lett. **58**, 134 (1975).
38. C. C. TANG, D. DAVALIAN, P. HUANG, and R. BRESLOW. J. Am. Chem. Soc. **100**, 3918 (1978).

Can. J. Chem. Downloaded from www.nrcresearchpress.com by 210.87.254.42 on 09/05/12
For personal use only.

Theoretical study of magnetic susceptibilities of small molecules by SCF-LCAO-MO-MINDO/3 method

PRABHAT K. K. PANDEY AND P. CHANDRA

Department of Chemistry, Banaras Hindu University, Varanasi-221005, India

Received March 27, 1979[1]

PRABHAT K. K. PANDEY and P. CHANDRA. Can. J. Chem. **58**, 767 (1980).

Magnetic susceptibilities of small hydrocarbons and water are calculated by employing gauge-invariant atomic orbitals within MINDO/3 approximation. A comparison with available INDO calculations indicates that MINDO/3 gives reasonable values for diamagnetic contribution, but in general overestimates the paramagnetic contribution to magnetic susceptibility.

PRABHAT K. K. PANDEY et P. CHANDRA. Can. J. Chem. **58**, 767 (1980).

On a calculé les susceptibilités magnétiques des petites molécules d'hydrocarbures et de l'eau en utilisant un étalon invariable d'orbitales atomiques à l'intérieur d'une approximation MINDO/3. Une comparaison avec les calculs INDO disponibles indiquent que MINDO/3 donne des valeurs raisonables pour la contribution diamagnétique, mais surestime en général la contribution paramagnétique à la susceptibilité magnétique.

[Traduit par le journal]

Can. J. Chem. Downloaded from www.nrcresearchpress.com by 210.87.254.5 on 09/05/12
For personal use only.

Introduction

The general theory of magnetic susceptibilities was first developed by Van Vleck (1) using Raleigh–Schrodinger perturbation theory up to second order. Further developments in these calculations were hampered because of the lack of the knowledge of the excited state wavefunctions although there have been quite a few attempts in this direction employing average energy approximation (2). In recent years few *ab initio* calculations utilizing both variational (3) as well as SCF perturbation theories (4) have been carried out. Ditchfield *et al.* (5) and Arrighini *et al.* (6) have used minimal and fairly extended basis sets, respectively, in their calculations. Their calculated results agree only moderately well with experiments. Moreover, these results were dependent on the choice of the origin of the coordinate system. The use of gauge-invariant atomic orbitals (GIAO's) avoids these difficulties and an SCF perturbation theory along these lines was developed by Davies (7) and by Hall and Hardisson (8), but their formulation was restricted to π-electron systems only. All these theories constitute the basis of an extensive review by Ditchfield (9). The general SCF perturbation theory of magnetic susceptibilities using GIAO's was first proposed by Ditchfield (10) and by Hall (11). The theory at *ab initio* level (12) is fairly complicated and costly to implement even for small molecules. We have, therefore, employed MINDO/3 (13) approximation within the framework of above theory and have compared the results with those obtained (14–16) by CNDO and INDO approximation (17). This study was a part of our plan of studying various molecular properties (18), e.g. dipole moments, dipole moment derivatives (19), esr isotropic hyperfine couplings (20), and nmr spin–spin couplings (21) employing MINDO/3 approximation.

[1]Revision received December 3, 1979.

Theory

The details of MINDO/3 approximation (13) and those of magnetic susceptibility calculations are described elsewhere (9, 10, 15). Employing GIAO's together with London's approximation (22), we obtain the following expressions for magnetic susceptibility in terms of its components (15).

$$[1]\quad (\chi)_{zz} = (\chi^{p})_{zz} + (\chi^{d})_{zz} = (\chi)_{zz}(\text{local}) + (\chi)_{zz}(\text{non-local})$$

$$[2]\quad (\chi)_{zz}(\text{local}) = (\chi)_{zz}(\text{intra}) + (\chi)_{zz}(\text{cross})$$

$$[3]\quad (\chi)_{zz}(\text{non-local}) = (\chi^{d})_{zz}(\text{inter}) + (\chi^{p})_{zz}(\text{two-centre})$$

$$[4]\quad (\chi^{p})_{zz}(\text{two-centre}) = (\chi^{p})_{zz}(\text{inter}) + (\chi)_{zz}{}^{R}(\text{cross})$$

$$[5]\quad (\chi)_{zz}(\text{intra}) = (\chi^{d})(\text{intra}) + (\chi^{p})(\text{intra})$$

where

$$[6]\quad (\chi^{d})_{zz}(\text{intra}) = -\sum_{A}\sum_{\mu\nu}^{A} P_{\mu\nu}{}^{(0)}(H_{\mu\nu}{}^{(2,0)})_{zz}$$

$$[7]\quad (\chi^{p})_{zz}(\text{intra}) = -\sum_{A}\sum_{\mu\nu}^{A} (P_{\mu\nu}{}^{(1)})_{z}{}^{L}(H_{\mu\nu}{}^{(1,0)})_{z}$$

$$[8]\quad (\chi^{d})_{zz}(\text{inter}) = -\sum_{A>B}\sum_{\mu}^{A}\sum_{\nu}^{B} P_{\mu\nu}{}^{(0)}(H_{\mu\nu}{}^{(2,0)})_{zz}$$

0008-4042/80/080767-05$01.00/0

©1980 National Research Council of Canada/Conseil national de recherches du Canada

Can. J. Chem. Downloaded from www.nrcresearchpress.com by 210.87.254.5 on 09/05/12
For personal use only.

TABLE 1. MINDO/3 calculated magnetic susceptibilities of some small molecules*

Molecule	Diamagnetic			Paramagnetic			Total			Average	Exp. (ref. 23)
	xx	*yy*	*zz*	*xx*	*yy*	*zz*	*xx*	*yy*	*zz*		
CH_4	−13.40	−13.40	−13.40	4.32	4.32	4.32	−9.08	−9.08	−9.08	−9.08	
	[−13.60]	[−13.60]	[−13.60]	[2.71]	[2.71]	[2.71]	[−10.89]	[−10.89]	[−10.89]	[−10.89]	−17.4
	−15.6	−15.6	−15.6	(3.8)	(3.8)	(3.8)	−11.8)	(−11.8)	(−11.8)	(−11.8)	
C_2H_4	−21.84	−29.71	−21.80	28.06	17.24	16.24	6.22	−12.47	−5.56	−3.94	
	(−24.5)	(−24.5)	(−24.5)	(7.8)	(6.8)	(15.5)	(−16.7)	(−17.7)	(−9.2)	(−14.6)	
†	—	—	—	—	—	—	(−9.6)	(−20.5)	(−17.0)	(−15.7)	
		(−21.36‡)			(27.23‡)						−18.8
C_2H_2	−18.90	−18.90	−19.28	18.62	18.62	0.0	−0.28	−0.28	−19.28	−6.61	
	[−18.94]	[−18.94]	[−19.24]	[19.88]	[19.88]	[0.0]	[0.94]	[0.94]	[−19.24]	[−5.79]	
	(−21.3)	(−21.3)	(−21.5)	(9.9)	(9.9)	(0.0)	(−11.4)	(−11.4)	(21.5)	(−14.8)	
†	—	—	—	—	—	—	(−11.2)	(−11.2)	(−21.7)	(−14.7)	−20.8
C_2H_6	−34.91	−34.91	−23.8	19.99	19.99	8.54	−14.92	−14.92	−15.34	−15.06	
	(−27.9)	(−27.9)	(−27.7)	(7.5)	(7.5)	(7.2)	(−20.4)	(−20.4)	(−20.4)	(−20.4)	
†	—	—	—	—	—	—	(−24.4)	(−24.4)	(24.2)	(−24.4)	−26.8
cyclo-C_3H_6	−48.78	−42.99	−48.01	27.02	25.99	32.80	−27.76	−17.00	−15.21	−17.99	−39.2
H_2O	−9.06	−8.49	−8.92	6.18	4.73	6.60	−2.88	−3.76	−2.32	−2.99	
	(−10.3)	(−9.7)	(−10.1)	(4.0)	(5.0)	(6.0)	(−6.3)	(−4.7)	(−4.1)	(−5.0)	−13.0

*Units are erg G^{-2} mol^{-1} × 10^{-6}; MINDO/3 values corresponding to $\rho_H = 1.0$ are given in square brackets; INDO values, two-centre terms neglected given in parentheses (9).
†INDO values, two-centre terms included (15).
‡Discrepancy between INDO calculated values reported in ref. 9 and those calculated by us.

TABLE 2. Average one-centre and two-centre contributions to calculated susceptibilities

Molecule	χ^d(intra)	χ^p(intra)	χ^L(cross)	χ^R(cross)	χ^p(inter)
CH_4	−13.65 [−13.75]	5.09 [5.03]	0.33 [−0.59]	−1.04 [−1.96]	—0.06 [0.23]
C_2H_4	−21.73	15.87	1.99	−0.85	3.51
C_2H_2	−19.03 [−19.04]	11.33 [12.17]	1.08 [1.08]	0.0 [0.0]	0.0 [0.0]
C_2H_6	−24.43	10.40	0.13	−2.51	8.15
cyclo-C_3H_6	−32.54	17.09	−0.19	−4.57	16.29
H_2O	−8.82	4.08	1.78	−0.02	0.0

[9] $$(\chi^p)_{zz}(\text{inter}) = -\sum_{A>B}\sum_{\mu}^{A}\sum_{\nu}^{B}(P_{\mu\nu}{}^{(1)})_z{}^R(H_{\mu\nu}{}^{(1,0)})_z$$

[10] $$(\chi)_{zz}{}^L(\text{cross}) = -\sum_{A}\sum_{\mu\nu}^{A}(P_{\mu\nu}{}^{(1)})_z{}^R(H_{\mu\nu}{}^{(1,0)})_z$$

[11] $$(\chi)_{zz}{}^R(\text{cross}) = -\sum_{A>B}\sum_{\mu}^{A}\sum_{\nu}^{B}(P_{\mu\nu}{}^{(1)})_z{}^L(H_{\mu\nu}{}^{(1,0)})_z$$

$P_{\mu\nu}{}^{(0)}$ being the unperturbed density matrix. The perturbed density matrix $P_{\mu\nu}{}^{(1)}$ is obtained by using SCF perturbation theory. The matrix elements of $H_{\mu\nu}{}^{(1,0)}$ and $H_{\mu\nu}{}^{(2,0)}$ are obtained following the procedure outlined by Ditchfield (9).

Results and Discussion[2]

The experimental geometries were employed in our calculations. In ethane, ethylene, and acetylene the C—C bond axis was chosen to be z-axis with origin at the centre of the C—C bond. Ethylene molecule was assumed to lie in x–z plane. In cyclopropane, the ring was assumed to lie in x–y plane with origin at the centre of one of the C—C bonds which was assumed to be along the x-axis. Water molecule was taken in x–z plane with origin at oxygen atom and the z-axis being the C_2-axis.

The calculated values of MINDO/3 magnetic susceptibilities for various molecules are presented in Tables 1 to 4. Wherever possible, INDO values are listed for comparison and are given in parentheses. We have also repeated MINDO/3 calculations with hydrogen orbital exponent, $\zeta_H = 1.0$, for two molecules, and these values are given in square brackets in each table.

Table 1 lists the diamagnetic and paramagnetic contributions to susceptibilities in xx, yy, and zz directions. In most of the cases (except ethylene) considered, it is seen that whereas MINDO/3 and INDO diamagnetic contributions are comparable, the MINDO/3 paramagnetic contributions to susceptibilities are invariably larger compared to their INDO counterparts. Thus although MINDO/3 predicts all the molecules studied to be diamagnetic in agreement with experiment (23) the total susceptibilities are less negative compared to the calculated INDO values as well as experimental data. On the other hand INDO values are seen to be in fair agreement with experiment.

Table 2 lists one- and two-centre contributions to the magnetic susceptibilities as defined in eqs. [6] to [11]. It is clear from this table that the major contribution to susceptibilities comes from one-centre terms. This can be better visualized by a glance at Table 3, which shows that the local contributions account for about 90% of the total susceptibilities. An atomwise analysis of susceptibility data is presented in Table 4, which again shows the dominance of intra atomic terms (χ^d)(intra) and (χ^p)(intra) over cross contributions. These conclusions of MINDO/3 calculations are in agreement with those of the INDO calculations.

In order to understand the difference between MINDO/3 and INDO susceptibilities, it is worthwhile to examine the orbital energies of these molecules as obtained by the above two approximations. These orbital energies, for three molecules, are shown in Fig. 1. As is obvious from this figure, the separation of various occupied orbitals in MINDO/3 and INDO methods are comparable, although INDO orbital energies are consistently lower than MINDO/3 orbital energies. The diamagnetic contribution to the magnetic susceptibility which depends only on unperturbed density matrix (which in turn depends upon occupied orbitals only) are thus comparable in the two methods. The χ^d for CH_4 is −13.4 and −15.6 in MINDO/3 and INDO respectively (Table 1). Similar trends are observed in other molecules given in Table 1. We also carried out INDO calculations on CH_4, C_2H_4, and C_2H_2 molecules and find perfect agree-

[2]All susceptibility values are given in units of (erg G^{-2} mol^{-1} × 10^{-6}). The conversion factor to SI unit (m^3/mol) is 10^{-12}.

Can. J. Chem. Downloaded from www.nrcresearchpress.com by 210.87.254.5 on 09/05/12
For personal use only.

TABLE 3. Average local and non-local contributions to the calculated susceptibilities

Molecule	intra	local	(χ^d) (two-centre)	(χ^p) (two-centre)	χ(non-local)
CH_4	−8.56 [−8.72]	−8.23 [−9.31]	0.25 [0.15]	−1.10 [−1.73]	−0.85 [−1.58]
C_2H_4	−5.86	−3.87	−2.72	2.66	−0.06
C_2H_2	−7.70 [−6.87]	−6.62 [−5.79]	0.0 [0.0]	0.0 [0.0]	0.0 [0.0]
C_2H_6	−14.03	−13.90	−6.81	5.64	−1.17
cyclo-C_3H_6	−15.45	−15.64	−14.05	11.72	−2.33
H_2O	−4.74	−2.96	0.0	−0.02	−0.02

TABLE 4. Average atomic contributions to the calculated susceptibilities

	C				H
Molecule	χ^d(intra)	χ^p(intra)	χ^L(cross)	χ(local)	χ(local)
CH_4	−7.97 [−8.35]	5.09 [5.03]	0.33 [−0.59]	−2.55 [−3.91]	−1.42 [−1.35]
C_2H_4	−8.09	7.93	0.99	−0.83	−1.39
C_2H_2	−8.26 [−8.29]	5.67 [6.09]	0.54 [0.54]	−2.05 [−1.66]	−1.25 [−1.23]
C_2H_6	−7.92	5.20	0.07	−2.65	−1.43
cyclo-C_3H_6	−8.03	5.70	−0.06	−2.39	−1.41
H_2O	−6.72	4.08	1.78	−0.86	−1.05

ment with Ditchfield's (9) reported values except in the *yy* component of ethylene where our INDO value turns out to be $(\chi^d)_{yy} = -21.36$ and $(\chi^p)_{yy} = 27.23$ in contrast to the values reported in ref. 9 ($(\chi^d)_{yy} = -24.5$ and $(\chi^p)_{yy} = 6.8$). The reason for this discrepancy is not clear.

It is also seen from Fig. 1 that the separation of virtual orbitals from occupied orbitals is smaller in MINDO/3 compared to that in INDO method. Furthermore, MINDO/3 virtual orbitals are more closely spaced than INDO virtual orbitals. The paramagnetic contribution to the susceptibility depends on first order density matrix. The calculation of perturbed eigenvectors and hence perturbed density matrix involves terms containing $(\varepsilon_l^{(0)} - \varepsilon_j^{(0)})^{-1}$, where $\varepsilon_l^{(0)}$ and $\varepsilon_j^{(0)}$ refer to energies of *l*th unoccupied and *j*th occupied orbitals, respectively. Since these quantities are much larger in MINDO/3 than in INDO, the paramagnetic contribution to susceptibilities from these two methods should be very different. This fact is reflected in our calculations where the MINDO/3 paramagnetic susceptibilities are found to be almost always greater than the corresponding INDO values.

In his CNDO calculations of susceptibilities Bley (15) has shown that the calculated susceptibilities were sensitive to hydrogen orbital exponent, ρ_H. We have repeated our MINDO/3 calculations with hydrogen orbital exponent value of 1.0 (instead of usual 1.3) for two molecules and the results are given in square brackets in Tables 1 to 4. These results indicate that MINDO/3 susceptibilities are rather insensitive to hydrogen orbital exponent variation. Bley's (15) calculations further show that CNDO and INDO ($\rho_H = 1.2$) susceptibilities do not differ significantly. Thus these susceptibilities are insensitive to one-centre exchange integrals. Since MINDO/3 and INDO exchange integrals are similar ($(sp|sp)_{INDO} = 0.08924$, $(sp|sp)_{MINDO/3} = 0.08931$, $(pp'|pp')_{INDO} = 0.02085$, $(pp'|pp')_{MINDO/3} = 0.02279$ au, for carbon) the difference in MINDO/3 and INDO calculated susceptibilities cannot be attributed to these integrals.

In conclusion we might say that since virtual orbitals are described rather poorly by MINDO/3, the use of MINDO/3 should be restricted to only those properties which do not require the use of virtual orbitals. These conclusions are further supported from our studies on spin–spin couplings (21).

Can. J. Chem. Downloaded from www.nrcresearchpress.com by 210.87.254.5 on 09/05/12
For personal use only.

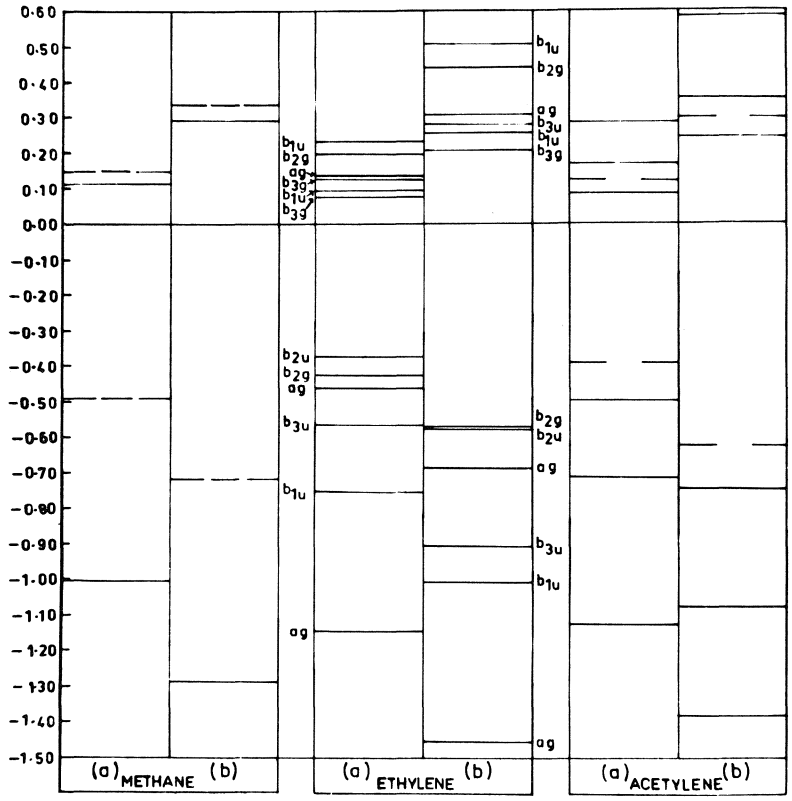


FIG. 1. Orbital energies in au: (*a*) MINDO/3; (*b*) INDO.

Acknowledgements

We thank the staff of Computer Centres I.I.T., Madras, and I.I.T., Kanpur, for their cooperation and C.S.I.R., New Delhi, for financial assistance.

1. J. H. VAN VLECK. Electric and magnetic susceptibilities. Oxford University Press. 1932.
2. J. H. VAN VLECK and A. FRANK. Proc. Natl. Acad. Sci. U.S. **15**, 539 (1929).
3. M. KARPLUS and H. J. KOLKER. J. Chem. Phys. **35**, 2235 (1961); **38**, 1263 (1963).
4. R. M. STEVENS and W. N. LIPSCOMB. J. Chem. Phys. **40**, 2238 (1964); **41**, 184 (1964); **41**, 3710 (1964); **42**, 3666 (1965); **42**, 4302 (1965).
5. R. DITCHFIELD, D. P. MILLER, and J. A. POPLE. J. Chem. Phys. **53**, 613 (1970).
6. G. P. ARRIGHINI, M. MAESTRO, and R. MOCCIA. J. Chem. Phys. **49**, 882 (1968); **52**, 6411 (1970); Chem. Phys. Lett. **1**, 351 (1970).
7. D. W. DAVIES. Trans. Faraday Soc. **57**, 2081 (1961).
8. G. G. HALL and A. HARDISSON. Proc. R. Soc. A**268**, 328 (1962).
9. R. DITCHFIELD. MTP International Review of Science. Physical Chemistry Series One. Vol. 2. *Edited by* G. Allen. Butterworth. 1972. p. 91.
10. R. DITCHFIELD. J. Chem. Phys. **56**, 5688 (1972).
11. G. G. HALL. Int. J. Quantum Chem. **7**, 15 (1973).
12. P. LAZZERETTI, R. ZANASI, and B. CADIOLI. J. Chem. Phys. **67**, 382 (1977).
13. R. C. BINGHAM, M. J. S. DEWAR, and D. H. LO. J. Am. Chem. Soc. **97**, 1285 (1975).
14. W. R. BLEY. Mol. Phys. **16**, 303 (1969).
15. W. R. BLEY. Mol. Phys. **20**, 491 (1971).
16. D. W. DAVIES. Mol. Phys. **20**, 605 (1971).
17. J. A. POPLE and D. L. DEVERIDGE. Approximate molecular orbital theory. McGraw-Hill, New York. 1970.
18. P. K. K. PANDEY. Ph.D. Thesis, Banaras Hindu University, Varanasi, India. 1977.
19. P. K. K. PANDEY, P. CHANDRA, P. L. PRASAD, and S. SINGH. Chem. Phys. Lett. **49**, 353 (1977).
20. P. K. K. PANDEY and P. CHANDRA. Can. J. Chem. **57**, 3126 (1979).
21. P. K. K. PANDEY and P. CHANDRA. Theor. Chim. Acta, **50**, 211 (1978).
22. F. LONDON. J. Phys. Radium, **8**, 397 (1937).
23. C. BARTER, R. C. MEISENHEIMER, and D. P. STEVENSAN. J. Phys. Chem. **64**, 1312 (1960).

Can. J. Chem. Downloaded from www.nrcresearchpress.com by 210.87.254.5 on 09/05/12
For personal use only.

An examination of parameters describing the dependence of rate constants on temperature for solvolysis of various organic esters in water and aqueous mixtures

MICHAEL JESSE BLANDAMER,[1] ROSS ELMORE ROBERTSON,[2] AND JOHN MARSHALL WILLIAM SCOTT[3]

Department of Chemistry, University of Calgary, Calgary, Alta., Canada T2N 1N4

Received July 30, 1979[4]

MICHAEL JESSE BLANDAMER, ROSS ELMORE ROBERTSON, and JOHN MARSHALL WILLIAM SCOTT. Can. J. Chem. **58**, 772 (1980).

The consequences are examined of fitting rate constants and temperatures for a solvolytic reaction to the equation $\log k = A/T + B \log T + C$. The coefficients A, B, and C for 150 reactions involving organic derivatives are linearly dependent. Possible mechanistic reasons for this underlying pattern of behaviour are considered. The linearity stems from the least squares analysis used to obtain the coefficients and as a result these quantities are not truly independent. Consequently, the validity of employing this type of analysis based on the three parameter equation is questioned.

MICHAEL JESSE BLANDAMER, ROSS ELMORE ROBERTSON et JOHN MARSHALL WILLIAM SCOTT. Can. J. Chem. **58**, 772 (1980).

On a examiné les conséquences de l'introduction des constantes de vitesse et de la température des réactions de solvolyse dans l'équation: $\log k = A/T + B \log T + C$. Les coefficients A, B et C pour 150 réactions impliquant des dérivés organiques dépendent linéairement les uns des autres. On considère les raisons possibles qui du point de vue du mécanisme expliqueraient ce type fondamental de comportement. Cette linéarité provient de l'analyse des moindres carrés utilisée pour obtenir ces coefficients et il en résulte que ces quantités ne sont pas réellement indépendantes. En conséquence la validité de l'utilisation de ce type d'analyse fondée sur les trois paramètres de l'équation est remise en question.

[Traduit par le journal]

In recent years, Robertson and co-workers (1, 2) have reported first order rate constants, k, as a function of temperature, T, for a range of solvolytic reactions in water and in aqueous mixtures. One of the first (3) features to be identified concerned the curvature of plots of $\log k$ against T^{-1}. This turned out to be a common feature for this class of reactions in water (1), confirming the earlier observation reported by Glew and Moelwyn-Hughes (4). The latter authors described the dependence of k on T in terms of an energy of activation, E_A, and the corresponding temperature coefficient, dE_A/dT. However, Robertson (1) expressed the latter quantity in terms of a heat capacity of activation, $\Delta C_p^{\ddagger}$, derived using transition state theory (5). One aim of this series of studies (1) has been to link the magnitude of $\Delta C_p^{\ddagger}$ (generally negative) with either the nature of the solute undergoing hydrolysis or the effect of added cosolvent (e.g. *tert*-butyl alcohol (6)) on a given solvolytic reaction. The heat capacities, $\Delta C_p^{\ddagger}$, together with corresponding enthalpies, $\Delta H^{\ddagger}$, and entropies, $\Delta S^{\ddagger}$, of activation are calculated from a set of parameters (i.e., A_i, B_i, and C_i) obtained by fitting the dependence of n rate constants at n temperatures for a given reaction i, to eq. [1] where $n \geq 8$

$$[1] \quad \log k_{in} = A_i/T_n + B_i \log T_n + C$$

The justification for using an equation of this form was based on the similarity with the Valentiner equation (7) which has been used extensively to describe the dependence of acid dissociation constants on temperature (8, 9). In practice the kinetic data were fitted to eq. [1] using conventional least squares technique (see below). Then, by invoking the formalism of transition state theory (5) $\Delta C_p^{\ddagger}$ can be calculated (1) from B_i, while at a given temperature $\Delta H^{\ddagger}$ can be calculated from A_i and B_i, $\Delta S^{\ddagger}$ from B_i and C_i. In this paper we do not consider this aspect of the calculation and the assumptions underlying transition state theory. Rather we concentrate attention on the analysis of the raw kinetic data using eq. [1]. We review the reasons which prompted this reconsideration and then consider some of the features associated with fitting the data to eq. [1] which are perhaps not immediately apparent. Finally we comment on the significance of our findings in the context of the analysis of kinetic data for solvolytic reactions in water and aqueous mixtures.

Correlations between Derived Parameters

In this paper, we confine our attention to the data reported by Robertson and co-workers (1, 2). For a given solvolytic reaction i, the first order rate constants at ambient pressure, k_{in}, are the arithmetic mean of 3 or 4 determinations, the overall standard deviation being less than 1%. The temperatures were

[1]Permanent address: Department of Chemistry, The University, Leicester, England.

[2]Author to whom correspondence should be addressed.

[3]Memorial University, St. John's, Nfld., Canada.

[4]Revision received December 17, 1979.

0008-4042/80/080772-05$01.00/0

©1980 National Research Council of Canada/Conseil national de recherches du Canada

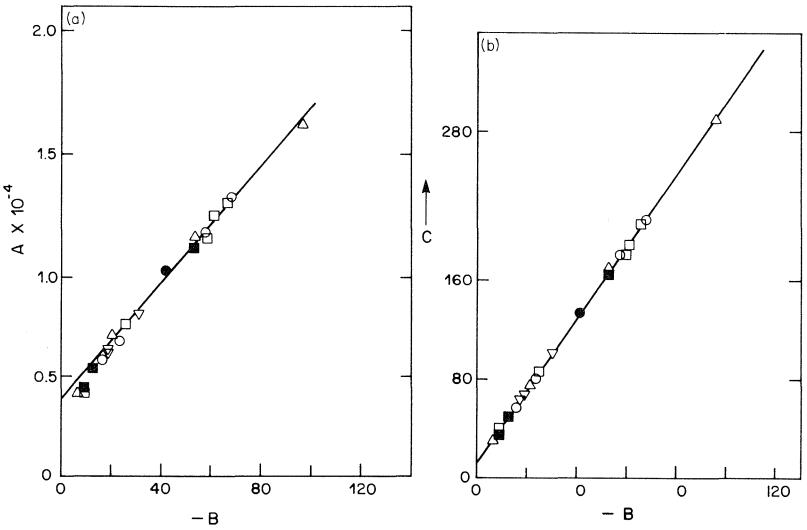


FIG. 1. Derived coefficients for solvolysis of *tert*-butyl chloride in water and in aqueous mixtures; (*a*) plot of A against B and (*b*) plot of C against B; solvent systems are (1) water (●; ref. 10), and aqueous mixtures where the cosolvent is (2) ethyl alcohol (○; ref. 11); (3) isopropyl alcohol (□; ref. 6); (4) *tert*-butyl alcohol (△; ref. 11); (5) acetonitrile (▽; ref. 12); and (6) tetrahydrofuran (■; ref. 11).

measured to a precision better than ± 0.001 K, in the majority of cases, and held constant to better than ± 0.01 K. The rate constants for each reaction were measured over a range >20 K (within the overall limiting range $273.15 \leq T \leq 383$ K) at temperatures which were *roughly* equally spaced but the individual temperatures were not set at predetermined values.

Many of the sets of kinetic data (1, 2) were refitted to eq. [1] using a FORTRAN program for the CDC computers at the Universities of either Calgary or Leicester (England). We were then able to check previously reported values of A_i, B_i, and C_i. In all cases, the agreement was good. Reassessment of eq. [1] was prompted by consideration of the coefficients describing the effects of various cosolvents on the kinetics of hydrolysis of *tert*-butyl chloride in water. We recall that for a given system, the accepted basis for a least square analysis is the independence of the derived coefficients. It was of interest to discover that for the complete set of data describing these solvent effects, the plots of A_i against B_i and C_i against B_i form two straight lines, Fig. 1. Within this pattern there are a number of interesting features which we discuss below. However, even more unexpected was the discovery that the parameters characterizing the solvolysis of 121 organic compounds in water shared a similar pattern. We show a selection of the data points in Fig. 2. There is some slight scatter in the plot of A_i against B_i but the data points in the plot of C_i against B_i fall very close to a straight line, bearing in mind that these parameters cover the following ranges: $-0.4 \times 10^4 \leq A_i \leq -2.93 \times 10^4$; $-194 \leq B_i \leq 19$; $24 \leq C_i \leq 576$. A least squares analysis gave the following two equations for 121 systems.

$$[2] \quad \begin{cases} A_i = (140.0 \pm 4.8)B_i - ((48.4 + 1.7) \times 10^2) \\ C_i = -(2.882 \pm 0.003)B_i + (14.2 \pm 1.2) \end{cases}$$

Indeed, with little change in these standard deviations it is possible to include, in the same correlation, the coefficients for reactions in mixed solvents making a total of 150 systems. It also follows that for these 150 systems, A_i is a linear function of C_i. Since the data cover a wide variety of reactions, mechanisms, and solvent systems, numerous speculations and interpretations are prompted. Such patterns are often sought because they summarize a lot of information in a convenient form. At the same time, however, the question is often raised as to their physical significance. We have in mind here the reevaluation by Exner (14) of isokinetic relationships and similar plots of $\Delta H^{\ominus}$ against $\Delta S^{\ominus}$ for equilibrium parameters. In the present case, we were concerned that the correlations (eq. [2]) were somehow predetermined by the way in which the data were analysed. This is the problem which we address in the remainder of this paper. We have assumed that the input experimental data are correct, but we wish to consider the consequence of using a least square analysis to fit the data to eq. [1].

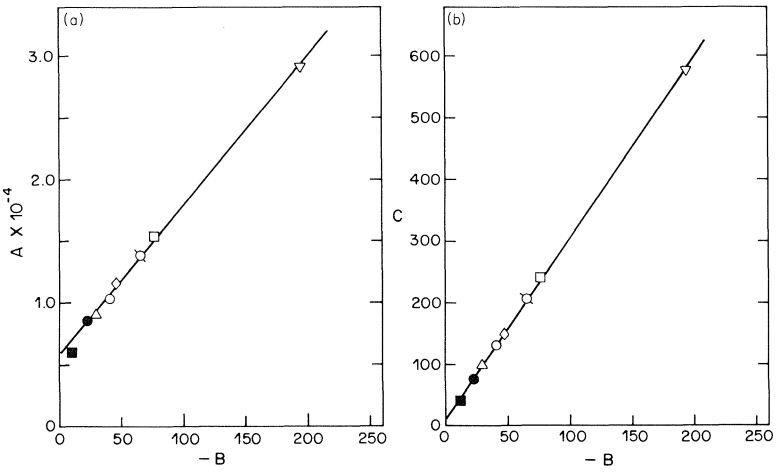


FIG. 2. Derived coefficients for solvolysis of various organic compounds in water; (*a*) plot of A against B and (*b*) plot of C against B; the data points refer to (1) methyl bromide (●; ref. 1); (2) *tert*-butyl chloride (○; ref. 10); (3) 1-adamantyl nitrate (□; ref. 12); (4) 2,4-dimethylbenzyl nitrate (▽; ref. 13); (5) allyl bromide (△; ref. 1); (6) *n*-butylmethane sulphonate (■; ref. 1); (7) 2-chloro-2-bromopropane (◇; ref. 1); (8) 2,6-dimethylbenzyl nitrate (⌀; ref. 13).

Analysis of Analytical Procedures

As a first step, we set up an ideal data set of pairs of rate constants and temperatures: k_1, T_1, k_2, $T_2 \ldots k_n$, T_n. These n points describe the rate data for a given compound in a given solvent at n temperatures, the latter being at constant intervals e.g., 5 K. We now assume that each rate constant is modified by some multiplicative perturbation to produce a new set of rate constants such that $k_{1w} = P_1k_1$, $k_{2w} = P_2k_2 \ldots k_{nw} = P_nk_n$, all being measured at the same n temperatures. Possible origins of these perturbations are discussed below.

If the ideal data set is fitted to eq. [1] using the least squares technique to obtain the three coefficients A, B, and C, then in matrix notation we obtain the following equation.

$$[3]\quad \begin{bmatrix} \sum_n \ln k_i \\ \sum_n \ln k_i \ln T_i \\ \sum_n T_i^{-1} \ln k_i \end{bmatrix} = \begin{bmatrix} A \\ B \\ C \end{bmatrix} \begin{bmatrix} \sum_n T_i^{-1} & \sum \ln T_i & n \\ \sum_n T_i^{-1} \ln T_i & \sum_n (\ln T_i)^2 & \sum_n \ln T_i \\ \sum_n (T_i^{-1})^2 & \sum T_i^{-1} \ln T_i & \sum_n T_i^{-1} \end{bmatrix}$$

We now suppose that the perturbed set of data is fitted to eq. [1], the coefficients A_i, B_i, and C_i being obtained. Then it is readily shown that

$$[4]\quad \begin{bmatrix} x \\ y \\ z \end{bmatrix} = \begin{bmatrix} \Delta A \\ \Delta B \\ \Delta C \end{bmatrix} \begin{bmatrix} \lambda_1 & \lambda_2 & n \\ \lambda_3 & \lambda_4 & \lambda_2 \\ \lambda_5 & \lambda_3 & \lambda_1 \end{bmatrix}$$

where

$$[5]\quad \Delta A = A_1 - A, \Delta B = B_1 - B, \text{ and } \Delta C = C_1 - C$$

and

$$[6]\quad \sum_n \ln P_i = x$$

$$[7]\quad \sum_n \ln P_i \ln T_i = y$$

$$[8]\quad \sum_n T_i^{-1} \ln P_i = z$$

The λ-coefficients are defined as follows

$$[9]\quad \sum_n T_i^{-1} = \lambda_1$$

$$[10]\quad \sum_n \ln T_i = \lambda_2$$

$$[11]\quad \sum_n T_i^{-1} \ln T_i = \lambda_3$$

$$[12]\quad \sum_n (\ln T_i)^2 = \lambda_4$$

$$[13]\quad \sum_n (T_i^{-1})^2 = \lambda_5$$

Standard matrix inversion and manipulation yields

the following equation for the three Δ-quantities

$$[14]\quad \begin{bmatrix}\Delta A\\ \Delta B\\ \Delta C\end{bmatrix} = \begin{bmatrix}x\\ y\\ z\end{bmatrix} \begin{bmatrix}a & b & 0\\ c & 0 & b\\ 0 & c & a\end{bmatrix}$$

where

$$[15]\quad a = (\lambda_4\lambda_1 - \lambda_3\lambda_2)/\text{det}$$

$$[16]\quad b = (\lambda_3 n - \lambda_2\lambda_1)/\text{det}$$

$$[17]\quad c = (\lambda_5\lambda_2 - \lambda_3\lambda_1)/\text{det}$$

and det is the determinant related to the 3 × 3 matrix on the right-hand side of eq. [4]. We note that the quantities a, b, and c depend solely on the temperatures and the value of n. If these do not change irrespective of the form of the perturbation quantities, $P_i \ldots P_n$, we conclude that the quantities det_i, a_i, b, and c are fixed. Equation [14] can be written in linear form

$$[18]\quad \Delta A = ax + by$$

$$[19]\quad \Delta B = cx + bz$$

$$[20]\quad \Delta C = cy + az$$

Equations [18], [19], and [20] can be solved to yield

$$[21]\quad c\Delta A - a\Delta B + b\Delta C = 2bcy$$

This is the required relation which shows that ΔA, ΔB, and ΔC are linearly related to the perturbation variable y or, by other manipulations of [18], [19], and [20], to x and z.

Discussion

The major finding of this work concerns the recognition that the changes in A, B, and C, are linearly related to the perturbation variable y. This further means these changes must be individually related to y or linearly related to each other. It is possible to identify a number of factors described by the perturbation parameters, P_1, P_2, . . . P_n.

With reference to the solvolytic reactions in water, the common denominator is the solvent and the manner in which this solvent plays a key role in the solvolytic reaction (1). In addition, the overall pattern observed between the coefficients A, B, C may indicate that there is a common feature associated with the activation process. Thus we have stressed the role of the solvent in solvating the developing anion formed as the R—X bond stretches on going from the initial to the transition state. Indeed, we have argued that the transition state is characterized by a critical degree of charge development on the developing anion. Through a series of solvolytic reactions in water we can identify the perturbation parameters as describing substituent effects on the alkyl group R. Thus the position of a given point on the A, B, C, vector summarizing the kinetics of solvolysis of a particular solute may be taken as a reference. Data points for other solutes on this vector may be characterized by a δ_R-parameter along the lines suggested by Leffler and Grunwald (15).

A similar analysis to that outlined above may be used to describe medium effects, δ_m (15), with reference to the effect of added cosolvent on the kinetic data for a given solvolytic reaction, e.g. solvolysis of *tert*-butyl chloride in water. It is interesting to note that small amounts of an organic solvent (e.g., *tert*-butyl alcohol) move the parameters A, B, C in a direction which characterizes those cosolvents which initially enhance water–water interactions (16). However, as the mole fraction of these cosolvents increases to beyond a critical mole fraction, there is a breakdown in water–water interactions. The coefficients A, B, and C now move in the opposite direction relative to their values in water. Indeed, the new trend is consistent with the change in coefficients produced when acetonitrile is added, a solvent which operates to disrupt water–water interactions even at low mole fractions (16).

These arguments, based on the importance of substituent or solvent effects on the A, B, and C parameters are tempting and attractive. However, they overlook the original key premise of the least squares analysis, namely that the derived A, B, and C quantities are independent. These quantities are not independent. In fact even if the perturbation quantities P_i describe some consistent or random experimental error, the analysis conspires to produce derived coefficients which are simply related. Clearly we need to reconsider certain aspects of the way in which the kinetic data have been analysed. The key question concerns the extent to which the data can be regressed to obtain a set of independent coefficients. For example, we need to know if such an analysis would significantly alter the values of $\Delta C_p^{\ddagger}$ which have been used in discussions of reaction mechanism. The development of an analytical technique with this essential requirement and applicable to kinetic data will form the basis of another communication from this laboratory.

Acknowledgements

Two authors, M.J.B. and J.M.W.S., wish to thank the University of Calgary for hospitality and financial assistance during the spring and summer of 1979. The former also wishes to thank the University of Leicester for granting a sabbatical leave of absence during the same period. Both R.E.R. and J.M.W.S.

wish to thank the National Research Council of Canada for financial support of this work.

1. R. E. ROBERTSON. Prog. Phys. Org. Chem. **4**, 213 (1967).
2. S. SINGH and R. E. ROBERTSON. Can. J. Chem. **55**, 2582 (1977).
3. R. E. ROBERTSON. Can. J. Chem. **33**, 1536 (1955).
4. D. N. GLEW and E. A. MOELWYN-HUGHES. Proc. R. Soc. London, Ser. A, **211**, 254 (1952).
5. S. GLASSTONE, K. J. LAIDLER, and H. EYRING. The theory of rate processes. MacMillan, New York. 1941.
6. R. E. ROBERTSON and S. E. SUGAMORI. J. Am. Chem. Soc. **91**, 7254 (1969).
7. H. S. HARNED and B. B. OWEN. The physical chemistry of electrolytic solutions. 3rd ed. Reinhold, New York. 1958.
8. D. H. EVERETT and W. F. K. WYNNE-JONES. Trans. Faraday Soc. **35**, 1380 (1939).
9. E. J. KING. Acid–base equilibria. Pergamon Press, New York. 1965.
10. E. A. MOELWYN-HUGHES, R. E. ROBERTSON, and S. E. SUGAMORI. J. Chem. Soc. 1965 (1965).
11. R. E. ROBERTSON and S. E. SUGAMORI. Can. J. Chem. **50**, 1353 (1972).
12. K. M. KOSHY, R. K. MOHANTY, and R. E. ROBERTSON. Can. J. Chem. **55**, 1314 (1977).
13. K. M. KOSHY, R. E. ROBERTSON, G. S. DYSON, and S. SINGH. Can. J. Chem. **54**, 3614 (1976).
14. O. EXNER. Prog. Phys. Org. Chem. **10**, 411 (1973).
15. J. E. LEFFLER and E. GRUNWALD. Rates and equilibria of organic reactions. Wiley, New York. 1963.
16. M. J. BLANDAMER. Adv. Phys. Org. Chem. **14**, 203 (1977).

The crystal and molecular structure of tetrabenzocyclodecan-1,6-dione

T. STANLEY CAMERON[1] AND CHRISTINE CHAN
Department of Chemistry, Dalhousie University, Halifax, N.S., Canada B3H 4J3
AND
DAVID G. MORRIS AND ALISTAIR G. SHEPHERD
Department of Chemistry, University of Glasgow, Glasgow G12 8QQ, Scotland

Received October 29, 1979

T. STANLEY CAMERON, CHRISTINE CHAN, DAVID G. MORRIS, and ALISTAIR G. SHEPHERD. Can. J. Chem. **58**, 777 (1980).

The crystals belong to the orthorhombic space group $C222$, with $a = 9.226$, $b = 12.092$, $c = 16.513$ Å, $Z = 4$. A single crystal X-ray diffraction analysis has shown that the title compound, in which all carbon atoms are sp^2 hybridized, exists with the ten membered ring in a slightly twisted tub conformation. The ^{13}C nmr spectrum is also reported.

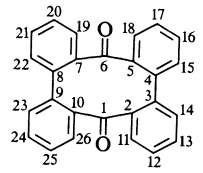
T. STANLEY CAMERON, CHRISTINE CHAN, DAVID G. MORRIS et ALISTAIR G. SHEPHERD. Can. J. Chem. **58**, 777 (1980).

Les cristaux de la molécule de tétrabenzocyclodécanedione-1,6 sont orthorhombiques avec $a = 9.226$, $b = 12.092$, $c = 16.513$ Å, groupe d'espace $C222$, $Z = 4$. Une analyse par diffraction de rayon-X sur un cristal unique a montré que le composé étudié, dans lequel tous les atomes de carbone sont dans l'état d'hybridation sp^2, a le cycle à 10 atomes sous une conformation bateau légèrement croisée. On donne également le spectre rmn du ^{13}C de la molécule.

[Traduit par le journal]

Introduction

The conformational properties of a large number of medium ring cycloalkanes have been determined by a combination of X-ray diffraction analysis and nmr spectroscopy, aided by strain energy calculations particularly in respect of even-membered rings; within this range of ring size a number of diversely substituted compounds has also been studied (1, 2). These studies have prompted us to determine the solid state conformation of tetrabenzocyclodecan-1,6-dione **1**, chosen because the carbons of the ten-membered ring in particular are all sp^2 hybridized.



1

Experimental

Crystals of **1** were prepared according to ref. 3 and were recrystallized from toluene to fine colourless needles.
Crystal data:

$C_{26}H_{16}O_2$ fw = 360.4
Orthorhombic, $C222_1$, $a = 9.226(1)$, $b = 12.092(4)$, $c = 16.513(3)$ Å, $V = 1842$ Å^3, $Z = 4$, $\rho_c = 1.299$ g cm^{-3} (18 ± 2°C; CuK$_{\alpha 1}$, $\lambda = 1.54051$ Å (graphite monochromator), $\mu = 5.6$ cm^{-1}), $F(000) = 752$.

The crystal system and approximate cell dimensions were determined from Weissenberg photographs. Systematic extinctions $h\,k\,l$, $h + k \neq 2n$, $00l$, $l \neq 2n$ uniquely indicated space group $C222_1$. The cell dimensions were refined on a Picker FACS-1 four circle diffractometer from twelve general reflections with 2θ between 65 and 70°; 802 unique reflections with $2\theta < 120$° measured of which 725 had $I > 3\sigma(I)$. The data were reduced to a common scale by a routine procedure (4) and were corrected for Lorentz and polarization but not for absorption or extinction factors.

The structure was solved by a multisolution application of the tangent formula (5) and was refined by a large block least squares ($\Sigma W(\Delta F)^2 = \min$). The weights were calculated from $W = (\sigma^2|F_o| + 0.000225F_o^2)^{-1}$ where σ is the individual esd for each reflection calculated from the diffractometer counting statistics. This program is part of an X-ray system written by Sheldrick (6). The positions of the hydrogen atoms were determined from a difference Fourier synthesis calculated when the conventional R was 0.12. The subsequent refinement in which the carbon and oxygen but not hydrogen atoms had anisotropic temperature factors used 715 reflections (ten reflections were removed on account of extinction effects) and it converged[2] with $R = 0.039$, $w_R = 0.039$, and $R = 0.068$ for all measured reflections.

The scattering factors were taken from International Tables for X-ray crystallography (7) and were corrected for the anomalous dispersion effect.

Atomic parameters are given in Table 1. Interatomic distances and bond angles are given in Table 2. Figure 1 shows a single molecule and Fig. 2 gives the packing in the unit cell.

Discussion

The crystal is constructed from isolated molecules **1** with each molecule containing one of the C_2 symmetry axes of the unit cell. The presence of this C_2 axis presents a problem for the numbering of the atoms in the compound. By chemical convention

[1]Author to whom correspondence should be addressed.

[2]A list of structure factors and complete atomic parameters is available, at a nominal charge, from the Depository of Unpublished Data, CISTI, National Research Council of Canada, Ottawa, Ont., Canada K1A 0S2.

0008-4042/80/080777-03$01.00/0
©1980 National Research Council of Canada/Conseil national de recherches du Canada

Can. J. Chem. Downloaded from www.nrcresearchpress.com by 210.87.254.105 on 09/05/12
For personal use only.

Can. J. Chem. Downloaded from www.nrcresearchpress.com by 210.87.254.105 on 09/05/12
For personal use only.

TABLE 1. Atomic parameters ($\times 10^4$, except $\times 10^3$ for hydrogen) with estimated standard deviations in parentheses

Name	*X*/*a*	*Y*/*b*	*Z*/*c*	Mod (*U*)
O	3211(3)	1534(3)	1499(2)	664
C(1)	2061(4)	1559(3)	1855(2)	363
C(2)	851(4)	2265(3)	1543(2)	314
C(3)	−86(4)	2851(3)	2048(2)	287
C(9)	648(4)	264(3)	2775(2)	339
C(10)	1888(4)	881(3)	2607(2)	323
C(11)	668(5)	2339(3)	700(2)	418
C(12)	−406(5)	2982(3)	373(2)	462
C(13)	−1321(5)	3566(3)	876(2)	461
C(14)	−1161(4)	3507(3)	1706(2)	379
C(23)	628(5)	−414(3)	3456(3)	447
C(24)	1793(5)	−443(3)	3975(2)	504
C(25)	3014(4)	180(4)	3823(2)	479
C(26)	3068(4)	825(3)	3134(2)	401
H(11)	130(4)	189(3)	32(2)	
H(12)	−59(6)	304(6)	−23(4)	
H(13)	−224(4)	391(3)	65(2)	
H(14)	−178(4)	402(3)	211(2)	
H(23)	−31(5)	−82(4)	352(3)	
H(24)	179(4)	−87(3)	448(2)	
H(25)	386(4)	16(3)	418(2)	
H(26)	402(5)	123(4)	301(3)	

TABLE 2. Interatomic distances and interbond angles with the estimated standard deviations in parentheses

Bond	Length (Å)	Bonds	Angle (deg)
O—C(1)	1.214(5)	O—C(1)—C(2)	119.9(3)
C(1)—C(2)	1.497(5)	O—C(1)—C(10)	118.8(3)
C(1)—C(10)	1.496(5)	C(2)—C(1)—C(10)	121.3(3)
C(2)—C(3)	1.394(5)	C(1)—C(2)—C(3)	123.1(3)
C(2)—C(11)	1.405(5)	C(1)—C(2)—C(11)	117.8(3)
C(3)—C(3)	1.501(5)	C(3)—C(2)—C(11)	119.1(3)
C(3)—C(14)	1.390(5)	C(2)—C(3)—C(3)	122.0(3)
C(9)—C(9)	1.503(5)	C(2)—C(3)—C(14)	119.3(3)
C(9)—C(10)	1.394(5)	C(3)—C(3)—C(14)	118.6(3)
C(9)—C(23)	1.392(5)	C(9)—C(9)—C(10)	122.2(3)
C(10)—C(26)	1.395(5)	C(9)—C(9)—C(23)	118.6(3)
C(11)—C(12)	1.370(6)	C(10)—C(9)—C(23)	119.2(3)
C(12)—C(13)	1.379(6)	C(1)—C(10)—C(9)	123.1(3)
C(13)—C(14)	1.380(6)	C(1)—C(10)—C(26)	117.5(3)
C(23)—C(24)	1.375(6)	C(9)—C(10)—C(26)	119.3(3)
C(24)—C(25)	1.378(6)	C(2)—C(11)—C(12)	120.9(4)
C(25)—C(26)	1.380(6)	C(11)—C(12)—C(13)	119.7(4)
		C(12)—C(13)—C(14)	120.5(4)
		C(3)—C(14)—C(13)	120.6(3)
		C(9)—C(23)—C(24)	120.5(4)
		C(23)—C(24)—C(25)	120.7(4)
		C(24)—C(25)—C(26)	119.3(4)
		C(10)—C(26)—C(25)	120.9(4)

the atoms of the ring should be numbered sequentially first, starting with the carbonyl carbon atom, and then followed by the remaining atoms of the phenyl groups. This gives the numbering scheme shown in **1**. However the two-fold axis bisects the C(3)—C(4) and C(8)—C(9) bonds so that crystallographically C(3) is equivalent to C(4), C(8) to C(9), etc. The chemical nomenclature has been maintained in Table 1 and readers should refer to **1** to establish which are the crystallographically equivalent atoms.

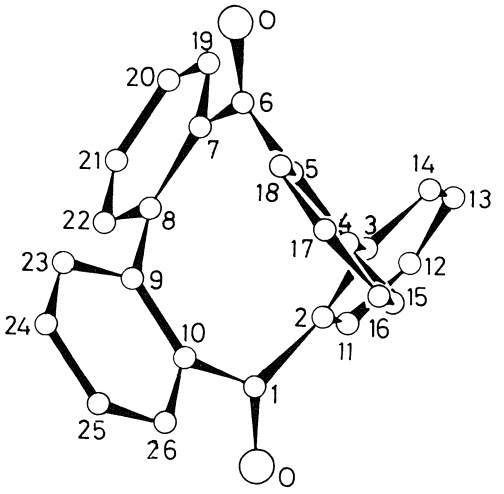


FIG. 1. View of a single molecule.

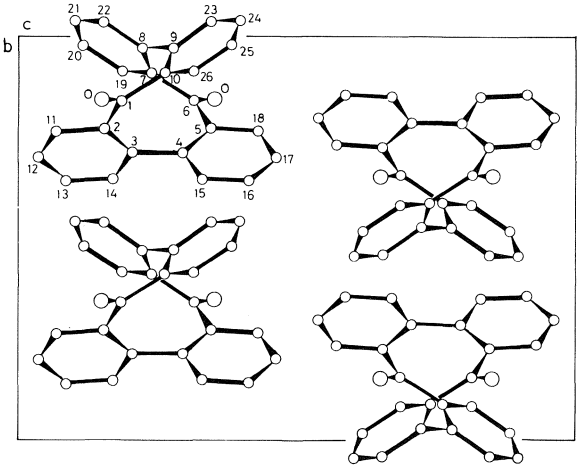


FIG. 2. Unit cell viewed along *a*.

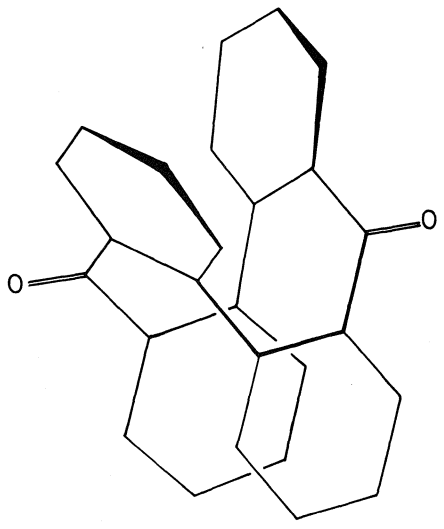
The molecule contains no improper rotation axes and so is optically active. The unit cell too has neither mirror planes nor inversion centres and therefore the sample appears to be an example of the spontaneous resolution of optical isomers (8).

The planes of the two phenyl rings connected by C(3)—C(4) and by C(8)—C(9) are inclined at a mean angle of 84(2)° and the planes of the phenyl groups are inclined at a mean angle of 39(2)° to the plane of the carbonyl group. Within the ten-membered ring, there are three distinct types of carbon–carbon bonds; two biphenylic bonds link the phenyl groups, four phenone bonds join the phenyl and carbonyl groups, and finally there are four aromatic bonds which are also part of the phenyl rings. The

Can. J. Chem. Downloaded from www.nrcresearchpress.com by 210.87.254.105 on 09/05/12
For personal use only.

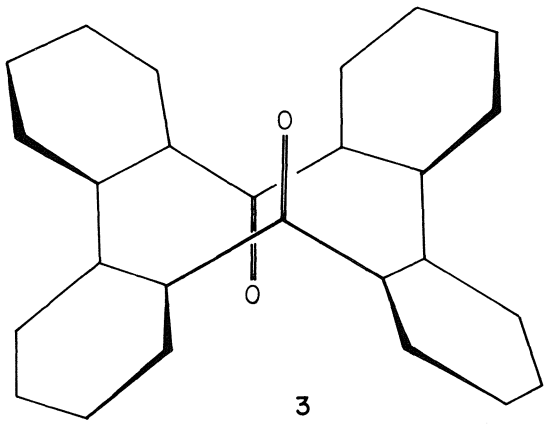
two biphenylic bond lengths are both 1.506(5) Å and compare with 1.496(3) Å in biphenyl itself (9) where the two rings are co-planar and with mean values (10) of 1.496(5) and 1.498(5) Å in the two forms of 9,10,19,20-tetrahydrobenzo[*a*,*c*,*g*,*i*]-cyclododecane where the planes of the rings are inclined at 85° and 63° respectively. The two unique phenone C—C bond lengths are 1.498(5) and 1.499(5) Å. These are not significantly different from those observed (11) in benzophenone (mean 1.48(2) Å) where the carbonyl and phenyl planes are each inclined at 30°. The endocyclic phenyl C—C bond lengths are 1.396(5) and 1.394(5); these are towards the long end of the range of C—C lengths (1.410(5)–1.371(5) Å) found in these phenyl groups but the distinction is not significant. Similarly the carbonyl C=O length of 1.215(5) Å is unexceptional.

A close known structural analogue (10) for the compound is 9,10,19,20-tetrahydrobenzo[*a*,*c*,*g*,*i*]-cyclododecane. The unit cell of the dodecane however does possess an inversion centre and so both optical isomers are present in the one cell. A second crystal form of the dodecane is known (10), in this case the molecule adopts a different conformation and is itself centrosymmetric. The conformation of the ten-membered ring **1** is a slightly twisted "tub" (**2**) with the carbonyl dipoles



2

oriented in opposite directions. An examination of a molecular model suggests that a *meso* form is also possible for the present compound (**3**); this conformation has a mirror plane along the two C=O bonds and has an inversion centre in the middle of the ring. A rough physical measurement on the model suggests that the planes of the phenyl and carbonyl groups would be mutually inclined at 65° and there are no severe non-bonded hydrogen interactions. Thus there seems to be no intrinsic reason why the



3

meso form cannot be prepared; so far, however, it has not been observed.

The ^{13}C nmr spectrum of **1** has been determined (Varian XL100, 0.1 *M* in $CDCl_3$). A single set of signals is obtained at 197.74 C(1), C(6) with aromatic absorptions at 140.20(s), 138.47(s), 130.94(d), 130.24(d), 129.64(d), and 127.97(d) ppm; the parenthesized letters denote multiplicity in the proton noise decoupled spectrum.

Acknowledgements

We thank the Natural Sciences and Engineering Research Council of Canada for a grant to T. S. Cameron, the Science Research Council for a postgraduate award to A. G. S., Dr. D. S. Rycroft for the ^{13}C nmr spectrum of **1**, and Professor R. A. Raphael, F.R.S. for a discussion.

1. J. DALE. Top. Stereochem. **9**, 199 (1976); J. D. DUNITZ. *In* Perspectives in structural chemistry. Vol. 2. *Edited by* J. D. Dunitz and J. A. Ibers. Wiley, New York, NY. 1968. p. 1.
2. F. A. L. ANET and T. N. RAWDAH. J. Am. Chem. Soc. **100**, 5003 (1978); **100**, 7166 (1978); J. DALE. Acta Chem. Scand. **27**, 1115 (1973); **27**, 1130 (1973); G. BORGEN and J. DALE. Acta Chem. Scand. Ser. B, **30**, 711 (1976); H. J. SCHNEIDER and F. THOMAS. Tetrahedron, **32**, 2005 (1976).
3. K. SUZUKI. Bull. Chem. Soc. Jpn. **35**, 735 (1962); R. E. ERICKSON and D. SCHNIPP. Chem. Ind. 161 (1966).
4. T. S. CAMERON and R. E. CORDES. Acta Crystallogr. Sect. B, **35**, 748 (1979).
5. J. KARLE and I. L. KARLE. Acta Crystallogr. **21**, 849 (1966).
6. G. SHELDRICK. X-ray system report. University Chemical Laboratory, Lensfield Rd., Cambridge, England, 1976.
7. International tables for X-ray crystallography. Vol. IV. The Kynoch Press, Birmingham, England. 1974.
8. A. COLLET, M. J. BRIENNE, and J. JACQUES. Bull. Soc. Chim. Fr. 127 (1972); 494 (1977).
9. G. P. CHARBONNEAU and Y. DELUGEARD. Acta Crystallogr. Sect. B, **32**, 1420 (1976).
10. U. VOLL, H. BURZLAFF, and H.-J. BESTMANN. Chem. Ber. **109**, 1324 (1976).
11. G. M. LOBANOVA. Kristallografiya, **13**, 984 (1968).

Linnett double quartet theory in organic chemistry: structure, reactivity and resonance

RICHARD FRANCIS LANGLER,[1] JUNE ELLEN TRENHOLM, AND JOHN SPENCER WASSON
Department of Chemistry, Dalhousie University, Halifax, N.S., Canada B3H 4J3

Received June 4, 1979

RICHARD FRANCIS LANGLER, JUNE ELLEN TRENHOLM, and JOHN SPENCER WASSON. Can. J. Chem. **58**, 780 (1980).

A reexamination of Linnett's nonpairing spatial orbital theory, as it is qualitatively employed, has led to a number of conclusions. Firstly, in our view the theory has been inconsistently applied to the prediction of molecular geometries and may be ambiguous in dealing with saturated systems. Secondly, it does not provide a guide to chemical reactivity, in contrast to claims made for it. Finally, NPSO theory does provide a useful extension of resonance theory as it is qualitatively employed in organic chemistry, contrary to an existing claim that NPSO theory makes resonance theory obsolete.

RICHARD FRANCIS LANGLER, JUNE ELLEN TRENHOLM et JOHN SPENCER WASSON. Can. J. Chem. **58**, 780 (1980).

Une nouvelle étude de la théorie des orbitales spatiales non appariées de Linnett, telle qu'elle est qualitativement employée, a conduit à plusieurs conclusions. Premièrement, la théorie est à notre avis utilisée indûment à prédire les géométries moléculaires et elle peut être ambigue dans le cas des systèmes saturés. Deuxièmement, la théorie ne constitue pas un guide de réactivité chimique contrairement à ce qui a été dit à ce sujet. Finalement, la théorie OSNA, loin de rendre désuette la théorie de la résonance telle qu'elle est employée qualitativement en chimie organique, en constitue plutôt un prolongement pratique.

[Traduit par le journal]

In 1961 Linnett (1) proposed a new structural theory which he named the Nonpairing Spatial Orbital (NPSO) theory but which is much more frequently referred to as Linnett Double Quartet (LDQ) theory. LDQ theory acknowledges the tendency of the elements in the "First Short Period" to achieve octets in forming stable molecules but presumes that "the importance of the pairing of electrons" has been overemphasized.

LDQ octets are not visualized as four spin pairs occupying four regions in space. Instead an octet is regarded as the sum of two tetrahedral quartets of electrons. A quartet contains electrons of the same spin (one quartet for electrons of spin $+\frac{1}{2}$ and one quartet for electrons of spin $-\frac{1}{2}$). The two quartets are *independently oriented*.

Molecular structures[2] are elaborated by maximizing electronic separations and minimizing electronic repulsions. Priority, it is assumed, must be given to maximizing the separation of electrons having the same spin.

Subsequent to the publication of the parent article a substantial number of papers and books have appeared which present and extend LDQ theory (2–25). NPSO theory has been developed as a valence bond approach to the electronic structure of molecules and provides results which are in excellent agreement with full configuration interaction analyses for π systems in small molecules (24). Apparently LDQ theory is not easily applied to molecules as large as naphthalene (24).

Qualitatively, LDQ theory has been applied to predicting bond lengths, bond angles, stabilities of various species, paramagnetism/diamagnetism of molecules, and regioselectivity in Diels–Alder reactions.

In previous discussions of O_2 (1, 22, 23) three structures[3] have been considered i.e., **1**–**3**. The relative stabilities of these structures, as indeed is the case for all LDQ structures, are assessed by assuming that the electrons are spatially fixed points. The lowest energy structure is that which offers the greatest separation of these fixed point electrons.[4] Structure **1** is assigned to the $^1\Sigma_g^+$ state of O_2 and structure **2** is assigned to the $^1\Delta_g$ state of O_2. Notwithstanding the presence of six "close pairs" in structure **1**, each of which has, at least nominally, an infinite repulsive force operant, **1** is a modest 15.1 kcal/mol higher in energy than **2**. Structure **2**, on the other hand, has a slightly greater total electronic repulsion than structure **3** but is supposed to be 22.6 kcal/mol higher in energy than **3**.[5] Thus analysis of apparent electronic separations is qualitatively helpful but can be somewhat misleading quantitatively.

The construction of LDQ structures for molecules is approached by developing separate structures for the molecule under consideration: one

[1]Correspondence should be directed to Dr. R. F. Langler, Chemistry Department, Mount Allison University, Sackville, N.B., Canada E0A 3C0.

[2]The role of the nuclei is ignored.

[3]We have adopted Linnett's convention of using x and o to represent electrons of opposed spins.

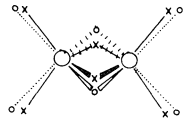
[4]Luder (23) has used Coulomb's law to evaluate the stabilities of the various O_2 structures.

[5]From time to time one or both quartets have their centres shifted from the nucleus (1, 10*b*), viz. structure **3**. This device has received no comment from the advocates of LDQ theory and no rules have been proposed for its use in qualitative structural deductions.

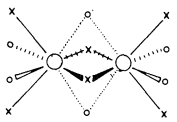
0008-4042/80/080780-06$01.00/0
©1980 National Research Council of Canada/Conseil national de recherches du Canada

Can. J. Chem. Downloaded from www.nrcresearchpress.com by 210.87.254.5 on 09/05/12
For personal use only.

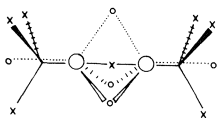
Can. J. Chem. Downloaded from www.nrcresearchpress.com by 210.87.254.5 on 09/05/12
For personal use only.



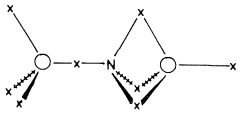
1



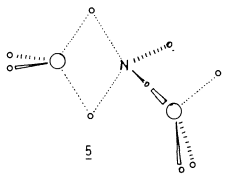
2



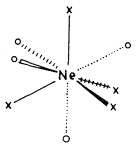
3



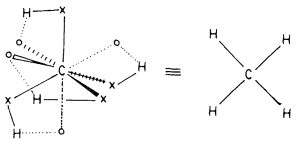
4



5



6



7

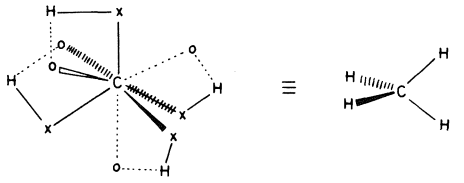
structure has only x electrons and the other has only o electrons. The two component structures for NO_2 are shown as **4** and **5**. Structure **4** requires an ONO angle of 180° while structure **5** requires an ONO angle of 125°. While the conclusion that the ONO angle is between 125–180° is not very precise, LDQ structures commonly offer reasonable bond angle predictions. A comparison of some predicted bond angles made by LDQ theory and by Pauling's hybridization approach are presented in Table 1. It should be noted that Linnett's restriction of LDQ theory to compounds primarily involving elements of the "First Short Period" makes it less useful than either Pauling's approach (26) or Gillespie's VSEPR theory (27). Although Luder (23) has extended LDQ theory to deal with geometries more complex than the tetrahedron, he has made no systematic attempt to compare predicted bond angles with observed bond angles in real molecules.

Structure and Reactivity

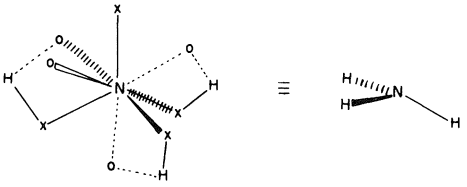
LDQ theory provides models for the repulsion minimized arrangement of sets of electrons which have the same spin viz. doublet (linear), triplet (trigonal planar), quartet (tetrahedral), quintet (trigonal bipyramidal), and sextet (octahedral). In this way repulsive interactions between electrons of the same spin are always minimized. To deduce molecular structures one must find the arrangement for the two valence shell spin sets which minimizes repulsions between them without altering the basic geometry for each spin set since "distortions will result in an increase of energy" (1).

Therefore the LDQ structures for Ne, F^-, O^{2-}, N^{3-}, and C^{4-} locate each valence electron in a corner of a cube which maintains the tetrahedral arrangement of each spin set while optimizing the separation of the two quartets (see structure **6**). Similarly the double singlet of $H:^-$ would be linear (as depicted by Luder for the double singlet of Be (10)). One would then expect to draw structure **7** or structure **8** as repulsion minimized LDQ structures for methane. Linnett (1) suggests that the x and o quartets should be superimposed, thus introducing four "close pairs" and facilitating the choice of tetrahedral geometry for methane, although such a procedure has "some resulting increase in inter-electron repulsion energy" (1). Since, for O_2 the best structure i.e., **3** was selected on the grounds that "the electrons, on an average, are more widely separated" (1), the choice of **7** or **8** for methane would seem to be more readily made than would be the case if the electrons were "close paired" first. Structure **8** could then be selected on the grounds that it reduces internuclear repulsions between the protons.

An analysis of possible structures for ammonia would bring one to the choice between **10** and **12** in a self-consistent way. The difficulty of selecting **12** over **10** is not tied to LDQ theory since commonly recognized structural features such as internuclear



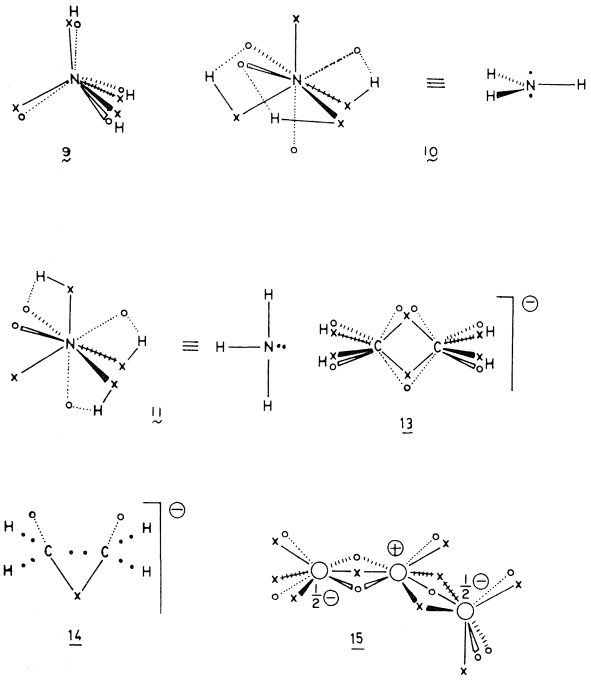
8



12

TABLE 1. Bond angles

Compound	Angles	Pauling prediction	LDQ prediction	Actual angle (Reference)
O_3	OOO	120°	125°	117° (22)
HCO_2H	OCO	120°	120–125°	123° (27)
CH_3N_3	CNN	120°	125°	120° (27)
NO_2	ONO	120°	125–180°	134° (27)
H_2CCH_2	HCH	120°	109°	117° (26)
H_2CCH_2	HCC	120°	125°	121° (27)



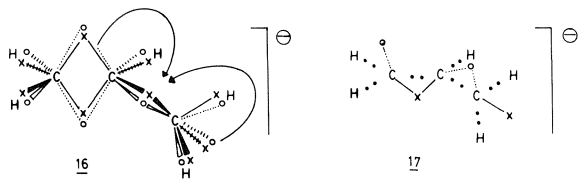
repulsions/steric effects dictate the incorrect choice of **10** independent of the bonding theory applied. In fact this approach to the use of LDQ structures would better prepare one for the information that amines are optically unstable, racemizing through a low energy trigonal transition state. Furthermore, it overcomes the difficulty of assuming that the lone pair is initially "close paired" and separates somewhat after formation of the ammonia molecule (13).

A similar analysis for water avoids the necessity to assume separation of "close pairs" after molecular formation (13).

In many cases LDQ structures must have σ bonding electrons spatially separated. For example, the one-electron reduction of ethylene would furnish a radical anion which could have the LDQ structure **13**. Such a structure is completely unacceptable, requiring, as it does, three spatially coincident electrons (two of which must have the same spin!). Separation of the electrons in the σ bonds would provide some release of the intolerable electronic repulsions in **13** (see **14**).

Ozone has a structure which is easily deduced from LDQ theory (structure **15**). Since the allyl anion is isoelectronic with O_3, Linnett (22) has suggested that they have the same structures. However, if the σ bonds have "close paired" electrons a structure for the allyl anion analogous to that for ozone is precluded. Instead the allyl anion would have structure **16**. Close pairing of the bonding electrons in **16** makes it physically impossible, in terms of a model, for the central carbon atom to share three electrons with each terminal methylene.[6] Again separation of the bonding electrons permits an electronically viable structure, viz. **17**.

Electronic separations in two-electron bonds are commonly assumed in cationic structures, viz. $H_2S_2^+$. It should be noted that such electronic separation in two electron bonds distorts the geometry somewhat.



Reactivity

Linnett has suggested that some chemical reactions may be understood in terms of the resistance that species with "remote pairs" might have to the formation of products which require "close pairs". Several examples have been advanced (1, 22).

[1] $2NO \rightarrow ONNO$ $\quad \Delta H > 0$

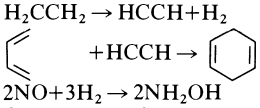
[2] $3(^1\Sigma_g^+O_2) \rightarrow 2O_3$ $\quad \Delta H < 0$

[3] $2(CH_3)_2CO \rightarrow C(CH_3)_4 + CO_2$ $\quad \Delta H < 0$

[6] The position of the electrons in structure **16** is indicated in the standard way. The arrows show where the electron and the orbitals should be if there are to be two CC bonds of bond order 1.5 each.

Can. J. Chem. Downloaded from www.nrcresearchpress.com by 210.87.254.5 on 09/05/12
For personal use only.

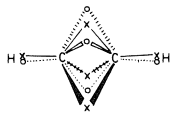
TABLE 2. ΔH predictions based on electronic separations

Reaction	ΔCP*	Predicted ΔH	Observed ΔH (kcal/mol)
1. $H_2 + O_2 \rightarrow HOOH$	+6	>0	−32.58
2. $H_2+N_2 \rightarrow HN{=}NH$	+3	>0	+48.7
3. $H_2CCH_2 \rightarrow HCCH+H_2$	−3	<0	+41.7
4. 	+3	>0	−40.8
5. $2NO+3H_2 \rightarrow 2NH_2OH$	+11	>0	−30.8
6. $CO_2+H_2 \rightarrow HCO_2H$	+1	>0	+4.0
7. $2H_2+CH_3CN \rightarrow C_2H_5NH_2$	+3	>0	−31.1
8. $4S_2 \rightarrow S_8$	+24	>0	−98.2
9. $CH_3NC+2H_2 \rightarrow (CH_3)_2NH$	+3	>0	−40.1
10. $H_2+CO \rightarrow H_2CO$	+3	>0	−1.5

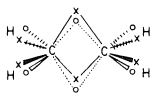
*ΔCP represents the change in the number of "close paired" electron pairs: ΔCP > 0 means the reaction creates close pairs and ΔCP < 0 means the reaction results in the separation of close pairs.

In eq. [1], it was argued, the total number of bonding electrons is constant but the formation of ONNO results in the creation of "close pairs" not present in two molecules of NO. The formation of O_3 from the $^1\Sigma_g^+O_2$ state would be exothermic because the product has much greater electronic separation than the starting material. Equation [3] is rationalized in the same way as eq. [2]. Table 2 presents a selection of reactions to which we have applied this type of analysis. The results in Table 2 clearly establish that there is no correlation between the hypothetical change in electronic separations and the ΔH for these reactions.

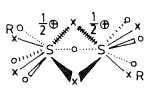
LDQ theory has been used to predict the relative bond strength of a single species in cases where there are a number of structural possibilities with different bond orders. However, there has been no examination of its implications for bond strengths in related but different ground state molecules. The presently accepted structures for acetylene and ethylene are given as **18** and **19**. Ethane and



18



19



20

ethylene have all bonding electrons "close paired". Acetylene has only the CH electrons "close paired". It should follow[7] that acetylene, which has the greatest electronic separation in the CC bond, has the greatest bond strength per pair of bonding electrons. Moreover ethylene and ethane should have essentially the same CC bond strength per pair of bonding electrons since both compounds have "close paired" CC bonding electrons (requiring a destabilization of 6 kcal/mol for each close pair). In fact acetylene has a CC bond strength of 64.6 kcal/mol per bonding pair, ethylene has a CC bond strength of 73.5 kcal/mol per bonding pair, and ethane has a CC bond strength of 83.1 kcal/mol per bonding pair (27). A similar analysis leads to an erroneous conclusion about the relative CN bond strengths per bonding pair for a carbon–nitrogen triple bond in comparison with a carbon–nitrogen double bond (C≡N, 69 kcal/mol per bonding pair and C=N 73.5 kcal/mol per bonding pair (27)).

The erroneous assumptions implicit in the LDQ structures for CC and CN multiple bonds could be responsible for the failure of the theory to anticipate the signs of ΔH for reactions 3 and 7 (Table 2). It seems likely that these assumptions are at fault as well in at least some of the other cases in Table 2.

If the electrons of the ethylenic four-electron bond were permitted to separate spatially, which could be readily achieved by allowing some separation of the electrons in the CH bonds, then the apparent differences in electronic repulsions for ethylene and acetylene would be removed. The result would be that the LDQ technique for predicting the sign of ΔH would no longer be applicable to reaction 3 in Table 2. An extension to systems containing four-electron bonds involving oxygen and nitrogen would remove still more cases from Table 2.

LDQ theory offers some advantages in rationalizing the stability of some radical cations. For example, structure **20** can be drawn for the disulfide radical cations which are unusually stable radical cations. Two features of these species are immediately clearer from such a structure than would be the case with a structure involving a Pauling "three-electron bond," viz. the bond order of 1.5 for the SS linkage and the equal electron densities of the two sulfur atoms. In structure **20**, as

[7]This conclusion presupposes that electronic correlation is the major factor controlling bond energies.

Can. J. Chem. Downloaded from www.nrcresearchpress.com by 210.87.254.5 on 09/05/12
For personal use only.

Can. J. Chem. Downloaded from www.nrcresearchpress.com by 210.87.254.5 on 09/05/12
For personal use only.

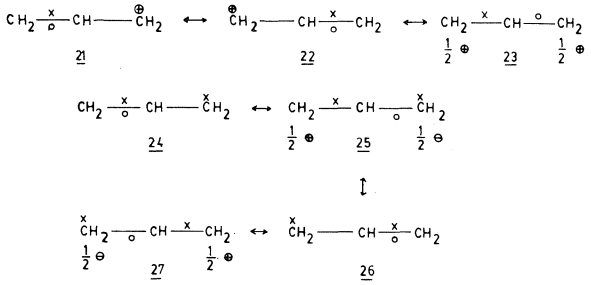
with all LDQ structures where, in MO terms, the HOMO is doubly occupied and the LUMO singly occupied, one antibonding electron and one bonding electron are depicted as two non-bonding electrons. This device causes occasional difficulties as we have shown during the discussion of the ethylene anion (**13**) if one attempts to keep all σ bonding electrons "close paired".

Resonance

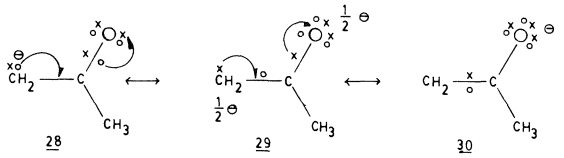
Qualitative utilization of resonance theory, as it is commonly employed, requires the formulation of a structure from which other structures are generated by electron pair delocalization through atomic *p* orbitals. It has proved to be a very powerful tool for understanding molecular structure and chemical reactions.

LDQ theory, it has been claimed (10, 11, 23, 25) reduces the number of resonance contributors describing a given π system. In fact, LDQ theory increases the number of resonance contributors available for the description of real species.[8] For example, the allyl cation is conventionally discussed in terms of the resonance contributors **21** and **22**. LDQ theory adds contributor **23** to the melée.[9] The allyl cation is adequately described electronically by contributor **23** alone. A completely parallel discussion can be advanced for the allyl anion.

The allyl radical would have contributors **24–27** available. In this case the addition of LDQ contributors **25** and **27** adds nothing to the insight offered by the conventional forms **24** and **26**. As a final example of the application of LDQ contributors to qualitative resonance considerations,



we have considered the acetonyl anion (shown as structures **28–30**). In this case the best description of the electronic distribution in the anion would be obtained by utilizing the LDQ contributor **29** and the conventional contributor **30**.



It should now be clear that LDQ contributors do not reduce the number of contributors available to describe π systems and are not systematically superior to conventional contributors. Whether the most useful description of a particular system is obtained by (*i*) LDQ contributors alone, (*ii*) a combination of LDQ contributors and conventional contributors, or (*iii*) by conventional contributors alone depends entirely upon the system under consideration. The advent of LDQ theory has not brought about "the time to abandon the hypothesis of resonance hybrids" (23).

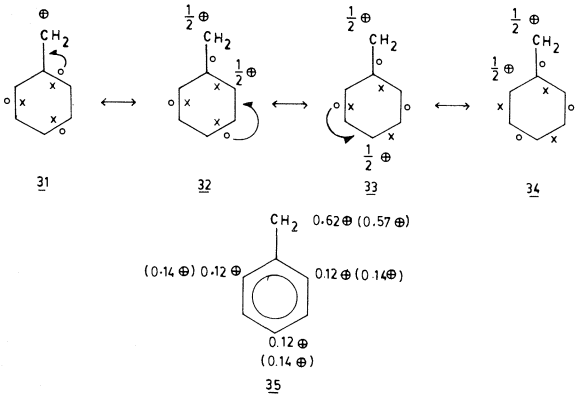
The strength of LDQ theory lies in providing descriptions of the electronic structures of molecules, particularly those with π systems. LDQ resonance contributors offer greater precision than conventional contributors for those systems in which atoms have fractional charges. This greater precision holds the promise of rapid and convenient resonance analyses which are more quantitative than analyses which are presently carried out without the aid of detailed numerical calculations.

A case in point is provided by the benzyl cation. Conventional resonance contributors depict a full positive charge localized on the benzylic carbon, the *ortho* carbon atoms, and the *para* carbon atom. Quantitatively, the problem then becomes how to assess the relative importance of the various contributors. It is clear that the form with the full charge on the benzylic carbon is the most important contributor since in attaching greater weight to that contributor one minimizes the disruption of the aromatic sextet. LDQ contributors offer a simple way to reduce the disruption of the π system in the ring, thus simplifying the problem of weighing the contributors. Thus equal weight for the contributors **31–34** leads to the conclusion shown in structure **35**. The results of simple HMO calculations for electron densities in the benzyl cation are shown in brackets after the LDQ conclusions.

Unfortunately, greater precision in the representation of resonance contributors does not *ipso facto* result in greater accuracy in the conclusion obtained. Resonance contributors have been widely used in rationalizing the results of chemical reactions. Such analyses frequently presume that the outcome of a reaction is completely dependent

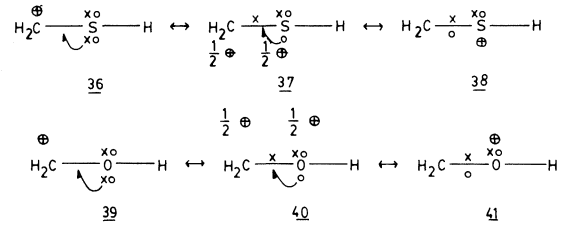
[8]From this point, we shall adopt Linnett's practice of a conventional line to represent two spin paired σ bonding electrons, but we shall retain the xo convention for non-bonding and π electrons.

[9]While contributors such as **21** and **22** can be understood as conventional structures or as LDQ structures, structure **23** is uniquely obtained from LDQ theory. Therefore we shall refer to **21** and **22** as conventional contributors and **23** as an LDQ contributor.



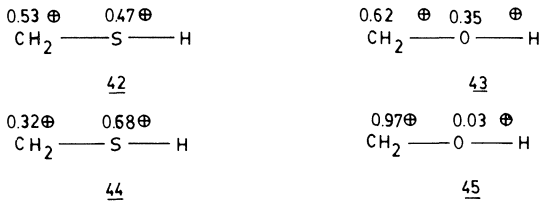
upon the nature of the transition state/intermediate which is described in resonance terms without reference to other features of the reaction (particularly the nature of the solvent involved). The inevitable consequence has been that resonance theory has been used to derive oversimplified descriptions which have introduced errors in the handling of contributors.

A case in point is provided by carbocations substituted by oxygen or sulfur. Two simple systems are shown as structures **36–38** and **39–41**. It has



been suggested that π bonding "should be more effective for oxygen than sulfur because of the more diffused nature of the sulfur orbital" (28). However, it seems likely that this view, which was derived from the results of reactions in solution, is in error. The conclusions of Wolfe and co-workers (29) for the π electron densities, based on a non-empirical SCF–MO treatment of these cations, are shown in structures **42** and **43**; **42** is **37**. Structure **43** can be obtained approximately by equal weighing of contributors **39** and **40**. Thus greater precision and accuracy are available if LDQ contributors are added to the basic set of resonance contributors which are employed in describing a π system. However, if rules are to be developed which permit a general semiquantitative assessment of π systems, it is essential that more theoretical calculations be done.

Finally, resonance contributors which deal primarily with electrons in π systems should lead to conclusions such as **42** and **43**. Often resonance arguments are not accompanied by careful assessment of inductive effects. Such omissions can lead to serious error. Structures **44** and **45** are included to illustrate the drastic alteration of electronic distribution which can result from inclusion of inductive effects.



Acknowledgements

The authors are pleased to acknowledge the assistance of Mr. A. R. Jurgens. Professor A. Whitla has provided helpful discussions which are gratefully acknowledged. We are grateful to Dalhousie University for financial support in the form of a grant from the Research Development Fund.

1. J. W. LINNETT. J. Am. Chem. Soc. **83**, 2643 (1961).
2. P. B. EMPEDOCLES and J. W. LINNETT. Theor. Chim. Acta, **4**, 377 (1966).
3. D. P. CHONG and J. W. LINNETT. Mol. Phys. **8**, 151 (1964).
4. D. M. HIRST and J. W. LINNETT. J. Chem. Soc. 1035 (1962).
5. D. M. HIRST and J. W. LINNETT. J. Chem. Soc. 3844 (1962).
6. R. D. GOULD and J. W. LINNETT. Trans. Faraday Soc. **59**, 1001 (1963).
7. D. M. HIRST and J. W. LINNETT. J. Chem. Phys. **43**, 574 (1965).
8. H. C. BOWEN and J. W. LINNETT. Trans. Faraday Soc. **60**, 1185 (1964).
9. P. B. EMPEDOCLES and J. W. LINNETT. Proc. R. Soc. London, Ser. A, **282**, 166 (1964).
10. (*a*) W. F. LUDER. J. Chem. Educ. **44**, 206 (1967); (*b*) S. ZUFFANTI and W. F. LUDER. Educ. Chem. **9**, 12 (1972).
11. (*a*) S. ZUFFANTI and W. F. LUDER. Educ. Chem. **9**, 187 (1972); (*b*) W. F. LUDER. J. Chem. Educ. **44**, 269 (1967).
12. R. A. FIRESTONE. Tetrahedron Lett. 971 (1968).
13. R. A. FIRESTONE. J. Org. Chem. **34**, 2621 (1969).
14. R. A. FIRESTONE. J. Chem. Soc. A, 1570 (1970).
15. R. A. FIRESTONE. J. Org. Chem. **36**, 702 (1971).
16. R. A. FIRESTONE. J. Org. Chem. **37**, 2181 (1972).
17. R. A. FIRESTONE. J. Chem. Soc. Chem. Commun. 163 (1973).
18. F. SERRATOSA. J. Chem. Educ. **50**, 402 (1973).
19. R. A. FIRESTONE. J. Org. Chem. **41**, 2212 (1976).
20. R. A. FIRESTONE. Tetrahedron Lett. 735 (1976).
21. R. A. FIRESTONE. Tetrahedron, **33**, 3009 (1977).
22. J. W. LINNETT. The electronic structure of molecules. Methuen, London. 1964.
23. W. F. LUDER. The electron-repulsion theory of the chemical bond. Reinhold, New York, NY. 1967.
24. R. PAUNCZ. Alternant molecular orbital method. W. B. Saunders, Philadelphia, PA. 1967.
25. J. E. HUHEEY. Inorganic chemistry. Harper and Row, New York, NY. 1972. p. 144.
26. L. PAULING. The chemical bond. Cornell University Press, Ithaca, NY. 1967.
27. R. J. GILLESPIE. Molecular geometry. Van Nostrand Reinhold, London. 1972.
28. W. TAGAKI. *In* Organic chemistry of sulfur. *Edited by* S. Oae. Plenum Press, New York, NY. 1977. p. 254.
29. F. BERNARDI, I. G. CSIZMADIA, H. B. SCHLEGEL, and S. WOLFE. Can. J. Chem. **53**, 1144 (1975).

Can. J. Chem. Downloaded from www.nrcresearchpress.com by 210.87.254.5 on 09/05/12
For personal use only.

Effet de cation sur la réactivité ambidente des anions: la nette tendance à la O-alkylation manifestée par les énolates de lithium de composés β-dicarbonylés

P. SARTHOU,[1] G. BRAM ET F. GUIBE[2]

Groupe de Recherche No 12, Centre National de la Recherche Scientifique, B.P. 28, 94320 Thiais, France

Reçu le 27 septembre 1979

P. SARTHOU, G. BRAM et F. GUIBE. Can. J. Chem. **58**, 786 (1980).

L'étude de la réactivité spécifique des paires d'ions d'énolates alcalins de composées β-dicarbonylés montre que les énolates de lithium, en dépit de la forte interaction enolate–cation qui les caractérise, présentent, notamment par rapport à ceux de sodium, une tendance marquée à la O-alkylation. Cette forte O-/C-nucléophilie de la paire d'ion lithium n'est pas sensiblement affectée par la polarité du milieu (du DME ou THF au DMF) mais dépend de la nature du réactif alkylant: elle est maximum lorsque celui-ci est un sulfonate ou un sulfate d'alkyle de réactivité électrophile modérée; elle est atténuée dans le cas des halogénures d'alkyle et des sulfonates d'alkyle très électrophiles (triflates). Il est proposé que la tendance à la O-alkylation manifestée par l'énolate de lithium est pour partie la conséquence d'une interaction Li^+ – groupe partant de l'électrophile (cas des sulfonates notamment) et pour partie une propriété intrinséque de la paire d'ions énolate–lithium; celle-ci est interprétée en terme de pouvoirs de solvatation comparés des états de transition de la C- et de la O-alkylation vis à vis des cations.

Certains des résultats concernant la réactivité nucléophile des paires d'ions dans le DMF sont en désaccord avec des résultats antérieurs de la littérature. Les raisons de ce désaccord sont examinées.

P. SARTHOU, G. BRAM, and F. GUIBE. Can. J. Chem. **58**, 786 (1980).

The study of the specific reactivity of the ion pairs of alkaline enolates of β-dicarbonyl compounds shows that the lithium enolates, in spite of their characteristically strong enolate–cation interactions display, especially when compared to sodium enolates, a marked tendency towards O-alkylation. This strong O-/C-nucleophilicity of the lithium ion pairs is not very sensitive to changes in medium polarity (from THF or DME to DMF) but depends on the nature of the alkylating agent, being enhanced with moderately electrophilic alkyl sulfonates or sulfate but lessened with alkyl halides or with very electrophilic sulfonates (triflate). It is suggested that the lithium enolate tendency towards O-alkylation is partly the result of a Li^+ – leaving group interaction (especially in the case of the sulfonates) and partly an intrinsic property of the enolate–lithium ion pair; this latter property is discussed in terms of the respective solvation abilities towards cations of the C- and O-alkylation transition states.

Some of our results about the nucleophilic reactivity of ion pairs in DMF are at variance with previous reports in the literature. The origin of the discrepancy is discussed.

L'orientation des réactions d'alkylation d'ions ambidents énolate–carbeniate est soumise à différents facteurs: solvant, nature du cation associé, nature du réactif alkylant, etc. (1–8). En ce qui concerne l'effet du cation associé, il est généralement admis que plus forte est l'interaction énolate–cation, plus grande est la tendance à la C-alkylation; ainsi dans la série des énolates alcalins on observe habituellement que le rapport C/O alkylation croit dans l'ordre $N^+R_4 < Cs^+ < K^+ < Na^+ < Li^+$, l'interaction anion–cation étant d'autant plus énergique que la taille du cation est réduite (1–5, 7, 8). Toutefois, en nous intéressant *spécifiquement* à la réactivité des *paires d'ions* nous avons pu montré que l'énolate de lithium de l'acétylacétate d'éthyle conduit, dans le diméthoxyéthane (DME) et avec TsOEt à un rapport C/O alkylation nettement supérieur à ceux des énolates de Na^+ et K^+ et proche de celui de la paire d'ions Cs^+ (9). Cette O-nucléophilie relative importante de l'énolate de lithium a ensuite été confirmée sur toute une série de réactifs alkylants à groupe partant sulfonate ou sulfate (10).

Cette propriété de la paire d'ion lithium ne peut être imputée à un relachement de l'interaction énolate–cation; celle-ci est au contraire considérablement renforcée comme en témoignent par exemple les résultats cinétiques dans le DME (9) qui montrent que l'énolate de lithium de l'acétylacétate d'éthyle est beaucoup moins réactif que l'énolate de sodium vis à vis de TsOEt ou d'autres agents alkylants. Dès 1955, Kornblum *et al.* avait montré (12) que les nitrites d'argent conduisaient avec les halogénures (bromure et iodure) d'alkyle à un rapport O/N alkylation très élevé et interprété ce résultat par une interaction Ag^+-groupe partant halogénure. Par analogie, nous avions proposé (9–10) l'existence d'une interaction lithium – groupe partant tosylate ou sulfate pour rendre compte de nos résultats.[3] Une telle interaction, susceptible d'une part de diminuer d'autant

[1]Ce travail fait partie de la Thèse d'Etat de P. Sarthou, Paris XI, 1978.

[2]Auteur à qui toute correspondance doit être adressée.

[3]On peut noter que l'interaction Li^+-sulfonate du type dur–dur tout comme l'interaction Ag^+-iodure ou Ag^+-bromure du type mou–mou, sont toutes deux des interactions favorables selon la théorie HSAB de Pearson (11).

0008-4042/80/080786-08$01.00/0

©1980 National Research Council of Canada/Conseil national de recherches du Canada

Can. J. Chem. Downloaded from www.nrcresearchpress.com by 210.87.254.5 on 09/05/12
For personal use only.

Can. J. Chem. Downloaded from www.nrcresearchpress.com by 210.87.254.5 on 09/05/12
For personal use only.

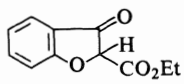
l'interaction énolate–cation dans l'état de transition et d'autre part de polariser la liaison carbone – groupe partant et de conduire ainsi à une réaction à "caractère S_N1" (12) plus marqué devrait en effet favoriser l'alkylation sur le site le plus électronégatif de l'énolate ambident.

Dans le but de vérifier le bien-fondé de l'explication proposée et de façon plus générale de préciser les facteurs qui déterminent le comportement ambident des formes associées des énolates alcalins (lithium notamment) de composés β-dicarbonylés, nous avons poursuivi notre étude en nous intéressant à la nature du groupe partant de l'électrophile et aux effets de milieu.

Effet du groupe partant de l'électrophile

Il paraissait important tout d'abord de vérifier si la tendance à la O-alkylation de l'énolate de lithium des composés β-dicarbonylés se manifestait seulement vis à vis de réactifs alkylants à groupe partant oxygéné dur tels que sulfonate ou sulfate ou si cette propriété s'étendait aussi aux électrophiles plus mous tels que les iodures d'alkyle.

Les taux de O-alkylation obtenus dans les réactions des énolates alcalins de l'acétylacétate d'éthyle avec les halogénures d'alkyle sont de façon générale très faible; aussi avons-nous utilisé pour cette étude l'énolate de la carbéthoxycoumaranone-3 **1** qui présente une forte tendance à la O-alkylation (13, 14). Le solvant choisi est le THF, l'énolate de lithium de **1** s'étant révélé insuffisamment soluble dans le DME.



1

Les résultats obtenus (analyse par chromatographie en phase gazeuse) sont représentés dans le tableau 1. A des fins de comparaison, nous avons reporté dans le tableau 2 certains des résultats (10) concernant les énolates de l'acétylacétate d'éthyle vis à vis de sulfonates ou de sulfate d'alkyle dans le DME. Les données du tableau 1 montrent que l'énolate de lithium de **1** conduit à une proportion d'éther d'énol plus élevé que celle de l'énolate de sodium et du même ordre de grandeur que celle de l'énolate de potassium. La présence dans le milieu de perchlorate à cation commun ne modifie pas sensiblement les rapport C-/O-alkylation obtenus. Ceci montre, comme celà avait déjà été fait dans le cas de l'acétylacétate d'éthyle sur la base de la structure des éthers d'énol obtenus (cf. réf. 9 et paragraphe suivant) que l'espèce réactive est la

TABLEAU 1. Alkylation des énolates de Li^+, Na^+ et K^+ de la carbéthoxycoumaranone-3 par EtI 0.4 *M* dans le THF. Rapports C/O; [énolate] = 0.05 *M*; *T* = 100°C

Enolate	C/O	
Li^+	1.8	2.0[b]
Na^+	2.5	2.5[b]
K^+[a]	2.0	—
$(C/O)_{Na^+}/(C/O)_{Li^+}$:	1.40	1.25

[a][Enolate] = 2×10^{-3} *M*.
[b]En présence de $ClO_4^-M^+$ 0.1 *M* ($M^+ = Li^+, Na^+$).

TABLEAU 2. Alkylation des énolates de lithium et de sodium de l'acétylacétate d'éthyle (EM) dans le DME. Effets de groupes partants sur les rapports C/O; [énolate] = 0.05 *M*; *T* = 40°C

	ELi	ENa	$(C/O)_{Na}/(C/O)_{Li}$
CH_3SO_3Et	2.4	8.6	3.6
$pCH_3OC_6H_4SO_3Et$	1.9	6.5	3.4
$pCH_3C_6H_4SO_3Et$	2.2	6.0	2.7
$C_6H_5SO_3Et$	2.2	6.0	2.7
$EtOSO_3Et$	2.2	4.8	2.20
FSO_3Et	3.0	3.5	1.15
CF_3SO_3Et[a]	3.6	3.8	1.05
$EtOSO_2Et$[b]	3.8	14	3.7

[a]*T* = 20°C.
[b]*T* = 100°C.

paire d'ions, à la quasi-exclusion de l'énolate dissocié.

La valeur du rapport $R = (C/O)_{Na^+}/(C/O)_{Li^+}$ permet de caractériser l'accroissement de la O-nucléophilie de l'énolate de lithium relativement à celle de l'énolate de sodium. La valeur de ce rapport (environ 1.25) pour le système **1**-EtI est voisine de celle observée pour l'acétylacétate d'éthyle avec les sulfonates très électrophiles (trifluorométhane-sulfonate, fluorosulfonate). Elle reste nettement inférieure à celle observée (de 2.2 à 3.7) pour l'acétylacétate d'éthyle avec le sulfite d'éthyle, le sulfate d'éthyle et les sulfonates d'éthyle de réactivité modérée (méthane sulfonate, *p*-toluène sulfonate).

En résumé, la tendance à la O-alkylation des enolates de lithium dépend de façon substantielle de la nature du groupe partant de l'électrophile. Elle est maximum avec les groupes partants oxygénés durs à faible pouvoir nucléofuge. Toutefois, elle se manifeste également, quoique à un moindre degré, lorsque le groupe partant est une entité molle telle que I^-.

Effet de solvant. Alkylation des énolates de l'acétylacétate d'éthyle dans le DMF

Dans les solvants éthérés comme le THF ou le DME de faible pouvoir dissociant, l'agrégation des espèces ioniques en édifices complexes (agrégats

Can. J. Chem. Downloaded from www.nrcresearchpress.com by 210.87.254.5 on 09/05/12
For personal use only.

TABLEAU 3. Alkylation des énolates de lithium et de sodium de l'acétylacétate d'éthyle (EM) par EtOTs et EtBr dans le DMF à 25°C. Pourcentages des produits de réaction[a]; [enolate] = 0.3 *M*; [RX] = 0.3 *M*

EM + RX	Sel	C	O_{cis}[b]	O_{trans}	Di-C
	0	47	42.0	11.0	0
ELi + EtOTs	$LiClO_4$ 0.1 *M*	51.0	40.0	7.0	0
	$LiClO_4$ 0.3 *M*	53.0	41.5	5.5	0
	0	45	16	39	0
ENa + EtOTs	$NaClO_4$ 0.1 *M*	53.5	21.5	25.0	0
	$NaClO_4$ 0.3 *M*	61.5	19.5	18.5	0
	0	86.5	3.0	2.5	8.0
ELi + EtBr	$LiClO_4$ 0.1 *M*	86.0	4.0	2.0	8.0
	$LiClO_4$ 0.3 *M*	87.0	4.0	1.5	7.5
	0	79.0	2.0	8.5	10.5
ENa + EtBr	$NaClO_4$ 0.1 *M*	80.0	2.5	5.5	12.0
	$NaClO_4$ 0.3 *M*	81.0	2.0	4.0	13.0

[a]Avancement des réactions compris entre 75 et 80% sauf pour ELi + EtOTs (50%).
[b]Les proportions de O_{cis} reportées ici sont nettement plus élevées que celles obtenues par Kurts et coll. (17, 18) dans des conditions similaires. Pour une interprétation de ces différences, voir partie expérimentale.

de paires d'ions, ions triples) est un phénomène fréquent (5); il s'observe notamment dans le cas des énolates alcalins de l'acétylacétate d'éthyle ainsi que le montrent des résultats cinétiques (9) ou spectrométriques ir (15). La question se posait donc de savoir si ces phénomènes étaient capables d'influer de façon significative sur l'orientation des réactions d'alkylation; dans le même ordre d'idées il a été montré par exemple (16) que l'orientation de l'alkylation d'ions phénates était fortement influencée par le caractère homogène ou hétérogène du milieu réactionnel. Nous avons donc effectué une étude de l'alkylation des énolates de lithium et de sodium de l'acétylacétate d'éthyle par le tosylate et le bromure d'éthyle dans le DMF. Ce solvant est suffisamment polaire pour rendre peu vraisemblable la formation d'agrégats de paires d'ions mais, contrairement à ce qui a lieu dans un solvant plus dissociant comme le HMPT (17, 18), on peut encore y observer à côté de la réactivité des ions dissociés, celle des paires d'ions (19, 20). L'analyse des produits a été réalisée par chromatographie en phase gazeuse. Les résultats de cette étude sont reportés dans le tableau 3.

La réaction d'alkylation conduit à quatre produits: les produits de mono-C- et di-C-alkylation et les deux isomères O-*cis* et O-*trans* de l'éther d'énol (Schéma 1). La présence de ces deux isomères montre (5, 9, 15, 18, 19) qu'il y a réaction concurrente de la paire d'ions et de l'énolate dissocié. En effet la géométrie de l'ion énolate est conservée durant la réaction d'alkylation[4] et la paire d'ions chélate (énolate en U) conduit à l'éther d'énol O-*cis* tandis que l'ion dissocié à structure transoïde (W ou S-*trans*) conduit à l'éther d'énol *trans*.

A partir du schéma d'Acree (8, 20, 21) appliqué à la réaction de l'énolate (Schéma 1), il est possible en se basant sur les résultats bruts du tableau 3 d'accéder au rapport C-/O-alkylation caractéristique de la paire d'ions (rapport $k_{C,pi}/k_{O,pi}$). Désignons par O_{pi} et O_i les concentrations en éther d'énol et par C_{pi} et C_i les concentrations en produit de C-alkylation provenant respectivement de la paire d'ions (pi) et de l'énolate dissocié (i). Les réactions du schéma 1 sont toutes bimoléculaires; α désignant le coefficient de dissociation de l'énolate, E_T l'énolate total, les équations cinétiques sont donc de la forme:

$$[1] \quad dO_{pi}/dt = (1 - \alpha(t))k_{O,pi}E_T(t)$$

$$[2] \quad dO_i/dt = \alpha(t)k_{O,i}E_T(t)$$

$$[3] \quad dC_{pi}/dt = (1 - \alpha(t))k_{C,pi}E_T(t)$$

$$[4] \quad dC_i/dt = \alpha(t)k_{C,i}E_T(t)$$

De [1] et [2], on tire, après intégration:

$$[5] \quad \frac{k_{C,pi}}{k_{O,pi}} = \frac{C_{pi}}{O_{pi}}$$

et le rapport des concentrations de C_{pi} et O_{pi} est donc constant et égal au rapport $k_{C,pi}/k_{O,pi} = k_C/k_{Opi}$ caractéristique de la paire d'ions.

La détermination de O_{pi} (et de O_i) est immédiate puisque, compte tenu de ce qui précède, on a:

$$O_{pi} = O_{cis} \text{ et } O_i = O_{trans}$$

Le cas de la C-alkylation est plus complexe; la structure du produit C-alkylé est en effet unique, qu'il provienne de l'énolate dissocié ou de la paire

[4]Dans le cas des formes associées, ceci n'est strictement valable que pour les paires d'ions Li^+ et Na^+. En ce qui concerne les cations plus volumineux, le problème est plus complexe et a été discuté dans le cadre du principe de Curtin-Hammet (ref. 9, note de la p. 3145).

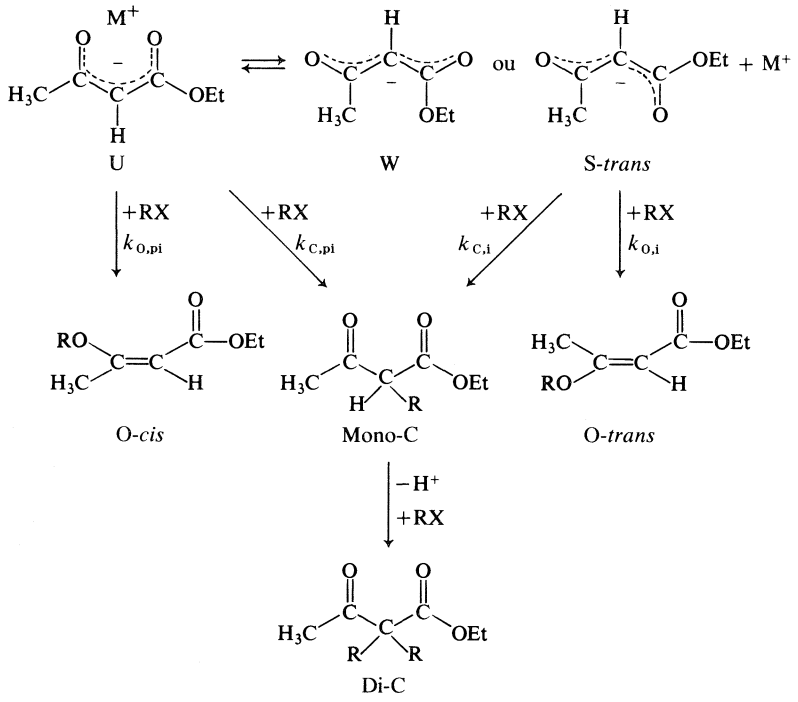


SCHÉMA 1

d'ions. On peut écrire:

$$C_i = O_i \cdot C_i/O_i = O_{trans} \cdot (C/O)_i$$

$(C/O)_i$ représentant le rapport C-/O-alkylation de l'énolate dissocié. Comme $C_{pi} = C_{total} - C_i$ il vient:

$$C_{pi} = C_{total} - O_{trans} \cdot (C/O)_i$$

et le rapport $(C/O)_{pi}$ caractéristique de la paire d'ions est finalement égal à:

$$[6] \quad (C/O)_{pi} = \frac{C_{total} - O_{trans}(C/O)_i}{O_{cis}}$$

C_{total} désigne la somme des concentrations en produit mono- et di-C-alkylé, ce dernier provenant en fait de la réaction ultérieure d'une partie du produit mono-C-alkylé.

La relation [6] montre qu'il est possible de calculer le rapport $(C/O)_{pi} = k_{C,pi}/k_{O,pi}$ à partir des seules données du tableau 3 si l'on connait la valeur de $(C/O)_i$. Nous avons pris pour modèle de l'énolate dissocié l'énolate de potassium crypté (cryptand (2.2.2) spécifique du potassium) pour lequel on sait que l'interaction énolate–cation est très faible (15). On a ainsi:

$$(C/O)_i = (C/O)_{E^-(K^+2.2.2)} = 1.6$$

pour EtBr (à 25°C)

$$(C/O)_i = (C/O)_{E^-(K^+2.2.2)} = 0.15$$

pour EtOTs (à 25°C).

L'éther d'énol résultant de l'alkylation de l'énolate de potassium crypté a une structure exclusivement *trans* en accord avec le caractère très relaché de l'interaction énolate–cation dans ce complexe. Notons que la valeur C/O = 0.15 obtenue avec TsOEt est très proche de celle de l'énolate dissocié dans le HMPT (C/O = 0.13) reporté par Kurts et coll. (17).

Les valeurs des rapports $(C/O)_{pi}$ calculés à l'aide de la relation [6] sont reportées sur le tableau 4. Les résultats des tableaux 3 et 4 conduisent aux commentaires suivants.

Bien que l'addition de sels inertes à cation commun (perchlorate) entraine dans tous les cas une augmentation des rapports C/O et O-*cis*/O-*trans* (régression de l'équilibre de dissociation d'Acree vers la paire d'ions) les rapports $(C/O)_{pi}$ correspondants ne sont pas sensiblement modifiés; ceci n'est pas surprenant puisque la présence de sel ajouté est peu susceptible de modifier l'interaction anion–cation au sein d'une paire d'ions déjà formée. En retour la quasi-constance du rapport $(C/O)_{pi}$, aux erreurs expérimentales près, nous paraît confirmer le bien-fondé de la méthode utilisée dans l'estimation de la réactivité des paires d'ions.

Dans le DMF comme dans le DME la paire d'ions lithium conduit à plus de O-alkylation que la paire d'ions sodium. Ceci est manifeste avec TsOEt où le rapport $R = (C/O)_{Na^+,pi}/(C/O)_{Li^+,pi} = 2.20$ est voisin de celui (R = 2.7) observé dans le

Can. J. Chem. Downloaded from www.nrcresearchpress.com by 210.87.254.5 on 09/05/12
For personal use only.

Can. J. Chem. Downloaded from www.nrcresearchpress.com by 210.87.254.5 on 09/05/12
For personal use only.

TABLEAU 4. Alkylation des énolates de lithium et de sodium de l'acétylacétate d'éthyle par EtOTs et EtBr dans le DMF à 25°C. Valeurs des rapports $(C/O)_{pi}$ des paires d'ions

EM	RX	ClO_4M	$(C/O)_{pi}$
		0	1.1
ELi	EtOTs	0.1 *M*	1.2
		0.3 *M*	1.3
		0	2.5
ENa	EtOTs	0.1 *M*	2.3
		0.3 *M*	3.0
		0	30
ELi	EtBr	0.1 *M*	23
		0.3 *M*	23
		0	38
ENa	EtBr	0.1 *M*	33
		0.3 *M*	44

DME (tableau 2). Avec EtBr les taux de O-alkylation sont faibles et les risques d'erreur importants. Néanmoins on observe là encore une diminution du taux de O-alkylation (R = 1.5) en passant de l'énolate de lithium à l'énolate de sodium, ce qui semble confirmer les résultats obtenus précédemment avec l'énolate de la carboethoxycoumaranone-3 (R = 1.25).

Pour une paire d'ions donnée, le taux de O-alkylation est plus élevé (2 fois environ) dans le DMF que dans le DME. Ceci peut s'expliquer par le meilleur pouvoir solvatant des cations du premier solvant; les paires d'ions, tout en conservant leur structure de chélate, seraient plus relachées dans le DMF d'où une tendance accrue à la O-alkylation. La baisse du taux de O-alkylation dans le THF peut aussi être liée à la formation d'agrégats; dans le cas de phénates, Kornblum et Lurie ont montré que le taux de O-alkylation était diminué lorsque la réaction était conduite en milieu hétérogène (16).

Notons qu'une estimation de la réactivité des paires d'ions des énolates alcalins (K^+, Na^+) de l'acétylacétate d'éthyle dans le DMF a été proposée avant nous par d'autres auteurs (22, 23). La méthode utilisée n'est pas basée sur l'analyse des éthers d'énol obtenus mais pour l'essentiel sur des mesures cinétiques. Les constantes de nucléophilie totale des paires d'ions $k_{t,pi} = k_{O,pi} + k_{C,pi}$ et le coefficient α de dissociation des énolates sont déterminés à partir de mesures de réactivité effectuées à diverses concentrations en énolate ou en présence de quantités variables de sels chimiquement inertes à cation commun (tetraphénylborates alcalins). La constante de nucléophilie totale de l'ion libre $k_{t,i} = k_{O,i} + k_{C,i}$ et son rapport C-/O-alkylation sont obtenus à partir de mesures de réactivité effectuées sur l'énolate de potassium en présence d'agents complexants (éther-couronnes). Le rapport $(C/O)_{pi}$ est alors calculé à l'aide de la relation [7]

$$[7] \quad (C/O)_{\text{expérimental}} = A(C/O)_i + B(C/O)_i$$

où

$$A = \alpha(k_{t,i}/k_{\text{expérimental}})$$

et

$$B = (1-\alpha)k_{t,pi}/k_{\text{expérimental}}$$

représentent les contributions respectives de l'énolate dissocié et de la paire d'ions à la réaction. La valeur de $(C/O)_{pi}$ ainsi trouvée pour l'énolate de sodium (0.61) est considérablement plus faible que la nôtre (environ 2.25). Nous pensons que cette différence résulte du caractère erroné de la relation [7]. La stricte application de la relation d'Acree, à savoir $k_t = \alpha k_i + (1-\alpha)k_p$, au rapport $(C/O)_{\text{expérimental}}$ conduit à la relation [8]:

$$[8] \quad (C/O)_{exp} = \frac{\alpha k_{C,i} + (1-\alpha)k_{C,p}}{\alpha k_{O,i} + (1-\alpha)k_{O,p}}$$

qui ne peut se ramener à une combinaison linéaire, telle que [7], des rapports $k_{C,i}/k_{O,i} = (C/O)_i$ et $k_{C,p}/k_{O,p} = (C/O)_p$. Une telle impossibilité traduit le fait que, dans des conditions de milieu données, les contributions respectives de la forme dissociée et de la forme associée à la réaction de C-alkylation d'une part et à la réaction de O-alkylation d'autre part ne sont pas les mêmes. Ceci apparait clairement lorsqu'on relie les rapports C_{pi}/C_i et O_{pi}/O_i, qui mesurent ces contributions, à l'aide de la relation:

$$C_{pi}/C_i = O_{pi}/O_i \frac{C_{pi}/O_{pi}}{C_i/O_i}$$

soit

$$[9] \quad C_{pi}/C_i = (O_{pi}/O_i)\frac{(C/O)_{pi}}{(C/O)_i}$$

$(C/O)_{pi}$ étant toujours supérieur à $(C/O)_i$ quel que soit le cation (9) il s'ensuit que la contribution de la paire d'ions est plus importante dans le cas de la C-alkylation.

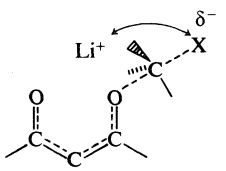
Discussion generale et conclusion

L'ensemble des résultats de cette étude confirme le caractère fortement O-nucléophile de l'énolate de lithium des β-ceto esters. Cette tendance à la O-alkylation ne parait pas dépendre de la polarité du milieu; elle n'est pas sensiblement affectée lorsqu'on passe du DME ou du THF au DMF. Ce fait parait exclure l'hypothèse selon laquelle la réaction de O-alkylation conduisant à l'éther d'énol

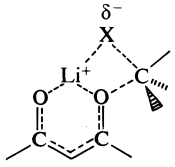
Can. J. Chem. Downloaded from www.nrcresearchpress.com by 210.87.254.5 on 09/05/12
For personal use only.

cis se déroulerait au sein d'agrégats ioniques complexes; les résultats observés traduisent donc très vraisemblablement la réactivité intrinsèque des paires d'ions monomères.

Les rapports C-/O-alkylation observés dépendent par contre de façon marquée du réactif alkylant. La tendance à la O-alkylation de l'énolate de lithium (comparée à celle de l'énolate de sodium) est particulièrement exaltée lorsque l'électrophile est un tosylate ou un sulfate de réactivité faible ou modérée; il est vraisemblable que dans ces cas une interaction Li^+ – groupe partant oxygéné joue un rôle dans l'orientation de la réaction, comme celà avait déjà été suggéré (9). La tendance à la O-alkylation de l'énolate de lithium (toujours comparée à celle de l'énolate de sodium) persiste néanmoins, quoique à un degré moindre, avec les autres agents alkylants et notamment les halogénures. Ceci rend à notre sens difficile une explication basée exclusivement sur l'existence d'une interaction lithium – groupe partant de l'électrophile et ce pour plusieurs raisons. Une telle interaction, vraisemblable en milieu de polarité modérée (DME, THF) et dans le cas où le groupe partant est une base oxygénée dure telle que TsO^- (l'effet ionisant de sels de lithium sur certains tosylates à radical R allylique ou β-aryléthylique a été mis en évidence à diverses reprises (24, 25)), parait beaucoup plus problématique avec un groupe partant tel que I^- ou Br^-, particulièrement au sein d'un solvant aussi polaire que le DMF capable lui-même de solvater énergiquement le cation Li^+. L'interaction Li^+ – groupe partant est en outre difficile à concilier avec un arrangement colinéaire du groupe entrant, du carbone siège de la substitution et du groupe partant lorsque ce dernier est monoatomique comme I^- ou Br^- (cf. **2**). Cette colinéarité apparait pour-



2

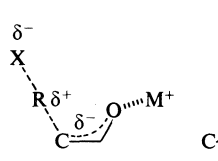


3

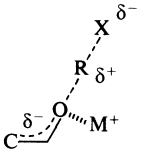
tant, après les travaux de Eschenmoser et coll. (26) comme une condition fondamentale de la réaction S_N2.

En l'absence de résultats concernant des réactifs alkylants chiraux, un processus assisté avec rétention de configuration selon un mécanisme à quatre centre (cf. **3**) ne peut être définitivement rejeté. A notre connaissance toutefois il n'existe pas dans la littérature d'exemples de tel processus dans le cas de réaction S_N2 sur le carbone et les études théoriques montrent que le processus S_N2 avec rétention de configuration doit être considérablement défavorisé par rapport au processus conduisant à l'inversion de configuration (27, 28). Georgoulis et coll. ont cependant mis récemment en évidence (29) une rétention partielle de configuration dans la réaction S_N2 de l'éthylate de lithium sur le chloro-3 butène-1 dans l'éthanol; dans ce dernier cas, la structure allylique et secondaire du radical R de l'électrophile, favorable à la formation d'un état de transition à caractère fortement carbocationique, rend la liaison carbone–chlore particulièrement sensible à l'effet ionisant du cation lithium de la paire d'ion $EtOLi^+$.

Pour l'ensemble des raisons invoquées ci-dessus la forte O/C-nucléophilie de l'énolate de lithium est vraisemblablement *en partie* une propriété propre à la paire d'ions et indépendante de la nature de l'électrophile. Nous suggérons que cette propriété est liée à la structure β-dicétonique chélatante de l'énolate et peut s'expliquer en termes de solvatation du cation par les états de transition. Dans le cas d'un énolate de monocétone (ou d'un phénate) l'entité énolate doit mieux solvater le cation dans l'état de transition **4** conduisant à la C-alkylation et où l'atome d'oxygène n'est pas directement impliqué dans la réaction avec l'électrophile que dans l'état de transition **5** conduisant à la O-alkylation.

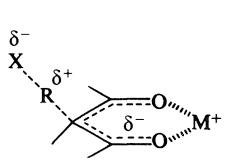


4

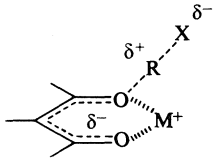


5

En d'autres termes l'affinité de **4** pour le cation est supérieure à celle de **5**; on s'attend donc à ce que la C-alkylation soit favorisée en présence de cation et ce d'autant plus que la tendance à l'association de ce dernier est forte, c'est-à-dire dans l'ordre $Li^+ > Na^+ > K^+$ ... etc. Dans le cas des composés β-dicarbonylés qui possèdent un site oxygéné supplémentaire, les deux états de transition **6** et **7**



6



7

ont tous deux une structure permettant encore une solvatation efficace du cation et aucune prédiction simple ne peut plus être faite quant à l'influence de ce dernier. Les variations du rapport C-/O-

Can. J. Chem. Downloaded from www.nrcresearchpress.com by 210.87.254.5 on 09/05/12
For personal use only.

alkylation observées en passant d'un cation à un autre vont traduire les variations des capacités respectives de solvatation des deux états de transition vis à vis des cations considérés. Notamment la *nette tendance* à la O-alkylation manifestée par la paire d'ions lithium traduit à notre sens une affinité marquée de l'état de transition **7** pour Li^+.[5] Dans cette optique, il serait intéressant d'étudier la compétition C-/O-alkylation au niveau *spécifique des paire d'ions* d'énolates de monocétones ou de phénates alcalins pour lesquels on doit s'attendre (cf. ci-dessus) à un rapport C/O maximum dans le cas de Li^+. Malheureusement leur faible tendance à l'association, comparée à celle des énolates de composés β-dicarbonylés, ainsi que l'impossibilité de contrôler dans ce cas les contributions respectives des paires d'ions et des ions dissociés par l'étude des produits de la réaction rend un tel projet difficile à mettre en œuvre.

Partie experimentale

I. Matières premières

Le THF anhydre (Merck) est agité en présence d'alumine (type 507 C, Fluka, 100 g/L de solvant) pendant plusieurs heures; après filtration il est distillé juste avant utilisation sur $LiAlH_4$ et sous azote. Le DMF est distillé sous vide (20 Torr) avant l'utilisation. L'iodure, le bromure et le tosylate d'éthyle (Merck) ont été distillés; pé(EtOTs) = 173°C/15 Torr.

$LiClO_4$ (Fluka) est séché sous vide 24 h à 100°C avant utilisation. $NaClO_4$ (Merck) est séché à 90°C et conservé sur P_2O_5 dans un dessicateur. L'acétylacétate d'éthyle (Merck-Schuchardt) est distillé avant emploi; pé = 81°C/20 Torr. La carbéthoxycoumaranone-3 **1** est préparée en trois étapes à partir de l'acide salicylique selon Brandström et Forsblad (30). La préparation des énolates alcalins de l'acétylacétate d'éthyle a déjà été décrite (9). La même méthode est utilisée pour ceux de la carbéthoxycoumaranone-3.

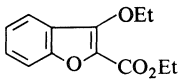
II. Analyses spectroscopiques

Les spectres rmn ont été réalisés sur un appareil Varian T-60 en utilisant le TMS comme référence interne. Les spectres infrarouges ont été enregistrés sur un appareil Perkin-Elmer 457. Les spectres de masse ont été réalisés sur un appareil AEI MS 30 opérant à 70 ev. Les spectres uv ont été enregistrés sur un appareil Beckman DB-GT.

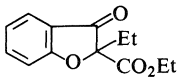
III. Préparation et caractérisation des dérivés éthylés

La préparation et la caractérisation des divers produits d'éthylation de l'acétylacétate d'éthyle a déjà été décrite (9).

Les dérivés O- et C-éthylé **8** et **9** de la carbéthoxycoumaranone-3 ont été préparés par action de l'iodure d'éthyle sur l'énolate de sodium dans l'éthanol. La carbéthoxycoumaranone-3 (3.4×10^{-3} mol) est ajoutée à une solution d'éthylate de sodium équimolaire dans l'éthanol (5 mL). Le mélange, qui prend rapidement en masse, est agité à chaud pendant quelques



8



9

minutes pour permettre la formation quantitative de l'énolate. Après addition de EtI (2×10^{-2} mol, excés), le mélange réactionnel est porté au reflux pendant 6 h. Après évaporation de l'éthanol, les produits organiques sont dissous dans un mélange éther–pentane 1:1, et la phase organique extraite au carbonate de sodium aqueux 10% pour éliminer la carbéthoxycoumaranone-3 n'ayant pas réagi. Cette dernière opération doit être réalisée rapidement pour éviter toute décarbéthoxylation (31) du produit C-éthylé **9**. Le rendement brut en produits d'alkylation, composés de **8** et **9** dans le rapport 1:2 environ (rmn), est pratiquement quantitatif. A partir de ce mélange, des échantillons purs de **8** et **9** on été obtenus par chromatographie préparative sur couche mince (gel de silice, élutions répétées au mélange hexane – éther éthylique 9:1). Le dérivé O-éthylé **8** a par ailleurs été obtenu seul, à l'exclusion de **9**, par réaction de l'énolate de sodium (5×10^{-2} mol) avec le sulfate d'éthyle équimolaire dans le DMSO (20 mL) à température ambiante pendant 18 h.

*Caractéristiques des produits **8** et **9***

*Carbéthoxy-2 éthoxy-3 coumarone (**8**)*

Huile (cristallisant en dessous de 10°C); uv (EtOH) λ_{max} (ε): 286 nm (34 000) (litt. (32): acide coumarone carboxylique-2 λ_{max} (EtOH): 274.5 nm); ir (CCl_4) ν: 1712 (C=O) cm^{-1} (litt. (31): carbéthoxy-2 méthoxy-3 coumarone ν: 1706 (C=O) cm^{-1}); rmn ($CDCl_3$) δ: 7.9–7.1 (4H, m, protons aromatiques), 4.55 (2H, q), 4.51 (2H, q), 1.47 (3H, t), 1.43 (3H, t, protons des groupements éthoxy) ppm; spectrométrie de masse *m/e*: 234 (M^+, 82%), 206 (25%), 161 ($M-CO_2C_2H_5$, 35%) 160 (100%).

*Carbéthoxy-2 éthyl-2 coumaranone-3 (**9**)*

Huile; uv (EtOH) λ_{max} (ε): 253 nm (12 000), 328 nm (5 000) (litt. (33): diméthyl-2,6 coumaranone-3 λ_{max} (EtOH): 260 nm, 327 nm); ir (CCl_4) ν: 1729 (C=O) cm^{-1} (cétone) et 1758 cm^{-1} (ester); rmn: $CDCl_3$ δ: 7.95–7.1 (4H,m, protons aromatiques), 2.65–1.93 (2H, m), 0.93 (3H, t), protons du groupement éthyle sur le carbone (système ABX_3), 4.31 (2H, q), 1.27 (3H, t, protons du groupement carbéthoxy); spectrométrie de masse *m/e*: 234 (M^+, 100%), 206 (58%), 162 (71%), 161 ($M-CO_2C_2H_5$, 97%), 147 (88%).

IV. Dosage par chromatographie en phase gazeuse

Appareil Perkin Elmer F11 à ionisation de flamme d'hydrogène. Gaz vecteur: azote. Colonne SE 30 15% sur Chromosorb W HMDS (80–100 mesh) de diamètre $\frac{1}{8}$ in. et de longeur 2 m. Dosage des dérivés de l'acétylacétate d'éthyle: température 103°C, pression d'azote en tête de colonne: 1.4 bar. Dosage des dérivés de la carbéthoxycoumaranone-3: température 200°C, pression: 1.4 bar.

La technique de dosage par cpg, notamment des deux isomères *cis* et *trans* de l'éther d'énol de l'acétylacétate d'éthyle a déjà été décrite en détail (9). La principale difficulté provient de l'isomérisation possible de l'isomère *cis* en isomère *trans* durant le dosage. On peut vérifier si l'appareil isomérise ou non un moment de l'analyse, et ainsi savoir si les résultats obtenus sont significatifs, en injectant les produits d'alkylation de l'énolate de lithium par TsOEt où l'éther d'énol est entièrement *cis* (9).

Il est possible que les proportions plus élevées d'éther d'énol *trans* observées par Kurts et coll. dans des conditions similaires aux notres (18, 19) soient dues à ce phénomène d'isomérisation.

1. H. O. House. Modern synthetic reactions. Benjamin, New York. 1972. p. 520 et suivantes.

[5]L'affinité plus marquée de l'état de transition **7** pour Li^+ (comparée à celle de **6** pour Li^+) pourrait s'expliquer par une plus grande densité électronique de **7** si on considère que même dans le produit final (produit alkylé) la densité électronique de l'ether d'énol O-*cis* dérivé de **7** est sans doute plus élevée que celle de la β-dicétone (mono-C) dérivée de **6**. Nous remercions l'un des examinateurs pour cette suggestion.

2. S. A. SHEVELEV. Russ. Chem. Rev. **39**, 844 (1970).
3. R. GOMPPER. Angew. Chem. Int. Ed. Engl. **3**, 560 (1964).
4. W. J. LE NOBLE. Synthesis, **1**, 6 (1970).
5. L. M. JACKMAN et B. C. LANGE. Tetrahedron, **33**, 2737 (1977).
6. N. KORNBLUM, P. J. BERRIGAN et W. J. LE NOBLE. J. Am. Chem. Soc. **85**, 1141 (1963).
7. N. KORNBLUM, R. SELTZER et P. HABERFIELD. J. Am. Chem. Soc. **85**, 1148 (1963).
8. F. GUIBE et G. BRAM. Bull. Soc. Chim. Fr. 933 (1975).
9. F. GUIBE, P. SARTHOU et G. BRAM. Tetrahedron, **30**, 3139 (1974).
10. G. BRAM, F. GUIBE et P. SARTHOU. C. R. Acad. Sci. Ser. C, **277**, 429 (1973).
11. R. G. PEARSON. J. Chem. Ed. **45**, 581 (1968); **45**, 643 (1968).
12. N. KORNBLUM, R. A. SMILEY, R. K. BLACKWOOD et D. C. IFFLAND. J. Am. Chem. Soc. **77**, 6269 (1955).
13. I. FORSBLAD. Ark. Kemi, **15**, 403 (1960).
14. G. BRAM, F. GUIBE et M. F. MOLLET. Tetrahedron Lett. 2951 (1970).
15. C. CAMBILLAU, G. BRAM, J. CORSET, C. RICHE et C. PASCARD-BILLY. Tetrahedron, **34**, 2675 (1978).
16. N. KORNBLUM et A. P. LURIE. J. Am. Chem. Soc. **81**, 2705 (1959).
17. A. L. KURTS, A. MACIAS, I. P. BELETSKAYA et O. A. REUTOV. Tetrahedron, **27**, 4769 (1971).
18. A. L. KURTS, A. MACIAS, I. P. BELETSKAYA et O. A. REUTOV. Tetrahedron Lett. 3037 (1971).
19. A. L. KURTS, A. MACIAS, I. P. BELETSKAYA et O. A. REUTOV. Dokl. Akad. Nauk SSSR (Engl.), **197**, 310 (1971).
20. S. F. ACREE et J. M. JOHNSON. Am. Chem. J. **38**, 258 (1907).
21. S. F. ACREE. Am. Chem. J. **48**, 352 (1912).
22. A. L. KURTS, S. M. SAKEMBAEVA, I. P. BELETSKAYA et O. A. REUTOV. Dokl. Akad. Nauk SSSR (Engl.), **210**, 144 (1973).
23. A. L. KURTS, S. M. SAKEMBAEVA, I. P. BELETSKAYA et O. A. REUTOV. J. Org. Chem. USSR, **9**, 1579 (1973).
24. S. WINSTEIN, S. SMITH et D. DARWISH. J. Am. Chem. Soc. **81**, 5551 (1959).
25. P. H. BOYLE, J. H. COY et H. W. DOBBS. J. Chem. Soc. Perkin Trans. I, 1617 (1972).
26. L. TENUD, S. FAROOQ, J. SEIBL et A. ESCHENMOSER. Helv. Chim. Acta, **53**, 2059 (1970).
27. L. SALEM. Chem. Br. **5**, 449 (1969).
28. N. L. ALLINGER, J. C. TAI et F. T. WU. J. Am. Chem. Soc. **92**, 579 (1970).
29. P. CAYZERGUES, C. GEORGOULIS et G. VILLE. J. Chem. Res. 325 (1978).
30. A. BRANDSTRÖM et I. FORSBLAD. Acta Chem. Scand. **11**, 914 (1957).
31. I. FORSBLAD. Ark. Kemi, **13**, 349 (1958).
32. L. LANG. Absorption spectra in the ultraviolet and visible region. Vol. 2. Publishing House of the Hungarian Academy of Sciences, Budapest. 1961. p. 259.
33. F. M. DEAN, P. HALEWOOD, S. MONGOLSUK, A. ROBERTSON et W. WHALEY. J. Chem. Soc. 1250 (1953).

Can. J. Chem. Downloaded from www.nrcresearchpress.com by 210.87.254.5 on 09/05/12
For personal use only.

Intramolecular Michael-type additions.[1] II.[2] Synthesis of derivatives of 7-thia-2-azabicyclo[3.2.1]oct-3-ene, a novel heterocyclic ring system

MARION E. M. BAGGS AND BRIAN GREGORY[3]

Department of Chemistry, Memorial University of Newfoundland, St. John's, Nfld., Canada A1B 3X7

Received July 12, 1979[4]

MARION E. M. BAGGS and BRIAN GREGORY. Can. J. Chem. **58**, 794 (1980).

The isothiouronium salt derived from dimethyl 4-chloromethyl-1,4-dihydro-2,6-dimethylpyridine-3,5-dicarboxylate reacted with ammonium hydroxide to give dimethyl 7-thia-2-aza-1,3-dimethylbicyclo[3.2.1]oct-3-ene-4,8-dicarboxylate, which could be converted back to a dihydropyridine using iodomethane. Replacement of ammonium hydroxide by sodium hydroxide afforded a tetrahydro- and a dihydrothieno[3,4-*c*]pyridine as by-products. 3,5-Diacetyl-4-chloromethyl-1,4-dihydro-2,6-dimethylpyridine reacted with thiourea, followed by ammonium hydroxide, to give 3-acetyl-2-methylpyrrole, 4-acetyl- and 4,8-diacetyl-7-thia-2-aza-1,3-dimethylbicyclo[3.2.1]oct-3-ene. The structure and stereochemistry of the novel 7-thia-2-azabicyclo[3.2.1]octenes are established using spectroscopic methods. The mechanism of their formation is discussed in terms of Baldwin's rules.

MARION E. M. BAGGS et BRIAN GREGORY. Can. J. Chem. **58**, 794 (1980).

Les sels d'isothiouronium dérivés du chlorométhyl-4-dihydro-1,4 diméthyl-2,6 pyridine dicarboxylate-3,5 de méthyle réagissent avec l'hydroxyde d'ammonium pour donner le thia-7 aza-2 diméthyl-1,3 bicyclo[3.2.1]octène-3 dicarboxylate-4,8 de méthyle, qui peut être retransformé en dihydropyridine à l'aide de l'iodométhane. L'emploi de l'hydroxyde de sodium au lieu de l'hydroxyde d'ammonium fournit comme produits secondaires le tétrahydro et le dihydro thiéno[3,4-*c*] pyridine. La diacétyl-3,5 chlorométhyl-4 dihydro-1,4 diméthyl-2,6 pyridine réagit avec la thiourée suivie de l'hydroxyde d'ammonium pour conduire aux dérivés acétyl-3 méthyl-2 pyrrole, acétyl-4 et diacétyl-4,8 thia-7 aza-2 diméthyl-1,3 bicyclo[3.2.1] octène-3. On a établi la structure et la stéréochimie des nouveaux thia-7 aza-2 bicyclo[3.2.1] octènes en utilisant des méthodes spectroscopiques. On discute du mécanisme de leur formation en fonction des règles de Baldwin.

[Traduit par le journal]

The acid-catalysed intramolecular addition of nucleophiles to dihydropyridines is well-known, having provided challenges in structure elucidation, e.g., the primary acid product from NADH (4), and useful synthetic routes to indole alkaloid skeleta (5). In contrast, intramolecular Michael-type addition to the dihydropyridine system is rare.[5] Thus, a 4-carboxy Hantzsch ester has been observed to readily form diethyl 1,3,5-trimethyl-7-oxa-2-aza-6-oxobicyclo[3.2.1]oct-3-en-4,8-dicarboxylate in acid media, presumably by β-protonation, followed by intramolecular Michael-type addition of the carboxylate anion to the iminium salt (7).

Based on the examination of Dreiding and space-filling molecular models, we concluded that 4-thiolmethyl-1,4-dihydropyridines **3***a–c* should, in basic media, undergo intramolecular Michael-type addition to generate 7-thia-2-azabicyclo-[3.2.1]oct-3-enes **4***a–c*. We are unaware of any previous reports of compounds containing this ring system. Although it had been claimed that reaction of the 4-chloromethyl-1,4-dihydropyridine **1***b* with sodium hydrosulfide gave the 4-thiolmethyl compound **3***b* (8), more recent work has shown that the product is, in fact, the 8-thia-2-azabicyclo[3.2.1]octene **5***b* (9). Similar bicyclic products have been obtained from other 4-chloroalkyl-1,4-dihydropyridines (3, 10, 11). It is clear that in the basic reaction conditions employed, ring expansion takes place to give an intermediate 4,5-dihydroazepine-4-thiol, which then undergoes intramolecular Michael-type addition. Ring expansion at such an early stage obviously precludes this reaction sequence as a route to **4**.

It is well known that thiols may be obtained by base-catalyzed decomposition of isothiouronium salts (12). Earlier, we have shown (13) that the chloromethyl-1,4-dihydropyridines **1***a–c* react with thiourea without ring expansion and give the isothiouronium salts **2***a–c* (Scheme 1). When the salt **2***a* was refluxed with sodium hydroxide in aqueous ethanol, a complex mixture was obtained. The major component was a colorless solid $C_{12}H_{17}NO_4S$ which showed infrared bands attributable to saturated and unsaturated ester carbonyl groups and NH, while the ultraviolet absorption spectrum resembled that of a 1,4,5,6-tetrahydronicotinic ester (14), thus eliminating 1,4-di-

[1]Although the term Michael addition (1) originally applied to the addition of anions derived by removal of a proton α to a carbonyl group, to unsaturated esters, ketones, etc., the scope has since broadened. The use of the term Michael-type addition in this and subsequent publications in this area follows that of March (2).

[2]Reference 3 may be regarded as Part I of this series.

[3]Author to whom all correspondence should be addressed.

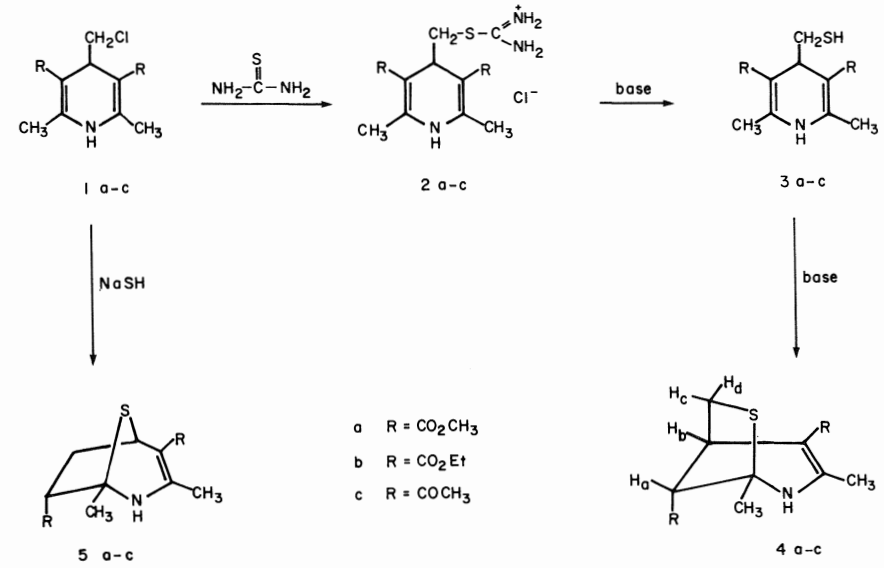
[4]Revision received January 16, 1980.

[5]For a recent review of dihydropyridine chemistry see ref. 6.

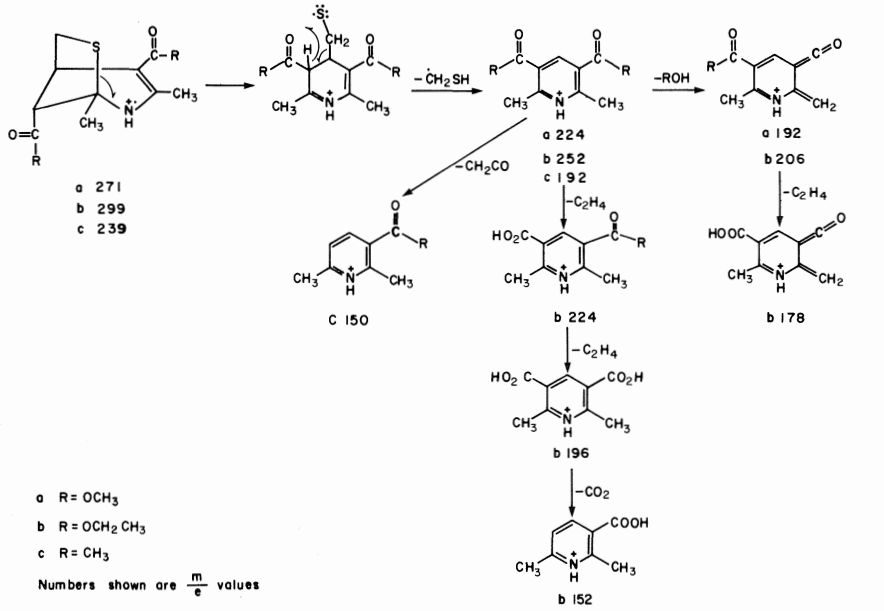
0008-4042/80/080794-09$01.00/0

©1980 National Research Council of Canada/Conseil national de recherches du Canada

Can. J. Chem. Downloaded from www.nrcresearchpress.com by 210.87.254.105 on 09/05/12
For personal use only.



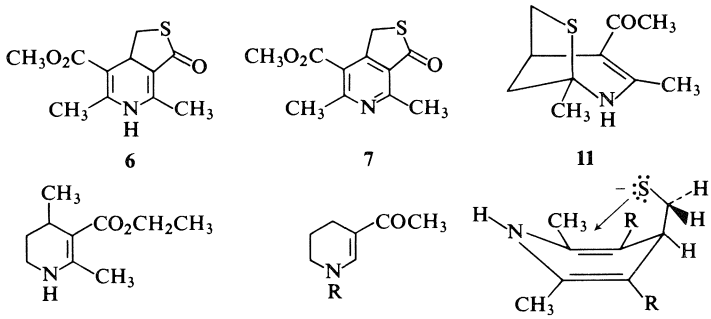
SCHEME 1



SCHEME 2

hydropyridine (15–17) and 4,5-dihydroazepine (16) structures. The mass spectrum was dominated by intense peaks corresponding to the molecular ion and loss of CH_2SH radical. Such a fragmentation pattern could have arisen from the 1,4-dihydropyridine structure **3***a* (cf. 18), which is inconsistent with the ultraviolet data, or from the 7-thia-2-azabicyclo[3.2.1]oct-3-ene structure **4***a* by initial C—S bond cleavage followed by hydrogen radical transfer and loss of CH_2SH radical as shown in Scheme 2. The fragmentation was quite different to that observed for the 8-thia-2-azabicyclo-[3.2.1]oct-3-enes (3, 9–11). In addition to singlets due to two non-equivalent methyl esters and two methyl groups attached to sp^3 (δ 1.80) and sp^2 (δ 2.11) carbon atoms, the ^{1}Hmr spectrum showed a broad singlet (NH), one-proton and two-proton doublets, and a broadened one-proton quartet. The latter multiplets clearly denote the presence of a —CH—CH—CH_2— moiety, consis-

Can. J. Chem. Downloaded from www.nrcresearchpress.com by 210.87.254.105 on 09/05/12
For personal use only.



6 7 11

15 16 R = H 17 R = CH_3 12

tent with structure **4***a*, although, surprisingly, the protons of the methylene group are apparently equivalent. In the belief that the spectroscopic properties of this compound were best represented by structure **4***a*, and that the protons of the methylene group were accidentally equivalent (19), it was resolved to synthesize analogues in which the methoxycarbonyl groups were replaced by other electron-withdrawing groups in the hope that one or more would show non-equivalent methylene protons (see below).

Minor products isolated from the action of aqueous ethanolic sodium hydroxide on **2***a* included the yellow crystalline 1,3,5,7a-tetrahydrothieno[3,4-*c*]-pyridine-3(1*H*)-one **6**, clearly formed by attack of the thiolate anion derived from **3***a* on a neighbouring ester, and the corresponding oxidation product 7.[6] The oxidation of **6** to **7** was accomplished, in a separate experiment, by the action of dilute nitric acid. No evidence was found in the ^{1}Hmr spectrum of **7** for the presence of the fully-aromatic enol tautomer (20). When ammonium hydroxide was used to decompose the isothiouronium salt **2***a*, the yield of the bicyclic compound **4***a* was considerably improved and this method was used in subsequent work.

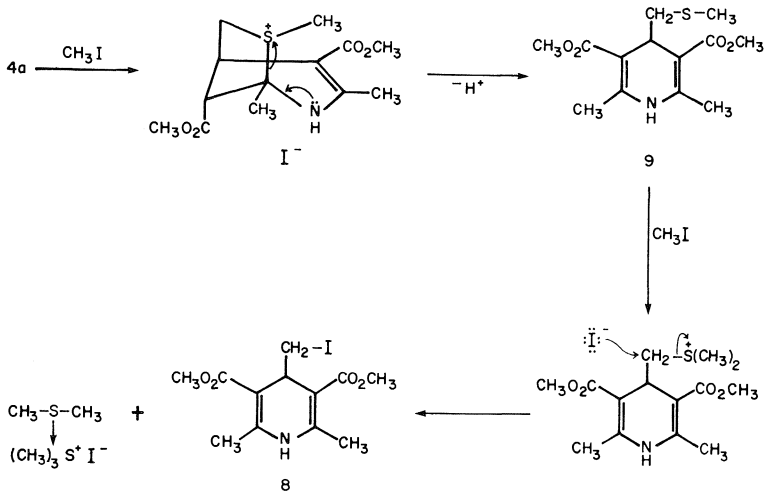
Further evidence to support structure **4***a* has been obtained through chemical studies. When compound **4***a* was heated at 74°C in a sealed tube with iodomethane in dimethylformamide, predictably the products were trimethylsulfonium iodide and the 4-iodomethyl-1,4-dihydropyridine **8**. These compounds are believed to be formed by methylation at sulfur, followed by C—S cleavage assisted by the nitrogen lone pair as shown in Scheme 3. Loss of proton would give the 4-methylthiomethyl-1,4-dihydropyridine **9** which, after methylation at sulfur, displacement of dimethyl sulfide by iodide anion, and final methylation of dimethyl sulfide, accounts for the products. The ease of regeneration of the dihydropyridine ring system precludes the involvement of a gross rearrangement in the base-catalysed decomposition of **2***a* and thus provides support for **4***a*.

When the diethyl ester **2***b* was reacted with ammonium hydroxide, the spectroscopic properties of the product were again in accord with the bicyclic structure **4***b*, although the ^{1}Hmr spectrum showed that the protons attached to C(6) were, once more, equivalent.

Separation of the mixture produced by the action of ammonium hydroxide on the diacetyl compound **2***c* afforded, as major product, a colorless crystalline product $C_{12}H_{17}NO_2S$ whose spectroscopic properties were in complete accord with structure **4***c*. Thus the ultraviolet absorption spectrum exhibited a major long-wavelength band at 325 nm. The bathochromic shift of about 22 nm by comparison with the corresponding esters is a reflection of the increased efficiency of electron acceptance from the nitrogen lone pair shown by a ketone carbonyl compared with an ester carbonyl. Such an effect has been observed previously with acyclic and cyclic compounds containing 4-aminopent-3-en-2-one or 3-aminocrotonate chromophores (see Table 1). A comparison of the ultraviolet spectra of the 7-thia compounds **4***a–c* with the 8-thia compounds **5***a,c* shows that the major absorption band occurs 10–12 nm to longer wavelength for the former compounds. The reason for this is not clear at the present time, since the chromophore is perfectly planar (as judged from Dreiding models) in each ring system; the possibility of interaction of the enamine system with orbitals on sulfur in **4** cannot be ruled out. The infrared spectrum of **4***c* exhibited stretching vibrations due to NH (3423 cm^{-1}), saturated ketone (1707 cm^{-1}), and an unsaturated ketone absorption at 1628 cm^{-1}, con-

[6]Benary (8) has obtained the ethyl ester of **7** by the action of potassium hydrosulfide on diethyl 4-iodomethyl-2,6-dimethylpyridine-3,5-dicarboxylate. For recent reviews of thienopyridines see refs. 20 and 21.

Can. J. Chem. Downloaded from www.nrcresearchpress.com by 210.87.254.105 on 09/05/12
For personal use only.



SCHEME 3

TABLE 1. Ultraviolet absorption data

Compound	Solvent*	λ_{max}nm(ε)	Reference
Ethyl 3-aminocrotonate	A	274 (20 400)	22
4-Aminopent-3-en-2-one	M	316 (15 100)	23
15	A	285 (17 800)	14
16	A	301 (21 150)	24
17	A	315 (31 300)	25
5*a*	A	290 (14 100)	9
5*c*	A	315 (14 100)	10
4*a*	E	268 (3 900) 303 (10 900)	
4*b*	E	262 (3 800) 302 (9 200)	
4*c*	E	273 (2 600) 325 (13 400)	
11	E	273 (2 000) 325 (9 100)	

*Solvent: A is absolute alcohol, E is 95% ethanol, M is methanol.

siderably lowered due to conjugative interaction with the lone pair on nitrogen in the manner characteristic of β-amino-αβ-unsaturated ketones (26). The most significant features of the ^{1}Hmr spectrum of **4***c* were the signals due to the —CH—CH—CH_2— system. In particular, the hydrogens of the methylene group were nonequivalent and appeared as a doubled AB quartet (see Fig. 1). The low field half of this latter signal appeared at δ 3.36 and showed coupling constants of 9.52 Hz, due to geminal coupling,[7] and 4.39 Hz due to coupling with the hydrogen at C(5). The high field half appeared at δ 3.19 and showed again the geminal coupling of 9.52 Hz and an additional coupling of 0.7 Hz. Examination of a Dreiding molecular model of **4***c* showed that the dihedral angle between H_d and H_b was near to 90° resulting in a value of *J* near to zero, while the dihedral angle between H_c and H_b was approximately 35°. Accordingly, the signal at δ 3.19 (*J* values 9.52 Hz and 0.7 Hz) was assigned to H_d, while the signal at δ 3.36 (*J* values 9.52 Hz and 4.39 Hz) was assigned to H_c. In addition to these signals, the spectrum showed a doublet at δ 3.06 (J = 3.17 Hz) due to H_a at C(8) and a multiplet, closely resembling a broadened triplet, at δ 4.07 due to H_b at C(5). The

[7]Although no attempts have been made to determine the sign of the geminal coupling, such couplings, with the exception of epoxides and ethyleneimines, are usually negative (ref. 19, p. 270).

Can. J. Chem. Downloaded from www.nrcresearchpress.com by 210.87.254.105 on 09/05/12
For personal use only.

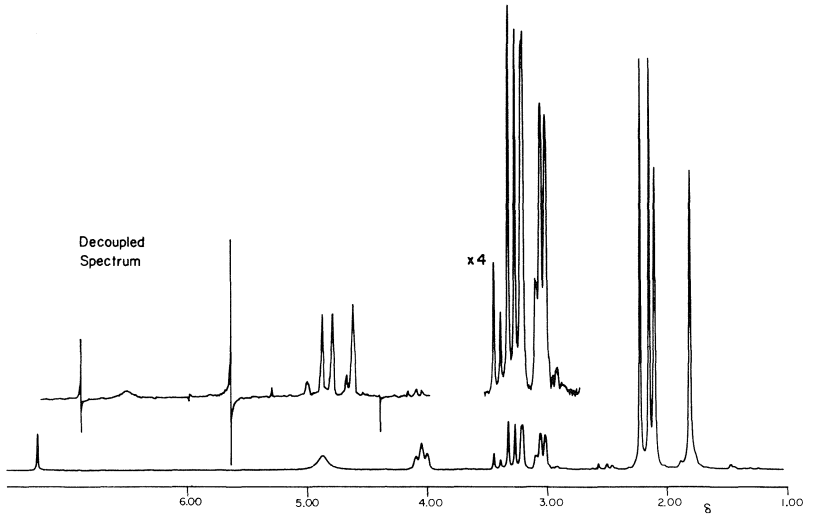


FIG. 1. ^{1}Hmr spectrum of **4***c*.

dihedral angle of 55° made by H_a with H_b is in good agreement with the observed coupling constant of 3.17 Hz; accordingly the acetyl group at C(8) is assigned the *endo* configuration. Irradiation at δ 4.07 caused the doublet at δ 3.06 to collapse to a singlet, while the doubled AB signal collapsed to an AB double doublet (see Fig. 1 inset).

In addition to compound **4***c*, other products isolated from this reaction include 2-methyl-3-acetylpyrrole, whose origin in this reaction is presently under investigation, and a compound $C_{10}H_{15}NOS$. The structure of this latter compound follows from the similarity of its ultraviolet absorption spectrum with that of **4***c*, the lack of one of the 3-proton acetyl absorptions found in the ^{1}Hmr spectrum of **4***c* and the lack of the saturated carbonyl absorption found in **4***c*.[8] The ^{1}Hmr surprisingly shows 2-proton doublets for protons at C(6) and C(8). This minor product is assigned structure **11** and probably results from retroaldolization at some stage of the reaction sequence.

A comparison of the uv (Table 1) and ^{1}Hmr (Table 2) spectra of **4***a–c* and **11** demonstrates the close similarity of the data and leaves little doubt they they all contain the same ring system. Further, the similarity of J_{ab} in **4***a–c* shows that the substituent at C(8) occupies the same configuration in each compound and is assigned an *endo* configuration; it is likely that this is the more thermodynamically stable configuration (cf. ref. 3).

[8]A weak absorption at 1710 cm^{-1} was observed in the ir spectrum of **11**. The origin of this peak is not clear; no spurious singlet due to impurity was observed in the nmr and repeated purification by preparative tlc failed to remove the band at 1710 cm^{-1}.

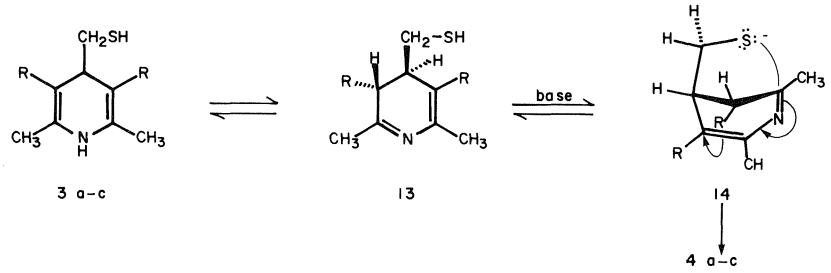
TABLE 2. ^{1}H magnetic resonance of 7-thia-2-azabicyclo-[3.2.1]oct-3-enes*

	4*a*	**4***b*	**4***c*	**11**
C(1)—CH_3	1.80	1.76	1.83	1.75
C(3)—CH_3	2.11	2.06	2.13	2.16
NH	4.52	4.79	4.88	4.70
H_a	3.04	2.98	3.06	2.27
H_b	3.79	3.77	4.07	3.50
H_c	3.22	3.16	3.36	3.39
H_d	3.22	3.16	3.19	3.39
J_{ab}	3.30	3.15	3.17	2.44
J_{bc}	2.64	2.70	4.39	2.93
J_{bd}	2.64	2.70	0.70	2.93
J_{cd}	0	0	9.52	0

*Chemical shift values (δ) are expressed in ppm downfield from internal TMS; coupling constants (*J*) are expressed in Hz.

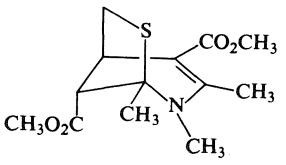
Attention has recently been drawn by Baldwin *et al.* to the importance of the Dunitz angle (27) in addition reactions to the carbonyl group and this has been extended to general rules for the prediction of the ease of cyclization reactions. In particular, cyclizations designated 5-*endo*-trig are disfavored (28, 29) although this may not hold when the nucleophilic atom or group is derived from a second row element (29). In the case of the formation of the 7-thia-2-azabicyclo[3.2.1]oct-3-enes, the Michael addition depicted in **12** may be regarded as, at once, a 5-*endo*-trig cyclization from the viewpoint of the thus formed 5-ring, but 7-*exo*-trig when the thus formed 7-ring is considered. In such a situation, it is clear that the disfavored 5-*endo*-trig cyclization is the more important and that the formation of the bicyclic system should not be facile, although the second-row nucleophile may invalidate these considerations. However, examination of a model of **12**

Can. J. Chem. Downloaded from www.nrcresearchpress.com by 210.87.254.105 on 09/05/12
For personal use only.



SCHEME 4

shows that the approach of the nucleophile is in a direction far removed from a Dunitz-type angle. For these reasons we considered the possibility that the formation of **4***a–c* may involve the formation of an equilibrium amount of the tautomer **13** followed by cyclization of its conjugate base **14** as shown in Scheme 4.[9] Such a pathway would offer several advantages, e.g., tautomerism to give **13**, which has the bulky thiolmethyl and R groups *trans*, and would automatically lead to the 8-*endo*-esters and ketones. Further, the intramolecular nucleophilic addition to the imine carbon is a simultaneous 5-*exo*-trig/7-*endo*-trig cyclization onto the potent Michael-acceptor iminoacrylate system. Examination of Dreiding models of **14** shows that the sulfide anion can approach the imine carbon closely and from a Dunitz angle. Since the *N*-methyl derivative of **3***a* would be incapable of tautomerism to a 3,4-dihydropyridine analogous to **13**, we have reacted dimethyl 4-chloromethyl-1,4-dihydro-1,2,6-trimethyl-pyridine-3,5-dicarboxylate with thiourea followed by ammonium hydroxide. The formation of the *N*-methyl bicyclic compound **18**, albeit in low yield,



18

shows that if the tautomerism **3** to **13** takes place at all, it is certainly not essential for the formation of the bicyclic compounds **4***a–c*.

[9]In a related study, we have shown that dimethyl 4-(diacetylmethyl)-4,5-dihydro-2,7-dimethylazepine-3,6-dicarboxylate cyclizes in basic media to give an 8,8-diacetyl-2-azabicyclo-[3.2.1]oct-3-ene (30). We have suggested that this reaction may involve initial tautomerism to a 4,5-dihydro-3*H*-azepine followed by 5-*exo*-trig/6-*endo*-trig Michael-type addition to the iminocrotonate system (30), rather than disfavored 5-*endo*-trig addition to the aminocrotonate system of a 4,5-dihydro-1*H*-azepine.

Experimental

Melting points were determined using a Fisher-Johns melting point apparatus. Infrared spectra were obtained in chloroform solution using a Perkin-Elmer 237B grating infrared spectrometer. Ultraviolet spectra were measured on a Unicam SP800D using solutions in 95% ethanol. Spectra were calibrated using the bands at 2850.7 and 1601.4 cm^{-1} of polystyrene (ir) or at 279.4 and 360.9 nm of a holmium oxide filter (uv). The ^{1}Hmr spectra were obtained using Bruker WP80DS Fourier Transform (designated (A)) or Varian EM360 (designated (B)) nmr spectrometers, using deuterochloroform as solvent unless specified otherwise. All chemical shifts are expressed in parts per million downfield from internal tetramethylsilane. Mass spectra were determined at 70 eV ionizing energy using a Hitachi-Perkin-Elmer RMU-6E mass spectrometer. Only the most intense peaks are listed; normalized intensities are given in parentheses. Initial and final total ion current values differed by $< 5\%$. Accurate mass measurements were obtained relative to known accurate masses of perfluorokerosene peaks using a Varian MAT 311 mass spectrometer. New compounds were homogeneous by tlc and elemental analyses were performed by Atlantic Microlab, Inc., Atlanta, GA. The identity of known compounds was established by mp, mixture mp, and comparisons of ir, ^{1}Hmr, and ms with those of authentic specimens. All evaporations were carried out using a rotary evaporator operating at 12 Torr and using a bath temperature of $\geq 40°C$.

Dimethyl 7-Thia-2-aza-1,3-dimethylbicyclo[3.2.1]oct-3-ene-4,8-dicarboxylate, **4**a

(*a*) Dimethyl 4-chloromethyl-1,4-dihydro-2,6-dimethyl-pyridine-3,5-dicarboxylate **1***a* (5 g) and thiourea (2 g) were refluxed in ethanol (95%, 125 mL) for 3.7 h. The solution was then cooled and evaporated *in vacuo* to yield the solid isothiouronium salt **2***a*, which, without further purification, was heated with concentrated ammonium hydroxide (25 mL) at 85°C for 1 h. After cooling, the reaction mixture was extracted using ethyl acetate (1 × 75 mL, 1 × 30 mL). The bulked organic layer was washed with water (3 × 10 mL), dried ($MgSO_4$), filtered, and evaporated to give an oil (4.445 g) which was shown using tlc to consist of one major component and several minor ones. Trituration of the oil with ethyl acetate induced crystallization, and filtration afforded crystalline product (0.878 g). The mother liquors were evaporated and the residue chromatographed on a column of silica gel N (300 g) using 60–80°C petroleum ether/ethyl acetate as elution solvent to give a further quantity of crystalline **4***a* (2.166 g). The combined yield of the chromatographically homogeneous product was 3.044 g (61%). After one crystallization from ethyl acetate and sublimation at 90°C/0.01 Torr, the colorless crystalline bicyclic compound **4***a* had mp 115–117°C; uv λ_{max} (ε): 268 nm (sh, 3900), 303 nm (10 900); ir ν_{max}: 3422 (NH s, free), 1739 (saturated ester), 1688 (unsaturated ester) cm^{-1}; ^{1}Hmr (A) δ:1.80 (s, 3H, methyl at C(1)), 2.11 (s, 3H, methyl at C(3)), 3.04 (d, 1H, $J = 3.30$ Hz, H at

Can. J. Chem. Downloaded from www.nrcresearchpress.com by 210.87.254.105 on 09/05/12
For personal use only.

Can. J. Chem. Downloaded from www.nrcresearchpress.com by 210.87.254.105 on 09/05/12
For personal use only.

C(8)), 3.22 (d, 2H, J = 2.64 Hz, H's at C(6)), 3.62 (s, 3H, methyl ester), 3.63 (s, 3H, methyl ester), 3.79 (br q, 1H, J approx. 2.8 Hz, H at C(5)), and 4.52 (br s, 1H, NH); ms *m/e*: 271(28, M^+), 240(11), 239(9), 225(13), 224(100), 211(7), 208(6), 196(6), 192(15), 180(10), 166(70), 134(15), 115(16), 107(12), 106(26), 84(7), 79(8), 77(8), 65(7), 59(10), and 42(12). *Anal.* calcd. for $C_{12}H_{17}NO_4S$: C 53.13, H 6.32, N 5.16, S 11.79; found: C 53.17, H 6.35, N 5.22, S 11.79.

(*b*) To the crude isothiouronium salt **2***a* prepared from the chloromethyl-1,4-dihydropyridine **1***a* (9 g) as in the previous experiment, was added ethanol (63 mL, 95%) followed by sodium hydroxide (2.259 g) in water (27 mL). After refluxing for 2 h in an oil bath at 105°C, the ethanol was removed by evaporation *in vacuo* and water (45 mL) was added. The aqueous reaction mixture was extracted using benzene (360 mL, 300 mL, and then 200 mL) and the bulked benzene extract washed with water, dried ($MgSO_4$), filtered, and evaporated to give a pale yellow oily solid (3.816 g) which, after chromatography on silica gel, yielded dimethyl 7-thia-2-aza-1,3-dimethylbicyclo[3.2.1]oct-3-ene-4,8-dicarboxylate, **4***a* (2.5 g, 28%) identical with the product from the previous experiment. The aqueous sodium hydroxide extract, which had contained a solid near the aqueous sodium hydroxide/benzene interface, was filtered to yield a yellow solid (1.935 g), which tlc showed to consist of two compounds. Separation was achieved by dissolution in chloroform (50 mL) followed by extraction with hydrochloric acid (5 × 15 mL, 6 *M*). The chloroform extract was washed with water (2 × 25 mL), dried ($MgSO_4$), and evaporated to give a solid which was further purified by recrystallization from ethyl acetate to yield yellow crystals of methyl 1,3,5,7a-tetrahydro-4,6-dimethylthieno[3,4-*c*]-pyridin-3(1*H*)-one-7-carboxylate **6** (1.63 g, 21%) mp 227–227.5°C; uv λ_{max} (ε): 236 (11 900), 241.5 (sh, 11 600), 267 (10 700), 391 nm (6300); ir ν_{max}: 3415 (NH, free), 3295 (NH, bonded), 1698 (vinylogous urethane), 1675 (vinylogous thiolurethane), 1640 (C=C) and 1611 (C=C) cm^{-1}; ^{1}Hmr (B) ($CDCl_3$/DMSO-d_6) δ: 2.11 (s, 3H, C-methyl), 2.17 (s, 3H, C-methyl), 3.62 (s, 3H, methyl ester), 3.67 (d, 2H, CH_2), 3.90 (t, 1H, CH); signals at 3.62, 3.67, and 3.90 were partly obscured due to overlapping; ms *m/e*: 239(22, M^+), 238(6), 224(24), 211(8), 208(11), 193(12), 185(10), 178(8), 165(100), 150(14), 134(15), 133(8), 106(7), 105(7), 77(6), 67(6), and 42(11). *Anal.* calcd. for $C_{11}H_{13}NO_3S$: C 55.21, H 5.48, N 5.85, S 13.40; found: C 55.28, H 5.53, N 5.84, S 13.33.

The aqueous acid layer was washed once with chloroform (20 mL), made slightly basic using sodium carbonate, and then extracted using chloroform (3 × 25 mL). The bulked chloroform extract was washed with water (5 mL), dried ($MgSO_4$), filtered, and evaporated to give an almost colorless residue (0.3 g, 4%) of methyl 1,3-dihydro-4,6-dimethylthieno[3,4-*c*]pyridin-3(1*H*)-one-7-carboxylate **7** which was sublimed at 70°C/0.01 Torr and then resublimed at 90°C/0.01 Torr to give colorless **7** mp 130–131°C; uv λ_{max} (ε): 215 (17 900), 239 (sh, 9400), 264 (sh, 6900), 285 (sh, 5300); ir ν_{max}: 1725 (aryl ester) and 1685 (unsaturated γ-thiol-lactone) cm^{-1} (31); ^{1}Hmr (B) δ: 2.76 (s, 3H, C-methyl), 2.84 (s, 3H, C-methyl), 3.96 (s, 3H, methyl ester), and 4.57 (s, 2H, CH_2); ms *m/e*: 237(98, M^+), 222(39), 206(39), 205(100), 194(14), 178(21), 177(75), 176(18), 149(14), 108(18), and 91(18). *Anal.* calcd. for $C_{11}H_{11}NO_3S$: C 55.70, H 4.67, N 5.90, S 13.49; found: C 55.76, H 4.70, N 5.94, S 13.49.

Oxidation of Methyl 1,3,5,7a-Tetrahydro-4,6-dimethylthieno[3,4-c]pyridin-3(1H)-one-7-carboxylate, 6

The tetrahydrothienopyridine **6** (60 mg) was shaken with dilute nitric acid (1.9 mL, 4 *M*) until dissolution was complete, and then for a further 5 min. The reaction mixture was quickly adjusted to pH 8–8.5 by addition of sodium carbonate solution and then extracted using ether (3 × 10 mL). The bulked ether extract was washed with water (2 mL), dried ($MgSO_4$), filtered, and evaporated. Sublimation of the residue at 70°C/0.01 Torr gave colorless needles of methyl 1,3-dihydro-4,6-dimethylthieno[3,4-*c*]pyridin-3(1*H*)-one-7-carboxylate **7** (32 mg, 54%) mp 130–131°C, and was identical with the compound obtained in the previous experiment.

Reaction of Dimethyl 7-Thia-2-aza-1,3-dimethylbicyclo[3.2.1]-oct-3-ene-4,8-dicarboxylate **4***a with Iodomethane*

A solution of the bicyclic compound **4***a* (0.506 g) and iodomethane (2.5 mL) in dry dimethylformamide (2.5 mL) was heated at 74°C for 2 h in a sealed tube during which time crystals were deposited. After cooling and addition of dry benzene (30 mL), filtration afforded pale yellow crystals which, after recrystallization from ethanol, gave colorless crystals of trimethylsulfonium iodide (0.202 g, 53%) mp 206–207°C (lit. (32) mp 203–207°C) undepressed on admixture with authentic material; ^{1}Hmr (B) (trifluoracetic acid) δ: 3.03 (s).

The benzene filtrate was washed with water (2 mL), sodium thiosulfate solution (2 × 2 mL, 10%), water (7 × 2 mL), dried ($MgSO_4$), filtered, and evaporated to give colorless crystals of dimethyl 1,4-dihydro-4-iodomethyl-2,6-dimethylpyridine-3,5-dicarboxylate **8** (0.335 g, 49%) mp 153–154°C (lit. (10) 155–157°C) which was not depressed on admixture with authentic material synthesized by the action of sodium iodide on the corresponding chloromethyl compound **1***a* in acetonitrile (ref. 33). The ir, ms, and ^{1}Hmr spectra of the iodomethyl compound obtained from the bicyclic compound **4***a* were identical with those of the iodomethyl compound obtained from **1***a* and with those reported by Ashby and Eisner (9) with the exception of the signal due to the methylene group which appears at δ 3.29 (d, J = 5.0 Hz) (Ashby and Eisner report δ 2.24).

Diethyl 7-Thia-2-aza-1,3-dimethylbicyclo[3.2.1]oct-3-ene-4,8-dicarboxylate, **4***b*

Diethyl 4-chloromethyl-1,4-dihydro-2,6-dimethylpyridine-3,5-dicarboxylate **1***b* (2.2 g) and thiourea (0.8 g) in ethanol (50 mL, 95%) were refluxed for 3.5 h, cooled, and evaporated *in vacuo*. The crude isothiouronium compound **2***b*, without further purification, was heated at 80–85°C with concentrated ammonium hydroxide (10 mL) for 1 h, cooled, and worked up, as in previous experiments, to give a brown oily product (1.699 g) which was purified by preparative tlc on silica gel plates using ethyl acetate/60–80°C petroleum ether (1:1) to give bicyclic compound **4***b* as a colorless glass (1.37 g, 63%); uv λ_{max} (ε): 262 (3800), 302 nm (9200); ir ν_{max}: 3423 (NH), 1730 (saturated ester), 1680 (unsaturated ester), 1595, 1475 cm^{-1}; ^{1}Hmr (A) δ: 1.13 (t, 3H, J = 7.04 Hz, methyl of saturated ethyl ester), 1.18 (t, 3H, J = 7.07 Hz, methyl of unsaturated ethyl ester), 1.76 (s, 3H, methyl at C(1)), 2.06 (s, 3H, methyl at C(3)), 2.98 (d, 1H, J = 3.15 Hz, H at C(8)), 3.16 (d, 2H, J = 2.70 Hz, H's at C(6)), 3.77 (br q, J approx. 2.9 Hz, H at C(5)), 4.05, 4.07 (overlapping q, 4H, J = 7.04 Hz, CH_2's of ethyl esters), 4.79 (br s, 1H, NH); ms *m/e*: 299(36, M^+), 252(100), 224(47), 208(13), 206(7), 196(40), 180(75), 152(37), 134(7), 129(20), 125(7), 108(9), 107(10), 106(15), 84(11), 57(14), and 42(12); m* 199 (252 → 224), 171.5 (252 → 208). Accurate mass on molecular ion: calcd. for $C_{14}H_{21}NO_4S$: 299.11908; found: 299.11902.

The Reaction of the Isothiouronium Salt from 3,5-Diacetyl-4-chloromethyl-1,4-dihydro-2,6-dimethylpyridine with Ammonium Hydroxide

3,5-Diacetyl-4-chloromethyl-1,4-dihydro-2,6-dimethyl-pyridine **1***c* (1.2 g) and thiourea (0.42 g) were refluxed, with stirring, in ethanol (95%, 25 mL) for 2.5 h. The solution was then cooled and evaporated *in vacuo*. The crude, solid isothiouronium salt **2***c* was then, without further purification, heated with concentrated ammonia (10 mL) at 74°C for 1 h.

Can. J. Chem. Downloaded from www.nrcresearchpress.com by 210.87.254.105 on 09/05/12
For personal use only.

After cooling, the solution was extracted with ethyl acetate (2 × 35 mL) and the bulked organic extract washed with water (10 mL), dried ($MgSO_4$), filtered, and evaporated to give a residual brown oil (0.789 g) which was shown by tlc to contain at least 5 components. Separation was achieved by preparative tlc on three 20 cm × 20 cm × 0.15 cm silica gel GF_{254} plates using ethyl acetate/60–80°C petroleum ether (1:1). The following components, in order of decreasing R_f, were isolated and characterized.

(*i*) 3-Acetyl-2-methylpyrrole (0.073 g, 12%) purified by recrystallization from 60–80°C petroleum ether and then sublimation at 64°C/0.05 Torr to give colorless needles, mp 90–90.5°C (lit. (34–36) mp 94–95, 86–87, 75°C); uv λ_{max} (ε): 210 (8300), 243 (8000), 282 nm (6300); ir ν_{max}: 3453 (NH, free), 3288 (NH, bonded), 1650 (carbonyl) cm^{-1}; ^{1}Hmr (B) δ: 2.41 (s, 3H, methyl), 2.53 (s, 3H, methyl), 6.46 (d, 1H, $J_{4,5}$ = 4 Hz, H at C(4)), 6.54 (d, 1H, $J_{4,5}$ = 4 Hz, H at C(5)), 9.39 (br s, 1H, NH); ms *m/e*: 123 (65, M^+), 108(100), 80(17), 53(20), 53.5(9), 52(7), 51(5), 43(8), and 39(8); m* at 94.9 (123 → 108 req m* 94.83), 59.5 (108 → 80 req m* 59.3), and 35.2 (80 → 53 req m* 35.11).

(*ii*) 4-Acetyl-7-thia-2-aza-1,3-dimethylbicyclo[3.2.1]oct-3-ene **11** (0.034 g, 3%) mp 180–181.5°C, purified by repeated preparative tlc; uv λ_{max} (ε): 273 (2000), 325 nm (9100); ir ν_{max}: 3415 (NH), 1710 (weak), 1632 (sh), 1627 (aminoenone carbonyl), 1565, 1462 cm^{-1}; ^{1}Hmr (A) δ: 1.75 (s, 3H, methyl at C(1)), 2.16 (s, 3H, methyl at C(3)), 2.21 (s, 3H, acetyl), 2.27 (d, 2H, *J* = 2.44 Hz, H's at C(8)), 3.39 (d, 2H, *J* = 2.93 Hz, H's at C(6)), 3.50 (br t, 1H, *J* = 2.93 Hz clearly discernible, H at C(5)), 4.70 (br s, 1H, NH); ms *m/e*: 197(44, M^+), 164(9), 154(17), 151(16), 150(100, $C_9H_{12}NO$ requires 150.0920; found 150.0915), 136(16), 121(9), 108(16), 107(11), 106(8), 99(10), 84(10), 58(9), 57(80), 44(9), 43(33), and 42(16). Accurate mass on molecular ion: calcd. for $C_{10}H_{15}NOS$: 197.08741; found: 197.0879.

(*iii*) 4,8-Diacetyl-7-thia-2-aza-1,3-dimethylbicyclo[3.2.1]-oct-3-ene **4***c* (0.323 g, 27%) mp 174–175°C; uv λ_{max} (ε): 273 (2600), 325 nm (13 400); ir ν_{max}: 3423 (NH), 1707 (saturated ketone), 1632 (sh), 1628 (aminoenone carbonyl), 1591, 1470 cm^{-1}; ^{1}Hmr (A) δ: 1.83 (s, 3H, methyl at C(1)), 2.13 (s, 3H, methyl at C(3)), 2.16 (s, 3H, acetyl), 2.25 (s, 3H, acetyl), 3.06 (d, 1H, *J* = 3.17 Hz, H at C(8)), 3.19 (dd, 1H, *J* = 0.7 Hz, *J* = 9.52 Hz, H at C(6)), 3.36 (dd, 1H, *J* = 4.39 Hz, *J* = 9.52 Hz, H at C(6)), 4.07 (br t, 1H, *J* approx. 3.7 Hz, H at C(5)), 4.88 (br s, 1H, NH); irradiation at δ 4.07 caused the double doublets at δ 3.19 and δ 3.36 to collapse to an AB dd, while the doublet at δ 3.06 collapsed to a singlet; ms *m/e*: 239(39, M^+), 222(25), 221(9), 206(12), 196(31), 193(13), 192(100), 179(12), 178(14), 154(17), 150(88), 108(9), 107(13), 106(10), 99(17), 84(13), 43(43), and 42(8); accurate mass on molecular ion; calcd. for $C_{12}H_{17}NO_2S$: 239.09797; found: 239.09781.

*Dimethyl 7-Thia-2-aza-1,2,3-trimethylbicyclo[3.2.1]oct-3-ene-4,8-dicarboxylate, **18***

Dimethyl 4-chloromethyl-1,4-dihydro-1,2,6-trimethylpyridine-3,5-dicarboxylate (37) (0.632 g) and thiourea (0.240 g) were refluxed in ethanol (95%, 15 mL) for 4½ h. The resulting solution was cooled, evaporated *in vacuo*, and the solid residue extracted with dry ether (2 × 15 mL) to remove an oily impurity. The solid was then heated at 100°C for 1 h with concentrated ammonium hydroxide (3 mL). After cooling, the reaction mixture was extracted using ethyl acetate (2 × 35 mL) and the organic extract washed with water (3 × 10 mL), dried ($MgSO_4$), filtered, and evaporated to give a pale brown oil (0.266 g). Purification was effected by preparative tlc twice on one 20 cm × 20 cm × 0.15 cm silica gel GF_{254} plate. When the almost pure product was held at 70°C/0.01 Torr for 15 min, a more volatile impurity was removed. Distillation of the residue at 95°C/0.01 Torr afforded an oil which solidified on standing to give colorless crystalline **18** (0.090 g, 14%) mp 78–80°C; uv λ_{max} (ε): 261 (2800), 316 nm (12 200); ir ν_{max}: 1735 (saturated ester) and 1675 cm^{-1} (unsaturated ester); ^{1}Hmr (A) δ: 1.90 (s, 3H, methyl at C(1)), 2.28 (s, 3H, methyl at C(3)), 2.88 (s, 3H, N-methyl), 3.18 approx. (m, 3H, H's at C(6) and C(8)), 3.65 (s, 3H, methyl ester), 3.66 (s, 3H, methyl ester), and 3.83 (overlapping broadened triplets, 1H, H at C(5)); ms *m/e*: 285(57, M^+), 254(22), 238(79), 226(24), 194(14), 181(13), 180(100), 129(85), 120(15), 98(21), and 56(16); accurate mass on molecular ion: calcd. for $C_{13}H_{19}NO_4S$: 285.10347; found: 285.10307.

Acknowledgements

The authors wish to express their gratitude to Memorial University of Newfoundland for financial support, Dr. W. Snedden for accurate mass measurements, and Dr. C. R. Jablonski for spectra measured on the Bruker nmr spectrometer.

1. A. Michael. J. Prakt. Chem. **35**, 349 (1887).
2. J. March. Advanced organic chemistry. McGraw-Hill, New York, NY. 1977. p. 679.
3. B. Gregory, E. Bullock, and T-S. Chen. Can. J. Chem. **57**, 44 (1979).
4. N. J. Oppenheimer and N. O. Kaplan. Biochemistry, **13**, 4675 (1974).
5. M. Lounasmaa, H. Merikallio, and M. Puhakka. Tetrahedron, **34**, 2995 (1978), and references therein.
6. U. Eisner and J. Kuthan. Chem. Rev. **72**, 1 (1972).
7. J. F. Biellmann and H. J. Callot. Tetrahedron, **26**, 4809 (1970).
8. E. Benary. Ber. **51**, 567 (1918).
9. J. Ashby and U. Eisner. J. Chem. Soc. C, 1706 (1967).
10. J. Ashby, L. A. Cort, J. A. Elvidge, and U. Eisner. J. Chem. Soc. C, 2311 (1968).
11. U. Eisner, M. Z. Haq, J. Flippen, and I. Karle. J. Chem. Soc. Perkin Trans. I, 357 (1972).
12. J. L. Wardell. *In* The chemistry of the thiol group. Part I. *Edited by* S. Patai. Wiley, London. 1974. p. 163.
13. E. Bullock, B. Gregory, and M. T. Thomas. Can. J. Chem. **55**, 693 (1977).
14. K. Tsuda, Y. Satch, N. Ikekawa, and H. Mishima. J. Org. Chem. **21**, 800 (1956).
15. D. Hofmann, E. M. Kosower, and K. Wallenfels. J. Am. Chem. Soc. **83**, 3314 (1961).
16. P. J. Brignell, E. Bullock, U. Eisner, B. Gregory, A. W. Johnson, and H. Williams. J. Chem. Soc. 4819 (1963).
17. P. J. Brignell, U. Eisner, and P. G. Farrell. J. Chem. Soc. B, 1083 (1966).
18. G. Schroll, S.-P. Nygaard, S.-O. Lawesson, A. M. Duffield, and C. Djerassi. Ark. Kemi, **29**, 525 (1968).
19. L. M. Jackman and S. Sternhell. Applications of nuclear magnetic resonance spectroscopy in organic chemistry. Pergamon Press, Oxford. 1969. pp. 119–120.
20. J. M. Barker. *In* Advances in heterocyclic chemistry. Vol. 21. *Edited by* A. R. Katritzky and A. J. Boulton. Academic Press, New York, NY. 1977. pp. 65–118.
21. S. W. Schneller. Int. J. Sulfur Chem. Part B, **7**, 309 (1972).
22. S. A. Glickman and A. C. Cope. J. Am. Chem. Soc. **67**, 1017 (1945).
23. D. L. Ostercamp. J. Org. Chem. **35**, 1632 (1970).
24. M. Freifelder. J. Org. Chem. **29**, 2895 (1964).
25. E. Wenkert, K. G. Dave, F. Haglid, R. G. Lewis, T. Oishi, R. V. Stevens, and M. Terashima. J. Org. Chem. **33**, 747 (1968).

26. N. H. CROMWELL, F. A. MILLER, A. R. JOHNSON, R. L. FRANK, and D. J. WALLACE. J. Am. Chem. Soc. **71**, 3337 (1949).
27. H. B. BÜRGI, J. D. DUNITZ, J. M. LEHN, and G. WIPFF. Tetrahedron, **30**, 1563 (1974).
28. J. E. BALDWIN. J. Chem. Soc. Chem. Commun. 734 (1976).
29. J. E. BALDWIN, J. CUTTING, W. DUPONT, L. KRUSE, L. SILBERMAN, and R. C. THOMAS. J. Chem. Soc. Chem. Commun. 736 (1976).
30. B. GREGORY, E. BULLOCK, and T. S. CHEN. J. Chem. Soc. Chem. Commun. 1070 (1979).
31. L. J. BELLAMY. Advances in infrared group frequencies. Methuen, London. 1968. p. 262.
32. I. HEILBRON and H. M. BUNBURY. Dictionary of organic compounds. Eyre and Spottiswoode, London. 1938.
33. P. J. BRIGNELL, U. EISNER, and H. WILLIAMS. J. Chem. Soc. 4226 (1965).
34. J. W. CORNFORTH. J. Chem. Soc. 1091 (1958).
35. C. E. LOADER and H. J. ANDERSON. Tetrahedron, **25**, 3879 (1969).
36. F. G. GONZALEZ and R. DE CASTRO BRZEZICKI. Chem. Abstr. **45**, 6183 (1951).
37. R. F. CHILDS and A. W. JOHNSON. J. Chem. Soc. C, 1950 (1966).

Can. J. Chem. Downloaded from www.nrcresearchpress.com by 210.87.254.105 on 09/05/12
For personal use only.

Spin trapping for hydroxyl in water: a kinetic evaluation of two popular traps[1]

PAUL R. MARRIOTT, M. JOHN PERKINS,[2] AND DAVID GRILLER
Division of Chemistry, National Research Council of Canada, Ottawa, Ont., Canada K1A 0R6

Received November 19, 1979

PAUL R. MARRIOTT, M. JOHN PERKINS, and DAVID GRILLER. Can. J. Chem. **58**, 803 (1980).

Two spin traps, 4-(*N*-methylpyridinium)*tert*-butyl nitrone (4-MePyBN) and 5,5-dimethyl-1-pyrroline-1-oxide (DMPO) were examined for their effectiveness at trapping hydroxyl in water. At pH 6 and 22°C, rate constants for trapping hydroxyl were found to be $0.5 \times 10^9\ M^{-1}\ s^{-1}$ (4-MePyBN) and $2.0 \times 10^9\ M^{-1}\ s^{-1}$ (DMPO). The hydroxyl adduct of DMPO decayed by a first order process with a half-life of 870 s. This was at least three times greater than that of the 4-MePyBN adduct. These and other results suggest that DMPO is the superior trap for this particular application and is well suited for use in biological systems.

PAUL R. MARRIOTT, M. JOHN PERKINS et DAVID GRILLER. Can. J. Chem. **58**, 803 (1980).

On a examiné deux pièges à spin la (*N*-méthylpyridinium)-4 *tert*-butyl nitrose (MePy-4BN) et l'oxyde-1 de diméthyl-5,5 pyrroline-1 (ODMP), pour leur efficacité dans la capture du groupe hydroxyle dans l'eau. On a trouvé, à 22°C et à un pH = 6, que les constantes de vitesse de la capture du groupe hydroxyle dans l'eau sont de: $0.5 \times 10^9\ M^{-1}\ s^{-1}$ (MePy-4BN) et $2.0 \times 10^9\ M^{-1}\ s^{-1}$ (ODMP). L'adduit hydroxyle du ODMP se décompose selon une réaction du premier ordre avec une demi-vie de 870 s. Cette période est au moins trois fois plus élevée que celle de l'adduit du MePy-4BN. Ces résultats ainsi que d'autres suggèrent que le ODMP est le piège idéal dans cette application particulière et il est indiqué pour être utilisé dans les systèmes biologiques.

[Traduit par le journal]

Introduction

The technique of spin trapping (1) was developed and proved in the general area of organic chemistry. However, it has recently seen increasing use in the biological field (2) where direct detection of free radicals is made extremely difficult by the complex nature of the systems under study. For example, spin trapping has been used to detect superoxide, $O_2^{-}\cdot$, formation in chloroplasts (3) in aerobic microsomal reduction of nitro-compounds (4) and in melanin photoreactions (5). It has also been used to identify hydroxyl radical production in systems involving aminoquinone antibiotics (6), bleomycin and iron(II) (7), photooxidation of chlorophylls (8), and microsomal lipid peroxidation (9).

In essence, the spin trapping experiment involves capture of a short-lived radical, R·, by a spin trap, to give a persistent spin adduct, SA·, which can be detected by epr spectroscopy. Most often the trap is a nitrone or nitroso compound and therefore the spin adducts are nitroxides.

$$R\cdot + \text{trap} \rightarrow SA\cdot$$

Although spin trapping is conceptually simple, the results can be misleading if they are not quantified. For example, a positive result can arise in systems where radicals are involved in a minor side reaction. Conversely, failure to observe a spin adduct does not prove the absence of radicals. It may simply reflect low rates of trapping or the formation of a short-lived spin adduct.

For the results of a trapping experiment to be of significance several criteria should be met and, where possible, quantified. These are: (*a*) the spin trap must be inert towards all reagents in the system except free radicals; (*b*) radicals should react rapidly with the spin trap so that competing reactions which destroy them are minimized; (*c*) the spin adducts must be long lived so that they can easily be detected; and (*d*) the epr parameters of the spin adducts must be sensitive to the nature of the radicals trapped.

Each of these four criteria has been examined in a few specific systems but rarely in a completely systematic way. As examples we note: (*a*) the failure of a spin trap due to its oxidation in a hydroperoxide–hematin system (10); (*b*) the measurement of rate constants[3] for spin trapping of benzoyloxy (11), alkoxycarbonyl (12), alkoxyl (13), phenyl (14), and alkyl radicals (15) although in media which are not always appropriate to biological work (16); (*c*) the measurement of the half-lives of spin adducts (15, 17) such as that of $O_2^{-}\cdot$ to 5,5-dimethyl-1-pyrroline-1-oxide (17); and (*d*) the extensive discussion of the sensitivity of epr parameters to the nature of the trapped radical particularly when phenyl-*tert*-butyl nitrone (PBN) was the spin trap (18).

[1]NRCC No. 18063.

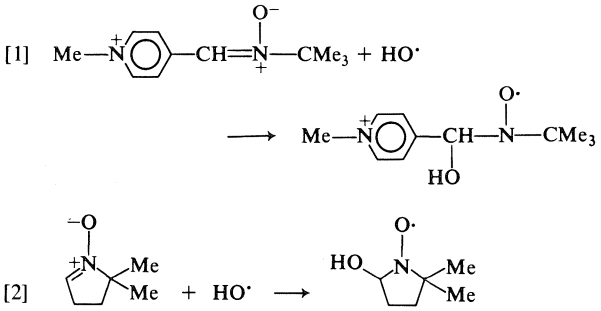
[2]Visiting scientist 1979; permanent address: Department of Chemistry, Chelsea College, University of London, Manresa Road, London, England SW3 6LX.

[3]These experiments have all been based on competitive reaction schemes and thus depend on the reliability of absolute rate constants drawn from other sources. Their accuracy should be assessed with this in mind.

0008-4042/80/080803-05$01.00/0
©1980 National Research Council of Canada/Conseil national de recherches du Canada

Can. J. Chem. Downloaded from www.nrcresearchpress.com by 210.87.254.40 on 09/05/12
For personal use only.

In this work we have evaluated factors (*a*)–(*d*) for an important biological application of spin trapping, that of detecting hydroxyl radicals in water. Two traps have been investigated; 4-(*N*-methylpyridinium)*tert*-butyl nitrone (4-MePyBN) (19) which is a water soluble trap representative of the PBN family and 5,5-dimethyl-1-pyrroline-1-oxide (DMPO) (20). The results suggest that DMPO is the superior reagent in this particular application.



Experimental

Materials

4-MePyBN and DMPO were obtained from Spin Trap Producers (Guelph, Ontario) and Aldrich respectively. DMPO required purification before use (17) (see below). All other materials were reagent grade and were used without further purification.

Electron Paramagnetic Resonance Measurements

Radicals were generated by photolyzing samples directly in the cavity of a Varian E 104 EPR spectrometer using a high pressure mercury arc lamp. The output of the lamp was filtered through an aqueous mixture of cobalt and nickel sulphates which removed much of the visible and most of the infrared radiation. The lamp was deliberately defocused to ensure uniform irradiation across the sample and the light intensity was adjusted using neutral density filters so that the rate of growth of spin adducts could be easily adjusted. Radical concentrations were determined using a standard procedure (21).

Sample Preparation

Samples were prepared in the dark and under nitrogen. Reagents were purged with nitrogen before mixing. In a typical experiment, a 1% aqueous hydrogen peroxide solution (sodium phosphate buffered) containing spin trap (~0.1 *M*) and (as required) organic substrate (~0.1 *M*) was transferred to a standard aqueous epr sample cell (0.2 mm id) and was then photolyzed in the cavity of the spectrometer. Under the low light intensities used in these experiments, photolysis of solutions in the absence of hydrogen peroxide gave no signals in the case of 4-MePyBN and *exceedingly* weak signals with DMPO which were not sufficiently strong to interfere with any of the experiments. However, samples containing hydrogen peroxide and 4-MePyBN gave weak signals before photolysis at pH 6 due to the ·OH adduct in the absence of methanol and to the $\cdot CH_2OH$ adduct when methanol was present in excess. This problem became progressively worse with increasing pH to the extent that at pH 7–8 the kinetic experiments could not be carried out. These results indicate that there is a slow, direct reaction between the trap and hydrogen peroxide which liberates hydroxyl. Under similar conditions, weak signals were observed with DMPO but were always < 1% of the final signal intensity. Despite these epr observations, nmr spectra of reaction mixtures at pH 6 showed no detectable change over the timescale of the experiment (1 h).

In order to remove the coloured impurity associated with DMPO (17), sample solutions containing this trap were shaken with activated charcoal and were filtered through glass wool prior to photolysis. This purification procedure tends to remove a small amount (~10%) of the spin trap itself. Therefore, in kinetic experiments the relative concentrations of trap and organic substrate were measured by nmr integration before epr experiments were carried out. We caution against the practice of storing stock solutions of spin traps since these often deteriorate with time (17).

Results and Discussion

The spin trapping experiments carried out in this work are described by the following reaction scheme:

$$[3]\quad HOOH \xrightarrow{h\nu} 2HO\cdot$$

$$[4]\quad HO\cdot + \text{trap} \xrightarrow{k_4} SA(HO\cdot)$$

$$[5]\quad HO\cdot + RH \xrightarrow{k_5} H_2O + R\cdot$$

$$[6]\quad R\cdot + \text{trap} \xrightarrow{k_6} SA(R\cdot)$$

Clean spectra of SA(HO·) and SA(R·) were generated respectively in the absence or in the presence of a large excess of an organic substrate. Samples of this kind were used to measure epr parameters and the decay kinetics of the spin adducts. For measurements of rate constants for spin trapping (k_4), the concentrations of RH and trap were adjusted so that the respective spin adducts were formed at similar rates and could both be detected in the same sample.

At the concentrations used in these experiments, no signals were observed due to the HOO· spin adduct although these have been reported when higher concentrations of hydrogen peroxide and lower concentrations of spin trap were used (18*a*). These results are consistent with the relatively slow rate of reaction between hydroxyl and hydrogen peroxide ($k_7 = 4.5 \times 10^7\ M^{-1}\ s^{-1}$ at pH 7) (22) as compared with the much faster rate constant for spin trapping (see below).

$$[7]\quad HO\cdot + H_2O_2 \xrightarrow{k_7} H_2O + HOO\cdot$$

Electron Paramagnetic Resonance Parameters

Electron proton resonance parameters for the spin adducts studied are given in Table 1 and where comparison was possible were in good agreement with literature data. Parameters for the 4-MePyBN spin adducts show a very small dependence on the type of radical being trapped. The consequences of this situation are illustrated in Fig. 1 which shows the spectrum of a solution containing the HO· and $\cdot CH_2OH$ spin adducts of 4-MePyBN. The simulation shown in the figure was obtained by adding spectra calculated from the epr parameters of the

Can. J. Chem. Downloaded from www.nrcresearchpress.com by 210.87.254.40 on 09/05/12
For personal use only.

TABLE 1. Electron paramagnetic resonance parameters for the spin adducts of DMPO and 4-MePyBN at pH 6

Trap	Radical scavenged	a^N(G)[a]	a^H(G)[a]
4-MePyBN	·OH	14.81[b]	1.45[b]
4-MePyBN	·CH_2OH	15.23	2.59[c]
DMPO	·OH	15.00	15.00[d]
DMPO	·CH_2OH	15.95	22.69[e]
DMPO	·CMe_2OH, ·$CH_2CH(Me)OH$	15.98	23.95[f]

[a]Measured at 22°C.
[b]Compare with ref. 19; *g*-value 2.00577; $a^H(OH) = 0.38$ G.
[c]*g*-value 2.00563.
[d]Compare with ref. 18*a*.
[e]Compare with ref. 26.
[f]See ref. 8.

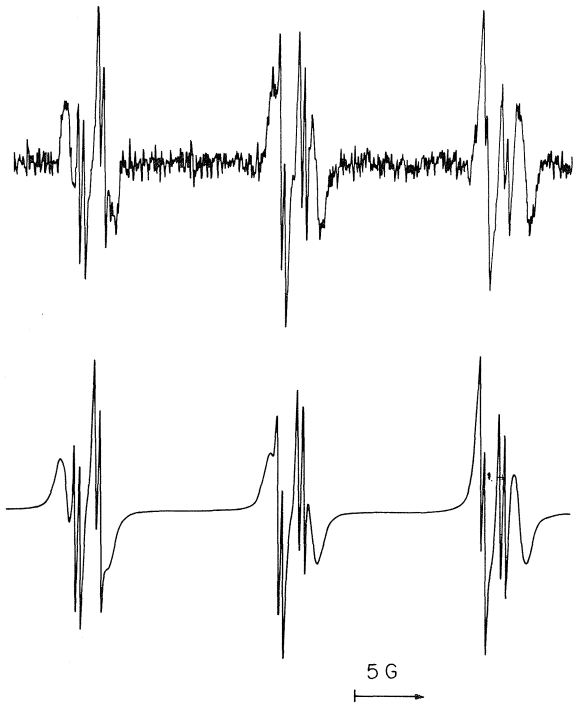


FIG. 1. Upper trace: epr spectrum of ·OH and ·CH_2OH spin adducts of 4-MePyBN. Lower trace: computer simulation.

individual spin adducts and confirms the analysis. However, it is quite clear that the similarity of spectra for spin adducts of 4-MePyBN will cause difficulties in identifying the nature of the trapped radicals and in quantifying relative radical concentrations. This problem of spectral clarity is often encountered with PBN type traps (18) and must be regarded as a serious disadvantage.[4] By way of

[4]As a further illustration, trapping of hydroxyl by PBN in a dimethylsulphoxide based solvent has been reported (6) although the observed hyperfine parameters were slightly different to those normally observed for the hydroxyl adduct (18). A similar experiment with DMPO (P. R. Marriott, unpublished results) shows that the radical trapped was more likely to have been methyl; a result consistent with the rapid reaction of hydroxyl with dimethylsulphoxide (23).

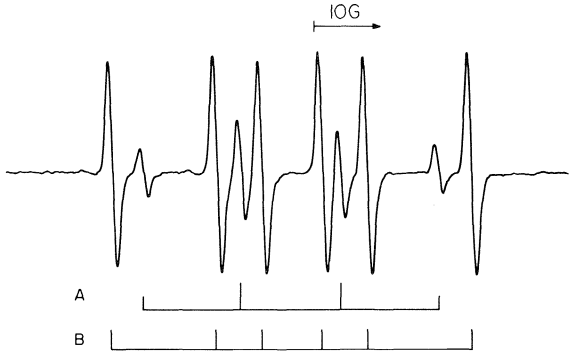


FIG. 2. Electron paramagnetic resonance spectrum of ·OH (*A*) and ·CH_2OH (*B*) spin adducts of DMPO.

comparison, Fig. 2 shows the analogous spectrum obtained using DMPO as trap. Its simplicity and clarity contrast sharply with the case of 4-MePyBN. The higher signal-to-noise ratio in the spectrum is a consequence of kinetic properties.

Decay Kinetics of Spin Adducts

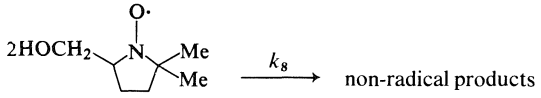
Rate constants for the decay of the hydroxyl adduct of DMPO at various pH are given in Table 2. At concentrations less than 4×10^{-5} *M* the decay was first order with a half-life of 870 s and the rate constants were independent of the concentrations of spin trap and hydrogen peroxide when each of these was varied by a factor of five. At higher concentrations the decay tended towards second order kinetics. The half-life of the hydroxyl adduct of DMPO is at least an order of magnitude greater than that of the O_2^{-}· adduct which is pH dependent ($\tau_{1/2} \sim 80$ s at pH 6 and ~35 s at pH 8 (17)).

TABLE 2. First order rate constants for the decay of the hydroxyl adduct of DMPO at 22°C

pH	Initial radical concentration (*M*)	Rate constant (s^{-1})
6.0	1.5×10^{-5}	4.7×10^{-4}
7.0	5.4×10^{-5}	8.4×10^{-4}
8.0	5.4×10^{-5}	9.8×10^{-4}

Can. J. Chem. Downloaded from www.nrcresearchpress.com by 210.87.254.40 on 09/05/12
For personal use only.

The $\cdot CH_2OH$ spin adduct of DMPO was far more persistent than that for hydroxyl and decayed with second order kinetics. The rate constant for the decay, k_8, was found to be 184 M^{-1} s^{-1} at pH 7.



[8]

The kinetic order for the decay of the hydroxyl adduct of 4-MePyBN could not be accurately determined because the maximum attainable concentration was not high enough for the decay to be monitored over several half-lives. However, an indication of the longevity of the spin adduct is that a 1.4×10^{-6} M solution decayed with a half-life of ~270 s at 22°C. By contrast the $\cdot CH_2OH$ adduct of 4-MePyBN was quite persistent, although this may in part reflect slow radical generation via the thermal reaction of hydrogen peroxide and trap (see Experimental section).

Rate Constants for Spin Trapping

Rate constants for spin trapping were determined in competition experiments where the known rate constant for reaction of hydroxyl with methanol (k_5) (ref. 24, taking the average of rate constants obtained by a variety of techniques) was chosen as a suitable kinetic standard. The concentrations of spin trap and methanol were varied until both $\cdot OH$ and $\cdot CH_2OH$ spin adducts could be detected in the same sample. The incident light intensity was also adjusted so that the growth in the spin adduct concentrations from the start of photolysis took place over a convenient time scale (ca. 5 min) for measurements to be taken. Near to the start of photolysis the chemistry of the system can be described by reactions [3]–[6]. This is because the time scale of this experiment is short compared to that for the unimolecular decay of the spin adducts and spin adduct concentrations are so low that radical–radical reactions do not contribute to the reaction scheme. Furthermore, since $R\cdot$ is efficiently trapped and its concentration is small compared to those of other components in the system, it follows that at the start of photolysis,

$$[9] \quad d[R\cdot]/dt = k_5[HO\cdot][RH] - k_6[R\cdot][trap] = 0$$

while

$$[10] \quad d[SA(R\cdot)]/dt = k_6[R\cdot][trap]$$

and

$$[11] \quad d[SA(HO\cdot)]/dt = k_4[HO\cdot][trap]$$

Combining these equations, we obtain

$$[12] \quad \frac{k_4}{k_5} = \frac{d[SA(HO\cdot)]/dt}{d[SA(R\cdot)]/dt} \cdot \frac{[RH]}{[trap]}$$

Since k_5, [RH], and [trap] are known, k_4, the rate constant for spin trapping is determined by measuring the initial rate of growth of the spin adducts.

Rate constants for trapping hydroxyl by DMPO and 4-MePyBN are given in Table 3. They were independent of the ratio of trap-to-methanol concentrations when this was varied by a factor of five. Experiments with 4-MePyBN were restricted to pH 6 because of problems with the "dark spectra" (see above) and must have greater error limits than those with DMPO because of the difficulties of integration.

As a check on the efficacy of this experimental procedure, the rate constant for attack of hydroxyl at 2-propanol was determined using 2-propanol instead of methanol as the organic substrate. Using the value of k_4 obtained above the rate constant k_5 for reaction at 2-propanol was found to be 1.5×10^9 M^{-1} s^{-1}, in excellent agreement with pulse radiolysis data ($k_5 = 1.5 \times 10^9$ M^{-1} s^{-1} (24)). It should be noted that attack at 2-propanol occurs at both methyl and methine hydrogen atoms (reactions [13], [14]) (25), although only one spectrum was detected, presumably because the spin adducts due the two carbon centered radicals have similar epr parameters.

$$[13] \quad HO\cdot + (CH_3)_2CHOH \rightarrow H_2O + \dot{C}H_2(CH_3)CHOH$$

$$[14] \quad HO\cdot + (CH_3)_2CHOH \rightarrow H_2O + (CH_3)_2\dot{C}OH$$

These results suggest that the rate constant for spin trapping of hydroxyl by DMPO is a satisfactory standard for measuring rates of reaction of hydroxyl with organic substrates by the above spin trapping method.

Summary

In this work we have evaluated the use of two spin traps, DMPO and 4-MePyBN, as scavengers for hydroxyl radicals in water using criteria (*a*)–(*d*). We find that DMPO is the superior trap because (*a*) it is unaffected by changing pH while 4-MePyBN is

TABLE 3. Rate constants (k_4) for the spin trapping of hydroxyl at 22°C

Spin trap	pH	k_4/k_5[a]	$k_4 \times 10^{-9}$ (M^{-1} s^{-1})
4-MePyBN	6	1.1	0.5
DMPO	6	4.1	2.0
DMPO	7	5.5	2.7
DMPO	8	5.3	2.6

[a]Using methanol as competitor, $k_5 = 4.8 \times 10^8$ M^{-1} s^{-1} (24).

Can. J. Chem. Downloaded from www.nrcresearchpress.com by 210.87.254.40 on 09/05/12
For personal use only.

Can. J. Chem. Downloaded from www.nrcresearchpress.com by 210.87.254.40 on 09/05/12
For personal use only.

not; (*b*) it scavenges hydroxyl 4.0 times more rapidly than 4-MePyBN; (*c*) its hydroxyl spin adduct is 3.2 times longer lived than that of 4-MePyBN; and (*d*) the epr spectra of DMPO spin adducts are more sensitive to the nature of the adduct radical than those of 4-MePyBN.

These results show that the outcome of spin trapping experiments are likely to be particularly sensitive functions of the properties of the spin traps. They suggest that a more quantitative approach to spin trapping and careful selection of the spin traps for particular applications is likely to yield more reliable results.

Acknowledgements

Two of us (D.G., M.J.P.) would like to thank NATO for the award of a research grant which made this collaboration possible. We would also like to thank Dr. K. U. Ingold for helpful discussions.

1. M. J. Perkins. *In* Essays in free radical chemistry, Chemical Society Special Publication 24. 1970. pp. 97–115; E. G. Janzen. Acc. Chem. Res. **4**, 31 (1971); C. Lagercrantz. J. Phys. Chem. **75**, 3466 (1971).
2. H. Aoshima, T. Kajiwara, A. Hatanaka, and H. Hatano. J. Biochem. **82**, 1559 (1977); J. L. Poyer, R. A. Floyd, P. B. McCay, E. G. Janzen, and E. R. Davis. Biochim. Biophys. Acta, **539**, 402 (1978); A. Joshi, H. Moss, and P. Riesz. Int. J. Radiat. Biol. **34**, 165 (1978); B. W. Griffin and P. L. Ting. FEBS Lett. **89**, 196 (1978); K. Mamino. J. Phys. Chem. **83**, 2520 (1979).
3. J. R. Harbour and J. R. Bolton. Biochem. Biophys. Res. Commun. **64**, 803 (1975); H. Aoshima, J. Sekiya, T. Kajiwara, and A. Hatanaka. Agric. Biol. Chem. **41**, 1787 (1977).
4. R. C. Sealy, H. M. Swartz, and P. L. Olive. Biochem. Biophys. Res. Commun. **82**, 680 (1978).
5. C. C. Felix, J. S. Hyde, T. Sarna, and R. C. Sealy. Biochem. Biophys. Res. Commun. **84**, 335 (1978).
6. J. W. Lown, S. K. Sim, and H.-H. Chen. Can. J. Biochem. **56**, 1042 (1978).
7. Y. Sugiura and T. Kikuchi. J. Antibiot. **31**, 1310 (1978); L. W. Oberley and G. R. Buettner. FEBS Lett. **97**, 47 (1979).
8. J. R. Harbour and J. R. Bolton. Photochem. Photobiol. **28**, 231 (1978).
9. C.-S. Lai and L. H. Piette. Arch. Biochem. Biophys. **190**, 27 (1978); A. N. Saprin and L. H. Piette. Arch. Biochem. Biophys. **180**, 480 (1977).
10. R. A. Floyd and L. M. Soong. Biochem. Biophys. Res. Commun. **74**, 79 (1977); see also R. A. Hood, R. H. Prince, and K. A. Robinson. Chem. Commun. 300 (1978).
11. E. G. Janzen, C. A. Evans, and Y. Nishi. J. Am. Chem. Soc. **94**, 8236 (1972).
12. M. J. Perkins and B. P. Roberts. Chem. Commun. 173 (1973); J. Chem. Soc. Perkin II, 297 (1974).
13. E. G. Janzen and C. A. Evans. J. Am. Chem. Soc. **95**, 8205 (1973); F. P. Sargent. J. Phys. Chem. **81**, 89 (1977).
14. E. G. Janzen and C. A. Evans. J. Am. Chem. Soc. **97**, 205 (1975); M. Kamimori, H. Sakuragi, K. Sawatari, T. Suehiro, K. Tokumaru, and M. Yoshida. Bull. Chem. Soc. Jpn. **52**, 2339 (1979).
15. T. Doba, T. Ichikawa, and H. Yoshida. Bull. Chem. Soc. Jpn. **50**, 3124 (1977); P. Schmid and K. U. Ingold. J. Am. Chem. Soc. **99**, 6434 (1977); **100**, 2493 (1978); Y. Maeda and K. U. Ingold. J. Am. Chem. Soc. **101**, 4975 (1978).
16. Y. Maeda, P. Schmid, D. Griller, and K. U. Ingold. Chem. Commun. 525 (1978).
17. G. R. Buettner and L. W. Oberley. Biochem. Biophys. Res. Commun. **83**, 69 (1978).
18. (*a*) J. R. Harbour, V. Chow, and J. R. Bolton. Can. J. Chem. **52**, 3549 (1974); (*b*) E. G. Janzen, D. E. Nutter, E. R. Davis, and B. J. Blackburn. Can. J. Chem. **56**, 2237 (1978); (*c*) P. H. Kasai and D. McLeod. J. Phys. Chem. **82**, 619 (1978); (*d*) E. G. Janzen, R. L. Dudley, E. R. Davis, and C. A. Evans. J. Phys. Chem. **82**, 2445 (1978).
19. E. G. Janzen, R. L. Dudley, and R. V. Shetty. J. Am. Chem. Soc. **101**, 243 (1979); E. G. Janzen, Y. Y. Wang, and R. V. Shetty. **100**, 2923 (1978); E. G. Janzen and R. V. Shetty. Tetrahedron Lett. 3229 (1979).
20. M. Iwamura and N. Inamoto. Bull. Chem. Soc. Jpn. **40**, 702 (1967); **43**, 856 (1970); E. G. Janzen and J. I.-P. Liu. J. Magn. Reson. **9**, 510 (1973); E. G. Janzen, C. A. Evans, and J. I.-P. Liu. J. Magn. Reson. **9**, 513 (1973).
21. G. B. Watts and K. U. Ingold. J. Am. Chem. Soc. **94**, 491 (1972).
22. H. A. Schwartz. J. Phys. Chem. **66**, 255 (1962).
23. W. T. Dixon, R. O. C. Norman, and A. Buley. J. Chem. Soc. 3625 (1964); G. Meissner, A. Henglien, and G. Beck. Z. Naturforsch. **22b**, 13 (1967); C. Lagercrantz and S. Forshult. Acta Chem. Scand. **23**, 811 (1969); B. C. Gilbert, R. O. C. Norman, and R. C. Sealy. J. Chem. Soc. Perkin II, 303 (1975).
24. M. Anbar and P. Neta. Int. J. Appl. Radiat. Isot. **18**, 493 (1967).
25. R. O. C. Norman and P. R. West. J. Chem. Soc. B, 389 (1969); C. E. Burchill and P. W. Jones. Can. J. Chem. **49**, 4005 (1971).
26. F. P. Sargent and E. M. Gardy. Can. J. Chem. **54**, 275 (1976).

The bromination and chlorination of 2,3-dialkylindoles. Isolation of 3-bromo- and 3-chloro-2,3-dialkylindolenines and acid catalyzed conversion to 3-methoxyindolenines[1]

GARY I. DMITRIENKO,[2] EDWARD A. GROSS, AND SUSAN F. VICE

The Guelph–Waterloo Centre for Graduate Work in Chemistry, Waterloo Campus, Department of Chemistry, University of Waterloo, Waterloo, Ont., Canada N2L 3G1

Received November 8, 1979

GARY I. DMITRIENKO, EDWARD A. GROSS, and SUSAN F. VICE. Can. J. Chem. **58**, 808 (1980).

The bromination of 2,3-dimethylindole in acetic acid followed by hydrolysis has been shown to yield the known dimer **16** of 3-hydroxy-2,3-dimethylindolenine **15** and not 3-hydroxymethyl-2-methylindole **12** as reported previously by others. Bromination of 2,3-dimethylindole in the presence of triethylamine has yielded 3-bromo-2,3-dimethylindolenine **17** as a crystalline solid which is stable at room temperature in a nitrogen atmosphere in the presence of triethylamine but decomposes vigorously in the absence of base. Under mildly acidic conditions **17** reacts rapidly with methanol to yield 3-methoxy-2,3-dimethylindolenine **3** in good yield. With *tert*-butyl hypochlorite in the presence of triethylamine, 2,3-dimethylindole gives 3-chloro-2,3-dimethylindolenine **2** which has chemical properties similar to **17** reacting readily with methanol to give **3**. Similarly tetrahydrocarbazole was converted to the analogous chloroindolenine **5** and bromoindolenine **18** both of which readily underwent methanolysis to give **6** in good yield. A mechanism for the acid catalyzed methanolysis of 3-chloro- and 3-bromoindolenines is proposed.

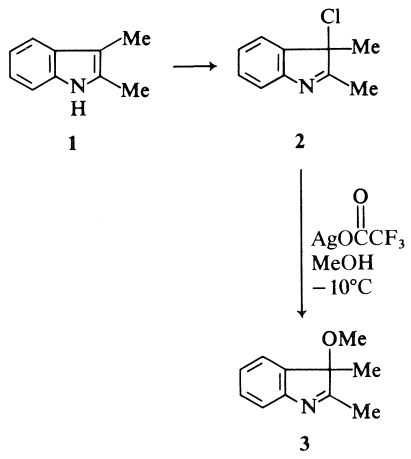
GARY I. DMITRIENKO, EDWARD A. GROSS et SUSAN F. VICE. Can. J. Chem. **58**, 808 (1980).

On a montré que la bromation du diméthyl-2,3 indole dans l'acide acétique, suivie d'une hydrolyse, conduit au dimère connu **16** de l'hydroxy-3 diméthyl-2,3 indolénine **15** et non à l'hydroxyméthyl-3 méthyl-2 indole **12** tel que rapporté antérieurement. La bromation du diméthyl-2,3 indole en présence de triéthylamine conduit au dérivé bromo-3 diméthyl-2,3 indolénine **17** sous forme d'un solide cristallin stable à température normale sous atmosphère d'azote et en présence de triéthylamine mais il se décompose rapidement en l'absence de base. Dans des conditions légèrement acides, le composé **17** réagit rapidement avec le méthanol pour conduire au méthoxy-3 diméthyl-2,3 indolénine **3** avec un bon rendement. Le diméthyl-2,3 indole réagit avec l'hypochlorite de *tert*-butyle en présence de triéthylamine pour donner le chloro-3 diméthyl-2,3 indolénine **2** dont les propriétés chimiques sont semblables à celles du composé **17**. Il réagit rapidement avec le méthanol pour conduire au composé **3**. De la même manière, la tétrahydrocarbazole se transforme en chloro et bromoindolénine (**5** et **18**) qui par méthanolyse fournissent chacun avec un bon rendement le composé **6**. On propose un mécanisme pour expliquer la méthanolyse catalysée par un acide des chloro-3 et bromo-3 indolénines.

[Traduit par le journal]

In the course of studies aimed at the synthesis of biologically active indole derivatives, we sought a simple route to 3-alkoxy-2,3-dialkylindoles. A survey of the literature revealed two relatively recent reports of the preparation of 3-alkoxyindolenines. Gassman *et al.* have reported that treatment of 2,3-dimethylindole with *tert*-butyl hypochlorite or sodium hypochlorite at low temperature yields a thermally unstable compound with spectroscopic characteristics compatible with its formulation as the 3-chloroindolenine **2** (1). Treatment of this compound with an equivalent of silver trifluoroacetate in methanol was reported to yield the 3-methoxyindolenine **3** in good yield (Scheme 1).

Since our synthetic objective required the preparation of relatively large amounts of methoxyindolenines, the requirement in this procedure for a relatively expensive reagent, silver trifluoroacetate, was unattractive.



SCHEME 1

More recently, Owellen has modified Gassman's procedure and applied it to the synthesis of the methoxyindolenine of tetrahydrocarbazole (2). Thus, treatment of tetrahydrocarbazole (Scheme 2) at low temperature in benzene or methylene chloride with *tert*-butyl hypochlorite and triethylamine, yielded a solution of the chloroin-

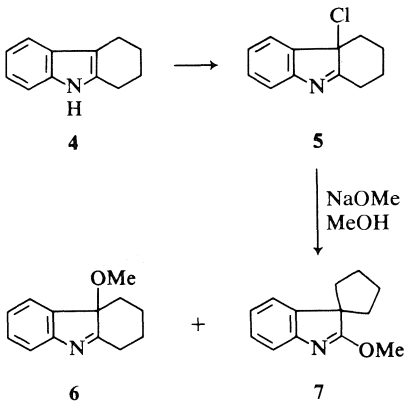
[1]Presented in part at the 62nd Annual Conference of the Chemical Institute of Canada, Vancouver, B.C., June 3–6, 1979.

[2]Author to whom all correspondence should be addressed.

0008-4042/80/080808-07$01.00/0

©1980 National Research Council of Canada/Conseil national de recherches du Canada

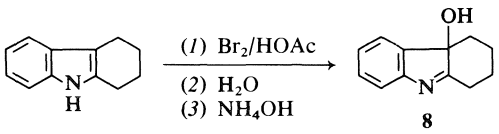
Can. J. Chem. Downloaded from www.nrcresearchpress.com by 210.87.254.40 on 09/05/12
For personal use only.



SCHEME 2

dolenine **5** which reacted with sodium methoxide in methanol to give largely the methoxyindolenine **6** accompanied by smaller amounts (about 20%) of the imido ether product **7**. The formation of an imido ether by-product limits the usefulness of this approach to the synthesis of 3-methoxyindolenines.

No other reports of the preparation of 3-alkoxy-2,3-dialkylindolenines could be found in the literature. There was, however, a report by Plant and Tomlinson of a rather simple preparation of 11-hydroxytetrahydrocarbazolenine, **8** (Scheme 3) by bromination–hydrolysis of tetrahydrocarbazole.[3] It was felt that this procedure might be changed into a synthesis of alkoxyindolenines rather than hydroxyindolenines simply by replacement of water by an appropriate alcohol.

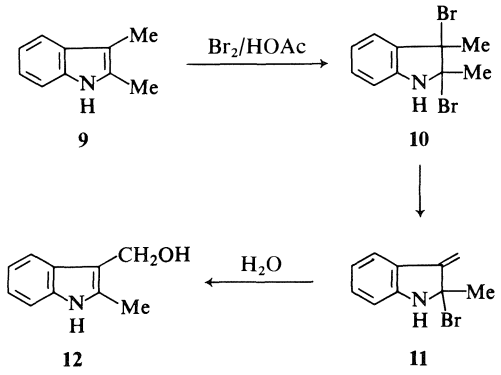


SCHEME 3

Since we were interested in a general synthetic approach, we were perplexed by another report by Plant and Tomlinson which indicated that application of the bromination–hydrolysis sequence to 2,3-dimethylindole gave not the 3-hydroxyindolenine but rather, 3-hydroxymethyl-2-methylindole **12** (6). Examination of the reported experimental details revealed that the structural assignment of this product rested on elemental analytical data and on an assumed mechanism illustrated in Scheme 4. It was assumed that the initial product was a dibromide **10** which underwent elimination of HBr to give the indicated allylic bromide **11** which in turn reacted with water by an S_N1' or S_N2' reaction to give 3-hydroxymethyl-2-methylindole.

In more recent work, Leete has synthesized authentic 3-hydroxymethyl-2-methylindole and has shown that the physical properties of this material are grossly different from those of Plant and Tomlinson's compound **12** (7). Unfortunately, Leete's observation has often been ignored in discussions of the bromination of 2,3-dimethylindole in recent review articles (8).

In order to clarify the situation, we have now repeated the bromination–hydrolysis of 2,3-dimethylindole as reported by Plant and Tomlinson.[4] We have found that bromination of 2,3-



SCHEME 4

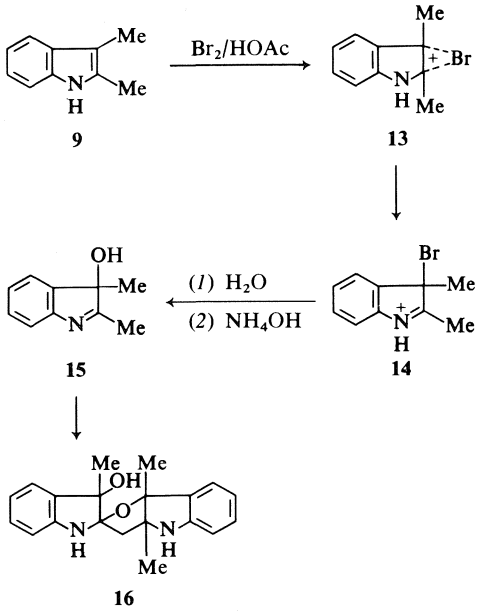
dimethylindole in glacial acetic acid followed by the addition of water and basic aqueous workup gives a crude product from which a crystalline solid mp 225°C (lit. (6) mp 225°C) could be obtained in 36% yield by fractional crystallization. This product was easily identified as the known dimer **16** by comparison with an authentic sample (10). The dimer was shown unambiguously to have the structure **16** some years ago on the basis of chemical studies by Berti *et al.* (10*c*) and Dave and Warnhoff (10*b*) and by an X-ray crystallographic study by McLean *et al.* (10*a*). No 3-hydroxymethyl-2-methylindole could be detected by nmr analysis of the crude product.

The most obvious mechanistic rationale for the formation of the dimer was that indicated in Scheme 5. It was felt that bromination likely yielded a protonated 3-bromoindolenine **14**, perhaps via a bromonium ion **13**. Nucleophilic substitution of bromide by water could give the 3-hydroxyindolenine **15** which could dimerize to give

[3]Plant and Tomlinson initially assigned the structure of this product as 10-hydroxy-1,2,3,10-tetrahydrocarbazole (3). Sometime later, Patrick and Witkop (4) and also Plant and Tomlinson (5) revised the structure to 11-hydroxy-2,3,4,11-tetrahydrocarbazole.

[4]For a preliminary account of some of this work see ref. 9.

Can. J. Chem. Downloaded from www.nrcresearchpress.com by 210.87.254.40 on 09/05/12
For personal use only.



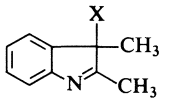
SCHEME 5

16 in a well known process (10, 11). Thus the reaction of 2,3-dimethylindole with bromine is not anomalous and appears to proceed in the same fashion as reported for tetrahydrocarbazole. The nature of the ultimate product is different because of the unusual tendency of 2-methyl-3-alkyl-3-hydroxyindolenines to dimerize (11).

Since this approach to the formation of 3-hydroxyindolenines appeared to have some generality after all, we next turned our attention to the preparation of 3-alkoxyindolenines in an analogous manner. We have now found that treatment of a methanol solution of 2,3-dimethylindole with an equimolar amount of bromine in acetic acid or methylene chloride at −5°C followed by basic aqueous workup yields the 3-methoxyindolenine **3** as an oil identical with the material prepared by the method of Gassman *et al.* (1). Similarly, tetrahydrocarbazole has been found to give the corresponding methoxyindolenine **6** uncontaminated by the spiro imido ether **7**.

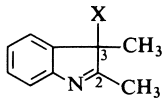
In our initial study, we assumed the intermediacy of a 3-bromoindolenine in the bromination–hydrolysis and bromination–methanolysis of 2,3-dimethylindole (9). Further investigation has led to the isolation of this intermediate. We have now found that treatment of 2,3-dimethylindole in methanol or methylene chloride with an equimolar amount of bromine in methylene chloride in the presence of an excess of triethylamine followed by basic aqueous workup yields 3-bromo-2,3-dimethylindolenine as a crystalline solid. The structure of this product follows from nmr, ir, and

TABLE 1. Indolenines: infrared spectra



X	$\bar{\nu}$(cm^{-1}) C=N— (Nujol)
OH	1590 (10*c*)
OOH	1600 (10*c*)
OMe	1601
Cl	1585
Br	1605

TABLE 2. Indolenines: nuclear magnetic resonance spectra



nmr ($CDCl_3$)

X	*J*(ppm) C2—CH_3	C3—CH_3
OH	1.89	1.39 (10*b*)
OOH	2.17	1.40 (10*b*)
OMe	2.20	1.41
Cl	2.42	1.75
Br	2.43	1.83

uv spectral data. The ir spectrum shows no signal for indole N—H stretch but instead a band at 1605 cm^{-1} which can be assigned to an indolenine C—N stretch (see Table 1 for comparison with other indolenines). In the nmr spectrum there are two 3-proton singlets; one at δ 1.83 (C3—CH_3) and one at δ 2.43 ppm (C2—CH_3). The chemical shift of the C3—CH_3 group in the bromoindolenine **17** agrees reasonably well with that calculated (δ 1.90) on the basis of empirical substituent effects on chemical shifts (see Table 2) (12). Under the same conditions tetrahydrocarbazole gives an analogous bromoindolenine **18** (cf. Scheme 6).

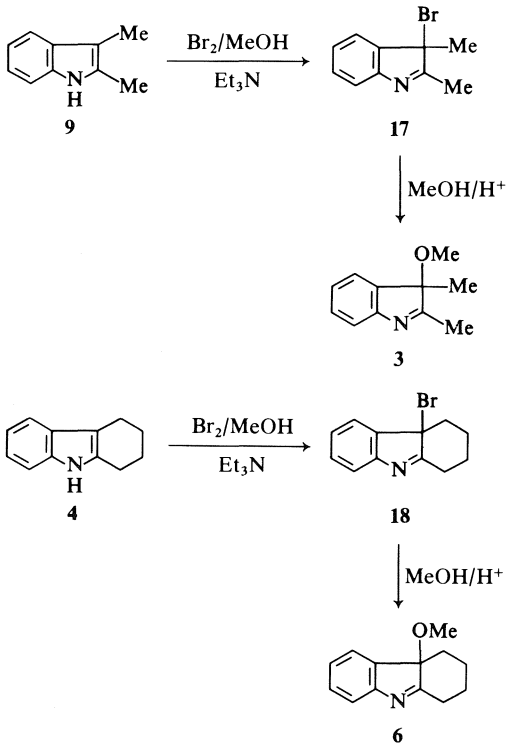
Treatment of a methylene chloride solution of **17** or **18** with methanol followed by basic aqueous workup gave the corresponding methoxyindolenines in good yield. The best yields of methoxyindolenines were obtained by treatment of a methylene chloride solution of **17** or **18** with methanol containing sufficient *p*-toluene sulfonic acid to neutralize all triethylamine present.

The fact that **17** and **18** do not react with methanol in the presence of triethylamine but react readily in the absence of base strongly suggests that methanolysis of 3-bromoindolenines is an acid catalyzed process and thus likely proceeds via an

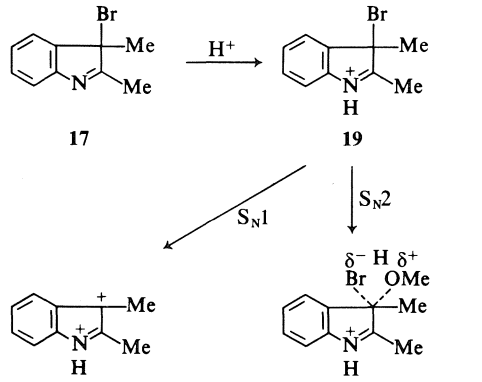
Can. J. Chem. Downloaded from www.nrcresearchpress.com by 210.87.254.40 on 09/05/12
For personal use only.

Can. J. Chem. Downloaded from www.nrcresearchpress.com by 210.87.254.40 on 09/05/12
For personal use only.

N-protonated bromoindolenine intermediate (Scheme 7). The S_N2 displacement of bromide ion from **19** is highly unlikely for steric reasons. Furthermore the positive charge in **19** would strongly disfavour development of additional positive charge as would be required in a simple S_N2 or S_N1 transition state.

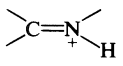


SCHEME 6



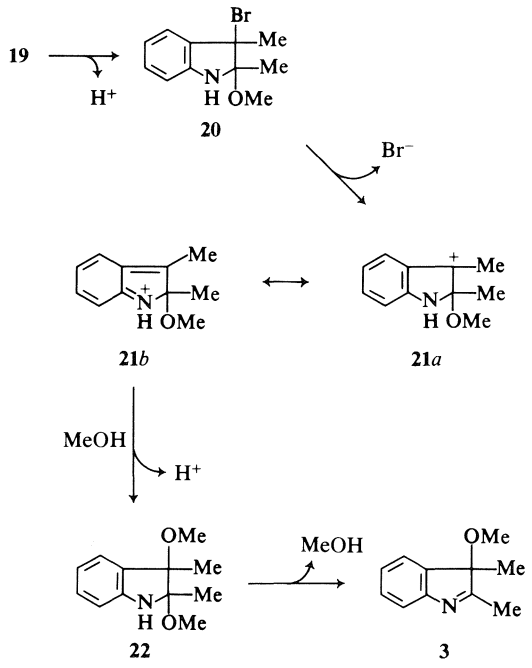
SCHEME 7

One reaction which would be expected to be favoured by protonation of the indolenine nitrogen is addition of methanol to the



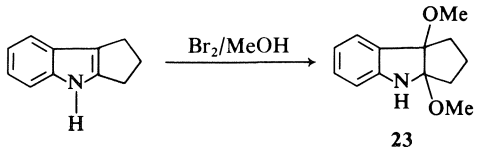
bond to give, after deprotonation, the 2-methoxy-3-bromoindoline **20** (see Scheme 8). S_N1-type ionization of **20** would be expected to occur readily yielding a highly resonance stabilized carbonium ion **21**.

Addition of methanol followed by deprotonation would yield **22** which upon elimination of methanol



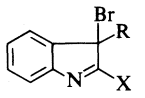
SCHEME 8

would give the observed methoxyindolenine. The failure of the reaction to proceed in the presence of base could be due to the failure to form significant amounts of the addition product **20** in the absence of acid catalysis. Consistent with this reaction scheme is the isolation of the 2,3-dimethoxyindoline **23** from the bromination–methanolysis of 2,3-cyclopentanoindole.[5]



Although a number of 3-bromoindolenines **24** possessing a heteroatom substituent at C-2 have been reported (13), **17** and **18** are the first 3-bromo-2,3-dialkyl indolenines to be isolated. As a result, some comments on the stability of **17** and **18**, especially in comparison with known 3-chloro-2,3-dialkylindolenines, are in order.

[5]Unpublished observation by E. Gross in this laboratory.



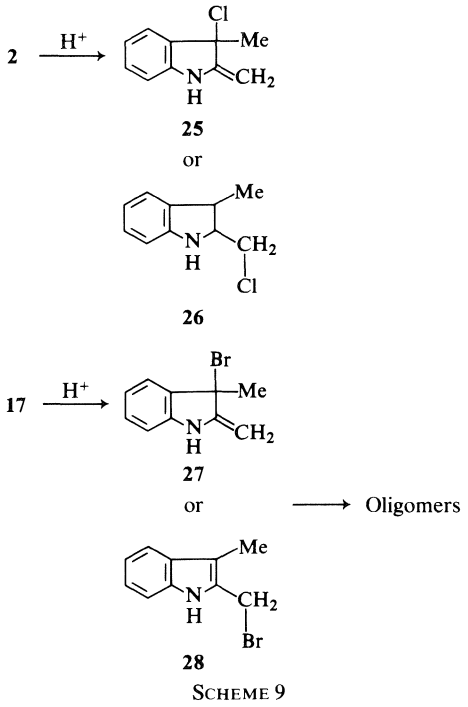
24

	R	X
a	Me	SEt
b	Me	SO_2Et
c	Ph	SEt
d	Ph	SO_2Et
e	Ph	Br

The bromoindolenine **17** is stable in the solid state at −78°C for at least several weeks. In the presence of small amounts of triethylamine **17** undergoes negligible decomposition after several hours at room temperature. Upon complete removal of triethylamine (as judged by nmr) *in vacuo*, **17** is stable in the solid form for at least forty minutes at room temperature if kept in a dry nitrogen atmosphere but decomposes with vigorous evolution of HBr to a deep blue-purple, highly insoluble solid upon exposure to a normal atmosphere.

The corresponding 3-chloroindolenine **2** has been detected in methylene chloride solution (1). It has been reported to be highly unstable, undergoing complete rearrangement to **25** or **26** upon brief warming from −78 to +15°C followed by rapid cooling in methylene chloride. Evaporation of a methylene chloride solution of **2** to dryness was reported to give an intractable product (1). The apparent instability of **2** relative to the 3-bromoindolenine **17** was puzzling. One possible explanation of this phenomenon lay in the fact that **17** was produced in the presence of base and solutions of **17** which were evaporated to dryness contained at least traces of triethylamine whereas solutions of **2** as prepared by Gassman and co-workers (1) did not contain base. To test this possibility, we have now prepared **2** by treatment of 2,3-dimethylindole with *tert*-butyl hypochlorite and triethylamine in methylene chloride followed by basic aqueous workup. The chloroindolenine **2** prepared in this way was isolated as a crystalline solid with stability comparable to that described for **17**. It seems clear now that the rearrangement process which converts **2** to **25** or **26** is an acid catalyzed process. The instability of the bromoindolenine **17** in the absence of base is likely due to initial rearrangement analogous to that reported for **2**, followed by as yet ill-defined, oligomerization reactions of **27** or **28** (Scheme 9).

It has been pointed out by Owellen (2) that solutions of the chloroindolenine **5** are unusually stable relative to **2**, undergoing no detectable decomposition at 70°C in benzene. Our observations suggest that this phenonmenon may be due to the fact that



SCHEME 9

benzene solutions of **5** were generated in the presence of triethylamine whereas the methylene chloride solutions of **2** were base free.

The chloroindolenines formed by chlorination of complex tryptamine-derived alkaloids have been reported to be relatively stable materials which can be recrystallized from alcohols without difficulty (14). It is interesting to speculate, based on our observations, that the stability of these compounds is due, at least in part, to the presence of a basic nitrogen atom within the chloroindolenine molecules themselves which inhibits acid catalyzed modes of decomposition.

The ease with which the 3-bromoindolenine **17** reacted with methanol to give the 3-methoxyindolenine **3** prompted us to question the reported need (1) for silver trifluoroacetate to catalyze the methanolysis of the 3-chloroindolenine **2**. We have now found that the crystalline chloroindolenine **2** reacts with methanol, containing no silver salts, very readily to give **3** in high yield. Similarly we have prepared the 3-chloroindolenine of tetrahydrocarbazole **5** by our method and converted it to the methoxyindolenine **6** simply by reaction with methanol.

It is clear now that the bromination of simple 2,3-dialkylindoles such as 2,3-dimethylindole and tetrahydrocarbazole proceeds via a 3-bromoindolenine which is a stable isolable compound in the presence of base. In the presence of acid 3-

Can. J. Chem. Downloaded from www.nrcresearchpress.com by 210.87.254.40 on 09/05/12
For personal use only.

Can. J. Chem. Downloaded from www.nrcresearchpress.com by 210.87.254.40 on 09/05/12
For personal use only.

bromoindolenines are unstable yielding highly coloured oligomeric products in an inert solvent and giving high yields of 3-methoxyindolenines in methanol. The latter reaction is clearly the method of choice for the preparation of simple 3-methoxy-2,3-dialkylindolenines. Chlorination of 2,3-dialkylindoles with *tert*-butyl hypochlorite gives high yields of 3-chloroindolenines which behave in an analogous manner to the 3-bromoindolenines. Experiments aimed at determining the limitations of the bromination–methanolysis route to methoxyindolenines and at exploring the reaction of 3-bromoindolenines with nucleophiles other than simple alcohols are in progress.

Experimental

Melting points were determined on a Fisher Mel-temp melting point apparatus and are uncorrected. Infrared spectra were recorded on a Beckman IR-10 spectrometer and the frequency (cm^{-1}) of significant peaks is reported. A Beckman Model 35 spectrophotometer was used for uv spectra and wavelengths (nm) of absorption bands are reported followed by extinction coefficients (ε) in parentheses. Nuclear magnetic resonance spectra were recorded on a Varian T-60 spectrometer (chloroform-*d* solvent unless otherwise indicated) and chemical shifts are reported on the δ scale, followed in parentheses by an account of the multiplicity and number of protons concerned. Mass spectra were recorded on a Varian CH-7 or VG-7070 mass spectrometer.

Indoles

2,3-Dimethylindole and tetrahydrocarbazole were prepared by Fischer cyclization of the appropriate phenylhydrazone by the method of Dave and Warnhoff (11*b*) and had physical constants in agreement with literature values.

Bromination–Hydrolysis of 2,3-Dimethylindole

Bromination–hydrolysis of 2,3-dimethylindole was performed essentially according to the method of Plant and Tomlinson (6).

To a rapidly stirred solution of 2,3-dimethylindole (0.522 g, 3.6 mmol) in glacial acetic acid (2 mL) at 0°C in a nitrogen atmosphere was added an equimolar amount of bromine in glacial acetic acid (2 mL). The whole was rapidly diluted with ice-water and the mixture was made basic with aqueous ammonia. The basic mixture was extracted with ether. The ether extract was washed with saturated aqueous sodium chloride, dried over anhydrous sodium sulfate, and evaporated to dryness on a rotary evaporator to yield a tan coloured solid. The nmr spectrum of the crude product indicated the complete absence of 3-hydroxymethyl-2-methylindole. Recrystallization of the crude product from ether gave a crystalline product (0.209 g, 36% yield) mp 224–225°C identical in all respects with the dimer **16** prepared by autoxidation of 2,3-dimethylindole (10).

*Preparation of 3-Bromo-2,3-dimethylindolenine **17***

2,3-Dimethylindole (0.45 g, 3.1 mmol) was dissolved in anhydrous methanol (20 mL) containing triethylamine (1 mL). The solution was cooled to −5°C and a solution of bromine (1 equivalent) in methylene chloride (4 mL) was added dropwise with stirring in a nitrogen atmosphere. After 5 minutes, water was added and the mixture was extracted with methylene chloride. The dried organic phase was evaporated to dryness *in vacuo* at room temperature to yield a pale yellow crystalline solid (0.68 g, 3.0 mmol) which was stable at room temperature in a nitrogen atmosphere or in a stoppered flask at −78°C. Infrared (Nujol): 1605; uv (0.1% Et_3N in CH_2Cl_2): 285 (2860), 291 (sh); nmr: 1.83 (s, 3), 2.43 (s, 3), 6.9–7.5 (m, 4).

*Preparation of 3-Chloro-2,3-dimethylindolenine (**2**)*

2,3-Dimethylindole (0.450 g, 3.1 mmol) was dissolved in methylene chloride (20 mL). The solution was cooled to −11°C in a nitrogen atmosphere and *tert*-butyl hypochlorite (3.1 mmol) in methylene chloride (9 mL) was added dropwise with stirring followed by triethylamine (1 mL). After stirring for an additional five minutes the workup was as described for **17** to give **2** as a pale yellow solid which was stored at room temperature in a nitrogen atmosphere and was used for subsequent reactions without further purification; ir (Nujol): 1585; uv (0.1% Et_3N/CH_2Cl_2): 285 (2800), 308 (sh); nmr: 1.75 (s, 3), 2.42 (s, 3), 6.96–7.60 (m, 4).

*Preparation of 3-Methoxy-2,3-dimethylindolenine by Methanolysis of **17***

3-Bromo-2,3-dimethylindolenine **17** (0.473 g, 2.11 mmol) was dissolved in methylene chloride (10 mL) and the solution cooled to −5°C in a nitrogen atmosphere. Methanol (20 mL) was added in 1 mL portions with stirring. The solution was stirred an additional 5 minutes. Water (75 mL) was added, the mixture was made basic with 10% aqueous ammonia and extracted with methylene chloride. Removal of solvent from the dried organic phase gave a colourless oily product (0.37 g) which was chromatographically pure and identical in all respects with 3-methoxy-2,3-dimethylindolenine prepared by the method of Gassman and co-workers (1).

*Preparation of 3-Methoxy-2,3-dimethylindolenine by Methanolysis of the Chloroindolenine **2***

Treatment of the chloroindolenine **2** with methanol as described for **17**, gave a quantitative yield of 3-methoxy-2,3-dimethylindolenine.

Preparation of 3-Methoxy-2,3-dimethylindolenine from 2,3-Dimethylindole

2,3-Dimethylindole (0.500 g, 3.45 mmol) was dissolved in a mixture of methylene chloride (20 mL) and triethylamine (1 mL). A solution of bromine (4.11 mmol) in methylene chloride (5.3 mL) was added dropwise with stirring to the cooled (−5°C) solution in a nitrogen atmosphere. The mixture was stirred an additional five minutes and methanol (20 mL) was added. A solution of *p*-toluenesulfonic acid monohydrate in methanol was added dropwise until a permanent orange-red colour was obtained. After 5 min, basic aqueous workup yielded the methoxy indolenine **4** (0.549 g, 3.14 mmol) identical in all respects with material prepared by the method of Gassman *et al.* (1).

*Preparation of Bromotetrahydrocarbazolenine (**18**)*

Tetrahydrocarbazole (0.530 g, 2.92 mmol) was dissolved in methylene chloride (20 mL) and triethylamine (1 mL) was added. One equivalent of bromine in methylene chloride (4 mL) was added dropwise at room temperature in a nitrogen atmosphere. The mixture was stirred a further 5 minutes and then partitioned between water (75 mL) and methylene chloride (50 mL). Removal of solvent from the dried organic phase *in vacuo* at room temperature left a pale yellow oil (0.60 g, 2.4 mmol) which was used without further purification for subsequent reactions; ir (neat): 1590; nmr: 0.9–3.3 (m, 8), 6.9–7.6 (m, 4).

*Preparation of Chlorotetrahydrocarbazolenine (**5**)*

Treatment of tetrahydrocarbazole (0.50 g, 2.69 mmol) with *tert*-butyl hypochlorite in the same manner as described in the preparation of **2** gave the chloroindolenine **5** as a pale yellow

solid (0.522 g, 2.54 mmol) which was used without further purification for subsequent reactions; ir (neat): 1595; uv (0.1% Et_3N/CH_2Cl_2): 264 (approx. 2250), 290 (sh); nmr: 1.19–2.95 (m, 8), 6.75–8.07 (m, 4).

Preparation of Methoxytetrahydrocarbazolenine

From the Chloroindolenine 5

Treatment of a methylene chloride solution of the chloroindolenine **5** with methanol as described for **2** gave the methoxyindolenine **6** as a homogeneous colourless oil (0.27 g, 1.34 mmol) identical in all respects with the methoxytetrahydrocarbazolenine prepared by the method of Owellen (2).

From the Bromoindolenine 18

Treatment of a methylene chloride solution of **18** (prepared from 0.53 g of tetrahydrocarbazole) with methanol as described for **17** gave the methoxyindolenine **6** as a thick oil (0.56 g).

From Tetrahydrocarbazole

Tetrahydrocarbazole (0.53 g, 3.1 mmol) was dissolved in methylene chloride (20 mL) containing triethylamine (1.0 mL). The solution was cooled in ice and one equivalent of bromine in methylene chloride (4 mL) was added dropwise over a period of 5 minutes. After the addition of anhydrous methanol (20 mL), a solution of *p*-toluenesulfonic acid monohydrate (0.780 g) in methanol (5 mL) was added dropwise. Basic aqueous workup as described previously yielded a pale yellow oil (0.57 g) consisting of **6** contaminated with a small amount of tetrahydrocarbazole. Column chromatography of the crude product on silica gel with elution by 10% v/v diethyl ether – petroleum ether (60–80) gave a colourless oil which solidified on standing (0.45 g). This material was identical with an authentic sample of **6** prepared by the method of Owellen (2).

Acknowledgements

We would like to thank the Natural Sciences and Engineering Research Council of Canada and the University of Waterloo for financial support of this work. A very timely gift of laboratory equipment from Merck–Frosst Laboratories, Kirkland, P.Q. is especially appreciated. We would also like to thank the Guelph–Waterloo Centre for Graduate Work in Chemistry for an Undergraduate Research Scholarship (to S.F.V.) and the Government of Ontario for an Experience '79 Grant (to E.A.G.).

1. P. G. Gassman, S. A. Campbell, and G. Mehta. Tetrahedron, **28**, 2749 (1972).
2. R. J. Owellen. J. Org. Chem. **39**, 69 (1974).
3. S. G. P. Plant and M. L. Tomlinson. J. Chem. Soc. 298 (1933).
4. J. B. Patrick and B. Witkop. J. Am. Chem. Soc. **72**, 633 (1950).
5. S. G. P. Plant and M. L. Tomlinson. J. Chem. Soc. 2127 (1950).
6. S. G. P. Plant and M. L. Tomlinson. J. Chem. Soc. 955 (1933).
7. E. Leete. J. Am. Chem. Soc. **81**, 6023 (1959).
8. R. M. Acheson. The chemistry of heterocyclic compounds. 3rd ed. John Wiley and Sons, New York. 1976. p. 97; J. C. Powers. *In* Indoles. Part 2. *Edited by* W. J. Houlihan. John Wiley and Sons, New York. 1972. p. 135.
9. G. I. Dmitrienko. Heterocycles, **12**, 1141 (1979).
10. (*a*) S. McLean, E. K. Strøm-Gundersen, K. S. Dichmann, J. K. Fawcett, and S. C. Nyburg. Tetrahedron Lett. 2645 (1970); (*b*) V. Dave and E. W. Warnhoff. Can. J. Chem. **49**, 1911 (1971); (*c*) G. Berti, A. Da Settimo, G. DiColo, and E. Nannipieri. J. Chem. Soc. C, 2703 (1969).
11. (*a*) S. McLean and G. I. Dmitrienko. Can. J. Chem. **49**, 3642 (1971); (*b*) V. Dave and E. W. Warnhoff. Can. J. Chem. **54**, 1015 (1976).
12. R. M. Silverstein, G. C. Bassler, and T. C. Morrill. Spectrometric identification of organic compounds. 3rd ed. John Wiley and Sons, New York. 1974. p. 215.
13. (*a*) T. Hino and M. Nakagawa. Heterocycles, **6**, 1680 (1977); (*b*) T. Hino, M. Endo, M. Tonozuka, Y. Hashimoto, and M. Nakagawa. Chem. Pharm. Bull. Jpn. **25**, 2350 (1977).
14. (*a*) W. O. Godtfredson and S. Vangedal. Acta Chem. Scand. **10**, 1414 (1956); (*b*) N. Finck and W. I. Taylor. J. Am. Chem. Soc. **84**, 3871 (1962); (*c*) G. E. Büchi and R. E. Manning. J. Am. Chem. Soc. **88**, 2532 (1966).

Can. J. Chem. Downloaded from www.nrcresearchpress.com by 210.87.254.40 on 09/05/12
For personal use only.

Synthesis, X-ray structure determination, and formation of 3,4,5-trichloroguaiacol occurring in kraft pulp spent bleach liquors

K. LINDSTRÖM AND F. ÖSTERBERG

Swedish Forest Products Research Laboratory, Box 5604, S-114 86 Stockholm, Sweden

Received October 2, 1979

K. LINDSTRÖM and F. ÖSTERBERG. Can. J. Chem. **58**, 815 (1980).

3,4,5-Trichloroguaiacol, which is formed during bleaching of chemical pulp and shown to bioaccumulate in fish, has been synthesized. The structure of the compound has been determined by means of X-ray analysis. The values of the ^{13}C nmr chemical shifts and melting point differ from those previously reported. A reaction mechanism is suggested for the formation of 3,4,5- and 4,5,6-trichloroguaiacol.

K. LINDSTRÖM et F. ÖSTERBERG. Can. J. Chem. **58**, 815 (1980).

On a synthétisé le trichloro-3,4,5 guaiacol, composé qui se forme lors du blanchissage des pulpes chimiques et qui s'accumule dans le poisson. On en a déterminé la structure au moyen de l'analyse par rayon-X. Les valeurs des déplacements chimiques par rmn du ^{13}C et du point de fusion diffèrent de celles rapportées antérieurement. On suggère un mécanisme réactionnel pour expliquer la formation des trichloro-3,4,5 et trichloro-4,5,6 guaiacol.

[Traduit par le journal]

Can. J. Chem. Downloaded from www.nrcresearchpress.com by 210.87.254.5 on 09/05/12
For personal use only.

Introduction

After chemical pulping residual lignin gives rise to a brownish colour. Bleaching with chlorine as an oxidizing agent depolymerizes the residual lignin and makes it more hydrophilic by the introduction of ionizable functional groups such as carboxylic and phenolic groups. Since native lignin consists of a network of guaiacylpropane units, aromatic electrophilic substitution can occur during bleaching. Hence, the effluent from an alkaline extraction stage contains salts of various chlorinated high and low molecular weight aromatic acids and phenolic compounds.

Introduction of modern analytical techniques such as gas chromatography – mass spectrometry in combination with computers (gc–ms–com) and an increase in the environmental impact of industrial wastes during the last decade have raised interest in looking for hazardous substances in the environment. In particular, chlorinated organics of low or relatively low polarity have a high affinity for fat in living organisms and may therefore remain for longer periods in the body. Thus, native lignin degradation products like chlorinated guaiacols could be expected at least in low concentrations in fatty tissues of aquatic organisms.

In 1973 Rogers and Keith (1, 2) identified trichloroguaiacol and tetrachloroguaiacol in mixed bleachery effluents. A comprehensive analytical study was carried out to establish the structure of the trichloroguaiacol isomer. Out of four possible trichlorinated isomers they established the isolated trichloroguaiacol to be a mixture of the 3,4,5- and the 4,5,6-trichloro compounds.

Investigations of the low molecular weight chlorophenolic compounds in the chlorination (C-stage) and caustic extraction stages (E-stage) was carried out by Lindström and Nordin (3) using glass open-tubular columns in gc–ms analysis. By laboratory bleaching trials they also determined various chlorinated phenols, guaiacols, and catechols in relation to pulp yield. Chlorocatechols were found mainly in the C-stage and chloroguaiacols in the E-stage (3).

In 1975 Leach and Thakore (4) claimed to have isolated and identified 3,4,5-trichloroguaiacol which was shown to be toxic to juvenile rainbow trout. This led us to carry out a comprehensive investigation of the bioaccumulation of chlorophenolic compounds originating in spent bleach liquors (5).

By chlorination of guaiacol in chloroform we found, in agreement with Rogers and Keith (2), that basically only 4,5,6-trichloroguaiacol was formed (cf. also ref. 6). The ^{13}C nmr chemical shifts of this substance did not, however, agree with those reported by Thakore and Oehlschlager (7) who declared that they had isolated and determined the structures of the 3,4,5- and the 4,5,6-isomers.

The occurrence of isomeric trichloroguaiacols in spent bleach liquors, together with their property of facile bioaccumulation in fish, led us to synthesize and to determine the structure of the most abundant isomer.

This paper describes the synthesis, the structural determination, and the probable mode of formation of 3,4,5-trichloroguaiacol occurring in spent bleach liquors.

0008-4042/80/080815-08$01.00/0

©1980 National Research Council of Canada/Conseil national de recherches du Canada

Can. J. Chem. Downloaded from www.nrcresearchpress.com by 210.87.254.5 on 09/05/12
For personal use only.

Results and Discussion

In a previous paper (3) the identity of three possible trichloroguaiacol isomers appearing in the ether extract of the kraft pulp mill caustic extraction stage was discussed. Gas chromatography (gc) on capillary columns gave poor resolution of two peaks of an ethylated phenolic fraction. Mass spectrometry (ms) of both the main peak and of a shoulder on that peak showed similar fragmentation patterns. However, the abundances of the typical isotopic chlorine clusters differed. The column used was a 25 m SE-30. By changing columns (25 m OV-17) all three peaks appeared well separated under isothermal conditions (200°C).

All four possible trichlorinated isomeric guaiacols are listed in Fig. 1. Figure 2 shows a limited reconstructed gas chromatogram (lmrgc, *m/e* 226; $M^+ - 28$) of an ethylated phenolic fraction from an ether extract of a caustic extraction stage. Since native lignin consists of mainly guaiacylpropane units where the propyl chain occupies the 4-position in the aromatic ring, this position must be chlorinated to yield free chloroguaiacols from lignin. Hence the number of isomers is reduced to three (**1**–**3**).

From a chemical point of view (see later) the 3,4,5- (**1**) and the 4,5,6-isomer (**2**) should be predominant in the liquor relative to the 3,4,6-isomer. Therefore peaks 3 and 4 (Fig. 2) were suspected to correspond to **1** and **2** or vice versa.

Chlorination of guaiacol in dichloromethane yields only one trichlorinated isomer corresponding to peak 4. Evaporation and recrystallization three times from petroleum ether yielded a compound with gc–ms data identical to that of peak 4 indicating the most likely isomer **2** (6).

Catechol was chosen instead of guaiacol as starting material for the synthesis of 3,4,5-trichloroguaiacol (1). The chlorination time required for obtaining an optimal yield of the

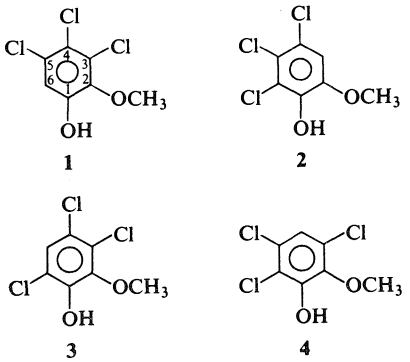


FIG. 1. Trichloroguaiacol isomers.

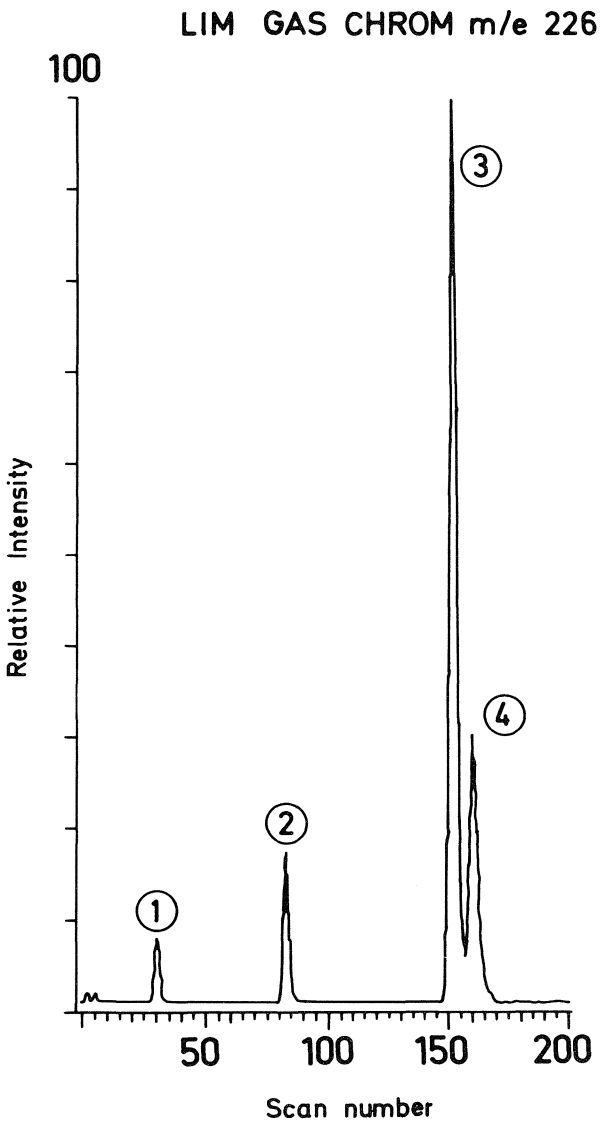


FIG. 2. A limited reconstructed gas chromatogram (lmrgc, *m/e* 226) of an ethylated ether extract of a caustic extraction stage phenolic fraction.

trichlorinated product is 10 min. After partial methylation (Fig. 3) the reaction mixture was separated by means of hplc as described under Experimental. As shown in Fig. 4 the two trichloroguaiacol isomers separated very well. The mass spectrum and retention time of peak 4′ indicated this substance to be identical to **2**. Peak 1′ was not fully resolved from peak 2′ (dichloroguaiacol isomer). After preparative chromatographic separation, the trichloroguaiacol isomer was easily removed from the dichloro impurity by repeated crystallization from petroleum ether (3 times).

To get complete information of the structure the

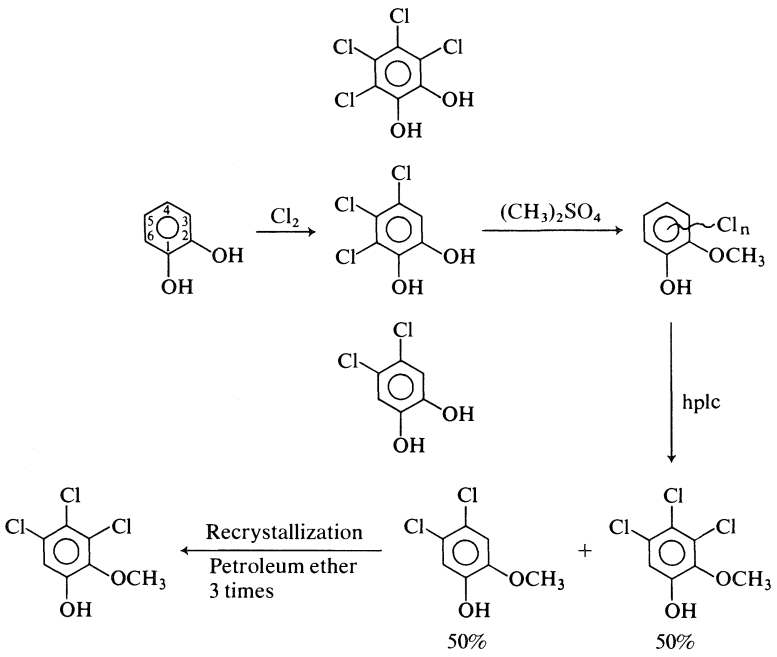


FIG. 3. Synthesis and purification of 3,4,5-trichloroguaiacol.

purified isomer was taken to X-ray analysis. As can be seen from Fig. 9 (Appendix) the substance studied is the 3,4,5-trichloroguaiacol isomer (1).

Upon methylation of the substances of peaks 1′ and 4′ (**1** and **2** in Fig. 1) capillary column gc gave only one distinct peak corresponding to 3,4,5-trichloroveratrol (Fig. 5) available at our laboratory. This indicates that peak 4 arises from the 4,5,6-trichloroguaiacol isomer (**2**).

Since the structure of **1**, and thereby indirectly that of **2**, was confirmed by means of X-ray analysis, values of the ^{13}C nmr chemical shifts and tentative assignments can now be presented for these two compounds as well as the corresponding melting points. The chemical shifts and the melting point of **1** do not agree with the values reported by Thakore and Oehlschlager (7). Whereas they reported a melting point of 127–128°C for **1**, we found 81–83°C; they found 105–107°C for **2** which is more in agreement with ours (112–114°C).

The ^{13}C nmr chemical shifts and tentative assignments are listed in Table 1. Due to deshielding by oxygen substituents $^{13}C1$ and $^{13}C2$ are shifted downfield relative to chlorine-bonded ^{13}C carbons. The reverse is true for hydrogen-bonded ^{13}C carbons which are relatively shielded. It seems likely that the relative positions of the signals of $^{13}C1$ and $^{13}C2$ for **1** are reversed to those of **2**. Probably a non-chlorine-bonded carbon is deshielded by an adjacent chlorine-bonded carbon so that $^{13}C2$ of compound **1** shifts to lower field compared to that of $^{13}C2$ of compound **2**. It is, however, likely that the differences in the shifts of $^{13}C4$ and $^{13}C5$ in isomers **1** and **2** should be very small.

Only the value of the ^{13}C chemical shift of C6 (isomer **1**, 115.5 ppm) reported by Thakore and Oehlschlager (7) is in agreement with those found by us. The differences in ^{13}C chemical shifts are up to 10 ppm. For instance, the value of $^{13}C3$ (isomer **1**) is reported to be 125.5 ppm compared to 131.0 ppm found by us. Similarly they reported a ^{13}C chemical shift of $^{13}C3$ (isomer **2**) at 120.8 ppm whereas we found a value of 110.8. The deviations of their values from ours of the ^{13}C chemical shifts and melting point are of such a magnitude that the compounds could not possibly be identical.

Usually isomer **1** predominates in kraft pulp mill spent bleach liquors (E-stage) yet isomer **2** is formed almost exclusively from chlorination of guaiacol. In an attempt to explain this phenomenon a dimeric substance (1-(4-acetoxy-3-*tert*-butyl-5-methoxyphenyl)-ethylene glycol-2-*O*-guaiacyl ether) was chlorinated in ethanol–water 1:1. Figure 6 shows a poor yield of about equal amounts of **1** and **2**. This supports the theory that, since the guaiacyl unit prior to and during chlorination is a 1,2-diether, chlorination proceeds initially at about equal rates in the 3- and 6-positions. Due to formation of hydrochloric acid pH decreases giving rise to a vinylic ether in the 1-position which is acid

Can. J. Chem. Downloaded from www.nrcresearchpress.com by 210.87.254.5 on 09/05/12
For personal use only.

Can. J. Chem. Downloaded from www.nrcresearchpress.com by 210.87.254.5 on 09/05/12
For personal use only.

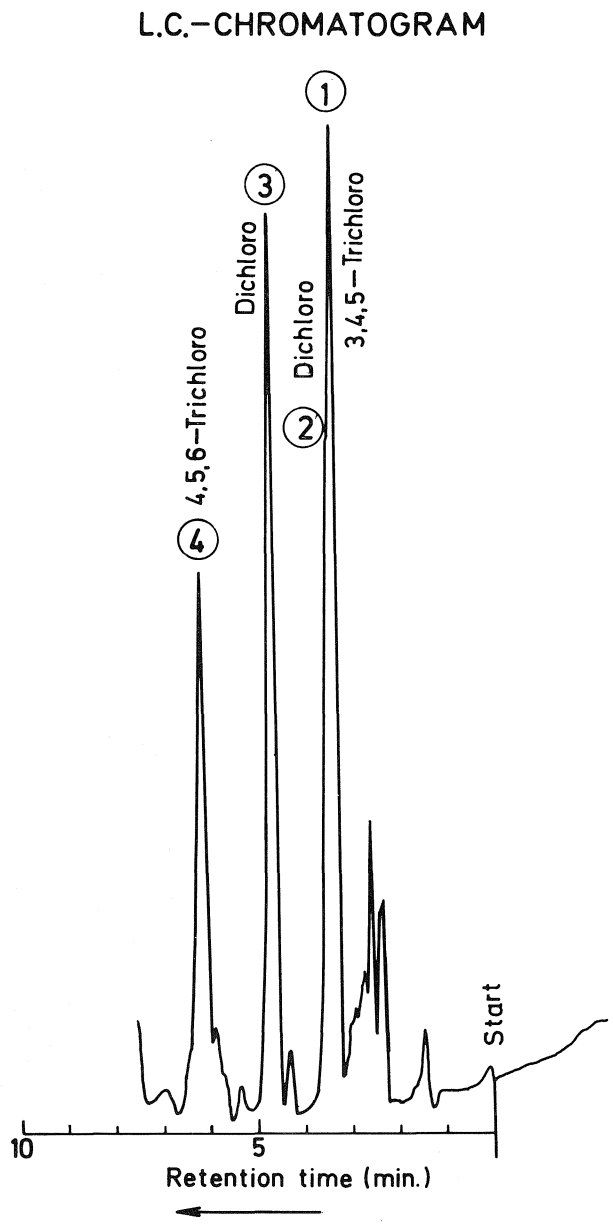


FIG. 4. The hplc separation of the reaction mixture.

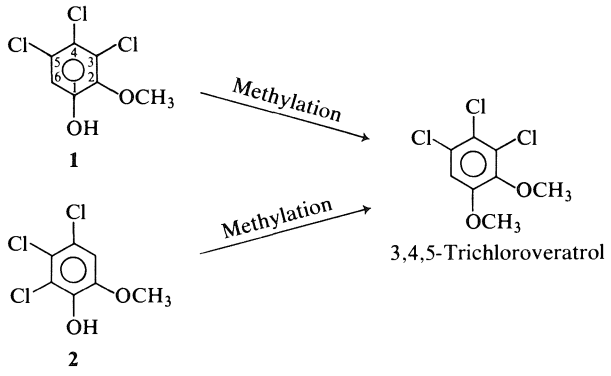


FIG. 5. Methylation of 3,4,5- and 4,5,6-trichloroguaiacol.

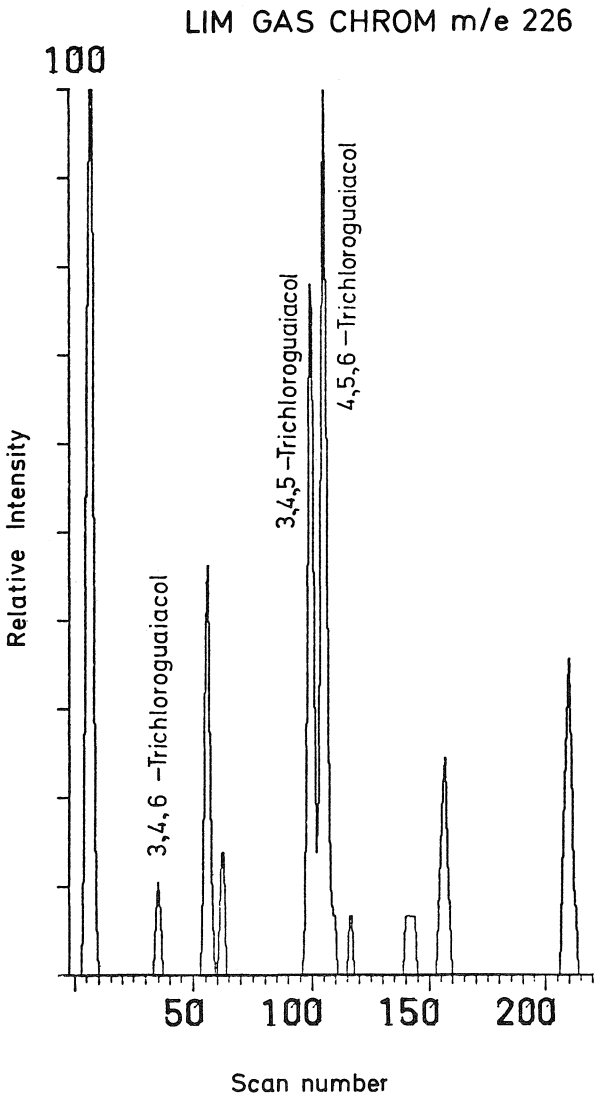


FIG. 6. The lmrgc (*m/e* 226) of an ether extract of a reaction mixture obtained from chlorination of 1-(4-acetoxy-3-*tert*-butyl-5-methoxyphenyl)-ethylene glycol-2-*O*-guaiacyl ether.

labile and decomposes mainly to **1** and **2** (Fig. 7). In native lignin, however, steric hindrance might occur in the 6-position (Fig. 8) which should favour formation of **1**.

If the pulp is not well washed, so that residual free guaiacol from the cooking stage remains in the pulp, then the 4,5,6-isomer (**2**) should predominate. It seems that bleached sulphite pulp yields more **2** but the reverse is true for bleached kraft pulp. Due to cooking to lower κ number more free guaiacol is formed during sulphite pulping and therefore formation of **2** exceeds that of **1**. During kraft pulping

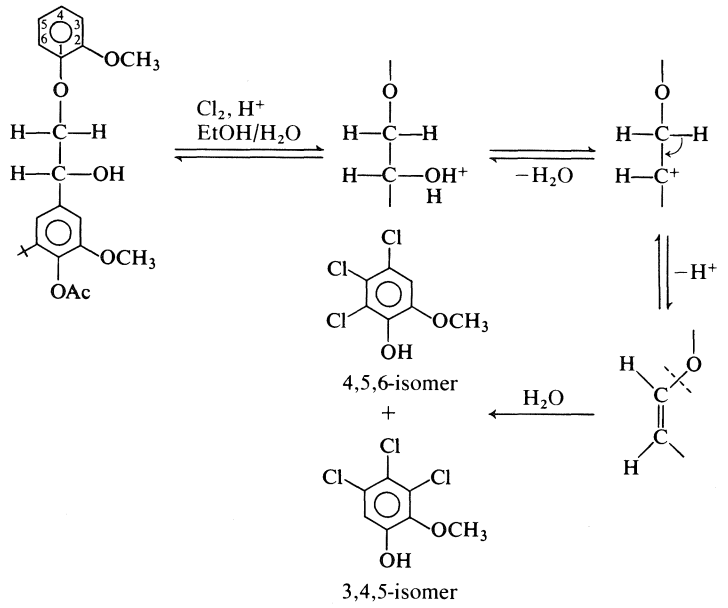


FIG. 7. Suggested mechanism of formation of trichloroguaiacol isomers.

TABLE 1. ^{13}C nmr chemical shifts of 3,4,5- and 4,5,6-trichloroguaiacol

Isomer	C1	C2	C3	C4	C5	C6	C(CH_3)
3,4,5	143.5	148.4	131.0	129.3	128.8	115.6	61.26
4,5,6	145.8	142.3	110.8	123.8	123.8	119.6	56.69

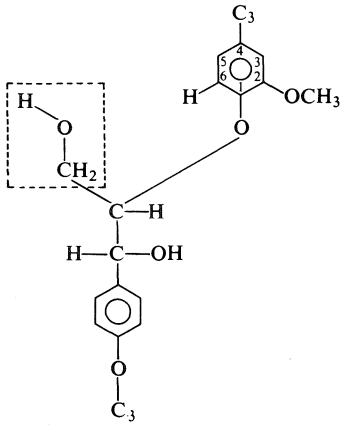


FIG. 8. Steric hindrance in the 6-position relative to the 3-position in lignin.

the higher κ number means that the macromolecular residual lignin is more effectively sterically hindered in the 6-position.

Experimental

Nuclear magnetic resonance spectra, ^1H and ^{13}C, were determined in deuterochloroform using a Varian CFT-20 60 MHz instrument. Tetramethylsilane was added to obtain a reference line. The gc–ms–com analysis was carried out using a 0.25 mm × 25 m OV-17 glass open-tubular column in a Finnigan gas chromatograph (9500) – mass spectrometer (3200F) with an on-line computer (6000). Helium carrier gas flow rate was 0.5 mL/min, split ratio 1:30, column temperature 200°C, injector temperature 250°C, and transfer line 250°C. Mass spectra were recorded every 2 s with a speed of 200 amu/s up to 400 amu at an electron energy of 70 eV.

The hplc separation, analytical scale, was carried out on a Waters high-performance liquid chromatograph equipped with double pumps and a solvent programmer. Chromatographic conditions: column, 3.2 × 250 mm Lichrosorb, 5 μm; flow rate, 2 mL/min; mobile phase (isocratic elution), petroleum ether – ethyl acetate – acetic acid, 175:25:1, all solvents freshly distilled; detector, 8 μL uv cell, measuring the absorption at 250 nm.

Preparative separation was carried out on the same instrument. Chromatographic conditions: column, Silicagel −60 (Merck) size C; flow rate, 9 mL/min; mobile phase, petroleum ether – ethyl acetate, initially 95:5 with a linear gradient elution to a final composition of 80:20 during 7.5 h; detector Uvicord II (LKB) with 100 μL cell measuring the absorption at 280 nm; fractionation, LKB Ultrorac 7000.

Synthesis and Purification

Six grams of catechol was dissolved in 100 mL of dichloromethane in a 250 mL three-neck round bottom flask equipped with a condenser and an inlet tube. Gaseous chlorine was bubbled violently through the solution for 10 min, followed by washing with 2 portions of 50 mL of slightly acidified water. Organic acids were eliminated by extraction with 2 × 50 mL aqueous sodium bicarbonate (0.1 mol per L). The reaction mixture was evaporated under reduced pressure and the residue redissolved in 100 mL ethanol. A small portion (0.1 mL) was taken out for gas chromatographic analysis. A 20% (1.2 g) recovery (estimated by gc) of 3,4,5-trichlorocatechol was obtained.

One equivalent, corresponding to 1 equiv. of estimated (gc) chlorocatechols, of an aqueous solution of sodium hydroxide (1 mol per L) was mixed with the ethanol solution in a 250 mL three-neck round bottom flask equipped with a dropping funnel, a condenser, and a magnetic stirrer; 0.5 equiv. of dimethylsulphate was dissolved in 10 mL ethanol. The solution was added

Can. J. Chem. Downloaded from www.nrcresearchpress.com by 210.87.254.5 on 09/05/12
For personal use only.

Can. J. Chem. Downloaded from www.nrcresearchpress.com by 210.87.254.5 on 09/05/12
For personal use only.

into the flask during 0.5 h. The reaction mixture was refluxed (1 h), cooled, and made alkaline (pH 11). Minor amounts of veratroles were extracted by 2 × 100 mL diethyl ether and discarded. After acidification with hydrochloric acid to pH 2 the ethanol solution was extracted with 2 × 100 mL diethyl ether. The ether extract was dried over anhydrous sodium sulphate, filtered, and evaporated. The residue was redissolved in ethyl acetate (3 mL).

One half of the ethyl acetate solution was injected onto the preparative column. A fraction starting after 170 min was collected during 25 min and the solvent evaporated under reduced pressure. The yield was 0.3 g (10%). Recrystallization was carried out three times from petroleum ether.

3,4,5-Trichloroguaiacol

The compound, white crystals, had mp 81–83°C; ^{1}H nmr δ: 7.05 (1 H, singlet, aromatic), 5.78 (1 H, singlet, OH), and 3.92 (3 H, singlet, OCH_3); ms *m/e* (% relative intensity): 230 (14) $M^+ + 4$, 228 (46) $M^+ + 2$, 226 (50) M^+, 215 (29) $M^+ - 11$, 213 (97) $M^+ - 13$, 211 (100) $M^+ - 15$.

Acknowledgements

We thank Dr Georg Johansson and Professor Ingemar Grenthe for the X-ray analysis. Professor Joseph Gierer is also acknowledged for valuable discussions and advice.

The Syntex $P2_1$ diffractometer is a gift from the Knut and Alice Wallenberg Foundation to the Department of Chemistry at the Royal Institute of Technology, Stockholm, Sweden.

1. I. H. Rogers. Pulp Paper Mag. Can. **74**, 111 (1973).
2. I. H. Rogers and L. H. Keith. *In* Identification and analysis of organic pollutants in water. Identification of two chlorinated guaiacols in kraft bleaching wastewaters. *Edited by* L. H. Keith. Ann Arbor Science, Ann Arbor, MI. 1976.
3. K. Lindström and J. Nordin. J. Chromatogr. **128**, 13 (1976).
4. J. M. Leach and A. N. Thakore. J. Fish. Res. Board Can. **32**, 1249 (1975).
5. L. Landner, K. Lindström, M. Karlsson, J. Nordin, and L. Sörensen. Bull. Environ. Contam. Toxicol. **18**, 663 (1977).
6. R. Fort, J. Sleziona, and L. Denivelle. Bull. Soc. Chim. Fr. 810 (1955).
7. A. N. Thakore and A. C. Oehlschlager. Can. J. Chem. **55**, 3298 (1977).

Appendix

X-ray Structure Determination

Three-dimensional X-ray intensity data were collected at 25 ± 2°C by using a Syntex $P2_1$ four-circle diffractometer. The compound has a fairly large vapour pressure and had to be mounted in a capillary in order to be preserved during the data collection. The space group was determined by axial photographs and the monoclinic symmetry was checked by measuring reflections $h\,k\,l$ and $h\,\bar{k}\,l$. The unit cell parameters were refined by least-squares methods using reflections obtained with the diffractometer. Unit cell dimensions and details of the data collection are given in Table 2.

TABLE 2. Crystal data, details of data collection and refinement

Mol formula: $C_7H_5O_2Cl_3$

Space group: $P2_1/c$ (monoclinic)

Unit cell parameters: a = 14.50(1) Å; b = 4.076(2) Å; c = 18.38 (1) Å; β = 123.46(7)°

Crystal habit and size: needle 0.2 × 0.05 × 0.01 mm^3

Radiation used: Graphite monochromatized MoKα λ = 0.71069 Å

V(Å^3); Z; D_c(g/cm^3); μ(cm^{-1}): 905(1); 4; 1.77; 9.7

Scan technique and part of (θ − 2θ) scan; quadrant reflection sphere investigated: with 2θ < 35°

Max. and min. scan speed: 29.3 and 2.0 deg/min

Scan interval: 1.2 deg

Total number of reflections; total number of independent reflections; reflections with $I < 1.96\sigma(I)$: 1179; 560; 403

Check reflections measured: Four after every 50th reflection, constant within ±3%

Data reduction and refinement

Type of absorption correction: None

Scattering factors: For neutral atoms, Cl with anomalous dispersion corrections

Model, R^a ($R_w{}^b$), S^c: All atoms isotropic 0.088, —, 2.45 Non-hydrogen anisotropic, hydrogen atoms isotropic 0.052, 0.045, 1.34

[a]Function minimized: $\sum_i w_i(|F_o| - |F_c|)^2$ where

$w_i = [\sigma^2_{count} + 0.02|F_o|^2]^{-1}$

[b]Reflections with $I \leq 1.96\sigma(I)$ ($|F_o| < 3.92\sigma\,|F_o|$) are given zero weight.

[c]S is the standard deviation of an observation of unit weight.

TABLE 3. Final fractional atomic positional parameters with estimated standard deviations within parentheses. The hydrogen atom positional coordinates are taken from the difference electron density maps

Atom	$x \times 10^4$	$y \times 10^4$	$z \times 10^4$
Cl1	6603(3)	1613(8)	1088(2)
Cl2	709(3)	3095(8)	4618(2)
Cl3	8951(3)	4374(8)	1723(2)
O1	4793(7)	3696(20)	1904(5)
O2	2776(7)	1199(20)	1379(7)
C1	3905(14)	4206(36)	1064(11)
C2	2869(16)	3015(33)	800(10)
C3	1972(11)	1495(30)	4933(12)
C4	2129(11)	−135(36)	4342(8)
C5	6826(16)	3612(27)	365(10)
C6	5938(13)	889(37)	4512(13)
C7	2396(22)	2788(63)	1858(15)
H(C6)	5150	1839	4400
H1(C7)	1700	3920	1440
H2(C7)	2990	4728	2020
H3(C7)	1820	290	1840
H(O1)	4890	2530	2520

To check the stability of the crystal and the diffractometer, four check reflections were measured at regular intervals during the data collection, see Table 2. The methods for background measurement and intensity calculation have been described

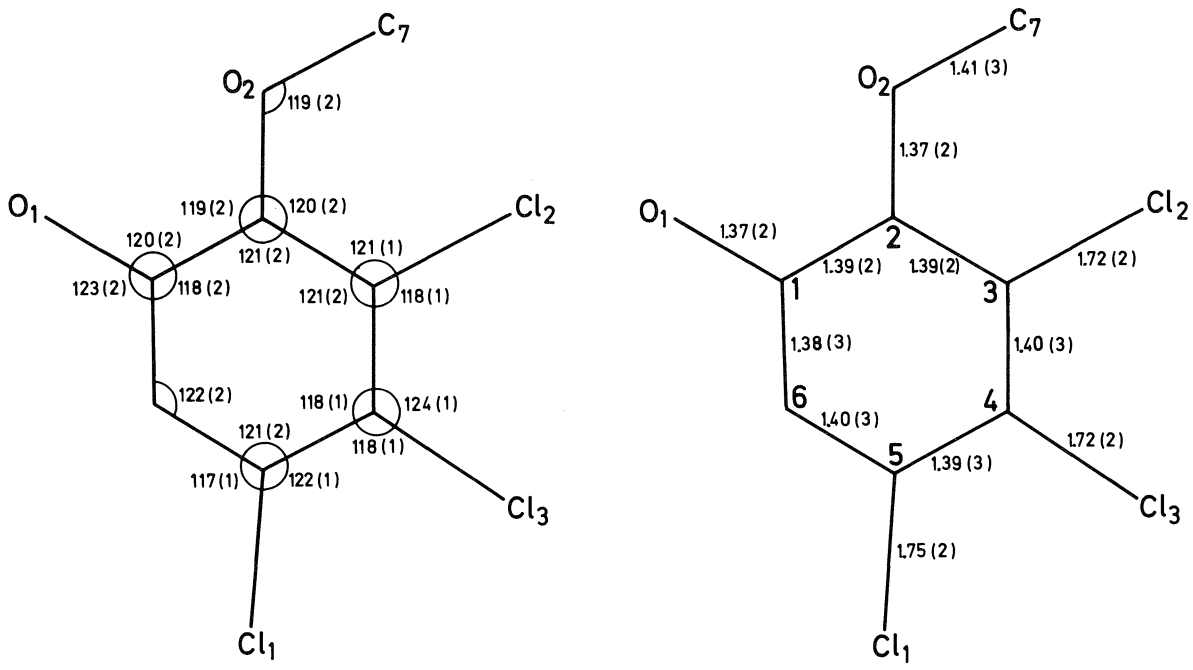


FIG. 9. Interatomic bond distances and angles within the molecule. Standard deviations are given within parentheses.

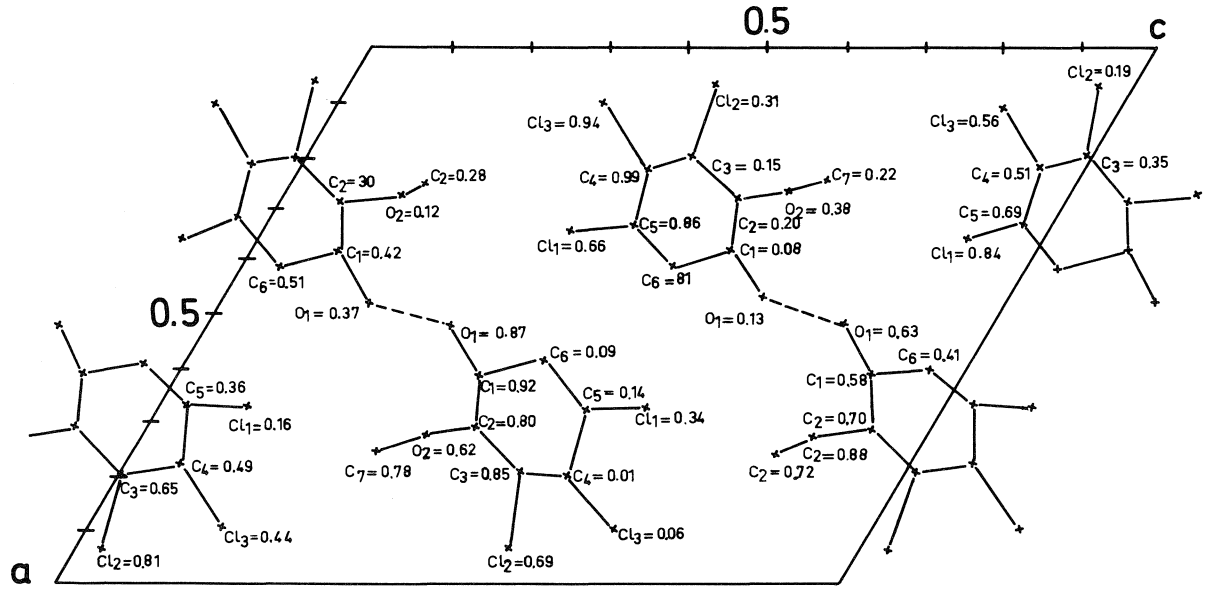


FIG. 10. Projection of the unit cell of the 3,4,5-structure. Hydrogen atoms have been excluded for clarity. The dashed lines indicate the location of an intermolecular hydrogen bond; $a = 14.50$; $b = 4.076$; $c = 18.38$; $\beta = 123.46°$; nr 14 = $P2_1/c$.

according to the procedure of the Syntex $P2_1$. The crystal used was small and had $\mu = 9.6$ cm^{-1}, hence no absorption correction was made on the intensity data. Only very thin crystals could be prepared so the reflections were weak and had to be measured over a long time for satisfactory counting statistics. The intensity decreases even further with increasing θ; because of this only the range $2\theta < 35°$ could be investigated.

Structure Determination and Refinement

A set of solutions was generated by the program MULTAN, using 95 reflections with E-values larger than 1.4.

Can. J. Chem. Downloaded from www.nrcresearchpress.com by 210.87.254.5 on 09/05/12
For personal use only.

All non-hydrogen atoms except the methoxy carbon C7 were located in the *E*-map. The remaining carbon and hydrogen atoms were located in different Fourier maps obtained after isotropic refinement of the atom parameters found in the *E*-map. In the final model, a total of 109 parameters (one scale factor, 36 positional parameters, and 72 anisotropic thermal parameters on all non-hydrogen atoms), were refined to the following *R*-values: $R = 0.052$, $R_w = 0.045$. If reflections with $I \leq 1.96\sigma(I)$ are included, the residuals are: $R = 0.077$, $R_w = 0.049$. The parameters are given in Table 3. Because of the small number of reflections recorded, no attempt was made to refine the positions and thermal parameters of the hydrogen atoms. The positional parameters for these atoms taken from the electron density maps are given in Table 3. These parameters and an estimated isotropic thermal parameter, $B = 5.0$ for all hydrogen atoms, were included as fixed parameters in the final least-squares refinement.

Details of the refinement models are given in Table 2. Tables of $|F_o|$ and $|F_c|$ values may be obtained from the authors.

Distances and angles, shown in Fig. 9, are in good agreement with the expected values. The intermolecular hydrogen bond is 2.77 Å and the shortest intermolecular Cl–Cl distance 3.43 Å.

Structure Description

The X-ray study shows conclusively that the compound studied is the 3,4,5-isomer. The structure is built of planar molecules stacked approximately parallel to the *ac*-plane (see Fig. 10). The molecules are held together by an intermolecular hydrogen bond between H(O1) and a symmetry related O1 in an adjacent molecule.

Can. J. Chem. Downloaded from www.nrcresearchpress.com by 210.87.254.5 on 09/05/12
For personal use only.

The electronic spectra of coordinated nitrite ion: correlation between spectra and structure

IAN M. WALKER[1] AND A. B. P. LEVER
Department of Chemistry, York University, Downsview, Ont., Canada M3J 1P3
AND
PAUL J. MCCARTHY
Department of Chemistry, Canisius College, Buffalo, NY 14208, U.S.A.

Received November 21, 1979

IAN M. WALKER, A. B. P. LEVER, and PAUL J. MCCARTHY. Can. J. Chem. **58**, 823 (1980).

The characteristic electronic spectrum of the nitrite ion survives when the ion is bonded to metal ions through the oxygen atoms. The vibrational fine structure associated with the $n \rightarrow \pi^*$ electronic transition in the near uv region has been examined at 10 K in single crystals of $K_3[Hg(O_2N)_4](NO_3)$ and in a series of nickel complexes with *N*-alkylated ethylenediamines. When either non-coordinated, monodentate oxygen coordinating, or bidentate chelating through oxygen, nitrite ion in the crystals shows vibronic features which depend on nitrite environment. It is suggested that the electronic spectra of the nitrite ion may constitute a useful tool in structure elucidation.

IAN M. WALKER, A. B. P. LEVER et PAUL J. MCCARTHY. Can. J. Chem. **58**, 823 (1980).

Le spectre électronique caractéristique de l'ion nitrite est présent même quand il est lié aux ions métalliques par l'intermédiaire des atomes d'oxygène. On a examiné la structure fine vibrationnelle, associée à la transition électronique $n \rightarrow \pi^*$ dans la région du proche uv à 10 K, d'un monocristal de $K_3[Hg(O_2N)_4](NO_3)$ et dans une série de composés du nickel complexé avec des éthylènediamines *N*-alkylés. Quelque soit leur état de coordination, soit non-coordonné, coordonné par l'intermédiaire de l'oxygène, ou chélaté bidentate via l'oxygène, l'ion nitrite dans des cristaux présente des caractéristiques vibrationnelles qui dépendent de l'environnement du nitrite. On suggère que les spectres électroniques de l'ion nitrite peuvent constituer un outil pratique pour la détermination de structure.

[Traduit par le journal]

Introduction

In several recent articles we have been concerned with details of crystal field splitting in complexes of nickel(II) (1, 2) and cobalt(II) (3) having lower than cubic symmetry. More recently we have studied some nickel ethylenediamine complexes having a *cis*-NiN_4O_2 chromophore in which the nitrite ligand coordinates through oxygen, and in which we encountered several spectral features which are characteristic of internal transitions of the nitrite ion. At the low temperatures used (10 K) many vibronic details of the electronic bands were found to be highly resolved. The nitrite ion in crystals and solutions of alkali nitrites possesses three characteristic spin-allowed absorption bands: two relatively weak transitions at 27.8 and 35.7 kK, which can be assigned as $n \rightarrow \pi^*$, and a strong $\pi \rightarrow \pi^*$ transition at 47.6 kK (4). The $n \rightarrow \pi^*$ transition of lowest energy shows considerable vibrational fine structure.

Vibronic details of coordinated nitrite ion in transition metal complexes have received little attention in the past. In 1967, Fee, Garner, and Harrowfield (5) noted that chromium(III) nitrite complexes of amines always show a structured absorption in the near uv with maximum absorption at ~350 nm (28.6 kK). This band is also found in the spectra of organic nitrites (RONO) and has been assigned to the $n \rightarrow \pi^*$ transition on the nitrite group in both cases (5). Fee *et al.* (5) believed that the n-level is located primarily on the nitrogen. The vibrational structure arises from progressions in the totally symmetric stretching and bending vibrations of the nitrito-group; this gives the absorption feature a highly characteristic appearance. The suggestion was made that the appearance of a structured uv band be taken as conclusive evidence of coordination through oxygen (O-coordination), and the authors assigned the structure of the chromium nitrito-complexes on this basis (5). On the other hand, the structured $n \rightarrow \pi^*$ transition is not generally observed in nitro compounds. This has been ascribed to the involvement of the lone pair on nitrogen in bonding to the metal (5). The near uv spectrum in nitro complexes is dominated by ligand-to-metal charge transfer processes (6–8).

In this article we present the spectra of nitrite ion in single crystals of complexes exhibiting several types of nitrite coordination, along with an account of what we believe to be the causes of the interesting variations in spectral detail encountered. The structural information available on these complexes is illustrated in idealized form in Table 1.

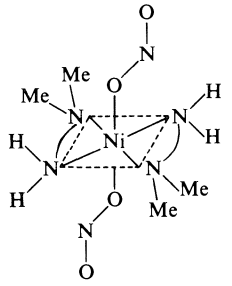
A remarkable additional feature of these spectra is the appearance of an additional absorption band around 22 kK in a number of the complexes

[1]To whom all correspondence should be addressed.

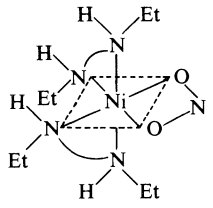
0008-4042/80/080823-10$01.00/0
©1980 National Research Council of Canada/Conseil national de recherches du Canada

Can. J. Chem. Downloaded from www.nrcresearchpress.com by 210.87.254.40 on 09/05/12
For personal use only.

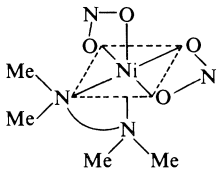
TABLE 1. Idealised[a] structures of nitrito complexes[b]



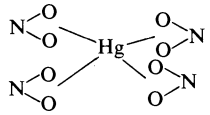
I[c]
$[Ni(a\text{-}Me_2en)_2(ONO)_2]$



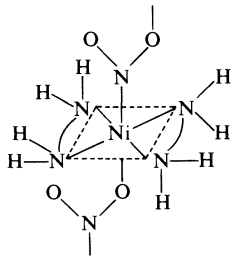
II[d]
$[Ni(s\text{-}Et_2en)_2(O_2N)]X$
$X = NO_2, BF_4$



III[e]
$[Ni(TMen)(O_2N)_2]$



IV[f]
$K_3[Hg(O_2N)_4]NO_3$



V[g]
$[Ni(en)_2(NO_2)]ClO_4$

[a] O—M—O angles of chelating nitrite are less than 90° (~60°) in all cases.
[b] (O_2N) indicates chelating nitrito-, (ONO) indicates unidentate nitrito-, and (NO_2) indicates nitro-coordination.
[c] *a*-Me_2en is *N,N*-dimethylethylenediamine. Structural data from ref. 15.
[d] *s*-Et_2en is *N,N'*-diethylethylenediamine. Structural data for NO_2^- salt from ref. 16 and for BF_4^- salt from ref. 17.
[e] TMen is *N,N,N',N'*-tetramethylethylenediamine. Structural data from ref. 18.
[f] Structural data from refs. 12 and 19.
[g] en is ethylenediamine. Structural data from ref. 20.

studied. This band also shows vibrational fine structure. We will argue that it can reasonably be attributed to a spin-forbidden n → π* transition of the coordinated nitrite ion gaining significant additional intensity under certain circumstances.

Experimental

Substituted ethylenediamines were obtained from Koch-Light (UK) or Aldrich (USA) and distilled before use. *meso*-Stilbenediamine was prepared and purified according to Irving and Parkins (9), and converted into the bis nitrito complex according to Goodgame and Hitchman (10). Single crystals of this compound were grown from a supersaturated solution of the complex in 50% v/v aqueous acetonitrile by seeding. Nitrito complexes of the substituted ethylenediamines were prepared by literature methods (10, 11). Single crystals were grown by slow evaporation of anhydrous methanol, ethanol, or acetonitrile solutions. $K_3[Hg(O_2N)_4]NO_3$ was prepared according to the method of Power *et al.* (12); single crystals were grown from an aqueous solution. Nickel analyses were performed by EDTA back titration using $ZnSO_4$ as titrant and eriochrome black T as indicator. (In the following, *a*-Et_2en is *N,N*-diethylethylenediamine, *m*-stien is *meso*-stilbenediamine; for the other abbreviations see Table 1.) *Anal.*: complex, % Ni calcd., % Ni found: $[Ni(a\text{-}Me_2en)_2(ONO)_2]$, 16.53, 16.74; $[Ni(a\text{-}Et_2en)_2(ONO)_2]$, 15.32, 15.42; $[Ni(s\text{-}Et_2en)_2(O_2N)]NO_2$, 15.32, 15.02; $[Ni(s\text{-}Et_2en)_2(O_2N)]BF_4$, 13.85, 13.87; $[Ni(TMen)(O_2N)_2]$, 21.99, 21.50; $[Ni(m\text{-stien})_2(O_2N)]NO_2$, 10.20, 10.02; $[Ni(en)_2(NO_2)]ClO_4$, 18.10, 17.85. Polarized crystal spectra were obtained on a Cary-14 spectrophotometer using a Displex cryogenic refrigerator and the procedure described earlier (1).

Results

We discuss first the uv–visible spectrum of sodium nitrite, after which we will examine data for some transition metal complexes. The low-energy edge of the n → π* ($^1A_1 \rightarrow {}^1B_2$) transition in alkali nitrites is indicative of what may be obtained from the uv spectrum under optimum conditions of resolution (13). In crystals of sodium nitrite at 4 K, progressions in 632 cm^{-1}, corresponding to the bending mode in the $^1B_2$ excited state, and 1018 cm^{-1}, corresponding to the symmetric stretch, are observed (13). It should be noted that these values are considerably reduced from those associated with the ground state vibrational frequencies (ν_{bend} = 829 cm^{-1}, $\nu_{stretch}$ = 1325 cm^{-1}). This appears to be due to the presence of an electron in the antibonding π* orbital in the excited state. These progressions are accompanied by lattice modes of 65, 110, 155, 180, and 218 cm^{-1}; this results in a very complex spectrum. The origin (0–0) line is extremely weak, but nonetheless de-

Can. J. Chem. Downloaded from www.nrcresearchpress.com by 210.87.254.40 on 09/05/12
For personal use only.

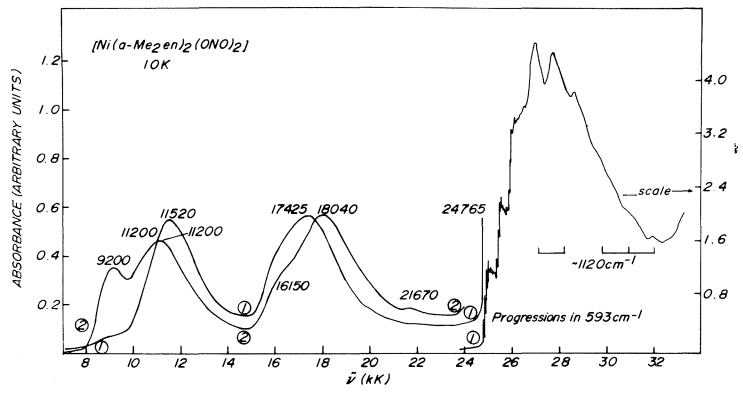


FIG. 1. Polarized crystal spectra at 10 K of $[Ni(a\text{-}Me_2en)_2(ONO)_2]$. In the near uv region the band is strongly polarized. Only the weaker polarization is shown, since the other appears to be almost 10 times as strong.

tectable at 25977 cm^{-1}. The band is polarized perpendicular to the plane of the anion, as expected from the symmetries of the states. The nitrite ions are well separated in the crystal, so no effects due to interionic coupling or exciton formation could be detected (13).

The spin-forbidden $n \rightarrow \pi^*$ ($^1A_1 \rightarrow {}^3B_2$) transition in $NaNO_2$ was identified in the visible region by Allen and Dixon (14). At 20 K the origin occurs at 18959 cm^{-1} and vibrational progressions in 644 and 1112 cm^{-1} are in evidence. These values are somewhat larger than those associated with the spin-allowed transition.

[Ni(a-$Me_2en)_2(ONO)_2$]

Crystals of this complex belong to space group $P2_1/c$ (15). The chromophore contains two monodentate nitrito groups *trans* to one another and possesses a center of symmetry. The polarized spectra of two crystals obtained along orthogonal extinction axes were recorded; the spectra at 10 K are shown in Fig. 1. As in all the nickel complexes, the vibrational structure above 24 kK is superimposed on a strongly polarized absorption due to the third ligand field transition of nickel ($^3A_2 \rightarrow {}^3T_1$(P) in O_h symmetry). The fine structure begins with a sharp spike at 24.77 kK; this can reasonably be assigned to the electronic origin (0–0) of the $n \rightarrow \pi^*$ transition. The position of the origin is about 1 kK lower in energy than the origin in $NaNO_2$, an effect which is undoubtedly due to coordination but is otherwise difficult to explain.

In polarization *1* at least 45 bands can be seen between 24.77 and 33 kK. The prominent vibration is the upper state ONO bend (593 ± 5 cm^{-1}); three members of this progression are visible. Above 27 kK one, or perhaps two, short progressions in the N—O stretch (1120 ± 20 cm^{-1}) are visible. Lattice modes are strongly in evidence here. There are 19 lines immediately following the origin line; these seem to be progressions in 47 and 71 cm^{-1}. A list of the sharp lines is given in the Appendix. The ligand field bands will be analyzed in a subsequent article (28).

[Ni(s-$Et_2en)_2(O_2N)$]NO_2

This compound belongs to space group $P\bar{1}$, and the *cis*-NiN_4O_2 chromophore contains a chelating O-bonded nitrito group (16). The X-ray structure shows that all four of the ligated nitrogens are hydrogen-bonded to the anionic nitrites in the lattice. In Fig. 2 *a* and *b* the whole spectrum is shown, but in this paper we discuss only the part above 20 kK; the rest will be treated elsewhere (29). The vibrational features are quite different from those of the preceding compound. Lattice modes are absent, but there appears to be more than one progression in the upper state bending mode. The three "origins" are at 25.23, 25.34, and 26.20 kK and the resulting progressions can be seen in both polarizations. The progression beginning at 26.20 kK may represent a combination ($\nu_{stretch} + n\nu_{bend}$) based on the origin at 25.23 kK. A combination progression has been observed with frequencies ($\nu_{bend} + n\nu_{stretch}$) in $NaNO_2$ (13). A short progression starting at 29.33 kK is in the N—O stretching mode (1015 cm^{-1}).

Between 20 and 25 kK lies a band comparable in strength to the crystal field bands. It contains poorly resolved structure in about 690 ± 80 cm^{-1}. This frequency seems to represent the upper state NO_2 bending mode. A comparable band is *not* found in the spectra of $[Ni(a\text{-}Me_2en)_2(ONO)_2]$. This band cannot be accounted for by any reasonable set of crystal field parameters. The vibrational feature of lowest energy is seen at about 20.2 kK, close to its position in $NaNO_2$ (14). It is not found in the corresponding isostructural nitrate salt (29) and

Can. J. Chem. Downloaded from www.nrcresearchpress.com by 210.87.254.40 on 09/05/12
For personal use only.

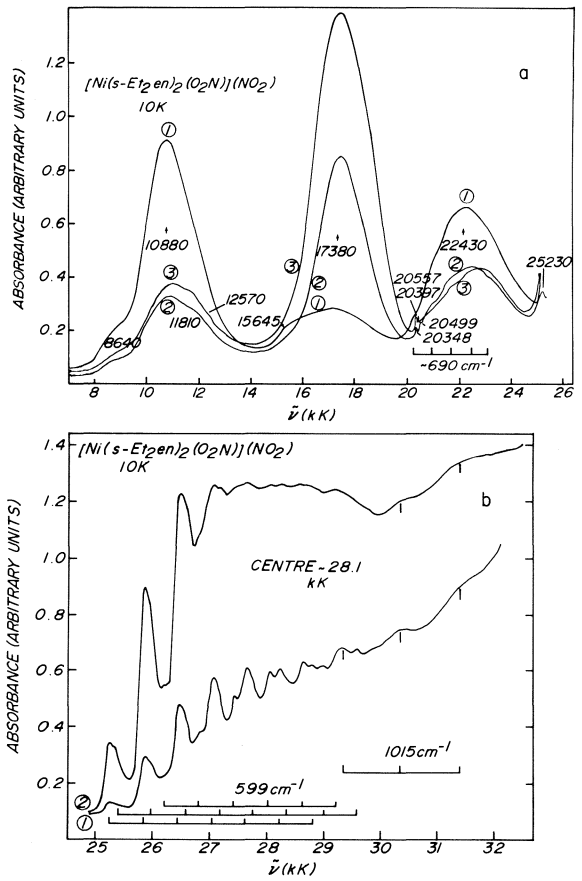


FIG. 2. Polarized crystal spectra at 10 K of [Ni(*s*-$Et_2en)_2(O_2N)]NO_2$. (*a*) 7–26 kK, (*b*) 25–32 kK. One intensity unit in (*b*) ≅ 1.3 units in (*a*).

is therefore most reasonably assigned to the singlet–triplet n → π* transition of nitrite. The mechanism governing the intensity of this band will be discussed below.

*[Ni(*s-$Et_2en)_2(O_2N)]BF_4$

The space group of crystals of this compound is $P2_1/c$ (17). The structure differs from that of the previous compound principally in having a lattice nitrite replaced by a tetrafluoroborate ion. As can be seen in Fig. 3, the vibrational structure in the uv of this compound presents a completely different aspect from that of the preceding compound. Well-resolved progressions in 600 cm^{-1} are absent from the near uv region, and only three progressions in the stretching mode are well resolved. The first begins at ca. 25.8 kK and the second and third progressions lie about 0.34 and 0.59 kK above the first. We therefore strongly suspect that the well-defined progressions in 599 cm^{-1} in [Ni(*s*-$Et_2en)_2(O_2N)]NO_2$ are due to the free nitrite in the lattice.

This compound also shows the structured band near 22 kK, and it contains vibrational structure in the NO_2 bending mode. The ligand field spectra of this compound will be discussed elsewhere (29).

*[Ni(*m-*stien)*$_2(O_2N)]NO_2$*

On the basis of a crystal field analysis we concluded that this compound has a *cis*-NiN_4O_2 chromophore. This has been confirmed by an X-ray crystallographic study.[2] Spectra of the complex are shown in Fig. 4. There appears to be an electronic origin at 24.89 kK and a strong progression in 600 ± 5 cm^{-1}. This is accompanied by six other progressions in 600 cm^{-1} built on the first progression plus lattice modes or low-energy vibrations of the chromophore. A second weaker progression begins at 25.89 kK. This may be a combination ($\nu_{stretch} + n\nu_{bend}$) progression, as was found in [Ni(*s*-$Et_2en)_2(O_2N)]NO_2$. This is also accompanied by three other progressions in 600 cm^{-1}. In all, we were able to record about 50 lines, the frequencies of which are given in the Appendix. While the individual vibronic components have the same energies in the two polarizations, the intensities vary. This causes the overall spectra to have a different appearance in the two polarizations.

The weak band near 22 kK is also present in this compound. It shows vibrational structure corresponding to the bending vibration (606 ± 15 cm^{-1}). The crystal field spectra of this complex will be discussed elsewhere (29).

[Ni(TMen)$(O_2N)_2]$

This complex is known from X-ray crystallography to belong to space group $P2_1/n$, and to possess two O-chelating nitrite groups (18). The spectra of this complex (Fig. 5) show the structured band near 22 kK on the low-energy side of the 26 kK band. The progression is in 660 ± 30 cm^{-1}. The uv region is masked by the onset of very intense absorption beginning about 28 kK. One can nonetheless see a small feature at 27.58 kK. In addition, there is a weak shoulder on the uv rise (not shown here) that is 1125 cm^{-1} above the 27.58 kK band. This appears to signal the onset of the spin-allowed n → π* transition of the nitrite ion. No strong progressions in 600 cm^{-1} are found in the near uv. This is consistent with the absence of free nitrite ion in the lattice.

*[Ni(*a-$Et_2en)_2(ONO)_2]$

Although the structure of this complex is unknown, previous studies characterize it as having O-bonded nitrite (10). The overall spectra of this compound (Fig. 6) show more similarity to those of

[2]M. Hitchman. Private communication.

Can. J. Chem. Downloaded from www.nrcresearchpress.com by 210.87.254.40 on 09/05/12
For personal use only.

Can. J. Chem. Downloaded from www.nrcresearchpress.com by 210.87.254.40 on 09/05/12
For personal use only.

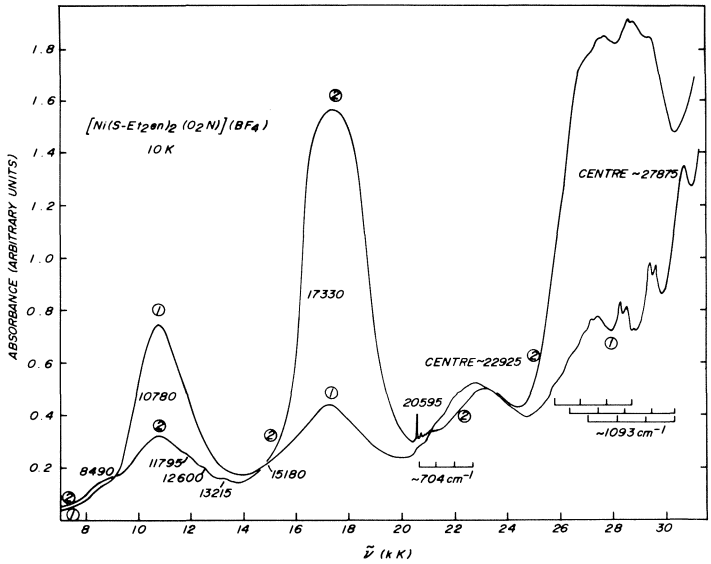


FIG. 3. Polarized crystal spectra at 10 K of $[Ni(s\text{-}Et_2en)_2(O_2N)]BF_4$.

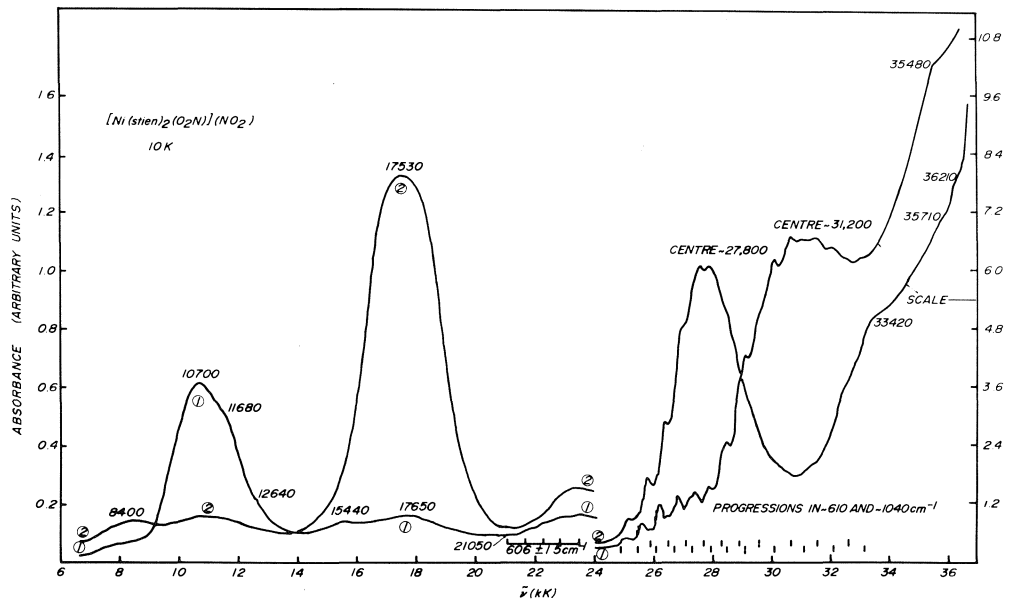


FIG. 4. Polarized crystal spectra at 10 K of $[Ni(m\text{-stien})_2(O_2N)]NO_2$.

$[Ni(a\text{-}Me_2en)_2(ONO)_2]$ than to the compounds known to have a *cis*-NiN_4O_2 chromophore. This is consistent with the presence of an all-*trans* rhombically distorted $NiN_2N_2'O_2$ chromophore which in turn implies monodentate nitrite. The vibrational structure (612 ± 20 cm^{-1}) in the near uv begins with two weak features ("origins") at 25.18 and 25.43 kK. This separation of ca. 250 cm^{-1} may indicate the presence in the lattice of two complexed nitrite ions which differ in symmetry. The vibrational structure on the weak band at 21 kK (631 ± 23 cm^{-1}) also suggests two distinct electronic origins separated by about 230 cm^{-1} with progressions in the nitrite bending vibration associated with each origin. A noteworthy feature of the spectra is the strong progression in 1064 ± 32 cm^{-1}, five members of which can be seen beginning at 27.99 kK.

$K_3[Hg(O_2N)_4]NO_3$

The compound belongs to space group *Pnma* (12). The structure of the complex anion has been

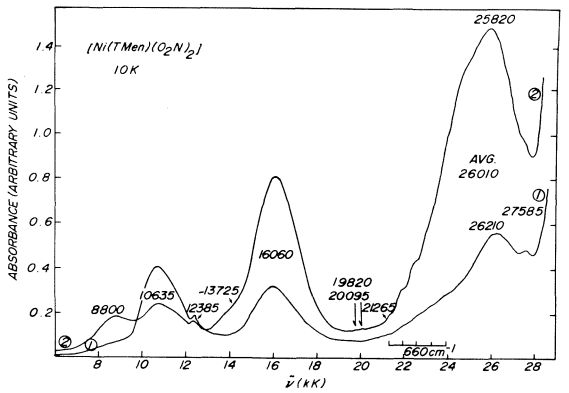


FIG. 5. Polarized crystal spectra at 10 K of [Ni(TMen)-$(O_2N)_2$].

shown from X-ray (19) and neutron diffraction studies (12) to consist of four chelating nitrito groups arranged in a roughly tetrahedral disposition about the central mercury. A mirror plane passes through the mercury atom and contains one nitrite. There are thus three non-equivalent chelating nitrites in the complex anion. The crystal spectrum at 10 K (Fig. 7) shows a single weak band centered at 24.1 kK with eight vibronic components; the progression is in 614 ± 15 cm^{-1}. This is readily assigned to the singlet–triplet n → π* transition.

The singlet–singlet transition is not visible in its entirety because of its enormous intensity in this crystal. There appear to be three "origin" lines at 26.00, 26.13, and 26.25 kK. It is tempting to assign these to each of the three non-equivalent chelating nitrite ions, although an explanation in terms of lattice modes must also be considered. A shoulder at 26.63 kK may be ascribed to the first member of a progression in the bending vibration.

$[Ni(en)_2(NO_2)]ClO_4$

The compound is isomorphous with $[Ni(en)_2(NO_2)]BF_4$, which is orthorhombic and belongs to space group $Pn2_1a$ (20). The $Ni(en)_2$ groups have approximate tetragonal symmetry and are joined into infinite chains by NO_2 groups bonding through oxygen and nitrogen. As expected, coordination of the lone pair on nitrogen totally changes the appearance of the spectrum in the near uv region (see Fig. 8). No structured band is present near 23 kK. There are many weak features on the crystal field bands, but these are best attributed to spin-forbidden transitions and/or vibronic crystal-field features. The overall positions of the bands are consistent with the nature of the chromophore, and are reminiscent of the spectrum of $Ni(en)_2(NO_2)_2$ studied by Bertini *et al.* (7). The exact nature of the band near 20 kK is, however, not certain. In $Ni(NH_3)_4(NO_2)_2$ and $[Ni(m\text{-stien})_2NO_2H_2O]ClO_4$ it has been assigned by Hitchman and Rowbottom to be due most probably to a nickel to nitrite π* transition.[2]

Discussion

Early workers (5, 13) in this area explained the absence of significant spectral shifts in the n → π* transition O-coordinated nitrite by reasoning that the highest non-bonding MO is chiefly nitrogen in character. Since nitrogen is not involved in coordination, the energy levels should not be shifted. This seemed logical, since the structured n → π* transition disappears and is replaced by intense ligand →

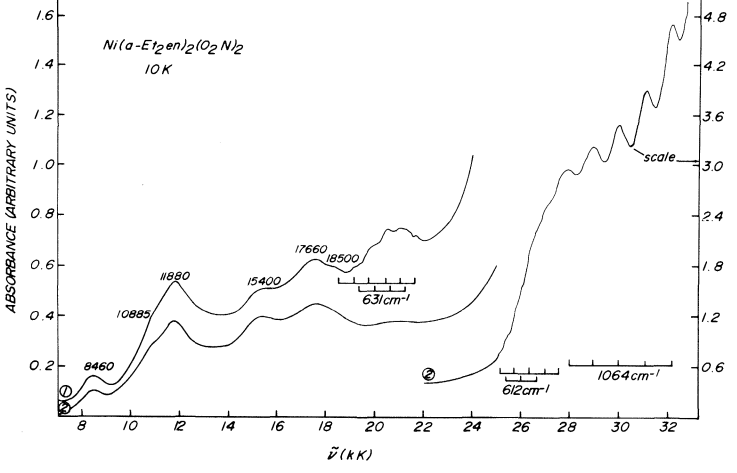


FIG. 6. Polarized crystal spectra at 10 K of $[Ni(a\text{-}Et_2en)_2(ONO)_2]$. Above 25 kK polarization *1* is similar to, but 2.5 times as intense as, polarization *2*.

Can. J. Chem. Downloaded from www.nrcresearchpress.com by 210.87.254.40 on 09/05/12
For personal use only.

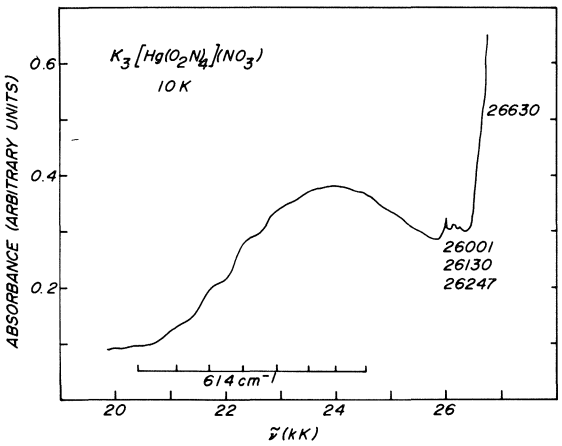


FIG. 7. Polarized crystal spectrum at 10 K of $K_3[Hg(O_2N)_4]NO_3$. Both polarizations are identical.

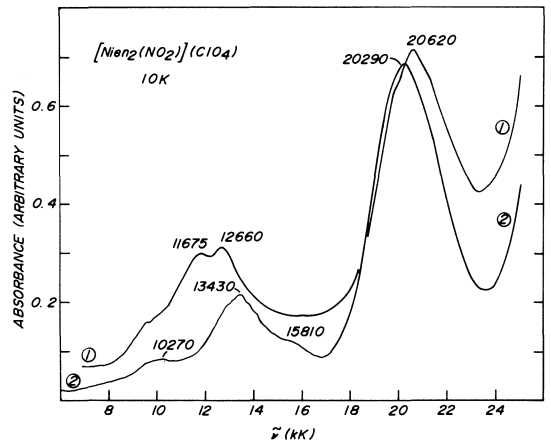


FIG. 8. Polarized crystal spectra at 10 K of $[Ni(en)_2(NO_2)]ClO_4$.

metal charge transfer bands once the n-level is tied up by bonding of nitrogen to a metal.

Strickler and Kasha (4), however, postulated that the highest-lying non-bonding MO's must be made up principally of oxygen AO's in order to explain the behavior of the n → π* transition in hydroxylic solvents. Their conclusions are in agreement with the early MO calculations of McEwen (21). More recent calculations (22) confirm this conclusion that the highest non-bonding MO's in NO_2^- are chiefly composed of oxygen 2*p* atomic orbitals.

In this work we present three examples in which chelating nitrite is present unobscured by non-coordinated nitrite, namely, $[Ni(s\text{-}Et_2en)_2O_2N]BF_4$, $[Ni(TMen)(O_2N)_2]$, and $K_3[Hg(O_2N)_4]NO_3$. In these three cases, the basic features of the spectra are substantially those of free nitrite, the only substantive modifications being in intensities of individual lines. It remains somewhat surprising to us that spectroscopic features dependent on oxygenic AO's should remain so unaffected when oxygen coordinates to nickel.

Our assignment of these transitions as n → π* for both the spin-allowed and spin-forbidden bands follows those of Barnes, Duncan, and Peacock (8) for metal ions which are non-oxidisable (e.g., Hg^{2+}, Y^{3+}, and Cd^{2+}).

The Band at 23 kK

The spin-forbidden n → π* singlet–triplet transition has attracted experimental attention for a number of years (23, 24). It is observed in aqueous solutions of a number of nitrite complexes at about 23 kK. It is normally extremely weak ($f \cong 10^{-7}$), but its intensity increases dramatically when the nitrite is coordinated in solution to heavy metal ions, such as Ag^+, Cd^{2+}, Pb^{2+}, or Tl^+ (23). The band is also much enhanced and vibrational structure is very well resolved in the cubic $Cs_2NaLn(NO_2)_6$ compounds (Ln = lanthanide cation) at 80 K (25). The nitrite ion is believed to coordinate via the nitrogen in these latter compounds. The bonding to the lanthanide is quite weak, and so the nitrite energy levels are not much perturbed.

In a recent article (24) calculations of oscillator strength have shown that the intensification mechanism for this band in crystals of $AgNO_2$ and $NaAg(NO_2)_2$ comes from spin–orbit induced mixing of nitrite states with appropriate states of the heavy metal. Substantial spin–orbit coupling constants and low-lying metal-to-ligand or ligand-to-metal charge-transfer states are shown to be of key importance. The increase of intensity, which is of the order of a thousand, is reasonably well reproduced by calculation.

That this band gains intensity in nickel complexes is undoubtedly due in part to the substantial spin–orbit coupling constant of nickel. The influence of nitrite geometry is also crucial. The band is clearly observed in our five compounds known to have chelating nitrito groups, and absent from $[Ni(en)_2(NO_2)]ClO_4$, which contains bridging NO_2 groups. The band does *not* appear in $[Ni(a\text{-}Me_2en)_2(ONO)_2]$ but *does* appear in $[Ni(a\text{-}Et_2en)_2(ONO)_2]$, even though we postulate that both contain the same basic coordination geometry. The reason for this is not clear. It may possibly be related to the fact that of all the O-coordinated nitrite studied here only the *a*-Me_2en complex is *known* to have the metal atom lying on

Can. J. Chem. Downloaded from www.nrcresearchpress.com by 210.87.254.40 on 09/05/12
For personal use only.

TABLE 2. "Origin" of progressions in spin-allowed n → π* transition in nitrito compounds[a]

Compound	Reference	"Origin" energy (kK)	ν(stretch) (cm^{-1})	ν(bend) (cm^{-1})
$NaNO_2$	13	25.977	1018	632 (644)[b]
KNO_2	13	25.412	1015	616
KNO_2 in KCl	27	25.5		
$[Ni(s\text{-}Et_2en)_2(O_2N)]NO_2$	This work	25.23	1015	599 (690)
$[Ni(s\text{-}Et_2en)_2(O_2N)]BF_4$	This work	25.8	1093	(704)
$[Ni(m\text{-}stien)_2(O_2N)]NO_2$	This work	24.890	1040	610 (606)
$[Ni(a\text{-}Me_2en)_2(ONO)_2]$	This work	24.776	1120	593
$[Ni(a\text{-}Et_2en)_2(ONO)_2]$	This work	25.18	1064	612 (631)
$[Cr(en)_2(ONO)_2]ClO_4$	5[c]	25.3		
$[Ni(TMen)(O_2N)_2]$	This work			(660)
$K_3[Hg(O_2N)_4]NO_3$	This work	26.00		629 (614)

[a]"Origin" means lowest energy absorption feature of vibrational progression. The frequencies listed for the upper state vibrations in the Ni complexes are averages, and have a precision of ±20 cm^{-1} in most cases.
[b]Bending frequencies observed in the singlet–triplet band are in parentheses. All data from this work except $NaNO_2$ (14).
[c]Spectrum at 20–25°C in DMF.

an inversion centre. The presence of this symmetry element may restrict the coupling of the metal and nitrite states which would augment the intensity of this spin-forbidden band.

We note that all our chosen examples of chelating nitrito groups are acentric. It would be interesting to observe whether a chelating nitrito group in a centrosymmetric nickel complex would also exhibit this band. Unfortunately, we are unaware of any such complex.

When this band was observed in solid $NaNO_2$, Allen and Dixon (14) noted that the intensity distribution of the fine structure was similar to that observed by Sidman (13) for the singlet transition, with the most notable feature a long progression in the bending vibration. In all the compounds in which we observe the band, only progressions in the bending vibration are observed.

The Spin-allowed Band

In $NaNO_2$ at 4 K the origin of this band is found at 25977 cm^{-1}, and in KNO_2 at 4 K it is found to be 565 cm^{-1} to lower energy (13). Sidman has proposed an explanation of the shift in terms of the nitrite MO's and the polarizability of the positive ions.

In the compounds studied here, the lowest observable feature in this spin-allowed band is in general slightly lower than in $NaNO_2$ (see Table 2). there is no apparent correlation between the energy of the first band and the nitrite environment.

Comparison of the spectra of the compounds in this study, however, brings out two pertinent observations. First, all the compounds containing nitrite coordinating through oxygen show some progression(s), usually short, in the N—O stretch. Thus, as expected, $[Ni(en)_2(NO_2)]ClO_4$ shows none. While $K_3[Hg(O_2N)_4]NO_3$ appears to be an exception, since no N—O stretching vibration is observed, it should be remembered that the crystal's absorption is so intense that we were not able to observe the spectrum in the region where this type of progression is expected.

The second observation is that only those compounds containing monodentate O-bonded or free nitrite ion show *significant* progressions in the ONO bending mode. Such progressions are accordingly very strong in $[Ni(s\text{-}Et_2en)_2(O_2N)]NO_2$, $[Ni(m\text{-}stien)_2(O_2N)]NO_2$, and $[Ni(a\text{-}Me_2en)_2(ONO)_2]$, and are quite visible but more poorly resolved in $[Ni(a\text{-}Et_2en)_2(ONO)_2]$. They are not observed in $[Ni(en)_2NO_2]ClO_4$, nor in the spectra of the BF_4 and TMen complexes. Again an apparent exception is the Hg complex. But only two members of a possible progression are seen, and then only in a very thick crystal. It is accordingly quite possible that such progressions might also be in the BF_4 and TMen crystals, but are swamped out by the more obvious progressions in the N—O stretch. So the presence of *measurable* or *significant* progressions of about 600 cm^{-1} might be used as diagnostic for the presence of monodentate O-coordinated or free nitrite ion.

The absence of strong progressions in the upper state bending vibration when the nitrite ion is chelating requires some comment. In free (ionic) or unidentate nitrite ion, the bending motion is essentially a property of the ONO group. In chelating nitrite, on the other hand, the bending motion is expected to be strongly coupled to the motions of

Can. J. Chem. Downloaded from www.nrcresearchpress.com by 210.87.254.40 on 09/05/12
For personal use only.

Can. J. Chem. Downloaded from www.nrcresearchpress.com by 210.87.254.40 on 09/05/12
For personal use only.

the framework of the complex; this could result in substantial changes in transition probabilities.

There is a slight reduction of the frequency of the upper state bending vibration from the values in $NaNO_2$, 632 and 644 cm^{-1} for the singlet and triplet transitions, respectively. From the best-resolved spectra in the present study the values are about 600 and 630 cm^{-1}, respectively (Table 2). The former value is more reliable because of the better resolution of the structure on the singlet–singlet transition. The difference in value between the monodentate and free nitrite is small, but the former (593 cm^{-1}) is the lowest value observed. This is in line with the fact that δ(ONO) in the ground state of $NaNO_2$ is 839 cm^{-1} (13), while the values for several Ni–nitrito complexes vary from 813 to 827 cm^{-1} (10, 26). The slight lowering may be associated with the reduction of electron density in the N—O bonds due to coordination. This would tend to reduce the bending frequency. Because of poor resolution in the fine structure associated with the upper state N—O stretching frequency, there is rather large variation in the values observed. Therefore, the data offer no clear indication of the effect that coordination has on the N—O stretching frequency.

Finally, no clear correlation could be made between the structural parameters of the nitrite group and the various observed vibrational frequencies or the origin of the $n \rightarrow \pi^*$ transition.

Conclusions

We have shown that the low-temperature crystal spectra of complexes containing the NO_2^- group give some indication of the mode of attachment of the NO_2^- group to the metal ion. Specifically, in N-coordinated complexes, the native $n \rightarrow \pi^*$ transition on the nitrite group with attendant vibrational structure is absent (5). The same is true of complexes in which the NO_2^- is ligated to two metal atoms, e.g., $[Ni(en)_2(NO_2)]ClO_4$. When the NO_2^- ion is either uncoordinated or monodentate O-coordinated, the spin-allowed $n \rightarrow \pi^*$ transition shows considerable structure in the bending vibration. Chelating nitrito-groups show an enhanced singlet–triplet $n \rightarrow \pi^*$ transition, but in the singlet–singlet transition, only strong progressions in the stretching vibration. These observations may eventually be useful in identifying the types of nitrite groups present in a given complex.

Acknowledgements

P.J.M. is grateful to the Research Corporation for a grant for the purchase of the Displex Cryogenic Refrigerator, while I.M.W. and A.B.P.L. are grateful to the National Research Council of Canada for their support.

1. A. B. P. Lever, G. London, and P. J. McCarthy. Can. J. Chem. **55**, 3172 (1977).
2. A. B. P. Lever, I. M. Walker, and P. J. McCarthy. Spectrosc. Lett. **12**, 739 (1979).
3. A. B. P. Lever, I. M. Walker, and P. J. McCarthy. Inorg. Chim. Acta, **39**, 81 (1980).
4. S. J. Strickler and M. Kasha. J. Am. Chem. Soc. **85**, 2899 (1963).
5. W. W. Fee, C. S. Garner, and J. N. M. Harrowfield. Inorg. Chem. **6**, 87 (1967).
6. K. G. Caulton and R. F. Fenske. Inorg. Chem. **6**, 562 (1967).
7. I. Bertini, O. Gatteschi, and A. Scozzafava. Inorg. Chem. **15**, 203 (1976).
8. J. C. Barnes, C. S. Duncan, and R. D. Peacock. J. Chem. Soc. Dalton, 1875 (1972).
9. M. N. H. Irving and R. M. Parkins. J. Inorg. Nucl. Chem. **27**, 270 (1965).
10. D. M. L. Goodgame and M. A. Hitchman. Inorg. Chem. **3**, 1389 (1964).
11. D. M. L. Goodgame and M. A. Hitchman. Inorg. Chem. **4**, 721 (1965).
12. L.F. Power, J. A. King, and F. H. Moore. J. Chem. Soc. Dalton, 93 (1976).
13. J. W. Sidman. J. Am. Chem. Soc. **79**, 2669 (1957).
14. W. C. Allen and R. N. Dixon. Trans. Faraday Soc. **65**, 1168 (1969).
15. M. G. B. Drew, D. M. L. Goodgame, M. A. Hitchman, and D. Rogers. Proc. Chem. Soc. 363 (1964).
16. M. J. Goldberg and R. E. Marsh. Acta Crystallogr. B**35**, 960 (1979).
17. R. Birdy, D. M. L. Goodgame, J. C. McConway, and D. Rogers. J. Chem. Soc. Dalton, 1730 (1977).
18. M. G. B. Drew and D. Rogers. Chem. Commun. 476 (1965).
19. D. Hall and R. V. Holland. Inorg. Chim. Acta, **3**, 235 (1969).
20. M. G. B. Drew, D. M. L. Goodgame, M. A. Hitchman, and D. Rogers. Chem. Commun. 477 (1965).
21. K. L. McEwen. J. Chem. Phys. **34**, 547 (1961).
22. M. Considine, J. A. Connor, and I. H. Hillier. Inorg. Chem. **16**, 1392 (1977).
23. H. J. Maria, A. Wahlborg, and S. P. McGlynn. J. Chem. Phys. **49**, 4925 (1968).
24. T. P. Carsey and S. P. McGlynn. J. Am. Chem. Soc. **101**, 1728 (1979), and references therein.
25. J. C. Barnes and R. D. Peacock. J. Chem. Soc. Dalton, 558 (1971).
26. L. El-Sayed and R. O. Ragsdale. Inorg. Chem. **6**, 1644 (1967).
27. E.Hutchinson and P. Pringsheim. J. Chem. Phys. **23**, 1113 (1955).
28. A. B. P. Lever, I. M. Walker, and P. J. McCarthy. To be published.
29. A. B. P. Lever, I. M. Walker, and P. J. McCarthy. Inorg. Chem. To be published.

Appendix

Sharp line spectral features observed in the near uv region at 10 K for the complexes indicated.

Shoulders are cited in parentheses. Data for the other complexes are clearly indicated on the figures.

[Ni(*a*-Me_2en)$_2$($ONO)_2$]: 24776, 24882, 24844, 24882, (24908), 24918, 24965, 24985, 25008, 25025, 25045, 25061, 25110, 25127, 25152, 25183, 25211, 25251, 25272, 25329, 25366, 25436, 25516, 25580, 25652, 25711, 25821, 25890, 25965, 26043, 26170, 26631, 27088, 27872, (28159), 28705, 30198, 30965, 32121.

[Ni(*m*-stien)$_2$(O_2N)]NO_2: 24890, 24929, 24957, 24988, 25027, 25074, 25122, 25497, 25534, 25567, 25592, 25631, 25671, 25725, 25895, 25933, 25991, 26028, 26093, 26131, 26162, 26190, 26227, 26263, 26328, 26491, 26533, 26587, 26628, 26699, 26738, 26769, 26797, 26833, 26867, 27087, 27128, 27181, 27223, 27294, 27339, 27396, 27438, 27483, 27672, 27720, 27783, 27816, 27933.

Can. J. Chem. Downloaded from www.nrcresearchpress.com by 210.87.254.40 on 09/05/12
For personal use only.

Field ionisation/field desorption mass spectrometry of polynuclear metal carbonyls

DENNIS G. TUCK, GORDON W. WOOD, AND SAMUEL ZHANDHIRE
Department of Chemistry, University of Windsor, Windsor, Ont., Canada N9B 3P4

Received November 13, 1979

DENNIS G. TUCK, GORDON W. WOOD, and SAMUEL ZHANDHIRE. Can. J. Chem. **58**, 833 (1980).

Field ionisation/field desorption mass spectra are reported for $Mn_2(CO)_{10}$, $Cd[Co(CO)_4]_2$ and some adducts, $In[Co(CO)_4]_3$, bipy·$Zn[Co(CO)_4]_2$, and bipy·$M[Mn(CO)_5]_2$ (M = Zn, Cd). The spectra are extremely simple, and the small number of easily identified species includes the molecular ion in some cases. The relative abundance of the fragments is discussed in terms of known stabilising factors in such compounds. No spectra could be obtained from $Co_2(CO)_8$ or $Fe_2(CO)_9$, which may be the result of their carbonyl-bridged structures.

DENNIS G. TUCK, GORDON W. WOOD et SAMUEL ZHANDHIRE. Can. J. Chem. **58**, 833 (1980).

On rapporte les spectres d'ionisation de champ et les spectres de masse par désorption de champ des composés suivants: $Mn_2(CO)_{10}$, $Cd[Co(CO)_4]_2$ et de quelques adduits tels: $In[Co(CO)_4]_3$, bipy·$Zn[Co(CO)_4]_2$, et bipy·$M[Mn(CO)_5]_2$ (M = Zn, Cd). Les spectres sont extrêmement simples et le petit nombre d'espèces facilement identifiées comprennent dans certains cas l'ion moléculaire. On discute de l'abondance relative des fragments en fonction des facteurs connus de stabilisation dans de tels composés. On n'a pas pu obtenir les spectres du $Co_2(CO)_8$ ou du $Fe_2(CO)_9$ ce qui peut être attribué aux structures de leurs groupes carbonyles pontés.

[Traduit par le journal]

Introduction

The use of mass spectrometry in inorganic and organometallic chemistry, although not as widespread as in the study of organic compounds, has increased considerably in recent years. The advantages of the technique, and some of the problems inherent in the interpretation of the results, have been discussed in various reviews (1). In terms of molecular weight or structure determination by electron impact mass spectrometry, some potentially serious problems include the low abundance of the molecular ion, which in some cases is not observed at all; the extensive fragmentation which frequently accompanies the high energy ionisation; and the high temperatures which are sometimes required to achieve a significant vapour pressure, and at which thermal decomposition may become significant.

The field ionisation mode of mass spectrometry adds a further dimension to such studies in that the much lower energies involved lead to simpler spectra than in electron impact work. Although a considerable literature exists on the application of this and the corresponding field desorption technique in the organic and biochemical areas (2), relatively few attempts have been made to investigate the behaviour of inorganic or organometallic molecules. Games *et al.* (3) have recently studied cationic complexes of some transition metals, and commented upon the simplicity of the spectra so obtained. We now report that the field ionisation/field desorption mass spectra of dinuclear and heteronuclear metal carbonyls, and of some simple adducts, emphasize the considerable promise which this field offers in the identification of organometallic compounds.

Experimental

Materials

The dinuclear carbonyls of manganese, iron, and cobalt were obtained from Alfa Inorganics. The remaining compounds were prepared by the electrochemical oxidation of zinc, cadmium, or indium in the presence of $Mn_2(CO)_{10}$ or $Co_2(CO)_8$ in organic media. Details of the preparation and characterisation of this latter group of compounds have been given elsewhere (4).

Mass Spectrometry

Mass spectra were obtained on a Varian MAT CH5 DF instrument interfaced to an INCOS 2000 data system. Sufficiently volatile samples were introduced through the direct inlet probe and field ionised; the remainder were applied to the field anode in solution and field desorbed. Details of these experimental procedures have been published elsewhere (5).

Results and Discussion

The results for the various compounds studied are collected together in Tables 1–8. The following detailed comments should be read in the light of those results.

$Mn_2(CO)_{10}$, $Fe_2(CO)_9$, and $Co_2(CO)_8$

The results for these binuclear carbonyls illustrates both the power of field ionisation mass spectrometry and one of its chief limitations. Thus for $Mn_2(CO)_{10}$, the molecular ion dominates the very simple spectrum (Fig. 1) in which the only other ion of significance is $Mn(CO)_5^{+\cdot}$ (1.5%). This result is in contrast to electron impact studies (6, 7) where $Mn_2(CO)_m^+$ ions ($10 > m > 0$), as well as $Mn_2^{+\cdot}$, were detected. Unfortunately, the structurally useful information in the spectrum of $Mn_2(CO)_{10}$ could not be duplicated for either the iron or the

0008-4042/80/080833-06$01.00/0
©1980 National Research Council of Canada/Conseil national de recherches du Canada

Can. J. Chem. Downloaded from www.nrcresearchpress.com by 210.87.254.6 on 09/05/12
For personal use only.

Can. J. Chem. Downloaded from www.nrcresearchpress.com by 210.87.254.6 on 09/05/12
For personal use only.

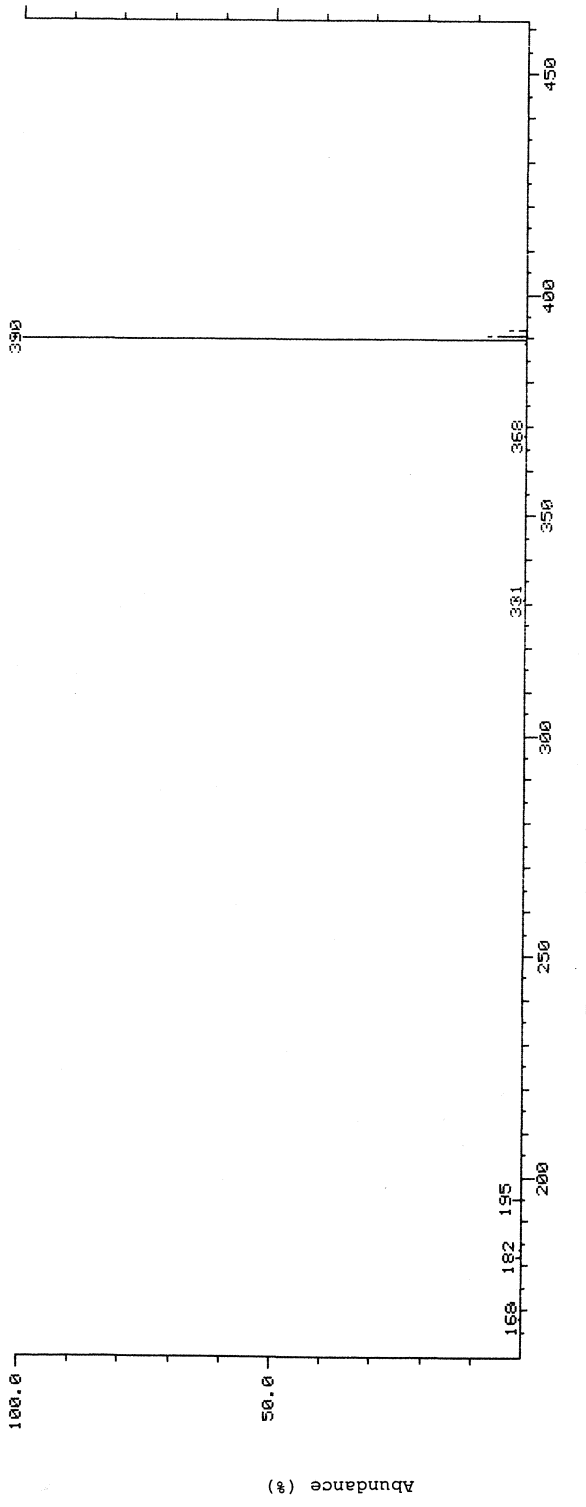


FIG. 1. Field ionisation mass spectrum of $Mn_2(CO)_{10}$.

cobalt compound, since it proved impossible to achieve the smooth vaporisation which is a prerequisite for FIMS with its relatively slow scanning rate (900 amu in 8–12 s in these experiments). After several trials, one sample of $Fe_2(CO)_9$ produced weak ions at m/z 197 and 147. Since the major isotopic species of $Fe(CO)_5^{+\cdot}$ has m/z 195.9, it is tempting to speculate that this species with an extra hydrogen may give rise to the m/z 197 base peak, but m/z 147 does not correspond to any combination of Fe, and CO and H. Even with numerous trials with samples from different sources, we were not successful in recording a reproducible spectrum of $Co_2(CO)_8$. In one experiment with slits open (nominal resolution ca. 200), we observed weak signals near m/z 342 and 171 on one scan, but at this resolution mass assignments cannot be made with certainty. Both color differences among samples and varying evaporation behavior from the probe strongly suggest that the introduction of this compound into the mass spectrometer is preceded by some decomposition.

Since $Fe_2(CO)_9$ and $Co_2(CO)_8$ are unique amongst the compounds studied in possessing bridging CO groups, as well as being the only failures experienced, it may be that there are reasons related to structural stability which prevent the generation of an adequate ion current in this mode of mass spectrometry.

Cd[Co(CO)$_4$]$_2$

The most abundant species in the spectra is the molecular ion, unambiguously identified by the manifold of ions arising from the presence of the various cadmium isotopes (Table 1), plus the ion at m/z = 457, which reflects the contribution of ^{13}C-containing molecules. The only other ions of detectable abundance are $Cd[Co(CO)_4]^+$, $Co(CO)_4^{+\cdot}$, and $Co(CO)_3^{+\cdot}$, consistent with a low probability dissociation pattern

$$Cd[Co(CO)_4]_2 \rightarrow Cd[Co(CO)_4] + Co(CO)_4 \rightarrow Co(CO)_3$$

From a structural point of view, it is interesting to note that the ion $Cd[Co(CO)_4]^+$ is not a radical cation, but rather a species in which the d^{10} Cd^{2+} ion is singly coordinated by a $Co(CO)_4^-$ ligand, and in which cobalt has an 18-electron configuration. Derivatives of this ion could well be stable in the solid state.

One final result in this spectrum concerns the peaks at m/z = 734.9, 735.7, 736.9, and 740.9, which correspond to the isotopic forms of $Cd_2[Co(CO)_4]_3^+$. Such species have not apparently been reported previously, but the formation of

TABLE 1. Field ionisation mass spectrum of $Cd[Co(CO)_4]_2$ (M = 455.73 for ^{114}Cd)

$Co(CO)_3^{+\cdot}$, $Co(CO)_4^{+\cdot}$		$Cd[Co(CO)_4]^+$		$Cd[Co(CO)_4]_2^{+\cdot}$		Cd isotopes	
m/z	Rel. int.	*m/z*	Rel. int.	*m/z*	Rel. int.	*m*	Rel. int.
142.9	5.8			448.0	2.3	106	4.2
170.9	6.7			449.9	3.4	108	3.1
		280.9	0.4	452.0	40.6	110	42.9
		282.0	0.8	453.0	45.6	111	44.2
		282.8	0.6	454.0	84.1	112	83.4
		283.9	1.0	455.0	52.1	113	42.5
		284.9	1.9	456.0	*100*	114	100
				457.0	8.2		
				458.0	25.5	116	26.3

similar cluster ions is common in FDMS. Structures in which each cobalt achieves an 18-electron configuration can be written for this ion, and further investigations of this species, and of its mode of formation, appear warranted.

$In[Co(CO)_4]_3$

Again, the spectrum of this high molecular weight species (M = 627.63) is dominated by the molecular ion base peak and the $In[Co(CO)_4]_2^+$ ion (14.2%), with $Co(CO)_4^{+\cdot}$ the only other detectable species. The isotope distribution for the $In[Co(CO)_4]_3^{+\cdot}$ ion agrees with the calculated intensities (see Table 2). This spectrum illustrates clearly how a field ionisation mass spectrum of such a molecule can provide complete and unambiguous characterisation, in that $InL_3^{+\cdot}$, InL_2^+, and $L^{+\cdot}$ ions are observed. The $InL_3^{+\cdot}$ ion is formally an indium(IV) species, of which no examples are known in the solid state; InL_2^+ is an indium(III) derivative, requiring no unpaired electrons, formally analogous to the $InMe_2^+$ cation (8, 9), and isoelectronic with the neutral $Cd[Co(CO)_4]_2$. It is worth noting that InL_2^+ species are the most abundant ions of the electron ionization mass spectra of indium(III) halides (10, 11).

Adducts of $Cd[Co(CO)_4]_2$

We have examined the neutral adducts with 2,2′-bipyridine (bipy) and *N,N,N′,N′*-tetramethylethylenediamine (TMED), and it should be pointed out here that these compounds almost certainly involve four coordination at cadmium (cf. the compound bipy·$Cd[Mn(CO)_5]_2$ discussed below).

Few attempts have been made to study the EI mass spectra of molecules of this type, and we therefore record in Table 3 the spectrum of $Cd[Co(CO)_4]_2$·TMED. The presence of the ions $TMED^+$, and $(CH_3)_2NCH_2^+$ demonstrate the extensive decomposition of the parent molecule and of the bidentate ligand in this mode of ionisation; in addition, $Cd[Co(CO)_4]^+$, Cd·$TMED^+$ and decomposition products of $Co(CO)_4$ are also observed. A total of more than 30 different species can be detected in the EI spectrum, but we have not attempted to identify these beyond the assignments shown in Table 3. In contrast, the field desorption spectrum of the same compound (Table 4) is extremely simple. The two ions TMED·$Cd[Co(CO)_4]^+$ (base peak) and $Cd[Co(CO)_4]_2^{+\cdot}$ represent the loss of $Co(CO)_4$ and TMED respectively from the parent complex; the cadmium-free fragments include $TMED^{+\cdot}$ and $Co(CO)_n^{+\cdot}$ (n = 3 or 4) clearly derived by the decomposition of the parent molecule. There is no information at present on whether this decomposition is the result of the ionisation process, or involves thermal decomposition prior to ionisation. Finally, we note that a weak molecular ion peak was observed in some spectra at 571.94 (calcd for ^{114}Cd species 571.86).

TABLE 2. Field ionisation mass spectrum of $In[Co(CO)_4]_3$ (M = 627.63 for ^{115}In)

m/z	Rel. int.	Assignment
114.9	0.03	In^+
171.0	5.8	$[Co(CO)_4]^{+\cdot}$
454.7	0.2	
456.7	14.2	$^{115}In[Co(CO)_4]_2^+$
457.7	0.7	
625.3	4.4	
627.3	*100*	$^{115}In[Co(CO)_4]_3^{+\cdot}$ [a]
628.3	13.4	
629.3	2.6	

[a]Isotope peaks for $M^{+\cdot}$, agree with calculated intensities: ^{113}In, *m/z* 625, 4.4%; ^{13}C, *m/z* 628, 13.2%; $^{13}C_2 + {}^{18}O$, *m/z* 629, 3.3%.

The spectra of the bipy adduct is similar to that just discussed (see Table 5), with bipy·$Cd[Co(CO)_4]^+$ (base peak), $Cd[Co(CO)_4]_2^{+\cdot}$, and $Cd[Co(CO)_4]^+$ ions from the parent molecule by removal of ligands, and $bipy^{+\cdot}$ and $Co(CO)_n^{+\cdot}$ (*n*

Can. J. Chem. Downloaded from www.nrcresearchpress.com by 210.87.254.6 on 09/05/12
For personal use only.

Can. J. Chem. Downloaded from www.nrcresearchpress.com by 210.87.254.6 on 09/05/12
For personal use only.

TABLE 3. Electron impact mass spectrum of TMED·Cd[Co(CO)$_4$]$_2$ (M = 571.86 for ^{114}Cd)[a]

m/z	Rel. int.	Assignment	m/z	Rel. int.	Assignment	m/z	Rel. int.	Assignment
28.0	35	$CO^{+\cdot}$	196.8	2		340.8	1	
58.1	*100*	$(CH_3)_2NCH_2^+$	197.8	1		341.7	1	
58.9	8	Co	198.8	5		343.8	1	
59.1	5		199.8	1		345.9	5	
70.1	2		200.8	5	CdCo(CO)	368.9	1	
71.1	2		201.8	11	$Co_2(CO)_3$	369.9	1	
72.1	4		202.8	1		370.9	2	
86.9	12	Co(CO)	203.1	33	TMEDCo(CO)	371.9	1	
99.1	1		204.1	2		372.9	2	
102.0	2		224.8	1		374.9	1	
104.0	1		226.8	1		396.9	3	
111.9	2		227.8	2		397.9	3	
112.9	1		228.8	3		398.9	9	
113.9	2	Cd	229.8	24	TMEDCd	399.9	4	
114.9	10	$Co(CO)_2$	230.8	2		400.9	10	$TMEDCdCo(CO)_4$
115.9	1		231.7	3		401.9	1	
115.1	1		234.0	16	$TMEDCo_2$	402.9	1	
116.1	11	$TMED^{+\cdot}$	235.0	1		424.7	1	
117.1	1		257.8	4		425.7	2	
117.8	10	Co_2	259.7	1		426.7	1	
130.0	2		262.0	4		427.7	2	$Cd[Co(CO)_4][Co(CO)_3]$
142.9	3	$Co(CO)_3$	285.8	3		451.7	1	
145.8	2		286.7	1		452.7	2	
147.0	7		287.9	1		453.7	5	
168.8	2		289.9	7		454.7	2	
169.8	2		311.7	1		455.7	6	$Cd[Co(CO)_4]_2$
170.8	5		313.8	8	$TMEDCd(CO)_3$	457.7	1	
171.8	2		314.8	2				
172.8	5	CdCo	315.7	3				
173.8	9	$Co_2(CO)_2$	316.9	1				
174.8	1		317.9	9				
175.1	9	TMEDCo	319.0	1				

[a]Isotopic species in braces.

TABLE 4. Field desorption mass spectrum of TMED·Cd[Co(CO)$_4$]$_2$ (M = 571.86 for ^{114}Cd)

Cd-free fragments			TMED·Cd[Co(CO)$_4$]$^+$		Cd[Co(CO)$_4$]$_2^{+\cdot}$		Cd isotopes	
m/z	Rel. int.	Assignment	m/z	Rel. int.	m/z	Rel. int.	m	Rel. int.
58.0	10.8	$(CH_3)_2NCH_2^+$	392.9	1.7			106	4.2
116.2	50.8	$TMED^{+\cdot}$					108	3.1
117.1	4.2		397.0	46.7	451.8	12.5	110	42.9
142.2	5.0		398.0	28.3	452.9	14.2	111	44.2
142.9	8.3	$Co(CO)_3^{+\cdot}$	399.0	65.8	453.8	16.7	112	83.4
144.2	2.5		400.0	36.7	454.7	9.2	113	42.5
170.9	44.2	$Co(CO)_4^{+\cdot}$	401.0	*100*	455.8	35.0	114	100
174.1	6.7		402.0	16.7				
280.8	1.7		403.0	20.0	457.8	2.5	116	26.3
298.8	2.5							

= 3 or 4) ions from the ligands. As in the earlier spectra, the characteristic mass pattern of the cadmium isotopes makes for an easy and unambiguous identification of ions containing this element.

Bipy·Zn[Co(CO)$_4$]$_2$

The spectrum of this compound was of unusually low intensity, but a recognizable $M^{+\cdot}$ (390.9 ± 0.2) was found in most scans.

Bipy·M[Mn(CO)$_5$]$_2$ (M = Zn, Cd)

For the zinc compound, the base peak is bipy·Zn[Mn(CO)$_5$]$^+$, which Zn[Mn(CO)$_5$]$_2^{+\cdot}$ as the only other zinc species identified (see Table 6). The

Can. J. Chem. Downloaded from www.nrcresearchpress.com by 210.87.254.6 on 09/05/12
For personal use only.

TABLE 5. Field desorption mass spectrum of bipy·Cd[Co(CO)$_4$]$_2$ (M = 611.80 for ^{114}Cd)

Low mass fragments			Cd[Co(CO)$_4$]$^+$		Bipy·Cd[Co(CO)$_4$]$^+$		Cd[Co(CO)$_4$]$_2^{+\cdot}$		Cd isotopes	
m/z	Rel. int.	Assignment	m/z	Rel. int.	m/z	Rel. int.	m/z	Rel. int.	m	Rel. int.
78.0	3.3	Bipy^{2+}			433.0	1.0	447.8	1.3	106	4.2
143.0	1.7	Co(CO)$_3^{+\cdot}$			434.9	2.7			108	3.1
156.1	52.2	Bipy$^{+\cdot}$	280.9	0.7	436.9	28.6	451.7	13.6	110	42.9
157.1	7.3		281.8	1.7	437.9	51.5	452.8	8.0	111	44.2
171.0	10.3	Co(CO)$_4^{+\cdot}$			438.9	84.7	453.8	17.6	112	83.4
185.5	1.3				439.9	44.2	454.8	16.6	113	42.5
186.0	2.0		284.8	2.0	440.9	*100*	455.8	24.9	114	100
263.6	1.7				442.0	13.3	456.7	1.7		
					442.9	17.9	457.8	8.6	116	26.3
					443.8	3.0				

TABLE 6. Field desorption mass spectrum of bipy·Zn[Mn(CO)$_5$]$_2$ (M = 609.82 for ^{64}Zn)

Low mass fragments			Bipy·Zn[Mn(CO)$_5$]$^+$		Zn[Mn(CO)$_5$]$_2^{+\cdot}$		Zn isotopes	
m/z	Rel. int.	Assignment	m/z	Rel. int.	m/z	Rel. int.	m	Rel. int.
156.1	7	Bipy$^{+\cdot}$	414.9	*100*	453.8	13	64	100
157.2	1		415.9	14	454.8	1		
195.0	14	Mn(CO)$_5^{+\cdot}$	416.9	49	455.7	6	66	56.9
196.0	1		417.9	17	456.7	2	67	8.4
295.2	13	BipyMn(CO)$_3^{+\cdot}$	418.9	44	457.8	3	68	38.0
296.2	3		419.9	5	458.7	1		
			420.9	4	459.7	0.1	70	1.3
			421.8	1	460.8	0.1		
			422.9	1				
			423.9	0.2				

TABLE 7. Field desorption mass spectrum of bipy·Cd[Mn(CO)$_5$]$_2$ (M = 659.80 for ^{114}Cd)

Low mass fragments			Bipy·Cd[Mn(CO)$_5$]$^+$		Cd[Mn(CO)$_5$]$_2^{+\cdot}$		Bipy·Cd[Mn(CO)$_5$]$_2^{+\cdot}$		Cd isotopes	
m/z	Rel. int.	Assignment	m/z	Rel. int.	m/z	Rel. int.	m/z	Rel. int.	m	Rel. int.
155.8	12	Bipy					651.7	4	106	4.2
194.7	4	Mn(CO)$_5$								
308.5	2	CdMn(CO)$_5$							108	3.1
391.3	4	[Mn(CO)$_5$]$_2$								
421.2	2		460.7	21	499.5	4			110	42.9
422.3	3		461.7	30	500.5	6	656.3[a]	74	111	44.2
440.4	3		462.7	66	501.5	17	657.6	79	112	83.4
			463.7	47	502.6	21	658.7	90	113	42.5
			464.7	74	503.6	12	659.7	*100*	114	100
			465.8	4			661.3	13		
			466.7	23			662.8	10	116	26.3
			467.8	2						
			468.8	2						

[a]This intense peak intermediate between the expected m/z 655.6 and 656.6 no doubt reflects a computer error in combining these two separate peaks.

cadmium analogue (Table 7) in contrast has the molecular ion as the base peak, with loss of Mn(CO)$_5$ or bipy leading to the other significant cadmium species.

General

The first and most important conclusion from this work must be that the use of field desorption and/or ionisation mass spectrometry leads to sim-

TABLE 8. Relative abundance of ions from adducts of Zn and Cd complexes

Compound = DML_2	Relative abundance			
	$DML_2^{+\cdot}$	$ML_2^{+\cdot}$	DML^+	ML^+
Bipy·Zn[Co(CO)$_4$]$_2$	n.d.	n.d.	100	n.d.
Bipy·Cd[Co(CO)$_4$]$_2$	n.d.	26.6	100	1.3
TMED·Cd[Co(CO)$_4$]$_2$	n.d.	32.2	100	0.6
Bipy·Zn[Mn(CO)$_5$]$_2$	n.d.	38.7	100	n.d.
Bipy·Cd[Mn(CO)$_5$]$_2$	100 (139)	16.0 (22.3)	71.9 (100.0)	0.4

ple and easily interpreted spectra, which should allow clear identification of unknown neutral organometallic compounds. Taken together with the earlier work on desorption of cationic species from cationic coordination complexes (3), the broad applicability of this technique is thus established.

Secondly, it is useful to compare the species produced in the case of the neutral adducts of the zinc and cadmium DML_2 compounds (L = $Co(CO)_4$ or $Mn(CO)_5$). Table 8 shows that in each case other than bipy·Cd[Mn(CO)$_5$]$_2$, the predominant ion is DML^+ (D = bidentate donor, M = Zn or Cd, L = metal carbonyl group); even in the exception noted, this ion is highly abundant. The stability of this species is easily understood; the Co or Mn atom achieves an 18-electron configuration, as does the 3-coordinate Zn or Cd, and there are no unpaired electrons. In the next abundant ion, $ML_2^{+\cdot}$, the most stable structure would involve neutral metal carbonyl ligands with the inert gas configuration at the transition metal bonded to a two-coordinate +1 zinc or cadmium ion. The molecular ion $DML_2^{+\cdot}$ is important only for bipy·Cd[Mn(CO)$_5$]$_2$, and it is worth noting that the spectrum here is for a cold source, field ionisation experiment; it may well be that the difference between this result and those for the other molecules relates to different degrees of thermal decomposition prior to ionisation. This substance apart, the spectra are remarkably similar, and the ratios DML^+:$ML_2^{+\cdot}$:ML^+ are surprisingly constant throughout, implying that the relative stabilities of these ions are but little affected by change of bidentate ligand or metal carbonyl, within the range examined.

Acknowledgements

This work was supported in part by Operating Grants from the National Research Council of Canada. One of us (S.Z.) acknowledges the award of a scholarship from the Canadian International Development Agency. We thank Mr. A. Osman for help in handling dinuclear metal carbonyl samples and Mr. A. Thibert for recording the spectra.

1. (*a*) J. LEWIS and B. F. G. JOHNSON. Acc. Chem. Res. **1**, 245 (1968); (*b*) M. R. LITZOW and T. R. SPALDING. Mass spectrometry of inorganic and organometallic compounds. Elsevier, New York. 1973; (*c*) J. M. MILLER and G. L. WILSON. Adv. Inorg. Chem. Radiochem. **18**, 229 (1976).
2. H. D. BECKEY. Principles of field ionization and field desorption mass spectrometry. Pergamon, Oxford. 1977. Chapt. 5 and references therein.
3. D. E. GAMES, J. L. GOWER, and L. A. P. KANE-MAGUIRE. J. Chem. Soc. Chem. Commun. 757 (1978).
4. J. J. HABEEB, D. G. TUCK, and S. ZHANDIRE. Can. J. Chem. **57**, 2196 (1979).
5. G. W. WOOD, E. J. OLDENBURG, P.-Y. LAU, and D. L. WADE. Can. J. Chem. **56**, 1372 (1978).
6. R. E. WINTERS and R. W. KISER. J. Phys. Chem. **69**, 1618 (1965).
7. J. LEWIS, A. R. MANNING, J. MILLER, and J. M. WILSON. J. Chem. Soc. A, 1663 (1966).
8. C. W. HOBBS and R. S. TOBIAS. Inorg. Chem. **9**, 1998 (1970).
9. J. S. POLAND and D. G. TUCK. J. Organomet. Chem. **42**, 315 (1972).
10. G. G. DEVYATYKH, V. G. RACHOV, and I. L. AGAFONOV. Russ. J. Inorg. Chem. **13**, 1497 (1968).
11. P. DOBUD and D. G. TUCK. Unpublished results.

Can. J. Chem. Downloaded from www.nrcresearchpress.com by 210.87.254.6 on 09/05/12
For personal use only.

An investigation into the origins of polar substituent effects upon ^{19}F chemical shifts, using 4-substituted β,β-difluorostyrenes

WILLIAM F. REYNOLDS, VICTORIA G. GIBB, AND NICK PLAVAC
Department of Chemistry, University of Toronto, Toronto, Ont., Canada M5S 1A1

Received November 14, 1979

WILLIAM F. REYNOLDS, VICTORIA G. GIBB, and NICK PLAVAC. Can. J. Chem. **58**, 839 (1980).

^{19}F, ^{13}C, and ^{1}H chemical shifts have been determined for β,β-difluorostyrene and eight 4-substituted derivatives. The β-fluorine chemical shift difference, $\Delta\delta_F$, is used to evaluate the constant in the Buckingham equation. $A = 3.0 \times 10^{-11}$ esu for C—F bonds which is in excellent agreement with the value derived by Adcock and Khor. This allows accurate estimates of direct field effect contributions to ^{19}F chemical shifts in aryl fluorides. Substituent parameter correlations demonstrate that the primary polar effect on ^{19}F chemical shifts is field-induced π polarization. *Ab initio* molecular orbital calculations confirm that the substituent-induced ^{19}F chemical shifts reflect changes in fluorine π electron density.

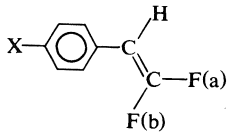
WILLIAM F. REYNOLDS, VICTORIA G. GIBB et NICK PLAVAC. Can. J. Chem. **58**, 839 (1980).

On a déterminé les déplacements chimiques du ^{19}F, du ^{13}C et du ^{1}H des β,β-difluorostyrènes et de 8 dérivés substitués en position 4. On utilise la différence de déplacement chimique, $\Delta\delta_F$, d'un fluor en β pour évaluer la constante de l'équation de Buckingham. Cette constante a pour valeur $A = 3.0 \times 10^{-11}$ ues dans le cas des liaisons C—F ce qui est en parfait accord avec la valeur calculée par Adcock et Khor. Ceci permet une évaluation précise des contributions de l'effet de champ direct sur le déplacement chimique du ^{19}F dans les fluorures d'aryles. Les corrélations des paramètres de substituant démontrent que l'effet polaire primaire, sur les déplacements chimiques du ^{19}F, est une polarisation π induite par le champ. Des calculs *ab initio* des orbitales moléculaires confirment le fait que les déplacements chimiques du ^{19}F induits par le substituant réflètent un changement de la densité des électrons π du fluor.

[Traduit par le journal]

Introduction

While in the past there has been considerable controversy about the origins of polar substituent effects upon ^{19}F chemical shifts in aryl fluorides (1, 2), recent work on several model systems has demonstrated that the main polar effect (except at very close range) is field-induced polarization of the aromatic π electron system (3–8). However, there is still uncertainty concerning the exact magnitude of the minor contributions to ^{19}F chemical shifts due to direct field effects (3–8). As previously pointed out (3), an excellent system for evaluating direct field effects is a series of 4-substituted β,β-difluorostyrenes, **I**:



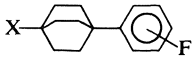
I

Assuming identical through-bond contributions to $\delta_{F(a)}$ and $\delta_{F(b)}$ (9), $\Delta\delta_F (\equiv \delta_{F(a)} - \delta_{F(b)})$ should provide a monitor of direct (through-space) field effects.[1] This allows evaluation of the constant, A, in the Buckingham equation (11):

$$[1] \quad \Delta\delta_F = A(\Delta E_z)$$

where ΔE_z ($\equiv E_z$(C—F(a)) − E_z(C—F(b))) is the difference in electric field components acting along the two C—F bonds.[2] In turn, A can be used in the estimation of field effects in other systems.

This approach has been tried (3), using previously reported data for **I** (12). However, the data were not entirely satisfactory for this purpose since individual chemical shifts were only reported to ±0.1 ppm, compared to a total range of $\Delta\delta_F$ of only 0.9 ppm. In addition, only one strongly polar substituent (CN) was included in the data set (12). Adcock and Khor have independently estimated a value of A from data for phenylbicyclo[2.2.2]octanes, **II** (4):



II

However, Ewing and Toyne have also investigated **II** and concluded that direct field effects were negligible in this and similar systems (6, 8). Consequently a careful reinvestigation of **I** seemed justified in order to compare estimated values of A from two different systems. It was felt that this would remove the final uncertainty concerning

[1]This approach, when applied to the corresponding 4-substituted styrenes (9), has been cited as providing convincing proof for direct field effects on ^{1}H chemical shifts (10).

[2]The Buckingham equation also contains a term in E^2 (11). However this should make a neglible contribution at the distances involved (9). In addition, the Buckingham equation was derived for axially symmetric bonds. While strictly speaking this is not true for the C—F bonds in both **I** and aryl fluorides, this should not introduce any significant error.

0008-4042/80/080839-07$01.00/0
©1980 National Research Council of Canada/Conseil national de recherches du Canada

Can. J. Chem. Downloaded from www.nrcresearchpress.com by 210.87.254.42 on 09/05/12
For personal use only.

TABLE 1. ^{19}F, ^{13}C, and vinyl ^{1}H chemical shifts for 4-substituted β,β-difluorostyrenes

X	Chemical shift									
	$\delta_{F(a)}$[a]	$\delta_{F(b)}$	$\Delta\delta_F$[b]	$\delta_{C(4)}$[c]	$\delta_{C(3,5)}$	$\delta_{C(2,6)}$	$\delta_{C(1)}$	$\delta_{C(\alpha)}$	$\delta_{C(\beta)}$	δ_H[c]
H	−85.48	−83.70	−1.78	126.79	128.43	127.44	130.07	82.08	156.16	5.122
$N(CH_3)_2$	−89.27	−87.29	−1.98	149.05	112.43	128.23	118.15	81.70	155.38	5.015
OCH_3	−87.77	−86.10	−1.67	167.28	113.97	128.53	122.33	81.49	155.69	5.056
CH_3	−86.47	−84.47	−2.00	136.13	129.13	127.36	127.17	81.88	156.01	5.080
F	−85.87	−84.60	−1.27	166.55	115.58	128.98	126.08	81.16	156.06	5.099
Cl	−84.52	−82.91	−1.61	132.98	—[d]	—[d]	—[d]	81.32	156.25	5.090
CF_3	−82.39	−81.00	−1.39	—[e]	125.45	127.45	133.74	81.49	156.77	5.183
CN	−81.07	−79.60	−1.47	117.05	132.06	127.75	134.58	81.64	156.82	5.188
NO_2	−80.41	−79.23	−1.18	—[e]	123.76	127.73	136.46	81.42	156.98	5.241

[a]In ppm relative to internal $CFCl_3$. High field shifts are negative.
[b]$\Delta\delta_F = \delta_{F(a)} - \delta_{F(b)}$.
[c]In ppm relative to internal $Si(CH_3)_4$. Low field shifts are positive.
[d]Overlapping peaks near δ 128.8.
[e]Not observed.

contributions of direct field effects to ^{19}F chemical shifts.

There is also uncertainty about the relationship between field effects upon ^{19}F chemical shifts and upon fluorine electron densities (3, 4). While CNDO/2 molecular orbital calculations for **I** proved some insight into this relationship, the calculated changes in atomic charges were, in many cases, comparable to the uncertainties in the charges. Consequently, it was decided to carry out more accurate *ab initio* (STO-3G minimal basis set (13)) calculations on **I** since this type of calculation has already proved very useful for understanding ^{19}F chemical shifts (14). Results of the experimental investigation and calculations are reported below.

Results

^{19}F chemical shifts and ^{19}F–^{19}F coupling constants were determined by analysis of the AB ^{19}F spectra obtained with ^{1}H decoupling. ^{1}H chemical shifts and ^{1}H–^{19}F coupling constants were determined by ABX analysis of the ^{1}H and ^{19}F spectra for the difluorovinyl groups. ^{19}F–^{13}C coupling constants were also determined by ABX analysis, using the ^{19}F parameters from the AB analysis in conjunction with the ^{19}F–^{13}C splittings observed in the ^{1}H-decoupled ^{13}C spectra. Chemical shifts are tabulated in Table 1 and coupling constants in Table 2.

Substituent-induced changes in calculated fluorine and vinyl carbon atomic charges as well as changes in σ and π components of these charges are summarized in Table 3.

Discussion

(a) Chemical Shifts

Taft's σ_I and σ_R substituent constants (15) can be used to separate polar and resonance contributions

TABLE 2. ^{19}F–^{19}F, ^{1}H–^{19}F, and ^{13}C–^{19}F coupling constants (in Hz) for 4-substituted β,β-difluorostyrenes

X	Coupling constants				
	F–F	H–F(a)	H–F(b)	C–F(a)	C–F(b)
H	+32.4	+3.8	+25.9	−288.8	−298.8
$N(CH_3)_2$	+41.2	+4.0	+26.5	−286.1	−295.3
OCH_3	+37.9	+3.7	+26.1	−287.0	−296.4
CH_3	+34.7	+3.8	+26.2	−287.6	−297.4
F	+33.5	+3.7	+25.6	−288.6	−297.5
Cl	+30.3	+3.5	+25.6	−289.1	−298.5
CF_3	+25.5	+3.3	+25.5	−291.1	−300.0
CN	+22.3	+3.3	+25.3	−292.6	−301.2
NO_2	+20.2	+3.2	+25.2	−292.6	−301.3

to chemical shifts. Results of these correlations are summarized in Table 4. In the case of the ^{19}F chemical shift correlations, significantly better correlations are obtained when the fluoro derivative is omitted (e.g. correlation coefficient, r, for $\delta_{F(b)}$ is respectively 0.993 and 0.997 with and without the fluoro derivative). However, the ρ_I and ρ_R values change to an insignificant degree. While the origins of the abnormal behaviour are unclear, similar problems have been noted in previous investigations, e.g. see ref. 9 where similar deviations were noted for vinyl ^{1}H chemical shifts in 4-fluorostyrene.

The correlations for $\delta_{F(a)}$ and $\delta_{F(b)}$ show the expected pattern of substituent effects. ρ_R is very similar for each fluorine, confirming that through bond effects are nearly equal for the two fluorines. ρ_I is 17% larger for $\delta_{F(a)}$ than for $\delta_{F(b)}$. σ_I provides a measure of the field effect of a substituent (16, 17). Since the field effect depends upon the component of the electric field acting along the C—F bond (11) and since this is greater for $\delta_{F(a)}$ (3), the enhanced ρ_I value for this fluorine can be attributed to direct field effects.

Although ρ_R values are very similar for $\delta_{F(a)}$ and

Can. J. Chem. Downloaded from www.nrcresearchpress.com by 210.87.254.42 on 09/05/12
For personal use only.

Can. J. Chem. Downloaded from www.nrcresearchpress.com by 210.87.254.42 on 09/05/12
For personal use only.

TABLE 3. Net atomic charges ($\times 10^4$) and σ and π components of these charges ($\times 10^4$) for the vinyl group of β,β-difluorostyrene and substituent-induced changes in these parameters ($\times 10^4$) for 4-substituted β,β-difluorostyrenes

Parameter	q_{net}[a] H	Δq[b] NH_2	OH	CH_3	F	CF_3	CN	NO_2
q_H	+692	−33	−11	−4	+1	+25	+41	+52
$q_{C(\alpha)}$	−1178	+27	+13	+6	+5	−14	−22	−27
$q_{C(\alpha)\sigma}$	−187	−63	−20	−17	+4	+48	+78	+100
$q_{C(\alpha)\pi}$	−991	+90	+33	+23	+1	−62	−100	−127
$q_{C(\beta)}$	+2841	−110	−47	−26	+11	+65	+107	+135
$q_{C(\beta)\sigma}$	+3317	+73	+35	+16	+36	−36	−58	−74
$q_{C(\beta)\pi}$	−475	−183	−83	−42	−25	+100	+165	+209
$q_{F(a)}$	−1197.1	−47.6	−15.5	−12.0	+1.8	+36.1	+60.8	+76.4
$q_{F(a)\sigma}$	−1969.3	−20.8	−4.2	−5.7	+4.2	+18.9	+31.5	+39.5
$q_{F(a)\pi}$	+772.2	−26.8	−11.3	−6.3	−2.4	+17.2	+29.3	+36.9
$q_{F(b)}$	−1218.3	−46.7	−22.4	−10.7	−8.0	+24.7	+40.9	+52.3
$q_{F(b)\sigma}$	−2001.5	−19.7	−9.7	−4.5	−3.8	+9.3	+15.0	+19.4
$q_{F(b)\pi}$	+783.2	−27.0	−12.7	−6.2	−4.2	+15.4	+25.9	+32.9
Δq_F[c]	+21.2	−0.9	+6.9	−1.3	+9.8	+11.4	+19.9	+24.1
$\Delta q_{F\sigma}$	+32.2	−1.1	+5.5	−1.2	+8.0	+9.6	+16.5	+20.1
$\Delta q_{F\pi}$	−11.0	+0.2	+1.4	−0.1	+1.8	+1.8	+3.4	+4.0

[a]Atomic charge relative to neutral atom ($\times 10^4$). Negative sign corresponds to increased electron density.
[b]Substituent-induced changes in atomic charges ($\times 10^4$).
[c]$\Delta q = q_{F(a)} - q_{F(b)}$.

TABLE 4. Substituent parameter correlations for experimental chemical shifts and coupling constants and calculated charge densities for 4-substituted β,β-difluorostyrenes

Variable	Substituent parameter	$\rho_I(\rho_F)$[a]	ρ_R[a]	r[b]	F[c]
$\delta_{F(a)}$[d]	σ_I, σ_R^0	5.75 ± 0.26	8.21 ± 0.27	0.999	1346
$\delta_{F(b)}$[d]	σ_I, σ_R^0	4.90 ± 0.40	7.92 ± 0.41	0.997	490
$\Delta\delta_F$[d]	σ_I, σ_R^0	0.85 ± 0.16	0.29 ± 0.17	0.953	34
$\delta_{C(1)}$	σ_I, σ_R^0	5.7 ± 1.1	20.4 ± 1.1	0.995	274
$\delta_{C(\alpha)}$	σ_I, σ_R^0	−1.09 ± 0.16	0.65 ± 0.16	0.945	25
$\delta_{C(\beta)}$	σ_I, σ_R^0	0.85 ± 0.06	1.61 ± 0.07	0.997	606
δ_H	σ_I, σ_R^0	0.11 ± 0.02	0.22 ± 0.02	0.977	73
$^2J_{F-F}$	σ_I, σ_R^0	−13.3 ± 0.9	−19.2 ± 0.9	0.998	665
$^1J_{C-F(a)}$	σ_I, σ_R^0	−4.45 ± 0.48	−6.46 ± 0.49	0.992	204
$^1J_{C-F(b)}$	σ_I, σ_R^0	−2.81 ± 0.38	−6.58 ± 0.39	0.993	252
$q_{F(a)\sigma}$	T_F, T_R^0	(3.68 ± 0.30) × 10^{-3}	(3.18 ± 0.41) × 10^{-3}	0.993	200
$q_{F(b)\sigma}$	T_F, T_R^0	(1.68 ± 0.20) × 10^{-3}	(3.06 ± 0.27) × 10^{-3}	0.993	201
$q_{F(a)\pi}$	T_F, T_R^0	(3.29 ± 0.25) × 10^{-3}	(4.25 ± 0.34) × 10^{-3}	0.996	322
$q_{F(b)\pi}$	T_F, T_R^0	(2.89 ± 0.24) × 10^{-3}	(4.23 ± 0.33) × 10^{-3}	0.996	320

[a]Weighting factors in correlation equation variable = $\rho_I\sigma_I + \rho_R\sigma_R^0 + C$ or variable = $\rho_F T_F + \rho_R T_R^0 + C$.
[b]Correlation coefficient.
[c]F test of variance.
[d]Fluoro derivative omitted from correlation (see text).

$\delta_{F(b)}$, there is a sufficient difference (ca. 4%) to result in a noticeable resonance contribution to $\Delta\delta_F$ (particularly for the $N(CH_3)_2$ derivative). Consequently $\Delta\delta_F$ is not a precise measure of direct field effects. However, field effects for individual substituents can be estimated from $\rho_I\sigma_I$ for the $\Delta\delta_F$ correlation. These can be compared with values of ΔE_z estimated by classical electrostatic calculations. E_z values were estimated assuming that the substituent acts as a point dipole and using R—X aliphatic group dipole moments for hydrocarbon solvents (18). Calculations were carried out using standard geometries, except that the C(1)—C(α)—C(β) angle was taken as 128.5° (see Details of Calculations). Results are summarized in Table 5. A correlation of $\rho_I\sigma_I$ versus ΔE_z yields:[3]

$$[2] \quad \rho_I\sigma_I = (3.01 \pm 0.12) \times 10^{-11}\Delta E_z \qquad (r = 0.996)$$

However, since the calculations are sensitive to the assumed geometry (3), a more reasonable estimate of the uncertainity in A is probably (3.0 ± 0.5) ×

[3]The corresponding correlation of $\Delta\delta_F$ versus ΔE_z gives A = 3.3 × 10^{-11} esu (r = 0.947), within these error limits.

TABLE 5. Calculated electric field components used in evaluating A for Buckingham equation

X	μ_x[a]	r[b]	E_z(A)[c]	E_z(B)[d]	ΔE_z[e]	$\rho_I\sigma_I$[f]
H	0	0	0	0	0	0
CH_3	−0.30	0.76	-0.198×10^{-4}	-0.019×10^{4}	-0.0179×10^{4}	−0.034
Cl	1.97	0.85	1.248×10^{4}	0.105	1.143×10^{4}	0.388
CF_3	2.32	1.72[g]	1.378×10^{4}	0.093×10^{4}	1.285×10^{4}	0.379
CN	3.6	2.02[h]	1.427×10^{4}	-0.030×10^{4}	1.457×10^{4}	0.472
NO_2	3.32	1.02	1.951×10^{4}	0.127×10^{4}	1.824×10^{4}	0.548

[a]RX aliphatic group dipole moment (16).
[b]Assumed distance of point dipole (in Å) along C(1)—X bond.
[c]Electric field component (in esu) acting along C—F(a) bond.
[d]Electric field component (in esu) acting along C—F(b) bond.
[e]$\Delta E_z = E_z(A) - E_z(B)$.
[f]Estimated electric field component to $\Delta\delta_F$. $\rho_I = 0.85$ (see Table 4).
[g]Along C(1)—C bond at midpoint of C—F bonds. μ_x taken as equal to dipole moment for CH_3CF_3 (29).
[h]At midpoint of C≡N bond.

10^{-11} esu.[4] This is in excellent agreement with the estimate of Adcock and Khor of $(2.5–3.1) \times 10^{-11}$ based on ^{19}F chemical shifts for **II** (4). Therefore, it is felt that A is now sufficiently well defined for fluorine attached to sp^2 carbons that it is possible to make nearly quantitative calculations of direct field contributions to ^{19}F chemical shifts in aryl fluorides, thus resolving more than ten years of controversy in this area.

The electrostatic calculations predict negligible field effects for $\delta_{F(b)}$ since the field acts almost at right angles to C—F(b). However the σ_I,σ_R^0 correlation gives a significant ρ_I value for $\delta_{F(b)}$ (Table 4). This must reflect the field-induced π polarization (the π polarization effect of a polar substituent is also proportional to σ_I (16)). In the absence of direct field effects, substituent-induced changes in carbon π electron density result in proportional changes in π electron density and chemical shift of the fluorine bonded to carbon (3). This must be true for $\delta_{F(b)}$ since this parameter is directly proportional to $\delta_{C(\beta)}$ (9) for the corresponding styrene derivatives:

$$[3]\quad \delta_{F(b)} = (0.95 \pm 0.03)\delta_{C(\beta)}(\text{styrene}) \quad (r = 0.997)$$

If ρ_I for $\delta_{F(b)}$ is assigned entirely to π polarization, then the ρ_I value for $\delta_{F(a)}$ indicates that the polar effect for this probe is about 85% (4.90/5.75) due to π polarization and ca. 15% (0.85/5.75) due to direct field effects. This is consistent with previous conclusions about the relative importance of field and π polarization effects in similar systems (3–8), although indicating a slightly greater contribution from field effects than suggested by Toyne and Ewing (6).

$\delta_{C(1)}$, $\delta_{C(\alpha)}$, and δ_H for **I** give substituent parameter correlations (Table 4) which are very similar to previously reported correlations for styrenes (9, 19), suggesting that the two fluorines do not significantly alter the substituent effects in styrene derivatives. However, the range of $\delta_{C(\beta)}$ for **I** is very significantly reduced comparted to 4-substituted styrenes (9), although still proportional to $\delta_{C(\beta)}$ for the latter system:

$$[4]\quad \delta_{C(\beta)}(\mathbf{I}) = (0.185 \pm 0.036)\delta_{C(\beta)}(\text{styrene}) \quad (r = 0.996)$$

Non-additive ^{13}C chemical shifts are now well documented for *para*-disubstituted benzene derivatives (19–22) and to a lesser extent for 4,β-disubstituted styrenes (23). However, eq. [4] illustrates what is apparently the most extreme example of non-additivity yet found (perfect additivity would require unit slope). In 4,β-disubstituted styrenes, non-additivity has been attributed to variable electron demand by the β-substituted vinyl group (23). However, this cannot be the case for **I** since this should lead to a non-linear relationship for eq. [4], while the actual correlation shows no evidence of non-linearity. Rather, the fluorines must alter the shift-to-charge ratio for ^{13}C chemical shifts (22). This point is further discussed in part *c*.

(b) ^{19}F–^{19}F, ^{1}H–^{19}F, and ^{13}C–^{19}F Coupling Constants

The *geminal* (^{19}F–^{19}F) and *vicinal* (^{1}H–^{19}F) vinyl coupling constants for **I** closely parallel the corresponding ^{1}H–^{1}H coupling constants in styrene (9) in that the *geminal* coupling constant is much more sensitive to substituent effects than either *vicinal* coupling constant (see Table 2). $^2J_{F-F}$ is sensitive to both polar and resonance effects (Table 4). It is not possible to unambiguously assign the two $^1J_{C-F}$ coupling constants to F(a) and F(b) since the ^{13}C satellite peaks in the ^{19}F spectra were too weak to be observed. However, the two coupling constants show a similar pattern of substituent effects as $\delta_{F(a)}$ and $\delta_{F(b)}$ (similar ρ_R values but a larger ρ_I value for one coupling). In view of this parallel, it seems

[4]To convert A to SI units, this value should be multiplied by 0.33×10^{-4} after which its units are mV^{-1}.

Can. J. Chem. Downloaded from www.nrcresearchpress.com by 210.87.254.42 on 09/05/12
For personal use only.

Can. J. Chem. Downloaded from www.nrcresearchpress.com by 210.87.254.42 on 09/05/12
For personal use only.

logical to assign the coupling which is more sensitive to polar effects as $^1J_{C-F(a)}$. This is consistent with the corresponding $^{13}C-^1H$ coupling constants in 4-substituted styrenes (24). $^1J_{C-F(a)}$ should be more sensitive to field-induced σ bond polarization (24).

(c) Calculated Electron Densities and Comparison with ^{19}F and ^{13}C Chemical Shifts

The *ab initio* molecular orbital calculations for β,β-difluorostyrene (Table 3) indicate that the difluorovinyl group acts as a weak π donor to the phenyl group (total π electron transfer of 0.0088 electrons) and a weak σ acceptor (total σ electron transfer of 0.0134 electrons). These competing effects result in a minimal overall effect for the difluorovinyl group.

The most interesting result concerns the relationship between δ_F and the fluorine π charge density $q_F\pi$. Figure 1 shows that there is an excellent linear relationship between these parameters. The most impressive feature of Fig. 1 is that it involves a plot of actual chemical shifts for two different fluorines in the same molecule against their actual calculated π charge density rather than a plot of substituent-induced changes in chemical shifts and π charge densities. This is possible because the calculations give a π charge density difference for the parent compound (−0.0110), corresponding to a calculated chemical shift difference, $\Delta\delta_F$ (−1.63 ppm), which is in excellent agreement with the experimental value for this compound ($\Delta\delta_F$ = −1.78 ppm). We believe that Fig. 1 represents the clearest evidence yet obtained for a linear relation between ^{19}F chemical shifts and fluorine π charge densities in a system where the fluorine is bonded to an sp^2 carbon.

By contrast, the fluorine total atomic charges do not predict $\Delta\delta_F$ for the parent compound, since the difference in atomic charge between F(a) and F(b) has the wrong sign (+0.00322). Consequently, one can only plot substituent-induced chemical shifts versus substituent-induced changes in atomic charges (i.e. defining $\delta_{F(a)}$, $\delta_{F(b)}$, $q_{F(a)}$, and $q_{F(b)}$ all as zero for X = H). When this is done, it is found that these are different slopes for $\delta_{F(a)}$ (758 ± 44 ppm/unit charge) and $\delta_{F(b)}$ (890 ± 45 ppm/unit charge). The σ charge densities in Table 3 suggest that two slopes are obtained because the calculations indicate field-induced σ-bond polarization which is relatively much greater than the observed field effects upon chemical shifts. This can be confirmed by correlating $q_F\sigma$ and $q_F\pi$ with the theoretical field, T_F, and resonance, T_R^0 substituent

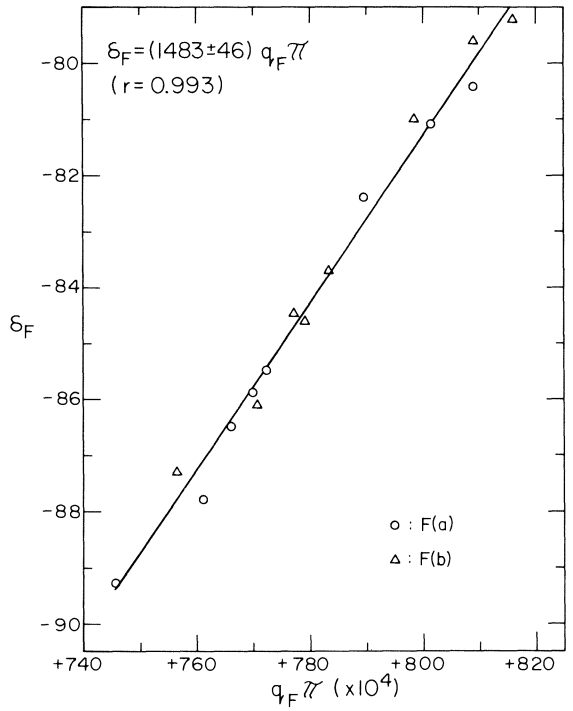


FIG. 1. Plot of ^{19}F chemical shifts (δ_F) for β,β-difluorostyrenes versus calculated π components of net atomic charges for fluorine ($q_F\pi$) (× 10^4). Positive sign of $q_F\pi$ corresponds to decreased electron density relative to a neutral fluorine atom.

parameters which have been derived for use with calculated charge densities (16, 17). The correlations (Table 4) show a much greater polar effect for $q_{F(a)}\sigma$ relative to $q_{F(b)}\sigma$ ($\rho_{F(a)}/\rho_{F(b)}$ = 2.19) compared to the corresponding chemical shift correlations ($\rho_{F(a)}/\rho_{F(b)}$ = 1.17). However, the correlations for $q_F\pi$ closely parallel the chemical shift correlations. This confirms that ^{19}F chemical shifts respond to π rather than total or σ charge density changes (14). It also provides an answer for an apparent dichotomy in the literature (3, 4). It appears that the main field effect upon fluorine atomic charges is due to field-induced σ bond polarization while the main field effect upon the ^{19}F chemical shifts is due to the weaker polarization of the partial C—F π bond (as previously suggested (4)).

$q_{F(b)}\pi$ gives an extremely precise linear relationship with $q_{C(\beta)}\pi$:

$$[5]\quad q_{F(b)}\pi = (0.154 \pm 0.002)q_{C(\beta)}\pi \qquad (r = 0.9997)$$

This confirms that, as suggested in part (*a*), $\delta_{F(b)}$ simply reflects substituent-induced changes in carbon π electron density and concomitant changes in fluorine π electron density.

Correlation of $q_{C(\beta)}\pi$ for **I** versus the corresponding parameter for styrene (16) yields:

[6] $q_{C(\beta)}\pi(\mathbf{I}) = (0.78 \pm 0.02)q_{C(\beta)}\pi(\text{styrene})$ $(r = 0.997)$

This demonstrates that the decreased substituent dependence for $\delta_{C(\beta)}$ shown in eq. [4] is only partly due to decreased substituent effects on $q_{C(\beta)}\pi$. Correlations of chemical shifts with π charge densities shown:

[7] $\delta_{C(\beta)}(\text{styrene}) = 193q_{C(\beta)}\pi(\text{styrene})$ $(r = 0.988)$

[8] $\delta_{C(\beta)}(\mathbf{I}) = 44q_{C(\beta)}\pi(\mathbf{I})$ $(r = 0.989)$

The former correlation gives a typical value for the shift-to-charge ratio (25, 26) while eq. [8] shows an abnormally small value. While the theoretical reasons for substituent-induced variations in the empirical shift-to-charge ratio are as yet unclear (21, 22), eq. [7] strongly suggests that it is the decrease in this parameter which is mainly responsible for the non-additive C(β) chemical shifts in **I**.

Summary and Conclusion

Consideration of field effects on the ^{19}F chemical shift difference, $\Delta\delta_F$, for 4-substituted β,β-difluorostyrenes yields a value of the constant in the Buckingham equation, $A = 3.0 \times 10^{-11}$ esu, in excellent agreement with a previous independent estimate from another system (4). Therefore it is now possible to make near quantitative estimates of direct field effects on ^{19}F chemical shifts in aryl fluorides. Clear evidence is presented for a linear relationship between ^{19}F chemical shifts and fluorine π electron density and further evidence is obtained that non-additive ^{13}C chemical shifts are mainly due to changes in the shift-to-charge ratio.

Experimental and Details of Calculations

4-Substituted β,β-difluorostyrenes were generally synthesized by the method of Naae (27) which involves a Wittig reaction of $(C_6H_5)_3P$ plus CF_2Br_2 with the appropriate 4-substituted benzaldehyde. Dry CH_2Cl_2 was used as a solvent. The reaction mixture was dumped into rapidly stirred pentane. The pentane layer was separated and the pentane was evaporated off. The β,β-difluorostyrene was then purified, either by distillation (X = H, CH_3, OCH_3, F, Cl, CF_3) or by thin layer chromatography (X = CN, NO_2, $N(CH_3)_2$). $[(CH_3)_2N]_3P$ was used in place of triphenylphosphine for the synthesis of the $N(CH_3)_2$ derivative, using glyme as solvent.

The compounds which, with the exception of the CF_3 derivative, were known compounds were characterized by their ^1H and ^{19}F spectra which showed characteristic ABX spectra for the difluorovinyl groups and AA′BB′ spectra for the *para*-disubstituted benzene functions. Purities were confirmed by ^{13}C nmr spectra.

^{19}F and ^1H spectra were obtained on a Varian XL-100 operating in continuous wave mode at respective frequencies of 94.19 and 100.06 MHz and at 31°C. Solutions contained 1 mol% compound in C_6D_{12} with 1% $CFCl_3$ and 0.1% $Si(CH_3)_4$ as reference peaks. Peak positions were obtained as averages of several measurements with a precision of 0.001 ppm. Further dilution of the parent compound and NO_2 and $N(CH_3)_2$ derivatives indicated that the observed chemical shifts differed from infinite dilution values by no more than 0.01 ppm. ^{13}C spectra were obtained on the same spectrometer operating in pulsed Fourier Transform mode. Samples were 0.4 *M* solutions of the compound in CCl_4 containing 8% C_6D_{12} as a lock signal.

Ab initio (STO-3G minimal basis set (13)) molecular orbital calculations were carried out on a SEL 32/75 computer using the program SUPERGAUSS 78, a modified version of GAUSSIAN 76 (28), developed by M. R. Peterson and R. A. Poirier. A partial energy minimization gave a value of the C(1)—C(α)—C(β) angle of 128.5°. Other geometries were identical to those given previously (16, 17). Planar NH_2 and OH were used in place of $N(CH_3)_2$ and OCH_3 for reasons of computational economy.

Acknowledgements

Financial support from the Natural Sciences and Engineering Research Council of Canada is gratefully acknowledged. We thank Professor P. Yates for helpful discussions concerning synthesis, M. R. Peterson and R. A. Poirier for help with the calculations, and Professor R. W. Taft for supplying a preprint prior to publication.

1. J. Fukunaga and R. W. Taft. J. Am. Chem. Soc. **97**, 1612 (1975).
2. W. Adcock and B. O. Gupta. J. Am. Chem. Soc. **97**, 6871 (1975).
3. W. F. Reynolds and G. K. Hamer. J. Am. Chem. Soc. **98**, 7296 (1976).
4. (*a*) W. Adcock and T. C. Khor. Tetrahedron Lett. 2063 (1976); (*b*) W. Adcock and T. C. Khor. J. Am. Chem. Soc. **100**, 7799 (1978).
5. W. F. Reynolds. Tetrahedron Lett. 675 (1977).
6. (*a*) D. F. Ewing, S. Sotheeswaran, and K. J. Toyne. Tetrahedron Lett. 2041 (1977); (*b*) D. F. Ewing and K. J. Toyne. J. Chem. Soc. Perkin II, 243 (1979).
7. W. Kitching, M. Bullpitt, D. Gartshore, W. Adcock, T. C. Khor, D. Doddrell, and I. D. Rae. J. Org. Chem. **42**, 2411 (1977).
8. D. F. Ewing. Org. Magn. Reson. **12**, 499 (1979).
9. G. K. Hamer, I. R. Peat, and W. F. Reynolds. Can. J. Chem. **51**, 897 (1973); **51**, 915 (1973).
10. W. T. Raynes. *In* The chemical society specialist reports on nuclear magnetic resonance. Vol. 3. *Edited by* R. K. Harris. The Chemical Society, London. 1974. p. 16.
11. A. D. Buckingham. Can. J. Chem. **38**, 300 (1960).
12. I. D. Rae and L. K. Smith. Aust. J. Chem. **25**, 1465 (1972).
13. W. J. Hehre, R. F. Stewart, and J. A. Pople. J. Chem. Phys. **51**, 2657 (1969).
14. W. J. Hehre, R. W. Taft, and R. D. Topsom. Prog. Phys. Org. Chem. **12**, 159 (1976).
15. S. Ehrenson, R. T. C. Brownlee, and R. W. Taft. Prog. Phys. Org. Chem. **10**, 1 (1973).
16. W. F. Reynolds, P. G. Mezey, and G. K. Hamer. Can. J. Chem. **55**, 522 (1977).
17. P. G. Mezey and W. F. Reynolds. Can. J. Chem. **55**, 1567 (1977).
18. C. W. N. Cumper. Tetrahedron, **25**, 3131 (1969).
19. R. A. McClelland and W. F. Reynolds. Can. J. Chem. **55**, 536 (1977).

Can. J. Chem. Downloaded from www.nrcresearchpress.com by 210.87.254.42 on 09/05/12
For personal use only.

20. J. BROMILOW, R. T. C. BROWNLEE, R. D. TOPSOM, and R. W. TAFT. J. Am. Chem. Soc. **98**, 2020 (1976).
21. B. M. LYNCH. Can. J. Chem. **55**, 541 (1977).
22. R. W. TAFT. Private communication.
23. D. A. R. HAPPER and G. J. WRIGHT. J. Chem. Soc. Perkin II, 694 (1979).
24. W. F. REYNOLDS, I. R. PEAT, and G. K. HAMER. Can. J. Chem. **52**, 3415 (1974).
25. P. C. LAUTERBUR. J. Am. Chem. Soc. **83**, 1838 (1961).
26. H. SPIESECKE and W. G. SCHNEIDER. Tetrahedron Lett. 468 (1961).
27. D. NAAE. Ph.D. Thesis, University of Iowa, Iowa City, IA. 1972.
28. GAUSSIAN 76, Quantum Chemistry Program Exchange Program No. 168, University of Indiana, Bloomington, IN.
29. A. L. MCCLELLAN. Tables of experimental dipole moments. W. H. Freeman and Co., San Francisco, CA. 1963.

Can. J. Chem. Downloaded from www.nrcresearchpress.com by 210.87.254.42 on 09/05/12
For personal use only.

Complete and partial miscibility in ternary system: triethylamine–methylethylketone–water

ALAN N. CAMPBELL

Department of Chemistry, University of Manitoba, Winnipeg, Man., Canada R3T 2N2

Received September 12, 1979

ALAN N. CAMPBELL. Can. J. Chem. **58**, 846 (1980).

The equilibrium diagram of the system triethylamine–methylethylketone–water has been investigated completely with respect to the occurrence of solid phases and of the lower and upper solution temperatures of the $L_1 \leftrightharpoons L_2$ equilibria, where L_1 and L_2 are equilibrium liquid phases. The $L_1 \leftrightharpoons L_2$ surface is not completely realizable because this surface is intersected by the $L \leftrightharpoons V$ surface. In this respect the system forms a contrast to the previously investigated system nicotine–methylethylketone–water, where the complete $L_1 \leftrightharpoons L_2$ surface is realizable experimentally.

ALAN N. CAMPBELL. Can. J. Chem. **58**, 846 (1980).

On a effectué une étude détaillée du diagramme de phase triéthylamine–méthyléthylcétone–eau du point de vue de l'existence des phases solides et de la plus faible et de la plus haute température atteinte par la solution dans les équilibres $L_1 \leftrightharpoons L_2$ où L_1 et L_2 sont les phases liquides à l'équilibre. La surface $L_1 \leftrightharpoons L_2$ n'est pas complètement réalisable parce qu'elle rencontre la surface $L \leftrightharpoons V$. Sous ce rapport, le système est en opposition avec le système suivant déjà étudié: nicotine–méthyléthylcétone–eau (1) où la surface complète $L_1 \leftrightharpoons L_2$ est réalisable expérimentalement.

[Traduit par le journal]

Introduction

The system nicotine–water represented by a completely closed oval is to be found in most elementary text books of physical chemistry. It is not so well known that the system methylethylketone–water is almost identical, almost, but not quite, since the lower part of the oval is cut off by the ice-line. The two binary systems together yield the ternary system nicotine–methylethylketone–water, and this has been studied by Campbell, Kartzmark, and Falconer (1). The two zones of heterogeneity unite in a tunnel, in the solid model, without temperature maximum.

The system triethylamine–water is equally well known in elementary text books as the standard example of a binary system with lower critical solution temperature: the system methylethylketone–water has an upper critical solution temperature. The triethylamine–water system is also interesting in that while miscibility is complete below 18°C, immediately above that temperature, say at 20°C, the gap is large and extends over 58 wt.% triethylamine. It was thought that the addition of a small amount of triethylamine to the methylethylketone–water system would produce complete miscibility and indeed this has been found to be the case.

Experimental

Triethylamine was estimated conductimetrically by titration with standard hydrochloric acid. The densities of all possible homogenous mixtures, at 16°C, were determined and plotted on a very large triangular diagram (21.5 inch side). From a knowledge of the triethylamine content and the density of any given homogenous mixture the composition could be obtained from the intersection of the horizontal representing the triethylamine content and the line of density. The densities were determined in a pyknometer of 50 cm^3 capacity, and are therefore not good enough for the determination of partial molar volume. In any case, the amounts of equilibrium layers available were limited so that for the determination of densities 5 cm^3, or sometimes 2 cm^3, pyknometers were used.

The densities are to be found in the Depository of Unpublished Data.[1] For all three binary systems, the plot of molar volume vs. mole fraction is, within the limits of experimental accuracy, a straight line.

The densities were plotted around the periphery of a triangular diagram. Points of equal density were joined by straight lines. Fortunately for the accuracy of the method, these lines formed sharp angles with the horizontals representing triethylamine content. Large part of the diagram at 25°C was heterogeneous so that, in some cases, weighed quantities of suitable component had to be added to ensure homogeneity.

For temperatures up to 70°C, mixtures were stirred magnetically overnight in a completely closed glass apparatus. The apparatus was immersed in a thermostat at the required temperature. After the attainment of equilibrium, samples were removed by means of air pressure. For temperatures above 70°C, the apparatus of Fig. 1 was used. At these temperatures, the vapour pressure is above 1 atm and samples of both layers could be withdrawn by opening the appropriate cock: the liquid passed immediately into a water condenser and was bottled off. Because of the danger of explosion the apparatus was completely enclosed in an electric furnace, whose temperature was controlled by a powerstat to a constancy of 1 or 2°C. The apparatus was charged at room temperature, using such volumes as would ensure that no mixing would occur when samples were withdrawn at high temperature. To the objection that there was no stirring it can be urged that the area of contact is large and the

[1]Complete set of data may be obtained, at a nominal charge, from the Depository of Unpublished Data, CISTI, National Research Council of Canada, Ottawa, Ont., Canada K1A 0S2.

0008-4042/80/080846-05$01.00/0

©1980 National Research Council of Canada/Conseil national de recherches du Canada

Can. J. Chem. Downloaded from www.nrcresearchpress.com by 210.87.254.40 on 09/05/12
For personal use only.

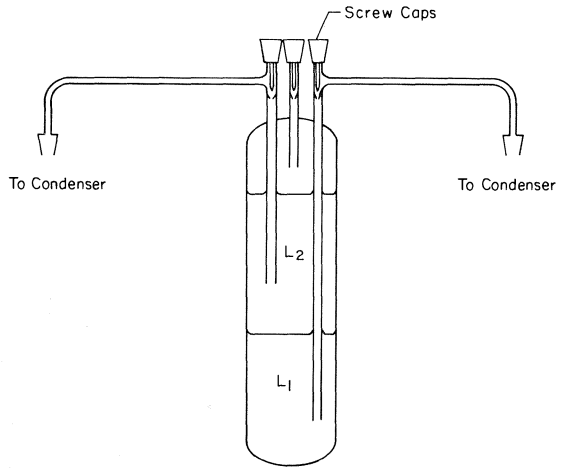


FIG. 1. High temperature apparatus.

rate of diffusion high at elevated temperatures. At any rate, the uniformity of the results seems to dispose of any contention that equilibrium was not attained. The experimental results are to be found in Depository and are expressed graphically in Figs. 2 and 3.

The solid model is terminated in the direction of lower temperature by the occurrence of the areas representing solid triethylamine, solid methylethylketone, and solid water: there are no compounds of the three components. The binary eutectic troughs should, and no doubt do, meet in a ternary eutectic point. It has been shown, however, by Randall and McKenna (2) that the binary eutectic of the system methylethylketone–water lies at −88.88°C and 99.91% methylethylketone, i.e. 9.9 wt.% water depresses the freezing point of methylethylketone about 2°C. The system triethylamine–methylethylketone had not been investigated and this was done by the author. Freezing point curves were determined with a copper–constantan thermocouple, cooling being done with liquid nitrogen. The data are in Depository and are represented graphically in Fig. 4. The eutectic lies at −130°C and 96.5 wt.% triethylamine. Obviously then the ternary eutectic lies close to this point, and is probably indistinguishable from it, since Randall and McKenna's eutectic contains so little water.

Since complete homogeneity in the ternary system was not attained at 160°C, the author turned to an apparatus which he had previously designed for a study of the L ⇆ V critical temperatures (3). The advantage of this apparatus is that thick-walled capillaries can be used and high temperatures and pressures attained. In the present study, two critical temperatures exist, viz. that of the equilibrium $L_1 \leftrightarrows L_2$ and that of the equilibrium $L_2 \leftrightarrows V$, i.e. in the field of view of the telescope used to follow the course of the experiment, two menisci are visible. If the temperature of homogeneity of the $L_1 \leftrightarrows L_2$ equilibrium lies below that of the $L_2 \leftrightarrows V$ equilibrium, the $L_1 \leftrightarrows L_2$ meniscus will disappear, leaving the $L_2 \leftrightarrows V$ meniscus. For concentrations below 30% of triethylamine, this was the case and for this range of concentration, the surface of homogeneity could be outlined. The work of Campbell and Kartzmark (3) showed that the critical temperatures L ⇆ V of ternary mixtures lie on a smooth surface connecting the critical temperatures of the three components. The critical temperature of water is 374°C, that of triethylamine is quoted as 262°C (4). If the approximate rule that the boiling point on the Kelvin scale is roughly two-thirds of the critical temperature, also on the Kelvin scale, is applied the following approximate critical temperatures are obtained: triethylamine, t_c = 270.9°C, methylethylketone, t_c = 256.0°C. From these approximate data it is apparent that the $L_1 \leftrightarrows L_2$ critical temperature (L_1 and L_2 equilibrium liquid phases) cannot be observed if it is higher than say 250 to 370°C, depending on composition. When this is the case, the $L_2 \leftrightarrows V$ meniscus disappears, leaving $L_1 \leftrightarrows V$. It was found experimentally that for mixtures having more than 30% triethylamine, the $L_1 \leftrightarrows L_2$ temperature could not be observed, in other words, the $L_1 \leftrightarrows L_2$ surface passes through the L ⇆ V surface about this limit of concentration. The method of experiment was to prepare a series of mixtures with fixed triethylamine content, and to find the temperatures of disappearance of the $L_1 \leftrightarrows L_2$ meniscus. In some cases, the temperature of disappearance of the L ⇆ V meniscus was also observed.

Another temperature to be considered is that below which homogeneity is attained. As this is invariably in the neighbourhood of room temperature it was sufficient to cool in ice water or, occasionally, to warm slightly. The method finally adopted was to use constant quantities of triethylamine (4, 8, and 16%) and vary the amounts of water and methylethylketone. The composition was then calculated on the basis of the sum of water and methylethylketone only (with constant triethylamine content). For each mixture, two and occasionally three temperatures were observed at which menisci disappeared. The numerical results are to be found in Depository and are expressed graphically in Fig. 5.

Discussion

Figures 2 and 3 represent the effect of rising temperature on the ternary equilibrium. At 0°C, at which temperature the binary system triethylamine–water is completely homogeneous, but the binary system methylethylketone–water is not, it is apparent that the addition of a few percent of triethylamine renders the methylethylketone–water system completely homogeneous. At 25°C, where both binary systems are heterogeneous, over a large area of composition, there is still a large area of the diagram which represents homogeneity. At 50°C, the two areas of heterogeneity have fused, leaving only small homogeneous areas; the curve MEK–TriE is always richer in triethylamine than the equilibrium curve H_2O–TriE. At 70°C, the same is true. The diagrams for 100, 120, 140, and 160°C are very similar. There is no approach to homogeneity with rising temperature.

Figure 4 represents the results of the thermal analysis of the methylethylketone–triethylamine system. The eutectic lies at −130°C and 96.5 wt.% triethylamine.

Examination of Fig. 5 shows that with increase of triethylamine content, the temperature of disappearance of the $L_1 \leftrightarrows L_2$ meniscus rises so that the $L_1 \leftrightarrows L_2$ surface passes through the L ⇆ V surface somewhat beyond 16% triethylamine. This means that though the $L_1 \leftrightarrows L_2$ dome is completely realisable for the system nicotine–methylethylketone–

Can. J. Chem. Downloaded from www.nrcresearchpress.com by 210.87.254.40 on 09/05/12
For personal use only.

Can. J. Chem. Downloaded from www.nrcresearchpress.com by 210.87.254.40 on 09/05/12
For personal use only.

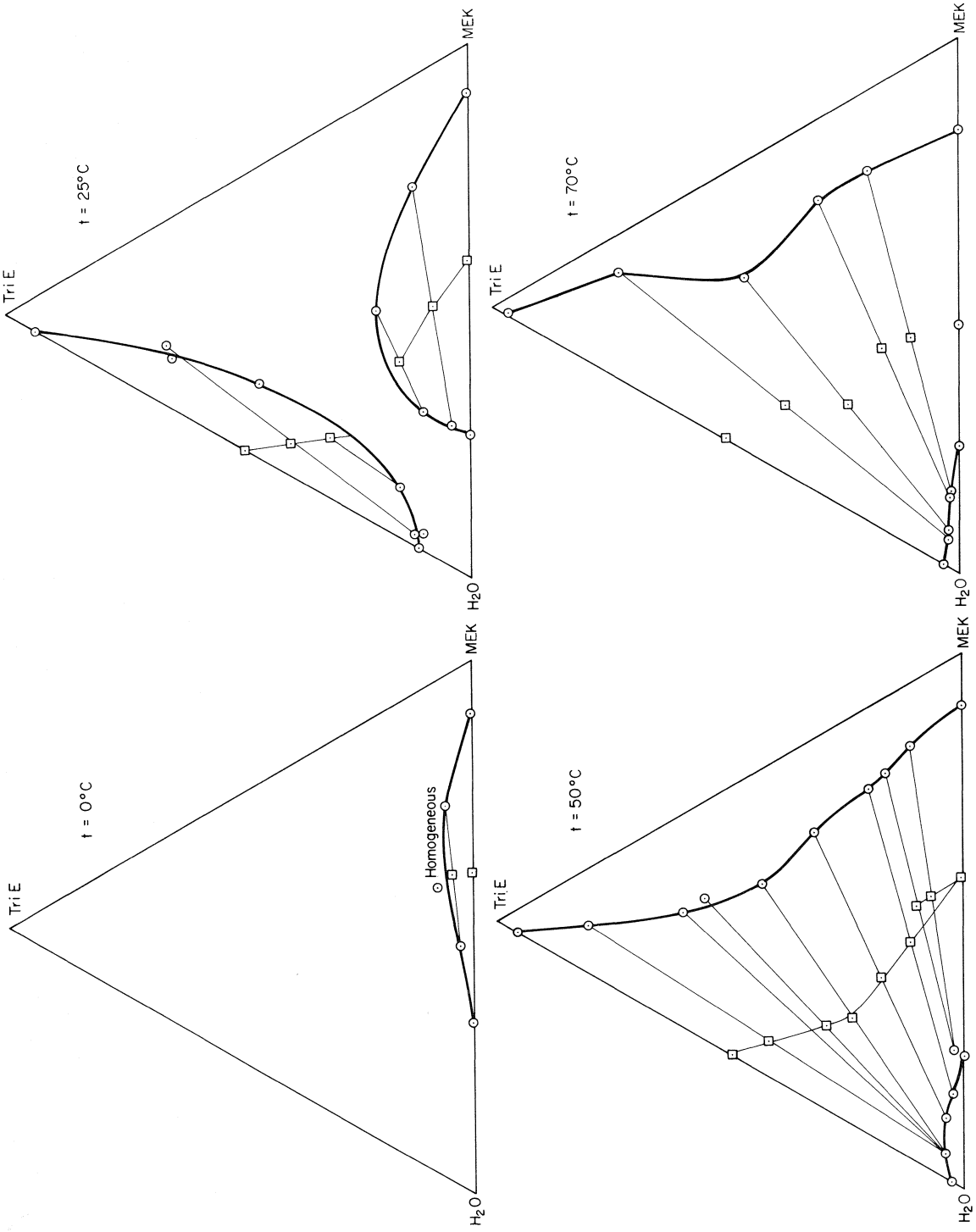


FIG. 2. The system triethylamine–methylethylketone–H_2O at 0°C, 25°C, 50°C, and 70°C.

Can. J. Chem. Downloaded from www.nrcresearchpress.com by 210.87.254.40 on 09/05/12
For personal use only.

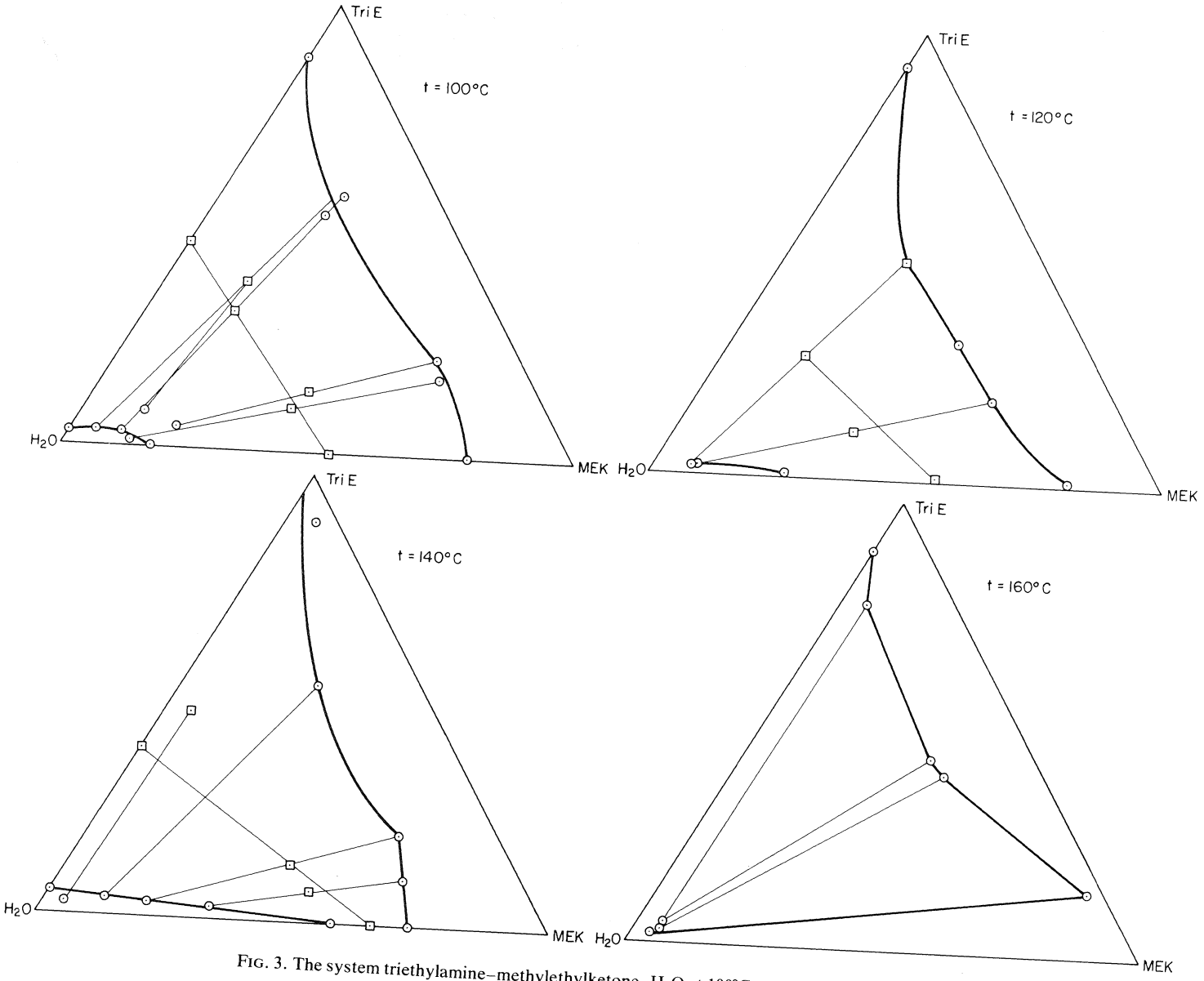


FIG. 3. The system triethylamine–methylethylketone–H_2O at 100°C, 120°C, 140°C, and 160°C.

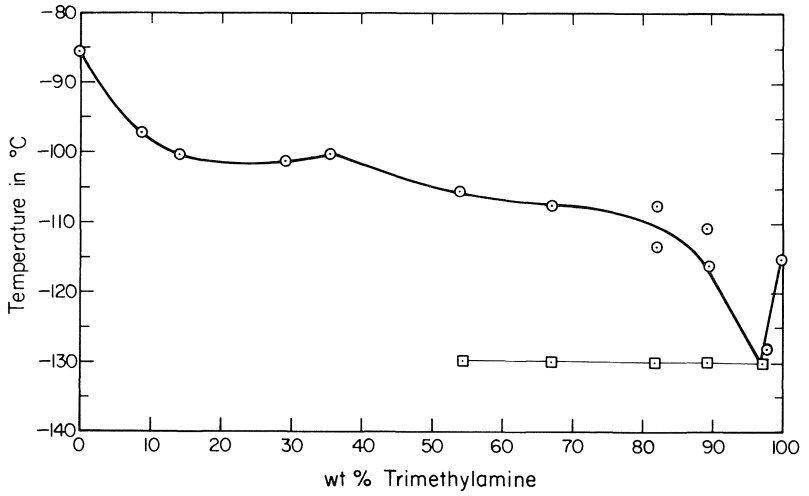


FIG. 4. Freezing point diagram for the system methylethylketone–triethylamine.

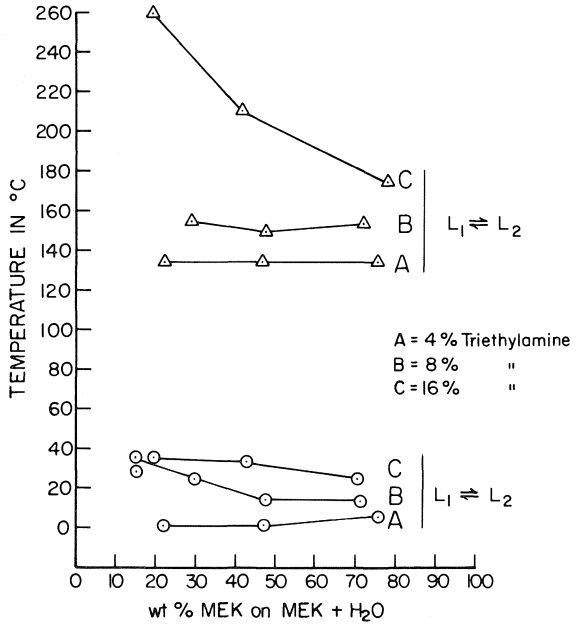


FIG. 5. Critical points L ⇌ V and $L_1 \rightleftharpoons L_2$ in the system methylethylketone–triethylamine–water for various fixed contents of triethylamine.

water (1), it has only a partial existence for the present system.

With 4 and 8% triethylamine, the content of methylethylketone has little effect on the temperature of disappearance of the $L_1 \leftrightharpoons L_2$ meniscus but, with 16% triethylamine, the temperature rises sharply with increasing water content. The low temperature disappearance of the $L_1 \leftrightharpoons L_2$ meniscus is but little influenced by triethylamine content but it is lowest for 4% triethylamine. The critical temperature L ⇋ V appears to be around 320°C, in the presence of 16% triethylamine.

From the data of the previous paper (1) on nicotine–methylethylketone–water a solid model was constructed which has been used in teaching here. A similar model can be constructed from the data of this paper.

Acknowledgement

I am indebted to Dr. J. E. Desnoyers for the following comment: "Your systems approach what is now called microemulsions. For example, we have shown that triethylamine–water mixtures exist as microphases at low temperatures and I suspect that methylethylketone is stabilizing these microstructures."

1. A. N. CAMPBELL, E. M. KARTZMARK, and W. E. FALCONER. Can. J. Chem. **36**, 1475 (1958).
2. N. RANDALL and F. E. MCKENNA. J. Am. Chem. Soc. **73**, 4859 (1951).
3. A. N. CAMPBELL and E. M. KARTZMARK. Can. J. Chem. **41**, 1088 (1963).
4. HANDBOOK OF CHEMISTRY AND PHYSICS. 39th ed. Chemical Rubber Publishing Company, Cleveland. 1958. p. 2125.

Can. J. Chem. Downloaded from www.nrcresearchpress.com by 210.87.254.40 on 09/05/12
For personal use only.

The X-ray crystal structures of $SeBr_3SbF_6$ and $TeBr_3AsF_6$

JACK PASSMORE, E. KEITH RICHARDSON, TOM K. WHIDDEN, AND PETER S. WHITE

Department of Chemistry, University of New Brunswick, P.O. Box 4400, Fredericton, N.B., Canada E3B 5A3

Received August 27, 1979

JACK PASSMORE, E. KEITH RICHARDSON, TOM K. WHIDDEN, and PETER S. WHITE. Can. J. Chem. **58**, 851 (1980).

The crystal structures of $SeBr_3SbF_6$ and $TeBr_3AsF_6$ were determined by X-ray diffraction methods. Single crystals of $SeBr_3SbF_6$ are orthorhombic, space group $P2_12_12_1$ with $a = 9.454(5)$ Å, $b = 12.623(6)$ Å, $c = 8.272(4)$ Å, and $Z = 4$. Single crystals of $TeBr_3AsF_6$ are monoclinic, space group $P2_1/c$, with $a = 7.994(3)$ Å, $b = 10.118(3)$ Å, $c = 12.306(3)$ Å, $\beta = 99.66(2)°$, and $Z = 4$. The cations in each salt have essentially C_{3v} symmetry and the average Se—Br distance in $SeBr_3SbF_6$ is 2.269(8) Å and the average Br—Se—Br angle is 100.9(3)°. Analogous data for $TeBr_3AsF_6$ are: Te—Br = 2.432(3) Å; Br—Te—Br = 97.92(9)°. Anions in each salt are essentially octahedral. The bond angles in isoelectronic Group V and Group VI trihalide molecules and cations are compared and found to be very similar. However, those found for Group VI trihalide cations are greater than (5 pairs) those observed in isoelectronic Group V molecules determined in the solid state, and angles estimated for Group VI cations in gas phase are greater (8 pairs) than those found for the related gas phase Group V trihalide partners. This result implies that geometries, at least in part, are determined by the relative sizes of the constituent atoms. The crystallography of the related salts $SeBr_3AsF_6$ and SBr_3MF_6 (M = As, Sb) was studied by single crystal and powder diffraction methods. Salts containing the same anion were found to be isostructural.

JACK PASSMORE, E. KEITH RICHARDSON, TOM K. WHIDDEN et PETER S. WHITE. Can. J. Chem. **58**, 851 (1980).

On a déterminé la structure des cristaux du $SeBr_3SbF_6$ et du $TeBr_3AsF_6$ par la méthode de diffraction de rayons-X. Les cristaux uniques du $SeBr_3SbF_6$ sont orthorhombiques, groupe d'espace $P2_12_12_1$ avec $a = 9.454(5)$ Å, $b = 12.623(6)$ Å, $c = 8.272(4)$ Å et $Z = 4$. Les cristaux uniques du $TeBr_3AsF_6$ sont monocliniques, groupe d'espace $P2_1/c$ avec $a = 7.994(3)$ Å, $b = 10.118(3)$ Å, $c = 12.306(3)$ Å, $\beta = 99.66(2)°$ et $Z = 4$. Les cations dans chacun des sels ont essentiellement une symétrie C_{3v} avec une distance moyenne de liaison SeBr, dans le $SeBr_3SbF_6$, de 2.269(8) Å et un angle moyen Br—Se—Br de 100.9(3)°. Dans le cas du $TeBr_3AsF_6$ ces données sont de: Te—Br = 2.432(3) Å et Br—Te—Br = 97.92(9)°. Dans chaque sel les anions sont essentiellement octaédriques. On a comparé les angles de liaisons des molécules isoélectroniques trihalogénées et des cations des groupes V et VI et on a trouvé des valeurs identiques. Cependant dans le cas des cations trihalogénés du groupe VI ces valeurs sont plus grandes (5 paires) que celles observées dans le cas des molécules isoélectroniques du groupe V et déterminées à l'état solide; les angles évalués pour les cations du groupe VI en phase gazeuse sont plus grands (8 paires) que celles trouvées pour les dérivés trihalogènes du groupe V à l'état gazeux. Ce résultat montre que les grandeurs relatives des atomes du composé déterminent les structures, au moins en partie. On a étudié la cristallographie des sels apprentés: $SeBr_3AsF_6$ et SBr_3MF_6 (M = As, Sb) par les méthodes de diffraction des cristaux uniques et des poudres. On a trouvé que les sels contenant les mêmes anions sont isostructuraux.

[Traduit par le journal]

Introduction

The structures of a number of MX_3^+ derivatives of the Group VI tetrahalides have been characterized by X-ray diffraction methods. The known structures which contain essentially discrete MX_3^+ ions include SF_3BF_4 (1), SeF_3MF_6 (M = Nb, Ta) (2), $SeF_3Nb_2F_{11}$ (3), $TeF_3Sb_2F_{11}$ (4), SCl_3ICl_4 (5), $SeCl_3AlCl_4$ (6), and $TeCl_3AlCl_4$ (7). In all cases cations have essentially C_{3v} symmetry with very small or no differences in the M—X bond lengths and the internally similar X—M—X angles about the central metal atom. Interionic contacts are generally weak and complete an octahedral environment around the central Group VI atom.

Recently SBr_3MF_6, $SeBr_3MF_6$, and $TeBr_3AsF_6$ (M = As, Sb) have been prepared (8) as stable crystalline solids. Raman spectra were consistent with an ionic formulation and C_{3v} symmetry for the cations. Single crystals of $SeBr_3SbF_6$ and $TeBr_3AsF_6$ were obtained and the structures of these salts were determined by X-ray diffraction methods and are reported below along with the unit cell parameters of the other tribromochalcogen salts listed above.

Experimental

Preparation of Single Crystals of $SeBr_3AsF_6$, $SeBr_3SbF_6$, and $TeBr_3AsF_6$

A detailed account of the preparation of the above salts is presented in ref. 8. Single crystals of $SeBr_3AsF_6$ were obtained by recrystallizing the product of the reaction of elemental selenium, bromine, and AsF_5 in SO_2 by adding a small amount of AsF_3 (SO_2:AsF_3 = 5:1), holding the solution at room temperature and slowly distilling off the solvent (3–5 h) into a cold trap held at 0°C. Crystals of $SeBr_3SbF_6$ were obtained directly as the product of the reaction of $Se_4(SbF_6)_2$, Br_2, and AsF_5 in SO_2 solution. Crystals of $TeBr_3AsF_6$ were also obtained directly as the product of the reaction of tellurium, bromine, and AsF_5 in SO_2 solution.

Crystal Data for SBr_3MF_6, $SeBr_3MF_6$, and $TeBr_3AsF_6$ (M = As, Sb)

Single crystals of $SeBr_3MF_6$ and $TeBr_3AsF_6$ were mounted and sealed in rigorously dried Pyrex capillaries as described in ref. 9. Unit cell parameters (Table 1) were obtained by photographic methods and, for $SeBr_3SbF_6$ and $TeBr_3AsF_6$, were refined from diffractometer data. Unit cell data for $SeBr_3AsF_6$ were refined by a least-squares procedure (10) using 21 out of 33 observed spacings on an X-ray powder photograph as input.[1]

[1]Tables of observed and calculated $1/d^2$ values for $SeBr_3AsF_6$, SBr_3AsF_6, and SBr_3SbF_6 are available at a nominal charge from the Depository of Unpublished Data, CISTI, National Research Council of Canada, Ottawa, Ont., Canada K1A 0S2.

0008-4042/80/080851-07$01.00/0

©1980 National Research Council of Canada/Conseil national de recherches du Canada

Can. J. Chem. Downloaded from www.nrcresearchpress.com by 210.87.254.5 on 09/05/12
For personal use only.

TABLE 1. Unit cell parameters and crystal data for the $M^{VI}Br_3M^{V}F_6$ salts

Parameter	Value				
	SBr_3AsF_6[a,c]	SBr_3SbF_6[a,d]	$SeBr_3AsF_6$[a]	$SeBr_3SbF_6$[b]	$TeBr_3AsF_6$[b]
System	Monoclinic	Orthorhombic	Monoclinic	Orthorhombic	Monoclinic
Space group	$P2_1/c$	$P2_12_12_1$	$P2_1/c$	$P2_12_12_1$	$P2_1/c$
Molecular weight	460.70	507.51	507.60	554.36	556.24
Cell dimensions: a	7.967(2) Å	9.784(9) Å	7.941(4) Å	9.454(5) Å	7.994(3) Å
b	9.721(3) Å	11.87(1) Å	9.643(3) Å	12.623(6) Å	10.118(3) Å
c	11.865(4) Å	7.961(6) Å	12.280(3) Å	8.272(4) Å	12.306(3) Å
β	97.61(3)°		99.28(4)°		99.66(2)°
Cell volume	910.9 Å^3	924.5 Å^3	928.1 Å^3	987.2 Å^3	981.19 Å^3
Density (calcd)	3.359 g/cm^3	3.646 g/cm^3	3.632 g/cm^3	3.729 g/cm^3	3.765 g/cm^3
Z	4	4	4	4	4
μ(MoKα)	181.44 cm^{-1}	170.16 cm^{-1}	220.05 cm^{-1}	195.53 cm^{-1}	196.94 cm^{-1}
F(000)	832	904	904	976	976
$a \sin\beta : b : c \sin\beta$	1:1.230:1.489	1.229:1.491:1	1:1.236:1.548	1.143:1.526:1	1:1.284:1.539

[a]Parameters refined from powder film data.
[b]Parameters refined from diffractometer data.
[c]Starting parameters from single crystal photographs: $a = 7.941$ Å, $b = 9.64$ Å, $c = 12.28$ Å, $\beta = 99.5°$ for $P2_1/c$.
[d]Starting parameters are those of $SeBr_3AsF_6$: $a = 9.64$ Å, $b = 12.08$ Å, $c = 7.94$ Å.

TABLE 2. Detailed information concerning the collection of X-ray intensity data for $SeBr_3SbF_6$ and $TeBr_3AsF_6$

Parameter	Value	
	$SeBr_3SbF_6$	$TeBr_3AsF_6$
Background time	10 s	10 s
Type of scan	ω−2θ	ω−2θ
Scan width	2° (corrected for dispersion)	2° (corrected for dispersion)
Scan rate	1 deg min^{-1}	1 deg min^{-1}
Maximum 2θ	55°	50°
No. of standards/interval	1/25	3/100
No. of reflections measured	1110	1726
No. of reflections observed ($I > 3\sigma(I)$)	798	1044
Maximum/minimum transmission factor	0.075/0.027	0.263/0.062
Crystal dimensions (cm)	0.025 × 0.021 × 0.050	0.036 × 0.036 × 0.007
λ (Å)	0.71069	0.71069
μ(MoK_α)	195.53 cm^{-1}	196.94 cm^{-1}
F(000)	976	976

$SeBr_3AsF_6$ and $TeBr_3AsF_6$ were monoclinic with systematically absent reflections that uniquely defined the space group as $P2_1/c$ (C_{2h}^5, No. 14, ref. 11) and $SeBr_3SbF_6$ was orthorhombic with absences uniquely defining its space group as $P2_12_12_1$ (D_4^2, No. 19, ref. 11).

The crystal data for SBr_3MF_6 (M = As, Sb; Table 1) were obtained from X-ray powder photographs using a least-squares fit (10) of the cell parameters to the observed spacings.[1] The crystal system and space group of the salts were unknown and therefore each was refined using the corresponding $SeBr_3MF_6$ unit cell dimensions as starting values in both $P2_1/c$ and $P2_12_12_1$ and the space group which gave the best fit of observed to calculated $1/d^2$ values assumed to be correct. Due to the diffuse nature of the powder patterns and consequent inaccuracy of the spacing measurements, only 14 out of 27 spacings were included in the refinement procedure for SBr_3AsF_6 and for SBr_3SbF_6 13 out of 24 spacings were included. The small number of observations in each procedure (~3 times the number of adjustable parameters) suggests that the final error estimates (Table 1) are over-optimistic.

X-ray intensity data for $SeBr_3SbF_6$ and $TeBr_3AsF_6$ were collected in the manner described in ref. 12 (experimental details presented in Table 2). The standard reflection measured during data collection for $SeBr_3SbF_6$ had a maximum deviation from its mean value of 2.3σ where $\sigma = (\Delta I^2/n)^{1/2}$. During the collection for $TeBr_3AsF_6$ three reflections were measured and their combined net intensity used as a standard. The maximum deviation from the mean for this figure was 3.76σ for one very different standard. When this figure was not included in the calculation the maximum deviation was reduced to 2.11σ.

The Determination of the Structure of $SeBr_3SbF_6$

Data reduction and structure refinement utilized the X-RAY76 program package (13). Atomic scattering factors for neutral atoms were taken from Cromer and Mann (14) and those for selenium, bromine, and antimony were corrected for anomalous dispersion (15). Corrections for Lorentz, polarization, and absorption factors (16) were made in the pre-treatment of data (see Table 2). A total of 124 reflections with $E \geq 1.50$ were used as input to MULTAN (17) and an E-map phased on the solution with the highest combined figure of merit revealed the atomic co-ordinates of the selenium, bromine, and antimony atoms. These positions were refined by least-squares after which an F_o synthesis gave the positions of the six fluorine atoms. With all atoms included in the calculation the least-squares procedure converged at a value of 0.170 for the conventional residual

Can. J. Chem. Downloaded from www.nrcresearchpress.com by 210.87.254.5 on 09/05/12
For personal use only.

Can. J. Chem. Downloaded from www.nrcresearchpress.com by 210.87.254.5 on 09/05/12
For personal use only.

TABLE 3. Final atomic positional parameters (fractional $\times 10^4$) with estimated standard deviations in parentheses for $SeBr_3SbF_6$ and $TeBr_3AsF_6$

Atom	x/a	y/b	z/c
	$SeBr_3SbF_6$		
Se1	−4656(6)	4698(3)	1330(6)
Br1	−4880(7)	3700(4)	3613(8)
Br2	−3167(6)	6001(4)	2091(8)
Br3	−6755(7)	5572(6)	1432(11)
Sb1	370(4)	8150(2)	3116(4)
F1	470(40)	9350(30)	1770(40)
F2	2160(40)	8570(20)	3860(50)
F3	−460(40)	8990(40)	4730(50)
F4	1180(50)	7390(50)	1480(50)
F5	560(40)	6930(30)	4440(60)
F6	−1400(40)	7810(40)	2450(60)
	$TeBr_3AsF_6$		
Te1	1891(1)	1674(1)	1931.9(8)
Br1	2401(3)	3944(2)	2535(2)
Br2	4313(3)	1523(2)	975(2)
Br3	3112(3)	532(2)	3608(1)
As1	1615(2)	7661(2)	772(1)
F1	2360(20)	6170(10)	510(10)
F2	−380(20)	7320(20)	113(9)
F3	2090(20)	8280(10)	−438(8)
F4	950(20)	9180(10)	1080(10)
F5	3620(20)	8050(20)	1460(10)
F6	1030(10)	7080(10)	1964(6)

function $R = \sum w(|F_o| - |F_c|)/\sum w|F_o|$ with $w = 1$. The weights in the procedure were changed to $1/[\sigma(F_o)^2 + 0.03F_o^2]$ where $\sigma(F_o)$ is derived from counter statistics (18). A minimum net intensity of 40 counts was used to define unobserved reflections. The refinement procedure converged at $R = 0.104$, $R_w = 0.142$ for 798 observed reflections. A ΔF synthesis showed a maximum residual electron density in the unit cell of 2.87 $e^-/Å^3$ at a position 0.83 Å from Sb1. The average shift/error value for the final cycle of refinement was 0.114 with a maximum shift/error of 0.581 associated with a fluorine thermal parameter. The quality of the crystals appeared too poor for any further improvement in the data set. Final atomic positional parameters for $SeBr_3SbF_6$ are presented in Table 3. Final anisotropic thermal parameters and tables of calculated and observed structure factors have been put in the Depository of Unpublished Data.[2]

The Determination of the Structure of $TeBr_3AsF_6$

Pre-treatment of data and structure refinement was carried out in a manner similar to that for $SeBr_3SbF_6$ except that the absorption correction was applied when $R = 0.130$ to ensure that the correction improved the model. The initial positional parameters for tellurium were determined using Patterson methods. An F_o synthesis phased with this position gave atomic co-ordinates for 4 large peaks which, from chemical considerations, were identified as the bromine and antimony atoms. Subsequent least-squares refinement and F_o synthesis gave the positions of the six fluorine atoms and with all atoms included in the calculation refinement converged at $R = 0.130$. The absorption correction was applied (Table 2 lists the transmission factors) and the weights in the least-squares procedure changed from 1 to $1/\sigma(F)^2$ where $\sigma(F)$ is directly derived from $\sigma(I)$ (18). The final residuals for 1726 reflections with 1044 classed as observed are $R = 0.048$, $R_w = 0.054$. The average shift/error for the final cycle of refinement was 0.022 with a maximum shift/error of 0.136 associated with a fluorine atom. The maximum residual electron density in the unit cell is 1.42 $e^-/Å^3$ at a position 1.97 Å from Br2. Final atomic positional parameters for $TeBr_3AsF_6$ are presented in Table 3. Final anisotropic thermal parameters and tables of calculated and observed structure factors have been deposited.[2]

Results and Discussion

Relevant bond lengths and angles for $SeBr_3SbF_6$ and $TeBr_3AsF_6$ are presented in Tables 4 and 5 respectively. Figures 1 and 2 show the crystal packing in $SeBr_3SbF_6$ and $TeBr_3AsF_6$. The three strongest anion–cation contacts in each structure complete a distorted octahedron about the central Group VI atom. The vertex-sharing packing of these anion and cation octahedra gives rise to an infinite three-dimensional net in $SeBr_3SbF_6$ (Fig. 1) and to a layered structure in $TeBr_3AsF_6$ (Fig. 2) where the cation octahedra form very distorted close-packed layers parallel to the *bc* plane with anions present in interstitial sites on either side of the layer. In terms of a VSEPR model (19), these contacts would be grouped around the lone pair of the MBr_3^+ cation. However, the relatively low average value of the F—M—F angles between the interionic contacts (86° in $SeBr_3SbF_6$; 93.2° in $TeBr_3AsF_6$) would suggest that, if the lone pair is stereochemically active in these cations, its activity is less than in the Group VI trifluoride cations. The

TABLE 4. Bond lengths (Å)[a] with estimated standard deviations in parentheses for $SeBr_3SbF_6$ and $TeBr_3AsF_6$

$SeBr_3SbF_6$		$TeBr_3AsF_6$	
Bond	Distance	Bond	Distance
Se1—Br1	2.280(8)	Te1—Br1	2.428(2)
—Br2	2.254(7)	—Br2	2.438(3)
—Br3	2.272(8)	—Br3	2.430(2)
Sb1—F1	1.88(4)	As1—F1	1.68(1)
—F2	1.88(4)	—F2	1.70(1)
—F3	1.88(5)	—F3	1.72(1)
—F4	1.82(5)	—F4	1.69(1)
—F5	1.90(4)	—F5	1.73(1)
—F6	1.81(4)	—F6	1.72(1)
Se1—F1	2.83(4)	Te1—F2	2.80(1)
—F2	2.76(3)	—F4	2.78(1)
—F5	2.72(4)	—F6	2.93(1)
		—F3	3.40(1)
Br1—F4	3.01(5)		
Br2—F6	2.85(5)	Br1—F5	3.34(1)
Br3—F4	3.02(6)	Br2—F3	3.07(1)
		Br3—F1	3.05(1)

[a]All interactions significantly less than the sum of van der Waals radii are included ($r_{Se} = 1.87$ Å, $r_{Te} = 2.06$ Å, $r_{Br} = 1.85$ Å, $r_F = 1.50$ Å from Bondi, ref. 20).

[2]Tables of observed and calculated structure factors and of anisotropic thermal parameters for $SeBr_3SbF_6$ and $TeBr_3AsF_6$ have been placed in the Depository of Unpublished Data, CISTI, National Research Council of Canada, Ottawa, Ont., Canada K1A 0S2.

Can. J. Chem. Downloaded from www.nrcresearchpress.com by 210.87.254.5 on 09/05/12
For personal use only.

TABLE 5. Bond angles (deg) with estimated standard deviations in parentheses for $SeBr_3SbF_6$ and $TeBr_3AsF_6$[a]

$SeBr_3SbF_6$		$TeBr_3AsF_6$	
Bonds	Angle	Bonds	Angle
Br1—Se1—Br2	103.3(3)	Br1—Te1—Br2	95.86(9)
—Br3	99.0(3)	—Br3	99.52(8)
Br2—Se1—Br3	100.4(3)	Br2—Te1—Br3	98.38(8)
F1—Sb—F2	86(2)	F1—As—F2	93.3(7)
—F3	90(2)	—F3	91.2(7)
—F4	88(2)	—F4	177.2(7)
—F5	172(2)	—F5	88.5(8)
—F6	93(2)	—F6	90.7(6)
F2—Sb—F3	89(2)	F2—As—F3	89.0(6)
—F4	91(2)	—F4	89.5(7)
—F5	87(2)	—F5	178.2(7)
—F6	176(2)	—F6	88.5(5)
F3—Sb—F4	177(2)	F3—As—F4	89.4(6)
—F5	95(2)	—F5	91.5(6)
—F6	88(2)	—F6	176.9(6)
F4—Sb—F5	88(2)	F4—As—F5	88.8(7)
—F6	92(2)	—F6	88.7(6)
F5—Sb—F6	94(2)	F5—As—F6	91.0(6)
F5—Se1—Br1	91.7(9)	F4—Te1—Br1	173.1(2)
—Br2	155.2(9)	—Br2	86.9(3)
—Br3	96.4(9)	—Br3	86.3(2)
—F2	81(1)	—F2	86.6(4)
—F1	79(1)	—F6	96.7(4)
F1—Se1—Br1	171.0(8)	F2—Te1—Br1	87.6(3)
—Br2	85.2(8)	—Br2	81.0(3)
—Br3	82.1(9)	—Br3	172.9(3)
—F2	98(1)	—F6	96.4(3)
F2—Se1—Br1	81.0(9)	F6—Te1—Br1	80.3(2)
—Br2	81.8(7)	—Br2	175.5(3)
—Br3	177.7(8)	—Br3	84.6(2)
Se1—Br1—F4	161(1)	Te1—Br2—F3	162.1(2)
—Br2—F6	169(1)	—Br3—F1	145.2(3)
—Br3—F4	159(1)	—Br1—F5	87.6(3)

[a]Mean ∠F—Sb—F, 90.08; mean ∠F—As—F, 90.01; mean ∠Br—Se—Br, 100.97; mean ∠Br—Te—Br, 97.91.

comparable angles in SF_3BF_4 (1), SeF_3NbF_6 (2) and $SeF_3Nb_2F_{11}$ (3) (average), and $TeF_3Sb_2F_{11}$ (4) are significantly larger, with values of 97°, 97.6°, and 100.9° respectively.

Contact between layers in $TeBr_3AsF_6$ consists of weak Br–F interactions (3.07 Å, 8.4% less than the sum of van der Waal's radii, 3.35 Å, ref. 20). Slightly stronger Br–F contacts are present in $SeBr_3SbF_6$ (2.96 Å). The Te–F contacts in $TeBr_3AsF_6$ (average 2.84 Å, 20.2% less than the sum of van der Waal's radii) are somewhat stronger than the Se–F contacts in $SeBr_3SbF_6$ (average 2.77 Å, 17.9% less than the sum of van der Waal's radii), consistent with tellurium having a greater positive charge than selenium and the more basic nature of AsF_6^- relative to SbF_6^-. The crystal data in Table 1 show that MBr_3AsF_6 salts are isomorphous and monoclinic (SeI_3AsF_6 has also been found to be isomorphous with the AsF_6^- salts studied herein (9)) and MBr_3SbF_6 salts are isomorphous and orthorhombic. Alkali metal $[AsF_6]^-$ and $[SbF_6]^-$ salts are also structurally different (21).

The cations are pyramidal with essentially C_{3v} symmetry. M—Br bond distances within each cation (Table 4) are statistically equivalent (average Se—Br distance, 2.269(8) Å; average Te—Br distance, 2.432(3) Å) while the Br—M—Br bond angles (Table 5) show minor differences. The average bond distances in $SeBr_3^+$ and $TeBr_3^+$ are significantly shorter than that in the isoelectronic species $AsBr_3$ (2.324(2) Å) and $SbBr_3$ (2.490(3) Å). Similar relationships are found between other trihalochalcogens and isoelectronic Group V trihalides (Table 6). The reduction in bond distance between isoelectronic pairs is reflected in changes in stretching forces constants (8) and presumably can be attributed to the difference in effective nuclear charge on the central atoms of the isoelectronic pairs.

The order of bond angle changes observed in Table 6, i.e. $XI_3 > XBr_3 > XCl_3 > XF_3$ (X = N, P, As, Sb, S^+, Se^+, Te^+) and $NX_3 > PX_3 > AsX_3 > SbX_3$ and $SX_3^+ > SeX_3^+ > TeX_3^+$ (X = F, Cl, Br, I) are explicable either by VSEPR theory (19) or by consideration of the relative sizes of the constituent atoms of the molecules or cations. The observation has been made (1) that molecules and cations that are isoelectronic pairs, e.g. PF_3 and SF_3^+, have the same bond angles despite the bond shortening in the cation. This conclusion was based on a comparison of data between the molecular species in the gas phase and the ion in the solid state. It is more meaningful, however, to compare the bond angles of isoelectronic pairs in the same environment, e.g., both in the gas phase. Bond angles for the Group V trihalides are smaller in the solid state than in the gas phase, with the exception of phosphorus and arsenic triiodides. The magnitudes of these differences (Δ) are shown in Table 7. The more electropositive the central atom and the greater the electronegativity of the halide, the greater the intermolecular interactions and the more the species tends towards having a polymeric structure with an octahedral environment about the central atom (90° angles). As the cation–anion interactions for the corresponding Group VI species are generally stronger than interactions between neutral Group V molecules (see Table 7), the bond angle in the isolated cation is reasonably predicted to be greater than that observed in the solid state by at least the difference observed for analogous data in isoelectronic Group V trihalides. If the corrections, Δ, in Table 7 are added to the Group VI trihalide angles the angles in all eight cases are

Can. J. Chem. Downloaded from www.nrcresearchpress.com by 210.87.254.5 on 09/05/12
For personal use only.

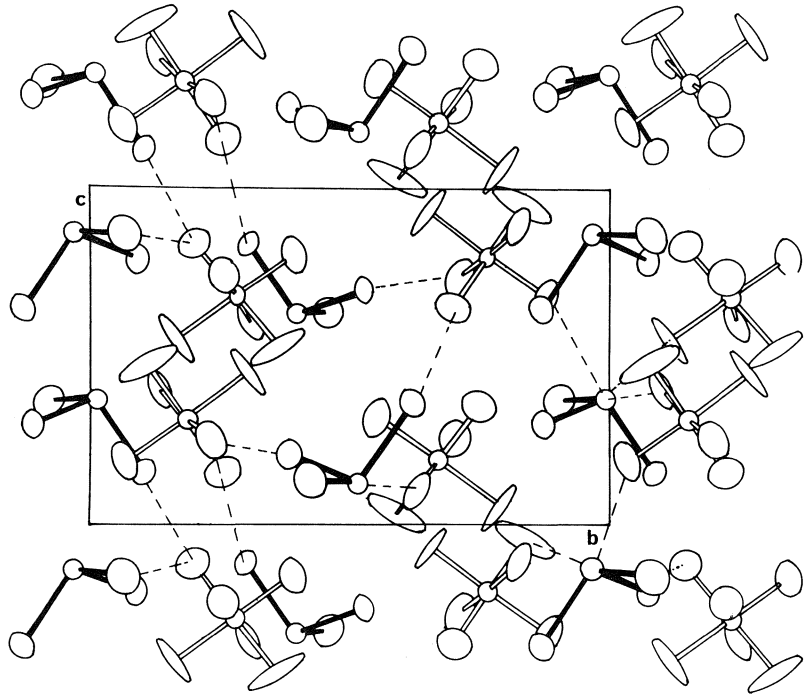


FIG. 1. The crystal packing in $SeBr_3SbF_6$.

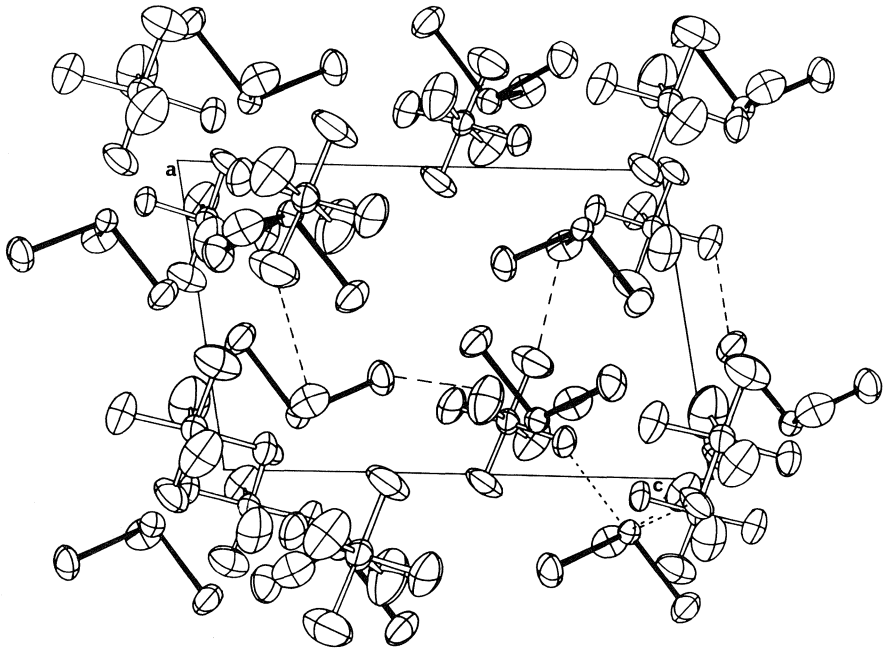


FIG. 2. The crystal packing in $TeBr_3AsF_6$.

greater than those observed for the gas phase isoelectronic Group V trihalide species. Alternatively, angles determined for Group V trihalides in the solid state may be compared with those of their Group VI congeners and, for the five cases in which data are available, the cation angles are larger. Thus, notwithstanding relatively large errors in the data, for all related pairs, the Group VI trihalide

Can. J. Chem. Downloaded from www.nrcresearchpress.com by 210.87.254.5 on 09/05/12
For personal use only.

TABLE 6. Average bond lengths (Å) and bond angles (deg) observed in the isoelectronic Group V and Group VI trihalide species

Group V			Group VI		
Compound	Bond length/angle	Reference	Compound	Bond length/angle	Reference
NF_3(g)	1.365(2)/102.37(3)	24	OF_3^+[a]		
NCl_3(g)	1.759(2)/107.1(5)	25	OCl_3^+[a]		
PF_3(g)	1.570(1)/97.8(2)	26	SF_3^+(s)	1.496(2)/97.5(1)	1
PCl_3(g)	2.0426(5)/100.10(2)	27	SCl_3^+(s)	1.988(3)/101.3(1)	5
PBr_3(g)	2.220(3)/101.0(4)	28*a*	SBr_3^+[b]	2.164(5)/101.1(0.9)[c]	
(s)	2.213(4)/100.5(2)	28*b*			
PI_3(g)	2.43(3)/102(3)	29*a*	SI_3^+[a]	2.368[c]/102.7[c]	
(s)	2.463(5)/102.0(3)	29*b*			
AsF_3(g)	1.707(2)/96.0(3)	30*a*[e]	SeF_3^+(s)	1.66(2)/94.2(1.7)	3
(s)[f]	1.70(3)/93(1)	30*b*,*c*			
$AsCl_3$(g)	2.162(1)/98.6(4)	31	$SeCl_3^+$(s)	2.103(13)/99.3[d]	6
$AsBr_3$(g)	2.324(2)/99.6(1)	22*a*	$SeBr_3^+$(s)	2.269(8)/100.9(3)	
(s)	2.364(0.015)/97.7(3)	22*b*			
AsI_3(g)	2.557(5)/100.2(4)	32*a*	$^{II}SeI_3^+$[b]	2.492(5)[c]/101.0[c]	
(s)	2.556(4)/102.0(1)	32*b*			
SbF_3(g)	1.879(4)/95.0(8)	33*a*	TeF_3^+(s)	1.84(4)/90.3(1.8)	4
(s)	1.92(2)/87.8(1.6)	33*b*			
$SbCl_3$(g)	2.333(3)/97.2(9)	34*a*	$TeCl_3^+$(s)	2.276(2)/95.0(2)	7
(s)	2.358(2)/94.13(5)	34*b*			
$SbBr_3$(g)	2.490(3)/98.2(6)	23*a*	$TeBr_3^+$(s)	2.432(3)/97.92(9)	
(s)	2.49(3)/95.5(2.4)	23*b*			
SbI_3(g)	2.719(1)/99.1(2.0)	35*a*	TeI_3^+[a]	2.650[c]/99.2[c]	
(s)	2.87(1)/95.8(3)	35*b*			

[a]Compounds containing this cation have not been prepared.
[b]Structural information not available.
[c]Estimated, see text.
[d]Standard deviations not quoted in original publication.
[e]Distance and angles for AsF_3(g) are an average of those reported in ref. 30*a*.
[f]Distances and angles for AsF_3(s) are an average of those found in $Te_6(AsF_6)_4 \cdot 2AsF_3$ (30*b*) and $S_{14}I_3(AsF_6)_3 \cdot AsF_3$ (30*c*).

TABLE 7. Δ and *r* values for trihalides

Group V trihalide	Δ[a]	*r*[b]	Group VI trihalide cation	Δ[d]	*r*
PF_3[c]			SF_3^+	1.0	0.78
PCl_3			SCl_3^+	0.7	0.86
PBr_3	0.5	1.05	SBr_3^+	0.4	—
PI_3	0.0	0.98			
AsF_3	3.6	0.93	SeF_3^+	3.0	0.72
$AsCl_3$			$SeCl_3^+$	2.5	0.84
$AsBr_3$	1.9	1.02	$SeBr_3^+$	2.0	0.83
AsI_3	−1.8	0.92		—	—
SbF_3	7.2	0.72	TeF_3^+	5.0	0.73
$SbCl_3$	3.1	0.90	$TeCl_3^+$	4.0	0.80
$SbBr_3$	2.7	0.90	$TeBr_3^+$	3.0	0.80
SbI_3	3.3	0.81	TeI_3^+	2.0	—

[a]Δ = angle in gas phase − angle in solid state.
[b]*r* = intermolecular contact/Σ van der Waals' radii.
[c]Data obtained from references given in Table 6.
[d]These are estimates of the correction (deg) necessary to derive bond angles for isolated trihalide cations from solid state data.

angles are greater than those of the isoelectronic Group V partners. This result is consistent with a model in which the geometry, at least in part, is determined by the relative sizes of the constituent atoms (36–38). The replacement of the Group V atom by a unipositive Group VI atom of smaller size naturally leads to a larger angle. In the context of VSEPR theory, this observation implies that the strength of bond–bond repulsions relative to that of lone pair-bond repulsions is greater in the cation than in the neutral Group V congener. This result does not obviously follow from simple electrostatics. It is of interest to note that the bond angles in Group VI dihalides (with two lone pairs) are generally equal to or greater than those of the corresponding Group V trihalides, having one lone pair (39). Although the wide usefulness of the VSEPR theory is acknowledged, this and other difficulties with the application of a second-order VSEPR model have been the subject of recent interest (40).

The data in Table 6 allow some predictions as to the bond lengths and angles in as yet uncharacterized species. There is a reduction in bond length by a factor of 1.026 ± 0.002 in going from the neutral to the charged species. The data therefore predict a bond length of 2.164(5) Å for SBr_3^+, 2.368(5) Å for SI_3^+, 2.492(5) Å for SeI_3^+, and 2.650(5) Å for TeI_3^+. During our exploration of a hard sphere model of these species a number of simple relationships between ligand–ligand separation and various other observables were explored. In one such relationship it was found that a relatively constant ratio (0.920 ± 0.006) exists

between the chlorine–chlorine separation in neutral or charged trichlorides and the bromine–bromine distance in comparable tribromides. The predicted Br—Br distance in SBr_3^+ is thus 3.355 Å and, from simple trigonometry, the bond angle is predicted to be 101.1 ± 0.9°. Similarly, the bond angles in the Group VI tri-iodide cations can be estimated from the ratio between ligand–ligand separations in the Group V tribromides and triiodides, assuming that the ratio is the same for Group V molecules and Group VI cations (see Table 6).

The anions in both $SeBr_3SbF_6$ and $TeBr_3AsF_6$ are, within experimental error, regular octahedra. Some distortions would be expected due to the anion–cation contacts but, within the accuracy of the experiment, none was observed. The average Sb—F and As—F distances are 1.86(4) Å and 1.71(1) Å respectively. Average F—Sb—F and F—As—F bond angles are 90(2)° and 90.0(7)°, respectively.

NOTE ADDED IN PROOF: The structure of TeI_3AsF_6 has recently been determined in our laboratory and the distances and angles were found to be consistent with those estimated.

Acknowledgement

The authors wish to thank the National Research Council of Canada for financial assistance.

1. D. D. GIBLER, C. J. ADAMS, M. FISCHER, A. ZALKIN, and N. BARTLETT. Inorg. Chem. **11**, 2325 (1972).
2. A. J. EDWARDS and G. R. JONES. J. Chem. Soc. A, 1891 (1970).
3. A. J. EDWARDS and G. R. JONES. J. Chem. Soc. A, 1491 (1970).
4. A. J. EDWARDS and P. TAYLOR. J. Chem. Soc. Dalton, 2150 (1973).
5. A. J. EDWARDS. J. Chem. Soc. Dalton, 1723 (1978).
6. B. A. STORK-BLAISSE and C. ROMERS. Acta Crystallogr. B**27**, 386 (1971).
7. B. KREBS, B. BUSS, and D. ALTENA. Z. Anorg. Allg. Chem. **386**, 257 (1971).
8. W. V. F. BROOKS, J. PASSMORE, and E. K. RICHARDSON. Can. J. Chem. **57**, 3230 (1979).
9. J. PASSMORE and P. TAYLOR. J. Chem. Soc. Dalton, 804 (1976).
10. H. J. EVANS, JR., D. E. APPLEMAN, and D. S. HANDWERKER. American Crystallographic Association Meeting. 1963. Abstracts 42 and 43.
11. International tables for X-ray crystallography. Vol. I. Kynoch Press, Birmingham. pp. 99, 105.
12. J. PASSMORE, P. TAYLOR, T. K. WHIDDEN, and P. S. WHITE. Can. J. Chem. **57**, 968 (1979).
13. J. M. STEWART (*Editor*). The X-ray system-version of 1976. Technical Report TR-446 of the Computer Science Centre, University of Maryland, College Park, MD.
14. D. T. CROMER and J. B. MANN. Acta Crystallogr. A**24**, 321 (1968).
15. C. H. DAUBEN and D. H. TEMPLETON. International tables for X-ray crystallography. Vol. III. Kynoch Press, Birmingham. 1968. p. 213. Table 3.3.2A.
16. W. R. BUSING and H. A. LEVY. Acta Crystallogr. **10**, 180 (1957).
17. G. GERMAIN, P. MAIN, and M. M. WOOLFSON. Acta Crystallogr. A**27**, 368 (1971).
18. P. W. R. CORFIELD, R. J. DOEDENS, and J. A. IBERS. Inorg. Chem. **6**, 197 (1967).
19. R. J. GILLESPIE. *In* Molecular geometry. Van Nostrand, Rheinhold, London. 1972.
20. A. BONDI. J. Phys. Chem. **68**, 441 (1964).
21. R. D. W. KEMMITT, D. R. RUSSEL, and D. W. A. SHARP. J. Chem. Soc. 4408 (1963).
22. (*a*) S. SAMDAL, D. M. BARNHART, and K. HEDBERG. J. Mol. Struct. **35**, 67 (1976); (*b*) J. TROTTER. Z. Kristollogr. **122**, 230 (1965).
23. (*a*) S. KONAKA and M. KIMURA. Bull. Chem. Soc. Jpn. **46**, 413 (1973); (*b*) D. W. CUSHAN and R. HULME. J. Chem. Soc. 4162 (1964).
24. M. OTAKE, C. MATSUMURA, and Y. MORINO. J. Mol. Spectrosc. **28**, 316 (1968).
25. H. B. BÜRGI, D. STEDMAN, and L. S. BARTELL. J. Mol. Struct. **10**, 31 (1971).
26. Y. MORINO, K. KUCHITSU, and T. MORTANI. Inorg. Chem. **8**, 867 (1969).
27. G. GAZZOLI. J. Mol. Spectrosc. **53**, 37 (1974).
28. (*a*) K. KUCHITSU, T. SHIBATA, A. YOKOZEKI, and C. MATSUMURA. Inorg. Chem. **10**, 2584 (1971); (*b*) R. ENJALBERT and J. GALY. Acta Crystallogr. B**35**, 546 (1979).
29. (*a*) S. M. SWINGLE. Acta Crystallogr. **3**, Pt. 1, 46 (1950); (*b*) E. T. LANCE, J. M. HASCHKE, and D. R. PEACOR. Inorg. Chem. **15**, 780 (1976).
30. (*a*) F. B. CLIPPARD and L. S. BARTELL. Inorg. Chem. **9**, 805 (1970); S. KONAKA and M. KIMURA. Bull. Chem. Soc. Jpn. **43**, 1693 (1970); (*b*) R. C. BURNS, R. J. GILLESPIE, W.-C. LUK, and D. R. SLIM. Inorg. Chem. **18**, 3086 (1979); (*c*) J. PASSMORE, G. SUTHERLAND, and P. WHITE, J. Chem. Soc. Chem. Commun. In press.
31. S. KONAKA. Bull. Chem. Soc. Jpn. **43**, 3107 (1970).
32. (*a*) Y. MORINO, T. UKAJI, and T. ITO. Bull. Chem. Soc. Jpn. **39**, 71 (1966); (*b*) J. TROTTER. Z. Kristallogr. **121**, 81 (1965).
33. (*a*) C. MATSUMURA and H. TAKEO. Symposium on molecular structure. Fukuoka. Oct. 15, 1969; (*b*) A. J. EDWARDS. J. Chem. Soc. A, 2751 (1970).
34. (*a*) S. KONAKA and M. KIMURA. Bull. Chem. Soc. Jpn. **46**, 404 (1973); (*b*) A. LIPKA. Acta Crystallogr. B**35**, 3020 (1979).
35. (*a*) A. ALMENNINGEN and T. BJORVATTEN. Acta Chem. Scand. **17**, 2573 (1963); (*b*) J. TROTTER and T. ZOBEL. Z. Kristallogr. **123**, 67 (1966).
36. L. S. BARTELL. J. Chem. Phys. **32**, 827 (1960).
37. C. GLIDEWELL. J. Chem. Phys. **20**, 113 (1976).
38. C. GLIDEWELL. Inorg. Chim. Acta, **12**, 219 (1975).
39. A. F. WELLS. *In* Structural inorganic chemistry. 4th ed. Clarendon Press, Oxford. 1975. Chapt. 16. p. 575.
40. A. SCHMIÉDEKAMP, D. W. J. CRUIKSHANK, S. SKAARUP, P. PULSEY, I. HARGITTAI, and J. E. BOGGS. J. Am. Chem. Soc. **101**, 2002 (1979).

Can. J. Chem. Downloaded from www.nrcresearchpress.com by 210.87.254.5 on 09/05/12
For personal use only.

Can. J. Chem. Downloaded from www.nrcresearchpress.com by 210.87.254.5 on 09/05/12
For personal use only.

Synthesis of maytansinoids: synthesis of an intermediate from D-glucose for the construction of maytansine[1]

PAK-TSUN HO

Division of Chemistry, National Research Council of Canada, Ottawa, Ont., Canada K1A 0R6

Received December 20, 1979

This paper is dedicated to Prof. Karel Wiesner on the occasion of his 60th birthday

PAK-TSUN HO. Can. J. Chem. **58**, 858 (1980).

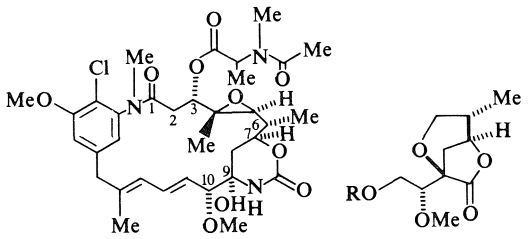
D-Glucose was converted to the lactone **1**, an intermediate containing the appropriate functionalities and correct stereochemistry for the construction of maytansine.

PAK-TSUN HO. Can. J. Chem. **58**, 858 (1980).

On transforme le D-glucose en lactone **1**, un intermédiaire contenant les fonctions et la stéréochimie appropriées en vue de la synthèse de la maytansine.

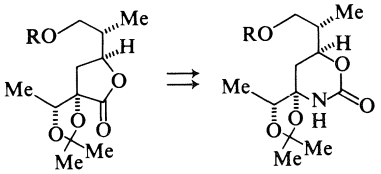
[Traduit par le journal]

Maytansine **I** is one of the clinically interesting macrolide maytansinoids (1). Because of the extremely low isolation yields of maytansine and its congenors, multifaced synthetic approaches toward this complex macrolide have been carried out by a number of research groups in the past several years (2), and the successful synthesis of *N*-methylmaysenine has recently been reported from two research groups (3). Earlier work in this laboratory on the model studies for the synthesis of maytansine led to the stereocontrolled preparation of the model lactone **i** and the simple conversion **i** to compound **ii**, a cyclic carbamate unit of maytansine (4). In the present communication we describe the efficient synthesis of the γ-lactone **1** from D-glucose. The promising lactone intermediate now has both correct relative and absolute stereochemistry and suitable functionalities for further elaboration to maytansine.

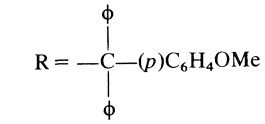


I

1



i **ii**



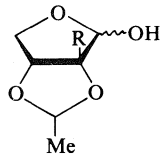
The starting material in the synthesis was the readily available sugar **2** for which a convenient synthesis from D-glucose had been developed in this laboratory (5). Reaction of **2** with tosyl chloride (1 equiv.) in pyridine at 0°C gave the tosylate **3**[2] in excellent yield. Treatment of compound **3** with *p*-toluenesulfonic acid (20% by weight) in anhydrous methanol at refluxing temperature for 3 days, followed by addition of methanolic potassium hydroxide at room temperature, led to the formation of the epoxide **4** (two glycosides) in 80% yield. For characterization, the two methyl glycosides **4** were easily separated by chromatography on silica gel (acetone–chloroform–hexane 1:6:3) to give the β- and α-glycoside in a ratio 8:2. The crystalline β-methyl glycoside had mp 60°C $[\alpha]_D$ −272° (*c* 1.0, chloroform), and it gave ^{1}H nmr signals at δ 4.80 (1H, s, C-1 proton), 3.42 (3H, s, methoxyl), and 3.20 ppm (2H, ABq, epoxide). The α-methyl glycoside was an oil, $[\alpha]_D$ +74.1° (*c* 1.2, chloroform), and gave ^{1}H nmr signals at δ 4.78 (1H, s, C-1 proton), 3.40 (3H, s, methoxyl), and 3.04 ppm (2H, ABq, epoxide). Compound **5** was

[1]Issued as NRCC No. 18122.

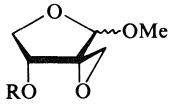
[2]Satisfactory physical and spectral data have been obtained for all new compounds.

0008-4042/80/080858-03$01.00/0

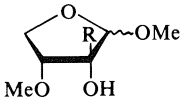
© 1980 National Research Council of Canada/Conseil national de recherches du Canada



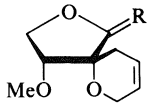
2 R = CH_2OH
3 R = CH_2OTs



4 R = H
5 R = Me



6 R = $CH_2C{\equiv}CCH_2OTHP$
7 R = $CH_2C{\equiv}CCH_2OH$
8 R = $CH_2CH{=}CHCH_2OH$



10 R = OMe, H
11 R = OH, H
12 R = O

obtained in 80% yield by reaction of **4** with sodium hydride and excess methyl iodide in anhydrous tetrahydrofuran at 0°C. Condensation of **5** with 3-tetrahydropyranyloxy-1-propynyl dimethyl alane (4 equiv.) in toluene solution (10°C, 1.5 days) resulted in the formation of the oily compound **6** in 80% yield (6). Removal of the tetrahydropyranyl group from **6** with catalytic amount of *p*-toluenesulfonic acid in 90% aqueous methanol (40°C, 1 h) furnished quantitatively the alcohol **7**. For the β-glycoside, $[\alpha]_D$ −86° (*c* 1.5, chloroform), ^{1}H nmr signals at δ 4.73 (1H, s, C-1 proton), and 4.22 ppm (2H, broad s, —CH_2OH); for the α-glycoside, $[\alpha]_D$ +80.3° (*c* 3.6, chloroform), ^{1}H nmr signals at δ 4.53 (1H, s, C-1 proton), and 4.21 ppm (2H, broad s, —CH_2OH). Hydrogenation of compound **7** on 5% Pd–$CaCO_3$ in benzene solution in the presence of a small amount of quinoline yielded the olefin **8** as a syrup in 92% yield.

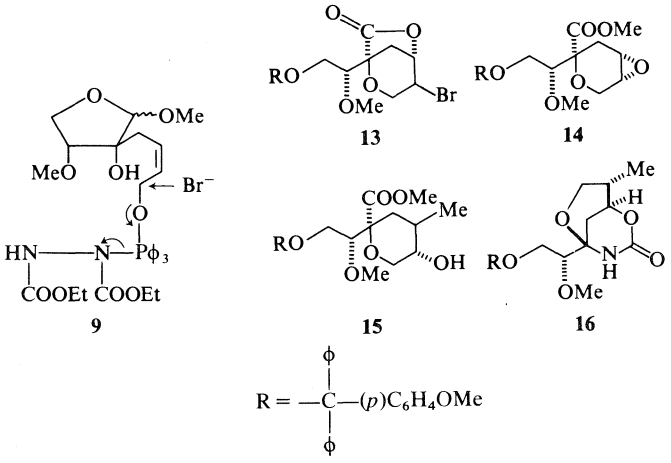
The operation which faced us now was the formation of the unsaturated spiroheterocyclic system by cyclization of the unsaturated diol **8**. After considerable experimentation, a simple and efficient cyclization procedure was developed. A solution of diethyl azodicarboxylate (2 equiv.) in tetrahydrofuran was added to a solution of **8**, triphenylphosphine (2 equiv.), and anhydrous lithium bromide (2.5 equiv.) in tetrahydrofuran at 0°C under argon. After stirring 30 min, anhydrous methanol was added to the reaction mixture and the solution was allowed to stir for an additional 2 h at room temperature. Purification on silica gel yielded the cyclization product **10** as a syrup in 87% yield. For the β-glycoside, $[\alpha]_D$ −132.8° (*c* 1.4, chloroform), ^{1}H nmr signals at δ 5.78 (2H, m, vinylic protons), 4.82 (1H, s, C-1 proton), 4.35 (2H, broad s, C=C—CH_2—O—), and 2.34 ppm (2H, broad s, C=C—CH_2—); for the α-glycoside, $[\alpha]_D$ +108.2° (*c* 1.1, chloroform), ^{1}H nmr signals at δ 5.80 (2H, m, vinylic protons), 4.60 (1H, s, C-1 proton), 4.30 (2H, broad s, C=C—CH_2—O—), and 2.10 ppm (2H, broad s, C=C—CH_2—). The use of lithium bromide and methanol in this one-step cyclization process is essential. When the reaction was carried out without lithium bromide, a nitrogen-containing compound was isolated and there was no desired product formed.[3] The cyclization reaction presumably proceeds via a bromide intermediate, formed by the attack of lithium bromide on the complex, or an adduct such as **9**, followed by ring closure resulting from a nucleophilic attack by the tertiary hydroxyl under basic conditions. The high efficiency of this one-step cyclization reaction may provide a useful method for the synthesis of a variety of unsaturated heterocycles. The utilization and generality of the cyclization reaction will be discussed elsewhere.

Compound **10**, on treatment with 70% aqueous trifluoroacetic acid at room temperature for 30 h, afforded quantitatively **11**, which was oxidized with a mixture of dimethyl sulfoxide and acetic anhydride (1:1) at room temperature to the corresponding γ-lactone **12** in 87% yield, mp 85°C, $[\alpha]_D$ −122.8° (*c* 1.7, chloroform); ν_{max}: 1790 (lactone) cm^{-1}; ^{1}H nmr signals at δ 5.80 (2H, m, vinylic protons), 4.35 (4H, m, —CH_2—$\overset{O}{\overset{\|}{C}}$O— and C=C—$CH_2$—O—), 3.80 (1H, t, C-3 proton), 3.44 (3H, s, methoxyl), and 2.28 (2H, broad s, C=C—CH_2—) ppm.

Further elaboration of the spirolactone **12** was accomplished in the following way. Reaction of **12** with potassium hydroxide in aqueous methanol at room temperature, followed by treatment of the resulting hydroxyacid with *p*-anisyldiphenylmethyl chloride (1.2 equiv.) in pyridine yielded the crude product which was dissolved in aqueous potassium hydroxide (pH 9.5) and reacted with a small excess of bromine – potassium bromide at 5°C to give the crystalline bromolactone **13** in 72% yield, mp 156°C; $[\alpha]_D$ −24.3° (*c* 1.0, chloroform); ν_{max}: 1790 (lactone) cm^{-1}. The epoxide **14** was obtained quantitatively by treatment of **13** with $LiOH \cdot H_2O$ (2 equiv.) in methanol at room temperature for 2 h. Its infrared spectrum showed ν_{max}: 1730 cm^{-1} for the ester. Finally, compound **14**, on treatment with lithium dimethylcuprate (2 equiv.) in ether solution (5 h, 0°C), was converted in 80% yield to a mixture

[3]Reactions of diols with diethyl azodicarboxylate and triphenyl phosphine to give cyclic ethers have been reported (see ref. 7).

Can. J. Chem. Downloaded from www.nrcresearchpress.com by 210.87.254.5 on 09/05/12
For personal use only.



containing 65% of the desired compound **1** accompanied by the regio-isomer hydroxyester **15**. The lactone **1** showed $[\alpha]_D$ −3.5 (*c* 1.0, chloroform) and ν_{max}: 1780 (γ-lactone) cm^{-1}. It gave ^1H nmr signals at δ 4.65 (1H, q, —C(=O)—O—CH—), 3.75 (3H, s, aromatic methoxyl), 3.48 (3H, s, methoxyl), and 1.03 ppm (3H, d, methyl). Thus, construction of the promising intermediate **1** for the synthesis of maytansine was completed. Further, the lactone **1**, under the same conditions described in the model investigation (4), was converted in good yield to the carbamate **16**, ν_{max}: 3410 (NH), 1710 (carbamate) cm^{-1}; ^1H nmr signals at δ 6.20 (1H, s, NH exchanged with D_2O), 4.38 (1H, q, —CH—O—C(=O)—NH—), and 1.05 ppm (3H, d, methyl). In accordance with the chemistry of maytansinoids, the correct stereochemistry of hydroxyl at C-9 will be readily produced by acid-catalyzed hydration (1*a*). The utilization of the intermediate **1** in the total synthesis of maytansine is currently underway.[4]

[4]A novel synthesis of "western–southern" region of maytansine has been accomplished and is reported in the accompanying communication.

Acknowledgements

The author wishes to thank Dr. O. E. Edwards for reading this manuscript and Mr. H. Seguin for analyses.

1. (*a*) S. M. Kupchan, Y. Komoda, W. A. Court, G. J. Thomas, R. M. Smith, A. Karin, C. J. Gilmore, R. C. Haltiwanger, and R. F. Bryan. J. Am. Chem. Soc. **94**, 1354 (1972); (*b*) B. Chabner, A. S. Levine, B. L. Johnson, and R. C. Young. Cancer Treat. Rep. **62**, 429 (1978).
2. (*a*) A. I. Meyers, K. Tomioka, D. M. Roland, and D. Comins. Tetrahedron Lett. 1375 (1978); (*b*) J. E. Roy and B. Ganem. Tetrahedron Lett. 775 (1977); (*c*) E. J. Corey, M. G. Bock, A. P. Kozikowski, A. V. RamaRao, D. Floyd, and B. Lipshutz. Tetrahedron Lett. 1051 (1978); (*d*) E. Götschi, F. Schneider, H. Wagner, and K. Bernauer. Helv. Chim. Acta, **60**, 1416 (1977); (*e*) W. J. Elliot and J. Fried. J. Org. Chem. **41**, 2469 (1976); (*f*) M. Isobe, M. Kitamura, and T. Goto. Tetrahedron Lett. 3465 (1979); (*g*) R. Bonjouklian and B. Ganem. Carbohydr. Res. **76**, 245 (1979).
3. (*a*) E. J. Corey, L. O. Weigel, D. Floyd, and M. G. Bock. J. Am. Chem. Soc. **100**, 2916 (1978); (*b*) A. I. Meyers, D. M. Roland, D. L. Comins, R. Henning, M. P. Fleming, and K. Shimizu. J. Am. Chem. Soc. **101**, 4732 (1979); (*c*) A. I. Meyers, D. Comins, D. M. Roland, R. Henning, and K. Shimizu. J. Am. Chem. Soc. **101**, 7104 (1979).
4. O. E. Edwards and P.-T. Ho. Can. J. Chem. **55**, 371 (1977).
5. P.-T. Ho. Tetrahedron Lett. 1623 (1978).
6. J. Fried, C. H. Lin, and S. H. Ford. Tetrahedron Lett. 1379 (1969).
7. J. T. Carlock and M. P. Mack. Tetrahedron Lett. 5153 (1978).

Can. J. Chem. Downloaded from www.nrcresearchpress.com by 210.87.254.5 on 09/05/12
For personal use only.

Synthesis of maytansinoids: the aromatic moiety of maytansine[1]

PAK-TSUN HO
Division of Chemistry, National Research Council of Canada, Ottawa, Ont., Canada K1A 0R6

Received January 17, 1980

PAK-TSUN HO. Can. J. Chem. **58**, 861 (1980).

A simple and novel synthesis of the tetrasubstituted aromatic compound related to the "western–southern" region of maytansine has been achieved.

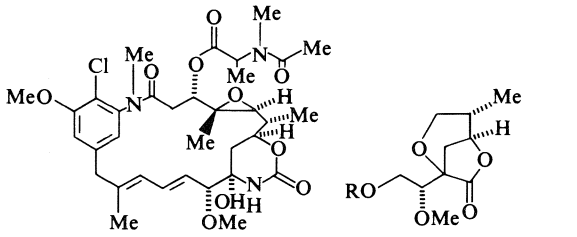
PAK-TSUN HO. Can. J. Chem. **58**, 861 (1980).

On a réalisé une synthèse simple et nouvelle d'un composé aromatique tétrasubstitué relié à la région "sud–ouest" de la maytansine.

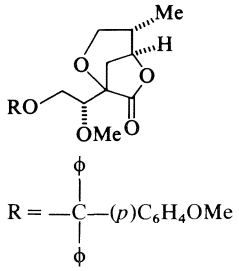
[Traduit par le journal]

In the studies toward the total synthesis of clinically interesting maytansine **I**, we have described recently the stereospecific synthesis of optically active lactone **II** and its derived carbamate as synthons for construction of maytansine (1). We now report a novel and efficient synthesis of the tetrasubstituted aromatic intermediate **1** which serves as the crucial synthon of the "western–southern" region of maytansine.[2]

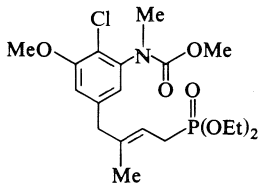
Compound **2**[3] was prepared in almost quantitative yield by reaction of commercially available 6-amino-*m*-cresol with trimethylacetyl chloride in methylene dichloride and aqueous sodium bicarbonate at room temperature, followed by methylation with potassium carbonate and methyl iodide in acetone at refluxing temperature. When **2** was treated with *n*-butyllithium (2.2 equiv.) in tetrahydrofuran at room temperature for 6 h, dilithiation of **2** occurred in the position *ortho* to the amino group (3). Reaction of the dianion with carbon dioxide at −70°C resulted in the formation of the crystalline acid **3** (mp 160°C) in 86% yield, based on **2** consumed; ν_{max}: 3440 (NH), 3300–2500 (acid), and 1690 (acid and amide) cm^{-1}; ^1H nmr signals at δ 10.12 (1H, broad s, COOH exchanged with D_2O), 8.23 (1H, broad s, NH exchanged with D_2O), 7.30 (1H, s, aromatic proton), and 6.90 ppm (1H, s, aromatic proton). The two singlets at 7.30 and 6.90 ppm for the two aromatic protons in the ^1H nmr spectrum of compound **3** clearly indicate that the carboxylic function is correctly located in the position *ortho* to the amide group. Hydrolysis of **3** with 25% aqueous hydrochloric acid under reflux for 16 h furnished the aniline hydrochloride derivative **4** in 95% yield, mp 162°C. Conversion of **4** to the chloro derivative **5** (mp 152°C) was accomplished in 90% yield by treatment with sodium nitrite (1 equiv.) in aqueous hydrochloric acid at 0°C, followed by heating the resulting solution with cuprous chloride (1.5 equiv.) at 60°C for 2 days. Consecutive treatment of compound **5** with ethyl chloroformate (1.5 equiv.) – triethylamine in acetone and sodium azide – water at 0°C gave the corresponding acyl azide. Curtius rearrangement of the crude azide in benzene (60°C, 30 min), followed by addition of methanol to the resulting



I



II R = —C(φ)(φ)—(*p*)C_6H_4OMe



1

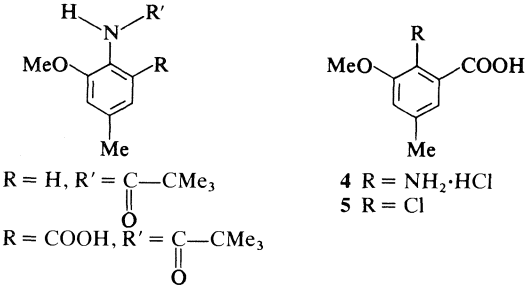
[1]Issued as NRCC No. 18189.

[2]For other approaches to the aromatic intermediate of maytansine, see ref. 2.

[3]Satisfactory physical and spectral data have been obtained for all new compounds.

0608-4042/80/080861-03$01.00/0

©1980 National Research Council of Canada/Conseil national de recherches du Canada

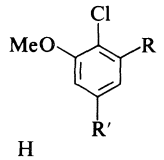


2 R = H, R′ = C(=O)—CMe$_3$

3 R = COOH, R′ = C(=O)—CMe$_3$

4 R = NH_2·HCl

5 R = Cl



6 R = N(H)—COOMe, R′ = Me

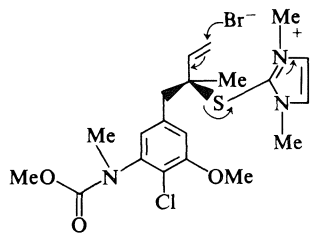
7 R = N(Me)—COOMe, R′ = Me

8 R = N(Me)—COOMe, R′ = CH_2Br

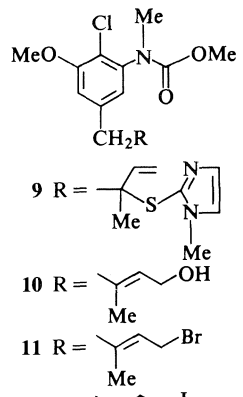
isocyanate (80°, 1 h) led to the isolation of the crystalline urethane derivative **6**, mp 79°C; ν_{max}: 3410 (NH) and 1730 (urethane) cm^{-1}. Methylation of compound **6** with sodium hydride and methyl iodide in tetrahydrofuran solution at 0°C gave the *N*-methyl derivative **7** (mp 101°C). The yield from **5** was 82%. When **7** was treated with *N*-bromosuccinimide (1.1 equiv.) in carbon tetrachloride, either with irradiation using a sunlamp or in the presence of catalytic amount of benzoyl peroxide under reflux for 4 h, the crystalline bromide **8** (mp 91°C) was obtained in 80% yield. The overall yield from starting material **2** was 49%.

The aromatic compound **8**, now readily available in good quantities, contains all substituents for further elaboration to the trisubstituted olefin **1**. Condensation of **8** with the lithium salt (1.2 equiv.), prepared from 1-methylimidazo-2-yl α-methylallyl sulfide and *n*-butyllithium (4), in tetrahydrofuran at −70°C for 1 h produced compound **9** as the α-alkylated product in 95% yield, ^{1}H nmr signals at δ 6.73 (2H, 2 overlapping s, aromatic protons), 5.98 (1H, m, vinylic proton), 4.83 (2H, m, vinylic protons), 3.03 (2H, s, benzylic protons), and 1.32 ppm (3H, s, methyl). It has been shown that [2,3]-sigmatropic rearrangement of trisubstituted allylic sulfoxides produces *trans*-trisubstituted allylic alcohols with high degree of stereoselectivity (4, 5). Oxidation of compound **9** to the corresponding sulfoxide with *m*-chloroperbenzoic acid (1 equiv.) in methylene dichloride at 0°C, followed by addition of diethylamine in methanol at room temperature overnight, afforded a mixture of the *E*- and *Z*-allylic alcohols (ratio 64:36) in 75% yield. The desired *E*-allylic alcohol **10** could be separated from its *Z*-isomer (ether, silica gel) as white crystals (mp 86°C). Treatment of **10** with *N*-bromosuccinimide – triphenyl phosphine complex (1.2 equiv.) in benzene (25°C, 2.5 h) gave the bromide **11** in 75% yield, ^{1}H nmr signals at δ 6.73 (2H, 2 overlapping s, aromatic protons), 5.70 (1H, t, vinylic proton), 4.04 (2H, d, C=C—CH_2Br), and 3.03 ppm (2H, s, benzylic protons).

The low stereoselectivity in the [2,3]-sigmatropic process was not satisfactory, so an efficient and highly stereoselective alternate synthesis of the bromide **11** was developed. When compound **9** was treated with a large excess of methyl bromide in dimethylformamide containing anhydrous lithium bromide (20°C, 10 h),[4] the material which was obtained in 60% yield was the *E*-allylbromide **11** contaminated with about 10% of its *Z*-isomer.[5] In a similar manner, reaction of compound **9** with methyl iodide in dimethylformamide in the presence of sodium iodide produced the rather unstable



A



9 R =

10 R =

11 R =

12 R =

iodide **12** in better yield (80∼85%). A possible pathway for this facile reaction was that the first stage of the reaction is quaternization of the basic nitrogen of imidazole to form the reactive intermediate **A**, which, by the attack of bromide anion on the double bond, would then proceed to yield the allylic rearrangement product **11**. The above simple procedure with high stereoselectivity may provide a useful general method for the preparation of *trans*-trisubstituted allylhalides.

Reaction of **12** with triethyl phosphite (1.2

[4]Reaction of 2-alkylthiothiazoline with methyl iodide in DMF to give alkyliodide has been reported (see ref. 6).

[5]Determined by comparison with the ^{1}H nmr of a standard solution of *E*- and *Z*-isomers.

equiv.) in toluene under reflux for 1.5 h afforded the phosphonate derivative **1** in 90% yield, ^{1}H nmr signals at δ 6.71 (2H, 2 overlapping s, aromatic protons), 5.35 (1H, t, vinylic proton), and 2.60 ppm (2H, q, C=C—CH_2—P—). With the intermediate **II** and **1** now readily available, further work directed at the construction of maytansine and its eventual total synthesis is in progress.

Acknowledgements

The author thanks Dr. O. E. Edwards for reading this manuscript and Mr. H. Seguin for analyses.

1. P.-T. Ho. Can. J. Chem. **58**, 858 (1980).
2. (*a*) E. Götschi, F. Schneider, H. Wagner, and K. Bernauer. Helv. Chim. Acta, **60**, 1416 (1977); (*b*) J. E. Foy and B. Ganem. Tetrahedron Lett. 775 (1977); (*c*) A. I. Meyers and J. M. Kane. Tetrahedron Lett. 771 (1977); (*d*) E. J. Corey, H. F. Wetter, A. P. Kozikowski, and A. V. RamaRao. Tetrahedron Lett. 777 (1977).
3. W. Fuhrer and H. W. Gschwend. J. Org. Chem. **44**, 1133 (1979).
4. D. A. Evans and G. C. Andrews. Acc. Chem. Res. **7**, 147 (1974).
5. D. A. Evans, G. C. Andrews, T. Fujimoto, and D. Wells. Tetrahedron Lett. 1389 (1973).
6. K. Hirai and Y. Kishida. Tetrahedron Lett. 2743 (1972).

Bimolecular production of gas phase ionic hydrates by ion cyclotron resonance spectroscopy

R. L. Clair and T. B. McMahon

Department of Chemistry, University of New Brunswick, Fredericton, N.B., Canada E3B 5A3

Received December 27, 1979

R. L. Clair and T. B. McMahon. Can. J. Chem. **58**, 863 (1980).

The gas phase ion–molecule reactions of α,α,α′,α′ tetrafluorodimethyl ether both alone and in mixtures with water have been examined. The dominant feature of the ion chemistry of these mixtures is the sequential bimolecular production of the hydrated hydronium ion, $H_5O_2^+$. Two independent mechanistic pathways for production of $H_5O_2^+$ are outlined arising from reaction of H_3O^+ with $(CF_2H)_2O$ and from CF_2H—O=CHF^+ with H_2O. Implications for examination of solvent switching equilibria are discussed.

R. L. Clair et T. B. McMahon. Can. J. Chem. **58**, 863 (1980).

On a examiné les réactions en phase gazeuse de l'ion moléculaire de l'éther α,α,α′,α′ tétrafluorodiméthylique pur ou mélangé à l'eau dans différentes proportions. Le fait dominant de la chimie de l'ion dans ces mélanges est la production bimoléculaire séquentielle de l'ion hydronium hydraté, $H_5O_2^+$. On propose deux mécanismes indépendants de production de $H_5O_2^+$ provenant de la réaction de H_3O^+ avec $(CF_2H)_2O$ et de la réaction de CF_2H—O=CHF^+ avec l'eau. On discute des implications de ces réactions pour l'examen du solvant dans l'établissement de l'équilibre.

[Traduit par le journal]

Examination of gas phase ion–molecule clustering equilibria, such as reaction [1], provides valuable information concerning the *absolute* energetics of solvation of ions, A^+, by solvents, S (1).

[1] $A^+ + S \overset{[M]}{\rightleftharpoons} AS^+$

The study of such equilibria is usually inaccessible to trapped-ion ion cyclotron resonance (ICR) experiments since stabilizing collisions with the excited $(AS^+)^*$ initially formed must take place within a time which is shorter than the intrinsic lifetime of $(AS^+)^*$ (2, 3). This condition usually necessitates the use of pressures which are sufficiently high to prevent efficient trapping of ions in the ICR cell (4). In the present communication we wish to report several *sequential bimolecular reactions* which lead to efficient production of cluster ions, AS^+, which can subsequently participate in solvent switching equilibria, reaction [2], to allow determination of accurate relative solvation energetics (5, 6).

[2] $AS_1^+ + S_2 \rightleftharpoons AS_2^+ + S_1$

As part of a continuing program of investigation of gas phase proton affinities of molecules less basic than water, the gas phase ion chemistry of α,α,α′,α′ tetrafluorodimethyl ether and binary mixtures of $(CH_2H)_2O$ with weak bases was recently examined. At 70 eV electron energy, the dominant ion in the mass spectrum of $(CF_2H)_2O$ is

0008-4042/80/080863-03$01.00/0

©1980 National Research Council of Canada/Conseil national de recherches du Canada

equiv.) in toluene under reflux for 1.5 h afforded the phosphonate derivative **1** in 90% yield, ^{1}H nmr signals at δ 6.71 (2H, 2 overlapping s, aromatic protons), 5.35 (1H, t, vinylic proton), and 2.60 ppm (2H, q, C=C—CH_2—P—). With the intermediate **II** and **1** now readily available, further work directed at the construction of maytansine and its eventual total synthesis is in progress.

Acknowledgements

The author thanks Dr. O. E. Edwards for reading this manuscript and Mr. H. Seguin for analyses.

1. P.-T. Ho. Can. J. Chem. **58**, 858 (1980).
2. (*a*) E. Götschi, F. Schneider, H. Wagner, and K. Bernauer. Helv. Chim. Acta, **60**, 1416 (1977); (*b*) J. E. Foy and B. Ganem. Tetrahedron Lett. 775 (1977); (*c*) A. I. Meyers and J. M. Kane. Tetrahedron Lett. 771 (1977); (*d*) E. J. Corey, H. F. Wetter, A. P. Kozikowski, and A. V. RamaRao. Tetrahedron Lett. 777 (1977).
3. W. Fuhrer and H. W. Gschwend. J. Org. Chem. **44**, 1133 (1979).
4. D. A. Evans and G. C. Andrews. Acc. Chem. Res. **7**, 147 (1974).
5. D. A. Evans, G. C. Andrews, T. Fujimoto, and D. Wells. Tetrahedron Lett. 1389 (1973).
6. K. Hirai and Y. Kishida. Tetrahedron Lett. 2743 (1972).

Can. J. Chem. Downloaded from www.nrcresearchpress.com by 210.87.254.40 on 09/05/12
For personal use only.

Bimolecular production of gas phase ionic hydrates by ion cyclotron resonance spectroscopy

R. L. Clair and T. B. McMahon

Department of Chemistry, University of New Brunswick, Fredericton, N.B., Canada E3B 5A3

Received December 27, 1979

R. L. Clair and T. B. McMahon. Can. J. Chem. **58**, 863 (1980).

The gas phase ion–molecule reactions of α,α,α′,α′ tetrafluorodimethyl ether both alone and in mixtures with water have been examined. The dominant feature of the ion chemistry of these mixtures is the sequential bimolecular production of the hydrated hydronium ion, $H_5O_2^+$. Two independent mechanistic pathways for production of $H_5O_2^+$ are outlined arising from reaction of H_3O^+ with $(CF_2H)_2O$ and from CF_2H—O=CHF^+ with H_2O. Implications for examination of solvent switching equilibria are discussed.

R. L. Clair et T. B. McMahon. Can. J. Chem. **58**, 863 (1980).

On a examiné les réactions en phase gazeuse de l'ion moléculaire de l'éther α,α,α′,α′ tétrafluorodiméthylique pur ou mélangé à l'eau dans différentes proportions. Le fait dominant de la chimie de l'ion dans ces mélanges est la production bimoléculaire séquentielle de l'ion hydronium hydraté, $H_5O_2^+$. On propose deux mécanismes indépendants de production de $H_5O_2^+$ provenant de la réaction de H_3O^+ avec $(CF_2H)_2O$ et de la réaction de CF_2H—O=CHF^+ avec l'eau. On discute des implications de ces réactions pour l'examen du solvant dans l'établissement de l'équilibre.

[Traduit par le journal]

Examination of gas phase ion–molecule clustering equilibria, such as reaction [1], provides valuable information concerning the *absolute* energetics of solvation of ions, A^+, by solvents, S (1).

[1] $A^+ + S \overset{[M]}{\rightleftharpoons} AS^+$

The study of such equilibria is usually inaccessible to trapped-ion ion cyclotron resonance (ICR) experiments since stabilizing collisions with the excited $(AS^+)^*$ initially formed must take place within a time which is shorter than the intrinsic lifetime of $(AS^+)^*$ (2, 3). This condition usually necessitates the use of pressures which are sufficiently high to prevent efficient trapping of ions in the ICR cell (4). In the present communication we wish to report several *sequential bimolecular reactions* which lead to efficient production of cluster ions, AS^+, which can subsequently participate in solvent switching equilibria, reaction [2], to allow determination of accurate relative solvation energetics (5, 6).

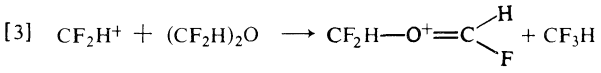
[2] $AS_1^+ + S_2 \rightleftharpoons AS_2^+ + S_1$

As part of a continuing program of investigation of gas phase proton affinities of molecules less basic than water, the gas phase ion chemistry of α,α,α′,α′ tetrafluorodimethyl ether and binary mixtures of $(CH_2H)_2O$ with weak bases was recently examined. At 70 eV electron energy, the dominant ion in the mass spectrum of $(CF_2H)_2O$ is

0008-4042/80/080863-03$01.00/0
©1980 National Research Council of Canada/Conseil national de recherches du Canada

Can. J. Chem. Downloaded from www.nrcresearchpress.com by 210.87.254.40 on 09/05/12
For personal use only.

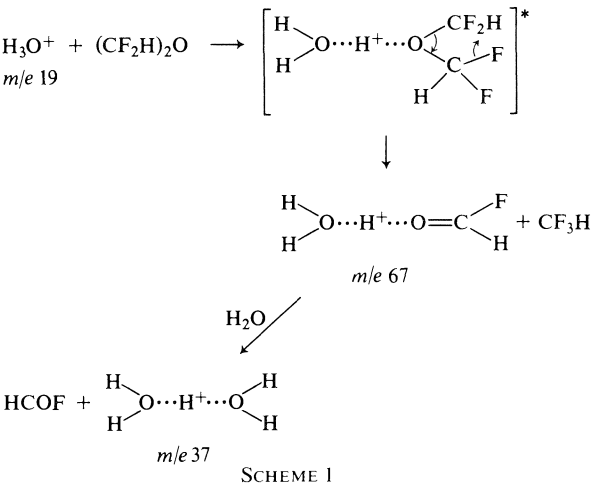
the difluoromethyl cation, CF_2H^+, which is found to react rapidly with the parent ether to produce an ion at *m/e* 99, reaction [3].



[3] $CF_2H^+ + (CF_2H)_2O \longrightarrow CF_2H{-}O^+{=}C(H)(F) + CF_3H$

This ion is found to be unreactive toward the ether. If, however, H_2O is added to the system, a rich and varied ion chemistry results as demonstrated by the variation of relative ionic abundances with time shown in Fig. 1 for a 2:1 mixture of $(CF_2H)_2O$ and H_2O at 70 eV and 3×10^{-6} Torr total pressure. The ultimate ionic product in this mixture is a species at *m/e* 37 which is revealed by a combination of ICR double resonance and deuterium labelling (D_2O) experiments to be the hydrated hydronium ion, $H_5O_2^+$. These experiments revealed that two independent pathways exist for sequential bimolecular production of $H_5O_2^+$ (for other examples of bimolecular production of gas phase cluster ions, see ref. 7).

The first of these pathways, outlined in Scheme 1, is initiated by reaction of the hydronium ion, H_3O^+, which reacts with $(CF_2H)_2O$ to form an intermediate proton bound dimer of water and tetrafluorodimethyl ether followed by elimination of CF_3H to yield a proton bound dimer of water and formylfluoride, HCOF. This species subsequently undergoes a nucleophilic displacement reaction in which the weak base, formylfluoride, is displaced from H_3O^+ by the stronger base, H_2O.



SCHEME 1

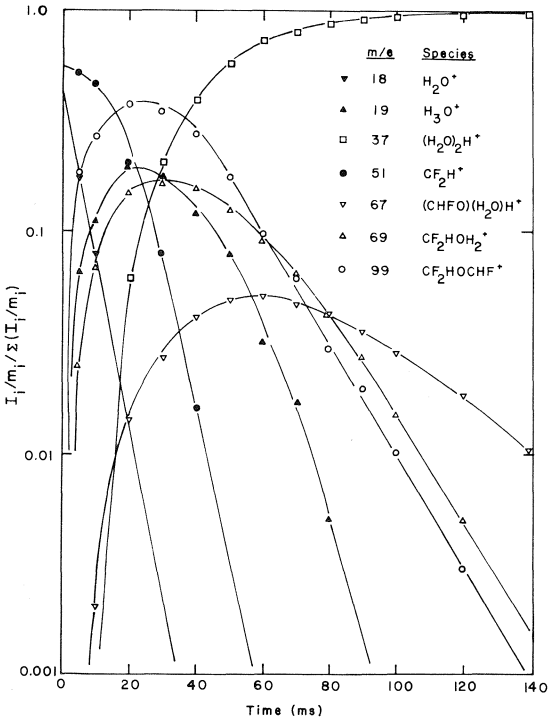
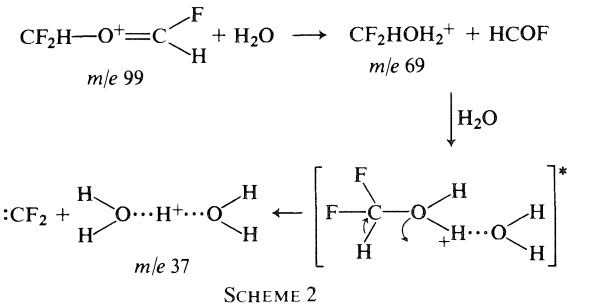
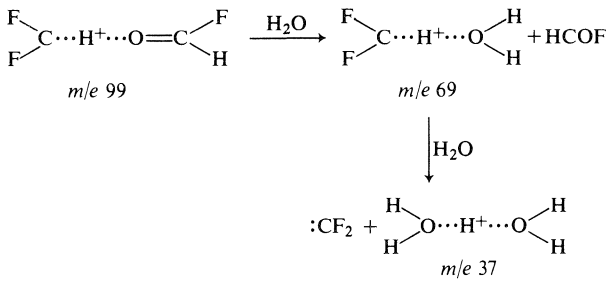


FIG. 1. Variation of relative ionic abundances with reaction time for a 2:1 mixture of $(CF_2H_2)_2O$ and H_2O at a total pressure of 3×10^{-6} Torr following a 6 ms 70 eV ionizing electron beam pulse.

The second sequence of reactions leading to production of $H_5O_2^+$ is initiated by *m/e* 99 produced in reaction of CF_2H^+ with $(CF_2H)_2O$, reaction [3]. The mechanistic details of this sequence are dependent on the assumed structure of *m/e* 99 which in turn depends on the nature of the reactivity of CF_2H^+. The difluoromethyl cation may be regarded either as an electrophilic carbonium ion, or, as has been recently suggested, as protonated difluorocarbene (8). As an electrophile, CH_2H^+ may react with the ether either via fluoride abstraction (9) or by addition to the basic oxygen (10) followed by elimination of CF_3H. In either case, the ion at *m/e* 99 will have the structure of a difluoromethyl cation co-ordinated with formyl fluoride and will undergo the series of reactions with H_2O outlined in Scheme 2. The first step of this mechanism involves nucleophilic displacement of HCOF by H_2O from CF_2H^+ to produce an ion at *m/e* 69 which may be regarded as protonated difluoromethanol. This



SCHEME 2



SCHEME 3

species then undergoes addition of H_2O followed by elimination of difluorocarbene to yield $H_5O_2^+$.

Alternatively, if CF_2H^+ reacts as protonated difluorocarbene, *m/e* 99 may be regarded as a proton bound dimer of difluorocarbene and formylfluoride giving rise to the sequence of reactions outlined in Scheme 3. In this case, both steps involve displacement of a base (either HCOF or $:CF_2$) by H_2O. The latter reaction is exothermic even though $:CF_2$ is known to be a stronger proton base than water (8), because of the exceptionally strong linkage involved in [—O···H···O—] proton bonds (1). Further investigations involving $^{13}CF_2H^+$ and CF_2D^+ are planned to deduce which of these schemes is operative in this system.

We are currently extending our studies of bimolecular production of cluster ions to the gas phase ion chemistry of other weak bases with tetrafluorodimethyl ether and other polyfluorinated ethers, with the ultimate aim of developing a scale of relative solvation energetics based on examination of equilibria such as reaction [2].

Acknowledgements

The generous financial support of the Natural Sciences and Engineering Research Council of Canada and the University of New Brunswick is gratefully acknowledged. R.L.C. thanks the O'Brien Foundation for Fellowship support.

1. P. KEBARLE. Ann. Rev. Phys. Chem. **28**, 445 (1977).
2. W. N. OLMSTEAD, M. LEV-ON, D. M. GOLDEN, and J. I. BRAUMAN. J. Am. Chem. Soc. **99**, 992 (1977).
3. M. MEOT-NER and F. H. FIELD. J. Am. Chem. Soc. **99**, 998 (1977).
4. T. E. SHARP, J. R. EYLER, and E. LI. Int. J. Mass Spectrom. Ion Phys. **9**, 421 (1972).
5. K. HIRAOKA and P. KEBARLE. Can. J. Chem. **55**, 24 (1977).
6. K. TANAKA, G. I. MACKAY, and D. K. BOHME. Can. J. Chem. **56**, 193 (1978).
7. J. L. BEAUCHAMP, M. C. CASERIO, and T. B. MCMAHON. J. Am. Chem. Soc. **96**, 6243 (1974).
8. J. VOGT and J. L. BEAUCHAMP. J. Am. Chem. Soc. **97**, 6682 (1975).
9. R. J. BLINT, T. B. MCMAHON, and J. L. BEAUCHAMP. J. Am. Chem. Soc. **96**, 1269 (1974).
10. P. AUSLOOS, S. G. LIAS, and J. R. EYLER. Int. J. Mass Spectrom. Ion Phys. **18**, 261 (1975).

Can. J. Chem. Downloaded from www.nrcresearchpress.com by 210.87.254.40 on 09/05/12
For personal use only.

Canadian Journal of Chemistry

Published by
THE NATIONAL RESEARCH COUNCIL OF CANADA

Volume 58 Number 9 May 1, 1980

Journal canadien de chimie

Publié par
LE CONSEIL NATIONAL DE RECHERCHES DU CANADA

Volume 58 numéro 9 1 mai 1980

Infrared spectra of the ammonium ion in crystals. Part VIII. Spectroscopic criteria of highly-bent hydrogen bonds [1,2]

OSVALD KNOP AND WOLFGANG J. WESTERHAUS
Department of Chemistry, Dalhousie University, Halifax, N.S., Canada B3H 4J3

AND

MICHAEL FALK
Atlantic Regional Laboratory, National Research Council of Canada, Halifax, N.S., Canada B3H 3Z1

Received November 9, 1979

OSVALD KNOP, WOLFGANG J. WESTERHAUS, and MICHAEL FALK. Can. J. Chem. **58**, 867 (1980).

Available evidence suggests that (*1*) the stretching frequencies of highly-bent hydrogen bonds decrease with increasing temperature, regardless of whether the bonds are static or dynamic in character, to a single acceptor or to several competing acceptors; and (*2*) departures from symmetric trifurcation (or bifurcation) toward asymmetric situations lower the stretching frequency. In further support of these criteria isotopic probe ion spectra between 10 K and room temperature have been obtained for taurine and for trigonal $(NH_4)_2MF_6$ (M = Si, Ge, Sn, Ti). Evidence of a low-temperature transition at 100(10) K in trigonal $(NH_4)_2SnF_6$ is presented, and existence of the previously reported transition at 38.6 K in trigonal $(NH_4)_2SiF_6$ is confirmed. Symmetry changes associated with these transitions are discussed.

OSVALD KNOP, WOLFGANG J. WESTERHAUS et MICHAEL FALK. Can. J. Chem. **58**, 867 (1980).

Les preuves disponibles suggèrent (*1*) que les fréquences de vibration des liaisons hydrogène fortement coudées décroissent avec une augmentation de la température que les liaisons aient un caractère statique ou dynamique, que l'on ait un accepteur unique ou plusieurs accepteurs en concurrence, et (*2*) que les écarts par rapport à une trifurcation (ou bifurcation) symétrique vers des situations asymétriques diminuent la fréquence de vibration. Comme preuves supplémentaires à l'appui de ces critères, nous avons déterminé les spectres, entre 10 K et la température de la pièce, de la sonde isotopique NH_3D^+ dans la taurine et dans les composés $(NH_4)_2MF_6$ trigonaux (M = Si, Ge, Sn, Ti). On met en évidence l'existence d'une transition à 100(10) K du $(NH_4)_2SnF_6$ trigonal et on confirme l'existence de la transition à 38.6 K du $(NH_4)_2SiF_6$ antérieurement signalée. On discute des changements de symétrie associés à ces transitions.

In Part VII (1) we investigated the ir spectra of the NH_3D^+ probe ion in NH_4SnF_3, NH_4CuSO_3, cubic $(NH_4)_2SiF_6$, and $(NH_4)_2SnCl_6$ between 10 K and room temperature. The ammonium ion in the first two crystals is situated on a threefold axis in such a way that one of the N—H bonds, N—H_a, is required to be on this axis; this follows from the site symmetry of the ion as determined by the non-hydrogenic portion of the crystal structure. The axial hydrogen H_a will then be equidistant from three equivalent acceptor atoms X related by the threefold axis. In cubic $(NH_4)_2SiF_6$ and $(NH_4)_2SnCl_6$ the site symmetry T_d requires all four N—H bonds to be on threefold axes and each H atom to have three equivalent acceptors X related by the respective threefold axis. In all four compounds the $\nu_1(NH_3D^+)$ frequency[3] decreases with increasing temperature. From this observation we concluded the following. At $T \rightarrow 0$ K the axial hydrogens are indeed confined to the threefold axes, i.e. the N—H···3X hydrogen bonds are symmetrically trifurcated. With increasing temperature the hydrogen-bond strength increases, the H atom becomes progressively more associated with *one* acceptor atom at a time, and the hydrogen bond acquires a pronouncedly dynamic character. The decrease of the ND stretching frequency $\nu_1(NH_3D^+)$ with increasing temperature is the opposite of the temperature behaviour of normal N—H···X bonds, for which $d\nu_1/dT \geq 0$.

[1]For Part VII, see ref. 1.
[2]NRCC No. 18124.
[3]For notation of NH_3D^+ fundamentals, see ref. 12.

0008-4042/80/090867-08$01.00/0
©1980 National Research Council of Canada/Conseil national de recherches du Canada

Can. J. Chem. Downloaded from www.nrcresearchpress.com by 210.87.254.5 on 09/05/12
For personal use only.

Can. J. Chem. Downloaded from www.nrcresearchpress.com by 210.87.254.5 on 09/05/12
For personal use only.

However, the existence of a negative temperature coefficient of the hydrogen stretching frequency is not restricted to the specific situations in the four ammonium compounds. There are indications that the sign of dv/dT in fact provides a diagnostic criterion for distinguishing, not only between normal and symmetrically trifurcated hydrogen bonds, but between normal and *all highly bent* (and thus weak, cf. ref. 2) hydrogen bonds, regardless of whether the bonds are static or dynamic in character, to a single acceptor or to several competing acceptors. Furthermore, we suggest that departures from symmetric trifurcation (or bifurcation) toward asymmetric situations will lower the stretching frequency. Thus when a crystal contains hydrogen bonds of several types but chemically similar, the $\nu_T \rightarrow 0$ K stretching frequency[4] that corresponds to a symmetrically trifurcated (or bifurcated) bond will be the highest. The following observations may be cited in support; some of them have been discussed in these terms previously (3), whilst those under *3* and *6* are new.

(*1*) The axial component $\nu_1(a)$ of the $\nu_1(NH_3D^+)$ absorption in NH_4SnF_3 and NH_4CuSO_3 has a much higher frequency than the nonaxial component $\nu_1(n)$ (1). The former corresponds to a symmetrically trifurcated N—H···3X bond, the latter to strong normal N—H···X bonds.

(*2*) The $\nu_1(NH_3D^+)$ frequencies in cubic $(NH_4)_2SiF_6$ and $(NH_4)_2SnCl_6$ are among the highest observed in ammonium fluorides and chlorides respectively (4).

(*3*) *Taurine*, $^+H_3N{\cdot}CH_2CH_2SO_3^-$, is known to contain two normal N—H···O and one asymmetrically bifurcated N—H···2O bonds (5). The highest-frequency ND stretching component of the $^-O_3S{\cdot}CH_2CH_2NH_2D^+$ probe ion in the ir spectrum of this crystal decreases significantly with increasing temperature (Fig. 1), whilst the peak frequencies of all the other bands in the ND stretching region remain stationary or increase slightly.

(*4*) $K_2SnCl_4{\cdot}H_2O$ contains a single type of water molecule. Its hydrogen-bonding engagement can be represented as Cl···H—O—H···2Cl. The bifurcated bond is symmetric. Those isotopically isolated OH and OD stretching frequencies that decrease with increasing temperature are higher than the OH and OD stretching frequencies that increase with temperature (3).

(*5*) $BaCl_2{\cdot}2H_2O$ contains water molecules of two types, one engaged in two normal O—H···Cl bonds and the other, in one normal O—H···Cl and one asymmetrically bifurcated O—H···2Cl bond. The highest of the four ν_{OH} (HDO) frequencies, and the highest of the four ν_{OD} (HDO) frequencies, in the ir spectrum of the isotopically isolated HDO molecule decreases on warming the crystal from 95 K to room temperature, whereas the other ν_{OH} (HDO) and ν_{OD} (HDO) frequencies increase (6, 7); these changes are parallelled in the Raman spectrum (7). Thus there can be no doubt that the frequencies with a negative dv/dT correspond to the bifurcated bond.

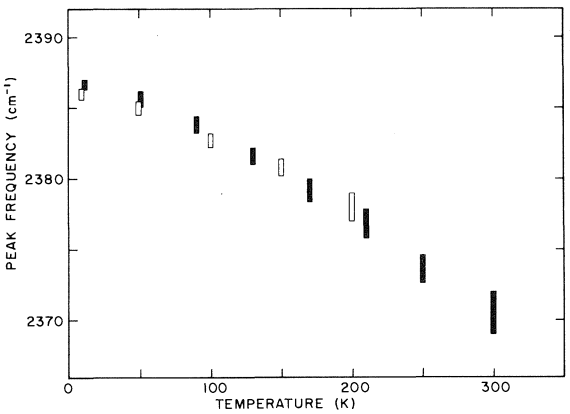


FIG. 1. Temperature variation of the frequency of the ND stretching absorption of the $^-O_3S{\cdot}CH_2CH_2NH_2D^+$ probe ion corresponding to the bifurcated N—H···2O hydrogen bond in taurine. Open rectangles, 1% D; full rectangles, 5% D.

(*6*) *Trigonal* $(NH_4)_2MF_6$ fluorides afford a further example of ammonium ions exhibiting anomalous behaviour. We have investigated the temperature dependence of the NH_3D^+ probe spectrum in several of these compounds. Because of their fairly detailed nature the results are described separately in the next section. They support the above generalization and are consistent with the conclusions drawn by Sergienko *et al.* (8–10) for trigonal $(NH_4)_2SiF_6$ and $(NH_4)_2GeF_6$ from the temperature variation of the integrated ir intensities of $\nu_3(NH_4^+)$ and $\nu_4(NH_4^+)$ bands.

Trigonal $(NH_4)_2MF_6$ *(M = Si, Ge, Sn, Ti)*

The coordination geometry of the ammonium ion in the trigonal $(NH_4)_2MF_6$ fluorides is favourable to the formation of a symmetrically trifurcated N—H···3F bond. The site symmetry of the ion is C_{3v}, hence a $\nu_1(NH_3D^+)$ doublet with an idealized 1:3 intensity ratio is expected and observed.[5] The

[4]In the absence of low-temperature transitions. If a transition occurs, the frequency values to be compared are those just above T_{tr}.

[5]At 10 K the intensity ratio for the Ti and Ge compounds is much smaller than the ideal value, but it increases rapidly to about $\frac{1}{4}$ for the titanate at 100 K and about $\frac{1}{3}$ for the germanate (Fig. 2). This behaviour is consistent with the expected dependence of the ND oscillators on the hydrogen-bond strength and on its temperature variation.

Can. J. Chem. Downloaded from www.nrcresearchpress.com by 210.87.254.5 on 09/05/12
For personal use only.

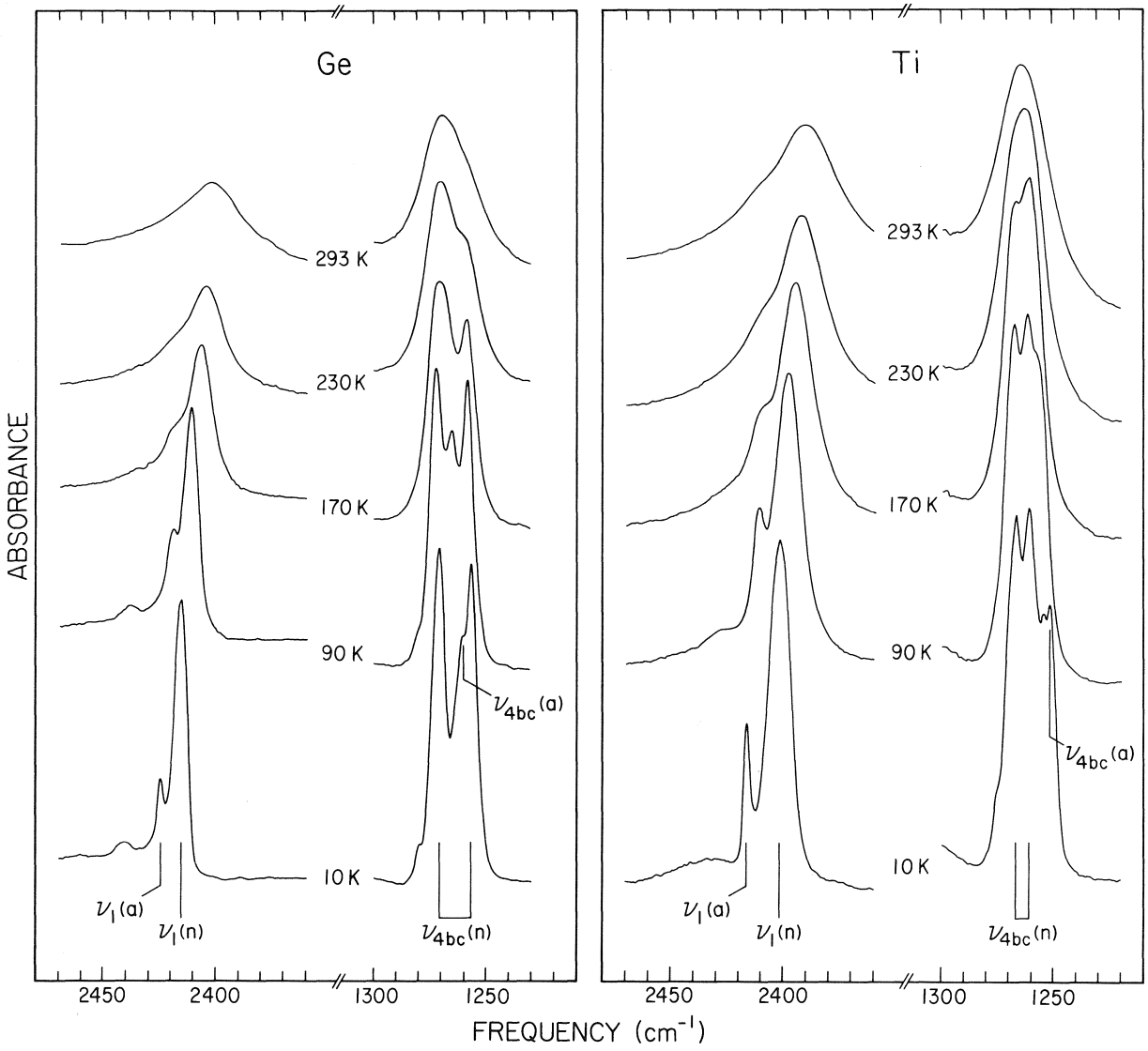


FIG. 2. The ND stretching and bending regions of the spectrum of $(NH_4)_2GeF_6$ and $(NH_4)_2TiF_6$ (2% D) at different temperatures. Features other than those identified as components of the ν_1 and ν_{4bc} fundamentals of NH_3D^+ originate in the secondary isotopic species $NH_2D_2^+$ or in the coupling of vibrations of neighbouring NH_3D^+ ions in the crystal.

weaker component thus unambiguously corresponds to $\nu_1(a)$, i.e. to the symmetrically trifurcated bond. In the four compounds investigated to date (M = Si, Ge, Sn, Ti) (4, 11, 12) the frequency of $\nu_1(a)$ is always higher than that of $\nu_1(n)$, the $\nu_1(a) - \nu_1(n)$ difference at 100 K ranging from 8.5 to 12.5 cm^{-1} (Table 1). The frequencies of both components decrease in the order Si > Ge > Ti > Sn. The 100 K values of $\nu_1(a)$ correlate linearly with the effective ionic radii r^{vi} (M^{4+}) (13): $\nu_1(a) = 2458.8 - 76.0r^{vi}$, $r^2 = 0.96$, $\sigma = 2.0$ cm^{-1}; for $\nu_1(n)$ the trend is evident but the correlation is not as high. The frequency decrease attendant on varying M is thus attributable to a volume effect.

The ν_1 and ν_{4bc} absorptions in the four compounds at different temperatures are shown in Figs. 2–4, and the temperature dependence of the frequencies and halfwidths (= full width at half height) is represented in Figs. 5–7. As would be expected for a symmetrically trifurcated bond, the $\nu_1(a)$ frequency falls off with increasing temperature,[6] by an amount comparable to the decrease in cubic $(NH_4)_2SiF_6$ (1). However, the $\nu_1(n)$ frequency *also* decreases with increasing temperature, which indi-

[6]A corresponding decrease in the frequencies of the $\nu_3(NH_4^+)$ ir absorption in trigonal $(NH_4)_2SiF_6$ and $(NH_4)_2GeF_6$ is reported in ref. 8, the band maxima shifting, between 150 and 300 K, by −14 and −12 cm^{-1} respectively.

Can. J. Chem. Downloaded from www.nrcresearchpress.com by 210.87.254.5 on 09/05/12
For personal use only.

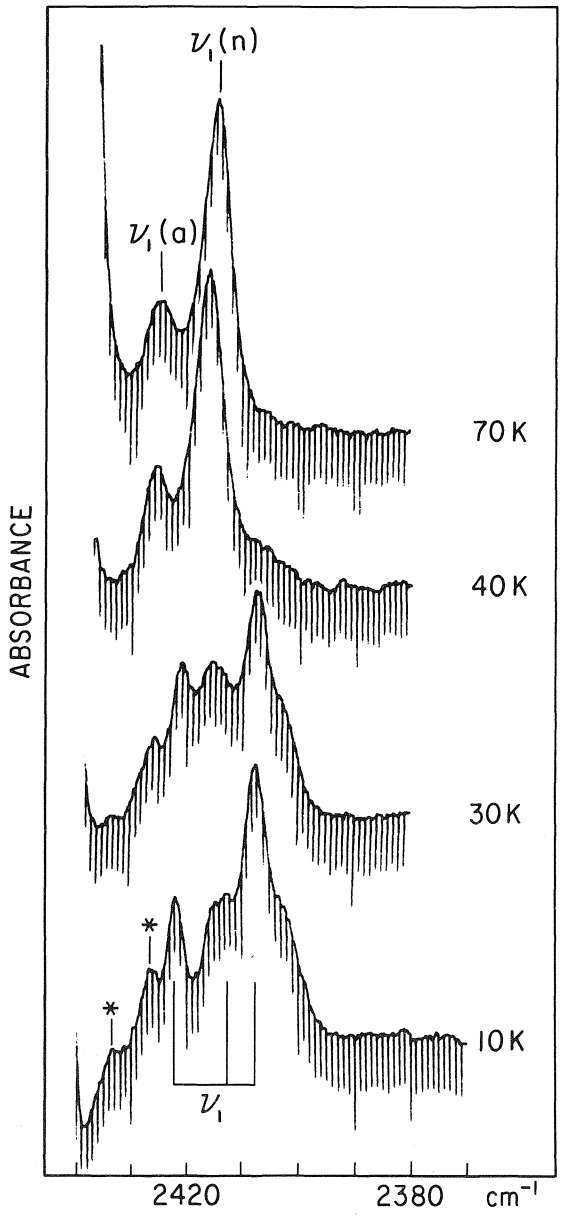


FIG. 3. The ND stretching region of the spectrum of trigonal $(NH_4)_2SiF_6$ (2% D) above and below the phase transition at 38.6 K (cf. caption of Fig. 2). Features marked with an asterisk are due to satellites of the ND stretching of cubic $(NH_4)_2SiF_6$ near 2442 cm^{-1} (not shown).

cates that the three equivalent nonaxial N—H_n···F bonds are highly bent. Examination of Fig. 1 of ref. 12 shows that in the most symmetric possible orientation the N—H_n bond would be in asymmetrically trifurcated situations N—H_n···(2F + F′)[7] but effectively closer to symmetric bifurcation,

[7]In the hexafluorosilicate, H_n···F ~ 2.08 Å, NH_nF ~ 144°; H_n···F′ ~ 2.42 Å, NH_nF' ~ 133°. For the symmetrically trifurcated bond, H_a···F″ ~ 2.31 Å, NH_aF'' ~ 123°.

TABLE 1. Frequencies (cm^{-1}) of the NH_3D^+ probe ion in trigonal $(NH_4)_2MF_6$ (M = Si, Ge, Ti, Sn) at 100 K

Vibration	Frequency			
	Si	Ge	Ti	Sn
$\nu_1(a)$	2424.5(5)	2419.3(5)	2410.7(5)	2407.2(8)
$\nu_1(n)$	2412.7(5)	2410.8(8)	2398.2(5)	2396.5(8)
$\nu_{4bc}(a)$	1275.3*	1266.0(5)	1259.7(8)	1256.0(5)
$\nu_{4b}(n)$, $\nu_{4c}(n)$	1278.2* 1256.8*	1272.3(5) 1258.5(5)	1268.3(5) 1262.2(5)	1267.7(8)

*From ref. 4. Estimated uncertainty, ±1 cm^{-1}.

analogous to orientation C in NH_4CuSO_3 (Fig. 2 of ref. 1). This orientation would be compatible with the observation that $\nu_1(a) > \nu_1(n)$ and $d\nu_1(n)/dT < 0$; it also receives support from a recent ^1H and ^{19}F nmr study of the hexafluorotitanate (14). Orientations analogous to A and A′ in NH_4CuSO_3, corresponding to a N—H_n···F bond in a plane passing through the threefold axis and thus to a normal N—H···F bond (H_n···F ~ 1.95 Å, NH_nF ~ 171°), on the other hand, would be expected to have a positive $d\nu_1(n)/dT$ and a considerably lower $\nu_1(n)$ frequency.

Schlemper and Hamilton (15), in their account of a crystal-structure determination of trigonal $(NH_4)_2SiF_6$ at room temperature by neutron diffraction, suggest that the ammonium ion occurs in two orientations (related by reflection in a plane perpendicular to the threefold axis through the N atom) disordered at room temperature and not necessarily in a 1:1 abundance ratio because of the polarity of the threefold axis; the transition observed at 38.6 K (16) may then correspond to an ordering of the two orientations. If this were the case, one would expect the $\nu_1(a)$ and $\nu_1(n)$ components of $\nu_1(NH_3D^+)$ to be split, or at least the absorption to be broadened, at temperatures above T_{tr}.

Only single, sharp ($\Delta\nu_{1/2}$ = 6–7 cm^{-1} at 40 K) $\nu_1(a)$ and $\nu_1(n)$ bands were observed in the probe spectra of trigonal $(NH_4)_2SiF_6$ between 40 and 150 K (Figs. 3 and 5),[8] confirming the previously reported result for 80 K (12). If orientational disorder of the ammonium ion occurs above T_{tr}, the $\nu_1(a)$ and $\nu_1(n)$ frequency differences corresponding to the two orientations at 40 K must each be less than about 4 cm^{-1}, the limit of visual recognition of an unresolved 1:1 Gaussian doublet of the observed total halfwidth. This limit would be larger if the intensity ratio differed from 1:1 as a consequence of unequal abundance of the two orientations. However, the appreciable dissimilarity of the fluorine

[8]See Experimental for the reason why the temperature range was not extended beyond 150 K.

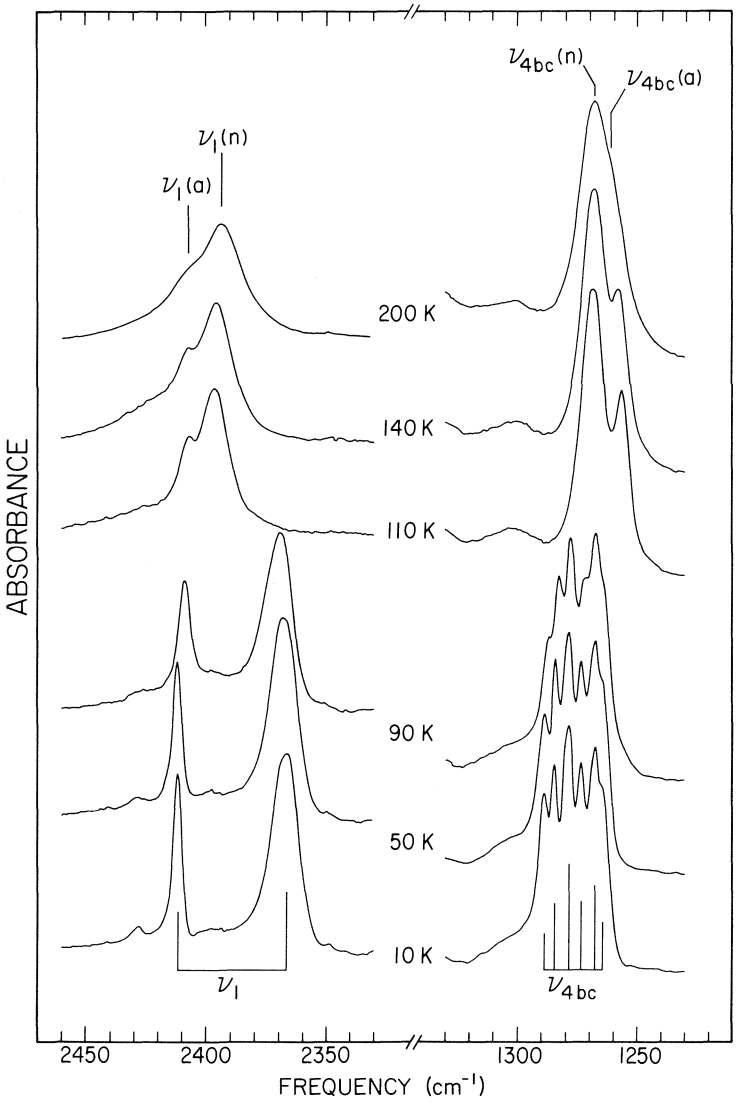


FIG. 4. The ND stretching and bending regions of the spectrum of trigonal $(NH_4)_2SnF_6$ (1% D) above and below the phase transition at ca. 100 K (cf. caption of Fig. 2).

environments of the NH_4^+ ion above and below the plane through N and perpendicular to C_3 would make us expect a splitting that is readily recognizable.

Below 40 K the 1:3 ν_1 doublet is transformed into a composite absorption (Fig. 4 and Table 2) which we interpret as a 1:1:2 triplet corresponding to site symmetry C_{2h} or C_s of the ammonium ion. Reduction of the site symmetry of the ion from T_d associated with low-temperature transitions of cubic $(NH_4)_2MX_6$ to lower-symmetry polymorphs has been detected by the NH_3D^+ probe spectra in several compounds (ref. 4 and results to be published), but the transition in trigonal $(NH_4)_2SiF_6$ appears to be the first such transition to be observed on cooling an $(NH_4)_2MX_6$ crystal that is trigonal at room temperature. Inasmuch as analogous transitions occur in cubic A_2MX_6 in which $A \neq NH_4$, it is almost certain that in the trigonal hexafluorosilicate the ammonium ion at $T \leq T_{tr}$ merely responds to a distortion (and possibly a rotational displacement) of the SiF_6 octahedra; its presence in the crystal cannot be regarded, by itself, as the cause of the transition. This agrees with the view of Stephenson *et al.* (16) but is contrary to the explanation proffered by Schlemper and Hamilton.

A hitherto unreported transition was detected in trigonal $(NH_4)_2SnF_6$ (Figs. 4 and 7). The ν_1 absorption below T_{tr} was a 1:3 doublet, with a splitting of 45 cm^{-1} at 10 K (Table 2). The ν_{4bc} absorption con-

Can. J. Chem. Downloaded from www.nrcresearchpress.com by 210.87.254.5 on 09/05/12
For personal use only.

Can. J. Chem. Downloaded from www.nrcresearchpress.com by 210.87.254.5 on 09/05/12
For personal use only.

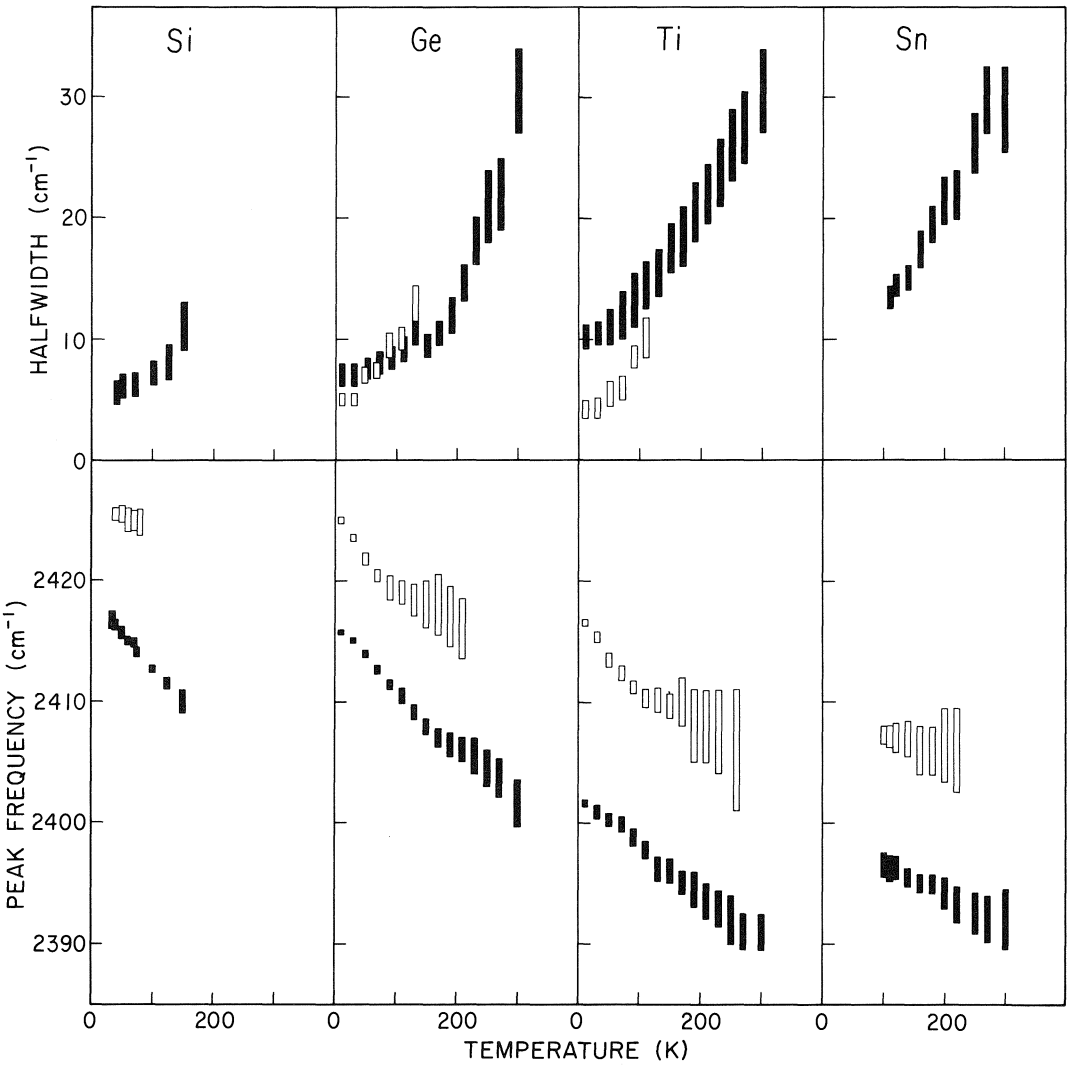


FIG. 5. Temperature variation of the component ND stretching frequencies and halfwidths of trigonal $(NH_4)_2MF_6$ (M = Si, Ge, Ti, Sn). Open rectangles, $\nu_1(a)$; full rectangles, $\nu_1(n)$.

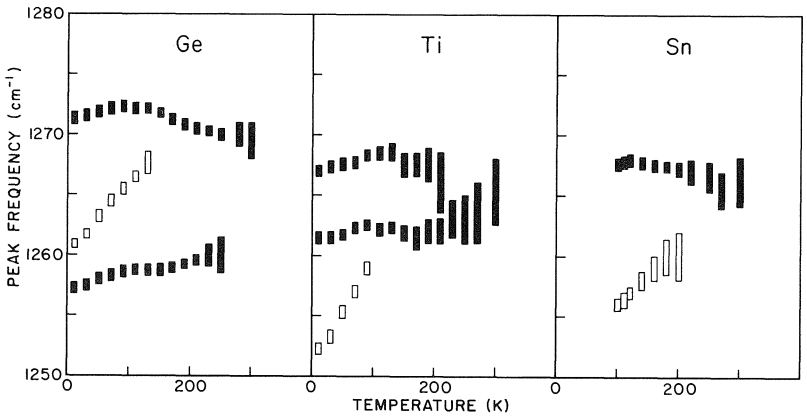


FIG. 6. Temperature variation of the ND bending frequencies of trigonal $(NH_4)_2MF_6$ (M = Ge, Ti, Sn).

Can. J. Chem. Downloaded from www.nrcresearchpress.com by 210.87.254.5 on 09/05/12
For personal use only.

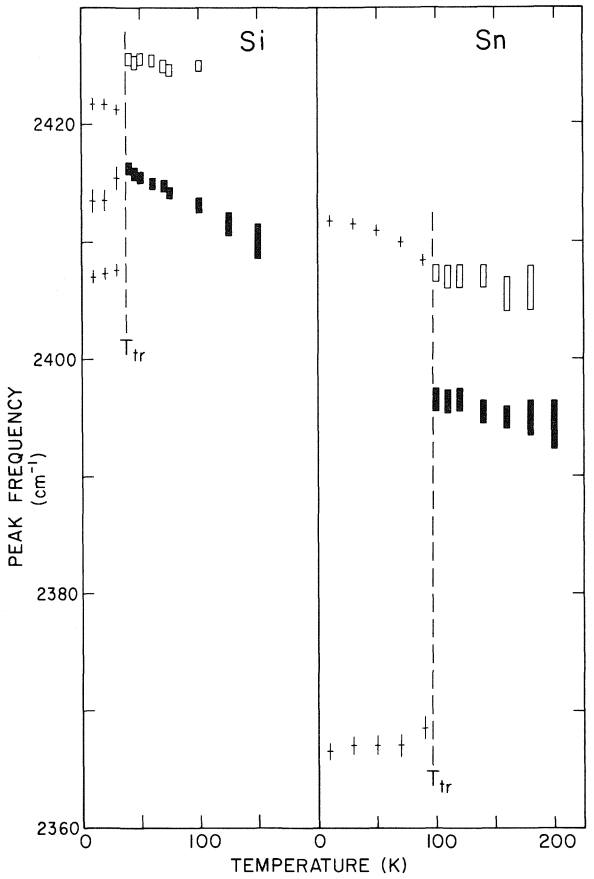


FIG. 7. Temperature variation of the component ND stretching frequencies of trigonal $(NH_4)_2SiF_6$ and $(NH_4)_2SnF_6$ above and below the respective transition temperatures. Open rectangles, $\nu_1(a)$; full rectangles, $\nu_1(n)$.

sisted of six components, two of which had approximately twice the unit intensity. It was interpreted as an octet corresponding to an ammonium ion at a site of symmetry C_1, which makes the apparent 1:3 ν_1 doublet an unresolved quartet. The symmetry of the low-temperature phase is thus not the same as in the low-temperature phase of the hexafluorosilicate. The large splitting of the ν_1 absorption and the temperature variation of the two component frequencies are noteworthy (Fig. 7). The narrow minor band has a high frequency which decreases with increasing temperature and at T_{tr} merges with the $\nu_1(a)$ frequency of the trigonal phase. The peak frequency of the more intense, composite band, on the other hand, is substantially lower and increases with temperature. The weighted mean frequency below T_{tr} is nearly stationary and appreciably lower than the weighted mean frequency above T_{tr}, which indicates an overall strengthening of the hydrogen-bond interaction in the low-temperature phase. The strengthening is

TABLE 2. Frequencies (cm^{-1}) of the NH_3D^+ probe ion at 10 K in the low-temperature phases of $(NH_4)_2SiF_6$ and $(NH_4)_2SnF_6$

Vibration	Frequency	
	Si	Sn
ν_1	2421.7 2413.5 2407.1†	2411.7 2366.5*
ν_{4bc}	‡	1288.8 1284.7 1278.6† 1273.6 1267.6† 1264.6

*Band of approximately three times the unit intensity (composite band).
†Band of approximately twice the unit intensity.
‡Interference with the ν_{4bc} band of the cubic phase.

also observed in the silicate, but the frequency difference in that case amounts to only about one sixth of that in the stannate. Furthermore, on the assumption that to a high ν_1 frequency there corresponds a low ν_{4bc} frequency and vice versa, the point obtained by plotting the average of the two highest ν_{4bc} component frequencies of the stannate against the lower ν_1 component frequency in the ν_{4bc} vs. ν_1 plot for ammonium halides (Fig. 3 of ref. 4) falls close to the point for NH_4AlF_4 (C.N. 8, normal hydrogen bonds), whilst the point corresponding to the average of the four lowest ν_{4bc} component frequencies and to the higher ν_1 frequency remains in the region characteristic of trigonal $(NH_4)_2MF_6$ above T_{tr}.[9] One thus concludes that on passage through T_{tr} the character of the axial N—H_a bond in the trigonal phase remains preserved, but the three N—H_n bonds change from asymmetric trifurcation (quasi-bifurcation) to normal N—H_n···F bonds of a strength appropriate to the acceptor strength of F in a composite MF_6 anion. In this respect the low-temperature phase of trigonal $(NH_4)_2SnF_6$ resembles more closely NH_4SnF_3 and NH_4CuSO_3 than the low-temperature phase of trigonal $(NH_4)_2SiF_6$, quite apart from the difference in the site symmetries of the ammonium ion and thus in the crystallographic symmetry of the two phases.

The NH_3D^+ probe spectrum of $(NH_4)_2GeF_6$ leaves no doubt of the absence of an NH_4^+ disorder analogous to that proposed for trigonal $(NH_4)_2SiF_6$ in ref. 15. The 80 K spectrum reported previously (12) and, more fully, the 10–293 K spectra presented in Fig. 2 and the frequencies and bandwidths

[9]Averaging the three highest ν_{4bc} frequencies and the three lowest ν_{4bc} frequencies respectively changes the positions of the points only slightly.

Can. J. Chem. Downloaded from www.nrcresearchpress.com by 210.87.254.5 on 09/05/12
For personal use only.

plotted in Fig. 5 show no indication of a transition in this temperature range and no evidence of $\nu_1(a)$ or $\nu_1(n)$ splitting. A similar observation is made for $(NH_4)_2TiF_6$ (refs. 4 and 11; Figs. 2 and 5), except that the $\nu_1(n)$ band is significantly broadened. However, no evidence of a transition between 4.2 and 400 K was observed in a recent ^1H and ^{19}F nmr study of this compound (14). Furthermore, it was concluded that reorientation of TiF_6 octahedra is unimportant below 250 K, so that the observed broadening of $\nu_1(n)$ could not be attributed to this source. We do not have an explanation of the broadening at present.

Although no use is made of the ν_{4bc} absorption in the above arguments, the frequency of the $\nu_{4bc}(a)$ component in the germanate and titanate increases with temperature (Fig. 6) and thus reflects the anomalous behaviour of the ammonium ion. The increase is consistent with the observed negative $d\nu_1/dT$ in these crystals and further strengthens the views presented in the preceding section. The temperature variation of the $\nu_{4b}(n)$ and $\nu_{4c}(n)$ frequencies is much smaller. The order of the components in the (ideally) 2:3:3 triplet is not the same in the four trigonal $(NH_4)_2MF_6$: it is 3:2:3 for Si and Ge but 2:(3 + 3) for Sn and 2:3:3 for Ti. This and the broadening of the $\nu_1(n)$ absorption seem to suggest that the ammonium ion in the hexafluorotitanate may differ somewhat in its behaviour from the ammonium ion in the Group IVA compounds.

Finally, we wish to correct the account of our earlier results on trigonal $(NH_4)_2MF_6$ (4) on two points. The systematic examination of the probe-ion spectra from 10 K up, in conjunction with the improved control of sample temperature obtainable with our current cryogenic system, reveals that the frequencies reported earlier refer in fact to a temperature closer to 100 K than to 77 K (cf. Table 1 for the new 100 K values). Because of the proximity of the actual sample temperature in the earlier runs to T_{tr} the ν_{4bc} absorption in the spectra of the hexafluorostannate contained the component bands of both phases. This admixture, however, was not recognized, as we were not aware of the existence of the transition at the time. As a result the $\nu_{4bc}(a)$ band of the trigonal (high-temperature) phase was assigned wrongly. The $\nu_{4bc}(a)$ frequency as assigned in Table 1 has a temperature behaviour appropriate to a symmetrically trifurcated N—H···3F bond (Fig. 6).

Experimental

Trigonal $(NH_4)_2SnF_6$ was prepared by dissolving freshly precipitated stannic acid in 48% HF and adding the requisite amount of NH_4F dissolved in a minimum volume of water. The first crystals formed by slow evaporation on a steam bath were collected and carefully handpicked. The other compounds used in this investigation were from commercial sources. They were purified by recrystallization and authenticated by comparison with previously reported ir spectra. Details of deuteration and ir apparatus and technique (hydrocarbon mulls) will be found in refs. 1 and 4.

It was difficult to avoid contamination of sample of trigonal $(NH_4)_2SiF_6$ with the cubic polymorph attendant on even the gentlest grinding of handpicked crystals of the pure trigonal form (cf. ref. 12). Crushing at liquid-nitrogen temperature reduced the problem but did not eliminate it completely.

As seen in Fig. 2, the three components of ν_{4bc} and the two components of ν_1 in the spectra of the trigonal $(NH_4)_2MF_6$ are well resolved at low temperatures but overlap at higher temperatures. The frequency and halfwidth of each component were estimated by allowing roughly for the effect of the overlap; they become increasingly uncertain at higher temperatures. This is reflected in the increasing size of the error bars which represent twice the estimated standard error, and in the discontinuation of the plots in Figs. 5 and 6 above certain temperatures. The ν_1 doublet of trigonal $(NH_4)_2SiF_6$ was in addition increasingly overlapped at higher temperatures by the ν_1 singlet of the cubic form, so that the region of reasonably accurate frequency values was greatly diminished and the halfwidth of the axial component could not be accurately determined. Similarly, the ν_{4bc} bands of the trigonal form were so much overlapped by the corresponding band of the cubic form that no analysis was attempted.

The assignments of the two nonaxial and one axial components of ν_{4bc} were aided by the large shift of the latter toward higher frequencies with increasing temperature (Fig. 6).

The transition temperature in the hexafluorosilicate could be bracketted, from the ir spectra, between 35 and 40 K, in good agreement with the calorimetric value, 38.6 K (16). In the hexafluorostannate T_{tr} was estimated to be 100 K with an uncertainty of ±10 K.

Acknowledgment

The investigation was supported by a research grant from the National Research Council of Canada to the first-named author.

1. O. KNOP, W. J. WESTERHAUS, and M. FALK. Can. J. Chem. **58**, 270 (1980).
2. I. D. BROWN. Acta Crystallogr. A, **32**, 24 (1976).
3. M. FALK, C.-H. HUANG, and O. KNOP. Can. J. Chem. **52**, 2380 (1974).
4. O. KNOP, I. A. OXTON, and M. FALK. Can. J. Chem. **57**, 404 (1979); **57**, 2003 (1979).
5. Y. OKAYA. Acta Crystallogr. **21**, 726 (1966).
6. G. BRINK. Spectrochim. Acta, **28A**, 1151 (1972).
7. H. F. LUTZ, W. POBITSCHKA, B. FRISCHEMEIER, and R.-A. BECKER. Appl. Spectrosc. **32**, 541 (1978).
8. V. I. SERGIENKO, L. N. IGNATIEVA, and S. F. BOGDAN. Spectrosc. Lett. **11**, 891 (1978).
9. V. I. SERGIENKO, P. S. GORDIENKO, M. F. EIBERMAN, and S. F. BOGDAN. Spectrosc. Lett. **11**, 877 (1978).
10. V. I. SERGIENKO, L. N. IGNATIEVA, and A. G. MIROCHNIK. Spectrosc. Lett. **11**, 855 (1978).
11. I. A. OXTON, O. KNOP, and M. FALK. J. Phys. Chem. **80**, 1212 (1976).
12. I. A. OXTON, O. KNOP, and M. FALK. Can. J. Chem. **53**, 3394 (1975).
13. O. KNOP and J. S. CARLOW. Can. J. Chem. **52**, 2175 (1974).
14. A. WATTON, E. KOSTER, H. S. SANDHU, and H. E. PETCH. J. Chem. Phys. **70**, 5197 (1979).
15. E. O. SCHLEMPER and W. C. HAMILTON. J. Chem. Phys. **45**, 408 (1966).
16. C. C. STEPHENSON, C. A. WULFF, and O. R. LUNDELL. J. Chem. Phys. **40**, 967 (1964).

A new synthesis of 2,10,11-trioxatricyclo[4.4.4.0^{1,6}]tetradecane

NORMAND BEAULIEU[1] AND PIERRE DESLONGCHAMPS

Laboratoire de Synthèse Organique, Département de Chimie, Faculté des Sciences, Université de Sherbrooke, Sherbrooke, (Qué.), Canada J1K 2R1

Received December 3, 1979

NORMAND BEAULIEU and PIERRE DESLONGCHAMPS. Can. J. Chem. **58**, 875 (1980).

A simple and convenient synthesis of tricyclic orthoester **1** (2,10,11-trioxatricyclo[4.4.4.0^{1,6}]tetradecane) is described.

NORMAND BEAULIEU et PIERRE DESLONGCHAMPS. Can. J. Chem. **58**, 875 (1980).

Une synthèse simple de l'orthoester tricyclique **1** (trioxa-2,10,11 tricyclo[4.4.4.0^{1,6}]tétradécane) est rapportée.

Can. J. Chem. Downloaded from www.nrcresearchpress.com by 210.87.254.5 on 09/05/12
For personal use only.

2,10,11-Trioxatricyclo[4.4.4.0^{1,6}]tetradecane (**1**) is an interesting tricyclic orthoester which was found to be unusually resistant toward acid hydrolysis (1). This low reactivity was predicted on the basis of the stereoelectronic rules which we have proposed for hydrolytic reactions (1, 2).

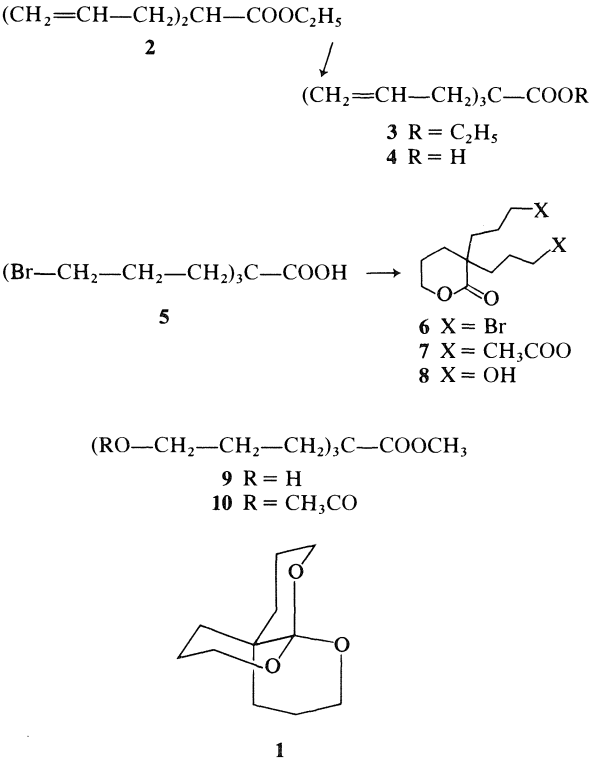
This compound, whose structure has recently been confirmed by X-ray analysis (3), was synthesized in 1955 by McElvain and McKay (4) using a very ingenious route. Their strategy includes "entre autres", three Diels–Alder condensations between the highly reactive, but rather sensitive, ketene acetal functionality and acrolein. We wish to report a new synthesis of tricyclic orthoester **1** in which there is improvement on the number of steps, reaction conditions, ease of product isolation, and overall yield.

Ethyl bis-allyl acetate **2**, which can be conveniently prepared by alkylation of diethyl malonate (5) with allyl bromide followed by decarboxylation (NaCl in DMSO–H_2O, (6)), was used as starting material.

Ethyl bis-allyl acetate **2** was alkylated (LDA, CH_2=CH—CH_2—Br, HMPT, −78°C, (7)) to give ethyl tri-allyl acetate **3** (≥90% yield). Basic hydrolysis of **3** (KOH, C_2H_5OH, reflux, 15 days) gave the corresponding carboxylic acid **4** (95% yield) which was converted into the known (4) tribromocarboxylic acid **5** (≥90% yield) by the photochemically induced addition of hydrogen bromide (*hν*, pentane, (8)). Treatment of tribromocarboxylic acid **5** with triethylamine in dichloromethane furnished the expected dibromolactone **6** (≥90% yield) which was further transformed (CH_3COONa, HMPT, room temperature, 2 h, (9)) into the diacetate lactone **7** (50% yield).

Basic hydrolysis of diacetate lactone **7** (K_2CO_3, CH_3OH, room temperature, 30 min) followed by the addition of excess acid (HCl, 2 *N*) gave crude diol lactone **8** which yielded tricyclic orthoester **1** (88%) upon reflux in benzene. The tricyclic orthoester **1** was also obtained (66%) by treatment of diacetate lactone **7** under acidic conditions 2.4 *N* HCl – DME (1:1), room temperature, 2 h) followed by the addition of benzene and distillation.

Diacetate lactone **7** was also hydrolysed with triethylamine in methanol (4 days, room temperature, (10)) to yield crude triol methyl ester **9** which was characterized spectroscopically and by its conversion into triacetate methyl ester **10**. Treatment of triol methyl ester **9** with *p*-toluenesulfonic



[1]Holder of a Natural Sciences and Engineering Research Council of Canada (NSERCC) postgraduate scholarship.

0008-4042/80/090875-03$01.00/0

©1980 National Research Council of Canada/Conseil national de recherches du Canada

Can. J. Chem. Downloaded from www.nrcresearchpress.com by 210.87.254.5 on 09/05/12
For personal use only.

acid in benzene at room temperature gave also tricyclic orthoester **1** (95%).

Tricyclic orthoester **1** was unchanged after treatment with a mixture of hydrochloric acid (0.1 *N*) and dimethoxyethane at room temperature. However, after 3 h at reflux under these conditions, orthoester **1** was converted into diol lactone **8**.

The above results, which are in accord with the report of McElvain and McKay (4), confirm our previous observation that compound **1** is a remarkably stable orthoester towards acid hydrolysis.

Experimental

The ir spectra were taken on a Perkin-Elmer 257 spectrophotometer. Vapor phase chromatographic (vpc) analyses were carried out on a Varian Aerograph instrument, model 920 (column: SE-30%, Chromosorb W, 60–80, 5 ft × $\frac{1}{4}$ in.). Proton nuclear magnetic resonance (nmr) spectra were recorded on a Varian A-60 or a Bruker WP-60 spectrometer. Chemical shifts are reported in δ values relative to tetramethylsilane as internal standard. The mass spectra (ms) were taken on a Hitachi-Perkin-Elmer RMU-6 and a Vg Micromass ZAB-2F mass spectrometer.

Ethyl Bis-allyl Acetate 2

Sodium metal (5.75 g) was added to absolute ethanol (250 mL). When the sodium had completely reacted, diethyl malonate (40 g, 0.25 mol) was slowly added. Allyl bromide (32 g, 0.27 mol) was then added dropwise during 90 min and the mixture was refluxed for 30 min. The mixture was then acidified with glacial acetic acid, filtered, and evaporated. The residue was mixed with water (50 mL) and the mixture was extracted with ether (4 × 40 mL). The ethereal extract was dried over sodium sulfate, filtered, and evaporated to yield diethyl monoallyl malonate (42.4 g, 85%); nmr ($CDCl_3$) δ: 1.35 (6H, triplet, J = 8 Hz, O—CH_2CH_3), 2.6–2.9 (2H, multiplet, allylic CH_2), 3.4–3.7 (1H, multiplet, CH), 4.1–4.5 (4H, quadruplet, J = 8 Hz), and 5.1–6.3 (3H, multiplet, olefinic H).

Using a similar procedure (Na (5.1 g), absolute ethanol (150 mL), and allyl bromide (29 g)), diethyl monoallyl malonate (42.4 g) was converted into diethyl bis-allyl malonate (38.6 g, 76%); nmr ($CDCl_3$) δ: 1.3 (6H, triplet, J = 8 Hz, O—CH_2CH_3), 2.75 (4H, doublet, J = 8 Hz, allylic CH_2), 4.1–4.5 (4H, quadruplet, J = 8 Hz, OCH_2), and 5.0–6.2 (6H, multiplet, olefinic H).

Diethyl bis-allyl malonate (10.0 g, 0.04 mol) was mixed with sodium chloride (3 g, 0.05 mol), water (2.7 g, 0.15 mol), and dimethylsulfoxide (40 mL) and the mixture was refluxed during 100 h. After cooling at room temperature, water (150 mL) was added and the mixture was extracted with ether (3 × 75 mL). The ethereal extract was dried over sodium sulfate, filtered, and evaporated to dryness. The oil obtained was distilled under reduced pressure to yield pure ethyl bis-allyl acetate **2** (5.46 g, 78%); bp 70°C, 4 Torr vpc retention time: 4 min (110°C); ir ($CHCl_3$): 1731 and 1642 cm^{-1}; nmr ($CDCl_3$) δ: 1.35 (3H, triplet, J = 8 Hz, CH_2CH_3), 2.3–3.0 (5H, multiplet), 4.32 (2H, quadruplet, J = 8 Hz, CH_2CH_3), and 5.24 – 6.4 (6H, multiplet, olefinic H); ms m/e: 168 (M^+). *Anal.* calcd. for $C_{10}H_{16}O_2$: C 71.43, H 9.53; found: C 71.16, H 9.73.

Ethyl Triallyl Acetate 3

n-Butyl lithium (25 mmol, 1.6 *M* in hexane) was added dropwise to a solution of diisopropylamine (3.3 mL, 25 mmol) in tetrahydrofuran (60 mL) under an atmosphere of nitrogen. After 15 min at room temperature, the solution was cooled to −78°C and a solution of ethyl bis-allyl acetate **2** (3.36 g, 20 mmol) in tetrahydrofuran (50 mL) was added dropwise. After 30 min, a solution of allyl bromide (3.2 g, 26 mmol) in hexamethylphosphoramide (28 mmol) was added and the reaction mixture was left at −78°C during 2 h. A saturated solution (40 mL) of ammonium chloride was added and the mixture was left to warm up to room temperature. The mixture was then extracted with ether (100 mL). The organic extract was washed with hydrochloric acid (5%, 2 × 50 mL), brine (50 mL), dried with magnesium sulfate, filtered, and evaporated. Distillation of the residue gave pure ethyl triallyl acetate **3** (4.06 g, 97%); vpc retention time: 14.5 min (110°C); ir ($CHCl_3$): 1730 and 1645 cm^{-1}; nmr ($CDCl_3$) δ: 1.3 (3H, triplet, J = 9 Hz, OCH_2CH_3), 2.4 (6H, doublet, J = 8 Hz, allylic CH_2), 4.2 (2H, quadruplet, J = 9 Hz, OCH_2CH_3), 4.9–6.4 (9H, multiplet, olefinic H); ms m/e: 208 (M^+, weak), and 163 ($M^+ - OC_2H_5$).

Triallyl Acetic Acid 4

Ethyl triallyl acetate **3** (4.06 g, 20 mmol) was mixed with ethanol (95%, 150 mL) and potassium hydroxide (5.6 g) and the mixture was heated at reflux for 15 days. After evaporation of the ethanol, water (50 mL) was added and the mixture was extracted with ether (2 × 50 mL). The aqueous phase was acidified with concentrated hydrochloric acid and extracted with ether (4 × 100 mL). This ethereal extract was dried with sodium sulfate, filtered, and evaporated to yield crude triallyl acetic acid **4** (3.25 g, 93%); ir ($CHCl_3$): 3600–2400, 1715, and 1645 cm^{-1}; nmr ($CDCl_3$) δ: 2.0–2.8 (6H, broad singlet, allylic CH_2), 4.8–6.3 (9H, multiplet, olefinic H), and 10.7 (1H, singlet, OH); ms (chemical ion – isobutane, 100 eV): 180 (M^+).

Tribromocarboxylic Acid 5

Triallyl carboxylic acid **4** (1.52 g, 9.05 mmol) was dissolved in pentane (300 mL). (The pentane used was treated with concentrated sulfuric acid during 4 days followed by washing with water, drying with magnesium sulfate, and distillation over calcium hydride.) Nitrogen gas was bubbled through the solution during 5 min. Hydrogen bromide gas was then bubbled through the solution (40 min) which was exposed to the radiation of an ultraviolet lamp (450 W). Nitrogen gas was again bubbled through the solution, ether (200 mL) was added, and the organic phase was washed with sodium thiosulfate (10%, 4 × 75 mL) and brine (50 mL). The organic phase was dried with magnesium sulfate, filtered, and evaporated to yield an oil which was crystallized from hexane (4.5 g, 95%); mp 91.5–93°C (lit. (4) mp 92–94°C); ir ($CHCl_3$): 3600–2400 and 1700 cm^{-1}; nmr ($CDCl_3$) δ: 1.5–2.0 (12 H, broad multiplet), 3.3–3.5 (6H, multiplet, CH_2Br), and 10.6 (1H, singlet, OH); ms (chemical ion − isobutane, 100 ev): 421, 423, 425, 427 (1:3:3:1) (M^+), 374, 376, 378, 380 (1:3:3:1) ($M^+ - CO_2H$), 341, 343, 345 (1:2:1) (M^+ − Br), and 180 (M^+).

Dibromolactone 6

Triethylamine (200 μL) was added to a solution of tribromocarboxylic acid **5** (235 mg, 0.55 mmol) in dichloromethane (25 mL) and the mixture was left at room temperature during 3 h. The organic solution was washed with water, dried with magnesium sulfate, filtered, and evaporated to yield essentially pure dibromolactone **6** (189 mg, 99%); ir ($CHCl_3$): 1730 cm^{-1}; nmr ($CDCl_3$) δ: 1.6–2.0 (12 H, multiplet), 3.2–3.5 (4H, broad triplet, CH_2Br), and 4.1–4.4 (2H, broad triplet, CH_2O); ms m/e (70 eV): 260, 261 (1:1) (M^+ − HBr).

Diacetate Lactone 7

Sodium acetate (820 mg, 10 mmol) was added to a solution of dibromolactone **6** (189 mg, 0.63 mmol) in hexamethylphosphoramide (30 mL) and the mixture was heated at 60°C during 2 h. After cooling to room temperature, dichloromethane (60 mL) was added. The organic phase was washed with hy-

drochloric acid (10%, 4 × 40 mL), dried with magnesium sulfate, filtered, and evaporated. Residual hexamethylphosphoramide was removed by distillation *in vacuo*. The residue was purified by preparative thin layer chromatography (tlc) on silica gel using ether as eluant to yield pure diacetate lactone **7** (87 mg, 52%); ir ($CHCl_3$): 1740 cm^{-1}; nmr ($CDCl_3$) δ: 1.5–1.9 (12 H, multiplet), 2.0 (6H, singlet, CH_3CO), 3.9–4.2 (4H, broad triplet, CH_2OAc), and 4.1–4.4 (2H, broad triplet, CH_2O); ms *m/e*: 240 ($M^+ - OCOCH_3$).

Tricyclic Orthoester 1

Method A

Potassium carbonate (10 mg) was added to a solution of lactone diacetate **7** (11 mg, 0.037 mmol) in methanol (3 mL) and the mixture was left for 30 min. Hydrolysis was complete, as shown by tlc, the solution was acidified with hydrochloric acid (2 *N*) and left for 24 h (no change on tlc). The mixture was refluxed for 3 h, and again there was no sign of orthoester **1** (tlc). Benzene was added and the mixture was refluxed for 4 h using a Dean-Stark water separator. Evaporation of the benzene solution gave tricyclic orthoester **1** which was purified by preparative thin layer chromatography (silica gel, ether) (5.8 mg, 88%).

Method B

Lactone diacetate **7** (6.1 mg, 0.02 mmol) was dissolved in a mixture of hydrochloric acid (2.4 *N*, 0.5 mL) and dimethoxyethane (0.5 mL) and the solution was left at room temperature for 2 h. Thin layer chromatography showed complete hydrolysis. Benzene was added and the mixture was refluxed for 2 h using a Dean-Stark water separator. After evaporation of the solvent and purification by preparative tlc, the tricyclic orthoester **1** was obtained pure (2.5 mg, 66%).

Method C

Lactone diacetate **7** (4.7 mg, 0.016 mmol) was dissolved in a mixture of methanol (5 mL) and triethylamine (50 μL) and left at room temperature for 4 days. Evaporation gave a crude product identified as the triol ester **9**; ir ($CHCl_3$): 3650–3200, and 1730 cm^{-1}; nmr ($CDCl_3$) δ: 1.4–1.9 (15 H, multiplet), 3.5–3.8 (6H, broad triplet, CH_2O), and 3.7 (3H, singlet, CH_3O).

The triol ester **9** was dissolved in benzene (1 mL) in the presence of *p*-toluenesulfonic acid (11 mg) and the mixture was left at room temperature for 2 h. Formation of orthoester **1** was complete as shown by tlc. Potassium carbonate (100 mg) was added, the mixture was stirred for 30 min and evaporated to dryness. Water (10 mL) was added and the aqueous solution was extracted with ether (3 × 20 mL). The organic phase was dried over sodium sulfate, filtered, and evaporated to yield tricyclic orthoester **1** (2.7 mg, 95%).

Large Scale Preparation of Tricyclic Orthoester 1

The tricyclic orthoester **1** (216 mg, 56%) was prepared from tribromocarboxylic acid **5** (834 mg, 1.97 mmol) by utilizing method A described above. Orthoester **1**: mp 114–115°C (lit. (4) mp 114–115°C); nmr ($CDCl_3$) δ: 1.66 (12 H, multiplet), and 3.98 (6H, multiplet, CH_2O); ms *m/e*: 198 (M^+).

Triacetate Ester 10

Lactone diacetate **7** (5.5 mg, 0.018 mmol) was mixed with methanol (5 mL) and triethylamine (50 μL) and left at room temperature for 4 days. Evaporation of the solvent gave crude triol ester **9**. Acetic anhydride (3 mL) and pyridine (3 mL) were added and the mixture was left for 15 h. Evaporation gave a mixture of diacetate lactone **7** (1.1 mg, 20%) and triacetate ester **10** (3.9 mg, 56%) which were separated by tlc. Triacetate ester **10**: ir ($CHCl_3$): 1730 cm^{-1}; nmr ($CDCl_3$) δ: 1.4–1.9 (12 H, multiplet), 2.0 (9H, singlet, CH_3CO), 3.5–3.8 (6H, broad triplet, CH_2O) and 3.7 (3H, singlet, CH_3O); ms (chemical ion – isobutane, 100 eV): 315 ($M^+ - CH_3CO_2$).

Hydrolysis of Tricyclic Orthoester 1

Orthoester **1** (8.2 mg, 0.042 mmol) was mixed with dimethoxyethane (4 mL) and hydrochloric acid (0.1 *N*, 1 mL) and left for 5 h at room temperature. The analysis indicated that hydrolysis of **1** did not take place. The mixture was then heated at reflux for 3 h and tlc indicated complete hydrolysis. The solvent was evaporated and a mixture of acetic anhydride (2 mL) and pyridine (2 mL) was added. After 15 h at room temperature, the solution was evaporated and the residue was purified by tlc to yield pure diacetate lactone **7** (8.5 mg, 68%).

Acknowledgements

Support for this work by the Natural Sciences and Engineering Research Council of Canada (NSERCC) and by the Ministère de l'Education, Québec, is gratefully acknowledged.

1. P. DESLONGCHAMPS, R. CHENEVERT, R. J. TAILLEFER, C. MOREAU, and J. K. SAUNDERS. Can. J. Chem. **53**, 1601 (1975).
2. P. DESLONGCHAMPS. Pure Appl. Chem. **43**, 351 (1975); Tetrahedron, **31**, 2463 (1975); Heterocycles, **7**, 1271 (1977).
3. S. H. BANYARD and J. D. DUNITZ. Acta Crystallogr. Sect. B, **32**, 318 (1976).
4. S. M. MCELVAIN, E. R. DEGGINGER, and J. D. BEHUN. J. Am. Chem. Soc. **76**, 5736 (1954); S. M. MCELVAIN and G. R. MCKAY, JR. J. Am. Chem. Soc. **77**, 5601 (1955).
5. R. F. B. COX and S. M. MCELVAIN. *In* Org. Synth. Coll. Vol. II. John Wiley and Sons, Inc., New York. 1943. p. 279.
6. A. P. KRAPCHO and A. J. LOVEY. Tetrahedron Lett. 957 (1973); A. P. KRAPCHO, J. F. WEIMASTER, J. M. ELDRIDGE, E. G. E. JAHNGEN, JR., A. J. LOVEY, and W. P. STEPHENS. J. Org. Chem. **43**, 138 (1978).
7. R. J. CREGGE, J. L. HERRMANN, C. S. LEE, J. E. RICHMAN, and R. H. SCHLESSINGER. Tetrahedron Lett. 2425 (1973).
8. H. O. HOUSE, C.-Y. CHU, W. V. PHILLIPS, T. S. B. SAYER, and C.-C. YAU. J. Org. Chem. **42**, 1709 (1977).
9. N. IKOTA and B. GANEM. J. Am. Chem. Soc. **100**, 351 (1978).
10. T. L. NAGABHUSHAN. Can. J. Chem. **48**, 383 (1970).

Can. J. Chem. Downloaded from www.nrcresearchpress.com by 210.87.254.5 on 09/05/12
For personal use only.

The preparation and oxidation of disulfides as a route to sulfone-sulfides

TERENCE PATRICK AHERN, HARVEY OWEN FONG, RICHARD FRANCIS LANGLER,[1] AND PETER MICHAEL MASON

Chemistry Department, Dalhousie University, Halifax, N.S., Canada B3H 4J3

Received December 3, 1979

TERENCE PATRICK AHERN, HARVEY OWEN FONG, RICHARD FRANCIS LANGLER, and PETER MICHAEL MASON. Can. J. Chem. **58**, 878 (1980).

Mercaptide/alkoxide competition in substitution and addition reactions is discussed as it applies to the preparation of disulfides. Oxidation of an asymmetric disulfide with H_2O_2 is shown to exhibit high regioselectivity which may be rationalized in the same terms employed for other sulfide oxidations, viz. substituent electron withdrawing ability (X_p) and steric effects.

TERENCE PATRICK AHERN, HARVEY OWEN FONG, RICHARD FRANCIS LANGLER et PETER MICHAEL MASON. Can. J. Chem. **58**, 878 (1980).

On discute de la compétition existant entre les thiolates et les alcoolates lors des réactions d'addition et de substitution, telles qu'elles sont appliquées à la préparation des disulfures. On a montré que l'oxydation d'un disulfure asymétrique par H_2O_2 est hautement régiosélective et qu'elle peut être expliquée comme dans le cas des oxydations d'autres sulfures, par l'effet des substituants électroattracteurs (X_p) et des effets stériques.

[Traduit par le journal]

Can. J. Chem. Downloaded from www.nrcresearchpress.com by 210.87.254.6 on 09/05/12
For personal use only.

Introduction

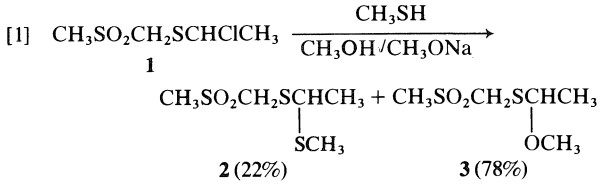
In connection with our work on the chlorinolyses of sulfur compounds (1–10), we have become interested in the preparation of β-sulfone-sulfides. These compounds permit the assessment of sulfonyl moieties as directing groups in asymmetric sulfide chlorinations (3). We have recently reported (2) the results generated by our approach to sulfone-sulfide synthesis via mercaptosulfone intermediacy.

The present report details results on the preparation and oxidation of disulfides with a view to obtaining the corresponding β-sulfone-sulfides. The conversion of a disulfide to a β-sulfone-sulfide requires the intermediacy of a β-sulfoxide-sulfide. While there are a variety of reagents (11–16) which permit the conversion of disulfides to β-sulfoxide-sulfides, very few reagents will accomplish the conversion of a sulfoxide-sulfide to a sulfone-sulfide.

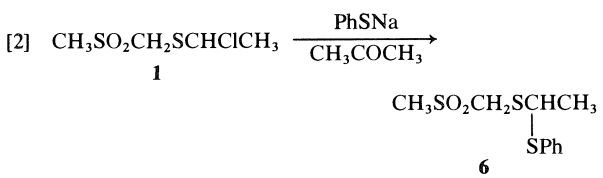
Results and Discussion

Disulfides may be prepared by condensation of a mercaptan with an aldehyde or ketone (17–19) or by base catalyzed condensation of a mercaptan and an α-chlorosulfide.[2]

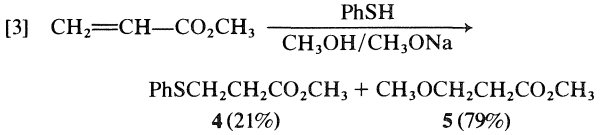
Although some mercaptide anions and α-chlorosulfides may be cleanly condensed in an alcoholic medium (4), eq. [1] illustrates one possible complication.



The results shown in eq. [1] can be rationalized by presuming an S_N1 mechanism which becomes dominant due to the enhanced stability of an alkyl substituted sulfenium ion over an unsubstituted sulfenium ion (4). Consistent with this proposal, **6** is formed, without complication, in acetone.



In a related Michael addition reaction (eq. [3]) a similar complication has been observed.



The results in eq. [3] may be rationalized by presuming that mercaptide anion addition is rever-

[1]Enquiries should be directed to Dr. R. F. Langler, Chemistry Department, Mount Allison University, Sackville, N.B., Canada E0A 3C0.

[2]The desired α-chlorosulfide may be prepared by chlorination of the desired sulfide with sulfuryl chloride or *N*-chlorosuccinimide, provided due consideration is given to substituent electronegativities. (3).

0008-4042/80/090878-06$01.00/0

©1980 National Research Council of Canada/Conseil national de recherches du Canada

sible while alkoxide anion addition is not.[3] In any case it is clear that alcoholic media may present unwelcome complications in these condensation reactions.

We have selected the symmetric disulfide **7** to begin our examination of disulfide oxidations.

[4] $PhCH(SCH_3)_2$ (**7**) $\xrightarrow[\text{Dioxane}]{30\%H_2O_2}$ $PhCH(SO_2CH_3)(SCH_3)$ (**8**, 8%)

The formation of **8** from oxidation of **7** as shown in eq. [4] is rather surprising since peroxidic oxidations normally give exclusively disulfoxides as outlined in eq. [5].

[5] $(CH_3O_2CCH_2S)_2CH_2$ (**9**) $\xrightarrow[\text{Dioxane}]{30\%H_2O_2}$ $(CH_3O_2CCH_2SO)_2CH_2$ (**10**, 58%)

The twofold oxidation of **9** produced no detectable amount of sulfone-sulfide in accord with a previous study of sulfide oxidations (22). Clearly, the oxidation of disulfides with peroxides is an unsuitable approach to the preparation of sulfone-sulfides.[4]

Sodium permanganate in aqueous dioxane has been reported (23) to permit the selective oxidation of sulfoxides in preference to sulfides. In that paper some difficulty was encountered with solvent oxidation. We have elected to employ potassium permanganate in aqueous THF[5] as a reagent system with somewhat improved availability and stability. To test this modified reagent system we have prepared[6] and oxidized the sulfoxide-sulfide **11**. The results are depicted in Scheme 1. The conversion of **11** to **13** illustrates the importance of the reaction conditions.

It was our objective to examine the oxidation of **6** which could, in principle, form a pair of regioisomeric sulfone-sulfoxide-sulfides each of which would exist as a pair of diastereomers. We have chosen to begin this portion of the work by examining a simpler system in order to establish a way to distinguish between regioisomers and diastereomers. We, therefore, subjected the sulfone-sulfide **1** to oxidation with one equivalent of *m*-chloroperbenzoic acid (mCPBA) as shown in Scheme 2. Nuclear magnetic resonance indicated that the sulfone-sulfoxide **14**[7] was an equimolar mixture of two compounds. Oxidation of **14** furnished the homogeneous disulfone **15** in greater than 90% yield, thereby establishing that **14**, as expected (25–27), was a mixture of diastereomers.

We were now prepared to examine the oxidation of **6** to assess regioselectivity in that reaction. While the problem of regioselectivity in 1,3-disulfide oxidations does not appear to have been scrutinized previously, that of regioselectivity in 1,2-disulfide oxidations has been.

Bhattacharya and Hortmann (28) have reported the disulfide oxidations shown in eq. [6] to be regiospecific.

They have concluded that "oxidation appeared to occur (in the absence of steric effects) at the sulfur atom farthest removed from the relatively

[6] $PhCH_2SSPh + mCPBA \longrightarrow PHCH_2SO_2SPh$

$CH_3CH_2SSPh + mCPBA \longrightarrow CH_3CH_2SO_2SPh$

more electron withdrawing group." Oxidation of 1,2-disulfides, as these authors point out, may proceed through 1,2-disulfoxides (29). In the closely related sodium metaperiodate oxidations of 1,2-disulfides Oae *et al.* (30) report no indication of 1,2-disulfoxide formation. These same factors, viz. steric effects and the electron withdrawing ability of substituents, have been cited to rationalize peroxydisulfate oxidations of simple sulfides (31).

Application of these factors to **6** leads to the expectation that oxidation should occur with high regioselectivity, at the sulfur bearing the phenyl group on the grounds that (*i*) a mesylmethyl group is more electronegative than a phenyl group ($X_pCH_3SO_2CH_2 = 2.85$, $X_pPh = 2.49$ (3)), and (*ii*) the central sulfur atom is much closer to the bulky mesyl group[8] than is the thiophenyl sulfur atom.

Oxidation of **6** with an equivalent of H_2O_2 afforded a mixture **16** of two compounds which displayed different chemical shifts for all corresponding non-aromatic protons, e.g., two doublets (all lines approximately equal in intensity) appeared at δ 1.23 and two singlets appeared at δ 3.03 in the nmr spectrum. Oxidation of the mixture with $KMnO_4/H_2O/THF$ afforded an homogeneous disulfone-sulfide, tentatively assigned structure **17** in about 50% yield. Crude **16** from another run was

[3]The sulfide ester **4** was prepared in good yield when the reaction was conducted in pyridine (2).

[4]A paper has appeared (21) which reports that $KMnO_4$ in cold acetone furnishes sulfone-sulfides from symmetric disulfides. Reaction times are 8–10 days.

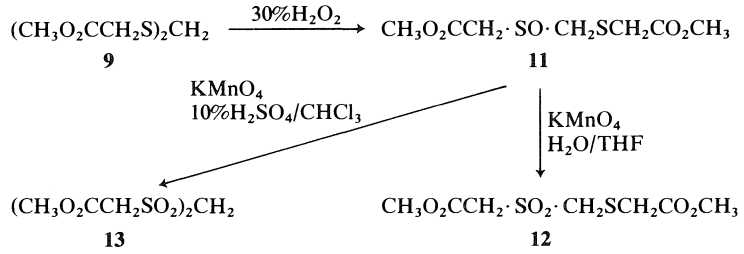
[5]Even dioxane freshly distilled from $KMnO_4$ reacted significantly faster with permanganate than THF.

[6]Sulfoxide-sulfides may also be obtained from sulfinate esters (24).

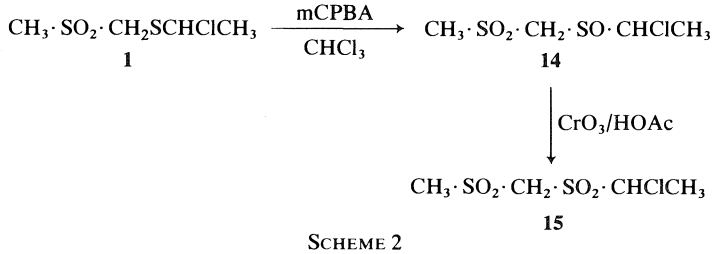
[7]Compound **14** was shown to be free of unreacted **1** and disulfone **15** by the addition of authentic samples of each to **14** which gave rise to the expected new signals in the nmr.

[8]The nature of the steric effect of the mesyl (or methylsulfonyl) group has been discussed previously (1).

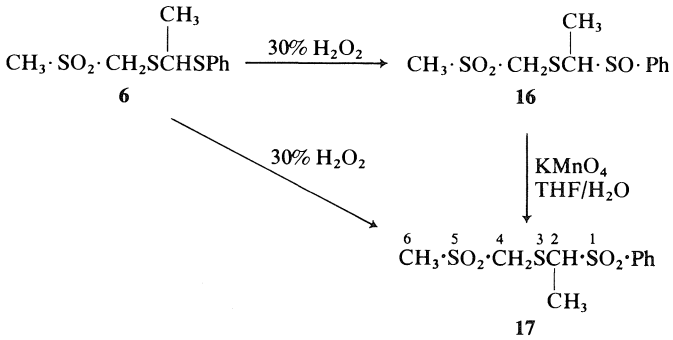
Can. J. Chem. Downloaded from www.nrcresearchpress.com by 210.87.254.6 on 09/05/12
For personal use only.



SCHEME 1



SCHEME 2



SCHEME 3

subjected to column chromatography which furnished a homogeneous sample of one diastereomer. Permanganate oxidation of the homogeneous diastereomer furnished the same disulfone-sulfide **17** in essentially the same yield as obtained from the diastereomeric mixture (*vide* Scheme 3). These results establish that **16** was indeed a diastereomeric mixture and that oxidation of **6** was highly regioselective.

The first evidence concerning which sulfur atom of **6** was oxidized to yield **16** was obtained from the mass spectrum of **16**. A moderate intensity ion was observed at *m/e* 125 (relative abundance ca. 50%) in accord with the presence of a phenylsulfinyl group. The mass spectrum of **17** showed the base peak at *m/e* 153 ($M^{\ddagger} - PhSO_2$). The loss of substituted sulfonyl groups as neutral fragments from molecular ions has been amply precedented (32–34). Furthermore, the aromatic regions in the nmr spectra of **6** and **16** show broad singlets whereas the nmr of **17** shows two distinct aromatic signals in accord with the presence of an electronegative SO_2 group attached directly to the phenyl ring.

A brief deuterium exchange experiment furnished polydeuterated **17**. The nmr and mass spectrum indicated about 70% exchange at C4 and 11% exchange at C2. This result is clearly inconsistent with the alternative disulfone-sulfide structure for **17**. The selectivity in the exchange experiment on **17** could be rationalized on the basis of a slightly greater acidity for the methylene protons than for the methine proton.

In conclusion we have found that (*i*) nucleophilic competitions make substitution and addition reactions in alcohols unreliable when mercaptide anions are the intended nucleophiles, and (*ii*) regioselectivity in a 1,3-disulfide oxidation appears to be subject to the same considerations advanced for 1,2-disulfide oxidations, i.e., the electron withdrawing ability (X_p) of substituents and steric effects.

Can. J. Chem. Downloaded from www.nrcresearchpress.com by 210.87.254.6 on 09/05/12
For personal use only.

Can. J. Chem. Downloaded from www.nrcresearchpress.com by 210.87.254.6 on 09/05/12
For personal use only.

Experimental

General

The ir spectra were recorded on a Perkin-Elmer 237B grating spectrophotometer. The nmr spectra were obtained on a Varian T60 instrument using TMS as the internal standard. The mass spectra were recorded on a Dupont-CEC model 21-104 mass spectrometer. Samples were directly introduced using an all glass probe and the spectra run at 30 eV with a source temperature of 150°C. Melting points were determined on a Fisher-Johns melting point apparatus and are uncorrected.

*Reaction of **1** with Sodium Methyl Mercaptide in Methanol*

Sodium metal (0.155 g) was dissolved in methanol (25 mL) and the solution cooled to 5°C. Methanethiol (3 mL) was slowly distilled into the solution. The α-chlorosulfide **1** (1.236 g) (3) was added and the reaction mixture stirred at ambient temperature for 24 h. Water (25 mL) was added and the resultant mixture washed with chloroform (five 50 mL aliquots). The combined organic layers furnished a mixture of the sulfone-sulfide-ether **3** and the sulfone-disulfide **2**. The mixture was chromatographed on silica gel (100 g) with diethyl ether elution (100 mL aliquots).

Fraction 3 (108.2 mg) was sulfone-disulfide **2**, ir ($CHCl_3$): 1315 and 1110 cm^{-1}; nmr ($CDCl_3$) δ: 4.46 (1H, q, J = 6 Hz), 4.30 (1H, d, J = 14 Hz), 3.90 (1H, d, J = 14 Hz), 2.96 (3H, s), 2.03 (3H, s), and 1.60 (3H, d, J = 6 Hz); ms *m/e*: 200 (M^+, 23.9%) and 75 (100%).

Fraction 4 (194.6 mg) was an equimolar mixture of **2** and **3**. Fractions 5–8 were combined and concentrated affording the sulfone-sulfide-ether **3** (585 mg), ir ($CHCl_3$): 1315 and 1115 cm^{-1}; nmr ($CDCl_3$) δ: 5.03 (1H, q, J = 6 Hz), 3.96 (2H, s), 3.36 (3H, s), 3.00 (3H, s), and 1.53 (3H, d, J = 6 Hz); ms *m/e*: 184 (M^+, 1.5%) and 59 (100%).

Reaction of Methyl Acrylate and Sodium Thiophenoxide in Methanol

Sodium metal (4.224 g) was dissolved in methanol (200 mL) and benzenethiol (19.8 g) added. The solution was cooled and methyl acrylate (15.62 g) in methanol (50 mL) was added dropwise over 0.5 h. The reaction mixture was refluxed 1 h. Water (250 mL) was added and the resultant mixture washed with methylene chloride (four 200 mL aliquots). The combined organic layers afforded a mixture of the ether-ester **5** and the sulfide-ester **4**. The mixture was rectified at reduced pressure affording **5** (9.949 g, bp 32–34°C/3 Torr) and **4** (4.524 g).

The sulfide-ester **4** was identical with previously described material (2).

The ether-ester **5** had ir ($CHCl_3$): 1730 cm^{-1}; nmr ($CDCl_3$) δ: 3.73 (3H, s), 3.73 (2H, t), 3.39 (3H, s) and 2.60 (2H, t); ms *m/e*: 118 (M^+, 28.5%), 59 (28.5%), and 45 (100%).

*Preparation of **6***

A solution of sodium thiophenate (0.912 g) in acetone (3 mL) was added to a solution of the chlorosulfone-sulfide **1** (1.000 g) (3) in acetone (9 mL) and the reaction mixture stirred at ambient temperature for 24 h. Water (25 mL) was added and the resultant mixture washed with chloroform (four 50 mL aliquots). The combined organic layers were dried and concentrated affording crude sulfone-disulfide **6** (1.282 g). The crude product was chromatographed on silica gel (100 g) employing 4:1 ether–chloroform (50 mL fractions). Fractions 6–8 were combined and concentrated and the residue recrystallized affording clean **6** (0.901 g, mp 40–41°C); ir ($CHCl_3$): 1320 and 1120 cm^{-1}; nmr ($CDCl_3$) δ: 7.30 (5H, broad s), 4.80 (1H, q, J = 6 Hz), 4.33 (1H, d, J = 14 Hz), 3.90 (1H, d, J = 14 Hz), 2.96 (3H, s), and 1.60 (3H, d, J = 6 Hz); ms *m/e*: 262 (M^+, 19.6%), 137 (86.0%), 109 (54.2%), and 73 (100%). *Anal.* calcd. for $C_{10}H_{14}O_2S_3$: C 45.77, H 5.37; found: C 45.63, H 5.59.

*Peroxidation of **7***

The disulfide **7** (10 g) (19) was dissolved in pyridine (100 mL), triethylamine (10 mL), and water (10 mL). After stirring overnight the reaction mixture was diluted with chloroform, acid washed, dried, and rectified at reduced pressure affording acid free disulfide (7.76 g, bp 144°C/5 Torr).

The disulfide (4.661 g) was dissolved in dioxane (50 mL) and H_2O_2 (30%, 2.870 g) added. The reaction mixture was refluxed for 0.5 h, after which it was concentrated and chromatographed on silica gel (400 g). Elution of the column with chloroform (100 mL aliquots) furnished the sulfone-sulfide **8** (0.438 g) from fractions 20–28. After recrystallization from 95% ethanol the sulfone-sulfide had mp 109–111°C and R_f 0.25 (with chloroform development); ir ($CHCl_3$): 1320 and 1120 cm^{-1}; nmr ($CDCl_3$) δ: 7.43 (5H, s), 4.86 (1H, s), 2.86 (3H, s), and 2.46 (3H, s); ms *m/e*: 137 (100%) and 121 (25%). *Anal.* calcd. for $C_9H_{12}O_2S_2$: C 49.97, H 5.59; found: C 50.17, H 5.48.

*Peroxidation of **9***

The disulfide-diester **9** (5.007 g) (35) was dissolved in dioxane (25 mL) and H_2O_2 (30%, 2.522 g) was added. The reaction was refluxed for 0.5 h and the solvent evaporated. The residue was recrystallized from methanol affording disulfoxide-diester **10** (3.347 g, mp 90–94°C); ir ($CHCl_3$): 1740 and 1050 cm^{-1}; nmr ($CDCl_3$) δ: 4.36 (6H, m) and 3.86 (6H, s); ms *m/e*: 106 (16.9%), 74 (33.8%), 59 (61.9%), and 45 (100%). *Anal.* calcd. for $C_7H_{12}O_6S_2$: C 32.80, H 4.71; found C 32.76, H 4.59.

*Preparation of **11***

The disulfide-diester **9** (5.005 g) (35) was dissolved in dioxane (25 mL) and H_2O_2 (30%, 2.522 g) was added. The reaction was refluxed for 0.5 h and the solvent evaporated. The crude product was chromatographed on silica gel (350 g) employing 9:1 diethyl ether – methanol (100 mL aliquots) as eluent. Fractions 13–17 were combined and concentrated affording clean diester-sulfoxide-sulfide **11** (2.376 g) as an oil; ir ($CHCl_3$): 1745, 1740, and 1050 cm^{-1}; nmr ($CDCl_3$) δ: 4.30 (1H, d, J = 12 Hz), 4.20 (1H, d, J = 12 Hz), 3.90 (1H, d, J = 12 Hz), 3.80 (1H, d, J = 12 Hz), 3.80 (3H, s), 3.76 (3H, s), and 3.57 (2H, s); ms *m/e*: 119 (84.7%), 91 (23.6%), and 45 (100%).

*Permanganate Oxidation of **11** in THF*

The diester-sulfoxide-sulfide **11** (1.000 g) in THF (5 mL) was added to a mixture of $KMnO_4$ (0.444 g) in 20% v/v aqueous THF (100 mL). The reaction mixture was stirred at ambient temperature for 10 min. Water (100 mL) was added and the resultant mixture washed with chloroform (four 100 mL aliquots). The combined organic layers were dried and concentrated. The crude diester-sulfone-sulfide (0.962 g) was chromatographed on silica gel employing diethyl ether (50 mL fractions) as eluent. Fractions 7–12 were combined and concentrated affording clean diester-sulfone-sulfide **12** (0.680 g) as an oil; ir ($CHCl_3$): 1750, 1328, and 1110 cm^{-1}; nmr ($CDCl_3$) δ: 4.37 (2H, s), 4.33 (2H, s), 3.83 (3H, s), 3.77 (3H, s), and 3.67 (2H, s); ms *m/e*: 197 (7.5%), 119 (100%), 91 (30%), and 45 (88.6%).

*Conversion of **11** to **13***

A solution of the diester-sulfoxide-sulfide **11** (1.003 g) in chloroform (25 mL) was added to 10% v/v sulfuric acid in water (35 mL) dropwise over 15 min. During the addition $KMnO_4$ (5.024 g) was added in small portions. Upon completion of the additions, the reaction mixture was stirred at room temperature for 1 h. The reaction mixture was cooled and sodium bisulfite added until the mixture became colorless. The layers were separated and the aqueous layer washed with chloroform. The combined chloroform layers were dried and concentrated affording the diester-disulfone **13** (1.15 g). Upon recrystallization the disulfone **13** had ir ($CHCl_3$): 1750, 1350, and 1120 cm^{-1}; nmr ($CDCl_3$) δ: 5.33 (2H, s), 4.46 (4H, s), and 3.90 (6H, s); ms *m/e*: 288 (M^+, 13%), 151 (100%), 79 (46.5%), and 74 (60.5%). Other properties were in accord with a previous report (36).

Can. J. Chem. Downloaded from www.nrcresearchpress.com by 210.87.254.6 on 09/05/12
For personal use only.

Preparation of ***14***

A solution of the chlorosulfone-sulfide **1** (2.241 g) (3) in chloroform (50 mL) was cooled to −6°C and *m*-chloroperbenzoic acid (85%, 2.534 g) added in small portions. The ice in the cooling bath was allowed to melt and the reaction mixture was stirred overnight. Chloroform (150 mL) was added and the resultant solution washed with 1% NaOH (two 50 mL aliquots). The organic layer was dried and concentrated. The residue was recrystallized from 95% ethanol affording diastereomeric chlorosulfone-sulfoxide **14** (0.799 g, mp 78–80°C); ir ($CHCl_3$): 1325, 1150, and 1060 cm^{-1}; nmr ($CDCl_3$) δ: 5.26 (0.5H, q, J = 7 Hz), 5.00 (0.5H, q, J = 7 Hz), 4.33 (2H, broad s), 3.23 (3H, s), and 1.93 (3H, d, J = 7 Hz); ms *m/e*: 141 (12.6%), 127 (11.5%), and 63 (100%).

Oxidation of ***14***

The chlorosulfone-sulfoxide **14** (0.100 g) in glacial acetic acid (1 mL) was added to a mixture of chromium trioxide (0.065 g) in glacial acetic acid (2 mL). The reaction mixture was heated to 90–100°C for 0.5 h. Water (15 mL) was added and the resultant mixture washed with chloroform (three 25 mL aliquots). The combined organic layers were washed with 2.5% w/v NaOH (two 25 mL aliquots), dried, and concentrated. The product was homogeneous chlorodisulfone **15** (by nmr) (0.097 g). Upon recrystallization it was shown to be identical with previously prepared chlorodisulfone **15** (3) by nmr, ir, mp, and mixture mp.

Oxidative Conversion of ***6*** *to* ***17***

Hydrogen peroxide (30%, 0.432 g) was added to a solution of the sulfone-disulfide **7** (0.500 g) in dioxane (25 mL) and the solution refluxed for 0.5 h. The solvent was evaporated and the residue chromatographed on silica gel (50 g) employing diethyl ether (50 mL fractions) as eluent. Fractions 5–7 were combined and concentrated affording the disulfone-sulfide **17** (0.137 g, mp 147–148°C); ir ($CHCl_3$): 1320 and 1150 cm^{-1}; nmr ($CDCl_3$) δ: 8.03 (2H, m), 7.70 (3H, m), 4.86 (1H, q, J = 7 Hz), 4.73 (1H, d, J = 14 Hz), 3.90 (1H, d, J = 14 Hz), 3.03 (3H, s), and 1.50 (3H, d, J = 7 Hz); ms *m/e*: 294 (M^+, 1.9%), 153 (100%), 125 (28.2%), and 73 (96.1%). *Anal.* calcd. for $C_{10}H_{14}O_4S_3$: C 40.79, H 4.79; found: C 40.83, H 4.61.

Preparation of ***16***

The sulfone-disulfide **6** (2.023 g) was added to a solution of hydrogen peroxide (30%, 0.874 g) in dioxane (100 mL) and the reaction mixture refluxed for 0.5 h. The solvent was evaporated and the residue chromatographed on silica gel (200 g) employing diethyl ether (100 mL fractions) for elution. Fractions 34–36 were combined and concentrated affording one of the diastereomers of **16** as a pure oil (0.317 g); ir ($CHCl_3$): 1320, 1110, and 1060 cm^{-1}; nmr ($CDCl_3$) δ: 7.63 (5H, broad s), 4.60 (1H, q, J = 6 Hz), 4.36 (1H, d, J = 14 Hz), 3.90 (1H,d, J = 14 Hz), 3.10 (3H, s), and 1.33 (3H, d, J = 6 Hz); ms *m/e*: 155 (40.3%), 125 (48.3%), 109 (100%), and 73 (32.2%).

The other diastereomer differed principally in its nmr spectrum which was obtained by subtraction of the nmr of the pure diastereomer from the nmr of a mixture of diastereomers. the second diastereomer had nmr ($CDCl_3$) δ: 7.53 (5H, s, broad), 4.43 (1H, q, J = 6 Hz), 4.36 (1H, d, J = 14 Hz), 3.80 (1H, d, J = 14 Hz), 2.96 (3H, s), and 1.36 (3H, d, J = 6 Hz).

Oxidation of **6** (2 g) furnishes ca. 1:1 mixture of diastereomers (1.92 g).

Conversion of ***16*** *to* ***17***

Both the crude diastereomeric mixture **16** and the purified diastereomer described above gave essentially the same results outlined below.

The sulfone-sulfoxide-sulfide **16** (0.202 g) in THF (5 mL) was added to potassium permanganate (0.076 g) in 20% v/v aqueous THF (100 mL). The reaction was stirred at ambient temperature for 10 min. Water (100 mL) was added and the mixture washed with chloroform (four 100 mL aliquots). The organic layers afforded disulfone-sulfide **17** (0.173 g) which was homogeneous by tlc and nmr. Recrystallization afforded **17** which was identical with previously obtained material by ir, nmr, mp, and mixture mp.

Acknowledgements

The authors are indebted to Mr. D. G. Kay and Mr. Z. A. Marini for some technical assistance. We thank Dr. J. H. Kim for running the mass spectra. We are grateful to Dalhousie University for financial support in the form of a grant from the Research Development Fund.

1. D. G. Kay, R. F. Langler, and J. E. Trenholm. Can. J. Chem. **57**, 2185 (1979).
2. H. O. Fong, W. R. Hardstaff, D. G. Kay, R. F. Langler, R. H. Morse, and D. N. Sandoval. Can. J. Chem. **57**, 1206 (1979).
3. T. P. Ahern, D. G. Kay, and R. F. Langler. Can. J. Chem. **56**, 2422 (1978).
4. R. F. Langler, Z. A. Marini, and J. A. Pincock. Can. J. Chem. **56**, 903 (1978).
5. R. F. Langler and J. A. Pincock. Can. J. Chem. **55**, 2316 (1977).
6. J. S. Grossert, W. R. Hardstaff, and R. F. Langler. Can. J. Chem. **55**, 421 (1977).
7. J. S. Grossert and R. F. Langler. Can. J. Chem. **55**, 407 (1977).
8. R. F. Langler. Can. J. Chem. **54**, 498 (1976).
9. J. R. Jardine and R. F. Langler. J. Chromatogr. **116**, 211 (1976).
10. W. R. Hardstaff, R. F. Langler, J. Leahy, and M. J. Newman. Can. J. Chem. **53**, 2664 (1975).
11. J. J. Rigau, C. C. Bacon, and C. R. Johnson. J. Org. Chem. **35**, 3655 (1970).
12. B. G. Cox and A. Gibson. J. Chem. Soc. Perkin Trans. II,1355 (1973).
13. R. Curci, F. Difuria, R. Testi, and G. Modena. J.Chem. Soc. Perkin Trans. II, 752 (1974).
14. M. Hojo and R. Masuda. Tetrahedron Lett. 613 (1976).
15. K. T. Liu and Y. C. Tong. J. Org. Chem. **43**, 2717 (1978).
16. P. B. Roush and W. K. Musker. J. Org. Chem. **43**, 4295 (1978).
17. T. H. Chan and B. S. Ong. Synth. Commun. **7**, 283 (1977).
18. H. E. Westlake, Jr. and G. Dougherty. J. Am. Chem. Soc. **63**, 658 (1941).
19. R. F. Langler, W. S. Mantle, and M. J. Newman. Org. Mass Spectrom. **10**, 1135 (1975).
20. J. B. Hendrickson, D. J. Cram, and G. S. Hammond. Organic chemistry. 3rd ed. McGraw-Hill, New York, NY. 1970.
21. M. Poje and K. Balenovic. Tetrahedron Lett. 1231 (1978).
22. N. J. Leonard and C. R. Johnson. J. Org. Chem. **27**, 282 (1962).
23. H. B. Henbest and S. A. Kahn. Chem. Commun. 1036 (1968).
24. L. Colombo, C. Gennari, and E. Narisano. Tetrahedron Lett. 3861 (1978).
25. J. F. King, R. P. Beatson, and J. M. Buchshriber. Can. J. Chem. **55**, 2323 (1977).
26. G. Canalini, G. Maccagnani, and F. Taddei. Tetrahedron Lett. 3035 (1971).

27. R. P. GUPTA, J. S. PIZEY, and K. SYMEONIDES. Tetrahedron, **32**, 1917 (1976).
28. A. K. BHATTACHARYA and A. G. HORTMANN. J. Org. Chem. **43**, 2728 (1978).
29. M. M. CHAU and J. L. KICE. J. Am. Chem. Soc. **98**, 7711 (1976).
30. S. OAE, Y. H. KIM, T. TAKATA, and D. FUKUSHIMA. Tetrahedron Lett. 1195 (1977).
31. C. SRINIVASAN, P. KUTHALINGAM, and N. ARUMUGAM. Can. J. Chem. **56**, 3043 (1978).
32. P. P. DAVIS, J. S. GROSSERT, R. F. LANGLER, and W. S. MANTLE. Org. Mass Spectrom. **12**, 659 (1977).
33. R. F. LANGLER, W. S. MANTLE, and M. J. NEWMAN. Org. Mass Spectrom. **10**, 1135 (1975).
34. W. R. HARDSTAFF and R. F. LANGLER. Org. Mass Spectrom. **10**, 215 (1975).
35. (*a*) G. G. STONER and G. DOUGHERTY. J. Am. Chem. Soc. **63**, 987 (1941); (*b*) A. MARTANI. Ann. Chim. **49**, 1844 (1959).
36. R. L. SHRINER, J. M. CROSS, and T. DOBRATZ. J. Am. Chem. Soc. **61**, 2001 (1939).

Can. J. Chem. Downloaded from www.nrcresearchpress.com by 210.87.254.6 on 09/05/12
For personal use only.

Erratum: Pseudozoanthoxanthins from gold coral

ROBERT E. SCHWARTZ, MARK B. YUNKER, AND PAUL J. SCHEUER
Department of Chemistry, University of Hawaii at Manoa, Honolulu, HI 96822, U.S.A.
AND
TOR OTTERSEN
Department of Chemistry, University of Oslo, Blindern, Oslo 3, Norway

(Ref.: Can. J. Chem. 57, 1707 (1979))
Received February 4, 1980

In Table 1, the uv spectral data for compound **5** in MeOH and MeOH—H^+ are incorrect. They should read:

Compound	Solvent	Wavelength, nm (log ε)				
5	MeOH	425(4.12)	306(4.22)	289(4.22)	259(4.31)	224(4.21)
5	MeOH—H^+	419(4.23)	291(4.35)		257(4.18)	226(4.18)

In Table 2, compound **4**[a] does not have an NHMe 3H singlet at δ 3.42. In compound **7**[a], the two overlapping singlets at δ 3.62 and δ 3.54 are not 3H singlets, but rather 6H singlets.

0008-4042/80/090883-01$01.00/0
©1980 National Research Council of Canada/Conseil national de recherches du Canada

The migratory aptitudes of some aryl groups in triarylvinyl cations[1]

CHOI CHUCK LEE AND ERIC C. F. KO

Department of Chemistry and Chemical Engineering, University of Saskatchewan, Saskatoon, Sask., Canada S7N 0W0

AND

ZVI RAPPOPORT

Department of Organic Chemistry, The Hebrew University of Jerusalem, Jerusalem, Israel

Received October 19, 1979

CHOI CHUCK LEE, ERIC C. F. KO, and ZVI RAPPOPORT. Can. J. Chem. **58**, 884 (1980).

Errors reported in the literature on the migratory aptitudes of some aryl groups in triarylvinyl cations have been corrected. From the corrected as well as some new data, the relative migratory aptitudes for Ph:Tol:An in triarylvinyl cations in acetic acid media are calculated to be 1:4 – 5:162, based on $k_{r(Tol)}/k_{r(Ph)}$ derived from migrations in the tritolylvinyl and 2-phenyl-1,2-ditolylvinyl cations and $k_{r(An)}/k_{r(Ph)}$ derived from migrations in the 2-anisyl-1,2-diphenylvinyl and triphenylvinyl cations.

CHOI CHUCK LEE, ERIC C. F. KO et ZVI RAPPOPORT. Can. J. Chem. **58**, 884 (1980).

On corrige les erreurs publiées dans la littérature lors de l'étude des aptitudes migratoires de quelques groupes aryles dans les cations triarylvinyles. A partir des données corrigées aussi bien qu'à partir de nouvelles données, on a calculé les aptitudes migratoires relatives Ph:Tol:An dans les cations triarylvinyles en milieu acide acétique et on a trouvé une valeur de 1:4 – 5:162 en se basant sur la valeur $k_{r(Tol)}/k_{r(Ph)}$ déduite des migrations dans les cations tritolylvinyle et phényl-2 ditolyl-1,2 vinyle et sur la valeur $k_{r(An)}/k_{r(Ph)}$ dérivée des migrations dans les cations anisyl-2 diphényl-1,2 vinyle et triphénylvinyle.

[Traduit par le journal]

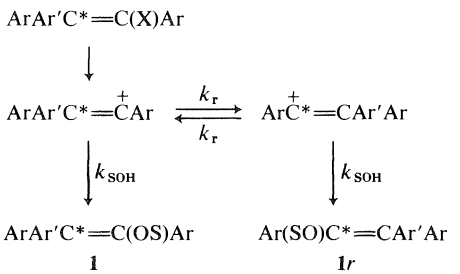
In studies of degenerate rearrangements arising from 1,2-aryl shifts across the double bond in triarylvinyl cations generated from isotopically labeled triarylvinyl substrates, when the mechanism as shown in Scheme 1 applies, a treatment by the method of Bonner and Collins (1) would give, after complete reaction, the relationship shown in eq. [1]. When Ar and Ar′ are the same, a statistical factor of 2 should be applied and for substrates of

$$[1] \quad [\mathbf{1}]/[\mathbf{1r}] = 1 + (k_{SOH}/k_r)$$

the type $(Ar)_2C^*{=}C(X)Ar$, eq. [1] should be modified to eq. [2]. In our previous work, this

$$[2] \quad [\mathbf{1}]/[\mathbf{1r}] = 1 + (k_{SOH}/2k_r)$$

statistical factor has, however, been neglected and eq. [1] was used to calculate values of k_{SOH}/k_r whether Ar and Ar′ are the same or different (2–6). When a single triarylvinyl system is being considered, such as the effect of different solvent compositions on the extent of isotopic scrambling in the solvolysis of triphenyl[2-^{14}C]vinyl bromide (**2**-Br-*2*-^{14}*C*) in aqueous acetic acid (6), values of k_{SOH}/k_r calculated from eq. [1] would give a set of internally consistent data for comparison. However, when different triarylvinyl systems are being compared, as in calculations of migratory aptitudes (2, 5), errors have resulted because the statistical factor of 2 has been omitted. An objective of the present paper is to correct these errors.



SCHEME 1

Rappoport *et al.* (2) have studied the degenerate rearrangement arising from 1,2-anisyl shifts in the 2-anisyl-1,2-diphenylvinyl cationic system using a deuterated phenyl group as label. Among the results reported was the finding that reaction of *trans*-2-anisyl-1-phenyl-2-($^2H_5$)phenylvinyl bromide (*trans*-**3**-Br-2-Ph-d_5) with HOAc–AgOAc resulted in 92.7 ± 1.8% degenerate rearrangement (46.3% scrambling of the Ph-d_5 label from C-2 to C-1), giving a $k_{r(An)}/k_{SOH}$ ratio, in HOAc, of 6.35 (equivalent to $k_{SOH}/k_{r(An)}$ of 0.16 calculated from eq. [1]). A comparison was then made with the results from the acetolysis of triphenyl[2-^{14}C]vinyl triflate (**2**-OTf-*2*-^{14}*C*) (7), or the reaction of triphenyl[2-^{14}C]-vinyl bromide (**2**-Br-*2*-^{14}*C*) with HOAc–AgOAc (8), both of which gave 6–7% scrambling of the ^{14}C-label from C-2 to C-1. Using eq. [1], $k'_{SOH}/k_{r(Ph)}$ in

[1]Vinyl cations from solvolysis. Part 31. From the Hebrew University of Jerusalem.

0008-4042/80/090884-05$01.00/0

©1980 National Research Council of Canada/Conseil national de recherches du Canada

Can. J. Chem. Downloaded from www.nrcresearchpress.com by 210.87.254.105 on 09/05/12
For personal use only.

Can. J. Chem. Downloaded from www.nrcresearchpress.com by 210.87.254.105 on 09/05/12
For personal use only.

HOAc was calculated to be about 13 for the triphenylvinyl cationic system. Assuming that k_{SOH} for *trans*-**3**-Br-2-Ph-d_5 and k'_{SOH} for **2**-OTf-*2*-^{14}C or **2**-Br-*2*-^{14}C were about equal in the HOAc solvent, a ratio for the relative migratory aptitudes, $k_{r(An)}/k_{r(Ph)}$, of 13/0.16 or 81 was obtained (2). In this treatment, however, a statistical factor of 2 should have been applied in the triphenylvinyl system. Using eq. [2], $k'_{SOH}/2k_{r(Ph)}$ is 13 and the corrected ratio for $k_{r(An)}/k_{r(Ph)}$ is 162 instead of 81.

In a similar way, Lee *et al.* (5) have compared the 1.5–2.0% scrambling obtained in the reaction of HOAc–AgOAc with *cis*- or *trans*-2-phenyl-1,2-di-*p*-tolyl[2-^{13}C]vinyl bromide (*cis*- or *trans*-**4**-Br-*2*-^{13}C) with the 13–14% scrambling observed in the analogous reaction of HOAc–AgOAc with tri-*p*-tolyl[2-^{13}C]vinyl bromide (**5**-Br-*2*-^{13}C) (4). Using eq. [1] and the mean values of 1.7 and 13.5% scramblings, respectively, for the reactions of *cis*- or *trans*-**4**-Br-*2*-^{13}C and **5**-Br-*2*-^{13}C, the $k_{SOH}/k_{r(Ph)}$ and $k'_{SOH}/k_{r(Tol)}$ ratios obtained would be 57 and 5.4. Again assuming k_{SOH} and k'_{SOH} to be about equal, the relative migratory aptitudes for $k_{r(Tol)}/k_{r(Ph)}$ would be 57/5.4 or about 10. Since the statistical factor of 2 should have been applied in the tri-*p*-tolylvinyl system, $k'_{SOH}/2k_{r(Tol)}$ is 5.4 and the corrected ratio for $k_{r(Tol)}/k_{r(Ph)}$ should be 57/(2 × 5.4) or about 5.

As the results discussed above were obtained from reactions in HOAc in the presence of AgOAc, it is of interest to evaluate another migration ratio using data from another reaction. A 3:2 mixture of *cis*- and *trans*-**4**-Br-*2*-^{13}C as well as **5**-Br-*2*-^{13}C were solvolyzed in 70% HOAc – 30% H_2O (by volume), one of the solvents used in a recent study with **2**-Br-*2*-^{14}C (6). The reaction product was the ketone (eq. [3]); any acetate product that might have been formed would be hydrolyzed under the reaction conditions. The ketone was reduced with $LiAlH_4$ to the corresponding 1,2,2-triarylethanol. Analysis of the alcohol by ^{13}C nmr as described previously (4, 5) gave the extent of scrambling of the ^{13}C-label from C-2 to C-1. The results are summarized in Table 1.

$$[3]\quad Ar(Ar')^{13}C{=}CBrAr \xrightarrow[30\%\ H_2O]{70\%HOAc} Ar(Ar')^{13}CHCOAr + Ar^{13}COCH(Ar')Ar$$

It is also of interest to ascertain whether there is any significant extent of return from isotopically scrambled ionic intermediates to scrambled unconsumed reactant. Since ^{13}C nmr cannot be used to analyze the ^{13}C contents in the vinylic carbons by the method used in the present study (4, 5) because of the lack of nuclear Overhauser enhancement, the corresponding ^{14}C-labeled *cis*- and *trans*-**4**-Br-*2*-^{14}C and **5**-Br-*2*-^{14}C were subjected to solvolysis in 70% HOAc – 30% H_2O under conditions that would give about 50 and 75% reaction. $LiAlH_4$ reduction of the mixture of reaction product and unconsumed reactant gave a mixture of 1,2,2-triarylethanol and triarylethene, the latter being derived from the unreacted triarylvinyl bromide (9). Separation of the ethylene from the alcohol was effected by passage through an alumina column, and ozonolysis of the ^{14}C-labeled triarylethene, with added carrier if necessary, showed that in all 4 experiments (Table 1, footnote *b*) there was no significant scrambling of the label in the recovered unconsumed reactant. Thus similar to the behavior of **2**-Br-*2*-^{14}C in aqueous acetic acid (6), in the solvolysis of *cis*- and *trans*-**4**-Br-*2*-^{14}C and of **5**-Br-*2*-^{13}C in 70% HOAc – 30% H_2O, the return process apparently could not compete with product formation, and the extent of scrambling did not change with reaction time. Therefore the mechanism shown in Scheme 1, in which the cation formation from the substrate is irreversible as far as scrambling is concerned, should hold in these systems and eqs. [1] and [2] can be applied in treating the data of Table 1.

Using the mean values of 3.5 and 18.6% scrambling, respectively, for the reactions of *cis*- and *trans*-**4**-Br-*2*-^{13}C and **5**-Br-*2*-^{13}C in 70% HOAc – 30% H_2O (Table 1), eqs. [1] and [2] would give $k_{SOH}/k_{r(Ph)}$ as 26.6 and $k'_{SOH}/2k_{r(Tol)}$ as 3.4. Again assuming $k_{SOH} = k'_{SOH}$, $k_{r(Tol)}/k_{r(Ph)}$ would be 26.6/(2 × 3.4) or about 4. It has been pointed out (2, 3) that $k_{SOH}/k_{r(Ar)}$ calculated from expressions such as eq. [1] may involve large errors, especially when the observed extent of scrambling is very small or very large. Instead of using mean values, if the observed

TABLE 1. Isotopic scramblings from solvolyses of a 3:2 mixture of *cis*- and *trans*-2-phenyl-1,2-di-*p*-tolyl[2-^{13}C]vinyl bromide (*cis*- and *trans*-**4**-Br-*2*-^{13}C) and of tri-*p*-tolyl[2-^{13}C]vinyl bromide (**5**-Br-*2*-^{13}C) in 70% HOAc – 30% H_2O at 150° ± 1°C

Substrate	Reaction time (min)	% Reaction[a] Run 1	% Reaction[a] Run 2	^{13}C scrambling from C-2 to C-1 (%) Run 1	^{13}C scrambling from C-2 to C-1 (%) Run 2
cis + *trans*-**4**-Br-2-^{13}C	70	52	51	3.2	4.0[b]
	140	73	72	4.0	3.4[b]
	360	95	97	3.1	3.2 (3.5)[c]
5-Br-2-^{13}C	50	48	48	17.7	18.6[b]
	90	74	75	19.3	18.1[b]
	240	94	95	19.0	18.7 (18.6)[c]

[a]From titration of the liberated bromide.
[b]Under analogous conditions using the corresponding ^{14}C-labeled substrate, the recovered unconsumed reactant showed no isotopic scrambling.
[c]Mean value.

Can. J. Chem. Downloaded from www.nrcresearchpress.com by 210.87.254.105 on 09/05/12
For personal use only.

extremes of 4.0 and 3.1% scrambling for *cis*- and *trans*-**4**-Br-*2*-^{13}C were utilized in calculations with eq. [1], $k_{SOH}/k_{r(Ph)}$ would range between 23.0 and 30.3. Similarly, for the extremes of 19.3 and 17.7% scrambling for **5**-Br-*2*-^{13}C, the calculated $k'_{SOH}/2k_{r(Tol)}$ would be 6.4 to 7.3, and $k_{r(Tol)}/k_{r(Ph)}$ would range between 3.2 and 6.4, rather than the value of 4 derived from using the mean scrambling values in the calculations. In the same way, for the reactions in HOAc–AgOAc (5), the use of the observed extreme values of 1.5 to 2.0% scrambling for *cis*- and *trans*-**4**-Br-*2*-^{13}C and 13–14% scrambling for **5**-Br-*2*-^{13}C would give $k_{r(Tol)}/k_{r(Ph)}$ ranging between 4.2 and 6.3, instead of 5 calculated using the mean scrambling values. Thus with the data from these two reactions in HOAc–AgOAc and in 70% HOAc – 30% H_2O, the calculated migration ratios for Tol/Ph are within experimental errors. Considering these results together with the corrected value for $k_{r(An)}/k_{r(Ph)}$ of 162 as discussed earlier, the relative migratory aptitudes of Ph:Tol:An in triarylvinyl cations in acetic acid media would be 1:4 – 5:162. These values are certainly of the order expected when compared with the well-known migratory aptitudes of these aryl groups reported for pinacol–pinacolone type of rearrangements in saturated carbocationic systems (10,11). It should be pointed out, however, that this set of migratory aptitudes for Ph:Tol:An is based on $k_{r(Tol)}/k_{r(Ph)}$ derived from migrations in the tritolylvinyl and 2-phenyl-1,2-ditolylvinyl cations, in which the migration terminus has an α-tolyl substituent, and $k_{r(An)}/k_{r(Ph)}$ derived from migrations in the 2-anisyl-1,2-diphenylvinyl and triphenylvinyl cations, in which the migration terminus has an α-phenyl substituent. It would be of interest to evaluate additional data on relative migration ratios from the 2-anisyl-1,2-ditolylvinyl and 2-tolyl-1,2-diphenylvinyl cationic systems in order to ascertain what effects the migration terminus may have on these migratory aptitudes.

Another evaluation of $k_{r(Tol)}/k_{r(Ph)}$ has been made by Lee *et al.* (5) using data from reactions of *cis*- and *trans*-**4**-Br-*2*-^{13}C and **5**-Br-*2*-^{13}C with CF_3COOH–CF_3COOAg but without taking into account the statistical factor of 2 for the reaction with **5**-Br-*2*-^{13}C. From the reported 34–35% and 46–47% scramblings, respectively, for *cis*- and *trans*-**4**-Br-*2*-^{13}C, and **5**-Br-*2*-^{13}C, the recalculated $k_{r(Tol)}/k_{r(Ph)}$, in trifluoroacetic acid, ranges between 2.5 and 3.6. This range of values appears to be somewhat lower than those obtained for reactions in HOAc–AgOAc or 70% HOAc – 30% H_2O, but it still overlaps with the range of 3.2 to 6.4 for the reaction in 70% HOAc – 30% H_2O. Since the stability and lifetime of a triarylvinyl cation should affect the extent of aryl migrations in the cation, some solvent dependency for migratory aptitudes might be expected. For the $k_{r(Tol)}/k_{r(Ph)}$ ratios discussed in the present work, no solvent dependency is found in HOAc–AgOAc and in 70% HOAc – 30% H_2O. However, in the more polar CF_3COOH–CF_3COOAg, when compared with HOAc media, the effect is apparently becoming observable, although the large range of values obtained may still fall within the extremes of the regions of experimental errors.

It should also be pointed out that in the work with *cis*- and *trans*-**3**-Br-2-Ph-d_5 (2), an An/Ph migration ratio has been calculated based on the processes given in Scheme 2, in which solvolysis in aqueous EtOH is used as an illustration. From Scheme 2, using the treatment of Bonner and Collins (1) and neglecting isotope effects, eqs. [4] and [5] were derived (2), eq. [5] being a specific example of the more general eq. [1]. For solvolysis in 60% EtOH,

$$[4]\quad [\mathbf{8}\text{-2-Ph-}d_5]/([\mathbf{9}\text{-2-Ph-}d_5] + [\mathbf{9}\text{-1-Ph-}d_5]) = k_{r(Ph)}/k_{SOH}$$

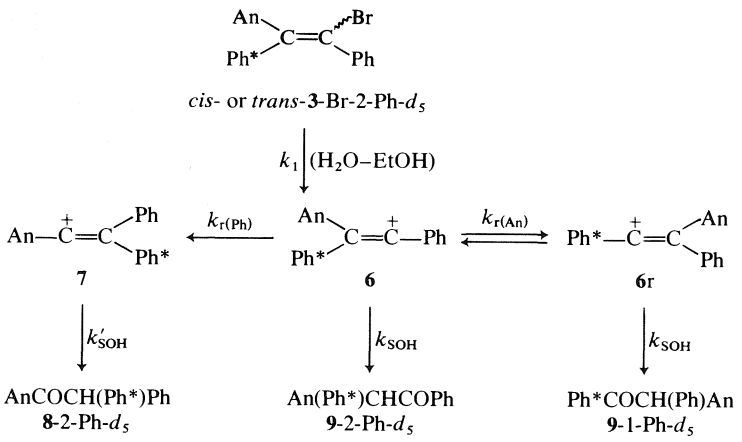
$$[5]\quad [\mathbf{9}\text{-2-Ph-}d_5]/[\mathbf{9}\text{-1-Ph-}d_5] = 1 + (k_{SOH}/k_{r(An)})$$

since **8** and **9** were formed to the extent of 5 and 95%, respectively (2,12), using eq. [4], $k_{SOH}/k_{r(Ph)}$ was calculated to be 19. The extent of degenerate rearrangement (2 × % scrambling of the Ph-d_5 label from C-2 to C-1 in **9**) in 60% EtOH was found to be 88.6–90.7%, and using eq. [5], $k_{r(An)}/k_{SOH}$ was found to be about 4.0. Hence the order of reactivity for $k_{r(An)}$:k_{SOH}:$k_{r(Ph)}$ in 60% EtOH was 76:19:1. In a similar way, using data from the reaction of *cis*- and *trans*-**3**-Br-2-Ph-d_5 with HOAc–AgOAc, the ratios for $k_{r(An)}$:k_{SOH}:$k_{r(Ph)}$ were calculated to be 120:19:1. Thus it was concluded that the migration ratio of An/Ph in rearrangement processes in the 2-anisyl-1,2-diphenylvinyl cation (**6**) was in the range of 76–120 (2).

On checking the integration using the method of Bonner and Collins (1) for the processes in Scheme 2, an error was found in eq. [4], which should be

$$[4a]\quad [\mathbf{8}\text{-2-Ph-}d_5]/[\mathbf{9}\text{-2-Ph-}d_5] = k_{r(Ph)}/k_{SOH}$$

corrected to [4*a*]. For solvolysis in 60% EtOH, with a degenerate rearrangement of 88.6–90.7%, the product distribution for **8**-2-Ph-d_5, **9**-2-Ph-d_5, and **9**-1-Ph-d_5 should be about 5, 52, and 43%, respectively. Thus from eq. [4*a*], $k_{SOH}/k_{r(Ph)}$ is about 10, instead of the reported 19, and the ratios for $k_{r(An)}$:k_{SOH}:$k_{r(Ph)}$ should be 40:10:1, not the reported 76:19:1. Similarly, for the reaction with HOAc–AgOAc, the corrected ratios for



SCHEME 2

$k_{r(An)}$:k_{SOH}:$k_{r(Ph)}$ should be 63:10:1. These corrected values suggest that in the rearrangement processes in cation **6**, the An/Ph migration ratio is in the range of 40–63, not the reported 76–120.

It is not surprising that the An/Ph migration ratio of 40–63, evaluated from the processes in Scheme 2, is much lower than the value of 162 derived earlier from the data obtained in the reactions of *trans*-**3**-Br-2-Ph-d_5 and **2**-Br-*2*-^{14}C with HOAc–AgOAc. In the rearrangement processes depicted in Scheme 2, there is a greater driving force for the $k_{r(Ph)}$ process since the 1,2-phenyl shift from the α-phenyl substituted cation **6** gives rise to a more stable α-anisyl substituted cation **7**, whereas the $k_{r(An)}$ process results in a degenerate rearrangement between α-phenyl substituted cations **6** and **6r**, both of which have the same energy. When the data from reactions of *trans*-**3**-Br-2-Ph-d_5 and **2**-Br-*2*-^{14}C with HOAc–AgOAc are compared, the scramblings arise from degenerate rearrangements in both reactions, which differ only in the migrating An and Ph groups, the phenyl substituents at the migration origin and migration terminus being the same. There is no inherently higher driving force for $k_{r(Ph)}$ over $k_{r(An)}$ as in Scheme 2, and hence the higher value of 162 was obtained for $k_{r(An)}/k_{r(Ph)}$.[2]

Experimental

Solvolyses of cis- *and* trans-*2-phenyl-1,2-di*-p-*tolyl[2-*^{13}C*]-vinyl Bromides (*cis- *and* trans-*4-Br*-2-^{13}C*) or Tri*-p-*tolyl-[2-*^{13}C*]vinyl Bromide (5-Br*-2-^{13}C*) in 70% HOAc – 30% H_2O*

A 3:2 mixture of *cis*- and *trans*-**4**-Br-*2*-^{13}C as well as **5**-Br-*2*-^{13}C were prepared as reported previously (4, 5). The solvolyses were carried out in a similar way as was described for the analogous reactions with triphenyl[2-^{14}C]vinyl bromide (**2**-Br-*2*-^{14}C) (6). A general procedure is given below.

A solution (47 m*M*) of 690 mg (1.9 mmol) of *cis*- and *trans*-**4**-Br-*2*-^{13}C or 712 mg (1.9 mmol) of **5**-Br-*2*-^{13}C in 40 mL of 70% HOAc – 30% H_2O (by volume) was placed in a sealed tube and heated in an oil bath at 150 ± 1°C for the desired length of time as recorded in Table 1. After cooling in an ice bath the tube was opened, H_2O was added, and the mixture was extracted three times with 25 mL portions of $CHCl_3$. The extract was washed with H_2O and dried over $MgSO_4$. The liberated bromide ion in the combined aqueous phase was determined by potentiometric titration (12) to give the extent of reaction. From the organic extract, removal of the $CHCl_3$ gave an oil which may contain the product, triarylethanone, as well as the unconsumed reactant, triarylvinyl bromide. $LiAlH_4$ reduction (4, 5) would convert the product to the corresponding 1,2,2-triarylethanol and any unconsumed reactant to triarylethene (9). Separation of the alcohol from the olefin was effected by passage through an alumina column in a similar way as recently described for the separation of 1,2,2-trianisyl[1,2-^{14}C]ethanol and 1,2,2-trianisyl[1,2-^{14}C]ethene (13). The triarylethanols so obtained from the reactions with *cis*- and *trans*-**4**-Br-*2*-^{13}C and with **5**-Br-*2*-^{13}C were analyzed by ^{13}C nmr in the same way as reported earlier (4, 5) to give the results summarized in Table 1.

Studies with cis- *and* trans-*4-Br*-2-^{14}C *and with 5-Br*-2-^{14}C

The ^{14}C-labeled substrates were prepared in the same way as the analogous ^{13}C-labeled bromides. Four solvolyses in 70% HOAc – 30% H_2O at 150 ± 1°C in sealed tubes were carried out with 47 m*M cis*- and *trans*-**4**-Br-*2*-^{14}C for 70 and 140 min and with 47 m*M* **5**-Br-*2*-^{14}C for 50 and 90 min, and these correspond to about 50 and 75% reactions for each substrate (Table 1). Work up of the reaction mixture was effected in the same way as described for the experiments with the ^{13}C-labeled substrates. After $LiAlH_4$ reduction and separation of the alcohol from the olefin through the alumina column, the 1,2,2-triaryl[2-^{14}C]ethene, derived from the unconsumed reactant, was diluted with inactive carrier and subjected to degradation by ozonolysis (13) to give the corresponding diaryl ketone, whose ^{14}C activity indicated no appreciable scrambling of the label in the recovered reactant in all four experiments.

[2]The corrected values from the present work have also been given in a recent book (14).

Acknowledgment

The financial support given by the Natural Sciences and Engineering Research Council of Canada is gratefully acknowledged.

1. W. A. BONNER and C. J. COLLINS. J. Am. Chem. Soc. **78**, 5587 (1956).
2. Z. RAPPOPORT, E. NOY, and Y. HOUMINER. J. Am. Chem. Soc. **98**, 2238 (1976).

Can. J. Chem. Downloaded from www.nrcresearchpress.com by 210.87.254.105 on 09/05/12
For personal use only.

3. Y. HOUMINER, E. NOY, and Z. RAPPOPORT. J. Am. Chem. Soc. **98**, 5632 (1976).
4. C. C. LEE, A. J. PAINE, and E. C. F. KO. Can. J. Chem. **55**, 2310 (1977).
5. C. C. LEE, A. J. PAINE, and E. C. F. KO. J. Am. Chem. Soc. **99**, 7267 (1977).
6. C. C. LEE and E. C. F. KO. Can. J. Chem. **56**, 2459 (1978).
7. C. C. LEE, A. J. CESSNA, B. A. DAVIS, and M. OKA. Can. J. Chem. **52**, 2679 (1974).
8. F. H. A. RUMMENS, R. D. GREEN, A. J. CESSNA, M. OKA, and C. C. LEE. Can. J. Chem. **53**, 314 (1975).
9. C. C. LEE and U. WEBER. J. Org. Chem. **43**, 2721 (1978).
10. W. E. BACHMANN and R. H. MOSER. J. Am. Chem. Soc. **54**, 1124 (1932).
11. W. E. BACHMANN and J. W. FERGUSON. J. Am. Chem. Soc. **56**, 2081 (1934).
12. Z. RAPPOPORT and Y. HOUMINER. J. Chem. Soc. Perkin Trans. II, 1506 (1973).
13. C. C. LEE, U. WEBER, and C. A. OBAFEMI. Can. J. Chem. **57**, 1384 (1979).
14. P. J. STANG, Z. RAPPOPORT, M. HANACK, and L. R. SUBRAMANIAN. Vinyl cations. Academic Press, New York, NY. 1979.

Can. J. Chem. Downloaded from www.nrcresearchpress.com by 210.87.254.105 on 09/05/12
For personal use only.

Synthesis and physical studies of pyridine and imidazole containing tridentate metal binding ligands

R. S. BROWN AND J. HUGUET

Department of Chemistry, University of Alberta, Edmonton, Alta., Canada T6G 2G2

Received September 26, 1979

R. S. BROWN and J. HUGUET. Can. J. Chem. **58**, 889 (1980).

Several tridentate ligands incorporating pyridine and substituted imidazoles were prepared and their physical properties studied as models for the enzyme carbonic anhydrase (CA). The H^+ and M^{2+} binding abilities (pK_a and $pK_{M^{2+}}$) were determined. In the case of the imidazole ligands, *N*-methylation reduces the metal binding ability of the ligand by some 3–4 $pK_{M^{2+}}$ units over the analogues in which the imidazole has N—H. ^{1}H-nmr studies of the simple ligands as a function of $[Zn^{2+}]$ show that the ligands are bound symmetrically as 1:1 and 2:1 complexes depending upon the ligand/metal ratio. Increasing the steric bulk of the ligands by introduction of 4,5-diisopropyl substituents on the imidazole inhibits the 2:1 (ligand/metal) complex. Titration experiments of several ligands bound to equimolar Zn^{2+} and Co^{2+} are described and analysed.

R. S. BROWN et J. HUGUET. Can. J. Chem. **58**, 889 (1980).

On a préparé plusieurs ligands tridentates incorporant la pyridine et des imidazoles substituées et on a étudié leurs propriétés physiques en tant que modèles de l'enzyme anhydrase carbonique (AC). On a déterminé les capacités de liaison H^+ et M^{2+} (pK_a et $pK_{M^{2+}}$. Dans le cas des ligands de l'imidazole, la capacité de liaison du métal par le ligand des produits *N*-méthylés est réduite de quelques 3–4 unités $pK_{M^{2+}}$ par rapport aux analogues non méthylés. Les études de rmn du ^{1}H sur les ligands simples en fonction de la $[Zn^{2+}]$ montrent que les ligands sont liés symétriquement sous la forme de complexes 1:1 et 2:1 dépendant du rapport ligand/métal. L'augmentation de l'encombrement stérique du ligand par l'introduction des substituants diisopropyle-4,5 sur l'imidazole inhibe le complexe 2:1 (ligand/métal). On décrit et analyse des expériences de titrage de plusieurs ligands liés équimoléculairement au Zn^{2+} et Co^{2+}.

[Traduit par le journal]

Can. J. Chem. Downloaded from www.nrcresearchpress.com by 210.87.254.40 on 09/05/12
For personal use only.

Introduction

Some time ago we initiated a project to synthesize and study synthetic analogues for the Zn^{2+}-binding site of Carbonic Anhydrase (CA) (1).[1] X-ray diffraction studies of CA suggest the active site consists of a Zn^{2+}-ion coordinated pseudotetrahedrally to three histidine imidazoles; the fourth ligand site is said to be occupied by an ionizable H_2O believed important for the catalytic process (2).

Our intent was to construct a series of tridentate ligands (**1–9**) and through their study provide some verification for any of the several proposed mechanisms of action of CA (2–5).[2] The ligands were screened by subjecting them to the following physical studies prior to the initiation of any catalysis studies. Firstly, the ligands must be shown to have a high affinity for divalent metals so the metal binding constants for Zn^{2+}, Co^{2+}, Ni^{2+}, and Cu^{2+} were determined. Secondly one must show that the ligands are indeed (symmetrically) tridentate when bound to Zn^{2+} so the ^{1}H-nmr spectra of the simple ligands (**1–4**) in D_2O containing varying ligand: Zn^{2+} ratios were obtained.

Lastly, the hydration ability of CA is tied to an ionizable group with a $pK_a \sim 7$ with the basic form being most active (1*e*). While the ionization of a Zn^{2+}—OH_2 is attractive mechanistically (for a compendium of literature pertaining to this point, see ref. 7) it has (to our knowledge) never been demonstrated that simple Zn^{2+} coordination can reduce the pK_a of H_2O so drastically (8).[3] Although the following account shows that each of ligands **1–9** possesses some deficiency which casts considerable doubt on their applicability as "models" for CA, several important observations are reported which provide information defining the minimum features such models must possess.

Results and Discussion

(i) H^+ and M^{2+} Binding Constants

Hydrogen (pK_a) and metal ($pK_{M^{2+}}$) binding con-

[1] CA is a metallo-enzyme which catalyses the hydration of CO_2, certain aldehydes (1*a*), and hydrolysis of esters such as *p*-nitrophenylacetate (1*b*, *c*) and 2-hydroxy-5-nitrotoluenesulfonic acid sultone (1*d*).

[2] While this study was in progress a report on the synthesis and preliminary study on two tris-imidazole carbinols appeared which in some respects paralleled this work (2-TIC or tris(2-imidazolyl) carbinol, $pK_{1\ Zn^{2+}} = 6.77$, $pK_{1\ Co^{2+}} = 7.20$; $pK_1 = 6.12$, $pK_2 = 3.59$, ref. 6). NOTE ADDED IN PROOF: Recently Boggess and Boberg (25) reported some first row transition metal complexes of tris-2-pyridyl carbinol, and some of their physical properties.

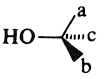
[3] Two reported examples for 5-coordinate Zn^{2+} show pK_a's for Zn^{2+}—OH_2 of 9.0 (8) and 8.69 (3*b*). That reported for $(NH_3)_5Co^{3+}$—OH_2 is 6.4 (5), the lower value presumably being due to the greater metal charge. A referee has suggested that the change in ligand field experienced by the d^6 Co^{3+} in passing from CO^{3+}—OH_2 to Co^{3+}—OH^- is also an important factor.

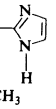
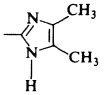
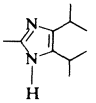
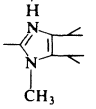
0008-4042/80/090889-13$01.00/0

©1980 National Research Council of Canada/Conseil national de recherches du Canada

Can. J. Chem. Downloaded from www.nrcresearchpress.com by 210.87.254.40 on 09/05/12
For personal use only.

TABLE 1. Compounds **1** to **9**



Compound	Substituents
1	a = b = c = 
d-1	a = b = c = 
2	a = b =  ; c = 
d-2	a = b =  ; c = 
3	a =  ; b = c = 
4	a = b = c = 
5	a = b =  ; c = 
6	a = b = c = 
7	a = b = c = 
8	a = b = c = 
9	a = b =  ; c = —CH₂— 

stants were determined by potentiometric titration methods outlined by Alberts and Serjeant (*9a*) and Rossotti and Rossotti (*9b*). Data were analysed by a modified computer version[4] of the Simms' method (10) and the pK_a's are presented in Table 2 while the metal stability constants for ligands **1**–**9** are presented in Table 3.

From Table 2, one sees no predictable trend in the basicities for **1**–**4** although on the average the *N*-methylimidazoles are more basic. Where comparison can be made between those ligands containing N—CH_3 and N—H imidazoles (i.e., **2** and **5**; **4** and 2-TIC (6)) the latter appears to be more basic at least at pK_1 and pK_2. The pK_a's of the 4,5-disubstituted imidazoles were determined in increasingly organic media for reasons of solubility and therefore cannot rigorously be compared with those values determined in water. As can be seen from the two sets of data reported for **6**, in the more organic environment the pK_a's are on the average lower, consistent with expectations based on solvent polarity, and clearly 4,5-substitution increases the basicity as expected.[5]

Ligand **9**, in which the 4,5-dimethylimidazole is extended from carbinol centre by a methylene unit, is the most basic particularly at pK_2 and pK_1. Presumably the large pK_2 value (when compared with **6**, **7**, or **8**) is due to increased separation of the positive charges (6).

From Table 3, the general ordering for metal stability constants for **1**–**6** is $Zn^{2+} < Co^{2+} < Ni^{2+} < Cu^{2+}$ and a first and second binding constant indicative of a 1:1 (L:M^{2+}) and 2:1 (L:M^{2+}:L) complex was obtained for each. Ligands **7** and **8** with 4,5-diisopropyl substituents appear from space-filling models to encapsulate the metal sufficiently to inhibit 2:1 complexation, and the stability constants obtained indicate *no* second binding constant. It is worthy of note that for CA_1 the order of stability constants is $Cu^{2+} > Zn^{2+} > Ni^{2+} > Co^{2+}$ at pH 5.5 (11) and the metal–ligand geometry is demonstrated to be distorted tetrahedral at least for Zn^{2+} and Co^{2+} (11). While we have no details for the coordination numbers for **1**–**6**:M^{2+} complexes

TABLE 2. pK_a's for ligands **1**–**9** determined by potentiometric titration[a]

Ligand	pK_3	pK_2	pK_1
1	1.5	2.1	4.7
2	1.5	2.1	5.4
3	1.6	2.65	5.6
4	1.7	2.5	5.5
5[b]	1.44 ± 0.04	2.87 ± 0.1	6.46 ± 0.05
6[c]	2.85 ± 0.03	5.12 ± 0.03	7.54 ± 0.03
6[d]	2.58 ± 0.02	4.78 ± 0.02	7.40 ± 0.02
7[d]	2.33 ± 0.04	4.49 ± 0.03	—[e]
8[f]	< 1.5	3.80 ± 0.05	6.90 ± 0.05
9[g]	2.45 ± 0.05	4.7 ± 0.1	8.2 ± 0.2

[a]Generally determined in solution comprised of 3.0 mL 0.25 *M* KNO_3, 1.0 mL of 0.025 *M* ligand and either 0.50 or 1.00 mL of 0.1095 *M* HNO_3, and have a ±0.1 unit precision unless noted.
[b]3 mL (1:1 acetone/H_2O), 0.25 *M* KNO_3, 1.0 mL of 0.025 *M* ligand in acetone, and 1.0 mL of 0.1095 *M* HNO_3.
[c]Determined in 3 mL, 0.25 *M* KNO_3, 1.0 mL of 0.025 *M* ligand containing 0.1095 mmol of HNO_3.
[d]3 mL of 1:1 acetone/H_2O, 0.25 *M* KNO_3, 1.0 mL of ligand (0.025 *M*) containing 0.1095 mmol HNO_3.
[e]pK_1 could not be determined due to precipitation in this medium.
[f]3 mL of 75:25 acetonitrile/H_2O, 0.25 *M* KNO_3, 1.0 mL of 0.1042 *M* HNO_3, 1.0 mL of 0.0269 *M* ligand in ethanol.
[g]3 mL of 1:1 acetone–H_2O, 0.25 *M* in KNO_3; 1.0 mL of 0.0245 *M* ligand in methanol, 1.0 mL of 0.1042 *M* HNO_3.

[4] The basic computer version was kindly supplied by Professor R. Breslow of Columbia University and was modified to be utilized for ligands which possess one, two, or three pK_a's.

[5]Whereas 2-methylimidazole has a pK_a of 7.85, that of 2,4,5-trimethylimidazole is 8.92 (24).

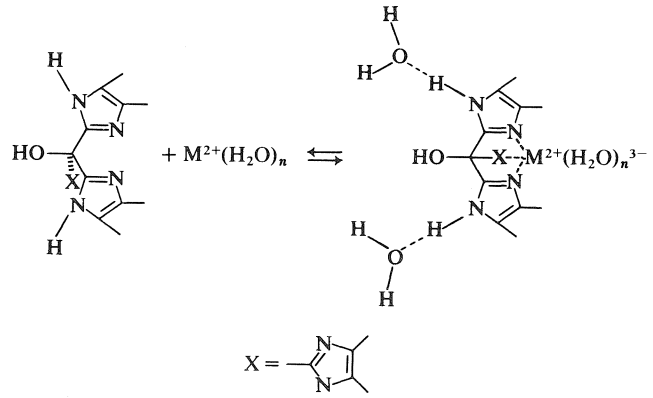
TABLE 3. Metal stability constants for ligands **1**–**9**[a,b]

Ligand	Parameter	Value			
		Zn^{2+}	Co^{2+}	Ni^{2+}	Cu^{2+}
1	pK_1	5.4	6.4	6.2	6.6
	pK_2	4.9	5.1	5.7	6.35
2	pK_1	5.9	6.6	7.1	7.5
	pK_2	5.1	6.2	6.6	7.0
3	pK_1	5.0	5.2	6.8	7.2
	pK_2	4.3	4.5	6.2	5.6
4	pK_1	3.15	—	4.8	—
	pK_2	2.7	—	3.5	—
5	pK_1	7.50 ± 0.05	8.67 ± 0.01	—	>10.5
	pK_2	6.67 ± 0.17	8.10 ± 0.10	—	>10
6[c]	pK_1[d]	8.86 ± 0.10	9.46 ± 0.07	—	11.91 ± 0.06
6[e]	pK_1	8.81 ± 0.03	9.65 ± 0.03	9.90 ± 0.05	11.41 ± 0.03
	pK_2	7.53 ± 0.03	8.93 ± 0.04	8.70 ± 0.15	9.64 ± 0.7
7[f]	pK_1	7.50 ± 0.04	<7.0	ppte	9.28 ± 0.2
8[g]	pK_1	4.0 ± 0.1	4.0 ± 0.1	—	—
9[h]	pK_1	6.0	4.3	4.5	7.7
Human CAB[i]	pK_1	10.5	7.2	9.5	11.6

[a]25.0°C, 3.0 mL of 0.25 *M* KNO_3, 1.0 mL of 0.025 *M* ligand containing 0.1095 mmol HNO_3, 0.5 mL of 0.011 *M* metal.
[b]Precision of ±0.1 units unless noted.
[c]Determined as in *a*.
[d]Precipitation prevented pK_2 determination.
[e]3.0 mL (1:1 acetone/H_2O) of 0.25 *M* KNO_3, 1.0 mL of 0.025 *M* ligand in 0.1095 *M* HNO_3, and 0.5 mL of 0.011 *M* metal.
[f]3.0 mL (1:1 acetone/H_2O) of 0.25 *M* KNO_3, 1.0 mL of 0.025 *M* ligand in acetone, 1.0 mL of 0.1095 *M* HNO_3, and 0.5 mL of 0.011 *M* metal.
[g]3.0 mL (75:25 CH_3CN/H_2O) 0.25 *M* KNO_3, 1.0 mL of 0.0269 *M* ligand in ethanol, 0.5 mL of 0.1042 *M* HNO_3, 0.5 mL of 0.11 *M* metal.
[h]3 mL 1:1 acetone–H_2O.
[i]Reference 14.

other than those implied from uv studies with Co^{2+} (*vide infra*), **7**, **8**, and **9** appear from models only to allow tetrahedral geometry if they are bound symmetrically. It would appear from Table 3 that Zn^{2+} is bound to **7** and **9** stronger than is Co^{2+} perhaps as a result of the enforced tetrahedral geometry. The data for **8** seem to indicate that Zn^{2+} and Co^{2+} binding are equivalently weak. Finally it is of note that **9** binds metal in the order $Cu^{2+} > Zn^{2+} > Ni^{2+} > Co^{2+}$ parallel to that for CA_1, although the former values are about 4 p*K* units lower than those for the enzyme.

A pattern emerges when one considers the stability constants for N—CH_3 imidazole derivatives **2**, **8**, and **4** when compared to their N—H imidazole analogues (**5**, **7**, and 2-TIC (**6**)) respectively. In every case *N*-methylation reduces the metal binding ability of the ligands by some 3–4 p*K* units. While we have no unambiguous reason for the stronger binding ability of N—H vs. N—CH_3 imidazoles, the phenomenon may be related to a better solvation of the former when bound to metal as in reaction [1].

[1] 

Can. J. Chem. Downloaded from www.nrcresearchpress.com by 210.87.254.40 on 09/05/12
For personal use only.

Can. J. Chem. Downloaded from www.nrcresearchpress.com by 210.87.254.40 on 09/05/12
For personal use only.

(ii) Nuclear Magnetic Resonance Studies

^{1}H-nmr spectra of roughly 10^{-2} *M* solutions of ligands **1–4** were determined in D_2O as a function of increasing [$ZnBr_2$]. After subsequent additions of Zn^{2+}, the pD (pD = pH(meter reading) + 0.4, ref. 12) of the test solutions decreased due to release of protons from the ligand accompanying metal binding, and the pD of the solutions at the end of the Zn^{2+} additions was in the order of 4. This is important since the previous (*vide supra*) potentiometric titrations to determine $pK_{Zn^{2+}}$ constants invariably showed the complexes to be fully formed by pH ~3.5. Chemical shifts for ligands **1–4** and the Zn^{2+} complexes for **1** and **2** are given in Table 4.

Some interesting trends that provide information about the structure of the complexes are apparent from consideration of the data for **1**; the pyridine-H spectral region is illustrated in Fig. 1. Assignments are easily verified by comparing the spectra of **1** and d-**1** (Fig. 2). Subsequent additions of Zn^{2+} showed the build-up of an additional set of resonances at the expense of those for **1**, and finally when the **1**/Zn^{2+} ratio was 2, a clean spectrum was produced indicative of a symmetrically bound 2:1 complex (Fig. 1). Now it appears that H_D is the low field resonance at δ 8.54 coupled to H_C at δ 8.25 (J_{CD} = 7.6 Hz). By elimination H_A in the 2:1 complex is shifted *upfield* to δ 7.7 and is coupled to H_B at δ 7.40 (J_{AB} = 5.4 Hz). This upfield shift probably occurs because H_A in the 2:1 complex lies very close to and above the plane of a pyridine group of a second ligand,[6] (13) and is therefore shielded by the latter's ring current. Unambiguous confirmation of these assignments is provided by the spectrum of the analogous 2:1 complex of d-**1** in Fig. 2.

These observations are important when considering the spectra for **2** and its Zn^{2+} complexes illustrated in Fig. 3. The middle spectrum again shows downfield shifts for H_D and H_C and an upfield shift for H_A; the position of H_B remains roughly unchanged. A sizeable downfield shift of 0.74 ppm is observed for the imidazole N—CH_3, as well as some small signals attributable to some residual uncomplexed **2**. Increasing [Zn^{2+}] causes a new set of resonances to appear at the expense of those from **2** and its 2:1 complex, until a symmetric pattern is obtained when the Zn^{2+}/**2** ratio is 15. We believe this final spectrum is that of the 1:1 complex of **2** and note that the pyridine H_A has shifted downfield once it is removed from the proximity with the second ligand. The spectral parameters for d-**2** confirm the assignments (Table 4 and Fig. 4).

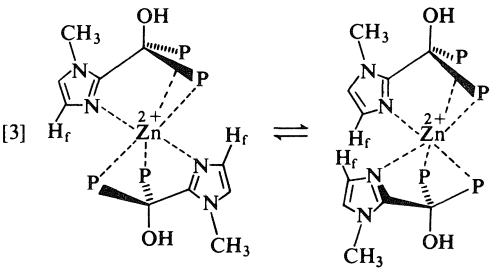
From the above, one can reasonably conclude that these molecules exist as symmetrically bound complexes in solution, and that both the 2:1 and 1:1 complexes exist depending on the ligand: Zn^{2+} ratio. It is noteworthy that for the equilibrium (reaction [2]),

$$[2]\quad 2L + Zn^{2+} \rightleftarrows \underset{\text{(1:1 complex)}}{L + L{:}Zn^{2+}} \rightleftarrows \underset{\text{(2:1 complex)}}{L{:}Zn^{2+}{:}L}$$

the rate of interchanging the species is slow on the nmr timescale since separate resonances are observed for each species.

Rotation within the 2:1 Complex of 2

From the middle spectra in Fig. 3 and Fig. 4 it can be seen that the imidazole hydrogens, H_e and H_f, appear as a singlet at δ 7.10 and a pair of fortuitously equal intensity broadened singlets at δ 6.44 and δ 6.62 respectively. Variable temperature ^{1}H-nmr studies on this sample showed that at temperatures above 320 K, the latter two peaks coalesce into a singlet centred at δ 6.52. From reaction [3] in the symmetrically bound 2:1 complex H_f of one imidazole can be positioned between two pyridines of the second ligand (**10**) or between an imidazole and a pyridine of the second ligand (**11**). This should give rise to two different shieldings for H_f.[7]

[3] 

10 **11**

From $\Delta\nu_{H_f}$ (20 cps at 100 MHz) and a coalescence temperature of 320 K, one can calculate[8] that site exchange (**10** ⇄ **11**) occurs with a rate constant of 44 s^{-1} and that the activation energy for the process is about 16 kcal/mol.

(iii) Complex Titration

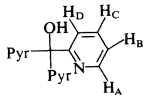
Of particular importance to the activity of CA, and therefore to any system designed to mimic CA, is the activity related ionization of a group with a pK_a of 7 (3). Tetrahedrally coordinated Zn^{2+}—OH_2 has been theorized to have such a low pK_a in the

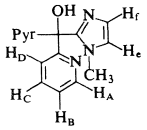
[6]This same effect has been noted before in the nmr spectrum of [$Fe^{II}Bipyr_3$]Cl_2 (13).

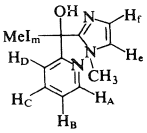
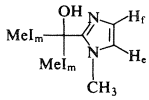
[7]At a temperature of 5°C, the high resolution ^{1}H-nmr spectrum of this complex shows two equal intensity imidazole N-CH_3 resonances separated by 2 Hz, in agreement with an equilibrium mixture of **10** and **11** as well as two sets of aromatic resonances very close together.

[8]For equal populations of two equilibrating species A and B (**10** and **11**) the residence time (τ) in site A or B is given as $\tau = 0.225/\Delta\nu$ where $\Delta\nu = \nu_A - \nu_B$ (23).

TABLE 4. Chemical shift values and assignments for ligands **1**–**5** and their Zn^{2+} complexes determined in D_2O solution

Ligand	δ and *J* value			
	H_A	H_B	H_C	H_D
1 	8.58 ddd J_{AB} = 5.0 Hz	7.45 ddd	7.94 ddd J_{CD} = 7.60 Hz	7.57 ddd J_{DC} = 7.60 Hz
Zn^{2+}/**1** = 0.5	7.77 ddd J_{AB} = 5.40 Hz	7.40 ddd	8.25 ddd J_{CD} = 7.60 Hz	8.54 ddd J_{DC} = 7.60 Hz
d-**1**	—	7.45 dd J_{BC} = 7.6 Hz J_{BD} = 1.0 Hz	7.92 dd J_{CD} = 7.6 Hz J_{CD} = J_{CB} = 7.6 Hz	7.54 dd J_{DC} = 7.6 Hz J_{DB} = 1.0 Hz
Zn^{2+}/d-**1** = 0.5	—	7.43 dd J_{BC} = 7.6 Hz J_{BD} = 1.0 Hz	8.26 dd J_{CD} = J_{CB} = 7.6 Hz	8.56 dd J_{DC} = 7.6 Hz J_{DB} = 1.0 Hz

Ligand	δ and *J* value						
	CH_3	H_f	H_e	H_A	H_B	H_C	H_D
2 	3.47 s	7.24 s	6.93 s	8.57 dm	7.46 m	7.95 dd	7.51 dm
Zn^{2+}/**2** = 0.5	4.21 s	6.44 s 6.62 s	7.10 s	8.04 dm	7.42 m	8.22 td	8.46 dm
Zn^{2+}/**2** = 15	4.08 s	7.18 d (or H_e)	7.12 d (or H_f)	8.78 dm	7.63 ddd	8.30 overlapping	8.08
d-**2**	3.48 s	7.24 s (br)	6.94 s (br)	—	7.52 dd J_{BC} = 5.2 Hz	7.96 dd J_{CD} = J_{CB} = 5.2 Hz	7.52 dd
d-**2**/Zn^{2+} = 0.5	4.27 s	7.08 s (br)	6.42 s 6.60 s	—	7.40 d (br) J_{BC} = 5.2 Hz	8.20 dd J_{CD} = J_{CB} = 5.2 Hz	8.45 d (br)
d-**2**/Zn^{2+} = 15	4.08 s	7.19	7.14 s		7.65 dd J_{BC} = 4.8 Hz J_{BD} = 1.6 Hz	8.30 overlapping	8.08

Ligand	δ value						
	CH_3	H_f	H_e	H_A	H_B	H_C	H_D
3 	3.52 s	7.31 d	7.01 d	8.71 dm	7.62 dd	8.07 dd	7.40 dm
4 	3.43 s	7.24 d	7.00 d	—	—	—	—

enzyme, and most recent work has favored this process (3, 7). Arguments against the ionization of Zn^{2+}—OH_2 centre on the lack of precedent (1*a*, 14) and ideas that Zn^{2+}—$\bar{O}H$ may not be sufficiently nucleophilic to account for the rate of hydration of CO_2 by CA.

On the other hand, ionization of Zn^{2+}-bound imidazole has been proposed to account for the low pK_a (4) with some experimental justification in simple complexes (4*a*), although it is observed in comparison of $(NH_3)_5Co^{3+}OH_2$ and $(NH_3)_5Co^{3+}$Im—H that Co^{3+} coordination in the latter reduces the

Can. J. Chem. Downloaded from www.nrcresearchpress.com by 210.87.254.40 on 09/05/12
For personal use only.

Can. J. Chem. Downloaded from www.nrcresearchpress.com by 210.87.254.40 on 09/05/12
For personal use only.

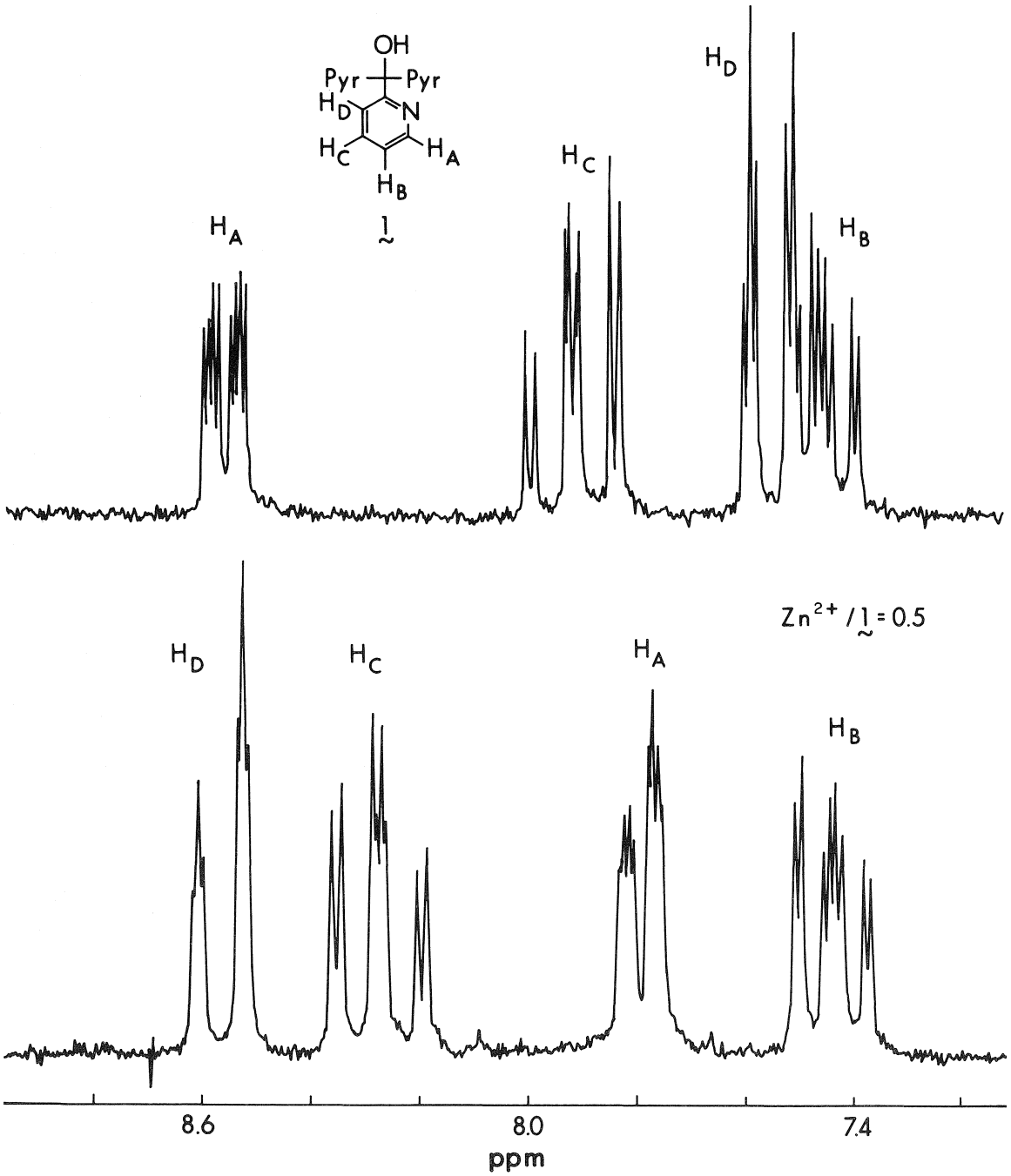


FIG. 1. The ^{1}H-nmr spectra of **1** and its 2:1 Zn^{2+} complex in D_2O. See Table 3.

ImH pK_a from 14 to only 10 while the pK_a of H_2O in the former is reduced from 15.5 (accounting for H_2O concentration) to 6.4 (5).

In order to cast some light on the above question, ligands **2** and **5**, differing only by *N*-methylation of the imidazole, were complexed to an equivalent amount of M^{2+} and titrated with NaOH. In both cases, titration of the free bases (0.025 mmol) in a solution containing 0.1095 mmol HNO_3 showed complete release of all added protons after pK_1 had been passed, and that this process was completely reversible. When bound to equimolar Zn^{2+}, **5** showed complete release of added H^+ by ~pH 3.5 indicating that metal binding was complete by that

Can. J. Chem. Downloaded from www.nrcresearchpress.com by 210.87.254.40 on 09/05/12
For personal use only.

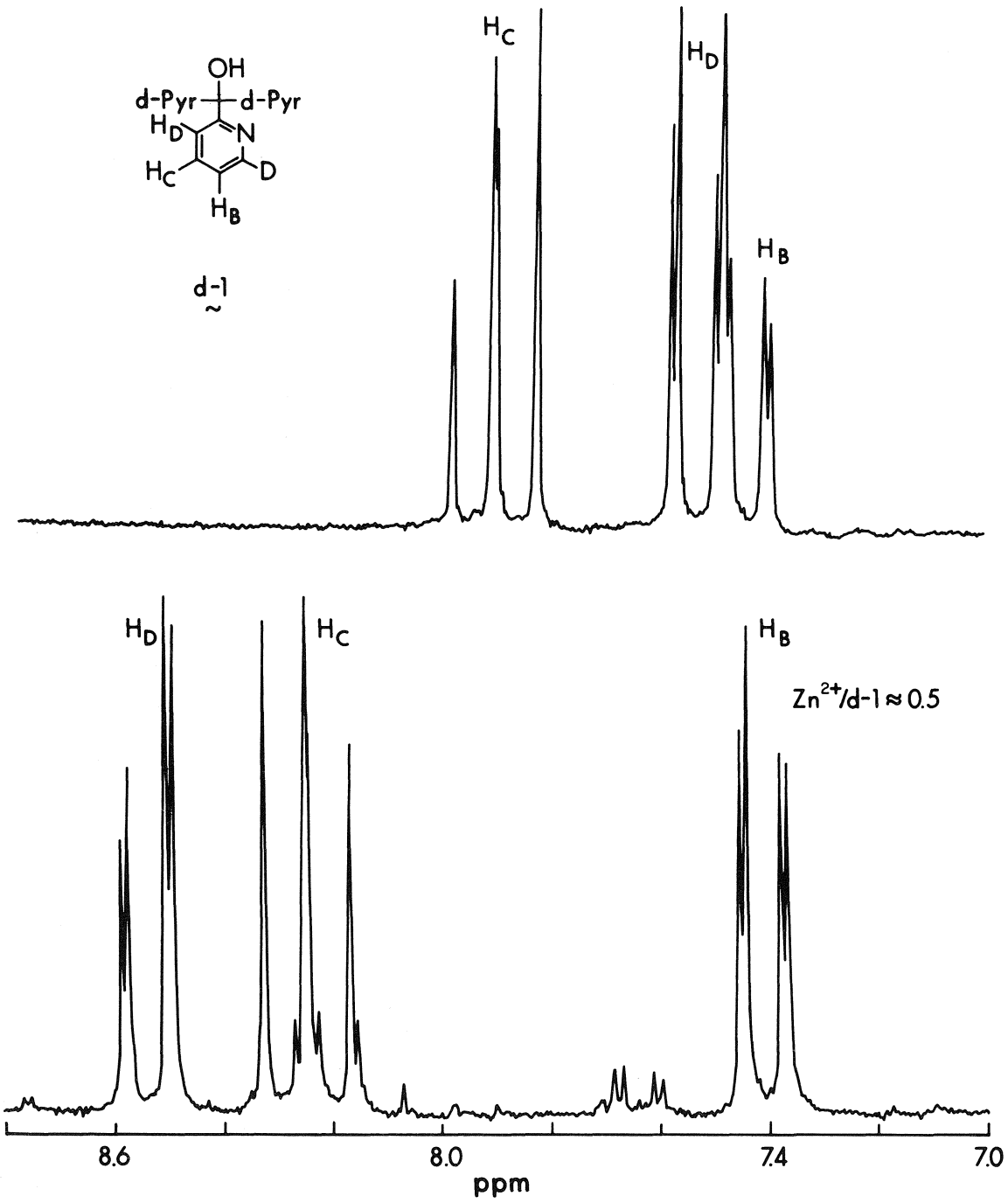


FIG. 2. The ^{1}H-nmr spectra of d-**1** and its 2:1 Zn^{2+} complex in D_2O. See Table 3.

point, and the additional release of 0.025 mmol H^+ (1.0 equiv. based on **5**:Zn^{2+}) upon further titration indicative of Zn^{2+}—OH_2 *or* Zn^{2+}—ImH ionization with an apparent pK_a of 6.98. Ultraviolet spectra of the solution on either side of the apparent pK_a showed no substantial changes and the solution remained clear until at least pH 10, indicating the free [Zn^{2+}] was very low. Analogous titration of **2** in the presence of Zn^{2+} curiously showed the release of only 0.8 equiv. (based on **2**—Zn^{2+}—OH_2) of H^+ at the apparent pK_a of 6.50 and not the expected 1.0. The inability to account for all the H^+ as-

Can. J. Chem. Downloaded from www.nrcresearchpress.com by 210.87.254.40 on 09/05/12
For personal use only.

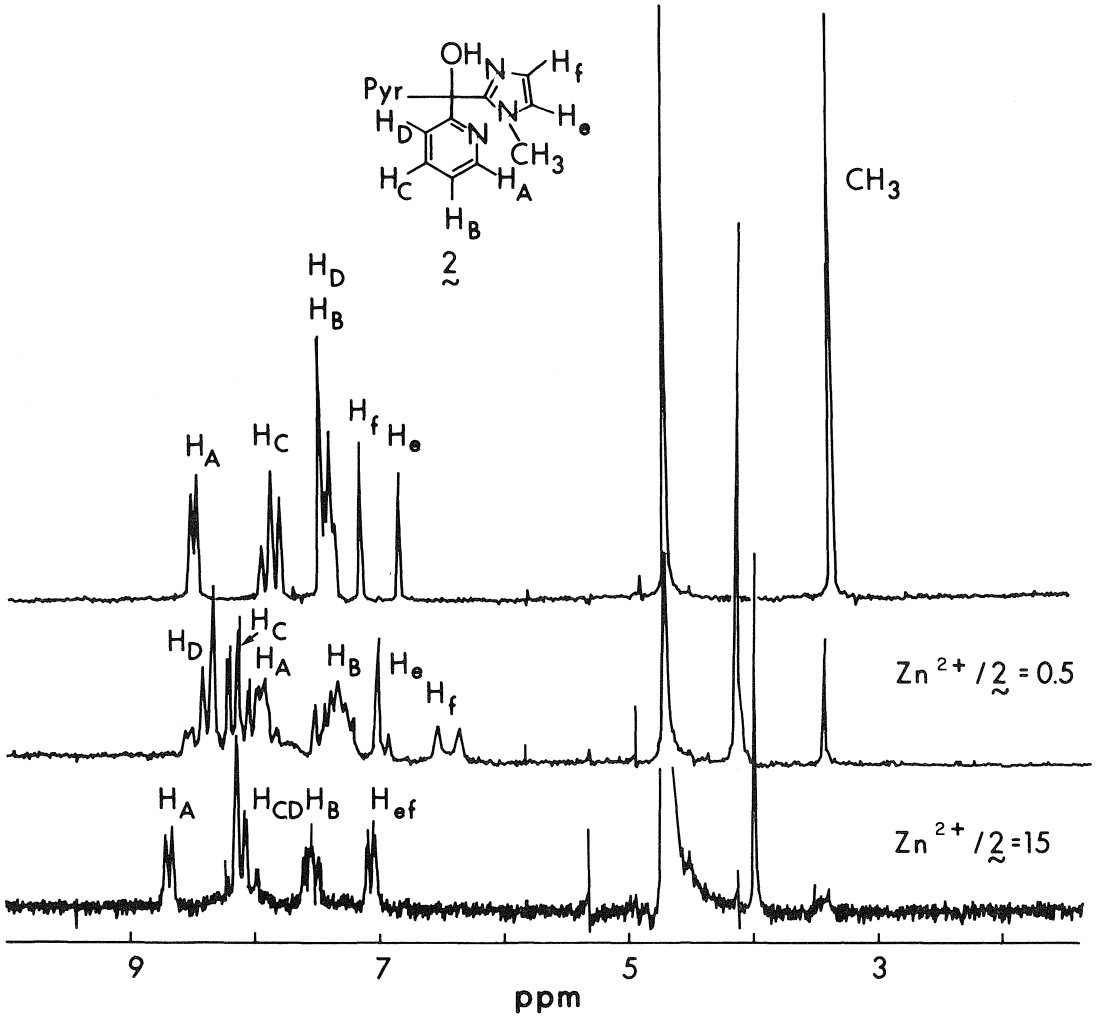


FIG. 3. The ^{1}H-nmr spectrum of **2** as a function of increasing $[Zn^{2+}]$. See text and Table 3 for assignments. The resonance at δ 4.8 is attributable to HOD.

sociated ionization of the complex *may* be associated with either incomplete formation of a 1:1 complex (i.e., some free ligand and some 2:1 complex which is not expected to have such a low pK_a (3*b*, 15)) or an equilibrium distribution of 4,5- and 6-coordinate Zn^{2+}:ligand complexes, the latter two not having such a low pK_a (15). Again, uv spectra of the solutions above and below the apparent pK_a showed minimal differences.

One might on the basis of these observations conclude that the apparent pK_a is best explained by ionization of a Zn^{2+}—OH_2, but this is almost certainly suspect since neither titration is reversible. ^{1}H-nmr spectra of Zn^{2+}:**2** and Zn^{2+}:**5** which had been titrated past the apparent pK_a's showed that the species formed was symmetric on the nmr timescale, although the ^{1}H-nmr absorptions were too broad to be definitive. We tentatively speculate that one possible explanation for the irreversibility of the titrations might be dimer formation as in path *a* or *b* of reaction [4], although one would think that these "dimers" would revert back to L:Zn^{2+}—OH_2 quickly in acid solution.

While some precedence for the existence of oxy and hydroxy bridged Zn^{2+} dimers is available (16) such bridged species are more commonly found with first row transition elements such as Co^{II}, Cu^{II}, Ni^{II}, and Fe^{III} (17).

The Co^{2+} complexes of **2** and **5** also show an apparent pK_a at 8.75 and 8.04 respectively. Ultraviolet spectra of each above and below the apparent pK_a do not show evidence of tetrahedrally bound Co^{2+} since no blue color is observed (18). Hence in these systems what appears to be simple

Can. J. Chem. Downloaded from www.nrcresearchpress.com by 210.87.254.40 on 09/05/12
For personal use only.

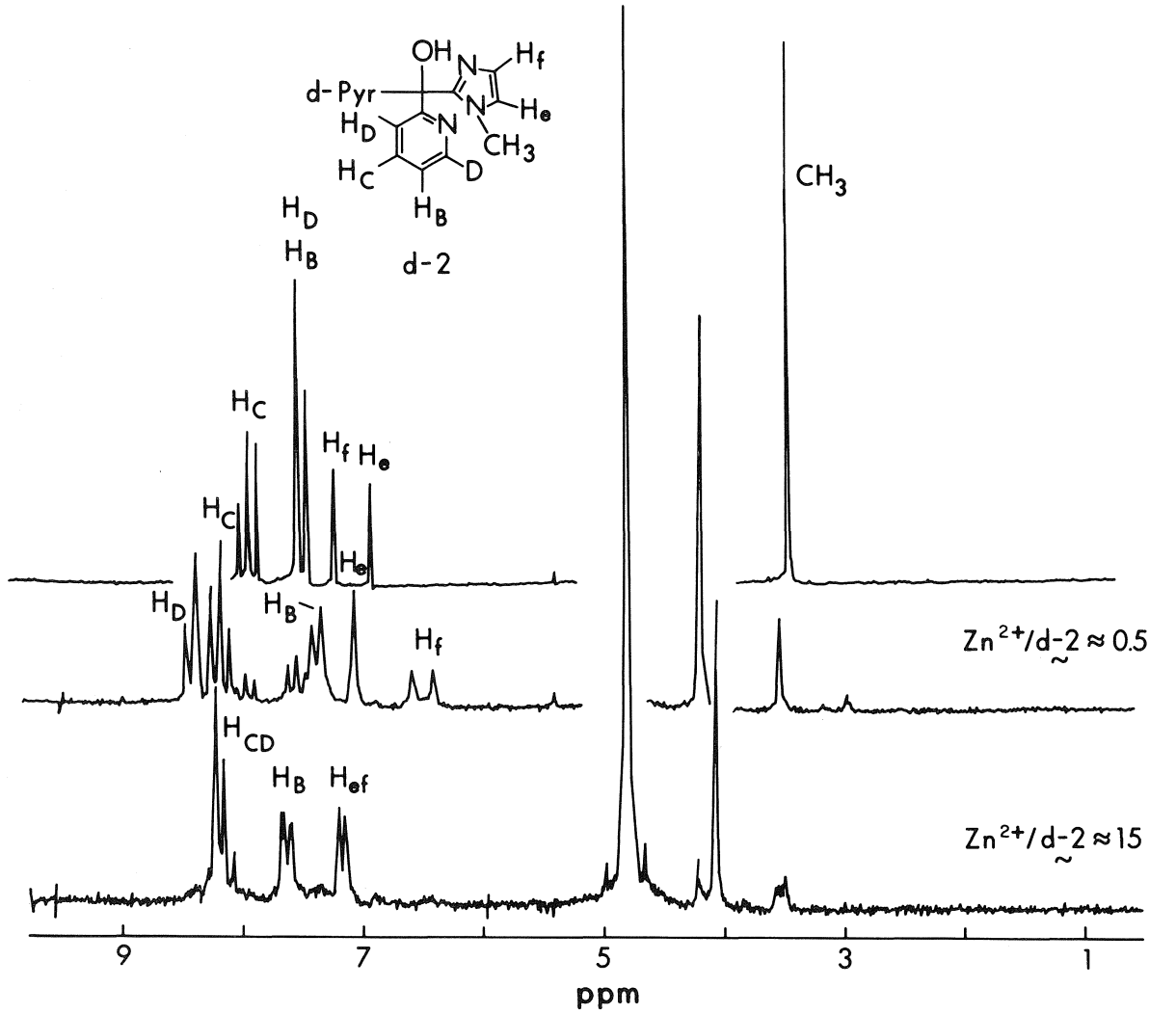
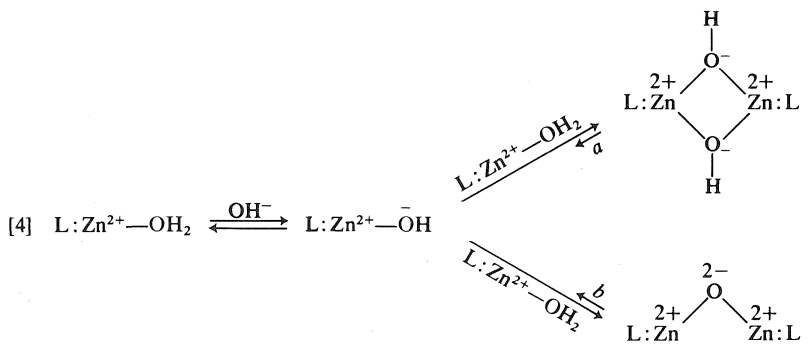


FIG. 4. The ^1H nmr of d-**2** as a function of increasing $[Zn^{2+}]$. The large resonance at δ 4.8 is attributable to HOD. For a discussion of the resonances attributable to H_f see text.

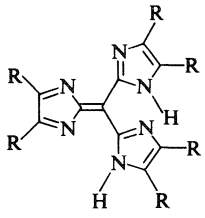
M^{2+}—OH_2 titration is not sufficient to enforce a tetrahedral geometry for Co^{2+}, but does not rule out that possibility for Zn^{2+}.

In order to circumvent this irreversibility ligands **6**–**8** having progressively bulkier substituents at the 4,5-positions were investigated. From space filling models, not only do **7** and **8** enforce tetrahedral binding for the metal, but the possibility of oxy-



Can. J. Chem. Downloaded from www.nrcresearchpress.com by 210.87.254.40 on 09/05/12
For personal use only.

bridged dimers is reduced since there should be severe buttricing between the isopropyl groups on adjacent ligands. Titration of Zn^{2+}:**6** performed analogously to those of Zn^{2+}:**5** and Zn^{2+}:**2** showed the consumption of 1.0 equiv. of ^{-}OH at about pH 7, but this was tied to the reversible formation of an intensely blue-colored solution which indicates the ligand itself suffers some modification. Ligand **7**, even at acid pH, when complexed with Zn^{2+} gave a bright pink solution. We note that upon drying (for microanalytical purposes) both **6** and **7** tended to dehydrate (as evidenced by the buildup of an M^{+}—H_2O peak in the mass spectrum) to form intensely colored crystals which appear to possess extensive conjugation as might be expected for a fulvene-like **12** (reaction [5]). ^{1}H-nmr experiments on these crystals in $CDCl_3$ solution showed complete molecular symmetry as expected if the alkyl groups were tautomerically equivalent on the nmr timescale.

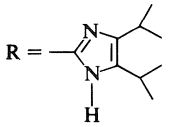
[5] **6** or **7** $\xrightarrow[\Delta]{-H_2O}$ 

12

R = CH_3, $CH(CH_3)_2$

In order to circumvent this dehydration, the OH group was replaced with H according to the scheme in reaction [6].

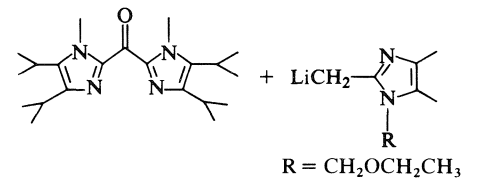
[6] **7** $\xrightarrow[\Delta]{NaOH/H_2O,\ Na_2S_2O_4}$ 

R = 

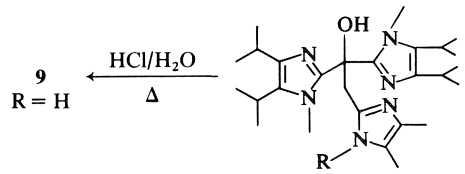
The corresponding methane was present as evidenced by a ^{1}H-nmr singlet at δ 5.4, and the material appeared reasonably stable as its HCl salt. Unfortunately in basic media, the methine H proved extremely susceptible to air oxidation which reconverted it back to **7** which again suffered deleterious dehydration to form what we believe is **12**.

Ligand **8** on the other hand showed no propensity to form colored solutions (again supporting dehydration of **6** or **7**) and was therefore titrated (for reasons of solubility **8** required a titration medium of 80% aqueous dioxane) in the presence of equimolar Zn^{2+}. In this case, curiously at "pH" 7 two equivalents of $\bar{O}H$ were consumed and the process was reversible. Control experiments under the same conditions but in the absence of **8** showed again the consumption of 2 equivalent $\bar{O}H$ at a "pH" of 7 which is clearly tied to the formation of $Zn(OH)_2 \cdot xH_2O$, but the latter species appears quite soluble in the medium. Thus it would appear that because Zn^{2+} binds to **8** only weakly ($pK_{Zn^{2+}} \simeq$ 4, Table 2) that at elevated "pH", OH^{-} simply sequesters the metal away from the ligand.

Our final ligand in this series (**9**) from the above experiences was designed to prevent 2:1 ($L:M^{2+}$) binding, oxy or hydroxy-bridged dimers, and the deleterious dehydration in the presence of Zn^{2+} and OH^{-}. As well, for reasonable metal binding, at least one imidazole (NH) was required, and **9** was prepared as shown in reaction [7].

[7] 

R = $CH_2OCH_2CH_3$



13

R = $CH_2OCH_2CH_3$

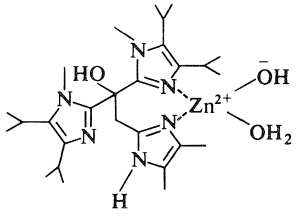
9 R = H

Deprotection of **13** in refluxing 10% HCl water proved to be very slow, requiring nearly two weeks to completely form **9**.

In 60% aqueous dioxane an equimolar mixture of **9** and Co^{2+} gave a blue colored solution (λ_{max} 580 nm, $\varepsilon_{min} = 60$ assuming complete 1:1 binding). Normally ε_{max} for tetrahedral cobalt is between 100 and 1000, depending on the system (18). In the presence of equimolar Zn^{2+}, **9** was titrated and showed the reversible consumption of 1 equiv. of OH^{-} at an apparent pK_a of 5.8 in the above medium. In the absence of **9**, Zn^{2+} under the same conditions showed precipitation of $Zn(OH)_2$ and the consumption of 2 equiv. of OH^{-} at around "pH" 7.

Interaction of **9** with Zn^{2+} is strong enough to hold the latter in solution, and the consumption of OH^{-} is consistent with Zn^{2+}:OH_2 titration (although the "pK_a" seems too low) or more likely

with ^-OH displacement of one of the weakly bound N—CH_3 imidazoles as in reaction [8].

[8] **9**:$Zn^{2+}OH_2 + OH^-$ ⇄ 

At this point we attempted some catalysis studies on solutions of **9**:Zn^{2+}—OH_2 at various "pH's" for both the hydrolysis of *p*-nitrophenyl acetate, and the hydration of acetaldehyde. Comparison of the reaction rates with metal, metal + ligand, and ligand at "pH" values between 5 and 10 showed no substantial differences so the complex present in this medium is not catalytically viable.

Conclusion

Although for various reasons, each of ligands **1–9** has some serious deficiency in terms of their ability to be considered as "models" for the metal binding site of CA, several important observations have been made which cast light on the minimum features such "models" should possess.

(*1*) N—CH_3 imidazole ligands bind metal rather poorly when compared with their N—H analogues. One clearly requires large $pK_{M^{2+}}$ values for a potential "model" for CA so that the metal will not be sequestered away from the ligand at elevated pH.

(*2*) Deleterious 2:1 (L:M^{2+}) binding can be overcome by placing large alkyl groups at the 4,5-imidazole positions. However such substitution in the tris-imidazole carbinol series appears to lead to facile dehydration to produce highly colored fulvene-like materials. Such dehydration can be overcome by removing the carbinol OH group, or methylating the imidazole nitrogen, however the former substitution of OH by H produces an extremely easily air-oxidized methane, and the latter *N*-methylation leads to rather poor metal binding ability.

(*3*) The small ligands **1–4** from nmr studies in D_2O solution can exist as 2:1 or 1:1 (L:M^{2+}) species, the latter being favored at high [metal].

Experimental Section

Routine ir and nmr spectra were obtained using a Nicolet FT-IR Spectrophotometer ($CHCl_3$ cast film) and a Varian A-60 spectrometer (D_2O or $CDCl_3$). Ligand/Zn^{2+} ^{1}H-nmr spectra were determined on a Varian HA-100-15 spectrometer with Fourier transform modifications provided by a Digilab FTS NMR-3 System. pK_a determinations were performed in a jacketted cell kept at 30 ± 0.1°C and under a nitrogen atmosphere. The pH was measured using a Radiometer TTT2 titrator and PHA 943 B titration module in conjunction with a Radiometer 6K2402B combined electrode, and recorded as a function of added 0.1000 *N* NaOH (delivered by a Radiometer ABU 12 autoburette), on a Radiometer SBR 3 titrigraph. Standard pH 4 and pH 7 buffers were used to check the electrode linearity and standardize the pH meter at the beginning of each series of experiments. The ionic strength was maintained constant by using a medium 0.16 *M* in KNO_3. Data were analysed by a computer version[4] of the Simm's method (10) and reported pK_a's are the average of at least three determinations. Metal binding constants were determined analogously to those reported (6). Stock solutions of Co^{2+}, Ni^{2+}, Zn^{2+}, and Cu^{2+} were prepared from their reagent grade hydrated nitrate salts and were standardized by EDTA titration. Typically a three to four-fold excess of ligand over metal was titrated as above and the data analysed to give metal binding constants which are reported as the average of three determinations.

*Bis(2-pyridyl)-2-(*N*-methylimidazolyl)carbinol (2)*

A solution of 0.9 g (0.11 mol) of *N*-methylimidazole (19) in 50 mL dry ether under N_2 was cooled to −30°C (suspension) and treated with 7.5 mL of 1.6 *M* *n*-butyllithium in hexane, followed by stirring at room temperature for 30 min. It was then cooled to −40°C and a solution of bis-2-pyridyl ketone (20) in 5 mL ether and 5 mL THF was added dropwise. After stirring at room temperature overnight the mixture was quenched with H_2O and the product was isolated by chloroform extraction. The combined extracts were dried ($MgSO_4$), and stripped of solvent to give a paste which was decolorized with charcoal and recrystallized from Skelly B / benzene to give 1.8 (61%) of white crystals: mp 153–155°C; ir 3350 (br), 1590, 1430, 1360, 1100 cm^{-1}; nmr (D_2O) Table 3; mass spectrum *m/e* 266 (M^+), 249 (M^+ − OH); *Anal.* calcd. for $C_{15}H_{14}N_9O$: C 67.67, H 5.26, N 21.05; found: C 67.98, H 5.37, N 21.07.

*Bis(2-pyridyl-6-*d*)-2-(*N*-methylimidazolyl)carbinol (d-2)*

It was prepared analogously to **2** but using bis-(2-pyridyl-6*d*) ketone. Nuclear magnetic resonance (D_2O) Table 3; mass spectrum *m/e* 268 (M^+), 251 (M^+ − OH).

*Bis-(2-pyridyl-6*d*)ketone*

A solution of 21 g (0.132 mol) of 2-bromopyridine-6*d* in 300 mL dry ether under N_2 was treated with 90 mL of 1.6 *M* *n*-butyllithium in hexane at −65°C. After two cycles of allowing the solution to warm to −45°C, and recooling to −65°C, 8 mL (0.067 mol) of diethylcarbonate was added keeping the temperature at −60°C. Stirring was continued for 2 h (−65°C) and then at room temperature overnight. Workup consisted of the addition of 8 g H_2SO_4 in 10 mL H_2O, followed by ether extraction. The combined extracts were dried (Na_2SO_4), and stripped of solvent to give a dark oil which after distillation gave a yellow oil, bp 120–140°C/0.15 Torr. Crystallization from toluene at −60°C afforded 6 g (24%) of off-white crystals, mp 51–53°C; ir 1680, 1575, 1430, 1320, 1300 cm^{-1}; ^{1}H-nmr ($CDCl_3$) δ 7.5 (2H, dd), 7.91 (2H, dd), 8.13 (2H, dd); mass spectrum *m/e* 186 (M^+), 79 (M^+ − *d*-Pyr—C=O).

*2-Bromopyridine-6*d

6-Bromo-2-lithiopyridine (21) was quenched at −40°C with an excess of methanol-d_1, and the mixture after workup, afforded 2-bromopyridine-6-*d*, in 82% yield. ^{1}H-nmr showed complete absence of the 2-H.

*Tris-(2-pyridyl-6-*d*)carbinol (d-1)*

In a procedure analogous to that described by Wibaut *et al.* (20) for the preparation of **1**, 2-lithiopyridine-6-*d* and bis-(2-pyridyl-6*d*)ketone were reacted to give 41% of d-**1**, mp 128–129°C (lit. (20) 127–128°C for **1**); ^{1}H-nmr (D_2O) Table 3;

Can. J. Chem. Downloaded from www.nrcresearchpress.com by 210.87.254.40 on 09/05/12
For personal use only.

Can. J. Chem. Downloaded from www.nrcresearchpress.com by 210.87.254.40 on 09/05/12
For personal use only.

mass spectrum *m/e* 266 (M^+), 249 ($M^+ - OH$), 187 (M^+ − 6-*d* pyr).[9]

*Bis(2-*N*-methylimidazolyl)-2-pyridyl Carbinol (**3**)*

To a suspension of 0.5 mol of 2-*N*-methylimidazolyl lithium in 600 mL dry ether at 0°C was added 0.25 mol of ethyl picolinate and the mixture was stirred 4 h. It was then decomposed with 20 mL of 10% H_2SO_4 and extracted with chloroform. The combined extracts were dried ($MgSO_4$) and solvent removed to give an oil from which unreacted *N*-methyl imidazole was removed by distillation (55°C/3 Torr). The residue was recrystallized from Skelly B/benzene to give 6 g (9%) of **3**, mp 131–133°C; ^{1}H-nmr ($CDCl_3$) Table 3; mass spectrum *m/e* 269 (M^+), 191 (M^+ − pyr); *Anal.* calcd. for $C_{14}H_{15}N_5O$: C 62.45, H 5.57, N 26.02; found: C 62.80, H 5.75, N 26.12.

*Bis(2-pyridyl)-2-(*N*-ethoxymethyl)imidazolyl Carbinol (**5**b)*

To a solution of 0.04 mol of 2-(*N*-ethoxymethyl)imidazolyl lithium (6) in 200 mL THF at −60°C was added a solution of 7.36 g (0.04 mol) of bis(2-pyridyl) ketone in 50 mL THF. After addition the deep blue solution was stirred an additional hour at −60°C and then overnight at room temperature. Quenching with H_2O, followed by several ethylacetate extractions which were combined and dried ($MgSO_4$) and then stripped of solvent yielding an oily paste which was recrystallized from ether to give 4.5 g (36%) of the product, mp 62–63.5°C; ^{1}H-nmr ($CDCl_3$) δ 0.95 (3H, t), 3.20 (2H, q), 5.20 (2H, s), 7.07 (2H, d), 7.25 (3H, m), 7.75 (4H, m), 8.50 (2H, d).

*Bis(2-pyridyl)-2-imidazolyl Carbinol (**5**)*

Deprotection of **5***b* (see above) was accomplished according to published procedure (6), and the free base liberated by basification, mp 225–235°C (decomp.): ^{1}H-nmr (D_2O) Table 3; ir 3200 (br), 1570, 1430, 744 cm^{-1}; mass spectrum *m/e* 252 (M^+), 235 ($M^+ - OH$), 185 (M^+ − imidazolyl), 146 (M^+ − pyr). Ligands **4**, **6**, **7**, and **8** were synthesized analogously to published procedure (6) the latter three starting from either 4,5-dimethylimidazole (22) or 4,5-diisopropylimidazole (22).

*Tris-2-[(*N*-ethoxymethyl)-4,5-dimethylimidazolyl]carbinol (**6**b)*

From 15.4 g (0.091 mol) of 2-(*N*-ethoxymethyl-4,5-dimethylimidazolyl) lithium reacted with 3.6 g (0.03 mol) diethyl carbonate in 200 mL THF at −60°C was isolated 7.5 g crude orange crystals (50%) which were recrystallized from hexane/ether to give **6***b*, mp 114–116.5°C: 90 MHz, ^{1}H-nmr ($CDCl_3$) δ 0.98 (3H, t), 2.03 (3H, s), 2.15 (3H, s), 3.15 (2H, q), 5.13 (2H, 5), 6.31 (1H, br); mass spectrum *m/e* 488 (M^+) 443 ($M^+ - OCH_2CH_3$) 429 ($M^+ - CH_2OCH_2CH_3$). The free ligand (**6**) was liberated analogously to published procedure (6) followed by basification, mp > 275°C (darkens): ^{1}H-nmr (D_2O) δ 2.26 (s). *Anal.* calcd. for $C_{25}H_{40}N_6O_4$: C 61.45, H 8.25, N 17.20; found: C 61.27, H 8.15, N 17.44.

*Tris-[2-(*N*-ethoxymethyl)-4,5-diisopropylimidazolyl]carbinol (**7**b)*

From 13.5 g (0.064 mol) of 2-lithio-*N*-ethoxymethyl-4,5-diisopropyl imidazole and 2.40 mL (0.021 mol) of diethyl carbonate was isolated 8.5 g (62%) of **7***b* (recrystallized from ethyl acetate), mp 121–123°C: ^{1}H-nmr ($CDCl_3$) δ 1.15 (45H, m), 3.05 (12H, m), 5.20 (6H, s), 6.75 (1H, br): mass spectrum *m/e* 656 (M^+), 639 ($M^+ - OH$), 597 ($M^+ - CH_2OCH_2CH_3$). The free base (**7**) was isolated analogously as for **6**: ^{1}H-nmr ($CDCl_3$) δ 1.26 (36 H, d), 3.01 (6H, hept.). *Anal.* calcd. for $C_{28}H_{46}N_6O$: C 69.70, H 9.54, N 17.43; found: C 69.33, H 9.54, N 17.49.

*Tris-2-(*N*-methyl-4,5-diisopropylimidazolyl)carbinol (**8**)*

From 0.058 mol of 2-(*N*-methyl-4,5-diisopropylimidazolyl) lithium and 0.019 mol diethylcarbonate was isolated ~50% of an oil containing **8** and its analogous ketone. One gram of this mixture was chromatographed over silica gel (ethylacetate) to give the desired **8** as an oil: ^{1}H-nmr (acetone-d_6) δ 1.15 (18H, d), 1.32 (18H, d), 3.5 (6H, m), 3.27 (9H, m), 6.42 (1H, s, br); *Anal.* calcd. for $C_{31}H_{52}N_6O$: C 70.99, H 9.92, N 16.03; found: C 71.17, H 10.04, N 14.64.

*Bis-2-[*N*-methyl-4,5-diisopropylimidazolyl]ketone*

Heating of neat **8** at 180°C/atm pressure for 5 min yielded an oil which was recrystallized from ether, mp 197–199°C; ^{1}H-nmr ($CDCl_3$) δ 1.23 (12H, d), 1.34 (12H, d), 3.1 (4H, m), 3.85 (6H, s); mass spectrum, *m/e* 358 (M^+), 343 ($M^+ - CH_3$); *Anal.* calcd. for $C_{21}H_{34}N_4O$: C 70.39, H 9.49, N 15.64; found: C 70.23, H 9.50, N 15.60.

*Bis-2-[*N*-methyl-4,5-diisopropylimidazolyl]-2-[*N*-methoxymethyl-4,5-dimethylimdazolylmethyl]carbinol, **9***

To 1.29 g (0.0084 mol) *N*-methoxymethyl-2,4,5-trimethylimidazole in 180 mL dry THF at −60°C was added 1 equiv. (0.0084 mol) *n*-BuLi in hexane. To this mixture was added 3.09 g (0.0084 mol) of bis-2-[*N*-methyl-4,5-diisopropylimidazolyl]-ketone in 10 mL THF. After workup, and recrystallization from ether, 2.7 g (63%) of the product was obtained, mp 133–134°C. ^{1}H-nmr ($CDCl_3$) δ 1.11 (12H, d), 1.26 (12H, d), 1.98 (3H, s), 2.09 (3H, s), 2.93 (4H, m), 3.23 (9H, d), 3.87 (2H, s), 5.35 (2H, s); mass spectrum, *m/e* 512 (M^+), 497 ($M^+ - CH_3$) 359 (M^+ − *N*-methoxymethyl-4,5-dimethylimidazolylmethyl). *Anal.* calcd. for $C_{29}H_{48}N_6O_2$: C 67.83, H 9.35, N 16.37; found: C68.03, H 9.42, N 16.51.

The free base (**9**) was obtained by refluxing the above material in 10% HCl for two weeks and basification, mp 168–170°C (darkens). ^{1}H-nmr ($CDCl_3$) δ 1.23 (24H, d), 2.10 (6H, s), 2.93 (10H, m), 3.57 (2H, s); mass spectrum, *m/e* 468 (M^+), 450 ($M^+ - H_2$), 359 (M^+ − 4,5-dimethylimidazolylmethyl).

Tris-2-[4,5-diisopropylimidazolyl]methane

Under nitrogen, 100 mg of the tris-2-[4,5-diisopropylimidazolyl]carbinol·*x*HCl salt was dissolved in 10 mL 3 *N* NaOH and 10 mL ethanol and brought to reflux, before 100 mg of sodium dithionite dissolved in the minimum amount of H_2O was added in one portion. After 1 min, the mixture was acidified with concentrated HCl, and then all volatiles were removed under vacuum. The residue was triturated with acetone which was filtered and evaporated to afford a yellowish solid, mp 120–180°C (decomp.), mass spectrum, *m/e* 466 ($M^+ - x$HCl), 451 ($M^+ - x$HCl − CH_3).

This material proved to be relatively stable as the HCl salt but upon basification in the presence of air discolored badly due to air oxidation followed by dehydration.

[9]Reference 20 reports a preparation of bis-(2-pyridyl) ketone in 10% yield from 2-pyridyl lithium and ethyl picolinate.

Acknowledgements

The authors are indebted to the National Sciences and Engineering Research Council of Canada and the University of Alberta for financial support. We are also indebted to Professor R. Breslow (Columbia University) who supplied copies of the computer programs for pK_a and $pK_{M^{2+}}$ analyses.

1. (*a*) Y. POCKER and J. E. MEANY. J. Am. Chem. Soc. **87**, 1809 (1965); (*b*) R. E. TASHIAN, C. C. PLATO, and T. B. SHOWS. Science, **140**, 53 (1963); (*c*) Y. POCKER and J. T. STONE. J. Am. Chem. Soc. **87**, 5497 (1965); (*d*) E. T. KAISER and K.-W. LO. J. Am. Chem. Soc. **91**, 4912 (1969); (*e*) Y. POCKER, J. E. MEANY, and B. C. DAVIS. Biochemistry, **13**, 1411 (1974).

2. (*a*) S. LINDSKOG *et al. In* The enzymes. Vol. 5. 3rd ed. 1971. p. 587; (*b*) K. K. KANNAN *et al.* Proc. Natl. Acad. Sci. U.S.A. **72**, 51 (1975).
3. (*a*) R. P. DAVIS. *In* The enzymes. Vol. 5. 2nd ed. 1962. p. 545; (*b*) P. WOOLEY. Nature, **258**, 677 (1975) and references therein; (*c*) S. LINDSKOG and J. E. COLEMAN. Proc. Natl. Acad. Sci. U.S.A. **70**, 2505 (1973); (*d*) D. W. APPLETON and B. SARKAR. Bioinorg. Chem. **7**, 211 (1977).
4. (*a*) D. W. APPLETON and B. SARKAR. Proc. Natl. Acad. Sci. U.S.A. **71**, 1686 (1974); (*b*) J. M. PESANDO. Biochemistry, **14**, 675 (1975); **14**, 681 (1975); (*c*) J. M. PESANDO and A. P. GROLLMAN. Biochemistry, **14**, 689 (1975); (*d*) R. K. GUPTA and J. M. PESANDO. J. Biol. Chem. **250**, 2630 (1975).
5. J. MACB. HARROWFIELD, V. NORRIS, and A. M. SARGESON. J. Am. Chem. Soc. **98**, 7282 (1976).
6. C. C. TANG, D. DAVALIAN, P. HUANG, and R. BRESLOW. J. Am. Chem. Soc. **100**, 3918 (1978).
7. (*a*) M. F. DUNN. Struct. Bonding, Berlin, **23**, 61 (1975); (*b*) S. LINDSKOG. Struct. Bonding, Berlin, **8**, 153 (1970); (*c*) J. E. COLEMAN. J. Biol. Chem. **242**, 5212 (1967).
8. J. H. COATES, G. J. GENTLE, and S. F. LINCOLN. Nature, **249**, 773 (1974).
9. (*a*) A. ALBERT and E. P. SERJEANT. Ionization constants of acids and bases. J. Wiley and Sons, New York, NY. 1962; (*b*) F. J. C. ROSSOTTI and H. ROSSOTTI. Determination of stability constants. McGraw-Hill. 1961.
10. H. S. SIMMS. J. Am. Chem. Soc. **48**, 1239 (1920).
11. S. LINDSKOG and P. O. NYMAN. Biochim. Biophys. Acta, **85**, 462 (1964).
12. P. K. GLASOE and F. A. LONG. J. Phys. Chem. **64**, 188 (1960).
13. S. CASTELLANO, H. GÜNTHER, and S. EBERSOLE. J. Phys. Chem. **69**, 4166 (1965).
14. S. LINDSKOG. J. Biol. Chem. **238**, 945 (1963).
15. R. H. PRINCE and P. R. WOOLEY. Nature Phys. Soc. **240**, 117 (1972).
16. (*a*) W. HAASE, R. MERGEHENN, and R. ALLMAN. Acta Crystallogr. B**31**, 1184 (1975); (*b*) M. ISHIMORI, T. HAGIWARA, T. TSURUTA, and Y. KAI. Bull. Chem. Soc. Jpn. **49**, 1165 (1976).
17. (*a*) J. A. BERTAUD and P. G. ELLER. Prog. Inorg. Chem. **21**, 29 (1976); (*b*) D. J. HODGSON. Prog. Inorg. Chem. **19**, 173 (1975).
18. (*a*) R. L. CARLIN. *In* Transition metal chemistry. Vol. 1. Marcel Dekker, New York. 1965; (*b*) M. CIAMPOLINE. Struct. Bonding, Berlin, **6**, 52 (1969).
19. A. M. ROE. J. Chem. Soc. 2195 (1963).
20. J. P. WIBAUT, A. P. DEJONGE, H. G. P. VAN DER VOORT, and P. PH. H. L. OTTO. Recl. Trav. Chim. Pays Bas, **70**, 1054 (1951).
21. J. E. PARKS, B. E. WAGNER, and R. H. HOLM. J. Organomet. Chem. **56**, 53 (1973).
22. H. BREDERECK and E. THEILIG. Chem. Ber. **86**, 88 (1953).
23. F. A. BOVEY. Nuclear magnetic resonance spectroscopy. Academic Press, New York, NY. 1969. Chapt. VII.
24. M. R. GRIMMETT. *In* Advances in heterocyclic chemistry. Vol. 12. *Edited by* A. R. Katritsky and A. J. Boulton. 1970. p. 104.
25. R. K. BOGGESS and S. J. BOBERG. J. Inorg. Nucl. Chem. **42**, 21 (1980).

Can. J. Chem. Downloaded from www.nrcresearchpress.com by 210.87.254.40 on 09/05/12
For personal use only.

Solvent effect on the rate of N(III)/Cl(V) reaction

SAMIR S. EMEISH[1]

Department of Chemistry, Bedford College, London NW1 4NS, U.K.

Received October 19, 1979

SAMIR S. EMEISH. Can. J. Chem. **58**, 902 (1980).

Kinetics of the reaction between N(III) and Cl(V) have been studied in water and water–dioxan solutions. The rate equation of the reaction in each solvent could be written as

$$\text{Rate} = k_3[HNO_2][ClO_3^-][H^+]$$

and the rate rises as the dielectric constant of the medium is lowered. This observation is in accord with suggested mechanistic details involving the intermediate H_2NClO_5.

SAMIR S. EMEISH. Can. J. Chem. **58**, 902 (1980).

On a étudié la cinétique de la réaction entre N(III) et Cl(V) dans l'eau et dans des solutions eau–dioxanne. On peut exprimer l'équation de vitesse de la réaction sous la forme suivante

$$\text{Vitesse} = k_3[HNO_2][ClO_3^-][H^+]$$

La vitesse augmente quand la constante diélectrique du milieu diminue. Cette observation est en accord avec le mécanisme suggéré qui implique un intermédiaire du type H_2NClO_5.

[Traduit par le journal]

Can. J. Chem. Downloaded from www.nrcresearchpress.com by 210.87.254.6 on 09/05/12
For personal use only.

Introduction

The oxidation of N(III) by Cl(V) in buffered aqueous acidic media has been studied extensively (1). The mechanistic details of the reaction are well established and the activated complex H_2NClO_5 has been proposed (2). Few studies investigating the effect of progressive variation in the solvent upon the rate of reaction have been reported.

The effect of variation of dielectric constant of the medium by addition of dioxan to aqueous solvent (3) on the rate of N(III)/Cl(V) reaction is presented in this work.

Experimental

Chemicals used were of the Analar grade (except for technical grade HCl). Analar dioxan was freed from possible traces of H_2O_2 by being run through chromatographic alumina before being used. Stock solutions of nitrite were stabilised by traces of NaOH.

The reaction was studied in water, 34 wt% dioxan, and 67 wt% dioxan. Table 1 gives some properties of these three solvents used. The diminution in V_{total} was determined by separate experiments at 25°C and this diminution has been taken into account in expressing concentrations. The values of the dielectric constant (D) were calculated from the results of Akerlof and Short (4).

Reproducible results were obtained, in each solvent, under normal laboratory conditions. Reaction was initiated in thermostatted solutions by thoroughly mixing sodium nitrite and potassium chlorate plus hydrochloric acid. Samples were taken at intervals and analysed for N(III) by the Shinn method as modified by Kershaw and Chamberlin (5).

[1]Present address: P.O. Box 2385, Amman, H. K. Jordan.

TABLE 1. Some properties of the water–dioxan solutions

V_{H_2O} (cm³)	V_{dioxan} (cm³)	V_{total} (cm³)	$Mass_{total}$ (g)	$Wt\%_{dioxan}$	D (25°C)
60	—	60.00	59.82	—	78.3
40	20	59.70	60.44	34.02	48.38
20	40	59.25	61.06	67.34	20.45

Results

N(III) in dilute aqueous acidic solutions ($[H^+] \approx 0.02$ mol dm^{-3}) will be present as HNO_2 and NO_2^-. The ionization constant of nitrous acid in aqueous solutions is well known. Corresponding constants of the acid in water–dioxan solutions have not been reported. Therefore the ionization constant of nitrous acid was determined spectrophotometrically in water and water–dioxan solutions similar to those used in the kinetic study of the reaction.

Nitrite and nitrous acid absorb in the same wavelength region, but with different molar absorption coefficients at the same wavelength. The absorption spectrum of nitrite in the region 400–300 nm consists of one featureless band with a peak at 354 nm. That of nitrous acid in the same region shows five peaks at 386, 372, 358, 346, and 336 nm with three well marked intervening troughs at 380, 364, and 357 nm (see Fig. 1). This observation corresponds well with the published data (6). General aspects of these features are maintained over the three media investigated although minor shifts in the wavelengths of absorption occur, e.g.,

0008-4042/80/090902-04$01.00/0
©1980 National Research Council of Canada/Conseil national de recherches du Canada

TABLE 2. Molar absorption coefficients (ε, in $m^2 mol^{-1}$) of NO_2^- and HNO_2

	Water		34 wt% dioxan		67 wt% dioxan	
Species	ε_{373}	$\varepsilon_{352.5}$	ε_{373}	$\varepsilon_{352.5}$	ε_{360}	ε_{354}
NO_2^-	15.1	23.1	18.8	27.4	30.3	29.5
HNO_2	55.4	34.5	61.4	35.4	70.9	33.2

TABLE 3. Values for pK_I of HNO_2 in the three media at 25°C*

$10^3[NaNO_2]_0$ (mol dm^{-3})	$10^3[HCl]_0$ (mol dm^{-3})	$10^3[HNO_2]$ (mol dm^{-3})	$10^3[NO_2^-]$ (mol dm^{-3})	$10^4[H^+]$ (mol dm^{-3})	$10^2F(I)$†	pK_I
			In water			
11.24	5.500	4.834	6.370	6.300	9.529	3.08
7.907	7.333	5.479	2.416	18.42	8.841	3.09
			In 34 wt% dioxan			
15.37	14.75	12.52	2.727	21.07	11.24	3.34
15.37	3.689	3.556	11.79	1.090	10.64	3.44
7.715	4.373	4.061	3.706	3.640	8.046	3.48
6.173	4.373	4.051	2.248	4.480	7.350	3.60
4.630	4.373	3.821	1.033	7.760	6.490	3.68
			In 67 wt% dioxan			
4.672	4.413	3.895	0.9171	6.781	6.670	3.81
4.672	4.413	3.895	0.9171	6.781	22.78	3.81
4.672	10.59	4.602	0.1401	60.58	21.98	3.74

*Values for $[HNO_2]$ and for $[NO_2^-]$ were calculated from the absorption spectrum of the corresponding acidified nitrite solution, via

$$A = \varepsilon_1 c_1 l + \varepsilon_2 c_2 l$$

and the values for $[H^+]$ were then calculated from

$$[H^+] = [Cl^-]_0 + [NO_2^-] - [Na^+]_0$$

†$F(I) = [I^{1/2}/(1 + I^{1/2})] - 0.25I$.

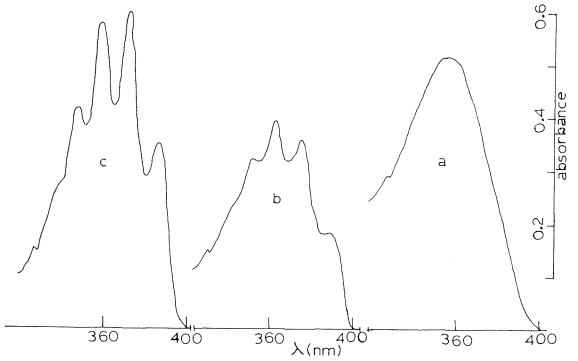


FIG. 1. Absorption spectra of N(III) in different acidic aqueous media: (*a*) 2.248 × 10^{-2} mol dm^{-3} $NaNO_2$; (*b*) 1.124 × 10^{-2} mol dm^{-3} $NaNO_2$ + 5.50 × 10^{-3} mol dm^{-3} HCl; (*c*) 1.124 × 10^{-2} mol dm^{-3} $NaNO_2$ + 5.50 × 10^{-2} mol dm^{-3} HCl.

the strongest absorption appears to lie at 372 nm in water while the corresponding peak is at 373 nm in 34 wt% dioxan and at 374 nm in 67 wt% dioxan.

Determined values for the molar absorption coefficients (ε) of nitrite and of nitrous acid in the three media are listed in Table 2. The values for ε of HNO_2 were determined by recording the spectra of solutions of NO_2^- containing excess HCl in the region 400–310 nm at timed intervals after acidification (Fig. 1). The absorption values (A) at the desired wavelength were then plotted vs. time and the curve was extrapolated to $t = 0$ to yield (A_0) corresponding to the initial concentration of the acid. This was done to minimize errors due to the loss of HNO_2 through decomposition. Table 3 gives the values for pK_I of nitrous acid in the three media. These values were calculated by

$$pK_I = -\log [H^+][NO_2^-]/[HNO_2]$$

where K_I is the concentration equilibrium constant at the ionic strength I.

The confidence in the technique adopted for the determination of K_I of HNO_2 is justified because the average value 3.08_5 for pK_I in aqueous solution (Table 3) compares favourably with 3.05 obtained through the equation of Tumavuori and Lumme (7). This equation has been used in the calculation of pK_I of the acid in water solutions at any I required in the present work. Furthermore, the same technique was used to determine pK_I of benzoic acid in

Can. J. Chem. Downloaded from www.nrcresearchpress.com by 210.87.254.6 on 09/05/12
For personal use only.

Can. J. Chem. Downloaded from www.nrcresearchpress.com by 210.87.254.6 on 09/05/12
For personal use only.

TABLE 4. Mean values of k_3 at 25°C and I = 0.033 mol dm^{-3}

Reaction medium	k_3 (dm^6 mol^{-2} s^{-1})
Water	2.32±0.07
34 wt% dioxan	3.58±0.11
67 wt% dioxan	14.34±0.27

TABLE 5

(*a*) Initial concentrations

Medium	10^4[HNO_2] (mol dm^{-3})	10^3[$KClO_3$] (mol dm^{-3})	10^2[H^+] (mol dm^{-3})
Water	3.646	6.587	1.782
34 wt% dioxan	4.538	8.304	1.930
67 wt% dioxan	3.486	4.109	8.881

(*b*) Effect of temperature on rate constant at I = 0.03 mol dm^{-3}

T (°C)	k_3 (dm^6 mol^{-2} s^{-1}) In water	In 34 wt% dioxan	In 67 wt% dioxan
10	0.60	—	5.15
15	0.97	1.47	—
20	1.55	2.41	10.8
25	2.42	3.74	14.93
30	4.00	6.00	21.73
35	6.18	8.73	31.18
40	9.52	12.52	46.32

close agreement with the literature value of 4.16. In 25 wt% dioxan a value for pK_I of benzoic acid of 4.6 (average of four experiments) also compares well with the results of Lynch and LaMer (8).

The rate of reaction between N(III) and Cl(V), in each solvent, at constant T and I (maintained by $NaNO_3$), may be represented by

$$-\mathrm{d[N(III)]}/\mathrm{d}t = k_3[HNO_2][ClO_3^-][H^+]$$

which is the same rate equation reported for this reaction when studied in aqueous buffered solutions (1, 2). The mean (± standard deviation) values of the rate constant, k_3, in the three media are shown in Table 4. These values were calculated by the above rate equation, at various concentrations of reactants at 25°C.[2]

Application of the Arrhenius relation on the effect of variation of temperature, at constant I, upon the rate of reaction, in each solvent (see Table 5) produced the following values for the activation energy of the reaction between N(III) and Cl(V): in aqueous media, 68.3 kJ mol^{-1}; in 34 wt% dioxan, 64.3 kJ mol^{-1}; in 67 wt% dioxan, 59.0 kJ mol^{-1}. These results indicate that the higher value for activation energy is obtained in the more polar medium (9).

[2]Details of the range of concentrations of reactants and the values of initial rates in each medium may be obtained, at a nominal charge, from the Depository of Unpublished Data, CISTI, National Research Council of Canada, Ottawa, Ont., Canada K1A 0S2.

Discussion

Basically, the kinetic observations of the reaction in aqueous buffered and in aqueous non-buffered acidic solutions are similar. A mechanism of the reaction has been proposed (2) to proceed through the formation of an overall equilibria producing the complex H_2NClO_5 as

[1*a*] $H^+ + HNO_2 + ClO_3^-$

[1*b*] $H^+ + HNClO_5^-$ ⇌ H_2NClO_5

[1*c*] $H_2NO_2^+ + ClO_3^-$

[1*d*] $HNO_2 + HClO_3$

followed by overall transformations,

[2] $H_2NClO_5 \xrightarrow{\text{r.d.s.}} NO_3^- + ClO_2^- + 2H^+$

[3] $ClO_2^- + HNO_2 \longrightarrow NO_3^- + ClO^- + H^+$

[4] $ClO^- + HNO_2 \longrightarrow NO_3^- + Cl^- + H^+$

The last two preequilibria steps ([1*c*] and [1*d*]) seem worth consideration as mechanistic steps because each is a two-body collision and definite concentrations of $H_2NO_2^+$ and $HClO_3$ could be maintained proportional to HNO_2 and ClO_3^- respectively in an acidic solution containing both species. The electron transfer in the oxidation process, as represented by the above schemes, probably takes place in the activated complex, and the electron transfer might be virtually uninfluenced by the medium.

The dependence of the rate of reaction on the dielectric constant (D) of the medium is governed by

$$\ln k = \ln k_0 - Nz_a z_b e^2/DRTr$$

which predicts a linear plot of ln k vs. $1/D$ with a positive slope for oppositely charged ions. Figure 2 shows the linearity produced by plotting ln k_3 vs. $1/D$ as obtained in the present study. The straight line has a positive slope and the value of k_3 at $D = \infty$ is 1.35 dm^6 mol^{-2} s^{-1}.

It has been observed (10) that water–dioxan mixtures should be more basic than water, so that an intrinsic increase in the dissociation constant of a weak acid (such as HNO_2) as dioxan is increased in the mixture is expected. However, it is also important to consider the relatively large effects of solvation and whilst all the species, HNO_2, H^+, and

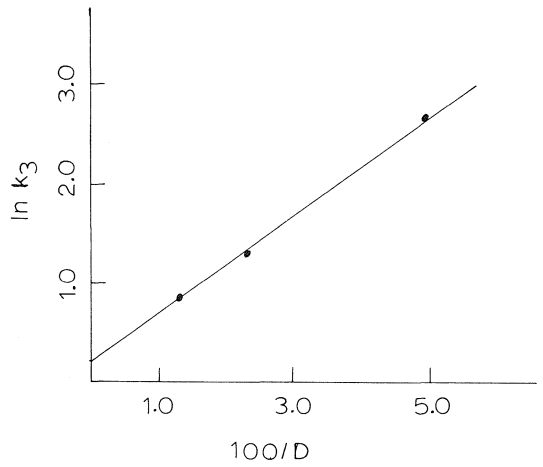


FIG. 2. Relation between the rate constant of reaction and the dielectric constant of medium.

NO_2^- have sites which can interact with the oxygen or hydrogen atoms of the solvent, the ionic species are undoubtedly the more involved in solvation. This selective effect should act to lower the dissociation constant as dioxan is increased. The diminution in volume observed when water is mixed with dioxan implies an appreciable interaction between the two components of the solvent, thus ions would be in competition with dioxan for water. Hence, at the outset, it is not at all clear how change of solvent would affect the concentration of HNO_2.

Variation in D from 80 to 20 has little effect on rate. The involvement of several preequilibria prior to the rate determining step makes it difficult to use the effect of variation of the dielectric constant of the medium in a unique way to pin-point the species actually interacting to produce the activated complex. Thus, supposing

$$H_2NO_2^+ + ClO_3^- \rightleftharpoons H_2NClO_5$$

represents the detail, where this step would be enhanced by a fall in D as is observed, but, for example,

$$H^+ + HNClO_5^- \rightleftharpoons H_2NClO_5$$

has the same charge characteristics and therefore would not be eliminated by the observations.

It has already been established that $2H^+$, NO_2^-, and ClO_3^- are in overall equilibrium with the activated complex. One H^+ is required for the protonation of NO_2^- and a second is mechanistically required per activated complex. This second H^+ would be more freely available in the more basic solvent. However, the major identified feature of the present work is a rise in pK of HNO_2 (rather as expected) leading to a rise in $[HNO_2]$, coupled with a rise in the overall rate constant. The rise in rate constant has been calculated for the "actually existing" reactant species.

Acknowledgement

The author is indebted to Dr. K. E. Howlett for his continuous encouragement, advice, and assistance in the experimental design and discussion of the results.

1. J. O. EDWARDS. Chem. Rev. **50**, 455 (1952).
2. M. M. ABDUL-JAWAD. Ph.D. Thesis, Bedford College, London. 1974.
3. E. S. AMIS. J. Chem. Educ. **28**, 635 (1951).
4. G. AKERLOF and O. A. SHORT. J. Am. Chem. Soc. **58**, 1241 (1936).
5. N. F. KERSHAW and N. S. CHAMBERLIN. Ind. Eng. Chem. Anal. Ed. **14**, 312 (1942).
6. J. V. L. LONGSTAF and K. SINGER. J. Chem. Soc. 2604 (1954).
7. J. TUMAVUORI and P. J. LUMME. Acta Chem. Scand. **22**, 2003 (1968).
8. C. C. LYNCH and V. K. LAMER. J. Am. Chem. Soc. **60**, 1252 (1938).
9. A. A. FROST and R. G. PEARSON. Kinetics and mechanism. John Wiley and Sons, NY. 1961. p. 139.
10. D. FEAKINS. Physico-chemical progress in mixed aqueous solvents. *Edited by* F. Franks. Heinemann, London. 1967. p. 71.

Can. J. Chem. Downloaded from www.nrcresearchpress.com by 210.87.254.6 on 09/05/12
For personal use only.

The dynamic structure of acenaphthalene in the solid state: pulse nuclear magnetic resonance measurements[1,2]

W. E. SANFORD,[3] G. J. KUPFERSCHMIDT, C. A. FYFE, AND R. K. BOYD

Guelph–Waterloo Centre for Graduate Work in Chemistry, Guelph Campus, University of Guelph, Guelph, Ont., Canada N1G 2W1

AND

J. A. RIPMEESTER

Division of Chemistry, National Research Council of Canada, Ottawa, Ont., Canada K1A 0R9

Received July 12, 1979[4]

W. E. SANFORD, G. J. KUPFERSCHMIDT, C. A. FYFE, R. K. BOYD, and J. A. RIPMEESTER. Can. J. Chem. **58**, 906 (1980).

Pulse nmr has been used to determine the temperature dependence of T_1 at 9.2, 18, and 60 MHz and also $T_{1\rho}$ at 9.2 MHz and T_{1D} at 18 MHz, for the proton resonance of solid acenaphthalene. The data indicate a discontinuity at ~130 K, coincident with the main thermal anomaly in the specific heat curve, and suggest the occurrence of two distinct molecular motions with activation energies 14.2 kJ mol^{-1} and 18.9 kJ mol^{-1}. Calculations using non-bonded atom–atom potential functions explain qualitatively the results of the nmr study and it is suggested that the two motional processes may be due to two sets of crystallographically different acenaphthalene molecules.

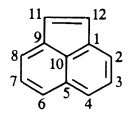
W. E. SANFORD, G. J. KUPFERSCHMIDT, C. A. FYFE, R. K. BOYD et J. A. RIPMEESTER. Can. J. Chem. **58**, 906 (1980).

On a utilisé la rmn à impulsion pour déterminer l'effet de la température sur T_1, à 9.2, 18 et 60 MHz et également sur $T_{1\rho}$ à 9.2 MHz et sur T_{1D} à 18 MHz dans le cas de la résonance du proton de l'acénaphtalène solide. Les données indiquent une discontinuité à ~ 130 K coincidant avec la principale anomalie thermique dans la courbe de chaleur spécifique et suggère l'existence de deux mouvements moléculaires distincts avec des énergies d'activation de 14.2 et 18.9 kJ mol^{-1}. Les calculs utilisant les fonctions de potentiel atome–atome non liés expliquent qualitativement les résultats de l'étude de rmn et on suggère que les deux mouvements peuvent être dus à deux ensembles de molécules d'acénaphtalène différents du point de vue cristallographique.

[Traduit par le journal]

Introduction

Acenaphthalene (**1**) was chosen for study because previous wide-line nmr investigations (1) indicated that an in-plane motion of the molecules occurred in the solid state at about 130 K (on an nmr timescale). Since the molecule has no symmetry axis for in-plane motions, any motion must involve disorder. The wide-line nmr results rule out motion about a two-fold axis, and the disorder introduced must be extreme. This is confirmed by the lack of success of



1

attempted investigations of the room-temperature structure by X-ray diffraction techniques (2–4). A low temperature structure (85 K) was determined by Wellberry (5) using film data. There were two quite different sites for the molecules in the low temperature structure, and a phase transition was indicated from photographs to occur at about 130 K. However, even knowing the low-temperature structure, it was not possible to unambiguously determine the room-temperature structure (5).

The purpose of the present work was to obtain more quantitative data concerning the motion of the acenaphthalene molecules in the solid state and, if possible, to relate these data to the low-temperature X-ray structure of Wellberry (5). The relaxation times of nuclei in the solid state are very sensitive to the presence of molecular motions, as these provide a relaxation mechanism for the nuclear spins. Furthermore, the temperature dependence of the nuclear relaxation times may be quantitatively related to the activation energy for the reorientation process (6). In the present work we have investigated the temperature dependence of T_1 (the spin–lattice relaxation time) at several frequencies, $T_{1\rho}$ (the spin–lattice relaxation time in the rotating frame) and T_{1D} (the dipolar relaxation time). The quantitative description of these parameters and their relationships to each other will be described in detail in the text.

Also, we have recently found it possible to predict the barriers to rotation in molecular solids using the crystal structure and non-bonded atom–atom potential functions to describe the lattice energy. The

[1]NRCC No. 18125.

[2]Taken in part from the M.Sc. thesis of W. E. Sanford, University of Guelph, 1975.

[3]Present address: Mohawk College of Applied Arts and Technology, Department of Chemistry, 135 Fennell Avenue West, Hamilton, Ont., Canada L8N 3T2.

[4]Revision received February 5, 1980.

0008-4042/80/090906-07$01.00/0

©1980 National Research Council of Canada/Conseil national de recherches du Canada

Can. J. Chem. Downloaded from www.nrcresearchpress.com by 210.87.254.105 on 09/05/12
For personal use only.

Can. J. Chem. Downloaded from www.nrcresearchpress.com by 210.87.254.105 on 09/05/12
For personal use only.

approach has had some success for planar aromatic compounds (7), cage-like aliphatic compounds (8), adamantane and hexamethylenetetramine (9), and several planar heterocyclic molecules (10–12). In the case of admantane it was possible to deduce a molecular mechanism for the order–disorder process which occurs in the solid (9). We have employed these calculations in the present work to attempt to relate the results of the relaxation time measurements to the low-temperature X-ray structure.

Experimental

Acenaphthalene was purified as previously described (1). Pulse nmr measurements were made at 18.0 MHz using a home-built spectrometer (10) and at 60 and 9.2 MHz using a Bruker SXP variable frequency spectrometer. Each separate relaxation time was obtained from a least-squares fit to the appropriate experimental data. Calculations of the theoretical temperature dependence of the different relaxation times and of the lattice energies were performed using Fortran IV programs written by the authors.

Results and Discussion

A. Spin–Lattice Relaxation Time Measurements

The effect of a single motion process on the spin–lattice relaxation time of a nucleus is described by eq. [1]

$$[1] \quad \frac{1}{T_1} = C\left[\frac{\tau_c}{1 + \omega_0^2\tau_c^2} + \frac{4\tau_c}{1 + 4\omega_0^2\tau_c^2}\right]$$

where ω_0 is the frequency of measurement, τ_c is the characteristic correlation time of the motion, and C is a constant characteristic of the motion (6, 13).

If the correlation times for the motional process obey an Arrhenius-type temperature dependence, eq. [2], the temperature dependence of T_1 may be related to an activation energy for the motional process (6, 13):

$$[2] \quad \tau_c = \tau_0 e^{-E_a/RT}$$

Thus a plot of log T_1 vs. $1/T$ should yield a "V" shaped curve with a minimum where $\omega_0\tau_c = 0.62$ and with limiting low- and high-temperature slopes equal to E_a/R and $-E_a/R$, respectively. As the frequency of measurement is increased, the minimum in the curve which occurs when $\omega_0\tau_c = 0.62$ will shift to higher temperature, and measurements at a series of frequencies will yield a series of curves with different minima which are all coincident when $\omega_0\tau_c \ll 1$ at high temperatures. Often, if a minimum is not found at one frequency, it may be observed by making measurements at another.

The spin–lattice relation times of acenaphthalene have been measured over the temperature range 100 to 290 K at 9.2, 18, and 60 MHz and are shown in Fig. 1. As can be seen from Fig. 1, all vary markedly with temperature, confirming the conclusion of the previous wide-line nmr investigation (1) that motion of the acenaphthalene molecules is occurring. However, the situation is more complex than the case of a single, simple motional process discussed above. There is evidence in each set of measurements of a discontinuity at 130 K which coincides with the major thermodynamic transition recently observed (14, 15). The T_1 curves are not simple "V" shapes, but indicate two distinct minima, seen most clearly in the 60 MHz curve where both minima lie on the high temperature side of the discontinuity. The data thus qualitatively suggest the possibility that supercooling of a high temperature phase, or some similar lack of thermal equilibration, might give rise to a false second minimum. This possibility was investigated by rapidly cooling the sample to 129 K, then warming it rapidly to 273 K. At both temperatures the results of the T_1 measurements were the same as those obtained previously using precautions to ensure thermal equilibration.

B. $T_{1\rho}$ and T_{1D} Measurements

For a single motional process, $T_{1\rho}$ is defined (16)

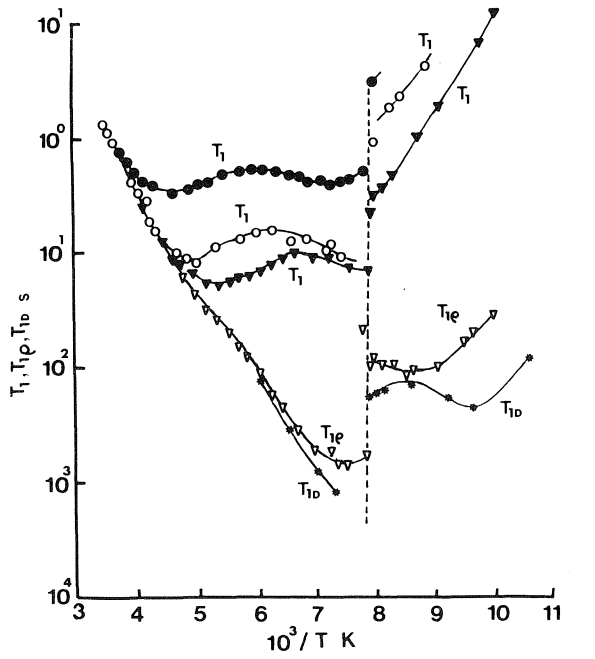


FIG. 1. Experimental temperature dependence of T_1 at 9.2 MHz ●; 18.0 MHz ○; and 60.0 MHz ▼; and of $T_{1\rho}$ at 9.2 MHz ▽; and of T_{1D} at 18.0 MHz *, for the proton resonance of acenaphthalene in the solid state. The curves indicated in the figure are for clarity only. Vertical dashed line corresponds to phase transition at 130 K.

Can. J. Chem. Downloaded from www.nrcresearchpress.com by 210.87.254.105 on 09/05/12
For personal use only.

as in eq. [3]:

$$[3] \quad \frac{1}{T_{1\rho}} = C\left[\frac{5}{2}\frac{\tau_c}{1+\omega_0^2\tau_c^2} + \frac{\tau_c}{1+4\omega_0^2\tau_c^2} + \frac{3}{2}\frac{\tau_c}{1+\omega_1^2\tau_c^2}\right]$$

H_1 is typically of the order of 1–50 G. A plot $T_{1\rho}$ vs. $1/T$ is again a "V" shaped curve, but the $T_{1\rho}$ minimum occurs when $\omega_1\tau_c = 0.5$ (usually in the same temperature region as the C.W. nmr line-narrowing transition). The temperature dependence of T_{1D} is less well described than that of T_1 or $T_{1\rho}$. In the high-temperature limit, it is described (17) by an equation similar to that for $T_{1\rho}$ (eq. [4*a*]),

$$[4a] \quad \frac{1}{T_{1D}} = C_1\left[\frac{\tau_c}{1+\omega_0^2\tau_c^2} + C_2\frac{\tau_c}{1+4\omega_0^2\tau_c^2}\right] + C_3\tau_c$$

where C_1, C_2, C_3 are constants dependent on the strength of the dipolar interaction. Evaluation of these constants experimentally is difficult. In the low temperature limit ($\tau_c > T_2$), the relaxation may be described (18) by eq. [4*b*]:

$$[4b] \quad \frac{1}{T_{1D}} = \frac{2(1-P)}{\tau_c}$$

where $(1 - P)$ is a geometrical parameter which accounts for any correlation in the local fields before and after the motion has occurred. The behaviour of T_{1D} in the transition region between these two limiting situations, i.e., at the minimum in the log T_{1D} vs. $1/T$ curve, is much less well understood.

Thus, both $T_{1\rho}$ and T_{1D} are more sensitive to low frequency motions than is T_1, and were measured, particularly in the region of the transition, to see if they could provide additional information about the motional processes. These data are shown also in Fig. 1. The data are consistent with the T_1 results, coinciding with them in the high temperature limit (Fig. 1). Both curves show two minima; that corresponding to the low energy occurs at temperatures below the temperature of the main heat capacity anomaly.

Qualitatively, these data indicate that there are two distinct motional processes occurring in the acenaphthalene crystal, since two distinct minima are apparent in Fig. 1. If just one unique motion were occurring, the theory predicts a single minimum in the curve for each different relaxation time (Fig. 1).

C. Analysis of the Relaxation Time Data in Terms of Two Motional Processes

The present analysis is based on the assumption that the spin exchange is fast enough to average the relaxation due to the two processes and that the relaxtion of all ^1H nuclei in the sample can be described by a single exponential (as is observed within experimental error), with a time constant given by eq. [5]:

$$[5] \quad \frac{1}{T_{1\ \mathrm{obs}}} = \frac{f_a}{T_1(a)} + \frac{f_b}{T_1(b)}$$

where $T_1(a)$ and $T_1(b)$ are the relaxation times of the nuclei due to the two motional processes if they occurred alone, and f_a and f_b are the relative fractions of nuclei participating in the two processes (19, 20). Both $T_{1(a)}$ and $T_{1(b)}$ have the form indicated in eq. [1] and are characterized by unique correlation times $\tau_c(a)$ and $\tau_c(b)$.

Similarly, $T_{1\rho}$ may be defined as in eq. [6] where $T_{1\rho(a)}$ and $T_{1\rho(b)}$ are each defined as in eq. [3]:

$$[6] \quad \frac{1}{T_{1\rho}} = \frac{f_a}{T_{1\rho(a)}} + \frac{f_b}{T_{1\rho(b)}}$$

Since the theory for T_{1D} in the region of the transition is ill defined, the T_{1D} data have not been quantitatively interpreted.

Figure 2 shows the complete experimental results of the T_1 and $T_{1\rho}$ measurements together with the theoretical curves calculation using eqs. [5] and [6] and assuming that $f_a = f_b$; the values used for the parameters relating to the two motions are given in Table 1. A reasonable fit to the experimental data is found (Fig. 2). The model yields activation energies of 14.2 kJ mol^{-1} and 18.9 kJ mol^{-1} for the two motions and adequately accounts for all the high temperature experimental results for T_1 at different frequencies and also the $T_{1\rho}$ and T_{1D} data, i.e., it explains the high energy motion quite well. The low temperature portion of each curve down to the discontinuity is also well fitted. However, the region of the curve between the two minima is fitted much less well, the experimental separation of the two minima being much less complete than predicted. This could be caused by a distribution of correlation times, mainly in the low energy motion, which arise from the same general type of motion with a distribution of energies and environments within the sample. This would result in the minimum due to the low energy motion being broader and flatter than predicted by eqs. [1] and [3]. This effect would be carried over into eqs. [5] and [6] and the agreement between the observed and calculated data would improve. This type of fitting was not attempted, as it was felt that it would not add significantly to the phycial understanding of the problem and that the estimates of the activation energies were in general adequate without this additional parametrization.

Can. J. Chem. Downloaded from www.nrcresearchpress.com by 210.87.254.105 on 09/05/12
For personal use only.

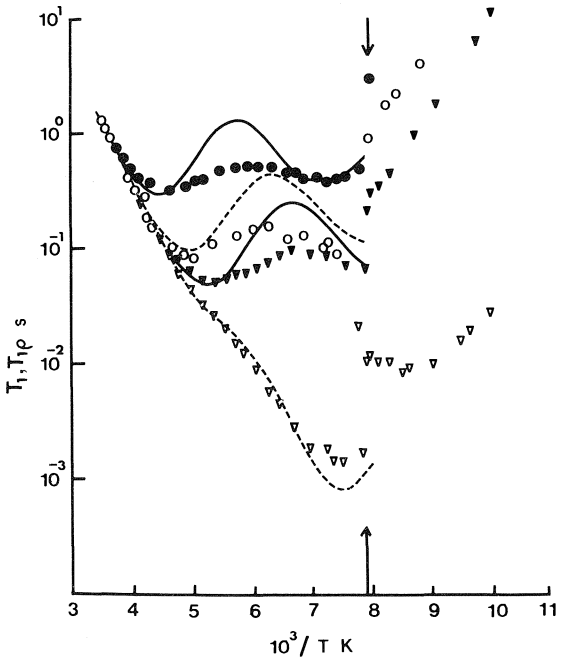


FIG. 2. Experimental temperature dependence of T_1 at 9.2, 18.0, and 60.0 MHz and of $T_{1\rho}$ at 9.2 MHz for the proton resonance of acenaphthalene in the solid state together with the theoretical temperature dependencies of these parameters (solid curves) calculated using the parameters given in Table 1.

TABLE 1. Parameters used to compute the theoretical T_1 and $T_{1\rho}$ curves from application of eqs. [1], [2], [3], and [5] with $f_a = f_b$ in eq. [5]

	E_a (kJ mol^{-1})	τ_0 (s)	C (s^{-2})
Motion 1	14.2	0.65×10^{-14}	0.7×10^9
Motion 2	18.9	0.70×10^{-13}	0.82×10^9

Thus, the relaxation time data indicate the occurrence of two different types of motions in solid acenaphthalene with similar activation energies. One further piece of information may be extracted from these data concerning the general nature of these two motional processes. The two minima occur at approximately the same values of T_1 (seen best in the 60 MHz T_1 data in Fig. 2). This is reflected in the similarity of the constants C (Table 1) for the two processes. C may be related to the change in the intermolecular contribution to the second moment (ΔSM) as in eq. [7]:

$$[7] \quad C = (2/3)\gamma^2\Delta\mathrm{SM}$$

Thus the two motional processes must cause similar reductions in the second moment. One situation which would fit this requirement would be the existence of two crystallographically different types of acenaphthalene molecules in the lattice, which could undergo very similar motions. These motions would be such as to cause similar reductions in the intermolecular contribution to the second moment, but would have slightly different energy barriers. Such a situation has indeed been reported by Wellberry (5) for the low temperature phase of this molecule, and it may be that each of the disordering motions involves half of the molecules in the lattice.

An alternative explanation of the relaxation-time data is that each of the two motional processes detected may each be due to just one quarter of the molecules, the remaining one-half of the molecules moving too quickly for their motion to be detected by the relaxation-time data (i.e., $\omega_0\tau_c \ll 1$ just above the transition). This explanation gives better agreement with the absolute values of the reduced second moments from the C.W. nmr study (eq. [7]). In this case, the activation energies for the two observed motions would be given as in Table 1, and the remaining molecules would move with activation energies less than 8 kJ mol^{-1}.

D. Potential Energy Calculations of the Rotational Barriers in Solid Acenaphthalene

As indicated in the Introduction, these calculations have been successful in a number of instances in predicting the barriers to rotation in molecular solids. Calculations have been performed on acenaphthalene using the low temperature crystal structure data of Wellberry (5) to investigate firstly if there are different barriers for crystallographically different acenaphthalene molecules as indicated by the nmr data above, and secondly, to try to predict the number of sites for each molecule in the high temperature phase. The previous C.W. nmr investigations (1) ruled out the possibility of the motion being about a two-fold axis as this would not average the intramolecular contribution to the second moment.

The low-temperature structure found at 85 K is an ordered structure with eight molecules per unit cell, involving four crystallographically different types labelled A, B, C, D packed in the characteristic "herring bone" type of arrangement. The lattice sites of the A and B molecules are similar as are those of the C and D molecules. The model for the calculations was exactly as described previously and the interatomic potentials used were the "exp-6" type (eq. [8]).

$$[8] \quad V_{ij} = -A/r_{ij}^6 + B\exp C/r_{ij}$$

The parameters A, B, C for each of the interatomic interactions H$\cdots$H, H$\cdots$C, and C$\cdots$C were taken from the work of Williams (21).

The inspection of the experimental atomic co-ordinates (5) revealed that the molecules were all non-planar and quite non-symmetric except where re-

Can. J. Chem. Downloaded from www.nrcresearchpress.com by 210.87.254.105 on 09/05/12
For personal use only.

quired by the space group. In the absence of any gas-phase data on the molecular structure, idealized molecules were generated using the best defined molecule from the X-ray data. It was thought that the type "C" molecule, apart from its slight non-planarity, was the most reasonable approximation to the true structure. This molecule was made exactly planar, the other molecules generated from it and the hydrogen atoms generated 1.08 Å on each carbon such that the C—H vector bisected the C—C—C angle of the central carbon to which it was attached.

The sublimation energy for the low temperature lattice was calculated to be 86.2 kJ mol^{-1}, in reasonable agreement with the experimental value of 71.2 kJ mol^{-1} (high temperature form). Calculations were then performed in which the test acenaphthalene molecule was rotated around a chosen axis and the potential between it and the lattice evaluated as a function of rotation angle, the rest of the molecules in the lattice being kept fixed at their positions of minimum potential. Several qualitative conclusions may be drawn from the initial calculations. Firstly, the rotation of the molecules must be in their molecular planes and, secondly, the axis for the rotation must be through the centre of gravity of the molecule which is approximately C_{10}. All other choices of axis gave rotation potentials which quickly became extremely repulsive.

The calculated potential energies of each of an A, B, C, and D molecule (5), as a function of angle of in-plane rotation, are shown in Fig. 3. The A and B molecules are quite similar to one another in this respect, and are qualitatively different from the C and D molecules which have much lower barriers to in-plane rotation. This qualitative finding is promising, in view of the conclusions drawn above from the nmr results. However, the quantitative results are unfortunately ambiguous. The energy barrier to rotation is *twice* the difference between peaks and valleys in the profiles of Fig. 3, (22, 23). The predicted energy barriers for A, B, and C or D molecules are thus 40–60 kJ mol^{-1}, and <20 kJ mol^{-1} respectively, appreciably higher than the experimentavalues (Table 1). The potential parameters used in the calculations (21) were those with the "hard" repulsive contributions. The calculated energy barriers could be lowered somewhat through use of an alternative parametrization incorporating "soft" repulsions, now thought (23) to be superior. However, even this would not resolve the ambiguity in the interpretation of the nmr data, viz. do the two motions observed correspond to the motion of first half of the molecules (probably C and D) followed at higher temperatures by the other half (A and B), or are one-half of the molecules (C plus D) already

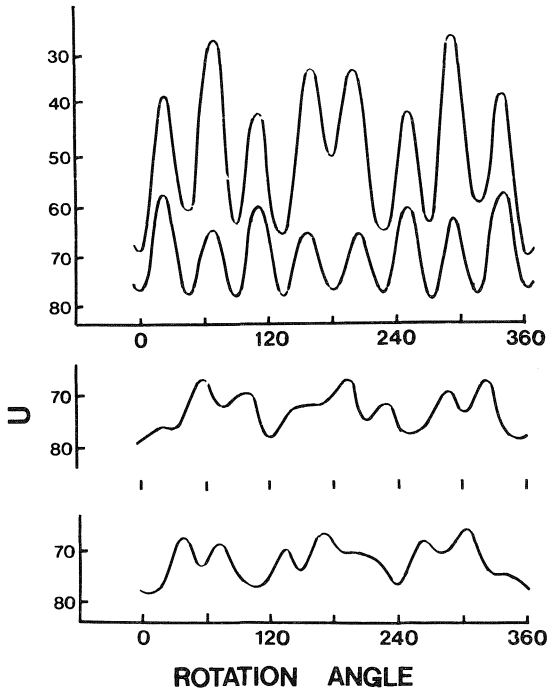


FIG. 3. Calculated potential energy curves for the movement of an acenaphthalene molecule in its molecular plane. From top to bottom, types A, B, C, D molecules as given in the low temperature crystal structure (5). U (kJ mol^{-1}) is lattice sum for a central molecule calculated using atom–atom approximation (7). Minima correspond to sublimation energy, and differences between maxima and minima to *half* the activation energy (22, 23).

in motion at the lowest temperature available (Fig. 2), and the two *observed* motions due to first the B and at higher temperatures the A molecules moving on the nmr timescale?

Even the effective order of the axis around which the molecules move is unclear from these calculations. For each molecule there are a number of minima which occur during the rotation, but it was felt that small differences between these could be critical in determing the order of the axis of rotation. Due to inadequacies in the model (correlated motions may well be important in determining the disordered structure), and more importantly in the present case, in the atomic coordinates, the calculations could not be considered to be of sufficient accuracy to be used for this purpose. It is thought, however, that if an accurate low-temperature structure becomes available that calculations of this type would then be useful for determining the order of the rotation axis and thus in predicting the nature of the room-temperature structure. The available experimental evidence on the nature of the disorder axis is that the wide-line nmr results (1) rule out a two-fold axis, and

Can. J. Chem. Downloaded from www.nrcresearchpress.com by 210.87.254.105 on 09/05/12
For personal use only.

recent calorimetric results (14, 15) yield a total entropy change corresponding to $R \ln 4$ for the transition region. In one of these studies (15) the transition region was consistent with a contribution from two transitions, each corresponding to $\Delta S = R \ln 2$. This is in agreement with a situation where half of the molecules (presumably C and D) move around a four-fold axis at lower temperatures followed by the other half (A and B), also around a four-fold axis, at higher temperatures.

One other comparison between the experimental results (Fig. 1) and the potential energy calculations (Fig. 3) seems capable of providing some additional insight. The observation of the $T_{1\rho}$ and T_{1D} minima, at temperatures below the phase transition at about 130 K, clearly indicates the existence of a large-amplitude motion in the low-temperature phase, as discussed above. These minima are relatively shallow, a factor of ~ 8 more so than the corresponding minima observed for the high-temperature phase.

One possible explanation for this qualitative difference could involve the participation of motion between inequivalent sites, in the case of the low-temperature phase (Fig. 3). It is known (24–26) that motion between inequivalent sites (i.e. "non-random" motion (24–26)) tends to decrease the relaxation efficiency. It can be shown that, for a simplified two-site model:

$$\frac{T_1(\text{min}) \text{ for random motion}}{T_1(\text{min}) \text{ for non-random motion}} = \frac{4 \exp(\Delta E/RT)]^2}{[1 + \exp(\Delta E/RT)}$$

where ΔE is the energy difference between the two sites (potential energy minima). On the basis of this admittedly over-simplified model, ΔE must be about 0.8 kcal mol^{-1} to account for the difference in the two $T_{1\rho}$ minima (Fig. 1), if the entire difference is ascribed to this effect operating in the low temperature phase only. This suggestion seems to be qualitatively in agreement with the calculated potential energy profiles (Fig. 3). The statistical population of such sites (about 5% at 130 K) could readily have been missed in the X-ray diffraction experiments of Welberry (5).

Conclusions

The pulse nmr investigation of the dynamic structure of acenaphthalene has made more quantitative our understanding of the order–disorder phase transition, clearly identifying two separate motional processes of activation energies 14.2 kJ mol^{-1} and 18.9 kJ mol^{-1}. These are tentatively assigned to the motion of two sets of acenaphthalene molecules in crystallographically different sites in the crystal. Studies of molecular motion in crystalline acenapthalene have also been made via dielectric measurements, and yield results in good general agreement with the present nmr data (27).

Investigation of the disordering by potential energy calculations has met with only limited success. Qualitatively the axis of rotation has been determined and the molecules in the unit cell appear to fall into two groups in terms of their barriers to rotation. However, it is felt that the results are not accurate enough to permit the determination of the order of the disordering axis due to the inadequate nature of the atomic co-ordinates. It is suggested that a redetermination of the low temperature structure be made and also a determination of the disordered structure just above the phase transition where the room-temperature disorder will exist, but the real thermal errors may be low enought to permit the complete determination of the structure in high temperature phase.

Acknowledgments

The authors wish to acknowledge the financial assistance of the National Research Council of Canada in personal research grants (R.K.B., C.A.F.) and the award of a National Research Council Scholarship (W.E.S.). They also thank the Province of Ontario for the award of a scholarship (G.J.K.) and the Research Advisory Board of the University of Guelph. They acknowledge the help of D. Sproat and A. Hays in the construction of one of the pulse spectrometers used in this study.

1. C. A. FYFE and G. J. KUPFERSCHMIDT. Mol. Cryst. Liquid Cryst. **28**, 179 (1975).
2. M. D. COHEN, I. RON, G. M. SCHMIDT, and J. M. THOMAS. Nature London, **224**, 167 (1969).
3. R. D. GORDON and R. F. YANG. J. Mol. Spectrosc. **34**, 266 (1970).
4. (*a*) H. GYULA, G. KOVACS, F. CSER, and G. KOSIJTERSYITY. Magy. Kem. Foly. **77**, 11 (1971); (*b*) F. CSER. Acta Chem. Acad. Sci. Hungary, **80**, 317 (1974).
5. T. R. WELLBERRY. Proc. R. Soc. London, **334A**, 19 (1973).
6. A. ABRAGAM. Principles of magnetic resonance. Clarendon Press, Oxford. 1961. Chapt. 8.
7. R. K. BOYD, C. A. FYFE, and D. A. WRIGHT. J. Phys. Chem. Solids, **35**, 1355 (1974).
8. C. A. FYFE and D. HAROLD-SMITH. J. Chem. Soc. Faraday Trans. II, **71**, 967 (1975).
9. C. A. FYFE and D. HAROLD-SMITH. Can. J. Chem. **54**, 769 (1976).
10. W. E. SANFORD and R. K. BOYD. Can. J. Chem. **54**, 2773 (1976).
11. W. E. SANFORD, R. K. BOYD, and J. A. RIPMEESTER. Mol. Cryst. Liq. Cryst. **46**, 121 (1978).
12. J. A. RIPMEESTER and R. K. BOYD. Can. J. Chem. **57**, 128 (1979).
13. P. S. ALLEN. N.M.R. studies of molecular motion in solids.

M.T.P. International Reviews of Science, Physical Chemistry, Series 1, Vol. 4, 1972.
14. R. K. BOYD, C. A. FYFE, and D. A. WRIGHT. To be published.
15. E. F. WESTRUM, JR. Private communication.
16. (*a*) G. P. JONES. Phys. Rev. **148**, 332 (1966); (*b*) D. C. LOOK and I. J. LOWE. J. Chem. Phys. **44**, 2995 (1966).
17. R. VAN STEENWINKEL. Z. Naturforsch. **24**a, 1526 (1969).
18. C. P. SLICHTER and D. AILION. Phys. Rev. **135**A, 1526 (1964).
19. S. ALBERT, H. S. GUTOWSKY, and J. A. RIPMEESTER. J. Chem. Phys. **56**, 2844 (1972).
20. D. E. O'REILLY and T. TSANG. J. Chem. Phys. **46**, 1291 (1967).
21. D. E. WILLIAMS. J. Chem. Phys. **47**, 4680 (1967).
22. W. R. BUSING. J. Phys. Chem. Solids, **39**, 691 (1978).
23. R. K. BOYD and C. A. FYFE. J. Phys. Chem. Solids, **39**, 693 (1978).
24. D. C. LOOK and I. J. LOWER. J. Chem. Phys. **44**, 3437 (1966).
25. J. E. ANDERSON. J. Magn. Reson. **11**, 398 (1973).
26. M. POLAK and D. C. AILION. J. Chem. Phys. **67**, 3029 (1977).
27. S. R. GOUGH. Private communication.

Can. J. Chem. Downloaded from www.nrcresearchpress.com by 210.87.254.105 on 09/05/12
For personal use only.

Etude paramétrique de l'enrichissement en carbone-13 dans la décomposition polyphotonique de CF_3Cl[1]

M. GAUTHIER, C. WILLIS ET P. A. HACKETT

Groupe de photochimie laser, Division de chimie, Conseil national de recherches du Canada, Ottawa (Ont.), Canada K1A 0R6

Reçu le 21 novembre 1979

M. GAUTHIER, C. WILLIS et P. A. HACKETT. Can. J. Chem. **58**, 913 (1980).

Le rendement et la teneur en ^{13}C du produit C_2F_6 ont été mesurés suite à la décomposition polyphotonique infrarouge de CF_3Cl. On a étudié ces facteurs en fonction de la fréquence d'activation ω, de la pression P de CF_3Cl, de la température T et de l'énergie incidente E_0. Comme pour CF_3Br et CF_3I, le rendement augmente selon $P^2E_0{}^2$.

M. GAUTHIER, C. WILLIS, and P. A. HACKETT. Can. J. Chem. **58**, 913 (1980).

The yield and ^{13}C content of the product C_2F_6 were measured following the multiphoton infrared decomposition of CF_3Cl. These factors were studied as a function of the activation frequency ω, of the pressure of CF_3Cl, of the temperature T, and of the incident energy E_0. As in the case of CF_3Br and CF_3I the yield increases according to $P^2E_0{}^2$.

[Journal translation]

Can. J. Chem. Downloaded from www.nrcresearchpress.com by 210.87.254.42 on 09/05/12
For personal use only.

Introduction

L'intérêt n'a cessé de s'accroître ces dix dernières années pour les nouvelles méthodes de séparation isotopique sous rayonnement laser (1). En particulier, l'absorption sélective de la radiation intense d'un laser CO_2 par les halocarbures polarise l'attention dans la recherche d'un procédé rentable pour la séparation du ^{13}C (2, 3). Nous résumons dans cet article une étude paramétrique complète de la décomposition polyphotonique du CF_3Cl, faisant suite aux premiers résultats déjà présentés sur CF_3X, X = Cl, Br, I (4–6).

Ambartzumian et coll. (7, 8) ont d'abord montré que la décomposition du CCl_4 donne les produits C_2Cl_4 et C_2Cl_6 enrichis en ^{13}C par irradiation infrarouge de la bande $\nu_4 + \nu_1 + \nu_2$. Plusieurs halométhanes ont ensuite été étudiés pour la séparation des isotopes du carbone par la décomposition sélective des molécules contenant ^{12}C (9, 10) ou des molécules contenant l'isotope ^{13}C dont l'abondance naturelle est seulement 1.11% (2–8). Bittenson et Houston (9) ont décomposé sélectivement $^{12}CF_3I$ avec un laser CO_2 et obtiennent un "facteur de séparation" près de 600 à basse pression (0.1 Torr) et basse température (−80°C). Knyazev et coll. (10) ont aussi décomposé sélectivement $^{12}CF_3I$ mais en séparant cette fois l'activation polyphotonique sélective par un laser infrarouge de la dissociation des molécules activées par un laser ultraviolet, un processus intéressant pour la décomposition des isotopes lourds.

Nous avons déjà montré que la décomposition sélective de $^{13}CF_3Br$ par un laser infrarouge à la température ambiante donnait des facteurs de séparation encore plus grands que pour la décomposition de $^{12}CF_3I$ à basse température (4).

Le rendement et la sélectivité de la décomposition dépendent des quatre paramètres fondamentaux: la fréquence ω et la fluence F de la radiation, la pression P, et la température T de l'absorbant. De plus, la géométrie de l'irradiation détermine le domaine de fluences auquel sera soumis le gaz à décomposer et affecte les mécanismes de la décomposition (6, 11, 12).

Partie expérimentale

Montage

Le schéma du montage est représenté à la fig 1. Un cylindre en Pyrex de 5 cm de diamètre et de 18 cm de longueur est fermé à chaque bout par une fenêtre de NaCl (Harshaw Laser Grade). Le faisceau d'un laser TEA CO_2 (Lumonics, modèle 103) passe par une ouverture de 1.4 cm de diamètre pour s'assurer de prendre la partie centrale qui a une densité d'énergie uniforme et est focalisé dans la cuve par une lentille en germanium (f = 10 cm).

Pour les irradiations à basse température, nous avons utilisé une cuve modifiée de mêmes dimensions mais pourvue à l'intérieur d'un tube de Pyrex de 8 mm hélicoidal avec une dixaine de tours qui était refroidi avec un courant d'azote de débit ajustable produit de l'évaporation d'azote liquide.

L'énergie incidente et l'énergie transmise sont mesurées avec des détecteurs pyroélectriques. Dans toutes les expériences une fréquence de 40 impulsions à la minute a été utilisée.

Analyse

Le CF_3Cl (Matheson) est purifié peu avant l'utilisation par distillation à basse température jusqu'à l'élimination de toute impureté détectable au spectromètre de masse. La cuve est raccordée directement au spectromètre de masse (Hitachi Perkin-Elmer RMU-6D) et aux pressions supérieures à 0.5 Torr, on analyse les produits après avoir piégé une partie du CF_3Cl dans un bain d'isopentane à −160°C. A cette température la tension de vapeur de l'hexafluoroéthane est de 75 mTorr, bien supérieure à la quantité produite. Les rendements et les teneurs en ^{13}C sont tirés des hauteurs des pics m/e 119, 120 et 121 de l'ion $C_2F_5{}^+$. Le CF_3Cl ne contribuera en aucun cas à ces masses. L'étalonnage donne une relation linéaire entre la hauteur des

[1]CNRC No. 18087.

0008-4042/80/090913-05$01.00/0

©1980 National Research Council of Canada/Conseil national de recherches du Canada

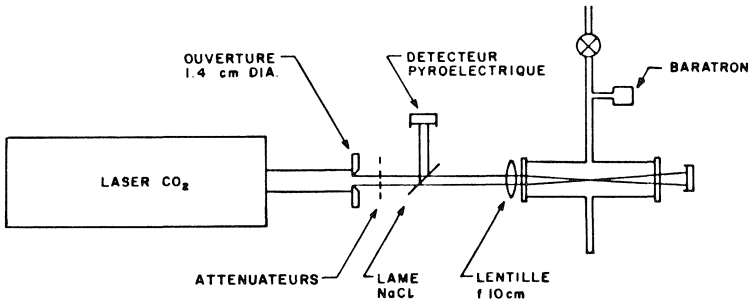


FIG. 1. Schéma du montage.

pics 119 + 120 + 121 et la pression de C_2F_6 à l'entrée du spectromètre.

La teneur en ^{13}C du produit s'exprime selon

$$[1] \quad x' = \frac{I_{121} + \frac{1}{2}I_{120}}{I_{119} + I_{120} + I_{121}}$$

Les résultats sont présentés sous la forme suivante

$$[2] \quad {}^{13}N = x'N$$

$$[3] \quad {}^{12}N = (1 - x')N$$

où N est le nombre de moles d'hexafluoroéthane produit par impulsion. Dans toutes les expériences, la décomposition est maintenue inférieure à 1% et le facteur de séparation primaire peut s'exprimer selon

$$[4] \quad \beta = \frac{x'}{x}\frac{1 - x}{1 - x'}$$

où $x = 0.0111$ est la teneur en ^{13}C du produit naturel (13).

Résultats

Comme pour CF_3Br (6), le rendement N est indépendant du nombre d'impulsions utilisé. La seule diminution observée est facilement explicable par la diminution de la pression de CF_3Cl.

Dépendance spectrale de la décomposition

Le spectre de la bande de valence ν_1 de CF_3Cl à 1106 cm^{-1} est montré à la fig. 2*a*. La bande d'absorption du $^{13}CF_3Cl$ apparaît à basse température (fig. 2*b*) avec un déplacement isotopique de 29 cm^{-1}. Une irradiation à des fréquences correspondant à cette absorption donne un produit enrichi en ^{13}C et le facteur de séparation augmente à mesure que l'absorption de $^{13}CF_3Cl$ devient prépondérante (5).

La décomposition de $^{12}CF_3Cl$ représentée par la courbe de ^{12}N à la fig. 2 diminue considérablement à mesure que la fréquence d'activation s'éloigne de la bande ν_1. Par contre la décomposition de $^{13}CF_3Cl$ passe par un maximum qui apparaît déplacé vers le rouge de 7 cm^{-1} par rapport au centre de la bande d'absorption de $^{13}CF_3Cl$ à 1077 cm^{-1}.

Pour étudier l'influence des autres paramètres, nous utiliserons une irradiation à 1077.3 cm^{-1}, correspondant au centre de la bande ν_1 de $^{13}CF_3Cl$, donc dans la région intermédiaire entre les maxima des deux spectres de décomposition des deux variétés isotopiques.

Influence de la pression

Le rendement en hexafluoroéthane en fonction de la pression apparaît à la fig. 3. Remarquons d'abord l'augmentation en P^2 pour ^{13}N aussi bien que pour ^{12}N pour la gamme de pressions utilisées. L'influence de la pression sur le facteur de séparation (qui est proportionnel à $^{13}N/^{12}N$) est moins

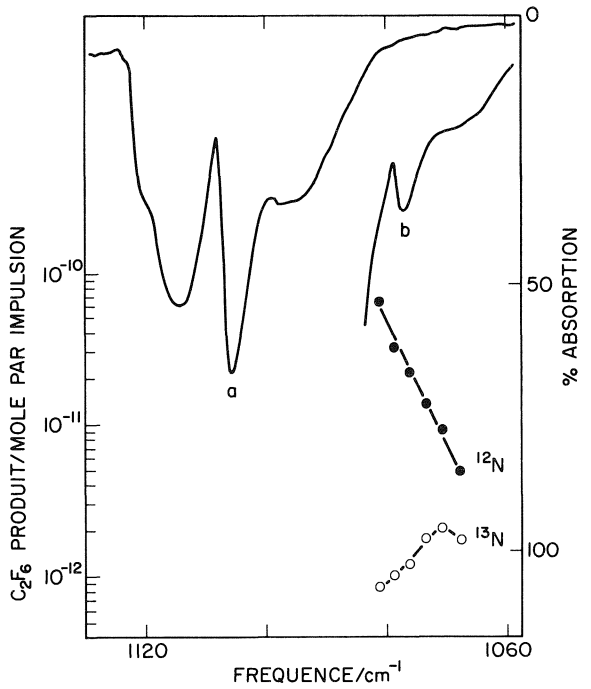


FIG. 2. Production d'hexafluoroéthane en fonction de la fréquence d'activation pour une pression de CF_3Cl de 0.5 Torr, une énergie incidente de 1.8 J et une température de 22°C. A une fréquence de 1081.1 cm^{-1}, la décomposition est pratiquement non sélective mais le facteur de séparation augmente rapidement pour atteindre $\beta = 45$ à 1067.5 cm^{-1} (5). On montre aussi les spectres d'absorption infrarouge de CF_3Cl dans une cuve de 5 cm de longueur: *a*: pression: 1.5 Torr et température: 22°C; *b*: pression: 100 Torr et température: −67°C.

Can. J. Chem. Downloaded from www.nrcresearchpress.com by 210.87.254.42 on 09/05/12
For personal use only.

Can. J. Chem. Downloaded from www.nrcresearchpress.com by 210.87.254.42 on 09/05/12
For personal use only.

importante pour CF_3Cl que pour CF_3Br (6). Bien que la pente de ^{13}N soit un peu plus faible, aucun nivellement n'est observé montrant que la réaction de mélange isotopique n'est pas importante au-dessous de 2 Torr.

[5] $^{13}CF_3 + {}^{12}CF_3Cl \rightarrow {}^{13}CF_3Cl + {}^{12}CF_3$

Qualitativement on peut donc proposer un mécanisme identique de production de l'hexafluoroéthane léger et de l'hexafluoroéthane enrichi.

Influence de l'énergie incidente

On montre à la fig. 4, l'augmentation du rendement en hexafluoroéthane en fonction de l'énergie incidente. Ce rendement en E_0^2 a été démontré clairement aussi pour CF_3Br et CF_3I. De même pour le facteur de séparation qui est indépendant de l'énergie incidente pour les trois trifluorométhanes. Comme on l'a déjà souligné (6), on n'a aucune raison de prévoir un comportement différent pour $^{13}CF_3Cl$ ou $^{12}CF_3Cl$ quant à la probabilité de décomposition en fonction de l'énergie incidente. En effet, sans qu'il soit nécessaire d'établir un modèle, par exemple un modèle géométrique de décomposition donnant les fluences-seuils (3), les

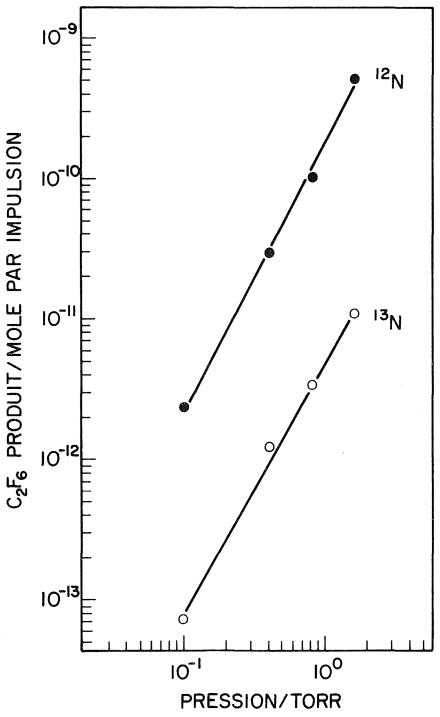


FIG. 3. Production d'hexafluoroéthane en fonction de la pression de CF_3Cl pour une fréquence d'activation de 1077.3 cm^{-1}, une énergie incidente de 1.8 J et une température de 22°C. Le facteur de séparation passe de $\beta = 3$ à $\beta = 1$ quand la pression augmente de 0.1 à 2 Torr.

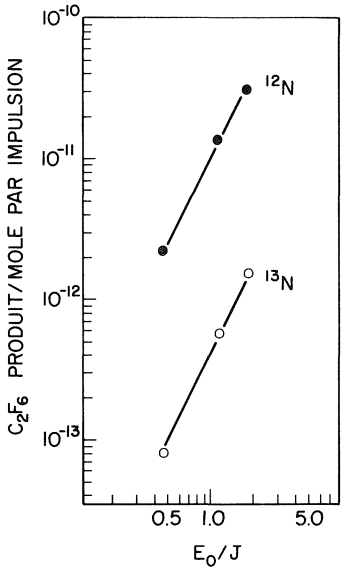


FIG. 4. Production d'hexafluoroéthane en fonction de l'énergie incidente pour une fréquence d'activation de 1077.3 cm^{-1}, une pression de 0.5 Torr et une température de 22°C. Dans ces conditions, le facteur de séparation est constant à 3.8 ± 0.4.

probabilités de décomposition peuvent être établies comme des volumes de réactions qui augmentent au même rythme pour les deux espèces isotopiques si on augmente l'énergie incidente, de sorte que le rapport de ces volumes, donc le facteur de séparation, ne varie pas.

Influence de la température

La fig. 5 représente la variation observée de ^{13}N et ^{12}N en fonction de la température. Ces résultats sont différents de ce qui est obtenu avec CF_3COCF_3 (3) à cause du mécanisme de décomposition différent. Puisque la décomposition de $^{13}CF_3Cl$ diminue aussi à basse température, il ne s'agit donc pas seulement d'un effet spectroscopique tel que suggéré ultérieurement (5) ou tel qu'observé dans d'autres systèmes (3).

Discussion

De toute évidence, le modèle du double cône de décomposition ($N \propto PE_0^{3/2}$) ne s'applique pas pour CF_3Cl qui donne un rendement en

[6] $N \propto P^2E_0^2$

Le mécanisme proposé est le suivant. L'activation polyphotonique se fait selon les réactions [7] et [8].

[7] $^{13}CF_3Cl \xrightarrow{\langle^{13}n\rangle\hbar\omega} {}^{13}CF_3Cl^*$

[8] $^{12}CF_3Cl \xrightarrow{\langle^{12}n\rangle\hbar\omega} {}^{12}CF_3Cl^*$

Dans nos expériences, le choix de la fréquence d'activation, mais aussi le choix de la pression, et de l'énergie incidente tendent à favoriser la réac-

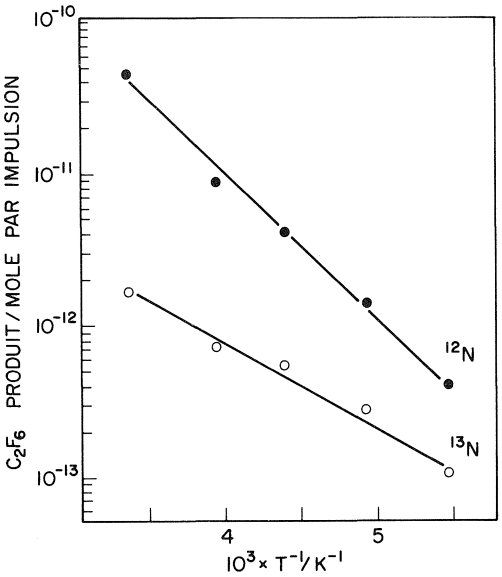


FIG. 5. Production d'hexafluoroéthane en fonction de la température pour une fréquence d'activation de 1077.3 cm^{-1}, une concentration dans la zone irradiée de 2.7×10^{-8} mol cm^{-3} et une énergie incidente de 1.8 J. Le facteur de séparation augmente jusqu'à $\beta = 25$ si on diminue la température jusqu'à $-90°C$.

tion [7] pour activer sélectivement, en vue de la décomposition, les molécules qui contiennent l'isotope ^{13}C. Les quantités $\langle {}^{13}n \rangle$ et $\langle {}^{12}n \rangle$ sont les nombres moyens de photons absorbés par molécule de chaque espèce isotopique. Ces quantités ne sont pas mesurables mais il est possible par contre de mesurer $\langle n \rangle$, le nombre moyen de photons absorbés par molécule irradiée soit par simple absorption (3) ou par un moyen optoacoustique (14).

Ces molécules possédant une activation vibrationnelle peuvent soit se décomposer spontanément, la réaction [9], si elles ont atteint un niveau d'énergie suffisant, soit se décomposer à la suite d'une collision avec une autre molécule activée, la réaction [10], et contribuer ainsi à la formation du produit hexafluoroéthane par recombinaison des radicaux trifluorométhyle.

[9] $CF_3Cl^* \rightarrow CF_3 + Cl$

[10] $CF_3Cl^* + CF_3Cl^* \rightarrow CF_3 + Cl + CF_3Cl$

[11] $CF_3 + CF_3 \rightarrow C_2F_6$

Une activation sélective de $^{13}CF_3Cl$ sera traduite par un produit C_2F_6 enrichi en ^{13}C. D'autre part, les molécules activées peuvent être perdues soit par collision avec une molécule "froide", la réaction [12], soit par diffusion hors du "volume actif", la réaction [13].

[12] $CF_3Cl^* + CF_3Cl \rightarrow CF_3Cl + CF_3Cl$

[13] $CF_3Cl^* \rightarrow CF_3Cl$

La réaction [13] inclut de même la diffusion de molécules froides dans le volume irradié et c'est cette réaction qui domine la compétition avec la réaction [10] dans notre système pour donner les bons exposants dans l'expression [6]. La formation d'hexafluoroéthane est contrôlée par les constantes de vitesse des réactions [11], [14] et [15].

[14] $CF_3 + Cl \rightarrow CF_3Cl$

[15] $Cl + Cl \rightarrow Cl_2$

Même si la vitesse de production de C_2F_6 à partir des radicaux trifluorométhyle dépend des concentrations réelles de CF_3, le rendement par impulsion N doit être indépendant de la concentration à moins que des réactions du type de la réaction [16] soient importantes.

[16] $CF_3 + Cl_2 \rightarrow CF_3Cl + Cl$

Cette réaction n'est pas importante dans ce mécanisme de même que la réaction [5] qui ne doit pas affecter le rendement en C_2F_6 mais ne changerait que le facteur de séparation (4–6). Aucune indication n'apparaît dans les présents résultats pour postuler la présence de deux sources de produits comme dans le cas de CF_3Br (6).

En somme le mécanisme se résume comme suit: (*a*) production d'une distribution de molécules activées ^{13}A et ^{12}A (= $[^{13}CF_3Cl^*]_i$ et $[^{12}CF_3Cl^*]_i$) dans un volume actif en forme de double cône, (*b*) décomposition, principalement par collision entre deux molécules activées, et (*c*) compétition de cette réaction avec la diffusion hors du volume actif. Tel que démontré précédemment (15), le nombre de molécules décomposées par impulsion suit la formule empirique $aP + bP^2$ où l'importance des coefficients a et b dépend fortement de l'énergie incidente. D'autre part, 70% de l'énergie de l'impulsion laser est comprise dans le pic initial de 80 ns FWHM (3) et les molécules activées subsistent pour une période relativement plus longue, plusieurs microsecondes (16). On peut donc supposer que chaque impulsion du laser produit la quantité $^{13}A + {}^{12}A$ de molécules activées; cette quantité augmente selon PV, le produit de la pression de l'absorbant et V, le volume actif, donné par la géométrie de l'irradiation. Dans le cas présent, on peut imaginer un certain volume à l'intérieur duquel le pompage est effectif: posons F comme la fluence à la surface de ce volume. F dépend de la nature de l'absorbant, de ω et de T mais est indépendant de P (17). Donc,

[17] $F = E_0/\pi r^2$

où E_0 est l'énergie incidente et r est le rayon du cône. On peut alors montrer facilement que

[18] $V \propto E_0^{3/2}$

Can. J. Chem. Downloaded from www.nrcresearchpress.com by 210.87.254.42 on 09/05/12
For personal use only.

Can. J. Chem. Downloaded from www.nrcresearchpress.com by 210.87.254.42 on 09/05/12
For personal use only.

une relation importante observée dans plusieurs systèmes pour l'activation polyphotonique en régime focalisé. Le pompage se fait alors à une vitesse proportionnelle à $PE_0^{3/2}$. La fraction de A $(= {}^{13}A + {}^{12}A)$ qui mène à la décomposition est donnée par le mécanisme selon

$$[19] \quad f = \frac{k_{10}A^2}{k_{10}A^2 + k_{13}AS}$$

où S est la surface de diffusion du volume actif. D'après l'expression [17],

$$[20] \quad S \propto E_0$$

Par substitution, on obtient alors une vitesse de décomposition

$$[21] \quad v \propto (1 + (k'PE_0^{1/2})^{-1})^{-1}PE_0^{3/2}$$

où $k' \propto k_{10}/k_{13}$. Deux cas limites peuvent se présenter (6) et les résultats présents ($v \propto P^2E_0^2$) montrent que l'expérience se situe à des rapports surface/volume élevés où la perte par diffusion des molécules activées est importante.

L'influence de la température représentée à la fig. 5 confirme ce mécanisme. En effet, pour une énergie incidente constante, on aura

$$[22] \quad N = c({}^{13}A + {}^{12}A)^2$$

où c est une constante indépendante de la température qui inclut la stoichiométrie et qui tient compte de la recombinaison éventuelle des radicaux selon la réaction [14]. De cette expression on obtient directement une relation entre les nombres de molécules activées ${}^{13}A$ et ${}^{12}A$ et les rendements ${}^{13}N$ et ${}^{12}N$.

$$[23] \quad ({}^{13}A)^2 = x^{13}N/a$$

$$[24] \quad ({}^{12}A)^2 = (1 - x)^{12}N/a$$

Si les raisonnements sur la fréquence d'activation développés pour CF_3COCF_3 sont applicables ici, on prévoit alors que l'activation de ${}^{13}A$ ne variera pas avec T et que l'activation de ${}^{12}A$ diminuera avec T puisque la fréquence d'activation se situe du côté bleu de la bande d'absorption polyphotonique de ${}^{13}CF_3Cl$ et du côté rouge pour ${}^{12}CF_3Cl$. La quantité $(x^{13}N)^{1/2}$ doit donc être constante et c'est ce qui est représenté à la fig. 6 (${}^{13}A$). De plus, la variation de $((1 - x)^{12}N)^{1/2}$ représentée à la fig. 6 (${}^{12}A$) donne une pente d'Arrhenius correspondant à une énergie d'activation de $795 \pm 25\ cm^{-1}$ qui concorde avec l'une des fréquences fondamentales de la molécule: 350, 478, 560, 762, 1106 et 1217 cm^{-1} (18).

En somme, ces résultats montrent que l'effet de la température combine l'influence des bandes chaudes et du mécanisme cinétique et résulte en une perte de produits enrichis en ${}^{13}C$. Le facteur de séparation augmente si on diminue la température mais au dépend du rendement puisque la probabilité de décomposition diminue non seulement pour ${}^{12}CF_3Cl$ mais aussi pour ${}^{13}CF_3Cl$. A part les différences spectroscopiques qui sont au détriment de CF_3I (5) les trois molécules CF_3X obéissent aux mêmes mécanismes de décomposition et se comportent de la même façon dans une étude paramétrique. L'efficacité de la production de ${}^{13}C$ par photon absorbé est présentement à l'étude.

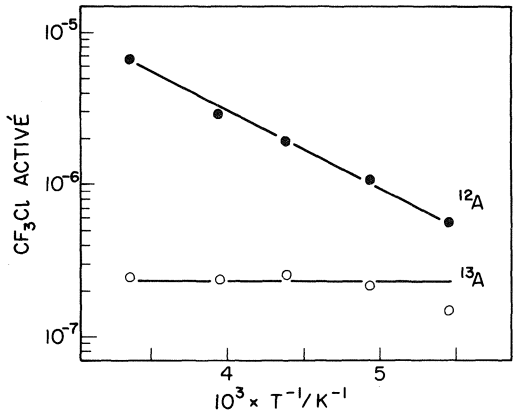


FIG. 6. Activation sélective de CF_3Cl aux conditions de la fig. 5, voir le texte.

1. V. S. LETOKHOV. Nature, **277**, 605 (1979).
2. J. B. MARLING et I. P. HERMAN. Contribution 4.2, 1979 IEEE/OSA Conference of Laser Engineering and Applications, Washington, DC, 30 Mai – 1 Juin, 1979.
3. P. A. HACKETT, C. WILLIS et M. GAUTHIER. J. Chem. Phys. **71**, 2682 (1979).
4. M. GAUTHIER, P. A. HACKETT, M. DROUIN, R. PILON et C. WILLIS. Can. J. Chem. **56**, 2227 (1978).
5. M. DROUIN, M. GAUTHIER, R. PILON, P. A. HACKETT et C. WILLIS. Chem. Phys. Lett. **60**, 16 (1978).
6. M. GAUTHIER, P. A. HACKETT et C. WILLIS. Chem. Phys. **45**, 39 (1980).
7. R. V. AMBARTZUMIAN, YU. A. GOROKHOV, V. S. LETOKHOV et A. A. PURETSKII. JETP Lett. **22**, 177 (1975).
8. R. V. AMBARTZUMIAN, YU. A. GOROKHOV, V. S. LETOKHOV, G. N. MAKAROV et A. A. PURETSKII. Phys. Lett. **56A**, 183 (1976).
9. S. BITTENSON et P. L. HOUSTON. J. Chem. Phys. **67**, 4819 (1977).
10. I. N. KNYAZEV, YU. A. KUDRIAVTZEV, N. P. KUZMINA, V. S. LETOKHOV et A. A. SARKISIAN. Appl. Phys. **17**, 427 (1978).
11. N. R. ISENOR, V. MERCHANT, R. S. HALLSWORTH et M. C. RICHARDSON. Can. J. Phys. **51**, 1281 (1973).
12. P. A. HACKETT, M. GAUTHIER, C. WILLIS et R. PILON. J. Chem. Phys. **71**, 546 (1979).
13. M. BENEDICT et T. H. PIGFORD. Nuclear chemical engineering. McGraw-Hill, New York, NY. 1957.
14. M. GAUTHIER, D. RAYNER, C. WILLIS et P. A. HACKETT. Chem. Phys. Lett. A paraître.
15. P. A. HACKETT, M. GAUTHIER et C. WILLIS. J. Chem. Phys. **69**, 2924 (1978).
16. M. GAUTHIER, W. S. NIP, P. A. HACKETT et C. WILLIS. J. Chem. Phys. A paraître.
17. M. GAUTHIER, C. WILLIS et P. A. HACKETT. Résultats non publiés.
18. AA. S. SUDBO, P. A. SCHULZ, E. R. GRANT, Y. R. SHEN et Y. T. LEE. J. Chem. Phys. **70**, 912 (1979).

Photochemical reactions of charge-transfer complexes. The irradiation of the charge-transfer complexes between 1,4-, 1,5-, and 2,3-dimethoxynaphthalenes and 1,2-dicyanoethylenes[1]

P. C. WONG AND D. R. ARNOLD[2]

Department of Chemistry, Dalhousie University, Halifax, N.S., Canada B3H 4J3

Received September 12, 1979

P. C. WONG and D. R. ARNOLD. Can. J. Chem. **58**, 918 (1980).

The first part of this paper describes the experimental search for a donor which would complex preferentially one of the isomers of 1,2-dicyanoethylene. This involved measuring the association constants (K_c^{DA}) of the charge-transfer (ct) complexes of several dimethoxynaphthalenes (DMN) with maleonitrile (MN) and fumaronitrile (FN). From the measured K_c^{DA}, we found that MN complexes more strongly than FN with 1,4- and 1,5-DMN but that FN complexes more strongly with 2,3-DMN than does MN. These results are explained in terms of more than one favourable geometry for the ct complexes, since the donors are relatively large compared to the acceptors.

Irradiation of the ct complexes between 1,4-, 1,5-, or 2,3-DMN and 1,2-dicyanoethylene led to isomerization of the olefins. The photostationary state depends on the absorption spectra of the ct complexes formed between the donor and the isomeric olefins. From spectroscopic and photo-CIDNP studies, we find evidence that the isomerization in polar solvents takes place via the triplet state of the olefin. The triplet is formed from the radical ion pair resulting after excitation of the ct complex.

P. C. WONG et D. R. ARNOLD. Can. J. Chem. **58**, 918 (1980).

La première partie de cette publication décrit la recherche expérimentale d'un donneur qui complexerait préférentiellement l'un des isomères du dicyano-1,2 éthylène. Cette recherche implique la mesure des constantes d'association (K_c^{DA}) des complexes de transfert de charge (tc) de plusieurs diméthoxynaphtalènes (DMN) avec le maléonitrile (MN) et le fumaronitrile (FN). Nous trouvons, à partir des mesures de K_c^{DA}, que les complexes du MN avec le DMN-1,4 et -1,5 sont plus stables que ceux du FN, mais les complexes du FN avec le DMN-2,3 sont plus stables que ceux du MN. On explique ces résultats en fonction de plus d'une géométrie favorable des complexes de tc puisque les donneurs sont relativement plus nombreux par rapport aux accepteurs.

L'irradiation des complexes de tc entre les DMN-1,4, -1,5 ou -2,3 et le dicyano-1,2 éthylène conduit à une isomérisation des oléfines. L'état photostationnaire dépend des spectres d'absorption des complexes de tc formés entre le donneur et les oléfines isomères. A partir des études spectroscopiques de photo-PNDIC nous trouvons la preuve que l'isomérisation dans les solvants polaires se fait via un état triplet de l'oléfine. Le triplet se forme à partir de la paire d'ions radicalaires résultant de l'excitation du complexe de tc.

[Traduit par le journal]

Introduction

We have previously reported (1) that the direct irradiation of the charge-transfer (ct) complexes between 1,2,3-triphenylcyclopropene and fumaronitrile (FN), and between *trans*-stilbene (TS) and FN, lead to *trans–cis* isomerization of the olefin. The proposed mechanism for the isomerization involves the triplet state of the olefin which is formed from the excited ct complexes. In the stilbene – 1,2-dicyanoethylene system, irradiation of the TS–FN ct complex leads to a mixture rich (>85%) in *cis*-stilbene (CS) which forms a weaker ct complex with FN than TS (both smaller association constant (K_c^{DA}) and ct transition extinction coefficient (ε_λ^{DA})).

This has encouraged us to search, in general, for donors (or acceptors) which would complex preferentially one of the acceptor (or donor) olefin isomers. Irradiation of the ct complex would then lead to enrichment of the other olefin isomer. The present approach may become a new synthetically useful method for obtaining a specific olefin isomer. Furthermore, if the ct bands of the two complexes formed from the *trans* and the *cis* olefin with a common donor (or acceptor) are well separated, then the *trans*:*cis* ratio of the photostationary state mixture can be "fine-tuned" upon varying the excitation wavelengths. This then affords a new photochromic system which is potentially useful.

In spite of the large body of theoretical studies on ct complexes, it is still difficult to predict the strength of the ct complex being formed (K_c^{DA}), the extinction coefficient of the ct transition (ε_λ^{DA}), and the relative orientation of the two components within the complex in solution (2). In the systems we have studied, we hoped to see differences in the complexing ability between the isomeric donors and acceptors as a function of the position and configuration of the substituents. Maleonitrile (MN) and fumaronitrile (FN) have nearly identical reduction potentials (1*a*, 3); therefore we expected that any difference in the relative complexing abil-

[1]A portion of this work was carried out at the University of Western Ontario, London, Ont., Canada N6A 5B7. Contribution No. 230 from the Photochemistry Unit.

[2]Author to whom correspondence should be addressed.

0008-4042/80/090918-10$01.00/0

©1980 National Research Council of Canada/Conseil national de recherches du Canada

Can. J. Chem. Downloaded from www.nrcresearchpress.com by 210.87.254.6 on 09/05/12
For personal use only.

Can. J. Chem. Downloaded from www.nrcresearchpress.com by 210.87.254.6 on 09/05/12
For personal use only.

ity toward a common donor molecule would come mainly from the difference in their geometries. We reasoned that if the attractive interactions favour the eclipsed form, with the electron withdrawing substituents in the acceptor aligning with the electron donating substituents in the donor, then, MN should be a stronger acceptor than FN towards donors like 2,3-dimethoxynaphthalene (2,3-DMN) and 1,4-DMN while the opposite would be true towards 1,5-DMN. Actually, there is some evidence that the eclipsed form results in a stronger ct interaction than does the staggered form in a similar system. Staab and co-workers have synthesized and recorded the absorption spectra of a series of [2.2]- (4) and [3.3]-paracyclophanes (5) bearing two electron donating substituents on one aromatic ring and two electron withdrawing substituents on the other. The intramolecular ct spectra of the "pseudo geminal" (eclipsed form) isomers differ remarkedly from those of the "pseudo ortho" (staggered form) isomers. Upon analysing their absorption spectra, using a HMO calculation, they found that the former compounds are stabilized relative to the latter compounds by ct interaction (6).

In this paper, we report the association constants (K_c^{DA}) and extinction coefficients (ε_λ^{DA}) of the ct complexes formed between isomeric donors (1,4-DMN, 1,5-DMN, and 2,3-DMN) and isomeric acceptors (FN and MN). The photochemistry and photophysics of these ct complexes have also been investigated. Irradiation of the ct complexes leads to isomerization of the olefins. The photostationary state ratio of the olefin isomers is dependent on the absorption spectra of the ct complexes. The photophysical processes leading to the isomerization have been examined using spectroscopic and photochemically induced dynamic nuclear polarization (photo-CIDNP) techniques.

Results

Both the ultraviolet–visible spectrophotometric (uv–vis) method and the proton nuclear magnetic resonance (^{1}Hmr) method were employed in measuring the association constants (K_c^{DA}) of the dimethoxynaphthalene – 1,2-dicyanoethylene ct complexes. Chloroform was used as the solvent for this part of the study so that comparison with reported data is possible (7). Irradiations were carried out using benzene as solvent . There is significant difference in the ct absorption spectra for the complexes formed between a common donor and FN and MN. Figures 1, 2, and 3 show these spectra in chloroform; similar spectra were observed in benzene solution. The absorbance (optical density,

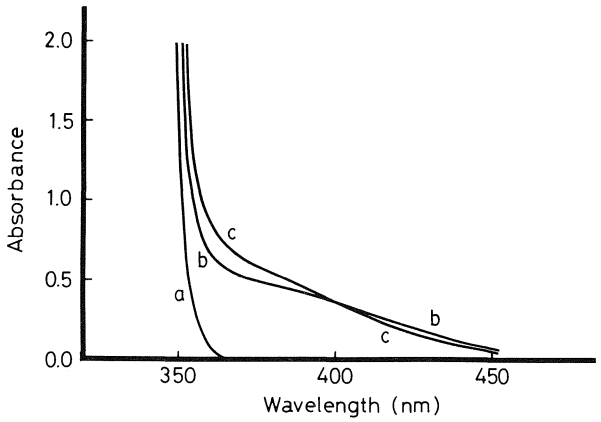


FIG. 1. Absorption spectra for: (*a*) 1,4-DMN (8.03 m*M*), (*b*) 1,4-DMN (8.03 m*M*) + FN (0.32 *M*), and (*c*) 1,4-DMN (8.03 m*M*) + MN (0.32 *M*) in chloroform solution.

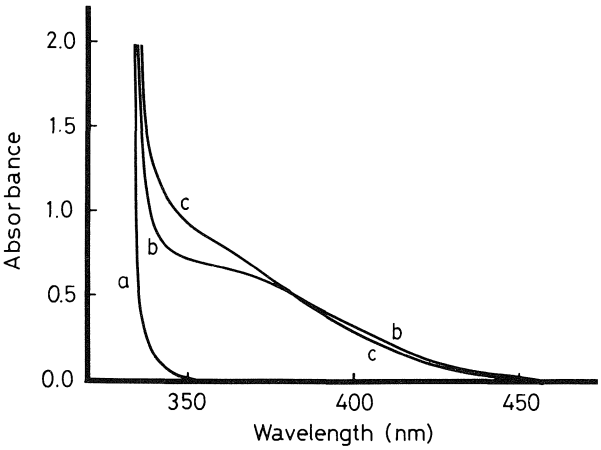


FIG. 2. Absorption spectra for: (*a*) 1,5-DMN (7.78 m*M*), (*b*) 1,5-DMN (7.78 m*M*) + FN (0.35 *M*), and (*c*) 1,5-DMN (7.78 m*M*) + MN (0.35 *M*) in chloroform solution.

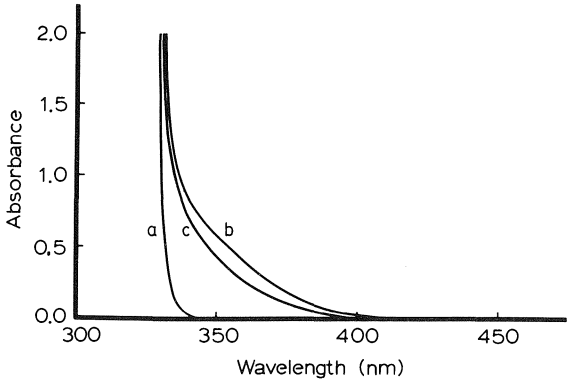


FIG. 3. Absorption spectra for: (*a*) 2,3-DMN (7.76 m*M*), (*b*) 2,3-DMN (7.76 m*M*) + FN (0.32 *M*), and (*c*) 2,3-DMN (7.76 m*M*) + MN (0.32 *M*) in chloroform solution.

TABLE 1. Ultraviolet–visible spectrophotometric evaluation of the association constants for the charge-transfer complexes between dimethoxynaphthalene 1,2-dicyanoethylene in chloroform solution with $[A]_0 \gg [D]_0$

Donor	Acceptor	Method	K_c^{DA} (M^{-1}) at different wavelengths 370	375	380	385	390	400 (nm)	Average K_c^{DA} (M^{-1})[a]
1,4-DMN	MN	B—H	0.843	0.918	0.892	0.846	0.855	0.807	0.860
		F—H—W	0.832	0.884	0.865	0.840	0.863	0.813	0.850
1,4-DMN	FN	B—H	0.370	0.370	0.388	0.398	0.450	0.485	0.401
		F—H—W	0.357	0.371	0.378	0.405	0.441	0.475	0.405
1,5-DMN	MN	B—H	0.894	0.849	0.831	0.786	0.812	0.813	0.831
		F—H—W	0.879	0.844	0.828	0.842	0.781	0.769	0.824
1,5-DMN	FN	B—H	0.522	0.566	0.567	0.500	0.573	0.544	0.545
		F—H—W	0.527	0.561	0.591	0.583	0.596	0.640	0.593

Donor	Acceptor	Method	K_c^{DA} (M^{-1}) at different wavelengths 345	350	355	360 (nm)	Average K_c^{DA} (M^{-1})
2,3-DMN	MN	B—H	0.595	0.552	0.552	—	0.566
		F—H—W	0.577	0.546	0.543	—	0.555
2,3-DMN	FN	B—H	0.510	0.570	0.671	0.633	0.593
		F—H—W	0.529	0.561	0.611	0.636	0.584

[a] $K_c^{DA} \pm 0.04\ M^{-1}$.

TABLE 2. Ultraviolet–visible spectrophotometric evaluation of the extinction coefficients of various wavelengths for the charge-transfer complexes between dimethoxynaphthalene and 1,2-dicyanoethylene in chloroform solution with $[A]_0 \gg]D]_0$

Donor	Acceptor	ε_λ^{DA} 370	375	380	385	390	400 (nm)
1,4-DMN	MN	373	322	302	288	259	214
1,4-DMN	FN	594	568	519	481	406	325
1,5-DMN	MN	362	335	297	270	217	145
1,5-DMN	FN	513	448	413	419	328	260

Donor	Acceptor	ε_λ^{DA} 345	350	355	360 (nm)
2,3-DMN	MN	430	367	290	—
2,3-DMN	FN	603	465	340	294

OD) is higher in the long wavelength region (i.e., between 350–380 nm) with the 1,4-DMN (or 1,5-DMN) – MN complex than the 1,4-DMN (or 1,5-DMN) – FN complex. On the other hand, when 2,3-DMN is the donor, the OD of the 2,3-DMN – FN complex is higher than that of the 2,3-DMN – MN complex in this region.

With the uv–vis method two experimental conditions were employed: (*1*) with $[A]_0 \gg [D]_0$ and (*2*) with $[D]_0 \gg [A]_0$ (where $[A]_0$ and $[D]_0$ are the total concentrations of the acceptor and the donor respectively). Two different approaches for evaluating the K_c^{DA} and ε_λ^{DA} were used, namely, the Benesi–Hildebrand (B–H) method (8) and the Foster–Hammick–Wardley (F–H–W) method (9). The results are summarized in Tables 1, 2, and 3.

Using the ^{1}Hmr method, the analogous B–H plots (7) also gave linear relationships. The results are summarized in Table 4. The K_c^{DA} values for the 1,5-DMN complexes were not measured due to the relative insolubility of 1,5-DMN. The heats of formation for the 1,4-DMN complexes were obtained from van't Hoff plots of the temperature dependent K_c^{DA} values determined by the ^{1}Hmr method.

Irradiation ($\lambda > 360$ nm) of the 1,4-DMN – FN ct complex in benzene solution caused little chemical change other than isomerization of the olefin. The quantum yield of isomerization of FN to MN was 2.4×10^{-3} ($\pm 10\%$) at 362 ± 6 nm. Prolonged irradiation led to a photostationary state of FN:MN = 63:37 in this solvent. The isomerization also occurred upon irradiation at $\lambda > 400$ nm; however,

Can. J. Chem. Downloaded from www.nrcresearchpress.com by 210.87.254.6 on 09/05/12
For personal use only.

Can. J. Chem. Downloaded from www.nrcresearchpress.com by 210.87.254.6 on 09/05/12
For personal use only.

TABLE 3. Ultraviolet–visible spectrophotometric evaluation of K_c^{DA} and ε_λ^{DA} for the charge-transfer complexes between 1,4-dimethoxynaphthalene and 1,2-dicyanoethylene in chloroform and acetonitrile solution with $[D]_0 \gg [A]_0$

Acceptor	Solvent		K_c^{DA} (M^{-1}) at different wavelengths 390	395	400	410 (nm)	Average K_c^{DA} (M^{-1})[d]
MN	$CHCl_3$	[a]	—	0.650	0.650	0.700	0.667
		[b]	—	0.600	0.611	0.694	0.635
		[c]	—	310	272	191	
FN	$CHCl_3$	[a]	—	0.460	0.453	0.424	0.446
		[b]	—	0.430	0.438	0.472	0.447
		[c]	—	361	334	284	
MN	CH_3CN	[a]	0.32	0.35	0.36	—	0.34
		[b]	0.31	0.35	0.34	—	0.33
		[c]	143	118	105	—	
FN	CH_3CN	[a]	0.27	0.27	0.28	—	0.27
		[b]	0.22	0.22	0.23	—	0.22
		[c]	200	167	142	—	

[a] K_c^{DA} evaluated from B—H method.
[b] K_c^{DA} evaluated from F—H—W method.
[c] ε_λ^{DA} evaluated from B—H method.
[d] $K_c^{DA} \pm 0.04\ M^{-1}$.

TABLE 4. Proton nuclear magnetic resonance evaluation of the association constants for the charge-transfer complexes between dimethoxynaphthalene and 1,2-dicyanoethylene[a] at various temperatures with $[D]_0 \gg [A]_0$

Donor	B Acceptor	K_c^{DA} (M^{-1})[b] 0.0°	29.0°	60.0° (±0.5°C)	Δ_0^{DA} (ppm)	ΔH^θ (kcal mol^{-1})
1,4-DMN	MN	0.83	0.67	0.57	1.67	−1.14
1,4-DMN	FN	0.63	0.54	0.47	0.43	−0.89
2,3-DMN	MN	—	0.61	—	1.10	—
2,3-DMN	FN	—	0.66	—	1.03	—

[a] The solvent was 5:95 (v/v) cyclohexane-d_{12} – chloroform.
[b] $K_c^{DA} \pm 0.04\ M^{-1}$.

TABLE 5. Fluorescence quenching parameters obtained at room temperature in benzene solution

Fluorophor	Quencher	Fluorescence lifetime, τ_0 (ns) (25°C)	$k_q\tau_0$ (M^{-1})	k_q ($s^{-1}M^{-1}$) × 10^{10}	K' (M^{-1})
1,4-DMN	FN	5.2	128	2.46	10
1,4-DMN	MN	5.2	121	2.33	18
2,3-DMN	FN	16.8	303	1.80	9
2,3-DMN	MN	16.8	284	1.69	10

since very little light is absorbed in this region, it was not possible to determine accurately the photostationary state. Irradiation ($\lambda > 360$ nm) of the 1,4-DMN – FN ct complex in acetonitrile also gave rise to isomerization. In this case also the approach to equilibrium was very slow.

Irradiation ($\lambda > 360$ nm) of the 1,5-DMN – FN ct complex in benzene solution likewise gave a photostationary state of FN:MN = 63:37. However, the photostationary state was FN:MN = 44:56 when the 2,3-DMN – FN ct complex was irradiated under these conditions. All the above photostationary states were reproducible starting from MN or a mixture of FN and MN while other reactions were negligible (< 5%).

The fluorescence lifetimes (τ_0) of the dimethoxynaphthalenes and the parameters obtained from the fluorescence quenching of the DMN's by the dinitriles are listed in Table 5. The Stern–Volmer plots at high quencher concentration were curved slightly upward. This is probably due to absorption of the incident light by the ground state ct complex. The quenching rate constants (k_q) in these cases were obtained by a method estab-

Can. J. Chem. Downloaded from www.nrcresearchpress.com by 210.87.254.6 on 09/05/12
For personal use only.

lished by Ware and co-workers (10):

$$[1] \quad K_{SV} = (I_0/I - 1)\,(1/[Q]) = K' + k_q\tau_0 + K'k_q\tau_0[Q]$$

$$[2] \quad K' = K_c^{DA}(\varepsilon_\lambda^{DA}/\varepsilon_\lambda^{D})$$

By plotting K_{SV} against [Q], a linear relationship was obtained. The K' and $k_q\tau_0$ values could then be obtained from the y-intercept and the slope of the straight line. The k_q's are all essentially diffusion controlled (see Table 5).

The photo-CIDNP experiments were performed with acetonitrile-d_3 as the solvent. In benzene-d_6 solution no CIDNP signal was observed under the same conditions. When a solution of 1,4-DMN and FN (or MN) was irradiated, the signal of the donor broadened (especially broadened are the 2,3,5,8 and the methoxy protons (Fig. 4)) in the initial period. At the same time we observed an emission signal for MN (or FN) while the FN (or MN) signal was not noticeably affected. The spectrum returned to its normal form gradually (minutes) after the light was switched off.

Discussion

By definition, an exciplex is a molecular complex which only exists in the excited state. An excited ct complex can be produced by either irradiation of the ct absorption band or by excitation of one of the uncomplexed components.

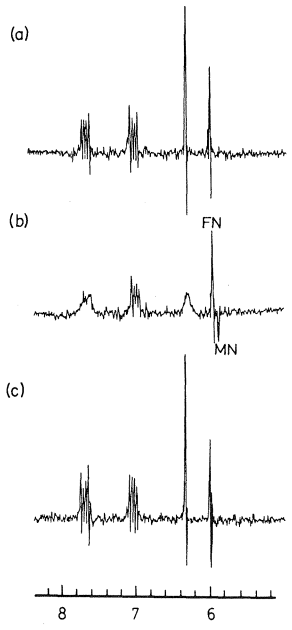


FIG. 4. Photo-CIDNP study of the 1,4-DMN – 1,2-dicyanoethylene system in acetonitrile-d_3; (*a*) before irradiation, (*b*) during irradiation, and (*c*) after irradiation.

A ground state ct complex is generally only slightly (a few kcal mol^{-1}) more stable than the free components. Direct irradiation of the ct band gives rise to a nonrelaxed state which possesses a lower energy content than the first excited singlet state of the components. This nonrelaxed state may also be obtained by exciting a free component (say the acceptor, A) to its first excited singlet state ($^1A^*$) and formation of an encounter complex with the donor (D) upon diffusion. The nonrelaxed state can (*a*) relax to an equilibrium state, which is called the ct fluorescence state in the ct complex system and the exciplex fluorescence state in the exciplex system, through reorientation of the components and the solvent molecules (11, 12), (*b*) decay in a radiationless manner back to the ground state, (*c*) give rise to triplet formation (13–15), or, (*d*) dissociate into the solvent-separated radical ions through the radical ion pair (15–17).

It is known that K_c^{DA} and ε_λ^{DA} obtained from the uv–vis method are often dependent upon the concentration conditions (e.g. $[D]_0 \gg [A]_0$, $[A]_0 \gg [D]_0$, or $[D]_0 = [A]_0$) while the product $(K_c^{DA} \cdot \varepsilon_\lambda^{DA})$ is not (7). Practically, since these two constants are essentially inversely related, an overestimation of one causes a corresponding underestimation of the other. The K_c^{DA} obtained from the ^{1}Hmr method is not concentration dependent; however, it is not useful for establishing ε_λ^{DA} which is of course important for photochemical studies. Therefore, it is desirable to use both methods whenever possible.

The only association constants for the ct complexes formed between a common donor (benzene) and both MN and FN have been reported by Schuler and Heusinger (18). They found that the K_c^{DA} for benzene–MN (0.43 M^{-1}) is larger than that of benzene–FN (0.16 M^{-1}) while the extinction coefficient of the former complex (ε_λ(275 nm) = 302) is less than that of the latter complex (ε_λ(275 nm) = 895). Using the ^{1}Hmr method, they obtained a slightly larger K_c^{DA} value (0.173 M^{-1}) for the benzene–FN complex which they attributed to the magnetic anisotropic effect of the benzene molecule on the substrate. This latter value is, in our opinion, unreliable since the observed chemical shift change was referred to the solvent (chloroform) signal which would also be shifted upfield as the concentration of the donor (benzene) increased. We have demonstrated in our case that the chloroform signal indeed shifted significantly as the concentration of the donor (e.g. 1,4-DMN) was increased. Therefore, in our ^{1}Hmr experiment, we took advantage of the deuterium lock for accurate chemical shift readings, referring to an inert internal reference (tetramethylsilane).

As shown in Tables 1, 3, and 4, there is generally

Can. J. Chem. Downloaded from www.nrcresearchpress.com by 210.87.254.6 on 09/05/12
For personal use only.

good agreement of the K_c^{DA} values for the DMN – 1,2-dicyanoethylene complexes using the uv–vis method and the ^{1}Hmr method. The only exceptions are two cases, 1,4- and 1,5-DMN with FN using the uv–vis method when $[A]_0 \gg [D]_0$. Possible causes for these anomalies may involve deviation in activity coefficients from unity, the presence of isomeric 1:1 complexes, contact ct complex, termolecular complexes, deviation from Beer's law, etc. (7, 19). Based upon our experimental results, it is difficult to choose from among these possibilities.

The relation between the ct extinction coefficient and the heat of formation of ct complex (ΔH^θ) has been considered by several authors (2, 19*a*, 20). There seems to be no consistent relationship between ε_λ^{DA} and ΔH^θ. We have also found that this is the case in our system (e.g. ε_λ^{DA} is larger for the 1,4-DMN–FN complex than the 1,4-DMN–MN complex but the opposite is true for the ΔH^θ values).

Our results indicate that MN has a greater complexing ability (larger K_c^{DA}) towards the donors, 1,4- and 1,5-DMN while the reverse is true when 2,3-DMN is the donor. This is in contrast with what we expected initially. Nevertheless, the results *do* prove that the relative complexing ability of the isomeric acceptors *is* dependent upon the structure of the donor. This is not easily rationalized from Mulliken's theory.

Based upon Mulliken's theory one would expect that the complexing power of structurally similar acceptors complexed to a common donor depends chiefly on their electron affinity (or reduction potential). Since FN and MN have essentially the same reduction potentials, the K_c^{DA} values for the DMN–FN complexes would be equivalent to those of the DMN–MN complexes. The observed difference in the K_c^{DA} values must then arise from the differences in the geometry of the components.

The difficulties involved in predicting the complexing abilities of the isomeric acceptors may result from the fact that the smaller acceptor can complex with the larger donor (DMN) in more than one region. The observed stability of these complexes would then be the average of all these various geometries. This problem may be minimized if the complexing regions of the donor and acceptor are of comparable size. For example, the ct complex formed between stilbene and tetracyanoethylene (TCNE) has the main ct interaction located at the central double bonds. We found that FN is a stronger acceptor ($K_c^{DA} = 0.17\,M^{-1}$) (16) than MN ($K_c^{DA} = 0.10\,M^{-1}$)[3] towards TS in benzene solution. These results favour a geometry of the ct complex where the two olefins are parallel and oriented at the central double bonds. The effects on K_c^{DA} values due to geometric factors are under further investigation in this laboratory for donors of smaller sizes or with additional steric effects, 1,3-benzodioxole and 2,3-dimethoxy-[2.2.2]bicyclooctene-2 for example.

Benzene was used as the solvent for the photochemical studies. The absorption spectra of the ct complexes in this solvent were essentially the same as in chloroform solution, shown in Figs. 1–3.

Prolonged irradiation ($\lambda > 360$ nm) of the ct band of the complex between FN and 1,4- or 1,5-DMN yielded a photostationary state which consisted of FN:MN = 63:37. On the other hand, the photostationary state was FN:MN = 44:56 when 2,3-DMN was the donor. An attempt to study the variation in the photostationary state as a function of excitation wavelength was abandoned because of the inefficiency of the isomerization as the result of the low absorbance of the complexes at longer wavelengths.

We have evidence that the photoisomerization is mainly due to the olefin triplet derived from the excited ct complex. Firstly, 2,3-DMN (0.3 *M*) does not absorb light with wavelengths > 360 nm and isomerization does occur upon irradiation at this wavelength. Secondly, even if a small amount of unfiltered light reaches free 2,3-DMN molecules, the singlet excited molecules of 2,3-DMN would be quenched by FN (under our experimental conditions, knowing the singlet quenching rate constants, we calculate that 99% of the singlet 2,3-DMN would be quenched by formation of the excited ct complex). Furthermore, the photostationary state in this case is different from that derived from triplet–triplet energy transfer employing high energy sensitizers (with the triplet energy, E_T, of the sensitizer > 50 kcal mol^{-1}, the photostationary state is FN:MN = 60:40 (1*a*)). These results can be fully accounted for with the mechanism described in Scheme 1.

In the present system, it is assumed that the triplets (^{3}*cis*-A* and ^{3}*trans*-A*) of the *cis*- and the *trans*-acceptor (A) olefins are of lower energies than the donor (D) triplet. It is also assumed that both *cis*-A and *trans*-A form ct complexes with D reversibly (steps 1 and 2). Excitation of the ct complexes (steps 3 and 6) lead to the corresponding excited ct complexes ([D.*cis*-A]* and [D.*trans*-A]*). Deactivation of these complexes (steps 4 and 7) gives the planar (more or less) olefin triplets which are known to promote isomerization via a common twisted triplet state (TTS) (steps 5 and 8) to give a fixed ratio of the ground state *trans*- and *cis*-A (step 9). From Fig. 3, one would expect

[3]P. C. Wong and D. R. Arnold. Unpublished results.

Can. J. Chem. Downloaded from www.nrcresearchpress.com by 210.87.254.6 on 09/05/12
For personal use only.

1. Donor(D) + *cis*-Acceptor(A) $\rightleftarrows$ [D · *cis*-A]
2. D + *trans*-A $\rightleftarrows$ [D · *trans*-A]
3. [D · *cis*-A] $\xrightarrow{h\nu}$ [D · *cis*-A]*
4. [D · *cis*-A]* $\rightarrow$ D + ^{3}*cis*-A*
5. ^{3}*cis*-A* $\rightarrow$ TTS
6. [D · *trans*-A] $\xrightarrow{h\nu}$ [D · *trans*-A]*
7. [D · *trans*-A]* $\rightarrow$ D + ^{3}*trans*-A*
8. ^{3}*trans*-A* $\rightarrow$ TTS
9. TTS $\rightarrow \alpha$(*trans*-A) + (1 − α) (*cis*-A)

SCHEME 1

that the photostationary state would favour a higher ratio of MN upon excitation of the 2,3-DMN – 1,2-dicyanoethylene complexes. This is in accord with the observed photostationary state with FN:MN = 44:56.

With the 1,4-DMN – 1,2-dicyanoethylene system, we can not rule out the involvement of the triplet–triplet transfer mechanism for the photoisomerization of the dinitriles since the photostationary state observed is similar to that of the triplet sensitized mechanism (FN:MN = 60:40) and the quantum yield of isomerization of FN is small (2.4×10^{-3}). We favour Scheme 1, however, since the isomerization occurred upon excitation at wavelengths > 400 nm where 1,4-DMN does not absorb. Even in the event 1,4-DMN is being irradiated, we calculate that 97% of the singlet 1,4-DMN would be quenched under the experimental conditions. Furthermore, the photostationary state ratio of the dinitriles can be explained in the same way as the 2,3-DMN case. The 1,4-DMN – MN complex has higher adsorbance than the 1,4-DMN – FN (Fig. 1) in the actinic light region. The same arguments are also applicable to the 1,5-DMN – 1,2-dicyanoethylene case (Fig. 2).

The detailed mechanism for the formation of triplets upon irradiation of the ct complex has been examined. The first step upon decay of the non-relaxed excited state, $^1(D^+A^-)^{\neq}$, of the ct complex is the formation of the singlet radical ion pair (in polar solvent). This step is supported by the favourable free energy charge (ΔG) (Table 6) estimated through the use of the Weller equation [3] (details of this calculation have been described before (1*a*)) and the observed fluorescence quenching rate constants, k_q, which are all diffusion controlled (Table 5).

$$[3]\quad \Delta G = 23.06[E_{1/2}^{ox}(D) - E_{1/2}^{red}(A) - e_0^2/\varepsilon\alpha] - \Delta^1E_{0,0}\ \text{kcal mol}^{-1}$$

The amount of energy within the bracket in eq. [3] is the free energy of the radical ion pair (E(RIP)).

The singlet radical ion pair can recombine to give the ground states D and A, dissociate to solvated ions, and/or undergo intersystem crossing via hyperfine interaction to give a triplet radical ion pair. If the energy of the triplet radical ion pair is above the sum of the energies of a triplet excited component and a ground state of the other component, then the triplet radical ion pair can recombine to give this set of triplet and ground state components. Confirmation of these processes in exciplex systems where the triplet state can be observed spectroscopically has been successfully demonstrated through studies of the external magnetic field effect on triplet formation yields (15). Since the triplet state of olefins is normally very short-lived, it would be difficult to trace their formation mechanism by normal spectroscopic techniques. Photo-CIDNP affords the best technique for the present studies. It can distinguish the radical ion mechanism from the exciplex mechanism or the triplet–triplet energy transfer mechanism for the formation of olefin triplets, since the latter two mechanisms would not give rise to polarization. The photo-CIDNP results confirm the radical ion pair mechanism (Fig. 5) in polar solvents. The observed polarization is interpreted in terms of the modified Kaptein rule (21) described below.

Our photo-CIDNP results, on the 1,4-DMN – 1,2-dicyanoethylene system, are very similar to Taylor's results cited by Roth (22). Irradiation of a solution of 1,4-DMN and FN brought about broadening of the signals for 1,4-DMN (especially broadened are the 2,3,5,8 and methoxy protons), not much change for the FN signal, and an emission for maleonitrile (Fig. 4). Similar results were observed when 1,4-DMN – MN was irradiated (i.e., not much change for MN signal and an emission for fumaronitrile).

The signal broadening for 1,4-DMN indicates the existence of the 1,4-DMN radical cation which exchanges electrons with 1,4-DMN at a fast rate (23). The observed emission for MN (or FN) can be accounted for with the aid of the modified Kaptein rule, assuming that the triplet olefin is derived from the radical ion pair (Fig. 5). $\Gamma n_i = \mu \cdot \varepsilon \cdot a_i \cdot \Delta g \cdot \gamma =$ − (emission for α-H of MN (or FN)), since $\mu =$ − (singlet origin), $\varepsilon =$ + (cage product), a(α-H) = −, $\Delta g = 2.004–2.0031 =$ + (22, 24), and $\gamma =$ − (triplet exit channel). The reason for the FN (or MN) signal being unaltered may be that the polarization due to decay from the singlet radical ion pair and the triplet radical ion pair essentially cancel each other, since they have opposite polarization according to this rule.

TABLE 6. The free energy charge (ΔG) for the formation of the radical ion pair calculated from the Weller equation[a] (acetonitrile solution)

D	A	$E_{1/2}^{ox}$(D),[b] V	$\Delta^1E_{0,0}$(D), kcal mol^{-1}	E_T(D), kcal mol^{-1}	E(RIP), kcal mol^{-1}	ΔG, kcal mol^{-1}
1,4-DMN	FN[c]	0.75[d]	83.6[e]	58.6[f]	53.6	−30.0
2,3-DMN	FN	1.04[d]	88.3[e]	64.0[f]	60.3	−28.0

[a]See ref. 33.
[b]Reference electrode $Ag/AgNO_3$ (0.1*M*).
[c]$E_{1/2}^{red}$(A) = −1.63 V and $E_T \sim$ 50 kcal mol^{-1}.
[d]Corrected values from ref. 34.
[e]Estimated from the overlap of the absorption and fluorescence spectra.
[f]Estimated from the first peak of the phosphorescence spectra.

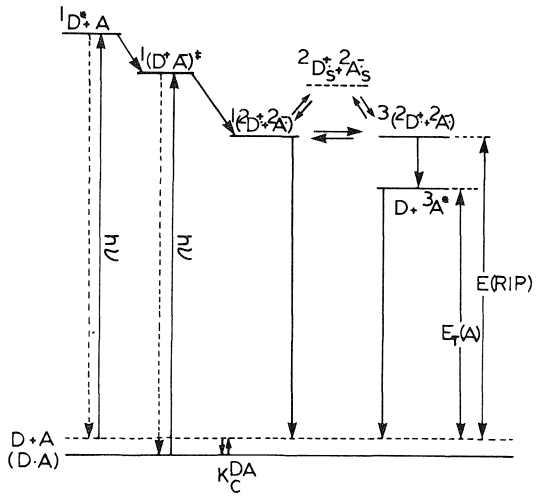


FIG. 5. Energy diagram for the formation of triplets upon direct excitation of a charge-transfer complex or upon photosensitized (electron-transfer) excitation in polar solvent.

The mechanism we propose is consistent with the studies of the effect of oxygen on the rate and quantum yield enhancement for the isomerization of olefins reported during the progress of this work. Hayashi and Nagakura (25) irradiated (at $\lambda >$ 300 nm) a solution of aromatic hydrocarbon and FN in both benzene and acetonitrile. They found rate enhancement for MN formation in the presence of oxygen. In benzene solution, with phenanthrene and triphenylene as the donor, they found that the exciplex fluorescence lifetime and the transient absorption lifetime of the radical ions were of the same magnitude, both of which decreased in the presence of oxygen. In acetonitrile solution, the transient absorption of the radical ions decays as a sum of a fast and slow component. These results suggest that, in nonpolar solvent, the exciplex (fluorescent ct state) which is rather polar is responsible for the triplet formation. In polar solvent, the radical ion pair which is the fast decay transient is responsible for the triplet formation. The presence of oxygen increases the intersystem crossing rate of the singlet exciplex and the singlet radical ion pair. Similar conclusions have been drawn by Lewis and Simpson (26) from a study on the isomerization of *trans*-stilbene upon irradiation of the TS–FN ct complex. They found that the quantum yield of isomerization of TS was larger in oxygenated solution than in degassed solution with both polar and nonpolar solvents.

Summary

From the measured K_c^{DA}, we found that maleonitrile (MN) complexes more strongly with 1,4- and 1,5-DMN than does fumaronitrile (FN), while the opposite is true when 2,3-DMN is the donor. These results are interpreted in terms of more than one favourable geometry for the ct complexes since the donors are relatively large compared to the acceptors.

Irradiation of the ct complexes between 1,4- (or 1,5- and 2,3-DMN) and 1,2-dicyanoethylene led to isomerization of the olefins. The photostationary state ratio of the olefin isomers depends upon the absorption spectra of the ct complexes. From the spectroscopic and photo-CIDNP studies, we have confirmed that the olefin isomerization in polar solvents involves the olefin triplet which is derived from the radical ion pair.

Experimental

General

Fumaronitrile (FN) (Aldrich Chemical Co.) was freshly sublimed twice under vacuum before use. Maleonitrile (MN) was prepared by iodine-catalyzed thermal isomerization of FN (27), and was purified by fractional distillation, column chromatography on neutral alumina (Woelm activity I) eluting with a 1:1 mixture of benzene and hexanes, followed by recrystallization from ether–pentane.

1,4-Dimethoxynaphthalene (1,4-DMN), 1,5-DMN, and 2,3-DMN were prepared from the corresponding dihydroxynaphthalenes (28) (Eastman Kodak Co.). 2,3-DMN was purified by recrystallization from methanol. 1,4-DMN was purified by column chromatography (neutral Woelm alumina activity I eluted with 5% benzene in hexanes) followed by recrystallization from methanol. 1,5-DMN was chromatographed (neutral Woelm alumina activity I eluted with benzene), vacuum sublimed, and recrystallized from 2-propanol three times before use.

Chloroform (Fisher spectroscopic grade) was dried and distilled over calcium chloride. Benzene (Fisher spectroscopic grade) was purified using the procedure employed by Kochevar

Can. J. Chem. Downloaded from www.nrcresearchpress.com by 210.87.254.6 on 09/05/12
For personal use only.

Can. J. Chem. Downloaded from www.nrcresearchpress.com by 210.87.254.6 on 09/05/12
For personal use only.

and Wagner (29). Acetonitrile (Aldrich Gold Label) was refluxed over calcium hydride under a dry nitrogen atmosphere for 12 h and distilled.

Ultraviolet–visible absorption spectra were recorded on either a Cary 118 or a Cary 219 spectrophotometer at room temperature (23°C) with 1 cm cuvettes. A Varian XL-100 nmr spectrometer equipped with deuterium lock and probe temperature control was employed for the ^{1}Hmr studies.

All irradiations were carried out using a General Electric 1 kW medium pressure mercury lamp with a quartz cooling jacket (Photochemical Research Associates). All solutions were placed in Pyrex irradiation vessels flushed with dry nitrogen and sealed with rubber septa. The progress of the reactions were followed by ^{1}Hmr (Varian T-60). Two filter systems were employed in the irradiations: filter A, a 1 cm saturated aqueous solution of sodium nitrite which transmits all light of wavelength > 400 nm, and filter B, a Corning 0-51 glass filter (4 mm) which transmits light > 360 nm.

Determination of Association Constants of Charge-transfer Complexes by Ultraviolet–Visible Method

Both cases where $[D]_0 \gg [A]_0$ and $[A]_0 \gg [D]_0$ were studied using the same procedure, therefore only the latter case is described below.

A chloroform solution of the donor (ca. 10 m*M*) was first prepared. Then a series of five solutions as prepared by weighing various amounts of the acceptor (ca. 0.15 *M* to 1.0 *M*) in 5 mL volumetric flasks before introducing 3 mL of the above solution through a pipette. The absorption spectrum of each of the above solutions was measured immediately after preparation.

Evaluation of the K_c^{DA} and ε_λ^{DA}, in all cases, employed both the Benesi–Hildebrand and Foster–Hammick–Wardley methods. The slopes and *y*-intercepts of the plots were computed using a standard linear least-squares program. The correlation coefficients are generally better than 0.99 and 0.96 for the B–H and the F–H–W method respectively.

Determination of Association Constants of Charge-transfer Complexes by ^{1}Hmr Method

This method was employed only in the $[D]_0 \gg [A]_0$ case since the dicyanoethylene concentration dependence of the substituted naphthalene chemical shifts was small in the $[A]_0 \gg [D]_0$ case. The same procedure as in the uv–vis method was employed in preparing the solutions except that the present solvent is a 1:19 v/v mixture of cyclohexane-d_{12} – chloroform containing 0.02% (by weight) of tetramethylsilane (TMS). The deuterated solvent was used to provide a field lock so that accurate chemical shift values could be obtained. The chemical shifts of the dicyanoethylene protons were determined relative to the chloroform ^{13}C satellite which is in turn relative to TMS. Since the chemical shift of the chloroform proton shifts upfield upon increasing the concentration of the donor, the observed changes in the acceptor chemical shift relative to chloroform must be corrected before use. Evaluation of K_c^{DA} and Δ_0^{DA} were performed in the same fashion as the analogous uv–vis method.

Irradiation of the 1,4-Dimethoxynaphthalene – 1,2-Dicyanoethylene Charge-transfer Complex

A benzene solution of 1,4-DMN (0.3 *M*) and FN (0.3 *M*) was irradiated through filter B. The reaction was followed by ^{1}Hmr. After prolonged irradiation (600 h), a photostationary state mixture of FN:MN = 62:38 was obtained. Other reactions were relatively unimportant (< 5%). This photostationary state was also obtained starting either from MN or a synthetic mixture of FN:MN = 64:36.

Isomerization of the dinitrile was also observed under the same conditions using filter A (>400 nm), irradiating in a region where the individual components are transparent. The isomerization appeared to be slower in acetonitrile solution than in benzene solution under the same conditions.

Prolonged irradiation (290 h) of a benzene solution of 1,4-DMN (0.3 *M*) through a Pyrex reaction vessel did not lead to any observable product.

Irradiation of the 1,5-Dimethoxynaphthalene – 1,2-Dicyanoethylene Charge-transfer Complex

Prolonged irradiation of a benzene solution of 1,5-DMN (0.08 *M*) and FM (0.6 *M*) through filter B gave a photostationary state mixture of FN:MN = 63:37. This mixture was also obtained starting either from MN or from a synthetic mixture of FN:MN (64:36) under identical conditions. The formation of other products was negligible (< 5%) after prolonged irradiation.

Isomerization of the dinitrile was also observed when acetonitrile was the solvent. 1,5-DMN was stable in benzene solution (0.08 *M*) upon prolonged irradiation through a Pyrex filter.

Irradiation of the 2,3-Dimethoxynaphthalene – 1,2-Dicyanoethylene Charge-transfer Complex

Irradiation of a benzene solution of FN (or MN) (0.3 *M*) and 2,3-DMN (0.3 *M*) through filter B led to isomerization of the alkene. The photostationary state obtained either from FN or MN or a mixture of FN and MN (50:50) consisted of FN:MN = 44:56. Isomerization of the dinitriles also occurred in acetonitrile solution. In all cases, the formation of other products was negligible (< 5%).

Quantum Yield Measurements

Quantum yield measurements were performed using a Jasco CRM-FA quantum yield apparatus with a 2 kW mercury–xenon lamp as the light source. The irradiation wavelength was 362 ± 6 nm. Ferrioxalate actinometry was employed (30). The sample, consisting of 1,4-DMN (80 m*M*) and fumaronitrile (80 m*M*) in benzene solution, was degassed (3 freeze–pump–thaw cycles) and sealed. All light was being absorbed (OD > 2.0 at all times). At 1.6% conversion, the quantum yield for isomerization of FN to MN was 2.4×10^{-3} (±10%).

Spectroscopic Studies

Fluorescence spectra were recorded on a Perkin-Elmer MPF-4 fluorescence spectrophotometer at room temperature (23°C). The samples were degassed under high vacuum using three freeze–pump–thaw cycles. Stern–Volmer plots were obtained by plotting the intensity of the spectra at the maximum versus concentration of the quencher.

Fluorescence life times (25°C) were measured by the single photon counting technique, details of which have been described elsewhere (31). The excitation source was a Photochemical Research Associates deuterium nanosecond flash lamp system. The decay curves were deconvoluted by iterative deconvolution.

The phosphorescence spectra were recorded on a spectrometer described before (32).

Photo-CIDNP Experiment

The light source was an Oriel Corporation 200 W Hg–Xe lamp focused and passed through a quartz light pipe into the solution in a 5 mm nmr tube which was spinning inside the probe of a Varian XL-100 nmr spectrometer (field strength 23.5 kG). Solutions were degassed by purging thoroughly with dry nitrogen. The concentration range was kept between 10 to 130 m*M*. The CIDNP signals were able to survive for minutes after the light was switched off. The amount of isomerized alkenes was negligible.

Acknowledgements

This work was supported by a grant from the

Natural Sciences and Engineering Research Council of Canada. We gratefully acknowledge the assistance of Ms. H. Schroeder in obtaining the 100 MHz ^{1}Hmr spectra, and Dr. S. K. Wong for his help with the photo-CIDNP studies.

1. (*a*) P. C. WONG and D. R. ARNOLD. Can. J. Chem. **57**, 1037 (1979); (*b*) D. R. ARNOLD and P. C.WONG. J. Am. Chem. Soc. **101**, 1894 (1979).
2. M. W. HANNA and J. L. LIPPERT. *In* Molecular complexes. Vol. 1. *Edited by* R. Foster. Crane, Russak & Co., Inc., New York, NY. 1973.
3. S. K. SMIRNOV, I. G. SEVASTIJANOVA, A. P. TOMILOV, L. A. FEDOROVA, and O. G. STRUKOV. Zh. Org. Khim. **5**, 1392 (1969).
4. (*a*) H. A. STAAB and W. REBAFKA. Chem. Ber. **110**, 3333 (1977); (*b*) H. A. STAAB, C. P. HERZ, and H.-E. HENKE. Chem. Ber. **110**, 3351 (1977); (*c*) H. A. STAAB and H. HAFFNER. Chem. Ber. **110**, 3358 (1977); (*d*) H. A. STAAB and V. TAGLIEBER. Chem. Ber. **110**, 3366 (1977).
5. H. A. STAAB and C. P. HERZ. Angew. Chem. Int. Ed. Engl. **16**, 799 (1977).
6. H. V. G. EGE and H. A. STAAB. Tetrahedron, **31**, 2441 (1975).
7. R. FOSTER. Organic charge-transfer complexes. Academic Press, New York, NY. 1969.
8. H. A. BENESI and J. H. HILDEBRAND. J. Am. Chem. Soc. **71**, 2703 (1949).
9. R. FOSTER, D. LL. HAMMICK, and A. A. WARDLEY. J. Chem.Soc. 3817 (1953).
10. (*a*) W. R. WARE, P. R. SKUKLA, P. J. SULLIVAN, and R. V. BREPLIS. J. Chem. Phys. **55**, 4048 (1971); (*b*) W. R.WARE and T. L. LEWIS. Chem. Phys. Lett. **15**, 290 (1972); (*c*) W. R. WARE. Pure Appl. Chem. **41**, 635 (1975).
11. Y. SHIROTA, I. TSUSHI, and H. MIKAWA. Bull. Chem. Soc. Jpn. **47**, 991 (1974).
12. M. IRIE, S. TOMIMOTO, and K. HAYASHI. J. Phys. Chem. **76**, 1419 (1976).
13. N. ORBACH, R. POTASHNIK, and M. OTTOLENGHI. J. Phys. Chem. **76**, 113 (1972).
14. Y. TANIGUCHI, Y. NISHINA, and N. MATAGA. Bull. Chem. Soc. Jpn. **45**, 764 (1972).
15. (*a*) M. E. MICHEL-BEYERLE. Z. Naturforsch. Teil A, **31**, 499 (1976); (*b*) M. E. MICHEL-BEYERLE, R. HABERKORN, W. BUBE, E. STEFFENS, H. SCHRODER, H. J. NEUSTER, E. W. SCHLAG, AND H. SEIDLITZ. Chem. Phys. **17**, 139 (1976); (*c*) K. SCHULTEN, H. STAERK, A, WELLER, H.-J. WERNER, and B. NICKEL. Z. Phys. Chem. (Frankfurt am Main), **101**, 371 (1976).
16. J. HINATU, H. MASUHARA, N. MATAGA, Y. SAKATA, and S. MISUMI. Bull. Chem. Soc. Jpn. **51**, 1032 (1978).
17. R. POTASHNIK, C. R.GOLDSCHMIDT, and M. OTTOLENGHI. J. Phys. Chem. **73**, 3171 (1979).
18. P. SCHULER and H. HEUSINGER. J. Mol. Struct. **28**, 25 (1975).
19. (*a*) R. S. MULLIKEN and W. B. PERSON. Molecular complexes. Wiley, New York, NY. 1969; (*b*) R. FOSTER. *In* Molecular complexes. Vol. 2. *Edited by* R. Foster. Paul Elek (Scientific Books) Ltd., London. 1974.
20. G. BRIEGLEB. Electronen-donator-acceptor-komplexe. Springer Verlag, Berlin. 1961.
21. (*a*) G. L. CLOSS and M. S. CZEROPSKI. J. Am. Chem. Soc. **99**, 6127 (1977); (*b*) J. BARGON. J. Am. Chem. Soc. **99**, 8350 (1977).
22. H. D. ROTH. Mol. Photochem. **5**, 91 (1973).
23. (*a*) H. D. ROTH. *In* Chemically induced magnetic polarization. *Edited by* L. T. Muns *et al.* D. Reidel Publishing Co., Dordrecht-Holland. 1977.
24. P. D. SULLIVAN. J. Phys.Chem. **74**, 2563 (1970).
25. H. HAYASHI and S. NAGAKURA. Chem. Phys. Lett. **53**, 201 (1978).
26. F. D. LEWIS and J. T. SIMPSON. J. Phys. Chem. **83**, 2015 (1979).
27. G. E. FICKEN, R. P. LINSTEAD, E. STEPHEN, and M. WHALLEY. J. Chem. Soc. 3879 (1958).
28. B. R. BAKER and G. H. CARLSON. J. Am. Chem. Soc. **64**, 2662 (1942).
29. I. E. KOCHEVAR and P. J. WAGNER. J. Am. Chem. Soc. **94**, 3859 (1972).
30. C. G. HATCHARD and C. A. PARKER. Proc. R. Soc. London, Ser. A, **235**, 518 (1956).
31. (*a*) W. R. WARE. *In* Creation and detection of the excited state. Vol. 1. *Edited by* A. Lamola. Marcel Dekker, New York, NY. 1971. pp. 213–302; (*b*) C. LEWIS, W. R. WARE, L. J. DOEMENY, and T. L. NEMZEK. Rev. Sci. Instrum. **44**, 107 (1973); (*c*) W. R. WARE, L. J. DOEMENY, and T. L. NEMZEK. J. Phys. Chem. **77**, 2038 (1973).
32. D. R. ARNOLD and R. J. BIRTWELL. J. Am. Chem. Soc. **95**, 4599 (1973).
33. D. REHM and A. WELLER. Isr. J. Chem. **8**, 259 (1970).
34. A. ZWEIG, L. H. MAVREV, and B. G. ROBERTS. J. Org. Chem. **32**, 1322 (1967).

Can. J. Chem. Downloaded from www.nrcresearchpress.com by 210.87.254.6 on 09/05/12
For personal use only.

Axial dissymmetry induced magnetic nonequivalence in the ^{13}C nuclear magnetic resonance spectra of allenes[1]

PIERRE L. BEAULIEU, VERONIQUE M. MORISSET, AND DENNIS G. GARRATT[2]

Department of Chemistry, University of Ottawa, Ottawa, Ont., Canada K1N 9B4

Received May 1, 1979[3]

PIERRE L. BEAULIEU, VERONIQUE M. MORISSET, and DENNIS G. GARRATT. Can. J. Chem. **58**, 928 (1980).

The observation of the magnetic nonequivalence of isopropyl methyl carbon resonances as a result of axial dissymmetry in 27 appropriately substituted allenes is reported. The magnitude of the nonequivalence Δ is more dependent upon the adjacent substituent group than upon the substituents which are bonded to the remote sp^2 carbon of the allene. A mechanism based upon the transmission of substituent effects from the remote substituents to the collinear π orbitals is proposed.

PIERRE L. BEAULIEU, VERONIQUE M. MORISSET et DENNIS G. GARRATT. Can. J. Chem. **58**, 928 (1980).

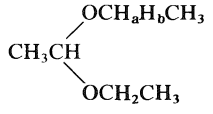
La non équivalence magnétique des carbones des méthyles du groupe isopropyle dans 27 allènes adéquatement substitués est due à une dissymétrie axiale. L'amplitude, Δ, de la non équivalence dépend d'avantage des substituants adjacents que des substituants liés au carbone sp^2 le plus éloigné de l'allène. On propose un mécanisme basé sur la transmission des effets des substituants éloignés jusqu'aux orbitales π disposées en ligne droite.

[Traduit par le journal]

The presence of a nearby center of molecular asymmetry is known to induce magnetic nonequivalence of the protons in methylene and isopropyl groups, although accidental degeneracy is frequently encountered, the protons appearing to be equivalent in the spectrum (1). The analogous effect of molecular centrodissymmetry on carbon-13 chemical shifts has been reported by Roberts and co-workers using compounds of the general type: $(CH_3)_2CH(CH_2)_nCHRR'$ (2).

It is not necessary, however, that a molecule be chiral for carbons or protons to be diastereotopic. A typical example from ^1H nmr spectroscopy is the diethyl acetal of acetaldehyde. Replacement of H_a by deuterium creates two chiral centres, the resulting molecule being a diastereomer of the species in which H_b is replaced by deuterium (1*e*, 3).

In contrast to the above, one may study compounds in which the lack of symmetry is not connected with the presence of asymmetrically substituted atoms, but results from an axis of dissymmetry such as is found in biphenyls, allenes, alkylidenecycloalkanes, and spiranes (4). For example, Martin and co-workers (5) have studied a number of allenic compounds with respect to the axial dissymmetry induced magnetic nonequivalence of methylene and isopropyl methyl proton resonances. The absolute magnitude of these nonequivalences is, however, quite small. In view of the greater sensitivity of ^{13}C nmr spectroscopy, and since to our knowledge, no one has investigated this phenomena by this technique, we have carried out a series of measurements of the chemical shift nonequivalence of isopropyl methyl carbon resonances as induced by the axial dissymmetry of 27 appropriately substituted allenes (6).[4]



Experimental

The allenes used during this investigation were synthesized by standard literature procedures (7) as part of another series of investigations. Full spectroscopic characterization of these compounds is to be reported separately. The ^{13}C nmr spectra were recorded using a Varian Associates FT80 spectrometer with a broad band probe, operating at 20.000 MHz, with 16K memory. Initial proton decoupled spectra were run with a spectral width of 4505 Hz. Subsequent spectra were recorded using spectral widths of 2000–2809 Hz dependent upon fold-back problems. A pulse width of 5 μs corresponding to a flip angle of approximately 21.5° was routinely employed. All samples were run in $CDCl_3$ at concentrations of 35% w/v at a probe temperature of 31°C. Chemical shifts are reported in units of δ downfield from an internal TMS standard, ± 0.02 ppm.

[1]Issued as NRCC No. 18138.

[2]Author to whom correspondence may be addressed at the Division of Chemistry, National Research Council of Canada, Ottawa, Ont., Canada K1A 0R6.

[3]Revision received January 18, 1980.

[4]Krudy and Macomber (6*a*) have reported that the chirality of the dimethyl allenic phosphonic ester, $(CH_3O)_2$-P(O)C(*t*Bu)=C=CH*t*Bu, renders the two methoxy groups on phosphorous nonequivalent. Unfortunately only an averaged chemical shift was reported. Runge and Firl (6*b*) list three trisubstituted allenes containing isopropyl groups, where in two cases the isopropyl methyl carbons have a chemical shift difference of 0.1 ppm and the remaining compound shows apparent accidental coincidence.

0008-4042/80/090928-04$01.00/0

©1980 National Research Council of Canada/Conseil national de recherches du Canada

Can. J. Chem. Downloaded from www.nrcresearchpress.com by 210.87.254.5 on 09/05/12
For personal use only.

Can. J. Chem. Downloaded from www.nrcresearchpress.com by 210.87.254.5 on 09/05/12
For personal use only.

Results and Discussion

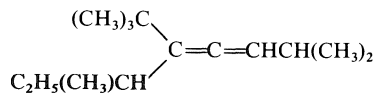
The ^{13}C nmr chemical shifts of the methyl carbons of isopropyl groups appear in Table 1. The degree of nonequivalence, Δ, of the methyl carbons *a* and *b* (where the designations *a* and *b* are more or less arbitrary) is seen to be very dependent upon the substituent pattern, the group bonded *geminal* to the isopropyl having the greatest influence. For example, when R = R″ = H and R′ is varied through the series: methyl–ethyl–isopropyl–*tert*-butyl (entries 1–4), the change in Δ is quite dramatic, 0.03 to 0.18 ppm, whereas when R = CH_3, R″ = H, and R′ is similarly varied (entries 10–14) Δ is relatively constant at 0.15 ± 0.02 ppm within experimental error. When R = *i*-C_3H_7 or *t*-C_4H_9, R″ = H (entries 19–22 and 24–27, respectively), a similar variation in R′ shows some fluctuations but with a general tendency towards larger values of Δ. The effect of changing R while holding R′ and R″ constant is perhaps best seen using entries 4, 14, 22, and 27. The variation of R from H to methyl–isopropyl–*tert*-butyl in this set gives values of Δ of: 0.18, 0.15, 0.38, and 0.83. The decrease between the values given for hydrogen and methyl suggests that there is a reversal in the factors giving rise to the shift difference. This is again suggested by the set of entries 7, 15, 18, and 30, where the absolute values of Δ are, respectively, 0.18, 0.14, 0.00, and 0.21.

TABLE 1. The observed ^{13}C nuclear magnetic resonance chemical shifts of diastereotopic isopropyl methyl carbons in allenes ($(CH_3)_2CHCR{=}C{=}CR'R''$)

	Allene			Chemical shifts (δ ± 0.02 ppm)		
Entry	R	R′	R″	δ_a	δ_b	$\Delta = \delta_a - \delta_b$
1	H	CH_3	H	22.63	22.60	0.03
2	H	C_2H_5	H	22.45	22.40	0.05
3	H	*i*-C_3H_7	H	22.61	22.44	0.17
4	H	*t*-C_4H_9	H	22.59	22.41	0.18
5	H	CH_3	C_2H_5	22.63	22.53	0.10
6	H	CH_3	*i*-C_3H_7	22.75	22.57	0.18
7	H	CH_3	*t*-C_4H_9	22.65	22.47	0.18
8	H	C_2H_5	*t*-C_4H_9	22.59	22.59	0.00
9	H	*i*-C_3H_7	*t*-C_4H_9	22.54	22.51	0.03
10	CH_3	CH_3	H	21.60	21.44	0.16
11	CH_3	C_2H_5	H	21.70	21.55	0.15
12	CH_3	*i*-C_3H_7	H	21.69	21.54	0.15
13	CH_3	C_6H_{11}	H	21.74	21.57	0.17
14	CH_3	*t*-C_4H_9	H	21.70	21.55	0.15
15	CH_3	CH_3	*t*-C_4H_9	21.64	21.50	0.14
16	CH_3	C_2H_5	*t*-C_4H_9	21.72	21.72	0.00
17	CH_3	*i*-C_3H_7	*t*-C_4H_9	21.96	21.64	0.32
18	C_2H_5	CH_3	*t*-C_4H_9	21.99	21.99	0.00
19	*i*-C_3H_7	CH_3	H	22.50	22.21	0.29
20	*i*-C_3H_7	C_2H_5	H	22.57	22.31	0.26
21	*i*-C_3H_7	*i*-C_3H_7	H	22.73	22.39	0.34
22	*i*-C_3H_7	*t*-C_4H_9	H	22.73	22.35	0.38
23	*i*-C_3H_7	*i*-C_3H_7	*t*-C_4H_9	21.83	21.26	0.57
24	*t*-C_4H_9	CH_3	H	24.85	24.31	0.54
25	*t*-C_4H_9	C_2H_5	H	24.94	24.39	0.55
26	*t*-C_4H_9	*i*-C_3H_7	H	24.87	24.21	0.66
27	*t*-C_4H_9	*t*-C_4H_9	H	25.17	24.34	0.83
28	*t*-C_4H_9	CH_3	C_2H_5	24.95	24.95	0.00
29	*t*-C_4H_9	CH_3	*i*-C_3H_7	25.11	24.82	0.29
30	*t*-C_4H_9	CH_3	*t*-C_4H_9	24.98	24.77	0.21

We observed in total four cases of apparent accidental coincidence of the methyl carbon resonances (entries 8, 16, 18, and 28). Of interest is the observation that entries 16, 18, and 28 are all tetrasubstituted allenes, each of which contains the methyl, ethyl, isopropyl, and *tert*-butyl groups, but in different spatial arrangements. There are, furthermore, two cases (entries 1 and 9) where the value of Δ, 0.03 ppm, was just at our level of detectability.

In general Δ will be the summation of two terms: $\Delta = \Delta_{CP} + \Delta_{ID}$, where Δ_{CP} is dependent on conformer populations, and Δ_{ID} results from the intrinsic diastereotopism of the averaged environments of the isopropyl methyl carbons, and which will be as a consequence independent of conformer populations (8). The contribution of intrinsic diastereotopism to the magnetic nonequivalence of the diastereotopic carbons is determinable only in those cases where the individual conformers are observable. This, however, we have not been able to achieve. Since the contribution of intrinsic nonequivalence is usually small, the magnitude of the nonequivalence observed seems most reasonably to result from factors which enhance the local dissymmetry inherent in the molecule. One must be careful, however. For example, Raban (8) has shown that the value of Δ_{ID} may be small as a result of the fortuitous cancelling of large terms of opposite sign. Of interest in this respect is our observation that the (RS,RS) and (RS,SR) diastereomers of allene **31** (2,6-dimethyl-5-*tert*-butyl-3,4-octadiene) are readily distinguished from each other via ^{13}C nmr.

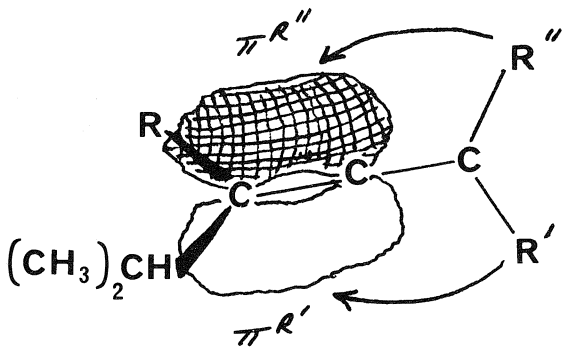


31

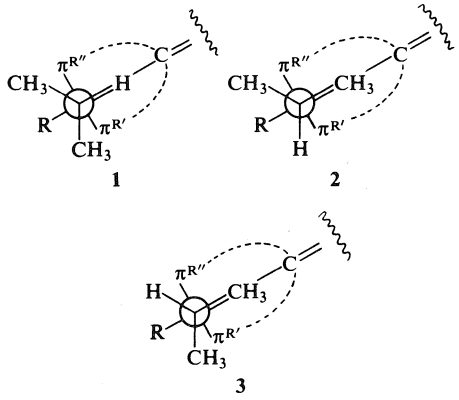
Examples of factors which may enhance the local dissymmetry are preferred conformations and hindrance to free rotation resulting from steric effects or conformational restrictions due to specific solvent interactions which alter the average molecular geometry.

Can. J. Chem. Downloaded from www.nrcresearchpress.com by 210.87.254.5 on 09/05/12
For personal use only.

One notes upon examining Dreiding molecular models that the substituents in the 1 and 3 positions of an allene (propadiene) are sufficiently remote that in most conformations the spatial orientation of one group should not influence the other by a direct steric interaction. As a result we anticipate that each group must very nearly achieve what might be termed time-averaged conformational symmetry with respect to the pertinent molecular plane of the allene (for example, the CH_2—C_{sp2}—H plane assuming non-spherical substituents such as C_2H_5 and n-C_3H_7). We therefore make the hypothesis that any conformational effects which are a result of the remote groups are transmitted via perturbations of the collinear π orbitals, $\pi^{R'}$ and $\pi^{R''}$, as is shown below:



Assuming that perturbations in these π orbitals reflect steric and electronic effects of the groups R′ and R″, one is able to envision the three staggered conformations, **1**–**3**.

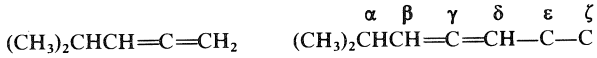


Of note is the fact that R is oriented perpendicular to both $\pi^{R'}$ and $\pi^{R''}$. This effect, which is intrinsic to the allenic functionality, results in the groups which are *gauche* to the substituent R (for example, both methyls in conformer **1**) experiencing large interactions with $\pi^{R'}$ and $\pi^{R''}$. Furthermore, a staggered conformation with respect to the group R leads to an eclipsing of the third substituent (H in **1**, CH_3 in **2** and **3**) with the *sp*-hybridized allenic carbon. The relatively small values of Δ we believe reflect attenuation of the substituent effects with transmission of the dissymmetry over the two bonds of the allenic system.

It seems apparent from an examination of conformers **1**–**3** that variation of the group R will give rise to a larger effect than the corresponding substitutions at either R′ or R″, as is observed. Thus when R is a bulky substituent, such as *tert*-butyl, conformers **2** and **3** should be favoured over **1**. If the perfect staggered arrangements in **2** and/or **3** are retained, the methyls will experience very different local environments, and therefore exhibit a large Δ (see for example entries 19–22). However, a large methyl–R interaction may cause sufficient departure from these purely staggered arrangements, diminishing the immediate magnetic interaction between methyl and R, but causing an essential eclipsing interaction of the methyls and $\pi^{R'}$, $\pi^{R''}$. Under such conditions very little difference in chemical shifts may be anticipated (entry 28), unless R′ and R″ are quite different with respect to their ability to perturb the π orbitals (compare entries 28–30 with 24–27). It is noteworthy in this respect that a number of fluctuations or reversals are observed in Table 1, as was mentioned earlier.

One may, however, argue that the methyls do not deform enough to go into the conformation implied above because of angle strain. In this alternative scenario the near-zero values of Δ presumably arise from nearly equal contributions from **2** and **3**, but with opposite signs. A variation on this hypothesis arises if one considers the possibility that perturbations in $\pi^{R'}$ and $\pi^{R''}$ may be quite small. Under such circumstances, with equal contributions from **2** and **3** and R = *tert*-butyl, the value of Δ may reflect a relatively large contribution from the Δ_{ID} term rather than a conformational effect.

Given that the isopropyl methyl carbon resonance in 4-methyl-1,2-pentadiene, **32**, is $\delta = 22.9$, we observe a diamagnetic ε-substituent effect of approximately 0.3 ppm for both methyl carbons (entry 1) and a ζ-substituent effect of approximately 0.2 ppm, also to higher field (entries 2–4). Of note here is the observation that δ_a and δ_b in species **3** and **4** show the two extremes as represented in entries **1** and **2**. Unfortunately we were not able at this time to obtain definitive conformational data based upon existing correlations between stereo-



32

chemical factors in the allenes and ^{13}C nmr chemical shifts. Studies related to this problem are, however, in progress.

In summary these data reflect the probable conformational origin of axial dissymmetry induced chemical shift nonequivalence of isopropyl methyl carbons in allenic systems.

Acknowledgements

The continued financial support of the Natural Sciences and Engineering Research Council of Canada is gratefully acknowledged, as is a Province of Ontario Graduate Scholarship 1978–1980 to one of us (PLB). We also wish to thank Dr. R. R. Fraser for useful discussions with respect to the probable cause of the observed nonequivalence.

1. (*a*) P. M. NAIR and J. D. ROBERTS. J. Am. Chem. Soc. **79**, 4565 (1957); (*b*) H. S. GUTOWSKY. J. Chem. Phys. **37**, 2196 (1962); (*c*) W. F. REYNOLDS and T. SCHAEFER. Can. J. Chem. **42**, 2119 (1964); (*d*) M VON GORKOM and G. E. HALL. Q. Rev. (London), **22**, 14 (1968); (*e*) K. MISLOW and M. RABAN. *In* Topics in stereochemistry. Vol. 1. *Edited by* Allinger and E. L. Eliel. Interscience, New York. 1967. pp. 1–38.
2. J. I. KROSCHWITZ, M. WINOKUR, H. J. REICH, and J. D. ROBERTS. J. Am. Chem. Soc. **91**, 5927 (1969).
3. J. B. LAMBERT, H. F. SHURVELL, L. VERBIT, R. G. COOKS, and G. H. STOUT. *In* Organic structural analysis. MacMillan Publishing Co., Inc., New York. 1976. p. 56.
4. E. L. ELIEL. *In* Stereochemistry of carbon compounds. McGraw-Hill Book Co., London. 1962. Chapt. 11. p. 307.
5. (*a*) M. L. MARTIN, R. MANTIONE, and G. J. MARTIN. Tetrahedron Lett. 3185 (1965); (*b*) M. L. MARTIN, R. MANTIONE, and G. J. MARTIN. Tetrahedron Lett. 3873 (1966); (*c*) M. L. MARTIN, R. MANTIONE, and G. J. MARTIN. Tetrahedron Lett. 4809 (1967).
6. (*a*) G. A. KRUDY and R. S. MACOMBER. J. Org. Chem. **43**, 4656 (1978); (*b*) W. RUNGE and J. FIRL. Ber. Bunsenges. Phys. Chem. **79**, 913 (1975).
7. (*a*) P. VERMEER, H. WESTMUZE, H. KLEIJN, and L. A. VAN DUCK. Recl. J. R. Neth. Chem. Soc. **97**, 56 (1978); (*b*) P. VERMEER, J. MEIJER, and L. BRANDSMA. Recl. Trav. Chim. Pays-Bas, **94**, 112 (1975); (*c*) W. VON E. DOERING and P. M. LAFLAMME. Tetrahedron, **2**, 75 (1958); (*d*) L. SKATTEBOL. Acta Chem. Scand. **17**, 1683 (1963).
8. M. RABAN. Tetrahedron Lett. 3105 (1966), and references cited therein.

Can. J. Chem. Downloaded from www.nrcresearchpress.com by 210.87.254.5 on 09/05/12
For personal use only.

On the nature of the radical pairs involved in the Grignard reaction

BAREND JOHANNES SCHAART, CORNELIS BLOMBERG, OTTO SJOUKE AKKERMAN, AND FRIEDRICH BICKELHAUPT

Scheikundig Laboratorium der Vrije Universiteit, De Boelelaan 1083, 1081 HV Amsterdam–Buitenveldert, The Netherlands

Received November 13, 1979

This paper is dedicated to Prof. Karel Wiesner on the occasion of his 60th birthday

BAREND JOHANNES SCHAART, CORNELIS BLOMBERG, OTTO SJOUKE AKKERMAN, and FRIEDRICH BICKELHAUPT. Can. J. Chem. **58**, 932 (1980).

During the simultaneous reaction of alkyl bromides and of *p*-halosubstituted benzyl bromides with magnesium in THF/C_6D_6 (1:4), CIDNP net effects (emission) are observed in the ^1H nmr spectrum. The effects are opposite to those occurring during the reaction of preformed ethylmagnesium bromide and the benzyl bromides. These results constitute firm evidence that only alkyl radical pairs $\overline{R{\cdot\cdot}R}$ are responsible for the CIDNP effects, and that the radicals R· are generated in the Grignard reaction proper, rather than in unrelated side reactions such as Wurtz coupling or metal halogen exchange.

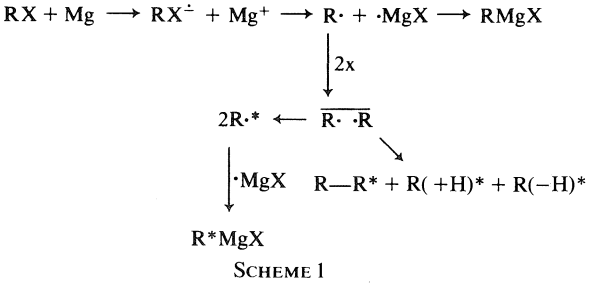
BAREND JOHANNES SCHAART, CORNELIS BLOMBERG, OTTO SJOUKE AKKERMAN et FRIEDRICH BICKELHAUPT. Can. J. Chem. **58**, 932 (1980).

On a observé dans le spectre rmn du ^1H des effets globaux de polarisation nucléaire dynamique induite chimiquement (PNDIC) qui apparaissent pendant la réaction silmultanée entre le magnésium dans un mélange THF/C_6H_6 (1:4) et des bromures d'alkyles et des bromures de benzyles substitués en position *para* par un halogène. Les effets sont en opposition à ceux observés lors de la réaction des bromures d'éthylmagnésium et des bromures de benzyles préformés. Ces résultats constituent une preuve tangible du fait que seuls les paires de radicaux alkyles $\overline{R{\cdot\cdot}R}$ sont responsables des effets PNDIC et du fait que les radicaux R· sont générés par la réaction de Grignard proprement dite plutôt que par des réactions secondaires indépendantes telles qu'un couplage de Wurtz ou une réaction d'échange métal–halogène.

[Traduit par le journal]

Introduction

In recent years strong support has been obtained (1–3) for the mechanism of formation of Grignard compounds in the reaction of alkyl halides with magnesium metal (henceforth called the Grignard reaction) as presented in Scheme 1.



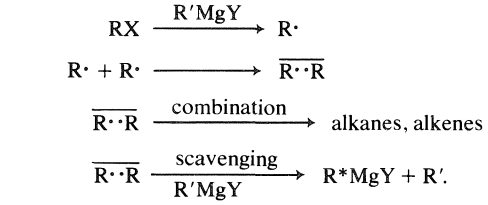
SCHEME 1

The evidence was based on product analysis and on a study of the influence of the solvent (2, 3*a*), on kinetic studies (3*b–d*), and in particular on the observation of CIDNP effects in the ^1H nmr spectrum (2). However, some problems remained.

In the first place, two radical pairs were originally considered as plausible precursors of the polarized products in the reaction, i.e., $\overline{R{\cdot\cdot}MgX}$ (**1**) and $\overline{R{\cdot\cdot}R}$ (**2**). Unfortunately, the *g*-factor of MgX· is not known, but it is likely to be different from the *g*-factor of R·. With $\Delta g \neq 0$, the occurrence of **1** as polarizing radical pair should have given rise to net effects (4). This was not the case; only multiplet effects were observed in the Grignard reagent. Consequently **1** was considered to be unlikely, but additional evidence was clearly desirable.

In the second place, Lawler and Livant (5) have shown that the polarization in the Grignard compound could in principle also arise from a catalyzed halogen–metal exchange reaction of the newly formed Grignard reagent with the alkyl halide (Scheme 2). Although evidence has been presented that this latter reaction was not responsible for the major part of the polarization observed in the Grignard reaction (1), an unequivocal confirmation of the proposed scheme was deemed necessary.

In the present investigation conclusive evidence on these problems is presented. The novel approach applied involved the study of the Grignard reaction using mixtures of halides which produce radicals with different *g*-factors.



SCHEME 2

0008-4042/80/090932-06$01.00/0
©1980 National Research Council of Canada/Conseil national de recherches du Canada

Can. J. Chem. Downloaded from www.nrcresearchpress.com by 210.87.254.5 on 09/05/12
For personal use only.

Can. J. Chem. Downloaded from www.nrcresearchpress.com by 210.87.254.5 on 09/05/12
For personal use only.

Results and Discussion

The Unique Involvement of Radical Pairs of Type $\overline{R\cdot\cdot R}$ *(2)*

The ^{1}H nmr spectrum was recorded on a Varian A56/60 D spectrometer during the reaction of ethyl bromide and *p*-chlorobenzyl bromide with magnesium in a mixture of tetrahydrofuran and perdeuterobenzene (1:4), eq. [1]; this spectrum is shown in Fig. 1.

[1] $CH_3CH_2Br + p\text{-}ClC_6H_4CH_2Br + Mg \xrightarrow[C_6D_6]{THF} CH_3CH_2MgBr + p\text{-}ClC_6H_4CH_2MgBr + \text{other products}$

Besides the formation of small amounts of *p*-$ClC_6H_4CH_2MgBr$ (CH, δ = 1.78 ppm), a clear net emission (E) superimposed on a multiplet effect E/A for the CH_2-group of CH_3CH_2MgBr (δ = −0.03 ppm) is observed. This can be explained by invoking the radical pairs

$\overline{p\text{-}ClC_6H_4CH_2\cdot\cdot CH_2CH_3}$ and $\overline{CH_3CH_2\cdot\cdot CH_2CH_3}$

as precursors of polarized CH_3CH_2MgBr. With $g_{CH_3CH_2\cdot}$ = 2.0025 (6) and $g_{p\text{-}ClC_6H_4CH_2\cdot}$ = 2.0027 (4*a*), application of Kaptein's sign rules (7) predicts the polarization observed for the CH_2 group of CH_3CH_2MgBr; in particular a net emission (E) and an E/A multiplet are expected ($\Gamma = \mu\cdot\varepsilon\cdot A_i\cdot\Delta g$ = +·−·−·−=−: E since μ = + (F-pair), ε = − (escape reaction), A_i = −22.4 (6), and $\Delta g = g_{CH_3CH_2\cdot} - g_{p\text{-}ClC_6H_4CH_2\cdot}$ = −; $\Gamma = \mu\cdot\varepsilon\cdot A_iA_j\cdot J_{ij}\cdot\delta_{ij}$ = +·−·−·+·+·+=+: E/A since μ = + (F-pair), ε = − (escape reaction), A_j = + 26.9 (6), J_{ij} = +, δ_{ij} = + (both nuclei *i* and *j* reside on the same radical).

Even more clearly, the net effect is demonstrated in the analogous reaction of CH_3I and *p*-$ClC_6H_4CH_2Br$ with magnesium in THF-d_8/C_6D_6 (Fig. 2). In this case a multiplet effect is not possible and a pure net emission is observed for CH_3MgI and for ethane (δ = −1.0 ppm and δ = 0.8 ppm respectively; $g_{CH_3\cdot}$ = 2.0025 (6)). Methane could not be detected in this reaction.

The cage product *p*-$ClC_6H_4CH_2CH_3$, however, is observed with a net polarization in agreement with Kaptein's sign rule (δ = 1 ppm, triplet, A, CH_3; δ = 2.3 ppm, quartet, E, CH_2). No net polarization was observed when either CH_3I or *p*-$ClC_6H_4CH_2Br$ were separately reacted with magnesium under identical conditions. It is obvious that ·MgBr cannot have the same *g*-factor as both $CH_3\cdot$ and *p*-$ClC_6H_4CH_2\cdot$; therefore, radical pairs

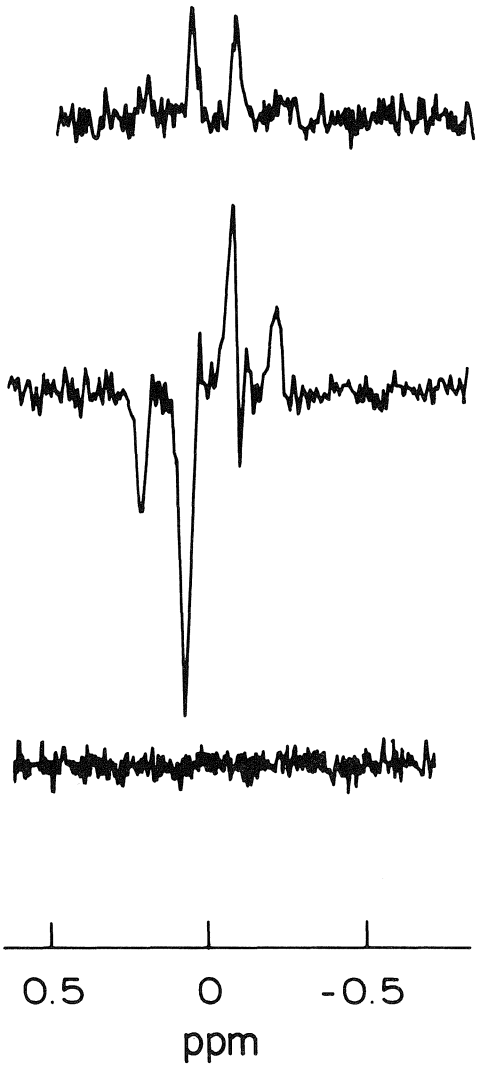


FIG. 1. Part of the 60 MHz ^{1}H nmr spectrum recorded during the reaction of C_2H_5Br and *p*-$ClC_6H_4CH_2Br$, with Mg in THF/C_6D_6 (1:4). (*a*) *t* = 0; (*b*) *t* = 0.5 min; (*c*) *t* = 4 min.

$\overline{R\cdot\cdot MgX}$ (type **1**) cannot be the source of the observed net effect.

So the CIDNP effects in the simultaneous reaction of CH_3I (or CH_3CH_2X, X = Br, I) and *p*-$ClC_6H_4CH_2Br$ with magnesium not only constitute the first example of net polarization observed in a Grignard reagent, but, by exclusion, also provide conclusive evidence that radical pairs originating from the alkyl groups of the alkyl halides (type **2**) are directly and exclusively involved as intermediates in the process leading to polarization in the Grignard reaction.

As stated earlier (2*b*), it is surprising that radical

Can. J. Chem. Downloaded from www.nrcresearchpress.com by 210.87.254.5 on 09/05/12
For personal use only.



FIG. 2. Part of the 60 MHz ^{1}H nmr spectrum recorded during the reaction of CH_3I and p-$ClC_6H_4CH_2Br$ with Mg in THF-d_8/C_6D_6 (1:4). (*a*) $t = 0$; (*b*) $t = 2$ min; (*c*) $t = 3$ min; (*d*) $t = 7$ min.

pairs of type **1**, although they must necessarily be postulated in the mechanism of Scheme 1, do not give rise to observable polarization. Several possible explanations can be advanced. According to the diffusional model of Adrian (8), the maximum net effect in a given magnetic field is reduced if large differences in the g-factor occur (less than 20% of the maximum enhancement may be found for $[\Delta g] > 20.10^{-3}$). Determination of the g-factor of ·MgBr is necessary to decide if this explanation is appropriate. Alternatively, rapid electron spin relaxation could be responsible for the absence of nuclear polarization (9) from the type **1** radical pairs.

The Origin of Polarizing Radical Pairs of Type 2

It has been shown in the previous section that in the simultaneous reaction of CH_3CH_2Br and p-$ClC_6H_4CH_2Br$ with magnesium, the CIDNP may be explained by invoking a diffusive encounter alkyl radical pair, e.g. $\overline{R \cdot\cdot R}$. With respect to the origin of such a radical pair, it has been pointed out in the introduction that the source of the radicals involved is to a certain extent subject to controversy (1, 5). These radicals might in principle be produced either by electron transfer from the metal to the alkyl halide (Scheme 1), in which case the polarization would reveal information on the Grig-

Can. J. Chem. Downloaded from www.nrcresearchpress.com by 210.87.254.5 on 09/05/12
For personal use only.

nard process proper (1, 2), or the radicals might be produced in a secondary reaction between the Grignard compound and the alkyl halide (Scheme 2), in which case polarization is irrelevant with regard to the principal steps of the Grignard reaction (5).

However, it has now been unequivocally shown that in the present case Scheme 2 is not to any observable extent responsible for the polarization effects occurring during the Grignard reaction, by performing the reaction of Scheme 2 separately, i.e., by adding p-$ClC_6H_4CH_2Br$ to a solution of preformed CH_3CH_2MgBr in THF/C_6D_6 at 40°C (Fig. 3). In this reaction, an absorption effect (A) is recognized in the CH_2-group of the Grignard reagent, which is opposite to the emission observed in the Grignard reaction!

The same effect is observed when the reaction is performed with p-$BrC_6H_4CH_2Br$ ($g_{p\text{-}BrC_6H_4CH_2\cdot} = 2.0047$) (4*a*), although in this case the effect is less obvious. This is completely in agreement with the prediction of the relative intensities of the lines in the multiplet by the method of Müller (10) (Fig. 4).

By the same arguments as given in the previous section, net polarization again implies that $\overline{p\text{-}ClC_6H_4CH_2\cdot\cdot CH_2CH_3}$ must be the polarizing radical pair. Moreover, as can be seen in Fig. 5, CH_3CH_2Br is produced simultaneously, and it also shows net absorption (CH_2, $\delta = 2.92$ ppm; A). Application of Kaptein's sign rule (7) for net effects (CH_3CH_2MgBr and CH_3CH_2Br, quartet, A, $\Gamma = \mu\cdot\varepsilon\cdot A_i\cdot\Delta g = \mu\cdot-\cdot-\cdot-$, so $\mu = -$; singlet precursor) indicates that both CH_3CH_2MgBr and CH_3CH_2Br are escape products from radical pairs from *singlet precursors*.[1]

Evidently, the following reactions occur (Scheme 3):

$$CH_3CH_2MgBr + p\text{-}ClC_6H_4CH_2Br \xrightarrow{S} \overline{p\text{-}ClC_6H_4CH_2\cdot\cdot CH_2CH_3}$$

$$\overline{p\text{-}ClC_6H_4CH_2\cdot\cdot CH_2CH_3} \longrightarrow CH_3CH_2Br\ (A) + CH_3CH_2MgBr\ (A)$$

SCHEME 3

The mechanism of incorporation of the polarized ethyl radicals into CH_3CH_2MgBr and CH_3CH_2Br is uncertain at the moment. However, the observed effects may be of great importance for a better understanding of metal–halogen exchange and Wurtz-type reactions. The occurrence of singlet precursors during the reaction of alkyl halides (11) and benzyl halides (12) with organolithium compounds has been reported, but CIDNP was observed in the side products only and not in the organolithium reagent. The CIDNP observed in our Grignard compound confirms the occurrence of radicals during the metal halogen exchange reaction.

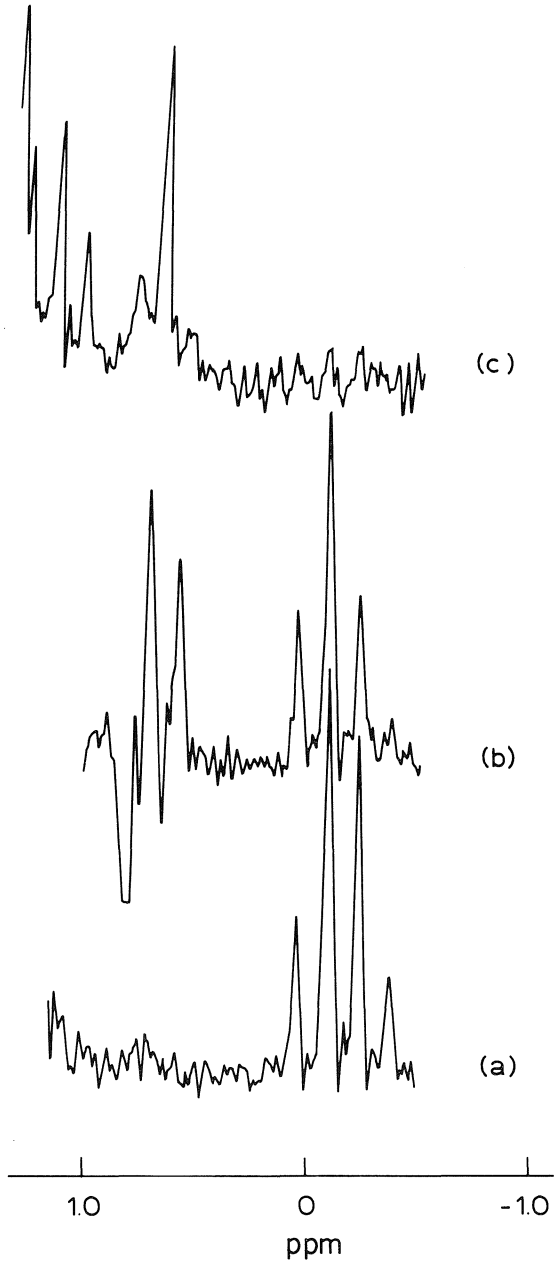


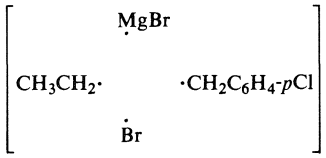
FIG. 3. Part of the 60 MHz ^1H nmr spectrum recorded during the reaction of C_2H_5MgBr with p-$ClC_6H_4CH_2Br$ in THF/C_6D_6 (1:4). (*a*) Before, (*b*) during, (*c*) after the reaction.

[1]If catalytic impurities are responsible for CIDNP during the Grignard reaction, they should give the same polarization in the reaction of the benzyl halide with a preformed Grignard reagent since these impurities are still present in the latter.



FIG. 4. The 60 MHz ^{1}H nmr spectrum of the methylene protons of C_2H_5MgBr recorded during the reaction with p-$BrC_6H_4CH_2Br$ in THF/C_6D_6 (1:4).

Both the product formation and the polarization effects described in this reaction are consistent with the occurrence of a caged system in the reaction of Scheme 3:



An extensive discussion of this aspect is beyond the scope of the present investigation. However, whatever the details of the mechanism of the metal–halogen exchange reaction may be, it does not significantly contribute to the polarization; Scheme 1 represents the only mechanism of the Grignard reaction compatible with the experimental results.

It should finally be pointed out that while opposite CIDNP net effects are observed in the Grignard reaction and in the metal–halogen exchange reaction in the case of added benzyl halide, Lawler and Livant have shown that if the halide and the Grignard reagent both carry alkyl groups, the Grignard and the exchange reaction exhibit CIDNP multiplet effects of the same sign (5). This inconsistency may be related to the catalyzed character of Lawler and Livant's reaction; moreover, there still exists some controversy on the mechanism of the Wurtz reaction (13), and also in this respect the observed phenomena deserve further investigation.

Acknowledgments

Financial support (B.J.S.) from the Netherlands Organization for the Advancement of Pure Research (Z.W.O.) via the Netherlands Foundation of Chemical Research (S.O.N.) is gratefully acknowledged.

1. B. J. SCHAART, H. W. H. J. BODEWITZ, C. BLOMBERG, and F. BICKELHAUPT. J. Am. Chem. Soc. **98**, 3712 (1976).
2. (*a*) H. W. H. J. BODEWITZ, C. BLOMBERG, and F. BICKELHAUPT. Tetrahedron Lett. 218 (1972); (*b*) Tetrahedron,

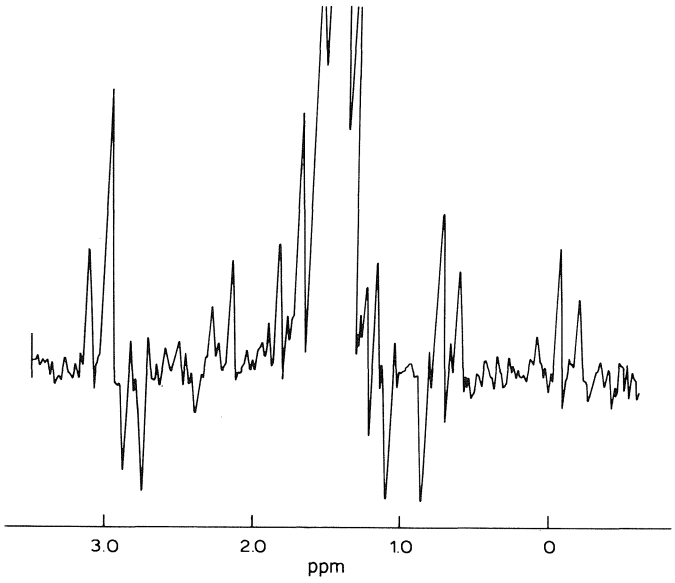


FIG. 5. Part of the 60 MHz ^{1}H nmr spectrum recorded during the reaction of C_2H_5MgBr with p-$ClC_6H_4CH_2Br$ in THF/C_6D_6 (1:4).

Can. J. Chem. Downloaded from www.nrcresearchpress.com by 210.87.254.5 on 09/05/12
For personal use only.

29, 719 (1973); (*c*) Tetrahedron, **31**, 1053 (1975); (*d*) Tetrahedron Lett. 2003 (1975); (*e*) H. W. H. J. BODEWITZ. Thesis, Vrije Universiteit, Amsterdam, 1975; (*f*) H. W. H. J. BODEWITZ, B. J. SCHAART, J. D. VAN DER NIET, C. BLOMBERG, F. BICKELHAUPT, and J. A. DEN HOLLANDER. Tetrahedron, **34**, 2523 (1978).

3. (*a*) H. M. WALBORSKY and M. S. ARONOFF. J. Organomet. Chem. **51**, 31 (1973); (*b*) R. J. ROGERS, H. L. MITCHELL, Y. FUJIWARA, and G. M. WHITESIDES. J. Org. Chem. **39**, 857 (1974); (*c*) E. A. VOGLER, R. L. STEIN, and J. M. WAGNER. J. Am. Chem. Soc. **100**, 3163 (1978); (*d*) M. HORAK, V. PALM, and V. SOOGENBITS. Reakts. Sposobn. Org. Soedin. **11**, 709 (1975); **11**, 721 (1975); Chem. Abstr. **84**, 73330b (1976); **84**, 734359q (1976).
4. (*a*) G. L. CLOSS. *In* Chemically induced magnetic polarization. *Edited by* A. R. Lepley and G. L. Closs. Wiley, New York. 1973; (*b*) R. G. LAWLER. *In* Progress in nuclear magnetic resonance. Vol. 9. *Edited by* J. W. Emsley, J. Feeney, and L. M. Sutcliffe. Pergamon Press, Oxford. 1973; (*c*) C. RICHARD and P. GRANGER. *In* NMR basic principles and progress. Vol. 8. *Edited by* P. Diehl, E. Fluck, and R. Kosfeld. Springer, Berlin. 1974.
5. R. G. LAWLER and P. LIVANT. J. Am. Chem. Soc. **98**, 3711 (1976).
6. R. W. FESSENDEN and R. H. SCHULER. J. Chem. Phys. **39**, 2147 (1963).
7. R. KAPTEIN. Chem. Commun. 732 (1971).
8. F. J. ADRIAN. J. Chem. Phys. **53**, 3374 (1970).
9. J. A. DEN HOLLANDER and R. KAPTEIN. Chem. Phys. Lett. **41**, 257 (1976).
10. K. MÜLLER. Chem. Commun. 45 (1972).
11. R. B. ALLAN, R. G. LAWLER, and H. R. WARD. J. Am. Chem. Soc. **95**, 1692 (1973).
12. R. Z. SAGDEEV, YU. N. MOLIN, K. M. SALIKOV, T. V. LESHINA, M. A. KAMKA, and S. M. SHEIN. Org. Magn. Reson. **5**, 599 (1973).
13. I. P. BELETSKAYA, G. A. ATAMKINA, and O. A. REUTOV. Russ. Chem. Rev. **45**, 330 (1976).

Can. J. Chem. Downloaded from www.nrcresearchpress.com by 210.87.254.5 on 09/05/12
For personal use only.

Thermochemistry of the lower bromides of tantalum

ALAN D. WESTLAND

Department of Chemistry, University of Ottawa, Ottawa, Ont., Canada K1N 9B4

Received August 23, 1979

ALAN D. WESTLAND. Can. J. Chem. **58**, 938 (1980).

The standard enthalpy of formation of tantalum(IV) bromide has been determined by solution calorimetry: $\Delta H_f^0(TaBr_4(c)\ 298\ K) = -125.6 \pm 0.5$ kcal mol^{-1}. Experimental estimates of the enthalpies of formation of tantalum(III) bromide and tantalum(II,III) bromide were also obtained. Estimates of the entropies and heat capacities of the compounds are also given.

ALAN D. WESTLAND. Can. J. Chem. **58**, 938 (1980).

On a déterminé, par calorimétrie en solution, l'enthalpie standard de formation du bromure de tantale(IV); $\Delta H_f^0(TaBr_4(c)\ 298\ K) = -125.6 \pm 0.5$ kcal mol^{-1}. On a également obtenu des évaluations expérimentales des enthalpies de formation des bromures de tantale(III) et de tantale(II,III). On donne également des évaluations des entropies et des capacités calorifiques de ces composés.

[Traduit par le journal]

Can. J. Chem. Downloaded from www.nrcresearchpress.com by 210.87.254.40 on 09/05/12
For personal use only.

Thermochemical data are lacking for the lower bromides of tantalum. The present work reports a solution calorimetric determination of the standard enthalpy of formation of tantalum(IV) bromide. Measurement of the enthalpies of solution of $TaBr_4$ and $TaBr_5$ in aqueous hydrofluoric acid enables one to relate the enthalpy of formation of one compound to that of the other. An estimate of the enthalpy of formation of the lower bromides can be based on the equilibria

$$2TaBr_4(c) \rightleftharpoons TaBr_3(c) + TaBr_5(g)$$

and

$$5TaBr_3(c) \rightleftharpoons 4TaBr_{2.5}(c) + TaBr_5(g)$$

(A) Calorimetric Determination of the Standard Enthalpy of Formation of Tantalum(IV) Bromide

Schäfer and Kahlenberg have shown that Ta(IV) chloride reacts quantitatively with hydrofluoric acid to form Ta(V) solution and hydrogen (1). Those authors incorporated H_2PtCl_6 into the solution to serve as a catalyst and cautioned that the reaction should be carried out in an argon atmosphere in order to prevent catalyzed oxidation of the hydrogen by air. The present author found that $TaBr_4$ reacted completely in the absence of catalyst within approximately 10 min. Reactions were carried out in the calorimeter both with and without added platinum and no difference in the time of reaction was observed. The presence of platinum was therefore deemed not to be necessary but outgassing of the acid with argon for 1–2 h was essential.

Experimental Section

Tantalum Bromides

These were prepared from tantalum sheet (Fansteel Metals 99.95%) and purified bromine. The pentabromide was prepared from the elements at 450°C in a previously evacuated and sealed system. Bromine in the samples was determined by totally hydrolyzing the compound in a closed container with aqueous hydroxide and completing the determination by the Volhard method. *Anal.* calcd. for $TaBr_5$: Br 68.83; found: Preparation 1, 68.81; Preparation 2, 68.79. The tetrabromide was prepared by reduction of $TaBr_5$ with aluminium foil (Ventron, 99.997%) at 250°C (2). Many attempts to prepare the compound led to material which, while exhibiting acceptable analytical purity, failed to dissolve completely and reproducibly in the calorimeter. It was found that in the final step of the synthesis, which consisted of subliming away excess $TaBr_5$, surface decomposition of the product occurred and this led to the production of sparingly soluble lower bromide. The best procedure consisted in carrying out the reduction of $TaBr_5$ with slightly less than the stoichiometric quantity of aluminium at 250°C for 7 days and then subliming away the unwanted bromides at 180°C over a period of several days. Two preparations dissolved with the required rapidity. *Anal.* calcd. for $TaBr_4$: Br 63.86; found: Preparation 1, 63.23; Preparation 2, 63.41. The tetrabromide appeared to be much more hygroscopic than the corresponding chloride.

Hydrofluoric Acid

Two solutions were prepared from 48% acid (Baker). The concentrations were determined by alkalimetric titration of weighed portions. (*a*) Hydrofluoric acid containing 7.80 ± 0.02% w/w HF. The 350 g portions used in the calorimeter contained 1.364 mol of HF and 17.91 mol of H_2O. (*b*) Hydrofluoric acid containing 8.98 ± 0.02% w/w HF. The 261.8 g portions used in partial processes [3*b*] and [3*c*] below contained 1.175 mol HF and 13.23 mol H_2O.

Hydrobromic Acid

A 0.697 ± 0.002% w/w HBr solution was prepared from the concentrated acid. The 40.00 g portions of this solution used in partial process [3*b*] contained 0.00345 mol HBr and 2.204 mol H_2O.

Calorimeter

The apparatus was identical to that described previously (3) except that the calibration heater had been replaced with a carbon resistor having a resistance of 112.1 ± 0.05 ohm. This was enclosed in a gold-plated copper sheath which was attached to a polyethylene tube in such a manner that it could be completely immersed in the calorimeter acid. A trial measurement of the heat of solution of tris(hydroxymethylamino)methane (THAM) in 0.1 *N* HCl gave $\Delta H_{solution} = -58.7$ cal g^{-1}.

0008-4042/80/090938-04$01.00/0

©1980 National Research Council of Canada/Conseil national de recherches du Canada

Can. J. Chem. Downloaded from www.nrcresearchpress.com by 210.87.254.40 on 09/05/12
For personal use only.

Montgomery *et al.* report a weighted mean value of -58.685 ± 0.01 cal g^{-1} (4). The THAM used in the present work was Fisher Brand Certified Primary Standard (99.9%) which was heated in air prior to use.

The solid samples were sealed in thin-walled quartz bulbs which could be crushed under the calorimeter acid. The bulbs were coated with wax. The dissolving of $TaBr_4$ was complete in about 10 min; $TaBr_5$ dissolved more quickly. The temperature readings were corrected for heat loss or gain by the method of Kubaschewski *et al.* (5). The measurement of enthalpies of mixing was carried out by means of an adaptation described previously (3).

The Partial Processes

The method involves relating $TaBr_4$ to $TaBr_5$ for which the standard enthalpy of formation is known accurately (3, 6). The various partial processes used in the Hess's Law treatment are described by the equations which follow. The relative quantities shown refer to the typical case in which 2.0 g of $TaBr_4$ are dissolved in 350 g of 7.80% HF solution but the reactions are written for 1 mol tantalum. Braces enclose solution compositions expressed in moles. The concentrations were chosen rather arbitrarily and the weights of solute and solvent used were governed by the capacity and range of the calorimeter.

[1] $\{TaF_5; 336.5HF; 5HBr; 4483.6H_2O\} \overset{\Delta H_1}{\rightleftharpoons} TaBr_5(c) + \{341.5HF; 4483.6H_2O\}$

[2] $TaBr_4(c) + \{341.5HF; HBr; 4483.6H_2O\} \overset{\Delta H_2}{\rightleftharpoons} \{TaF_5; 336.5HF; 5HBr; 4483.6H_2O\} + \frac{1}{2}H_2$

[3] $\frac{1}{2}H_2 + \frac{1}{2}Br_2 + \{341.5HF; 4483.6H_2O\} \overset{\Delta H_3}{\rightleftharpoons} \{341.5HF; HBr; 4483.6H_2O\}$

These reactions sum to give

$$TaBr_4(c) + \tfrac{1}{2}Br_2 \overset{\Delta H_4}{\rightleftharpoons} TaBr_5(c)$$

where $\Delta H_4 = \Delta H_1 + \Delta H_2 + \Delta H_3$.

Results

Process 1. The Dissolving of $TaBr_5$(c) in 7.80% Hydrofluoric Acid

In a previous study (3) it was shown that the enthalpy of dissolving $TaBr_5$ in hydrofluoric acid was essentially independent of sample size at the low concentrations of interest here (ca. 1.5 g $TaBr_5$ in 350 g solvent). The values of ΔH_1 obtained were 93.0_1, 93.0_5, 92.8_7, 93.2_1, and 92.9_0 kcal mol^{-1}. The mean value is $\Delta H_1 = 93.0 \pm 0.14$ kcal mol^{-1}. The uncertainty range here as elsewhere below indicates the standard deviation of the individual values from the mean value.

Process 2. The Dissolving of $TaBr_4$(c) in 7.80% Hydrofluoric Acid

Process 2 requires that 2.0 g of $TaBr_4$ be dissolved in 350 g of 7.80% HF which also contains 1 mol HBr per mol of $TaBr_4$ employed. The requisite amount of HBr was added to the calorimeter acid in the form of an aqueous solution. The resulting slight change in the concentration of HF was compensated for in earlier runs by using slightly more concentrated HF solution but in the absence of such compensation the resulting error was shown to be <0.05 kcal mol^{-1}. It was not convenient to prepare exactly 2.0 g samples of $TaBr_4$ as indicated by the ideal partial process 2. Instead, various quantities were dissolved in 7.80% hydrofluoric acid and the mean value of the observed enthalpies was chosen. There was, as with $TaBr_5$, no indication that the enthalpy of solution was influenced by sample size. The values of ΔH_2 obtained were 83.0, 82.3, 81.9, 82.1, and 82.3 kcal mol^{-1}. The mean value is 82.3 ± 0.5 kcal mol^{-1}.

The reaction produced 0.5 mol H_2 per mol of $TaBr_4$ dissolved. The gas was evolved saturated with water vapour and HF. According to the vapour pressure data of Brosheer *et al.* (7), 0.014 mol water was thereby removed from the solution which therefore entailed a correction of -0.15 kcal mol^{-1} $TaBr_4$. The values of ΔH_2 given include the correction.

Process 3. The Enthalpy of Formation of Hydrogen Bromide in Solution

Reaction 3 refers to a process which cannot be measured readily. However, this reaction may be replaced by three others which when added together give reaction 3.

[3*a*] $\frac{1}{2}H_2 + \frac{1}{2}Br_2 + 640.7H_2O \overset{\Delta H_{3a}}{\rightleftharpoons} \{HBr; 640.7H_2O\}$

[3*b*] $\{HBr; 640.7H_2O\} + \{341.5HF; 3842.9H_2O\} \overset{\Delta H_{3b}}{\rightleftharpoons} \{341.5HF; HBr; 4483.6H_2O\}$

[3*c*] $\{341.5HF; 4483.6H_2O\} \overset{\Delta H_{3c}}{\rightleftharpoons} \{341.5HF; 3842.8H_2O\} + 640.7H_2O$

The enthalpy ΔH_{3a} (-28.94 ± 0.02 kcal) was obtained from a standard compilation (8). ΔH_{3b} and ΔH_{3c} were determined by mixing [3*b*]: 40.00 g 0.697% HBr solution and [3*c*]: 39.72 g H_2O with 261.8 g 8.98% HF solution in the calorimeter. The enthalpies obtained were as follows: ΔH_{3b}, -1.40, -1.48, and -1.47 kcal; mean $= -1.45 \pm 0.04$ kcal; ΔH_{3c}, $+2.42$, $+2.37$, $+2.38$, and $+2.40$ kcal. Mean $= +2.39 \pm 0.02$ kcal.

TABLE 1. Thermodynamic values for $TaBr_4$ at 298 K

State	ΔH_f^0 (kcal mol^{-1})	S^0 (cal K^{-1} mol^{-1})	ΔG_f^0 (kcal mol^{-1})	C_p
Solid	-125.6 ± 0.5	56 ± 2	-118 ± 2	$25 + 15 \times 10^{-3}T$
Gaseous	-95 ± 3	104 ± 5	-101 ± 3	$26 - 2 \times 10^{5}T^{-2}$

The Addition of the Partial Processes

The enthalpy of the process $TaBr_4(c) + \frac{1}{2}Br_2(l) \rightleftharpoons TaBr_5(c)$ is obtained from the individual enthalpies:

$$\Delta H_1 = +93.01 \pm 0.14 \text{ kcal}$$

$$\Delta H_2 = -82.3 \pm 0.5 \text{ kcal}$$

$$\Delta H_{3a} = -28.94 \pm 0.02 \text{ kcal}$$

$$\Delta H_{3b} = -1.45 \pm 0.04 \text{ kcal}$$

$$\Delta H_{3c} = +2.39 \pm 0.02 \text{ kcal}$$

whence $\Delta H_4 = -17.3 \pm 0.5$ kcal. The error limit on ΔH_4 is the root-mean-square of the values for the individual ΔH_i. The error limits on subsequent enthalpy values are similarly defined.

By combining this value with the standard enthalpy of formation of solid $TaBr_5$ (3, 6): $\Delta H_f^0(TaBr_5(c)) = -142.9$ kcal mol^{-1}, we obtain the enthalpy of formation of solid $TaBr_4$:

$$Ta(c) + 2Br_2(l) \rightleftharpoons TaBr_4(c)$$

$$\Delta H_f^0(TaBr_4(c)), 298 \text{ K} = -125.6 \pm 0.5 \text{ kcal mol}^{-1}$$

(B) Thermochemistry of $TaBr_4$, $TaBr_3$, and $TaBr_{2.5}$

Until now it has not been possible to survey the thermochemistry of the lower bromides of tantalum. A phase equilibrium study has revealed the temperature ranges for the existence of $TaBr_4$, $TaBr_{2.83}$, $TaBr_{2.5}$, and $TaBr_{2.33}$ (2). The thermochemistry of the last of these remains unexamined still but we are able to make estimates concerning the others.

The tribromide appears to possess a fairly broad homogeneity range, the lower limit of which has the composition $TaBr_{2.83}$ and which is obtained by equilibration with $TaBr_{2.5}$. When the phase is equilibrated with $TaBr_4$ it has a composition close to $TaBr_{3.16}$ (9).

(1) $TaBr_4$

The above reported enthalpy of formation of solid $TaBr_4$ may be combined with other estimated quantities to give the set of values in Table 1 which may be used in thermodynamic calculations of a somewhat approximate nature.

The estimates have been made by employing Kopp's Law and the established values of heat capacities of similar compounds as found in standard compilations (8, 10). It is a corollary of this principle that one may estimate entropies of solids by an additivity rule. A formula suggested by Geiseler provides estimates of entropies for vapours (11).

Unfortunately, vapour pressure data for $TaBr_4$ are not available, owing no doubt to the difficulty of measurement. We can therefore provide only a rough estimate of the enthalpy of sublimation. The following considerations are useful. The enthalpies of sublimation of $ZrBr_4$ and $HfBr_4$ are reported to be 25.5 and 24.1 kcal mol^{-1} (12, 13). Similarly the ΔH_{subl} values for $NbBr_5$ and $TaBr_5$ are 26.5 and 25.4 kcal mol^{-1} respectively (14). We assume that the ΔH_{subl} value for $TaBr_4$ is likewise about 1.3 kcal mol^{-1} less than that for $NbBr_4$. A previous estimate gives $\Delta H_{subl}(NbBr_4) = 30$–$35$ kcal mol^{-1} (15). We therefore obtain $\Delta H_f^0(TaBr_4(g))$ given in Table 1 with the same range of uncertainty as $\Delta H_{subl}(NbBr_4)$.

The heat capacities were derived from $ZrBr_4(c)$ and $TiBr_4(g)$ by subtracting the heat capacities of the metals at 298 K. The halogen contribution so obtained was then added to the heat capacity of tantalum metal. The related compounds UCl_4, UBr_4, and $ThBr_4$ enable us to infer the standard entropies of $TaBr_4$ by making use of the observation that if we have S_{298}^0 for a chloride, the increment in entropy which would result by replacing Cl by Br is the same in all analogous compounds, e.g. UCl_4 and UBr_4.

The empirical formula of Geiseler (11) gives the value for $S^0(TaBr_4(g)\ 298\ K) = 104.3$ cal K^{-1} mol^{-1}.

(2) $TaBr_{3.16}$

Tantalum tribromide possesses a fairly broad range of nonstoichiometry at ≥ 325°C which extends from $TaBr_{2.83}$ to $TaBr_{3.16}$ (2, 9). We consider first the upper range limit.

Recommended values are

$$\Delta H_f^0\ (TaBr_{3.16}(c)\ 298\ K) = -114.7 \pm 3 \text{ kcal mol}^{-1}$$

$$S^0\ (TaBr_{3.16}(c)\ 298\ K) = 45 \pm 3 \text{ cal K}^{-1} \text{ mol}^{-1}$$

$$C_p\ (TaBr_{3.16}(c)) = 21 + 12 \times 10^{-3}T$$

Schäfer *et al.* (9) have provided the information that at 625 ± 10 K, $TaBr_{3.16}$ was found to be in equilibrium with $TaBr_4(c)$ and $TaBr_5(g)$ at a pressure of 0.39 atm. The calculations were thus based upon

Can. J. Chem. Downloaded from www.nrcresearchpress.com by 210.87.254.40 on 09/05/12
For personal use only.

Can. J. Chem. Downloaded from www.nrcresearchpress.com by 210.87.254.40 on 09/05/12
For personal use only.

the equilibrium

$$1.19TaBr_{3.16}(c) + TaBr_5(g) \rightleftharpoons 2.19TaBr_4(c)$$

The estimated entropy utilized the reported values for UBr_3 and $TiBr_3$.

(3) $TaBr_{2.83}$

Recommended values are

$$\delta H_f^0\,(TaBr_{2.83}(c)\ 298\ K) = -103 \pm 4\ kcal\ mol^{-1}$$

$$S^0\,(TaBr_{2.83}(c)\ 298\ K) = 41 \pm 3\ cal\ K^{-1}\ mol^{-1}$$

$$C_p\,(TaBr_{2.83}(c)) = 19 + 10 \times 10^{-3}T$$

McCarley and Boatman (2) have shown that when the tribromide is equilibrated with $TaBr_{2.5}$, material with the lower composition limit, $TaBr_{2.83}$, is obtained. We may estimate the enthalpy of formation of this phase from the observation that the enthalpies of formation per equivalent of $NbCl_{2.67}$ and $NbCl_{3.13}$ are nearly equal, i.e. 47 and 46 kcal respectively. If we assume that the tantalum tribromide phase is similar in this respect we obtain

$$\Delta H_f^0(TaBr_{2.83}) = (2.83/3.16)\,\Delta H_f^0(TaBr_{3.16})$$

(4) $TaBr_{3.0}$

The stoichiometric tribromide is not distinguished by any particular stability. However, thermochemical calculations may be carried out with the following provisional values:

$$\Delta H_f^0\,(TaBr_3(c)\ 298\ K) = -109 \pm 4\ kcal\ mol^{-1}$$

$$S^0\,(TaBr_3(c)\ 298\ K) = 43 \pm 3\ cal\ K^{-1}\ mol^{-1}$$

$$C_p\,(TaBr_3(c)) = 20 + 11 \times 10^{-3}T$$

The enthalpy value was obtained by linear interpolation between the values for the upper and lower phase limits.

(5) $TaBr_{2.5}$

Recommended values are

$$\Delta H_f^0\,(TaBr_{2.5}(c)\ 298\ K) = -95 \pm 4\ kcal\ mol^{-1}$$

$$S^0\,(TaBr_{2.5}(c)\ 298\ K) = 38 \pm 3\ cal\ K^{-1}\ mol^{-1}$$

$$C_p\,(TaBr_{2.5}(c)) = 18 + 9 \times 10^{-3}T$$

Schäfer *et al.* (9) found that for the process

$$6.58TaBr_{2.5}(c) + TaBr_5(g) \rightleftharpoons 7.58TaBr_{2.83}(c)$$

the $TaBr_{2.5}$ phase was in equilibrium at 713 K with 0.83 atm of $TaBr_5$ vapour. The entropy estimate was based on the assumption that $TaBr_{2.5}$ could be regarded as equivalent to $TaBr_2$ plus $TaBr_3$ in the way that $S^0(Fe_3O_4)$ is nearly equal to $S^0(FeO) + S^0(Fe_2O_3)$. $PbBr_2$ and UBr_3 were used as the model compounds.

Acknowledgements

This work was supported by the Natural Sciences and Engineering Research Council. Preliminary experiments performed by Dr. R. Makhija led to the design of the experimentation used.

1. H. Schäfer and F. Kahlenberg. Z. Anorg. Allgem. Chem. **305**, 178 (1960).
2. R. E. McCarley and J. C. Boatman. Inorg. Chem. **4**, 1486 (1965).
3. A. D. Westland. Can. J. Chem. **57**, 2665 (1979).
4. R. L. Montgomery, R. A. Melaugh, C.-C. Lau, G. H. Meier, H. H. Chan, and F. D. Rossini. J. Chem. Thermodyn. **9**, 915 (1977).
5. O. Kubaschewski, E. Ll. Evans, and C. B. Alcock. Metallurgical thermochemistry. Pergamon, Oxford. 1967.
6. P. Gross, C. Hayman, D. L. Levi, and G. L. Wilson. Trans. Faraday Soc. **58**, 890 (1962).
7. J. C. Brosheer, F. A. Lenfesty, and K. L. Elmore. Ind. Eng. Chem. **39**, 423 (1947).
8. D. D. Wagman, W. H. Evans, V. B. Parker, I. Halow, S. M. Bailey, and R. H. Schumm. Selected values of chemical thermodynamic properties. Technical note 270-3. National Bureau of Standards, Washington, DC. 1968.
9. H. Schäfer, R. Gerken, and H. Scholz. Z. Anorg. Allgem. Chem. **335**, 96 (1965).
10. F. D. Rossini. Selected values of chemical thermodynamic properties. Circular 500, National Bureau of Standards, Washington, DC. 1952.
11. G. Geiseler. Z. Phys. Chem. **202**, 424 (1954).
12. A. S. Normanton and R. A. J. Shelton. Trans. Faraday Soc. **66**, 33 (1970).
13. R. Makhija and A. D. Westland. J. Chem. Soc. Dalton, 1707 (1977).
14. S. S. Berdonosov, A. V. Lapitskii, and E. K. Bakov. Russ. J. Inorg. Chem. **10**, 173 (1965).
15. D. Lal and A. D. Westland. J. Chem. Soc. Dalton, 2505 (1974).
16. H. Schäfer and F. Kahlenberg. Z. Anorg. Allgem. Chem. **305**, 291 (1960).

Thermodynamic and transport properties of binary liquid systems

SHEO PRAKASH, KANDIMALLA SIVANARAYANA, AND OM PRAKASH

Chemical laboratories, University of Allahabad, Allahabad, India

Received June 20, 1979[1]

SHEO PRAKASH, KANDIMALLA SIVANARAYANA, and OM PRAKASH. Can. J. Chem. **58**, 942 (1980).

Densities, viscosities, and sound velocities were determined for the system *o*-chlorophenol + acetone and *o*-chlorophenol + ethyl methyl ketone at 25°C. From the experimental results, the deviation in isentropic compressibility K_S, excess molar volume V^E, excess viscosity η^E, and excess molar free energy of activation of flow G^{*E} were calculated. The deviations from ideality of the thermodynamic and transport functions are explained on the basis of molecular interactions between the components of the mixture.

SHEO PRAKASH, KANDIMALLA SIVANARAYANA et OM PRAKASH. Can J. Chem. **58**, 942 (1980).

On a déterminé les densités, les viscosités et les vitesses du son dans les systèmes *o*-chlorophénol + acétone et *o*-chlorophénol + éthyl méthylcétone à 25°C. Utilisant les résultats expérimentaux, on a calculé la déviation de compressibilité isentropique, K_s, le volume molaire en excès, V^E, l'excès de viscosité, η^E et G^{*E} l'énergie d'activation molaire libre en excès de l'écoulement. On explique les déviations par rapport aux fonctions thermodynamique et de transport idéales en se basant sur les interactions moléculaires entre les composants du mélange.

[Traduit par le journal]

Introduction

The variation of ultrasound velocities, isentropic compressibilities, intermolecular free lengths, and free volumes of binary liquid mixtures of protic, aprotic, and associating liquids with changing mole fraction of one of the components has been investigated by some of the workers (1–5). The trends of changes have been interpreted by these workers in terms of difference in size of molecules and the strength of interaction taking place between the components of the mixtures. The measurement of the ultrasound velocity in mixtures formed by liquid components reveals the degree of deviations from ideality, eventual molecular associations, if any, as well as important correlations with various parameters. This paper deals with our investigations of the thermodynamic and transport properties of binary liquid mixtures and is in continuation of our previous studies (6–8). From the experimental results of densities, sound velocities, and viscosities for the systems *o*-chlorophenol + acetone and *o*-chlorophenol + ethyl methyl ketone at 25°C, the thermodynamic and transport functions: deviation in isentropic compressibility K_S, excess molar volume, V^E, excess viscosity η^E, and excess molar free energy of activation of flow G^{*E}, have been computed.

Experimental

Density

Densities of pure liquids and their mixtures were determined by using a double walled pyknometer having narrow bore and provided with ground glass stoppers. The pyknometer was calibrated against pure benzene and acetone. Densities are accurate to within ± 0.0001 g cm^{-3}.

Sound Velocity

The continuous wave interferometric technique was used for the measurement of ultrasonic velocity (9). The ultrasound waves of 2 MHz frequency produced by a gold plated quartz crystal fixed at the bottom of a cell are passed through the medium and are reflected by a moveable metallic plate kept parallel to the crystal. When the separation between the crystal and the plate is exactly a whole multiple of sound wave length, standing waves are produced. Acoustic resonance due to these standing waves gives rise to an electrical reaction to the generator driving the quartz plate and the anode current of the generator becomes maximum. The micrometer screw is raised slowly to note maximum anode current. The wave length was determined with the help of total distance moved by the micrometer for 20 maximum readings of the anode current. The product of wavelength and the frequency gives the ultrasound velocity. The accuracy in velocity measurements was ±0.18%.

Viscosity

Viscosities were determined with a viscometer similar to Cannon-Ubbehlohde viscometer calibrated against pure liquids (acetone and benzene) and the accuracy was found to be ±0.005 cP.

All the measurements were carried out at a constant temperature 25°C, and for that purpose a thermostatically controlled bath constant to ±0.01°C was used.

Materials and Solutions

o-Chlorophenol (RDSH, Germany) was fractionally distilled over Zn Powder, the middle fraction redistilled over BaO, and the middle colourless fraction collected. Acetone (SM) and ethyl methyl ketone (SM) were redistilled and further purified by standard methods described by Weissberger (10). The purities of the chemicals were checked by comparing the values of the density with those reported in the literature. *o*-Chlorophenol, $\rho(25°C) = 1.25854\,g\,cm^{-3}$ (lit. 1.25770 g cm^{-3} (11)), acetone, $\rho(25°C) = 0.78513\,g\,cm^{-3}$ (lit. 0.78502 g cm^{-3} (12), 0.7851 g cm^{-3}(2)), and ethyl methyl ketone, $\rho(30°C) = 0.79419\,g\,cm^{-3}$ (lit. 0.79452 g cm^{-3} (12)). At the time of preparing the mixtures care was taken to avoid loss of liquids by evaporation.

Results

The values of density ρ, sound velocity v, and

[1]Revision received November 21, 1979.

0008-4042/80/090942-04$01.00/0

©1980 National Research Council of Canada/Conseil national de recherches du Canada

Can. J. Chem. Downloaded from www.nrcresearchpress.com by 210.87.254.42 on 09/05/12
For personal use only.

TABLE 1. Experimental values of density ρ (g cm^{-3}), sound velocity v (m s^{-1}), and viscosity η (cP) at 25°C

o-Chlorophenol + acetone				*o*-Chlorophenol + ethyl methyl ketone			
x_1*	ρ	v	η	x_1*	ρ	v	η
0.0000	0.78513	1164	0.316	0.0000	0.80097	1198	0.404
0.1010	0.85770	1206	0.442	0.1005	0.85848	1230	0.517
0.2004	0.92529	1252	0.644	0.1961	0.91298	1264	0.700
0.2997	0.98007	1286	0.857	0.3003	0.96005	1292	0.913
0.4006	1.03644	1320	1.217	0.3994	1.01715	1328	1.322
0.5000	1.08355	1348	1.666	0.5010	1.06856	1354	1.744
0.5999	1.12954	1370	2.190	0.6001	1.11146	1374	2.277
0.6997	1.16708	1386	2.712	0.6991	1.14902	1386	2.736
0.7988	1.20027	1396	3.086	0.8006	1.19073	1396	3.091
0.9003	1.22962	1400	3.303	0.8991	1.22649	1398	3.315
1.0000	1.25854	1402	3.381	1.0000	1.25854	1402	3.381

*x_1 is mole fraction of *o*-chlorophenol.

TABLE 2. Values of coefficients a_0, a_1, and a_2 determined by the method of least squares and the standard error of estimate (σ)

System	Function	a_0	a_1	a_2	σ
o-Chlorophenol + acetone	K_s	−66.29	28.56	−7.78	0.28
	V^E	−8.35	2.02	1.87	0.18
	η^E	−0.61	3.08	1.52	0.05
	G^{*E}	1115	529	−143	12.47
o-Chlorophenol + ethyl methyl ketone	K_s	−49.46	13.14	1.68	0.40
	V^E	−8.25	−0.19	1.06	0.22
	η^E	−0.49	3.11	1.24	0.04
	G^{*E}	912	675	−319	12.04

viscosity η for the two systems are listed in Table 1. Isentropic compressibility k_S, molar volume V, and deviation in isentropic compressibility K_S were obtained from the expressions

$$[1] \quad k_S = v^{-2}\rho^{-1}$$

$$[2] \quad V = (X_1M_1 + X_2M_2)/\rho$$

$$[3] \quad K_S = k_S - [X_1k_{S,1} + X_2k_{S,2}]$$

where M_1, M_2 are molecular weights of the components 1 and 2 and X_1 and X_2 are their mole fractions. k_S, $k_{S,1}$, and $k_{S,2}$ are the isentropic compressibilities of the mixtures and the pure components 1 and 2, respectively.

The excess viscosity η^E, excess molar volume V^E, and excess molar free energy of activation of flow G^{*E} were calculated from the following equations (13):

$$[4] \quad \eta^E = \eta - (X_1\eta_1 + X_2\eta_2)$$

$$[5] \quad V^E = V - (X_1V_1 + X_2V_2)$$

$$[6] \quad G^{*E} = RT[\ln \eta V - (X_1 \ln \eta_1V_1 + X_2 \ln \eta_2V_2)]$$

where η and V are the viscosity and molar volume respectively of the mixtures; η_1, η_2 and V_1, V_2 are the viscosities and molar volumes of the pure components 1 and 2, respectively; R is the gas constant; and T is the absolute temperature.

Each set of results was best fitted with an empirical equation of the form

$$[7] \quad A/X_1X_2 = a_0 + a_1(X_1 - X_2) + a_2(X_1 - X_2)^2$$

The method of least squares was used to determine the values of the coefficients a_0, a_1, and a_2 of the functions K_S, V^E, η^E and G^{*E}, represented by A in eq. [7]. The values of these coefficients along with the standard error of estimate (σ) have been given in Table 2.

Figures 1, 2, 3, and 4 show the values of K_S, V^E, η^E, and G^{*E} as a function of the mole fraction of *o*-chlorophenol. The continuous curves were obtained by substituting the coefficients a_0, a_1, and a_2 in eq. [7].

Discussion

The choice of *o*-chlorophenol has been based on its limited polymerization through intermolecular hydrogen bonding in the pure state. The addition of ketones causes the rupture of intramolecular and intermolecular hydrogen bonding in *o*-

Can. J. Chem. Downloaded from www.nrcresearchpress.com by 210.87.254.42 on 09/05/12
For personal use only.

Can. J. Chem. Downloaded from www.nrcresearchpress.com by 210.87.254.42 on 09/05/12
For personal use only.

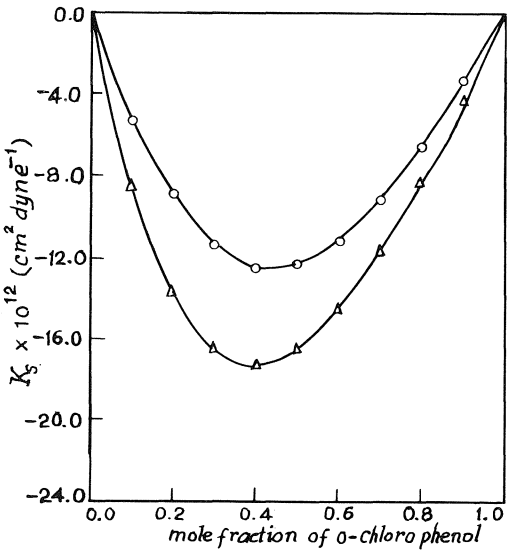


FIG. 1. Plot of K_S as a function of composition for *o*-chlorophenol + acetone (△) and *o*-chlorophenol + ethyl methyl ketone (○).

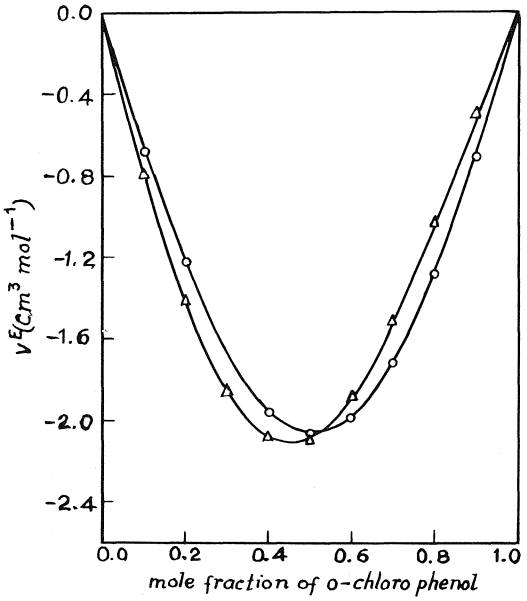


FIG. 2. Plot of V^E as a function of composition for *o*-chlorophenol + acetone (△) and *o*-chlorophenol + ethyl methyl ketone (○).

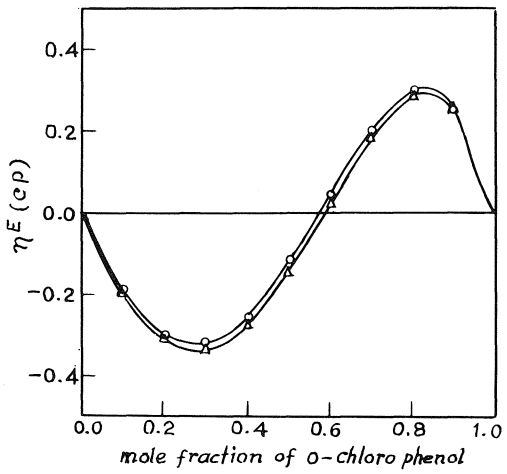


FIG. 3. Plot of η^E as a function of composition for *o*-chlorophenol + acetone (△) and *o*-chlorophenol + ethyl methyl ketone (○).

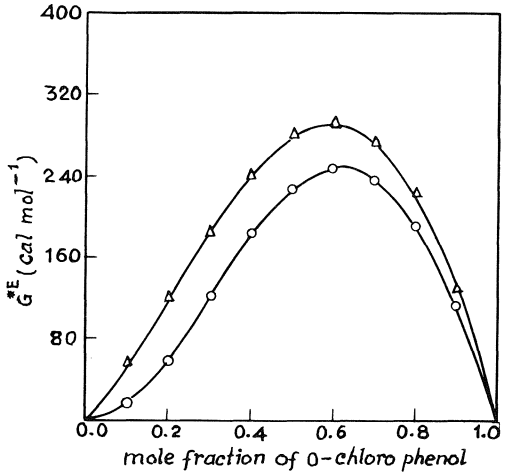


FIG. 4. Plot of G^{*E} as a function of composition for *o*-chlorophenol + acetone (△) and *o*-chlorophenol + ethyl methyl ketone (○).

chlorophenol and this will be followed by association of unlike molecules through intermolecular hydrogen bonding.

In most theories of the behaviour of non-electrolyte solutions the major contribution to the deviation from ideal mixing are attributed to the dispersion forces (14). In such theories the deviations are expected to be positive. Negative deviations from ideal behaviour in mixtures of molecules different in size can be accounted for by geometric considerations (15).

Attempts have been made to explain the behaviour of liquid mixtures on the basis of sign and magnitude of the excess volume V^E, and deviation in isentropic compressibility K_S. A negative value of K_S and V^E indicates strong interaction between the components of the mixtures while their positive values are indicative of weaker interaction. When the strength of interaction between the unlike molecules increases, K_S and V^E become increasingly negative.

Figures 1 and 2 show negative K_S and V^E with well marked maxima at 0.4 and 0.5 mole fractions of *o*-chlorophenol respectively. The negative values of V^E for the liquid systems are well explained by Prigogine (16) in terms of different size of the molecules or the dipole–dipole interaction between them. In the present case the observed values of V^E and K_S indicate that the association between unlike molecules predominates over dissociation of *o*-chlorophenol aggregates.

According to Fort and Moore (17) the values of η^E are negative for the systems in which dispersion forces are dominant, becoming less negative and then increasingly positive as the strength of interaction increases. Figure 3 shows that the values of η^E are negative at first but become positive when mixtures are rich in *o*-chlorophenol. The values of G^{*E} are positive over the entire range of composition with maxima at 0.6 mole fraction of *o*-chlorophenol (Fig. 4).

From these observations one can infer that the interactions in *o*-chlorophenol + acetone are stronger than that in *o*-chlorophenol + ethyl methyl ketone.

Acknowledgement

One of us (K.S.) is thankful to the C.S.I.R., New Delhi, for the award of a Junior Research fellowship.

1. E. A. Moelwyn Hughes and P. L. Thorpe. Proc. R. Soc. London, 268 (1964); 574 (1964).
2. D. D. Deshpande and L. G. Bhatgadde. J. Phys. Chem. **72**, 261 (1968).
3. W. J. Snyder and J. R. Snyder. J. Chem. Eng. Data, **19**, 270 (1974).
4. S. Prakash and S. B. Srivastava. J. Chem. Thermodyn. **7**, 997 (1975).
5. R. Vilcu and A. Simion. Rev. Roum. Chim. **21**, 177 (1976).
6. S. Prakash, S. B. Srivastava, and O. Prakash. Ind. J. Pure Appl. Phys. **13**, 791 (1975).
7. S. Prakash, R. Singh, and N. Prasad. Acta Chim. Hung. **88**, 371 (1976).
8. S. Singh, K. Sivanarayana, R. Kushwaha, and S. Prakash. J. Chem. Eng. Data, **24**, 279 (1979).
9. S. Prakash, S. Singh, N. Prasad, and R. Singh. Rev. Acoust. **9**(1-2), 34 (1978).
10. A. Weissberger, E. S. Proskaur, J. A. Riddick, and E. E. Toops. Organic solvents. Vol. VII. 2nd ed. Interscience Publishers, New York. 1955. pp. 379, 385.
11. R. R. Dreisbach. Adv. Chem. Ser. 15 (1955).
12. J. Timmermans. Physico-chemical constants of pure organic compounds. Elsevier Publishing Co., Inc., New York. 1950. pp. 353, 360.
13. Horacio N. Solimo, Roque Riggio, Franco Davolio, and Miguel Katz. Can. J. Chem. **53**, 1258 (1975).
14. J. O. Hirschfelder, C. F. Curtis, and R. B. Bird. Molecular theory of gases and liquids. John Wiley and Sons, Inc., NY. 1954. p. 25.
15. E. A. Guggenhaim. Mixtures. Oxford University Press, Oxford. 1952. p. 29.
16. I. Prigogine. The molecular theory of solutions. North Holland Publishing Co., Amsterdam. 1957.
17. R. J. Fort and W. R. Moore. Trans. Faraday Soc. **62**, 1112 (1966).

Can. J. Chem. Downloaded from www.nrcresearchpress.com by 210.87.254.42 on 09/05/12
For personal use only.

Etude par resonance magnétique multinucléaire d'intermédiaires réactionnels électrophiles. Partie 8. Action des acides de Lewis chlorés $COCl_2$, $POCl_3$, $(CH_3)_2N{=}CHCl^+Cl^-$ et Cl_2 sur l'hexaméthylphosphotriamide (HMPT)

S. POIGNANT, J. R. GAUVREAU ET G. J. MARTIN

Laboratoire de Chimie Organique Physique, Equipe de Recherche Associée au CNRS no. 315, Faculté des Sciences, 44072 Nantes, France

Reçu le 4 juillet 1979[1]

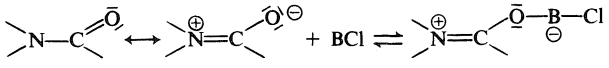
S. POIGNANT, J. R. GAUVREAU et G. J. MARTIN. Can. J. Chem. **58**, 946 (1980).

L'étude de la structure des intermédiaires électrophiles issus de carboxamides et d'acides de Lewis chlorés a été étendue au cas des amides phosphoriques. L'action de $COCl_2$ et $POCl_3$ sur l'hexaméthylphosphotriamide (HMPT) peut conduire à l'obtention d'un sel de chlorophosphonium (**3***a*) qui a été mis en évidence et caractérisé par rmn (^1H, ^{13}C, ^{31}P, ^{15}N). Un mécanisme de formation semblable à celui du chlorure de chloroiminium (réactif de Vilsmeier) obtenu avec les amides a été proposé. L'action du chlore sur le HMPT ne conduit pas à un sel stable du même type mais essentiellement au produit de substitution (**2**). Un nouveau composé biphosphoré (**6**) a pu être identifié dans le cas de l'action d'un excès de chlore.

S. POIGNANT, J. R. GAUVREAU, and G. J. MARTIN. Can. J. Chem. **58**, 946 (1980).

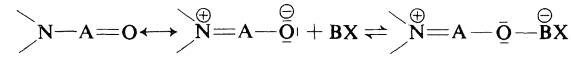
The structural study of the electrophilic intermediates obtained from carboxamides and chlorinated Lewis acids is extended to the phosphoric amides. The action of $COCl_2$ and $POCl_3$ on hexamethylphosphotriamide (HMPT) can lead to a chlorophosphonium salt (**3***a*) the structure of which is proved by nmr spectroscopy (^1H, ^{13}C, ^{31}P, ^{15}N). The mechanism of formation is comparable to that of the chloroiminium chloride (Vilsmeier reagent) from the corresponding amides. The action of chlorine on HMPT does not lead to a stable salt of the same kind but essentially to the substitution product (**2**). A new biphosphorylated compound (**6**) has been identified when an excess of chlorine is reacted with HMPT.

L'interaction entre des amides tertiaires et des acides de Lewis conduit à la formation de sels d'iminium, réactifs électrophiles, intermédiaires de réaction dans la formylation de Vilsmeier–Haack. Nous avons étudié la structure (1*a*), la cinétique de formation (1*b*, *c*) et les réactions d'échanges de nucléophiles (1*d*) des sels de chloroiminium obtenus à partir du *N,N*-diméthylformamide (DMF) et des oxychlorures minéraux. Ce travail a ensuite été étendu aux carboxamides *N,N*-bisubstitués (1*e*) et aux analogues sulfurés des amides (*N,N*-diméthylthioamides) et des acides de Lewis ($CSCl_2$, $PSCl_3$) (1*f*). Dans tous les cas, on obtient des composés salins qui présentent une activité électrophile importante et dont les applications synthétiques sont très nombreuses (2). La formation des sels d'iminium à partir des amides (ou des thioamides) s'explique par le caractère dipolaire de ces dernières qui leur permet de s'associer, dans un premier stade, aux acides de Lewis.

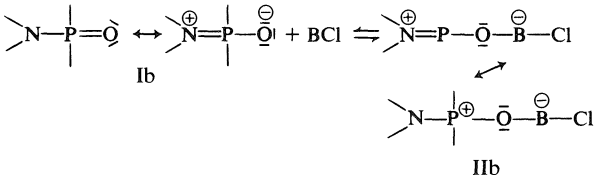


Ia IIa

Il est donc intéressant de considérer le cas d'autres bases oxygénées de grande polarité pour tenter de préparer de nouveaux types de réactifs électrophiles et d'en préciser la structure. A cet égard, les nitrosamines et les amides phosphoriques offrent des exemples intéressants:

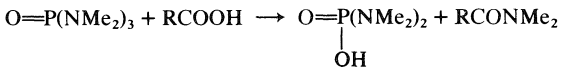


Les nitrosamines (A≡N) sont effectivement alkylées aisément en sels de diazenium (3*a*) ou protonés par les acides forts (3*b*), et nous envisageons maintenant le cas de l'hexaméthylphosphoramide

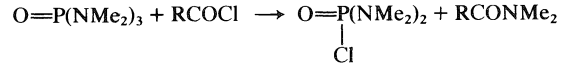


Ib IIb

Les acides organiques (4*a*) conduisent au remplacement d'un ou plusieurs groupements N—Me_2 soit par un OH dans le cas d'un acide carboxylique:



soit par un chlore dans le cas d'un chlorure d'acide:



Les acides minéraux se complexent également avec le HMPT pour donner, soit des complexes stables comme HMPT, BF_3 (4*b*) soit une substitution

[1]Révision reçue le 19 décembre 1979.

0008-4042/80/090946-07$01.00/0

©1980 National Research Council of Canada/Conseil national de recherches du Canada

Can. J. Chem. Downloaded from www.nrcresearchpress.com by 210.87.254.105 on 09/05/12
For personal use only.

d'un ou plusieurs groupements NMe_2 (HMPT, oxychlorures). Comme avec le chloroforme (3,5) le HMPT conduit à des complexes 1–1 stables avec les phénols (4, 6):

$$Ar—O—H + O{=}P(NMe_2)_3 \rightleftharpoons Ar—O—H^{\delta-}\cdots O^{\delta+}{=}P(NMe_2)_3$$

Cependant, le HMPT peut subir, comme les carboxamides, des attaques nucléophiles d'organolithiens (7):

$$RLi + HCH_2N(CH_3O)P[N(CH_3)_2]_2 \rightarrow RH + LiCH_2N(CH_3O)P[N(CH_3)_2]_2$$

$$\downarrow$$

$$LiOP[N(CH_3)_2]_2 + CH_2{=}NCH_3$$

de même que l'interaction d'une base forte (6, 8):

$$B^{\ominus} + HCH_2N(CH_3O)P[N(CH_3)_2]_2 \rightleftharpoons BH + {}^{\ominus}CH_2N(CH_3O)P[N(CH_3)_2]_2$$

Nous nous sommes limités dans ce travail à l'action des oxychlorures d'acides minéraux, du chlore et du sel de chloroiminium sur le HMPT et nous avons pu préparer et caractériser de nouveaux sels de phosphonium halogénés. Ces résultats apportent des données structurales originales qui peuvent permettre de préciser le mécanisme d'action des acides de Lewis halogénés en milieu HMPT.

Action des oxychlorures minéraux sur le HMPT

Alors que l'oxychlorure de phosphore $POCl_3$ est connu pour provoquer le remplacement d'un ou plusieurs groupements diméthylamino (9) par des atomes de chlore, Normant et Deshayes (10) utilisent le chlorure de thionyle avec le HMPT pour chlorer des alcools mais n'observent en rmn aucune complexation du HMPT:

$$ROH + SOCl_2 \xrightarrow{HMPT} RCl + SO_2 + HCl$$

Nous n'avons effectivement pu mettre en évidence aucune entité comparable au sel d'iminium obtenu par action de $SOCl_2$ sur le diméthylformamide (DMF). Par contre avec le phosgène, $COCl_2$, et l'oxychlorure de phosphore, $POCl_3$, un sel de phosphonium a pu être caractérisé (Tableau 1).

Action du phosgène $COCl_2$

L'action du phosgène sur le HMPT conduit probablement à un intermédiaire électrophile **1***a* instable, qui évolue, suivant la température de réaction, vers deux composés phosphorés distincts (**2** et **3***a*) que la rmn nous a permis de mettre en évidence et de caractériser.

Les paramètres rmn figurent dans le Tableau 1. Le déplacement à champs faibles des protons NMe_2 du sel est tout à fait comparable à celui observé dans les sels d'iminium, de même que l'exaltation du couplage $^1J_{^{13}C—H}$ (1*e*) et ceci reflète la nature ionique du composé. Le couplage J_{PNCH} est également exalté par rapport à sa valeur dans le HMPT de départ.

L'évolution des composés **2** et **3***a* est différente et dépend de la température. Dans le premier cas (*A*), le chlorure de carbamoyle formé réagit extemporanément avec le phosgène pour donner le chlorure de phosgéniminium $>N^{+}{=}CCl_2Cl^-$ déjà étudié dans un autre contexte par Viehe (11). Le chlorure de chlorophosphonium **3***a* est stable et difficilement hydrolysable, cependant une hydrolyse basique conduit à la formation de HMPT et de HCl. A température ambiante, la réaction conduit à un mélange des composés **2** et **3***a* avec prédominance de **3***a* (voir Partie expérimentale).

Action de l'oxychlorure de phosphore $POCl_3$

L'action de $POCl_3$ sur le HMPT conduit également à un sel de phosphonium. Il se forme très probablement un intermédiaire instable (analogue à **1***a*) lequel évolue en fonction de la température soit vers le sel **3***b* soit vers le composé covalent **2** déjà évoqué.

Notons qu'en opérant à froid et à partir d'un mélange équimoléculaire HMPT/$POCl_3$, il est possible d'obtenir du sel de phosphonium **3***b* en quantité pratiquement stœchiométrique. Comme dans le cas de **3***a* l'hydrolyse basique de **3***b* conduit à la formation de HMPT, $OPOCl_2^-$ et Cl^-. Avec un excès de HMPT et en opérant à chaud le produit covalent **2** devient alors prépondérant.

Les spectres ^1H, ^{13}C et ^{31}P du composé **3***b* (Tableau 1) sont tout à fait cohérents avec la structure proposée et s'expliquent avec les mêmes arguments qui ont été évoqués dans le cas de l'action du phosgène. Notons que l'anion n'influe pas sur les valeurs de $\delta_{^1H}$ et $\delta_{^{31}P}$ du cation, contrairement au cas des sels de chloroiminium; l'encombrement stérique autour de l'atome de phosphore chargé positivement est probablement responsable de ce fait. En effet, même si nous sommes en présence de paires d'ions intimes, l'anion est probablement trop loin du centre positif pour que son effet se fasse sentir.

Les valeurs $\delta_{^{31}P}$ sont conformes aux données de la littérature (12) obtenues sur des composés similaires. La complexation provoque un déplacement à champ faible du phosphore de l'amide

Can. J. Chem. Downloaded from www.nrcresearchpress.com by 210.87.254.105 on 09/05/12
For personal use only.

Can. J. Chem. Downloaded from www.nrcresearchpress.com by 210.87.254.105 on 09/05/12
For personal use only.

TABLEAU 1. Paramètres rmn du HMPT et de ses produits de réaction avec les acides $COCl_2$, $POCl_3$ et avec le chlore. Solvant: $CH_2Cl_2/CDCl_3$. Une augmentation algébrique du déplacement chimique correspond à une diminution de l'écran électronique

Composés		$\delta_{^1H}$	$\delta_{^{13}C}$	$J_{^{13}C-H}$	$\delta_{^{31}P}$	J_{PNCH}	$\delta_{^{15}N}$	$^1J_{^{15}N-^{31}P}$
No.	Formule	ppm/TMS	ppm/TMS	(Hz)	ppm/PO_4H_3	(Hz)	ppm/CH_3NO_2	(Hz)
1	$((CH_3)_2N)_3P{=}O$	2.55	36.7	136	+24.5	9.6	−357.9	29.3
2	$(CH_3)_2N{-}\overset{\overset{O}{\|}}{\underset{\underset{Cl}{\|}}{P}}{-}N(CH_3)_2$	2.67 3.26*	36.8	138.5	+31	13	−343.4	22
3*a*	$((CH_3)_2N)_3\overset{+}{P}Cl,\ Cl^-$	2.93	37.4	141.5	+53.8	13	−346.6	29.3
3*b*	$((CH_3)_2N)_3\overset{+}{P}Cl,\ OPOCl_2^-$	2.90	37.2	141.5	+53.8 −8.5	13	−346.9	30.8
6	$\underbrace{((CH_3)_2N)_2P(O){-}O{-}}_{(1)}\underbrace{P(Cl)(N(CH_3)_2)_3}_{(2)}$	(*1*) 3.30* (*2*) 3.40*	36.8	138	(*1*) 12.7 (*2*) 28.5	10.8	—	—

*Les spectres ont été réalisés en présence de chlore ce qui provoque un déplacement paramagnétique des groupes méthyles des composés **2** et **6**. Cet effet a pu être évalué à 0.6 ppm dans le cas du composé covalent **2**. Pour le composé **6** les déplacements chimiques ^{31}P sont conformes aux données de la littérature (12)

$([(CH_3)_2N]_2\overset{\overset{O}{\|}}{P})_2{-}O$, $\delta_{^{31}P}$ = 11 à 12 ppm)

On mesure également $^2J_{POP}$ = 19.5 Hz.

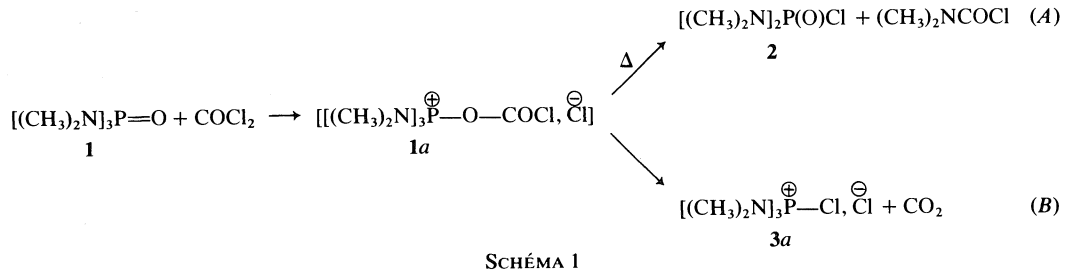


SCHÉMA 1

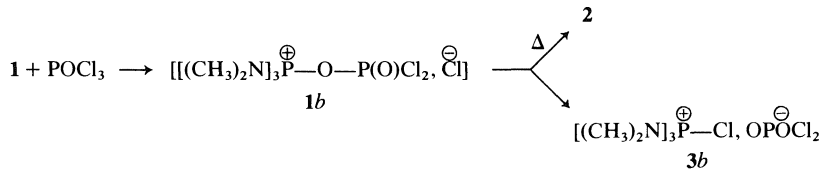


SCHÉMA 2

TABLEAU 2. Variations comparatives des paramètres rmn du DMF, du HMPT et des chlorures correspondants

Groupement	Δδ ou ΔJ		DMF → $(CH_3)_2\overset{+}{N}CHCl\ Cl^-$	HMPT → $[(CH_3)_2N]_3\overset{+}{P}Cl\ Cl^-$
$N(CH_3)_2$	$\Delta(^1J_{^{13}C-H})$	Hz	+7	+5.5
	$\Delta\delta_{^{13}C}$	ppm	+12	+0.7
	$\Delta\delta_{^{15}N}$	ppm	+59.4	+11.3
CCl/C=O	$\Delta\delta_{^{13}C}$	ppm	+5	—
PCl/P=O	$\Delta\delta_{^{31}P}$	ppm	—	+29.3

engagé dans le carbocation (+53.8 ppm). L'existence de l'anion $OPOCl_2^-$ est confirmée par le signal à −8.5 ppm déjà attribué dans le sel de chloroiminium (1*e*). Les variations des divers déplacements chimiques et couplages, comparativement entre la complexation du DMF et celle de l'HMPT, sont rassemblées dans le tableau 2. Il est notamment intéressant de comparer les $\Delta\delta_{^{15}N}$ et $\Delta\delta_{^{13}C}$. On ne retrouve pas, en série phosphorée, l'important effet paramagnétique sur l'écran de l'azote lorsqu'on passe de l'amide au sel de Vilsmeier. Sur la base des relations entre $\delta_{^{15}N}$ et la barrière à la rotation autour des liaisons N—X que nous avons établies précédemment (3*c*, 3*b*), il est possible de supposer que la variation de la délocalisation N—P ne doit pas être très accentuée entre le

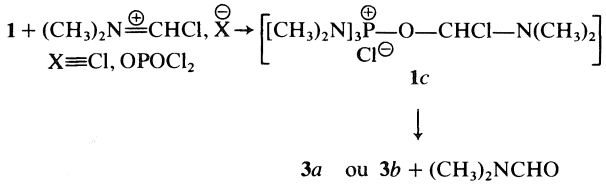


SCHÉMA 3

HMPT et les complexes **3**. L'effet paramagnétique observé en résonance du phosphore correspond au changement d'électronégativité des substituants et de la conjugaison p_π–d_π entre le substituant et l'atome de phosphore. Ce comportement traduit l'augmentation du caractère électrophile du phosphore dans **3**, qui reste cependant moins important que celui de l'atome de carbone dans le sel de chloroiminium.

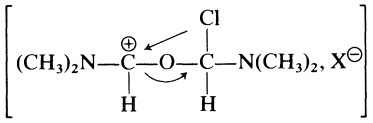
Action du chlorure de chloroiminium (réactif de Vilsmeier) $(CH_3)_2\overset{+}{N}{=}CHCl,\ Cl^-$

Lors de nos travaux sur les phénomènes d'échange (1*d*) intervenant lors de la réaction de formation du complexe de Vilsmeier nous avons montré que ce complexe était lui-même un acide de Lewis plus fort que $SOCl_2$, $POCl_3$ ou $COCl_2$.

Cette remarque se vérifie ici car l'action de $(CH_3)_2\overset{+}{N}{=}CHCl\ Cl^-$ sur le HMPT est rapide et complète.

L'intermédiaire instable **1***c* conduit au sel de chlorophosphonium **3***a* ou **3***b* probablement par un mécanisme de prototropie du chlore identique à celui envisagé dans l'échange intermoléculaire DMF – sel d'iminium (1*d*, *e*).

Can. J. Chem. Downloaded from www.nrcresearchpress.com by 210.87.254.105 on 09/05/12
For personal use only.



Dans ce cas l'équilibre est totalement déplacé vers la formation du sel de phosphonium beaucoup moins réactif que le complexe de Vilsmeier. Appel et Willms (13) ont d'ailleurs utilisé la forte réactivité du chlorure de chloroiminium dans le domaine de la synthèse peptidique, confirmant ce que nous avions prévu lors de nos précédents travaux.

Action du chlore Cl_2

Les halogènes (Cl_2, Br_2) peuvent être utilisés en milieu HMPT soit pour oxyder des alcools (14) en cétone soit pour les additionner sur des composés tels que les alcènes (15) et obtenir, par addition *trans*, des dibromoalcanes. Nous avons étudié l'action du chlore sur le HMPT en l'absence de tout autre réactif afin de tenter de caractériser un intermédiaire de réaction, comme dans le cas des oxychlorures minéraux. Le sel de chlorophosphonium du type **3** ne se forme pas mais un sel d'oxyphosphonium **5** a été caractérisé. Les intermédiaires **4***a* ou **4***b* expliqueraient parfaitement les phénomènes observés.

En l'absence d'autre réactif le complexe **4***a* évolue vers l'espèce **2** déjà caractérisée avec $POCl_3$.

De plus lorsque la réaction est effectuée en excès de chlore, nous pouvons mettre en évidence le caractère acide de Lewis du composé **2**. En effet au fur et à mesure de sa formation **2** réagit sur le HMPT pour former un intermédiaire instable **1***d* voisin de **1***b* envisagé avec $POCl_3$.

Aucun réarrangement ne conduit à un sel de phosphonium stable comme avec $POCl_3$; par contre un excès de chlore catalyse la formation d'un composé bi-phosphoré covalent très stable **6**. L'identification du composé **6** a été facilitée par l'utilisation de la rmn ^{31}P et des techniques d'irradiation sélective (cf. Tableau 1 et Fig. 1).

Enfin, il faut noter qu'à température plus élevée ou en présence d'un excès de HMPT, il se forme plusieurs produits difficilement identifiables qui sont probablement des composés de polymérisation.

Conclusion

La réaction entre un acide de Lewis et une amide tertiaire a pu être étendue avec succès au cas de l'hexaméthylphosphotriamide, à basse température. En effet les oxychlorures $COCl_2$ et $POCl_3$, de même que le complexe de Vilsmeier lui-même, se complexent toujours sur l'atome d'oxygène basique du HMPT. Un mécanisme général rend compte de l'évolution d'un premier intermédiaire du type "oxonium" vers un sel contenant l'atome de chlore.

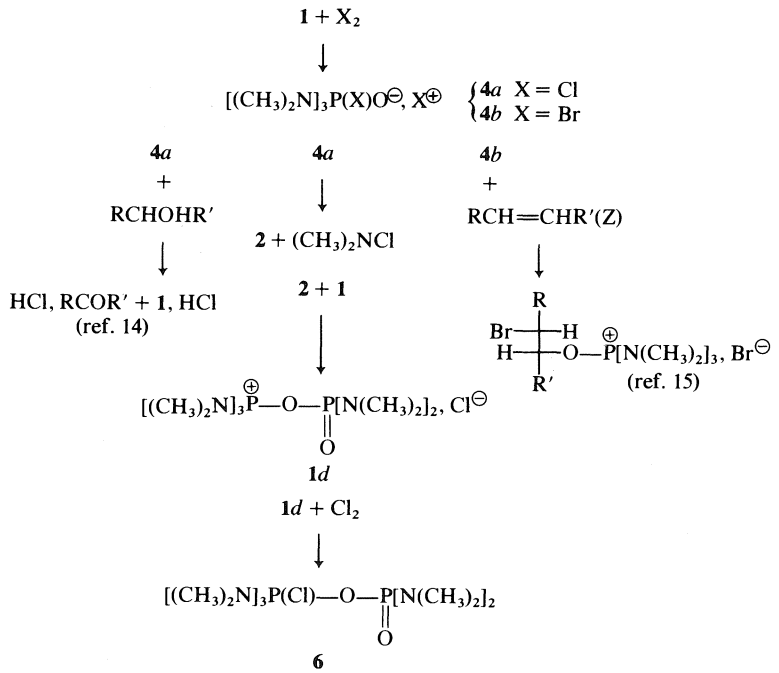


SCHÉMA 4

Can. J. Chem. Downloaded from www.nrcresearchpress.com by 210.87.254.105 on 09/05/12
For personal use only.

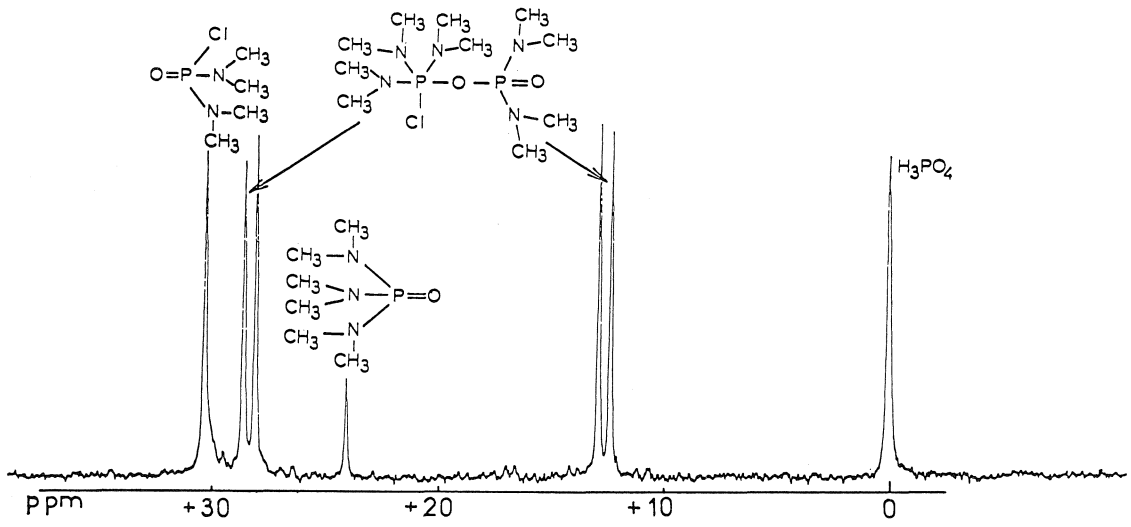


FIG. 1. Action du chlore sur le HMPT; spectre rmn ^{31}P (36.44 MHz); solvant: CH_2Cl_2; $T = 200$ K. La double irradiation sélective du composé **6** a été effectuée à 36.44 MHz tandis que la résonance du proton était observée à 90 MHz. L'irradiation des deux atomes de phosphore a ainsi permis l'identification des signaux de résonance protonique des groupes $(CH_3)_2N$.

Sel de chloroiminium avec le DMF : $\left[\begin{matrix}\diagdown\\ \diagup\end{matrix}N{=}C{-}Cl\right]^{\oplus}\ X^{\ominus}$

Sel de chlorophosphonium avec le HMPT : $\left[\begin{matrix}\diagdown\\ \diagup\end{matrix}N{=}P{-}Cl\right]^{\oplus}\ X^{\ominus}$

Le sel de phosphonium est nettement moins réactif que le sel d'iminium puisque la réaction de ce dernier avec la base de départ (le HMPT) est complète. Par ailleurs, ce sel de phosphonium présente un faible caractère électrophile car il n'attaque pas plus le DMF qu'il ne s'échange avec le HMPT lui-même. La présence d'un sel de chlorophosphonium similaire a été postulée comme intermédiaire réactionnel de la formation d'alkoxytrisdiméthylaminophosphonium (TDAP). (16). La variation des paramètres rmn (notamment δ_{15N}) est en accord avec les observations de réactivité chimique. Le chlore ne peut remplacer les acides de Lewis chlorés mentionnés précédemment car il ne conduit pas à un sel de phosphonium mais plutôt au produit monochloré de substitution par l'intermédiaire d'un complexe d'un autre type. Toutefois il faut noter que son utilisation en synthèse en qualité d'agent chlorant ou oxydant en milieu HMPT, peut s'accompagner de la formation de produits polyphosphorés qui résulte de son action directe sur la phosphoramide.

Partie expérimentale

Préparation des produits

Les réactifs et solvants ont été soigneusement séchés et distillés avant chaque manipulation. L'appareillage est purgé par un courant d'azote sec.

Sels de chlorophosphonium **3***a et* **3***b*

A 0°C une solution de 0.05 mol de phosgène ou d'oxychlorure de phosphore dans 30 cm³ de chlorure de méthylène est additionnée au moyen d'une ampoule de Mariotte à une solution de 0.05 mol (8.7 cm³) de HMPT dans 50 cm³ d'éther. Une agitation est maintenue tout au long de l'addition. Le sel de phosphonium cristallise. A la fin de la réaction le solvant est évaporé, les cristaux sont lavés plusieurs fois à l'éther puis séchés. On obtient ainsi avec un rendement de 100% 11.7 g de sel **3***a* et 16.6 g de sel **3***b*.

Les résultats de microanalyse[2] confirment les formules **3***a* et **3***b*. *Anal.* calc. (**3***a*): C 30.8, H 7.8, Cl 30.3, N 18.0, P 13.2; trouvée: C 30.4, H 8.1, Cl 29.9, N 17.9, P 13.2. *Anal.* calc. (**3***b*): C 21.7, H 5.5, Cl 32.0, N 12.6, O 9.6, P 18.6; trouvée: C 21.9, H 5.7, Cl 31.5, N 12.5, O 9.8, P 18.2.

Si la température de réaction est supérieure à 0°C, il se forme du composé **2**, la proportion de **2** augmentant avec la température. Dans ce cas le résidu liquide peut être distillé (point ébullition 112°C sous 12 Torr). Il est intéressant de noter que l'hexaéthylphosphoramide $((C_2H_5)N)_3P{=}O$ ne réagit pas sur $COCl_2$ ou $POCl_3$ dans les mêmes conditions que le HMPT.

Hydrolyse des sels de chlorophosphonium **3***a et* **3***b*

A 10 g de sel **3***a* ou **3***b* sont additionnés 50 cm³ d'une solution d'eau saturée en K_2CO_3. Après 24 heures d'agitation, on constate par rmn du ^{31}P que l'hydrolyse est totale et qu'il s'est formé du HMPT.

Réaction du réactif de Vilsmeier sur le HMPT

A partir de 5 g de diméthylformamide on prépare le réactif de Vilsmeier selon la méthode habituelle (1*a*). Puis on additionne la quantité stœchiométrique de HMPT en suivant le même mode opératoire que pour la préparation de **3***a* et **3***b*.

Réaction du chlore sur le HMPT

A −70°C, une solution de 0.01 mol (1.83 cm³) de HMPT dans 2 cm³ de $CDCl_3$ est additionnée goutte à goutte à 5 cm³ d'une solution de $CDCl_3$ contenant 0.02 mol de chlore. Une agitation

[2]Les analyses quantitatives élémentaires ont été réalisées par le centre de microanalyses du Centre National de la Recherche Scientifique à Caen.

Can. J. Chem. Downloaded from www.nrcresearchpress.com by 210.87.254.105 on 09/05/12
For personal use only.

est maintenue tout au long de l'addition. Des prélèvements sont effectués et étudiés en rmn à la même température.

Spectres de résonance magnétique nucléaire

Les spectres ^1H ont été réalisés à 60 MHz au moyen d'un spectromètre Varian A 60 A.

Les spectres ^{13}C ont été enregistrés à 25.18 MHz en utilisant un spectromètre Varian XL 100-12 (temps d'acquisition At = 2s, angle d'impulsion $\theta = 30°$). Les déplacements chimiques ^1H et ^{13}C ont été mesurés par rapport au tétraméthylsilane (TMS) utilisé en référence interne. Les spectres ^{31}P à 36.44 MHz (At = 1.365 s, $\theta = 25°$, référence interne H_3PO_4) et ^{15}N à 9.117 MHz (At = 0.683 s, $\theta = 45°$, référence interne CH_3NO_2) ont été réalisés au moyen d'un spectromètre Bruker WH 90 DS. Les spectres ont été réalisés pour le proton dans CH_2Cl_2 et pour les autres noyaux dans $CDCl_3$ avec des concentrations de l'ordre de 2 mol L^{-1}. Chaque spectromètre est en outre équipé d'une sonde à température variable qui a été utilisée pour étudier à basse température les intermédiaires instables.

1. (*a*) G. J. Martin et M. L. Martin. Bull. Soc. Chim. Fr. 1637 (1963); (*b*) G. J. Martin, S. Poignant, M. L. Filleux et M. T. Quemeneur. Tetrahedron Lett. **58**, 5061 (1970); (*c*) G. J. Martin et S. Poignant. J. Chem. Soc. Perkin Trans. II, 1964 (1972); (*d*) G. J. Martin et S. Poignant. J. Chem. Soc. Perkin Trans. II, 642 (1974); (*e*) M. L. Martin, G. Ricolleau, S. Poignant et G. J. Martin. J. Chem. Soc. Perkin Trans. II, 182 (1976); (*f*) M. L. Martin, M. H. Helbert et S. Poignant. J. Chem. Soc. Perkin Trans. II, 1243 (1977).
2. H. G. Viehe et H. Bohme (*Editeurs*). Iminium salts in organic chemistry. Part 1. Wiley, New York. 1976.
3. (*a*) A. Burgermeister. Thèse de Doctorat, Ratisbonne, RFA. 1978; (*b*) J. P. Gouesnard et G. J. Martin. Org. Magn. Reson. **12**, 263 1979; (*c*) G. J. Martin, J. P. Gouesnard, J. Dorie et M. L. Martin. J. Am. Chem. Soc. **93**, 1381 (1977).
4. (*a*) H. Normant. Bull. Soc. Chim. Fr. 791 (1968); (*b*) J. Normant. Thèse de Doctorat, Paris. 1963.
5. L. F. Andrieth et R. Steinman. J. Am. Chem. Soc. **63**, 2115 (1941).
6. H. Normant et T. Cuvigny. Bull. Soc. Chim. Fr. 3344 (1966).
7. A. G. Abatjoglou et E. L. Eliel. J. Org. Chem. **39**, 3042 (1974).
8. T. Cuvigny et H. Normant. Bull. Soc. Chim. Fr. 1867 (1965).
9. P. Lester. U.S. Patent No. 2,678,335. 1954; Chem. Abstr. **49**, 6300 (1955).
10. J. F. Normant et H. Deshayes. Bull. Soc. Chim. Fr. 2854 (1972).
11. H. G. Viehe. Angew. Chem. **12**, 806 (1973).
12. M. M. Crutchfield, C. H. Dungan, J. H. Letcher, V. Mark et J. R. van Wazer. Topics in phosphorus chemistry. Vol. 5. Interscience Publishers, New York. 1967. pp. 19, 358.
13. R. Appel et L. Willms. Chem. Ber. **112**, 1057 (1979).
14. M. Al Neirabeyeh, J. C. Ziegler, B. Gross et P. Caubere. Synthesis, **12**, 811 (1976).
15. C. Anselmi, G. Berti, B. Macchia, F. Macchia et L. Monti. Tetrahedron Lett. **13**, 1209 (1972).
16. (*a*) B. Castro, M. Nacro et C. Selve. Tetrahedron, **35**, 481 (1979); (*b*) J. R. Dormoy et B. Castro. Tetrahedron Lett. 3321 (1979).

Can. J. Chem. Downloaded from www.nrcresearchpress.com by 210.87.254.105 on 09/05/12
For personal use only.

Solvent effect on the protonation of some alkylamines[1]

ALFONSO MUCCI, ROBERT DOMAIN, AND ROBERT L. BENOIT
Département de Chimie, Université de Montréal, Montréal (Qué.), Canada H3C 3V1

Received August 31, 1979

ALFONSO MUCCI, ROBERT DOMAIN, and ROBERT L. BENOIT. Can. J. Chem. **58**, 953 (1980).

Thermodynamic data were obtained at 25°C for the solution and protonation of six bases B: ammonia, three methylamines, and monoethyl and *n*-propylamines in dimethylsulfoxide (Me_2SO) and propylene carbonate (PC). Vapour pressure, potentiometric, and calorimetric determinations were carried out. The solvent effect on the basicity order and protonation of the amines is analysed by using gas phase data and comparing the solution thermodynamics of gaseous B and BH^+. The heat of solution of B in both solvents is close to its heat of condensation. The solution data for BH^+ are discussed in terms of two recent hydration data interpretations.

ALFONSO MUCCI, ROBERT DOMAIN et ROBERT L. BENOIT. Can. J. Chem. **58**, 953 (1980).

On a obtenu des données thermodynamiques sur la dissolution et la protonation à 25°C de six bases B: l'ammoniac, les trois méthylamines et les monoéthyl et *n*-propylamines dans le diméthylsulfoxyde (Me_2SO) et le carbonate de propylène (PC). On a effectué des déterminations de pression de vapeur, potentiométrie et calorimétrie. L'effet de solvant sur l'ordre de basicité et la protonation des amines est analysé en utilisant des données en phase gazeuse et en comparant la thermodynamique de solution de B et BH^+ gazeux. La chaleur de solution de B dans les deux solvants est voisine de sa chaleur de condensation. Les données sur la solution de BH^+ sont examinées en relation avec deux interprétations récentes de données sur l'hydratation.

Trends in the reactivity of chemical species belonging to related series, when referred to condensed phases, may differ widely from the more regular trends observed in the gas phase. For instance, it is well known that the gas phase basicity of NH_3 and the methylamines B as deduced from proton affinities varies according to $NH_3 < MeNH_2 < Me_2NH < Me_3N$, while in aqueous solution the order based on enthalpy of protonation is $NH_3 < MeNH_2 > Me_2NH > Me_3N$ (1). The apparently anomalous order in water has been shown to result from two opposite trends, one for B where its solution exothermicity increases in the order $NH_3 < MeNH_2 < Me_2NH \sim Me_3N$, while for BH^+ the trend reverses with $-\Delta H^0_w$ (BH^+) decreasing according to $NH_4^+ > MeNH_3^+ > Me_2NH_2^+ > Me_3NH^+$.

Using relevant thermodynamic data and Born–Haber type cycles, several authors (refs. 1 and 2 and references cited therein) carried out detailed analyses of the relations between gas phase and aqueous basicity of related series of amines. The major factor responsible for the basicity sequence in aqueous solution was found to be the change in hydration enthalpy of the ammonium ions ΔH^0_w (BH^+) within a related series. For this, two explanations have been proposed. On the one hand, following an earlier qualitative proposal (3), Jones and Arnett (1) attributed the major part of this variation in ΔH^0_w (BH^+) to the change of the number of N^+—H hydrogen bonds available for solvation. On the other hand, Aue *et al.* (2), in their recent analysis, accounted for the changes in ΔH^0_w (BH^+) (after suitable corrections) in terms of the simple classical Born electrostatic theory.

Given the complex nature of the interactions between both solutes B and BH^+ and solvent water, a thermodynamic study of the protonation of a series of amines in selected non-aqueous solvents should be of interest since it might provide a test of the previously proposed models and should give further insight into the solvent effect on an important proton transfer reaction. We are presenting here the results of such a study in which the solvents dimethylsulfoxide (Me_2SO) and propylene carbonate (PC) were used. These solvents, which belong to the dipolar aprotic class, were selected for several reasons. First, solute–solvent interactions in these non-hydrogen-bonded media are likely to be simpler than in water. Then, the relevant bulk properties of the solvents, dielectric constant and basicity, are sufficiently different for a meaningful test of their effect on the protonation and solvation data. Finally, the same solvents were also used by Krishnan and Friedman (4) for a related study of the heats of solution of amine salts as well as of hydrocarbons and alcohols. The amines we studied include ammonia, the methylamines ($MeNH_2$, Me_2NH, Me_3N), monoethylamine ($EtNH_2$), and *n*-propylamine (*n*-$PrNH_2$).

Experimental

Materials

PC (Anachemia) was doubly distilled under vacuum and middle portions were collected. Me_2SO (BDH) was reagent grade. Both solvents were dried and stored over activated 4A molecu-

[1]Presented in part at the 2nd Joint Conference of the Chemical Institute of Canada and the American Chemical Society, Montreal, P.Q., May 29 – June 2, 1977.

0008-4042/80/090953-06$01.00/0
©1980 National Research Council of Canada/Conseil national de recherches du Canada

Can. J. Chem. Downloaded from www.nrcresearchpress.com by 210.87.254.105 on 09/05/12
For personal use only.

Can. J. Chem. Downloaded from www.nrcresearchpress.com by 210.87.254.105 on 09/05/12
For personal use only.

lar sieves. Trifluoromethanesulfonic acid from 3M Co. had a purity of 99.5%. The gaseous amines (Canadian Liquid Air) were the best grades available and their purity was NH_3 (99.9%), $MeNH_2$ (98.0%), Me_2NH, (99.0%), Me_3N (99.0%), $EtNH_2$ (98.5%). Liquid *n*-$PrNH_2$ was a white label product from Eastman Kodak. Tetraethylammonium iodide (NEt_4I) (Baker) was dried in a vacuum oven at 50°C for 24 h.

Calorimetry

The heat of solution of the gaseous amines in 200 mL Me_2SO was determined at 25°C. The gas calorimeter and procedure have been described in an earlier publication (5). The concentration of the amines dissolved after each calorimetric run was determined by addition of a known volume of solution to an excess of aqueous standard HCl solution and back titration with standard NaOH. From 3–7 determinations were carried out for each amine. The heat of protonation of the gaseous amines in Me_2SO was obtained similarly by dissolving the amines in an excess of 0.1 *M* solution of HCF_3SO_3, a strong acid in this solvent (6). The amount of amine reacted was deduced after titration of the remaining excess acid. The heats of solution and protonation of liquid *n*-$PrNH_2$ were measured with an LKB Model 8725-2 Isoperibol calorimeter previously described (7), the amount of amine dissolved or reacted being known from the weights of the glass ampoules. Some difficulties were met in the calorimetric work in PC since the primary and secondary amine solutions proved to be unstable at 25°C because of the formation of carbamates (8). For example, the least stable solution, that of $MeNH_2$, was 40% decomposed in 25 min at 25°C, but the decomposition was reduced to 7% for the same duration at 10°C. An ancillary study of the kinetics of amine decomposition showed that the ratio $(amine)_t/(amine)_0$, as measured by acid–base titration, decreased linearly with time, at least initially. This ratio was also proportional to the shift of the OH ⇌ NH proton nmr resonance signal. We found that the reaction rates for the different amines varied according to $MeNH_2 \sim Me_2NH \gg EtNH_2 \sim$ *n*-$PrNH_2$. On the basis of these results, the calorimetric measurements of the heats of solution in PC were carried out at 10°C for $MeNH_2$ and Me_2NH and at 25°C for $EtNH_2$ and *n*-$PrNH_2$ (9). Corrections were also used to determine the amount of amine dissolved in the calorimetric runs and to calculate the heat involved since the formation of carbamate is exothermic.

Vapour Pressure Measurements

Solution vapour pressures were measured with a precision quartz gauge (Texas Instruments) whose quartz spiral was kept at 60°C. The 60 mL cell containing the magnetically agitated solution was kept in a water bath regulated to ±0.005°C. The glass tubing connecting the cell with the gauge was thermally jacketed. The solutions were degassed by repeated freezing and evacuation. The concentration of the amines in solution was determined by acid–base titration after each measurement.

Potentiometry

Potentiometric titration of Me_2SO solutions of the amines with HCF_3SO_3 in Me_2SO were carried out at 25°C in a thermostated cell placed in a glovebox under a stream of dry nitrogen. An essentially constant ionic strength was maintained by making the solution initially 0.100 *M* in Et_4NI. The pair of electrodes used were a Radiometer G202 B glass electrode and an I^-/I_3^- reference electrode consisting of a platinum wire in a Me_2SO solution 10^{-2} *M* in I_2 and 2×10^{-2} *M* in I^- (10). The junction connecting the reference electrode to the cell was a 10^{-1} *M* Et_4NClO_4 solution in Me_2SO. The potential measurements were made with a Tacussel potentiometer. Stable readings were obtained within 1 min. The glass electrode was calibrated with a series of HCF_3SO_3 solutions in Me_2SO containing 0.100 *M* Et_4NI.

Results

Energetics of Solution of NH_3 and Amines

Enthalpy

The heats of solution, Q, of the bases in Me_2SO and PC were determined for varying quantities of each amine (1 to 5×10^{-2} mol for NH_3 and the gaseous amines and 2 to 8×10^{-3} mol in the case of liquid *n*-$PrNH_2$). The values of Q were plotted against the number of moles, and the slopes of the least-squares lines gave the molar enthalpy of solution. Since no concentration dependence was observed within the limits of error, these molar enthalpies of solution can be taken as the infinite dilution values ΔH_s^0 (B). In the case of liquid *n*-$PrNH_2$, ΔH_s^0 (B) was obtained by subtraction from the heat of solution, the heat of vaporization at 25°C, 7.44 kcal mol^{-1} (11). Our values of ΔH_s^0 (B) (kcal mol^{-1}) and the enthalpy of solution of B in Me_2SO and PC are given in Table 1. Also included in this table are literature values of ΔH_s^0 (B) in water.

Free Energy

The total vapour pressure of NH_3 and amine solutions in Me_2SO was measured at 25°C as a function of concentration, usually 0.1–2.0 *M*. In view of the very low vapour pressure of Me_2SO, 0.60 Torr, the vapour pressures of the solutes, 40–400 Torr, were calculated by subtracting from the total vapour pressure the solvent vapour pressure obtained from Raoult's law. The plots of P_B vs. the mole fraction X_B were linear and least-squares analyses gave values of Henry's constants, K_x, with their standard deviations (less than 2% of K_x). The free energies of solution were calculated from ΔG_s^0 (B) = RT ln K_c, where K_c, Henry's law constant, is in atm. mole L^{-1} so that comparisons could be made with water. Table 2 presents our values of ΔG_s^0 (B) (standard deviation less than 0.01) for Me_2SO as well as literature data for water as solvent. Because of complications arising from the reaction of some of the amines with PC, no measurements of vapour pressure were made in this solvent.

Energies of Protonation of NH_3 and Amines

Enthalpy

The heats of solution, Q, of the bases in Me_2SO containing an excess of HCF_3SO_3 were determined for varying amounts of the amines (1 to 12×10^{-3} mol). The plots of Q vs. the number of moles of base were linear and the least-squares slopes gave $\Delta H_{n,s}^0$, the heat of neutralization of gaseous B (liquid *n*-$PrNH_2$), according to reaction [1]:

[1] $B(g) + H^+(s) = BH^+(s)$ $\quad \Delta H_{n,s}^0$

Values of $\Delta H_{n,s}^0$ were combined with those of ΔH_s^0

Can. J. Chem. Downloaded from www.nrcresearchpress.com by 210.87.254.105 on 09/05/12
For personal use only.

TABLE 1. Enthalpies of solution of gaseous amines and their heats of condensation (kcal mol^{-1}) at 25°C

B	$-\Delta H^0_s$(B) H_2O[a]	Me_2SO	PC	ΔH^0_v(B)[b]
NH_3	8.42	5.42 ± 0.06	4.98 ± 0.02	4.85
$MeNH_2$	10.82	6.42 ± 0.03	6.7[c] ± 0.2	5.79
Me_2NH	12.69	5.96 ± 0.09	6.0[c] ± 0.1	5.65
Me_3N	12.60	4.73 ± 0.08	5.35 ± 0.03	5.46
$EtNH_2$	13.05	6.86 ± 0.02	6.55 ± 0.05	6.47
n-$PrNH_2$	13.37	7.13 ± 0.01	6.81 ± 0.04	7.44

[a]Reference 1.
[b]Reference 11.
[c]10°C.

TABLE 2. Free energies (kcal mol^{-1}) and entropies (cal mol^{-1} deg^{-1}) of solution of gaseous amines at 25°C

B	$-\Delta G^0_s$(B) H_2O[a,b]	Me_2SO[b]	$-\Delta S^0_s$(B) H_2O	Me_2SO
NH_3	2.43	0.30	20.1	17.2
$MeNH_2$	2.67	0.77	27.3	18.9
Me_2NH	2.41	0.65	34.5	17.8
Me_3N	1.34	−0.07	37.8	16.1
$EtNH_2$	2.61	1.03	35.0	19.5
n-$PrNH_2$	2.51	1.56	36.4	18.7

[a]Reference 1.
[b]Standard state defined as: B (real gas, 1 atm) → B (hypothetical 1 *M*, s).

(B), the heat of solution of gaseous or liquid B, to yield $\Delta H^0_{p,s}$, the heat of protonation of B in Me_2SO:

[2] $B(s) + H^+(s) = BH^+(s)$ $\Delta H^0_{p,s}$

with $\Delta H^0_{p,s} = \Delta H^0_{n,s} - \Delta H^0_s$ (B). Our values of $\Delta H^0_{p,s}$, the enthalpy of protonation of the solute bases in Me_2SO, are given in Table 3 together with the corresponding literature values for these bases in water as solvent.

Because of the limited stability of HCF_3SO_3 and of some amines in PC, the values of $\Delta H^0_{p,s}$ in PC were obtained indirectly from published data by combining enthalpies for the following three reactions:

[3] $HCl(g) = H^+(s) + Cl^-(s)$

[4] $BH^+(s) + Cl^-(s) = BHCl(c)$

[5] $B(g) = B(s)$

Data for reactions [3] and [4] are taken from refs. 5 and 4, respectively. By combining these three reactions, we obtain enthalpy data for reaction [6]:

[6] $HCl(g) + B(g) + BH^+(s) = H^+(s) + B(s) + BHCl(c)$ $\sum \Delta H_s$

in both water and PC for each amine. Finally values of $\Delta H^0_{p,s}$ for reaction [2] in PC are deduced from:

[7] $\Delta H^0_{p,pc} = \Delta H^0_{p,w} - \sum \Delta H_{pc} + \sum \Delta H_w$

Using the values of $\Delta H^0_{p,w}$ from Table 3, the values of $\Delta H^0_{p,pc}$ thus computed are listed in Table 3.

TABLE 3. Enthalpies of protonation of amines (kcal mol^{-1}) at 25°C

B	$-\Delta H^0_{p,s}$ H_2O[a]	Me_2SO	PC	$-\Delta H^0_{p,q}$ Gas phase[b]
NH_3	12.49	19.2 ± 0.5	31.9	202.3
$MeNH_2$	13.18	18.9 ± 0.3	31.6	211.3
Me_2NH	12.04	17.6 ± 0.3	31.3	217.9
Me_3N	8.82	14.4 ± 0.3	29.0	222.1
$EtNH_2$	13.71	19.1 ± 0.1	33.6	214.0
n-$PrNH_2$	13.84	18.9 ± 0.1	33.4	215.5

[a]Reference 1.
[b]Reference 13.

Free Energy

The values of the equilibrium constant *K* for reaction [2] for NH_3 and the amines in Me_2SO were deduced from our potentiometric curves obtained from the neutralization of 10^{-2} *M* solutions of B by 0.1 *M* HCF_3SO_3. The solutions were also made 0.100 *M* in Et_4NI. The slopes of the least-squares plots of the potential of the glass electrode against log [BH^+]/[B] varied between 60.1 and 61.6 mV according to the nature of B. These values are in satisfactory agreement with the slope of 61.5 mV obtained when plotting ΔE vs. log [HCF_3SO_3] between 2×10^{-4} and 3×10^{-2} *M* acid in a 0.100 *M* Et_4NI Me_2SO solution. The p*K* values calculated from the half-neutralization potentials, and the corresponding free energies $\Delta G^0_{p,s}$ are listed in Table 4, together with the p*K* literature values given for water as solvent. No corrections were made for the effect of the ionic strength which would be small for this type of protonation reaction. The p*K* values obtained for NH_3 and $EtNH_2$ are within 0.1 unit of the values determined by Kolthoff *et al.* (12) using a glass electrode and a silver – 0.01*M* silver nitrate reference electrode calibrated with buffer solutions of known pH.

Discussion

Our data in Tables 3 and 4 for the enthalpy and free energy of protonation emphasize the fact that the basicity order of the substituted amines is solvent dependent. While the order based on $\Delta H^0_{p,s}$ is $NH_3 < MeNH_2 > Me_2NH > Me_3N$ and $NH_3 < MeNH_2 < EtNH_2 \sim$ *n*-$PrNH_2$ in water, the sequence found in Me_2SO or PC is $NH_3 \sim MeNH_2 \sim$ (or <) $EtNH_2 \sim$ *n*-$PrNH_2 > Me_2NH > Me_3N$. These trends are at variance with the gas phase order $NH_3 < MeNH_2 < EtNH_2 <$ *n*-$PrNH_2 < Me_2NH < Me_3N$ which corresponds to the proton affinities (13) listed in Table 3. If we now choose as basicity parameter the free energy or protonation $\Delta G^0_{p,s}$ (or p*K*) (Table 4) instead of $\Delta H^0_{p,s}$, the gas phase basicity order remains the same but the solution basicity order is modified. A complete analysis

TABLE 4. Thermodynamic functions for the protonation of amines at 25°C

B	pK^e		$-\Delta G^0_{p,s}$(kcal mol^{-1})			$\Delta S^0_{p,s}$(cal deg^{-1} mol^{-1})	
	$H_2O^{a,b}$	Me_2SO^b	$H_2O^{a,c}$	Me_2SO^c	Gas phase^d	H_2O^a	Me_2SO
NH_3	9.24	10.4	12.61	14.2	193.7	+0.4	−16.8
$MeNH_2$	10.65	11.0	14.53	15.0	202.9	+4.5	−13.1
Me_2NH	10.78	10.3	14.70	14.0	209.7	+8.9	−12.1
Me_3N	9.80	8.4	13.37	11.5	214.3	+5.2	−9.7
$EtNH_2$	10.68	10.9	14.57	14.9	205.6	+2.9	−14.1
n-$PrNH_2$	10.57	10.7	14.42	14.6	207.2	+1.9	−14.7

[a]Reference 1.
[b]pK values are for proton ionization.
[c]Standard state defined as a molar solution behaving as an ideal solution.
[d]References 2 and 13.
[e]See note added in proof.

of the complex solvent effect on the protonation thermodynamic functions $\Delta H^0_{p,s}$ and $\Delta G^0_{p,s}$ can best be carried out by using corresponding data for the gas phase and comparing the thermodynamics of solution of H^+, B, and BH^+. To broaden our discussion, we will also consider literature data for the same processes in water (1, 2).

If we look first at the solvent effect on the solution of the gaseous amines B, the enthalpy data in Table 1 show that for a given amine ΔH^0_s (B) varies little when passing from Me_2SO to PC, but much more when passing to H_2O. Furthermore, when considering the effect of the nature of B, ΔH^0_s (B) is much less exothermic and changes less for Me_2SO or PC than for H_2O. The free energies of solution ΔG^0_s (B) in Table 2 reflect the smaller solubilities of B in Me_2SO but show less difference between Me_2SO and H_2O than ΔH^0_s (B). The entropies of solution ΔS^0_s (B) in Table 2 are smaller for Me_2SO than for H_2O and vary little for Me_2SO with the nature of B, in contrast with the large variations for H_2O. A good Barclay–Butler (ΔH^0_s–ΔS^0_s) plot (14) with a 600 K slope is obtained for the solution of 5 amines in Me_2SO, *n*-$PrNH_2$ remaining off the line. Krishnan and Friedman (15) have shown that for many solvents the heat of solution of gaseous alkanes and aliphatic alcohols of increasing chain length could be explained in terms of group contributions. Our data for Me_2SO and our series of primary amines showed a smaller —CH_2— group contribution. These authors (15) have also proposed a general equation which we have used to calculate the heat of solution of the amines in Me_2SO with literature values for the solutes and solvent physical parameters. The values thus obtained for ΔH^0_s (B) were systematically 1–2 kcal mol^{-1} less exothermic than the experimental values. However, both observed trends, increasing exothermicity with increasing chain length for primary amines and decreasing exothermicity with increasing number of methyl substituents for the methylamines, were correctly predicted. The same calculations carried out for PC as solvent led to a poorer agreement with our experimental data for the primary amines. More valuable information can be obtained by comparing the heat of solution of the amines and their heat of condensation $-\Delta H^0_v$ (B). Table 1 shows very similar $-\Delta H^0_s$ and ΔH^0_v values for both Me_2SO and PC. Thus if we look at the solution process of the amines B as a two-step process, condensation of B followed by mixing of liquid B with Me_2SO or PC, the previous observation indicates a very small heat of mixing of liquid B with both solvents. Considering the polar nature of both solute and solvent molecules, this is somewhat unexpected, although we have obtained similar results in a recent study of the thermodynamics of solution of SO_2, a polar solute, in some polar aprotic solvents (16). Data in Table 1 show clearly that when water is the solvent the picture is entirely different, the much more exothermic heat of solution of the amines in H_2O reflecting in part the contribution from the hydrophobic-type interactions of the carbon chain of the alkylamines with water.

Turning now to the solvent effect on the solution of the gaseous ions BH^+, the values of the enthalpies of solution ΔH^0_s (BH^+) were calculated by means of a relation derived from the thermodynamic cycles relating protonation processes in the gas phase and in the solvents.

$$\Delta H^0_s(BH^+) = \Delta H^0_{p,s} - \Delta H^0_{p,g} + \Delta H^0_s(B) + \Delta H^0_s(H^+)$$

The value of the enthalpy of solvation of the gaseous proton $\Delta H^0_s(H^+)$ selected for water is −270.0 kcal mol^{-1} while the corresponding values for Me_2SO and PC are derived from the above and from the enthalpies of transfer of H^+ between H_2O and Me_2SO and PC. These latter values were in turn obtained from experimental values for reaction [3] and the enthalpies of transfer of Cl^- between H_2O and Me_2SO (5) and PC (14) based on

Can. J. Chem. Downloaded from www.nrcresearchpress.com by 210.87.254.105 on 09/05/12
For personal use only.

Can. J. Chem. Downloaded from www.nrcresearchpress.com by 210.87.254.105 on 09/05/12
For personal use only.

the tetraphenylborate–tetraphenylarsonium extrathermodynamic assumption. The values of $\Delta H_s^0(BH^+)$ thus calculated are listed in Table 5. Similar calculations were carried out for $\Delta G_s^0(BH^+)$ in H_2O and Me_2SO using data in Tables 2 and 4 and for $\Delta G_s^0(H^+)$, the values -261.0 kcal mol^{-1} in water and -265.5 kcal mol^{-1} in Me_2SO, the latter one calculated from the free energy of transfer between H_2O and Me_2SO obtained by Kolthoff (17). The values of $\Delta G_s^0(BH^+)$ as well as those of $\Delta S_s^0(BH^+)$ are given in Table 6.

Let us now consider the solvent effect on the energetics of solution of the gaseous ions BH^+ in relation to the bulk dielectric constant D of the solvents Me_2SO (46.6), PC (65.1), and H_2O (78.5). First, the values of $-\Delta G_s^0(BH^+)$ are consistently higher in Me_2SO than in H_2O. This is opposite to what would be qualitatively expected on the basis of the simple Born equation relating $-\Delta G_s^0$ and D. Second, if we calculate $-\Delta G_s^0$ for a given ion BH^+ such as NH_4^+, using the ionic radius $r_{NH_4^+} = 1.70$ Å and a previously established relation (18), we obtain for $-\Delta G_s^0(NH_4^+)$ in Me_2SO 95.6 kcal mol^{-1}, in contrast to our value 86.3 kcal mol^{-1}. The failure of the simple Born treatment to account for the effect of a change in the dielectric constant of the solvent on the free energy of solvation of BH^+ ions can also be shown to extend to the enthalpy of solvation $\Delta H_s^0(BH^+)$. However, Aue *et al.* (2) recently concluded that by modifying this electrostatic approach they could satisfactorily explain their thermodynamic results derived from gas phase and aqueous data for the protonation of a large series of nitrogen bases. Aue *et al.* essentially subtracted from the thermodynamic parameter for the solution in water of gaseous BH^+ ions a non-electrostatic contribution assumed to be equal to the corresponding parameter for the solution of B. The remaining electrostatic contributions ΔH^{el} and ΔG^{el} were said to follow the expected dependence on suitably calculated values of $1/r_{BH^+}$. In order to test this approach, using our data in Tables 5 and 6, we deduced values of $-\Delta H_s^0(BH^+)^{el}$ for Me_2SO and PC and compared these values with those calculated from the simple Born equation using the values of r_{BH^+} calculated by Aue *et al.* (2). Poor agreement was found, the calculated values being higher than the experimental ones for NH_4^+ but consistently lower by up to 25–35 kcal mol^{-1} (the difference increasing with r_{BH^+} for all other BH^+ ions. It therefore seems that this modified electrostatic approach fails to provide a quantitative picture of the solvent effect for the solution enthalpies of the BH^+ ions we have studied here.

TABLE 5. Enthalpies of solution of gaseous ammonium ions and proton (kcal mol^{-1}) at 25°C

	$-\Delta H_s^0(BH^+)$		
BH^+	H_2O	Me_2SO	PC
NH_4^+	88.6	98.4	93.7
$MeNH_3^+$	82.7	90.1	86.1
$Me_2NH_2^+$	76.8	81.8	78.5
Me_3NH^+	69.3	73.1	71.4
$EtNH_3^+$	82.2	88.1	85.2
n-$PrNH_3^+$	81.7	86.6	83.8
H^+	270.0	276.1	259.1

TABLE 6. Free energies (kcal mol^{-1}) and entropies (cal mol^{-1} deg^{-1}) of solution of gaseous ammonium ions and proton at 25°C

	$-\Delta G_s^0(BH^+)$		$-\Delta S_s^0(BH^+)$	
BH^+	H_2O	Me_2SO	H_2O	Me_2SO
NH_4^+	82.3	86.3	21.1	40.6
$MeNH_3^+$	75.3	78.4	24.8	39.3
$Me_2NH_2^+$	68.4	70.5	28.2	37.9
Me_3NH^+	61.4	62.6	26.5	35.2
$EtNH_3^+$	72.6	75.8	33.9	41.3
n-$PrNH_3^+$	70.8	74.6	36.6	40.3
H^+	261.0	265.5	30.2	35.6

The second approach we have considered to explain the solvent effect on our values of $\Delta G_s^0(BH^+)$ and $\Delta H_s^0(BH^+)$ is non-electrostatic and is an extension of the proposal of Trotman-Dickenson (3) developed by Jones and Arnett (1). These workers attributed the variation of free energy and enthalpy of hydration of $R_nNH_{4-n}^+$ ions essentially to the change in the number $(4-n)$ of H bound to N which can form H-bonds to water. Looking at our data for Me_2SO and PC in Tables 5 and 6, we first note a gradual decrease in the values of $-\Delta G_s^0(BH^+)$ and $-\Delta H_s^0(BH^+)$ when passing from NH_4^+ to $MeNH_3^+$, $Me_2NH_2^+$ and Me_3NH^+. There is an average decrease per H-bond of 7.9 kcal mol^{-1} and 8.4 kcal mol^{-1} in Me_2SO for ΔG^0 and ΔH^0, respectively, and 7.3 kcal mol^{-1} in PC for ΔH^0. However, when we consider the ions $MeNH_3^+$, $EtNH_3^+$, and n-$PrNH_3^+$, which could all form three H-bonds, both ΔG^0 and ΔH^0 values in Me_2SO and PC show some decrease with the size of the substituent. Thus, contributions from the carbon chain to the solvation process of BH^+ ions in Me_2SO and PC cannot be entirely neglected, making the H-bond picture a qualitative one. The values of the ionic entropies of solvation $\Delta S_s^0(BH^+)$ listed in Table 6 show only minor and regular variations for Me_2SO but large changes for water. Considering now the effect of the solvent on the solvation thermodynamics of each ion BH^+, our values for $-\Delta G_s^0(BH^+)$ in Table 6 are higher in Me_2SO than

in water by about 1.0 kcal mol^{-1} per possible H-bond. This is in line with the higher basicity of Me_2SO. When we include the data for PC in Table 5 we also find that BH^+ solvation enthalpy is more exothermic in Me_2SO than in PC, in accordance with the higher basicity of Me_2SO. However, the exothermicity is lower in water than in both Me_2SO and PC, although the basicity of water as defined by $\Delta H^0_s(H^+)$ is between that of Me_2SO and PC. The anomalous position of water and of other H-bonding solvents in such relationships between two basicity parameters has already been discussed (19).

In concluding this discussion, we can say that our analysis has brought into focus the complex interplay of the many factors which control the effect of a change of solvent on the basicity order and the protonation thermodynamic functions of a series of substituted bases. The complexity of the solvent effect is magnified when protonation data ($\Delta G^0_{p,s}$ and $\Delta H^0_{p,s}$) are compared for solvents belonging to different classes such as dimethylsulfoxide and water (12). Thus, the unexpectedly small and irregular pK ($\Delta G^0_{p,s}$) differences for the series of amines B in Me_2SO and H_2O (Table 4) result from irregular entropy compensations of nearly constant $\Delta H^0_{p,s}$ differences. Furthermore, the higher exothermicity of $\Delta H^0_{p,s}$ in Me_2SO (Table 3) is in turn due to both variable but more exothermic $\Delta H^0_s(BH^+)$ and less exothermic $\Delta H^0_s(B)$ values in Me_2SO, which are in part opposed by a more exothermic $\Delta H^0_s(H^+)$ in Me_2SO. Our analysis shows clearly that attempts to rationalize pK differences with such a pair of solvents in terms of one simple solvent parameter such as the proton transfer activity coefficient were bound to be unsuccessful.

NOTE ADDED IN PROOF: The pK values of the BH^+ ions in PC may be calculated from known values in acetonitrile since ΔpK for related BH^+ ions in both solvents appears to be constant (20). However, there are discrepancies in pK values in PC reported by two groups of workers (20, 21).

Acknowledgement

The financial assistance of the National Research Council of Canada is gratefully acknowledged.

1. F. M. JONES and E. M. ARNETT. *In* Progress in physical organic chemistry. Vol. II. *Edited by* A. Streitwieser, Jr. and R. W. Taft. Interscience, New York, NY. 1974.
2. D. H. AUE, H. M. WEBB, and M. T. BOWERS. J. Am. Chem. Soc. **98**, 318 (1976).
3. A. F. TROTMAN-DICKENSON. J. Chem. Soc. 1293 (1949).
4. C. V. KRISHNAN and H. L. FRIEDMAN. J. Phys. Chem. **74**, 3900 (1970).
5. R. DOMAIN, M. RINFRET, and R. L. BENOIT. Can. J. Chem. **54**, 2101 (1976).
6. R. L. BENOIT and C. BUISSON. Electrochim. Acta, **18**, 105 (1973).
7. R. L. BENOIT, M. RINFRET, and R. DOMAIN. Inorg. Chem. **11**, 2603 (1972).
8. H. NAJER, P. CHABRIER, and R. GIUDICELLI. Bull. Soc. Chim. Fr. 1142 (1954).
9. A. MUCCI. M.Sc. Thesis, Université de Montréal, Montréal (Qué.), Canada. 1977.
10. R. L. BENOIT, M. F. WILSON, and S. Y. LAM. Can. J. Chem. **55**, 792 (1977).
11. R. R. DREISBACH. *In* Physical properties of chemical compounds. *Edited by* R. F. Gould. Adv. Chem. Ser. 29 (1961).
12. I. M. KOLTHOFF, M. K. CHANTOONI, JR., and S. BHOWMIK. J. Am. Chem. Soc. **90**, 23 (1968).
13. P. KEBARLE. Ann. Rev. Phys. Chem. **28**, 445 (1977).
14. C. V. KRISHNAN and H. L. FRIEDMAN. *In* Solute–solvent interactions. *Edited by* D. Ritchie and C. F. Coetzee. M. Dekker, New York, NY. 1976.
15. C. V. KRISHNAN and H. L. FRIEDMAN. J. Phys. Chem. **75**, 3598 (1971).
16. R. L. BENOIT and E. MILANOVA. Can. J. Chem. **57**, 1319 (1979).
17. I. M. KOLTHOFF. J. Phys. Chem. **76**, 2024 (1976).
18. G. CHOUX and R. L. BENOIT. J. Am. Chem. Soc. **91**, 6221 (1969).
19. R. L. BENOIT and C. LOUIS. *In* The chemistry of non-aqueous solvents. Vol. VA. *Edited by* J. J. Lagowski. Academic Press, New York, NY. 1978.
20. K. IZUTSU, T. NAKAMURA, and I. IIJIMA. Bull. Chem. Soc. Jpn. **52**, 2721 (1979).
21. J. TALARMIN, M. L'HER, and J. COURTOT-COUPEZ. C. R. Acad. Sci. Ser. C, **287**, 105 (1978).

Can. J. Chem. Downloaded from www.nrcresearchpress.com by 210.87.254.105 on 09/05/12
For personal use only.

Canadian Journal of Chemistry
Published by
THE NATIONAL RESEARCH COUNCIL OF CANADA

Journal canadien de chimie
Publié par
LE CONSEIL NATIONAL DE RECHERCHES DU CANADA

Volume 58 Number 10 May 15, 1980 Volume 58 numéro 10 15 mai 1980

Can. J. Chem. Downloaded from www.nrcresearchpress.com by 210.87.254.42 on 09/05/12
For personal use only.

Volumetric and thermochemical properties of ionic surfactants: sodium decanoate and octylamine hydrobromide in water

ROSARIO DE LISI,[1] GÉRALD PERRON, AND JACQUES E. DESNOYERS[2]
Department of Chemistry, Université de Sherbrooke, Sherbrooke (Qué.), Canada J1K 2R1
Received November 20, 1979

ROSARIO DE LISI, GÉRALD PERRON, and JACQUES E. DESNOYERS. Can. J. Chem. **58**, 959 (1980).

The heat capacities per unit volume and the densities of sodium decanoate (NaDec) in water were measured as a function of concentration and temperature in the range 0.5 to 45°C. Similar data were obtained for octylamine hydrobromide at 5 and 15°C. Enthalpies of dilution of NaDec in water were measured at 25°C. From these and previously published data the apparent and partial molal heat capacities, expansibilities, volumes, and relative enthalpies were determined as a function of temperature and concentration. The concentration dependence of $\bar{V}_2$ and $\bar{L}_2$ is similar to that of other surfactants such as alkyltrimethylammonium bromides and sodium dodecyl sulfate, but in contrast with the other surfactants, $\bar{C}_{P,2}$ goes through a sharp maximum in the micellization region at the lower temperatures. These thermodynamic properties can be analysed with a phase-separation model to give the changes in volume, heat capacity, and enthalpy during micellization as a function of temperature. The limitations of this model are also discussed.

ROSARIO DE LISI, GÉRALD PERRON et JACQUES E. DESNOYERS. Can. J. Chem. **58**, 959 (1980).

Les capacités calorifiques par unité de volume et les masses volumiques du décanoate de sodium (NaDec) dans l'eau ont été mesurées en fonction de la concentration et de la température dans la région 0.5 à 45°C. Des données semblables ont été obtenues pour le bromhydrate d'octylamine à 5 et 15°C. Les enthalpies de dilution de NaDec ont été mesurées à 25°C. A partir de ces données et d'autres obtenues auparavant, les capacités calorifiques, les enthalpies, les expansibilités et les volumes molaires apparents et partiels ont été déterminés en fonction de la température et de la concentration. La dépendance de $\bar{V}_2$ et $\bar{L}_2$ sur la concentration est qualitativement semblable à d'autres surfactants, tels les bromures d'alkyltriméthylammonium et le dodécyl sulfate de sodium. Par contre, $\bar{C}_{P,2}$ passe par un maximum étroit dans la région de la micellisation aux basses températures, contrairement à d'autres surfactants. Ces fonctions thermodynamiques peuvent être analysées au moyen d'un modèle de changement de phase pour obtenir les changements de volume, de capacité calorifique et d'enthalpie durant la micellisation en fonction de la température. Les limites de ce modèle sont aussi discutées.

Introduction

In a continuing study on the thermodynamic properties of aqueous surfactants we have examined systematically the alkylamines hydrobromides (1, 2) and nonyl and decyltrimethylammonium bromides in water (3–5). With the former system the effect of chain length was investigated, mostly with the aim of understanding the properties of surfactants in the dispersed state, i.e. in the pre-micellar region. The two alkyltrimethylammonium bromides were investigated thoroughly in the micellar region. It was thus possible to examine the temperature dependence of the thermodynamic functions and in particular of the heats, entropies, volumes, and heat capacities of micellization. All these functions were shown to be self-consistent and should prove very useful in checking quantitatively various models and theories.

Anionic surfactants were also investigated. The volumes and heat capacities of some alkyl sulfates (6) and alkyl carboxylates (7) were reported at 25°C. Of these, the carboxylates seem most interesting since they show very sharp changes near the critical micelle concentration (CMC). We therefore felt that carboxylate surfactants might be promising as model systems to investigate microphase transitions in surfactant solutions.

The alkyl carboxylates have been extensively studied in the literature. The thermodynamic studies have been concerned with the determination of the CMC under various conditions (8, 9), the volumetric

[1]On leave of absence from Instituto Di Chimica-Fisica, Dell'Universita Di Palermo, Italie.
[2]To whom all correspondence should be addressed.

0008-4042/80/100959-11$01.00/0
©1980 National Research Council of Canada/Conseil national de recherches du Canada

Can. J. Chem. Downloaded from www.nrcresearchpress.com by 210.87.254.42 on 09/05/12
For personal use only.

properties (10, 11), the heat capacities (12), and the enthalpies (13). However, most of these studies were limited to the determination of the thermodynamic functions of micellization and a detailed study of the properties in the micellar region were usually not made. Since it is through a careful study of this region that models for the various equilibria in solution will eventually be established these systems need further investigation.

The useful working range of most of our thermodynamic techniques is above 0.01 mol kg^{-1}. The CMC must therefore be well above this concentration limit if the micellization region is to be studied thoroughly. Therefore the highest homolog that can be investigated conveniently is sodium decanoate (NaDec) which has a CMC above 0.08 mol kg^{-1} at 25°C. In this paper we will report heat capacities, enthalpies, volumes, and expansibilities of NaDec over a wide temperature range. In a following paper (14) the activities and entropies will be presented. Since the volumes and compressibilities have also been investigated thoroughly by Vikingstad *et al.* (10, 11), as in the case of the two alkyltrimethylammonium bromides, all the thermodynamic properties will be known with this system in water.

As it was mentioned above, the alkylamine hydrobromides were investigated primarily in the pre-micellar region and over the whole concentration range at 25°C only. Measurements were therefore repeated at 5 and 15°C for octylamine hydrobromide (OABr), mostly in the micellar region. It will thus be possible to investigate the temperature dependence of the thermodynamic functions with this system also.

Experimental

The purification procedure for OABr was reported previously (2). The NaDec was prepared by titrating decanoic acid (Aldrich, gold label), purified by fractional recrystallizations, with NaOH solution. Then water was removed with a flash evaporator. All solutions were prepared by weight with deionized (Continental Deionized Water System) distilled water. The solutions were titrated to a pH of 9.2 to suppress hydrolysis as much as possible (15). Still, a slight cloudiness appeared in the solutions below the CMC suggesting the existence of traces of free decanoic acid or high molecular weight alcohols, which were probably solubilized in the micelles above the CMC. Repeated purification did not eliminate this. Similar effects were observed by Høiland and Vikingstad (16). However, the high reproducibility of the data, the excellent group additivity between data for various carboxylates, and the excellent agreement between the present data on volumes and those of Vikingstad *et al.* (11) and Kale and Zana (17) suggest that these traces of impurities do not have a significant effect on the thermodynamic properties. Still, freshly prepared solutions were used whenever possible, and, if they had to be kept for an extended period, they were kept in a refrigerator in tightly closed bottles.

With the exception that the injection in the flow microcalorimeter was made with a Gilson peristaltic pump (Minipuls 2), the techniques used, the procedure and the precision of the measurements are the same as those reported in previous studies on surfactants (5) and do not require further discussion.

Results

The apparent molal volumes ϕ_V and heat capacities at constant pressure ϕ_C were calculated from the differences in densities and in heat capacities per unit volume. The temperature of measurement of ϕ_V is lower than that of ϕ_C by a constant amount (0.35 K) as a consequence of the two instruments being placed in series. However, the error introduced by this temperature difference in the calculation of ϕ_C is well within the experimental uncertainty. Measurements were made at 0.5 (a few data points), 2, 5, 10, 15, 25, 40 (a few data points), and 45°C for NaDec and at 5 and 15°C for OABr. Enthalpies of dilution of NaDec were obtained at 25°C only. The original data are given elsewhere[3] but the data at even molalities are given in Table 1.[4] The experimental ϕ_V and ϕ_C in the pre-micellar region can be fitted in molality m by the equation

$$[1] \quad \phi_Y = \phi_Y^0 + A_Y m^{1/2} + B_Y m$$

where Y stands for V or C and A_Y are the limiting slopes calculated from the Debye–Hückel theory. The parameters ϕ_Y^0 and B_Y, obtained from a least-squares fit, are given in Table 2.

The apparent molal relative enthalpies ϕ_L are derived from the enthalpies of dilution in the usual way (2) and can be expressed as a polynomial in $m^{1/2}$ in the pre-micellar region:

$$[2] \quad \phi_L = A_L m^{1/2} + B_L m + C_L m^{3/2} + \ldots$$

where again A_L is the limiting Debye–Hückel slope for relative enthalpies.

Volumes

The concentration dependence of ϕ_V (not shown) of NaDec and OABr is similar to that of other surfactants (3–7, 10, 11, 17); ϕ_V does not change much in the pre-micellar region, increases sharply at the CMC, and levels off slowly at higher concentration. The value at infinite dilution ϕ_V^0, which is equal to the standard partial molal volume $\bar{V}_2^0$, is shown as a function of temperature in Fig. 1 and compared

[3]Complete set of the actual experimental data is available, at a nominal charge, from the Depository of Unpublished Data, CISTI, National Research Council of Canada, Ottawa, Ont., Canada K1A 0S2.

[4]The Publishing Department of the Canadian Journal of Chemistry would appreciate readers' views on this experimental method of presenting tabular matter in microprint in the journal as an alternative to placing it in the Depository of Unpublished Data, CISTI, National Research Council of Canada, Ottawa.

Can. J. Chem. Downloaded from www.nrcresearchpress.com by 210.87.254.42 on 09/05/12
For personal use only.

TABLE 1. Volumetric and thermochemical data of sodium decanoate and octylamine hydrobromide in water

m	ϕ_V	$\bar{V}_2$	ϕ_C	$\bar{C}_{P2}$	ϕ_L	$\bar{L}_2$
			NaDec 5°C			
0.01	156.89	157.05	758.9	711.0	227	393
0.02	157.03	157.30	710.8	314.4	583	696
0.03	157.16	157.54	732.5	217.6	543	995
0.04	157.28	157.76	714.1	170.4	698	1298
0.05	157.40	157.98	715.6	123.7	845	1609
0.06	157.51	158.19	717.3	125.9	977	1918
0.07	157.63	158.39	718.6	728.6	1153	2236
0.08	157.73	158.60	720.0	731.3	1309	2520
0.09	157.84	158.80	721.4	731.9	1530	2825
0.10	157.95	159.00	722.8	736.5	1751	3142
0.11	158.05	159.20	724.1	739.0	2041	3440
0.12	158.16	159.40	725.5	741.5	2170	3750
0.13	158.26	159.59	736.9	1315	2341	4590
0.14	158.36	159.79	804.6	2110	3150	8496
0.15	158.86	160.52	811.4	1455	3650	12727
0.16	159.27	161.92	862.9	1031	4247	16437
0.17	159.70	166.93	888.2	804	5046	18774
0.18	160.17	167.57	876.8	609	5850	20344
0.19	160.53	168.02	859.3	509	6623	20972
0.20	160.95	168.39	891.6	405	7346	21480
0.22	161.68	168.95	980.7	266	8645	21934
0.25	162.60	169.38	910.3	275	10246	22096
0.30	163.75	169.71	855.3	263	12207	22068
0.35	164.67	169.87	599.3	261	13634	21912
0.40	165.29	169.96	557.6	263	14653	21695
0.50	166.21	170.12	495.8	273	15995	21134
0.60	166.87	170.27	456.1	282	16895	20562
0.70	167.37	170.43	431.8	289	17315	20082
0.80	167.76	170.58	414.1	295	17631	19626
1.00	168.38	170.90	391.2	301	17951	18798
			NaDec 10°C			
0.01	159.94	160.07	745.6	748.6	261	449
0.02	160.06	160.28	748.4	753.5	441	793
0.03	160.16	160.48	750.9	758.1	613	1126
0.04	160.26	160.64	753.2	762.5	782	1442
0.05	160.35	160.80	755.5	766.8	950	1850
0.06	160.44	160.96	757.8	771.0	1119	2143
0.07	160.52	161.12	760.0	775.2	1289	2491
0.08	160.61	161.27	762.1	779.3	1460	2805
0.09	160.69	161.42	764.2	783.4	1696	3140
0.10	160.77	161.56	766.4	787.4	1876	3485
0.11	160.85	161.71	768.5	1062	2303	5818
0.12	161.13	164.01	835.1	1370	2669	8768
0.13	161.60	164.00	827.9	910	3256	11496
0.14	162.05	168.12	837.9	822	3953	13716
0.15	162.51	169.70	831.1	642	4642	15203
0.16	162.96	170.63	818.5	567	5347	16551
0.17	163.43	170.96	798.0	434	6058	17641
0.18	163.76	171.18	777.3	373	6711	18058
0.19	164.25	171.30	758.2	347	7311	18313
0.20	164.61	171.40	737.6	328	7861	18458
0.22	165.23	171.55	648.9	305	8823	18616
0.25	165.99	171.71	651.0	286	10095	18657
0.30	166.94	171.89	590.8	273	11424	18562
0.35	167.66	172.02	547.1	271	12447	18333
0.40	168.23	172.13	510.8	275	13162	18106
0.50	169.01	172.27	464.9	297	14085	17598
0.60	169.57	172.41	436.3	307	14619	17123
0.70	169.99	172.59	418.6	309	14967	16706
0.80	170.32	172.75	406.0	310	15153	16396
1.00	170.84	173.08	387.1	313	15314	15926
			NaDec 5°C			
0.01	157.58	157.77	724.3	726.0	231	414
0.02	157.70	157.94	726.7	733.0	404	729
0.03	157.82	158.14	729.0	737.4	564	1038
0.04	157.92	158.33	731.1	741.7	727	1352
0.05	158.02	158.53	733.1	745.8	879	1689
0.06	158.12	158.69	735.3	749.8	1036	1992
0.07	158.21	158.86	737.3	753.7	1197	2320
0.08	158.30	159.03	739.0	757.6	1358	2674
0.09	158.39	159.20	740.9	761.4	1484	2929
0.10	158.48	159.37	742.8	765.1	1810	3255
0.11	158.57	159.54	744.7	768.9	2105	3610
0.12	158.75	161.39	746.5	772.6	2465	6405
0.13	158.99	162.51	790.1	1404	2892	9367
0.14	159.25	163.92	842.4	1410	3416	11687
0.15	159.65	165.12	875.2	1234	4027	14286
0.16	160.04	166.64	873.8	735	4757	16947
0.17	160.47	167.48	869.6	654	5547	18607
0.18	160.91	168.07	648.1	435	6268	19739
0.19	161.36	168.76	833.4	375	7006	20359
0.20	161.76	169.34	800.5	335	7667	20651
0.22	162.53	169.77	758.8	325	8835	20754
0.25	163.44	170.10	706.5	305	10262	20825
0.30	164.52	170.31	636.7	292	12006	20581
0.35	165.35	170.43	584.0	295	13270	20192
0.40	166.01	170.56	546.3	292	14120	20304
0.50	166.99	170.73	493.5	283	15340	19789
0.60	167.57	170.89	458.5	290	16048	19281
0.70	168.07	171.08	434.0	302	16476	18829
0.80	168.45	171.24	420.0	312	16743	18359
1.00	169.04	171.55	399.8	321	16998	17592
1.20	169.49	171.86	385.3	328		
			NaDec 15°C			
0.01	161.63	161.76	763.5	765.8	284	486
0.02	161.75	161.97	765.6	769.6	477	851
0.03	161.85	162.16	767.5	773.0	660	1204
0.04	161.95	162.31	769.3	776.2	831	1559
0.05	162.03	162.47	771.0	779.3	1017	1916
0.06	162.12	162.62	772.6	782.3	1196	2237
0.07	162.20	162.77	774.2	785.2	1375	2543
0.08	162.28	162.91	775.7	788.0	1555	2870
0.09	162.36	163.05	777.3	790.9	1800	3325
0.10	162.44	163.19	780.0	913	2093	6090
0.11	162.73	165.80	801.3	1586	2426	9209
0.12	163.20	168.27	813.9	892	2987	10124
0.13	163.64	169.46	812.8	765	3638	12234
0.14	164.09	170.45	826.7	653	4301	13664
0.15	164.54	171.08	792.0	547	4950	14554
0.16	164.99	171.56	772.8	444	5576	15229
0.17	165.43	172.02	750.1	373	6179	15696
0.18	165.81	172.37	728.3	353	6727	16124
0.19	166.16	172.62	708.3	339	7228	16278
0.20	166.48	172.82	689.9	328	7680	16349
0.22	167.07	172.94	656.1	312	8461	16409
0.25	167.78	173.10	612.6	299	9415	16370
0.30	168.71	173.18	562.2	299	10552	16179
0.35	169.35	173.28	520.0	286	11365	15874
0.40	169.81	173.35	492.1	288	11820	15764
0.50	170.52	173.50	453.6	301	12632	15344
0.60	171.03	173.64	428.5	313	13057	14924
0.70	171.42	173.78	413.1	324	13294	14639
0.80	171.74	173.93	402.6	333	13479	14364
1.00	172.21	174.22	390.3	348	13508	13879
			NaDec 25°C			
0.01	164.26	164.40	732.6	733.6	335	539
0.02	164.36	164.52	733.5	734.6	523	923
0.03	164.48	164.61	734.2	735.5	719	1297
0.04	164.57	165.09	734.7	735.7	910	1669
0.05	164.65	165.25	735.2	736.0	1099	2043
0.06	164.72	165.81	735.7	736.2	1288	2420
0.07	164.80	165.96	736.1	736.2	1477	2807
0.08	164.87	166.10	736.4	856	1866	3145
0.09	164.94	166.89	760.9	877	1850	4315
0.10	165.25	167.31	765.2	784	2320	6785
0.11	165.64	168.53	781.8	727	2765	8110
0.12	166.00	171.67	782.5	633	3190	10000
0.13	166.49	172.32	767.4	528	3690	11050
0.14	166.95	173.39	745.5	427	4415	11410
0.15	167.39	173.90	723.2	402	4877	11650
0.16	167.81	174.24	702.8	384	5305	11820
0.17	168.20	174.44	683.6	364	5698	11930
0.18	168.55	174.55	665.8	357	6050	12000
0.19	168.86	174.65	648.6	343	6363	12040
0.20	169.12	174.73	632.9	338	6645	12050
0.22	169.65	174.83	605.1	332	7158	11990
0.25	170.25	175.00	572.3	329	7690	11860
0.30	171.09	175.19	533.9	329	8373	11620
0.35	171.70	175.33	504.4	331	8838	11410
0.40	172.19	175.38	482.8	335	9150	11230
0.50	172.80	175.57	455.7	346	9533	10930
0.60	173.26	175.74	436.9	358	9735	10630
0.70	173.57	175.88	427.0	366	9845	10340
0.80	173.87	176.05	418.9	372	9892	10040
1.00	174.33	176.34	411.1	384	9867	9440
1.20	174.69	176.64	406.5	395	9743	8870
1.50	175.19	177.10	405.0	404	9445	7840
1.80	175.51	177.55	405.8	408	9040	6900
			NaDec 5°C			
0.01	167.77	167.92	724.3	726.0	231	414
0.02	167.89	168.11	726.7	733.0	404	729
0.03	168.01	168.33	729.0	737.4	564	1038
0.04	168.12	168.53	731.1	741.7	727	1352
0.05	168.22	168.73	733.1	745.8	879	1689
0.06	168.32	168.89	735.3	749.8	1036	1992
0.07	168.41	169.06	737.3	753.7	1197	2320
0.08	168.50	169.23	739.0	757.6	1358	2674
0.09	168.59	169.40	740.9	761.4	1484	2929
0.10	168.68	169.57	742.8	765.1	1810	3255
0.11	168.77	169.74	744.7	768.9	2105	3610
0.12	168.95	171.59	746.5	772.6	2465	6405
0.13	169.19	172.71	790.1	1404	2892	9367
0.14	169.45	174.12	842.4	1410	3416	11687
0.15	169.85	175.32	875.2	1234	4027	14286
0.16	170.24	176.84	873.8	735	4757	16947
0.17	170.67	177.68	869.6	654	5547	18607
0.18	171.11	178.27	648.1	435	6268	19739
0.19	171.56	178.96	833.4	375	7006	20359
0.20	171.96	179.54	800.5	335	7667	20651
0.22	172.73	179.97	758.8	325	8835	20754
0.25	173.64	180.30	706.5	305	10262	20825
0.30	174.72	180.51	636.7	292	12006	20581
0.35	175.55	180.63	584.0	295	13270	20192
0.40	176.21	180.76	546.3	292	14120	20304
0.50	177.19	180.93	493.5	283	15340	19789
0.60	177.77	181.09	458.5	290	16048	19281
0.70	178.27	181.28	434.0	302	16476	18829
0.80	178.65	181.44	420.0	312	16743	18359
1.00	179.24	181.75	399.8	321	16998	17592
1.20	179.69	182.06	385.3	328		
			NaDec 15°C			
0.01	161.63	161.76	763.5	765.8	284	486
0.02	161.75	161.97	765.6	769.6	477	851
0.03	161.85	162.16	767.5	773.0	660	1204
0.04	161.95	162.31	769.3	776.2	831	1559
0.05	162.03	162.47	771.0	779.3	1017	1916
0.06	162.12	162.62	772.6	782.3	1196	2237
0.07	162.20	162.77	774.2	785.2	1375	2543
0.08	162.28	162.91	775.7	788.0	1555	2870
0.09	162.36	163.05	777.3	790.9	1800	3325
0.10	162.44	163.19	780.0	913	2093	6090
0.11	162.73	165.80	801.3	1586	2426	9209
0.12	163.20	168.27	813.9	892	2987	10124
0.13	163.64	169.46	812.8	765	3638	12234
0.14	164.09	170.45	826.7	653	4301	13664
0.15	164.54	171.08	792.0	547	4950	14554
0.16	164.99	171.56	772.8	444	5576	15229
0.17	165.43	172.02	750.1	373	6179	15696
0.18	165.81	172.37	728.3	353	6727	16124
0.19	166.16	172.62	708.3	339	7228	16278
0.20	166.48	172.82	689.9	328	7680	16349
0.22	167.07	172.94	656.1	312	8461	16409
0.25	167.78	173.10	612.6	299	9415	16370
0.30	168.71	173.18	562.2	299	10552	16179
0.35	169.35	173.28	520.0	286	11365	15874
0.40	169.81	173.35	492.1	288	11820	15764
0.50	170.52	173.50	453.6	301	12632	15344
0.60	171.03	173.64	428.5	313	13057	14924
0.70	171.42	173.78	413.1	324	13294	14639
0.80	171.74	173.93	402.6	333	13479	14364
1.00	172.21	174.22	390.3	348	13508	13879
			NaDec 25°C			
0.01	164.26	164.40	732.6	733.6	335	539
0.02	164.36	164.52	733.5	734.6	523	923
0.03	164.48	164.61	734.2	735.5	719	1297
0.04	164.57	165.09	734.7	735.7	910	1669
0.05	164.65	165.25	735.2	736.0	1099	2043
0.06	164.72	165.81	735.7	736.2	1288	2420
0.07	164.80	165.96	736.1	736.2	1477	2807
0.08	164.87	166.10	736.4	856	1866	3145
0.09	164.94	166.89	760.9	877	1850	4315
0.10	165.25	167.31	765.2	784	2320	6785
0.11	165.64	168.53	781.8	727	2765	8110
0.12	166.00	171.67	782.5	633	3190	10000
0.13	166.49	172.32	767.4	528	3690	11050
0.14	166.95	173.39	745.5	427	4415	11410
0.15	167.39	173.90	723.2	402	4877	11650
0.16	167.81	174.24	702.8	384	5305	11820
0.17	168.20	174.44	683.6	364	5698	11930
0.18	168.55	174.55	665.8	357	6050	12000
0.19	168.86	174.65	648.6	343	6363	12040
0.20	169.12	174.73	632.9	338	6645	12050
0.22	169.65	174.83	605.1	332	7158	11990
0.25	170.25	175.00	572.3	329	7690	11860
0.30	171.09	175.19	533.9	329	8373	11620
0.35	171.70	175.33	504.4	331	8838	11410
0.40	172.19	175.38	482.8	335	9150	11230
0.50	172.80	175.57	455.7	346	9533	10930
0.60	173.26	175.74	436.9	358	9735	10630
0.70	173.57	175.88	427.0	366	9845	10340
0.80	173.87	176.05	418.9	372	9892	10040
1.00	174.33	176.34	411.1	384	9867	9440
1.20	174.69	176.64	406.5	395	9743	8870
1.50	175.19	177.10	405.0	404	9445	7840
1.80	175.51	177.55	405.8	408	9040	6900
			NaDec 5°C			
0.01	169.66	169.77	609.2	610.9	212	338
0.02	169.70	169.74	610.5	613.0	333	574
0.03	169.71	169.74	611.7	614.6	457	811
0.04	169.72	169.72	612.6	616.0	585	1048
0.05	169.71	169.69	613.4	617.2	718	1291
0.06	169.71	169.65	614.1	618.1	856	1546
0.07	169.69	169.60	614.8	619.3	998	2021
0.08	169.66	169.55	615.4	620.3	1148	2372
0.09	169.64	169.50	616.0	621.2	1304	2761
0.10	169.64	169.45	616.5	631	1470	3152
0.11	169.63	169.42	617.0	645	1654	3559
0.12	169.62	169.39	619.4	664	1831	3940
0.13	169.61	169.36	621.8	697	1715	3910
0.14	169.60	169.33	625.1	756	1825	4230
0.15	169.59	170.38	632.5	862	1630	4902
0.16	169.63	173.70	649.5	984	3060	5823
0.17	169.87	176.98	658.5	759	2190	8519
0.18	170.09	178.69	657.3	535	2631	10248
0.19	170.31	177.74	650.1	443	2713	10940
0.20	170.56	177.51	643.0	395	2999	11074
0.22	170.76	177.82	633.3	326	3279	11820
0.25	171.02	178.06	622.7	308	3557	12030
0.30	171.34	178.25	613.0	299	3854	12145
0.35	171.63	178.34	595.2	290	4185	12270
0.40	172.52	179.51	556.1	280	5291	12135
0.50	173.24	179.08	525.5	275	6048	11620
0.60	173.61	179.13	499.5	275	6630	11690
0.70	174.45	179.13	458.2	275	7488	11470
0.80	175.31	179.31	427.7	275	8033	11280
1.00	175.78	179.31	414.0	275	8428	11160
1.20	176.45	179.31	384.2	275	8975	10940
			NaDec 15°C			
0.01	171.82	171.90	623.6	625.4	246	389
0.02	171.88	171.96	625.1	627.8	381	647
0.03	171.93	171.98	626.2	629.2	516	926
0.04	171.93	172.00	627.1	630.6	653	1211
0.05	171.95	172.00	627.9	631.8	796	1506
0.06	171.94	172.00	628.6	632.8	939	1821
0.07	171.96	171.98	629.5	633.8	1088	2156
0.08	171.96	171.97	629.9	634.7	1244	2513
0.09	171.96	171.94	630.5	635.5	1406	2914
0.10	171.96	171.92	631.1	636.3	1576	3358
0.11	171.96	171.90	631.8	636.7	1669	3612
0.12	171.95	171.89	631.6	703	1761	3800
0.13	171.95	171.87	637.5	754	1845	4419
0.14	171.95	175.50	641.8	665	1958	5799
0.15	172.24	177.50	641.3	564	2077	8302
0.16	172.45	178.36	615.8	499	2266	9158
0.17	172.65	178.91	627.7	382	2467	8084
0.18	172.89	179.27	618.8	355	2680	8468
0.19	173.09	179.54	608.7	341	2882	8673
0.20	173.20	179.75	599.3	330	3085	8818
0.22	173.52	179.90	590.5	322	3264	8930
0.25	173.73	180.54	581.9	315	3445	9055
0.30	173.83	180.16	574.0	310	3609	9060
0.35	174.14	180.32	558.3	302	3923	9100
0.40	176.06	180.56	525.3	297	4568	8845
0.45	175.66	180.64	490.5	288	5036	8605
0.50	176.16	180.64	488.0	477	5182	8375
0.60	176.88	180.64	464.5	288	5872	8105
0.70	177.44	180.64	452.3	288	6178	7965
0.80	177.84	180.64	445.6	288	6396	7845
1.00	178.40	180.64	441.4	288	6673	7645
			NaDec 5°C			
0.01	701.6	703.4			169.47	168.64
0.02	703.2	706.2			168.62	168.65
0.03	704.7	708.7			169.38	169.30
0.04	706.0	711.0			168.86	169.30
0.05	707.2	713.3			168.97	169.49
0.06	708.4	715.5			169.07	169.68
0.07	709.6	717.6			169.17	169.86
0.08	710.7	719.6			169.27	170.03
0.09	711.8	721.7			169.36	170.20
0.10	712.9	723.7			169.63	170.53
0.11	714.0	725.7			170.07	170.42
0.12	715.0	727.6			170.41	170.10
0.13	716.1	729.6				
0.14	753	1076				
0.15	832	1575				
0.16	863	1132				
0.17	870	866				
0.18	864	683				
0.19	851	566				
0.20	834	475				

Units: ϕ_V, J K^{-1} mol^{-1}; $\bar{V}_2$, J mol^{-1}; ϕ_C, J K^{-2} mol^{-1}; $\bar{C}_{P2}$, J K^{-2} mol^{-1}; m, mol kg^{-1}.

All ϕ_V data are at 0.39°C lower (see text).

m	ϕ_V	$\bar{V}_2$	ϕ_C	$\bar{C}_{P2}$	ϕ_L	$\bar{L}_2$
			NaDec 25°C			
0.01	173.95	174.04	625.8	627.5	221	430
0.02	174.02	174.14	627.2	629.4	422	717
0.03	174.07	174.19	628.1	630.7	587	1055
0.04	174.10	174.22	628.9	631.7	733	1302
0.05	174.13	174.24	629.6	632.5	861	1607
0.06	174.15	174.26	630.1	633.2	1012	1931
0.07	174.17	174.26	630.6	633.8	1161	2274
0.08	174.18	174.26	631.0	634.2	1328	2643
0.09	174.19	174.26	631.4	634.7	1495	3043
0.10	174.19	174.25	631.7	635.0	1672	3494
0.11	174.20	174.25	631.9	635.2	1765	3751
0.12	174.20	174.24	632.1	635.3	1861	4019
0.13	174.19	177.60	632.0	687	1961	4309
0.14	174.14	179.02	630.0	506	2065	6441
0.15	174.16	180.34	622.0	410	2173	4951
0.16	175.00	180.71	617.4	385	2289	5305
0.17	175.23	180.93	603.9	369	2425	5610
0.18	175.45	181.12	593.5	356	2530	5800
0.19	175.64	181.28	581.0	343	2640	5990
0.20	175.83	181.41	579.3	339	2753	5945
0.22	176.19	181.63	571.4	333	2853	5885
0.25	176.16	181.64	564.2	328	2955	5810
0.30	176.32	181.72	557.2	328	3045	6310
0.35	176.62	181.89	543.3	317	3213	5915
0.40	177.78	182.20	514.0	310	3549	5655
0.45	177.84	182.36	490.8	308	3762	5565
0.50	178.30	182.44	477.2	307	3908	5330
0.60	179.01	182.44	463.5	307	4097	4960
0.70	179.50	182.44	454.5	307	4182	4720
0.80	179.87	182.44	449.3	307	4250	4600
1.00	180.40	182.44	388.0	307	4320	4400

Can. J. Chem. Downloaded from www.nrcresearchpress.com by 210.87.254.42 on 09/05/12
For personal use only.

TABLE 2. Thermodynamic parameters for sodium decanoate and octylamine hydrobromide in water

(*a*) NaDec

Parameter	Value						
	2°C	5°C	10°C	15°C	25°C	40°C	45°C
ϕ_V^0 (cm^3 mol^{-1})	156.66	157.36	159.72	161.41	164.08	168.20	168.54
B_V (cm^3 mol^{-2} kg)	8.2	6.4	5.4	4.9	3.0	5.8	16.0
ϕ_C^0 (J K^{-1} mol^{-1})	705.7	720.5	739.8	759.8	770		762
B_C (J K^{-1} mol^{-1} kg)	103	152	172	108	−37.5		−114
CMC[a] (mol kg^{-1})	0.128	0.118	0.108	0.098	0.085		0.075
ΔV_m (cm^3 mol^{-1})	9.74	10.40	9.93	9.72	9.6		6.4
ΔC_m (J K^{-1} mol^{-1})	−480	−470	−480	−460	−430		−370
$\Delta H_{m,graph}$ (J mol^{-1})	18810	17960	15520	13400	8750		650
$\Delta H_{m,calcd}$ (J mol^{-1})	19355	17930	15550	13200	—		750

(*b*) OABr

Parameter	Value[b]				
	5°C	15°C	25°C	35°C	45°C
ϕ_V^0	169.50	171.62	173.72	175.18	177.54
B_V	−2.7	−2.1	−1.8	−0.5	−0.6
ϕ_C^0	606	620	622	612	614
B_C	2.5	2.5	−16	−45	−130
CMC[a]	0.24	0.22	0.22	0.23	0.26
ΔV_m	9.8	8.8	8.1	6.9	6.1
ΔC_m	−349	−348	−332	(−310)	(−225)
$\Delta H_{m,graph}$	8700	5280	1975	(−1320)	(−4125)
$\Delta H_{m,calcd}$	8860	5375	—	(−1235)	(−4025)

[a]From $\bar{V}$ data.
[b]Values in parentheses are extrapolated values.

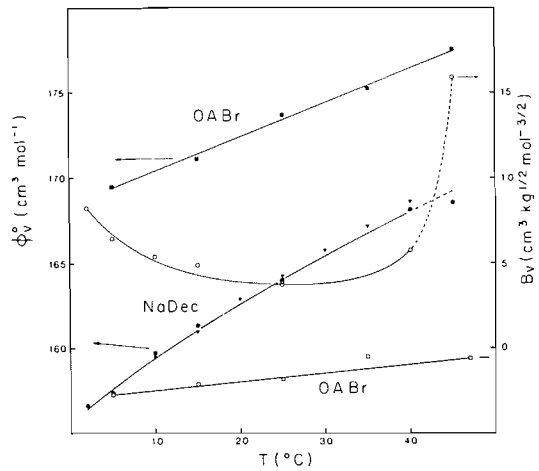


FIG. 1. Temperature dependence of the parameters ϕ_V^0 and B_V of eq. [1] for sodium decanoate and octylamine hydrobromide: ϕ_V^0, ● and ■, present results, ▽, Kale and Zana (17), ▼, Vikingstad *et al.* (11); B_V, ○ and □, present results.

with the data of Vikingstad *et al.* (11) on NaDec. The mean deviation between both sets of data is 0.2 cm^3 mol^{-1} up to 25°C, which is excellent agreement. On the other hand our ϕ_V^0 at 45°C is lower by 1.5 cm^3 mol^{-1} from the value extrapolated from Vikingstad. A close examination of our data and procedure leads us to suspect that the thermostat for our densimeter might not have been functioning properly at 45°C as a result of the instruments being placed in series. Consequently the actual temperature of measurement could have been lower by one or two degrees. Some data were measured at 40°C in the pre-micellar region checking the temperature in the densimeter and the agreement with Vikingstad was now excellent (see Fig. 1). This error at 45°C could have an important effect on the parameter B_V and on the CMC but should not affect the data at high concentration too much. Also an error of 1.5 cm^3 mol^{-1} could affect our ϕ_C data by about 6 J K^{-1} mol^{-1}, but fortunately the effect on the concentration dependence of ϕ_C will be much smaller.

Another indication of the accuracy of the present data comes from the group additivity of the homologous series RCOONa at 25°C. The difference in $\bar{V}_2^0$ of NaDec and Na octanoate (7) is 31.8 cm^3 mol^{-1} which is twice the average CH_2 contribution, 15.9 cm^3 mol^{-1}, of other similar homologous series (1, 18).

The increase of ϕ_V^0 with temperature is typical of hydrophobic solutes in water. This will be discussed further through expansibilities.

The parameter B_V, which is a measure of the deviation from the Debye–Hückel theory, is also

Can. J. Chem. Downloaded from www.nrcresearchpress.com by 210.87.254.42 on 09/05/12
For personal use only.

shown in Fig. 1. The sign and temperature dependence of B_V of OABr are typical of surfactants and other hydrophobic solutes (4). On the other hand B_V of NaDec are positive like other carboxylates (7) suggesting that the carboxylate group plays an important role in the solute–solute interactions. If ${\phi_V}^0$ of NaDec was too negative at 45°C, B_V could then be too positive. It would therefore be dangerous to put too much weight on the large increase in B_V of NaDec at 45°C.

The partial molal volumes $\overline{V}_2$, obtained from a plot of $\Delta(\phi_V m)/\Delta m$ against the mean molality (3), are shown at three temperatures in Fig. 2. The initial break in the curves are taken as the CMC. This graph can be used to calculate the change in volume during micellization (4), ΔV_m. Essentially the linear part of $\overline{V}_2$ beyond the CMC is extrapolated to the CMC and the difference between this value of $\overline{V}_2$ and the value of $\overline{V}_2$ at the initial break is taken as ΔV_m. These values are given in Table 2. In general the values for NaDec are about 1 $cm^3\ mol^{-1}$ smaller than those of Vikingstad *et al.* (11). Vikingstad

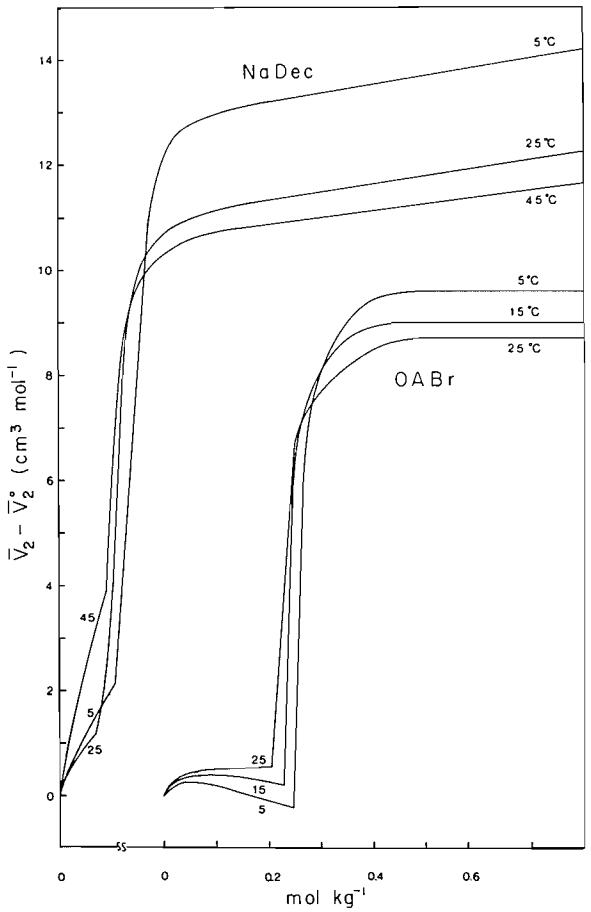


FIG. 2. Partial molal volumes of sodium decanoate and octylamine hydrobromide.

calculated the volume of the surfactant in the micellar state V_m directly from the apparent molal volumes, i.e.

$$[3] \quad \phi_V = \frac{\mathrm{CMC}}{m} V_s + \frac{m - \mathrm{CMC}}{m} V_m$$

where V_s is the molar volume of the surfactant in the dispersed state. It can readily be shown that this method is equivalent to the one used above. The total volume of the solutions above the CMC is given by

$$[4] \quad V = \sum_i n_i \overline{V}_i$$
$$= n_w \overline{V}_w + n_s \overline{V}_s + n_m \overline{V}_m$$
$$= 55.51 V_w + \mathrm{CMC}\,\overline{V}_s + (m - \mathrm{CMC})\,\overline{V}_m$$

where the subscript w refers to water. Equation [4] implies that the concentration of monomers remains constant beyond the CMC. The value of ${\overline{V}_2}^a$ above the CMC is then given by

$$[5] \quad {\overline{V}_2}^a = (\partial V/\partial m)_{T,P}$$
$$= \overline{V}_m + 55.51(\partial \overline{V}_w/\partial m) + \mathrm{CMC}(\partial \overline{V}_s/\partial m) + (m - \mathrm{CMC})(\partial \overline{V}_m/\partial m)$$

In the pre-micellar region the volumes of the solution is given by

$$[6] \quad V = 55.51 \overline{V}_w + m \overline{V}_s$$

and the value ${\overline{V}_2}^b$ below the CMC is given by

$$[7] \quad {\overline{V}_2}^b = \overline{V}_s + 55.51\partial(\overline{V}_w/\partial m) + m(\partial \overline{V}_s/\partial m)$$

Combining eq. [5] and eq. [7]

$$[8] \quad {\overline{V}_2}^a - {\overline{V}_2}^b = \overline{V}_m - \overline{V}_s + (m - \mathrm{CMC}) \times \partial(\overline{V}_m - \overline{V}_s)/\partial m$$
$$= \Delta V_m + (m - \mathrm{CMC})\partial \Delta V_m/\partial m$$

At the CMC it is therefore correct to identify ${\overline{V}_2}^a - {\overline{V}_2}^b$ with ΔV_m.

The partial molal volume $\overline{V}_2$ can also be calculated from ϕ_V, given by eq. [3],

$$[9] \quad {\overline{V}_2}^a = (\partial(\phi_V m)/\partial m)_{T,P}$$
$$= V_m + \mathrm{CMC}(\partial V_s/\partial m) + (m - \mathrm{CMC}) \times (\partial V_m/\partial m)$$

Similarly in the pre-micellar region

$$[10] \quad {\overline{V}_2}^b = V_s + m(\partial V_s/\partial m)$$

Again, combining eq. [9] and eq. [10],

$$[11] \quad {\overline{V}_2}^a - {\overline{V}_2}^b = V_m - V_s + (m - \mathrm{CMC}) \times \partial(\overline{V}_m - \overline{V}_s)/\partial m$$
$$= \Delta V_m + (m - \mathrm{CMC})(\partial \Delta V_m/\partial m)$$

Can. J. Chem. Downloaded from www.nrcresearchpress.com by 210.87.254.42 on 09/05/12
For personal use only.

Although the parameters V_m and V_s used by Vikingstad *et al.* (10) are apparent molal volumes, they lead to the same ΔV_m as in our procedure provided the data are extrapolated to the CMC. If the data are not extrapolated, then larger values for ΔV_m can result since $\bar{V}_2$ increases slightly with m above the CMC (Fig. 2). This difficulty would not arise with OABr since $\bar{V}_2$ is essentially constant beyond the CMC (Fig. 2).

As it had been observed with other surfactants (2, 3, 5) ΔV_m generally decreases as the temperature increases.

Heat Capacities

There are no data in the literature which can be used to compare with our ϕ_C data. On the other hand some idea of the accuracy of the present data can be obtained from group additivity. The difference in $\bar{C}_{P,2}{}^0$ between NaDec and sodium octanoate (7, 19) is 176 J K^{-1} mol^{-1}, in very close agreement with twice the accepted value for the methylene group, 88–90 J K^{-1} mol^{-1} (2, 18–20).

The apparent molal heat capacities of NaDec and OABr, contrary to those of alkyltrimethylammonium bromides (5), show a pronounced hump in ϕ_C in the micellization region at low temperatures. These humps disappear at 45°C for NaDec and at 25°C for OABr. In Fig. 3 the experimental ϕ_C values in the hump region are plotted against m for three temperatures. The magnitude of the hump as a function of the temperature does not change in a regular way. In order to fix this, some data points were measured in the hump region at 0.5°C. The humps at low temperatures were missed for OABr in our earlier work (2) since very few data points were obtained in the CMC region.

As in the case of volumes, $\bar{C}_{P,2}$ were calculated from ϕ_C and are shown for three temperatures in Fig. 4. Here the changes in $\bar{C}_{P,2}$ are very large near the CMC and are nearly discontinuous at low temperature.

The temperature dependence of $\phi_C{}^0$ and B_C, shown in Fig. 5, is similar to that of other hydrophobic electrolytes such as the larger tetraalkylammonium halides (21) and surfactants (4).

The concentration at the first break in $\bar{C}_{P,2}$ was taken as the CMC, which in general is slightly lower from those derived from $\bar{V}_2$. The CMC and the concentration at the maximum in $\bar{C}_{P,2}$ are plotted against temperature in Fig. 6. These critical concentrations tend to the same value at higher temperatures but diverge significantly at lower temperatures.

The ΔC_m was calculated from an extrapolation of the relatively linear regions below and above the CMC region, ignoring the hump for this purpose.

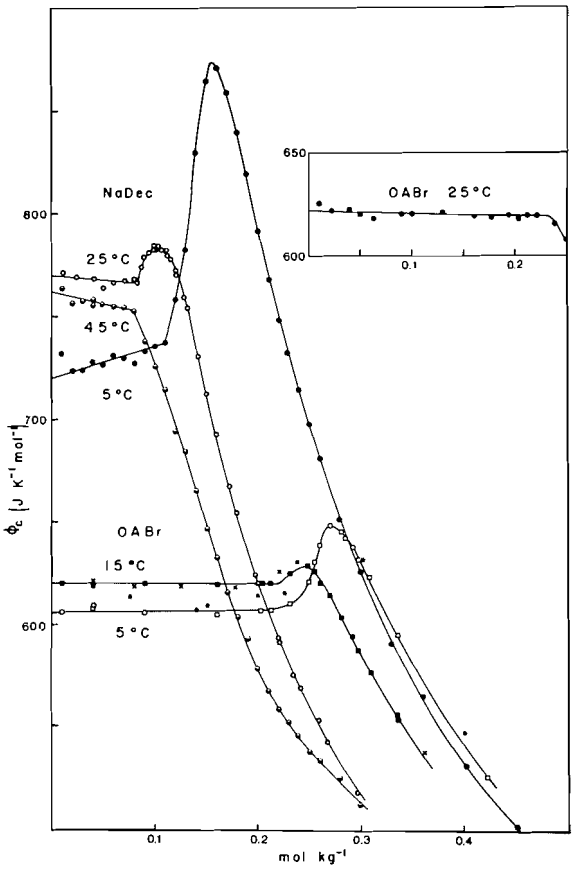


FIG. 3. Apparent molal heat capacities of sodium decanoate and octylamine hydrobromide.

These ΔC_m are given in Table 2, and, as in the case of ΔV_m, they decrease in magnitude as the temperature increases.

Enthalpies

The apparent molal relative enthalpies of NaDec were measured at 25°C and are shown in Fig. 7. The partial molal relative enthalpies $\bar{L}_2$ were then calculated at various temperatures from the heat capacities (4) and are also shown for 5, 25, and 45°C in Fig. 7. The enthalpies of OABr have been reported elsewhere at 25°C (2). Using the $\bar{C}_{P,2}$ data at 5, 15, and 25°C, $\bar{L}_2$ were also calculated at various temperatures and are shown in Fig. 8. As with alkyltrimethylammonium bromides (5) the relatively linear region of $\bar{L}_2$ below and above the CMC were extrapolated to the CMC and the differences were taken as ΔH_m; they are reported in Table 2. These ΔH_m obtained graphically at temperatures other than 25°C are compared in Table 2 with those calculated from

$$[12] \quad \Delta H_m{}^T = \Delta H_m{}^{298} + \int_{298}^{T} \Delta C_m \mathrm{d}T$$

Can. J. Chem. Downloaded from www.nrcresearchpress.com by 210.87.254.42 on 09/05/12
For personal use only.

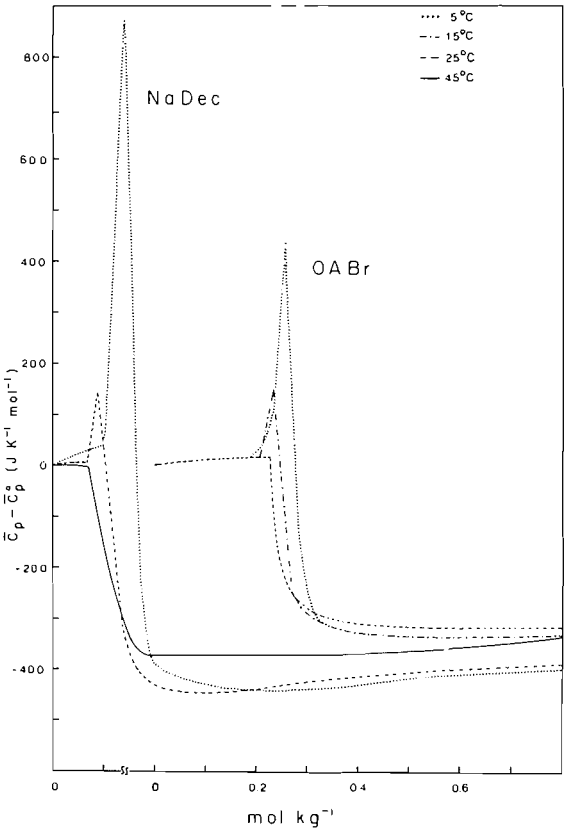


FIG. 4. Partial molal heat capacities of sodium decanoate and octylamine hydrobromide.

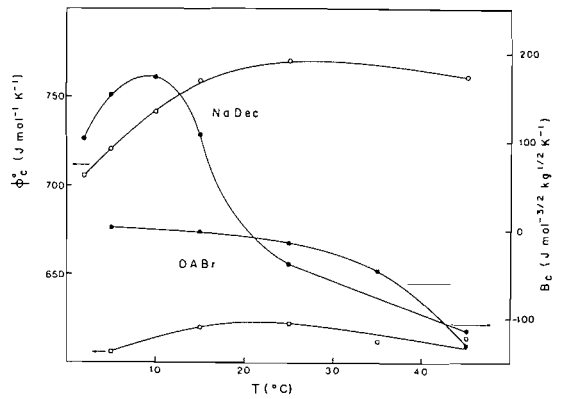


FIG. 5. Temperature dependence of the parameters ϕ_c^0 and B_c of eq. [1] for sodium decanoate and octylamine hydrobromide.

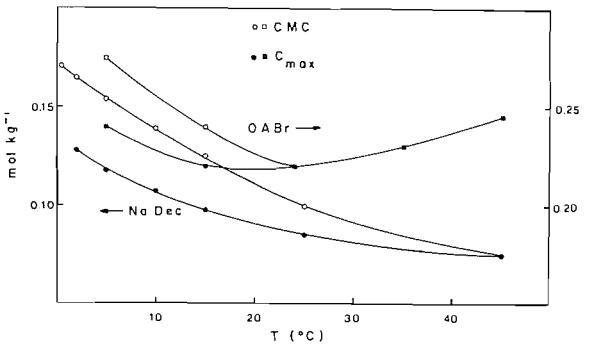


FIG. 6. Temperature dependence of the CMC and the concentration corresponding to the maximum heat capacity of sodium decanoate.

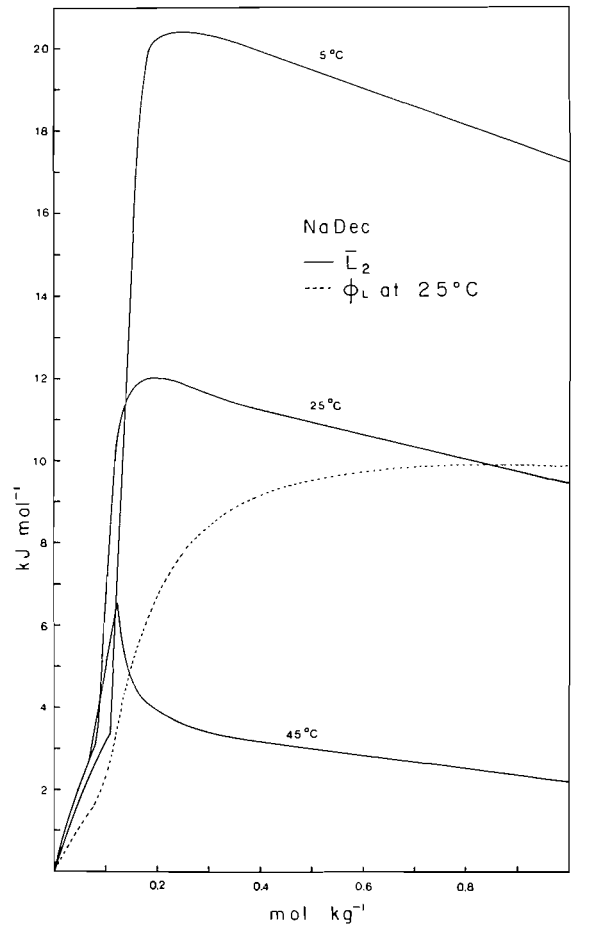


FIG. 7. Apparent and partial molal relative enthalpies of sodium decanoate.

The agreement is excellent, showing the self-consistency of the calculations.

As in the case of heat capacities no values of ΔH_m by calorimetric determination are reported in the literature, and consequently it is impossible to test the accuracy of these parameters. The concentration dependence of $\bar{L}_2$ of NaDec has the same general shape as K octanoate (13).

Discussion

The main objective in this work was to investigate the thermodynamic functions in the CMC region.

Can. J. Chem. Downloaded from www.nrcresearchpress.com by 210.87.254.42 on 09/05/12
For personal use only.

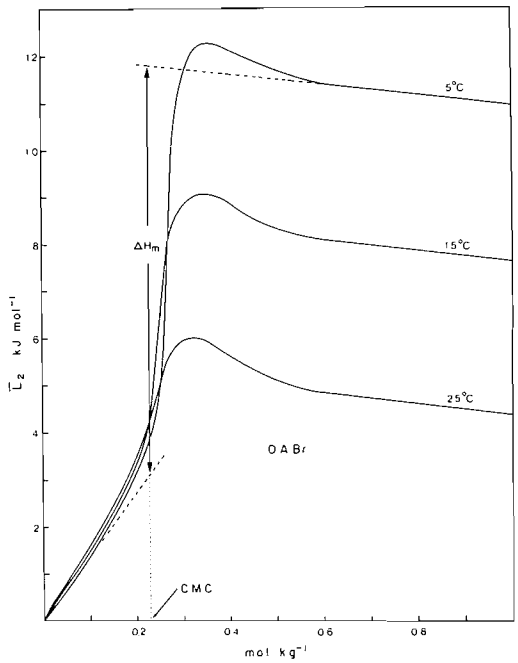


FIG. 8. Partial molal relative enthalpies of octylamine hydrobromide: ΔH_m, experimentally determined enthalpy of micellization at 5°C.

The parameter B_C of alkyltrimethylammonium bromides (3, 5) were positive, especially at low temperatures, but ϕ_C or $\bar{C}_{P,2}$ showed no hump near the CMC. The pronounced humps with NaDec and OABr at low temperatures were also observed with aqueous solutions of *tert*-butanol (22), *n*-butoxyethanol (23), diethylmethylamine and triethylamine (24), and tetrabutylammonium octanoate (7).

The method of measuring ΔV_m, described above, is based on a phase separation model. Essentially the CMC is considered equivalent to a solubility and the micelles to a reservoir of surfactant molecules or microphases. This is why the model predicts that at the CMC there will be a sudden change in $\bar{V}_2$, and any additional solute molecule will dissolve in the micelles. In actual fact $\bar{V}_2$ reaches the value of $\bar{V}_m$ at concentrations which are at 2 to 4 times the CMC. Obviously this means that phase transition models are only approximately valid for micellization, especially for shorter-chain surfactants, and micellization occurs over a range of concentration. Therefore, depending on the method of definition used, one or more CMC can be observed and different methods of extrapolating the data may lead to different values of the CMC (25). For example, Zimmels and Lin (9) identify up to three CMC's with NaDec and Markins *et al.* (26), two. The usually quoted CMC of NaDec is close to 0.10 mol kg^{-1} (8, 27) which fall in between the initial break and the leveling-off region. Obviously micellization is a complex phenomenon and more refined theoretical approaches, such as multiple equilibria, would be required to account for the change in thermodynamic functions in the CMC region. Still the phase transition approach is a convenient way of defining ΔV_m.

The treatment used for ϕ_V and $\bar{V}_2$ can readily be extended to enthalpies. Corresponding to eqs. [3] and [8] we now have

$$[13]\quad \phi_H = \frac{\text{CMC}}{m} H_s + \frac{m - \text{CMC}}{m} H_m$$

$$[14]\quad \phi_L = \frac{\text{CMC}}{m} L_s + \frac{m - \text{CMC}}{m} L_m$$

and

$$[15]\quad \bar{L}_2^a - \bar{L}_2^b = \Delta H_m + (m - \text{CMC})\partial\Delta H_m/\partial m$$

Therefore, the present method of measuring ΔH_m is consistent with the phase-separation approach. In view of the large concentration dependence of ϕ_L and $\bar{L}_2$ in the pre- and post-micellar regions, many of the calorimetric determinations of ΔH_m based on integral heats of dilution or of mixing are erroneous and may even lead to the wrong sign (25, 28, 29).

The interpretation of the concentration dependence of heat capacities does not seem as straightforward as $\bar{V}_2$ and $\bar{L}_2$ since, with NaDec and OABr at low temperatures, $\bar{C}_{P,2}$ goes through a large hump near the CMC. Some idea of the origin of this hump can be obtained from Fig. 9 where $\bar{C}_{P,2}$ is compared with $\bar{L}_2$ for NaDec at 10°C. The first break of the two curves coincide and both functions reach their micellar value at about the same concentration. The values of $\bar{L}_2$ at 5 and 15°C are also shown in Fig. 9. Since $\bar{C}_{P,2}$ is the temperature dependence of $\bar{L}_2$, it follows that the hump arises because both ΔH_m and the CMC decrease significantly with temperature.

Recently Benson (30) was able to account nearly quantitatively for the high heat capacity of water from a simple two-species model. Hvidt (31) also applied independently a similar model to the expansibility and compressibility of water. Jolicoeur *et al.* (32), through a similar approach, predicted quantitatively the shape and the maximum of ϕ_C accompanying the complexation of K^+ with a crown ether. Applying the same reasoning to the phase-transition model for micellization, it is possible to account for the hump in ϕ_C of some surfactants. Equation [13] can be derived with respect to T,

$$[16]\quad \phi_C = \frac{\text{CMC}}{m} C_{ps} + \frac{m - \text{CMC}}{m} C_{pm} - \frac{\Delta H_m}{m} \frac{\partial\,\text{CMC}}{\partial T}$$

Can. J. Chem. Downloaded from www.nrcresearchpress.com by 210.87.254.42 on 09/05/12
For personal use only.

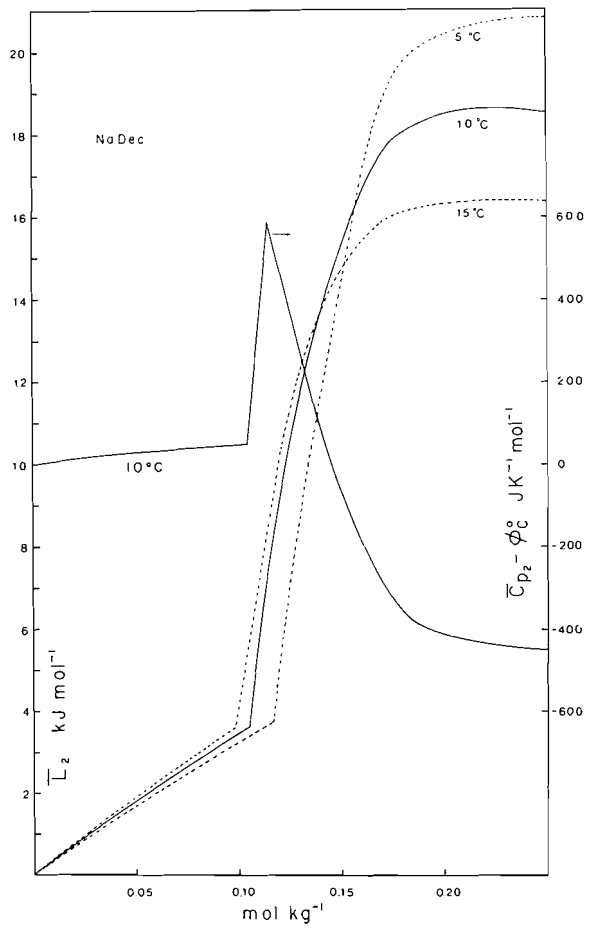


FIG. 9. Comparison of the partial molal heat capacities and relative enthalpies of sodium decanoate at 10°C.

If the CMC is considered the concentration of the monomers in equilibrium with micelles, then it is generally accepted that the standard free energy for micelle formation is proportional to $(1 + \beta)RT \times \ln \text{CMC}$, where β is the degree of dissociation. From the Gibbs–Helmholtz equation it then follows that

$$[17] \quad \Delta H_m = -(1 + \beta)RT^2 \frac{\partial \ln \text{CMC}}{\partial T}$$

if β does not vary with temperature. Replacing $\partial \text{CMC}/\partial T$ from eq. [17] into eq. [16], it follows that

$$[18] \quad \phi_C = \frac{\text{CMC}}{m} C_{ps} + \frac{m - \text{CMC}}{m} C_{pm} + \frac{\text{CMC}}{(1 + \beta)mRT^2} (\Delta H_m)^2$$

At $m = \text{CMC}$, the magnitude of the hump should then be $(\Delta H_m)^2/(1 + \beta)RT^2$.

Taking the data in Table 2 for NaDec at 5°C the predicted hump for full dissociation ($\beta = 1$) is 251 J K^{-1} mol^{-1} while the experimental value is 147 J K^{-1} mol^{-1}, which is of the same magnitude.

The value of $\bar{C}_{P,2}$ can be obtained from the differentiation of eq. [18] and the hump is now given by

$$[19] \quad \bar{C}_P(\text{relax}) = \frac{2\text{CMC}\,\Delta H_m(\partial \Delta H_m/\partial m)}{(1 + \beta)RT^2}$$

For an ideal micellar system ΔH_m should be constant and consequently no hump (but a discontinuity) should be observed with $\bar{C}_{P,2}$. Therefore this hump is a direct measurement of the deviation from the phase-transition model. It should therefore be possible from the shape of the concentration dependence of ϕ_C or $\bar{C}_{P,2}$ in the CMC region to obtain quantitative information on the various equilibria involved in the micellization process. Obviously alkyltrimethylammonium bromides do not micellize in the same way as sodium carboxylates or alkylamine hydrobromides since their ϕ_C go through a maximum at the CMC but show no hump.

The above simple model suggests that the hump should increase continuously as the temperature is lowered. In actual fact this is not so. The temperature dependence of the maximum ϕ_C of NaDec is shown in Fig. 10, and it can be seen that the hump goes through a maximum somewhere between 2 and 5°C. This temperature region also corresponds to the region where B_C goes through a maximum. It is also interesting to note that B_C of Pen_4NBr also goes through a maximum in D_2O at low temperature (21) and that the association constant of tetraalkylammonium halides obtained from conductivity also seem to pass through a maximum somewhere around the temperature of maximum density of water (33).

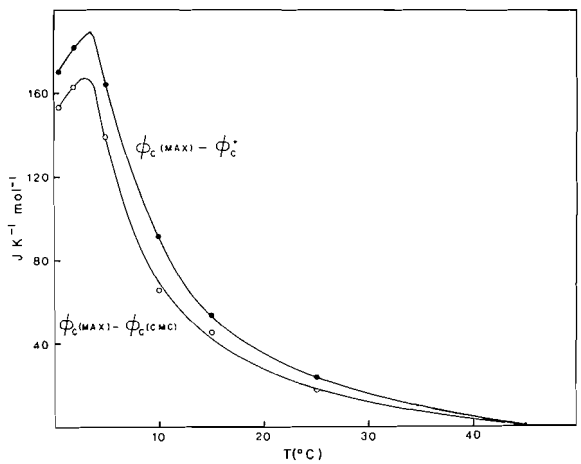


FIG. 10. Temperature dependence of the maximum value of ϕ_C of NaDec.

Can. J. Chem. Downloaded from www.nrcresearchpress.com by 210.87.254.42 on 09/05/12
For personal use only.

The partial molal expansibilities $\bar{E}_2$ obtained from the temperature dependence of $\bar{V}_2$ are shown as a function of m and of T on Fig. 11. Despite the larger uncertainty with this function, definite trends are apparent. $\bar{E}_2$ of most organic solutes in water go through a maximum (23). However, at low temperatures this maximum becomes a well-defined hump. As with heat capacities the existence of this hump can be predicted with the phase-transition model. By analogy with eq. [18], the apparent molal expansibility after the CMC is given by

$$[20]\quad \phi_E = \frac{\mathrm{CMC}}{m} E_s + \frac{m - \mathrm{CMC}}{m} E_m + \frac{\mathrm{CMC}}{(1 + \beta)mRT^2} \Delta H_m \Delta V_m$$

The size of the hump in ϕ_E will therefore depend on the sign and magnitude of ΔH_m and ΔV_m. Since for most surfactants at low temperature both ΔH_m and ΔV_m are positive, a positive hump is predicted. Our data on $\bar{E}_2$ of NaDec are not precise enough to ascertain if the hump goes through a maximum, as in the case of $\bar{C}_{ps}$, or not. The sign of ΔE_m is negative for NaDec but it is difficult to say if ΔE_m changes with T or not in view of the experimental uncertainty.

Vikingstad *et al.* (11) have studied the adiabatic compressibility of NaDec; $\bar{K}_{S,2}{}^0$ is negative and increases with temperature, but $\Delta K_{S,m}$ is positive and decreases in magnitude with temperature. These trends are consistent with the other thermodynamic properties. Unfortunately the concentration dependence of ϕK_S or $\bar{K}_{S,2}$ are not given. It is therefore difficult to say if any maximum or hump is present or absent in the CMC region.

The temperature dependence of the CMC can in principle be predicted from ΔH_m and ΔC_m. If ΔC_m is assumed to vary linearly with temperature, $\partial \Delta C_m / \partial T = B$, it was shown then (3) that

$$[21]\quad (1 + \beta)R \ln \frac{\mathrm{CMC}}{(\mathrm{CMC})_0} = \left(\Delta H_m{}^0 - T_0 \Delta C_m{}^0 + \frac{BT_0{}^2}{2}\right)\left(\frac{1}{T} - \frac{1}{T_0}\right) - (\Delta C_m{}^0 - BT_0) \ln \frac{T}{T_0} - \frac{B}{2}(T - T_0)$$

where the reference state is taken as 298.15 K. Equation [21] can be solved for different values of β and it turns out that no single value of β can account for the experimental CMC given in Table 2 and in Fig. 6 (defined as the initial break). To fit the data, β has to be assumed to be around 0.2 at low temperatures and zero at high temperatures. A value for the CMC intermediate between the initial break and the final one is required to fit the data with a single β. Very good agreement with literature was obtained for the temperature dependence of the CMC of sodium dodecylsulfate (3) since in this case micellization is sharp. With NaDec or OABr the CMC is ill-defined and it is more difficult to apply eq. [21]. Again this stresses the importance of finding better quantitative models for micellization.

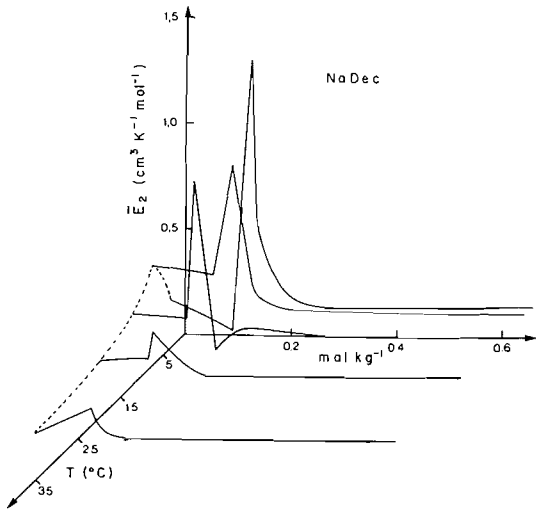


FIG. 11. Temperature and concentration dependence of the partial molal expansibilities of sodium decanoate.

Acknowledgements

We are grateful to the National Sciences and Engineering Research Council of Canada and to the Quebec Ministry of Education for financial assistance. One of us (R.D.) is also indebted to Canada Council for a fellowship which allowed him to come to Canada.

1. J. E. DESNOYERS and M. AREL. Can. J. Chem. **45**, 359 (1967).
2. P.-A. LEDUC, J.-L. FORTIER, and J. E. DESNOYERS. J. Phys. Chem. **78**, 1217 (1974).
3. G. M. MUSBALLY, G. PERRON, and J. E. DESNOYERS. J. Colloid Interface Sci. **54**, 80 (1976).
4. J. E. DESNOYERS, R. DE LISI, C. OSTIGUY, and G. PERRON. *In* Solution chemistry of surfactants. Vol. 1. *Edited by* K. L. Mittal. Plenum Press, New York. 1979. p. 221.
5. R. DE LISI, C. OSTIGUY, G. PERRON, and J. E. DESNOYERS. J. Colloid Interface Sci. **71**, 147 (1979).
6. G. M. MUSBALLY, G. PERRON, and J. E. DESNOYERS. J. Colloid Interface Sci. **48**, 494 (1974).
7. P.-A. LEDUC and J. E. DESNOYERS. Can. J. Chem. **51**, 2993 (1973).
8. P. MUKERJEE and K. J. MYSELS. Critical micelle concentration of aqueous surfactant systems. NSRDS-NBS-36-USA. 1971.
9. Y. ZIMMELS and I. J. LIN. Colloid Polym. Sci. **252**, 594 (1974).
10. E. VIKINGSTAD, A. SKAUGE, and H. HØILAND. J. Colloid Interface Sci. **66**, 240 (1978).

11. E. VIKINGSTAD, A. SKAUGE, and H. HØILAND. J. Colloid Interface Sci. **72**, 59 (1979).
12. P. WHITE and G. C. BENSON. J. Phys. Chem. **64**, 599 (1960).
13. P. WHITE and G. C. BENSON. Trans. Faraday Soc. **54**, 1025 (1959).
14. R. DE LISI, G. PERRON, J. E. DESNOYERS, K. M. KALE, and D. F. EVANS. To be published.
15. E. EAGLAND and F. FRANKS. Trans. Faraday Soc. **61**, 2468 (1965).
16. H. HØILAND and E. VIKINGSTAD. Private communication.
17. K. M. KALE and R. ZANA. J. Colloid Interface Sci. **61**, 312 (1977).
18. C. JOLICOEUR and G. LACROIX. Can. J. Chem. **54**, 624 (1976).
19. J. E. DESNOYERS, C. DE VISSER, G. PERRON, and P. PICKER. J. Solution Chem. **5**, 605 (1976).
20. N. NICOLS and I. WADSÖ. J. Chem. Thermodyn. **7**, 329 (1975).
21. G. PERRON, N. DESROSIERS, and J. E. DESNOYERS. Can. J. Chem. **54**, 2163 (1976).
22. C. DE VISSER, G. PERRON, and J. E. DESNOYERS. Can. J. Chem. **55**, 856 (1977).
23. G. ROUX, G. PERRON, and J. E. DESNOYERS. J. Solution Chem. **7**, 639 (1978).
24. G. PERRON, G. ROUX, D. ROBERTS, and J. E. DESNOYERS. J. Solution Chem. To be published.
25. J. E. DESNOYERS, R. DE LISI, and G. PERRON. Pure Appl. Chem. **52**, 433 (1980).
26. Z. N. MARKINA, N. Z. KOSTOVA, and P. A. REBINDER. Dokl. Akad. Nauk SSSR, **177**, 640 (1967).
27. T. S. BRUN, H. HØILAND, and E. VIKINGSTAD. J. Colloid Interface Sci. **63**, 590 (1978).
28. G. C. KRESHECK. *In* Water: a comprehensive treatise. Vol. 4. *Edited by* F. Franks. Plenum Press, New York. 1975. Chapt. 2.
29. H. WENNERSTRÖM and B. LINDMAN. Phys. Rep. **52**, 1 (1979).
30. S. W. BENSON. J. Am. Chem. Soc. **100**, 5640 (1978).
31. A. HVIDT. Acta Chem. Scand. A**32**, 675 (1978).
32. C. JOLICOEUR, L. L. LEMELIN, and R. LAPALME. J. Phys. Chem. **83**, 2806 (1979).
33. R. DE LISI, M. GOFFREDI, and V. TURCO LIVERI. To be published.

Can. J. Chem. Downloaded from www.nrcresearchpress.com by 210.87.254.42 on 09/05/12
For personal use only.

Thermodynamics of ionization of 2,4- and 2,5-dinitrophenol in dimethylsulfoxide

KOK-SIONG SIOW AND KOK-PENG ANG[1]

Department of Chemistry, University of Singapore, Bukit Timah Road, Singapore 1025

Received October 2, 1979

KOK-SIONG SIOW and KOK-PENG ANG. Can. J. Chem. **58**, 970 (1980).

Ionization constants of 2,4- and 2,5-dinitrophenol in dimethylsulfoxide were measured by the conductance method at five temperatures ranging from 20 to 40°C. The ionization constants of 2,4-dinitrophenol are much larger than those of 2,5-dinitrophenol, and in both cases they increase with temperature. The thermodynamic functions of ionization are discussed in terms of Hepler's theory for substituent and solvent effects. The ionization of phenols in dimethylsulfoxide is controlled by the enthalpy factor, both internal and environmental, which is in contrast to the entropy-controlled process in water.

KOK-SIONG SIOW et KOK-PENG ANG. Can. J. Chem. **58**, 970 (1980).

On a mesuré les constantes d'ionisation des dinitrophénols-2,4 et -2,5 dans le diméthylsulfoxyde, par la méthode de la conductivité à 5 températures allant de 20 à 40°C. Les constantes d'ionisation du dinitro-2,4 phénol sont plus élevées que celles du dinitro-2,5 phénol et, dans les deux cas, elles augmentent avec la température. On discute des fonctions thermodynamiques de l'ionisation en fonction de la théorie de Hepler relative aux effets du substituant et du solvant. Le facteur d'enthalpie interne et externe contrôle l'ionisation des phénols dans le diméthylsulfoxyde ce qui est à l'opposé de la réaction en phase aqueuse dont le facteur déterminant est l'entropie.

[Traduit par le journal]

Introduction

Dimethylsulfoxide (DMSO) is a dipolar aprotic solvent with a high dielectric constant (46.4). Its large dipole moment (3.9 D) and polarizability (n_D^{20} is 1.478) enable it to stabilize molecules and ions through dipole and induced-dipole interactions. It solvates strongly protons and other cations, as it has a high electron density on the unscreened oxygen atom in its molecules. Thus as a solvent, the properties of DMSO complement those of water which is typically protic, and it has been suggested that "DMSO is destined to achieve an importance as a solvent for quantitative work in organic chemistry comparable to that of water in inorganic chemistry" (1).

Ionization constants in DMSO have been determined for a fairly large number of substances. Few studies, however, have been made on the thermodynamics of ionization of acids in this solvent. In view of the importance of DMSO as a solvent, it would be desirable to have more data of enthalpies and entropies of ionization so as to achieve a better understanding of the ionization process in this solvent. Thus, with this in mind, measurements were made of the ionization constants of two dinitrophenols in DMSO as a function of temperature to evaluate their ΔH and ΔS of ionization. The results are discussed in terms of Hepler's theory for substituent and solvent effects (2). Finally, a comparison between DMSO and water is also made with respect to their effects on the ionization process.

Experimental

Materials

2.4- and 2,5-Dinitrophenol (Merck Chemicals) were purified by repeated crystallization from ethanol until constant melting point (2,4-dinitrophenol, 113–114°C and 2,5-dinitrophenol 105–106°C).

AnalaR grade potassium chloride was recrystallized twice from conductance water and dried overnight at 180°C.

Dimethylsulfoxide (Aldrich Chemical Co.) was purified by passage through a column of activated alumina (Merck's chromatographic grade in basic form). The solvent from the column was collected into a distillation flask and vacuum fractionated at a pressure of a few Torr. A first fraction amounting to about 10% of the total was rejected and the second fraction of about 75% was collected. The purified DMSO had a specific conductance of less than 9×10^{-8} ohm^{-1} cm^{-1} at 25°C.

Conductance water for KCl solutions: deionised water was heated with alkaline permanganate and distilled into an all glass still for a further stage of distillation in an atmosphere of nitrogen. The specific conductance of the conductance water ranged from 6 to 8×10^{-7} ohm^{-1} cm^{-1}.

Apparatus

Conductances of solutions were measured with the Wayne Kerr B642 Autobalance Universal Bridge. For the conductance range studied, the instrument has an accuracy of 0.1%.

Two conductance cells of different dimensions were used. The electrodes of the cells were lightly platinized according to the technique of Jones and Bollinger (3). The cell constants were determined with standard KCl solutions (4) in the usual manner.

Temperature control was provided by a thermostatic water bath maintained to ±0.02°C.

Procedure

Solutions of dinitrophenols in DMSO were prepared in a nitrogen-filled dry box. All the solutions, including KCl solutions, were prepared by weight corrected to their vacuum values. Concentration in volume was then calculated from weight concentration and density. Solutions of different concentrations were prepared by successive dilution of a stock solution. Transfer

[1]To whom all correspondence should be addressed.

0008-4042/80/100970-04$01.00/0

©1980 National Research Council of Canada/Conseil national de recherches du Canada

Can. J. Chem. Downloaded from www.nrcresearchpress.com by 210.87.254.42 on 09/05/12
For personal use only.

TABLE 3. Limiting molar conductance, ionization constant,* and thermodynamic functions for 2,4-dinitrophenol in DMSO

Temperature (°C)	Λ_0	$K \times 10^5$	ΔG^0 (cal mol^{-1})	ΔH^0 (cal mol^{-1})	ΔS^0 (cal deg^{-1} mol^{-1})
20	19.8	0.973	6720		
25	23.0	0.995	6830	814	−20.2
30	26.6	1.02	6930	1010	−19.5
35	30.5	1.05	7020	1210	−18.9
40	34.9	1.08	7110		

*The literature pK values for 2,4-dinitrophenol in DMSO are: 5.2, from ref. 7; 5.4, from ref. 8.

TABLE 4. Limiting molar conductance, ionization constant, and thermodynamic functions for 2,5-dinitrophenol in DMSO

Temperature (°C)	Λ_0	$K \times 10^7$	ΔG^0 (cal mol^{-1})	ΔH^0 (cal mol^{-1})	ΔS^0 (cal deg^{-1} mol^{-1})
20	19.0	1.21	9280		
25	22.2	1.33	9380	3560	−19.5
30	25.7	1.48	9480	3760	−18.9
35	29.9	1.64	9570	3970	−18.2
40	34.5	1.82	9660		

of DMSO solutions to the conductance cells was performed in the dry box; the cells were stoppered before being taken out of the dry box for immersion in the thermostatic bath. Conductance readings were recorded when they became invariant with time; this took about 1 h for each measurement.

Values of the viscosity, density, and dielectric constant of the solvent were interpolated from the data of Yao and Bennion (5).

Results

The molar conductance data for dinitrophenol solutions together with the specific conductances of solvent at different temperatures are shown in Tables 1 and 2.[2] The data were evaluated according to the method of Fuoss and Shedlovsky (6). The following equation was used

$$[1] \quad 1/\Lambda S(z) = 1/\Lambda_0 + c\Lambda S(z)f^2/K\Lambda_0^2$$

The plot of $1/\Lambda S(z)$ versus $c\Lambda S(z)f^2$ was linear; the limiting molar conductance, Λ_0, and the ionization constant, K, were obtained from the intercept and the slope. The values are summarized in Tables 3 and 4. The values of the ionization constant calculated directly from the equation at various concentrations also show satisfactory consistency.

For the purpose of calculating the thermodynamic functions, the experimental data at various temperatures were fitted to an equation of the following form

$$[2] \quad \ln K = a + bT + cT^2$$

by the method of least-squares to yield thermodynamic functions of ionization as shown in Tables 3 and 4. The values for ΔH are quoted only for 25, 30, and 35°C, since ΔH is derived from the temperature dependence of ln K and it is expected that there is more uncertainty at the extremes of the temperature range. As an independent check on these ΔH values, the experimental ln K values were plotted versus $1/T$ and the slopes of the curves were estimated graphically. The results so obtained agreed with those calculated to within 10 to 20 cal mol^{-1}.

Discussion

As we are more interested in the relative acidities of the two phenols, we may begin our discussion with the following equation

$$[3] \quad \text{2,4-D} + \text{2,5-D}^- \rightleftharpoons \text{2,4-D}^- + \text{2,5-D}$$

where 2,4-D$^-$ and 2,5-D$^-$ indicate the anions of the respective dinitrophenols. Following Hepler's method of separating the thermodynamic functions into the "internal" and "environmental" contributions, and making the assumption (9) that ΔS_{int} for a symmetrical reaction, such as the one above, is nearly zero and can be neglected, we obtain for the reaction

$$[4] \quad \delta\Delta G = (\Delta H_{2,4\text{-D,int}} - \Delta H_{2,5\text{-D,int}}) + (\Delta H_{2,4\text{-D,env}} - \Delta H_{2,5\text{-D,env}}) - T(\Delta S_{2,4\text{-D,env}} - \Delta S_{2,5\text{-D,env}}) = \delta\Delta H_{int} + \delta\Delta H_{env} - T\delta\Delta S_{env}$$

$$[5] \quad \delta\Delta G = \delta\Delta H_{int} \text{ (in the absence of solvent)}$$

[2]Complete set of data is available, at a nominal charge, from the Depository of Unpublished Data, CISTI, the National Research Council of Canada, Ottawa, Ont., Canada K1A 0S2.

Can. J. Chem. Downloaded from www.nrcresearchpress.com by 210.87.254.42 on 09/05/12
For personal use only.

where ΔH's and ΔS's refer to the enthalpies and entropies of ionization of the two phenols.

Values of ΔH_{int} at 25°C for *p*- and *m*-nitrophenol in relation to the unsubstituted phenol[3] have been found (11) to be -3690 and -2130 cal mol^{-1} respectively. If it is assumed that the additivity principle of substituent effects (12) applies here, the difference (-1560 cal mol^{-1}) between the above two ΔH_{int} values may then be taken as the value of $\delta\Delta H_{int}$ in our case. Comparing it with the experimental $\delta\Delta G$ value (-2550 cal mol^{-1}), this means that about 60% of the overall difference in acidity of the two dinitrophenols in DMSO is accounted for by the substituent effects.

The effects of solvent may be illustrated in a convenient way by referring to the following scheme

[6]

$$\begin{array}{ccc} \text{2,4-D (g)} + \text{2,5-D}^- \text{(g)} & \xrightarrow{\delta\Delta G_g} & \text{2,4-D}^- \text{(g)} + \text{2,5-D (g)} \\ \downarrow \Delta G_s(\text{2,4-D}) \quad \downarrow \Delta G_s(\text{2,5-D}^-) & & \downarrow \Delta G_s(\text{2,4-D}^-) \quad \downarrow \Delta G_s(\text{2,5-D}) \\ \text{2,4-D (DMSO)} + \text{2,5-D}^- \text{(DMSO)} & \xrightarrow{\delta\Delta G_s} & \text{2,4-D}^- \text{(DMSO)} + \text{2,5-D (DMSO)} \end{array}$$

At 25°C the values of ΔS of the two compounds are nearly equal, suggesting that $\delta\Delta S_{env} \approx 0$ and hence $[\Delta S_s(\text{2,4-D}^-) - \Delta S_s(\text{2,4-D})] \approx [\Delta S_s(\text{2,5-D}^-) - \Delta S_s(\text{2,5-D})]$ for the above scheme. This indicates that the relative entropy of solvation for 2,4-D$^-$ and that for 2,5-D$^-$ with reference to their respective parent compounds are about the same. The ΔH data, on the other hand, show that

$$\begin{aligned} \delta\Delta H_{env} &= \delta\Delta H - \delta\Delta H_{int} \\ &\approx -2750 - (-1560) \\ &\approx -1190 \text{ cal mol}^{-1} \end{aligned}$$

where

$$\begin{aligned} \delta\Delta H_{env} = {} & [\Delta H_s(\text{2,4-D}^-) - \Delta H_s(\text{2,4-D})] \\ & - [\Delta H_s(\text{2,5-D}^-) - \Delta H_s(\text{2,5-D})] \end{aligned}$$

Thus, in relation to their respective parent compounds the 2,4-D$^-$ anion is stabilized by solvation by DMSO to a greater extent than is the 2,5-D$^-$ anion. The effect of solvation accounts for the remaining 40% of the overall difference in acidity of the two phenols in DMSO. As mentioned earlier, DMSO solvates anions through dipole and induced-dipole interactions and its solvation power increases with the size and polarizability of the ions. The negative charge on the anion of 2,4-D is spread over the phenolic oxygen and the oxygen atoms of both the nitro groups and hence is more delocalized than is the case for the anion of 2,5-D. It is to be expected, therefore, that the former would be solvated by DMSO more strongly than the latter. That the delocalization of the anion confers enhanced acidity on the acid in DMSO has also been noted by Bordwell *et al.* (13).

It would be interesting to compare the results here with those in aqueous solutions. Hepler (11) has shown that the stronger acidity of *p*-nitrophenol over *m*-nitrophenol in water is due almost entirely to its favourable entropy of ionization. The ΔH ($= \Delta H_{int} + \Delta H_{env}$) values for these two phenols (in water) were about equal, although the ΔH_{int} of *p*-nitrophenol is expected to be less positive as its anion is stabilized by resonance to a greater extent. Thus, the two results in DMSO and in water are totally in contrast with each other, showing that the two solvents complement one another in their solvent capabilities. In water, the solvent will interact more strongly with the anion of *m*-nitrophenol which has a relatively concentrated negative charge compared with the more diffuse charge on the resonance stabilized anion of *p*-nitrophenol. This stronger interaction results in a more negative ΔH_{env} value for *m*-nitrophenol which almost completely off-sets the favourable ΔH_{int} of *p*-nitrophenol. At the same time, however, it makes the entropy of solvation for *m*-nitrophenol less favourable than for *p*-nitrophenol, owing to the loss in translational freedom of the water molecules bound to it.

It has also been noted (14) that for the series: phenol, 4-nitrophenol, 2,6-dinitrophenol, and 2,4,6-trinitrophenol, the acidity in DMSO increases along the series faster than in water. This is demonstrated by a progressive drop in ΔpK ($pK_{DMSO} - pK_{H_2O}$) for the series from 6.5 to 3.8 to 1.3 and to ca. -1.3. This fact can now be explained in terms of the differential properties of the two solvents. As the

[3]McMahon and Kebarle (10) have recently measured ΔG^0 (taken as $\approx \Delta H^0$ on the assumption that $\Delta S^0 \approx 0$) for the same reactions in gas phase. Their values were, however, obtained at 327°C.

Can. J. Chem. Downloaded from www.nrcresearchpress.com by 210.87.254.42 on 09/05/12
For personal use only.

degree of delocalization in the anions increases along the series, their stabilization by induced-dipole interactions will become stronger and stronger in DMSO relative to that in water.

From the above argument it may be concluded that the ionization of phenols in DMSO is controlled by the enthalpy of ionization, both internal and environmental. This is in contrast to the entropy-controlled process for the ionization of phenols in water.

1. W. S. MATTHEWS, J. E. BARES, J. E. BARTMESS, F. G. BORDWELL, F. J. CORNFORTH, G. E. DRUCKER, Z. MARGOLIN, R. J. MCCALLUM, G. J. MCCOLLUM, and N. R. VANIER. J. Am. Chem. Soc. **97**, 7006 (1975).
2. J. W. LARSON and L. G. HEPLER. *In* Solute–solvent interactions. *Edited by* J. F. Coetzee and C. D. Ritchie. M. Dekker, London. 1969. Chapt. 1.
3. G. JONES and D. M. BOLLINGER. J. Am. Chem. Soc. **57**, 280 (1935).
4. J. E. LIND, J. J. ZWOLENIK, and R. M. FUOSS. J. Am. Chem. Soc. **81**, 1557 (1959).
5. N. P. YAO and D. N. BENNION. J. Electrochem. Soc. **118**, 1097 (1971).
6. R. M. FUOSS and T. SHEDLOVSKY. J. Am. Chem. Soc. **71**, 1496 (1949).
7. B. CLARE, D. COOK, S. KO, Y. MAC, and A. J. BAKER. J. Am. Chem. Soc. **88**, 1911 (1966).
8. M. K. CHANTOONI, JR. and I. M. KOLTHOFF. J. Phys. Chem. **80**, 1306 (1976).
9. K. S. PITZER. J. Am. Chem. Soc. **59**, 2365 (1937).
10. T. B. MCMAHON and P. KEBARLE. J. Am. Chem. Soc. **99**, 2222 (1977).
11. L. G. HEPLER. J. Am. Chem. Soc. **85**, 3089 (1963).
12. C. D. JOHNSON. The Hammett equation. Cambridge University Press, London. 1973.
13. F. G. BORDWELL, J. E. BARTMESS, G. E. DRUCKER, Z. MARGOLIN, and W. S. MATTHEWS. J. Am. Chem. Soc. **97**, 3226 (1975).
14. I. M. KOLTHOFF, M. K. CHANTOONI, JR., and S. BHOWMIK. J. Am. Chem. Soc. **90**, 23 (1968).

Can. J. Chem. Downloaded from www.nrcresearchpress.com by 210.87.254.42 on 09/05/12
For personal use only.

The solution conformation of prostacyclin as determined by high field proton magnetic resonance techniques[1]

GEORGE KOTOVYCH,[2] GERDY H. M. AARTS, TOM T. NAKASHIMA, AND GLEN BIGAM
Department of Chemistry, University of Alberta, Edmonton, Alta., Canada T6G 2G2

Received November 12, 1979

GEORGE KOTOVYCH, GERDY H. M. AARTS, TOM T. NAKASHIMA, and GLEN BIGAM. Can. J. Chem. **58**, 974 (1980).

The proton magnetic resonance (^{1}H nmr) spectrum at 400 MHz of prostacyclin at pH 10.4 in glycine buffer has been completely analyzed utilizing homonuclear double resonance, inversion recovery, and difference nOe experiments. The spectral analysis shows that the two protons at C-4 are non-equivalent even though they are removed from the asymmetric centres at C-8 and C-9 by five bonds. The difference nOe measurements verify the configuration at C-5.

Proton longitudinal relaxation times (T_1) were measured at 400 and 200 MHz. From the T_1 frequency dependence, effective rotational correlation times ranging from 2.3×10^{-10} to 3.0×10^{-10} s were calculated for H-5, H-9, H-11, and H-15. This indicates that the portion of the molecule encompassed by these protons has a longer correlation time than is observed for the C-2 and the C-17 to C-19 protons, for which the average correlation time is 1.2×10^{-10} s. Hence the aliphatic side chains have more segmental motion.

GEORGE KOTOVYCH, GERDY H. M. AARTS, TOM T. NAKASHIMA et GLEN BIGAM. Can. J. Chem. **58**, 974 (1980).

On a analysé complètement le spectre de résonance magnétique du ^{1}H de la prostacycline à 400 MHz, à un pH de 10.4 dans un tampon de glycine, en utilisant la double résonance homonucléaire, l'inversion de récupération et des expériences de différences de enO. L'analyse spectrale révèle que les deux protons en position C-4 ne sont pas équivalents même s'ils sont éloignés des centres asymétriques C-8 et C-9 par 5 liaisons. Des mesures de différence enO permettent de vérifier la configuration au niveau du carbone en position 5.

On a mesuré les temps de relaxation longitudinale (T_1) à 400 et 200 MHz. En se basant sur l'effet de fréquence sur T_1, on a calculé les temps de corrélation rotationnelle efficace pour les protons H-5, H-9, H-11 et H-15 qui varient entre $2.3 - 10^{-10}$ et $3 - 10^{-10}$ s. Ceci indique que la portion de la molécule entourée par ces protons a un temps de corrélation plus grand que celui observé pour les protons portés par les carbones 2 et 17 à 19 pour lesquels le temps moyen de corrélation est de 1.2×10^{-10} s. En conséquence les chaînes latérales aliphatiques ont plus de mouvement segmentaire.

[Traduit par le journal]

Introduction

The metabolic pathway of arachidonic acid proceeds via the cyclic endoperoxides which are then rapidly converted into thromboxane, prostacyclin (PGI_2), and other prostaglandins. Prostacyclin (Fig. 1) was discovered by Moncada *et al.* (1). It inhibits platelet aggregation and relaxes vascular smooth muscle (2). (The structure of PGI_2 was first presented in 1976 (ref. 2, pp. 179–187).) On the other hand, thromboxane A_2 induces platelet aggregation and causes contraction of arteries (ref. 2, pp. 133–154). Hence there exists in blood vessels a delicate balance involving prostacyclin, which, in the circulatory system, is generated by the vessel walls (3) and thromboxane A_2, which is produced by the platelets (4). In fact, clinical studies have shown that low doses of aspirin (160 mg per day) present an effective, nontoxic, antithrombic regimen in man. These prevent pathologic thromboses by blocking platelet synthesis of thromboxane without affecting the synthesis of vascular prostacyclin (5).

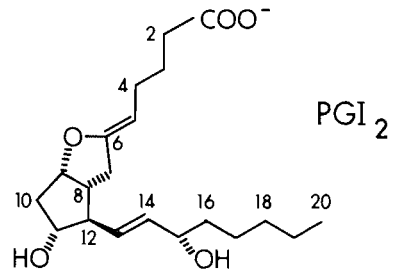


FIG. 1. Structure of prostacyclin (PGI_2).

Because of the diverse functions of these two compounds, we have studied the conformation of PGI_2 in solution using high-field ^{1}H nmr techniques. We have previously studied thromboxane B_2 in $CDCl_3$ and CD_3OD solutions (G. Kotovych and G. H. M. Aarts, Can. J. Chem. 1980, in press) as the biologically active thromboxane A_2 has a half-life of only about 32 s (ref. 2, pp. 133–154). In this way we hope to correlate the structure and activity of these compounds in solution.

Materials and Methods

The sodium salt of prostacyclin was a gift from Dr. John Pike of the Upjohn Co., Kalamazoo, MI. The present measurements were carried out in glycine-d_5 buffer (0.02 *M*) in D_2O and the pH of the buffer was adjusted to 10.4 (uncorrected meter reading)

[1]This is paper No. 3 in a series of high-field nmr studies on vitamins and prostaglandins. For paper No. 1 see ref. 16; paper No. 2 is in press.

[2]Formerly Kotowycz.

0008-4042/80/100974-10$01.00/0
©1980 National Research Council of Canada/Conseil national de recherches du Canada

Can. J. Chem. Downloaded from www.nrcresearchpress.com by 210.87.254.5 on 09/05/12
For personal use only.

Can. J. Chem. Downloaded from www.nrcresearchpress.com by 210.87.254.5 on 09/05/12
For personal use only.

using 40% (w/w) NaOD in D_2O. A high pH was used for these studies since even at a pH of 7.6, PGI_2 is rapidly hydrolyzed to 6-ketoprostaglandin $F_{1\alpha}$ (6). The buffer solution was vacuum degassed using the freeze–pump–thaw technique. The sodium salt of PGI_2 was weighed out into the nmr tube and the required volume of the buffer solution was added. With the exception of the pH adjustment, the complete preparation was carried out in a dry box under a nitrogen gas atmosphere. The final PGI_2 concentration was 0.02 *M*. The samples were then vacuum degassed and sealed. All glassware was cleaned extensively, including a nitric acid wash, to eliminate paramagnetic impurities. To check for the presence of these impurities, one sample was prepared with ~0.5 mol% EDTA and the measured relaxation times remained unchanged.

The nmr measurements were carried out in the Fourier transform mode using the Bruker WH-400/DS and the Bruker WH-200/DS nmr spectrometers and the Aspect 2000 Data System utilizing 16 or 32K of data memory. With the exception of the difference nOe measurements, all of the experiments were carried out at 277 K to maintain sample stability. The deuterium resonance of the solvent D_2O was used as the lock signal. The homonuclear decoupling experiments were also performed in the pulse mode. The chemical shifts, with respect to the methyl resonance of TSP, and coupling constants, were calculated to first order (with the exception of H-4 and 4*) at 400 MHz and are reported with an accuracy of about ±0.010 ppm and ±0.20 Hz, respectively. For maximum accuracy, spectra were expanded to a width of 2 Hz/cm.

The proton longitudinal relaxation rates were obtained using the 180°–τ–90° two pulse sequence. Usually 10 τ values were included in the analysis of the data, based on the initial slope of a plot of $\ln((M_\infty - M_\tau)/(M_\infty))$ vs. τ. These *M* values were obtained from the measurement of the sum of the peak heights of a multiplet corresponding to a given proton. Three M_∞ values were measured for maximum accuracy. Data are not reported where there was significant overlap of resonances due to different protons. The relaxation rates were obtained from a computer analysis of the data using a least-squares program. The T_1 values are reproducible from one sample to a second sample with an accuracy of ±5%. Consequently, the error limits on the $T_{1D}(400)/T_{1D}(200)$ quotient are ±10%. The difference nOe experiments were carried out in the standard manner (7) at both frequencies at 298 K since at the higher temperature the proton rotational correlation times are shorter and provide larger enhancements (7–9).

Results

Four different techniques were required to assign the proton resonances and to determine the proton chemical shifts. These are: characteristic proton chemical shifts, double resonance techniques, inversion recovery spectra, and difference nOe experiments. The resonances for H-2, H-13 and 14, H-17 to 19, and H-20 were assigned on the basis of their characteristic chemical shifts. Many of the other proton resonances, including H-9, H-5, H-15, and H-11, were assigned on the basis of homonuclear proton decoupling experiments. For example, irradiation of H-9 (Fig. 2B) simplifies the resonances due to H-10α, H-10β, and H-8. This experiment also shows that the coupling between H-7α and H-8β is nearly zero, which indicates a dihedral angle of almost 90°. Irradiation of the H-10α and the H-3 multiplet confirms the chemical shift of H-2 and H-10β as well as the coupling constants J(9-10α) and J(10α-11) (Fig. 2C). Finally, irradiation of H-4 and 4* confirms the chemical shift of H-5 and H-3 (Fig. 2D).

Assignments based on the difference nOe experiments are shown in Fig. 3. These experiments are based on the fact that protons in close proximity to the irradiated proton will be observed, even if these proton resonances are hidden by other resonances. As seen in Fig. 3B, upon saturating H-5, a large nOe is observed for H-7α and H-4 and 4*. This experiment allowed the assignment of H-7α, since from molecular models this proton is closest to H-5. It also appears that H-2 and H-3 are slightly enhanced, which is probably not surprising. Decoupling experiments carried out on H-5 showed that the low field H-7 resonance is due to the C-7 proton in the β position because of the allylic long-range coupling between H-7β and H-5 (10). In Fig. 3C, when H-11 is saturated, an nOe is observed for the other protons that are β to the ring, namely H-10β and H-8β, proving that the 10β proton resonance is to low field of the 10α proton resonance. In addition, an nOe is observed for H-13 and H-14. In an additional experiment, H-9 was saturated and an nOe was observed for H-10β and H-8, all of which are β to the ring. An enhancement was not observed for H-11. Finally, saturation of the overlapping H-8 and H-7α multiplets (Fig. 3D) yields an nOe for H-7β, H-12, H-11, and H-9, as expected. An nOe is also observed for H-13 and H-14. An nOe for H-13 and H-14 in these two experiments is consistent with freedom of rotation about the C12—C13 bond. This was confirmed by an nOe experiment in which H-13 and H-14 were saturated and ring protons H-8, H-11, and H-12 showed an nOe enhancement.

To confirm that H-10β does in fact resonate to low field of H-10α, further difference nOe experiments were carried out. These are shown in Fig. 4. In Fig. 4B, the H-10β multiplet is saturated and an nOe is observed for the nearest protons, namely H-10α and H-11. The nOe at H-9 cannot be confirmed due to the residual HDO signal. However, when the H-10α multiplet is saturated, a large nOe is observed for H-10β, as expected, but a very weak effect is now observed for H-11, which is β to the ring. These experiments confirm the H-10α and H-10β assignments.

Finally, chemical shifts were also obtained from the inversion recovery spectra by selective nulling of overlapping multiplets. As seen in Fig. 5, the

Can. J. Chem. Downloaded from www.nrcresearchpress.com by 210.87.254.5 on 09/05/12
For personal use only.

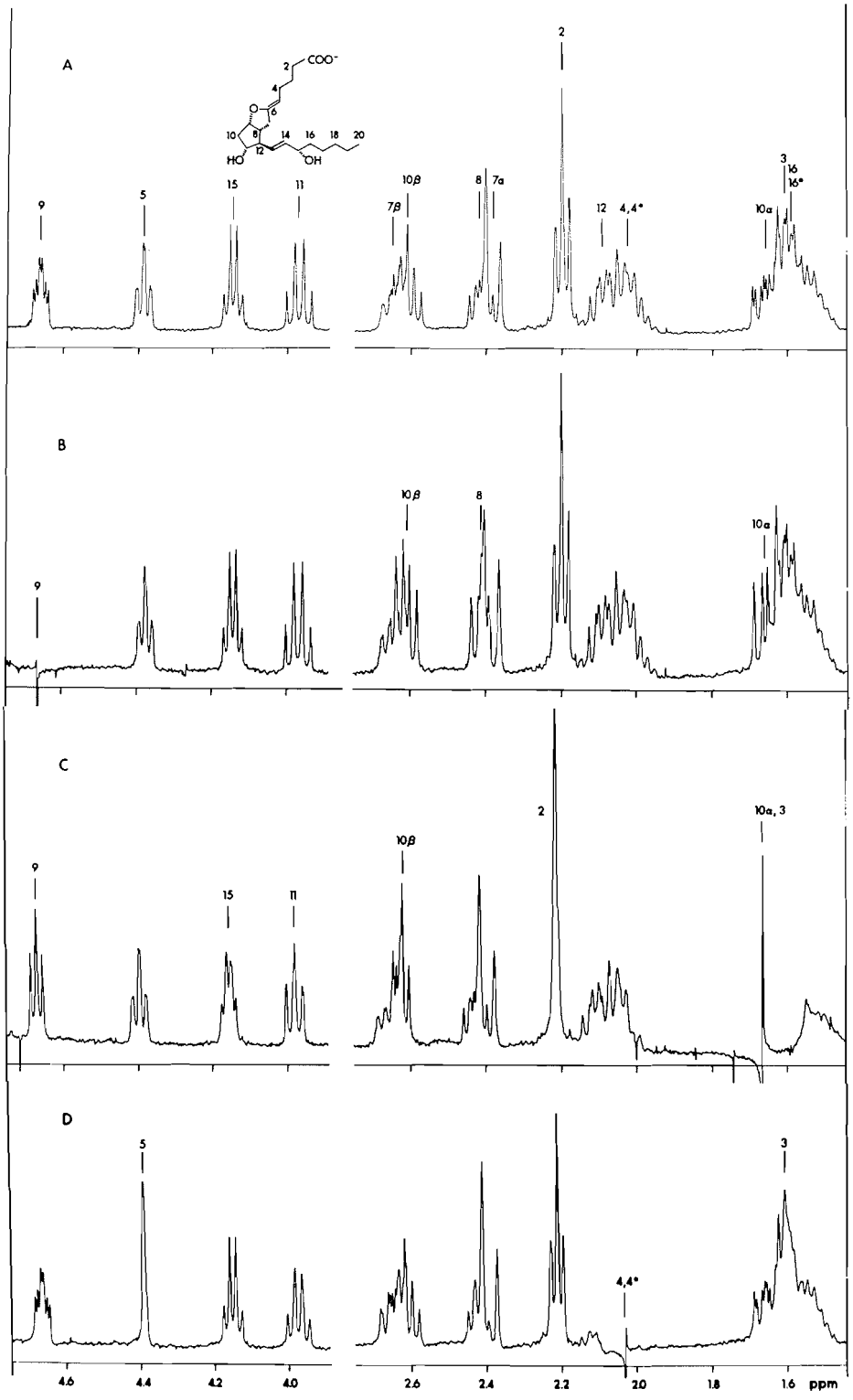


FIG. 2. Results of the homonuclear decoupling experiments at 400 MHz at 277 K. Spectrum A is the normal spectrum. In B, the H-9 multiplet is irradiated. In C, the multiplet corresponding to H-10α and H-3 is irradiated whereas in D, the H-4,4* multiplet is decoupled. The protons affected by the irradiation are indicated in spectra 2B–2D.

Can. J. Chem. Downloaded from www.nrcresearchpress.com by 210.87.254.5 on 09/05/12
For personal use only.

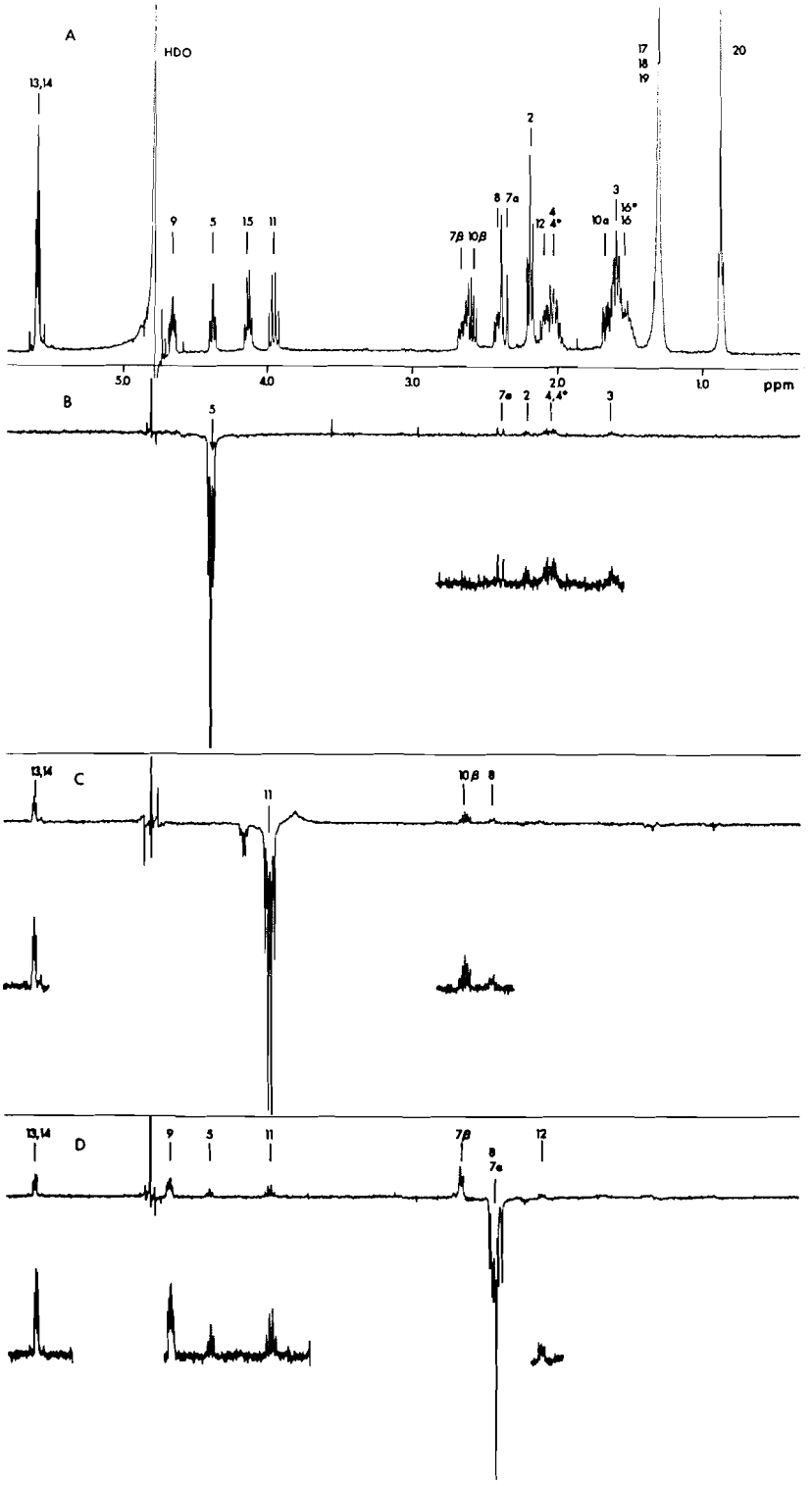


FIG. 3. Results of the difference nOe experiments performed at 400 MHz at 298 K. The normal spectrum is seen in A. In B, H-5 is saturated and an nOe is observed for H-7α, H-4,4* and a smaller nOe is observed for H-2 and H-3. In C, H-11 is saturated and an nOe is observed for H-13, H-14, H-10β, and H-8. In spectrum D, H-7α and H-8 are saturated and the protons experiencing the nOe are indicated. For these experiments, 16K data points were used together with 800 scans, a 90° pulse width of 10.7 μs and a delay time of 6 s.

Can. J. Chem. Downloaded from www.nrcresearchpress.com by 210.87.254.5 on 09/05/12
For personal use only.

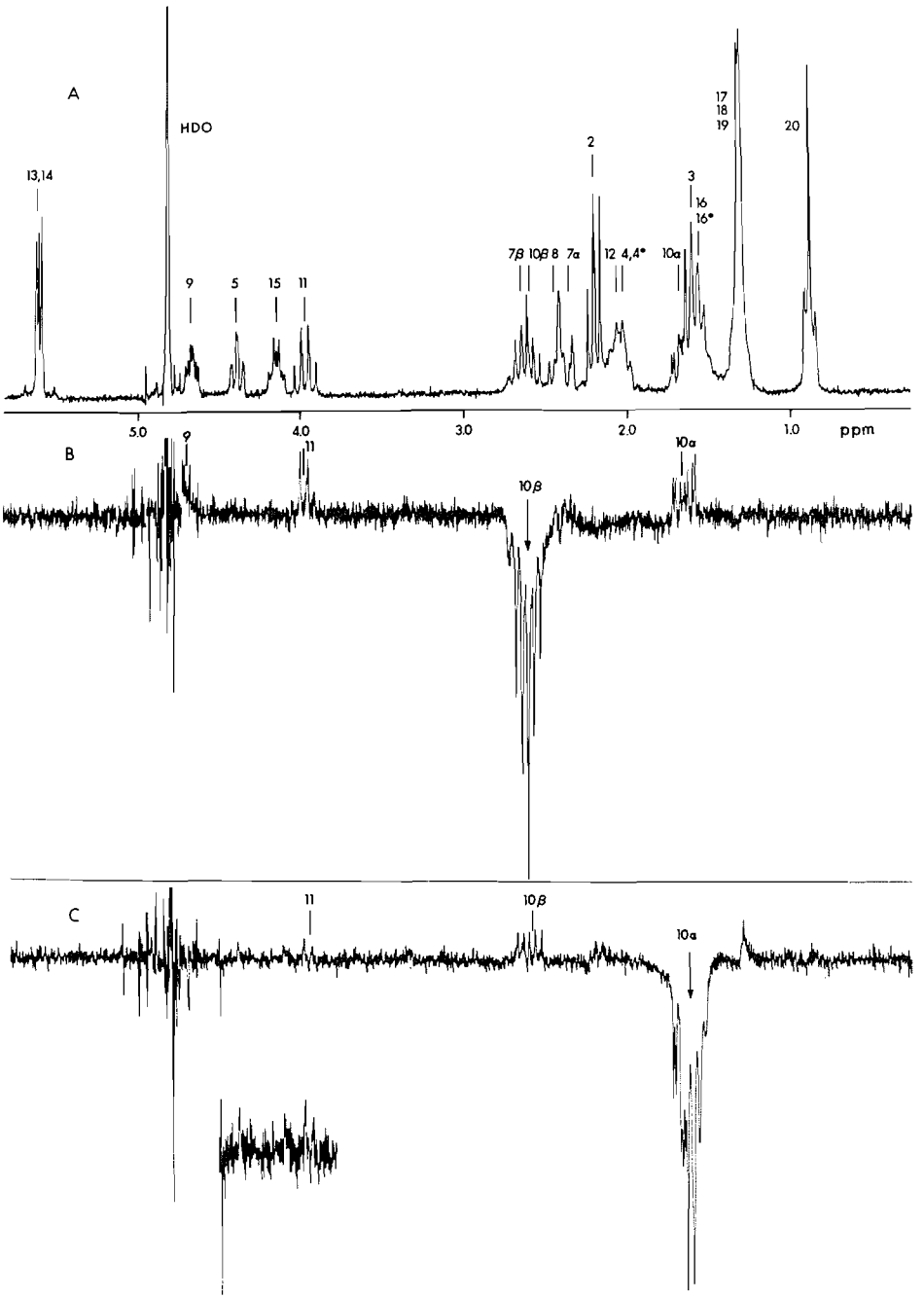


FIG. 4. The difference nOe experiments performed at 200 MHz at 298 K. The normal spectrum is seen in A, whereas in B H-10β was saturated. An nOe is observed for H-10α and H-11β. In C, H-10α is saturated and a large nOe is observed for H-10β and a small nOe for H-11. 16K data points were used together with 800 scans, a 90° pulse width of 5.2 μs and a delay time of 6 s.

multiplet corresponding to H-4 and 4* is readily visible when a τ value of 0.6 s is used in the 180°–τ–90° two-pulse sequence since H-12, having a longer T_1 value, is nulled. Similarly, the doublet corresponding to H-7α is clearly visible from the spectrum with a τ value of 0.4 s, since the resonances corresponding to H-8 are now nulled.

On the basis of the above experiments, the chemical shifts of all the protons were assigned and these are tabulated in Table 1, together with the

Can. J. Chem. Downloaded from www.nrcresearchpress.com by 210.87.254.5 on 09/05/12
For personal use only.

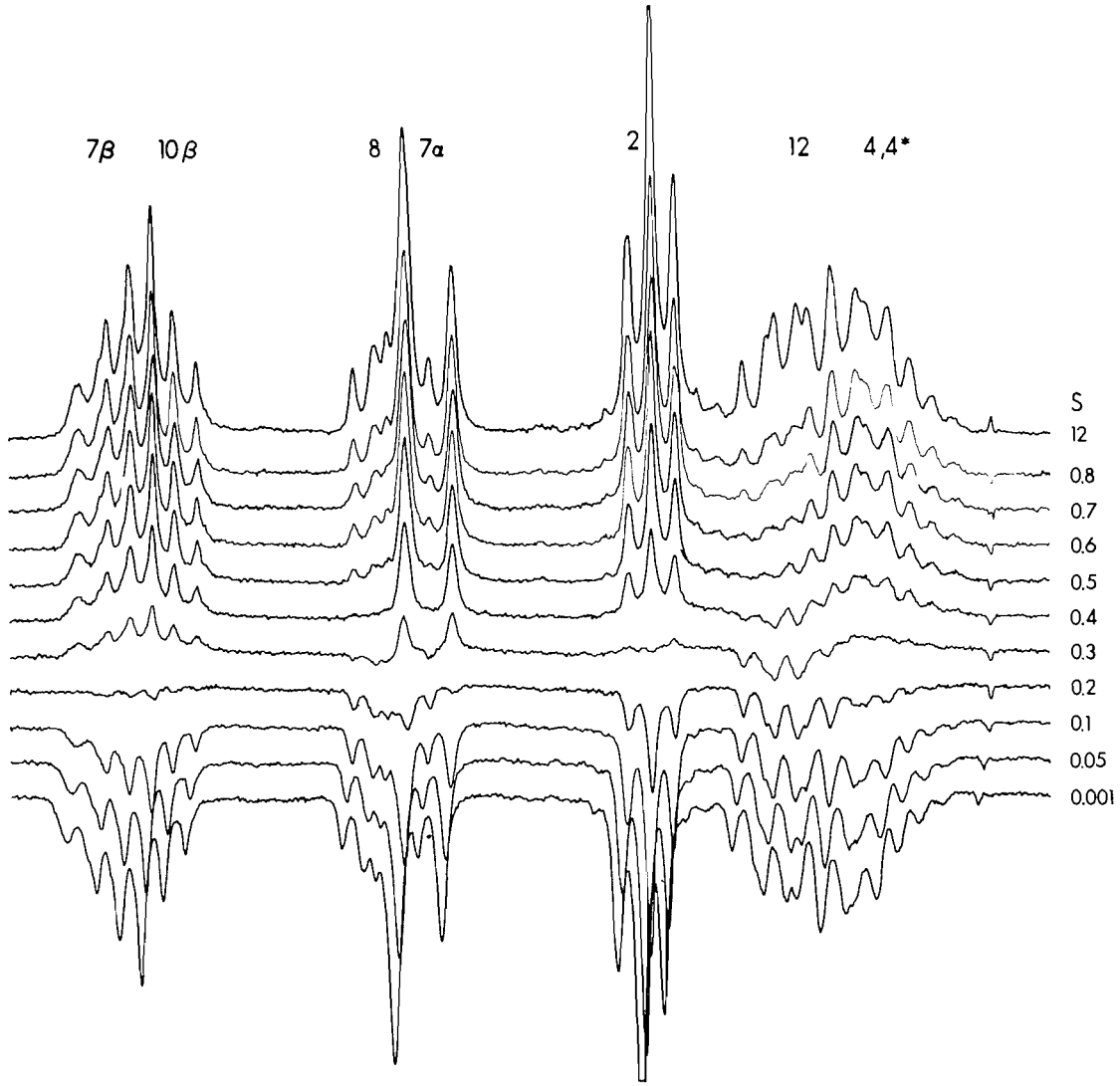


FIG. 5. The 180°–τ–90° inversion recovery spectra of prostacyclin in glycine buffer at 277 K obtained at 400 MHz; 48 scans were used to obtain each spectrum together with 32K data points.

coupling constants. A most interesting aspect of the analysis was the observation of the chemical nonequivalence of the two protons at C-4, even though they are removed by five bonds from two asymmetric centres at C-8 and C-9. The observed and calculated spectra are shown in Fig. 6 and the chemical shift difference between these two protons is 21 Hz at 400 MHz. The spectra represent the AB portion of an ABM_2X system, where the two C-3 protons are represented by M_2, and H-5 is represented by X. The agreement between the calculated and observed spectra is excellent, considering that the line width at half height of the C-4 protons is about 4 Hz, and the observed spectrum is obtained from an inversion recovery experiment.

The results of the proton longitudinal relaxation times, based on the initial slope approximation, are given in Table 2, at 200 and 400 MHz. Since the samples were degassed and prepared in a deuterated buffer, and one sample contained EDTA to check on the absence of paramagnetic impurities, the initial rates are very nearly equal to $1/T_{1D}$, where T_{1D} is the longitudinal relaxation time due to the dipolar interaction.

Discussion

The analysis of the 400 MHz spectrum of prostacyclin yields two important results. The first is the observation that the chemical shift of H-10β is to low field of the chemical shift for H-10α. Our

Can. J. Chem. Downloaded from www.nrcresearchpress.com by 210.87.254.5 on 09/05/12
For personal use only.

TABLE 1. Chemical shifts and coupling constants for PGI_2 in D_2O glycine buffer, pH 10.4, at 4°C[a]

Proton	Chemical shifts (ppm)	Coupling constants (Hz)
2	2.20	$J(2-3) = 7.5$
3	1.61	$J(2-3) = 7.5$
4, 4*	2.051, 1.999[b]	$J(3-4) = J(3-4^*) = 7.2$[b] $J(4-4^*) = -14.5$[b] $J(4-5) = J(4^*-5) = 7.2$
5	4.39	$J(4-5) = J(4^*-5) = 7.2$ $J(5-7\beta) = 1.6$
7α	2.38	$J(7\alpha-7\beta) = 15.5$ $J(7\alpha-8) = 0$
7β	2.64	$J(5-7\beta) = 1.6$ $J(7\alpha-7\beta) = 15.5$ $J(7\beta-8) = 7.6$
8	2.41	$J(7\alpha-8) = 0$ $J(7\beta-8) = 7.6$ $J(8-9) = 6.5$ $J(8-12) = 10.7$
9	4.66	$J(8-9) = 6.5$ $J(9-10\alpha) = 3.0$ $J(9-10\beta) = 7.2$
10α	1.66	$J(9-10\alpha) = 3.0$ $J(10\alpha-10\beta) = 14.3$ $J(10\alpha-11) = 8.7$
10β	2.61	$J(9-10\beta) = 7.2$ $J(10\alpha-10\beta) = 14.3$ $J(10\beta-11) = 8.7$
11	3.97	$J(10\alpha-11) = 8.7$ $J(10\beta-11) = 8.7$ $J(11-12) = 8.7$
12	2.09	$J(8-12) = 10.7$ $J(11-12) = 8.7$
13	5.60[c]	
14	5.60[c]	
15	4.15	$J(14-15) = 6.5$ $J(15-16) = 6.5$
16, 16*	~1.6	
17, 18, 19	1.30	
20	0.874	$J(19-20) = 6.7$

[a]The chemical shifts, with respect to TSP, and the coupling constants, are calculated to first order except for H-4 and 4* where these parameters were obtained from the simulated spectrum. The H-12 and H-15 multiplets cannot be analyzed to first order due to virtual coupling arising from the very small chemical shift between H-13 and H-14 as well as between H-16 and H-16*. Therefore measured splittings for the H-15 multiplet are reported (6.5 Hz).
[b]From the simulated spectrum carried out using the Bruker Software and Aspect 2000 Data System.
[c]Centre of multiplet.

assignment is based on the difference nOe experiments and is consistent with the torsion angle dependency of chemical shifts published previously (11). The torsion angle between C(H)—OH and C(10)—H-10α is ~0°, and hence the OH group is expected to shield H-10α by 0.25 ppm and to deshield H-10β by 0.25 ppm. The ether oxygen at C-9 is also *cis* to H-10α and hence a chemical shift difference of 0.95 ppm is observed between H-10α and H-10β. A shift difference of 0.90 ppm between similar protons has been observed in 1,3-disubstituted five-membered prostanoid precursors (11).

TABLE 2. Proton T_1 data and effective rotational correlation times for PGI_2 at 4°C[a]

Proton	$T_{1D}(200)$	$T_{1D}(400)$	τ_R (s)
2	0.41	0.48	1.1×10^{-10}
5	0.69	1.09	2.3×10^{-10}
9	0.57	0.96	2.5×10^{-10}
11	0.50	0.92	3.0×10^{-10}
15	0.49	0.83	2.6×10^{-10}
17, 18, 19	0.45	0.56	1.3×10^{-10}

[a]The average errors in τ_R are about $\pm 0.4 \times 10^{-10}$ s, based on the ±10% error in the $T_{1D}(400)/T_{1D}(200)$ quotient.

Secondly, protons 4 and 4* are chemically nonequivalent. The observed and calculated spectra which are shown in Fig. 6 are in excellent agreement and the chemical shift difference is 21 Hz. This non-equivalence is probably enhanced by the presence of the oxygen at C-9 and is due to the asymmetric centers at C-8 and C-9. Examples of long-range nonequivalence have been previously documented (ref. 10, p. 377).

The chemical shifts of H-9, H-5, H-15, and H-11 are in the same order as those observed for the PGI_2 methyl ester in $CDCl_3$ (12). In fact, the presence of the H-9 multiplet in the range of 4.45–4.55 ppm has been used (13) to assign compounds stereochemically related to (6*S*)-5,6-dihydroprostacyclin. However, in the present study, the chemical shifts are to lower field than those observed in $CDCl_3$ due to the solvent D_2O.

The results of the proton relaxation measurements are shown in Table 2. Due to multiplet overlap, correlation times could not be obtained for all protons. Typical spectra used for this analysis are shown in Fig. 7.

The frequency dependence for $1/T_{1D}$ has been worked out by Solomon (14) for two interacting spins and the equation for the general case may be written as (ref. 15, and references therein):

$$\frac{1}{T_{1D,j}} = \sum_{i \neq j} \frac{C^6}{r_{ij}^{\,6}} \left(\frac{\tau_R}{1 + \omega_I^{\,2}\tau_R^{\,2}} + \frac{4\tau_R}{1 + 4\omega_I^{\,2}\tau_R^{\,2}} \right)$$

In this equation, C is a product of physical constants, r_{ij} are the internuclear distances in Å, ω_I is the proton resonance frequency in rad/s, and τ_R represents the average rotational correlation time. This formula assumes dipole–dipole relaxation, isotropic motion, and no internal motion (15).

There are two unknowns in this equation, τ_R and r_{ij}. When relaxation rates at two frequencies are known, for example at 200 and 400 MHz, the correlation time, τ_R, for a given proton can be evaluated from a plot of τ_R vs. the $T_{1D}(400)/T_{1D}(200)$ quotient. This plot has previously been applied to the analysis of relaxation times of Vitamin D de-

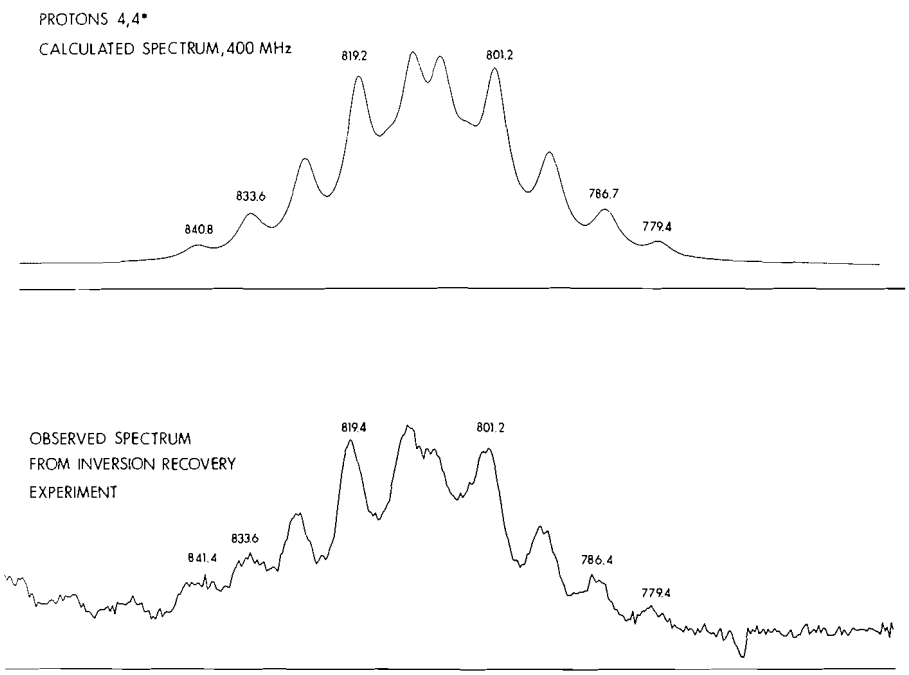


FIG. 6. The observed spectrum for H-4 and 4* obtained from the inversion recovery experiment shown in Fig. 5 ($\tau = 0.6$ s). The simulated spectrum is also shown and is in excellent agreement with the observed spectrum. The chemical shift difference between these two protons is 21 Hz. A line width at half height of 4 Hz was used in the calculation. Six representative observed and calculated frequencies are indicated. In the spectral simulation, $J(3–4) = J(3–4^*)$ was set at 7.20 Hz and $J(4–4^*)$ was set at 14.5 Hz.

rivatives (16) and thromboxane B_2 in $CDCl_3$ solution (G. Kotovych and G. H. M. Aarts, Can. J. Chem. 1980, in press). A similar approach, but at 220 and 100 MHz, has previously been applied in the measurement of the correlation times for the propionyl–CoA protons (17). In the present study, initial relaxation rates are obtained from coupled spectra. However, as first order spectra are observed for most of the multiplets, errors associated with interpreting initial relaxation rates due to cross relaxation are minimized (18, 19).

Using the calibration graph published previously (16), the effective rotational correlation times for the protons listed in Table 2 were evaluated. These range from 2.3×10^{-10} to 3.0×10^{-10} s for the rigid portion of the molecule encompassing protons 5–15. However, for H-2, H-17, H-18, and H-19 the frequency dependence is very small and the correlation times are shorter by a factor of two than for the other measured protons. The present results are in agreement with the ^{13}C relaxation measurements on prostaglandin $F_{2\alpha}$ (20) and its methyl ester (21). The ^{13}C results indicate that the prostaglandin molecule possesses rigidity encompassing carbon atoms 5–15, but carbon atoms 2–4 and 16–20 possess a greater flexibility, as would a butyric acid or an *n*-pentyl side-chain. The agreement between these studies and the present study is excellent, considering the fact that prostaglandin $F_{2\alpha}$ has only one five-membered ring.

The nOe is proportional to r^{-6}, where r is the distance between the irradiated and the observed protons. The present difference nOe data shows that saturation of H-5 causes an enhancement for H-7α (Fig. 3B). This confirms that H-5 is *cis* to C-7 and not *trans*. This configuration of H-5 was previously shown on the basis of chemical shift additivities (12), an empirical approach, whereas the nOe is quantitative in determining points of configuration. Finally, saturation of H-11 proves that H-12 is α to the ring, as expected, since an nOe is not observed for H-12 (Fig. 3C).

In conclusion, homonuclear decoupling experiments, inversion recovery experiments, as well as difference nOe measurements were required to completely assign the 400 MHz ^1H nmr spectrum of prostacyclin. The two protons at C-4 are nonequivalent even though they are removed by 5 bonds from the asymmetric centres at C-8 and C-9. The effective rotational correlation times indicate that the portion of the molecule from H-5 to H-15 possesses a greater rigidity than the side chain protons H-2 or H-17 to H-19. Finally, the difference nOe measurements verify the configuration at C-5.

Can. J. Chem. Downloaded from www.nrcresearchpress.com by 210.87.254.5 on 09/05/12
For personal use only.

Can. J. Chem. Downloaded from www.nrcresearchpress.com by 210.87.254.5 on 09/05/12
For personal use only.

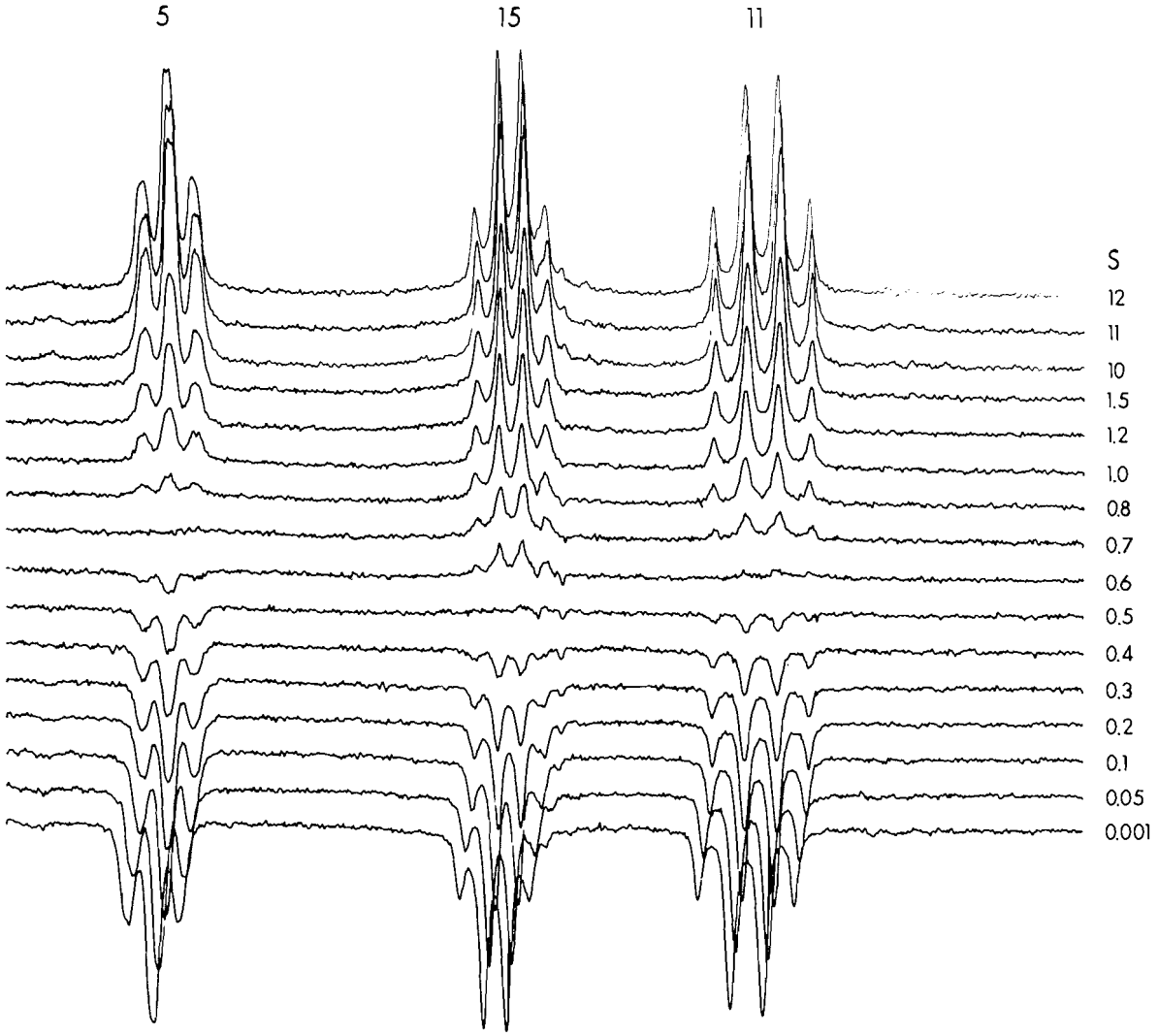


FIG. 7. The 180°–τ–90° inversion recovery spectra of prostacyclin in glycine buffer at 277 K obtained at 400 MHz. These experiments were used to calculate the initial relaxation rates ($1/T_{1D}$).

Acknowledgements

The authors wish to thank Dr. John Pike of the Upjohn Company in Kalamazoo, MI for providing us with the Na^+ salt of prostacyclin, Dr. B. D. Sykes for valuable suggestions, and the Natural Sciences and Engineering Research Council of Canada and the University of Alberta for generous financial assistance. We also thank the Natural Sciences and Engineering Research Council of Canada for a grant that made possible the purchase of the 400 MHz nmr spectrometer.

1. S. MONCADA, R. GRYGLEWSKI, S. BUNTING, and J. R. VANE. Nature (London), **263**, 663 (1976).
2. N. KHARASCH and J. FRIED (*Editors*). Biochemical aspects of prostaglandins and thromboxanes. Academic Press, New York, NY. 1977. pp. 155–177.
3. R. J. GRYGLEWSKI, S. BUNTING, S. MONCADA, R. J. FLOWER, and J. R. VANE. Prostaglandins, **12**, 685 (1976).
4. M. HAMBERG, J. SVENSSON, and B. SAMUELSSON. Proc. Natl. Acad. Sci. U.S.A. **72**, 2994 (1975).
5. H. R. HARTER, J. W. BURCH, P. W. MAJERUS, N. STANFORD, J. A. DELMEZ, C. B. ANDERSON, and C. A. WEERTS. New Engl. J. Med. **301**, 577 (1979).
6. R. A. JOHNSON, D. R. MORTON, J. H. KINNER, R. R. GORMAN, J. C. MCGUIRE, F. F. SUN, N. WHITTAKER, S. BUNTING, J. SALMON, S. MONCADA, and J. R. VANE. Prostaglandins, **12**, 915 (1976).
7. R. RICHARZ and K. WÜTHRICH. J. Magn. Reson. **30**, 147 (1978).
8. J. H. NOGGLE and R. E. SCHIRMER. The nuclear Overhauser effect. Academic Press, New York, NY. 1971.
9. J. D. GLICKSON, S. L. GORDON, T. P. PITNER, D. G. AGRESTI, and R. WALTER. Biochemistry, **15**, 5721 (1976).
10. L. M. JACKMAN and S. STERNHELL. Applications of nuclear magnetic resonance spectroscopy in organic chemis-

try. 2nd ed. Pergamon Press, Oxford, England. 1969. p. 316.
11. M. ANTEUNIS and D. DANNEELS. Org. Magn. Reson. **7**, 345 (1975).
12. R. A. JOHNSON, F. H. LINCOLN, J. L. THOMPSON, E. G. NIDY, S. A. MIZSAK, and U. AXEN. J. Am. Chem. Soc. **99**, 4182 (1977).
13. R. A. JOHNSON, F. H. LINCOLN, E. G. NIDY, W. P. SCHNEIDER, J. L. THOMPSON, and U. AXEN. J. Am. Chem. Soc. **100**, 7690 (1978).
14. I. SOLOMON. Phys. Rev. **99**, 559 (1955).
15. R. ROWAN III, J. A. MCCAMMON, and B. D. SYKES. J. Am. Chem. Soc. **96**, 4773 (1974).
16. G. KOTOWYCZ, T. T. NAKASHIMA, M. K. GREEN, and G. H. M. AARTS. Can. J. Chem. **58**, 45 (1980).
17. C. H. FUNG, R. J. FELDMANN, and A. S. MILDVAN. Biochemistry, **15**, 75 (1976).
18. R. L. VOLD and R. R. VOLD. Prog. Nucl. Magn. Reson. Spectrosc. **12**, 79 (1978).
19. I. D. CAMPBELL and R. FREEMAN. J. Magn. Reson. **11**, 143 (1973).
20. W. W. CONOVER and J. FRIED. Proc. Natl. Acad. Sci. U.S.A. **71**, 2157 (1974).
21. C. CHACHATY, Z. WOLKOWSKI, F. PIRION, and G. LUKACS. J. Chem. Soc. Chem. Commun. 951 (1973).

Can. J. Chem. Downloaded from www.nrcresearchpress.com by 210.87.254.5 on 09/05/12
For personal use only.

The reaction of some nuclear substituted acyclic conjugated styryl ketones and related Mannich bases with ethanethiol

J. R. DIMMOCK[1] AND L. M. SMITH

College of Pharmacy, University of Saskatchewan, Saskatoon, Sask., Canada S7N 0W0

AND

P. J. SMITH

Department of Chemistry and Chemical Engineering, University of Saskatchewan, Saskatoon, Sask., Canada S7N 0W0

Received November 19, 1979

J. R. DIMMOCK, L. M. SMITH, and P. J. SMITH. Can. J. Chem. **58**, 984 (1980).

The second order rate constants for the reaction of ethanethiol with a number of conjugated nuclear-substituted styryl ketones and related Mannich bases in 50% aqueous acetonitrile was undertaken. Variation of the alkyl group adjacent to the carbonyl function was accompanied by altered avidity to ethanethiol which was explained as being due in part to the varying inductive effects of the alkyl groups which would, in turn, affect the stability of the reaction intermediates. The greatest disparity in reactivity between groups of compounds was between the ketones and analogous Mannich bases which was in accord with the marked difference in bioactivities between these two groups of compounds.

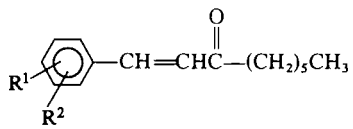
J. R. DIMMOCK, L. M. SMITH et P. J. SMITH. Can. J. Chem. 58, 984 (1980).

On a entrepris l'étude des constantes de vitesse de deuxième ordre de la réaction de l'éthanethiol avec un certain nombre de styrylcétones conjuguées ayant des substituants sur le noyau, et avec les bases de Mannich apparentées dans l'acétonitrile aqueux à 50%. Un changement du groupe alkyle adjacent au carbonyle s'accompagne d'une altération de l'avidité pour l'éthanethiol. Ce fait est attribué en partie au changement d'effets inductifs des groupes alkyles qui a leur tour affecte la stabilité des intermédiaires de la réaction. Du point de vue de la réactivité entre les groupes de composés, on observe la plus grande disparité entre les cétones et les bases de Mannich analogues ce qui est en accord avec la différence profonde de bioactivités entre ces groupes de composés.

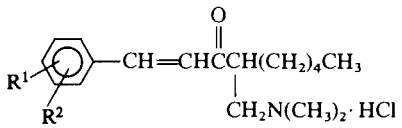
[Traduit par le journal]

Introduction

A large number of α,β-unsaturated ketones have a wide spectrum of biological activities (1) including antitumour properties (2–4). Some of the enones prepared in our laboratories and evaluated as candidate anticancer drugs were the styryl ketones **1** and their corresponding Mannich bases **2**, which showed a marked disparity in biological properties (2). While the ketones were either inactive or possessed only marginal potencies versus a tumour cell line in mice and were bereft of murine toxicity, the Mannich bases **2** were active in an *in vitro* screen, showed pronounced toxicities to mice, and certain of the compounds displayed significant potencies against tumours in mice. The question was therefore raised as to the reason for this dramatic change in biological activities produced by molecular modification of **1** to the Mannich bases **2**.



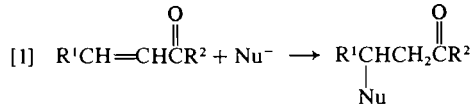
1 (R = H, Cl, $N(CH_3)_2$)



2 (R = H, Cl)

The biological activities of molecules containing the α,β-unsaturated carbonyl group have been attributed to reactivity towards cellular thiols (5–7). It was decided, therefore, to react certain members of series **1** and **2** with a model thiol, ethanethiol, under similar reaction conditions. A similar reactivity of **1** and **2** with the thiol would lead one to assume that other chemical or physicochemical parameters may be important in explaining the differences in bioactivities of **1** and **2**, while a marked increase in chemical reactivity of **2** would imply a greater reactivity for certain cellular nucleophiles.

Nucleophilic attack by anions on α,β-unsaturated carbonyl compounds, eq. [1], is known



[1] $R^1CH{=}CHCR^2 + Nu^- \longrightarrow R^1CHCH_2CR^2$ (Nu)

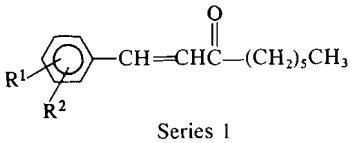
as the Michael reaction and has been extensively studied primarily because of its synthetic usefulness (8–12). To our knowledge there have been

[1]Author to whom correspondence should be addressed.

0008-4042/80/100984-08$01.00/0

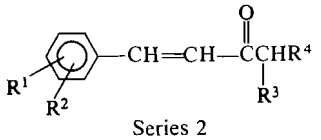
©1980 National Research Council of Canada/Conseil national de recherches du Canada

Can. J. Chem. Downloaded from www.nrcresearchpress.com by 210.87.254.5 on 09/05/12
For personal use only.



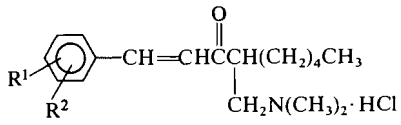
Series 1

3 $R^1 = R^2 = H$
4 R^1 = 2-Cl; $R^2 = H$
5 R^1 = 3-Cl; $R^2 = H$
6 R^1 = 4-Cl; $R^2 = H$
7 R^1 = 2-Cl; R^2 = 4-Cl
8 R^1 = 2-Cl; R^2 = 6-Cl
9 R^1 = 3-Cl; R^2 = 4-Cl
10 $R^1 = 4\text{-}CH_3$; $R^2 = H$
11 $R^1 = 4\text{-}OCH_3$; $R^2 = H$



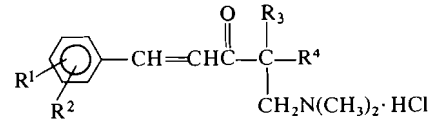
Series 2

12 $R^1 = R^2 = H$; $R^3 = CH_3$; $R^4 = (CH_2)_3CH_3$
13 R^1 = 3-Cl; R^2 = 4-Cl; $R^3 = CH_3$; $R^4 = (CH_2)_3CH_3$
14 $R^1 = R^2 = R^3 = R^4 = H$
15 R^1 = 3-Cl; R^2 = 4-Cl; $R^3 = R^4 = H$



Series 3

16 $R^1 = R^2 = H$
17 R^1 = 2-Cl; R^2 = 6-Cl
18 R^1 = 3-Cl; R^2 = 4-Cl



Series 4

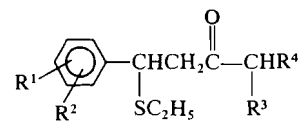
19 $R^1 = R^2 = H$; $R^3 = CH_3$; $R^4 = (CH_2)_3CH_3$
20 R^1 = 3-Cl; R^2 = 4-Cl; $R^3 = CH_3$; $R^4 = (CH_2)_3CH_3$
21 $R^1 = R^2 = R^3 = R^4 = H$
22 R^1 = 3-Cl; R^2 = 4-Cl; $R^3 = R^4 = H$

very few kinetic studies on the reaction of a neutral nucleophile on an α,β-unsaturated ketone (13, 14). Accordingly, the present investigation involved firstly the reaction of ethanethiol with a series of ring-substituted hexyl styryl ketones, **3–11**, series 1, as well as several styryl ketones possessing varying alkyl groups **12–15**, series 2, and secondly the reaction of some of the corresponding Mannich bases **16–21**, series 3 and 4, in buffered solution at several pH values in order to evaluate the electronic and stereochemical factors which govern the rate of the addition reaction.

Results

A series of α,β-unsaturated ketones **3–15** were prepared and in all cases they were shown to be the *E*-isomer. The rate constants, k_2, for the reactions of these compounds with ethanethiol in a buffered 50% acetonitrile–water[2] solvent at 37°C at several pH values are shown in Table 1.

It was found in all cases that the substrates were stable under the conditions employed in the absence of thiol and, as well, the adducts **23** were formed quantitatively and did not undergo elimination under the reaction conditions. The reactions were studied under pseudo first order conditions with the thiol present in large excess.



23 $R^1 = R^2 = H$, Cl; $R^3 = H$, CH_3; $R^4 = H$, $(CH_2)_4CH_3$, $(CH_2)_3CH_3$

A Hammett plot of log k/k_0 versus σ was carried out for the reaction of the styryl ketones **3–11** from which a ρ value of $+1.59 \pm 0.07$ was obtained. It should be noted that compounds with *ortho* substituents are less reactive than the analogous *para*-substituted isomer. The Hammett ρ value for the reaction of ethanethiol with **12** and **13** was calculated to be +1.56 and with **14** and **15** it was found to be +1.16.

Several Mannich bases corresponding to the styryl ketones **3–15** were prepared and their rate constants determined under the same conditions as for the ketones except that the increased reactivity of the Mannich salts relative to the ketones necessitated the use of a lower concentration of the thiol. The Mannich bases, like the ketones, were shown to be the *E*-isomers. The rate constants, k_2, are shown in Table 2.

All of the Mannich salts **16–20** were stable in the solvent system employed in the absence of thiol. However, in the case of **21**, elimination occurred at a significant rate in the absence of ethanethiol to give the corresponding olefin, eq. [2].

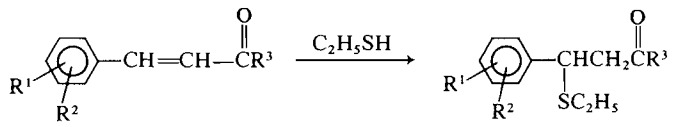
The reaction of the Mannich salts with ethanethiol in buffered solution was not as straightforward as the reaction of the corresponding ketones. While the ketones reacted smoothly with thiol to completion and an excellent pseudo

[2]This solvent was necessary in order to permit solubility of the reactants and buffer salts.

Can. J. Chem. Downloaded from www.nrcresearchpress.com by 210.87.254.5 on 09/05/12
For personal use only.

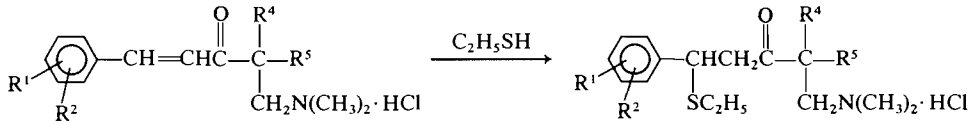
Can. J. Chem. Downloaded from www.nrcresearchpress.com by 210.87.254.5 on 09/05/12
For personal use only.

TABLE 1. Rate constants for the reaction of a series of α,β-unsaturated ketones with ethanethiol in buffered 50% acetonitrile–water at several pH values at 37°C



Compound No.	R^1	R^2	R^3	pH	10^4k_2 (M^{-1} s^{-1})
3	H	H	Hexyl	7.4	1.67
3	H	H	Hexyl	7.0	0.697
3	H	H	Hexyl	6.4	0.179
4	2-Cl	H	Hexyl	7.4	3.71
5	3-Cl	H	Hexyl	7.4	4.78
6	4-Cl	H	Hexyl	7.4	3.91
10	4-CH_3	H	Hexyl	7.4	0.788
11	4-OCH_3	H	Hexyl	7.4	0.483
7	2-Cl	4-Cl	Hexyl	7.4	8.46
8	2-Cl	6-Cl	Hexyl	7.4	4.58
9	3-Cl	4-Cl	Hexyl	7.4	12.3
9	3-Cl	4-Cl	Hexyl	7.0	5.44
9	3-Cl	4-Cl	Hexyl	6.4	1.15
12	H	H	1-Methylpentyl	7.4	0.814
13	3-Cl	4-Cl	1-Methylpentyl	7.4	6.98
14	H	H	Methyl	7.4	5.10
15	3-Cl	4-Cl	Methyl	7.4	25.2

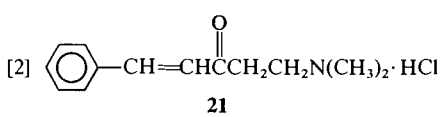
TABLE 2. Rate constants for the reaction of a series of Mannich bases **16–20** with ethanethiol in buffered 50% acetonitrile–water at several pH values at 37°C



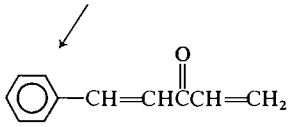
Compound No.	R^1	R^2	R^4	R^5	pH	$10k_2$ (M^{-1} s^{-1})
16	H	H	H	Pentyl	7.4	0.457
16	H	H	H	Pentyl	7.0	0.245
16	H	H	H	Pentyl	6.4	0.0995
17	2-Cl	6-Cl	H	Pentyl	7.4	1.00
18	3-Cl	4-Cl	H	Pentyl	7.4	1.90
18	3-Cl	4-Cl	H	Pentyl	7.0	1.02
18	3-Cl	4-Cl	H	Pentyl	6.4	0.273
19	H	H	CH_3	Butyl	7.4	0.303
20	3-Cl	4-Cl	CH_3	Butyl	7.4	1.30

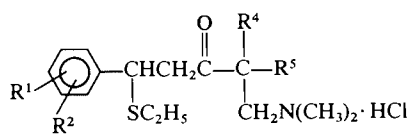
first order plot was obtained up to at least two half-lives, the corresponding addition reaction of the Mannich salts did not proceed to completion and the kinetic plot was linear to only approximately 30% of the reaction. As well, the thiol addition products **24** and **25** eliminated ethanethiol under the reaction conditions to give starting material. The addition product of the Mannich salt **16** eliminated C_2H_5SH to give **16** with a rate constant of $k_1 = 1.42 \times 10^{-4}$ s^{-1} at 37°C.

A Hammett plot of log k/k_0 versus σ was obtained for the reaction of the Mannich salts **16–18** and the ρ

[2] 

21





24 $R^1 = R^2 = H$
25 R^1 = 3-Cl; R^2 = 4-Cl

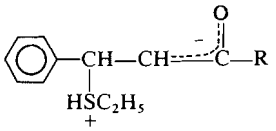
Can. J. Chem. Downloaded from www.nrcresearchpress.com by 210.87.254.5 on 09/05/12
For personal use only.

value was found to be $+1.01 \pm 0.13$. The Hammett value for the reaction of compounds **19** and **20** with ethanethiol was calculated to be +1.06.

Discussion

As Table 1 indicates, the rate constants for the thiol addition increase as the alkyl moiety of the ketones is varied from 1-methylpentyl to *n*-hexyl to methyl; i.e., the k_2 values for **12**, **3**, and **14** are 0.814, 1.67, and 5.10, respectively. Since it has been established that all the ketones exist exclusively as the *E*-isomer, molecular models reveal that steric variation of the alkyl group would be unlikely to affect the rate of attack of the thiol at the olefinic carbon atom. It is noteworthy that for the reaction of the ring-substituted ketones in series 1, the only point which fell significantly from the Hammett plot was that of the 2,6-dichloro compound, **8**. Presumably a steric effect is involved for reaction of this substrate with thiol.

It is reasonable to suggest that the alkyl groups to some degree affect the rate of reaction by an inductive effect. A consideration of the Taft σ^* values indicates that the 1-methylpentyl side chain is a better electron donor than the *n*-hexyl and methyl groups. The possible intermediate, **26**, in the addition process will consequently be of higher energy when the electron donating power of R is increased and hence the rate of reaction will be decreased.



26

It is unlikely, however, that the alkyl side chain R affects the rate of formation of **26** purely by an inaffects the rat of formation of **26** purely by an inductive effect. Undoubtedly, to some degree, the change in the R group leads to a change in the rate by means of a solvation effect. The larger alkyl groups will cause a greater disruption of solvent structure than methyl and also a reduction in solvent stabilization of the developing negative charge at the transition state.

Examination of the ρ values obtained for the three series of ketones where the alkyl group was changed is consistent with the effect of the R groups on the rate of reaction. The 1-methylpentyl and hexyl groups confer lower reactivity on the conjugated α,β-unsaturated ketones than the methyl group and hence the reactivity of the two former series of compounds will be more dependent on nuclear substituents and a larger ρ value would be predicted. The observed ρ values for the ketones in which the alkyl group is 1-methylpentyl, *n*-hexyl, and methyl were found to be 1.56, 1.59, and 1.16, respectively, and the results obtained are therefore in accord with the reactivity–selectivity principle (15, 16).

In order to gain an insight into the nature of the attacking nucleophile onto the α,β-unsaturated ketones, the second order rate constant for the addition reaction of **3** and **9** was determined at pH values of 7.4,[3] 7.0, and 6.4 (Table 1). It was found that the k_2 values for **3** and **9** at pH 7.0 and 6.4 were approximately 40% and 10% of the value obtained at pH 7.4. This observation may be rationalized in that by lowering the pH the concentration of ethanethiol anion, $C_2H_5S^-$, is also lowered and hence attack at the olefinic carbon is retarded.

A comparison of the rate constants for addition to the ketones, Table 1, with the corresponding rate constants for addition to the Mannich salts, Table 2, shows that the Mannich bases are considerably more reactive to thiol addition than the related ketones. Since the nitrogen of the Mannich salt will be significantly protonated at the pH values of the present experiments, the protonated ammonium group will inductively stabilize the intermediate of addition **26** leading to a faster reaction. It should be noted that for the Mannich salts **16** and **19** where R^3 is changed from hydrogen to methyl, a rate decrease is observed, Table 2, in agreement with the observations noted for the corresponding ketones. It is reasonable to expect that solvation effects are important for the reaction of the Mannich bases, as for the ketones. Such effects probably account, to a significant extent, for the difference of reactivity noted for the ketones and their corresponding Mannich bases.

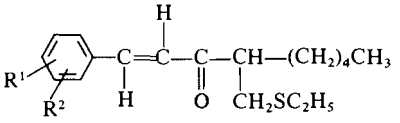
The ρ values for the two Mannich systems, namely series 3, compounds **16–18**, and series 4, compounds **19** and **20**, were found to be 1.01 and 1.06, respectively. The decrease in ρ value when the electron-withdrawing ammonium group is placed in the alkyl side chain compared to that for the analogous ketones is reasonable since this electron-withdrawing group increased the rate of reaction and hence the selectivity, as measured by ρ, is decreased.

The Mannich salts, like the ketones, were less reactive with ethanethiol when the pH of the buffered solution was lowered. As the results in Table 2 indicate, the reactivity of the thiol with two of the Mannich bases **16** and **18** at pH 7.0 and 6.4 was approximately 50% and 20%, respectively, of that of the rate at pH 7.4. This would support the view of

[3]Experiments were initially performed at pH 7.4 in order to simulate physiological conditions.

Can. J. Chem. Downloaded from www.nrcresearchpress.com by 210.87.254.5 on 09/05/12
For personal use only.

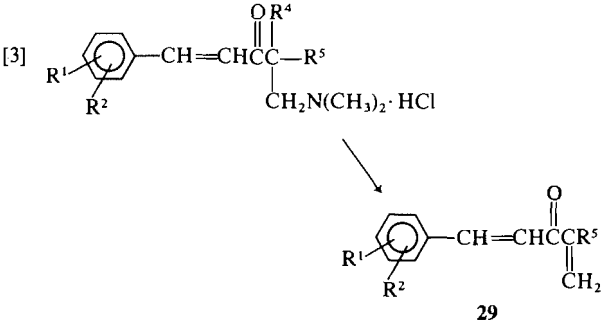
the ethylthio anion, $C_2H_5S^-$, being the nucleophile in the addition reaction of the styryl ketones as well as the related Mannich bases. The literature describes the reaction of thiolate ions with unactivated aryl halides in hexamethylphosphoramide (17) but no evidence of nucleophilic aromatic substitution by the $C_2H_5S^-$ anion in the case of the ring-chlorinated ketones or Mannich bases was found. In addition, while the possibility exists of the direct displacement of the onium group in the Mannich salts by thiol to produce **27** and **28**, this did not occur in the present study.



27 $R^1 = R^2 = H$
28 R^1 = 3-Cl; R^2 = 4-Cl

The possible role of the nitrogen atom of the Mannich bases acting as a nucleophile with intramolecular attack of the α,β-unsaturated group must be considered. This effect would be more pronounced at higher pH values and, indeed, the rate is greater for reactions carried out at pH 7.4 rather than at 6.4. That the amine nitrogen is not involved as a nucleophile, however, is shown by the fact that the quaternary ammonium analogue of Mannich salt **18**, prepared by quaternization of the Mannich base with methyl halide, was only slightly less reactive than **18**; i.e., $k_2 = 0.0801$ and 0.190 for the quaternary ammonium compound and **18**, respectively.

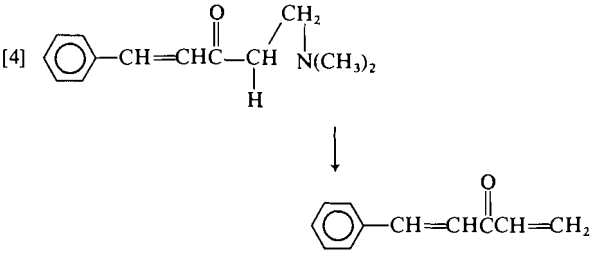
As indicated previously, the reaction of the Mannich salts with thiol is more complex than the corresponding reaction with the ketones. While the ketone reaction was straightforward and proceeded to completion, the reaction of the Mannich bases with thiol gave a linear kinetic plot to only 30% reaction and this process did not reach completion. A consideration of the possible elimination reaction of the Mannich salts when $R^4 = H$ to give the alkene



29

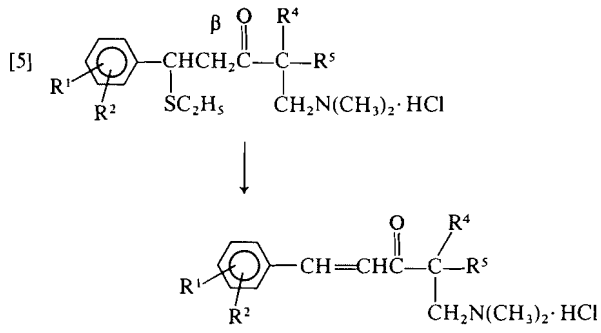
29 must be considered, eq. [3]. That this elimination process is not significant is shown by the fact that the Mannich salts, where $R^4 = H$ and CH_3, have similar reactivities and behave kinetically in an identical manner. When $R^4 = CH_3$, elimination to give **29** is not possible.

It has been proposed (18, 19) that elimination from Mannich salts proceeds intramolecularly with the free amine nitrogen acting as the abstracting base. Even though the amine nitrogen would be significantly protonated under the pH conditions of the current study, it was found that the Mannich salt **21**, where $R^4 = R^5 = H$, underwent elimination at a very fast rate in the absence of thiol, eq. [2], whereas **16** with $R^4 = H$ and R^5 = pentyl was stable under the same conditions. Presumably, the ability of the nitrogen base to remove the hydrogen would be more favoured sterically when $R^4 = R^5 = H$, eq. [4], if the reaction proceeds intramolecularly.



The addition of thiol to the Mannich salts did not proceed to completion but, in fact, equilibrium was attained. The addition product from the reaction of salt **16** with thiol eliminated to give the α,β-unsaturated carbonyl compound **16**, i.e., $k_r = 1.42 \times 10^{-4}$ s^{-1}. The equilibrium constant $K = k_2/k_r$ is therefore 3.2×10^2 M^{-1}. The reversal of the addition process is more favourable for the Mannich salts than for the ketone series possibly due to the increased acidity of the β-hydrogen when the strong electron-withdrawing ammonium group is incorporated into the molecule, eq. [5].

In conclusion, these studies indicate that dramatic differences in avidity of a model nucleophile, ethanethiol, exist between styryl ketones and the related Mannich bases. Thus the five Mannich bases **16–20** react on average approximately 240 times more quickly than the analogous ketones **3**, **8**, **9**, **12**, and **13**, respectively, and this differential in chemical reactivity may explain the marked difference in bioactivities between the two series of compounds. It should be noted, however, that the rate of attack of ethanethiol by the Mannich bases is appreciably slower than the rate of attack by an established SH-alkylator, *N*-ethylmaleimide.



Experimental

Nuclear magnetic resonance spectroscopy was carried out using a Varian T-60 spectrometer by running the spectrum of the compound in deuterochloroform, unless otherwise stated, at room temperature with tetramethylsilane as the internal standard. Infrared spectra were run as films using a Beckman AccuLab 4 machine. Ultraviolet spectroscopy was undertaken utilizing a Gilford 250 spectrophotometer. Mass spectra were determined with an MS-12 spectrometer by Christine Nicholaichuk, Department of Chemistry and Chemical Engineering, University of Saskatchewan, Saskatoon. Melting points and boiling points are uncorrected. Elemental analyses were obtained by R. E. Teed, Department of Chemistry and Chemical Engineering, University of Saskatchewan, Saskatoon. Organic extracts were washed with water, dried over anhydrous magnesium sulphate, and the solvent removed *in vacuo* with a rotary film evaporator. Fisher reagent grade acetonitrile was dried (anhydrous calcium chloride) and distilled prior to use while the *N*-ethylmaleimide employed in this study was the gold label variety purchased from Aldrich. Thin-layer chromatography was undertaken using Eastman chromatogram alumina sheets of 100 μm thickness.

Syntheses of Nuclear Substituted Styryl Ketones (3–15) and Related Mannich Bases (16–22)

Compounds **3**, **4**, **6–9**, and **11** were prepared by the literature procedure (20), compound **5** by the previously reported method (2), compounds **12** and **13** were obtained by the method described earlier (21), and compound **14** by the literature method (22). The Mannich bases **16–18** were prepared by the literature procedure (23), **19** and **20** by a previously described method (21), and **21** by the literature method (24). The quaternary ammonium compound derived from the free base of **18** was prepared according to the literature procedure (22). The remaining compounds were prepared as follows and the physical data are given in Table 3.

1-(*p*-Methylphenyl)-1-nonen-3-one, **10**, was prepared by the literature procedure (20), crystallizing from petroleum ether (bp 30–60°C), as shiny, colourless plates.

1-(3,4-Dichlorophenyl)-1-buten-3-one, **15**, was prepared as follows. A mixture of 3,4-dichlorobenzaldehyde (0.5 g, 0.003 mol) and 1-triphenylphosphoranylidene-2-propanone (1.0 g, 0.003 mol) in benzene (50 mL) was heated under reflux for 24 h. Evaporation of the solvent produced a semisolid which was triturated with ether. The solid was removed by filtration, and evaporation of the ether gave a yellow oil which solidified on cooling. Recrystallization of the solid from petroleum ether (bp 30–60°C) gave **15** as beige needles.

1-(3,4-Dichlorophenyl)-5-dimethylamino-1-penten-3-one hydrochloride **22** was prepared from **17** by the literature method (23) and crystallized from acetone as pale yellow granular crystals. No melting point was obtained as the compound decomposed on heating.

Preparation of the Thiol Adducts of Nuclear Substituted Styryl Ketones 23, and Related Mannich Bases 24, 25

Thiol adducts of the unsaturated ketones **3**, **4**, **6**, **7–9**, and **12–15** were prepared in quantitative yield and the structures verified by elemental analysis.[4] Details of the preparation of one of the compounds, **23** ($R^1 = R^2 = R^3 = H$; $R^4 = (CH_2)_5CH_3$), exemplifies the generality of this reaction.

A mixture of 1-phenyl-1-nonen-3-one, **3** (20 g, 0.09 mol) and ethanethiol (5.6 g, 0.09 mol) in benzene (75 mL) containing two to three drops of piperidine was heated under reflux for 24 h. Evaporation of the solvent gave a yellow oil, which on distillation produced 1-ethylthio-1-phenyl-nonan-3-one, as a pale yellow oil. Mass spectrum *m/e*: 278 (M^+), 218, 113.

The Mannich bases **16** and **18** were converted to the corresponding thiol adducts by the following general method. A mixture of the Mannich bases as the hydrochloride salts (0.01 mol) and ethanethiol (0.015 mol) in ethanol (50 mL) containing two to three drops of piperidine was heated at 40°C for 48 h. The solvent was removed and, on cooling, the resultant solid was triturated with petroleum ether (bp 30–60°C) to give waxy yellow solids which were recrystallized from acetone as fluffy colourless crystals producing **24** and **25**. The physical data for these two compounds is found in Table 3.

Syntheses of 4-Ethylthiomethyl-1-phenyl-1-nonen-3-ones 27, 28

The following general method was employed in preparing these thio derivatives from **16** and **18**, respectively. A mixture of the Mannich base (0.01 mol) and ethanethiol (0.015 mol) was heated under reflux in xylene (50 mL) for 5 h. The solvent was removed, giving a viscous oil which was distilled producing the desired products **27** and **28** as pale yellow oils. The physical data for these two compounds are found in Table 3.

Determination of the Rates of Reaction of Ethanethiol with the Nuclear Substituted Styryl Ketones 3–21

The ketones **3–15** were reacted with ethanethiol under the following conditions. The appropriate ketone (10^{-3} *M*) was dissolved in approximately 23 mL of the acetonitrile–phosphate buffer in a 25 mL volumetric flask heated in a water bath at 37 ± 0.1°C. At the commencement of the reaction ($T = 0$), ethanethiol (300 μL) was added and the volume of the reaction mixture adjusted to 25 mL. At regular time intervals, a 1.0 mL aliquot was diluted to 10.0 mL with 50% aqueous ethanol and 1.0 mL of this solution was further diluted to 25 mL. Absorbance readings of this solution were taken at the appropriate absorption maxima of the ketone.

In the case of the Mannich bases **16–20**, the appropriate compound as the hydrochloride salt (10^{-3} *M*) was dissolved in the acetonitrile–phosphate buffer mixture and the volume adjusted to 25.0 mL. In a separate flask, ethanethiol (100 μL) was dissolved in the same solvent and diluted to 25.0 mL. A portion of the Mannich base salt solution (1.0 mL) was placed in 25.0 mL volumetric flask heated at 37°C in a water bath. At the commencement of the reaction, ethanethiol solution (1.0 mL) was added to the heated solution and the volume adjusted to 25.0 mL. At regular time intervals, aliquot portions (1.0 mL) of the mixture were diluted to 10.0 mL with 50% aqueous ethanol and the absorbance recorded at the absorbance maxima of the

[4]Details of the boiling points and elemental analyses of these thiol adducts are available at a nominal charge from the Depository of Unpublished Data, CISTI, National Research Council of Canada, Ottawa, Ont., Canada K1A 0S2.

Can. J. Chem. Downloaded from www.nrcresearchpress.com by 210.87.254.5 on 09/05/12
For personal use only.

TABLE 3. Physical data of some styryl ketones and related Mannich bases and thio derivatives

Compound No.	Melting point (°C) or boiling point (°C/Torr)	Yield (%)	Elemental analyses Calculated (%) C	Calculated (%) H	Found (%) C	Found (%) H
10	46–47	43	83.42	9.63	82.91	9.72
15[a]	55	44	55.84	3.75	56.58	3.71
22[b]	dec.	52	50.59	5.23	50.22	5.20
24[c]	118–119.5	26	64.57	9.21	65.05	9.25
25[d]	126–127	22	54.48	7.32	53.92	7.28
27[e]	181–183/0.85	38	74.43	9.02	73.49	9.20
28[f]	174–180/0.5	29	60.16	6.73	60.99	6.66

[a]Nuclear magnetic resonance δ: 7.70–7.30 (4H, m, C_6H_3, C_1H), 6.70 (1H, d, C_2H), 2.40 (3H, s, C_4H_3).
[b]*Anal.* calcd. for $C_{13}H_{16}Cl_3NO$: N 4.54; found: N 4.53; nmr (CF_3COOH) δ: 7.78–7.30 (4H, m, C_6H_3 and C_1H), 6.85 (1H, d, C_2H), 3.50 (4H, s, C_4H_2 and C_5H_2), 3.02 (6H, d, $N(CH_3)_2$).
[c]*Anal.* calcd. for $C_{20}H_{34}ClNOS$: N 3.77; found: N 3.79; nmr δ: 7.20 (5H, s, C_6H_5), 4.39 (1H, t, C_1H), 3.85–2.00 (13H, m, C_2H_2, C_4H, CH_2N, $N(CH_3)_2$, S—CH_2), 1.70–0.70 (14H, m, C_5H_{11}, SCH_2CH_3).
[d]Anal. calcd. for $C_{20}H_{32}Cl_3NOS$: N 3.18; found: N 3.22; nmr δ: 7.60–7.30 (3H, m, C_6H_3), 4.38 (1H, t, C_1H), 3.79–2.10 (13H, m, C_2H_2, C_4H, CH_2N, $N(CH_3)_2$, S—CH_2), 1.70–0.63 (14H, m, C_5H_{11}, SCH_2CH_3).
[e]Infrared (film): 1700, 1670 (C=O), 1620, 985 cm^{-1} (olefinic group); peak at 2750 cm^{-1} ($HN(CH_3)_2$) absent; nmr δ: 7.72–7.20 (6H, m, C_6H_5, C_1H), 6.78 (1H, d, C_2H), 3.20–2.10 (5H, m, C_4H, $CH_2SC_2H_5$, SCH_2CH_3), 2.10–0.75 (14H, m, C_5H_{11}, SCH_2CH_3).
[f]The infrared spectrum was similar to **27**; nmr δ: 7.53–7.00 (4H, m, C_6H_3, C_1H), 6.82 (1H, d, C_2H), 2.82–2.00 (5H, m, C_4H, $CH_2SC_2H_5$, SCH_2CH_3), 1.95–0.65 (14H, m, C_5H_{11}, SCH_2CH_3).

Mannich base hydrochlorides. The kinetic data were obtained during the early stages of the reaction and the optical density at infinity was taken as zero, assuming the reaction proceeded to completion. The rate constants obtained by this procedure agreed very well with the rate constants determined by the initial slope method and hence can be ascribed to the forward reaction.

The kinetic runs were carried out in triplicate under pseudo first order conditions. The best fit of the line to the points was obtained by a least-squares treatment of the data using an HP 2000 computer. The second order rate constants, k_2, were obtained by dividing the values of k_1 by the concentration of ethanethiol. The acetonitrile–phosphate buffer mixtures were prepared as follows. A solution of monobasic sodium phosphate monohydrate (9.30 g) in double distilled water was adjusted to 1000 mL (solution A) and a solution of dibasic sodium phosphate heptahydrate was prepared by dissolving the salt (17.88 g) in water and diluting to 1000 mL (solution B).

A mixture of acetonitrile (500.0 mL) and solution A (280.0 mL) was placed in a 1000 mL volumetric flask and solution B was added to 1000 mL. The pH of the resultant solution was 7.40. The acetonitrile buffer solutions of 7.00 and 6.40 were prepared in a similar manner, except that the amounts of solution A were 389.0 and 490.0 mL respectively. These buffer solutions were stable for a period of at least two months. No sodium chloride was added to these solutions due to its preventing complete solubility of the ketones.

The products obtained by reacting ethanethiol with the styryl ketones and Mannich bases were identified as follows. Reaction between 1-phenyl-1-nonen-3-one and ethanethiol occurred under identical conditions to that of the kinetic procedure. The mixture was extracted with chloroform and removal of the solvent produced an oil shown by infrared and nmr spectroscopy as well as mass spectrometry to be 1-ethylthio-1-phenyl-nonan-3-one.

Reaction of ethanethiol and 1-(3,4-dichlorophenyl)-4-dimethylaminomethyl-1-nonen-3-one hydrochloride, **18**, occurred as described previously whereby approximately 30% of the Mannich base had reacted. The reaction mixture was extracted with chloroform and evaporation of the solvent *in vacuo* produced an oil which was examined by thin-layer chromatography. Using petroleum ether (bp 60–80°C) as the developing solvent, four spots with R_f values of 0.41, 0.62, 0.68, and 0.80 were observed. Under these conditions, 1-(3,4-dichlorophenyl)-4-dimethylaminomethyl-1-ethylthio-1-nonane, **25**, gave an R_f value of 0.68 and the hydrochloride salt a value of 0.62. The unreacted Mannich free base had an R_f value of 0.80 and the hydrochloride salt one of 0.41 under these conditions, while both 1-(3,4-dichlorophenyl)-4-methylene-1-nonen-3-one, **29** (R^1 = 3-Cl; R^2 = 4-Cl, $R^5 = (CH_2)_4CH_3$), and 1-(3,4-dichlorophenyl)-4-ethylthiomethyl-1-nonen-3-one, **28**, move with the solvent front. In order to confirm the absence of these latter two compounds, thin-layer chromatography using petroleum ether (bp 30–60°C) of the reaction product was undertaken and four spots with R_f values of 0.26, 0.32, 0.38, and 0.47 were observed. Under these conditions, 1-(3,4-dichlorophenyl)-4-methylene-1-nonen-3-one and 1-(3,4-dichlorophenyl)-4-ethylthiomethyl-1-nonen-3-one had R_f values of 0.54 and 0.36, respectively, and the unreacted free Mannich base and hydrochloride salt had R_f values of 0.47 and 0.26, respectively, while the free Michael adduct and its hydrochloride salt had R_f values of 0.38 and 0.32, respectively.

An examination of the stability of the reactants and products was undertaken. The ketones **3**, **9**, **12–15**, as well as the Mannich base hydrochlorides **16–20**, were dissolved in the acetonitrile–phosphate buffer solution, pH 7.40, and heated at 37°C for the length of the period of the reaction. No change in absorbance was observed. In addition, the thiol adducts of the ketone, **23**, were found to be stable under the reaction conditions. The thiol adduct of the Mannich base, **25**, reverted slowly to the precursor Mannich base, **18**, under the same conditions as the reaction of the Mannich bases with ethanethiol. The k_1 value for this adduct was found to be $1.42 \times 10^{-4}\ s^{-1} \pm 5.78\%$ by following the increasing absorbance of the Mannich base.

The order of reaction between ethanethiol and these enones under the experimental conditions employed was investigated. Three different concentrations of the styryl ketone **3** (2.28, 3.87, and 5.75×10^{-3} *M*) were reacted with the same concentration of ethanethiol, namely 1.62×10^{-1} *M*, while three different concentrations of the Mannich base **16** (1.08, 1.85, and 2.63×10^{-4} *M*) were each reacted with ethanethiol (6.49×10^{-3} *M*). The order of reaction of both compounds with respect to ethanethiol was shown to be one. Similarly, three different concentrations of ethanethiol (1.62, 2.16, and 2.70×10^{-1} *M*) were reacted with **3** (5.55×10^{-3} *M*) and three different concentrations of ethanethiol (6.49, 7.57, and 8.65×10^{-4} *M*) were reacted with **18** (2.10×10^{-5} *M*) and the order of reaction was likewise shown to

Can. J. Chem. Downloaded from www.nrcresearchpress.com by 210.87.254.5 on 09/05/12
For personal use only.

be one. In all of these experiments, the concentration of thiol was at least twentyfold in excess.

N-Ethylmaleimide was shown to be stable in the acetonitrile–phosphate buffer mixture, pH 7.40, over a 24-h period at 37°C. Reaction of *N*-ethylmaleimide with ethanethiol under the reaction conditions employed for thiol reaction with the ketones **3–15** showed that the reaction proceeded too fast to measure in the same manner as previously undertaken. However the reduction in the absorption maxima of *N*-ethylmaleimide at 300.5 nm was observed (25) and indicated that the reaction was at least 97% complete within 64 s.

Acknowledgement

The authors thank the Medical Research Council of Canada for an operating grant to J. R. Dimmock (MA 5538).

1. J. R. DIMMOCK and M. C. L. WONG. Can. J. Pharm. Sci. **11**, 35 (1976).
2. J. R. DIMMOCK and W. G. TAYLOR. J. Pharm. Sci. **64**, 241 (1975).
3. O. K. KABIEV and S. M. VERMENICHEV. Izv. Akad. Nauk Kaz. SSR, Ser. Biol. **9**, 72 (1971); Chem. Abstr. **75**, 47091u (1971).
4. A. FURST, W. C. CUTTING, and R. H. DREISBACH. Stanford Med. Bull. **12**, 190 (1954); Chem. Abstr. **49**, 515e (1955).
5. D. A. KOECHEL, S. A. SMITH, and E. J. CAFRUNY. J. Pharmacol. Exp. Ther. **203**, 272 (1977) and references cited therein.
6. C. H. LANTZ, J. LARNER, R. M. SCHUBERT, G. A. HOWIE, and S. M. KUPCHAN. Cancer Biochem. Biophys. **1**, 229 (1976).
7. R. L. HANSON, H. A. LARDY, and S. M. KUPCHAN. Science, **168**, 328 (1970).
8. N. WANG, S. SU, and L. TSEI. Tetrahedron Lett. **13**, 1121 (1979).
9. G. DIONNE and C. H. R. ENGEL. Can. J. Chem. **56**, 419 (1978).
10. H. HART, B. CHEM, and M. JEFFARES. J. Org. Chem. **44**, 2722 (1979).
11. G. A. KRAUS and J. O. PEZZANITE. J. Org. Chem. **44**, 2480 (1979).
12. K. HERMANN and H. WYNBERG. J. Org. Chem. **44**, 2238 (1979).
13. C. E. LOUGH, D. J. CURRIE, and H. L. HOLMES. Can. J. Chem. **46**, 771 (1968).
14. R. B. PRITCHARD, C. E. LOUGH, D. J. CURRIE, and H. L. HOLMES. Can. J. Chem. **46**, 775 (1968).
15. A. PROSS. Adv. Phys. Org. Chem. **14**, 69 (1977).
16. D. J. MCLENNAN. Tetrahedron, **34**, 2331 (1978).
17. P. COGOLLI, F. MAIOLO, L. TESTAFERRI, M. TINGOLI, and M. TIECCO. J. Org. Chem. **44**, 2642 (1979).
18. J. A. MOLLICA, J. B. SMITH, I. M. NUNES, and H. K. GOVAN. J. Pharm. Sci. **59**, 1770 (1970).
19. P. CARSKY, P. ZUMAN, and V. HORAK. Coll. Czech. Chem. Commun. **29**, 3044 (1964).
20. P. J. SMITH, J. R. DIMMOCK, and W. G. TAYLOR. Can. J. Chem. **50**, 871 (1972).
21. J. R. DIMMOCK and L. M. SMITH. J. Pharm. Sci. In press.
22. J. R. DIMMOCK, N. W. HAMON, K. W. HINDMARSH, D. G. MILLS, L. E. NEGRAVE, G. H. RANK, and A. J. ROBERTSON. J. Pharm. Sci. **65**, 482 (1976).
23. J. R. DIMMOCK and W. G. TAYLOR. J. Pharm. Sci. **63**, 69 (1974).
24. J. R. DIMMOCK, A. M. QURESHI, L. M. NOBLE, P. J. SMITH, and H. A. BAKER. J. Pharm. Sci. **65**, 38 (1976).
25. J. D. GREGORY. J. Am. Chem. Soc. **77**, 3922 (1955).

Can. J. Chem. Downloaded from www.nrcresearchpress.com by 210.87.254.5 on 09/05/12
For personal use only.

Standard electrode potentials of the chloranil electrode in formamide at different temperatures

UPENDRA NATH DASH AND SURENDRA KUMAR NAYAK
Department of Chemistry, G. M. College, Sambalpur (Orissa), India

Received September 13, 1979

UPENDRA NATH DASH and SURENDRA KUMAR NAYAK. Can. J. Chem. **58**, 992 (1980).

From the emf measurements of the buffered cell

$$Ag,AgCl/KCl(m_3),KOBz(m_2),HOBz(m_1),chloranil/Pt$$

the standard potentials of the chloranil electrode have been determined in formamide at 15, 25, 35, and 45°C. The standard molal potential of the chloranil electrode has been expressed through the equation

$$E_m^0 = (3.8042 \pm 0.0001) - (10.538 \pm 0.0003) \times 10^{-2}T + (183.455 \pm 0.001) \times 10^{-4}T \ln T - (61.049 \pm 0.006) \times 10^{-6}(T^2/2)$$

The standard thermodynamic quantities, ΔG^0, ΔH^0, ΔS^0, and ΔC_p^0 for the electrode reaction have been calculated from the standard molal potential, E_m^0 of the electrode at these temperatures.

UPENDRA NATH DASH et SURENDRA KUMAR NAYAK. Can. J. Chem. **58**, 992 (1980).

On a déterminé les potentiels normaux d'une électrode de chloranil dans le diméthylformamide à 15, 25, 35 et 45°C à partir des mesures de la fem d'une cellule tamponée de

$$Ag,AgCl/KCl(m_3),KOBz(m_2),HOBz(m_1),chloranil/Pt$$

Le potentiel molaire normal de l'électrode de chroranil peut être représenté par l'équation:

$$E_m^0 = (3.8042 \pm 0.0001) - (10.538 \pm 0.0003) \times 10^{-2}T + (183.455 \pm 0.001) \times 10^{-4}T \ln T - (61.049 \pm 0.006) \times 10^{-6}(T^2/2)$$

On a calculé les quantités thermodynamiques ΔG^0, ΔH^0, ΔS^0, et ΔC_p^0 pour la réaction à l'électrode à partir du potentiel molaire normal, E_m^0, de l'électrode à ces températures.

[Traduit par le journal]

Introduction

A survey of the literature (1, 2) shows that the chloranil electrode in conjunction with the hydrogen or the silver – silver chloride electrodes has been studied in aqueous, mixed aqueous, and non-aqueous media at 25°C, and the standard potential of this electrode was reported in water (0.664 V), 50% aqueous alcohol (0.664 V), glacial acetic acid (0.680 V), and 50% aqueous dioxane (0.715 V) at this temperature. But the original study of the chloranil electrode by Conant *et al.* (1) led to the assumption that the potential of the saturated chloranil electrode against the hydrogen electrode is independent of the solvent, and for some time this might be a plausible factor for its study in other solvents. However, later studies reporting different values for the potential of this electrode in glacial acetic acid and in 50% aqueous dioxane indicated invalidity of this assumption and inspired the present authors to study this electrode in formamide, a solvent closely resembling water from the point of dielectric constant and viscosity.

The cells without liquid junction involving silver – silver chloride and quinhydrone electrodes have been widely used in formamide (3) for the determination of ionization constants of various acids in this solvent. The acetic acid – acetate and benzoic acid – benzoate buffer cells have been successfully employed in this solvent for evaluation of the standard potentials of the silver – silver halides (4) and the silver – silver thiocyanate electrodes (3*e*) by using the quinhydrone electrode as the standard reference half-cell in these buffer cells.

In the present study, we have employed the benzoic acid – benzoate buffer cell involving the silver – silver chloride and chloranil electrodes, and accordingly the cell studied was

[A] $Ag,AgCl/KCl(m_3),KOBz(m_2),HOBz(m_1),chloranil/Pt$

Experimental

The preparation of silver – silver chloride electrode has been described earlier (5). Chloranil electrodes were prepared according to Hall *et al.* (6). Chloranil was a "Loba Chemie Wien – Fischamend Austranal-Praparate" sample. The cell vessels are of the type recommended by Harned and Wright (7).

Benzoic acid, potassium benzoate, and potassium chloride were the same samples as used in earlier studies (3*e*). Formamide (B.D.H., L.R.) was purified as described elsewhere (8).

Solutions for emf measurements were prepared by dissolving

0008-4042/80/100992-04$01.00/0
©1980 National Research Council of Canada/Conseil national de recherches du Canada

Can. J. Chem. Downloaded from www.nrcresearchpress.com by 210.87.254.40 on 09/05/12
For personal use only.

Can. J. Chem. Downloaded from www.nrcresearchpress.com by 210.87.254.40 on 09/05/12
For personal use only.

the appropriate weighed amounts of salts and acid in known weights of formamide.

The setting up of the cell [A] was similar to that of the cell involving the quinhydrone and silver – silver chloride electrodes (*3a*) except that the saturated solution of chloranil – formamide salts and acid was warmed to 50°C in order to have an adequate saturation of chloranil and then cooled to room temperature (*6c*) and subsequently transferred to the chloranil compartment of the cell in which the platinized platinum electrode had previously been placed under a dry nitrogen atmosphere. The silver – silver chloride electrode was placed in the appropriate cell compartment which had first been thoroughly rinsed and then filled with formamide solution which was previously warmed to 50°C and cooled to room temperature with a view to having an identical experimental condition with that of the chloranil solution. After filling, the cell was kept in the thermostat at the required temperature with an accuracy of ±0.1°C.

Electromotive force measurements were made with a Bajaj (India) potentiometer in conjunction with a dc galvanometer (OSAW) and a Western standard cell (Muirhead and Co., England). The reproducibility was of the order of ±0.2 mV.

Results and Discussion

A summary of emf data of the buffered cell was presented in Table 1 along with other data at 15, 25, 35, and 45°C.

Standard potential of the chloranil electrode from the study of the buffered cell was found by almost an identical procedure as adopted in previous studies (*3e*, 4).

The auxiliary function, $E_m^{0\prime}$, was calculated with the help of the equation

$$[1]\quad E_m^{0\prime} = E_m^0(\mathrm{Ag/AgCl}) - E + 2.3026(RT/F) \times [\mathrm{p}K_a - \log(m_1 m_3/m_2)] = E_m^0 - 2.3026(RT/F)\log[\gamma(\mathrm{HOBz}) \times \gamma(\mathrm{Cl^-})/\gamma(\mathrm{OBz^-})] = E_m^0 + f(I)$$

and the standard molal potential, E_m^0, of the chloranil electrode was found by method of extrapolating (9–11) $E_m^{0\prime}$ (Fig. 1) to zero ionic strength, $I = 0$ (here, $I = m_2 + m_3$), as $\log[\gamma(\mathrm{HOBz})\gamma(\mathrm{Cl^-})/\gamma(\mathrm{OBz^-})]$ tends to zero. The symbols in eq. [1] have their usual significance. The values of E_m^0(Ag/AgCl) and that of pK_a for benzoic acid needed for calculation are known in formamide at the temperatures under investigation (*3b*, *3e*, 12).

The values of E_m^0 of the chloranil electrode, thus obtained are presented in Table 1. The values of the standard deviations calculated by the least-squares method are also included in Table 1. The values for the standard potential on the molar (E_c^0) and mole-fraction (E_N^0) scales have also been calculated at experimental temperatures by the usual equations (13)

$$[2]\quad E_N^0 = E_m^0 - 2(2.3026RT/F)\log(1000/M)$$

and

$$E_c^0 = E_m^0 + 2(2.3026RT/F)\log\rho$$

where M and ρ are the molecular weight and density, respectively, of formamide. The variation of the standard potential in molal (E_m^0), molar (E_c^0), and mole-fraction (E_N^0) scales with temperature has been expressed through the equations of the type,

$$[3]\quad E_x^0 = A + BT + CT\ln T + DT^2/2$$

where x is m, c, or N, and T is the temperature in K. The parameters A, B, C, and D in eq. [3] on different scales are presented in the following chart along with their standard deviations calculated by least-squares method.

x	A	-10^2B	10^4C	-10^6D
m	3.8042±0.0001	10.538±0.0003	183.455±0.001	61.049±0.006
c	12.0532±0.0003	41.932±0.002	733.944±0.014	244.738±0.707
N	3.8265±0.0001	10.608±0.001	183.486±0.002	60.559±0.828

A comparison of the standard potential of the chloranil electrode obtained in formamide at 25°C (0.8360 V) with those reported in water (0.664 V), 50% aqueous alcohol (0.664 V), glacial acetic acid (0.680 V), and 50% aqueous dioxane (0.715 V) at this temperature shows that the E_m^0 value is higher in formamide than in other solvents.

It is thus clear that these differences in the E_m^0 values obtained in different media are due to the fact that tetrachlorohydroquinone is solvated in certain solvents and any change in E_m^0 value on passing from water or other solvents to formamide will be due to variation of solvation. It is, however, known (2) that in glacial acetic acid tetrachlorohydroquinone forms the solid solvate $C_6Cl_4(OH)_2 \cdot 2CH_3COOH$, while in 50% aqueous dioxane it forms the solid solvate $C_6Cl_4(OH)_2 \cdot C_4H_8O_2$. Unfortunately, the present work does not provide a means of examining

TABLE 1. Summary of emf data of the buffered cell

T (°C)	$m_1 \times 10^2$ (mol kg^{-1})	$m_2 \times 10^2$ (mol kg^{-1})	$m_3 \times 10^2$ (mol kg^{-1})	$-E$ (V)	$I \times 10^2$ (mol kg^{-1})	$E_m^{0\prime}$ (V)	E_m^0 (V)
15	1.425	1.080	2.476	0.1599	3.556	0.8332	
	1.334	1.057	2.796	0.1626	3.853	0.8340	
	1.398	1.094	2.843	0.1619	3.937	0.8326	
	1.194	0.993	3.471	0.1639	4.464	0.8311	
	1.367	1.014	3.880	0.1676	4.894	0.8292	0.8432±0.0004
	1.361	1.161	4.596	0.1667	5.757	0.8276	
	1.346	1.096	5.012	0.1694	6.108	0.8270	
	1.334	1.017	5.317	0.1720	6.334	0.8265	
	1.353	1.104	5.521	0.1704	6.625	0.8257	
	1.346	1.063	5.809	0.1714	6.872	0.8246	
25	1.780	1.296	2.120	0.1652	3.416	0.8305	
	1.732	1.314	2.862	0.1666	4.176	0.8253	
	1.612	1.299	3.842	0.1737	5.141	0.8264	
	1.828	1.400	5.785	0.1802	7.181	0.8215	
	1.794	1.400	6.629	0.1823	8.029	0.8201	0.8360±0.0006
	1.799	1.443	7.274	0.1824	8.717	0.8186	
	1.879	1.501	8.293	0.1848	9.794	0.8175	
	1.814	1.350	8.709	0.1849	10.059	0.8145	
	1.833	1.357	9.352	0.1881	10.709	0.8157	
	1.875	1.457	10.389	0.1853	11.846	0.8115	
35	1.191	0.935	2.648	0.1482	3.583	0.8230	
	1.336	1.084	4.491	0.1568	5.575	0.8185	
	1.355	1.033	5.000	0.1619	6.033	0.8166	0.8289±0.0008
	1.794	1.400	6.629	0.1631	8.029	0.8134	
	1.799	1.443	7.274	0.1654	8.717	0.8140	
	1.814	1.350	8.709	0.1684	10.059	0.8102	
45	1.340	1.052	1.763	0.1441	2.815	0.8181	
	1.191	0.935	2.648	0.1533	3.583	0.8161	
	1.332	1.000	3.301	0.1599	4.301	0.8155	0.8216±0.0007
	1.339	0.966	4.882	0.1686	5.848	0.8124	
	1.355	1.033	5.500	0.1711	6.533	0.8131	
	1.397	1.065	6.021	0.1722	7.086	0.8116	

the solid phase in equilibrium with the saturated solution in formamide, however, the ΔG^0 values computed at 25°C from the relation,

$$[4] \quad \Delta G^0 = -nFE_m^0$$

for the electrode reaction

$$\text{Tetrachlorobenzoquinone(s)} + H_2(g) + \text{solvent} \rightleftharpoons \text{tetrachlorohydroquinone(solvated)} + 2e$$

in water (-128.14 kJ mol^{-1}), glacial acetic acid (-131.23 kJ mol^{-1}), 50% aqueous dioxane (-137.98 kJ mol^{-1}), and formamide (-161.33 kJ mol^{-1}) show that any change in ΔG^0 on passing from water to formamide will be due to variation of free energy of solvation. The higher free energy due to solvation of tetrachlorohydroquinone in formamide in comparison with those in water, glacial acetic acid, or 50% aqueous dioxane may be due to the fact that tetrachlorohydroquinone is more solvated in formamide than in other media. This is consistent with the result obtained in the case of quinhydrone electrode in formamide (9).

The standard Gibbs energy change, ΔG^0, for the electrode reaction calculated on the molal scale by means of eq. [4] at different temperatures is expressed by the equation,

$$[5] \quad \Delta G^0 = -A' - B'T - C'T \ln T - D'T^2/2$$

in J mol^{-1}, where A', B', C', and D' are, respectively, nF times A, B, C, and D, the constants in eq. [3]. As usual, the values of the standard entropy change, ΔS^0, were evaluated from the relation

$$\Delta S^0 = -\partial(\Delta G^0)/\partial T$$

and are fitted to the equation,

$$[6] \quad \Delta S^0 = B' + C' + C' \ln T + D'T$$

in J mol^{-1} K^{-1}. Using the ΔG^0 and ΔS^0 values so obtained in the Gibbs–Helmholtz equation ($\Delta G^0 = \Delta H^0 - T\Delta S^0$), the values of ΔH^0 were calculated at different temperatures and have been expressed through the equation

$$[7] \quad \Delta H^0 = -A' + C'T + D'T^2/2$$

in J mol^{-1}. The ΔC_p^0 values were computed for the electrode reaction at different temperatures from

Can. J. Chem. Downloaded from www.nrcresearchpress.com by 210.87.254.40 on 09/05/12
For personal use only.

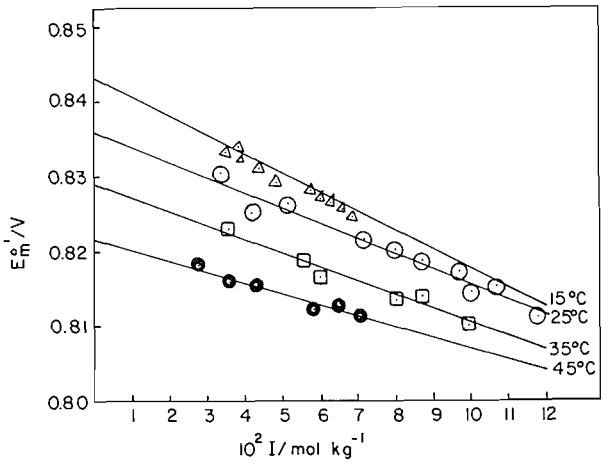


FIG. 1. Plot of ionic strength versus $E_m^{o\prime}$.

the relation

$$\Delta C_p^0 = \partial(\Delta H^0)/\partial T$$

and are fitted to the equation

[8] $\Delta C_p^0 = C' + D'T$

in J mol^{-1} K^{-1}. The values of the constants A', B', C', and D' (eqs. [5]–[8]) were found to be (734.148 ± 0.004) × 10^3, −(20.3366 ± 0.0005) × 10^3, 3540.37 ± 0.03, and −11.7814 ± 0.0012, respectively.

1. J. B. CONANT, L. F. SMALL, and B. S. TAYLOR. J. Am. Chem. Soc. **47**, 1959 (1925).
2. B. O. HESTON and N. F. HALL. J. Am. Chem. Soc. **55**, 4729 (1933); **56**, 1462 (1934).
3. (*a*) B. NAYAK and U. N. DASH. Aust. J. Chem. **26**, 111 (1973); **26**, 115 (1973); (*b*) U. N. DASH and B. NAYAK. Aust. J. Chem. **28**, 793 (1975); **28**, 797 (1975); **28**, 1649 (1975); (*c*) U. N. DASH. Aust. J. Chem. **28**, 1653 (1975); **29**, 1609 (1976); **30**, 2621 (1977); (*d*) U. N. DASH. Thermochim. Acta, **27**, 379 (1978); (*e*) U. N. DASH. Thermochim. Acta, **30**, 73 (1979); (*f*) U. N. DASH. J. Electroanal. Chem. **98**, 1297 (1979).
4. U. N. DASH and B. NAYAK. Aust. J. Chem. **28**, 1657 (1975).
5. R. K. AGARWAL and B. NAYAK. J. Phys. Chem. **70**, 2568 (1966).
6. (*a*) N. F. HALL and J. B. CONANT. J. Am. Chem. Soc. **49**, 3047 (1927); **49**, 3062 (1927); (*b*) N. F. HALL and T. H. WERNER. J. Am. Chem. Soc. **50**, 2367 (1928); (*c*) D. J. G. IVES and G. J. JANZ (*Editors*). Reference electrode. Academic Press, London. 1961. p. 448.
7. H. S. HARNED and D. D. WRIGHT. J. Am. Chem. Soc. **55**, 4849 (1933).
8. U. N. DASH and B. NAYAK. Indian J. Chem. **8**, 659 (1970).
9. B. NAYAK and D. K. SAHU. Electrochim. Acta, **16**, 1957 (1971); **18**, 271 (1973).
10. U. N. DASH and B. NAYAK. J. Electroanal. Chem. **41**, 323 (1973).
11. U. N. DASH. Electrochim. Acta, **21**, 289 (1976); **21**, 1061 (1976).
12. U. N. DASH. Ph.D. Thesis. Indian Institute of Technology, Kharagpur. 1973.
13. R. A. ROBINSON and R. H. STOKES. Electrolyte solutions. Butterworths, London. 1959.

Can. J. Chem. Downloaded from www.nrcresearchpress.com by 210.87.254.40 on 09/05/12
For personal use only.

Reactions of bis(ditertiaryphosphine) complexes of rhodium(I) with carbon monoxide, dioxygen, dihydrogen, and hydrogen chloride[1]

BRIAN R. JAMES AND DEVINDER MAHAJAN

Department of Chemistry, University of British Columbia, Vancouver, B.C., Canada V6T 1Y6

Received November 20, 1979

BRIAN R. JAMES and DEVINDER MAHAJAN. Can. J. Chem. **58**, 996 (1980).

The products, resulting from addition under mild conditions of the gaseous molecules CO, O_2, H_2, and HCl, to some rhodium(I)–bis(ditertiaryphosphine) complexes, are described; the P⌒P phosphines used were $Ph_2P(CH_2)_nPPh_2$, n = 1–4, and (+)-diop (diop = 2,3-*O*-isopropylidene 2,3-dihydroxy-1,4-bis(diphenylphosphino)butane). Monocarbonyls were isolated from addition of CO to $Rh(P⌒P)_2^+BF_4^-$ complexes (n = 1 and 3), the reactions being reversible; there was no reaction with the n = 2 system, while the n = 4 and diop systems absorbed > 1 mol of CO per Rh to give mixtures of products. The same cation precursors add O_2 to yield *cis*-$Rh(P⌒P)_2O_2^+BF_4^-$ adducts (n = 1–3), the binding being reversible for the n = 2 system; pure products were not isolated with the n = 4 cation which absorbs 3 mol O_2/Rh; the diop system was unreactive toward O_2. Reversible additions of 1 mol H_2 yield isolable *cis*-$H_2Rh(P⌒P)_2^+BF_4^-$ complexes with the n = 3 and diop systems; the n = 1 and 2 $Rh(P⌒P)_2^+$ cations are unreactive toward H_2, while a mixture of hydrides is formed from the n = 4 species. The chlorohydrido cations $HRh(P⌒P)_2Cl^+A^-$ (A = Cl, BF_4, PF_6, SbF_6), n = 1–3, were prepared via routes involving addition of gaseous HCl to precursor $Rh(P⌒P)_2Cl$ complexes; however, the reactions with the n = 4 and diop systems did not yield pure products.

The solution structures of all the isolated five- and six-coordinate addition products have been determined using ^1H and variable temperature ^{31}P nmr. The five-coordinate carbonyl with n = 1 shows equivalent phosphines from −50 to 25°C, while the n = 3 system shows inequivalent phosphines resulting from a trigonal bipyramidal structure with an equatorial carbonyl. The $HRh(P⌒P)_2Cl^+$ cation, n = 3, has *cis* geometry, while *trans*-structures are preferred for the n = 1 and 2 species.

BRIAN R. JAMES et DEVINDER MAHAJAN. Can. J. Chem. **58**, 996 (1980).

On décrit les produits résultant de l'addition, dans des conditions douces, de molécules de CO, O_2, H_2 et HCl à l'état gazeux sur quelques complexes de rhodium(I) bis(ditertiaryphosphines). On a utilisé les phosphines P⌒P suivantes: $Ph_2P(CH_2)_nPPh_2$, n = 1–4 et (+)-diop (diop = *O*-isopropylidène-2,3 dihydroxy-2,3 bis(diphénylphosphino)-1,4 butane). On a isolé des produits monocarbonylés résultant de l'addition réversible de CO sur les complexes $Rh(P⌒P)_2^+BF_4^-$ (n = 1 et 3). On n'obtient pas de réaction avec le système n = 2 tandis que dans les systèmes où n = 4 et où le groupe diop absorbé est > 1 mol de CO/Rh, on obtient un mélange de produits. Les mêmes précurseurs cationiques additionnent de l'oxygène pour conduire à l'adduit $Rh(P⌒P)_2O_2^+BF_4^-$ *cis* (n = 1–3); le mode de liaison est réversible dans le cas du système n = 2. On n'a pas isolé de produits purs dans le cas du cation n = 4 qui absorbe 3 mol de O_2/Rh. Le système diop ne réagit pas avec l'oxygène. Les additions réversibles de 1 mol de H_2 donnent les complexes $H_2Rh(P⌒P)_2^+BF_4^-$ *cis* que l'on peut isoler avec n = 3 et le système diop. Les cations $Rh(P⌒P)_2^+$ où n = 1 et 2 ne réagissent pas avec H_2 tandis qu'on obtient un mélange d'hydrures à partir des espèces où n = 4. On a préparé les cations chlorohydrido $HRh(P⌒P)_2Cl^+A^-$ (A = Cl, BF_4, PF_6, SbF_6), n = 1–3 en utilisant l'addition de HCl gazeux sur les complexes précurseurs $Rh(P⌒P)_2Cl$. Cependant les réactions avec les systèmes n = 4 et diop ne donnent pas des produits purs.

On a déterminé la structure des solutions de tous les produits d'addition penta et hexacoordonnés en utilisant la rmn du ^1H et celle du ^{31}P à température variable. Les composés carbonylés pentacoordonnés avec n = 1 présentent des phosphines équivalentes entre −50 et 25°C, tandis que les systèmes où n = 3 présentent des phosphines non équivalentes résultant d'une structure trigonale bipyramidale avec un carbonyle en position équatoriale. Le cation $HRh(P⌒P)Cl^+$, n = 3 a une géométrie *cis* tandis que la structure *trans* est privilégée pour les espèces où n = 1 et 2.

[Traduit par le journal]

Introduction

We are currently interested in the activation of small gas molecules by bis(tertiaryphosphine) $Ph_2P(CH_2)_nPPh_2$ complexes of rhodium(I), and reactivity patterns as a function of n, and have reported recently (1) on the synthesis of $Rh(P⌒P)_2X$ complexes,[2] where X is a coordinated or associated anionic moiety including H, Cl, BF_4, PF_6, SbF_6. The complexes effect catalytic hydrogenation of unsaturated carboxylic acids (1), and a report on catalytic decarbonylation of aldehydes using $Rh(P⌒P)_2^+$ cations (P⌒P = dpe and 1,3-bis(diphenylphosphino)propane) appeared (2) after completion of the CO work described in the present paper. The complex $HRh(dpe)_2Cl^+Cl^-$ was noted some years ago to be an extremely effective catalyst for hydrogenation of terminal olefins (3), while the crystal structure of *trans*-$HRh(dpm)_2Cl^+BPh_4^-$ was reported (4) during the preparation of this manuscript. $Rh(dpe)_2O_2^+PF_6^-$ was one of the first reported dioxygen adducts characterized by crystallography (5).

In this paper, we describe the synthesis and the

[1]Presented in parts at a Symposium on Rhodium in Homogeneous Catalysis, Veszprém, Hungary, 1978, and at the 62nd Canadian Chemical Conference of the Chemical Institute of Canada, Vancouver, Canada, 1979.

[2]Ligand abbreviations used for $Ph_2P(CH_2)_nPPh_2$: n = 1, bis(diphenylphosphino)methane or dpm; n = 2, 1,2-bis(diphenylphosphino)ethane or dpe; n = 3, 1,3-bis(diphenylphosphino)propane or dpp; n = 4, 1,4-bis(diphenylphosphino)butane or dpb. P⌒P signifies generally a chelating diphosphine, including (+)-diop.

0008-4042/80/100996-09$01.00/0

©1980 National Research Council of Canada/Conseil national de recherches du Canada

Can. J. Chem. Downloaded from www.nrcresearchpress.com by 210.87.254.105 on 09/05/12
For personal use only.

Can. J. Chem. Downloaded from www.nrcresearchpress.com by 210.87.254.105 on 09/05/12
For personal use only.

characterization of rhodium complexes obtained by addition of CO, O_2, H_2, and HCl to a range of $Rh(\widehat{P\ P})_2X$ complexes. The studies are pertinent to the known catalytic hydrogenation and decarbonylation properties and to any potential carbonylation and oxygenation properties. The general synthetic procedures described have been used earlier to synthesize especially a range of corresponding iridium complexes (5–12), while such studies on the rhodium systems have been more limited and less systematic (5, 9, 13–16). There has been particular interest in the solution structure of the five- and six-coordinate iridium complexes (8, 10–12), and we also report here the solution structure of some corresponding rhodium systems. The paper by Baird's group (16) appeared after submission of the present work.

Experimental

Most of the materials, apparatus, and experimental techniques used were described previously in conjunction with the synthesis of the precursor $Rh(\widehat{P\ P})_2X$ complexes, X = Cl, BF_4 (1 and references therein). The gases CO (C.P. grade), HCl (Technical), and H_2 (Prepurified), were Matheson products and were used as provided. O_2 was obtained as Extra Dry grade from Canadian Liquid Air. The stoichiometries of the gas/Rh solution reactions were measured using the constant pressure apparatus described previously (17).

PPh_3 in an appropriate solvent was used as a reference for the low temperature ^{31}P nmr, although all the ^{31}P shifts are reported in ppm (upfield positive) from 85% H_3PO_4.

Carbonyl Complexes

$Rh(\widehat{P\ P})_2CO^+BF_4^-$ ($\widehat{P\ P}$ = dpm, dpp)

CO was bubbled through a CH_2Cl_2 solution (5 mL) of $Rh(dpm)_2^+BF_4^-$ (0.28 g, 0.29 mmol) or $Rh(dpp)_2^+BF_4^-$ (0.30 g, 0.30 mmol). Addition of diethyl ether precipitated a yellow complex that was filtered at 0°C, washed with ether, dried, and stored under a CO atmosphere.

The $Rh(dpe)_2^+BF_4^-$ complex under the same conditions was unreactive toward CO. $Rh(dpb)_2^+BF_4^-$ yielded a yellow complex contaminated with a white powder, ν(CO) at 1962 and 2003 cm^{-1}. Attempts to synthesize $Rh(dpb)_2CO^+Cl^-$ via an exchange reaction using *trans*-$RhCl(CO)(PPh_3)_2$ with excess dpb, a method found successful for iridium analogues (11), also gave a mixture of products with ν(CO) at 1910 and 1941 cm^{-1}.

$Rh(diop)_2^+BF_4^-$ with CO in CH_2Cl_2 again yielded an inseparable mixture with ν(CO) bands at 1976 and 2015 cm^{-1}. Reaction of $Rh(diop)_2Cl$ with CO in benzene followed by addition of ether yielded a yellow complex, **A**, with CO bands at 1926 and 1974 cm^{-1} and a band at 308 cm^{-1} assignable to ν(Rh—Cl), different to that of the starting complex at 284 cm^{-1}; the same CO bands have been reported for the five-coordinate complex[3] $Rh(diop)(diop^*)(CO)_2^+Cl^-$, **B**, prepared by a different route (15). We repeated the literature preparation and obtained a complex with an ir identical to that of **A**. The analyses of the products obtained by either method were always 2–3% low in carbon to correspond to complex **B**.

[3]diop* represents the monodentate diphosphine.

Dioxygen Complexes

Slight modifications of a literature procedure (5) were used to prepare the dioxygen complexes.

$Rh(\widehat{P\ P})_2O_2^+BF_4^-$ ($\widehat{P\ P}$ = dpm, dpe, dpp)

O_2 was bubbled through an orange methanol solution (20 mL) of $Rh(dpm)_2^+BF_4^-$ (0.22 g, 0.23 mmol); the brown solid that separated after a few minutes was filtered, washed with methanol, and dried *in vacuo*. The dpe and dpp analogues at corresponding concentrations separated out on concentrating to a 5 mL volume at 0°C; the filtered solids were washed with diethyl ether and dried *in vacuo*.

A deep red methanol solution (20 mL) of $Rh(dpb)_2^+BF_4^-$ (0.25 g, 0.24 mmol) slowly became brown under O_2 over ~20 h; addition of diethyl ether yielded an impure brown solid with ir bands at 851 cm^{-1} and 1120 cm^{-1}, likely attributable to ν(O_2) and ν(P—O), respectively (18, 19). The $Rh(diop)_2^+BF_4^-$ complex was essentially unreactive toward O_2 under similar conditions.

Dihydride Complexes

$H_2Rh(\widehat{P\ P})_2^+BF_4^-$ ($\widehat{P\ P}$ = dpp and (+)-diop)

H_2 was bubbled for a few minutes through a red CH_2Cl_2 solution (10 mL) of $Rh((\widehat{P\ P})_2^+BF_4^-$ (0.35 mmol). Addition of diethyl ether to the pale yellow solution at 0°C induced crystallization of the white dihydrides. The crystals were filtered, washed with ether, dried, and stored under H_2.

The same procedure using dpb gave a mixture that almost certainly contained some of the $H_2Rh(dpb)_2^+BF_4^-$ complex (ν(Rh—H) 2072 cm^{-1}, τ20.3 (pair of multiplets in $CDCl_3$ at 25°C)). The $Rh(dpm)_2^+$ and $Rh(dpe)_2^+$ cations were unreactive toward H_2 under similar conditions.

Chlorohydrido Complexes

$HRh(\widehat{P\ P})_2Cl^+A^-$ ($\widehat{P\ P}$ = dpm, dpe, dpp; A = Cl, BF_4, PF_6, SbF_6)

The $HRh(dpm)_2Cl^+Cl^-$ complex was obtained as white crystals on bubbling HCl(g) through an orange solution of $Rh(dpm)_2Cl$ or $Rh(dpm)_2^+BF_4^-$ (0.33 mmol) in methanol (15 mL); the solid was filtered, washed with methanol, and dried *in vacuo*. The dpe and dpp analogues were similarly made using ethanol solutions (15 mL) of $Rh(\widehat{P\ P})_2Cl$ (0.40 mmol), but after stirring for a few minutes, excess HCl(g) was removed by a flow of Ar. Concentration to ~5 mL, followed by addition at 0°C of 20 mL diethyl ether, yielded light yellow crystals that were filtered, washed with ether, and dried *in vacuo*. The $HRh(dpe)_2Cl^+Cl^-$ complex has been prepared previously from a precursor Rh(III)–alkyl complex (3).

The $HRh(P\ P)_2Cl^+A^-$ (A = BF_4, PF_6, SbF_6) complexes with dpm, dpe, and dpp, were prepared from CH_2Cl_2 solutions (5 mL) of the chlorides (0.15 mmol) by addition of the AgA salt (0.15 mmol in 5 mL acetone); after filtering off the AgCl, the solution was concentrated to ~2 mL and 3 mL THF then added. Addition of diethyl ether gave products that were filtered, washed with ether, and dried *in vacuo*. Attempts to prepare the $HRh(\widehat{P\ P})_2Cl^+A^-$ complexes by treatment of the chlorides with aqueous HA solutions, a method successful for the iridium analogues (11, 12), were unsuccessful. Addition of 2 mol of AgA salt per $HRh(\widehat{P\ P})_2Cl^+Cl^-$ also yielded the $HRh(\widehat{P\ P})_2Cl^+A^-$ complexes, instead of the expected (12) dicationic species $HRh(\widehat{P\ P})_2^{2+}2A^-$.

Attempts to synthesize pure $HRh(\widehat{P\ P})_2Cl^+A^-$ (A = Cl, BF_4) complexes with dpb and diop proved unsuccessful. The reaction of HCl(g) with solutions of $Rh(dpb)_2Cl$ appeared to yield light yellow mixtures, although ir bands at 2150 cm^{-1}, assignable to ν(Rh—H), and 280 and 290(sh) cm^{-1}, assignable to ν(Rh—Cl), indicated the presence of $HRh(dpb)_2Cl^+Cl^-$, as did a high field broad multiplet at τ26.5 in the ^1H nmr in $CDCl_3$ at 25°C. Simi-

Can. J. Chem. Downloaded from www.nrcresearchpress.com by 210.87.254.105 on 09/05/12
For personal use only.

TABLE 1. Analytical and molar conductivity (Λ) data for the rhodium complexes

Complex	Decomposition point (°C)[a]	Analysis (%) Found		Analysis (%) Calculated		Λ[b] (ohm^{-1} cm^2 mol^{-1})
$Rh(dpm)_2CO^+BF_4^-$	168	61.7	4.4	62.09	4.46	85[c]
$Rh(dpp)_2CO^+BF_4^-$	179–182	63.4	4.1	63.34	4.99	81[c]
$Rh(dpm)_2O_2^+BF_4^-$	209–211	61.0	4.5	60.62	4.44	83
$Rh(dpe)_2O_2^+BF_4^-$	164–167	61.3	4.7	61.31	4.72	84
$Rh(dpp)_2O_2^+BF_4^-$	197–201	61.5	5.2	61.97	4.97	81
$Rh(dpp)_2H_2^+BF_4^-$	86	63.7	5.2	63.80	5.32	81[d]
$Rh(diop)_2H_2^+BF_4^-$	153	61.2[e]	5.7	62.64	5.56	79[d]
$HRh(dpm)_2Cl^+Cl^-$	144	59.0[f]	4.7	63.64	4.77	67
$HRh(dpe)_2Cl^+Cl^-$	136	60.8[f]	5.0	64.28	5.05	68
$HRh(dpp)_2Cl^+Cl^-$	152	62.3[f]	5.4	64.88	5.31	68
$HRh(dpm)_2Cl^+BF_4^-$	204	60.0	4.6	60.35	4.53	95
$HRh(dpe)_2Cl^+BF_4^-$	184	60.9	4.9	61.06	4.79	96
$HRh(dpp)_2Cl^+BF_4^-$	164–167	59.4[e]	5.0	67.71	5.05	95

[a]Uncorrected, in air.
[b]10^{-3} *M* in CH_3NO_2 at 25°C under Ar unless stated otherwise; values for 1:1 electrolytes 75–95 ohm^{-1} cm^2 mol^{-1} (20).
[c]Under CO.
[d]Under H_2.
[e]Low carbon due to presence of CH_2Cl_2 detected in nmr.
[f]Low carbon probably due to HCl impurity (see text); for the dpe salt, Cl, 8.1% (calcd. 7.3).

TABLE 2. ^{1}H nmr and infrared data for the rhodium complexes

Complex	τ_{Rh-H}[a]	δ(H)[b] aliphatic; phenyl	Infrared (cm^{-1})[c]
$Rh(dpm)_2CO^+BF_4^-$	—	4.5; 7.5[d,e]	1948
$Rh(dpp)_2CO^+BF_4^-$	—	—	1930
$Rh(dpm)_2O_2^+BF_4^-$	—	3.8, 4.5; 7.3[f]	881
$Rh(dpe)_2O_2^+BF_4^-$	—	2.2; 7.3[f]	888
$Rh(dpp)_2O_2^+BF_4^-$	—	1.7, 2–3; 7.4[f]	896
[g]$H_2Rh(dpp)_2^+BF_4^-$	18.5[h,i]	1.9, 2.3, 3.1; 7.0, 7.3, 7.5, 7.9, 8.1[e,i]	2052
[j]$H_2Rh(dpb)_2^+BF_4^-$	20.3[h,i]	—	2072
[k]$H_2Rh(diop)_2^+BF_4^-$	20.0[h,i]	1.2s, 2.3, 2.9, 3.3; 7.5[i]	2020, 2080
[l]$HRh(dpm)_2Cl^+X^-$	22.0[m]	4.6, 5.0; 7.3	2064[m]
[l]$HRh(dpe)_2Cl^+X^-$	26.0[n]	2.3, 2.8; 7.3	2085[n]
[l]$HRh(dpp)_2Cl^+X^-$	25.0[o]	1.6, 2.3, 2.8; 7.4	2100[o]
[j]$HRh(dpb)_2Cl^+Cl^-$	26.5	—	2150
[j]$HRh(diop)_2Cl^+Cl^-$	22.0	—	2130

[a]In $CDCl_3$ at 25°C.
[b]Measured in ppm (downfield positive) from TMS in $CDCl_3$, unless stated otherwise; all multiplets unless designated s, singlet.
[c]ν(CO) for the carbonyls; ν(O_2) for the dioxygen complexes; ν(RhH) for the hydrido complexes; Nujol.
[d]Under CO; under Ar, the multiplets of $Rh(\widehat{P\ P})_2^+$ are seen also (1).
[e]In acetone-d_6.
[f]Under O_2; the dpe data refer to $Rh(dpe)_2^+$ due to loss of O_2.
[g]Reference 16 gives τ 18.6 for an *in situ* species.
[h]Pair of multiplets.
[i]Under H_2.
[j]Impure complex.
[k]Reference 13 gives τ 21.5 and ν(Rh—H) 2030 cm^{-1} for the PF_6^- salt.
[l]Data essentially identical for X = Cl or BF_4.
[m]J_{Rh-H} 18.0, J_{P-H} 13.0 Hz, agrees with literature data for the BPh_4^- salt (4); ref. 4 gives ν(Rh—H) = 2080 cm^{-1}.
[n]J_{Rh-H} 15.0, J_{P-H} 6.0 Hz, agrees with literature data (3); ref. 3 gives ν(Rh—H) = 2048 cm^{-1}.
[o]$J_{Rh-H} = J_{P-H}$ = 13.0 Hz agrees with literature data (16); ref. 16 gives ν(Rh—H) = 2090 cm^{-1}.

larly, the presence of $HRh(diop)_2Cl^+Cl^-$ in a mixture was indicated by spectral data: ir at 2130 cm^{-1}, ν(Rh—H); and 278, 290 cm^{-1}, ν(Rh—Cl); ^{1}H nmr ($CDCl_3$ at 25°C) at τ22.0, br multiplet.

Results and Discussion

Oxidative addition or just simple addition of the XY molecules (XY = CO, O_2, H_2, and HCl) to the four- or five-coordinate rhodium(I) complexes $Rh(\widehat{P\ P})_2A$, $\widehat{P\ P}$ = dpm, dpe, dpp, dpb, and diop; A = Cl, BF_4 (1), has been used to synthesize rhodium(I) and rhodium(III) complexes of the type $Rh(\widehat{P\ P})_2(XY)_m^+A^-$. Pure complexes were isolated when m = 1, and Tables 1–3 list analytical, conductivity, and spectroscopic data for these species. The gas:Rh stoichiometry was measured in several solvents for formation of the carbonyl, dioxygen, and dihydride complexes listed in Table 1, and was found to be ~1.0 under 1 atm gas at 25°C in all cases

TABLE 3. $^{31}P\{^1H\}$ nmr data for the rhodium complexes[a]

Complex	δ[b]	J_{Rh-P}, Hz	J_{P-P}, Hz	T, °C
[c]$Rh(dpm)_2CO^+BF_4^-$	+22.59	97.5	—	25
	+19.80	97.1	—	−50
[c]$Rh(dpp)_2CO^+BF_4^-$	−15.13, +12.87	122.5, 85.1	30	25
	−15.14, +9.94	91.6, 114.7	46	−50[d]
$Rh(dpm)_2O_2^+BF_4^-$	+14.39, +30.80	112.4, 82	38	25
$Rh(dpe)_2O_2^+Cl^-$	−51.3, −44.3	126, 92	7.7	−80[e]
$Rh(dpp)_2O_2^+BF_4^-$	−14.90, +12.68	122.5, 84.9	30	25[f]
[g]$H_2Rh(dpp)_2^+BF_4^-$	−19.96, −9.12	99.6, 82.2	30	−50
[h]$H_2Rh(diop)_2^+BF_4^-$	−21.40, −6.4	103, 90	19.7	−50
[i]$HRh(dpm)_2Cl^+X^-$	+16.70	84.3	—	25[j]
	+15.40	82.6	—	−60
[i]$HRh(dpe)_2Cl^+X^-$	−51.80	93.8	—	25
	−56.46	94.2	—	−60
[i]$HRh(dpp)_2Cl^+X^-$	−2.34	91	—	25
	−16.0, +6.4	[k]	[k]	−85

[a]Measured in ppm (upfield positive) from 85% H_3PO_4. Shifts for the free ligands ($CDCl_3$ or CH_2Cl_2) occur at +22.25 (dpm), +12.52 (dpe), +17.25 (dpp), +15.95 (dpb), and +22.50 (diop).
[b]In CH_2Cl_2/acetone-d_6 (2:1 v/v).
[c]Under CO.
[d]Reference 15 gives δ −15.2, + 12.5; J_{Rh-P} 115, 86; J_{P-P} = 46 for an impure Cl^- salt in CD_2Cl_2.
[e]Data from ref. 11.
[f]Reference 16 gives essentially same data for the Cl^- salt formed *in situ* in CH_2Cl_2.
[g]Under H_2 ref. 16 gives δ −17.0, −6.3; J_{Rh-P} 99.80; J_{P-P} = 30 for the Cl^- salt formed *in situ* in $CDCl_3$.
[h]Under H_2. Slight changes in δ with temperature.
[i]Data essentially identical for X = Cl, or BF_4.
[j]Reference 4 gives δ 15.8 (J = 83) for the BPh_4^- salt.
[k]Doublet of doublet of triplets, not well resolved. Reference 16 gives δ −12.3, +8.9; J_{Rh-P} = 90, 93; J_{P-P} = 35 for the Cl^- salt at −70°C. At room temperature the doublet was at δ −1.9 (J = 90 Hz).

except the $Rh(dpe)_2^+/O_2$ system; the O_2-binding for this system was readily reversible under these conditions and the stoichiometry corresponded, for example, to an equilibrium constant of ~0.5 atm^{-1} (21).

Carbonyl Complexes

The nonreactivity of the $Rh(dpe)_2^+$ cation as a chloride salt toward 1 atm CO has been noted previously (15). The pure $Rh(\widehat{P\ P})_2CO^+$ cations ($\widehat{P\ P}$ = dpm, dpp) have been isolated for the first time as the BF_4^- salts, although the dpp complex has been made by Sanger via a different procedure (15) as the Cl^- salt in a mixture with the binuclear complex $[RhCl(CO)(dpp)_2]_2$. The $Rh(\widehat{P\ P})_2CO^+BF_4^-$ complexes are stable in the solid state, but in solution readily lose CO in a reversible manner to generate the $Rh(\widehat{P\ P})_2^+$ cations (1), as evidenced by loss of the terminal CO band in the ir, and by changes in the visible spectra from continua (increasing absorption on going from 450–350 nm) to λ_{max} at 385 and 446 nm for the dpm salt, and at 412 nm for the dpp salt (1). The $^{31}P\{^1H\}$ nmr data for $Rh(dpp)_2CO^+BF_4^-$ under Ar at 25°C correspondingly show the doublet of the $Rh(dpp)_2^+$ species (1). Under CO at 25°C, the spectrum is a doublet of doublet of triplets broadened at the base suggesting some fluxionality, but this sharpens at −50°C (Fig. 1) to the A_2B_2X pattern expected for a trigonal bipyramidal structure with an equatorial carbonyl ligand. Sanger (15) had reached a similar conclusion from ^{31}P data on his impure chloride product; the two sets of data are in good agreement.

The ^{31}P spectrum for the $Rh(dpm)_2CO^+BF_4^-$ complex under CO is a sharp doublet at 25°C and −50°C. The equivalent P atoms can result from a square pyramidal (with apical CO) or a fluxional bipyramidal (tbp) structure. The latter is favoured. The corresponding $Ir(dpm)_2CO^+Cl^-$ complex also exhibits a single ^{31}P resonance even at −92°C, while the dpe analogue is tbp at this temperature (and in the solid state (7)) but is fluxional at −21°C, and a decrease in rearrangement barrier between square pyramid and tbp structures in the order dpp > dpe > dpm has been suggested (11). Under Ar at 25°C, two overlapping ^{31}P doublets measured for $Rh(dpm)_2CO^+$ result from an equilibrium mixture with the decarbonylated product; at −50°C, two well defined doublets confirm the presence of both $Rh(dpm)_2^+$ (δ 20.83, J_{Rh-P} = 115 Hz, cf. ref. 1) and $Rh(dpm)_2CO^+$. The ^1H nmr for the methylene protons similarly shows the equilibrium mixture in the absence of the CO atmosphere.

The $Rh(\widehat{P\ P})_2^+BF_4^-$ ($\widehat{P\ P}$ = dpb, diop) complexes in solution absorbed 1.3–1.7 mol CO per Rh, and this, together with the ir data, is consistent with some dicarbonyl product in the isolated mixtures. Sanger was also unable to prepare a pure $Rh(dpb)_2CO^+Cl^-$ complex using a different route, and as reported (15), we also found the ^{31}P spectra of the mixtures too complicated to be of value. Complex **A** obtained from carbonylation of

Can. J. Chem. Downloaded from www.nrcresearchpress.com by 210.87.254.105 on 09/05/12
For personal use only.

Can. J. Chem. Downloaded from www.nrcresearchpress.com by 210.87.254.105 on 09/05/12
For personal use only.

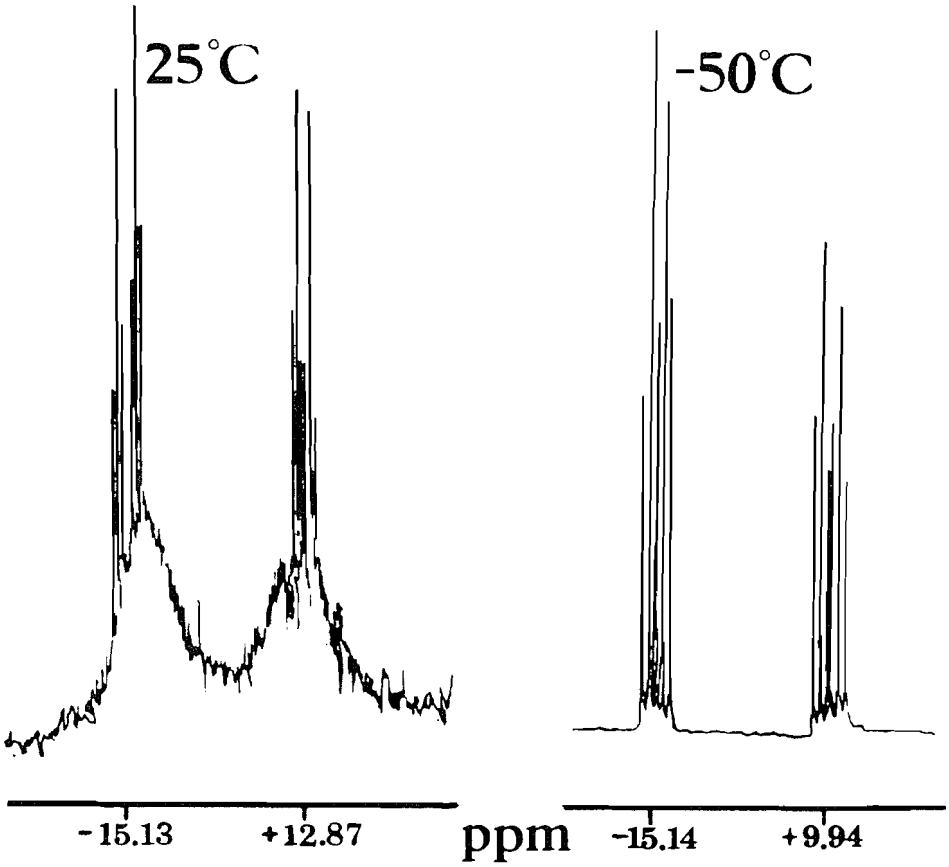
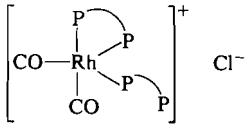


FIG. 1. ^{31}P nmr of $Rh(dpp)_2(CO)^+BF_4^-$ in CH_2Cl_2/acetone-d_6 under CO at 25 and −50°C.

$Rh(diop)_2Cl$ appears to be a mixture containing some $Rh(diop)(diop^*)(CO)_2^+Cl^-$, **B** (15), but the 308 cm^{-1} band, conductivity data (for formula **B**, Λ = 28 under Ar, and 37 ohm^{-1} cm^2 mol^{-1} under CO, at 25°C in nitromethane), the gas uptake stoichiometry, and carbon analysis, suggest contamination with neutral complexes such as $[RhCl(CO)(diop)]_2$ (15) or $RhCl(CO)(diop)(diop^*)$. Dimeric species such as $[(diop)(CO)_2Rh(\widehat{P\ P})Rh(CO)_2(diop)]^{2+}$ could also be present.



B

Dioxygen Complexes

The $Rh(\widehat{P\ P})_2O_2^+BF_4^-$ complexes are obtained analytically pure by oxygenation of the $Rh(\widehat{P\ P})_2^+$ cations with dpm, dpe, and dpp. The ir bands in the 880–900 cm^{-1} region are typical of side-on coordinated peroxide (19), and the complexes are formally six-coordinate rhodium(III) species. The anion of the previously characterized $Rh(dpe)_2O_2^+PF_6^-$ complex obscures the $\nu(O_2)$ region (5). In solution the $Rh(dpe)_2O_2^+$ cation readily loses O_2 (5), and this is readily monitored spectrophotometrically by a change from a continuum to an absorption maximum at 407 nm (1). The dpm and dpp systems show much stronger O_2-binding that is irreversible in solution at ambient temperatures.

The ^{31}P spectra (Fig. 2) show the expected doublet of doublet of triplets A_2B_2X pattern. The dpm and dpp complexes are nonfluxional at 25°C; the dpe system shows just the simple doublet of the $Rh(dpe)_2^+$ cation (1), due to loss of O_2, although ^{31}P nmr at −80°C has revealed previously (11) the expected pattern of a rigid $Rh(dpe)_2O_2^+$ species. The substantially larger downfield shifts noted for the dpe dioxygen complex (and the HCl adduct, see below) provide a further example of extra deshielding apparent in five-membered ring systems (16, 22). A recent report (16) notes ^{31}P nmr data for a $Rh(dpp)_2O_2^+Cl^-$ species formed *in situ*, initially inadvertently; agreement is excellent.

The $Rh(dpb)_2^+BF_4^-$ complex in dichloroethane

Can. J. Chem. Downloaded from www.nrcresearchpress.com by 210.87.254.105 on 09/05/12
For personal use only.

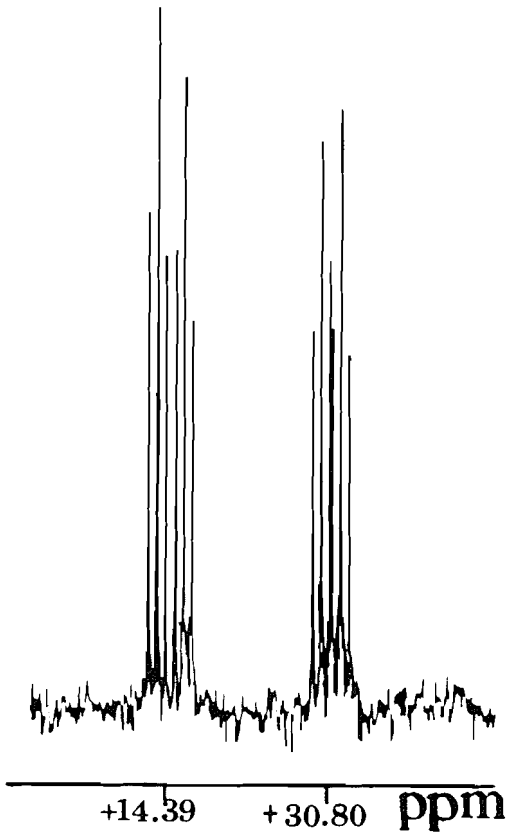


FIG. 2. ^{31}P nmr of $Rh(dpm)_2O_2^+ BF_4^-$ in CH_2Cl_2/acetone-d_6 at 25°C.

solution at 25°C absorbed ~2.8 mol O_2 per Rh and this, coupled with the ir of the product obtained from methanol solutions (see Experimental), would be consistent with the formulation $Rh(dpbO_2)_2O_2^+BF_4^-$ in which all the phosphines have been converted to the oxide, but the carbon analysis is ~6% too low. Such complexes containing coordinated phosphine oxides are known, for example $[RhCl(OPPh_3)_{0.67}O_2]_n$ (23) and *cis*-$Rh(PPh_3)_2[OPPh_2C(S)NPh]O_2$ (24), and a nonstoichiometric compound formed after some loss of the phosphine oxide into solution could be formulated for the dpb product. However, the complex ^{31}P nmr spectra are more consistent with an impure compound.

Dihydride Complexes

The well known nonreactivity of $Rh(dpe)_2^+$ toward 1 atm H_2 (25, 26) is obtained also for the dpm analogue. However, the dpp and diop analogues are readily isolated as the *cis*-$H_2Rh(\widehat{P\ P})_2^+BF_4^-$ complexes; both complexes on dissolving in solution under Ar readily lose H_2. The dihydrides are comparable to the known *cis*-$H_2Rh[P(CH_3)_3]_4^+$ complex (27), and show ν(Rh—H) in the ir, a pair of multiplets in the high-field ^1H nmr at 25°C, and two resonances in the $^{31}P\{^1H\}$ nmr; based on the literature data (27), the lower field resonance for each system is attributed to the mutually *trans* P atoms, and that at higher field to the P atoms *trans* to the hydrides. The presence of two P resonances at all temperatures rules out the *cis–trans* rearrangement that has been observed in complexes of the type H_2ML_4 (M = Fe, Ru; L = phosphine, phosphite (28, 29)). The ^{31}P data possibly suggest some temperature dependence in terms of line-width for the higher field resonance, although a relatively poor signal-to-noise ratio in the 25°C spectra clouds the issue somewhat; such broadening could result from mutual exchange of the two P atoms *trans* to hydrides; as judged by the inability of rhodium(I) mono(ditertiaryphosphine) complexes to add H_2, a P atom *trans* to hydride is not favoured, at least thermodynamically (14, 30).

The $H_2Rh(diop)_2^+$ cation has been characterized previously as the ClO_4^- and PF_6^- salts, although ^{31}P nmr data were not studied (13). The carbon analysis in our sample was slightly low due to the presence of some CH_2Cl_2 solvent in the crystals. A previous attempt to isolate $H_2Rh(dpp)_2^+$ as the chloride salt was unsuccessful (14, 16), but nmr data on a system formed *in situ* (16) agree well with ours.

The impure $H_2Rh(dpb)_2^+BF_4^-$ complex isolated is likely contaminated with the starting complex, since solution gas-uptake data showed a H_2:Rh stoichiometry of ~0.6.

Chlorohydrido Complexes

Oxidative addition of HCl(g) to $Rh(\widehat{P\ P})_2Cl$ leads to the formation of $HRh(\widehat{P\ P})_2Cl^+$ cations with $\widehat{P\ P}$ = dpm, dpe, and dpp. The isolated chloride salts give low analyses for carbon (Table 1), but pure salts with BF_4^-, PF_6^-, and SbF_6^- anions are readily made from the chloride using the appropriate silver salt. Analogous iridium(III) chloride complexes, prepared via the oxidative addition procedure, also show low carbon content due to contamination by HCl (6), and a somewhat high chloride analysis for the $HRh(dpe)_2Cl^+Cl^-$ complex (Table 1, footnote *f*) suggests a similar explanation for the rhodium systems, especially since the ^{31}P spectra were clean (see below). Further recrystallizations did not improve the elemental analyses.

The dpe and dpp chlorohydrido complexes lose HCl in *N*,*N*-dimethylacetamide (DMA), a relatively basic solvent, to generate the $Rh(\widehat{P\ P})_2^+$ cations (1), while the $HRh(dpm)_2Cl^+$ complex does not decompose. The hydride in the $HRh(\widehat{P\ P})_2Cl^+$ cations is readily detected in the ir, and ^1H nmr high field at 25°C (Table 2). The latter appears as a

Can. J. Chem. Downloaded from www.nrcresearchpress.com by 210.87.254.105 on 09/05/12
For personal use only.

doublet of quintets for the dpm and dpe systems, and as a sextet for the dpp system that is explicable if $J_{P-H} \sim J_{Rh-H}$; these 25°C data reveal equivalent P atoms which can result from either a *trans* chlorohydrido structure or a fluxional *cis* structure.

The corresponding doublet of the $^{31}P\{^1H\}$ nmr at 25°C for the dpp cation broadens on cooling, and at −85°C approximates to two doublets of triplets, characteristic of a non-rigid structure with *cis*-geometry for the H and Cl atoms (11, 12, 16, 31). The ^{31}P spectra for the dpm and dpe cations showed a doublet that was unchanged from 25 to −60°C. The crystal structure of $HRh(dpm)_2Cl^+$-BPh_4^- (made inadvertently via a reaction in which ethanol is the hydride source) shows a *trans* geometry (4); the ^1H and ^{31}P nmr data reported are identical to ours, although the ν(Rh—H) band is observed at 2080 cm^{-1}, some 15 cm^{-1} higher than our value. A higher stretching frequency is expected for a hydride *trans* to chloride rather than phosphine, but usually the differences are much larger (32) and a difference in the associated anion is sufficient (33) to account for the ir discrepancy. A *trans*-geometry is considered more likely then for our $HRh(dpm)_2Cl^+$ salt, and the dpe analogue due to the similar ν(Rh—H) value. However, this remains somewhat equivocal since rearrangement barriers do decrease as *n* decreases (11, 12), and the ν(Rh—H) values for *trans* geometries, at least neglecting ring size effects, might be expected to be greater than that of 2100 cm^{-1} measured for *cis*-$HRh(dpp)_2Cl^+$.

Pure $HRh(\widehat{P\ P})_2Cl^+$ species with $\widehat{P\ P}$ = dpb and diop were not isolated, although their presence in mixtures is strongly indicated by spectroscopic data (see Experimental); a broad band around 3500 cm^{-1} in the solid isolated with the diop system could be a ν(OH) band resulting from acid cleavage of the ligand acetal group. Such a reaction has been observed in ruthenium systems containing a sulfoxide analogue of diop (—PPh_2 replaced by —$SOCH_3$ (34, 35)).

It should be noted that for the $HRuCl(diop)_2$ complex, ^{31}P and ^1H nmr data, which revealed inequivalent P atoms, were initially interpreted as usual in terms of a *cis* geometry; however, an X-ray analysis revealed a *trans* structure, the inequivalence being due to a distortion resulting from the presence of the dioxolane ring in the diop. The comparable $HRuCl(dpb)_2$ complex, and the dpp and dpe analogues, show C_{4v} symmetry down to −60°C as judged by the high-field ^1H nmr, and have been assumed to have *trans* structures (31, 35–37).

A claim that $HRh(dpe)_2Cl^+Cl^-$ is an extremely active catalyst for hydrogenation of terminal olefins (3) prompted us to test the potential activity of the $HRh(\widehat{P\ P})_2Cl^+A^-$ complexes ($\widehat{P\ P}$ = dpm, dpe, dpp; A = Cl, BF_4) described here. Under conditions comparable to those reported in the literature (3), we observed no hydrogenation of olefinic substances. However, addition of a base, or use of DMA as solvent, removes the HCl and generates the active $Rh(\widehat{P\ P})_2^+$ catalysts (1). The literature procedure use for isolation of the catalytic $HRh(dpe)_2Cl^+Cl^-$ involved separation from insoluble black residues (3); traces of contaminant metal could account for the observed catalytic hydrogenation.

General

Despite our systematic study of the reactions of small gas molecules with $Rh(\widehat{P\ P})_2^+$ cations as the length of the —$(CH_2)_n$— carbon chain increases between the ligating P atoms, it is difficult to discern any definite reactivity patterns, although the *n* = 4 and diop systems gave mixtures of products in every case except the diop/H_2 reaction. Ligands of the type $A(CH_2)_nA'$, where $n \geq 5$ and A and A′ are donor groups, tend to bridge metal atoms in preference to forming a chelate ring, but this depends very much on the bulk of the substituents on A and A′ (38, 39). In rhodium systems containing one diphosphine per Rh, the tendency to form diphosphine-bridged dimers is marked even with *n* = 1, 3, and 4; in fact, the *n* = 2 appears exceptional in giving a chelate ring, reflecting presumably the extra stability of the five-membered ring (4, 15). Thus, some dissociation of one diphosphine ligand from our $Rh(\widehat{P\ P})_2^+$ systems could lead to formation of a dimeric species, for example, $[RhCl(CO)(diop)]_2$ in the CO reaction. The bis(diop) complexes $HRh(diop)_2$ and $Rh(diop)_2^+$ yield active hydrogenation catalysts via processes that do involve dissociation of a phosphine moiety (1, 40, 41). Such dissociation can also lead to gas uptake: metal stoichiometries of >1.0, as exemplified by formation of the $Rh(diop)(diop^*)(CO)_2^+$ species. Our results then imply that the Ph_2P—C_4—PPh_2 ring systems dissociate more readily than the *n* = 1–3 systems. A recent study using platinum(II) diphosphine – $SnCl_2$ complexes as hydroformylation catalysts revealed maximum activity for the *n* = 4 system, and this was similarly attributed to a loose *cis*-coordination of the diphosphine in the strained seven-membered chelate ring (42).

Within the series $Rh(\widehat{P\ P})_2O_2^+$, ν(O—O) increases from 881–896 cm^{-1} as *n* goes from 1 to 3,

Can. J. Chem. Downloaded from www.nrcresearchpress.com by 210.87.254.105 on 09/05/12
For personal use only.

while only the $n = 2$ system shows reversible O_2-uptake behaviour. This adds further indirect support (43) against a widely accepted correlation between O—O bond strength (and length) and O_2 lability (44), which would require reversible behaviour by the $n = 1$ system also.

The $n = 2$ cation also appears anomalous in the $n = 1$–3 series in not binding CO, especially since the iridium analogue does (26). Of the $n = 1$–3 cations, only the $n = 3$ forms a dihydride, although the $n = 1$ system with dimethyl- instead of diphenylphosphino moieties is known to add H_2 (45). We are currently studying the kinetics and the thermodynamics of the reactions described in this paper, and this should help in unravelling the subtleties involved. Otsuka and co-workers (46, 47) have been studying the structure and reactivity of the nickel subgroup *cis*-$M[PR_2(CH_2)_nPR_2]X_2$ complexes (X = O, H), and have suggested a possible correlation between lability of X_2 and the interligand angle PMP; the steric bulk of the R groups appears dominant.

The regular trend in decreasing ν(Rh—H) values with decreasing ring size within the $HRh(P\frown P)_2Cl^+$ cations could possibly be rationalized within a *cis*-series (H *trans* to P) by an increased *trans* influence as a result of a more easily attained linear H—Rh—P arrangement, at least as n decreases from 4–2 (cf. ref. 46). However, the situation must be much more complex considering the likely different *cis* and *trans* geometries within the series. Kinetic and thermodynamic details on the HCl binding would again be of value in explaining, for example, the respective irreversible and reversible character of the reaction in DMA for the apparently *trans* dpm and dpe systems.

In view of the proved or potential catalytic activity of the $Rh(P\frown P)_2^+$ species generally (see Introduction), a more systematic attempt to acquire crystallographic data is also being made.

Acknowledgements

We thank the National Research Council of Canada for support of this research, and Johnson, Matthey Ltd. for the loan of $RhCl_3 \cdot 3H_2O$.

1. B. R. James and D. Mahajan. Can. J. Chem. **57**, 180 (1979).
2. D. H. Doughty and L. H. Pignolet. J. Am. Chem. Soc. **100**, 7083 (1978).
3. F. Pruchnik. Inorg. Nucl. Chem. Lett. **10**, 661 (1974).
4. M. Cowie and S. K. Dwight. Inorg. Chem. **18**, 1209 (1979).
5. J. A. McGinnety, N. C. Payne, and J. A. Ibers. J. Am. Chem. Soc. **91**, 6301 (1969).
6. L. Vaska and D. L. Catone. J. Am. Chem. Soc. **88**, 5324 (1966).
7. J. A. J. Jarvis, R. H. B. Mais, P. G. Owston, and K. A. Taylor. J. Chem. Soc. Chem. Commun. 906 (1966).
8. S. D. Ibekwe and K. A. Taylor. J. Chem. Soc. A, 1 (1970).
9. L. Vaska, L. S. Chen, and W. V. Miller. J. Am. Chem. Soc. **93**, 6671 (1971).
10. W. M. Bedford and G. Rouschias. J. Chem. Soc. Dalton Trans. 2531 (1974).
11. J. S. Miller and K. G. Caulton. J. Am. Chem. Soc. **97**, 1067 (1975).
12. M. J. Hopkinson and J. F. Nixon. J. Organomet. Chem. **148**, 201 (1978).
13. D. Sinuo and H. B. Kagan. J. Organomet. Chem. **114**, 325 (1976).
14. D. A. Slack and M. C. Baird. J. Organomet. Chem. **142**, C69 (1977).
15. A. R. Sanger. J. Chem. Soc. Dalton Trans. 120 (1977).
16. D. A. Slack, I. Greveling, and M. C. Baird. Inorg. Chem. **18**, 3125 (1979).
17. B. R. James and G. L. Rempel. Discuss. Faraday Soc. **46**, 48 (1968); Can. J. Chem. **44**, 233 (1966).
18. R. L. Augustine, R. J. Pellet, J. F. Van Peppen, and J. P. Mayer. Adv. Chem. Ser. **132**, 111 (1974).
19. J. Lyons. *In* Aspects of homogeneous catalysis. Vol. 3. *Edited by* R. Ugo. Reidel, Dordrecht. 1977. p.1.
20. W. J. Geary. Coord. Chem. Rev. **7**, 81 (1971).
21. B. R. James and D. Mahajan. To be published.
22. P. E. Garrou. Inorg. Chem. **14**, 1435 (1975).
23. G. L. Geoffroy, D. A. Denton, M. E. Keeney, and R. R. Bucks. Inorg. Chem. **15**, 2382 (1976).
24. A. W. Gal and F. G. A. Bolder. J. Organomet. Chem. **142**, 375 (1977).
25. A. Sacco, M. Rossi, and C. F. Nobile. J. Chem. Soc. Chem. Commun. 589 (1966).
26. M. C. Hall, B. T. Kilbourn, and K. A. Taylor. J. Chem. Soc. A, 2539 (1970).
27. R. R. Schrock and J. A. Osborn. J. Am. Chem. Soc. **93**, 2397 (1971).
28. F. N. Tebbe, P. Meakin, J. P. Jesson, and E. L. Muetterties. J. Am. Chem. Soc. **92**, 1068 (1970).
29. P. Meakin, L. J. Guggenberger, J. P. Jesson, D. H. Gerlach, F. N. Tebbe, W. G. Peet, and E. L. Muetterties. J. Am. Chem. Soc. **92**, 3482 (1970).
30. J. Halpern, D. P. Riley, A. S. C. Chan, and J. J. Pluth. J. Am. Chem. Soc. **99**, 8055 (1977) and references therein.
31. R. C. Ball, B. R. James, J. Trotter, D. K. W. Wang, and K. R. Dixon. J. Chem. Soc. Chem. Commun. 460 (1979).
32. J. P. Jesson. Stereochemistry and stereochemical nonrigidity in transition metal hydrides. Transition metal hydrides. *Edited by* E. L. Muetterties. Marcel Dekker, New York. 1971. p. 89.
33. A. D. Allen, T. Eliades, R. O. Harris, and P. Reinsalu. Can. J. Chem. **47**, 1605 (1969).
34. B. R. James and R. S. McMillan. Can. J. Chem. **55**, 3927 (1977).
35. B. R. James, R. S. McMillan, R. H. Morris, and D. K. W. Wang. Adv. Chem. Ser. **167**, 122 (1978).
36. B. R. James and D. K. W. Wang. Inorg. Chim. Acta, **19**, L17 (1976).
37. D. K. W. Wang. Ph.D. dissertation. University of British Columbia, Vancouver. 1978.
38. N. A. Al-salem, H. D. Empsall, R. Markham, B. L. Shaw, and B. Weeks. J. Chem. Soc. Dalton Trans. 1972 (1979).

39. A. CONSTABLE, W. S. MCDONALD, and B. L. SHAW. J. Chem. Soc. Dalton Trans. 496 (1979).
40. B. R. JAMES and D. MAHAJAN. Isr. J. Chem. **15**, 214 (1977).
41. B. R. JAMES, D. MAHAJAN, and D. K. W. WANG. Proc. IXth Intern. Conf. Organometal. Chem. Dijon. 1979. Abstr. D29.
42. Y. KAWABATA, T. HAYASHI, and I. OGATA. J. Chem. Soc. Chem. Commun. 462 (1979).
43. M. LAING, M. J. NOLTE, and E. SINGLETON. J. Chem. Soc. Chem. Commun. 660 (1975).
44. F. A. COTTON and G. WILKINSON. Advanced inorganic chemistry. 3rd ed. Wiley, New York. 1972. pp. 635, 783.
45. J. CHATT and S. A. BUTTER. J. Chem. Soc. Chem. Commun. 501 (1967); J. Chem. Soc. A, 1411 (1970).
46. T. YOSHIDA, T. YAMAGATA, T. H. TULIP, J. A. IBERS, and S. OTSUKA. J. Am. Chem. Soc. **100**, 2063 (1978).
47. S. OTSUKA. Proc. IXth Intern. Conf. Organomet. Chem. Dijon. 1979. Abstr. S14.

Can. J. Chem. Downloaded from www.nrcresearchpress.com by 210.87.254.105 on 09/05/12
For personal use only.

Electrophilic cleavage of cyclopropanes. The areneselenenylation of tetracyclo[3.2.0.0^{2,7}.0^{4,6}]heptane (quadricyclene)[1,2]

PIERRE L. BEAULIEU, VERONIQUE M. MORISSET, AND DENNIS G. GARRATT[3]

Department of Chemistry, University of Ottawa, Ottawa, Ont., Canada K1N 9B4

Received October 2, 1979

PIERRE L. BEAULIEU, VERONIQUE M. MORISSET, and DENNIS G. GARRATT. Can. J. Chem. **58**, 1005 (1980).

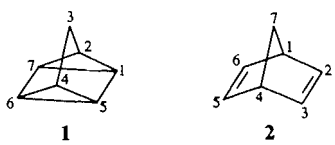
The reaction of benzeneselenenyl chloride with tetracyclo[3.2.0.0^{2,7}.0^{4,6}]heptane (quadricyclene) yields, under conditions of kinetic control, adducts of both 1,3- and conjugative 1,6-addition, the latter being formed preferentially. Electrophilic cleavage of the cyclopropane ring occurs by both retention and inversion of configuration. In agreement with the known propensity for bond cleavage in this system only the C5—C6 and/or the C1—C7 bonds are broken. The rate of cyclopropane ring cleavage is found to follow second order kinetics, first order in quadricyclene and first order in selenenyl chloride; k_{obs} = 1850 vs. 12 300 dm^3 mol^{-1} s^{-1} for bicyclo[2.2.1]hepta-2,5- diene at 24.5°C in methylene chloride solvent. The use of nucleophilic solvents such as HOAc, CH_3OH, and CH_3CN gives products of solvent-incorporation, preferentially via 1,3-addition.

PIERRE L. BEAULIEU, VERONIQUE M. MORISSET et DENNIS G. GARRATT. Can. J. Chem. **58**, 1005 (1980).

La réaction du chlorure de benzènesélénènyle avec le tétracyclo[3.2.0.0^{2,7}.0^{4,6}]heptane (quadricyclène) donne, sous contrôle cinétique, les adduits résultants d'une addition-1,3 ainsi que d'une addition conjuguée-1,6. L'addition conjuguée-1,6 est préférentielle. Le clivage électrophile du cyclopropane se produit à la fois avec rétention et inversion de configuration. Conformément à la tendance connue pour ce système à rompre les liaisons, seules les liaisons C5—C6 et/ou C1—C7 se rompent. On a trouvé que la vitesse d'ouverture du cyclopropane a une cinétique de second ordre. Elle est d'ordre 1 dans le cas du quadricyclène et d'ordre 1 dans le cas du chlorure de sélénènyle; k_{obs} = 1850 vs. 12 300 dm^3 mol^{-1} s^{-1} dans le cas du bicyclo[2.2.1]heptane diène-2,5 à 24.5°C dans le chlorure de méthylène. L'utilisation de solvants nucléophiles, tels que AcOH, CH_3OH et CH_3CN donne de préférence des produits d'incorporation du solvant par l'intermédiaire d'une addition-1,3.

[Traduit par le journal]

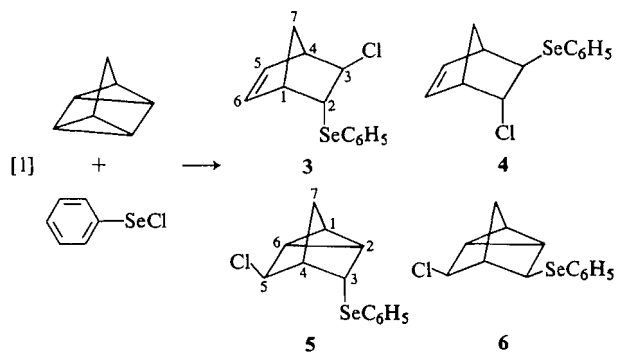
Electrophilic additions of areneselenenyl halides (1) and pseudohalides (2) to carbon–carbon double and triple bonds have received considerable interest of late. No attention has, however, been devoted to the possible reaction of these electrophiles with carbon–carbon single bonds in, for example, cyclopropanes. In this article we wish to report the results of a detailed examination of the cyclopropane ring cleavage of tetracyclo[3.2.0.0^{2,7}.0^{4,6}]heptane, **1**, using benzeneselenenyl chloride as the electrophilic reagent. The choice of **1** as substrate was made from a consideration of its anticipated high reactivity with selenium electrophiles. Both **1** and the isomeric olefin bicyclo[2.2.1]hepta-2,5-diene, **2**, normally display high reactivity (3), presumably as a result of their large strain energies, 78.7 and 25.6 kcal mol^{-1}, respectively (4). Earlier studies involving the reaction of benzeneselenenyl chloride with **2** substantiate these expectations (5); the specific rate constants for the reactions of **2** and the less strained olefin, cyclohexene, with benzeneselenenyl chloride in methylene chloride solution at 25°C being, respectively, 12 400 and 272 dm^3 mol^{-1} s^{-1}.



1 **2**

Results

The reaction of **1** with benzeneselenenyl chloride was initially studied in methylene chloride solution at 23–25°C. The reaction is essentially instantaneous, the deep red coloration of the selenenyl chloride solution disappearing immediately upon mixing. Immediate ^1H and ^{13}C nmr analysis of the crude product mixture, after work-up, shows the presence of four adducts **3–6** in the relative proportions 62:30:5:3. No evidence was found for prod-



3 **4** **5** **6**

[1]NRCC No. 18144.

[2]We have chosen to use the nomenclature as given instead of that initially proposed: quadricyclo[2.2.1.0^{2,6}.0^{3,5}]heptane.

[3]Author to whom correspondence may be addressed at the Division of Chemistry, National Research Council of Canada, 100 Sussex Dr., Ottawa, Ont., Canada K1A 0R6.

0008-4042/80/101005-09$01.00/0

©1980 National Research Council of Canada/Conseil national de recherches du Canada

Can. J. Chem. Downloaded from www.nrcresearchpress.com by 210.87.254.6 on 09/05/12
For personal use only.

TABLE 1. Solvent dependence of the product ratio under conditions of kinetic control for the cyclopropane ring cleavage of tetracyclo[3.2.0.0^{2,7}.0^{4,6}]heptane by benzeneselenenyl chloride at 23–25°C

Solvent	ε[a]	% Composition 3	4	5	6	7	8	Ratio A[b]	Ratio B[c]
n-C_5H_{12}	1.84 (20°C)	63	26	5	6	—	—	68:32	89:11
CCl_4	2.23	61	27	4	8	—	—	65:35	88:12
Et_2O	4.34 (20°C)	54	23	9	14	—	—	63:37	77:33
CH_2Cl_2	8.9	62	30	5	3	—	—	67:33	91:9
CH_3CN	36.2	15	6	11	9	54	5	80:20	21:79
HOAc	6.19	20	9	0	0	48	23	68:32	29:71
CH_3OH	32.6	0	0	0	0	74	26	74:26	0:100

[a]Dielectric constant at 25°C, except as indicated in parentheses, for the pure liquid.
[b]Ratio A: the ratio of edge-on attack to corner or end-on attack.
[c]Ratio B: the ratio of conjugative 1,6-addition to 1,3-addition.

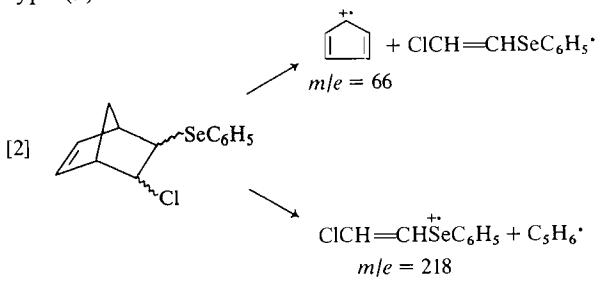
ucts of Wagner–Meerwein type rearrangement or alternative configurations with respect to 1,3- or conjugative 1,6-addition.

Similar results are observed when the solvent is *n*-pentane, carbon tetrachloride, or diethyl ether, as is shown in Table 1. The effect of polar hydroxylic solvents such as alcohols and carboxylic acids, wherein substantial amounts of solvent-incorporated products may be formed, was also investigated. Results obtained using methanol, acetonitrile, and acetic acid as solvent are also given in Table 1.

Assignment of structures, as shown in eq. [1], follows from an analysis of their spectral properties and a comparison of these data (ir, ms, and ^{1}H, ^{13}C nmr) with those of the known sulphur analogues (6). For example, the two tricyclo[2.2.1.0^{2,6}]heptanes, **5** and **6**, each have seven aliphatic carbon resonances in their respective ^{13}C nmr spectra, three of which resonate at higher field than those normally associated with the bicyclo[2.2.1]heptane ring system (7). The presence of these high field carbons indicates that only one of the two cyclopropane rings in **1** has been cleaved during the formation of these species. Additional support for these assignments is found in the ir spectra in the form of weak–medium absorptions in the range 12.2–12.6 μm (8).

The structure of **5** is clearly the C3 epimer of **6** as determined by ^{13}C nmr analysis. The *endo* orientation of the phenylseleno moiety at C3 in **5** follows from the observed paramagnetic shift of C3 in **5** relative to **6** and a diamagnetic shift of C5, albeit a small one, in **5** relative to **6**. The small absolute value of this latter shift difference was unanticipated but presumably results from a combination of the expected γ-*gauche* interaction and an anisotropy effect from the phenyl ring operating in the opposite sense. A similar observation has been made with respect to the analogous sulphur compounds.

Compounds **3** and **4** both have five aliphatic carbons and two olefinic carbons as determined by ^{13}C nmr spectroscopy. Mass spectral analysis of samples of each species shows molecular ions at *m/e* 284 (calcd. 283.657). A major fragmentation path for each compound is the mass spectrometric equivalent of a "retro Diels–Alder reaction" giving rise to a very strong peak at *m/e* 66 which corresponds to a $C_5H_6^{+\cdot}$ fragment. The presence of an intense ion cluster at *m/e* 218 (calcd. 217.559 C_8H_7SeCl) indicates that either fragment may carry the positive charge. This observation is strong evidence for norbornenyl derivatives with only protons in positions C1, 4, 5, 6 and C7, thus ruling out skeletal rearrangements of the Wagner–Meerwein type (9).

[2] 

The ^{1}H nmr spectrum of **4** has two triplets situated at δ 4.30 and 3.05 ppm. Associating the low field triplet with a proton geminal to chlorine and the high field triplet with a proton geminal to the phenylseleno group allows one to tentatively assign the proton geminal to chlorine as *exo* and that geminal to the phenylseleno moiety as *endo* (10).[4] In contrast, **3** has apparent triplets at δ3.86 and 3.62 ppm. If one again associates the low field triplet with the proton geminal to chlorine and the high field triplet with the proton geminal to the

[4]This follows from a comparison of the spectral properties of the adduct derived from benzeneselenenyl chloride and bicyclo[2.2.1]hept-2-ene, the data for which are given in the Experimental.

Can. J. Chem. Downloaded from www.nrcresearchpress.com by 210.87.254.6 on 09/05/12
For personal use only.

TABLE 2. A comparison of the specific rate constants for the reactions of benzeneselenenyl chloride and benzenesulphenyl chloride with tetracyclo[3.2.0.0^{2,7}.0^{4,6}]heptane and bicyclo[2.2.1]hepta-2,5-diene in methylene chloride solution at 24.5°C

	Tetracyclo[3.2.0.0^{2,7}.0^{4,6}]heptane, **1**			Bicyclo[2.2.1]hepta-2,5-diene, **2**		
Reactant	k_{obs}[a]	k_{edge}	k_{corner} (dm^3 mol^{-1} s^{-1})	k_{obs}[b]	k_{endo}	k_{exo} (dm^3 mol^{-1} s^{-1})
C_6H_5SeCl	1850	1239.5	610.5	12300	4674	7626
C_6H_5SCl	270	113	157	1600	1392	208

[a] $k_{obs} = k_{edge} + k_{corner}$. [b] $k_{obs} = k_{endo} + k_{exo}$.

Parameter	Value (kcal mol^{-1}) Compound **1**	Compound **2**
ΔH_f^0 (condensed phase, 25°C)[c]	+51.70	+42.72
Strainless ΔH_f (gas phase)	−18.09	+25.0
Strain energy	78.7	25.6

[c] $\Delta H_i = \Delta\Delta H_f = [\Delta H_f^0\,(\mathbf{2}) - \Delta H_f^0\,(\mathbf{1})] = 42.72 - 51.70 = -8.98$ kcal mol^{-1}. ΔH_f^0 are from enthalpy of combustion data for the condensed phase at 25°C.

Reactant	k_{obs} **1**/k_{obs} **2**	$\Delta\Delta G^{\ddagger}$ (kcal mol^{-1})[d]	k_{edge}/k_{endo}	$\Delta\Delta G^{\ddagger}$	k_{corner}/k_{exo}	$\Delta\Delta G^{\ddagger}$
C_6H_5SeCl	0.150	−1.12	0.163	−1.07	0.131	−1.20
C_6H_5SCl	0.169	−1.05	0.543	−0.36	0.113	−1.29

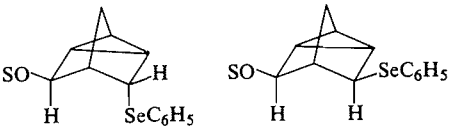
[d] $\Delta\Delta G^{\ddagger} = [\Delta G^{\ddagger}\,(\mathbf{2}) - \Delta G^{\ddagger}\,(\mathbf{1})] = RT \ln (k_{obs}\ \mathbf{1}/k_{obs}\ \mathbf{2})$.

phenylseleno group, and notes that the chemical shifts of *endo* protons are usually shifted upfield relative to *exo* protons, all else being equal, it is apparent that in this case the chlorine atom is oriented *exo* and the phenylseleno moiety is oriented *endo*, the opposite to **4**.

In view of the relatively large ratio of olefinic to cyclopropyl adducts ((**3** + **4**)/(**5** + **6**) = 91:9 in, for example, CH_2Cl_2) it is important to know the possibility regarding isomerization of **1** and **2** under our reaction conditions. Control experiments using an excess of **1** show only the presence of unreacted **1**, thereby suggesting that the products arise solely via ionic cleavage of the cyclopropane rings of **1**. As a further probe in this regard we have determined the rate of reaction of **1** with benzeneselenenyl chloride.

The rate of cyclopropane ring cleavage by benzeneselenenyl chloride in methylene chloride solution at 24.5°C was followed by the stopped-flow technique using a Durrum–Gibson stopped-flow spectrophotometer. The rate of disappearance of benzeneselenenyl chloride was followed by measuring the decrease in its absorption at 433 nm. The cyclopropane ring cleavage was found to exhibit second order kinetics, first order in quadricyclene **1**, and first order in selenenyl chloride, to at least 80% completion of the reaction. For comparison the specific rate constants for the addition to the isomeric olefin **2** and the analogous results for the reactions of benzenesulphenyl chloride are given in Table 2.

When hydroxylic solvents were used, the only products of solvent-incorporation isolated or observed were the C3 epimeric tricyclo[2.2.1.0^{2,6}]heptanes, **7** and **8**, formed with inversion



7 **8**

SO = CH_3O
CH_3CO_2

of configuration at C5, the site of nucleophilic attack by the solvent. No evidence was found for conjugative 1,6-addition or products of Wagner–Meerwein rearrangement.

In order to ascertain whether or not the electrophile was indeed still the selenenyl chloride,[5] a series of control experiments were carried out under equivalent conditions but in the absence of the substrate **1**. While both acetic acid and methanol will react with benzeneselenenyl chloride, the former albeit extremely slowly, we were able to determine that the substrate **1** reacts many orders of magnitude faster. To ensure that benzeneselenenyl chloride would be the predominant, if not the only, electrophilic species, we always added the powdered selenenyl chloride or a concentrated solution of it in methylene chloride

[5]Selenenyl halides are known to react with alcohols to give selenenic esters (11).

Can. J. Chem. Downloaded from www.nrcresearchpress.com by 210.87.254.6 on 09/05/12
For personal use only.

Can. J. Chem. Downloaded from www.nrcresearchpress.com by 210.87.254.6 on 09/05/12
For personal use only.

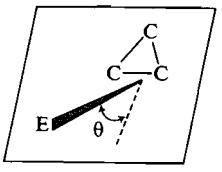
(the minimum volume possible was used), with vigorous stirring, to a solution of **1** in the appropriate solvent.

The use of acetonitrile, a more basic but somewhat less nucleophilic solvent, yields a mixture of all four chloro adducts plus two acetamides, resulting from nucleophilic attack by the nitrogen atom of the solvent followed by hydrolysis under conditions of an aqueous work-up.

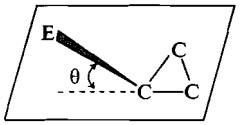
Discussion

Conceptually there exist two distinct modes whereupon a strained carbon–carbon single bond might interact with an electrophile EN. For example, the electrophile and the strained bond may approach each other orthogonally, ie. edge-on attack. In the case of cyclopropane itself one would anticipate the maximum interaction of orbitals to occur when the electrophile approaches the single bond in the same plane as the three carbons which define the ring, as is shown in Scheme 1 for $\theta = 0°$. In the case of a substituted cyclopropane as is found in the substrate **1**, the best angle of approach with respect to this plane may be significantly different, although values of θ as large as 90° seem very unlikely if one accepts the Walsh model for the orbitals in cyclopropanes. The major point to be noted is that this type of interaction leads to retention of configuration at the carbon atom, wherein the new bond is formed with the electrophilic portion of the reagent (E of EN).

Alternatively, the electrophile may approach the corner of the strained bond along an extended axis joining the two carbon atoms, that is to say, collinearly or end-on, the interaction ultimately resulting in inversion of configuration at the carbon atom forming the new bond with E. Once again, we note that in the case of an unsymmetrically substituted cyclopropane, as in **1**, the preferred orbital interaction may lead to an angle of approach somewhat different from the idealized situation of collinearity. The possible product configurations resulting from these scenarios are shown in Scheme 2 using **1** as substrate.



Edge-on Attack
retention of configuration at carbon
in plane $\theta = 0°$



Corner or End-on Attack
inversion of configuration at carbon
in plane $\theta = 0°$, equivalent to collinear attack

SCHEME 1

This classical approach may be unnecessarily restrictive as initial attack may in fact involve an *edge which does not finally suffer cleavage*, with subsequent cleavage occurring after edge-to-corner isomerization (3*c*). Such a scenario, however, exchanges one problem for another, that is, how does one distinguish whether or not attack occurs on a bond which *is not* subsequently cleaved or in some other way altered? Since no attempts in this laboratory or elsewhere, to our knowledge, have succeeded, we propose to consider our results in terms of the concepts just developed.

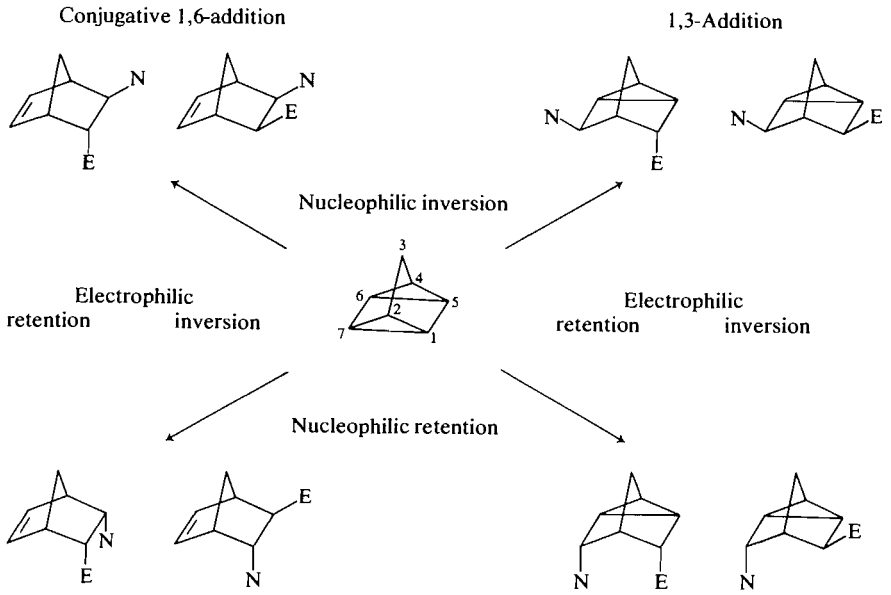
From a mechanistic viewpoint, the results given in Table 1 may be explained in terms of the two classical competitive pathways on the reaction hypersurface as shown in Scheme 3 for the specific case of areneselenenylation.

The reasonableness of this scheme is readily demonstrated by an examination of the available data. The observation of second order kinetics, first order in both selenenyl chloride and cyclopropane, **1**, serves to define the composition of the

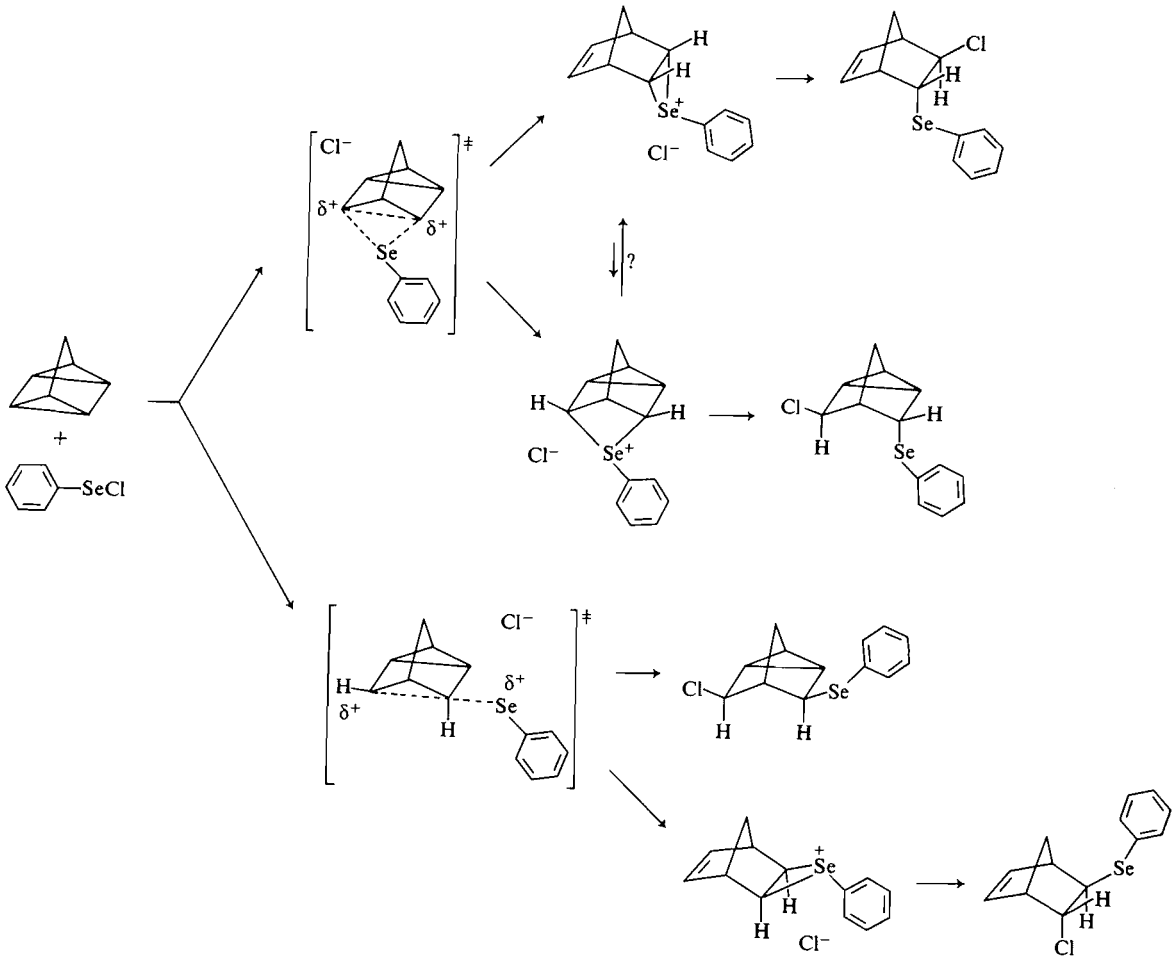
$$[3] \quad -d[C_6H_5SeCl]/dt = k_{obs}[C_6H_5SeCl][\mathbf{1}]$$

rate determining transition state(s) as containing one molecule of each species. In accord with our previous discussion, the observation of products with both *exo* and *endo* phenylseleno groups implies two different modes of approach and interaction. In this respect it becomes clear that our rate constant k_{obs} may be partitioned into at least two terms, k_{edge} and k_{corner}. The values of these terms may be estimated from the observed product distributions under conditions of kinetic control. This necessitates that we make the assumption that the reverse reaction(s) are much slower than the primary interaction and that the activation energy for product formation is very small compared with the barrier height for interconversion among the intermediate ions, which seems reasonable. The ratio of the products is then equal to the ratio of the population of the starting states.

On this basis, since 67% of the attack is edge-on, and 33% of the attack is corner, we obtain $k_{edge} = 1239.5$, and $k_{corner} = 610.5\ dm^3\ mol^{-1}\ s^{-1}$, respectively. A similar partitioning of the k_{obs} for the reaction of benzeneselenenyl chloride with **2** and the corresponding data for benzenesulphenyl chloride are given in Table 2.



SCHEME 2



SCHEME 3

Can. J. Chem. Downloaded from www.nrcresearchpress.com by 210.87.254.6 on 09/05/12
For personal use only.

Can. J. Chem. Downloaded from www.nrcresearchpress.com by 210.87.254.6 on 09/05/12
For personal use only.

An analysis of these reactivity data is quite instructive. Bicyclo[2.2.1]hepta-2,5-diene, **2**, is known to be more stable than **1**. The strain inherent in these polycyclic systems results in a value of ΔH_f^0 for **1** which is larger than that for **2** by 8.98 kcal mol^{-1} in the condensed phase at 25°C and 9.95 kcal mol^{-1} in the gas phase (12). The strainless $\Delta\Delta H_f^0$ is calculated to be approximately 43.1 kcal mol^{-1} which leads to a calculated difference in strain energies of 52.1–53.1 kcal mol^{-1} (13). The question thus arises as to the extent to which this difference in enthalpies, or strain energies, is retained at the rate determining and product determining transition states.

If relief of all or some part of this ground state strain difference occurs, the difference in the free energy of activation, $\Delta\Delta G^{\ddagger}$ ($=\Delta G^{\ddagger}(\mathbf{2}) - \Delta G^{\ddagger}(\mathbf{1}) \equiv RT \ln[k_{obs}\mathbf{1}/k_{obs}\mathbf{2}]$), will be positive. On the other hand, an increase in the ground state strain difference will lead to a negative value for $\Delta\Delta G^{\ddagger}$. This latter scenario corresponds to a negative value of $\ln[k_{obs}\mathbf{1}/k_{obs}\mathbf{2}]$ or a value for $k_{obs}\mathbf{1}/k_{obs}\mathbf{2}$ of less than one. Such an observation would be indicative of an opening of the free energy gap between the initial isomer pair where ΔG_i, the free energy of isomerization for the process $\mathbf{1} \rightarrow \mathbf{2}$, is less than zero.

As can be seen from the analysis in Table 2, both benzeneselenenyl chloride and benzenesulphenyl chloride react with **1** and **2** in a similar fashion giving rise to values of $\Delta\Delta G^{\ddagger}$ of -1.12 and -1.05 kcal mol^{-1}, respectively. Values of $\Delta\Delta G^{\ddagger}$ based upon a partitioning of the data in terms of *edge-on* and *endo* attack or *corner* and *exo* attack are also negative, indicative therefore of rate determining transition states with apparently little or no release of the strain energy inherent in **1** relative to that of **2**. Phrased somewhat differently, the available data are indicative of a higher activation energy for the reaction of these electrophiles with **1**.

Mechanistically, we interpret these data as reflecting the expected much lower reactivity of a cyclopropyl single bond relative to an olefinic double bond. The difference in reactivity is apparently so large that even the possible release of 53 kcal mol^{-1} of strain energy is not able to force a reversal of the normal trend. Alternatively, if one views the electrophilic interaction of these reagents with **1** and **2** as examples of nucleophilic displacement at bivalent selenium or sulphur, it is possible to interpret our data in terms of the cyclopropane single bond reacting as a poorer nucleophile than the π orbital of the olefinic double bond.

Considering the observed product distributions, Table 1, we observe a number of trends. For example, in all solvent systems studied the proportion of edge-on attack is greater than that of corner or end-on attack. In particular, the percentage of edge-on attack is relatively constant, 66 ± 3%, for solvents with a dielectric constant, ε, less than 10, where the effect of the dielectric constant of the medium is approximately comparable to that of its specific solvating action (14). In the case of methanol, where the dielectric constant is 32.6, the effect of the dielectric constant appears to be of minor importance compared with the specific solvating action (14, 15). This latter point is perhaps best demonstrated by the greater proportion of edge-on attack, 74% vs. 66%, and the complete absence of products of conjugative 1,6-addition. We note that the latter are observed to predominate when non-nucleophilic solvents are used.

In acetonitrile, a solvent system which may be considered slightly more polar and more basic, but less nucleophilic, than either acetic acid or methanol, we observe an even larger ratio of edge-on attack to corner attack, 80:20. In contrast to methanol, we observe products of conjugative 1,6-addition in the product mixtures obtained from acetonitrile and acetic acid, plus the chloro adducts, **5** and **6**, in acetonitrile. These latter results are interpreted as reflecting the lower nucleophilicities of these solvents compared to methanol. Of particular note are the enhanced yields of tricyclo[2.2.1.0^{2,6}]heptanes in the nucleophilic solvents, and the observation that these tricyclic adducts are almost exclusively products of solvent-incorporation. The presence of solvent-incorporated products of 1,3-addition and the absence of the analogous species of conjugative 1,6-addition presumably reflects the ability of these solvents to effectively trap the first formed cationic intermediates before rearrangement is possible.

The predominance of edge-on attack during areneselenenyl chloride addition is interpreted as the result of a combination of the very good neighbouring group ability of bivalent selenium (16) and the high electron density along the edge of the cyclopropane defined by the C1—C7 and C5—C6 bonds of **1**.

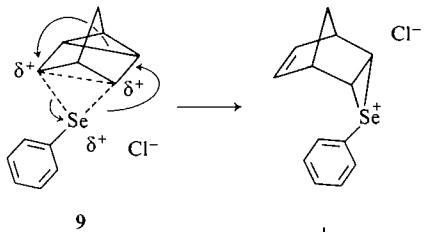
The products of conjugative 1,6-addition are of some interest since they serve to establish the orientation of ring opening in the second cyclopropane system as occurring stereospecifically with *inversion* of configuration at C3 when the electrophilic portion, E = C_6H_5Se, attacks with *retention* of configuration at C2, but with *retention* of configuration at C3 when E(=C_6H_5Se) forms a new bond with *inversion* at C2. This stereospecificity may be explained by the isomerization of the initially formed selenonium ions, **9** (a selenetanium ion) and **10**, to *endo* and *exo* norbor-

Can. J. Chem. Downloaded from www.nrcresearchpress.com by 210.87.254.6 on 09/05/12
For personal use only.

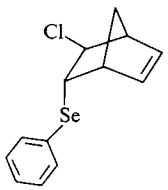
nenyl seleniranium ions (eqs. [4] and [5]) followed by nucleophilic attack by chloride ion. In this regard we note that the tricyclic adducts **5**–**8** are *exo* at C5, implying inversion of configuration at carbon, which is indicative, using Cristol *et al.*'s criteria of the absence of free carbonium ions on the reaction hypersurface (17).

The configurational results given above are similar to those obtained when one uses the analogous sulphenyl chloride as the electrophile (18, 19).

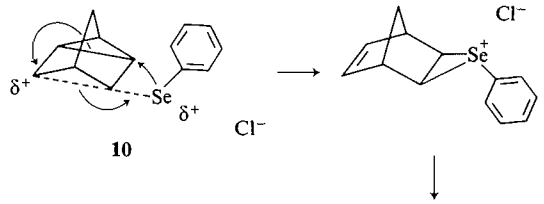
[4]



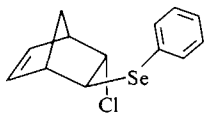
9



[5]



10



In comparing our data for areneselenenylation with that for arenesulphenylation a number of important differences are immediately obvious (19). Firstly the ratio of edge-on attack to corner attack favours corner attack, 42:58, these data contrasting with the 67:33 ratio found during this investigation. Secondly, 1,3-addition is favoured over conjugative 1,6-addition, 76:24, during arenesulphenylation compared to a value of 9:91 during areneselenenylation. Thirdly, no product of conjugative 1,6-addition resulting from edge-on attack is observed during the addition of arenesulphenyl chlorides to **1**, while the analogous species is the major adduct formed during the areneselenenyl chloride addition reaction! This result is very significant since it appears to indicate that the conjugative cyclopropyl group is unable to compete with neighbouring bivalent sulphur for stabilization of positive charge at C5 during edge-on attack, but does compete very effectively with bivalent selenium. This rationale, which suggests that bivalent sulphur is a better neighbouring group than bivalent selenium leads, however, to a contradiction, in that the preference for the selenenyl chloride to attack edge-on while sulphenyl chlorides prefer corner attack seems to be indicative of bivalent selenium being the more effective neighbouring group. We interpret this difference in product distributions in terms of isomerizations of the type shown in eq. [4]. The data given herein suggest that in nonpolar media the *endo* norbornenyl seleniranium ion is favored over the selenetanium ion, whereas during sulphenylation the analogous thietanium ion is the more stable species.

Experimental

General

^{1}H nuclear magnetic resonance spectra were recorded on Varian Associates T-60 and HA-100 spectrometers; ^{13}C nmr spectra were recorded on a Varian FT80-16K spectrometer using chloroform-*d* as an internal lock and reference. All spectral parameters are referenced to TMS as an internal standard and all spectra were run in sealed tubes. Infrared spectra were run in NaCl cavity cells as CCl_4 solutions using a Unicam 1100 spectrophotometer.

Benzeneselenenyl chloride was available commercially (Aldrich). This material contains a small amount of phenylselenium trichloride and must be recrystallized prior to use.

Tetracyclo[3.2.0.0^{2,7}.0^{4,6}]heptane, **1**, was purchased from Aldrich and used without further purification. The purity of **1** was established via nmr and glc. All analytical and preparative tlc separations were performed on Analtech or Macherery–Nagel precoated plates, silica gel GF, using CH_2Cl_2 as eluant. Spot visualization was accomplished using uv, iodine, and phosphomolbydic acid – EtOH.

Caution

Scrupulous avoidance of contact with the materials used during this study is essential. All reactions were carried out in an isolation glove box equipped with a filter system suitable for use with carcinogenic or radioactive material, with a reduced atmospheric pressure inside the box. This procedure was used because of medical problems which arose during the course of study of the analogous reaction with **2** *approximately four years previously. Within twelve hours of carrying out the areneselenenylation reaction with norbornadiene, the author suffered an acute attack of asthmatic bronchitis. This attack resulted in hospitalization of the experimenter. There had been no prior history of attacks of this nature. The medical diagnosis* suggests *that the attack may have resulted from a chemical irritant. Subsequent increased sensitivity towards lung problems has been noted by the author, particularly with respect to norbornenyl and nortricyclyl compounds. The physical and toxicological properties of these selenium compounds have not been fully investigated. Organoselenium compounds are, in general, somewhat malodorous and have in some cases been reported as carcinogenic.*

Can. J. Chem. Downloaded from www.nrcresearchpress.com by 210.87.254.6 on 09/05/12
For personal use only.

The Reaction of Benzeneselenenyl Chloride with Tetracyclo[3.2.0.0^{2,7}.0^{4,6}]heptane

A solution of C_6H_5SeCl (0.575 g, 3.00 mmol) in 20 mL anhydrous CH_2Cl_2 was added dropwise to a stirred solution containing **1** (0.276 g, 3.00 mmol) in 30 mL of anhydrous CH_2Cl_2 at room temperature. The red coloration of the selenenyl chloride disappeared immediately. The solvent was removed at room temperature and the crude yellow oil stored under nitrogen. This oil, which corresponded to a quantitative yield, was analyzed by nmr. A similar procedure was used in the cases involving *n*-pentane, diethyl ether, cyclohexane, and carbon tetrachloride. When acetonitrile or acetic acid was used as solvent the reaction mixture, including solvent, was extracted from aqueous medium and neutralized with sodium carbonate, using methylene chloride. Adduct mixtures were dried over magnesium sulphate and isolated as above. The solvent methanol was removed by evaporation at 45°C. Control experiments indicate that methanolysis of chloro adducts under these conditions is negligible.

Exo-*3-phenylseleno*-exo-*5-chlorotricyclo[2.2.1.0^{2,6}]heptane* **6** gave ir (CCl_4, NaCl): 12.35 μm (nortricyclene); ^{1}H nmr δ: 3.96 (bs, 2H, C3*H*, C5*H*); ^{13}C nmr δ: 14.8 (d, C1), 16.7 (d, C2), 49.8 (d, C3), 42.8 (d, C4), 64.8 (d, C5), 20.5 (d, C6), 34.2 (t, C7).

Endo-*3-phenylseleno*-exo-*5-chlorotricyclo[2.2.1.0^{2,6}]heptane* **5** gave ir (CCl_4, NaCl): 12.3 μm; ^{1}H nmr δ: 4.02 (m, 1H, C5*H*Cl), 3.82 (m, 1H, C3*H*Se); ^{13}C nmr δ: 12.2 (d, C1), 17.3 (d, C2), 50.2 (d, C3), 41.0 (d, C4), 62.4 (d, C5), 19.6 (d, C6), 30.2 (t, C7).

Endo-*3-chloro*-exo-*2-phenylselenobicyclo[2.2.1]hept-5-ene* **4** gave ^{1}H nmr δ: 3.10 (m, H1), 3.05 (t, H2), 4.30 (t, H3), 3.2 (m, H4), 6.36 (dt, H5), 6.24 (dt, H6), 1.76 (m, 2H, H7), $J_{2,3}$ = 3.6 Hz; $J_{1,2}$ = 0.32 Hz; $J_{3,4}$ = 3.2 Hz; $J_{2,7\text{-}anti}$ = 3.0 Hz; $J_{5,6}$ = 6.5 Hz; ^{13}C nmr δ: 49.5 (d, C1), 50.6 (d, C2), 64.9 (d, C3), 49.6 (d, C4), 134.9 (d, C5), 137.0 (d, C6), 46.3 (t, C7).

Endo-*2-phenylseleno*-exo-*3-chlorobicyclo[2.2.1]hept-5-ene* **3** gave ^{1}H nmr δ: 3.16 (m, H1), 3.62 (dt, H2), 3.86 (dt, H3), 3.22 (m, H4), 6.27 (dt, H5), 6.13 (dt, H6), 1.9 (m, 2H, H7), $J_{2,3}$ = 3.5 Hz; $J_{1,2}$ = 3.5 Hz; $J_{3,4}$ = 0.3 Hz; $J_{2,7\text{-}anti}$ = 1.2 Hz; $J_{3,7\text{-}anti}$ = 3.8 Hz; $J_{5,6}$ = 5.2 Hz; ^{13}C nmr Δ: 52.2 (d, C1), 53.0 (d, C2), 65.8 (d, C3), 47.7 (d, C4), 137.6 (d, C5), 131.8 (d, C6), 46.7 (t, C7).

Endo-*3-chloro*-exo-*2-phenylselenobicyclo-[2.2.1]heptane*

To a solution of 0.0942 g (1 mmol) of bicyclo[2.2.1]hept-2-ene dissolved in 25 mL of anhydrous methylene chloride was added a solution of 0.1915 g (1 mmol) benzeneselenenyl chloride. The reaction mixture was briefly stirred until no further colour change (red → colourless) was observed. The solvent was evaporated to give an orange to yellow oil in essentially quantitative yield (96–100%); ^{1}H nmr δ: 2.37 (m, H1), 3.06 (dd, H2), 4.15 (dt, H3), 2.43 (m, H4), 1.3–2.1 (m, H5,6), 1.57 (m, H7); $J_{2,3}$ = 4.0 Hz; $J_{3,4}$ = 3.2 Hz; $J_{2,7\text{-}anti}$ = 2.8 Hz; $J_{3,5\text{-}exo}$ = 0.8 Hz; $J_{1,2}$ = 0.0; ^{13}C nmr δ: 44.5 (d, C1), 54.2 (d, C2), 68.0 (d, C3), 44.6 (d, C4), 21.6 (t, C5), 29.6 (t, C6), 36.3 (t, C7).

Exo-*3-phenylseleno*-exo-*5-methoxytricyclo[2.2.1.0^{2,6}]heptane* gave ir ($CHCl_3$, NaCl) μm: 12.2 (m, nortricyclene); ^{1}H nmr δ: 3.54 (m, 1H, C*H*Se), 3.96 (m, 1H, C*H*OCH$_3$), 1.2–2.5 (m, 6H), 3.25 (s, 3H, CH$_3$O); ^{13}C nmr δ: 14.2 (d, C1), 16.9 (d, C2), 46.4 (d, C3), 38.2 (d, C4), 86.0 (d, C5), 17.4 (d, C6), 29.0 (t, C7), 56.6 (q, CH$_3$O).

Endo-*3-phenylseleno*-exo-*5-methoxytricyclo[2.2.1.0^{2,6}]heptane* gave ir ($CHCl_3$, NaCl) μm: 12.2 (m, nortricyclene); ^{1}H nmr δ: 3.50 (m, 1H, C*H*Se), 3.80 (m, 1H, C*H*OCH$_3$), 1.2–2.5 (m, 6H), 3.29 (s, 3H, CH$_3$O); ^{13}C nmr δ: 12.2 (d, C1), 17.3 (d, C2), 46.6 (d, C3), 38.2 (d, C4), 84.3 (d, C5), 19.5 (d, C6), 27.7 (t, C7), 56.5 (q, CH$_3$O).

Exo-*3-phenylseleno*-exo-*5-acetyltricyclo[2.2.1.0^{2,6}]heptane* gave ir ($CHCl_3$, NaCl) μm: 12.2 (m, nortricyclene), 5.74 (s, acetate, C=O); ^{13}C nmr δ: 14.8 (d, C1), 17.3 (d, C2), 46.0 (d, C3), 42.5 (d, C4), 79.6 (d, C5), 19.3 (d, C6), 30.0 (t, C7), 170.7 (s, C=O), 21.1 (q, *C*H$_3$CO$_2$).

Endo-*3-phenylseleno*-exo-*5-acetyltricyclo[2.2.1.0^{2,6}]-heptane* gave ir ($CHCl_3$, NaCl) μm: 12.2 (m, nortricyclene), 5.74 (s, acetate, C=O); ^{13}C nmr δ: 12.4 (d, C1), 19.9 (d, C2), 46.3 (d, C3), 42.6 (d, C4), 77.7 (d, C5), 20.7 (d, C6), 28.3 (t, C7), 170.7 (s, C=O), 20.7 (q, *C*H$_3$CO$_2$).

Endo-*3-phenylseleno*-exo-*5-acetamidotricyclo[2.2.1.0^{2,6}]-heptane* gave ir ($CHCl_3$, NaCl) μm: 5.96 (s, RCONH), 2.85 (m, NH), 2.96 (bm, NH), 6.25 (s, NH), 6.55 (s, NH), 12.2 (m, nortricyclene); ^{13}C nmr δ: 11.5 (d, C1), 17.0 (d, C2), 47.4 (d, C3), 39.4 (d, C4), 54.2 (d, C5), 18.1 (d, C6), 27.6 (t, C7), 170.0 (s, NH*C*=O), 22.9 (q, *C*H$_3$CONH); ms *m/e*: M$^+$ 307. All samples gave satisfactory elemental analyses and mass spectra in addition to the ir and nmr data given above.

Kinetic Studies

All kinetic runs were carried out on a Durrum–Gibson stopped-flow spectrophotometer. Prior to any set of kinetic runs the instrument was allowed to stabilize for at least 2 h. A constant temperature bath was maintained at 24.50 ± 0.03 °C. The instrument was checked out and calibrated prior to each set of runs. Zero and 100% transmittance lines were determined by running pure solvent vs. the cyclopropane solution. Kinetic runs with each solution were carried out until a reproducible trace was stored on the oscilloscope. Measurements were carried out in the standard way. The specific rate constant for the reaction of benzeneselenenyl chloride with methanol in methylene chloride, under conditions equivalent to those used to determine k_{obs} for **1**, is 0.011 dm^3 mol^{-1} s^{-1}. Thus benzeneselenenyl chloride reacts with **1** approximately 1.7 × 10^5 times faster than it does with methanol. Since pure methanol is 24.7 mol dm^{-3}, the kinetic excess, or factor by which **1** will be preferred under our reaction conditions, [**1**] = 0.04 mol dm^{-3}, is approximately 274.

Acknowledgements

The continued financial support of the Natural Sciences and Engineering Research Council of Canada is gratefully acknowledged, as is a Province of Ontario Scholarship to one of us (PLB) 1978–1980. Useful discussions with Drs. G. H. Schmid, University of Toronto, R. R. Fraser, University of Ottawa, and O. E. Edwards, the Division of Chemistry, National Research Council of Canada, Ottawa are also greatly appreciated.

1. (*a*) D. G. Garratt and G. H. Schmid. J. Org. Chem. **42**, 1776 (1977); (*b*) D. G. Garratt. Can. J. Chem. **56**, 2184 (1978); (*c*) G. H. Schmid and D. G. Garratt. Tetrahedron Lett. 3991 (1975); (*d*) K. B. Sharpless and R. F. Lauer. J. Org. Chem. **39**, 429 (1974); (*e*) S. Raucher. J. Org. Chem. **42**, 2950 (1977); (*f*) F. Lautenschlaeger. J. Org. Chem. **34**, 4002 (1969); (*g*) D. L. J. Clive, G. Chittattu, and C. K. Wong. Can. J. Chem. **55**, 3894 (1977); (*h*) E. G. Kataev, T. G. Mannafov, E. A. Berdnikov, and O. A. Komarovskaya. Zh. Org. Khim. **9**, 1983 (1973); (*i*) E. G. Kataev, T. G. Mannafov, and Yu.Yu. Samitov. Zh. Org. Khim. **11**, 2324 (1975); (*j*) S. Raucher. Tetrahedron Lett. 3909 (1977); (*k*) D. L. J. Clive, G. Chittattu, N. J. Curtis, W. A. Kiel, and C. K. Wong. J. Chem. Soc. Chem. Commun. 725 (1977); (*l*) N. S. Zefirov, L. G. Gurvich, A. S. Shahkov, and V. A. Smit. Zh. Org. Khim. **10**, 1786 (1974); (*m*) G. H. Schmid and D. G. Garratt. Chem. Scr. **10**, 76 (1976); (*n*) G. H. Schmid and D. G. Garratt. Tetrahedron, **34**, 2869 (1978).
2. (*a*) G. Hölzle and W. Jenny. Helv. Chim. Acta, **41**, 593

(1958); (*b*) W. JENNY. Helv. Chim. Acta, **36**, 1278 (1953); (*c*) D. L. J. CLIVE. J. Chem. Soc. Chem. Commun. 100 (1974); (*d*) H. J. REICH. J. Org. Chem. **39**, 428 (1974); (*e*) D. G. GARRATT and G. H. SCHMID. Can. J. Chem. **52**, 3599 (1974); (*f*) D. G. GARRATT, M. D. RYAN, and M. UJJAINWALLA. Can. J. Chem. **57**, 2145 (1979); (*g*) D. G. GARRATT. Can. J. Chem. **57**, 2180 (1979).

3. (*a*) S. J. CRISTOL and R. T. LALONDE. J. Am. Chem. Soc. **80**, 4355 (1958); (*b*) S. J. CRISTOL, J. K. HARRINGTON, T. C. MORRILL, and B. E. GREENWALD. J. Org. Chem. **36**, 2773 (1971); (*c*) T. C. MORRILL, S. MALASANTA, K. M. WARREN, and B. E. GREENWALD. J. Org. Chem. **40**, 3032 (1975); (*d*) T. C. MORRILL and B. E. GREENWALD. J. Org. Chem. **36**, 2769 (1971); (*e*) S. J. CRISTOL and R. L. SNELL. J. Am. Chem. Soc. **76**, 5000 (1954); (*f*) W. G. DAUBEN and R. L. CARGILL. Tetrahedron, **15**, 197 (1961); (*g*) G. F. KOSER, P. R. PAPPAS, and S.-M. YU. Tetrahedron Lett. 4943 (1973); (*h*) S. F. NELSON, J. P. GILLESPIE, and P. J. HINTZ. Tetrahedron Lett. 2361 (1971); (*i*) G. S. HAMMOND, N. J. TURRO, and A. FISHER. J. Am. Chem. Soc. **83**, 4674 (1961); (*j*) S. J. CRISTOL, J. K. HARRINGTON, and M. S. SINGER. J. Am. Chem. Soc. **88**, 1529 (1966); (*k*) S. F. NELSON, J. P. GILLESPIE, P. J. HINTZ, and E. D. SEPPANEN. J. Am. Chem. Soc. **95**, 8380 (1973); (*l*) S. F. NELSON and J. C. CALABROSE. J. Am. Chem. Soc. **95**, 8385 (1973).
4. (*a*) H. K. HALL, JR., C. D. SMITH, and J. H. BALDT. J. Am. Chem. Soc. **95**, 3197 (1973); (*b*) R. B. TURNER, W. R. MEADOR, and R. E. WINKLER. J. Am. Chem. Soc. **79**, 4116 (1957); (*c*) P.V.R. SCHLEYER, J. E. WILLIAMS, and K. R. BLANCHARD. J. Am. Chem. Soc. **92**, 2377 (1970).
5. D. G. GARRATT. Ph.D. thesis, University of Toronto, Toronto, Ont., Canada. 1975.
6. (*a*) D. G. GARRATT, and P. L. BEAULIEU. J. Org. Chem. **44**, 3555 (1979); (*b*) S. J. CRISTOL, R. P. ARGANBRIGHT, G. D. BRINDELL, and R. M. HEITZ. J. Am. Chem. Soc. **79**, 6035 (1957); (*c*) G. H. SCHMID and T. C. MORRILL. Private communication; (*d*) N. S. ZEFIROV, N. K. SADOVAYA, R.SH. AKHOMEDOVA, and V. BODRIKOV. Zh. Org. Khim. **14**, 662 (1978); Chem. Abstr. **89**, 42641 (1978).
7. (*a*) E. LIPPMAA, T. PEHK, and J. PAASIVIRTA. Org. Magn. Reson. **5**, 277 (1973); (*b*) Y. MARINO, K. KIRCHITAU, and A. YONOZEKI. Bull. Chem. Soc. Jpn. **40**, 1552 (1967); (*c*) J. F. CHIANG, C. F. WILCOS, and S. H. BAUER. J. Am. Chem. Soc. **90**, 3149 (1968); (*d*) A. W. MCCULLOCH, A. G. MCINNES, D. G. SMITH, and J. A. WALTER. Can. J. Chem. **54**, 2013 (1976).
8. (*a*) J. D. ROBERTS, E. R. TRUMBALL, W. BENNETT, and R. ARMSTRONG. J. Am. Chem. Soc. **72**, 3116 (1950); (*b*) H. KWART and R. K. MILLER. J. Am. Chem. Soc. **78**, 5680 (1956); (*c*) J. D. ROBERTS, W. BENNETT, and R. ARMSTRONG. J. Am. Chem. Soc. **72**, 3329 (1950); (*d*) E. R. LIPPINCOTT. J. Am. Chem. Soc. **73**, 2001 (1951).
9. S. J. CRISTOL, R. A. SANCHEZ, and T. C. MORRILL. J. Org. Chem. **31**, 2738 (1966).
10. (*a*) D. LIOTTA and G. ZIMA. Tetrahedron Lett. **19**, 4977 (1978); (*b*) D. G. GARRATT and A. KABO. Can. J. Chem. This issue.
11. O. BEHAGHEL and W. MULLER. Ber. **68**, 1540 (1935); W. S. COOK and R. A. DONIA. J. Am. Chem. Soc. **73**, 2275 (1951).
12. (*a*) H. K. HALL, JR., C. D. SMITH, and J. H. BALDT. J. Am. Chem. Soc. **95**, 3197 (1973); (*b*) K. B. WIBERG and R. A. FENOGLIO. J. Am. Chem. Soc. **90**, 3395 (1968).
13. P. V. R. SCHLEYER, J. E. WILLIAMS, and K. R. BLANCHARD. J. Am. Chem. Soc. **92**, 2377 (1970).
14. L. P. HAMMETT. *In* Physical organic chemistry; reaction rates, equilibria, and mechanisms. 2nd ed. McGraw-Hill, New York. 1970. pp. 221–262.
15. (*a*) K. FREDENHAGEN and J. DEHMLOS. Z. Anorg. Allg. Chem. **179**, 77 (1929); (*b*) K. FREDENHAGEN. Z. Anorg. Allg. Chem. **186**, 1 (1930).
16. S. P. MCMANUS and D. H. LAM. J. Org. Chem. **43**, 650 (1978).
17. S. J. CRISTOL, J. K. HARRINGTON, and M. S. SINGER. J. Am. Chem. Soc. **88**, 1529 (1966).
18. T. C. MORRILL, S. MALASAVTA, K. M. WARREN, and B. E. GREENWALD. J. Org. Chem. **40**, 3032 (1975).
19. P. L. BEAULIEU, A. KABO, and D. G. GARRATT. Can. J. Chem. This issue.

Can. J. Chem. Downloaded from www.nrcresearchpress.com by 210.87.254.6 on 09/05/12
For personal use only.

Electrophilic cleavage of cyclopropanes. II. Concerning the effect of increasing electron demand upon the product-determining transition state in the reaction of 4-substituted-2-nitrobenzenesulphenyl chlorides and benzenesulphenyl chlorides with tetracyclo[3.2.0.0^{2,7}.0^{4,6}]heptane (quadricyclene)[1]

PIERRE L. BEAULIEU, ANN KABO, AND DENNIS G. GARRATT[2]

Department of Chemistry, University of Ottawa, Ottawa, Ont., Canada K1N 9B4

Received October 3, 1979

PIERRE L. BEAULIEU, ANN KABO, and DENNIS G. GARRATT. Can. J. Chem. **58**, 1014 (1980).

The effect of increasing electron demand upon the product-determining transition state in the reaction of arenesulphenyl chlorides with tetracyclo[3.2.0.0^{2,7}.0^{4,6}]heptane has been investigated. As the electron donating ability of the remote substituents on the phenyl ring of the sulphenyl chloride is varied from nitro to methoxy the relative proportion of adducts derived from edge-on attack is found to increase relative to that of adducts derived from corner attack. An *ortho*-nitro group was found to lead to a stabilizing interaction only in the case of 2,4-dinitrobenzenesulphenyl chloride. A mechanism involving the competition between the two conceptual modes of approach is suggested.

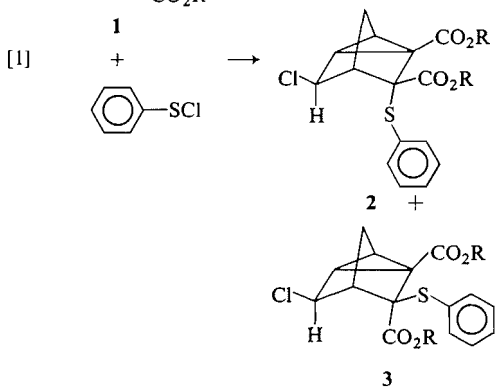
PIERRE L. BEAULIEU, ANN KABO et DENNIS G. GARRATT. Can. J. Chem. **58**, 1014 (1980).

On a étudié l'effet d'une augmentation de l'affinité électronique sur l'état de transition conduisant au produit principal lors de la réaction des chlorures d'arènesulphényles avec le tétracyclo[3.2.0.0^{2,7}.0^{4,6}]heptane. Comme la tendance à donner des électrons par des substituants dans des positions éloignées du cycle phényle du chlorure de sulphényle varie du groupe nitro au groupe méthoxy, on a trouvé que la proportion relative d'adduits résultant d'une attaque sur le côté augmente par rapport à celle des adduits résultant d'une attaque au sommet. On a trouvé qu'un groupe nitro en position *ortho* conduit à une interaction stabilisante uniquement dans le cas du chlorure de dinitro-2,4 benzènesulphényle. On suggère un mécanisme qui fait intervenir une compétition entre ces deux types d'approches.

[Traduit par le journal]

Considerable attention has been given to the mechanism of arenesulphenylation of carbon–carbon double and triple bonds (1). A survey of the literature, however, indicates a paucity of data with respect to the analogous electrophilic cleavage of carbon–carbon single bonds in strained systems such as cyclopropanes. The reaction of sulphenyl halides with simple alkyl- or aryl-substituted cyclopropanes is generally quite sluggish even in the presence of Lewis acids such as $AlCl_3$ and BF_3.[3] An apparent exception to these observations is the report of Morrill and co-workers (2) of the facile ionic cyclopropane ring cleavage in the highly strained quadricyclene systems tetracyclo[3.2.0.0^{2,7}.0^{4,6}]-heptane-1,5-dicarboxylic acid **1***a* and its dimethyl ester **1***b* by benzenesulphenyl chloride (eq. [1]) to give *exo*-5-chloro-*endo*-3-phenylthiotricyclo-[2.2.1.0^{2,6}]heptane-2-*exo*-3-dicarboxylic acid, **2***a*, the C3 epimer **3***a*, and the corresponding dimethyl esters, **2***b* and **3***b*, in approximately equal amounts, the addition of 4-toluenesulphenyl chloride, under

a R = H
b R = CH_3



equivalent conditions, giving analogous results (3).[4] These data were interpreted in terms of the

[1]NRCC No. 18145.

[2]Author to whom correspondence may be addressed at the Division of Chemistry, National Research Council of Canada, Ottawa, Ont., Canada K1A 0R6.

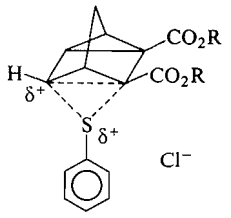
[3]D. G. Garratt and A. Kabo, unpublished results; B. B. Jarvis, University of Maryland, private communication; and G. Mandrapilias and K. Yates, University of Toronto, private communication.

[4]We have extended the *endo–exo* terminology beyond its original usage in norbornane systems (3*a*) to nortricyclenes in accord with the suggestion of Cristol and Lalonde (3*b*), by referring configurations with respect to the unsubstituted methano bridge. We agree with Cristol and Lalonde that the use of the terms *endo* and *exo* in these connotations is better than coining new terms, even though the original derivations are not precisely applicable.

0008-4042/80/101014-07$01.00/0

© 1980 National Research Council of Canada/Conseil national de recherches du Canada

Can. J. Chem. Downloaded from www.nrcresearchpress.com by 210.87.254.105 on 09/05/12
For personal use only.



4

absence of a bridged sulphonium ion, **4**, as the sole intermediate prior to the product-determining transition state.

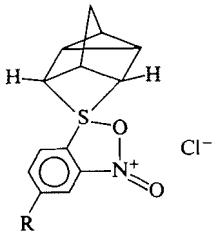
These results were very unexpected. Theoretical considerations based upon the Walsh model for cyclopropane (4) led one to predict that edge-on attack would be preferred over corner or end-on attack during electrophilic ring cleavage (5). The excellent neighbouring group ability (6) of bivalent sulphur, giving rise to species such as **4**, was expected to enhance this edge-on attack. These concepts have been discussed in detail in the preceding article.

The absence of epimers at C5 in Morrill *et al.*'s work is also of note since Cristol and co-workers have given evidence that the subsequent attack by the nucleophilic portion, N of EN, proceeds by inversion, unless a carbonium ion-like intermediate is formed on the reaction hypersurface prior to the product-determining transition state (7). Presumably both retention and inversion would have been observed if C5 obtained carbonium ion character, although the presence of ion-pairs, the importance of which has not been estimated, may lead to a situation favouring one epimeric form almost to the exclusion of the other.

A further intriguing aspect of Morrill *et al.*'s results with **1***a* and **1***b* is the absence of products derived from conjugative 1,6-addition. While such results appear common for the systems **1***a* and **1***b*, ionic cleavage of tetracyclo[3.2.0.$0^{2,7}$.$0^{4,6}$]heptane, **5**, usually gives substantial amounts of 2,3-disubstituted bicyclo[2.2.1]hept-2-enes as well as 3,5-disubstituted tricyclo[2.2.1.$0^{2,6}$]heptanes and, in some cases, products of Wagner–Meerwein type rearrangement (8).

In this article we report our observations of cyclopropane ring cleavage in **5** using a series of arenesulphenyl chlorides. The substrate **5** was chosen to allow comparisons to be made with a previous study from this laboratory, which utilized the isomeric olefin bicyclo[2.2.1]hepta-2,5-diene (9). Our aim here and in the previous study (9) is to demonstrate the variable product ratios which result from making minor changes in the electrophilicity of the sulphenyl chloride while holding the steric factors in the product-determining transition state constant. In effect we use the tool of increasing electron demand (10). The relative proportions of the *endo*-2-arylthio-3-chlorobicyclo-[2.2.1]hept-5-enes, the adducts of conjugative 1,6-addition derived from edge-on attack, to the *endo*-3-arylthio-5-chlorotricyclo[2.2.1.$0^{2,6}$]-heptanes as a function of the substituents R^2 and R^4 (see Table 1) should give a measure of the electron demand on the sulphur atom towards stabilizing charge development on C3 and C5 of the system. A second measure of the electron demand on sulphur will be reflected in the ratio of *endo*-arylthio adducts to *exo*-arylthio adducts, i.e., products derived from edge-on attack versus those derived from corner attack, since only the stability of a bridging species such as **4** would be expected to be affected by a change in the electrophilicity of the sulphenyl halide. In this respect one expects to observe an increase in the proportion of *endo*-arylthio adducts as the electrophilicity of the sulphenyl chloride is increased through electron donating substituents.

The use of three subseries of arenesulphenyl chlorides, namely those possessing the *ortho*-nitro substituent and those with only a *para* substituent or an *ortho* substituent other than nitro, was the result of our interest in the possible bonding interaction of an oxygen atom from an *ortho*-nitro group with the adjacent sulphur atom leading to a spirosulphurane intermediate **6** instead of the commonly hypothesized sulphonium ion **4**.



6

Studies involving the reaction of arenesulphenyl halides with carbon–carbon double bonds, which correlate thiiranium ion structure with product geometry, have provided considerable insight into the nature of the ionic intermediates and have demonstrated that simple alkane- and arenesulphenyl halides often react in a manner quite different from that of *ortho*-nitro substituted arenesulphenyl halides (11). Thus of paramount importance, in addition to the effect of increasing electron demand, is the determination of what effect, if any, the *ortho*-

Can. J. Chem. Downloaded from www.nrcresearchpress.com by 210.87.254.105 on 09/05/12
For personal use only.

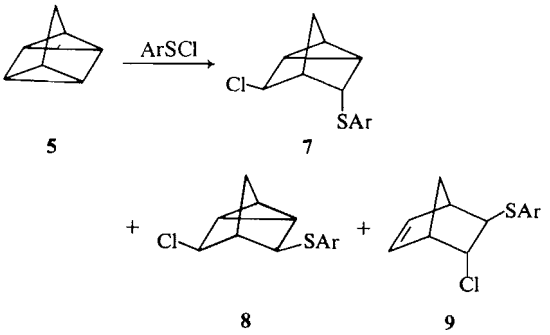
TABLE 1. Effect of increasing electron demand on the kinetically controlled product distributions for the addition of arenesulphenyl chlorides to tetracyclo[3.2.0.$0^{2,7}$.$0^{4,6}$]heptane

Entry	R^2	R^4	4	66	30	Ratio of attack: Edge-on/ end-on	1,3-Addition edge-on/ end-on	End-on 1,3-addition/ 1,6-addition
1	NO_2	NO_2	4	66	30	4:96	6:94	69:31
2	NO_2	Cl	8	46	46	8:92	14:86	50:50
3	NO_2	H	9	49	42	9:91	15:85	53:47
4	NO_2	CH_3	11	48	41	11:89	16:84	54:46
5	NO_2	CH_3O	23	42	35	23:77	36:64	54:46
6	H	NO_2	0	62	38	0:100	0:100	62:38
7	H	CF_3	14	55	31	14:86	20:80	64:36
8	H	Br	32	46	22	32:68	41:59	67:33
9	H	Cl	38	38	24	38:62	50:50	61:39
10	H	F	49	33	18	49:51	44:56	65:35
11	H	H	42	34	24	42:58	55:45	59:41
12	H	CH_3	54	36	10	54:46	60:40	78:22
13	H	C_2H_5	52	37	11	52:48	58:42	78:22
14	H	t-C_4H_9	55	35	10	55:45	61:39	78:22
15	H	CH_3O	57	25	18	57:43	70:30	58:42
16	CH_3	NO_2	7	51	42	7:93	12:88	55:45
17	CH_3	CH_3	59	25	16	59:41	69:31	61:39

nitro substituent is really contributing to the reactions under consideration. For example, one can envision a destabilization through inductive electron withdrawal, and/or a steric interaction, instead of the aforementioned stabilization of positive charge on sulphur.

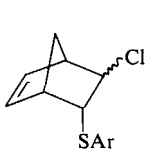
Results and Discussion

We have found that reaction of **5** with arenesulphenyl chlorides under ionic conditions gives two or all three of the adducts **7–9** (eq. [2]), when

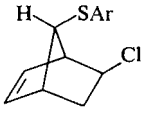
[2] 

5 **7** **8** **9**

methylene chloride is used as solvent at ambient temperature. No evidence was found for products of edge-on conjugative 1,6-addition, **10**, or Wagner–Meerwein rearrangement, **11**. The very different product compositions and distributions obtained from **5** and its isomeric olefin bicyclo[2.2.1]hepta-2,5-diene, indicate the absence



10



11

of common intermediates and of thermal isomerization of the type **5** ⇌ diene.

Product analyses were based upon previously defined criteria utilizing ^1H and ^{13}C nmr spectroscopy (9, 12). All compounds in addition gave mass and infrared spectra in accord with their structures. The ^{13}C nmr data for species **7** and **8** indicated three cyclopropyl methine carbons with characteristic high-field chemical shifts (12) and high $^1J_{^{13}C-^1H}$ values (13). The remaining carbon resonances, methine *geminal* to chlorine or sulphur and the methylene bridge, were readily identified on the basis of their chemical shifts and multiplicities. The ^1H nmr spectra also exhibit shifts and coupling constants in accord with literature values for tricyclo[2.2.1.$0^{2,6}$]heptanes. In addition we were able to compare these spectral data for **8** and **9** with those of authentic samples prepared during the analogous investigation using bicyclo[2.2.1]-hepta-2,5-diene.

The structure of **7** is clearly the C3 epimer of **8** as determined by ^{13}C nmr analysis. The *endo* orientation of the arylthio moiety at C3 follows from the observed paramagnetic shift of C3 in **7** relative to **8**

Can. J. Chem. Downloaded from www.nrcresearchpress.com by 210.87.254.105 on 09/05/12
For personal use only.

Can. J. Chem. Downloaded from www.nrcresearchpress.com by 210.87.254.105 on 09/05/12
For personal use only.

and a diamagnetic shift of C5, albeit a small one, in **7** relative to **8**. The small absolute value of this latter shift difference was unanticipated but presumably results from a combination of the expected γ-*gauche* interaction and an anisotropy effect from the phenyl ring operating in the opposite sense.

The kinetically controlled product distributions were determined by immediate ^{1}H and ^{13}C nmr analysis of the reaction mixtures (Table 1). In each case it was possible to observe and integrate non-overlapping resonances from each species, thereby allowing product ratios to be readily determined. Control experiments using individual samples of the respective adducts, obtained via preparative tlc and/or column chromatography on silica gel, indicate that subsequent isomerizations are much slower than the initial addition process. Product distributions, however, could not be determined from the isolated yields obtained via these separation procedures. The compounds are not entirely stable under our chromatography conditions. The isolation of up to four additional species, unidentified at present, in yields of less than 2–5% of the total reaction mixture employed for separations was observed. These species are believed to be artifacts of the chromatographic procedure and *not* true products of the initial additions.

An examination of the primary product distributions (Table 1) shows a number of trends. A very significant result is the absence of even traces of *endo*-2-arylthio-3-chlorobicyclo[2.2.1]hept-2-enes, **10**, since this indicates that the conjugative cyclopropyl group is unable to compete with neighbouring bivalent sulphur for stabilization of positive charge at C5, during edge-on attack. Our ascertainment of the absence of even traces of the olefins **10** is substantiated by a series of control analyses performed using independently synthesized samples of the olefins **10** (9). Secondly, the observation and isolation of only one olefinic product derived from corner attack is important since it establishes the orientation of ring opening in the second cyclopropane system as occurring stereospecifically with *retention* of configuration at C3. That the two tricyclic adducts, **7** and **8**, are *exo* at C5, implying inversion of configuration at carbon, is in accord with Morrill *et al.*'s results and is furthermore indicative, using Cristol and co-workers' criteria, of the absence of free carbonium ions on the reaction hypersurface.

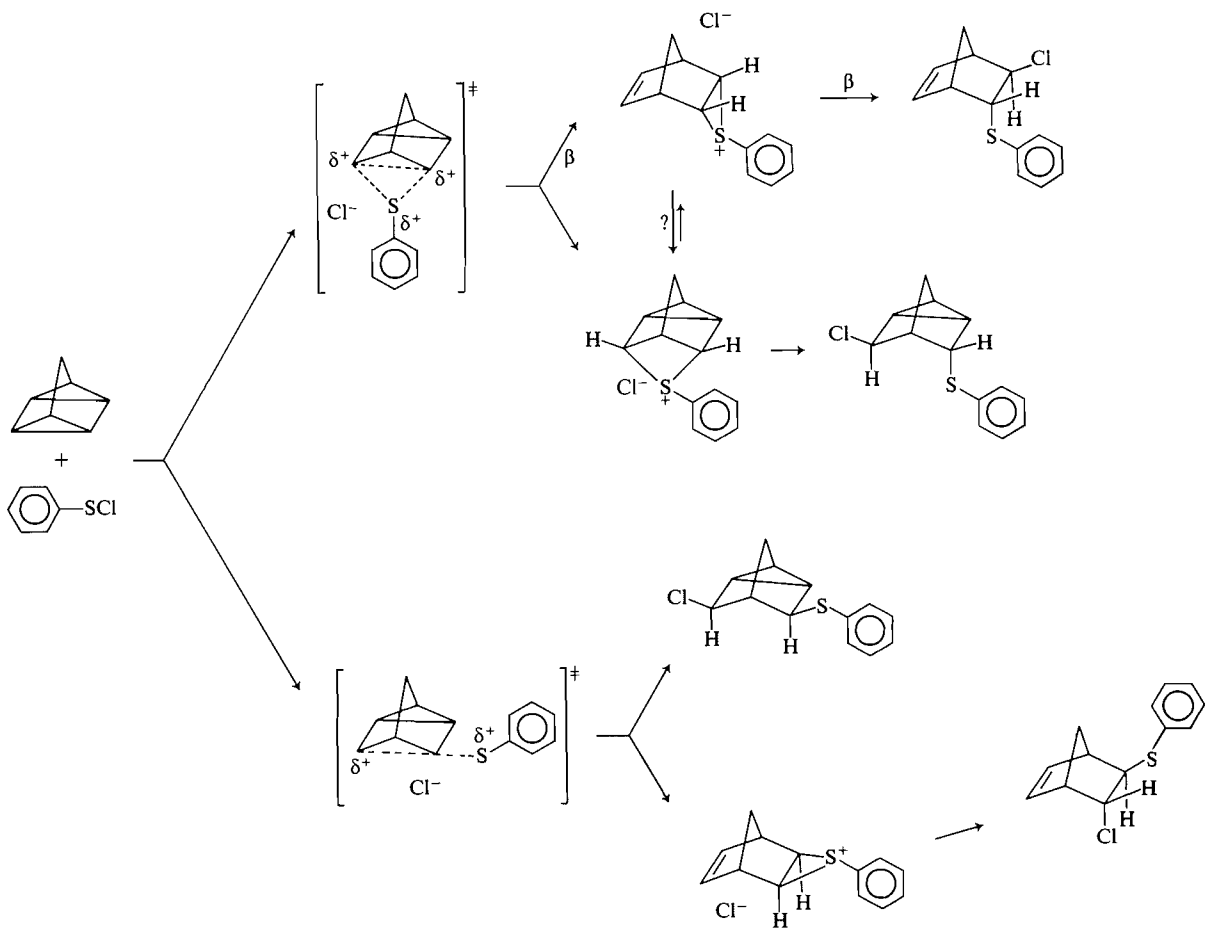
Regarding the results from *ortho*-nitro substituted benzenesulphenyl chlorides (entries 1–5), one observes that the ratio of edge-on attack to end-on or corner attack, 7:(8 + 9), increases as the electron donating ability of the *para* substituent on the arenesulphenyl chloride is varied from nitro, a poor donor, to methoxy, a good donor. This type of variation is much more dramatic in the absence of the *ortho*-nitro substituents as is shown in entries 6–15, the change going from 0:100 to 57:43.

It is interesting to observe here that 2,4-dinitrobenzenesulphenyl chloride (entry 1) appears to be somewhat better at stabilizing charge development on sulphur, as reflected in the proportion of edge-on attack, than 4-nitrobenzenesulphenyl chloride (entry 6). We interpret this difference as a result of neighbouring group assistance for a weakly stabilized, or perhaps non-stabilized sulphonium ion of type **4**. A further examination of Table 1 indicates that little, if any, extra stabilization is obtained from an *ortho*-nitro group when the *para* substituent is more electron donating than nitro. Thus, comparing entries 2 and 9, 3 and 11, 4 and 12, or 5 and 15, we see significant increases in the percentage of edge-on attack in the absence of the *ortho*-nitro group. These data suggest that, if anything, in these cases the *ortho*-nitro substituent leads to a destabilization of charge development on sulphur in the product-determining transition state. This is of course reasonable since nitro groups are generally considered as electron withdrawing.

On the basis of the above it appears that only in the case of 2,4-dinitrobenzenesulphenyl chloride does the *ortho*-nitro substituent lead to a stabilizing interaction, possibly via formation of a spirosulphurane intermediate such as **6**. This neighbouring group assistance by the *ortho*-nitro substituent appears to occur as a result of the dual electron withdrawal of both nitro groups, since as we have noted above, in the presence of more electron donating substituents in the *para* position one observes only the electron withdrawing properties of the *ortho*-nitro group.

This scenario is further supported by a comparison of entries 4 and 16 where the relative orientation of methyl and nitro substituents is reversed. It is not clear at this time whether or not the small decrease in the percentage of edge-on attack on going from entry 4 to 16 results from a stronger destabilizing effect of a *para*-nitro group relative to an *ortho*-nitro group, from a stronger stabilizing effect of a *para*-methyl group relative to an *ortho*-methyl group, or from different steric interactions in the transition state for methyl and nitro. Comparing entries 12 and 17 one notes that a second methyl group leads to an increase in the amount of edge-on attack, but that this increase, 5%, is relatively small.

If one compares the ratio of edge-on attack to



SCHEME 1

corner attack for 1,3-addition the variations as a function of R^2, R^4 are much larger. The validity for such a partition of data is, however, questionable since, as an examination of the last column of Table 1 shows, the relative proportion of 1,3-addition to conjugative 1,6-addition during corner attack is not constant, and indeed does not appear to rigorously follow any set pattern. For example, regarding only entries 6, 9, 11, 12, and 15, we observe values of 60:40 ± 2 in every case but 12, which is 78:22. Looking only at column 6, which represents the proportion of species **9**, one observes that these values fall between 30 and 46% when there is a nitro group or another strong electron withdrawing group, e.g., CF_3, present. If the only substituents present are good donors such as methyl, ethyl, *tert*-butyl, and methoxy, the proportion of **9** drops to 10–18%. This also holds for +T substituents[5] such as the halogens F, Cl, and Br. In the case of fluorine the +T effect appears to override the −I or electron-withdrawing inductive effect as is seen in the small proportion, 18%, of olefinic product and the higher ratio of edge-on to corner attack (compare entries 10 and 11). Considering the data as a whole, we observe a general increase in the percentage of conjugative 1,6-addition resulting from corner attack as the ability of the substituents to stabilize charge development on sulphur is decreased.

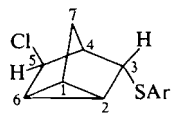
Unfortunately our data base is too small to allow us to convincingly explain this observation.

The results reported herein may be explained in terms of the two classical competitive pathways on the reaction hypersurface as shown in Scheme 1. We have indicated two product types resulting from each hypothetical intermediate. Route β, which corresponds to the formation of an olefinic product from edge-on attack, was included despite the absence of such adducts in this solvent system. We note that related studies with the corresponding

[5] +T is Ingold's symbol for the effect wherein substituents like NH_2 and OCH_3 can supply electrons by resonance (14).

Can. J. Chem. Downloaded from www.nrcresearchpress.com by 210.87.254.105 on 09/05/12
For personal use only.

TABLE 2. Carbon-13 nuclear magnetic resonance parameters (δ, ppm) for the *endo*-3-arylthio, *exo*-5-chloro nortricyclenes synthesized during this investigation



	C1	C2	C3	C4	C5	C6	C7	Other carbons (excluding aromatics)
Ar = 2-NO_2, 4-NO_2	13.3	21.0	49.3	41.7	64.2	17.9	34.2	
2-NO_2, 4-Cl	15.0	20.8	49.5	41.7	64.2	17.9	34.2	
2-NO_2	15.1	21.2	49.4	41.7	64.2	17.9	34.1	
2-NO_2, 4-CH_3	13.9	21.4	49.6	41.8	64.4	18.2	34.1	20.1q
2-NO_2, 4-CH_3O	14.2	21.0	49.1	41.9	64.5	17.5	34.0	53.5q
4-Br	14.6	20.3	50.4	42.0	64.4	16.6	33.7	
4-Cl	14.6	21.2	50.5	41.9	64.2	16.6	33.6	
4-F	14.6	20.6	51.1	42.0	63.8	16.7	33.6	
4-H	15.3	20.4	51.0	42.0	64.5	16.7	33.7	
4-CH_3	14.6	20.6	51.1	42.1	64.2	16.8	33.5	21.0q
4-C_2H_5	15.3	20.3	51.1	42.1	64.4	17.2	33.6	15.3q, 28.4t
4-tC_4H_9	14.6	20.3	51.2	42.2	64.2	16.8	33.6	{31.3q 34.5s
4-CH_3O	15.1	20.7	50.9	41.9	64.1	17.2	33.5	55.6q
2-CH_3, 4-NO_2	14.3	21.0	50.6	42.0	64.3	18.5	33.5	
2-CH_3, 4-CH_3	14.7	21.1	51.1	41.9	64.6	18.4	33.6	{20.5q 20.9q

areneselenenyl chlorides have indicated that the product compositions in these ring cleavages are very sensitive to subtle changes in solvent properties. On this basis we anticipate the formation of such species with the proper choice of solvent.

Summary

Our studies show that the electrophilic cleavage of cyclopropane rings by arenesulphenyl chlorides in systems such as **5** can be accounted for in terms of two competing reaction orientations. Small variations in the molecular structure of the electrophile are seen to result in a change in neighbouring group participation, while retaining an essentially identical steric environment within the vicinity of the reaction site. The degree of neighbouring group participation is found to be a function of the electron demand of the incipient ionic species, the kinetically controlled product distributions reflecting the effect of this electron demand upon the product-determining transition state.

Experimental

General

All melting points were measured on a Fisher-Johns block and are reported uncorrected. The ^1H nmr spectra were recorded on Varian Associates T-60 and HA-100 spectrometers; ^{13}C nmr spectra were recorded on a Varian FT80-16K spectrometer, using chloroform-*d* as an internal lock and reference. All spectral parameters are referenced to TMS as an internal standard.

Tetracyclo[3.2.0.0^{2,7}.0^{4,6}]heptane was purchased from Aldrich and used without further purification. The purity was confirmed via nmr and glc; ^{13}C nmr ($CDCl_3$) δ: 32.0 (t(dd), C3, $^1J_{C,H}$ = 131.4 Hz, $^2J_{C,H} \simeq {}^3J_{C,H}$ = 4.0 Hz), 23.0 (d(tt), C2, C4, $^1J_{C,H}$ = 166.0 Hz, $^2J_{C,H}$ = 8.6, 3.3 Hz), 14.8 (d(ddt) C1, C5, C6, C7, $^1J_{C,H}$ = 184.7 Hz).

2,4-Dinitrobenzenesulphenyl chloride was prepared by the method of Lawson and Kharasch (15) from bis(2,4-dinitrophenyl) disulphide. Recrystallized from CCl_4, mp 96–96.5°C (lit. (15) mp 97–98°C).

2-Nitro-4-chlorobenzenesulphenyl chloride was prepared by the method of Turner and Conner (16) using 1,4-dichlorobenzene as starting material; mp 98°C (lit. (16) mp 97.5–98°C).

2-Nitrobenzenesulphenyl chloride was commercially available (Aldrich). Recrystallized from CCl_4, mp 76°C (lit. (16) mp 75.4–75°C).

2-Nitro-4-methylbenzenesulphenyl chloride was prepared from the analogous aniline by the procedure of Zincke and Rose (17). Recrystallized from CCl_4, mp 89–90°C.

2-Nitro-4-methoxybenzenesulphenyl chloride was prepared from the analogous aniline as above. Crystallized as brilliant orange needles from CCl_4, mp 106–107°C.

The remaining arenesulphenyl chlorides were prepared from the corresponding commercially available thiols or disulphides by chlorination with molecular chlorine in CCl_4 with cooling (0–4°C). All physical data were as expected (18).

General Reaction Procedure

Product studies were carried out as previously described (19). In the cases of 2-nitro-4-substituted benzenesulphenyl chlorides ^1H nmr analysis was carried out during the course of the reactions and thereafter to ensure the establishment of kinetically controlled product distributions. Because of the essentially instantaneous nature of the reactions of arenesulphenyl chlorides which lack the *ortho*-nitro substituent, only the slow isomerizations *post*-addition were observable by ^1H nmr. Samples of individual adducts were isolable via preparative tlc on silica gel

Can. J. Chem. Downloaded from www.nrcresearchpress.com by 210.87.254.105 on 09/05/12
For personal use only.

using CH_2Cl_2 or 80:20 cyclohexane – ethyl acetate as eluant depending upon the substituents. ^{13}C nuclear magnetic resonance parameters for adducts of type **7** are listed in Table 2; ^{13}C nmr parameters for adducts of types **8** and **9** have been reported previously (9).

Acknowledgements

Continued financial support from the Natural Sciences and Engineering Research Council of Canada is appreciated, as is a Province of Ontario Scholarship to one of us (PLB) 1978–1980.

1. (*a*) G. H. SCHMID and D. G. GARRATT. *In* The chemistry of the functional groups: Supplement A: the chemistry of double-bonded functional groups. *Edited by* S. Patai. John Wiley and Sons, London. 1977. pp. 828–854; (*b*) P. B. D. DE LA MARE and R. BOLTON. Electrophilic addition to unsaturated systems. Elsevier, New York. 1966; (*c*) R. C. FAHEY. *In* Topics in stereochemistry. Vol. 3. *Edited by* E. L. Eliel and N. L. Allinger. Interscience, New York. 1968. pp. 299–305; (*d*) G. H. SCHMID. *In* The chemistry of the carbon–carbon triple bond. *Edited by* S. Patai. John Wiley and Sons, Chichester, England. 1978. pp. 306–312.
2. T. C. MORRILL, S. MALASANTA, K. M. WARREN, and B. E. GREENWALD. J. Org. Chem. **40**, 3032 (1975).
3. (*a*) J. BREDT. J. Prakt. Chem. **121**, 153 (1929); (*b*) S. J. CRISTOL and R. T. LALONDE. J. Am. Chem. Soc. **80**, 4355 (1958).
4. (*a*) W. L. JORGENSEN and L. SALEM. *In* The organic chemists book of orbitals. Academic Press, New York. 1973. pp. 19–23; (*b*) H. BASCH, M. B. ROBIN, N. A. KUEBLER, C. BAKER, and D. W. TURNER. J. Chem. Phys. **51**, 52 (1969); (*c*) R. M. STEVENS, E. SWITKES, E. A. LAWS, and W. N. LIPSCOMB. J. Am. Chem. Soc. **93**, 2603 (1971).
5. (*a*) S. J. CRISTOL, W. Y. LIM, and A. R. DAHL. J. Am. Chem. Soc. **92**, 4013 (1970); (*b*) G. KLOPMAN. J. Am. Chem. Soc. **91**, 89 (1969); (*c*) G. A. OLAH and A. M. WHITE. J. Am. Chem. Soc. **91**, 3954 (1969); **91**, 3956 (1969).
6. B. CAPON and S. P. MCMANUS. *In* Neighbouring group participation. Plenum Press, New York, NY. 1976.
7. S. J. CRISTOL, J. K. HARRINGTON, and M. S. SINGER. J. Am. Chem. Soc. **88**, 1529 (1966).
8. (*a*) S. J. CRISTOL, J. K. HARRINGTON, T. C. MORRILL, and B. E. GREENWALD. J. Org. Chem. **36**, 2773 (1971); (*b*) S. J. CRISTOL and R. T. LALONDE. J. Am. Chem. Soc. **80**, 4355 (1958); (*c*) T. C. MORRILL and B. E. GREENWALD. J. Org. Chem. **36**, 2769 (1971); (*d*) A. W. MCCULLOCH, A. G. MCINNES, D. G. SMITH, and J. A. WALTER. Can. J. Chem. **54**, 2013 (1976); (*e*) S. J. CRISTOL and R. L. SNELL. J. Am. Chem. Soc. **76**, 5000 (1954); (*f*) G. F. KOSER, P. R. PAPPAS, and S.-M. YU. Tetrahedron Lett. 4943 (1973); (*g*) S. F. NELSEN, J. P. GILLESPIE, and P. J. HINTZ. Tetrahedron Lett. 2361 (1971); (*h*) S. F. NELSEN, J. P. GILLESPIE, P. J. HINTZ, and E. D. SEPPANEN. J. Am. Chem. Soc. **95**, 8380 (1973).
9. D. G. GARRATT and P. L. BEAULIEU. J. Org. Chem. **44**, 3555 (1979).
10. (*a*) C. D. JOHNSON. J. Org. Chem. **43**, 1814 (1978); (*b*) P. G. GASSMAN and A. F. FENTIMAN. J. Am. Chem. Soc. **92**, 2549 (1970); (*c*) H. C. BROWN and M. RAVINDRANATHAN. J. Org. Chem. **43**, 1709 (1978); (*d*) G. A. OLAH, G. K. PRAKASH, and G. LIANG. J. Am. Chem. Soc. **99**, 5683 (1977).
11. (*a*) D. C. OWSLEY, G. K. HELMKAMP, and M. F. RETTIG. J. Am. Chem. Soc. **91**, 5239 (1969); (*b*) D. R. HOGG. Mech. React. Sulfur Compd. **5**, 87 (1970); (*c*) E. N. GIVENS and H. KWART. J. Am. Chem. Soc. **90**, 378 (1968); **90**, 386 (1968); (*d*) N. KHARASCH. *In* Organic sulfur compounds. Vol. 1. *Edited by* N. Kharasch. Pergammon Press, Oxford. 1961. p. 379; (*e*) W. H. MUELLER and P. E. BUTLER. J. Am. Chem. Soc. **88**, 2866 (1966); (*f*) W. H. MUELLER and P. E. BUTLER. J. Am. Chem. Soc. **90**, 2075 (1968); (*g*) W. A. THALER. J. Org. Chem. **34**, 871 (1969).
12. (*a*) E. LIPPMAA, T. PEHK, and J. PAASIVIRTA. Org. Magn. Reson. **5**, 277 (1973); (*b*) Y. MARINO, K. KIRCHITAU, and A. YONAZEKI. Bull. Chem. Soc. Jpn. **40**, 1552 (1967); (*c*) J. F. CHIANG, C. F. WILCOS, and S. H. BAUER. J. Am. Chem. Soc. **90**, 3149 (1968).
13. (*a*) V. S. WATTS and J. H. GOLDSTEIN. J. Chem. Phys. **46**, 4165 (1967); (*b*) K. TACI, R. MUNEYUKI, and H. TANIDA. Can. J. Chem. **41**, 3142 (1963); (*c*) K. M. CRECELY, V. S. WATTS, and J. H. GOLDSTEIN. J. Mol. Spectrosc. **30**, 184 (1969); (*d*) G. SCHRUMPF and W. LÜTTKE. Tetrahedron Lett. 2635 (1965).
14. L. P. HAMMETT. *In* Physical organic chemistry. McGraw-Hill Book Co., Toronto. 1970. p. 359.
15. D. LAWSON and N. KHARASCH. J. Org. Chem. **24**, 857 (1956).
16. R. A. TURNER and R. CONNER. J. Chem. Soc. **69**, 1009 (1947).
17. T. ZINCKE and H. ROSE. Ann. **406**, 103 (1914); **406**, 127 (1914).
18. N. KHARASCH. Intra-Science Chemistry Reports. Vol. 1. Number 4. 1969.
19. (*a*) D. G. GARRATT and P. L. BEAULIEU. Can. J. Chem. **57**, 119 (1979); (*b*) D. G. GARRATT. Can. J. Chem. **56**, 2184 (1978); (*c*) G. H. SCHMID, C. L. DEAN, and D. G. GARRATT. Can. J. Chem. **54**, 1253 (1976).

Can. J. Chem. Downloaded from www.nrcresearchpress.com by 210.87.254.105 on 09/05/12
For personal use only.

Addition of arenesulphenyl chlorides to 2-methylenebicyclo[2.2.1]hept-5-ene: effect of increasing electron demand upon the rate and product determining transition states[1]

DENNIS G. GARRATT,[2] PIERRE L. BEAULIEU, AND VERONIQUE M. MORISSET
Department of Chemistry, University of Ottawa, Ottawa, Ont., Canada K1N 9B4

Received October 3, 1979

DENNIS G. GARRATT, PIERRE L. BEAULIEU, and VERONIQUE M. MORISSET. Can. J. Chem. **58**, 1021 (1980).

The rates and products of addition of a series of sixteen arenesulphenyl chlorides to 2-methylenebicyclo[2.2.1]hept-5-ene, **7**, and the *E*, *Z* isomeric 2-ethylidenebicyclo[2.2.1]hept-5-enes, **8** and **9**, have been determined in methylene chloride solution. The major species from attack on **7** is always *endo*-3-arylthio-1-chloromethyltricyclo[2.2.1.$0^{2,6}$]heptane, the product of *exo* attack upon the *endocyclic* double bond with homoallylic participation of the *exocyclic* π system. No evidence was found for initial electrophilic attack upon the *exocyclic* double bond.

DENNIS G. GARRATT, PIERRE L. BEAULIEU et VERONIQUE M. MORISSET. Can. J. Chem. **58**, 1021 (1980).

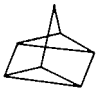
On a déterminé la vitesse de formation des produits d'addition d'une série de 16 chlorures d'arènesulphényles sur le méthylène-2 bicyclo[2.2.1]heptène-5 (**7**) et sur les isomères (*E*) et (*Z*) des éthylidènes-2 bicyclo[2.2.1]heptènes-5 **8** et **9** en solution dans le chlorure de méthylène. Le produit principal résultant de l'attaque du composé **7** est toujours l'arylthio-3 chlorométhyl-1 tricyclo[2.2.1.$0^{2,6}$]heptane *endo*, produit qui provient d'une attaque *exo* sur la double liaison *endocyclique* avec une participation homoallylique du système π *exocyclique*. On n'a pas trouvé de preuves d'une attaque électrophile initiale sur la double liaison *exocyclique*.

[Traduit par le journal]

In two previous articles (1, 2) we have discussed the effect of increasing electron demand (3) upon the product determining transition state in the reaction of arenesulphenyl chlorides with carbon–carbon double bonds and single bonds using respectively bicyclo[2.2.1]hepta-2,5-diene, **1**, and tetracyclo[3.2.0.$0^{2,7}$.$0^{4,6}$]heptane, **2**, as substrates.



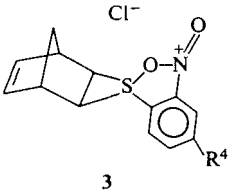
1



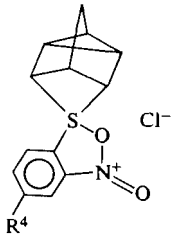
2

The aim of these studies was two-fold. Firstly, we desired to ascertain the effect of varying the electrophilicity of the sulphenyl halide while retaining an essentially constant steric environment in the product determining transition state. In this way we would obtain a measure of the degree of charge development on the substrate within this transition state as a function of two neighbouring group effects, the neighbouring groups being the arylthio moiety and the homoallylic double bond in **1** or the conjugative cyclopropyl moiety in **2**. Secondly, we wished to obtain information with respect to the possible bonding interaction of an oxygen atom from the *ortho* nitro group, in *ortho* nitro substituted arenesulphenyl chlorides, with the adjacent sulphur atom which could lead to spirosulphurane intermediates of type **3** and **4** instead of the commonly accepted sulphonium ions **5** and **6** (4).

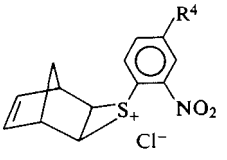
In regard to this latter point, we observed a stabilizing interaction only in the case of 2,4-dinitrobenzenesulphenyl chloride, presumably as a result of the dual electron withdrawal of both nitro groups, since in the presence of more electron donating substituents in the *para* position one observes only the electron withdrawing properties of the *ortho* nitro group.



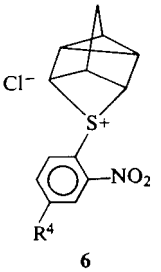
3



4



5



6

[1]NRCC No. 18153.

[2]Author to whom correspondence may be addressed at the Division of Chemistry, National Research Council of Canada, 100 Sussex Dr., Ottawa, Ont., Canada K1A 0R6.

0008-4042/80/101021-09$01.00/0

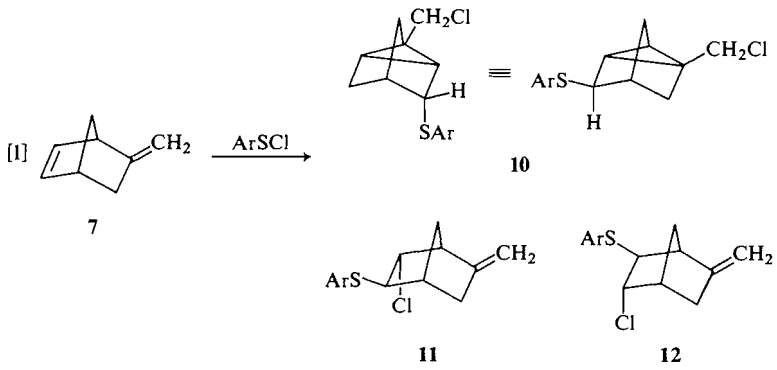
©1980 National Research Council of Canada/Conseil national de recherches du Canada

Can. J. Chem. Downloaded from www.nrcresearchpress.com by 210.87.254.40 on 09/05/12
For personal use only.

Can. J. Chem. Downloaded from www.nrcresearchpress.com by 210.87.254.40 on 09/05/12
For personal use only.

TABLE 1. Effect of increasing electron demand upon the kinetically controlled product distributions for the addition of arenesulphenyl chlorides to 2-methylenebicyclo[2.2.1]hept-5-ene in methylene chloride solution at 23–25°C

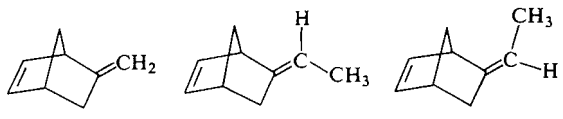
Entry	R^2	R^4	10	11	12	Ratio of attack 10:(11+12)	Ratio of attack 10:11
1	NO_2	NO_2	100	0	0	100:0	100:0
2	NO_2	Cl	100	0	0	100:0	100:0
3	NO_2	H	100	0	0	100:0	100:0
4	NO_2	CH_3	100	0	0	100:0	100:0
5	NO_2	CH_3O	100	0	0	100:0	100:0
6	H	NO_2	99	1	0	99:1	99:1
7	H	CF_3	98	2	0	98:2	98:2
8	H	Br	98	2	0	98:2	98:2
9	H	Cl	96	3	1	96:4	97:3
10	H	F	95	4	1	95:5	96:4
11	H	H	93	5	2	93:7	95:5
12	H	CH_3	88	8	4	88:12	92:8
13	H	tC_4H_9	88	8	4	88:12	92:8
14	H	CH_3O	70	15	15	70:30	82:18
15	$3,4\text{-}(Cl)_2C_6H_3SCl$		98	2	0	98:2	98:2
16	$2,5\text{-}(Cl)_2C_6H_3SCl$		98	2	0	98:2	98:2



As an extension of these studies we report herein the analogous series of reactions using 2-methylenebicyclo[2.2.1]hept-5-ene, **7**, and the *E*,*Z* isomeric 2-ethylidenebicyclo[2.2.1]hept-5-enes, **8** and **9**, respectively. Our interest in this system stems from the possibility of determining the relative propensity for attack upon an *exocyclic* vs. an *endocyclic* double bond as a function of the electrophilicity of the sulphenyl halide while simultaneously obtaining a measure of the relative neighbouring group efficiency of the arylthio moiety and the homoallylic double bond. Furthermore, this system is of interest since it allows one to ascertain the regiochemistry of the reaction. The importance of this latter point has been discussed in a number of recent reviews (5, 6).

Results and Discussion

We have found that the reaction of **7** with arenesulphenyl chlorides under ionic conditions in methylene chloride solution gives one, two, or all three of the adducts **10–12** (eq. [1]). In all cases species **10**, *endo*-3-arylthio-1-chloromethyltricyclo[2.2.1.$0^{2,6}$]heptane, the product of *exo* attack upon the *endocyclic* double bond with homoallylic participation of the *exocyclic* π system, is the major adduct (see Table 1).[3] No evidence is found for the presence of products derived from *endo* attack upon the *endocyclic* double bond, **13–15**, or for

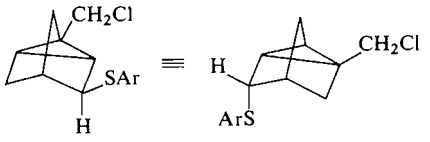


[3]We have extended the *exo–endo* terminology beyond its original usage in bicyclo[2.2.1]heptane systems (*7a*) to nortricyclenes in accord with the suggestion of Cristol and Lalonde (*7b*) by referring configuration with respect to the unsubstituted methano bridge at carbon 7.

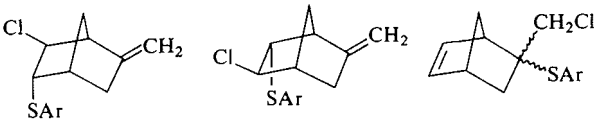
Can. J. Chem. Downloaded from www.nrcresearchpress.com by 210.87.254.40 on 09/05/12
For personal use only.

initial attack upon the *exocyclic* double bond, **16** and **17**. The absence of products of *endo* addition, possibly the result of a steric interaction with the C3 *endo* proton, is in contrast to our results and those of others with substrate **1**.

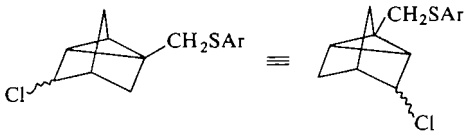
The reactions of arenesulphenyl chlorides with



13

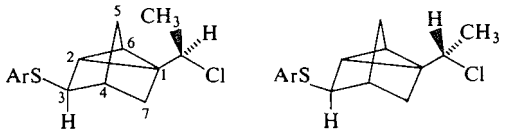


14 **15** **16**



17

the *E*,*Z* isomeric dienes **8** and **9** similarly give rise to products of *exo* attack upon the *endocyclic* double bond with homoallylic rearrangement. Of note is the observation that while the electrophilic attack is apparently stereospecific, subsequent nucleophilic attack by chloride ion is non-stereospecific, giving rise to essentially equal mixtures of the 3-*RS*,8-*RS* and 3-*RS*,8-*SR* diastereoisomeric nortricyclenes, **18** and **19**. This result is important since the only



18 **19**

related case of homoallylic rearrangement during a sulphenyl chloride addition, which dealt with bicyclo[2.2.1]hepta-2,5-diene, **1**, gives a single adduct via an apparent "homo-S_N2'" attack by chloride ion on the intermediate thiiranium ion (1).

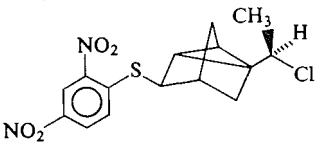
Product analyses are based upon previously defined criteria utilizing ^{1}H nmr and ^{13}C nmr spectroscopy (1, 2, 8). All compounds in addition give mass and infrared spectra in accord with their structures (9).

For example, the ^{1}H nmr spectrum of adduct **20**, derived from the addition of 2,4-dinitrobenzenesulphenyl chloride with **7**, has an AB quartet centered at δ 3.84 ($^2J_{AB}$ = 10 Hz), integrating as two protons, assigned to the —CH_2Cl moiety, and a broad singlet at δ 3.55 (1H, $W_{1/2}$ = 3.5 Hz) assigned to the proton geminal to the arylthio group. No evidence was found for olefinic protons.

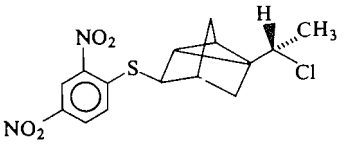
The ^{13}C nmr data for **20** indicate two cyclopropyl methine carbons with the characteristic high-field chemical shifts (10), δ 19.7 and 22.5, and large $^1J_{C,H}$ values, 175.4 and 179.1 Hz, respectively.[4] An additional high-field quaternary carbon, δ 28.3, consistent with a cyclopropyl center is also observed. The remaining carbons (methine bridgehead, methylene bridges, and the methine carbon, which is bonded to the arylthio group) are readily assigned on the basis of their chemical shifts and multiplicities.

The electron-impact mass spectrum of **20** has a low intensity molecular ion cluster at *m*/*e* 340. Characteristic fragments include the loss of a chlorine atom ($M^+ - {}^{35}Cl$; *m*/*e* 305), loss of the arylthio group ($M^+ - 199$; *m*/*e* 141) followed by loss of CH_2Cl ((*m*/*e* 141) − 49; *m*/*e* 92) and a retro Diels–Alder fragmentation with loss of ethylene to give a C_6H_6Cl fragment ((*m*/*e* 141) − 28; *m*/*e* 113). The loss of an oxygen atom or a NO fragment from the molecular ion was also of note.

The regiochemistry of the addition was confirmed by an examination of the analogous products derived from dienes **8** and **9**. Thus in the ^{1}H nmr spectra, we observe quartets at δ 4.18 and 4.27 which are readily assigned to the methine protons geminal to the chlorine atoms in diastereomers **21** and **22**. The protons geminal to the arylthio group in the diastereomers have virtually magnetically equivalent environments, resonating at δ 3.53 and 3.55, respectively. We note that no attempt has been made on our part to rigorously assign the relative configuration of adducts **21** and **22** (**18** and **19**) at this time.



21



22

A comparison of the ^{13}C nmr spectra of **20**, **21**, and **22** is most instructive. The carbons directly bonded to chlorine resonate at δ 59.4 and 59.0 in **21** and **22**. This represents paramagnetic shifts of 12.8

[4]See ref. 10*a*, Chapt. 10.

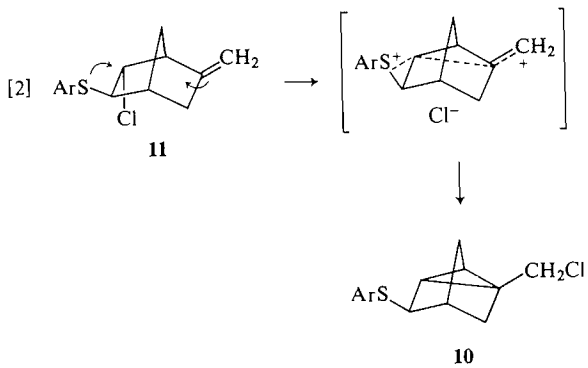
Can. J. Chem. Downloaded from www.nrcresearchpress.com by 210.87.254.40 on 09/05/12
For personal use only.

and 12.4 ppm, respectively, upon the substitution of a methyl group for a proton, in accord with the anticipated α effect.[5] In contrast, the methine carbons geminal to sulphur show essentially a constant magnetic environment, δ 51.2 in **20** vs. δ 50.9, 51.2 for **21**, **22**. These shift differences would be reversed if a regiochemistry such as is found in species **17** were present.

In accord with the above, the mass spectra of **21** and **22** have intense molecular ions at *m/e* 354. Characteristic fragmentations include the loss of HCl ($M^+ - 36$; *m/e* 318), the loss of C_2H_4Cl (α-cleavage, $M^+ - 63$; *m/e* 291), and the loss of ArS ($M^+ - 199$; *m/e* 155). This latter fragment further fragments via loss of ethylene (retro Diels–Alder, (*m/e* 155) − 28; *m/e* 127) followed by loss of HCl ((*m/e* 127) − 36; *m/e* 91) to give the very stable C_7H_7 cation-radical.

The presence of adducts of type **11** and **12** derived from *exo–anti* attack upon the *endocyclic* double bond is also quite instructive. The assignment of configuration in these cases is made by a comparison of the spectral parameters (^1H, ^{13}C nmr, ir, ms) of samples of the phenylthio and anisylthio forms of **11** and **12** with the analogous samples of *exo*-2-arylthio-*endo*-3-chlorobicyclo-[2.2.1]heptane prepared via the addition of benzenesulphenyl and 4-methoxybenzenesulphenyl chlorides to bicyclo[2.2.1]hept-2-ene, **23**. The spectral parameters of these compounds have been previously reported (11, 12). The assignment of the arylthio group in species **11** as *exo* is very important. This piece of data in conjuction with the observation that adducts of type **11** isomerize to the nortricyclene adducts **10** (presumably by way of a thiiranium ion-like intermediate resulting from neighbouring group assistance of carbon–chlorine bond cleavage by the arylthio group) allows one to assign the configuration in **10** as *endo*.[3]

An examination of the primary product distributions (Table 1) shows a number of trends. Regarding first of all the results from *ortho* nitro-substituted benzenesulphenyl chlorides (entries 1–5), one observes the formation of adducts of type **10** only. This is very important because it indicates that a homoallylic *exocyclic* double bond is more efficient at stabilizing charge development at C6 of **7** than is the neighbouring 2-nitroarylthio group. This is true even when that group has a methoxy substituent in the *para* position (entry 5)! These data contrast very strongly with our previous results with substrate **1** (1), wherein we observed that a homoallylic *endocyclic* double bond is in general less efficient than the neighbouring 2-nitroarylthio group at stabilizing charge development on carbon. In this study we find that even where very efficient electron donors are involved, as in entries 12–14, the homoallylic *exocyclic* double bond is more efficient than sulphur towards such stabilization. This is perhaps most dramatically demonstrated for the isomeric 2-ethylidenebicyclo[2.2.1]hept-5-enes, **8** and **9**, where only products of homoallylic rearrangement are isolable or observed spectroscopically.



Furthermore, in contrast to the reactions with substrates **1** and **2**, we do not observe any evidence for a stabilizing interaction from an *ortho* nitro substituent even in the case of 2,4-dinitrobenzenesulphenyl chloride (1, 2). A comparison of entries 1 and 6, 2 and 9, 3 and 11, 4 and 12, and 5 and 14 shows that in each case the *ortho* nitro substituent contributes a destabilizing effect upon the thiiranium ion-like intermediate as it approaches the product determining transition state.

In order to gain a more complete idea of the electronic factors affecting this reaction, we have carried out a series of kinetic studies using as substrates compounds **1**, **2**, **7**, **8**, and **23**. The rates of addition of the arenesulphenyl chlorides which lack the *ortho* nitro substituent were measured in methylene chloride solution at 24.5°C by means of the stopped-flow technique using a Durrum-Gibson stopped-flow spectrophotometer. The rate of disappearance of the sulphenyl chlorides was followed by measuring the decrease in their absorptions at 392.5 nm. All the rates (Table 2) were measured under pseudo first order conditions. The data from all runs gave linear first order plots. The second order rate constants were obtained by dividing the pseudo first order rate constants by the substrate concentrations.

On examination of Table 2 one recognizes immediately the rather unanticipated result, that for any given substrate the rate constants, k_2, are essentially constant. There is little, if any, correlation between the rates of addition and the electron

[5]See ref. 10*a*, Chapt. 2.

TABLE 2. Specific rate constants for the reaction of some ring-substituted arenesulphenyl chlorides with substrates **7**, **8**, **1**, **2**, and **23** in methylene chloride solution at 24.5°C

	k_2 (dm^3 mol^{-1} s^{-1})				
Sulphenyl chloride	**7**	**8**	**1**	**2**	**23**
3,4-$(Cl)_2C_6H_3SCl$	1050	2050	2400	290	2100
2,5-$(Cl)_2C_6H_3SCl$	900	1950	2500	350	2100
4-BrC_6H_4SCl	1050	2200	2600	320	2400
4-ClC_6H_4SCl	1000	1700	2300	340	2450
4-FC_6H_4SCl	1050	2000	2100	350	1900
C_6H_5SCl	850	1750	1700	270	1600
4-$CH_3C_6H_4SCl$	1000	1900	1950	250	1700
4-$CH_3OC_6H_4SCl$	1090	2100	2300	290	2000
2,4,6-$(CH_3)_3C_6H_2SCl$	750	1500	1950	650	1900

donating or electron withdrawing ability of the ring-substituents on the sulphenyl chloride. In terms of σ–ρ linear free energy relationships, one finds values of ρ which are essentially *zero*, perhaps slightly negative or slightly positive! These data must be interpreted in terms of the virtual absence of charge development upon sulphur in the rate determining transition state! In the cases of substrates **7** and **8** one might also state that there is apparently little, if any, charge development on sulphur in the product determining transition state. Yet our earlier investigations dealing with substrates **1** and **2** showed a very strong dependence in the product determining states for the electron donating or withdrawing abilities of the ring-substituents, an observation indicative, when coupled with the kinetic data, of different rate and product determining transition states.

It is, furthermore, very important that in the case of substrate **23**, only products of *exo–anti* addition have been isolated or observed, since this rules out σ participation as playing a significant role (11–13). One must not, however, rule out the significance of *anti* addition, particularly since electrophilic attack upon the bicyclo[2.2.1]heptyl system very frequently occurs *syn* (14)!

The available data suggest a bridged rate determining transition state. This transition state must, however, have little or no charge development on sulphur if our interpretation of the rate data (Table 2) is correct. The need for a bridged rate determining transition state follows from the absence of products of *exo–syn* or Wagner–Meerwein type rearrangement (σ participation) which would presumably result were an open carbonium ion (norbornyl carbonium ion, etc.) present on the reaction hypersurface. This argument is based on the concept that if the rate determining transition state is not bridged, the succeeding intermediate should lose its configurational integrity and thereby give rise to additional products. The absence of such products therefore indicates a bridged rate determining transition state.

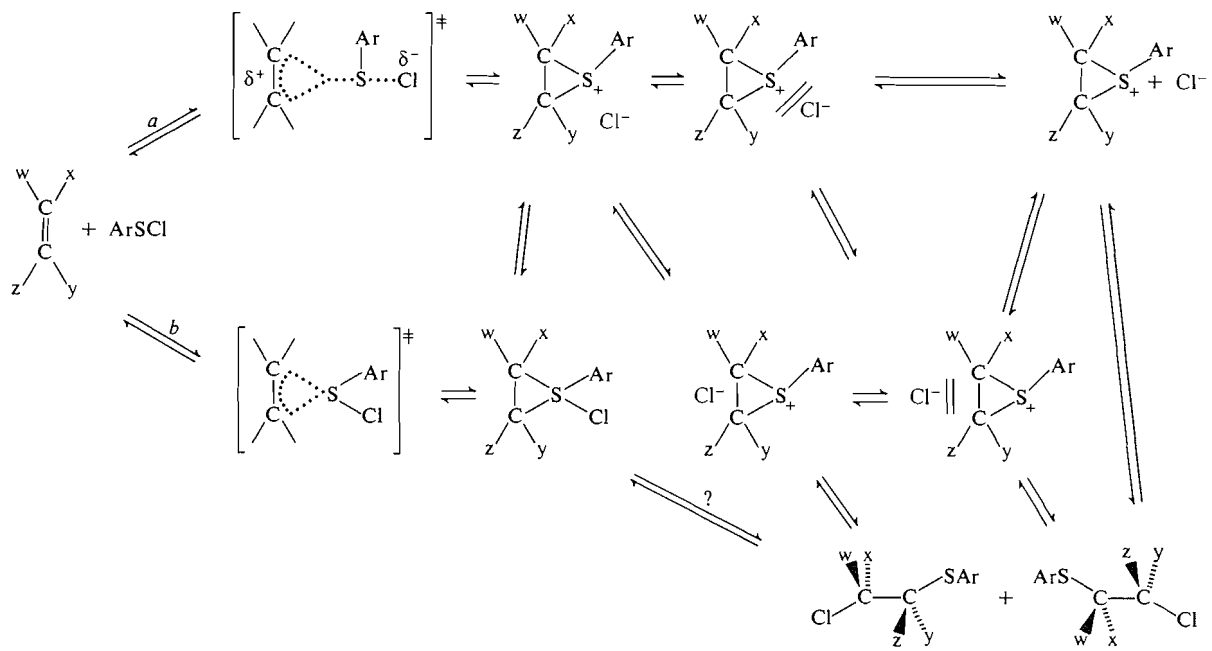
On the basis of these data and the plethora of results previously published (5, 6, 15), a mechanism involving at least one intermédiate and two transition states is required. Although many variations on the following scenarios are conceptually possible, two mechanisms have received the most attention (see Scheme 1). Path *a* in Scheme 1 is the sulphur analogue of the S_N2 mechanism. Path *b* involves a different angle of approach between the substrate molecule and the sulphenyl chloride and leads to an episulphurane species which may ionize to the thiiranium ion or may proceed directly to products.

While the rate data in Table 2 readily rule out a mechanism involving initial dissociation of the sulphenyl halide to a sulphenium ion, ArS^+, followed by attack on the olefinic double bond,[6] to give a thiiranium ion (16), it is clear that both paths *a* and *b* can accommodate these results. In path *a* a rate determining transition state structure of the S_N2 sort is anticipated to have a charge distribution leading to a ρ value which is zero or slightly positive, in analogy to S_N2 displacement at carbon. In path *b* the formation of an episulphurane intermediate may occur in such a way that little or no charge develops on sulphur in the transition state, despite the obvious redox nature of the reaction. Although conclusive evidence is lacking, at this time, as to which path most correctly corresponds to the actual reaction hypersurface, it is clear that given the dissociation of the sulphur–chlorine bond in an episulphurane-like intermediate one arrives at the same series of thiiranium ion-pairs, which serve to define the probable product determining transition state structures (5, 6).

Of importance in regard to the nature of the product determining transition state is the observation of non-stereospecific attack by chloride ion on the intermediates derived from dienes **8** and **9**. From this result it would appear that a concerted rearrangement of episulphuranes such as **24** and **25** to product does not occur, or that **24** and **25** are not the sole precursors. One must, however, be careful. A consideration of the possible bonding modes for an episulphurane type species suggests a trigonal bipyramid configuration (17, 18). Thus even in the case of "stereospecific" *exo* attack upon the olefinic double bonds of, for example, **8**, two

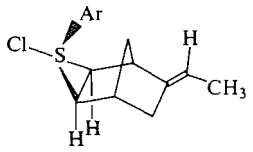
[6]Rate limiting formation of a sulphenium ion, RS^+, from RSCl may be considered as the sulphur analogue of an S_N1 displacement at carbon.

Can. J. Chem. Downloaded from www.nrcresearchpress.com by 210.87.254.40 on 09/05/12
For personal use only.

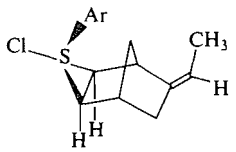


SCHEME 1

isomeric episulphuranes may be formed: **24** and **24'**. If both **24** and **24'** are formed in equivalent amounts, it would be possible for **18** and **19** to be formed via concerted rearrangements of the form



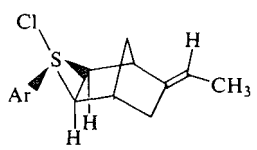
24



25

24 → **18**, **24'** → **19**, or vice versa. Such a scenario ([**24**] = [**24'**]), however, seems very unlikely to us on both electronic and steric grounds. Our own preference is for product formation at the intimate or solvent-separated ion-pair stage. Further studies, however, will be necessary to clearly define the reaction hypersurface.

In terms of comparing these results for 2-methylenebicyclo[2.2.1]hept-5-ene with those of others for different electrophiles, it is of note that Hassner and co-workers (19) have shown preferential iodination of the *endocyclic* double bond using IN_3 and INCO, whereas von Schleyer and O'Conner report (20) the preferential protonation of the *exocyclic* double bond, both series of reactions leading to nortricyclic products. The difference between von Schleyer's results and those of Hassner and of ourselves is readily interpreted in terms of ion stabilities.



24'

Protonation of the *exocyclic* double bond of **8** leads to a tertiary carbonium ion, whereas the analogous attack upon the *endocyclic* double bond would give only a secondary species, albeit one which could be stabilized by both σ and π participation. Alternatively one can view the differentiation between the two π systems in terms of kinetics. Protonation of a 1,1-disubstituted alkene is known to occur many orders of magnitude faster than attack upon a 1,2-disubstituted alkene (21). An extension of this scenario explains the preferential attack by electrophiles such as IN_3, INCO, and ArSCl on the *endocyclic* double bond. It is known that where bridged rate determining transition states are common, a *cis*-1,2-disubstituted double bond generally reacts faster than a similarly substituted 1,1-disubstituted alkene (22, 23).

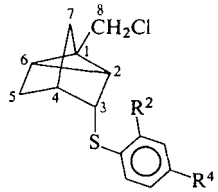
Experimental

All melting points were measured on a Fisher-Johns block and are reported uncorrected. The ^1H nmr spectra were recorded on Varian Associates T-60 and HA-100 spectrometers in chloroform-*d*, the TMS resonance being used to provide the field-frequency lock; ^{13}C nmr spectra at 20.000 MHz were obtained on a Varian FT80-16K spectrometer. Samples (100–300 mg/1 mL) in chloroform-*d* were contained in 10 mm tubes. The deuterium resonance from the solvent was used for the field-frequency lock. A spectral width of 4000 Hz with an acquisition time of 1.023 s, using 2-40K transforms, was em-

Can. J. Chem. Downloaded from www.nrcresearchpress.com by 210.87.254.40 on 09/05/12
For personal use only.

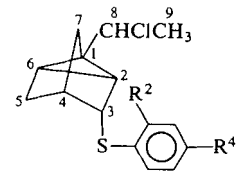
Can. J. Chem. Downloaded from www.nrcresearchpress.com by 210.87.254.40 on 09/05/12
For personal use only.

TABLE 3. Carbon-13 nmr parameters (δ, ppm) for the *endo*-3-arylthio-1-chloromethyltricyclo[2.2.1.$0^{2,6}$]heptanes synthesized during this investigation



R^2	R^4	C1	C2	C3	C4	C5	C6	C7	C8
NO_2	NO_2	28.3	22.5	51.2	36.5	35.6	19.7	31.8	46.6
NO_2	Cl	28.2	22.8	51.2	36.5	35.6	19.7	31.6	46.9
NO_2	H	28.2	22.9	51.1	36.6	35.6	19.7	31.6	47.1
NO_2	CH_3	28.1	23.0	51.4	36.6	35.6	19.7	31.5	47.1
NO_2	CH_3O	28.2	23.1	52.2	36.7	35.5	19.6	31.5	47.2
H	NO_2	28.1	22.9	51.3	36.6	35.3	19.4	31.5	46.8
H	Br	28.1	23.0	51.3	36.6	35.3	19.4	31.5	46.9
H	Cl	28.1	23.4	53.7	36.8	35.3	19.4	31.2	47.2
H	F	28.0	23.5	53.8	36.7	35.4	19.5	31.3	47.4
H	H	28.1	23.6	53.4	36.9	35.3	19.4	31.3	47.4
H	CH_3	28.1	23.7	54.2	36.8	35.2	19.4	31.2	47.4
H	tC_4H_9	28.0	23.9	55.0	36.9	35.2	19.3	31.2	47.5
H	CH_3O	28.0	24.1	56.2	37.1	35.3	19.2	31.1	47.6

TABLE 4. Carbon-13 nmr parameters (δ, ppm) for the diastereoisomeric *endo*-3-arylthio-1-(1′-chloroethyl)tricyclo-[2.2.1.$0^{2,6}$]heptanes synthesized during this investigation



R^2	R^4	C1	C2	C3	C4	C5	C6	C7	C8	C9
NO_2	NO_2	33.4	22.7	50.9	36.1	33.6	19.5	31.8	59.4	23.4
		33.3	21.7	51.2	36.2	34.4	19.4	31.6	59.0	23.5
NO_2	Cl	33.2	22.9	51.0	36.1	33.5	19.4	31.6	59.6	23.5
		33.1	22.1	51.3	36.1	33.5	19.4	31.3	59.2	23.5
NO_2	H	33.2	23.1	50.8	36.1	33.6	19.4	31.6	59.8	23.5
		33.1	22.2	51.1	36.1	34.2	19.4	31.3	59.5	23.6
NO_2	CH_3	33.2	23.1	51.1	36.2	33.6	19.4	31.6	59.9	23.5
		33.2	22.3	51.4	36.2	34.2	19.4	31.3	59.6	23.6
NO_2	CH_3O	33.2	23.3	51.9	36.3	33.5	19.4	31.5	59.9	23.5
		33.2	22.5	52.3	36.3	34.0	19.4	31.2	59.7	23.6
H	NO_2	33.4	22.5	51.3	36.3	33.7	19.3	31.9	59.6	23.3
		33.3	21.6	51.9	36.5	34.6	19.4	31.6	59.4	23.5
H	Cl	33.2	23.5	53.4	36.4	33.4	19.0	31.3	60.0	23.5
		33.2	22.9	53.8	36.4	33.6	19.2	31.0	59.8	23.5
H	CH_3O	33.2	23.5	53.9	36.5	33.6	18.7	31.0	61.2	23.6
		33.3	22.5	54.3	36.5	34.9	19.0	30.8	59.9	23.7

ployed. Coupling constants ($J_{^{13}C-^1H}$) were measured from high resolution spectra enhanced by applying the noise modulated decoupling field between data acquisition periods to retain the nOe. Signal assignments were made with the assistance of off-resonance, single-frequency decoupled spectra. All chemical shifts are expressed (δ, ppm) from internal TMS. Representative parameters are given in Tables 3 and 4. Mass spectra were recorded using an MS-9. Infrared spectra were recorded using a Unicam 1100 spectrometer, with matched NaCl 0.1071 mm cavity cells as CCl_4 or $CHCl_3$ solutions. All analytical and preparative tlc separations were performed on Analtech or Macherey-Nagel precoated plates, silica gel GF. Visualization of the tlc spots was accomplished by I_2, uv (254 nm), and phosphomolybdic acid – EtOH.

2-Methylenebicyclo[2.2.1]hept-5-ene was purchased from Aldrich and used without further purification. The purity was confirmed via ir, nmr, and glc; ir (CCl_4) μm: 3.12(w), 3.21(m), 3.3–3.4(bs), 3.45(m), 5.65(bw), 5.98(m), 6.32(bw), 6.88(bm),

Can. J. Chem. Downloaded from www.nrcresearchpress.com by 210.87.254.40 on 09/05/12
For personal use only.

7.4(m), 9.8(w), 10.0(w), 10.4(w), 10.6(m), 11.0(m), 11.2(s), 11.6(m); ^{1}H nmr ($CDCl_3$) δ: 5.22(m, 2H), 4.18(m, 1H), 3.02(m, 1H), 2.37(m, 1H), 0.93–2.2(m, 4H); ^{13}C nmr ($CDCl_3$) δ: 150.9(s, C2), 136.4(d, C6), 134.3(d, C5), 103.3(t, C8), 51.0(d, C1), 50.2(t, C7), 42.1(d, C4), 33.6(t, C3).

2-Ethylidenebicyclo[2.2.1]hept-5-ene was purchased from Aldrich. Analysis via nmr and glc indicated that this material was a 78:22 mixture of the *E* and *Z* isomers. Separation was accomplished on an analytical scale using glc/SE-30 column. Only exploratory product studies were carried out on isomerically pure samples, since reactivity studies indicated nonstereospecific addition. E *isomer*: ^{1}H nmr partial ($CDCl_3$) δ: 4.85(q, 1H, $=CHCH_3$); ^{13}C nmr ($CDCl_3$) δ: 50.5(d, C1), 142.0(s, C2), 31.1(t, C3), 41.8(d, C4), 134.4(d, C5), 135.9(d, C6), 50.3(t, C7), 112.7(d, C8), 14.8(q, d, C9). Z *isomer*: ^{1}H nmr partial ($CDCl_3$) δ: 4.48(q, 1H, $=CHCH_3$); ^{13}C nmr ($CDCl_3$) δ: 44.8(d, C1), 141.4(s, C2), 33.6(t, C3), 41.4(d, C4), 133.7(d, C5), 136.9(d, C6), 49.5(t, C7), 113.1(d, C8), 14.6(q, d, C9).

Arenesulphenyl chlorides were prepared as previously described (1, 2). Bicyclo[2.2.1]hept-2-ene, bicyclo[2.2.1]hepta-2,5-diene, and tetracyclo[3.2.0.0^{2,7}.0^{4,6}]heptane were the commercial products. These materials were analyzed as previously described (1, 2) and used without further purification.

General Procedure was as previously described (1, 2). Kinetic studies were carried out as previously described (23). Melting points of crystalline *endo*-3-arylthio-1-chloromethyltricyclo[2.2.1.0^{2,6}]heptanes are Ar = 2,4-$(NO_2)_2$: 101–105°C; 2-NO_2, 4-Cl : 76–78°C; 2-NO_2 : 77–79°C; 2-NO_2, 4-CH_3 : 59–61°C; 2-NO_2, 4-CH_3O : 62–63°C.

Elemental analysis (C, H, S) was carried out on all new compounds and found to be within ± 0.35% of the theoretical values. Isomerization of species **11** and **12** to **10** was observed by recording the ^{1}H and ^{13}C nmr spectra of the crude reaction mixtures over a period of two months. While it was immediately clear that **11** isomerizes to **10**, the simultaneous isomerization of **12** to **11** made it difficult to determine at this time whether or not **12** is able to go to **10** directly.

Acknowledgements

The continued financial support of the Natural Sciences and Engineering Research Council of Canada is gratefully acknowledged, as is a Province of Ontario Scholarship to one of us (PLB) 1978–1980.

1. D. G. GARRATT and P. L. BEAULIEU. J. Org. Chem. **44**, 3555 (1979).
2. P. L. BEAULIEU, A. KABO, and D. G. GARRATT. Can. J. Chem. **58**, 1014 (1980).
3. (*a*) C. D. JOHNSON. J. Org. Chem. **43**, 1814 (1978); (*b*) P. G. GASSMAN and A. F. FENTIMAN. J. Am. Chem. Soc. **92**, 2549 (1970); (*c*) H. C. BROWN and M. RAVINDRANATHAN. J. Org. Chem. **43**, 1709 (1978); (*d*) G. A. OLAH, G. K. PRAKASH, and G. LIANG. J. Am. Chem. Soc. **99**, 5683 (1977).
4. (*a*) D. C. OWSLEY, G. K. HELMKAMP, and M. F. RETTIG. J. Am. Chem. Soc. **91**, 5239 (1969); (*b*) D. R. HOGG. Mech. React. Sulfur Compd. **5**, 87 (1970); (*c*) E. N. GIVENS and H. KWART. J. Am. Chem. Soc. **90**, 378 (1968); **90**, 386 (1968); (*d*) N. KHARASCH. *In* Organic sulphur compounds. Vol. 1. *Edited by* N. Kharasch. Pergamon Press, Oxford. 1961. p. 379; (*e*) W. H. MUELLER and P. E. BUTLER. J. Am. Chem. Soc. **88**, 2866 (1966); (*f*) W. H. MUELLER and P. E. BUTLER. J. Am. Chem. Soc. **90**, 2075 (1968); (*g*) W. A. THALER. J. Org. Chem. **34**, 871 (1969); (*h*) D. G. GARRATT and P. L. BEAULIEU. Can. J. Chem. In press.
5. (*a*) G. H. SCHMID and D. G. GARRATT. *In* The chemistry of functional groups. Supplement A: The chemistry of double-bonded functional groups. *Edited by* S. Patai. Wiley & Sons, London. 1977. pp. 828–854; (*b*) G. H. SCHMID. *In* Topics in sulfur chemistry. *Edited by* A. Senning and P. S. Magee. Georg Thieme Publishers, Stuttgart. 1977. p. 103.
6. W. A. SMIT, N. S. ZEFIROV, I. V. BODRIKOV, and M. Z. KRIMER. Acc. Chem. Res. **12**, 282 (1979).
7. (*a*) J. BREDT. J. Prakt. Chem. **121**, 153 (1929); (*b*) S. J. CRISTOL and R. T. LALONDE. J. Am. Chem. Soc. **80**, 4355 (1958).
8. A. W. MCCULLOCH, A. G. MCINNES, D. G. SMITH, and J. A. WALTER. Can. J. Chem. **54**, 2013 (1976); (*b*) E. LIPPMAA, T. PEHK, and J. PAASIVISTA. Org. Magn. Reson. **5**, 277 (1973).
9. (*a*) J. D. ROBERTS, E. R. TRUMBALL, W. BENNETT, and R. ARMSTRONG. J. Am. Chem. Soc. **72**, 3116 (1950); (*b*) H. KWART and R. K. MILLER. J. Am. Chem. Soc. **78**, 5680 (1956); (*c*) J. D. ROBERTS, W. BENNETT, and R. ARMSTRONG. J. Am. Chem. Soc. **72**, 3329 (1950); (*d*) E. R. LIPPINCOTT. J. Am. Chem. Soc. **73**, 2001 (1951); (*e*) S. J. CRISTOL, R. A. SANCHEZ, and T. C. MORRILL. J. Org. Chem. **31**, 2738 (1966).
10. (*a*) J. B. STOTHERS. *In* Carbon-13 NMR spectroscopy. Academic Press, New York. 1972. Chapt. 5; (*b*) G. C. LEVY and G. L. NELSON. Carbon-13 nuclear magnetic resonance for organic chemists. Wiley & Sons, New York. 1972. Chapt. 3; (*c*) G. M. WHITESIDES and J. SAN FILIPPO. J. Am. Chem. Soc. **92**, 6611 (1970); (*d*) S. MASSON and A. THUILLIR. Bull. Soc. Chim. Fr. 3508 (1971); (*e*) R. S. NEALE and E. B. WHIPPLE. J. Am. Chem. Soc. **86**, 3130 (1964).
11. (*a*) D. G. GARRATT, M. D. RYAN, and M. UJJAINWALLA. Can. J. Chem. **57**, 2145 (1979); (*b*) H. C. BROWN, S. IKEGAMI, and J. H. KAWAKAMI. J. Am. Chem. Soc. **92**, 6914 (1970); (*c*) S. J. CRISTOL, R. P. ARGANBRIGHT, G. D. BRINDELL, and R. M. HEITZ. J. Am. Chem. Soc. **79**, 6035 (1957); (*d*) H. KWART and L. J. MILLER. J. Am. Chem. Soc. **83**, 4552 (1961); (*e*) W. H. MUELLER and P. E. BUTLER. J. Am. Chem. Soc. **88**, 2866 (1966).
12. N. S. ZEFIROV, N. K. SADOVAJA, A. M. MAGGERAMOV, I. V. BODRIKOV, and V. R. KASRTASHOV. Tetrahedron, **31**, 2948 (1975); Zh. Org. Khim. **10**, 2620 (1974).
13. (*a*) H. C. BROWN and J. H. KAMAKAMI. J. Am. Chem. Soc. **95**, 8665 (1973); **97**, 5521 (1975); (*b*) H. C. BROWN and K.-T. LIU. J. Am. Chem. Soc. **97**, 600 (1975); **97**, 2469 (1975).
14. (*a*) F. A. L. ANET. Tetrahedron Lett. 3393 (1964); (*b*) K. C. PANDE and S. WINSTEIN. Tetrahedron Lett. 3399 (1964); (*c*) A. MCKILLOP and M. E. FORD. J. Org. Chem. **39**, 2434 (1974); (*d*) R. D. BACH and R. F. RICHTER. J. Am. Chem. Soc. **94**, 4747 (1972); (*e*) T. G. TRAYLOR. Acc. Chem. Res. **2**, 152 (1968); (*f*) B. E. SMART. J. Org. Chem. **38**, 2027 (1973); (*g*) R. CAPLE, G. M. S. CHEN, and J. D. NELSEN. J. Org. Chem. **36**, 2870 (1971); (*h*) D. R. MARSHALL, P. REYNOLDS-WARNHOFF, E. W. WARNHOFF, and J. R. ROBINSON. Can. J. Chem. **49**, 885 (1971); (*i*) H. C. BROWN, S. IKEGAMI, and J. H. KAWAKAMI. J. Am. Chem. Soc. **92**, 1990 (1970); (*j*) H. C. BROWN, J. H. KAWAKAMI, and K.-T. LIU. J. Am. Chem. Soc. **95**, 2209 (1973); (*k*) W. FLIEGE and R. HUISGEN. Justus Liebigs Ann. Chem. 2038 (1973); (*l*) J. K. STILL and R. D. HUGHES. J. Org. Chem. **36**, 340 (1971).
15. (*a*) G. H. SCHMID and T. T. TIDWELL. J. Org. Chem. **43**, 460 (1978); (*b*) W. A. SMIT, A. S. GYBIN, V. S. BOGDANOV, M. Z. KRIMER, and E. A. VOROBIEVA. Tetrahedron Lett. 1085 (1978); (*c*) G. H. SCHMID and V. M. CSIZMADIA. Can. J. Chem. **44**, 1338 (1966); (*d*) G. H. SCHMID and P. H. FITZGERALD. J. Am. Chem. Soc. **93**, 2547 (1971); (*e*) G. H. SCHMID and V. M. CSIZMADIA. Can. J. Chem. **50**, 2465 (1972); (*f*) G. H. SCHMID and V. J. NOWLAN. J. Org. Chem. **37**, 3086 (1972); (*g*) K. IZAWA, T. OKUYAMA, and T.

FUENO. Bull. Soc. Chem. Jpn. **47**, 1480 (1974); (*h*) E. DUNKELBLUM. Tetrahedron, **30**, 3991 (1974); (*i*) M. OKI, W. NAKANISHI, M. FUKUNAGA, G. D. SMITH, W. L. DUAX, and Y. OSAWA. Chem. Lett. 1277 (1975); (*j*) G. M. BEVERLY and D. R. HOGG. J. Chem. Soc. Chem. Commun. 138 (1966); (*k*) W. H. MUELLER and P. E. BUTLER. J. Am. Chem. Soc. **90**, 2075 (1968); (*l*) W. A. THALER, W. H. MUELLER, and P. E. BUTLER. J. Am. Chem. Soc. **90**, 2069 (1968); (*m*) G. H. SCHMID and D. G. GARRATT. Can. J. Chem. **52**, 1807 (1974); **52**, 2463 (1974); (*n*) G. H. SCHMID, D. G. GARRATT, and S. YEROUSHALMI. J. Org. Chem. **43**, 3764 (1978); (*o*) D. G. GARRATT and P. BEAULIEU. Can. J. Chem. **57**, 119 (1979); (*p*) N. S. ZEFIROV, N. K. SADOVAJA, L. A. NOVGORODTSEVA, R. SH. ACHMEDOVA, S. V. BARANOV, and I. V. DODRIKOV. Tetrahedron, **35**, 2759 (1979).

16. J. L. KICE. *In* Sulfur in organic and inorganic chemistry. Vol. 1. *Edited by* A. Senning. Marcel Dekker, New York. 1971. Chapt. 6. p. 176.
17. (*a*) M. M. L. CHEN and R. HOFFMANN. J. Am. Chem. Soc. **98**, 1647 (1976); (*b*) Y. KIKUZONO, T. YAMABE, S. NAGATA, H. KATO, and K. FUKUI. Tetrahedron, **30**, 2197 (1974); (*c*) D. G. GARRATT, G. H. SCHMID, and I. G. CSIZMADIA. J. Mol. Struct. **22**, 117 (1974).
18. (*a*) J. C. MARTIN and T. M. BALTHAZOR. J. Am. Chem. Soc. **99**, 152 (1977); (*b*) T. M. BALTHAZOR and J. C. MARTIN. J. Am. Chem. Soc. **97**, 5634 (1975); (*c*) E. F. PEROZZI and J. C. MARTIN. J. Am. Chem. Soc. **101**, 1155 (1979).
19. (*a*) A. HASSNER, R. P. HOBLITT, C. HEATHCOCK, J. E. KROPP, and M. LORBER. J. Am. Chem. Soc. **92**, 1326 (1970); (*b*) A. HASSNER and J. S. TEETER. J. Org. Chem. **35**, 3397 (1970).
20. P. VON SCHLEYER and R. E. O'CONNER. 134th National Meeting, American Chemical Society, Chicago, IL. Sept. 1958. Abstr. p. 39.
21. (*a*) P. RIESZ, R. W. TAFT, JR., and R. H. BOYD. J. Am. Chem. Soc. **79**, 3724 (1957); (*b*) R. D. BACH and J. W. HOLUBKA. J. Am. Chem. Soc. **96**, 7814 (1974); (*c*) F. R. MAYO and J. J. KATZ. J. Am. Chem. Soc. **69**, 1339 (1947); (*d*) F. R. MAYO and M. G. SAVOY. J. Am. Chem. Soc. **69**, 1348 (1947); (*e*) Y. POCKER, K. D. STEVENS, and J. J. CHEMPOUX. J. Am. Chem. Soc. **91**, 4199 (1969); (*f*) T. OKUYAMA, K. IZAWA, and T. FUENO. J. Am. Chem. Soc. **95**, 6749 (1973).
22. G. COLLIN, U. JAHNKE, G. JUST, G. LORENZ, W. PRITZKOW, M. ROLLIG, L. WINGUTH, P. DIETRICH, G.-E. DORING, H. G. HAUTHAL, and A. WIEDENHOFT. J. Prakt. Chem. **311**, 238 (1969).
23. (*a*) G. H. SCHMID, C. L. DEAN, and D. G. GARRATT. Can. J. Chem. **54**, 1253 (1976); (*b*) C. L. DEAN, D. G. GARRATT, T. T. TIDWELL, and G. H. SCHMID. J. Am. Chem. Soc. **96**, 4958 (1974); (*c*) G. H. SCHMID and D. G. GARRATT. Can. J. Chem. **51**, 2463 (1973); **52**, 1807 (1974); (*d*) T. R. CERKSUS, V. M. CSIZMADIA, G. H. SCHMID, and T. T. TIDWELL. Can. J. Chem. **56**, 205 (1978).

Can. J. Chem. Downloaded from www.nrcresearchpress.com by 210.87.254.40 on 09/05/12
For personal use only.

Factors influencing the nature of seleniranium ions in selenenyl chloride additions to alkenes: the use of methanol as solvent[1]

DENNIS G. GARRATT[2] AND ANN KABO

Department of Chemistry, University of Ottawa, Ottawa, Ont., Canada K1N 9B4

Received October 4, 1979

DENNIS G. GARRATT and ANN KABO. Can. J. Chem. **58**, 1030 (1980).

The reaction of benzeneselenenyl chloride with some simple alkylsubstituted acyclic and cyclic alkenes has been investigated using methanol as the solvent. Products of solvent-incorporation, β-methoxyalkyl phenyl selenides, are normally favoured over the analogous chloro species, but exceptions have been noted. The observation of products of solvent-incorporation, Wagner–Meerwein rearrangement, and homoallylic rearrangement is in accord with an Ad_E2 mechanism involving both intimate and solvent-separated ion-pairs prior to the product forming step.

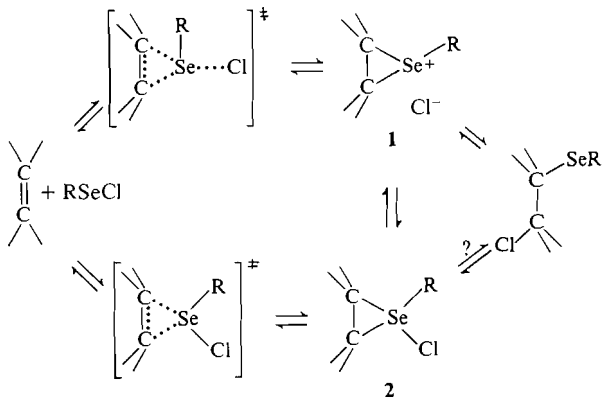
DENNIS G. GARRATT et ANN KABO. Can. J. Chem. **58**, 1030 (1980).

On a étudié la réaction du chlorure de benzènesélènènyle avec quelques alcènes simples acycliques et cycliques ayant un substituant alkyle en utilisant le méthanol comme solvant. Les produits résultant de l'incorporation du solvant, les phénylsélénures de β méthoxyalkyles, sont normalement favorisés par rapport aux analogues chlorés, mais on a noté quelques exceptions. L'observation des produits résultant de l'incorporation du solvant, de transpositions de Wagner–Meerwein, de transpositions homoallyliques, est en accord avec un mécanisme Ad_E2 impliquant des paires d'ions liés et des paires d'ions séparés par le solvant avant l'étape de formation des produits.

[Traduit par le journal]

Considerable attention has been given to the reactions of areneselenenyl halides with carbon–carbon double bonds (1). The addition reaction has been found to be *anti*-stereospecific by numerous investigators (2). This observation in addition to supplementary kinetic evidence (3) has been used as the basis for postulating a mechanism (see Scheme 1) involving a seleniranium ion, [3] **1**, and/or an episelenurane, **2**, intermediate prior to the product forming step (4, 5). In a recent article (6), we reported that an open cationic species may exist prior to the product forming step in additions to vinyl ethers such as 3,4-dihydro-2*H*-pyran. The intermediacy of a bridged species was, however, evident from an analysis of kinetic data, suggesting therefore that a seleniranium ion-like species precedes any cation of the open structure.

Such data are generally interpreted in terms of an Ad_E2 mechanism (7). The usual criteria of such a two-step mechanism, solvent-incorporated or rearranged products, are, however, quite rare in selenenyl halide additions. For example, the reaction of 2,4-dinitrobenzeneselenenyl chloride with *E*- or *Z*-1-phenylpropene in acetic acid, which is albeit a poor or weak nucleophilic solvent, fails to give acetate products under conditions of kinetic control (2*a*). Similar results have been reported by others using the somewhat stronger electrophiles, benzeneselenenyl chloride and bromide (1*f*, 2*b*). Furthermore, bicyclo[2.2.1]hept-2-ene, an olefin prone to skeletal rearrangements during electrophilic attack, gives only the products of *exo–anti* addition when reacted with benzeneselenenyl chloride or thiocyanate in methylene chloride solution (8).



SCHEME 1

The use of more nucleophilic solvents, such as

[1]NRCC No. 18146.

[2]Author to whom correspondence may be addressed at the Division of Chemistry, National Research Council of Canada, 100 Sussex Dr., Ottawa, Ont., Canada K1A 0R6.

[3]We note that the use of the term *seleniranium ion*, particularly in Scheme 1, was not and is not intended to imply a dissociated ion. It has always been our belief that a series of ion-pairs is to be found on the reaction hypersurface. This statement is not, however, intended to suggest that a dissociated ion is not formed under some circumstances. The authors wish by this note to remove any possible confusion which might exist over the usage of such nomenclature in the future as apparently currently exists with respect to the use of thiiranium or episulphonium ion in the analogous reactions of sulphenyl chlorides (see for example ref. 1*a*, pp. 828–854, and ref. 10).

0008-4042/80/101030-12$01.00/0

©1980 National Research Council of Canada/Conseil national de recherches du Canada

Can. J. Chem. Downloaded from www.nrcresearchpress.com by 210.87.254.105 on 09/05/12
For personal use only.

Can. J. Chem. Downloaded from www.nrcresearchpress.com by 210.87.254.105 on 09/05/12
For personal use only.

alcohols, has been ignored, primarily it would appear because of the leitmotif of organic chemistry that one can not, or at least should not, carry out reactions in a medium which itself readily reacts with one of the reagents.

In this case the reaction of selenenyl halides with alcohols to give selenenic esters (selenenyl alkoxides) has been known for over forty years (9). We observe the reaction of benzeneselenenyl chloride with methanol to be bimolecular, the rate of disappearance of selenenyl chloride following second order kinetics, first order in both selenenyl chloride and methanol in methylene chloride solution. Comparing k_2 for the reaction of benzeneselenenyl chloride with methanol to that of k_2' for the *analogous* reaction with ethylene (3), $k_2 = 0.011$ $dm^3\ mol^{-1}\ s^{-1}$ vs. $k_2' = 498$ $dm^3\ mol^{-1}\ s^{-1}$, CH_2Cl_2/25°C, indicates that the π orbital of a carbon–carbon double bond is a more effective nucleophile than the oxygen atom of an alcohol as far as nucleophilic displacement at bivalent selenium is concerned!!

If one makes the assumption, the validity of which is unfortunately not known, that the difference in relative reactivity of ethylene vs. methanol, $\simeq$ 45 250:1, is the same in methanol as in methylene chloride, and if one notes that the concentration of methanol in pure methanol is approximately 24.7 mol dm^{-3}, it becomes apparent that under normal reaction conditions, wherein the alkene concentration in the solvent is in the range of 0.04–0.12 mol dm^{-3}, the probability of the selenenyl chloride reacting preferentially with the alkene is at least 70–200:1. Such a scenario will be valid for any alkene which is more reactive than ethylene.

On the basis of these observations and calculations it became apparent that one should be able to carry out reactions between benzeneselenenyl chloride and simple alkenes in polar and nucleophilic solvents such as methanol.[4] It was anticipated that by virtue of the greater polarity and nucleophilic nature of methanol one would be able to draw further mechanistic conclusions with respect to the importance of ion-pairs during the reaction of selenenyl halides with alkenes.[3] Furthermore, it was felt that the use of methanol or other alcohols as solvents might open up a new series of potentially useful synthetic reagents for the introduction, both stereo- and regiospecifically, of an ether functionality into an organic substrate.

We wish to present experimental data which have a direct bearing upon this problem.

[4]Methanol has been used as a solvent for other nucleophilic substitutions at selenenyl selenium (11).

Results and Discussion

In the early stages of this investigation we examined the effect of increased solvent polarity and nucleophilicity using simple *E*- and *Z*-1,2-dialkylsubstituted ethylenes, such as the isomeric 3-hexenes, and 2,5-dimethyl-3-hexenes. In each case a mixture of methoxy- and chloro-adducts is isolable; the products being formed by net *anti*-stereospecific addition (see Table 1). Assignments are based upon both ^1H and ^{13}C nmr spectroscopy (Tables 2 and 3, and Experimental). The ratio of methoxy- to chloro-adducts, $[ROCH_3]/[RCl]$, is found to be generally greater than one, but some exceptions are apparent, as in, for example, the case of *Z*-2,5-dimethyl-3-hexene.

Control experiments demonstrate that the reaction of selenenyl chloride with methanol is much slower than the additions and that samples of chloroadducts are not solvolyzed under our reaction conditions. Supplementary data of this form are also available from the literature (12). McManus and Lam have determined that the methanolysis of 2-chloroethyl phenyl selenide follows first order kinetics, $k = 2.94 \times 10^{-4}\ s^{-1}$, which corresponds to $\tau_{1/2} = 39$ min. The essentially instantaneous nature of these additions, $\tau_{1/2}$ = a few milliseconds to seconds, dependent upon concentrations, thus rules out methanolysis of the chloroadducts as being significant.

When unsymmetrically substituted ethylenes, such as the 4,4-dimethyl-2-pentenes, are reacted under these conditions, attack by methanol is highly regioselective, occurring at the least sterically hindered position to give the *anti*-Markownikoff adducts.[5] These data are indicative of the importance of steric factors towards directing the approach of the solvent molecule, CH_3OH, to the least hindered secondary site of the initially formed intermediate, although the importance of nonrepulsive electronic effects can not be totally ruled out.

The use of *Z*- and *E*-1-phenylpropene as substrates is particularly instructive. The addition is *anti*-stereospecific and regiospecific in the Markownikoff sense in accord with earlier studies (2*a*,

[5]In the tables we use the designation Markownikoff, *M*, and *anti*-Markownikoff, *aM*, to distinguish between regioisomeric adducts. Since such nomenclature is confusing for adducts derived from 1,2-disubstituted or tetrasubstituted ethylenes, we have adopted the convention that when both olefinic carbon atoms contain the same number of *alkyl groups* the Markownikoff isomer is defined as that one in which the chloride or methoxide moiety is bonded to the carbon whose sum of Taft's inductive substituent constants, $\Sigma\sigma^*$, is the more negative. This method of nomenclature has been previously employed (19).

Can. J. Chem. Downloaded from www.nrcresearchpress.com by 210.87.254.105 on 09/05/12
For personal use only.

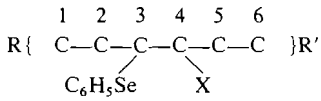
TABLE 1. The kinetically controlled product distributions for the addition of benzeneselenenyl chloride to a series of alkenes in methylene chloride and methanol solvents at 25°C

		RCl (%)		$ROCH_3$ (%)	
Alkene	Solvent	M*	aM*	M*	aM*
Z-3-Hexene	CH_2Cl_2	100			
	CH_3OH	12		88	
E-3-Hexene	CH_2Cl_2	100			
	CH_3OH	26		74	
Z-2,5-Dimethyl-3-hexene	CH_2Cl_2	100			
	CH_3OH	52		48	
E-2,5-Dimethyl-3-hexene	CH_2Cl_2	100			
	CH_3OH	16		84	
Z-Cyclooctene	CH_2Cl_2	100			
	CH_3OH	0		100	
Z-2-Pentene	CH_2Cl_2	55	45		
	CH_3OH	4	3	27	66
E-2-Pentene	CH_2Cl_2	62	38		
	CH_3OH	8	4	30	58
Z-4-Methyl-2-pentene	CH_2Cl_2	30	70		
	CH_3OH	33	10	0	57
E-4-Methyl-2-pentene	CH_2Cl_2	25	75		
	CH_3OH	25	9	0	66
Z-4,4-Dimethyl-2-pentene	CH_2Cl_2	0	100		
	CH_3OH	0	11	0	89
E-4,4-Dimethyl-2-pentene	CH_2Cl_2	8	92		
	CH_3OH	7	25	0	68
Z-1-Phenylpropene	CH_2Cl_2	100	0		
	CH_3OH	5	0	95	0
E-1-Phenylpropene	CH_2Cl_2	100	0		
	CH_3OH	43	0	57	0
2-Methyl-2-butene	CH_2Cl_2	100	0		
	CH_3OH	75	0	25	0
2-Methyl-1-butene	CH_2Cl_2	100	0		
	CH_3OH	47	0	53	0
2,3-Dimethyl-1-butene	CH_2Cl_2	100	0		
	CH_3OH	37	0	63	0
2,4-Dimethyl-1-pentene	CH_2Cl_2	100	0		
	CH_3OH	20	0	80	0
2,3-Dimethyl-1-pentene	CH_2Cl_2	100	0		
	CH_3OH	21	0	79	0
2,4,4-Trimethyl-1-hexene	CH_2Cl_2	100	0		
	CH_3OH	0	0	100	0

Product ratios for some polycyclic alkenes

Alkene	Solvent	Product ratios
Cis-bicyclo[3.3.0]oct-2-ene	CH_2Cl_2	**8**:**9**:**10**:**11**:**12**:**13**:**14**:**15** = 57:7:12:24:0:0:0:0
	CH_3OH	**8**:**9**:**10**:**11**:**12**:**13**:**14**:**15** = 3:0:0:4:17:9:17:50
Bicyclo[2.2.1]hept-2-ene	CH_2Cl_2	**17**:**18**:**19**:**20**:**21** = 100:0:0:0:0
	CH_3OH	**17**:**18**:**19**:**20**:**21** = 63:25:4:4:4
Bicyclo[2.2.1]hepta-2,5-diene	CH_2Cl_2	**27**:**28**:**29**:**30**:**31**:**32** = 8:0:0:0:31:61
	CH_3OH	**27**:**28**:**29**:**30**:**31**:**32** = 2:3:19:76:0:0
2-Methylenebicyclo[2.2.1]hept-5-ene	CH_2Cl_2	**38**:**39**:**40**:**41** = 54:0:6:40
	CH_3OH	**38**:**39**:**40**:**41** = 20:80:0:0
2-Ethylidenebicyclo[2.2.1]hept-5-ene	CH_2Cl_2	**46**:**47**:**48**:**49** = 50:50:0:0
	CH_3OH	**46**:**47**:**48**:**49** = 15:15:35:35

TABLE 2. Carbon-13 nmr parameters for the products of addition of benzeneselenenyl chloride to a series of 1,2-disubstituted ethylenes in methanol

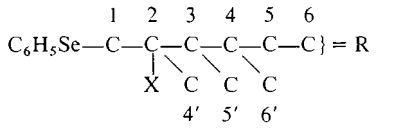


Compound				Chemical shift assignments (δ, ppm)						
R	R'	Configuration	X	C1	C2	C3	C4	C5	C6	CH_3O
Et	Et	3-*RS*, 4-*RS*	Cl	13.4 q	24.9 t	55.6 d	68.8 d	28.0 t	11.9 q	
			CH_3O	13.2 q	25.1 t	52.1 d	85.4 d	24.1 t	10.7 q	57.8 q
Et	Et	3-*RS*, 4-*SR*	Cl	12.2 q	25.5 t	54.8 d	69.2 d	29.9 t	11.1 q	
			CH_3O	13.0 q	24.5 t	52.5 d	85.3 d	24.5 t	10.0 q	57.9 q
*i*Pr	*i*Pr	3-*RS*, 4-*RS*	Cl	21.8 q 20.7 q	33.0 d	60.8 d	73.0 d	33.7 d	21.1 q 19.9 q	
			CH_3O	21.0 q 20.0 q	32.0 d	60.0 d	87.5 d	31.9 d	20.5 q 17.7 q	60.7 q
*i*Pr	*i*Pr	3-*RS*, 4-*SR*	Cl	22.8 q 17.0 q	29.5 d	61.5 d	73.9 d	30.9 d	21.8 q 14.7 q	
			CH_3O	23.0 q 19.1 q	31.3 d	60.0 d	89.6 d	27.9 d	20.9 q 16.6 q	61.8 q
Me	Et	2-*RS*, 3-*RS*	Cl		17.2 q	46.0 d	69.3 d	27.1 t	11.9 q	
			CH_3O		17.7 q	42.4 d	86.1 d	23.7 t	10.3 q	57.8 q
Me	Et	2-*RS*, 3-*SR*	Cl		18.3 q	44.8 d	70.0 d	30.1 t	11.2 q	
			CH_3O		17.1 q	43.2 d	85.8 d	24.6 t	10.1 q	58.3 q
Me	*i*Pr	2-*RS*, 3-*RS*	Cl		19.6 q	45.4 d	75.3 d	33.3 d	21.6 q	
			CH_3O		Unknown				20.8 q	
Me	*i*Pr	2-*RS*, 3-*SR*	Cl		19.4 q	43.2 d	75.4 d	32.7 d	20.9 q	
			CH_3O		Unknown				17.3 q	
Me	*t*Bu	2-*RS*, 3-*RS*	Cl		24.2 q	42.1 d	78.1 d	37.9 s	29.0 q	
			CH_3O		Unknown					
Me	*t*Bu	2-*RS*, 3-*SR*	Cl		17.9 q	42.3 d	77.7 d	37.7 s	27.8 q	
			CH_3O		Unknown					
Me	C_6H_5	1-*RS*, 2-*RS*	Cl		18.3 q	46.7 d	67.1 d	Aromatic		
			CH_3O		18.7 q	44.6 d	87.6 d	Aromatic		56.9 q
Me	C_6H_5	1-*RS*, 2-*SR*	Cl		19.2 q	45.6 d	68.6 d	Aromatic		
			CH_3O		24.7 q	45.7 d	86.3 d	Aromatic		57.5 q
Et	Me	2-*RS*, 3-*RS*	Cl	13.2 q	23.7 t	56.0 d	61.1 d	20.8 q		
			CH_3O	13.1 q	24.4 t	53.7 d	79.1 d	16.3 q		56.5 q
Et	Me	2-*RS*, 3-*SR*	Cl	12.6 q	25.8 t	56.7 d	61.8 d	24.3 q		
			CH_3O	12.9 q	24.9 t	54.6 d	79.4 d	17.0 q		56.6 q
*i*Pr	Me	2-*RS*, 3-*RS*	Cl	22.0 q 21.8 q	31.3 d	64.0 d	60.9 d	23.0 q		
			CH_3O	21.6 q 21.2 q	31.6 d	62.4 d	78.5 d	18.0 q		56.3 q
*i*Pr	Me	2-*RS*, 3-*SR*	Cl	22.6 q 17.7 q	30.1 d	65.2 d	61.5 d	25.2 q		
			CH_3O	22.1 q 17.8 q	28.8 d	62.8 d	78.7 d	19.4 q		56.4 q
*t*Bu	Me	2-*RS*, 3-*RS*	Cl	29.4 q	37.9 s	67.3 d	59.6 d	26.7 q		
			CH_3O	29.1 q	36.6 s	68.4 d	76.4 d	19.1 q		55.7 q
*t*Bu	Me	2-*RS*, 3-*SR*	Cl	28.1 q	38.0 s	71.1 d	49.0 d	23.8 q		
			CH_3O	29.4 q	35.3 s	67.3 d	77.4 d	19.1 q		56.0 q

NOTE: The configuration (*RS*, *RS*) = *threo*; (*RS*, *SR*) = *erythro*.

Can. J. Chem. Downloaded from www.nrcresearchpress.com by 210.87.254.105 on 09/05/12
For personal use only.

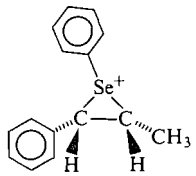
TABLE 3. Carbon-13 nmr parameters for the products of addition of benzeneselenenyl chloride to a series of 1,1-disubstituted ethylenes in methanol



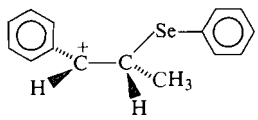
Compound	X	C1	C2	C3	C4	C5	C6	C4'	C5'	C6'	CH_3O
Et	Cl	42.6 t	74.4 s	35.8 t	9.1 q			29.5 q			
	CH_3O	37.4 t	76.8 s	30.1 t	8.0 q			22.4 q			49.3 q
*i*Pr	Cl	42.5 t	78.1 s	37.3 d	18.0 q			27.9 q	18.0 q		
	CH_3O	36.4 t	78.7 s	33.9 d	17.6 q			18.8 q	17.3 q		49.1 q
*i*Bu	Cl	44.0 t	73.9 s	51.4 t	30.3 d	23.2 q		25.2 q		23.1 q	
	CH_3O	38.6 t	77.2 s	45.7 t	24.6 d	24.3 q		23.5 q		24.1 q	49.3 q
$CH_2C(Me)_2Et$	CH_3O	40.4 t	78.0 s	46.9 t	37.0 s	34.8 t	8.5 q	26.8 q	28.0 q 27.8 q		49.1 q
*s*Bu*	Cl	44.5 t	78.1 s	42.5 d	27.9 t	12.5 q		24.5 q	23.3 q		
	Cl	44.3 t	77.8 s	42.5 d	27.9 t	12.3 q		24.4 q	23.4 q		
	CH_3O	41.2 t	79.0 s	36.7 d	24.3 t	13.8 q		12.7 q	19.5 q		49.0 q
	CH_3O	41.1 t	78.8 s	36.7 d	23.5 t	13.2 q		12.7 q	19.1 q		49.0 q

*(2-*RS*, 3-*RS*) and (2-*RS*, 3-*SR*) diastereoisomers.

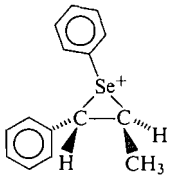
13). It is clear from these observations that the increased polarity of the medium is not able to shift the relative order of stabilities between isomeric β-phenylseleno benzylic carbonium ions, **3** and **4** (usually the less stable species), and seleniranium ions, **5** and **6**. Alternatively, we can make the hypothesis that if **3** and **4** are formed on the reaction hypersurface, they collapse to products faster than rotation about the C1—C2 single bond, i.e., faster than isomerization and equilibration of the form: **3**⇄**4**. The exclusive formation of products of *anti*-addition would then be, presumably, the result of retardation of *syn* attack because of the bulk of the β-phenylseleno group, as seems reasonable.



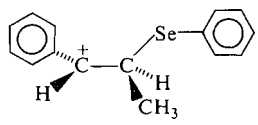
5



3



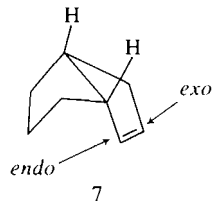
6



4

With 1,1-disubstituted and trisubstituted ethylenes, benzeneselenenyl chloride reacts regiospecifically in the Markownikoff sense, electronic factors apparently overriding steric hindrance to approach in contrast to our observations for 1,2-dialkylsubstituted ethylenes (eqs. [1] and [2], Table 1). In comparison, we note that areneselenenyl chlorides show an equivalent regiospecificity in methylene chloride solution, whereas arenesulphenyl chlorides add regioselectively in the opposite, i.e., *anti*-Markownikoff sense.

The configurational-selectivity,[6] ie, the ability of the selenenyl chloride to preferentially attack one face of the olefinic π system, is demonstrated by the reaction of benzeneselenenyl chloride with *cis*-bicyclo[3.3.0]oct-2-ene, **7**. The ratio of *exo* to *endo* attack is found to favour the sterically least hindered *exo* face in both methanol and methylene chloride solution (eq. [5]), $(exo/endo)_{CH_3OH}$ = 74:26, $(exo/endo)_{CH_2Cl_2}$ = 81:19. Of note, however, is the relative distribution of regioisomers. For example, the major species from the reaction of benzeneselenenyl chloride with **7** in methanol is the

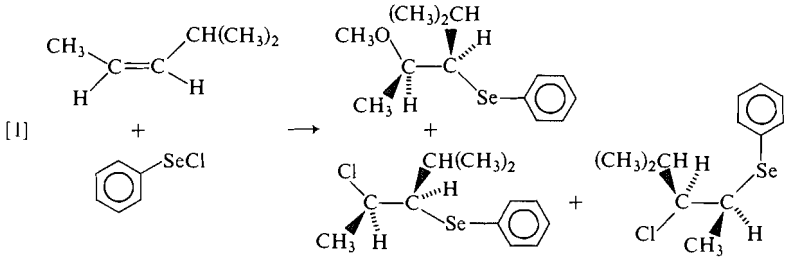


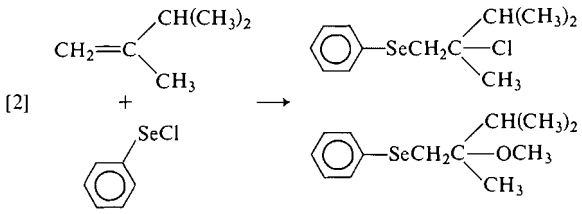
7

Markownikoff adduct of *exo* attack with solvent-incorporation, **15**. This compound plus its chloro analogue, **11**, account for 54% of the reaction mix-

[6]The term configurational-selectivity was originally coined in reference to a problem in allene chemistry in which it became necessary to distinguish which face or faces of the orthogonal π systems was/were being attacked (20). The extension of the use of this term to problems such as *exo* and *endo* attack seems to us quite reasonable.

Can. J. Chem. Downloaded from www.nrcresearchpress.com by 210.87.254.105 on 09/05/12
For personal use only.





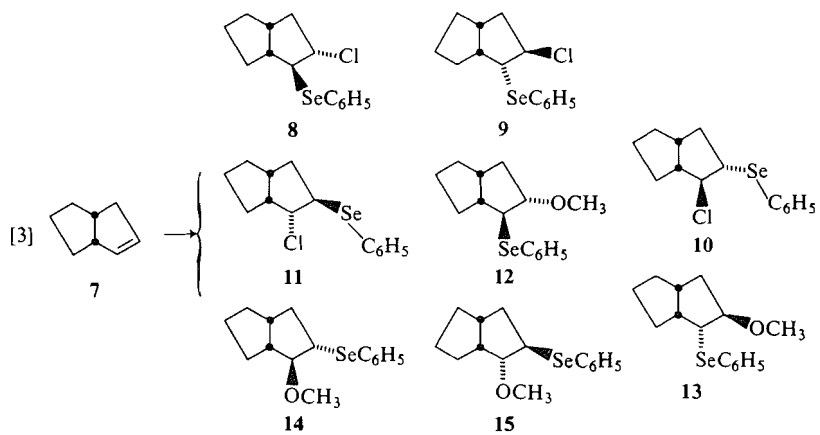
ture, the *anti*-Markownikoff adducts of *exo* attack, **8** and **12**, accounting for another 20%. In methylene chloride solution, *anti*-Markownikoff attack, on the *exo* face, compound **8**, accounts for 57% compared to 24% Markownikoff, **11**, the reverse of the situation in methanol! These observations are more striking if one compares the product distribution from **7** with those from the acyclic alkene, *Z*-4-methyl-2-pentene (Table 1). In the latter case we observe only a marginal change in the ratio of Markownikoff to *anti*-Markownikoff adducts upon changing the solvent. Furthermore, attack by methanol is regiospecific in the *anti*-Markownikoff sense. Clearly there are no gross preferences involved, but rather some subtle admixture of factors, most likely involving series of ion-pairs.

The reaction of benzeneselenenyl chloride with bicyclo[2.2.1]hept-2-ene, **16**, is most instructive in this regard. In methylene chloride solution only the product of *exo–anti* addition, **17**, is isolable or observed. In contrast, we find five products, **17–21**, when methanol is the solvent (eq. [4]). In addition to the products of *exo–anti* addition, we observe minor amounts of *exo*-2-methoxy-*syn*-7-phenylselenobicyclo[2.2.1]heptane, **20**, and *exo*-2-chloro-*syn*-7-phenylselenobicyclo[2.2.1]heptane, **21**, the result of Wagner–Meerwein rearrangement, plus *exo*-2-phenylseleno-*exo*-3-methoxybicyclo[2.2.1]-heptane, **19**, a product of *exo–syn* addition! No evidence was found for products of elimination, such as nortricyclenes.

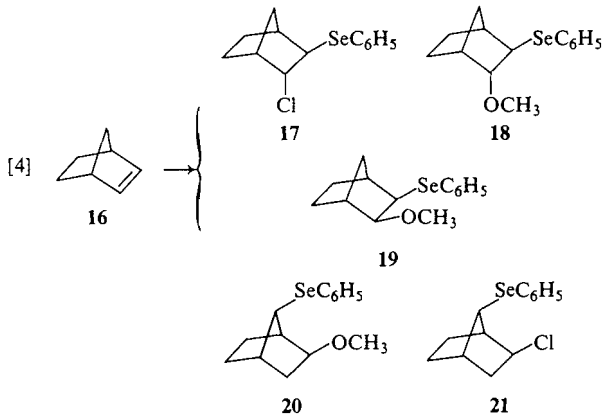
To account for the data discussed up to this point we require a more complex reaction hypersurface, such as is shown in Scheme 2. In terms of this scheme we interpret the results from **16** as reflecting competitive attack by chloride ion and methanol on a seleniranium ion species at the intimate ion-pair, **22**, and solvent-separated ion-pair, **23**, stage. The ratio of chloro adduct **17** to the methoxy adduct **18** ([**17**]/[**18**] = 72:28) presumably reflects a higher rate of collapse to product from the intimate ion-pair **22**, than is possible for the alternative species **23**.

The observation of Wagner–Meerwein rearrangement and *exo–syn* addition is indicative of the presence of a relatively low barrier towards interconversion of seleniranium ion **23** and solvent-separated norbornyl carbonium ions, such as **24** and **25** (eq. [5]).

The reaction of benzeneselenenyl chloride with the analogous olefin, bicyclo[2.2.2]oct-2-ene,



Can. J. Chem. Downloaded from www.nrcresearchpress.com by 210.87.254.105 on 09/05/12
For personal use only.

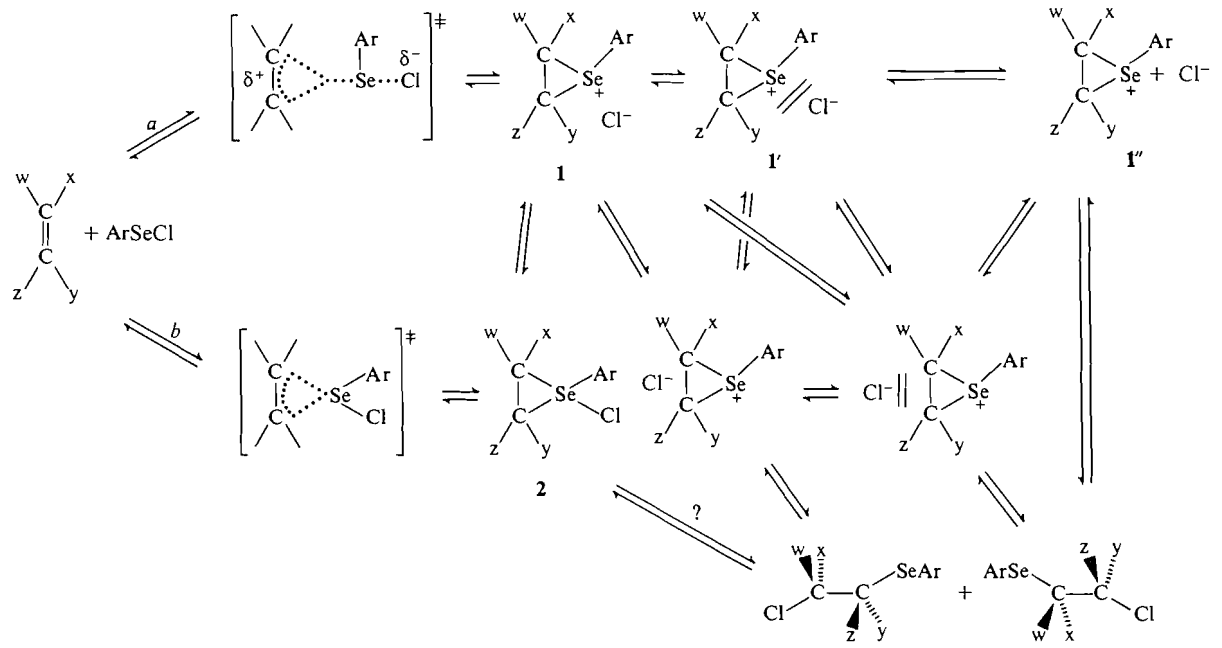


yields only products of simple 1,2-*anti* addition, as is shown in eq. [6]. Attempts to force a series of rearrangements by use of elevated temperatures were unsuccessful.

The reaction of benzeneselenenyl chloride with bicyclo[2.2.1]hepta-2,5-diene, **26**, shows a number of interesting trends which are quite distinct from those already discussed. Thus in methanol solution, four species, all the result of homoallylic attack, **27–30**, are isolable. Of primary importance is the observation of adducts arising from both *exo* and *endo* addition, and the predominance of *endo* attack: [**27** + **29**]/[**28** + **30**] = [*exo*]/[*endo*] = 21:79. These observations contrast with those described earlier for the reaction with **16** which proceeds exclusively with *exo*-configurational-specificity (eq. [7]).

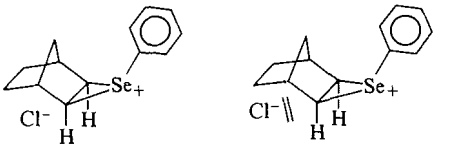
In methylene chloride solution the reaction of **26** with benzeneselenenyl chloride also yields adducts of *exo* and *endo* attack, [*exo*]/[*endo*] = [**27** + **31**]/[**32**] = 39:61, but in this case products of simple 1,2-addition (*exo–anti* and *endo–anti*) are found to predominate. One interpretation of these solvent-oriented differences is collapse to products in methylene chloride solution from intimate ion-pairs, such as **33** and **34**, before π participation by the homoallylic double bond is able to become important. To explain the exclusive formation of nortricyclenes in methanol, it appears sufficient to infer that attack upon the homoallylic double bond of the first formed intimate ion-pairs **35** and **36** by methanol occurs preferentially. Such a scenario also accounts for the high ratio of methoxy to chloro adducts, [$ROCH_3$]/[RCl] = 95:5, since the solvent molecules do not have to enter the sterically hindered zone near selenium in order to react, and since the chloride ion does not have to migrate to the far side of the reacting system. The formation of *exo*-chloro nortricyclenes may be rationalized in the same way by assuming an intermolecular attack by chloride ion instead of rearrangement of the first formed ion-pair. This of course necessitates that the chloride ion which attacks the ion-pair originates from a different ion-pair.

The absence of *endo*-chloro and *endo*-methoxy nortricyclenes, and of products of Wagner–Meerwein rearrangement, is indicative, using Cristol's criteria, of the absence of free or dissociated carbonium ions on the reaction hypersurface (14). It is



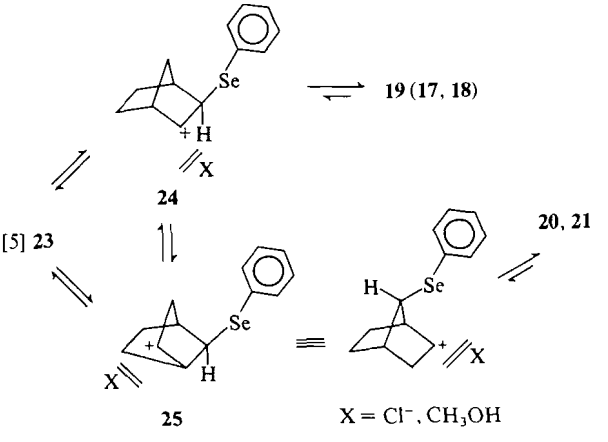
SCHEME 2

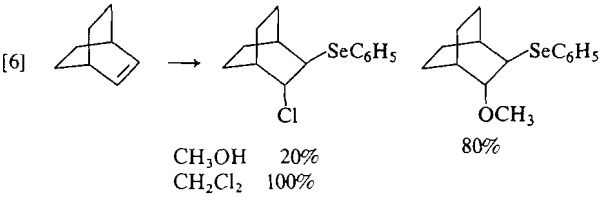
Can. J. Chem. Downloaded from www.nrcresearchpress.com by 210.87.254.105 on 09/05/12
For personal use only.

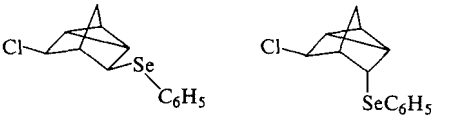


22 23

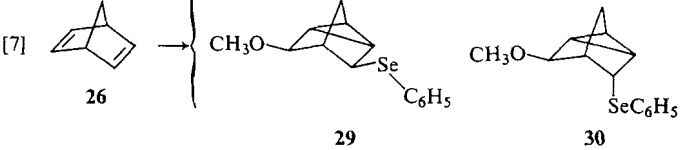
not immediately obvious, however, why species **28** is found in methanol but not in methylene chloride. Once again, very subtle factors appear to be responsible. We note that precedence for *endo* attack upon substrate **26** is to be found in the literature, although rarely is *endo* attack favoured over that of *exo* (15).

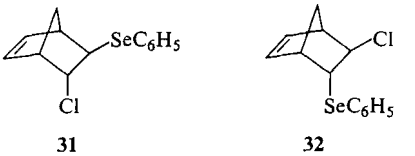






27 28





31 32

The high yields of products derived from homoallylic rearrangement in the latter example suggested to us that a more detailed investigation of dienes containing properly aligned double bonds might be most fruitful. We therefore studied the reactions of benzeneselenenyl chloride with 1,4-cyclohexadiene (eq. [12]), bicyclo[4.4.0]deca-1(6),3-diene (eq. [13]), bicyclo[4.3.0]nona-1(6),3-diene (eq. [14]), *Z,Z*-1,5-cyclooctadiene (eq. [15]), 2-methylenebicyclo[2.2.1]hept-5-ene, **37** (eq [16]), and the *E,Z* isomeric 2-ethylidenebicyclo-[2.2.1]hept-5-enes, **44** and **45** (eq. [17]).

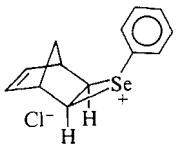
As can be seen from eqs. [12]–[15], for the first four substrates only products of net 1,2-*anti* addition are observed or isolated in both methanol and methylene chloride solutions. Similar results have been reported for related electrophiles such as arenesulphenyl halides (16, 17). These results are significant inasmuch as they are indicative that an open carbonium ion is not involved at any stage in the reaction mechanism.

The reaction of benzeneselenenyl chloride with **37** (eq. [16]) is very interesting for we observe only marginal chemoselectivity in methylene chloride solution, attack upon the *endocyclic* double bond being preferred over attack upon the *exocyclic* double bond by a ratio of 60:40. In methanol, however, the reaction is chemospecific, attack occurring exclusively on the endocyclic double bond. This observation is indicative of a change in the relative reactivities of 1,2- and 1,1-disubstituted double bonds as the polarity and nucleophilicity of the solvent is varied.

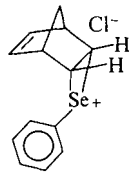
Of further note is the observation that the homoallylic products, **38** and **39**, are the result of attack upon the *endocyclic* double bond. While species **40** readily isomerizes and solvolyzes to

Can. J. Chem. Downloaded from www.nrcresearchpress.com by 210.87.254.105 on 09/05/12
For personal use only.

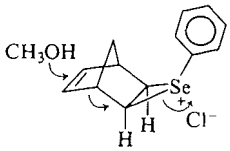
Can. J. Chem. Downloaded from www.nrcresearchpress.com by 210.87.254.105 on 09/05/12
For personal use only.

[8]  → 27 + 31

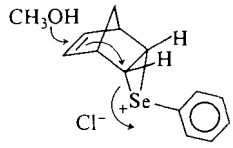
33

[9]  → 32

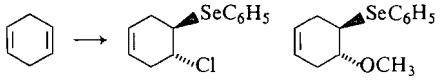
34

[10]  → 29

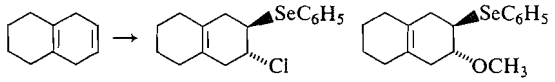
35

[11]  → 30

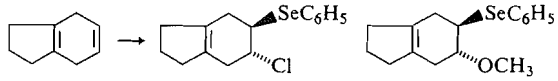
36

[12] 

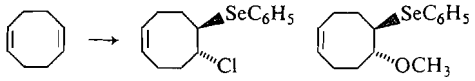
CH_3OH 24% 76%
CH_2Cl_2 100%

[13] 

CH_3OH 10% 90%
CH_2Cl_2 100%

[14] 

CH_3OH 12% 88%
CH_2Cl_2 100%

[15] 

CH_3OH 0% 100%
CH_2Cl_2 100%

give **38** and **39** at elevated temperatures (refluxing methanol), attempts to convert **41** into nortricyclenes **42** and **43** failed. Only adducts **38** and **39** were isolated from an attempted methanolysis of **41**. We interpret this result in terms of a reversible addition sequence, in which **37** and benzeneselenenyl chloride are regenerated and then reacted, forming the thermodynamically preferred adducts **38** and **39**.

In the case of the isomeric 2-ethylidenebicyclo[2.2.1]hept-5-enes, **44** and **45** (eq. [17]), only products of *exo* attack upon the *endocyclic* double bond with homoallylic rearrangement are observed in both methanol and methylene chloride. Of note is the observation that while the electrophilic attack is configurationally specific-*exo*, subsequent nucleophilic attack by chloride ion or methanol is non-stereospecific, giving rise to essentially equal amounts of the 3-*RS*,8-*RS* and 3-*RS*,8-*SR* diastereoisomeric nortricyclenes, **46**, **48** and **47**, **49**, respectively.

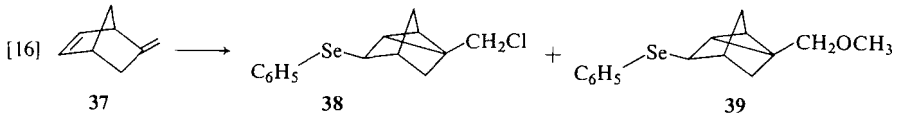
While homoallylic carbonium ions, such as **50** and **51**, or equilibrating free carbonium ions, such as **52**, **53**, and **54**, may exist on the reaction hypersurface, the absence of further products, particularly those resulting from attack β to the phenylseleno moiety, **55** and **56**, and those arising from Wagner–Meerwein rearrangements, tends to rule out their importance. A more plausible scenario, from the point of view of the authors, is a *non*-configurationally-selective attack by chloride ion or methanol upon seleniranium ions such as **57** and **58**. A similar route presumably is required for diene **37** in methanol solution.

Conclusions

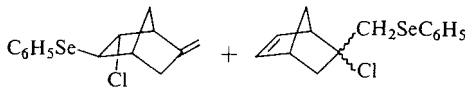
In summary, benzeneselenenyl chloride shows chemical behaviour in methanol which is similar in many cases to that found in less polar media, such as methylene chloride, but with a few marked differences. In particular, these results are indicative of the need for a relatively complex reaction mechanism such as Scheme 2. It should be noted that the main difference between Schemes 1 and 2 is the expansion of the concept of a seleniranium ion intermediate into three forms: the intimate ion-pair, **1**, solvent-separated ion-pairs, **1′**, and the free or dissociated ion, **1″**. The sum of the evidence for areneselenenylation of alkenes in methanol is most consistent with a mechanism wherein these intermediates are all rather close in energy. The need for two types of intimate and solvent-separated ion-pairs follows from the observation of *anti*-stereospecific addition since in the absence of a freely rotating carbonium ion the counter ion must migrate to the far side of the substrate ion. While all of these ion types may not exist for any given reaction, the results obtained during this study show the need for at least two of them.

The data presented in this study can not, however, be used at this time to specify a less ambiguous reaction hypersurface, particularly with re-

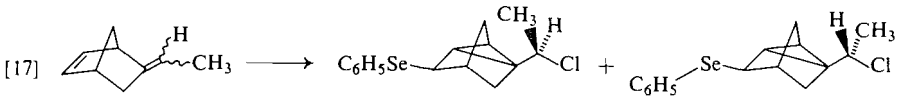
Can. J. Chem. Downloaded from www.nrcresearchpress.com by 210.87.254.105 on 09/05/12
For personal use only.



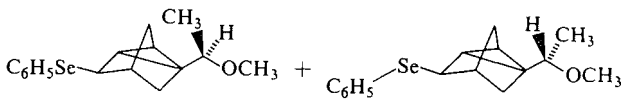
37 38 39



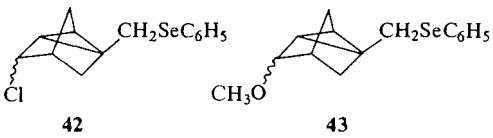
40 41



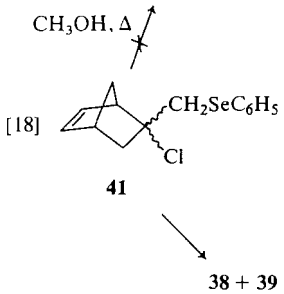
44 or 45 46 47



48 49



42 43



spect to the rate limiting step. This arises in part from the absence of kinetic data, particularly the kinetic order of the reaction. While we have determined that the reaction follows second order kinetics (first order in both benzeneselenenyl chloride and alkene, in methylene chloride, chloroform, acetic acid, and nitromethane), third order kinetics, second order in selenenyl chloride, have been observed in ethyl acetate (3, 18). Thus the nature of the solvent may affect the outcome of the addition more dramatically than is often anticipated. Kinetic studies in methanol solution are currently under active investigation in this laboratory.

Experimental

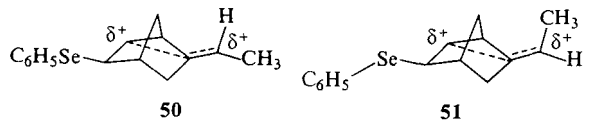
General

Proton and carbon-13 nmr spectra were run on Varian Associates HA-100, T-60, and FT80-16K spectrometers using chloroform-*d* as an internal standard and lock. All spectral parameters are referenced to TMS as an internal standard. Infrared spectra were run in matched NaCl cavity cells, 0.1071 mm, as $CHCl_3$ solutions using a Unicam 1100 spectrophotometer.

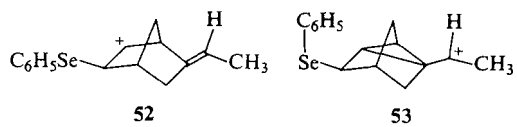
Benzeneselenenyl chloride was commercially available (Aldrich). This material contains a small amount of phenylselenium trichloride and must be recrystallized prior to use; mp 63–64.5°C. Olefins used during this study were commercially available from either Aldrich or Chemical Samples. Their purity in each case was determined by nmr, ir, and glc. All analytical and preparative tlc separations were performed on Analtech or Macherey–Nagel precoated plates, silica gel GF or alumina GF, using methylene chloride as eluant.

General Procedure

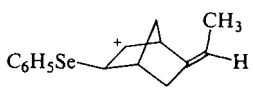
To a quantity (1.0–4.0 mmol) of alkene in 35–95 mL of absolute methanol (ACS) was added dropwise a solution of benzeneselenenyl chloride in methylene chloride which contained the minimum volume possible of solvent for the molar equiv-



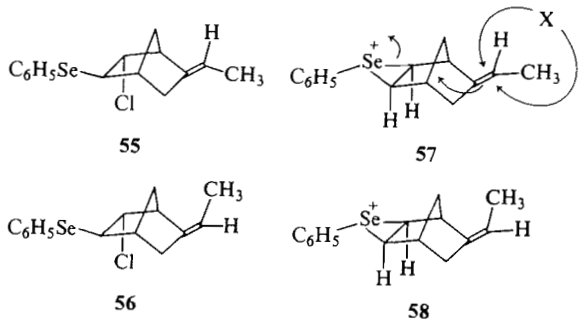
50 51



52 53



54



55 57

56 58

X = Cl^-, CH_3OH

alent of electrophile. The reaction mixture was stirred until the bright red coloration of the reagent disappeared. General reaction times were less than 2 min. Immediate evaporation of the solvent (35–45°C) yielded colourless to pale yellow oils. All compounds were immediately analyzed by nmr, ir, glc, and ms. Isolated yields were essentially quantitative, the mixture of methoxy and chloro adducts accounting for 98%+ of the starting equivalents of alkene during preparative scale reactions.

Product Data for Cyclic and Polycyclic Adducts

Caution: Scrupulous avoidance of contact with the adducts of benzeneselenenyl chloride and bicyclo[2.2.1]hepta-2,5-diene, **26**, is essential! All reactions were carried out in an isolation glove-box equipped with a filter system suitable for use with carcinogenic or radioactive material, with a reduced atmospheric pressure inside the box. This procedure was used because of medical problems which arose during the preliminary study of this reaction during 1975. Within twelve hours of carrying out the areneselenenylation reaction, the author (DGG) suffered an acute attack of asthmatic bronchitis. This attack resulted in hospitalization of the experimenter. There had been no prior history of attacks of this nature. The medical diagnosis *suggests* that the attack may have resulted from a chemical irritant. Subsequent increased sensitivity towards lung problems has been noted by the author, particularly with respect to norbornenyl and nortricyclic compounds.

Exo-*3-phenylseleno*-exo-*5-methoxytricyclo[2.2.1.0^{2,6}]heptane*, ***29***, gave ir μm: 12.2 (m, nortricyclene); ^{1}H nmr δ: 3.54 (m, 1H, C*H*Se), 3.96 (m, 1H, C*H*OCH$_3$), 1.2–2.5 (m, 6H), 3.25 (s, 3H, C*H*$_3$O); ^{13}C nmr δ: 14.1 (d, C1), 16.7 (d, C2), 46.3 (d, C3), 38.0 (d, C4), 85.8 (d, C5), 19.3 (d, C6), 28.8 (t, C7), 56.4 (q, CH_3O).

Endo-*3-phenylseleno*-exo-*5-methoxytricyclo[2.2.1.0^{2,6}]heptane*, ***30***, gave ir μm: 12.2 (m, nortricyclene); ^{1}H nmr δ: 3.50 (m, 1H, C*H*Se), 3.84 (m, 1H, C*H*OCH$_3$), 1.2–2.5 (m, 6H), 3.29 (s, 3H, CH_3O); ^{13}C nmr δ: 12.0 (d, C1), 19.3 (d, C2), 46.4 (d, C3), 38.0 (d, C4), 84.1 (d, C5), 17.2 (d, C6), 27.6 (t, C7), 56.3 (q, CH_3O).

Exo-*3-phenylseleno*-exo-*5-chlorotricyclo[2.2.1.0.^{2,6}]heptane*, ***27***, gave ir (CCl_4, NaCl): 12.35 μm; ^{1}H nmr δ: 3.96 (bs, 2H, C3*H*, C5*H*); ^{13}C nmr δ: 14.8 (d, C1), 17.3 (d, C2), 46.2 (d, C3), 42.8 (d, C4), 64.8 (d, C5), 20.5 (d, C6), 30.0 (t, C7).

Endo-*3-phenylseleno*-exo-*5-chlorotricyclo[2.2.1.0^{2,6}]heptane*, ***28***, gave ir (CCl_4, NaCl): 12.3 μm; ^{1}H nmr δ: 4.02 (m, 1H, C*H*Cl), 3.82 (m, 1H, C*H*Se); ^{13}C nmr δ: 12.2 (d, C1), 19.9 (d, C2), 46.6 (d, C3), 42.6 (d, C4), 62.4 (d, C5), 20.7 (d, C6), 28.3 (t, C7).

Endo-*3-chloro*-exo-*2-phenylselenobicyclo[2.2.1]hept-5-ene*, ***31***, ^{1}H nmr δ: 3.10 (m, H1), 3.05 (t, H2), 4.30 (t, H3), 3.2 (m, H4), 6.36 (dt, H5), 6.24 (dt, H6), 1.76 (m, 2H, H7); $J_{2,3}$ = 3.6 Hz; $J_{1,2}$ = 0.3 Hz; $J_{3,4}$ = 3.2 Hz; $J_{2,7\text{-}anti}$ = 3.0 Hz; $J_{5,6}$ = 6.5 Hz; ^{13}C nmr δ: 49.5 (d, C1), 50.6 (d, C2), 64.9 (d, C3), 49.6 (d, C4), 134.9 (d, C5), 137.0 (d, C6), 46.3 (t, C7).

Endo-*2-phenylseleno*-exo-*3-chlorobicyclo[2.2.1]hept-5-ene*, ***32***, ^{1}H nmr δ: 3.16 (m, H1), 3.62 (dt, H2), 3.86 (dt, H3), 3.22 (m, H4), 6.27 (dt, H5), 6.13 (dt, H6), 1.9 (m, 2H, H7); $J_{2,3}$ = 3.5 Hz; $J_{1,2}$ = 3.5 Hz; $J_{3,4}$ = 0.3 Hz; $J_{2,7\text{-}anti}$ = 1.2 Hz; $J_{3,7\text{-}anti}$ = 3.8 Hz; $J_{5,6}$ = 5.2 Hz; ^{13}C nmr δ: 52.2 (d, C1), 53.0 (d, C2), 65.8 (d, C3), 47.7 (d, C4), 137.6 (d, C5), 131.8 (d, C6), 46.7 (t, C7).

Trans-*1-phenylseleno-2-methoxycyclooctane*, ^{13}C nmr δ: 50.0 (d, C1), 85.1 (d, C2), 29.3, 28.9, 26.5, 26.1, 25.5, 24.5 (t, C3—C8), 130.2 (s, C_{Se}), 134.7 (d, C_o), 128.5 (d, C_m), 126.9 (d, C_p), 56.4 (q, CH_3O).

Trans-*1-phenylseleno-2-chlorocyclooct-5-ene*, ^{13}C nmr δ: 50.2 (d, C1), 65.5 (d, C2), 36.2 (t, C3), 23.0 (t, C4), 129.5 (d, C5), 130.9 (d, C6), 24.7 (t, C7), 34.4 (t, C8), 134.2 (d, C_o), 129.0 (d, C_m), 127.6 (d, C_p).

Trans-*1-phenylseleno-2-methoxycyclooct-5-ene*, ^{13}C nmr δ: 48.8 (d, C1), 83.7 (d, C2), 31.0 (t, C3), 22.9 (t, C4), 128.4 (d, C5), 130.1 (d, C6), 25.5 (t, C7), 33.0 (t, C8), 57.8 (q, CH_3O), 130.3 (s, C_{Se}), 134.8 (d, C_o), 128.7 (d, C_m), 127.0 (d, C_p).

Trans-*1-phenylseleno-2-chlorocyclohex-4-ene*, ^{13}C nmr δ: 43.4 (d, C1), 58.0 (d, C2), 31.8 (t, C3), 122.5 (d, C4), 124.1 (d, C5), 28.3 (t, C6), 128.6 (s, C_{Se}), 134.8 (d, C_o), 129.2 (d, C_m), 128.0 (d, C_p).

Trans-*1-phenylseleno-2-methoxycyclohex-4-ene*, ^{13}C nmr δ: 41.8 (d, C1), 78.0 (d, C2), 30.6 (t, C3), 123.8 (d, C4), 125.1 (d, C5), 29.4 (t, C6), 56.2 (q, CH_3O), 128.9 (s, C_{Se}), 134.6 (d, C_o), 128.7 (d, C_m), 127.2 (d, C_p).

Trans-3-*phenylseleno-4-methoxybicyclo[4.4.0]deca-1(6)-ene*, ^{13}C nmr δ: 126.3 (s, C1), 35.7 (t, C2), 42.6 (d, C3), 78.7 (d, C4), 34.7 (t, C5), 124.9 (s, C6), 29.5 (t, C7), 22.6 (t, C8,9), 29.7 (t, C10), 56.2 (q, CH_3O), 128.9 (s, C_{Se}), 134.6 (d, C_o), 128.6 (d, C_m), 127.1 (d, C_p).

Trans-*3-phenylseleno-4-chlorobicyclo[4.4.0]deca-1(6)-ene*, ^{13}C nmr δ: 125.5 (s, C1), 33.8 (t, C2), 44.5 (d, C3), 59.2 (d, C4), 37.2 (t, C5), 123.9 (s, C6), 29.6 (t, C7), 22.8 (t, C8,9), 29.8 (t, C10), 134.8 (d, C_o), 129.1 (d, C_m), 127.8 (d, C_p).

Trans-*3-phenylseleno-4-chlorobicyclo[4.3.0]nona-1(6)-ene*, ^{13}C nmr δ: 131.2 (s, C1), 35.7 (t, C2), 44.3 (d, C3), 58.9 (d, C4), 35.5 (d, C5), 129.6 (s, C6); 29.1 (t, C7), 21.6 (t, C8), 32.7 (t, C9).

Trans-*2-phenylseleno-3-methoxybicyclo[2.2.2]octane*, ^{13}C nmr δ: 30.2 (d, C1), 50.3 (d, C2), 85.3 (d, C3), 28.4 (d, C4), 17.9 (t, C5), 23.0 (t, C6), 20.9 (t, C7), 26.6 (t, C8); 56.3 (q, CH_3O), 129.2 (s, C_{Se}), 133.6 (d, C_o), 128.8 (d, C_m), 126.9 (d, C_p).

Trans-*2-phenylseleno-3-chlorobicyclo[2.2.2]octane*, ^{13}C nmr δ : 31.4 (d, C1), 53.8 (d, C2), 66.6 (d, C3), 34.0 (d, C4), 18.5 (t, C5), 24.9 (t, C6), 20.2 (t, C7), 24.9 (t, C8), 129.2 (s, C_{Se}), 134.2 (d, C_o), 128.9 (d, C_m), 127.9 (d, C_p).

Exo-*2-phenylseleno*-endo-*3-methoxybicyclo[2.2.1]heptane*, ^{13}C nmr δ: 40.3 (d, C1), 50.5 (d, C2), 88.7 (d, C3), 43.7 (d, C4), 19.5 (t, C5), 29.8 (t, C6), 35.2 (t, C7), 57.1 (q, CH_3O).

Exo-*2-phenylseleno*-endo-*3-chlorobicyclo[2.2.1.]heptane*, ^{1}H nmr δ: 2.37 (m, H1), 3.06 (dd, H2), 4,15 (dt, H3), 2.43 (m, H4), 1.3–2.1 (m, H5,6), 1.57 (m, H7); $J_{2,3}$ = 4.0 Hz ; $J_{3,4}$ = 3.2 Hz; $J_{2,7\text{-}anti}$ = 2.8 Hz; $J_{3,5\text{-}exo}$ = 0.8 Hz; $J_{1,2}$ = 0.0; ^{13}C nmr δ: 44.3 (d, C1), 54.0 (d, C2), 67.9 (d, C3), 44.5 (d, C4), 21.5 (t, C5), 29.5 (t, C6), 36.2 (t, C7).

Syn-*7-phenylseleno*-exo-*2-methoxybicyclo[2.2.1]heptane*, ^{13}C nmr δ: 46.8 (d, C1), 90.6 (d, C2), 27.4 (t, C3), 35.3 (d, C4), 24.6 (t, C5,6), 55.8 (d, C7), 56.3 (q, CH_3O).

Syn-*7-phenylseleno*-exo-*2-chlorobicyclo[2.2.1]heptane*, ^{13}C nmr δ: 42.6 (d, C1), 69.2 (d, C2), 26.8 (t, C3), 35.9 (d, C4), 24.1 (t, C5), 24.5 (t, C6), 56.7 (d, C7).

Exo-*2-phenylseleno*-exo-*3-methoxybicyclo[2.2.1]heptane*, ^{13}C nmr δ: 41.6 (d, C1), 49.9 (d, C2), 84.3 (d, C3), 44.6 (d, C4), 29.4 (t, C5), 29.7 (t, C6), 37.2 (t, C7).

Endo-*3-phenylseleno-1-chloromethyltricyclo[2.2.1.0^{2,6}]heptane*, ^{13}C nmr δ: 28.3 (s, C1), 24.2 (d, C2), 49.7 (d, C3), 37.4 (d, C4), 35.2 (t, C5), 19.5 (d, C6), 32.1 (t, C7), 47.3 (t, C8, CH_2Cl).

Can. J. Chem. Downloaded from www.nrcresearchpress.com by 210.87.254.105 on 09/05/12
For personal use only.

Can. J. Chem. Downloaded from www.nrcresearchpress.com by 210.87.254.105 on 09/05/12
For personal use only.

Endo-*3-phenylseleno-1-methoxymethyltricyclo[2.2.1.0.^{2,6}]heptane*, ^{13}C nmr δ: 26.0 (s, C1), 21.3 (d, C2), 49.7 (d, C3), 37.1 (d, C4), 35.1 (t, C5), 16.4 (d, C6), 31.5 (t, C7), 72.6 (t, C8, CH_2OCH_3), 58.3 (q, CH_3O), 130.4 (s, C_{Se}), 133.2 (d, C_o), 129.0 (d, C_m), 126.6 (d, C_p).

Exo-*2-phenylseleno*-endo-*3-chloro-5-methylenebicyclo[2.2.1]heptane*, ^{13}C nmr δ : 44.9 (d, C1), 53.2 (d, C2), 66.9 (d, C3), 48.5 (d, C4), 134.7 (s, C5), 31.0 (t, C6), 36.9 (t, C7), 104.8 (t, C8, $=CH_2$).

Exo-*2-phenylselenomethyl*-endo-*2-chlorobicyclo[2.2.1]hept-5-ene*, ^{13}C nmr δ: 55.6 (d, C1), 78.8 (s, C2), 43.3 (t, C3), 42.9 (d, C4), 133.2 (d, C5), 139.8 (d, C6), 45.1 (t, C7), 49.3 (t, C8, CH_2Se).

(3-RS, *8*-RS) *and (3*-RS, *8*-SR)-endo-*3-phenylseleno-1-(1'-chloroethyl)tricyclo[2.2.1.0^{2,6}]heptanes*, ^{13}C nmr δ: 33.4 (s, C1), 23.4, 23.6 (d, C2), 49.5, 49.7 (d, C3), 37.0 (d, C4), 33.4 (t, C5), 19.0, 19.4 (d, C6), 31.8, 32.1 (t, C7), 59.9 (d, C8), 24.2, 23.7 (q, C9), 130.3 (s, C_{Se}), 133.3 (d, C_o), 128.9 (d, C_m), 126.8 (d, C_p).

(3-RS, *8*-RS) *and (3*-RS, *8*-SR)-endo-*3-phenylseleno-1-(1'-methoxyethyl)tricyclo[2.2.1.0^{2,6}]heptanes*, ^{13}C nmr δ: 33.4 (s, C1), 19.5, 22.8 (d, C2), 49.5, 49.8 (d, C3), 36.8 (d, C4), 32.5 (t, C5), 18.0, 18.4 (d, C6), 29.9, 31.4 (t, C7), 76.2, 76.3 (d, C8), 14.7 (q, C9), 56.3 (q, CH_3O).

Exo-*2-phenylseleno*-endo-*3-chloro*-cis-*bicyclo[3.3.0]octane*, ^{13}C nmr δ: 48.8 (d, C1), 56.9 (d, C2), 63.2 (d, C3), 42.5 (t, C4), 40.0 (d, C5), 32.2 (t, C6), 24.9 (t, C7), 33.7 (t, C8).

Exo-*3-phenylseleno*-endo-*2-chloro*-cis-*bicyclo[3.3.0]octane*, ^{13}C nmr δ: 49.8 (d, C1), 69.4 (d, C2), 53.2 (d, C3), 40.8 (t, C4), 39.6 (d, C5), 33.3 (t, C6), 27.4 (t, C7), 31.1 (t, C8).

Exo-*3-phenylseleno*-endo-*2-methoxy*-cis-*bicyclo[3.3.0]octane*, ^{13}C nmr δ: 48.1 (d, C1), 87.6 (d, C2), 53.2 (d, C3), 37.0 (t, C4), 39.3 (d, C5), 33.8 (t, C6), 25.1 (t, C7), 32.6 (t, C8), 57.3 (q, CH_3O).

Acknowledgements

The continued financial support of the Natural Sciences and Engineering Research Council of Canada is gratefully acknowledged.

1. (*a*) G. H. SCHMID and D. G. GARRATT. *In* The chemistry of double bonded functional groups. Supplement A. Part 2. *Edited by* S. Patai. Wiley & Sons, London. 1977. pp. 854–866; (*b*) N. N. YAROVENKO, V. N. SHEMANINA, and G. B. GAZIEVA. Zh. Obshch. Khim. (Engl.), **29**, 922 (1959); (*c*) N. N. YAROVENKO, G. B. GAZIEVA, V. N. SHEMANINA, and N. A. FEDOROVA. Zh. Obshch. Khim. (Engl.), **29**, 922 (1959); (*d*) W. JENNY. Helv. Chim. Acta, **36**, 1278 (1953); (*e*) W. JENNY. Helv. Chim. Acta, **41**, 593 (1958); (*f*) E. G. KATAEV, T. G. MANNAFOV, E. A. BERDNIKOV, and O. A. KOMAROVSKAYA. Zh. Org. Khim. **9**, 1983 (1973); (*g*) N. S. ZEFIROV, L. G. GARVICH, A. S. SHASHKOV, and V. A. SMIT. Zh. Org. Khim. **10**, 1786 (1974); (*h*) C. D. HURD and O. FANCHER. Int. J. Sulfur Chem. Part A, **1**, 18 (1971); (*i*) S. RAUCHER. Tetrahedron Lett. 3909 (1977); (*j*) S. RAUCHER. J. Org. Chem. **42**, 2950 (1977); (*k*) H. J. REICH. J. Org. Chem. **39**, 428 (1974); (*l*) I. KAWAJIMA and M. SHIMIZU. Tetrahedron Lett. 1277 (1978).
2. (*a*) D. G. GARRATT and G. H. SCHMID. Can. J. Chem. **52**, 3599 (1974); (*b*) K. B. SHARPLESS and R. F. LAUER. J. Org. Chem. **39**, 429 (1974); (*c*) F. LAUTENSCHLAEGER. J. Org. Chem. **34**, 4002 (1969); (*d*) D. L. J. CLIVE. J. Chem. Soc. Chem. Commun. 100 (1974).
3. G. H. SCHMID and D. G. GARRATT. Tetrahedron, **34**, 2869 (1978).
4. (*a*) G. H. SCHMID and D. G. GARRATT. Tetrahedron Lett. 3991 (1975); (*b*) B. LINDGREN. Tetrahedron Lett. 4347 (1974).
5. (*a*) D. G. GARRATT and G. H. SCHMID. Can. J. Chem. **52**, 1027 (1974); (*b*) D. G. GARRATT. Tetrahedron Lett. 1915 (1978).
6. D. G. GARRATT. Can. J. Chem. **56**, 2184 (1978).
7. C. K. INGOLD. Structure and mechanism in organic chemistry. 2nd ed. Cornell University Press, Ithaca, NY. 1969.
8. D. G. GARRATT, M. D. RYAN, and M. UJJAINWALLA. Can. J. Chem. **57**, 2145 (1979).
9. (*a*) O. BEHAGHEL and W. MULLER. Ber. **68**, 1540 (1935); (*b*) W. S. COOK and R. A. DONIA. J. Am. Chem. Soc. **73**, 2275 (1951); (*c*) G. HOLZLE and W. JENNY. Helv. Chim. Acta, **41**, 331 (1958); (*d*) W. JENNY. Helv. Chim. Acta, **35**, 1429 (1952); (*e*) D. D. LAWSON and N. KHARASCH. J. Org. Chem. **24**, 857 (1959); (*f*) W. JENNY. Helv. Chim. Acta, **35**, 845 (1952); (*g*) W. JENNY. Helv. Chim. Acta, **41**, 317 (1958).
10. W. A. SMIT, N. S. ZEFIROV, I. V. BODRIKOV, and M. Z. KRIMER. Acc. Chem. Res. **12**, 282 (1979); G. H. SCHMID. *In* Topics in sulphur chemistry. *Edited by* A. Senning and P. S. Magee. Georg Thieme Publishers, Stuttgart. 1977. p. 103.
11. T. AUSTAD. Acta Chem. Scand. Ser. A, **29**, 895 (1975) and references cited therein.
12. S. P. MCMANUS and D. H. LAM. J. Org. Chem. **43**, 650 (1978).
13. D. G. GARRATT. Can. J. Chem. **57**, 2180 (1979).
14. S. J. CRISTOL, J. K. HARRINGTON, and M. S. SINGER. J. Am. Chem. Soc. **88**, 1529 (1966).
15. (*a*) J. T. LUMB and G. H. WHITHAM. J. Chem. Soc. 1189 (1964); (*b*) J. MEINWALD, S. S. LABANA, L. L. LABANA, and G. H. WAHL, JR. Tetrahedron Lett. 1789 (1965); (*c*) A. GAGNEUX and C. A. GROB. Helv. Chim. Acta, **42**, 2006 (1959).
16. (*a*) M. SIMONETTA and S. WINSTEIN. J. Am. Chem. Soc. **76**, 18 (1954); (*b*) E. E. VAN TAMELEN. J. Am. Chem. Soc. **77**, 1704 (1955); (*c*) G. H. SCHMID. Can. J. Chem. **46**, 3757 (1968); (*d*) H. J. FRANZ, W. HOBOLD, R. HOHN, G. MULLER-HAGEN, R. MULLER, W. PRITZKOW, and H. SCHMIDT. J. Prakt. Chem. **312**, 622 (1970); (*e*) J. LABOWS and D. SWERN. J. Org. Chem. **37**, 3004 (1972); (*f*) J. G. TRAYHAM, G. R. FRANZEN, G. A. KNESEL, and D. J. NORTHINGTON. J. Org. Chem. **38**, 368 (1973); (*g*) W. PRITZKOW. Wiss. Z. Univ. Heidelberg, **16**, 120 (1974).
17. A. HASSNER, R. P. HOBLITT, C. HEATHCOCK, J. E. KROPP, and M. LAUBER. J. Am. Chem. Soc. **92**, 1326 (1970).
18. (*a*) D. G. GARRATT. Can. J. Chem. **56**, 2184 (1978); (*b*) D. G. GARRATT. Ph.D. Thesis, University of Toronto, Toronto, Ont. 1975; (*c*) E. G. KATAEV, T. G. MANNOFOV, and M. K. MANNANOV. Kinet. Katal. **9**(5), 1161 (1968).
19. (*a*) G. H. SCHMID, C. L. DEAN, and D. G. GARRATT. Can. J. Chem. **54**, 1253 (1976); (*b*) D. G. GARRATT, M. D. RYAN, and M. UJJAINWALLA. Can. J. Chem. **57**, 2145 (1979).
20. D. G. GARRATT, P. L. BEAULIEU, and M. D. RYAN. Tetrahedron. In press.

Preparation and structure of *mer*-trichloro(acetonitrile)bis-(triphenylphosphine)osmium(III)

R. L. PARKES AND N. C. PAYNE[1]

Chemistry Department, University of Western Ontario, London, Ont., Canada N6A 5B7

AND

E. O. SHERMAN

Department of Chemistry, Eastern Illinois University, Charleston, IL 61920, U.S.A.

Received July 31, 1979

R. L. PARKES, N. C. PAYNE, and E. O. SHERMAN. Can. J. Chem. **58**, 1042 (1980).

An air-stable, red, crystalline, N-bonded acetonitrile complex of Os(III), $OsCl_3(NCCH_3)(P(C_6H_5)_3)_2$, has been prepared and characterized by elemental analysis, magnetic susceptibility, and a single crystal X-ray structure determination. Crystals are monoclinic, space group $P2_1/c$, cell dimensions $a = 10.029(2)$, $b = 15.233(2)$, $c = 25.246(4)$ Å, $\beta = 113.65(1)°$, and $Z = 4$. Three dimensional X-ray diffraction intensity data were collected on an automatic four circle diffractometer using Cu radiation. Full-matrix least-squares refinement on F converged at $R = 0.038$ for 4384 unique observations. The Os atom has a slightly distorted octahedral coordination geometry, with *trans* phosphine ligands, mean Os—P 2.406(2) Å. The acetonitrile ligand is σ-bonded through the N atom, Os—N 2.038(6) Å. The bond *trans* to the acetonitrile ligand, Os—Cl(1) 2.364(2) Å, is not significantly different from the mean of the *cis* Os—Cl bonds, 2.361(2) Å.

R. L. PARKES, N. C. PAYNE et E. O. SHERMAN. Can. J. Chem. **58**, 1042 (1980).

On a préparé un complexe cristallin rouge, stable à l'air de Os(III)–acétonitrile lié par l'azote: $OsCl_3(NCCH_3)(P(C_6H_5)_3)_2$ et on l'a caractérisé par l'analyse élémentaire, la susceptibilité magnétique et par une détermination structurale par diffraction des rayons-X sur un monocristal. Les cristaux sont monocliniques, groupe d'espace $P2_1/c$ et les dimensions de la maille sont respectivement $a = 10.029(2)$, $b = 15.233(2)$, $c = 25.246(4)$ Å, $\beta = 113.65(1)°$ et $Z = 4$. Les intensités diffractées ont été mesurées à l'aide d'un diffractomètre automatique à 4 cercles en utilisant la radiation du cuivre. L'affinement, basé sur 4384 facteurs de structures,conduit par moindres carrés (matrice entière), a été conclu lorsque $R(F) = 0.038$. L'atome d'osmium a une coordination octaédrique légèrement déformée avec les ligands phosphines en position *trans*. La longueur moyenne de la liaison Os—P est de 2.406(2) Å. Le ligand acétonitrile est lié à l'osmium par une liaison σ, par l'atome d'azote; Os—N = 2.038(2) Å. La liaison en position *trans* par rapport au ligand acétonitrile Os—Cl(1) 2.364(2) Å ne diffère pas de façon significative de la valeur moyenne 2.361(2) Å de la liaison Os—Cl en position *cis*.

[Traduit par le journal]

Introduction

Although halide complexes of osmium(III) of general formula $OsX_3(R_3P)_3$ with monodentate alkyl, dialkylaryl, and alkyldiaryl tertiary phosphines are well known (1), the corresponding complexes with triaryl phosphines have not been reported. During the preparation of dichlorotris(triphenylphosphine)osmium(II) by the method of Oudeman, Van Rantwijk, and Van Bekkum (2), a red crystalline solid was isolated, which by elemental and spectroscopic analysis appeared to contain triphenylphosphine, acetonitrile, and chloride ligands in the ratio 2:1:3, respectively. Subsequent X-ray examination of this material has shown that this compound is *mer*-trichloro-(acetonitrile)bis(triphenylphosphine)osmium(III). The preparation and structure of this compound are described in this paper.

Experimental

All solvents were thoroughly deaerated with nitrogen by the freeze–pump–thaw method. Reactions were carried out under nitrogen in a closed apparatus or in a nitrogen filled dry box.

Disodium hexachloroosmate(IV) was prepared from osmium tetroxide (Fisher Chemical Co.) by the standard literature procedure (3). Triphenylphosphine (Eastman Chemicals Co.) was recrystallized twice from absolute ethanol before use.

Magnetic susceptibility measurements were made with a Cahn, Model 7600 Faraday balance at 23.0 ± 0.5°C. Melting points were determined under vacuum in sealed capillaries and are uncorrected. Infrared spectra were obtained on a Perkin Elmer, Model 621, Grating Spectrometer as Nujol mulls between KBr plates. Elemental analyses were performed by Galbraith Laboratories, Inc., Knoxville, TN, U.S.A. Mass spectra were obtained with a Varian MAT 311A Spectrometer directly on the solid sample in a heated probe.

Preparation of Trichloro(acetonitrile)bis-(triphenylphosphine)osmium(III)

A modification of the procedure reported by Oudeman *et al.* (2) was used. A solution of disodium hexachloroosmate(IV) (2.35 g, 4.85 mmol) in 95% ethanol (100 mL) was added dropwise to a refluxing, stirred solution of triphenylphosphine (11.45 g, 43.65 mmol) in 95% ethanol (100 mL). After heating for 1.5 h, dark green dichlorotris(triphenylphosphine)osmium(II) was deposited from the brown–green reaction mixture. The mixture was cooled and transferred to the dry box where the osmium(II) complex (2.71 g, 53.3%) was removed by filtration. The remaining filtrate was then refluxed for an additional 5 h under nitrogen and yielded a grey–green solid in a yellow–brown solution. The solid material was separated and treated with acetonitrile (5 mL) to produce a red slurry. This mixture was chromatographed in the dry box on a 2.5 × 30 cm alumina

[1]To whom all correspondence should be addressed.

0008-4042/80/101042-04$01.00/0

©1980 National Research Council of Canada/Conseil national de recherches du Canada

Can. J. Chem. Downloaded from www.nrcresearchpress.com by 210.87.254.105 on 09/05/12
For personal use only.

Can. J. Chem. Downloaded from www.nrcresearchpress.com by 210.87.254.105 on 09/05/12
For personal use only.

column. Elution with methylene chloride yielded a mobile bright red fraction which was collected and an immobile yellow band which was discarded. Evaporation of the methylene chloride solvent produced 2.00 g (47.8%) of a red solid which was dried under vacuum (10^{-3} Torr) at 60°C. The material was recrystallized from methylene chloride/hexane (1:1 v/v) yielding bright red crystals mp 250°C (decomp.). *Anal.* calcd. for $Os(CH_3CN)[P(C_6H_5)_3]_2Cl_3$: C 52.93, H 3.87, Cl 12.33, N 1.62; found: C 52.40, H 3.53, Cl 12.70, N 1.54. Magnetic moment: 2.0 BM.

Collection and Reduction of X-ray Data

A photographic examination showed monoclinic symmetry and systematic absences of $h0l$ for l odd and $0k0$ for k odd, uniquely defining the space group as $P2_1/c$. Precise cell dimensions and an orientation matrix were determined at 22°C by a least-squares procedure, employing the diffractometer setting angles of 27 carefully centered reflections with $35° < 2\theta < 56°$. Crystal data for $OsCl_3(CH_3CN)(P(C_6H_5)_3)_2$ are as follows

$C_{38}H_{33}Cl_3NP_2Os$ fw = 862.2
a = 10.029(2) Å, b = 15.233(2) Å, c = 25.246 Å, Z = 4, β = 113.65(1)°, V = 3533 Å, μ = 93.9 cm^{-1}, $F(000)$ = 1685 e, D_{obsd} = 1.64(1) g cm^{-3} (by neutral buoyancy in CCl_4 and CH_2BrCH_2Br), D_{calcd} = 1.621 g cm^{-3}.

A total of 6506 observations was recorded by the θ–2θ scan technique at a scan rate of 2° per min out to a 2θ maximum of 130° on a Picker FACS-1 diffractometer operating under the Vanderbilt disc system (4). Prefiltered (Ni foil, 0.018 mm) Cu radiation was used ($\lambda(K\alpha_1)$ = 1.54056 Å). Stationary counts of 10 s were recorded at the scan limits. Crystal quality, as evidenced by ω scans of 0.10° width at half-height, and the regular recording of six standard reflections, 100, 110, 020, 0$\bar{2}$0, 012, and 006, remained unchanged during the 13 day period required to record the data. After corrections for background, Lorentz and polarization effects, $\sigma(I)$ values were assigned as described elsewhere (5). Since the approximate crystal dimensions were 0.20 × 0.06 × 0.06 mm^3 the data were corrected for absorption using the analytical method of de Meulenaer and Tompa in the program AGNOST (6). The crystal had 6 faces, the forms {100} and {001}, (0$\bar{1}$0) and a fractured face best described as (153). Transmission coefficients varied from 0.357 to 0.655. All computing was carried out on the CDC Cyber 73/14 at the University of Western Ontario, using the programs described in detail elsewhere (7).

Structure Solution and Refinement

The structure was solved by Patterson and Fourier techniques using 4384 unique observations with $I > 3\sigma(I)$ that were considered "observed". Refinement was by full-matrix least-squares techniques on F, minimizing $\Sigma\omega(|F_o| - |F_c|)^2$, where $\omega = 4F_o^2/\sigma^2(F_o)^2$. Scattering factors for Os, Cl, P, C, and N were taken from the International Tables (8), those for H from Stewart *et al.* (9), and anomalous contributions calculated by Cromer and Liberman (10) were included for the Os, Cl, and P atoms. Refinement proceeded smoothly, and in the final cycle the Os, Cl, P, N, and acetonitrile C atoms were assigned anisotropic thermal parameters, while the phenyl C atoms were refined isotropically. The contributions of the 33 H atoms, all located earlier in a difference Fourier synthesis, were included in idealised positions. Refinement converged (4384 observations, 226 variables, maximum coordinate shift 0.07 esd) with agreement factors $R_1 = \Sigma(|F_o| - |F_c|)/\Sigma|F_o| = 0.038$ and $R_2 = (\Sigma\omega(|F_o| - |F_c|)^2/\Sigma\omega F_o^2)^{1/2} = 0.042$. The error on an observation of unit weight was 1.34 electrons. Secondary extinction was not present, and a statistical study indicated a suitable weighting scheme. The highest peak in a total difference Fourier synthesis was 1.1(1) e $Å^{-3}$, at (0.448, 0.000, 0.346), and of no chemical significance. Of the 2122 unused data, none differed by more than 4σ from the calculated value.

Atomic coordinates are given in Table 1 for the non-hydrogen atoms. Thermal parameters for these atoms, hydrogen atom parameters, and observed and calculated structure amplitudes (in electrons, × 10), are available.[2]

Thus a satisfactory refinement was achieved assuming a N-bonded acetonitrile ligand. To confirm this assignment, an attempt was made to refine the three atom species as an isonitrile ligand, coordinated through a C atom. However non-positive definite thermal parameters were observed for the atom coordinated to Os, so the original formulation was retained.

Results and Discussion

The air stable red compound has not been previously reported. The presence of acetonitrile as suggested by elemental analysis was also apparent in the mass spectrum of the products of thermal decomposition of the complex at 250°C. In addition to the acetonitrile peak at mass 41, peaks due to triphenylphosphine and its fragmentation products were also observed. No parent peak or other osmium containing fragment was detected. The X-ray analysis (*vide infra*) unequivocally demonstrates that the compound is correctly formulated as *mer*-trichloro(acetonitrile)bis(triphenylphosphine)-osmium(III). The effective magnetic moment of 2.0 BM agrees well with the magnetic properties of similar low spin, d^5 osmium(III) compounds (1). The octahedral coordination observed in this compound parallels that reported for other osmium compounds (1) and for the mixed complex, $OsCl_3(NH_3)[P(C_6H_5)_3]_2$ (11). It should be noted that no infrared band attributable to the nitrile stretching vibration of acetonitrile coordinated to osmium is observed in the region 2500–1800 cm^{-1} in which such absorptions usually occur (12, 13). The absence of a nitrile stretching band has been reported for a Re analogue (14) and other species containing N-bonded acetonitrile ligands (15).

The crystals are built up from independent molecules of the acetonitrile complex depicted in Fig. 1. The shortest intermolecular non-bonding contact is 2.32 Å between H atoms attached to phenyl C atoms C(14) and C(46). Intramolecular dimensions are given in Table 2; in this and all other tables estimated standard deviations are given in parentheses.

The Os atom has a distorted, octahedral coordination geometry, with *trans* phosphine ligands,

[2]Lists of hydrogen atom parameters, anisotropic thermal parameters, and structure factors are available, at a nominal charge, from the Depository of Unpublished Data, CISTI, National Research Council of Canada, Ottawa, Ont., Canada K1A 0S2.

Can. J. Chem. Downloaded from www.nrcresearchpress.com by 210.87.254.105 on 09/05/12
For personal use only.

TABLE 1. Atomic positional ($\times 10^4$) parameters for $OsCl_3(NCCH_3)(P(C_6H_5)_3)_2$

Atom	x	y	z	Atom	x	y	z
Os	1110.6(3)	2298.3(2)	1521.2(1)	C(33)	4604(9)	1068(6)	632(4)
Cl(1)	−492(2)	3502(1)	1360(1)	C(34)	3989(9)	272(6)	428(4)
Cl(2)	3237(2)	3171(1)	1908(1)	C(35)	2543(9)	141(6)	249(4)
Cl(3)	−755(2)	1244(1)	1155(1)	C(36)	1636(8)	813(5)	264(3)
P(1)	1075(2)	2490(1)	570(1)	C(41)	2287(8)	1129(5)	2824(3)
P(2)	1121(2)	2048(1)	2465(1)	C(42)	1739(9)	276(6)	2665(4)
N(1)	2507(7)	1267(4)	1664(2)	C(43)	2677(12)	−437(7)	2933(5)
C(1)	3241(9)	681(5)	1751(3)	C(44)	4054(12)	−281(8)	3323(5)
C(2)	4186(10)	−81(6)	1860(4)	C(45)	4587(12)	517(7)	3458(5)
C(11)	−672(8)	2353(5)	−51(3)	C(46)	3714(9)	1247(6)	3201(4)
C(12)	−697(9)	2149(6)	−595(4)	C(51)	1739(7)	2943(4)	2991(3)
C(13)	−2023(11)	2062(6)	−1075(4)	C(52)	2120(8)	2779(5)	3579(3)
C(14)	−3274(11)	2162(6)	−1011(4)	C(53)	2484(8)	3472(5)	3966(3)
C(15)	−3300(10)	2375(6)	−486(4)	C(54)	2472(8)	4312(5)	3786(3)
C(16)	−1976(9)	2463(5)	2(3)	C(55)	2107(8)	4480(5)	3209(3)
C(21)	1713(8)	3521(5)	378(3)	C(56)	1766(7)	3798(5)	2814(3)
C(22)	1545(8)	4304(5)	611(3)	C(61)	−612(7)	1777(4)	2518(3)
C(23)	1883(9)	5096(5)	420(4)	C(62)	−1881(8)	2145(5)	2132(3)
C(24)	2389(10)	5097(6)	−9(4)	C(63)	−3178(9)	2041(5)	2211(4)
C(25)	2582(11)	4332(7)	−250(5)	C(64)	−3193(9)	1527(6)	2651(4)
C(26)	2236(10)	3537(6)	−52(4)	C(65)	−1959(10)	1123(6)	3021(4)
C(31)	2220(8)	1651(5)	458(3)	C(66)	−639(8)	1247(5)	2961(3)
C(32)	3718(9)	1769(5)	658(3)				

TABLE 2. Selected interatomic distances (Å) and angles (deg)

Bond	Length	Bond	Length
Os—P(1)	2.405(2)	C(1)—C(2)	1.454(10)
Os—P(2)	2.408(2)	P(1)—C(11)	1.836(7)
Os—Cl(1)	2.364(2)	P(1)—C(21)	1.833(8)
Os—Cl(2)	2.366(2)	P(1)—C(31)	1.816(7)
Os—Cl(3)	2.355(2)	P(2)—C(41)	1.817(7)
Os—N	2.038(6)	P(2)—C(51)	1.830(7)
N—C(1)	1.121(9)	P(2)—C(61)	1.842(7)

Bonds	Angle	Bonds	Angle
N—Os—Cl(1)	179.5(2)	Os—P(1)—C(11)	117.8(2)
N—Os—Cl(2)	85.3(2)	Os—P(1)—C(21)	120.1(2)
N—Os—Cl(3)	85.7(2)	Os—P(1)—C(31)	108.3(2)
N—Os—P(1)	90.3(2)	Os—P(2)—C(41)	111.2(2)
N—Os—P(2)	88.4(2)	Os—P(2)—C(51)	117.8(2)
Cl(1)—Os—Cl(2)	94.17(7)	Os—P(2)—C(61)	118.5(2)
Cl(1)—Os—Cl(3)	94.78(7)	C(11)—P(1)—C(21)	100.8(3)
Cl(1)—Os—P(1)	89.84(6)	C(11)—P(1)—C(31)	103.4(3)
Cl(1)—Os—P(2)	91.45(6)	C(21)—P(1)—C(31)	104.6(3)
Cl(2)—Os—Cl(3)	171.04(7)	C(41)—P(2)—C(51)	104.4(3)
P(1)—Os—P(2)	177.83(6)	C(41)—P(2)—C(61)	103.1(3)
Os—N—C(1)	177.2(6)	C(51)—P(2)—C(61)	99.7(3)
N—C(1)—C(2)	179.6(9)		

Table 2. Bond distances and bond angles within the molecule are very similar to those observed in $OsCl_3(NH_3)(P(C_6H_5)_3)_2$ (11), *mer*-$OsCl_3(P(CH_3)_2(C_6H_5))_3$ (16), and the Re analogue, $ReCl_3(CH_3CN)(P(C_6H_5)_3)_2$ (14). The solid state deviations from octahedral geometry at the Os atom are most apparent in the displacement of Cl(2) and Cl(3) away from Cl(1) towards the CH_3CN ligand, Cl(2)—Os—Cl(3) 171.04(7)°. Furthermore, the angles at the two P atoms are significantly distorted to permit rings 3 and 4 (Fig. 1) to "sandwich" the CH_3CN ligand. This is particularly apparent in the Os—P(1)—αC angles of 108.3(2) and 111.2(2)° for rings 3 and 4, compared to values ranging from 117.8(2) to 120.1(2)° for the other four phenyl rings. Similar distortions have been attri-

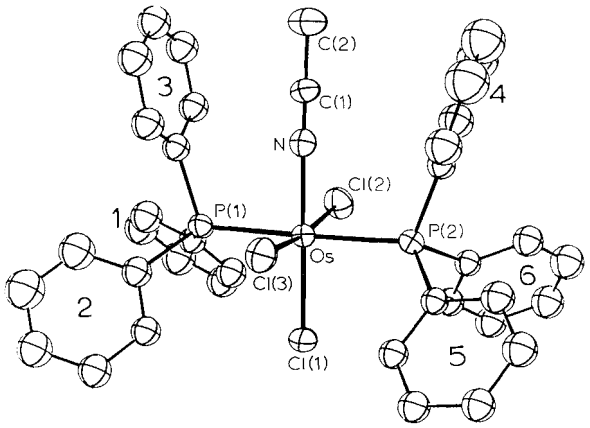


FIG. 1. An illustration of the molecule, drawn with thermal ellipsoids at the 50% probability level. H atoms have been omitted, and atoms C(11) through C(16) form ring 1, etc.

buted to steric crowding (11). Dimensions within the phenyl rings are unexceptional.

The acetonitrile ligand is σ-bonded to the Os atom, Os—N—C(1) 177.2(6)°, and remains linear, N—C(1)—C(2) 179.6(9)°. There is no significant lengthening of the C≡N bond, 1.121(9) Å, compared to that of free acetonitrile, 1.15(3) Å (17). The Os—Cl(1) bond length of 2.364(2) Å *trans* to the acetonitrile ligand is not significantly different from the mean of the *cis* Os—Cl bonds, 2.361(2) Å, indicating a *trans* influence for the acetonitrile ligand comparable to that of Cl. The Os—N bond, 2.038(6) Å, is significantly shorter (9σ) than that of 2.136(9) Å observed in $OsCl_3(NH_3)(P(C_6H_5)_3)_2$, much of which is presumably due to the different hybridizations at the N atom.

Acknowledgement

We thank the Natural Sciences and Engineering Research Council of Canada for financial support of this work.

1. J. CHATT, G. J. LEIGH, D. M. P. MINGOS, and R. J. PASKE. J. Chem. Soc. A, 2636 (1968).
2. A. OUDEMAN, F. VAN RANTWIJK, and H. VAN BEKKUM. J. Coord. Chem. **4**, 1 (1974).
3. F. P. DWYER and J. W. HOGARTH. Inorg. Synth. **5**, 20 (1957).
4. P. G. LENHERT. J. Appl. Crystallogr. **8**, 568 (1975).
5. R. G. BALL, N. J. BOWMAN, and N. C. PAYNE. Inorg. Chem. **15**, 1704 (1976).
6. D. CAHEN and J. A. IBERS. J. Appl. Crystallogr. **5**, 298 (1972).
7. R. G. BALL and N. C. PAYNE. Inorg. Chem. **16**, 1187 (1977).
8. International tables for X-ray crystallography. Vol. IV. Kynoch Press, Birmingham, England. Table 2.2B.
9. R. F. STEWART, E. R. DAVIDSON, and W. T. SIMPSON. J. Chem. Phys. **42**, 3175 (1965).
10. D. T. CROMER and D. LIBERMAN. J. Chem. Phys. **53**, 1891 (1970).
11. D. BRIGHT and J. A. IBERS. Inorg. Chem. **8**, 1078 (1969).
12. R. A. WALTON. Q. Rev. **19**, 126 (1965).
13. M. F. FARONA and K. F. KRAUS. Inorg. Chem. **9**, 1700 (1970).
14. M. G. B. DREW, D. G. TISLEY, and R. A. WALTON. Chem. Commun. 600 (1970).
15. G. ROUSCHIAS and G. WILKINSON. J. Chem. Soc. A, 993 (1967).
16. L. ASLANOV, R. MASON, A. G. WHEELER, and P. O. WHIMP. Chem. Commun. 30 (1970).
17. Interatomic distances. Special Publication No. 11, Chemical Society, London.

Can. J. Chem. Downloaded from www.nrcresearchpress.com by 210.87.254.105 on 09/05/12
For personal use only.

Substituent positional effect on radiative lifetimes of anthracene sulphonates

A. K. GUPTA, SEKHAR BASU, AND K. K. ROHATGI-MUKHERJEE
Physical Chemistry Section, Jadavpur University, Calcutta-700032, India

Received August 30, 1979

A. K. GUPTA, SEKHAR BASU, and K. K. ROHATGI-MUKHERJEE. Can. J. Chem. **58**, 1046 (1980).

Excited state lifetimes of anthracene-1-sulphonate, anthracene-2-sulphonate, anthracene-1,5-disulphonate, and anthracene-1,8-disulphonate have been studied by photoselection and single photon counting methods. Experimental lifetimes are compared with theoretical values. For anthracene- monosulphonates, exciplex formation with water is proposed. In the case of anthracene-1,8-disulphonate, distortion in molecular geometry is found responsible for the higher non-radiative decay constant. Summation of nonradiative decay constants, Σk_i, increase in the series 1-AS < 2-AS < 1,5-AS ≪ 1,8-AS. The sharp increase for 1,8-AS is perhaps due to distortion of the molecular geometry due to steric effect of two bulky and charged $-SO_3^-$ groups on the same side of the anthracene skeleton.

A. K. GUPTA, SEKHAR BASU et K. K. ROHATGI-MUKHERJEE. Can. J. Chem. **58**, 1046 (1980).

On a étudié par sélection photochimique et par les méthodes de dénombrement de photon unique, les durées de vie de l'état excité des sulfonate-1, sulfonate-2, disulfonate-1,5 et disulfonate-1,8 d'anthracène. On a comparé les durées de vie expérimentales aux valeurs théoriques. On propose la formation d'un exciplex avec l'eau dans le cas des monosulfates d'anthracène. Quant au disulfonate-1,8 d'anthracène, on a trouvé que la distorsion de la géométrie moléculaire est responsable de la forte constante de désintégration non radiative. La sommation des constantes de désintégration non radiative Σk_i, augmente dans la série S-1A < S-2A < S-1,5A ≪ S-1,8A. La forte augmentation dans le cas du disulfonate-1,8 d'anthracène est peut être due à la distorsion de la géométrie moléculaire provoquée par l'effet stérique des deux groupes chargés et volumineux SO_3^- du même côté du squelette anthracène.

[Traduit par le journal]

Introduction

Anthracene sulphonates exhibit interesting variations in their excited state properties depending upon the number and the position of sulphonate (SO_3^-) groups introduced in the anthracene moiety. In aqueous solution, anthracene-1-sulphonate (1-AS) gives structureless and anthracene-2-sulphonate (2-AS) gives nearly structureless fluorescence spectra. On the other hand, fluorescence spectra for anthracene-1,5-disulphonate (1,5-AS), and anthracene-1,8-disulphonate (1,8-AS) have vibrational features and the mirror-image symmetry relationship between absorption and emission spectra is preserved. In aprotic solvents the vibrational structures in the emission spectra of monosulphonates are restored and the spectrum shifts towards the blue (1). The quantum yields of fluorescence also depends strongly on the nature of solvent and 1-AS has been suggested as a suitable probe for polarity (2). These observations provide a necessary rationale for systematic investigations into the radiative and nonradiative processes in these interesting molecules.

A knowledge of natural radiative lifetime, actual radiative lifetime, and fluorescence quantum yields can throw some light on the photophysical behaviour of these molecules. The mean radiative lifetime τ^0 is defined as the time spent by the atom or the molecule in the excited state after electronic excitation if unperturbed by the environment. It is measured by the time required for the intensity of fluorescence to fall to 1/eth of its initial value and is given by

$$[1] \quad \tau^0 = 1/k_f$$

where k_f is the unimolecular rate constant for fluorescence emission. However, in a real system other competitive processes occur and the measured lifetime τ is much less than the mean radiative lifetime.

The observed lifetime is given by

$$[2] \quad \tau = \frac{1}{k_f + \sum k_i} = \frac{\tau^0 k_f}{k_f + \sum k_i}$$

and

$$[3] \quad \tau = \tau^0 \phi_f$$

where Σk_i is the summation of rate constants for all modes of deactivation of the excited state by nonradiative pathways and ϕ is the quantum yield of fluorescence.

Several formulae have been derived to relate the mean radiative lifetime τ^0 to the absorption and emission bands of large polyatomic molecules. A relationship given by Förster (3) assumes a mirror image symmetry between the absorption and emission bands. But the formula due to Strickler and Berg (4) avoids such assumption. Their expression is

0008-4042/80/101046-05$01.00/0
©1980 National Research Council of Canada/Conseil national de recherches du Canada

Can. J. Chem. Downloaded from www.nrcresearchpress.com by 210.87.254.42 on 09/05/12
For personal use only.

Can. J. Chem. Downloaded from www.nrcresearchpress.com by 210.87.254.42 on 09/05/12
For personal use only.

$$[4] \quad \tau^0 = 2.88 \times 10^{-9} \frac{n_f^3}{n_a} \frac{\int F d\bar{\nu}}{\int (F/\bar{\nu}^3) d\bar{\nu}} \int (\varepsilon_{\bar{\nu}}/\bar{\nu}) d\bar{\nu}$$

where F is the relative fluorescence quantum intensity at wave number $\bar{\nu}$ cm^{-1}; n_f and n_a are refractive indices of the solvent over fluorescence and absorption bands. Therefore, if ϕ_f, the quantum yield of fluorescence, is known then eq. [4] together with eq. [3] can be used to determine the actual lifetimes of electronically excited molecules.

Another important method for the measurement of actual lifetimes is by the method of photoselection, that is, by the study of depolarization of fluorescence emission. An expression connecting the degree of polarization of fluorescence and excited state lifetime due to Perrin (5) is given by

$$[5] \quad 1/p = 1/p_0 + (1/p_0 - 1/3)(RT/\eta V)\tau$$

where p and p_0 are degrees of polarization at viscosities η and ∞ respectively; τ is the excited state lifetime; and V is the molar volumes of the fluorescing molecule; R and T have their usual significance. The degree of polarization, p_0, at infinite viscosity can be calculated from the intercept when $1/p$ is plotted against $1/\eta$ (Perrin's plot). This expression is based on Brownian movement of rotation in a solvent of viscosity η.

The most direct method of estimating τ is the time correlated single photon counting technique (6) in which every emitted photon is counted as a function of time. In this technique, the time of emission of individual photons is measured in terms of the amplitude of the pulse triggered by the photon. Photons of various heights are counted in a multichannel analyser. The plot of the number of pulses as a function of time gives the decay curve from which the lifetime or the decay constant can be computed.

Material and Methods

Anthracene 1-, 2-monosulphonates and 1,5-, 1,8-disulphonates abbreviated as 1-AS, 2-AS, 1,5-AS, and 1,8-AS were prepared from corresponding quinones. The method has been described earlier (7).

The absorption spectra were measured manually in a Beckmann Spectrophotometer Model DU4700. The same instrument with spectrofluorimetric attachment was used for fluorescence measurement. The excitation source was a 6-W Hg-vapour lamp with a filter (Beckmann 22630) to isolate 365 nm radiation.

Quantum efficiency and polarization measurements were made with a Brice Phoenix Universal Light Scattering Photometer Model 1000 series. For the measurement of quantum efficiency, the solution was purged with N_2. Measurements were repeated a number of times before the data were accepted. The set of polarizer and analyzer was supplied with the instrument. The exciting radiation of wave length 365 nm was isolated by inserting a Wood's glass filter in the incident beam. The detector unit was a 1P28 photomultiplier tube attached to a rotating shaft so that it could be positioned at any angle. The polarization was measured at 90° to the incidence direction. No correction as suggested by Azumi and McGlynn (8) was considered necessary since the intensity ratio with the polarizer oriented in vertical and horizontal directions was unity when a solution of anthracene sulphonate was taken in a low viscosity solvent such as water. Each polarization measurement was repeated five times and the average value was taken.

The measurement of actual lifetime, τ, by single photon counting technique were performed by Dr. G. Beddard and Dr. T. Harriman at the Royal Institution of Great Britain, London. The solutions were 10^{-5} M in water and not deaerated. Oxygen concentration in aerated solution is of the order of 10^{-4} M under the partial pressure of O_2 in the atmosphere and temperature of experiment. It can cause a change of about 2% in measured lifetime in the nanosecond range as can be shown from oxygen quenching data (9). The τ value was obtained by data-fitting technique assuming exponential decay curve.

Results

Determination of Mean Radiative Lifetime

The mirror image relationship between absorption and emission does not hold good for 1-AS and 2-AS although for disulphonates the relationship is applicable. For the former the emission spectra are structureless and red shifted in aqueous solution. Therefore for the determination of mean radiative lifetime τ^0, from integrated areas under the absorption and emission bands, the equation of Strickler and Berg was preferred. The integrals $\int F d\bar{\nu}$, $\int (F/\bar{\nu}^3) d\bar{\nu}$, and $\int (\varepsilon_{\bar{\nu}}/\bar{\nu}) d\bar{\nu}$ were calculated by measuring the areas under the respective curves (Figs. 1 and 2) using a planimeter. The natural

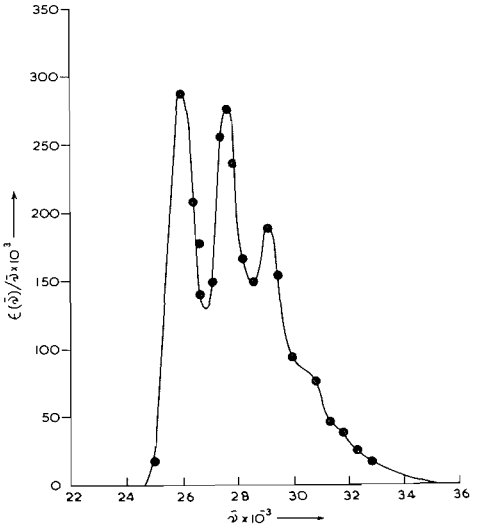


FIG. 1. Plots of $F(\bar{\nu})$ vs. $\bar{\nu}$ and $F(\bar{\nu})/\bar{\nu}^3$ vs. $\bar{\nu}$ for anthracene-1-Na sulphonate. $F(\bar{\nu})$ is the relative fluorescence quantum intensity at wave number $\bar{\nu}$ cm^{-1}.

TABLE 1. Mean natural radiative lifetime of anthracene and its sulphonates (according to the formula of Strickler and Berg (4))

Compound	Solvent	$\int F\,d\bar{\nu} \times 10^{-3}$	$\int F/\bar{\nu}^3\,d\bar{\nu} \times 10^{10}$	$\int \varepsilon_{\bar{\nu}}/\bar{\nu}\,d\bar{\nu} \times 10^{-3}$	$\tau^0 \pm 0.9$ (ns)	$k_f \times 10^7\ s^{-1}$
Anthracene	Benzene	2.25	1.72	1.05	12.7	7.9
1-AS	Water	3.71	2.95	1.13	13.7	7.3
2-AS	Water	3.47	2.59	1.24	11.8	8.4
1,5-AS	Water	3.44	2.69	1.06	14.5	6.8
1,8-AS	Water	2.65	1.82	0.33	40.8	2.4

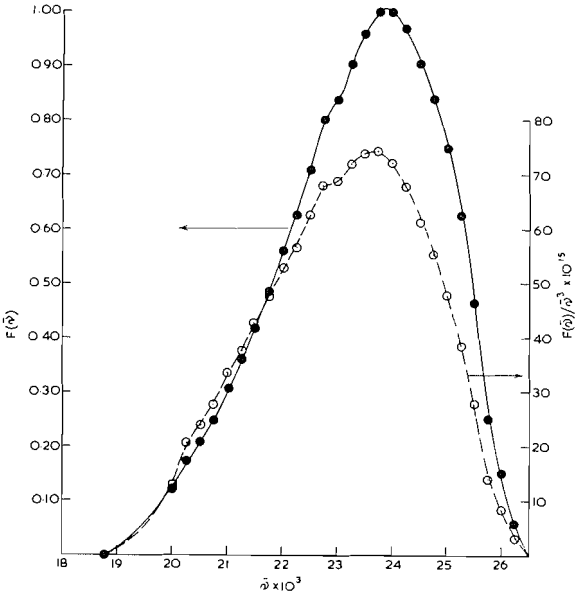


FIG. 2. Plot of $\varepsilon(\bar{\nu})/\bar{\nu}$ vs. $\bar{\nu}$ for anthracene-1-Na sulphonate. $\varepsilon(\bar{\nu})$ is the molar extinction coefficient at wave number $\bar{\nu}$ cm^{-1}.

radiative lifetimes so computed are presented in Table 1. It is evident from Table 1 that anthracene, 1-AS, 2-AS, and 1,5-AS have very nearly the same values for mean natural radiative lifetime τ^0 with an average deviation of ± 0.9 in the nanosecond range. But the value differs largely for 1,8-AS.

The dilute solution values of quantum yield of fluorescence, ϕ_f^0, were determined by using anthracene in benzene as fluorescence standard ($\phi_f^0 = 0.29$) (10). All the solutions were of identical optical density at wave length 365 nm. The ϕ_f^0 values are almost equal for all the sulphonates and are also close to that for anthracene in benzene (Table 2). This is indicative of the fact that the SO_3^- groups do not have a large perturbation effect on the energy levels of anthracene. Knowing ϕ_f^0 and τ^0, the actual lifetime τ can be calculated from eq. [3].

Lifetime Measurements from Polarization Studies

The polarization of fluorescence was measured as a function of viscosity η. The viscosity was varied by adding different proportions of water to glycerol and the corresponding values obtained from the Handbook of Chemistry and Physics. The Perrin plot obtained by plotting $1/p$ vs. $1/\eta$ are given in Fig. 3. The values of p_0 calculated therefrom are tabulated in Table 3. Equation [5] was utilized to calculate τ, the actual lifetime, for the four anthracene sulphonates. The molar volumes of the compounds necessary for calculation of τ were obtained from their respective solid state density data (11). However, the correctness of using solid state molar volumes in the expression is questionable, since the volume together with its solvation envelop is involved in the Brownian movement of rotation. But, as anthracene is a big molecule with hydrophobic character even though the $-SO_3^-$ group is hydrophilic, the overall degree of solvation may be considered to be small as the charge density is low. The calculated values of τ from polarization studies have been tabulated in Table 3. The concentration of the fluorescer was such that concentration depolarization was avoided ($c = 10^{-5}$ *M*).

Table 4 compares the values of τ for various anthracene sulphonates determined by different methods. The τ values obtained by single-photon counting technique are included and are given in column 4. In the last column are given the ratios of τ_{cal} to τ_{photon}.

Discussion

Anthracene is an interesting molecule from the viewpoint of spectroscopy because a number of energy levels of different symmetry type and spin multiplicity are located near the first allowed absorption band (12). Slight variation in their posi-

TABLE 2. The quantum yield of fluorescence ϕ_f^0 and actual lifetime τ in ns of anthracene in benzene and its sulphonate derivatives in aqueous solution

Compound	ϕ_f^0	τ (ns)
Anthracene	0.29	3.68
1-AS	0.25	3.42
2-AS	0.40	4.72
1,5-AS	0.26	3.77
1,8-AS	0.16	6.53

Can. J. Chem. Downloaded from www.nrcresearchpress.com by 210.87.254.42 on 09/05/12
For personal use only.

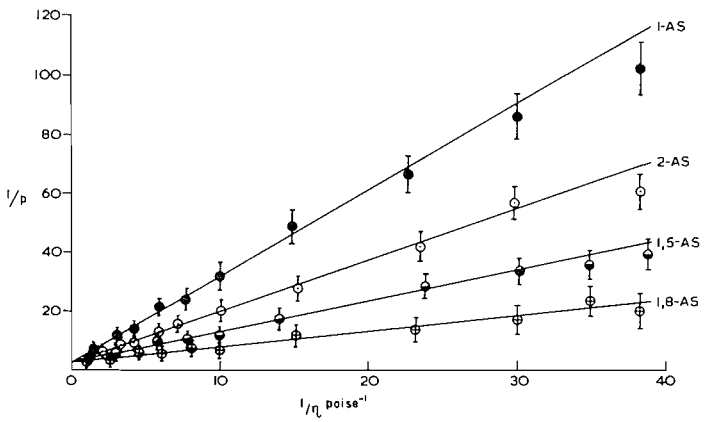


FIG. 3. Plot of $1/p$ vs. $1/\eta$ for different anthracene sulphonates solution in glycerol–water mixtures at 30°C.

TABLE 3. The degree of limiting polarization P_0 and the actual lifetime τ calculated from Perrin's plot

Compound	P_0	$\tau \pm 0.5$ (ns)
1-AS	0.33	8.6
2-AS	0.33	5.3
1,5-AS	0.33	4.2
1,8-AS	0.33	2.2

TABLE 4. Values of τ for various anthracene sulphonates determined by different methods

Compound	τ_{calcd}* (ns)	τ_{pol}† (ns)	τ_{photon}‡ (ns)	$\frac{\tau_{calcd}}{\tau_{photon}}$
1-AS	3.4	8.6	7.30	0.47
2-AS	4.7	5.3	4.50	1.05
1,5-AS	3.8	4.2	3.22	1.16
1,8-AS	6.5	2.2	1.46	4.64

*Calculated from eqs. [3], [4].
†From eq. [5].
‡From single photon counting technique.

tions, which may be brought about by physical parameters such as temperature and solvent or by substitution in different positions of the anthracene skeleton, can alter their photophysical properties by changing their oscillator strength, transition dipole directions, extent of vibronic mixing with the background levels or by switching over of energy levels etc. These changes will eventually be reflected in the lifetimes of the species.

It is interesting to note from Table 4 that the polarization method and the single photon counting technique yield τ values with similar trends. But calculated values differ widely for 1-AS, which is much less than the observed value, and for 1,8-AS, which is much greater than the observed value. For 1,8-AS, the molar extinction coefficient is considerably reduced which is apparent in large τ^0 (Table 1). Two bulky and similarly charged —SO_3^- groups on the same side of the ring may cause distortion of the planar hydrocarbon skeleton leading to reduced absorption probability and consequently enhanced calculated natural radiative lifetime. The ratio τ_{cal}/τ_{photon} (i.e. single photon value) as recorded in column 5 of Table 4 brings out the trend clearly. The Strickler–Berg (4) expression is not very suitable for molecules with weak transition ($\varepsilon < 8000\ cm^2\ mol^{-1}$) and if the geometry of the molecule changes on excitation. In the case of 1,8-AS, the extinction coefficient is low ($\varepsilon_{max} \simeq 3000\ cm^2\ mol^{-1}$) but there is no indication of any difference in geometry in the excited and the ground state energy levels from absorption and emission spectra.

From the lifetime data available, it is possible to calculate the radiative k_f and nonradiative (Σk_i) decay constants (Table 5) for these molecules from the following expression obtained by rearrangement of expression [2].

$$[6] \quad 1/\tau - 1/\tau^0 = \Sigma k_i$$

The single photon counting technique is one of the most reliable methods for measuring decay constants. The τ^0 values used were obtained from τ_{photon} and measured values of quantum yield ϕ_f according to eq. [3] and k_f from eq. [1].

A large increase in nonradiative decay constant for 1,8-AS suggests additional degradative path-

TABLE 5. k_f and Σk_i values of 1-AS, 2-AS, 1,5-AS, and 1,8-AS

Parameter	Value			
	1-AS	2-AS	1,5-AS	1,8-AS
$k_f \times 10^{-7}\ s^{-1}$	3.4	8.9	8.1	10.9
$\Sigma k_i \times 10^{-7}\ s^{-1}$	10.3	13.3	22.9	57.6

Can. J. Chem. Downloaded from www.nrcresearchpress.com by 210.87.254.42 on 09/05/12
For personal use only.

Can. J. Chem. Downloaded from www.nrcresearchpress.com by 210.87.254.42 on 09/05/12
For personal use only.

ways in this molecule. Distorsion may bring about the possibility of internal conversion $S_1 \rightsquigarrow S_0$ or enhancement of the intersystem crossing ($S_1 \rightsquigarrow T$) rate, k_{isc}. For 1,8-dimethylnaphthalene, the increase in k_{isc} has been attributed to distortion of the naphthalene planar configuration due to steric effect of adjacent methyl groups (13). On the other hand, reduction in fluorescence yield for 6-hydroxy-9-phenylfluoron (HPF) in 0.01 *M* KOH as compared to fluorescein has been explained by Lindquist and Lundeen (14) as due to the possibility of molecular distortion in HPF which increases internal conversion. In HPF, the —COOH group of fluorescein is replaced by H and absorption and emission spectra remain unchanged.

Such discrepancy between calculated and observed values may also arise if the $^1L_b \leftarrow A$ transition is hidden under the intense $^1L_a \leftarrow A$ transition and absorbing and emitting states are different. For example, for biphenyl in cyclohexane the experimental value is 89 ns, whereas the calculated value is only 2.9 ns (15); the discrepancy has been explained by assuming involvement of hidden transitions. However, this kind of situation would introduce negative polarization in the fluorescence emission. But p_0 values for all the four anthracene sulphonates under study are the same at infinite viscosity ($p_0 = 0.33$). This indicates that the emission dipole has the same direction for all these compounds. The deviation of p_0 from the ideal value (i.e. $p_0 = 0.5$) is yet to be explained. However, Perrin (16) obtained $p_0 \simeq 0.25$ for anthracene. Such a decrease from the ideal value could also be due to the involvement of some torsional vibrations or to exciplex formation as suggested by Valeur and Weber (17) for indole molecule.

The loss of structure in fluorescence spectra as well as the discrepancy between calculated and observed values of τ in the case of 1-AS clearly indicates that the emitting state is not the pure S_1 state of the compound. The possibility of emission from an exciplex between excited 1-AS and H_2O molecules may be considered. Since in non-aqueous media the emission band is quite structured and a mirror image of the absorption band, complexation in the excited state, is specific for H_2O only. The absence of a pH effect on fluorescence spectra does not support the possibility of internal or external proton transfer in the excited state. In the case of indole a similar exciplex between H_2O and the excited molecule was observed (18). Khalil *et al.* (19) have reported increase in fluorescence intensity of exciplex formed between polar molecules with an increase in solvent polarity. This further supports our conclusion that loss of structure in emission spectra in aqueous solution for monosulphonates is due to specific solute–solvent interactions in the excited state.

Acknowledgements

We are deeply indebted to Drs. G. Beddard and T. Harriman of the Royal Institution of Great Britain for determining the lifetimes of our samples by single-photon counting technique. This has also given confidence in our polarization data. We also thank the University Grants Commission for providing Junior Fellowship to A.K.G and S.B., and financial assistance for the Research Project.

1. K. K. ROHATGI and B. P. SINGH. J. Phys. Chem. **75**, 595 (1971).
2. S. K. ASH and K. K. ROHATGI-MUKHERJEE. Indian J. Biophys. Biochem. **16**, 28 (1979).
3. TH. FÖRSTER. Fluoreszenz Organischer Verbindungen. Vandenhoeck and Ruprecht, Gottingen. 1951. p. 153.
4. S. J. STRICKLER and R. A. BERG. J. Chem. Phys. **37**, 814 (1962).
5. F. PERRIN. Ann. Phys. **12**, 169 (1929).
6. W. R. WARE. Creation and detection of excited states. Vol. 1. *Edited by* A. A. Lamola. Marcel Dekker. p. 239.
7. K. K. ROHATGI-MUKHERJEE and A. K. GUPTA. Indian J. Chem. **14A**, 723 (1976).
8. T. AZUMI and S. P. MCGLYNN. **37**, 2413 (1962).
9. A. K. GUPTA. Ph.D. Thesis, Jadavpur University, Calcutta. 1978.
10. F. WEBER and J. W. F. TEALE. Trans. Faraday Soc. **53**, 646 (1957).
11. A. K. GUPTA, B. P. SINGH, and K. K. ROHATGI-MUKHERJEE. J. Indian Chem. Soc. **LV**, 382 (1978).
12. D. M. FRIEDRICH, R. MATHEIS, and A. C. ALBRECHT. J. Mol. Spectrosc. **51**, 166 (1974).
13. T. R. WRIGHT and H. REISER. IV IUPAC Symp. Photochemistry. Baden-Baden. 1972.
14. L. LINDQUIST and G. W. LUNDEEN. J. Chem. Phys. **44**, 1711 (1966).
15. I. B. BERLMAN and O. J. STEINGRABER. J. Chem. Phys. **43**, 2140 (1965).
16. P. PRINGSHEIM. Fluorescence and phosphorescence. Interscience Publishers Ltd., London. 1949. Chapt. IV.
17. B. VALEUR and G. WEBER. Photochem. Photobiol. **25**, 441 (1977).
18. M. S. WALKER, T. W. BEDNAR, and R. LUMRY. J. Chem. Phys. **47**, 1020 (1967).
19. O. S. KHALIL, H. HOFLER, and S. P. MCGLYNN. Chem. Phys. Lett. **17**, 479 (1972).

Oxidative cleavage of conformationally rigid vinyl orthoesters. Evidence for primary and secondary stereoelectronic control in the cleavage of tetrahedral intermediates

PIERRE DESLONGCHAMPS, NORMAND BEAULIEU,[1] ROBERT CHÊNEVERT, AND ROBERT A. DICKINSON[2]

Laboratoire de Synthèse Organique, Département de Chimie, Faculté des Sciences, Université de Sherbrooke, Sherbrooke (Qué.), Canada J1K 2R1

Received December 10, 1979

PIERRE DESLONGCHAMPS, NORMAND BEAULIEU, ROBERT CHÊNEVERT, and ROBERT A. DICKINSON. Can. J. Chem. **58**, 1051 (1980).

Permanganate oxidation of either axial vinyl orthoester **1** or equatorial vinyl orthoester **7** yields essentially hydroxy ester **5** only. These results can be interpreted on the basis of stereoelectronic effects which control the cleavage of tetrahedral intermediates **2** and **8**.

PIERRE DESLONGCHAMPS, NORMAND BEAULIEU, ROBERT CHÊNEVERT et ROBERT A. DICKINSON. Can. J. Chem. **58**, 1051 (1980).

L'oxydation au permanganate de l'orthoester vinylique axial **1** ou équatorial **7** donne l'hydroxy ester **5** principalement. Ces résultats peuvent être expliqués en tenant compte des effets stéréoélectroniques qui contrôlent la fragmentation des intermédiaires tétraédriques **2** et **8**.

Can. J. Chem. Downloaded from www.nrcresearchpress.com by 210.87.254.5 on 09/05/12
For personal use only.

In 1972 we elaborated a new theory stating that the stereochemistry of the tetrahedral intermediate is a determining factor in the formation of products during the hydrolysis of esters and amides (1–3). We have postulated that the precise conformation of tetrahedral intermediates is very important because their specific decomposition is controlled by the orientation of the non-bonded electron pairs of the heteroatoms (stereoelectronic control).

We have since then obtained experimental evidence in favor of this principle from four different types of experiments: (*a*) the oxidation of acetals by ozone (4), (*b*) the acid hydrolysis of cyclic orthoesters (1, 5), (*c*) the hydrolysis of *syn* and *anti* *N,N*-dialkylated imidate salts (6), and (*d*) the concurrent carbonyl–oxygen exchange during the hydrolysis of esters and amides (7).

Each of these different types of experiments has furnished strong evidence, and taken together, they provide rather convincing arguments in favor of the principle of stereoelectronic control.[3] However, they cannot be considered absolute proof for this theory. This is because, in each of these experiments, the knowledge of the precise stereochemistry of the tetrahedral intermediate is gained by the application of the principle of stereoelectronic control which is then reused to predict the breakdown of that same tetrahedral intermediate. Consequently there is some ambiguity, as the theory is used to predict both the stereochemistry of the tetrahedral intermediate as well as its breakdown.

We therefore looked for an experiment in which the assignment of the stereochemistry of the tetrahedral intermediate would be independent of the stereoelectronic theory. Such an experiment, if successful, could confidently be considered as unambiguous proof.

We wish now to report a study on the oxidation of conformationally rigid bicyclic vinyl orthoesters **1** and **7** which appeared to fulfil these requirements.[4]

We chose the bicyclic axial vinyl orthoester **1** (Scheme 1) in the hope that we could find a reagent to transform **1** into the intermediate **2**. This intermediate **2** with the OH group in the axial position is equivalent to the intermediate which we have postulated in the ozonolysis of acetals **3** and in the hydrolysis of orthoester **4**, and should thus behave similarly during its cleavage, yielding only the hydroxy ester product **5**. The other possible product, the bicyclic lactone **6**, should again not be observed.

This new approach was also quite interesting because the isomeric bicyclic equatorial vinyl orthoester **7** could also presumably be prepared and it should give, with an appropriate reagent, the intermediate **8** having an equatorial OH group. This investigation of the cleavage of vinyl orthoesters could therefore not only confirm the fragmentation behavior of the intermediate **2** but it would also be valuable for the complementary experiment of observing the breakdown of intermediate **8** with the OH group in the equatorial position.

Results

Synthesis of Orthoesters 1 and 7

The syntheses of axial and equatorial vinyl orthoesters **1** and **7** are described in Scheme 2. Reaction of the known dioxenium salt **10** (5) in dichloromethane containing 2-chloroethanol and

[1]Holder of a Natural Sciences and Engineering Research Council of Canada (NSERCC) Postgraduate Scholarship, 1978–1980.

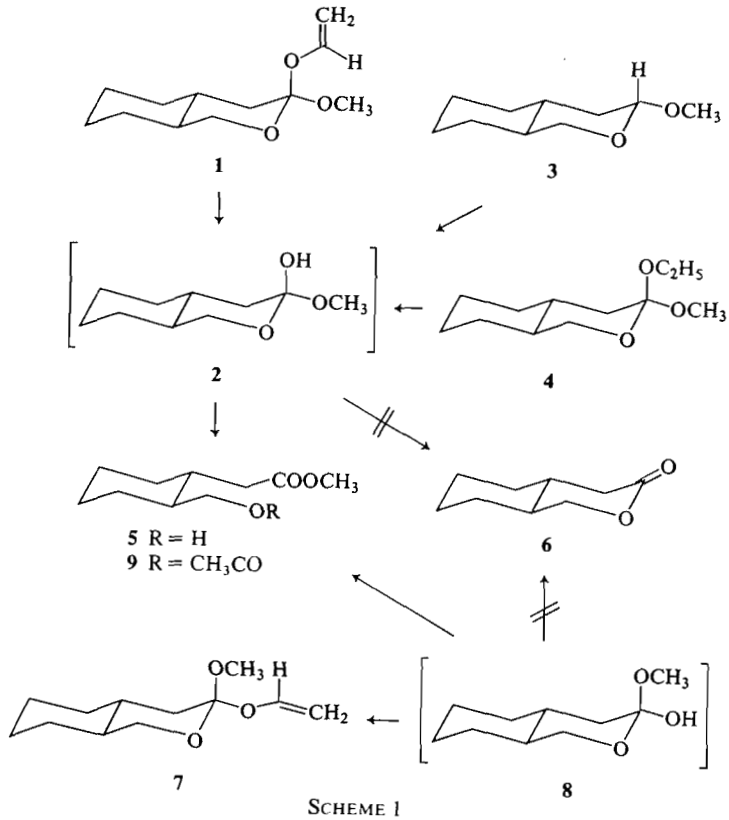
[2]NRCC Postdoctorate Fellow, 1974.

[3]For theoretical work on this subject, see ref. 8.

[4]This work was reported in part in ref. 3, see pp. 1290–1306.

0008-4042/80/101051-08$01.00/0

©1980 National Research Council of Canada/Conseil national de recherches du Canada



SCHEME 1

triethylamine at −78°C gave axial chloroethyl equatorial methyl orthoester **11**. Treatment of crude **11** with potassium *tert*-butoxide in tetrahydrofuran gave axial vinyl methyl orthoester **1**.

Dichloroethyl dioxenium fluoroborate salt **13** was prepared *in situ* by the reaction of boron trifluoride etherate and trichloroethyl orthoformate (**12**) (9). The reaction of unpurified **13** with bicyclic lactone **6** gave the corresponding chloroethyllactonium salt **14** which was not purified. Treatment of crude **14** with methanol in dichloromethane containing triethylamine (5) gave crude equatorial chloroethyl axial methyl orthoester **15**. Treatment of crude **15** with potassium *tert*-butoxide in tetrahydrofuran gave equatorial vinyl methyl orthoester **7** contaminated with dimethyl orthoester **16** (4%) (5) and with axial methyl equatorial ethyl orthoester **17** (10%) (5).[5] Purification by low temperature vpc gave equatorial vinyl methyl orthoester **7** containing 8% of axial methyl equatorial ethyl orthoester **17**. Compound **7**[6] was not purified further and was used as such.

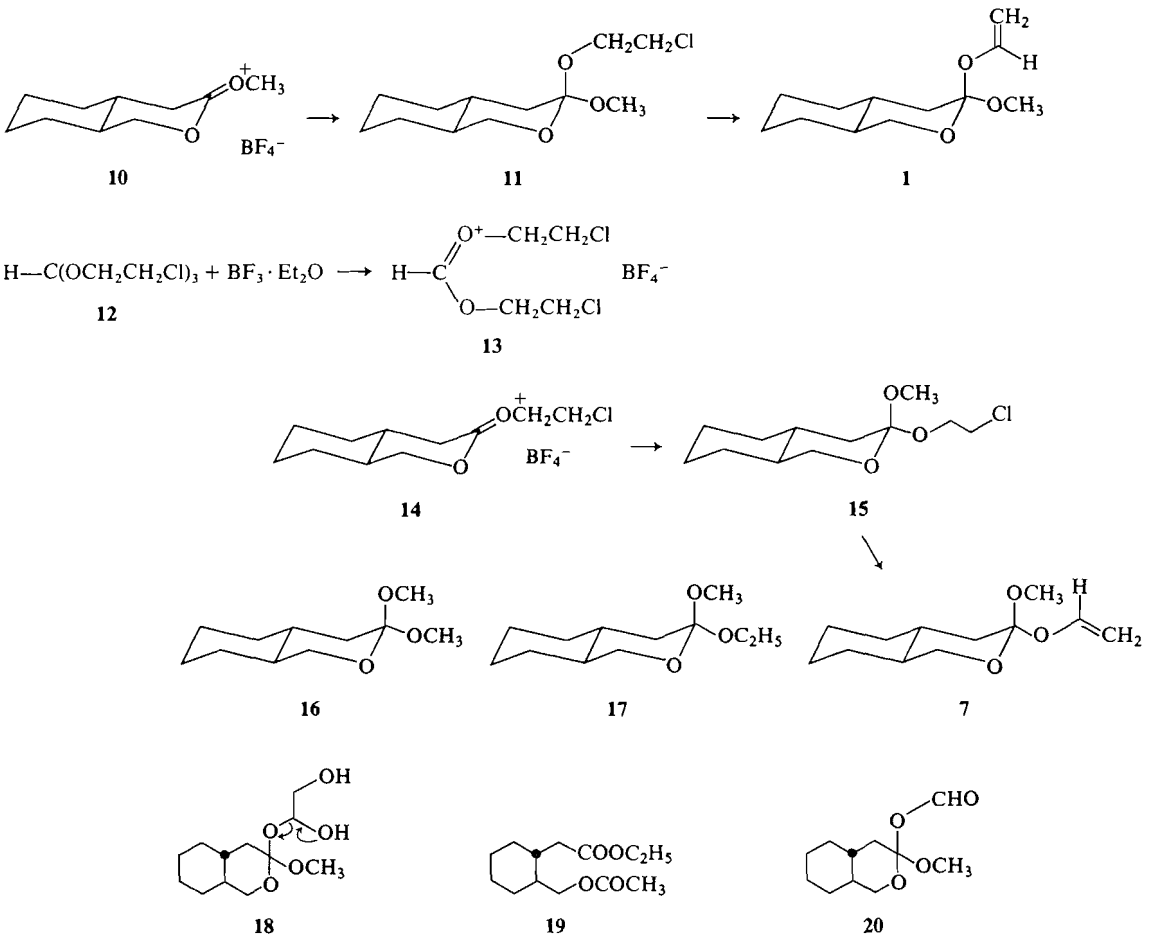
Oxidative Cleavage of Vinyl Orthoesters 1 and 7

The two vinyl orthoesters **1** and **7** were each treated during 3 min with potassium permanganate in a buffered solution containing ^{18}O-labelled water (≈32% ^{18}O) mixed with acetonitrile. Under these conditions, both vinyl orthoesters had reacted completely. This operation was then followed by the addition of a large excess of pyridine and acetic anhydride. It was anticipated that under those conditions potassium permanganate would react with vinyl orthoesters **1** and **7** to generate the tetrahedral intermediates **2** and **8** respectively (via an intermediate such as **18** (10)). The intermediates **2** and **8** would then break down to give either hydroxy ester **5** or bicyclic lactone **6**. The hydroxy ester **5**, if formed, would then be esterified and isolated as the acetate methyl ester **9**. The use of an ^{18}O-labelled solvent was to verify that the permanganate oxidation yielded the intermediates **2** and **8** via the expected intermediate **18** or its equivalent.

[5]The formation of **17** is presumably a result of an exchange between the dichloroethyl dioxenium fluoroborate **13** and diethyl ether which was present as a by-product. This exchange must have produced some of the corresponding diethyl dioxenium fluoroborate which in turn alkylated the lactone with an ethyl group instead of a chloroethyl group.

[6]The assignment of stereochemistry for the two vinyl orthoesters **1** and **7** is based on the method of synthesis (5), and on the proton nmr chemical shift of the OCH_3 group of orthoesters (5).

Can. J. Chem. Downloaded from www.nrcresearchpress.com by 210.87.254.5 on 09/05/12
For personal use only.



SCHEME 2

Under the above conditions (buffer pH = 13), axial vinyl orthoester **1** gave acetate methyl ester **9** (98%) and bicyclic lactone **6** (2%). Mass spectral analysis showed that acetate methyl ester **9** contained 9% of ^{18}O, which corresponds to a theoretical incorporation of 28%. Under similar conditions (buffer pH = 10), the equatorial vinyl orthoester **7** (containing 8% of **17**) gave acetate methyl ester **9** (88%), bicyclic lactone **6** (3%), and acetate ethyl ester **19** (9%). Mass spectral analysis showed that acetate methyl ester **9** contained 13% of ^{18}O which corresponds to a theoretical incorporation of 41%.

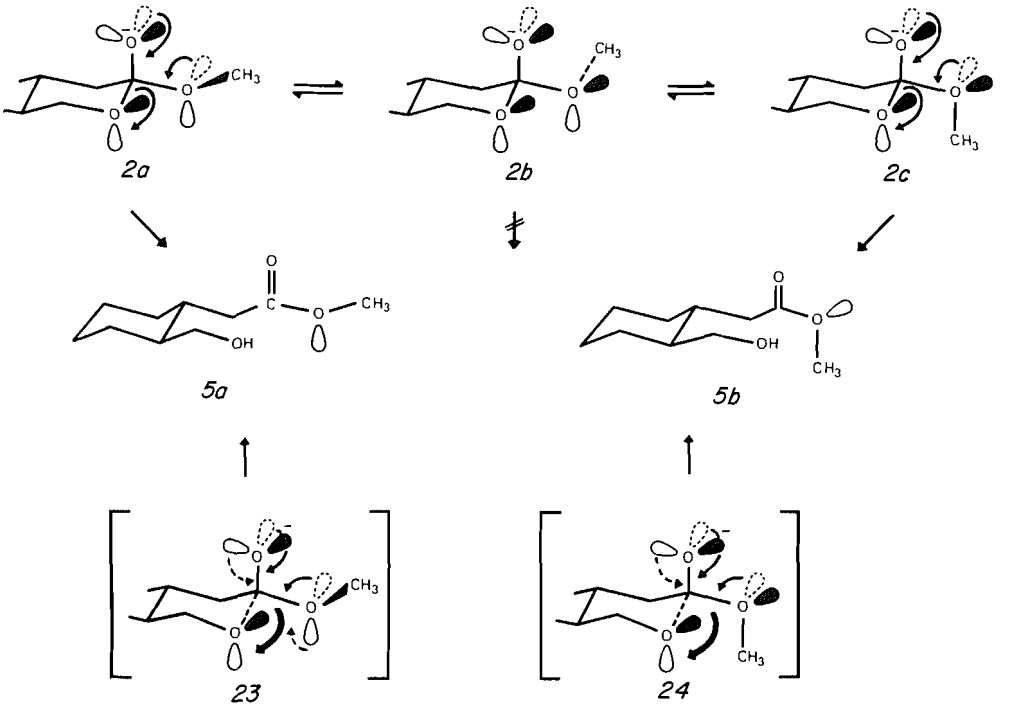
Pure orthoester **17** was found to be resistant to potassium permanganate under the above conditions, but it was transformed into acetate ethyl ester **19** by treatment with pyridine and acetic anhydride. It can therefore be concluded that both the axial and the equatorial vinyl orthoesters **1** and **7** gave essentially only hydroxy ester **5**.

The partial ^{18}O incorporation shows that there must be two pathways by which the vinyl orthoesters **1** and **7** give hydroxy ester **5**. In one pathway, the oxygen of the vinyl ether in **1** and **7** must be lost. One possibility is that **1** and **7** would form in part the ion **10** which would then react with the solvent to give labelled hydroxy ester **5** via the intermediate **2**[7] (5). In the other pathway, the vinyl orthoesters **1** and **7** must have formed the desired intermediates **2** and **8** respectively, with retention of the oxygen atom of the vinyl ether function.

The oxidation of equatorial vinyl orthoester **7** was repeated, except that the reaction time for the $KMnO_4$ oxidative reaction was changed from 3 to 35 min. Under those conditions, **7** gave a mixture of bicyclic lactone **6** (29%), acetate methyl ester **9** (63%), and acetate ethyl ester **19** (8%). The ^{18}O incorporation in **6** (55%) and **9** (53%) was essentially the same. This result shows that hydroxy

[7]For instance, it is conceivable that $KMnO_4$ would react with the vinyl ether function to yield in part the corresponding orthoester formates **20**. These formates (**20**) derived from **1** and **7** could then easily give the dioxenium salt **10**.

Can. J. Chem. Downloaded from www.nrcresearchpress.com by 210.87.254.5 on 09/05/12
For personal use only.



SCHEME 3

ester **5** was formed from intermediate **8**, and **5** was then partly transformed into bicyclic lactone **6** prior to the acetic anhydride – pyridine treatment.

We have concluded from this set of experiments that vinyl orthoesters **1** and **7** have yielded *in situ* the intermediates **2** and **8** respectively and that these two intermediates are cleaved to yield hydroxy methyl ester **5** only.

Discussion

Both tetrahedral intermediates **2** and **8** yield the hydroxy ester **5** in preference to the bicyclic lactone **6**. This result may appear to be unusual because the formation of the bicyclic lactone **6** should presumably be easier; indeed, in the formation of **6**, two molecules are formed (**6** and CH_3OH) and the ring is not broken, while in the formation of **5** only one molecule is formed and the ring is cleaved. It is therefore evident that there must be some parameters which lower specifically the energy of the transition state for the formation of hydroxy ester **5**.

We think that these parameters are of stereoelectronic nature. It is possible to explain the formation of hydroxy ester **5** from intermediate **2** by considering the principle of stereoelectronic control. However, the principle of stereoelectronic control cannot explain the exclusive formation of hydroxy ester **5** from intermediate **8** because it allows both processes. It is, however, possible to understand the preference for the formation of hydroxy ester **5** from intermediate **8** by considering the importance of another stereoelectronic effect which can be related to the anomeric effect (11).

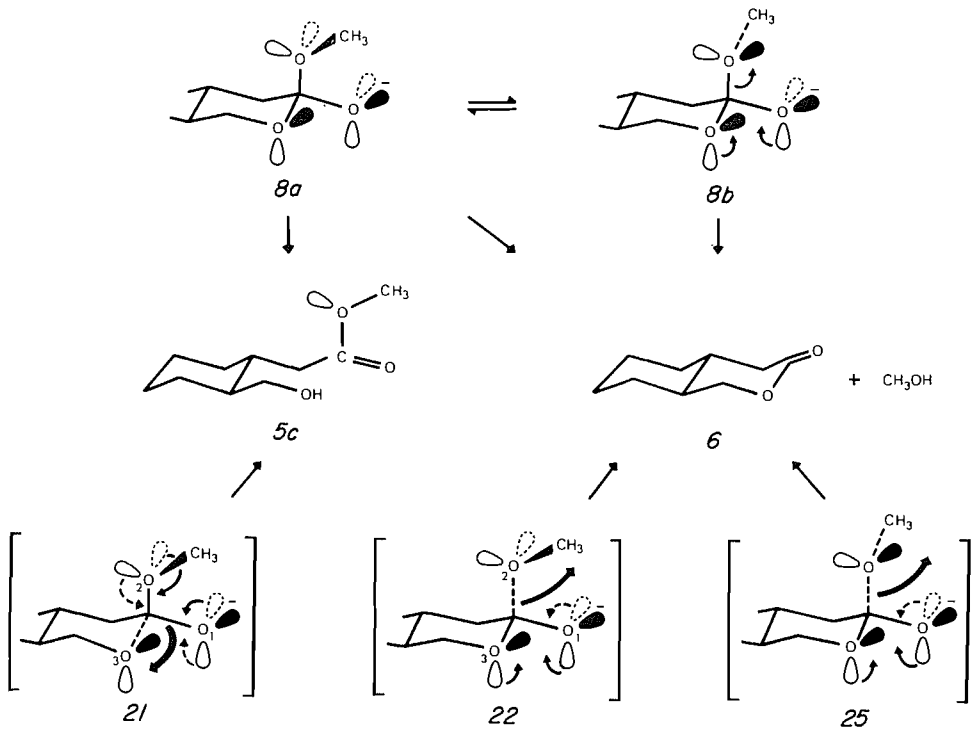
Thus, two effects must now be considered in the stereoelectronic theory: primary stereoelectronic control as previously defined (two oxygens having each an electron pair oriented antiperiplanar to the leaving group) and secondary stereoelectronic control[8] as defined by the anomeric effect.

We will first consider the possible cleavages of the axial intermediate **2** which is derived from orthoester **1**. The intermediate **2** can exist in the three conformations **2***a*, **2***b*, and **2***c* (Scheme 3) and stereoelectronic control predicts the following results: **2***a* can only give the hydroxy ester in the Z conformation **5***a*, **2***b* cannot break down; whereas **2***c* can only produce the hydroxy ester in the *E* conformation **5***b*. Thus, stereoelectronic control predicts the formation of hydroxy ester **5** only, a result identical to the observed one.

It must be added at this stage, but for reasons to be discussed later, that it is very likely that if the

[8]This classification is justified by the fact that these two effects have their origin in the same chemical principle, orientation in space of non-bonded electron pairs. We also think that the primary stereoelectronic effect is a stronger effect than the secondary stereoelectronic effect (*vide infra*).

Can. J. Chem. Downloaded from www.nrcresearchpress.com by 210.87.254.5 on 09/05/12
For personal use only.



SCHEME 4

three conformers **2***a*, **2***b*, and **2***c* are produced, they must be interconvertible[9] by rotation, and the formation of hydroxy ester **5** should occur from **2***a* only. Indeed, we will later argue that a transition state yielding an *E* ester (**2***c* → **5***b*) cannot compete with a transition state which yields a *Z* ester (**2***a* → **5***a*).

Examination of the possible stereoelectronically controlled cleavages of the equatorial intermediate **8** derived from orthoester **7** leads to the following conclusions. The equatorial intermediate **8** can take two different conformations, **8***a* and **8***b* (Scheme 4). The conformer **8***a* can cleave to yield either the hydroxy ester **5** or the lactone **6** and intermediate **8***b* can break down in only one direction to yield the lactone **6**. Thus stereoelectronic control allows the formation of both products, the hydroxy ester **5** and the lactone **6**, but only the former is observed experimentally. Consequently, this result indicates that the energy barrier for the formation of the hydroxy ester **5** is lower than that for the formation of the lactone **6**. Again, it is likely that if both conformers **8***a* and **8***b* are formed, they must be interconvertible by rotation, and the formation of hydroxy ester **5** should occur from the cleavage of **8***a*.

The next task is to rationalize the fact that the energy barrier for the formation of hydroxy ester **5** is lower than that for bicyclic lactone **6**. We think that it is due to an electronic effect which is similar to the anomeric effect observed in acetals (11).

For this analysis, it is necessary to consider the orientation of *all the electron pairs on the two oxygens which will eventually form the ester function* in **5** and in **6**. Formulas **21** and **22** describe the two transition states of conformer **8***a* which lead to the hydroxy ester **5***c* and to the bicyclic lactone **6** respectively. In both of them, there are two oxygens (O1 and O2 in **21**, and O1 and O3 in **22**) having each an electron pair antiperiplanar to the bond to be cleaved (C—O3 in **21**, and C—O2 in **22**). This is the stereoelectronic effect that we have previously discussed (1–3) which can now be defined as the primary stereoelectronic driving force for the cleavage reaction.

There are, however, other secondary stereoelectronic effects which are operating in both transition states **21** and **22**. In **21**, the axial oxygen (O2) has an electron pair antiperiplanar to the equatorial C—O1 bond, thus this electron pair can

[9]We have previously postulated the lack of conformational change prior to the breakdown of the tetrahedral intermediate (2). We no longer believe that it is necessary to invoke this postulate for hemiorthoesters. For a discussion see pp. 1303–1308 in ref. 3. For cases where this postulate applies see ref. 7.

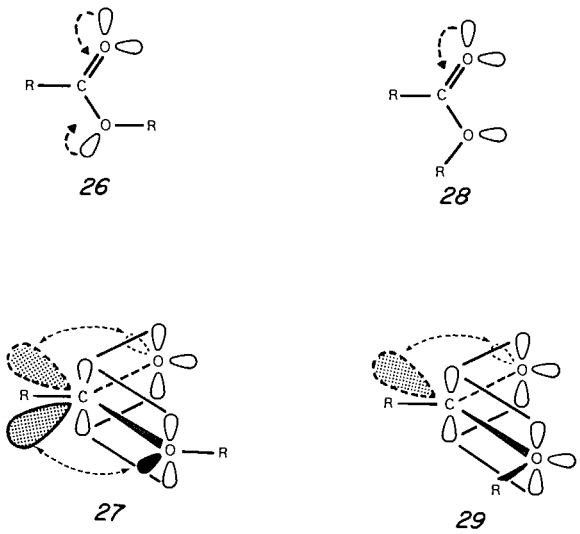
Can. J. Chem. Downloaded from www.nrcresearchpress.com by 210.87.254.5 on 09/05/12
For personal use only.

Can. J. Chem. Downloaded from www.nrcresearchpress.com by 210.87.254.5 on 09/05/12
For personal use only.

be delocalized into the antibonding orbital (σ^*) of the C—O1 bond (12). This electronic delocalization confers a double bond character to the C—O2 bond, as is believed to be the case for acetals (11). Similarly, the equatorial oxygen (O1) also has an electron pair antiperiplanar to the axial C—O2 bond. In transition state **22**, the equatorial oxygen (O1) has an electron pair oriented antiperiplanar to the C—O3 bond, but in the ring oxygen (O3) one electron pair is not oriented antiperiplanar to a polar bond. Thus, in addition to the primary stereoelectronic effect (symbolized by ⌒) which occurs in both transition states, transition state **21** has two additional secondary electronic effects (symbolized by ⌒) whereas transition state **22** has only one. It is therefore reasonable to expect that the reaction via transition state **21** is a lower energy process than that via **22**.

It is also interesting to note that **21** leads to the stable *Z* form of an ester (**5***c*) while **22** leads to the less stable *E* form (**6**) (13). Therefore, a correlation seems possible between the energy of the transition state and the geometrical form of the ester produced. Indeed, it can be seen that a transition state leading to a *Z* ester will always have two secondary stereoelectronic effects and that leading to an *E* ester will always have only one. For instance, the conversion of **2***a* into **5***a* (a *Z* ester), will occur via transition state **23** (Scheme 3) which has, besides primary stereoelectronic control (⌒), two secondary electronic effects (⌒). On the other hand, the conversion of **2***c* to **5***b* (an *E* ester) will occur through transition state **24** which has only one secondary electronic effect (⌒). A similar situation is observed in the **8***b* → **6** transformation (cf. **25** in Scheme 4).[10]

We think that this type of secondary electronic delocalization is also operative in the two geometrical forms of the ester function. In the *Z* form of an ester, each oxygen has an electron pair involved in the π system (primary stereoelectronic control). There are two additional electron pairs (one on each oxygen) which are each antiperiplanar to a C—O bond, and can therefore be delocalized in the antibonding orbital (σ^*) of these two C—O σ bonds (secondary stereoelectronic control). In the *E* form of an ester, besides the two electron pairs which form the π system, there is only one electron pair (on the C=O oxygen) which can be delocalized.



SCHEME 5

Thus, in the *Z* form, there are two secondary electronic effects, illustrated in two dimensions by **26** and in three dimensions by **27** (Scheme 5). In the *E* form, there is only one secondary electronic effect, as shown in two dimensions by **28** and in three dimensions by **29**. The *Z* form is more stable than the *E* form in esters (13) and we think that this difference in stability is due mainly to the additional electronic delocalization present in the *Z* form only.

We have recently studied (14) the iodine ion displacement reaction on unsymmetrical cyclic dioxenium salts and the results obtained could be rationalized on the basis of secondary stereoelectronic effect. This secondary stereoelectronic effect in esters is similar to the anomeric effect observed in acetals (2). The only difference is that the central carbon is trigonal (sp^2 hybridized) in esters and tetrahedral (sp^3 hybridized) in acetals.

Experimental

The ir spectra were taken on a Perkin-Elmer 257 spectrophotometer. Proton nmr spectra were recorded on a Varian A-60 or a Bruker WP-60 instrument. Chemical shifts are reported in δ values relative to tetramethylsilane as internal standard. The following abbreviations have been used: s, singlet, m, multiplet. ^{13}C nmr spectra were obtained with a Bruker H-90 instrument. Vapor phase chromatographic (vpc) analyses were carried out on a Varian Aerograph instrument, model 920. (Column A: SE-30, 10% Chromosorb W, 60–80 mesh and column B: SE-30, 5% Chromosorb W, 100–120 mesh.) Mass spectral assays were obtained using a Hitachi-Perkin-Elmer RMU-6A instrument at 70 ev.

Bicyclic lactone **6** was obtained by Baeyer–Villiger oxidation of *trans*-hydrindanone-2 (15).

[10]It is interesting to note that secondary stereoelectronic effects can also influence the leaving group ability of an alkoxide group. For instance, in the competing transition states **21** and **22**, the ring oxygen in **21** which has only one anomeric effect should be a better leaving group than the OCH_3 group in **22** which has two anomeric effects. This effect lowers again the energy of transition state **21** by comparison with transition state **22**. In the other transition states **23**, **24**, and **25**, the leaving group oxygen has only one anomeric effect.

Can. J. Chem. Downloaded from www.nrcresearchpress.com by 210.87.254.5 on 09/05/12
For personal use only.

Axial Chloroethyl Equatorial Methyl Bicyclic Orthoester 11

Trimethyloxonium tetrafluoroborate (470 mg, 3.0 mmol) (16) was added to a solution of bicyclic lactone **6** (170 mg, 1.1 mmol) in anhydrous dichloromethane (10 mL). This mixture was magnetically stirred at room temperature for 15 h in a dry box containing an atmosphere of nitrogen and was then added to a cooled solution (−78°C) of 2-chloroethanol (2 mmol) and triethylamine (3 mmol) in dichloromethane (30 mL). The reaction mixture was left for 30 min at −78°C and left to warm up to room temperature. A saturated solution (20 mL) of sodium carbonate was added. The organic phase was separated and the aqueous phase was extracted with dichloromethane (2 × 25 mL). The combined organic extract was dried with potassium carbonate, filtered, and evaporated to yield crude orthoester **11** (206 mg, 75%); vpc (column A, temperature: injector, 170°C; detector, 100°C; column, 115°C): retention time, 7.0 min; ir (CCl_4): 1000–1200 cm^{-1}; nmr (CCl_4) δ: 1.0–1.2 (12H, m), 3.38 (3H, s, OCH_3), and 3.70 (6H, m, —OCH_2CH_2Cl and OCH_2); ms *m/e* (70 ev): 248, 250 (ratio 3:1, M^+), 217, 219 ($M^+ - OCH_3$), 169 ($M^+ - OC_2H_4Cl$).

Trichloroethyl Orthoformate (12)

Triethyl orthoformate (7.41 g, 50 mmol) was mixed with 2-chloroethanol (24.15 g, 300 mmol), benzene (200 mL), and a catalytic amount of *p*-toluenesulfonic acid. The mixture was refluxed overnight. The solution was then washed with a solution of sodium bicarbonate, dried over sodium carbonate, filtered, and evaporated to dryness. Distillation *in vacuo* gave pure trichloroethyl orthoformate (**12**) (7.75 g, 62%); bp 145°C/12 Torr, (lit. (17) bp 157°C/14 Torr); nmr ($CHCl_3$) δ: 5.48 (1H, s, CH) and 3.87 (12H, m, OCH_2CH_2Cl); ms *m/e* (70 ev): 250, 252 (M^+).

Equatorial Chloroethyl Axial Methyl Bicyclic Orthoester 15

Trichloroethyl orthoformate (**12**) (1.0 g, 4 mmol) was mixed with boron trifluoride etherate (5 mmol, 600 μL) in a dry box under an atmosphere of nitrogen. The mixture was magnetically stirred for 20 min, bicyclic lactone **6** (265 mg, 1.72 mmol) was added and the mixture was left for 90 min. Anhydrous ether (10 mL) was added and the mixture was stirred for 5 min. The mixture was left and then the ether was decanted to leave an insoluble residue. This residue was washed once more with ether. The reddish residue was dissolved in anhydrous dichloromethane (10 mL) and was added to a cooled solution (−78°C) of methanol (5 mmol), triethylamine (5 mmol), and dichloromethane (25 mL). After 30 min at −78°C, the reaction mixture was warmed up to room temperature and a saturated solution of sodium carbonate (20 mL) was added. The two phases were separated, the aqueous phase was extracted with dichloromethane (2 × 25 mL), and the combined organic phase was dried with potassium carbonate. Filtration and evaporation gave crude equatorial chloroethyl axial methyl bicyclic orthoester **15** which was distilled *in vacuo* (328 mg, 78%); bp 120°C/1 Torr; ir ($CHCl_3$): 1000–1200 cm^{-1}; nmr ($CDCl_3$) δ: 1.0–2.0 (12H, m), 3.30 (3H, s, OCH_3), and 3.80 (6H, m, —OCH_2CH_2Cl and OCH_2); ms *m/e* (70 ev): 248, 250 (ratio 3:1, M^+), 217–219 ($M^+ - OCH_3$).

Axial Vinyl Bicyclic Orthoester 1

A solution of freshly sublimed potassium *tert*-butoxide (225 mg, 2 mmol) in anhydrous tetrahydrofuran (10 mL) was slowly added to a solution of axial chloroethyl equatorial methyl bicyclic orthoester **11** (150 mg, 0.6 mmol) in tetrahydrofuran (5 mL). The mixture was then refluxed for 2 h. Most of the solvent was removed *in vacuo*, the residue was mixed with a solution (5 mL) of sodium bicarbonate (5%) and the aqueous mixture was extracted with ether (3 × 25 mL). The organic extract was dried on potassium carbonate, filtered, and evaporated to yield axial vinyl bicyclic orthoester **1** (110 mg, 88%); vpc (column B, temperature: injector, 118°C; detector, 112°C; column, 100°C): retention time, 28.5 min; ir (CCl_4): 1635 and 1000–1200 cm^{-1}; nmr (CCl_4) δ: 1.0–2.0 (12H, m), 3.29 (3H, s, OCH_3), 3.6 (2H, m, CH_2O), 4.13, 4.56, and 6.5 (1H, 1H, 1H, ABX system, $J_{AX(cis)}$ = 6.5 Hz, $J_{BX(trans)}$ = 15 Hz, and $J_{AB(gem)}$ = 1 Hz); ^{13}C nmr δ: 143.8 (C11), 112.6 (C1), 91.6 (C12), 68.4 (C5), 48.7 (C10), 40.7 (C4), 37.7 (C2), 36.5 (C3), 32.5 (C9), 27.0 (C6), and 25.9 (C7 and C8); ms *m/e* (70 ev): 212 (M^+, absent), 181 ($M^+ - OCH_3$), 169 ($M^+ - OC_2H_3$).

Equatorial Vinyl Bicyclic Orthoester 7

A solution of freshly sublimed potassium *tert*-butoxide (250 mg, 2.2 mmol) in anhydrous tetrahydrofuran (10 mL) was slowly added to a solution of equatorial chloroethyl axial methyl bicyclic orthoester **15** (339 mg, 1.37 mmol) in tetrahydrofuran (8 mL) and the mixture was refluxed for 1 h. The solvent was then removed *in vacuo* and a solution (5 mL) of sodium bicarbonate (5%) was added. The aqueous phase was extracted with ether (3 × 25 mL), the organic extract was dried with potassium carbonate, filtered, and evaporated. The residue was distilled *in vacuo* to yield a mixture (251 mg, 84%) of dimethyl bicyclic orthoester **16** (4%, retention time 20.3 min, (5)), equatorial vinyl orthoester **7** (86%, retention time 28.3 min, (5)), and equatorial methyl axial ethyl orthoester **17** (10%, retention time 29.2 min); vpc (column A, temperature: injector, 112°C; detector, 122°C; column, 105°C). Purification by vpc gave equatorial vinyl orthoester **7** containing 8% of equatorial methyl axial ethyl orthoester **17**; ir (CCl_4): 1640 and 1000–1200 cm^{-1}; nmr (CCl_4) δ: 1.0–2.1 (12H, m), 3.33 (3H, s, OCH_3), 3.6 (2H, m, CH_2O), 4.07, 4.47, and 6.50 (1H, 1H, 1H, ABX system, $J_{AX(trans)}$ = 15 Hz, $J_{BX(cis)}$ = 6.5 Hz, $J_{AB(gem)}$ = 1.5 Hz); ^{13}C nmr δ: 144.3 (C11), 112.6 (C1), 91.8 (C12), 68.3 (C5), 47.4 (C10), 40.8 (C4), 38.9 (C2), 37.2 (C3), 32.4 (C9), 27.1 (C6), and 25.2 (C7 and C8); ms *m/e* (70 ev): 212 (M^+, absent), 181 ($M^+ - OCH_3$), 169 ($M^+ - OC_2H_3$).

Oxidation of Axial Vinyl Bicyclic Orthoester 1

A. A solution of axial vinyl bicyclic orthoester **1** (80 mg, 0.37 mmol) in anhydrous acetonitrile (0.5 mL) was rapidly added to a mixture of potassium permanganate (1.0 mmol), acetonitrile (1 mL), buffer (60 μL, $NaHCO_3$–NaOH, pH = 13), and ^{18}O-labelled water (30 μL, 96.5% ^{18}O), and the mixture was magnetically stirred for 3 min. Pyridine (10 mL) and acetic anhydride (8 mL) were added and the mixture was left for 15 h. Ether (60 mL) was added and the organic phase was washed with hydrochloric acid (10%, 3 × 40 mL). The organic phase was dried with magnesium sulfate, filtered through Celite, and evaporated (64 mg, 74%). Analysis by vpc (column B, temperature 150°C) showed a mixture of bicyclic lactone **6** (2%, retention time, 9.5 min) and acetate methyl ester **9** (98%; retention time, 15.0 min) which were identified with authentic samples (5). Acetate methyl ester **9** was obtained pure by vpc and mass spectral analysis and showed an ^{18}O incorporation of 9.0% which corresponds to 28% theoretical incorporation.

B. Axial vinyl orthoester **1** (79 mg, 0.37 mmol) in acetonitrile (0.5 mL) was added to a mixture of potassium permanganate (3 mmol), buffer (0.1 mL), and acetonitrile (1 mL). The mixture was left for 3 min and a solution (50 mL) of potassium bicarbonate (5%) was added. The mixture was extracted with ether (3 × 50 mL), the organic extract was dried over potassium carbonate, filtered, and evaporated to dryness (46 mg). Analysis by ^1H nmr showed the absence of axial vinyl orthoester **1**.

Oxidation of Equatorial Vinyl Bicyclic Orthoester 7

A. Equatorial vinyl orthoester **7** (150 mg, 0.71 mmol) containing 8% of equatorial ethyl axial methyl orthoester **17** was oxidized by a procedure similar to that described for compound **1**, except that the buffer was at pH = 10. It yielded a mixture

(127 mg, 79%) of bicyclic lactone **6** (3%; retention time, 10 min), acetate methyl ester **9** (88%; retention time, 15 min), and acetate ethyl ester **19** (9%; retention time, 21 min) identified by comparison with authentic samples (5); vpc (column B, temperature: 152°C). Acetate methyl ester **9** was obtained pure by vpc and mass spectral analysis showed an ^{18}O incorporation of 13.2% which corresponds to 41% theoretical incorporation.

B. Equatorial vinyl orthoester **7** (81 mg, 0.38 mmol) containing 11% of equatorial ethyl axial methyl orthoester **17** was oxidized by a procedure similar to that described above except that the reaction time for the oxidation was 35 min. After acetylation with pyridine and acetic anhydride, it yielded after workup a mixture (57 mg) of bicyclic lactone **6** (29%), acetate methyl ester **9** (63%), and acetate ethyl ester **19** (8%). Bicyclic lactone **6** and acetate methyl ester **9** were obtained pure by vpc (column B) and mass spectral analysis showed a theoretical ^{18}O incorporation of 55% in bicyclic lactone **6** (^{18}O = 17.7%) and 53% in acetate methyl ester **9** (^{18}O = 17.1%).

Oxidation of Axial Methyl Equatorial Ethyl Orthoester 17

A solution of axial methyl equatorial ethyl orthoester **17** (110 mg, 0.5 mmol) in acetonitrile (3 mL) was added to a mixture of potassium permanganate (1.0 mmol) and buffer (pH = 10, 90 μL). The mixture was left for 3 min and a solution (30 mL) of sodium bicarbonate (5%) was added. The mixture was extracted with dichloromethane (3 × 25 mL), the organic extract was dried with potassium carbonate, filtered, and evaporated to dryness to give axial methyl equatorial ethyl orthoester **17** unchanged (103 mg).

Reaction of Axial Methyl Equatorial Ethyl Orthoester 17 with Pyridine and Acetic Anhydride

A solution of axial methyl equatorial ethyl orthoester **17** (90 mg, 0.42 mmol) in acetonitrile (3 mL) was mixed with buffer (pH = 10, 90 μL). Pyridine (10 mL) and acetic anhydride (5 mL) were added and the mixture was left for 15 h. The solvent was removed *in vacuo* and dichloromethane (50 mL) was added. The organic solution was washed with water (2 × 25 mL), dried with magnesium sulfate, filtered, and evaporated to yield a mixture (94 mg) of acetate ester **9** (93%, retention time: 27.5 min) and bicyclic lactone **6** (7%, retention time: 11.2 min); vpc (column B, 146°C).

Acknowledgements

We wish to thank Professor J. K. Saunders for the interpretation of ^{13}C nmr spectra.

This research was supported by the Natural Sciences and Engineering Research Council of Canada (NSERCC) and by the Ministère de l'Education of Québec.

1. P. DESLONGCHAMPS, P. ATLANI, D. FREHEL, and A. MALAVAL. Can. J. Chem. **50**, 3405 (1972).
2. P. DESLONGCHAMPS. Pure Appl. Chem. **43**, 351 (1975); Tetrahedron, **31**, 2463 (1975).
3. P. DESLONGCHAMPS. Heterocycles, **7**, 1271 (1977).
4. P. DESLONGCHAMPS and C. MOREAU. Can. J. Chem. **49**, 2465 (1971); P. DESLONGCHAMPS, C. MOREAU, D. FREHEL, and P. ATLANI. Can. J. Chem. **50**, 3402 (1972); P. DESLONGCHAMPS, P. ATLANI, D. FREHEL, A. MALAVAL, and C. MOREAU. Can. J. Chem. **52**, 3651 (1974); P. DESLONGCHAMPS, C. MOREAU, D. FREHEL, and R. CHENEVERT. Can. J. Chem. **53**, 1204 (1975).
5. P. DESLONGCHAMPS, R. CHENEVERT, R. J. TAILLEFER, C. MOREAU, and J. K. SAUNDERS. Can. J. Chem. **53**, 1601 (1975).
6. P. DESLONGCHAMPS, C. LEBREUX, and R. J. TAILLEFER. Can. J. Chem. **51**, 1665 (1973); P. DESLONGCHAMPS, S. DUBE, C. LEBREUX, D. R. PATTERSON, and R. J. TAILLEFER. Can. J. Chem. **53**, 2791 (1975); P. DESLONGCHAMPS and R. J. TAILLEFER. Can. J. Chem. **53**, 3029 (1975); P. DESLONGCHAMPS, U. O. CHERIYAN, J.-P. PRADERE, P. SOUCY, and R. J. TAILLEFER. Nouv. J. Chim. **3**, 343 (1979); P. DESLONGCHAMPS, U. O. CHERIYAN, and R. J. TAILLEFER. Can. J. Chem. **57**, 3262 (1979).
7. P. DESLONGCHAMPS, U. O. CHERIYAN, A. GUIDA, and R. J. TAILLEFER. Nouv. J. Chim. **1**, 235 (1977); P. DESLONGCHAMPS, P. GERVAL, U. O. CHERIYAN, A. GUIDA, and R. J. TAILLEFER. Nouv. J. Chim. **2**, 631 (1978).
8. J. M. LEHN and G. WIPFF. Helv. Chim. Acta, **61**, 1274 (1978); J. Am. Chem. Soc. **96**, 4048 (1974).
9. H. MEERWEIN, K. BODENBENNER, P. BORNER, F. KUNERT, and K. WUNDERLICH. Ann. Chem. **632**, 38 (1960).
10. K. B. WIBERG and K. A. SAEGEBARTH. J. Am. Chem. Soc. **79**, 2822 (1957).
11. R. U. LEMIEUX and S. KOTO. Tetrahedron, **30**, 1933 (1974) and references quoted therein.
12. C. ALTONA. Ph.D. Thesis, University of Leiden, The Netherlands. 1964; C. ROMERS, C. ALTONA, H. R. BUYS, and E. HAVINGA. *In* Topics in stereochemistry. Vol. 4. *Edited by* E. L. Eliel and N. L. Allinger. Wiley-Interscience, New York, NY. 1969. p. 39.
13. R. HUISGEN and H. OTT. Tetrahedron **6**, 253 (1959); G. I. JONES and N. L. OWEN. J. Mol. Struct. **18**, 1 (1973).
14. N. BEAULIEU and P. DESLONGCHAMPS. Can. J. Chem. **58**, 164 (1980).
15. G. A. HAGGIS and L. N. OWEN. J. Chem. Soc. 389 (1953); E. ALI and L. N. OWEN. J. Chem. Soc. 2111 (1958); W. HUCKEL and W. EGERER. Ann. Chem. **645**, 162 (1961).
16. H. MEERWEIN. *In* Organic synthesis. Vol. 46. John Wiley and Sons, Inc., New York, NY. 1966. pp. 113 and 120.
17. J. HEBKY. Collect. Czech. Chem. Commun. **13**, 442 (1948).

Can. J. Chem. Downloaded from www.nrcresearchpress.com by 210.87.254.5 on 09/05/12
For personal use only.

Canadian Journal of Chemistry
Published by
THE NATIONAL RESEARCH COUNCIL OF CANADA

Journal canadien de chimie
Publié par
LE CONSEIL NATIONAL DE RECHERCHES DU CANADA

Volume 58 Number 11 June 1, 1980 Volume 58 numéro 11 1 juin 1980

Photoelimination from a γ-substituted α,β-unsaturated ketone

JAMES L. CHARLTON AND GERALD N. LYPKA
Department of Chemistry, University of Manitoba, Winnipeg, Man., Canada R3T 2N2
Received November 5, 1979

JAMES L. CHARLTON and GERALD N. LYPKA. Can. J. Chem. **58**, 1059 (1980).

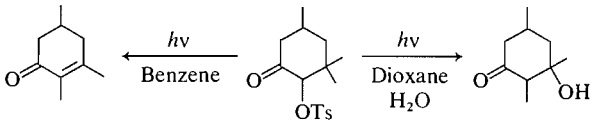
During a study of unsaturated six membered ring sultones (1), it was found that irradiation of the sultone **7** in methanol gave the esters **8** and **9** as primary photoproducts. These esters, on continued irradiation, led to a completely aromatic compound which has now been identified as 12-hydroxy-11-phenylbenzo(*j*)fluoranthene **10**.

JAMES L. CHARLTON et GERALD N. LYPKA. Can. J. Chem. **58**, 1059 (1980).

Lors de l'étude des sultones contenant un cycle à 6 non saturé (1), on a trouvé que l'irradiation de la sultone **7** dans le méthanol donne les esters **8** et **9** comme produits principaux. Ces esters sous irradiation continue se transforment en un composé complètement aromatique identifié comme étant l'hydroxy-12 phényl-11 benzo[*j*]fluoranthène (**10**).

[Traduit par le journal]

The photoelimination of the substituents from ketones has been the subject of several recent investigations. α-Tosyloxyketones have been examined by Iwasaki and Schaffner (2) who reported that irradiation in the $n\pi^*$ absorption band of the 2,5-*cis*-tosyloxyketone **1** led to the cyclohexanone **2** in benzene solution and to ketol **3** in aqueous dioxane.

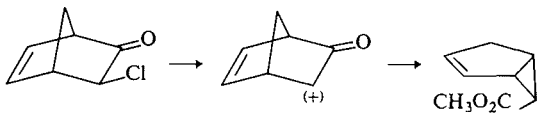


2 1 3

An α-keto carbonium ion was proposed as an intermediate. In later work Schaffner and co-workers extended the scope of this reaction to include electrophilic substitution on aromatic nuclei (3). Similarly Lai, in his study of tosyloxyketones, proposed an α-ketocarbonium ion pathway leading to a Favorski-type process (4).

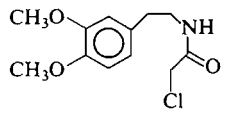
The photolysis of α-chloroketones has been studied by a number of groups (5). As an example, Kaplan and Hartwig photolized the ketone **4**, in methanol, to give **5** in 95% yield (5*a*). As in tosyloxyketones, a carbonium ion was postulated as an intermediate.

Yonemitsu and co-workers have conducted several studies on the photochemistry of *N*-chloroacetamides (6). For instance, photolysis of 3,4-dimethoxy phenethylamide **6** caused expulsion of the chlorine to yield both radical and cationic intermediates (7).



4 5, 95%

A vinyl analogue of these α-photoelimination reactions is reported here. Extensive irradiation of the sultone **7** gave a compound which analysed for $C_{26}H_{16}O$ and exhibited a signal for only one non-



6

aromatic proton at δ 5.42 in the nuclear magnetic resonance spectrum. This signal disappeared on the addition of deuterium oxide. As well, the carbon-13 nuclear magnetic resonance spectrum exhibited only one carbon down-field at δ 148.6 with the rest all falling in the aromatic region between δ 119.1 and δ 137.8. The infrared spectrum showed hydroxyl absorption at 3530 cm^{-1} and the

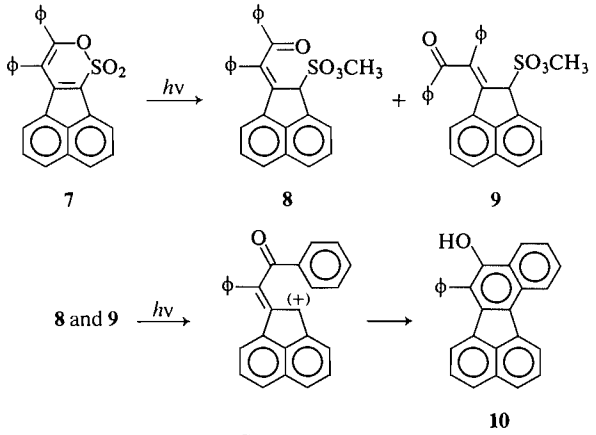
0008-4042/80/111059-02$01.00/0
©1980 National Research Council of Canada/Conseil national de recherches du Canada

Can. J. Chem. Downloaded from www.nrcresearchpress.com by 210.87.254.105 on 09/05/12
For personal use only.

mass spectrum gave a molecular ion peak at *m/e* 344.

Ozonolysis in ethyl acetate at −20°C and sublimation of the products, after oxidative workup, led to the isolation of benzoic acid and phthalic anhydride.

The most reasonable interpretation of these data is represented by the structure 12-hydroxy-11-phenylbenzo(*j*)fluoranthene, **10**, and the following mechanism is proposed:



7 8 9 10

SCHEME I

The intermediacy of the esters **8** and **9** was established by their isolation (1) and conversion, by photolysis, to the phenol **10**. While we have represented the intermediate in this reaction as cationic, we have no direct evidence for its existence and a radical mechanism cannot be excluded.

The structure of **10** was further substantiated by the similarity of its ultraviolet spectrum to that of benzo(*j*)fluoranthene (8) and by the expected bathochromic shift of the ultraviolet spectrum on going from neutral to basic medium.

Experimental

Melting points were determined on a Kofler hot stage and are uncorrected. Infrared spectra were obtained with a Beckman IR-10 instrument and nuclear magnetic resonance spectra were recorded on a Varian EM-360 (^{1}Hmr) or a Bruker WH90-DS (^{13}Cmr) instrument. Chemical shifts are reported in ppm downfield from tetramethylsilane. Mass spectra were recorded on a Finnegan 1015 mass spectrometer.

Irradiation of Sultone 7

Sultone **7** (1) (198 mg) was dissolved in methanol (150 cm^3) and irradiated, under nitrogen, for 3 h with a 450 W medium pressure mercury lamp, using a pyrex filter. The reaction was followed by thin layer chromatography (Camag DSF-5 silica gel, eluent ethyl acetate – petroleum ether 1:4). The solvent was removed under vacuum and the residue chromatographed on silica gel (eluent ethyl acetate – petroleum ether, 1:4) to give yellow crystals (130 mg, 78% yield) which recrystallized from benzene, melting point 180–183°C; λ_{max} (CH_3OH) (ε): 432(3 000), 385 (6 500), 366 (4 950), 333 (27 200), 318 (30 400), 236 (50 000), and 224 (ε 47 000) nm; λ_{max} (0.7 *N* KOH/CH_3OH) (ε): 513 (5 000 nm; ν_{max}($CHCl_3$): 3530 and 1570 cm^{-1}; ^{1}Hmr ($CDCl_3$) δ: 5.42(s), 7.5(m); ^{13}Cmr ($CDCl_3$) δ: 148.7, 137.8–119.1 (overlapping signals); *Anal.* calcd. for $C_{26}H_{16}O$: C 90.67, H 4.68; found: C 90.70, H 4.59.

Ozonolysis of 10

The photoproduct **10** (90 mg) was dissolved in ethyl acetate (30 cm^3) and treated at −20°C with ozone until the yellow colour disappeared. Hydrogen peroxide (5 cm^3; 30% solution) and sodium hydroxide (15 cm^3; 1 *N*) were added and the solution refluxed for 5 min. It was then acidified (1 *N* HCl) and extracted with ether. These extracts were dried ($MgSO_4$) and evaporated to leave a residue that could be partially separated by fractional sublimation, one compound subliming at 25–50°C (0.004 Torr) and the other at 50–130°C (0.004 Torr). Recrystallization of the former from chloroform – light petroleum gave a compound, mp 119–120°C. A mixture melting point with benzoic acid showed no depression. Recrystallization of the second compound from chloroform – light petroleum gave crystals, mp 128–130°C. A mixture melting point of this compound with phthalic anhydride showed no depression. Infrared spectra of the above compounds were identical to those of authentic samples.

Acknowledgements

We gratefully acknowledge the financial assistance of the National Sciences and Engineering Research Council of Canada.

1. J. L. CHARLTON and P. DE MAYO. Can. J. Chem. **46**, 55 (1968).
2. S. IWASAKI and K. SCHAFFNER. Helv. Chim. Acta, **51**, 557 (1968).
3. A. TUINMAN, G. IWASAKI, K. SCHAFFNER, and O. JEGER. Helv. Chim. Acta, **51**, 1778 (1968).
4. H. K. LAI. Ph.D Thesis, University of Manitoba, Winnipeg. 1975.
5. (*a*) B. E. KAPLAN and A. L. HARTWIG. Tetrahedron Lett. **55**, 4855 (1970); (*b*) G. JONES II and L. P. MCDONNELL. J. Am. Chem. Soc. **98**, 620 (1976); (*c*) R. S. GIVENS and L. STREKOWSKI. J. Am. Chem. Soc. **97**, 5867 (1975).
6. M. IDEDA, K. HIRAO, Y. OKUNO, N. NANAO, and O. YONEMITSU. Tetrahedron, **33**, 489 (1977) and references cited.
7. O. YONEMITSU, Y. OKUNO, Y. KANAOKA, I. A. KARLE, and B. WITKOP. J. Am. Chem. Soc. **90**, 6522 (1968).
8. B. BOSSENBROCK, D. C. SANDERS, H. M. CURRY, and H. SHECHTER. J. Am. Chem. Soc. **91**, 371 (1969).

Can. J. Chem. Downloaded from www.nrcresearchpress.com by 210.87.254.105 on 09/05/12
For personal use only.

Stereocontrolled catalytic hydrogenations of 3-oxocholestanes and some related compounds to the corresponding axial 3-alcohols

MASAYOSHI ISHIGE AND MICHIO SHIOTA

Chemical Laboratory, Ochanomizu University, Otsuka, Bunkyo-ku, Tokyo, Japan

Received November 19, 1979

Can. J. Chem. Downloaded from www.nrcresearchpress.com by 210.87.254.105 on 09/05/12
For personal use only.

MASAYOSHI ISHIGE and MICHIO SHIOTA. Can. J. Chem. **58**, 1061 (1980).

Catalytic hydrogenations of 5α-cholestan-3-ones and related compounds with Urushibara nickel A catalyst in cyclohexane gave a distinct preponderance of unstable axial 3α-ols. Product ratios of axial alcohols decreased with increasing solvent polarity. For 3-oxo-5α-steroids, the cobalt catalyst was less selective for the axial alcohol formation. On the other hand, conversion of 5β-cholestan-3-one into the corresponding axial 3β-ol was most successfully attained by hydrogenation catalyzed by Urushibara cobalt A catalyst in methanol. For such a 5β-ketone, alcoholic media with higher polarities were more favorable for giving the product rich in axial alcohol. The stereochemistry of the products obtained from hydrogenations conducted in nonpolar solvents may be understood in terms of the steric congestion around the ketone carbonyl group. However, when alcohols were used as solvents, the product ratios obtained did not correlate well with the congestion ratios of substrates.

MASAYOSHI ISHIGE et MICHIO SHIOTA. Can. J. Chem. **58**, 1061 (1980).

L'hydrogénation catalytique des cholestane-5α ones-3 et de composés apparentés au moyen du catalyseur de nickel A de Urushibara dans le cyclohexane a conduit à la formation prépondérante des alcools-3α axiaux instables. La proportion d'alcool axial décroît quand on augmente la polarité du solvant. Dans le cas des oxo-3 stéroides-5α, le catalyseur au cobalt est moins sélectif quant à la formation d'alcool axial. D'autre part, la transformation de la cholestane-5β one-3 en l'alcool-3β axial correspondant se fait plus facilement par hydrogénation catalytique en présence du cobalt A de Urushibara dans le méthanol. Dans le cas de la cétone 5β, l'utilisation d'un milieu alcoolique à forte polarité favorise grandement la formation de l'alcool axial. On peut comprendre la stéréochimie des produits d'hydrogénation dans des solvants non polaires en fonction d'une compression stérique autour du groupe carbonyle de la cétone. Cependant, quand on utilise des alcools comme solvants, la proportion de produits obtenus ne correspond pas tout à fait aux taux de compression des substrats.

[Traduit par le journal]

Introduction

With synthetic methods in hand for preparing steroid axial 3-alcohols from the corresponding ketones (1–8), we are interested in examining the stereoselectivity of catalytic hydrogenation of 3-oxo-steroids.

Compared with the syntheses of equatorial alcohols, the preparation of the axial isomers has generally been troublesome. It is well known that the catalytic hydrogenation of unhindered cyclic ketones in acidic media gives a preponderance of the axial alcohols (9–11). However, the method is limited in its application to various kinds of steroids, not only because the selectivity of the products is not always satisfactory, but also because the use of strong acids often leads to the formation of by-products. In neutral solvents, nearly equal amounts of isomeric alcohol are frequently obtained (11); the reason proposed is that the attack of hydrogen occurs equally from either side of the molecule in those compounds in which there is little difference in steric hindrance around the carbonyl group. However, the preponderance of steroid axial 3-alcohols obtained by catalytic hydrogenation using neutral solvents under mild conditions (1–6) suggests that this reductive technique will provide a convenient route for preparing axial 3-ols because of the ease of the procedure and the high selectivity for less stable axial alcohols. Furthermore, the data collected, which contravene the general tendency,[1] are helpful in understanding the stereochemistry of catalytic hydrogenation of unhindered alicyclic ketones.

The purpose of the present work is twofold: first, to investigate the finding that some 5α-cholestan-3-ones can be favorably hydrogenated to the 3α-ols using Urushibara nickel A catalyst in cyclohexane and to check the general applicability of this method to the preparation of steroid axial 3-alcohols; second, to compare the ratios of axial to equatorial alcohols obtained in order to find the controlling factors of stereoselectivity of the catalytic hydrogenation.

Results and Discussion

Hydrogenations of 5α- and 5β-Cholestan-3-ones (1 and 2)

In a previous publication (3), we have described in part the effects of solvents and catalysts on the product ratios in the hydrogenation of 5α-cholestan-3-one (**1**). Among the catalysts tested, Urushibara nickel A (abbreviated to U-Ni-A

[1]For the general rule to predict stereochemistry of catalytic hydrogenation of cyclic ketones, see ref. 9, footnote 23.

0008-4042/80/111061-08$01.00/0

©1980 National Research Council of Canada/Conseil national de recherches du Canada

TABLE 1. Effect of solvents on the product ratios (axial alcohol %) in the hydrogenations of 5α- and 5β-cholestan-3-ones with Urushibara catalysts

Ketone	Catalyst	Axial alcohol %				
		MeOH	EtOH	*i*-PrOH	*t*-BuOH	Cyclohexane
5α-Cholestan-3-one	U-Ni-A	42	47	48	53	87
	U-Co-A	33	34	47	60	73
	U-Cu-A	—	—	—	11	26
5β-Cholestan-3-one	U-Ni-A	72	76	60	51	57
	U-Co-A	99	89	75	72	52
	U-Cu-A	—	—	—	65	47

hereafter), which was prepared by the acid treatment of precipitated nickel, appeared to be most promising for the preferential production of the axial 3α-ol when it was used in hydrocarbon solvents. By using some other Urushibara catalysts, we have now examined more extensively the effects of these reagents on the selectivity of reduction of 5α- and 5β-cholestan-3-ones (**1** and **2**). According to the procedure described previously, the reactions were carried out at 30–35°C under high pressure. The stereochemistry of hydrogenation in neutral media is very sensitive to contamination and to the catalyst. A trace of water in the reaction causes a great diminution of the proportion of axial alcohol. Thus the water in the reaction system must be carefully removed. The results are summarized in Table 1.

It can be recognized from the table that in the presence of U-Ni-A and U-Co-A, the change in the product ratio with solvent presents a striking contrast between the 5α- and 5β-ketones. The formation of axial 3α-ol (**3**) from the 5α-ketone **1** was not favorable in alcohol media with higher polarities, while the same ketone gave products predominant in axial alcohol when a nonpolar solvent such as cyclohexane was used. A tendency to increase the 3α-ol ratio with decrease of solvent polarity can be more clearly seen when the data for the reduction of the 5α-ketone in ether are considered (3). On the other hand, the 5β-ketone **2** was preferentially hydrogenated to the axial 3β-ol (**4**) in more polar media.

The catalysts play another important role for selectivity. Although the properties of the nickel and cobalt catalysts used appear similar, the difference in selectivity of the metals can be noticed when the product ratios are examined in detail. In the reactions of 5α-cholestan-3-one, nickel was more selective for the formation of axial 3α-ol than cobalt. With 5β-cholestan-3-one, on the contrary, cobalt more effectively favored the formation of the axial 3β-ol **4** than nickel. Therefore the best result for axial alcohol formation from 5α-cholestan-3-one was obtained under the conditions with U-Ni-A in cyclohexane, whereas the 5β-ketone **2** was most preferentially hydrogenated to the corresponding axial alcohol in the presence of U-Co-A in methanol.

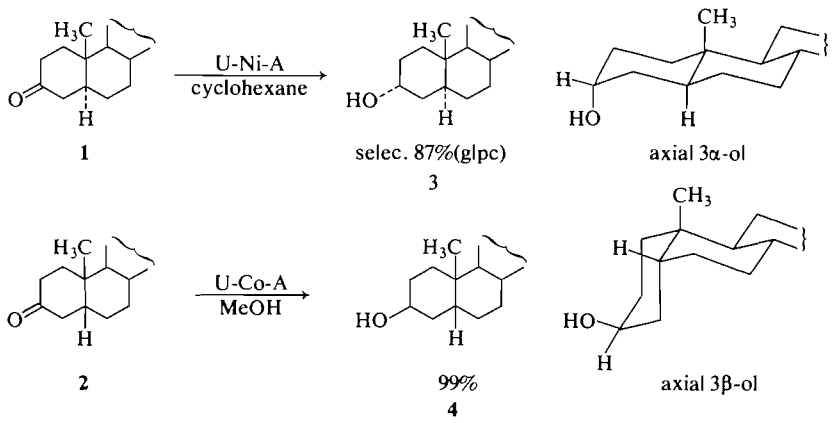
These findings may imply that in the presence of the nickel and cobalt catalysts, 5α-cholestan-3-one is more likely to give the corresponding equatorial 3β-ol through the adsorbed transition complex which is stabilized in more polar solvents, whereas the reduction of the 5β-ketone to the axial 3β-ol proceeds through the species stabilized in similar polar media. If this is the case, it would mean that the adsorbed transition complexes of nickel are generally less polar than those of cobalt, although the polarities of the complexes vary with substrates and solvents.

More distinct examples of opposite stereoselectivities have been reported in the palladium or platinum catalyzed hydrogenation of 5α- and 5β-cholestan-3-ones (5). The reduction of 5α-cholestan-3-one with palladium in *t*-BuOH gives the equatorial 3β-ol in 98% selectivity, while the reduction of the 5β-ketone results in the formation of the axial 3β-ol in 95% selectivity under the same conditions. Similar results are also obtained with *i*-PrOH and tetrahydrofuran, but not with cyclohexane. Platinum catalysts have a similar selectivity, but are somewhat less selective than palladium.

Hydrogenations of 5-Cholesten-3-one (5) and 5α-Cholest-6- and -7-en-3-ones (6 and 7)

The hydrogenation with U-Ni-A in hydrocarbon solvents has proved most useful when the method is applied to 5-cholesten-3-one (**5**), since **5** is liable to isomerize to the conjugated ketone in the presence of acids. A unique characteristic of U-Ni-A reduction is that the yield of epicholesterol (5-cholesten-3α-ol) (**8**) is superior to those observed with most other methods of preparation (1, 12–21). The yield of the U-Ni-A reactions varies widely if contaminants, one of which is frequently water

Can. J. Chem. Downloaded from www.nrcresearchpress.com by 210.87.254.105 on 09/05/12
For personal use only.



1 3 2 4

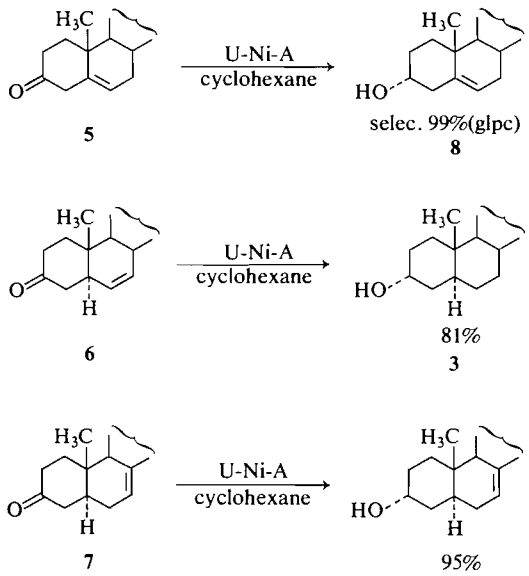
SCHEME 1

contained in the reaction system, are present. When water is thoroughly removed, the yield is found to be improved over that previously reported (94% (3) up to about 99%).

The hydrogenation of 5α-cholest-6-en-3-one (**6**) under the same conditions gave a mixture of saturated 3α-ol and 3β-ol in the ratio of 81:19. The C=C double bond of the ketone appeared more readily hydrogenated than the carbonyl group, and the reduction may proceed mainly through 5α-cholestan-3-one as an initial reduction product. The product ratio from this ketone is, in fact, analogous to that from 5α-cholestan-3-one.

In the reaction of 5α-cholest-7-en-3-one (**7**), the ethylenic double bond remained unreacted and only the carbonyl group was selectively converted into the 3α-hydroxyl group.

Compared with the results of saturated ketones,



5 8 6 3 7

SCHEME 2

the higher selectivities of axial 3α-ol from the unsaturated ketones are related to the presence of C=C double bonds in the B-ring. The geometry of the unsaturated steroidal ketones might participate in the preponderance of the axial alcohols, but the pronounced preference for a 3α-hydroxyl group is difficult to explain on the basis of steric control alone.

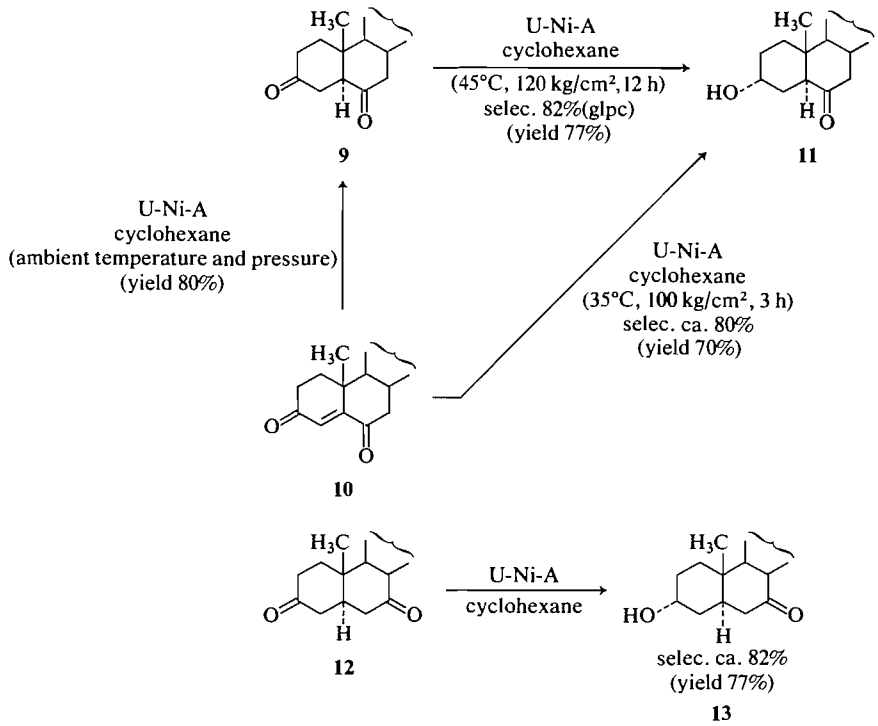
Hydrogenations of 5α-Cholestan-1-one, -2-one, -4-one, and -6-one

In order to investigate the relationship between the positions of carbonyl groups and the selectivities, the hydrogenations of 5α-cholestan-1-one, -2-one, -4-one, and -6-one with U-Ni-A in cyclohexane were attempted. The 1-one, 4-one, and 6-one did not undergo hydrogenation after a long reaction time. Only the 2-one was readily hydrogenated to give the axial 2β-ol in a good yield (Table 2). In this case, the strong preference for axial alcohol formation seems to be caused by the exclusive α-face attack of hydrogen on the carbonyl group because the approach of catalyst from the β-side is hindered by the presence of a *syn*-axial angular methyl group. However, from the fact that the hydrogenation using *t*-butyl alcohol solvent showed the diminution of the 2β-ol ratio, it is rather questionable to consider that a strong preference is exclusively a consequence of steric hindrance to β-face attack upon the ketone.

TABLE 2. The product ratio in the hydrogenation of 5α-cholestan-2-one with U-Ni-A

Solvent	Product ratio (%)	
	2β (axial)	2α (equatorial)
Cyclohexane	98	2
t-BuOH	80	20
EtOH	80	20

Can. J. Chem. Downloaded from www.nrcresearchpress.com by 210.87.254.105 on 09/05/12
For personal use only.



SCHEME 3

Hydrogenations of 4-Cholestene-3,6-dione (10) and 5α-Cholestane-3,6- and -3,7-diones (9 and 12)

A previous paper has described the preparation of 3α-hydroxy-5α-cholestan-6-one (**11**) and -7-one (**13**) from the corresponding diones with U-Ni-A in cyclohexane (4). Striking features of the reactions are represented both by the exclusive reduction of the 3-carbonyl group and by the selective formation of the axial 3α-hydroxyl group. However, since the 3,6-dione **9** is intrinsically less reactive, the reaction must be effected for a long time under slightly more drastic conditions than usual. Inspection of a model of this dione shows that a conformational change of the A-ring caused by a change from sp^2 to sp^3 at C3 gives rise to a slight clockwise rotation of bonds attached to C5 relative to those at C10. This rotation tends to force a further decrease on the originally small torsion angle between C5—C6 and C9—C10 bonds. The distortions opposed to those stemming from C3 will retard the reduction of compound **9**. On the other hand, the 3,7-dione **12** will not be affected so greatly, as indicated in the experiments, by a geometry deformation involving the reaction, because the separation of the 7-carbonyl group from C5 by a methylene enables the B-ring to accommodate the small skeletal deformations around the C5—C10 bond.

The unreactivity of the carbonyl group at the 6- and 7-positions may be ascribed to steric hindrance. In this connection, 5α-cholestan-6-one and 3β-acetoxy- and 3β-hydroxy-5α-cholestan-6-ones were found to undergo no hydrogenation under the same conditions. However, when *t*-BuOH solvent was used instead of cyclohexane, 3β-hydroxy-5α-cholestan-6-one and -7-one were readily hydrogenated into the mixtures containing 5α-cholestane-3β,6β- and -3β,7β-diols respectively. Likewise each 3β-hydroxy ketone is known to be converted into the diols with U-Ni-B in EtOH (22).

These results suggest that steric hindrance will predominately control stereochemistry in nonpolar solvents whereas it will not always prevail in alcohol media.

The preparation of 3α-hydroxy-5α-cholestan-6-one (**11**) could be easily attained by the hydrogenation of 4-cholestene-3,6-dione (**10**) with U-Ni-A in cyclohexane under high pressure. Generally the use of alcohol solvent is undesirable as the yield of the product decreases. However, even at ambient temperature and pressure, it happened that Δ^4-3,6-dione **10** gave the desired product in *t*-BuOH in a good yield, but further examination to obtain reproducible results is needed. The reduction in cyclohexane at atmospheric pressure yielded 5α-cholestane-3,6-dione as a major product.

Although the analysis of the stereochemical results of the reduction of this conjugated ketone is

Can. J. Chem. Downloaded from www.nrcresearchpress.com by 210.87.254.105 on 09/05/12
For personal use only.

Can. J. Chem. Downloaded from www.nrcresearchpress.com by 210.87.254.105 on 09/05/12
For personal use only.

not clear, it is evident that reaction to form 3α-hydroxy-6-one **11** does not proceed via the intermediate 5α-cholestane-3,6-dione **9** because the reaction of the dione **9** is very slow (see Scheme 3). The formation of the desired hydroxy ketone may be envisaged as resulting from either rapid isomerization of the 5β-isomer or partial reduction of a species of 3,5-diene-3,6-diolate coordinating with the metal.

Hydrogenation of 5-Hydroxy-5α-cholestan-3-one (14)

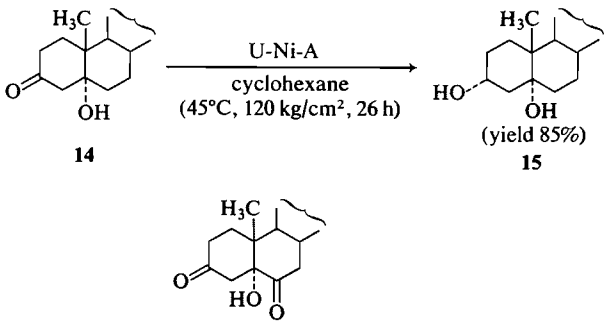
A unique character in the reduction of 5-hydroxy-5α-cholestan-3-one (**14**) is the highly selective conversion of the 3-carbonyl group into the axial 3α-hydroxyl group; 5α-cholestane-3α,5-diol (**15**) was thus obtained as the only product. However, as the hydroxy ketone **14** reacted very slowly, the reaction had to be carried out for a long time at a more elevated temperature under higher pressure. The situation was almost independent of solvents and catalysts. Therefore it is probable that the stereoselectivity is exclusively determined by steric factors.

In addition, we found that the hydrogenation of 5-hydroxy-5α-cholestane-3,6-dione (**16**) does not take place under these drastic conditions.

Hydrogenations of 5,6α-Epoxy-5α- and 5,6β-Epoxy-5β-cholestan-3-ones (17 and 18)

The examination of the behavior of epoxy ketones to catalytic hydrogenation under neutral conditions is of interest, and the reduction of some 5,6-epoxy ketones with U-Ni-A in cyclohexane were attempted.

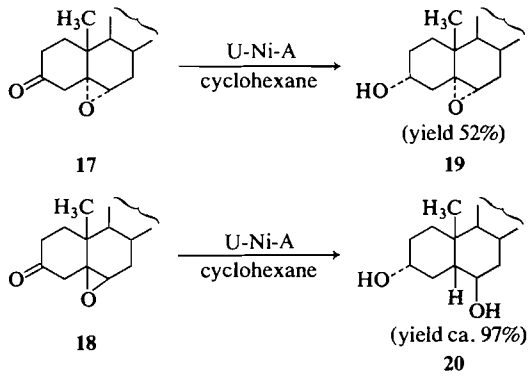
In preliminary experiments, we found that 5,6α-epoxy-5α-cholestan-3-one (**17**) was characteristically converted into different products depending on the reaction conditions employed. For example, the epoxy ketone **17** gave 6α-hydroxy-4-cholesten-3-one as a major product when stirred in ethanol in the presence of alumina, whereas 5α-cholestane-3,6-dione was produced when cyclohexane was used instead of ethanol.



SCHEME 4

Under the conditions using cyclohexane solvent in the presence of U-Ni-A but without hydrogen gas, the α-epoxy ketone **17** changed into an oily mixture which appeared to contain mainly 4-cholestene-3α,6α-diol. On the other hand, under the hydrogen atmosphere, 5,6α-epoxy-5α-cholestan-3α-ol (**19**) was the main component obtained from a crude oily product, which was easily isolated as a crystalline solid (mp 120–121°C, 52% yield) by column chromatography on silica gel. Subsequent oily material eluted was composed of several minor compounds, which were produced through the cleavage of the epoxy ring. Since the epoxy alcohol obtained was stable as compared with the starting epoxy ketone, it is suggested that the rate of reduction of the carbonyl group is comparable to that of epoxide-ring cleavage.

The epoxide ring of 5,6β-epoxy-5β-cholestan-3-one (**18**) was more labile, opening under the influence of the metal. The hydrogenation of this β-epoxy ketone **18** under the same conditions as above afforded crude crystals, from which 5β-cholestane-3α,6β-diol (**20**) was obtained in a ca. 97% yield by recrystallization, mp 142–143.5°C. It is probable that the diol is the hydrogenation product of an intermediate 6β-hydroxy-4-cholesten-3-one.



SCHEME 5

Steric Control in the Reduction of Ketones

Although the interpretation of the stereochemistry of addition reactions of ketones in terms of steric factors has been the subject of some controversy,[2] the importance of this factor operating in the reduction of ketones has been well recognized since the 1950's.

The concept of steric approach control in the addition reactions of hindered cyclic ketones has

[2]For recent reviews concerning the stereochemical mechanism, see ref. 23.

Can. J. Chem. Downloaded from www.nrcresearchpress.com by 210.87.254.105 on 09/05/12
For personal use only.

been well accepted since proposed by Dauben *et al.* (24), and additional explanations advanced for unhindered cyclic ketones have been offered by many workers (21–28).

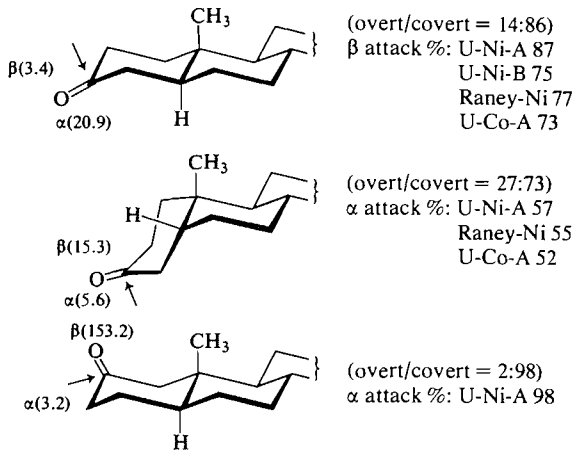
Recently two types of approach to estimate the steric environment about a reaction center have been offered, based on the theoretical calculations.

Perlberger and Müller pointed out that the rates for the reduction of ketones are interpreted in terms of two parameters derived from force-field calculations (29). However, the parameters concerning steroid ketones are not available from the reported papers.

Wipke and Gund have shown that the steric congestions calculated with molecular mechanics correlate well with the stereoselectivity of ketone additions by large nucleophiles, or in highly congested substrates (30). For addition of small nucleophiles to uncongested ketones, the torsion-corrected functions are successfully used to reproduce the stereoselectivity of the reduction. The values of overt (β) and covert (α) congestions of 5α-cholestan-3-one are 3.4 and 20.9 respectively. The ratio of these congestions (14:86) is fairly close to the product ratios obtained in the nickel-catalyzed hydrogenation in cyclohexane (β attack %: U-Ni-A 87, U-Ni-B 75, Raney-Ni 77). In the case of 5α-cholestan-2-one, good correlation between the experimental product ratio (98% α attack) and the congestion functions (3.2α, 153.2β or 2:98) was also observed. These findings thus suggest that the selectivity in the reactions is dominated by steric control with reagents, meaning that the slow step is in an early (reactant-like) transition state. This consideration consistently explains the facts that highly congested ketones, such as 5α-cholestan-1-one, -4-one, and -6-one, resist reaction in a nonpolar solvent. However, neither the congestions (5.6α, 15.3β or 27:73) nor the torsion-corrected ones (ratio of overt/covert, 13:87) of 5β-cholestan-3-one seem to reflect as well the observed ratios (β attack %: U-Ni-A 57, Raney-Ni 55).

It is reasonably conceivable that the A-ring of a 5β-ketone, in which the C4—C5 bond is axial with regard to the B-ring, is in a somewhat higher energy level relative to that of a 5α-ketone, being torsionally strained to minimize the energy in the ground state. This torsion strain is probably less than the strain predicted from the Chérest and Felkin's concept (31). Therefore the discrepancy between the observed and calculated product ratios in the 5β-ketone might be diminished by correcting the congestion function by using parameters suitable for torsion in the ground state.

The cobalt-catalyzed reductions in a nonpolar solvent give similar results to those obtained with nickel. Thus, the preference for attacking direction of reagents is, to a large extent, predictable by the congestions of ketones.



NOTE: Arrow denotes the direction of preferable attack of hydrogen on carbonyl carbon. The figures in parentheses represent the congestion values.

SCHEME 6

The aspects of reactions in polar alcoholic solvents are more enigmatic. Considering that the congestion or corrected congestions do not correlate well with the product ratios, most stereochemical results do not obviously appear to reflect a steric or torsion effect. With the 5β-ketone, torsional effects involving solvation may not prevail, because the assignment of stereochemistry based on the torsional-corrected congestions is the reverse of the observed preferred direction of hydrogen addition to the carbonyl carbon. Additionally, from the viewpoint of steric hindrance, 5α-cholestan-2-one is of interest, in that the ratio of the equatorial 2α-ol tends to increase in alcohol media, though the attack from the β-side is strongly hindered. In such cases, it may be rather questionable that steric control is a principal factor in determining the stereochemistry. In addition, it is evident that a concept of "product development control" does not explain the predominant formation of the products. The alcoholic solvents can probably play various roles in the reaction processes, such as association with a substrate, adsorption on the catalyst metal, and proton donation.

Experimental

All the melting points were determined on a Yanagimoto hot-stage and are uncorrected. The nmr spectra were recorded with a JEOL C-60 HL nmr spectrometer using chloroform-*d* solvent containing TMS as an internal standard unless otherwise stated. The ir spectra were measured on a JASCO IR-G spectrometer using KBr discs. The product ratios were determined with a Shimadzu GC-4APF gas chromatograph by using either a

Can. J. Chem. Downloaded from www.nrcresearchpress.com by 210.87.254.105 on 09/05/12
For personal use only.

3 m glass column packed with 1.5% Silicone OV-17 on silanized Shimalite (80–100 mesh) or a 50 m glass capillary column (0.3 mm id; Silicone OV-101; Scott-type).

Catalysts

The catalysts used were prepared according to the procedure described previously (3). In order to remove the water completely from the catalyst surface, the crystallites, which were thoroughly washed with water and then with *t*-BuOH, were suspended once in the solvent by means of an ultrasonic cleaner, then precipitated by centrifugation, and separated out from the liquid by decantation. The procedures were carried out repeatedly. The catalysts thus obtained were used immediately.

Hydrogenation

According to the procedure described in the previous paper (3), the hydrogenations were usually effected at 30–35°C under a high pressure of 70–100 kg/cm². For preparative purposes, the hydrogenations of 5α-steroids were usually carried out with U-Ni-A catalyst in cyclohexane, whereas the reactions of the 5β-series were performed with U-Co-A in methanol.

Hydrogenation of 5α-Cholestan-3-one (1)

A typical example of the hydrogenation of 5α-cholestan-3-one with U-Ni-A in cyclohexane was reported previously (3). The crude product was chromatographed on silica gel with hexane–ether (8:2) to give pure 5α-cholestan-3α-ol (**3**) in 72% yield; mp 188–189°C (lit. (32) mp 186–187°C). Successive elution with hexane–ether (1:1) afforded 5α-cholestan-3β-ol; mp 141–142°C (lit. (33) mp 142–143°C).

Hydrogenation of 5β-Cholestan-3-one (2)

A typical example will be described. 5β-Cholestan-3-one (100 mg) was hydrogenated with U-Co-A (freshly prepared from 1.5 g of precipitated cobalt) in methanol (3 mL) for 2.5 h in a similar manner to that with the 5α-ketone. The product was purified by column chromatography on silica gel with hexane–ether (19:1) to give 5β-cholestan-3β-ol (**4**) in 75% yield; mp 101–102°C (lit. (15) mp 106°C); ir: 3280 (strong) and 1030 (sharp, strong) cm⁻¹; nmr (δ): 4.03 (3α-H), 0.95 (19-H), and 0.65 (18-H).

Hydrogenations of 5-Cholesten-3-one (5) and 5α-Cholest-6-en- and -7-en-3-ones (6 and 7)

Preparation of 5-cholesten-3α-ol (epicholesterol) (**8**) from 5-cholesten-3-one using U-Ni-A in cyclohexane was presented in a previous report (3). The crude crystals gave 5-cholesten-3α-ol (**8**) (92% yield) when they were chromatographed on silica gel using hexane–ether (9:1); mp 139–140°C (lit. (1) mp 141°C).

5α-Cholest-6-en-3-one (**6**) (100 mg) was hydrogenated with U-Ni-A (from 1 g of precipitated nickel) in cyclohexane (3 mL) for 2.5 h at 35°C under the pressure of 90 kg/cm². After purification of the product by column chromatography on silica gel, the spectroscopic data and melting point revealed that 5α-cholestan-3α-ol (**3**) was the major component, which was found to be contained in the crude product in a proportion of 81% by means of gas chromatographic analysis.

The hydrogenation of 5α-cholest-7-en-3-one (**7**) was carried out for 5 h under the same conditions as above. Gas chromatographic analysis showed that the product consisted of two compounds in the ratio of 95:5. 5α-Cholest-7-en-3α-ol was isolated in 88% yield by column chromatography on silica gel with hexane–ether (9:1); mp 174–175°C (lit. (34) mp 175–176°C); ir: 3300 (strong), 1660 (weak), 1045, and 1005 (sharp, strong) cm⁻¹; nmr (δ): 5.10 (7-olefinic H) and 4.00 (3α-H).

Hydrogenations of 5α-Cholestane-3,6-dione (9) and 4-Cholestene-3,6-dione (10)

The preparative procedure of 3α-hydroxy-5α-cholestan-6-one (**11**) from these ketones was described previously (4). 5α-Cholestane-3,6-dione was hydrogenated under slightly more drastic conditions than usual. The crude product gave compound **11** in 77% yield after purification by column chromatography; mp 163–164°C (lit. (35) mp 159–160.5°C). The reduction of 4-cholestene-3,6-dione gave the same 3α-hydroxy ketone **11** in 70% yield.

Hydrogenation of 5α-Cholestane-3,7-dione (12)

The procedure to prepare 3α-hydroxy-5α-cholestan-7-one (**13**) is given in our previous paper (4). The desired 3α-hydroxy-7-one **13** was obtained from 5α-cholestane-3,7-dione (**12**) in 77% yield; mp 197–198°C.

Hydrogenation of 5-Hydroxy-5α-cholestan-3-one (14)

5-Hydroxy-5α-cholestan-3-one (**14**) (100 mg) was reduced in cyclohexane (3 mL) with U-Ni-A (from 3 g of precipitated nickel) at 45°C for 26 h under the pressure of 120 kg/cm². The product was recrystallized twice from ethanol to give 5α-cholestane-3α,5-diol (**15**) in 85% yield; mp 197–198°C (lit. (36) mp 199°C); ir: 3300 (strong), 1120 (sharp, strong), 1100 (shoulder), 1075, 1033 (sharp, strong), 1110 (sharp), and 1000 cm⁻¹; nmr (δ): 4.00 (3β-H).

Hydrogenations of 5,6α-Epoxy-5α- and 5,6β-Epoxy-5β-cholestan-3-ones (17 and 18)

5,6α-Epoxy-5α-cholestan-3-one (**17**) was prepared from 5,6α-epoxy-5α-cholestan-3β-ol by Pfitzner and Moffatt's oxidation method (37). To a solution of 5,6α-epoxy-5α-cholestan-3β-ol (1.209 g, 3 mmol), dimethyl sulfoxide (5 mL), benzene (10 mL), pyridine (0.24 mL), and dicyclohexylcarbodiimide (1.85 g) was added 0.12 mL of trifluoroacetic acid with swirling. The mixture was allowed to stand overnight at room temperature. Water (ca. 25 mL) was added to the yellowish mixture and the insoluble dicyclohexylurea was removed by filtration. The organic phase was then extracted with water (50 mL × 6), dried over sodium sulfate, and evaporated. The residue was dissolved in ether and a small amount of precipitate was filtered. After evaporation of the solvent, the crude product was twice recrystallized from ethanol to give 624 mg of 5,6α-epoxy-5α-cholestan-3-one **17** (first crop) (52%); mp 120–121.5°C (lit. (38) mp 122–123°C); ir: 1720 cm⁻¹; nmr (pyridine-d_5) δ: 3.24 (d, 1H, J = 15 Hz, 4α-H), 2.87 (d, 1H, J = 4 Hz, 6β-H), 1.28 (19-H), and 0.65 (18-H) (39).[3]

The hydrogenation of this ketone **11** (100 mg) was carried out with U-Ni-A (prepared from 1 g of precipitated nickel) in cyclohexane (3 mL) at 35°C for 3 h under a pressure of 100 kg/cm². The oily material formed was chromatographed on silica gel (15 g) with hexane–ether (9:1). The first fraction gave 5,6α-epoxy-5α-cholestan-3α-ol (**19**) in a yield of 53 mg (52%); mp 120–121°C (lit. (41) mp 122–123°C); ir: 3550, 1050, 1020, 1010, and 940 cm⁻¹; nmr (pyridine-d_5) δ: 3.95 (broad, 1H, $W_{1/2}$ ca. 8 Hz, 3β-H), 2.74 (d, 1H, J = 4 Hz, 6β-H), 1.01 (19-H), and 0.61 (18.H).[3] The subsequent fractions gave a yellow oil, which was found to be a mixture of several compounds by gas chromatography.

According to the same procedure as described above, 5,6β-epoxy-5β-cholestan-3-one (**18**)[4] was obtained by the oxidation of 5,6β-epoxy-5β-cholestan-3β-ol (605 mg, 1.5 mmol). The yield of first crop was 214 mg (36%); mp 128–129°C; ir: 1720 cm⁻¹;

[3]The calculated values of chemical shifts of 19-H for 5α,6α-epoxy ketone and 5α,6α-epoxy-3α-ol by Zürcher's method (ref. 40) are 1.267 and 1.025 ppm respectively. The parameters of 18-H for 5,6-epoxides are not given in the literature.

[4]Only a limited number of papers have reported that 5,6β-epoxy-5β-cholestan-3-one is detectable in the mixture resulting from the epoxidation of 5-cholesten-3-one with *m*-chloroperbenzoic acid. The practical preparation of this compound does not appear to have been described (ref. 42).

nmr[5] (pyridine-d_5) δ: 3.03 (d, 1H, J = 15 Hz, 4β-H), 2.90 (d, 1H, J = 2.5 Hz, 6α-H), 1.08 (19-H), and 0.62 (18-H). *Anal.* calcd. for $C_{27}H_{44}O_2$: C 80.94, H 11.07; found: C 80.97, H 10.95.

The hydrogenation of β-epoxy ketone **18** (100 mg) was performed under the same conditions as in the case of the α-epoxy ketone. The crude crystalline product with mp 127–128°C was recrystallized from acetone–methanol (1:1) to give 97.6 mg of 5β-cholestane-3α,6β-diol (**20**) (ca. 97%); mp 142–143.5°C (lit. (43) mp 134–136°C); ir: 3470, 1090, 1062, 1038, 1019, and 965 cm^{-1}; nmr[6] δ: 3.70 ($W_{1/2}$ ca. 8 Hz, 6α-H), 3.50 ($W_{1/2}$ ca. 15 Hz, 3β-H), 1.11 (19-H), and 0.68 (18-H).

Acknowledgments

We are grateful to Miss Akiko Kono for the syntheses of 5,6-epoxy ketones. Thanks are also due to Miss Ritsuko Omachi for the preparation of 5α-cholestan-2-one.

1. L. RUZICKA and M. W. GOLDBERG. Helv. Chim. Acta, **19**, 1407 (1936).
2. M. ISHIGE and M. SHIOTA. Synthesis, 171 (1973).
3. M. ISHIGE and M. SHIOTA. Can. J. Chem. **53**, 1700 (1975).
4. M. ISHIGE, M. SHIOTA, and F. SUZUKI. Can. J. Chem. **54**, 2581 (1976).
5. S. NISHIMURA, M. ISHIGE, and M. SHIOTA. Chem. Lett. 535 (1977).
6. S. NISHIMURA, M. ISHIGE, and M. SHIOTA. Chem. Lett. 963 (1977).
7. (*a*) Y. M. Y. HADDAD, H. B. HENBEST, J. HUSBANDS, and T. R. B. MITCHELL. Proc. Chem. Soc. 361 (1964); (*b*) P. A. BROWN and D. N. KIRK. J. Chem. Soc. C, 1653 (1969); (*c*) J. C. ORR, M. MERSEREAU, and A. SANFORD. J. Chem. Soc. Chem. Commun. 162 (1970); (*d*) H. B. HENBEST and A. ZURQIYAH. J. Chem. Soc. Perkin Trans. I, 604 (1974).
8. R. CONTRERAS and L. MENDOZA. Steroids, **34**, 121 (1979).
9. D. H. R. BARTON. J. Chem. Soc. 1027 (1953).
10. J. H. BREWSTER. J. Am. Chem. Soc. **76**, 6361 (1954).
11. R. L. AUGUSTINE. Catalytic hydrogenation. Marcel Dekker, Inc., New York. 1965. pp. 86–87.
12. R. E. MARKER, T. S. OAKWOOD, and H. M. CROOKS. J. Am. Chem. Soc. **58**, 481 (1936).
13. R. E. MARKER, O. KAMM, T. S. OAKWOOD, and J. F. LAUCIUS. J. Am. Chem. Soc. **58**, 1948 (1936).
14. PL. A. PLATTNER and W. LANG. Helv. Chim. Acta, **27**, 1872 (1944).
15. C. W. SHOPPEE and G. H. R. SUMMERS. J. Chem. Soc. 687 (1950).
16. B. BELLEAU and T. F. GALLAGHER. J. Am. Chem. Soc. **73**, 4458 (1951).
17. W. G. DAUBEN and J. F. EASTHAM. J. Am. Chem. Soc. **73**, 4463 (1951).
18. R. B. CLAYTON, H. B. HENBEST, and M. SMITH. J. Chem. Soc. 1982 (1957).
19. K. D. BINGHAM, T. M. BLAIKLOCK, R. C. B. COLEMAN, and G. D. MEAKINS. J. Chem. Soc. C, 2330 (1970).
20. Y. HOUMINER. J. Org. Chem. **40**, 1361 (1975).
21. E. J. COREY, K. C. NICOLAOU, M. SHIBASAKI, Y. MACHIDA, and C. S. SHINER. Tetrahedron Lett. 3183 (1975).
22. S. NISHIMURA. Nippon Kagaku Zasshi, **77**, 340 (1956).
23. (*a*) E. J. GOLLER. J. Chem. Educ. **51**, 182 (1974); (*b*) E. C. ASHBY and J. T. LAEMMLE. Chem. Rev. **75**, 521 (1975); (*c*) D. C. WIGFIELD. Tetrahedron, **35**, 449 (1979).
24. (*a*) W. G. DAUBEN, G. J. FONKIN, and D. S. NOYCE. J. Am. Chem. Soc. **78**, 2579 (1956); (*b*) W. G. DAUBEN, E. J. BLANZ, J. JIU, and R. A. MICHELI. J. Am. Chem. Soc. **78**, 3752 (1956).
25. (*a*) J.-M. CENSE. Tetrahedron Lett. 2153 (1972); (*b*) P. R. JONES, E. J. GOLLER, and W. J. KAUFFMAN. J. Org. Chem. **34**, 3566 (1969); (*c*) R. RICKBORN and M. T. WUESTHOFF. J. Am. Chem. Soc. **92**, 6894 (1970); (*d*) M. CHÉREST, H. FELKIN, and C. FRAJERMAN. Tetrahedron Lett. 379 (1971); (*e*) M. CHÉREST and H. FELKIN. Tetrahedron Lett. 383 (1971).
26. E. L. ELIEL and Y. SENDA. Tetrahedron, **26**, 2411 (1970).
27. P. GENESTE, G. LAMATY, and J.-P. ROQUE. Tetrahedron Lett. 5007 (1970).
28. (*a*) E. C. ASHBY, S. H. YU, and P. V. ROLING. J. Org. Chem. **37**, 1918 (1972); (*b*) W. T. WIPKE and P. GUND. J. Am. Chem. Soc. **98**, 8107 (1976); (*c*) G. D. MEAKINS, R. K. PERCY, E. E. RICHARDS, and R. N. YOUNG. J. Chem. Soc. C, 1106 (1968).
29. (*a*) P. MÜLLER and J. C. PERLBERGER. J. Am. Chem. Soc. **97**, 6862 (1975); (*b*) P. MÜLLER and J. C. PERLBERGER. J. Am. Chem. Soc. **98**, 8407 (1976); (*c*) P. MÜLLER and J. C. PERLBERGER. Helv. Chim. Acta, **59**, 1880 (1976); (*d*) J. C. PERLBERGER and P. MÜLLER. J. Am. Chem. Soc. **99**, 6316 (1977).
30. W. T. WIPKE and P. GUND. J. Am. Chem. Soc. **96**, 299 (1974); **98**, 8107 (1976).
31. M. CHÉREST and H. FELKIN. Tetrahedron Lett. 2205 (1968).
32. C. W. SHOPPEE. J. Chem. Soc. 1138 (1946).
33. Org. Synth. Coll. Vol. II. 1943. pp. 191–193.
34. D. H. EVANS and G. H. R. SUMMERS. J. Chem. Soc. 4821 (1956).
35. R. M. DODSON and B. RIEGEL. J. Org. Chem. **13**, 424 (1948).
36. A. J. FUDGE, C. W. SHOPPEE, and G. H. R. SUMMERS. J. Chem. Soc. 958 (1954).
37. K. E. PFITZNER and J. G. MOFFATT. J. Am. Chem. Soc. **87**, 5661 (1965); **87**, 5670 (1965).
38. B. ELLIS and V. PETROW. J. Chem. Soc. 4417 (1956).
39. A. D. CROSS. J. Am. Chem. Soc. **84**, 3206 (1962).
40. R. F. ZÜRCHER. Helv. Chim. Acta, **46**, 2054 (1963).
41. PL. A. PLATTNER, A. FÜRST, F. KOLLER, and H. H. KUHN. Helv. Chim. Acta, **37**, 258 (1954).
42. (*a*) Y. HOUMINER. J. Chem. Soc. Perkin Trans. I, 1663 (1975); (*b*) R. B. D. DE LA MARE and R. D. WILSON. J. Chem. Soc. Perkin Trans. II, 975 (1977).
43. Y. URUSHIBARA and K. MORI. Bull. Chem. Soc. Jpn. **31**, 1068 (1958).

[5]The chemical shift of 19-H for 5β,6β-epoxy ketone is calculated at 1.067 ppm.

[6]For 5β-cholestane-3α,6β-diol, the calculated chemical shifts of 19-H and 18-H are 1.108 and 0.692 ppm respectively.

Can. J. Chem. Downloaded from www.nrcresearchpress.com by 210.87.254.105 on 09/05/12
For personal use only.

Structural determination of the capsular polysaccharide of *Streptococcus pneumoniae* type-19 (19F)[1,2]

HAROLD J. JENNINGS, KARL-GUNNAR ROSELL, AND DENNIS J. CARLO

Division of Biological Sciences, National Research Council of Canada, Ottawa, Ont., Canada K1A 0R6

AND

Applied Microbiology Department, Merck Sharp and Dohme, Rahway, NJ 07065, U.S.A.

Received November 8, 1979

HAROLD J. JENNINGS, KARL-GUNNAR ROSELL, and DENNIS J. CARLO. Can. J. Chem. **58**, 1069 (1980).

The structure of the *Pneumococcus* type-19 (19F) capsular polysaccharide has been reinvestigated using nmr spectroscopy. It is composed of residues of 2-acetamido-2-deoxy-D-mannose, D-glucose, L-rhamnose, and phosphate in the molar ratio of 1:1:1:1. The polysaccharide is linear and is composed of the above components in a repeating unit of the following structure: →4)-β-D-ManNAc*p*-(1→4)-α-D-Glc*p*-(1→2)-α-L-Rha*p*-(1-PO_4^-)→.

HAROLD J. JENNINGS, KARL-GUNNAR ROSELL et DENNIS J. CARLO. Can. J. Chem. **58**, 1069 (1980).

On a étudié de nouveau la structure du polysaccharide capsulaire *Pneumococcus* type 19 (19F) en utilisant la rmn. Il est composé d'unités d'acétamido-2 déoxy-2 D-mannose, de D-glucose, de L-rhamnose et de phosphate dans un rapport molaire de 1:1:1:1. Le polysaccharide est linéaire et le monomère contient les constituants mentionnés ci-dessus dans la séquence suivante: →4)-β-D-ManNAc*p*-(1→4)-α-D-Glc*p*-(1→2)-α-L-Rha*p*-(1-PO_4^-)→.

[Traduit par le journal]

Introduction

The pneumococcal polysaccharides have recently assumed importance due to their use in a multivalent vaccine against pneumococcal infections (1, 2). Because of the diversity of pneumococcal types the choice of capsular polysaccharides used in the vaccine was based on serological surveys of the most prevalent types among pneumococcal isolates (2). However most of these surveys have been carried out using typing sera which do not differentiate between cross-reacting types (3). Types 19 (19F) and 57 (19A) are in this category, being highly cross-reactive and both being implicated in pneumococcal infections (3, 4). Component analysis has revealed that type 19 (19F) contains 2-acetamido-2-deoxy-D-mannose, D-glucose, L-rhamnose, and phosphate (4, 5), whereas type 57 (19A) contains the former plus 2-acetamido-2-deoxy-D-glucose and D-galactose as additional components (4). The structural basis for this cross-reaction is of special interest for vaccine production (3) and is probably based on a structural unit involving the components common to both types. We now report the complete structural elucidation of the type 19 (19F) polysaccharide which was accomplished using ^{13}C and ^{1}H nmr spectroscopic techniques. Some preliminary structural features of this polysaccharide have been previously published (5, 6).

Experimental

Materials

Pneumococcal capsular polysaccharide type 19 (19F) was prepared from pneumococcal strains obtained from Robert Austrian and the capsular type of the strain was confirmed by quellung reactions with factor antisera from the SSI by Robert Austrian, University of Pennsylvania. The organisms were grown in a fermenter and the polysaccharides were extracted and purified as previously described (4). Alkaline phosphatase (calf intestine, 2-8 unit/mg) was obtained from Schwarz/Mann, Orangeburg, NY.

General Methods

Solutions were concentrated under reduced pressure below 50°C. Optical rotations were determined on a Perkin-Elmer 141 instrument with 10 mm semi-micro cells at 23±1°C. Gas liquid chromatography (gc) was performed on a Hewlett-Packard 5830A instrument equipped with a flame ionization detector and a model 18850A electronic integrator. The glass columns (180 × 0.15 cm) used contained the following liquid phases on 100–200 mesh gas Chromosorb Q: (*i*) 3% ECNSS-M at 190°C for alditol acetates and at 170°C for partially methylated alditol acetates, (*ii*) 3% OV-17 at 190°C for amino-sugar derivatives, (*iii*) 3% OV-1 at 230°C for permethylated oligosaccharide derivatives, and (*iv*) 1% ECNNS-M from 160–220°C at 3°C per min for alditol acetates. Combined gas liquid chromatography – mass spectrometry (gc–ms) was carried out on a Finnigan 3100D instrument using the above columns and an ionization potential of 70 eV.

The ^{13}C nmr spectra were recorded in 10 mm tubes at 37°C on a Varian CFT20 spectrometer operating at 20 MHz in the pulsed Fourier transform mode with complete proton decoupling. Chemical shifts are reported in parts per million (ppm) downfield from external tetramethylsilane and the ^{2}H resonance of deuterium oxide was used as a field-frequency lock signal. The samples were run as deuterium oxide solutions at concentrations of approximately 50 mg per mL.

The ^{1}H nmr spectra were measured at 85°C on a Varian CFT 20 spectrometer operating in the pulsed Fourier transform mode. Samples were lyophylised (×2) from 99.7% D_2O and run

[1]NRCC No. 18170.

[2]The U.S. system of nomenclature is used throughout followed in some cases by the Danish equivalent in brackets.

0008-4042/80/111069-06$01.00/0

©1980 National Research Council of Canada/Conseil national de recherches du Canada

Can. J. Chem. Downloaded from www.nrcresearchpress.com by 210.87.254.105 on 09/05/12
For personal use only.

Can. J. Chem. Downloaded from www.nrcresearchpress.com by 210.87.254.105 on 09/05/12
For personal use only.

in the same solvent. The apparent first-order coupling constants (Hz) were measured directly and the chemical shifts (δ) are expressed relative to internal sodium 3-trimethylsilylpropionate-2,2,3,3-d_4.

Analytical Methods

Analyses for amino sugar were performed using a Technicon Autoanalyser in which the hydrolysates were first incubated with alkaline phosphatase. Acid hydrolysis of the polysaccharide was carried out using 4 *M* HCl at 100°C, at intervals between 4 and 24 h and the total 2-amino-2-deoxy-mannose content was determined by extrapolation to zero time. Phosphorus was determined by the method of Chen *et al.* (7).

Monosaccharide Composition

The polysaccharide (5 mg) was hydrolysed with 2 *N* HCl in a sealed ampoule for 4 h at 100°C. The HCl was removed by codistillation from water and the resultant residue was divided into two equal parts. One part was deaminated (8) with water (0.6 mL), acetic acid (1.0 mL), and 5% aqueous sodium nitrite (1.0 mL) for 1 h at room temperature. During these conditions the 2-amino-2-deoxy-D-mannose was converted to D-glucose (9). The solution was passed through a Dowex 50 (H+) ion-exchange column and lyophylised. The aldoses were then converted to alditol acetates (10) and analysed by gc–ms analysis using column (*i*). The remaining part of the residue was subjected to the same procedures as above, omitting the deamination step.

Some previous glycose analyses were also performed both with and without deamination as described above except for the use of milder acidic conditions (0.25 *M* H_2SO_4 at 100°C for 16 h).

Methylation Analysis

The polysaccharide (3 mg) was methylated with methyl iodide in the presence of methyl sulfinyl anion according to the method of Hakomori (11). The methylated product was recovered by partitioning the reaction mixture between water and chloroform and the chloroform phase was concentrated to dryness. The permethylated polysaccharide was treated with 90% formic acid at 100°C for 2 h and the hydrolysate was concentrated to dryness following which the residue was further hydrolysed with 0.25 *M* H_2SO_4 at 100°C for 16 h. Following neutralisation ($BaCO_3$) and filtration, the hydrolysate was concentrated to dryness. The residual partially methylated reducing sugars were converted into partially methylated alditol acetate derivatives which were analysed by gc–ms analysis (12,13) using columns (*i*) and (*ii*). An identical procedure was used for the methylation analysis of the trisaccharide alditol except that prior to acid hydrolysis some of the permethylated trisaccharide alditol was subjected directly to gc–ms analysis using column (*iii*).

Partial Hydrolysis of the Polysaccharide

The type 19 polysaccharide (80 mg) of $[\alpha]_D$ +41° (*c*, 0.5 in water) was treated with 0.1 *M* HCl (5 mL) at 100°C for 20 min. After neutralization with 1 *M* NaOH the solution was concentrated to small volume and applied to a Sephadex G-25 column (90 × 2 cm) and eluted with water. Monitoring of the eluate using a Waters Associates differential refractometer (model R 403) and by treating portions of the eluate with phenol–H_2SO_4 (14) yielded one single phosphorylated trisaccharide component of $[\alpha]_D$ +55° (*c*, 1.0 in water) which contained 5.2% P. The phosphorylated trisaccharide was treated with $NaBH_4$ (100 mg) and the solution was left for 3 h at room temperature. The solution was then neutralized with acetic acid and the resultant phosphorylated trisaccharide alditol was purified by the application of this concentrated solution to a Sephadex G-25 column as described above. The phosphorylated trisaccharide alditol was treated with alkaline phosphatase (5 mg) in 0.1 *M* $(NH_4)_2CO_3$ (3 mL) at pH 9.0 for 5 days at 37°C. The solution was extracted with 90% aqueous phenol at room temperature and following centrifugation to promote phase separation the aqueous layer was removed. A further aqueous layer was obtained using identical procedures following an additional aqueous washing of the phenol layer using an equal volume of water. The two aqueous layers were combined, concentrated to small volume and the resultant dephosphorylated trisaccharide alditol was purified by the application of this concentrated solution to a Sephadex G-25 column as previously described. The resultant lyophylised material contained only 0.1% P.

Configuration of Glycosidic Linkages

The trisaccharide alditol (10 mg) was acetylated with pyridine – acetic anhydride (1:1) (1 mL) for 4 h at 90°C. After evaporation to dryness the product was purified on a Sephadex LH 20 column (25 × 2 cm) using chloroform–acetone (2:1) as eluant. The eluate was monitored by using chloroform–methanol (6:1) as the irrigant.

The peracetylated trisaccharide alditol was then dissolved in acetic anhydride (1 mL) and oxidized with chromic acid (100 mg) essentially by previously described methods (15,16). After 1 h at 50°C in an ultrasonic bath, water (4 mL) was added to the cooled reaction mixture and the product was recovered by chloroform extraction (3 × 5 mL). The combined chloroform extracts were then concentrated to dryness and hydrolysed with 0.5 *M* trifluoroacetic acid (1 mL) for 16 h at 100°C. The resulting sugars were converted into alditol acetates and analysed by gc–ms using column (*iv*).

Results and Discussion

Analyses of the type 19 polysaccharide demonstrated that it contained 2-acetamido-2-deoxy-D-mannose, D-glucose, L-rhamnose, and phosphate in the molar ratio of 1:1:1:1 thus indicating that it is composed of a trisaccharide repeating unit. These sugar components have been previously identified in a type 19 pneumococcal polysaccharide (5, 6), although the particular strain of the type 19 organism used in these experiments was not mentioned. Hydrolyses performed using strongly acidic conditions (2 *N* HCl) with and without deamination yielded a glucose/rhamnose molar ratio of 2:1 and 1:1 respectively, the additional glucose in the former experiment originating from the deamination of the 2-amino-2-deoxy-D-mannose residue (9). All hydrolyses using milder acidic conditions gave lower glucose contents due to the acid-stability of the amino–sugar linkage and thus indicated that 2-acetamido-2-deoxy-D-mannose was probably linked glycosidically to the glucose residue.

Methylation of the type 19 polysaccharide and subsequent hydrolysis of the permethylated product yielded equal proportions of 2,3,6-tri-*O*-methyl-D-glucopyranose and 3,4-di-*O*-methyl-L-rhamnopyranose identified as their alditol acetate derivatives by gc–ms (12). This indicated the presence of both 2-linked rhamnopyranose and 4-linked glucopyranose residues in the polysaccharide. The methylated mannosamine derivative was not detected in this analysis due to the presence of a

Can. J. Chem. Downloaded from www.nrcresearchpress.com by 210.87.254.105 on 09/05/12
For personal use only.

retained phosphate substituent. However, this derivative was detected in the methylation analysis of the reduced dephosphorylated trisaccharide originally obtained by the partial acid hydrolysis of the polysaccharide.

Methylation of the trisaccharide alditol ($NaBD_4$ reduced) and subsequent gc–ms analysis of the permethylated produce indicated a single component which gave a fragmentation pattern in its mass spectrum consistent with the structure shown in Fig. 1. The following fragments with their relative intensities (in brackets) were obtained: *m/e* 45(61), 46(18), 59(100), 71(57), 48(43), 88(64), 101(48), 103(21), 111(23), 115(38), 129(59), 134(21), 142(39), 155(21), 174(4), 196(3), 206(32), 228(18), 260(3). The sequence of the sugars in the reduced trisaccharide was divulged by the masses 206 and 260 which are indicative of the rhamnopyranose and 2-acetamido-2-deoxy-D-mannopyranose being situated at the reducing and non-reducing end respectively of the original trisaccharide repeating unit of the polysaccharide. This structure was also confirmed by hydrolysis of the permethylated trisaccharide alditol which yielded 1,3,4,5-tetra-*O*-methyl-L-rhamnitol, 2,3,6-tri-*O*-methyl-D-glucose, and 2-deoxy-3,4,6-tri-*O*-methyl-2-(*N*-methylacetamido)-D-mannopyranose. The mode of linkage of the phosphate diester to the trisaccharide repeating unit and the configuration of the other linkages was determined by ^{13}C and ^{1}H nmr spectroscopy.

The ^{13}C nmr spectrum of the type 19 polysaccharide is shown in Fig. 2 and indicates that it is composed of a trisaccharide phosphate repeating unit depicted in Fig. 2. Some of the assigned chemical shifts for the polysaccharide and the reduced trisaccharide repeating units are listed in Table 1, together with $^{13}C—^{31}P$ coupling constants. The three anomeric signals of the polysaccharide at 95.1, 98.9, and 100.6 ppm were assigned to C-1″,

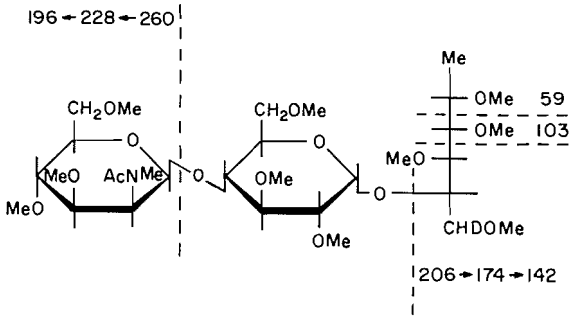


FIG. 1. Reduced methylated oligosaccharide obtained from the type 19 polysaccharide and some characteristic fragments in the mass-spectrum.

TABLE 1. Carbon-13 chemical shifts of the type 19 pneumococcal polysaccharide and the phosphorylated and dephosphorylated reduced trisaccharide repeating units[a]

	C-1	C-1′	C-1″	C-2	C-2″	C-4′	C-5	C-6	C-6′	CH_3	CH_3 $NHCOCH_3$	C=O $NHCOCH_3$
Native polysaccharide	98.9	100.6	95.1 (5.3)[b]	54.3	78.1 (8.7)[c]	79.9	76.8 (4.6)[c]	61.6[d]	61.0[d]	17.8	23.2	176.7
Reduced phosphorylated trisaccharide	98.4	100.6	60.8[d]	53.8	79.0	79.8	77.0 (—)[e,f]	61.6[d]	61.1[d]	19.9	23.2	176.5
Reduced dephosphorylated trisaccharide	98.4	100.6	60.6[d]	54.4	79.0	79.8	77.9	61.6[d]	61.1[d]	19.8	23.0	176.6

[a]In ppm from external tetramethylsilane.
[b]$^2J(^{31}P—^{13}C)$.
[c]$^3J(^{31}P—^{13}C)$.
[d]Tentative assignments.
[e]Not resolved.

Can. J. Chem. Downloaded from www.nrcresearchpress.com by 210.87.254.105 on 09/05/12
For personal use only.

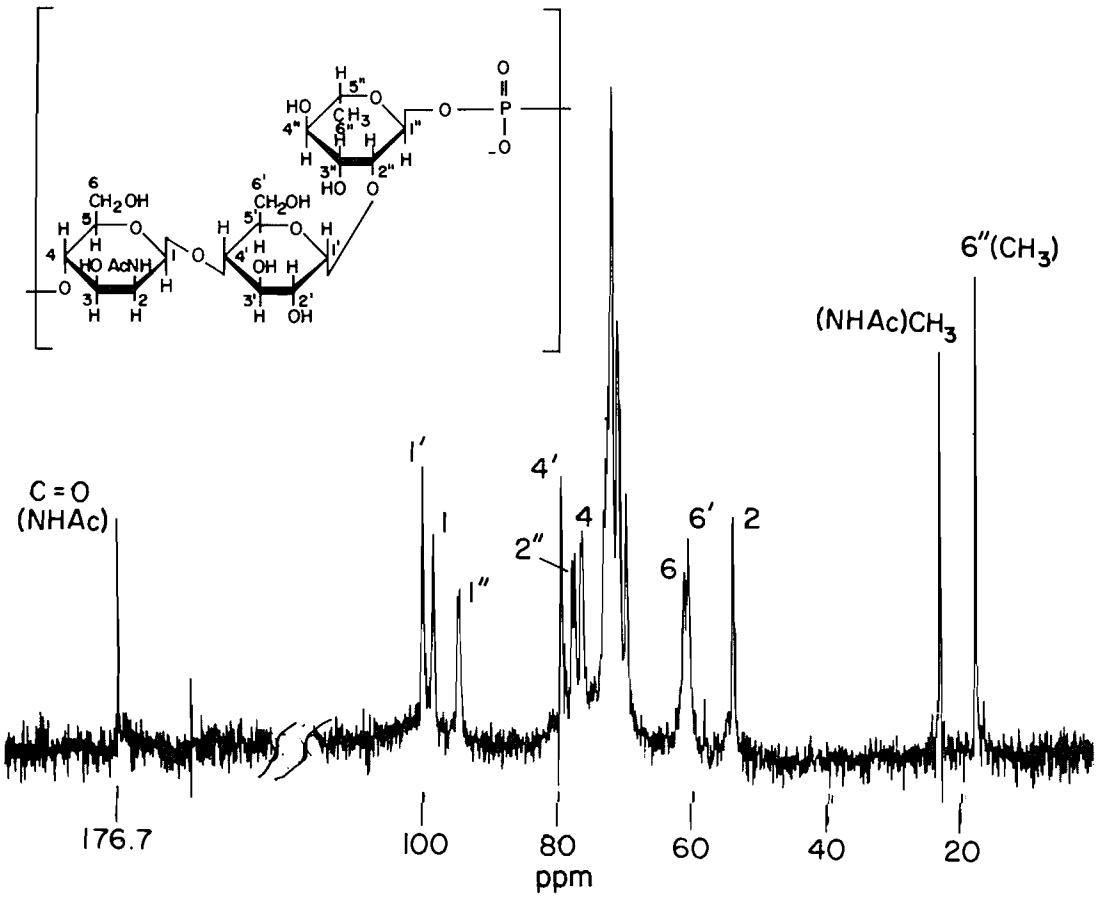


FIG. 2. Fourier-transformed ^{13}C nmr spectrum of the native type 19 pneumococcal polysaccharide taken with an aquisition time of 0.5 s and spectral width of 4 kHz. The number of free induction decays was 114 000. Inset: The repeating unit of the type 19 polysaccharide.

C-1, and C-1′ respectively on the following evidence. Because of $^{13}C—^{31}P$ coupling the signal at 95.1 ppm was assigned to C-1″ ($^2J_{C\text{-}1'',P} = 5.6$ Hz) of the rhamnopyranose residue and confirmation of this assignment was obtained when this C-1″ signal was changed from a doublet to an uncoupled singlet at 61.0 ppm in the ^{13}C nmr spectrum of the trisaccharide with the reduced rhamnopyranose endgroup. On the basis of the previous assignments (17) the signal at 100.6 ppm was assigned to C-1′ of the α-D-glucopyranose residue and by difference the remaining anomeric signal at 98.9 ppm could be assigned to C-1 of the 2-acetamido-2-deoxy-D-mannopyranose residue.

That the phosphate diester was linked to C-4 of the 2-acetamido-2-deoxy-D-mannopyranose residue could be deduced from the ^{13}C nmr spectrum of the polysaccharide. The presence of two exocyclic hydroxymethyl signals at 61.6 and 61.0 ppm indicated that C-6 is unsubstituted (18) and the fact that in comparison with monomer models (19) C-2 is not significantly shielded and is not involved in $^3J_{C\text{-}2,P}$ coupling eliminates the possibility of a 3-linkage. Of the two $^{13}C—^{31}P$ coupled signals in the linkage region of the ^{13}C nmr spectrum of the polysaccharide (Fig. 2) at 78.1 and 76.8 ppm, the former was assigned to C-2″ of the rhamnopyranose residue ($^3J_{C\text{-}2'',P} = 8.7$ Hz) because this doublet was shifted to an uncoupled singlet at 79.0 ppm in the ^{13}C nmr spectrum of the phosphorylated reduced trisaccharide (Table 1). In contrast the coupled signal at 76.8 ppm remained virtually unchanged in both the above ^{13}C nmr spectra and therefore it could be attributed to a $^{13}C—^{31}P$ coupled signal of one of the carbons of the 2-acetamido-2-deoxy-D-mannopyranose residue. Although this latter residue is known to be linked at C-4 it was deduced that the low-field signal at 76.8 ppm could not be attributed to C-4 but could be assigned to the unlinked C-5 of the same residue. This was because this signal which had remained virtually unchanged in the ^{13}C nmr spectra of both

Can. J. Chem. Downloaded from www.nrcresearchpress.com by 210.87.254.105 on 09/05/12
For personal use only.

polysaccharide and the phosphorylated reduced trisaccharide became an uncoupled singlet which had undergone a characteristic small downfield shift (1.1 ppm) in the ^{13}C nmr spectrum of the dephosphorylated reduced trisaccharide (Table 1). Had this signal been associated with the linkage carbon (C-4) one would have expected a substantial upfield shift (approximately 4 ppm) in this carbon on dephosphorylation based on chemical shift differences between the related 2-acetamido-2-deoxy-D-glucopyranose (19) and its 4-phosphate derivative (20). That this signal at 77.9 ppm in the ^{13}C nmr spectrum of the dephosphorylated reduced trisaccharide is due to C-5 of the non-reducing terminal 2-acetamido-2-deoxy-mannopyranose residue is only consistent with this residue being in the β-D-configuration because it has been established using monomer models (19) that C-5 of this residue in the α-D-configuration would be more shielded and thus would occur at a higher field position (73.2 ppm) in the ^{13}C nmr spectrum. The assignment of the β-D-configuration to the 2-acetamido-2-deoxy-mannopyranose residue is also consistent with the results of chromic acid oxidation of the peracetylated dephosphorylated reduced trisaccharide where the above residue was destroyed leaving only the glucose and rhamnitol residues in a 1:1 ratio as determined by gc analysis. It has been previously demonstrated that pyranose sugars in which the aglycone is in an equatorial position (β-D-configuration) are readily oxidized while those in an axial position (α-D-configuration) are not (16). This result also confirmed the assignment of the α-D-configuration to the glucopyranose residue. Yadomae *et al.* (6) using ^{13}C nmr spectroscopy have also recently established the β-D-configuration of the non-reducing terminal 2-acetamido-2-deoxy-mannopyranose residue of a disaccharide obtained from the type 19 polysaccharide. The remaining uncoupled signal in the linkage region of the ^{13}C nmr spectrum of the type 19 polysaccharide at 79.9 ppm could be assigned to C-4′ of the α-D-glucopyranose residue which is consistent with previous assignments on other 4-linked α-D-glucopyranose residues (17). In addition, because this residue is the middle residue of the trisaccharides obtained from the type 19 polysaccharide, the uncoupled signal at 79.9 ppm remains virtually unchanged in the ^{13}C nmr spectra of the polysaccharide and both the phosphorylated and dephosphorylated reduced trisaccharides (Table 1).

The remaining assignment of the anomeric configuration of the L-rhamnopyranose residues of the type 19 polysaccharide could not be deduced from chemical shift data because of the lack of sensitivity of the anomeric signals of glycopyranoses in the *manno*-configuration (21, 22). That these rhamnopyranose residues were in the α-L-configuration was indicated by an increase in specific rotation when the polysaccharide of $[\alpha]_D$ +41° was hydrolysed to the phosphorylated trisaccharide of $[\alpha]_D$ +55°. Such a positive increase is due to the newly formed β-L-rhamnopyranose residues in the resultant equilibrium mixture of trisaccharides with reducing rhamnose residues (23). Also the ^1H nmr spectrum of the polysaccharide gave an anomeric signal (doublet of doublets) at δ5.68 ($J_{H\text{-}1'',H\text{-}2''}$ = 1.3 Hz) which could be assigned to the L-rhamnopyranose residue due to the presence of 3-bond $^1H—^{31}P$ coupling ($^3J_{H\text{-}1'',P}$ = 6.7 Hz). Due to their relative insensitivity to changes in anomeric configuration these coupling constants were unsatisfactory for assigning the anomeric configuration of glycopyranoses in the *manno*-configuration (24). However on the basis of studies on mannopyranosyl phosphates (24) the low-field position (δ 5.68) of the doublet of doublets is indicative of the rhamnopyranose residue having the α-L-configuration. The ^1H nmr spectrum of the polysaccharide also has two other anomeric doublets at δ 5.18 ($J_{H\text{-}1',H\text{-}2'}$ = 3.8 Hz) and δ 5.04 ($J_{H\text{-}1,H\text{-}2}$ = 1.6 Hz), the coupling constants of which are consistent with those expected for α-D-glucopyranose and 2-acetamido-2-deoxy-β-D-mannopyranose residues respectively. Thus the type 19 polysaccharide is composed of the repeating unit depicted in Fig. 2. This structure is identical to one recently proposed for the pneumococcal type 19 polysaccharide in an independent study.[3]

Acknowledgments

We wish to thank Fred Cooper for obtaining the mass-spectra.

1. P. SMIT, D. OBERHOLZER, S. HAYDEN-SMITH, H. J. KOORNHOF, and M. R. HILLEMAN. J. Am. Med. Assoc. **238**, 2613 (1977).
2. R. AUSTRIAN. J. Infect. Dis. **136**, S38 (1977).
3. J. B. ROBBINS. Immunochemistry, **15**, 839 (1978).
4. T. KRISHNAMURTHY, C-J. LEE, J. HENRICHSEN, D. J. CARLO, T. M. STOUDT, and J. B. ROBBINS. Infect. Immun. **22**, 727 (1978).
5. T. MIYAZAKI and T. YADOMAE. Carbohydr. Res. **16**, 153 (1971).
6. T. YADOMAE, N. OHNO, and T. MIYAZAKI. Carbohydr. Res. **75**, 191 (1979).
7. P. S. CHEN, J. Y. TORIBA, and H. WARNER. Anal. Chem. **28**, 1756 (1956).
8. L. V. DMITRIEV, V. L. BACKINOWSKI, V. L. LVOV, N. K.

[3]Professor T. Miyazaki. Personal communication.

KOTCHETKOV, and I. L. HOFMAN. Eur. J. Biochem. **50**, 539 (1975).
9. D. HORTON and K. D. PHILIPS. Carbohydr. Res. **21**, 417 (1972).
10. J. S. SAWARDEKER, J. H. SLONEKER, and A. R. JEANES. Anal. Chem. **37**, 1602 (1965).
11. S. HAKOMORI. J. Biochem. (Tokyo), **55**, 205 (1964).
12. B. LINDBERG. Methods Enzymol. **28B**, 178 (1972).
13. K. STELLNER, H. SAITO, and S. HAKOMORI. Arch. Biochem. Biophys. **155**, 461 (1973).
14. M. DUBOIS, K. A. GILLES, J. K. HAMILTON, P. A. REBERS, and F. SMITH. Anal. Chem. **28**, 350 (1956).
15. S. J. ANGYAL and K. JAMES. Carbohydr. Res. **12**, 147 (1970).
16. J. HOFFMAN, B. LINDBERG, and S. SVENSSON. Acta Chem. Scand. **26**, 661 (1972).
17. P. COLSON, H. J. JENNINGS and I. C. P. SMITH. J. Am. Chem. Soc. **96**, 8081 (1974).
18. H. J. JENNINGS and I. C. P. SMITH. Methods Enzymol. **50**, 39 (1978).
19. D. R. BUNDLE, H. J. JENNINGS, and I. C. P. SMITH. Can. J. Chem. **51**, 3812 (1973).
20. D. R. BUNDLE, H. J. JENNINGS, and I. C. P. SMITH. J. Biol. Chem. **249**, 2275 (1974).
21. A. S. PERLIN, B. CASU, and H. J. KOCH. Can. J. Chem. **48**, 2596 (1970).
22. P. COLSON and P. R. KING. Carbohydr. Res. **47**, 1 (1976).
23. E. FISCHER. Ber. **29**, 324 (1896).
24. J. V. O'CONNOR, H. A. NUNEZ, and R. BARKER. Biochemistry, **18**, 500 (1979).

Can. J. Chem. Downloaded from www.nrcresearchpress.com by 210.87.254.105 on 09/05/12
For personal use only.

Reactions of cyclopropylcarbinol in dilute hydrochloric acid

CHOI CHUCK LEE AND ALLAN J. CESSNA

Department of Chemistry and Chemical Engineering, University of Saskatchewan, Saskatoon, Sask., Canada S7N 0W0

Received December 5, 1979

CHOI CHUCK LEE and ALLAN J. CESSNA. Can. J. Chem. **58**, 1075 (1980).

The treatment of cyclopropylcarbinol (**1**-OH) with dilute HCl has been used as a method for the preparation of cyclobutanol (**2**-OH). While **2**-OH is the major product in this reaction, a careful investigation showed the presence of a total of 13 products, namely, the alcohols **1**-OH, **2**-OH, and allylcarbinol (**3**-OH), cyclopropylcarbinyl, cyclobutyl and allylcarbinyl chlorides (**1**-Cl, **2**-Cl and **3**-Cl, respectively), dicyclopropylcarbinyl, cyclobutyl cyclopropylcarbinyl, allylcarbinyl cyclopropylcarbinyl, dicyclobutyl and allylcarbinyl cyclobutyl ethers (**1**-O-**1**, **2**-O-**1**, **3**-O-**1**, **2**-O-**2**, and **3**-O-**2**, respectively), as well as butyraldehyde and isobutyraldehyde. The alcohols, chlorides, and ethers likely arose from reactions of the bicyclobutonium ion with available nucleophiles in the reaction mixture. The minor amounts of the two aldehydes may be due to a ring opening isomerization of 2-methylcyclopropanol, the latter in turn resulted from a net 1,3-hydride shift in the cyclopropylcarbinyl cation, probably via an edge-protonated cyclopropane-type of species. Treatment of [α-^{14}C]cyclopropylcarbinol (**1**-OH-α-^{14}C) with dilute HCl gave samples of **1**-OH-*x*-^{14}C,**2**-OH-*x*-^{14}C, and **3**-OH-*x*-^{14}C the degradation of which showed that all three methylene groups in these alcohols have become equivalent, indicating a complete equilibration between isotope-position labeled bicyclobutonium ions.

CHOI CHUCK LEE et ALLAN J. CESSNA. Can. J. Chem. **58**, 1075 (1980).

On a utilisé l'action de l'acide chlorhydrique dilué sur le cyclopropylcarbinol (OH-**1**) comme méthode de préparation du cyclobutanol (OH-**2**). Bien que l'alcool OH-**2** soit le produit majoritaire, une étude soignée indique la présence de 13 produits qui sont les alcools OH-**1**, OH-**2** et l'allylcarbinol (OH-**3**), les chlorures de cyclopropylcarbinyle, de cyclobutyle et d'allylcarbinyle (respectivement Cl-**1**, Cl-**2** et Cl-**3**), les éthers de dicyclopropylcarbinyle, de cyclobutyle et de cyclopropylcarbinyle, d'allylcarbinyle et de cyclopropylcarbinyl, de dicyclobutyle et finalement d'allylcarbinyle et de cyclobutyle (respectivement **1**-O-**1**, **2**-O-**1**, **3**-O-**1**, **2**-O-**2** et **3**-O-**2**) ainsi que le butyraldéhyde et l'isobutyraldéhyde. Les alcools, les chlorures et les éthers proviennent de la réaction entre l'ion bicyclobutonium avec les agents nucléophiles disponibles dans le mélange réactionnel. Les faibles quantités d'aldéhydes obtenues peuvent être dues à une isomérisation du produit résultant de l'ouverture du cycle du méthyl-2 cyclopropanol; ce dernier à son tour provient d'une transposition-1,3 d'hydrure dans le cation cyclopropylcarbinyle probablement par l'intermédiaire d'espèces du type cyclopropane protoné à la périphérie. L'action du HCl dilué sur le cyclopropylcarbinol[α ^{14}C] (OH-**1** α ^{14}C) donne des échantillons de OH-**1**-*x* ^{14}C, OH-**2**-*x* ^{14}C et OH-**3**-*x* ^{14}C); leur dégradation révèle que les trois groupes méthylènes de ces alcools deviennent équivalents et qu'il en résulte un équilibre complet entre les ions cyclobutonium margués par des isotopes dans certaines positions.

[Traduit par le journal]

It has been known since 1960 that the treatment of cyclopropylcarbinol (**1**-OH) with dilute HCl is a good method for the preparation of cyclobutanol (**2**-OH) (1). In our recent study on exchange reactions between cyclobutane and tritiated trifluoromethanesulfonic acid (2), we have used this method to prepare **2**-OH as a carrier to aid the identification of products after the mixture from the exchange reaction was quenched with H_2O. In the purification of **2**-OH prepared from **1**-OH (1), it was noted from vpc analysis that while **2**-OH was the main product, many other products were also present and this led us to undertake a further investigation of the reaction.

Roberts and co-workers (1) treated **1**-OH with about 1 *N* HCl to give a 72% yield of product which analyzed by vpc as 97% **2**-OH and 3% allylcarbinol (**3**-OH). In the present study, preliminary experiments were carried out to test the effect of HCl concentration on the relative compositions of **1**-OH, **2**-OH, and **3**-OH and the results are summarized in Table 1. In the subsequent work, either 1.4 or 2.0 *N* HCl was utilized.

Figure 1 shows the chromatogram from the vpc analysis of the products after **1**-OH was treated with 2.0 *N* HCl at 85°C for 1.5 h (Expt. 1). The identities of the various components and their relative yields for Expt. 1 and similar data from other experiments are given in Table 2. The identification of the various products was carried out by fractionation into broad fractions each containing several components and the individual compounds in each of these fractions were identified by nmr

TABLE 1. Relative amounts of cyclopropylcarbinol (**1**-OH), cyclobutanol (**2**-OH), and allylcarbinol (**3**-OH) from vpc analysis after treatment of **1**-OH with HCl at 85°C for 1.5 h

	Relative composition (%)		
HCl(*N*)	**1**-OH	**2**-OH	**3**-OH
0.53	31.8	63.1	5.2
0.95	8.7	84.6	6.6
1.14	5.3	88.0	6.7
1.38	2.9	90.0	7.1
1.56	2.2	90.6	7.2
1.78	1.4	91.2	7.4
1.98	1.3	91.3	7.5

0008-4042/80/111075-05$01.00/0

©1980 National Research Council of Canada/Conseil national de recherches du Canada

Can. J. Chem. Downloaded from www.nrcresearchpress.com by 210.87.254.6 on 09/05/12
For personal use only.

Can. J. Chem. Downloaded from www.nrcresearchpress.com by 210.87.254.6 on 09/05/12
For personal use only.

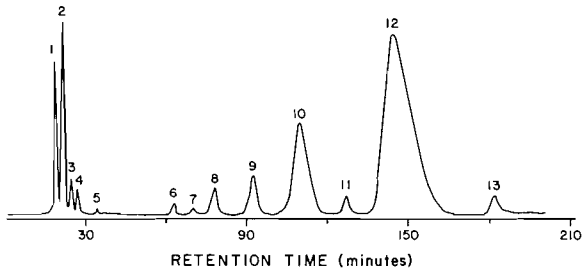


FIG. 1. Vapor phase chromatogram of products from the treatment of cyclopropylcarbinol (**1**-OH) with 2.0 *N* HCl at 85°C for 1.5 h.

and by peak reenforcement with authentic samples. The authentic samples prepared for this purpose, besides **1**-OH, **2**-OH, and **3**-OH, were the cyclopropylcarbinyl, cyclobutyl, and allylcarbinyl chlorides (**1**-Cl, **2**-Cl and **3**-Cl, respectively), dicyclopropylcarbinyl ether (**1**-O-**1**), cyclobutyl cyclopropylcarbinyl ether (**2**-O-**1**), and allylcarbinyl cyclopropylcarbinyl ether (**3**-O-**1**). Figure 2 gives the nmr spectra of these chlorides and ethers, showing the very characteristic absorptions of the cyclopropylcarbinyl, cyclobutyl, and allylcarbinyl groups.

The facile interconversion between cyclopropylcarbinyl, cyclobutyl, and allylcarbinyl cations was first reported by Roberts and Mazur (3), and these interconversions presumably proceed via the bicyclobutonium ion **4** (4). The early literature

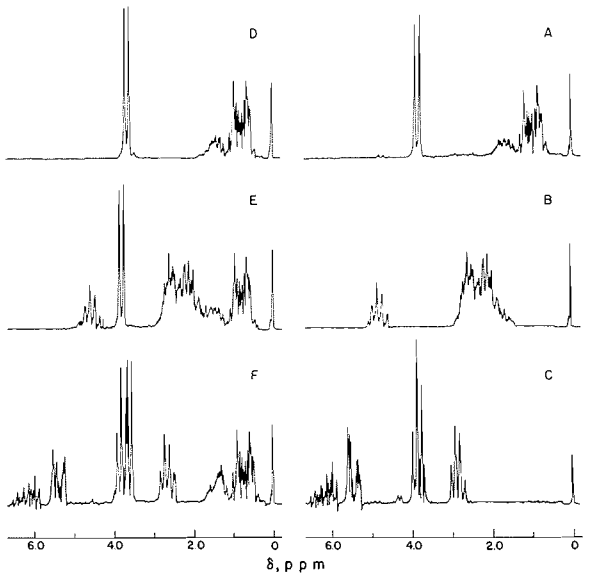
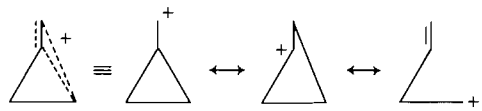


FIG. 2. ^{1}H nmr spectra, A, B, C, D, E, F, are, respectively, the spectra of cyclopropylcarbinyl chloride (**1**-Cl), cyclobutyl chloride (**2**-Cl), allylcarbinyl chloride (**3**-Cl), dicyclopropylcarbinyl ether (**1**-O-**1**), cyclobutyl cyclopropylcarbinyl ether (**2**-O-**1**), allylcarbinyl cyclopropylcarbinyl ether (**3**-O-**1**).



4

on these systems has been reviewed (5), and recent studies with low temperature ^{13}C nmr have been reported by Olah, Roberts, and their co-workers (6, 7). Most of the products given in Table 2 may be readily accounted for by reactions of **4** with available nucleophiles during the treatment of **1**-OH with dilute HCl.

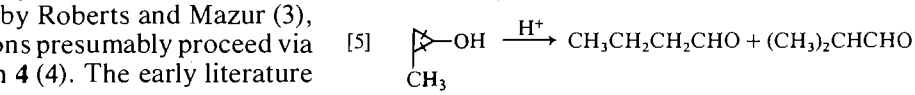
[1] $\mathbf{4} + Cl^- \longrightarrow \mathbf{1}\text{-Cl} + \mathbf{2}\text{-Cl} + \mathbf{3}\text{-Cl}$

[2] $\mathbf{4} + H_2O \xrightarrow{(-H^+)} \mathbf{1}\text{-OH} + \mathbf{2}\text{-OH} + \mathbf{3}\text{-OH}$

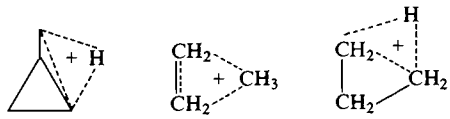
[3] $\mathbf{4} + \mathbf{1}\text{-OH} \xrightarrow{(-H^+)} \mathbf{1}\text{-O-}\mathbf{1} + \mathbf{2}\text{-O-}\mathbf{1} + \mathbf{3}\text{-O-}\mathbf{1}$

[4] $\mathbf{4} + \mathbf{2}\text{-OH} \xrightarrow{(-H^+)} \mathbf{2}\text{-O-}\mathbf{1} + \mathbf{2}\text{-O-}\mathbf{2} + \mathbf{3}\text{-O-}\mathbf{2}$

Of interest is the origin of the two other minor products, butyraldehyde and isobutyraldehyde. Since cyclopropanol is known to isomerize to propionaldehyde under hydrolytic conditions (8, 9), it is likely that these two 4-carbon aldehydes arose from acid catalyzed isomerization of 2-methylcyclopropanol (eq. [5]). This conclusion is

[5] 

supported by the observation that when an attempt was made to prepare 2-methylcyclopropanol from the treatment of 2-methylcyclopropylmagnesium bromide with O_2 followed by decomposition of the resulting complex with 2% H_2SO_4, the major products were butyraldehyde and isobutyraldehyde. The formation of 2-methylcyclopropanol would involve an overall 1,3-hydride shift in the cyclopropylcarbinyl cation. Thus it may be speculated that this suggests a possible minor involvement of edge-protonated cyclopropane **5**, and in this context **4** and **5** may be regarded as analogous to corner- and edge-protonated cyclopropanes **6** and **7**, respectively (10).



5 **6** **7**

Using isotopic labeling, various degrees of equivalence among the three methylene groups in the cyclopropylcarbinyl, cyclobutyl, and allylcarbinyl products have been observed (1, 4, 5), and these findings have been attributed to equilibra-

TABLE 2. Yields of products as measured by vpc after treatment of **1**-OH with dilute HCl

Vpc peaks[a]	Identity[b]	Relative yields (%)				
		Expt. 1[c]	Expt. 2[d]	Expt. 3[e]	Expt. 4[f]	Expt. 5[g]
1	**3**-Cl	3.1	Trace	—	Trace	Trace
2	**2**-Cl	4.1	2.8	2.8	1.0	1.5
3	$(CH_3)_2CHCHO$	0.7	0.1	—	0.5	0.3
4	**1**-Cl	0.2	0.1	0.2	0.1	0.1
5	$CH_3CH_2CH_2CHO$	0.1	Trace	—	Trace	Trace
6	**3**-O-**2**[h]	0.5	0.1	0.2	0.2	0.2
7	**3**-O-**1**	0.2	0.1	0.2	0.1	0.1
8	**2**-O-**2**[h]	2.4	1.2	1.7	0.1	0.5
9	**2**-O-**1**	3.7	1.5	0.2	0.6	1.7
10	**3**-OH	10.8	7.3	10.7	1.2	3.7
11	**1**-O-**1**	1.8	0.2	—	0.7	1.0
12	**2**-OH	70.3	83.9	82.7	19.3	61.5
13	**1**-OH	2.1	2.6	1.3	76.2	29.2

[a]As illustrated by Fig. 1.
[b]**1**-Cl, **2**-Cl, and **3**-Cl are, respectively, cyclopropylcarbinyl, cyclobutyl, and allylcarbinyl chlorides; 1-OH, 2-OH, and 3-OH are, respectively, cyclopropylcarbinol, cyclobutanol, and allylcarbinol; 1-O-1, 2-O-1, 3-O-1, 2-O-2, and 3-O-2 are, respectively, dicyclopropylcarbinyl ether, cyclobutyl cyclopropylcarbinyl ether, allylcarbinyl cyclopropylcarbinyl ether, dicyclobutyl ether, and allylcarbinyl cyclobutyl ether.
[c]In 2.0 *N* HCl at 85°C for 1.5 h.
[d]In 1.4 *N* HCl at 85°C for 1.5 h.
[e]In 1.4 *N* HCl at 85°C for 10 h.
[f]In 1.4 *N* HCl at 60°C for 2 h.
[g]In 1.4 *N* HCl at 60°C for 10 h.
[h]Tentative identification.

TABLE 3. ^{14}C distributions in the recovered cyclopropylcarbinol (**1**-OH-*x*-^{14}C), cyclobutanol (**2**-OH-*x*-^{14}C), and allylcarbinol (**3**-OH-*x*-^{14}C) after treatment of [α-^{14}C]cyclopropylcarbinol (**1**-OH-α-^{14}C) in 1.4 *N* HCl at 85°C for 1.5 h

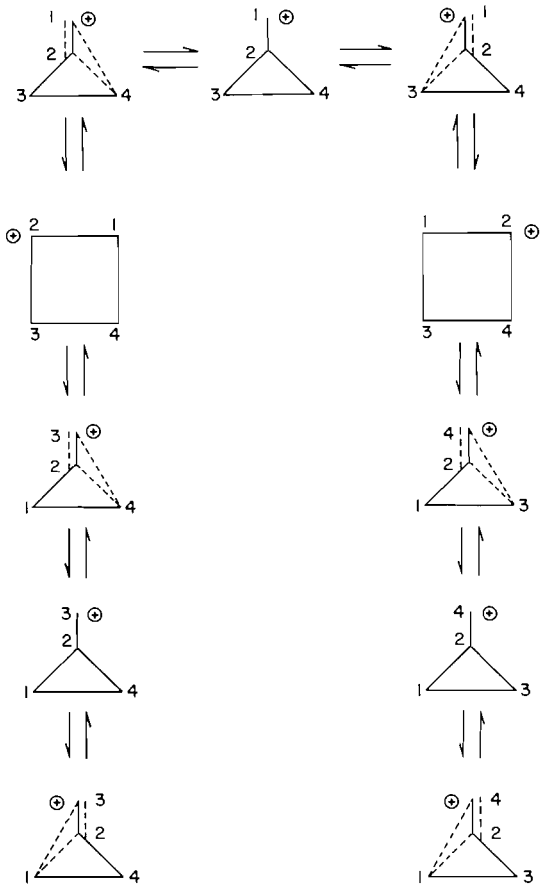
Reaction product	Degradation product	Specific activity (dpm/mmol)		^{14}C distribution (%)	
		Run 1	Run 2	Run 1	Run 2
1-OH-*x*-^{14}C		37 700	34 400	100	100
		12 300	12 000	32.6	34.9
2-OH-*x*-^{14}C		521 000	560 000	100	100
		348 000	373 000	66.8	66.6
3-OH-*x*-^{14}C		27 900	40 700	100	100
	HCHO[e]	9 230	13 700	33.1	33.7
		8 070	9 540	100	100
		5 410	6 580	67.0	69.0

[a]Analyzed as the *N*-phenylamide (anilide).
[b]Analyzed as the benzamide.
[c]Analyzed as the dibenzamide.
[d]Analyzed as the α-naphthylurethane.
[e]Analyzed as the dimedon derivative.

tions between bicyclobutonium ions as illustrated in Scheme 1 (5). In the treatment of [α-$^2H_2$]cyclopropylcarbinol (**1**-OH-α-d_2) with dilute HCl (1), it was inferred from the nmr spectrum of the cyclobutanone obtained from oxidation of the **2**-OH-d_2 product that the D-labeled methylene group was statistically distributed among the C-2, -3, -4 positions of the cyclobutanol.

In an attempt to verify the nmr results observed by Roberts and co-workers, isotopic scrambling studies using the ^{14}C-tracer technique were carried out. After [α-^{14}C]cyclopropylcarbinol (**1**-OH-α-^{14}C) was treated with 1.4 *N* HCl at 85°C for 1.5 h (conditions used in Expt. 2, Table 2), degradation by known methods (see Experimental) of the recovered **1**-OH-*x*-^{14}C, **2**-OH-*x*-^{14}C, and **3**-OH-*x*-^{14}C gave the data summarized in Table 3. These results, showing $\frac{1}{3}$ of the ^{14}C-activity on each of the three methylene groups, unequivocally demonstrated the equivalence of these methylene groups

Can. J. Chem. Downloaded from www.nrcresearchpress.com by 210.87.254.6 on 09/05/12
For personal use only.



SCHEME 1

in all three alcoholic products, thus confirming the earlier observation of Roberts and co-workers and indicating that complete equilibration as shown in Scheme 1 had taken place.

Experimental

Treatment of 1-OH with Dilute HCl

As an illustration of the experimental procedure, Expt. 1 (Table 2) is described below.

A mixture of 15.0 g (0.21 mol) of **1**-OH and 85 mL of 2.0 *N* HCl was heated at 85°C for 1.5 h. The material was then neutralized with 2.0 *N* KOH and then continuously extracted with ether for 24 h. The extract was dried over $MgSO_4$ and the ether was removed to give a residue which on vpc analysis (25 ft, $\frac{1}{8}$-inch copper column packed with 25% β,β′-oxidipropionitrile on 60/80 mesh Chromosorb P-AW) gave the chromatogram shown in Fig. 1. Subsequently, the residue was fractionated to give 2.6 g of fraction 1, bp 72–88°C, containing peaks 1 to 5 (chlorides and aldehydes), 9.8 g of fraction 2, bp 118–128°C, containing peaks 10, 12, and 13 (alcohols), and 1.8 g of fraction 3, bp 140–148°C, containing peaks 6–9 and 11 (ethers). The presence of various components in each of the three fractions was indicated by their nmr spectra and individual components were identified by peak reenforcement with authentic samples on vpc analysis. In fraction 3, peaks 7, 9, and 11, respectively, were identified as the ethers **3**-O-**1**, **2**-O-**1** and **1**-O-**1**. Since authentic samples of other possible ethers were not prepared, tentative assignments for peaks 6 and 8 were based on nmr and vpc considerations. Integration of the nmr spectrum of fraction 3 showed the presence of relatively more cyclobutyl group than was suggested by the vpc peak area of **2**-O-**1** relative to that of **1**-O-**1**. Hence the other ethers present likely contained the cyclobutyl group, and peaks 6 and 8 were assigned to **3**-O-**2** and **2**-O-**2**, respectively.

Preparation of Authentic Compounds

The alcohols, **1**-OH, **2**-OH, and **3**-OH, were prepared by previously reported methods of Roberts and co-workers, **1**-OH from the $LiAlH_4$ reduction of cyclopropanecarboxylic acid (3), **2**-OH from the vpc purified major fraction in the present work (1), and **3**-OH from $LiAlH_4$ reduction of vinylacetic acid (11). The nmr spectra of these alcohols are essentially the same as those reported by Servis and Roberts (11).

Previous preparations of **1**-Cl, such as those from the chlorination of methylcyclopropane (3) and from the reaction of **1**-OH with $SOCl_2$ (1), generally gave various mixtures of **1**-Cl, **2**-Cl, and **3**-Cl. Pure **1**-Cl was prepared in the present work by the treatment of **1**-OH in CCl_4 with triphenylphosphine (12, 13).

Triphenylphosphine (14.7 g, 56 mmol) was added in one batch to a stirred solution of 4.0 g (56 mmol) of **1**-OH in 25 ml of CCl_4. The mixture was refluxed for 2 h, cooled, and 50 mL of ether was added. After filtration and thorough washing of the solid material with more ether, the filtrate was washed with H_2O, dried over $MgSO_4$, and then fractionally distilled to give 2.5 g (51%) of product, bp 79–83°C. Vapor phase chromatographic analysis using a 10 ft, $\frac{1}{8}$-inch stainless steel column packed with 25% FFAP on Chromosorb P showed the presence of about 5% CCl_4 as impurity. After purification by preparative vpc, the **1**-Cl obtained, bp 83°C, gave the nmr spectrum shown in Fig. 2A.

In a similar way, **2**-Cl was prepared from **2**-OH, triphenylphosphine, and CCl_4 in 32% yield, bp 81–82°C (lit. (3) bp 82–83°C). Using the method described by Roberts and Mazur (3), **3**-Cl was prepared from the reaction of **3**-OH with $SOCl_2$ in the presence of pyridine; it boiled at 75°C (lit. (3) bp 73–74°C). The nmr spectra of **2**-Cl and **3**-Cl are shown in Fig. 2, B and C.

The ethers, **1**-O-**1**, **2**-O-**1**, and **3**-O-**1**, were prepared by the reaction of the appropriate alkoxide with cyclopropylcarbinyl bromide (**1**-Br), the latter being prepared from the treatment of **1**-OH with triphenylphosphine in CBr_4 (12, 13) as in the analogous preparation of **1**-Cl.

Sodium cyclopropylmethoxide was prepared by the portionwise addition of 1.84 g (80 mmol) of Na to a stirred solution of 5.0 g (70 mmol) of **1**-OH in 100 mL of anhydrous ether. After stirring for an hour, the alkoxide solution was decanted into a flask containing 9.4 g (70 mmol) of **1**-Br and fitted with a reflux condenser and a drying tube. The mixture was heated under reflux for 5 h. At this point, vpc analysis of the reaction mixture showed the presence of a substantial amount of unreacted **1**-Br. In order to raise the reaction temperature, 50 mL of dry acetone was introduced, most of the diethyl ether was removed by fractional distillation, and the remaining material was refluxed for a further 5 h when vpc analysis showed that essentially all of the **1**-Br had disappeared. The reaction mixture was then diluted with 50 mL of ether and filtered. The filtrate was washed with H_2O, dried over $MgSO_4$, and fractionated to give 4.1 g of crude product which contained about 5% **1**-OH and about 15% mesityl oxide as impurities. After purification by preparative vpc, the desired product, **1**-O-**1**, bp 148–149°C, gave the nmr spectrum shown in Fig. 2D.

In the preparation of **2**-O-**1** and **3**-O-**1**, the reaction of sodium cyclobutoxide or sodium allylmethoxide with **1**-Br was again utilized. Both reactions were carried out at about the same time and in both cases acetone rather than ether was directly used as

Can. J. Chem. Downloaded from www.nrcresearchpress.com by 210.87.254.6 on 09/05/12
For personal use only.

the initial solvent. After work-up as described in the preparation of **1**-O-**1**, it was found that the major product was mesityl oxide, derived from the condensation of acetone. Sufficient amounts of the desired products, **2**-O-**1** and **3**-O-**1**, however, were recovered from preparative vpc for subsequent peak reenforcement studies. Their nmr spectra are given in Fig. 2, E and F.

Attempted Synthesis of 2-Methylcyclopropanol (8)

By analogy with the synthesis of cyclopropanol from the reaction of the Grignard reagent with O_2 (14), an attempt was made to prepare **8** from the reaction of 2-methylcyclopropylmagnesium bromide with O_2. 2-Methylcyclopropyl bromide (8.2 g, 61 mmol), prepared as described by Kirmse and Wedel (15), was converted to the Grignard reagent in about 150 mL of anhydride ether. O_2 was then bubbled through the reaction mixture until precipitation of the white solid complex had apparently ceased. A 2% H_2SO_4 solution (75 mL) was added and the mixture was stirred overnight. Upon work-up, the major products as shown by vpc were butyraldehyde and isobutyraldehyde, presumably derived from ring opening isomerization of **8**. Unreacted 2-methylcyclopropyl bromide and some minor components were also present, but no attempt was made to identify the minor compounds.

Experiments with [α-^{14}C]cyclopropylcarbinol (1-OH-α-^{14}C)

The **1**-OH-α-^{14}C was prepared as previously described (4). To 40 mL of 1.4 *N* HCl was added 0.98 g (14 mmol) of **1**-OH-α-^{14}C and the mixture was heated at 85°C for 1.5 h. The resulting material was neutralized with dilute KOH and about 1.0 g each of ordinary **1**-OH, **2**-OH, and **3**-OH were added as carriers. After continuous extraction with ether and work-up as described earlier, the three alcohols, **1**-OH-*x*-^{14}C, **2**-OH-*x*-^{14}C, and **3**-OH-*x*-^{14}C, were recovered by preparative vpc and then degraded to give the isotopic scramblings recorded in Table 3.

The degradation of **1**-OH-*x*-^{14}C and **2**-OH-*x*^{14}C (4) were carried out via $KMnO_4$ oxidation to cyclopropanecarboxylic acid and succinic acid, respectively. Schmidt reactions on these two acids gave, respectively, cyclopropylamine and ethylenediamine which were converted to the corresponding benzamide and dibenzamide for activity determination. The procedures for these degradative reactions have been described previously (4).

Cleavage of the double bond in **3**-OH-*x*-^{14}C to give HCHO, recovered as the dimedon derivative, was effected by oxidation with performic acid followed by treatment with periodate, using the procedures previously described for similar reactions with allylcarbinyl chloride (4). The **3**-OH-*x*-^{14}C was also hydrogenated to give 1-butanol which was in turn oxidized to butyric acid and then degraded to propylamine, again using previously reported procedures (16, 17).

Acknowledgement

The financial support given by the Natural Sciences and Engineering Research Council of Canada is gratefully acknowledged.

1. M. C. Caserio, W. H. Graham, and J. D. Roberts. Tetrahedron, **11**, 171 (1960).
2. C. C. Lee and E. C. F. Ko. Can. J. Chem. **58**, 1 (1980).
3. J. D. Roberts and R. H. Mazur. J. Am. Chem. Soc. **73**, 2509 (1951).
4. R. H. Mazur, W. N. White, D. A. Semenov, C. C. Lee, M. S. Silver, and J. D. Roberts. J. Am. Chem. Soc. **81**, 4390 (1959).
5. R. Breslow. *In* Molecular rearrangements. Part 1. *Edited by* P. de Mayo. Interscience Publishers, New York. 1963. pp. 233–294.
6. J. S. Staral, I. Yavari, J. D. Roberts, G. K. S. Prakash, D. J. Donovan, and G. A. Olah. J. Am. Chem. Soc. **100**, 8016 (1978).
7. J. S. Staral and J. D. Roberts. J. Am. Chem. Soc. **100**, 8018 (1978).
8. C. W. Stahl and D. L. Cottle. J. Am. Chem. Soc. **65**, 1783 (1943).
9. C. H. DePuy and L. R. Mahoney. J. Am. Chem. Soc. **86**, 2653 (1964).
10. C. C. Lee. Prog. Phys. Org. Chem. **7**, 129 (1970).
11. K. L. Servis and J. D. Roberts. J. Am. Chem. Soc. **86**, 3773 (1964).
12. J. B. Lee and I. M. Downie. Tetrahedron, **23**, 359 (1967).
13. J. Hooz and S. S. H. Gilani. Can. J. Chem. **46**, 86 (1968).
14. J. D. Roberts and V. C. Chambers. J. Am. Chem. Soc. **73**, 3176 (1951).
15. W. Kirmse and B. G. v. Wedel. Ann. **676**, 1 (1964).
16. C. C. Lee and I. Y. Z. Ponce. Can. J. Chem. **50**, 3179 (1972).
17. C. C. Lee, A. J. Cessna, E. C. F. Ko, and S. Vassie. J. Am. Chem. Soc. **95**, 5688 (1973).

Can. J. Chem. Downloaded from www.nrcresearchpress.com by 210.87.254.6 on 09/05/12
For personal use only.

Novel molybdenum and tungsten carbonyl compounds containing the bidentate chelating thiomethoxymethyl group and tridentate chelating gallate ligands: crystal and molecular structures of $[Me_2Ga(N_2C_3H_3)(OCH_2CH_2NMe_2)]Mo(CO)_2(\eta^2\text{-}CH_2SMe)$ and $[Me_2Ga(N_2C_5H_7)(OCH_2CH_2NMe_2)]Mo(CO)_2(\eta^2\text{-}CH_2SMe)$

KENNETH S. CHONG, STEVEN J. RETTIG, ALAN STORR, AND JAMES TROTTER

Department of Chemistry, University of British Columbia, Vancouver, B.C., Canada V6T 1Y6

Received November 5, 1979

KENNETH S. CHONG, STEVEN J. RETTIG, ALAN STORR, and JAMES TROTTER. Can. J. Chem. **58**, 1080 (1980).

Details of the synthesis and physical properties of novel molybdenum and tungsten carbonyl compounds containing the bidentate chelating thiomethoxymethyl group and tridentate chelating gallate ligands are described. Crystals of $[Me_2Ga(N_2C_3H_3)(OCH_2CH_2NMe_2)]Mo(CO)_2(\eta^2\text{-}CH_2SMe)$ are triclinic, $a = 8.144(1)$, $b = 9.150(1)$, $c = 13.731(1)$ Å, $\alpha = 96.155(6)$, $\beta = 98.83(1)$, $\gamma = 108.73(1)°$, $Z = 2$, space group $P\bar{1}$ and crystals of $[Me_2Ga(N_2C_5H_7)(OCH_2CH_2NMe_2)]Mo(CO)_2(\eta^2\text{-}CH_2SMe)$ are monoclinic, $a = 8.1754(7)$, $b = 15.074(1)$, $c = 16.708(1)$ Å, $\beta = 94.365(6)°$, $Z = 4$, space group $P2_1/c$. The structures were solved by Patterson and Fourier syntheses and were refined by full-matrix least-squares procedures to final R values of 0.021 and 0.033 for 3679 and 4362 reflections with $I \geq 3\sigma(I)$ respectively. The Mo atoms in both structures are best described as heptacoordinate with bidentate η^2-CH_2SMe ligands. Important bond lengths (corrected for libration) are: Mo—S, 2.4750(6), Mo—C(S), 2.202(3), Mo—O, 2.248(2), Mo—N(pyrazolyl), 2.192(2), Mo—N(amino), 2.394(2), Mo—C(O), 1.903(3) and 1.957(3), Ga—O, 1.912(2), Ga—N, 2.020(2), and Ga—C, 1.962(4) and 1.969(4) Å for $[Me_2Ga(N_2C_3H_3)(OCH_2CH_2NMe_2)]Mo(CO)_2(\eta^2\text{-}CH_2SMe)$; corresponding distances for $[Me_2Ga(N_2C_5H_7)(OCH_2CH_2NMe_2)]Mo(CO)_2(\eta^2\text{-}CH_2SMe)$ are 2.4906(8), 2.211(3), 2.263(2), 2.205(2), 2.403(3), 1.906(3), 1.958(3), 1.918(2), 2.014(3), 1.963(4), and 1.966(4) Å.

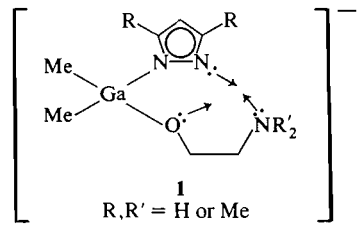
KENNETH S. CHONG, STEVEN J. RETTIG, ALAN STORR et JAMES TROTTER. Can. J. Chem. **58**, 1080 (1980).

On décrit la synthèse et les propriétés physiques des nouveaux composés carbonylés du molybdène et du tungstène contenant le groupe thiométhoxyméthyle comme agent chélatant bidentate et des ligands gallate chélatés de façon tridentate. Les cristaux de $[Me_2Ga(N_2C_3H_3)(OCH_2CH_2NMe_2)]Mo(CO)_2(\eta^2\text{-}CH_2SMe)$ sont triclinques $a = 8.144(1)$, $b = 9.150(1)$, $c = 13.731(1)$ Å, $\alpha = 96.155(6)$, $\beta = 98.83(1)$, $\gamma = 108.73(1)°$, $Z = 2$, groupe d'espace $P\bar{1}$ et les cristaux de $[Me_2Ga(N_2C_5H_7)(OCH_2CH_2NMe_2)]Mo(CO)_2(\eta^2\text{-}CH_2SMe)$ sont monocliniques $a = 8.1754(7)$, $b = 15.074(1)$, $c = 16.708(1)$ Å, $\beta = 94.365(6)°$, $Z = 4$, groupe d'espace $P2_1/c$. On a résolu les structures par les synthèses de Patterson et de Fourier et on les a affinées par la méthode des moindres carrés (matrice complète) jusqu'à des valeurs respectives R de 0.021 et de 0.033 pour 3679 et 4362 réflexions avec $I \geq 3\sigma(I)$. Les atomes de molybdène dans les deux structures sont heptacoordonnés avec les ligands bidentates η^2-CH_2SMe. Les longueurs importantes de liaisons (corrigées pour la libration) sont: Mo—S, 2.4750(6), Mo—C(S), 2.202(3), Mo—O, 2.248(2), Mo—N(pyrazolyl), 2.192(2), Mo—N(amino), 2.394(2), Mo—C(O), 1.903(3) et 1.957(3), Ga—O, 1.912(2), Ga—N, 2.020(2) et Ga—C, 1.962(4) et 1.969(4) Å pour $[Me_2Ga(N_2C_3H_3)(OCH_2CH_2NMe_2)]Mo(CO)_2(\eta^2\text{-}CH_2SMe)$; les distances correspondantes pour $[MeGa(N_2C_5H_7)(OCH_2CH_2NMe_2)]Mo(CO)_2(\eta^2\text{-}CH_2SMe)$ sont 2.4906(8), 2.211(3), 2.263(2), 2.205(2), 2.403(3), 1.906(3), 1.958(3), 1.918(2), 2.014(3), 1.963(4) et 1.966(4) Å.

[Traduit par le journal]

Introduction

Recently sulfur ligand transition metal complexes have attracted considerable attention (1–4). Those of molybdenum have merited special interest since there is evidence that redox reactions which are catalyzed by molybdoenzymes occur at sites where the molybdenum is coordinated by one or more sulfur atoms (5). Our continuing investigations into the coordinating properties of organogallate ligands of the type **1** (6–9), has resulted in a series of carbonyl complexes of molybdenum and tungsten containing both the ligand **1** and the organosulfur ligand "CH_2SMe". The complexes have been probed to determine the nature of the sulfur–metal bonding and definitive structural parameters, resulting from crystal structure determinations, are presented for the complexes $[Me_2Ga(N_2C_3H_3)(OCH_2CH_2NMe_2)]Mo(CO)_2(\eta^2\text{-}CH_2SMe)$ and $[Me_2Ga(N_2C_5H_7)(OCH_2CH_2NMe_2)]Mo(CO)_2(\eta^2\text{-}CH_2SMe)$.



1

R,R' = H or Me

Experimental

Starting Materials

Air-sensitive materials were handled in a glove box under an atmosphere of oxygen-free dry nitrogen or in a nitrogen-blanketed apparatus or on a high-vacuum line. Tetrahydrofuran (THF) was dried by refluxing over Na/benzophenone and was used immediately following distillation. Benzene was dried by refluxing over molten potassium followed by distillation. Pyrazole and 3,5-dimethylpyrazole (K and K Laboratories) and

0008-4042/80/111080-11$01.00/0

©1980 National Research Council of Canada/Conseil national de recherches du Canada

Can. J. Chem. Downloaded from www.nrcresearchpress.com by 210.87.254.40 on 09/05/12
For personal use only.

Can. J. Chem. Downloaded from www.nrcresearchpress.com by 210.87.254.40 on 09/05/12
For personal use only.

sodium hydride (Alfa Inorganic) were used as supplied. Ethanolamine and *N,N*-dimethylethanolamine were refluxed over anhydrous $CaSO_4$ and distilled prior to use. Thiomethoxymethyl chloride was prepared using a literature method (10) and gallium trimethyl was prepared as previously described (11). Molybdenum and tungsten hexacarbonyls were used as supplied (Strem) and $(MeCN)_3M(CO)_3$ (M = Mo or W) were prepared by a literature method (12).

Preparations

The ligands **1** were prepared as sodium salts in THF solution by the method already described (6–8). The tricarbonyl anions, $LM(CO)_3^-$ (M = Mo or W), incorporating these ligands were prepared, again as sodium salts in THF solution, by adding a THF solution of the ligand salt, NaL, to an equimolar amount of $(MeCN)_3M(CO)_3$ and refluxing for about 1 h. After cooling to −78°C a THF solution of $ClCH_2SMe$ was added dropwise with stirring to the air-sensitive yellow solution of the anion. The mixture was warmed to room temperature and the solvent removed under vacuum. The brown residue was extracted with benzene and the mixture filtered. Evaporation of the filtrate left an oily solid which was washed with methanol to produce a yellow powder. Recrystallization from benzene gave bright yellow crystals of the product. Yields of purified crystals were 15–25%. Analytical data, selected ir frequencies, and ^1H nmr data for the eight compounds are collected in Table 1. The compound $MeGa(N_2C_3H_3)_3Mo(CO)_2(\eta^2\text{-}CH_2SMe)$ was prepared similarly from the ligand $Na^+MeGa(N_2C_3H_3)_3^-$ (13). *Anal.* calcd.: C 33.7, N 16.8, H 3.4; found: C 33.9, N 16.6, H 3.4. ν_{CO}: 1942, 1805 (CH_2Cl_2); 1924, 1776 (Nujol); 1955, 1948, 1835, 1822 (cyclohexane). ^1H nmr (C_6D_6): τ 9.99 s (GaMe); 8.61 s (SMe); 6.77 d, 6.07 d, relative intensity 1:1 (CH_2—S); 4.11, 4.01 relative intensity 1:2 (^4H); 2.97, 2.84 relative intensity 1:2 (^5H); 2.29, 2.10, 1.71 relative intensity 1:1:1 (^3H). Mass spectrum: parent ion (22%); P − CO (16%); P − 2CO (100%).

Spectra

Mass spectra were recorded on a Varian MAT CH4 mass spectrometer at 70 eV with an ion source temperature of 100–180°C. Infrared spectra were recorded on a Perkin-Elmer 457 spectrophotometer and ^1H nmr spectra on a Varian XL-100 spectrometer using FT techniques.

X-ray Crystallographic Analyses

*[Dimethyl(*N,N*-dimethylethanolamino)(1-pyrazolyl)gallato-(*N(2),O,N(3)*)](*η²*-thiomethoxymethyl)dicarbonylmolybdenum*

The crystal chosen was mounted in a general orientation and had dimensions of ca. 0.425 × 0.138 × 0.226 mm. Unit-cell parameters were refined by least-squares on 2 sin θ/λ values for 25 reflections measured on a diffractometer with Mo K_α radiation (λ = 0.71073 Å). Crystal data (at 22°C) are:

$C_{13}H_{24}GaMoN_3O_3S$ fw = 468.08

Triclinic, a = 8.144(1), b = 9.150(1), c = 13.731(1) Å, α = 96.155(6), β = 98.83(1), γ = 108.73(1)°, V = 944.0(3) Å^3, Z = 2, ρ_c = 1.647 g cm^{-3}, $F(000)$ = 472, μ(Mo K_α) = 22.7 cm^{-1}. Absent reflections: none. Space group $P\bar{1}$ (C_i^1, No. 2) from structure analysis.

Intensities were measured with graphite monochromatized Mo K_α radiation on an Enraf-Nonius CAD4-F diffractometer. An ω scan at 0.91–6.71° min^{-1} over a range of (0.55 + 0.35 tan θ) degrees in ω (extended by 25% on both sides for background measurement) was employed. Data were measured to 2θ = 55°. The intensities of three check reflections, measured every 3600 s throughout the data collection, remained constant to within 2%. After data reduction, an absorption correction was applied using the Gaussian integration method (14, 15). Transmission factors ranged from 0.566 to 0.758. Of the 4315 independent reflections measured, 3679 (85%) had intensities greater than 3σ(I) above background where $\sigma^2(I) = S + 2B + (0.04(S - B))^2$ with S = scan count and B = background count.

Analysis was initiated in the centrosymmetric space group $P\bar{1}$ on the basis of the E-statistics. The positions of the Mo, Ga, and S atoms were determined from the three-dimensional Patterson function and those of the remaining non-hydrogen atoms from a subsequent difference map. After full-matrix least-squares refinement of all non-hydrogen atoms with anisotropic thermal parameters to R = 0.034, a difference map gave the positions of all 24 hydrogen atoms which were included in subsequent cycles of refinement with isotropic thermal parameters. The scattering factors of ref. 16 were used for non-hydrogen atoms and those of ref. 17 for hydrogen atoms. Anomalous scattering factors from ref. 18 were used for the Mo, Ga, and S atoms. The weighting scheme, $w = 1/\sigma^2(F)$ where $\sigma^2(F)$, is derived from the previously defined $\sigma^2(I)$ gave uniform average values of $w(|F_o| - |F_c|)^2$ over ranges of $|F_o|$ and was employed in the final stages of refinement. An isotropic Type I extinction correction (Thornley–Nelmes definition of mosaic anisotropy with a Lorentzian distribution) was applied (19–21). The final value of g was 1.97(11) × 10^4. Convergence was reached at R = 0.021 and R_w = 0.028 for 3679 reflections with $I \geq 3\sigma(I)$. For all 4315 reflections R = 0.030 and R_w = 0.029.

On the final cycle of refinement the mean and maximum parameter shifts corresponded to 0.11 and 0.79σ, respectively. The mean error in an observation of unit weight was 0.9165. A final difference map showed maximum fluctuations of ±0.4 e Å^{-3} near the heavy atoms and ±0.2 e Å^{-3} elsewhere. The final positional and thermal parameters appear in Tables 2 and 3 respectively. Measured and calculated structure factors have been placed in the Depository of Unpublished Data.[1]

*[Dimethyl(*N,N*-dimethylethanolamino)(3,5-dimethyl-1-pyrazolyl)gallato(*N(2),O,N(3)*)](*η²*-thiomethoxymethyl)-dicarbonylmolybdenum*

Details of the structure analysis are the same as for $[Me_2Ga(N_2C_3H_3)(OCH_2CH_2NMe_2)]Mo(CO)_2(\eta^2\text{-}CH_2SMe)$ except where noted. Crystal dimensions were 0.15 × 0.53 × 0.62 mm. Forty-seven reflections were used in the refinement of the unit-cell parameters. Crystal data are:

$C_{15}H_{28}GaMoN_3O_3S$ fw = 496.13

Monoclinic, a = 8.1754(7), b = 15.074(1), c = 16.708(1) Å, β = 94.365(6)°, V = 2053.0(3) Å^3, Z = 4, ρ_c = 1.605 g cm^{-3}, $F(000)$ = 1008, μ(Mo K_α) = 19.4 cm^{-1}. Absent reflections: $0k0$, $k \neq 2n$, and $h0l$, $l \neq 2n$ define uniquely the space group $P2_1/c$ (C_{2h}^5, No. 14).

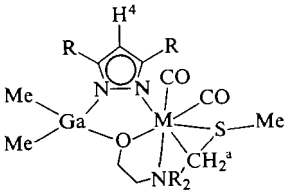
An ω–2θ scan at 1.55–10.08° min^{-1} over a range of 0.70 + 0.35 tan θ° in ω was employed. Of 5927 independent reflections measured (to 2θ = 60°), 4362 (73.6%) had intensities greater than 3σ(I) above background. An absorption correction was applied, transmission factors ranging from 0.276 to 0.633.

The coordinates of the Mo, Ga, and S atoms were determined from the Patterson function and those of the remaining non-hydrogen atoms from a subsequent difference map. Refinement of the non-hydrogen atoms with anisotropic thermal parameters gave R = 0.042. All 28 hydrogen atoms were located from a difference map at this point and were included in subsequent

[1]The structure factor table and Table 3 (thermal parameters) are available, at a nominal charge, from the Depository of Unpublished Data, CISTI, National Research Council of Canada, Ottawa, Ont., Canada K1A 0S2.

Can. J. Chem. Downloaded from www.nrcresearchpress.com by 210.87.254.40 on 09/05/12
For personal use only.

TABLE 1. Analytical, ^{1}H nmr, and ir data for the complexes



M	R	R′	Found, % calculated, % C	H	N	τ(ppm)* (C_6D_6 solution) S-Me	H^4	H^a	R	R′	Ga-Me	Approximate isomer ratio	ν_{CO} (cm^{-1}) CH_2Cl_2	Nujol	C_6H_{12}	ν_{NH} (cm^{-1}) Nujol
Mo	H	H	30.3	4.6	9.4	8.42s	3.82t†	6.26d‡, 7.16d‡	2.19d†, 2.73d†	— —	9.92s, 10.26s	4	1933	1920	i	3360
			30.0	4.6	9.5	8.67s	3.73t†	6.16d‡, 7.20d‡	1.96d†, 2.58d†	— —	10.14s, 10.31s	1	1782	1775	i	3301
Mo	H	Me	33.4	5.3	9.1	8.39s	3.91t†	6.41d‡, 7.22d‡ (br)	2.49s, 2.77d† (br)	7.45s, 8.26s	9.93s, 10.16s	7	1923	1910	1950	—
													1785	1780	1924	—
			33.4	5.2	9.0	—	3.85t†	— —	— —	7.49s, 8.22s	10.08s, 10.19s	1	—	—	1811	—
Mo	Me	H	33.7	5.2	8.9	8.40s	4.20s	6.29d‡, 7.23d‡	7.46s, 7.98s	— —	9.90s, 10.22s	9	1933	1900	i	3359
			33.4	5.2	9.0	8.70s	—	— —	7.38s, 7.93s	— —	10.14s, 10.30s	1	1784	1773	i	3310
Mo	Me	Me	36.4	5.5	8.4	8.40s	4.25s	6.45?, 7.29d‡ (br)	7.44s, 7.98s (br)	7.44s, 8.12s (br)	9.93s, 10.13s (br)	20	1923	1911	1945	—
													1781	1780	1921	—
			36.3	5.7	8.5	—	—	— —	— —	— —	10.10s, 10.17s	1	—	—	1810	—
															1806	—
W	H	H	25.1	3.8	7.9	8.20s	3.92t†	6.36d‡, 6.96d‡	2.14d†, 2.83d†	— —	9.94s, 10.31s	4	1924	1890	i	3338
			25.0	3.8	8.0	8.44s	3.82t†	6.25d‡, 7.04d‡	1.90d†, 2.80d†	— —	10.18s, 10.38s	1	1768	1750	i	3261
W	H	Me	27.4	4.3	7.3	8.15s	3.98t†	6.41d‡, 6.96d‡	2.46s, 2.83d† (br)	7.24s, 8.27s	9.95s, 10.21s	6	1911	1903	1939	—
													1769	1765	1917	—
			28.1	4.4	7.6	—	3.90t†	— —	— —	7.29s, 8.24s	10.11s, 10.24s	1	—	—	1800	—
															1795	
W	Me	H	27.8	4.4	7.4	8.17s	4.23s	6.37d‡, 7.01d‡	7.44s, 8.03s	— —	9.90s, 10.23s	10	1921	1888	i	3338
			28.1	4.4	7.6	8.46s	—	— —	7.34s, 7.98s	— —	10.13s, 10.33s	1	1765	1757	i	3288
W	Me	Me	31.2	4.9	7.2	8.17s	4.27s	6.52d‡, 7.03d‡	7.53s, 8.01s (br)	7.25s, 8.13s (br)	9.93s, 10.16s (br)	25	1914	1898	1937	—
													1768	1760	1914	—
			30.9	4.8	7.2	—	—	— —	— —	— —	10.10s, 10.21s	1	—	—	1799	—
															1792	

*τ values refer to $\tau_{C_6H_6}$ = 2.84 ppm, s = singlet, d = doublet, t = triplet, i = insoluble.
†J_{HCCH} = 2 Hz.
‡J_{HCH} = 6 Hz.

Can. J. Chem. Downloaded from www.nrcresearchpress.com by 210.87.254.40 on 09/05/12
For personal use only.

TABLE 2. Final positional parameters (fractional: O, N, and C × 10^4, Mo, Ga, and S × 10^5, H × 10^3) with estimated standard deviations in parentheses

Atom	*x*	*y*	*z*
$[Me_2Ga(N_2C_3H_3)(OCH_2CH_2NMe_2)]Mo(CO)_2(\eta^2\text{-}CH_2SMe)$			
Mo	48808(2)	74996(2)	20576(1)
Ga	21134(4)	39086(3)	23826(2)
S	63567(10)	72224(8)	6408(5)
O(1)	1631(3)	8456(3)	1317(2)
O(2)	6555(4)	11089(2)	2448(2)
O(3)	4213(2)	4902(2)	1910(1)
N(1)	3606(3)	7191(2)	3349(1)
N(2)	2655(3)	5726(2)	3491(1)
N(3)	7297(3)	7186(3)	3133(2)
C(1)	2799(4)	8041(3)	1586(2)
C(2)	5896(4)	9716(3)	2296(2)
C(3)	2266(8)	2135(4)	3040(4)
C(4)	116(5)	3850(5)	1362(3)
C(5)	4116(4)	6984(4)	420(2)
C(6)	7468(9)	9065(6)	278(5)
C(7)	3605(4)	8196(3)	4129(2)
C(8)	2708(4)	7410(4)	4795(2)
C(9)	2132(4)	5874(4)	4360(2)
C(10)	5733(4)	4496(3)	2232(2)
C(11)	6758(4)	5483(4)	3206(2)
C(12)	8946(4)	7634(5)	2731(3)
C(13)	7716(6)	8094(6)	4150(3)
H(3a)	139(6)	187(5)	329(4)
H(3b)	318(7)	238(6)	356(4)
H(3c)	239(6)	133(6)	258(3)
H(4a)	−7(6)	313(5)	80(4)
H(4b)	29(7)	479(7)	114(4)
H(4c)	−80(7)	344(6)	152(4)
H(5a)	341(4)	587(4)	20(2)
H(5b)	379(4)	766(4)	−1(2)
H(6a)	686(7)	969(6)	38(4)
H(6b)	738(10)	891(8)	−33(6)
H(6c)	848(10)	939(8)	63(5)
H(7)	419(4)	931(4)	411(2)
H(8)	262(5)	781(4)	541(3)
H(9)	144(5)	492(4)	458(3)
H(10a)	650(4)	474(4)	175(2)
H(10b)	540(4)	347(4)	230(2)
H(11a)	592(4)	527(3)	372(2)
H(11b)	779(5)	524(4)	340(2)
H(12a)	880(5)	685(5)	204(3)
H(12b)	991(5)	761(4)	320(3)
H(12c)	921(5)	875(4)	267(3)
H(13a)	877(5)	801(4)	457(3)
H(13b)	673(5)	780(4)	444(3)
H(13c)	803(7)	908(6)	409(4)
$[Me_2Ga(N_2C_5H_7)(OCH_2CH_2NMe_2)]Mo(CO)_2(\eta^2\text{-}CH_2SMe)$			
Mo	44863(3)	28338(2)	39138(1)
Ga	27097(4)	7691(2)	39578(2)
S	66230(11)	30320(7)	50393(5)
O(1)	1258(3)	3737(2)	4351(2)
O(2)	4991(4)	4769(2)	3396(2)
O(3)	4671(2)	1402(1)	4286(1)
N(1)	2782(3)	2339(2)	2933(1)
N(2)	2337(3)	1453(2)	2929(1)
N(3)	6532(3)	2220(2)	3122(1)
C(1)	2441(4)	3371(2)	4207(2)
C(2)	4783(4)	4024(2)	3578(2)
C(3)	3181(8)	−474(3)	3725(3)

TABLE 2 (*Concluded*)

Atom	*x*	*y*	*z*
C(4)	1091(6)	1120(3)	4700(3)
C(5)	4540(5)	3036(3)	5223(2)
C(6)	7295(8)	4164(4)	5149(4)
C(7)	2121(4)	2702(2)	2246(2)
C(8)	1291(4)	2050(3)	1786(2)
C(9)	1448(4)	1282(2)	2236(2)
C(10)	6208(5)	1030(3)	4127(3)
C(11)	6574(5)	1236(3)	3285(2)
C(12)	8167(5)	2615(4)	3332(3)
C(13)	6159(6)	2320(4)	2247(2)
C(14)	2273(8)	3660(3)	2048(3)
C(15)	789(8)	374(4)	2038(4)
H(3a)	208(7)	−84(4)	370(3)
H(3b)	386(7)	−69(4)	411(4)
H(3c)	375(7)	−54(4)	333(4)
H(4a)	−5(10)	101(5)	444(4)
H(4b)	87(9)	168(5)	475(5)
H(4c)	139(9)	84(4)	522(4)
H(5a)	415(5)	364(3)	548(2)
H(5b)	431(5)	251(3)	552(2)
H(6a)	851(9)	424(4)	482(4)
H(6b)	743(10)	428(5)	554(5)
H(6c)	654(7)	447(4)	489(4)
H(8)	74(4)	216(2)	126(2)
H(10a)	720(6)	135(3)	452(3)
H(10b)	607(5)	37(3)	420(2)
H(11a)	556(6)	93(3)	293(3)
H(11b)	766(5)	110(3)	327(2)
H(12a)	904(6)	235(3)	299(3)
H(12b)	806(5)	318(3)	316(3)
H(12c)	861(9)	245(5)	394(4)
H(13a)	501(6)	200(3)	211(3)
H(13b)	699(6)	196(3)	200(3)
H(13c)	602(5)	300(3)	214(3)
H(14a)	140(7)	377(4)	166(4)
H(14b)	208(7)	402(3)	256(3)
H(14c)	314(7)	379(4)	200(3)
H(15a)	163(9)	−3(5)	185(4)
H(15b)	27(7)	39(4)	158(4)
H(15c)	12(9)	15(5)	254(5)

cycles of refinement with isotropic thermal parameters. The final value of the extinction parameter g was 0.68(10) × 10^4. Convergence was reached at $R = 0.033$ and $R_w = 0.039$ for 4362 reflections with $I \geq 3\sigma(I)$. For all 5927 reflections $R = 0.054$ and $R_w = 0.042$. The mean and maximum parameter shifts on the final cycle of refinement corresponded to 0.12 and 1.5σ respectively and the mean error in an observation of unit weight was 1.1480.

The thermal motions of both molecules have been analysed in terms of rigid-body modes of translation, libration, and screw motion (22) using the computer program MGTLS. For $[Me_2Ga(N_2C_3H_3)(OCH_2CH_2NMe_2)]Mo(CO)_2(\eta^2\text{-}CH_2SMe)$, **2** (rms σU_{ij} = 0.0016 Å^2), analysis of all non-hydrogen atoms except carbonyl oxygens and methyl carbons C(3), C(4), and C(6) gave physically reasonable rigid-body parameters and rms ΔU_{ij} = 0.0028 Å^2. For $[Me_2Ga(N_2C_5H_7)(OCH_2CH_2NMe_2)]Mo(CO)_2(\eta^2\text{-}CH_2SMe)$, **3** (rms σU_{ij} = 0.0019 Å^2), three separate analyses were employed. All non-hydrogen atoms except carbonyl oxygen atoms and methyl carbons C(3), C(4), and C(12)–C(15) gave rms ΔU_{ij} = 0.0044 Å^2, but indicated significant independent motion of the Ga and N(3) tetrahedra, these being analysed separately giving rms ΔU_{ij} = 0.0019 and

Can. J. Chem. Downloaded from www.nrcresearchpress.com by 210.87.254.40 on 09/05/12
For personal use only.

TABLE 4. Bond lengths (Å) with estimated standard deviations in parentheses

(*a*) Non-hydrogen atoms

Bond	Length (Å) Uncorr.	Corr.	Bond	Length (Å) Uncorr.	Corr.
			$[Me_2Ga(N_2C_3H_3)(OCH_2CH_2NMe_2)]Mo(CO)_2(\eta^2\text{-}CH_2SMe)$		
Mo —S	2.4732(6)	2.4750	O(1) —C(1)	1.157(3)	1.157
Mo —O(3)	2.241(2)	2.248	O(2) —C(2)	1.178(3)	1.178
Mo —N(1)	2.187(2)	2.192	O(3) —C(10)	1.423(3)	1.426
Mo —N(3)	2.387(2)	2.394	N(1) —N(2)	1.367(3)	1.371
Mo —C(1)	1.952(3)	1.957	N(1) —C(7)	1.336(3)	1.339
Mo —C(2)	1.898(3)	1.903	N(2) —C(9)	1.336(3)	1.337
Mo —C(5)	2.196(3)	2.202	N(3) —C(11)	1.496(4)	1.500
Ga —O(3)	1.908(2)	1.912	N(3) —C(12)	1.482(4)	1.483
Ga —N(2)	2.014(2)	2.020	N(3) —C(13)	1.476(4)	1.478
Ga —C(3)	1.969(4)	1.969	C(7) —C(8)	1.376(4)	1.378
Ga —C(4)	1.960(4)	1.962	C(8) —C(9)	1.365(4)	1.368
S —C(5)	1.741(3)	1.744	C(10)—C(11)	1.488(5)	1.492
S —C(6)	1.803(4)	1.804			
			$[Me_2Ga(N_2C_5H_7)(OCH_2CH_2NMe_2)]Mo(CO)_2(\eta^2\text{-}CH_2SMe)$		
Mo —S	2.4853(8)	2.4906	O(2) —C(2)	1.178(4)	1.178
Mo —O(3)	2.249(2)	2.263	O(3) —C(10)	1.420(4)	1.424
Mo —N(1)	2.199(2)	2.205	N(1) —N(2)	1.384(3)	1.389
Mo —N(3)	2.396(3)	2.403	N(1) —C(7)	1.348(4)	1.351
Mo —C(1)	1.954(3)	1.958	N(2) —C(9)	1.344(4)	1.345
Mo —C(2)	1.901(3)	1.906	N(3) —C(11)	1.507(5)	1.518
Mo —C(5)	2.206(3)	2.211	N(3) —C(12)	1.481(5)	1.491
Ga —O(3)	1.910(2)	1.918	N(3) —C(13)	1.479(5)	1.490
Ga —N(2)	2.009(3)	2.014	C(7) —C(8)	1.391(5)	1.392
Ga —C(3)	1.958(4)	1.966	C(7) —C(14)	1.489(5)	1.490
Ga —C(4)	1.954(4)	1.963	C(8) —C(9)	1.382(5)	1.384
S —C(5)	1.753(4)	1.756	C(9) —C(15)	1.498(6)	1.499
S —C(6)	1.799(5)	1.802	C(10)—C(11)	1.493(5)	1.499
O(1)—C(1)	1.155(4)	1.155			

(*b*) Distances involving hydrogen atoms

Compound	C—H (Å)	Mean
$[Me_2Ga(N_2C_3H_3)(OCH_2CH_2NMe_2)]Mo(CO)_2(\eta^2\text{-}CH_2SMe)$	0.80–1.09(3–7)	0.93(7)
$[Me_2Ga(N_2C_5H_7)(OCH_2CH_2NMe_2)]Mo(CO)_2(\eta^2\text{-}CH_2SMe)$	0.68–1.18(4–8)	0.97(11)

0.0021 Å^2 respectively. The appropriate bond distances have been corrected for libration (23), using shape parameters q^2 of 0.08 for all atoms involved. Corrected bond lengths for both molecules appear in Table 4 along with the uncorrected values. Corrected bond angles do not differ from the uncorrected values listed in Table 5 by more than 1σ. Intra-annular torsion angles are given in Table 6 and possible weak hydrogen bonds are listed in Table 7.

Results and Discussion

The experimental evidence summarized in Table 1 together with mass spectral data (see below) suggests a monomeric pseudo-octahedral structure for the compounds studied, both in solution and in gas phase. As with previous carbonyl complexes utilizing these gallate ligands (8, 9) it is conjectured that the tridentate chelating ligands are *fac* ligands in all the complexes herein reported. The proposed monomeric pseudo-octahedral structure incorporating a *fac* gallate ligand has been proven conclusively for the $[Me_2Ga(N_2C_3H_3)(OCH_2CH_2NMe_2)]Mo(CO)_2(\eta^2\text{-}CH_2SMe)$ and $[Me_2Ga(N_2C_5H_7)(OCH_2CH_2NMe_2)]Mo(CO)_2(\eta^2\text{-}CH_2SMe)$ complexes in the solid state through crystal structure determinations (see below).

Infrared Spectra

The infrared spectra of the complexes in CH_2Cl_2 solutions and as Nujol mulls (Table 1) show two equally strong broad bands in the carbonyl stretching region of the spectrum indicating a *cis*

Can. J. Chem. Downloaded from www.nrcresearchpress.com by 210.87.254.40 on 09/05/12
For personal use only.

TABLE 5. Bond angles (deg) with estimated standard deviations in parentheses
(*a*) Non-hydrogen atoms

Bonds	Angle (deg)	Bonds	Angle (deg)
$[Me_2Ga(N_2C_3H_3)(OCH_2CH_2NMe_2)]Mo(CO)_2(\eta^2\text{-}CH_2SMe)$			
S —Mo—O(3)	83.89(4)	Mo —S —C(5)	59.59(9)
S —Mo—N(1)	166.25(5)	Mo —S —C(6)	113.2(2)
S —Mo—N(3)	88.73(6)	C(5) —S —C(6)	106.1(2)
S —Mo—C(1)	108.57(7)	Mo —O(3) —Ga	112.59(7)
S —Mo—C(2)	93.10(8)	Mo —O(3) —C(10)	111.7(2)
S —Mo—C(5)	43.32(8)	Ga —O(3) —C(10)	118.0(2)
O(3)—Mo—N(1)	82.98(6)	Mo —N(1) —N(2)	120.4(1)
O(3)—Mo—N(3)	75.72(2)	Mo —N(1) —C(7)	132.6(2)
O(3)—Mo—C(1)	111.37(9)	N(2) —N(1) —C(7)	106.9(2)
O(3)—Mo—C(2)	168.8(1)	Ga —N(2) —N(1)	118.6(1)
O(3)—Mo—C(5)	83.39(9)	Ga —N(2) —C(9)	133.3(2)
N(1)—Mo—N(3)	84.08(7)	N(1) —N(2) —C(9)	107.7(2)
N(1)—Mo—C(1)	80.17(9)	Mo —N(3) —C(11)	106.1(2)
N(1)—Mo—C(2)	99.0(1)	Mo —N(3) —C(12)	112.5(2)
N(1)—Mo—C(5)	138.33(9)	Mo —N(3) —C(13)	113.7(2)
N(3)—Mo—C(1)	161.63(9)	C(11)—N(3) —C(12)	108.7(3)
N(3)—Mo—C(2)	93.5(1)	C(11)—N(3) —C(13)	108.6(3)
N(3)—Mo—C(5)	129.67(9)	C(12)—N(3) —C(13)	107.2(3)
C(1)—Mo—C(2)	79.8(1)	Mo —C(1) —O(1)	175.9(2)
C(1)—Mo—C(5)	68.7(1)	Mo —C(2) —O(2)	178.8(3)
C(2)—Mo—C(5)	101.8(1)	Mo —C(5) —S	76.8(1)
O(3)—Ga —N(2)	92.24(7)	N(1) —C(7) —C(8)	110.6(3)
O(3)—Ga —C(3)	112.2(2)	C(7) —C(8) —C(9)	104.2(2)
O(3)—Ga —C(4)	106.8(2)	N(2) —C(9) —C(8)	110.5(3)
N(2)—Ga —C(3)	106.0(2)	O(3) —C(10)—C(11)	110.1(2)
N(2)—Ga —C(4)	109.7(1)	N(3) —C(11)—C(10)	111.1(2)
C(3)—Ga —C(4)	125.0(2)		
$[Me_2Ga(N_2C_5H_7)(OCH_2CH_2NMe_2)]Mo(CO)_2(\eta^2\text{-}CH_2SMe)$			
S —Mo—O(3)	82.97(6)	C(5) —S —C(6)	105.8(3)
S —Mo—N(1)	166.81(7)	Mo —O(3) —Ga	111.3(1)
S —Mo—N(3)	89.09(7)	Mo —O(3) —C(10)	111.6(2)
S —Mo—C(1)	109.0(1)	Ga —O(3) —C(10)	119.0(2)
S —Mo—C(2)	90.7(1)	Mo —N(1) —N(2)	118.8(2)
S —Mo—C(5)	43.4(1)	Mo —N(1) —C(7)	133.4(2)
O(3)—Mo—N(1)	84.61(8)	N(2) —N(1) —C(7)	107.4(2)
O(3)—Mo—N(3)	75.34(8)	Ga —N(2) —N(1)	117.9(2)
O(3)—Mo—C(1)	111.7(1)	Ga —N(2) —C(9)	132.5(2)
O(3)—Mo—C(2)	168.7(1)	N(1) —N(2) —C(9)	108.4(2)
O(3)—Mo—C(5)	82.1(1)	Mo —N(3) —C(11)	106.7(2)
N(1)—Mo—N(3)	83.50(9)	Mo —N(3) —C(12)	111.7(2)
N(1)—Mo—C(1)	79.7(1)	Mo —N(3) —C(13)	114.0(2)
N(1)—Mo—C(2)	100.8(1)	C(11)—N(3) —C(13)	110.2(3)
N(1)—Mo—C(5)	138.6(1)	C(11)—N(3) —C(13)	106.2(3)
N(3)—Mo—C(1)	161.0(1)	C(12)—N(3) —C(13)	107.9(3)
N(3)—Mo—C(2)	95.3(1)	Mo —C(1) —O(1)	175.5(3)
N(3)—Mo—C(5)	129.7(1)	Mo —C(2) —O(2)	177.7(3)
C(1)—Mo—C(2)	79.2(1)	Mo —C(5) —S	76.8(1)
C(1)—Mo—C(5)	69.3(1)	N(1) —C(7) —C(8)	109.3(3)
C(2)—Mo—C(5)	99.7(2)	N(1) —C(7) —C(14)	123.2(3)
O(3)—Ga—N(2)	93.4(1)	C(8) —C(7) —C(14)	127.5(3)
O(3)—Ga —C(3)	111.2(2)	C(7) —C(8) —C(9)	105.7(3)
O(3)—Ga —C(4)	106.1(2)	N(2) —C(9) —C(8)	109.2(3)
N(2)—Ga —C(3)	109.9(2)	N(2) —C(9) —C(15)	121.9(4)
N(2)—Ga —C(4)	109.8(2)	C(8) —C(9) —C(15)	129.0(4)
C(3)—Ga —C(4)	122.6(2)	O(3) —C(10) —C(11)	109.8(3)
Mo —S —C(5)	59.8(1)	N(3) —C(11) —C(10)	111.8(3)
Mo —S —C(6)	112.5(2)		

Can. J. Chem. Downloaded from www.nrcresearchpress.com by 210.87.254.40 on 09/05/12
For personal use only.

TABLE 6. Intra-annular torsion angles (deg) five-membered chelate rings

Bond	Obs.	Bond	Obs.
$[Me_2Ga(N_2C_3H_3)(OCH_2CH_2NMe_2)]Mo(CO)_2(\eta^2\text{-}CH_2SMe)$			
Mo —O(3)	30.67(7)	Mo —O(3)	−19.1(2)
O(3)—Ga	−35.78(8)	O(3) —C(10)	46.5(2)
Ga —N(2)	29.2(1)	C(10)—C(11)	−57.6(3)
N(2)—N(1)	−10.0(2)	C(11)—N(3)	37.4(2)
N(1)—Mo	−11.9(1)	N(3) —Mo	−10.1(2)
$[Me_2Ga(N_2C_5H_7)(OCH_2CH_2NMe_2)]Mo(CO)_2(\eta^2\text{-}CH_2SMe)$*			
Mo —O(3)	27.92(9)	Mo —O(3)	−23.0(2)
O(3)—Ga	−35.87(9)	O(3) —C(10)	49.2(3)
Ga —N(2)	34.7(2)	C(10)—C(11)	−56.0(3)
N(2)—N(1)	−18.0(2)	C(11)—N(3)	33.1(2)
N(1)—Mo	−5.8(2)	N(3) —Mo	−5.9(2)

*Coordinates used in this calculation are related to those in Table 2 by inversion through the centre of symmetry for direct comparison with the values obtained for 2.

TABLE 7. Hydrogen-bond data* (distances in Å and angles in deg)

D—H...A	H...A	D...A	∠DHA
$[Me_2Ga(N_2C_3H_3)(OCH_2CH_2NMe_2)]Mo(CO)_2(\eta^2\text{-}CH_2SMe)$			
C(5)—H(5a)...S[1]	3.01(3)	3.841(3)	143(2)
C(10)—H(10a)...S	2.88(3)	3.457(3)	118(2)
C(12)—H(12a)...S	2.68(4)	3.198(4)	109(2)
C(13)—H(13b)...N(1)	2.60(4)	3.162(5)	120(3)
$[Me_2Ga(N_2C_5H_7)(OCH_2CH_2NMe_2)]Mo(CO)_2(\eta^2\text{-}CH_2SMe)$			
C(6)—H(6a)...O(1)[2]	2.55(8)	3.457(6)	155(5)
C(10)—H(10a)...S	2.73(5)	3.386(4)	117(3)
C(12)—H(12c)...S	2.69(7)	3.267(5)	113(5)
C(13)—H(13a)...N(1)	2.42(4)	3.069(5)	118(3)

*Superscripts refer to atoms at positions: [1] $1-x, 1-y, -z$; [2] $1+x, y, z$.

arrangement of the two CO ligands in the complexes. For those four complexes soluble in cyclohexane four sharp bands of roughly equal intensity were observed in this region of the spectrum. A similar phenomenon was evident in CS_2 solution ir measurements. These results suggest the presence of positional or orientational isomers in these two solvents. Positional isomers could arise if the "CH_2SMe" moiety were to be substituted for CO at different octahedral positions in the decarbonylation reaction in the final stage of the synthesis. However, molecular models indicate that the most favored position of substitution, sterically, should be the one opposite the pyrazolyl nitrogen atom, and this is indeed shown to be so in the two solid state structures described below. The second type of isomerism possible, orientational, would arise if the CH_2SMe ligand in a fixed octahedral position were oriented differently in the two isomers. Here there are two distinct possibilities, one involving a rotation of the sulfur ligand about the CH_2–S bond axis to place the S—Me group in different up or down positions in two isomers, the other, a rotation of the sulfur ligand about the midpoint of the CH_2—S bond which would give the ligand two different "bites" relative to the remainder of the unsymmetrical octahedral molecule. It is noteworthy that the ^1H nmr results (C_6D_6 solution) also indicate the presence of two isomers in solution but with a significantly different ratio than those indicated by the ir results for cyclohexane or CS_2 solutions. The synthesis and study of the molecule $MeGa(N_2C_3H_3)_3Mo(CO)_2(\eta^2\text{-}CH_2SMe)$ was undertaken to help clarify the above observations. In this complex we have a symmetrical tridentate chelating ligand and positional isomerism is not possible. The ^1H nmr results for this compound (C_6D_6 solution) indicate the presence of one isomer, whereas the ir results (cyclohexane solution), with 4 ν_{CO} bands, indicate the presence of two isomers of approximately equal concentration. With this molecule a different "bite" for the sulfur ligand should not give rise to more than two ν_{CO} bands for a mixture of the two conformers. To explain the spectrum different orientations of the S—Me group towards and away from the gallate ligand in the two isomers is a distinct possibility. It is interesting to compare the above results with those reported for the analogous compound (η^5-C_5H_5)$Mo(CO)_2(\eta^2\text{-}CH_2SMe)$ (24–26). For this compound only two ν_{CO} bands are reported both for halocarbon oil mull (24) (1922, 1838 cm^{-1}) and cyclohexane solution (25) (1952, 1869 cm^{-1}) spectra, indicating just one isomer for this complex. Again in this molecule positional and "bite" isomerism are not possible and evidently the highly unfavorable arrangement with the SMe group oriented towards the η^5-C_5H_5 ring is not observed. The ir results for the complexes (Table 1) with unsymmetrical gallate ligands may equally satisfactorily be explained on the basis of two different isomers in solution with the S—Me group pointing away from the gallate ligand in one isomer and in the opposite direction in the other isomer.

The presence of isomers so clearly shown in cyclohexane and CS_2 solutions but not in CH_2Cl_2 may be due to a solvent effect or to the fact that the ν_{CO} bands in CH_2Cl_2 are broad and the bands for different isomers, if present, may be unresolvable. It is not uncommon, however, in this type of complex for the isomer ratio to be drastically altered by merely changing the solvent (27, 28). In C_6H_6 solvent the ν_{CO} bands are not well resolved, due to interference from solvent absorptions but in the spectrum of the complex where R = R′ = Me

Can. J. Chem. Downloaded from www.nrcresearchpress.com by 210.87.254.40 on 09/05/12
For personal use only.

(Table 1) it does appear that one isomer is greatly favored with two strong ν_{CO} bands detectable at 1914 and 1786 cm^{-1}, a result in keeping with the ^1H nmr results.

As with previous results (8, 13, 24, 25, 29, 30), ν_{CO} values for the tungsten complexes are 10–15 cm^{-1} lower than those for the corresponding molybdenum compounds. In the relevant complexes in the present series the ν_{NH} values show the same trend to lower values for the tungsten compounds.

^1H Nuclear Magnetic Resonance Spectra

These results, collected in Table 1, were obtained using C_6D_6 solutions. For all the complexes (excepting $MeGa(N_2C_3H_3)_3Mo(CO)_2(\eta^2\text{-}CH_2SMe)$) the spectra indicate the presence of two isomers in solution. Each isomer can be readily associated with a particular set of proton signals due to the quite different relative amounts of each isomer present in the solution. Table 1 lists approximate isomer ratios obtained from the relative integrations of the two sets of Ga—Me signals for each complex. It is evident that the fewer the methyl substituents on the gallate ligand (i.e. R = R′ = H) the closer the isomer distribution (4:1). With R = H, R′ = Me or R = Me, R′ = H, the effect is relatively the same, the isomer ratio now about 8:1. When R = R′ = Me the preference of one isomer over the other is much larger, about 20:1.

It is tempting to rationalize these results on the same basis as the ir results, viz. two orientational isomers in solution. It might be expected, however, that interconversion of such isomers would be influenced by temperature and that eventually at higher temperatures an "average" spectrum would be observed. The four Ga—*Me* signals displayed by the complexes at room temperature are very sharp and remain so at elevated temperatures (80°C) with no noticeable broadening. This result suggests that either the interconversion process for the rotational isomers is not very facile or that the ^1H nmr experiment is showing the presence of two positional isomers in C_6D_6 solution. Unfortunately the complexes which gave isomer ratios closest to unity in the ^1H nmr experiments were not soluble in cyclohexane or CS_2 to enable a search for an expected 8 ν_{CO} bands due to 4 orientational isomers (2 for each positional isomer). Those complexes which were soluble in these solvents would most probably have relatively too little of the less abundant isomer to show up in the ir spectrum.

The isomer distributions should be compared with those observed in the corresponding nitrosyl complexes (8). In the latter, the isomer ratio (necessarily positional isomers) depends greatly on the position of methyl substitution. Thus if R = H, R′ = Me the isomer ratio is 1:1, but if R = Me, R′ = H the ratio is 5:1. In the present series of complexes the corresponding ratios are much less variant (see Table 1). An argument in favor of the orientational isomer explanation is the fact that well formed crystalline samples of the pure complexes were easily obtained (compare the poor crystalline samples of the corresponding nitrosyl complexes) and even samples used in X-ray studies when examined in solution gave the above ir and ^1H nmr results.

The non-equivalence of the two CH_2 protons of the CH_2SMe moiety is clearly demonstrated in the AX patterns observed for these protons in all the complexes ($J \approx 6.0$ Hz). This is consistent with the mode of bonding of this ligand in the solid state structures (see below) in which the "CH_2SMe" group and the Mo atom are involved in a three-membered metallocyclic ring with a "tetrahedral" CH_2 grouping.

Mass Spectra

Although the fragmentation patterns were similar for all compounds, the relative intensities of the various signals within a particular fragmentation pattern differed markedly for analogous molybdenum and tungsten derivatives. For all the compounds the monomer parent ion signal was the highest *m/e* recorded. The four molybdenum compounds displayed as their strongest signals the ions corresponding to the parent minus two CO groups (P − 2CO) with P − 2CO − Me (90%) and P (40%) being quite strong. P − CO and P − Me were observed as weak signals. In contrast, for the four tungsten compounds the signal corresponding to the P − 2CO − Me was the strongest with P − CO (70%) and P (40%). P − 2CO and P − Me were observed but weak. Another noteworthy feature of the set of spectra was the strong signal corresponding to P − 2CO − Me_2S (60%) observed in all four compounds containing the "$OCH_2CH_2NMe_2$" moiety but the very weak signal due to this ion or its complete absence in the four compounds containing the "$OCH_2CH_2NH_2$" fragment.

In all eight spectra the intensity ratios of the individual peaks in multi-peak signals agree closely with theoretical predictions based on the percentage isotope composition of the contributing metal atoms.

X-ray Crystallographic Analyses of $[Me_2Ga(N_2C_2H_3)(OCH_2CH_2NMe_2)]Mo(CO)_2(\eta^2\text{-}CH_2SMe)$, 2, and $[Me_2Ga(N_2C_5H_7)(OCH_2CH_2NMe_2)]Mo(CO)_2(\eta^2\text{-}CH_2SMe)$, 3

With the exception of one weak intermolecular interaction for each structure (C—H···S for **2** and

Can. J. Chem. Downloaded from www.nrcresearchpress.com by 210.87.254.40 on 09/05/12
For personal use only.

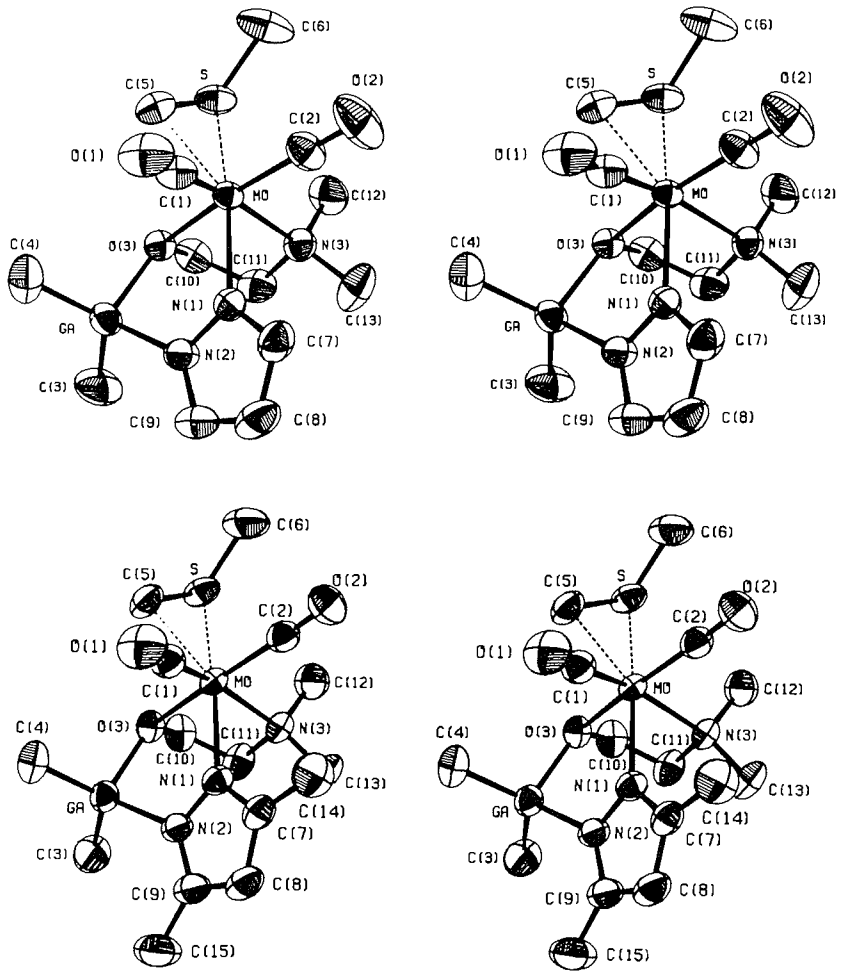


FIG. 1. Stereo views of the [dimethyl(*N*,*N*-dimethylethanolamino)(1-pyrazolyl)gallato(*N*(2),*O*,*N*(3))](η^2-thiomethoxymethyl)dicarbonylmolybdenum (top) and [dimethyl(*N*,*N*-dimethylethanolamino)(3,5-dimethyl-1-pyrazolyl)gallato(*N*(2),*O*,*N*(3))]-(η^2-thiomethoxymethyl)dicarbonylmolybdenum (bottom) molecules.

C—H···O for **3**, see Table 7), the solid state structures of both complexes consist of discrete molecular units separated by normal van der Waals distances.

The coordination about molybdenum in both molecules may be regarded as distorted octahedral with the η^2-CH_2SMe ligand occupying one coordination site or as heptacoordinated with a bidentate η^2-CH_2SMe ligand (see Fig. 1). The latter description is consistent with the observed angles between the carbonyl groups (79.8(1)° for **2**, 79.2(1)° for **3**) (26 and references therein). The η^2-CH_2SMe ligand is situated opposite the pyrazolyl nitrogen atom as predicted from molecular model studies. Molecules **2** and **3** are stereochemically equivalent to the related allyl complex $[Me_2Ga(N_2C_5H_7)(OCH_2CH_2NH_2)]Mo(CO)_2(\eta^3\text{-}C_4H_7)$, **4** (9). Bond lengths and angles in the $Mo(CO)_2$ moieties in **2**, **3**, and **4** are equal within experimental error and, as noted earlier (9), there are significant differences between the pairs of Mo—C(O) and C—O distances. The Mo—C(O) distances *trans* to oxygen are shorter than those *trans* to nitrogen by an average of 0.055 Å as a result of both steric and *trans* effects. The substituents of the gallate ligands, **1**, influence the bond lengths to the chelated metal. The Mo—N(amino) distance in **4** (R′ = H) is 2.285(2) Å and in the present structures (R′ = Me) the corresponding Mo—N distances increase to a mean value of 2.399(5) Å. When R changes from H to Me, the Mo—O distances increase slightly, but significantly, from 2.248(2) Å in **2** to a mean of 2.266(3) Å in **3** and **4**. The Mo—N(pyrazolyl) distances in **2** and **3** (2.192(2) and 2.205(2) Å) are slightly, but significantly, shorter than the corresponding distance of 2.222(2) Å in **4**, reflecting a

Can. J. Chem. Downloaded from www.nrcresearchpress.com by 210.87.254.40 on 09/05/12
For personal use only.

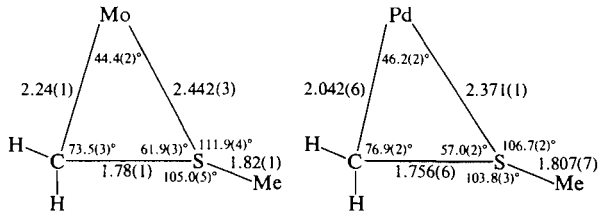
small electronic difference between the η^3-C_4H_7 and η^2-CH_2SMe ligands.

The steric requirements of the asymmetric gallate ligand were found to force an unusual orientation of the 2-methylallyl ligand in **4** (9) in which the methyl group was oriented toward the carbonyl ligands. This also occurs in both **2** and **3** as well as in the related molecule (η^5-C_5H_5)Mo(CO)$_2$(η^2-CH_2SMe) (26), all of which have the SMe group directed toward the carbonyl ligands. Unlike in solution, where orientational isomerism involving the η^2-CH_2SMe ligand is indicated, only one such isomer is present in the solid state. Weak intramolecular C—H···S hydrogen bonds (see Table 7) may be responsible for the predominance of one of the isomers in solution (see Table 1) and in combination with intermolecular C—H···S interactions in **2** and C—H···O interactions in **3** are sufficient to completely eliminate the minor isomer in the solid.

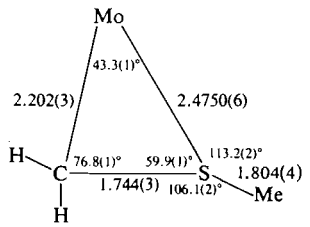
The M(η^2-CH_2SMe) systems in **2** and **3** are compared with those in (η^5-C_5H_5)Mo(CO)$_2$(η^2-CH_2SMe) (26) and (Ph_3P)PdCl(η^2-CH_2SMe) (31) in Fig. 2. The Mo—S distances in **2** and **3** differ significantly and both are longer than the corresponding distance in (η^5-C_5H_5)Mo(CO)$_2$(η^2-CH_2SMe) (26) while the Mo—C distances in **2** and **3** are somewhat shorter than in the cyclopentadienyl complex although these differences are not significant. Steric effects are most likely responsible for these differences, the S atoms in **2** and **3** being separated by less than the sum of van der Waals radii from both C(10) and C(12) of the gallate ligand. The C—S distances of all four complexes shown in Fig. 2 are equal within experimental error, those in the MCS ring being significantly shorter than the S—Me distances by a weighted mean of 0.054 Å. This shortening of the CH_2—S bonds corresponds to only a minimal amount of double bond character. The bond angles at C(5) in both of the present structures are equal within experimental error to the corresponding values observed in the low-temperature structure of (Ph_3P)PdCl(η^2-CH_2SMe) (31), confirming tetrahedral coordination for this atom. The Mo—C(5) distances (2.202(3) and 2.211(3) Å) in the present structures are significantly shorter than the terminal Mo—C(allyl) distances of 2.324(3) and 2.335(3) Å in **4** (which are shorter than the central Mo—C(allyl) bond, 2.372(3) Å). The above evidence indicates that the best description of the MCS system involves the formation of a three-membered metallocyclic ring containing an M—C σ-bond and lone-pair donation by S to the metal as noted previously (31).

The gallium atoms have distorted tetrahedral coordination geometry with bond angles ranging

(C_5H_5)Mo(CO)$_2$(CH_2—S—Me) (Ph_3P)PdCl(CH_2—S—Me)



($Me_2Ga(N_2C_3H_3)OCH_2CH_2NMe_2$)Mo(CO)$_2$($CH_2$—S—Me)



($Me_2Ga(N_2C_5H_7)OCH_2CH_2NMe_2$)Mo(CO)$_2$($CH_2$—S—Me)

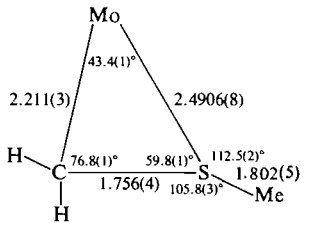


FIG. 2. Bond lengths (Å) and angles in the M(η^2-CH_2SMe) moiety.

from 92.24(7) to 125.0(2)°. All bond lengths and angles in the asymmetric gallate ligand are in good agreement with those observed in related structures (6, 7, 9, 32, 33) and the ligand conformation is similar to other structures in which the ligand is facially coordinated (7, 9, 32). The pyrazolyl groups in both structures are significantly nonplanar (χ^2 = 24.6 and 26.4 for **2** and **3** respectively) with the metal atoms considerably displaced from the N_2C_3 planes (Mo by −0.1336(2) and −0.2270(2), Ga by 0.2070(3) and 0.3722(4) Å for **2** and **3** respectively).

Acknowledgments

We thank the Natural Sciences and Engineering Research Council of Canada for financial support and the University of British Columbia Computing Centre for assistance. We are grateful to Mr. P. Borda for C, H, N analyses and to Dr. S. Chan for ^{1}H nmr spectra.

1. M. DI VAIRA, S. MIDOLLINI, and L. SACCONI. Inorg. Chem. **17**, 816 (1978).
2. G. H. BARNETT, M. K. COOPER, M. MCPARTLIN, and G. B. ROBERTSON. J. Chem. Soc. Dalton Trans. 587 (1978).
3. S. D. KILLOPS, S. A. R. KNOW, G. H. RIDING, and A. J. WELCH. J. Chem. Soc. Chem. Commun. 486 (1978).

4. Y. P. TSAO, C. J. FRITCHIE, JR., and H. A. LEVY. J. Am. Chem. Soc. **100**, 4089 (1978).
5. R. C. BRAY. *In* The enzymes. Vol. 2. 3rd ed. *Edited by* P. D. Boyer. Academic Press, New York. 1975. p. 299.
6. K. S. CHONG, S. J. RETTIG, A. STORR, and J. TROTTER. Can. J. Chem. **55**, 4166 (1977).
7. K. S. CHONG, S. J. RETTIG, A. STORR, and J. TROTTER. Can. J. Chem. **56**, 1212 (1978).
8. K. S. CHONG and A. STORR. Can. J. Chem. **57**, 167 (1979).
9. K. S. CHONG, S. J. RETTIG, A. STORR, and J. TROTTER. Can. J. Chem. **57**, 1335 (1979).
10. F. G. BORDWELL and B. M. PITT. J. Am. Chem. Soc. **77**, 572 (1955).
11. A. STORR and B. S. THOMAS. Can. J. Chem. **48**, 3667 (1970).
12. D. P. TATE, W. R. KNIPPLE, and J. M. AUGL. Inorg. Chem. **1**, 433 (1962).
13. K. R. BREAKELL, S. J. RETTIG, D. L. SINGBEIL, A. STORR, and J. TROTTER. Can. J. Chem. **56**, 2099 (1978).
14. P. COPPENS, L. LEISEROWITZ, and D. RABINOVICH. Acta Crystallogr. **18**, 1035 (1965).
15. W. R. BUSING and H. A. LEVY. Acta Crystallogr. **22**, 457 (1967).
16. D. T. CROMER and J. B. MANN. Acta Crystallogr. Sect. A, **24**, 321 (1968).
17. R. F. STEWART, E. R. DAVIDSON, and W. T. SIMPSON. J. Chem. Phys. **42**, 3175 (1965).
18. D. T. CROMER and D. LIBERMAN. J. Chem. Phys. **53**, 1891 (1970).
19. P. J. BECKER and P. COPPENS. Acta Crystallogr. Sect. A, **30**, 129 (1974); **30**, 148 (1974); **31**, 417 (1975).
20. P. COPPENS and W. C. HAMILTON. Acta Crystallogr. Sect. A, **26**, 71 (1970).
21. F. R. THORNLEY and R. J. NELMES. Acta Crystallogr. Sect. A, **30**, 748 (1974).
22. V. SCHOMAKER and K. N. TRUEBLOOD. Acta Crystallogr. Sect. B, **24**, 63 (1969).
23. D. W. J. CRUICKSHANK. Acta Crystallogr. **9**, 747 (1956); **9**, 754 (1956); **14**, 896 (1961).
24. R. B. KING and M. B. BISNETTE. Inorg. Chem. **4**, 486 (1965).
25. R. B. KING. Inorg. Chem. **5**, 2243 (1966).
26. E. R. DEGIL and L. F. DAHL. J. Am. Chem. Soc. **91**, 3751 (1969).
27. J. CALDERON, F. A. COTTON, and A. SHAVER. J. Organomet. Chem. **37**, 127 (1972).
28. J. CALDERON, F. A. COTTON, and A. SHAVER. J. Organomet. Chem. **38**, 105 (1972).
29. S. TROFIMENKO. J. Am. Chem. Soc. **91**, 588 (1969).
30. S. TROFIMENKO. Inorg. Chem. **10**, 504 (1971).
31. K. MIKI, Y. KAI, N. YASUOKA, and N. KASAI. J. Organomet. Chem. **135**, 53 (1977).
32. K. S. CHONG, S. J. RETTIG, A. STORR, and J. TROTTER. Can. J. Chem. **57**, 3113 (1979).
33. K. S. CHONG, S. J. RETTIG, A. STORR, and J. TROTTER. Can. J. Chem. **57**, 3107 (1979).

Can. J. Chem. Downloaded from www.nrcresearchpress.com by 210.87.254.40 on 09/05/12
For personal use only.

Synthesis and characterization of octahedral and trigonal bipyramidal transition metal complexes incorporating chelating gallate ligands: crystal and molecular structure of $[Me_2Ga(N_2C_5H_7)(OCH_2CH_2NMe_2)]Ni[(N_2C_5H_7)_2GaMe_2]$

KENNETH S. CHONG, STEVEN J. RETTIG, ALAN STORR, AND JAMES TROTTER

Department of Chemistry, University of British Columbia, Vancouver, B.C., Canada V6T 1Y6

Received November 19, 1979

Can. J. Chem. Downloaded from www.nrcresearchpress.com by 210.87.254.40 on 09/05/12
For personal use only.

KENNETH S. CHONG, STEVEN J. RETTIG, ALAN STORR, and JAMES TROTTER. Can. J. Chem. **58**, 1091 (1980).

The preparation and physical properties of octahedral and trigonal bipyramidal complexes incorporating the tris-chelating ligands $[Me_2Ga(N_2C_5H_7)(OCH_2CH_2NR'_2)]^-$ (R' = H or Me) are described. Crystals of [dimethylbis(3,5-dimethyl-1-pyrazolyl) gallato ($N(2)$, $N'(2)$)][dimethyl (3, 5 - dimethyl - 1 - pyrazolyl) (N, N - dimethylethanolamino(gallato ($N(2)$, O, $N(3)$)]nickel(II) are triclinic, $a = 20.8562(11)$, $b = 9.1536(4)$, $c = 8.2798(4)$ Å, $\alpha = 100.204(3)$, $\beta = 85.513(4)$, $\gamma = 101.989(3)°$, $Z = 2$, space group $P\bar{1}$. The structure was solved by Patterson and Fourier syntheses and was refined by full-matrix least-squares procedures to $R = 0.048$ and $R_w = 0.078$ for 5508 reflections with $I \geq 3\sigma(I)$. The coordination about the Ni atom is distorted trigonal bipyramidal with the two nitrogen atoms from the $Me_2Ga(N_2C_5H_7)_2$ ligand occupying equatorial positions. The tridentate $Me_2Ga(N_2C_5H_7)(OCH_2CH_2NMe_2)$ ligand is meridionally coordinated with the oxygen in the equatorial and the two nitrogens in the axial positions. Important bond lengths (corrected for libration) are: Ni—N(eq), 2.005(3) and 2.006(3), Ni—O, 1.993(3), Ni—N(pz—ax), 2.072(3), Ni—N(amino), 2.229(3), Ga—O, 1.913(3), Ga—N, 1.971(3)–1.989(3), and Ga—C, 1.961(10)–1.986(6) Å.

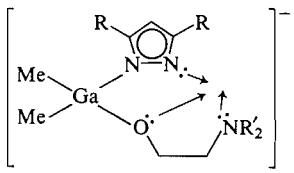
KENNETH S. CHONG, STEVEN J. RETTIG, ALAN STORR et JAMES TROTTER. Can. J. Chem. **58**, 1091 (1980).

On décrit la préparation et les propriétés physiques de complexes octaédriques et trigonaux bipyramidaux incorporant les ligands trichélatés $[Me_2Ga(N_2C_5H_7)(OCH_2CH_2NR'_2)]^-$ (R' = H ou Me). Les cristaux de [diméthylbis(diméthyl-3,5) pyrazolyl-1)-gallato($N(2)$,$N'(2)$)][diméthyl(diméthyl-3,5 pyrazolyl-1)(N,N-diméthyléthanolamino)gallato($N(2)$,O,$N(3)$)] nickel(II) sont triclinques avec $a = 20.8562(11)$, $b = 9.1536(4)$, $c = 8.2798(4)$ Å, $\alpha = 100.204(3)$, $\beta = 85.513(4)$, $\gamma = 101.989(3)°$, $Z = 2$ groupe d'espace $P\bar{1}$. On a résolu la structure par les synthèses de Patterson et de Fourier et on l'a affinée par la méthode des moindres carrés (matrice complète) jusqu'à des valeurs conventionnelles $R = 0.048$ et $R_w = 0.078$ pour 5508 réflexions avec $I \geq 3\sigma(I)$. La coordination autour de l'atome de nickel est déformée de façon trigonale bipyramidale avec les deux atomes d'azote du ligand $Me_2Ga(N_2C_5H_7)_2$ en positions équatoriales. Le ligand tridentate $Me_2Ga(N_2C_5H_7)(OCH_2CH_2NMe_2)$ est coordonné de façon méridionale avec l'oxygène équatorial et les deux atomes d'azote en positions axiales. Les longueurs importantes de liaison (corrigés pour la libration) sont: Ni—N(eq), 2.005(3) et 2.006(3), Ni—O, 1.993(3), Ni—N(pz—ax), 2.072(3), Ni—N(amino), 2.229(3), Ga—O, 1.913(3), Ga—N, 1.971(3)–1.989(3) et Ga—C, 1.961(10)–1.986(6) Å.

[Traduit par le journal]

Introduction

A series of four anionic tridentate chelating ligands of the type **1** has been synthesized. Previous reports dealt with octahedral complexes of the first row transition elements (Mn → Zn) incorporating the ligand **1** where R = H and R' = H (1), binuclear



1, R = H or Me; R' = H or Me

transition metal complexes (Co → Zn) using the ligand **1** where R = H and R' = Me (2), and carbonyl compounds of Mo, W, and Mn using all four ligands (3). The present account investigates the coordinating properties of the two ligands where R = R' = Me and where R = Me and R' = H towards divalent transition metal ions M^{2+} (where M = Fe, Co, Ni, Cu, and Zn). Depending on the ligand a series of trigonal bipyramidal five-coordinate transition metal complexes (R = R' = Me) or a series of six-coordinate octahedral transition metal complexes (R = Me and R' = H) were isolated. Steric factors, which in the main determine the geometry adopted about the transition metal ion, are discussed, and the crystal structure of the five-coordinate nickel(II) complex is presented.

Experimental

Starting Materials

Air-sensitive materials were handled in a glove box under an atmosphere of oxygen-free dry nitrogen or in a nitrogen-blanketed apparatus. Tetrahydrofuran (THF) was dried by refluxing over lithium aluminum hydride and was used immediately following distillation. Benzene was dried by refluxing over molten potassium followed by distillation. 3,5-Dimethylpyrazole (K and K laboratories) and sodium hydride (Alfa Inorganic) were used as supplied. Ethanolamine and N,N-dimethylethanolamine were refluxed over anhydrous $CaSO_4$ and distilled prior to use. Gallium trimethyl (4) and $FeCl_2 \cdot 1.5$ THF (5) were prepared as described previously.

Preparative Details

Ligand Synthesis

The two ligands employed in this study were synthesized by

0008-4042/80/111091-10$01.00/0

©1980 National Research Council of Canada/Conseil national de recherches du Canada

Can. J. Chem. Downloaded from www.nrcresearchpress.com by 210.87.254.40 on 09/05/12
For personal use only.

the same general route described previously for 1 where R = R' = H (1) and where R = H and R' = Me (2). Thus, sodium 3,5-dimethylpyrazolide was prepared in THF by reacting sodium hydride with 3,5-dimethylpyrazole. One molar equivalent of trimethyl gallium was then added followed by either ethanolamine or *N*,*N*-dimethylethanolamine depending on which ligand 1 was required. Refluxing at this final stage produced a clear THF solution of the desired ligands. These solutions were used in the subsequent preparations of the transition metal complexes. The purity of the ligand solutions was evident from the high-yield syntheses of numerous complexes incorporating one ligand per metal centre (3).

Preparation of the Complexes

The preparations of the complexes listed in Table 1 were all very similar and can be summarized by the following procedure. The transition metal starting materials for all the preparations are given in Table 1, together with physical data for the isolated complexes.

To one equivalent of a stirred solution or suspension of the transition metal salt in THF was added two[1] equivalents of ligand in the same solvent. The resulting precipitate was allowed to settle and the clear solution isolated. The THF solvent was then removed *in vacuo* and the solid remaining recrystallized from xylene or bezene to yield well-formed crystals in each case.

Spectra

A Varian MAT CH4 spectrometer was used to record mass spectra at 70 eV with an ion source temperature of 100–180°C. Infrared spectra were recorded on a Perkin-Elmer 457 spectrophotometer as Nujol mulls and electronic absorption solution spectra on a Cary 14 spectrometer.

X-ray Crystallographic Analysis of [Dimethylbis(3,5-dimethyl-1-pyrazolyl)gallato(N(2),N'(2))][dimethyl(3,5-dimethyl-1-pyrazolyl)(N,N-dimethylethanolamino)gallato-(N(2),O,N(3))]nickel(II)

The crystal chosen was mounted in a general orientation and had dimensions of ca. 0.70 × 0.48 × 0.42 mm. Unit-cell parameters were refined by least-squares on 2 sin θ/λ values for 25 reflections measured on a diffractometer with Cu K_α radiation (λ = 1.54184 Å). Crystal data (at 22°C) are:

$C_{23}H_{43}Ga_2N_7NiO$ fw = 631.80
Triclinic, a = 20.8562(11), b = 9.1536(4), c = 8.2798(4) Å, α = 100.204(3), β = 85.513(4), γ = 101.989(3)°, V = 1520.3(1) Å^3, Z = 2, ρ_c = 1.380 g cm^{-3}, $F(000)$ = 656, μ(Cu K_α) = 27.74 cm^{-1}. Absent reflections: none. Space group $P\bar{1}$ (C_i^1, No. 2) from structure analysis.

Intensities were measured with graphite monochromatized Cu K_α radiation on a Enraf-Nonius CAD4-F diffractometer. An ω–2θ scan at 1.26–10.06° min^{-1} over a range of (0.70 + 0.14 tan θ) degrees in ω (extended by 25% on both sides for background measurement) was employed. Data were measured to 2θ = 150°. The intensities of 3 check reflections, measured every 3600 s throughout the data collection, remained constant to within ±2.5%.

After data reduction, an absorption correction was applied using the Gaussian integration method (6, 7). Transmission factors ranged from 0.224 to 0.449 for 480 sampling points. Of the 6233 independent reflections measured, 5508 (88.4%) had intensities greater than 3σ(I) above background where $\sigma^2(I) = S + 2B + (0.04(S - B))^2$ with S = scan count and B = background count.

Analysis was initiated in the centrosymmetric space group $P\bar{1}$ on the basis of the E-statistics. The coordinates of the gallium and nickel atoms were determined from the Patterson function and those of the remaining non-hydrogen atoms from subsequent Fourier syntheses. The "ethanolamine" carbon atoms C(17), C(22), and C(23) were found to be twofold disordered; site occupancies were estimated from relative peak heights on a Fourier map to be 0.70 for "a" sites and 0.30 for "b" sites. Isotropic refinement of the disordered carbon atoms with the occupancy factors fixed resulted in nearly equal thermal parameters for corresponding pairs, thus the site occupancies were kept fixed at these values throughout the refinement. All of the ordered non-hydrogen atoms and the three disordered carbon atoms with 0.70 occupancy were refined with anisotropic thermal parameters and the remaining disordered carbon atoms with isotropic thermal parameters to R = 0.058. A difference map gave positions for all ordered hydrogen atoms which were subsequently refined with isotropic thermal parameters. Ideal positions (C—H = 0.98 Å, $B_H = B_C + 1.1$) were calculated for the disordered hydrogen atoms which were included as fixed atoms in the final stages of the refinement.

The scattering factors of ref. 8 were used for non-hydrogen atoms and those of ref. 9 for hydrogen atoms. Anomalous scattering factors from ref. 10 were used for the Ga and Ni atoms. The weighting scheme, $w = 1/\sigma^2(F)$ where $\sigma^2(F)$ is derived from the previously defined $\sigma^2(I)$ gave uniform average values of $w(|F_o| - |F_c|)^2$ over ranges of $|F_o|$ and was employed in the final stages of refinement. An isotropic Type I extinction correction (Thornley–Nelmes definition of mosaic anisotropy with a Lorentzian distribution) was applied (11–13). The final value of g was 0.60(4) × 10^4. Convergence was reached at R = 0.048 and R_w = 0.078 for 5508 reflections with $I \geq 3\sigma(I)$. For all 6263 reflections R = 0.052 and R_w = 0.078. The function minimized was $\Sigma w(|F_o| - |F_c|)^2$, $R = \Sigma||F_o| - |F_c||/\Sigma|F_o|$, and $R_w = (\Sigma w(|F_o| - |F_c|)^2/\Sigma w|F_o|^2)^{1/2}$.

On the final cycle of refinement the mean and maximum parameter shifts corresponded to 0.36 and 3.5σ (oscillating hydrogen thermal parameter) respectively. The mean error in an observation of unit weight was 2.89. A final difference map showed maximum fluctuations of ±1.0 e Å^{-3} near the gallium atoms and ±0.4 e Å^{-3} elsewhere. The final positional and thermal parameters appear in Tables 2 and 3[2] respectively. Measured and calculated structure factors have been placed in the Depository of Unpublished Data.[2]

The ellipsoids of thermal motion for the non-hydrogen atoms are shown in Fig. 1. The thermal motion has been analysed in terms of the rigid-body modes of translation, libration, and screw motion (14) using the computer program MGTLS. The rms standard error in the temperature factors U_{ij} (derived from the least-squares analysis) is 0.0033 Å^2. Analysis of all non-hydrogen atoms excluding methyl carbon atoms and C(16) gave rms U_{ij} = 0.0046 Å^2 and physically reasonable rigid-body parameters. The appropriate bond distances have been corrected for libration (15), using shape parameters q^2 of 0.08 for all atoms involved. Corrected bond lengths appear in Table 4 along with the uncorrected values and corrected bond angles do not differ by more than 1σ from the uncorrected values listed in Table 5. Intra-annular torsion angles defining the conformations of the chelate rings are given in Table 6.

Results and Discussion

Mass Spectra

The mass spectra of the octahedral complexes,

[1]In the preparation of the five-coordinate copper complex it was necessary to use a 3:1 ligand to metal salt stoichiometry as a 2:1 ratio produced intractable oils only.

[2]The structure factor table and Table 3 (thermal parameters) are available, at a nominal charge, from the Depository of Unpublished Data, CISTI, National Research Council of Canada, Ottawa, Ont., Canada K1A 0S2.

Can. J. Chem. Downloaded from www.nrcresearchpress.com by 210.87.254.40 on 09/05/12
For personal use only.

TABLE 1. Analytical data

Compound	M	Color	Transition metal precursor	Analysis (%) found/calcd C	H	N	Comments
$[Me_2Ga(N_2C_5H_7)(OCH_2CH_2NH_2)]_2M$	Fe	Orange	$FeCl_2 \cdot 1.5THF$	39.3 38.2	7.1 6.8	14.5 14.8	Extremely moisture and air sensitive
	Co	Magenta	$CoCl_2$	38.5 38.0	6.9 6.7	14.2 14.8	Solution air sensitive
	Ni · benzene	Blue	$Ni(BF_4)_2 \cdot 6H_2O$	44.8 44.6	6.9 6.9	13.0 13.0	Air stable
	Ni · acetone	Turquoise	$Ni(BF_4)_2 \cdot 6H_2O$	40.6 40.2	7.2 7.1	13.4 13.4	Air stable
$[Me_2Ga(N_2C_5H_7)_2]$ M $[Me_2Ga(N_2C_5H_7)(OCH_2CH_2NMe_2)]$	Fe	Pale yellow	$FeCl_2 \cdot 1.5THF$	41.5 43.9	6.9 6.9	14.2 15.6	Extremely air sensitive
	Co	Dark purple	$CoCl_2$	43.6 43.7	6.9 6.9	15.8 15.5	Air stable
	Ni	Emerald green	$Ni(BF_4)_2 \cdot 6H_2O$	43.8 43.7	6.7 6.9	15.6 15.5	Air stable
	Cu	Blue–green	$CuBr_2$	43.2 43.4	6.8 6.8	15.3 15.4	Air stable
	Zn	White	$ZnCl_2$	42.7 43.3	6.4 6.8	16.0 15.4	Air sensitive

Can. J. Chem. Downloaded from www.nrcresearchpress.com by 210.87.254.40 on 09/05/12
For personal use only.

TABLE 2. Final positional parameters (fractional; O, N, and C × 10^4, Ga and Ni × 10^5, H × 10^3) with estimated standard deviations in parentheses

Atom*	x	y	z
Ga(1)	10058(2)	19529(5)	34287(7)
Ga(2)	40486(2)	71815(6)	23915(7)
Ni	26320(3)	44890(6)	23655(7)
O	3441(1)	5524(4)	1276(4)
N(1)	1140(2)	3841(3)	2502(5)
N(2)	1722(1)	4826(3)	2228(4)
N(3)	1904(1)	1781(3)	3886(4)
N(4)	2483(1)	2776(3)	3641(4)
N(5)	3485(1)	7105(3)	4406(4)
N(6)	2874(1)	6172(3)	4367(4)
N(7)	2626(2)	2968(4)	−53(4)
C(1)	643(2)	4473(5)	2160(7)
C(2)	905(3)	5828(5)	1659(7)
C(3)	1575(2)	6026(4)	1725(5)
C(4)	−58(3)	3687(8)	2346(14)
C(5)	2096(3)	7300(6)	1321(8)
C(6)	2040(2)	682(4)	4634(5)
C(7)	2695(2)	946(5)	4842(5)
C(8)	2962(2)	2264(4)	4228(5)
C(9)	1515(3)	−558(6)	5124(8)
C(10)	3659(2)	3090(7)	4166(8)
C(11)	3557(2)	7953(5)	5902(5)
C(12)	2996(2)	7591(4)	6846(5)
C(13)	2581(2)	6471(4)	5848(4)
C)14)	4166(3)	9116(8)	6325(9)
C(15)	1901(2)	5690(6)	6227(6)
C(16)	3589(3)	4945(8)	−393(7)
C(17a)′	2986(4)	4034(9)	−1133(8)
C(18)	536(3)	2298(8)	5588(10)
C(19)	667(3)	264(6)	1662(9)
C(20)	4043(6)	9026(12)	1504(13)
C(21)	4862(4)	6484(13)	2639(21)
C(22a)′	1958(6)	2388(15)	−716(12)
C(23a)′	2959(8)	1765(11)	−7(11)
C(17b)″	3318(7)	3220(16)	−656(19)
C(22b)″	2207(16)	3242(35)	−1158(38)
C(23b)″	2407(10)	1281(21)	64(25)
H(2)	59(5)	608(11)	100(12)
H(4a)	−17(7)	332(17)	364(18)
H(4b)	−26(5)	403(12)	149(12)
H(4c)	−10(5)	229(12)	193(13)
H(5a)	251(4)	689(9)	99(11)
H(5b)	198(3)	777(8)	66(9)
H(5c)	229(9)	821(24)	193(22)
H(7)	289(3)	54(7)	546(8)
H(9a)	148(3)	−21(7)	640(9)
H(9b)	105(4)	−66(9)	444(10)
H(9c)	154(4)	−154(11)	529(11)
H(10a)	401(3)	279(6)	462(7)
H(10b)	371(3)	333(7)	306(8)
H(10c)	368(3)	413(8)	463(9)
H(12)	293(2)	795(6)	794(7)
H(14a)	450(8)	860(20)	652(22)
H(14b)	446(6)	963(15)	511(16)
H(14c)	418(3)	954(7)	765(8)
H(15a)	183(3)	610(7)	711(8)
H(15b)	161(3)	563(5)	540(7)
H(15c)	182(3)	472(7)	602(7)
H(16a)′	377	580	−99
H(16b)′	393	432	−45
H(16c)″	340	545	−113
H(16d)″	408	514	−60
H(17a)′	309	344	−220
H(17b)′	269	470	−133
H(18a)	52(5)	365(13)	595(13)
H(18b)	13(6)	198(13)	559(14)
H(18c)	74(3)	193(7)	629(8)
H(19a)	27(6)	−43(12)	194(13)
H(19b)	52(5)	53(11)	64(12)
H(19c)	78(5)	−34(11)	174(13)
H(20a)	437(5)	1005(11)	193(11)
H(20b)	422(7)	870(15)	75(18)
H(20c)	381(6)	929(12)	143(14)
H(21a)	498(4)	691(9)	364(10)
H(21b)	489(4)	569(11)	181(12)
H(21c)	504(6)	690(15)	225(16)
H(17c)″	357	270	−8
H(17d)″	334	280	−185
H(22a)′	202	220	−198
H(22b)′	169	172	−29
H(22c)′	175	342	−60
H(23a)′	317	142	−116
H(23b)′	344	235	56
H(23c)′	280	103	53
H(22d)″	218	244	−211
H(22e)″	175	307	−57
H(22f)″	232	421	−138
H(23d)″	245	65	−103
H(23e)″	267	98	84
H(23f)″	194	105	43

*Prime denotes occupancy 0.70, double primes denote occupancy 0.30.

$[Me_2Ga(N_2C_5H_7)(OCH_2CH_2NH_2)]_2M$, display signals due to the parent ions in addition to signals from ions arising from predictable fragmentation patterns. In each case the most intense signal was due to the ion $[MeGa(N_2C_5H_7)_2(OCH_2CH_2NH_2)M]^+$. No ions of higher mass than the octahedral parent ion were observed in the spectra, a result which substantiates the presence of monomeric species in the gas phase.

In the case of the five-coordinate complexes, the signal corresponding to the parent ion was either very weak or absent. The strongest signal in the majority of the spectra corresponded to the ion $[MeGa(N_2C_5H_7)_2(OCH_2CH_2NMe_2)M]^+$. The one exception was the Cu complex which gave as its strongest signal that corresponding to the ion $[MeGa(N_2C_5H_7)(OCH_2CH_2NMe_2)Cu]^+$. This ion was not present in the fragmentation patterns of the remaining five-coordinate complexes. As in the case of the octahedral complexes, no signals due to ions of higher mass than the monomeric five-coordinate species were observed.

In both sets of spectra the relative intensities of the individual peaks in multi-line signals agreed well with those predicted on the basis of the natural isotope compositions of the contributing metal atoms.

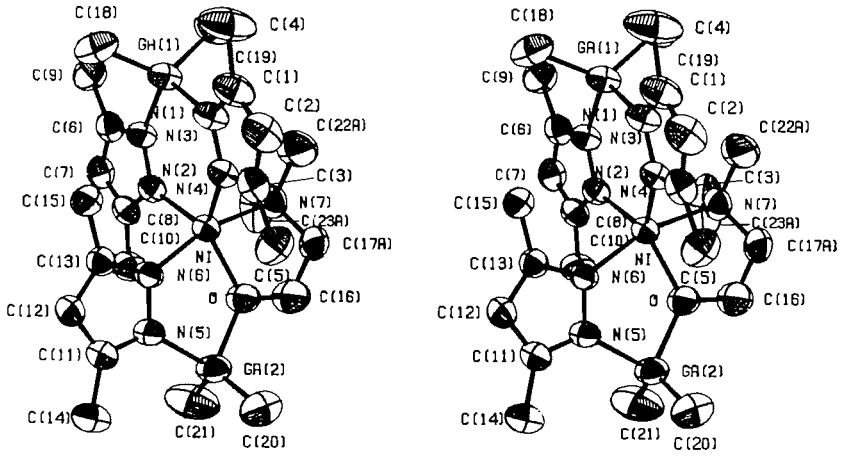


FIG. 1. Stereo view of the [dimethylbis(3,5-dimethyl-1-pyrazolyl)gallato(*N*(2),*N*′(2))][dimethyl(3,5-dimethyl-1-pyrazolyl)(*N*,*N*-dimethylethanolamino)gallato(*N*(2),*O*,*N*(3))]nickel](II) molecule, 50% thermal ellipsoids are shown for the non-hydrogen atoms.

TABLE 4. Bond lengths (Å) with estimated standard deviations in parentheses
(*a*) Non-hydrogen atoms

Bond	Length (Å)		Bond	Length (Å)	
	Uncorr.	Corr.		Uncorr.	Corr.
Ga(1)—N(1)	1.972(3)	1.975	N(5) —C(11)	1.341(5)	1.342
Ga(1)—N(3)	1.984(3)	1.989	N(6) —C(13)	1.337(5)	1.340
Ga(1)—C(18)	1.978(7)	1.978	N(7) —C(17a)	1.489(8)	1.490
Ga(1)—C(19)	1.984(6)	1.986	N(7) —C(22a)	1.495(11)	1.497
Ga(2)—O	1.910(3)	1.913	N(7) —C(23a)	1.425(9)	1.427
Ga(2)—N(5)	1.967(3)	1.971	N(7) —C(17b)	1.475(15)	
Ga(2)—C(20)	1.960(10)	1.961	N(7) —C(22b)	1.401(30)	
Ga(2)—C(21)	1.969(9)	1.969	N(7) —C(23b)	1.535(19)	
Ni —O	1.989(3)	1.993	C(1) —C(2)	1.369(7)	1.370
Ni —N(2)	2.000(3)	2.006	C(1) —C(4)	1.500(8)	1.501
Ni —N(4)	2.001(3)	2.005	C(2) —C(3)	1.377(7)	1.378
Ni —N(6)	2.068(3)	2.072	C(3) —C(5)	1.485(7)	1.488
Ni —N(7)	2.227(3)	2.229	C(6) —C(7)	1.356(6)	1.358
O —C(16)	1.424(6)	1.424	C(6) —C(9)	1.494(6)	1.495
N(1) —N(2)	1.383(4)	1.386	C(7) —C(8)	1.385(6)	1.386
N(1) —C(1)	1.357(5)	1.357	C(8) —C(10)	1.494(6)	1.496
N(2) —C(3)	1.340(5)	1.341	C(11)—C(12)	1.370(6)	1.373
N(3) —N(4)	1.377(4)	1.380	C(12)—C(14)	1.498(6)	1.499
N(3) —C(6)	1.358(5)	1.359	C(12)—C(13)	1.388(5)	1.390
N(4) —C(8)	1.344(5)	1.346	C(13)—C(15)	1.485(6)	1.488
N(5) —N(6)	1.378(4)	1.381	C(16)—C(17a)	1.468(10)	1.470
			C(16)—C(17b)	1.544(16)	

Infrared Spectra

The infrared spectra of the octahedral complexes display N—H vibrations identical to the *meridional* octahedral complexes formed with the ligand **1** where R = R′ = H (1). It is therefore not unreasonable to assign this same arrangement to the gallate ligands in the present complexes. The visible spectrum (see below) of the Ni derivative provides further evidence for this assignment for this complex.

The infrared spectra of the five-coordinate complexes fell into two groups. The Fe, Ni, and Zn complexes formed one group with very similar spectra whilst the Co and Cu complexes formed the second group. These two groups displayed marked differences in their ir spectra in the region 1600–400 cm^{-1} (see Fig. 2). These differences between the spectra of the two groups of complexes probably arise from different molecular geometries. A trigonal bipyramidal geometry has been demonstrated for the Ni complex through an X-ray structure determination (see below) whereas a severely distorted trigonal bipyramidal geometry is suggested for the Co complex by its visible spectrum.

Can. J. Chem. Downloaded from www.nrcresearchpress.com by 210.87.254.40 on 09/05/12
For personal use only.

Can. J. Chem. Downloaded from www.nrcresearchpress.com by 210.87.254.40 on 09/05/12
For personal use only.

TABLE 5. Bond angles (deg) for non-hydrogen atoms with estimated standard deviations in parentheses

Bonds	Angle (deg)	Bonds	Angle (deg)
N(1) —Ga(1)—N(3)	103.9(1)	Ni —N(6) —N(5)	120.0(2)
N(1) —Ga(1)—C(18)	107.5(2)	Ni —N(6) —C(13)	132.4(2)
N(1) —Ga(1)—C(19)	107.2(2)	N(5) —N(6) —C(13)	106.9(3)
N(3) —Ga(1)—C(18)	106.3(3)	Ni —N(7) —C(17a)	101.3(3)
N(3) —Ga(1)—C(19)	108.2(2)	Ni —N(7) —C(22a)	113.8(4)
C(18)—Ga(1)—C(19)	122.2(3)	Ni —N(7) —C(23a)	111.4(4)
O —Ga(2)—N(5)	89.7(1)	C(17a)—N(7) —C(22a)	106.5(7)
O —Ga(2)—C(20)	109.9(3)	C(17a)—N(7) —C(23a)	111.7(7)
O —Ga(2)—C(21)	108.5(3)	C(22a)—N(7) —C(23a)	111.5(9)
N(5) —Ga(2)—C(20)	110.7(4)	Ni —N(7) —C(17b)	104.3(6)
N(5) —Ga(2)—C(21)	110.3(5)	Ni —N(7) —C(22b)	113.5(12)
C(20)—Ga(2)—C(21)	122.7(5)	Ni —N(7) —C(23b)	113.7(8)
O —Ni —N(2)	126.3(1)	C(17b)—N(7) —C(22b)	112.5(15)
O —Ni —N(4)	131.1(1)	C(17b)—N(7) —C(23b)	107.8(9)
O —Ni —N(6)	85.4(1)	C(22b)—N(7) —C(23b)	105.1(15)
O —Ni —N(7)	79.5(1)	N(1) —C(1) —C(2)	108.8(4)
N(2) —Ni —N(4)	102.3(1)	N(1) —C(1) —C(4)	120.9(5)
N(2) —Ni —N(6)	95.6(1)	C(2) —C(1) —C(4)	130.3(5)
N(2) —Ni —N(7)	94.5(1)	C(1) —C(2) —C(3)	106.7(4)
N(4) —Ni —N(6)	95.3(1)	N(2) —C(3) —C(2)	109.1(4)
N(4) —Ni —N(7)	93.5(1)	N(2) —C(3) —C(5)	121.4(4)
N(6) —Ni —N(7)	164.8(1)	C(2) —C(3) —C(5)	129.5(4)
Ga(2)—O —Ni	123.2(2)	N(3) —C(6) —C(7)	108.9(4)
Ga(2)—O —C(16)	118.6(3)	N(3) —C(6) —C(9)	122.0(4)
Ni —O —C(16)	118.1(3)	C(7) —C(6) —C(9)	129.2(4)
Ga(1)—N(1) —N(2)	128.5(2)	C(6) —C(7) —C(8)	106.5(3)
Ga(1)—N(1) —C(1)	123.8(3)	N(4) —C(8) —C(7)	109.3(3)
N(2) —N(1) —C(1)	107.5(3)	N(4) —C(8) —C(10)	121.2(4)
Ni —N(2) —N(1)	127.1(2)	C(7) —C(8) —C(10)	129.5(4)
Ni —N(2) —C(3)	124.8(3)	N(5) —C(11) —C(12)	108.9(3)
N(1) —N(2) —C(3)	108.0(3)	N(5) —C(11) —C(14)	121.8(4)
Ga(1)—N(3) —N(4)	127.5(2)	C(12) —C(11) —C(14)	129.3(5)
Ga(1)—N(3) —C(6)	124.1(3)	C(11) —C(12) —C(13)	105.7(4)
N(4) —N(3) —C(6)	108.2(3)	N(6) —C(13) —C(12)	109.7(3)
Ni —N(4) —N(3)	127.8(2)	N(6) —C(13) —C(15)	121.4(3)
Ni —N(4) —C(8)	124.6(3)	C(12) —C(13) —C(15)	128.8(4)
N(3) —N(4) —C(8)	107.1(3)	O —C(16) —C(17a)	108.8(4)
Ga(2)—N(5) —N(6)	120.2(2)	O —C(16) —C(17b)	107.2(7)
Ga(2)—N(5) —C(11)	130.7(3)	N(7) —C(17a)—C(16)	111.4(6)
N(6) —N(5) —C(11)	108.8(3)	N(7) —C(17b)—C(16)	108.0(9)

Electronic Spectra

The electronic spectra of the complexes were recorded in the range 300–1400 nm and are listed and assigned in Tables 7 and 8.

The spectra of the octahedral nickel and cobalt complexes are as expected for high-spin Ni(II) and Co(II) complexes, and have been analysed on the basis of the energy levels discussed in ref. 16. D_q and B values are listed in Table 7. The observed ν_2 and ν_3 bands of the nickel complexes were used in the calculation of these parameters. This leads to a calculated value of 10.4 kK for ν_1 for both nickel complexes. The expected $\rightarrow {}^1E_g$ transitions are 13.1 kK ($C/B = 4.5$ has been assumed for the calculation of the ${}^1E_g$ transition (16)) in close agreement with the 12.9 kK experimental values. Similarly ν_1 and ν_3 have been used to calculate D_q and B of the cobalt complex. This leads to a calculated value of 19.8 kK for ν_2 for the complex. Comparison of the D_q values of the present complexes with those for the octahedral complexes of Ni(II) and Co(II) using the ligand **1** where R = R′ = H (1) shows the present values to be slightly lower than the previous ones, suggesting a weaker crystal field in these new complexes. Comparison of the ε values of the absorptions for the new nickel complexes with those reported earlier for the *fac* and *mer* octahedral complexes where R = R′ = H (2) suggests a *meridional* arrangement of the ligand in the present complexes. This postulation is also supported by the Nujol ir spectrum which shows three distinct bands in the ν_{NH} region of the spectrum.

Can. J. Chem. Downloaded from www.nrcresearchpress.com by 210.87.254.40 on 09/05/12
For personal use only.

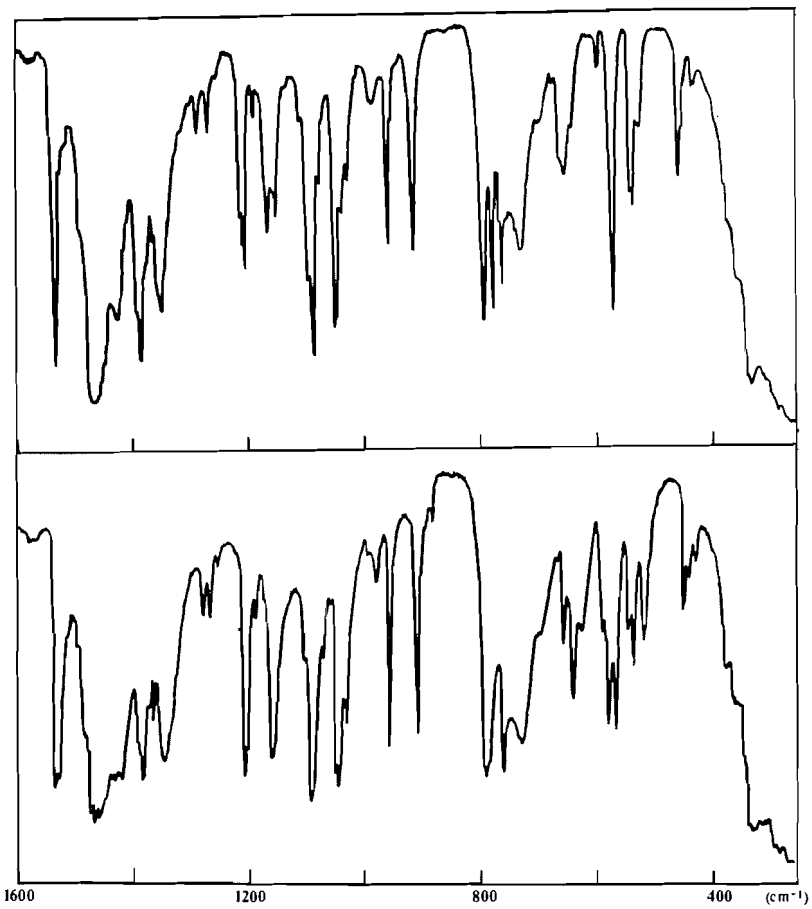


FIG. 2. Infrared spectra (Nujol) of the five-coordinate complexes $[Me_2Ga(N_2C_5H_7)(OCH_2CH_2NMe_2)]M[Me_2Ga(N_2C_5H_7)_2]$. Upper: M = Fe, Ni, Zn. Lower: M = Co, Cu.

TABLE 6. Intra-annular torsion angles (deg) for chelate rings

Bond	Angle (deg)	Bond	Angle (deg)
Ga(1) —N(1)	0.0(2)	Ga(2) —O	−1.6(1)
N(1) —N(2)	10.2(3)	O —Ni	6.6(1)
N(2) —Ni	−17.2(2)	Ni —N(6)	−12.1(2)
Ni —N(4)	18.6(2)	N(6) —N(5)	14.6(2)
N(4) —N(3)	−12.8(3)	N(5) —Ga(2)	−7.8(2)
N(3) —Ga(1)	1.3(2)		
Ni —O	4.6(3)	Ni —O	4.6(3)
O —C(16)	20.5(5)	O —C(16)	−30.9(7)
C(16) —C(17a)	−47.1(6)	C(16) —C(17b)	51.3(8)
C(17a)—N(7)	47.3(4)	C(17b)—N(7)	−45.7(8)
N(7) —Ni	−27.8(3)	N(7) —Ni	23.7(6)

The spectra of the five-coordinate Ni, Co, and Cu complexes are presented in Fig. 3. The nickel spectrum has been assigned on the basis of the crystal field model discussed by Ciampolini (17). With the exception of the splitting of one band the spectrum can be interpreted in terms of a trigonal bipyramidal model. The splitting of the band around 11.5 kK into two components indicates a reduction of symmetry from the idealized D_{3h} on which the model is based. Reduction to C_{3v} symmetry would give two bands as transitions to $^3A_1(F)$ and $^3A_2(F)$ instead of degenerate transitions to $^3A_1'' + {}^3A_2''$ in D_{3h} symmetry. The spectrum of the present compound is almost identical to that of $[Ni(trenMe)Cl]^+$ where trenMe = tris(2-dimethylaminoethyl)amine (18), the bromo analog of which has been shown by X-ray crystallography to possess C_{3v} microsymmetry (19). The only notable difference in the present spectrum is the shift of all the bands to higher energy (NiN_4O chromophore vs. NiN_4Cl chromophore).

The overall shape of the cobalt spectrum did not fit ligand field models for either trigonal bipyramidal or square pyramidal geometries. This is no doubt due to severe distortions from these idealized geometries in the present complex. Indeed it is well

Can. J. Chem. Downloaded from www.nrcresearchpress.com by 210.87.254.40 on 09/05/12
For personal use only.

TABLE 7. Electronic spectra for $[Me_2Ga(N_2C_5H_7)(OCH_2CH_2NH_2)]_2M$ complexes

M	Energy (kK)	ε	D_q (cm^{-1})	B (cm^{-1})	Assignment
Ni (in benzene)	9.5	10.2	1035	790	$^3A_{2g} \rightarrow {}^3T_{2g}$
	12.9	0.5			$^3A_{2g} \rightarrow {}^1E_g$
	16.5	10.5			$^3A_{2g} \rightarrow {}^3T_{1g}(F)$
	26.5	20.5			$^3A_{2g} \rightarrow {}^3T_{1g}(P)$
Ni (in acetone)	9.5	10.7	1035	790	$^3A_{2g} \rightarrow {}^3T_{2g}$
	12.9	0.5			$^3A_{2g} \rightarrow {}^1E_g$
	16.5	9.7			$^3A_{2g} \rightarrow {}^3T_{1g}(F)$
	26.5	18.7			$^3A_{2g} \rightarrow {}^3T_{1g}(P)$
Co (in benzene)	9.2	5.2	1050	850	$^4T_{1g}(F) \rightarrow {}^4T_{2g}$
	[14.7	0.9			$^4T_{1g}(F) \rightarrow {}^2T_{2g}, {}^2T_{1g}]$
	19.8	38			$^4T_{1g}(F) \rightarrow {}^4A_{2g}$
	20.6 (sh)*	37			$^4T_{1g}(F) \rightarrow {}^4T_{1g}(P)$

*sh = shoulder.

TABLE 8. Electronic spectra for $[Me_2Ga(N_2C_5H_7)(OCH_2CH_2NMe_2)]M[(N_2C_5H_7)_2GaMe_2]$ complexes*

M	Energy (kK)	ε	Assignment
Ni	7.4	15.0	$^3E' \rightarrow {}^3E''(F)$
	11.3	30	$^3E' \rightarrow {}^3A_1'', {}^3A_2''$
	12.4	24	
	14.9	35	$^3E' \rightarrow {}^3A_2'(F)$
	20.6 (sh)	—	$^3E' \rightarrow {}^3E''(P) + {}^3A_2'(P)$
	24.2	130	
Co	7.3	9	$^4A_2' \rightarrow {}^4E''$
	9.6	15	$^4A_2' \rightarrow {}^4E'$
	13.7	13	$^4A_2' \rightarrow {}^4A_2'(P)$
	17.6	198	$^4A_2' \rightarrow {}^4E''(P)$
	19.8 (sh)	—	
	20.7 (sh)	—	
Cu	13.5	135	$^2A_1' \rightarrow {}^2E(1) + {}^2E(2)$
	9.0 (sh)	—	

*Benzene solutions, sh = shoulder.

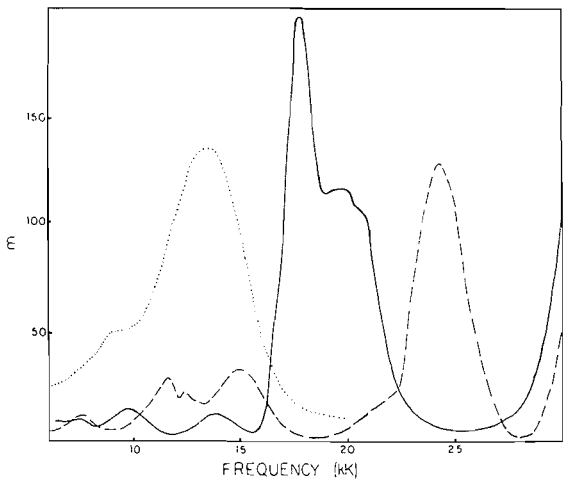


FIG. 3. Electronic spectra of the five-coordinate Ni, Co, and Cu complexes (- - - Ni, — Co, · · · Cu).

known that trigonal bipyramidal cobalt(II) complexes are commonly more distorted toward the tetrahedron than their Ni(II) analogs (20). The band positions for the present complex correlate closely with those of the complex $\{Co(NP_3)Br\}^+PF_6^-$, where NP_3 = tris(2-diphenylphosphinoethyl)-amine, which has been shown by X-ray crystallography to possess an extremely distorted trigonal bipyramidal geometry (21).

The assignment of the bands given in Table 8 is based on the ligand field model proposed by Wood (22) for idealized high-spin trigonal bipyramidal Co(II) complexes. The expected singlet band for the transition $4A_2' \rightarrow 4E''$ is replaced in the spectrum of the present compound by a complex band envelope, no doubt due to the aforementioned distortions from the idealized geometry.

The spectrum of the five-coordinate copper derivative shows essentially one band with a shoulder to lower energy. The spectrum does not in itself point to a particular geometry for the complex but it is not inconsistent with a highly distorted geometry similar to the one proposed for the cobalt compound. It has already been pointed out that the two complexes have identical ir spectra, suggestive of similar molecular geometries.

The mechanism of formation of the present five-coordinate complexes is not obvious. A previous study (2) using the $[Me_2Ga(N_2C_3H_3)(OCH_2CH_2NMe_2)]^-$ ligand demonstrated that bis-ligand octahedral complexes could not be formed. In that study binuclear five-coordinate metal complexes were produced and a plausible mechanism proposed. It was not surprising, therefore, that the more sterically demanding ligand $[Me_2Ga(N_2C_5H_7)(OCH_2CH_2NMe_2)]^-$ did not lead to octahedral complexes. Further, it is again

Can. J. Chem. Downloaded from www.nrcresearchpress.com by 210.87.254.40 on 09/05/12
For personal use only.

thought that the five-coordinate complexes formed with this ligand must arise from a decomposition of the second (and subsequent) incoming ligands. The absence of the ligand $Me_2Ga(N_2C_5H_7)_2^-$ in the starting materials was evidenced by the complete lack of production of the previously characterized $\{Me_2Ga(N_2C_5H_7)_2\}_2Cu$ compound (23, 24).

X-ray Crystallographic Analysis of $[Me_2Ga(N_2C_5H_7)(OCH_2CH_2NMe_2)]$-$Ni[(N_2C_5H_7)_2GaMe_2]$

The structure of $[Me_2Ga(N_2C_5H_7)(OCH_2CH_2NMe_2)]Ni[(N_2C_5H_7)_2GaMe_2]$ consists of discrete molecular units separated by normal van der Waals distances. There are a number of short intramolecular C—H···O and C—H···N interactions which may correspond to weak hydrogen bonds present in the structure (O···H(5a) 2.57(8), N(2)···H(15b) 2.60(5), N(2)···H(22c) 2.47, N(2)···H(22e) 2.58, and N(4)···H(23e) 2.65 Å). In any case these interligand contacts are indicative of steric crowding about the central metal.

The coordination geometry about the nickel atom is distorted trigonal bipyramidal. The tridentate $Me_2Ga(N_2C_5H_7)(OCH_2CH_2NMe_2)$ ligand is meridionally coordinated with the oxygen occupying an equatorial position and the two nitrogen atoms are in the axial sites. The two remaining equatorial positions are occupied by the two nitrogen donors of the $Me_2Ga(N_2C_5H_7)_2$ ligand. The angle between the axial groups is 164.8(1)°.

The nature of complexes formed by the reaction of the gallate ligands L, **1**, with divalent metals of the first transition series is determined by steric factors. When R′ = H and R = H (2) or Me (Table 1), octahedral complexes L_2M are formed. When R′ = Me and R = H binuclear five-coordinate complexes $(\mu\text{-}N_2C_3H_3)_2(LM)_2$ were isolated (1) and the present study shows that when R = R′ = Me mononuclear five-coordinate species $[Me_2Ga(N_2C_5H_7)_2]ML$ are obtained.

The complex (Fig. 1) contains two systems of three fused rings which have the Ni atom in common and are approximately at right angles to one another. The central six-membered $Ga(2)N_4Ni$ ring is significantly non-planar, the Ni atom being displaced from the plane defined by the other five atoms in the ring (see Table 6 for torsion angles). The $[Me_2Ga(N_2C_5H_7)_2]Ni$ system is slightly folded, the angle between normals to the two pyrazolyl mean planes being 9.1(1)°. This is intermediate between the markedly folded systems observed in the square planar complexes $[Me_2Ga(N_2C_3H_3)_2]_2M$, M = Cu (24) and Ni (25) and the nearly planar arrangement found in the tetrahedral complex $[Me_2Ga(N_2C_5H_7)_2]_2Cu$ (24). The ligand **1** has internal geometry and conformation similar to that observed for other "meridionally" coordinated ligands **1** (1, 2, 26). All three pyrazolyl rings are planar within experimental error ($\chi^2 = 1.9$, 5.5, and 0.6 for N_2C_3 rings containing N(1), N(3), and N(5) respectively) and in each case the metal atoms are displaced significantly from the mean planes (Ga(1) −0.1463(5), Ni 0.1297(6) from the N(1) ring; Ga(1) −0.1112(5), Ni 0.2284(6) from the N(3) ring and Ga(2) 0.1894(6), Ni −0.2581(6) Å from the N(5) ring).

The equatorial Ni—N bond distances (2.006(3) and 2.005(3) Å) are equal within experimental error and are both significantly longer than the mean Ni—N(pz) distance of 1.895(4) Å in the square planar complex $[Me_2Ga(N_2C_3H_3)_2]_2Ni$ (25). The Ni—O, Ni—N(pz), and Ni—N(amino) distances involving the $Me_2Ga(N_2C_5H_7)(OCH_2CH_2NMe_2)$ ligand are 1.993(3), 2.072(3), and 2.229(3) Å. These values may be compared to corresponding distances of 2.037(3), 2.112(3), and 2.279(3) Å in trigonal bipyramidal $[Me_2Ga(N_2C_5H_7)(OCH_2CH_2NMe_2)]Fe(NO)_2$ (26); 1.981(3), 2.023(4), and 2.173(3) Å (all basal) in the binuclear square pyramidal complex $(\mu\text{-}N_2C_3H_3)_2(CuL)_2$ (1) and mean values of 2.047(2), 2.097(6), and 2.152(4) Å in octahedral *mer*-L_2Ni (2).

Acknowledgments

We thank the Natural Sciences and Engineering Research Council of Canada for financial support and the University of British Columbia Computing Centre for assistance. We are grateful to Mr. P. Borda for C, H, N analyses and to Mr. J. Nip for mass spectra.

1. K. S. CHONG, S. J. RETTIG, A. STORR, and J. TROTTER. Can. J. Chem. **56**, 1212 (1978).
2. K. S. CHONG, S. J. RETTIG, A. STORR, and J. TROTTER. Can. J. Chem. **55**, 4166 (1977).
3. K. S. CHONG and A. STORR. Can. J. Chem. **57**, 167 (1979).
4. A. STORR and B. S. THOMAS. Can. J. Chem. **48**, 3667 (1970).
5. M. ARESTA, C. F. NOBILE, and D. PETRUZZELLI. Inorg. Chem. **16**, 1817 (1977).
6. P. COPPENS, L. LEISEROWITZ, and D. RABINOVICH. Acta Crystallogr. **18**, 1035 (1965).
7. W. R. BUSING and H. A. LEVY. Acta Crystallogr. **22**, 457 (1967).
8. D. T. CROMER and J. B. MANN. Acta Crystallogr. Sect. A, **24**, 321 (1968).
9. R. F. STEWART, E. R. DAVIDSON, and W. T. SIMPSON. J. Chem. Phys. **42**, 3175 (1965).
10. D. T. CROMER and D. LIBERMAN. J. Chem. Phys. **53**, 1891 (1970).

11. P. J. BECKER and P. COPPENS. Acta Crystallogr. Sect. A, **30**, 129 (1974); **30**, 148 (1974); **31**, 417 (1975).
12. P. COPPENS and W. C. HAMILTON. Acta Crystallogr. Sect. A, **26**, 71 (1970).
13. F. R. THORNLEY and R. J. NELMES. Acta Crystallogr. Sect. A, **30**, 748 (1974).
14. V. SCHOMAKER and K. N. TRUEBLOOD. Acta Crystallogr. Sect. B, **24**, 63 (1969).
15. D. W. J. CRUICKSHANK. Acta Crystallogr. **9**, 747 (1956); **9**, 754 (1956); **14**, 896 (1961).
16. A. P. B. LEVER. Inorganic electronic spectroscopy. Elsevier, New York. 1968.
17. M. CIAMPOLINI. Inorg. Chem. **5**, 35 (1966).
18. M. CIAMPOLINI and N. NARDI. Inorg. Chem. **5**, 41 (1966).
19. P. L. ORIOLI and M. DIVAIRA. Inorg. Chem. **6**, 955 (1967).
20. L. SACCONI. Coord. Chem. Rev. **8**, 351 (1972).
21. M. DIVAIRA. J. Chem. Soc. Dalton Trans. 1575 (1975).
22. J. S. WOOD. Inorg. Chem. **7**, 852 (1968).
23. K. R. BREAKELL, D. J. PATMORE, and A. STORR. J. Chem. Soc. Dalton Trans. 749 (1975).
24. D. J. PATMORE, D. F. RENDLE, A. STORR, and J. TROTTER. J. Chem. Soc. Dalton Trans. 718 (1975).
25. D. F. RENDLE, A. STORR, and J. TROTTER. J. Chem. Soc. Dalton Trans. 176 (1975).
26. K. S. CHONG, S. J. RETTIG, A. STORR, and J. TROTTER. Can. J. Chem. **57**, 3113 (1979).

Can. J. Chem. Downloaded from www.nrcresearchpress.com by 210.87.254.40 on 09/05/12
For personal use only.

Electrochemical oxidation of carboxylic acid anions in the presence of some mono- and di-substituted olefins[1]

PHILIPPE J. CHAMPAGNE[2] AND ROGER N. RENAUD

Division of Chemistry, National Research Council of Canada, Ottawa, Ont., Canada K1A 0R6

Received December 12, 1979

PHILIPPE J. CHAMPAGNE and ROGER N. RENAUD. Can. J. Chem. **58**, 1101 (1980).

The anodic oxidation of the sodium salts of acetic, propionic, and isovaleric acids was performed in the presence of a series of ethylenic compounds bearing electron-withdrawing substituents. The results showed that under certain experimental conditions the electrogenerated radicals added to the ethylenic double bond to give mainly 1,2-dialkylated products.

The stereoisomers obtained were separated and, whenever possible, identified. Their physical properties are reported.

PHILIPPE J. CHAMPAGNE et ROGER N. RENAUD. Can. J. Chem. **58**, 1101 (1980).

Les sels sodés des acides acétique, propanoïque et méthyl-2 propanoïque ont été oxydés électrochimiquement en présence de composés éthyléniques ayant des substituents électroattracteurs. Les résultats ont démontrés que, sous certaines conditions expérimentales, les radicaux formés attaquent la double liaison pour donner principalement des composés dialkylés.

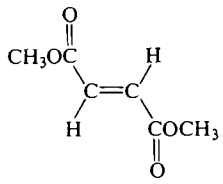
Les stéréoisomères obtenus ont été séparés et, dans certain cas, identifiés. Leurs propriétés physiques sont rapportées.

In the previous paper in this series (1) we reported the dimethylation of some symmetrical 1,2-disubstituted ethylenes via electrochemically generated methyl radicals.

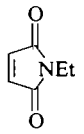
$$ZCH{=}CHZ \xrightarrow[\text{electrolysis}]{CH_3CO_2Na} ZCH(CH_3){-}CH(CH_3)Z$$

This reaction proceeded cleanly in high yields (55–88%) and in each case gave a 1:1 mixture of *meso* and *racemic* stereoisomers. The purpose of the present study was to investigate the generality of this reaction both in terms of the nature of the alkyl radical and the nature of the electron-withdrawing substituents on the ethylene molecule. As well as for the symmetrically disubstituted ethylenes (**1–3**), we have investigated the reactivity of the radicals derived from acetic, propionic, and isovaleric acids in the presence of an unsymmetrical disubstituted ethylene (**4**) and a monosubstituted ethylene (**5**).

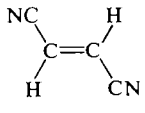
The only interesting 1,2-dialkylation of olefinic compounds reported in the literature is via the dialkyl copperlithium addition to α,β-ethylenic ketones (2). The electrochemical approach described in this paper is useful for alkylation of olefins substituted with a variety of electron-withdrawing groups.



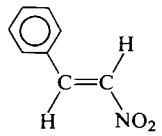
1



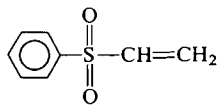
2



3



4



5

Experimental

Starting materials **2**, **3**, and **4** and sodium benzenesulfinate were commercially available. The dimethylester **1** was readily synthesized from fumaric acid (3). The vinyl sulfone **5** was prepared by a method developed in this laboratory and detailed below. All melting points are uncorrected. The cell used in this study and the general procedure for electrolysis of the sodium carboxylate in the presence of ethylenic substrates have been reported earlier (1). Gas–liquid chromatographic analyses and separations were performed respectively on a Fisher/Victoreen Series 4400 with a 6% SE 30 on Anakrom ABS 90/30 column and an aerograph Autoprep model A-700 using a 20 ft × 3/8 in. column, 30% SE 30 on 45/60 chromosorb P. Proton magnetic resonance spectra were taken in deuteriochloroform on a Varian Associates spectrometer model EM 360 and are reported in the δ scale. The mass spectra were obtained from a Finnigan 4000 GC-MS mass spectrometer.

Phenyl Vinyl Sulfone (5)

A solution of benzenesulfinic acid, sodium salt (11.2 g, 63.4 mmol), and 1-bromo-2-chloroethane (38.0 g, 236 mmol) in absolute ethanol (500 mL) was refluxed for 3 days, cooled, and then filtered to remove most of the sodium bromide. The ethanol was removed on a rotary evaporator and the white solid residue was extracted with CH_2Cl_2. After filtering and evaporation of the solvent, a white solid was obtained (11.6 g) which, by ^1H nmr, contained a mixture of the expected β-chloroethyl phenyl sulfone and the disubstituted product 1,2-bis-(phenylsufonyl)ethane. This mixture was treated directly with

[1]NRCC No. 18141.

[2]Present address: Department of Energy, Mines and Resources, Canmet, Energy Research Laboratories, Coal Liquifaction Laboratory, Ottawa, Ont., Canada K1A 0G1.

0008-4042/80/111101-05$01.00/0

©1980 National Research Council of Canada/Conseil national de recherches du Canada

Can. J. Chem. Downloaded from www.nrcresearchpress.com by 210.87.254.6 on 09/05/12
For personal use only.

Can. J. Chem. Downloaded from www.nrcresearchpress.com by 210.87.254.6 on 09/05/12
For personal use only.

triethylamine (10 mL) in CH_2Cl_2 (100 mL) and successively refluxed overnight, washed with water, dried over $MgSO_4$, and filtered. On evaporation of the solvent, an off-white solid (9.6 g) was obtained. This solid was recrystallized from a minimum amount of ethanol to give a white crystalline solid (3.4 g) which proved to be the disubstitution product $C_6H_5SO_2CH_2CH_2SO_2C_6H_5$, mp 184–186°C (lit. (4) 183–184°C). *Anal.* calcd. for $C_{14}H_{14}S_2O_4$: C 54.19, H 4.52, S 20.64; found: C 54.03, H 4.75, S 20.36.

The filtrate, after evaporation of the ethanol, gave a sticky yellowish solid (6.2 g). This solid was recrystallized from benzene in a Craig tube and repeated cooling and centrifuging yielded pure phenyl vinyl sulfone (4.0 g, 34%), mp 69.5–70.5°C (lit. (5) 68.5°C); ^{1}H nmr: 7.85 (2 H, m, ArH *o* to SO_2), 7.55 (3 H, m, ArH *m* and *p* to SO_2), 5.87–7.00 (3 H, m, olefinic). *Anal.* calcd. for $C_8H_8SO_2$: C 57.10, H 4.76, S 19.05; found: C 57.30, H 4.93, S 18.94.

Anodic Oxidation of Acetic Acid Anion[3]

(*A*) In the presence of **4** (1.49 g, 0.03 *M*)

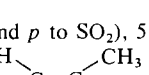
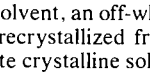
The extracted oil was distilled at 10^{-2} Torr and 25°C to remove volatile matter, then at 100°C to give a viscous yellow oil (1.22 g) which by vpc showed two major peaks, the faster moving peak being slightly larger than the slower one and having the same retention time as the starting material **4**. However, ^{1}H nmr indicated the presence of only a very small amount of **4**. On the Autoprep this fraction gave three peaks, the smallest having the same retention time as **4**. The two slowest moving peaks, approximately equal in area, were separated on the Autoprep and shown to be *threo*- and *erythro*-2-phenyl-3-nitrobutane (**6**) in a total yield of 37%. First peak (*threo*- or *erythro*-**6**); ^{1}H nmr: 7.20 (5 H, broad s, Ph), 4.63 (1 H, m, methine α to NO_2), 3.20 (1 H, m, methine α to Ph), 1.30 (6 H, d, J = 7.0 Hz, methyls). *Anal.* calcd. for $C_{10}H_{13}NO_2$: C 67.05, H 7.28, N 7.82; found: C 67.17, H 7.65, N 7.56. Second peak (*threo*- or *erythro*-**6**); ^{1}H nmr: 7.2 (5 H, s, Ph), 4.72 (1 H, m, methine α to NO_2), 3.40 (1 H, m, methine α to Ph), 1.59 (3 H, d, J = 7.0 Hz, methyl), 1.33 (3 H, d, J = 7.0 Hz, methyl). *Anal.* found for $C_{10}H_{13}NO_2$: C 67.54, H 7.64, N 7.58.

After treatment with NaOMe in MeOD in an nmr tube each of the above isomers gave the same nmr spectrum with no apparent methine absorptions and two 3 proton methyl singlets at 1.32 and 1.45.

(*B*) In the presence of **5** (3.69 g, 0.066 *M*)[4]

The extracted oil (4.30 g) was vacuum distilled at 10^{-2} Torr and 25°C to remove traces of volatile material, then at 110°C to give a colourless viscous oil (3.80 g), and at 200°C to give a colourless oil (0.30 g) which formed white crystals on standing at room temperature.

Column chromatography of the 110°C fraction on silica gel using a mixture of hexane/ethyl acetate (4:1) as eluent gave, as a first fraction, 2-phenylsulfonylbutane (**7**) (2.95 g, 69%); ^{1}H nmr: 7.80 (2 H, m, ArH *o* to SO_2), 7.52 (3 H, m, ArH *m* and *p* to SO_2), 2.85 (1 H, m, methine α to SO_2), 1.82 (2 H, m, methylene), 1.19 (3 H, d, CH_3C—, J = 6.8 Hz), 0.88 (3 H, t, CH_3CH_2—, J = 6.8 Hz). *Anal.* calcd. for $C_{10}H_{14}SO_2$: C 60.60, H 7.05, S 16.16; found: C 60.83, H 7.20, S 16.28.

Further elution with the same solvent system gave phenyl 1-propenyl sulfone (**8**), mp 65.5–66.0°C (lit. (6) 67–68°C); ^{1}H nmr: 7.83 (2 H, m, ArH *o* to SO_2), 7.53 (3 H, broad s, ArH *m* and *p* to SO_2), 5.9–7.4 (2 H, m, ), 1.9 (3 H, d,  , J = 6.8 Hz).[5] *Anal.* calcd. for $C_9H_{10}SO_2$: C 59.34, H 5.49, S 17.58; found: C 59.55, H 5.63, S 17.70.

The white solid obtained from distillation was shown to be 3,4-bis(phenylsulfonyl)hexane (**9**) as a mixture of isomers resulting from dimerization of the β-methylated radical intermediate, mp 112–114°C; ^{1}H nmr: 7.78 (4 H, m, ArH *o* to SO_2), 7.50 (6 H, broad s, ArH *m* and *p* to SO_2), 3.58 (2 H, t, methines α to SO_2), 1.98 (4 H, m, methylene), 0.90 (6 H, 2t, methyls, J = 7.0 Hz). *Anal.* calcd. for $C_{18}H_{22}S_2O_4$: C 59.02, H 6.01, S 17.49; found: C 59.10, H 6.19, S 17.39.

Anodic Oxidation of Propionic Acid Anion[6]

(*C*) In the presence of **1** (1.49 g, 0.03 *M*)

The extracted oil was distilled at 10^{-2} Torr and 25°C to remove volatile components and then at 80°C to give a colourless oil (2.20 g) which on vpc showed two major peaks equal in area and a few other minor peaks. The two major peaks were separated on the Autoprep and shown to be the *meso*- and *dl*-3,4-dicarbomethoxyhexane (**10**) (1.29 g, 64%). Both isomers were oils at ambient temperature. The ^{1}H nmr spectra of the two peaks collected together and collected separately were superimposable and all agreed well with the expected spectrum for **10**: (*meso*, *dl*, and *meso* + *dl*) 3.67 (6 H, s, methoxyls), 2.61 (2 H, m, methines), 1.60 (4 H, m, methylenes), 0.88 (6 H, t, methyls, J = 7.0 Hz). *Anal.* calcd. for $C_{10}H_{18}O_4$: C 59.50, H 8.90; found: (first peak) C 59.62, H 8.79; (second peak) C 60.02, H 8.62; (combined peaks) C 59.21, H 8.67.

(*D*) In the presence of **2** (1.25 g, 0.03 *M*)

The extracted oil was distilled at 10^{-2} Torr and 25°C to remove volatiles, then at 100°C to give 1.34 g of a colourless oil. The vpc of this oil showed two major peaks equal in area, which were separated on the Autoprep and shown to be the *trans* and *cis* isomers[7] of 2,3-diethyl-*N*-ethylsuccinimide (**11**) (0.65 g, 36%). First peak (*trans*-**11**); ^{1}H nmr: 3.55 (4 H, q, N-CH_2CH_3, J = 7.0 Hz), 2.53 (2 H, m, methines), 1.79 (4 H, m, CH_3CH_2CH), 1.15 (3 H, t, NCH_2CH_3, J = 7.0 Hz), 1.00 (6 H, t, CH_3CH_2CH). *Anal.* calcd. for $C_{10}H_{17}NO_2$: C 65.60, H 9.28, N 7.66; found: C 65.53, H 9.30, N 7.82. Second peak (*cis*-**11**); ^{1}H nmr: 3.52 (4 H, q, NCH_2CH_3, J = 7.0 Hz), 2.75 (2 H, m, methines), 1.70 (4 H, m, CH_3CH_2CH), 1.15 (3 H, t, NCH_2CH_3, J = 7.0 Hz), 1.02 (6 H, t, CH_3CH_2CH, J = 7.0 Hz). *Anal.* found: C 65.32, H 9.16, N 7.90.

(*E*) In the presence of **3** (1.00 g, 0.0386 *M*)

The extracted oil was distilled at 10^{-2} Torr and 25°C to remove volatile materials, then at 70°C to give 1.0 g of colourless oil which by vpc was shown to consist of > 90% of an approximately 1:1 mixture of *meso* and *dl* isomers of 2,3-diethylsuccinonitrile (**12**) (total yield 52%). These products could be separated either on the Autoprep or on a silica gel column (hexane/ethyl acetate 4:1). The stereoisomers were indistinguishable by ^{1}H nmr but could be identified tentatively by melting points (8). First peak

[3]The general procedure for the oxidation reaction and initial workup is given elsewhere (1) and includes, after the electrolysis, evaporation of solvents, extraction from water with CH_2Cl_2, and evaporation of CH_2Cl_2.

[4]The substrate concentration in this case was increased to allow separation of some dimer.

[5]The ^{1}H nmr spectrum of the olefinic region and that of the methyl doublet are essentially identical to those regions in the spectrum of crotonic acid.

[6]This run and all subsequent runs were prepared as described in ref. 1 with substitution of the relevant acid for acetic acid.

[7]As utilized previously (1), the *cis* and *trans* isomers can be assigned according to the nmr shifts of the methine protons. As for 2,3-dimethyl-*N*-phenylsuccinimide (7) the methine protons are shifted to lower field for the *cis* isomer and to higher field for the *trans* isomer.

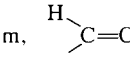
Can. J. Chem. Downloaded from www.nrcresearchpress.com by 210.87.254.6 on 09/05/12
For personal use only.

(*meso*-**12**) mp 51–52°C after being treated with a 5% solution of NaOH and sublimed (lit. (8*a*) 45–50°C); ^{1}H nmr: 2.74 (2 H, m, methines), 1.90 (4 H, m, methylenes), 1.20 (6 H, t, methyls, J = 7.0 Hz). *Anal.* calcd. for $C_8H_{12}N_2$: C 70.59, H 8.82, N 20.59; found: C 70.29, H 8.70, N 20.29. Second peak (*dl*-**12**) mp 54–56°C (lit. (8*b*) 56–57°C); ^{1}H nmr: 2.74 (2 H, m, methines), 1.90 (4 H, m, methylenes), 1.20 (6 H, t, methyls, J = 7.0 Hz). *Anal.* found: C 70.28, H 8.72, N 20.36.

(*F*) In the presence of **4** (1.49 g, 0.03 *M*)

The yellow extracted oil was distilled at 10^{-2} Torr and 25°C to remove volatile materials. Increasing the temperature to 100°C gave 1.74 g of viscous slightly yellow oil which showed several minor peaks on the vpc along with a peak having the same retention time as **4** (28%) and the expected doublet of peaks of nearly equal area. These two peaks were separated by preparative tlc (silica gel, hexane/ethyl acetate 4:1) and identified as the *threo* and *erythro* isomers of 3-nitro-4-phenylhexane (**13**) (0.85 g, 41%). First peak (*threo*- or *erythro*-**13**); ^{1}H nmr: 7.25 (5 H, m, Ph), 4.55 (1 H, m, methine α to NO_2), 2.90 (1 H, m, methine α to Ph), 1.60 (4 H, broad m, methylenes), 0.81 (3 H, t, methyl, J = 7.0 Hz), 0.70 (3 H, t, methyl, J = 7.0 Hz); ms *m/e*: 207 $(M)^+$. *Anal.* calcd. for $C_{12}H_{17}NO_2$: C 69.57, H 8.21, N 6.76; found: C 69.88, H 8.42, N 6.81. Second peak (*erythro*- or *threo*-**13**); ^{1}H nmr: 7.19 (5 H, m, Ph), 4.58 (1 H, m, methine α to NO_2), 2.95 (1 H, m, methine α to Ph), 1.82 (4 H, m, methylenes), 0.94 (3 H, t, methyl, 7.0 Hz), 0.74 (3 H, t, methyl, J = 7.0 Hz); ms *m/e*: 207 $(M)^+$. *Anal.* found: C 69.79, H 8.44, N 6.62.

(*G*) In the presence of **5** (1.68 g, 0.03 *M*)

The light yellow extracted oil was distilled at 10^{-2} Torr and 25°C to remove volatile materials (mostly propionic acid) and at 130°C to give 2.18 g of colourless viscous oil which showed three main peaks on the vpc. This oil was separated on a silica gel column (hexane/ethyl acetate 4:1) to give three fractions. The first fraction corresponded to 3-phenylsulfonylhexane (**14**) (1.03 g, 37%) as an oil; ^{1}H nmr: 7.87 (2 H, m, ArH *o* to SO_2), 7.59 (3 H, m, ArH *m* and *p* to SO_2), 2.89 (1 H, m, methine), 1.57 (6 H, m, methylene), 0.97 (6 H, t, methyls, J = 6.8 Hz). *Anal.* calcd. for $C_{12}H_{18}SO_2$: C 63.70, H 7.86, S 14.15; found: C 63.87, H 8.04, S 14.06. The second fraction corresponded to *trans*-1-phenylsulfonyl-1-butene (**15**) (0.566 g, 29%); ^{1}H nmr: 7.87 (2 H, m, ArH *o* to SO_2), 7.58 (3 H, m, ArH *m* and *p* to SO_2), 6.79[8] (2 H, m, ), 2.24 (2 H, m, methylene), 1.02 (3 H, t, methyl, J = 7.0 Hz). *Anal.* calcd. for $C_{10}H_{12}SO_2$: C 61.20, H 6.12, S 16.16; found: C 61.31, H 6.32, S 16.16. The third fraction was a white crystalline compound corresponding to the starting material **5** (0.057 g).

Anodic Oxidation of Isovaleric Acid Anion

(*H*) In the presence of **1** (1.44 g, 0.03 *M*)

The extracted oil was washed with a saturated $NaHCO_3$ solution, then distilled at 10^{-2} Torr and 35°C to remove volatiles and at 75°C to give 3.27 g of a colourless mixture of solid and oil which formed a gel on standing. The vpc of this fraction in ether showed several high vapour pressure peaks and a doublet of peaks of nearly equal area. The gel was repeatedly cooled in a Craig tube and centrifuged at 1500 rpm to give 0.48 g (19%) of a white solid which, after recrystallizing from ethanol, melted at 86.0–87.5°C and was shown to be one isomer of the dialkylation product, dimethyl 2,3-diisobutylsuccinate (**16**); ^{1}H nmr: 3.66 (6 H, s, methoxyls), 2.68 (2 H, m, methines α to carbonyl), 1.59 (6 H, m, methylenes and methines δ to carbonyl), 0.89 (12 H, d, $(CH_3)_2CH$—, J = 5.5 Hz). *Anal.* calcd. for $C_{14}H_{26}O_4$: C 65.08, H 10.14; found: C 64.92, H 10.13. The residual oil contained a trace of the solid by vpc and a second major peak with a longer retention time which was separated on the Autoprep as an oil. This oil was shown to be the other isomer of **16** (0.44 g, 17%); ^{1}H nmr: the same as for the first peak. *Anal.* found: C 64.91, H 10.13.

(*I*) In the presence of **2** (1.25 g, 0.03 *M*)

The extracted oil was washed with a saturated solution of $NaHCO_3$ to remove excess acid, then distilled at 10^{-2} Torr and 25°C to remove volatiles and at 60°C to give 4.65 g of a colourless oil which contained several low vapor pressure components by vpc analysis and a doublet of peaks of nearly equal area at longer retention time. The two slower moving components were separated on the Autoprep as oils and shown to be the *cis* and *trans* isomers of 2,3-diisobutyl-*N*-ethylsuccinimide (**17**) (1.58 g, 66%). First peak (*trans*-**17** (7)); ^{1}H nmr: 3.47 (2 H, q, NCH_2CH_3, J = 7.0 Hz), 2.48 (2 H, m, methines α to carbonyl), 1.70 (6 H, m, methylenes, and methines of isobutyl groups), 1.18 (3 H, t, NCH_2CH_3, J = 7.0 Hz), 0.98 (12 H, d, methyls of isobutyl groups, J = 6.0 Hz). *Anal.* calcd. for $C_{14}H_{25}NO_2$: C 70.40, H 10.45, N 5.86; found: C 70.06, H 10.34, N 5.76. Second peak (*cis*-**17**); ^{1}H nmr: 3.47 (2 H, q, NCH_2CH_3, J = 7.0 Hz), 2.87 (2 H, m, methines α to carbonyl), 1.70 (6 H, m, methylenes and methines of isobutyl groups), 1.18 (3 H, t, NCH_2CH_3, J = 7.0 Hz), 0.98 (12 H, m, methyls of isobutyl groups, J = 6.0 Hz). *Anal.* found: C 70.28, H 10.61, N 5.83.

(*J*) In the presence of **3** (1.0 g, 0.038 *M*)

The extracted oil was washed with a saturated solution of $NaHCO_3$, then distilled at 10^{-2} Torr and 25°C for 6 h to remove volatile materials. Increasing the temperature to 70°C gave a solid which was shown by vpc to be almost pure *meso*- and *dl*-2,3-diisobutylsuccinonitrile **18** in equal amounts (1.10 g, 45%); ^{1}H nmr: 2.70 (2 H, m, methines α to C≡N), 1.02 (6 H, m, methylenes and methines of isobutyl groups), 0.92 (12 H, d of d's, methyls, J = 6.0 Hz). *Anal.* calcd. for $C_{12}H_{20}N_2$: C 75.00, H 10.40, N 14.60; found: C 75.12, H 10.39, N 14.49.

The two components of the mixture were separated on the Autoprep and their ^{1}H nmr spectra were identical with that of the mixture. First peak (*meso*- or *dl*-**18**) mp 104.5–106°C. *Anal.* found: C 75.13, H 10.55, N 14.39. Second peak (*meso*- or *dl*-**18**) mp 94–95°C. *Anal.* found: C 74.80, H 10.37, N 14.71.

(*K*) In the presence of **4** (1.49 g, 0.03 *M*)

The extracted oil was washed with a saturated solution of $NaHCO_3$ to remove excess acid and distilled at 10^{-2} Torr and 25°C for 6 h to remove volatile materials. The viscous residue was distilled in a Späth bulb at 125°C to give 1.3 g of yellow oil which by vpc showed several minor peaks along with three peaks of nearly equal area. The slowest one could not be identified but the other two corresponded to *threo*- and *erythro*-2,7-dimethyl-4-nitro-5-phenyloctane (**19**). These stereoisomers were separated by preparative tlc to give a total yield of 0.60 g (23%) of products. First peak (*threo*- or *erythro*-**19**); ^{1}H nmr: 7.29 (5 H, m, Ph), 4.68 (1 H, m, methine α to NO_2), 3.07 (1 H, m, methine α to Ph), 1.49 (6 H, broad m, methylenes and methines of isobutyl groups), 0.81 (12 H, m, methyls); ms *m/e*: 263 $(M)^+$. *Anal.* calcd. for $C_{16}H_{25}NO_2$: C 73.00, H 9.51, N 5.32; found: C 73.16, H 9.71, N 5.22. Second peak; ^{1}H nmr: 7.20 (5 H, m, Ph), 4.70 (1 H, m, methine α to NO_2), 3.09 (1 H, m, methine α to Ph), 1.55 (6 H, broad m, methylenes and methines of isobutyl groups), 0.88 (12 H, m, methyls); ms *m/e* 263 $(M)^+$. *Anal.* found: C 73.18, H 9.75, N 5.12.

[8]This is assumed to be the *trans* isomer by analogy with **9** since both **9** and **15** are most likely formed by the same mechanism and their ^{1}H nmr spectra in the olefinic regions are nearly identical, being centered around 6.79 ppm.

TABLE 1. Electrochemical oxidation of carboxylic acid anions in the presence of substituted olefinic substrates

$$XCH{=}CHY \xrightarrow[\text{electrolysis}]{RCOO^-} XCH(R){-}CH(R)Y$$

Substrate	%[a] 1,2-dialkylated product[b]		
	R = CH_3	R = CH_2CH_3	R = $CH_2CH(CH_3)_2$
Dimethyl fumarate (**1**)	80(1)	(*C*)**10**, 64	(*H*)**16**, 36
N-Ethyl maleimide (**2**)	88(1)	(*D*)**11**, 36	(*I*)**17**, 66
Fumaronitrile (**3**)	55(1)	(*E*)**12**, 52	(*J*)**18**, 45
β-Nitrostyrene (**4**)	(*A*)[c]**6**, 37	(*F*)**13**, 41[e]	(*K*)**19**, 23
Phenyl vinyl sulfone (**5**)	(*B*)**7**, 69[d]	(*G*)**14**, 37[f]	(*L*)**20**, 41[g]

[a]Due to the important formation of Kolbe products, 20-fold excess of current was used in each run. The current efficiencies were then all less than 5% and no attempt was made to optimize the efficiency. All yields reported are based on the original concentration of olefinic substrate.
[b]The ratio of *cis*/*trans* addition in each case was ≈ 1:1.
[c]The letter refers to each experimental run.
[d]Plus 20% of the olefinic product (*B*) **8** and 8% of the dimer (*B*) **9**.
[e]Plus 28% of starting compound **4**.
[f]Plus 29% of the olefinic product (*G*) **15**.
[g]Plus 24% of the olefinic product (*L*) **21** and 17% of the starting compound **5**.

(*L*) In the presence of **5** (1.68 g, 0.03 *M*)

The extracted oil was washed with a saturated $NaHCO_3$ solution and distilled at 10^{-2} Torr and 75°C to remove volatile materials. Further distillation at 150°C gave 2.07 g of a crude viscous slightly yellow oil. This oil was fractionated on a silica gel column (hexane/ethyl acetate 4:1) to give as a first fraction 1.15 g (41%) of a colourless oil corresponding to 4-phenylsulfonyl-2,7-dimethyloctane (**20**); ^{1}H nmr: 7.85 (2 H, m, ArH *o* to SO_2), 7.56 (3 H, m, ArH *m* and *p* to SO_2), 2.90 (1 H, m, methine α to SO_2), 1.48 (8 H, m, methylenes and methines of alkyl chains), 0.85 (12 H, d of d's, unresolved methyls). *Anal.* calcd. for $C_{16}H_{26}SO_2$: C 68.10, H 9.22, S 11.34; found: C 68.26, H 9.40, S 11.50.

A second fraction was obtained in 24% yield (0.528 g) which was shown to be the monoalkylated elimination product, *trans*-1-phenylsulfonyl-4-methyl-pent-1-ene (**21**);[9] ^{1}H nmr: 7.81 (2 H, m, ArH *o* to SO_2), 7.51 (3 H, m, ArH *m* and *p* to SO_2), 6.1–7.3 (2 H, m, $\overset{H}{\diagdown}C{=}C\overset{}{\diagup}$), 1.69 (3 H, broad m, methylene and methine), 0.90 (6 H, d of d's, methyls, J = 6.0 Hz). *Anal.* calcd. for $C_{12}H_{16}SO_2$: C 64.30, H 7.14, S 14.30; found: C 64.45, H 7.32, S 14.24.

The third fraction obtained was identified as the starting material **5** (0.29 g).

Results and Discussion

The electrochemical oxidation of various carboxylic acid anions in the presence of olefinic substrates bearing electron-withdrawing substituents (Table 1) can be seen to give acceptable yields of dialkylated products. The reaction appears to be quite general to a large variety of acids and substrates. While there is a fairly wide variation in the yields obtained from different combinations of acid and substrate, it must be noted that all reactions were carried out under the same experimental conditions, including current and time of electrolysis. The yields obtained in each case are a function of the reactivity of the olefin, the reactivity of the radical, and the tendency for the reagents to undergo side reactions such as (*a*) dimerization by the radicals, (*b*) loss of a second electron by the radicals to form carbonium ions which can react with the solvent, and (*c*) loss of an H atom by the radical intermediate to form the monoalkylated olefin. The conversion of substrate to products was not always quantitative and the unconverted starting material was either recovered or detected in the reaction mixture. This means that the yields of dialkylated products could be increased substantially by the addition of more carboxylic acid and a longer reaction time.

It has been shown previously that for monosubstituted olefins bearing electron-withdrawing groups such as carboxylic esters (9) the initial radical attack occurs at the terminal carbon, β to the electronegative substituents. There has been considerable discussion as to whether this occurs because of stabilization of the resulting α radical by the substituent (product-like transition state) or because of a polar effect guiding the direction of initial attack (transition state similar to starting material) (10). The results obtained from the reaction of **5** with methyl radicals show that the initial radical attack occurs exclusively on the olefinic carbon atom β to the sulfone, since only the β-alkylated elimination (or abstraction) product **8** and the dimer **9**, resulting from combination of two α-sulfonyl radicals, are formed aside from the dialkylated product **7**. The

[9]As for compounds **9** and **15**, the olefinic region in the ^{1}H nmr spectrum of **21** is nearly identical to that of *trans*-crotonic acid.

Can. J. Chem. Downloaded from www.nrcresearchpress.com by 210.87.254.6 on 09/05/12
For personal use only.

relative instability of an α-sulfonyl radical is indicated by the large amount of olefinic product **8** formed. These results are an indication that for addition of alkyl radicals to α,β-unsaturated sulfones, the transition state for the first radical addition occurs quite early on the reaction coordinate.

The ratio of *cis* to *trans* addition resulting in *meso/dl* or *threo/erythro* mixtures was approximately 1:1 in all cases and no further effort was made to differentiate between the stereoisomers.

In summary, the electrochemical oxidation of carboxylic acid anions in the presence of olefins bearing electron-withdrawing groups appears to be a useful and unparalleled method of dialkylation of double bonds. Several aspects of this reaction are currently under study and will be reported later. One limitation of the dialkylation reaction appears to be the bulk of the attacking radicals. The formation of isopropyl radicals in the presence of **1** under the present reaction conditions resulted in a yield of < 10% of dialkylation product while *t*-butyl radicals gave very small yields of dimeric and polymeric products.

Acknowledgements

We wish to thank Mr. J. C. Stephens for his technical assistance, Mr. H. Séguin for the elemental analysis, and Mr. M. E. Bednas for the mass spectral determination.

1. R. N. RENAUD and P. J. CHAMPAGNE. Can. J. Chem. **57**, 990 (1979).
2. (*a*) R. K. BOEKMAN, JR. J. Org. Chem, **38**, 4450 (1973); (*b*) R. M. COATES and L. O. SANDEFUR. J. Org. Chem. **39**, 275 (1974); (*c*) G. H. POSNER and C. M. LENTZ. Tetrahedron Lett. 3215 (1977).
3. P. K. KADABA. Synthesis, 317 (1971).
4. F. MONTANARI and A. NEGRINI. Gazz. Chim. Ital. **87**, 1061 (1957).
5. A. H. FORD-MOORE, R. A. PETERS, and R. W. WAKELIN. J. Chem. Soc. 1754 (1949).
6. W. E. PARHAM, F. D. BLAKE, and D. R. THEISSEN. J. Org. Chem. **27**, 2415 (1962).
7. J. BODE and H. BROCKMANN, JR. Chem Ber. **105**, 34 (1972).
8. (*a*) L. EBERSON. Acta Chem. Scand. **17**, 1196 (1963); (*b*) R. V. WITELEY, JR. and R. S. MARIANELLI. Synthesis, 392 (1978).
9. M. CHKIR and D. LELANDAIS. Chem. Commun. 1369 (1971).
10. E. BLOCK. Reactions of organosulfur compounds. Academic Press, New York. 1978. Chapt. 5.

Can. J. Chem. Downloaded from www.nrcresearchpress.com by 210.87.254.6 on 09/05/12
For personal use only.

The structure of an unusual disulfide, formed from reaction between a sulfene–amine zwitterion and thionyl chloride

J. STUART GROSSERT,[1] MADAN M. BHARADWAJ, J. BRIAN FAUGHT, AND ARIS TERZIS[2]

Department of Chemistry, Dalhousie University, Halifax, N.S., Canada B3H 4J3

Received December 28, 1978[3]

J. STUART GROSSERT, MADAN M. BHARADWAJ, J. BRIAN FAUGHT, and ARIS TERZIS. Can. J. Chem. **58**, 1106 (1980).

Thionyl chloride has been shown to react with the zwitterion from dimeric sulfene and triethylamine to give bis(methylsulfonyl dichloromethyl) disulfide, **3**. The structure of **3** was determined from its spectral properties and was confirmed by an X-ray crystal structure analysis. Dechlorination of **3** gave bis(methylsulfonylmethyl) disulfide, **4**. Raman spectra of **3** and **4**, as well as of **5** and **6**, two related sulfones derived from 2,4,6-trithiaheptane, are reported.

J. STUART GROSSERT, MADAN M. BHARADWAJ, J. BRIAN FAUGHT et ARIS TERZIS. Can. J. Chem. **58**, 1106 (1980).

On a montré que le chlorure de thionyle réagit avec les paires d'ions du sulfène dimère et la triéthylamine pour conduire au bis(méthylsulfonyle dichlorométhyl) disulfure **3**. On a déterminé la structure du composé **3** à partir de ses propriétés spectrales et on l'a confirmée par une analyse de la structure du cristal à l'aide de rayon-X. La déchloration de **3** donne le bis(méthylsulfonylméthyl) disulfure **4**. On donne les spectres Raman des composés **3** et **4** aussi bien que ceux de **5** et **6** qui sont deux sulfones apparentées provenant du trithia-2,4,6 heptane.

[Traduit par le journal]

Thionyl chloride, **1**, has been shown to react with a wide variety of organic molecules (1, 2). We report here the formation of a novel disulfide, **3**, from the reaction between **1** and a solution of the zwitterion, **2**, formed *in situ* when sulfene dimerizes and complexes with triethylamine (3, 4).

Elemental analysis of **3** required that it be assigned the formula $C_4H_6Cl_4O_4S_4$, which indicates that a reduction at sulfur in the conversion **2** → **3** had occurred. The infrared spectrum showed characteristic sulfonyl stretching bands at 1160 and 1340 cm^{-1}. The presence of a methanesulfonyl group was confirmed by an ^1H nmr singlet at δ 3.30 and a quartet in the off-resonance ^{13}C nmr spectrum at δ 43.8. The latter spectrum showed also a quaternary carbon, bound to electronegative substituents, at δ 109.6. These chemical shifts compare with those of similar compounds (5), and the symmetry of the molecule is clearly shown by the simplicity of the nmr spectra.

The mass spectrum of **3** was in accord with the proposed structure, although no molecular ion could be observed (*vide infra*). The ions at *m/e* 161, 146, and 114 all clearly contained 2 chlorine atoms whereas the ion at *m/e* 79 contained only one chlorine atom. The ions at *m/e* 114 and 79 could reasonably be attributed to the species $CCl_2S^{+\cdot}$ and $CClS^+$ respectively. It is interesting to note that although the peak at *m/e* 79 ($CH_3SO_2^+$) is prevalent in the mass spectra of compounds containing methanesulfonyl groups (5), in this case the peak-height ratio of *m/e* 79:81 corresponds closely to that expected for an ion containing one chlorine atom, which suggests that formation of $CH_3SO_2^+$ is not an important fragmentation in the mass spectrum of **3**. The ions at *m/e* 161, 146, 114, and 79 provide good evidence for the presence of the $CH_3SO_2CCl_2SS$— fragment in **3**. Some similarities in fragmentation patterns have been observed in the mass spectra of bis(trichloromethyl) disulfide (6) and bis(chloromethyl) disulfide.[4]

The ultraviolet spectrum of **3** showed only end absorption. At first sight, this was surprising since most dialkyl disulfides exhibit uv absorption around 250 nm (7–10). However, it may be noted that di-*tert*-butyl disulfide shows only end absorption (8, 9), and that although changes in the torsion angle (ω) about the C—S—S—C bond have a major influence in the value of λ_{max} (9), it is not clear exactly what role the electronegativity of substituents will play. For instance, bis(trifluoromethyl) disulfide has λ_{max} = 237 nm, but this compound has only been studied by electron diffraction in the gas phase (10) and ω has not been determined.

Reductive removal of the chlorines from **3** with a classical HI/P procedure gave **4**. The structure of **4** was apparent from its elemental analysis and from simple ^1H and ^{13}C nmr spectra which required the presence of two $CH_3SO_2CH_2$— groups in a simple, symmetrical molecule. The sulfonyl groups in **4**

[1]Author to whom communications should be addressed.

[2]Present address: The National Research Foundation, 48 Vassileos Constantinou Avenue, Athens 501/1, Greece.

[3]Revision received February 14, 1980.

[4]J. S. Grossert and R. F. Langler, unpublished work.

0008-4042/80/111106-05$01.00/0

©1980 National Research Council of Canada/Conseil national de recherches du Canada

Can. J. Chem. Downloaded from www.nrcresearchpress.com by 210.87.254.6 on 09/05/12
For personal use only.

Can. J. Chem. Downloaded from www.nrcresearchpress.com by 210.87.254.6 on 09/05/12
For personal use only.

were clearly indicated by infrared absorptions at 1305 and 1110 cm^{-1}. The mass spectrum of **4** showed a molecular ion at *m/e* 250 and a base peak at *m/e* 45 (CHS^+). The ultraviolet spectrum of **4** showed a clean absorption maximum at 243 nm.

Although the foregoing evidence constituted reasonable proof for the structure of **3**, it was deemed advisable to undertake an X-ray crystal structure analysis, particularly given the rather novel reaction which led to its formation. The interatomic distances and bond angles in **3** are given in Fig. 1 (see Experimental for structure data). There is good agreement between the dimensions of the two halves of the molecule. Equivalent bond lengths differ by about 1 esd from their average values with the exception of the C—Cl distances which differ by as much as 2.5 esd's.

The C—S—S—C torsion angle in **3**, ω, was found to be 113.3°. Repulsion between the lone-pair electrons on the sulfur atoms in disulfides is expected to be a minimum when ω = 90° (7, 9), although values of ω outside the range of 80–100° are well documented (11, 12).

The S—S bond distance in **3** was found to be 2.018(2) Å which may be compared with the S—S bond distance of 2.060(3) Å in orthorhombic sulfur (13). The S—S bond distance in disulfides is known to depend both on the value of ω and on the electronegativity of the substituents attached to sulfur (12). As in the case of the ultraviolet spectra, it is not clear what role electronegativity of substituents on sulfur will play in affecting bond length of disulfides since, unlike the relation between ω and bond length (12), no systematic study of this relationship appears to have been reported. However, the S—S bond distance in **3** is quite reasonable when compared with values of 2.05 ± 0.019 Å

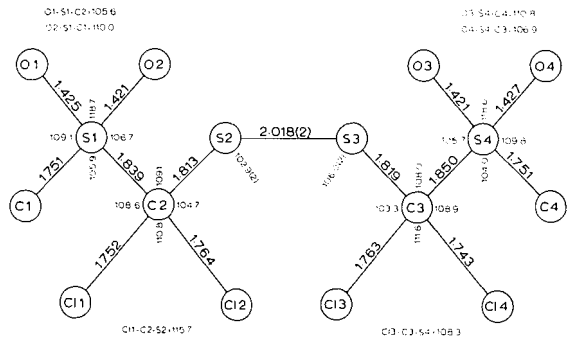


FIG. 1. Numbering and structural parameters for bis(methylsulfonyldichloromethyl) disulfide, **3**. Bond lengths (Å) and bond angles (°) of the non-hydrogen atoms are shown. The error in bond lengths and bond angles is 0.005 Å and 0.3° respectively, unless otherwise noted in parentheses.

found for bis(trifluoromethyl) disulfide (10) and 2.022(2) or 2.012(2) Å for bis(succinimidoyl) disulfide (14). These are examples of disulfides with substituents of greater electronegativity than alkyl groups.

It is noteworthy that three sets of C—S bond lengths were observed in **3** and that the differences between the sets are significant. The sum of the covalent radii of carbon and sulfur is 1.81 Å (15), and the average bond length of 1.816(2) Å observed for C(2)—S(2) and C(3)—S(3) is not significantly different. The longest C—S bond distance in **3** was observed for the equivalent C(2)—S(1) and C(3)—S(4) bonds which average 1.845(5) Å. This is consistent with the nonobservance of a molecular ion in the mass spectrum of **3**; in fact, the ion at highest *m/e* (307) corresponds to $M^{\ddagger} - CH_3SO_2$, i.e. to cleavage of the C(2)—S(1) or C(3)—S(4) bond.

$$MeSO_2Cl + Et_3N$$

$$\downarrow$$

$$MeSO_2CHSO_2\overset{+}{N}Et_3 \quad (2)$$

$$\downarrow SOCl_2 \quad (1)$$

$$MeSO_2CCl_2SSCCl_2SO_2Me \quad (3)$$

$$\downarrow HI/P/HOAc$$

$$MeSO_2CH_2SSCH_2SO_2Me \quad (4)$$

$$MeSO_2CH_2SO_2CH_2SO_2Me \quad (5)$$

$$MeSO_2CCl_2SO_2CCl_2SO_2Me \quad (6)$$

$$MeSO_2CH(SOCl)SO_2\overset{+}{N}Et_3\bar{Cl} \quad (7)$$

$$MeSO_2CCl(SCl)SO_2Cl \quad (8)$$

$$MeSO_2CCl_2SCl \quad (9)$$

In recent years, the value of the S—S stretching frequencies of disulfides, as observed in the Raman spectrum, has become increasingly important in correlations with the disulfide structure (7, 16). Most disulfides show the S—S stretching frequency as an intense band in the range of 510–540 cm^{-1}, and this value has been correlated with the magnitude of the C—S—S—C torsion angle, ω (16). Since compounds **3** and **4** represent disulfides with novel substituents, it was deemed worthwhile to examine their Raman spectra. It appeared that the appropriate bands were present, but since assignment of these bands is not always straightforward (17), the Raman spectra of the cor-

Can. J. Chem. Downloaded from www.nrcresearchpress.com by 210.87.254.6 on 09/05/12
For personal use only.

TABLE 1. The Raman spectral absorption maxima* of compounds **3–6**

$(MsCCl_2S)_2$† **3**	$(MsCH_2S)_2$† **4**	$(MsCH_2)_2SO_2$† **5**	$(MsCCl_2)_2SO_2$† **6**
1151(m)	1106(w)	1381(w)	1352(m)
800(w)	682(m)	1168(m)	1168(vs)
777(w)	503(s)	1157(m)	1156(w)
719(m)	378(w)	1106(w)	838(m)
542(m)‡	328(w)	785(m)	770(m)
491(m)‡	305(br)	706(s)	741(m)
401(vs)		506(m)	705(m)
380(m)		500(sh)	542(m)
334(m)		474(w)	524(w)
305(m)		444(m)	502(w)
		390(w)	491(s)
		385(sh)	399(s)

*Absorption maxima are reported in units of cm^{-1}; intensities (in parentheses) are given using standard abbreviations.
†Ms = $MeSO_2$.
‡Both these two bands were shown to be strongly polarized when the spectrum was studied using a benzene solution of **3**.

responding sulfones **5** and **6** derived from 2,4,6-trithiaheptane (5) were run also. The results are recorded in Table 1. From these it is apparent that a clear-cut assignment of the S—S stretching frequency in **3** and **4** is not a simple problem, and the obvious cautionary note about making untested assignments of such peaks in molecules with more complex functionalities should be made. Similar problems have been encountered previously, even with relatively simple dialkyl disulfides (18).

In conclusion, it is intriguing to speculate on the mechanism by which **3** may be formed. It is probable that initial reaction between **2** and **1** yields an intermediate,**7**, conversion of which into the sulfenyl chloride, **9**, can be postulated to proceed via **8**. The conversion **7** → **8** is supported by the work of Krubsack and co-workers (2),[5] whereas the desulfonylation **8** → **9** has a precedent in work by Fusco *et al.* (19). Reduction of sulfenyl chlorides to disulfides (**9** → **3**) is amply documented (8).

Experimental

General

Most details have been provided previously (5). The Raman spectra were run in the solid phase using an Argon ion laser at 4880 Å excitation in conjunction with a Spex 1401 double monochromator.

Preparation of Bis(methylsulfonyldichloromethyl) Disulfide, 3[6]

A solution of triethylamine (20.7 mL, 0.15 mol) in acetonitrile (100 mL) was cooled to −40°C. With continuous stirring, a solution of methanesulfonyl chloride (7.8 mL, 0.1 mol) in acetonitrile (15 mL) was added over a 30-min period, and the mixture was stirred for a further 2 h. The mixture was filtered rapidly, purified thionyl chloride, **1**, (20) (25 mL) was added to the filtrate, and the resulting solution was stirred at room temperature for 15 h. The solvent was rotary evaporated to give a yellow solid which was partitioned between $CHCl_3$ and water. The $CHCl_3$ extract (washed and dried) gave a yellow oil which crystallized from MeOH to give **3** as colorless plates,yield 4.6 g, 47%, mp 119–120°C; ir(KBr) ν_{max}: 3030 w, 2940 w, 2930 w, 1320 vs, 1145 vs, 955 m, 940 m, 780 m, 695 m cm^{-1}; for Raman spectrum see Table 1; uv showed only end absorption; for nmr see text; ms *m/e*: 313(2.2), 311(7.8), 309(13.3), 307(10.7), 163(5.6), 161(7.1),. 151(7.1), 149(8.9), 148(3.3), 147(6.7), 146(4.4), 116(6.6), 114(8.9), 111(22.2), 95(17.3), 81(33.2), 79(100), 63(28.0), 48(14.4), 47(26.6), 45(17.8), 44(13.7), 38(8.9), 36(26.6); *Anal.* calcd. for $C_4H_6Cl_4O_4S_4$: C 12.38, H 1.56, Cl 36.53, S 33.04%, M 388.13; found: C 12.28, H 1.46, Cl 37.06, S 33.08%, M (cryoscopic) 380.

Crystal Data of 3

$C_4H_6Cl_4O_4S_4$ fw = 388.14

Orthorhombic, a = 20.999(3), b = 12.347(2), c = 10.585(1) Å, V = 2744.4 Å^3, Z = 8, ρ_c = 1.878 g cm^{-3}, (18°C, CuK_α, λ = 1.54051 Å).

Preliminary photographic data showed the crystals to be orthorhombic, with the following systematic absences: *h*0*l*, $l = 2n + 1$; *hk*0, $h = 2n + 1$; 0*kl*, $k = 2n + 1$. These absences uniquely identify the space group as P_{bca} (No. 61).

Data were collected from a crystal (0.13 × 0.11 × 0.18 mm) mounted with the *c* axis nearly parallel to the ϕ axis of a Picker FACS-1 automatic diffractometer, fitted with a graphite monochromator. The reflections were measured using the θ–2θ scan technique from a point 0.95° below the calculated 2θ position for $CuK_{\alpha 1}$ to 0.95° above the position calculated for $CuK_{\alpha 2}$ at the rate of 1° min^{-1}. Stationary-crystal, stationary-counter background counts of 20 s were recorded at each limit of the scan range. During the data collection, three standard reflections were measured at a period of 30 reflections. The intensity of 2 1 7 decreased by 32%, 8 7 3 by 40%, and 12 4 0 by 21%. A linear correction factor was applied to the data. A total of 2378 intensity measurements were recorded in the form *hkl* with $2\theta < 120°$ and reduced to a set of 2041 independent reflections. The integrated intensity was calculated as

$$I_{(net)} = I_{(scan)} - 0.5(t_T/t_B)(B_1 + B_2)$$

where $I_{(scan)}$ is the number of counts over the scan range, t_T is the scan time, t_B is the time for each background count B_1 and B_2. The standard deviations $\sigma(I)$ were calculated according to the expression

[5]We thank a referee for pointing out that although the conversion $R.SO_2\overset{+}{N}R_3' \rightarrow R.SO_2Cl$ has apparently not been reported on, it has been observed in the referee's laboratory.

[6]This compound may be named as 3,3,5,5-tetrachloro-2,4,5,7-tetrathiaoctane-2,2,7,7-tetraoxide also. Naming it as a disulfide has merit in that it draws attention to the dominant functional group.

TABLE 2. Positional and thermal parameters* (esd's) for $C_4H_6S_4O_4Cl_4$ ($\times 10^4$)

Atom	x/a	y/b	z/c	U_{11}	U_{22}	U_{33}	U_{12}	U_{13}	U_{23}
Cl1	328(1)	8518(1)	8829(1)	657(9)	872(10)	657(9)	−194(8)	53(7)	247(8)
Cl2	332(1)	8639(1)	6097(1)	820(10)	991(11)	603(9)	−32(9)	−213(8)	−315(8)
Cl3	2240(1)	8950(1)	11337(1)	600(8)	105(11)	391(7)	1(8)	−3(6)	−51(7)
Cl4	1877(1)	7370(1)	9442(1)	620(8)	504(7)	806(10)	−129(7)	−64(7)	70(7)
S1	264(1)	10620(1)	7578(1)	378(6)	620(8)	655(9)	−17(6)	−48(6)	−31(7)
S2	1455(1)	9333(1)	7338(1)	480(7)	762(9)	388(7)	38(7)	20(6)	33(6)
S3	1743(1)	9792(1)	9076(1)	516(7)	515(7)	607(8)	48(6)	−142(6)	−76(7)
S4	3006(1)	8713(1)	9042(1)	458(6)	540(7)	512(7)	13(6)	65(6)	49(6)
O1	504(2)	11083(3)	8716(4)	506(20)	766(25)	789(27)	−11(20)	−106(19)	−306(22)
O2	416(2)	11125(3)	6410(4)	688(25)	864(28)	818(29)	13(23)	−34(22)	30(24)
O3	2943(2)	8394(4)	7757(4)	791(27)	1061(32)	492(23)	25(25)	133(20)	143(22)
O4	3251(2)	9765(3)	9313(3)	482(20)	522(20)	811(27)	−97(17)	72(18)	−28(20)
C1	−561(3)	10457(6)	7711(6)	344(28)	930(44)	1029(50)	35(32)	−90(30)	−86(39)
C2	598(2)	9245(4)	7512(4)	434(27)	507(28)	374(27)	−70(23)	−38(21)	−54(22)
C3	2193(2)	8656(4)	9710(5)	457(26)	350(25)	426(27)	−19(22)	−26(22)	−5(21)
C4	3428(3)	7738(4)	9904(6)	560(26)	552(35)	1027(50)	137(29)	−128(33)	5(36)

*The form of the anisotropic vibration is $\exp[-2\pi^2(a^{*2}h^2U_{11} + \ldots + a^*b^*hkU_{12} + \ldots)]$.

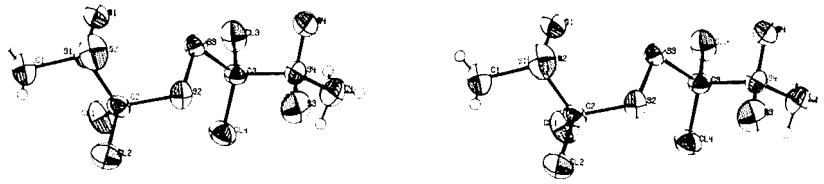


FIG. 2. A stereoscopic view of bis(methylsulfonyldichloromethyl) disulfide, **3**, showing ORTEP-generated 50% probability ellipsoids.

$$\sigma(I) = [N_T + 0.25\, t_T/t_B\,(B_1 + B_2) + C(I)^2 + 0.01^2\,(I - I_c)^2]^{1/2}$$

where N_T is the total net integrated scan count obtained in the time t_T, C is a factor to account for, among other things, instrument stability during data collection (for this structure C was 0.035), I is the net intensity, and I_c is I corrected for absorption. The last term in the expression is a factor accounting for errors in the absorption correction.

An absorption correction[7] was applied and the calculated transmission coefficients based on a linear absorption coefficient of 132.7 cm^{-1} for CuK_α radiation ranged from 0.210 to 0.346. Lorentz and polarization corrections were applied; 1522 reflections with $I > 2\sigma(I)$ were used in the refinement of the structure.

Solution and Refinement of the Structure of 3

The structure was determined using the direct-phasing program MULTAN (22). Two solutions were attempted from seven starting phases and the correct solution was chosen from the lowest Karle R factor. From the E-map all but two non-hydrogen atoms were located. These two atoms were found from the subsequent Fourier map, phased on the trial structure. A structure factor calculation based on this model gave a conventional R factor of 0.21 where

$$R = (\Sigma||F_o| - |F_c||)/\Sigma|F_o|$$

Temperature and scale factors were taken from the Wilson plot. Block-diagonal, (9 × 9) least-squares refinement with unit weights and isotropic thermal parameters for all non-hydrogen atoms converged at $R = 0.124$. Refinement, minimizing $\Sigma(w|F_o| - |F_c|)^2$, was continued with anisotropic thermal parameters for the chlorine and sulfur atoms, and isotropic thermal parameters for the oxygen and carbon atoms. A weighting scheme was introduced ($w = 1/[\sigma^2(F_o)]$) as well as a secondary extinction correction (26). The R factor at convergence was 0.065. The inclusion of anisotropic thermal parameters for all atoms except the two methyl carbon atoms reduced R to 0.057. After final refinement, positional and anisotropic thermal parameters for all non-hydrogen atoms, and positional and isotropic thermal parameters for the six hydrogen atoms were calculated when $R = 0.057$. The six hydrogen atoms were located by a difference Fourier synthesis. The final R index on data with $I > 2\sigma(I)$ was 0.037; R_2, defined as $([\Sigma(w|F_o| - |F_c|)^2]/[\Sigma w|F_o|^2])^{1/2}$ was 0.048. The final "goodness of fit", $\{[\Sigma(w|F_o| - |F_c|)^2]/(m - n)\}^{1/2}$ was 0.83, where m is the number of observations and n is the number of refined parameters. The scattering factors for all atoms were taken from Cromer and Mann (27). Sulfur and chlorine were corrected for the real part of the anomalous dispersion (28).

Atomic positions and thermal parameters for the non-hydrogen atoms of **3** are presented in Table 2. Table 3, containing the hydrogen atom positional and thermal parameters, as well as bond lengths and angles involving hydrogen, Table 4, the structure factor table, and Table 5, the correct starting set of reflections with their phases, are in the Depository of Unpublished Data.[8] The bond lengths and angles for non-hydrogen atoms in **3** are detailed in Fig. 1. Figure 2 shows a stereoscopic view of **3**, and Fig. 3 gives a stereoscopic view of the molecular packing.

[7]The computer programs used were locally modified versions of the following: NRC-2 (data reduction) (21); NRC-3 (absorption correction) (21); MULTAN (22); FORDAP (23); NUCLS (24); ORTEP (25).

[8]This information can be obtained, at a nominal charge, from the Depository of Unpublished Data, CISTI, National Research Council of Canada, Ottawa, Ont., Canada K1A 0S2.

Can. J. Chem. Downloaded from www.nrcresearchpress.com by 210.87.254.6 on 09/05/12
For personal use only.

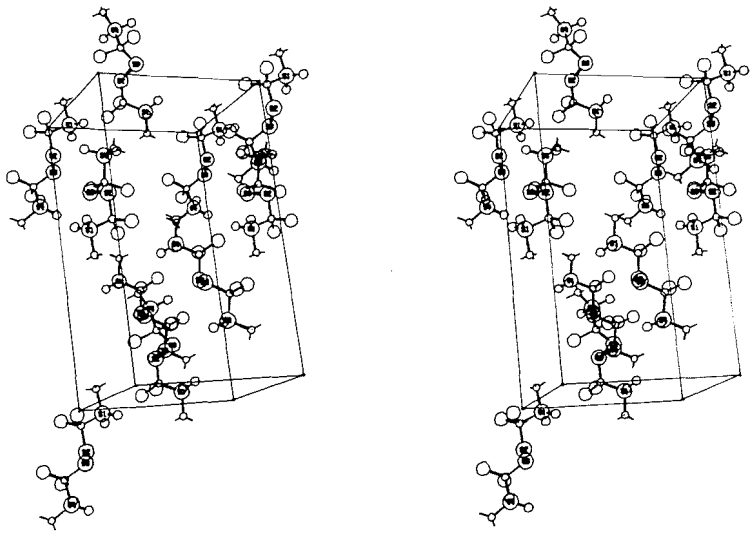


FIG. 3. A stereoscopic view of the crystal packing of bis(methylsulfonyldichloromethyl) disulfide, **3**. The sulfur atoms in each molecule are marked.

Preparation of Bis(methylsulfonylmethyl) Disulfide, 4

A mixture of **3** (1.0 g, 2.58 mmol) and red phosphorus (1 g) was refluxed in a solution of HI(55%, 10 mL) and HOAc (glacial, 10 mL) for 6 h. After filtering the hot solution through Celite, the filtrate was rotary evaporated to a dark brown oil, from which crystals could be obtained by extraction with MeOH. Recrystallization (MeCN–MeOH) gave **4** as white needles, (190 mg, 29%) mp 171–173° C; uv λ_{max} (MeCN):243 nm, ε 720; ir(KBr) ν_{max}:2980 m, 2920 m, 1305 vs, 1110 vs, 970 m, 850 s, 840 s cm^{-1}; for Raman spectrum, see Table 1; ^1H nmr (CD_3CN) δ(TMS): 3.04 (s), 4.44 (s); ^{13}C nmr (DMSO-d_6) δ (DSS): 41.1 (CH_3), 61.0 (CH_2); ms *m/e*: 250(1.3), 171(6.3), 125(4.2), 111(19), 94(42), 91(17), 80(16), 79(13), 65(38), 47(38), 46(35), 45(100), m* 116.5; *Anal.* calcd. for $C_4H_{10}S_4O_4$: C 19.19, H 4.03, S 51.22%, M 250.4; found: C 19.30, H 4.16, S 51.40%, M(cryoscopic) 240.

Acknowledgements

We thank the National Research Council of Canada for financial support and Dalhousie University for an Izaak Walton Killam Scholarship (to M. M. B.). Special thanks are due to Dr. C. H. Warren for his interest in running the Raman spectra.

1. K. OKA and S. HARA. Tetrahedron Lett. 2783 (1976); J. S. PIZEY. Synthetic reagents. Vol. 1. Ellis Horwood – J. Wiley, Chichester. 1974. p. 321.
2. A. SENNING. Bull. Soc. Chim. Belg. **86**, 675 (1977); T. HIGA and A. J. KRUBSACK. J. Org.Chem. **40**, 3037 (1975).
3. J. S. GROSSERT and M. M. BHARADWAJ. J. Chem. Soc. Chem. Commun. 144 (1974).
4. J. F. KING. Acc. Chem. Res. **8**, 10 (1975).
5. J. S. GROSSERT, M. M. BHARADWAJ, R. F. LANGLER, T. S. CAMERON, and R. CORDES. Can. J. Chem. **56**, 1183 (1978).
6. S. KAAE and A. SENNING. Acta Chem. Scand. **22**, 159 (1968).
7. B. PANIJPAN. J. Chem. Educ. **54**, 670 (1977), and references therein.
8. L. FIELD. *In* Organic chemistry of sulfur. *Edited by* S. Oae. Plenum, New York. 1977. p. 303.
9. D. B. BOYD. J. Am. Chem. Soc. **94**, 8799 (1972); D. B. BOYD. J. Phys. Chem. **78**, 1554 (1974).
10. G. A. R. BRANDT, H. J. EMELÉUS, and R. N. HASZELDINE. J. Chem. Soc. 2198 (1952); 2549 (1952); R. N. HASZELDINE and J. M. KIDD. J. Chem. Soc. 3219 (1953); H. J. M. BOWEN. Trans. Faraday Soc. **50**, 452 (1954).
11. D. D. JONES, I. BERNAL, M. N. FREY, and T. K. KOETZLE. Acta Crystallogr. Sect. B, **30**, 1220 (1974).
12. A. HORDVIK. Q. Rep. Sulfur Chem. **5**, 21 (1970).
13. A. CARON and J. DONOHUE. Acta Crystallogr. **18**, 562 (1965).
14. MAZHAR-UL-HAQUE and M. BEHFOROUZ. J. Chem. Soc. Perkin Trans. II, 1459 (1974).
15. L. PAULING. The nature of the chemical bond. 3rd ed. Cornell University Press, Ithaca, NY. 1960. p. 224.
16. H. E. VAN WART, H. A. SCHERAGA, and R. B. MARTIN. J. Phys. Chem. **80**, 1832 (1976), and references therein.
17. H. A. CARTER, C. S-C. WANG, and J. M. SHREEVE. Spectrochim. Acta, Part A, **29**, 1479 (1973).
18. F. R. DOLLISH, W. G. FATELY, and F. F. BENTLEY. Characteristic Raman frequencies of organic compounds. Wiley, New York. 1974. Chapt. 5.
19. R. FUSCO, S. ROSSI, S. MAIORANA, and G. PAGANI. Gazz. Chim. Ital. **97**, 774 (1965).
20. L. F. FIESER and M. FIESER. Reagents for organic synthesis. Vol. 1. Wiley, New York. 1967. p. 1158.
21. F. R. AHMED, S. R. HALL, M. E. PIPPY, and C. P. HUBER. NRC-crystallographic programs for the IBM/360 system. National Research Council of Canada, Ottawa, Ont. 1970.
22. G. GERMAINE, P. MAIN, and M. M. WOOLFSON. Acta Crystallogr. Sect. A, **27**, 368 (1971).
23. Z. ZALKIN. FORDAP, a Fortran program for Fourier calculations. University of California, Berkeley, CA. 1965.
24. J. SYGUSCH, F. R. BRISSE, and S. HANESSIAN. Acta Crystallogr. Sect. B, **30**, 40 (1974).
25. C. K. JOHNSON. ORTEP, Report ORNL-3794. Oak Ridge, TN. 1965.
26. P. COPPENS and W. C. HAMILTON. Acta Crystallogr. Sect. A, **26**, 71 (1970).
27. D. T. CROMER and J. B. MANN. Acta Crystallogr. Sect. A, **24**, 321 (1968).
28. D. H. TEMPLETON. *In* International tables for X-ray crystallography. Vol. III. *Edited by* C. H. MacGillavry and G. D. Rieck. The Kynoch Press, Birmingham, England. 1962. pp. 213–216.

Can. J. Chem. Downloaded from www.nrcresearchpress.com by 210.87.254.6 on 09/05/12
For personal use only.

A high field proton magnetic resonance study of the solution conformation of thromboxane B_2[1]

GEORGE KOTOVYCH[2] AND GERDY H. M. AARTS
Department of Chemistry, University of Alberta, Edmonton, Alta., Canada T6G 2G2

Received September 12, 1979

GEORGE KOTOVYCH and GERDY H. M. AARTS. Can. J. Chem. **58**, 1111 (1980).

The solution conformation of thromboxane B_2 (TXB_2) has been studied using high-field nuclear magnetic resonance techniques. In $CDCl_3$, both anomers are present in solution with 76% 11α-OH TXB_2 and 24% 11β-OH TXB_2. In CD_3OD, the predominant anomer is 11β-OH TXB_2 (80%) while the concentration of 11α-OH TXB_2 is 20%. The proton resonances were assigned at 400 MHz using double resonance techniques. The analysis of the vicinal coupling constants indicates that the six-membered ring is present in solution in a chair conformation with both of the aliphatic side chains equatorial. Proton longitudinal relaxation times were measured at 25°C in $CDCl_3$ for H-2, H-11β, H-12, H-13, H-14, and H-17 to H-19, both at 200 MHz and at 400 MHz. From the frequency dependence of these dipolar relaxation times, the rotational correlation times were evaluated. Within experimental error, all of the values are similar in magnitude ($\sim 2.0 \times 10^{-10}$ s) indicating that this is the molecular rotational correlation time.

GEORGE KOTOVYCH et GERDY H. M. AARTS. Can. J. Chem. **58**, 1111 (1980).

On a étudié la conformation du thromboxane B_2 (TXB_2) en solution, en utilisant les techniques de rmn à haut champ. Les deux anomères sont présents en solution dans le $CDCl_3$ dans la proportion de 76% de OH-11α TXB_2 et 24% OH-11β TXB_2. Dans le CD_3OD, l'anomère prédominant est le OH-11β TXB_2 (80%), le OH-11α TXB_2 est à une concentration de 20%. On a attribué les résonances du proton à 400 MHz en utilisant les techniques de double résonance. L'analyse des constantes de couplage vicinal indique que le cycle à 6 chaînons est présent en solution sous une conformation chaise avec les deux chaînes latérales aliphatiques en position équatoriale. On a mesuré les temps de relaxation longitudinale du proton à 25°C dans le $CDCl_3$ pour H-2, H11β, H-12, H-13, H-14 et de H-17 à H-19 à 200 et à 400 MHz. A partir de l'effet de la fréquence sur les temps de relaxation dipolaire, on a évalué le temps de corrélation rotationnelle. A l'intérieur des erreurs expérimentales, toute les valeurs sont du même ordre de grandeur ($\sim 2 \times 10^{-10}$ s) indiquant ainsi qu'il s'agit du temps de corrélation rotationnelle moléculaire.

[Traduit par le journal]

Introduction

The metabolic pathway of arachidonic acid involves the formation of cyclic endoperoxides which are rapidly converted into thromboxane A_2 (TXA_2), prostacyclin, and other prostaglandins (1, 2). TXA_2 was identified by Samuelsson and coworkers (2) (Fig. 1) and is a highly unstable compound. It has a half life of about 30–40 s before its conversion to thromboxane B_2 (TXB_2). TXA_2 possesses pronounced biological activity, and thromboxanes have been identified in many tissues including platelets, leucocytes, spleen, inflammatory granuloma, brain, and kidney (3). They are of considerable pathophysiological interest in thromboembolic diseases, anaphylactic reactions, and have a physiological role in normal hemostatis. TXA_2 is a strong platelet aggregating factor (3). In contrast, prostacyclin, which has been isolated and its structure has been determined (4, 5), is able to disaggregate platelets after the induction of platelet aggregation by ADP or arachidonic acid (5).

Because of the diverse functions of these prostaglandins, we have carried out a study of the conformation of TXB_2 using high field nuclear magne-

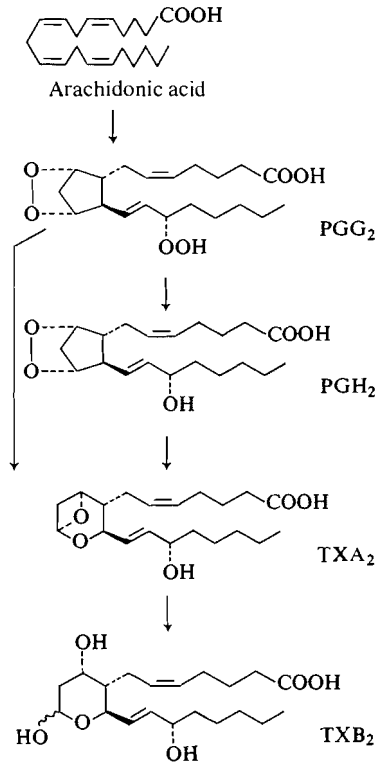


FIG. 1. The conversion of arachidonic acid to TXB_2.

[1]This is paper No. 2 in a series of high-field nmr studies on vitamins and prostaglandins. Paper No. 1 is ref. 14.

[2]Formerly Kotowycz.

0008-4042/80/111111-07$01.00/0
©1980 National Research Council of Canada/Conseil national de recherches du Canada

Can. J. Chem. Downloaded from www.nrcresearchpress.com by 210.87.254.42 on 09/05/12
For personal use only.

Can. J. Chem. Downloaded from www.nrcresearchpress.com by 210.87.254.42 on 09/05/12
For personal use only.

tic resonance (nmr) techniques. As the lifetime of TXA_2 is too short for these studies, the present studies have centred on TXB_2. The detailed solution conformation may serve as an aid in the understanding of the action of TXA_2. In a related study, the conformation of prostacyclin has also been reported (6). In the solid state, diffraction experiments have shown that for TXB_2 there are two crystallographically independent molecules in the unit cell (7). The α chains (at C-8) are bent sharply in the middle and the carboxyl group is positioned either above or below the mean plane of the rest of the molecule.

In a recent review article (8), nmr data on thromboxanes were not mentioned. In the discussion of the synthesis of TXB_2 (ref. 5, pp. 103–113), Nelson *et al.* discussed the equilibrium of the α- and β-hydroxy forms that lead to a mixture of C-11 epimers in solution. From ^{13}C nmr data for TXB_2 in $CDCl_3$ (with a few percent of CD_3OD), about 35% of the α-hydroxy anomer and 65% of the β-hydroxy anomer were found. But detailed nmr studies of the proton chemical shifts, coupling constants, and proton longitudinal relaxation rates have not been carried out. However, Conover and Fried (9) have measured the proton chemical shifts for $PGF_{2\alpha}$ in phosphate buffer together with the proton–proton coupling constants for the cyclopentane ring. The magnitudes of the coupling constants were analyzed using the Karplus equation, and a half-chair conformation was proposed for this prostaglandin with only the hydroxyl group at C-9 in the pseudo-axial orientation.

In the present study, the conformation of the sugar-like TXB_2 six-membered ring is analyzed on the basis of the vicinal proton–proton coupling constants. Both 11α-OH TXB_2 and 11β-OH TXB_2 are present in solution and the concentrations of the two anomeric forms are determined from the spectra, both in CD_3OD and $CHCl_3$. The individual protons are assigned using double resonance techniques. As well, correlation times of individual protons in the molecule are determined from the measurement of the frequency dependence of the proton relaxation rates.

Materals and Methods

Thromboxane B_2 was a gift from Dr. John Pike, the Upjohn Co., Kalamazoo, MI. The thromboxane B_2 solutions were prepared in $CDCl_3$, 99.8% deuterated (from SCI-Graphics) at a concentration of approximately 2 mg per 0.35 mL $CDCl_3$. For the relaxation time measurements two concentrations, 4 mg and 2 mg per 0.35 mL of $CDCl_3$ were used. All materials were handled in a dry box in a nitrogen gas atmosphere. The $CDCl_3$ was purified by treating it with Al_2O_3 (B.D.H. Chemicals) and then vacuum degassing it several times (freeze–pump–thaw technique). The thromboxane was dried *in vacuo* overnight at a temperature of 60°C. The purified solvent was added to the dried thromboxane, the solution was then transferred to an nmr tube, and was vacuum degassed several times using the freeze–pump–thaw technique. Subsequently, the nmr tube was sealed. For all of the above experiments, the glassware was cleaned extensively to eliminate paramagnetic impurities. The same procedure was used in preparing the CD_3OD (from SCI-Graphics) solutions, except the treatment with Al_2O_3 was omitted.

The nmr measurements were carried out at 298 K using the Bruker WH-400/DS and the Bruker WH-200/DS nmr spectrometers operating at proton frequencies of 400 and 200 MHz, respectively. The experiments were carried out in the pulsed Fourier transform mode using the Bruker Aspect 2000 computer, 16K data points, and a pulse width of 5 μs (pulse angle = 42°) for the determination of the chemical shifts and coupling constants at 400 MHz. The repetition time of the pulse cycle was 2.0 s. The deuterium resonance of the solvents was used as the lock signal. The homonuclear decoupling experiments were performed in the pulsed mode using the same pulse width. The chemical shifts and coupling constants were calculated to first order and are reported with an accuracy of about 0.010 ppm (±4 Hz at 400 MHz) and about 0.20 Hz, respectively. For maximum accuracy, spectra were expanded to a width of 2 Hz/cm, the peaks were then bisected by vertical lines and from these spectra average values of chemical shifts and coupling constants were determined.

The proton longitudinal relaxation rates were obtained at both frequencies using the 180°–τ–90° inversion recovery sequence (10). Delay times of 12 s at 400 MHz and 10 s at 200 MHz were used. Usually 10 τ values were included in the analysis of the data, based on the initial slope of a plot of $\ln((M_\infty - M_\tau)/(M_\infty))$ vs. τ. In this plot, M_∞ is the equilibrium value of the magnetization and M_τ is the value of the magnetization at time τ between the 180° and 90° pulse sequence. These M values were obtained from the measurement of the sum of the peak heights of a multiplet corresponding to a given proton. Three M_∞ values were always measured for maximum accuracy and 30–50 scans were used for these measurements. The relaxation rates were obtained from a computer analysis of the data using a least-squares program. The T_1 values are reproducible from one sample to a second sample with an accuracy of ±5% at 400 MHz and ±10% at 200 MHz. Some overlap of multiplets corresponding to different protons was observed, mainly at 200 MHz, and hence the larger error limits at this frequency. Data are not reported where there was significant overlap of resonances corresponding to different protons. The one exception is for protons 17–19, which have identical chemical shifts. The relaxation rate for these protons is reported as it provides a probe of the mobility of this side chain.

Results

The complete 400 MHz proton magnetic resonance spectra of TXB_2 in $CDCl_3$ and CD_3OD are shown in Fig. 2. From the spectra (Figs. 2 and 3), it can be seen that both the α- and β-anomers are present in solution. In $CDCl_3$, the predominant anomer has the OH group at C-11 in the α configuration, hence H-11 is β to the ring (Fig. 4). In CD_3OD, the OH group at C-11 in the predominant anomer has the β configuration. The proton resonances were assigned on the basis of homonuclear proton decoupling experiments. Proton resonances corresponding to the minor anomers in $CDCl_3$ are

Can. J. Chem. Downloaded from www.nrcresearchpress.com by 210.87.254.42 on 09/05/12
For personal use only.

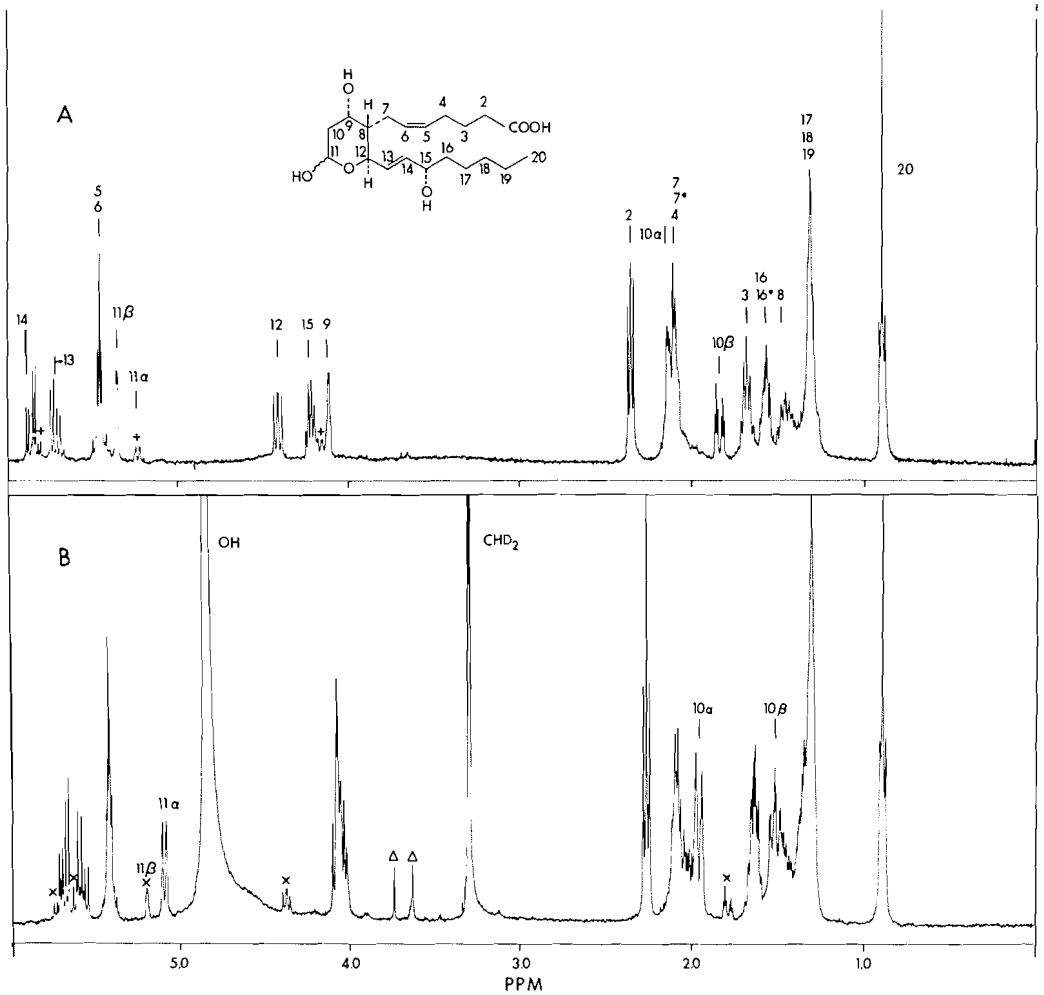


FIG. 2. A. The 400 MHz proton magnetic resonance spectrum of TXB_2 in $CDCl_3$. The assignment of the proton resonances is shown in the figure. Peaks indicated by a + are from the minor anomer. B. The 400 MHz proton magnetic resonance spectrum of TXB_2 in CD_3OD. Peaks indicated by an × are due to the minor anomer. The Δ represents artifacts.

indicated by a (+) in Fig. 2A and in CD_3OD by a (×) in Fig. 2B.

The chemical shifts and coupling constants for TXB_2 in $CDCl_3$ are listed in Table 1. TXB_2 is present in $CDCl_3$ solutions mainly as the 11α-OH TXB_2 anomer. Integration of the 11α and 11β proton resonances (Fig. 2A) indicates that the major anomer is present at a concentration of 76% while the minor anomer is present at a concentration of 24%. On the other hand, when CD_3OD is used as the solvent (Fig. 2B), the concentration of the 11α-OH anomer drops to 20% while the predominant anomer is now 11β-OH at a concentration of 80%.

A wide range of decoupling experiments were performed but only several representative experiments will be described. Decoupling of H-15 (4.22 ppm) in $CDCl_3$ solution yields a quartet for H-14 (5.86 ppm) due to the couplings J(13—14) and J(12—14). This experiment (Fig. 3B) also allows the assignment of the protons at C-16 (1.56 ppm) and establishes the chemical shift of H-14 for the minor anomer. Irradiation of H-11β allows the assignment of H-10α at 2.11 ppm and H-10β at 1.84 ppm. Then irradiation of H-12 (4.41 ppm) results in a doublet for H-13 and a change in the H-8 multiplet. The exact chemical shift of H-8 (1.48 ppm) was established by irradiating this multiplet over a range of frequencies until maximum decoupling for H-9 and H-12 was observed. Irradiation of H-2 (2.35 ppm) results in the assignment of H-3 at 1.68 ppm.

Upon irradiating the region between 2.1 and 2.2 ppm, the following changes in the spectrum were observed (Fig. 3C): a singlet for H-5 and H-6;

Can. J. Chem. Downloaded from www.nrcresearchpress.com by 210.87.254.42 on 09/05/12
For personal use only.

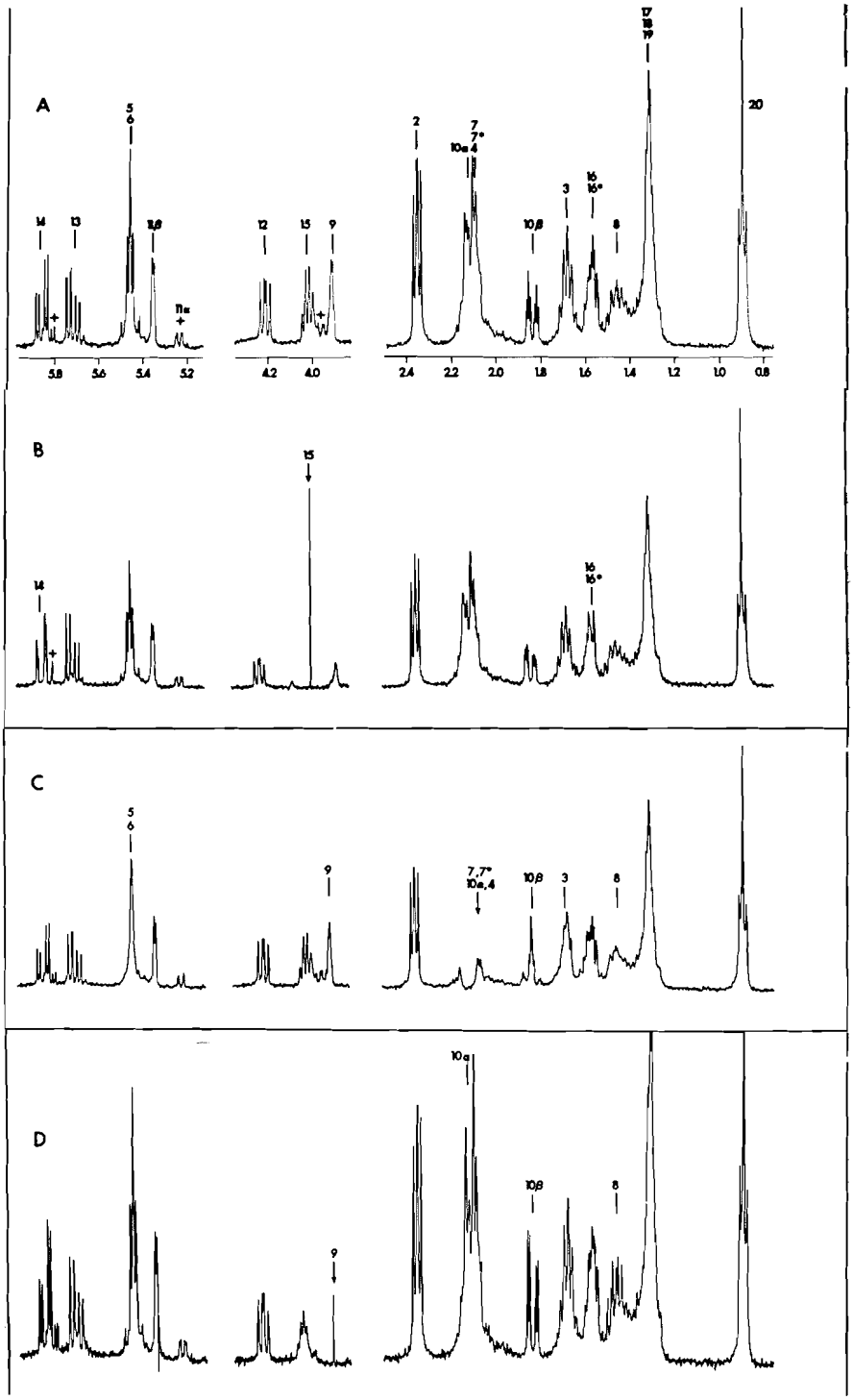
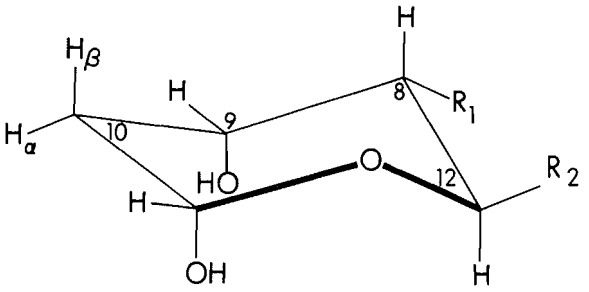


FIG. 3. Results of the proton homonuclear decoupling experiments on TXB_2 in $CDCl_3$ at 400 MHz. Spectrum A is the normal spectrum. In spectrum B, the H-15 multiplet is decoupled; in spectrum C, the region between 2.1 and 2.2 ppm is decoupled; whereas in spectrum D, the H-9 multiplet is irradiated.



11α-OH TXB_2

FIG. 4. The conformation of the predominant anomer of TXB_2 in $CDCl_3$, 11α-OH TXB_2. This is the conformation of the minor anomer in CD_3OD. The symbols R_1 and R_2 are: R_1 = —CH_2CH=$CHCH_2CH_2CH_2COOH$; R_2 = —CH=CH—$HC(OH)CH_2$-$CH_2CH_2CH_2CH_3$.

a sharpening of the resonances assigned to H-11β and H-11α, a singlet for H-9 (4.11 ppm), and a simplification of the H-10β, the H-3, and the H-8 multiplets. This arises since 5 protons are in this region. Finally, irradiation of H-9 (Fig. 3D) affects the H-8, H-10α, and the H-10β resonances and confirms their assignment.

Decoupling experiments were also performed on TXB_2 in CD_3OD and several of these will be summarized. When H-11α is irradiated, then H-10α and H-10β are identified for the 11β-OH anomer. This allows the measurement of J(10α—10β) and J(9—10α) and J(9—10β). When H-10α is irradiated, then H-11α collapses to a doublet, corresponding to J(10β—11α). The H-10β resonance also changes, giving a doublet of doublets, thus confirming the coupling J(9—10β) and J(10β—11α). Detailed measurements in CD_3OD were carried out only on the protons affected by the change of configuration at the anomeric center, and these data on the chemical shifts and coupling constants are presented in Table 2.

The results of the proton longitudinal relaxation time measurements, both at 200 MHz and at 400 MHz, are given in Table 3. The experiments were carried out on TXB_2 solutions in $CDCl_3$ at two concentrations, namely 2 mg and 4 mg per 0.35 mL of $CDCl_3$. The lowest possible concentrations were used so that only intramolecular dipolar interactions would be important. Relaxation mechanisms due to paramagnetic impurities have been minimized by careful cleaning of all glassware and the degassing of all samples. The deuterated solvent was used to eliminate solute–solvent dipolar interactions. The initial slope approximation was used in the analysis of the data. The sum of all the

TABLE 1. Chemical shifts and coupling constants for TXB_2 in $CDCl_3$ for both the 11α-OH TXB_2 and the 11β-OH TXB_2[a]

Proton	Chemical shifts (ppm)	Coupling constants Hz
	A 11α-OH (76%)	
2	2.35	J(2—3) = 6.5
3	1.68	J(2—3) = 6.5 J(3—4) = 7.1[b]
4	2.14[b]	
5,6	5.46	
7,7*	2.10[b]	
8	1.48[b]	J(8—9) = small[b]
9	4.11	J(8—9) = small[b] J(9—10α) = 3.2[b] J(9—10β) = 2.9[b]
10α	2.11	J(9—10α) = 3.2[b] J(10α—10β) = 14.2 J(10α—11β) = small[b]
10β	1.836	J(9—10β) = 2.9[b] J(10α—10β) = 14.2 J(10β—11β) = 3.6[b]
11β	5.35	J(10α—11β) = small[b] J(10β—11β) = 3.6[b]
12	4.41	J(8—12) = 10.5 J(12—13) = 7.4
13	5.72	J(12—13) = 7.4 J(13—14) = 15.6 J(13—15) = 1.0
14	5.86	J(13—14) = 15.6 J(14—15) = 5.5
15	4.22	J(13—15) = 1.0 J(14—15) = 5.5 J(15—16) = 6.2
16,16*	~1.56[b]	J(15–16) = 6.2
17, 18, 19	1.31	
20	0.893	J(19—20) = 6.9
	B 11β-OH (24%)	
10α	[c]	
10β	[c]	
11α	5.23	J(10α—11α) = 1.7[b] J(10β—11α) = 9.4[b]
12	4.15	J(8—12) = 11.0 J(12—13) = 8.2
13	[c]	
14	~5.83	J(13—14) = 15.2 J(14—15) = 5.5

[a]The chemical shifts and coupling constants were obtained at 400 MHz from a first order analysis of the spectra. Internal TMS was used as the reference compound. The average values of the coupling constants, obtained from both multiplets wherever possible, are reported.
[b]Calculated from decoupled spectra.
[c]Could not be measured due to multiplet overlap.

Can. J. Chem. Downloaded from www.nrcresearchpress.com by 210.87.254.42 on 09/05/12
For personal use only.

Can. J. Chem. Downloaded from www.nrcresearchpress.com by 210.87.254.42 on 09/05/12
For personal use only.

TABLE 2. Chemical shifts and coupling constants for TXB_2 in CD_3OD obtained at 400 MHz for both the 11α-OH TXB_2 and the 11β-OH TXB_2[a]

Proton	Chemical shifts (ppm)	Coupling constants (Hz)
	A 11α-OH (20%)	
10α	[b]	
10β	1.795	$J(10\alpha—10\beta) = 13.7$
11β	5.20	
12	4.38	$J(8—12) = 9.8$ $J(12—13) = 7.6$
13	5.61	$J(12—13) = 7.6$ $J(13—14) = 15.2$
14	5.73	$J(13—14) = 15.2$ $J(14—15) = 6.6$
	B 11β-OH (80%)	
10α	1.97	$J(10\alpha—10\beta) = 13.6$ $J(10\alpha—11\alpha) = 2.1$
10β	1.52	$J(10\beta—10\alpha) = 13.6$ $J(10\beta—11\alpha) = 9.7$
11α	5.10	$J(10\alpha—11\alpha) = 2.1$ $J(10\beta—11\alpha) = 9.7$
12	~4.08	
13	5.58	$J(12—13) = 7.7$ $J(13—14) = 15.3$
14	5.69	$J(13—14) = 15.3$ $J(14—15) = 6.5$

[a]The chemical shifts and coupling constants are obtained from a first order analysis of the spectra. Internal TMS was used as the reference compound.
[b]Could not be measured due to multiplet overlap.

lines of a multiplet corresponding to a given proton was used to obtain the total intensity at a given τ value (11), as required for a coupled system. Consequently, the initial rates are very nearly equal to $1/T_{1D}$, where T_{1D} is the longitudinal relaxation time due to the intramolecular dipolar interaction. As the spin rotation mechanism must be considered in the relaxation of the methyl protons, the relaxation of these protons is not considered in the present study.

The frequency dependence for $1/T_{1D}$ has been worked out by Solomon (12) for two interacting spins, and equations for $1/T_{1D}$ relaxation in the general case have also been worked out (13, and references therein). When relaxation rates at two frequencies are known, for example at 200 MHz and at 400 MHz, the rotational correlation time τ_R for a given proton can be evaluated from a plot of τ_R vs the $T_{1D}(400)/T_{1D}(200)$ quotient. This plot has previously been applied to the analysis of relaxation times of Vitamin D derivatives (14). Using the calibration graph published previously (14), the correlation times for the protons listed in Table 3 were evaluated. These range from 1.7 to 2.2 × 10^{-10} s for all protons listed in the table at both TXB_2 concentrations. The one exception is for protons 17–19 at the lower TXB_2 concentration, where only a small frequency dependence for T_{1D} was observed, and a correlation time of ~1 × 10^{-10} s is calculated. In addition, these protons have the same chemical shift and this may affect the relaxation times. Hence, within experimental error, the correlation times for the measured protons are all equal. The error limits for the correlation times were obtained by taking the $T_{1D}(400)/T_{1D}(200)$ quotient ±15%, and evaluating the upper and lower limit values for the correlation times. These are given in Table 3. The value of ±15% was chosen, since the uncertainty in the T_1 data at 200 MHz is about 10%, and at 400 MHz it is about 5%.

Discussion

The H-11α multiplet is to high field of the H-11β multiplet in both solvents (Fig. 2). As well, H-10α resonates to low field of the H-10β. These results are consistent with the observation for carbohydrates that equatorially oriented protons resonate at lower field than chemically similar but axially oriented protons (15). As well, when a proton under consideration is axial, a shift of 0.30 ppm to low field is observed for each neighboring axial hydroxyl group in D_2O. In the present study, the 10β proton in CD_3OD resonates at 1.80 ppm for the 11α-OH TXB_2 anomer (11α-OH is axial) but shifts

TABLE 3. Proton longitudinal relaxation times (s) for TXB_2 in $CDCl_3$ at 298 K

Proton	$T_{1D}(200)$[a]	$T_{1D}(400)$[a]	τ_R(s)	$T_{1D}(200)$[b]	$T_{1D}(400)$[b]	τ_R(s)
2	0.40	0.61	$2.1 \pm 0.6 \times 10^{-10}$	0.35	0.54	$2.2 \pm 0.7 \times 10^{-10}$
11β	0.74	1.09	$2.0 \pm 0.7 \times 10^{-10}$	0.57	0.88	$2.2 \pm 0.7 \times 10^{-10}$
12	0.50	0.77	$2.2 \pm 0.7 \times 10^{-10}$	0.42	0.66	$2.2 \pm 0.7 \times 10^{-10}$
13	0.81	1.11	$1.7 \pm 0.6 \times 10^{-10}$	0.62	0.92	$2.0 \pm 0.7 \times 10^{-10}$
14	0.80	1.17	$1.9 \pm 0.6 \times 10^{-10}$	0.65	0.91	$1.8 \pm 0.6 \times 10^{-10}$
17–19	1.04	1.20	$\sim 1 \times 10^{-10}$	0.75	1.07	$1.9 \pm 0.6 \times 10^{-10}$

[a]The TXB_2 concentration was 2 mg per 0.35 mL of $CDCl_3$.
[b]The TXB_2 concentration was 4 mg per 0.35 mL of $CDCl_3$.

Can. J. Chem. Downloaded from www.nrcresearchpress.com by 210.87.254.42 on 09/05/12
For personal use only.

to 1.52 ppm in the 11β-OH TXB_2 anomer (shift difference = 0.28 ppm). This is in excellent agreement with the predicted chemical shift difference.

Coupling constants for vicinal hydrogens are related to the torsion angle and Karplus (16, 17) has proposed a relationship of the form $^3J(H1, H2) = a \cos^2 \phi + b$ for saturated systems (H1—C1—C2—H2), where ϕ is the angle between the H1—C1—C2 and the H2—C2—C1 planes, and a and b are constants for the particular system under study. Other forms of this equation have been proposed but in all cases these equations must be used with care in determining torsion angles from coupling constants due to the difficulties in determining values for the constants for any one specific kind of structure (17, 18). Observed values of vicinal coupling constants for chair forms of a variety of carbohydrates have been tabulated (19). Coupling constants between vicinal diaxial protons have a mean value of 9.63 Hz and a range from 8.6–11.5 Hz, between diequatorial protons the mean value is 1.54 Hz (the range is 0.6–3.5 Hz) while the coupling constants between an axial proton and an equatorial proton fall in the range 1.5–5.8 Hz with a mean value of 3.66 Hz.

The vicinal coupling constants presented in Tables 1 and 2 indicate that TXB_2 is present in solution with the six-membered ring in a chair conformation and with both side chains equatorial. For 11α-OH TXB_2 (Tables 1*A* and 2*A*), the large values of 10.5 Hz for $^3J(8—12\alpha)$ in $CDCl_3$ and 9.8 Hz in CD_3OD indicate that these protons are diaxial and the dihedral angle involving these protons is close to 180°. Similarly, for 11β-OH TXB_2 the $^3J(10\beta—11\alpha)$ coupling constant is 9.4 Hz in $CDCl_3$ and 9.7 Hz in CD_3OD (Tables 1*B* and 2*B*). The magnitudes of J(axial–equatorial) and J(equatorial–equatorial) are as expected for both anomers in both solvents.

The results of the proton longitudinal relaxation time measurements are presented in Table 3. As expected, when the concentration of TXB_2 is doubled, the T_{1D} values decrease uniformly. This is due to intermolecular association which has been previously observed (9) for ^{13}C T_1 data on $PGF_{2\alpha}$. From the frequency dependence of the data, correlation times ranging from 1.7×10^{-10} to 2.2×10^{-10} s were evaluated for the protons listed in the table. These correlation times are similar in magnitude, within experimental error, at both TXB_2 concentrations. These data indicate that the molecular rotational correlation time is $\sim 2.0 \times 10^{-10}$ s.

Finally, the conformation of 11α-OH TXB_2 (Fig. 4) as determined in this study should be similar to that expected for TXA_2 since both bonds in the latter compound (Fig. 1) from the C-9 and C-11 carbon atoms to the bridging oxygen atom are α to the ring. The major anomer in $CDCl_3$ also has both of the C-9 and C-11 OH groups α to the ring.

Acknowledgements

The authors acknowledge valuable discussions with Dr. T. T. Nakashima and Mr. G. Bigam, Dr. O. Maryniak of the University of Alberta Hospital for his suggestions concerning the prostaglandins, Dr. John Pike of the Upjohn Company in Kalamazoo, MI. for providing us with thromboxane B_2, and the Natural Sciences and Engineering Research Council of Canada and the University of Alberta for generous financial assistance.

1. J. R. VANE. *In* Advances in prostaglandin and thromboxane research. Vol. 4. *Edited by* F. Coceani and P. M. Olley. Raven Press, New York. 1978. pp. 27–44.
2. M. HAMBERG, J. SVENSSON, and B. SAMUELSSON. Proc. Natl. Acad. Sci. U.S.A. **72**, 2994 (1975); see also B. Samuelsson *et al.*, ref. 1, pp. 1–25.
3. B. SAMUELSSON, M. GOLDYNE, E. GRANSTRÖM, M. HAMBERG, S. HAMMARSTRÖM, and C. MALMSTEN. Annu. Rev. Biochem. **47**, 997 (1978).
4. S. MONCADA, R. GRYGLEWSKI, S. BUNTING, and J. R. VANE. Nature, **263**, 663 (1976).
5. N. KHARASCH and J. FRIED (*Editors*). Biochemical aspects of prostaglandins and thromboxanes. Academic Press, New York, NY. 1977. See S. Moncada and J. R. Vane. pp. 155–177; see also Sun *et al.* pp. 179–187.
6. G. KOTOVYCH, G. H. M. AARTS, T. T. NAKASHIMA, and G. BIGAM. Can. J. Chem. **58**, 974 (1980).
7. D. A. LANGS, G. T. DETITTA, M. G. ERMAN, and S. FORTIER. *In* Abstracts, Fourth International Prostaglandin Conference. Washington, DC. May 27–31, 1979. p. 66.
8. A. A. AKREM and E. V. KOROLEVA. NMR spectroscopy in the chemistry of prostaglandins. *In* Vestsi Akad. Navuk BSSR, Ser. Khim. Navuk. No. 6, 103–118 (1978).
9. W. W. CONOVER and J. FRIED. Proc. Natl. Acad. Sci. U.S.A. **71**, 2157 (1974).
10. R. L. VOLD, J. S. WAUGH, M. P. KLEIN, and D. E. PHELPS. J. Chem. Phys. **48**, 3831 (1968).
11. R. L. VOLD and R. R. VOLD. Prog. Nucl. Magn. Reson. Spectrosc. **12**, 79 (1978).
12. I. SOLOMON. Phys. Rev. **99**, 559 (1955).
13. R. ROWAN III, J. A. MCCAMMON, and B. D. SYKES. J. Am. Chem. Soc. **96**, 4773 (1974).
14. G. KOTOWYCZ, T. T. NAKASHIMA, M. K. GREEN, and G. H. M. AARTS. Can. J. Chem. **58**, 45 (1980).
15. R. U. LEMIEUX and J. D. STEVENS. Can. J. Chem. **44**, 249 (1966).
16. M. KARPLUS. J. Chem. Phys. **30**, 11 (1959).
17. M. KARPLUS. J. Am. Chem. Soc. **85**, 2870 (1963).
18. G. KOTOWYCZ and R. U. LEMIEUX. Chem. Rev. **73**, 669 (1973).
19. B. COXON. Methods Carbohydr. Chem. **6**, 513 (1972).

Interaction of divalent metal ions with pyridoxal phosphate. I. Nuclear magnetic resonance studies of cobalt(II) binding[1]

TENKASI S. VISWANATHAN AND TERRENCE J. SWIFT[2]

Chemistry Department, Case Western Reserve University, University Circle, Cleveland, OH 44106, U.S.A.

Received November 1, 1979

TENKASI S. VISWANATHAN and TERRENCE J. SWIFT. Can. J. Chem. **58**, 1118 (1980).

The binding of Co(II) to pyridoxal phosphate (PLP) at neutral pH was investigated with ^{31}P, ^{1}H, and ^{13}C nmr spectroscopy. The proton and phosphorus spin–lattice relaxation times of PLP were measured in the absence of Co(II) and with increasing amounts of the metal ion. The shifting and the relaxation enhancement of the phosphorus resonance in the presence of Co(II) have indicated the binding of the metal ion to the phosphate of PLP. The addition of metal ion also shifted and broadened the proton and carbon resonances. The shifting and broadening was the largest for the 4-CHO proton with other protons following the order 4-CHO ≫ 2-methyl > 5-methylene > 6-H. At neutral pH Co(II) shifted only the 5-methylene proton resonance of pyridoxamine phosphate (PMP) indicating binding of Co(II) only to the 5′-phosphate of PMP at this pH. Comparison of the shifting and broadening of the proton resonances of PLP with similar shifts in model compounds has indicated a structure for the 1:1 PLP:Co(II) complex in which the metal ion is simultaneously bound to the phosphate and the aldehyde oxygen. The proton spin–lattice relaxation times and the isotropic shifts of the ^{13}C resonances in the 1:1 PLP:Co(II) complex support this conclusion.

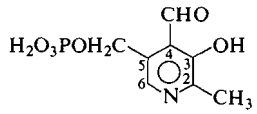
TENKASI S. VISWANATHAN et TERRENCE J. SWIFT. Can. J. Chem. **58**, 1118 (1980).

On a étudié le mode de liaison du Co(II) avec le phosphate de pyridoxale (PPL) à pH neutre en utilisant la spectroscopie de rmn du ^{31}P, du ^{1}H et du ^{13}C. On a mesuré les temps de relaxation spin–réseau du proton et du phosphore du PPL en l'absence de Co(II) et avec les quantités croissantes d'ion métallique. Le déplacement chimique et l'accroissement de relaxation de la résonance du phosphore en présence du Co(II) indiquent que l'ion métallique se lie au phosphate de PPL. L'addition de l'ion métallique provoque également un déplacement et transforme en massif la résonance du proton et du carbone. Cet effet de déplacement et d'élargissement est maximal dans le cas du proton du CHO en position 4 et décroît dans l'ordre CHO ≫ méthyl-2 > méthylène-5 > H-6. A pH neutre, le Co(II) ne déplace que la résonance du proton du méthylène en position 5 du phosphate de pyridoxamine indiquant ainsi que le Co(II) n'est lié qu'au phosphate-5′ de pyridoxamine (PPM) à ce pH. La comparaison du déplacement chimique et de l'élargissement de résonance du proton du PPL avec d'autres déplacements chimiques dans des composés types indique que le complexe PPL:Co(II) a une structure 1:1 dans laquelle l'ion métallique est lié simultanément au phosphate et à l'oxygène de l'aldéhyde. Le temps de relaxation spin–réseau du proton et les déplacements chimiques isotopiques du ^{13}C dans le complexe PPL:Co(II) 1:1 confirment cette conclusion.

[Traduit par le journal]

Introduction

Pyridoxal phosphate containing enzymes catalyze many biological reactions of amino acids. These include transamination, decarboxylation, deamination, and racemization. Most of the enzymatic reactions of PLP (**1**) have been duplicated by nonenzymatic model reactions in which pyridoxal or other appropriate hydroxyaldehydes and a divalent or trivalent metal ion serve as catalysts.



1 Pyridoxal phosphate

A general mechanism for PLP-catalyzed reactions proposed by Metzler and Snell (1) implies the formation of a Schiff base from PLP and an amino acid. In the nonenzymatic model systems the metal ion stabilizes the Schiff bases by chelation. In the ternary model systems involving PLP, an amino acid and a divalent metal ion, binary amino acid – metal ion and PLP – metal ion complexes are formed under certain conditions. The metal ion complexes of amino acids have been extensively studied. On the other hand, not much is known about the PLP – metal ion complexes. A recent attempt (2) to isolate and characterize these complexes yielded an insoluble polymeric solid. In a previous communication (3) we described a nuclear magnetic resonance spectroscopic method of studying these complexes at low concentrations with the aid of paramagnetic metal ions.

Paramagnetic complexes derived from biological ligands with multiple binding sites and metal ions such as Co(II), Ni(II), Cu(II), and Mn(II) lend themselves to detailed investigation of their structure by nmr spectroscopy. The effect of a paramagnetic metal ion on the chemical shifts and the rates of relaxation of the neighboring nuclei is so large that the ion is an exceptionally good probe of its surroundings. This paper describes the results of our studies on the binding of Co(II) to PLP and related compounds by ^{31}P, ^{1}H, and ^{13}C nmr spectroscopy. This metal ion forms well defined com-

[1]Based on the Ph.D. thesis of T.S.V., 1975.

[2]To whom all correspondence should be addressed.

0008-4042/80/111118-07$01.00/0

©1980 National Research Council of Canda/Conseil national de recherches du Canada

Can. J. Chem. Downloaded from www.nrcresearchpress.com by 210.87.254.5 on 09/05/12
For personal use only.

Can. J. Chem. Downloaded from www.nrcresearchpress.com by 210.87.254.5 on 09/05/12
For personal use only.

plexes with PLP in aqueous solutions and the complexes are sufficiently labile to investigate their structure by nmr spectroscopy at high ligand-to-metal ratios.

Experimental

PLP, PMP, and AMP were purchased from Sigma Chemical company. The transition metal impurities in the commercial AMP sample were removed by passage of a solution of this sample through a cation exchange (chelex-100, Na form) column. Constancy of ^{31}P linewidth over a wide temperature range was taken as the criterion for the absence of transition metal ion contamination. The concentration of AMP employed for the ^{31}P nmr work was 0.21 *M*. The concentration of PLP and PMP for the ^{31}P nmr studies was about 0.25 *M* and it was about 0.5 *M* for ^{13}C nmr determinations. Stock solutions of Co(II) in deuterium oxide were prepared from reagent grade $Co(NO_3)_2 \cdot 6H_2O$ purchased from J. T. Baker Chemicals.

Most of the proton nmr studies described here were done at the ambient probe temperature of 37°C on a Varian A60A NMR spectrometer. Some proton studies were done at 100 MHz on a Varian HA-100 NMR spectrometer and proton T_1 measurements were done at 60 MHz on a TT-14 NMR spectrometer equipped with a Nicolet 1080 computer. All the ^{13}C and ^{31}P nmr work was done on a Varian XL-100 NMR spectrometer in the pulsed FT/proton noise decoupled mode. The temperature of the XL-100 probe was determined by inserting a calibrated thermometer inside the spectrometer probe. Internal tetramethylammonium (TMA) chloride was used as the reference for proton and carbon nmr studies. The reference used for ^{31}P nmr was hexamethylphosphoramide (HMPA) contained in a coaxial 4 mm tube. The susceptibility corrections to the chemical shift were negligible at the maximum concentration ($< 2 \times 10^{-3}$ *M*) of Co(II) used in this experiment. All resonances with frequency greater than the resonance frequency of the chosen reference material were given a positive sign for the chemical shift.

Theory

The actual nmr spectrum of ligands bound to a paramagnetic metal ion is often unobservable because of the large linewidths associated with such species. In general, the spectrum of the paramagnetic complex is obtained by the addition of small amounts of the paramagnetic metal ion to a solution containing the ligand molecules. The resultant shifting and broadening are extrapolated to obtain the spectrum for the pure complex.

Paramagnetic Relaxation by Cobalt(II)

The contribution T_{2p}^{-1} of the paramagnetic metal ion to the observed transverse relaxation rate T_2^{-1} of a ligand nucleus is given by

$$[1] \quad T_{2p}^{-1} = T_2^{-1} - T_{2o}^{-1}$$

where T_{2o}^{-1} is the contribution of other mechanisms. The equations for T_{2p}^{-1} for ligand nuclei in a solution containing only a fraction of coordinated ligand molecules have been derived by Swift and Connick (4). The longitudinal relaxation rate for ligand resonances in such systems is given by the equations of Bloembergen and Morgan (5) and Luz and Meiboom (6).

$$[2] \quad T_{1p}^{-1} = T_1^{-1} - T_{1o}^{-1} = f/(T_{1M} + \tau_M)$$

where f is the ratio [Co(II)]/[ligand], T_{1M} is the longitudinal relaxation rate of ligand nuclei in the complex and τ_M is the average residence time of the ligands in the bound form. The quantities T_{1p}^{-1}, T_1^{-1}, and T_{1o}^{-1} are defined as for T_2.

The relaxation rates T_{1M}^{-1} and T_{2M}^{-1} for ligand nuclei in the coordination sphere of Co(II) can be calculated theoretically from the Solomon–Bloembergen equation (7, 8).

$$[3] \quad T_{1M}^{-1} = T_{2M}^{-1} = \left[\frac{4}{3}\frac{s(s+1)g^2\beta^2\gamma_I^2}{r^6} + \frac{2}{3}\frac{s(s+1)A^2}{\hbar^2}\right]\tau_s$$

where τ_s is the electron spin relaxation time, A is the coupling constant for the electron–nucleus scalar interaction, and r is the electron–nuclear distance. For values of A/h, g, S, and r derived from X-ray crystallographic studies Shulman *et al.* (10) calculated a value of $T_{1M}^{-1} = T_{2M}^{-1} = 5.7 \times 10^2\ s^{-1}$ for the phosphorus nuclei in the Co(II)-bound phosphates. Comparing the experimentally determined T_{1M}^{-1}, T_{2M}^{-1} and the shifting values in PLP–Co(II) system with the theoretical values would indicate whether the complexation involves direct binding of the metal ion to the phosphate.

Paramagnetic Shifting by Cobalt(II)

Paramagnetic shifting by Co(II) may take place either by a dipolar mechanism or Fermi contact mechanism. A detailed discussion of these shift mechanisms may be found elsewhere (9). Contact shifts arise only if there is a significant amount of unpaired spin density at the resonating nucleus and the observation of contact shifts for ligand nuclei provides evidence for metal–ligand covalency. The dipolar shifts occur only in complexes in which the electronic magnetic moment is anisotropic. An accurate knowledge of the geometry of the complex is important to the quantitative separation of contact and dipolar contributions to the isotropic shift.

Results and Discussion

1. ^{31}P Nuclear Magnetic Resonance Studies of PLP–Co(II) System

The addition of cobalt nitrate solution to a 0.25 *M* solution of PLP at pD 6.2 results in considerable shifting and broadening of the phosphorus resonance of PLP. The temperature dependence of the

Can. J. Chem. Downloaded from www.nrcresearchpress.com by 210.87.254.5 on 09/05/12
For personal use only.

shifting and broadening for a [Co(II)]/[PLP] ratio of 2.4×10^{-3} is shown in Fig. 1. The curves are typical of diamagnetic $\rightleftharpoons$ paramagnetic exchange systems (4, 11) and indicate complexation between PLP and Co(II). Whether this complexation involves the phosphate group or not could be decided by comparing the shifting and broadening of PLP–Co(II) system with the corresponding data for an authentic phosphate–Co(II) complex such as AMP–Co(II). Shulman *et al.* (10) have studied the AMP–Co(II) system by continuous wave ^{31}P nmr at 24.31 MHz and concluded that the metal ion binds to the phosphate of AMP. We have reproduced their results under the conditions (pulse nmr at 40.5 MHz) employed in our studies.

Comparison of the data for AMP–Co(II) and PLP–Co(II) showed that the limit of very fast exchange does not exist for both systems simultaneously in the available temperature range, making accurate comparison of the shift $\Delta\omega$ difficult. However, the shift $\Delta\omega/f$ at the point of maximum shift in the curves should be comparable if the Co(II) binds directly to the phosphate of PLP as in AMP–Co(II). The value of $\Delta\omega$ was taken as the difference between the shift of the metal complex solution of known f at the point of maximum shift and the shift of the metal-free solution at the temperature of the maximum shift in the metal-containing solutions. Both shifts were referenced to an external HMPA contained in a coaxial capillary tube. The values of $\Delta\omega/f$ calculated by this method for AMP–Co(II) and PLP–Co(II) are 3.8×10^4 Hz and 3.3×10^4 Hz respectively. The good agreement indicates that Co(II) binds directly to the phosphate. The value of $\Delta\omega/f$ for PMP–Co(II) is slightly less than for PLP–Co(II). Potentiometric studies have indicated that the logarithm of the stability constants for 1:1 complexes of cobalt(II) with ribose phosphate (12), AMP (13), and PLP (12) are 2.08, 2.19, and 2.39 respectively. The close values also indicate that the primary mode of binding of Co(II) in these complexes is through the phosphate.

Since the PLP–Co(II) system does not enter the very fast exchange region in the temperature range studied, the line broadening data do not provide any structural information. However, they shed some light on the kinetics of the exchange of free and bound PLP molecules. The temperature dependence of T_{2p}^{-1} at temperatures 10° below the temperature of T_2^{-1} maximum (50°C) derives mainly from the temperature dependence of the term τ_M. In the slow exchange region Swift–Connick equation for T_{2p}^{-1} reduces to $T_{2p}^{-1} = f\tau_M^{-1}$. From the full linewidth at half height of 36.5 and 62.0 Hz at 278.2 and 288.6 K respectively an activation energy of 8 kcal can be calculated for the ligand exchange in the PLP–Co(II) system. The residence time τ_M at 5°C is 2.4×10^{-5} s.

The direct binding of Co(II) to the phosphate of PLP was also established from the measurement of the T_1 relaxation time of phosphorus in the complex. The point of maximum signal broadening for the PLP–Co(II) system occurs at 50°C. At temperatures 70°C and above $\tau_M \ll T_{2M}$, $\Delta\omega_M$ leading to the fast exchange limit. Since $T_{1M} = T_{2M}$ for the coordinated phosphate $\tau_M \ll T_{1M}$. Under these conditions eq. [2] reduces to $T_{1p}^{-1} = fT_{1M}^{-1}$. Figure 2 shows the linear dependence of T_{1p}^{-1}, T_{2p}^{-1}, and $\Delta\omega_p$ on f at 70°C. The value of T_{1M}^{-1} obtained by

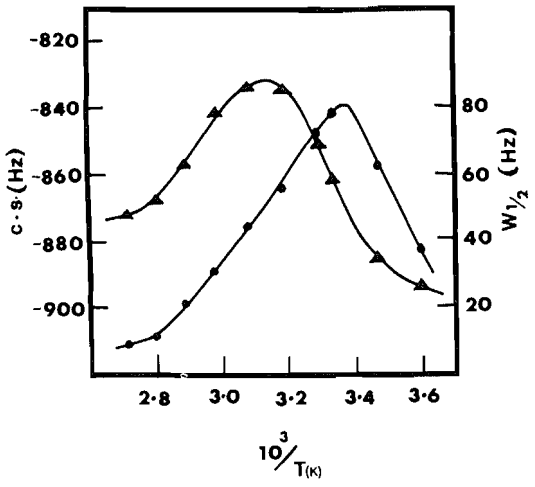


FIG. 1. Plot of the full linewidth at half maximum intensity (●) and the shift (▲) in Hz from hexamethylphosphoramide (HMPA) of the ^{31}P resonance of PLP–Co(II) at 40.5 MHz versus reciprocal temperature (K); $f = 2.4 \times 10^{-3}$.

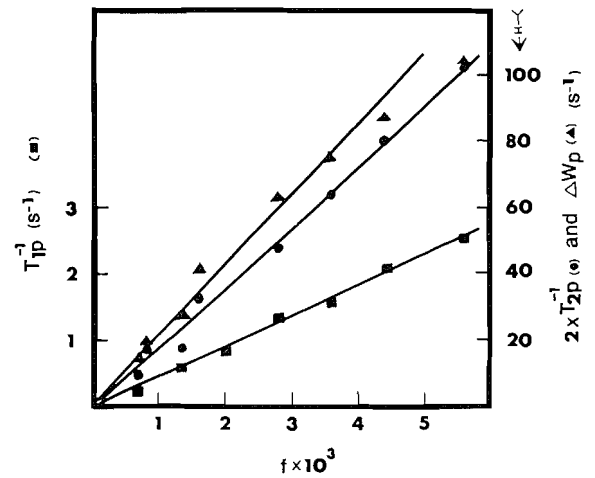


FIG. 2. The dependence of T_{1p}^{-1}, T_{2p}^{-1}, and the shift $\Delta\omega_p$ of the ^{31}P resonance of PLP–Co(II) on the concentration of Co(II) at 70°C.

Can. J. Chem. Downloaded from www.nrcresearchpress.com by 210.87.254.5 on 09/05/12
For personal use only.

extrapolation from this plot is $4.5 \times 10^2\ s^{-1}$, which is in good agreement with the value of $5.7 \times 10^2\ s^{-1}$ calculated for a Co(II)-bound phosphate from eq. [3]. Thus, the shift and T_1 data indicate that Co(II) binds directly to the phosphate of PLP. It also indicates that there is only one bound phosphate per Co(II) in the PLP–Co(II) complex. The phosphorus nmr study does not, however, indicate whether the metal binds to other sites in PLP. This question is answered by our proton and carbon nmr studies of this system.

2. Proton Nuclear Magnetic Resonance Studies

The proton nmr spectrum of PLP has been well studied. At pD 6.2 a cobalt-free solution gives sharp peaks for all the protons of PLP at 37°C. Progressive addition of Co(II) solution to PLP solution results in selective shifting and broadening of the resonances. The shifting and broadening increase linearly with the concentration of the metal ion. From the slope of the linear plots (not shown) values for $\Delta\omega_p$ and T_{2p}^{-1} were calculated for each of the proton resonances in a 1:1 PLP:Co(II) complex and they are shown in Table 1.

Table 1 shows that the extent of broadening and shifting is largest for the aldehyde proton and follows the order 4-CHO $\gg$ 2-CH_3 > 5-CH_2 $\approx$ 6-H. The 5-methylene protons are split by the phosphorus (J = 6 Hz) and the addition of metal ion collapses this coupling in addition to the broadening of this signal. In such cases it is difficult to be sure how to measure the linewidth and it was not measured. For calculation of the shift, the center of the doublet was used as the position of this resonance for small values of f. In PMP only the 5-methylene protons show considerable shifting at pD 6.2 and other protons exhibit negligible shift. At this pD the 4′-amino group of PMP remains protonated and chelation of the metal ion by the 3-O^- and the amino moieties is not likely to take place. Under these conditions the primary binding site for Co(II) in PMP would be the phosphate and the selective shifting of the 5-methylene manifests this interaction. The shift of 5-methylene in PMP–Co(II) and PLP–Co(II) are comparable. The large shifts of the 4-CHO and 2-methyl protons observed in PLP–Co(II) probably indicates a definite interaction of the Co(II) with the ring in PLP.

TABLE 1. Proton shift and broadening data at 60 MHz of 1:1 complexes of Co^{2+} and some phosphate-containing vitamins

Compound	Nucleus	Shift (Hz)	Full linewidth at half height (Hz)
Pyridoxal phosphate	4-CHO	8576	9328
	5-CH_2	214	—
	6-H	135	17
	2-CH_3	1398	285
Pyridoxamine[a] phosphate	5-CH_2	349	—
Thiamine[b] monophosphate	6′-H	136	—
	2′-CH_3	−20	—
Thiamine[b] pyrophosphate	6′-H	70	—
	2′-CH_3	−25	—
Thiamine[b] triphosphate	6′-H	3	—
	2′-CH_3	−13	—

[a]The shifting and the broadening of other protons are negligible.
[b]Reference 14.

The temperature dependence of the shifting and broadening of the PLP proton resonances by Co(II) was also studied to ascertain the contribution of rate effects to the observed linewidths. The 2-methyl and 6-H resonances are well into the fast exchange region at 37°C and the shifting has reached the weighted average value. The net shifting $\Delta\omega_p$ caused by the metal ion is nearly temperature independent for these resonances. The logarithm of the shifting and broadening of the 4-CHO resonance by Co(II) alone as a function of the inverse temperature is shown in Fig. 3. The figure shows that at 37°C the linewidth of this resonance has considerable contribution from the diamagnetic $\rightleftharpoons$ paramagnetic exchange rate term. No attempt was made to obtain structural information from proton linewidths because of this uncertainty and the lack of detailed knowledge about the

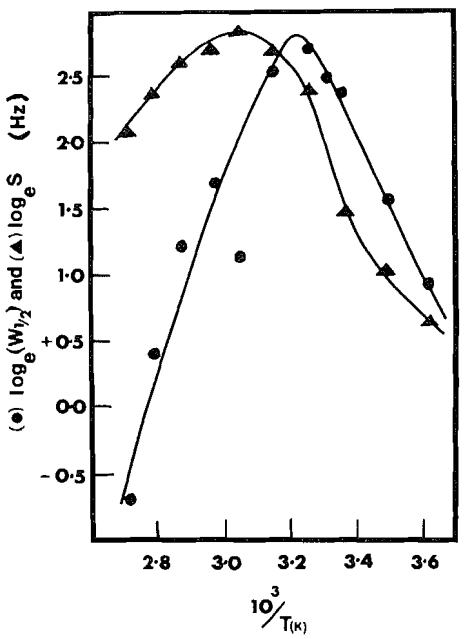


FIG. 3. The full linewidth at half height (●) and the shift (▲) of the CHO proton of PLP–Co(II) ($f = 1.2 \times 10^{-3}$) after correcting for the CHO $\rightleftharpoons$ $CH(OH)_2$ exchange.

Can. J. Chem. Downloaded from www.nrcresearchpress.com by 210.87.254.5 on 09/05/12
For personal use only.

mechanism for the proton transverse relaxation enhancement in this system.

The shifting of 6-H and 2-methyl protons in PLP–Co(II) are quite different from the shifts of 6-H and 2-methyl protons of α-picoline (15) in α-picoline complexes of cobalt(II) acetylacetonates indicating that Co(II) does not bind to the heterocyclic nitrogen of PLP at pD 6.2. It is not surprising since the nitrogen remains protonated at pD 6.2. But, raising the pD to 10 does not change the relative values of the shifting and broadening of the PLP resonances. Briggs (12) has observed that the metal ion was not competing with the final dissociating proton for a binding site in potentiometric titrations of 1:1 PLP:Co(II) solutions. An examination of space filling molecular models shows that the phosphate-bound metal cannot form a direct σ-bond with the heterocyclic nitrogen in a 1:1 PLP:Co(II) complex since it requires the metal ion to lie along the C_4—N axis in the plane of the ring. The sign and the relative shifts of the 6-H and 2-methyl protons in PLP–Co(II) are also not in accordance with the formation of an outersphere complex (11, 14) consisting of a trapped water molecule hydrogen bonded to the nitrogen and simultaneously coordinated to the metal ion. On the contrary, the large shifting and broadening of the formyl proton suggests that the interaction of the metal ion with the ring is through the CHO or 3-O^- or both.

The aldehyde group of PLP can exist in two forms, the free form, —CHO, and the hydrated form, —$CH(OH)_2$. The exchange rate for the CHO $\rightleftharpoons$ $CH(OH)_2$ equilibrium is very low at the pD and the temperature employed in our measurements. The free form is the dominant form and the hydrated form constitutes about 5% of the total PLP. Sharp resonances are obtained for both species. The 2-methyl signal of the two forms are superimposed on each other at 60 MHz in metal-free solutions but the addition of cobalt solution to PLP selectively shifts the 2-methyl resonance of the free aldehyde form downfield. The 2-methyl resonance of the hydrated form is also shifted downfield and broadened but the shifting is only 1/7-th of the shift of the 2-methyl in the free aldehyde form. The smaller shifting of the 2-methyl of the hydrated PLP by Co(II) is still about ten times the shift of the methyl resonance of PMP. The observed shifting of the 2-methyl resonance could not have been derived from the

$$\text{PLP–Co(II)} \rightleftharpoons \text{PLP} \rightleftharpoons \text{PLP}(H_2O)$$

exchange since the latter is extremely slow at the pD and the temperature employed in these studies.

TABLE 2. The observed proton spin–lattice relaxation times (60 MHz) and metal–proton distances in 1:1 PLP:Co(II) solutions (0.05 *M*) at 22°C

Nuclei	T_{1p}^{-1}	r (Å)
4-CHO	346.1	3.89
5-CH_2	108.0	4.73
6-H	25.4	6.02
2-CH_3 (free)	26.4	5.98
2-CH_3 (hydr)	21.8	6.17

Thus, the methyl shift data indicate that the phosphate-bound metal ion interacts to varying degrees with the ring in PLP, hydrated PLP, and in PMP. This conclusion is reinforced by a kinetic study (12) of the PLP–Ni(II) system. The study revealed the presence of both PLP(H_2O)–Ni(II) and PLP–Ni(II) complexes. The author has shown that the Ni(II) binds more strongly to the unhydrated form than to the hydrated species and the hydration of the free PLP is more favorable than the hydration of the metal complex. Thus, both the kinetic and nmr evidence indicate a specific interaction of the metal ion with the carbonyl functional group of the free PLP.

There are two possibilities for the phosphate-bound Co(II) to form a direct bond with the ring in the PLP:Co(II) complex: (*1*) The metal may bind to both 4-CHO and 3-O^- functional groups of another PLP molecule in a 2:1 PLP:Co(II) complex. (*2*) The metal could form a direct bond with the aldehyde oxygen in a 1:1 complex. The first possibility was ruled out by comparing the shift of the aldehyde proton of PLP and salicylaldehyde. Fritz *et al.* (16) studied the isotropic shifts of the proton resonances in a series of compounds of the type (X-salad)$_2$$CoB_2$ where X-salad is a substituted salicylaldehyde and B is a pyridine base. They observed that the CHO proton is shifted approximately 2.1×10^4 Hz downfield at 60 MHz compared to the shift in salicylaldehyde. These studies were repeated by Croasmun (17) in our laboratories and from his results an identical value was calculated for the shift of the CHO protons of salicylaldehyde in the coordination sphere of Co(II).

The shift of 0.86×10^4 Hz observed for the CHO proton in a 1:1 PLP:Co(II) complex is only 40% of the shift in a 1:1 salad:Co(II) complex. The smaller shift of CHO suggests that it is unlikely that Co(II) binds to the hydroxyaldehyde in PLP and salicylaldehyde in the same way. However, the shift of CHO is too large to be accounted for by a weak interaction with these groups. The smaller shift for the CHO of PLP as compared with the shift in salicylaldehyde may arise if the phosphate-bound

Can. J. Chem. Downloaded from www.nrcresearchpress.com by 210.87.254.5 on 09/05/12
For personal use only.

metal binds only to the aldehyde oxygen of PLP in a 1:1 complex. A covalent binding of the metal to the carbonyl group of free PLP will provide a mechanism for spin delocalization, which in turn will lead to large contact shifts. This model is consistent with the observation of small dipolar shifts due to the phosphate-bound metal in PLP(H_2O):Co(II) and PMP:Co(II) and large contact shifts in PLP:Co(II).

The spin–lattice relaxation times of the protons of PLP were also measured at 60 MHz and 22°C in the absence of any metal ion and with various concentrations of cobalt. The addition of cobalt(II) results in the selective enhancement of the T_1^{-1} of the PLP protons and the enhancement is linear with the concentration of cobalt(II). The values of T_{1P}^{-1} extrapolated for a 1:1 PLP:Co(II) complex are shown in Table 2. Since $\tau_M \ll T_{1M}$ at this temperature, the T_{1P}^{-1} values actually represent T_{1M}^{-1} values.

The cobalt(II) induced proton shifts shown in Table 1 are all to lower fields and they are all small. Therefore, the scalar term in eq. [3] would be much too small to account for the observed T_{1M} values. Hence, T_{1M} for PLP:Co(II) is dipolar determined and can be used to determine "r" the metal–nuclear distance. In Table 2 we list the value of r derived from the proton T_{1M} values assuming $S = 3/2$, $g = 2.8$, and a τ_s of 5×10^{-13} s, the same value used to interpret the phosphorus data and used by Shulman *et al.* (10) in Co–AMP and Co–ATP studies. The close r values for the 2-methyl protons in the PLP–Co(II) and PLP(H_2O)–Co(II) confirms that the T_1 relaxation of the protons is dipolar determined since the distance between the 2-methyl protons and the phosphate-bound metal ion should be nearly equal in both complexes. The differential shift of the 2-methyl protons in these two complexes should originate from a Fermi contact mechanism since the dipolar shift term should be nearly equal for both complexes. Thus, the shift and relaxation data collectively imply a covalent interaction of the metal ion with the ring in PLP–Co(II). The relative distances of the 5-methylene, 6-H, and 4-CHO from the metal ion indicate that the metal is probably forming a bond with the oxygen of the carbonyl group.

3. Carbon Nuclear Magnetic Resonance Studies

The ^{13}C nmr spectrum of PLP has been well studied (18). The shifting of the carbon resonances upon addition of Co(II) solution to a 0.5 *M* PLP solution at pD 6.2 was studied at 35°C. The results are shown in Table 3. The temperature dependence of these shifts was not studied and nothing is known about the mechanism of these carbon shifts. The cobalt(II) induced shifts are difficult to interpret since a combination of σ- and π-delocalisation of the unpaired electron coupled with the correlation effects and dipolar shifts would result in a complex shift pattern for large systems such as PLP–Co(II). Table 3 shows that the shifting of all the carbon resonances except the C-5 are downfield. The upfield shifting of the C-5 resonance might be the result of binding to the phosphate. The predominantly lowfield shift of the ^{31}P, ^{1}H, and ^{13}C resonances indicates that the delocalization of the odd electron takes place through σ-bonds. Examination of the molecular models shows that when Co(II) is bound to the phosphate and the aldehyde oxygen, the favored conformation would be one in which the CHO oxygen is directed away from the 3-O^-. This model allows enough mobility about the C4—C4′ bond to keep the CHO group in the plane of the pyridine ring. The odd electron could be transported to the ring through π-electrons and through a σ–π configuration interaction mechanism, but the lack of detailed knowledge about mechanism of ^{13}C isotropic shifts allows only speculations of possible mechanisms of spin transport.

TABLE 3. The isotropic shift of the carbon-13 resonances in the 1:1 PLP:Co^{2+} complex in aqueous solution at 35°C

Nucleus	Shift (ppm)	Shift (Hz) at 25.16 MHz	Relative shift
C-2	690.48	17 372	13
C-3	436.36	10 979	8
C-4	263.16	6 621	5
C-5	−55.15	−1 388	−2
C-6	56.82	1 430	2
2-CH_3	27.75	698	1
5-CH_2	25.24	635	1
4-CHO	52.54	1 322	2

In conclusion, the present nmr study of the PLP–Co(II) system indicates that Co(II) binds to PLP through the phosphate and it also indicates the presence of an additional interaction with the ring. The interaction with the ring does not appear to be a chelate formation with the 3-hydroxy-4-aldehyde moiety. The proposed structure for the PLP–Co(II) complex is similar to the structure proposed for the PLP–Mn(II) complex (3) and both structures are in good agreement with the structure proposed for these complexes from a potentiometric study (12) of pyridoxal phosphate – divalent metal ion solutions.

1. D. E. METZLER and E. E. SNELL. J. Am. Chem. Soc. **77**, 2431 (1955).
2. M. E. FARAGO, M. M. MCMILLAN, and S. S. SABIR. Inorg. Chim. Acta, **14**, 207 (1975).

3. T. S. VISWANATHAN and T. J. SWIFT. Can. J. Chem. **57**, 1050 (1979).
4. T. J. SWIFT and R. E. CONNICK. J. Chem. Phys. **37**, 307 (1962).
5. N. BLOEMBERGEN and L. O. MORGAN. J. Chem. Phys. **34**, 842 (1961).
6. Z. LUZ and S. MEIBOOM. J. Chem. Phys. **40**, 2686 (1964).
7. I. SOLOMON. Phys. Rev. **99**, 559 (1955).
8. N. BLOEMBERGEN. J. Chem. Phys. **27**, 572 (1957).
9. J. P. JESSON. *In* NMR of paramagnetic molecules. *Edited by* G. N. LaMar, W. DeW. Horrocks, Jr., and R. H. Holm. Academic Press. 1973.
10. R. G. SHULMAN, H. STERNLICHT, and B. J. WYLUDA. J. Chem. Phys. **43**, 3116 (1965).
11. T. A. GLASSMAN, C. COOPER, L. W. HARRISON, and T. J. SWIFT. Biochemistry, **10**, 843 (1971).
12. T. N. BRIGGS. Ph.D. Thesis, Case Western Reserve University. 1976.
13. H. SIGEL and H. BRINTZINGER. Helv. Chim. Acta, **47**, 1701 (1964).
14. A. A. GALLO, I. L. HANSEN, H. Z. SABLE, and T. J. SWIFT. J. Biol. Chem. **247**, 5913 (1972).
15. J. A. HAPPE and R. L. WARD. J. Chem. Phys. **39**, 1211 (1963).
16. H. P. FRITZ, W. C. GRETNER, H. J. KELLER, and K. E. SCHWARZHANS. Z. Naturforsch. B, **23**, 906 (1968).
17. W. CROASMUN and T. J. SWIFT. Unpublished results.
18. T. S. VISWANATHAN and T. J. SWIFT. Bioorg. Chem. **8**, 191 (1979).

Can. J. Chem. Downloaded from www.nrcresearchpress.com by 210.87.254.5 on 09/05/12
For personal use only.

Synthetic and oxidation studies of ruthenium(II) phthalocyanine complexes

DAVID DOLPHIN, BRIAN R. JAMES,[1] ALAN J. MURRAY, AND JOHN R. THORNBACK

Department of Chemistry, University of British Columbia, Vancouver, B.C., Canada V6T 1Y6

Received November 5, 1979

DAVID DOLPHIN, BRIAN R. JAMES, ALAN J. MURRAY, and JOHN R. THORNBACK. Can. J. Chem. **58**, 1125 (1980).

Ruthenium(II) phthalocyanine complexes of the type $RuPcL_2$ (Pc = the phthalocyaninato dianion, L = various pyridines, imidazole, dimethylformamide, dimethylsulfoxide, and acetonitrile) may be prepared generally in solution by photolysis of RuPc(CO)L′ complexes in the presence of excess L (L′ may be the same as L or may be a different ligand), and in some cases as solids by extraction of crude RuPc with L. The solid RuPc(CO)L monocarbonyls can be formed from reaction of the $RuPcL_2$ complexes with carbon monoxide, as well as via an extraction procedure using L with crude RuPc(CO) formed from $Ru_3(CO)_{12}$ and phthalocyanine.

Chemical or electrochemical oxidation of the $RuPcL_2$ or monocarbonyl complexes generates a cationic ruthenium(II) phthalocyanine radical species and not ruthenium(III), as evidenced by esr and visible spectroscopy.

DAVID DOLPHIN, BRIAN R. JAMES, ALAN J. MURRAY et JOHN R. THORNBACK. Can. J. Chem. **58**, 1125 (1980).

Les complexes phthalocyanine de ruthénium(II) du type $RuPcL_2$ (Pc = dianions phthalocyaninato, L = différentes pyridines, imidazole, diméthylformamide, diméthylsulfoxyde et acétonitrile) peuvent généralement être préparés en solution par photolyse des complexes de RuPc(CO)L′ en présence d'un excès de L (L′ peut être identique à L ou peut être un ligand différent) et dans certains cas ils peuvent être préparés sous forme solide par extraction du RuPc brut avec L. Le solide monocarbonylé RuPc(CO)L peut être formé par la réaction des complexes $RuPcL_2$ avec le monoxyde de carbone aussi bien que par le procédé d'extraction utilisant L avec le RuPc(CO) brut formé à partir de $Ru_3(CO)_{12}$ et la phthalocyanine.

L'oxydation chimique ou électrochimique de $RuPcL_2$ ou des complexes monocarbonylés génère un radical cationique de phthalocyanine de ruthénium(II) et non de ruthénium(III) tel que mis en évidence par la rpe et la spectroscopie visible.

[Traduit par le journal]

Introduction

Continuing our interests in models for biological oxygenation and their potential for catalysis via O_2 activation (1–4), we are studying the chemistry of ruthenium(II) complexes with macrocyclic N_4 ligand systems. This paper reports studies on phthalocyanine complexes; the phthalocyaninato dianion (Pc) is a tetraazoporphyrinato ligand, the bridging methine positions and pyrrole rings of the porphyrin skeleton having been replaced by nitrogen, and benzpyrrole groups, respectively.

Although there have been several literature reports on the synthesis of ruthenium phthalocyanines, most of the complexes were not well-characterized. The reaction of *o*-cyanobenzamide with $RuCl_3 \cdot 3H_2O$ is reported to give "RuPc", which on extraction with aniline gives a crystalline solid, $RuPc \cdot 6C_6H_5NH_2$ (5, 6). Corresponding complexes were isolated with other amines such as *n*-butylamine and pyridines (7).[2] Extraction of the same crude "RuPc" with dmso and dmf also gives complexes of the same RuPc·6L stoichiometry (8). The dmso complex has been used as an nmr shift reagent (8). With concentrated H_2SO_4, "RuPc" is said to give $[RuPcH]^+$, protonation occurring on a non-coordinating nitrogen atom (9).

Ruthenium(III) species formulated ClRuPc and ClRu(PcCl) are said to be formed via reaction of $RuCl_3 \cdot 3H_2O$ with *o*-dicyanobenzene (10) or phthalocyanine, H_2Pc (11), respectively. Species formulated ClRuPc(L), where L = *o*-dicyanobenzene, *o*-cyanobenzamide, or py, have also been described (10). A recent report (12), which appeared after the completion of our studies, questions the existence of the ruthenium(III) phthalocyanines and describes the characterization of a diamagnetic ruthenium(II) species $Ru(ClPc) \cdot py_2 \cdot 4py$, which was previously formulated (10) as the ruthenium(III) species ClRuPc(py)·5py, as well as a $Ru(ClPc)(PPh_3)_2$ complex. Part of the work described in this paper has been reported briefly elsewhere (13).

Experimental

All synthetic reactions were carried out under an atmosphere of argon using standard vacuum line and Schlenk tube techniques. The ^1H nmr spectra were measured on a Varian XL-100 operating in the Fourier transform mode. The esr spectra were recorded at 77 K on a Varian E-3, no signals being observed at room temperature. Infrared spectra were measured on a Perkin Elmer 457, and electronic spectra on a Cary 17D.

Cyclic voltammograms were obtained using an H-cell with the three compartments separated by sintered glass frits. Potentials were measured at a platinum electrode against a Ag/AgCl reference electrode at 25 ± 2°C. The $^nBu_4N^+PF_6^-$ electrolyte (TBAH) was synthesized (14), recrystallized from ethanol, and dried under vacuo at 70°C. A polarographic analyzer (M.I. As-

[1] To whom all correspondence should be addressed.

[2] Ligand abbreviations used: py = pyridine, Im = imidazole, dmf = *N,N′*-dimethylformamide, dmso = dimethylsulfoxide, thf = tetrahydrofuran, acac = acetylacetonato, OEP = octaethylporphyrin dianion, TPP = tetraphenylporphyrin dianion, porp = a general porphyrin dianion.

0008-4042/80/111125-08$01.00/0

©1980 National Research Council of Canada/Conseil national de recherches du Canada

Can. J. Chem. Downloaded from www.nrcresearchpress.com by 210.87.254.6 on 09/05/12
For personal use only.

Can. J. Chem. Downloaded from www.nrcresearchpress.com by 210.87.254.6 on 09/05/12
For personal use only.

sociates) in conjunction with an oscilloscope (Tektronix Inc.) measured the voltammograms at a scan speed of 250 mV/s. Coulometric experiments were carried out in a flow cell which enabled continuous monitoring of the visible spectrum of the solution during electrolysis. The coulometry was carried out in solution identical to those used for cyclic voltammetry, using a PAR-173 module with an HDC-371 integrator attachment.

Dmf, dmso, py, CH_3CN, and CH_2Cl_2 were freshly distilled, the CH_2Cl_2 being distilled from CaH_2. Other solvents and chemicals were used as reagent grade. *Ortho*-cyanobenzamide was synthesized using a literature procedure (15). Ruthenium trichloride trihydrate was obtained from Johnson Matthey Ltd. $Ru_3(CO)_{12}$ was a Strem Chemicals product.

Chemical oxidations for dilute solutions were carried out by a spectrophotometric titration procedure using Br_2 solutions.

Photolysis experiments were carried out under vacuum using a 650 W visible photo-flood lamp.

All the complexes synthesized gave satisfactory microanalytical data (P. Borda, this department). Reference 13 lists typical data for the $RuPcL_2$ and RuPc(CO)L complexes.

Preparation of Complexes

The details for the synthesis of crude "RuPc" from $RuCl_3 \cdot 3H_2O$ and *o*-cyanobenzamide, and the subsequent extraction procedure with pyridines to give well-characterized crystalline $RuPcL_2$ complexes, were given in our earlier report (13). The procedure for their carbonylation using 1 atm CO to give RuPc(CO)L, and isolation of the same carbonyls via an extraction procedure on crude RuPc(CO) made from $Ru_3(CO)_{12}$ and H_2Pc were also described (13).

*Carbonyl(*N,N'*-dimethylformamide)phthalocyaninatoruthenium(II)*

"RuPc" (1 g) was refluxed in dmf for 5 h and the resulting solution filtered. The resulting deep blue solution was then added to an alumina column containing hexane and the column eluted with hexane until all the dmf had been removed. Elution with diethyl ether and evaporation to a low volume yielded red-purple crystals of the complex (v(CO) = 1943 cm^{-1}, Nujol). Yield ca. 20%.

Bis(dimethylsulfoxide)- and Carbonyl(dimethylsulfoxide)-phthalocyaninatoruthenium(II)

"RuPc" (1 g) was refluxed in dmso for 3 h and the mixture filtered. Evaporation of the solution to low volume yielded purple crystals. Washing with hexane removes the excess dmso of crystallization, giving $RuPc(dmso)_2$. Yield ca. 40%. Carbonylation using 1 atm CO in dmso at 100°C (5 h) gives solutions that yield, after chromatography, RuPc(CO)(dmso) (v(CO) = 1955 cm^{-1}, Nujol).

*Bis(acetonitrile)-, Bis(imidazole)-, and Bis(*N,N'*-dimethylformamide)phthalocyaninatoruthenium(II) Species*

The bis(acetonitrile) species was readily formed *in situ* in dilute solution (10^{-4} *M*) by degassing an acetonitrile solution of $RuPc(dmso)_2$ and irradiating *in vacuo* with a 650 W tungsten lamp for ~15 min; other precursor complexes such as $RuPc(py)_2$, RuPc(CO)(py), or crude RuPc(CO) could be used with somewhat longer reaction times. Solutions of $RuPc(dmf)_2$ were prepared similarly from $RuPc(dmso)_2$ or RuPc(CO)(dmf). The bis(imidazole) species is readily formed via photolysis of $RuPc(dmso)_2$ in CH_2Cl_2 containing excess Im.

Results and Discussion

Synthetic Studies

An efficient route to the solid diamagnetic $RuPcL_2$ complexes involves Soxhlet extraction into L of crude "RuPc" formed from $RuCl_3 \cdot 3H_2O$ and *o*-cyanobenzamide. The method has been used with L = py, 4-Mepy, and 4-^{t}Bupy. The useful $RuPc(dmso)_2$ precursor complex can be obtained after a procedure involving refluxing "RuPc" in dmso; a similar procedure using dmf yields the monocarbonyl RuPc(CO)(dmf) formed presumably by decarbonylation of the amide, a process not uncommon for ruthenium (16, 17).

The RuPc(CO)L monocarbonyls are more generally prepared by treatment of $RuPcL_2$ solutions with 1 atm CO over prolonged periods at ≥ 100°C. The corresponding reactions for iron(II) systems are very fast even at room temperature (18). A less reliable method for making RuPc(CO)L complexes involves reaction of L with a crude RuPc(CO) product (13); this latter species is formed by refluxing $Ru_3(CO)_{12}$ with the neutral H_2Pc ligand in toluene under N_2, a procedure that has proved successful for synthesizing corresponding solvated Ru(porphyrin)(CO) complexes (19, 20). The phthalocyanine reaction probably gives RuPc(CO) (v(CO) = 1945 cm^{-1}, Nujol), but the method was somewhat irreproducible, and sometimes gave additional weak ir bands in the carbonyl region; chemical analyses were also variable.

Several other methods were tried in attempts to incorporate Ru(II) directly into the Pc ligand. These involved the reaction of chlororuthenate(II) solutions (21, 22), and more well-characterized precursors such as *cis*-$RuCl_2(dmso)_4$ (23), $Ru(dmso)_6^{2+}$ (24), $RuCl_2(PPh_3)_3$ (25), and $Ru(acac)_3$ (26), with M_2Pc (M = H, Na, Li), but only a small amount of metallation was apparent.

Photolysis of either RuPc(CO)L or $RuPcL_2$ in a solution of the appropriate ligand L′ leads to ready *in situ* formation of $RuPcL_2'$ species. The $RuPc(dmso)_2$ is a particularly useful precursor since the dmso ligands are readily photolabile, although the quantum yield of the process is low (< 0.01). Although a photo-flood lamp was used in these reactions, some experiments employing laser radiation have shown that only radiation < 400 nm is effective for the photochemical reactions (27). Stynes (28) has synthesized $RuPc(CH_3CN)_2$ via photolysis in CH_3CN of a species formed by reaction of $Ru_3(CO)_{12}$ with *o*-dicyanobenzene; the intermediate is again likely to be RuPc(CO), and it is of interest that Calderazzo's group has recently synthesized an iron analogue, FePc(CO)(dmf), by reaction of $Fe(CO)_5$ or $Fe(CO)_9$ with *o*-dicyanobenzene in dmf solution (29, 30).

Figure 1 summarizes the various reactions that we have studied. The species show characteristic visible spectra (Table 1) and the solution reactions are readily monitored spectrophotometrically.

Can. J. Chem. Downloaded from www.nrcresearchpress.com by 210.87.254.6 on 09/05/12
For personal use only.

TABLE 1. Spectral data and electrochemical data for RuPc species

Complex	λ_{max}nm ($\varepsilon \times 10^{-4}$, M^{-1} cm^{-1})[a]	$E_{1/2}$(V)[b]	g (band width)[c]
$RuPc(py)_2$	622(7.4), 567(2.9), 375(2.6), 315(12)	0.77	—
[d]	~700(~1), 530(3.2), 300(~9)	1.40	2.010(25)
RuPc(CO)(py)	637(16.5), 578(3.7), 342(2.8), 297(12)	0.91	—
[d]	703(3.5), 529(3.5), 381(3.0), 280(11.5)	—	2.006(7.1)
$RuPc(4\text{-Mepy})_2$	622(6.7), 560(2.8), 375(2.8), 310(11)	0.74	—
[d]	~690(~1), 535(3.4), 300(~7)	1.40	2.007(27)
RuPc(CO)(4-Mepy)	640(15.2), 580(4.1), 342(2.9), 295(8)	0.88	—
[d]	[e]	—	2.006(9.2)
$RuPc(4\text{-}^tBupy)_2$	621(6.5), 567(2.8), 370(3.0), 310(8.5)	0.70	—
[d]	~690(~1), 530(3.0), 300(7)	1.32	2.009(32)
RuPc(CO)(4-^{t}Bupy)	640(17.0), 579(3.5), 345(2.8)	[e]	—
$RuPc(Im)_2$	621(9.0), 566(3.1), 312(11.5)	[e]	—
[d]	[e]	—	2.008(15)
$RuPc(CH_3CN)_2$	633(9.0), 578(4.5), 312(10.5)	0.72	—
$RuPc(dmf)_2$	622(6.8), 568(2.9), 382(3.2), 312(10.4)	0.80	—
[d]	695(2.5), 529(2.4)		2.004(7.7)
RuPc(CO)(dmf)	638(12), 575(3.9), 344(2.6), 291(12)	0.90	—
[d]	704(4.3), 510(3.7)	—	2.004(5.3)
$RuPc(dmso)_2$	637(8.8), 578(3.3), 381(3.5), 318(11.3)	0.89	—
[d]	688(3.7), 519(3.5), 379(3.1)	—	2.007(11.2)
RuPc(CO)(dmso)	645(12.3), 583(4.3), 344(2.9), 293(13)	[e]	—
[d]	695(4.1), 516(4.2), 383(3.0)	—	2.005(7.1)

[a]In CH_2Cl_2; shoulders not listed.
[b]Measured as $\frac{1}{2}(E_{p,c} + E_{p,a})$ for one-electron process, and listed relative to a sce at 25°C.
[c]Isotropic g value at 77 K; band width in G.
[d]One-electron oxidation product of complex listed immediately above.
[e]Not measured.

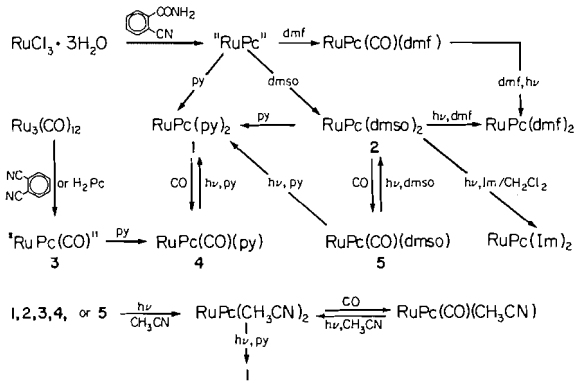


FIG. 1. Synthesis of Ru(II) phthalocyanine complexes; py here stands for pyridine, 4-methyl- and 4-tertiarybutylpyridine. The $Ru_3(CO)_{12}$/*o*-dicyanobenzene reaction is the work of Stynes (28).

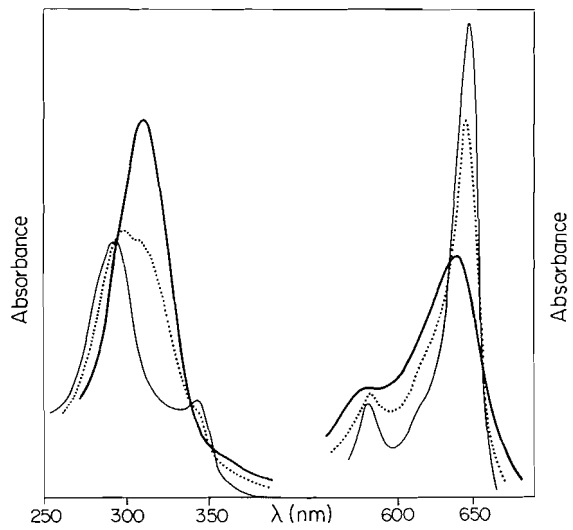


FIG. 2. Visible spectral changes during photolysis of RuPc(CO)(4-Mepy) (—) in CH_3CN giving $RuPc(CH_3CN)_2$ (—).

Photolysis in the coordinating solvents (pyridines, dmso, dmf, CH_3CN), or in CH_2Cl_2 with added ligand, always gave clean visible spectral changes with several isosbestic points; examples are shown in Figs. 2 and 3, as well as in the figure in ref. 13. In non-coordinating solvents in the absence of added ligand, the photolysis decolourized the solutions irreversibly due to decomposition of the Pc ligand, possibly to phthalimide.

The displacement of the dmso ligands in $RuPc(dmso)_2$ by pyridines to give $RuPc(py)_2$ occurred readily, in the absence of irradiation, by simply warming for a few minutes a pyridine solution of the bis(dmso) complex.

The complexes (Table 1) all show an intense absorption in the visible region (620–645 nm) together with a weaker band(s) at slightly higher energy (560–585 nm), and this is characteristic of metal phthalocyanine complexes (31, 32). Absorp-

Can. J. Chem. Downloaded from www.nrcresearchpress.com by 210.87.254.6 on 09/05/12
For personal use only.

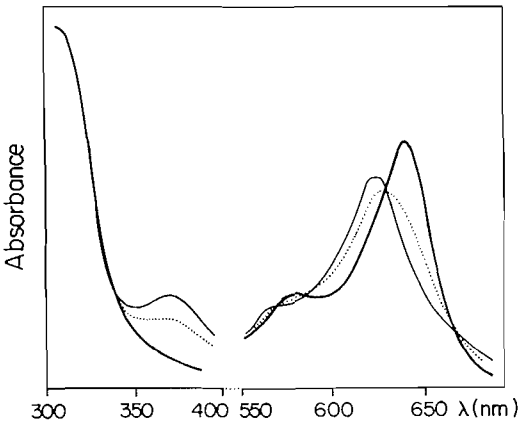


FIG. 3. Visible spectral changes during photolysis of $RuPc(CH_3CN)_2$ (—) in pyridine giving $RuPc(py)_2$ (—).

tion bands are also generally observed in the Soret region (340–380 nm) together with more intense ones around 290–315 nm. The RuPc(CO)L species, in the systems that we have studied, always have their intense visible absorption band at ca. 10–20 nm higher than, and with an extinction coefficient at least twice as large as, that of the corresponding $RuPcL_2$ species. The Soret band of the monocarbonyls studied appears at 30–40 nm below that of the corresponding bis(L) species. The bis(imidazole) and bis(acetonitrile) complexes appear exceptional in apparently not showing a Soret band, although this is probably masked by the more intense 312 nm band. In the related Ru(porphyrin)L_2 systems, replacement of one L by CO again gives a marked red-shift in the visible region, but the blue-shift in the Soret region is small (1, 33).

The ir spectrum of $RuPc(dmso)_2$ showed bands in the 1100 cm^{-1} region, possibly indicative of *S*-bonded dmso (24), although there are also Pc bands in this region; some weaker bands at 920–930 cm^{-1} could be due to *O*-bonded dmso, but this region is complicated by the presence of methyl rocking modes (34), and we have not synthesized the d_6-dmso analogue which would help to eliminate this ambiguity. A recent structure determination of the iron(II) analogue, $FePc(dmso)_2$, shows a somewhat unexpected and interesting result in that both dmso ligands are *S*-bonded (35); both Fe(II) and Ru(II) are considered to be border-line cases in the hard–soft acid classification (36) but, based on the iron data, the $RuPc(dmso)_2$ will almost certainly contain just *S*-bonded sulfoxide (see below). The ^1H nmr spectrum in $CDCl_3$ was not very satisfactory for this complex because of a solubility limitation, but the other complexes showed two pairs of doublets centered in the τ regions 0.6–0.9 and 1.8–2.1 (13), a typical pattern assigned to the α and β benz-protons of diamagnetic metallophthalocyanines (37). The absence of paramagnetic shifts in the ^1H nmr of $CHCl_3$ present in the solutions also shows the complexes to be diamagnetic (38).

A Faraday balance measurement on the $RuPc(4\text{-}^tBupy)_2$ complex confirmed the diamagnetism in this one case ($\chi_m = -860 \times 10^{-6}$ cgs at 20°C, the diamagnetic correction being about $+550 \times 10^{-6}$ cgs).

Oxidation Studies

Cyclic voltammograms were measured for a number of the ruthenium(II) complexes in 0.05 *M* TBAH–CH_2Cl_2 solution. The bis(pyridine) species show two chemically reversible one-electron oxidations (Fig. 4, Table 1), while the other species reveal just a single reversible one-electron oxidation (Table 1). Visible and esr spectral data (Table 1) demonstrate that the first oxidation occurs at the porphyrin ring, and the half-wave potentials (0.70–0.91 V) are formal reduction potentials for reaction [1]:

[1] $Ru^{II}[Pc(1-)]L_2^+ + e \rightarrow Ru^{II}(Pc)L_2$

(Pc itself refers to the dianion)

Solutions of the ruthenium phthalocyanine cations were prepared by exhaustive electrolysis in the TBAH–CH_2Cl_2 solution. The one-electron oxidations (±10%) proceed cleanly and reversibly over many cycles provided the potential is not significantly increased above the first oxidation potential; the solutions change from blue to red-purple and the visible spectral changes reveal several isosbestic points (Figs. 5, 6). All the oxidized species have two broad absorptions in the (510–535) and 700 nm regions, although the band at ~700 nm is less evident for the bis(pyridine) cations (Figs. 5, 6). The spectral changes are very similar to those observed for the one-electron oxidation of copper(II) phthalocyanine species to the $Cu[Pc(-1)]^+$ cation (39), and the general broadening of spectra with decreased intensity of the visible

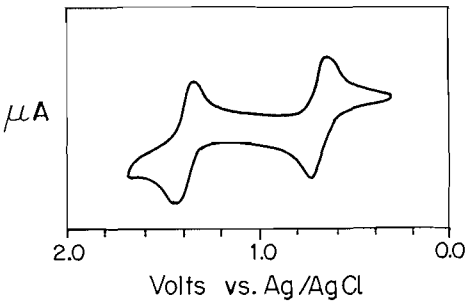


FIG. 4. Cyclic voltammogram for $RuPc(4\text{-}Mepy)_2$ in 0.05 *M* TBAH-CH_2Cl_2 vs. Ag/AgCl.

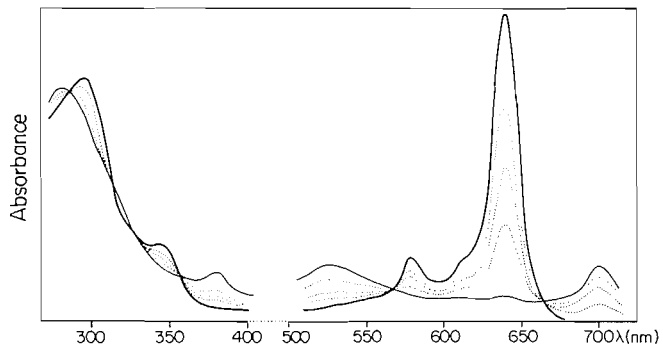


FIG. 5. Visible spectral changes during the one-electron oxidation (at 0.92 V with respect to a sce) of RuPc(CO)(py) (—) to cation (—) in 0.05 *M* TBAH–CH_2Cl_2.

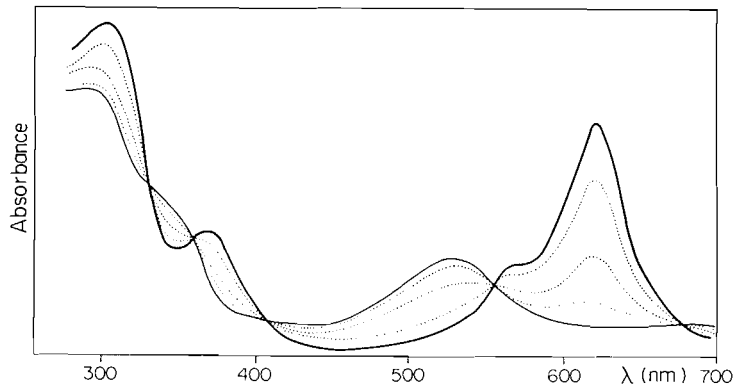


FIG. 6. Visible spectral changes during the one-electron oxidation (at 0.72 V with respect to a sce) of RuPc(4-^{t}Bupy)$_2$ (—) to cation (—) in 0.05 *M* TBAH–CH_2Cl_2.

bands is typical of that found for ligand oxidation in metallo-phthalocyanines and -porphyrins (40–42).

The esr spectra obtained for frozen solutions of the monocations at 77 K (Table 1) confirm that an electron has been removed from the phthalocyanine π-system to give the radical [Pc(1−)] ligand. The isotropic g values are close to the free electron value of 2.0 and are characteristic of oxidation at the phthalocyanine ring (40). Oxidation at the metal center to give $Ru^{III}Pc^+$ d^5 monocations would likely not give esr signals. Relatively few Ru^{III} complexes have been subjected to esr studies (44–47); there are difficulties in observing the signals due to fast relaxation times (48), and signals were not observed with $Ru^{III}(porp)(py)_2^+$ systems (43). The band-width of the $g = 2.0$ signal for a $Ru^{II}[Pc(-1)](CO)L^+$ monocarbonyl is invariably smaller than that of the corresponding bis(L) species (Table 1), and this can be used as a diagnostic tool, particularly for the pyridine systems where the effect is quite marked (e.g. for pyridine itself, 7.1 vs. 25 G). The differing degrees of line-broadening may result from interaction with the pyridine-nitrogen(s); no hyperfine splitting is observed in the signals.

The nature of the dication product from the second oxidation observed with the bis(pyridine) systems (1.32–1.40 V) has not been elucidated. Although stable on the cyclic voltammetric time scale, the dications could not be generated by electrolysis since decomposition occurred. The second oxidation could occur at the metal giving $Ru^{III}[Pc(-1)]L_2^{2+}$, or at the Pc giving $Ru^{II}[Pc(-2)]L_2^{2+}$.

A similar difficulty in elucidation of the dicationic species was encountered in a study of $Ru^{II}(porp)(CO)(py)$ complexes, where again the first oxidation pertained to formation of a porphyrin radical species $Ru^{II}[porp(-1)](CO)(py)^+$ (43, 49). A major difference in the porphyrin systems, however, is that a one-electron oxidation of carbonyl-free $Ru^{II}(porp)(py)_2$ species occurs *at the metal* to give $Ru^{III}(porp)L_2^+$ cations (43, 49). The introduction of CO in the porphyrins causes large anodic shifts for the first oxidation, e.g., $E_{1/2}[Ru(TPP)(CO)(py)] - E_{1/2}[Ru(TPP)(py)_2] =$

Can. J. Chem. Downloaded from www.nrcresearchpress.com by 210.87.254.6 on 09/05/12
For personal use only.

Can. J. Chem. Downloaded from www.nrcresearchpress.com by 210.87.254.6 on 09/05/12
For personal use only.

TABLE 2. Redox couples for some metallo-phthalocyanine and -porphyrin complexes[a]

Complex	M(III)/M(II)	M(II)L$^+$/M(II)[b]	Reference[c]
RuPc(CO)(py)	—	0.91	tw
$RuPc(py)_2$	—	0.77	tw
Ru(TPP)(CO)(py)	—	0.81	43
$Ru(TPP)(py)_2$	0.21	—	43
Ru(TPP)(CO)	0.93[d]	0.82	43, 53
Ru(OEP)(CO)(thf)	—	0.61	43, 49
$Ru(OEP)(py)_2$	0.08	—	49
$Ru(OEP)(CH_3CN)_2$	0.28	—	1
$Ru(TPP)(PEt_3)_2$	0.36	—	53
$Ru(TPP)(PPh_3)_2$	0.50	—	53
$Ru(TPP)(P(OMe)_3)_2$	0.59	—	53
$Ru(TPP)(^tBuNC)_2$	0.65	—	53
$FePc(py)_2$	—	0.70	50
CrPc/py	0.52	—	50
ZnPc/py	—	0.68	50
CoPc/py	0.22	—	50
MnPc/py	0.01	—	50

[a]All potentials in V vs. a sce at 25°C.
[b]Redox process involves Pc or porphyrin ligand.
[c]tw = this work; refs. 43, 49; data in 0.1 *M* TBAH–CH_2Cl_2; ref. 53, 0.1 *M* TBAH–CH_3CN/benzene; ref. 1, 0.1 *M* TBAH–CH_3CN; ref. 49, ClO_4^-–py.
[d]This assignment (ref. 53) seems incorrect.

0.60 V (Table 2), making the carbonyl complexes harder to oxidize and, indeed, this results in the change in oxidation site. The $\Delta E_{1/2}$ value for the Pc systems, $E_{1/2}$[RuPc(CO)(py)] − $E_{1/2}$[$RuPc(py)_2$], is only 0.14 V (0.10 V for the dmf system), and is more consistent with oxidation at the same site, namely, the phthalocyanine ligand. The level of the Pc π_{mo} must be higher than the metal *d* orbital in both monocarbonyl and bis(L) species; unlike in the porphyrin systems (43, 49), difference in π-back bonding ability between CO and, for example, pyridine is not sufficient to invert the relative positions of metal *d* and Pc π_{mo} levels, and this is possibly consistent with evidence that phthalocyanine ligands compared to porphyrins are exceptionally good π-acceptors (ref. 50). This also accounts for a general finding of metal phthalocyanine complexes being more stable towards oxidation than corresponding porphyrins (ref. 50, Table 2). The oxidation of the various bis(pyridine)ruthenium(II) phthalocyanines to species containing the [Pc(−1)] radical cation at 0.7–0.8 V (Table 1) is consistent with data (Table 2) showing oxidation of the Pc ligand in ZnPc solutions at 0.68 V (50, 51) and in FePc in py/ClO_4^- solutions at 0.7 V (50). Oxidation at 0.52 V in a CrPc/py system was assigned as a Cr(III)/Cr(II) couple (50). Compared to porphyrin systems, considerable stabilization of the low-spin Fe(II) and Cr(II) was attributed to π-back donation into the Pc ring (50). For low-spin Ru(II) such an effect would be even more marked, and reduction potentials are higher than for corresponding iron–Pc and –porphyrin systems (49, 52). Consistent with this is that the reported oxidation of $FePc(dmso)_2$ at 0.47 V occurs at the metal and not at the ligand (50). With MnPc– and CoPc–pyridine systems, the oxidation at much lower potentials (0.01 and 0.22 V, respectively) is again consistent with oxidation at the metal (50). The data indicate that ligand oxidation will occur in Pc systems at ≥0.60 V. With porphyrin systems, the presence of an axial CO ligand may raise the potential into the region of porphyrin ligand oxidation and again, at least with TPP and OEP, this could be in the same 0.6 V range (43, 49). Orbital descriptions on replacement of an axial amine ligand by CO in porphyrins of the Fe subgroup, and the implications for heme-based redox processes, have been presented (49, 52).

The limited data in Table 1 show the expected stabilization of the lower valency state by incorporation of a CO ligand (see also Table 2), and stabilization of the higher valency state by electron-donor substituents within pyridines (^{t}Bu > Me > H). The somewhat higher potential of the bis(dmso) complex, compared to the bis(dmf) *O*-bonded and the bis(CH_3CN) *N*-bonded systems could be consistent with stabilization of Ru(II) via π-backbonding through *S*-bonded sulfoxides. Other recent data on ruthenium porphyrins (Table 2) show similar trends: lower potentials with more basic phosphines, higher potentials with π-acceptor ligands (phosphites, isocyanides). Some of the higher potentials of the TPP derivatives reported by Boschi *et al.* (Table 2, ref. 53) are in the range where ligand oxidation could occur, although a different solvent

Can. J. Chem. Downloaded from www.nrcresearchpress.com by 210.87.254.6 on 09/05/12
For personal use only.

system was employed; the evidence for metal oxidation was lack of an esr signal, but the measurements appear to have been done at room temperature where the signal of the porphyrin radical is not detected (ref. 43 and this work). Visible spectra were not presented, and thus the site of oxidation is not well established. The suggested metal oxidation at 0.93 V for the Ru(TPP)(CO) complex (53) is almost certainly incorrect (43).

The one-electron oxidation products in our Pc systems could be formed in solution by chemical oxidation with bromine solutions. The esr spectra (including bandwidths) of the products were identical to those of the electrochemically generated species, indicating that the products are $Ru[Pc-(1-)]L_2^+$ with no incorporation of bromide. Dithionite readily reduced the oxidized species to the starting materials. Iodine, and also Ce^{4+} and $Fe(phen)_3^{3+}$, were ineffective oxidants, while chlorine gave irreversible oxidation beyond the first oxidation as evidenced via detection of the purple radical cation intermediates. Attempts to isolate the product of the Br_2 oxidation gave only mixtures which included the starting material.

The lack of reactivity of the Ru(II) phthalocyanine complexes toward O_2 in CH_2Cl_2 is consistent with the relatively high potentials listed in Table 1. The Fe(III)/Fe(II)–Pc couples have been shown to vary considerably with solvent and counter ion (50) and, although we do not yet have any corresponding data, this may well be true for the Ru couples. The $RuPc(dmf)_2$ in dmf, for example, does react with O_2 with loss of the visible absorption bands and a decrease in intensity of the Soret band; no esr signal is detected and irreversible oxidation of the Pc ligand is indicated. Since the ability to form a dioxygen complex is governed to some extent by the reduction potential of the metal system (2, 4, 54), we are hoping to "tune" the Ru(III)/Ru(II)–Pc couple for such reactivity (cf. ref. 50). Reversible O_2-binding by iron(II) phthalocyanine systems, after some controversial claims (55), has been accomplished recently (56–60), including a dmso system (58–60).

Our limited studies on cathodic reduction of the Ru(II) phthalocyanines were not successful, the systems showing somewhat irreversible and irreproducible behaviour. Some potentials in the range -1.7 to -1.9 V have been reported recently for $Ru(TPP)L_2$ systems (L = tertiary-phosphines, -phosphites, ^{t}BuNC) and attributed to the Ru(II)/Ru(I) couple, although the lower valent species were unstable chemically (53). Studies on the electrochemical reduction of Fe(II)Pc systems have been reported recently (61, 62).

Acknowledgements

This work is a contribution from the Bioinorganic Chemistry Group and is supported by grants from the Natural Sciences and Engineering Research Council of Canada and the University of British Columbia. We thank Dr. J. Van Houten for carrying out the laser photochemical reactions, Dr. R. C. Thompson for the magnetic susceptibility measurements, and Johnson Matthey Ltd. for the loan of ruthenium. One of us (B.R.J.) would like to thank Professor F. Calderazzo of the Istituto di Chimica Generale, Università di Pisa, for discussions, and for the facilities and cooperation of the Institute during the writing of the paper.

1. D. Dolphin, N. P. Farrell, and B. R. James. J. Am. Chem. Soc. **100**, 324 (1978).
2. B. R. James. Interaction of dioxygen with metalloporphyrins. The porphyrins. Vol. V. *Edited by* D. Dolphin. Academic Press, New York. 1978. p. 205.
3. B. R. James. Adv. Chem. Ser. In press.
4. B. R. James, A. W. Addison, M. Cairns, D. Dolphin, N. P. Farrell, D. R. Paulson, and S. Walker. Progress in dioxygen complexes of metalloporphyrins. Fundamental research in homogeneous catalysis. Vol. 3. *Edited by* M. Tsutsui. Plenum Press, New York. 1979. p. 751.
5. P. C. Krueger and M. E. Kenney. J. Inorg. Nucl. Chem. **25**, 303 (1963).
6. J. W. van Eek. Private communication.
7. J. E. Maskasky. Ph.D. thesis, Case Western Reserve University. 1974.
8. C. K. Choy and M. E. Kenney. Office of Naval Res. Contract No. N00014-75-C-0693, Project No. NR356-590, Tech. Report No. 3, 1977.
9. B. D. Berezin. Zh. Obshch. Khim. **43**, 2738 (1973).
10. I. M. Keen and B. W. Malerbi. J. Inorg. Nucl. Chem. **27**, 1311 (1965).
11. B. D. Berezin and G. V. Sennikova. Dokl. Akad. Nauk SSSR, **159**, 117 (1964).
12. L. J. Boucher and P. Rivera. Inorg. Chem. In press.
13. N. P. Farrell, A. J. Murray, J. R. Thornback, D. H. Dolphin, and B. R. James. Inorg. Chim. Acta, **28**, L144 (1978).
14. W. Lange and E. Müller. Chem. Ber. **63**, 1058 (1930).
15. G. T. Byrne, R. P. Linstead, and A. R. Lowe. J. Chem. Soc. 1017 (1934).
16. S. A. Fouda, B. C. Y. Hui, and G. L. Rempel. Inorg. Chem. **17**, 3213 (1978).
17. B. R. James. Inorg. Chim. Acta Rev. **4**, 73 (1970).
18. D. V. Stynes and B. R. James. J. Am. Chem. Soc. **96**, 2733 (1974).
19. D. R. Paulson, A. W. Addison, D. Dolphin, and B. R. James. J. Biol. Chem. **254**, 7002 (1979).
20. J. J. Bonnet, S. S. Eaton, G. R. Eaton, R. H. Holm, and J. A. Ibers. J. Am. Chem. Soc. **95**, 2141 (1973).
21. B. C. Hui and B. R. James. Can. J. Chem. **52**, 348 (1974).
22. J. D. Gilbert, D. Rose, and G. Wilkinson. J. Chem. Soc. A, 2765 (1970).
23. A. Mercer and J. Trotter. J. Chem. Soc. Dalton, 2480 (1975).
24. A. R. Davies, F. W. B. Einstein, N. P. Farrell, B. R. James, and R.S. McMillan. Inorg. Chem. **17**, 1965 (1978).
25. T. A. Stephenson and G. Wilkinson. J. Inorg. Nucl. Chem. **28**, 945 (1966).

26. W. P. GRIFFITH. The chemistry of the rarer platinum metals. Interscience, London. 1967. p. 156.
27. J. VAN HOUTEN. Unpublished data.
28. D. V. STYNES. Private communication.
29. F. CALDERAZZO, D. VITALI, G. PAMPALONI, and I. COLLAMATI. J. Chem. Soc. Chem. Commun. 221 (1979).
30. G. PAMPALONI. Tesi di laurea, University of Pisa. 1979.
31. D.L. LEDSON and M. V. TWIGG. Inorg. Chim. Acta, **13**, 43 (1975).
32. A. B. P. LEVER. Adv. Inorg. Chem. Radiochem. **7**, 27 (1965).
33. F. R. HOPF, T. P. O'BRIEN, W. R. SCHEIDT, and D. G. WHITTEN. J.Am. Chem. Soc. **97**, 277 (1975).
34. B. R. JAMES and R. H. MORRIS. Spectrochim. Acta, **34A**, 577 (1978).
35. F. CALDERAZZO, G. PAMPALONI, D. VITALI, I. COLLAMATI, G. DESSY, and V. FARES. J. Chem. Soc. In press.
36. J. E. HUHEEY. Inorganic chemistry: principles of structure and reactivity. Harper and Row, London. 1975. p. 225.
37. T. J. MARKS and D. R. STOJOKOVIE. J. Am. Chem. Soc. **100**, 1695 (1978).
38. D. F. EVANS. J. Chem. Soc. 2003 (1959).
39. A. E. CAHILL and H. TAUBE. J. Am. Chem. Soc. **73**, 2847 (1951).
40. J. F. MYERS, G. W. RAYNER CANHAM, and A. B. P. LEVER. Inorg. Chem. **14**, 461 (1975).
41. J. H. FUHRHOP. Struct. Bonding, Berlin, **18**, 1 (1974).
42. D. DOLPHIN and R. H. FELTON. Acc. Chem. Res. **7**, 26 (1974).
43. G. M. BROWN, F. R. HOPF, J. A. FERGUSON, T. J. MEYER, and D. G. WHITTEN. J. Am. Chem. Soc. **95**, 5939 (1973).
44. A. HUDSON and M. J. KENNEDY. J. Chem. Soc. A, 1116 (1969).
45. R. E. DESIMONE. J. Am. Chem. Soc. **95**, 6238 (1973).
46. P. T. MANOHARAN, P. K. MEHROTRA, M. M. TAQUI KHAN, and R. K. ANDAL. Inorg. Chem. **12**, 2753 (1973).
47. U. AGARWALA and O. K. MEDHI. Private communication.
48. B. A. GOODMAN and J. B. RAYNOR. Adv. Inorg. Chem. Radiochem. **13**, 278 (1970).
49. G. M. BROWN, F. R. HOPF, T. J. MEYER, and D. G. WHITTEN. J. Am. Chem. Soc. **97**, 5385 (1975).
50. A. B. P. LEVER and J. P. WILSHIRE. Can. J. Chem. **54**, 2514 (1976).
51. A. WOLBERG and J. MANASSEN. J. Am. Chem. Soc. **92**, 2982 (1970).
52. A. ANTIPAS, J. W. BUCHLER, M. GOUTERMAN, and P. D. SMITH. J. Am. Chem. Soc. **100**, 3015 (1978).
53. T. BOSCHI, G. BONTEMPELLI, and G.-A. MAZZOCCHIN. Inorg. Chim. Acta, **37**, 155 (1979).
54. R. D. JONES, D. A. SUMMERVILLE, AND F. BASOLO. J. Am. Chem. Soc. **100**, 4416 (1978).
55. G. MCLENDON and A. E. MARTELL. Inorg. Chem. **16**, 1812 (1977).
56. H. PRZYWARSKA-BONIECKA, L. TRYNDA, and E. ANTONINI. Eur. J. Biochem. **52**, 567 (1975).
57. C. ERCOLANI, F. MONACELLI, and G. ROSSI. Inorg. Chem. **18**, 712 (1979).
58. C. ERCOLANI and F. MONACELLI. Private communication.
59. J. G. JONES and M. V. TWIGG. Private communication.
60. I. COLLAMATI. Inorg. Chim. Acta, **35**, L303 (1979).
61. A. B. P. LEVER and J. P. WILSHIRE. Inorg. Chem. **17**, 1145 (1978).
62. K. M. KADISH, L. A. BOTTOMLEY, and J. S. CHENG. J. Am. Chem. Soc. **100**, 2731 (1978).

Can. J. Chem. Downloaded from www.nrcresearchpress.com by 210.87.254.6 on 09/05/12
For personal use only.

A study of the donor properties of the phenoxachalcogenines II: 7,7,8,8-tetracyanoquinodimethane as the acceptor

DAVID P. RAINVILLE AND RALPH A. ZINGARO
Department of Chemistry, Texas A&M University, College Station, TX 77843, U.S.A.
AND
JOHN P. FERRARIS
Department of Chemistry, University of Texas at Dallas, Richardson, TX 75080, U.S.A.

Received November 19, 1979

DAVID P. RAINVILLE, RALPH A. ZINGARO, and JOHN P. FERRARIS. Can. J. Chem. **58**, 1133 (1980).

The phenoxachalcogenines have been studied as donors towards 7,7,8,8-tetracyanoquinodimethane. For the 1:1 complexes studied, the equilibrium constants, K, vary over the range 4–16; the enthalpy, ΔH^0, is about -2.0 kcal/mol; the free energy, ΔG^0, is -1.4 to -1.0 kcal/mol, and the entropy change, ΔS^0, is -7.3 to -3.5 eu. The entropy change is greatest in the case of the dibenzo-1,4-dioxane – 7,7,8,8-tetracyanoquinodimethane charge-transfer complex. This is attributed to the planarity of the dibenzo-1,4-dioxane molecule. The extinction coefficient, ε_c, for the series studied varies from 115 to 230, and no regularity in the trend has been noted.

The lack of any significant changes (with change in the chalcogen atom) in the thermodynamic values for the phenoxachalcogenine – 7,7,8,8-tetracyanoquinodimethane charge-transfer complexes is interpreted in terms of a similar π to π type interaction involving a delocalized π orbital of the phenoxachalcogenine rather than a localized n orbital of the hetero atom.

The room temperature four-probe dc conductivities of single crystals of PSe–TCNQ and PS–TCNQ were found to be 4×10^{-8} and 3×10^{-7} ohm^{-1} cm^{-1}, respectively.

DAVID P. RAINVILLE, RALPH A. ZINGARO et JOHN P. FERRARIS. Can. J. Chem. **58**, 1133 (1980).

On a étudié les phénoxachalogénines en tant que donneurs vis-à-vis des tétracyano-7,7,8,8 quinodiméthanes. Dans le cas des complexes du type 1:1 étudiés, la constante d'équilibre K varie de 4 à 16, l'enthalpie ΔH^0 est d'environ -2.0 kcal/mol, l'énergie libre, ΔG^0 est de -1.4 à 1.0 kcal/mol et la variation d'entropie ΔS^0 est de -7.3 à 3.5 ue. La variation d'entropie est maximale dans le cas du complexe de transfert de charge entre le dibenzodioxanne-1,4 et le tétracyano-7,7,8,8 quinodiméthane. On attribue ce fait à la planéarité de la molécule de dibenzodioxanne-1,4. Dans les séries étudiées, le coefficient d'extinction ε_c varie de 115 à 230 et on n'a noté aucune régularité.

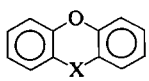
On interprète l'absence de tout changement significatif (avec le changement dans l'atome de chalcogène) dans les valeurs thermodynamiques du complexe de transfert de charge du phénoxachalcogénine tétracyano-7,7,8,8 quinodiméthane, en fonction d'une interaction de type $\pi \rightarrow \pi$ impliquant une orbitale π délocalisée de la phénoxachalcogénine plutôt qu'une orbitale localisée n l'hétéroatome.

Sur la base de quatre essais de conductivité dc à température ambiante sur un mono cristal de PSe–TCNQ et PS–TCNQ, on a trouvé les valeurs suivantes 4×10^{-8} et 3×10^{-7} ohm^{-1} cm^{-1} respectivement.

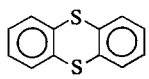
[Traduit par le journal]

Introduction

The phenoxachalcogenines (**1**) and related compounds such as thianthrene (**2**) have been studied with respect to their donor properties towards various acceptor molecules. A review of these studies can be found in a previous paper (1) in which the donor properties of the phenoxachalcogenines towards tetracyanoethylene and chloranil were reported.



1



2

X = O	dibenzo-1,4-dioxane	DBDO	thianthrene	PSS
X = S	phenoxathiin	PS		
X = Se	phenoxaselenine	PSe		
X = Te	phenoxatellurine	PTe		

In the present study, the preparation of crystalline compounds with tellurium and selenium heterocyclic compounds using the well-known acceptor molecule 7,7,8,8-tetracyanoquinodimethane (TCNQ) (2) was sought. The choice of TCNQ as an acceptor molecule was made because of the high electron affinity of the polyene system conferred by the powerful electron withdrawing effect of the four cyano groups and because of the report of a 1:1 complex formed between TCNQ and tetrathiafulvalene (TTF) (3). This complex possesses one of the largest reported electrical conductivities of any known organic compound (3).

During the course of our investigations the donor properties of the phenoxachalcogenines (**1**) towards TCNQ were studied. The results of this study as well as the electrical conductivity measurements of several crystalline complexes formed between the phenoxachalcogenines and TCNQ are reported.

0008-4042/80/111133-05$01.00/0
©1980 National Research Council of Canada/Conseil national de recherches du Canada

Can. J. Chem. Downloaded from www.nrcresearchpress.com by 210.87.254.105 on 09/05/12
For personal use only.

Can. J. Chem. Downloaded from www.nrcresearchpress.com by 210.87.254.105 on 09/05/12
For personal use only.

TABLE 1. Calculated values for the equilibrium constants and extinction coefficients[a]

Donor	Acceptor	λ_{max} (Å)	Temperature	ε_c	Average ε_c	K^{-1}	K L mol^{-1}
PTe	TCNQ	7350–7550	10.0	104.1		0.065	15.49
			20.0	124.9	135.3	0.085	11.76
			30.0	176.8		0.115	8.67
PSe	TCNQ	6700–6900	10.0	237.5		0.146	6.87
			20.0	173.4	188.8	0.166	6.02
			30.0	155.5		0.171	5.86
PS	TCNQ	6950–7150	10.0	232.5		0.224	4.47
			20.0	258.0	233.0	0.267	3.75
			30.0	208.6		0.297	3.37
DBDO	TCNQ	6500–6700	10.0	134.0		0.155	6.44
			20.0	107.0	116.7	0.189	5.29
			30.0	109.2		0.224	4.46

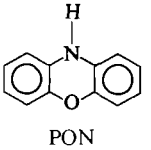
[a]By the method of Rose and Drago, see ref. 5.

Results and Discussion

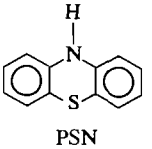
Job's plots were prepared for each of the phenoxachalcogenine–TCNQ systems. In each case, a fairly broad maximum was observed at a mole fraction of 0.5 suggesting the formation of a weak 1:1 complex. The plots were symmetrical on either side of the maxima indicating the absence of higher complexes at the temperatures and concentrations used in these studies (4). These observations, however, do not preclude the possibility of the formation of higher complexes at different temperatures and concentrations.

The stoichiometry of the charge-transfer complex which forms between phenoxazine (PON) and TCNQ was also found to be 1:1 by Job's method. The maximum in the Job's plot of the PON–TCNQ system is not as broad as that observed in the phenoxachalcogenine–TCNQ systems, indicating that the PON–TCNQ complex has a somewhat larger equilibrium constant and is therefore less dissociated than the phenoxachalcogenine–TCNQ complexes.

Solid complexes were isolated for the four phenoxachalcogenine–TCNQ systems. In addition, solid complexes were also obtained from the phenoxazine (PON)- and phenothiazine (PSN)–TCNQ systems. The stoichiometry of these complexes was determined by chemical analysis of the isolated complex, and was found to be 1:1 in all cases.



PON



PSN

The equilibrium constants, K, and the extinction coefficients for the four phenoxachalcogenine–TCNQ complexes were calculated using the method of Rose and Drago (5). Examinations of the values for the equilibrium constants and the extinction coefficients for these systems show that they are relatively small. This indicates that the complexes formed in dichloromethane solution are relatively weak, probably of the $\pi-\pi$ charge-transfer type (4). We cannot exclude, however, the occurrence of a stronger charge-transfer band at higher frequencies arising from the large absorbances of both TCNQ and the phenoxachalcogenine in this region.

Table 2 shows the calculated values of the standard enthalpy changes for the four phenoxachalcogenine–TCNQ systems obtained by plotting log K vs. $1/T$ and determining the best fit for each line by the linear least squares method. The standard free entropy changes of formation for the four phenoxachalcogenine–TCNQ complexes were also determined using basic thermodynamic relationships and are reported in Table 2.

An examination of the data in Tables 1 and 2 for the values of K, ε_c, ΔH^0, and ΔS^0 leads to several conclusions. Among the four phenoxachalcogenines studied the entropy loss which accompanies the formation of the DBDO–TCNQ charge-transfer complex is greater than values measured for the other three complexes. Dibenzo-1,4-dioxane has been shown to possess an almost

TABLE 2. Calculated values for the standard enthalpy and entropy changes for the formation of the four phenoxachalcogenine–TCNQ charge transfer complexes

Donor	ΔH^0 kcal/mol	ΔS^0 eu (20°C)
Phenoxatellurine	−4.93	−3.49
Phenoxaselenine	−1.36	−1.02
Phenoxathiin	−2.41	−5.58
Dibenzo-1,4-dioxane	−3.12	−7.35

Can. J. Chem. Downloaded from www.nrcresearchpress.com by 210.87.254.105 on 09/05/12
For personal use only.

planar structure with the oxygen atoms displaced 0.16 to 0.17 Å from the plane (this would correspond to an angle of 164° about the O—O axis) (6), which would classify it as possessing D_{2h} symmetry if it were totally planar and C_{2v} symmetry if it were folded about the oxygen–oxygen axis. Furthermore, the DBDO–TCNQ complex has been studied in the solid state by X-ray diffraction analysis, which indicates that the DBDO molecules are essentially planar (7). In this study, it was shown that a relatively large separation of 3.46 Å exists between the planes of adjacent stacked TCNQ and DBDO molecules. This suggests that any charge-transfer interaction present in the solid state is weak. While DBDO has been shown to be almost planar, phenoxathiin (8) and phenoxatellurine (9) are folded along the O—S and O—Te axes at an angle of 138°. Phenoxaselenine probably has a similar angle about the O—Se axis due to its isomorphism (10) with phenoxatellurine and phenoxathiin. In view of these observations, the greater loss in entropy observed for formation of the DBDO–TCNQ complex compared with the phenoxachalcogenine–TCNQ complexes is expected. However, it should be noted that the geometry of dibenzo-1,4-dioxane in solution may differ from that in the solid state. If this is true, the greater entropy loss for the formation of the DBDO–TCNQ complex cannot be explained by the geometry of the DBDO molecule. No meaningful trend is observed for the entropies of formation among the other phenoxachalcogenine–TCNQ complexes. The value for the standard entropy of formation for the PTe–TCNQ charge-transfer complex exhibits a greater magnitude of change in comparison with the values for the PS–TCNQ and PSe–TCNQ complexes. This is expected because of the larger equilibrium constant for the PTe–TCNQ complex.

When the values of K, ε_c, ΔH^0, and related quantities are examined, it is apparent that no correlation can be made with the electronegativities of the chalcogen atom in the series O > S > Se > Te. Since oxygen is the most electronegative, the magnitude of ΔH for the DBDO–TCNQ complex should be less than that observed for the other complexes. This is not observed, indicating that the electronegativity of the chalcogen heteroatom is not the primary factor which determines the magnitude of the charge-transfer interaction. This suggests that the type of interaction for the phenoxachalcogenine series toward TCNQ is basically of the same type, involving a delocalized π orbital of the phenoxachalcogenine rather than a localized n-orbital of the chalcogen atom. This is corroborated by the observed mixed-stack arrangement of the DBDO–TCNQ complex (7) which is typical for donor–acceptor π to π type complexes (11). This conclusion is in agreement with that reached by Heller *et al.* (1), but differs from that reached by Hetnarski and Grabowska (12).

Hillebrand *et al.* (13) postulated in their study of the interaction of PS with TCNE that the absorption band at 6700–6800 Å is due to the transition from the highest occupied molecular orbital (HOMO) on the donor to the lowest unoccupied molecular orbital (LUMO) on the acceptor. The absorption peak at 4300–4500 Å was assigned to a somewhat higher energy transition from the second highest filled molecular orbital on the donor to the lowest unfilled orbital on the acceptor.

The phenoxachalcogenine–TCNQ complexes in dichloromethane exhibit absorption maxima from 6500–7550 Å. The observation of an absorption band below 4500 Å is precluded by the fact that TCNQ itself possesses strong absorption at wavelengths shorter than about 4500 Å. It is, however, reasonable to assume that the absorption bands at the wavelengths 6500–7350 Å are due to a HOMO–LUMO transition (13).

An examination of the work of Hetnarski and co-workers (12, 14), Hillebrand and co-workers (13, 15), Heller *et al.* (1), and this study, indicates that the type of donor interactions of the phenoxachalcogenines in charge-transfer systems involving TCNQ as the acceptor are of the π to π type.

Voltammetry (vs. SCE; 0.1 *M* Et_4NClO_4; MeCN; Pt electrode; 25°C) yields the following one electron oxidation potentials ($E_{\frac{1}{2}}$): PTe, +0.76 V; PSe, +1.10 V; PS, +1.18 V. The large differences between the first oxidation potentials of the phenoxachalcogenine donors and the first reduction potential of the acceptor (TCNQ, +0.14 V) suggests the complexes will possess a non-ionic ground state[1] and hence be insulating. Not surprisingly, the room temperature four-probe dc conductivities of single crystals of PSe–TCNQ and PS–TCNQ are 4×10^{-8} and 3×10^{-7} ohm^{-1} cm^{-1}, respectively. The use of a stronger, but related acceptor (FTCNQ) (16) whose first reduction potential is +0.26 V also affords insulating complexes with PTe, PSe, and PS ($\sigma < 6 \times 10^{-7}$ ohm^{-1} cm^{-1}, 300 K). Even the very strong acceptor DDQ ($E_{\frac{1}{2}} =$ 0.51 V) only raises the conductivity to ca. 10^{-6} ohm^{-1} cm^{-1}.

Other charge transfer complexes with donor

[1]G. Saito and J. P. Ferraris. Unpublished results.

Can. J. Chem. Downloaded from www.nrcresearchpress.com by 210.87.254.105 on 09/05/12
For personal use only.

atoms towards TCNQ were isolated in the solid state. Phenoxazine–TCNQ with a λ_{max} at 7500 Å probably is similar to the phenoxachalcogenine–TCNQ complexes with π to π type charge transfer. As previously pointed out this is a 1:1 complex in dichloromethane solution. The analogous phenothiazine molecule readily forms a charge transfer complex with TCNQ. When solutions of TCNQ and phenothiazine are mixed together, the phenothiazine–TCNQ precipitates out of solution in the form of black needles. Because the complex precipitates so readily, solution studies were not performed. The solid complex has been shown to be a 1:1 complex by chemical analysis. In addition, the phenothiazine–TCNQ complex is also an insulator. Since phenoxazine is isomorphous with phenothiazine, the PON–TCNQ complex probably exhibits electrical properties similar to those of the phenothiazine–TCNQ complex.

Experimental

General Methods

All reactions of organometallic compounds were carried out in flame-dried glassware under pre-purified nitrogen using standard techniques (17). The ^{1}H nmr spectra were recorded on a Varian T-60 NMR spectrometer. The ^{13}C nmr were recorded on a JEOL Model JNM-PS-100 high resolution nmr spectrometer equipped with a Nicolet 1080 E data processing system in the T-1 mode. A sweep width of 5617.977 Hz (224.4 ppm), a sweep frequency of 25.0344 MHz (obsd), and an irradiating frequency of 99.5388 MHz at 10 W power were used. $CDCl_3$ was the source of an internal deuterium lock. Routine infrared spectra were recorded on a Beckman IR-8 spectrophotometer. Visible spectra were recorded on a Cary 14 spectrophotometer. Three electrode voltammetry measurements were conducted in an acid-washed all-glass cell equipped with O-ring seals and inert atmosphere purge. The potentiostat was an MPI System 1000 and I-V curves were displayed on an Omniscribe XY recorder. Electrical conductivity measurements were made on single crystals attached to four 25 μm gold wires with conducting silver paint. Ten microamps from a constant current source were passed through the sample and the voltage drop measured with a Keithley digital electrometer. Melting points were taken on a Büchi SMP-20 melting point apparatus and are uncorrected. Elemental analyses were performed by Galbraith Laboratories Inc., Knoxville, TN.

Reagents

Dichloromethane was purchased from Fisher Scientific Company and purified by distillation from P_2O_5 under nitrogen prior to use. Phenoxathiin was purchased from Eastman Organic Chemicals and recrystallized from methanol. It had a melting point of 56–57°C (lit. (10) mp 58°C); ir(KBr): 3075(w), 1540(m), 1400, 1280(w), 1270, 1200, 920, 855, 805, and 740 cm^{-1}; ^{1}H nmr ($CDCl_3$) δ(ppm): 6.97(m); ^{13}C nmr ($CDCl_3$) δ(ppm): 155.685(s), 134.921(s), 129.085(s), 125.497(s), 119.580(s), 101.528(s). Phenoxazine was purchased from Aldrich Chemical Company and recrystallized from diphenyl ether. It had a melting point of 154–156°C (lit. (18) mp 156°C). Phenothiazine was purchased from Aldrich Chemical Company and recrystallized from ethanol to a melting point of 186°C (lit. (19) mp 186–187°C). 7,7,8,8-Tetracyanoquinodimethane was purchased from Aldrich Chemical Company. It was recrystallized twice from spectral grade acetonitrile and sublimed to a melting point of 294–296°C (lit. (2) mp 293.5–296°C). Other solvents and reagents (reagent grade) were purchased from commercial sources.

Phenoxatellurine was prepared by the method of Drew (20) in 34.1% yield; mp 76–77°C (lit. (20) mp 77°C); ^{1}H nmr ($CDCl_3$) δ(ppm): 7.5(d, 2H), 7.3(m 6H); ^{13}C nmr ($CDCl_3$) δ(ppm): 151.96(s), 127.47(s), 126.59(s), 124.29(s), 119.96(s), 117.61(s); ir (KBr): 1422, 1280(s), 1252(m), 1200, 1105(m), 930(s), 856, 790, 748(s), 709 cm^{-1}.

Phenoxaselenine was prepared by the method of Drew (21) in 72% yield; mp 86–87°C (lit. (21) mp 87–88°C); ^{1}H nmr ($CDCl_3$) δ(ppm): 7.1(m); ^{13}C nmr ($CDCl_3$) δ(ppm): 152.836(s), 129.223(s), 128.072(s), 124.839(s), 118.539(s), 116.128(s); ir (KBr): 3075(w), 1432(d, m), 1280(w), 1260, 1220, 1110(w), 930(w), 860(6), 800, and 750 cm^{-1}.

Dibenzo-1,4-dioxane was prepared by the method of Gilman and Dietrich (22) in 7% yield; mp 119–120°C (lit. (22) mp 119°C); ^{1}H nmr ($CDCl_3$) δ(ppm): 6.85(s); ^{13}C nmr ($CDCl_3$) δ(ppm): 141.998(s), 123.579(s), 116.128(s).

1:1 Donor Acceptor (TCNQ) Complexes

A typical procedure for the formation of TCNQ charge-transfer complexes is illustrated by the following procedure for the preparation of the phenoxatellurine – 7,7,8,8-tetracyanoquinodimethane complex.

In a 100 mL round bottomed flask were placed 0.7238 g (2.4486 mmol) of phenoxatellurine and 0.5000 g (2.4486 mmol) of 7,7,8,8-tetracyanoquinodimethane. To the flask was added 60 mL of spectral grade acetonitrile. The resulting solution was refluxed, with stirring, for 0.5 h. After the reflux period, the solution was cooled and the acetonitrile was evaporated *in vacuo* to leave 1.2238 g (2.4486 mmol, 100%) of PTe–TCNQ. *Anal.* calcd. for $C_{24}H_{12}N_4OTe$: C 57.62, H 2.40, N 11.21; found: C 57.44, H 2.34, N 11.46.

Charge-transfer complexes were also formed between TCNQ and the phenoxachalcogenines: phenoxaselenine, phenoxathiin, dibenzo-1,4-dioxane, as well as between TCNQ and the phenochalcogenazines: phenoxazine and phenothiazine. The yields for all of these preparations were quantitative. The crystalline products were all analytically pure.[2]

Solutions

Solutions of phenoxatellurine, phenoxaselenine, phenoxathiin, dibenzo-1,4-dioxane, phenoxazine, and 7,7,8,8-tetracyanoquinodimethane in dichloromethane were prepared by weighing the required amounts of the respective solids into clean weighing bottles. The solids were then transferred quantitatively into clean, dry volumetric flasks and diluted with the required amount of dry dichloromethane.

Solutions were prepared which yielded data amenable to the Rose–Drago method (5) for the calculation of equilibrium constants and extinction coefficients. The solutions were prepared by adding the required amount of the donor stock solution with a buret to a 10.0 mL volumetric flask and then evaporating the solvent. Ten milliliters of the TCNQ solution was then added to produce the required concentration of both components. A combined volume of 10.0 mL was generally used for Job's method studies. The visible spectra were obtained using cells thermostated at 10, 20, and 30°C.

All stock solutions were prepared using a water bath at 20°C. The change in volume of dichloromethane with temperature was calculated using the data of Heller (23) who determined that 1.000 mL of dichloromethane at 20°C occupies a volume of 1.014 mL at 30°C and 0.987 mL at 10°C.

[2]D. P. Rainville and R. A. Zingaro. Unpublished results,

Acknowledgements

We would like to thank the Robert A. Welch Foundation and the Selenium–Tellurium Development Association, Inc. for their financial support of this research.

1. C. A. HELLER, R. A. ZINGARO, and E. A. MEYERS. Can. J. Chem. **52**, 3814 (1974).
2. D. S. ACKER and W. R. HERTLER. J. Am. Chem. Soc. **84**, 3370 (1962).
3. (*a*) J. FERRARIS, D. O. COWAN, V. WALATKA, JR., and J. PERLSTEIN. J. Am. Chem. Soc. **95**, 948 (1973); (*b*) L. B. COLEMAN, M. J. COHEN, D. J. SANDMAN, F. G. YAMAGISHI, A. F. GARITO, and A. J. HEEGER. Solid State Commun. **12**, 1125 (1973).
4. R. S. MULLIKEN and W. B. PERSON. Molecular complexes. Wiley–Interscience, New York. 1969. p. 304.
5. N. J. ROSE and R. S. DRAGO. J. Am. Chem. Soc. **81**, 6138 (1959).
6. A. W. CORDES and C. K. FAIR. Acta Crystallogr. Sect. B, **30**, 1621 (1974).
7. I. GOLDBERG and U. SHMUELI. Acta Crystallogr. Sect. B, **29**, 432 (1973).
8. S. HOYA. Acta Crystallogr. **20**, 429 (1966).
9. M. R. SMITH, M. M. MANGION, R. A. ZINGARO, and E. A. MEYERS. J. Heterocycl. Chem. **10**, 527 (1973).
10. R. G. WOOD, C. H. MCCALE, and G. WILLIAMS. Philos. Mag. **31**, 71 (1941).
11. (*a*) C. K. PROUT and J. D. WRIGHT. Angew. Chem. Int. Ed. Engl. **7**, 659 (1968); (*b*) T. H. HERBSTEIN. Perspectives in structural chemistry. Vol. IV. Wiley, New York. 1971. pp. 166–395.
12. (*a*) B. HETNARSKI and A. GRABOWSKA. Bull. Acad. Pol. Sci. Ser. Sci. Chim. **17**, 333 (1969); (*b*) B. HETNARSKI and A. GRABOWSKA. Rocz. Chem. **44**, 1713 (1970).
13. M. HILLEBRAND, O. MAIOR, and V. EM. SAHINI. Rev. Roum. Chim. **15**, 149 (1970).
14. B. HETNARSKI and W. HOFMAN. Bull. Acad. Pol. Sci. Ser. Sci. Chim. **17**, 1 (1969).
15. M. HILLEBRAND, O. MAIOR, V. EM. SAHINI, and E. VOLANSCHI. J. Chem. Soc. B, 1489 (1969).
16. J. P. FERRARIS and G. SAITO. J. Chem. Soc. Chem. Commun. 992 (1978).
17. H. C. BROWN. Organic syntheses via boranes. Wiley, New York. 1975.
18. K. MARUYAMA. Bull. Chem. Soc. Jpn. **37**, 553 (1964).
19. H. MUSSO. Chem. Ber. **92**, 2862 (1959).
20. H. D. K. DREW. J. Chem. Soc. 223 (1926).
21. H. D. K. DREW. J. Chem. Soc. 511 (1928).
22. H. GILMAN and J. J. DIETRICH. J. Am. Chem. Soc. **79**, 1439 (1957).
23. C. A. HELLER. Ph.D. Dissertation, Texas A&M University, College Station, TX. 1972.

Can. J. Chem. Downloaded from www.nrcresearchpress.com by 210.87.254.105 on 09/05/12
For personal use only.

The mechanism of oxidation of acetals by ozone. I. Stoichiometry, order of the reaction, solvent effects, and substituent effects

ROLAND J. TAILLEFER,[1] SHIRLEY E. THOMAS, AND YVES NADEAU[2]
Département de chimie, Université de Sherbrooke, Sherbrooke (Qué.), Canada J1K 2R1
AND
S. FLISZÁR[1] AND HERVÉ HENRY
Département de chimie, Université de Montréal, Montréal (Qué.), Canada H3C 3V1
Received December 16, 1979

ROLAND J. TAILLEFER, SHIRLEY E. THOMAS, YVES NADEAU, S. FLISZÁR, and HERVÉ HENRY. Can. J. Chem. **58**, 1138 (1980).

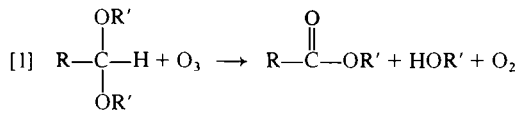
A systematic investigation of the reaction between ozone and acetals to form acetal hydrotrioxides **A** has been undertaken. The stoichiometry of the reaction has been shown to be 1:1 in each reactant and the order of the reaction was also one in each reactant. Substituent effects measured in a variety of systems and under several conditions of temperature and solvent were found to be small ($\rho = -1.10$ to -1.58). Solvent polarity was also found to have little effect on the rate of the reaction. Mechanistically, these facts are interpreted in terms of a 1,3-dipolar insertion of ozone into the C—H bond of the acetal function.

ROLAND J. TAILLEFER, SHIRLEY E. THOMAS, YVES NADEAU, S. FLISZÁR et HERVÉ HENRY. Can. J. Chem. **58**, 1138 (1980).

Une étude systématique de la réaction de l'ozone avec les acétals pour former les acétals hydrotrioxides **A** a été entreprise. On a trouvé que la stoechiométrie et l'ordre de la réaction étaient de un dans chacun des réactifs. L'effet des substituents sur la vitesse de réaction, mesuré dans plusieurs systèmes et sous différentes conditions de températures et de solvants est faible ($\rho = -1.10$ à -1.58) de même que l'effet de la polarité des solvants. Ces faits sont interprétés en invoquant un mécanisme d'addition 1,3-dipolaire de l'ozone dans le lien C—H de la fonction acétale.

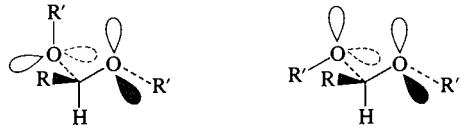
Introduction

In 1971, it was first reported (1) that aldehyde acetals reacted with ozone to give esters in high yield (reaction [1]).



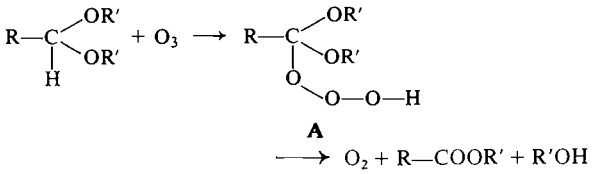
Experimental evidence was also provided (2–4) to suggest that for oxidation to proceed, it is required that one non-bonded electron pair on each oxygen of the acetal function lies antiperiplanar to the C—H bond of the acetal function (Scheme 1). Recently, it was shown (5) that an acetal hydrotrioxide (**A**, Scheme 2) is an intermediate in the reaction, and that singlet oxygen is produced during its unimolecular decomposition (5).

What is known now about the mechanism of the reaction can then be written as described in Scheme



Unreactive conformation Reactive conformation

SCHEME 1



SCHEME 2

2. This paper presents the results of a systematic investigation of the first step of this reaction, the oxidation step.

Experimental

The acetals used in this study were prepared by standard procedures or were commercial products. Their physical properties corresponded to literature values and their spectral properties were in accord with their structure. Vapor phase chromatographic analyses were carried out on a Hewlett-Packard F and M 5750 instrument with flame ionization detection, or Varian Aerograph instruments: model 2800 with thermal conductivity detector and temperature programming, or model 600 D with flame detector. Columns of various loadings (5%, 10%, 15%) and dimensions (6 ft × $\frac{1}{8}$ in., 5 ft × $\frac{1}{8}$ in., 10 ft × $\frac{1}{4}$ in., 15 ft × $\frac{1}{4}$ in.) were employed with the liquid phases XE-60, UCW-98, SE-30, carbowax-20 M, and PPE (OS-138). Peak intensities were measured either with a planimeter or by triangulation. Ozone was produced from a Welsbach Ozonator model T-816. Low temperature baths were either an acetone – dry ice mixture (−78°C) or a Neslab low temperature bath, model LTE-9 (−70°C – 0°C). Solvents used were spectrograde carbon tetrachloride, methylene chloride, or hexane previously treated with ozone, or spectrograde ethyl acetate.

[1]To whom all correspondence should be addressed.
[2]Undergraduate summer student 1977.

0008-4042/80/111138-06$01.00/0
©1980 National Research Council of Canada/Conseil national de recherches du Canada

Can. J. Chem. Downloaded from www.nrcresearchpress.com by 210.87.254.40 on 09/05/12
For personal use only.

Can. J. Chem. Downloaded from www.nrcresearchpress.com by 210.87.254.40 on 09/05/12
For personal use only.

Stoichiometry and Order of the Reaction

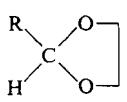
The fast reacting dioxolane acetals (**1**) were used for these experiments. The rate of ozone production was measured iodometrically by absorbing the ozone–oxygen flow in an aqueous solution of potassium iodide (4%) during 300 s. The ozone–oxygen stream was passed through 10 mL of solvent (CCl_4 or CH_2Cl_2) before the KI solution to reproduce the reaction conditions. A solution of acetal in CCl_4 or CH_2Cl_2 (ca. 0.1 *M*) at 0°C was then introduced in place of the solvent above and the same procedure was repeated. The absorbed ozone can then be obtained by difference. A dry ice – acetone trap was placed between the reaction vessel and the KI vessel to remove any solvent losses. Acetal concentrations were assayed by vpc.

Kinetics

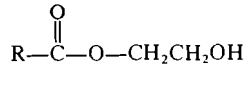
The kinetic method used to measure slow rates at low temperatures in ethyl acetate as solvent has been described previously (4). Rapid rates (solvent CCl_4; 0–35°C, dioxolane acetals **1**) were measured by stop-flow techniques using a Durrum-Gibson D-130 instrument, equipped with a reaction cuvette of 20 mm, a Jarrel-Ash 0.25 m monochromator with deuterium lamp. Optical densities were recorded on a Techtronic 535 oscilloscope equipped with a Polaroïd C-12 camera. Rates were measured by following the disappearance of ozone at 280 or 290 nm, where the extinction coefficients in carbon tetrachloride are 670 and 789 M^{-1} respectively (6). The competition method used to obtain relative rates for the dioxolane acetals **1** was that described by Hammett (7).

Results

The stoichiometry of the reaction of oxidation of 2-phenyl-1,3-dioxolane (**1**, R = C_6H_5) by ozone was first studied by Deslongchamps *et al.* (2) at −78°C in ethyl acetate as solvent. They found that in excess acetal, ozone oxidized 1 mol acetal to produce 1 mol oxygen and 1 mol hydroxy ester **2** (R = C_6H_5). The stoichiometry was further verified by the following experiments. A solution of acetal in excess concentration was reacted in an ozone–oxygen stream at 0°C. The acetals were assayed by vpc, and the absorbed ozone by iodometric titrations. The results are shown in Table 1. Similarly, a solution of acetal was reacted with excess ozone in carbon tetrachloride at 25°C under the conditions of a kinetic experiment. Ozone concentrations were measured spectrophotometrically. The results are shown in Table 2.



1



2

The results therefore show that under conditions where either ozone or acetal is in excess concentration, the stoichiometry of the reaction is clearly 1:1.

Order of the Reaction

The stoichiometry of the reaction, now being clearly established, suggests a second order reaction. Under the conditions where ozone is in slight excess, eq. [2] should apply (8)

$$[2]\quad \frac{1}{[O_3]_0 - [A]_0} \ln \frac{[O_3][A]_0}{[O_3]_0[A]} = kt$$

where $[O_3]$ is the concentration of ozone as determined spectrophotometrically, [A] the concentration of acetal deduced from the stoichiometry, and the subscript 0 refers to initial concentrations. Typical results are shown in Fig. 1 for the reaction of 2-methyl-1,3-dioxolane (**1**, R = CH_3) in carbon tetrachloride at 25°C. Other results obtained at different concentrations of ozone and acetal are shown in Table 3. These data suggest that the reaction is first order in both ozone and acetal.

Under the conditions where the acetal is in large excess, the reaction should become pseudo-first order in ozone. Again, for the case of the reaction of 2-methyl-1,3-dioxolane (**1**, R = CH_3) with ozone in carbon tetrachloride at 25°C, good linearity was observed as illustrated in Fig. 2. Table 4 shows the results obtained for different initial concentrations of ozone and acetal. The consistency of the second order rate constant and the identity of this rate with that obtained from second order kinetics clearly demonstrate that the reaction order is one in ozone and one in acetal.

Activation Parameters

The effect of temperature on the rate of oxidation of different acetals under various conditions is shown in Table 5. The activation parameters, found by plotting ln (k/T) vs. $1/T$, for these and other acetals are listed in Table 6.

Substituent Effects

The influence of substituents on the reactivity of various types of acetals was also investigated. Relative rate of oxidation of 2-alkyl substituted- and

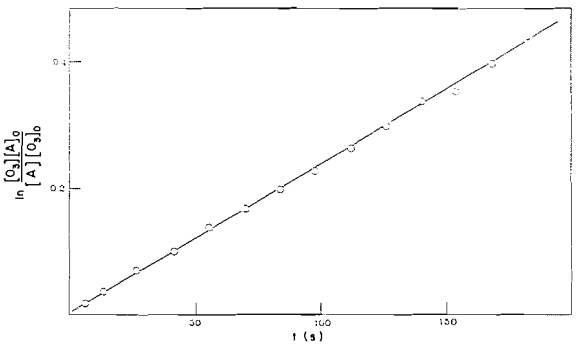


FIG. 1. Second order plot for the oxidation by ozone of 2-methyl-1,3-dioxolane (**1**, R = CH_3).

Can. J. Chem. Downloaded from www.nrcresearchpress.com by 210.87.254.40 on 09/05/12
For personal use only.

TABLE 1. Stoichiometry of the reaction of ozone with dioxolane acetals **1** at 0°C

R	Acetal (mmol) Initial	Acetal (mmol) Final	Absorbed ozone (mmol)	Solvent	Absorbed ozone / Consumed acetal
CH_3	22.8	19.7	3.18	CH_2Cl_2	1.00
	17.4	13.8	3.46	—	0.94
	13.6	8.3	5.84	—	1.09
C_6H_5	16.2	11.5	5.00	—	1.06
	12.3	9.4	2.69	—	0.95
	9.2	4.4	4.79	—	1.01
p-$CH_3C_6H_4$	12.3	9.3	2.92	CCl_4	0.97
	9.1	2.6	6.68	—	1.03

TABLE 2. Stoichiometry of the reaction of ozone with dioxolane acetals **1** in CCl_4 at 0°C

R	[Acetal] × 10^4, M	$[O_3]$ × 10^4, M Initial	$[O_3]$ × 10^4, M Final	Ozone / Acetal
C_6H_5	7.1	9.4	2.3	1.00
	5.0	6.4	1.5	0.98
	3.7	5.8	2.0	1.03
CH_3	5.0	6.0	1.2	0.96
	3.0	6.2	3.3	0.97
	3.0	3.6	0.5	1.03

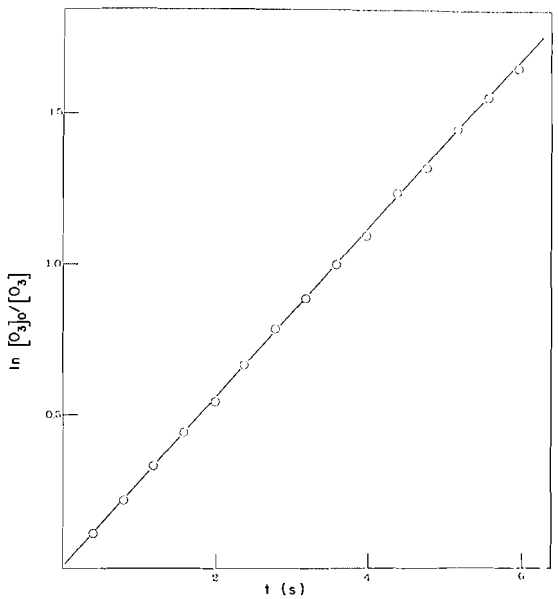


FIG. 2. Pseudo-first order plot for the oxidation by ozone of 2-methyl-1,3-dioxolane (**1**, R = CH_3).

2-aryl substituted-1,3-dioxolanes, determined by a competition method in CCl_4 at 0°C are listed in Table 7. Rates for alkyl substituted dimethoxymethanes and 2-alkyl substituted-1,3-dioxanes determined in ethyl acetate at −78°C are listed in Table 8. These data were correlated with

TABLE 3. Influence of initial concentrations of ozone and 2-methyl-1,3-dioxolane on the second order rate constants in CCl_4 at 25°C

$[O_3]_0$ × 10^4, M	$[A]_0$ × 10^4, M	k, M^{-1} s^{-1}
6.2	3.00	27.5
4.4	3.00	29.4
3.1	3.00	28.1
6.1	5.00	27.6
5.9	5.00	Ave. 28.1±1.0

TABLE 4. Influence of the initial concentrations of ozone and 2-methyl-1,3-dioxolane under pseudo-first order conditions on the rate constant in carbon tetrachloride at 25°C

$[A]_0$ (M)	$[O_3]_0$ × 10^4 (M)	k'^a (s^{-1})	k^b (M^{-1} s^{-1})
9.8×10^{-3}	5.4	0.280	28.6
4.1×10^{-2}	6.5	1.16	28.3
4.1×10^{-2}	3.7	1.22	29.9
6.5×10^{-2}	5.1	1.84	28.3
3.5×10^{-1}	5.9	10.5	30.0
3.5×10^{-1}	5.4	10.5	30.0
			Ave. 29.2±1.0

[a]Pseudo-first order constants.
[b]Second order rate constants.

TABLE 5. Effect of temperature on the rate of oxidation by ozone of different acetals

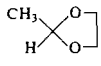
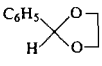
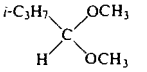
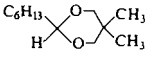
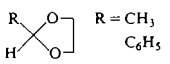
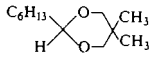
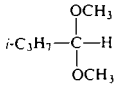
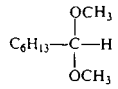
Acetal	Solvent	T (°C)	k (M^{-1} s^{-1})
	CCl_4	15	19.1±1.2
		25	28.5±1.2
		35	37.2±1.2
	CCl_4	15	50.5±2.5
		25	73.4±2.0
		35	104.0±2.3
	EtOAc	−40	(3.48±0.10)× 10^{-2}
		−50	(1.53±0.04)× 10^{-2}
		−78	(6.87±0.14)× 10^{-4}
	Hexane	−50	(11.70±0.40)× 10^{-2}
		−60	(5.90±0.10)× 10^{-2}
		−78	(7.40±0.30)× 10^{-3}

TABLE 6. Activation parameters for the reaction of ozone with different acetals

Acetal	Solvent	$\Delta H^{\neq}$(kJ mol^{-1})	$\Delta S^{\neq}$(J mol^{-1} K^{-1})
	CCl_4	22.6±2.9	−141±10
	CCl_4	24.9±0.4	−125±2
	Hexane	34.3±3.5	−106±17
	EtOAc[a]	33.3±2.5	−106±12
	EtOAc	37.4±0.7	−110±3
	EtOAc[a]	35.2±1.6	−121±7

[a]Reference 4.

TABLE 7. Relative rate of oxidation of 2-substituted-1,3-dioxolanes in CCl_4 at 0°C

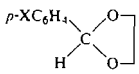
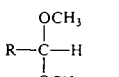
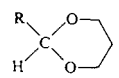
	k_{rel}		k_{rel}
R = *t*-Bu	2.510±0.100	X = MeO	2.090±0.070
i-Pr	1.540±0.140	Me	1.520±0.050
Et	1.270±0.100	H	1.000
Me	1.000	Cl	0.520±0.030
H	0.420±0.010	NO_2	0.144±0.015
C_6H_5	2.200±0.120		
CH_2Cl	0.067±0.007		

TABLE 8. Pseudo-first order rate constants for the oxidation of alkyl-substituted dimethoxymethanes and 2-alkyl substituted-1,3-dioxanes in ethyl acetate, by ozone at 4.40×10^{-2} *M* at −78°C

Acetal	R	Rate constant (s^{-1})	Deviation[a] (%)
	*t*-C_4H_9	8.53×10^{-6}	4.2
	i-C_3H_7	3.02×10^{-5}	2.1
	n-C_6H_{13}	2.82×10^{-5}	0.1
	CH_3OCH_2	3.15×10^{-6}	1.3
	$ClCH_2$	8.12×10^{-7}	
	*t*-C_4H_9	8.36×10^{-4}	2.5
	i-C_3H_7	7.12×10^{-4}	0.6
	n-C_6H_{13}	3.38×10^{-4}	0.1
	CH_3OCH_2	2.80×10^{-5}	4.2

[a]Deviation from average of at least two results.

the appropriate Taft or Hammett substituent constants (9) and the results of these correlations are listed in Table 9. It should be noted that for 2-alkyl substituted-1,3-dioxolanes (Table 7), R = C_6H_5 did not fit the line and was omitted from the correlation. The same is true for the R = *t*-C_4H_9 compound in the dimethoxymethanes series (Table 8). The σ^* value for the *n*-hexyl group (Table 8) was taken as that of the *n*-propyl group.

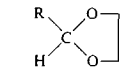
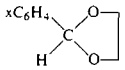
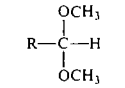
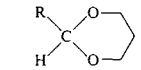
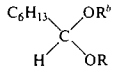
Solvent Effects

The influence of solvent polarity on the rate of

Can. J. Chem. Downloaded from www.nrcresearchpress.com by 210.87.254.40 on 09/05/12
For personal use only.

Can. J. Chem. Downloaded from www.nrcresearchpress.com by 210.87.254.40 on 09/05/12
For personal use only.

TABLE 9. Correlation of the rate data with Hammett or Taft substituent constants

Acetal	Solvent	T(°C)	ρ	r^a
	CCl_4	0	−1.16	0.995
	CCl_4	0	−1.10	0.998
	EtOAc	−78	−1.27	0.998
	EtOAc	−78	−1.58	0.980
	EtOAc	−78	−1.31	0.910

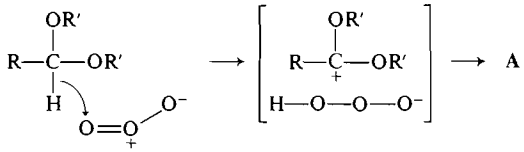
[a]Correlation coefficient.
[b]log k vs. $2\sigma^*$ of the R group. Data taken from ref. 4.

oxidation of ozone of 2-hexyl-5,5-dimethyl-1,3-dioxane was investigated at two temperatures. The results are shown in Table 10. The concentration of ozone in the different solvents was determined as previously published (4).

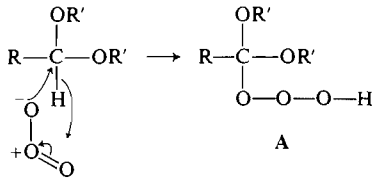
Discussion

Several mechanisms can be envisaged for the oxidation of the C—H bond of the acetal function by ozone to form the acetal hydrotrioxide **A**. These are depicted in Scheme 3. The possibility that the hydride transfer mechanism (Scheme 3*a*) might be operative arises from the strong conformational effects observed in these reactions (2–4). Antiperiplanar lone pairs will elongate the C—H bond as well as stabilize the incipient dioxonium ion. The 1,3-diplolar insertion mechanism (Scheme 3*b*) has been postulated for the ozonation of ethers (10–12), aldehydes (13, 14), and hydrocarbons (15, 16). Ozone attack on oxygen (Scheme 3*c*) is similar to that proposed for the ozonation of certain amines

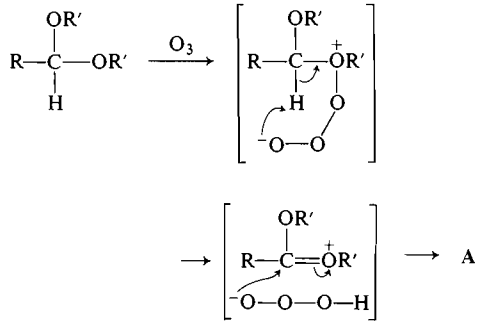
(*a*) Hydride transfer mechanism



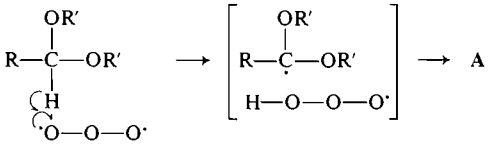
(*b*) 1,3-Dipolar insertion mechanism



(*c*) Attack on an ether oxygen



(*d*) Radical mechanism

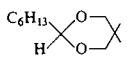


SCHEME 3

(17), sulfides (18), and ethers (12). Finally, radical mechanisms (Scheme 3*d*) have been proposed for the ozonation of certain hydrocarbons (19–21) and alcohols (21) as well as ethers at high temperatures (11).

The highly negative entropies of activation found

TABLE 10. Effect of solvent on the rate of oxidation by ozone of 2-hexyl-5,5-dimethyl-1,3-dioxane

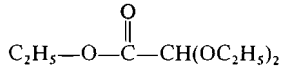


T (°C)	Solvent	k_1 (s^{-1})[a]	Deviation[b] (%)	$[O_3]$ (mol L^{-1})	k_2 (M^{-1} s^{-1})[c]
−78	Hexane	2.82×10^{-4}	4.4	3.80×10^{-2}	7.43×10^{-3}
	Freon-11	3.35×10^{-4}	2.7	4.21×10^{-2}	8.11×10^{-3}
	EtOAc	5.21×10^{-4}	1.2	4.40×10^{-2}	1.18×10^{-2}
−50	Hexane	1.62×10^{-3}	3.5	1.39×10^{-2}	1.17×10^{-1}
	EtOAc	2.61×10^{-3}	1.5	1.48×10^{-2}	1.76×10^{-1}
	Ac_2O	2.61×10^{-3}	3.3	1.21×10^{-2}	2.16×10^{-1}

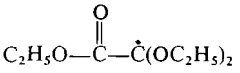
[a]Pseudo-first order rate constants.
[b]Deviation from average of at last two results.
[c]Second order rate constants.

Can. J. Chem. Downloaded from www.nrcresearchpress.com by 210.87.254.40 on 09/05/12
For personal use only.

for these reactions (Table 6) suggest a highly ordered transition state. Further, electron donation in the substituent accelerates the rates (Tables 7 to 9). These facts are compatible with all the mechanisms proposed in Scheme 3, except perhaps the radical mechanism (Scheme 3*d*) where one would expect a less negative entropy of activation (22). Although this criterion is not convincing by itself the fact that compound **3**, which would produce the stabilized radical **4**, did not react at all with ozone at room temperature for 3 h in ethyl acetate (2), strongly militates against a radical pair mechanism.



3



4

All ρ values (Table 9) are small in magnitude no matter what the experimental conditions (temperature and solvent). This can be interpreted by invoking either the argument that the charge created in the transition state is mainly stabilized by the oxygen atoms of the acetal function and to a much lower extent by the substituent, or else little charge is created in the transition state. This latter reason would be in accord with the observed solvent effects (Table 10). At −50°C for example, the observed acceleration is only a factor of 2 in going from the non-polar hexane solvent to the very polar acetic anhydride solvent. The same is true at −78°C (hexane to ethyl acetate). These facts would tend to eliminate highly polar transition states and/or intermediates described in Scheme 3*a* and 3*c*.

The most likely mechanism would then be the insertion mechanism (Scheme 3*b*).[3] Further evidence for this mechanism will be provided from a study of primary and secondary isotope effects presently underway.

Acknowledgments

Support for this work by the National Research Council of Canada and by "le Ministère de l'Education", Québec, is gratefully acknowledged.

[3] This mechanism would apply whether the ozone structure is a dipole or a singlet diradical (23). The present work does not permit us to differentiate between the two.

1. P. DESLONGCHAMPS and C. MOREAU. Can. J. Chem. **49**, 2465 (1971).
2. P. DESLONGCHAMPS, P. ATLANI, D. FRÉHEL, A. MALAVAL, and C. MOREAU. Can. J. Chem. **52**, 3651 (1974).
3. P. DESLONGCHAMPS, C. MOREAU, D. FRÉHEL, and P. ATLANI. Can. J. Chem. **50**, 3402 (1972); P. DESLONGCHAMPS, C. MOREAU, D. FRÉHEL, and R. CHÊNEVERT. Can. J. Chem. **53**, 1204 (1975).
4. R. J. TAILLEFER, S. E. THOMAS, Y. NADEAU, and H. BEIERBECK. Can. J. Chem. In press.
5. F. KOVAC and B. PLESNICAR. J. Chem. Soc. Chem. Commun. 122 (1978); J. Am. Chem. Soc. **101**, 2677 (1979).
6. T. W. NAKAGAWA, L. J. ANDREWS, and R. M. KEEFER. J. Am. Chem. Soc. **82**, 269 (1960).
7. L. P. HAMMETT. Physical organic chemistry. 2nd ed. McGraw-Hill, New York. 1970. p. 91.
8. K. J. LAIDLER. Chemical kinetics. McGraw-Hill, New York. 1965. Chapt. 1.
9. J. HINE. Physical organic chemistry. 2nd ed. McGraw-Hill, New York. 1962. Chapt. 4.
10. C. C. PRICE and A. L. TUMOLO. J. Am. Chem. Soc. **86**, 4691 (1964).
11. R. E. ERICKSON, R. T. HANSEN, and J. HARKINZ. J. Am. Chem. Soc. **90**, 6777 (1968).
12. P. S. BAILEY and D. A. LERDAL. J. Am. Chem. Soc. **100**, 5820 (1978).
13. R. E. ERICKSON, D. BAKALIK, C. RICHARDS, M. SCANLON, and G. HUDDLESTON. J.Org. Chem. **31**, 461 (1966).
14. H. M. WHITE and P. S. BAILEY. J. Org. Chem. **30**, 3037 (1965).
15. J. E. BATTERBEE and P. S. BAILEY. J. Org. Chem. **32**, 3899 (1967).
16. D. TAL, E. KEINAN, and Y. MAZUR. J. Am. Chem. Soc. **101**, 502 (1979).
17. P. S. BAILEY, D. A. LERDAL, and T. CARTER. J. Org. Chem. **43**, 2662 (1978) and references therein.
18. P. S. BAILEY and A. Y. KHASHAB. J. Org. Chem. **43**, 675 (1978) and references therein.
19. G. A. HAMILTON, B. S. RIBNER, and T. M. HELLMAN. Adv. Chem. Ser. **77**, 15 (1968).
20. T. M. HELLMAN and G. A. HAMILTON. J. Am. Chem. Soc. **96**, 1530 (1974).
21. M. C. WHITING, A. J. N. BOLT, and H. H. PARISH. Adv. Chem. Ser. **77**, 4 (1968).
22. G. A. RUSSEL. *In* Free radicals. Vol. 1. *Edited by* J. K. Kochi. 1973. Chapt. 7, p. 292; M. L. POUTSMA. *In* Free radicals. Vol. 2. *Edited by* J. K. Kochi. 1973. Chapt. 15, p. 168.
23. W. R. WADT and W. A. GODDARD III. J. Am. Chem. Soc. **97**, 3004 (1975) and refs. 10 and 11 therein.

Regioselectivity in cycloaddition reactions on solid phases[1]

VARDA YEDIDIA AND CLIFFORD C. LEZNOFF
Department of Chemistry, York University, Downsview, Ont., Canada M3J 1P3

Received November 23, 1979

VARDA YEDIDIA and CLIFFORD C. LEZNOFF. Can. J. Chem. **58**, 1144 (1980).

A 1% crosslinked divinylbenzene–styrene copolymer, incorporating benzyl acrylate groups, reacted in normal Diels–Alder reactions with *E*-1-phenyl-1,3-butadiene or methyl *E*-2,4-pentadienoate to give their respective polymer-bound benzyl cyclohexenecarboxylates. Polymer-bound benzyl propiolate and polymer-bound benzyl phenylpropiolate reacted with benzonitrile oxide in a typical 1,3-dipolar addition reaction to give their respective polymer-bound isoxazoles. Cleavage of the polymer-bound Diels–Alder adducts and the polymer-bound 1,3-dipolar addition adduct derived from polymer-bound benzyl propiolate gave mixtures of *ortho* and *meta* regiomers similar to those produced in analogous reactions in solution. Cleavage of the polymer-bound 1,3-dipolar addition adduct, derived from polymer-bound benzyl phenylpropiolate, followed by esterification, gave a solitary adduct, 4-carbomethoxy-3,5-diphenylisoxazole, but an analogous solution 1,3-dipolar addition yielded a 1:1 ratio of the two possible regiomers.

VARDA YEDIDIA et CLIFFORD C. LEZNOFF. Can. J. Chem. **58**, 1144 (1980).

Un copolymère styrène–divinylbenzène réticulé à 1% incorporant des groupes acrylate de benzyle réagit selon une réaction normale de Diels–Alder avec le phényl-1-*E* butadiène-1,3 ou le pentadièn-2,4 oate de méthyle pour donner leurs cyclohexènecarboxylates de benzyle respectifs liés aux polymère. Le propiolate de benzyle et phénylpropiolate de benzyle liés au polymère réagissent avec l'oxyde de benzonitrile selon une addition dipolaire-1,3 typique pour conduire à leurs isoxazoles respectifs liés au polymère. Le clivage des adduits de Diels–Alder du polymère auxquels ils sont liés ainsi que des adduits dipolaires-1,3 provenant du propiolate de benzyle liés au polymère conduit à des mélanges de régioisomères *ortho* et *méta* semblables à ceux obtenus lors des réactions analogues en solution. Le clivage du polymère de l'adduit dipolaire-1,3 qui provient du phénylpropiolate de benzyle lié au polymère suivi d'une estérification conduit à un seul produit, le carbométhoxy-4 diphényl-3,5 isoxazole; toutefois une réaction analogue en solution fournit les deux régioisomères possibles dans un rapport 1:1.

[Traduit par le journal]

Introduction

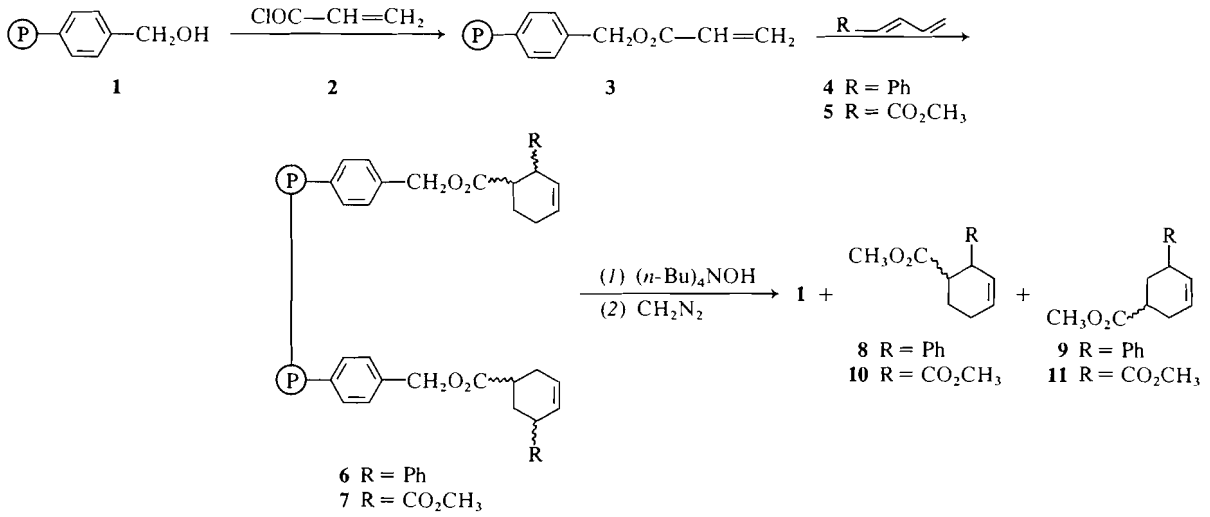
Cycloaddition reactions involving preformed insoluble polymer supports are rare. Blazka and Harwood (3) reacted a polymer-bound maleamide with cyclopentadiene to give a polymer-bound Diels–Alder adduct for possible use as a handle in enzymatic studies. Nieuwstad *et al.* (4) used a series of polymer-bound dienes in cyclo addition reactions with sulfur dioxide for the purpose of removing sulfur dioxide from waste and flue gases. In both of these cases the cycloaddition adducts were not liberated from the polymer support. In some mechanistic studies, Rebek and Gaviña and Gaviña *et al.* (5) have achieved the trapping of reactive intermediates with polymer-bound substrates and the Diels–Alder-like adducts were cleaved from the polymer and isolated.

Our interest in studying cycloaddition reactions on insoluble polymer supports results from the fact that we have achieved the synthesis of several types of *alicyclic* compounds in multistep syntheses on solid phases including chalcones (6), carotenoids (7), and insect pheromones (8) and wish to extend the synthetic possibilities to include the vast array of natural products containing cyclic systems. Only a few cyclization reactions have been accomplished on solid phases (9, 10). In addition, we felt that cycloaddition reactions performed on solid phases could result in cycloadducts having an altered ratio of regiomers compared to their solution phase analogs. It is well known that 1-substituted-1,3-butadienes react with 1-substituted alkenes containing an electron withdrawing group to give a great predominance of the *ortho* adduct over the *meta* adduct (11–13), often to the exclusion of the *meta* adduct entirely (14). In fact the problem of obtaining the disfavoured *meta* adducts has recently been addressed by Danishefsky *et al.* (15). We felt that the attachment of the dienophile or diene to an insoluble polymer support, necessarily through the substituent group, would increase the steric bulk of the substituent so that the *meta* adduct would become favoured over the *ortho* adduct. We also hoped that the yields of Diels–Alder reactions on insoluble polymer supports would increase compared to their analogous reactions in solution phase due to the decreased probability of intraresin reactions leading to polymeric products (10, 16). Furthermore, the Diels–Alder adducts could be efficiently isolated from the reaction mixture by simple filtration leaving excess reactants and by products in the solution phase (17). To ensure that formation of a *meta* adduct was not fun-

[1]The use of polymer supports in organic synthesis. Part XXII. For Parts XXI and XX, see refs. 1 and 2 respectively.

0008-4042/80/111144-07$01.00/0
©1980 National Research Council of Canada/Conseil national de recherches du Canada

Can. J. Chem. Downloaded from www.nrcresearchpress.com by 210.87.254.6 on 09/05/12
For personal use only.



SCHEME 1.

damentally electronically disfavoured we selected known examples of Diels–Alder reactions in solution which gave at least some, however small, *meta* adduct and adapted those reactions to the solid phase conditions.

It was envisioned that altered regioselectivity of polymer-bound Diels–Alder reactions (compared to similar reactions in the solution phase) due to the steric bulk of the polymer may be difficult to achieve as most suitable Diels–Alder reactions are performed at moderately high temperatures where polymer mobility is high. For this reason we also wished to examine cycloaddition reactions at room temperature or lower. The 1,3-dipolar additions of nitrile oxides with alkenes or alkynes (18, 19) is carried out below room temperature and examples exist in which mixtures of regiomers are obtained. Furthermore, 1,3-dipolar additions are more sensitive to the polarity of the solvent in which the reaction occurs and it is possible that local solvent effects of the insoluble polymer at the reaction site could influence the regioselectivity of the 1,3-dipolar cycloadditions.

Results and Discussion

Diels–Alder Cycloadditions

A suspension of a 1% crosslinked divinylbenzene–styrene copolymer, containing benzyl alcohol functional groups, (**1**) (20), in tetrahydrofuran (THF) was treated with an excess of acryloyl chloride (**2**) and stirred for 18 h under argon at room temperature. Filtration of the mixture yielded the polymer-bound benzyl acrylate (**3**), suitable as a polymer-bound dienophile in Diels–Alder reactions (3). Treatment of a suspension of **3** with *E*-1-phenyl-1,3-butadiene (**4**) in hot xylene or methyl *E*-2,4-pentadienoate (**5**) in hot toluene gave the polymer-bound Diels–Alder cyclohexene adducts (**6**) and (**7**) respectively. Cleavage of **6** with tetra-*n*-butylammonium hydroxide in THF and subsequent esterification of the crude products yielded a mixture of *cis* and *trans* isomers of methyl 2-phenyl-3-cyclohexenecarboxylates (**8**) and *cis* and *trans* isomers of methyl 5-phenyl-3-cyclohexenecarboxylates (**9**) (21, 22). Similar treatment of **7** gave a mixture of *cis* and *trans* isomers of dimethyl 3-cyclohexene-1,2-dicarboxylates (**10**) and *cis* and *trans* isomers of dimethyl 3-cyclohexene-1,3-dicarboxylates (**11**) (14) (Scheme 1). Polymer **1** was recovered from both cleavage reactions and was capable of being recycled with little loss of capacity. The quantity of **2** bound to **1** was determined by cleavage of **3** with K_2CO_3 in methanol (23) to give solely 3-methoxypropanoic acid (**12**), the cleaved addition product. The amount of **12** recovered from **3** is consistent with the capacity of similar polymers (23), even though it is possible that some acrylic acid itself was formed and lost in the work-up through polymerization or evaporation. Thus the determined capacity of **3** for **2** represents a minimum value.

We have generally cleaved polymer-bound esters under basic conditions using initially (24) tetra-*n*-butylammonium hydroxide or K_2CO_3 in methanol but latterly exclusively the K_2CO_3 method (23) as it is simple and results in fewer by-products. Unfortunately attempted cleavage of **6** with K_2CO_3 in methanol gave some of **8** and **9** but even after 48 h, an infrared spectrum of the resulting polymer exhibited an absorption band at 1725

Can. J. Chem. Downloaded from www.nrcresearchpress.com by 210.87.254.6 on 09/05/12
For personal use only.

Can. J. Chem. Downloaded from www.nrcresearchpress.com by 210.87.254.6 on 09/05/12
For personal use only.

cm^{-1} indicating that complete cleavage had not occurred. Cleavage of **6** with tetra-*n*-butylammonium hydroxide in THF resulted in complete removal of the ester functionality.

Although we had successfully prepared cyclohexenes on solid phases by two Diels–Alder reactions we were interested in knowing whether we had changed the ratio of regiomers **8** to **9** and **10** to **11** compared to similar reactions not involving the polymer. Although Nazarov *et al.* (22) had previously reacted *methyl* acrylate (**13**) with **4** to give **8** and **9** in a 97:3 ratio and Overman *et al.* (14) reacted **13** with **5** to give **10** and **11** in an 82:18 ratio, we felt that even better control solution reactions would be the Diels–Alder reactions of *benzyl* acrylate (**14**) with **4** and **5** respectively. Thus **14** reacted with **4** to give a crude mixture of benzyl 2-phenyl-3-cyclohexenecarboxylates and benzyl 5-phenyl-3-cyclohexenecarboxylates which were cleaved and esterified in a manner identical to that of the polymer-bound adduct **6**. Isolation and purification of the products by preparative thin-layer chromatography (tlc) gave a mixture of **8** and **9**. The mixture of **8** and **9** could be readily analyzed by its nuclear magnetic resonance (nmr) spectrum which exhibited distinct $-OCH_3$ resonances for the two diastereomers of **8** and the two of **9**. Gas chromatography (gc) of the mixture exhibited four peaks of which the two fast moving ones of **8** were distinctly separated from the slower moving peaks of **9**. In addition the mixture of **8** and **9** was dehydrogenated as before (22) to give methyl 2-phenylbenzoate (**15**) and methyl 3-phenylbenzoate (**16**), which were compared by nmr and gc to authentic **15** and **16**, prepared by esterification of commercially available 2-phenylbenzoic acid and 3-phenylbenzoic acid. In a similar manner **14** reacted with **5** in a solution phase Diels–Alder reaction to give a mixture of the two diastereomers of **10** and the two of **11**, as shown by gc and nmr analysis. Hydrogenation of the mixture of **10** and **11** yielded a mixture of the saturated *cis*- and *trans*-dimethyl cyclohexane-1,2-dicarboxylates (**17**) and *cis*- and *trans*-dimethyl cyclohexane-1,3-dicarboxylates (**18**). Authentic *cis*-**17** and *trans*-**17** were prepared from the commercially available diacids. An authentic mixture of *cis*- and *trans*-**18** was readily prepared by oxidation of the commercially available mixture of cyclohexane-1,3-dimethanols by the method of Corey and Schmidt (25). The mixture of Diels–Alder adducts, **10** and **11**, obtained for the polymer-bound acrylate **3** and **5** was also hydrogenated to give a mixture of *cis*- and *trans*-**17** and *cis*- and *trans*-**18** which were compared to authentic **17** and **18** prepared above. The gc data of the *cis* and *trans* isomers of **8**, **9**, **17**, and **18** show the ratios of **8**:**9** and **17**:**18** for both the solid phase and solution Diels–Alder reactions (Table 1).

TABLE 1. Comparisons of the regioselectivity and yields in Diels–Alder reactions on solid phases and in solution

Diene	Dienophile	Products	Yield (%)	Regioselectivity[a] ratio
4	**3**	**8**+**9**[b]	80	94:6
4	**14**	**8**+**9**[b]	—	94:6
4	**13**	**8**+**9**	61	97:3[c]
5	**3**	**10**+**11**[b]	52	77:23
5	**14**	**10**+**11**[b]	—	88:12
5-Acid[d]	**13**	**10**+**11**	—	82:18[e]

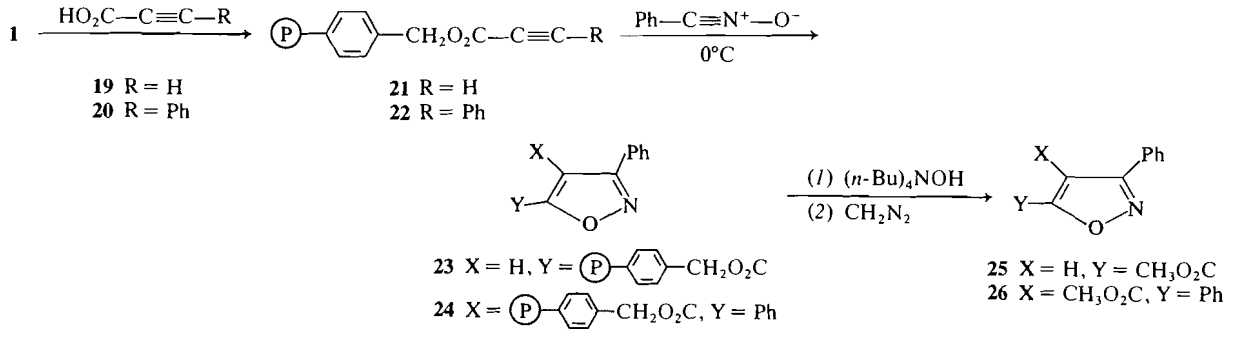
[a]This value represents the ratio of *ortho* compared to *meta* adducts.
[b]See Experimental section for reaction conditions.
[c]From ref. 22.
[d]*E*-2,4-Pentadienoic acid.
[e]From ref. 14.

As we can see from the data in Table 1, the Diels–Alder reactions performed herein on solid phases are similar to those done in a homogeneous phase with respect to distribution of regiomers and absolute yields of products.[2]

1,3-Dipolar Cycloadditions

Since it was felt that the lack of extensive alterations in regioselectivity in the Diels–Alder reactions on solid phases compared to their solution analogs (Table 1) was a result of the high temperatures of the Diels–Alder reactions, we decided to examine a cycloaddition reaction that occurs readily at lower temperatures but still gives a mixture of regiomers. Thus polymer **1** reacted with propiolic acid (**19**) or phenylpropiolic acid (**20**) to give the polymer-bound benzyl propiolate (**21**) and polymer-bound benzyl phenylpropiolate (**22**). Treatment of **21** and **22** with benzonitrile oxide, generated *in situ* from α-chlorobenzaldoxime, at 0°C in THF yielded the polymer-bound benzyl isoxazoles (**23**) and (**24**) respectively. Base cleavage of **23** and **24** as before, followed by esterification with CH_2N_2, gave *solely* methyl 3-phenylisoxazole-5-carboxylate (**25**) and *only* methyl 3,5-diphenylisoxazole-4-carboxylate (**26**) respectively in reasonable yield (Scheme 2). Although Huisgen *et al.* (26, 27) have shown that *methyl* propiolate and *methyl* phenylpropiolate reacted in a 1,3-dipolar addition addition reaction to give a *72:28 mixture* of **25** and methyl 3-phenyl-

[2]In this paper we were particularly interested in the possible change in *regioselectivity* of adducts in going to solid phase Deils–Alder reactions from their solution analogs and were less interested in changes in enantioselectivity. In addition, our base cleavage method is likely to cause *cis–trans* isomerization of the cycloadducts (22) and hence the *original* ratio of *cis* to *trans* isomers obtained in the solid phase reactions could not be accurately determined.



SCHEME 2.

isoxazole-4-carboxylate (**27**) and a *99:1 mixture* of **26** and methyl 3,4-diphenylisoxazole-5-carboxylate (**28**) respectively under almost identical conditions we believed that model reactions more similar to the polymer would use *benzyl* propiolate (**29**) and *benzyl* phenylpropiolate (**30**). Thus treatment of **29** and **30** with benzonitrile oxide as before yielded mixtures of crude benzyl isoxazoles. Base cleavage of the crude mixtures, derived from **29** and **30**, under conditions identical to those under which **23** and **24** were cleaved, followed, as before, by treatment with CH_2N_2 and purification by preparative tlc yielded pure **25** and 1:1 mixture of **26** and **28** respectively. The products were analyzed by nmr and gc and the results are summarized in Table 2. It is interesting to note that the regioselectivity of the 1,3-dipolar addition of **21** and **29** with benzonitrile oxide is identical and completely regioselective to give, after hydrolysis and reesterification, solely **25** while the reported addition of benzonitrile oxide to methyl propiolate gave a 3:1 *mixture* of regiomers **25** and **27**. We originally proposed that a bulky ester functionality on the alkyne would disfavour the normal "*ortho*" adduct compared to the "*meta*" adduct in cycloaddition reactions. The above experiments justified this hypothesis but showed that a polymer-bound benzyl ester group does *not* necessarily make the dienophile bulkier than a *simple* benzyl ester. On this basis we were very surprised to find that the 1,3-dipolar cycloaddition of polymer **22** with benzonitrile oxide proceeded to give *exclusively* the more hindered "*ortho*" adduct **26**, while the simple benzyl analog **30** yielded an expected mixture of **26** and **28**. Thus the bulky benzyl ester **30** yielded more of the "*meta*" isomer than the reported use of methyl propiolate which gave almost no "*meta*" adduct. Thus the course of the 1,3-dipolar cycloaddition of **30** proceeded in the right direction, but the reaction of polymer **22** with benzonitrile oxide proceeded in the opposite direction on the basis of the steric effect. It is known that reactions occurring on insoluble polymer supports

TABLE 2. Comparisons of the regioselectivity in benzonitrile oxide reactions with alkynoic esters on solid phases and in solution

Alkynoic ester	Products	Yield (%)	Regioselectivity[a] ratio
21	**25**[b]	80	100:0
29	**25**[b]	30	100:0
Methyl propiolate	**25**+**27**	98	72:28[c]
22	**26**[b]	81	0:100
30	**26**+**28**[b,d]	66	55:45
30	**26**+**28**[b,e]	54	72:28
Methyl phenylpropiolate	**26**+**28**	94	1:99

[a]This value represents the ratio of isoxazole 5-carboxylates compared to isoxazole 4-carboxylates.
[b]See Experimental section for reaction conditions.
[c]See ref. 27.
[d]In THF.
[e]In toluene.

can proceed in a solvent environment quite different than that of the bulk of solution (28) and that 1,3-dipolar cycloadditions are solvent dependent (13). It is thus possible that in the reactions of **22** with benzonitrile oxide the solvent at the reaction site is not THF, the bulk solvent, but the polymer itself which is toluene-like. To test this hypothesis we conducted the solution analog reaction of **30** with benzonitrile oxide in *toluene* to more closely simulate the possible solvent environment at the reactive site of the polymer. Cleavage of the crude product as above and treatment with CH_2N_2 actually afforded a mixture of **26** and **28** in a *decreased* ratio (1:2.5). Thus the local environment at the reaction site is *not* toluene-like and the true reason for the exclusive formation of **26** in the polymer-supported 1,3-dipolar addition remains conjecture at this time.

Conclusions

Our idea that a polymer-bound benzyl group is so bulky compared to a simple benzyl group that the regioselectivity of polymer-bound cycloaddition reactions can be altered compared to its solution analog is not valid and it appears that the polymer-

Can. J. Chem. Downloaded from www.nrcresearchpress.com by 210.87.254.6 on 09/05/12
For personal use only.

Can. J. Chem. Downloaded from www.nrcresearchpress.com by 210.87.254.6 on 09/05/12
For personal use only.

bound benzyl group is no more bulky than a simple benzyl group, at least, for Diels–Alder reactions at high temperatures. We have shown, however, that a benzyl ester group itself can alter the regioselectivity of cycloaddition reactions compared to simple methyl esters. We have demonstrated that the polymer can alter the regioselectivity of 1,3-dipolar cycloaddition reactions compared to its solution analog. Finally, we have demonstrated that cycloaddition reactions can be routinely performed on solid phases in yields comparable to or better than those in solution.

Experimental

A chloromethylated 1% divinylbenzene (DVB) – styrene copolymer, containing 1.09 mequiv. Cl/g of resin, obtained from Sigma Chemical Company was used as the starting resin in all resin transformations. Filtration was done under vacuum using sintered glass Büchner funnels. Suspensions and solutions were stirred using magnetic stirrers. Matheson high purity argon was used to maintain inert atmosphere conditions. Infrared (ir) spectra were recorded on a Pye Unicam SP1000 infrared spectrophotometer using KBr discs for solids or as neat films between NaCl discs. Nuclear magnetic resonance (nmr) spectra were recorded on a Varian LM 360 spectrometer using deuterochloroform as solvent and tetramethylsilane as the internal standard. The positions of the signals are reported in δ units. (The splittings of the signals are described as singlets (s), doublets (d), triplets (t), quartets (q), or multiplets (m).) Mass spectra (ms) were recorded at 70 eV on a Hitachi Perkin Elmer RMU 6E mass spectrometer, attached to a Perkin Elmer 902 gas chromatograph (gc) fitted with a Scot 50-ft stainless steel OV 225 column. The number in parentheses after the indicated ion shows the percentage of the base peak represented by that ion. Melting points (mp) were determined using a Kofler hot stage melting point apparatus and are uncorrected. Thin-layer chromatography (tlc) was performed using silica gel G as the adsorbent. Other gas chromatography (gc) was recorded on a Varian aerograph (series 1700) gas chromatograph with a Varian aerograph (model 20) recorder. The column was a 7-ft column, 6% SE 30, 4% QF 1 on acid washed HMDS. Helium was used as the gas carrier with a 1 mL/s flow rate. The chart speed was 1.7 cm/s. The retention times are given in cm.

Preparation of Polymer-bound Acrylate (3)

A suspension of 5 g of 1% crosslinked divinylbenzene–styrene copolymer containing benzyl alcohol groups (**1**) in 100 mL of dry THF was stirred with 4.0 mL (49.3 mmol) of acryloyl chloride (**2**) under an argon atmosphere at room temperature for 18 h. The polymer was filtered, washed twice with THF, twice with methanol, twice with THF, twice with ether, and air dried to yield the polymer-bound acrylate (**3**); ir (KBr): 1725 (CO_2R), 1635, and 1415 cm^{-1} ($RCH{=}CH_2$).

The quantity of acryloyl chloride bound to polymer **1** was determined by cleavage of polymer **3** with K_2CO_3 in methanol (23) to yield 3-methoxypropionic acid from which the loading capacity of **3** was calculated. Thus polymer **3** contained 0.58 mmol of acrylate per gram of polymer.

Preparation of Polymers 6 and 7

A suspension of 3.5 g of polymer-bound acrylate (**3**) and 2.7 g (20.8 mmol) of *E*-1-phenyl-1,3-butadiene (**4**) (29) in 40 mL of xylene was refluxed for 18 h at 140°C in the presence of 0.05 g of phenyl-β-naphthylamine. The solution was cooled and the polymer was filtered and washed three times with benzene and twice with ether to give polymer **6**; ir (KBr): 1730 cm^{-1} (CO_2R).

In a similar manner polymer **3** was allowed to react with methyl *E*-2,4-pentadienoate (**5**)[3] in toluene at 110°C for 24 h in the presence of 4-*tert*-butylcatechol (14) to yield polymer **7**; ir (KBr): 1720–1740 cm^{-1} (CO_2R).

Preparation of the Cyclohexene Diels–Alder Adducts 8 and 9 from Polymers 6 and 10, and 11 from Polymer 7

A suspension of 0.4 g of polymer **6** was cleaved with 8.5 mmol of tetra-*n*-butylammonium hydroxide in 10 mL THF (30), and the crude product was esterified with CH_2N_2. The product was purified by preparative tlc using hexane–benzene (1:1) as the eluant to give 40 mg (80%) of a mixture of compounds consisting of **8** and **9** as an oil; ir (neat): 1710–1745 (CO_2R), 1655 (C=C), 1600 (ArC=C), and 1170 cm^{-1} (C—O); nmr δ: 7.18 (m, aromatic), 5.6–5.85 (m, vinylic), 3.85 (m, PhC*H*C=C), 3.65, 3.52, and 3.47 (s, OCH_3), 1.8–2.8 (m, allylic CH_2 and CH_2).

Gas chromatography (gc) (column temperature 180°C) indicated the presence of four isomers with the following retention times: $t_1 = 8.7$, $t_2 = 9.6$, $t_3 = 11.1$, $t_4 = 12.1$.

The mass spectrum (ms) of all the four isomers, obtained directly from gc–ms, showed molecular ions at *m/e* 216 and fragment ions at 156, 115, and 91.

Using a mixture of the *cis* and *trans* isomers of **8** and also a total mixture of the four isomers of **8** and **9** obtained as reported (22), it was established (using the peak enhancement method) that the first two peaks in the gc are due to the *cis* and *trans* isomers of **8** while the latter two minor peaks are due to the *cis* and *trans* isomers of **9** (Table 1).

The mixture of **8** and **9** liberated from polymer **6** was dehydrogenated as before (22) to give a mixture containing methyl 2-phenylbenzoate (**15**) and methyl 3-phenylbenzoate (**16**). Authentic **15** and **16** were obtained by esterification with CH_2N_2 of commercially available (K & K Fine Chemicals) 2-phenyl- and 3-phenylbenzoic acids respectively. Comparison of **15** and **16** obtained via **8** and **9** with authentic **17** and **18** by gc showed the compounds to have identical retention times, t(**15**) = 9.0, t(**16**) = 16.2.

Similarly (except that the purification was done using ether–hexane (1:1) as the eluant) 1 g of polymer **7** gave 60 mg (52%) of a mixture of **10** and **11** as an oil; ir (neat): 1710–1750 (3 shoulders, CO_2R); 1660 (C=O), and 1170 cm^{-1} (C—O); nmr δ: 5.8 (m, vinylic), 3.71 and 3.69 (s, OCH_3), 1.95–2.5 (m, CH_2).

The mixture was converted to the corresponding dimethyl cyclohexanedicarboxylates using 20 mg of 10% palladium on charcoal in 3 mL ethanol under 1 atm of hydrogen. The completion of the reaction was indicated by the disappearance of the vinylic protons in the nmr spectrum.

Authentic *cis*- and *trans*-dimethyl cyclohexane-1,2-dicarboxylates (**17**) were prepared from the commercially available (Aldrich) diacids by esterification with CH_2N_2, while a mixture of *cis*- and *trans*-dimethyl cyclohexane-1,3-dicarboxylates (**18**) was obtained by oxidation (25).

The gc analysis (column temperature 150°C) indicated the presence of 3 peaks. The peak enhancement method established that the first peak (t = 7.6) is due to the *cis* and *trans* isomers of (**17**) (76.5%) and the other two peaks ($t_1 = 8.6$, $t_2 = 10.0$) are due to the *cis* and *trans* isomers of (**18**) (23.5%).

The Use of Benzyl Acrylate (14) in the Preparation of the Diels–Alder Adducts 8 and 9 from 4 and the Adducts 10 and 11 from 5

To 2 g (12.3 mmol) or benzyl acrylate (**14**), prepared by the method of Banks *et al.* (31), in 5 mL of xylene was added 2.0 g

[3]Obtained from Tridom Chemicals and redistilled before use.

Can. J. Chem. Downloaded from www.nrcresearchpress.com by 210.87.254.6 on 09/05/12
For personal use only.

(15.4 mmol) of *E*-1-phenyl-1,3-butadiene (**4**) (29) and the mixture reacted under conditions similar to those used in the preparation of polymer **6**. Xylene and the unreacted starting materials were distilled under reduced pressure. A portion of 0.3 g of the crude residue was stirred with 5 mmol of tetra-*n*-butylammonium hydroxide in 10 mL of THF for 48 h. The THF was then evaporated and the residue was diluted with 20 mL of water and washed four times with 20 mL of ether. The ether was dried over $MgSO_4$ and evaporated. No unhydrolyzed material was detected by nmr.

The water layer was acidified with HCl and extracted three times with ether. The ether was dried over $MgSO_4$ and evaporated. The product was then esterified and purified as before to yield 215 mg of the cyclohexene diesters. Analysis by gc indicated the presence of 94.4% of a mixture of *cis* and *trans* **8** and 5.6% of a mixture of *cis* and *trans* **9** (Table 1).

Similarly, 1 g (6.2 mmol) of **14** and 0.7 g (6.2 mmol) of methyl *E*-2,4-pentadienoate (**5**) were refluxed in 4 mL of toluene at 110°C for 24 h in the presence of 0.05 g of 4-*tert*-butylcatechol (14) to give a crude mixture of **10** and **11**.

Hydrolysis, hydrogenation, and esterification with CH_2N_2 of a portion of the product as before yielded a mixture containing 88.2% of a *cis* and *trans* mixture of **17** and 11.8% of a *cis* and *trans* mixture of **18**.

Preparation of Polymer-bound Propiolate 21 and Phenyl Propiolate 22

In a typical experiment, 3.5 g of **1**, 2.2 mL (35 mmol) of propiolic acid (**19**), and ~0.2 g of *p*-toluenesulfonic acid (32) in 150 mL benzene were placed in a round-bottomed flask of a Soxhlet extractor in which molecular sieves (3 Å) had been placed in a thimble. The suspension was refluxed for 24 h. The polymer was then filtered and washed twice with benzene, twice with methanol, once with water, once with methanol, once with dioxane, and twice with ether to give the polymer-bound propiolate (**21**); ir (KBr): 3280 (C≡C—H), 2140(C≡C), and 1715 cm^{-1} (CO_2R).

Similarly, **1** reacted with phenyl propiolic acid (**20**) to give the polymer-bound phenyl propiolate (**22**); ir (KBr): 2240 (C≡C—Ph) and 1710–1730 cm^{-1} (CO_2R).

Base hydrolysis of polymers **21** and **22** with tetra-*n*-butylammonium hydroxide in THF yielded regenerated polymer **1** and the respective propiolic acid from which the loading capacities of **21** and **22** were determined. Thus polymers **21** and **22** contained 0.43 mmol/g of **19** and 0.48 mmol/g of **20** respectively.

Preparation of the Polymer-bound 1,3-Dipolar Adducts 23 and 24

A suspension of 2.5 g polymer-bound propiolate (**19**) and 2.7 g (17.5 mmol) of benzohydroximoyl chloride (33) in 75 mL of dry THF was cooled in an ice bath under an argon atmosphere. To this mixture, 2.8 mL (20 mmol) of freshly distilled triethylamine in 15 mL of dry THF was added dropwise while stirring during a 20 min period. After the addition the reaction mixture was cooled for another hour and then allowed to warm to room temperature and stirred for 20 h. The polymer was filtered and washed twice with THF, twice with methanol, once with water, twice with dioxane, and twice with ether. The ir spectrum of **23** exhibited a band at 1740 cm^{-1} (CO_2R) and no absorptions at 3280 and 2140 cm^{-1} due to residual propiolate.

Similarly, polymer **22** was allowed to react with benzonitrile oxide, prepared *in situ* as above. After the reaction mixture was stirred for 20 h at room temperature a second equivalent amount of benzohydroximoyl chloride was added to the solution. The addition of the triethylamine was repeated as before and the reaction mixture was stirred at room temperature for another 20 h. The ir spectrum of 24 exhibited a band at 1730 cm^{-1} and no band at 2240 cm^{-1} (C≡C—Ph).

Preparation of Methyl 3-Phenylisoxazole-5-carboxylate 25 and Methyl 3,5-Diphenylisoxazole-4-carboxylate (26)

A suspension of 2.5 g of polymer **23** was cleaved with tetra-*n*-butylammonium hydroxide in THF and the product was esterified with CH_2N_2 as before to yield 256 mg of crude methyl 3-phenylisoxazole-5-carboxylate (**25**) as a solid. The solid was recrystallized from methanol to give 175 mg of pure **25**, mp 108–109°C (lit. (27) mp 109–110°C); ir (KBr): 1730(CO_2R), 1602, 1592, 1577 (phenyl and isoxazole ring), and 1150 cm^{-1} (C—O); nmr δ: 7.37–7.9 (m, 5, aromatic *H*), 7.25 (s, 1, *H*C=C), 4.0 (s, 3, OCH_3); ms *m/e*: 203(88) (M^+), 116(72) 104(100), 77(83).

Similarly, **24** yielded methyl 3,5-diphenylisoxazole-4-carboxylate (**26**) (27), mp 97–98°C (lit. (27) mp 98–99°C); ir (KBr): 1725 (CO_2R), 1610, 1595, 1570 (phenyl and isoxazole ring), and 1130 (C—O); nmr δ: 7.25–7.98 (m, 10, aromatic *H*), 3.67 (s, 3, OCH_3): ms *m/e*: 279(18) (M^+), 142(100), 115(95), 77(78).

Preparation of Isoxazoles 25, 26, and 28 from the Solution 1,3-Dipolar Addition to Benzyl Propiolate (29) and Benzyl Phenylpropiolate (30)

A solution of 1 g (6.25 mmol) of benzyl propiolate (**29**) (34), prepared in the same manner as **21**, was treated with the equivalent amount of benzonitrile oxide using the same procedure as used for the preparation of polymer **23**. After the reaction was completed the THF or toluene was evaporated and the crude residue was dissolved in 20 mL of ether. The ether layer was washed three times with water, dried over $MgSO_4$ and the ether evaporated. A portion of 0.32 g of the crude product was then hydrolyzed with tetra-*n*-butylammonium hydroxide in THF and esterified with CH_2N_2 as before to yield 165 mg of crude **25** as the sole product, which was then purified on preparative tlc using benzene–hexane (6:4) as the eluant to give 100 mg of pure **25**.

Benzyl phenylpropiolate (**30**) was prepared by a described method for related compounds (32). The product was distilled at 160°C at 0.03 Torr to give **30** in 50% yield; ir (neat): 2200 (C≡C), 1700–1730 (CO_2R), and 1590–1610 cm^{-1} (phenyl); nmr δ: 7.32 (m, 10, aromatic *H*) and 5.17 (s, 2H, PhCH_2O_2C); ms *m/e*: 236(10) (M^+), 129(98), 102(100), 91(99), 77(40). *Anal.* calcd. for $C_{16}H_{12}O_2$: C 81.34, H 5.12; found: C 81.19, H 5.10.

In a manner similar to that described for **29**, **30** was allowed to react twice with equivalent amounts of benzonitrile oxide using the procedure used for the preparation of polymer **24**. Base hydrolysis and an identical work-up as above gave a mixture of products. The composition of the mixture was determined by the O—CH_3 singlets absorption in the nmr spectrum and was found to consist of 41% of **26**, 51% of **28**, and 8% of methyl phenylpropiolate; ir (KBr): 1705–1725 (CO_2R), 1610, 1590, 1570, and 1490 (phenyl and isoxazole ring), and 1120 cm^{-1} (C—O); nmr δ: 7.75–8.05 (m, *ortho*-aromatic *H*), 7.3–7.57 (m, aromatic *H*), 3.88, 3.8, and 3.67 (s, OCH_3). In one experiment toluene was used as solvent instead of THF to give a mixture consisting of **26** and **28** in a 28:72 ratio.

Acknowledgement

We are grateful for the financial assistance of the Natural Sciences and Engineering Research Council of Canada for the support of this research.

1. C. C. LEZNOFF and V. YEDIDIA. Can. J. Chem. **58**, 287 (1980).
2. P. M. WORSTER, C. R. MCARTHUR, and C. C. LEZNOFF. Angew. Chem. **91**, 255 (1979); Angew. Chem. Int. Ed. Engl. **18**, 221 (1979).
3. S. J. BLAZKA and H. J. HARWOOD. Polym. Prepr. Am.

Chem. Soc. Div. Polym. Chem. **16**, 633 (1975); S. J. BLAZKA. Diss. Abstr. Int. B, **37**, 2285 (1976).
4. T. J. NIEUWSTAD, A. P. G. KIEBOOM, A. J. BREIJER, J. VAN DER LINDEN, and H. VAN BEKKUM. Recl. Trav. Chim. Pays-Bas, **95**, 225 (1976).
5. J. REBEK and F. GAVIÑA. J. Am. Chem. Soc. **96**, 7112 (1974); F. GAVIÑA, P. GIL, and B. PALAZÓN. Tetrahedron Lett. 1333 (1979).
6. C. C. LEZNOFF and J. Y. WONG. Can. J. Chem. **51**, 3756 (1973).
7. C. C. LEZNOFF and W. SYWANYK. J. Org. Chem. **42**, 3203 (1977).
8. C. C. LEZNOFF and T. M. FYLES. J. Chem. Soc. Chem. Commun. 251 (1976); C. C. LEZNOFF, T. M. FYLES, and J. WEATHERSTON. Can. J. Chem. **55**, 1143 (1977); T. M. FYLES, C. C. LEZNOFF, and J. WEATHERSTON. Can. J. Chem. **55**, 4135 (1977); T. M. FYLES, C. C. LEZNOFF, and J. WEATHERSTON. J. Chem. Ecol. **4**, 109 (1978); P. I. SVIRSKAYA, C. C. LEZNOFF, J. WEATHERSTON, and J. E. LAING. J. Chem. Eng. Data, **24**, 152 (1979).
9. M. FRIDKIN, A. PATCHORNIK, and E. KATCHALSKI. J. Am. Chem. Soc. **87**, 4646 (1965); J. I. CROWLEY and H. RAPOPORT. J. Am. Chem. Soc. **92**, 6363 (1970); F. CAMPS, J. CASTELLS, and J. PI. AN. Quim. **70**, 848 (1974); J. M. VANEST, M. GORSANE, V. LUBERT, J. PECHER, and R. H. MARTIN. Chimia, **29**, 343 (1975); C. C. LEZNOFF and P. I. SVIRSKAYA. Angew. Chem. **90**, 1001 (1978); Angew. Chem. Int. Ed. Engl. **17**, 947 (1978).
10. C. C. LEZNOFF. Acc. Chem. Res. **11**, 327 (1978).
11. K. N. HOUK. J. Am. Chem. Soc. **95**, 4092 (1973); O. EISENSTEIN, J. M. LEFOUR, N. T. ANH, and R. F. HUDSON. Tetrahedron, **33**, 523 (1977).
12. J. FEUER, W. C. HERNDON, and L. H. HALL. Tetrahedron, **24**, 2575 (1968).
13. K. N. HOUK. Acc. Chem. Res. **8**, 361 (1975).
14. L. E. OVERMAN, G. F. TAYLOR, K. N. HOUK, and L. N. DOMELSMITH. J. Am. Chem. Soc. **100**, 3182 (1978).
15. S. DANISHEFSKY, M. P. PRISBYLLA, and S. HINER. J. Am. Chem. Soc. **100**, 2918 (1978).
16. J. I. CROWLEY and H. RAPOPORT. Acc. Chem. Res. **9**, 135 (1976).
17. R. B. MERRIFIELD. J. Am. Chem. Soc. **85**, 2149 (1963); R. L. LETSINGER and M. J. KORNET. J. Am. Chem. Soc. **85**, 3045 (1963).
18. R. HUISGEN. J. Org. Chem. **41**, 403 (1976).
19. M. CHRISTL and R. HUISGEN. Chem. Ber. **106**, 3345 (1973).
20. J. M. STEWART and J. D. YOUNG. Solid phase peptide synthesis. W. H. Freeman Ltd., San Francisco, CA. 1969. pp. 27–28; J. M. J. FRÉCHET, M. D. DE SUET, and M. J. FARRALL. J. Org. Chem. **44**, 1774 (1979).
21. J. S. MEEK, F. J. LORENZ, and S. J. CRISTOL. J. Am. Chem. Soc. **71**, 1830 (1949).
22. I. N. NAZAROV, A. TITOV, and A. I. KUZNETSOVA. Izz. Akad. Nauk SSSR, 1224 (1959).
23. J. M. GOLDWASSER and C. C. LEZNOFF. Can. J. Chem. **56**, 1562 (1978).
24. C. C. LEZNOFF and J. M. GOLDWASSER. Tetrahedron Lett. 1875 (1977).
25. E. J. COREY and G. SCHMIDT. Tetrahedron Lett. 399 (1979).
26. K. BUST, M. CHRISTL, R. HUISGEN, W. MACK, and R. SUSTMANN. Chem. Ber. **106**, 3258 (1973).
27. M. CHRISTL, R. HUISGEN, and R. SUSTMANN. Chem. Ber. **106**, 3275 (1973).
28. S. L. REGEN. J. Am. Chem. Soc. **96**, 5275 (1974).
29. I. E. MUSKAT and M. HERRMAN. J. Am. Chem. Soc. **53**, 252 (1931); O. GROMMITT and F. J. CHRISTOPH. J. Am. Chem. Soc. **73**, 3479 (1951).
30. T. M. FYLES, C. C. LEZNOFF, and J. WEATHERSTON. Can. J. Chem. **56**, 1031 (1978).
31. A. R. BANKS, R. F. FIBIGER, and T. JONES. J. Org. Chem. **42**, 3965 (1977).
32. T. HORIUCHI, A. FUJINAMI, K. NOTERA, T. OZAKI, S. YAMAMOTO, T. WAKATSUKI, and Y. NISHIZAWA. Chem. Abstr. **74**, 125196*c* (1971).
33. A. WERNER and H. BUSS. Chem. Ber. **27**, 2193 (1894).
34. J. H. BOWIE, D. H. WILLIAMS, P. MADSEN, G. SCHROLL, and S. O. LAWESSON. Tetrahedron, **23**, 306 (1967).

Can. J. Chem. Downloaded from www.nrcresearchpress.com by 210.87.254.6 on 09/05/12
For personal use only.

Can. J. Chem. Downloaded from www.nrcresearchpress.com by 210.87.254.105 on 09/05/12
For personal use only.

COMMUNICATION

Dissociation kinetics of potassium anion in methylamine

Y. HARIMA, H. KURIHARA, AND S. AOYAGUI[1]

Faculty of Engineering, Tokyo Institute of Technology, Ohokayama, Meguro-ku, 152 Tokyo, Japan

Received January 2, 1980

Y. HARIMA, H. KURIHARA, and S. AOYAGUI. Can. J. Chem. **58**, 1151 (1980).

The potential-sweep voltammograms of solvated electrons in methylamine containing KI as the supporting electrolyte demonstrate the coexistence of one- and two-electron species in equilibrium. The $it^{1/2}$ vs. log t curve obtained with potential-step chronoamperometry exhibits a transient part between two plateaux. The analysis of this curve yields the approximate value of 10^2 s^{-1} for the first-order rate constant of the dissociation of the two-electron species, K^-.

Y. HARIMA, H. KURIHARA et S. AOYAGUI. Can. J. Chem. **58**, 1151 (1980).

On a mesuré les voltammogrammes à variation linéaire de potentiel des électrons solvatisées dans la méthylamine qui contient le KI comme l'électrolyte. Ils démontrent la coexistence des espèces à un- et deux-électrons en équilibre. La courbe $it^{1/2}$ vs. log t qui a été tracée à l'aide de la chronoampèrométrie exhibe une région de passage entre deux plateaux. Faisant l'analyse de cette courbe, on a obtenu ainsi la valeur approximative de 10^2 s^{-1} pour la constante du premier ordre de la dissociation des espèces à deux-électrons, K^-.

Dissolution of alkali metals, M, into certain amines, amides or ethers and pulse radiolysis of alkali amides in these solvents yield various chemical species that may be called alkali metal species or solvated electron species. They may be any of the one-electron species, e.g. e_s^- and $(M^+ \cdot e_s^-)$, and the two-electron species, e.g. $(M^+ \cdot e_s^-)_2$ and M^-, where e_s^- is the free solvated electron and the parentheses mean the ion-pair. Kinetic studies on the formation of these species in amines and ethers have recently been developed extensively by means of pulse radiolysis in conjunction with optical detection of the reactants or products (1). This technique, however, has no potentiality in the direct measurement of dissociation rates. It has been obtained only indirectly by using the dissociation constant. When the optical distinction of alkali metal species is hardly possible, as is the case with liquid ammonia solutions (2), the formation rate constant cannot be obtained even with the pulse radiolysis technique. An attempt was made to measure the dissociation rate constant in this solvent by an electrochemical method, but it was beyond the accessible limit of this technique (3).

This note deals with the potential-step chronoamperograms and potential-sweep voltammograms of solvated electrons in methylamine containing KI. They indicate the electron-transfer process coupled with a chemical reaction, consequently promising the electrochemical elucidation of the dissociation kinetics of the two-electron species, possibly K^-. In this solvent the formation process of K^- from e_s^- and K^+ is too slow to be followed by pulse radiolysis (4).

Methylamine was prepared and purified according to the method of Yamamoto *et al.* (5). The procedures of handling the solvent and preparing KI solutions were the same as described elsewhere (3). An air-tight electrolysis cell was used. Solvated electrons were generated by electrolysis. Potential-sweep voltammetric and potential-step chronoamperometric experiments were carried out in the way described previously (3). In all chronoamperometric experiments the electrode potential was stepped by 100 mV towards the anodic direction from the equilibrium potential. Measurements were made at -50 ± 1°C.

Figure 1 shows log i vs. E plots in potential-sweep voltammetry of the cathodic generation of solvated electrons in a 0.5 M KI solution of methylamine, where i and E are respectively the current density and the electrode potential. The experimental points in region I lie on a straight line whose slope is equal to that of the diffusion-controlled electron-transfer process with $n = 1$, n being the number of electrons transferred. In region II, they come to deviate from it and tend to lie on a straight line with $n = 2$. These curves have the same characteristics as those obtained with liquid ammonia solutions (3), except that the current density at which the straight lines of $n = 1$ and 2 cross is two orders of magnitude lower than the corresponding one in the latter curves. In liquid ammonia it has been concluded that a two-electron species is

[1]To whom all correspondence should be addressed.

0008-4042/80/111151-03$01.00/0

©1979 National Research Council of Canada/Conseil national de recherches du Canada

Can. J. Chem. Downloaded from www.nrcresearchpress.com by 210.87.254.105 on 09/05/12
For personal use only.

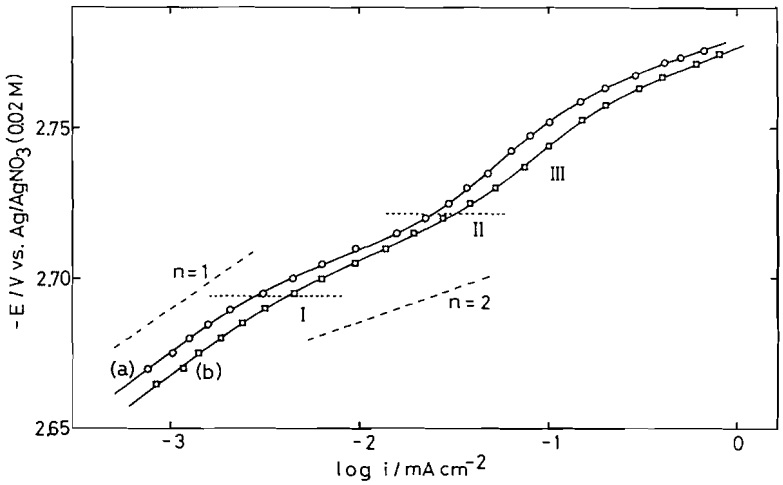


FIG. 1. Plots of log i vs. E in potential-sweep voltammetry for the cathodic generation of solvated electrons in 0.5 M KI solutions of methylamine at −50°C. Sweep rate: (*a*) 12.5 and (*b*) 25.0 mV s^{-1}. Broken lines show the theoretical slopes for the n-electron transfer reactions.

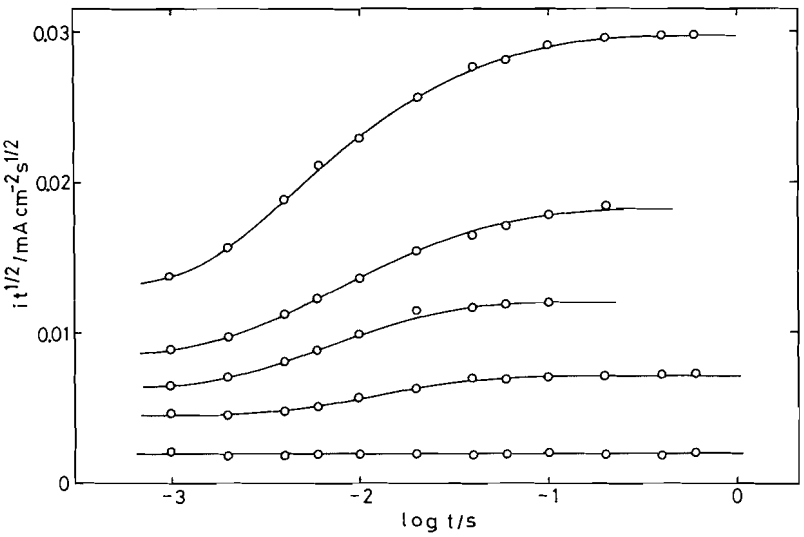


FIG. 2. Plots of $it^{1/2}$ vs. log t in potential-step chronoamperometry for the oxidation of 0.005 (lowermost)–0.1 (uppermost) mM solvated electrons in 0.5 M KI solutions of methylamine at −50°C. Potential-step height: +100 mV.

formed at potentials of region II, on the basis of such log i vs. E curves and also some other findings (3). From its analogy, it is very likely that the region II reaction in methylamine is also the formation of certain two-electron species.

Although region III is beyond the scope of this work, the concomitance of the potassium deposition may be strongly suggested by the poor reproducibility of the curves in this region and the poor solubility of this metal (6). It will be discussed in a separate paper on the basis of cyclic voltammetry.

Since it prevails to consider that the most probable two-electron species in alkylamines is M^- (7), the following reaction schemes can be written for regions I and II.

Region I:

$$[1]\qquad \begin{aligned} e_M^- &\rightleftharpoons e_s^- \\ e_s^- + K^+ &\underset{k_1}{\rightleftharpoons} (K^+ \cdot e_s^-) \end{aligned}$$

Region II:

$$[2]\qquad \begin{aligned} 2e_M^- &\rightleftharpoons 2e_s^- \\ 2e_s^- + 2K^+ &\rightleftharpoons 2(K^+ \cdot e_s^-) \underset{k_2}{\rightleftharpoons} K^- + K^+ \end{aligned}$$

where e_M^- is the electron in electrode metal and k's are the rate constants.

Figure 2 shows $it^{1/2}$ vs. log t plots in potential-step chronoamperometry obtained with 0.5 M KI solutions whose total solvated electron concentra-

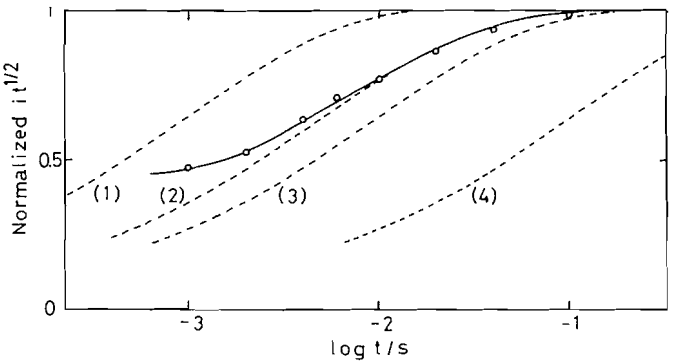


FIG. 3. Normalized $it^{1/2}$ vs. log t curves in potential-step chronoamperometry calculated with various α values. The circles reproduce the uppermost plot in Fig. 2. α = (*1*) 100, (*2*) 20, (*3*) 10, and (*4*) 1 s^{-1}.

tion, c_t, ranges from ca. 0.005 to 0.1 m*M*. In the lowermost curve corresponding to region I, the $it^{1/2}$ values are independent of time, as in liquid ammonia. This fact suggests that the electrode reaction in the solution containing only one-electron species is seemingly a simple diffusion-controlled process and the lower limit of the dissociation rate constant of $(K^+ \cdot e_s^-)$ is thus around 10^3 s^{-1} which is the reciprocal of the time-window of the technique employed. In solutions of higher c_t where K^- coexists with the one-electron species, e_s^- and $(K^+ \cdot e_s^-)$, each $it^{1/2}$ vs. log t curve has two plateaux and a transient region between them. At the first plateau the current density is considered to be controlled by the diffusuion of the one-electron species. The increase in $it^{1/2}$ with time in the transient region may be attributed to the kinetic current due to the formation of $(K^+ \cdot e_s^-)$ from K^-. For the sake of convenience in analysis, eq. [2] is rewritten in the following schematic form:

$$[3] \quad \begin{matrix} B \overset{k}{\rightleftharpoons} 2A \\ A \pm e_M^- \rightarrow C \end{matrix}$$

where k is the rate constant and B and A correspond respectively to K^- and the composite species whose concentration and diffusion coefficient are $[e_s^-] + [(K^+ \cdot e_s^-)]$ and D_{av}, respectively. Here the brackets mean the concentration and D_{av} the weighted mean of the diffusion coefficients of e_s^- and $(K^+ \cdot e_s^-)$. Figure 3 shows a comparison between the normalized experimental plot of $it^{1/2}$ vs. log t reproduced from the uppermost curve in Fig. 2 and the theoretical curve calculated from the analytical equation given by Tokuda and Matsuda (8) with various values for the parameter α defined by

$$[4] \quad \alpha = (1/3\pi)(D_A/D_B)([A]/[B])k$$

or in terms of $[e_s^-]$ and $[(K^+ \cdot e_s^-)]$, by

$$[5] \quad \alpha = (1/3\pi)(D_{av}/D_{K^-})k_2[K^+]([e_s^-] + [(K^+ \cdot e_s^-)])/[K^-]$$

where D's are the diffusion coefficients of the species subscript. The experimental curve was fitted best with the theoretical one of $\alpha = 20$ s^{-1}. The pseudo-first-order rate constant for the dissociation of K^-, $k = k_2[K^+]$, thus obtained was around 10^2 s^{-1}. The disagreement at low $it^{1/2}$ values may arise because the analytical equation was derived under the condition $[A]/[B] \ll 1$ which was not realized in the test solutions employed.

1. J. W. FLETCHER and W. A. SEDDON. J. Phys. Chem. **79**, 3055 (1975).
2. G. RUBINSTEIN, T. R. TUTTLE, JR., and S. GOLDEN. J. Phys. Chem. **77**, 2872 (1973).
3. Y. HARIMA and S. AOYAGUI. Israel J. Chem. **18**, 81 (1979).
4. J. W. FLETCHER, W. A. SEDDON, J. J. JEVCAK, and F. C. SOPCHYSHYN. Can. J. Chem. **57**, 3571 (1975).
5. M. YAMAMOTO, Y. NAKAMURA, and M. SHIMOJI. Trans. Faraday Soc. **67**, 2292 (1971).
6. Y. NAKAMURA, M. YAMAMOTO, S. SHIMOKAWA, and M. SHIMOJI. Bull. Chem. Soc. Jpn. **44**, 3212 (1971).
7. S. MATALON, S. GOLDEN, and M. OTTOLENGHI. J. Phys. Chem. **73**, 3098 (1969).
8. K. TOKUDA and H. MATSUDA. Rev. Polarogr. Kyoto, **25**, 15 (1979) (Abstracts of the 25th Polarographic Meeting, Kobe).

Can. J. Chem. Downloaded from www.nrcresearchpress.com by 210.87.254.105 on 09/05/12
For personal use only.

Canadian Journal of Chemistry
Published by
THE NATIONAL RESEARCH COUNCIL OF CANADA

Journal canadien de chimie
Publié par
LE CONSEIL NATIONAL DE RECHERCHES DU CANADA

Volume 58 Number 12 June 15, 1980 Volume 58 numéro 12 15 juin 1980

Can. J. Chem. Downloaded from www.nrcresearchpress.com by 210.87.254.6 on 09/05/12
For personal use only.

Water attack at an sp^2 hybridized-carbon: the hydroxyl σ-complex of 4,6-dinitrobenzofuroxan in water–DMSO–tetramethylammonium chloride mixtures

FRANÇOIS TERRIER
Département de Chimie, Faculté des Sciences de Rouen, F 76130, Mont Saint Aignan, France

AND

HABIB ACHASSI SORKHABI, FRANÇOIS MILLOT, JEAN-CLAUDE HALLE, AND ROBERT SCHAAL
Laboratoire de Physicochimie des Solutions, LA CNRS 161, E.N.S.C.P. 11 rue Pierre et Marie Curie F 75231, Paris, France

Received December 5, 1979

FRANÇOIS TERRIER, HABIB ACHASSI SORKHABI, FRANÇOIS MILLOT, JEAN-CLAUDE HALLE, and ROBERT SCHAAL. Can. J. Chem. **58**, 1155 (1980).

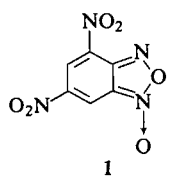
The kinetics of formation and decomposition of the hydroxyl-σ adduct **2** derived from 4,6-dinitrobenzofuroxan **1** have been studied in various water – dimethylsulphoxide (DMSO) – tetramethylammonium chloride ($I = 0.5\ M$) mixtures. At pH < 7, the formation of **2** occurs exclusively from water attack at the 7-carbon of **1**. This process is strongly favored by DMSO: the first-order rate constant $k_1^{H_2O}$ changes from $1.9 \times 10^{-2}\ s^{-1}$ in water to $1.33\ s^{-1}$ in 90% DMSO. Taking into account the decrease in the water content of the solutions, and assuming that only one water molecule participates in the reaction, this increase in $k_1^{H_2O}$ reflects a 10^3-fold increase in the ability of a water molecule to act as a nucleophile. This interesting result compares well with previous data reported by Murto for the solvolysis of 2,4-dinitrofluorobenzene in the same solvent mixtures.

FRANÇOIS TERRIER, HABIB ACHASSI SORKHABI, FRANÇOIS MILLOT, JEAN-CLAUDE HALLE et ROBERT SCHAAL. Can. J. Chem. **58**, 1155 (1980).

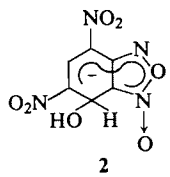
La formation et la décomposition du complexe hydroxylé **2** dérivé du dinitro-4,6 benzofuroxanne **1** ont été étudiées cinétiquement dans divers mélanges eau – diméthylsulfoxide – chlorure de tétraméthylammonium ($I = 0.5\ M$). Aux pH < 7, la formation de **2** résulte exclusivement de l'attaque de l'eau sur le carbone-7 de **1**. Cette réaction est très accélérée par le DMSO: la constante du premier ordre $k_1^{H_2O}$ est égale à $1.9 \times 10^{-2}\ s^{-1}$ dans l'eau et $1.33\ s^{-1}$ dans 90% DMSO. En tenant compte de la diminution de la concentration de l'eau des solutions et en supposant qu'une seule molécule d'eau participe à la réaction, on constate que cette augmentation de $k_1^{H_2O}$ reflète en réalité une augmentation de l'ordre de 1000 de la nucléophilie de l'eau. Ce résultat est en bon accord avec les données précédemment publiées par Murto pour la solvolyse du dinitro-2,4 fluorobenzène dans les mêmes mélanges.

Introduction

In aqueous solution, 4,6-dinitrobenzofuroxan **1** gives a very stable Meisenheimer-type complex which was previously identified by nmr and visible spectroscopy and which is completely formed at pH 5.5 (1). The kinetics of formation and decomposition of **2** have been thoroughly investigated between pH 1 and 13 ($I = 0.2\ M$) in pure water (1). The results showed that the formation of **2** arises exclusively from the attack of water molecules on the parent substrate **1** at pH < 7. Since there is no other report of this kind in the field of Meisenheimer complexes, it was of interest to study this reaction in water–DMSO mixtures. Such a study should provide information on the extent to which DMSO may affect the ability of water to act as a nucleophile in a nucleophilic aromatic substitution reaction. The results are compared with the data obtained for the solvolysis of 2,4-dinitrofluorobenzene in the same solvent mixtures (2).



1



2

0008-4042/80/121155-06$01.00/0
©1980 National Research Council of Canada/Conseil national de recherches du Canada

Can. J. Chem. Downloaded from www.nrcresearchpress.com by 210.87.254.6 on 09/05/12
For personal use only.

Results

4,6-Dinitrobenzofuroxan **1** ($\lambda_{max}^{water} = 415$ nm, $\varepsilon = 7050\ M^{-1}\ cm^{-1}$) behaves similarly in water and water–DMSO–NMe_4Cl 0.5 *M* mixtures and gives rapidly the very stable yellow-colored complex **2** ($\lambda_{max}^{water} = 462.5$ nm, $\varepsilon = 24\,400\ M^{-1}\ cm^{-1}$) according to Scheme 1.

$$[1]\quad \mathbf{1} + H_2O \underset{k_{-1}}{\overset{k_1^{H_2O}}{\rightleftharpoons}} \mathbf{2} + H^+ \qquad K_a = [\mathbf{2}][H^+]/[\mathbf{1}]$$

$$[2]\quad \mathbf{1} + OH^- \underset{k_{-2}}{\overset{k_2}{\rightleftharpoons}} \mathbf{2} \qquad k_2 = [\mathbf{2}]/[\mathbf{1}][OH^-]$$

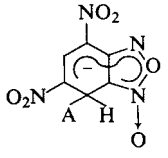
SCHEME 1

The thermodynamics and kinetics of formation and decomposition of **2** have been investigated in mixtures containing 30, 50, 70, 80, and 90% DMSO (by volume). Dilute hydrochloric acid solutions, various buffer solutions, and dilute tetramethylammonium hydroxide solutions were used. The ionic strength *I* was always kept constant at 0.5 *M* by adding tetramethylammonium chloride as needed. The solutions were the same as those recently used to build an acidity scale in water–DMSO–NMe_4Cl mixtures ($I = 0.5\ M$) (3). The pH values are relative to the standard state in this ternary solvent.

The pH values corresponding to the half-formation of **2** in every solvent mixture have been determined by plotting the variations at 465 nm of the optical density obtained at equilibrium as a function of pH. These $pH_{1/2}$ values, which denote the pH at which the parent molecule **1** and the complex **2** are present at equal concentrations, correspond to the pK_a values for the reversible formation of **2** (reaction [1]). The K_a values are summarized in Table 2 together with the values of the equilibrium constant K_2 calculated from eq. [3]; K_S^I is the autoprotolysis constant of water–DMSO mixtures containing Me_4NCl at the ionic strength 0.5 *M* (3*a*).

$$[3]\quad K_a = K_2 K_S^I$$

Kinetic determinations were carried out over a large pH range of 1–13 in 30 and 50% DMSO. The logarithmic values of the observed first-order rate constant k_{obsd} for the combined formation and decomposition of **2** in these solvent mixtures are plotted in Fig. 1 as a function of pH. Also presented are the k_{obsd} values measured in water at the same ionic strength ($I = 0.5\ M$). At the low buffer concentrations used in this study ($[A^-] + [AH] \leq 4 \times 10^{-2}$), no appreciable catalysis of the reactions was observed for the most acidic buffers (chloroacetate, 2-chlorobenzoate, benzoate, acetate). In contrast, we could detect some catalysis by the basic species A^- of the phosphate, 2-cyano, and 4-cyano phenoxide buffers in the three solvents. The k_{obsd} values used between pH 6 and 8.5 in the pH-rate profiles of Fig. 1 were therefore those extrapolated to zero buffer concentrations, but we did not further investigate this catalysis. The influence of the phenol buffers used above pH 8.5 (2-bromo phenol, 4-chloro phenol, and phenol) was different. The oscilloscope pictures taken in a stopped-flow apparatus revealed that the appearance of **2** is preceded by the very fast formation of short-lived species which are presumably the Meisenheimer-type adducts **3** arising from nucleophilic attack of the phenoxide anions A^- at the 7-carbon of **1** (1, 4–6). Because of these reactions, we were not able to perform measurements of k_{obsd} in these buffers. The k_{obsd} values at pH > 11 were measured in tetramethylammonium hydroxide solutions.



3

In 70, 80, and 90% DMSO, all the organic buffers, including carboxylate buffers, appeared to react with **1**. As a consequence, our kinetic determinations were confined to the hydrochloric acid solutions. The corresponding k_{obsd} values are summarized in Table 1.

The rate constant k_{obsd} reflects the rate of approach to equilibrium between **1** and **2** and is the sum of the individual pseudo-first-order rate constants k_f and k_d for the formation and decomposition of **2** respectively. As shown previously (1) k_f and k_d may be calculated from eqs. [4] and [5]. Figures 2 and 3 show the pH–rate profiles of k_f and k_d in various water–DMSO mixtures.

$$[4]\quad k_f = \frac{k_{obsd}}{1 + 10^{-pH}/10^{-pH_{1/2}}}$$

$$[5]\quad k_d = \frac{k_{obsd}}{1 + 10^{-pH_{1/2}}/10^{-pH}}$$

These pH–rate profiles are consistent with eqs. [6] and [7]:

$$[6]\quad k_f = k_1^{H_2O} + k_2[OH^-] = k_1^{H_2O} + k_2 K_S^I/[H^+]$$

$$[7]\quad k_d = k_{-1}[H^+] + k_{-2}$$

Scheme 1 shows the reactions to which the various constants, viz. k_2 and $k_1^{H_2O}$, refer to hydroxide ion and water attack of **1**, respectively, while k_{-2} and k_{-1} refer to non-catalyzed and H^+-catalyzed

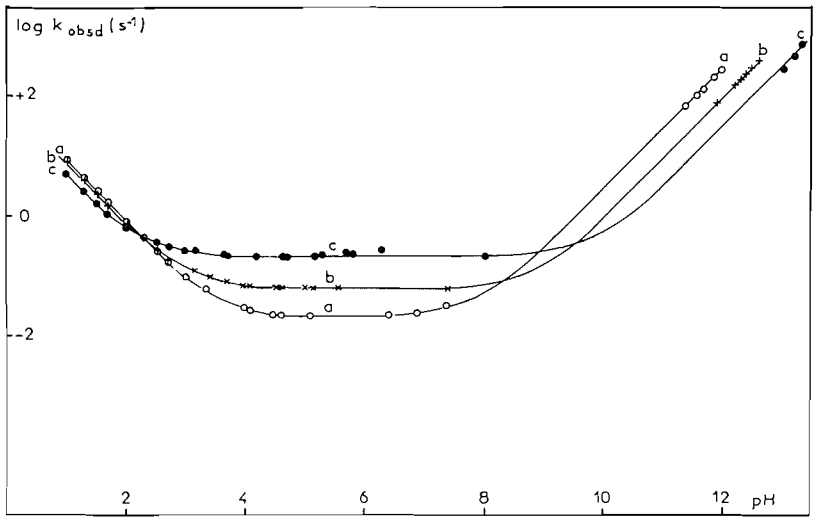


FIG. 1. pH dependence of k_{obsd} (s^{-1}) for the formation and decomposition of the adduct **2** in water – DMSO – tetramethylammonium chloride ($I = 0.5$ *M*) mixtures at 20°C. The plots *a*, *b*, *c* refer to water, 30% DMSO – 70% water, and 50% DMSO – 50% water (v/v), respectively.

TABLE 1. Experimental and calculated pseudo-first-order rate constants k_{obsd}, k_f, and k_d for the formation and/or decomposition of the adduct **2** in 70% – 30%, 80% – 20%, and 90% – 10% DMSO–water (v/v) mixtures ($I = 0.5$ *M* NMe_4Cl, $t = 20$°C)

70% DMSO $pK_a = 1.75$, $pK_s^I = 18.06$				80% DMSO $pK_a = 1.48$, $pK_s^I = 19.94$				90% DMSO $pK_a = 1.50$, $pK_s^I = 22.36$[a]			
pH	k_{obsd} (s^{-1})	$k_f \times 10^2$ (s^{-1})	k_d (s^{-1})	pH	k_{obsd} (s^{-1})	$k_f \times 10^2$ (s^{-1})	k_d (s^{-1})	pH	k_{obsd} (s^{-1})	$k_f \times 10^2$ (s^{-1})	k_d (s^{-1})
1	3.93	59.3	3.34	0.70	8.45	120	7.25	0.71	9.52	132	8.19
1.12	3.11	59.1	2.52	0.82	6.33	113	5.19	0.83	7.70	135	6.35
1.30	2.30	60.2	1.70	1.00	4.64	115	3.49	1.01	5.00	122	3.78
1.40	2.02	62.4	1.40	1.30	3.03	120	1.82	1.16	4.02	126	2.76
1.52	1.68	62.2	1.06	1.52	2.34	122	1.12	2.01	1.96	149	0.463
1.70	1.39	65.5	0.735	1.70	2.10	131	0.79				
2.00	1.04	66.5	0.374								
2.30	0.87	67.8	0.191								

[a] pK_s^I unknown at $I = 0.5$ *M*; $pK_s^I = 22.36$ at $I = 0.2$ *M* (3*a*).

decomposition of **2**, respectively. In water, 30 and 50% DMSO, the various rate coefficients were easily determined from the linear portions of each of k_f and k_d pH–rate profiles (high and low pH regions of each, respectively). In 70, 80, and 90% DMSO where our measurements were limited to the acidic region, the k_f and k_d pH–rate profiles are identical to a plateau and a straight line of slope −1 which give the $k_1^{H_2O}$ and k_{-1} values respectively. The various rate coefficients are summarized in Table 2. Also given are the K_a values calculated from the ratio $k_1^{H_2O}/k_{-1}$; as can be seen, they are in good agreement with those thermodynamically determined.

Discussion

The pK_a for formation of the adduct **2** changes from 3.62 in water to 1.5 in 90% DMSO. This 130-fold increase in K_a is due to the well-known tendency of DMSO to stabilize large polarizable anions such as **2** (7–12). Because of the strong dependence of the ionic product K_S^I upon the DMSO concentration (3*a*), the increased stabilization of **2** is, however, best measured by looking at the changes in the equilibrium constant K_2. As can be seen in Table 2, K_2 increases by a factor of 10^8 when going from water to 80% DMSO. This is the consequence of an increase in the rate constant k_2 for hydroxide ion attack on **1** and a concomitant de-

Can. J. Chem. Downloaded from www.nrcresearchpress.com by 210.87.254.6 on 09/05/12
For personal use only.

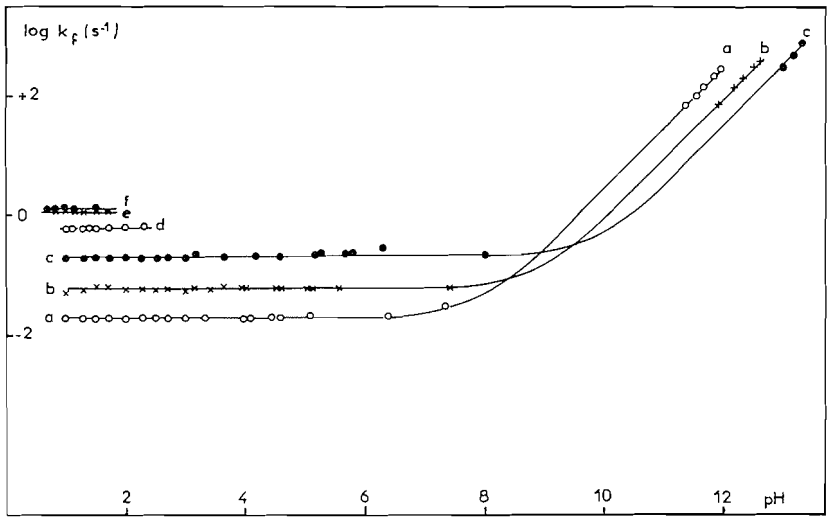


FIG. 2. pH dependence of k_f (s^{-1}) for the formation of the adduct **2** at 20°C. The plots *a, b, c, d, e, f* refer to water, and the mixtures containing 30, 50, 70, 80, and 90% DMSO by volume, respectively.

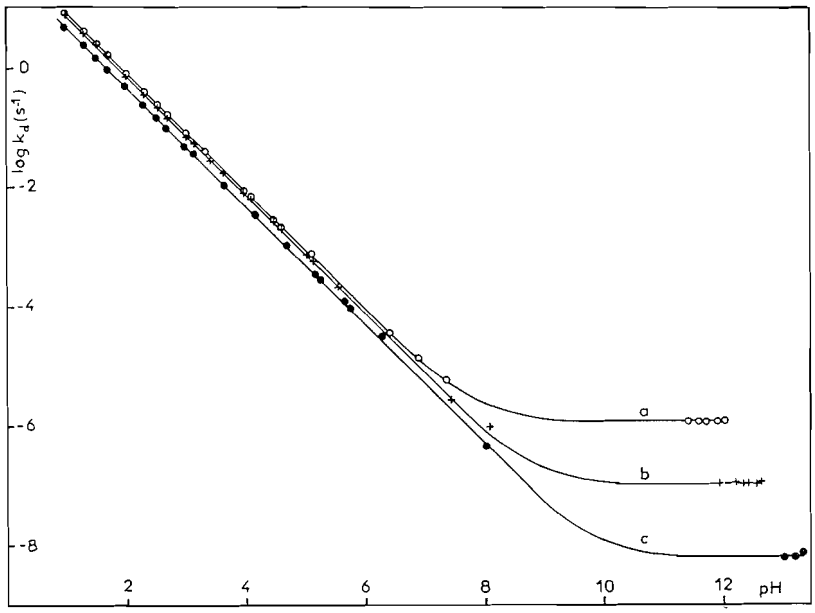


FIG. 3. pH dependence of k_d (s^{-1}) for the decomposition of the adduct **2** at 20°C. The plots *a, b, c* refer to water, 30% DMSO – 70% water, and 50% DMSO – 50% water (v/v), respectively.

crease in the rate constant k_{-2} for the spontaneous decomposition of **2**. DMSO has been found to affect similarly the rate and equilibrium constants for formation and decomposition of the hydroxyl σ-adducts derived from substituted 1-X-3,5-dinitro benzenes (13) and the reasons for this behaviour have been extensively discussed (9, 10, 14).

Comparison of the k_{obsd} pH–rate profiles with the k_f and k_d pH–rate profiles clearly shows that the formation of the adduct **2** arises exclusively from the attack of water molecules on **1** at the lower pH in water–DMSO mixtures. This result is largely the consequence of the very strong electron-withdrawing character of the furoxan ring (1, 15, 16) which is demonstrated by the very high thermodynamic stability of the adduct **2**. We note in particular that **2** is almost completely formed in a hydrochloric acid solution 0.001 *M* in 70, 80, and 90% DMSO.

As previously pointed out (1), the fact that water reacts so efficiently with 4,6-dinitrobenzofuroxan to give the anionic σ-complex **2** is the only report of

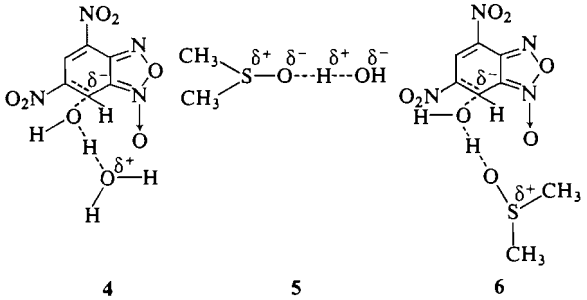
Can. J. Chem. Downloaded from www.nrcresearchpress.com by 210.87.254.6 on 09/05/12
For personal use only.

TABLE 2. Kinetic and equilibrium parameters for the formation and decomposition of **2** in various water–DMSO–NMe_4Cl 0.5 *M* mixtures at 20°C (I = 0.50 *M*)

	Value at solvent composition = [a]					
Parameter	0[b] 0	30 0.097	50 0.195	70 0.355	80 0.486	90 0.70
$k_1^{H_2O}$, s^{-1}	0.019	0.056	0.191	0.603	1.175	1.334
$k_1'^{H_2O}$, M^{-1} s^{-1}	3.4×10^{-4}	1.5×10^{-3}	7×10^{-3}	3.8×10^{-2}	0.108	0.264
k_{-1}, M^{-1} s^{-1}	80	71	46.6	31.8	33.4	37
k_2, M^{-1} s^{-1}	2.7×10^{4}	7.7×10^{4}	3.3×10^{5}	—	—	—
k_{-2}, s^{-1}	1.15×10^{-6}	1.12×10^{-6}	6.5×10^{-9}	—	—	—
K_a, thermodynamical	2.4×10^{-4}	8.1×10^{-4}	3.98×10^{-3}	1.78×10^{-2}	3.31×10^{-2}	3.16×10^{-2}
kinetics[d]	$2.37_5 \times 10^{-4}$	7.88×10^{-4}	4.1×10^{-3}	1.89×10^{-2}	3.52×10^{-2}	3.60×10^{-2}
K_2, M^{-1}	2.4×10^{10}	6.89×10^{11}	4.47×10^{13}	2.04×10^{16}	2.88×10^{18}	7.25×10^{20}[c]

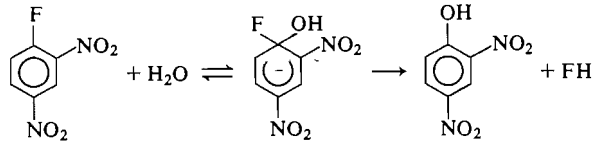
[a]First entry, % DMSO by volume; second entry, molar fraction of DMSO.
[b]At 0.2 *M*, t = 20°C: $k_1^{H_2O}$ = 0.0245 s^{-1}, k_{-1} = 100 M^{-1} s^{-1}, k_2 = 27400 M^{-1} s^{-1}, $k_{-2} = 1.35 \times 10^{-6}$ s^{-1} (1).
[c]Calculated from the ratio $K_2 = K_a/K_s'$ by using the K_s' value determined at I = 0.2 *M*. pK_s' = 22.36 (3*a*).
[d]Calculated from the ratio $k_1^{H_2O}/k_{-1}$.

this sort in the field of Meisenheimer complexes. Of particular interest therefore is the effect of DMSO on the rate of water attack on **1**. As can be seen in Table 2, there is an approximate 67-fold increase in the observed first-order rate constant $k_1^{H_2O}$ when going from water to 90% DMSO – 10% water. However, this increase in $k_1^{H_2O}$ does not give a right evaluation of the effect of DMSO since one must take into account the decrease in the water content as well as the number of water molecules participating in the reaction. Assuming that only one water molecule is involved in the transition state for complex formation on the whole range of the DMSO–water mixtures studied, calculation of the ratio $k_1^{H_2O}/[H_2O]$ gives the values of the second-order rate constant $k_1'^{H_2O}$ indicated in Table 2. One thus see that $k_1'^{H_2O}$, and consequently the nucleophilic power of a water molecule, increases about thousandfold when the solvent changes from water to 90% DMSO. DMSO would have a still more important effect on the rate of water attack if two or more water molecules are present in the transition state.



4 **5** **6**

From buffer catalysis and isotope effects (1), it has been shown that the reaction of water with **1** in aqueous solution proceeds via a transition state such as **4** which represents general base catalyzed water attack with a second water molecule acting as a base catalyst. DMSO has a well-known high tendency to associate with water to form hydrogen-bonded structures such as **5** in which the basic character of the water molecules is strongly enhanced (5, 17). On this basis, one can reasonably expect the reaction in water–DMSO mixtures to proceed faster via a transition state such as **6** where the DMSO molecule would be the base catalyst. Also noteworthy is the fact that the DMSO influence on the rate constant $k_1^{H_2O}$ for water attack on **1** is very close to the one observed by Murto on the rate constant for the water hydrolysis of 2,4-dinitrofluorobenzene **7** in the same experimental conditions (2). This similarity suggests that the rate-determining step of this latter reaction is, indeed, the formation of the corresponding intermediate σ-complex **8**, and not the expulsion of the fluoride ion, over the whole range of water–DMSO mixtures. Such a conclusion is in agreement with the fact that fluoride ion is a much better leaving group than hydroxide ion (18).



7 **8**

Experimental Section

Materials

4,6-Dinitrobenzofuroxan was prepared by the procedure of Drost (19); mp 172°C (lit. (19) 172°C). Buffer solutions were made up from the best available commercial grades of reagents. HCl solutions were made from Titrisol, tetramethylammonium hydroxide solutions from commercial (Eastman) 25% aqueous solutions.

Rate and pH Measurements

Stopped-flow determinations were performed on a Durrum

Can. J. Chem. Downloaded from www.nrcresearchpress.com by 210.87.254.6 on 09/05/12
For personal use only.

stopped-flow spectrophotometer, the cell compartment of which was maintained to ±0.5°C. All kinetic runs were carried out under pseudo-first-order conditions with substrate concentrations of about 3×10^{-5} *M*. Rate constants are accurate to ±3%.

The pH was measured with a Tacussel Model Isis 20000 pH meter by using a cell involving a hydrogen electrode, as previously described (3). The pH values are relative to the standard state in the water–DMSO–NMe_4Cl 0.5 *M* mixtures.

1. F. TERRIER, F. MILLOT, and W. P. NORRIS. J. Am. Chem. Soc. **98**, 5883 (1976), and references therein.
2. J. MURTO and A. M. HIIRO. Suom. Kemistil. B, **37**, 177 (1964).
3. H. ACHASSI SORKHABI, J. C. HALLE, and F. TERRIER. J. Chem. Res. (*a*) (S) 108; (M) 1371 (1978); (*b*) (S) 196; (M) 2542 (1978).
4. C. F. BERNASCONI and M. C. MULLER. J. Am. Chem. Soc. **100**, 5530 (1978).
5. S. M. SHEIN and O. C. BYVAL'KEVICH. Zh. Org. Khim. **8**, 328 (1972).
6. E. BUNCEL, A. JONCZYK, and J. G. K. WEBB. Can. J. Chem. **53**, 3761 (1975).
7. A. J. PARKER. Chem. Rev. **69**, 1 (1969).
8. (*a*) J. H. FENDLER, E. J. FENDLER, and C. E. GRIFFIN. J. Org. Chem. **34**, 689 (1969); (*b*) E. J. FENDLER, J. H. FENDLER, C. E. GRIFFIN, and J. W. LARSEN. J. Org. Chem. **35**, 287 (1970).
9. (*a*) W. L. HINZE, L. J. LIU, and J. H. FENDLER. J. Chem. Soc. Perkin Trans. 2, 1751 (1975); (*b*) J. H. FENDLER, W. L. HINZE, and J. L. LIU. J. Chem. Soc. Perkin Trans. 2, 1768 (1975).
10. (*a*) F. TERRIER, F. MILLOT, and R. SCHAAL. J. Chem. Soc. Perkin Trans. 2, 1192 (1972); (*b*) F. TERRIER, A. P. CHATROUSSE, and R. SCHAAL. J. Org. Chem. **37**, 3010 (1972); (*c*) F. TERRIER and F. MILLOT. Bull. Soc. Chim. Fr. 1743 (1970); (*d*) F. TERRIER and F. MILLOT. Bull. Soc. Chim. Fr. 3897 (1971).
11. (*a*) M. R. CRAMPTON and H. A. KHAN. J. Chem. Soc. Perkin Trans. 2, 1173 (1972); (*b*) M. R. CRAMPTON, M. A. EL GHARIANI, and H. A. KHAN. J. Chem. Soc. Perkin Trans 2, 1178 (1972).
12. E. A. SYMONS and E. BUNCEL. Can. J. Chem. **50**, 1729 (1972).
13. (*a*) F. TERRIER, F. MILLOT, and M. P. SIMONNIN. Tetrahedron Lett. 2933 (1971); (*b*) F. MILLOT and F. TERRIER. Bull. Soc. Chim. Fr. 1823 (1974); (*c*) A. P. CHATROUSSE and F. TERRIER. Bull. Soc. Chim. Fr. 4549 (1972).
14. F. TERRIER, F. MILLOT, and J. MOREL. J. Org. Chem. **41**, 3892 (1976).
15. (*a*) G. AH-KOW, F. TERRIER, and F. LESSARD. J. Org. Chem. **43**, 3578 (1979); (*b*) A. P. CHATROUSSE and F. TERRIER. C. R. Acad. Sci. Paris Ser. C, **23**, 195 (1976).
16. E. BUNCEL, N. CHUAQUI-OFFERMANS, R. Y. NOIR, and A. R. NORRIS. Can. J. Chem. **57**, 494 (1979).
17. K. H. KHOO. J. Chem. Soc. A, 2932 (1971).
18. J. F. BUNNETT and R. E. ZAHLER. Chem. Rev. **49**, 275 (1951).
19. P. DROST. Justus Liebigs Ann. Chem. **307**, 49 (1899).

Can. J. Chem. Downloaded from www.nrcresearchpress.com by 210.87.254.6 on 09/05/12
For personal use only.

Capture du paradiméthoxyorthoquinodiméthane: synthèses de quinones et d'un intermédiaire de la daunomycinone

JOËLLE LADURANTY, LUCETTE LEPAGE ET YVES LEPAGE
Laboratoire de chimie organique A, 123, rue A. Thomas, 87060 Limoges, France

Reçu le 12 décembre 1979

JOËLLE LADURANTY, LUCETTE LEPAGE et YVES LEPAGE. Can. J. Chem. **58**, 1161 (1980).

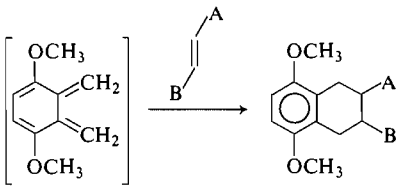
Les auteurs décrivent de nouveaux dérivés *para*-diméthoxylés et acétoxylés des séries naphtalénique, anthracénique, naphtacénique, naphto(2,3-*c*) thiophénique et benzo(*c*) thiophénique par capture d'*ortho*-quinodiméthanes à l'aide de philodiènes variés. Parmi eux, un intermédiaire dans la synthèse de la daunomycinone a été préparé et a pu être oxydé en une benzoquinone qui permettrait l'accès à de nouveaux composés du même type que cet important produit "antileucémique".

JOËLLE LADURANTY, LUCETTE LEPAGE, and YVES LEPAGE. Can. J. Chem. **58**, 1161 (1980).

New *para*-dimethoxyl and *para*-diacetoxy derivatives in the naphthalene, anthracene, naphthacene, naphtho (2,3-*c*) thiophene and benzo-*c*-thiophene series are synthesized via the trapping of *o*-quinodimethanes by various dienophiles. Among these compounds, an intermediate for the synthesis of daunomycinone has been prepared and can be oxidized to a benzoquinone which provides access to new analogues of this important antileukemic agent.

[Journal translation]

La capture, par des philodiènes, des *ortho*-quinodiméthanes préconisée par Cava *et al.* (1) devient de plus en plus utilisée en synthèse (2–4). Nous nous sommes proposés de synthétiser un certain nombre de composés *para*-diméthoxylés à l'aide de l'*o*-xylylène correspondant **1**, en particulier des quinones pouvant autoriser l'accès aux acènes diméthoxylés en 1,4, composés aux multiples usages potentiels: notamment le diméthoxy-1,4 anthracène (5*a*, *b*) a été utilisé comme capteur de benzyne (6) et a fait l'objet de mesures d'électroluminescence (7).



1

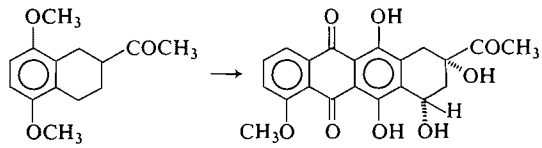
D'autre part, les groupements "méthoxy" sur ces positions permettent un accès facile aux quinones et hydroquinones correspondantes.

Nous avons effectué la synthèse de nouveaux dérivés *para*-diméthoxylés des séries naphtalénique, anthracénique, naphtacénique, naphto-(2,3-*c*) thiophénique et benzo(*c*) thiophénique par capture d'orthoquinodiméthanes à l'aide de philodiènes variés.

Nous donnons, d'autre part, une nouvelle préparation d'un intermédiaire **2** (8*a*, *b*, *c*) de la synthèse de la daunomycinone **3** (9) aglycone d'un composé antitumoral très étudié actuellement (10–16).

Il faut remarquer que cette cétone **2**, isolée par Wong et coll. (8*a*, *b*), a été aussi préparée récemment par une autre voie rapide par Blade et Hodge (8*c*).

A notre connaissance, lorsque nous avons débuté ce travail, aucune étape de la synthèse de la daunomycinone et des composés du même type ne



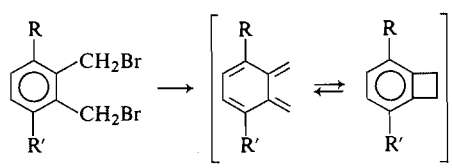
2 **3**

comprenait cette réaction de capture. Depuis, quelques synthèses différentes très récentes (17–19) utilisent des dienes instables.

Les *ortho*-quinodiméthanes ont le plus souvent été préparés par pyrolyse des sulfones (20), par pyrolyse des tétrahydrophtalazines (21) et par action de l'iodure de sodium sur les dérivés dibromés ou tétrabromés (1, 3, 4).

C'est cette dernière méthode que nous avons choisie; nous avons fait la réduction des composés monométhoxylé **4***c*, diacétoxylé **4***b* et diméthoxylé en 3,6 **4***a*.

Notons que seul le dérivé monométhoxylé **4***c*



4

a R = R′ = OCH_3; *b* R = R′ = $OCOCH_3$; *c* R = OCH_3, R′ = H

0008-4042/80/121161-07$01.00/0

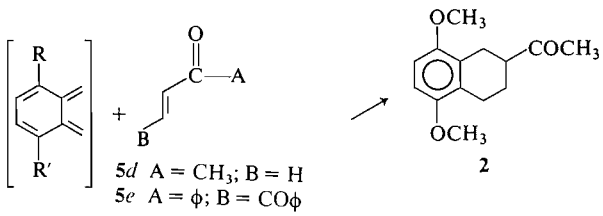
©1980 National Research Council of Canada/Conseil national de recherches du Canada

Can. J. Chem. Downloaded from www.nrcresearchpress.com by 210.87.254.42 on 09/05/12
For personal use only.

Can. J. Chem. Downloaded from www.nrcresearchpress.com by 210.87.254.42 on 09/05/12
For personal use only.

n'était pas connu; il a été préparé par action du *N*-bromosuccinimide sur le méthoxy-3 *ortho*-xylène.

La capture de ces dienes instables par la méthylvinylcetone **5***d* et par le *trans*-dibenzoyléthylène **5***e* nous a permis d'obtenir les produits d'addition attendus **2**, **9***a* et **9***b*.



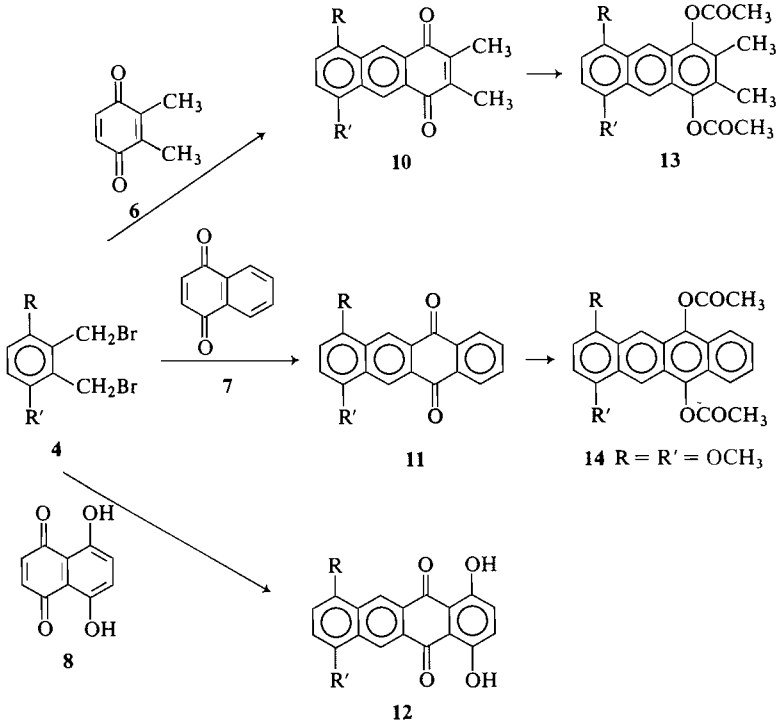
a R = R′ = OCH_3; *b* R = R′ = $OCOCH_3$; *c* R = OCH_3, R′ = H

Par contre ces *o*-xylylènes piégés par la diméthyl-2,3 benzoquinone **6** (22), la naphtoquinone **7** et la naphtazarone **8**[1] (23) ne nous ont pas donné les produits d'addition mais les quinones anthracéniques **10***a*, **10***b* et **10***c* ainsi que les quinones naphtacéniques **11***a*, **11***b*, **12***a* et **12***b* par suite d'une déshydrogénation dans le milieu réactionnel et aromatisation du noyau formé.

Les quinones **10***a*, **10***b*, **10***c* et **11***a* ont été réduites (en milieu acétylant) en les diesters phénoliques **13***a*, **13***b*, **13***c* et **14**. Les esters phénoliques **13** présentent une structure fine dans la zone 400–350 nm ainsi qu'une forte fluorescence bleu-turquoise au jour, caractéristiques des dérivés anthracéniques diméthoxylés. Quant au naphtacène **14**, la structure fine vers 450–500 nm très caractéristique de ce type de composés a pu être observée ainsi qu'une forte fluorescence orange au jour.

Nous avons soumis les composés *para*-diméthoxylés, **2**, **9**, **10***a* et **11***a* à une oxydation déméthylante à l'aide du nitrate d'ammonium et de cérium (CAN) (réactif préconisé par P. Jacob et coll. (24)); nous avons ainsi obtenu les quinones cétoniques **15** et **16** ainsi que les diquinones **17***a* et **17***b*. La quinone **15** devrait permettre un accès facile à des dérivés de la daunomycinone.

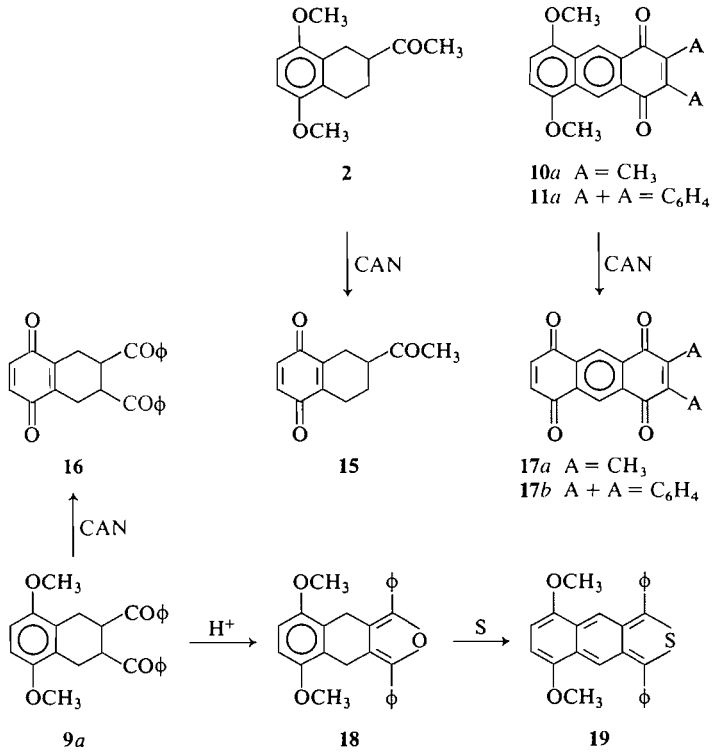
Le composé dibenzoylé **9***a* se cyclise facilement sous l'action des acides pour conduire au dihydronaphto(2,3-*c*) furanne **18** qui permet, par



a R = R′ = OCH_3; *b* R = R′ = $OCOCH_3$; *c* R = OCH_3 R′ = H

[1]Nous adressons nos bien vifs remerciements à Monsieur le Professeur Otto Bayer et à Monsieur Gangneux, Directeur de la Société Ugine-Kuhlmann qui nous ont fourni gracieusement la naphtazarone et la naphtoquinone-1,4.

Can. J. Chem. Downloaded from www.nrcresearchpress.com by 210.87.254.42 on 09/05/12
For personal use only.

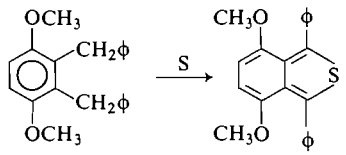


action du soufre, l'obtention du naphto(2,3-*c*) thiophène diméthoxylé **19** dont la réactivité et les caractéristiques spectrales sont voisines des autres composés, peu nombreux, de cette série (25, 26).

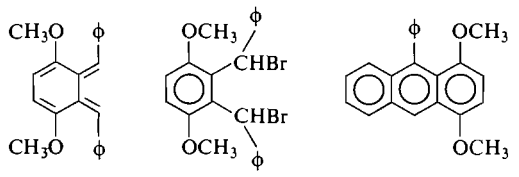
Nous avons voulu voir s'il nous était possible de piéger un *ortho*-quinodiméthane encombré, en l'occurence le diène **20**. A cet effet, nous avons isolé un nouveau composé dibenzylé, le dibenzyl-2,3 diméthoxy-1,4 benzène **21** obtenu par action du bromure de phénylmagnesium sur le composé dibromé **4***a*. Malheureusement, l'action du *N*-bromosuccinimide sur ce dérivé **21** n'a pas conduit au dérivé halogéné **22** attendu, mais à un composé bromé anthracénique dont la réduction a abouti au produit **23**, isolé il y a longtemps, par l'un de nous (*5b*).

Nous avons profité de ce résultat pour voir si l'action du soufre sur ce composé **21** conduisait préférentiellement à une carbocyclisation comme cela avait déjà été remarqué dans le cas du dibenzyl-2,3 *para*-terphényle (27), ou à une hétérocyclisation comme dans les cas d'encombrement stérique faible (27). En fait, nous n'obtenons pratiquement que le benzo(*c*) thiophène **24**.

Enfin, nous avons examiné si cette réaction de

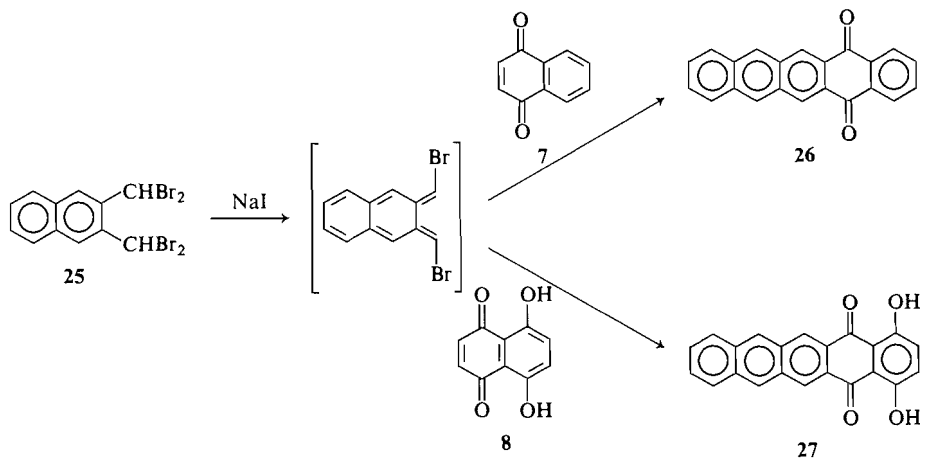


capture à partir de dérivés di- ou tétrahalogénés pouvait s'étendre aux benzologues supérieurs, en particulier aux dérivés tétrabromés du diméthyl-2,3 naphtalène **25**. Cette réaction avait toutes les chances de réussir, car Cava et Shirley (28) avaient bien obtenu un adduit en traitant la sulfone naphtalénique en présence de *N*-phénylmaléimide. Nous avons donc traité le bis(dibromométhyl)-2,3 naphtalène **25** par l'iodure de sodium en présence de naphtoquinone **7** ou de naphtazarone **8** et nous avons ainsi obtenu les deux pentacènequinones **26** ou **27** correspondantes, décrites récemment (29).



Conclusion

Parmi les composés *para*-diméthoxylés décrits se trouve un intermédiaire important de la synthèse de la daunomycinone. Ce dernier composé a été transformé en une quinone nouvelle qui pourrait permettre un accès facile à de nombreux pro-



duits du même type que celui de cette très intéressante quinone cétonique.

Partie expérimentale

Les points de fusion instantanés ont été déterminés au bloc chauffant de Kofler ou de Maquenne. Les identifications de produits ont toujours été faites par trois méthodes différentes: épreuve du point de fusion du mélange, spectres infrarouge et ultraviolet–visible identiques. Les spectres infrarouge ont été enregistrés avec un spectrographe Perkin Elmer 297. Les spectres d'absorption uv–visible ont été enregistrés avec un spectrographe Beckman Acta M VI.

Nous sommes heureux d'exprimer notre gratitude à M. le Professeur Penicaut de l'U.E.R. des Sciences Médicales et Pharmaceutiques de Limoges qui vient de mettre à notre disposition un spectrographe Varian E.M. 360. Ces spectres sont pris dans $CDCl_3$ avec le tétraméthylsilane comme référence interne; les δ sont exprimés en ppm.

Les analyses élémentaires ont été effectuées par M. Leger (Laboratoire R. Bellon) ou par le service de Microanalyse du C.N.R.S. que nous remercions bien vivement.

Derives dibromométhylés **4**a *(30),* **4**b *(30) et* **4**c

Les dérivés dibromés **4***a* (30), **4***b* (30) et **4***c* ont été obtenus de façon classique par action du *N*-bromosuccinimide en présence de peroxyde de benzoyle sur les composés diméthylés correspondants.

*Méthoxy-1 bis(bromométhyl)-2,3 benzene (***4**c*)*

Un mélange de 10 g de diméthyl-2,3 anisole (10.4 cm^3), 300 cm^3 de tétrachlorure de carbone anhydre, 26.10 g de *N*-bromosuccinimide et 100 mg de peroxyde de benzoyle est porté à ébullition jusqu'à ce que le succinimide surnage (24 h). Après filtration à chaud, la solution est lavée à l'eau chaude jusqu'à ce que la phase aqueuse soit limpide. La phase organique est séchée sur sulfate de sodium, évaporée. D'une huile dense reprise par l'éther de pétrole (40–65°C) cristallisent 17.3 g de cristaux incolores, rdt 80%, pf inst 80°C (éther de pétrole). *Anal.* calc. pour $C_9H_{10}Br_2O$: C 36.77, H 3.43, Br 54.36; trouvée: C 36.84, H 3.56, Br 54.35.

Technique générale de capture de diènes (1)

Un gramme de dérivé dibromé, une quantité équimoléculaire de quinone ou autres philodiènes, 2 g d'iodure de sodium mis en présence dans 10 cm^3 de diméthylformamide anhydre sont maintenus à 90°C pendant 24 h. La solution brune obtenue est précipitée par l'eau contenant du bisulfite de sodium. Le produit est essoré, séché puis extrait au chloroforme (Soxhlet). Après évaporation, les cristaux sont lavés soit à l'éther soit à l'acétone.

*Dibenzoyl-2,3 diméthoxy-5,8 tétrahydro-1,2,3,4 naphtalène (*9a)

Dix grammes de dérivé dibromé **4***a* et 7.40 g de *trans*-dibenzoyl éthylène **5***e* traités par la méthode précédente pendant 6 h à 70°C permettent d'obtenir 5.64 g de cristaux, rdt 68%, pf inst 219–220°C (*n*-propanol); uv (CH_2Cl_2) λ_{max} en nm (log ε): 285 (3.83), 244 (4.56); ir (KBr) ν(C=O): 1685 cm^{-1}; rmn ^1H: δ en ppm: 7.3–8.2 (l, 10H, φC=O), 6.68 (s, 2H, aromatiques, H-6, H-7), 2.36–4.36 (l, 6H, CH_2 et CH), 3.73 (s, 6H, OCH_3). *Anal.* calc. pour $C_{26}H_{24}O_4$: C 77.98, H 6.14; trouvée: C 77.90, H 6.18.

*Diacétoxy-5,8 dibenzoyl-2,3 tétrahydro-1,2,3,4 naphtalène (*9b)

Deux grammes de dérivé dibromé **4***b* et 1.24 g de *trans*-dibenzoyléthylène **5***e* sont traités pendant 6 h à 70°C suivant la technique générale décrite plus haut; 1.3 g de cristaux incolores précipitent par addition d'éther, rdt 54%, pf inst 208–209°C (benzène); ir (KBr) ν(C=O): 1760 et 1680 cm^{-1}; rmn ^1H δ: 7.72 (l, 10H, φC=O), 6.97 (s, 2H, aromatiques, H-6, H-7), 4.17 (l, 2H, CHCO), 2.84 (l, 2H, CH_2), 2.20 (s, 6H, $OCOCH_3$). *Anal.* calc. pour $C_{28}H_{24}O_6$: C 73.67, H 5.30; trouvée: C 73.82, H 5.42.

*Dihydro-4,9 diméthoxy-5,8 diphenyl-1,3 naphto(2,3-*c*) furanne (***18***)*

Dans un litre d'un mélange acide acétique – acide chlorhydrique (4:1) sont dissous à chaud 5 g de composé dibenzoylé **9***a*. Après un reflux d'une heure, le furanne **18** précipite par refroidissement du milieu et 4.05 g de cristaux incolores sont filtrés, rdt 84%, pf inst 242°C (chloroforme à froid). Les cristaux fondent en rougissant. Ultraviolet ($CH_3C{\equiv}N$) λ_{max} (log ε): 350 inf, 332 (4.51), 318 inf, 297 (4.24), 240 inf; rmn ^1H δ: 7.60 (m, 10H, aromatiques, φ), 6.73 (s, 2H, aromatiques, H-6, H-7), 4.07 (s, 2H, CH_2), 3.87 (s, 6H, OCH_3). *Anal.* calc. pour $C_{26}H_{22}O_3$: C 81.65, H 5.80; trouvée: C 81.74, H 5.81.

*Diméthoxy-5,8 diphenyl-1,3 naphto(2,3-*c*) thiophene (***19***)*

Un mélange intime de 1 g de naphto(2,3-*c*) furanne **18** et de 0.280 g de soufre est chauffé pendant 25 min à 270°C. Après extraction au chloroforme R.P. et évaporation, le produit dissous dans le benzène est purifié par filtration sur colonne de silice. La solution rouge foncé à forte fluorescence orange est évaporée. Après lavage à l'éther, on recueille 0.640 g de cristaux rouges, rdt 62%, pf inst 223–224°C (benzène); uv et visible ($CH_3C{\equiv}N$) λ_{max} (log ε): 522 (3.86), 510 inf (3.85), 352 (3.75), 290 (4.46), 278 inf, 265 (4.52); rmn ^1H δ: 8.80 (s, 2H, aromatiques, H-4, H-9), 7.70 (l, 10H, aromatiques, φ), 6.28 (s, 2H, aromatiques, H-6, H-7), 3.96 (s, 6H, OCH_3). *Anal.* calc. pour $C_{26}H_{20}O_2S$: C 78.77, H 5.09, S 8.07; trouvée: C 78.55, H 5.20, S 8.20.

*Dibenzoyl-6,7 tétrahydro-5,6,7,8 naphtoquinone-1,4 (***16***)*

A 0.100 g de dibenzoyl-2,3 diméthoxy-5,8 tétrahydro-1,2,3,4

Can. J. Chem. Downloaded from www.nrcresearchpress.com by 210.87.254.42 on 09/05/12
For personal use only.

Can. J. Chem. Downloaded from www.nrcresearchpress.com by 210.87.254.42 on 09/05/12
For personal use only.

naphtalène **9***a* dissous dans 100 cm³ d'acétonitrile est ajouté 0.411 g de nitrate de cérium et d'ammonium en solution dans 6 cm³ d'eau. Après agitation de 30 min, extraction au chloroforme, lavage à l'eau, la phase organique est séchée sur sulfate de sodium, évaporée; 0.93 g de cristaux "jaune pâle" sont essorés après addition d'éther, rdt 86%, pf inst 233–234°C (diméthylformamide). Ultraviolet (CH_2Cl_2) λ_{max} (log ε): 330 (faible), 259 (4.05); ir ν(C=O): 1670 et 1650 cm^{-1}; rmn ^1H δ: 7.33–8.13 (l, 10H, φCO), 6.79 (s, 2H, C=C), 2.03–4.30 (l, 6H, $2CH_2$ et 2H en α du CO). *Anal.* calc. pour $C_{24}H_{18}O_4$: C 77.82, H 4.90; trouvée: C 77.50, H 5.06.

*Dibenzyl-2,3 diméthoxy-1,4 benzene (**21**)*

Trente grammes de diméthoxy-1,4 bis(bromométhyl)-2,3 benzène **4***a* dissous dans 500 cm³ de benzène anhydre sont ajoutés goutte à goutte à la solution benzénique bouillante de bromure de phenylmagnésium (préparée préalablement à partir de 96 cm³ de bromobenzène, 24 g de magnésium, 230 cm³ d'éther anhydre. Ce dernier a été remplacé en fin de réaction par un volume équivalent de benzène sec, puis distillé). Le reflux est maintenu pendant 15 h. Après traitement habituel et entraînement à la vapeur d'eau, des cristaux incolores sont isolés par addition de méthanol (16.5 g), rdt 56%, pf inst 111°C (méthanol); uv (CH_2Cl_2) λ_{max} (log ε): 296 inf, 291 (3.68), 269; rmn ^1H δ: 7.12 (l, 10H, φ), 6.80 (s, 2H, aromatiques, H-5, H-6), 3.97 (s, 4H, CH_2), 3.73 (s, 6H, OCH_3). *Anal.* calc. pour $C_{22}H_{22}O_2$: C 82.96, H 6.96; trouvée: C 82.90, H 6.88.

*Diméthoxy-1,4 phenyl-9 anthracène (**23**) (réf. 5*b*)*

A 2 g de dibenzyl-2,3 diméthoxy-1,4 benzène **21** dissous dans 250 cm³ de tétrachlorure de carbone anhydre sont ajoutés 3.4 g de *N*-bromosuccinimide et 0.100 g de peroxyde de benzoyle. Après un reflux de 2.5 h, le succinimide surnageant est filtré à chaud. La phase organique est lavée à l'eau chaude, séchée sur sulfate de sodium et évaporée; une huile orange cristallise par addition d'éther (1.1 g de cristaux jaunes). Le spectre uv–visible de ces cristaux présente une structure fine vers 400 nm, caractéristique de la structure anthracénique. Ce composé n'a pas été étudié plus précisément. Il a été réduit par la technique suivante.

A 0.300 g d'hydrure de lithium et d'aluminium en suspension dans l'éther anhydre est ajouté 0.250 g du composé précédent. Après agitation de 2 h, apparition d'une fluorescence bleu-turquoise (uv), hydrolyse sur glace, extraction à l'éther, la phase organique est séchée sur sulfate de sodium et évaporée. Les cristaux "jaune vert" (140 mg) sont lavés avec du méthanol, pf inst 159°C (litt. (*5b*) pf 158–159°C (acétone)); uv et visible (CH_2Cl_2) λ_{max} (log ε): 394 (3.80), 368 (3.86), 350 (3.58), 272 (4.63).

*Diméthoxy-4,7 diphenyl-1,3 benzo(*c*) thiophène (**24**)*

Un mélange de 0.500 g de dibenzyl-2,3 diméthoxy-1,4 benzène **21** (15.7×10^{-4} mol) et de 0.170 g de soufre (53.1×10^{-4} mol) est chauffé à 270°C pendant une heure. Après extraction au chloroforme et évaporation du solvant, le produit est purifié par élution d'une solution cyclohexanique sur une colonne d'alumine neutre. La solution jaune orange à forte fluorescence verte est évaporée; 0.120 g de cristaux jaunes sont filtrés après lavage à l'éther de pétrole (40–65°C); pf inst. 161°C (xylène), rdt 22%; uv et visible (CH_2Cl_2) λ_{max} (log ε): 397 (4.11), 335 (3.50), 257 (4.36); rmn ^1H δ: 7.52 (l, 10H, φ), 6.20 (s, 2H, aromatiques, H-6, H-5), 3.68 (s, 6H, OCH_3). *Anal.* calc. pour $C_{22}H_{18}O_2S$: C 76.28, H 5.24, S 9.24; trouvée: C 76.08, H 5.16, S 9.36.

*Acétyl-2 diméthoxy-5,8 tétrahydro-1,2,3,4 naphtalène (**2**)*

A 5 g de dérivé dibromé **4***a* dissous dans 50 cm³ de diméthylformamide anhydre sont ajoutés 15 cm³ de méthylvinylcétone **5***d* (en excès) et 10 g de iodure de sodium et ce mélange est laissé à 60°C pendant 5 jours.

La résidu huileux obtenu par précipitation du milieu réactionnel dans l'eau "bisulfitique" est extrait à l'acétate d'éthyle. Après traitement classique, une solution benzénique est éluée sur colonne de silice et évaporée; 1.63 g est recueilli après lavage à l'éther de pétrole, rdt 45%, pf inst 81°C (éther de pétrole), (litt. (8) pf 81–82°C).

*Acétyl-7 tétrahydro-5,6,7,8 naphtoquinone-1,4 (**15**)*

A 0.800 g de composé diméthoxylé **2** dissous dans 15 cm³ d'acétonitrile sont ajoutés par petites fractions 5.7 g de nitrate d'ammonium et de cerium en solution dans 15 cm³ d'eau. Après 30 min d'agitation, le milieu réactionnel est extrait au chloroforme, le traitement habituel nous permet d'isoler 0.600 g de cristaux, rdt 80%, pf inst 76°C (cyclohexane–benzène 3:1). Ultraviolet–visible (EtOH) λ_{max} (log ε): 336 (faible), 257 (3.81); ir (KBr) ν(C=O): 1705–1650 cm^{-1}; rmn ^1H δ: 6.76 (s, 2H, C=C), 2.30 (s, 3H, $COCH_3$), 2.37 (m, 7H, CH_2 et CH). *Anal.* calc. pour $C_{12}H_{12}O_3$: C 70.57, H 5.92; trouvée: C 70.44, H 5.97.

*Diméthoxy-5,8 diméthyl-2,3 anthraquinone-1,4 (**10**a)*

Un mélange de 2 g de dérivé dibromé **4***a* et 0.84 g de diméthyl-2,3 benzoquinone **6** est traité suivant la technique générale: 0.75 g de cristaux rouges sont essorés, rdt 41%, pf inst 277–278°C (xylène); uv et visible (CH_2Cl_2) λ_{max} (log ε): 473 (3.73), 355 (3.34), 256 (4.81); ir (KBr) ν(C=O): 1670 cm^{-1}; rmn ^1H δ: 8.95 (s, 2H, aromatiques, H-9, H-10), 6.82 (s, 2H, aromatiques, H-6, H-7), 3.95 (s, 6H, OCH_3), 2.20 (s, 6H, CH_3). *Anal.* calc. pour $C_{18}H_{16}O_4$: C 72.96, H 5.44; trouvée: C 73.13, H 5.24.

*Diacétoxy-1,4 diméthoxy-5,8 diméthyl-2,3 anthracène (**13**a)*

A 1.5 g de zinc en poudre préalablement activé est ajouté 1.5 g de quinone **10***a* en solution dans 10 cm³ d'un mélange d'anhydride acétique – pyridine (5:1) puis laissé à reflux pendant 5 min. On verse sur glace et on reprend le zinc par 2-fois 5 cm³ d'acide acétique et on extrait au chloroforme. Après traitement habituel, on récupère 1.80 g de cristaux jaunes, rdt 96%, pf inst 232°C (benzène); uv et visible: ($CH_3C{\equiv}N$) λ_{max} (log ε): 394 (3.65), 369 (3.68), 264 (4.71), 248 (4.81); ir (KBr) ν(C=O): 1765 cm^{-1}; rmn ^1H δ: 8.62 (s, 2H, aromatiques, H-9, H-10), 6.60 (s, 2H aromatiques, H-6, H-7), 4.00 (s, 6H, OCH_3), 2.57 (s, 6H, $OCOCH_3$), 2.30 (s, 6H, CH_3). *Anal.* calc. pour $C_{22}H_{22}O_6$: C 69.10, H 5.80; trouvée: C 69.19, H 5.99.

*Diméthoxy-7,10 naphtacènequinone-5,12 (**11**a)*

On traite selon la technique générale 2 g de dérivé dibromé **4***a* et 0.975 g de naphtoquinone **7** (purifiée par sublimation). On obtient 0.73 g de cristaux oranges qu'on lave à l'acétone, rdt 37%, pf inst 279–280°C. Ultraviolet et visible ($CH_3C{\equiv}N$) λ_{max} (log ε): 458 (3.85), 300 (3.98), 259 (4.94); ir (KBr) ν(C=O): 1680 cm^{-1}; rmn ^1H δ: 9.17 (s, 2H, aromatiques, H-6, H-11), 8.33 (m, 2H, aromatiques, H-1, H-4), 7.74 (m, 2H, aromatiques, H-2, H-3), 6.82 (s, 2H, aromatiques, H-8, H-9), 3.98 (s, 6H, OCH_3). *Anal.* calc. pour $C_{20}H_{14}O_4$: C 75.46, H 4.43; trouvée: C 75.57, H 4.22.

*Diacétoxy-6,11 diméthoxy-1,4 naphtacène (**14**)*

Une solution de 0.710 g de quinone **11***a* dans 10 cm³ de mélange anhydride acétique – pyridine (5:1) est portée à reflux 5 min en présence de poudre de zinc préalablement activée. Après filtration du zinc, la liqueur rouge est versée sur de la glace pilée; le zinc est lavé par 2-fois 3 cm³ d'acide acétique chaud. Après extraction à l'acétate d'éthyle, lavage de la phase organique au bicarbonate de sodium et à l'eau, évaporation du solvant, on obtient 0.72 g de cristaux rouges, rdt = 80%, pf inst 229–230°C (benzène). Ultraviolet et visible (CH_2Cl_2) λ_{max} (log ε): 510 (3.64), 480 (3.70), 460 inf (3.52), 430 inf, 401 (3.90), 379 (3.36), 368 (3.34), 295 (5.04), 285 (4.89), 272 (4.90); ir (KBr) ν(C=O): 1765 cm^{-1}; rmn ^1H δ: 8.95 (s, 2H, aromatiques, H-5, H-12), 7.7 (l, 4H, aromatiques, H-7, H-8, H-9, H-10), 6.55 (s,

Can. J. Chem. Downloaded from www.nrcresearchpress.com by 210.87.254.42 on 09/05/12
For personal use only.

2H, aromatiques, H-2, H-3), 4.03 (s, 6H, OCH_3), 2.72 (s, 6H, $OCOCH_3$). *Anal.* calc. pour $C_{24}H_{20}O_6$: C 71.28, H 4.99; trouvée: C 71.04, H 5.08.

*Dihydroxy-1,4 diméthoxy-7,10 naphtacènequinone-5,12 (12*a)

Un mélange de 2 g de dérivé dibromé **4***a* et de 1.29 g de naphtazarone **8** (fraichement purifiée) est traité suivant la technique générale; 0.9 g de cristaux rouges sont recueillis, rdt 41%, pf inst 353°C (diméthylformamide et subl.). Ultraviolet et visible (CH_2Cl_2) λ_{max} (log ε): 505 inf (3.84), 498 (3.84), 285 inf, 267 (4.61); ir (KBr) ν(C=O): 1635 cm^{-1}. *Anal.* calc. pour $C_{20}H_{14}O_6$: C 68.57, H 4.03; trouvée: C 68.58, H 4.26.

*Diacétoxy-5,8 diméthyl-2,3 anthraquinone-1,4 (10*b)

A partir de 2 g de dérivé dibromé **4***b* et de 0.72 g de quinone **6**, on peut obtenir par la méthode précédente 0.67 g de cristaux jaunes, rdt 36%, pf inst 278°C (diméthyl formamide). Ultraviolet et visible (CH_2Cl_2) λ_{max} (log ε): 405 (3.67), 310 inf (3.75), 297 (4.93), 284 (5.06), 273 (5.11); ir (KBr) ν(C=O): 1785, 1775–1665 cm^{-1}; rmn ^1H δ: 8.69 (s, 2H, aromatiques, H-9, H-10), 7.43 (s, 2H, aromatiques, H-6, H-7), 2.53 (s, 6H, $OCOCH_3$), 2.19 (s, 6H, CH_3). *Anal.* calc. pour $C_{20}H_{16}O_6$: C 68.18, H 4.58; trouvée: C 67.92, H 4.58.

*Diméthyl-2,3 tétraacétoxy-1,4,5,8 anthracène (13*b)

La solution de 0.92 g de quinone **10***b* dans 10 cm^3 d'un mélange anhydride acétique – pyridine (5:1) est chauffée à reflux pendant 5 min en présence de poudre de zinc préalablement activée. Le milieu réactionnel se décolore et présente en fin de réaction une fluorescence bleue. Après traitement classique des réductions acétylantes, on essore 0.960 g de cristaux jaunes, rdt 84%, pf inst 290°C (diméthylformamide). Ultraviolet et visible (CH_2Cl_2) λ_{max} (log ε): 396 (3.76), 375 (3.86), 357 (3.72), 339 (3.48), 325 inf, 262 (4.72); ir (KBr) ν(C=O): 1760 cm^{-1}; rmn ^1H δ: 8.23 (s, 2H, aromatiques, H-9, H-10), 7.30 (s, 2H, aromatiques, H-6, H-7), 2.48 (s, 6H, $OCOCH_3$ en 5.8), 2.43 (s, 6H, $OCOCH_3$ en 1.4), 2.27 (s, 6H, CH_3). *Anal.* calc. pour $C_{24}H_{22}O_8$: C 65.74, H 5.06; trouvée: C 65.80, H 5.06.

*Diacétoxy-7,10 naphtacènequinone-5,12 (11*b)

A partir de 4.21 g de dérivé dibromé **4***b* et de 1.75 g de naphtoquinone **7** (purifié par sublimation sous vide à 120°C), la méthode précédente nous permet d'isoler 1.71 g de cristaux jaunes, rdt 41%, pf inst 277–278°C (diméthylformamide). Ultraviolet et visible (CH_2Cl_2) λ_{max} (log ε): 398 (3.70), 316 inf (3.84), 295 (4.53), 283 (4.55), 272 (4.54), 265 (4.53); ir (KBr) ν(C=O): 1770–1680 cm^{-1}; rmn ^1H δ: 8.93 (s, 2H, aromatiques, H-6, H-11), 8.39 (m, 2H, aromatiques, H-1, H-4), 7.81 (m, 2H, aromatiques, H-2, H-3), 7.50 (s, 2H, aromatiques, H-8, H-9), 2.56 (s, 6H, $OCOCH_3$). *Anal.* calc. pour $C_{22}H_{14}O_6$: C 70.58, H 3.77; trouvée: C 70.33, H 3.87.

*Diacétoxy-7,10 dihydroxy-1,4 naphtacènequinone-5,12 (12*b)

Le dérivé dibromé **4***b* (3 g) et la naphtazarone **8** (1.5 g) purifiée par extraction au Soxhlet conduisent par la méthode de capture de diène à 1.25 g de cristaux rouges, rdt 39%, pf inst 309°C (diméthylformamide et subl.). Ultraviolet et visible (CH_2Cl_2) λ_{max} (log ε): 512 inf (3.98), 498 inf (4.14), 480 inf (4.24), 470 (4.25), 301 (4.46), 290 (4.53), 280 (4.58), 265 inf (4.47); ir (KBr) ν(C=O): 1775, 1645, 1620 cm^{-1}; rmn ^1H δ: 13 (s, 2H, OH), 8.97 (s, 2H, aromatiques, H-6, H-11), 7.53 (s, 2H, aromatiques, H-8, H-9), 7.37 (s, 2H, aromatiques, H-2, H-3), 2.57 (s, 6H, $OCOCH_3$). *Anal.* calc. pour $C_{22}H_{14}O_8$: C 65.05, H 3.47; trouvée: C 65.30, H 3.70.

*Diméthyl-2,3 méthoxy-5 anthraquinone-1,4 (10*c)

On chauffe 3 g de dérivé dibromé **4***c* et 1.39 g de quinone **6** dans les conditions précédentes et on traite suivant la même méthode; on essore 1.40 g de cristaux jaunes, rdt 52%, pf inst 219–220°C (diméthylformamide). Ultraviolet et visible (CH_2Cl_2) λ_{max} (log ε): 433 (3.75), 324 (3.56), 297 (4.13), 281 (4.34), 261 (4.41); ir (KBr) ν(C=O): 1660 cm^{-1}; rmn ^1H δ: 9.03 (s, 1H, aromatique, H-10), 8.53 (s, 1H, aromatique, H-9), 7.55 (d, 2H, aromatiques, H-5, H-6), 6.93 (t, 1H, aromatique, H-7), 4.06 (s, 3H, OCH_3), 2.26 (s, 6H, CH_3). *Anal.* calc. pour $C_{17}H_{14}O_3$: C 76.67, H 5.30; trouvée: 76.56, H 5.39.

*Diacétoxy-1,4 diméthyl-2,3 méthoxy-5 anthracène (13*c)

On fait bouillir pendant deux minutes 0.290 g de quinone **10***c*, 0.3 g de zinc en poudre activé dans 4 cm^3 d'un mélange anhydride acétique – pyridine (5:1). La liqueur présente une fluorescence bleu. Après précipitation par l'eau, extraction, lavage au carbonate de sodium, la phase organique est séchée et évaporée. On isole 0.370 g de cristaux "jaune pâle", rdt 96%, pf inst 201–202°C (benzène). Ultraviolet et visible (CH_2Cl_2) λ_{max} (log ε): 396 (3.68), 376 (3.81), 364 (3.69), 357 (3.71), 266 (4.68), 264 (4.67); ir (KBr) ν(C=O): 1760 cm^{-1}; rmn ^1H δ: 8.66 (s, 1H, aromatique, H-9), 8.16 (s, 1H, aromatique, H-10), 7.46 (d, 2H, aromatiques, H-7, H-8), 6.70 (m, 1H, aromatique, H-6), 4.30 (s, 3H, OCH_3), 2.56 (s, 6H, $OCOCH_3$), 2.30 (s, 6H, CH_3). *Anal.* calc. pour $C_{21}H_{20}O_5$: C 71.58, H 5.72; trouvée: C 71.50, H 5.88.

Pentacènequinone-5,14 (26) (réf. 29)

Un gramme de bis(dibromométhyl)-2,3 naphtalène **25** (31) est traité (48 h) en présence de naphtoquinone **7**. Nous avons obtenu 0.2 g de cristaux jaunes, rdt 36%, pf inst 374°C (diméthylformamide) (litt. (29) pf 375°C (subl.)).

Dihydroxy-1,4 pentacènequinone-5,14 (27) (réf. 29)

On traite 1 g de dérivé tétrabromé du diméthylnaphtalène **25** (31) en présence de 0.400 g naphtazarone **8** et d'iodure de sodium pendant 48 h. On isole 0.16 g de cristaux rouges, rdt 20%, pf inst 384°C (subl.) (litt. (29) pf 385°C (subl.)).

*Anthracènetétrone-1,4,5,8 (17*a)

A 0.600 g de quinone diméthoxylée **10***a* dissous dans 210 cm^3 d'un mélange acétonitrile–acétone (1:5) sont ajoutés goutte à goutte 3.40 g de nitrate d'ammonium et de cérium en solution dans 10 cm^3 d'eau. Après extraction au chloroforme, lavage à l'eau, la phase organique est séchée sur sulfate de sodium puis évaporée. On isole 0.31 g de cristaux "jaune pâle", rdt 58%, pf inst 224°C (acétonitrile). Ultraviolet et visible (CH_2Cl_2) λ_{max} (log ε): 360 inf. (3.65), 355 (3.67), 304 inf (3.56), 252 (4.65); ir (KBr) ν(C=O): 1660 cm^{-1}; rmn ^1H δ: 8.86 (s, 2H, aromatiques, H-9, H-10), 7.13 (s, 2H, aromatiques, H-2, H-3), 2.26 (s, 6H, CH_3). *Anal.* calc. pour $C_{16}H_{10}O_4$: C 72.18, H 3.79; trouvée: C 71.70, H 3.90.

*Naphtacènetétrone-1,4,6,11 (17*b)

Une solution de 2.58 g de nitrate de cérium et d'ammonium dans 6 cm^3 d'eau est versée lentement sur 0.4 g de quinone diméthoxylée **11***a* dissous dans 360 cm^3 d'un mélange acétone–acétonitrile (5:1). Après une demi-heure d'agitation, extraction au chloroforme et traitement habituel, on essore 0.19 g de cristaux, rdt 52%, pf inst 262°C (diméthylformamide). Ultraviolet et visible (CH_2Cl_2) λ_{max} (log ε): 357 inf (3.79), 348 (3.84), 300 (3.74), 259 (4.75); ir (KBr) ν(C=O): 1670 cm^{-1}; rmn ^1H δ: 9.04 (s, 2H, aromatiques, H-5, H-12), 7.73–8.56 (m, 4H, aromatiques, H-7, H-8, H-9, H-10), 7.17 (s, 2H, aromatiques, H-2, H-3). *Anal.* calc. pour $C_{18}H_8O_4$: C 75.00, H 2.80; trouvée: C 74.45, H 3.01.

Remerciements

Les auteurs expriment leur gratitude à la Délégation Générale à la Recherche Scientifique et Technique pour la bourse accordée à l'un d'entre eux.

1. M. P. CAVA, A. A. DEANA et K. MUTH. J. Am. Chem. Soc. **81**, 6458 (1959).
2. K. ALDER et M. FREMERY. Tetrahedron, **14**, 190 (1961).
3. J. F. W. MACOMIE et D. H. PERRY. Synthesis, **7**, 416 (1973).
4. L. LEPAGE et Y. LEPAGE. C.R. Acad. Sci. Sér. C, **280**, 847 (1975).
5. (*a*) A. ETIENNE et Y. LEPAGE. C.R. Acad. Sci. **240**, 1233 (1955); (*b*) Y. LEPAGE. Ann. Chim. (Paris), 1150 (1959); 1152 (1959).
6. B. H. KLANDERMAN et T. H. R. CRISWELL. J. Am. Chem. Soc. **91**, 510 (1969).
7. D. L. MARICLE et M. RAUHUT. Belg. Patent No. 666,750, (Jan. 12, 1966); U.S. Appl. July 13, 1964; Chem. Abstr. **65**, 11 769 g (1966).
8. (*a*) C. M. WONG, D. POPIEN, R. SCHWENK et J. TERAA. Can. J. Chem. **49**, 2712 (1971); (*b*) C. M. WONG, R. SCHWENK, D. POPIEN et T. L. HO. Can. J. Chem. **51**, 466 (1973); (*c*) R. J. BLADE et P. HODGE. J. Chem. Soc. Chem. Commun. 85 (1979).
9. R. H. THOMSON. Naturally occurring quinones. Academic Press, London and New York. 1971. p. 563.
10. A. S. KENDE, J. E. MILLS et Y. G. TSAY. U.S. Patent No. 4,021,457 (3 mai 1977); Appl. 632,939 (18 nov. 1975).
11. (*a*) F. ARCAMONE, L. BERNARDI, B. PATELLI et A. DI MARCO. Ger. Patent No. 2,601,785 (28 juil. 1976); Brit. Appl. 75/2, 691 (22 janv. 1975); (*b*) L. BERNARDI, P. GIARDINO, B. PATELLI et F. ARCAMONE. Ger. Patent No. 2,727,341 (22 déc. 1977); Brit. Appl. 76/25, 517 (19 juin 1976).
12. R. D. GLEIM, S. TRENBEATH, R. S. D. MITTAL et C. J. SIH. Tetrahedron Lett. **38**, 3385 (1976).
13. F. ARCAMONE, L. BERNARDI, P. GIARDINO, B. PATELLI, A. DI MARCO, A. M. CASAZZA, G. PRATESI et P. REGGIANI. Cancer Treat. Rep. **60**, 829 (1976).
14. (*a*) A. S. KENDE, Y. G. TSAY et J. E. MILLS. J. Am. Chem. Soc. **98**, 1967 (1976); (*b*) A. S. KENDE, J. BELLETIRE, T. J. BENTLEY, E. HUME et J. AIREY. J. Am. Chem. Soc. **97**, 4425 (1975).
15. W. W. LEE, A. P. MARTINEZ, T. H. SMITH et D. W. HENRY. J. Org. Chem. **41**, 2297 (1976).
16. F. ARCAMONE, L. BERNARDI, B. PATELLI, P. GIARDINO, A. DI MARCO, A. M. CASAZZA, C. SORANZO et G. PRATESI. Experientia, **34**, 1255 (1978).
17. F. A. J. KERDESKY et M. P. CAVA. J. Am. Chem. Soc. **100**, 3635 (1978).
18. J. R. WISEMAN, N. I. FRENCH, R. K. HALLMARK et K. G. CHIONG. Tetrahedron Lett. **40**, 3765 (1978).
19. (*a*) T. KAMETANI, M. TAKESHITA, H. NEMOTO et K. FUKUMOTO. Chem. Pharm. Bull. **26**, 556 (1978); (*b*) A. AMARO, M. C. CARRENO et F. FARINA. Tetrahedron Lett. **41**, 3983 (1979); (*c*) R. K. BOECKMAN, JR., M. H. DELTON, T. NAGASAKA et T. WATANABE. J. Org. Chem. **42**, 2946 (1977).
20. M. P. CAVA et A. A. DEANA. J. Am. Chem. Soc. **81**, 4266 (1959).
21. T. J. LEVEK et E. F. KIEFFER. J. Am. Chem. Soc. **98**, 1875 (1976).
22. C. SANNIE, J. J. PANOUSE et S. VERTALIER. Bull. Soc. Chim. Fr. 1039 (1955).
23. A. K. MACBETH, J. R. PRICE et F. L. WINZOR. J. Chem. Soc. 325 (1935).
24. P. JACOB III, P. S. CALLERY, A. T. SHULGIN et N. CASTAGNOLI, JR. J. Org. Chem. **41**, 3627 (1976).
25. M. P. CAVA et J. P. VAN METER. J. Org. Chem. **34**, 538 (1969).
26. L. LEPAGE et Y. LEPAGE. J. Heterocycl. Chem. **15**, 793 (1978).
27. L. LEPAGE et Y. LEPAGE. J. Heterocycl. Chem. **15**, 1185 (1978).
28. M. P. CAVA et R. L. SHIRLEY. J. Am. Chem. Soc. **82**, 654 (1959).
29. B. SERPAUD et Y. LEPAGE. Bull. Soc. Chim. Fr. 539 (1977).
30. L. HORNER, P. V. SUBRAMANIAN et K. EIBEN. Justus Liebigs Ann. Chem. **714**, 91 (1968).
31. W. RIED et H. BODEM. Chem. Ber. **89**, 708 (1956).

Can. J. Chem. Downloaded from www.nrcresearchpress.com by 210.87.254.42 on 09/05/12
For personal use only.

Réactions d'addition nucleophiles sur les cétones. Une méthode directe, simple, rapide et précise de mesure de vitesse de formation et de décomposition des combinaisons bisulfitiques

BERNARD BOYER, GÉRARD LAMATY ET JEAN PIERRE ROQUE

Laboratoire de Chimie Organique Physique, Université des Sciences et Techniques du Languedoc, Place Eugène Bataillon, 34060 Montpellier, France

Reçu le 21 février 1980

BERNARD BOYER, GÉRARD LAMATY et JEAN PIERRE ROQUE. Can. J. Chem. **58**, 1168 (1980).

Description d'une méthode qui permet, en une seule expérience, de mesurer directement la constante de vitesse d'addition de l'ion sulfite sur les carbonyles et la constante de vitesse de décomposition des combinaisons bisulfitiques.

BERNARD BOYER, GÉRARD LAMATY, and JEAN PIERRE ROQUE. Can. J. Chem. **58**, 1168 (1980).

A method is described which allows, with a single experiment, the determination of the rate constants of formation and decomposition of bisulfite addition compounds.

Can. J. Chem. Downloaded from www.nrcresearchpress.com by 210.87.254.105 on 09/05/12
For personal use only.

Les travaux entrepris depuis plusieurs années au laboratoire nous ont conduit à proposer que la position de l'état de transition le long du chemin réactionnel dépendait de la nature du nucléophile (1). Certains, tels les ions BH_4^- et CN^-, donnent un état de transition plutôt tardif, d'autres comme le mercaptoéthanol ou l'hydroxylamine un état de transition plutôt précoce. L'ion sulfite est un autre exemple de nucléophile à état de transition précoce et il a été plusieurs fois utilisé tant par nous (2) que par d'autres auteurs (3).

Cependant, nous étant intéressé récemment à sa réactivité vis-à-vis de cétones encombrées, nous nous sommes heurtés à des difficultés expérimentales qui ne nous ont pas permis d'utiliser la technique cinétique volumétrique mise au point par l'un de nous (2); cette technique, outre le fait qu'elle est grosse consommatrice de produit, n'est pas applicable aux composés dont la combinaison bisulfitique est trop instable.

L'examen de la littérature, même la plus récente (3*d*, 3*e*) nous a montré qu'il n'existait aucune méthode de *mesure directe* de la constant de vitesse d'addition, k_a, de l'ion sulfite sur les carbonyles; toutes les méthodes décrites à ce jour consistent à mesurer la constante d'équilibre, K, et la constante de vitesse, k_d, de décomposition des combinaisons bisulfitiques et à égaler k_a au rapport k_d/K. Si la précision sur k_d est généralement bonne, celle sur K est beaucoup plus modeste ($\pm 5\%$ dans le meilleur des cas) et l'incertitude sur K se répercute sur k_a, ce qui rend cette technique indirecte impropre à l'un des usages que nous voulions en faire: mesurer les effets isotopiques cinétiques secondaires du deutérium, qui sont généralement faibles, sur des cétones encombrées pour lesquelles k_a est forcément petit.

Nous avons donc été amenés à essayer de mettre au point une méthode *directe*, et *précise* de mesure de k_a; au cours du déroulement de nos essais, nous nous sommes aperçus qu'il était possible de mesurer directement, sur le *même échantillon*, *et* k_a *et* k_d avec une précision tout à fait satisfaisante. C'est cette technique que nous décrivons dans ce mémoire; elle a l'avantage d'être simple à mettre en oeuvre, de consommer peu de produit et nous pensons qu'elle peut être utile aux autres groupes de chercheurs intéressés par l'étude de ce type de réaction.

Principe de la méthode

Elle consiste à étudier *directement* la réaction d'addition en ajoutant une quantité adéquate de cétone à une solution concentrée de bisulfite de Na et en suivant, par spectrophotométrie uv, la disparition de la cétone. Lorsque l'équilibre est atteint, on détruit le bisulfite restant par un réactif approprié que l'on ajoute en léger excès; la combinaison bisulfitique se décompose alors, libérant la cétone dont on suit l'apparition par uv et du bisulfite de Na qui est aussitôt neutralisé par l'excès de réactif.

Une telle méthode, pour pouvoir être appliquée, doit satisfaire aux conditions suivantes.

(1) Il faut que les solutions de sulfite soient stables au moins pendant la durée de la mesure. Nous avons constaté, par dosages iodométriques (4) répétés, qu'une solution de SO_3HNa, environ 0.5 *M*, à pH 5.41 dans un tampon acétique, perdait 3% de son titre environ en 10 jours; on peut donc raisonnablement admettre qu'elle évoluera très peu au cours d'une expérience qui dure au maximum quelques heures.

(2) Il faut que l'on puisse trouver une longueur d'onde adéquate. Les solution de bisulfite absorbent légèrement ($\varepsilon = 11$ à 256 nm) dans la région du

0008-4042/80/121168-04$01.00/0

©1980 National Research Council of Canada/Conseil national de recherches du Canada

Can. J. Chem. Downloaded from www.nrcresearchpress.com by 210.87.254.105 on 09/05/12
For personal use only.

spectre (bande $n \rightarrow \pi^*$) du carbonyle. Il est toutefois possible, dans le domaine de concentrations utilisées, de trouver une longueur d'onde permettant d'observer la disparition et la réapparition de la cétone; nous avons constaté qu'à la longueur d'ordre de 295 nm les variations de densité optique ($\simeq 0.2$) étaient suffisantes pour suivre correctement l'évolution de la concentration en cétone.

(3) Il faut que l'on trouve un réactif qui consomme instantanément et totalement l'excès de sulfite. L'addition de l'ion sulfite étant réalisée, il fallait trouver un réactif qui éliminerait tout le sulfite libre, déplaçant ainsi l'équilibre vers la cétone. Notre choix s'est porté sur le formol 35%, neutralisé au préalable par une solution de soude 1 *N*; il est très réactif vis-à-vis du sulfite et donne instantanément un produit d'addition très stable. De plus, en solution aqueuse, il est présent sous forme d'hydrate et n'absorbe pas dans la région considérée ($\lambda = 295$ nm).

(4) Il faut qu'il existe un pH auquel les réactions d'addition et de décomposition aient approximativement la même vitesse. Afin de réaliser consécutivement, *sur le même échantillon et* l'addition de l'ion sulfite *et* la décomposition de la combinaison bisulfitique, il était nécessaire que les deux constantes de vitesse expérimentales soient à peu près du même ordre de grandeur.

Notre expérience antérieure nous a montré que dans le domaine de pH 5–6, cette dernière condition était remplie. Les composés carbonylés étant peu solubles dans l'eau, nous avons utilisé comme solvant un mélange H_2O/EtOH 60:40 en volume dans un tampon acétique, [AcOH] = 0.05 *M*, de pH égal à 5.41 (5).

Description de la méthode

Nous représenterons sur le schéma ci-dessous (fig. 1) un exemple de cinétique réunissant à la fois les variations de densité optique de la réaction d'addition de l'ion sulfite et celles de la réaction de décomposition des combinaisons bisulfitiques.

Réaction d'addition (partie (a) de la courbe enregistrée)

Nous nous sommes placés dans des conditions cinétiques du pseudopremier ordre; la concentration en sulfite est au moins 10 à 15 fois supérieure à la concentration en cétone ($[SO_3HNa]_0 \simeq 0.25\ M$; $[C{=}O]_0 \simeq 1.5 \times 10^{-2} M$).

L'avancement de la réaction se traduit par une décroissance de l'absorption du groupe carbonyle. On suit la disparition de la cétone jusqu'à ce que la courbe D = f(t) tende vers une valeur constante; l'équilibre est alors atteint.

La partie (a) de cette cinétique nous donne une constante de vitesse expérimentale du pseudo-

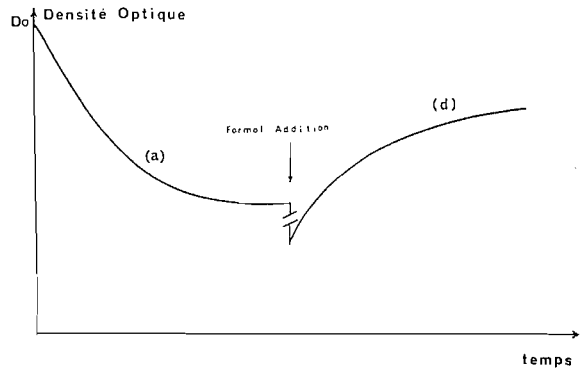


FIG. 1. Variation de la densité optique en function du temps.

premier ordre, k_f qui représente en fait la somme des constantes d'addition k_a, et de décomposition, k_d, puisque la réaction est équilibrée.

Réaction de décomposition (partie (d) de la courbe envisagée)

Lorsque l'équilibre est atteint, nous ajoutons dans la cuve 100 µL de formol neutre à 35% qui réagit avec le sulfite en excès et le fixe ensuite irréversiblement au fur et à mesure de sa formation, déplaçant ainsi l'équilibre vers la cétone.

Nous observons d'abord une chute brutale de la densité optique, résultant de la disparition de l'excès de SO_3HNa, puis une augmentation lente de la densité optique due à l'apparition de la cétone. On enregistre la courbe D = f(t).

Nous avons vérifié que la vitesse de la réaction de décomposition était indépendante de la quantité de formol ajouté, à condition qu'il soit en excès par rapport au sulfite total. Les constantes de vitesse de formation et de décomposition dépendant du pH utilisé, nous avons vérifié également qu'il n'y avait pas de variation de pH au cours de la réaction et en particulier lors de la fixation, par le formol, du sulfite en excès.

Nous mesurons alors la vitesse de disparition du composé d'addition, cette réaction est du premier ordre par rapport au substrat.

Détermination des constantes de vitesse de formation et de décomposition

Le mécanisme détaillé de la réaction correspond au schéma suivant (6):

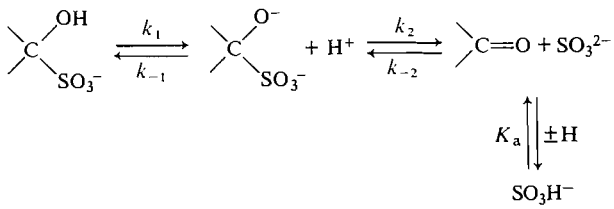


SCHÉMA I

Can. J. Chem. Downloaded from www.nrcresearchpress.com by 210.87.254.105 on 09/05/12
For personal use only.

On démontre (8) que les constantes de vitesse de formation, k_f, et de décomposition, k_d, mesurées *expérimentalement*, sont reliées à la constante d'addition réelle k_a par l'expression:

$$k_f = k_a[SO_3H^-] + k_d \text{ avec:}$$
$$k_d = k_1k_2/k_{-1}[H^+] \text{ et } k_a = k_{-2}K_a/[H^+]$$

La lissage, par la méthode des moindres carrés (7), des exponentielles obtenues sur les parties (a) et (d) des courbes (fig. 1) conduit aux valeurs k_f et k_d.

Connaissant la concentration exacte en SO_3HNa, obtenue par dosage iodométrique, k_f et k_d, nous pouvons alors déduire la constante de vitesse d'addition k_a, ainsi que la constante d'équilibre $K = k_d/k_a$ de décomposition de la combinaison bisulfitique.

Résultats

A titre d'exemple, nous donnons ci-dessous les résultats obtenus avec trois cétones encombrées, une cétone non encombrée et son homologue deutérié.

Pour chaque cétone, nous indiquons la concentration en ion sulfite, la constante de formation k_f, celle de décomposition k_d, celle d'addition k_a et enfin la constante d'équilibre de décomposition $K = k_d/k_a$. Toutes les valeurs des constantes de vitesse sont multipliées par 10^3 et sont exprimées en s^{-1} (k_f et k_d) ou $M^{-1}s^{-1}$ (k_a)

Norbornanone-2 $[HSO_3Na] = 0.223\ M$
k_f : 4.92, 4.94, 4.83, 4.88, 4.88, 4.92
k_d : 2.56, 2.55, 2.64, 2.62, 2.58, 2.61 $\quad \bar{k}_d = 2.593 \pm 0.036$
k_a : 10.58, 10.72, 9.82, 10.13, 10.31, 10.36 $\quad \bar{k}_a = 10.32 \pm 0.32$
$K = 0.25\ M^{-1}$

Méthyl-1 norbornanone-2 $[HSO_3Na] = 0.231\ M$
k_f : 3.63, 3.67, 3.68, 3.62
k_d : 3.35, 3.40, 3.40, 3.36 $\quad \bar{k}_d = 3.378 \pm 0.026$
k_a : 1.21, 1.17, 1.21, 1.13 $\quad \bar{k}_a = 1.18 \pm 0.04$
$K = 2.86\ M^{-1}$

Triméthyl-3,3,5 cyclohexanone $[HSO_3Na] = 0.249\ M$
k_f : 11.5, 11.6, 11.1, 11.2, 11.2, 11.1
k_d : 2.37, 2.36, 2.43, 2.37, 2.45, 2.42 $\quad \bar{k}_d = 2.400 \pm 0.038$
k_a : 36.66, 37.10, 34.82, 35.46, 35.14, 34.86 $\quad \bar{k}_a = 35.68 \pm 0.97$
$K = 0.067\ M^{-1}$

Cyclohexanone $[HSO_3Na] = 0.223\ M$
k_f : 41.9, 41.6, 41.7, 41.9, 41.5
k_d : 0.528, 0.525, 0.530, 0.523, 0.523 $\quad \bar{k}_d = 0.526 \pm 0.003$
k_a : 185.5, 184.2, 184.6, 185.5, 183.8 $\quad \bar{k}_a = 184.7 \pm 0.80$
$K = 2.80 \times 10^{-3}\ M^{-1}$

Cyclohexanone-2,2,6,6-d_4 $[HSO_3Na] = 0.223\ M$
k_f = 45.7, 45.6, 45.3, 45.8, 45.7, 45.6
k_d : 0.482, 0.482, 0.483, 0.487, 0.483, 0.485 $\quad \bar{k}_d = 0.484 \pm 0.002$
k_a : 202.8, 202.3, 201.0, 203.2, 202.8, 202.3 $\quad \bar{k}_a = 202.40 \pm 0.76$

Effets isotopiques:
$k_a^H/k_a^D = 0.913 \pm 0.008$ $\quad k_d^H/k_d^D = 1.087 \pm 0.010$

Partie expérimentale

Toutes les mesures ont été effectuées à 25.0 ± 0.1°C sur un spectrophotomètre uv Gilford-250. Les différentes solutions ont été préparées somme suit.

Solution A $[SO_3HNa] \simeq 0.5\ M$

Dans un ballon de 100 mL, on introduit 9.5055 g de pyrosulfite de sodium anhydre RP et on ajuste le volume par le tampon acétique. Cette solution est étalonnée au moment de l'utilisation.

Solution B $[C{=}O] \simeq 3 \times 10^{-2}\ M$

On pèse la quantité nécessaire de cétone pour préparer dans le même tampon 20 mL d'une solution dont la concentration initiale est voisine de $3 \times 10^{-2}\ M^{-1}$. Les solutions A et B sont plongées dans un bain thermostaté à 25.0 ± 0.1°C. Après l'équilibre thermique on met (*a*) dans la cuve de référence: 2 mL tampon; (*b*) dans la cuve de mesure: 1 mL solution A + 1 mL solution B.

Discussion

Les résultats présentés ci-dessus montrent qu'il

est possible de mesurer directement la constante de vitesse d'addition de l'ion sulfite sur un carbonyle avec une précision généralement très bonne; les déviations standards vont de 0.3% dans le meilleur des cas à 3.5% dans le plus mauvais. Contrairement à ce que l'on pourrait craindre les solutions concentrées de sulfite sont stables et l'absorption de l'ion SO_3^{2-} ne masque pas totalement celle du carbonyle. La méthode décrite ci-dessus est donc utilisable pour toutes les cétones, mêmes celles qui donnent une combinaison bisulfitique très instable (méthyl-1 norbornanone-2) dès lors que l'on ne se propose que d'étudier l'influence de la structure de la cétone sur k_a donc qu'une précision de l'ordre de 5% est suffisante.

En revanche si on est intéressé par le mesure des effets isotopiques secondaires, le plus souvent faibles, cette technique ne peut être utilisée qu'avec les cétones assez réactives, donnant une combinaison bisulfitique stable et pour lesquelles k_f et k_d sont très différentes l'une de l'autre. Pour cette raison, nous n'avons même pas essayé de mesuré les constantes de vitesse de la méthyl-1 norbornanone-2 deutériée, car les effets isotopiques que nous aurions pu calculer auraient été dépourvus de toute signification.

1. P. GENESTE, G. LAMATY et J. P. ROQUE. Tetrahedron Lett. 5007 (1970).
2. P. GENESTE, G. LAMATY et J. P. ROQUE. Tetrahedron, **27**, 5539 (1971).
3. (*a*) T. D. STEWART et L. H. DONALLY. J. Am. Chem. Soc. **54**, 2333 (1932); **54**, 3559 (1932); (*b*) D. A. BLACKADDER et C. HINSHELWOOD. J. Chem. Soc. 2720 (1948); 2782 (1948); (*c*) C. G. GREEN et J. HINE. J. Org. Chem. **39**, 3897 (1974); (*d*) P. R. YOUNG and W. P. JENCKS. J. Am. Chem. Soc. **99**, 1206 (1977); (*e*) P. R. YOUNG and W. P. JENCKS. J. Am. Chem. Soc. **100**, 1228 (1978).
4. G. CHARLOT. Les méthodes de la chimie analytique. Masson. Paris. 1961. p. 915.
5. D. D. PERRIN et B. DEMPSEY. Buffers for pH and metal-ion control. Chapman and Hall, London. 1974. p. 77.
6. C. N. CAUGHLAN et H. V. TARTAR. J. Am. Chem. Soc. **63**, 1265 (1941).
7. D. E. DEMING. Statistical adjustment of data. J. Wiley and Sons, New York. 1948.
8. B. BOYER. Thèse de Doctorat d'Etat, Montpellier, France. 1978.

Can. J. Chem. Downloaded from www.nrcresearchpress.com by 210.87.254.105 on 09/05/12
For personal use only.

Cyclisation during an attempted Meyer–Schuster rearrangement

PAUL CACHIA, NICHOLAS DARBY, THOMAS C. W. MAK,[1] THOMAS MONEY, AND JAMES TROTTER
Chemistry Department, The University of British Columbia, 2075 Wesbrook Mall, Vancouver, B.C., Canada V6T 1W5

Received January 23, 1980

PAUL CACHIA, NICHOLAS DARBY, THOMAS C. W. MAK, THOMAS MONEY, and JAMES TROTTER. Can. J. Chem. **58**, 1172 (1980).

The structure of a tricyclic diketone produced during Meyer–Schuster rearrangement has been established by chemical and X-ray crystallographic evidence.

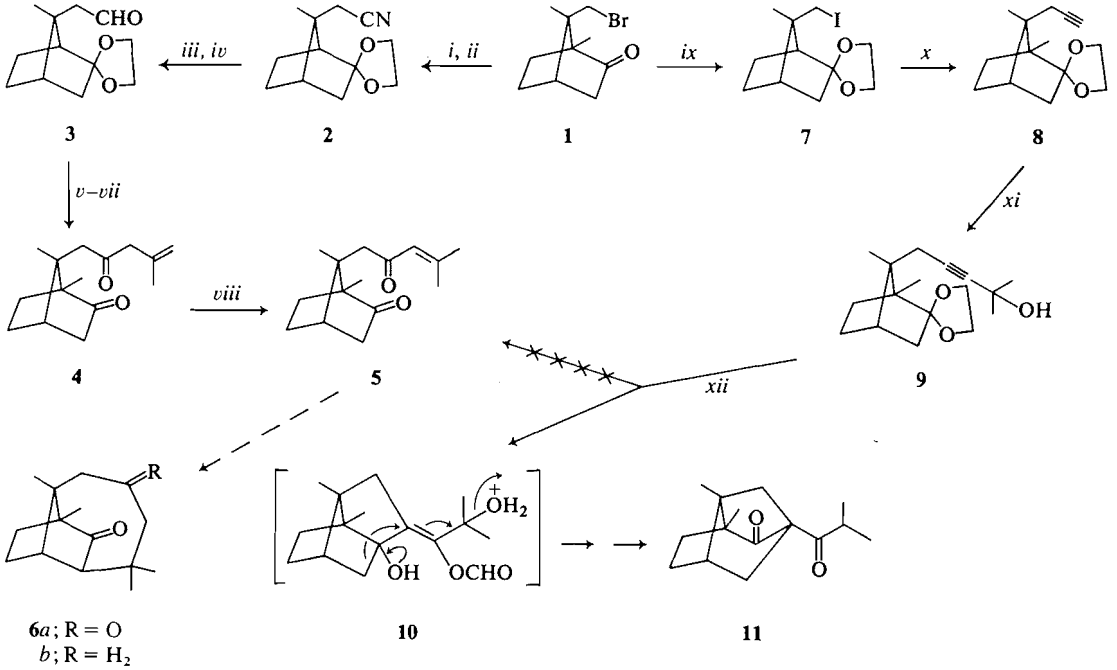
PAUL CACHIA, NICHOLAS DARBY, THOMAS C. W. MAK, THOMAS MONEY et JAMES TROTTER. Can. J. Chem. **58**, 1172 (1980).

Les preuves fournies par la radiocristallographie ont permis d'établir la structure de la dicétone tricyclique produite au cours de la transposition de Meyer–Schuster.

[Traduit par le journal]

Can. J. Chem. Downloaded from www.nrcresearchpress.com by 210.87.254.5 on 09/05/12
For personal use only.

The development of simple synthetic routes from camphor to a variety of monoterpenoids and sesquiterpenoids has been the subject of recent investigations in our laboratory (1–3). One objective of our general synthetic scheme (1) was the conversion of camphor to longicamphor (**6***b*) (4) and the subsequent use of this compound as an intermediate in the synthesis of related sesquiterpenoids. Our initial synthetic approach to longicamphor (**6***b*) depended on the successful cyclisation of an intermediate enedione (**5**) to diketone (**6***a*) followed by selective reduction of the more accessible carbonyl group in this compound. A simple synthesis of enedione (**5**) from 8-bromocamphor (**1**) was subsequently achieved (cf. Scheme 1) but our preliminary attempts to cyclise this compound were unsuccessful. During investigations of an alternative synthetic route to enedione (**5**), however, an interesting new reaction occurred. In this alternative route, treatment of 8-iodocamphor ethylene acetal (**7**) (1, 2) with lithium acetylide provided an 8-ethynyl derivative



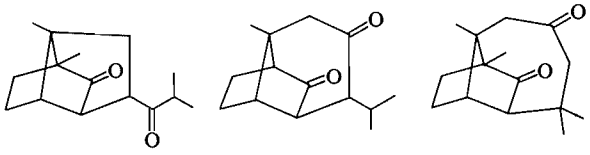
SCHEME 1. *i*, KCN/HMPA; *ii*, $(CH_2OH)_2$, H^+; *iii*, DIBAL/C_6H_{12}; *iv*, HCl/Rochelle salt; *v*, $CH_2{=}C(CH_3)CH_2MgBr$; *vi*, H_3O^+, dioxane; *vii*, CrO_3/C_5H_5N; *viii*, Al_2O_3; *ix*, NaI/HMPA; *x*, $LiC{\equiv}CH{:}H_2NCH_2CH_2NH_2$/HMPA/$Et_2O$; *xi*, *n*-BuLi/$Et_2O$/$Me_2CO$/0–25°C; *xii*, 98%$HCO_2H$/95°C/7 h.

[1]On sabbatical leave from The Chinese University of Hong Kong, Shatin, New Territories, Hong Kong.

0008-4042/80/121172-06$01.00/0
©1980 National Research Council of Canada/Conseil national de recherches du Canada

Can. J. Chem. Downloaded from www.nrcresearchpress.com by 210.87.254.5 on 09/05/12
For personal use only.

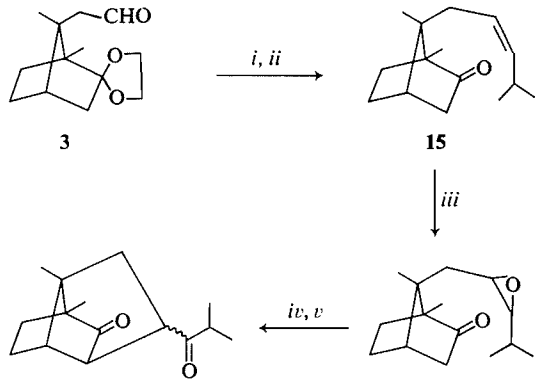
(**8**) whose lithium salt condensed with acetone to give acetylenic alcohol (**9**). It was expected that this compound would undergo Meyer–Schuster rearrangement (5) to the enedione (**5**). In the event, treatment of acetylenic alcohol (**9**) with 98% formic acid led to the formation of a crystalline product (mp 49–51°C (sealed tube); $[\alpha]_D$ +32.5 (c. 1.19, abs. EtOH); 50% yield (glc yield ~68–80%)) whose spectroscopic properties (λ_{max} end absorption, ν_{max} 1701, 1745 cm^{-1}; $\delta(CCl_4)$ 0.98 (6H, s), 1.05 (6H, s), 2.84 (1H, septet); *m/e* (relative intensity), 234 (M^+) (42), 191 (100), 163 (51) were inconsistent with the expected enedione structure (**5**). The absence of a 1415 cm^{-1} band in the ir spectrum and vinyl hydrogen signals in the nmr spectrum led us to consider that cyclisation had occurred during the formic acid treatment. Of three possible tricyclic diketone structures for this compound **12** was rejected by independent synthesis (cf. Scheme 2) and structure **14** was inconsistent with the presence of



12 **13** **14**

an $M - C_3H_7$ (isopropyl) peak in the mass spectrum and the septet at 2.84 δ in the nmr spectrum. Structure **13** was difficult to rationalise on mechanistic grounds and was also inconsistent with the presence of an $M - C_3H_7CO$ peak in the mass spectrum. A final solution to this structural problem was provided by X-ray crystallographic analysis which demonstrated that the diketone was a tricyclo[4.2.1.$0^{3,7}$]nonane derivative (**11**).

The bond lengths and a perspective view of **11** are shown in Fig. 1 and the bond angles are listed in Table 1. Atoms C(1), C(2), C(4), and C(5) (cf. Fig. 1) are co-planar, as are C(1), C(5), C(6), and C(7), and the cycloheptane skeleton C(1)—C(7) has the chair conformation. The [4.2.1.$0^{3,7}$]nonane system deviates considerably from idealized $m(C_s)$ symmetry as a result of ring substitution and the strain is reflected mainly in the small bond angles involving the bridge atoms C(3), C(8), and C(9). The crystal structure consists of well-separated molecules with the shortest intermolecular contacts corresponding to normal van der Waals' interactions.



3 **15** **16** **12**

SCHEME 2. *i*, $Me_2CHCH{=}PPh_3$; *ii*, Me_2CO/6 *N* HCl; *iii*, MCPBA/C_6H_6; *iv*, Me_3COH/Me_3COK; *v*, $CrO_3/H_2SO_4/H_2O/Me_2CO$.

Thus treatment of acetylenic alcohol (**9**) with formic acid results in cyclisation as well as rearrangement of the original bicyclo[2.2.1]heptane framework. A possible mechanism for this novel transformation[2] is shown in Scheme 1.

Experimental

Unless otherwise stated the following are implied. Melting points (mp) were determined on a Thomas Hoover capillary melting point apparatus and are uncorrected. Gas chromatography was carried out on a Hewlett-Packard Model 5831-A gas chromatograph using 6 ft × 1/8 in. columns and nitrogen as carrier gas. The following columns were employed:

Column	Dimensions	Stationary phase	Support	Mesh
A	6 ft × 1/8 in.	3% OV-17	Chromosorb W (HP)	80/100
B	6 ft × 1/8 in.	3% OV-101	Chromosorb W(HP)	80/100

The carrier gas flow rate was about 35 mL/min. The 60 MHz nmr spectra were recorded on a Varian Associates Model T-60. The 100 MHz spectra were recorded on a Varian Associates Model HA-100 or Model XL-100 and the 270 MHz spectra were recorded on a 270 MHz instrument (7) constructed from a Bruker console, a Nicolet computer Model 293A with a Diablo disk, and a 270 MHz super conducting magnet supplied by Oxford Instruments. Signal positions are given in delta (δ) with tetramethyl silane (TMS) as an internal reference. Signal multiplicity and integrated area are indicated in parentheses. Infrared spectra were recorded on a Perkin-Elmer 137 spec-

[2]In terms of Baldwin's Rules (6), this transformation, in the initial stage, could be described as a 5-*exo*-dig cyclisation.

Can. J. Chem. Downloaded from www.nrcresearchpress.com by 210.87.254.5 on 09/05/12
For personal use only.

TABLE 1. Bond angles (deg) with estimated standard deviations in parentheses

Bonds	Angle (deg)	Bonds	Angle (deg)
C(2)—C(1)—C(11)	109.2(2)	C(4)—C(5)—C(8)	102.4(2)
C(7)—C(1)—C(11)	114.6(3)	C(6)—C(5)—C(8)	104.9(2)
C(8)—C(1)—C(11)	116.7(3)	C(5)—C(6)—C(7)	104.8(2)
C(2)—C(1)—C(7)	109.4(2)	C(6)—C(7)—C(1)	107.1(2)
C(2)—C(1)—C(8)	100.6(2)	C(1)—C(8)—C(5)	99.6(2)
C(7)—C(1)—C(8)	105.1(2)	C(1)—C(8)—C(9)	104.6(2)
C(1)—C(2)—C(3)	107.1(2)	C(1)—C(8)—C(10)	115.6(2)
C(1)—C(2)—O(1)	125.5(2)	C(5)—C(8)—C(9)	103.2(2)
C(3)—C(2)—O(1)	127.4(2)	C(5)—C(8)—C(10)	114.0(2)
C(2)—C(3)—C(4)	103.8(2)	C(9)—C(8)—C(10)	117.5(2)
C(2)—C(3)—C(9)	100.3(2)	C(3)—C(9)—C(8)	96.4(2)
C(2)—C(3)—C(12)	112.1(2)	C(3)—C(12)—C(13)	118.3(2)
C(4)—C(3)—C(9)	100.9(2)	C(3)—C(12)—O(2)	120.4(2)
C(4)—C(3)—C(12)	117.4(2)	C(13)—C(12)—O(2)	121.2(2)
C(9)—C(3)—C(12)	119.9(2)	C(12)—C(13)—C(14)	110.6(3)
C(3)—C(4)—C(5)	104.6(2)	C(12)—C(13)—C(15)	110.0(3)
C(4)—C(5)—C(6)	115.0(3)	C(14)—C(13)—C(15)	111.7(3)

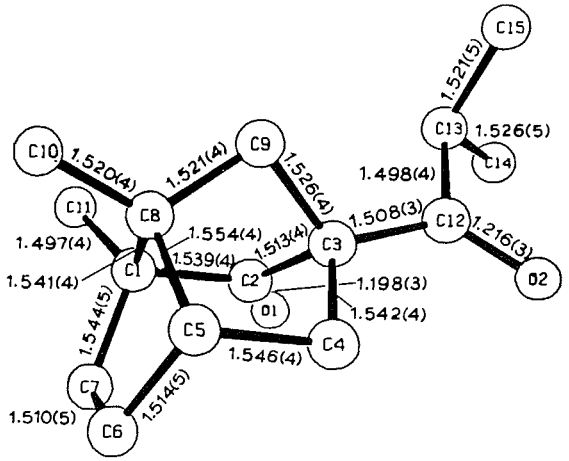


FIG. 1. Perspective view of **11** (crystallographic numbering) showing bond distances (Å) with their estimated standard deviations in parentheses. The atom numbering corresponds to those of Table 1.

trophotometer and optical rotations were measured with either a Perkin-Elmer Model 141 polarimeter or a Perkin-Elmer Model 241 MC polarimeter. Low resolution mass spectra were recorded on a Varian/Mat Model CH4B mass spectrometer and high resolution mass spectra were determined on the AEI Model MS902 or Model MS550 instrument. Microanalyses were performed by Mr. P. Borda, Microanalytical Laboratory, University of British Columbia, Vancouver. All the solvents used for nmr, ir, and optical rotations were of spectral grade. Dry solvents were obtained in the following way: ether by distillation from sodium; hexamethylphosphoramide (HMPA), benzene, *t*-butanol, and hexanes by distillation from CaH_2; acetone by distillation from 4A molecular sieves; tetrahydrofuran (THF) by distillation from $LiAlH_4$.

(+)-8-Cyanocamphor Ethylene Acetal (2)

(+)-8-Bromocamphor ethylene acetal (10.0 g, 36.4 mmol) and sodium cyanide (10.70 g, 0.218 mol) were dissolved in dry hexamethylphosphoramide (HMPA) (100 mL) and the reaction mixture heated at 100°C for 4 days under a nitrogen atmosphere. Addition of water (200 mL) followed by extraction with petroleum ether (30–60) (5 × 50 mL) and workup in the usual way provided (+)-8-cyanocamphor ketal (**2**) (7.0 g, 88% yield) as a colourless oil; bp 85–87°C/10^{-2} mm; $[\alpha]_D^{26} = +5.06$ (c 2.35, 95% EtOH): $\delta(CCl_4)$ 0.76 (s, 3H), 1.05 (s, 3H), 2.13 (d, 1H, J = 17 Hz), 2.86 (d, 1H, J = 17 Hz), 3.79 (m, 4H) $\nu_{max}(CCl_4)$ 2247 and 1420 cm^{-1}; *m/e* 221 (M^+), 181, 113, 95 (base peak) M.W. calcd. for $C_{13}H_{19}NO_2$: 221.1415. Found (high resolution mass spectrometry): 221.1422. *Anal.* calcd. for $C_{13}H_{19}NO_2$: C 70.54, H 8.66, N 6.33; found: C 70.44, H 8.50, N 6.20.

8-Formylcamphor Ethylene Acetal (3)

8-Cyanocamphor ethylene acetal (**2**) (2.33 g, 10.6 mmol) was dissolved in dry hexane (30 mL) and the solution cooled (dry ice – acetone) to −50°C. Diisobutylaluminum hydride (DIBAL) (Alfa, 20% in hexane, 1 molar solution, 13.2 mL, 13.2 mmol) was added via syringe under a nitrogen atmosphere and the reaction was warmed to room temperature over 2 h.

The reaction mixture was carefully added to a mixture of saturated Rochelle salt and water (1:1; 150 mL). Hydrochloric acid (6 *N*) was added (5 mL) and this mixture was stirred vigorously for 2 h. Finally, saturated sodium bicarbonate (6 mL) was added and the solution separated into two distinct layers. The organic layer was separated and washed with saturated sodium chloride (50 mL), dried (sodium sulphate), and the solvent was evaporated to yield 8-formylcamphor ketal (**3**) as a clear colourless oil. The oil was chromatographed on alumina (Alumina Woelm Neutral; activity grade III) (50 g) and 8-formylcamphor ethylene acetal (**3**) was eluted from the column using 10% ether – 90% petroleum ether (30–60) as eluant (200 mL), (2.07 g, 88% yield). Removal of solvent provided **3** as a clear colourless oil which was used immediately without further purification; $\delta(CCl_4)$ 0.74 (s, 3H), 0.90 (s, 3H), 3.76 (m, 4H), 9.74 (t, 1H); $\nu_{max}(CCl_4)$ 2717, 1721, and 1404 cm^{-1}.

8-(3-Methyl-1-oxo-3-butenyl)camphor (4)

8-Formylcamphor ketal (**3**) (765 mg, 3.42 mmol) in ether (10 mL) was added to a 1 *M* ether solution of 2-methyl-2-propenyl magnesium chloride (15 mL; 15 molar equivalents) at 4°C (ice–water bath). The reaction was stirred for 20 min at 4°C and then for 45 min at room temperature. Careful hydrolysis was accomplished by dropwise addition of saturated ammonium chloride solution (50 mL) and the aqueous mixture was extrac-

Can. J. Chem. Downloaded from www.nrcresearchpress.com by 210.87.254.5 on 09/05/12
For personal use only.

ted with ether (2 × 25 mL). The organic layers were combined and washed with saturated sodium chloride (1 × 10 mL) and dried over magnesium sulphate. Evaporation of the solvent gave 8-(1-hydroxy-3-methyl-3-butenyl)camphor ethylene acetal as a colourless oil (630 mg, 66% yield) after chromatography on silica gel (Silica Gel Woelm 100–200; activity grade III; 20% ether:80% petroleum ether (30–60) as eluant); δ(CCl_4) 3.78 (m, 4H), 4.80 (bm, 2H); ν_{max}(film) 3472, 1645, and 893 cm^{-1}.

8-(1-Hydroxy-3-methyl-3-butenyl)camphor ethylene acetal was deketalized in dioxane (15 mL) and 1 *N* hydrochloric acid (1.5 mL) for 17 h at room temperature. Workup provided a colourless oil (515 mg, 97% yield); δ(CCl_4) 0.87 (s, 3H), 1.10 (s, 3H), 3.53 (bs, 1H), 3.75 (bm, 1H), 4.82 (d, 2H, J = 7 Hz); ν_{max}(CCl_4) 3448, 1645, 1740, 1410, and 890 cm^{-1} which was oxidized immediately by dissolving in acetone (50 mL) and treatment with Jones reagent until a permanent orange colour remained in the solution. Workup in the usual manner gave 8-(3-methyl-1-oxo-3-butenyl)camphor (**4**) as a colourless oil (500 mg, 98% yield); ν_{max}(film) 1740, 1725, 1650, 1408, and 895 cm^{-1}.

8-(3-Methyl-1-oxo-2-butenyl)camphor (5)

A solution of 8-(3-methyl-1-oxo-3-butenyl)camphor (**4**) (50 mg, 0.21 mmol) in petroleum ether (30–60) (6 mL) containing wet ether (10 drops) was treated with alumina (Alumina Woelm Basic; activity grade one) (150 mg) for 19 h at room temperature.

The alumina was filtered, washed carefully with ether, and the total filtrate evaporated to yield 8-(3-methyl-1-oxo-2-butenyl)-camphor (**5**) (45 mg, 90% yield) as a colourless oil which crystallized on standing. This material was purified by sublimation (90°C/10 mm) to yield colourless crystals (mp 43–55°C); δ(CCl_4) 0.83 (s, 3H), 1.02 (s, 3H), 1.87 (d, 3H, J = 2 Hz), 2.12 (d, 3H, J = 2 Hz), 2.70 (dd, 1H), 5.93 (m, 1H); ν_{max}(CCl_4) 1739, 1692, 1618, and 1408 cm^{-1}; λ_{max}(MeOH) 238 (ε = 12 800); *m/e* 234 (M^+), 218, 206, 153, 136 (base peak), 95. *Anal.* calcd. for $C_{15}H_{22}O_2$: C 76.88, H 9.46; found: C 76.66, H 9.53.

8-Ethynylcamphor Ethylene Acetal (8)

A solution of 8-iodocamphor ethylene acetal (**7**) (1) (3.36 g, 10.4 mmol) in dry ether:HMPA (1:1) (20 mL) was added under nitrogen to a suspension of lithium acetylide ethylenediamine complex (Foote Mineral Company: 1.30 g, 14.1 mmol) in dry ether:HMPA (1:1) (40 mL). The reaction mixture was stirred at room temperature for 24 h and then added to saturated ammonium chloride (100 mL). Extraction with petroleum ether (30–60) (5 × 25 mL) and workup in the usual way yielded 8-ethynylcamphor ethylene acetal (**8**) (2.45 g) as an orange oil which was purified by vacuum distillation (bp, 68°C/5 × 10^{-3} mm) (1.24 g, 54% yield); δ(CCl_4) 0.78 (s, 3H), 1.02 (s, 3H), 2.62 (bm, 1H), 2.90 (bm, 1H), 3.77 (bm, 4H); ν_{max}(CCl_4) 3279 and 2128 cm^{-1}; *m/e* 220 (M^+), 205, 195, 181, 126, 113, 95 (base peak). M.W. calcd. for $C_{14}H_{20}O_2$: 220.1463. Found (high resolution mass spectrometry): 220.1459.

8-(3-Hydroxy-3-methyl-1-butynyl)camphor Ethylene Acetal (9)

A solution of 8-ethynylcamphor ethylene acetal (**8**) (1.77 g, 8.05 mmol) in dry ether (25 mL) was cooled at 4°C (ice–water) and then treated with *n*-butyllithium (3.94 mL; Alfa, 2.45 molar in hexanes; 1.2 equivalents) over 5 min. The reaction mixture was stirred at 4°C for 45 min, dry acetone (0.70 g, 12 mmol) was added, and the solution stirred at room temperature for 2.5 h.

The reaction mixture was poured into saturated ammonium chloride (100 mL), extracted with ether (2 × 25 mL) and the combined extracts washed with water (1 × 25 mL) and saturated sodium chloride (1 × 25 mL). Drying (magnesium sulphate) and evaporation yielded 8-(3-hydroxy-3-methyl-1-butynyl)-camphor ethylene acetal (**9**) (2.29 g) as a yellow oil. The crude product (Alumina Woelm Neutral; activity grade III) was applied to an alumina column in 5% ether – 95% petroleum ether (30–60). Elution with 50% ether – petroleum ether yielded 8-(3-hydroxy-3-methyl-1-butynyl)camphor ethylene acetal (**9**) (1.42 g, 63.4% yield) as a pale yellow oil; δ(CCl_4) 0.77 (s, 3H), 0.98 (s, 3H), 1.43 (s, 6H), 3.82 (bm, 4H); ν_{max}(CCl_4) 3448 and 2232 cm^{-1}; *Anal.* calcd. for $C_{17}H_{26}O_3$: C 73.33, H 9.42; found: C 73.04, H 9.52.

(+)3,7-Dimethyl-1-1-(2-methyl-1-oxopropyl)-tricyclo-[4.2.1.$0^{3,7}$]nonan-2-one (11)

A solution of 8-(3-hydroxy-3-methyl-1-butynyl)camphor ethylene acetal (**9**) (1.70 g, 6.12 mmol) in 98% formic acid (15 mL) was refluxed for 21 h. The reaction mixture was poured into water (50 mL), extracted with ether (3 × 20 mL) and the combined extracts washed with water (2 × 20 mL), saturated sodium bicarbonate (3 × 20 mL), water (1 × 20 mL), and saturated sodium chloride (2 × 20 mL). Drying (magnesium sulphate) and evaporation of the solvent yielded an orange oil (1.24 g, 79% pure by glc on column A at 150°C) which was purified by column chromatography on alumina (Alumina Woelm Neutral; activity grade III). Elution with petroleum ether (30–60) (400 mL) yielded **11** (1.0 g, 70% yield) as a pale yellow oil which crystallized on standing overnight. Recrystallization from petroleum ether (30–60) at −20°C gave **11** as colourless rods, mp 51–52°C. (sealed tube): δ($CDCl_3$) 1.09 (d, 3H, J = 7 Hz), 1.13 (s, 3H), 1.14 (d, 3H, J = 7 Hz), 1.40 (s, 3H), 2.89 (septet, 1H, J = 7 Hz); ν_{max}(CCl_4) 1745, and 1701 cm^{-1}; *m/e* 234 (M^+), 191, 163, 145, 135, 107, 95 (base peak); M.W. calcd. for $C_{15}H_{22}O_2$: 234.1620. Found (high resolution mass spectrometry): 234.1625. *Anal.* calcd. for $C_{15}H_{22}O_2$: C 76.88, H 9.46; found: C 77.09, H 9.48.

8-(3-Methyl-1-butenyl)camphor (15)

8-Formylcamphor ketal (**3**) (2.07 g, 9.24 mmol) in dry THF (40 mL) was added over 10 min to a clear orange solution containing isobutylphosphonium bromide (5.26 g, 13.2 mmol, 1.25 equivalents) and *n*-butyllithium (5.17 mL; Alfa, 2.25 molar in hexanes) in dry THF (40 mL). The reaction was stirred at room temperature for 8 h and excess ylide was destroyed with methanol (0.5 mL). The reaction mixture, preadsorbed on silica gel (Silica Gel Woelm, 100–200; activity grade III) (25 g), was then chromatographed on silica gel of the same activity (50 g). Elution with 20% ether – 80% petroleum ether (30–60) provided 8-(3-methyl-1-butenyl)camphor ethylene acetal as a colourless oil (1.94 g, 80% yield) (bp 82–83°C/2 × 10^{-3} mm); δ(CCl_4) 0.76 (s, 3H), 0.80 (s, 3H) 0.93 (d, 6H, J = 7 Hz), 3.80 (m, 4H), 5.23 (m, 2H); *Anal.* calcd. for $C_{17}H_{28}O_2$: C 77.21, H 10.68; found: C 76.93, H 10.53.

Deketalization was accomplished by dissolving the ketal olefin in a mixture of acetone (25 mL) and 6 *N* hydrochloric acid (10 drops) and stirring at room temperature for 8 h. Extraction of the diluted reaction product with ether and workup in the usual way provided 8-(3-methyl-1-butenyl)camphor (**15**) as a colourless oil (1.08 g, quantitative) (bp 75°C/10^{-3} mm); δ(CCl_4) 0.90 (s, 6H), 0.94 (s, 3H), 0.97 (s, 3H), 5.30 (m, 2H): ν_{max}(CCl_4) 1739, 1408, and 1370 cm^{-1}; *m/e* 220 (M^+), 138, 137, 136, 135, 125, 124, 122, 109 (base peak). M.W. calcd. for $C_{15}H_{24}O$: 220.1827. Found (high resolution mass spectrometry): 220.1811.

8-(1,2-Epoxy-3-methylbutyl)camphor (16)

A solution of *meta*-chloroperbenzoic acid (1.12 g, 6.5 mmol, 1.1 equivalents, 85% pure) in benzene (30 mL) was added over 30 min to a solution of 8-(3-methyl-1-butenyl)camphor (**15**) (1.3 g, 5.9 mmol) in dry benzene (30 mL) at 4°C (ice–water). The reaction was stirred at 4°C for an additional 0.5 h and then allowed to warm to room temperature over 2 h. Extraction of the benzene solution with small portions of saturated sodium bisulphite (5 mL portions) was continued until a negative starch–iodide test was obtained. Evaporation of the washed solvent

Can. J. Chem. Downloaded from www.nrcresearchpress.com by 210.87.254.5 on 09/05/12
For personal use only.

yielded 8-(1,2-epoxy-3-methylbutyl)camphor (**16**) as a clear colourless oil (1.4 g, quantitative) (bp 84°C/10^{-3} mm); $\delta(CCl_4)$ 0.83 (s, 3H), 0.90 (d, 3H, J = 6 Hz) 1.04 (d, 3H, J = 6 Hz), 1.05 (s, 3H), 2.88 (m, 2H); $\nu_{max}(CCl_4)$ 1739, 1408, 1255, 948, and 881 cm^{-1}; *m/e* 236 (M^+), 193, 153 (base peak), 137, 136, 135, 123, 121, 109, 108, 107, 95, 94, 93; M.W. calcd. for $C_{15}H_{24}O_2$: 236.1775. Found (high resolution mass spectrometry): 236.1786.

1,6-Dimethyl-2-oxo-4-(1-oxo-2-methylpropyl)-tricyclo-[4.3.0^{1,6}.0^{3,7}]nonane (12)

8-(1,2-Epoxy-3-methylbutyl)camphor (**16**) (1.09 g, 4.24 mmol) was treated with dry *tert*-butanol (100 mL) containing potassium *tert*-butoxide (6.70 g, 59.8 mmol, 14 equivalents) at reflux under nitrogen for 8 h.

The reaction mixture was poured into water (200 mL) and extracted with petroleum ether (30–60) (4 × 25 mL). The organic layers were combined and washed with water (2 × 25 mL) and saturated sodium chloride (1 × 25 mL). Drying (sodium sulphate) and evaporation of the solvent yielded 1,6-dimethyl-2-oxo-4-(1-hydroxy-2-methylpropyl)tricyclo[4.3.0.^{1,6}0^{3,7}]nonane which was purified by chromatography on silicic acid (Malinckrodt Silicic Acid, 100 mesh) (40 g) using, at first, chloroform (100 mL) and then 1.5% ethanol (95%) – 98.5% chloroform (130 mL) as eluants. This yielded a mixture of diastereomeric alcohols (986 mg); $\delta(CCl_4)$ 0.82 (d, 3H, J = 7 Hz), 0.88 (s, 3H), 0.96 (s, 3H), 0.97 (d, 3H, J = 7 Hz), 2.24 (m, 1H), 2.68 (bs, 1H), 3.07 (bm, 2H); $\nu_{max}(CCl_4)$ 3413 and 1739 cm^{-1} which was oxidized in acetone using Jones reagent until a permanent orange colour remained in solution. Excess reagent was destroyed with a few drops of methanol and the reaction mixture was poured into water (100 mL). The product was isolated by extraction with diethyl ether (3 × 25 mL). The organic layers were combined and washed with saturated sodium bicarbonate (1 × 25 mL) and saturated sodium chloride (1 × 25 mL). Drying (magnesium sulphate) and evaporation of the solvent yielded 1,6-dimethyl-2-oxo-4-(1-oxo-2-methylpropyl)tricyclo[4.3.0^{1,6}.0^{3,7}]nonane (**12**) as a mixture of two diastereomers; $\delta(CCl_4)$ 0.89 (s, 3H), 0.98 (s, 3H), 1.06 (d, 6H, J = 7 Hz), 2.14 (bm, 1H), 2.50 (bs, 1H), 2.76 (m, 2H); $\nu_{max}(CCl_4)$ 1739 and 1710 cm^{-1}; *m/e* 234 (M^+), 163, 153 (base peak), 135, 107, 93, 79; M.W. calcd. for $C_{15}H_{22}O_2$: 284.1619. Found (high resolution mass spectrometry): 234.1612.

X-ray Crystallographic Analysis of 11

Upon exposure to air at ambient temperatures, a freshly prepared crystalline sample of **11** gradually turned into an amorphous solid in the course of 3–4 days. Several crystals were used in taking preliminary X-ray photographs and in the collection of intensity data. Unit-cell parameters were refined by least-squares on 2 sin θ/λ values for 25 high-angle reflections measured on a diffractometer with MoK_α radiation (λ = 0.71069 Å). The crystal data at 22°C are:

Orthorhombic, a = 19.521(2), b = 10.238(2), c = 6.881(2) Å, V = 1375.2 Å^3, Z = 4, ρ_c = 1.132 g cm^{-3}, $\mu(MoK_\alpha)$ = 0.79 cm^{-1}. Systematic absences: $h00$ with h odd, $0k0$ with k odd, and $00l$ with l odd determine the space group uniquely as $P2_12_12_1$ (D_2^4, No. 19).

Intensities were recorded to 2θ = 53° with graphite monochromatized MoK_α radiation on an Enraf-Nonius CAD-4 diffractometer. A variable speed ω scan over a range of r = (0.85 + 0.35 tan θ) degrees in ω was employed. The scan was extended at both ends by r/4 for background measurement. Crystal orientation was monitored every 100 reflections and the intensities of three standard reflections checked hourly throughout the data collection. Of the 1662 independent reflections measured, 1015 (61%) had intensities greater than 3.5σ(I) above background where $\sigma^2(I) = S + B + (0.04S)^2$, with S = scan count and B = normalized background count. The data were corrected for Lorentz and polarization factors but absorption correction was considered unnecessary.

TABLE 2. Final positional parameters (fractional × 10^4) with estimated standard deviations in parentheses, and mean U_{ii} (Å^2 × 10^2)

Atom	x	y	z	Mean U_{ii}
C(1)	852(1)	2914(3)	269(4)	6.3
C(2)	1622(1)	2744(3)	679(4)	5.9
C(3)	2004(1)	3358(2)	−1002(4)	5.3
C(4)	1851(1)	4828(3)	−792(5)	7.3
C(5)	1076(1)	4953(3)	−1210(5)	7.4
C(6)	638(2)	5272(3)	542(6)	9.0
C(7)	561(1)	3991(4)	1606(4)	9.0
C(8)	877(1)	3533(3)	−1771(4)	6.2
C(9)	1529(1)	2999(3)	−2680(4)	6.8
C(10)	220(1)	3432(4)	−2948(5)	9.7
C(11)	503(2)	1618(4)	445(8)	12.0
C(12)	2746(1)	2948(3)	−1055(4)	5.9
C(13)	2909(1)	1557(3)	−1548(5)	7.3
C(14)	3445(2)	1012(4)	−153(7)	11.6
C(15)	3141(2)	1457(4)	−3653(6)	10.2
O(1)	1862(1)	2257(3)	2107(3)	9.1
O(2)	3197(1)	3735(2)	−726(4)	8.6

The structure was solved by direct methods using MULTAN (8). After full-matrix anisotropic refinement (local adaptations of ORFLS and FORDAP) of all 17 non-hydrogen atoms to R = 0.091, a difference map revealed the positions of all 22 hydrogen atoms, which were included in subsequent least-squares cycles with isotropic thermal parameters (B = 8.5 Å^2 for methyl H, 7.0 Å^2 for methylene and methine H).

Literature scattering factors of non-hydrogen atoms (9) and hydrogen atoms (10) were used and the function minimized was $\Sigma w(|F_o| - |F_c|)^2$, with $w = 1/\sigma^2(F)$. Convergence was reached at R = 0.042 for 1015 observed reflections.

The final positional parameters of C and O atoms are given in Table 2. Lists of hydrogen atomic coordinates, thermal parameters, and structure factors have been placed in the Depository of Unpublished Data.[3]

Acknowledgements

We are grateful to the National Research Council of Canada and the University of British Columbia for generous financial support.

1. C. R. ECK, G. L. HODGSON, D. F. MACSWEENEY, R. W. MILLS, and T. MONEY. J. Chem. Soc. Perkin I, 1938 (1974); G. L. HODGSON, D. F. MACSWEENEY, and T. MONEY. J. Chem. Soc. Perkin I, 2113 (1973).
2. C. R. ECK, R. W. MILLS, and T. MONEY. J. Chem. Soc. Perkin I, 251 (1975); P. CACHIA, N. DARBY, C. R. ECK, and T. MONEY. J. Chem. Soc. Perkin I, 359 (1976).
3. (*a*) N. DARBY, N. LAMB, and T. MONEY. Can. J. Chem. **57**,

[3]This material (19 pages) is available, at a nominal charge, from the Depository of Unpublished Data, CISTI, National Research Council of Canada, Ottawa, Ont., Canada K1A 0S2.

742 (1979); (*b*) M. S. ALLEN, N. DARBY, P. SALISBURY, E. R. SIGURDSON, and T. MONEY. Can. J. Chem. **57**, 733 (1979) and references therein; (*c*) M. S. ALLEN, N. LAMB, and T. MONEY. J. Chem. Soc. Chem. Commun. 112 (1979).

4. S. C. WELCH and R. L. WALTERS. Synth. Commun. **3**, 15 (1973); **3**, 419 (1973); J. Org. Chem. **39**, 2665 (1974).
5. (*a*) H. PAULING, D. A. ANDREWS, and N. C. HINDLEY. Helv. Chim. Acta, **59**, 1233 (1976) and references therein; (*b*) M. EDENS, D. BOERNER, C. R. CHASE, D. NASS, and M. D. SCHIAVELLI. J. Org. Chem. **42**, 3403 (1977); (*c*) S. SWAMINATHAN and K. V. NARAYANAN. Chem. Rev. **71**, 429 (1971); (*d*) P. B. D. DE LA MARE. *In* Molecular rearrangements. Part I. *Edited by* P. de Mayo. Interscience, New York. 1963. pp. 87–89.
6. J. E. BALDWIN. J. Chem. Soc. Chem. Commun. 734 (1976); 736 (1976).
7. A. G. MARSHALL, L. D. HALL, M. HATTON, and J. SALLOS. J. Magn. Reson. **13**, 392 (1974).
8. G. GERMAIN, P. MAIN, and M. W. WOOLFSON. Acta Crystallogr. Sect. A, **27**, 368 (1971).
9. D. T. CROMER and J. B. MANN. Acta Crystallogr. Sect. A, **24**, 321 (1968).
10. R. F. STEWART, E. R. DAVIDSON, and W. T. SIMPSON. J. Chem. Phys. **42**, 3175 (1965).

Can. J. Chem. Downloaded from www.nrcresearchpress.com by 210.87.254.5 on 09/05/12
For personal use only.

Conformational preferences of the fluoromethyl group in *p*-methylbenzyl fluoride and some derivatives

TED SCHAEFER, WALTER P. NIEMCZURA,[1] RUDY SEBASTIAN, LEONARD J. KRUCZYNSKI, AND WERNER DANCHURA[2]

Department of Chemistry, University of Manitoba, Winnipeg, Man., Canada R3T 2N2

Received December 13, 1979

TED SCHAEFER, WALTER P. NIEMCZURA, RUDY SEBASTIAN, LEONARD J. KRUCZYNSKI, and WERNER DANCHURA. Can. J. Chem. **58**, 1178 (1980).

The coupling over seven bonds between ^{19}F nuclei and protons in *p*-methylbenzyl fluoride and a series of ring-substituted derivatives is used to estimate the value for a conformation in which the C—F bond lies in a plane perpendicular to the benzene ring. The *J* method is then used to show that in CS_2 solution, the conformational preference of the fluoromethyl group is very weak in 3,5-dichloro-4-methylbenzyl fluoride and in 3,5-dibromo-4-methylbenzyl fluoride. The barrier to rotation about the exocyclic carbon–carbon bond is perhaps as large as 0.2 kcal/mol. In *p*-methylbenzyl fluoride, the C—F bond prefers a plane perpendicular to the benzene plane by ca. 0.9 kcal/mol. Good agreement is found with the conformational preferences based on couplings over six or seven bonds between the methylene protons and the *para* ring or methyl protons. The deductions are compared with calculations at various levels of molecular orbital theory.

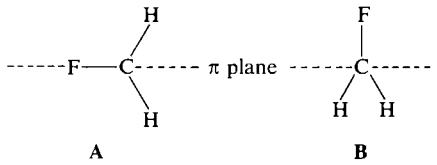
TED SCHAEFER, WALTER P. NIEMCZURA, RUDY SEBASTIAN, LEONARD J. KRUCZYNSKI et WERNER DANCHURA. Can. J. Chem. **58**, 1178 (1980).

On a utilisé les couplages à travers sept liaisons, entre le ^{19}F et les protons du fluorure de *p*-méthylbenzyle et d'une série de dérivés cycliques substitués dans le but de déterminer cette valeur pour une conformation de la liaison C—F qui se situe dans le plan perpendiculaire au noyau benzénique. On a alors utilisé la méthode *J* pour montrer qu'en solution dans le CS_2, la préférence conformationnelle du groupe fluorométhyle est très faible dans le cas du fluorure des dichloro-3,5, et dibromo-3,5 méthyl-4 benzyles. La barrière à la rotation autour de la liaison exocyclique carbone–carbone est peut être de 0.2 kcal/mol. Dans le cas du fluorure de *p*-méthylbenzyle, la liaison C—F se situe de préférence dans le plan perpendiculaire à celui du benzène avec une barrière à la rotation de 0.9 kcal/mol. On a trouvé que ces résultats s'accordent parfaitement avec les préférences conformationnelles évaluées sur la base des couplages à travers 6 ou 7 liaisons entre les protons méthyléniques et les protons situés en position *para* sur le cycle ou les protons du groupe méthyle. On a comparé les déductions ainsi faites avec des calculs d'orbitales moléculaires effectués à divers niveaux.

[Traduit par le journal]

Introduction

The internal barrier to rotation in toluene is only 0.014 kcal/mol (1) and, at 0.010 kcal/mol, is even lower in benzotrifluoride (2). Substitution in the methyl group to give a CH_2X or a CHX_2 sidechain changes the sixfold barrier for a CH_3 group to one of a predominantly twofold nature. These twofold barriers have been investigated in solution for X = F, Cl, Br, I, CH_3 (3–5) and a variety of other X substituents (6, 7). The investigations are mainly based on the $\sin^2\theta$ dependence of $^6J_p^{H,CH}$, the coupling constant over six bonds between protons in the sidechain and a *para* ring proton; θ is the angle by which the C—H bond twists out of the benzene plane (the *J* method). For 3,5-dichlorobenzyl fluoride, on the other hand, the determination of the twofold internal barrier was based on an assumed $\sin^2\theta$ dependence of $^6J_p^{H,CF}$ and yielded 0.26 kcal/mol (3). Conformations **A** and **B** were of low and high energy, respectively. These results



A **B**

were in satisfactory agreement with *ab initio* STO 3G calculations (3, 8) as well as with computations (3) based on MINDO MO methods. On the other hand, CNDO/2 and INDO MO calculations gave barriers an order of magnitude larger than these (3, 9), although they found **A** as the stable conformer.

Subsequent vibrational spectra (10) in solution were interpreted as arising from a large number of conformers, a result of free or nearly free internal rotation. The photoelectron spectra of benzyl halides have been interpreted in terms of a *gauche* conformation in which an α C—H bond prefers the benzene plane (11).

Whereas there exists satisfactory evidence for a sole $\sigma-\pi$ mechanism for $^6J_p^{H,CH}$ and hence for its $\sin^2\theta$ dependence (12), it was pointed out by Dr. R. Wasylishen that the $\sin^2\theta$ dependence of $^6J_p^{F,CH}$ in benzyl fluoride is not firmly established. While it is

[1]Present address: Department of Biochemistry, University of Wisconsin, Madison, WI 53706, U.S.A.

[2]Present address: Department of Chemistry, University of Winnipeg, Winnipeg, Man., Canada R3B 2E9.

0008-4042/80/121178-05$01.00/0

©1980 National Research Council of Canada/Conseil national de recherches du Canada

Can. J. Chem. Downloaded from www.nrcresearchpress.com by 210.87.254.105 on 09/05/12
For personal use only.

Can. J. Chem. Downloaded from www.nrcresearchpress.com by 210.87.254.105 on 09/05/12
For personal use only.

true that INDO MO FPT calculations yield such a dependence (and also agree quantitatively with observed $^6J_p^{H,CH}$ values), a non σ–π component in $^6J_p^{F,CH}$ may exist. This component would then introduce an error into the barrier determination.

In view of the disagreement among the experimental and theoretical results above and of some recent evidence (13, 14) for small σ contributions to ^1H, ^{19}F couplings over six bonds, further work is in order. In addition, if the conformational preferences of the fluoromethyl group are indeed weak and are influenced by hyperconjugative interactions of the C—F bond with the aromatic π system (9, 15), then substituents may alter these preferences. The previous conclusions from the J method are related to 3,5-dichlorobenzyl fluoride and therefore need not hold for benzyl fluoride. Unfortunately, the ^1H nmr spectrum of benzyl fluoride would be intractable even at 400 MHz. Accordingly, we now examine *p*-methylbenzyl fluoride and a series of its derivatives. These compounds are amenable to spectral analysis and have the advantage that the $^7J_p^{CH_2,CH_3}$ and $^7J_p^{F,CH_3}$ can be treated as σ–π couplings.

Experimental

The fluoromethyl group was produced from the bromomethyl or chloromethyl groups by treatment with KF in the presence of 18-crown-6 ether (Aldrich) (16). The benzyl fluoride derivatives, the physical properties of some of which have been given by Béguin and Meary-Tertian (17) and by Schaefer and co-workers (3), were easily identified from their ^1H nmr spectra. In particular, the characteristic $^2J^{H,F}$ of 47 to 48 Hz in the methylene proton spectra confirmed the presence of the fluoromethyl group. Because of polymerization problems, the pure derivatives were not isolated.

A typical procedure went as follows. To 20 mL of acetonitrile (dried over Type 5A sieve, from Fisher) were added 1.55 g (9.2 m*M*) of 2,4,6-trimethylbenzyl chloride (Aldrich), 1.07 g (1.8 m*M*) of KF (dried at 250°C for 24 h), and 0.24 g (0.9 m*M*) of 18-crown-6 ether. The mixture was gently refluxed at 80°C with *vigorous* stirring for 90 h. The solution was decanted from KF and KCl and evaporated to a viscous mass. Extraction with petroleum ether left most of the crown ether behind. Subsequent removal of the petroleum ether resulted in a colorless solid which polymerized in about 5 min. A small portion was retrieved before polymerization and was dissolved in CS_2 in a 5 mm od nmr tube. The sample was degassed and flame-sealed. Under these conditions, the benzyl fluoride derivative was indefinitely stable.

The ^1H nmr spectra of all benzyl fluoride derivatives in degassed CS_2 solutions were recorded on an HA100 spectrometer at a probe temperature of 305 K. They were calibrated in the frequency sweep mode by placing markers at 2 to 5 Hz intervals. The frequencies of the markers relative to the TMS lock frequency were obtained by reading sweep and lock oscillator frequencies. Sweep rates were 0.01 or 0.02 Hz/s at a spectral dispersion of 1 Hz/cm. In this way peak frequencies could be found with a rms error of 0.02 Hz or better. Strong and weak multiple irradiation experiments (18) gave the signs of the long-range couplings to ^{19}F relative to $^2J^{H,F}$, known to be positive.

STO 3G MO calculations were performed as previously described (3).

Results and Discussion

Spectral Analyses

These were done in the usual manner with the computer program LAME (19, 20). The spectra of 2,4,6-trimethylbenzyl fluoride and of *p*-methylbenzyl fluoride could not be completely analyzed. For the latter, the ring protons are almost isochronous in CS_2 solution, so that while an analysis was problematical, decoupling of the ring protons yielded good values of $^7J_p^{CH_2,CH_3}$. In benzene-d_6 solution, the magnitude of $^7J_p^{F,CH_3}$ was the same as in CS_2 solution.

Figure 1 displays half of the methylene proton resonance of *p*-methylbenzyl fluoride under conditions where the ring protons are decoupled.

In Table 1 some spectral parameters are given for compounds **1** to **4** and **6** to **10**.

The Value of $^7J_{90}^{F,CH_3}$ and the Internal Barrier

If $^7J_{90}$ in eq. [1] can be found

$$[1] \quad {}^7J_p^{F,CH_3} = {}^7J_{90}\langle \sin^2\theta \rangle$$

then, as discussed for a similar situation previously (3), the observed value of $^7J^{F,CH_3}$ yields $\langle \sin^2\theta \rangle$,

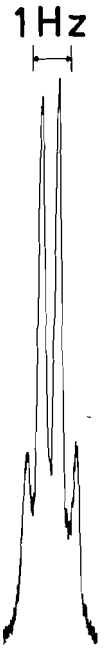


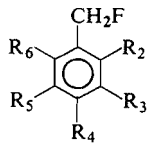
FIG. 1. This quartet is half the methylene proton resonance at 100 MHz and 305 K, obtained by decoupling the ring protons, of a ca. 10 mol% solution of *p*-methylbenzyl fluoride in CS_2. The quartet itself is centered at $\delta = 5.382_6$ ppm (TMS), $^2J^{H,F}$ is $48.1_2 \pm 0.05$ Hz and $\delta(CH_2)$ is 5.142_0 ppm.

Can. J. Chem. Downloaded from www.nrcresearchpress.com by 210.87.254.105 on 09/05/12
For personal use only.

TABLE 1. Some spectral parameters for some benzyl fluoride derivatives[a]

Compound[b]	δ_{CH_2}[c]	δ_{ring}[c]	δ_{CH_3}[c]	$^7J_p^{F,CH_3}$	$^2J^{H,F}$
1	5.471	7.037	2.254	2.83[d]	47.74
2	5.277	—	2.081	2.81	47.35
3	5.53	7.34	2.322	2.96	47.8
4	5.28	6.73	2.22	3.15	48.8
6	5.141	7.141	2.398	1.62	47.39
7	5.21	7.43	2.536	1.65	47.4
8	5.199	—	—	2.55_e	47.0[f]
9	5.30	7.52	—	2.60_e	46.9[f]
10	5.14	—	2.291	2.1_5	48.0

[a]Ca. 10 mol% solutions in CS_2 except for **2** which was 5 mol% in C_6D_6.
[b]The structures of **1** to **10** are in text.
[c]In ppm to low field of internal tetramethylsilane.
[d]Coupling constants in this column are accurate to 0.02 Hz except for $^7J_p^{F,CH_3}$ in **10**; its accuracy is 0.1 Hz.
[e]These are $^7J_p^{F,CH_2}$ values, the F nucleus being situated on the CH_2F group which is flanked by two halogen substituents.
[f]The values for the CH_2F group flanked by chlorine and bromine substituents are, respectively, 47.5 and 47.5 Hz.

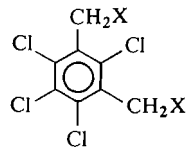


1, $R_2 = R_6 = Cl$; $R_4 = CH_3$
2, $R_2 = R_3 = R_5 = R_6 = Cl$; $R_4 = CH_3$
3, $R_2 = R_6 = Br$; $R_4 = CH_3$
4, $R_2 = R_4 = R_6 = CH_3$
6, $R_3 = R_5 = Cl$; $R_4 = CH_3$
7, $R_3 = R_5 = Br$; $R_4 = CH_3$
8, $R_3 = R_5 = Cl$; $R_4 = CH_2F$*
9, $R_3 = R_5 = Br$; $R_4 = CH_2F$*
10, $R_4 = CH_3$

relatable to V_2 for the fluoromethyl group. Various lines of evidence suggest that conformation **B** is the preferred conformer for **1** to **4** and that V_2 is greater than 4 kcal/mol. The nmr spectrum of 2,6-dichlorobenzyl fluoride in a nematic solvent suggests a V_2 of 4 to 5 kcal/mol (21). *Ab initio* calculations on this compound involve optimization of the C—C—F bond angle and find a V_2 of 6.8 kcal/mol (3). Dynamic nmr data (22) on **5** for X = Cl, Br, I (mean $\Delta G^{\ddagger}$ of 8.8, 10.7, and 12.1 kcal/mol, respectively, for reorientation of the CH_2X groups) can be plotted versus Van der Waals volumes (23) of the halogens and hydrogen (essentially a zero, sixfold, barrier for a methyl group). The smooth curve suggests a V_2 of ca. 5 kcal/mol for **1**.

The values of $^7J_p^{F,CH_3}$, in conjunction with calculations of $\langle \sin^2 \theta \rangle$, can now be used to place limits on $^7J_{90}$. If V_2 is infinite, $\langle \sin^2 \theta \rangle$ is unity for **1** and $^7J_{90}$ is 2.81 Hz. If V_2 is 4 kcal/mol, $\langle \sin^2 \theta \rangle$ is 0.91 and $^7J_{90}$ is 3.10 Hz. Actually, the $^7J^{F,CH_3}$ values for **3** and **4** suggest somewhat higher barriers than in **1** (there is some evidence (24) that *ortho* substituents in benzene derivatives hinder internal rotation as $CH_3 > Br > Cl$). In that event[3] the minimum value of $^7J_{90}$ is 3.15 Hz (V_2 is infinite) and the maximum is 3.43 Hz (if V_2 is 5 kcal/mol in **4**). If V_2 were 10 kcal/mol, $^7J_{90}$ would be 3.25 Hz. It seems reasonable, therefore, that $^7J_{90}$ is 3.34 ± 0.09 Hz.

In **6** and **7**, $^7J^{F,CH_3}$ is $1.63_5 \pm 0.02$ Hz. It follows that $\langle \sin^2 \theta \rangle$ is $1.63_5 \pm 0.02/3.34 \pm 0.09$ or 0.49 ± 0.02. Therefore V_2 is essentially zero, with the faint possibility that conformation **A** is favored by as much as 0.1_5 kcal/mol. Formally, V_2 is 0.06 kcal/mol, **A** favored.



5

$^7J^{CH_2,CH_3}$ *and the Internal Barrier in* **6** *and* **7**

In **6**, $^7J^{CH_2,CH_3}$ is 0.52 ± 0.01 Hz. For a vanishing V_2, $^7J_{90}$ would be 1.04 ± 0.02 Hz. As discussed in detail previously (3), $^7J_{90}$ is expected to be smaller than in *p*-xylene, where it is 1.24 Hz. INDO MO FPT calculations on benzyl fluoride suggest $^7J_{90}$ as 1.09 Hz. If true, then $\langle \sin^2 \theta \rangle$ is 0.48 and V_2 is 0.2 kcal/mol, **B** favored. If $^7J_{90}$ is 1.02 Hz, as previously assumed (3), V_2 becomes 0.1 kcal/mol, **A** favored. To within experimental error, then, $^7J^{CH_2,CH_3}$ is in agreement with the conclusions above, i.e., that the CH_2F group is nearly a free rotor in **6**.

A check on $^7J_{90}^{CH_2,CH_3}$ is available from the value

[3]It is interesting that INDO MO FPT calculations (3) find $^6J_{90}^{F,CH}$ as −3.18 Hz in conformation **B** of benzyl fluoride. This value should be equal in magnitude to $^7J_{90}^{F,CH_3}$ (12).

Can. J. Chem. Downloaded from www.nrcresearchpress.com by 210.87.254.105 on 09/05/12
For personal use only.

of $^7J_p^{*F,CH_2}$ in **8** and **9**, being 2.55 ± 0.04 and 2.60 ± 0.02 Hz, respectively. Assuming that V_2 of the "free" CH_2F group is the same as in **6** and **7**, i.e., essentially zero, the presence of the fluorine substituent in this group has decreased the seven-bond ^1H, ^{19}F couplings by factors of $2.55/2.81_5$ or 0.91 and 2.60/2.96 or 0.88. The mean reduction of 0.89_5 is then presumably caused by the polarization of the C—H bonds, leading to decreased overlap with the π orbitals in the $\sigma-\pi$ mechanism (reductions by a factor of 0.9 occurs in analogous β-fluoroethyl radicals (25)). In other words, one might expect $^7J_{90}^{CH_2,CH_3}$ in **6** and **7** to be smaller than $^7J_{90}^{CH_3,CH_3}$ in *p*-xylene by a factor of 0.89, close to the values discussed at the beginning of this section.

In summary, $^7J^{F,CH_3}$ and $^7J^{CH_2,CH_3}$ agree that V_2 in **6** and **7** is 0 to 0.2 kcal/mol. The conformational preference of the CH_2F group is smaller than RT.

Conformational Preference in p-*Methylbenzyl Fluoride*

$^7J_p^{F,CH_3}$ is $2.1_5 \pm 0.1$ Hz, corresponding to a $\langle \sin^2\theta \rangle$ of 0.64 ± 0.04. Therefore **B** is preferred and V_2 is 0.9 ± 0.3 kcal/mol. $^7J_p^{CH_2,CH_3}$ is 0.42 ± 0.02 Hz and $\langle \sin^2\theta \rangle$ is 0.40 ± 0.03 corresponding to **B** stable and V_2 of 0.9 ± 0.3 kcal/mol. It seems certain that the conformational preference is much more marked in this compound than in **6** and **7**.

In 3,5-dichlorobenzyl fluoride and its 4-methyl derivative, the magnitudes of $^6J_p^{H,CH_2}$ and $^7J_p^{CH_2,CH_3}$ are identical, showing that V_2 is the same in these compounds. Because $^6J_p^{H,CH_2}$ in benzyl fluoride is not available, a similar comparison with its 4-methyl derivative cannot be made. Measurements of $^5J^{F,C}$ in benzyl fluoride and some model compounds (26) *could* be interpreted as indicating a preferred conformation **B** and a V_2 of between 0.1 to 0.8 kcal/mol (depending on how much of the five-bond coupling arises from a pure $\sigma-\pi$ mechanism).

Comparison with Molecular Orbital Calculations

Semiempirical calculations at the CNDO/2 level of MO theory (9) suggest **A** as more stable than **B** by 2.95 kcal/mol for benzyl fluoride and that a *p*-methyl substituent drops this preference to 2.75 kcal/mol. An earlier INDO result gave 2.4 kcal/mol for benzyl fluoride (3). In our opinion, the absolute values represent a gross overestimate (these methods tend to find "closely-connected" conformations for groups containing polar bonds). Nevertheless, it is interesting that a *p*-methyl substituent apparently lowers the energy of a **B** conformation by 0.2 kcal/mol.

The original STO-3G computations for a standard geometry found **A** to be more stable by 0.25 kcal/mol in benzyl fluoride (8). Optimization of the C—C—F angle (111.5°) gives **A** more stable than **B** by 0.34 kcal/mol. A similar procedure (C—C—F angle of 111.2°) finds **A** more stable by 0.55 kcal/mol in 3,5-dichlorobenzyl chloride. Again, optimization of the C—C—F angle (111.5°) gave **A** more stable by 0.23 kcal/mol in *p*-methylbenzyl fluoride. Comparison of all the MO data with the *J* method suggests that the STO-3G results are to be preferred over the semiempirical results for these compounds.

Conclusions

The conformational preference of the CH_2F group in 3,5-dichlorobenzyl fluoride, in 3,5-dichloro- and 3,5-dibromo-4-methylbenzyl fluoride, is very weak in solution and the twofold barrier to internal rotation about the exocyclic carbon–carbon bond is perhaps as large as 0.2 kcal/mol. In contrast, in *p*-methylbenzyl fluoride the conformer in which the C—F bond lies in a plane perpendicular to the benzene ring is preferred by ca. 0.9 kcal/mol. Spectral difficulties disallow an estimate for benzyl fluoride. STO 3G MO calculations are more reliable than CNDO/2 or PCILO approaches in assessing the conformational preferences.

Acknowledgments

We thank Ms. Priscilla Wang for assistance with the synthesis of the bromine derivatives, Dr. Rod Wasylishen and Dr. W. Adcock for helpful comments, and the Natural Sciences and Engineering Council of Canada for financial aid.

1. H. Rudolph, J. Dreizler, A. Jaeschke, and P. Wendling. Z. Naturforsch. Teil A, **22**, 940 (1967).
2. T. Ogata and A. P. Cox. J. Mol. Spectrosc. **61**, 265 (1976).
3. T. Schaefer, J. B. Rowbotham, W. J. E. Parr, K. Marat, and A. F. Janzen. Can. J. Chem. **54**, 1322 (1976).
4. T. Schaefer, L. Kruczynski, and W. Niemczura. Chem. Phys. Lett. **38**, 498 (1976).
5. T. Schaefer, L. J. Kruczynski, and W. J. E. Parr. Can. J. Chem. **54**, 3210 (1976).
6. T. Schaefer, W. Danchura, and W. Niemczura. Can. J. Chem. **56**, 2229 (1978).
7. T. Schaefer, W. Niemczura, W. Danchura, and T. A. Wildman. Can. J. Chem. **57**, 1881 (1979).
8. W. J. Hehre, L. Radom, and J. A. Pople. J. Am. Chem. Soc. **94**, 1496 (1972).
9. C. Béguin and E. Gout-Malleret. J. Fluorine Chem. **8**, 279 (1976).
10. G. A. Crowder and J. J. Townsend. J. Fluorine Chem. **10**, 181 (1977).
11. J. Schmidt and A. Schweig. Tetrahedron Lett. 981 (1973).
12. T. Schaefer, W. Niemczura, and W. Danchura. Can. J. Chem. **57**, 355 (1979).
13. T. Schaefer and W. J. E. Parr. Can. J. Chem. **56**, 1717 (1978).

14. T. SCHAEFER, W. NIEMCZURA, C. M. WONG, and K. MARAT. Can. J. Chem. **57**, 807 (1979).
15. W. ADCOCK and A. N. ABEYWICKREMA. Tetrahedron Lett. 1809 (1979).
16. C. L. LIOTTA and H. P. HARRIS. J. Am. Chem. Soc. **96**, 2250 (1974).
17. C. BÉGUIN and A. MEARY-TERTIAN. Bull. Soc. Chim. Fr. 795 (1967).
18. R. FREEMAN and W. A. ANDERSON. J. Chem. Phys. **37**, 2053 (1962).
19. S. CASTELLANO and A. A. BOTHNER-BY. J. Chem. Phys. **41**, 3863 (1962).
20. C. W. HAIGH and J. M. WILLIAMS. J. Mol. Spectrosc. **32**, 398 (1969).
21. E. GOUT, C. BÉGUIN, D. CANET, and J. P. MARSHAL. Org. Magn. Reson. **7**, 633 (1975).
22. J. PEELING, J. B. ROWBOTHAM, L. ERNST, and T. SCHAEFER. Can. J. Chem. **52**, 2414 (1974).
23. H. FÖRSTER and F. VÖGTLE. Angew. Chem. Int. Ed. Engl. **16**, 429 (1977).
24. A. MANNSCHRECK and H. MÜNSCH. Tetrahedron Lett. 3227 (1968).
25. K. S. CHEN, P. J. KRUSIC, P. MEAKIN, and J. K. KOCHI. J. Phys. Chem. **78**, 2014 (1974).
26. W. ADCOCK and A. N. ABEYWICKREMA. Aust. J. Chem. In press.

Can. J. Chem. Downloaded from www.nrcresearchpress.com by 210.87.254.105 on 09/05/12
For personal use only.

The activity coefficients of some polar solutes in benzene

A. V. ANANTARAMAN AND SAUL GOLDMAN

Guelph–Waterloo Centre for Graduate Work in Chemistry, Guelph Campus, Department of Chemistry, University of Guelph, Guelph, Ont., Canada N1G 2W1

Received October 5, 1979

A. V. ANANTARAMAN and SAUL GOLDMAN. Can. J. Chem. 58, 1183 (1980).

Cryoscopy was used to determine the low concentration (< 1 molal) stoichiometric molal activity coefficients of: chlorobenzene, *m*-dichlorobenzene, *o*-dichlorobenzene, and nitromethane in benzene. The data were corrected to a fixed temperature (10°C) by using pre-existing heat of mixing data. The activity coefficients all showed negative deviations from Henry's law ideality, and some of the factors that contribute to this non-ideality were discussed.

A. V. ANANTARAMAN et SAUL GOLDMAN. Can. J. Chem. 58, 1183 (1980).

On a utilisé la cryoscopie pour déterminer les coefficients d'activité molaire stoechiométrique à faible concentration (1 molal) des *o*- et *m*-dichlorobenzènes et du nitrobenzène en solution dans le benzène. On a corrigé les données pour une température déterminée (10°C) en utilisant les données connues de chaleur de mélange. Tous les coefficients d'activité montrent des déviations négatives par rapport à la loi de Henry et on discute des facteurs qui contribuent au fait que les systèmes étudiés ne sont pas idéals.

[Traduit par le journal]

Introduction

Over the past half a century a large body of systematic data has been accumulated on the dilute solution activity coefficients of electrolytes in water. Since these data are sensitive to solute–solute and solute–solvent interactions at a molecular level, they have greatly contributed to our fundamental understanding of these interactions. In contrast to this, almost no systematic data on the low concentration activity coefficients of polar solutes in non-aqueous solvents exist. It is the purpose of this work to contribute data for these latter systems. The cryoscopic method is well-suited to the dilute solution regime, and so it was chosen in this investigation.

Experimental

Materials

The benzene (Fisher, B-245 reagent grade) was purified and dried as described elsewhere (1), and stored over molecular sieves (Fisher, 4 Å) for at least 10 days prior to use. Monochlorobenzene (Fisher, B-255 reagent grade) was purified by repetitively shaking with concentrated sulfuric acid until no colour appeared in the acid phase. It was then washed sequentially with water, aqueous potassium bicarbonate, and water. The product was dried with Drierite and then fractionally distilled; the middle half fraction was retained. *Ortho-* and *meta*-dichlorobenzene (Baker analyzed and BDH reagent grades respectively) were purified by repetitively shaking with concentrated sulfuric acid, water, 10% aqueous sodium hydroxide, and water. They were then dried with Drierite and fractionally distilled with the middle half fraction retained. Nitromethane (Fisher, N-98 reagent grade) was dried with Drierite and then fractionally distilled from Drierite with the middle half fraction retained. All the solutes were stored over Drierite for at least 10 days prior to use.

The densities of the materials used were determined at 25°C with a 25-mL long-stemmed pycnometer. The values found were as follows. Benzene 0.87362 (lit. 0.87368); nitromethane 1.13134 (lit. 1.13128); chlorobenzene 1.10082 (lit. 1.10098); *o*-dichlorobenzene 1.30042 (lit. 1.30033); *m*-dichlorobenzene 1.28305 (lit. 1.28280). The literature values were taken from a standard reference (2). The agreement with the literature values was considered to be satisfactory.

Freezing Point Apparatus

An adiabatic solution calorimeter, similar in design to one described elsewhere (3), was used. The principle features included a matched pair of thermistors immersed in oil in a U-shaped tube to determine temperature changes, an unsilvered glass Dewar flask, whose outer annular space could be readily evacuated or refilled with air, a stirrer shaft, a port consisting of a glass capillary tube for sampling and sample introduction, and a copper mesh tube which was used to contain molecular sieves. This tube was re-charged with fresh molecular sieves prior to each experimental run. The Dewar was surrounded by a transparent plexiglas can, and the entire apparatus was used in a constant temperature bath. The thermistors and accompanying circuitry (3) were sensitive to changes of 10^{-5}°C. They were calibrated with a standard platinum resistance thermometer (Rosemount Engineering Co., Model 162D).

Techniques

Dried solid benzene crystals were prepared by freezing benzene in the presence of molecular sieves. The solid was mixed with dried cold liquid benzene in the Dewar, and the apparatus was assembled and placed in a constant temperature bath set at about 5°C. The stirrer was started and the system (with air in the outer annular space of the Dewar) was allowed to approach equilibrium. After thermal drifting had slowed down, the annular space was evacuated and the final equilibrium state was approached. This procedure shortened the time required to reach equilibrium. Equilibrium was taken to exist when thermal drifting was reduced to 10^{-5}°C over a period of at least 10 min.

In preliminary experiments it was found that the temperature continuously drifted downward, and this was subsequently determined to be due to the gradual uptake of water by the system from the atmosphere. The use of molecular sieves contained in the copper mesh tube (which was immersed in the liquid phase) eliminated this drift (see below).

After equilibrium was established, liquid solute was added by means of a syringe fitted with a long needle through the glass capillary port. After the initial rapid temperature drop, a new

0008-4042/80/121183-05$01.00/0

©1980 National Research Council of Canada/Conseil national de recherches du Canada

Can. J. Chem. Downloaded from www.nrcresearchpress.com by 210.87.254.40 on 09/05/12
For personal use only.

Can. J. Chem. Downloaded from www.nrcresearchpress.com by 210.87.254.40 on 09/05/12
For personal use only.

TABLE 1. Freezing point depression of benzene by four solutes

Chlorobenzene (molal)	θ* (°C)	*o*-Dichlorobenzene (molal)	θ* (°C)	*m*-Dichlorobenzene (molal)	θ* (°C)	Nitromethane (molal)	θ* (°C)
0.0229	0.1168	0.0185	0.0940	0.0186	0.0949	0.1269	0.6274
0.0382	0.1949	0.0258	0.1292	0.0391	0.1982	0.1602	0.7729
0.0859	0.4358	0.0464	0.2283	0.0658	0.3308	0.1775	0.8617
0.1267	0.6390	0.0535	0.2640	0.0963	0.4828	0.2316	1.109
0.1529	0.7679	0.0696	0.3433	0.1223	0.6095	0.2329	1.133
0.1861	0.9331	0.0812	0.3996	0.1471	0.7321	0.2624	1.249
0.1907	0.9540	0.1069	0.5239	0.1716	0.8516	0.2829	1.344
0.2133	1.064	0.1149	0.5628	0.2039	1.010	0.3317	1.574
0.2174	1.085	0.1373	0.6724	0.2492	1.230	0.3970	1.864
0.2507	1.246	0.1448	0.7107	0.2740	1.352	0.4458	2.055
0.2926	1.450	0.1670	0.8181	0.3152	1.551	0.4734	2.189
0.3261	1.615	0.1758	0.8602	0.3628	1.776	0.5676	2.572
0.3372	1.666	0.1953	0.9547	0.4241	2.080	0.6724	2.986
0.3986	1.957	0.2052	1.004	0.4802	2.351	0.6824	2.978
0.4402	2.154	0.2354	1.150			0.7323	3.217
0.4847	2.357	0.2729	1.328			0.8044	3.495
0.5210	2.525	0.3099	1.506				
0.5634	2.720	0.3610	1.748				
0.6072	2.911	0.3933	1.903				
		0.4346	2.096				

*θ = freezing point depression of solution relative to pure benzene.

temperature plateau was re-established and a sample of the solution was immediately extracted with a syringe for analysis of its solute concentration. During sampling, the stirrer was momentarily stopped so as to reduce the likelihood of crystal intake by the sampling syringe. It was easy to avoid crystals (and to check on the adequacy of the stirring and the quantity of residual solid phase) because the entire apparatus was transparent so that the experimentor was always able to see the system. After a new temperature plateau was established additional solute was added, the system was sampled, etc. In all cases the freezing mixture concentrations were determined by comparison of the solution densities with those of a set of previously prepared standards. The densities were all determined with a Picker densimeter (Sodev, Model 02D). During the course of a run, as the system temperature dropped, the bath temperature was periodically re-adjusted downward so as to maintain, as nearly as possible, adiabatic conditions. The flatness of the temperature–time plateaus provided an index of this.

Because of the water absorption problem, the dissolved water concentration before and after a typical run was determined with an aquatest Karl Fischer Titrimeter (Photovolt, model 702). The molecular sieves were incapable, during the pre-equilibration period, of totally drying the system, but they did maintain a fairly constant water content. Typically, we found the water concentrations before and after a run (about 4 h) to be ~0.0017 and ~0.0019 molar respectively. Since this represents a change of only ~0.0002 molar in dissolved total water concentration, we believe that the freezing point depressions reported here were only slightly, if at all, affected by the presence of dissolved water.

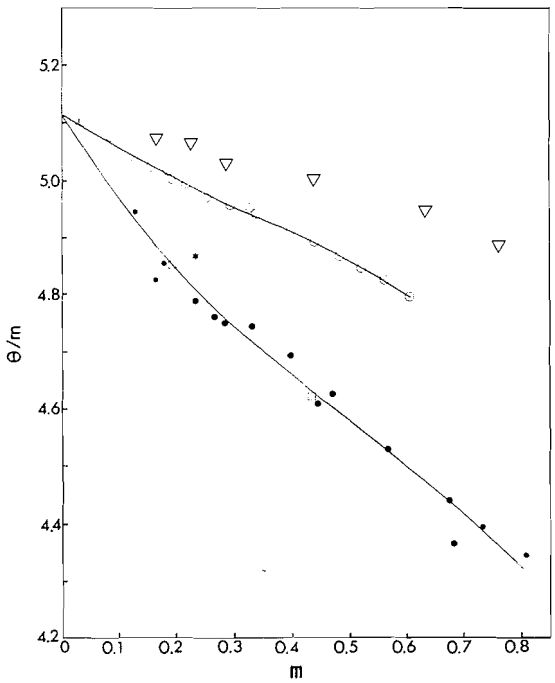


FIG. 1. Comparison with other data of the molal freezing point depression (θ/*m*) against molality (*m*). (●) This work, nitromethane; (□) ref. 4, nitromethane; (○) this work, chlorobenzene; (▽) ref. 5, chlorobenzene. The solid lines were calculated by eq. [1] and the least-squares constants in Table 2.

Results

The results obtained are entered in Table 1. For each system at least three independent runs were carried out. All these data can be smoothly extrapolated to $(\theta/m) = 5.113$ as $m \rightarrow 0$ (e.g. see Fig. 1). This is an indication that solid solutions of solute in benzene did not form. Comparisons with other data, for the two systems in which comparisons are possible, are shown in Fig. 1. In this figure we plot the molar freezing point depression (θ/*m*) rather than θ, against concentration, since the former plot

Can. J. Chem. Downloaded from www.nrcresearchpress.com by 210.87.254.40 on 09/05/12
For personal use only.

is much more sensitive to error than the latter. It is seen from Fig. 1 that for nitromethane our results agree very well indeed with those of Kraus *et al.* (4), but our chlorobenzene points fall significantly and consistently below those obtained by Bury and Jenkins for this system (5). The co-author of this article who did the experimental work (A.V.A.) was aware of this discrepancy and therefore repeated some of the chlorobenzene points several times, and under somewhat different conditions, to try to determine if some systematic error on his part was responsible for the discrepancy. The different conditions included: doing the experiments on different days, re-calibrating the densimeter frequently, arranging for the experimental runs to be of different lengths and injecting different quantities of solute during the run. No significant systematic error was found. We believe Bury and Jenkins' data on this system are in error, and that a likely source of this error was the way in which they tried to eliminate the effect of dissolved moisture. These authors used solid P_2O_5 immersed in their solutions to remove water. We feel that this is a poor method, since the H_3PO_4 formed from the reaction of water with P_2O_5 will dissolve in benzene and consequently influence the results.

Treatment of the Data

The freezing point data are treated in a conventional way (6, 7). It was found that the data in Table 1 could be represented by a Lewis and Randall j-function of the form

$$[1] \quad j = am + bm^2 + cm^3$$

where a, b, and c are constants, m is the solute molality,

$$j \equiv 1 - \theta/m\lambda$$

and θ is the freezing point depression corresponding to molality m.

$$\lambda = \frac{RT_0^2}{\bar{L}_0} \cdot \frac{W}{1000}$$

where T_0 = the freezing point of pure benzene, $\bar{L}_0$ = the latent heat of fusion of benzene at T_0, W = the molecular weight of benzene, and R is the gas constant. From a published study on the properties of benzene (8) we obtain the values $T_0 = 278.69$ K, $\bar{L}_0 = 2358$ cal/mol, and hence $\lambda = 5.113$ deg/molal.

The values of a, b, and c were found by fitting eq. [1] to the data in Table 1 by least-squares (9). The values thus found are entered in Table 2.

The connection between the j-function and the activity coefficient is (7):

TABLE 2. Least-squares estimates of constants in eq. [1]

Solute	a (molal)$^{-1}$	b (molal)$^{-2}$	c (molal)$^{-3}$
Chlorobenzene	0.125	−0.108	0.115
o-Dichlorobenzene	0.624	−2.651	3.560
m-Dichlorobenzene	0.258	−0.595	0.507
Nitromethane	0.319	−0.325	0.211

$$[2] \quad -\ln \gamma_{T_F} = j + \int_0^{[m]} j\,\mathrm{d} \ln [m] - \xi_1 \lambda I_1 - \xi_2 \lambda I_2$$

where γ_{T_F} = stoichiometric molal activity coefficient of the solute at the freezing point of the solution.

$$I_1 = \int_0^{\theta} (1 - j)\,\mathrm{d}\theta$$

$$I_2 = \int_0^{\theta} \theta(1 - j)\,\mathrm{d}\theta$$

$$\xi_1 = \left(\frac{2000}{WRT_0^2}\right)\left(\frac{\bar{L}_0}{T_0} - \frac{\bar{J}}{2}\right)$$

$$\xi_2 = \left(\frac{3000}{WRT_0^3}\right)\left(\frac{\bar{L}_0}{T_0} - \frac{2\bar{J}}{3}\right)$$

$\bar{J}$ is the difference between the molal heat capacities of liquid and solid benzene. It will be assumed to be invariant with temperature. This assumption is based on the dilute concentrations used and consequently on the small temperature range spanned by the experiments. From $J = 0.76$ cal/mol deg (8), and the previously given values of $\bar{L}_0$ and T_0 we find: $\xi_1 = 13.4 \times 10^{-4}$ molal/K^2; $\xi_2 = 7.103 \times 10^{-6}$ molal/K^3. Substituting eq. [1] into eq. [2] and doing the integrations provides a closed form expression for $\ln \gamma_{T_F}$ that is lengthy but straightforward enough to use (7). This expression, together with the entries in Table 2, provides the smoothed values of γ_{T_F} given at rounded molalities in Table 3.

Since the freezing temperatures of the solutions are composition-dependent the values of γ_{T_F} at different molalities refer to different temperatures. We now correct these γ_{T_F}'s to a fixed temperature by means of the thermodynamic relation (6):

$$[3] \quad \log_{10} \gamma_{T_S} = \log_{10} \gamma_{T_F} - \bar{L}_2 Y + \bar{J}_2 Z$$

where

$$Y = \frac{T_S - T_F}{2.303RT_ST_F}$$

and

$$Z = T_S Y - \frac{1}{R} \log_{10} \frac{T_S}{T_F}$$

TABLE 3. Activity coefficients at rounded molalities

	C_6H_6–C_6H_5Cl		C_6H_6–o-$C_6H_4Cl_2$		C_6H_6–m-$C_6H_4Cl_2$		C_6H_6–CH_3NO_2	
m[a]	γ_{T_F}[b]	γ_{10}[c]	γ_{T_F}[b]	γ_{10}[c]	γ_{T_F}[b]	γ_{10}[c]	γ_{T_F}[b]	γ_{10}[c]
0	1.0	1.0	1.0	1.0	1.0	1.0	1.0	1.0
0.05	0.990	0.990	0.950	0.950	0.978	(0.978)[d]	0.971	0.972
0.10	0.980	0.980	0.917	0.917	0.961	(0.961)	0.946	0.946
0.15	0.971	0.971	0.897	0.897	0.947	(0.947)	0.923	0.923
0.20	0.963	0.963	0.885	0.885	0.936	(0.936)	0.901	0.902
0.25	0.955	0.955	0.879	0.879	0.927	(0.927)	0.882	0.883
0.30	0.947	0.947	0.874	0.874	0.920	(0.921)	0.865	0.866
0.35	0.939	0.939	0.868	0.868	0.915	(0.915)	0.848	0.849
0.40	0.932	0.932	0.858	0.858	0.910	(0.911)	0.833	0.834
0.45	0.924	0.924	—	—	0.906	(0.907)	0.819	0.820
0.50	0.917	0.917	—	—	0.902	(0.903)	0.805	0.807

[a] m is the solute molality.
[b] γ_{T_F} is the molal activity coefficient of the solute at the freezing point of the solution; it was obtained by eq. [2].
[c] γ_{10} is the molal activity coefficient of the solute at 10°C; it was obtained by eqs. [3] and [5].
[d] These values are given in parentheses because they were obtained by assuming the same correction as was used for the C_6H_6–o-$C_6H_4Cl_2$ system.

In eq. [3] T_F is the freezing point of the solution, T_S is some fixed temperature, and $\bar{L}_2$ and $\bar{J}_2$ are the relative partial molal enthalpy and heat capacity, respectively, of the solute. In this work we can only do this correction approximately, because values of $\bar{J}_2$ are unavailable, and because $\bar{L}_2$ is known (in effect) by extrapolation from concentrated solution data. Fortunately however, if T_S is selected so as to be fairly close to T_F (in this case T_S will be 283.15 K so that $T_S - T_F$ will be between ~4 to 9 K) then the correction is very small, so that our approximation of it should be adequate.

We approximate $\bar{J}_2$ by zero. The only support we have for this approximation comes from heat of mixing work on the benzene–chlorobenzene system (10) in which it was found that no temperature-dependence could be detected for the heat of mixing curve over the range 30–60°C. Since $\bar{J}_2$ comes from the temperature derivative of $\bar{L}_2$, and $\bar{L}_2$'s can be obtained from the heat of mixing curve (below) this indicates that $\bar{J}_2$ is, within experimental error, zero for this system.

We found that for the systems for which heat of mixing data were available: C_6H_6–C_6H_5Cl, C_6H_6–o-$C_6H_4Cl_2$, C_6H_6–CH_3NO_2, the heat of mixing data, in the dilute solute region, could be approximated by the quadratic formula:

$$[4] \quad \Delta H^m = KX_1X_2$$

In eq. [4] ΔH^m is the enthalpy of mixing per mol of mixture, K is a constant, and X_1, X_2 are the mole fractions of solvent and solute respectively. By applying the usual thermodynamic relations (11) to eq. [4] it is easily shown that:

$$[5] \quad \bar{L}_2 = K(X_1^2 - 1)$$

The values of K (in cal/mol) that were selected for use were: −6.7, +210, +720 for the systems C_6H_6–C_6H_5Cl (10, 12), C_6H_6–o-$C_6H_4Cl_2$ (13), C_6H_6–CH_3NO_2 (14), respectively. These values of K, together with eqs. [3] and [5], were used to obtain the values for γ_{10} given in Table 3. The correction for the C_6H_6–m-$C_6H_4Cl_2$ system was obtained by using the same K value as was used for the C_6H_6–o-$C_6H_4Cl_2$ system (+210 cal/mol).

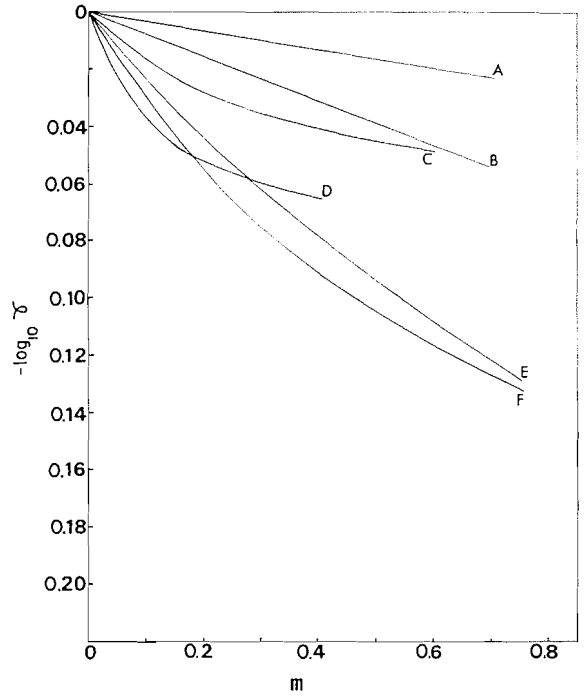


FIG. 2. Concentration-dependence of $\log_{10}\gamma$. The γ's are all corrected to 10°C. *A*, ideal solute behaviour;[2] *B*, chlorobenzene (this work); *C*, *m*-dichlorobenzene (this work); *D*, *o*-dichlorobenzene (this work); *E*, nitromethane (this work); *F*, nitrobenzene (7).

Can. J. Chem. Downloaded from www.nrcresearchpress.com by 210.87.254.40 on 09/05/12
For personal use only.

Can. J. Chem. Downloaded from www.nrcresearchpress.com by 210.87.254.40 on 09/05/12
For personal use only.

It is seen from Table 3 that the correction of the γ's from the freezing points of the solution temperatures to 10°C is an extremely small one, and in fact does not even effect the third decimal place for most of the entries in this table. Indeed, this correction is much smaller than the uncertainty in the γ's caused by the uncertainty in the value of λ (15).[1] Therefore for these systems, if one's purpose is merely to correct the γ's to a constant temperature that is close to the freezing point of the solvent, more elaborate efforts to get $\bar{L}_2$ and $\bar{J}_2$ accurately, are unjustified.

Discussion

The entries in Table 3 are displayed in log form in Fig. 2. For purposes of comparison we also include in this plot the function for an ideal solute,[2] and previous results for the system nitrobenzene in benzene (7), now corrected to 10°C.

Several principal features are apparent. (*1*) All the solutes show negative deviations from ideality in the low concentration region investigated. (*2*) In this concentration range, all the solutes, except chlorobenzene, show some upward curvature as the concentration rises. This behaviour (i.e. upward curvature with rising concentration) is reminiscent of electrolyte solution behaviour where it is caused by the increasing importance of repulsive forces between solute molecules. (*3*) The *o*- and *m*-dichlorobenzene systems seem to be part of a family of curves. The fact that the *ortho* curve is under the *meta* curve is consistent with their relative dipole moments (2.52 and 1.72 D for *o*-$C_6H_4Cl_2$ and *m*-$C_6H_4Cl_2$, respectively (16)).

The result that the activity coefficients of *o*-$C_6H_4Cl_2$ fall below those of $C_6H_5NO_2$ at low concentrations, despite the fact that $C_6H_5NO_2$ has a higher dipole moment than *o*-$C_6H_4Cl_2$ (4.27 vs. 2.52 D) and both molecules are similar in size and shape seems odd at first sight. We speculate that this *may* be a result of the effect of higher multiple moments (e.g. quadrupole, octupole, etc.) which at present are not known for these species. It is conceivable, for example, that dipole–quadrupole interactions between *o*-$C_6H_4Cl_2$ molecules are sufficiently more stabilizing (in a free energy sense) than the corresponding interactions between $C_6H_5NO_2$ molecules, to produce the results that were found (i.e., curves *D* and *F* under 0.2 molal). Unfortunately, since these higher multipole moments are not known, this must remain speculation.

We plan to extend these measurements to the solvent 1,4-dioxane, which is a slightly polar solvent (~0.50 D), in order to see how these activity coefficients are influenced by the nature of the solvent. This work will be reported as a separate communication.

Acknowledgment

We are grateful to the Natural Sciences and Engineering Research Council of Canada for financial support.

1. S. GOLDMAN. Can. J. Chem. **52**, 1668 (1974).
2. A. WEISSBERGER and E. S. PROSKAUER. Organic solvents. Vol. VII. 2nd ed. Interscience Publishers, Inc., New York, NY. 1955.
3. G. L. BERTRAND, R. D. BEATY, and H. A. BURNS. J. Chem. Eng. Data, **13**, 436 (1968).
4. B. C. BARTON, D. A. ROTHROCK, and C. A. KRAUS. J. Am. Chem. Soc. **74**, 786 (1952).
5. C. R. BURY and H. O. JENKINS. J. Chem. Soc. 688 (1934).
6. R. A. ROBINSON and R. H. STOKES. Electrolyte solutions. 2nd rev. ed. Butterworths, London. 1959. pp. 183–188.
7. S. GOLDMAN and W. C. DUER. Can. J. Chem. **52**, 3918 (1974).
8. G. D. OLIVER, M. EATON, and H. M. HUFFMAN. J. Am. Chem. Soc. **70**, 1502 (1948).
9. K. A. BROWNLEE. Statistical theory and methodology in science and engineering. 2nd ed. John Wiley and Sons, Inc., New York, NY. 1965. pp. 431–447.
10. S. N. BHATTACHARYA, A. V. ANANTARAMAN, and S. R. PALIT. Physica, **28**, 633 (1962).
11. I. M. KLOTZ. Chemical thermodynamics. Rev. ed. W. A. Benjamin Inc., New York, NY. 1964. p. 281.
12. J. CANNING and G. H. CHEESMAN. J. Chem. Soc. 1230 (1955).
13. E. M. TURNER, D. W. ANDERSON, J. A. REICH, and W. E. VAUGHAN. J. Phys. Chem. **74**, 1275 (1970).
14. I. BROWN and W. FOCK. Aust. J. Chem. **9**, 180 (1956).
15. S. GOLDMAN. Unpublished results.
16. Handbook of Chemistry and Physics. 41st ed. The Chemical Rubber Co., Cleveland, OH. 1959–1960. pp. 2532–2539.

[1]The uncertainty in the λ value of benzene is about 0.025 deg/molal (7). In the C_6H_6–*o*-$C_6H_4Cl_2$ system for example this uncertainty produces an uncertainty of about 0.020 units in γ when the concentration is 0.50 molal. At this concentration ($\gamma_{283} - \gamma_{T_c}$) = 0.0006 or ~30 times less than the uncertainty due to the uncertainty in λ. Similar results are obtained for the other systems.

[2]A solute that is ideal in the Henry's law sense has a *rational* activity coefficient of unity at all concentrations. From this, and the fact that the chemical potential is invariant with the concentration scale selected, one finds that: $\gamma = 1000/(1000 + Wm)$ where W is the molecular weight of the solvent. This equation (with $W = 78.114$) was used to obtain curve *A* in Fig. 2.

Synthesis of sugar-organometallic conjugates: ferrocenyl monosaccharide derivatives[1]

MICHAEL J. ADAM AND LAURANCE D. HALL

Department of Chemistry, University of British Columbia, Vancouver, B.C., Canada V6T 1W5

Received November 13, 1979

MICHAEL J. ADAM and LAURANCE D. HALL. Can. J. Chem. **58**, 1188 (1980).

Suitably blocked carbohydrates containing free thio **4**, amino **5**, and hydroxyl **10**, **19** nucleophilic functionalities have been treated with (*a*) ferrocenecarbonyl chlorides **2** and **3**, (*b*) *N*,*N*-dimethylaminomethylferrocene methiodide **12**, and (*c*) ferrocenyl tosylate **16** to form the ferrocenyl sugar derivatives **6**, **7**, **8**, **9**, **11**, **13**, **14**, **15**, and **20**. Direct conjugation of a free, water-soluble sugar to ferrocene was achieved by the formation of a Schiff's base between glucosamine hydrochloride **25** and ferrocene carboxaldehyde **24**. The synthesis of ferrocenyl sugars using bridging group technology is exemplified by the conjugation of the thio sugar **4** to ferrocene via the versatile coupling reagent cyanuric chloride **21** to form the *s*-triazine compound **23**. These products have been studied by ^{1}H nmr spectroscopy: chemical shifts, coupling constants, and proton spin–lattice relaxation measurements.

MICHAEL J. ADAM et LAURANCE D. HALL. Can. J. Chem. **58**, 1188 (1980).

On a traité des carbohydrates convenablement protégés contenant des fonctions nucléophiles libres (thio **4**, amino **5** et hydroxyle **10**, **19**) avec (*a*) les chlorures de ferrocènecarbonyle **2** et **3**, (*b*) avec l'iodométhylate de *N*,*N*-diméthylaminométhylferrocène **12** et (*c*) avec le tosylate de ferrocènyle **16** pour former les dérivés ferrocéniques **6**, **7**, **8**, **9**, **11**, **13**, **14**, **15** et **20** du sucre. On a réalisé la conjugaison directe d'un sucre libre soluble dans l'eau avec le ferrocène, par la formation d'une base de Schiff entre le chlorhydrate de glucosamine **25** et le carboxaldéhyde de ferrocène **24**. La synthèse de ferrocényles de sucres basée sur la technique de groupes servant de pont est démontrée par la conjugaison du thiosucre **4** avec le ferrocène par l'intermédiaire du chlorure cyanurique **21** un agent de couplage polyvalent qui conduit à la formation du composé *s*-triazine **23**. On a étudié ces produits par rmn ^{1}H: les déplacements chimiques, les constantes de couplage et les mesures de relaxation spin–réseau du proton.

[Traduit par le journal]

Introduction

Ferrocene **1** and its derivatives are finding (2) an ever-increasingly wide range of industrial and biochemical applications in areas ranging from the development of new iron-containing drugs (3) to the formation of ferrocene-modified polymers (4). Such derivatives are also of interest for a number of other reasons including the development of optically active catalysts (5), of metal compounds for new immunoassay techniques (6), of heavy metal probes for electron microscopy (7), of the synthesis of radiopharmaceuticals (8), and the modification of electrode surfaces (9). It might therefore be anticipated that these, and other, areas would be advanced in a variety of ways by the development of general routes to the synthesis of ferrocenyl sugar derivatives. And it might also be anticipated that the combined presence of the sugar and metal moieties would give these compounds interesting biological properties. Prompted by this, and by the fact that carbohydrates can be either water soluble, or when suitably substituted, soluble in organic media, we have investigated the synthesis of sugar–ferrocene conjugates in which the sugar moiety is covalently attached to the cyclopentadienyl ligand of the ferrocene complex.

We also document here the use of ^{1}H nmr spectroscopy to evaluate the primary structure of these compounds, and the effect that a proximal chiral sugar group has on the proton resonances of the cyclopentadienyl ring. Attention is also drawn to the use of proton spin–lattice relaxation measurements for the assignment of the proton resonances of substituted cyclopentadienyl rings.

Results and Discussion

Synthesis

A wide variety of ferrocene derivatives are susceptible to nucleophilic attack by the amino, hydroxyl, or thiol functional groups of suitably blocked carbohydrate derivatives. All of the reactions used here to form ferrocenyl sugar conjugates are of this type. The compounds formed were all crystalline (with exception of **20**) and were usually orange or red in color. This greatly facilitated their detection during thin layer chromatography (tlc) and as a result that technique provided a convenient method for following reactions; for the same reason it proved convenient to purify several compounds by silica-gel chromatography (see Experimental).

It was already known that the ferrocenoyl chlorides **2** and **3** (10) react readily with a variety of nucleophilic reagents, including thiols, amines, and alcohols, in dry organic solvents with a suitable base acceptor and it was a simple matter to treat **2** and **3** with a variety of blocked sugars, each containing one of these three functional groups. Reac-

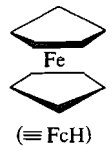
[1]For a preliminary communication, see ref. 1.

0008-4042/80/121188-10$01.00/0

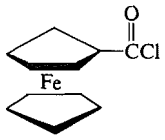
©1980 National Research Council of Canada/Conseil national de recherches du Canada

Can. J. Chem. Downloaded from www.nrcresearchpress.com by 210.87.254.5 on 09/05/12
For personal use only.

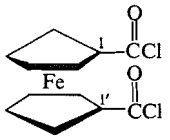
Can. J. Chem. Downloaded from www.nrcresearchpress.com by 210.87.254.5 on 09/05/12
For personal use only.



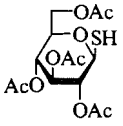
1



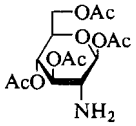
2



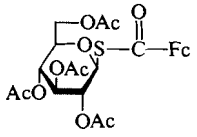
3



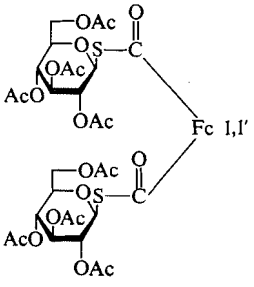
4



5



6

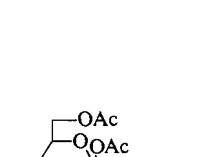


7

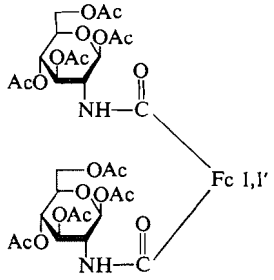
tion with 2,3,4,6-tetra-*O*-acetyl-1-thio-β-D-glucopyranose **4** (11), and 1,3,4,6-tetra-*O*-acetyl-2-amino-2-deoxy-β-D-glucopyranose **5** (12) occurred readily at room temperature in dry chloroform with either pyridine or triethylamine, as the base acceptor, to form the mono- and 1,1′-dithioesters **6**, **7** and amides **8**, **9**. In like fashion, reaction of the mono-ferrocenoyl chloride with 1,2:5,6-di-*O*-isopropylidene-α-D-glucofuranose **10** in dry pyridine overnight afforded the monosubstituted ester **11**.

N,N-Dimethylaminomethylferrocene methiodide **12** (13) also reacts with a variety of nucleophilic reagents by virtue of its benzyl-like structure and having the trimethylamine moiety as a gaseous leaving group. These reactions, however, require more vigorous conditions that those involving the acid chlorides, Thus, reaction with the 1-thio sugar **4** in boiling acetonitrile with anhydrous sodium carbonate was successful but a mixture of α and β anomers (40:60) was isolated (as determined by ^{1}H nmr), probably because of mutarotation of the 1-thio sugar under the basic reaction conditions. Fortunately, several recrystallizations from ethanol afforded the pure β compound **13**. Reaction of the 2-amino sugar **5** with two equivalents of the methiodide reagent **12** under the same conditions yielded the *N,N*-bis amine compound **14**. However this was not a good route to the secondary amine compound **15** since mixtures (as determined by tlc) of both **14** and **15** were always obtained even when a large excess of **5** was employed. All attempts to condense reagent **12** with sugar hydroxyl groups failed.

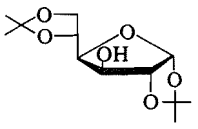
The ferrocenyl tosylate **16** was next evaluated as an alternative alkylating reagent to **12**. This compound does not appear to have been synthesized previously although its intermediacy was postulated in the formation of the ether **17** during reaction of the alcohol **18** with tosyl chloride in diethyl ether solution (14). This tosylate **16** proved to have the same high reactivity as other "benzylic" tosylates and as a result could not be prepared by the



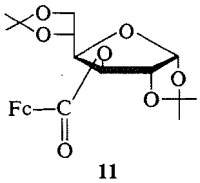
8



9

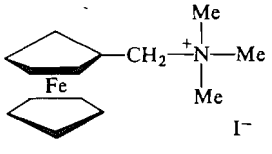


10

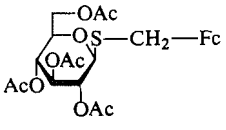


11

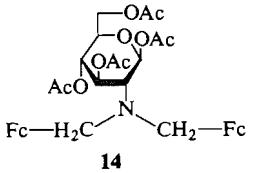
reaction of **18** with tosyl chloride in pyridine at ambient temperature. Instead it was prepared by the method of Kochi and Hammond (15) and used *in situ* (see Experimental) without isolation.



12

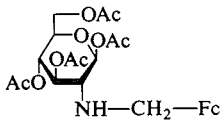


13

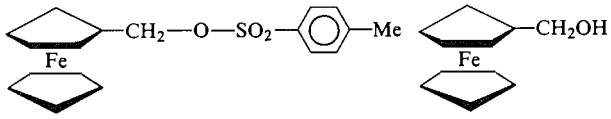


14

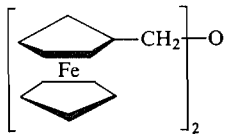
Can. J. Chem. Downloaded from www.nrcresearchpress.com by 210.87.254.5 on 09/05/12
For personal use only.



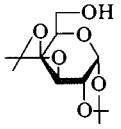
15



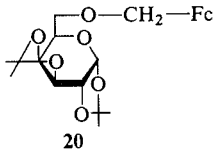
16 18



17



19



20

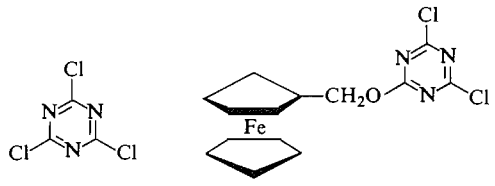
Reaction of **16** with the 1-thio sugar **4** at ambient temperature for 2 days gave **13** which was easily isolated since it crystallized readily from ethanol. The yield of **13** was much higher than that for the reaction between **4** and **12** and no evidence was found for the formation of the α anomer. With 1,2:3,4-di-*O*-isopropylidene-α-D-galactopyranose **19** reaction of **16** in an ether solution for two days at room temperature was also successful but the yield was much lower than that found for the thio sugar reaction. Since this product **20** was an oil, workup was more difficult and purification was performed on column chromatography. Reaction of the tosylate with the 2-amino sugar **5** was also low-yielding and the solution had to be heated under reflux for 2 days in a chloroform–ether solution. The product **15** was, however, easily isolated since it could be extracted into dilute acid and then extracted back into ether upon neutralization; the starting 2-amino sugar was separated from the product since it was not soluble in ether.

Impressed by the ease with which *s*-triazine derivatives react with carbohydrate derivatives (16) we also evaluated this approach to the synthesis of ferrocenyl–sugar conjugates. Reaction of hydroxymethylferrocene **18** (17) with cyanuric chloride **21** in basic aqueous acetone afforded the ferrocenyl triazine dichloride **22**: although **17** was also formed as a byproduct it could be readily removed by filtration prior to crystallization of **22**. The dichloride **22** was somewhat unstable but could be stored for several weeks in an evacuated desiccator and was suitable for further reactions without purification. Reaction of **22** with two equivalents of the 1-thio glucose sugar **4** occurred readily in acetonitrile with triethylamine to yield the ferrocenyl sugar compound **23**.

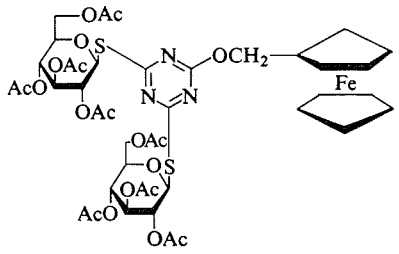
Two approaches were considered for the formation of water-soluble ferrocene–sugar conjugates: selective reaction of an unblocked sugar and deblocking of the above-described, blocked derivatives.

It is well known that amino sugars form Schiff's bases with aromatic aldehydes (18), and reaction of ferrocene carboxaldehyde **24** in ethanol with glucosamine hydrochloride **25** in the presence of triethylamine gave, as expected, the Schiff's base **26** in 70% yield. This reaction should find substantial generality. Unfortunately an initial attempt to stabilize the Schiff's base by reductive amination with sodium cyanoborohydride was unsuccessful; tlc of the reaction mixture indicated the formation of a mixture of compounds.

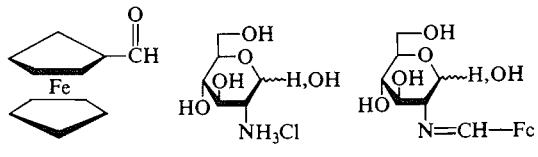
Attempts to deblock the substituted sugar conjugates were very disappointing since only two reactions gave acceptable yields. Thus de-*O*-acetylation of compounds **6** and **13** was successfully accomplished using sodium methoxide in methanol (19). Compound **13** was cleanly deacetylated and the product **27** crystallized readily from water as the monohydrate. Compound **6**, as expected under these conditions, was partially cleaved at the thio–ester linkage but the main prod-



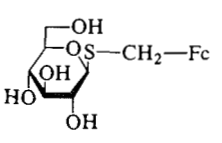
21 22



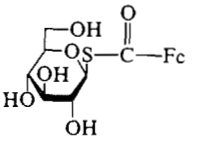
23



24 25 26



27



28

uct was the unblocked ferrocenyl derivative **28**; the product was easily purified by column chromatography and the methyl ferrocenecarboxylate was also isolated, and subsequently identified by ^{1}H nmr. Deacetylation of the 1,1′di-thio ester **7** proved to be very complex (tlc) and was not pursued further. More surprisingly, deacetylation of both the amides **8** and **9** with sodium methoxide in methanol was complex and no pure product could be isolated. Deacetylation of the amines **14** and **15** also proved disappointing; in each case two compounds which had very similar R_f values were detected by tlc and attempts to purify these compounds by preparative tlc or by column chromatography failed. The *s*-triazine derivative **23** was also exposed to these deacetylation conditions but again tlc showed the major product to be colorless (detection by H_2SO_4 charring), which suggests cleavage of either the thio sugar or ferrocene moieties from the triazine ring.

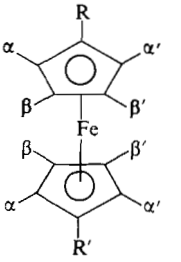
Removal of the isopropylidene blocking groups from **20** was also unsuccessful. The standard procedure of heating in dilute sulfuric acid could not be used since ferrocene compounds are readily oxidized under these conditions. Heating under reflux in aqueous methanol using IR 120 H^+ resin was tried but after 1 h the solution turned colorless and a colorless product having the same R_f value as the diacetone galactose precursor **19** was detected on tlc, suggesting that cleavage of the ether linkage was taking place. The resin had also turned green and it was thought that oxidation was occurring under these conditions as well.

Nuclear Magnetic Resonance Spectra

Proton Data

The ^{1}H chemical shifts and coupling constants for the ferrocenyl sugar derivatives **6**, **7**, **8**, **9**, **11**, **13**, **14**, **15**, **20**, **23**, **26**, **27**, and **28** are summarized in Table 1.

It is interesting to observe that a proximal chiral group renders all four protons of the substituted cyclopentadienyl ring inequivalent, as previously observed by Kursanov *et al.* (20) for cymantrene systems. The chiral group, in our case the sugar, renders the α,α′ and β,β′ protons diastereotopic and potentially four separate resonances can be observed. This turned out to be the case in the spectrum of compound **7**, but more usually only the



α protons are separated and the β protons remain overlapping as in the spectrum of compound **8**, Fig. 1. It should be noted that ^{13}C chemical shifts are more sensitive to this effect (21).

Assignment of the individual proton resonances of the substituted cyclopentadienyl rings of these chiral derivatives presents a problem. As we have reported elsewhere (22), a combination of ^{1}H—^{1}H spin-decoupling and ^{1}H spin–lattice relaxation measurements can give unequivocal results, and the assignments given in Table 1 are based on comparison with those given[2] previously (22).

From the ^{1}H chemical shifts and coupling constants of all the compounds synthesized, it seems probable that the sugar units have the same conformations as the sugar precursor. However compound **23** has a very interesting ^{1}H nmr spectrum indeed, Fig. 1(C), which merits separate discussion. The proton resonances of the two sugar rings in this compound are non equivalent in the ^{1}H nmr spectrum which implies that the molecule must favour a preferred set of conformations. Although there exist no formal symmetry elements in this molecule, it was argued initially that a pseudo-C_2 rotation axis, as shown, could be generated if there were free rotation (fast on the nmr time scale) about the bonds joining the substituents to the central triazine ring. However, the observed nonequivalences imply that steric hindrance prevents complete rotation about some of these bonds. In the insert Figure 1(E), of the acetate region, all eight acetate groups are resolved. Since the separation between two acetate resonances, common to both sugar rings, could not be more than 15 Hz, it would therefore be necessary for the bonds to rotate more slowly than $2\pi \times 15$ revolutions per second in order for separate resonances to be observed. This, however, would correspond to an unrealistically high barrier to rotation; it follows that our original argument is untenable. The following explanation appears to be preferable. It seems likely that the molecule favours a conformation in which the ferrocene moiety is oriented on

[2]Briefly it was shown that the β,β′-protons, each of which has two vicinal neighbours, relax at approximately twice the rate of the α,α′-protons which have only one neighbour.

Can. J. Chem. Downloaded from www.nrcresearchpress.com by 210.87.254.5 on 09/05/12
For personal use only.

Can. J. Chem. Downloaded from www.nrcresearchpress.com by 210.87.254.5 on 09/05/12
For personal use only.

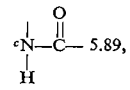
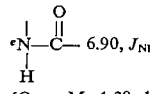
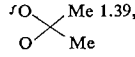
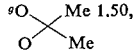
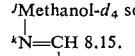
TABLE 1. Chemical shifts (ppm) and multiplet splittings (Hz) for the ferrocenyl monosaccharide compounds

Compound	(α, α′)[a]	(β, β′)[a]	Cp (unsubstituted)	H-1	H-2	H-3	H-4	H-5	H-6	H-6′	OAc	—CH_2
6[b]	4.77 4.68	3.99	3.97	5.72 $J_{1,2}$ 10.4	5.54 $J_{2,3}$ 10.4	5.48 $J_{3,4}$ 9.0	5.32 $J_{4,5}$ 10.0	3.34 $J_{5,6}$ 4.3	4.22 $J_{6,6'}$ 12.5	4.0 $J_{5,6'}$ 2.0	1.70 1.69 1.68 1.65	
7[b]	4.76 4.61 $J_{\alpha,\alpha'}$ 1.3 $J_{\alpha,\beta}$ 2.6	4.11 4.02 $J_{\beta,\beta'}$ 2.6		5.70 $J_{1,2}$ 10.5	ca. 5.5	ca. 5.5	5.35 $J_{4,5}$ 10.3	3.50 $J_{5,6}$ 4.3	4.29 $J_{6,6'}$ 12.6	4.05 $J_{5,6'}$ 2.0	1.79 1.71 1.69 1.65	
8[b,c]	4.71 4.68	4.01	4.05	5.90 $J_{1,2}$ 8.8	4.76 $J_{2,3}$ 10.0	5.42 $J_{3,4}$ 9.4	5.35 $J_{4,5}$ 9.4	3.64 $J_{5,6}$ 4.7	4.31 $J_{6,6'}$ 12.4	4.13 $J_{5,6'}$ 2.1	1.73 1.70 1.67 1.61	
9[d,c]	ca. 4.3	ca. 4.3		5.99 $J_{1,2}$ 8.8	4.48 $J_{2,3}$ 10.1	5.43 $J_{3,4}$ 9.5	5.23 $J_{4,5}$ 9.8	3.94 $J_{5,6}$ 4.4	4.35 $J_{6,6'}$ 12.4	4.16 $J_{5,6'}$ 2.1	2.14 2.12 2.10 2.09	
11[b,f]	4.97 4.72	4.07	4.10	5.73 $J_{1,2}$ 3.6	4.36	5.78 $J_{3,4}$ 2.0	4.51 $J_{4,5}$ 2.3	4.51 $J_{5,6}$ 5.3	4.11 $J_{6,6'}$ 8.7	4.24 $J_{5,6'}$ 3.5		
13[b]	4.15 4.09	3.93	3.99	5.37	4.23	5.37	5.25	3.24 $J_{5,6}$ 4.9	4.25 $J_{6,6'}$ 12.3	4.06 $J_{5,6'}$ 2.2	1.73 1.72 1.69 1.67	3.72 3.59 J_{gem} 12.7
14[b]	4.23 4.16	3.96	4.03	5.99 $J_{1,2}$ 8.9	3.34 $J_{2,3}$ 10.6	5.59 $J_{3,4}$ 9.1	5.26 $J_{4,5}$ 10.0	3.25 $J_{5,6}$ 4.1	4.28	4.0 $J_{5,6'}$ 1.9	1.80 1.70 1.68 1.65	3.90 3.70 J_{gem} 13.2
15[b]	4.11	3.93	4.02	5.72 $J_{1,2}$ 8.5	2.98 $J_{2,3}$ 10.0	5.20 $J_{3,4}$ 9.8	5.32 $J_{4,5}$ 9.3	3.32 $J_{5,6}$ 4.1	4.31 $J_{6,6'}$ 12.4	4.01 $J_{5,6'}$ 2.2	1.75 1.70 1.66 1.63	3.64 3.46 J_{gem} 13.2
20[b,g]			3.98	5.55 $J_{1,2}$ 5.0	4.17 $J_{1,3}$ 2.3			$J_{5,6}$ 2.3	$J_{6,6'}$ 7.9	4.51		
23[b,h]	4.59 4.33	3.87	3.92	*H*-1x 5.83 $J_{1x,2x}$ 10.5 H-1y 5.44 $J_{1y,2y}$ 10.5	H-2x 5.44 H-2y 5.34	H-3x 5.34 H-3y 5.34	H-4x 5.26 $J_{4x,5x}$ 10.2 H-4y 5.16 $J_{4y,5y}$ 10.1	H-5x 3.26 $J_{5x,6x}$ 5.2 H-5y 3.34 $J_{5y,6y}$ 4.2	4.16–4.18 4.16–4.18	4.03–4.08 $J_{5x,6'x}$ 2.0 4.03–4.08 $J_{5y,6'y}$ 2.1	1.86 1.74 1.71 1.69 1.68 1.67	4.83 4.09 J_{gem} 15.0

Can. J. Chem. Downloaded from www.nrcresearchpress.com by 210.87.254.5 on 09/05/12
For personal use only.

TABLE 1 (*Concluded*)

Compound	(α, α′)[a]	(β, β′)[a]	Cp (unsubstituted)	H-1	H-2	H-3	H-4	H-5	H-6	H-6′	OAc	—CH_2
23[i,h]	4.47		4.24	H-1x 5.86	H-2x 5.25	H-3x 5.54	H-4x 5.25				2.03	5.05
		4.18		$J_{1x,2x}$ 10.6	$J_{2x,3x}$ 9.3	$J_{3x,4x}$ 9.3		ca. 4.1	ca. 4.1	ca. 4.1	2.02	
	4.40			H-1y 5.76	H-2y 5.11	H-3y 5.47	H-4y 5.08				2.02	4.81
				$J_{1y,2y}$ 10.6	$J_{2y,3y}$ 9.4	$J_{3y,4y}$ 9.4					2.01	
											1.99	J_{gem} 15.1
											1.98	
											1.97	
											1.97	
26[i,k]			4.27		2.88	3.61			3.70	3.91		
				$J_{1,2}$ 10.2	$J_{2,3}$ 9.1	$J_{3,4}$ 9.2		$J_{5,6}$ 5.2	$J_{6,6'}$ 11.6	$J_{5,6'}$ 1.7		
27[i]	4.27	4.12	4.17	4.37	3.27	~3.4	~3.4	~3.4	3.69	3.89		3.84
				$J_{1,2}$ 9.6	$J_{2,3}$ 9.4			$J_{5,6}$ 5.4	$J_{6,6'}$ 12.2	$J_{5,6'}$ 2.2		3.71
												J_{gem} 13.2
28[i]	4.83	4.49	4.34	4.76	4.87	3.69	3.52	3.46	3.70	3.89		
				$J_{1,2}$ 9.8	$J_{2,3}$ 9.0	$J_{3,4}$ 9.7	$J_{4,5}$ 9.7	$J_{5,6}$ 5.1	$J_{6,6'}$ 12.0	$J_{5,6'}$ 2.2		

[a]Assignments were made by comparison to 6 and 7 (22); α and β resonances are assigned to high field of their α and β counterparts.
[b]Deuteriobenzene solution.
[c]  5.89, J_{NH,H_2} = 9.1 Hz.
[d]Deuteriochloroform solution.
[e]  6.90, J_{NH,H_2} = 9.3 Hz.
[f]  Me 1.39, 1.32, 1.23, 1.04.
[g]  Me 1.50, 1.42, 1.16, 1.04.
[h]Since there are two inequivalent sugar rings the notation H-1x, H-1y etc. is used.
[i]Deuterioacetone solution.
[j]Methanol-d_4 solution.
[k]  8.15.
[l]Deuterioacetone/D_2O, ca. 10:1 solution.

Can. J. Chem. Downloaded from www.nrcresearchpress.com by 210.87.254.5 on 09/05/12
For personal use only.

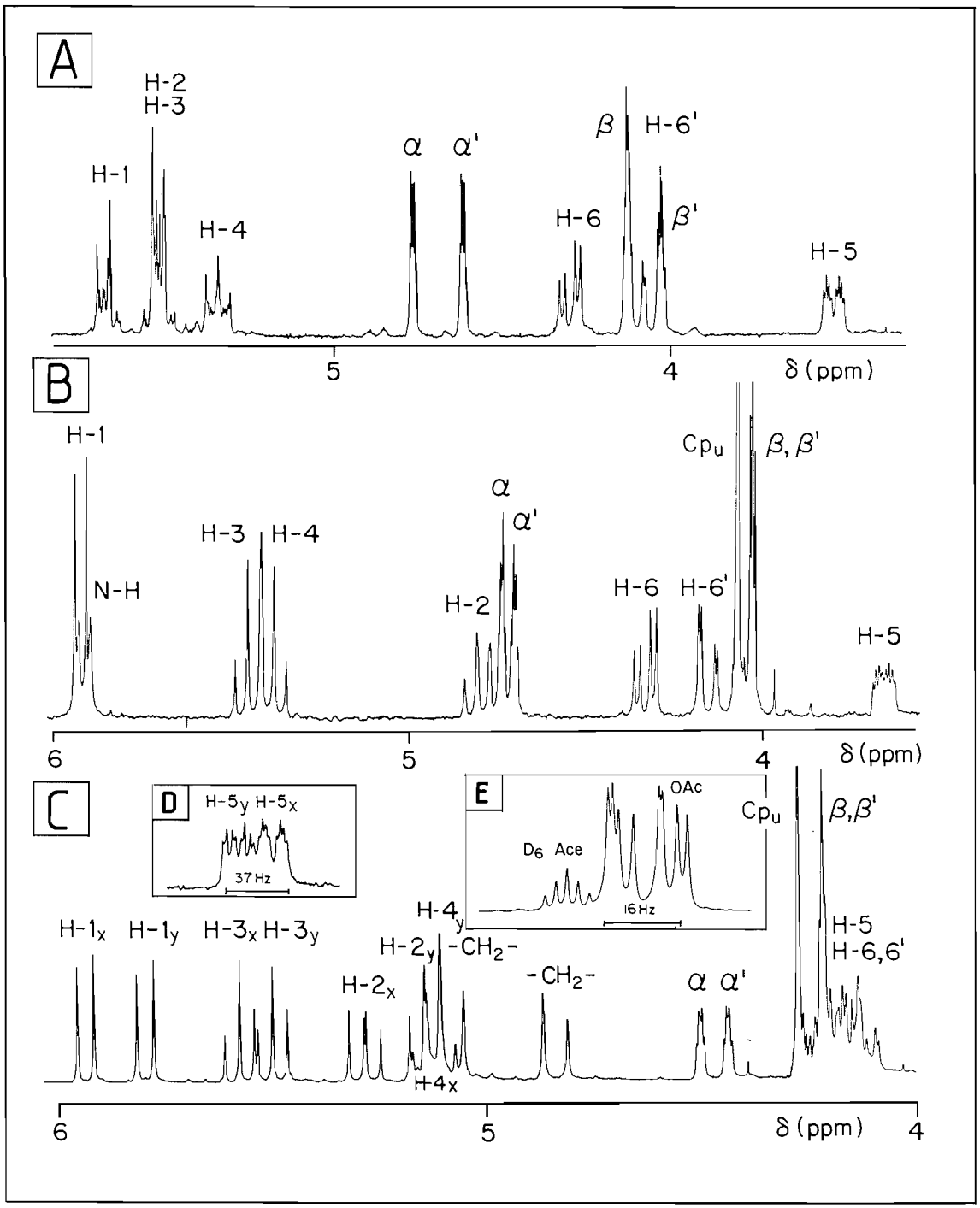
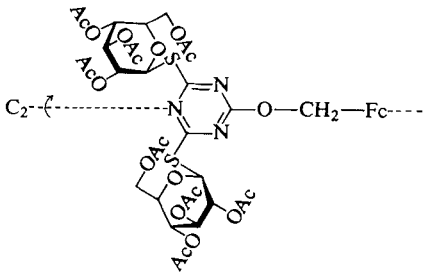
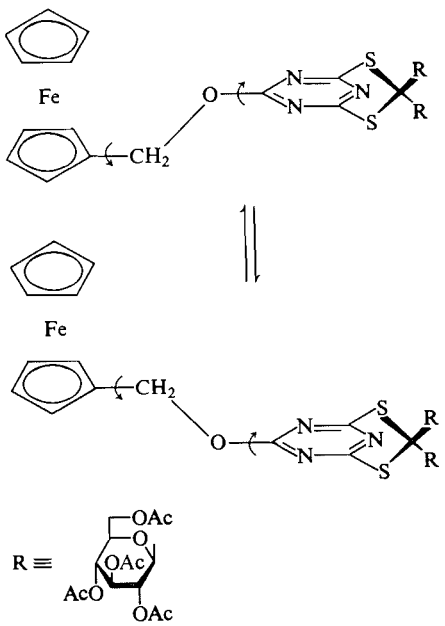


FIG. 1. Partial ^1H nmr spectra (270 MHz) of the sugar and cyclopentadienyl ring proton resonances of (A) compound **7** in deuteriobenzene (NA = 100), (B) compound **8** in deuteriobenzene (NA = 500), (C) compound **23** in deuterioacetone (NA = 50). The insert (D) shows the two H-5 resonances of compound **23** in deuteriobenzene (NA = 20) centered at 3.30 ppm and insert (E) shows the eight acetate resonances of compound **23** in deuterioacetone centered at 2.00 ppm. All spectra were accumulated at 32K data points with a sweep width of 3000 Hz and an acquisition time of 5.439 s at a temperature of 20°C. Cp_u refers to the singlet arising from the five protons of the unsubstituted cyclopentadienyl ring.

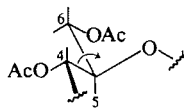


one side of the triazine ring as shown in the diagram. This would allow a rapid "cranking" motion about the bonds joining the ferrocene group to the triazine moiety which would be reasonable since this motion sweeps out only a small volume. It is then assumed that the bond rotations which would allow the ferrocene unit to tip over to the underside of the ring must be very slow. This seems also to be reasonable since a large inertial moment must be overcome in order for the bulky ferrocene group to make a 360° sweep through solvent molecules. It can then be seen from molecular models that the preferred conformation for the sugar units places one sugar unit above and one below the plane of the triazine ring as shown in the diagram. These two effects combined would then bring one sugar group much closer to the aromatic ring current of the ferrocene system than the other sugar group and result in a chemical shift difference between resonances of the two sugar moieties. This argument is supported by the spectrum in Fig. 1(C), since the sugar ring resonances $H_1 \rightarrow H_4$ for one



sugar group are all shifted in one direction with respect to the equivalent resonances of the other sugar group. That is, H_{1x} is to low field of H_{1y}, H_{2x} is to low field of H_{2y}, etc.

An interesting feature of the deuteriobenzene spectrum of **23** is that the H_5 resonances of the two sugar rings, shown in the insert Fig. 1(D), exhibit quite different coupling patterns. The H_{5y} resonance has a much larger $J_{5y,6y} = 5.2$ Hz than does the more usual value for H_{5x} of $J_{5x,6x} = 4.2$ Hz. This suggests that the bond joining C_{5y} and C_{6y}, as shown, is favouring preferred conformations, which reinforces the previous suggestion that this molecule is sterically crowded.



Experimental

All solutions were concentrated using a Buchi rotary evaporator. All melting points were determined using a Thomas Hoover Unimelt instrument (Model 6406-K) and are corrected. All optical rotations were determined using a Perkin-Elmer Polarimeter (model 241-MC).

Thin layer chromatography (tlc) was performed on silica gel plates (Baker-flex Silica gel 1B2-F) using the following solvents: (*A*) 1:1, toluene – ethyl acetate, (*B*) 4:1 toluene – ethyl acetate, (*C*) 1:5 methanol–chloroform. All blocked sugar ferrocenyl derivatives were checked for purity by tlc in solvents *A* or *B* and the unblocked compound in solvent *C*. Column chromatography was performed using 100–200 ASTM mesh silica (Fisher) packed in columns approximately 2.5 × 50 cm, and eluted with solvents *A*, *B*, or *C*. For reactions requiring anhydrous (dry) solvents the solvents were dried by standard methods, distilled, and stored under a nitrogen atmosphere.

Ferrocene was obtained from Sigma Chemical Company, Saint Louis, MO. All the ferrocene-derived starting materials were synthesized from known methods (see text) except for 1,1′-ferrocene dicarboxylic acid which was purchased from Strem Chemicals, Inc., Newburyport, MA. Sodium hydride was purchased from Alfa Products, Danvers, MA, as 50% dispersion in oil. *p*-Toluenesulfonyl chloride was purchased from Eastman Organic Chemicals, Rochester, NY, and purified by the method of Pelletier (23). Cyanuric chloride (97%) was purchased from Aldrich Chemical Co., Milwaukee, WI. All microanalyses were performed by Mr. P. Borda, of this Department. The mass spectra were obtained using an Atlas CH-4B mass spectrometer and high resolution determinations were obtained using an AEI MS-9 or an MS-50 mass spectrometer.

Proton nmr spectra were measured at 270 MHz with the prototype of a homebuilt spectrometer based on a Bruker WP-60 console, a Nicolet 1180 computer (32K), a Nicolet 293A pulse controller unit, a Diablo Disk, and an Oxford Instruments Superconducting solenoid. Concentrations of normal samples ranged from 0.01 to 0.10 *M* and T_1 measurements were performed in concentrations of < 0.05 *M*, with degassing achieved by 5 freeze–pump–thaw cycles. All deuterated solvents were obtained from Merck Sharp and Dohme, Montreal, Canada, and tetramethylsilane was used as a standard.

Can. J. Chem. Downloaded from www.nrcresearchpress.com by 210.87.254.5 on 09/05/12
For personal use only.

Can. J. Chem. Downloaded from www.nrcresearchpress.com by 210.87.254.5 on 09/05/12
For personal use only.

Reactions of 1-Ferrocenecarbonyl Chloride 2 and of 1,1'-Ferrocene Dicarbonyl Chloride 3 with Sugars 4, 5, and 10

Either 1 or 2 equivalents of the thio **4** or amino **5** sugars were added to a stirred solution of **2** or **3** (0.25 g) in dry chloroform (15 mL). Then 1 or 2 equivalents of either pyridine or triethylamine were added and the reaction allowed to stir for 15 min at room temperature. The mixture was then extracted twice with each of water, 5% sodium carbonate, and water again. The chloroform layer was dried over anhydrous sodium sulfate, filtered, and evaporated to dryness. The 1,2,5,6-di-*O*-isopropylidene-α-D-glucofuranose sugar **10** was treated with **2** in dry pyridine overnight and after concentration, chromatographed on a silica gel column using solvent *B*.

2,3,4,6-Tetra-O-*acetyl-1-deoxy-1*-S-*(1-ferrocenecarboxylate)*-β-D-*glucopyranose* **6** was obtained in 60% yield from ethanol, mp 186–187°C, $[\alpha]_D^{22}$ +35.0°(*c* 1, $CHCl_3$). *Anal.* calcd. for $C_{25}H_{28}FeO_{10}S$: C 52.11, H 4.86, S 5.56; found: C 52.02, H 4.92, S 5.80.

*1,1'-Bis-(*S-*(2,3,4,6-tetra*-O-*acetyl-1-deoxy-1-thio*-β-D-*glucopyranose)) ferrocenecarboxylate* **7** was obtained in 56% yield from ethanol, mp 213–214°C, $[\alpha]_D^{22}$ −36.0° (*c* 1, $CHCl_3$). *Anal.* calcd. for $C_{40}H_{46}FeO_{10}S$: C 49.71, H 4.76, S 6.64; found: C 49.56, H 4.76, S 6.55.

*(2-*N-*(1,3,4,6-tetra*-O-*acetyl-2-amino-2-deoxy*-β-D-*glucopyranose))-1-ferrocenecarboxamide* **8** was obtained in 50% yield from ethanol, mp 182–183°C, $[\alpha]_D^{22}$ −2.5° (*c* 1, $CHCl_3$). *Anal.* calcd. for $C_{25}H_{29}FeNO_{10}$: C 53.70, H 5.19, N 2.50; found: C 54.00, H 5.23, N 2.51.

*Bis-(2-*N-*(1,3,4,6-tetra*-O-*acetyl-2-amino-2-deoxy*-β-D-*glucopyranose))- 1,1- ferrocenecarboxamide* **9** was obtained in 60% yield from ethanol, mp 110–111°C, $[\alpha]_D^{22}$ +20.0° (*c* 1, $CHCl_3$). *Anal.* calcd. for $C_{40}H_{48}FeN_2O_{20}$: C 51.53, H 5.15, N 3.00; found: C 51.29, H 5.25, N 2.98.

*(3-*O-*(1,2:5,6-di*-O-*isopropylidene*-α-D-*glucofuranose))-1-ferrocene carboxylate* **11** was prepared in 50% yield from column chromatography using solvent *B* and crystallization from ethanol–H_2O, mp 110–111°C, $[\alpha]_D^{22}$ −55.5° (*c* 0.64, $CHCl_3$). *Anal.* calcd. for $C_{22}H_{28}FeO_6$: C 59.50, H 6.31; found: C 59.27, H 6.07.

Preparation of 1,3,4,6-Tetra-O-*acetyl-2*-N,N-*bis-(1-aminomethylferrocene)-2-deoxy*-β-D-*glucopyranose* **14**

A mixture of *N,N*-dimethylaminomethylferrocene methiodide (2.5 g, 6.5×10^{-3} mol), the 2-amino sugar **5** (0.9 g, 2.6×10^{-3} mol), and sodium carbonate (0.8 g, 7.5×10^{-3} mol) in acetonitrile (40 mL) was heated to reflux for 12 h. The mixture was then evaporated to dryness, dissolved in chloroform, and extracted five times with water. The chloroform layer was dried over anhydrous sodium sulfate, filtered, evaporated to dryness and after trituration with hexane, filtered to give 1.28 g (66%). The compound was recrystallized by dissolution in a minimum of benzene, followed by addition of a small amount of hexane and subsequent addition of petroleum ether (bp 30–60°C) until a slightly cloudy solution was obtained, and then cooling; mp 97–98°C, $[\alpha]_D^{22}$ +77.0° (*c* 1, $CHCl_3$). *Anal.* calcd. for $C_{36}H_{41}Fe_2NO_9$: C 58.19, H 5.52, N 1.88; found: C 57.88, H 5.56, N 1.93.

Preparation of 2,3,4,6-Tetra-O-*acetyl-1*-S-*(1-thiomethylferrocene)*-β-D-*glucopyranose 13 from 12*

A mixture of 2,3,4,6-tetra-*O*-acetyl-1-thio-β-D-glucopyranose (2 g, 5.5×10^{-3} mol) the methiodide **12** (2 g, 5.2×10^{-3} mol), and anhydrous sodium carbonate (0.6 g, 5.6×10^{-3} mol) in acetonitrile (50 mL) was refluxed for 12 h. The mixture was evaporated to dryness, dissolved in chloroform, and extracted five times with water. The chloroform layer was dried over anhydrous sodium sulfate, filtered, and evaporated to dryness. The product was then column chromatographed on silica gel using solvent *A* and crystallized from ethanol to give 0.5 g (17%) of **13**, mp 129–130°C, $[\alpha]_D^{22}$ +32.0° (*c* 0.85, $CHCl_3$). This product however was found by ^1H nmr to be a mixture of α- and β-anomers (40:60). Five repeated recrystallizations from ethanol gave the pure β anomer, mp 139–140°C, $[\alpha]_D^{22}$ −39.0° (*c* 1, $CHCl_3$). *Anal.* calcd. for $C_{25}H_{30}FeO_{10}S$: C 53.41, H 5.34, S 5.70; found: C 53.21, H 5.34, S 5.93.

Preparation of (1-Hydroxymethylferrocene)-p-*toluenesulphonyl Chloride* **16**

Sodium hydride (0.12 g, 2.5×10^{-3} mol) was placed in a 50 mL, two-necked flask and washed twice with anhydrous ether. Then dry ether was added (15 mL) along with dry 1-hydroxymethylferrocene (0.5 g, 2.3×10^{-3} mol). The mixture was then heated under reflux overnight under nitrogen. The stirred suspension of the alcoholate was cooled to −23°C and to this was added dropwise, over a period of 0.5 h, a solution of *p*-toluenesulphonyl chloride (0.44 g, 2.3×10^{-3} mol) in anhydrous ether (15 mL). The mixture was stirred at −10°C for two more hours and allowed to warm to room temperature for another hour. The mixture was then filtered under nitrogen through sintered glass and the resulting solution of the tosylate **16** used directly in subsequent reactions.

Preparation of 2,3,4,6-Tetra-O-*acetyl-1*-S-*(1-thiomethylferrocene)*-β-D-*glucopyranose 13 using the Tosylate 16*

1-Hydroxymethylferrocene (0.5 g, 2.3×10^{-3} mol) was converted into the tosylate **16**, to an ether solution of which was added a solution of the 1-thio sugar **4** (0.5 g, 1.4×10^{-3} mol) in dry chloroform (10 mL). The mixture was kept for 40 h at ambient temperature and was then filtered and evaporated to dryness. Upon addition of ethanol the product crystallized to give 0.67 g (87%) of **13**. One recrystallization from ethanol gave orange plates in 79% yield, mp 139–140°C. For further analytical data see the preparation via the methiodide **12**.

Preparation of 1,3,4,6-Tetra-O-*acetyl-2*-N-*(1-aminomethylferrocene)*-β-D-*glucopyranose* **15**

1-Hydroxymethylferrocene (0.5 g, 2.3×10^{-3} mol) was converted into the tosylate; to an ether solution of the tosylate was added a solution of the 2-amino sugar **5** in dry chloroform (20 mL). The mixture was heated under reflux for two days and was then filtered, evaporated to dryness, dissolved in ether, and extracted into 5% aqueous HCl. The aqueous layer was then neutralized with sodium bicarbonate and extracted with ether. The ether layer was dried over anhydrous sodium sulfate, evaporated to a small volume, and cooled. The compound **15** crystallized as fine needles in 30% yield, mp 126–127°C, $[\alpha]_D^{22}$ +8.0° (*c* 1, $CHCl_3$). *Anal.* calcd. for $C_{25}H_{31}FeNO_9$: C 55.08, H 5.69, N 2.57; found: C 54.79, H 5.54, N 2.69.

Preparation of 1,2:3,4-Di-O-*isopropylidene-3*-O-*(1-hydroxymethylferrocene)*-α-D-*galactopyranose* **20**

1-Hydroxymethylferrocene (0.5 g, 2.3×10^{-3} mol) was converted into the tosylate and to the ether solution was added the 6-hydroxy sugar **19** (0.45 g, 1.7×10^{-3} mol) in anhydrous ether (5 mL). The mixture was kept for two days and was then filtered, evaporated to dryness, and purified on silica gel column chromatography using solvent *A*, to give the compound as an oil in 20% yield, $[\alpha]_D^{22}$ −58.7° (*c* 0.8, $CHCl_3$). *Anal.* calcd. for $C_{23}H_{30}FeO_6$: C 60.30, H 6.55; found: C 60.16, H 6.59.

Preparation of 2-Deoxy-2-N-*(1-ferrocenecarboxaldehydeimine)*-α,β-D-*glucopyranose* **26**

A mixture of 1-ferrocenecarboxaldehyde (0.5 g, 2.3×10^{-3} mol), 2-amino-2-deoxy-α,β-D-glucopyranose hydrochloride (0.5 g, 2.3×10^{-3} mol), and triethylamine (0.24 g, 0.24×10^{-3} mol) in absolute ethanol (15 mL) was stirred vigorously for

Can. J. Chem. Downloaded from www.nrcresearchpress.com by 210.87.254.5 on 09/05/12
For personal use only.

15 h. The mixture was then evaporated to a small volume and an equal amount of acetone added. The mixture was cooled and filtered to give 0.68 g (71%) product which was recrystallized by dissolving in a minimum of ethanol, evaporating to about half its volume, adding hexane, and refrigeration; mp 161–162°C, $[\alpha]_D^{22}$ +66.7° (*c* 0.33, MeOH). *Anal.* calcd. for $C_{17}H_{21}FeNO_5$: C 54.39, H 5.64, N 3.73; found: C 54.09, H 5.90, N 3.90.

Preparation of 2,4-Dichloro-6-(1-hydroxymethylferrocene)-s-triazine **22**

To an ice cold stirred solution of cyanuric chloride (0.86 g, 4.6×10^{-3} mol) in acetone (20 mL), over a period of 45 min was added, simultaneously, a mixture of hydroxymethylferrocene (1 g, 4.6×10^{-3} mol) in acetone (40 mL) and a solution of sodium hydroxide (5 mL of 4%) in water (55 mL). The solution was then filtered to yield a compound which was identified as the ferrocene ether dimer. The filtrate was allowed to become acidic upon standing at 0°C and the resulting orange precipitate filtered after 2 h to give the compound in 50% yield. This product is sufficiently pure for further reactions and should be stored in an evacuated desiccator. Purification was achieved by column chromatography on silica gel using solvent *A* and crystallized from ether–hexane, mp 120°C (dec.). *Anal.* calcd. for $C_{14}H_{11}N_3OCl_2Fe$: C 46.21, H 3.02, N 11.54; found: C 46.68, H 3.18, N 11.24; ms (high resolution) calcd. for $C_{14}H_{11}N_3OCl_2Fe$: 362.9615 amu; found: 362.9265 amu. Bis-(1-hydroxymethylferrocene)-ether was obtained in 15% yield, mp 113–114°C. *Anal.* calcd. for $C_{22}H_{22}Fe_2O$: C 63.83, H 5.32; found: C 63.84, H 5.45; ms (low resolution) calcd. for $C_{22}H_{22}Fe_2O$: 414 amu; found: 414 amu.

Preparation of 2-(1-Hydroxymethylferrocene)-4,6-bis-S-(2,3,4,6-tetra-O-acetyl-1-deoxy-1-thio-β-D-glucopyranose)-s-triazine **23**

Triethylamine (0.2 g, 2.0×10^{-3} mol) in acetonitrile (2 mL) was added to a stirred solution of compound **22** (0.3 g, 8.3×10^{-3} mol) and 1-thio glucose **4** (0.6 g, 1.65×10^{-3} mol) in acetonitrile (25 mL). After 10 min the mixture was poured into ice water (100 mL) and extracted with chloroform. The chloroform layer was dried over anhydrous sodium sulfate, filtered, and evaporated to dryness. One recrystallization from isopropanol gave 0.6 g (74%), mp 120–121°C, $[\alpha]_D^{22}$ +25.4 (*c* 1, $CHCl_3$). *Anal.* calcd. for $C_{42}H_{49}FeN_3O_{19}S_2$: C 49.48, H 4.81, N 4.12; found: C 49.51, H 4.72, N 4.12; ms (high resolution) calcd. for $C_{42}H_{49}FeN_3O_{19}S_2$: 1019.1749 amu; found: 1019.1769 amu.

Preparation of 1-Deoxy-1-S-(1-thiomethylferrocene)-β-D-glucopyranose **27**

To a stirred solution of compound **13** (0.1 g) in methanol–chloroform (4 mL, 1:1) was added dry 0.2 *N* sodium methoxide (0.3 mL). After 30 min under nitrogen, the solution was neutralized with IR 120 H^+ ion exchange resin, filtered, evaporated to dryness, and crystallized from H_2O to give 52 mg (75%). Recrystallization from H_2O gave orange plates of the monohydrate, mp 145–146°C, $[\alpha]_D^{22}$ −43.2° (*c* 0.44, MeOH). *Anal.* calcd. for $C_{17}H_{22}FeO_5S$: C 49.55, H 5.82, S 7.78; found: C 49.84, H 5.65, S 7.70.

Preparation of 1-Deoxy-1-S-(1-ferrocenecarboxylate)-β-D-glucopyranose **28**

To a stirred solution of the thio ester **6** (0.1 g) in methanol–chloroform (4 ml, 1:1) was added 0.2 *N* sodium methoxide (0.7 mL) and the solution was stirred for 45 min under nitrogen. The solution was then neutralized with IR 120 H^+ resin and the mixture filtered, evaporated to dryness, and the compound chromatographed on a silica gel column using solvent *C* to give 35 mg (50%) from ethanol, mp 145–146°C, $[\alpha]_D^{22}$ −3.3° (*c* 0.3, $CHCl_3$). *Anal.* calcd. for $C_{17}H_{20}FeO_6S$: C 50.03, H 4.90; found: C 49.75, H 5.08.

Acknowledgments

It is a pleasure to thank the National Research Council of Canada for their support of this work via operating grants to L.D.H. (A-1905) and a Postgraduate Scholarship to M.A. (1977–1979). The authors would also like to thank Dr. Brian Kolthammer of this Department for helpful discussions relating to organometallic chemistry and to Dr. Jeremy Sanders, visiting here from Cambridge University, for assistance in the interpretation of the nmr spectrum of compound **23**.

1. M. Adam and L. D. Hall. J. Chem. Soc. Chem. Commun. 865 (1979).
2. B. W. Rockett and G. Marr. J. Organomet. Chem. **167**, 53 (1979).
3. E. I. Edwards, R. Epton, and G. Marr. J. Organomet. Chem. **107**, 351 (1976).
4. K. Tsubakihama, J. Matsua, T. Sasaki, K. Yoshida, T. Fujimura, and K. Araki. J. Polym. Sci. **17**, 173 (1979); A. Gal, M. Cais, and D. H. Kohn. J. Appl. Polym. Sci. **22**, 3449 (1978).
5. H. Brunner. Angew. Chem. Int. Ed. Engl. **10**, 249 (1971).
6. M. Cais, S. Dani, Y. Eden, O. Gandolfi, M. Horn, E. E. Isaacs, Y. Josephy, Y. Saar, E. Slovia, and L. Snarsky. Nature, **270**, 534 (1977).
7. G. Marr and B. W. Rockett. J. Organomet. Chem. **58**, 323 (1973).
8. M. Wenzel, E. Nipper, and W. Klose. J. Nucl. Med. **18**, 367 (1977).
9. M. S. Wrighton, M. C. Palazzotto, A. B. Bocarsly, J. M. Bolts, A. B. Fisher, and L. Nadjo. J. Am. Chem. Soc. **100**, 7264 (1978); J. M. Bolts, A. B. Bocarsly, M. C. Palazzotto, E. G. Walton, N. S. Lewis, and M. S. Wrighton. J. Am. Chem. Soc. **101**, 1378 (1979); Chem. Eng. News, Mar. 19, 1979, pp. 25; A. W. C. Lin, P. Yeh, A. M. Yacynych, and T. Kuwana. J. Electroanal. Chem. **84**, 411 (1977).
10. P. L. Pauson and W. E. Watts. J. Chem. Soc. 2990 (1963).
11. D. Horton. Methods in carbohydrate chemistry. Vol. 2. Academic Press, New York, NY. 1963. p. 433.
12. M. Bergmann and L. Zervas. Chem. Ber. **64B**, 975 (1931).
13. D. Lednicer and C. R. Hauser. Org. Synth. Coll. Vol. **V**, 434 (1973).
14. L. W. Hall, Jr. Diss. Abstr. **20**, 78 (1959).
15. J. K. Kochi and G. S. Hammond. J. Chem. Soc. 3443 (1953).
16. M. J. Adam and L. D. Hall. Carbohydr. Res. **68**, C17 (1979).
17. D. Lednicer, T. A. Mashburn, Jr., and C. R. Hauser. Org. Synth. Coll. Vol. **V**, 621 (1973).
18. D. Horton. *In* The amino sugars. Vol. 1A. *Edited by* R. W. Jeanloz. Academic Press, New York, NY. 1969. p. 70.
19. A. Thompson and M. L. Wolfrom. Methods in carbohydrate research. Vol. 2. Academic Press, New York, NY. 1963. p. 215.
20. D. N. Kursanov, N. Parnes, N. M. Loim, N. E. Kolobova, I. B. Zlotina, P. V. Petrovskii, and E. I. Fedin. J. Organomet. Chem. **44**, C15 (1972).
21. N. M. Loim, D. N. Kursanov, Z. N. Parnes, N. N. Sul Dino, and E. I. Fedin. J. Organomet. Chem. **52**, C33 (1973).
22. M. J. Adam and L. D. Hall. J. Organomet. Chem. **186**, 289 (1980).
23. S. W. Pelletier. Chem. Ind. 1034 (1953).

FOR ERRATA SEE
64 #12 10.86 P. 2477

Acylation of aromatic substrates with ketenes. An example of vinyl oxocation reactivity

K. R. FOUNTAIN,[1] PAMELA HEINZE,[2] MARK SHERWOOD,[3] DAVE MADDEX,[4] AND GREG GERHARDT[5]

Northeast Missouri State University, Kirksville, MO 63501, U.S.A.

Received December 14, 1979

K. R. FOUNTAIN, PAMELA HEINZE, MARK SHERWOOD, DAVE MADDEX, and GREG GERHARDT. Can. J. Chem. **58**, 1198 (1980).

Acylations of aromatic substrates with ketenes involve the reactivity of species similar to vinyl cations. Resonance stabilization of ketene – aluminum chloride complexes seems to make these complexes less reactive than corresponding vinyl cations.

The kinetic isotope effect of the reaction with dimethylketene and benzene is 1.06, compatible with vinylcation cases, but not with acylation with CH_3COBF_4 types of electrophiles.

Substrate specificity was determined from k (toluene)/k (benzene) values. It was 47.2 for dimethylketene and 173.7 for diphenylketene. The diphenylketene – aluminum chloride complex could be isolated.

K. R. FOUNTAIN, PAMELA HEINZE, MARK SHERWOOD, DAVE MADDEX et GREG GERHARDT. Can. J. Chem. **58**, 1198 (1980).

L'acylation de substrats aromatiques au moyen de cétènes fait intervenir la réactivité d'espèces semblables aux cations vinyliques. La stabilisation par résonance des complexes cétène – chlorure d'aluminium semble rendre ces complexes moins réactifs que les cations vinyliques correspondants.

L'effet isotopique cinétique de la réaction entre le diméthylcétène et le benzène est de 1.06. Il est compatible avec l'existence de cations vinyliques, mais il n'est pas compatible avec une acylation au moyen d'agents électrophiles du type CH_3COBF_4.

La spécifité du substrat est déterminée à partir des valeurs de k toluène/k benzène. Elle est de 47.2 pour le diméthylcétène et de 173.7 pour le diphénylcétène. On a pu isoler le complexe cétène – chlorure d'aluminium.

[Traduit par le journal]

Although acylations of aromatic rings with ketene have been known (1–4) for over forty years, no serious mechanistic study of this reaction has been undertaken. We report in this paper the results of experiments showing positional selectivity, the substrate selectivity, the intermolecularity of the transfer of the proton from the site of attack to the α position of the ketone, and the kinetic isotope effect. Experiments with both dimethyl and diphenyl ketenes were explored.

We used dimethylketene (DMK) prepared by Staudinger's method, pyrolysis of dimethylmalonic anhydride (5); it was redistilled before use. Diphenylketene (DPK) was prepared by the triphenylphosphine catalysed dehalogenation of 2-bromo-2,2-diphenylacetylbromide (6), and distilled before use. The yields from dimethylketene acylation with a variety of substrates are summarized in Table 1. (The low yields with benzene, in neat hydrocarbon, are in contrast to the modest yields of up to 45.0% reported by earlier workers for ketene (4).) The reaction mixtures for the reaction with benzene, by gas chromatography, revealed seven compounds besides the authentic ketone. These compounds were due to the reaction of dimethylketene with itself in the presence of aluminum chloride to give dimers, as was shown by comparing the nmr spectrum of the reaction mixture with a sample of dimethylketene which had been allowed to dimerize at room temperature. Other ill-defined materials which were nonaromatic (nmr) were not further examined. The low yields of isobutyrophenone obtained with benzene as a substrate are due to the faster rate of these side reactions compared to the rate of acylation of the aromatic nucleus. These side products were a constant feature of the reactions with less active aromatic substrates. They completely vanished in the cases of more active substrates such as toluene, which were exceptionally clean, giving only one ketone in most cases.

TABLE 1. Yields of ketones from acylation with dimethylketene at 25°C in neat hydrocarbon

Substrate	%Yield (based on dimethylketene)
1. Benzene	5 [a]
2. Toluene	28.7
3. *o*-Xylene	40.0[a]
4. Anisole	65.2[b]

[a]Yield determined by gas chromatography.
[b]*ortho*/*para* (*o*/*p*) ratio 4.47×10^{-3} by gas chromatography; no *meta* isomer (0.1% of isomers could be detected).

Position Selectivity

The dimethylketene – aluminum chloride complex is highly positionally selective even though one might suspect that it should be highly reactive.

The position selectivity of dimethylketene was contrasted to that of isobutyryl chloride by analyzing the isomer distribution of reactions of the

[1]Author to whom correspondence should be addressed.
[2]PRF Undergraduate Scholar, 1976, 1977.
[3]PRF Undergraduate Scholar, 1975.
[4]Project SEED Student, Summer 1977.
[5]PRF Undergraduate Scholar, 1977–1978.

0008-4042/80/121198-08$01.00/0
©1980 National Research Council of Canada/Conseil national de recherches du Canada

Can. J. Chem. Downloaded from www.nrcresearchpress.com by 210.87.254.105 on 09/05/12
For personal use only.

Can. J. Chem. Downloaded from www.nrcresearchpress.com by 210.87.254.105 on 09/05/12
For personal use only.

TABLE 2. Comparison of *o/p* ratios for acylations with isobutyryl chloride and dimethylketene

Substrate	*ortho/para* × 10^2	
	Isobutyryl chloride	Dimethylketene
1. Toluene	4.33	0.00
2. Anisole	1.30	0.447
3. Ethylbenzene	0.0734	0.000
4. Cumene	0.000	0.000

acid chloride with aromatic substrates at 25°C. The results are shown in Table 2 in which *ortho/para* (*o/p*) ratios are given. No *meta* isomers were observed. Control experiments showed that no isomerization of products occurred under the reaction conditions, and as little as 0.1% of the isomers could be detected.

The nmr spin patterns of the *ortho* isomers, collected by preparative scale gc, displayed ABCD patterns similar to that of *o*-methylacetophenone (7) and had carbonyl bands at 1680 cm^{-1}. With dimethylketene only *para* isomers in yields of 15–50% were observed except with anisole and *o*-methylanisole. With anisole the *o/p* ratio was 4.47×10^{-3}. With *o*-methylanisole a mixture of the 4-isomer and 5-isomer in the ratio of 29:5 was obtained. It was observed that allowing pure samples of these ketones to stand in contact with aluminum chloride caused no changes to include *ortho* or *meta* isomers. Hence, it is likely that these mixtures represent the products of kinetic control and are not thermodynamically controlled mixtures. Since the selectivity of a reagent in discriminating between *ortho*- and *para*-positions depends not only on polar but also on steric interactions (8), one may thus infer that the reagents involved in acylation with $AlCl_3$ (dimethyl or diphenylketene) have a larger steric requirement than for an ordinary acid chloride acylation.

In no case of acylation with ketene did we find any *meta* isomers. This is unexpected because an acylating agent consisting of an oxovinyl cation should be a reactive species similar to an acylium ion. Such selectivity from reagents thought to be highly reactive has recently been reported by Stang and Anderson from alkylations with the stereoelectronically similar vinyl cations (9). Their product distributions are given in Table 3.

Except for toluene no *meta* isomer was observed. The *ortho*, *para* selectivity was lower for these vinyl cations than for the ketenes of this study. Both vinyl cation selectivity and ketene selectivity are higher than for acylations in general.

TABLE 3. Isomer distribution of vinyl triflate with monosubstituted benzenes (C_6H_5X) at 120°C

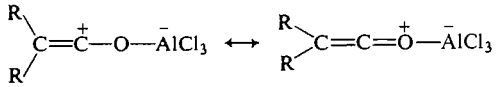
X	*ortho*	*meta*	*para*
CH_3O	11.3	0.0	88.7
CH_3	27.6	8.0	63.6
F	21.1	0.0	78.6
Cl	29.7	0.0	70.3

Substrate Selectivity

An indication of the substrate specificity of dimethylketene was obtained by competition experiments with benzene and toluene. In this case it was necessary to use an excess of benzene in the substrate mixture to ensure adequate detection of the isobutyrophenone in the rather complex gas chromatogram which arose due to the side products. The data on these experiments are summarized in Table 4. In each experiment a ratio of moles $AlCl_3$/moles dimethylketene of 2.5:1 was used.

The substrate specificity of 47.2[6] for dimethylketene found in this work contrasts with that found by Olah *et al.* (10) for acylation with $CH_3CO^+SbF_6^-$ or $CH_3CO^+SbCl_6^-$ which had toluene/benzene ratios of 125 and 121, respectively, for acylation in nitromethane at 25°C, and with acetyl chloride in nitromethane (11) which had a toluene/benzene ratio of 134. The dimethylketene – aluminum chloride reagent is thus actually more reactive than the other acylating agents cited in spite of the low yields with benzene and other moderately activated aromatic substrates. This finding supports the idea that the dimethylketene reacts more rapidly with itself in the presence of aluminum chloride than with a nonactivated or only moderately activated aromatic ring.

Our relative rates for toluene–benzene competitions compared with the value of 6.76 for vinyl cation alkylations (9) indicate that the substituted ketene – aluminum chloride complex is a great deal more substrate selective than the stereoelectronically similar vinyl cations. One might rationalize this greater substrate selectivity on the basis of structure **1** in which a mode of delocalization of charge is shown for the substituted ketene –



1

[6]51.69 was corrected to a mole per mole ratio by multiplying by mol. wt. phenyl ketone/mol. wt. tolyl ketone.

Can. J. Chem. Downloaded from www.nrcresearchpress.com by 210.87.254.105 on 09/05/12
For personal use only.

TABLE 4. Substrate selectivity for dimethylketene

Substrate ratio benzene/toluene	Substrate mols/ ketene mols	Ratios of areas (tolyl/phenyl)	Substrate ratio g/tolyl ketene: g/phenyl ketone
1:1	99	52.340	52.34
3:1	184	16.980	50.95
5:1	257	10.372	51.80
			Av. = 51.69

TABLE 5. Yields of ketones from acylation with diphenylketene

Substrate	Yield (%)
1. Benzene	10.0
2. Toluene	11.1
3. *o*-Xylene	47.0
4. Ethylbenzene	19.6
5. Cumene	6.26
6. Anisole	59.1
7. *o*-Methylanisole	49.1 (76.6 corrected)[a]
8. Chlorobenzene	1.07

[a]In this experiment an aliquot showed that only a 64% yield of the diphenylketene was obtained.

aluminum chloride complex which is not available for the analogous vinyl cation. Analogous "resonance" arguments are advanced for the known stability of carbocations from α-haloethers (12).

Diphenylketene Studies

Our study of acylation of various aromatic substrates with diphenylketene supports the picture of a ketene – aluminum chloride complex as a site selective reagent prone to react with other ketene molecules rather than aromatic rings. Table 5 shows the yield data. All of these reactions were found to produce polymeric tar from which the ketones had to be removed.

We examined the nature of the ketene–$AlCl_3$ complex as follows. To a 2.4 g solution of diphenylketene in 300 mL of ligroin was added one equivalent of aluminum chloride plus 10% excess, assuming reaction [1]. The mixture became cloudy and a ring of brown precipitate formed on the bottom. An additional 10% excess of $AlCl_3$ was added and a white solid was noted. A small aliquot of this solid was removed, rapidly filtered, and an ir spectrum taken (Nujol). The absence of ketene was noted by the lack of absorption at 2100 cm^{-1}. Instead, a medium band at 1620^{-1} appeared. The solution above this precipitate contained diphenylketene as shown by the yellow color and ir spectrum. To this mixture was then added 50 mL of anisole and the solution allowed to stand overnight. Decantation of the ligroin from the resultant brown complex was followed by dissolving the complex in CH_2Cl_2 and treatment with ice–HCl. Solvent removal yielded 2.16 g (58.3%) of the anisyl ketone. This compares very well with 59.1% of this ketone obtained by slowly adding an excess of aluminum chloride to anisole and diphenylketene.

These data are consistent with formulation of the $AlCl_3$–diphenylketene adduct **2** as in [1].

[1] $(C_6H_5)_2C{=}C{=}O + AlCl_3 \rightarrow (C_6H_5)_2C{=}C{-}O{-}AlCl_3$
2

The lack of any ketene bands in the precipitate and the appearance of a band at 1620 cm^{-1} would indicate that coordination to the O atom does indeed occur. These results parallel those reported by Hurd, who isolated a similar $AlCl_3$–ketene complex in CS_2 which also gave acylations with benzene and anisole (1).

The substrate specificity of the diphenylketene – aluminum chloride complex differs from that of dimethylketene as seen by comparing the data in Table 4 with those in Table 6. We regard the value from the 10:1 experiment as more valid because of difficulties in comparing greatly different areas with our integrator.

The value of 173.7 for the relative rate of toluene to benzene indicates the greater kinetic stability of the diphenylketene – aluminum chloride complex over that of the dimethylketene – aluminum chloride complex, as we observed in the isolation of the DPK complex. No isolation of the dimethylketene – aluminum chloride complex was possible. When we attempted to assay its relative stability by first adding $AlCl_3$ to a solution of dimethylketene in carbon disulfide, then adding anisole, no acylated anisole was found (96% recovery of starting anisole).

If one takes the relative rates of a toluene–benzene competition experiment as a measure of the kinetic stability of a species, one can order the vinyl type cations in the sequence below. This order allows one to think about structural variations

$$C_6H_5{-}\overset{+}{C}{=}CMe_2 < Cl_3\bar{A}l{-}O{-}\overset{+}{C}{=}CMe_2$$

$$< Cl_3\bar{A}l{-}O{-}\overset{+}{C}{=}C(C_6H_5)_2$$

TABLE 6. Substrate specificity for diphenylketene

Benzene/toluene	Substrate moles/ketene moles	Area ratio (mols/mol)	k(toluene)/k(benzene)
1:1	25	18.9	189
10:1	110	17.37	173.7

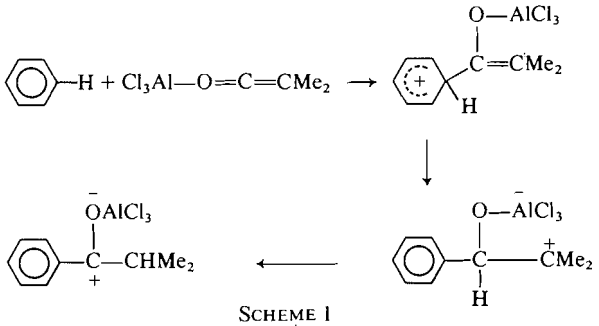
within the series in a consistent way. One can say that the phenyl ring attached directly to the charged carbon atom in the vinyl cation is less able to stabilize the charge than is the oxygen atom in the ketene complexes. This is certainly the order one would expect from consideration of the constants, say using σ^+ for OCH_3 as a model for —O—$AlCl_3$, and the σ^+ for C_6H_5(−0.78 vs. −0.18) (10).

The Intermolecularity of Proton Transfer

The unique stereoelectronic requirements of the dimethylketene – aluminum chloride complex, (if one accepts that coordination occurs at the oxygen as in **3**) allow intramolecular transfer of the proton on the benzene ring to the α-position in the final

$$(CH_3)_2C{=}C{=}\overset{+}{O}{-}\bar{A}lCl_3$$

ketone as in Scheme 1 to be formally considered. The driving force could be a combination of formation of a stable carbocation and rearomatization. Such 1,2 shifts are well known in carbonium ion chemistry. Despite early workers' claims (1–4) that evolution of HCl occurred with ketene, the present reactions with dimethylketene or diphenylketene showed no tendency to evolve HCl although a careful check was made to observe it. The question of how the ketone arises via proton transfer is thus an important one if one is to determine a kinetic isotope effect. When toluene-d_8 was acylated with dimethylketene, the label was retained to the extent of 98 ± 2% (by nmr integration) indicating that the α-proton in the final product ketone does not enter the molecule in the work-up step as would be necessary if aluminum chloride formed a complex like **4** as suggested by early workers for the case of ketene (2). Likewise acylating benzene-d_6 with



SCHEME 1

diphenylketene gave 97 ± 1% retention of deuterium.

$$Cl_2Al{-}CH_2{-}COCl$$

Control experiments using ketones labeled in the α-position showed that exchange under work-up conditions could have been 7 ± 5%.

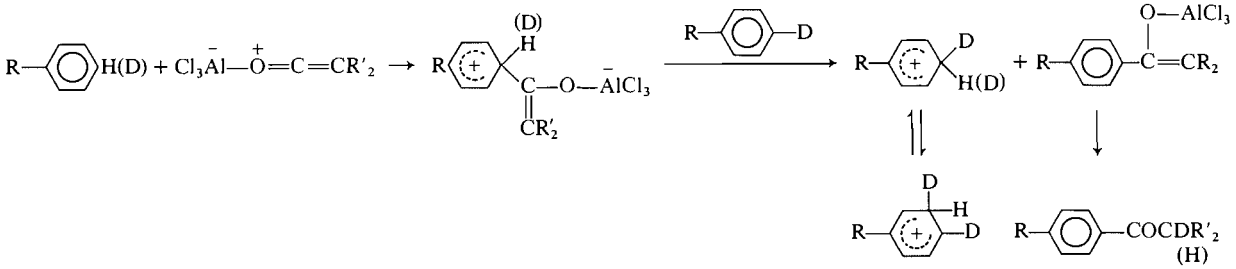
It was desirable to perform a crossover experiment in which one aromatic substrate was deuterated and the other was nondeuterated because the substrate itself in the foregoing experiments was the only source of deuterium (protium), hence allowing the probability that the result was predetermined. Accordingly, a 50:50 molar mixture of anisole and toluene-d_8 was acylated with dimethylketene with the result that each ketone was found to have deuterium at the α-position. The *p*-tolylketone was found to have ca. 70% protium at the α position. When *p*-toluene-*d* alone was acylated, label retention (D) occurred only to about 80% by nmr integration. These results clearly eliminate the formally possible Scheme 1 and point to a transfer of the proton via excess aromatic substrate as in Scheme 2.

When diphenylketene was used to acylate *p*-deuteriotoluene, the resulting ketone had a value of 72% protium at the α-position. This enhances the conclusions found for dimethylketene acylation in that extensive scrambling of the label occurs as in Scheme 2.

This mechanism is interesting because it allows the possibility of the observation of a large kinetic isotope effect. It is well documented that the absence of a base of sufficient strength to remove a proton easily leads to high kinetic isotope effects (13). One expects a high kinetic isotope effect in the present work due to the low basicity of the aromatic substrates (14, 15), i.e., more S_E3 character.

Following the method of Olah *et al.* (10), we determined the k_H/k_D for benzene acylation by comparing ratios of products from competition reactions with toluene–benzene and toluene – benzene-d_6. The reactions were run on mixtures having molar ratios of 5 mols of benzene-d_6 to one mol of toluene and 5 mols of benzene to one mol of toluene to circumvent difficulties in the analysis (see Experimental). The results are given in Table 7. The low value of 1.06 is contrasted with Olah's

Can. J. Chem. Downloaded from www.nrcresearchpress.com by 210.87.254.105 on 09/05/12
For personal use only.



SCHEME 2

value of 2.27 for acetylation with $CH_3CO^+SbF_6^-$ and CH_3COBF_4 complexes. This value is consistent with the great selectivity shown by the acylating agents from ketenes and is entirely consistent with the value of 0.98 ± 0.026 found by Stang and Anderson (9) for alkylation with vinyl cations.

A second paper reporting on Hammett–Brown (16) treatments of dimethylketene and diphenylketene acylations is in preparation.

Experimental

General

Infrared spectra were neat or Nujol mulls except where noted, and were run on a Beckman IR4. The nmr measurements were run in the solvents noted with TMS or DSS as internal standards. All chemicals were reagent grade Eastman or Aldrich products.

Preparation of Ketenes

Dimethylketene was prepared by the pyrolysis of dimethylmalonic anhydride as per Staudinger *et al.* (5). The material thus obtained was distilled twice before use and opened only to a dry nitrogen atmosphere.

Diphenylketene was made by debromination of α-bromodiphenylacetylbromide (7) with triphenyl phosphine in ligroin. The dibromotriphenyl phosphorane was filtered through a sintered glass funnel and hydroquinone (0.1 g) was added. The ligroin was removed by distillation under reduced pressure and the residue distilled to give yields of 60–85% of diphenylketene.

Preparation of Authentic Aryl Isopropyl Ketones

All authentic ketones were made by acylation with isobutyryl chloride and $AlCl_3$ in the aromatic substrate in excess as the solvent. The reactions were all at 25°C, and were catalysed by the addition of 2.5 equivalents of aluminum chloride per equivalent of acid chloride (4). The known isobutyrophenones were made into appropriate derivatives which were recrystallized to constant melting points. These compounds are summarized with their references in Table 8. The new isobutyrophenones synthesized in this work were also made into derivatives, and their analytical data appear below.

4-Methoxy-3-methylphenyl Isopropyl Ketone

Analysis for 2,4-DNP (mp 194–196°C). *Anal.* calcd. for $C_{18}H_{20}N_4O_5$: C 58.06, H 5.41, N 15.05; found: C 57.96, H 5.57, N 15.01.

3-Chloro-4-methylphenyl Isopropyl Ketone

Analysis for 2,4-DNP (mp 146–148°C). *Anal.* calcd. for $C_{17}H_{17}ClN_4O_4$: C 54.19, H 4.55, N 14.87; found: C 54.11, H 4.52, N 14.78.

4-Isopropylphenyl Isopropyl Ketone

Analysis for 2,4-DNP (mp 131–131.5°C). *Anal.* calcd. for $C_{19}H_{22}N_4O_8$: C 61.61, H 5.99, N 15.13; found: C 61.48, H 5.91, N 15.04.

4-Methoxy-3-bromophenyl Isopropyl Ketone

This material was a solid and was analyzed as obtained (mp 66.5–68.8°C). *Anal.* calcd. for $C_{11}H_{13}BrO_2$: C 51.38, H 5.10; found: C 51.37, H 5.12.

Procedure for Acylation with Dimethylketene

Typically the reaction was run at 25°C in a flask fitted for mechanical stirring with excess hydrocarbon as the substrate. The best results were obtained when, following Williams and Osborne (4), aluminum chloride was added portionwise to a mixture of hydrocarbon and dimethylketene under an N_2 atmosphere. Accordingly, in each case the pure dimethylketene was mixed with a 20-fold excess of hydrocarbon and a 2.5 molar excess of $AlCl_3$ added slowly. The reactions were stirred for an hour after the addition was completed, then the reaction mixtures were poured onto ice and 6 *M* HCl. Extracting with equal volumes of dichloromethane, water washing, 5% sodium bicarbonate washing, water washing, then drying over magnesium sulfate, gave oils in each case after solvent removal. When distilled, these oils gave derivatives which were identical to those from the known ketones from acid chloride preparations.

Spectral data include ir at 1680–1690 cm^{-1}, ν (C=O) for all ketones (neat), and nmr signals at δ ($CDCl_3$): 3.6–3.8 (broad heptet 1H), and 1.13–1.25 (doublet, 6H).

Deuterium Labelling Experiments

A 1.5 g (0.021 mol) sample of doubly distilled dimethylketene was treated with 10 g (0.075 mol) of anhydrous aluminum chloride from a fresh bottle and 10 g (0.1 mol) of toluene-d_8 (99+% isotopically pure). After the reaction had subsided, it was stirred for an additional hour and worked up by pouring onto H_2O–HCl (6 *M*) in ice and extracting with dichloromethane. Washing with water twice and drying over $MgSO_4$ gave the ketone, after solvent removal. The ketone was purified by preparative scale gc (Varian 920 Autoprep) using a 20 ft × ⅜ in. 15% SE 30 on 30/60 Chromosorb W column. The nmr showed only a singlet at 1.2 ppm with a trace of heptet at 3.40 ppm which corresponded to an exchange of 4.5% (ratio of 3.4 to 1.2 was 3/66). The amount of exchange during workup was determined as follows. The parent unlabelled ketone was treated with a 2.5 molar excess of aluminum chloride (4.0 g of ketone + 10.0 g of aluminum chloride) in toluene, and stirred for one hour. It was then poured into 25 mL of D_2O–DCl (from $SOCl_2$ and D_2O). The workup then proceeded as for the other experiments. The nmr integration gave for the parent compound, before exchange, the ratios 88:66.5 for the signals at 1.1–1.25 and 7.0 ppm for a ratio of 1.32 (theory 1.2). After the exchange, the ratio was 84:63.5 = 1.32. Taking the signal at 1.1–1.25 as worth 6H, one obtains a

Can. J. Chem. Downloaded from www.nrcresearchpress.com by 210.87.254.105 on 09/05/12
For personal use only.

TABLE 7. k_H/k_D Values for benzene

Experiment	Area ratio = (tolyl ketone / benzene ketone)	k_H/k_D
Benzene–toluene 5:1	10.371	1.06
Benzene-d_6 – toluene 5:1	11.051	

TABLE 8. Derivatives of ketones

Ketone	Derivative	Melting point (°C) Found	Lit.	Reference
Isobutyrophenone	2,4 DNP	162–163	163	Ref. 17
4-Methoxyisobutyrophenone	Semicarbazone	211–212	212–213	Ref. 18; II, **8**, 118
4-Methylisobutyrophenone	Oxime	90–91	90–91	Ref. 18; II, **7**, 254
3,4-Dimethylisobutyrophenone	Oxime	67–68	68	Ref. 18; **7**, 335

ratio of 14.0 units/proton. In the parent compound before the exchange the signal at 3.4 due to α-C—H was 14.5 ± 0.5 units. After the exchange, experimental ratios for three experiments gave an average of 0 ± 3% exchange. The worst case gave 9% exchange with two experiments giving no exchange. (Ratios of 3.4 signal were 14.6, 14.5, and 13.2.)

When 4.11 g (0.021 mol) of diphenylketene was treated with aluminum chloride in 20 mL of benzene-d_6 (99.9% isotopically pure), and the reaction worked up by washing only with water, the nmr showed the ratio of the signal at 5.95 ppm to the aromatic signal to be 1:35 (1:10 theory). One can say that exchange to the extent of ~3% occurred in workup. This was entirely consistent with our results from dimethylketene.

Reactions with p-*Deuteriotoluene*

With Dimethylketene

A 2.0 g (0.0280 mol) sample of dimethylketene was treated with 22 g (0.233 mol) of *p*-deuteriotoluene (see below) and 5.7 g (4.29×10^{-2} mol) of aluminum chloride. The workup was as described above. After separation via preparative scale gc the nmr of the ketone showed 20% protium signal at 3.4 ppm (compared to the signals at 1.2). The signal at 1.25 had three components corresponding to the methyl groups of the deuterated and undeuterated ketones. The yield of ketone was 25%.

With Diphenylketene

A 1.78 g (9.18×10^{-3} mol) sample of diphenylketene was dissolved in 25 mL of *p*-deuteriotoluene with mechanical stirring. A sample of 3.33 g ($2.5 \times 9.18 \times 10^{-3}$ mol) of anhydrous aluminum chloride was added portionwise through the reflux condenser. The workup was as recorded above, omitting the base wash. The nmr spectrum showed 20 integral units for the signal at 2.32 ppm and 5 units for the proton at 6.0 ppm (the α-proton). This corresponds to ~72% protium content at the α position. The yield was ca. 10%.

Preparation of p-*Deuteriotoluene*

A 1 mol sample of *p*-bromotoluene was dropped onto 1.5 g-atoms of magnesium in ether. After the reaction had subsided, the mixture was stirred 24 h, then quenched by addition of 99+% deuterium oxide. Distillation gave 80 g of hydrocarbon. The nmr consisted of an A_2B_2 signal at 7.38 (4H) and a singlet at 2.38 (3H) (in $CDCl_3$ and neat). The ratios of integration were 130:96 (4.06 protons). This corresponds to ~94% deuteration.

Competition Experiments with Dimethylketene

General Procedure

Dimethylketene generated and purified as reported above was added to a 20-fold excess of a 50 mol% mixture of each substrate. Aluminum chloride was added portionwise with stirring of the reaction, and the reactions were stirred one hour after the addition was completed. Workup was as recorded above.

Gas chromatographic analysis was done on a Perkin-Elmer 3920 instrument (TC Bridge) with a 6 ft 10% Carbowax 20 m on 80/100 Chromosorb W column at a temperature of 190°C, He flow rate of 30 mL/min.

Relative response factors (RRF) were determined by mixing known concentrations of ketones (in g/100 mL) and determining the ratios of areas. This procedure gives a relative response factor (RRF) of area per g of ketone I/area per g of ketone II. The RRF for tolyl ketone/phenyl ketone was 1.3250. All competitions were done by comparing the rates of reaction with toluene for experimental convenience (12). The rate constant ratios were determined by the formula

$$\frac{k_a}{k_b} = \frac{[AX]}{[BX]} \Big/ \frac{[A_0]}{[B_0]}$$

In all cases the substrate ratios to ketene were large enough to ensure small errors in the rate ratios. Integration was performed by a Spectra Physics electronic integrator.

Authentic samples of ketones were used in artificial mixtures as a check on the accuracy of the integration technique. It was found that at very high ratios the integrator consistently overestimated the amount of the smaller component. Corrections were applied where appropriate or the reaction run was redone using a larger amount of less active substrate.

The benzene/toluene ratios were determined in this way using ratios of benzene/toluene of 1:1, 3:1, and 5:1. These results are summarized in Table 4.

Reactions of Diphenylketene with Aromatic Substrates

A typical procedure is given using ethyl benzene as a substrate at 25°C. A 9.7 g (0.05 mol) sample of distilled diphenylketene was dissolved in 50 mL of pure ethyl benzene. While this solution was magnetically stirred, a 2.5-fold excess of aluminum chloride (16.6 g) was added portionwise through the reflux condenser. The reaction mixture was stirred overnight, then poured into HCl – ice water and washed with water repeatedly until the

Can. J. Chem. Downloaded from www.nrcresearchpress.com by 210.87.254.105 on 09/05/12
For personal use only.

TABLE 9. Analytical data for diphenylacetophenones

Compound	Melting point (°C)	Analysis: Calculated C	Calculated H	Found C	Found H	Yield (%)
α,α-Diphenylacetophenone	134–136[a]					>10
α,α-Diphenyl-*p*-methylacetophenone	98–99	88.08	6.33	87.81	6.38	11.1
α,α-Diphenyl-3,4-dimethylacetophenone	97–98	87.97	6.71	87.71	6.90	47.0
α,α-Diphenyl-4-methoxyacetophenone	126–128	83.45	6.00	83.18	6.12	59.1
α,α-Diphenylisopropyl acetophenone	116–119	87.86	7.05	87.62	6.96	6.26
α,α-Diphenyl-4-ethylacetophenone	101–103	87.97	6.71	87.82	6.88	19.6
α,α-Diphenyl-4-ethoxy-3-methylacetophenone	104–106	83.51	6.31	83.46	6.50	49.1 (76.6 corrected)[b]
α,α-Diphenylchloroacetophenone	140–145	78.30	4.93	78.49	5.18	1.07

[a]Literature (ref. 18, vol. 7, p. 522) mp 135–136°C.
[b]In this experiment an aliquot showed that only a 64% yield of the ketene was obtained.

washings gave a pH of six by pHydrion paper. The excess ethyl benzene was removed by distillation. The residual brown tar was extracted repeatedly with hot pentane. The combined extracts were concentrated to ~50% of their volume and allowed to stand. Crystals of the product formed slowly and were collected. They showed ν(Nujol): 1675 (C=O) cm^{-1}. This procedure was used for all the ketones. The effectiveness of this technique for recovery was tested by dissolving a known amount of a ketone in pentane at the boiling point, concentrating it, and collecting crystals.

In the case of more active substrates very little polymerization occurred and recovery with pentane (subsequent to distillation of most of the substrate–solvent) was simple, since the polar ketone is not very soluble in the cold pentane solvent. Recovery of pure anisyl ketone from hot pentane was 98.3%. In the case of cumenyl ketone, however, which turned out to be soluble in pentane, the solid was recovered by triturating it out of the polymer with pentane, and recrystallizing the crude solid which was contaminated with cumene, from ethanol. As a check on the recovery method some pure cumenyl ketone was dissolved in cumene and as much of the cumene was distilled off as possible. Subsequently recrystallization from ethanol was effected. Recovery of the pure ketone was 80%.

The yields, melting points, and microanalytical data are recorded in Table 9.

Competition of Toluene and Benzene for Diphenylketene

These experiments were performed in an analogous manner to those for dimethylketene except that the analysis of the reaction mixtures was done using a Waters high performance liquid chromatography apparatus consisting of two Model 6000 pumps, a U6K loop injector, a Model 440 Absorbance Detector connected to a Soltec Model 252A recorder, and a Model 660 Solvent programmer. Integrations were performed as with the dimethylketene experiments. The column was a Whatman ODS – Magnum 9 C_{18} reverse phase column. Flow rate was 2.5 mL/min of 25% water – methanol.

The relative response factor for the tolyl ketone relative to the phenylketone was 1.296 as determined by artificial mixtures. The values corrected by the relative response factor appear in Table 6 along with the relative rates.

Crossover Experiment with Anisole and Toluene-d_8

A mixture of 15 g (0.14 mol) of anisole and 15 g (0.15 mol) of toluene-d_8 was treated with 1.56 g of clean, triple distilled dimethylketene (0.022 mol) and 10 g (0.075 mol) of anhydrous aluminum chloride in a three-necked flask equipped with a drying tube, mechanical stirrer, and addition funnel. After the reaction had subsided the mixture was poured onto 300 g of 6 *M* HCl – ice water and extracted with three 100-mL portions of dichloromethane. After drying over magnesium sulfate the solvent was removed and the higher boiling excess organic substrates were removed under reduced pressure. The residue was fractionally distilled through a 3 in. Vigreux column to give ketone materials in fractions two and three (bp 98–140°C; 10.5 Torr). These ketones were separated by preparative scale gc and analyzed by mass spectra (Varian EM 600 calibrated by perfluorokerosine-H) and nmr.

The nmr spectrum of the anisyl isopropyl ketone showed considerable incorporation of D at the isopropyl group. The mass spectrum had (average of 5 scans) a ratio of M to $M + 1$ of $0.380 \pm 5.53 \times 10^{-2}$ (standard deviation). The expected M to $M + 1$ ratio was 0.122. These figures indicate a protium/deuterium value of 3.83 in the anisyl ketone.

The nmr spectrum of the tolyl ketone showed retention of only about 70% of the deuterium label at the position as indicated by a septet at $\delta = 3.4$ (compared to the methyl signal at 1.1–1.25). These data indicated that proton transfer from the aromatic ring to the α-position was intermolecular.

Acknowledgement

Acknowledgement is made to the donors of the Petroleum Research Fund, administered by the American Chemical Society, for support of this work.

1. C. HURD. J. Am. Chem. Soc. **47**, 2777 (1925).
2. K. PACKENDORFF, N. D. ZELINSKY, and L. LEDER-PACKENDORFF. Ber. **66**, 1069 (1933).
3. F. S. SPRING and T. VICKERSTAFF. J. Chem. Soc. (London), 1873 (1935).
4. J. W. WILLIAMS and J. M. OSBORN. J. Am. Chem. Soc. **61**, 3438 (1939).
5. H. STAUDINGER, H. SCHLUBACH, and H. SCHNEIDER. Helv. Chim. Acta, **6**, 287 (1923).
6. S. D. DARLING and R. L. KIDWELL. J. Org. Chem. **33**, 3974 (1968).
7. C. J. PRICHERT and J. R. CAMPBELL. The Aldrich library of NMR spectra. Aldrich Chemical Co., Milwaukee, WI. 1974. p. 20B.

Can. J. Chem. Downloaded from www.nrcresearchpress.com by 210.87.254.105 on 09/05/12
For personal use only.

8. E. LEFFLER and E. GRUNWALD. Rates and equilibria of organic reactions. John Wiley and Sons, Inc., New York. 1963. p. 200.
9. J. STANG and G. ANDERSON. J. Am. Chem. Soc. **100**, 1520 (1978).
10. G. A. OLAH, S. J. KUHN, S. H. FLOOD, and B. A. HARDIE. J. Am. Chem. Soc. **86**, 2203 (1964).
11. G. A. OLAH, M. E. MOFFATT, S. J. KUHN, and B. A. HARDIE. J. Am. Chem. Soc. **86**, 2198 (1964).
12. G. A. OLAH and J. M. BOLLINGER. J. Am. Chem. Soc. **89**, 2993 (1967) and references therein.
13. H. ZOLLINGER. Adv. Phys. Org. Chem. **2**, 163 (1964).
14. E. L. MOCKOR, A. HOFSTRA, and J. H. VAN DER WAALS. Trans. Faraday Soc. **54**, 186 (1958).
15. W. M. LAUER and G. STEDMAN. J. Am. Chem. Soc. **80**, 6439 (1958).
16. L. M. STOCK and H. C. BROWN. Adv. Phys. Org. Chem. **1**, 35 (1963).
17. R. L. SHRINER, R. C. FUSON, and D. Y. CURTIN. The systematic identification of organic compounds. 5th ed. John Wiley & Sons, Inc., New York. 1964. p. 363.
18. F. K. BEILSTEIN. Handbuch der organischen Chemie. Springer Verlag, Berlin. 1918.

Can. J. Chem. Downloaded from www.nrcresearchpress.com by 210.87.254.105 on 09/05/12
For personal use only.

A proton magnetic resonance nuclear Overhauser enhancement study. Application to vitamin D derivatives D_2 and D_3[1]

GEORGE KOTOVYCH[2] AND GERDY H. M. AARTS

Department of Chemistry, University of Alberta, Edmonton, Alta., Canada T6G 2G2

AND

KLAUS BOCK

Department of Organic Chemistry, The Technical University of Denmark, Lyngby, Denmark

Received December 31, 1979

GEORGE KOTOVYCH, GERDY H. M. AARTS, and KLAUS BOCK. Can. J. Chem. **58**, 1206 (1980).

Nuclear Overhauser effect difference experiments on vitamins D_2 and D_3 at 400 MHz allow an unambiguous assignment to be made for the H_E and H_Z protons bonded to the C-19 carbon. This assignment is especially important since the A ring, and hence the C-19 atom, undergoes a conformational interconversion. The results indicate the importance of proton nOe difference experiments in determining points of configuration and they indicate that the assignment of resonances based on allylic coupling constants in a molecule undergoing a conformational equilibrium can be incorrect.

GEORGE KOTOVYCH, GERDY H. M. AARTS et KLAUS BOCK. Can. J. Chem. **58**, 1206 (1980).

Des expériences de différence d'effet Overhauser nucléaire (eOn) effectuées sur des vitamines D_2 et D_3 à 400 MHz permettent d'identifier sans ambiguité les protons H_E et H_Z liés au carbone en position 19. Cette identification est spécialement importante puisque le cycle A, et par conséquent le carbone en position 19, subit une interconversion conformationnelle. Ces résultats témoignent de l'importance des expériences de différence de eOn sur les protons dans la détermination des sites de configuration et ils indiquent que les attributions de résonance basées sur les constantes de couplage allylique dans une molécule en équilibre conformationnelle peuvent être incorrectes.

[Traduit par le journal]

Introduction

Vitamin D compounds, which are extremely important for calcium and phosphorus metabolism (1), have been studied by nmr, especially to obtain information regarding the conformational equilibria of these molecules. Line assignments are extremely important, particularly if nOe measurements (2, and references therein) are to be used to obtain the conformation of these molecules in solution. For vitamin D_2, in CCl_4 solution, proton 19, with a chemical shift δ equal to 4.97 ppm, was assigned as the proton *cis* to the 5,6 double bond (3). This assignment was based on the predicted angular dependence of allylic coupling constants. Experimentally, however, the observed allylic coupling constant between this proton and the two protons at C-1 was about 1.0 Hz. The identical coupling constant is an average value and the averaging arises from the chair–chair interconversion of the A ring. The chemical shift for the second C-19 proton is 4.73 ppm. For vitamin D_3 (4), the same assignments for the multiplets corresponding to the two non-equivalent H-19 protons were made. These were also based on the coupling constant information. In addition, the H-19 resonance at low field was expected to be at lower field because of the possibility of mutual deshielding by the proximal 7-proton. The two H-19 resonances could not be assigned strictly on the basis of an $Eu(dpm)_3$ titration study of vitamin D_3 (4). The same assignments have been applied to a variety of vitamin D_3 derivatives (5, 6).

We have applied nOe difference spectroscopy to the study of vitamins D_2 and D_3 with the intention of obtaining information concerning distances in solution between individual protons (7). This technique was previously applied to gain information concerning the spatial structures of protein molecules, namely the basic pancreatic trypsin inhibitor (8) and for spectral assignments in lysozyme (9). The dependence of the homonuclear nOe, at two frequencies, on the correlation time has been elegantly discussed by Glickson *et al.* (10). While carrying out the present nOe difference experiments, an unambiguous assignment of the H_E and the H_Z protons at C-19 could be made. This is especially important in view of the fact that the C-19 carbon, bonded to the A ring, undergoes a conformational change due to the chair–chair interconversion of this ring.

Experimental

The nOe experiments were carried out at 400 MHz in the standard manner (8) using a Bruker WH-400/DS NMR spectrometer. The experimental procedure will be described briefly.

[1]This is paper number 4 in a series of high-field nmr studies on vitamins and prostaglandins. Paper numbers 2 and 3 are refs. 13 and 14.

[2]Formerly Kotowycz.

0008-4042/80/121206-05$01.00/0

©1980 National Research Council of Canada/Conseil national de recherches du Canada

Can. J. Chem. Downloaded from www.nrcresearchpress.com by 210.87.254.5 on 09/05/12
For personal use only.

Can. J. Chem. Downloaded from www.nrcresearchpress.com by 210.87.254.5 on 09/05/12
For personal use only.

The gated decoupler was set on resonance for a minimum time of greater than 4 times the longest T_1 value for the molecule (7) to effectively saturate the resonance of the irradiated nucleus. Four free induction decay signals were accumulated. The memory was then negated and the experiment was repeated with the gated decoupler off-resonance (control spectrum). The off-resonance frequency was chosen following the procedure described previously (2), namely by placing it exactly equidistant in the spectrum from the resonance frequency of the observed nucleus but in the opposite direction from the on-resonance irradiating frequency (2). These four free induction decay signals were thus compared with the original four. The total number of sequences was determined by the required signal-to-noise ratio. After collecting the FID's the signal was Fourier transformed. A 90° pulse was used in order to obtain the best S/N ratio and the pulse width was 10.7 μs. A total of 16K data points were used. The sample preparation, including purification of the solvent ($CDCl_3$) and degassing were discussed previously (7).

Results and Discussion

The results of the nOe measurements are given in Table 1. The % nOe was calculated using the irradiated inverted peak as the reference. All nOe values were evaluated by integration. The results for both vitamins are the same within experimental error (±10%). The most important conclusion obtained from these experiments concerns the assignment of the C-19 protons. When proton 7 is irradiated, the high-field C-19 proton experiences an nOe. It is closest to proton 7 (11) and is therefore labelled C-19 H_Z following standard rules of nomenclature (12) (Figs. 1 and 2). The multiplet at δ = 1.47 ppm also exhibits an nOe. As this multiplet could not be definitively assigned, from the structure it must correspond to protons 14 and/or 15. The assignment of the upfield C-19 proton as C-19 H_Z is confirmed by irradiating it. As expected, a large nOe is observed not only for the low-field C-19

TABLE 1. Selective nOe enhancements observed for vitamins D_2 and D_3 at 400 MHz

Proton		% nOe	
Irradiated	Observed	D_2	D_3
19Z	19E	27	26
	7	6	6
19E	19Z	29	28
7	19Z	8	6
	6	6[a]	6[a]
	Multiplet at δ = 1.47 ppm[b]	11	13
6	4α	8	7
	4β	7	6
	7	6[a]	4[a]
	9β	12	10

[a]A distorted signal is observed for these protons since they are tightly coupled to the protons being irradiated.
[b]This multiplet corresponds to protons 14 and possibly 15. A definite assignment could not be made.

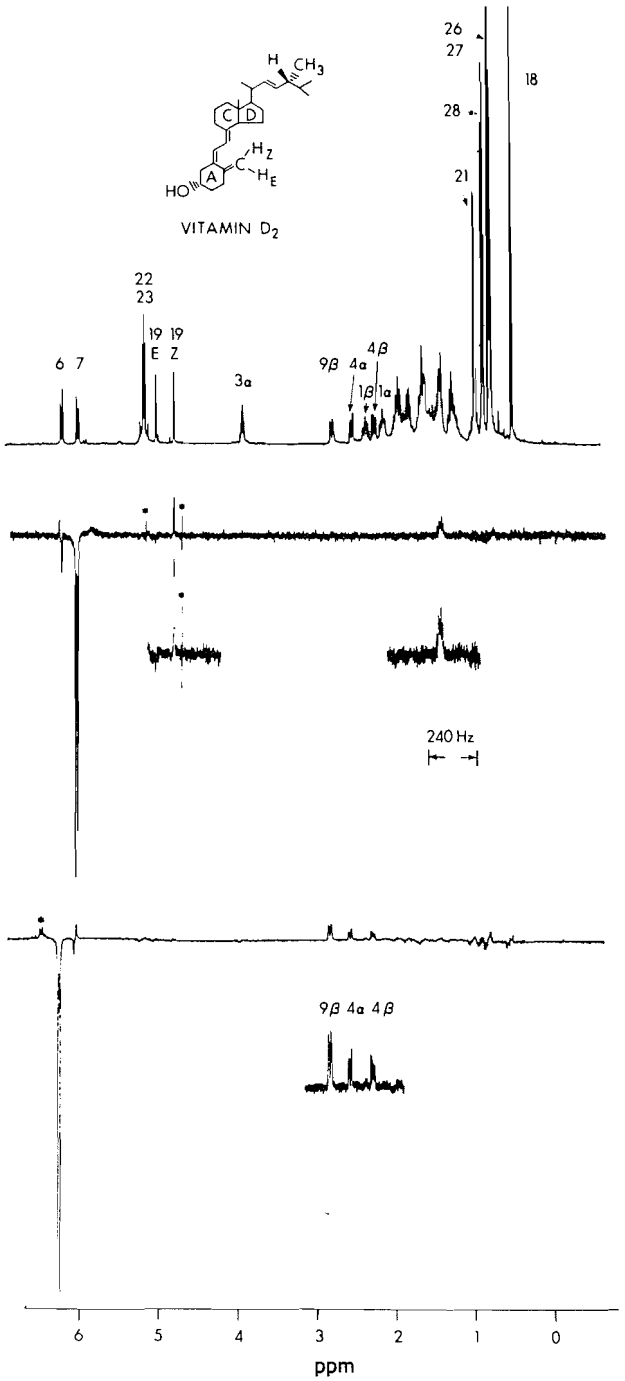


FIG. 1. The 400 MHz Fourier transform nmr spectrum for vitamin D_2 is seen at the top. The middle spectrum corresponds to the experiment where proton 7 is irradiated. An nOe is observed for the high-field proton at C-19, the doublet for proton 6 and the multiplet at δ = 1.47 ppm. The bottom spectrum corresponds to the experiment where proton 6 is irradiated. An nOe is observed for protons 4α, 4β, 7, and 9β. The * indicates instrumental artifacts.

Can. J. Chem. Downloaded from www.nrcresearchpress.com by 210.87.254.5 on 09/05/12
For personal use only.

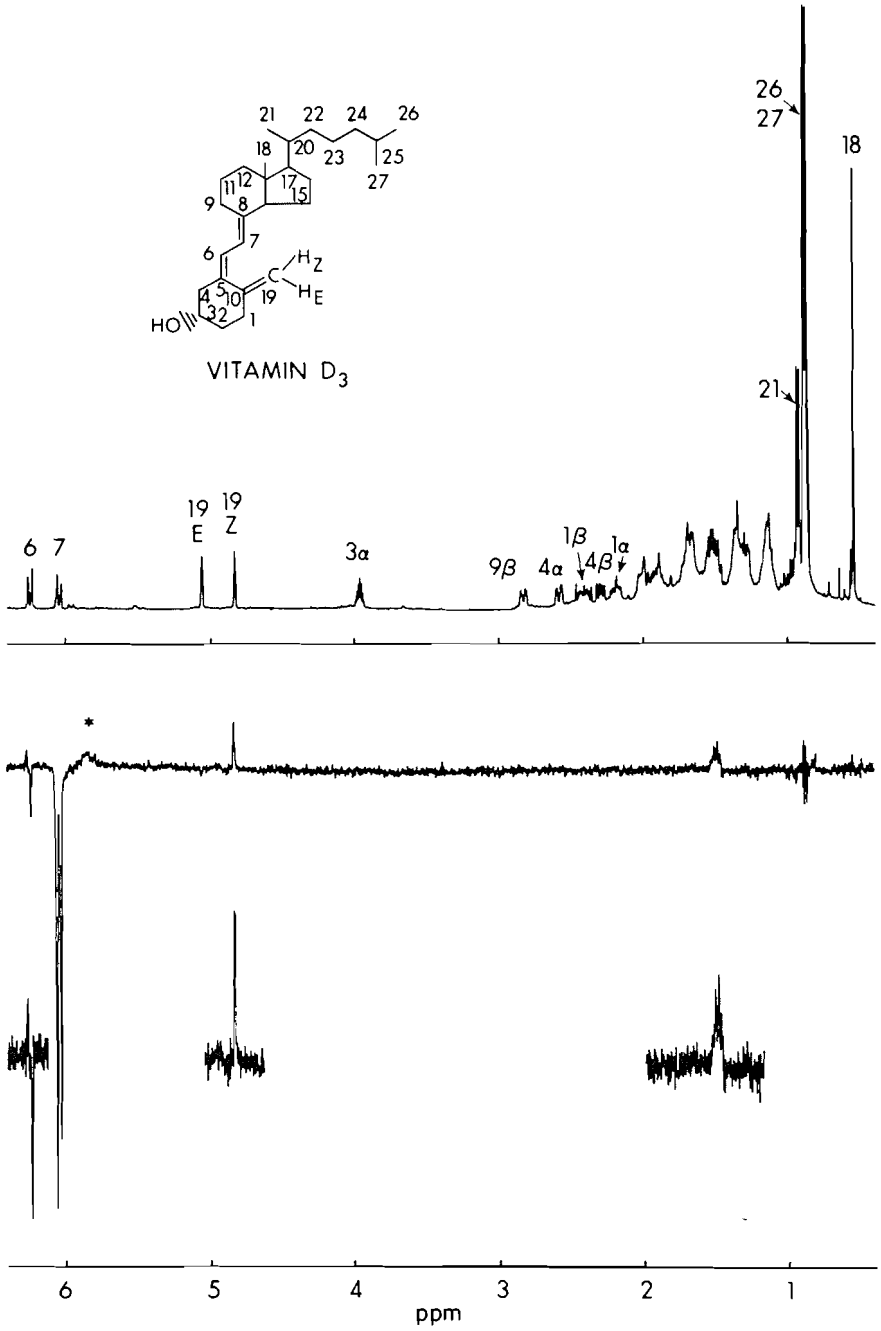


FIG. 2. The 400 MHz Fourier transform nmr spectrum for vitamin D_3 is seen at the top. The bottom spectrum corresponds to the experiment where proton 7 is irradiated. An nOe is observed for the high-field proton at C-19, the multiplet at $\delta = 1.47$ ppm and the doublet for proton 6. The * indicates experimental artifacts.

proton but also for proton 7 (Fig. 3). However, upon irradiation of the low-field C-19 proton, only the C-19 H_Z proton is observed to exhibit an nOe. This low-field proton is therefore labelled C-19 H_E. Finally, irradiation of proton 6 causes an nOe for protons 4α, 4β, and 9β. These protons are the closest to proton 6 and an nOe is expected (11). From the spectra (Figs. 1–3), it can be seen that small baseline effects can be observed in the high field region. At present these cannot be explained.

Irradiation of the H-6 proton doublet which forms an AB system with the H-7 proton produces a distorted resonance for the H-7 proton. A distorted signal for H-6 is also observed upon irradiation of

Can. J. Chem. Downloaded from www.nrcresearchpress.com by 210.87.254.5 on 09/05/12
For personal use only.

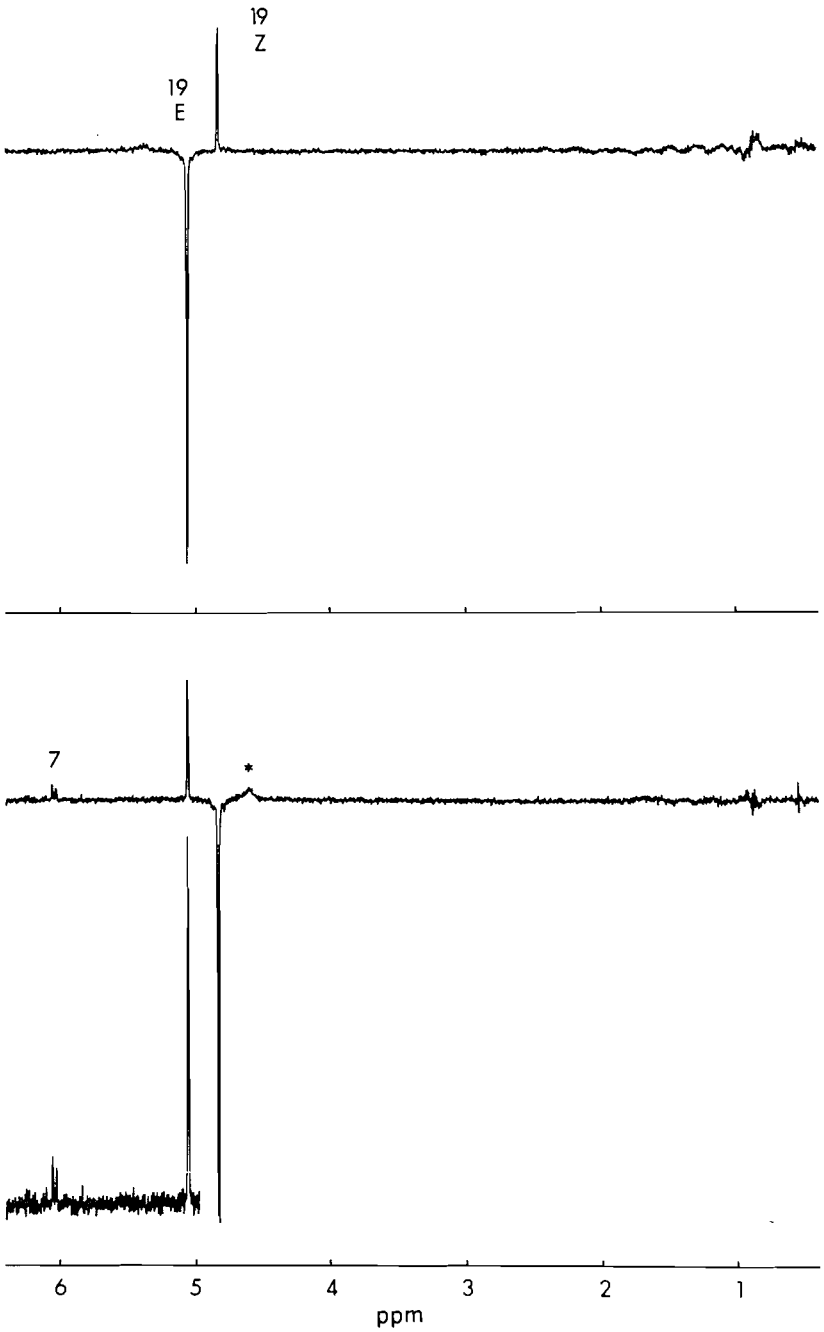


FIG. 3. NOe spectra for vitamin D_3. In the top spectrum, the low-field C-19 proton is irradiated and an nOe is observed for the high-field C-19 proton. In the bottom spectrum, the high-field C-19 proton is irradiated and proton 7 and the low field C-19 proton experience the nOe. The * indicates experimental artifacts.

the H-7 doublet. Similar effects were observed by carrying out the experiments with a small pulse angle of 10° (1.13 μs pulse width). As these two protons are tightly coupled, the observed nOe is smaller than expected (ref. 11, pp. 226–232). In addition, the power levels necessary for on-resonance saturation may affect the magnetization of both nuclei simultaneously and cause a distortion of the nucleus experiencing the nOe, especially if the lines irradiated are not subjected to the same saturation field. The latter condition may be difficult to obtain if the coupling constant between the two nuclei is large ($\geq$8 Hz) and at the same time the chemical shift difference is small.

In conclusion, we have shown the importance of the proton nuclear Overhauser effect difference experiment in determining points of configuration. This method has the distinct advantage that one experiment picks out all of the protons that are in close proximity to the irradiated proton even if these protons are hidden by some other resonances. Finally, the assignment of resonances based on allylic coupling constants in a molecule undergoing a conformational equilibrium, as does the A ring of vitamin D, can be incorrect.

Acknowledgements

K.B. expresses his appreciation to the Department of Chemistry, University of Alberta, for generous access to the high-field nmr facility. The generous financial assistance of the Natural Sciences and Engineering Research Council of Canada and the University of Alberta is gratefully acknowledged.

1. A. W. NORMAN, W. H. OKAMURA, E. J. FRIEDLANDER, H. L. HENRY, R. L. JOHNSON, M. N. MITRA, D. A. PROSCAL, and W. WECKSLER. Calcif. Tissue Res. **21**, 153 (1976).
2. R. ROWAN III, J. A. MACCAMMON, and B. D. SYKES. J. Am. Chem. Soc. **96**, 4773 (1974).
3. G. N. LA MAR and D. L. BUDD. J. Am. Chem. Soc. **96**, 7317 (1974).
4. R. M. WING, W. H. OKAMURA, A. REGO, M. R. PIRIO, and A. W. NORMAN. J. Am. Chem. Soc. **97**, 4980 (1975).
5. E. BERMAN, N. FRIEDMAN, Y. MAZUR, and M. SHEVES. J. Am. Chem. Soc. **100**, 5626 (1978).
6. M. SHEVES, E. BERMAN, Y. MAZUR, and Z. V. I. ZARETSKII. J. Am. Chem. Soc. **101**, 1882 (1979).
7. G. KOTOWYCZ, T. T. NAKASHIMA, M. KIRK GREEN, and G. H. M. AARTS. Can. J. Chem. **58**, 45 (1980).
8. R. RICHARZ and K. WÜTHRICH. J. Magn. Reson. **30**, 147 (1978).
9. G. E. CHAPMAN, B. D. ABERCROMBIE, P. D. CARY, and E. M. BRADBURY. J. Magn. Reson. **31**, 459 (1978).
10. J. D. GLICKSON, S. L. GORDON, T. P. PITNER, D. G. AGRESTI, and R. WALTER. Biochemistry, **15**, 5721 (1976).
11. J. H. NOGGLE and R. E. SCHIRMER. The nuclear Overhauser effect. Academic Press, New York, NY. 1971.
12. T. W. G. SOLOMONS. Organic chemistry. John Wiley and Sons, Inc., New York, NY. 1978. pp. 274–276.
13. G. KOTOVYCH and G. H. M. AARTS. Can. J. Chem. **58**, 1111 (1980).
14. G. KOTOVYCH, G. H. M. AARTS, T. T. NAKASHIMA, and G. BIGAM. Can. J. Chem. **58**, 974 (1980).

Can. J. Chem. Downloaded from www.nrcresearchpress.com by 210.87.254.5 on 09/05/12
For personal use only.

Carbon-13 chemical shift assignments of chromones and isoflavones

HEM CHANDRA JHA AND FRITZ ZILLIKEN

Institute of Physiological Chemistry, University of Bonn, Nußallee 11, D-5300 Bonn 1, West Germany

AND

EBERHARD BREITMAIER

Institute of Organic Chemistry and Biochemistry, University of Bonn, Gerhard-Domagk-Straße 1, D-5300 Bonn 1, West Germany

Received January 28, 1980

HEM CHANDRA JHA, FRITZ ZILLIKEN, and EBERHARD BREITMAIER. Can. J. Chem. **58**, 1211 (1980).

Carbon-13 chemical shifts of 8 chromones and 35 isoflavones variously substituted by hydroxy-, acetoxy-, and methoxy-groups are assigned. The applicability of chemical shift increments reflecting inductive and resonance effects is discussed. Some general relations between substitution patterns and carbon shielding useful for the identification of naturally occurring isoflavones are outlined. Typical C—H couplings of chromone and phenyl carbons are analyzed for a 4′,6,7-trisubstituted derivative.

HEM CHANDRA JHA, FRITZ ZILLIKEN et EBERHARD BREITMAIER. Can. J. Chem. **58**, 1211 (1980).

On a attribué les déplacements chimiques en rmn ^{13}C de 8 chromones et de 35 isoflavones substituées de manière diverse par des groupes hydroxy, acétoxy et méthoxy. On discute de la possibilité d'appliquer des incréments de déplacement chimique comme méthode d'évaluer des effets inducteurs de résonance. On souligne quelques relations générales entre les schémas de substitutions et de blindage du carbone qui sont utiles pour l'identification des isoflavones naturelles. On analyse des couplages typiques C—H des carbones de la chromone et du phényle dans un dérivé trisubstitué en position 4′, 6 et 7.

[Traduit par le journal]

Isoflavonoids are gaining considerable importance due to having potential contraceptive (1), antioxidative (2), and antifungal (3) properties. Their chief source of occurrence is in the leguminous plants, some of which are very much in use as food materials. Moreover, leguminous plants sometimes exhibit remarkable physiological activities attributable to their isoflavone contents. György and co-workers (2) found 4′,6,7-trihydroxyisoflavone to be the antioxidative substance of fermented soyabeans. A recent work ascribes hypolipidemic activity of Bengal gram (cicer arietinum) to the presence of biochanin A (4′-methoxy-5,7-dihydroxyisoflavone) and formononetin (4) (4′-methoxy-7-hydroxyisoflavone).

Structurally, isoflavonoids furnish a great variety in as much as natural products like isoflavanones, isoflavones, rotenoids, pterocarpans, coumestanes, 3-aryl-4-hydroxycoumarins, and coumaronochromones are all included in this group. The discovery and the structure elucidation of these substances have been to a large extent made possible due to application of spectroscopic methods. Among these, ^{13}C nmr has not yet been fully applied to study the isoflavone structure although the flavones as sister compounds have been subjected to much detailed investigations (5–8). Some of these works make only cursory reference to the spectra of specific isolated isoflavones. Recent papers (9, 10) describe the ^{13}C nmr spectra of selected isoflavones substituted in 4′,5,7-positions.

The present study concerns ^{13}C shifts of 43 chromones and isoflavones variously substituted in the rings A and B by methoxy-, hydroxy-, and acetoxy-groups (Table 1). As these substituents often occur in isoflavones and chromones isolated from plant material, the shift assignments outlined in Tables 2–6 may facilitate future work of determining the positions of oxygen functional groups in naturally occurring isoflavones and chromones.

Signals were assigned by comparing the ^{13}C shifts with literature data available for chromone (11), isoflavone (12), and its seven substituted derivatives (9, 10). In the aromatic carbon shift range, quaternary carbons were localized as sharp singlets by low power noise proton decoupling. Further straightforward assignment aids are the enhanced intensities observed for the C-2′,6′ and C-3′,5′ carbon pairs of the 4′-substituted derivatives and the inductive and mesomeric effects of hydroxy-, acetoxy-, and methoxy-groups (13).

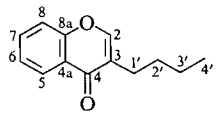
A coupled spectrum of 6-acetoxy-4′,7-dimethoxyisoflavone, **47**, was taken in order to support the assignments made for the 4′,6,7-trisubstituted representatives **34–50**. The largest C—H coupling (196.5 Hz) was measured for C-2 (153.3 ppm) which experiences a considerable positive polarization not only by the α-inductive effect of the oxygen but also due to a mesomeric electron withdrawing of the β carbonyl group. These data have diagnostic value when isoflavones (unsubstituted in the 2-position) have to be distin-

0008-4042/80/121211-09$01.00/0

©1980 National Research Council of Canada/Conseil national de recherches du Canada

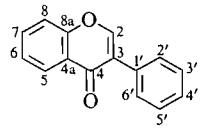
TABLE 1. Chromones and isoflavones **1–54**

(*a*) Chromones **1–9**



No.	Compound	Reference
1	Chromone	11
2	Chromone,7-hydroxy-3-methyl-	
3	Chromone,7-hydroxy-3-ethyl-	
4	Chromone,6,7-dihydroxy-3-methyl-	
5	Chromone,6,7-dihydroxy-3-ethyl-	
6	Chromone,6,7-dihydroxy-3-propyl-	
7	Chromone,6,7-dihydroxy-3-isopropyl-	
8	Chromone,6-hydroxy-7-methoxy-3-methyl-	
9	Chromone,7-hydroxy-6-methoxy-3-methyl-	

(*b*) Isoflavones **10–54**



No.	Compound	Reference
10	Isoflavone	12
11	Isoflavone,7-methoxy-	9
12	Isoflavone,2′,7-dimethoxy-	9
13	Isoflavone,2′-hydroxy-7-methoxy-	9
14	Isoflavone,2′-acetoxy-7-methoxy-	9
15	Isoflavone,6,7-dihydroxy-	
16	Isoflavone,7-hydroxy-6-methoxy-	
17	Isoflavone,6-hydroxy-7-methoxy-	
18	Isoflavone,6,7-dimethoxy-	
19	Isoflavone,7,8-dimethoxy-	
20	Isoflavone,4′,6-dimethoxy-	
21	Isoflavone,4′,7-dihydroxy-	10
22	Isoflavone,7-hydroxy-4′-methoxy-	9
23	Isoflavone,4′-hydroxy-7-methoxy-	9

guished from flavones. (*i*) No long-range couplings were resolved for the protonated chromone ring carbons as no three-bond interactions ($^3J_{CH}$) are possible within a 3,6,7-trisubstituted chromone ring present in 6,7-disubstituted isoflavones. The one-bond C—H couplings are 166.6 Hz for C-5 (112.9 ppm) and 164.8 Hz for C-8 (106.2 ppm). These couplings are larger than the values observed for the protonated phenyl carbons (C-2′,6′ at 130.1 ppm: J_{CH} = 160.5 Hz; C-3′,5′ at 113.8 ppm: J_{CH} = 160.8 Hz). The corresponding doublet signals are additionally split by three-bond couplings with *meta*-protons (7.3 and 4.6 Hz). (*ii*) A typical quartet due to two-bond coupling ($^2J_{CO—CH_3}$ = 7.2 Hz) localizes the carbonyl carbon of the acetoxy group at 167.8 ppm. (*iii*) The assignment given for C-1′ and C-3 is based on the larger nuclear Overhauser enhancement experienced by C-1′ (124.1 ppm) on proton broad-band decoupling due to two *ortho*-protons.

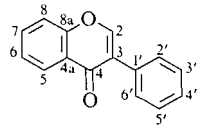
The assignments of the following carbon pairs in Tables 2 and 3 are interchangeable due to signal crowding: C-5 and C-6, in **1** and **10**; C-3 and C-4a, in **8**, **9**, **47**, and **48**; C-7 and C-8a, in **15–17**, **25**, **27**, **34–47**; C-2′(6′) and C-3′(5′), in **10–19** and **28**; C-3′ and C-4′, in **54**.

In order to derive the substitution pattern of an unknown isoflavone it is useful to check the additivity of the empirical substituent increments. Substituent increments have therefore been deduced for the chromone and phenyl ring carbons in Tables 7 and 8 on the basis of as much data as available from Tables 2 and 3.

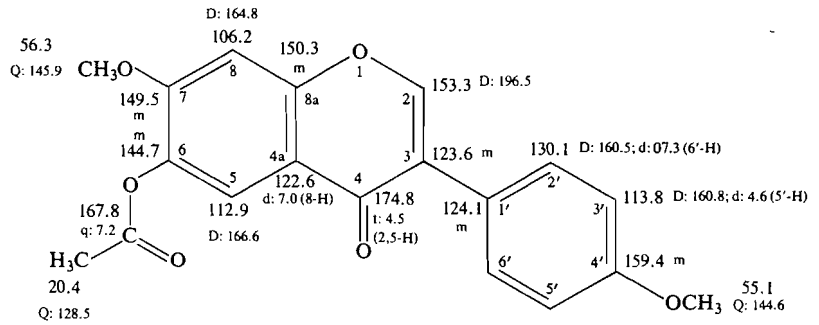
It turns out that electron releasing of a methoxy

TABLE 1 (*Concluded*)

(*b*) Isoflavones **10–54**



No.	Compound	Reference
24	Isoflavone,4′,7-dimethoxy-	9
25	Isoflavone,7-acetoxy-4′-methoxy-	9
26	Isoflavone,4′-acetoxy-7-methoxy-	9
27	Isoflavone,4′,7-diacetoxy-	
28	Isoflavone,5,7-dihydroxy-	10
29	Isoflavone,4′,5,7-trihydroxy-	10
30	Isoflavone,5,7-dihydroxy-4′-methoxy-	10
31	Isoflavone,4′,7-dimethoxy-5-hydroxy-	
32	Isoflavone,4′,5,7-trimethoxy-	10
33	Isoflavone,5,7-dihydroxy-3′,4′,5′-trimethoxy-	
34	Isoflavone,4′,6,7-trihydroxy-	
35	Isoflavone,6,7-dihydroxy-4′-methoxy-	
36	Isoflavone,6,7-dihydroxy-4′-ethoxy-	
37	Isoflavone,6,7-dihydroxy-4′-propyloxy-	
38	Isoflavone,6,7-dihydroxy-4′-isopropyloxy-	
39	Isoflavone,6,7-dihydroxy-4′-butyloxy-	
40	Isoflavone,4′,7-dihydroxy-6-methoxy-	
41	Isoflavone,4′,6-dihydroxy-7-methoxy-	
42	Isoflavone,6,7-dimethoxy-4′-hydroxy-	
43	Isoflavone,4′,6-dimethoxy-7-hydroxy-	
44	Isoflavone,4′,7-dimethoxy-6-hydroxy-	
45	Isoflavone,4′,6,7-trimethoxy-	
46	Isoflavone,7-benzyloxy-6-hydroxy-4′-methoxy-	
47	Isoflavone,6-acetoxy-4′,7-dimethoxy-	
48	Isoflavone,4′,6,7-triacetoxy-	
49	Isoflavone,6,7-diphenylmethylenedioxy-4′-hydroxy-	
50	Isoflavone,6,7-diphenylmethylenedioxy-4′-methoxy-	
51	Isoflavone,4′,7,8-trihydroxy-	
52	Isoflavone,7,8-dihydroxy-4′-methoxy-	
53	Isoflavone,4′,7,8-trimethoxy-	
54	Isoflavone,3′,4′,6,7-tetramethoxy-	



47 6-Acetoxy-4′,7-dimethoxyisoflavone

big type: ^{13}C chemical shifts in ppm; small type: $^{13}C—^{1}H$ coupling constants in Hz; D, Q: one-bond doublets and quartets; d, t, q: two-and three-bond doublets, triplets, and quartets; m: poorly resolved long-ranged multiplets.

TABLE 2. Chromone carbon shifts of chromones and isoflavones **1–54**

Compound	Shift								
	2	3	4	5	6	7	8	8*a*	4*a*
1	145.5	113.0	177.6	125.3	125.8	133.8	118.3	156.6	125.0
2	151.68	119.33	176.61	126.64	114.80	162.43	102.15	158.12	116.11
3	151.60	124.85	176.18	126.73	114.80	162.46	102.14	158.00	116.38
4	151.32	118.48	176.49	107.79	144.40	152.11	102.75	151.69	116.08
5	151.17	124.03	176.03	107.91	144.40	152.14	102.75	151.53	116.38
6	151.56	122.30	176.03	107.91	144.37	152.08	102.72	151.50	116.38
7	152.26	122.97	175.49	113.68	147.53	148.86	110.55	151.90	113.68
8	151.56	116.87	176.49	107.55	145.04	153.45	99.90	151.56	118.84
9	151.38	115.75	176.40	104.30	146.74	152.78	102.94	152.57	118.81
10	154.14	124.44	175.38	125.74	125.32	133.90	118.24	155.93	124.19
11	152.38	125.11	175.31	127.64	114.63	163.81	100.01	157.73	118.32
12	153.83	122.67	175.49	127.87	114.35	163.96	100.28	158.09	118.61
13	155.44	122.09	178.62	127.87	115.79	164.94	99.87	157.97	117.15
14	153.31	122.29	174.46	127.48	114.54	163.92	100.17	157.80	117.96
15	152.87	123.18	174.70	108.40	144.80	152.44	102.84	151.23	116.93
16	152.99	123.36	174.33	104.88	147.07	153.11	102.97	152.05	116.53
17	153.42	123.18	174.33	107.91	145.43	153.75	100.14	150.96	117.60
18	153.23	123.64	174.30	104.36	147.59	154.39	100.08	151.96	117.29
19	153.75	123.79	174.91	121.06	110.74	156.33	136.39	150.23	118.81
20	153.66	123.64	174.97	106.12	154.93	128.04	120.84	149.53	126.43
21	152.26	122.67	178.58	127.19	115.05	162.62	102.15	157.64	116.87
22	152.66	123.55	174.88	127.25	115.11	162.71	102.18	157.67	116.84
23	151.84	124.44	175.20	127.01	114.25	163.54	99.97	157.20	117.92
24	152.87	123.82	174.88	127.04	114.56	163.80	100.32	157.64	117.87
25	153.63	124.09	174.94	127.07	119.78	156.31	111.16	154.42	121.82
26	152.66	124.57	175.55	127.89	114.72	164.22	100.24	158.05	118.49
27	153.29	124.95	175.56	127.99	119.73	156.84	111.05	154.75	122.46
28	155.11	124.17	181.34	163.97	100.02	165.10	94.62	159.06	106.23
29	154.01	123.88	181.37	163.70	99.73	164.73	94.34	158.82	106.05
30	154.46	124.20	181.57	163.94	99.91	165.01	94.54	159.05	106.21
31	154.02	122.66	180.52	162.16	98.08	165.41	92.25	157.76	105.76
32	150.62	125.06	174.30	161.03	96.17	163.80	92.89	159.12	109.31
33	154.33	122.54	180.07	162.34	99.26	164.56	93.80	157.70	104.70
34	151.90	123.21	174.88	108.43	144.64	152.29	102.81	151.23	116.96
35	152.32	122.76	174.64	108.34	144.67	152.23	102.78	151.17	116.84
36	152.32	122.85	174.76	108.40	144.67	152.20	102.78	151.20	116.90
37	152.32	122.76	174.64	108.34	144.67	152.23	102.75	151.17	116.84
38	152.32	122.79	174.67	108.34	144.67	152.32	102.78	151.17	116.84
39	152.32	123.12	175.06	108.55	144.67	151.96	102.87	151.44	117.08
40	152.08	123.40	174.73	104.89	146.95	152.96	102.94	152.08	116.57
41	152.23	123.42	174.85	108.13	145.25	153.57	99.87	151.05	117.72
42	152.29	123.64	174.64	104.39	147.47	154.27	100.02	151.93	117.26
43	152.23	124.64	174.73	104.88	147.01	153.02	103.00	152.14	116.60
44	152.54	122.97	174.64	108.07	145.34	153.66	99.96	151.02	117.66
45	152.45	123.46	174.70	104.48	147.59	154.36	99.99	152.05	117.38
46	152.53	123.03	174.70	108.43	145.65	152.90	101.42	150.86	117.90
47	153.29	123.59	174.83	112.93	144.71	149.50	106.20	150.35	122.59
48	154.51	124.21	175.15	113.80	147.19	154.15	120.36	140.60	122.85
49	153.20	123.55	174.48	102.30	145.40	152.47	98.41	151.43	119.24
50	153.23	124.09	174.12	102.30	145.46	152.81	98.44	151.60	119.24
51	152.66	124.94	174.72	123.82	117.32	155.30	132.14	150.78	115.20
52	152.66	124.94	174.45	123.82	117.50	155.24	134.75	150.78	115.20
53	153.05	123.36	175.09	121.00	110.61	156.18	136.30	150.17	118.75
54	152.84	123.33	174.57	104.42	147.56	154.36	100.05	151.93	117.29

group at position 6 of the chromone ring is weakened at C-7 ($z_o = -5.9$ ppm) due to $-m$-electron withdrawing of the *para* carbonyl group while electron releasing of a methoxy- or hydroxy-group at C-7 is increased at C-8 ($z_o = -17.9$ and -16.1 ppm) due to the $+m$-effect of the *ortho* chromone oxygen. The average $(z_o + z_{o'})/2$ of both *o*-effects in each case corresponds approximately to the OH and OCH_3 increments known for the benzene shifts (Table 8).

TABLE 3. 3-Alkyl-, 3-phenyl-, and 4′-*o*-alkyl carbon shifts of chromones and isoflavones **1–54**

	Shift									
Compound	1′	2′	3′	4′	5′	6′	4′-OC_α	4′-OC_β	4′-OC_γ	4′-OC_δ
1										
2	10.71									
3	18.64	13.11								
4	10.86									
5	18.76	13.23								
6	27.38	21.46	13.66							
7	24.80	21.25								
8	10.87									
9	10.90									
10	132.02	128.20	128.96	127.90	128.96	128.20				
11	127.90	128.25	128.80	131.79	128.80	128.25				
12	121.11	157.66	111.37	131.84	120.60	129.74				
13	120.70	156.64	119.64	130.51	120.81	129.71				
14	125.03	149.02	125.82	131.42	122.79	129.38				
15	132.68	128.98	128.04	127.52	128.04	128.98				
16	132.50	128.95	128.07	127.58	128.07	128.95				
17	132.47	128.95	128.07	127.60	128.07	128.95				
18	132.32	128.92	128.10	127.67	128.10	128.92				
19	132.05	128.98	128.16	127.82	128.16	128.98				
20	123.94	130.04	113.71	159.37	113.71	130.04				
21	123.91	129.98	115.05	157.33	115.05	129.98				
22	124.40	130.04	113.56	159.12	113.56	130.34				
23	122.41	129.78	115.16	157.51	115.16	129.78				
24	124.18	130.04	113.59	159.18	113.59	130.04				
25	123.85	130.07	113.68	159.34	113.68	130.07				
26	129.68	130.11	121.67	150.71	121.67	130.11				
27	129.35	130.17	121.82	150.95	121.82	130.17				
28	132.17	129.95	129.07	128.90	129.07	129.95				
29	122.90	130.97	115.82	158.20	115.82	130.97				
30	123.84	131.09	114.54	160.70	114.54	131.09				
31	122.91	130.13	113.74	159.43	113.74	130.13				
32	124.43	130.26	113.44	159.55	113.44	130.26				
33	126.43	106.61	152.81	137.78	152.81	106.61				
34	123.12	130.04	115.08	157.24	115.08	130.04				
35	124.79	130.04	113.53	158.97	113.53	130.04				
36	124.67	130.04	114.05	158.33	114.05	130.04	63.08	14.66		
37	124.64	130.04	114.08	158.49	114.08	130.04	69.08	22.16	10.38	
38	124.55	130.07	115.29	157.24	115.29	130.07	69.27	21.89		
39	124.67	130.04	114.20	158.67	114.20	130.04	67.42	31.02	18.97	13.75
40	122.91	130.01	115.10	157.30	115.10	130.01				
41	122.91	130.01	115.08	157.30	115.08	130.01				
42	122.70	129.98	115.08	157.36	115.08	129.98				
43	123.15	130.04	113.59	159.12	113.59	130.04				
44	124.61	130.04	113.56	159.06	113.56	130.04				
45	124.45	130.07	113.65	159.24	113.65	130.07				
46	124.61	130.40	113.56	159.09	113.56	130.40				
47	124.13	130.11	113.76	159.42	113.76	130.11				
48	129.50	130.47	122.15	151.17	122.15	130.47				
49	122.36	130.01	115.11	157.45	115.11	130.01				
50	123.18	130.07	113.62	159.22	113.62	130.07				
51	125.19	130.10	113.65	159.30	113.65	130.10				
52	126.07	130.10	113.61	159.31	113.61	130.10				
53	124.09	130.07	113.62	159.21	113.62	130.07				
54	124.91	112.95	148.80	148.50	111.52	121.21				

The shieldings of 6,7-dimethoxy- and 7-hydroxy-6-methoxyisoflavones (Tables 2 and 7) show that deviations from increment additivity of up to 4 ppm have to be expected for *o*-disubstituted chromone rings in isoflavones, particularly for the substituted carbons themselves. To conclude, benzene shift increments cannot be used to predict accurately the shieldings of benzenoid carbons in multisubstituted chromone rings since cooperative effects occur with the carbonyl carbon, the ring

TABLE 4. Methoxy carbon shifts of chromones and isoflavones **1–54**

	Shift							
Compound	5-	6-	7-	8-	2′-	3′-	4′-	5′-OCH_3
8			56.06					
9		55.82						
11			55.74					
12					55.81			
13			56.01					
14			55.78					
16		55.85						
17			56.19					
18		55.82	56.28					
19			56.43	60.98				
20		56.31					55.09	
22							55.06	
23			55.69					
24			55.88				55.06	
25							55.09	
26			55.89					
30							55.60	
31			55.88				55.13	
32	56.13		55.79				55.06	
33						56.00	60.13	56.00
35							55.06	
40		55.88						
41			56.13					
42		55.82	56.16					
43		55.91					55.06	
44			56.16				55.06	
45		55.91	56.31				55.09	
46							55.06	
47			56.28				55.13	
48							55.09	
52							55.06	
53			56.37	60.95			55.06	
54		55.85	56.28			55.64	55.64	

TABLE 5. Acetoxy carbon shifts of chromones and isoflavones **1–54**

	Shift							
Compound	6-OAC		7-OAC		2′-OAC		4′-OAC	
14					168.96	20.90		
25			168.32	20.91				
26							169.45	21.14
27			168.62	21.15			169.50	21.15
47	167.80	20.42						
48	167.84	20.76	168.50	20.90			169.60	21.34

TABLE 6. Benzyloxy- and diphenylmethylenedioxy carbon shifts of chromones and isoflavones **46, 49, 50**

	Shift						
Compound	-O-C	1″	2″	3″	4″	5″	6″
46	70.63	136.08	127.77	128.46	128.07	128.46	127.77
49	118.51	138.94	125.95	128.55	129.62	128.55	125.95
50	118.54	138.91	125.94	128.56	129.62	128.56	125.94

TABLE 7. Hydroxy-, methoxy-, and combined substituent increments (ppm) of chromone ring carbons in isoflavones **10–55**

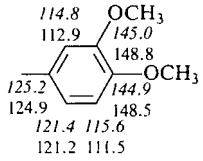
Data from compound(s)	Substituent(s) in position	z_2	z_3	z_4	z_5	z_6	z_7	z_8	z_{8a}	z_{4a}
21, 22	7-OH	−1.7±0.2	−1.3±0.4	0.5±1	1.5±0.1	−10.2±0.1	28.8±0.1	−16.1±0.1	1.7±0.1	−7.3±0.1
28, 29, 30, 33	5,7-Di-OH	0.3±0.5	−0.7±1.0	5.7±0.8	37.7±1	−25.6±0.4	30.9±0.3	−23.9±0.3	2.7±0.1	−18.4±0.4
15, 34–39	6,7-Di-OH	−1.9±0.3	−1.5±0.2	−0.6±0.3	−17.3±0.1	19.3±0.1	18.3±0.2	−15.4±0.1	−4.7±0.1	−7.3±0.2
51, 52	7,8-Di-OH	−1.5±0	0.5±0	−0.8±0.1	−1.9±0	−7.9±0.1	21.4±0.1	15.2±1.3	−5.1±0	−9.0±0
20	6-OCH_3	−0.5	−0.8	−0.4	−19.6	29.6	−5.9	2.6	−6.4	2.2
24	7-OCH_3	−1.3	−0.6	−0.5	−1.3	−10.8	29.9	−17.9	1.7	−6.3
Increment sum										
(*line 5 + 6*)	6,7-*Di-OCH*$_3$	*−1.8*	*−1.4*	*−0.9*	*−20.9*	*18.8*	*24.0*	*−15.3*	*−4.7*	*−4.1*
18, 42, 45, 55	6,7-Di-OCH_3	−1.4±0.4	−0.9±0.2	−0.8±0.2	−21.3±0.1	22.2±0.1	20.4±0.1	−18.2±0.1	−3.9±0.1	−6.9±0.1
32	5,7-Di-OCH_3	−3.5	0.6	−1.0	35.3	−29.0	29.9	−25.3	3.2	−14.9
19, 53	7,8-Di-OCH_3	−0.7±0.4	−0.9±0.3	−0.4±0.1	−4.7±0.1	−14.6±0.1	22.4±0.1	18.1±0.1	−6.2±0.5	−5.4±0.1
Increment sum										
(*line 1 + 5*)	7-*OH*-6-*OCH*$_3$	*−2.2*	*−2.1*	*0.1*	*−18.1*	*19.4*	*22.9*	*−13.5*	*−4.7*	*−5.1*
16, 40, 43	7-OH-6-OCH_3	−1.7±0.5	−0.8±0.6	−0.8±0.2	−20.8±0.1	21.7±0.1	19.1±0.1	−15.2±0.1	−3.8±0.1	−7.6±0.1
41, 44	7-OCH_3-6-OH	−1.7±0.2	−1.2±0.2	−0.6±0.1	−17.7±0.1	20.0±0.1	19.7±0.1	−4.9±0.1	−4.9±0.1	−6.5±0.1

TABLE 8. Hydroxy-, acetoxy-, and methoxy increments (ppm) of phenyl ring carbons in isoflavones

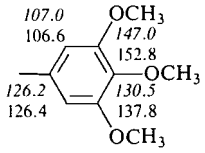
Representative(s)	Substituent in position	$z_{1(\alpha)}$	z_o	$\frac{z_o + z_{o'}}{2}$	$z_{o'}$	z_m	$\frac{z_m + z_{m'}}{2}$	$z_{m'}$	z_p
13	2′-OH	28.4	−11.3	*−10.3*	−9.3	2.6	*2.0*	1.5	−8.1
12	2′-OCH_3	29.5	−17.6	*−14.2*	−10.9	3.9	*2.7*	1.5	−8.3
14	2′-$OCOCH_3$	20.8	−7.0	*−6.6*	−6.2	3.5	*2.3*	1.2	−3.1
21, 23, 29, 34, 40, 41, 42, 49, 51	4′-OH	29.8±2.0		−14.0±1.0			1.9±0.5		−8.7±1.0
20, 24, 25, 31, 32, 35, 43, 44, 45, 46, 47, 50, 52, 53	4′-OCH_3	31.3±0.2		−15.3±0.2			1.9±0.1		−7.8±1.0
26, 27, 48	4-$OCOCH_3$	23.0±0.3		−7.1±0.3			2.0±0.2		−2.5±0.2
Benzene[a]	—OH	26.6		−12.8			1.6		−7.1
	—OCH_3	31.4		−14.4			1.0		−7.8
	—$OCOCH_3$	23.0		−6.4			1.3		−2.3

[a]Reference 13.

oxygen, and between the substituents. In 4′-substituted isoflavones the effects of hydroxy-, methoxy-, and acetoxy-groups on 3-phenyl carbon shifts are essentially those reported for benzene (Table 8). In the 2′-substituted derivatives (**12–14**), however, the *ortho*- and *meta*-effects z_o, $z_{o'}$, and z_m, $z_{m'}$, differ among each other (Table 8), while the average values $(z_o + z_{o'})/2$ and $(z_m + z_{m'})/2$ again approximately correspond to the benzenoid shift increments. Considerable deviations from increment additivity are observed for polysubstituted 3-phenyl rings of isoflavones, particularly at the centers of substitution, as is shown for the phenyl carbons of 3′,4′,6,7-tetramethoxy- and 5,7-dihydroxy-3′,4′,5′-trimethoxyisoflavone **54** and **33** (italic values for increment values and Roman values for experimental values).



54



33

Definitive assignment of the phenyl carbons C-2′ and C-5′ of the tetramethoxy derivative **54** follows from a long-range coupling of $^3J_{CH} = 6.7$ Hz due to a *meta* proton only observed for the signal at 112.9 ppm which, therefore, belongs to C-2′.

Thus, although giving good shift predictions for carbons apart from substitution centers, carbon shift increments in general rather permit the prediction of the signal sequence than of accurate shielding values for higher substituted derivatives. Despite these restrictions concerning increment additivity, some specific shift values found in Tables 2–6 are very characteristic of certain substitution patterns.

A carbonyl shift of 181 ± 1 ppm clearly identifies a 5-hydroxy-group, the deshielding of about 6 ppm relative to all other substituted isoflavones arising from intramolecular hydrogen bonding between C-5-hydroxy and C-4-carbonyl.

Two NOE enhanced signals (off-resonance doublets) at 98 ± 2 ppm and 93 ± 2 ppm are characteristic of C-6 and C-8 in a 5,7-di-*O*-substituted chromone ring, while C-5 and C-8 of 6,7-disubstituted derivatives will appear as strong signals at 106 ± 2 ppm and 101 ± 2 ppm.

A 4′-substituted isoflavone (OH, OCH_3, but not $OCOCH_3$) is well characterized by the signal sequence 123 ± 2 ppm, 130 ± 1 ppm (strong), 114 ± 1 ppm (strong), and 158 ± 2 ppm.

An off-resonance quartet at 55.1 ± 0.1 ppm is very likely due to a 4′-methoxy group while all other methoxy groups of isoflavones and chromones resonate near 56 ppm (Table 4). In the case of 6,7-dimethoxy derivatives two closely spaced methoxy signals at 55.9 (C-6-OCH_3) and 56.2 ppm (C-7-OCH_3) will be observed most likely. For the substitution pattern 6-OCH_3-7-OH, a methoxy shielding of 55.85 ± 0.1 ppm can be expected, while 56.1 ± 0.1 ppm appears to characterize 6-OH-7-OCH_3 (Table 4).

As can be seen in Table 5, the carbonyl carbon of the acetyl group also seems to reflect the acetoxy position (4′-$OCOCH_3$: 169.5; 2′-$OCOCH_3$: 169.0; 6-$OCOCH_3$: 167.8; 7-$OCOCH_3$: 168.5 ppm), but the number of data available is too small for establishing a general rule.

As chromone and phenyl ring are isolated from each other in terms of carbon shielding (8, 9), equally substituted benzene rings in chromones and isoflavones exhibit almost identical ^{13}C shifts (Table 2) independent of the group at positions 3 (alkyl or phenyl) and substituents thereon.

Experimental Section

All ^{13}C nmr spectra were taken in a 50:50 (v/v) mixture of $CDCl_3$ and $(CD_3)_2SO$ in order to exclude solvent effects as much as possible. Internal tetramethylsilane (2 vol.%) was used as reference. Solutions (1 mL) were prepared from 10–40 mg chromone and isoflavone samples. A Bruker WP-60-FT instrument operating at 15.08 MHz for ^{13}C and 60 MHz in the proton decoupling channel was used (except for the spectrum of **47** which was taken at 20.115 MHz). The deuterium signal of $(CD_3)_2SO$ served for field/frequency stabilization at 8.67 MHz. A total of 20 000 accumulated 45° pulse interferograms were exponentially multiplied for a line broadening of 0.4 Hz, zero-filled to 16 K, Fourier-transformed and phase-corrected by a BNC-128 computer (20 Bit) to the real parts of the ^{13}C nmr spectra. For a spectral width of 3.75 kHz distributed among 8 K data points, the digital resolution was 0.45 Hz or 0.03 ppm. Chemical shifts were calculated from the digitized spectra by the computer. The values given in Tables 2–6 can be rounded to the nearest 10th of a ppm.

Preparation of the Isoflavones

The isoflavones and chromones have been prepared via the deoxybenzoins obtained by condensation of required phenols with derivatives of arylacetic acids or appropriate aliphatic acids (14–17). The methods had to be selected from among the Friedel–Crafts reaction, Fries rearrangement, or Hoesch condensations, depending on the nature of phenols used. Formylation of the deoxybenzoins and the ring closure were achieved by ethylformate/sodium (18) or ethyloxalylchloride/pyridin (19) or ethylorthoformate/piperidine–pyridine (20) or borontrifluoride etherate/methylsulfonyl chloride (21). The identity of the substances, so far as known, has been ascertained by mp comparisons. The genuineness of the new compounds was verified by elemental analysis and by application of uv-, ir-, nmr-, and mass-spectrometry.

Demethylations, methylations, and acetylations of the isoflavones were performed according to conventional methods.

The full characterization and preparation procedures for new isoflavone derivatives will be published separately.

1. J. D. BIGGERS. *In* The pharmacology of plant phenolics. *Edited by* J. W. Fairbairn. Academic Press, New York, London. 1959. pp. 51–69.
2. P. GYÖRGY, K. MURATA, and H. IKEHATA. Nature, **203**, 870 (1964).
3. H. FUKAMI and M. NAKAJIMA. *In* Naturally occurring insecticides. *Edited by* M. Jacobsen and G. W. Grosby. Marcel Dekker Inc., New York. 1971. pp. 71–97.
4. R. D. SHARMA. Lipids, **14**, 535 (1979).
5. C. A. KINGSBURY and J. H. LOOKER. J. Org. Chem. **40**, 1120 (1975).
6. (*a*) B. TERNAI and K. R. MARKHAM. Tetrahedron, **32**, 565 (1976); **32**, 2607 (1976); (*b*) K. R. MARKHAM, B. TERNAI, R. STANLEY, H. GEIGER, and T. J. MARBY. Tetrahedron, **34**, 1389 (1978).
7. C.-J. CHANG. Loydia, **41**, 17 (1978).
8. (*a*) H. WAGNER, V. M. CHARI, and J. SONNENBICHLER. Tetrahedron Lett. **21**, 1799 (1976); (*b*) V. M. CHARI, H. WAGNER, and A. NESZMÉLYI. Proc. 5th Hung. Bioflavonoid Symp., Mátrafüred, Hungary. 1977. p. 49.
9. A. PELTER, R. S. WARD, and T. J. GRAY. J. Chem. Soc. Perkin I, 2475 (1976).
10. A. PELTER, R. S. WARD, and R. J. BASS. J. Chem. Soc. Perkin I, 666 (1978).
11. Z. DINYA, GY. LITKEI, A. LÉVAI, A. BÖLCSKEI, P. JÉKEL, S. ROCHLITZ, A. I. KISS, M. FARKAS, and R. BOGNAR. Proc. 5th Hung. Bioflavonoid Symp., Mátrafüred, Hung. 1977. p. 247.
12. M. S. CHAUHAN and J. W. STILL. Can. J. Chem. **53**, 2880 (1975).
13. J. B. STOTHERS. Carbon-13 NMR spectroscopy. Academic Press, New York, London. 1972; E. BREITMAIER and W. VOELTER. ^{13}C NMR spectroscopy. 2nd ed. Verlag Chemie, Weinheim, New York. 1978.
14. P. E. SPOERRI and A. S. DUBOIS. Org. React. **5**, 387 (1945).
15. Y. KAWASE, T. FUJIMOTO, and K. FUKUI. Bull. Chem. Soc. Jpn. **31**, 691 (1958).
16. S. S. KAMARKAR, K. H. SHAH, and K. VENKATRAMAN. Proc. Indian Acad. Sci. **41**A, 192 (1955).
17. W. D. OLLIS. The isoflavonoids in the chemistry of flavonoid compounds. *Edited by* T. A. Geissman. Pergamon Press. 1962, and references therein.
18. P. C. JOSHI and K. VENKATRAMAN. J. Chem. Soc. 513 (1934).
19. W. BAKER, J. B. HARBORNE, and W. D. OLLIS. J. Chem. Soc. 1860 (1953).
20. V. R. SATHE and K. VENKATRAMAN. Curr. Sci. **18**, 373 (1949).
21. R. J. BASS. J. Chem. Soc. Chem. Commun. 78 (1976).

Application de la spectrométrie infrarouge et Raman à l'étude des complexes en solution aqueuse: Fe^{3+}–$H_2C_2O_4$

MOHSEN JABER,[1] FRANÇOIS BERTIN ET GERMAINE THOMAS-DAVID

Laboratoire de Chimie Analytique II, Université Claude Bernard, Lyon I, 43 boulevard du 11 Novembre 1918, 69622 Villeurbanne, France

Reçu le 23 novembre 1979

MOHSEN JABER, FRANÇOIS BERTIN et GERMAINE THOMAS-DAVID. Can. J. Chem. **58**, 1220 (1980).

L'étude par spectrométrie Raman du système Fe^{3+}–$H_2C_2O_4$ en solution aqueuse montre très nettement la formation successive de trois complexes: $Fe(C_2O_4)^+$, $Fe(C_2O_4)_2^-$, $Fe(C_2O_4)_3^{3-}$, chaque espèce est caractérisée par un spectre Raman spécifique.

L'évolution de l'intensité des bandes Raman des trois complexes en fonction de la longueur d'onde de la raie excitatrice et la comparaison entre les spectres ir et Raman des trioxalates de fer(III) et d'aluminium montrent pour les oxalatoferrates un effet de pré-résonance Raman.

MOHSEN JABER, FRANÇOIS BERTIN, and GERMAINE THOMAS-DAVID. Can. J. Chem. **58**, 1220 (1980).

A study by Raman spectrometry of the system Fe^{3+}–$H_2C_2O_4$ in aqueous solution shows very clearly the successive formation of the three complexes: $Fe(C_2O_4)^+$, $Fe(C_2O_4)_2^-$, $Fe(C_2O_4)_3^{3-}$. Each species is characterised by a specific Raman spectrum.

The evolution of Raman band intensities with the range of exciting line, and the comparison between ir and Raman spectra of Fe(III) and Al(III) complexes, show for Fe(III) species a pre-resonance Raman effect.

Can. J. Chem. Downloaded from www.nrcresearchpress.com by 210.87.254.40 on 09/05/12
For personal use only.

La formation des oxalates complexes de fer(III) en solution aqueuse a fait l'objet de plusieurs investigations utilisant des techniques telles que la potentiométrie, la spectrophotométrie uv–visible, la polarographie ... (1–18). L'interprétation des résultats obtenus conduit la plupart des auteurs à proposer la formation de trois complexes mononucléaires $Fe(C_2O_4)^+$, $Fe(C_2O_4)_2^-$ et $Fe(C_2O_4)_3^{3-}$ (34). Toutefois Fronaeus (19), après examen des spectres infrarouges des solutions aqueuses d'oxalatoferrates, admet dans certains cas la formation de complexes polynucléaires; d'un autre côté Moorhead (20) et Bauer (21) par étude spectrophotométrique uv concluent à l'existence d'une espèce protonée $FeHC_2O_4^{2+}$. Il est possible que les divergences ainsi observées résultent de l'incertitude concernant le nombre de protons libérés par la formation des oxalates de Fe(III), surtout en milieu très acide.

Aucune étude complète n'a été effectuée par spectrométrie infrarouge et Raman sur ce système. D'une façon générale les oxalates complexes des métaux de transition sont des composés colorés qui absorbent fortement le rayonnement visible ou proche uv; ils n'ont pratiquement pas été étudiés par Raman à l'inverse de nombreux autres oxalates complexes incolores (22–28). Notons cependant les travaux de Vaisserman (27) et Gouteron (28) qui ont récemment publié les spectres de diffusion des oxalates de rhodium et d'iridium en utilisant une raie laser exitatrice dont la longueur d'onde est située en dehors de la région d'abosrption des composés; ces auteurs ne sont pas parvenus à obtenir le spectre Raman du trioxalate de Fe(III) et l'un d'eux (28) note une altération très rapide du composé lorsqu'il est soumis au rayonnement laser.

Dans le cadre d'un travail concernant l'application de la spectrométrie infrarouge et Raman à l'étude des équilibres complexes en solution aqueuse (29–33), nous présentons ici les résultats obtenus au cours de l'étude de la formation des différents complexes pour le système Fe^{3+}–$H_2C_2O_4$, en fonction de l'acidité des solutions et du rapport des concentrations analytiques en métal/coordinat. L'évolution des spectres met en évidence trois étapes successives qui présentent un léger phénomène de résonance Raman.

Conditions expérimentales

Solutions

Les solutions mères d'oxalate de fer(III) sont obtenues par dissolution, dans l'eau distillée, d'acide oxalique $H_2C_2O_4 \cdot 2H_2O$ et de chlorure ferrique $FeCl_3 \cdot 6H_2O$ dans des proportions adéquates; les réactifs utilisés sont des produits Merck pour analyses; on prépare des solutions de concentration 0.5 *M* en coordinat, avec un rapport métal/coordinat $t = 0$, 1, 1/2 et 1/3. Le degré d'acidité des échantillons examinés est fixé par addition d'acide chlorhydrique concentré Prolabo R. P. ou par neutralisation par de la soude concentrée (~10 *N*) et titrée; pour mesurer l'acidité de nos solutions nous avons utilisé la chaîne de mesures potentiométriques décrite précédemment (30–32).

Parallèlement aux solutions dans l'eau légère, on réalise des solutions deutériées de même concentration analytique (0.5 *M*) en coordinat par addition progressive de DCl 7.8 *N* à des échantillons obtenus par dissolution d'oxalate de sodium et de chlorure ferrique dans l'eau lourde, en quantités adéquates; tous ces réactifs sont des produits Merck pour analyses.

Pour chaque rapport $t = 0$, $t = 1$, 1/2 et 1/3, le domaine d'étude est limité par la précipitation de l'hydroxyde ferrique, soit pH ≤

[1]Boursier du C.N.R.S. Libanais.

0008-4042/80/121220-09$01.00/0

©1980 National Research Council of Canada/Conseil national de recherches du Canada

Can. J. Chem. Downloaded from www.nrcresearchpress.com by 210.87.254.40 on 09/05/12
For personal use only.

3.5 pour $t = 1/3$, pH $\leq 2.\overline{5}$ pour $t = 1/2$, pH ≤ 2.0 pour $t = 1$ et pH ≤ 1.5 pour $t = 0$, rapport qui correspond aux solutions de chlorure ferrique dépourvues d'ions oxalates.

Spectres

On a enregistré une soixantaine de spectres ir et Raman de solutions ainsi préparées.

Les conditions d'obtention des spectres ir et Raman sont identiques à celles décrites précédemment (30–33). Toutefois, compte tenu de la coloration jaune–vert des solutions, l'enregistrement des spectres Raman et l'exploitation des résultats obtenus nécessitent ici quelques précautions particulières. Pour éviter l'échauffement et l'altération des solutions par suite d'une absorption trop importante du rayonnement laser au cours de l'enregistrement, nous avons réalisé un dispositif de circulation continue de la solution dans un tube capillaire en quartz, disposé verticalement et perpendiculaire au faisceau; la circulation est assurée par une pompe péristaltique; un tel dispositif exige un assez grand volume de solution: 50 mL environ. La puissance du laser a été limitée à 200 mW. Afin de mettre en évidence le phénomène de résonance Raman, on utilise quatre fréquences excitatrices à 514.5; 488.0; 476.5 et 457.9 nm.

Nous mesurons les intensités des raies de diffusion des complexes avec une grande précision en utilisant comme étalons internes les ions ClO_4^- et NO_3^- en concentration 0.04 *M* dont les raies caractéristiques sont situées respectivement à 936 et à 1050 cm^{-1}. De plus, pour chaque échantillon, nous procédons à deux enregistrements successifs; nous pouvons ainsi vérifier qu'il n'y a pas eu d'évolution notable ni dans la physionomie du spectre, ni dans les intensités des bandes pendant l'éclairement de la solution. Les intensités mesurées sont corrigées de la réponse spectrale du détecteur et de l'absorption des faisceaux diffusés par l'échantillon (29, 39, 40).

Les spectres d'absorption uv–visible de l'échantillon sont obtenus au moyen d'un spectromètre-enregistreur BECKMAN DK 2 A, double faisceau en cuves parallèlépipédiques de quartz, d'épaisseur 0.1 et 0.5 cm, à la température ambiante; l'eau distillée est utilisée comme solution de référence. Ces enregistrements sont complétés par des mesure effectuées à l'aide d'un spectromètre OPTICA monofaisceau, ce qui permet d'obtenir une valeur précise de l'absorbance des solutions pour des longueurs d'onde bien définies.

Résultats expérimentaux

Spectres infrarouges des oxalates de fer(III) en solution

Quel que soit le rapport t étudié, les spectres ir présentent les mêmes bandes; la neutralisation des solutions entraîne une diminution des bandes du coordinat $H_2C_2O_4$ ou de ses formes dissociées; simultanément d'autres bandes, dues aux complexes oxalatoferrates apparaissent, situées à 1710, 1680, 1460(?), 1395, 1255, 930, 890 et 800 cm^{-1}, et augmentent d'intensité avec le pH. Aux pH limites avant la précipitation de l'hydroxyde ferrique, les spectres ont sensiblement la même allure quel que soit le rapport t, à l'exception de la bande à 1710 cm^{-1} qui semble plus intense pour le rapport $t = 1/3$. On ne peut donc pas utiliser les spectres ir pour suivre de façon significative l'évolution des équilibres dans cet exemple.

Evolution des spectres Raman en fonction du rapport t *et de l'acidité des solutions*

(a) Spectres du chlorure ferrique en l'absence du coordinat

A pH = 1, il apparaît une bande très intense à 317 cm^{-1} et quatre bandes de faible intensité à 173, 423, 493 et 601 cm^{-1}, signalées par Sharma et Harston (35–38), et qui peuvent être attribuées aux complexes chlorés du type $|Fe(H_2O)_xCl_y|^{(3-y)}$. Par acidification, les bandes 173 et 317 cm^{-1} gardent la même fréquence, les bandes 423, 493 et 601 cm^{-1} diminuent d'intensité et il apparait simultanément une bande large vers 433 cm^{-1}, également notée par Sharma.

(b) Spectres des complexes pour le rapport t = *1/3 (fig. 1)*

(*i*) Domaine d'acidité $|HCl_{eq}| > 7\ N$; le spectre comporte les bandes de diffusion de $H_2C_2O_4$ ainsi que celles qui caractérisent les complexes chlorés du fer(III) citées ci-dessus.

(*ii*) Domaine $7\ N > |HCl_{eq}| > 3.1\ N$; l'intensité des bandes du coordinat libre et des complexes chlorés diminue; tandis qu'il apparait des bandes à 270, 548, 795, 900, 1258, 1395, 1693 et 1713 cm^{-1}, dont l'intensité augmente quand l'acidité de la solution diminue. Ces bandes sont certainement dues aux complexes oxalatoferrates. Dans ce domaine on constate un déplacement progressif de la fréquence de la bande à 317 cm^{-1} vers 307 cm^{-1}, résultant sans doute de l'interférence entre deux bandes provenant l'une de l'ion $FeCl_4^-$ (37), l'autre des complexes oxalatoferrates. La fig. 1 présente l'évolution des spectres dans la région de fréquences la plus caractéristique. Lorsque $|HCl_{eq}| = 3.1\ N$ il apparait une bande à 260 cm^{-1} tandis que disparait celle à 307 cm^{-1} citée plus haut, révélant ainsi la présence d'une bande intense à 297 cm^{-1}.

(*iii*) Domaine $3.1\ N \geq |HCl_{eq}| \geq 1.3\ N$: on observe un déplacement progressif des bandes des complexes oxalatoferrates accompagné d'importantes modifications d'intensité. Lorsque $|HCl_{eq}| = 1.3\ N$, les bandes observées se trouvent ainsi à 260, 297, 363, 533, 555, 796, 900, 1256, 1394, 1698 et 1720 cm^{-1}. Parallèlement les bandes du coordinat non engagé dans les complexes diminuent régulièrement d'intensité mais restent encore visibles même pour $|HCl_{eq}| = 1.3\ N$.

(*iv*) Domaine d'acidité allant de $|HCl_{eq}| \leq 1.3\ N$ à pH ≤ 3: les bandes du coordinat finissent par disparaître complètement; la disparition de la raie située à 848 cm^{-1} permet de repérer une raie à 855 cm^{-1} due aux complexes. Cette évolution s'accompagne (fig. 1) d'une diminution d'intensité puis

Can. J. Chem. Downloaded from www.nrcresearchpress.com by 210.87.254.40 on 09/05/12
For personal use only.

d'une disparition de la bande à 297 cm^{-1} qui était apparue dans une région intermédiaire, ainsi que d'un élargissement et d'un déplacement progressif de la bande à 260 cm^{-1} qui s'achève par l'apparition d'une bande étroite, très intense située à 249 cm^{-1}. Parallèlement, d'autres bandes se déplacent en fréquence d'une façon continue pour atteindre à pH = 2.8: 358, 508, 535, 560, 795, 855, 903, 1257, 1399, 1705 et 1729 cm^{-1}. L'intensité des bandes à 249, 560 et 1729 cm^{-1} subit une augmentation considérable par rapport à celle des autres bandes du spectre. Il semble que les complexes possèdent aussi une bande proche de 1640 cm^{-1} dans le domaine de la bande de déformation de l'eau.

L'examen des différents spectres pour le rapport $t = 1/3$ nous permet donc de distinguer quatre domaines dont trois correspondent à la formation de différents complexes oxalatoferrates.

(c) Spectres pour le rapport t = *1/2*

(*i*) Pour $|HCl_{eq}| > 3.1\ N$, on observe les bandes des oxalatoferrates repérées pour le rapport $t = 1/3$ en milieu fortement acide, ainsi que celles du coordinat et des chlorures de Fe(III). Le même phénomène d'interférence entre les bandes à 307 et à 317 cm^{-1} apparaît ici.

(*ii*) Domaine d'acidité $|HCl_{eq}| < 3.1\ N$: les spectres présentent des bandes déjà observées pour $t = 1/3$ dans l'intervalle $3.1\ N > |HCl_{eq}| > 1.3\ N$: la bande à 307 cm^{-1} disparait, tandis que celle à 297 cm^{-1} apparait. On constate une disparition complète des fréquences imputables à l'acide oxalique; à pH ~ 2 les bandes situées à 260, 297, 363, 490(?), 533, 555, 796, 855, 900, 1256, 1394, 1698 et 1720 cm^{-1} passent par un maximum d'intensité, particulièrement accentué pour les bandes à 260, 297, 555 et 1720 cm^{-1}.

(d) Spectres pour le rapport t = *1*

Les spectres obtenus sur toute la gamme d'acidité comprise entre $|HCl_{eq}| = 7.5\ N$ et pH = 1.4 présentent les mêmes caractéristiques. Au fur et à mesure de la neutralisation, les bandes de l'acide oxalique et celle des chlorures de fer(III) diminuent puis disparaissent tandis qu'il apparait des bandes situées à 270, 307, 548, 795, 853, 900, 1258, 1395, 1693 et 1713 cm^{-1} qui augmentent continuellement d'intensité sans changer de fréquence. Ces bandes correspondent à celles observées pour les rapports $t = 1/3$ et $t = 1/2$ lorsque $|HCl_{eq}| > 3.1\ N$. Elles atteignent un maximum d'intensité pour $|HCl_{eq}| = 1.3\ N$.

La bande à 307 cm^{-1} est bien due aux complexes oxalates et non à l'ion $FeCl_4^-$. On le vérifie en enregistrant le spectre d'une solution, à pH = 1, de nitrate ferrique qui présente les mêmes bandes que celles citées ci-dessus, à l'exception des raies de NO_3^-.

Discussion

Identification des différents complexes

L'observation globale des spectres Raman pour les trois rapports t, fait nettement apparaître trois étapes sur la complexation de Fe(III) par les ions oxalates. Celles-ci sont caractérisées par trois spectres nettement différents surtout dans la région de basse fréquence (fig. 2). En effet, l'espèce présente à pH 2.8 pour le rapport $t = 1/3$, n'apparait jamais pour les rapports $t = 1$ et $t = 1/2$. Pour $t = 1/3$, la précipitation de $Fe(OH)_3$ n'a lieu qu'à pH élevé, ce qui signifie que la quasi-totalité des ions Fe(III) sont complexés par l'oxalate; comme les bandes du coordinat libre sont absentes, on en déduit que l'espèce qui se forme à ce moment renferme trois groupements oxalate par métal: il s'agit très probablement de $Fe(C_2O_4)_3^{3-}$.

En milieu très acide: $|HCl_{eq}| > 3.1\ N$, on observe la formation d'un complexe qui possède les mêmes fréquences de vibration quel que soit le rapport t. Comme ces fréquences sont présentes pour le rapport $t = 1/1$ juste avant la précipitation de $Fe(OH)_3$ et qu'à ce moment les bandes du coor-

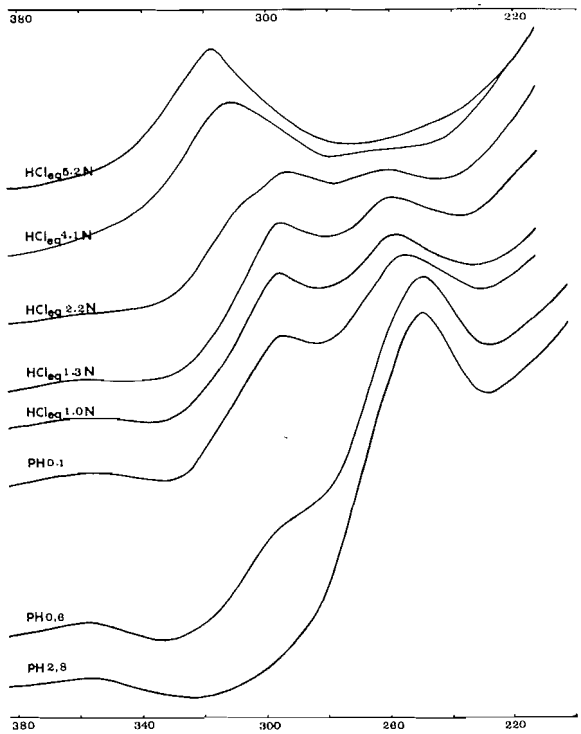


FIG. 1. Evolution des spectres Raman des oxalates complèxes de fer(III) en fonction de l'acidité de la solution pour $t = 1/3$ dans le domaine 380–200 cm^{-1}.

Can. J. Chem. Downloaded from www.nrcresearchpress.com by 210.87.254.40 on 09/05/12
For personal use only.

TABLEAU 1. Fréquences de vibration des oxalates complexes de fer(III) en solution aqueuse*

$Fe(C_2O_4)^+$				$Fe(C_2O_4)_2^-$				$Fe(C_2O_4)_3^{3-}$			
Raman		Ir		Raman		Ir		Raman		Ir	
270	Ep			260	F			249	TF		
307	TF			297	F			—			
—				363	tf			358	f		
				490	?						
								508	tf		
				533	Ep			535	m		
548	TF			555	TF			560	TF		
795	f	800	m	796	f	800	m	795	f	800	m
853	f			855	tf			855	f		
900	m	890	m	900	m	890	m	903	m	890	m
		930	Ep			930	Ep			930	Ep
1258	m	1255	m	1256	m	1255	m	1257	m	1255	m
1395	m	1395	F	1394	m	1395	F	1399	m	1395	F
		1460	?			1460	?			1460	?
1693	m	1680	TF	1698	Ep	1680	TF	1705	Ep	1680	TF
1713	F	1710	TF	1720	TF	1710	F	1729	TF	1710	F

*TF, très forte; F, forte; m, moyenne; f, faible; tf, très faible; Ep, épaule.

dinat ont disparu, on peut en conclure que ce complexe renferme un coordinat par métal: il s'agirait donc de $Fe(C_2O_4)^+$. La continuité qui existe entre les spectres de vibration des trois espèces semble exclure l'hypothèse de la formation d'une espèce protonée $FeHC_2O_4^{2+}$; de plus, dans ce complexe, les deux groupes carboxylates devraient être différents, ce qui est contraire aux observations spectrales.

Dans un domaine intermédiaire entre la formation de $Fe(C_2O_4)^+$ et celle de $Fe(C_2O_4)_3^{3-}$ il apparait un complexe dont les bandes ont été répertoriées. La fig. 1 montre que pour $t = 1/3$, ce complexe est prépondérant dans l'intervalle $3.1\ N \geq |HCl_{eq}| \geq 1.3\ N$; pour $t = 1/2$ ce complexe est pratiquement seul à pH ~ 0.5. Il est vraisemblable qu'il s'agit de l'espèce $Fe(C_2O_4)_2^-$.

La fig. 2 présente les spectres Raman de ces trois complexes dans le domaine 380–200 cm^{-1}; leurs fréquences de vibration ir et Raman sont rassemblées dans le tableau 1.

Il ne semble pas que les complexes polynucléaires du Fe(III) proposés par Fronaeus (19), se forment, du moins en quantité appréciable, car on devrait constater pour les pH élevés, surtout dans les rapports $t = 1/1$ et $t = 1/2$, une modification spectrale importante, comme cela se produit avec le système Be^{2+}–$H_2C_2O_4$ (31).

Remarques concernant le spectre Raman du complexe trioxalate

Nous indiquons, tableau 2, les fréquences ir et Raman des espèces $Fe(C_2O_4)_3^{3-}$ en solution et $Na_3Fe(C_2O_4)_3 \cdot 3H_2O$ cristallisé. Ce dernier composé a été préparé par évaporation très lente d'une solution d'oxalatoferrate dans un rapport $t = 1/3$ (pH = 2.8); son spectre Raman, enregistré pour plusieurs échantillons, est obtenu en utilisant le dispositif rétro-Raman et la raie excitatrice à 514.5 nm. Ce tableau donne par comparaison les fréquences ir du complexe $K_3Al(C_2O_4)_3 \cdot 3H_2O$ à l'état cristallisé et celles du spectre Raman du même complexe en solution. Les attributions sont celles données par Gouteron (28) et Vaisserman

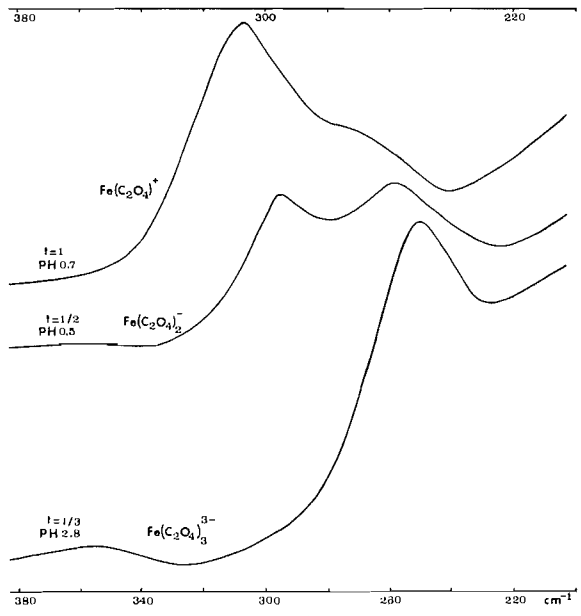


FIG. 2. Spectres Raman des oxalates complexes de fer(III) dans le domaine 380–200 cm^{-1}.

Can. J. Chem. Downloaded from www.nrcresearchpress.com by 210.87.254.40 on 09/05/12
For personal use only.

TABLEAU 2. Fréquences ir et Raman du complexe trioxalate de fer(III) et leurs attributions en comparaison avec celles de trioxalate d'aluminium incolore

$K_3Al(C_2O_4)_3 \cdot 3H_2O$ solide Fréq. ir (27, 28)	$Al(C_2O_4)_3^{3-}$ en solution Fréq. Raman	$K_3Fe(C_2O_4)_3 \cdot 3H_2O$ solide Fréq. ir et attribution (27–28)				$Fe(C_2O_4)_3^{3-}$ en solution		$Na_3Fe(C_2O_4)_3 \cdot 3H_2O$ solide Fréq. Raman
						Raman	Ir	
110								
136		120			Vibrations			
166		144			externes			
210 Ep		190	Ep					
268 f		217	m	E				
	270 f					249 TF		256 m
		328	m		Déformation			
365 f		346	F		des cycles			
374 f	369 m	365	m	E	et vibrations			
					M—O	358* f		
								390 Ep
								400 F
432 m	430 ?					430 ?		411 Ep
478 F	473 f			E				455 tf
494 F		500	F			508 tf		
583 F		532	F	E	ν(M—O)	535 Ep		536 f
	583 F			A_1		560 TF		562 F
596 Ep	608 Ep	580	m	E				
805 F		790	F	A_2	δ(O—C=O)	795* f		797 f
823 F	811 f	803	F	E			800 m	
	859 f					855 f		855 f
910 F		892	F	E	ν(C—C)		890 m	
	918 F		Ep	A_1		903 m	930 Ep	901 m
1270 F		1255	F	A_2		1257* F	1255 m	1258 F
1295 F	1273 tf	1270	F	E	ν(C—O)			
1405 F	1408 Ep	1390	F	E		1399 m	1395 m	1394 F
	1429 TF			A_1			1460 ?	1463 F
								1616 f
1680 F		1647	F	A_2				1668 f
1702 F	1688 F	1682	F	E	ν(C=O)		1680 F	1686 f
1723 F	1723 Ep	1712	F	E		1705 Ep	1710 F	1710 ?
	1746 F			A_1		1729 TF		1738 F

*Bandes dépolarisées.

TABLEAU 3. Variation de l'intensité I_A/I_e des bandes de diffusion du complexe $Fe(C_2O_4)_3^{3-}$ en solution en fonction de la longueur d'onde λ_0 de la raie excitatrice

Bandes de diffusion $\bar{\nu}_0 - \bar{\nu}$ (cm^{-1})		I_A/I_e à raie excitatrice λ_0 (nm)				
		514.5	488.0	476.5	457.9	$\rho = I_{vH}/I_{vv}$
1729	A_1	6.34	6.60	7.13	8.47	0.07
1399		0.20	0.22	0.23	0.39	0.55
1257	A_2	0.45	0.46	0.52	0.53	0.71
903	A_1	0.42	0.53	0.50	0.56	0.33
795	A_2	0.08	0.10	0.13	0.12	0.69
560	A_1	4.05	4.59	5.15	5.81	0.02
535	E	1.00	1.12	1.27	1.28	0.73
358	E	0.13	0.16	0.21	0.26	0.70
249	A_1	2.26	2.88	3.24	3.93	0.10

(27) dans l'hypothèse d'une symétrie D_3; on admet que ces attributions sont également valables pour les vibrations du trioxalate d'aluminium. Pour le groupe D_3 les vibrations de types A_1 et E sont actives en absorption.

En comparant le spectre Raman du complexe $Fe(C_2O_4)_3^{3-}$ en solution au spectre ir de $K_3Fe(C_2O_4)_3 \cdot 3H_2O$ et aux spectres du trioxalate d'aluminium que nous avons enregistré aussi, on remarque l'absence d'une bande de type A_1 correspondant à ν(C—O) qui devrait apparaître vers 1430 cm^{-1} (par comparaison avec $Al(C_2O_4)_3^{3-}$), alors qu'à l'état solide on aperçoit une bande intense à 1463 cm^{-1}; deux bandes dépolarisées apparaissent à 1257 et 795 cm^{-1} qui pourraient être attribuées aux modes ν_a(C—O) et δ(O—C=O) de type A_2 normalement interdites en Raman classique. Le fait le plus remarquable est une augmentation considérable d'intensité des bandes de type A_1 situées à 1729, 560 et 249 cm^{-1}. Par contre la bande à 358 cm^{-1} de type E subit le phénomène inverse. Il en est de même pour la bande moyenne à 1399 cm^{-1} pour laquelle la valeur de rapport de dépolarisation (0.55) laisse quelques doutes quant à la symétrie du mode mis en jeu attribuée à un mode E.

Ces observations sont compatibles avec l'existence d'un phénomène de résonance Raman pour le complexe $Fe(C_2O_4)_3^{3-}$.

Spectres d'absorption électronique du complexe trioxalate

Le spectre d'absorption électronique d'une solution de chlorure ferrique de concentration CM = 10^{-3} *M* à pH ~ 3 présente une bande large avec un maximum pour λ_A = 280 nm. Au même pH et pour une même concentration en Fe(III), la formation du trioxalate entraîne un déplacement du maximum vers 260 nm dont le cœfficient d'absorption molaire est de 2600 $mol^{-1}\,cm^{-1}$. Ceci est en bon accord avec les résultats donnés dans la littérature (3–5, 12). L'absorbance devient nulle pour $\lambda > 350$ nm. Par contre pour la solution concentrée étudiée (CM = 0.167 *M*) par spectrométrie Raman et ir l'absorption n'est pas nulle dans le domaine des fréquences excitatrices utilisées. Les valeurs des cœfficients d'absorption molaire k (en supposant que la loi de Beer–Lambert est toujours applicable dans nos conditions de concentration) aux fréquences de diffusion Raman $\bar{\nu}_0 - \bar{\nu}$ du complexe sont:

(*i*) Pour λ_0 = 514.5 nm, k = 0 pour toutes les raies Raman.

(*ii*) Pour λ_0 = 488.0 nm, k atteint la valeur 0.7 $mol^{-1}\,cm^{-1}$ pour la raie $\bar{\nu}_0 - \bar{\nu}$ = 249 cm^{-1}.

(*iii*) Pour λ_0 = 476.5 nm, k varie de 0.00 pour 1729 cm^{-1} à 1.52 $mol^{-1}\,cm^{-1}$ pour 249 cm^{-1}.

(*iv*) Pour λ_0 = 457.9 nm, k varie de 0.55 pour 1729 cm^{-1} à 6.84 $mol^{-1}\,cm^{-1}$ pour 249 cm^{-1}.

On note que la fréquence $\bar{\nu}$ d'une raie du spectre Raman est toujours inférieure à la fréquence $\bar{\nu}_A$ du maximum d'absorption du spectre électronique.

Mise en évidence d'un effet de résonance Raman des complexes oxalatoferrates

(a) Evolution de l'intensité des bandes Raman du complexe $Fe(C_2O_4)_3^{3-}$ en fonction de la fréquence de la raie excitatrice

Les intensités relatives I_A/I_e, mesurées par rapport à l'intensité I_e de la raie étalon de l'ion ClO_4^- située à 936 cm^{-1} et corrigées de la réponse spectrale et de l'absorption du faisceau laser, sont reportées au tableau 3 en fonction des différentes raies excitatrices utilisées. La dernière colonne du tableau donne le rapport de dépolarisation ρ de chaque bande; celui-ci est pratiquement constant, quelle que soit la fréquence du laser. Nous avons enregistré les spectres plusieurs fois sur différentes solutions de même composition (rapport t = 1/3;

Can. J. Chem. Downloaded from www.nrcresearchpress.com by 210.87.254.40 on 09/05/12
For personal use only.

Can. J. Chem. Downloaded from www.nrcresearchpress.com by 210.87.254.40 on 09/05/12
For personal use only.

TABLEAU 4. Variation de l'intensité I_A/I_e des bandes de diffusion du complexe $Fe(C_2O_4)^+$ en solution en fonction de la longueur d'onde λ_0 de la raie excitatrice

Bandes de diffusion $\bar{\nu}_0 - \bar{\nu}$ (cm^{-1})	I_A/I_e à raie excitatrice λ_0 (nm)				
	514.5	488.0	476.5	457.9	$\rho = I_{vH}/I_{vv}$
1713	2.88	2.75	2.46	1.82	0.10
1395	0.86	1.94	2.38	3.34	0.28
1258	0.51	0.60	0.59	0.51	0.65
900	0.44	0.57	0.71	0.96	0.25
795	0.20	0.21	0.35	0.83	0.52
548	3.36	4.01	4.52	5.53	0.05
307	4.38	5.87	7.51	13.54	0.10
270	1.67	2.24	2.95	6.35	0.07

CM = 0.167 *M*; pH = 2.8); les intensités des bandes sont constantes.

On constate que l'intensité de la plupart des bandes augmente quand la fréquence de la raie excitatrice $\bar{\nu}_0$ s'approche du maximum $\bar{\nu}_A$ de la bande d'absorption électronique de l'échantillon. Cette variation observée apparait plus nettement sur la fig. 3 qui présente les spectres d'une solution de $Fe(C_2O_4)_3^{3-}$ obtenus en utilisant les raies extrêmes 514.5 et 457.9 nm.

L'intensité des bandes de type A_1 situées à 1729, 560 et 249 cm^{-1} est exaltée par rapport à celles des autres raies du même spectre et des bandes de $Al(C_2O_4)_3^{3-}$. Ces trois bandes subissent une augmentation importante quand $\bar{\nu}_0$ tend vers $\bar{\nu}_A$; le domaine de fréquences du laser dont nous disposions est trop éloignée de $\bar{\nu}_A$ pour nous permettre de tracer le profil d'excitation. L'intensité de la bande dépolarisée de type *E* à 358 cm^{-1} est très faible, elle augmente aussi quand $\bar{\nu}_0$ s'approche de $\bar{\nu}_A$. La même variation est observée pour la bande à 1399 cm^{-1}. Enfin l'intensité de deux bandes dépolarisées situées à 1257 et 795 cm^{-1} attribuables à des modes de type A_2 augmente légèrement.

Ainsi pour le spectre du trioxalate ferrique, la variation de l'intensité des bandes et l'apparition de raies interdites sont certainement la traduction d'un phénomène de Raman de résonance. Cependant la fréquence excitatrice étant toujours très éloignée de la fréquence $\bar{\nu}_A$ du maximum d'absorption électronique, l'absorption n'a lieu que pour des concentrations élevées et nous pensons plutôt qu'il s'agit d'une pré-résonance.

(b) Evolution de l'intensité des bandes Raman des complexes $Fe(C_2O_4)^+$ et $Fe(C_2O_4)_2^-$ en fonction de la longueur d'onde de la raie excitatrice

Les spectres de diffusion de ces deux espèces montrent comme pour le trioxalate des intensités relatives de raies très différentes.

A pH ~ 3 les solutions de $Fe(C_2O_4)^+$ et $Fe(C_2O_4)_2^-$ (10^{-3} *M* en Fe^{3+}) présentent des maximums vers 270 et 265 nm respectivement. Les cœfficients d'absorption molaire sont plus élevés que ceux de $Fe(C_2O_4)_3^{3-}$ mais pas suffisamment pour nous permettre de travailler en solutions diluées. A ces concentrations les complexes sont transparents dans le domaine visible; par contre les valeurs des cœfficients d'absorption molaire *k* aux fréquences de diffusion Raman des solutions plus concentrées étudiées sont:

(*i*) Pour $Fe(C_2O_4)^+$, $1.10 < k < 45.03$ mol^{-1} cm^{-1}.

(*ii*) Pour $Fe(C_2O_4)_2^-$, $0.80 < k < 26.59$ mol^{-1} cm^{-1}.

Nous donnons dans les tableaux 4 et 5 les intensités relatives corrigées I_A/I_e des bandes de diffusion Raman (par rapport à la bande référence de ClO_4^-) pour les différentes longueurs d'onde du laser utilisé. La dernière colonne présente les rapports de dépolarisation des bandes. Les intensités ont été mesurées pour plusieurs solutions, les résultats étant reproductibles. Lorsque la fré-

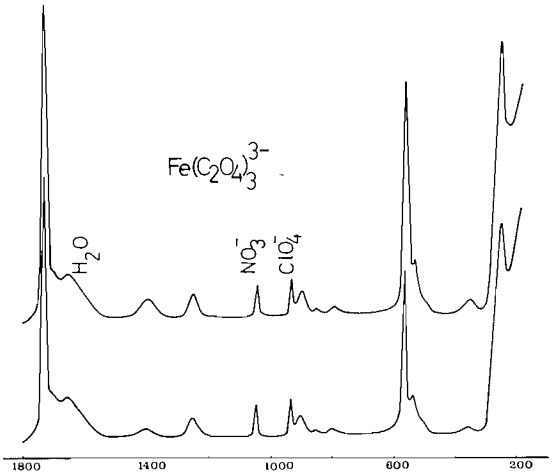


FIG. 3. Spectres Raman du complexe $Fe(C_2O_4)_3^{3-}$ enregistrés avec deux fréquences excitatrices: (*a*) raie 457.9 nm; (*b*) raie 514.5 nm.

Can. J. Chem. Downloaded from www.nrcresearchpress.com by 210.87.254.40 on 09/05/12
For personal use only.

TABLEAU 5. Variation de l'intensité I_A/I_e des bandes de diffusion du complexe $Fe(C_2O_4)_2^-$ en solution en fonction de la longueur d'onde λ_0 de la raie excitatrice

Bandes de diffusion $\bar{\nu}_0 - \bar{\nu}$ (cm^{-1})	I_A/I_e à raie excitatrice λ_0 (nm)				
	514.5	488.0	476.5	457.9	$\rho = I_{vH}/I_{vv}$
1720	4.07	4.68	4.66	5.92	0.08
1394	0.31	0.52	0.90	2.07	0.32
1256	0.48	0.55	0.62	0.72	0.66
900	0.40	0.46	0.51	0.59	0.27
796	0.09	0.15	0.15	0.19	0.67
555	3.60	5.07	5.07	7.06	0.03
297	1.78	2.31	3.08	4.03	0.06
260	1.36	1.83	2.23	3.07	0.07

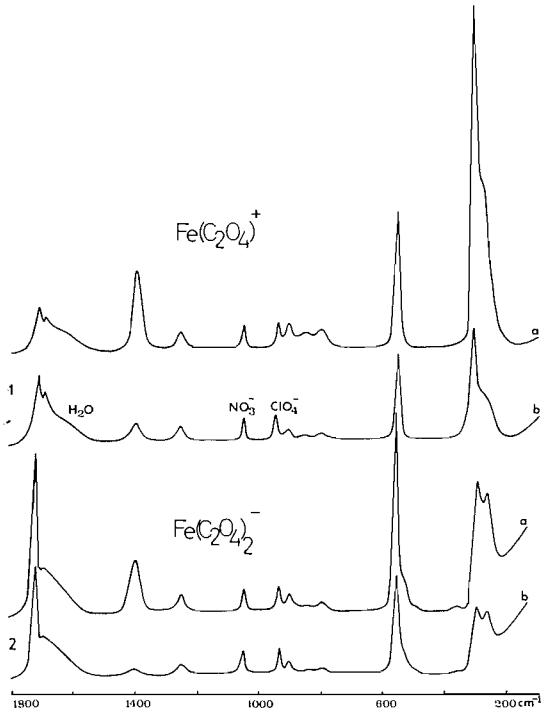


FIG. 4. Spectres Raman: (*1*) $Fe(C_2O_4)^+$; (*2*) $Fe(C_2O_4)_2^-$ enregistrés avec deux fréquences excitatrices ν_0: (*a*) raie 457.9 nm; (*b*) raie 514.5 nm.

quence $\bar{\nu}_0$ s'approche du maximum d'absorption $\bar{\nu}_A$:

(*iii*) Pour le complexe $Fe(C_2O_4)^+$, l'intensité des bandes situées à 1395, 900, 795, 548, 307 et 270 cm^{-1} augmente considérablement, tandis que celle de la bande à 1713 cm^{-1} diminue légèrement. L'intensité de la bande à 1258 cm^{-1} n'est pratiquement pas affectée.

(*iv*) Pour $Fe(C_2O_4)_2^-$ toutes les bandes augmentent d'intensité d'une manière significative, surtout celles à 1394, 555, 297 et 260 cm^{-1}.

Les phénomènes observés pour les deux composés sont dûs aussi à un effet de pré-résonance qui est plus important que dans le cas du trioxalate de fer(III). On présente fig. 4, les spectres Raman de pré-résonance de chaque espèce, enregistrés avec les raies extrêmes 514.5 et 457.9 nm et rapportés à une même intensité des bandes étalons. On voit nettement que par exemple pour $Fe(C_2O_4)^+$ l'intensité de deux bandes 1395 et 270 cm^{-1} est multipliée par 4 environ et celle à 1394 cm^{-1} du complexe $Fe(C_2O_4)_2^-$ est multipliée par 7.

Conclusion

L'étude systématique des solutions colorées d'acide oxalique et de chlorure de fer(III) par spectrométrie Raman, a permis de confirmer sans ambiguité la formation des trois complexes successifs: $Fe(C_2O_4)^+$, $Fe(C_2O_4)_2^-$, $Fe(C_2O_4)_3^{3-}$ et de rejeter l'existence d'une espèce protonée et celle d'une espèce polynucléaire, proposées antérieurement. L'enregistrement des spectres qui n'avait pu avoir lieu jusqu'à présent a été réalisé grâce à un dispositif particulier.

Chacune des espèces mises en évidence est caractérisée par un spectre Raman spécifique. Cependant, compte tenu de la nécessité de travailler à forte concentration et de la très grande stabilité des complexes qui se forment en milieu très acide, il n'a pas été possible de déterminer avec précision la concentration des espèces et d'en proposer une répartition en fonction du pH.

La comparaison entre les spectres ir et Raman des trioxalates de fer(III) et d'aluminium et l'évolution de l'intensité des bandes Raman des trois complexes en fonction de la longueur d'onde de la raie excitatrice du laser ont permis de montrer que les spectres de diffusion des oxalatoferrates présentent un effet de pré-résonance Raman.

1. J. LAMBLING. Bull. Soc. Chim. Fr. 495 (1949).
2. J. BADOZ-LAMBLING. Ann. Chim. Paris, **8**, 586 (1953).
3. A. BABKO et L. DUBOYENKO. Zh. Obshch. Khim. **26**, 660 (1956).

4. D. GRADDON. Chem. Ind. 80 (1956).
5. D. GRADDON. J. Inorg. Nucl. Chem. **3**, 308 (1956).
6. N. DUTT et B. BIMARES. Zh. Anorg. Allgem. Chem. **293**, 195 (1957).
7. V. PARAMONOVA et S. BARTENEV. Zh. Neorg. Khim. **8**, 157 (1963).
8. R. BAUER et M. VILLAFIORITTA. Gazzeta, **95**, 1247 (1965).
9. J. LLOPIS et R. POSADO. Electrochim. Acta, **13**, 1131 (1968).
10. M. DENEUX, R. MEILLEUR et R. BENOIT. Can. J. Chem. **46**, 1383 (1968).
11. V. ZOLOTUKHIN. Zh. Neorg. Khim. USSR, **13**, 702 (1968).
12. K. YAKULOV, V. PAL CHEYSCU, M. MANSUROV et V. KUVSHINOV. Dokl. Akad. Nauk Tadzh. **12**, 33 (1969).
13. J. SHAH et R. PATEL. J. Ind. Chem. Soc. **48**, 1075 (1971).
14. G. COOPER. Ph.D., University of Virginia, no 72-33, 230 (1972).
15. J. SHAH et R. PATEL. J. Prakt. Chem. **315**, 983 (1973).
16. J. SHAH et R. PATEL. Curr. Sci. **42**, 236 (1973).
17. I. MURGULESCU et J. PAUN. Rev. Roum. Chim. **20**, 1195 (1975).
18. M. PATEL, J. SHAH et R. PATEL. J. Ind. Chem. Soc. Vol. L11, 882 (1975).
19. S. FRONAEUS et R. LARSSON. Acta Chem. Scand. **14**, 1364 (1960).
20. E. MOORHEAD et N. SUTIN. Inorg. Chem. **5**, 1866 (1966).
21. R. BAUER et W. MACF SMITH. Can. J. Chem. **43**, 2755 (1965).
22. H. MURATA et K. KAWAI. J. Chem. Phys. **25**, 796 (1956).
23. R. GAUFRES et J. MATHIEU. C. R. Acad. Sci. Paris, **248**, 81 (1958).
24. J. MATHIEU et H. POULET. J. Chem. Phys. **59**, 369 (1962).
25. R. HESTER et R. PLANE. Inorg. Chem. **3**, 513 (1964).
26. V. SAMINI, R. BELDIE et M. DAMASCHIN. Rev. Roum. Chim. **11**, 1361 (1966).
27. J. VAISSERMAN. C. R. Acad. Sci. Paris S.B. **270**, 948 (1970).
28. J. GOUTERON. J. Inorg. Nucl. Chem. **38**, 55 (1976).
29. M. JABER. Thèse Lyon, no 78-01 (1978).
30. M. JABER, F. BERTIN et G. THOMAS-DAVID. Can. J. Chem. **55**, 3689 (1977).
31. M. JABER, F. BERTIN et G. THOMAS-DAVID. Can. J. Chem. **56**, 777 (1978).
32. M. JABER, F. BERTIN, G. THOMAS-DAVID et M. T. FOREL. C. R. Acad. Sci. Paris, **284**, 717 (1977).
33. M. JABER, F. BERTIN et G. THOMAS-DAVID. Spectrochim. Acta, **34A**, 1093 (1978).
34. L. SILLEN et A. MARTELL. Stability constants of metal-complexes 1964 et 1971, The Chemical Society, London.
35. S. SHARMA. J. Inorg. Chem. **35**, 3831 (1973).
36. S. SHARMA. J. Chem. Phys. **60**, 1368 (1974).
37. S. SHARMA, V. SEHGAL, H. BAMI et S. SHARMA. J. Inorg. Nucl. Chem. **37**, 2417 (1975).
38. A. MARSTON et S. BUSH. Appl. Spectrosc. **26**, 579 (1972).
39. T. STREKAS, D. ADAMS, A. PACKER et T. SPIRO. Appl. Spectrosc. **28**, 324 (1974).
40. T. MEJEAN, F. GRUEGE et M. T. FOREL. Nouv. J. Chim. **1**, 121 (1977).

Can. J. Chem. Downloaded from www.nrcresearchpress.com by 210.87.254.40 on 09/05/12
For personal use only.

Molecular rearrangements.[1] Part XVI. Thermolysis and photolysis of *N*-benzyldiphenylamine and *N*-phenylacetyldiphenylamine

M. Z. A. Badr, M. M. Aly, and A. M. Fahmy

Chemistry Department, Faculty of Science, Assiut University, Assiut, Egypt, A.R.E.

Received October 25, 1979

M. Z. A. Badr, M. M. Aly, and A. M. Fahmy. Can. J. Chem. **58**, 1229 (1980).

Heating *N*-phenylacetyldiphenylamine in a sealed tube at 360°C gave rise to carbon monoxide, bibenzyl, toluene, stilbene, diphenylmethane, aniline, carbazole, *N*-benzylcarbazole, acridine, 9-phenylacridine, 4-aminotriphenylmethane, diphenylamine, *p*-benzyldiphenylamine, and *o*-aminodiphenylmethane. A similar result was also obtained on heating *N*-benzyldiphenylamine, with the exception of carbon monoxide. Such results in addition to those obtained from photolysis of *N*-phenylacetyldiphenylamine are interpreted in terms of a free-radical mechanism.

M. Z. A. Badr, M. M. Aly et A. M. Fahmy. Can. J. Chem. **58**, 1229 (1980).

Le chauffage de la *N*-phénylacétyldiphénylamine dans un tube scellé à 360°C conduit à la formation des produits suivants: monoxyde de carbone, bibenzyle, toluène, stilbène, diphénylméthane, aniline, carbazole, *N*-benzylcarbazole, acridine, phényl-9 acridine, amino-4 triphénylméthane, diphénylamine, *p*-benzyldiphénylamine et *o*-aminodiphénylméthane. On obtient les mêmes résultats en chauffant la *N*-benzyldiphénylamine à l'exception de la formation du monoxyde de carbone.On interprète ces résultats en plus de ceux obtenus par la photolyse de la *N*-phénylacétyldiphénylamine en fonction d'un mécanisme faisant intervenir un radical libre.

[Traduit par le journal]

The pyrolysis of diphenylamine by passing through a red-hot tube was reported in 1916 (1) to lead to the formation of carbazole. The photoconversion of diphenylamines to carbazoles has been subjected to extensive investigation by many workers (2–4).

The present work throws light on the mechanistic behaviour of *N*-phenylacetyldiphenylamine and *N*-benzyldiphenylamine on their thermolysis and photolysis.

Thermolysis of *N*-phenylacetyldiphenylamine by heating in a sealed tube under nitrogen atmosphere at ca. 360°C for 7 days gives rise to the products shown in Table 1.

The nature of the products suggests the preliminary homolysis of the acyl—N bond giving phenylacetyl and diphenylaminyl radicals. The phenylacetyl radicals decarbonylate (5) forming benzyl radicals which subsequently contribute to the formation of toluene, bibenzyl, and *trans*-stilbene as discussed in a previous work (6) or substitute on diphenylamine (formed through H-abstraction by diphenylaminyl radicals) in the *ortho*- and *para*-positions giving *o*-benzyldiphenylamine and its *p*-isomer (Scheme 1).

9-Phenylacridine is supposed to be formed from its precursor *o*-benzyldiphenylamine through consecutive cyclization and dehydrogenation processes (Scheme 2).

Furthermore, the benzyl radicals may undergo a reversible C—N coupling with diphenylaminyl radicals forming *N*-benzyldiphenylamine that subsequently rearranges into α-anilinodiphenylmethane through N—C phenyl migration from the free radical (I) into (II), probably through a bridged radical intermediate. The rearranged product, α-anilinodiphenylmethane, in turn undergoes pyrolysis forming ultimately aniline, diphenylmethane, and 4-aminotriphenylmethane. This hypothesis was further confirmed by the similar results which were obtained on heating *N*-benzyldiphenylamine under the same conditions (cf. Table 1). Moreover, thermolysis of α-anilinodiphenylmethane affords the formation of aniline, 4-aminotriphenylmethane, and diphenylmethane through homolysis of the C—N bond into anilino and diphenylmethyl free radicals that selectively abstract H, forming aniline and diphenylmethane, respectively, and/or undergo C—C coupling in the *para*-position of aniline, forming 4-aminotriphenylmethane together with a resinous polymeric material of unidentified structure.

The *o*- and *p*-semidine derivatives obtained by Welzel *et al.* (7), due to C—N dimerization of diphenylaminyl radicals generated through thermolysis of tetraphenylhydrazine, were not detected by us, due to the presence of the relatively more reactive benzyl radicals that ultimately change the fate of diphenylaminyl radicals through coupling at the *ortho*- and *para*-positions, forming the benzyldiphenylamines identified among the products. On the other hand, the instability of the

[1]For Part XV see ref. 21.

0008-4042/80/121229-04$01.00/0

©1980 National Research Council of Canada/Conseil national de recherches du Canada

Can. J. Chem. Downloaded from www.nrcresearchpress.com by 210.87.254.40 on 09/05/12
For personal use only.

Can. J. Chem. Downloaded from www.nrcresearchpress.com by 210.87.254.40 on 09/05/12
For personal use only.

TABLE 1. Products of thermolysis of *N*-phenylacetyldiphenylamine and *N*-benzyldiphenylamine in g (%)

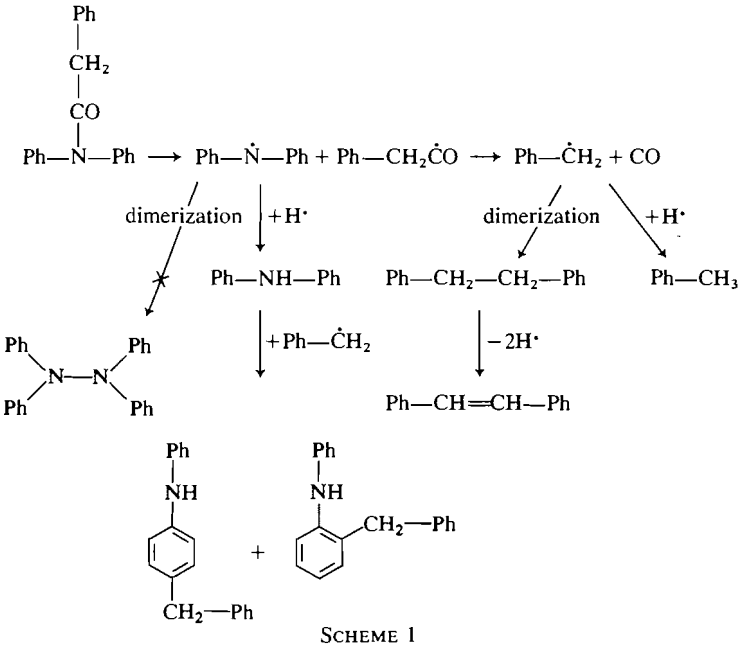
Products	Boiling point °C/Torr	*N*-Phenylacetyl-diphenylamine		*N*-Benzyl-diphenylamine	
Carbon monoxide		Evolved		—	
Toluene[a]	110/760	1.30	(4.48)	1.70	(6.54)
Diphenylmethane[b]	90–92/2	0.45	(1.55)	0.60	(2.31)
Bibenzyl[c]	98–100/2	1.50	(5.17)	2.10	(8.07)
trans-Stilbene[d]	130–135/2	1.70	(5.86)	2.20	(8.46)
Aniline[e]	47–55/2	0.42	(1.45)	[m]	
Diphenylamine[f]	132–138/2	5.30	(18.27)	6.20	(23.85)
o- and *p*-Aminodiphenylmethane[h]	145–150/2	1.87[h]	(6.45)	[n]	
Acridines[i]	210–215/2	3.70	(12.76)	4.30	(16.54)
p-Benzyldiphenylamine[j]	240–246/2	2.25	(7.75)	2.40	(9.23)
4-Aminotriphenylmethane[k]	252–255/2	1.30	(4.48)	[o]	
Carbazole and *N*-benzylcarbazole[l]	260–265/2	4.80	(16.55)	5.21	(20.04)
Residue	Non-volatile	1.80	(6.20)	1.25	(4.80)

[a] n_D^{20}: 1.4970; 2,4-dinitro derivative mixture mp 72°C.
[b] n_D^{27}: 1.5788; on oxidation with $K_2Cr_2O_7/H_2SO_4$ gave benzophenone; dinitrophenylhydrazone derivative mp, and mixture mp 237–238°C.
[c] Mixture mp 52°C; 4,4′-dinitro derivative mixture mp, 179–180°C.
[d] Mixture mp 124°C.
[e] n_D^{20}: 1.5836; acetyl derivative mp and mixture mp 113–114°C.
[f] Melting point and mixture mp 54°C, picrate mixture mp 182°C.
[h] Separated by column chromatography on silica gel (100–150 mesh) using benzene as eluent into *o*-isomer 0.15 g, acetyl derivative mixture mp 135°C and *p*-isomer 1.50 g, picrate mixture mp 179°C.
[i] 9-Phenyl acridine mixture mp 182–183°C, picrate mixture mp 185–186°C, and a trace amount of acridine as found by tlc, R_f values 0.54 and 0.65, respectively.
[j] Mixture mp 197–199°C.
[k] Mixture mp 199–200°C.
[l] Identified by preparative tlc using ether – petroleum ether (40–60°), 1:7 v/v, as eluent; carbazole R_f 0.35, picrate mp 185°C and *N*-benzylcarbazole R_f 0.27, picrate mp 104–105°C.
[m] Present as trace amount not more than 0.1% in diphenylamine fraction as found by preparative tlc; $R_{f(aniline)}$ 0.76, acetyl derivative mixture mp 113–114°C.
[n] Present as trace amount not more than 0.1% in acridine fraction as found by preparative tlc; $R_{f(ortho)}$ 0.72 and $R_{f(para)}$ 0.69 and their ir spectra are coincident with authentic samples.
[o] Present as trace amount not more than 0.1% in carbazole fraction as found by preparative tlc; R_f 0.46, and was further identified by coincidence of its ir spectrum with that of an authentic sample.

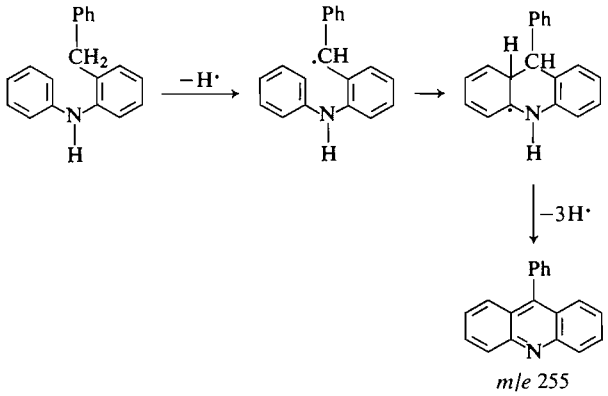
expected N—N coupling product tetraphenylhydrazine (7) under the conditions used must be responsible for its absence among the products.

The plausible explanation for carbazole formation is through cyclization of diphenylaminyl radicals (Scheme 4) and not from diphenylamine, since prolonged heating of diphenylamine under the same conditions does not afford carbazole.

The *o*- and *p*-aminodiphenylmethanes can reasonably be assumed to form through coupling of



SCHEME 1



SCHEME 2

benzyl and phenylaminyl radicals. The *o*-isomer undergoes cyclization into acridine as described in a previous work (8) whereas the *p*-isomer remains unattacked.

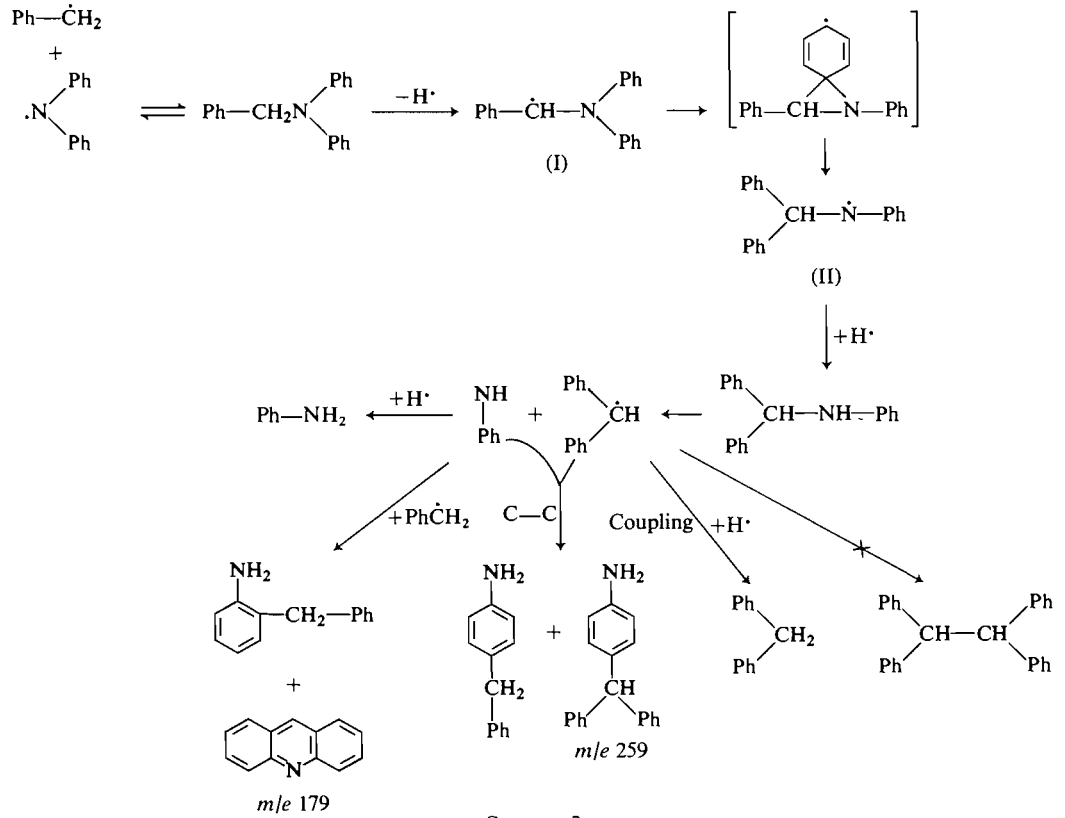
Thermolysis of *N*-benzyldiphenylamine by heating in a sealed tube at ca. 360°C for 7 days gives rise to the same products as those obtained from thermolysis of *N*-phenylacetyldiphenylamine with the exception of carbon monoxide. Although some of the products are present in trace amounts due to the variable rate of decay of the free radical intermediates, yet their presence is of great importance for mechanistic interpretation. Such results can be explained by homolysis of the benzyl—N bond, furnishing benzyl and diphenylaminyl radicals that follow the previously mentioned chain sequence.

Irradiation of *N*-phenylacetyldiphenylamine in carbon tetrachloride as an aprotic solvent for 60 h leads to the formation of diphenylamine, *N*-benzyldiphenylamine, carbazole, 9-phenylacridine, *N*-benzylcarbazole, and *p*-benzyldiphenylamine as the only amine products. It is noteworthy that aniline, 4-aminotriphenylmethane, *o*- and *p*-aminodiphenylmethanes are absent among the products as detected by tlc.

Such main differences between thermolysis and photolysis indicate that the benzyl and diphenylaminyl radicals are held together within the solvent cage following a route analogous to Schemes 1, 2, and 4 rather than forming α-anilinodiphenylmethane as a preliminary product.

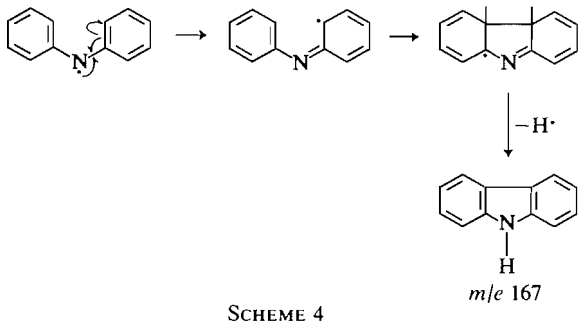
Experimental

All melting points are uncorrected. The ir spectroscopic analyses were carried out on a Pye-Unicam ir spectrophotometer, model SP 200G. The uv absorptions were carried out on a Pye-Unicam uv spectrophotometer, model SP 8000 using 95% ethanol as solvent. Gas–liquid chromatographic analysis was carried out on a Pye-Unicam gas chromatograph, "Series 104",



SCHEME 3

Can. J. Chem. Downloaded from www.nrcresearchpress.com by 210.87.254.40 on 09/05/12
For personal use only.



SCHEME 4

dual flame ionization detector, model 24, and the columns used were 4 ft × 5 mm packed with 20% SE30 on Chromosorb W (35–80 mesh) at 180°C and/or 10% SE30 on Celite (60–80 mesh). Thin-layer chromatography was carried out on plates covered with silica gel (25–40 mesh) and eluted with benzene–cyclohexane (3:1 v/v) or ether – petroleum ether (40–60°C) (1:7 v/v). Ultraviolet irradiation was carried out using a Mallinkrodt 150 W mercury discharge lamp.

Solvents used were of AnalaR grade and were used without further purification.

Molecular weight determinations of some reaction products were carried out by mass spectrophotometer, model A.E.I.M.S. 902.

Thermolysis of N-*Phenylacetyldiphenylamine and* N-*Benzyldiphenylamine*

N-Phenylacetyldiphenylamine (29 g, 0.1 mol) or *N*-benzyldiphenylamine (26 g, 0.1 mol) was heated in a sealed tube under nitrogen at about 360°C for 7 days. The tube was chilled in ice, opened, and the carbon monoxide formed in the case of *N*-phenylacetyldiphenylamine was detected by platinum chloride test paper and by absorption in a trap containing ammoniacal cuprous chloride (6). The products were separated as indicated in a previous work (6) and identified by elemental analysis, ir spectroscopy, and mixture mp determination with authentic samples and their derivatives, whenever possible, as summarized in Table 1.

Thermolysis of α-*Anilinodiphenylmethane*

α-Anilinodiphenylmethane (10 g) was heated in a sealed tube under nitrogen for 3 days and was worked up as mentioned previously to afford 4-aminotriphenylmethane (3.6 g, 36%), aniline (1.2 g, 12%), diphenylmethane (2.3 g, 23%), and a resinous polymeric material (2.4 g).

Photolysis of N-*Phenylacetyldiphenylamine*

N-Phenylacetyldiphenylamine (1 g) in carbon tetrachloride (100 mL) was irradiated at room temperature (25°C) for 60 h. The photolysate was separated into neutral and amine products. The neutral products were identified by glc as bibenzyl and stilbene in the ratio 1:2.5. The amine products were identified by tlc and their R_f values are indicated using ether – petroleum ether (40–60°C) (1:7, v/v) as eluent: diphenylamine (0.81), *p*-benzyldiphenylamine (0.76), *N*-benzyldiphenylamine (0.64), carbazole (0.35), *N*-benzylcarbazole (0.27), and 9-phenylacridine (0.21).

Preparation of Reference Compounds

N-*Benzyldiphenylamine* (ref. 9): needles from ethanol, mp 85–86°C.

N-*Phenylacetyldiphenylamine* (ref. 10): crystallized from ether, mp 73–74°C.

Bibenzyl (ref. 11): crystallized from ethanol, mp 52°C; 4,4′-dinitro derivative, mp 180°C.

trans-*Stilbene* (ref. 12): crystallized from ethanol, mp 123–124°C.

Diphenylmethane (ref. 13): crystallized from petroleum ether (40–60°C), mp 26°C, n_D^{27}: 1.5788.

9-Phenylacridine (ref. 14): yellow prisms from ethanol, mp 182–183°C; picrate, mp 185–186°C.

o-*Aminodiphenylmethane* (ref. 15): crystallized from petroleum ether (40–60°C), mp 51–52°C, acetyl derivative, 135°C.

p-*Aminodiphenylmethane* (ref. 16): crystallized from petroleum ether (40–60°C), mp 34–35°C; picrate, mp 179°C.

α-*Anilinodiphenylmethane* (ref. 17): prisms from ethanol, mp 58°C; bp 224°C/12 Torr; HCl salt, mp 202–203°C.

4-Aminotriphenylmethane (ref. 18): crystallized from ethanol, mp 199–201°C.

N-*Benzylcarbazole* (ref. 19): crystallized from ethanol, mp 114–116°C, picrate, mp 105°C.

p-*Benzyldiphenylamine* (ref. 20): crystallized from ethanol, mp 199°C.

1. H. MEYER and A. W. HOFFMANN. Monatsh. **37**, 681 (1916).
2. K. H. GRELLMAN, G. M. SHERMAN, and H. LINSCHITZ. J. Am. Chem. Soc. **85**, 1881 (1963).
3. E. J. BOWEN and J. H. D. ELAND. Proc. Chem. Soc. London, 202 (1963).
4. H. LINSCHITZ and K. H. GRELLMAN. J. Am. Chem. Soc. **86**, 303 (1964).
5. E. S. HUYSER. Free-radical chain reactions. J. Wiley, New York. 1970. p. 153, and references cited therein; M. Z. A. BADR, M. M. ALY, and F. F. ABDEL-LATIF. J. Org. Chem. **44**, 3244 (1979).
6. M. Z. A. BADR, M. M. ALY, and S. S. SALEM. Tetrahedron, **33**, 3155 (1977).
7. P. WELZEL. Chem. Ber. **103**, 1318 (1970); P. WELZEL, L. GUNTHER, and G. ECKHARDT. Chem. Ber. **107**, 3624 (1974); P. WELZEL, I. MUTHER, and H. VOLK. Tetrahedron Lett. **9**, 745 (1977).
8. M. Z. A. BADR and M. M. ALY. Can. J. Chem. **52**, 293 (1974).
9. R. MELDOLA. Ber. **14**, 1385 (1881); **15**, 1580 (1882).
10. W. WISLICENUS and R. ERBE. Ann. **421**, 119 (1920); Chem. Abstr. **15**, 503 (1921).
11. L. CANNIZARO and G. ROSSI. Ann. **251**, 121 (1862).
12. D. A. BALLARD and W. M. DEHN. J. Am. Chem. Soc. **54**, 3969 (1932).
13. A. I. VOGEL. Practical organic chemistry. Longmans, London. 1956. p. 513.
14. A. BERNTHREN. Ann. **224**, 13 (1884).
15. C. L. HEWETT, L. J. LERMIT, H. T. OPENSHOW, A. R. TODD, A. H. WILLIAMS, and F. N. WOODWARD. J. Chem. Soc. 292 (1948).
16. W. J. HICKINBOTTOM. J. Chem. Soc. 1119 (1937).
17. A. SKITA. Ber. **48**, 1685 (1915).
18. A. RINCK. Ber. **38**, 1767 (1905).
19. B. LEVY. Monatsh. **33**, 183 (1912).
20. R. MELDOLA. J. Chem. Soc. **41**, 198 (1882).
21. M. Z. A. BADR, M. M. ALY, G. M. EL-NAGAR, and A. M. FAHMY. Z. Naturforsch. Teil B, **34**, 1128 (1979).

Can. J. Chem. Downloaded from www.nrcresearchpress.com by 210.87.254.40 on 09/05/12
For personal use only.

The reaction of malondiamides with disulfur dichloride: a reinvestigation

GERALD W. KUTNEY AND IAN W. J. STILL
Erindale College, University of Toronto, Mississauga, Ont., Canada L5L 1C6

Received August 22, 1979

GERALD W. KUTNEY and IAN W. J. STILL. Can. J. Chem. **58**, 1233 (1980).

The reactions of a series of *N, N'*-dialkyl and *N,N'*-diaryl malondiamides with disulfur dichloride have been reinvestigated. The claim, made almost 60 years ago, that the products of this reaction are dithioketones R_2CS_2, is shown to be unfounded. The structures of these products are shown to be the symmetrically substituted 1,2,4,5-tetrathianes, **8***a–e*.

GERALD W. KUTNEY et IAN W. J. STILL. Can. J. Chem. **58**, 1233 (1980).

On a de nouveau étudié les réactions d'une série de *N,N'*-dialkyle et de *N,N'*-diaryle malonediamides avec le disulfure de chlore. Contrairement à ce qu'on pensait il y a de cela près de 60 ans, les produits de la réaction ne sont pas les dithiocétones R_2CS_2. On démontre que les produits sont les tétrathianes (**8***a–e*) substituées d'une façon symétrique en positions 1,2,4,5.

[Traduit par le journal]

Introduction

Although the first literature reports of the reaction of sulfur chlorides (S_2Cl_2 and SCl_2) with active methylene compounds are now almost 100 years old (1, 2), the apparent complexity of these reactions and the unusual nature of some of the products claimed have ensured a continuing, albeit sporadic, interest in the topic which has manifested itself in a number of recent publications (3–6). A closely related topic, which has also generated a good deal of recent interest, is the reaction of similar active methylene compounds with thionyl chloride (7–9).

The impetus for our present study, involving mainly the reactions of disulfur dichloride (sometimes referred to as sulfur monochloride) with active methylene compounds, was the intriguing, but so far unverified, report by Naik (10) that *N,N'*-diphenylmalondiamide **1***d* and related malondiamide derivatives afforded the "dithioketone" (thiosulfine) products **2**, formulated also by Naik as the dithiirane species **3**. The evidence for the "dithioketone" rested largely on the results of further chemical transformations of **2** and on the elemental analysis data. The fact that, almost 60 years later, no compound possessing the structural features of either **2** or **3** has been isolated [1] indicated to us that Naik's proposed structures were probably incorrect. In addition, the work of Hope and Wiles (4), which claimed that *N,N'*-diphenylmalondiamide and disulfur dichloride, when refluxed in benzene (the solvent used by Naik) in a 1:1 molar ratio, produced the tetrasulfide **4** ($n = 4$, $R = C_6H_5$) in 86% yield, appeared to be at variance not only with the results claimed by Naik but also with the behavior of another simple β-dicarbonyl compound, ethyl acetoacetate. Gompper *et al.* (3) had shown one year previously that ethyl acetoacetate on treatment with disulfur dichloride in a 2:1 molar ratio at 25°C in petroleum ether produced the simple symmetrical sulfide derivative **5**. Hope and Wiles (4) also demonstrated an apparent sensitivity of the reaction with disulfur dichloride to solvent effects by showing that malondiamide itself reacted only in refluxing dioxane, and not in refluxing benzene, to produce the trisulfide **4** ($n = 3$, $R = H$). Pizey and Symeonides (12) have very recently claimed the formation of di- or trisulfide type products on treatment of 2,4-pentanedione with disulfur dichloride, depending on the reaction conditions. Thus, all types of S_n-linked β-dicarbonyl compound from $n = 1$ to $n = 4$ have been reported. It seems clear, however, that a number of questions remain to be answered in this area and we have attempted to address these in the present paper.

[1]Several authors have claimed the intermediacy of such species in certain reactions. See, for example, one very recent report by Senning (11).

Results and Discussion

In order to investigate the reaction of β-dicarbonyl compounds of the *N,N'*-diphenylmalondiamide type with disulfur dichloride a series of *N,N'*-disubstituted malondiamides **1***a–h* was prepared by a standard literature route (13) by refluxing diethyl malonate with the appropriate primary amine. The products obtained, with the yields and some physical properties, appear in Table 1. Attempts to prepare the di-*tert*-butyl and di-4-nitrophenyl analogues by this route, or from malonyl dichloride, were unsuccessful. It will be noted from Table 1 that yields of the *N,N'*-dialkylmalondiamides were generally much higher than for their diaryl counterparts.

Preliminary examination of the products from

0008-4042/80/121233-06$01.00/0
©1980 National Research Council of Canada/Conseil national de recherches du Canada

Can. J. Chem. Downloaded from www.nrcresearchpress.com by 210.87.254.6 on 09/05/12
For personal use only.

Can. J. Chem. Downloaded from www.nrcresearchpress.com by 210.87.254.6 on 09/05/12
For personal use only.

TABLE 1. *N,N'*-Disubstituted malondiamides, **1***a–h*

R	Yield[a] (%)	Melting point (°C)	Lit. mp (ref.) (°C)	^{1}H nmr (δ)[b,c] —NH—	^{1}H nmr (δ)[b,c] —CH_2—	^{13}C nmr(δ)[b,c] —$COCH_2CO$—
n-C_3H_7, **1***a*	82	135–137	139(13)	7.1	2.9–3.3	—
iso-C_3H_7, **1***b*	28	109–114	115(14)	7.1	3.09	41.5
$C_6H_5CH_2$, **1***c*	84	133–135	142(13)	7.5	3.25	—
C_6H_5, **1***d*	69	225–227	225(13)	10.13	3.49	45.7
4-$CH_3C_6H_4$, **1***e*	35	251–253	250(13)	10.00	3.37	—
4-$CH_3OC_6H_4$, **1***f*	17	233–234	226–228(15)	10.09	3.78	45.4
n-C_4H_9, **1***g*	89	128–129	132(13)	7.55	3.0–3.4	—
2,4-$C_6H_3Cl_2$, **1***h*	13	210–212	214(16)	10.08	3.73	—

[a]Isolated yields of the diamides, recrystallized at least twice from ethanol.
[b]Spectra of compounds **1***a, b, c, g* were recorded in $CHCl_3$-*d*; those for entries **1***d, e, f, h* in DMSO-d_6.
[c]^{13}C nmr data showed δ for the C=O carbon consistently at 165–166 ppm.

the reaction of *N,N'*-disubstituted malondiamides with S_2Cl_2 in refluxing benzene (the conditions used by Naik (10)) indicated that these easily isolated, white crystalline solids were fully substituted on the central methylene carbon atoms, since no ^{1}H nmr signals attributable to —CO*CH*CO— or —COCH_2CO— groupings, or to enolic protons (17), were present (cf. Table 1 for nmr data of starting compounds). This seemed to indicate that the type of product **4**, reported by Hope and Wiles (4), was not formed under our conditions and we were thus left to conclude that (*a*) one of Naik's suggested structures **2** or **3** for these products was correct or (*b*) that some other structural feature which explained the ^{1}H nmr results must be present. In the latter case, we felt that the most reasonable structures to be considered were the 1,3-dithietane **6**, the 1,2,4-trithiolane **7**, or the 1,2,4,5-tetrathiane **8**. Around this time we were interested to discover a recent correction to a literature report of some 50 years earlier proposing the intriguing structure **9** for a reaction product. Berry *et al.* (18) have shown, using mass spectral and ^{125}Te Mössbauer studies, that **9** should in fact be formulated as the dimeric compound **10**. The obvious analogy between this situation and the one which we were investigating encouraged us to explore this possibility further. It is interesting to note in passing that the reaction of ethylamine with S_2Cl_2 has been reported to give the tetrathiane derivative **11***a* (19), while, more recently, Appel and Montenach (20) have reported the isolation of the analogue **11***b*, by the reaction of *N*-trimethylsilylbenzenesulfonamide with S_2Cl_2.

The results of the reactions of several malondiamide derivatives with S_2Cl_2 in a 1:2 molar ratio are summarized in Table 2, along with the major ^{1}H and ^{13}C nmr features of the products (*N,N'*-di-2,4-dichlorophenylmalondiamide gave a complex mixture of products in addition to a 36% recovery of the starting material). Elemental analysis data confirmed the empirical formulas to be as reported by Naik (10), which eliminates structures **6** and **7** from consideration. In the ^{1}H nmr spectra the main feature of interest concerns the chemical shift of the NH protons which appeared at around 7 ppm in the *N,N'*-dialkyl examples, as they had in the starting malondiamides, but at around 9 ppm in the diaryl examples. The apparent upfield shift (compared to

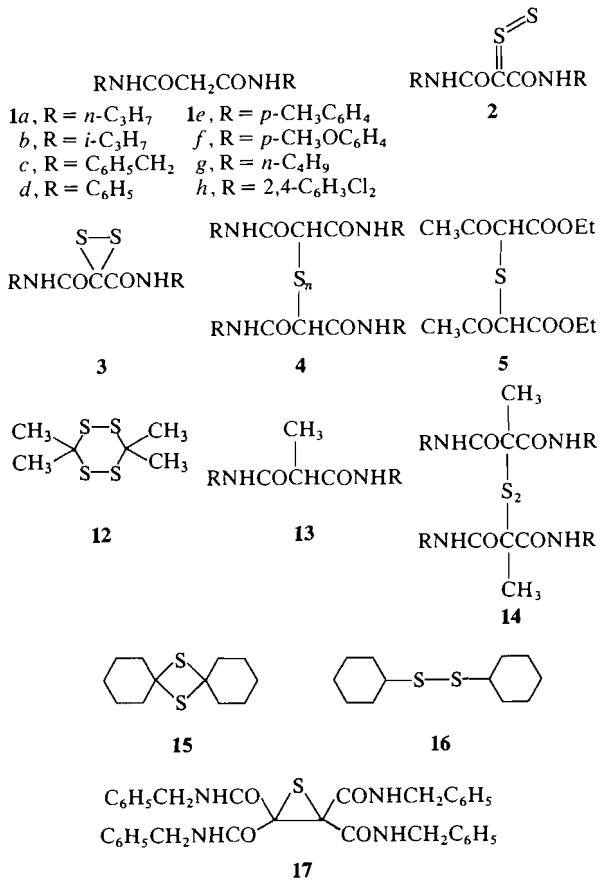


TABLE 2. Tetrathianes (**8***a–f*) from reactions of malondiamides (**1***a–f*) with S_2Cl_2

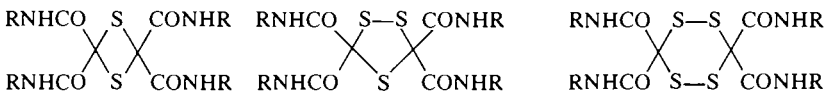
R	Yield[a] (%)	Melting point[b] (°C)	^{1}H nmr[c,d] N—H(δ)	^{13}C nmr[c,d] S,S (δ)	^{13}C nmr[c,d] C=O (δ)
n-C_3H_7, **8***a*	80	195–195.5	7.15	73.9	166.1
iso-C_3H_7, **8***b*	90	230 (dec.)	6.93	74.0	165.4
$C_6H_5CH_2$, **8***c*	92	194–195 (dec.)	(7.08–7.63)	73.9	162.2
C_6H_5, **8***d*	85	185–196 (dec.)	8.92	73.2[e]	[e]
4-$CH_3C_6H_4$, **8***e*	77	190–219 (dec.)	8.88	75.3	164.1
4-$CH_3OC_6H_4$, **8***f*	[f]	—	8.83	—	—

[a]Isolated, but unrecrystallized.
[b]Recrystallized three times from ethanol or until no impurities detectable by tlc or nmr.
[c]In $CHCl_3$-*d* unless otherwise stated.
[d]For full nmr spectra, see Experimental.
[e]In DMSO-d_6.
[f]This product appeared to be present from the ^{1}H nmr spectrum but decomposed upon (repeated) attempts at purification.

the starting compounds **1**) in the latter cases is almost certainly the result of a solvent change from DMSO-d_6 to $CHCl_3$-d_1. Not unexpectedly, we have also found the NH proton chemical shifts to vary significantly with concentration. The ^{13}C nmr chemical shifts for the fully-substituted central carbon atoms (former methylene group) and the carbonyl carbons also appear in Table 2. It should be noted that, although no data exist in the literature for direct comparison, the relatively high-field location of the former set of signals at ca. 73–75 ppm is much more in accord with the presence of an sp^3-hybridized carbon, such as is present in **8***a–e*, than the sp^2-hybridized carbon required by Naik's proposed structure **2**. Data have appeared in the literature for the ^{13}C nmr chemical shifts for a series of 2,2-disubstituted 1,3-dithianes (21), which appear in the range 45–54 ppm, and some ketone dithioacetals (22), with δ values even closer to those in Table 2, in the range 55–65 ppm. The model compound, 3,3,6,6-tetramethyl-1,2,4,5-tetrathiane **12**, was synthesized by a known procedure (23) and found to show a chemical shift of δ 59.1 for the quaternary carbons. In the series of tetrathianes **8***a–e* one would expect this value to be shifted to lower field by the presence of two carbonyl-bearing groups at each quaternary position.

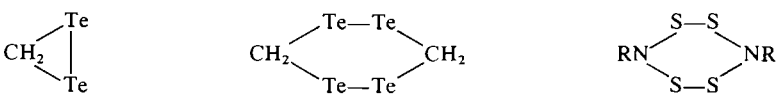
Clearly, the most effective method to distinguish the possible structure type **8** from the "monomeric" structures such as **2**, **3** proposed by Naik, is to determine the molecular weights of the products in Table 2. Mass spectral evidence for a molecular ion peak was obtained only in the case of the *N,N'*-diisopropyl analogue. Significantly, however, fragment ions at *m/e* values substantially greater than called for by molecular formulas of type **2** or **3** were found in all cases. We then turned to other methods of molecular weight determination and the results of some Rast camphor melting point depression measurements and osmometric determinations are collected in Table 3. The results are in very good agreement with the 1,2,4,5-tetrathiane structure **8** for the products in Table 2. Determinations were not made in all cases, given the already demonstrated similarities in the nmr spectra of these compounds (Table 2).

The remaining points of interest in this investigation concern a possible mechanism for the conversion of **1** by S_2Cl_2 into **8** and an explanation for the formation of the acyclic tetrasulfide products in the work of Hope and Wiles (4). We have carried



6 **7**

8*a*, R = *n*-C_3H_7 **8***d*, R = C_6H_5
b, R = *i*-C_3H_7 *e*, R = *p*-$CH_3C_6H_4$
c, R = $C_6H_5CH_2$ *f*, R = *p*-$CH_3OC_6H_4$



9 **10**

11*a*, R = C_2H_5
11*b*, R = $SO_2C_6H_5$

Can. J. Chem. Downloaded from www.nrcresearchpress.com by 210.87.254.6 on 09/05/12
For personal use only.

Can. J. Chem. Downloaded from www.nrcresearchpress.com by 210.87.254.6 on 09/05/12
For personal use only.

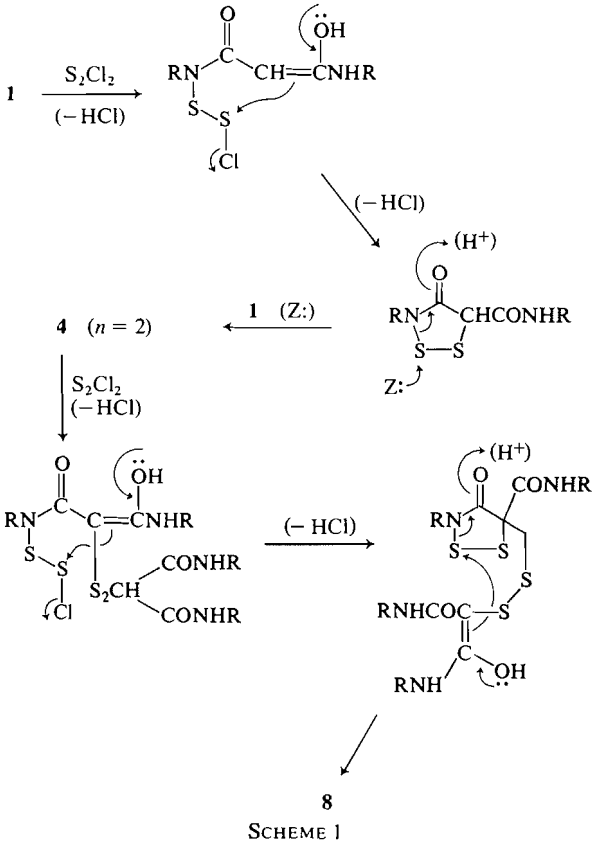
out a number of experiments using *N,N'*-dibenzylmalondiamide and S_2Cl_2, varying factors such as number of equivalents of S_2Cl_2, temperature, and reaction time. In no case was any product other than the tetrathiane **8***c* isolated, although lowering the reaction temperature and reducing the amount of disulfur dichloride present from 2 to 0.5 equivalents sharply reduced the yields obtained.[2] There was no evidence for the formation of any disulfide **4** ($n = 2$, R = $C_6H_5CH_2$), in accordance with Naik's results (10), nor could we detect any evidence for an intermediate monosubstituted malondiamide of this general type when the reaction was monitored throughout by nmr. It seems to us that those findings, and other features such as the lack of formation of tetrathianes with tertiary malondiamides and also the much greater reactivity (towards S_2Cl_2) of all the malondiamides studied than simple β-diketones such as 2,4-pentanedione,[3] can be accounted for by an initial *N*-sulfenylation step and the possible, although not essential, intermediacy of a 1,2,3-dithiazolidine, as shown in Scheme 1. *N*-Sulfenylation with S_2Cl_2 is well precedented, not only for amides (4) but also for aromatic amines (24) and, very recently, for ketone hydrazones (25) where, interestingly, the authors also propose a dithioketone intermediate. It is of interest to note that the methylmalondiamides **13** were reported to readily form disulfides **14** with disulfur dichloride, possibly via a similar pathway (10, 26).

One interesting observation which may explain the isolation of the acyclic tetrasulfide **4** ($n = 4$) by Hope and Wiles was our finding that increasing the reflux time employed in the reaction of *N,N'*-diphenylmalondiamide with S_2Cl_2 from 3 to 6 h (in benzene) produced a product which was clearly not the 1,2,4,5-tetrathiane **8***d* produced earlier, but a buff solid which was almost insoluble in all the common organic solvents and may be the tetrasulfide reported by Hope and Wiles. It was also found that a sample of the tetrathiane **8***d* when left exposed to air and light for several days appeared to give the same type of highly insoluble product. A mechanistic proposal for the apparent rearrangement at this stage would be conjectural but apparently involves a C—S bond cleavage of some sort

TABLE 3. Molecular weight determinations for 1,2,4,5-tetrathianes **8***a*, *c*

R	Calcd. mol. wt.	Rast[a]	Osmometry[b]
n-C_3H_7, **8***a*	496	527	—
$C_6H_5CH_2$, **8***c*	688	701	665

[a]The mean of several determinations.
[b]The mean of three determinations.



SCHEME 1

and has analogy in the interesting photochemical rearrangement of **15** to the disulfide **16** (27).

Attempts to study the chemical behavior of the tetrathianes **8***a–e* have been made, but with little success. For example, these compounds did not react with hydrogen peroxide in acetone after six days at 25°C, or on refluxing for several hours, and also showed no reaction with H_2O_2-acetic acid at room temperature for several days. In contrast, refluxing for relatively short periods of time under the latter set of conditions led to extensive decomposition. Attempted ring cleavage of the tetrathianes with 2-methyl-2-propanethiolate ion also led to extensive decomposition. Photochemical cleavage/rearrangement was not attempted on compounds **8***a–e* directly, but the irradiation of the model tetrathiane **12** with a 400-W medium pres-

[2]One of the referees has suggested that the molar ratio of the reactants may be critical in determining the products formed (cf. refs. 3 and 4). Our results do not support this view, although it is clear that the reactions appear to be sensitive to other changes in the reaction conditions, such as temperature, reaction time, solvent polarity, etc.

[3]I. W. J. Still and G. W. Kutney, unpublished findings from this laboratory.

Can. J. Chem. Downloaded from www.nrcresearchpress.com by 210.87.254.6 on 09/05/12
For personal use only.

sure mercury lamp, for 25 h in acetonitrile led to recovery of the starting material. More promisingly, the reaction of the *N,N'*-dibenzyl analogue **8***c* with triphenylphosphine in benzene led to the formation of the thiirane **17** in very good yield.[4] Further studies on this reaction of the tetrathiane derivatives are continuing.

Experimental

Infrared spectra were recorded with a Pye-Unicam SP1000 spectrometer and mass spectra on the Bell and Howell 21-490 instrument. The ^{1}H nmr spectra were recorded on a Varian EM-360 spectrometer and the ^{13}C nmr spectra on a Varian XL-100-15(FT) instrument at 25.16 MHz, operating at 32 ± 3°C, with acquisition times of 0.666 s and pulse widths of 12 μs (90° "flip angle" ≡ 55 μs). Melting points were determined using an Electrothermal Mark II apparatus and osmometric measurements on the Hewlett-Packard 302 Vapor Pressure Osmometer.

Synthesis of N,N'-*Disubstituted Malondiamides* **1**a–h

These were synthesized from diethyl malonate (see Table 1) by the general procedure of Whiteley and co-workers (13). Attempts to synthesize the *N,N'*-di-*tert*-butyl and *N,N'*-di-4-nitrophenyl analogs by this route, and others, were unsuccessful.

Reaction of Malondiamides with S_2Cl_2

(**8***a*): *N,N'*-Di-*n*-propylmalondiamide **1***a* (1.00 g, 5.38 mmol) and disulfur dichloride (1.50 g, 11.11 mmol) in 25 mL benzene were refluxed for 3 h. Evaporation of the solvent yielded the tetrathiane **8***a* (1.07 g, 80%). Recrystallization from hot absolute ethanol yielded white crystals: mp 195–195.5°C; ir ($CHCl_3$) ν: 3440 (NH), 1685 (C=O) cm^{-1}; ^{1}H nmr ($CDCl_3$) δ: 0.70–1.02 (t, 3), 1.18–1.86 (m, 2), 3.00–3.40 (q, 2), 6.98–7.30 (t, 1); ^{13}C nmr ($CDCl_3$) δ: 11.2 (CH_3), 22.5 (CH_2), 42.4 (CH_2NH), 73.9 (>C<), 162.2 (CO). *Anal.* calcd. for $C_{18}H_{32}N_4O_4S_4$: C 43.53, H 6.49, N 11.28, S 25.82; found: C 43.43, H 6.38, N 11.22, S 26.07.

(**8***b*): Prepared as **8***a* above. Infrared ($CHCl_3$) ν: 3420 (NH), 1680 (C=O) cm^{-1}; ^{1}H nmr ($CDCl_3$) δ: 1.08–1.40 (d, 6), 3.67–4.39 (q, 1), 6.80–7.06 (d, 1); ^{13}C nmr ($CDCl_3$) δ: 22.1 (CH_3), 43.2 (CH), 74.0 (>C<), 165.4 (CO). *Anal.* calcd. for $C_{18}H_{32}N_4O_4S_4$: C 43.53, H 6.49, N 11.28; found: C 42.91, H 6.44, N 11.19.

(**8***c*): Prepared as **8***a* above. Infrared ($CHCl_3$) ν: 3430 (NH), 1685 (C=O) cm^{-1}; ^{1}H nmr ($CDCl_3$) δ: 4.34–4.55 (d, 2), 7.08–7.63 (m, 6); ^{13}C nmr (DMSO-d_6) δ: 44.7 (CH_2), 73.9 (>C<), 127.5–136.7 (aromatic), 166.1 (CO). *Anal.* calcd. for $C_{34}H_{32}N_4O_4S_4$: C 59.28, H 4.68, N 8.13; found: C 58.85, H 5.24, N 7.76.

N,N'-Dibenzylmalondiamide **1***c* (0.11 g, 0.39 mmol) and disulfur dichloride (0.11 g, 0.81 mmol) in 2 mL $CDCl_3$ were placed in an nmr tube. The nmr spectrum was taken at approximately 5-min intervals. By monitoring the disappearance of the active methylene protons, it was determined that the reaction was over in 55 min at 25°C.

(**8***d*): Prepared as **8***a* above. Infrared (Nujol) ν: 3380, 3300 (NH), 1685, 1670 (C=O) cm^{-1}; ^{1}H nmr ($CDCl_3$) δ: 6.80–7.58 (m, 5), 8.92 (s, 1). *Anal.* calcd. for $C_{30}H_{24}N_4O_4S_4$: C 56.94, H 3.82, N 8.85; found: C 56.88, H 3.79, N 8.87.

N,N'-Diphenylmalondiamide (2.10 g, 8.33 mmol) and disulfur dichloride (1.13 g, 8.37 mmol) in 17 mL benzene were refluxed in an additional experiment for 6 h (4). Filtration yielded a buff colored solid (2.20 g). This compound was insoluble in all the common organic solvents. A sample of tetrathiane (prepared above) which had been left open to the air for several days changed dramatically in solubility characteristics and appeared finally to be identical with the insoluble product above.

(**8***e*): Prepared as **8***a* above. Infrared ($CHCl_3$) ν: 3430 (NH), 1685 (C=O) cm^{-1}; ^{1}H nmr ($CDCl_3$) δ: 2.29 (s, 3), 6.92–7.50 (m, 4), 8.88 (s, 1); ^{13}C nmr ($CDCl_3$) δ: 21.0 (CH_3), 75.3 (>C<), 120.5–135.6 (aromatic), 164.1 (CO). *Anal.* calcd. for $C_{34}H_{32}N_4O_4S_4$: C 59.28, H 4.68, N 8.13, S 18.62; found: C 58.72, H 4.79, N 8.09, S 18.61.

(**8***f*): *N,N'*-Di-4-methoxyphenylmalondiamide **1***f* (1.00 g, 3.18 mmol) and disulfur dichloride (0.89 g, 6.59 mmol) in 25 mL benzene were refluxed for 3 h. Removal of the solvent yielded a brown solid (1.18 g). Attempted purification by thick layer chromatography led to extensive decomposition upon addition of methanol.

3,3,6,6-Tetramethyl-1,2,4,5-tetrathiane **12**

This compound was prepared in 14% yield by the procedure of Magnusson (23); mp 92–95°C (lit. (28) mp 98°C).

Preparation of 2,2,3,3-Tetrabenzylcarbamoylthiirane **17**

The tetrathiane **8***c* (0.69 g, 1.00 mmol) and triphenylphosphine (0.52 g, 2.00 mmol) were stirred in benzene (20 mL) for 16 h at 25°C. Filtration yielded a white solid. Evaporation of the solvent yielded triphenylphosphine sulfide (0.35 g, 58%), mp 160–161°C (lit. (29) mp 157.5°C). Recrystallization of the white solid from 95% ethanol yielded the thiirane **17**, (0.32 g, 82% based on triphenylphosphine), mp 196–198°C. Infrared (Nujol) ν: 3315 (NH), 1680 (CO) cm^{-1}; ^{1}H nmr (DMSO) δ: 4.15–4.35 (d, 2), 7.20 (5H, s) 8.40 (1H, m). *Anal.* calcd. for $C_{34}H_{32}N_4O_4S$: C 68.88, H 5.44, N 9.46, S 5.41; found: C 68.21, H 5.92, N 9.18, S 5.28.

[4]We thank one of the referees for suggesting this experiment.

Acknowledgement

We thank the National Research Council of Canada for partial support of this investigation.

1. K. Buchka. Ber. **18**, 2090 (1885).
2. A. Delisle. Ber. **22**, 306 (1889).
3. R. Gompper, H. Euchner, and H. Kast. Justus Liebigs Ann. Chem. **675**, 151 (1964).
4. P. Hope and L. A. Wiles. J. Chem. Soc. 4583 (1965).
5. R. D. G. Jones and L. F. Power. Aust. J. Chem. **24**, 735 (1971).
6. S. K. Gupta. J. Org. Chem. **39**, 1944 (1974).
7. J. S. Pizey and K. Symeonides. Phosphorus Sulfur, **1**, 41 (1976).
8. K. Oka and S. Hara. Tetrahedron Lett. 695 (1977); 3059 (1977).
9. A. J. Krubsack, R. Sehgal, W. Loong, and W. E. Slack. J. Org. Chem. **40**, 3179 (1975).
10. K. G. Naik. J. Chem. Soc. **119**, 379 (1921); **119**, 1231 (1921).
11. A. Senning. Angew. Chem. **91**, 1006 (1979).
12. J. S. Pizey and K. Symeonides. Phosphorus Sulfur, **6**, 243 (1979).
13. J. V. Backes, R. W. West, and M. A. Whiteley. J. Chem. Soc. **119**, 359 (1921).
14. F. R. Benson and J. J. Ritter. J. Am. Chem. Soc. **71**, 4128 (1949).
15. A. K. Sen and P. Sengupta. J. Indian Chem. Soc. **46**, 858 (1969).
16. A. Baruffini, P. Borgna, and G. Pagani. Pharmacol. Ed. Sci. **22**, 769 (1967); Chem. Abstr. **68**, 77925s (1968).
17. D. H. Dewar, J. E. Fergusson, P. R. Hentschel, C. J. Wilkins, and P. P. Williams. J. Chem. Soc. 688 (1964).

18. F. J. BERRY, B. C. SMITH, and C. H. W. JONES. J. Organomet. Chem. **110**, 201 (1976).
19. L. A. WILES and Z. S. ARIYAN. Chem. Ind. 2102 (1962).
20. R. APPEL and M. MONTENACH. Chem. Ber. **111**, 759 (1978).
21. A. HOPPMANN, P. WEYERSTAHL, and W. ZUMMACK. Justus Liebigs Ann. Chem. 1547 (1977).
22. R. G. PETROVA, I. I. KANDROR, V. I. DOSTOVALOVA, T. D. CHURKINA, and R. K. FREIDLINA. Org. Magn. Reson. **11**, 406 (1978).
23. B. MAGNUSSON. Acta Chem. Scand. **13**, 1031 (1959).
24. D. H. R. BARTON and M. J. ROBSON. J. Chem. Soc. Perkin Trans. I, 1245 (1974).
25. R. OKAZAKI, K. INOUE, and N. INAMOTO. Tetrahedron Lett. 3673 (1979).
26. K. G. NAIK and Y. N. BHAT. Q. J. Indian Chem. **4**, 525 (1927).
27. J. D. WILLETT, J. R. GRUNWELL, and G. A. BERCHTOLD. J. Org. Chem. **33**, 2297 (1968).
28. C. WILLGERODT. Ber. **20**, 2467 (1887).
29. A. MICHAELIS and L. GLEICHMANN. Ber. **15**, 801 (1882).

Can. J. Chem. Downloaded from www.nrcresearchpress.com by 210.87.254.6 on 09/05/12
For personal use only.

Air oxidation of Reissert compounds

MARIA D. ROZWADOWSKA AND DANUTA BRÓZDA

Institute of Chemistry, Adam Mickiewicz University, Grunwaldzka 6, 60-780 Poznań, Poland

Received December 10, 1979

MARIA D. ROZWADOWSKA and DANUTA BRÓZDA. Can. J. Chem. **58**, 1239 (1980).

Reissert compounds undergo autoxidation in basic solution giving rise to isoquinaldo- or quinaldonitriles. Under the same reaction conditions, dihydroisoquinoline Reissert compounds undergo oxidative decyanation to dihydroisocarbostirils. The intermediacy of α-peroxycyanides is proposed in this transformation.

MARIA D. ROZWADOWSKA et DANUTA BRÓZDA. Can. J. Chem. **58**, 1239 (1980).

Les composés de Reissert subissent une autoxydation en solution basique pour conduire aux isoquinaldo- ou aux quinaldonitriles. Dans les mêmes conditions les composés de Reissert du type dihydroisoquinoléine subissent une décyanation oxydative conduisant aux dihydroisocarbostiriles. On propose des α-péroxycyanures comme intermédiaires dans cette transposition.

[Traduit par le journal]

Can. J. Chem. Downloaded from www.nrcresearchpress.com by 210.87.254.5 on 09/05/12
For personal use only.

In a previous paper (1) we described the tendency of various Reissert compounds to undergo autoxidation in basic solution and reported that the course of the reaction is dependent on the oxygenation state of the compound. This has also been confirmed by other authors (2).

In this paper we wish to report the results of our further study in this area, particularly concerning the formation of intermediates in the oxidation of Reissert compounds containing the *N*-benzoyl group. We have measured the amount of oxygen used as well as established the form in which the cyano substitutent is eliminated from dihydro derivatives.

From the experimental point of view the phase-transfer conditions (3), or rather the two-phase catalytic system (4), used for the generation of carbanions proved to be the most convenient method for the measurements. The oxygen was taken from the air, the consumed amount being determined from the difference in volume before and after the reaction. The experiments were carried out under atmospheric pressure and at room temperature. Only derivatives with the *N*-benzoyl group could be used, because *N*-alkoxycarbonyl derivatives appeared to release volatile components in the course of oxidation; similarly, the dimethylformamide – sodium hydride procedure, used for the generation of carbanions, had to be dismissed.

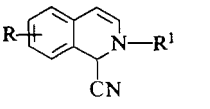
We have found that isoquinoline derived Reissert compounds **1***a* and **5***a* need only a half-molar equivalent of oxygen to be oxidized to isoquinaldonitrile and dihydroisocarbostiril, respectively. In the product mixtures benzoic acid (90% of theory) and hydrogen cyanide (determined as AgCN, 80% of theory) could be found.

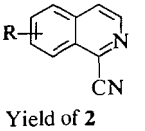
Oxidation of Reissert Compounds

It is well established that Reissert compounds **1**, **3** are readily converted into the corresponding heteroaromatic nitriles **2**, **4** in alkaline solutions (5–10). No mechanistic interpretation of this process has been given, although it has been suggested occasionally (9, 10) that the nitriles could have resulted from an interaction of Reissert anions with oxygen.

As can be seen from Schemes 1 and 2, Reissert compounds derived from isoquinolines **1** and quinolines **3** are oxidized to isoquinaldonitriles **2** and quinaldonitriles **4**, respectively, independently of the nature of the *N*-substituent. The yields are usually high, except for quinoline derivatives, where large amounts of insoluble polymers are formed.

In the case of *N*-sulfonyl derivatives **1***e*, *f*, these compounds could be transformed into isoquinaldonitriles even without the presence of oxygen. Among the products of this reaction corresponding sulfinic acid was found (5), which indicates that an internal red.–ox. process takes place.





1	R	R¹	Yield of **2** (%)
a	H	COC_6H_5	90
b	H	$COOC_2H_5$	90
c	H	$COCH_3$	97
d	6,7-OCH_3	$COOC_2H_5$	94
e	H	$SO_2C_6H_5$	65
f	H	$SO_2C_6H_4CH_3$	97

SCHEME 1. Oxidation of isoquinoline Reissert compounds in the two-phase catalytic system.

0008-4042/80/121239-04$01.00/0

©1980 National Research Council of Canada/Conseil national de recherches du Canada



3	R	R¹	Yield of **4** (%)
a	H	C_6H_5	45
b	H	OC_2H_5	45

SCHEME 2. Oxidation of quinoline Reissert compounds in the two-phase catalytic system.

The base-catalysed autoxidation of nitriles is well known (11–16). α-Alkylated arylacetonitriles or α-amino arylacetonitriles (to which belong Reissert compounds) undergo oxidative decyanation giving rise to ketones and isocyanates. However, only dihydro Reissert compounds behave in this way, being oxidized to carbonyl derivatives, whereas "normal" ones give the corresponding heteroaromatic nitriles. This difference can be explained if one considers that an alternative pathway of oxidizing a dihydro system versus an aromatic system exists.

A 2:1 molar ratio of Reissert compound to oxygen agrees well with the formation of 1 mol of benzoic acid and 1 mol of nitrile. We now would like to propose a plausible mechanism suggesting that the initially formed Reissert anion combines with molecular oxygen leading to a peroxy intermediate. In the two-phase catalytic system, the peroxy species decomposes immediately and oxidizes a second molecule of Reissert compound.

Although we were not able to perform a positive iodine–starch test at various stages of this reaction, we succeeded in oxidizing 2-benzoyl-1,2-dihydroisoquinaldonitrile **1***a* into isoquinaldonitrile **2***a* both by *m*-chlorperbenzoic acid and by hydrogen peroxide in the two-phase system and under an argon atmosphere. Benzoyl peroxide in catalytic amounts did not affect the rate of the autoxidation, but gave the same result when used in stoichiometric amounts.

Oxidation of Dihydro Reissert Compounds

The oxidation of *N*-benzoyl and *N*-alkoxycarbonyl dihydroisoquinoline Reissert derivatives **5***a–e* gave dihydroisocarbostiriles **6***a–e* or their *N*-acyl derivatives **8** (Scheme 3).

Hydrastinine pseudo-cyanide **5***h* was converted into oxyhydrastinine **6***h*, (NCH_3) in high yield.

N-benzenesulfonyl- and *N*-*p*-toluenesulfonyl-1-cyano-1,2,3,4-tetrahydroisoquinolines **5***f*, *g* as well as dihydroquinoline Reissert compounds **7** do not enter into the reaction with oxygen even at −76°C and with butyl lithium as the base.

In several experiments, in which the autoxidation of **5***a* and **5***d* was stopped immediately after the uptake of oxygen ceased, we were able to isolate the *N*-benzoyldihydroisocarbostiril **8**. This indicates that the initial oxidation is followed by hydrolysis.

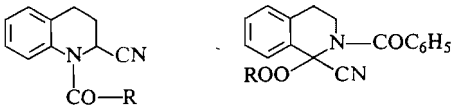


5	R	R¹	Yield of **6** (%)
a	H	COC_6H_5	75
b	H	$COOC_2H_5$	68
c	H	$COOCH_3$	47
d	6,7-O—CH_2—O—	COC_6H_5	80
e	6,7-O—CH_2—O—	$COOC_2H_5$	37 (19)
f	H	$SO_2C_6H_5$	No reaction with O_2
g	H	$SO_2C_6H_4CH_3$	No reaction with O_2
h	6,7-O—CH_2—O—	CH_3	92 (NCH_3 derivative)

SCHEME 3. Oxidation of dihydroisoquinoline Reissert compounds in the two-phase catalytic system.

As has been mentioned before, the action of molecular oxygen on dihydro Reissert compounds yields carbonyl derivatives in a way similar to that in which aryl acetonitriles or α-amino arylacetonitriles are oxidized to ketones (11–16). In the latter case the cyano group is oxidized as well and eliminated as an isocyanate. Intermediate α-hydroperoxy nitriles have been isolated (14, 16, 17) in reactions carried out at low temperatures, in anhydrous solvents, and in the presence of such bases as potassium *tert*-butoxide or lithium diisopropylamide. A detailed kinetic study (16) revealed that a further decomposition of the peroxy nitriles to the carbonyl derivatives and isocyanates proceeds via a four-membered dioxetane as an intermediate.

In the case of oxidation of dihydro Reissert compounds in the two-phase system, where only a

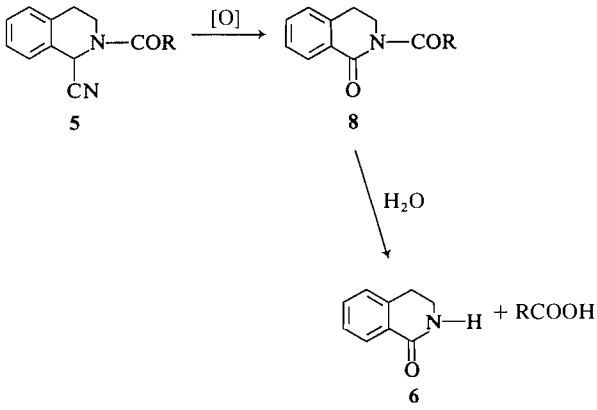


7
a R = C_6H_5
b R = OC_2H_5

9
a R = H
b R = $COCH_3$

half-molar equivalent of oxygen is consumed, one would expect the elimination of the cyanide rather than the isocyanate ion. Indeed, this was the case. We were able to precipitate silver cyanide in 80% yield from the reaction in which 2-benzoyl-1,2,3,4-tetrahydroisoquinaldonitrile **5***a* was oxidized. We also got a positive cyanide test simply by

Can. J. Chem. Downloaded from www.nrcresearchpress.com by 210.87.254.5 on 09/05/12
For personal use only.



treating the alkaline water layer, which was left after the separation of the organic phase, with ferrous sulfate and hydrochloric acid. At the same time the pyridine – cupric sulfate test (18) for the detection of isocyanates was negative.

Taking these facts into consideration, one could propose the following mechanism for the autoxidation of dihydro Reissert compounds in the two-phase system. The initial step also involves the formation of α-hydroperoxy cyanide, which then oxidizes a second molecule of the Reissert compound. In this way either a dimeric peroxide or two molecules of cyanohydrin are formed. The latter is known to readily undergo base-catalysed decomposition. However, we have not done any kinetic studies in order to confirm any of these suggestions.

In an experiment in which 2-benzoyl-1,2,3,4-tetrahydroisoquinaldonitrile **5***b* was oxidized at −76°C in tetrahydrofuran in the presence of butyl lithium, we observed the uptake of 1 mol of oxygen for oxidation of 1 mol of this compound. When this reaction was quenched with hydrochloric acid we isolated 1-hydroperoxy-2-benzoyl-1,2,3,4-tetrahydroisoquinaldonitrile **9***a* in good yield, whereas the addition of acetyl chloride, instead of hydrochloric acid, resulted in *O*-acetyl derivative **9***b*. Both crystalline peroxides were satisfactorily characterized by spectroscopic methods as well as by elemental analysis (see Experimental). Hydroperoxide **9***a* appeared to be unstable at temperatures above 0°C. When left overnight in acetone solution at room temperature it was converted into dihydroisocarbostiril **6***a* in 57% yield.

From these facts, one can come to the conclusion that the autoxidation of Reissert compounds may proceed via different mechanisms which are dependent on the reaction conditions. In the two-phase catalytic system, in which the reaction is run at room temperature and in the presence of aqueous sodium hydroxide and quaternary ammonium salts, the *in statu nascendi* formed hydroperoxide may serve as an oxidizing agent for the oxidation of a second molecule of Reissert compound. At low temperature and in anhydrous solvents the peroxy intermediate may be stable enough to be isolated and characterized.

Experimental

Melting points were determined on a Kofler block. Infrared spectra were measured in chloroform solution using 0.1 mm cells and approximately 0.2 *M* sample concentration on a Unicam SP 200G spectrometer and in KBr discs on a Beckman IR 4230 instrument. Chemical ionisation mass spectra (ci ms) were obtained using a Finnigan 1015D spectrometer with a model 6000 data collection system and electron ionization mass spectra (ei ms) were obtained with a JEOL MS 100-D instrument. Thin-layer chromatography (tlc) was run on precoated plates (Merck, silica gel 60 F 254).

The starting Reissert compounds were prepared according to the known procedure. Compounds **1**, **3** and dihydro analogs **5***a*, *d*, *e* were prepared from appropriate isoquinoline or quinoline derivatives by the modified procedure (20); dihydro Reissert compounds **5***b*, *c*, *f*, *g* by ionic hydrogenation of appropriate Reissert compounds (21); and derivatives **7** by a catalytic hydrogenation of quinoline Reissert compounds (23). Hydrastinine pseudocyanide **5***h* was prepared from hydrastinine and potassium cyanide according to ref. 22, yield 83%, mp 83–84.5°C (lit. (22) oil); ir: 2220 cm^{-1} (CN); ei ms *m/e*: 216(M^+), 215(M − 1), 190(M − CN), 188(M − CN − 2H), 173(M − CN − CH_3 − 2H) (base). *Anal.* calcd. for $C_{12}H_{12}N_2O_2$: C 66.67, H 5.56, N 12.97; found: C 66.83, H 5.81, N 12.83.

The following general procedure for air oxidation of Reissert compounds in the two-phase catalytic system was used. Air was bubbled into a well stirred two-phase system consisting of the Reissert derivative (1 mmol) in benzene (6–12 mL), 50% aqueous sodium hydroxide (1–2 mL), and 30 mg triethylbenzylammonium chloride (TEBA). After 1.5 h (or 20 h in the case of the dihydro Reissert compounds), the organic phase was separated and washed with water, dilute hydrochloric acid, and water. The solvent was evaporated and the residue was crystallized: isoquinaldonitrile from xylene, quinaldonitrile from ether – petroleum ether, and dihydroisocarbostiril from *n*-hexane. Products were characterized by their melting points, ir, and mass spectra, as well as by thin-layer chromatography, and compared with data published in the original literature.

Benzoic acid was determined in the following way. The aqueous phase that remained after the separation of the organic layer from the two-phase oxidation of **1***a* or **3***a* was rendered acidic and extracted with ether. After work-up, benzoic acid was obtained in 90 and 65% yield, respectively.

Silver cyanide was precipitated in the case of oxidation of compound **5***a*, when the aqueous layer was treated with silver nitrate, yield 80%.

Reactions in which the uptake of oxygen was measured were run in a closed system consisting of a 150 mL round-bottom flask connected to a gas buret.

Peroxides 9 from Dihydroisoquinoline Reissert Compound 5a

A solution consisting of 252 mg (1 mmol) of 2-benzoyl-1,2,3,4-tetrahydroisoquinaldonitrile **5***a* in tetrahydrofuran (5 mL) was placed in a 150 mL two-necked flask connected to a gas buret, which permitted the measurement of the volume of consumed oxygen. It was cooled to −76°C and 1 mmol of butyl lithium in hexane solution was added through a serum cup with

Can. J. Chem. Downloaded from www.nrcresearchpress.com by 210.87.254.5 on 09/05/12
For personal use only.

vigorous stirring. After 1 mmol of oxygen was used (ca. 1.5 h) the temperature was allowed to rise to ca. 0°C and dilute hydrochloric acid was added. This then was extracted with ether, etheral extracts dried, and solvent evaporated at room temperature to give 147 mg (52%) of crystalline **9***a*. It was recrystallized from tetrahydrofuran, mp 114–115.5°C; ir (KBr): 3180 (OOH), 2175 (CN), 1630 cm^{-1} (CO); ci ms (NH_3) *m/e*: 295($M^+ + 1$), 279($M - O + 1$), 252 (base) ($M - HNCO + 1$), 157($M - OOH - COC_6H_5 + 1$); ei ms *m/e*: 277($M - OH$), 262($M - O_2$), 156($M - O_2 - C_6H_5CHO$), 105 (base) ($C_6H_5CO^+$). *Anal.* calcd. for $C_{17}H_{14}N_2O_3$: C 69.39, H 4.76, N 9.53; found: C 69.51, H 4.81, N 9.41.

When the reaction was quenched with acetyl chloride, **9***b* was obtained after the usual work-up, yield 135 mg (40%); mp 134–135°C, after recrystallization from methylene chloride – hexane (1:1); ir (KBr): 1790 (CO), 1670 cm^{-1} (CO); ci ms (NH_3) *m/e*: 337($M^+ + 1$), 279($M - OCOCH_2 + 1$), 261($M - OOCOCH_3$), 252 (base) ($M - CN - OCOCH_3 + 1$). *Anal.* calcd. for $C_{19}H_{16}N_2O_4$: C 67.86, H 4.76, N 8.33; found: C 67.70, H 5.03, N 8.44.

2-Benzoyl-3,4-dihydroisocarbostiril (8, R = C_6H_5)

2-Benzoyl-1,2,3,4-tetrahydroisoquinaldonitrile **5***a* (1 mmol) was oxidized with air oxygen in the two-phase catalytic system in the manner described in the general procedure.

The reaction was stopped after 50 min and worked up in the usual way. 2-Benzoyl-3,4-dihydroisocarbostiril (**8**, R = C_6H_5) (180 mg, 72%) was obtained, mp 132°C (lit. (24) mp 132°C) after crystallization from ethanol; ir, ms, and tlc were identical with an authentic sample.

Hydrolysis of 2-Benzoyl-3,4-dihydroisocarbostiril (8, R = C_6H_5)

A two-phase system consisting of compound **8** (R = C_6H_5), (125.5 mg, 0.5 mmol) in benzene (4 mL), 50% aqueous sodium hydroxide (0.5 mL), and TEBA (20 mg) was stirred at room temperature for 24 h under an argon atmosphere. The standard work-up resulted in 40 mg (55%) of dihydroisocarbostiril (**6**, R = H).

Oxidation of 2-Benzoyl-1,2-dihydroisoquinaldonitrile **1***a in the Two-phase Catalytic System, under Argon*

(A) With m*-Chlorperbenzoic Acid*

A two-phase catalytic system was prepared from compound **1***a* (260 mg, 1 mmol), benzene (6 mL), TEBA (30 mg), and 50% aqueous sodium hydroxide (1 mL). A rapid stream of argon was introduced and 250 mg of 84% *m*-chlorperbenzoic acid in benzene (3 mL) was added. After 24 h this mixture was worked up giving 150 mg (97%) of isoquinaldonitrile (**2**, R = H).

(B) With Hydrogen Peroxide

The two-phase system containing 1 mmol of compound **1***a* was prepared in the way described above. Then 0.5 mL of 31% hydrogen peroxide was added dropwise, the interval between two successive drops being 0.5 h. A vigorous stream of argon was passed through and the reaction carried out for 24 h. Then it was worked up in the usual way, to yield quantitative amounts of isoquinaldonitrile (**2**, R = H).

(C) With Benzoyl Peroxide

When 75% benzoyl peroxide was used as the oxidizing agent using the same reaction conditions as well as the same amounts of reactants, isoquinaldonitrile (**2**, R = H) was obtained in quantitative yield after 24 h.

1. M. D. Rozwadowska and D. Brózda. Tetrahedron Lett. 589 (1978).
2. S. Ruchirawat and M. Chuankamnerdkarn. Heterocycles, 1345 (1978).
3. E. V. Dehmlow. Angew. Chem. **86**, 187 (1974); **89**, 521 (1977).
4. M. Makosza. Pure Appl. Chem. **43**, 439 (1975); Conference Paper Workshop, Interlaken, 23 (1976).
5. F. D. Popp. Adv. Heterocycl. Chem. **9**, 1 (1968); **24**, 187 (1979) and references cited therein.
6. F. D. Popp, L. E. Katz, C. W. Klinowski, and J. M. Wefer. J. Org. Chem. **33**, 4447 (1968).
7. J. Saito, Y. Kikugawa, and S. Yamada. Chem. Parm. Bull. **22**, 740 (1974).
8. F. D. Popp, R. E. Buhts, and D. K. Chesney. J. Heterocycl. Chem. **15**, 429 (1978).
9. G. W. Kirby, S. L. Tan, and B. C. Uff. Int. Congr. Pure Appl. Chem., Boston, 1971, Abstract 270, p. 113.
10. B. C. Uff, J. R. Kershaw, and S. R. Chhabra. J. Chem. Soc. Perkin Trans. I, 479 (1972).
11. M. S. Karasch and G. Sosnowsky. Tetrahedron, **3**, 97 (1958).
12. H. G. Aurich. Tetrahedron Lett. 657 (1964).
13. D. H. Bennett, G. W. Kirby, and V. A. Moss. Chem. Commun. 218 (1967); J. Chem. Soc. C, 2049 (1970).
14. S. J. Selikson and D. S. Watt. J. Org. Chem. **40**, 267 (1975).
15. J. Jarrousse and J. C. Raulin. C.R. Acad. Sci. Ser. C, **284**, 503 (1977).
16. Y. Sawaki and Y. Ogata. J. Am. Chem. Soc. **99**, 6313 (1977).
17. L. Dulog and W. Vogt. Tetrahedron Lett. 5169 (1966).
18. M. D. Rozwadowska. Can. J. Chem. **55**, 164 (1977).
19. E. A. Werner. J. Chem. Soc. **123**, 2577 (1923).
20. T. Koizumi, K. Takeda, K. Yoshida, and E. Yoshii. Synthesis, 497 (1977).
21. M. D. Rozwadowska and D. Brózda. Bull. Acad. Pol. Sci. Ser. Sci. Chim. **26**, 33 (1978).
22. A. Kaufmann. Ber. **51**, 116 (1918).
23. M. D. Rozwadowska. Rocz. Chem. **51**, 2321 (1977).
24. C. J. Cavallito and T. H. Haskell. J. Am. Chem. Soc. **66**, 1166 (1944).

Can. J. Chem. Downloaded from www.nrcresearchpress.com by 210.87.254.5 on 09/05/12
For personal use only.

Synthesis of substituted hydrindanes. Part II. Approaches to the synthesis of fawcettimine

ROBERT H. BURNELL, ALAIN HUMBLET, JACQUES PELLETIER, AND SANTYNAND BADRIPERSAUD
Département de Chimie, Université Laval, Québec (Qué.), Canada G1K 7P4

Received November 2, 1979

ROBERT H. BURNELL, ALAIN HUMBLET, JACQUES PELLETIER, and SANTYNAND BADRIPERSAUD. Can. J. Chem. **58**, 1243 (1980).

Several unsaturated hydrindanones have been prepared to assess various synthetic routes which could lead to the Lycopodium alkaloid fawcettimine. Comparison with an earlier model series starting from dimedone shows that this dihydroorcinol based sequence must be modified considerably.

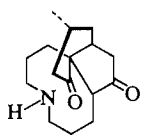
ROBERT H. BURNELL, ALAIN HUMBLET, JACQUES PELLETIER et SANTYNAND BADRIPERSAUD. Can. J. Chem. **58**, 1243 (1980).

On a préparé plusieurs hydrindanones non saturées dans le but d'évaluer les différentes sortes de synthèse pouvant conduire à l'alcaloide lycopodium fawcettimine. La comparaison avec des séries de modèles antérieurs provenant de la dimédone montre que la séquence basée sur le dihydroorcinol doit être modifiée considérablement.

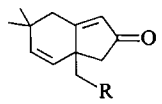
[Traduit par le journal]

Can. J. Chem. Downloaded from www.nrcresearchpress.com by 210.87.254.42 on 09/05/12
For personal use only.

In Part I of this series (1) we described the preparation of hydrindenones **2***a* and **2***b* as models for the synthesis of Lycopodium alkaloids such as fawcettimine **1**. Structural studies on the latter (2) show the more stable form of the alkaloid to be a hemi-aminal arising from transannular reaction of the six-membered ring carbonyl with the secondary amino residue. This equilibration would be inevitable if structure **1** were synthesised or of course impossible if the amino residue is *N*-acetylated. Our first synthetic models contained *gem*-dimethyl groups (**2***a* and **2***b*) while fawcettimine has but one methyl residue at this position, so we have examined the analogous syntheses starting from dihydroorcinol rather than dimedone, only to find that this trivial difference in starting material considerably changes the outcome.



1

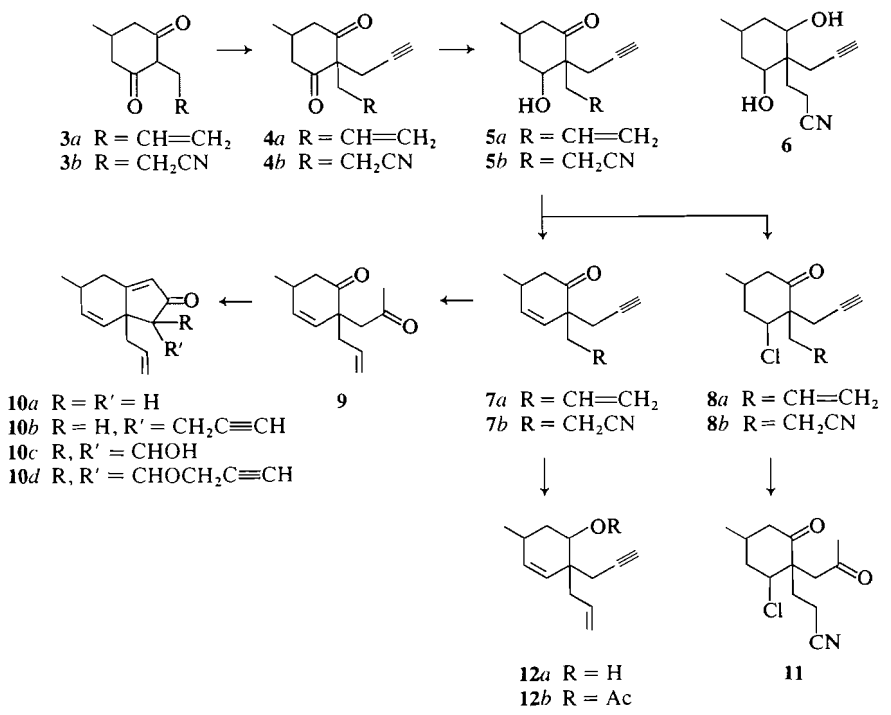


2*a* R = CH_2COOH
2*b* R = $CH{=}CH_2$

As shown in Scheme 1, allyl and cyanoethyl dihydroorcinols (**3***a* and **3***b*) were both readily alkylated with propargyl bromide to give the 2,2-disubstituted 1,3-cyclohexadiones (**4***a* and **4***b*). As in the earlier models the diones were partially reduced to the ketols **5***a* and **5***b* although the conditions found necessary to avoid complete reduction to the diols such as **6** not only differed from each other (**5***a*: lithium tri-*tert*-butoxy aluminium hydride at 0°C; **5***b*: sodium borohydride at 0°C) but also from previous models with the *gem*-dimethyl groups, where even above room temperature for 2 days only one of the carbonyl groups was reduced in the presence of sodium borohydride. While varying the conditions did enable us to obtain the ketols in good yield, dehydration of **5***a* and **5***b* only grudgingly afforded the olefins **7***a* and **7***b* which were in both cases extremely difficult to separate from, what we learned later to be, the chlorine-containing substitution products **8***a* and **8***b*. The 2-cyanoethyl-2-propargylcyclohexenone **7***b* was never obtained pure enough for satisfactory elemental analysis but careful distillation of the allyl analogue **7***a* afforded material which we were able to carry through to the hydrindenone **10***a*. Thus hydration of the propargyl triple bond to give the diketone **9** and cyclisation in degassed aqueous potassium hydroxide afforded **10***a*. Other methods for eliminating the oxygen functions in **5***a* and **5***b*, via the mesylates, the tosylates, or the chloro compounds (**8***a* and **8***b*) were met with no greater success. Thinking that elimination might be more readily achieved later in the synthesis, the chloroketone **8***b* was converted to the dione **11** but cyclisations attempted in aqueous or anhydrous bases lead to alternate cyclisation products.

The discouraging failure of the dihydroorcinol series to imitate the sequence from dimedone did provide us with a limited quantity of material (**10***a*) which we could use to test the behaviour of the hydrindenone system to alkylation, which would be the next step in the overall synthesis. The structures of the products were secured only by mass spectrometric and other spectral evidence but alkylation under kinetically controlled conditions (3) with propargyl bromide was found to be exclusively at the methylene carbon to yield **10***b*. The latter was also obtained via the hydroxymethylene derivative **10***c*, but in this case the *O*-alkylated product **10***d* was also isolated. Since **10***b* contains the complete fawcettimine carbon skeleton this approach offered a reasonable chance of success if the

0008-4042/80/121243-07$01.00/0
©1980 National Research Council of Canada/Conseil national de recherches du Canada



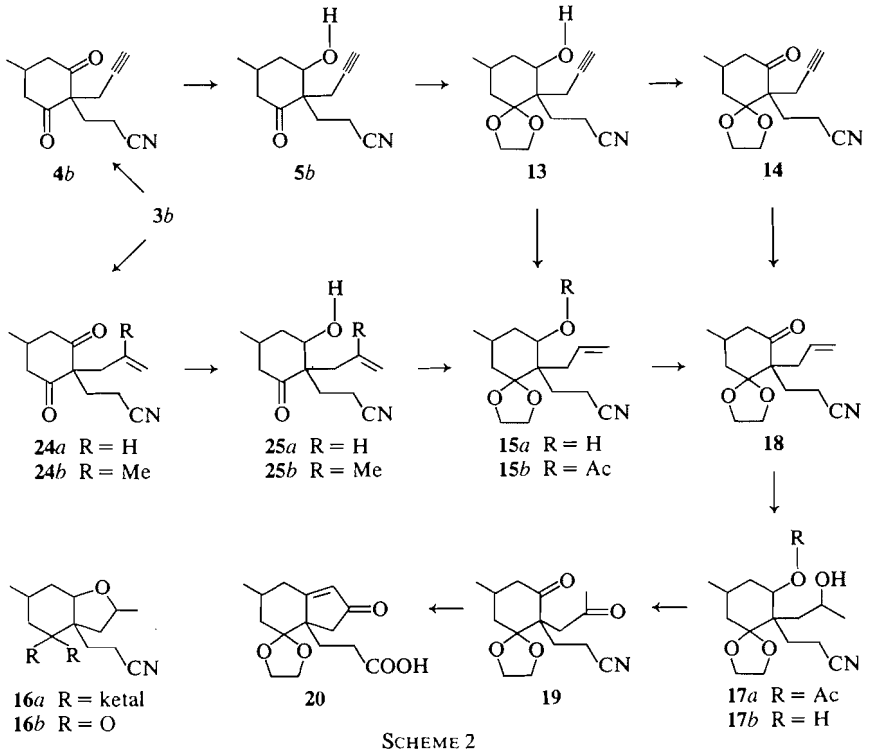
SCHEME 1

disastrous dehydration step could be avoided permitting an improvement in the overall yield (**3***a* → **10***a*; 11% overall). An alternate pathway involving the acetate **12***b* and the alcohol **12***a* was investigated but offered no advantage.

On eight previous occasions we had found that attempted ketalisation of 2,2-disubstituted cyclohexa-1,3-diones or 2,2-disubstituted 3-hydroxycyclohexanones under a variety of conditions lead only to the decomposition of the starting material, presumably by β-ketone fission or by retro-aldolisation. The hydroxy-ketone **5***b* proved to be an exception and the ketal-alcohol **13** was obtained in good yield by the classical method (Scheme 2). This not only renders the dehydration redundant but also preserves the potential carbonyl group necessary for fawcettimine. The hydroxyl group in **13** was oxidised affording the ketone **14** but attempted hydration of the triple bond also hydrolysed the ketal moiety which provoked cleavage of the ring. The hydroxy-ketal was hydrogenated over Lindlar catalyst to give the allyl derivative **15***a* but acetoxymercuration (4) of the latter gave the tetrahydrofuran **16***a* (characterised as the ketone **16***b*) whereas the acetyl derivative of **13** took 6 days to decolorise the reagent (normally less than 5 min suffices) and the yield of hydroxy-acetate **17***a* was poor. However, the ketone **18**, obtained by oxidation of alcohol **15***a* or by Lindlar-catalysed reduction of ketone **14**, reacted rapidly on acetoxymercuration and since sodium borohydride in sodium hydroxide was used to precipitate the mercury during the work-up, the intermediate diol **17***b* was oxidised by the Ratcliffe–Rodehorst method (5) to afford diketone **19**. The latter cyclised in aqueous potassium hydroxide to afford the hydrindenone **20** with concomitant hydrolysis of the nitrile.

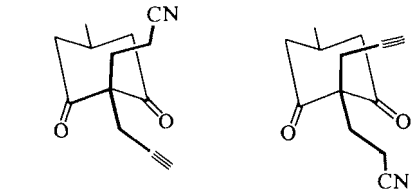
During the course of these syntheses certain stereochemical preferences had become evident while all compounds are necessarily racemic. For instance, the alkylation of **3***b* establishes the quaternary centre in **4***b* producing the geometrical isomers **4***bZ* and **4***bE* and the relationship of the cyanoethyl and methyl substituents is not changed during subsequent transformations. The nmr spectrum of the product shows two methyl doublets at 1.15 and 1.08 δ in the ratio of 2:1 respectively but in our hands these isomers were inseparable. Most peaks in the nmr spectra of many of the products were broad. We had hoped to separate the mixtures to continue the synthesis with that isomeric racemate which could lead to fawcettimine but the first product where this was possible was the ketal-ketone **18**. Lengthy chromatography of the latter did provide one pure racemate (mp 94–95°C) and the other somewhat less pure (mp 56–60°C) which still contained about 10% of the

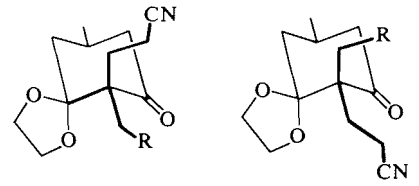
Can. J. Chem. Downloaded from www.nrcresearchpress.com by 210.87.254.42 on 09/05/12
For personal use only.

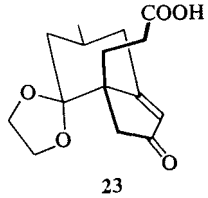


SCHEME 2

higher melting isomer. Before separation the nmr spectrum of the mixture showed two peaks for the methylene protons of the dioxolane ring at 3.98 and 3.93 δ in an approximate ratio of 2:1. The higher melting isomer showed only the 3.93 peak while the lower melting mixture showed mostly the 3.98 peak. The regions between 2.0 and 3.0 δ in the spectra were complex but distinctly different. It seemed hazardous to say which racemate corresponded to which of the structures **21***a* or **21***b*.







The diketone **19** proved easier to separate and the two racemates **22***a* and **22***b* could also be prepared from the purified samples of **21***a* and **21***b*. The main differences in properties were the melting points and the nmr signals for the methylene adjacent to the aliphatic ketone. In the spectrum of the higher melting diketone (mp 166–167°C) (obtained from the lower melting alkene) this methylene appeared as a singlet at 3.15 δ while in the other isomer (mp 113–115°C) this signal was lost in the complex system between 2.4 and 2.8 δ. The lower melting isomer decomposed on standing at room temperature. Examination of models suggests that the higher melting, more stable, and more abundant compound contains the stereochemistry required for (±)fawcettimine. Cyclisation of the diketone **19** before separation gave variable results but the pure racemic **22***a* afforded the cyclised acid without difficulty. This acid must have the structure shown in **23**. The overall yield from **3***b* to **23** was ca. 20% and this includes the loss incurred separating the diketone racemates.

Although fewer steps are involved Scheme 2 shows an alternate route to the hydrindenone acid

Can. J. Chem. Downloaded from www.nrcresearchpress.com by 210.87.254.42 on 09/05/12
For personal use only.

Can. J. Chem. Downloaded from www.nrcresearchpress.com by 210.87.254.42 on 09/05/12
For personal use only.

20 from the allyl-cyanoethylcyclohexa-1,3-dione **24***a* via the ketol **25***a* and the ketal **17** (mentioned earlier) but this offered no advantage in time or yield. A similar shorter synthesis involving the methallyl analog **24***b*, from which the methyl ketone can be readily obtained by ozonolysis, was abandoned when the hydroxy-ketone **25***b* failed to ketalise even under forcing conditions. This is hard to explain since the allyl compound **24***a* gave the corresponding ketal in 80% yield. After considerable experimentation we have found that the route can be shortened by partial ketalisation of the diketone **4***b* to the ketal **14** in 63% yield. Surprisingly neither of the similar diones **4***a* nor **24***b* afforded the ketal under the same or more vigorous conditions.

Recently, Inubushi and co-workers (6) have published a total synthesis of (±)fawcettimine.

Experimental

Unless otherwise stated the conditions and instruments for the spectra quoted are: uv, ethanol solutions, Beckman DK-1A; ir, Perkin–Elmer 457 and Beckman IR 12; nmr, Bruker HX 90, internal TMS standard, coupling constants in parentheses; ms, Varian M 66. Elemental analyses by the Pascher Laboratory, Bonn and Chemalytics, Arizona, U.S.A.

*2-Allyl-2-propargyl-5-methylcyclohexa-1,3-dione (**4**a)*

2-Allyl-5-methylcyclohexa-1,3-dione (**3***a*) (30 g) prepared by the method of Stetter and Dierichs (7) was added to a refluxing solution of potassium (7.5 g) in *t*-BuOH (500 mL) under nitrogen. After 5 h of reflux, propargyl bromide (18 mL) was added slowly to the cooled solution and the mixture was heated at 90°C for 10 h. After cooling, a crude oily product (containing some *O*-alkylated product) was obtained by adding dilute HCl and extracting with ether. To exclude the *O*-alkylated product, the oil was taken up in MeOH (200 mL) and treated with 10% HCl (300 mL) at reflux for 2 h. The neutral product obtained by extraction was distilled (84–86°C at 0.02 Torr) affording the diketone **4***a* (27 g, 74%); ν (film): 3280, 3080, 2120, 1730, 1700, and 1640 cm^{-1}; nmr (C_6D_6) δ: $CH_3C(H)$ d(6.5) 0.81, $HC{\equiv}C{-}CH_2$ t(3.0) 1.96 and d(3.0) 2.46, $CH_2{=}CH{-}$ m 5.0 and m 5.3; ms *m/e*: 204(M^+, weak), 134, 133, 91, and 69(base). *Anal.* calcd. for $C_{13}H_{16}O_2$: C 76.5, H 7.8; found: C 76.4, H 7.6.

*2-Allyl-2-propargyl-3-hydroxy-5-methylcyclohexanone (**5**a)*

To the diketone **4***a* (11 g) vigorously stirred in THF (300 mL) under nitrogen at 0°C was added very slowly a solution of lithium tri-*tert*-butoxy aluminium hydride (13 g) in THF (200 mL). After 5 h at 0°C saturated sodium sulfate solution (400 mL) was added and the resulting precipitate filtered (Celite). Evaporation afforded the hydroxy-ketone **5***a* (10.3 g, 94%). The minor product crystallised from CCl_4, mp 89–90°C; ν (KBr): 3550, 3300, 3110, 2130, 1715, and 1660 cm^{-1}; nmr ($CDCl_3$) δ: $CH_3C(H)$ d(6.0) 1.25, $HC{\equiv}C{-}CH_2$ t(3.0) 2.05, HOCH s 3.1 and dd(5.0 and 3.0) 4.2; ms *m/e*: 206(M^+), 165, 161, 121, 105, 91 and 78(base). *Anal.* calcd. for $C_{13}H_{18}O_2$: C 75.6, H 8.7; found: C 75.5, H 8.6.

The *major* product never crystallised but showed very similar spectral properties to those above except in the nmr where the C*H*—O(H) appears as dd(11.0 and 5.0) 4.15.

The *mesylate* prepared from the minor product, mp 98–99°C (from hexane). *Anal.* calcd. for $C_{14}H_{20}O_4S$: C 59.1, H 7.1, O 22.5; found: C 59.1, H 6.9, O 22.6.

The *tosylate* prepared from the minor product, mp 104–105°C (from EtOH). *Anal.* calcd. for $C_{26}H_{24}O_4S$: C 66.6, H 6.7, S 8.9; found: C 66.8, H 6.7, S 9.0.

*2-Allyl-2-propargyl-5-methylcyclohex-3-enone (7*a)*

The hydroxy-ketone **5***a* (20 g) in pyridine (500 mL) was cooled to 0°C. Phosphorus oxychloride (55 mL) was added dropwise and the temperature then kept at 70°C for 20 h. The cooled mixture was cautiously poured into stirred ice water and the crude product (17.5 g) obtained by $CHCl_3$ extraction. Vacuum distillation (Hempel column, 39°C at 0.02 Torr) afforded the cyclohexenone **7***a* (4.8 g, 28%) as a colourless oil, n_D^{25} 1.4955; ν (film): 3300, 3105, 3050, 2125, 1720, and 1650 cm^{-1}; nmr ($CDCl_3$) δ: $CH_3C(H)$ d(7.0) 1.05, $HC{\equiv}C{-}CH_2{-}$ t(3.0) 2.03 and d(3.0) 2.30, $-CH{=}CH-$ AB part of an ABX system ν_A 5.63 and ν_B 5.77 (10.0, 3.5, and 1.5); ms *m/e*: 188(M^+), 173, 147, 145(base), 131, 109, 107, 105, and 91. *Anal.* calcd. for $C_{13}H_{16}O$: C 82.9, H 8.6; found: C 83.0, H 8.5.

The residue from the first distillation was distilled with a shorter column (Vigreux) to give the chloroketone **8***a* (84°C at 0.02 Torr, 3 g), n_D^{25} 1.5053; ν (film): 3295, 3095, 2105, 1710, 1645, and 850 cm^{-1}; nmr ($CDCl_3$) δ: CH_3CH d(6.0) 1.05, $HC{\equiv}C{-}CH_2{-}$ t(2.0) 2.03 and d(2.0) 2.63, CH—Cl t(3.0) 4.63 (chloro substituent must be axial). *Anal.* calcd. for $C_{13}H_{17}OCl$: C 69.5, H 7.6, Cl 15.8; found: C 69.6, H 7.7, Cl 15.4.

The cyclohexenone **7***a* was also obtained from the chloroketone **8***a* (in 1,5-diazabicyclo[4.3.0]non-5-ene, 90°C, 2 h), from the mesylate (lithium bromide in DMF, this also gave the corresponding bromoketone), and from the tosylate (CCl_4, neutral alumina, reflux 4 h) but the best yields were 25, 30, and 45% respectively.

*2-Allyl-2-acetonyl-5-methylcyclohex-3-enone (**9**)*

The propargyl residue in **7***a* (6.6 g) was hydrated as described previously (1) (BF_3-etherate, trichloroacetic acid, MeOH, 20 h) and the crude oily product afforded the acetonyl compound **9** (73–74°C at 0.04 Torr, 5.1 g, 70%), n_D^{25} 1.4915; ν (film): 3075, 3020, 1720, 1715, and 1645 cm^{-1}; nmr ($CDCl_3$) δ: CH_3CH d(6.5), 1.10, CH_3CO s 2.02, $CH_2{=}CH{-}$ m 5.05 and m 5.66, $-CH{=}CH-$ AB part of ABX system ν_A 5.40 and ν_B 5.47 (9.5, 3.0, and 1.5); ms *m/e*: 206(M^+, weak), 164, 150, 149, 148, 124 (base), 122, 119, and 106. *Anal.* calcd. for $C_{13}H_{18}O_2$: C 75.6, H 8.7; found: C 75.4, H 8.8.

*8-Allyl-5-methylhydrinda-3,6-dien-2-one (**10**a)*

The diketone **9** (6.8 g) was cyclised using degassed aqueous KOH. Benzene–ether (5:2) elution of a neutral alumina column (activity III) afforded the liquid conjugated enone **10***a* (5.3 g, 85%), bp 80–82°C at 0.02 Torr, n_D^{25} 1.5249; λ_{max}: 234 (6500) nm; ν (film): 3100, 3040, 1715, 1650, and 1637 cm^{-1}; nmr ($CDCl_3$) δ: CH_3CH d(6.5) 1.15, CH_2CO ABq(18.0) centred at 2.28 (ν_A 2.14, ν_B 2.44), $CH_2{=}CH-$ m 5.02, $-CH{=}CH-$ AB part of ABX system ν_A 5.48 and ν_B 5.66 (9.0, 2.5, and 1.0), $=CHCO$ s 5.86 (broadened by allylic protons); ms *m/e*: 188(M^+), 147(base, $M-41$), 119, 117, 105, 91, 86, and 84.

2,4-Dinitrophenylhydrazone, mp 122–123°C. *Anal.* calcd. for $C_{19}H_{20}N_4O_4$: C 61.9, H 5.5, N 15.2; found: C 61.7, H 5.4, N 14.9.

*1-Propargyl-8-allyl-5-methylhydrinda-3,6-dien-2-one (**10**b)*

(*a*) Kinetically controlled alkylation of the hydrindadienone **10***a* (0.5 g) using essentially House *et al.*'s[3] method (lithium diisopropylamide, 1,2-dimethoxyethane, −20°C, rapid addition of propargyl bromide) afforded a coloured oil from which the propargyl-ketone **10***b* (0.235 g, 40%) was obtained by chromatography; λ_{max}: 234 (7150) nm; ν (film): 3300, 3080, 3020, 1705, 1645 (sh), and 1630 cm^{-1}; nmr ($CDCl_3$) δ: CH_3CH d(7.0) 1.16, $HC{\equiv}C{-}$ t(2.5) 2.05; ms *m/e*: 226(M^+), 185(base, $M-41$), 157, 147, 142, 119, and 115.

(*b*) The *hydroxymethylene derivative* **10***c* prepared using dry sodium methoxide in benzene, methyl formate and then adding **10***a*, solidified after evaporative distillation (yield 76%), mp 94–95°C (from petroleum ether); λ_{max}: 247 (9950) and 287 (7100) nm, λ_{max} (NaOH): 337 (10 450) nm; ν (KBr): 2800–2600, 1710,

Can. J. Chem. Downloaded from www.nrcresearchpress.com by 210.87.254.42 on 09/05/12
For personal use only.

1635, and 1580 cm^{-1}; nmr ($CDCl_3$) δ: CH_3CH d(6.5) 1.14, =CHCO s 6.0, =CH—OH s 7.11 and s 10.9; ms *m/e*: 216(M^+), 195, 175(base, $M-41$), 163, and 147.

Alkylation of the hydroxymethylene **10***c* (potassium *tert*-butoxide, benzene) afforded the same *C*-alkylated product **10***b* (0.060 g) which was separated by column chromatography from the *O-alkylated product* **10***d* (0.060 g): λ_{max}: 247 (6600) and 283 (sh, 4600) nm; ν(CCl_4): 3300, 3100, 3040, 2120, 1720, 1650, 1275–1200, and 1100 cm^{-1}; nmr ($CDCl_3$) δ: CH_3CH d(7.0) 1.15, $HC\equiv C-CH_2-$ t(2.0) 2.60 and d(2.0) 4.60, =CHCO s 6.10, —C=CH—O—R s 7.20.

2-Allyl-2-propargyl-5-methylcyclohex-3-enol (12a)

The cyclohexenone **7***a* (4.0 g) was reduced as described above for **5***a* but at room temperature affording the low melting alcohol **12***a* (3.6 g, 81%), mp ca. 40°C (from petroleum ether by cooling in dry ice); ν (film): 3500(broad), 3300, 3080, 3020, 2100, and 1640 cm^{-1}; nmr ($CDCl_3$) δ: CH_3CH d(7.0) 1.00, $-CH_2-CH(OH)-$ m 1.44 and dd(12.0 and 4.0) 3.83, $HC\equiv C-CH_2-$ t(3.0) 2.03 and d(3.0) 2.40, $CH_2=CH-$ m 5.11 and m 5.72, $-CH\equiv CH-$ s 5.50 (!).

Converted to the *O-acetyl derivative* **12***b* in the usual manner but this was also liquid (bp 60°C at 0.01 mm), n_D^{25} 1.4848. Spectral changes as expected ($\nu_{C=O}$ 1735 and 1250 cm^{-1} and nmr ($CDCl_3$) δ: CH_3CO s 2.02). *Anal.* calcd. for $C_{15}H_{20}O_2$: C 77.6, H 8.7; found: C 77.6, H 8.8.

2(β-Cyanoethyl)-5-methylcyclohexa-1,3-dione (3b)

Dihydroorcinol (34 g), EtOH (81 mL) triethylamine (54 mL), water (81 mL), and freshly distilled acrylonitrile (24.2 mL, 35% excess) were heated to reflux for 3.5 h. After cooling in ice, the mixture was acidified with 50% HCl and the precipitated cyanoethyl product **3***b* (28.7 g, 60%) was filtered and washed with water, mp 161–162°C (from acetone, lit. (8) mp 159–163°C): λ_{max}: 261 (14 500) nm; ν (KBr): 3250–2100, 2245, 1635, and 1570 cm^{-1}; nmr (acetone-d_6) δ: CH_3—CH d(4.5) 1.06. *Anal.* calcd. for $C_{10}H_{13}O_2N$: C 67.0, H 7.3, N 7.8; found: C 67.1, H 7.3, N 7.7.

2(β-Cyanoethyl)-2-propargyl-5-methylcyclohexa-1,3-dione (4b)

To the cooled solution of potassium (15.5 g) dissolved in anhydrous *t*-BuOH (1 L) was added 2-cyanoethylcyclohexa-1,3-dione **3***b* (64.6 g) and the mixture refluxed for 4 h. To the cooled solution was then added propargyl bromide (4 equiv., drop by drop) and the refluxing continued for 40 h. The cooled reaction mixture was poured into dilute HCl and the product obtained by $CHCl_3$ extraction. The oil was purified by chromatography over neutral alumina (III) and the diketone **4***b* obtained as a low melting solid (64.2 g, 82%), mp 51–52°C (from EtOH – water): ν (KBr): 3270, 2250, 2120, 1730, and 1700 cm^{-1}; nmr ($CDCl_3$) δ: CH_3—CH two d(7.0) 1.08 and 1.15 relative intensities 2:1 respectively and m 2.14, CH_2CO s 2.25. *Anal.* calcd. for $C_{13}H_{15}NO_2$: C 71.9, H 7.0, N 6.4; found: C 71.9, H 7.0, N 6.3.

2(β-Cyanoethyl)-2-propargyl-3-hydroxy-5-methylcyclohexanone 5b

The diketone **4***b* (39.8 g) was dissolved in MeOH (800 mL) and cooled to 0°C. Sodium borohydride (1.89 g) in water (35 mL) was added with rapid stirring during 15 min and agitation continued for a further 15 min after which the mixture was poured into water (2 L) containing acetic acid (10 mL). Methylene chloride extraction gave an oil which crystallised after neutral alumina (III) chromatography. The partially reduced product **5***b* (38.9 g, 96%) being eluted with benzene – 2% ethyl acetate, mp 117–118°C (from acetone–hexane): ν (KBr): 3420 and 3380 (two OH bands), 3305 and 3265 (two ≡CH bands), 2255 and 2245 (two C≡N bands), 2115, 1700, 1050, and 1020 cm^{-1}; nmr ($CDCl_3$) δ: CH_3—C two d(5.0) 0.98 and 1.06, CH_2—C≡C d(2.5) 2.56, OH s 2.86. The *CH*OH of the minor product (25% from integration) showed dd(11.0 and 3.5) 3.73 and the major product (75%) dd(11.0 and 4.5) 4.12. *Anal.* calcd. for $C_{13}H_{17}NO_2$: C 71.2, H 7.8, N 6.4, O 14.6; found: C 71.4, H 7.8, N 6.2, O 14.5.

The *mesylate* was prepared in quantitative yield in the normal manner, mp 111–112°C (from acetone–hexane): ν (KBr): 3290, 2260, 1710, 1350, 1170, 950–935 cm^{-1}; nmr ($CDCl_3$) δ: CH_3 d(6.0) 1.09, CH_3 (in mesylate) s 3.08, C*H*—OMs dd(10.0 and 5.0) 4.76. *Anal.* calcd. for $C_{14}H_{19}NO_4S$: C 56.6, H 6.4, N 4.7, O 21.6; found: C 56.5, H 6.3, N 4.6, O 21.5.

The *tosylate*, mp 181–182°C (from acetone): ν(KBr): 3300, 3100, 1710, 1605, and 1370 cm^{-1}; nmr ($CDCl_3$) δ: CH_3—C d(5.5) 1.04, CH_3 (tosylate) s 2.42, aromatic protons d(8.0) 7.35 and d(8.0) 7.83. *Anal.* calcd. for $C_{20}H_{23}NO_4S$: C 64.3, H 6.2, N 3.8; found: C 64.3, H 6.1, N 4.0.

2(β-Cyanoethyl)-2-propargyl-5-methylcyclohexa-1,3-diol 6

This was the only reduced product when the reaction described above (**5***b*) was performed at room temperature, mp 160–161°C: ν (KBr): 3420, 3320, 2255, 2115, and 1000 cm^{-1}; nmr (acetone-d_6) δ: CH_3 d(5.0) 0.97, $HC\equiv C-CH_2-$ t(2.5) 2.32 and d(2.5) 2.58, CHOH m 3.90 and s 2.94 (D_2O). *Anal.* calcd. for $C_{13}H_{19}NO_2$: C 70.6, H 8.7, N 6.3; found: C 70.4, H 8.7, N 6.4.

The *diacetate*, mp 154–156°C (from hexane–acetone): ν (KBr): 3300, 2235, 2115, 1740, 1725, 1260, and 1240 cm^{-1}; nmr ($CDCl_3$) δ: CH_3 d(6.0) 1.00, CH_3CO s 2.07 and CH—OR dd(11.0 and 3.5) 4.92. *Anal.* calcd. for $C_{17}H_{23}NO_4$: C 66.9, H 7.6, N 4.6; found: C 67.0, H 7.7, N 4.5.

Dehydration of Ketol 5b (Affording 7b and 8b)

To ketol **5***b* (3.54 g) in anhydrous pyridine (80 mL), cooled in ice, was slowly added phosphorus oxychloride (10 equiv.). The mixture was then heated at 64°C for 21 h, cooled, and cautiously poured into ice water (500 mL). Methylene chloride extraction afforded an oil (3 g) from which on trituration with a small volume of hexane precipitated the *chloro compound* **8***b* (2.58 g, 67%), mp 94–95°C (from acetone–hexane): ν (KBr): 3300, 2240, 2105, 1715, and 760 cm^{-1}; nmr ($CDCl_3$) δ: CH_3 d(6.0) 1.08, C*H*—Cl t(3.5) 4.56. *Anal.* calcd. for $C_{13}H_{16}NOCl$: C 65.7, H 6.8, N 5.9, Cl 14.9; found: C 65.4, H 6.8, N 5.8, Cl 14.8.

The *semicarbazone*, mp 205–206°C (from EtOH–water). *Anal.* calcd. for $C_{14}H_{19}N_4OCl$: C 57.0, H 6.5, N 19.0, Cl 12.0; found: C 56.8, H 6.4, N 19.3, Cl 11.8.

The mother liquors from above were evaporated and the oil purified by preparative tlc (silica gel) to give the dehydration product **7***b* (0.400 g), bp 80°C at 0.04 Torr: ν (film): 3300, 3030, 2270, 2140, and 1720 cm^{-1}; nmr ($CDCl_3$) δ: CH_3 d(6.5) 1.09, —CH=CH— dd(10.0 and 1.5) 5.42 and dd(10.0 and 1.5) 5.42 and dd(10.0 and 3.0) 5.89.

This same olefin (**7***b*) was obtained in low yield by heating the mesylate with lithium chloride in DMF, by refluxing the tosylate in pyridine for 4 days (40% yield after difficult purification), and by heating the tosylate with neutral alumina (activity I) in CCl_4 (yield 25%, the remainder being the alcohol **5***b*).

2(β-Cyanoethyl)-2-propargyl-3-ethylenedioxy-5-methylcyclohexanol 13

The ketol **5***b* (27.5 g), *p*-toluene sulfonic acid (1.0 g), and ethylene glycol (38.6 g) were refluxed in benzene (300 mL) for 48 h (Dean–Stark separator). After cooling the excess glycol was decanted and the ketal (80%) obtained by normal manipulation. To remove a small quantity of unreacted ketone **5***b*, the product was chromatographed over neutral alumina affording the ketal **13**, mp 113–114°C (acetone–hexane): ν (KBr): 3530, 3290, 2245, 2110, 1095, and 1025 cm^{-1}; nmr ($CDCl_3$) δ: CH_3 d(6.0) 0.92, HO—CH s 2.64 (D_2O) and dd(10.0 and 4.0) 3.67, $-OCH_2CH_2O-$ s 3.95. *Anal.* calcd. for $C_{15}H_{21}NO_3$: C 68.4, H 8.0, N 5.3, O 18.2; found: C 68.1, H 8.0, N 5.2, O 18.5.

The *tosylate*, mp 128–129°C (from ether–hexane): ν (KBr):

Can. J. Chem. Downloaded from www.nrcresearchpress.com by 210.87.254.42 on 09/05/12
For personal use only.

3285, 2245, 2120, 1605, 1340, 1185, 1170, and 1120–1050 cm^{-1}; nmr ($CDCl_3$) δ: CH_3 d(5.5) 0.91, aromatic CH_3 s 2.46, $—OCH_2CH_2O—$ s 3.97, $CH_{(ax)}$ OTs dd(11.5 and 4.5) 4.68, aromatic protons d(8.5) 7.38 and d(8.0) 7.83. *Anal.* calcd. for $C_{22}H_{17}NO_5S$: C 63.3, H 6.5, N 3.4, S 7.7; found: C 63.0, H 6.6, N 3.2, S 8.0.

2(β-Cyanoethyl)-2-propargyl-3-ethylenedioxy-5-methylcyclohexanone ***14***

(a) Ratcliffe–Rodehorst (5) Oxidation of Alcohol ***13***

Chromium trioxide (82.2 g) was added to a solution of pyridine (123 g) in methylene chloride (2 L). Stirring was continued for 10 min and then the alcohol **13** (36 g) in a minimum of methylene chloride was added all at once. After stirring for 1 h, the solution was decanted and the residue well washed with more methylene chloride. The combined organic solutions were washed and evaporation afforded the ketone **14** (36 g, quantitative), mp 101–102°C (softening at 91–92°C, from acetone–hexane): ν (KBr): 3280, 2250, 2120, 1710, and 1130–1040 cm^{-1}; nmr ($CDCl_3$) δ: CH_3 d(6.0) 1.04, $—OCH_2CH_2O—$ s 3.98. *Anal.* calcd. for $C_{15}H_{19}NO_3$: C 68.9, H 7.3, N 5.4; found: C 68.7, H 7.1, N 5.3.

(b) By Partial Ketalisation of ***4***b

To the diketone ***4b*** (10 g) in benzene (200 mL) was added ethylene glycol (18 mL) and *p*-toluene sulfonic acid (0.20 g). After 26 h of reflux in a Dean–Stark separator, the mixture was well washed, evaporated, and the ketal **14** (7.56 g; 63%) obtained by crystallisation from methanol–water.

2(β-Cyanoethyl)-2-allyl-3-ethylenedioxy-5-methylcyclohexanol ***15***a

(a) By Hydrogenation of ***13***

Lindlar catalyst (0.400 g) was hydrogenated in acetone (25 mL) containing quinoline (3 drops). The propargyl compound **13** (1.27 g) was added in a minimum of acetone and hydrogenation continued (uptake 1 mol). After filtering and washing the catalyst, evaporation afforded the crude product from which minor impurities were removed by chromatography over neutral alumina (activity III). The allyl compound ***15a*** (1.25 g, 97%) crystallised slowly from hexane–ether, mp 81–82°C: ν (KBr): 3460, 3080, 2250, 2240, 1645, and 1110–1025 cm^{-1}; nmr ($CDCl_3$) δ: CH_3 d(6.0) 0.94, HO—CH d(10.0) 3.28 and broad s 3.58 (D_2O), $—OCH_2CH_2O—$ s 3.90, $—CH=CH—$ m 5.1 and m 5.9. *Anal.* calcd. for $C_{15}H_{23}NO_3$: C 67.9, H 8.7, N 5.3; found: C 67.9, H 8.9, N 5.2.

The *acetate* ***15b*** crystallised from hexane, mp 77–78°C: ν (KBr): 3085, 2240, 1730, 1640, 1240, and 1090–1030 cm^{-1}; nmr ($CDCl_3$) δ: CH_3 d(6.0) 1.04, CH_3CO s 1.98, $—OCH_2CH_2O—$ two s 3.86 and 3.91. *Anal.* calcd. for $C_{17}H_{26}NO_4$: C 66.4, H 8.2, N 4.6; found: C 66.3, H 8.1, N 4.6.

The *3,5-dinitrobenzoate*, mp 140–141°C (from EtOH). *Anal.* calcd. for $C_{22}H_{25}N_3O_8$: C 57.5, H 5.5, N 9.2; found: C 57.6, H 5.6, N 9.4.

(b) By Ketalisation of ***25***a

Following the procedure described above for **13**, the ketol ***25a*** (see later) was converted to the allyl-ketal ***15a*** in 80% yield.

2,6-Dimethyl-4-ethylenedioxy-9-(β-cyanoethyl)-perhydrobenzofuran ***16***a

Mercuric acetate (1.45 g) was dissolved in water (5 mL) to which was added THF (5 mL). To this yellow solution was added the allyl derivative ***15a*** (1.2 g) in a minimum of THF (4). The color disappeared in 10–15 s and stirring was continued for 5 min. NaOH solution (5 mL of 3 *M*) followed by sodium borohydride (5 mL of a 0.5 *M* solution in aqueous sodium hydroxide 3 *M*) was added to precipitate the mercury. After decanting, the solution was saturated with NaCl and extraction afforded the liquid product ***16a*** (1.16 g, 97%): ν (film): 2240 and 1120–1040 cm^{-1}; nmr ($CDCl_3$) δ: CH_3 d(5.0) 0.92, $CH_3—CH—O$ d(6.5) 1.32, $—OCH_2CH_2O—$ s 3.97. For characterisation the ketal moiety in tetrahydrofuran ***16a*** was hydrolysed (MeOH, water, HCl, room temperature, 16 h) to the *ketone* ***16b*** (ν (film): 2250, 1710, and 1140–1050 cm^{-1}; nmr ($CDCl_3$) δ: CH_3 d(5.0) 1.04, $CH_3—CH—O$ d(6.0) 1.23 and m 4.0) which afforded a crystalline *semicarbazone*, mp 205–206°C (from ethanol). *Anal.* calcd. for $C_{14}H_{22}N_4O_2$: C 60.4, H 8.0, N 20.1; found: C 60.5, H 7.9, N 20.5.

2(β-Cyanoethyl)-2-allyl-5-methylcyclohexa-1,3-dione ***24***a

The nitrile ***3b*** (89.5 g) was alkylated with allyl bromide (4 equiv.) in the presence of potassium *tert*-butoxide (from potassium (21 g) in 1 L of *t*-BuOH) following the procedure outlined for ***4b***. The product ***24a*** (78%) showed bp 130–132°C at 0.04 Torr, n_D^{25} 1.4980; ν (film): 3095, 2245, 1728, 1700, 1650, and 937 cm^{-1}; nmr ($CDCl_3$) δ: CH_3 two d(6.0) 0.96 and (5.5) 1.14, allyl residue m 4.98–5.75 (3H). *Anal.* calcd. for $C_{13}H_{17}NO_2$: C 71.2, H 7.8, N 6.4; found: C 71.2, H 7.7, N 6.3.

2(β-Cyanoethyl)-2-allyl-3-hydroxy-5-methylcyclohexanone ***25***a

The diketone ***24a*** (71.2 g) was reduced by the method described for ***5b*** affording the ketol ***25a*** (70 g, 97%), bp 132–135°C at 0.05 Torr, n_D^{25} 1.5003; ν (film): 3480, 3050, 2250, 1705, 1648, and 925 cm^{-1}; nmr ($CDCl_3$) δ: CH_3 d(5.5) 1.06, HO—CH broad s 3.11 (D_2O) and for the minor product (ca. 25%) showed m 4.0 and the major product (ca. 75%), dd(11.0 and 5.0) 3.79, allyl residue m 4.96–6.0 (3H). *Anal.* calcd. for $C_{13}H_{19}NO_2$: C 70.6, H 8.7, N 6.3; found: C 70.3, H 8.7, N 6.3.

The *acetate*, mp 128–129°C (from MeOH); ν (KBr): 3090, 2245, 1730, 1705, 1645, and 1240 cm^{-1}; nmr ($CDCl_3$) δ: CH_3 d(6.0) 1.02, CH_3CO s 2.02, $—CH_2—CH=CH_2$ dt(5.5 and 1.5) 2.50, dt(5.5 and 1.5) 2.66, m 5.48–5.83 and m 5.0 (also contains $CH—OAc$). *Anal.* calcd. for $C_{15}H_{21}NO_3$: C 68.4, H 8.0, N 5.3; found: C 68.5, H 8.1, N 5.1.

The Hydroxy-acetate ***17***a

The acetyl derivative ***15b*** (1.20 g) was dissolved in a small volume of THF and added to a solution of mercuric acetate (1.245 g) in water (4 mL) and THF (4 mL). Decoloration of the mixture at room temperature took 6 days when the reaction was stopped by adding 3 *M* NaOH (4 mL) and sodium borohydride (4 mL of 0.5 *M* in aqueous NaOH). After decanting from the mercury, the solution was saturated with NaCl and methylene chloride extraction gave a mixture affording ***17a*** (9%) by chromatography (alumina activity IV), mp 135°C: ν (KBr): 3500, 2250, 1725, 1275, and 1100–1030 cm^{-1}; nmr ($CDCl_3$) δ: CH_3 d(6.0) 0.94, $CH_3—CHOH$ d(6.5) 1.34, CH_3CO s 2.05, $—OCH_2CH_2O—$ d(6.5) 3.87.

2(β-Cyanoethyl)-2-allyl-3-ethylenedioxy-5-methylcyclohexanone ***18***

The alcohol ***15a*** (1.5 g) was oxidised with chromium trioxide (3.4 g) in pyridine (5.4 mL) and methylene chloride (85 mL) as described for **14**. The product **18** (1.4 g, 95%) crystallised with difficulty so the analytical sample was sublimed, mp 84–85°C: ν (KBr): 3090, 2245, 1705, 1645, and 1135–1005 cm^{-1}; nmr ($CDCl_3$) δ: CH_3 d(6.5) 1.03, $—OCH_2CH_2O—$ s 3.93 and s 3.98 relative intensities 1:2, allyl residue 4.95–6.15 (3H). *Anal.* calcd. for $C_{15}H_{21}NO_3$: C 68.4, H 8.0, N 5.3; found: C 68.6, H 8.1, N 5.1.

This same product (**18**) was also prepared in quantitative yield by hydrogenating the corresponding propargyl compound **14** over Lindlar catalyst, as described for ***15a***.

Chromatography of **18** over silica gel gave, by slow elution with benzene – ethyl acetate 2%, fractions containing mostly the isomer ***21a*** in about 60% yield. The purest sample obtained showed mp 56–60°C (from ether–hexane), nmr ($CDCl_3$) δ: $—OCH_2CH_2O—$ s 3.98.

Can. J. Chem. Downloaded from www.nrcresearchpress.com by 210.87.254.42 on 09/05/12
For personal use only.

Further elution afforded pure **21***b* which crystallised from ether–hexane, mp 94–95°C, nmr ($CDCl_3$) δ: —OCH_2CH_2O— s 3.93.

In later experiments simply seeding a solution of the mixed racemates **18** with pure **21***b* provoked the crystallisation of the latter and the mother liquors were thus enriched in **21***a*. At best about 10% of **21***b* remained in the sample.

*2(β-Cyanoethyl)-2-acetonyl-3-ethylenedioxy-5-methylcyclohexanone **19** (via **17**b)*

The allyl ketone **18** (1.03 g) was hydrated as described for **17***a*, except that decoloration took only 8–10 s and stirring was continued for only 5 min. The usual work-up (borohydride–NaOH) only partially reduced the carbonyl functions and gave 0.897 g of a mixture of the diol **17***b* and the corresponding keto-alcohol which not even careful chromatography could separate. The diol mixture was oxidised as described in the preparation of **14**. The product (**19**, quantitative) crystallised but repeated recrystallisation from acetone–hexane effected the separation of the pure racemate **22***a*, mp 166–167°C: ν (KBr): 2240, 1720, 1700, and 1170–1040 cm^{-1}; nmr ($CDCl_3$) δ: CH_3 d(5.5) 1.02, CH_3COCH_2— s 2.21 and s 3.15 (2H), —OCH_2CH_2O— s 3.95 (4H). *Anal.* calcd. for $C_{15}H_{21}NO_4$: C 64.5, H 7.6, N 5.0; found: C 64.4, H 7.8, N 4.7.

Silica gel chromatography of the mother liquors gave the lower melting isomer **22***b*, mp 113–115°C. The spectral data were virtually identical with those for **22***a* except for the absence of the nmr singlet at 3.15 δ (2H) which now complicated the multiplet in the 2.4–2.8 δ region.

In separate experiments, pure **21***a* was found to lead to **22***a* and the **21***b* samples afforded **22***b*. Yields were comparable in all cases.

*3[9(2-Oxo-4-ethylenedioxy-6-methylhydrind-1(8)-en)yl] Propionic Acid **20** (**23**)*

Under nitrogen, potassium hydroxide (1.32 g) was dissolved in degassed water (25 mL) and the diketone **19** (0.540 g of **22***a*) was added. The mixture was gently refluxed (under nitrogen) for 24 h and the crude product obtained by methylene chloride extraction. Preparative tlc over silica gel (ethyl acetate) afforded the cyclised acid **20** (0.300 g, 56%), mp 137–138°C: λ_{max}: 238 (12 300) nm; ν (KBr): 3600–2400, 3040, 1715(broad), and 1630 cm^{-1}; nmr ($CDCl_3$) δ: CH_3CH d(6.0) 0.98, —OCH_2CH_2—O s 3.92 (4H), =CH— s 5.93, —COOH br s 9.30 (D_2O). *Anal.* calcd. for $C_{15}H_{20}O_5$: C 64.3, H 7.2; found: C 64.2, H 7.2.

The *methyl ester* was prepared with excess ethereal diazomethane or better with methyl iodide and potassium carbonate, mp 101–103°C (from methanol): nmr ($CDCl_3$) δ: CH_3 d(6.0) 1.0, $COOCH_3$ s (3H) 3.63, —OCH_2CH_2O— s (4H) 3.92 and =CH—CO s 5.92.

When the mixture of isomeric racemates of **19** was used as starting material, the crude product was difficult to purify and was normally converted to the methyl ester and chromatographed. Yields varied from 15–40%.

*2(β-Cyanoethyl)-2-acetonyl-3-chloro-5-methylcyclohexanone **11***

The chloro-containing propargyl derivative **8***b* (2.3 g) was hydrated as described above, mercuric oxide (0.140 g), BF_3–etherate (0.1 mL), trichloroacetic acid (0.010 g), and MeOH (2 mL). After 2.5 h, H_2SO_4 (250 mL of 2%) was added to hydrolyse the intermediates and the diketone **11** then isolated by extraction (2.1 g, 85%), mp 126–127°C (from acetone–hexane): ν (KBr): 2240, 1712, 1705, and 760 cm^{-1}; nmr ($CDCl_3$) δ: CH_3 d(5.5) 1.07, CH_3COCH_2— s 2.21 and ABq (20) ν_A 3.11 and ν_B 2.83, CH—Cl t(3.5) 4.88. *Anal.* calcd. for $C_{13}H_{18}NO_2Cl$: C 61.1, H 7.1, N 5.5, Cl 13.9; found: C 60.9, H 7.3, N 5.2, Cl 13.6.

Acknowledgements

We wish to acknowledge financial aid from both the Natural Sciences and Engineering Research Council of Canada and the Ministère de l'éducation (D.G.E.S.), Gouvernement du Québec.

1. A. Beth, J. Pelletier, R. Russo, M. Soucy, and R. H. Burnell. Can. J. Chem. **53**, 1504 (1975).
2. Y. Inubushi, H. Ishii, T. Harayama, R. H. Burnell, W. A. Ayer, and B. Altenkirk. Tetrahedron Lett. 1069 (1967).
3. H. O. House, M. Gall, and H. D. Olmastead. J. Org. Chem. **36**, 2361 (1971).
4. H. C. Brown and P. Geoghegan, Jr. J. Am. Chem. Soc. **89**, 1522 (1967).
5. R. Ratcliffe and R. Rodehorst. J. Org. Chem. **35**, 4000 (1970).
6. T. Harayama, M. Takatani, and Y. Inubushi. Tetrahedron Lett. 4307 (1979).
7. H. Stetter and W. Dierichs. Chem. Ber. **85**, 1061 (1952).
8. H. Reinshagen. Justus Liebigs Ann. Chem. **681**, 84 (1965).

Indirect determination of the protonation constants $pK_a(B/BH^+)$ of substituted pyrazoles and indazoles from electrochemical results on the corresponding pentacyanoferrates complexes

JEAN-LOUIS BRISSET AND VICTOR ILIMBI

Laboratoire de Physicochimie des Solutions, LA CNRS 161, E.N.S.C.P. 11 rue Pierre et Marie Curie, 75231 Paris, France

Received December 18, 1979

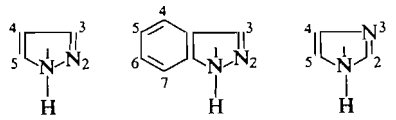
JEAN-LOUIS BRISSET and VICTOR ILIMBI. Can. J. Chem. **58**, 1250 (1980).

A linear correlation is found between the oxidation potentials of the pentacyano (L) ferrates(II) complexes, where L refers to various substituted pyrazoles and indazoles, and the protonation constants of the heterocyclic base L. This correlation allows the $pK_a(L/LH^+)$ of very weak bases in these series be estimated.

JEAN-LOUIS BRISSET et VICTOR ILIMBI. Can. J. Chem. **58**, 1250 (1980).

Une corrélation linéaire entre le potentiel d'oxydation des complexes de type $Fe^{II}(CN)_5L$ (L: pyrazole ou indazole substitué) et la constante de protonation de la base L a été établie. Cette corrélation permet d'estimer le $pK_a(L/LH^+)$ de bases très faibles choisies dans ces séries.

The association between the pentacyanoferrate (II) or (III) moiety $Fe(CN)_5$ and various nucleophilic reagents R, such as organic bases involving one nitrogen atom, has been examined in numerous papers. The complexes $Fe(CN)_5R$ in which R refers to an amine or a pyridine molecule have been carefully investigated, but the literature is rather scanty on the pentacyanoferrates coordinated to a heterocyclic molecule involving several nitrogen atoms. The *N*-methylpyrazinium complex has been investigated through kinetic studies, but the 5-membered heterocyclic molecules have received little attention. When two nitrogen atoms are involved, the corresponding parent molecules are the pyrazole (PZ) or the imidazole (IM), according to the position of the N atoms in the ring.



PZ Indazole IM

Some kinetic and electrochemical results referring to the imidazole ferrate can be found in a few papers (1–5), but a more general study shows that this family of complexes has a very particular behaviour. Spectrophotometric data relevant to some pyrazole complexes are available in a work by Larue (6) (see Table 1).

A previous study (7–9) of the electrochemical behaviour of a number of pyridine complexes showed that the oxidation potential was pH-independent in the range $3 < pH < 12$ for a given complex, which could be therefore characterized by means of the relevant value of the half-wave oxidation potential $E_{1/2}$*. In addition, it was also shown that the $E_{1/2}$* values were linearly correlated to the acidity constants $pK_a(Py/PyH^+)$ of the pyridine ligands.

In this paper we are concerned with the substituted pyrazoles and indazoles complexes, and we attempt to discover whether a similar correlation occurs between the protonation constants $pK_a(B/BH^+)$ and the electrochemical data (viz. the values of the redox potentials) in a similar way as for the pyridine ferrates.

Experimental

The complexes were prepared *in situ* by dissolving solid $Na_3Fe(CN)_5(NH_3)$ and the appropriate ligand in a ratio close to 1:5 in a 0.5 *M* electrolytic solution of KCl or $NaClO_4$. The pH was varied by small additions of strong acid or base and measured immediately after recording the voltammetric curves. The device used for the electrochemical study (dc polarography on a platinum rotating electrode) has been described (8). The ligands were commercially available chemicals purchased from Ega, Fluka, or Aldrich, except for 4-chloropyrazole, 1-methylpyrazole, and 1-acetylpyrazole which were prepared according to known methods (10–12).

The acidity constants pK_a of the ligands were determined potentiometrically in 0.5 *M* KCl solutions.

Results and Discussion

The current–voltage curves recorded for the oxidation of the complexes verify the usual criteria for reversibility:

One monoelectronic wave is observed and the difference $E_{3/4} - E_{1/4}$ is found to be 0.06 V according to the usual value at 20°C.

As a side phenomenon, a second wave is observed for some indazole ferrates (compounds **8–11**) at less positive potentials; this wave is not identified presently, since it is not observed for the pure ligand, or for the pure aquoferrate.

0008-4042/80/121250-03$01.00/0

©1980 National Research Council of Canada/Conseil national de recherches du Canada

Can. J. Chem. Downloaded from www.nrcresearchpress.com by 210.87.254.105 on 09/05/12
For personal use only.

Can. J. Chem. Downloaded from www.nrcresearchpress.com by 210.87.254.105 on 09/05/12
For personal use only.

TABLE 1. Characteristic half-wave potentials (mV, vs sce) of the complexes and protonation constants of the heterocyclic ligand

No.	Ligand LH	$E_{1/2}$		$pK_a(LH/LH_2^+)$	$pK_a'(LH/LH_2^+)$	λ_{max}[g]
1	*Pyrazole*	198		2.64[c]	2.47[c]	455(6)
2	3,Methyl-	148		3.73[b,c]	3.56[c]	485(6)
3	4-Chloro-	225		2.03[d]	1.86[f]	387
4	3,5-Dimethyl-	125		4.55[b,c]	4.38[c]	495(6)
5	1-Acetyl-	178		3.16[d]	2.99[f]	355 453
6	1-Methyl-	194		2.77[d]	2.04[c]	392
7	*Indazole*	254		1.39[c]	1.22[c]	660, 415 470(6)
8	4-Nitro-	292	54[a]	0.42[d]	0.25[f]	490
9	5-Nitro-	304	74[a]	0.13[d]	−0.04[f]	360
10	6-Nitro-	282	56[a]	0.66[d]	0.49[f]	455
11	7-Nitro-	344	88[a]	−0.83[d]	−1.00[f]	485
12	5,6-Dinitro-	340		−0.73[d]	−0.90[f]	335

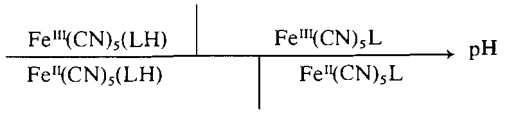
[a]For the 2nd plateau.
[b]Determined potentiometrically at ionic strength 0.5.
[c]Calculated from the thermodynamic constants pK' by correcting with 0.17 (14).
[d]Calculated from eq. [1] (ionic strength 0.5).
[e]Thermodynamic data taken from ref. 14.
[f]Thermodynamic, calculated from values in ref. 14 by correcting with 0.17.
[g]Wavelength (nm) of the absorption peaks of the complexes on the 1st plateau. A linear correlation can be found between $E_{1/2}$ and λ^{-1}, as previously found for the pyridine complexes (9). For the ligands considered, the equations are respectively: $E(V) = 127.5\lambda^{-1} - 0.111$ for PZ, with $r^2 = 0.72$. $E(V) = 51.2\lambda^{-1} + 0.176$ for indazole, with $r^2 = 0.87$. Complex **11** was not considered because of its particular behaviour as an acido-basic indicator.

The plot: $\log (i/i_{lim} - i) = f(E)$, is linear and the slope confirms that one electron is involved in the redox process.

Levich's law is obeyed, and this gives evidence that the electrochemical process is diffusion-controlled.

For each compound, the values of the half-wave potentials $E_{1/2}$ in oxidation are plotted against the corresponding pH values (Fig. 1). The general outline of these diagrams consists of two plateaus for which $E_{1/2}$ is pH-independent joined by a straight line of slope − 0.06 V per pH unit. This is consistent with the following predominance area diagram, where LH refers to the heterocyclic ligand and L to the relevant deprotonated molecule (charges are omitted for the sake of clearness).[1]

However, the second plateau is not observed for some particular ligands, probably because it is located in the high pH range (pH > 12) which has not been investigated (e.g. pH > 12.5 for the indazole complexes). In addition, one can verify that for the 1-substituted ligands for which no proton loss can be considered (e.g. 1-methylpyrazole), the half-wave oxidation potential is not pH-independent in the range 2–12 as expected. The acido-basic properties of the complexes might then be attributed to the OH^- ions which attack at the ligand LH in a similar way as suggested by Gillard (13). The predominance area diagram should then be modified by replacing $Fe(CN)_5L$ by $Fe(CN)_5(LHOH)$. Experiments are under way to get further informations.



In addition, the values of $E_{1/2}$ for the first plateau are linearly correlated to the protonation constants $pK_a(LH/LH_2^+)$ of the ligands. It is noticeable that the results for the substituted pyrazole and indazole complexes fit very well on the same plot. This indicates that the acidity of the sp^2 nitrogen atom is concerned, as has already been found for the pentacyano (pyridine) ferrates(II) for which such an experimental correlation was verified for more than 20 ligands (9). The equation:

[1] $E_{1/2}\,(mV/sce) = -41.65pK_a + 309.43$

can be suggested as the general relationship relevant to the pyrazole and indazole ferrates, with a correlation coefficient of 0.99. It is worthwhile to

[1]Except for acidic media (pH < 2) where protonation occurs on the cyanide groups, the various redox systems considered are, with increasing pH:

$Fe^{II}(CN)_5(LH) \rightleftharpoons Fe^{III}(CN)_5(LH) + e^-$

corresponding to the first plateau of the plot $E_{1/2}$* vs. pH.

$Fe^{II}(CN)_5(LH) \rightleftharpoons Fe^{III}(CN)_5L + H^+ + e^-$

corresponding to the slope of 0.06 V per pH unit.

$Fe^{II}(CN)_5L \rightleftharpoons Fe^{III}(CN)_5L + e^-$

corresponding to the second plateau.

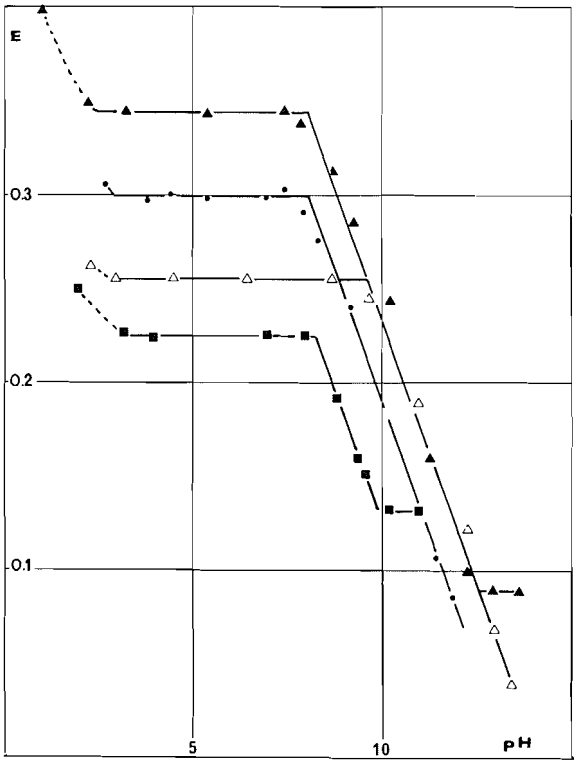


FIG. 1. Typical plots of the half-wave potentials vs. pH for the pentacyanoferrate complexes of 5-nitroindazole (●), 7-nitroindazole (▲), indazole (△), 4-chloropyrazole (■). E (V) is referred to the sce electrode.

mention that the slope of eq. [1] is about two times that of the pyridine correlation. As an immediate consequence, the protonation constants $pK_a(LH/LH_2^+)$ or very "acid" ligands taken in these series can be determined by means of eq. [1], provided one knows the $E_{1/2}$ vs. pH plots. We report in Table 1 the protonation constants pK_a of nitroindazoles and various substituted pyrazoles, which are otherwise too low to be determined potentiometrically.

The so-determined constants are not thermodynamic values since they are obtained from measurements performed at ionic strength 0.5 instead of zero. Assuming then that the ionic strength affects the constants $pK_a(LH/LH_2^+)$ in the same manner, one can estimate the thermodynamic values by calibrating against a given reference (e.g. unsubstituted indazole or pyrazole) or correcting the interpolated value by 0.17 according to ref. 14 (Table 1). The precision on the calculated values depends on the accuracy admitted for the polarographic measurements. Considering that $E_{1/2}$ is known with an accuracy of ±8 mV, then the pK_a values are determined within ± 0.2 pK units.

Acknowledgements

The non-commercially available ligands used in this study were synthesized in the Organic Research Laboratory of this Institute by Dr. Y. Vo Quang. We are also grateful to Dr. J. T. Edward (McGill University, Montreal) for help in writing this paper.

1. T. R. SULLIVAN, D. R. STRANKS, J. BURGESS, and R. I. HAINES. J. Chem. Soc. Dalton, 1460 (1977).
2. H. E. TOMA, J. M. MARTINS, and E. GIESBRECHT. J. Chem. Soc. Dalton, 1610 (1978).
3. R. E. SHEPHERD. J. Am. Chem. Soc. **98**, 3329 (1976).
4. H. E. TOMA and C. CREUTZ. Inorg. Chem. **16**, 545 (1977).
5. J. L. BRISSET and V. ILIMBI. To be published.
6. T. A. LARUE. Anal. Chem. **37**, 246 (1965).
7. M. BIQUARD, J. L. BRISSET, and R. GABORIAUD. C.R. Acad. Sci. **285**C, 459 (1977).
8. J. L. BRISSET, M. BIQUARD, and V. ILIMBI. C.R. Acad. Sci. **288**C, 513 (1979).
9. J. L. BRISSET and M. BIQUARD. To be published.
10. R. HUTTEL, O. SCHAFER, and G. WELZEL. Ann. **598**, 186 (1956).
11. G. DEDICHEN. Ber. **39**, 1845 (1906).
12. G. HUTTEL and J. KRATZER. Chem. Ber. **92**, 2014 (1959).
13. R. D. GILLARD. Coord. Chem. Rev. **16**, 67 (1975).
14. A. ALBERT. *In* Physical methods in heterocyclic chemistry. Vol. 1. *Edited by* A. R. Katritzky. Academic Press, New York. 1963. p. 1.

Can. J. Chem. Downloaded from www.nrcresearchpress.com by 210.87.254.105 on 09/05/12
For personal use only.

Activity corrections for ionic equilibria in aqueous solutions

MIAN S. SUN, DONALD K. HARRISS, AND VINCENT R. MAGNUSON

Department of Chemistry, University of Minnesota, Duluth, MN 55812, U.S.A.

Received July 30, 1979

MIAN S. SUN, DONALD K. HARRISS, and VINCENT R. MAGNUSON. Can. J. Chem. **58**, 1253 (1980).

Activity corrections for ionic equilibria in aqueous solutions at 25°C and ionic strengths up to 0.5 have been investigated. An empirical formula for activity corrections was generated by statistically fitting stability constant data for approximately 540 complexes, for which both thermodynamic and concentration stability constants were known, to a modified Debye–Hückel relationship. The general formula is

$$\Delta \log K = 0.51[\sqrt{I}/(1 + 1.50\sqrt{I}) - 0.09I]\chi - 0.09I$$

$\chi > 0$, where $\Delta \log K$ is the difference in the logarithms of the stability constants at infinite dilution and finite I ($I \leq 0.5$), and χ is an even integer dependent only on the stoichiometry and charge of the ions involved. Activity correction formulae for ionic equilibria involving classes of ligands (amino acid, inorganic, amine, and organic acid) also were developed. The general formula predicts stability constant corrections within 0.1 log unit for 87% of the data used at ionic strength 0.1 and 64% of the data at ionic strength 0.5. In addition, single ion activity coefficients as a function of ionic strength, $0 < I \leq 0.5$, are presented.

MIAN S. SUN, DONALD K. HARRISS et VINCENT R. MAGNUSON. Can. J. Chem. **58**, 1253 (1980).

On a étudié les corrections d'activité pour l'équilibre ionique en solution aqueuse à 25°C et à des forces ioniques allant jusqu'à 0.5. Les données relatives aux constantes de stabilité de 540 complexes pour lesquelles on connaît les constantes de stabilité thermodynamique et concentration, ajustées d'un point de vue statistique ont permis de produire une formule empirique du type Debye–Hückel de correction des activités. Cette formule générale est la suivante:

$$\Delta \log K = 0.51[\sqrt{I}/(1 + 1.50\sqrt{I}) - 0.09I]\chi - 0.09I$$

$\chi > 0$ dans cette formule $\Delta \log K$ est la différence des logarithmes des constantes de stabilité à dilution infinie et finie I ($I \leq 0.5$) et χ est un nombre entier pair qui dépend seulement de la stoechiométrie et de la charge des ions impliqués. On a également développé des formules de correction d'activité des équilibres ioniques qui font intervenir les classes de ligands (acide aminé, inorganique, amine et acide organique). La formule générale permet de prédire à 0.1 unité logarithmique près pour 87% des données utilisées les corrections de constantes de stabilité à une force ionique de 0.1 et pour 64% des données à une force ionique de 0.5. On présente de plus des coefficients d'activité d'un ion unique comme étant une fonction de la force ionique comprise entre $0 < I \leq 0.5$.

[Traduit par le journal]

Introduction

Utilization of literature data for aqueous ionic equilibria is hampered by the lack of ionic activity correction formulae of demonstrated validity for solutions of medium to high ionic strength. Recent data compilations (1, 2) provide a valuable resource with which to test the validity of existing formulae, and a means to develop an empirical formula applicable over a wide range of ionic strengths.

Correction to infinite dilution requires the knowledge of activity coefficients. The most commonly used formulae are the Debye–Hückel (3–5) and Davies (6, 7) equations. The former is said to be applicable at ionic strengths less than 0.1 (3) while the latter are said to be useful up to 0.5 (8). The reliability of these formulae for general application at higher ionic strengths remains questionable due to the lack of large-scale testing with experimental data.

Although the Debye–Hückel and Davies equations have been used extensively, many researchers have used a general equation of the same form to estimate single-ion activity coefficients at 25°C, e.g.,

$$[1] \quad \log \gamma = -0.51z^2\left(\frac{\sqrt{I}}{1 + A\sqrt{I}} + BI\right)$$

When $A = 1.0$ and $B = -0.2$ this equation is referred to as the Davies equation (6), although a value of -0.3 for B has been used in recent works (7). Equation [1] is referred to as the Debye–Hückel equation (3) when $A = 0.33a_0$ and $B = 0$ where a_0 is the effective ion diameter in Å; values of a_0 have been reported for a number of ions (9). Other values for these parameters have been suggested by Scatchard (5) ($A = 1.5$ and $B = 0$) and Güntelberg (4) ($A = 1.0$ and $B = 0$) with a suggested ionic strength less than 0.1.

In the compilation of Smith and Martell (1, 2), a great many stability constants are reported at $I = 0.1$ or 0.5, and for some, corresponding values at infinite dilution also are available. These data will be used to re-examine the parameters in eq. [1] and to establish guidelines for extrapolating the stability constant data at $0 < I \leq 0.5$ to infinite dilution.

Considering a reaction at equilibrium

$$a\mathrm{A} + b\mathrm{B} + \ldots . \rightleftharpoons p\mathrm{P} + q\mathrm{Q} + \ldots .$$

where all charges are omitted for simplicity, the thermodynamic equilibrium constant can be written

0008-4042/80/121253-05$01.00/0

©1980 National Research Council of Canada/Conseil national de recherches du Canada

Can. J. Chem. Downloaded from www.nrcresearchpress.com by 210.87.254.105 on 09/05/12
For personal use only.

Can. J. Chem. Downloaded from www.nrcresearchpress.com by 210.87.254.105 on 09/05/12
For personal use only.

TABLE 1. Average $\Delta \log K$ values with standard deviations, numbers in parentheses are sample size, $I = 0.1$, 25°C

					Calculated	
χ	Inorganic	Organic acids	Amino acids	Amines	a	b
−6				−0.73(1)		
−4				−0.55±0.05(3)		
−2				−0.26±0.03(36)		
0			0.02±0.03(17)	−0.05±0.04(71)[c]		
0				−0.11±0.11(14)[d]		
2	0.22±0.04(11)	0.21±0.03(16)	0.20±0.04(27)	0.21±0.05(9)	0.20	0.21
4	0.41±0.05(9)	0.42±0.06(15)	0.40±0.05(24)	0.40±0.08(5)	0.41	0.43
6	0.65±0.06(10)	0.64±0.11(16)	0.61±0.05(10)		0.62	0.64
8		0.82±0.09(45)		0.79±0.06(12)	0.83	0.86
10		1.13±0.16(4)			1.03	1.07
12		1.22±0.11(18)			1.24	1.29
14					1.45	1.50
16					1.65	1.72
18		1.92±0.11(14)			1.86	1.93

[a]This work, eq. [9].
[b]Davies, $B = -0.3$.
[c]Applicable to ML only.
[d]Applicable to ML_2 only.

$$k = \frac{[P]^p[Q]^q \cdots}{[A]^a[B]^b \cdots} \cdot \frac{\gamma_P{}^p\gamma_Q{}^q \cdots}{\gamma_A{}^a\gamma_B{}^b \cdots} = K_c K_\gamma$$

where K_c is the concentration equilibrium constant and K_γ the activity correction. The difference between logarithms of the thermodynamic equilibrium constant and the concentration equilibrium constant will be referred to as $\Delta \log K$,

$$[2] \quad \Delta \log K = (p \log \gamma_P + q \log \gamma_Q + \ldots) - (a \log \gamma_A + b \log \gamma_B + \ldots)$$

Assuming A and B in eq. [1] to be constants, independent of the nature of the ions, combination of eqs. [1] and [2] at 25°C yields

$$[3] \quad \Delta \log K = 0.51\left(\frac{\sqrt{I}}{1 + A\sqrt{I}} + BI\right)\chi$$

where

$$[4] \quad \chi = (az_A{}^2 + bz_B{}^2 + \ldots) - (pz_P{}^2 + qz_Q{}^2 + \ldots)$$

and the z's are charges for the ionic species. The χ values, as can be shown, take on only even integer values.

Using experimental data for $\Delta \log K$ at various values of χ and I, appropriate statistical treatments can be applied to eq. [3] to determine best values for A and B.

Treatment of Data

Stability constants, which were reported at both infinite dilution and $I = 0.1$ or 0.5, at 25°C for metal complexes over a wide range of metal ions and ligand types (amino acids, inorganic, organic acids, and amines), were selected from Smith and Martell. Approximately 850 $\Delta \log K$ values for metal complexes with $-6 \leq \chi \leq +18$ were collected. Average values of $\Delta \log K$ along with standard deviations at each χ value at 25°C for $I = 0.1$ and 0.5 are presented in Tables 1 and 2, respectively. A total of 47 different metals, including hydrogen, ranging in oxidation state from +1 to +4 and approximately 140 ligands were considered in this study. Data were not included for cases for which tetraalkylammonium salts were used as background electrolytes as use of these salts results in larger $\log K_c$ values than if salts such as $NaClO_4$ or KNO_3 are used (1, 2); also, approximately 15% of the possible data were rejected because of unreasonably high deviations from the means given in Tables 1 and 2.

With the exception of inorganic ligands, data at $\chi = 2$ are dominated by HL and H_2L. For $\chi \geq 4$ a variety of complexes with metal ions and/or protons are involved, except in the case of organic acids where the HL^- species yield the majority of values at $\chi = 4$. Negative values of χ were observed only for the amines due to positively charged ligands in reaction such as

$$M^{2+} + HL^+ \rightleftharpoons MHL^{3+}$$

Much of the data at $\chi = 0$ involves complex formation with neutral ligands. Data at $\chi = 0$ for other ligand categories either are lacking or highly uncertain (see Tables 1 and 2). The uncertainties in $\Delta \log K$, as indicated by the standard deviations, generally increase with χ and I.

TABLE 2. Average Δ log K values with standard deviations, numbers in parentheses are sample size, I = 0.5, 25°C

					Calculated	
χ	Inorganic	Organic acids	Amino acids	Amines	*a*	*b*
−4				−0.77±0.06(2)		
−2				−0.48±0.07(26)		
0	−0.05±0.09(7)	−0.05±0.31(17)	0.04±0.05(6)	−0.14±0.09(106)[c]		
0				−0.27±0.23(33)[d]		
0				−0.44±0.17(7)[e]		
2	0.34±0.10(12)	0.27±0.05(52)	0.25±0.04(12)	0.22±0.05(6)	0.26	0.27
4	0.58±0.09(34)	0.60±0.09(26)	0.49±0.07(11)	0.51±0.02(4)	0.56	0.54
6	0.83±0.11(34)	0.93±0.27(18)	0.72±0.07(9)		0.86	0.81
8	1.27±0.12(11)	1.27±0.17(27)		1.23±0.04(5)	1.17	1.08
10	1.50±0.13(6)				1.47	1.35
12	1.78±0.16(14)	1.77±0.31(9)			1.78	1.62
14					2.08	1.89
16	2.20±0.32(6)				2.38	2.16

[a]This work, eq. [9].
[b]Davies, B = −0.3.
[c]Applicable to ML only.
[d]Applicable to ML_2 only.
[e]Applicable to ML_3 only.

At constant ionic strength all Δ log K values at a given value of χ as calculated by eq. [3] should be the same; a plot of Δ log K versus χ should give a straight line through the origin. Weighted linear regressions were performed on Δ log $K = m\chi + b$ and Δ log $K = m\chi$ for the raw data ($\chi \neq 0$) at constant ionic strength, I = 0.1 or 0.5, with weighting factors based on the uncertainties shown in Tables 1 and 2. In all cases linearity between Δ log K and χ is indicated by Pearson correlation coefficients greater than 0.96. The best fits do not pass through the origin for the amines, the organic acids, and the general case.

The B values calculated from the slopes for the Davies equation are dependent upon ionic strength, decreasing in magnitude with the ionic strength. Thus, assuming that the intercept is a function of I, $Cf(I)$, eq. [3] can be replaced with

$$[5] \quad \Delta \log K = 0.51\left(\frac{\sqrt{I}}{1 + A\sqrt{I}} + BI\right)\chi + Cf(I)$$

For eq. [1] with A = 1, it has been shown that B is a function of I as given below, applicable up to I = 3.0 (10):

$$[6] \quad B = \alpha + \beta F(I)$$

and

$$[7] \quad F(I) = [1 - (1 + 2\sqrt{I} - 2I)\exp(-2\sqrt{I})]/4I$$

where α and β are constants (10). Thus, with A = 1 eq. [5] becomes

$$[8] \quad \Delta \log K = 0.51\left[\frac{\sqrt{I}}{1 + \sqrt{I}} + \alpha I + \beta I F(I)\right]\chi + Cf(I)$$

A weighted least-squares procedure (11) was applied to eqs. [5] and [8] to evaluate the parameters α, β, A, B, and C. The weighting factors included the variances in I, as well as the variances in Δ log K. In view of the low precision of the reported ionic strengths (one significant figure), the uncertainties in I were assumed to be ±10%. The statistically best fit was found for $f(I) = I$.

Results and Discussion

The calculated parameters for eqs. [5] and [8] are tabulated in Table 3. The C values are identical for both equations within the precision shown in Table 3 and eq. [5] is as reliable as eq. [8] in predicting Δ log K.

For the amino acid and inorganic ligand cases, there was no statistical difference whether the term $f(I)$ was included or not. Thus, for these two ligand types we report C to be equal to zero.

All complexes used in this study other than those containing amines involve negatively charged ligands and exhibit χ values greater than zero. For $\chi > 0$ the observed Δ log K values of all complexes including amines fall within a narrow range. Using values of A, B, and C from Table 3 in eq. [5], the general expression for calculation of Δ log K is

$$[9] \quad \Delta \log K = 0.51\left(\frac{\sqrt{I}}{1 + 1.50\sqrt{I}} - 0.09I\right)\chi - 0.09I \qquad \chi > 0$$

In Fig. 1, calculated Δ log K values at I = 0.1 vs. χ are shown along with the average observed data classified by ligand type. Also shown for comparison

Can. J. Chem. Downloaded from www.nrcresearchpress.com by 210.87.254.105 on 09/05/12
For personal use only.

TABLE 3. Summary of parameters evaluated for eqs. [5] and [8] with Wentworth's least-squares procedure, $\chi \neq 0$

Type of ligand	Cases	A	$-B$	$-\alpha$	$-\beta$	$-C^a$	SEE[b]
Inorganic	147	1.27±0.21	0.17±0.06	0.18±0.06	0.24±0.18	0	0.083
Organic acids	260	1.61±0.10	0.03±0.03	0.02±0.04	0.52±0.08	0.10±0.02	0.066
Amino acids	93	1.32±0.15	0.25±0.04	0.26±0.05	0.28±0.13	0	0.046
Amines	109	1.42±0.16	0.04±0.04	0.05±0.05	0.36±0.13	0.30±0.02	0.043
Overall ($\chi > 0$)	541	1.50±0.07	0.09±0.02	0.09±0.02	0.43±0.06	0.09±0.02	0.067

[a] $B = CI$.
[b] SEE = standard error of estimate.

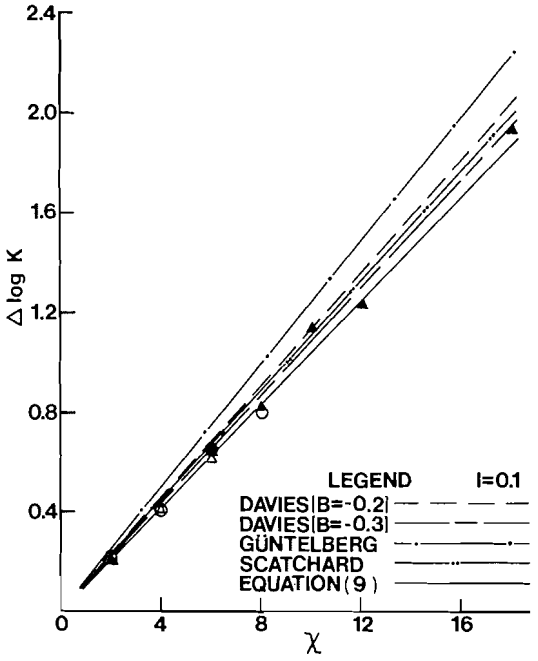


FIG. 1. Observed average $\Delta \log K$ values, $\chi > 0$, for metals complexing with organic acids (▲), inorganic (●), amino acids (△), and amines (○) at $I = 0.1$ and 25°C. The solid line is eq. [9] with $\Delta \log K$ plotted as a function of χ. Also shown for comparison is $\Delta \log K$ versus χ based on the Davies, Güntelberg, and Scatchard equations.

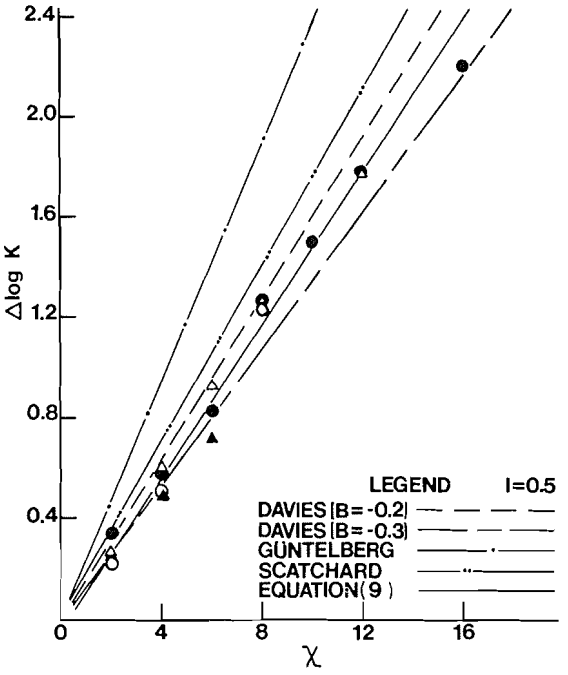


FIG. 2. Observed average $\Delta \log K$ values, $\chi > 0$, for metals complexing with organic acids (△), inorganic (●), amino acids (▲), and amines (○) at $I = 0.5$ and 25°C. The solid line is eq. [9] with $\Delta \log K$ plotted as a function of χ. Also shown for comparison is $\Delta \log K$ versus χ based on the Davies, Güntelberg, and Scatchard equations.

are the predicted $\Delta \log K$ values based on the Davies equations, both with $B = -0.2$ and -0.3, the Güntelberg equation, and the Scatchard equation. Similar plots are shown in Fig. 2 for the case $I = 0.5$. As can be seen from Fig. 1, both eq. [9] and the Davies equation with $B = -0.3$ successfully predict the observed values of $\Delta \log K$. However, at higher ionic strength (see Fig. 2, $I = 0.5$) eq. [9] clearly is superior in fitting the data.

A measure of the accuracy of eq. [9] can be obtained by noting that 87% of the $\Delta \log K$ values are predicted within ± 0.1 at $I = 0.1$ and 64% within these limits at $I = 0.5$. In terms of percentage errors in $\Delta \log K$, 89% and 74% are predicted within $\pm 20\%$ at $I = 0.1$ and $I = 0.5$, respectively.

The results for the amine complexes, as shown in Tables 1 and 2, appear to be unique. Metal amine complexes with values of $\chi > 0$, $\chi = 0$, and $\chi < 0$ correspond to complexes in which the ligands are negatively charged, neutral, and positive, respectively. The $\Delta \log K$ values at $\chi = 0$ divide into groups depending on the number of neutral ligands involved, and the $\Delta \log K$ ratios $-0.05 : -0.11 :: 1 : 2.2$ (Table 1, $I = 0.1$) and $-0.14 : -0.27 : -0.44 :: 1 : 1.9 : 3.1$ (Table 2, $I = 0.5$) indeed correspond to the number of ligands in ML, ML_2, and ML_3, respectively. The $\Delta \log K$ values are in fact the negative values of $\log \gamma_L$, $2 \log \gamma_L$, or $3 \log \gamma_L$ for the neutral ligands in these complexes. The logarithm of the activity coefficient for the neutral species should be proportional to the ionic strength (12), i.e.,

$$\log \gamma_L = cI$$

Can. J. Chem. Downloaded from www.nrcresearchpress.com by 210.87.254.105 on 09/05/12
For personal use only.

Can. J. Chem. Downloaded from www.nrcresearchpress.com by 210.87.254.105 on 09/05/12
For personal use only.

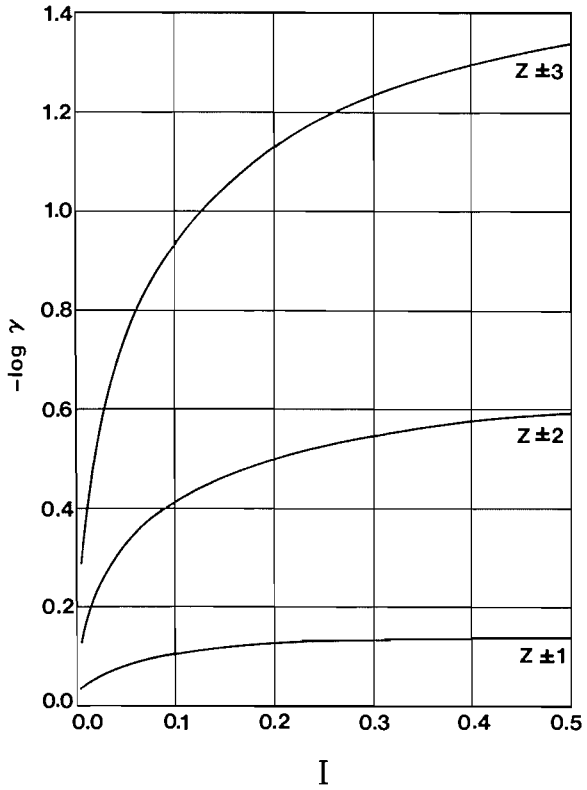


FIG. 3. Single ion activity coefficients predicted with smoothed $\Delta \log K$ values from eq. [9].

thus,

$$[10] \quad (\Delta \log K)_{\chi=0} = -ncI$$

where n is the number of neutral ligands in the complex and c is a constant. Using the data in Tables 1 and 2 for amines, the computed value of c is about 0.3. The reported values of $\Delta \log K$ at $\chi = 0$ for the silver(I) amine complexes, showing no discernible pattern, do not agree with the calculated values from eq. [10]. Using the parameters in Table 3, the equation for the amine complexes is

$$[11] \quad \log K = 0.51\left(\frac{\sqrt{I}}{1 + 1.42\sqrt{I}} - 0.41I\right)\chi - 0.30I \qquad \chi \neq 0$$

The activity coefficients for single ions can be estimated at a given ionic strength by fitting eq. [2] with smoothed $\Delta \log K$ values from eq. [9] using suitable linear combination of the logarithms of γ_1, γ_2, and γ_3 which are, respectively, the activity coefficients of singly, doubly, and triply charged ions. The results are shown in Fig. 3. Alternately, using the smoothed $\Delta \log K$ values from eq. [9] to fit eq. [3] with $I \leq 0.5$ and $\chi \leq 18$ leads to

$$[12] \quad \log \gamma = -0.51z^2\left(\frac{\sqrt{I}}{1 + 1.50\sqrt{I}} - 0.11I\right)$$

which reproduces the curves in Fig. 3 to the nearest 0.02 log unit. For singly and doubly charged ions these results differ slightly from those of Ringbom (13); however, the difference is much larger for the triply charged ions. For example, the activity coefficients (as $-\log\gamma$) for single ions with $z = \pm 3$ at ionic strengths 0.1, 0.3, and 0.5 are found to be 0.93, 1.23, and 1.34 in this work compared to 0.74, 0.96, and 1.03 in Ringbom's work.

Equations [9], [10], and [11] represent the best empirical choices to date for activity corrections in aqueous solutions for $I > 0.1$. They are recommended for use for the general case, neutral ligands ($\chi = 0$), and amines, respectively.

Acknowledgments

We thank the Environmental Protection Agency for financial support, University of Minnesota Computer Services for a computer research grant, and Dr. Michael Miller and Dr. Sara Ingle for helpful discussions.

1. R. M. SMITH and A. E. MARTELL. Critical stability constants. Plenum, New York. Vol. 2, 1975; Vol. 4, 1976.
2. A. E. MARTELL and R. M. SMITH. Critical stability constants. Plenum, New York. Vol. 1, 1974; Vol. 3, 1977.
3. R. A. ROBINSON and R. H. STOKES. Electrolyte solutions. Butterworths, London. 1965. p. 229.
4. E. GÜNTELBERG. Z. Phys. Chem. **123**, 199 (1926).
5. G. SCATCHARD. The structure of electrolytic solutions. *Edited by* W. J. Hamer. John Wiley and Sons, New York. 1959. p. 9.
6. C. W. DAVIES. J. Chem. Soc. 2093 (1938).
7. C. W. DAVIES. Ion association. Butterworths, Washington. 1962. p. 41.
8. J. N. BUTLER. Ionic equilibrium, a mathematical approach. Addison-Wesley, Reading. 1964. p. 437.
9. J. KIELLAND. J. Am. Chem. Soc. **59**, 1675 (1937).
10. C. F. BAES, JR. and R. E. MESMER. The hydrolysis of cations. Wiley-Interscience, New York. 1976.
11. W. E. WENTWORTH. J. Chem. Educ. **42**, 96 (1965).
12. H. S. HARNED and B. B. OWEN. The physical chemistry of electrolytic solutions. Reinhold, New York. 1950. p. 397.
13. A. RINGBOM. Complexation in analytical chemistry. Interscience, New York. 1963. p. 24.

Analysis of ^{13}C nuclear magnetic resonance chemical shifts of acyclic hydrocarbons

HELMUT BEIERBECK AND JOHN K. SAUNDERS

Département de chimie, Université de Sherbrooke, Sherbrooke (Qué.), Canada J1K 2R1

Received December 27, 1979

HELMUT BEIERBECK and JOHN K. SAUNDERS. Can. J. Chem. **58**, 1258 (1980).

The ^{13}C nmr chemical shifts of aliphatic hydrocarbons were derived from chemical shifts and probabilities of individual chain conformations. Conformer resonances were calculated with parameters developed for conformationally homogeneous cyclic molecules. Conformer populations were derived from bond rotation potentials and steric energy contributions, available from independent sources. This analysis contains non adjustable parameters. It represents a unified treatment of cyclic and acyclic hydrocarbon resonances, which is capable of dealing with molecular asymmetry and thus permits the determination of configuration in aliphatic hydrocarbons.

HELMUT BEIERBECK et JOHN K. SAUNDERS. Can. J. Chem. **58**, 1258 (1980).

Les déplacements chimiques en rmn de ^{13}C des hydrocarbures aliphatiques fûrent obtenus en combinant le déplacement chimique et la probabilité des conformations de la chaîne. Les résonances des conformères ont été calculés avec les paramètres utilisés pour les molécules cycliques conformationnellement homogènes. La population des conformères est obtenue des potentiels de rotation des liaisons et des contributions de l'énergie stérique; disponibles de source indépendante. Cette analyse ne contient pas de paramètre variable. Elle représente un traitement unique des résonances des hydrocarbures cycliques et acycliques, capable de s'ajuster à l'assymétrie moléculaire et ainsi permet la détermination de la configuration des hydrocarbures aliphatiques.

The early work by Grant and Paul (1) on aliphatic hydrocarbons provided one of the first demonstrations of the additivity of substituent effects on ^{13}C nmr chemical shifts. Unfortunately, their analysis was based on a topological, rather than geometric, description of molecular structure, and conformational interconversions were not explicitly taken into consideration. Consequently their substituent parameters could neither deal with molecular asymmetry, nor could they be applied to conformationally homogeneous cyclic substrates. Lindeman and Adams (2) later proposed an expanded and modified parameter set, but it too was topological and therefore incapable of dealing with molecular chirality.

Structure elucidation obviously includes the determination of configuration at asymmetric centers, and chemical shift parameters must be able to reproduce magnetic nonequivalence. Since chemical shift nonequivalence in asymmetric chains is the result of geometric nonequivalence in individual conformations, it cannot be understood without a knowledge of the physical properties of these conformations. In other words, the observed chemical shifts are conformational averages, and therefore have to be compared to conformational averages, calculated from conformer resonances and populations.

We have used such an approach to analyse the carbon chemical shifts of a series of saturated aliphatic hydrocarbons (3). The conformer resonances were calculated with a parametrization scheme developed for rigid cyclic substrates (4). The conformer populations were taken to be products of rotamer populations, and the rotational states of adjacent bonds were assumed to be independent. Steric contributions to conformer energies, although considered important (5), were ignored in order to simplify the analysis. Numerical values for the chemical shift and rotamer population parameters were derived by a least-squares fit of calculated to observed conformationally averaged resonances. The chemical shifts calculated from these conformer resonances and probabilities agreed reasonably well with the experimental values. However, magnetic nonequivalence in asymmetric molecules was greatly underestimated, and the rotamer populations derived by optimization did not agree too well with experimental values (6, 7).

The insensitivity of the calculated chemical shifts to molecular asymmetry turned out to be due to the neglect of steric contributions to the conformer energies, and these are now incorporated into the analysis. Secondly, it was decided to use experimentally determined rotational energies (6) and previously derived substituent parameter values for rigid cyclic systems (4) in place of parameter optimization.

The modified analysis of the ^{13}C nmr chemical shifts of saturated aliphatic hydrocarbons presented here contains no more adjustable parameters. It represents a unified treatment of cyclic and acyclic hydrocarbon resonances, which is capable

0008-4042/80/121258-08$01.00/0

©1980 National Research Council of Canada/Conseil national de recherches du Canada

Can. J. Chem. Downloaded from www.nrcresearchpress.com by 210.87.254.5 on 09/05/12
For personal use only.

Can. J. Chem. Downloaded from www.nrcresearchpress.com by 210.87.254.5 on 09/05/12
For personal use only.

of dealing effectively with molecular chirality, and thus permits the determination of configuration in aliphatic hydrocarbons.

Results and Discussion

The conformer resonances are calculated with a parameter set developed for rigid, conformationally homogeneous substrates (4). The chemical shifts for primary, secondary, tertiary, and quaternary carbons are based on four separate reference parameters P, S, T, and Q. An increment HC is added for every 1,3-diaxial hydrogen–hydrogen alignment, a parameter CC for every carbon–carbon *gauche* arrangement, and an increment δ for every *syn*-axial δ interaction. In the previous analysis (3) the numerical parameter values were obtained by a least-squares fit to a set of aliphatic hydrocarbon data. In the present version the numerical values from ref. 4 are used (Table 1).

In the previous analysis (3) the conformational energies were simply considered to be the sums of the rotational energies of the constituent bonds of the chain, and steric energy contributions were ignored. Now the conformer energies are taken to be the sums of rotational and steric energy contributions E_{ij} with associated statistical weights u_{ij}.

$$u_{ij} = \exp(-E_{ij}/RT)$$

The conformer statistical weights Ω_j are the products of m statistical weights u_{ij}, corresponding to m contributions E_{ij} to the energy of conformer j.

$$\Omega_j = \prod_{i=1}^{m} u_{ij}$$

Division of the n conformer statistical weights Ω_j by their sum, the conformational partition function Z, then gives the conformer populations p_j

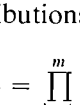
$$Z = \sum_{j=1}^{n} \Omega_j$$

$$p_j = \Omega_j/Z$$

There is rotational isomerism about four types of bonds. The three rotational states of bonds involving quaternary carbons are taken to be equally probable, with zero rotational energies and statistical weights of 1.0. The remaining three bond types correspond to butane, 2-methylbutane, and 2,3-dimethylbutane, whose rotational energy differences are available from Raman spectroscopic studies (6). The rotation potential for 2,3-dimethylbutane has been confirmed by low temperature ^{13}C nmr spectroscopy (7). The energies of the degenerate rotational states are set equal to zero, with statistical weights of 1.0, and the relative energies and corresponding statistical weights for the unique rotational states are given in Table 1.

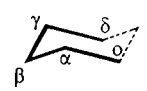
TABLE 1. Parameter definitions and numerical values[a]

Chemical shift parameters		Value (ppm)
P		7.44
S		17.62
T		24.17
Q		26.53
HC		4.55
CC		1.85
δ		2.56

Population parameters	Energy (kJ/mol)	Statistical weight u_{ij}
	−4.042	5.055
	3.385	0.257
	−0.226	1.095
	8.368	0.035

[a]The chemical shift parameters are taken from ref. 4. The rotation potentials, taken from ref. 6, are the energies of the unique, relative to the degenerate, rotational state. The δ energy contribution is taken from ref. 5. The statistical weights are calculated for 300 K.

Two types of steric effects are considered, namely δ and ε interactions. The statistical weights of conformations, which would contain ε interac-



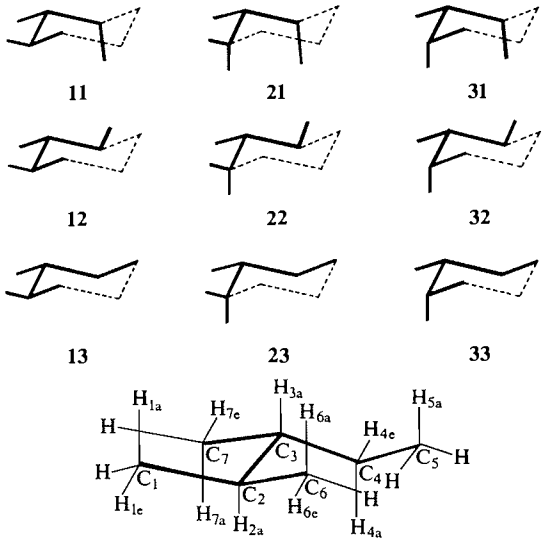
δ ε

tions, are set equal to zero. Each *syn*-axial δ interaction is taken to contribute 2.0 kcal/mol to the

Can. J. Chem. Downloaded from www.nrcresearchpress.com by 210.87.254.5 on 09/05/12
For personal use only.

conformational energy (5). The δ energy term and its corresponding statistical weight are included in Table 1. If there are neither δ nor ε interactions, the "steric" statistical weight is 1.0.

The derivation of the C_1 and C_6 resonances of 2,3-dimethylpentane may serve as numerical illustration. Rotation about bonds C_2—C_3 and C_3—C_4 gives rise to nine molecular conformations, denoted **11** to **33**.



In conformer **13**, for example, bond C_2—C_3 is in the unique rotational state of 2,3-dimethylbutane, bond C_3—C_4 in a degenerate rotational state of 2-methylbutane, and there is one δ interaction between C_5 and C_6. The statistical weight Ω_{13} for conformation **13** of 2,3-dimethylpentane is therefore

$$\Omega_{13} = 1.095 \times 1.000 \times 0.035 = 0.038$$

This value and the remaining conformer statistical weights are listed in Table 2. The sum of the conformer statistical weights Ω_j, the partition function Z, is equal to 4.468 in this case, and division of the Ω_j by that value gives the conformer populations p_j in the last column of Table 2.

The chemical shifts of C_1 and C_6 in conformation **13** of 2,3-dimethylpentane are determined by the following interactions:

C_1	P300			
	HC	H_{1a}–H_{3a}	H_{1e}–H_{6e}	H_{1a}–H_{6a}
	CC	—		
	δ	—		
C_6	P301			
	HC	H_{6e}–H_{1e}	H_{6a}–H_{1a}	H_{6a}–H_{3a}
	CC	—		
	δ	C_6—C_5		

The primary carbon C_1 is involved in three HC, zero CC, and zero δ interactions (abbreviated P300), and its chemical shift in that conformation is

$$7.44 + 3 \times 4.55 = 21.09 \text{ ppm}$$

The primary carbon C_6 is engaged in three HC, zero CC, and one δ interaction (abbreviated P301), and its chemical shift is

$$7.44 + 3 \times 4.55 + 2.56 = 23.65 \text{ ppm}$$

The nine sets of conformer resonances for C_1 and C_6 are given in Table 3. Multiplication of these conformer resonances by the conformer populations of Table 2 gives the conformer contributions shown in the last two columns of Table 3. Their sums are the conformationally averaged chemical shifts.

The procedure was again tested with the hydrocarbon data of Lindeman and Adams (2), and was able to reproduce the complete set of chemical shifts with a standard deviation of 1.59 ppm (Table 4). The experimental data of ref. 2 were found to require a few corrections. Firstly, calculations suggested a reversal of the assignments for C_2 and C_3 of

TABLE 2. Derivation of conformer populations for 2,3-dimethylpentane

Conformer	$u_{C_2-C_3}$	$u_{C_3-C_4}$	u_δ	Ω_j[a]	p_j[b]
11	1.095	0.257	1.000	0.282	0.063
12	1.095	1.000	1.000	1.095	0.245
13	1.095	1.000	0.035	0.038	0.009
21	1.000	0.257	0.035	0.009	0.002
22	1.000	1.000	1.000	1.000	0.224
23	1.000	1.000	1.000	1.000	0.224
31	1.000	0.257	0.035	0.009	0.002
32	1.000	1.000	1.000	1.000	0.224
33	1.000	1.000	0.035	0.035	0.008
			Z	4.468	

[a] $\Omega_j = u_{C_2-C_3} \times u_{C_3-C_4} \times u_\delta$.
[b] $p_j = \Omega_j / Z$.

TABLE 3. Derivation of conformer and conformationally averaged chemical shifts for C_1 and C_6 of 2,3-dimethylpentane

	Structural interactions[a]		Conformer resonances		Conformer contributions	
Conformer	C_1	C_6	C_1	C_6	C_1	C_6
11	P300	P300	21.09	21.09	1.33	1.33
12	P300	P300	21.09	21.09	5.17	5.17
13	P300	P301	21.09	23.65	0.18	0.20
21	P201	P300	19.10	21.09	0.04	0.04
22	P200	P300	16.54	21.09	3.70	4.72
23	P200	P300	16.54	21.09	3.70	4.72
31	P300	P201	21.09	19.10	0.04	0.04
32	P300	P200	21.09	16.54	4.72	3.70
33	P301	P200	23.65	16.54	0.19	0.13
				δ_{calcd}	19.07	20.05
				δ_{obsd}	17.7	20.0

[a] Structural interactions are given in the sequence: reference, n_{HC}, n_{CC}, n_δ.

Can. J. Chem. Downloaded from www.nrcresearchpress.com by 210.87.254.5 on 09/05/12
For personal use only.

2,3,3,4-tetramethylpentane, and this interchange was confirmed by off-resonance decoupling.[1] Secondly, the 2,4-dimethyl-3-ethylpentane data required two changes. With a 0.2 *m* $CDCl_3$ solution[1] at 30°C a chemical shift of 52.1 ppm was obtained for C_3, in place of 56.8 ppm (2). Furthermore, we found a pair of two carbon peaks at 19.4 and 21.5 ppm, and a one carbon signal at 20.2. Therefore the 20.0 ppm resonance of ref. 2 is assigned to C_7 and the 19.0 and 21.1 ppm peaks to C_1 and C_6.

Table 4 contains several examples of hydrocarbons with one or two asymmetric centers, and the presence of the chiral centers is clearly reflected in the calculated chemical shifts. Although magnetic nonequivalence is a consequence of chemical shift differences in individual chain conformations, it is essentially carried by population, rather than by chemical shift parameters. Consider the case of a chiral molecule with two magnetically nonequivalent carbons C_i and $C_{i'}$. Whatever the geometric relation of C_i to any other group R in any given molecular conformation *a*, i.e. whatever the contribution of R to the C_i resonance, another conformer *b* can always be found where $C_{i'}$ takes the place of C_i, i.e. where R makes the same chemical shift contribution to $C_{i'}$. The interactions of C_i and $C_{i'}$ with R may nevertheless lead to unequal contributions to the C_i and $C_{i'}$ resonances, since conformers *a* and *b* will generally occur with unequal probability. The analysis of the C_1 and C_6 resonances of 2,3-dimethylpentane, the simplest asymmetric aliphatic hydrocarbon, may serve as illustration. Clockwise 120° rotation about bond C_2—C_3 brings C_6 into a position previously occupied by C_1, relative to the rest of the molecule. Since this does not change the geometric relation between C_1 and C_6, the conformer shift of C_6 after rotation always equals the C_1 resonance before rotation. This is clearly seen in Table 3, where the C_6 conformer resonances repeat the C_1 values with a delay of three rows. That C_1 and C_6 are nevertheless nonequivalent is simply due to the fact that bond rotation changes the conformer populations. For example, the C_1 conformer shift in **13**, 21.09 ppm, equals the C_6 conformer shift in **23**, but the conformer contributions, 0.18 and 4.72 ppm, are quite different (Table 3).

The conformer populations are functions of rotation potentials as well as steric energy contributions, but it is the steric effects which transmit molecular asymmetry. The chiral center is always at least two bonds from C_i and $C_{i'}$, as in 2,3-dimethylpentane, and therefore the partial structure up to and including at least the γ carbons remains symmetric. It is of course precisely this molecular segment which makes the principal shift contributions, HC and CC, to the conformer resonances. Only the δ shift parameter originates outside this range. Now if $E_\delta = 0$, nothing perturbs the symmetry of this segment, and HC and CC interactions make equal contributions to C_i and $C_{i'}$. Magnetic nonequivalence is exclusively due to unequal probabilities of occurrence of δ shift contributions in this case. If $E_\delta \neq 0$, on the other hand, steric interactions will make some rotational states less probable, and thus destroy the symmetry of the rotamer populations. Now C_i and $C_{i'}$ are nonequivalent, because the much more important HC and CC interactions are no longer equally probable.

Consider again the case of 2,3-dimethylpentane.

$E_\delta = 0$. If the p_j are rederived by setting all $u_\delta = 1.0$ in Table 2, and the new conformer populations are used to weigh the conformer resonances in Table 3, a C_6–C_1 shift difference of only 20.12 – 20.08 = 0.04 ppm is obtained (Table 5). This difference is exclusively due to unequal δ shift contributions

$$(p_{13} + p_{31}) - (p_{21} + p_{33}) = 0.014$$

and 0.014 × 2.56 = 0.04 ppm. The case $E_\delta = 0$ corresponds to the previous version of the analysis (3). However, the chemical shifts have changed somewhat, since the parameters have changed.

$E_\delta = 8.368$ kJ/mol. *Syn*-axial δ interactions of C_1 and C_6 with C_5 destroy the symmetry of the rotational states of the C_2—C_3 bond.

State 1 $p_{11} + p_{12} + p_{13} = 0.317$

State 2 $p_{21} + p_{22} + p_{23} = 0.450$

State 3 $p_{31} + p_{32} + p_{33} = 0.234$

Bond C_2—C_3 is now more likely to be in rotational state 2, since this state is only once contained in a δ conformation, and state 3 twice. It is this population difference between rotational states 2 and 3 which is responsible for the nonequivalence of C_1 and C_6, since it leads to unequal HC interactions with C_3—H. In rotational state 1 both C_1 and C_6 are engaged in this HC interaction, in state 2 it is only C_6 and in state 3 only C_1. The resulting difference in HC contributions

$$(0.450 - 0.234) \times 4.55 = 0.98 \text{ ppm}$$

is precisely the difference between 20.05 ppm and 19.07 ppm (Table 5). It is clear from Table 5 that an underestimation of the value of E_δ should have no serious consequences for the derivation of chemical shifts, since the populations of conformations

[1]Samples of 2,3,3,4-tetramethylpentane and 2,4-dimethyl-3-ethylpentane were purchased from Chemical Samples Company.

Can. J. Chem. Downloaded from www.nrcresearchpress.com by 210.87.254.5 on 09/05/12
For personal use only.

TABLE 4. Observed and calculated conformationally averaged ^{13}C nmr chemical shifts for acyclic hydrocarbons[a]

Substrate	^{13}C nmr chemical shift								
	C(1)	C(2)	C(3)	C(4)	C(5)	C(6)	C(7)	C(8)	C(9)
Propane derivatives									
2,2-diMe	31.6	28.0							
	34.7	26.5							
Butane derivatives									
2-Me	21.9	29.9	31.6	11.5					
	23.1	30.3	32.8	11.5					
2,2-diMe	28.7	30.3	36.5	8.5					
	31.7	30.2	39.5	7.4					
2,3-diMe	19.2	34.0							
	19.6	35.2							
2,2,3-triMe	27.0	32.7	37.9	17.7					
	28.7	33.9	40.7	16.5					
2,2,3,3-tetraMe	25.6	35.0							
	25.6	37.6							
Pentane derivatives									
Nil	13.5	22.2	34.1						
	15.4	24.9	34.5						
2-Me	22.7	27.9	41.9	20.8	14.3				
	23.2	29.6	41.5	21.3	15.9				
3-Me	11.4	29.4	36.8			18.7			
	11.4	30.8	36.3			19.4			
2,2-diMe	29.5	30.6	47.3	18.1	15.1				
	31.7	30.2	48.6	17.7	16.5				
2,3-diMe	17.7	31.9	40.6	26.8	11.6	20.0	14.5		
	19.1	33.8	41.3	27.4	11.7	20.1	15.6		
2,4-diMe	22.7	25.7	49.0						
	23.4	26.2	48.6						
3,3-diMe	7.7	33.4	32.3			25.6			
	7.5	37.0	33.9			28.3			
2,2,3-triMe	27.1	33.0	45.4	24.4	13.0			13.3	
	28.7	33.9	47.1	24.2	12.1			12.1	
2,2,4-triMe	29.9	30.9	53.3	25.3	24.7				
	32.6	30.2	55.0	26.0	24.6				
2,3,3-triMe	17.1	35.1	34.9	32.6	7.9		23.3		
	16.6	38.9	37.6	34.2	7.5		24.8		
2,3,4-triMe	18.1	29.8	45.3			21.4	10.4		
	19.0	31.3	47.0			21.1	12.2		
2,2,3,3-tetraMe	25.6	36.0	37.3	28.8	9.0			20.6	
	25.7	37.6	41.3	30.7	7.6			21.2	
2,2,3,4-tetraMe	28.2	34.0	47.9	27.4	17.3			11.6	24.5
	29.5	33.9	52.2	31.2	20.2			9.9	22.4
2,2,4,4-tetraMe	31.8	32.4	56.5						
	33.4	30.2	61.4						
2,3,3,4-tetraMe	17.2	33.6	37.1				18.9		
	16.7	36.4	41.3				21.2		
3-Et	10.5	25.2	42.4						
	11.3	27.5	42.0						
2-Me, 3-Et	19.0	29.1	47.6	22.6	11.8				
	19.5	30.8	47.1	24.2	11.7				
3-Me, 3-Et	7.5	30.6	34.8			23.2			
	7.5	33.9	37.6			24.9			
3,3-diEt	7.1	27.1	37.1						
	7.6	30.8	41.3						
2,4-diMe, 3-Et	19.0	29.0	52.1[b]			21.1	20.0	14.5	
	20.4	30.8	52.7			21.0	22.9	13.0	
Hexane derivatives									
Nil	13.7	22.7	31.7						
	15.4	25.0	33.3						
2-Me	22.4	28.1	38.9	29.7	23.0	13.6			
	23.2	29.7	40.4	29.8	25.4	15.3			

TABLE 4 (*Continued*)

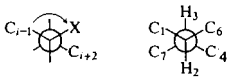
Substrate	^{13}C nmr chemical shift								
	C(1)	C(2)	C(3)	C(4)	C(5)	C(6)	C(7)	C(8)	C(9)
3-Me	10.9	29.5	34.3	39.0	20.2	13.9	18.8		
	11.4	30.9	35.7	39.5	21.3	15.9	19.5		
2,2-diMe	29.2	30.1	44.1	27.0	23.7	13.9			
	31.7	30.2	47.3	26.0	25.9	15.3			
2,3-diMe	17.8	32.8	38.5	36.7	20.7	14.0	20.0	15.1	
	19.1	33.8	40.7	36.1	21.6	15.8	20.0	15.6	
2,4-diMe	22.2	25.4	46.6	32.1	29.9	11.0	23.2	19.0	
	22.8	26.2	46.6	32.2	31.1	11.4	24.0	19.6	
2,5-diMe	22.4	28.4	36.9						
	23.1	30.0	36.7						
3,3-diMe	8.1	34.3	32.8	44.3	17.3	14.8	26.5		
	7.5	37.0	33.9	46.0	17.7	16.5	28.3		
3,4-diMe *meso*	11.8	25.8	39.5				15.8		
	11.8	27.0	40.3				15.9		
3,4-diMe *d,l*	11.8	27.6	38.5				13.8		
	11.8	27.8	39.7				15.3		
2,2,4-triMe	29.9	31.0	51.0	31.9	31.0	11.2			21.9
	32.6	30.2	53.0	32.0	32.0	11.3			21.1
2,2,5-triMe	29.3	30.1	42.0	33.9	28.9	22.5			
	31.7	30.2	43.5	32.8	30.3	23.1			
2,3,3-triMe	17.1	35.0	35.5	43.1	17.0	14.8		23.8	
	16.6	38.9	37.6	43.2	17.7	16.5		24.8	
2,3,5-triMe	17.8	32.4	36.2	43.9	25.7	21.9	20.0	15.3	23.5
	18.9	33.9	37.0	43.0	26.2	22.4	20.0	15.6	24.4
3-Et	10.6	25.6	40.6	35.4	20.0	14.1			
	11.3	27.5	41.4	36.3	21.2	15.9			
Heptane derivatives									
Nil	13.7	22.6	32.0	29.0					
	15.4	25.0	33.5	32.5					
2-Me	22.4	28.1	39.3	27.2	32.4	22.8	13.8		
	23.2	29.7	40.5	28.7	33.9	24.9	15.4		
3-Me	11.3	29.7	34.7	36.5	29.7	23.3	14.1	19.3	
	11.4	30.8	35.7	38.4	29.7	25.4	15.3	19.5	
4-Me	14.1	20.2	39.5	32.3				19.3	
	15.9	21.3	39.6	35.0				19.5	
2,2-diMe	29.2	30.2	44.4	24.4	33.0	22.8	13.8		
	31.7	30.2	47.4	24.9	34.4	24.9	15.4		
2,3-diMe	17.9	32.2	38.8	34.0	30.0	23.1	13.8	20.1	15.2
	19.1	33.8	40.7	34.9	30.0	25.4	15.3	20.0	15.6
2,4-diMe	22.1	25.3	47.0	30.2	39.9	19.9	14.0	23.1	19.4
	22.8	26.2	46.7	31.6	39.9	21.3	15.9	24.0	19.6
2,5-diMe	22.3	28.4	36.5	34.4	34.8	29.5	11.0	22.5	19.0
	23.1	30.0	36.7	34.7	36.0	30.8	11.4	23.2	19.4
2,6-diMe	22.4	28.1	39.5	25.2					
	23.2	29.7	40.9	25.1					
3,3-diMe	8.0	34.2	32.5	41.3	26.4	23.7	13.7	26.4	
	7.5	37.0	33.9	44.7	26.0	25.9	15.3	28.3	
3,4-diMe 3*R*, 4*S*	11.9	25.8	39.8	37.2	35.5	20.8	14.2	15.8	16.3
	11.8	26.9	40.3	39.6	35.6	21.6	15.8	15.9	15.9
3,4-diMe 3*R*, 4*R*	11.9	27.6	38.9	36.3	37.5	20.8	14.2	13.9	14.2
	11.8	27.8	39.7	39.0	36.5	21.6	15.8	15.3	15.3
3,5-diMe 3*R*, 5*R*	10.9	30.5	31.9	44.3				18.9	
	11.4	31.7	32.2	44.3				19.3	
3,5-diMe 3*R*, 5*S*	11.1	29.5	32.0	44.5				19.6	
	11.3	30.6	32.2	45.1				19.9	
4,4-diMe	14.9	17.3	44.8	32.8				27.0	
	16.5	17.7	46.0	33.9				28.3	
3-Et	10.6	25.6	40.7	32.7	29.2	23.1	13.7		
	11.3	27.5	41.4	35.1	29.6	25.4	15.3		

Can. J. Chem. Downloaded from www.nrcresearchpress.com by 210.87.254.5 on 09/05/12
For personal use only.

TABLE 4 (*Concluded*)

Substrate	^{13}C nmr chemical shift C(1)	C(2)	C(3)	C(4)	C(5)	C(6)	C(7)	C(8)	C(9)
Octane derivatives									
Nil	13.6	22.7	32.1	29.4					
	15.4	25.0	33.5	32.4					
2-Me	22.3	28.0	39.2	27.4	29.7	32.0	22.7	13.6	
	23.2	29.7	40.5	28.8	32.8	33.4	25.0	15.4	
3-Me	11.1	29.7	34.6	36.7	26.9	32.4	22.7	13.8	19.0
	11.4	30.8	35.7	38.5	28.6	33.9	24.9	15.4	19.5
4-Me	14.0	19.4	39.6	32.6	36.8	29.3	23.0	13.7	20.2
	15.9	21.3	39.6	35.1	38.4	29.7	25.4	15.3	19.5
Nonane derivatives									
Nil	13.8	22.7	32.0	29.4	29.6				
	15.4	25.0	33.5	32.4	32.5				

[a]The experimental values, taken from ref. 2, are given first. The standard error of fit for all hydrocarbons is 1.59 ppm. Numbering system for asymmetric hydrocarbons (somewhat different from the previous version): carbons 1 to *n* form an all-*trans* chain and the substituent at C(*i*) is found 120° clockwise from C(*i* − 1) on the Newman projection of C(*i*)—C(*i* + 1).



2,3-dimethylpentane

[b]The value of 52.1 ppm was obtained with a 0.2 *m* $CDCl_3$ solution at 30°C.

TABLE 5. Chemical shifts for C_1 and C_6 of 2,3-dimethylpentane, calculated as function of the *syn*-axial δ energy term

E_δ (kJ/mol)	$p_{13}+p_{21}+p_{31}+p_{33}$	Chemical shifts C_1	C_6
0.0	0.373	20.08	20.12
2.5	0.180	19.53	20.08
5.0	0.074	19.22	20.06
7.5	0.029	19.09	20.06
8.368	0.020	19.07	20.05
10.0	0.011	19.04	20.05
12.5	0.004	19.02	20.05
15.0	0.001	19.01	20.05
20.0	0.000	19.01	20.05

with δ interactions rapidly reach their limiting value of zero.

2,3-Dimethylpentane was discussed in detail, since it is the simplest asymmetric hydrocarbon chain, and the effect of asymmetry on chemical shifts is most clearly seen in this system. The procedure is of course equally applicable to the derivation of chemical shifts of carbons further from the site of asymmetry, or in chains with more than one chiral center. The principal cause of magnetic nonequivalence, intra- or intermolecular, remains unchanged. Steric interactions perturb the rotational states of the individual bonds in the chain, and these changes in rotamer populations are a function of chirality. The changes in rotamer populations in turn determine the signs and magnitudes of the chemical shift differences. The conformational transmission over several bonds is illustrated by the dimethylheptanes.

Compound		Chemical shift C_1	C_8
2,3-Dimethylheptane	Obsd	17.9	20.1
	Calcd	19.1	20.0
2,4-Dimethylheptane	Obsd	22.1	23.1
	Calcd	22.8	24.0
2,5-Dimethylheptane	Obsd	22.3	22.5
	Calcd	23.1	23.2

The assignment of configuration in chains with more than one chiral center is demonstrated for the diastereomeric 3,4-dimethylhexanes.

3,4-Dimethylhexanes		Chemical shift C_1	C_2	C_3	C_7
meso	Obsd	11.8	25.8	39.5	15.8
	Calcd	11.8	27.0	40.3	15.9
d,l	Obsd	11.8	27.6	38.5	13.8
	Calcd	11.8	27.8	39.7	15.3

The calculations predict that in the *meso* isomer one primary and the tertiary carbon signal are shifted upfield, and the secondary carbon signal downfield relative to the *d,l* isomer. This is indeed found to be the case (8).[2] It should be emphasized

[2]The signal assignments for the diastereometric 3,4-dimethylhexanes in this article are based on the spectrum of the stereospecifically synthesized *meso* isomer (9).

Can. J. Chem. Downloaded from www.nrcresearchpress.com by 210.87.254.5 on 09/05/12
For personal use only.

that spectra for both isomers are required for an assignment of configuration.

To conclude, the analysis presented here is based on the accepted model for the conformational behaviour of chain molecules (5). Aliphatic hydrocarbons adopt a variety of rapidly interconverting conformations, each with distinct physical properties, and their behaviour cannot be understood without a knowledge of conformer properties and probabilities. There are no fundamental structural differences between cyclic molecules and individual conformations of acyclic substrates, and methods for the derivation of chemical shifts for rigid systems are equally applicable to the derivation of chain conformer resonances. The conformer probabilities are functions of the conformer energies, and the conformer energies are the sums of rotation potentials and steric energy contributions, which are available from independent sources. No additional assumptions or adjustable parameters are required. The analysis of the ^{13}C nmr chemical shifts of aliphatic hydrocarbons, based on this model, automatically predicts magnetic nonequivalence in chiral molecules, and represents a unified treatment of cyclic and acyclic hydrocarbons.

Acknowledgments

We thank the National Research Council of Canada and the Ministère de l'Education du Québec for financial assistance.

1. D. M. GRANT and E. G. PAUL. J. Am. Chem. Soc. **86**, 2984 (1964).
2. L. P. LINDEMAN and J. Q. ADAMS. Anal. Chem. **43**, 1245 (1971).
3. H. BEIERBECK and J. K. SAUNDERS. Can. J. Chem. **55**, 771 (1977).
4. H. BEIERBECK, J. K. SAUNDERS, and J. W. APSIMON. Can. J. Chem. **55**, 2813 (1977).
5. P. J. FLORY. Statistical mechanics of chain molecules. Wiley, New York. 1969.
6. A. L. VERMA, W. F. MURPHY, and H. J. BERNSTEIN. J. Chem. Phys. **60**, 1540 (1974).
7. L. LUNAZZI, D. MACCIANTELLI, F. BERNARDI, and K. U. INGOLD. J. Am. Chem. Soc. **99**, 4573 (1977).
8. W. RITTER, W. HULL, and H. J. CANTOW. Tetrahedron Lett. 3093 (1978).
9. W. RITTER. Private communication.

Can. J. Chem. Downloaded from www.nrcresearchpress.com by 210.87.254.5 on 09/05/12
For personal use only.

Vapor phase Beckmann rearrangement of the cyclohexanone oxime catalyzed by $AlPO_4$–γAl_2O_3 systems

A. COSTA, P. M. DEYÁ, AND J. V. SINISTERRA
Organic Chemistry Department, Faculty of Science, University of Palma de Mallorca, Balearic Islands, Spain
AND
J. M. MARINAS
Organic Chemistry Department, Faculty of Science, University of Córdoba, Córdoba, Spain

Received October 3, 1979

A. COSTA, P. M. DEYÁ, J. V. SINISTERRA, and J. M. MARINAS. Can. J. Chem. **58**, 1266 (1980).

Beckmann rearrangement of cyclohexanone oxime has been carried out in vapor phase by means of a pulse reactor unit directly coupled to a gas chromatograph. The catalysts chosen gave good yields of ε-caprolactam. Apparent rate constants and activation energies were calculated in terms of the kinetic model of Bassett and Habgood. Selectivity studies, using pulse experiments interpreted by OPE curves, led to the conclusion that ε-caprolactam and 5-cyanopent-1-ene were competitive products. A reaction pathway is proposed which is in agreement with both the observed rates and selectivities.

A. COSTA, P. M. DEYÁ, J. V. SINISTERRA et J. M. MARINAS. Can. J. Chem. **58**, 1266 (1980).

On a effectué une transposition de Beckmann sur l'oxime de la cyclohexanone en phase gazeuse à l'aide d'un réacteur à impulsion relié directement à un appareil à chromatographie en phase gazeuse. Les catalyseurs choisis conduisent à l'ε-caprolactame avec de bons rendements. On a calculé les constantes de vitesse apparentes et les énergies d'activation en fonction du modèle cinétique de Bassett et Habgood. Des études de sélectivité, utilisant les expériences à impulsion interprétées par les courbes EPO, permettent de conclure qu'il y a formation compétitive de l'ε-caprolactame et du cyano-5 pentène-1. On propose un système de réaction qui est en accord avec les vitesses et les sélectivités observées.

[Traduit par le journal]

Introduction

The Beckmann rearrangement is a typical aniontropic rearrangement catalyzed by Brönsted and Lewis acids. It is of industrial importance in the conversion of cyclohexanone oxime to ε-caprolactam and catalysts for this application have often been described. However, only a few studies of the mechanism and kinetics in the vapor phase reaction have appeared in the literature (1, 2).

For years, we have used aluminium orthophosphates of the Kearby type (3) and other related systems as Friedel–Crafts type catalysts in different cationic organic processes with reagents in vapor phase (4–6). Among these is to be found the Beckmann rearrangement (7–9). For this paper we have chosen different bicomponent catalysts synthetized in a propylene oxide medium and described by us in a previous work (10), composed of aluminium orthophosphate and γ-alumina (75:25% by weight). These catalysts offer a greater surface acidity than other similar catalysts such as pure aluminium orthophosphate (11) or aluminium orthophosphate – silica systems (12). Furthermore, kinetics of the Beckmann rearrangement of cyclohexanone oxime on $AlPO_4$–γAl_2O_3 systems has been determined by using the Bassett and Habgood model (13). This model is applied to the first order processes in which the surface reaction is the controlling step and the partial pressure of the reactant is low.

Experimental

Synthesis of the Catalysts

(CBP)

A solution of 14.8 g of $Al(NO_3)_3 \cdot 9H_2O$ in 58 mL of doubly distilled water was cooled to 0°C and stirred mechanically while aqueous ammonia was added until complete precipitation of the aluminium hydroxide had occurred. At the same time a solution of 18.4 g of $AlCl_3 \cdot 6H_2O$ in 25 mL of doubly distilled water and 4.4 mL of H_3PO_4 (85% by weight) was cooled to 0°C and stirred mechanically while 26.5 mL of propylene oxide were added, causing an increase of the solution's viscosity. The last solution was added to the former precipitate and the resulting mixture was homogenized. Complete precipitation of the hydroxide and phosphate of aluminium was attained by the addition of aqueous ammonia until a gel was formed, which was left for 24 h at room temperature. After washing several times with isopropanol, the solid was collected by suction filtration and subsequently dried for 24 h at 100–110°C. Finally the catalyst was obtained by calcination for 3 h at 650 ± 10°C at 1 atm. The resulting catalyst can be stored indefinitely if reasonable precautions against basic vapors and moisture are observed.

(CBPU10), (CBPU20), (CBPO10), (CBPO20)

These systems were prepared in the same way as that of (CBP), except that, to the initial solution of $AlCl_3 \cdot 6H_2O$, 0.37 g of urea were added for (CBPU10), 0.74 g of urea for (CBPU20), 0.55 g of oxalic acid for (CBPO10), and 1.10 g of oxalic acid for (CBPO20).

0008-4042/80/121266-05$01.00/0
©1980 National Research Council of Canada/Conseil national de recherches du Canada

Can. J. Chem. Downloaded from www.nrcresearchpress.com by 210.87.254.105 on 09/05/12
For personal use only.

Can. J. Chem. Downloaded from www.nrcresearchpress.com by 210.87.254.105 on 09/05/12
For personal use only.

Apparatus

The equipment was similar to that described by Choudary (14). A gas chromatograph, Hewlett-Packard 5834A, was modified by introduction of a microreactor between the sample inlet and the chromatographic column. The fixed bed vertical reactor was made of 2.5 mm id and 45 mm long stainless steel and heated by an electrical microfurnace. The catalyst particles (0.125–0.250 mm) were held in place by two plugs of glass wool. The reaction temperature was measured with a NiCr–Ni Din thermocouple connected to a Getrosist 96 Phillips controller. Pulses of a solution (1.5 *M*) of cyclohexanone oxime in benzene were introduced in a nitrogen carrier stream (flow rate 30 mL/min) by means of a standard 10 μL syringe, and the chromatographic separation of reactants and products was then carried out by using a 2 m by 6 mm column, packed with 10% Ucon on Chromosorb W 60–80, heated from 150 to 200°C with a rate of 10°C/min.

Procedure

(a) Operation of the Microreactor Unit

Catalyst charges of 6.0 and 14.0 mg were used. The catalyst was stabilized by heating to 200°C for 12 h in flowing nitrogen. Experiments were carried out at temperatures ranging from 200 to 320°C by inserting several pulses of 6 μL at each temperature and charge of catalyst.

(b) Identification of the Reaction Products

Identification of the reaction products was performed under testing conditions that led to a maximum yield in ε-caprolactam for the maximum total conversion. In these conditions the chromatograms showed the presence of eleven different signals. Those showing a major entity were analyzed by gc-ms (HP 5992A). The definitive assignation was achieved by preparing different solutions of cyclohexanone oxime in benzene and adding to each of them a small amount (5% by weight), with regard to the cyclohexanone oxime, of each of the previously identified products. These solutions were injected into reactor at reacting temperatures where the total conversion of the oxime was small, and the increase of the corresponding signal was checked.

(c) Determination of the Textural and Acidity Properties of the Catalysts

From the adsorption–desorption nitrogen isothermes at liquid nitrogen temperature, the surface area (S_{BET}) and accumulated pore volume (ΣV_p) were determined by the B.E.T. method (15). The total acidity of the catalysts and the density of acid centers were measured by titration in a non-aqueous medium by applying the alterations to the original method (16) proposed by Benesi (17) and Balikova (18), using *p*-dimethylaminoazobenzene as Hammett indicator.

Results and Discussion

(a) General

The addition of oxalic acid and urea brings about an alteration of the textural and acidic properties of the systems used without varying their chemical composition. However this addition does not produce any improvement in the characteristics of the catalysts, and the original catalyst (CBP) is the one that offers the best overall properties. The total conversion of cyclohexanone oxime increases with both temperature and catalyst charges, ε-caprolactam being the main reaction product as shown in Table 1. The thermal process without catalyst never surpasses 2% of the oxime input, thereby showing the effectiveness of the catalyst in the process. Once its activity is stabilized deactivation of the catalyst is minimal, since at insertion of one hundred pulses at regular time intervals, an activity decrease of only 5% is produced, in the experimental conditions described below.

TABLE 1. Typical distribution of reaction products[a]

Product	Yield (%)
Cyclohexanone oxime	5.8
ε-Caprolactam	73.1
Cyclohexanone	3.6
5-Cyanopent-1-ene	5.4
2-Methylpyridine	2.8
2-Cyclohexenone	1.2
6-Methyl-δ-valerolactam, propylene, and polymeric products[b]	3.8

[a]Reaction temperature 320°C; charge of catalyst (CBP), 10 mg.
[b]Arising from ε-caprolactam.

(b) Apparent Rate Constants and Activation Energies

From the Bassett and Habgood equation [1] (13):

$$[1] \quad \ln \frac{1}{1-X} = RTkK\frac{W}{Q}$$

where X = molar fractionary conversion; R = gas constant (atm mL^{-1} mol^{-1}); T = reaction temperature (K); K = adsorption constant of the cyclohexanone oxime on the catalyst (mol atm^{-1} g^{-1}); k = rate constant of the surface process (s^{-1}); W = weight of catalyst (g); Q = flow rate of carrier gas (mL s^{-1}). It is possible to obtain the apparent rate constant (kK) at a fixed temperature by plotting $\ln [1/(1 - X)]$ vs. W, while the activation energy (E_a) of each catalyst was plotted representing $\ln \{\ln[1/(1 - X)]\}$ vs. W. The results are summarized in Table 2.

These results underscore the direct connection between the apparent rate constants and the total acidity of the catalysts, as indicated in Fig. 2, thereby verifying that other similar catalysts less acidic, i.e. pure aluminium orthophosphate (8), provide poorer results than the ones achieved with $AlPO_4$–γAl_2O_3 systems.

(c) Analysis of the OPE Selectivity Curves

The OPE selectivity curves were obtained by plotting the fractional conversion of a particular product against the total conversion, for different weight ratios of catalyst to introduced oxime (CAT/OX), such as has recently been described by Wojciechowski *et al.* (19). In this aspect the microcatalytic pulse technique is more advantageous than the conventional continuous flow technique in

Can. J. Chem. Downloaded from www.nrcresearchpress.com by 210.87.254.105 on 09/05/12
For personal use only.

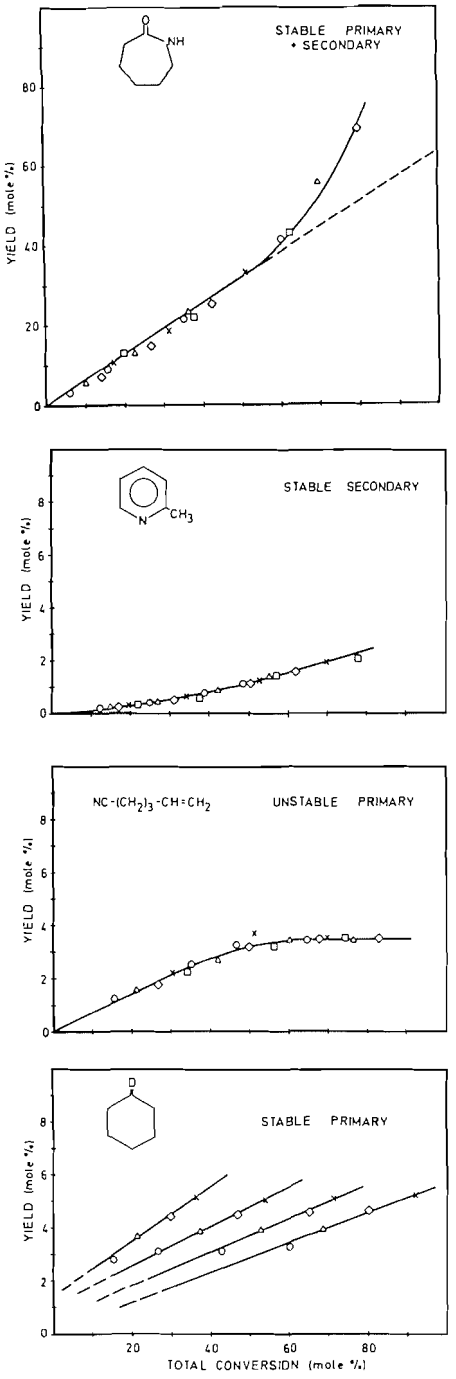
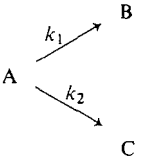


FIG. 1. OPE selectivity curves. The symbols represent the following CAT/OX ratios: 7.86 (○), 8.84 (△), 9.82 (◇), 11.79 (×), 12.85 (□).

several ways. The ratio (CAT/OX) is high whereas the duration of the reactant in the catalytic bed is very short. Consequently, the activity loss of the catalyst can be considered non-existant for any particular pulse. Thereby, as shown in Fig. 1, by applying this method to the main reaction products, it can be inferred that ε-caprolactam, 5-cyanopent-1-ene, and cyclohexanone are primary reaction products coming from cyclohexanone oxime. ε-Caprolactam and 5-cyanopent-1-ene adopt the behavior of stable and unstable primary products, respectively, at temperatures higher than 280°C. Cyclohexanone acts as a primary product although it has an unspecified catalytic effect, as the conversion of the cyclohexanone increases with the (CAT/OX) ratio but not with temperature.

To determine which of the above mentioned products are really competitors, we used the kinetic selectivity criterion of Wheeler (20), viz., that for a process such as is outlined, and the follows a first order kinetic,



can be written as:

$$\sigma = k_1/k_2 = X_B/X_C$$

where k_1 and k_2 = rate constants; X_B and X_C = fractional conversions in B and C respectively; σ = kinetic selectivity factor.

The application of this criterion allows us to draw the conclusion that ε-caprolactam and 5-cyanopent-1-ene are competitive products, a conclusion in agreement with the mechanism proposed by Grob (21) for the Beckmann rearrangement of cyclohexanone oxime in homogeneous phase. Furthermore, by plotting the selectivity factors vs. the total acidity of the catalysts, Fig. 2, it can be

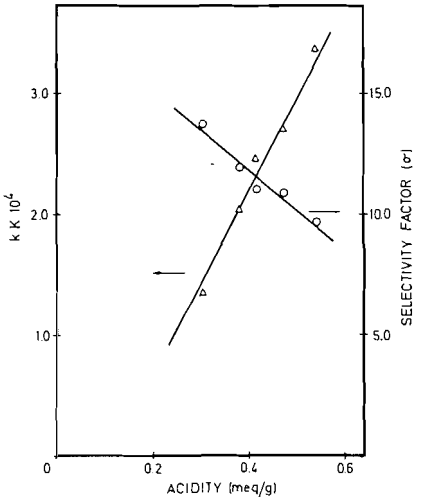
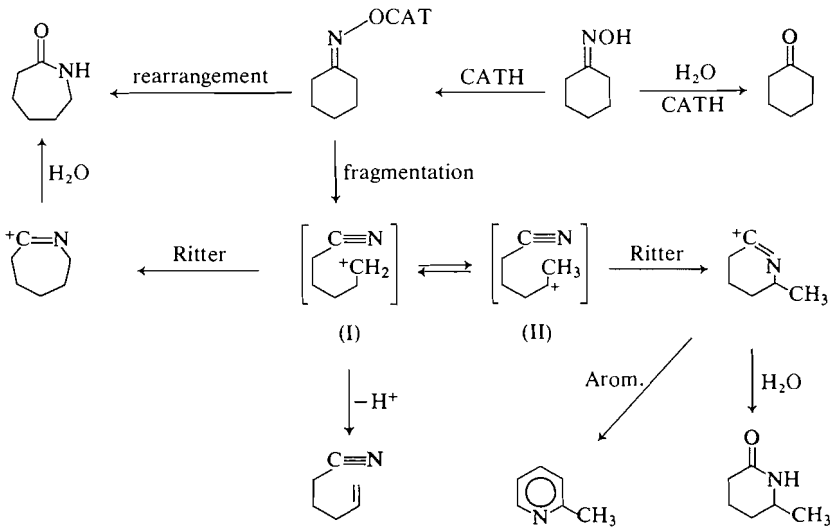


FIG. 2. Relationship between the total acidity of the catalyst, apparent kinetics constants, and selectivity factors.

TABLE 2. Summary of the most significant experimental variables for each catalyst

Catalyst	$kK\ 10^4$ (mol atm^{-1} g^{-1} s^{-1})	E_A (kcal mol^{-1})	σ	Acidity (mequiv. g^{-1})
CBP	3.37	20.19	9.65	0.55
CBPU10	2.73	21.56	10.91	0.48
CBPU20	2.06	15.77	11.61	0.38
CBPO10	2.44	19.26	10.97	0.42
CBPO20	1.31	17.35	13.63	0.31



seen that the catalytic activity increases as the process selectivity of ε-caprolactam diminishes, with an increase of the catalyst's acidity.

(d) Discussion of a Possible Reaction Pathway

The mechanism proposed below agrees with the experimental results and is an attempt to explain how each of the reaction products could be formed. The first step would imply the chemisorption of the cyclohexanone oxime on the catalyst, and then, either a rearrangement reaction could take place or a fragmentation process which would lead to the intermediate **I** being unstable. This in its turn could evolve to a more stable structure such as **II**.

The intermediate **II** would provide an explanation for the appearance of 2-methylpyridine, 6-methyl-δ-valerolactam as well as the existence of an alternative pathway for the formation of ε-caprolactam, according to its OPE curve. The appearance of 2-methylpyridine, through a way similar to that proposed by us, has been described (22) for this process in homogeneous phase using HMPT. Finally, 5-cyanopent-1-ene and cyclohexanone could be obtained, by proton loss from **I** and **II** and hydrolysis of the initial oxime, respectively.

Conclusion

The $AlPO_4$–γAl_2O_3 systems used in this study show promising catalytic activity for this process. The acidity of the catalyst is the main variable to be considered, but at the same time such an increase in acidity adds to the secondary process of fragmentation that disagrees with the proposal of rearrangement.

1. J. D. BUTTER and T. C. POLEŞ. J. Chem. Soc. Perkin II, 41 (1973).
2. K. L. SAMARIN, R. I. POMILENKO, and I. YA. TYURGAEV. Kinet. Katal. **16**, 896 (1975).
3. K. K. KEARBY. Actes Cong. Int. Catal. 2ºParis, **2**, 2267 (1960).
4. J. M. MARINAS and A. ALBEROLA. An. Quim. **67**, 37 (1971).
5. J. M. MARINAS, A. ALBEROLA, and M. S. ESTEBAN. An. Quim. **68**, 1295 (1972).
6. A. ALBEROLA, M. S. ESTEBAN, J. M. MARINAS, and R. PEREZ-OSSORIO. An. Quim. **70**, 944 (1977).
7. A. ALBEROLA, M. BLANCO, M. S. ESTEBAN, J. M. MARINAS, and R. PEREZ-OSSORIO. An. Quim. **72**, 887 (1976).
8. M. S. ESTEBAN and J. M. MARINAS. An. Quim. **74**, 1413 (1978).
9. A. COSTA, M. S. ESTEBAN, J. M. MARINAS, and R. PEREZ-OSSORIO. An. Quim. **73**, 1521 (1977).

Can. J. Chem. Downloaded from www.nrcresearchpress.com by 210.87.254.105 on 09/05/12
For personal use only.

10. J. M. CAMPELO, J. M. MARINAS, and R. PEREZ-OSSORIO. Proc. Vth Iber. Symp. Catal. **1**, 84 (1978).
11. A. ALBEROLA and J. M. MARINAS. An. Quim. **66**, 585 (1970).
12. J. V. SINISTERRA, J. M. MARINAS, and C. JIMENEZ. An. Quim. **73**, 561 (1977).
13. D. X. BASSETT and H. W. HABGOOD. J. Phys. Chem. **64**, 769 (1960).
14. V. R. CHOUDARY. J. Chromat. **152**, 208 (1978).
15. S. BRUNAUER, P. EMMETT, and E. TELLER. J. Am. Chem. Soc. **60**, 309 (1930).
16. O. JHONSON. J. Phys. Chem. **59**, 827 (1955).
17. H. A. BENESI. J. Phys. Chem. **61**, 970 (1957).
18. M. BALIKOVA. React. Kinet. Catal. Lett. **2**, 323 (1975).
19. D. BEST and H. W. WOJCIECHOWSKI. J. Catal. **47**, 11 (1977).
20. A. WHEELER. Adv. Catal. **3**, 250 (1951).
21. C. A. GROB *et al.* Helv. Chim. Acta, **47**, 1003 (1964).
22. N. O. VESTERAGER, E. B. PEDERSEN, and S. O. LANESSON. Tetrahedron, **30**, 2507 (1974).

Can. J. Chem. Downloaded from www.nrcresearchpress.com by 210.87.254.105 on 09/05/12
For personal use only.

The photochemistry of 4-phenyl-1-iodobutane and 4-phenyl-2-iodomethyl-1-butene

JAMES LESLIE CHARLTON,[1] GAYNOR JANE WILLIAMS, AND GERALD NICHOLAS LYPKA
Department of Chemistry, University of Manitoba, Winnipeg, Man., Canada R3T 2N2

Received November 5, 1979

JAMES LESLIE CHARLTON, GAYNOR JANE WILLIAMS, and GERALD NICHOLAS LYPKA. Can. J. Chem. **58**, 1271 (1980).

The photochemistry of 4-phenyl-1-iodobutane **3** and 4-phenyl-2-iodomethyl-1-butene **4** has been studied to investigate the effect of structure on the character of the intermediates generated on photolysis. The irradiation of the simple primary iodide **3** appears to yield only radical intermediates. By contrast the photolysis of the allylic iodide **4** yields products that are more consistent with cationic intermediates.

JAMES LESLIE CHARLTON, GAYNOR JANE WILLIAMS et GERALD NICHOLAS LYPKA. Can. J. Chem. **58**, 1271 (1980).

On a étudié la photochimie du phényl-4 iodo-1 butane (**3**) et du phényl-4 iodométhyl-2 butène-1 (**4**) dans le but d'examiner l'effet de la structure sur le caractère des intermédiaires engendrés par la photolyse. L'irradiation de l'iodure primaire **3** semble conduire uniquement à des intermédiaires radicalaires. La photolyse de l'iodure allylique **4** au contraire donne des produits qui sont compatibles avec des intermédiaires cationiques.

[Traduit par le journal]

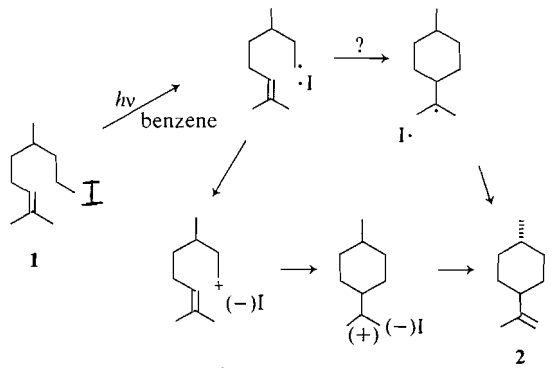
Can. J. Chem. Downloaded from www.nrcresearchpress.com by 210.87.254.40 on 09/05/12
For personal use only.

Introduction

Recent work by Kropp has shown that the photolysis of alkyl iodides can lead sequentially from free radical to ionic intermediates and that reaction products resulting from the ionic intermediates are often dominant (1).

$$RI \xrightarrow{h\nu} R\cdot \cdot I \rightarrow R(+)(-)I \rightarrow \text{products}$$

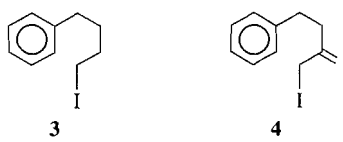
While Kropp has made use of this reaction to prepare unusual cations, others have used the photolysis of alkyl iodides to generate intermediates that have potential in organic synthesis. For instance, Gokhale has found that the irradiation of citronellyl iodide **1** yields *trans-p*-menth-8-ene **2** as illustrated in Scheme 1 (2).



SCHEME 1

This reaction may involve either radical or cationic cyclization with analogies existing for both modes, although in this case the orientation of the double bond in the product and the use of a nonpolar solvent would indicate a radical process is more likely (3). More extensive polyene cyclizations have been carried out using both radicals and cations as intermediates (3, 4) and it seems that alkyl iodides would make good starting materials for such processes.

In order to lay the ground work for such a project we have carried out an investigation of the photochemistry of 4-phenyl-1-iodobutane **3** and 4-phenyl-2-iodomethyl-1-butene **4**.



3 **4**

The 4-phenyl-1-iodo-butane **3** was chosen for study as extensive studies have been made on both the 4-phenylbutyl radical and cation generated by alternate methods. Iodide **4** was chosen as a model since the allylic radical is incapable of simple disproportionation by hydrogen atom transfer, a reaction which dominated the chemistry of the 4-phenylbutyl radical generated from **3** (*vide infra*).

Results and Discussion

The title compounds were irradiated in acetonitrile and/or benzene as outlined in Table 1 (for a preliminary report on this work see ref. 5).

Finely divided, anhydrous potassium carbonate was used as a scavenger for hydrogen iodide in acetonitrile whereas a separate aqueous phase was used to scavenge hydrogen iodide from benzene. Scheme 2 represents a general reaction mechanism for the photochemistry of **3**.

In the absence of HI and O_2 the major reaction of the initially formed radicals is the formation of the alkene **5**, both in benzene and in acetonitrile.

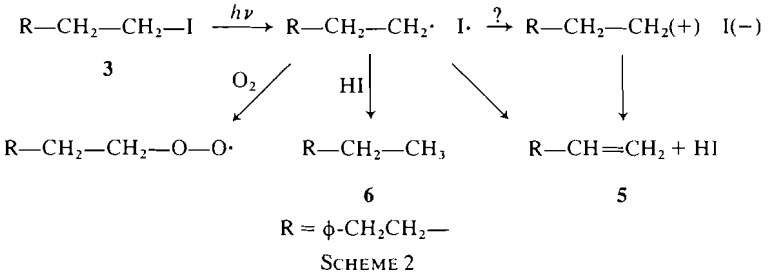
[1]To whom all correspondence should be addressed.

0008-4042/80/121271-04$01.00/0
©1980 National Research Council of Canada/Conseil national de recherches du Canada

Can. J. Chem. Downloaded from www.nrcresearchpress.com by 210.87.254.40 on 09/05/12
For personal use only.

TABLE 1. Products and conditions of irradiation

Compound	Solvent	HI Scavenger	N_2/O_2	Products	% Yield
3	CH_3CN	K_2CO_3	N_2	**5**	99
	CH_3CN	K_2CO_3	O_2	**5**	52
	Benzene	H_2O	N_2	**5**	88
	Benzene	None	O_2	**5**	51
	Benzene	None	N_2	**5**	61
				6	27
4	CH_3CN	K_2CO_3	N_2	**7**	28
				8	37



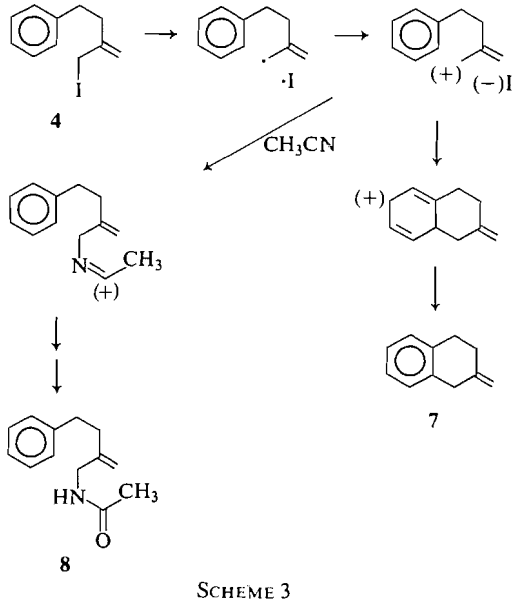
SCHEME 2

In the presence of oxygen the yield of alkene is reduced from 100% in acetonitrile and 88% in benzene to 52 and 51% respectively. A possible interpretation is that 50% of the initially formed radical pairs give alkene while the remainder dissociate and can be trapped by oxygen and hydrogen iodide. Since there is a small effect of changing solvent on the process leading to alkene, there may be some justification to invoke a disproportionation to ions before collapse to the alkene. In benzene, the presence of hydrogen iodide causes many of the 4-phenylbutyl radicals to be reduced to the alkane **6**.

The yield of tetralin from the photolysis of **3** in either benzene or acetonitrile at 25°C was determined to be less than 2%. The absence of tetralin in this experiment contrasts with the work of De Tar who prepared the 4-phenylbutyl radical from di-δ-phenylvaleryl peroxide and obtained a 28% yield of tetralin in refluxing benzene (6). Kochi obtained an 11% yield of tetralin in a similar experiment (80°C in benzene) (7). Since we are able to confirm the presence of the 4-phenylbutyl radical by trapping with oxygen, and reduction with hydrogen iodide, we can only conclude that the intramolecular addition to the phenyl ring is an activated process and does not compete with alternate processes at 25°C.

In contrast to iodide **3**, iodide **4** gives mainly ionic products as illustrated in Scheme 3.

The presence of a carbonium ion is proved by the formation of amide **8**, a reaction analogous to the Ritter reaction (1, 8). It seems reasonable to conclude that product **7** also arises from the carbonium ion and it seems less likely that it arises from the



SCHEME 3

radical since the 4-phenylbutyl radical did not cyclize under the same conditions. It seems that the addition of the allylic cation to the phenyl ring is reasonably slow and that nucleophilic trapping by acetonitrile competes effectively. It is hoped that more reactive aromatic or alkene substituents will increase the tendency towards intramolecular addition and provide a route to polycyclic organic compounds.

Experimental

Nuclear magnetic resonance (nmr) spectra were recorded on a Varian EM360 or A 56-60 spectrometer using tetramethylsilane

Can. J. Chem. Downloaded from www.nrcresearchpress.com by 210.87.254.40 on 09/05/12
For personal use only.

as internal standard and infrared (ir) spectra were recorded on a Unican SP1000. Mass spectra were recorded on a Finnigan 1015 mass spectrometer. All chromatography was carried out using the method described by Still *et al.* (9).

4-Phenyl-1-butanol

4-Phenyl butanoic acid (18 g, Aldrich) was reduced with lithium aluminum hydride (4.5 g) in ether (100 mL) in the usual way. Work up yielded 13.2 g of alcohol (91%).

4-Phenyl-1-iodobutane ***3***

4-Phenylbutanol (5.75 g), red phosphorous (0.5 g) and iodine (4.84 g) were refluxed in benzene to produce the iodide as outlined by Vogel (10). Work up yielded 6.7 g (67%) which could be further purified by chromatography (eluant, hexane): nmr (CCl_4) δ 1.53–2.0 (m, 4H), 2.45–2.83 (m, 2H), 2.96–3.3 (m, 2H), 7.15 (s, 5H); mass spectrum *m/e* (relative intensity) 260 (1), 133 (100), 91 (>100). *Anal.* calcd. for $C_{10}H_{13}I$: C 46.17, H 5.04; found: C 46.58, H 5.00.

4-Phenyl-2-methyl-1-butene

3-Chloro-2-methylpropene (35.5 g, 0.39 mol) in ether (50 mL) was added to benzyl magnesium chloride (from 49.1 g benzylchloride and 9.4 g magnesium, 0.39 mol) at room temperature. The mixture was refluxed 2 h, and worked up in the usual way by ether extraction to yield 54 g of crude product. Distillation under reduced pressure (130–135°C at 15 mm Hg) gave 37.7 g (66%) of a colourless oil: nmr (CCl_4) δ 1.72 (s, 3H) 2.0–2.9 (m, 4H), 4.61 (s, 2H), 7.05 (s, 5); mass spectrum *m/e* (relative intensity) 146 (5), 91 (100), 77 (7), 65 (20).

4-Phenyl-2-methyl-1-butene Oxide

m-Chloroperbenzoic acid (30 g, 0.17 mol) in methylene chloride (500 mL) was added to the alkene (20.5 g, 0.14 mol) in 100 mL of methylene chloride at a rate to maintain reflux. After addition of the peracid the solution was refluxed an additional 1/2 h, cooled to room temperature, filtered, and washed with 10% sodium bisulfite, then aqueous sodium bicarbonate. Drying ($MgSO_4$) and evaporation (*in vacuo*) yielded a colourless oil (21.8 g). Attempted distillation resulted in polymerization. Nmr (neat) δ 1.22 (s, 3H), 1.50–1.95 and 2.2–2.9 (m, 4H), 2.37 (s, 2H), 7.15 (s, 5H); mass spectrum *m/e* (relative intensity) 144 (32), 129 (100), 128 (65), 104 (35), 91 (88).

4-Phenyl-2-hydroxymethyl-1-butene

The alcohol was prepared from the epoxide (*vide supra*, 21.8 g, 0.135 mol) using lithium diethylamide (0.44 mol) according to the method of Crandall and Chang (11). The crude product (14 g) was chromatographed on silica gel (eluant benzene, benzene/ether 1:1) to give 5.0 g of a yellow oil (24%): nmr (CCl_4) δ 2.10–2.95 (m, 4H), 4.03 (broad s, 3H), 4.97 (d, 2H), 7.22 (s, 5H); mass spectrum *m/e* (relative intensity) 162 (2), 144 (2), 129 (6), 103 (100), 91 (75), 65 (31). *Anal.* calcd. for $C_{11}H_{14}O$: C 81.44, H 8.70; found: C 81.45, H 8.82.

4-Phenyl-2-tosyloxymethyl-1-butene

Toluenesulfonyl chloride (5.72 g, 0.03 mol) was added to a cooled solution of the alcohol (2.44 g, 0.015 mol) and pyridine (5.93 g, 0.075 mol) in methylene chloride (50 mL). After stirring 2 h and work up by extraction with ice water and aqueous bicarbonate, the dried ($MgSO_4$) organic layer was evaporated and the residue chromatographed on silica gel (eluant, hexane/benzene 1:1 then benzene) to yield the tosylate (1.23 g, 32%) as a colourless oil. Some alcohol (0.49 g) was also recovered. Nmr ($CDCl_3$) δ 1.95–2.77 (m, 4H), 2.32 (s, 3H), 2.32 (s, 2H), 4.95 (d, 2H), 7.12 (s, 5H), 7.47 (q, 4H): mass spectrum *m/e* (relative intensity) 190 (23), 155 (100), 144 (89), 129 (>100), 104 (45), 91 (>100). *Anal.* calcd. for $C_{18}H_{20}O_3S$: C 68.32, H 6.37; found: C 67.96, H 6.44.

4-Phenyl-2-iodomethyl-1-butene, ***4***

The iodide was prepared from the tosylate using a modification of the procedure of Tipson, Clapp, and Cretcher (12). NaI (0.9 g, 0.006 mol) was added to a solution of the tosylate (0.914 g, 0.003 mol) in acetone (20 mL) and stirred at room temperature for 1/2 h followed by filtration and evaporation of the acetone *in vacuo*. Chromatography on silica gel (eluant hexane/benzene 1:1) gave a pale violet oil (iodine contaminated, 0.6 g, 76%): nmr (CCl_4) δ 2.35–2.95 (m, 4H), 3.85 (s, 2H), 5.07 (d, 2H), 7.15 (s, 5H); mass spectrum *m/e* (relative intensity) 245 (1), 145 (53), 117 (16), 91 (100), 65 (24). *Anal.* calcd. for $C_{11}H_{13}I$: C 48.55, H 4.82; found: C 48.88, H 4.76.

Irradiations

Irradiations were carried out at 20–25°C in vycor or quartz vessels using either a low pressure mercury lamp (Ultraviolet Products PCQX1) or a medium pressure mercury lamp Hanovia, 450 W).

Photolysis of 4-Phenyl-1-iodobutane ***3***

In Acetonitrile

Anhydrous, powdered potassium carbonate was added to a solution of the iodide (0.185 g) in acetonitrile (15 mL), the system was flushed with dry nitrogen or oxygen and then irradiated with the Hanovia lamp at 20°C. Samples of the solution were analysed by a tandem gas chromatograph – mass spectrometer (10 ft × 1/8 in. SE30, 10% on chromosorb P, 160–220°C) and products were identified by comparison to authentic samples of 4-phenyl-1-butene and 1-phenylbutane (*vide infra*). Quantitative analysis was carried out by gas chromatography using naphthalene as internal standard. Yields were determined at 50–90% conversion and back corrected for unreacted iodide.

In Benzene

The iodide (200 mg) was dissolved in benzene (50 mL) and flushed with nitrogen or oxygen. In some samples, water was added (~20% the volume of benzene) to scavenge hydrogen iodide. Analysis was carried out as described above.

4-Phenyl-1-butene

Allyl bromide (47.8 g, 0.4 mol) was added to benzyl magnesium chloride (prepared from benzyl chloride, 50 g, and magnesium, 9.5 g) in ether at a rate to maintain reflux. After refluxing a further 45 min the reaction mixture was poured into 10% aqueous hydrochloric acid and the ether extract separated, dried, and evaporated. Distillation yielded a colourless oil 28.9 g (55%) (6).

4-Phenylbutane

Reduction of the alkene with hydrogen over palladium on charcoal (5%) gave the alkane in quantitative yield.

Photolysis of 4-Phenyl-2-iodomethyl-1-butene

Anhydrous, powdered potassium carbonate (1 g) was added to a solution of the iodide (0.438 g) in dry acetonitrile (100 mL). The solution was flushed with dry nitrogen and irradiated for 20 h using the Hanovia lamp. After filtration, and evaporation, chromatography on silica gel (eluant, hexane then acetone) yielded a colourless oil (51 mg), the iodide (94 mg) and with acetone, a yellow oil (194 mg). The yellow oil was further purified by silica gel chromatography (eluant, ether/acetone 49:1). The colourless oil eluted with hexane: nmr (CCl_4) δ 2.10–3.00 (m, 4H), 3.42 (s, 2H), 4.77 (s, 2H), 6.96 (s, 4H); mass spectrum *m/e* (relative intensity) 144 (96), 129 (>100), 115 (100), 91 (31), 77 (40), 63 (55), *Anal.* calcd. for $C_{11}H_{12}$: C 91.67, H 8.33; found: 91.18, H 8.72.

The oil eluted with acetone: nmr ($CDCl_3$), δ 2.00 (s, 3H), 2.15–3.03 (m, 5H), 3.90 (d, 2H), 4.96 (s, 2H), 7.27 (s, 5H); ir (neat 3300, 1645–1670 cm^{-1}; mass spectrum *m/e* (relative intensity) 203 (3), 144 (22), 129 (34), 122 (73), 91 (66), 70 (100).

4-Phenyl-3-aminomethyl-1-butene

The tosylate (300 mg) was stirred for 2 h at room temperature in a solution of acetonitrile – ammonium hydroxide (20 mL, 1:1). This was evaporated then taken up in ether and extracted with 3 *N* HCl. The HCl extract was made basic with aqueous bicarbonate and extracted with ether. Drying ($MgSO_4$) and evaporation yielded a colourless oil (62 mg): nmr (CCl_4) δ 2.13 (m, 6H), 3.0–3.3 (m, 2H), 4.90 (d, 2H), 7.17 (s, 5H); ir (neat) 3260–3440 cm^{-1}; mass spectrum *m/e* (relative intensity) 161 (2), 129 (31), 104 (21), 91 (100), 70 (> 100).

Synthesis of 4-Phenyl-2-acetamidomethyl-1-butene

The amine (*vide supra*, 62 mg) was dissolved in acetic anhydride (20 mL) and pyridine (2 mL), warmed on a steam bath for 1 h, and then evaporated to near dryness *in vacuo*. The residue was dissolved in ether, washed with 3 *N* HCl and aqueous bicarbonate, dried ($MgSO_4$), and evaporated to yield a colourless oil (68 mg). Chromatography on silica gel (eluant ether/acetone 49:1) yielded the amide, identical in every respect to that obtained from the photolysis of iodide **4** in acetonitrile (*vide supra*).

Acknowledgements

We would like to acknowledge the financial assistance of the Natural Sciences and Engineering Council of Canada and the technical assistance of W. Buchannon.

1. P. J. Kropp, T. H. Jones, and G. S. Poindexter. J. Am. Chem. Soc. **95**, 5420 (1973); G. S. Poindexter and P. J. Kropp. J. Am. Chem. Soc. **96**, 7142 (1974); P. J. Kropp, G. S. Poindexter, N. J. Pienta, and D. C. Hamilton. J. Am. Chem. Soc. **98**, 8135 (1976).
2. P. D. Gokhale, A. P. Joshi, R. Sahni, V. G. Naik, N. P. Damodaran, U. R. Nayak, and S. Dev. Tetrahedron, **32**, 1391 (1976).
3. R. Breslow, S. S. Olin, and T. Groves. Tetrahedron Lett. 1837 (1968); M. Julia. Pure Appl. Chem. **40**, 553 (1974).
4. W. S. Johnson. Biorg. Chem. **5**, 51 (1977); E. E. Van Tamelen. Acc. Chem. Res. **8**, 152 (1974).
5. J. L. Charlton and G. J. Williams. Tetrahedron Lett. 1473 (1977).
6. D. F. De Tar and C. Weiss. J. Am. Chem. Soc. **78**, 4296 (1956).
7. J. K. Kochi and R. D. Gilliom. J. Am. Chem. Soc. **86**, 5251 (1965).
8. L. J. Koumen and D. J. Cota. Org. React. **17**, 213 (1969).
9. W. S. Still, M. Kahn, and A. Mitra. J. Org. Chem. **43**, 2923 (1978).
10. A. I. Vogel. Practical organic chemistry. 3rd ed. Longmans, Green and Co. Ltd., London, England. 1964. p. 285.
11. J. K. Crandall and L.-H. Chang. J. Org. Chem. **32**, 435 (1967).
12. R. S. Tipson, M. A. Clapp, and L. H. Cretcher. J. Org. Chem. **12**, 133 (1947).

Can. J. Chem. Downloaded from www.nrcresearchpress.com by 210.87.254.40 on 09/05/12
For personal use only.

Electrophilic additions to allenes. IV. Concerning the nature of the *ortho*-nitro group effect in the reaction of arenesulphenyl chlorides with allenes[1,2]

DENNIS G. GARRATT[3] AND PIERRE L. BEAULIEU[4]

Department of Chemistry, University of Ottawa, Ottawa, Ont., Canada K1N 9B4

Received November 23, 1979

DENNIS G. GARRATT and PIERRE L. BEAULIEU. Can. J. Chem. **58**, 1275 (1980).

The reactions of twelve arenesulphenyl chlorides, five of which contained an *ortho*-nitro substituent, with ten 1,3-disubstituted allenes, using methylene chloride as solvent, are described. No evidence for a special *ortho*-nitro group effect involving a spirosulphurane type intermediate is observed. Variations in the chemoselectivity and configurational-selectivity of the additions are interpreted in terms of steric interactions in the product determining transition state.

DENNIS G. GARRATT et PIERRE L. BEAULIEU. Can. J. Chem. **58**, 1275 (1980).

On décrit les réactions, dans le chlorure de méthylène comme solvant, de 12 chlorures d'arènes-sulphényles, dont 5 contiennent un substituant nitro en position *ortho*, avec 10 allènes disubstitués en position 1,3. On n'a pas obtenu de preuve à l'effet que les groupes nitro en position *ortho* font intervenir un intermédiaire du type spirosulphurane. On interprète les variations de la chimiosélectivité et la sélectivité configurationnelle des additions en fonction d'interactions stériques dans l'état de transition déterminant la nature du produit.

[Traduit par le journal]

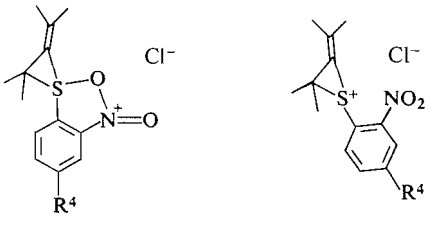
Introduction

Arenesulphenyl chlorides react with alkylsubstituted allenes to form products derived from exclusive attack by sulphur on the central allenic carbon. Rearranged or solvent-incorporated products have not been described, but sometimes products resulting from the loss of HCl are observed (2). The formation of 2:1 adducts, as a result of competitive addition of the sulphenyl halide to the first formed adduct, is normally not observed.

The rate law in polar solvents has been reported to be overall second order, first order in allene and first order in sulphenyl chloride (3). An Ad_E2 mechanism has been postulated in accord with that previously described for simple alkenes (4).

In the first article of this series we reported the observation that 2,4-dinitrobenzenesulphenyl chloride reacts with 1,3-disubstituted allenes, preferentially forming the *E* alkene (5). The ratio of *E* to *Z* alkene was found to increase as the bulk of the substituent group *cis* to the arylthio group increased. These results were interpreted in terms of steric approach control (6) leading to the formation of a series of alkylidenethiiranium ions or alkylideneepisulphuranes (3*b*, 7), in accord with the stereoselectivity previously reported by Jacobs and co-workers (2*e*).

Concern has been raised in a number of quarters (8) over the possible bonding interaction of an oxygen atom from the *ortho*-nitro group, in *ortho*-nitrobenzenesulphenyl halides, with the adjacent sulphur atom leading to a spirosulphurane intermediate **1** instead of the commonly accepted thiiranium ion **2**. Studies correlating thiiranium ion



1 **2**

structure with product geometry have provided considerable insight into the nature of thiiranium ions and have demonstrated that simple alkane- and arenesulphenyl halides often react in a manner quite different from that of *ortho*-nitro-substituted arenesulphenyl halides (8*e*, *f*, 9). However, while these sulphenyl chlorides may be considered atypical (8*h*, 10), the results previously obtained permit a reasonable starting point for the study of the ionic sulphenylation of allenes.

Of paramount importance is to determine what effect, if any, the *ortho*-nitro substituent is really contributing to the reactions under consideration. For example, in addition to the above mentioned *possible* stabilization of a positive charge on sulphur by delocalization into the adjacent nitro group, one can envision a destabilization through

[1]For Part III see ref. 1.

[2]Issued as NRCC No. 18218.

[3]Author to whom correspondence may be addressed at the Division of Chemistry, National Research Council of Canada, Ottawa, Ont., Canada K1A 0R6.

[4]Current address: Department of Chemistry, University of Alberta, Edmonton, Alta., Canada T6G 2G2.

0008-4042/80/121275-05$01.00/0

©1980 National Research Council of Canada/Conseil national de recherches du Canada

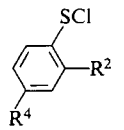
Can. J. Chem. Downloaded from www.nrcresearchpress.com by 210.87.254.42 on 09/05/12
For personal use only.

Can. J. Chem. Downloaded from www.nrcresearchpress.com by 210.87.254.42 on 09/05/12
For personal use only.

inductive electron withdrawal, and/or a steric effect. It is the purpose of this investigation to elucidate those factors which influence the nature of the product determining step in the reaction of arenesulphenyl chlorides with allenes.

Results and Discussion

In order to ascertain the degree and type of involvement of the *ortho*-nitro substituent, we have investigated the reactions of allenes **3–12** with a series of six *para*-substituted arenesulphenyl chlorides, χC_6H_4SCl (χ = NO_2, CF_3, Cl, H, CH_3, CH_3O) I–VI, the corresponding *ortho*-nitro, *para*-substituted arenesulphenyl chlorides, VII–XI, and one further *ortho*-substituted arenesulphenyl chloride, XII, lacking the *ortho*-nitro substituent and thus serving to demonstrate specific steric and electronic effects.

	RCH=C=CHR′				
	R	R′		R^2	R^4
3	CH_3	CH_3	I	H	NO_2
4	C_2H_5	C_2H_5	II	H	CF_3
5	iC_3H_7	iC_3H_7	III	H	Cl
6	tC_4H_9	tC_4H_9	IV	H	H
7	CH_3	C_2H_5	V	H	CH_3
8	CH_3	iC_3H_7	VI	H	CH_3O
9	CH_3	tC_4H_9	VII	NO_2	NO_2
10	C_2H_5	iC_3H_7	VIII	NO_2	Cl
11	C_2H_5	tC_4H_9	IX	NO_2	H
12	iC_3H_7	tC_4H_9	X	NO_2	CH_3
			XI	NO_2	CH_3O
			XII	CH_3	H

All reactions were carried out at ambient temperature except as noted (see Table 1) using methylene chloride as solvent. The kinetically controlled product distributions, Table 1, were determined by immediate ^1H nmr analysis of the reaction mixture. Reaction end-points were determined by the disappearance of the S—Cl chromophore ($\lambda_{max} \simeq 392$ nm) and/or a negative starch–iodide test (11) Analysis of the respective ^1H, ^{13}C nmr spectra and the mass spectral fragmentation patterns, using the criteria previously established (1, 5), indicates that the 1:1 adducts are formed via regiospecific attack of the arylthio moieties on the central allenic carbon (eq. [1]).

[1] $ArSCl + RCH{=}C{=}CHR' \rightarrow RCH{=}C(CHClR')(SAr) + R'CH{=}C(CHClR)(SAr)$

Qualitatively one observes that the 4-substituted 2-nitrobenzenesulphenyl chlorides, VII–XI, react many orders of magnitude slower than the analogous 4-substituted arenesulphenyl chlorides ($\tau_{\frac{1}{2}}$ 1–4 days at 0.05 *M* vs. a few milliseconds). Furthermore, the relative reactivity of the 4-substituted 2-nitrobenzenesulphenyl chlorides is observed to follow the order XI > X > IX > VIII > VII, in accord with the rate measurements of Brown and Hogg (12), using cyclohexene as substrate, and in accord with the predicted relative electrophilicities based upon the known charge stabilization characteristics of the 4-substituents. The much greater reactivity of those sulphenyl chlorides which lack the *ortho*-nitro functionality precluded any similar observations at this time.

Considering only the data applicable to the symmetrically substituted allenes, one observes the previously described increase in the *E*:*Z* ratios (5) as R and R′ are varied from methyl to ethyl ... isopropyl ... *tert*-butyl. In the absence of an *ortho*-nitro substituent (entries I–VI, XII) the *E*:*Z* ratios are fairly constant: R = CH_3, 50–55:50–45; R = C_2H_5, 69–72:31–28; R = iC_3H_7, 79–82:21–18; R = tC_4H_9, 97–100:3–0. When an *ortho* nitro substituent is present (entires VII–XI) these values are in general 5% to 10% larger: R = CH_3, 59–64:41–36; R = C_2H_5, 72–80:28–20; R = iC_3H_7, 92–100:8–0; R = tC_4H_9, 100:0.

While the above data suggest the possible interplay of a steric effect on the part of the *ortho* nitro group, no definitive indication of a specialized electronic stabilizing interaction is apparent. The available data for unsymmetrically 1,3-disubstituted allenes is, however, more instructive.

Firstly, let us consider the chemoselectivity of the reaction. By use of the term *chemoselective* we mean the proportion of attack upon one of the mutually perpendicular π bonds relative to the other. In Table 1 this is given as the ratio α:β. When R = CH_3 and R′ = C_2H_5 the value of α:β is relatively constant 53–55:47–45 (entries I–XII). However, when R = CH_3 and R′ = iC_3H_7, the proportion of attack next to R′ is found to be 5 to 10% less when an *ortho* nitro group is present, irrespective of the nature of the *para* substituent. This is more pronounced where R = CH_3 and R′ = tC_4H_9, the difference being 20-40%. Little variation is, however, observed within a given series. Compare, for example, entries I–VI or VII–XI. A possible set of anomalous data exists for ratios given under entry VI, the *para* methoxy species. We believe that these ratios may reflect thermodynamic control rather than kinetic control as a result of very fast isomerizations, most likely via allylic inter-

Can. J. Chem. Downloaded from www.nrcresearchpress.com by 210.87.254.42 on 09/05/12
For personal use only.

TABLE 1. Kinetically controlled product distributions for the reactions of arenesulphenyl chlorides with some 1,3-disubstituted allenes at ambient temperature in methylene chloride solution

		I 4-NO_2	II 4-CF_3	III 4-Cl	IV 4-H	V§ 4-CH_3	VI§ 4-CH_3O	VII 2-NO_2 4-NO_2	VIII 2-NO_2 4-Cl	IX 2-NO_2	X 2-NO_2 4-CH_3	XI 2-NO_2 4-CH_3O	XII§ 2-CH_3
(*a*) Symmetrically substituted allenes R = R′													
E:*Z*†	CH_3	50:50	53:47	55:45	55:45	55:45	55:45	64:36	60:50	59:41	61:39	59:41	56:44
	C_2H_5	69:31	70:30	72:28	72:28	—	—	80:20	78:22	72:28	76:24	79:21	72:28
	iC_3H_7	82:18	82:18	80:20	80:20	79:21	80:20	92:8	91:9	82:18	100:0	92:8	81:19
	tC_4H_9	100:0	100:0	97:3	97:3	100:0	100:0	100:0	100:0	100:0	100:0	100:0	100:0
(*b*) Unsymmetrically substituted allenes													
	R = CH_3 R′ = C_2H_5	55:45	57:43	53:47	53:47	—	—	53:47	53:47	53:47	53:47	53:47	—
	CH_3 iC_3H_7	62:38	57:43	55:45	55:45	63:37	—	52:48	51:49	48:52	50:50	53:47	66:34
	CH_3 tC_4H_9	65:35	62:38	59:41	59:41	55:45	73:27	42:58	36:64	33:67	45:55	37:63	48:52
α:β*	C_2H_5 iC_3H_7	51:49	57:43	50:50	47:53	49:51	44:56	46:54	45:55	46:54	44:56	46:54	47:53
	C_2H_5 tC_4H_9	50:50	62:38	49:51	55:45	53:47	80:20	33:67	36:64	31:69	26:74	30:70	43:57
	iC_3H_7 tC_4H_9	50:50	50:50	50:50	56:44	60:40	53:47	38:62	38:62	31:69	41:59	40:60	34:66
	CH_3 C_2H_5	53:47	58:42	56:44	56:44	—	—	66:34	58:42	60:40	60:40	64:36	—
	CH_3 iC_3H_7	53:47	54:46	57:43	57:43	55:45	—	65:35	59:41	65:35	64:36	66:34	67:33
α‡	CH_3 tC_4H_9	54:46	52:48	58:42	58:42	55:45	52:48	69:31	69:31	73:27	71:29	76:24	69:31
E:*Z*	C_2H_5 iC_3H_7	73:27	65:35	72:28	64:36	64:36	71:29	76:24	78:22	85:15	73:27	80:20	68:32
	C_2H_5 tC_4H_9	70:30	61:39	73:27	67:33	64:36	58:42	76:24	69:31	84:16	85:15	83:17	63:37
	iC_3H_7 tC_4H_9	82:18	72:28	70:30	77:23	66:34	72:28	100:0	89:11	84:16	100:0	88:12	87:13
	CH_3 C_2H_5	71:29	79:21	70:30	70:30	—	—	86:14	72:28	77:23	74:26	81:19	—
	CH_3 iC_3H_7	84:16	86:14	80:20	80:20	81:19	—	95:5	88:12	87:13	88:12	87:13	85:15
β‡	CH_3 tC_4H_9	100:0	100:0	88:12	88:12	100:0	100:0	100:0	100:0	100:0	100:0	100:0	100:0
E:*Z*	C_2H_5 iC_3H_7	90:10	79:21	84:16	73:27	73:27	55:45	100:0	89:11	91:9	88:12	100:0	77:23
	C_2H_5 tC_4H_9	92:8	100:0	100:0	100:0	100:0	100:0	100:0	100:0	100:0	100:0	100:0	100:0
	iC_3H_7 tC_4H_9	100:0	100:0	90:10	88:12	100:0	100:0	100:0	100:0	100:0	100:0	100:0	100:0

*The chemoselectivity.
†The configurational-selectivity.
‡The configurational-selectivity for the α and β double bonds, respectively.
§Reactions with allenes **3**, **4**, **7**, and **8** carried out 0°C and/or −70°C because of fast isomerizations $E \rightleftharpoons Z$ at ambient temperature. In those cases where no data are given the isomerizations were too fast even at −80°C.

Can. J. Chem. Downloaded from www.nrcresearchpress.com by 210.87.254.42 on 09/05/12
For personal use only.

mediates. Attempts to unambiguously prove this ascertainment have not thus far been successful.

The observed variations in the ratio α:β are quite important. In the first paper of this series (5) we noted that very little chemoselectivity, with respect to which of the mutually perpendicular π bonds of the allene system is attacked, was observed. We hypothesized, on this basis, the presence of an effective mechanism for the transmission of the inductive electron donation of the alkyl groups to the remote double bond. Using the more extensive basis set now available we can see that this interpretation was too limited in scope and that other factors must be interacting during the product determining transition state.

No systematic variations, as a function of the *para* substituents, are apparent from an examination of the α:β ratios. What is observed, is a decrease in the percentage of α attack, as reflected in a low value of α:β when R′ is bulky, particularly when R′ = *tert*-butyl, and when there is an *ortho* substituent on the arenesulphenyl chloride, be that substituent *nitro* or *methyl*! The observation of a similar effect for an *ortho* methyl substituent would appear to rule out the need to invoke a specialized spirosulphurane intermediate of type **1**. The somewhat larger effect of an *ortho* nitro group relative to methyl may result from its larger steric bulk. Minor variations as in the case of allene **12**, entries VII–XII are then interpreted in terms of conformational effects on the part of the planar nitro group. The α:β values are therefore also in accord with a steric interaction mechanism during "steric approach control".

The configurational selectivity, i.e. the *E*:*Z* ratio, for the α and β double bonds, shows trends very similar to those found for the symmetrically substituted allenes. The ratio of *E* to *Z* alkene is found to increase as the bulk of the substituent groups *cis* to the arylthio group increases. Furthermore, the *E*:*Z* ratio for 2-methyl- and 2-nitrobenzenesulphenyl chlorides are remarkably similar as is seen on comparing entries IX and XII. These effects are taken as indicative of a long-range steric interaction between the remote substituent, be it R or R′, and the approaching reagent in accord with steric approach control as previously described (5). These data therefore give additional support to our hypothesis of the predominance of a steric effect for the *ortho* nitro group. It is thus our ascertainment that on the basis of the 120 reactions studied and reported herein, there is no evidence to require a novel intermediate of the spirosulphurane variety on the reaction hypersurface for the arenesulphenylation of 1,3-disubstituted allenes. We also note that while there exists a great rate decrease upon substituting an *ortho* nitro group for an *ortho* hydrogen, there is little evidence for a similar dramatic change with respect to the product determining transition states! Of importance in this regard is the observation that 2-methylbenzenesulphenyl chloride reacts many orders of magnitude faster than 2-nitrobenzenesulphenyl chloride, yet shows similar configurational-selectivity!

Experimental

General

All melting points were recorded on a Fisher–Johns block and are uncorrected. The ^{1}H nmr spectra were run on Varian Associates T-60 and HA-100 spectrometers; ^{13}C nmr spectra were run on a Varian Associates FT-80 spectrometer using a 16K memory. Chloroform-*d* was used as an internal lock and reference. All spectral parameters are referenced to TMS as an internal standard. Tables of spectra data are available upon request from the authors.

Allenes

2,3-Pentadiene was commercially available. 2,3-Hexadiene, 5-methyl-2,3-hexadiene, 5,5-dimethyl-2,3-hexadiene, 3,4-heptadiene, and 2,6-dimethyl-3,4-heptadiene were prepared by standard literature procedures from the commercially available alkenes (Chemical Samples) (13). 2,2,6,6,-Tetramethyl-3,4-heptadiene, 2,2,6-trimethyl-3,4-heptadiene, 2,2-dimethyl-3,4-heptadiene, and 2-methyl-3,4-heptadiene were prepared by the method of Vermeer and co-workers (14).

2,4-Dinitrobenzenesulphenyl chloride was prepared by the method of Lawson and Kharasch (15) from bis(2,4-dinitrophenyl)disulphide. Recrystallized from CCl_4, mp 96–96.5°C (lit. (15) mp 97–98°C).

2-Nitro-4-chlorobenzenesulphenyl chloride was prepared by the method of Turner and Conner (16) using *p*-dichlorobenzene (Aldrich) as starting material; mp 98°C (lit. (16) mp 97.5–98°C).

2-Nitrobenzenesulphenyl chloride was commercially available (Aldrich). Recrystallized from CCl_4, mp 76°C (lit. (15) mp 74.5–75°C).

2-Nitro-4-methylbenzenesulphenyl chloride was prepared from the analogous aniline by the procedure of Zincke and Rose (17). Recrystallized from CCl_4, mp 89–90°C (lit. (17) mp 90°C).

2-Nitro-4-methoxybenzenesulphenyl chloride was prepared from the analogous aniline as above. Crystallized as brilliant orange needles from CCl_4, mp 106–107°C. The remaining *arenesulphenyl chlorides* were prepared from the corresponding thiol or disulphide by chlorination with molecular chlorine in CCl_4 with cooling (0–4°C). Physical properties were as previously reported (18).

Product Studies

These were carried out as previously described (1, 5). In the cases of 2-nitroarenesulphenyl chlorides, ^{1}H nmr analysis was carried out during the course of the reactions and thereafter to ensure the establishment of kinetically controlled product distributions. Because of the essentially instantaneous nature of the reactions of arenesulphenyl chlorides lacking the *ortho*-nitro group, only the slow isomerizations, post-addition, were observable by ^{1}H nmr.

Acknowledgements

The continued financial support of the Natural Sciences and Engineering Research Council of

Canada is gratefully acknowledged. We are also indebted to the Province of Ontario for a scholarship to P.L.B., 1978–1980.

1. D. G. GARRATT, P. L. BEAULIEU, and V. M. MORISSET. Tetrahedron Lett. **21**, 129 (1980).
2. (*a*) W. H. MUELLER and P. E. BUTLER. J. Org. Chem. **33**, 1533 (1968); (*b*) T. L. JACOBS and R. MACOMBER. J. Org. Chem. **33**, 2988 (1968); (*c*) D. J. PASTO, R. L. SMORADA, B. L. TURINI, and D. J. WAMPFLER. J. Org. Chem. **41**, 432 (1976); (*d*) D. J. PASTO and M. F. MILES. J. Org. Chem. **41**, 425 (1976); (*e*) T. L. JACOBS, R. MACOMBER, and D. ZUNKER. J. Am. Chem. Soc. **89**, 7001 (1967).
3. (*a*) K. ILZAWA, T. OKUYAWA, and T. FUENO. J. Am. Chem. Soc. **95**, 4090 (1973); (*b*) G. H. SCHMID, D. G. GARRATT, and S. YEROUSHALMI. J. Org. Chem. **43**, 3764 (1978).
4. G. H. SCHMID and D. G. GARRATT. *In* The Chemistry of functional groups, Supplement A: The chemistry of double-bonded functional groups. *Edited by* S. Patai. Wiley and Sons, London. 1977. pp. 828–858, and references cited therein.
5. D. G. GARRATT and P. BEAULIEU. Can. J. Chem. **57**, 119 (1979).
6. (*a*) D. J. PASTO and B. LEPESKA. J. Am. Chem. Soc. **98**, 1091 (1976); (*b*) W. G. DAUBEN, G. J. FOUKEN, and D. S. NOYCE. J. Am. Chem. Soc. **78**, 2579 (1956); (*c*) E. C. ASHBY and S. A. NODING. J. Org. Chem. **42**, 264 (1977).
7. W. R. MOORE and R. C. BERTELSON. J. Org. Chem. **27**, 4182 (1962).
8. (*a*) D. C. OWLSEY, G. K. HELMKAMP, and M. F. RETTIG. J. Am. Chem. Soc. **91**, 5239 (1969); (*b*) D. R. HOGG. Mech. React. Sulfur Compd. **5**, 87 (1970); (*c*) E. N. GIVENS and H. KWART. J. Am. Chem. Soc. **90**, 378 (1968); **90**, 386 (1968); (*d*) N. KHARASCH. *In* Organic sulfur compounds. Vol. 1. *Edited by* N. Kharasch. Pergamon Press, Oxford. 1961. p. 379; (*e*) W. H. MUELLER and P. E. BUTLER. J. Am. Chem. Soc. **88**, 2866 (1966); (*f*) W. H. MUELLER and P. E. BUTLER. J. Am. Chem. Soc. **90**, 2075 (1968); (*g*) W. A. THALER. J. Org. Chem. **34**, 871 (1969); (*h*) D. G. GARRATT and P. L. BEAULIEU. J. Org. Chem. **44**, 3555 (1979).
9. (*a*) W. H. MUELLER and P. E. BUTLER. Chem. Commun. 646 (1966); (*b*) W. A. THALER, W. H. MUELLER, and P. E. BUTLER. J. Am. Chem. Soc. **90**, 2068 (1968); (*c*) W. A. SMIT, A. S. GYBIN, V. S. BOGDANOV, M. Z. KRIMER, and E. A. VOROBIEVA. Tetrahedron Lett. 1085 (1978); (*d*) G. H. SCHMID. *In* Topics in sulfur chemistry. Vol. 3. *Edited by* A. Senning. George Thieme Publishers, Stuttgart. 1977. p. 103.
10. G. H. SCHMID, V. M. CSIZMADIA, V. J. NOWLAN, and D. G. GARRATT. Can. J. Chem. **50**, 2457 (1972).
11. N. KHARASCH. J. Chem. Educ. **33**, 585 (1956), and references cited therein.
12. C. BROWN and D. R. HOGG. J. Chem. Soc. B, 1262 (1968).
13. (*a*) W. VON DOERING and P. M. LAFLAMME. Tetrahedron, **2**, 75 (1958); (*b*) L. SKATTEBOL. Acta Chem. Scand. **17**, 1683 (1963); (*c*) W. R. MOORE and H. R. WARD. J. Org. Chem. **27**, 4179 (1962).
14. (*a*) P. VERMEER, H. WESTMIJZE, H. KLEIJN, and L. A. VON DIJCK. Recl. J. Royal Netherlands Chem. Soc. **97**, 56 (1978); (*b*) P. VERMEER, J. MEIJER, and L. BRANDSMA. Recl. Trav. Chim. Pays-Bas, **94**, 112 (1975).
15. D. LAWSON and N. KHARASCH. J. Org. Chem. **24**, 857 (1956).
16. R. A. TURNER and R. CONNER. J. Chem. Soc. **69**, 1009 (1947).
17. T. ZINCKE and H. ROSE. Ann. **406**, 103 (1914); **406**, 127 (1914).
18. N. KHARASCH. Intra-Sci. Chem. Rep. **1**, 340 (1969).

Can. J. Chem. Downloaded from www.nrcresearchpress.com by 210.87.254.42 on 09/05/12
For personal use only.

Canadian Journal of Chemistry

Published by
THE NATIONAL RESEARCH COUNCIL OF CANADA

Journal canadien de chimie

Publié par
LE CONSEIL NATIONAL DE RECHERCHES DU CANADA

Volume 58 Number 13 July 1, 1980

Volume 58 numéro 13 1 juillet 1980

Effect of the acyl substituent on the equilibrium constant for hydration of esters

J. PETER GUTHRIE[1] AND PATRICIA A. CULLIMORE

Department of Chemistry, University of Western Ontario, London, Ont., Canada N6A 5B7

Received December 10, 1979

J. PETER GUTHRIE and PATRICIA A. CULLIMORE. Can. J. Chem. **58**, 1281 (1980).

Heats of hydrolysis have been measured for the trimethyl orthoesters of isobutyric, propionic, benzoic, methoxyacetic, chloroacetic, and cyanoacetic acids using aqueous acid with an organic cosolvent where necessary, and of the corresponding esters in alkaline solution. Solubilities or free energies of transfer from gas to aqueous solution have been measured, permitting calculation of the free energies of formation of the aqueous orthoesters, and by methods which we have published previously, calculation of the free energies of formation of the covalent hydrates of the esters, and the free energy changes for hydration of these esters.

Using estimated pK_a values equilibrium constants were calculated for the addition of hydroxide to the esters. The data are in good agreement with the appropriate Marcus equation relating rate and equilibrium constants with a value for b of 8.99 ± 0.17. This line was used to estimate the equilibrium constant for addition of hydroxide, and thence of water, to some additional esters where only the rate constant was available. Rate constants for hydrolysis of methyl esters in aqueous solution at 25°C were calculated from literature data, correcting for the effect of other conditions as necessary. From the equilibrium constants for addition of water we could estimate the rate constants for uncatalyzed hydrolysis; for the cases where this rate constant has been measured, the agreement was satisfactory. For acid catalyzed hydrolysis the data permit a test of the two alternative mechanisms considered previously, namely specific acid catalysis and general acid catalysis with hydronium ion acting as a general acid. For esters the mechanism is clearly specific acid catalysis, but for aldehydes and ketones it appears very likely that the mechanism is general acid catalysis.

J. PETER GUTHRIE et PATRICIA A. CULLIMORE. Can. J. Chem. **58**, 1281 (1980).

On a mesuré les chaleurs d'hydrolyse des orthoesters triméthyliques des acides isobutyrique, propionique, benzoique, méthoxyacétique, chloroacétique et cyanacétique en utilisant une solution aqueuse acide avec un cosolvant organique lorsque cela s'avère nécessaire; on a aussi mesuré les chaleurs d'hydrolyse des esters correspondants en solution basique. On a mesuré les solubilités ou les énergies libres de transfert de la phase gazeuse à la solution aqueuse ce qui a permis de calculer les énergies libres de formation des orthoesters aqueux et de calculer, au moyen de méthodes publiées antérieurement, les énergies libres de formation des hydrates covalents des esters et les changements d'énergie libre d'hydratation de ces esters.

On a calculé les constantes d'équilibre de la réaction d'addition de l'hydroxyde sur les esters en utilisant les valeurs approximatives du pK_a. Les données sont en parfait accord avec l'équation appropriée de Marcus reliant la vitesse et les constantes d'équilibre avec une valeur de $b = 8.99 \pm 0.17$. Cette donnée est utilisée pour évaluer la constante d'équilibre de la réaction d'addition d'hydroxyde et par conséquent, celle de l'eau sur les quelques esters additionnels lorsque la constante de vitesse est la seule donnée disponible. On a calculé les constantes de vitesse d'hydrolyse des esters méthyliques en solution aqueuse à 25°C à partir des données de la littérature en corrigeant s'il y a lieu, pour tenir compte de l'effet des autres conditions. On peut évaluer les constantes de vitesse d'hydrolyse non catalysée à partir des constantes d'équilibre de la réaction d'addition de l'eau. Dans les cas où l'on a mesuré la constante de vitesse, l'accord est satisfaisant. En ce qui a trait à l'hydrolyse acide, les données permettent de vérifier les deux mécanismes alternatifs considérés antérieurement en particulier la catalyse acide spécifique et la catalyse acide générale à l'aide d'ion hydronium agissant comme un acide général. Dans le cas des esters, le mécanisme est nettement une catalyse acide spécifique mais pour les aldéhydes et les cétones il semble être plus communément du type catalyse acide générale.

[Traduit par le journal]

Introduction

We have previously reported potentially useful relations between rate and equilibrium constants for carbonyl reactions (1). In that work it was suggested that equilibrium constants for the addition of hydroxide to esters (or other carbonyl compounds) could be estimated from the Marcus (2–4) equation relating rate to equilibrium constant; it seemed important to increase the number of esters used to establish this relationship from the three which

[1]Alfred P. Sloan Fellow 1975–1979.

0008-4042/80/131281-14$01.00/0

© 1980 National Research Council of Canada/Conseil national de recherches du Canada

Can. J. Chem. Downloaded from www.nrcresearchpress.com by 210.87.254.105 on 09/05/12
For personal use only.

Can. J. Chem. Downloaded from www.nrcresearchpress.com by 210.87.254.105 on 09/05/12
For personal use only.

TABLE 1. Calorimetric results[a]

Compound	ΔH_r(kcal/mol)[b]	ΔH_{sol} (kcal/mol)[c]
$C_2H_5C(OCH_3)_3$	−12.37 (0.13)[d]	−5.55 (0.15)[e]
$C_2H_5COOCH_3$	−14.38 (0.22)[e]	−2.34 (0.06)[d]
C_2H_5COOH	−14.29 (0.03)[e]	
$(CH_3)_2CHC(OCH_3)_3$	−12.72 (0.28)[d]	
$(CH_3)_2CHCOOCH_3$	−14.72 (0.24)[f]	−2.21 (0.09)[d]
$(CH_3)_2CHCOOH$	−14.15 (0.04)[f]	
$ClCH_2C(OCH_3)_3$	−7.80 (0.26)[d]	
$ClCH_2COOCH_3$	−13.70 (0.70)[e]	−0.22 (0.09)[g]
$ClCH_2COOH$	−17.68 (0.15)[h]	+3.20 (0.10)[i]
$NC—CH_2–C(OCH_3)_3$	−6.14 (0.35)[d]	
$NC—CH_2—COOCH_3$	−12.97 (0.50)[e]	1.37 (0.18)[i]
$NC—CH_2—COOH$	−10.16 (0.16)[h]	4.07 (0.12)[d]
$CH_3O—CH_2—C(OCH_3)_3$	−12.53 (0.12)[d]	−6.72 (0.10)[e]
$CH_3O—CH_2—COOCH_3$	−15.67 (1.40)[e]	−2.42 (0.07)[d]
$CH_3O—CH_2—COOH$	−15.32 (0.20)[e]	−0.93 (0.24)[d]
$C_6H_5C(OCH_3)_3$	−4.13 (0.09)[j]	
$C_6H_5COOCH_3$	−17.44 (0.45)[h]	+3.41 (0.06)[j]
C_6H_5COOH	−14.09 (0.54)[k]	
H_2O		−0.06 (0.01)[d]
		−0.08 (0.01)[e]
		−0.07 (0.01)[f]
		−0.22 (0.01)[j]
		−1.36 (0.03)[k]
CH_3OH		−1.76 (0.03)[d]
		−1.84 (0.02)[e]
		−1.94 (0.01)[f]
		−0.32 (0.02)[j]
		−1.53 (0.04)[k]

[a]All at 25°C; standard deviations in parentheses.
[b]Heat of reaction with the solvent indicated; the reaction is either hydrolysis or neutralization.
[c]Heat of solution, without chemical reaction, in the solvent indicated.
[d]0.1 *N* HCl in water.
[e]0.1 *N* NaOH in water.
[f]1.0 *N* NaOH in water.
[g]0.001 *N* HCl in water.
[h]Calculated from ΔH sol'n and the heats of ionization of the acid (38) and water (38).
[i]Reference 39.
[j]0.1 *N* HCl in 50% methanol: 50% water (v/v).
[k]0.1 *N* tetraethylammonium hydroxide in 90% DMSO:10% water (v/v).

were then available. Accordingly we have prepared a series of orthoesters and measured their heats of hydrolysis as well as the heats of hydrolysis of the corresponding esters. Where necessary we have also measured the quantities necessary to calculate the free energies of transfer from gas to 1 *M* aqueous solution. Then, by methods which we have developed (5–8) it is possible to calculate the free energy of formation of the ester hydrate and thus the equilibrium constant for hydration of the ester. These new data confirm and extend our previous (1) findings, and now permit a definite answer to the question of the mechanism of acid catalyzed ester hydrolysis.

We have also been able to predict rate constants for various hydrolytic processes which have not yet been measured.

Results and Discussion

The calorimetric results obtained in this work are gathered in Table 1. The ideal heat of hydrolysis for an ester refers to the process:

[1] $RCOOCH_3(l) + H_2O(l) = RCOOH(l) + CH_3OH(l)$

The actual process measured calorimetrically is:

[2] $RCOOCH_3(l) + HO^-(aq) = RCOO^-(aq) + CH_3OH(aq)$

To transform eq. [2] into the form of eq. [1] requires that the enthalpy change for the reaction of acid (liquid or solid) with hydroxide ion, as well as the heats of solution of methanol and water be known. By combining these values we can calculate the overall enthalpy change for eq. [1], and then, if the standard heats of formation for the acid, methanol, and water are available, $\Delta H^0_f(l)$ for the ester can be calculated. For this work the standard enthalpies for formation of isobutyric, chloroacetic, cyanoacetic, and methoxyacetic acids were either of inadequate precision or unavailable, so that the standard enthalpies of formation (and subsequently calculated values for $\Delta H^0_f(g)$, $\Delta G^0_f(g)$, and $\Delta G^0_f(aq)$) for the corresponding esters and orthoesters, were reported as a sum with an unknown.

Similarly, the ideal heat of hydrolysis for the

TABLE 2. Free energies of transfer from gas to aqueous solution at 25°C[a]

Compound	Concentration (M)	Pressure (Torr)	ΔG_t (kcal/mol)
	(a) Calculated from solubility and vapour pressure		
$C_2H_5C(OCH_3)_3$	1.02 (0.041)[b]	12.9[c]	−2.43 (0.39)
$C_2H_5COOCH_3$	0.81 (0.08)[b,d]	97.8[c]	−1.09 (0.39)
$(CH_3)_2CH—C(OCH_3)_3$	0.048 (0.004)[b]	8.28[c]	−0.88 (0.39)
$(CH_3)_2CH—COOCH_3$	0.274 (0.010)[b]	61.7[c]	−0.72 (0.39)
$ClCH_2—C(OCH_3)_3$	0.396 (0.044)[b]	3.24[c]	−2.69 (0.39)
$ClCH_2—COOCH_3$	0.455 (0.023)[b]	9.96[c]	−2.10 (0.39)
$NC—CH_2—C(OCH_3)_3$	0.754 (0.112)[b]	0.290[c]	−4.50 (0.39)
$CH_3O—CH_2—C(OCH_2CH_3)_3$	0.380 (0.028)[b]	1.05[c]	−3.33 (0.39)
$C_6H_5—C(OCH_3)_3$	0.012 (0.001)[b]	0.248[c]	−2.14 (0.39)
$C_6H_5—COOCH_3$	0.011 (0.001)[b,e]	0.349[c]	−1.88 (0.18)
	(b) Determined by analysis of vapor and liquid phases		
$NC—CH_2—COOCH_3$	1.62 (0.06)[f,g,h]	0.35[f,g]	−4.84[g]
	1.72 (0.17)[f,g,h]	0.44[f,g]	−4.75[g]
	1.79 (0.12)[f,g,h]	0.37[f,g]	−4.87[g]
			Av. −4.82 (0.06)
$CH_3O—CH_2—C(OCH_3)_3$	0.088 (0.006)[f,i,j]	0.114[f,i]	−3.78[i]
			−3.87[k]
			Av. −3.83 (0.05)
$CH_3OCH_2—COOCH_3$	0.192 (0.004)[f,h,l]	0.323[f,l]	−3.63[l]
	0.202 (0.012)[f,h,l]	0.210[f,l]	−3.91[l]
	0.213 (0.011)[f,h,l]	0.199[f,l]	−3.97[l]
			Av. −3.84 (0.18)

[a]Standard states, hypothetical ideal gas at 1 atm pressure, and 1 M aqueous solution with an infinitely dilute reference state.
[b]Saturated solution; solubility determined in this work unless otherwise noted.
[c]Vapor pressure of the pure liquid, calculated from the boiling point as described in ref. 1.
[d]Reference 40; relative error assumed to be 10%.
[e]Reference 41; relative error assumed to be 10%.
[f]Determined by analysis of the solution and distillate, as described in the text.
[g]Solvent was 0.01 N HCl.
[h]Average of analyses taken before and after a run.
[i]Solvent was 0.1 N NaOH.
[j]Uncertainty calculated from the standard deviations of the integrals.
[k]Calculated from the free energy of transfer for $CH_3OCH_2—C(OCH_2CH_3)_3$ by subtracting the contributions for the three CH_2 groups.
[l]Solvent was pH 7 phosphate buffer.

orthoester refers to the process:

[3] $$RC(OCH_3)_3(l) + H_2O(l) = RCOOCH_3(l) + 2CH_3OH(l)$$

when the actual process measured was:

[4] $$RC(OCH_3)_3(l) + H_2O(aq) = RCOOCH_3(aq) + 2CH_3OH(aq)$$

To convert eq. [4] into the form of eq. [3] we must know the heats of solution of the ordinary ester, methanol, and water. The overall enthalpy change for eq. [3] and a value for $\Delta H^0_f(l)$ for the orthoester (pending a known value for ΔH^0_f for the corresponding acid) can be calculated as previously described.

Whenever possible aqueous solvents were used for calorimetric measurements. The usual solvents are aqueous 0.1 N HCl or 0.1 N NaOH; aqueous 1 N NaOH would be used if the rate of hydrolysis was slow in tenth normal base, or 0.001 N HCl would be used if acid catalyzed decomposition occurred too rapidly in tenth normal acid. Solubility problems sometimes necessitated the use of mixed solvent systems: 50 or 70% methanol in water, or 90% dimethyl sulfoxide in water. Methanolic solvents were often unsatisfactory for alkaline hydrolysis because although solubility was improved, the rate of reaction was markedly slower than in water.

Entropies of the gaseous compounds were estimated as described in the Calculations. Free energies of transfer were determined for all esters and orthoesters as described in the Experimental. The data and results from these experiments are summarized in Table 2. With these data in hand the free energies of formation could be derived; thermodynamic quantities used in this paper are collected in Table 3. In some cases the heat of formation of the parent carboxylic acid is unknown or only approximately known. In such a case the heats and free energies of formation of the ester and orthoester are unspecified by a constant unknown quantity, but values based on the difference be-

Can. J. Chem. Downloaded from www.nrcresearchpress.com by 210.87.254.105 on 09/05/12
For personal use only.

Can. J. Chem. Downloaded from www.nrcresearchpress.com by 210.87.254.105 on 09/05/12
For personal use only.

TABLE 3. Thermochemical data for compounds used in this paper[a]

(*a*) Compounds for which the free energy of formation in aqueous solution has not previously been reported

Compound	ΔH_f(g)[b]	S°(g)[c]	ΔG^0_f(g)	ΔHv[b,d]	ΔH^0_f(l or c)[b]	ΔG_t[b,e]	ΔG^0_f(aq)[b]
C_2H_5COOH	−108.91 (0.48)[h]	77.12 (1.5)[g]	−88.16 (0.65)[h]	13.15 (0.48)[i]	−122.06 (0.05)[f]	−4.58 (0.1)[j]	−92.74 (0.66)[h]
$C_2H_5COOCH_3$	−104.19 (1.03)[h]	89.26 (1.5)[g]	−77.34 (1.12)[h]	8.24 (1.00)[g]	−112.43 (0.23)[k]	−1.09 (0.39)[k]	−78.43 (1.19)[h]
$C_2H_5C(OCH_3)_3$	−141.43 (1.04)[h]	111.06 (1.5)[g]	−85.04 (1.13)[h]	10.15 (1.00)[g]	−151.58 (0.27)[k]	−2.43 (0.39)[k]	−87.48 (1.19)[h]
$(CH_3)_2CHCOOCH_3$	+18.69+i(1.03)[h,l]	85.88 (1.5)[g]	+43.57+i(1.12)[h,l]	8.69 (1.00)[g]	+10.00+i(0.25)[k,l]	−0.72 (0.39)[k]	+42.85+i(1.19)[h,l]
$(CH_3)_2CHC(OCH_3)_3$	−18.11+i(1.07)[h,l]	117.86 (1.5)[g]	+36.26+i(1.16)[h,l]	10.54 (1.00)[g]	−28.64+i(0.39)[k,l]	−0.88 (0.39)[k]	+35.38+i(1.23)[h,l]
$ClCH_2COOCH_3$	−15.93+l(1.23)[h,l]	34.93 (1.5)[g]	+52.56+l(1.31)[h,l]	10.37 (1.00)[g]	+5.56+l(0.72)[k,l]	−2.10 (0.39)[k]	+50.46+l(1.37)[h,l]
$ClCH_2C(OCH_3)_3$	−24.69+l(1.26)[h,l]	56.94 (1.5)[g]	+41.42+l(1.34)[h,l]	11.36 (1.00)[g]	−36.04+l(0.77)[k,l]	−2.69 (0.39)[k]	+38.73+l(1.39)[h,l]
$NCCH_2COOCH_3$	+25.78+y(1.13)[h,l]	91.63 (1.5)[g]	+44.78+y(1.22)[h,l]	13.43 (1.00)[g]	+12.35+y(0.53)[k,l]	−4.82 (0.06)[k]	+39.96+y(1.22)[h,l]
$NCCH_2C(OCH_3)_3$	−15.96+y(1.20)[h,l]	113.64 (1.5)[g]	+32.52+y(1.28)[h,l]	13.36 (1.00)[g]	−29.32+y(0.66)[k,l]	−4.50 (0.39)[k]	+28.03+y(1.34)[h,l]
$CH_3OCH_2COOCH_3$	+20.18+m(1.73)[h,l]	97.90 (1.5)[g]	+51.76+m(1.79)[h,l]	10.29 (1.00)[g]	+9.89+m(1.41)[k,l]	−3.84 (0.18)[k]	+47.92+m(1.80)[h,l]
$CH_3OCH_2C(OCH_3)_3$	−17.91+m(1.74)[h,l]	121.65 (1.5)[g]	+43.08+m(1.80)[h,l]	11.27 (1.00)[g]	−29.18+m(1.42)[k,l]	−3.83 (0.05)[k]	+39.25+m(1.80)[h,l]
C_6H_5COOH	−70.29 (0.38)[f]	88.19 (0.5)[m]	−51.22 (0.41)[h]	21.70 (0.35)[n]	−91.99 (0.14)[f]	−5.80 (0.19)[o]	−57.02 (0.45)[h]
$C_6H_5COOCH_3$	−64.37 (1.23)[h]	99.90 (1.5)[g]	−39.07 (1.31)[h]	13.28 (0.01)[f]	−77.51 (0.72)[k]	−1.88 (0.18)[k]	−40.95 (1.32)[h]
$C_6H_5C(OCH_3)_3$	−102.62 (1.24)[h]	121.95 (1.5)[g]	−47.86 (1.32)[h]	13.49 (1.00)[g]	−116.11 (0.73)[k]	−2.14 (0.39)[k]	−49.99 (1.37)[h]

(*b*) Compounds for which the free energy of formation in aqueous solution has been reported

Compound	ΔG^0_f(aq)
H_2O	−56.69[p]
CH_3OH	−41.88[q]

(*c*) Compounds for which only the free energy of formation in aqueous solution was calculated in this work

Compound	ΔG^0_f(aq)
$C_2H_5C(OCH_3)(OH)_2$	−122.24 (1.29)
$(CH_3)_2CHC(OCH_3)(OH)_2$	+0.39+i(1.32)[l]
$ClCH_2C(OCH_3)(OH)_2$	+2.86+l(1.52)[l]
$NCCH_2C(OCH_3)(OH)_2$	−8.70+y(1.47)
$CH_3OCH_2C(OCH_3)(OH)_2$	+3.81+m(1.88)[l]
$C_6H_5C(OCH_3)(OH)_2$	−83.89 (1.47)

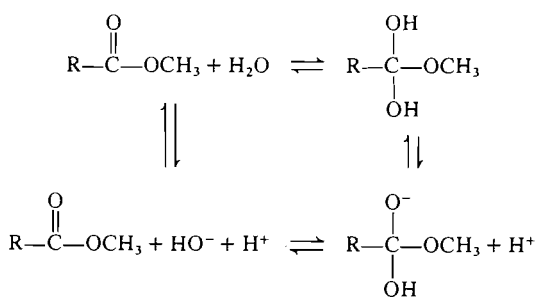
[a]At 25°C, standard states are ideal gas at 1 atm, pure liquid, and 1 *M* aqueous solution with an infinitely dilute reference state, unless otherwise noted; estimated standard deviations in parentheses. [b]In kcal mol^{-1}. [c]In cal deg^{-1} mol^{-1}. [d]Heat of vaporization. [e]Free energy of transfer, from gas at 1 atm to 1 *M* aqueous solution with an infinitely dilute reference state. [f]Reference 39. [g]Calculated as described in the text. [h]Calculated from other values in this table. [i]Reference 42, heat of vaporization, liquid to monomeric vapor. [j]Calculated from data in ref. 43. [k]Determined in this work. [l]The heat of formation of the corresponding acid is unknown, or not known to useful precision; i represents ΔH°_f(l)[$(CH_3)_2CHCOOH$], l represents ΔH°_f(c)[$ClCH_2COOH$]; y represents ΔH°_f(c)[$NCCH_2COOH$]; m represents ΔH°_f(l)-[CH_3OCH_2COOH]. [m]Reference 44. [n]Best value based on ref. 39. [o]Calculated from the vapor pressure derived from the results of ref. 45 and the solubility, ref. 46. [p]Reference 47. [q]Reference 5.

Can. J. Chem. Downloaded from www.nrcresearchpress.com by 210.87.254.105 on 09/05/12
For personal use only.

tween two such numbers as, for instance, the free energy change upon covalent hydration of an ester, are fully specified.

From the free energies of formation of the ester hydrates and the esters, we could calculate the free energy changes, and hence the equilibrium constants for the addition of water to the esters. Using the linear free energy relationships which we reported earlier (1) the pK_a for ionization of the ester hydrate to give the anionic tetrahedral intermediate could be readily calculated. Then, by means of the cycle shown in Scheme 1, the equilibrium constants for the addition of hydroxide to the esters may be calculated. Similarly, by estimating the appropriate pK_a values using the relations developed previously (1) we may derive the equilibrium constants for the addition of water to give the zwitterionic intermediate and for the reaction of ester with hydronium ion to give the cationic tetrahedral intermediate. The reaction of protonated ester with water to give this same cationic species is more of a problem because of the need to know the pK_{BH^+} value for the ester itself. Ester pK_{BH^+} values are often not yet available; we have used the available data and estimated further values from the appropriate linear free energy relations (see the Calculations).

All of the equilibrium constants so calculated are found in Table 4. For comparison with these equilibrium constants we required rate constants for the acid, base, and uncatalyzed hydrolysis of methyl esters in aqueous solution at 25°C. Although a vast amount of effort has been expended in the study of ester hydrolyses, many of the investigations have been in mixed solvents, or have involved other esters or other temperatures. For some esters only the esterification rate and not the hydrolysis rate has been measured. In order to obtain a set of rate constants for the same conditions as the equilibrium constants, we have made extensive use of linear free energy relationships to correct the rate constants from the literature to standard conditions. We have found that many of the linear free energy relationships have slopes differing from unity, so that it would not be correct to use rate ratios to correct from one set of conditions to another. All of the data upon which our final set of rate constants is based are to be found in the Supplementary Tables.[2] The rate constants for aqueous solution are found in Table 4, which also contains estimated values for those rate constants which have not yet been reported. The estimation procedures are described below.



SCHEME 1

Marcus and Cohen (2–4) derived an expression for the rate of reaction within an encounter complex which is equivalent to:

$$[5] \quad \log k = \log (k_B T/h) - b(1 - (\log K)/4b)^2$$

Following Hine (9), we have translated the original expression derived by Marcus, which was expressed in terms of free energies of activation and reaction into a form expressed in terms of rate and equilibrium constants. The dimensionless parameter b is a measure of the "intrinsic barrier", i.e. the kinetic barrier to reaction when the equilibrium constant is 1.0. This expression holds only for log K between $-4b$ and $+4b$; for very favorable reactions, $\log k = \log (k_B T/h)$, i.e. $d \log k/d \log K = 0.0$; and for very unfavorable reactions $\log k = \log (k_B T/h) + \log K$, i.e. $d \log k/d \log K = 1.0$. The expression describes a smooth curve between these two limiting lines, and has only one adjustable parameter. It should be stressed that the equation must be applied to a single reaction step, occurring within an encounter complex. An encounter complex will be assumed to mean two or more molecules confined within the same solvation cage, but not necessarily interacting either favorably or unfavorably.

Since most reactions involve diffusion steps either before or after the chemical reaction step, it is necessary to use somewhat more complicated expressions to describe the reactions in terms of the observable rate and equilibrium constants. We will now derive the appropriate expressions for those cases relevant to the present discussion. We will take explicit account of the possibility of changes in rate determining step as the chemical steps become fast enough to compete with diffusion steps: as Murdoch (14) has pointed out, this can lead to additional curvature in rate equilibrium correlations beyond that implied by eq. [5]. The theory has generally been discussed in terms of the rather

$$[6] \quad A + B \rightleftharpoons C + D$$

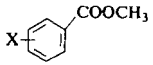
symmetrical type of reaction shown in [6], where

[2]Copies of the Supplementary Tables may be obtained, at a nominal charge, from the Depository of Unpublished Data, CISTI, National Research Council of Canada, Ottawa, Ont., Canada K1A 0S2.

Can. J. Chem. Downloaded from www.nrcresearchpress.com by 210.87.254.105 on 09/05/12
For personal use only.

TABLE 4. Rate and equilibrium constants for reactions of methyl esters[a]

Ester	σ_R^{*}[b]	log k_{OH^-}[c]	log K^{-}[d]	log k_w[e]	log K°[f]	log K^{zg}	log k_{H^+}[h]	log K_{gac}[i]	log K_+[j]	log k_+[k]	pK_{BH^+}[l]
$HCOOCH_3$	0.49[m]	1.58[n]	−3.8[o]	−6.2[p]	−6.6[q]	−17.9[o]	−2.62[r]	−9.97[o]	−4.76[o]	2.59[s]	−5.21[t]
CH_3COOCH_3	0.00[m]	−0.82[n]	−6.0[o]	−9.07[u]	−8.2[q]	−19.7[o]	−3.95[r]	−11.13[o]	−7.68[o]	−0.50[s]	−3.45[t]
CH_3CH_2—$COOCH_3$	−0.10[m]	−0.84[n]	−7.36[o]	(−8.9)	−9.43[v]	−20.35[o]	−3.96[r]	−12.27[o]	−8.18[o]	−0.14[s]	−4.10[t]
$(CH_3)_2CH$—$COOCH_3$	−0.19[m]	−1.05[n]	−8.47[o]	(−9.7)	−10.42[v]	−21.38[o]	−4.19[r]	−13.19[o]	−9.21[o]	−0.22[s]	−3.97[t]
$(CH_3)_3C$—$COOCH_3$	−0.30[m]	−1.50[n]	−8.25[w]	(−9.4)	−10.05[x]	−21.05[x]	−4.82[r]	−12.72[x]	−9.07[x]	−1.17[s]	(−3.65)[t]
$CH_3CH_2CH_2$—$COOCH_3$	−0.12[m]	−0.99[n]	−7.37[w]	(−8.8)	−9.42[x]	−20.34[x]	−4.11[r]	−12.24[x]	−8.28[x]	−0.15[s]	(−3.96)[t]
$(CH_3CH_2)_2CH$—$COOCH_3$	−0.23[m]	−1.69[n]	−8.57[w]	(−9.7)	−10.46[x]	−21.43[x]	−4.37[r]	−13.19[x]	−9.41[x]	−0.59[s]	(−3.78)[t]
$(CH_3CH_2)_3C$—$COOCH_3$	−0.34[y]	−2.70[z]	−10.23[w]	(−11.0)	−11.99[x]	−23.00[x]	−5.72[am]	−14.62[x]	−11.03[x]	−2.13[s]	(−3.59)[t]
$(CH_3)_3C$—CH_2—$COOCH_3$	−0.17[m]	−1.57[aa]	−8.37[w]	(−9.6)	−10.34[x]	−21.29[x]	−4.77[am]	−13.12[x]	−9.24[x]	−0.89[s]	(−3.88)[t]
Ph—CH_2—$COOCH_3$	+0.22[m]	−0.34[n]	−6.23[w]	(−8.2)	−8.72[x]	−19.50[x]	−4.11[r]	−11.85[x]	−7.05[x]	0.69[s]	−4.8[t]
Ph_2CH—$COOCH_3$	+0.41[m]	−1.62[n]	−8.45[w]	(−10.1)	−11.19[x]	−21.89[x]	−4.69[r]	−14.49[x]	−9.62[x]	0.19[s]	(−4.87)[t]
Ph_3C—$COOCH_3$	0.45[ab]	−4.64[ac]	−13.27	(−14.2)	−16.06[x]	−26.74[x]	(−9.4)	−19.40[x]	−14.46[x]	(−4.5)	(−4.94)[t]
CH_2=CH—$COOCH_3$	0.61[ab]	−0.73[n]	−6.92[w]	(−9.0)	−9.93[x]	−20.54[x]	−5.33[r]	−13.40[x]	−9.20[x]	−1.13[s]	(−4.2)[ad]
E-CH_3—CH=CH—$COOCH_3$	+0.36[m]	−1.05[n]	−7.48[w]	(−9.3)	−10.15[x]	−20.87[x]	−5.49[r]	−13.41[x]	−9.21[x]	−1.29[s]	−4.2[ae]
FCH_2—$COOCH_3$	1.10[m]	1.46[n]	−2.89[w]	(−6.2)	−6.54[x]	−16.94[x]	−4.06[r]	−10.46[x]	−4.41[x]	1.99[s]	(−6.05)[t]
F_2CH—$COOCH_3$	2.05[m]	3.81[n]	1.99[w]	−3.74[u]	−2.92[x]	−12.91[x]	−3.93[r]	−7.68[x]	−0.00[x]	3.75[s]	(−7.68)[t]
F_3C—$COOCH_3$	2.61[d]	5.64[n]	+4.7[o]	−2.02[u]	−0.9[af]	−11.3[o]	(−3.2)	−6.16[o]	2.48[o]	(5.4)	(−8.64)[b]
$ClCH_2$—$COOCH_3$	1.05[m]	+1.71[n]	−3.07[o]	−6.44[u]	−6.66[v]	−17.08[o]	−4.12[r]	−10.53[o]	−4.33[o]	2.08[s]	−6.2[t]
Cl_2CH—$COOCH$	1.94[m]	3.09[n]	0.42[w]	−4.66[u]	−4.34[x]	−14.38[x]	−3.67[r]	−9.00[x]	−1.43[x]	3.90[s]	−7.57[t]
							−4.91[r,ag]	−9.00[x]	−1.43[x]	2.66[s,ag]	
Cl_3C—$COOCH_3$	2.65[m]	3.57[n]	1.45[w]	−3.09[u]	−4.24[x]	−13.98[x]	−3.40[r]	−9.54[x]	−0.82[x]	5.32[s]	−8.72[t]
							−5.05[r,ag]	−9.54[x]	−0.82[x]	3.67[s,ag]	
$BrCH_2$—$COOCH_3$	1.00[m]	1.96[n]	−1.91[w]	(−5.4)	−5.43[x]	−15.87[x]	−4.12[r]	−9.25[x]	−3.37[x]	1.76[s]	(−5.88)[t]
Br_2CH—$COOCH_3$	1.91[ab]	2.62[n]	−0.57[w]	−5.41[u]	−5.29[x]	−15.34[x]	−4.97[r]	−9.92[x]	−2.48[x]	2.47[s]	(−7.44)[t]
ICH_2—$COOCH_3$	0.85[m]	1.45[n]	−2.91[w]	(−6.1)	−6.23[x]	−16.74[x]	−4.17[r]	−9.92[x]	−4.30[x]	1.45[s]	(−5.62)[t]
NC—CH_2—$COOCH_3$	1.30[m]	1.61[n]	−1.96[o]	(−5.7)	−5.87[v]	−16.19[x]	−4.77[r]	−9.97[o]	−4.06[o]	1.13[s]	−5.9[t]
$HOCH_2$—$COOCH_3$	0.56[m]	0.35[n]	−4.99[w]	(−7.5)	−7.93[x]	−18.56[x]	−3.92[r]	−11.36[x]	−6.37[x]	1.07[s]	(−4.99)[t]
CH_3O—CH_2—$COOCH_3$	0.60[m]	0.45[n]	−6.22[o]	(−8.4)	−9.21[v]	−19.83[o]	−4.21[r]	−12.68[o]	−7.37[o]	1.09[s]	(−5.30)[t]
CH_3OOC—$COOCH_3$	2.00[m]	4.47[n]	3.50[w]	−4.40[ah]	−1.34[x]	−11.36[x]	−3.48[r]	−6.06[x]	—	—	—
CH_3OOC—CH_2—$COOCH_3$	0.76[ab]	0.24[n]	−5.19[w]	(−7.7)	−8.39[x]	−18.94[x]	−4.76[an]	−12.00[x]	−6.03[x]	1.21[s]	(−5.97)[t]
^-OOC—$COOCH_3$	−1.06[al]	0.18[n]	−5.30[w]	(−6.6)	−6.10[x]	−17.43[x]	—	—	—	—	—
^-OOC—CH_2—$COOCH_3$	−0.06[al]	−1.63[n]	−8.47[w]	(−9.8)	−10.59[x]	−21.48[x]	—	—	—	—	—
^-O_3S—CH_2—$COOCH_3$	0.26[ab]	−0.69[n]	−6.85[w]	(−8.7)	−9.39[x]	−20.15[x]	—	—	—	—	—
^+H_3N—CH_2—$COOCH_3$	1.34[ab]	1.76[n]	−2.31[w]	(−6.0)	−6.27[x]	−16.57[x]	−5.60[r]	−10.40[x]	−2.40[x]	+2.40[s]	(−8.00)[t]
$(CH_3)_3N^+$—CH_2—$COOCH_3$	1.90[m]	1.99[n]	−1.85[w]	(−6.0)	−6.56[x]	−16.61[x]	−6.00[aj]	−11.18[x]	−3.76[x]	1.42[s]	(−7.42)[t]
$(CH_3)_2S^+$—CH_2—$COOCH_3$	2.05[ab]	2.62[n]	−0.57[w]	(−5.2)	−5.48[x]	−15.47[x]	(−4.8)	−10.23[x]	−2.55[x]	(2.9)	(−7.68)[t]



Can. J. Chem. Downloaded from www.nrcresearchpress.com by 210.87.254.105 on 09/05/12
For personal use only.

TABLE 4 (*Concluded*)

Ester	σ_R*[b]	log k_{OH^-}[c]	log K^{-}[d]	log k_w[e]	log K^{o}[f]	log K^{zg}	log k_{H^+}[h]	log K_{gas}[i]	log K_+[j]	log k_+[k]	pK_{BH^+}[l]
X = 4-CH_3—O—	0.61[ab]	−1.88[ak]	−8.89[w]	(−10.6)	−11.89[x]	−22.50[x]	−6.76[r]	−15.37[x]	−9.47[x]	−0.86[s]	(−5.9)[al]
4-CH_3—	0.60[ab]	−1.47[ak]	−8.20[w]	(−10.0)	−11.19[x]	−21.80[x]	−6.58[r]	−14.66[x]	−8.66[x]	−0.58[s]	(−6.0)[al]
H—	0.60[m]	−1.14[ak]	−7.08[o]	(−9.1)	−10.07[y]	−20.68[o]	−6.37[r]	−13.54[o]	−7.38[o]	−0.21[s]	−6.16[al]
4-Cl—	0.87[ab]	−0.89[ak]	−7.20[w]	(−9.4)	−10.55[x]	−21.05[x]	−6.53[r]	−14.26[x]	−7.86[x]	−0.13[s]	(−6.4)[al]
4-Br—	0.87[ab]	−0.83[ak]	−7.10[w]	(−9.3)	−10.44[x]	−20.94[x]	−6.52[r]	−14.15[x]	−7.75[x]	−0.12[s]	(−6.4)[al]
4-NO_2—	1.39[ab]	−0.08[ak]	−5.77[w]	(−8.6)	−9.78[x]	−20.06[x]	−6.34[r]	−13.93[x]	−6.93[x]	+0.66[s]	(−7.0)[al]
3-NO_2—	1.21[ab]	−0.21[ak]	−6.00[w]	(−8.7)	−9.80[x]	−20.15[x]	−6.49[r]	−13.81[x]	−6.91[x]	+0.41[s]	(−6.9)[al]
2-NO_2—	1.16[ab]	−0.70[ak]	−6.87[w]	(−9.3)	−10.60[x]	−20.97[x]	−7.68[r]	−14.57[x]	−6.27[x]	0.62[s]	−8.3)[al]
3,5-$(NO_2)_2$—	1.73[ab]	+0.72[ak]	−4.30[w]	(−7.7)	−8.78[x]	−18.91[x]	—	−13.26[x]	—	—	—
2,4-$(NO_2)_2$—	1.93[ab]	+0.19[ak]	−5.28[w]	(−8.6)	−10.03[x]	−20.07[x]	—	−14.68[x]	—	—	—

[a]All in aqueous solution at 25°C; values in parentheses have been estimated, as described. [b]Taft σ_R* value for R in R—$COOCH_3$. [c]Rate constant for hydroxide ion catalyzed hydrolysis, M^{-1} s^{-1}. [d]Equilibrium constant for addition of hydroxide ion to the ester to give the anionic tetrahedral intermediate, M^{-1}. [e]Rate constant for uncatalyzed hydrolysis, s^{-1}. [f]Equilibrium constant for addition of water to the ester to give the neutral tetrahedral intermediate; dimensionless. [g]Equilibrium constant for addition of water to the ester to give the zwitterionic tetrahedral intermediate; dimensionless. [h]Rate constant for acid catalyzed hydrolysis, M^{-1} s^{-1}. [i]Equilibrium constant for general acid catalyzed (hydronium ion as general acid) addition of water to give the protonated tetrahedral intermediate, M^{-1}. [j]Equilibrium constant for addition of water to the protonated tetrahedral intermediate; dimensionless. [k]Rate constant for addition of water to the protonated ester, s^{-1}. [l]Acid dissociation constant for the protonated ester, M. [m]Reference 48. [n]From Table S7. [o]Calculated from log K^{o} using pK_a values estimated as described in the text. [p]Reference 1. [q]Reference 5, 1. [r]From Table S8. [s]Calculated from log k_{H^+} using the pK_{BH^+} value given in this table. [t]From Table S16. [u]From Table S9. [v]Calculated from the free energies of formation in Table 3. [w]Estimated from log k_{OH^-}, using the Marcus curve for log k_{OH^-} vs. log K_{OH^-} as described in the text. [x]Calculated from log K^{-}, using pK_a values estimated as described in the text. [y]Estimated assuming that the increase in σ* on replacing the third H of acetic acid by Et is the same as for replacing the second H by Et; compare with the series Me, Et, *i*-Pr, *t*-Bu. [z]From Table S11. [aa]From Table S18. [ab]From Table S19. [ac]From Table S6. [ad]Assumed to be the same as methyl crotonate. [ae]Reference 23. [af]Reference 8, 1. [ag]Based upon esterification rates; see text. [ah]Reference 49. [ai]Reference 50. [aj]Reference 51. [ak]From Table S12. [al]From Table S17. [am]From Table S10. [an]Reference 52.

diffusion processes can become rate limiting for either forward or reverse reactions. Two other reaction types, which will be more useful for the present paper will be discussed below; for all three models we will consider the three cases: equilibrium constant very favorable in the forward direction, about unity, and very unfavorable in the forward direction. The full model for process [6] involves diffusion together of the reactants, reaction within the encounter complex, and diffusion apart of the products. It is necessary to make some allowance for the rate and equilibrium constant for the encounter complex formation and dissociation processes. Hine (9) has made the very reasonable proposal that the equilibrium constant for encounter complex formation should be about $0.017\ M^{-1}$; this was calculated assuming that the nucleophile could encounter the carbonyl group from either side, but had to be in a sphere of radius 1.5 Å (the van der Waal's radius of oxygen) touching the carbon, and that there was no special attraction or repulsion. We have employed this value for the equilibrium constant for the formation of all encounter complexes involving two solutes. If Hine's suggested value is adopted, then certain consequences follow; in particular, the rate of diffusion together of reactants must be less than the value for simple spherical reagents in order to cause the equilibrium constant to have the value required. We have endeavored to assign reasonable values to these rate constants in the following way. The encounter distance was taken as 3 Å and the rate constant for diffusional separation was calculated from the Eigen eq. [7] (10)

$$[7] \qquad k_{-1} = (3/R_{ij}^2)(D_i + D_j)$$

using a value of 1.5×10^{-5} cm^2 s^{-1} for the diffusion constants of both species.[3] The rate constant so calculated was 1.0×10^{11} s^{-1}. From this rate constant and the equilibrium constant we may calculate that k_1, the rate constant for diffusion together to form the complex, is 1.7×10^9 s^{-1}.[4] Although there are certainly objections possible to the way in which these values were estimated, they are logically consistent and there is no obvious way to derive more exact expressions. It seems preferable to us to use rather approximate values and accept a certain crudeness in the theory and degree of fit to experimental data in order to have only one adjustable parameter and no more.

[3]Values of about this magnitude are found for various small molecular species, and are not strongly sensitive to size of molecules; see ref. 11.

[4]This may be shown, by expressing the rate constant in terms of the Smoluchowski equation (12), to correspond to a solid angle for approach of the nucleophile of 3.14 rather than 4π.

Can. J. Chem. Downloaded from www.nrcresearchpress.com by 210.87.254.105 on 09/05/12
For personal use only.

With these considerations in mind we may then consider the three cases of interest. First, for reactions with two reactants and two products eq. [6] can be elaborated as eq. [8]. Reaction coordinate

[8] $A + B \rightleftharpoons A,B \rightleftharpoons C,D \rightleftharpoons C + D$

diagrams for each of the three cases for this model are illustrated in Fig. 1; the three cases shown are (*a*) reaction rate is diffusion controlled in the forward direction; (*b*) reaction rate is controlled by the rate of the chemical transformation, with ΔG related to ΔG^0; (*c*) reaction rate is diffusion controlled in the reverse direction. The figure helps make it clear that the equilibrium constant to be used in the Marcus expression for this process is the overall equilibrium constant for eq. [8] since in our approximation the equilibrium constants for the formation of the encounter complexes from starting materials and products are the same. This will not always be the case, but unless there are clear theoretical grounds for assuming that they are unequal (as when there is an electrostatic interaction) or there is convincing experimental evidence demanding such a conclusion it seems to us preferable to use an inexact expression in place of one which gives a better fit but uses numerous parameters not well determined by the data. This seems particularly important in the situation of interest for this paper where the data span wide ranges of rate and equilibrium constants, but in the latter case are of limited precision.

If the equilibrium constants for the diffusion together of substrates or diffusion apart of products, for the process in eq. [8], were markedly different, the equilibrium constant for the chemical step would no longer be that for the overall process. If the encounter process had a large barrier (a high "work term" to bring reactants together) then the limiting rate constant at very favorable equilibrium constant would be much less than the diffusion limit. There are numerous cases where sizeable "work terms" have been invoked (13) but this is always to explain one or two divergent points.

When the equation for the overall process is derived, making the steady state assumption for encounter complex, rather more complex equations than those previously employed are obtained. That one must consider changes from rate limited transport to rate limiting reaction, and that this can be an additional source of curvature in rate equilibrium correlations has been shown by Murdoch (14).

A somewhat different formulation is necessary for the case of carbonyl addition processes, where we wish to consider reactions such as [9], of the

[9] $A + B \rightleftharpoons C$

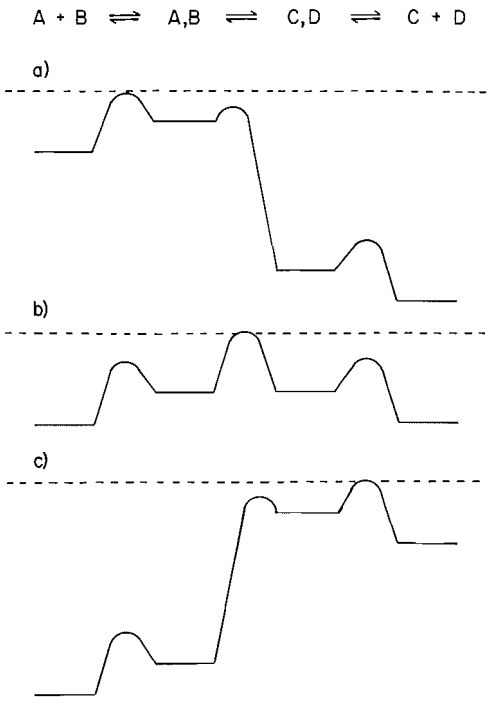


FIG. 1. Reaction coordinate diagrams for the case of two reactants and two products. (*a*) Equilibrium constant very favorable for product formation, diffusion together of reactions is rate limiting. (*b*) Equilibrium constant is of intermediate magnitude, chemical reaction step is rate limiting. (*c*) Equilibrium constant is very unfavorable for product formation, diffusion apart of products is rate limiting.

type where the forward reaction can be limited by the rates of diffusion together of A and B, as the equilibrium constant becomes very large in the direction favoring C, but the reverse reaction can in principle become as fast as a molecular vibration, 10^{13} s^{-1}, as the equilibrium constant for formation of C becomes very unfavorable. Equation [9] should be expanded to eq. [10].

[10] $A + B \underset{k_{-1}}{\overset{k_1}{\rightleftharpoons}} A,B \underset{k_{-2}}{\overset{k_2}{\rightleftharpoons}} C$

Figure 2 makes clear that our assumptions require the use of a different value for the equilibrium constant, reduced from the overall equilibrium constant by the equilibrium constant for encounter complex formation. This model leads to the overall eq. [11] which we have used in this paper for hydroxide addition to carbonyl compounds. This leads to slightly different numerical results from those previously reported, but does not change the qualitative conclusions.

[11] $k_{obs} = k_1/(1 + k_{-1}/k_2)$

$\log k_2 = 13 - b(1 - \log K/4b)^2$

Can. J. Chem. Downloaded from www.nrcresearchpress.com by 210.87.254.105 on 09/05/12
For personal use only.

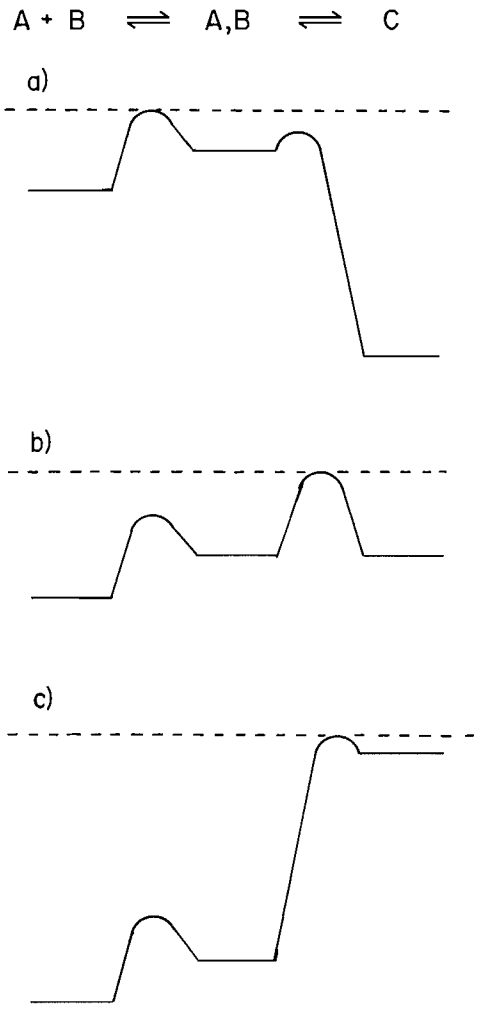


FIG. 2. Reaction coordinate diagrams for the case of two reactants and only one product. (*a*) Equilibrium constant very favorable for product formation, diffusion together of reactants is rate limiting. (*b*) Equilibrium constant is of intermediate magnitude, chemical reaction step is rate limiting. (*c*) Equilibrium constant is very unfavorable for product formation, rate constant for breakdown of the product is approaching the vibration limit.

There are additional problems when the nucleophile is water, since the solvent does not need to diffuse into contact with the carbonyl compound. However there is probably a need for a water molecule to reorient itself so that it is able to react; we indicate such a reoriented water as H_2O^* in [12].

[12] $A + H_2O \rightleftharpoons A, H_2O^* \rightleftharpoons C$

The only limitation on the forward rate as the equilibrium constant becomes very large in the direction favoring products is then the relaxational time of water molecules, which corresponds to a

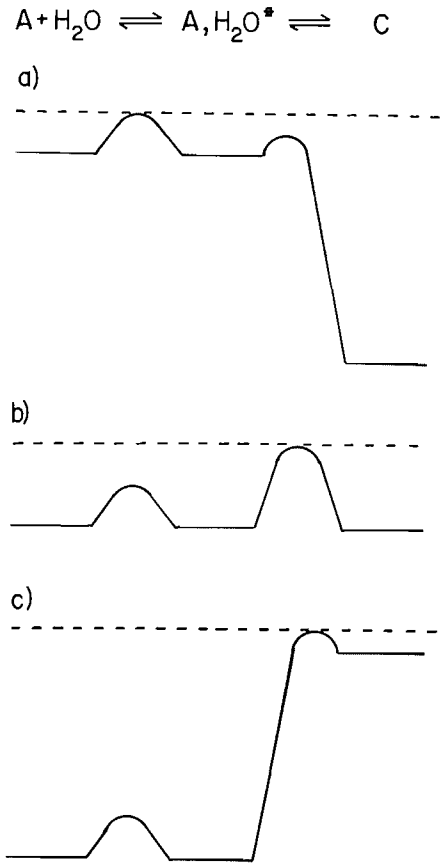


FIG. 3. Reaction coordinate diagrams for the case of two reactants, one of which is water, and only one product. (*a*) Equilibrium constant very favorable for product formation, relaxation of water to give a molecule of water in a reactive orientation is rate limiting. (*b*) Equilibrium constant is of intermediate magnitude, chemical reaction step is rate limiting. (*c*) Equilibrium constant is very unfavorable for product formation, rate constant for breakdown of product is approaching the vibration limit.

rate constant of about 10^{11} s^{-1}.[5] In the absence of any further information we have set the equilibrium constant for reorganization to 1.0 and applied eq. [11] to this case as well. Since the data do not fall in regions where solvent reorganization is likely to be rate limiting, this uncertainty should have little qualitative effect, although it does mean that the equilibrium constant will be in error by some unknown offset.

Figure 3 illustrates this case; there are several points which require discussion; first it is quite possible if not certain that a similar solvent reorganization step should be included in the cases

[5]This value is derived from various relaxation times reported for water molecules in liquid water, which seem to be in approximate agreement at about 3×10^{-12} s (ref. 15), implying a rate constant of about 10^{11} s^{-1} or a little larger.

Can. J. Chem. Downloaded from www.nrcresearchpress.com by 210.87.254.105 on 09/05/12
For personal use only.

discussed earlier. What is not certain is what the equilibrium constant for the reorganization process should be or what would constitute unambiguous evidence for such a process becoming an important contribution to the overall rate equation.

The effect of using these various forms of the Marcus equation upon the actual shape of the curves is relatively small for b values significantly greater than 1 if the equilibrium constants are neither very small nor very large. If the equilibrium constants are such that the curve begins to approach one of the asymptotes, then it clearly makes a very considerable difference which form of the equation is used.

The new thermochemical data reported in this paper permit the calculation of equilibrium constants for the addition of water or hydroxide to six additional esters, supplementing the three for which this was possible from our previous work (1). We may test these new equilibrium constants several ways. First we may show that the equilibrium constants for addition of hydroxide lead to a good correlation with the rate constants for attack of hydroxide and that the points fall on a line consistent with the Marcus eq. [11]. Figure 4 shows that this is indeed the case and that the points fall on a line within experimental error; the b value calculated by the method of least squares for the 9 points is 8.99 ± 0.17. This value differs from that reported earlier (1) because we are now fitting to a different equation. If the equation used in ref. 1 is used for the 9 esters for which data are now available, the b value obtained by least squares is very similar to that obtained for three esters (1). Secondly we may show that the rates of uncatalyzed attack of water on the esters are consistent with the equilibrium constants calculated for the addition of water to give the zwitterion, as was done previously (1). Unfortunately only one of the esters studied in the present work has had its water rate measured; Fig. 5, which includes other points obtained as described below, shows that for the esters for which data are available the agreement with eq. [11] is poorer if the reaction is assumed to proceed directly to the neutral tetrahedral species. Since we are using a different equation, the details of the fit are slightly changed, from that described in ref. 1, but the qualitative conclusion is unchanged, that only addition to give the zwitterion provides a satisfactory description of the data. Thirdly, we may plot the equilibrium constants for hydration against the Taft σ^* values for the acyl substituent; this plot, shown in Fig. 6, shows a reasonably good linear free energy relationship, with a reasonable ρ^* value of 3.02 with the correlation coefficient, $r = 0.944$ for 8 points.

Since the equilibrium constants derived from our thermochemical data seem to be in satisfactory agreement with the kinetic behavior of the esters,

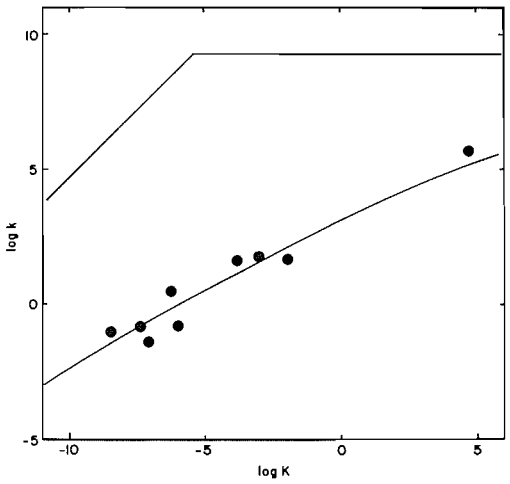


FIG. 4. Marcus curve for hydroxide attack on esters. The line through the points is drawn using the value of b determined by least squares, 8.99 ± 0.17. The limiting line corresponding to $b = 0$ is also shown.

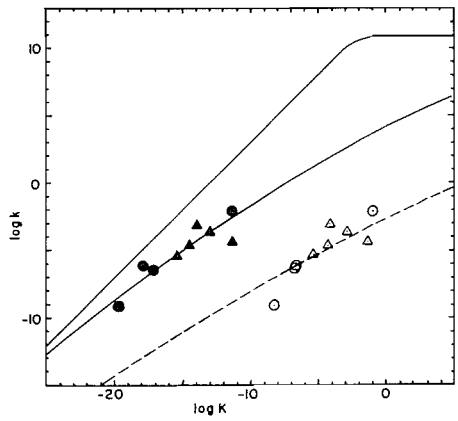


FIG. 5. Marcus curve for uncatalyzed hydrolysis of esters. (——) and open points, calculated assuming that the attack of water leads directly to the neutral tetrahedral intermediates, i.e. concerted proton transfer. (○) points where K^- was determined from thermochemical data; (△) points where K^- was determined from the curve relating rate and equilibrium constants for hydroxide attack. The line was determined by least squares, $b = 15.74 \pm 0.32$; the weighted sum of the squares of the deviations was 15.2 (points based on thermochemistry were given double weight). Note that two of the points derived from thermochemistry deviate badly. (—) and closed points, calculated assuming that the attack of water leads to the zwitterion, with fast subsequent proton transfer. The line was determined by least squares, $b = 8.81 \pm 0.28$; the weighted sum of the squares of the deviations was 7.81. Note that in this case the most serious deviation was for dimethyl oxalate, where the equilibrium constant was determined from the correlation for hydroxide reactions. The limiting line corresponding to $b = 0$ is also shown.

Can. J. Chem. Downloaded from www.nrcresearchpress.com by 210.87.254.105 on 09/05/12
For personal use only.

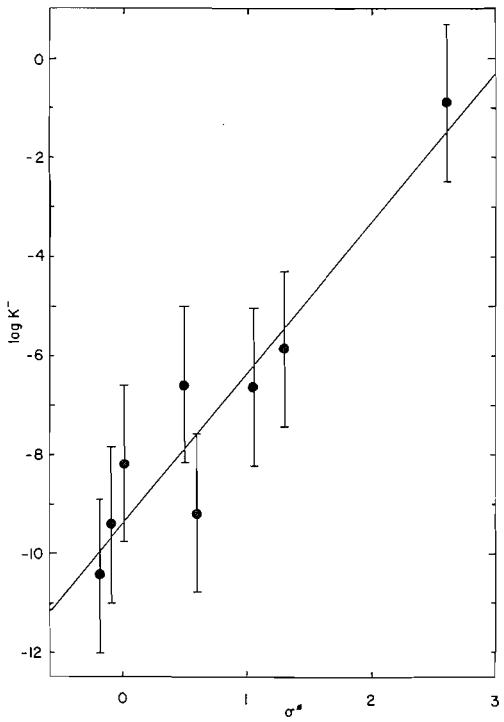
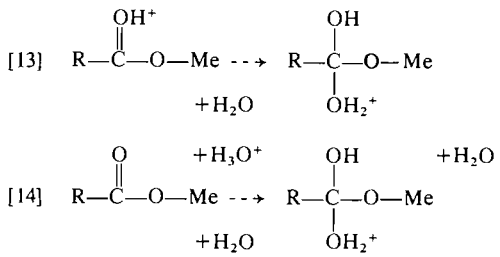


FIG. 6. Relationship between log K^0 and σ^* for aliphatic esters. The best line (least squares) is $\log K^0 = -9.336 + 3.02\sigma^*$.

we are emboldened to try using the Marcus relationship to derive further equilibrium constants from literature values of rate constants for the hydroxide ion catalyzed hydrolysis of esters. As we have previously pointed out (1) this reaction is mechanistically unambiguous (provided, as is generally the case, that the leaving group is as good a leaving group as hydroxide or better) and therefore is likely to be very satisfactory for this purpose. Equilibrium constants so estimated are found in Table 4, along with values derived more directly from experiment. This procedure allows us to obtain many more equilibrium constants. The derived data can be tested by looking at the correlation between rate and equilibrium constants for the water reaction, for which we now have five additional points; the agreement is seen from Fig. 5 to be satisfactory. Since no water rates are available for the aromatic esters, the equilibrium constants estimated for them cannot be tested in this way.

With significantly less confidence we can use these new equilibrium constants for addition to esters, derived from the rate constants for hydroxide attack, to estimate rate constants for the water reaction, where they have not been reported. These estimated rate constants are given in Table 4. Some at least are experimentally accessible, without requiring unreasonably prolonged reaction times.

Acid catalyzed hydrolysis of esters poses a problem, since there are two mechanisms which both lead to plausible fits of data to the Marcus equation with the limited set of data initially available (1), namely specific acid catalyzed[6] addition of water in which water adds to the protonated ester to give the protonated form of the tetrahedral intermediate, process [13], or general acid catalyzed[6] addition of water, with hydronium ion acting as general acid, so that water plus hydronium ion combines with the ester to give the protonated tetrahedral intermediate, process [14].



The difficulty with process [13] was that the best available values for the pK_{BH^+} values of carbonyl compounds led to some points falling in impossible regions, corresponding to rate constants exceeding the relaxation rate for water (1); this was not compelling because there is considerable uncertainty concerning the true pK_{BH^+} values for simple carbonyl compounds, and recent values for acetone have varied from −2.72 (16) to −5.37 (17). Only for the more negative values of the pK_{BH^+} for acetone and other simple carbonyl compounds do the points fall in forbidden regions. We have a strong preference for these more negative values since an analysis[7] of the published data for protonation of acetone showed that there was a two step protonation process, as proposed by Palm *et al.* (18). This analysis was used as a starting point for the pK_{BH^+} assignment of Cox *et al.* (17). For acetaldehyde and formaldehyde, the two compounds which could give a clear answer to the question, there are no accepted values for pK_{BH^+}, although several attempts have been made to measure them (19–21). From the data in ref. 21 a pK_{BH^+} value of −8.1 can be deduced for formaldehyde.[7]

With a larger set of equilibrium constants for hydration in hand we can endeavor to give a clearer

[6]Specific acid catalyzed and general acid catalyzed are used in the strict mechanistic (as opposed to kinetic) sense to mean that the proton is fully (specific) or partially (general) transferred at the transition state.

[7]J. P. Guthrie, unpublished calculations.

Can. J. Chem. Downloaded from www.nrcresearchpress.com by 210.87.254.105 on 09/05/12
For personal use only.

answer to the question. It must be borne in mind that in this attempt the only solidly established facts are the observed rate constants. The equilibrium constants for hydration are, we believe, reliable although imprecise, but most have not been tested. The pK_{BH^+} values for the esters, although various attempts have been made to measure them (22–24), are still plagued by the uncertainties which beset all measurements of ionization constants for very weak bases. We have extended the set of esters for which pK_{BH^+} values are available by the use of linear free energy relationships; see the Calculations. The pK_{BH^+} values for the tetrahedral intermediates are necessarily (since one cannot prepare a solution of these metastable species for titration) based upon extrapolation from simpler compounds using linear free energy relations which are bound to be imperfect. In the case of the protonated alcohol species, there are so few direct measurements that it was necessary to base the linear free energy relation (1) on indirectly measured basicities (25). Nevertheless, the values for pK_{BH^+} of the intermediate are probably fairly reliable since they were used in deriving the zwitterion content for the neutral intermediate in the successful correlation for uncatalyzed hydrolysis.

If we plot the observed rate constants for acid catalyzed reaction vs. the equilibrium constants calculated for process [14] we find a rather implausible looking graph, Fig. 7, with severe scatter of the data about the best line. A more detailed examination of structure reactivity relationships for esters makes this mechanism look very unsatisfactory. The well known fact that the rate constants for the acid catalyzed reactions of *meta*- and *para*-substituted benzoate esters are almost independent of substituent means, in terms of mechanism [14], that the effects of substituents on hydration and upon protonation of the neutral hydrate must almost cancel, since in terms of the Marcus equation, if the rate constants are independent of structure while falling short of diffusion controlled values, then the equilibrium constants must also be independent of structure. This leads to an unreasonable requirement that the ρ value for pK_{BH^+} of the tetrahedral intermediate be of the same magnitude as the ρ value for the hydration. Although the ρ value of 2.9 which we observe for hydration of aromatic esters appears quite reasonable for this process, which occurs at the carbon directly bonded to the benzene ring, it is far too large for an ionization at an atom separated from the ring by one carbon atom; for anilines ρ for pK_a is −2.81 (26) while for benzylamines it is −1.05 (27). Similarly for the aliphatic esters the ρ^* value for the acid catalyzed hydrolysis is ~0, so that ρ^* for ionization of the tetrahedral intermediate must have a magnitude of 2.4, which is again too large for a substituent effect with an intervening carbon atom; ρ^* for $R—NH_3^+$ is −3.15 (26) while for $R—CH_2—NH_3^+$ it is −1.75 (7). These arguments suggest that the general acid catalyzed mechanism is probably not correct, and force us to the specific acid catalyzed path.

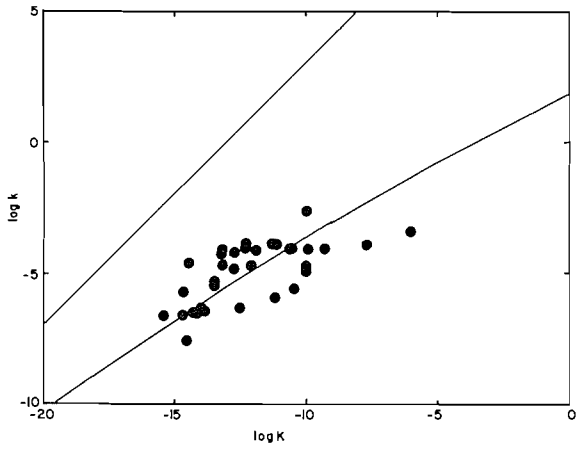


FIG. 7. Marcus curve for acid catalyzed ester hydrolysis assuming that this follows mechanism [14], with general acid catalysis by hydronium ion. The line is the best fit by least squares, but is not satisfactory, $b = 11.12 \pm 0.19$, sum of squares of deviations = 33.91. The limiting line corresponding to $b = 0$ is also shown.

Alternatively we may use the best available pK_{BH^+} values for the esters (see Calculations) and see how well the data obey the Marcus equation for mechanism [13]. When the data are plotted in this way, the points fall in reasonable accord with eq. [11] for $b = 8.45 \pm 0.10$. This supports the assumption of a simple specific acid catalyzed path for acidic hydrolysis of esters, but there remain the problems with the simple carbonyl compounds. These problems exist only if the assumption is made that these compounds should also fall on the same line as the esters, but this assumption seemed reasonable in view of the behavior seen for uncatalyzed and base catalyzed addition of water. Since the pK_{BH^+} values for all of acetone, acetaldehyde, and formaldehyde would have to be very close to 0.0 for these compounds to fall on the same line as the esters for the simple specific acid mechanism, this seems unlikely to be the correct description for them. Alternatively there may be a change in mechanism between the esters and the simple carbonyl compounds, with the former showing specific acid catalysis, and the latter showing general acid catalysis with hydronium ion acting as general acid.

Other investigations, to be reported separately,

Can. J. Chem. Downloaded from www.nrcresearchpress.com by 210.87.254.105 on 09/05/12
For personal use only.

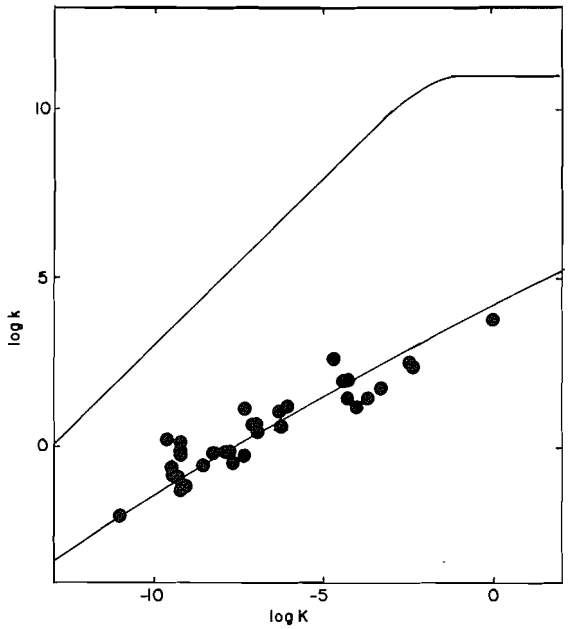


FIG. 8. Marcus curve for acid catalyzed ester hydrolysis assuming that this follows mechanism [13], with specific acid catalysis. The line is the best fit by least squares, and looks much better than for mechanism [14]. The b value is 8.76 ± 0.10, sum of squares of deviations = 9.09. The limiting line corresponding to $b = 0$ is also shown.

have independently led us to the conclusion that the acid catalyzed reactions of simple aldehydes and ketones are actually general acid catalyzed, while the analogous reactions of esters are specific acid catalyzed.

Assuming that the specific acid catalyzed path is indeed followed, we have estimated rate constants for these esters for which no values have been reported. These rate constants are found in Table 4.

Experimental

Materials

Trimethyl orthobenzoate (Aldrich, bp 87–88°C/7 Torr) was used as received. The trimethyl orthoesters of propionic, isobutyric, chloroacetic, and methoxyacetic acids were prepared by the method of McElvain and Nelson (28). The corresponding acids and esters were commercially available. Purity was evaluated by nmr spectroscopy, and compounds were distilled where necessary. The nmr spectra were recorded on a Varian T-60 spectrometer.

Methods

Heats of solution and reaction were measured using a simple calorimeter as previously described (29). Solubilities of organic liquids were measured as previously described (30) for concentrations $>0.03\,M$. For the less soluble compound, trimethylorthobenzoate, 200 mL of 0.001 N HCl were saturated with the orthoester and allowed to equilibrate with stirring at 25 ± 1°C. A 100 mL aliquot of the aqueous layer was drawn and shaken continuously for two minutes with each of five consecutive 4 mL portions of $CHCl_3$. After each extraction the chloroform layer was transferred to a 25 mL volumetric flask by syringe. A suitable reference standard was added and the solution was made up to the mark with $CHCl_3$. Concentrations were evaluated by electronic integration of their nmr spectra.

Free energies of transfer (ideal gas at 1 atm to 1 M aqueous solution with an infinitely dilute reference state) were calculated from solubilities and vapour pressures where possible. For the purpose of these calculations $< 1\,M$ compound will be assumed to behave ideally. For compounds with a solubility exceeding 1 M (i.e. trimethyl orthomethoxyacetate, methyl methoxyacetate, methyl cyanoacetate), a method was devised whereby the vapour pressure above a solution of known concentration at 25°C could be measured, thus giving the free energy of transfer directly. N_2 gas was passed into dilute aqueous solution of known concentration of compound through sintered glass, at a rate which would allow sufficient time for the gas to come to equilibrium with water and the compound (ca. 30 mL min^{-1}). The saturated N_2 gas was then passed through a trap which prevented direct transfer of entrained droplets, and then into a dry ice – acetone cooled condenser where water and compound were condensed. The flow rate was established using a gas flow meter at the end of the train. The water to compound mole ratio in the condensate was determined using nmr. At a gas flow rate of ca. 30 mL min^{-1}, it took ca. 19 h to collect 1 mL of condensate. It was assumed that the vapour pressure of water above the dilute solution was that of pure water.

Calculations

The standard entropy in the gas phase was estimated by the group contributions method of Benson (31). Following Benson we use C for tetrahedral carbon, C_B for aromatic carbon, and C_d for doubly bonded (alkene) carbon. If the desired group contribution was not available, a value was approximated by using one for a similar group. The effects of sp^3 oxygen and carbon on the S^0 for a group were regarded as being equal, so that the contribution for the group, [C $(O)_3$ (C)], could be substituted by the value for [C $(C)_4$]. For trimethyl orthobenzoate, where the group required [C $(O)_3$ (C_B)], the known value for [C $(C)_3$ (C_B)] was used. For methyl benzoate, S^0 values for the groups, [C_B (C_d)] and [CO (C) (O)], were used for the groups, [C_B (CO)] and [CO (C_B) (O)], respectively. It was also necessary to substitute the value of the group, [C (Cl) (C) $(H)_2$], for that of [C (Cl) (CO) $(H)_2$], for methyl chloroacetate.

Steric effects on the free energy change for the reaction:

[15] $\quad C—OCH_3 + H_2O = C—OH + CH_3OH$

were determined as previously described (32). For trimethyl orthoisobutyrate, it was also necessary to consider a sixth neighbour H—H interaction worth 2.00 kcal mol^{-1} (33), in addition to the usual interactions. For trimethyl orthobenzoate, we needed an approximate energy for the coaxial interaction of the π cloud with two hydrogens. Space filling models of trimethyl orthobenzoate show that phenyl cyclohexane (34) is not a good model to give us this energy. The maximum value for each interaction of this type would be that for a fifth neighbour hydrogen – lone pair interaction worth 0.15 kcal mol^{-1} (35). As the π cloud would be less "directed" than a lone pair, one would expect the energy for the former type of interaction to be smaller. Therefore, zero should be an acceptable value for the energy of this interaction.

Very few values for pK_{BH^+} values of esters have been reported. For aliphatic esters we have earlier reviewed the literature and selected values (1); from these data eq. [16] relating pK_{BH^+} to the Taft ρ^* value for the acyl substituent could be derived.

[16] $\quad pK_{BH^+} = -4.17 - 1.71\rho^*$

For aromatic esters, Edward and Wong have recently published

what should be a reliable value for ethyl benzoate, using characteristic vector analysis to correct for solvent effects (24); their value is −6.16. We assume that the ρ value for esters will be approximately equal to that reported for benzoic acids (using pK_{BH^+} values determined assuming that the acids were Hammett bases) namely −1.09 (36). This assumption can be tested by considering the ρ values for acetophenones using pK_{BH^+} values based upon the assumption of Hammett base behavior (37) ρ = −2.22, and using pK_{BH^+} values derived by characteristic vector analysis, $\rho^* = -1.69$ (17). The assumption is clearly only appproximately valid. Another estimate can be made assuming that ρ is the same as for benzamides, for which pK_{BH^+} values are available for the unsubstituted and *p*-nitro substituted derivatives (24). Both ρ values were used and the average was calculated, with the difference between the two estimates taken as the uncertainty in pK_{BH^+}. All of the data on which our estimated pK_{BH^+} values are based may be found in Supplementary Tables S16 and S17.[2]

1. J. P. GUTHRIE. J. Am. Chem. Soc. **100**, 5892 (1978).
2. A. O. COHEN and R. A. MARCUS. J. Phys. Chem. **72**, 4249 (1968).
3. R. A. MARCUS. J. Am. Chem. Soc. **91**, 7224 (1969).
4. R. A. MARCUS. Annu. Rev. Phys. Chem. **15**, 155 (1964), and references cited therein.
5. J. P. GUTHRIE. J. Am. Chem. Soc. **95**, 6999 (1973).
6. J. P. GUTHRIE. Can. J. Chem. **53**, 898 (1975).
7. J. P. GUTHRIE. J. Am. Chem. Soc. **96**, 3608 (1974).
8. J. P. GUTHRIE. Can. J. Chem. **54**, 202 (1976).
9. J. HINE. J. Am. Chem. Soc. **93**, 3701 (1971).
10. (*a*) M. EIGEN. Angew. Chem. Int. Ed. Engl. **3**, 1 (1964); (*b*) M. EIGEN. Z. Phys. Chem. (N.F.), **1**, 176 (1954).
11. (*a*) W. J. ALBERY, M. L. HITCHMAN, and J. ULSTRUP. Trans. Faraday Soc. **64**, 2831 (1968); (*b*) W. J. ALBERY, A. R. GREENWOOD, and R. F. KIBBLE. Trans. Faraday Soc. **63**, 360 (1967).
12. M. V. SMOLUCHOWSKI. Z. Phys. Chem. **92**, 129 (1917).
13. A. J. KRESGE. Rev. Chem. Soc. **2**, 475 (1973), and references cited therein.
14. J. R. MURDOCH. J. Am. Chem. Soc. **94**, 4410 (1972).
15. F. FRANKS (*Editor*). Water, a comprehensive treatise. Vol. 1. Plenum, New York. 1972.
16. (*a*) A. LEVI, G. MODENA, and G. SCORRANO. J. Am. Chem. Soc. **96**, 6585 (1974); (*b*) R. A. MCCLELLAND and W. F. REYNOLDS. Can. J. Chem. **54**, 718 (1976).
17. R. A. COX, C. R. SMITH, and K. YATES. Can. J. Chem. **57**, 2952 (1979). We thank Cox *et al.* for communicating this manuscript to us in advance of its publication.
18. V. A. PALM, U. L. HALDNA, and A. J. TALVIK. *In* The chemistry of the carbonyl group. *Edited by* S. Patai. Wiley, New York, NY. 1966. p. 444.
19. P. T. MCTIGUE and L. C. GRUEN. Aust. J. Chem. **16**, 177 (1963).
20. P. T. MCTIGUE and J. M. SIME. Aust. J. Chem. **16**, 592 (1963).
21. M. I. SILING and B. Y. AKSELROD. Russ. J. Phys. Chem. **42**, 1479 (1968).
22. E. M. ARNETT. Prog. Phys. Org. Chem. **1**, 223 (1963), and references cited therein.
23. D. G. LEE and M. H. SADAR. J. Am. Chem. Soc. **96**, 2862 (1974), and references cited therein.
24. J. T. EDWARD and S. C. WONG. J. Am. Chem. Soc. **99**, 4229 (1977).
25. L. S. LEVITT and B. W. LEVITT. Tetrahedron, **27**, 3777 (1971).
26. J. CLARK and D. D. PERRIN. Q. Rev. Chem. Soc. **18**, 295 (1964).
27. L. F. BLACKWELL, A. FISCHER, I. J. MILLER, D. D. TOPSOM, and J. VAUGHAN. J. Chem. Soc. 3588 (1964).
28. S. M. MCELVAIN and J. W. NELSON. J. Am. Chem. Soc. **64**, 1825 (1942).
29. J. P. GUTHRIE. J. Am. Chem. Soc. **96**, 3608 (1974).
30. J. P. GUTHRIE. J. Am. Chem. Soc. **95**, 6999 (1973).
31. S. W. BENSON. Thermochemical kinetics. 2nd ed. John Wiley & Sons, New York, NY. 1976.
32. J. P. GUTHRIE. Can. J. Chem. **53**, 898 (1975).
33. K. PIHLAJA. Acta Chem. Scand. **25**, 451 (1971).
34. J. HIRSCH. Top. Stereochem. **1**, 199 (1967).
35. K. PIHLAJA and J. KANKARE. Acta Chem. Scand. **23**, 1745 (1969); K. PIHLAJA. Acta Chem. Scand. **25**, 451 (1971).
36. R. STEWART and K. YATES. J. Am. Chem. Soc. **82**, 4059 (1960).
37. R. STEWART and K. YATES. J. Am. Chem. Soc. **80**, 6355 (1958).
38. J. W. LARSON and L. G. HEPLER. *In* Solute–solvent interactions. *Edited by* J. F. Coetzee and C. D. Ritchie. Marcel Dekker, New York. 1969. p. 1.
39. J. B. PEDLEY and J. RYLANCE. Sussex-NPL computer analyzed thermochemical data: organic and organometallic compounds. University of Sussex, Brighton, England. 1977.
40. C. HANSCH, J. E. QUINLAN, and G. L. LAWRENCE. J. Org. Chem. **33**, 347 (1968).
41. BEILSTEIN. Handbuch der organischen Chemie. **9** (3), 382.
42. J. KONICEK and I. WADSO. Acta Chem. Scand. **24**, 2612 (1970).
43. J. HINE and P. K. MOOKERJEE. J. Org. Chem. **40**, 292 (1975).
44. D. R. STULL, E. F. WESTRUM, JR., and G. C. SINKE. The chemical thermodynamics of organic compounds. Wiley, New York, NY. 1967.
45. L. MALASPINA, R. GIGLI, and G. BARDI. J. Chem. Phys. **59**, 387 (1973).
46. R. K. FREIER. Aqueous solutions. Vol. 1. Walter de Gruyter, Berlin. 1976.
47. F. D. ROSSINI, D. D. NAGMAN, W. H. EVANS, S. LEVINE, and I. JAFFE. Natl. Bur. Stand. (U.S.) Circ. No. 500 (1952).
48. R. W. TAFT. *In* Steric effects in organic chemistry. *Edited by* M. S. Newman. Wiley, New York. 1956. p. 619.
49. J. VUORI and J. KOSKIKALLIO. Suom. Kemistil. B, **42**, 136 (1969).
50. G. B. BARLIN and D. D. PERRIN. Q. Rev. Chem. Soc. **20**, 75 (1966).
51. M. R. WRIGHT. J. Chem. Soc. B, 707 (1969).
52. A. SKRABAL and D. MRAZEK. Monatsh. Chem. **39**, 495 (1918).

Can. J. Chem. Downloaded from www.nrcresearchpress.com by 210.87.254.105 on 09/05/12
For personal use only.

Etude par la résonance de l'azote 15 et du phosphore 31 de la liaison P—N dans des dérivés du phosphore trivalent; analyse statistique des données expérimentales

JEAN-PAUL GOUESNARD, JEAN DORIE et GÉRARD J. MARTIN

Laboratoire de Chimie Organique Physique, ERA CNRS 315, Faculté des Sciences, 44072 Nantes, France

Reçu le 10 juillet 1979[1]

JEAN-PAUL GOUESNARD, JEAN DORIE et GÉRARD J. MARTIN. Can J. Chem. **58**, 1295 (1980).

L'étude par rmn de l'azote 15 et du phosphore 31 et par rmn dynamique du carbone 13 d'une cinquantaine d'amino-phosphines a permis de systématiser le rôle des facteurs physico-chimiques qui gouvernent la distribution électronique de la liaison azote–phosphore(III). Une analyse factorielle et régressionnelle des paramètres rmn $\delta^{15}N$, $\delta^{31}P$ et $^1J_{P—N}$ appartenant à plusieurs séries d'amino-phosphines a permis de mettre en évidence l'existence de facteurs communs et de différentes corrélations dans les familles de composés et entre les variables rmn. Ces résultats statistiques ont été discutés en termes d'effets topologiques, électroniques et stériques des substituants. Le rôle des substituants de l'atome d'azote et de l'atome de phosphore sur les paramètres rmn ainsi que sur la barrière à la rotation autour de la liaison P—N, $\Delta G_T^{\neq}$, est interprété sur la base de considérations relatives à l'hybridation des atomes d'azote et de phosphore, à la conjugaison p_π–d_π et à la nature des états électroniques (terme ΔE^{-1}) du fragment P—N.

JEAN-PAUL GOUESNARD, JEAN DORIE, and GÉRARD J. MARTIN. Can. J. Chem. **58**, 1295 (1980).

Natural abundance ^{15}N and ^{31}P nmr and dynamic ^{13}C nmr have been applied to the study of about fifty aminophosphines, in order to generalize the influence of the chemical factors which govern the electronic distribution of the nitrogen–phosphorus III bond. Factor and regression analyses of $\delta^{15}N$, $\delta^{31}P$, and $^1J_{P—N}$ values performed on different series of aminophosphines have shown that common factors and various correlations exist between the nmr parameters in the different kinds of derivatives. The statistical results are discussed in terms of topologic, electronic, and steric contributions. The nature of the different substituents of the nitrogen or phosphorus atoms governs the observed changes in screening, coupling constants, and the rotational barriers $\Delta G^{\neq}$ around the P—N bond, which are explained in considering the type of nitrogen and phosphorus hybridization, the p_π–d_π donation and the electronic states (ΔE^{-1} approximation) of the P—N fragment.

Introduction

Les aminophosphines dérivant du phosphore trivalent présentent une grande activité chimique et biologique. Leur structure et leur comportement stéréochimique dynamique ont abondamment été étudiés en résonance magnétique nucléaire (rmn) du proton, du carbone et notamment du phosphore (1). Par contre, il existe très peu de résultats de mesures effectuées en résonance de l'azote 14 (2*a*) ou 15 (2*b*–*e*). Nous avons montré que le déplacement chimique $\delta^{15}N$ pouvait être, dans certaines conditions, une bonne sonde pour évaluer le degré de délocalisation électronique autour des liaisons N—X (3*a*) et nous avons appliqué cette méthode au cas des liaisons N—C (3*b*), N—Si (4), et N—N (5). Nous nous proposons ici d'analyser statistiquement les valeurs de $\delta^{15}N$, $\delta^{31}P$ et $^1J_{(^{31}P—^{15}N)}$ de plusieurs familles d'aminophosphines P(III) et de tenter d'interpréter les correspondances observées en termes d'effets électroniques (délocalisation) et stériques.

Résultats

A. Déterminations expérimentales

Les aminophosphines étudiées correspondent à la formule $X(Y)P—N(R)_2$ et sont définies dans le Tableau 1. La différence de nature des substituants R de l'atome d'azote définit 10 séries de composés numérotées de I à X, et dans chaque série, la nature des substituants X et Y du phosphore caractérise le composé. Ainsi l'aminophosphine IV **14** aura la formule $(iC_3H_7)_2N—P(Cl)C_6H_5$. Dans le Tableau 2, nous avons indiqué les valeurs des paramètres physico-chimiques représentant les effets électroniques et stériques des substituants X, Y et R du système P—N. Ces valeurs ont été extraites des mises au point récentes les plus fiables. Les paramètres σ_I et σ_{R^0} de Taft *et al.* (6*a*) compilés par Exner (6*b*), ont été préférés à ceux de Swain et Lupton car la séparation des effets de champ et de résonance est illusoire dans cette systématique (7). Le terme $R_{P—X}$ représente la polarisabilité électronique d'une liaison P—X (9) supposée être une mesure de la contribution du terme d'énergie d'excitation moyenne (ΔE^{-1}) à $\delta^{31}P$ pour différentes liaisons P—X. L'effet stérique, caractérisé par le paramètre E_S proportionnel au rayon de van der Waals a été introduit par Taft (8*b*) et compilé par Unger et Hansch (8*a*). Les paramètres rmn δ et J sont rassemblés dans les Tableaux 3 et 4. Le Tableau 3 regroupe les données relatives à toutes les séries de fragment aminé, pour deux types de substituants du phosphore **14** et **17**, et permet ainsi de comparer l'influence des substituants de l'atome d'azote sur les paramètres rmn. Le Tableau 4 offre au contraire la possibilité d'examiner le rôle joué

[1]Revision reçue le 7 février 1980.

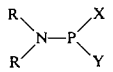
0008-4042/80/131295-10$01.00/0

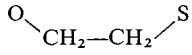
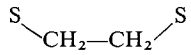
©1980 National Research Council of Canada/Conseil national de recherches du Canada

Can. J. Chem. Downloaded from www.nrcresearchpress.com by 210.87.254.40 on 09/05/12
For personal use only.

Can. J. Chem. Downloaded from www.nrcresearchpress.com by 210.87.254.40 on 09/05/12
For personal use only.

TABLEAU 1. Liste des composés étudiés groupés par série (I à X) de différents substituants de l'atome d'azote et par type de composé (**1** à **39**) représentant les différents substituants de l'atome de phosphore



Substituants de l'atome d'azote		Substituants de l'atome de phosphore					
							
Série	R	Composé	X	Y	Composé	X	Y
I	CH_3	**1**	CH_3	CH_3	**22**	$N(CH_3)_2$	Cl
		2	C_6H_5	C_6H_5	**23**	$N(CH_3)_2$	Br
II	C_2H_5	**3**	C_6H_5	iC_3H_7	**24**	$N(CH_3)_2$	$N(CH_3)_2$
		4	C_6H_5	$C{\equiv}C{-}CH_3$	**25**	$N(CH_3)_2$	$N(C_2H_5)_2$
III	nC_3H_7	**5**	CF_3	CF_3	**26**	$N(CH_3)_2$	$N(iC_3H_7)_2$
		6	F	CH_3	**27**	$N(CH_3)_2$	OC_2H_5
IV	iC_3H_7	**7**	F	C_6H_5	**28**	$N(C_2H_5)_2$	Cl
		8	F	F	**29**	$N(C_2H_5)_2$	$N(C_2H_5)_2$
V	nC_4H_9	**9**	Cl	CH_3	**30**	$N(C_2H_5)_2$	$N(iC_3H_7)_2$
		10	Cl	C_2H_5	**31**	$N(C_3H_{7i})_2$	Cl
VI	sC_4H_9	**11**	Cl	iC_3H_7	**32**	$N(C_3H_{7i})_2$	$N(iC_3H_7)_2$
		12	Cl	tC_4H_9	**33**	OCH_3	C_6H_5
VII	tC_4H_9	**13**	Cl	$CH(Si(CH_3)_3)_2$	**34**	OCH_3	OCH_3
		14	Cl	C_6H_5	**35**	OC_2H_5	OC_2H_5
VIII	$(CH_3)_3Si$	**15**	Cl	CH_2Cl	**36**		
		16	Cl	CF_3			
IX	$C_6H_5CH_2$	**17**	Cl	Cl	**37**		
		18	Br	CH_2Cl			
X	$C_6H_5CH_2$ / CH_3	**19**	Br	Br	**38**	(*o*) O—C_6H_4—O (*o*)	
		20	$N(CH_3)_2$	CH_3			
		21	$N(CH_3)_2$	C_6H_5	**39**	(*o*) S—$C_6H_3(CH_3)$—S (*o*)	

par les substituants du phosphore dans trois séries de référence I, II et IV. Le Tableau 5 rassemble les données accessibles de rmn dynamique relatives au processus de rotation restreinte autour de la liaison P—N. Les données de la littérature ont été complétées par des mesures que nous avons effectuées par rmn dynamique du carbone.

B. Calculs statistiques

(*a*) L'analyse factorielle des valeurs $\delta^{15}N$, $\delta^{31}P$ et $^1J_{P—N}$ a été effectuée sur 24 observations différentes correspondant à chacun des trois paramètres rmn associés aux composés **14**, **17**, **22**, **24**, **25**, **28**, **29** et **31** des séries I, II et IV. Dans ce type d'approche statistique (10*a*), utilisée initialement en rmn pour étudier les effets de solvant (10*b*–*e*) et les effets de substituants halogénés (10) sur δ, nous avons pu mettre en évidence le nombre et l'influence relative des facteurs liés au type de la substitution sur l'atome d'azote, qui gouvernent les paramètres $\delta^{15}N$, $\delta^{31}P$ et $^1J_{P—N}$. De plus, l'analyse factorielle nous a permis d'obtenir le degré d'autocorrélation

TABLEAU 2. Effets électroniques et stériques des substituants X ou Y du système $(R)_2N—P(X)Y$. Les valeurs de σ_I et σ_R ont été extraites de la compilation des effets de substituants réalisée par Exner (6*b*); elles correspondent aux déterminations effectuées par Taft *et al.* en rmn de ^{19}F (6*a*). $R_{P-X,Y}$ représente la réfraction de la liaison P—X ou P—Y; les valeurs de *R* ont été extraites de la mise au point de Le Fevre (9). Les valeurs du paramètre stérique de Taft (8*b*), E_S, sont issues du travail de Unger et Hansch (8*a*)

Substituant X ou Y	σ_I	σ_R	$R_{P-X,Y}$	E_S
CH_3	−0.08	−0.15	3.6	−1.24
C_6H_5	+0.08	−0.09	3.6	−1.01[a]
				−3.80[b]
Cl	+0.37	−0.18	8.8	−0.97
F	+0.52	−0.32	3.6	−0.46
CF_3	+0.41	+0.10	3.6	−2.40
CH_2Cl	+0.14	−0.03	3.6	−1.48
OC_2H_5	+0.20	−0.44	3.1	−0.55
$N(Me)_2$	+0.10	−0.54	3.4	−1.05
$N(Et)_2$	+0.08	−0.58	3.4	−1.20
$N(iC_3H_7)_2$	+0.08	−0.58	3.4	−1.40

[a]Epaisseur du cycle.
[b]Largeur du cycle.

TABLEAU 3. Paramètres rmn structuraux d'aminophosphines groupés en fonction de la nature du fragment aminé

Composés étudiés		Résultats $^{15}N^a$		Résultats ^{31}P	
Type P(X)Y	Série $(R)_2N$	$-\delta^{15}N$ (ppm/NO_3^-)	$^1J_{P-N}$ (Hz)	$\delta^{31}P$ (ppm/H_3PO_4 85%)	Conditions
14	I	332.7	76.2	141.0	*b*
	II	305.3	79.1	140.4	*b*
	III	308.7	80.6	140.1	*c*
	IV	286.0	82.0	131.0	*c*
	V	309.4	80.6	140.1	*c*
	VI	285.5	82.0	131.0	*c*
	IX	303.7	82.0	138.1	*d*
	X	319.7	77.6	142.7	*c*
17	I	320.0	89.4	166.0	*b*
	II	291.9	92.3	162.0	*b*
	IV	272.4	95.2	168.2	*c*
	VI	274.3	96.7	169.0	*c*
	X	306.7	90.8	162.6	*c*

[a]Composés étudiés en solution à 90% dans $CHCl_3$, en présence de 0.1 mL^{-1} de $Cr(AcAc)_3$ et à 301 K, $\delta(N/CH_3NO_2) = \delta(N/NO_3^-) - 1.5$ ppm.
[b]Valeurs extraites de la réf. 1*a*.
[c]Ce travail: produit pur.
[d]Ce travail: produit en solution à 30% $CHCl_3$.
[e]Ce travail: produit en solution à 30% dans un mélange 50:50 CS_2/CD_3COCD_3.

des variables rmn: $\delta^{15}N(I) = f[\delta^{15}N(II)]$, etc. Les résultats sont indiqués dans le Tableau 6.

(*b*) L'analyse régressionnelle des variables rmn entre elles $\delta^{15}N = f(\delta^{31}P)$, $\delta^{15}N = f(^1J_{P-N})$ et $\delta^{31}P = f(^1J_{P-N})$ (Tableau 7) nous a permis de mettre en évidence les analogies et les différences de comportement. Il est intéressant de noter à ce sujet que le nombre d'observations ne doit pas être nécessairement le même pour les trois séries, contrairement au cas de l'analyse factorielle décrite ci-dessus.

(*c*) Nous avons finalement essayé d'approfondir les interprétations structurales des analyses statistiques précédentes, en tentant d'obtenir des corrélations significatives entre les variables rmn et des paramètres structuraux traduisant le nombre des substituants de l'atome d'azote. En second lieu, nous avons essayé de mettre en évidence des corrélations entre les variables rmn et les paramètres de substituants σ_I, σ_R et E_S.

Discussion des résultats

A. Etude statistique de l'intercorrélation des paramètres rmn

(a) Analyse factorielle des données rmn relatives aux séries I, II et IV

L'analyse permet de mettre en évidence le degré de corrélation des variables entre elles et le nombre minimum de facteurs dont dépendent les variables. Les résultats du Tableau 6 montrent qu'un seul facteur suffit pratiquement pour exprimer $\delta^{15}N$ et $\delta^{31}P$ dans les trois familles étudiées. La matrice des données originales peut être reproduite avec une erreur moyenne sur chaque point inférieure à 0.3 ppm. La série IV se comporte d'une façon très légèrement différente des deux séries I et II. L'autocorrélation de $\delta^{15}N$ ou de $\delta^{31}P$ dans les trois séries considérées est en général très satisfaisante. Il est ainsi possible de prévoir le comportement de $\delta^{15}N$ et de $\delta^{31}P$ dans une série de référence. Ce résultat peut présenter un intérêt structural notable. Par contre, deux facteurs sont nécessaires pour rendre compte des valeurs de $^1J_{P-N}$ à ± 0.3 Hz et si les variables I et II se comportent d'une façon analogue, la série IV se différencie très nettement ici. Le degré de corrélation de $^1J_{P-N}$ dans les séries I et II est bon, mais est médiocre dans les deux autres cas, I et IV ou II et IV. Cette méthode n'est entachée d'aucun arbitraire, mais n'apporte cependant aucune explication physico-chimique sur la nature et l'origine des facteurs. Celle-ci sera réalisée dans le paragraphe B sur la base d'analyses régressionnelles de chaque paramètre rmn en termes d'effets de structure et de substituants.

(b) Analyse de l'interdépendance des paramètres rmn entre eux (Tableau 7)

$\delta^{15}N$ et $\delta^{31}P$

Il est intéressant de noter que les valeurs $\delta^{15}N$ sont bien corrélées au déplacement chimique du phosphore pour les trois séries considérées (Fig. 1). Les valeurs des pentes *b* des droites de régression indiquent que $\delta^{15}N$ varie environ deux fois moins que $\delta^{31}P$ et l'erreur moyenne sur l'estimation de $\delta^{15}N$ à partir de $\delta^{31}P$ est de 3 ppm. Ainsi, l'influence des effets électroniques des substituants X et Y du phosphore se traduit dans le même sens, sur $\delta^{15}N$ et

Can. J. Chem. Downloaded from www.nrcresearchpress.com by 210.87.254.40 on 09/05/12
For personal use only.

Can. J. Chem. Downloaded from www.nrcresearchpress.com by 210.87.254.40 on 09/05/12
For personal use only.

TABLEAU 4. Paramètres rmn structuraux d'aminophosphines groupés en fonction de la nature des substituants de l'atome de phosphore

Composés étudiés		Resultats ^{15}N[a]		Résultats ^{31}P	
Série $(R)_2N$	Type P(X)Y	$-\delta^{15}N$ (ppm/NO_3^-)	$^1J_{P-N}$ (Hz)	$\delta^{31}P$ (ppm/H_3PO_4)	Conditions
I	**1**	373.0	60.0	39.0	[b]
	2	370.7	61.8	63.9	[b]
	5	—	—	46.3	[b]
	7	—	—	159.8	[b]
	8	316.0[f]	—	144.0	[b]
	9	330.0	75.0	150.7	[b]
	14	332.7	76.2	141.0	[b]
	15	—	—	123.0	[b]
	17	320.0	89.4	166.0	[b]
	20	342.0[f]	—	86.0	[b]
	21	346.7	75.7	100.3	[b]
	22	330.1	77.6	159.0[g]	[c]
	24	349.4	60.1	122.0	[c,b]
	25	351.9	54.4	120.8	[c]
	26	357.5	51.5	105.9	[c]
	27	341.5	69.0	137.0	[b]
	28	326.0	79.5	155.5	[c]
	29	353.6	50.0	119.7	[c]
	30	357.8	52.9	104.7	[c]
	31	326.0	80.9	149.2	[c]
	35	333.5	75.0	144.7	[b]
II	**14**	305.3	79.1	140.4	[b]
	17	291.9	92.3	162.0	[b]
	22	305.5	79.4	155.5	[c]
	24	318.4	72.1	120.8	[c]
	25	321.4	66.2	119.7	[c]
	26	330.8	49.8	104.7	[c]
	28	303.0	80.9	154.0	[b]
	29	322.3	61.5	118.0	[b]
	30	330.9	52.9	103.9	[c]
	31	303.7	79.1	147.0	[c]
IV	**14**	286.0	82.0	131.0	[c]
	17	272.4	95.2	168.2	[c]
	22	287.3	83.0	149.2	[c]
	24	297.7	80.9	105.9	[c]
	25	299.0	81.0	104.7	[c]
	28	285.1	86.4	147.0	[c]
	29	300.6	83.8	103.9	[c]
	31	283.7	86.4	139.0	[d]

[a–d]Voir la légende du Tableau 3.
[f]Valeurs obtenues par spectroscopie ^{14}N et extraites de la réf. 2*a*.
[g]La valeur $\delta^{31}P$ du composé I 22 est de 160.0 Hz, réf. 1*a*.

sur $\delta^{31}P$ mais d'une façon atténuée dans le premier cas. Dans la série IV, la plus encombrée, l'atténuation des effets de X, Y sur $\delta^{15}N$ atteint presque 60%. Enfin, la croissance algébrique, des ordonnées à l'origine *a*, en fonction de la substitution alkyle sur l'atome d'azote est à mettre en relation avec l'effet β (cf. B).

$\delta^{15}N$ *et* $^1J_{P-N}$

Les corrélations sont très bonnes dans les deux séries (I, II) où ne se manifeste pas d'encombrement stérique, et les pentes ont des valeurs très voisines (Fig. 1). On constate que les points correspondant à la série IV ont une dispersion statistique importante, mais si on les répartit en deux familles, contenant les composés chlorés ou non chlorés, on obtient alors une bonne corrélation pour les deux types de molécule ($R = 0.95$) et des ordonnées à l'origine et pentes voisines ($a = -361.5$ et -370.0, $b = 0.91$ et 0.87 respectivement). Les composés I-**1**, **2** et **21** se comportent d'une façon anormale par rapport à la série considérée. En effet, dans les cas considerés, les substituants de l'atome de phosphore présentent soit un encombrement stérique notable, soit une faible electronegativité. Cet aspect est developpé par ailleurs (32).

Can. J. Chem. Downloaded from www.nrcresearchpress.com by 210.87.254.40 on 09/05/12
For personal use only.

TABLEAU 5. Valeurs des paramètres d'activation du processus de rotation restreinte autour de la liaison P—N. Tous les résultats, à l'exception de[h], ont été obtenus en rmn ^1H

Série	Composé	$\Delta\nu^\infty$ (Hz)	T_c (K)	$\Delta G_T^\ddagger$ (kJ mol^{-1})	Conditions	Réf.
I	**1**		<180	<33	Pur	[h]
	2		<143	<29	$CHFCl_2$	15
	3		<193	<37	CS_2	12
	4		<193	<37	CS_2	12
	5	7	168	36.8	CF_2Cl_2	15
	7	62.7	208	41.8	nC_5H_{12}	16
	8		<153	<29	$CHFCl_2$	15
	9	17	233	49.3	CH_2=CHCl 13%	11
		[a]	233	48.1[b]	$CFCl_3$ 13%	11
	10	[a]	217	[c]	CH_2=CHCl 19%	11
	11	[a]	206	[d]	CH_2=CHCl 20%	11
	12	17	189	39.7	$CHFCl_2$	20
		[a]	188	[e]	CH_2=CHCl 10%	11
	13	12	220	47.2	CH_2Cl_2 15%	19
	14	33	219	45.1	CS_2	12
		53	223±2	43.9[f]	$CDCl_3$	13
		52	223	45.1	CS_2	14
		53	223	45.6	$CFCl_3$	15
		122	233	45.6	CS_2	[h]
	15	27	229	47.6[g]	CH_2=CHCl 33%	11, 18
	16	13	203	43.9	$CFCl_3$	15
	17	4	160	35.1	$CHFCl_2$	15
	18	[a]	218	≃46.0	$CDCl_3$	11
	22		<193	<37	CS_2	12
			<133	<27	$CHFCl_2$	15
	33	42.9	174	35.1	$CFCl_3/CF_2Cl_2$	16
	34		<121	<27	$CFCl_3/CF_2Cl_2$	16
	36	[a]	143	≃28.0	CF_2=CCl_2	17
	37	[a]	161	31.8	$CHFCl_2$	17
	38	30.7	161	32.6	$CFCl_3/CF_2Cl_2$	16
	39	65.2	188	37.2	$CHFCl_2$	17
II	**2**		<153	<29	$CHFCl_2$	15
	5	[a]	[a]	41.8	[a]	21
	14	30	223	41.8	CS_2	14
		31	216	45.1	$CFCl_3/CDCl_3$	15
	17		193	37	$CHFCl_2$	15
III	**14**	34	218	45.1	CS_2	14
IV	**5**	[a]	[a]	61.9	[a]	21
	6	[a]	213	45.6	CH_2=CHCl 20%	11
	9	12	265	57.3	$C_6D_5CD_3$	20
	12	14	273	58.9	$CHFCl_2$	20
		18	222	46.4	CH_2Cl_2 15%	19
	13	20	248	53.1	CH_2Cl_2 15%	19
	14	46	268	55.2	CS_2	14
	17 CH	80	225	44.7	CS_2/CD_3COCD_3	[h]
	CH_3	105	228	44.7		
V	**14**	17	213	44.7	CS_2	14
VI	**6**	[a]	223	45.1	$CHClF_2$ 14%	11
	9	[a]	268	56.4	$CDCl_3$ 20%	11
	14	20	288	61.0	CS_2	14
	CH_2	100	280	55.6	CS_2	[h]
	CH_3	100	280	55.6		
	17 CH	60	220	44.3		
	CH_2	90	225	44.7	CS_2/CD_3COCD_3	[h]
	CH_3	125	228	44.7		
VII	**8**	10.4	226	48.9	$C_6H_5CH_3$ 20%	22
	17	15.3	338	73.1	$C_6H_5CH_3$ 20%	22
	19	17.0	346	74.4	$C_6H_5CH_3$ 20%	22
VIII	**5**	[a]	[a]	63.9	[a]	21
	8	[a]	[a]	<35	[a]	22
	12	5	200	44.3	CH_2Cl_2 15%	19
	17	[a]	[a]	41.0	[a]	22
		[a]	[a]	41.8	[a]	21
	19	[a]	[a]	41.8	[a]	22
IX	**14**	[a]	227	≃46.0	$CDCl_3$	15
X	**14**	45	225	46.4	CS_2	14

[a]Non-indiqué. Valeurs de $\Delta H^\ddagger$ (kJ mol^{-1}).
[b]48.1.
[c]45.1.
[d]40.5.
[e]39.3.
[f]E_a = 50.2.
[g]43.5.
[h]Ce travail; résultats de rmn dynamique ^{13}C.

TABLEAU 6. Résultat de l'analyse factorielle des données rmn relatives à trois séries (variables) de huit amino-phosphines **14, 17, 22, 24, 25, 26, 29** et **31**

Paramètre rmn soumis à l'analyse factorielle	Variables[a] factorisées	Caracteristiques des facteurs: Coefficients de la matrice factorielle V_1	V_2	V_3	Valeurs propres associées aux facteurs, en % de la variance F_1	F_2	F_3	Correlations des variables: Variables[b] corrélées	Pente	R
$\delta^{15}N$	Série I	0.987	−0.161	−0.012	2.955	0.042		I et II	1.22	0.978
	Série II	0.998	+0.039	−0.042	(98.5%)	(1.5%)		II et IV	1.11	0.994
	Série IV	0.992	+0.121	−0.030		[c]	[c]	IV et I	0.75	0.960
$\delta^{31}P$	Série I	0.999	−0.040	−0.029	2.986	0.012		I et II	1.05	0.998
	Série II	0.998	−0.049	+0.027	(99.5%)	(0.5%)		II et IV	0.73	0.990
	Série IV	0.996	+0.09	+0.002		[c]	[c]	IV et I	1.30	0.991
$^1J_{P-N}$	Série I	0.955	−0.272	−0.115	2.603	0.367	0.030	I et II	1.44	0.966
	Série II	0.975	−0.183	+0.127	(87%)	(12%)	(1%)	II et IV	1.51	0.743
	Série IV	0.860	+0.509	−0.016			[c]	IV et I	0.48	0.685

[a]Les variables i peuvent se mettre sous la forme linéaire $m_{i1}F_1 + m_{i2}F_2 + m_{i3}F_3$ et l'importance relative des facteurs est donnée en pourcentage de la variance totale.
[b]Pentes et coefficients des corrélations d'un paramètre rmn d'une variable en fonction du même paramètre rmn d'une autre variable.
[c]Facteur non significatif.

TABLEAU 7. Analyse régressionnelle linéaire $U = a + bV$ entre les variables rmn. S_U, S_a et S_b représentent les erreurs moyennes sur l'estimation de U, a et b. R est le coefficient de la corrélation et t le test de Student (voir partie expérimentale). N est le nombre de couples de valeurs U_i, V_i utilisées dans le calcul. Le groupe A correspond aux composés **9, 14, 17, 22, 24, 25, 26, 27, 28, 29, 30, 31, 35** (série I) et les groupes B et C contiennent tous les composés des séries II et IV respectivement du Tableau 4

Variables rmn U	V	Coefficient de la régression a	b	Ecarts-types sur les coefficients et tests de signification S_U	S_a	S_b	R	t_b	N	Série de composés étudiés: Série	Composés
$\delta^{15}N$	$\delta^{31}P$	−427.1	0.64	3.0	6.0	0.04	0.97	14.7	13	I	Groupe A
		−392.1	0.59	3.0	6.2	0.04	0.97	13.0	10	II	Groupe B
		−338.6	0.38	3.0	6.3	0.05	0.96	8.0	8	IV	Groupe C
		−420.0	0.61	3.9	5.6	0.04	0.95	14.7	23	I, II	Groupes A+B[a]
		−408.2	0.53	4.7	5.6	0.04	0.92	12.8	31	I, II, IV	Groupes A+B+C[a]
$\delta^{15}N$	$^1J_{P-N}$	−407.4	1.00	2.3	3.5	0.05	0.98	19.8	13	I	Groupe A
		−381.6	0.96	2.8	5.0	0.07	0.98	14.0	10	II	Groupe B
		—	—	—	—	—	[b]	[b]	8	IV	Groupe C
		−405.2	0.98	2.7	3.1	0.04	0.98	21.9	23	I, II	Groupes A+B[a]
		−400.8	0.89	5.2	5.6	0.08	0.91	11.6	31	I, II, IV	Groupes A+B+C[a]
$\delta^{31}P$	$^1J_{P-N}$	36.6	1.46	6.3	9.7	0.14	0.95	10.5	13	I	Groupe A
		23.7	1.53	7.1	12.7	0.17	0.95	8.7	10	II	Groupe B
		—	—	—	—	—	[b]	[b]	8	IV	Groupe C
		35.9	1.40	8.8	10.2	0.14	0.91	9.9	23	I, II	Groupes A+B[a]
		—	—	—	—	—	[b]	[b]	31	I, II, IV	Groupes A+B+C[a]

[a]Avec correction β pour les séries II ou IV.
[b]Résultat non significatif.

$\delta^{31}P$ et $^1J_{P-N}$

L'allure des droites de régression est comparable pour les deux séries I et II, et aucune corrélation significative ne peut être obtenue pour la série IV.

Ainsi le comportement de $\delta^{15}N$ et $\delta^{31}P$ vis à vis de $^1J_{P-N}$ est tout à fait semblable: $\delta^{15}N$ et $\delta^{31}P$ varient dans le même sens et une augmentation du déplacement chimique (effet paramagnétique) entraine une augmentation du couplage. Cependant $^1J_{P-N}$ ressent différemment les interactions électroniques et stériques des substituants R, X et Y.

B. Interprétation des variations des paramètres rmn en fonction de la structure moléculaire

(a) Influence des substituants de l'atome d'azote (R) sur $\delta^{15}N$ et $^1J_{P-N}$

Les résultats discutés précédemment peuvent s'expliciter en tenant compte de la substitution α, β et γ de l'atome d'azote. Les composés **14** des séries I à X ont été choisis comme molécules de référence et la matrice utilisée pour le calcul régressionnel a été construite sur la base des valeurs du Tableau 3 et du nombre n de substituants en α, β et γ.

Can. J. Chem. Downloaded from www.nrcresearchpress.com by 210.87.254.40 on 09/05/12
For personal use only.

Can. J. Chem. Downloaded from www.nrcresearchpress.com by 210.87.254.40 on 09/05/12
For personal use only.

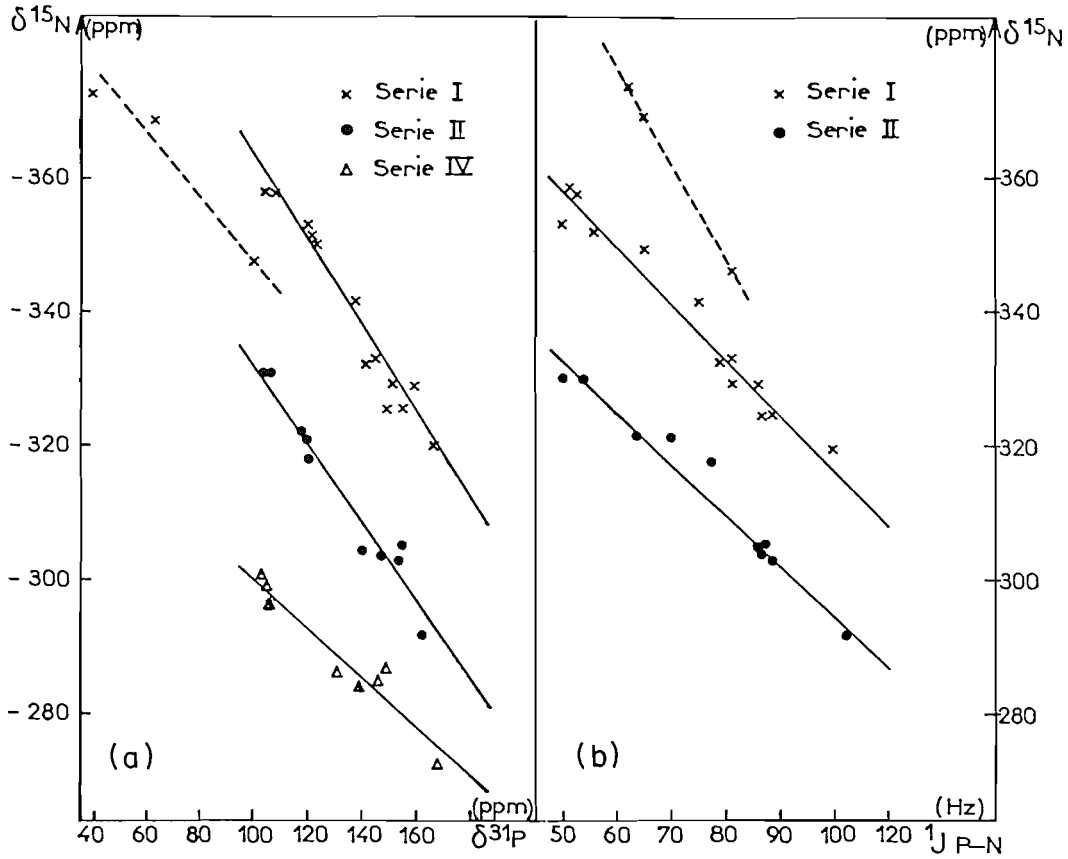
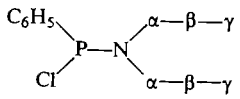


FIG. 1. (*a*) Variation du déplacement chimique de l'azote (en ppm/NO_3^-) par rapport à celui du phosphore (en ppm/H_3PO_4 85%) pour différentes séries $(CH_3)_2N$(I), $(C_2H_5)_2N$(II) et $(iC_3H_7)_2N$(IV) d'amino-phosphines; (*b*) variation du déplacement chimique de l'azote (en ppm/NO_3^-) en fonction de la constante de couplage phosphore–azote (en Hz). Une augmentation algébrique de δ correspond à une diminution de l'écran.



Les valeurs de $\delta^{15}N$ rapportées à la série $(CH_3)_2N—P<$ origine de la corrélation, sont convenablement exprimées au moyen du seul paramètre β. On calcule aussi un effet γ diamagnétique (−0.6 ppm) mais cet incrément n'est pas statistiquement significatif.

$$[1]\quad \delta^{15}N(\pm 1.7)\ \text{ppm} = -331.7(\pm 1.4) + 11.6(\pm 0.5)n(\beta)$$

$$R = 0.996 \quad t_b = 23 \quad N = 8$$

Ce résultat est en accord avec la valeur de l'incrément β_t déterminé pour des amines tertiaires (24*c*). Lorsque le calcul régressionnel est effectué sur une série plus variée de composés et en distinguant les différents types d'amines, la valeur de l'incrément β varie de 12 à 22 ppm. L'effet β n'est pas constant d'une série de composés à l'autre et dépend de la nature du groupe X (C(β)—C(α)—*N*—X ou C(β)—C(α)—*C*—X) directement lié à l'atome *N* (ou *C*) considéré (24*a*, *b*). Un comportement analogue a été souligné en résonance du carbone (25*a*) et il a été suggéré (25*b*) que la variation de l'effet β pouvait être relié à l'ordre de liaison π du fragment *C*···X. Cette observation est à rapprocher des corrélations que nous avons étudiées entre $\delta^{15}N$ et les valeurs de l'enthalpie libre d'activation du processus de rotation autour de la liaison N—X (3). La relation [1] permet d'expliquer les résultats de l'analyse factorielle au moyen d'un facteur topologique caractérisant un seul type de substituant β. On peut cependant affiner les prédictions de $\delta^{15}N$ dans toutes les séries de composés aminophosphorés dans lesquels les substituants X et Y du phosphore varient, en décomposant cet effet en deux incréments β′ et β″

Can. J. Chem. Downloaded from www.nrcresearchpress.com by 210.87.254.40 on 09/05/12
For personal use only.

représentant respectivement la première et la seconde substitution alkyle $\beta' = 13.6$ ppm et $\beta'' = 10.0$ ppm avec $\beta = \frac{1}{2}(\beta' + \beta'')$.

En ce qui concerne $^1J_{P—N}$, deux facteurs ont été mis en évidence par l'analyse factorielle et, en effet, cette constante de couplage ne peut s'exprimer correctement qu'en fonction de deux paramètres de substitution, β et γ ($R = 0.95$, $N = 8$).

$$[2] \quad {}^1J_{P—N}(\pm 0.8)\ \text{Hz} = 76.6 + 1.3(\pm 0.2)n(\beta) + 0.7(\pm 0.3)n(\gamma)$$

La constante $^1J_{P—N}$ augmente donc avec le nombre et la grosseur des substituants alkyles de l'atome d'azote.

Il faut noter que les valeurs de $\delta^{31}P$ ne changent pas en fonction de la substitution alkyle de l'atome d'azote ($\delta^{31}P = 140.4 \pm 0.5$ ppm pour les composés **14** des différentes séries) sauf lorsqu'il y a une double substitution $\beta\beta$ et dans ce cas $\delta^{31}P = 131 \pm 1$ ppm (effet diamagnétique).

(b) Influence des substituants X, Y de l'atome de phosphore sur les paramètres rmn

Tous les substituants X et Y, que nous avons considérés, à l'exception du groupe CH_3 (I.1) sont capables de se conjuguer par un mécanisme p_π–p_π ou p_π–d_π avec l'atome de phosphore. Il a été montré que l'environnement électronique de l'atome de phosphore III dépend étroitement de l'état d'hybridation de la paire libre d'électrons (26) et de la conjugaison p_π–d_π. Une augmentation du transfert $p_\pi \rightarrow d_\pi$ vers l'atome de phosphore se traduit par un effet diamagnétique notable sur $\delta^{31}P$ (28). Or, les modifications de la structure électronique de P se répercutent d'une façon analogue sur l'azote, car $\delta^{15}N$, $^1J_{P—N}$ et $\delta^{31}P$ varient dans le même sens (cf. A-b). Nous avons étudié les trois types d'effets décrits dans le paragraphe A: σ_I et σ_{R^0}, E_S et $R_{P—X}$.

Il est intéressant de constater que les valeurs de $\delta^{31}P$, $\delta^{15}N$ et $^1J_{P—N}$ sont corrélées d'une façon significative à σ_I, mais non à σ_{R^0} (13 points série I)

$$[3] \quad \delta^{31}P(\pm 10) = 102(\pm 6) + 103(\pm 16)\sigma_I(X, Y) \qquad R = 0.88 \quad t_b = 6.1$$

$$[4] \quad \delta^{15}N(\pm 6) = -327(\pm 4) + 69.5(\pm 10)\sigma_I(X, Y) \qquad R = 0.90 \quad t_b = 6.9$$

$$[5] \quad {}^1J_{P—N}(\pm 5) = 44(\pm 3) + 71(\pm 8)\sigma_I(X, Y) \qquad R = 0.93 \quad t_b = 8.3$$

Ces corrélations traduisent l'existence d'un effet paramagnétique sur le déplacement chimique et d'une augmentation du couplage avec l'accroissement des effets inducteurs attracteur des substituants X et Y. L'adjonction de σ_{R^0} à σ_I, n'augmente pas d'une façon statistiquement significative les corrélations avec $\delta^{15}N$, $\delta^{31}P$ et $^1J_{P—N}$ car le test F de Snedecor (31) reste inférieur à sa valeur théorique bien que la valeur du coefficient de corrélation R augmente sensiblement.

Les corrélations des variables rmn $\delta^{15}N$, $\delta^{31}P$ et $^1J_{P—N}$ avec le terme stérique E_S ne sont pas significatives si on considère les séries I, II ou IV dans leur ensemble. Cependant les valeurs de $\delta^{31}P$ peuvent se grouper en deux familles importantes correspondant à des molécules chlorées ou non chlorées, respectivement. La liaison P—Cl étant beaucoup plus polarisable que les autres, on doit attendre une influence paramagnétique du terme

ΔE^{-1} plus grande sur $\delta^{31}P$(Cl, X) que sur $\delta^{31}P$(X, Y)

(26). On peut alors calculer deux droites de régression pour ces deux familles de composés.

Composés chlorés:

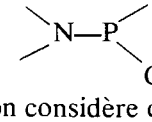
$$[6] \quad \delta^{31}P(\pm 2.6) = 258 + 32E_S \qquad R = 0.96 \quad 9\ \text{pts} \quad t_b = 8.4$$

Composés non chlorés:

$$[7] \quad \delta^{31}P(\pm 4.8) = 206 + 26E_S \qquad R = 0.95 \quad 9\ \text{pts} \quad t_b = 7.7$$

L'influence de l'encombrement stérique et de la polarisabilité de la liaison P—Cl se retrouve dans le comportement de $\delta^{15}N$ et $^1J_{P—N}$, car, à l'exception des composés chlorés, on observe une diminution de $\delta^{15}N$ (effet diamagnétique) et de $^1J_{P—N}$ avec la grosseur des substituants, liée aux modifications d'hybridation du fragment phosphore–azote par variation de l'encombrement stérique. Des substituants encombrants sur le phosphore tendent à rendre l'azote pyramidal et provoquent un effet diamagnétique sur $\delta^{15}N$ et une diminution de $^1J_{P—N}$. Au contraire, une augmentation de la grosseur des substituants de l'azote confère à celui-ci une hybridation à tendance sp^2 qui augmente $^1J_{P—N}$ et $\delta^{15}N$.

Les anomalies observées dans la série IV peuvent s'expliquer par l'existence d'une structure pyramidale privilégiée (27), conforme aux résultats d'une étude effectuée par RX sur la trimorpholinophosphine (30). Le cas des composés aromatiques



peut s'expliquer aisément si on considère que la valeur $E_S = -1.01$

Can. J. Chem. Downloaded from www.nrcresearchpress.com by 210.87.254.40 on 09/05/12
For personal use only.

utilisée (Tableau 2), correspond à une conformation d'encombrement minimum du cycle aromatique. En fait, comme le noyau phényle se conjugue partiellement avec P, son encombrement réel doit être plus important. Dans ce cas, le transfert p_π–d_π du cycle phényle vers le phosphore l'emporte sur celui du group $N(R)_2$ qui tend à adopter une disposition sp^3 (effet diamagnétique).

C. Relation entre les paramètres rmn et la barrière à la rotation autour de la liaison P—N

De nombreux auteurs (ref. du tableau 5) ont déterminé les valeurs $\Delta G^{\neq}$ et la référence (23) contient une discussion générale du phénomène de topoisomérisation. L'examen des valeurs d'enthalpie libre d'activation permet de mettre en évidence plusieurs traits caractéristiques du comportement des amino-phosphines. On constate notamment que la barrière augmente avec l'accroissement de la taille des substituants R sur l'atome d'azote et lorsque les substituants X et Y présentent des inerties différentes et des encombrements voisins, mais la grosseur intrinsèque de X, Y n'entraine qu'une faible diminution de $\Delta G_T^{\neq}$. Dans l'hypothèse de l'existence d'une géométrie trigonale de l'azote à l'état fondamental et tétraédrique dans l'état de transition, l'accroissement de la taille des substituants R de l'azote rend moins probable une géométrie non plane de l'azote, et entraine une augmentation de la barrière. Par contre l'augmentation de la taille des substituants X ou Y du phosphore favorise un azote pyramidal et entraine une faible diminution de la barrière, d'autre part lorsque les substituants X et Y ont des encombrements stériques sensiblement identiques on peut observer une dépendance de $\Delta G_T^{\neq}$ avec les effets électroniques des substituants ($\Delta G_T^{\neq}$ **I 1** < $\Delta G_T^{\neq}$ **I 17** par exemple).

Contrairement à ce que nous avons observé dans les séries N—X où X est un atome ne possédant pas d'orbitale *d* (e.g., X = C, N) (3), aucune corrélation simple n'apparaît entre $\delta^{15}N$ (ou $^1J_{P—N}$) et $\Delta G^{\neq}$. Cette absence de corrélation confirme aussi le rôle prépondérant de l'encombrement stérique dans l'état de transition sur le mécanisme de rotation autour de la liaison P—N. On peut cependant mettre en évidence une tendance de variation de la barrière avec $\delta^{31}P$; $\Delta G_T^{\neq}$ diminue avec l'écran du phosphore.

Série	$\Delta G_T^{\neq}$ (kJ mol^{-1})	$\delta^{31}P$ (ppm)
I, II, III, V, X	44 à 46	140 à 142.5
IV, VI	55 à 56	131

Cependant, le petit nombre de points correspondant à des valeurs différentes de $\Delta G^{\neq}$ et $\delta^{31}P$ ne permet pas de calculer une corrélation très significative.

L'effet diamagnétique observé sur $\delta^{31}P$ est en accord avec l'augmentation de la conjugaison p_π–d_π de l'azote vers le phosphore.

Partie expérimentale

Préparation des aminophosphines

Les aminophosphines sont obtenues par action de l'amine secondaire sur les chlorophosphines selon la réf. 29*a*. Le composé **I 1** a été synthétisé en faisant réagir le bromométhyl magnésium sur l'amino dichlorophosphine (29*a*). Les aminophosphines oxygénées **I 27** et **I 35** résultent de la réaction de l'éthanol sur la tris(diméthylamino) phosphine (29*b*). Certains composés triaminés ne se forment pas dans de bonnes conditions car de nombreuses réactions d'échange interviennent. Les structures des produits préparés ont été vérifiées par rmn ^1H, ^{13}C ou ^{31}P.

Résonance magnétique nucléaire

Les spectres ^{15}N ont été obtenus au moyen d'un spectromètre Bruker WH 90-DS, en abondance naturelle dans des liquides purs à 301 K après addition de 0.08 *M* de $Cr(AcAc)_3$ dissous dans 10% de $CHCl_3$; SW = 6000 Hz, At = 0.68 s, PW = 12 × 10^{-6} s, ν_0 = 9.117 MHz. Découplage large bande (2 W), nombre d'accumulation: 2 × 10^4 à 2 × 10^5 suivant la masse moléculaire. Les composés chlorés donnent des rapports signal-sur-bruit meilleurs que les autres composés. Les déplacements chimiques ont été repérés par rapport à une solution dans D_2O, H^+ de $^{15}NO_3$ Na enrichi à 30% contenue dans un tube coaxial de 4 mm centré dans un tube échantillon de 15 mm ($\delta(Ni/CH_3NO_2)$ = $\delta(Ni/NO_3^-)$ − 1.5 ppm). Les spectres ^{31}P ont été enregistrés sur un appareil Bruker WH 90-DS pour des produits purs ou en solution à 30% dans un mélange 50:50 $CS_2/CO(CD_3)_2$ (cas IV **17**) ou en solution à 30% dans $CHCl_3$ (cas IV **31** et IX **14**); SW = 12000 Hz, At = 0.34 s, PW = 7 × 10^{-6} s, ν_0 = 36.447 MHz, découplage large bande, nombre d'accumulations: 100. Les valeurs de $\delta^{31}P$ sont indiquées en ppm par rapport à H_3PO_4. Les expériences de rmn dynamique ont été réalisées au moyen du spectrographe Bruker WH 90-DS en résonance de ^{13}C (SW = 3000 Hz, At = 1.34 s, PW = 3 × 10^{-6} s, ν_0 = 22.635 MHz, découplage large bande, nombre d'accumulations = 10^3).

Calculs statistiques

Les analyses factorielles ont été effectuées au moyen des sous-programmes CORRE: matrice de corrélation, EIGEN et TRACE: valeurs propres et vecteurs propres, LOAD: matrice factorielle, sur calculatrice IBM 1130. Les régressions linéaires ont été effectuées au moyen d'un calculateur de bureau. Les paramètres statistiques ont les significations habituelles: $R_{x,y}$ coefficient de corrélation, *S* écart-type sur les coefficients de la régression, et $tb_x = b_x/Sb_x$. La valeur calculée tb_x doit être supérieure à la valeur t_F trouvée dans la table de Fischer en fonction de *N* et de la probabilité *P* d'existence dérivée pour la corrélation. Ainsi pour *P* = 99% et N = 8, 10, 13, 23 et 31 on trouve t_F = 3.3, 3.2, 3.0, 2.8 et 2.7. Le test *F* permet de vérifier si l'adjonction d'une seconde variable indépendante x_2 à la régression conduit à une amélioration significative de la corrélation. Si la valeur $F = S_y^2/S_y'^2$ (où S_y et S_y' représentent les écarts-types sur l'estimation par la corrélation à 1 et 2 variables respectivement) est plus grande que F_S, la corrélation bilinéaire est significative. F_S se trouve dans les tables de Snedecor en fonction de *N* et *N'* (31).

1. (*a*) M. M. Crutchfield, C. H. Dungan, J. H. Letcher, V. Mark et J. R. Van Wazer. ^{31}P Nuclear magnetic resonance. *Dans* Topics in phosphorus chemistry. Vol. 5. *Edité*

Can. J. Chem. Downloaded from www.nrcresearchpress.com by 210.87.254.40 on 09/05/12
For personal use only.

par M. Grayson and E. J. Griffith. Interscience, New York. 1967; (*b*) G. MAVEL. NMR studies of phosphorus compounds. *Dans* Annual reports on nmr spectroscopy. Vol. 5B. *Edité par* E. F. Mooney. Academic Press, New York. 1973; (*c*) P. S. PREGOSIN et R. W. KONZ. ^{31}P and ^{13}C NMR of transition metal phosphine complexes. *Dans* NMR basic principles and progress. Vol. 16. *Edité par* P. Diehl, E. Fluck et R. Kosfeld. Springer-Verlag, Heidelberg. 1979.

2. (*a*) K. BARLOS, H. NOTH et B. WRACKMEYER. Z. Naturforsch. Teil B, **33**, 515 (1978); (*b*) G. A. GRAY and T. A. ALBRIGHT. J. Am. Chem. Soc. **98**, 3857 (1976); **99**, 3243 (1977); (*c*) A. COGNE, J. B. ROBERT et L. WIESENFELD. Chem. Phys. Lett. **57**, 627 (1978); (*d*) B. THOMAS et G. GROSSMANN. Z. Anorg. Allg. Chem. **448**, 107 (1979); (*e*) J. H. HARGIS, S. D. WORLEY, W. B. JENNINGS et M. S. TOLLEY. J. Am. Chem. Soc. **99**, 8090 (1977).
3. (*a*) G. J. MARTIN, J. P. GOUESNARD, J. DORIE, C. RABILLER et M. L. MARTIN. J. Am. Chem. Soc. **99**, 1381 (1977); (*b*) J. DORIE, B. MECHIN et G. J. MARTIN. Org. Magn. Reson. **12**, 229 (1979).
4. M. L. FILLEUX-BLANCHARD et N. D. AN. Org. Magn. Reson. **12**, 12 (1979).
5. J. P. GOUESNARD et G. J. MARTIN. Org. Magn. Reson. **12**, 263 (1979).
6. (*a*) R. W. TAFT, E. PRICE, I. R. FOX, I. C. LEWIS, K. K. ANDERSEN et G. T. DAVIS. J. Am. Chem. Soc. **85**, 709 (1963); **85**, 3146 (1963); (*b*) O. EXNER. A critical compilation of substituent constants. Correlation analysis in chemistry. Recent advances. *Edité par* N. B. Chapman and J. Shorter. Plenum Press, New York. 1978. p. 500.
7. J. SHORTER. Multiparameter extensions of the Hammett equation. Correlation analysis in chemistry. Recent advances. *Edité par* N. B. Chapman et J. Shorter. Plenum Press, New York. 1978. p. 154.
8. (*a*) S. H. UNGER et C. HANSCH. Quantitative models of steric effects. Progress in physical organic chemistry. Vol. 12. *Edité par* R. W. Taft. Interscience, New York. 1976. p. 91; (*b*) R. N. TAFT. Steric effects in organic chemistry. *Edité par* M. S. Newman. Wiley, New York. 1956.
9. R. J. W. LE FEVRE. Molecular refractivity and polarizability. *Dans* Advances in physical organic chemistry. Vol. 3. *Edité par* V. Gold. Academic Press, New York. 1965. p. 1.
10. (*a*) H. H. HARMAN. Modern factor analysis. University Press, Chicago. 1976; (*b*) P. H. WEINER, E. R. MALINOWSKI et A. R. LEVINSTARE. J. Phys. Chem. **74**, 4537 (1970); (*c*) P. H. WEINER et E. R. MALINOWSKI. J. Phys. Chem. **75**, 1207 (1971); (*d*) G. J. MARTIN, D. LE BOTLAN, T. BERTRAND et J. M. LETOURNEUX. J. Chem. Res. (5), 408 (1979); (*e*) M. R. BACON et G. E. MACIEL. J. Am. Chem. Soc. **95**, 2413 (1973); (*f*) K. B. WIBERG, W. E. PRATT et W. F. BAILEY. Tetrahedron Lett. 4861 (1978).
11. S. DI STEFANO, H. GOLDWHITE et E. MAZZOLA. Org. Magn. Reson. **6**, 1 (1974).
12. M. P. SIMONNIN, J. J. BASSELIER et C. CHARRIER. Bull. Soc. Chim. Fr. 3544 (1967).
13. A. M. COWLEY, M. J. S. DEWAR et W. R. JACKSON. J. Am. Chem. Soc. **90**, 4185 (1968).
14. D. IMBERY et K. FRIEBOLIN. Z. Naturforsch. Teil B, **23**, 759 (1968).
15. A. M. COWLEY, M. J. S. DEWAR, W. R. JACKSON et S. W. D. JENNINGS. J. Am. Chem. Soc. **92**, 1085 (1970); **92**, 5206 (1970).
16. M. P. SIMONNIN et C. CHARRIER. Org. Magn. Reson. **4**, 113 (1972).
17. H. BOUDJEBEL, H. GONCALVES et F. MATHIS. Bull. Soc. Chim. Fr. 628 (1975).
18. H. GOLDWHITE et D. G. ROWSELL. Chem. Commun. 713 (1969).
19. H. GOLDWHITE et P. P. POWER. Org. Magn. Reson. **11**, 499 (1978).
20. J. BURDON, J. C. HOTCHKISS et W. B. JENNINGS. J. Chem. Soc. Perkin Trans. II, 1052 (1976).
21. R. H. NEILSON, R. C. Y. LEE et A. H. COWLEY. Inorg. Chem. **16**, 1455 (1977).
22. O. J. SCHERER et N. KUHN. Chem. Ber. **108**, 2478 (1975).
23. J. M. LEHN. Fortschr. Chem. Forsch. **15**, 311 (1970).
24. (*a*) J. P. WARREN et J. D. ROBERTS. J. Phys. Chem. **78**, 2507 (1974); (*b*) R. O. DUTHALER et J. D. ROBERTS. J. Am. Chem. Soc. **100**, 3889 (1978).
25. (*a*) J. B. STOTHERS. ^{13}C nmr spectroscopy. Academic Press, New York. 1972. Chapt. 3. p. 5; (*b*) L. ERNST. Angew. Chem. Int. Ed. Engl. **15**, 303 (1976).
26. (*a*) D. PURDELLA. Rev. Roum. Chim. **10**, 949 (1965); (*b*) B. I. IONIN. Zh. Obshch Khim. **38**, 1659 (1968); (*c*) S. P. IONOV et G. V. IONOVA. Russ. J. Phys. Chem. **43**, 458 (1969).
27. (*a*) L. D. QUIN et J. J. BREEN. Org. Magn. Reson. **5**, 17 (1973); (*b*) L. B. LITTLEFIELD et L. D. QUIN. Org. Magn. Reson. **12**, 199 (1979); (*c*) D. G. GORENSTEIN. J. Am. Chem. Soc. **99**, 2254 (1977).
28. E. MUYLLE et G. P. VAN DER KELEN. Spectrochim. Acta, Part A, **32**, 599 (1976).
29. (*a*) A. B. BURG et P. SLOTA. J. Am. Chem. Soc. **80**, 1107 (1958); (*b*) D. HOUALLA, M. SANCHEZ et R. WOLF. Bull. Soc. Chim. Fr. 2368 (1965).
30. C. ROMMING et J. SONGSTAD. Acta Chem. Scand. Ser. A, **32**, 689 (1978).
31. G. W. SNEDECOR. Statistical methods. The Iowa State University Press, Ames, IA. 1956. p. 246.
32. J. P. GOUESNARD et J. DORIE. J. Mol. Struct. A paraître.

Cinétique d'oxydation des oximes du benzaldéhyde et de l'acétophénone par l'ion thallique

ROBERT LORTIE ET MIKLOS ZADOR

Département de Chimie, Université de Montréal, C.P. 6210, Succursale A, Montréal (Qué.), Canada H3C 3V1

Reçu le 19 décembre 1979

ROBERT LORTIE et MIKLOS ZADOR. Can. J. Chem. **58**, 1305 (1980).

La cinétique d'oxydation des oximes du benzaldéhyde et de l'acétophénone par le Tl(III) a été étudiée en milieu aqueux. La réaction s'effectue par deux étapes consécutives: formation d'un intermédiaire nitroso et sa décomposition ultérieure. L'oxime forme un complexe interne avec le Tl(III), ce qui conduit à l'équation de vitesse: $-d[\text{oxime}]/dt = K_1k_2[\text{oxime}][\text{Tl(III)}]/(1 + K_1[\text{Tl(III)}])$. La formation du produit final carbonylé est inhibée par le Tl(III), dû à la formation d'un complexe résistant à la décomposition. La coordination du Tl(III) par les ions chlorure affecte de façon différente la vitesse des deux étapes. Le mécanisme de la réaction est discuté.

ROBERT LORTIE and MIKLOS ZADOR. Can. J. Chem. **58**, 1305 (1980).

The kinetics of oxidation of benzaldehyde and acetophenone oximes by Tl(III) in aqueous medium has been studied. The reaction occurs in two consecutive steps: formation of a nitroso intermediate and its decomposition. The oxime forms a complex with Tl(III) leading to the rate equation: $-d[\text{oxime}]/dt = K_1k_2[\text{oxime}][\text{Tl(III)}]/(1 + K_1[\text{Tl(III)}])$. The formation of the final carbonyl product is inhibited by Tl(III), a result of the formation of a complex resistant to decomposition. Coordination of Tl(III) by chloride ions affects the rate of the above two steps. The reaction mechanism is discussed.

[Journal translation]

Can. J. Chem. Downloaded from www.nrcresearchpress.com by 210.87.254.40 on 09/05/12
For personal use only.

L'utilisation de sels thalliques pour régénérer les dérivés carbonylés par oxydation des oximes, phenylhydrazones et semicarbazones constitue une méthode intéressante en synthèse (1). L'oxydation des oximes s'effectue d'après l'éq. [1].

$$[1]\quad R_1R_2C{=}NOH + Tl^{3+} + \tfrac{1}{2}H_2O \rightarrow R_1R_2CO + Tl^{+} + 2H^{+} + \tfrac{1}{2}N_2O$$

McKillop et ses collaborateurs ont montré qu'elle est rapide et sélective dans le cas d'un grand nombre d'oximes (1).

Le travail présent est consacré à l'étude de la cinétique et du mécanisme d'oxydation des oximes du benzaldéhyde et de l'acétophénone en milieu aqueux par le perchlorate thallique.

Partie expérimentale

Les solutions de perchlorate thallique ont été obtenues par dissolution du Tl_2O_3 (B.D.H.) dans l'acide perchlorique. La concentration en Tl(III) a été déterminée par iodométrie. L'oxime du benzaldéhyde est un produit commercial (Eastman), contenant les isomères *syn* et *anti* à l'équilibre. L'oxime du cyclohexanone et l'oxime *anti* de l'acétophénone ont été synthétisés et caractérisés par des méthodes standards (2).

L'acétoxy-1 nitroso-1 cyclohexane a été synthétisé comme suit: 1.45 g (~ 1.3 mmol) d'oxime du cyclohexanone sont dissous dans 10 mL de CCl_4 ajouté de quelques gouttes d'anhydride acétique. On y ajoute 5 g (~ 13 mmol) de $Tl(OAc)_3$ que l'on maintient en suspension en agitant à l'aide d'une barre magnétique. Après 15 min à reflux on obtient une solution verte qui ne contient plus du Tl(III). La solution est lavée par de l'eau, contenant du bicarbonate de sodium, filtrée et séchée sur du sulphate de magnésium.

A cause de son instabilité, le produit, l'acétoxy-1 nitroso-1 cyclohexane, est caractérisé directement en solution dans le CCl_4 par rmn, rpe et le spectre visible (rmn: multiplet du cycle δ = 1.7 ppm et δ = 2.3 ppm, singulet de l'acétoxy δ = 2.4 ppm; rpe: triplet I:1:1, a_n = 12.6 Oe, comparé à a_n = 13.2 Oe obtenu dans le CH_2Cl_2 (3); spectre visible λ_{max} = 667 nm, comparé à λ_{max} = 665 nm dans le CH_2Cl_2 (3)).

La cinétique d'oxydation a été suivie par spectrophotométrie soit en enregistrant les spectres à intervalles réguliers (Pye-Unicam model 1700), soit en enregistrant la variation d'absorbance à longueur d'onde constante (Zeiss PMQ II). Un grand excès de Tl(III) par rapport à l'oxime a été utilisé. Les constantes de vitesse d'ordre un ont été obtenues à partir de la relation $kt = \ln[(A_0 - A_\infty)/(A_t - A_\infty)]$, où A_0, A_t et A_∞ représentent les absorbances aux temps 0, t et infini respectivement. Les conditions expérimentales choisies sont discutées dans le chapitre Résultats.

La température de réaction a été maintenue constante à ± 0.1°C. La force ionique du milieu a été ajustée à 1 *M* à l'aide de perchlorate de sodium.

Lors de l'étude de l'influence d'ions chlorure, il a fallu procéder, dans certains cas, par addition de solution de chlorure de sodium pendant le déroulement de la réaction pour pouvoir étudier les deux étapes (voir plus loin).

Résultats

Les spectres uv du mélange réactionnel enregistrés à intervalles réguliers, révèlent clairement que l'on est en présence de deux réactions consécutives. Les spectres initial et final correspondent bien aux réactifs et aux produits carbonylés; cependant, comme l'indique la fig. 1, une bande plus intense apparait entre 240–250 nm en cours de réaction.

La fig. 2 montre un résultat typique obtenu en enregistrant la variation d'absorbance à longueur d'onde constante en fonction du temps. On observe d'abord une augmentation d'absorbance ce qui est suivie d'une diminution plus lente pour arriver à l'absorbance du produit carbonylé. Ces résultats indiquent la formation d'un intermédiaire réactionnel ce qui impose des précautions particulières

0008-4042/80/131305-06$01.00/0
©1980 National Research Council of Canada/Conseil national de recherches du Canada

Can. J. Chem. Downloaded from www.nrcresearchpress.com by 210.87.254.40 on 09/05/12
For personal use only.

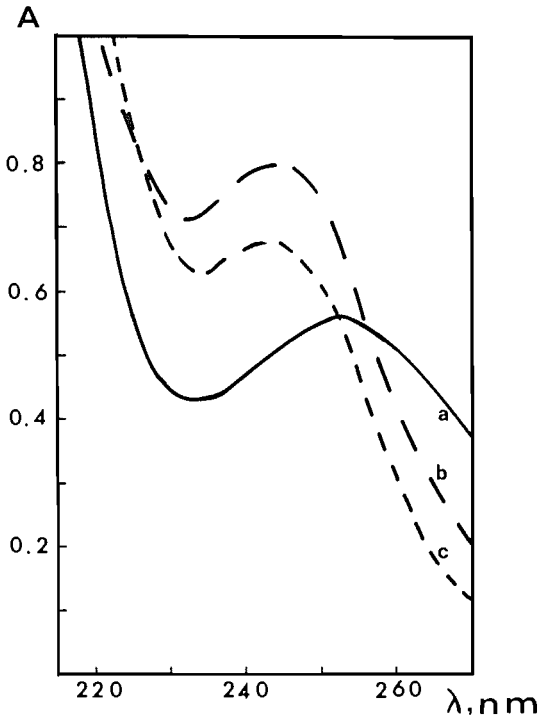


FIG. 1. Spectres d'absorption de la solution réactionnelle aux temps correspondant à la prédominance de (a) oxime du benzaldéhyde, (b) intermédiaire, (c) benzaldéhyde.

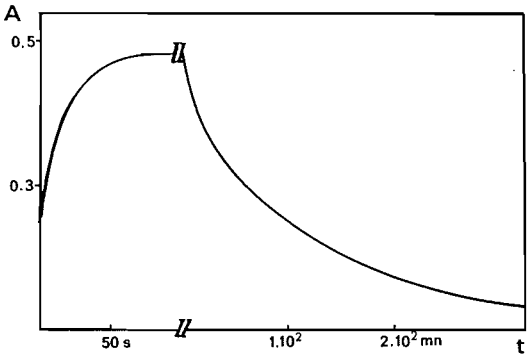


FIG. 2. Variation d'absorbance lors de l'oxydation de l'oxime du benzaldéhyde. T = 45°C; $[H^+]$ = 1 M; [Tl(III)] = 1.25 × 10^{-2} M; [oxime] = 5 × 10^{-4} M; λ = 290 nm.

pour l'étude cinétique d'autant plus que la vitesse relative des deux phénomènes varie, d'après les résultats préliminaires, de façon significative avec la concentration en Tl(III) et de ses ligands dans le milieu réactionnel.

Cinétique de la première étape

Pour l'étude de cette étape on a choisi une longueur d'onde où l'absorbance de l'intermédiaire et du produit final sont identiques (un point isobestique de la fig. 1). Ceci permet d'éliminer entièrement l'interférence de la deuxième étape. En présence d'un grand excès de Tl(III) ([Tl(III)] ≫ [oxime]) des cinétiques d'ordre un ont été observées.

La constante de vitesse expérimentale, k_{exp}, augmente d'abord avec la concentration en Tl(III) (Fig. 3); il y a ensuite une courbure conduisant vers un plateau. Ce comportement est caractéristique d'un mécanisme impliquant la formation d'un complexe entre les deux réactifs:

$$\text{Tl(III)} + \text{oxime} \rightleftharpoons \text{Tl(III)}\cdot\text{oxime} \qquad K_1, \text{ rapide}$$

$$\text{Tl(III)}\cdot\text{oxime} \rightarrow \text{intermédiaire} \qquad k_2, \text{ lent}$$

$$[2] \quad -\mathrm{d[oxime]}/\mathrm{d}t = k_2K_1[\text{oxime}][\text{Tl(III)}]/(1+K_1[\text{Tl(III)}])$$

Les résultats sont en accord avec l'éq. [3], qui représente l'expression habituelle de la constante de vitesse expérimentale d'un mécanisme à deux étapes dont le premier implique la formation rapide et réversible d'un complexe entre les deux réactifs.

$$[3] \quad k_{exp} = k_2K_1[\text{Tl(III)}]/(1 + K_1[\text{Tl(III)}])$$

L'ensemble des paramètres cinétiques est résumé au tableau 1, qui indique également l'accord obtenu entre k_{exp} et k_{calc} obtenu à l'aide de l'éq. [3]. La variation de la concentration en acide perchlorique de 0.25 à 1 M, à force ionique constante n'affecte pas de façon significative les constantes de vitesse.

Le complexe Tl(III)·oxime a été mis en évidence par spectrophotométrie; sa formation conduit à une augmentation appréciable d'absorbance par rapport à la somme de celle du Tl(III) et l'oxime entre 250 et 310 nm. Cependant, dû à sa nature peu stable et, en partie, à l'absorbance élevée du Tl(III) aux hautes concentrations, des bonnes valeurs de K_1 n'ont pas pu être obtenues par cette méthode.

Cinétique de la deuxième étape

L'intermédiaire formé se décompose avec diminution d'absorbance à 260–290 nm pour l'oxime

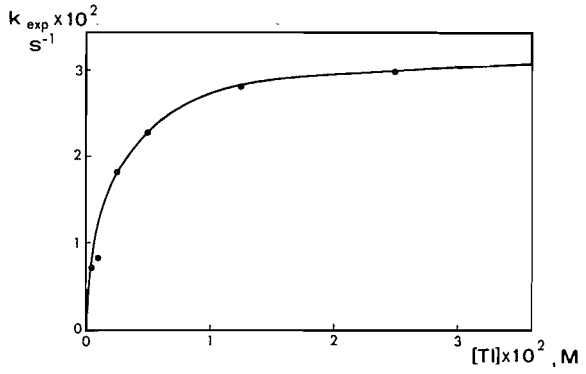


FIG. 3. Variation de k_{exp} avec la concentration en Tl(III). T = 45°C; $[H^+]$ = 0.5 M; [oxime du benzaldéhyde] = 5 × 10^{-5} M.

Can. J. Chem. Downloaded from www.nrcresearchpress.com by 210.87.254.40 on 09/05/12
For personal use only.

TABLEAU 1. Variations de k_{exp} avec la concentration en Tl(III) et paramètres cinétiques correspondants*

Oxime du benzaldéhyde			Oxime de l'acétophénone		
10^3[Tl(III)] M	10^2k_{exp} s^{-1}	10^2k_{calc} s^{-1}	10^3[Tl(III)] M	10^3k_{exp} s^{-1}	10^3k_{calc} s^{-1}
0.50	0.71	0.66	0.10	1.3	1.05
1.0	1.0	1.09	0.25	2.3	2.10
2.50	1.8	1.81	0.50	2.7	3.15
5.0	2.3	2.31	1.25	3.6	4.50
12.5	2.8	2.77	12.5	6.8	6.06
25	3.0	2.97	23.7	5.6	6.17
50	3.3	3.08			
$K_1 = (5.2 \pm 0.5)10^2\ M^{-1}$			$K_1 = (2 \pm 0.6)10^3\ M^{-1}$		
$k_2 = (3.2 \pm 0.3)10^{-2}\ s^{-1}$			$k_2 = (6.3 \pm 1.3)10^{-3}\ s^{-1}$		

*T = 45°C; [$HClO_4$] = 0.5 M; [oxime] = 5×10^{-5} M à 5×10^{-4} M; solvant = H_2O.

TABLEAU 2. Variation de k'_{exp} avec la concentration en Tl(III) et paramètres cinétiques correspondants*

Oxime du benzaldéhyde		Oxime de l'acétophénone	
10^3[Tl(III)] M	$10^3k'_{exp}$ s^{-1}	10^3[Tl(III)] M	$10^4k'_{exp}$ s^{-1}
1.0	2.8	1.0	5.5
2.5	1.20	1.5	1.8
5.0	0.55	2.5	1.4
12.5	0.23	5.0	1.0
25.0	0.12	7.5	0.70
		10.0	0.54
$k_4/K_3 = (3.0 \pm 0.3)10^{-6}\ M\ s^{-1}$		$k_4/K_3 = (5.9 \pm 1)10^{-7}\ M\ s^{-1}$	

*T = 45°C; [$HClO_4$] = 1.0 M; [oxime] = 5×10^{-5} à 5×10^{-4} M; solvant = H_2O.

du benzaldéhyde et à 230–270 nm pour l'oxime de l'acétophénone.

La constante de vitesse d'ordre un de cette étape k'_{exp} diminue avec l'augmentation de la concentration du Tl(III) en excès (voir tableau 2). De plus, l'addition du Tl(III) au mélange réactionnel pendant le déroulement de cette étape est suivie d'une diminution instantanée de la pente de la courbe absorbance vs. temps. La réaction est donc inhibée par le Tl(III). Par conséquent, à haute concentration en Tl(III) la formation de l'intermédiaire est beaucoup plus rapide que sa disparition, donc cette dernière étape a pu être étudiée facilement. A basse concentration en Tl(III) la nature consécutive de la réaction est apparente, les deux réactions ont alors des vitesses comparables. Comme même une contribution faible d'absorbance de la première étape influe significativement sur l'allure des courbes, de bonnes valeurs des constantes n'ont pas pu être obtenues à des concentrations en Tl(III) inférieures à celles du tableau 2. L'augmentation de l'acidité de 0.25 à 1.0M conduit à une diminution de 35% de k'_{exp}.

L'effet inhibiteur du Tl(III) a été interprété en admettant la formation d'un complexe de celui-ci avec l'intermédiaire (I) formé d'après le schéma suivant:

$$Tl(III) + I \rightleftharpoons Tl(III)\cdot I \qquad K_3, \text{ rapide}$$

$$I \rightarrow \text{produit carbonylé} \qquad k_4, \text{ lent}$$

Ceci conduit, en présence d'un excès de Tl(III) aux équations

$$[4] \quad d[\text{carbonyle}]/dt = k_4[I]_{total}/(1 + K_3[Tl(III)])$$

$$[5] \quad k'_{exp} = k_4/(1 + K_3[Tl(III)])$$

Le graphe de $1/k'_{exp}$ vs. [Tl(III)] donne une droite en accord avec l'éq. [5], permettant à déterminer la valeur de k_4/K_3. L'ordonnée à l'origine est très faible; par conséquent k_4 n'a pas pu être obtenu. Ceci implique que K_3[Tl(III)] > 1, donc l'intermédiaire est fortement complexé, beaucoup plus fortement que l'oxime ($K_3 \gg K_1$).

Influence des ions chlorure

L'influence des ions hydroxyles n'a pas pu être étudiée en détail, dû aux effets multiples (catalytiques et hydrolytiques) d'une variation de la concentration en H^+, et la faible solubilité du Tl(III) à pH élevé. L'influence de la coordination du Tl(III) a donc été étudiée au moyen d'ions chlorure dont l'affinité pour l'ion Tl^{3+} est bien connue (4).

Les ions chlorures influencent les deux étapes de l'oxydation de l'oxime du benzaldéhyde. Seul un domaine de concentration assez restreint a pu être étudié, dû à l'effet différent sur les deux étapes et l'absorbance élevée des complexes Tl(III)—Cl.

Les résultats présentés au tableau 3 montrent l'effet inhibiteur des ions chlorure sur k_{exp}. Les valeurs de k_{exp} ont pu être interprétés par l'éq. [6] analogue à l'éq. [3] contenant un terme dû à $TlCl^{2+}$.

$$[6] \quad k_{exp} = \frac{k_2K_1[Tl(III)] + k_{2,TlCl}K_{1,TlCl}[TlCl^{2+}]}{1 + K_1[Tl(III)] + K_{1,TlCl}[TlCl^{2+}]}$$

Can. J. Chem. Downloaded from www.nrcresearchpress.com by 210.87.254.40 on 09/05/12
For personal use only.

TABLEAU 3. Influence des ions chlorure sur les constantes de vitesse d'oxydation de l'oxime du benzaldéhyde*

$10^3[Cl^-]$ M	10^2k_{exp} s^{-1}	10^2k_{calc} s^{-1}	$10^3[Cl^-]$ M	k'_{Cl}/k'_0†
—	1.01	1.09	—	1.0
0.5	0.96	0.87	0.25	1.2
0.75	0.87	0.75	0.5	2.1
1.0	0.54	0.60	0.75	3.2
1.5	0.27	0.33	1.0	5.0
2.0	0.10	0.08	1.25	4.3
			1.5	1.4
			4.0	>20

*T = 45°C; $[HClO_4]$ = 0.5 M; [oxime] = 5×10^{-5} M; [Tl(III)] = 1.0×10^{-3} M; solvant = H_2O.
†Constantes de vitesse de décomposition de l'intermédiaire en présence d'ions chlorure (k'_{Cl}) par rapport à celle obtenue en l'absence d'ions chlorure (k'_0).

La régression pondérée, basée sur la distribution des espèces Tl—Cl obtenue en utilisant les constantes de stabilité de la littérature (4), a permis de déterminer les constantes: $K_{1,TlCl} = 200\,M^{-1}$ et $k_{2,TlCl} = 3.4 \times 10^{-2}\,s^{-1}$. Il est à noter, que les espèces $TlCl_2^+$ et $TlCl_3$ n'ont pas de contribution significative à l'éq. [6] ce qui cause la diminution importante de vitesse pour $Cl/Tl > 1$.

La constante de vitesse de décomposition de l'intermédiaire augmente avec la concentration d'ion Cl^- ajouté jusqu'à un rapport $Cl/Tl = 1$. Ceci s'explique en admettant que $TlCl^{2+}$ complexe moins fortement l'intermédiaire que Tl^{3+}, entraînant l'augmentation de la concentration de l'intermédiaire libre de l'éq. [4] et, par conséquent, l'augmentation de k'_{exp}. La diminution subséquente de la vitesse est assez difficile à expliquer sans des données sur la stabilité du complexe mixte de type $TlCl_2 \cdot L$. Ceci signifierait que $TlCl_2^+$ complexe plus fortement l'intermédiaire que $TlCl^{2+}$.

Il est très significatif cependant qu'en présence d'un excès de chlorure ($Cl/Tl \geq 4$), où $TlCl_3$ et $TlCl_4^-$ prédominent, la vitesse devient beaucoup plus grande en accord avec l'éq. [4], dû à l'impossibilité de former des complexes avec l'intermédiaire.

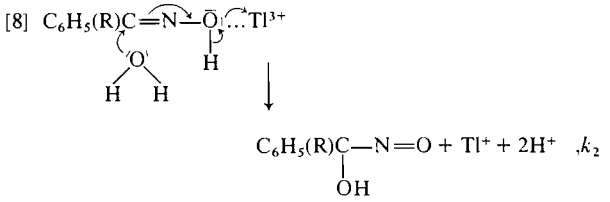
Discussion

Les résultats obtenus sont en accord avec le mécanisme postulé par McKillop *et al.*, qui ont montré pour la première fois, l'utilité de l'oxydation thallique des oximes en synthèse (1). Nos résultats ont apporté les preuves de ce mécanisme ainsi que les données sur la vitesse des différentes étapes. Le mécanisme proposé est le suivant:

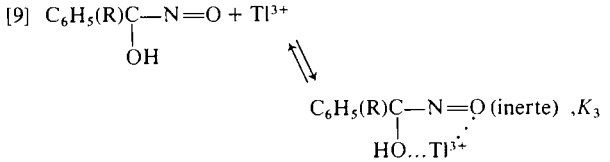
[7] $C_6H_5(R)C{=}NOH + Tl^{3+} \rightleftarrows C_6H_5(R)C{=}NO(H)Tl^{3+}$,K_1

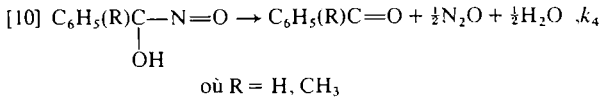
1

La formation du complexe Tl(III)· oxime (1) a été

[8] 

2

[9] 

[10] 

où R = H, CH_3

clairement démontrée et les constantes de formation K_1, déterminées. L'intervention de complexes internes avec le Tl(III) a été proposée, lors de l'oxydation d'autres substrats hydroxylés, tels l'acide formique (5) et de divers benzènediols (6), et récemment dans l'oxydation de l'acide mercapto-2 succinique (7).

L'absence d'inhibition par H^+ implique que le complexe est de type $> C{=}NO(H)Tl^{3+}$, donc il n'y a pas de départ de protons lors de la coordination, celle-ci mettant en jeu un doublet libre de l'oxygène. Ceci a été suggéré dans le cas de l'acide formique (5). Toutefois, l'équilibre:

$$Tl^{3+} + H_2O \rightleftarrows TlOH^{2+} + H^+$$

est déplacé vers la gauche avec l'augmentation de l'acidité, ce qui peut entraîner une variation de réactivité du Tl(III).

L'influence des ions chlorure montre que l'introduction du premier ligand ne réduit que peu la réactivité de l'espèce formée, $TlCl^{2+}$, envers l'oxime. Il est probable que ce soit similaire pour $TlOH^{2+}$, ce qui serait en accord avec l'influence négligeable de l'acidité.

Le remplacement de H par CH_3 en position α affecte de façon différente K_1 et k_2. Pour R = H on a $K_1 = 5.2 \times 10^2\,M^{-1}$ à comparer avec $K_1 = 2 \times 10^3\,M^{-1}$ pour R = CH_3. Cette augmentation est attendue, compte tenu de l'effet électron-donneur du CH_3, plus élevé que celui de H, et du caractère électrophile du Tl^{3+}. Il est cependant plus difficile à expliquer la diminution de k_2; $k_2 = 3.2 \times 10^{-2}\,s^{-1}$ (R = H) comparée à $6.3 \times 10^{-3}\,s^{-1}$ (R = CH_3). Il y a probablement un empêchement stérique du CH_3 lors de l'attaque de la molécule d'eau dans l'éq. [8]. De plus, cette attaque nucléophile nécessite une charge positive partielle sur ce carbone, qui est

Can. J. Chem. Downloaded from www.nrcresearchpress.com by 210.87.254.40 on 09/05/12
For personal use only.

surement plus faible en présence du groupe CH_3, ce qui peut contribuer également à la diminution de k_2.

Une réactivité similaire ou supérieure de TlX^{2+} (X = OH, Cl) par rapport à Tl^{3+} trouvé dans ce cas se retrouve dans l'oxydation d'autres substrats hydroxylés: dans le cas de benzènediols, ($k_{TlOH} > k_{Tl}$ (6)) et de la forme énolique du cyclohexanedione-1,2 ($k_{TlOH} > k_{Tl}$, $k_{TlCl} > k_{Tl}$ (8)). Ce comportement contraste avec celui observé lors de l'oxydation des oléfines ($k_{Tl} \gg k_{TlX}$ (9, 10)).

Cette différence s'explique par la possibilité de formation d'un complexe interne du thallium impliquant les doublets libres des oxygènes des hydroxyles et, dans le cas de l'oxime, la facilité de délocalisation des électrons du système $\diagdown C{=}N{-}O{-}Tl$, sous l'influence du thallium électrophile, nécessaire à l'étape 8. Dans le cas des oléfines, la formation du lien C—Tl nécessite la destruction du système π de l'oléfine; la réactivité du Tl^{3+}, plus électrophile, est donc largement supérieure à celle de TlX^{2+}.

La décomposition oxydative du produit d'oxythallation, qui présente certaines analogies avec l'étape 8, nécessite aussi le développement d'une charge positive sur l'atome de carbone en β, mais celui-ci est séparé du thallium par un lien σ (carbone–carbone) et la délocalisation des électrons est beaucoup moins aisée. Pour cette raison, la réduction de charge et du caractère électrophile, lors de la coordination du thallium, entraînent une diminution très importante de la réactivité (10). La réactivité négligeable de $TlCl_2^+$ est une caractéristique générale de l'oxydation de substrats organiques.

Le complexe Tl(III)·oxime n'a pas été observé dans une étude cinétique effectuée dans un mélange acide acétique – eau (11). Ceci est attribuable à la prédominance des complexes $Tl(OAc)_n^{3-n}$ qui présentent moins d'affinité pour les oximes. La différence importante de réactivité observée pour l'oxime de l'acétophénone ($k = 0.18 M^{-1}\,s^{-1}$ calculée pour 45°C dans l'acide acétique aqueux (11) à comparer à notre valeur de $k_2K_1 = 12 M^{-1}\,s^{-1}$) montre aussi que la coordination par les ions acétate diminue fortement la réactivité du Tl(III); il n'est cependant pas possible de dire si k_2 ou K_1 est la plus affectée.

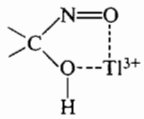
Les spectres rpe, pris sur le mélange réactionnel lors du déroulement de la réaction, n'ont pas permis la détection de radicaux iminoxy, $C_6H_5(R)C{=}NO^{\cdot}$ suggérés comme intermédiaires dans l'oxydation d'oximes par divers oxydants à un électron (3), et aussi dans le cas du Tl(III) en milieu acide acétique – eau (12).

L'intermédiaire nitroso (**2**) n'a pas pu être isolé dans les conditions expérimentales dû à son instabilité, causé par le groupe OH en position α.[1]

Nous avons pu isoler un intermédiaire nitroso en oxydant l'oxime du cyclohexanone par le $Tl(OAc)_3$, en utilisant le tétrachlorure de carbone comme solvant, ce qui empêche la solvolyse ultérieure et permet la caractérisation *in situ*. L'ion acétate participe à la réaction comme nucléophile et le produit obtenu est l'acétoxy-1 nitroso-1 cyclohexane, présentant le spectre rpe caractéristique en accord avec les données de la littérature (3).

Dû à la réactivité très faible de $Tl(OAc)_3$, l'oxydation d'oximes du benzaldéhyde et de l'acétophénone n'a lieu qu'à température élevée dans ce solvant où les dérivés nitroso correspondants, peu stables (13), se décomposent.

L'aspect le plus important de l'étape de décomposition de l'intermédiaire nitroso (**2**) dans cette séquence de réactions consécutives est l'inhibition par l'ion thallique. Elle s'explique en admettant la formation d'un complexe avec l'intermédiaire nitroso dont la vitesse de décomposition est négligeable. Dans ce cas il y a possibilité de formation d'un chélate à cinq atomes du type:



ce qui explique la stabilité accrue par rapport à l'oxime monodentate ($K_3 \gg K_1$).

La faible diminution de k'_{exp} avec l'augmentation de l'acidité s'explique qualitativement par le déplacement de l'équilibre d'hydrolyse:

$$Tl^{3+} + H_2O \rightleftarrows TlOH^{2+} + H^+$$

vers la formation de Tl^{3+} et son effet subséquent sur l'éq. [5]. Comme $TlCl^{2+}$ inhibe moins que Tl^{3+}, il est probable que ce soit similaire pour $TlOH^{2+}$.

Enfin, le schéma réactionnel implique que le rapport k_{exp}/k'_{exp} est fortement dépendant de la présence de ligands du Tl(III). En absence d'ions chlorure (à $[Tl(III)] \geq 5 \times 10^{-3} M$) on a un rapport $k_{exp}/k'_{exp} \geq 50$, ce qui se traduit par une accumulation de l'intermédiaire nitroso dont la cinétique de décomposition peut être étudiée. Par contre, en présence d'un excès d'ions chlorure (Cl/Tl ≥ 3) on

[1]L'absence de signal rpe aux faibles concentrations utilisées n'exclut pas la présence du dérivé nitroso. En effet, son spectre rpe est dû au radical-anion $N{-}O^{\cdot -}$, présent à très faible proportion (3, 13). Ce dernier est favorisé en présence de bases et un spectre rpe est alors obtenu. Ce spectre est cependant très compliqué dû à la formation de complexes avec le Tl(III) et dû aux couplages avec son spin nucléaire.

a l'inverse, $k_{exp}/k'_{exp} \ll 1$, et la formation de l'intermédiaire devient l'étape lente de la réaction.

Ces conclusions montrent encore une fois la nécessité de milieux non-complexants pour l'obtention du mécanisme détaillé de l'oxydation thallique.

Remerciements

Les auteurs remercient le Conseil de Recherches en Sciences Naturelles et en Génie du Canada pour l'octroi grâce auquel ce travail a pu être réalisé.

1. A. McKillop, J. D. Hunt, R. D. Naylor et E. C. Taylor. J. Am. Chem. Soc. **93**, 4918 (1971).
2. H. Metzger. *Dans* Methoden der organischen chemie. Vol. 10, t.4. *Edité par* E. Muller. Georg Thieme Verlag, Stuttgart. 1952. p. 56.
3. J. W. Lown. J. Chem. Soc. B, 441 (1966).
4. D. Peschanski et S. Valladas-Dubois. Bull. Soc. Chim. Fr. 1170 (1956); S. Ahrland, L. Grenthe, L. Johansson et B. Noren. Acta Chem. Scand. **17**, 1567 (1963).
5. H. N. Halvorson et J. Halpern. J. Am. Chem. Soc. **78**, 5562 (1956); S. D. Saxena et K. S. Gupta. Monatsh. Chem. **108**, 813 (1977).
6. E. Pelizetti, E. Mentasti et G. Saini. J. Chem. Soc. Dalton Trans. 721 (1974); E. Pelizetti, E. Mentasti et E. Pramauro. Gazz. Chim. Ital. **105**, 403 (1975).
7. Z. Amjad, J. G. Chambers et A. McAuley. Can. J. Chem. **55**, 3575 (1977).
8. R. Favier et M. Zador. Can. J. Chem. **48**, 2407 (1970).
9. P. M. Henry. J. Am. Chem. Soc. **88**, 1597 (1966); L. Nadon, M. Tardat, M. Zador et S. Fliszar. Can. J. Chem. **51**, 2366 (1973).
10. L. Nadon et M. Zador. Can. J. Chem. **55**, 3590 (1977).
11. A. Meenakshi, P. Maruthamuthu, K. V. Seshadri et M. Santappa. Indian J. Chem. **11**, 608 (1973).
12. T. Balakrishnan et M. Santappa. Int. J. Chem. Kinet. **10**, 883 (1978).
13. J. W. Lown. J. Chem. Soc. B, 664 (1966).

Can. J. Chem. Downloaded from www.nrcresearchpress.com by 210.87.254.40 on 09/05/12
For personal use only.

Magnitudes of ^{18}O isotope shifts in ^{13}C nuclear magnetic resonance spectra of ketones and alcohols

JAMES DIAKUR, THOMAS T. NAKASHIMA, AND JOHN C. VEDERAS[1]

Department of Chemistry, University of Alberta, Edmonton, Alta., Canada T6G 2G2

Received February 18, 1980

JAMES DIAKUR, THOMAS T. NAKASHIMA, and JOHN C. VEDERAS. Can. J. Chem. **58**, 1311 (1980).

The magnitudes of ^{18}O-induced isotope shifts in ^{13}C nmr spectra of ketones and aldehydes are dependent on structure and range from about 0.05 ppm to 0.03 ppm for the carbon attached to ^{18}O. An increase in negative charge density on the carbonyl oxygen or conjugation to an aromatic ring reduces the size of the upfield shift. The shifts in [^{18}O]alcohols are solvent-dependent, range from 0.03 ppm to 0.01 ppm, and tend to decrease in the order tertiary ≥ secondary ≥ primary ≥ phenols.

JAMES DIAKUR, THOMAS T. NAKASHIMA et JOHN C. VEDERAS. Can. J. Chem. **58**, 1311 (1980).

L'intensité des déplacements isotopiques induits par l'^{18}O dans les spectres rmn du ^{13}C des cétones et des aldéhydes dépend de la structure et se situe entre 0.05 et 0.03 ppm pour le carbone lié à l'^{18}O. Une augmentation de la densité de la charge négative de l'oxygène du carbonyle ou la conjugaison avec le noyau aromatique réduit l'ampleur du déplacement vers les champs forts. Les déplacements dans les alcools marqués à l'[^{18}O] dépendent du solvant et se situent entre 0.03 et 0.01 ppm et tendent à diminuer dans l'ordre tertiaire ≥ secondaire ≥ primaire ≥ phénols.

[Traduit par le journal]

Introduction

Isotopic substitution frequently causes a measurable change in the nmr chemical shifts of neighboring nuclei. Although the best-studied examples are the isotopic shifts induced by ^{2}H in ^{13}C nmr (1), a number of other systems are known, including ^{2}H and ^{13}C effects in ^{19}F nmr spectra (2), ^{13}C and ^{15}N in ^{59}Co nmr (3), ^{15}N in ^{1}H nmr and ^{13}C nmr (4), and ^{34}S in ^{13}C nmr (5). Oxygen-18 has been shown to produce such isotopic shifts in ^{55}Mn and ^{95}Mo nmr spectra (6) as well as the very useful effect in ^{31}P nmr (7). Recently we (8) and the research groups of Van Etten (9) and Darensbourg (10) independently confirmed theoretical predictions (11, 12) of ^{18}O-induced upfield shifts in ^{13}C nmr spectra.[2] The detection of such shifts using high field nmr permits direct observation of the position and extent of ^{18}O labeling in organic molecules. This methodology is especially useful with polyoxygenated substances where the usual mass spectrometric analysis (13) would require extensive degradations or preliminary specific labeling to ascertain the exact structures of the fragments. We recently applied the technique to a biosynthetic study of averufin, a precursor of aflatoxins (14).

The present study attempts to empirically explore some of the steric and electronic factors which determine the magnitude of the ^{18}O-induced isotope shifts in ^{13}C nmr in ketones and alcohols. Since changes in chemical shielding due to isotopic substitution are controlled by the dynamic state of the molecule (2, 12, 15), calculation of the magnitude of this effect requires exact knowledge of changes in molecular geometry and electron density. Nevertheless, general trends with predictive value are accessible by experimental methods. We have included some results from previous work (8) for comparison.

Experimental

^{13}C nmr Spectra

All ^{13}C nmr spectra were measured at 100.6 MHz on a Bruker WH 400 spectrometer in the Fourier Transform mode. In a typical experiment, 0.25 to 1.0 mmol of sample (30–50% ^{18}O, natural abundance ^{13}C) was dissolved in 2.5 mL of $CDCl_3$ containing tetramethylsilane, and the full proton-decoupled spectrum was obtained using a 10 mm probe. The normal conditions employed a 32K data block, 500 to 1000 scans, 25 000 Hz sweep width, 0.65 s acquisition time, and 45° pulse angle. Signals for carbons bearing oxygen were subsequently expanded using a 32K data block, 500 to 100 scans, 1000 Hz sweep width, 16.3 s acquisition time, and 45° pulse angle. A number of experiments were repeated at higher resolution to ensure reliable isotope shift values. Since all samples contained at least 50% unlabeled compound, the peaks due to carbons bearing ^{16}O provided an internal reference for measurement of the chemical shift change upon ^{18}O substitution.

Oxygen-18 Compounds

Unlabeled commercially-available ketones and aldehydes were purified as necessary by distillation or recrystallization prior to exchange with [^{18}O] water. The method of Radlick was used to prepare tropone (16). Dihydrodibenzo[*a*,*d*]cyclooctene-12(5*H*) one was synthesized according to Stewart and coworkers (17) from 2-(γ-phenylpropyl)benzoyl chloride. The latter compound was made by a modification of literature procedures (18); the keto group of the chalcone intermediate was reduced with sodium borohydride in methanol and the resulting lactone was hydrogenated with palladium on charcoal in acetic acid – ethanol to produce 2-(γ-phenylpropyl)benzoic acid.

[1]Author to whom correspondence should be addressed.

[2]Our initial measurements on pulegone were done by Drs. W. Conover and G. Sullivan in December 1977 using Stanford Magnetic Resonance Laboratory's HXS-360.

0008-4042/80/131311-05$01.00/0

©1980 National Research Council of Canada/Conseil national de recherches du Canada

Can. J. Chem. Downloaded from www.nrcresearchpress.com by 210.87.254.6 on 09/05/12
For personal use only.

Can. J. Chem. Downloaded from www.nrcresearchpress.com by 210.87.254.6 on 09/05/12
For personal use only.

The carbonyl compounds were labeled by reflux (3-96h) in a 1:1 mixture of [^{18}O]water[3] (30–60% isotopic purity) and dioxane or THF (19). Alcohols labeled with oxygen-18 were prepared by sodium borohydride reduction (4-fold excess, THF-methanol, 3h, 25°C) of the [^{18}O] carbonyl compounds. All purified products had chromatographic properties (vpc or tlc) identical with authentic unlabeled materials, and gave the expected spectra (ir, ^{1}H nmr, ^{13}C nmr, uv, and mass spectra). Isotopic content was mass spectrometrically determined for every sample on an AEI MS2 instrument.

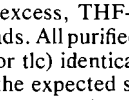
Results and Discussion

In a preliminary communication (8) we suggested that the magnitude of the isotope shift for carbonyl carbons attached to ^{18}O tends to decrease in the order: ketones ≥ aldehydes ≥ esters ≥ amides. Conjugation of the carbonyl to an aromatic system also appeared to decrease the shift size. The *para*-substituted acetophenones seemed suited for examination of electronic influences on isotope shift since their basicities had already been compared to carbonyl stretching frequencies and thermodynamic parameters (20). Hammett σ constants of *para*-substituents correlate well to ^{13}C and ^{15}N coupling constants and chemical shifts in several aromatic systems (21). Although carbonyl chemical shifts of *para*-substituted acetophenones (22) and benzaldehydes (23) do not show such a correlation with σ, the formyl proton chemical shifts of the benzaldehydes do. Mathias has suggested the *para*-substituent changes the electron density at the oxygen but not at the carbonyl carbon. The differences in isotope shift values for the acetophenones (Table 1) are too small to allow quantitative correlation with σ constants, but increasing electron donation by the *para* group coincides with decreasing isotope shift. This decrease in shift magnitude due to electron donation is illustrated by the two carbonyl groups of averufin (Fig. 1) (14). A shift of 4.17 Hz is observed in the 100.6 MHz ^{13}C nmr for C-10 of ^{18}O-labeled averufin; fluorenone and anthrone have similar shift sizes. However, the carbonyl at C-9 which has donation through the π system from the oxygens at C-1, C-3, C-6, and C-8 shows a shift of only 2.95 Hz, the smallest we have yet measured for a carbonyl group. As expected, this trend is not evident in the corresponding benzylic alcohols (Table 2) since the oxygen is not conjugated to the aromatic system. The low shift value of 1-(*p*-aminophenyl) ethanol may be due to hydrogen bonding or solvent effects.[4]

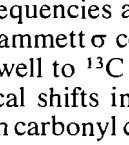
[3]The [^{18}O]water was generously donated by the Stable Isotopes Resource of Los Alamos National Laboratory, Los Alamos, NM, U.S.A.

[4]Although solvent has little effect on isotope shift magnitude in carbonyl groups, the effects on alcohols can be substantial (8); *vide infra*.

TABLE 1. Upfield shifts at 100.6 MHz of carbonyl carbons attached to ^{18}O[a]



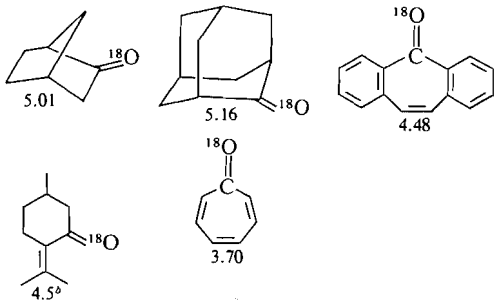
R^1	R^2	Shift in Hz
Cyclohexyl	CH_3	5.2[b]
Cyclohexyl	H	4.58
$CH_3(CH_2)_6$	H	4.8[b]
Phenyl	H	4.2[b]
Phenyl	Phenyl	4.6[b]
Phenyl	CH_3	4.70
p-OH-phenyl	CH_3	4.40
p-NH_2-phenyl	CH_3	4.45
p-OCH_3-phenyl	CH_3	4.58
p-CH_3-phenyl	CH_3	4.63
p-Cl-phenyl	CH_3	4.68
p-NO_2-phenyl	CH_3	4.78
m-CH_3-phenyl	CH_3	4.66
o-CH_3-phenyl	CH_3	4.76



n	Shift in Hz
3	4.94
4	5.11
5	5.22
6	5.12
7	5.22



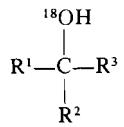
3*n*	Shift in Hz
0	4.10
1	4.12
2	4.82
3	4.42



[a]Spectra were run in $CDCl_3$; unless noted, shifts are ±0.06 Hz.
[b]Taken from ref. 8; shifts are ±0.1 Hz.

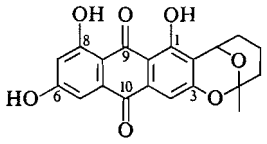
Comparison of the *ortho*, *meta*, and *para* methylacetophenones suggests some rotation of the carbonyl out of conjugation with the ring in the *ortho* isomer. Though complicated by other electronic factors, such steric inhibition of resonance can be observed in infrared (24), ultraviolet (25), and ^{13}C nmr spectra (22) of *ortho*-substituted acetophenones. Stewart and co-workers have shown that the *ortho–ortho* bridged diaryl ketones (Table 1) are useful for studying the effects of deconjugation on basicities and ultraviolet spectra

TABLE 2. Upfield shifts at 100.6 MHz of carbons attached to ^{18}O in alcohols[a]



R^1	R^2	R^3	Shift in Hz
CH_3	CH_3	CH_3	3.5[b]
Cyclohexyl	CH_3	CH_3	3.2[c]
	1-Methylcyclohexanol		3.12
			3.32[d]
			2.90[e]
Cyclohexyl	CH_3	H	2.6[c]
			2.80[d]
			Broad[e]
Phenyl	CH_3	H	2.28
			2.1[c,f]
			2.0[c,g]
			Broad[c,d]
p-NH_2-phenyl	CH_3	H	1.84[h]
p-OH-phenyl	CH_3	H	2.15[h]
p-OCH_3-phenyl	CH_3	H	2.16
p-CH_3-phenyl	CH_3	H	2.10
p-Cl-phenyl	CH_3	H	2.18
p-NO_2-phenyl	CH_3	H	2.15
Phenyl	Phenyl	H	2.0[c]
	Cyclooctanol		2.90
	Cycloheptanol		2.60
	Cyclohexanol		2.20
	Cyclopentanol		2.65
	Cyclobutanol		2.00
$CH_3(CH_2)_6$	H	H	2.1[c]
			1.90[d]
			Broad[e]
Phenyl	H	H	1.9[c]

[a]Unless noted, spectra are in $CDCl_3$ and shifts are ±0.06 Hz.
[b]Calculated from ref. 9.
[c]Taken from ref. 8; shifts are ±0.1 Hz.
[d]Methanol-d_4.
[e]*tert*-Butanol-d_{10}.
[f]Benzene-d_6.
[g]Pyridine-d_5.
[h]DMSO-d_6.



C-1: 1.13 Hz C-9: 2.95 Hz
C-6: 1.13 Hz C-10: 4.17 Hz
C-8: 1.05 Hz

FIG. 1. ^{18}O isotope shifts of carbonyl and hydroxyl carbons in 100.6 MHz ^{13}C nmr spectra of averufin.

(17). Kazakova *et al.* (26) have also investigated their reduction potentials and the esr spectra of their anion radicals as a function of ring size.[5] As the number of methylene groups in the bridge increases, at least one of the aromatic rings is forced out of conjugation with the carbonyl and the solution basicity decreases. Since isotope shift is dependent on molecular dynamics,[6] in particular anharmonic vibration and rotation (12, 15), it is not surprising that its correspondence to ultraviolet spectra, basicities, or reduction potentials is poor. The general trend, however, is a decrease in the magnitude of the isotope shift due to conjugation. Not only do saturated ketones display larger shifts than unsaturated ketones, but the planar fluorenone and nearly planar anthrone have similarly small shifts despite very different electronic properties. Benzophenone is less planar than anthrone (17) and shows a larger isotope shift as do the other bridged diaryl ketones. The reason for the

[5]The esr spectrum of the radical derived from 10,11-dihydro-5*H*-dibenzo[*a*,*d*]cyclohepten-5-one indicates a carbonyl–phenyl angle of 18–26° (27).

[6]The conformational behavior of 6,7-dihydro-5*H*-dibenzo-[*a*,*d*]cycloocten-12-one has been examined by nmr; see experimental part of ref. 28.

Can. J. Chem. Downloaded from www.nrcresearchpress.com by 210.87.254.6 on 09/05/12
For personal use only.

Can. J. Chem. Downloaded from www.nrcresearchpress.com by 210.87.254.6 on 09/05/12
For personal use only.

relative shift sizes of 10,11-dihydro-5*H*-dibenzo[*a*,*d*]cyclohepten-5-one ($n = 2$) and 6,7-dihydro-5*H*-dibenzo[*a*,*d*]cycloocten-12-one ($n = 3$) remains unestablished. Molecular models suggest that the preferred conformation of the latter compound may have one of the aromatic rings in conjugation with the carbonyl whereas that of the former does not, but this view is not supported by the studies described above (17,26). As expected, the highly basic planar tropone (29) has a much smaller shift than its folded derivative (30), 5*H*-dibenzo[*a*,*d*]cyclohepten-5-one.

Ring size effects were tested in the cyclic aliphatic ketone series since their ^{13}C nmr chemical shifts (31), ionization potentials (32), vibrational–rotational spectra, and geometries (33) had already been examined. The ^{18}O-induced isotope shifts in this group are very similar, although a slight decrease can be observed for cyclobutanone. Interestingly, the relative shift magnitudes vary considerably in the corresponding cyclic alcohols. This may be due to relative degrees of freedom and to changes in hybridization of the carbon–oxygen bond. Based on analogy with hydrocarbons (34), as the internal bond angle decreases, the carbon–carbon bonds acquire more *p* character while the carbon–oxygen bonds assume more *s* character. An increase in *s* character of a single bond holding an isotope is predicted to produce a decrease in nmr isotope shift (2, 15), and cyclobutanol does indeed show the smallest shift of the cyclic alcohols.[7] Conformational effects probably contribute to the irregular variation observed in this series.

In contrast to carbonyl compounds, alcohols show considerable solvent influence on ^{18}O isotope shift magnitude. Hydroxylic solvents such as D_2O, methanol-d_4, or *tert*-butanol-d_{10} frequently (but not always) broaden the signals for the ^{18}O-labeled and unlabeled species to a single peak encompassing the whole region. So far this phenomenon has not appeared with labeled tertiary alcohols, suggesting that the existence of multiple hydrogen-bonded forms in solution may be responsible for the effect. The magnitude of the shift decreases in the order: tertiary alcohols $\geq$ secondary alcohols $\geq$ primary alcohols $\geq$ phenols. Although the only phenols examined have been the hydroxyl groups of averufin (Fig. 1), we expect further work will show this order to be generally valid. It is interesting to note that as the number of alkyl groups on the carbon bearing the hydroxyl increases, the hardness of the oxygen as a base increases and the ionization potential decreases (36). Currently it is not possible to separate the through-bond electronic influences from steric bulk effects on isotope shift.

The present work establishes that the ^{18}O isotope shift is generally observable in high field (100.6 MHz) ^{13}C nmr, and that its magnitude depends on structure. These shifts on the carbons attached to oxygen in ketones and aldehydes range from approximately 0.05 ppm to 0.03 ppm, whereas those of alcohols span about 0.03 ppm to 0.01 ppm. Donation of negative charge to the labeled carbonyl oxygen or conjugation to an aromatic ring decreases the size of the effect. Saturated alcohols exhibit a substantial trend for an increasing isotope shift as the substitution at the carbinol carbon increases. Although the solvent has little influence on shift magnitude in ^{18}O carbonyls, this is not true for alcohols, presumably because of hydrogen bonding. In our preliminary communication (8) we also detected shifts at carbons β to the site of isotopic substitution in two esters, but those ketones and alcohols which were examined showed at best slight broadening due to the presence of both ^{18}O and ^{16}O species. Possibly spectrometers operating at even higher field may be able to resolve these signals.

[7]The geometry of cyclobutanol has been studied by microwave spectroscopy (35).

Acknowledgements

We gratefully acknowledge financial support from the Natural Sciences and Engineering Research Council of Canada, and generous gifts of [^{18}O]water from the Stable Isotopes Resource of Los Alamos National Laboratory. We thank Professor R. S. Brown for stimulating discussions.

1. J. B. STOTHERS. Top. Carbon 13 NMR Spectrosc. **1**, 299 (1974); S. C. HO, H. J. KOCH, and R. S. STUART. Carbohydr. Res. **64**, 251 (1978); P. E. PFEFFER, K. M. VALENTINE, and F. W. PARRISH. J. Am. Chem. Soc. **101**, 1265 (1979); M. J. SHAPIRO and A. D. KAHLE. Org. Magn. Reson. **12**, 235 (1979); R. A. NEWMARK and J. R. HILL. J. Magn. Reson **21**, 1 (1976); J. J. Led and S. B. Petersen. J. Magn. Reson. **33**, 603 (1979).
2. H. BATIZ-HERNANDEZ and R. A. BERNHEIM. Progr. Nucl. Magn. Reson. Spectrosc. **3**, 63 (1967).
3. P. C. LAUTERBUR. J. Chem. Phys. **42**, 799 (1965); A. LOWENSTEIN and M. SHPORER. Mol. Phys. **9**, 293 (1965).
4. L. N. KURKOVSKAYA. Zh. Strukt. Khim. **19**, 946 (1978); Chem. Abstr. **90**, 120552 (1979).
5. S. A. LINDE and H. J. JAKOBSEN. J. Magn. Reson. **17**, 411 (1975).
6. K. U. BUCKLER, A. R. HAASE, O. LUTZ, M. MULLER, and A. NOLLE. Z. Naturforsch. Teil A, **32**, 126 (1977).
7. M. COHN and A. HU. Proc. Natl. Acad. Sci. U.S.A. **75**, 200 (1978); R. L. VAN ETTEN and J. M. RISLEY. Proc. Natl. Acad. Sci. U.S.A. **75**, 4784 (1978); D. R. WEBB, G. G. MCDONALD, and D. R. TRENTHAM. J. Biol. Chem. **253**, 2908 (1978); J. BOCK and M. COHN. J. Biol. Chem. **253**, 4082

(1978); R. L. JARVEST and G. LOWE. J. Chem. Soc. Chem. Commun. 364 (1979); M. COHN and B. D. NAGESWARA RAO. Bull. Magn. Reson. 38 (1979).
8. J. C. VEDERAS. J. Am. Chem. Soc. **102**, 374 (1980).
9. J. M. RISLEY and R. L. VAN ETTEN. J. Am. Chem. Soc. **101**, 252 (1979).
10. D. J. DARENSBOURG. J. Organomet. Chem. **174**, C70 (1979); D. J. DARENSBOURG and B. J. BALDWIN. J. Am. Chem. Soc. **101**, 6447 (1979).
11. W. T. RAYNES and G. STANNEY. J. Magn. Reson. **14**, 378 (1974).
12. C. J. JAMESON. J. Chem. Phys. **66**, 4983 (1977).
13. E. R. KLEIN and P. D. KLEIN. Biomed. Mass Spectrom. **5**, 425 (1978).
14. J. C. VEDERAS and T. T. NAKASHIMA. J. Chem. Soc. Chem. Commun. 183 (1980).
15. R. A. BERNHEIM and H. BATIZ-HERNANDEZ. J. Chem. Phys. **45**, 2261 (1966).
16. P. RADLICK. J. Org. Chem. **29**, 960 (1964).
17. R. STEWART, M. R. GRANGER, R. B. MOODIE, and L. J. MUENSTER. Can. J. Chem. **41**, 1065 (1963).
18. C. D. GUTSCHE, E. F. JASON, R. S. COFFEY, and H. E. JOHNSON. J. Am. Chem. Soc. **80**, 5756 (1958).
19. D. SAMUEL and B. L. SILVER. Adv. Phys. Org. Chem. **3**, 123 (1965); M. BYRN and M. CALVIN. J. Am. Chem. Soc. **88**, 1916 (1966).
20. E. M. ARNETT, R. P. QUIRK, and J. W. LARSEN. J. Am. Chem. Soc. **92**, 3977 (1970).
21. C. H. YODER, R. H. TUCK, and R. E. HESS. J. Am. Chem. Soc. **91**, 539 (1969); T. AXENROD, M. J. WIEDNER, T. KHIN, G. A. WEBB, H. J. C. YEH, and S. BULUSU. Org. Magn. Reson. **12**, 1 (1979).
22. K. S. DHAMI and J. B. STOTHERS. Can. J. Chem. **43**, 479 (1965).
23. A. MATHIAS. Tetrahedron, **22**, 217 (1966).
24. H. H. FREEDMAN. J. Am. Chem. Soc. **82**, 2454 (1960).
25. G. D. HEDDEN and W. G. BROWN. J. Am. Chem. Soc. **75**, 3744 (1953).
26. V. M. KAZAKOVA, I. G. MAKAROV, A. I. SAMOKHVALOVA, and D. V. IOFFE. J. Struct. Chem. USSR (Engl. Ed.), **15**, 209 (1974).
27. S. KAZAMA, M. KAMIYA, Y. AKAHORI, and T. MASUDA. Yakugaku Zasshi, **98**, 242 (1978); Chem. Abstr. **88**, 189905e (1978).
28. F. E. ELHADI, W. D. OLLIS, and J. F. STODDART. J. Chem. Soc. Perkin Trans. I, 1415 (1978).
29. C. L. NORRIS, R. C. BENSON, P. BEAK, and W. H. FLYGARE. J. Am. Chem. Soc. **95**, 2766 (1973); A. SABLJIC and N. TRINAJSTIC. Croat. Chem. Acta, **51**, 249 (1978).
30. H. SHIMANOUCHI, T. HATA, and Y. SASADA. Tetrahedron Lett. 3573 (1968); M. ALLAN, E. HEILBRONNER, and E. KLOSTER-JENSEN. J. Electron Spectrosc. Relat. Phenom. **6**, 181 (1975); H. GUSTEN, L. KLASIN, T. TOTH, and J. V. KNOP. J. Electron Spectrosc. Relat. Phenom. **8**, 417 (1976).
31. J. B. STOTHERS and P. C. LAUTERBUR. Can. J. Chem. **42**, 1563 (1964).
32. D. CHADWICK, D. C. FROST, and L. WEILER. Tetrahedron Lett. 4543 (1971).
33. L. H. SCHARPEN and V. W. LAURIE. J. Chem. Phys. **49**, 221 (1968); H. J. GEISE and F. C. MIJHOFF. Recl. Trav. Chim. **90**, 577 (1971); Y. OHNISHI and K. KOZIMA. Bull. Chem. Soc. Jpn. **41**, 1323 (1968); D. F. BOCIAN and H. L. STRAUSS. J. Chem. Phys. **67**, 1071 (1977); T. C. ROUNDS and H. L. STRAUSS. J. Chem. Phys. **69**, 268 (1978).
34. R. A. ALDEN, J. KRAUT, and T. G. TRAYLOR. J. Am. Chem. Soc. **90**, 74 (1968).
35. J. N. MACDONALD, D. NORBURY, and J. SHERIDAN. Spectrochim. Acta Part A, **34**, 815 (1978).
36. I. A. BLAIR, J. H. BOWIE, and V. C. TRENERRY. J. Chem. Soc. Chem. Commun. 230 (1970).

Can. J. Chem. Downloaded from www.nrcresearchpress.com by 210.87.254.6 on 09/05/12
For personal use only.

1,2-Diphenyl-3,5-dimethyl-4-oxo-6,7-diazabicyclo[3.2.0]hept-2-ene, a nitrogen unsubstituted diazetidine with an unusually unreactive nitrogen

DEANE D. MCINTYRE, DONALD MACKAY, AND LICHIN L. WONG[1]

Guelph–Waterloo Centre for Graduate Work in Chemistry, Waterloo Campus, Department of Chemistry, University of Waterloo, Waterloo, Ont., Canada N2L 3G1

Received December 28, 1979

DEANE D. MCINTYRE, DONALD MACKAY, and LICHIN L. WONG. Can. J. Chem. **58**, 1316 (1980).

In the title ring system, the benzylic nitrogen (N_7), whether substituted or not, is abnormally unreactive. Hydrolysis of the di-urethanes **3***a* or *b* occurs readily at N_6 to give **10***a* or *b*, but not at all at N_7. In **3***d* Pd—H_2 removes very rapidly the benzyloxycarbonyl group at N_6 but only very slowly the one at N_7. The product **7** is the first example of a diazetidine unsubstituted on nitrogen which has been fully characterized.

N_6 in **7** or in **10***a* or *b* can be readily acylated (products **24**, **13**, **14**), acyloxylated (**23***a–c*, **3***a*, **3***b*, **11**, **12**), or methylated (**25**). All efforts to induce similar reactions at N_7 in **7** or in its monosubstituted derivatives **23** or **24** failed.

Diazetidine **7** is thermally very stable, but it is rapidly oxidized by a wide variety of reagents to 2,5-diphenyl-3,4-dimethylcyclopentadienone and nitrogen. There is no evidence for the intermediacy of the cyclic azo compound **19**, even when the oxidation is carried out at −50°C.

DEANE D. MCINTYRE, DONALD MACKAY et LICHIN L. WONG. Can. J. Chem. **58**, 1316 (1980).

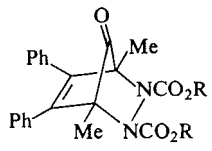
Dans le système cyclique mentionné dans le titre, l'azote benzylique (N_7) qu'il soit substitué ou non est anormalement peu réactif. L'hydrolyse des di-uréthanes **3***a* ou *b* se produit facilement au niveau de l'azote N_6 pour conduire à **10***a* ou *b*, mais pas du tout au niveau N_7. L'hydrogénation en présence de palladium du composé **3***d* enlève rapidement le groupe benzyloxycarbonyle en N_6 mais n'enlève que très lentement celui en N_7. Le produit **7** est le premier exemple d'une diazétidine non substituée sur l'azote qui soit entièrement caractérisée.

L'azote en position 6 du composé **7** ou des composés **10***a* ou *b* peut facilement subir une réaction d'acylation (produits **24**, **13**, **14**), d'acyloxylation (**23***a–c*, **3***a*, **3***b*, **11**, **12**) ou de méthylation (**25**). Tous les efforts en vue d'induire des réactions semblables sur l'azote en position 7 ou dans ses dérivés monosubstitués **23** ou **24** ont échoué. La diazétidine **7** est très stable thermiquement, mais elle est rapidement oxydée par un très grand nombre de réactifs en diphényl-2,5 diméthyl-3,4 cyclopentadiénone et en azote. Il n'y a pas de preuve de l'existence du composé azocyclique intermédiaire (**19**) même quand l'oxydation est réalisée à −50°C.

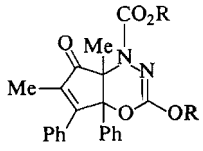
[Traduit par le journal]

We have previously shown that the cyclone 2,5-dimethyl-3,4-diphenylcyclopentadienone reacted with azo esters to give the bridged adducts **1**, which isomerized readily and reversibly to the 1,3,4-oxadiazines **2**, and more slowly but quantitatively to the 1,2-diazetidines **3** (1). The four-membered ring system is thus thermodynamically the most stable of the three isomers.

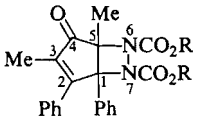
A quite different behaviour was observed when the cyclone reacted with azodiacyls. With azodibenzoyl, *p,p'*-dinitroazodibenzoyl (1), or azodiacetyl only the oxadiazines **5***a–c* were isolated, the yields being quantitative. If the reaction was monitored by ^{1}Hmr spectroscopy at 35°C, a slow process due to the low concentration of the cyclone monomer, the methyl singlets of the intermediates **4** were detectable to a maximum concentration of about 13% in the case of **4***a* in carbon tetrachloride, and 10% in the case of **4***b* in benzene. The oxadiazines were thermally very stable, **5***a* being unaffected when heated up to 170°C. Above 200°C complete decomposition occurred, there being no evidence of the diazetidines.



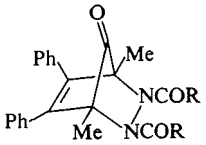
1



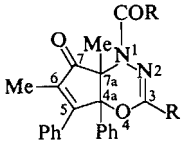
2



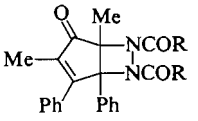
3



4



5



6

1–3, *a*, R = Me; *b*, R = Et; *c*, R = CH_2CCl_3; *d*, R = CH_2Ph
4–6, *a*, R = Me; *b*, R = Ph; *c*, R = $C_6H_4NO_2$-*p*

The equilibrium between **4** and **5** is obviously strongly towards the latter. A question of interest to us was whether the failure to observe the formation

[1]MDS Health Group, Rexdale, Ont., Canada M9W 4Z9.

0008-4042/80/131316-08$01.00/0

©1980 National Research Council of Canada/Conseil national de recherches du Canada

Can. J. Chem. Downloaded from www.nrcresearchpress.com by 210.87.254.5 on 09/05/12
For personal use only.

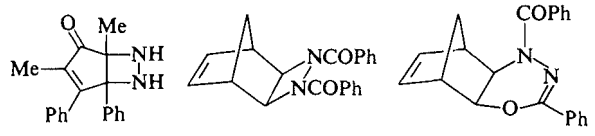
Can. J. Chem. Downloaded from www.nrcresearchpress.com by 210.87.254.5 on 09/05/12
For personal use only.

of **6** was due to a relative thermal instability of **6** (by contrast with **3**), or to the existence of too high a barrier to **6** from either of the isomers **4** or **5**.

An answer to this could be provided by an independent synthesis of a diazetidine such as **6**, to which one logical precursor would be the parent diazetidine **7**.

We report here on several synthetic approaches to the diacyldiazetidine containing ring system **6**. We also describe an efficient synthesis of the cyclic hydrazine **7**, the first example of a diazetidine unsubstituted on nitrogen which has been fully characterized.

That a 1,2-diacyldiazetidine is capable of independent existence was established in a recent report of the formation of **8** from azodibenzoyl and quadricyclane (2). Its structure was inferred from its ir peak at 1680 cm^{-1} and the symmetry in its ^{1}Hmr spectrum. To check the possibility that the oxadiazine **9** might account for these spectra, with fortuitous shift equivalence of stereochemically unrelated protons, the synthesis was repeated.[2] The uv spectrum of the product with a broad shoulder centred around 275 nm rigorously excluded structure **9** in which a strong band at 290–300 nm would be required (7). The ^{13}Cmr spectrum also confirmed the equivalence of all the expected carbons in **8**.

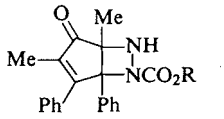


7 **8** **9**

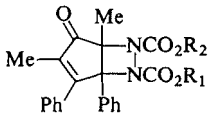
A notable feature in the ^{1}Hmr spectra of the series of urethanes **3***a–c* was the extraordinary shielding and broadening effects observed for the protons next to the acyloxy oxygen at the benzylic nitrogen (N_7).[3,4] We have attributed this (1) to the closeness of these groups to the face of the benzene ring at C_2. In the crystal of the *p,p'*-dibromo derivative of **3***a* the methyl carbon is, at the nearest point, less than 3.5 Å above the plane of the benzene ring (8); the methyl protons must rotate within 1 Å closer, thus accounting for the shielding effect. It is also evident that the ester group is somewhat embedded in a cavity created by the two benzene rings and the other ester group. As the present work will show, the protection afforded the environment round N_7 leads to greatly diminished reactivity at it or its substituents.[5]

An example of this effect already described is the alkaline hydrolysis of **3***a* and *b* which occurred easily at N_6 to give the basic esters **10***a* and *b*, but not at all at N_7 (9). Under more vigorous conditions the diazetidine ring was destroyed, giving the cyclone (with acid quite different reactions were observed both with **3***a* (10) and with **10***a* (9)).

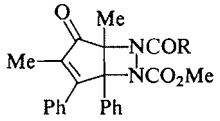
The NH group in **10***a* and *b* was normal in every way. Methyl chloroformate in pyridine regenerated **3***a* from **10***a*. The mixed isomeric diazetidines **11** and **12** were made by respective treatment of **10***a* and **10***b* with ethyl and methyl chloroformate. The ester methyl group in **11** and the methylene group in **12** showed the expected anomaly in the ^{1}Hmr spectrum.



10*a*, R = Me
b, R = Et
c, R = CH_2Ph



11, R_1 = Me, R_2 = Et
12, R_1 = Et, R_2 = Me



13, R = Me
14, R = Ph

Treatment of **10***a* with acetyl or benzoyl chloride gave **13** or **14**. These appeared to be potential precursors to a diacyldiazetidine like **6**, by a sequence of preferential urethane hydrolysis followed by acylation. In the event the urethane group was again the more resistant to hydrolysis, 1 *N* KOH in methanol giving an almost quantitative yield of **10***a* from **14**.

A compound like **13** or **14** is one of two possible isomeric diazetidines which could be formed in principle as thermal end products of the reaction of the cyclone with an acylazo ester. In view, how-

[2]Cases are known in which originally proposed 1,2-diacyl-1,2-diazetidine structures have been revised to 1,3,4-oxadiazines (3–5). The adduct of furan and azodibenzoyl has been assigned a diazetidine structure (6), but this is incorrect: we have shown (unpublished work) it to be an oxadiazine.

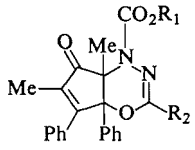
[3]In **3***a* the methyl group was shielded (ca. 0.9 ppm from the other methyl group) and slightly broadened. In each of **3***b* and *c* one of the methylene protons was normal and the other was shielded (Δδ0.9 and 2.2 ppm, respectively) and broadened.

[4]The Chemical Abstracts numbering system is used (see structure **3**). Earlier papers used a different system (1, 9). The numbering system for the 1,3,4-oxadiazines described here, **5** and **15–17**, is also amended (see structure **5**).

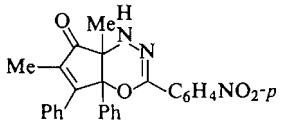
[5]Since the ring system is very stable these proximity effects cannot be destabilizing to the molecule. N_7 is not so much crowded as inaccessible.

Can. J. Chem. Downloaded from www.nrcresearchpress.com by 210.87.254.5 on 09/05/12
For personal use only.

ever, of the exclusive formation of oxadiazines **5***a–c* from azodiacyls the result when the cyclone was heated with methyl benzoylazocarboxylate or ethyl *p*-nitrobenzoylazocarboxylate was entirely predictable. Only **15** or **16** was isolated, the mode of regioisomeric fusion being confirmed for the latter. Its uv absorption at 338 nm, like that of **5***c* at 335 nm, is diagnostic of the *p*-$NO_2C_6H_4\overset{|}{C}{=}N$ chromophore (7). Hydrolysis with 1*N* alkali gave the base **17** which was converted into **5***c* with *p*-nitrobenzoyl chloride in pyridine.

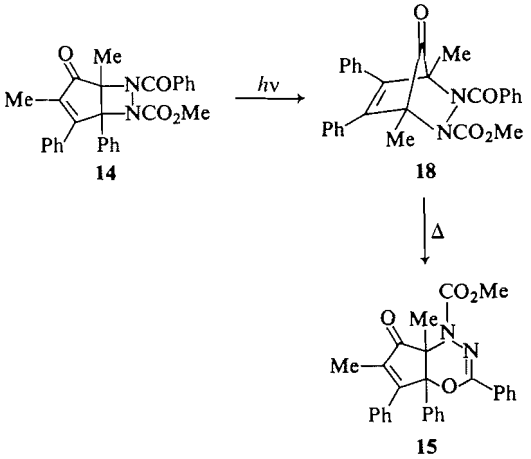


15, R_1 = Me, R_2 = Ph
16, R_1 = Et, R_2 = $C_6H_4NO_2$-*p*



17

The oxadiazine **15** could also be prepared by photolysis of the diazetidine **14** in benzene at 10°C, conditions known to convert **3** into the bridged adduct **1** (1). The bridged adduct **18** was in fact observable by ^{1}Hmr spectroscopy. After 1 h the solution contained about 30% **18**, 50% **15**, and 20% starting material; after 3.5 h the yield of **15** was quantitative. At no stage was there any indication of the presence of the regioisomer of either **15** or **14**. Presumably the only processes involved are the photoisomerization of **14** to **18**, followed by the thermal isomerization of the very labile **18** to **15** (Scheme 1).



SCHEME 1

Another potential route to **7**, and thence to **6**, might be by reductive cleavage of the trichloroethyl groups in **3***c*. This technique usually employs an acidic medium (Zn dust, acetic acid) (11), and since compounds **3** were unstable to acid (10) we elected instead to make the dibenzyl ester **3***d*, on which hydrogenolysis could be carried out under neutral conditions.

Good yields of **3***d* were obtained directly by refluxing the cyclone with dibenzyl azodicarboxylate in bromobenzene. It showed the expected ^{1}Hmr features in its methylene protons ($CDCl_3$), a normal position for the AB quartet of the N_6 ester group (5.23δ), and for the A doublet of the N_7 ester (4.99δ), but a broadened shielded X doublet (3.79δ) for the other proton.

Treatment of **3***d* with hydrogen over Pd–charcoal caused the rapid removal of the group at N_6, followed by the much slower (about 50-fold) removal of the group at N_7. The intermediate **10***c* was readily identified in the spectrum of the semihydrogenated material, by its methylene AX quartet (5.03, 3.81δ), but no effort was made to isolate it. Hydrogenolysis was complete in 16–20 h, furnishing the free 1,2-diazetidine **7**. The crude hydrazine could be purified by allowing a solution of it in ethyl acetate – hexane to evaporate slowly under nitrogen giving faintly yellow-green crystals, which decomposed between 110 and 115°C without a well defined mp. Its identity as **7** followed from its mass spectrum (M^+ = 290 and 292 for the normal and deuterated compound), its (weak) NH and single C=O absorption in the ir spectrum, the enone chromophore at 280 nm (1) and its ^{1}H and ^{13}Cmr spectra.

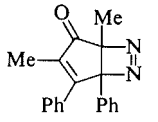
Earlier examples of 1,2-unsubstituted diazetidines have been prepared as precursors to cyclic azo compounds, and have either been oxidized without isolation (12), or isolated but not further characterized due to their instability (13). There have been passing references to 3,3,4,4-tetrafluorodiazetidine, but without any details regarding its properties (14).

Though impure **7** decomposed rather rapidly to the cyclone, purified samples kept well at room temperature. In the absence of oxidizing agents it is in fact a remarkably stable substance, having a half-life of 2.5 days in refluxing benzene, the cyclone being the only non-volatile product formed. Whether di-imide is also produced is not certain, since thermolysis in the presence of cyclohexene gave no detectable amounts of cyclohexane.

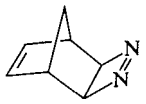
Oxidation of **7** to the cyclone occurred with great ease with a range of reagents: mercuric oxide in ether, ethereal hydrogen peroxide, and cupric chloride in buffered acid were used at room temperature. In an attempt to detect or intercept the intermediate diazetine **19** homogeneous oxidations were followed by low temperature ^{1}Hmr spectroscopy in $CDCl_3$. Benzoyl peroxide, diethyl

Can. J. Chem. Downloaded from www.nrcresearchpress.com by 210.87.254.5 on 09/05/12
For personal use only.

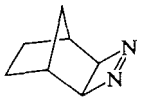
azodicarboxylate, and *p*-benzoquinone all smoothly oxidized **7**, but even at −50°C the only new peaks observed were those of the monomer and dimer of the cyclone.



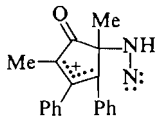
19



20



21



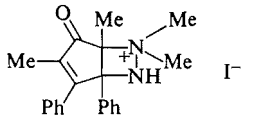
22

If oxidation does proceed through **19** its decomposition even at −50°C must be very rapid. This is in vivid contrast with the stability of the diazetines **20** and **21** whose half-lives are of the order of 10^5 and 10^6 days respectively at room temperature (12). Most of this stabilization has been attributed to the forbiddenness of the reaction (a retro 2+2 cycloaddition). Major differences here are the creation of a resonance stabilized (enone) group and the unsymmetrical nature of **7**. The latter may permit a polar, non-concerted, and low energy pathway for loss of nitrogen. For example, removal of hydride in a first oxidation step could produce the allylically stabilized nitrene **22**. In that case **19** would not be an intermediate at all.

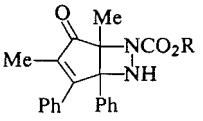
All other reactions of **7** support completely the view that it has a normal, reactive N atom and a very unreactive one.

A range of acyloxy and acyl groups could be introduced on N_6 using the appropriate chloride and pyridine. The methyl and ethyl esters **23***a* and *b* are the regioisomers of the hydrolysis products **10***a* and *b*. The benzyl ester **23***c* was prepared and hydrogenolyzed back to **7**, confirming the preservation of the diazetidine ring in the acylation reactions. The acetyl derivative **24**, along with **13** and **14**, shows that the diazetidine system is stable with at least one acyl group on nitrogen.

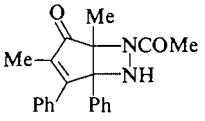
Even the use of an excess of methyl chloroformate in pyridine at room temperature or at 100°C failed to convert **23***a* into **3***a*. Similarly attempts to acetylate **24** to **6***a* were abortive. The reactions were monitored by ^{1}Hmr spectroscopy, with no evidence of any methyl peaks other than those due to **23***a* (an anomalous shift was of course expected for the N_7 acetyl group in **6***a*). Bases used without success were triethylamine, 1,5-diazabicyclo-[3.4.0] non-5-ene, potassium carbonate, sodium hydride, lithium di-isopropylamide, and *n*- and *tert*-butyllithium. Decomposition of the substrate occurred, especially with the inorganic bases. Phthaloyl chloride gave a complex reaction with **7**, but certainly none of the desired cyclic hydrazide derivative.



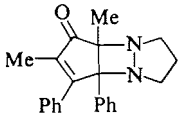
25



23*a*, R = Me
b, R = Et
c, R = CH_2Ph



24



26

Reaction of **7** with methyl iodide and potassium carbonate gave a dimethylation product, the stable quaternary iodide **25**, but no *N*,*N*′-dimethyl derivative. The use of 1,3-ditosyloxypropane led to recovery of **7**, and 1,3-dibromo and di-iodopropane caused oxidation to the cyclone; there was no evidence for the formation of compound **26**. Triethyloxonium fluoborate likewise gave the cyclone from **7**. Attempts to methylate the amide **24** with methyl iodide in the presence of either potassium carbonate or diazabicyclononene were also unsuccessful.

We have thus failed to replace the hydrogen on N_7 in any of the diazetidines **7**, **23**, or **24** with any substituent, other than deuterium in the case of **7**. In the failure specifically to replace it with an acyl group our original question of whether such a diazetidine is inherently unstable with respect to the isomeric oxadiazine is still unanswered.

Experimental

The following spectrometers were used: for ir, a Beckman IR10; for uv, a Unicam SP.800B; for ^{1}Hmr, a Varian T-60 or Perkin-Elmer R12B; for ^{13}Cmr, a Bruker WP-80; for ms, a Varian MAT CH-7. Melting points are uncorrected.

Ultraviolet and ^{13}Cmr Spectra of 3,4-Dibenzoyl-3,4-diazatricyclo[4.2.1.0^{2,5}]non-7-ene (8)

Compound **8** was prepared from quadricyclane and azodibenzoyl as described by Landis and Mitchell (2). It had: λ_{max}(EtOH) sh 275 nm (−NCOPh) (ε 6000); δ(^{13}C)($CDCl_3$): 40.6, 45.2 (C_1,C_6 or C_2,C_5), 67.1 (C_9), 128.5, 128.9, 132.2, 132.6 (Ph), 136.0 (C_7,C_8), 178.8 (C=O) ppm.

cis-*1-Acetyl-3,6,7a-trimethyl-4a,5-diphenyl-7-oxo-1,4a,7,7a-tetrahydrocyclopent[e][1,3,4]-oxadiazine (5a)*

The cyclone (1.30 g, 5 mmol) was refluxed for 12 h in a freshly prepared solution of azodiacetyl (7) (5.7 mmol) in tetrachloro-

Can. J. Chem. Downloaded from www.nrcresearchpress.com by 210.87.254.5 on 09/05/12
For personal use only.

ethylene (20 mL). The solvent was evaporated and the residue crystallized on addition of pentane. Filtration gave **5***a* (94%) which was twice crystallized from cyclohexane as prisms, mp 168–169°C; ν(CCl_4): 1736 (keto C=O), 1690 (amide C=O), 1677 (C=N) cm^{-1}; λ_{max}(EtOH): 242 (ε 15 600) (MeC=N), 283 (ε 12 600) (β-enone) nm; δ(CCl_4–$CDCl_3$): 7.5–6.9 (10H, Ph, m), 2.13 (6H, COMe and C_3—Me, fortuitous s), 1.77 (3H, C_6—Me, s), 0.97 (3H, C_{7a}—Me, s) ppm. *Anal.* calcd. for $C_{23}H_{22}N_2O_3$: C 73.78, H 5.92, N 7.48; found: C 73.55, H 5.90, N 7.69.

The reaction was also monitored by ^{1}Hmr spectroscopy in carbon tetrachloride at 35°C. After 90 h the methyl singlet due to the intermediate **4***a* accounted for about 13% of the total methyl absorption. Compound **4***a* had δ 2.22 (6H, OMe, s), 2.01 (6H, C—Me, s) ppm.

Samples of **5***a* (30 mg) were heated for 4 h in an evacuated sealed tube (*a*) *at 170°C*: the slightly discolored product was completely unreacted **5***a*; (*b*) *at 210°C*: the ^{1}Hmr spectrum of the black tarry product showed that profound degradation had occurred.

1,2-Diphenyl-3,5-dimethyl-6-ethoxycarbonyl-7-methoxycarbonyl-4-oxo-6,7-diazabicyclo[3.2.0]hept-2-ene (11)

The basic ester **10***a* (100 mg, 0.29 mmol) was kept at room temperature for 3 days in pyridine (1 mL) containing ethyl chloroformate (50 mg, 0.46 mmol). The solution was blown to dryness, and water was added giving the colorless diester (87 mg, 71%) (see Table 1 for further details).

6-Methoxycarbonyl-7-ethoxycarbonyl Compound 12 (Isomer of 11)

The basic ester **10***b* (157 mg, 0.43 mmol) and methyl chloroformate (200 mg, 2.1 mmol) in pyridine (1.5 mL) reacted to the extent of about 50% after 3 days at room temperature (work-up as for **11**). The half reacted material was treated with fresh chloroformate (2 mmol) in pyridine (2 mL) and left for 7 more days. Work-up gave the diester (148 mg, 80%) (Table 1).

1,2-Diphenyl-3,5-dimethyl-6-acyl-7-methoxycarbonyl-4-oxo-6,7-diazabicyclo[3.2.0]hept-2-ene (Table 1)

The 6-Acetyl Compound 13

Acetic anhydride (95 μL, 0.95 mmol) and **10***a* (9) (300 mg, 0.86 mmol) were refluxed for 1 h in pyridine (3 mL). Evaporation and addition of water gave crystalline **13** (294 mg, 88%).

The 6-Benzoyl Compound 14

A solution of benzoyl chloride (50 mg, 0.36 mmol) and **10***a* (116 mg, 0.33 mmol) in pyridine (2.5 mL) was kept at room temperature for 2 days. It was then worked up as for **13** giving a 90% yield of **14**.

Hydrolysis of 14

A solution of **14** (200 mg, 0.39 mmol) was dissolved in 1*N* potassium hydroxide in methanol (10 mL), kept for 12 h, and extracted with an ether–water mixture. The ether layer was washed repeatedly with water, to remove the methanol, and then dried and evaporated to give nearly pure **10***a*.

cis-*1-Methoxycarbonyl-3-phenyl-6,7a-dimethyl-7-oxo-1,4a,7,7a-tetrahydrocyclopent[e][1,3,4]-oxadiazine (15)*

(a) From Methyl Benzoylazocarboxylate

1-Methoxycarbonyl-2-benzoylhydrazine, mp 139–142°C, was synthesized from methyl chloroformate and benzhydrazide in pyridine, and was crystallized from dilute methanol. The hydrazine (1.0 g, 5.2 mmol), *N*-bromosuccinimide (0.93 g, 5.2 mmol), and pyridine (0.41 g, 5.2 mmol) were allowed to react in chloroform (10 mL). The clear orange solution which was immediately formed was allowed to stand for 15 min and was then shaken out thoroughly with water and dried. It was then evaporated in a stream of dry nitrogen to give the orange oily azo compound (0.86 g, 87%): δ($CDCl_3$): 8.1–7.8 (2H, *o*-Ph, m), 7.8–7.3 (3H, *m* + *p*-Ph, m), 4.08 (3H, OMe, s) ppm.

The azo compound (0.84 g, 4.4 mmol) and the cyclone (1.0 g, 3.9 mmol) were refluxed in benzene (100 mL) for 12 h. The almost colorless solution was evaporated to a residue which crystallized on addition of hexane containing a small amount of ether. The precipitate (1.7 g, 98%) had the ^{1}Hmr spectrum of analytically pure **15**, obtained by recrystallization as prisms, mp 150.5–152°C, from methanol; ν(CCl_4): 1745 (ester C=O), 1717 (keto C=O), 1656 (C=N) cm^{-1}; δ($CDCl_3$): 8.2–7.0 (15H, Ph, m, including 2 sharp s at 7.40 and 7.18), 3.87 (3H, OMe, s), 2.17 (3H, C_6—Me, s) 1.20 (3H, C_{7a}—Me, s) ppm. *Anal.* calcd for C_6—Me, s), 1.20 (3H, C_{7a}—Me, s) ppm. *Anal.* calcd. for $C_{28}H_{24}N_2O_4$: C 74.32, H 5.35, N 6.19; found: C 74.26, H 5.40, N 6.18.

(b) From Diazetidine 14

A solution of **14** (0.45 g, 1.0 mmol) in dry benzene (150 mL) was irradiated at 10°C through Pyrex with a 125-W Hanovia uv immersion lamp. Work-up of a portion after 1 h showed the presence of the intermediate **18**, as well as unreacted **14** and the final product **15**. The proportions of these as determined by ^{1}Hmr spectroscopy were **14**:**18**:**15** = 20:30:50%; after 2.5 h they were 10:30:60%. The reaction was complete in 3.5 h (compound **18** had Me absorptions at δ(CCl_4): 3.26 (3H, OMe, s), 1.87, 1.68 (each 3H, C—Me, s) ppm). Evaporation gave a crystalline residue of **15** in essentially quantitative yield. Recrystallization gave material identical with the product from (*a*).

cis-*1-Ethoxycarbonyl-3-*p*-nitrophenyl-6,7a-dimethyl-7-oxo-1,4a,7,7a-tetrahydrocyclopent[e][1,3,4]-oxadiazine (16)*

1-Ethoxycarbonyl-2-*p*-nitrobenzoylhydrazine, mp 196–196.5°C (lit. (15) mp 185–187°C), was converted into its mercuric salt (7). The salt (12 g, 26 mmol) in carbon tetrachloride (100 mL) was stirred while bromine (4.2 g, 26 mmol) was added. After 0.5 h, the whole was filtered and evaporated to give the azo compound (6.2 g, 95%) as an orange oil; δ(CCl_4): 8.42, 8.27, 8.13, 7.98 (4H, $NO_2C_6H_4$, q), 4.52 (2H, —OCH_2, q, J = 7 Hz), 1.49 (3H, CH_3, t) ppm.

A solution of the cyclone (1.48 g, 5.7 mmol) and the azo compound (1.43 mmol, 5.7 mmol) was refluxed in benzene (30 mL) for 3 h and evaporated. Addition of hexane caused formation of a pale yellow solid (2.48 g, 85%) which was crystallized from ethanol as pale yellow needles, mp 228.5–230°C; ν(CCl_4): 1746 (ester C=O), 1718 sh (keto C=O), 1646 (C=N) cm^{-1}; λ_{max}(EtOH): 287 (enone) (ε 21 000), 338 (*p*-$NO_2C_6H_4$C=N) (ε 10 000) nm; δ($CDCl_3$): 8.2–7.1 (14H, arom., m), 4.36 (2H, —OCH_2, q, J = 7 Hz), 2.17 (3H, C_6—Me, s), 1.40 (3H, ester Me, t), 1.23 (3H, C_{7a}—Me, s) ppm. *Anal.* calcd. for $C_{29}H_{25}N_3O_6$: C 68.09, H 4.93, N 8.21; found: C 68.43, H 5.07, N 8.14.

*Conversion of Oxadiazine 16 into Oxadiazine 5*c

A solution of **16** (256 mg, 0.50 mmol) in 1*N* potassium hydroxide in aqueous methanol (1:1, 60 mL) was kept for 1 day at room temperature, and then made just neutral to litmus. Extraction with methylene chloride gave a yellow solution which on evaporation afforded the base **17** (79 mg, 36%) as a yellow solid, used in the next step without further purification; ν(Nujol): 3270 (NH), 1700 (C=O) cm^{-1}; δ($CDCl_3$): 8.2–6.9 (14H, arom., m), 5.62 (1H, N—H, b), 2.13 (3H, C_6—Me, s), 0.96 (3H, C_{7a}—Me, s) ppm.

The base **16** (110 mg, 0.25 mmol) and *p*-nitrobenzoyl chloride (62 mg, 0.33 mmol) were allowed to react in pyridine (1.5 mL) at room temperature for 1 week. The solvent was evaporated and the residue crystallized by adding water. Recrystallization from benzene–pentane gave **5***c*, identical by mp and mixed mp with authentic **5***c* (1).

Can. J. Chem. Downloaded from www.nrcresearchpress.com by 210.87.254.5 on 09/05/12
For personal use only.

TABLE 1. Properties of 7-substituted and 6,7-disubstituted 1,2-diphenyl-3,5-dimethyl-4-oxo-6,7-diazabicyclo[3.2.0]hept-2-enes

Compound	N_6-group	N_7-group	Mp (°C)	$\nu_{NH/CO}(CCl_4)$ (cm^{-1})	δ($CDCl_3$) (ppm)[f] Ph[g]	C_3—Me	C_5—Me	N_6-group	N_7-group	Analysis (calcd/found) Compound	C	H	N
3d	CO_2CH_2Ph	CO_2CH_2Ph	147 –148[a]	1760, 1740 (ester), 1723 (oxo)	7.5 –6.8	2.07	1.14	5.33, 5.13 (CH_2, ABq, J = 13 Hz)	4.99, 3.79 (AXq, J = 14 Hz)	$C_{35}H_{30}N_2O_5$	75.25 74.94	5.41 5.43	5.02 5.03
11	CO_2Et	CO_2Me	189.5[b] –190	1755, 1726 (ester), 1710 (oxo)	7.8 –6.7	2.09	1.16	4.27q, 1.30t (J = 7 Hz)	2.93	$C_{24}H_{24}N_2O_5$	68.56 68.63	5.75 5.88	6.66 6.93
12	CO_2Me	CO_2Et	194 –196[a]	1768, 1741 (ester), 1724 (oxo)	7.6 –6.7	2.07	1.18	3.80	3.89, 2.95 (2 octets, AM of AMX_3, J_{AM} = 11, $J_{AX} = J_{MX}$ = 7 Hz), 0.76 (X_3, t)	$C_{24}H_{24}N_2O_5$	68.56 68.51	5.75 5.86	6.66 6.69
13	COMe	CO_2Me	176 –177[c]	1748 (ester), 1720 (oxo), 1682 (amide)	7.7 –6.8	2.12	1.23	2.12	2.93	$C_{23}H_{22}N_2O_4$	70.75 70.44	5.68 5.66	7.17 7.06
14	COPh	CO_2Me	199 –200[b]	1752 (ester), 1714 (oxo), 1687 (amide)	7.9 –6.9	2.20	0.76	Ph	3.12	$C_{28}H_{24}N_2O_4$	74.32 74.26	5.35 5.40	6.19 6.18
23a	CO_2Me	H	110 –112[d]	3225; 1772,[e] 1710, 1689	7.5 –7.1	2.23	1.17	3.77	5.4	$C_{21}H_{20}N_2O_3$	72.39 72.66	5.79 6.00	8.04 7.87
23b	CO_2Et	H	127–128.5[d]	3216; 1775,[e] 1714, 1691	7.4 –7.1	2.26	1.19	4.20q, 1.28t (J = 7 Hz)	5.4	$C_{22}H_{22}N_2O_3$	72.90 73.06	6.12 6.13	7.73 7.35
23c	CO_2CH_2Ph	H	145 –147[d]	3228; 1725 (ester), 1715 (oxo)	7.5 –7.2	2.22	1.19	5.23	5.5	$C_{27}H_{24}N_2O_3$	76.39 76.15	5.70 5.94	6.60 6.39
24	COMe	H	141 –142[d]	3218; 1703 (oxo), 1660 (amide)	7.4 –7.1	2.40	1.26	2.03	5.8	$C_{21}H_{20}N_2O_2$	75.88 75.72	6.06 6.18	8.43 8.38

[a]Recrystallized from $CHCl_3$–MeOH.
[b]Recrystallized from MeOH.
[c]Recrystallized from CCl_4–iso-octane.
[d]Recrystallized from ether–hexane.
[e]An additional C=O peak is present; the middle one is probably oxo.
[f]Singlets unless otherwise stated.
[g]Outer limits of absorptions; singlets were observed for C_1—Ph and CH_2Ph.

Can. J. Chem. Downloaded from www.nrcresearchpress.com by 210.87.254.5 on 09/05/12
For personal use only.

*1,2-Diphenyl-3,5-dimethyl-6,7-dibenzyloxycarbonyl-4-oxo-6,7-diazabicyclo[3.2.0]hept-2-ene (3*d)

We thank the Lucidol Division of Pennwalt Chemical Co., Buffalo, NY, for a generous gift of dibenzyl azodicarboxylate. It was recrystallized from ether – petroleum ether (bp 30–60°C) before use.

The azo compound (6.0 g, 20 mmol) and the cyclone 5.2 g (20 mmol) were refluxed together in bromobenzene (100 mL) for 16 h. The residue left on evaporation crystallized on addition of ether–isooctane. The crystals were washed with cold methanol and recrystallized from chloroform–methanol as colorless prisms (50%) (Table 1).

1,2-Diphenyl-3,5-dimethyl-4-oxo-6,7-diazabicyclo-[3.2.0]hept-2-ene (7)

A solution of **3***d* (2.0 g, 3.6 mmol) in ethyl acetate (30 mL) containing 5% Pd on charcoal (200 mg) was treated with hydrogen at room temperature for 16 h. Filtration and evaporation gave a light green oil which slowly crystallized on addition of hexane. The solid (0.75 g, 72%) was crystallized by allowing a solution of it in ethyl acetate – hexane to evaporate under nitrogen. The yellow-green prisms decomposed with melting between 110 and 115°C; $\nu(CCl_4)$: 3272 (NH), 1710 (C=O) cm^{-1}; λ_{max}(EtOH): 280 nm (enone) (13 400); *m/e* 290 (M^+), 260 (M—N_2H_2) (deuterated **7** had: *m/e* 292 (M^+)); $\delta(^1H)$ ($CDCl_3$): 7.4–6.8 (10H, Ph, m), 4.18 (2H, NH, b), 2.15 (3H, C_3—Me, s), 1.07 (3H, C_5—Me, s) ppm; $\delta(^{13}C)(CDCl_3)$: 206.8 (C_4), 137.5–126.5 (C_2, C_3, and Ph), 79.7 (C_1), 69.5 (C_5), 16.2 (C_3—Me), 10.8 (C_5—Me) ppm. *Anal.* calcd. for $C_{19}H_{18}N_2O$: C 78.59, H 6.25, N 9.65; found: C 78.84, H 6.57, N 9.45.

In the above hydrogenation, consumption of the first equivalent of hydrogen was rapid (ca. 20 min). In one run the reaction was interrupted at this stage and worked up as above. The residue consisted mainly of **10***c* (>80%) which was not further purified; $\delta(CDCl_3)$: 7.5–6.9 (15H, Ph, m), 5.03 (1H, A portion of CH_2 AX, d, J = 13 Hz), 3.81 (1H, X portion of CH_2 AX, broadened d) ppm.

Thermal Reactions of 7

(a) Half-life Measurement

A solution of **7** (60 mg, 0.4 *M*) in benzene was heated in refluxing benzene and its ^{1}Hmr spectrum periodically monitored. Decomposition to the cyclone, the only detectable product, was 50% complete in 2.5 days.

(b) Attempt to Detect Di-imide

A solution of **7** (60 mg) was refluxed in cyclohexene (1 mL) for one day by which time decomposition to cyclone was complete. Gas–liquid chromatographic analysis (6 ft × 1/8 in. column, 10% XE-60) failed to detect any cyclohexane in the cyclohexene.

Oxidation of 7

(a) Room Temperature

After completion of the reaction with the chosen oxidizing agent, in general using 60 mg (0.21 mmol) in 10 mL of solvent, the organic solution was filtered, if necessary, and then evaporated to dryness. The residue was examined by ^{1}Hmr spectroscopy and found to consist only of cyclone in each case. (*i*) Mercuric oxide (1 g) in ether. (*ii*) Ethereal hydrogen peroxide obtained by shaking the ether several times with 50% aq. hydrogen peroxide. (*iii*) Cupric chloride (50%) in a sodium acetate – acetic acid buffer at pH 5, and ether.

(b) Low Temperature ^{1}Hmr Experiments

In each case 60 mg of **7** and an equivalent of oxidizing agent were dissolved in $CDCl_3$ (0.5 mL) cooled down to at least −50°C. The solution was transferred rapidly to the chilled nmr tube which was immediately placed in the probe, previously cooled to the lowest temperature to be studied in the run. The temperature was raised as needed to a level at which reaction occurred at a convenient rate. In each case **7** gave only the monomer and dimer of the cyclone (at higher temperatures only the dimer). Any other new peaks were attributable to the reduced form of the oxidizing agent except in the case of (*iii*) when small amounts of the adduct of the cyclone and the quinone were detectable. (*i*) Benzoyl peroxide, −10°C. (*ii*) Diethyl azodicarboxylate, −50°C. Diethyl hydrazodicarboxylate was isolated at the end of the run. (*iii*) *p*-Benzoquinone, −10°C. The formation of the Diels–Alder adduct of the quinone and cyclone was confirmed by synthesis of a reference sample.

1,2-Diphenyl-3,5-dimethyl-6-acyl or acyloxy-4-oxo-6,7-diazabicyclo[3.2.0]hept-2-ene (Table 1)

*The 6-Methoxycarbonyl-, 6-Ethoxycarbonyl-, 6-Benzyloxycarbonyl Compounds (**23**a, **23**b, **23**c), and the 6-Acetyl Compound (**24**)*

To a solution of **7** (0.50 g, 1.72 mmol) in dry ether (40 mL) containing pyridine (2 mL) was added 5 equivalent of the appropriate acyl chloride. The whole was stirred for 30 min, the ether was evaporated, and water was added to the semi-solid residue to induce crystallization. The products were recrystallized from aqueous methanol and then from ether–hexane: **23***a*, 60%; **23***b*, 50%; **23***c*, 60%; **24**, 70%.

The use of 1 equivalent of acyl chloride led to rather slow formation of the above products.

*Hydrogenolysis of **23**c*

A solution of **23***c* (100 mg, 0.24 mmol) in ethyl acetate (10 mL) containing 5% Pd on charcoal (20 mg) was stirred with hydrogen for 1 h. Filtration and evaporation gave the diazetidine **7**.

Attempted Phthaloylation of 7

Phthaloyl chloride (42 mg, 0.21 mmol) and **7** (60 mg, 0.21 mmol) were kept in pyridine (1 mL) for 12 h. Evaporation, addition of water, and ether extraction led to an ether soluble fraction whose ^{1}Hmr spectrum was extremely complex.

*Attempted Acylation of **23**a and **24** with Pyridine as Base*

A solution of **23***a* (39 mg, 0.11 mmol) and methyl chloroformate (26 mg, 2.8 mmol) in pyridine (0.4 mL) was heated at 100°C in an nmr tube. There was no change in the spectrum over a period of 12 h. Work-up gave pure unreacted **23***a*.

Compound **24** was similarly treated with acetyl chloride, again without any change.

*Attempted Acetylation of **24** with Other Bases*

In general **24** (100 mg, 0.30 mmol), dissolved in a suitable solvent (5 mL), was treated with 1.2 equivalent of the base and then 1 equivalent of acetyl chloride. Work-up consisted of addition of ether and water, aqueous extraction, and evaporation of the ethereal solution. In all cases the ^{1}Hmr spectrum of the residues was very complex. (*i*) Sodium hydride, ether. (*ii*) Lithium di-isopropylamide, benzene. (*iii*) *n*-Butyllithium, benzene. (*iv*) *tert*-Butyllithium, benzene. All these reaction mixtures darkened badly within 0.5 h, except for reaction (*ii*). (*v*) Triethylamine, neat. (*vi*) 1,5-Diazabicyclo[3.4.0]non-5-ene, benzene. (*vii*) Potassium carbonate (2 g), methylene chloride. These reaction mixtures were stirred for 12 h.

N,N-*Dimethyldiazetidinium Iodide **25***

A solution of **7** (430 mg, 1.48 mmol) in methyl iodide (5 mL) was stirred with potassium carbonate (2 g) under nitrogen for 3 h, and ether (10 mL) was added. The heavy potassium salts settled to the bottom leaving a milky suspension of the organic iodide which was carefully decanted and filtered. The precipitate was washed with ether (460 mg, 70%). Compound **25** was a colorless solid, decomposing >160°C, freely soluble in water

and sparingly in $CDCl_3$; ν(Nujol): 3350 (NH), 1703 (C=O) cm^{-1}; λ_{max}(EtOH): 300 nm (enone) (8200); *m/e*: 319 ($C_{21}H_{23}N_2O^+$), 127 (I^+); δ($CDCl_3$): 7.5–7.2 (10H, Ph, broad s), 3.73 (3H, $\overset{+}{N}$—Me, s), 3.55 (3H, $\overset{+}{N}$—Me, s), 2.30 (3H, C_3—Me, s), 1.37 (3H, C_6—Me, s) ppm. *Anal.* calcd. for $C_{21}H_{23}IN_2O$: I 28.43; found: I 28.33.

Attempted Alkylations

(a) On 7

In each case **7** (60 mg, 0.21 mmol) was treated with the alkylating agent (1 equivalent) in a suitable solvent under nitrogen, and after 12 h the solution was filtered, if necessary, and evaporated.

(*i*) 1,3-Propaneditosylate, potassium carbonate (1 g), in methylene chloride: **7** was recovered there being no evidence of the formation of **26**. (*ii*) 1,3-Dibromopropane, potassium carbonate (1 g), in benzene, reflux: cyclone was formed; 1,2-diiodopropane, neat, behaved similarly. (*iii*) Triethyloxonium fluoborate, in methylene chloride: cyclone was formed.

(b) On 24

The *N*-acetyl compound (60 mg, 0.18 mmol) in methyl iodide (2 mL) was stirred under nitrogen for 12 h with potassium carbonate (1 g). Filtration and evaporation gave unreacted **24**. The same result was obtained when diazabicyclononene was used as base.

Acknowledgement

We thank the Natural Sciences and Engineering Research Council of Canada for financial assistance.

1. D. MACKAY, C. W. PILGER, and L. L. WONG. J. Org. Chem. **38**, 2043 (1973).
2. M. E. LANDIS and J. C. MITCHELL. J. Org. Chem. **44**, 2288 (1979).
3. C. F. HUEBNER, P. L. STRACHAN, E. M. DONOGHUE, N. CAHOON, L. DORFMAN, R. MARGERISON, and E. WENKERT. J. Org. Chem. **32**, 1126 (1967); C. F. HUEBNER, E. M. DONOGHUE, C. J. NOVAK, L. DORFMAN, and E. WENKERT. J. Org. Chem. **35**, 1149 (1970).
4. E. KOERNER VON GUSTORF and B. KIM. Angew. Chem. **76**, 592 (1964); E. KOERNER VON GUSTORF, D. V. WHITE, B. KIM, D. HESS, and J. LEITICH. J. Org. Chem. **35**, 1155 (1970).
5. L. MARCHETTI and G. TOSI. Tetrahedron Lett. 3071 (1971); J. FIRL and S. SOMMER. Tetrahedron Lett. 4193 (1971).
6. N. S. ZEFIROV and A. A. DUDINOV. Zh. Org. Khim. **3**, 428 (1967).
7. J. A. CAMPBELL, D. MACKAY, and T. D. SAUER. Can. J. Chem. **50**, 371 (1972).
8. P. C. CHIEH, D. MACKAY, and L. WONG. J. Chem. Soc. Perkin II, 2094 (1972).
9. D. MACKAY and L. L. WONG. Can. J. Chem. **53**, 1973 (1975).
10. D. MACKAY and C. W. PILGER. Can. J. Chem. **52**, 1114 (1974).
11. R. B. WOODWARD, K. HEUSLER, J. GOSTELI, P. NAEGLI, W. OPPOLZER, R. RAMAGE, S. RANGANATHAN, and H. VORBRUGGEN. J. Am. Chem. Soc. **88**, 852 (1966); T. B. WINDHOLZ and D. B. R. JOHNSTON. Tetrahedron Lett. 2555 (1967).
12. N. RIEBER, J. ALBERTS, J. A. LIPSKY, and D. M. LEMAL. J. Am. Chem. Soc. **91**, 5668 (1969).
13. S. MASAMUNE, N. NAKAMURA, and J. SPADARO. J. Am. Chem. Soc. **97**, 918 (1975).
14. S. RODKIN, A. YA. YAKUBOVICH, and S. D. MAKAROV. Zh. Org. Khim. **7**, 2271 (1971); M. A. ENGLIN, A. S. FILATOV, and N. F. ALEKSEEVA. Zh. Org. Khim. **7**, 2611 (1971).
15. G. D. SHARVIN, B. I. BUSYKIN, and R. KH. FASSAKLOV. Khim. Geterostsikl. Soedin. **13**, 741 (1977).

Can. J. Chem. Downloaded from www.nrcresearchpress.com by 210.87.254.5 on 09/05/12
For personal use only.

The reaction of potassium iodide in polyhydrogen fluoride – pyridine with two cage diols. A simple synthesis of tetracyclo[6.3.0.0^{4,11}.0^{5,9}]undeca-2,6-diene ("homohypostrophene")

DAO CONG DONG AND JOHN T. EDWARD

Department of Chemistry, McGill University, 801 Sherbrooke St. West, Montreal, P.Q., Canada H3A 2K6

Received January 14, 1980

DAO CONG DONG and JOHN T. EDWARD. Can. J. Chem. **58**, 1324 (1980).

The diol **2** was converted by treatment with potassium iodide in polyhydrogen fluoride – pyridine into a mixture of the diiodide **5** and homohypostrophene **6**. The diol **10** under the same conditions gave the ether **14**. Treatment of the mixture of **5** and **6** with sodium in boiling tetrahydrofuran gave an easily-separable mixture of **6** and **7**.

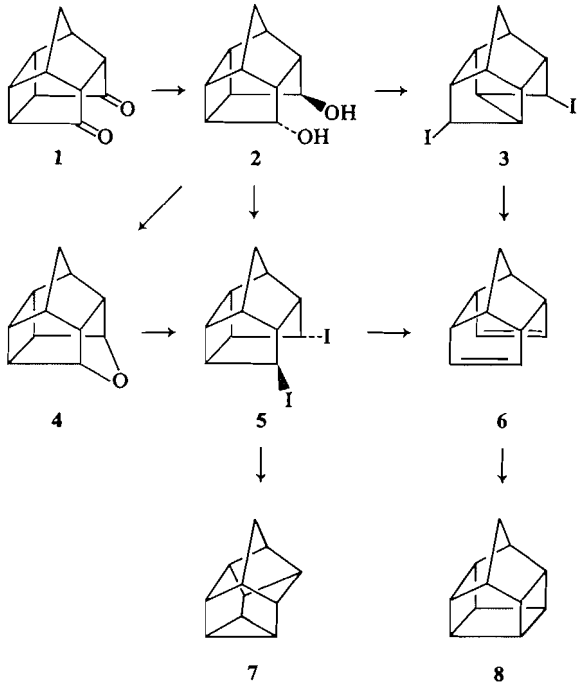
DAO CONG DONG et JOHN T. EDWARD. Can. J. Chem. **58**, 1324 (1980).

Le diol **2** traité par l'iodure de potassium dans une combinaison de polyfluorure d'hydrogène – pyridine est transformé en un mélange de diiodure **5** et d'homohypostrophène **6**. Le diol **10** dans les mêmes conditions donne l'éther **14**. Le mélange de **5** et **6** traité par le sodium dans le tétrahydrofuranne à l'ébullition fournit un mélange de **6** et de **7** que l'on peut facilement séparér.

[Traduit par le journal]

Introduction

Recently three groups (1–3) simultaneously described routes from the diketone **1** (4) to homohypostrophene **6** whence homopentaprismane **8** may be prepared by photocyclization (2, 3). Perhaps the simplest of these routes was the three-step procedure (Scheme 1: **1** → **2** → **3** → **6**) of Smith and Barborak (1). We now describe a variant of this procedure even simpler in practice. As before (1), the diketone was reduced to the *endo,endo*-diol **2** (1, 5). The latter was treated with potassium iodide in polyhydrogen fluoride – pyridine, a reagent recently developed by Olah and Welch (6), and the reaction was monitored by ^{1}H nmr. The diol **2** disappeared from the reaction mixture within 7 hours, and three products appeared: first the ether **4** ("oxabirdcage" (5, 7)) formed rapidly and then disappeared (20% after 2 h, 7% after 7 h, 0% after 24 h); then more slowly, the diiodide **5** and homohypostrophene **6**. After 24 h the mixture of **5** and **6** was isolated and, without separation, treated with sodium in boiling tetrahydrofuran, a reagent known to convert **5** to a mixture of **6** and **7** (2). In the event, final overall yields of 55% of **6** and 31% of **7** were obtained. These two products were easily separable by chromatography on silica impregnated with silver nitrate.



SCHEME 1

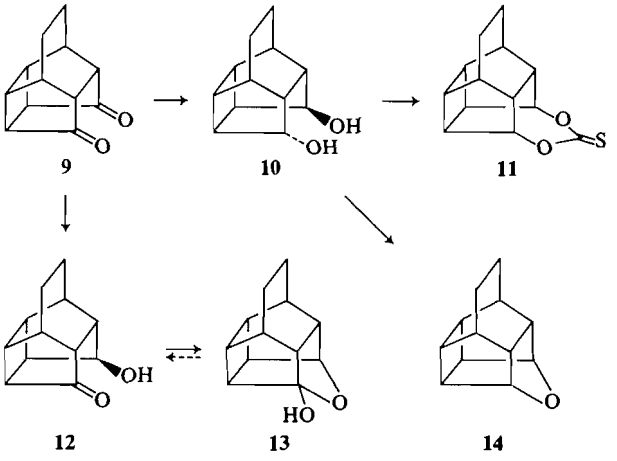
The attempt to obtain bishomohypostrophene from the homologous diketone **9** (4, 8, 9) by a similar series of reactions failed. Lithium aluminum hydride reduction of **9** gave a diol (10, 11) for which Dekker *et al.* (10) have established the *endo,endo* configuration (10) by reaction with thionyl chloride to form a cyclic sulfite; we have confirmed this by formation of the cyclic thiocarbonate **11**. Reaction of the diol **10** with potassium iodide in polyhydrogen fluoride – pyridine at room temperature gave the ether **14** as the only product, even after prolonged standing. Recently Nakazaki *et al.* (11) converted **10** into **14** by treatment with sulfuric acid in acetic acid at 120°C for 42 h. Evidently polyhydrogen fluoride – pyridine may prove advantageous in the conversion of some diols into ethers under mild conditions.

Dekker *et al.* (10) obtained **13** by treatment of **9** with sodium borohydride, or by formation of the monoethylene ketal of **9**, borohydride reduction,

0008-4042/80/131324-03$01.00/0

©1980 National Research Council of Canada/Conseil national de recherches du Canada

Can. J. Chem. Downloaded from www.nrcresearchpress.com by 210.87.254.105 on 09/05/12
For personal use only.



SCHEME 2

and acid hydrolysis, a sequence which obviously involved the hydroxy ketone **12** as an intermediate. We have confirmed these results, obtaining **13** by reduction of **9** with one equivalent or with a large excess of borohydride. The equilibrium **12** ⇄ **13** evidently lies far to the right (no C=O bond in ir spectrum). By contrast, Cookson *et al.* (4) found that treatment of **1** with one mol (4 equivalents) of sodium borohydride gave a mixture of mono- and di-reduction products, and that the former existed mainly as uncyclized hydroxy ketone (C=O in ir). Treatment of **1** with a large excess of borohydride gave a mixture of isomeric diols. These and other results (4, 10) indicate a considerably greater propensity for the formation of an ether bridge in the polycyclic compounds related to **9** than in their lower homologues related to **1**, a result in keeping with simple considerations based on ring strain (4, 12).

Experimental

Melting points were taken in capillary tubes using a Gallenkamp apparatus and are uncorrected. The nmr spectra were recorded on a Varian T-60A spectrometer in $CDCl_3$ containing tetramethylsilane (TMS) as internal standard. Infrared spectra were recorded in KBr pellets on a Perkin-Elmer 297 spectrophotometer. Mass spectra were recorded at 70 eV on a LKB 9000 or a Hewlett-Packard mass spectrometer. Elemental analyses were performed by Dr. C. Daessle of Montreal and Galbraith Laboratories, Inc., Knoxville, TN, U.S.A. Tetrahydrofuran was dried by refluxing over lithium aluminum hydride, followed by distillation.

Hexacyclo[5.4.0.0^{3,6}.0^{4,11}.0^{5,9}.0^{8,10}]undecane (7) and Tetracyclo[6.3.0.0^{4,11}.0^{5,9}]undeca-2,6-diene (6)

Diol **2** (4.0 g, 22.5 mmol) was added to a magnetically stirred solution of polyhydrogen fluoride – pyridine (75 g) containing potassium iodide (20.0 g, 120 mmol) in a polyethylene bottle. The reaction mixture was stirred for 24 h, quenched by pouring on to ice-water (200 g), and extracted with ether (3 × 100 mL). The ether layer was washed with aqueous sodium thiosulfate, dried (Na_2SO_4), and passed quickly through a short column of neutral alumina (30 g). Solvent was removed and the oily residue (8.5 g) was found by nmr to be a mixture of diolefin **6** (from singlet at δ 5.90; olefinic protons (2)) and diodide **5** (from AB pattern at δ 1.37, 1.78; methylene protons (1, 2)).

The oily mixture, dissolved in dry THF (30 mL) was added dropwise to a stirred suspension of sodium (4.0 g) in dry THF (40 mL) under nitrogen. The reaction mixture was then refluxed for 1.5 h, filtered, and the filtrate poured into ice-water. The aqueous layer was extracted with pentane, and the combined extracts were dried (Na_2SO_4). Careful removal of solvent gave 3.44 g of a colorless oil shown by nmr to be made up of **6** and **7** in the ratio 2:1. The mixture was separated by chromatography on 30% $AgNO_3$ – silica gel. Elution with pentane gave 1.0 g (31% from diol **2**) of hexacyclo[5.4.0.0^{3,6}.0^{4,11}.0^{5,9}.0^{8,10}]undecane **7**, mp 127–129°C (lit. (2) mp 132–134°C; nmr ($CDCl_3$) δ:1.42 (d, $J \simeq$ 1 Hz, 2H), 1.6–2.4 (complex m, 4H), 1.6–3.1 (complex m, 6H); mass spectrum *m/e*: 144(34) (molecular ion), 129(29), 116(12), 115(15), 80(22), 79(100), 78(55), 77(33), 66(51), 40(25). Elution with 20% Et_2O – pentane gave 1.8 g (55% from diol **2**) of **6**, mp 145–146°C (sublimed) lit. (1) mp 143–145°C, (ref. 2) mp 141.5–142.5°C, (ref. 3) mp 139–140°C, (ref. 7) mp 143.5–144.5°C); nmr ($CDCl_3$) δ:5.90 (s, $w_{\frac{1}{2}} \simeq$ 3 Hz, 4H, olefinic H), 3.20 (m, 2H, bridge head H), 2.37 (broad s, $w_{\frac{1}{2}} \simeq$ 5 Hz, 4H, 1, 4, 5, and 8 methine protons), 1.70 (broad s, $w_{\frac{1}{2}} \simeq$ 3 Hz, methylene protons); mass spectrum *m/e*:144(34) (molecular ion), 129(24), 128(16), 115(14), 91(4), 79(100), 78(30), 77(42).

When diol **2** was treated with polyhydrogen fluoride – pyridine containing potassium iodide for only 7 h under the conditions described above, and the reaction product then submitted to reduction by sodium in THF, the ether **4** (7%; characterized by ir, nmr, and mass spectrum) was isolated in addition to **6** and **7**.

Pentacyclo[6.4.0.0^{2,7}.0^{3,11}.0^{6,10}]dodecane-9,12-diol (10)

To a solution of **9** (11.52 g, 0.06 mol) in dry THF (350 mL) was added dropwise a suspension of lithium aluminum hydride (6.1 g, 0.16 mol) in dry THF (200 mL). The mixture was refluxed for 30 h. Dilute HCl (6%) was added to the cooled reaction mixture and an inorganic solid was filtered off. The organic layer was separated from the aqueous layer and the latter extracted with chloroform (6 × 100 mL). The extracts and organic layer were combined, dried (Na_2SO_4), and concentrated to afford **10** as a colorless solid (8.0 g, 70%) mp 149–153°C. Recrystallization from ethyl acetate raised the mp to 170–172°C (lit. (11) mp 168–170°C); nmr ($CDCl_3$) δ:5.45 (s, 2H, OH), 3.70 (br s, $w_{\frac{1}{2}} \simeq$ 6 hz, H9–H12), 2.4–3.0 (m, 6H), 1.3–1.9 (m, 6H); ir (KBr):3140 (br), 1510 (br), 1255 (s), 1150 (s), 1090 (s), 1063 (m) cm^{-1}; mass spectrum *m/e*: 192(4) (molecular ion), 174(68), 156(12), 146(58), 145(40), 118(31), 107(27), 104(40), 95(32), 91(100), 80(94), 79(81), 77(52). *Anal.* calcd. for $C_{12}H_{16}O_2$: C 74.97, H 8.39; found: C 75.11, H 8.56.

Pentacyclo[6.4.0.0^{2,7}.0^{3,11}.0^{6,10}]dodecane-9,12-thiocarbonate (11)

A solution of **10** (0.96 g, 5 mmol) and *N,N'*-thiocarbonyldiimidazole (1.00 g, 5 mmol) in dry toluene (40 mL) was refluxed with stirring under nitrogen for 1.5 h. The solvent was removed *in vacuo* and the residue was taken up in chloroform (150 mL). The resulting solution was washed successively with 5% HCl, water, saturated $NaHCO_3$ solution, and water. The organic layer was dried (Na_2SO_4) and concentrated *in vacuo*. A colorless solid was removed by filtration (1.00 g, 90%), mp 320–322°C; nmr ($CDCl_3$) δ:4.30 (broad s, $w_{\frac{1}{2}} \simeq$ 12 Hz, 2H, H9–H12), 3.27 (broad s, $w_{\frac{1}{2}} \simeq$ 18 Hz, 2H), 2.93 (broad s, $w_{\frac{1}{2}} \simeq$ 7 Hz, 2H), 2.70 (poorly resolved m, 2H), 1.60 (m, 6H); ir (KBr):2955 (m), 2915 (m), 2860 (m), 1425 (s), 1310 (s), 1250 (s), 1000 (s) cm^{-1}; mass spectrum *m/e*:234(m, 100), 174(24), 146(21),

Can. J. Chem. Downloaded from www.nrcresearchpress.com by 210.87.254.105 on 09/05/12
For personal use only.

130(15), 117(41), 118(20), 115(26), 79(91), 78(41), 77(44). *Anal.* calcd. for $C_{13}H_{14}O_2S$: C 66.63, H 6.02, S 13.68; found: C 66.91, H 6.11, S 13.69.

Reaction of Diol 10 with Potassium Iodide in Polyhydrogen Fluoride – Pyridine

Diol **10** (1.0 g, 5.3 mmol) was added to a stirred solution of polyhydrogen fluoride – pyridine (20 g) containing potassium iodide (7.5 g, 11.5 mmol) in a polyethylene bottle. The reaction mixture was stirred at room temperature for 24 h, quenched by pouring onto ice-water (100 g), and extracted with ether (3 × 50 mL). The ether extract was washed with aqueous sodium thiosulfate, dried (Na_2SO_4), and poured quickly through a short column of neutral alumina. The solvent was removed and the residue (0.90 g) was sublimed (100°C/8 Torr) to give 4-oxahexacyclo[5.4.2.$0^{2,6}$.$0^{3,10}$.$0^{5,9}$.$0^{8,11}$]tridecane **14** as a colorless solid (0.70 g, 76%), mp 178–179°C (lit. (11) mp 182–184°C); nmr ($CDCl_3$) δ:4.77 (m, 2H), 2.68 (m, 2H), 2.43 (m, 2H), 2.23 (m, 2H), 1.70 (m, 2H), 1.50 (broad s, 4H); ir (KBr):2950 (m), 2940 (m), 2860 (m), 1465 (w), 1335 (m), 1507 (m), 1255 (m), 1033 (s), 962 (s), 855 (s) cm^{-1}; mass spectrum *m/e*: 174(100) (molecular ion), 173(11), 146(34), 130(19), 131(23), 117(5), 104(34), 91(64), 79(78), 78(63), 77(40), 65(19). *Anal.* calcd. for $C_{12}H_{14}O$: C 82.72, H 8.10; found: C 82.55, H 8.28.

4-Oxahexacyclo[5.4.2.$0^{2,6}$.$0^{3,10}$.$0^{5,9}$.$0^{8,11}$]tridecane-3-ol (13)

Sodium borohydride (0.76 g, 20 mmol) was added to a stirred solution of the diketone **9** (1.88 g, 10 mmol) in 95% EtOH (20 mL). The solution was stirred at room temperature for 10 h, then water (15 mL) was added and the solution refluxed gently for 10 min on a steam bath. Thirty-five milliliters of water was added and the solution extracted with chloroform (4 × 50 mL). The combined organic extracts were dried (Na_2SO_4) and concentrated *in vacuo* to give the alcohol **13** as a colorless solid (1.46 g, 77%) mp 181–183°C. Sublimation at 130°C (8 Torr) gave material with mp 191–192°C; nmr ($CDCl_3$) δ:4.65 (t, $J \simeq$ 5 Hz, 1H, —CHO—), 4.45 (br band 1H, O*H*), 1.50 (br s, $w_{\frac{1}{2}} \simeq$ 5 Hz, 4H, methylene protons), 1.6–3.0 (complex m, 8H, methine protons); ir (KBr):3220 (broad s), 2915 (s), 2900 (s), 2865 (m), 1350 (2), 1325 (s), 1153 (s), 1120 (s), 1010 (s), 906 (s) cm^{-1}; mass spectrum *m/e*:190(22) (molecular ion), 172(8), 145(81), 144(19), 131(24), 130(24), 129(27), 118(46), 117(72), 107(23), 105(47), 99(29), 92(100), 91(99.8), 77(40.) *Anal.* calcd. for $C_{12}H_{14}O_2$: C 75.76, H 7.42; found: C 75.54, H 7.62.

With one equivalent of $NaBH_4$, the same reaction gave **13** in 80% yield.

Acknowledgements

The financial support of the Natural Sciences and Engineering Research Council of Canada and of the Ministère de l'Education du Québec is gratefully acknowledged.

1. R. C. SMITH and J. C. BARBORAK. J. Org. Chem. **41**, 1433 (1976).
2. A. P. MARCHAND, T.-C. CHOU, J. D. EKSTRAND, and D. VAN DER HELM. J. Org. Chem. **41**, 1438 (1976).
3. P. E. EATON, L. CASSAR, R. A. HUDSON, and D. R. HWANG. J. Org. Chem. **41**, 1445 (1976).
4. R. C. COOKSON, E. CRUNDWELL, R. R. HILL, and J. HUDEC. J. Chem. Soc. 3062 (1964).
5. T. SASAKI, S. EGUCHI, Y. KIRIYAMA, and O. HIROAKI. Tetrahedron, **30**, 2707 (1974).
6. G. A. OLAH and J. WELCH. Synthesis, 653 (1974).
7. G. R. UNDERWOOD and B. RAMAMOORTHY. Chem. Commun. 12 (1970); Tetrahedron Lett. 4125 (1970).
8. D. VALENTIN, N. J. TURRO, and G. S. HAMMOND. J. Am. Chem. Soc. **86**, 5202 (1964).
9. D. F. O'BRIEN and J. W. GATES, JR. J. Org. Chem. **50**, 2593 (1965).
10. J. DEKKER, J. J. DEKKER, L. FOURIE, and G. L. WENTELER. J. S. Afr. Chem. Inst. **28**, 321 (1975); Chem. Abstr. **86**, 120851a (1977).
11. M. NAKAZAKI, K. NAEMURA, N. ARASHIBA, and M. IWASAKI. J. Org. Chem. **44**, 2433 (1979).
12. DAO CONG DONG and J. T. EDWARD. J. Org. Chem. In press.

Can. J. Chem. Downloaded from www.nrcresearchpress.com by 210.87.254.105 on 09/05/12
For personal use only.

Electrophilic cleavage of cyclopropanes. III. The reaction of molecular bromine with tetracyclo[3.2.0.0^{2,7}.0^{4,6}]heptane[1,2]

DENNIS G. GARRATT[3]

Department of Chemistry, University of Ottawa, Ottawa, Ont., Canada K1N 9B4

Received October 19, 1979

DENNIS G. GARRATT. Can. J. Chem. **58**, 1327 (1980).

The ionic addition of molecular bromine to tetracyclo[3.2.0.0^{2,7}.0^{4,6}]heptane (quadricyclene) has been investigated in a variety of solvent systems. Depending upon the nature of the solvent, three or more of six dibromo and five solvent-incorporated adducts are isolable. A mechanism involving a series of ion-pairs and competitive edge-on vs. corner (end-on) attack is proposed.

DENNIS G. GARRATT. Can. J. Chem. **58**, 1327 (1980).

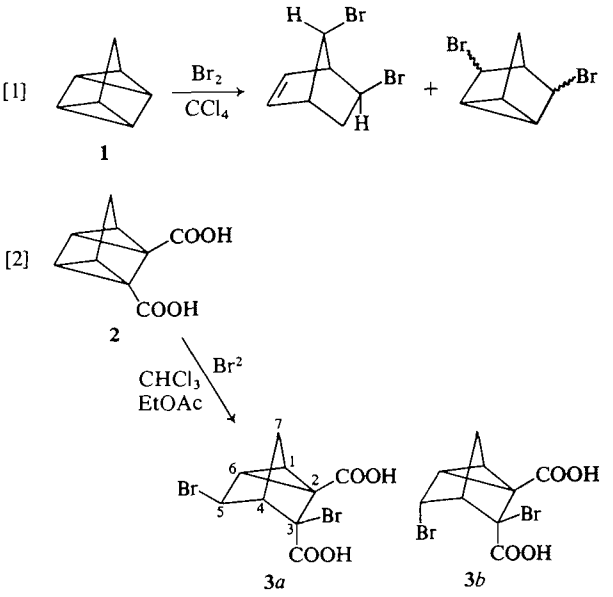
On a étudié l'addition ionique du brome moléculaire sur le tétracyclo[3.2.0.0^{2,7}.0^{4,6}]heptane (quadricyclène) dans plusieurs systèmes de solvants. Dépendant de la nature du solvant, on a pu isoler un minimum de 3 de 6 adduits dibromés et de 5 adduits incorporant le solvant. On propose un mécanisme impliquant une série de paires d'ions et des attaques compétitives par le côté ou par le sommet (end-on).

[Traduit par le journal]

Can. J. Chem. Downloaded from www.nrcresearchpress.com by 210.87.254.105 on 09/05/12
For personal use only.

The reaction of tetracyclo[3.2.0.0^{2,7}.0^{4,6}]heptane, **1**, with bromine in carbon tetrachloride solution has been reported by Dauben and Cargill (1) to yield a mixture of 3,5-dibromotricyclo[2.2.1.0^{2,6}]-heptanes and *exo*-2-*syn*-7-dibromobicyclo[2.2.1]-hept-5-ene. The relative proportions were, however, not reported not were data of unambiguous mechanistic utility forthcoming. A related study involving the bromination of tetracyclo-[3.2.0.0^{2,7}.0^{2,6}]heptane-1,5-dicarboxylic acid, **2**, has been reported (2) to give a nortricyclic dibromide, **3**, of indeterminate configuration at C5. Cristol and co-workers (3) subsequently provided evidence that in the absence of carbonium ion-like intermediates, nucleophilic attack during the second step of the reaction occurs with inversion of configuration at carbon. These data would then support the assignment of configuration at C5 in terms of an *exo* bromine atom, **3***a* (2, 4).

The results, while indicative of apparently stereospecific inversion of configuration at carbon during both electrophilic cleavage and subsequent nucleophilic attack, contrast with other reports (5) of more varied stereochemical pathways. For example, Skell and co-workers (6) have reported the ionic bromination of dehydroadamantane, **4**, in the presence of isoamyl nitrite to give a 59:41 mixture of the isomeric 2,6-dibromoadamantanes, **5** and **6**. They argued that since all aspects of ionic brominations of cyclopropanes point to formation



of a 1-bromo-3-carbonium ion, it is reasonable to attribute to the second step, the reaction with bromide ion, the proportioning between axial and equatorial approach.

An alternative rationalization of their data, however, would be a competitive attack by bromine, both from the edge and the corner, followed by stereospecific attack by bromide ion with inversion of configuration at carbon.

In their detailed mechanism, Skell and co-workers propose the ionic reaction of bromine with alkylcyclopropanes to occur at the least substituted position, with inversion, to produce a bromocarbonium ion – bromide ion-pair which undergoes

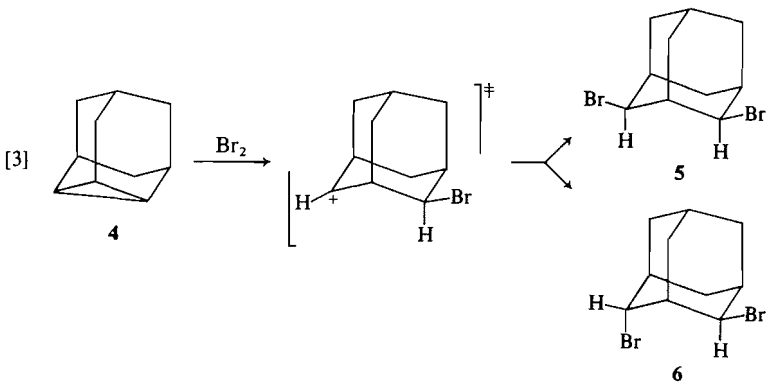
[1]Issued as NRCC No. 18368.

[2]For Part II, see ref. 12*b*.

[3]Author to whom correspondence may be directed at the Division of Chemistry, National Research Council of Canada, 100 Sussex Dr., Ottawa, Ont., Canada K1A 0R6.

0008-4042/80/131327-07$01.00/0

©1980 National Research Council of Canada/Conseil national de recherches du Canada



extensive sequential rearrangements, uncharacteristic of solvolysis-type intermediates (i.e. intimate or solvent-separated ion-pairs), but characteristic of the nonrelaxed or free carbonium ion-anion pairs (6). The question remains, however, as to how general this scheme is. For example, the known propensity for C5—C6 (C1—C7) bond cleavage in **1**, and the relatively good neighbouring group ability of bromine, suggests a driving force for edge-on attack and thus retention of configuration at carbon instead of inversion during the first step.

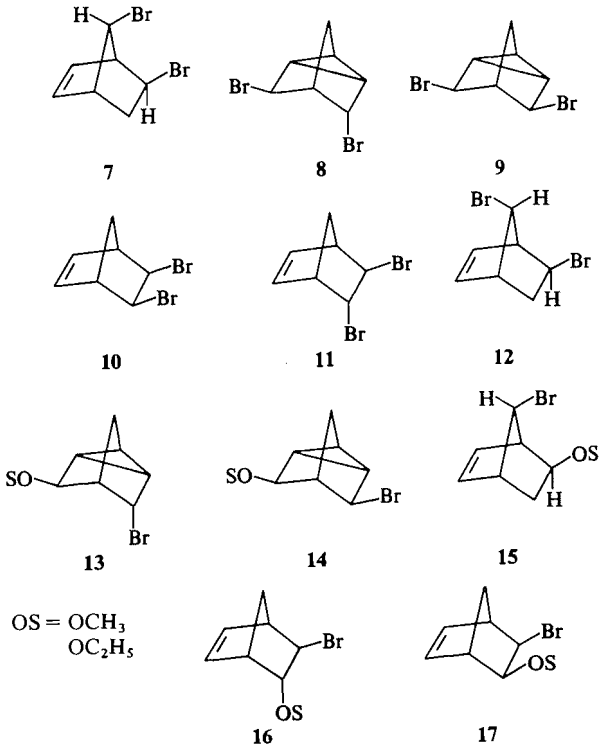
Our interest in the stereochemistries of arene-selenenylations and arenesulphenylations of cyclopropanes, in particular the tetracyclo-[3.2.0.0.^{2,7}.0^{4,6}]heptane system led us to re-examine the initial work of Dauben and Cargill and to extend the mechanistic probe to include an investigation of the effect of solvent upon the product determining step. In analogy with earlier work on alkenes and alkynes (7), the effect of protic solvents on the product composition and stereochemistry is anticipated to give important data with respect to the number and types of intermediates involved.

Results and Discussion

The reaction of equimolar quantities of bromine and **1** in methylene chloride solution at ambient temperature, 23–25°C, in the presence or absence of isoamyl nitrite, but in the dark, results in an essentially quantitative yield of crude dibromides, **7–9**. The reaction is exothermic and appears to occur essentially instantaneously, the red-brown coloration of bromine disappearing immediately to give a clear colorless solution. Characterization of the crude dibromides (isolated via evaporation of the solvent under nitrogen) by means of ^{1}H and ^{13}C nmr analysis confirms the initial assignments of Dauben and Cargill. It may be noted that these previous assignments were made in accord with the observations of Winstein and co-workers (8), which were based on the analogous bromination of bicyclo[2.2.1]hepta-2,5-diene.

One olefinic product is observed when the solvent is methylene chloride or carbon tetrachloride (see Table 1). This species is identified as *exo*-2-*syn*-7-dibromobicyclo[2.2.1]hept-5-ene, **7**, on the basis of its ^{13}C nmr spectrum and by comparison with an authentic sample prepared by the analogous bromination of bicyclo[2.2.1]hepta-2,5-diene in accord with the procedure of Winstein and co-workers (8).

The remaining two species, **8** and **9**, isolable from these solvents are isomeric nortricyclenes. Compound **8** exhibits seven aliphatic carbon resonances



Can. J. Chem. Downloaded from www.nrcresearchpress.com by 210.87.254.105 on 09/05/12
For personal use only.

TABLE 1. Solvent dependence of the product ratio under conditions of kinetic control for the addition of molecular bromine to tetracyclo[3.2.0.0^{2,7}.0^{4,6}]heptane at 23–25°C

Solvent	ε[a]	% Product distribution 7	8	9	10	11	12	13	14	15	16	17	Ratio A[b]	Ratio B[c]	N_{rel}[d]
c-C_6H_{12}	2.02^{20}	17	49	21	7	6	0						49:51	100:0	
CCl_4	2.23	20	64	16	0	0	0						64:36	100:0	
CH_2Cl_2	8.9	27	50	23	0	0	0						50:50	100:0	
EtOH	24.3	5	8	4	0	0	0	42	35	6	0	0	50:50	17:83	
MeOH	32.6	5	2	4	0	0	0	52	27	10	0	0	54:46	11:89	24 (25)
Mixed Solvents															
MeOH:CH_2Cl_2 (v/v)															
0.5:99.5		18	37	37	0	0	1	3	3	1	0	0	41:59	93:7	13 (20)
5:95		9	20	29	0	0	4	12	14	5	7	0	36:64	62:38	16 (16.5)
10:90		8	17	21	0	0	4	17	17	7	9	0	38:62	50:50	20 (20)
30:70		10	10	9	0	0	0	29	28	7	3	4	39:61	29:71	25 (20)
50:50		5	7	4	0	0	0	40	35	5	2	2	47:53	16:84	19 (19.5)

[a]Dielectric constant at 25°C, except as indicated by a superscript, for the pure liquid.
[b]Ratio A = the % edge-on attack vs. % corner or end-on attack.
[c]Ratio B = the % dibromo adducts vs. % solvent-incorporated adducts.
[d]N_{rel} = the relative nucleophilicities of bromide ion to methanol.

in its ^{13}C nmr spectrum, three of which resonate at higher field than that normally observed for norbornyl carbons and are thus readily assigned as the cyclopropyl carbon resonances. The absence of symmetry allows one to immediately assign **8** as *exo,endo*-3,5-dibromotricyclo[2.2.1.0^{2,6}]heptane. In contrast to **8**, compound **9** exhibits only five aliphatic resonances and therefore has a plane of symmetry which passes through C1, C4, and C7. Assignment of **9** as *exo,exo*-3,5-dibromotricyclo-[2.2.1.0^{2,6}]heptane follows from a comparison of this species' spectral properties, ^{1}H, ^{13}C nmr, and ir, with those of an authentic sample prepared from bicyclo[2.2.1]hepta-2,5-diene. The symmetric dibromide prepared in this way has been shown elsewhere (8), by means of dipole moment studies, to be di-*exo*.

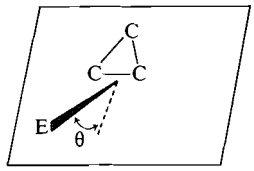
An examination of the ^{13}C nmr resonances at this point (see Experimental) leads to a rather surprising observation. If one considers the relative chemical shifts of C7 in **8** and **9**, one would expect C7 in **9** to resonate at higher field than the analogous methylene carbon in **8** because of the double γ *gauche* effect of two *exo* bromines in the case of **9** vs. only one *exo* bromine in **8** (9, 10, 11). We observe, however, C7 resonances at δ 30.1 and 33.2 for **8** and **9** respectively, the opposite of our initial expectations! A reexamination of our data for the analogous 3-arylthio, 5-chloro and 3-phenylseleno, 5-chloro nortricyclenes (12, 13, 14) also shows this trend. While a rationalization for this apparent reversal in the normal γ *gauche* effect is not immediately obvious, we note that some care must be exercised in making assignments in this ring system.

If cyclohexane is used as solvent, two further dibromo adducts, **10** and **11**, are observed. Both **10** and **11** are norbornenyl derivatives as is demonstrated by olefinic protons in the ^{1}H nmr spectra and olefinic carbon resonances at δ 137.4 and 137.2, 135.2, respectively. Compound **10** has only four resonances in its ^{13}C nmr spectrum and is thus assigned on the basis of its symmetry as *exo,exo*-2,3-dibromobicyclo[2.2.1]hept-5-ene. The presence of seven resonances in the analogous spectrum of **11** defines it as *exo,endo*-2,3-dibromobicyclo[2.2.1]hept-5-ene.

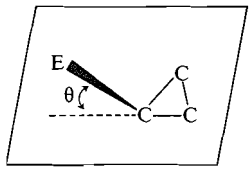
The use of hydroxylic solvents, such as methanol and ethanol, leads to products of solvent-incorporation, **13–15**, in addition to the normal dibromides, **7–9**. In both of these solvents, products of solvent-incorporation are found to predominate by a factor of 8 or 9 to 1 for a bromine concentration of 0.01–0.06 mol dm^{-3}.

In order to acquire further data with respect to the effect of changing the polarity and nucleophilicity of the solvent system, we carried out a number of reactions in mixtures of methanol and methylene chloride. As can be seen from an examination of Table 1, the percentage of dibromo adducts relative to the percentage of solvent-incorporated adducts decreases as one progresses from neat methylene chloride to neat methanol, as would be expected. Of particular interest, however, is the product distribution obtained in 0.5:99.5 methanol – methylene chloride. Under these reaction conditions the molar concentration of methanol was equivalent to that of molecular bromine. Our results indicate that, on a competitive basis, bromide ion is a more effective nucleophile

Can. J. Chem. Downloaded from www.nrcresearchpress.com by 210.87.254.105 on 09/05/12
For personal use only.



Edge-on Attack
retention of configuration at carbon
in plane $\theta = 0°$



Corner or End-on Attack
inversion of configuration at carbon
in plane $\theta = 0°$, equivalent to collinear attack

SCHEME 1

than methanol by a factor of at least 13 to 1. Also of note is the observation of a further, previously unknown, dibromo adduct **12**. On the basis of its ^{13}C nmr spectrum and its mass spectrum which exhibits a retro-Diels–Alder fragmentation to yield a C_5H_5Br cation-radical, we are able to assign the configuration as *exo,anti*-2,7-dibromobicyclo-[2.2.1]hept-5-ene.

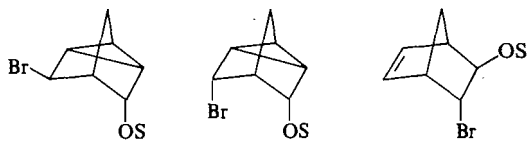
In order to elaborate on the importance of these observations, we note that conceptually there exist two distinct modes whereupon a strained carbon–carbon single bond might interact with an electrophile, EN. For example, the electrophile and the strained bond may approach each other orthogonally, i.e. edge-on attack. In the case of cyclopropane itself, one would anticipate the maximum interaction of orbitals to occur when the electrophile approaches the front lobe of the single bond in the same plane as the three carbons which define the ring, as is shown in Scheme 1 for $\theta = 0°$. In the case of a substituted cyclopropane, as is found in substrate **1**, the best angle of approach with respect to this plane may be significantly different, although values of θ as large as 90° seem very unlikely if one accepts the Walsh model for the orbitals in cyclopropanes. The major point to be noted is that this type of interaction leads to *retention* of configuration at the carbon atom, wherein the new bond is formed with the electrophilic portion of the reagent (E of EN).

Alternatively, the electrophile may approach the corner of the strained bond along an extended axis joining the two carbon atoms, that is to say, collinearly or end-on, the interaction between the rear lobe of the bond undergoing cleavage and the electrophile ultimately resulting in inversion of configuration at the carbon atom forming the new bond with E. Once again we note that in the case of an unsymmetrically substituted cyclopropane as in **1**, the preferred orbital interaction may lead to an angle of approach which is different from the idealized situation of collinearity.

This classical approach may be unnecessarily restrictive as initial attack may in fact involve an *edge which does not finally suffer cleavage*, with subsequent cleavage occurring after edge-to-corner isomerization (15). Such a scenario, however, exchanges one problem for another, that is, how does one distinguish whether or not attack occurs on a bond which *is not* subsequently cleaved or in some other way altered?

Such a classical approach is not without controversy. One referee, for example, has pointed out that LCAO SCF MO calculations of the electrostatic potential energy experienced by a unit positive charge as it interacts with the electrons and nuclei of cyclopropane (16) establish clearly, at least to his satisfaction, that an electrophile attacks a three-membered ring in an edge-wise fashion. It was further pointed out that this is not surprising because the electron density is concentrated in that region and that steric hindrance to approach of the electrophile towards corner attack must exist. In direct contrast are the results and interpretations of Skell and co-workers (6), who, as we have previously noted, prefer the alternate scenario of stereospecific corner attack.

It is our contention that the classical two-competitive-pathways approach best explains the data given in Table 1. Thus, species **12** and **13** are the result of edge-on attack, while **7**, **9**, **10**, and **14–17** result from corner attack. Compounds **8** and **11** are assigned as the products of edge-on and corner attack, respectively, in accord with the assignments of the solvent-incorporated species, **13** and **16**. In this respect we note the absence of such species as **18–20**.



18 **19** **20**

Considering the observed product distributions in Table 1, we observe a number of trends. For example, the ratio of edge-on attack to corner attack (ratio A) shows a smooth variation from neat methylene chloride, 50:50, to neat methanol, 54:46, passing through a minimum for the 5:95 methanol – methylene chloride solvent system. The overall effect of changing the polarity of the solvent system

Can. J. Chem. Downloaded from www.nrcresearchpress.com by 210.87.254.105 on 09/05/12
For personal use only.

Can. J. Chem. Downloaded from www.nrcresearchpress.com by 210.87.254.105 on 09/05/12
For personal use only.

either by using mixed solvents or neat solvents appears, however, to be minimal as judged by ratio A. This point is further demonstrated by comparing the relative nucleophilicities, N_{rel}, of bromide ion to methanol (column 16, Table 1) as the solvent polarity is varied. Although the values of N_{rel} vary from 13- to 25-fold preferences in favour of bromide ion over that of methanol, an error of 3 or 4% in the product distributions, which is quite reasonable for the nmr and glc techniques used, would be sufficient to average out these differences. To show this effect we have calculated the possible error in N_{rel} based upon an error of ±4% in the ratio B. These values are shown in Fig. 1. The mean values of N_{rel}, based upon these high–lows, are given in Table 1, column 16, in parentheses. The average of these values is 20.2 in very good agreement with the value of 19.5 calculated on the basis of our primary N_{rel} values. We therefore conclude that solvent polarity has little effect upon the relative nucleophilicities of bromide ion and methanol for attack on the intermediate species during the bromination of tetracyclo[3.2.0.$0^{2,7}$.$0^{4,6}$]heptane.

The relatively high percentage of nortricyclenes compared to olefinic products, in all solvent systems, presumably reflects the ability of bromide ion, and the alcohols, to effectively trap the first formed cationic intermediates before rearrangement is possible. These intermediates are in all likelihood intimate ion-pairs, **21** and **22**, or solvent-separated ion-pairs, **23** and **24**, as are shown in Scheme 2. The absence of *endo* methoxy and ethoxy nortricyclenes lends support to this scenario, in accord with Cristol *et al.*'s criteria (3). This observation also serves to rule out a stereochemical interpretation such as Skell's, at least in so far as solvent-incorporated products are concerned, unless one is willing to propose that the active electrophile is CH_3O^+, which seems very unlikely under our reaction conditions. Furthermore, it would appear even less likely that **8** is formed according to Skell's hypothesis when **18** is not observed or isolated.

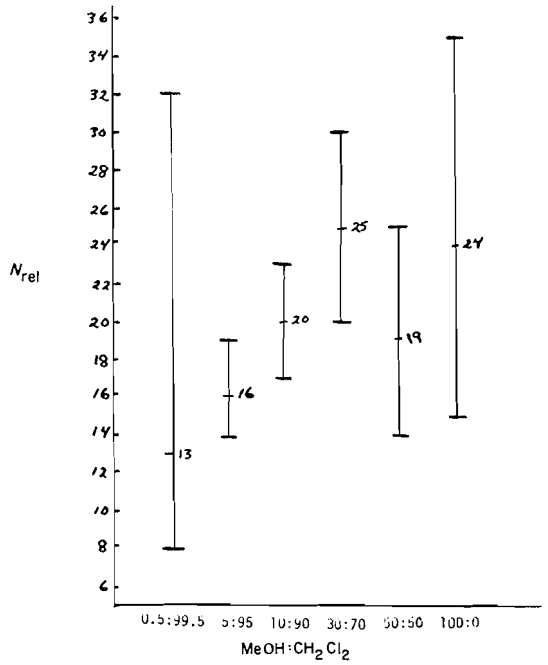


FIG. 1. Plot of N_{rel} as a function of mixed solvent ratio assuming an error of ±4% in the measurement of ratio B.

The further dissociation of ion-pairs **21–24** to free carbonium ions **25** and **26** is presumably followed by a fast isomerization to the isomeric unsaturated ions **27–30**. Species **28** appears to have a long enough life-time in some solvent systems to collapse to products **10**, **11**, **16**, and **17** while ion **27**, when it exists, seems to immediately undergo Wagner–Meerwein rearrangement to ion **29**.

The exact nature of the ionic species and their relationship to each other on the reaction hypersurface is not yet unambiguous. For example, it is conceivable that **25** and **26** might interconvert by a 6,2-hydrogen shift. If such an isomerization occurs the true origin of compounds **7**, **10–12**, and **15–17** must be considered in doubt. We stress however that the absence of adducts **18** and **19** rules out **25** and **26** as long-lived intermediates. This latter interpretation rests very strongly on the validity of Cristol's hypothesis (see ref. 3). If Cristol's hypothesis is true, our data require a mechanism involving both corner and edge-wise attack. A mechanism based upon only edge-wise attack may be ruled out!

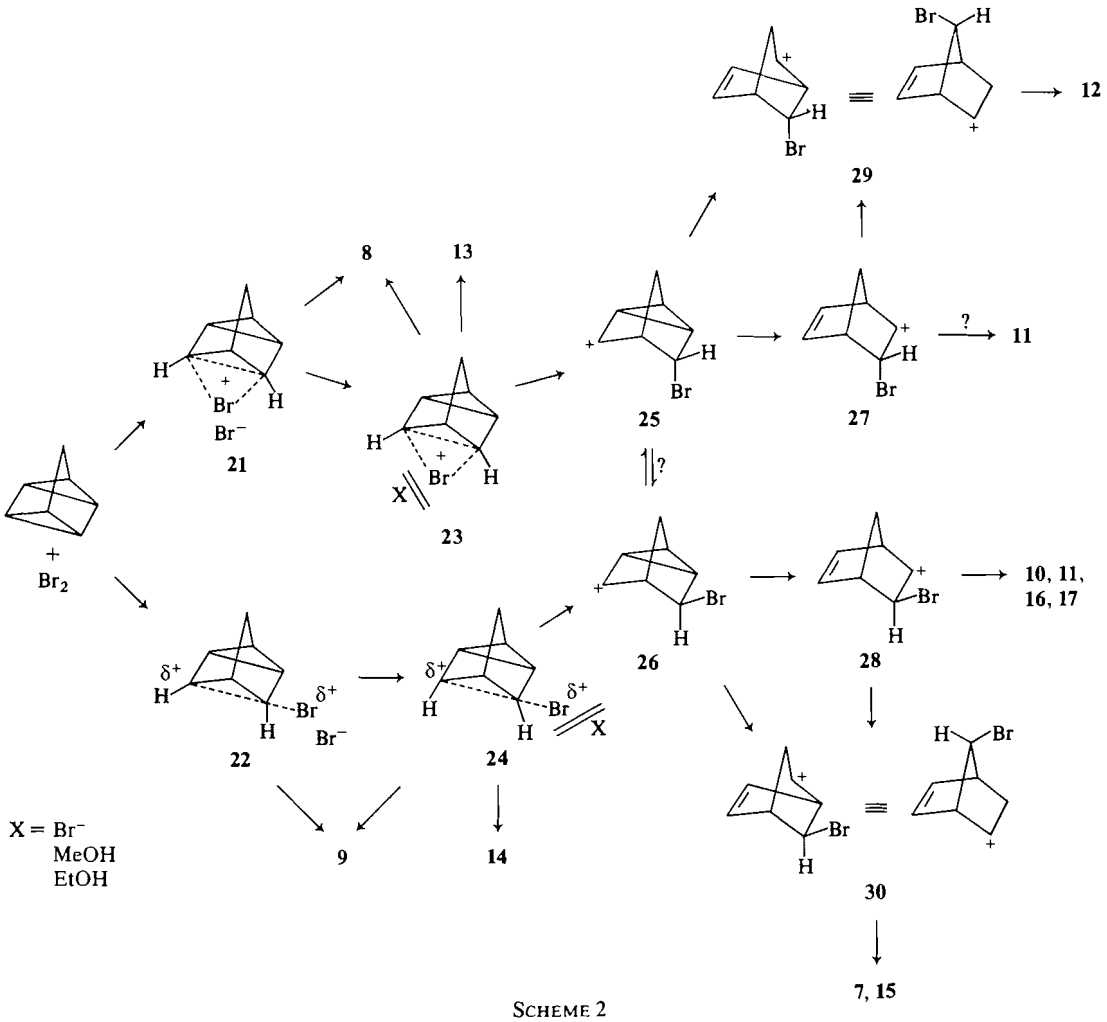
The interpretation suggested above, while quite different from that of Skell and co-workers, may only reflect the perhaps anomalous behaviour of this very novel and reactive ring system. We acknowledge that the mechanism of Skell and coworkers accounts very well for a plethora of data. In view of the results presented above we suggest, however, that their stereochemical interpretation may be incorrect.

Experimental

General

The ^{1}H nmr spectra were recorded on Varian Associates T-60 and HA-100 spectrometers. The ^{13}C nmr spectra were recorded on a Varian FT-80-16K spectrometer with a broad band probe, operating at 20 000 MHz, using chloroform-*d* as an internal lock and reference. All spectra were run in sealed tubes. Infrared spectra were run in NaCl cavity cells as $CHCl_3$ solutions, using a Unicam 1100 spectrometer. All analytical and preparative tlc separations were performed on Analtech precoated plates.

Can. J. Chem. Downloaded from www.nrcresearchpress.com by 210.87.254.105 on 09/05/12
For personal use only.



SCHEME 2

Tetracyclo[3.2.0.0^{2,7}.0^{4,6}]heptane, **1**, was available commercially from Aldrich. It was used without further purification. The purity of **1** was established by nmr and glc (SE-30 column).

Caution: Scrupulous avoidance of contact with the materials prepared during this investigation is essential! *At least two deaths of laboratory workers in Winstein's laboratory have been attributed to these compounds.* All samples were handled in this laboratory under conditions of continuous isolation, using a glove box equipped with a filter system suitable for use with carcinogenic and radioactive material!

The Reaction of Bromine with Tetracyclo[3.2.0.0^{2,7}.0^{4,6}]-heptane

A solution of bromine (1–3 mmol) in 20–30 mL of the appropriate solvent is added dropwise to a stirred solution containing a molar equivalent of **1** in 30–50 mL of the same solvent. The solvent is removed at room temperature by rotary evaporation (a temperature of 45°C was used with both MeOH and EtOH), and the crude yellow oils stored under nitrogen. These oils which corresponded to an essentially quantitative yield were analyzed by nmr and mass spectroscopy. Chromatographic separation of the various isomers was accomplished on silica gel. Product distributions could *not* be determined from these isolated yields, however, because of isomerization problems on the plates. The glc yields (SE-30) were, however, in agreement, ±2–3%, with the values calculated from both ^{1}H and ^{13}C nmr spectra. Because of the toxicity factors and handling difficulties associated with these compounds no attempt was made to obtain physical properties such as melting points, or elemental analysis.

Spectroscopic Properties

Values of ^{13}C nmr ($CDCl_3$) δ: *exo*-2-*syn*-7-dibromobicyclo-[2.2.1]hept-5-ene: 48.7 (d, C1), 54.1 (d, C2), 29.1 (t, C3), 44.0 (d, C4), 135.8 (d, C5), 137.8 (d, C6), 56.4 (d, C7). *Exo*-2-*anti*-7-dibromobicyclo[2.2.1]hept-5-ene: 51.4 (d, C1), 56.0 (d, C2), 33.0 (t, C3), 44.4 (d, C4), 133.0 (d, C5), 134.5 (d, C6), 59.2 (d, C7). *Exo,exo*-2,3-dibromobicyclo[2.2.1]hept-5-ene: 44.5 (d, C1, C4), 52.4 (d, C2, C3), 137.4 (d, C5, C6), 30.2 (t, C7). *Exo,endo*-2,3-dibromobicyclo[2.2.1]hept-5-ene: 44.5 (d, C1), 52.8 (d, C2(C3)), 52.6 (d, C3(C2)), 45.6 (d, C4), 135.2 (d, C5), 137.2 (d, C6), 30.2 (t, C7). *Exo,exo*-3,5-dibromotricyclo[2.2.1.0^{2,6}]-heptane: 13.5 (d, C1), 22.3 (d, C2, C6), 51.0 (d, C3, C5), 43.9 (d, C4), 33.2 (t, C7). *Exo,endo*-3,5-dibromotricyclo[2.2.1.0^{2,6}]-heptane: 15.5 (d, C1), 19.4 (d, C2), 53.7 (d, C3), 43.9 (d, C4), 54.3 (d, C5), 22.1 (d, C6), 30.1 (t, C7). *Exo*-2-methoxy-*syn*-7-bromobicyclo[2.2.1]hept-5-ene: 46.9 (d, C1), 82.2 (d, C2), 29.4 (t, C3), 43.9 (d, C4), 134.6 (d, C5), 139.0 (d, C6), 56.7 (d, C7), 56.8 (q,

CH_3O). *Exo*-2-bromo-*exo*-3-methoxybicyclo[2.2.1]hept-5-ene: 45.7 (d, C1), 54.0 (d, C2), 82.8 (d, C3), 46.1 (d, C4), 139.5 (d, C5), 133.0 (d, C6), 49.4 (t, C7), 56.4 (q, CH_3O). *Exo*-3-bromo-*exo*-5-methoxytricyclo[2.2.1.$0^{2,6}$]heptane: 14.6 (d, C1), 19.2 (d, C2), 54.6 (d, C3), 40.0 (d, C4), 85.2 (d, C5), 17.9 (d, C6), 28.6 (t, C7), 56.5 (q, CH_3O). *Endo*-3-bromo-*exo*-5-methoxytricyclo-[2.2.1.$0^{2,6}$]heptane: 12.8 (d, C1), 21.8 (d, C2), 52.6 (d, C3), 40.0 (d, C4), 81.8 (d, C5), 18.8 (d, C6), 27.5 (t, C7), 56.3 (q, CH_3O). *Exo*-2-ethoxy-*syn*-7-bromobicyclo[2.2.1]hept-5-ene: 47.0 (d, C1), 83.9 (d, C2), 29.2 (t, C3), 44.0 (d, C4), 134.8 (d, C5), 139.0 (d, C6), 57.0 (d, C7), 67.0 (t, CH_2O), 15.1 (q, CH_3CH_2O). *Exo*-3-bromo-*exo*-5-ethoxytricyclo[2.2.1.$0^{2,6}$]heptane: 14.6 (d, C1), 19.2 (d, C2), 55.2 (d, C3), 40.5 (d, C4), 83.7 (d, C5), 18.4 (d, C6), 28.8 (t, C7), 64.5 (t, CH_2O), 15.4 (q, CH_3CH_2O). *Endo*-3-bromo-*exo*-5-ethoxytricyclo[2.2.1.$0^{2,6}$]heptane: 13.0 (d, C1), 21.8 (d, C2), 53.1 (d, C3), 40.5 (d, C4), 80.3 (d, C5), 19.4 (d, C6), 27.8 (t, C7), 64.3 (t, CH_2O), 15.4 (q, CH_3CH_2O).

Acknowledgements

The continued financial support of the Natural Sciences and Engineering Research Council of Canada in terms of an annual operating grant during the author's tenure at the University of Ottawa is gratefully acknowledged. Useful discussions with Dr. O. E. Edwards, Division of Chemistry, National Research Council of Canada, are also greatly appreciated.

1. W. G. DAUBEN and R. L. CARGILL. Tetrahedron, **15**, 197 (1961).
2. S. J. CRISTOL and R. T. LALONDE. J. Am. Chem. Soc. **80**, 4355 (1958).
3. (*a*) S. J. CRISTOL, W. Y. LIM, and A. R. DAHL. J. Am. Chem. Soc. **92**, 4013 (1970); (*b*) S. J. CRISTOL, J. K. HARRINGTON, and M. S. SINGER. J. Am. Chem. Soc. **88**, 1529 (1966).
4. J. BREDT. J. Prakt. Chem. **121**, 153 (1929).
5. (*a*) R. T. LALONDE and A. D. DEBBOLI, JR. J. Org. Chem. **38**, 4228 (1973); (*b*) J. C. DAY, K. J. SHEA, and P. S. SKELL. J. Am. Chem. Soc. **95**, 5089 (1973); (*c*) N. C. DENO and D. N. LINCOLN. J. Am. Chem. Soc. **88**, 5357 (1966); (*d*) J. M. HOFFMANN, J. K. GRAHAM, and C. F. ROWELL. J. Org. Chem. **41**, 3005 (1975); (*e*) G. G. MAYNES and D. E. APPLEQUIST. J. Am. Chem. Soc. **95**, 856 (1973); (*f*) K. J. SHEA and P. S. SKELL. J. Am. Chem. Soc. **95**, 6728 (1973); M. S. KHARASCH, M. Z. FINEMAN, and F. R. MAYO. J. Am. Chem. Soc. **61**, 2139 (1939); (*h*) R. T. LALONDE, P. B. FERRARA, and A. D. DEBBOLI, JR. J. Org. Chem. **37**, 1094 (1972); (*i*) D. E. APPLEQUIST and L. F. MCKENZIE. J. Org. Chem. **41**, 2262 (1976); (*j*) L. B. LAMBERT and K. KOBAYASHI. J. Org. Chem. **41**, 671 (1976); (*k*) J. B. LAMBERT and B. A. IWANTZ. J. Org. Chem. **37**, 4082 (1972); (*l*) J. B. LAMBERT, R. D. H. BLACK, J. H. SHAW, and J. J. PAPAY. J. Org. Chem. **35**, 3214 (1970); (*m*) C. H. DEPUY, W. C. ARNEY, JR., and D. H. GIBSON. J. Am. Chem. Soc. **90**, 1830 (1968); (*n*) C. H. DEPUY. Fortschr. Chem. Forsch. **40**, 73 (1973).
6. P. S. SKELL, J. C. DAY, and K. J. SHEA. J. Am. Chem. Soc. **98**, 1195 (1976).
7. (*a*) G. H. SCHMID and D. G. GARRATT. *In* The chemistry of functional groups. Supplement A: The chemistry of double-bonded functional groups. *Edited by* S. Patai. John Wiley & Sons, London. 1977. pp. 764–785; (*b*) P. B. D. DE LA MARE and R. BOLTON. *In* Electrophilic additions to unsaturated systems. Elsevier, New York. 1966; (*c*) R. C. FAHEY. *In* Topics in stereochemistry. Vol. 3. *Edited by* E. L. Eliel and N. L. Allinger. Interscience, New York. 1968. p. 237; (*d*) G. H. SCHMID. *In* The chemistry of the carbon–carbon triple bond. *Edited by* S. Patai. John Wiley & Song, Chichester, England. 1978.
8. (*a*) S. WINSTEIN. J. Am. Chem. Soc. **83**, 1516 (1961); (*b*) S. WINSTEIN and M. SHATAVSKY. Chem. Ind. 56 (1956); (*c*) L. SCHMERLING, J. P. LUVISI, and R. W. WELCH. J. Am. Chem. Soc. **78**, 2819 (1956).
9. A. W. MCCULLOCH, A. G. MCINNES, D. G. SMITH, and J. A. WALTER. Can. J. Chem. **54**, 2013 (1976).
10. J. B. STOTHERS, C. T. TAN, and K. C. TEO. Can. J. Chem. **54**, 1211 (1976).
11. E. LIPPMAA, T. PEHK, and J. PAASIVIRTA. Org. Magn. Reson. **5**, 277 (1973).
12. (*a*) D. G. GARRATT and P. L. BEAULIEU. J. Org. Chem. **44**, 3555 (1979); (*b*) P. L. BEAULIEU, A. KABO, and D. G. GARRATT. Can. J. Chem. **58**, 1014 (1980); (*c*) D. G. GARRATT, P. L. BEAULIEU, and V. M. MORISSET. Can. J. Chem. **58**, 1021 (1980).
13. P. L. BEAULIEU, V. M. MORISSET, and D. G. GARRATT. Can. J. Chem. **58**, 1005 (1980).
14. D. G. GARRATT and A. KABO. Can. J. Chem. **58**, 1030 (1980).
15. (*a*) C. H. DEPUY, P. C. FÜNFSCHILLING, A. H. ANDRIST, and J. M. OLSON. J. Am. Chem. Soc. **99**, 6297 (1977); (*b*) T. C. MORRILL, S. MALASANTA, K. M. WARREN, and B. E. GREENWALD. J. Org. Chem. **40**, 3032 (1975); (*c*) J. B. HENDRICKSON and R. K. BOECKMAN, JR. J. Am. Chem. Soc. **91**, 3269 (1969); (*d*) A. NICKON and J. H. HAMMONS. J. Am. Chem. Soc. **86**, 3322 (1964).
16. R. BONACCORSI, E. SCROCCO, and J. TOMASI. J. Chem Phys. **52**, 5270 (1970).

Can. J. Chem. Downloaded from www.nrcresearchpress.com by 210.87.254.105 on 09/05/12
For personal use only.

A tunable pulsed Raman spectrometer capable of probing picosecond processes[1]

D. NICOLLIN, P. BERTELS, AND J. A. KONINGSTEIN
Department of Chemistry, Carleton University, Ottawa, Ont., Canada K1S 5B6

Received January 16, 1980

D. NICOLLIN, P. BERTELS, and J. A. KONINGSTEIN. Can. J. Chem. **58**, 1334 (1980).

A pulsed tunable laser Raman spectrometer is described. The relevant characteristics are: tunability in the range of 355–755 nm, peak power of > 100 kW, pulse duration 3.2 ns, spectral line width < 0.1 cm^{-1}. Raman pulses can be studied in real time with a resolution > 10 ns while Raman spectra can be recorded with an experimental slit width > 0.5 cm^{-1}. The overall performance of the instrument may be compared to that of a conventional cw laser Raman spectrometer having typical power levels of 100 mW. Spectroscopic measurements are discussed which demonstrate the capability of the apparatus to probe Raman processes which occur at the pico and microsecond time scale.

D. NICOLLIN, P. BERTELS et J. A. KONINGSTEIN. Can. J. Chem. **58**, 1334 (1980).

On décrit un spectromètre Raman au laser à impulsions que l'on peut ajuster. Les principales caractéristiques sont: la synthonisation dans l'intervalle de 355–755 nm, une puissance maximale > 100 kW, durée d'impulsion de 3.2 ns, la largeur de la ligne spectrale > 0.1 cm^{-1}. Les impulsions Raman peuvent être étudiées en temps réel avec une résolution > 10 ns tandis que les spectres Raman peuvent être enregistrés avec une largeur de pente > 0.5 cm^{-1}. La performance totale de l'instrument peut être comparée à celle d'un spectromètre Raman conventionnel au laser o.c. ayant un niveau typique de puissance de 100 mW. On discute des mesures spectroscopiques qui démontrent la capacité de l'appareil d'explorer les effets Raman qui se produisent dans des intervalles de temps de l'ordre de la pico et de la microseconde.

[Traduit par le journal]

I. Introduction

For all practical purposes it appears that pulsed laser Raman spectroscopy is apt to have a great impact in the study of short-lived intermediates, properties of electronic excited states including their lifetime (1–3). In order to explore these properties one has to make use of the frequency tunability of the pulsed laser radiation, its very high peak power combined with short duration, and narrow spectra line width. However, the above properties can only be fully evaluated if the scattered light can be monitored with a system having a detection capability including real time resolution, high spectral resolution, high sensitivity, and low noise. Although several reports have appeared in the literature dealing with pulsed Raman spectrometers, none of the systems described therein met all the above required characteristics simultaneously (4–7). In the present work we described a Raman spectrometer in which level of operation combines high performance in all mentioned characteristics. The organization of this paper is as follows. In section II the instrument is described in full detail and in section III a short discussion is presented of some relevant results unique to pulsed light scattering spectroscopy as obtained with the instrument.

II. Description of the Experimental Set-up

In this section the various components of the tunable pulsed laser Raman spectrometer are described.

A. The Laser Light Source and Optical Arrangement

The unit used in the present set-up (see Fig. 1) is composed of a N_2 laser which pumps a dye laser. The N_2 laser, model M2000 from Lambda Physik, generates light pulses having ~1 mW peak power with a duration of 4 ns and a variable repetition rate up to 50 Hz. This laser is used to pump a Lambda Physik FL 2000 dye laser which includes one amplifier stage. Relevant characteristics of the laser system are a high conversion efficiency (~10%) for dyes which produce stimulated emission in the spectral range of 355–755 nm. This can be extended to 217 nm with frequency doubling, with a spectral band width of ~1 cm^{-1} and this value can be reduced to a factor 10 by installing an etalon in the laser cavity while maintaining ~80% of the energy. Associated with the laser peak is a broad band emission spectrum due to superradiance of the dye laser oscillator stage, which is usually of such high intensity that it prevents the recording of weak Raman spectra. In order to overcome the effect of superradiance, a tunable grating filter (PTR optics model F 100 with variable slits) was placed between the sample and dye laser. This filter reduces the effective laser light level to an approximate average power level of 2.5 mW with the laser operating at a 25 pulses/s repetition rate (0.1 mJ/pulse). We found however that for certain samples, like transparent liquids or properly polished transparent single

[1]Research supported by the Natural Sciences and Engineering Research Council of Canada.

0008-4042/80/131334-10$01.00/0
©1980 National Research Council of Canada/Conseil national de recherches du Canada

Can. J. Chem. Downloaded from www.nrcresearchpress.com by 210.87.254.42 on 09/05/12
For personal use only.

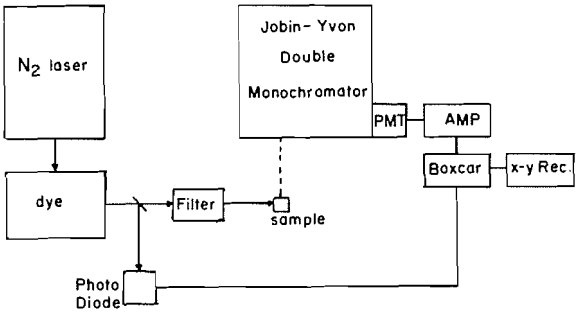


FIG. 1. Schematics of the pulsed laser Raman spectrometer. The tunable dye laser is built following a modular concept, that is, oscillator, amplifier cells, and dye reservoir are interchangeable. Not shown is the optical system for the collection of the scattered light.

crystals, spectra could be recorded some 10 nm away from the peaking frequency of the superradiance emission without the use of the filter. This is specially true if the laser emission occurred away from the center frequency of the superradiance band and towards longer wavelength.

The light from the laser was focussed into the sample. This caused some problems in that without the tunable grating filter in place and in employing a spherical lens with $f < 25$ cm the quartz cells containing liquid samples were damaged and cracks developed in even such hard crystals like rare earth garnets or ruby, causing a larger increase in the scattered light level. Damage to the sample was, however, eliminated if the spherical lens was used in combination with the filter or the lens itself replaced with a cylindrical one. This would, at the same time, prevent the possible occurrence of non linear effects (8). It is thus important to measure from time to time the light level of the laser pulses and this was achieved by using a GEN-TEC ED 100 Joule meter, or a GCO holographic radiometer to determine the average power of the pulses (the two instruments were in agreement to within 10%). Neutral density screens of pure nickel were employed in combination with the GCO radiometer to prevent saturation of the probe. Glass neutral density filters are of no use because they are immediately damaged by the powerful laser pulses. In our experiments the scattered light pulses were dispersed with a Jobin Yvon double monochromator equipped with curved holographic gratings. The stray light rejection rate of this instrument amounts to 10^{-14} if measured at 20 cm^{-1} away from a Rayleigh line and spectra were recorded in the 90° geometry.

B. The Detection System

It has previously been remarked that the recording of nanosecond signals requires constant advances in the state of the art (9, 10). In our system where the nanosecond signals are due to Raman scattering rather than fluorescence or phosphorescence processes, use was made of the following components: (*i*) a cooled photomultiplier, (*ii*) suitable amplification stages for the signals emerging from the photomultiplier, and (*iii*) a boxcar integrator. Among those the photomultiplier tube is by far the corner stone of the system. This tube should have a rise time faster than that of the signal pulses in order not to distort them. Also, the photocathode should have a high sensitivity in the spectral range of interest and in addition the PMT should also have a high gain. Several considerations made us choose the RCA C31034 photomultiplier tube. The small size of its cathode, rather broad spectral response, fast rise time (2.3 ns at 2000 V), high gain ($\sim 10^7$ at 2000 V), reasonable price, and availability made this tube a prime candidate for pulsed work. The popular and commonly used ITT FW 130 PM tube in cw experiments cannot be used in the present experimental arrangements (11) because of its slow rise time while other phototubes having a less than 1 ns rise time are considerably more expensive.

In Fig. 2 we display the time response behaviour of the RCA C31034 PMT due to a single photoelectron leaving the cathode. We note that the pulse shape of the signal due to the event has a fwhm of 3.2 ns which happens, in a fortuitous way, to be equal to the width of the light pulses coming from the dye laser system (these pulses are, according to the manufacturer, 20% shorter than the 4 ns pulses of the N_2 laser). There is a great deal of information available in the literature regarding the detection of fluorescence spectra excited with pulsed lasers (12–16). They and Raman signals from strongly scattering systems like CCl_4 etc. can be detected directly by feeding the signal of the PMT in a boxcar integrator. For example, we obtained a full scale output signal of the boxcar, without amplification of the Raman signal pulses, for the 996 cm^{-1} band of benzene excited by radiation of 0.3 mJ/pulse ($\lambda = 457.9$ nm) at 20 μm spectrometer slit widths (spectral slit width 0.5 cm^{-1}). However, in order to detect weaker Raman signals it is necessary to amplify first the anode pulses and then feed them into a boxcar integrator.

The amplification of the weak Raman signals was achieved by cascading fast pulsed amplifiers (LeCroy W 101 A). Two stages were incorporated in the system which resulted in an overall gain of 100, a total rise time of ~ 1 ns, and a noise output of 5 mV

Can. J. Chem. Downloaded from www.nrcresearchpress.com by 210.87.254.42 on 09/05/12
For personal use only.

Can. J. Chem. Downloaded from www.nrcresearchpress.com by 210.87.254.42 on 09/05/12
For personal use only.

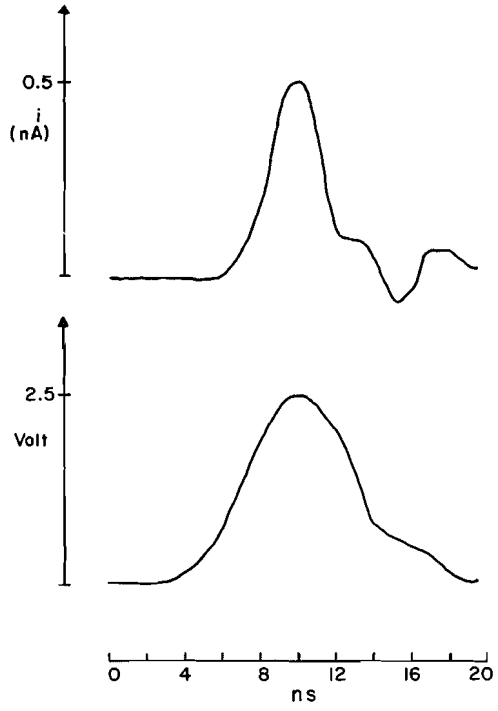


FIG. 2. Top: trace due to a single photoelectron response of the RCA C31034 PMT (HV = 2000 V) recorded with a A 7633 Textronix scope. The anode rise time is 2.3 ns and the fwhm is 3.2 ns. The behaviour of the tailing end of the pulse is due to ringing effects of the amplification system. Bottom: pulse due to Rayleigh-scattered light signals which were amplified by the cascading preamplifiers. The increase in fwhm is due to instrumental limitations of the boxcar integrator.

(10). Great care was taken in order to reduce, as much as possible, pickup of rf noise, generated by the N_2 laser placed only 2 m away from the detection system (12). Turning to the boxcar integrator EGG PAR model 162 (main frame) with gated integrator (model 164) we found that it was necessary to equip the main frame with a digital storage option to handle the low repetition rate of the light pulses so that the smallest aperture duration setting of ~10 ns could be used to obtain the best matching of the anode pulse. At this point it seems worthwhile to emphasize that this gate width determines the lowest time resolution capability of the system. A typical resulting shape of a light pulse due to Raman scattering is displayed in Fig. 2 and the fwhm amounts to ~6 ns. We feel this value to be of some importance because it permits real time studies of Raman signals, employing the 100 ns to 50 ms ranges of the boxcar integrator. The triggering of the model 162 was achieved in the following way. Although the power supply of the N_2 laser provides an electronic signal pulse which could be used for triggering purposes, we found that using these pulses did not result in real advantages. First of all the time delay between this pulse and the light pulse is ~500 ns which prevents one from using the highest time resolution scale of 100 ns (aperture delay range) of the boxcar if additional delay lines are to be eliminated. Secondly, due to changing characteristics of the thyratron of the N_2 laser, the time delay of ~500 ns is apt to change. These problems were circumvented by allowing part of the beam of the N_2 laser itself to fall on a EGG FND 100 ultra fast silicon photodiode (rise time < 1 ns), and by using the output signals for triggering purposes. The time required for the laser light pulses to reach the sample and then the photocathode of the PMT and from there via the amplification stages of the boxcar amounts to a total of ~75 ns. This delay is about equal to the dead time of the boxcar after the triggering signal from the photodiode has entered this instrument and therefore allows us to use all the aperture delay ranges (100 ns – 50 ms for lifetime measurement purposes). A Raman spectrum can now be recorded selecting the aperture duration of ~10 ns fixed in time and by letting the monochromator scan over a required spectra range. On the other hand, the signal can also be displayed in real time by setting the monochromator at a fixed wavelength and in letting the aperture duration scan within any of the ranges available on the model 162. The reproducibility of the instrument with regard to the latter option lifetime measurements can be seen in Fig. 3 where decay curves of the R_1 fluorescence line of ruby are shown.

III. Light Levels, Noise Characteristics, and Performance

It is clear from Fig. 3 that sensitivity problems do not interfere with a determination of the lifetime of strong signals like that due to phosphorescence but such can be quite different if a similar determination has to be carried out of a weaker (Raman) signal. Thus it seems worthwhile to present an evaluation of the performance of the system in comparison with that of the well known cw laser Raman systems.

A. Light Levels

The characteristics of the RCA c31034 PMT as given by the manufacturer are a typical 10% quantum efficiency in the green, a fwhm of 3.2 ns for the anode pulse, and a current gain G of 4×10^5 at 1520 V.

A quantum efficiency of 10% means that some 10 incoming photons are required to cause the ejection of 1 photoelectron from the photocathode. Given

Can. J. Chem. Downloaded from www.nrcresearchpress.com by 210.87.254.42 on 09/05/12
For personal use only.

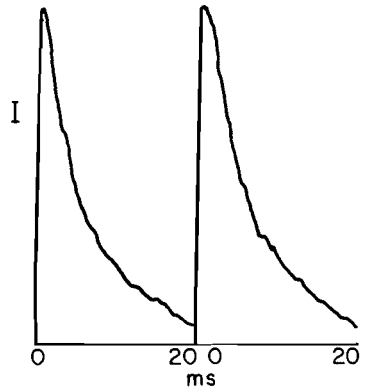


FIG. 3. Repetitive scans of pulses due to phosphorescence radiation at the frequency of the R_1 line of ruby. Phosphorescence was induced by the pulsed laser operating at $\lambda = 514.5$ nm. The long decay as compared to that of the laser light pulse (see Fig. 2) is due to the rather long lifetime of the excited state in which the phosphorescence transition originates.

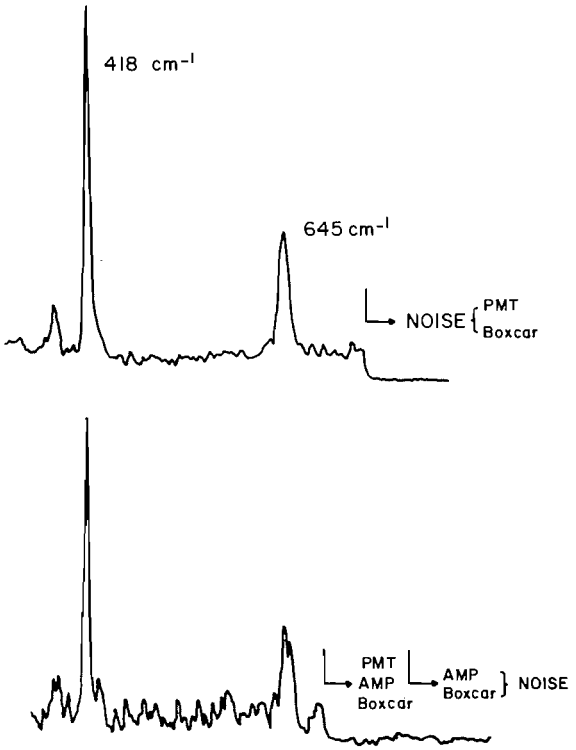


FIG. 4. Top: part of the Raman spectrum of ruby excited with the 514.5 nm radiation of the pulsed dye laser. The pulses due to Raman scattered light were fed directly from the PMT into the boxcar integrator. Also shown is the noise level due to PMT and boxcar only. Bottom: same part of the Raman spectrum with the laser intensity attenuated by a factor of 100 but now recorded with cascading amplifier *and* boxcar. Also shown is the noise level due to the various electronic components of the overall system.

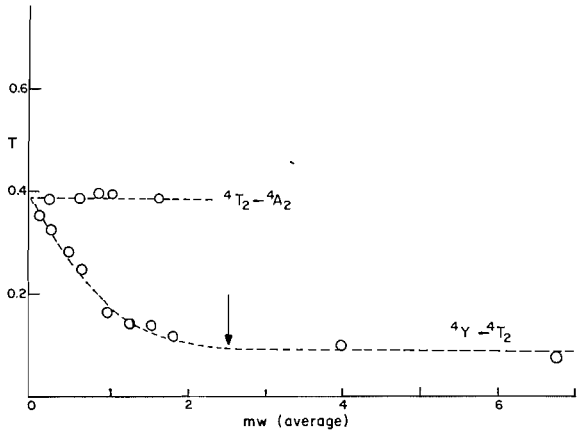


FIG. 5. Transmission at 457.9 nm of a 3.2×10^{-3} *M* solution of the complex $Cr(bpy)_3(ClO_4)_3$ in water as a function of the power of the pulsed laser. The horizontal line represents transmission characteristics due to the $^4T_2 \leftarrow {}^4A_2$ transition of $Cr(bpy)_3^{3+}$ with a cross section $\sigma = 8.89 \times 10^{-19}$ cm^2. Upon an increase of the power density (relative to the number of molecules in the irradiated area), achieved by focussing the laser light into the sample, the ground state $^4A_2$ becomes depopulated and the occurrence of excited state transitions of the type $^4Y \leftarrow {}^4T_2$ (with a cross section $\sigma = 2.56 \times 10^{-18}$ cm^2) causes the transmission to decrease and approach a constant value for I_L(average) > 2.5 mW. This behaviour is in the present analysis not interpreted in terms of bleaching of the $^4A_2$ ground state but rather, within the time frame of the duration of the pulse (~4 ns) the majority of the $Cr(bpy)_3^{3+}$ molecules are considered to be in the $^4T_2$ excited state (with an experimentally estimated lifetime of ~10 ps) and spectroscopic processes (like Raman or other optical transitions) associated with the $^4A_2$ ground state cannot be detected anymore.

the fwhm and gain G, we compute an output anode pulse current of 2×10^{-5} A, employing the relation $i = eg/\text{fwhm}$ (which assumes a triangular pulse shape) (9). This current being led across a 50 Ω load resistor generates a pulse of 1.0 mV at the input of the first amplification stage. The overall gain of the stages is 100, which means that an input voltage of 100 mV is applied to the gated integrator which, together with the main frame, produces an output voltage of 10 V. Hence the original 10 incoming photons give rise to a total signal of 10 V on a recorder if every single photon produces one volt! To check the validity of the above we carried out the following series of measurements. The output of the pulsed dye laser tuned to 514.5 nm was set at an average power of 10 mW (0.4 mJ energy per pulse at 25 Hz or 1.25×10^5 W peak power in 3.2 ns) which corresponds to 10^{15} photons. A Raman signal of CCl_4 was then generated by arbitrarily adjusting the slits of the J.Y. monochromator to yield 10 V (one photoelectron/pulse full scale recorder) signal. We compute a light scattering efficiency

Can. J. Chem. Downloaded from www.nrcresearchpress.com by 210.87.254.42 on 09/05/12
For personal use only.

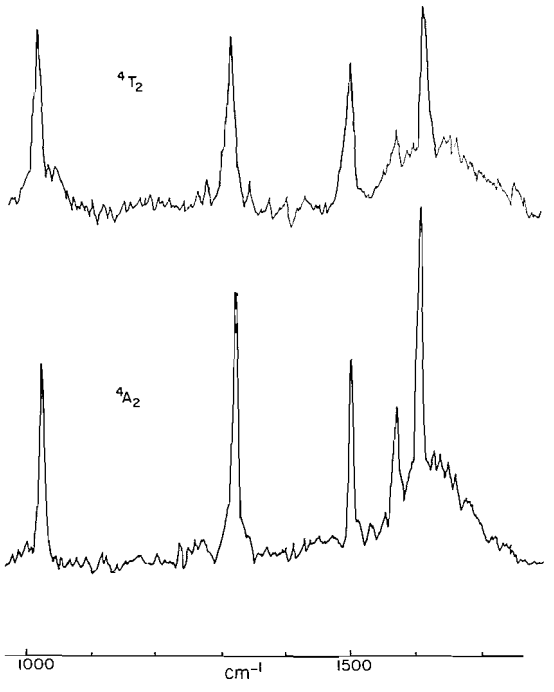


FIG. 6. Part of the Raman spectrum of $Cr(bpy)_3^{3+}$ recorded with the pulsed laser apparatus. The Raman shifts are due to normal modes involving motions of the atoms of the bipyridine rings. The top spectrum is that with the laser radiation >2.5 mV (average) focussed into the cell and consequently (see Fig. 5) Raman spectra are induced from $^4T_2$ only. The lower spectrum is that with the beam unfocussed (horizontal line in Fig. 5) and represents light scattering from $^4A_2$ only.

factor of 10^{-14}. Next, all parameters and, in particular, the geometrical arrangement were kept the same and the pulsed laser was replaced by a cw argon ion laser also operating at 514.5 nm with an average power of 400 mW corresponding to 10^{18} photons/s. Given the reduction factor of 10^{14} we now compute that 10^4 photons/s reach the photocathode and 1000 photoelectron/s are ejected. The calculated value for the current i follows from $i = NeG$ which in our example amounts to an average value of $i = 6.4 \times 10^{-11}$ A. By replacing the pulsed amplifiers and boxcar by a pico ammeter we measured a current precisely equal to the calculated value.

B. Noise Characteristics and Performance

Using the data sheet supplied by the manufacturer, that is 50_{cps} at $T = -30°C$ for the PMT, a typical number for the noise would be $1.6 = 10^{-7}$ counts/pulse as obtained by multiplying the dark count by the anode pulse width (5–7, 17). To evaluate the overall performance of the instrument versus the conventional cw systems we made use of the numbers given in the preceding section, hence:

$$[1]\quad \frac{(S/N)_{cw}}{(S/N)_{pulsed}} = \frac{\dfrac{1000_{cps}}{50_{cps}}}{\dfrac{1_{c/pulse}}{1.6 \times 10^{-7}{}_{c/pulse}}} = 3.2 \times 10^{-6}$$

This number for the ratios of the signal-to-noise in both systems appears to be precisely equal to the experiment ratio of the average power of the cw laser versus the pulsed laser peak power (6) (0.4 W vs. 25×10^5 W). However, this calculation really refers to an ideal case in the sense that, in our system, the computed noise would amount to 1/1000th of the width of the trace on the recorder paper. Furthermore eq. [1] overestimates the actual performance of the present system in that contrary to a cw system (in which the PMT noise is always larger than the noise of photon counting unit), the opposite holds for a pulsed amplified

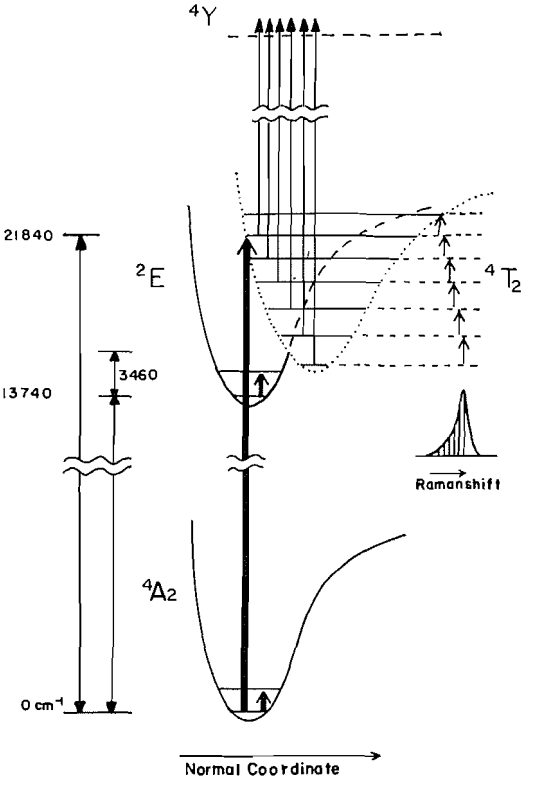


FIG. 7. Part of the energy level diagram of (2,2′-bipyridine)Cr(III) relevant to the present experiments. The energy of the pump (λ = 457.9 nm) reaches vibrational levels in the upper part of the $^4T_2$ electronic surface. Due to the larger number of photons delivered by the pulsed laser during the lifetime of these levels (and those in the bottom of the well) in comparison to the number of molecules in the irradiated area, population of these levels takes place and absorption transitions (at 457.9 nm) of the type ^4Y–$^4T_2$ takes place (see also Fig. 5). In addition Raman transitions are induced and due to the anharmonicity effect the band is expected to be broadened towards smaller shifts (see Fig. 8).

Can. J. Chem. Downloaded from www.nrcresearchpress.com by 210.87.254.42 on 09/05/12
For personal use only.

system. This is clearly demonstrated by the results displayed in Fig. 4, where spectra are shown recorded with and without the cascaded amplifiers. The upper trace (Fig. 4) shows a near flat response if the slits are closed, representing, in fact, boxcar ouput noise only. On the other hand the lower trace of Fig. 4 shows the effect of boxcar + amplifier

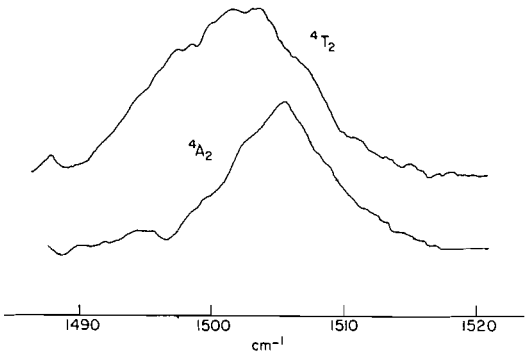


FIG. 8. A comparison of the band contours of a Raman effect of $^4T_2$ and $^4A_2$: $Cr(bpy)_3(ClO_4)$ in H_2O.

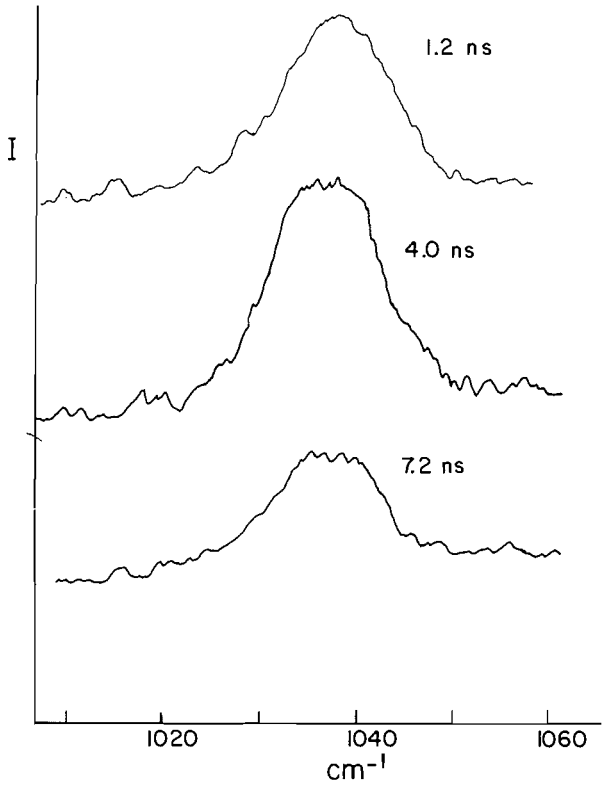


FIG. 9. Recordings of the Raman band at ~1040 cm^{-1} for different positions of the aperture duration (gate) of the boxcar integrator (at the 50 ns time scale). The recording shown in the middle is that where the center of the aperture duration (gate) coincides with the center (peak) of the pulse due to scattered light (see Fig. 8).

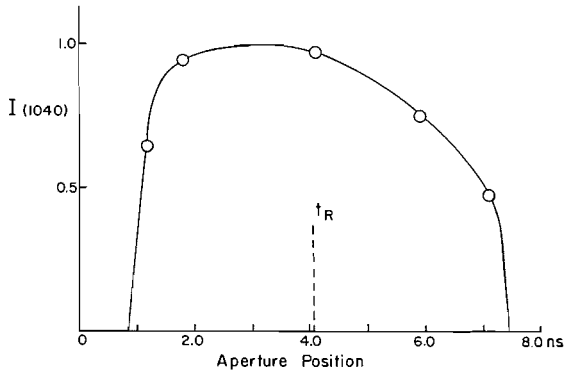


FIG. 10. The integrated intensity of the Raman band at ~1040 cm^{-1} of $Cr(bpy)_3^{3+}$ as a function of the position of the aperture of the boxcar in real time. Based on the real shape of the pulse of the dye laser (Fig. 2, bottom) one predicts an intensity distribution for the Raman signal which would favour that part of the curve with the position of the aperture $> t_R$. The experimental results represented by open circles indicate the opposite and the intensity distribution is due to the fact that during the rise time of the pulse ($t_R \approx 2.3$ ns), the time evolution of the population characteristics of the vibrational levels in the top part of the electronic surface of $^4T_2$ is favoured over those in the bottom and hence vibrational light scattering of those levels contribute to the overall intensity. The situation is reversed for $t > t_R$.

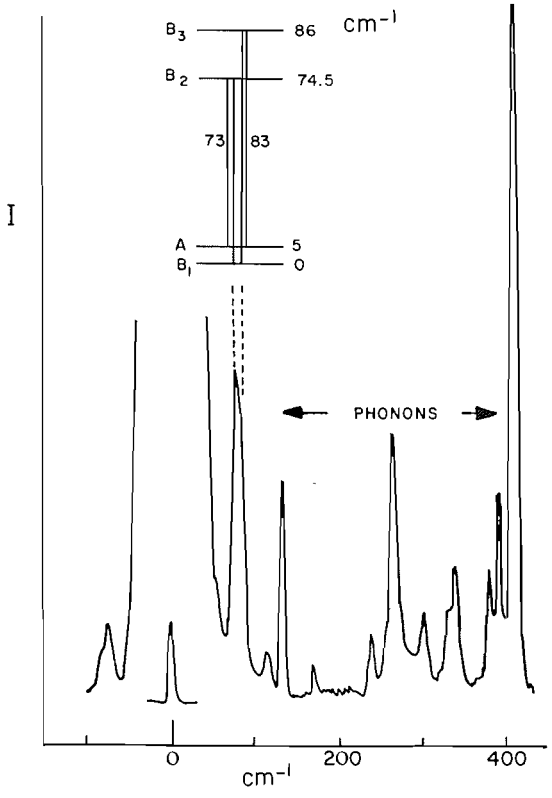


FIG. 11. Part of the Raman spectrum of terbium aluminum garnet ($TbAl_5O_{12}$) at 77 K recorded with the pulsed system (λ = 496.0 nm). Phonons and electronic Raman effects are indicated including the assignment of the electronic transitions.

noise. As anticipated, changes are not detectable if the high voltage of the PMT is switched off.

Taking advantage of the fact that the actual level due to PMT noise always remains below that of boxcar + cascaded amplifiers we increased the high voltage of the PMT to its maximum rating. By using the data of Fig. 4 we actually estimated an overall decrease of the (S/N) ratio by more than three orders of magnitude for the pulsed system (including amplification), with respect to the value used for $(S/N)_{pulsed}$ of eq. [1]. Taking into account also the fact that the availability of light levels for the pulsed system is always a thousand times smaller than that of a cw laser (operating at the ~1 W power range) we finally conclude that the effective performance (of the pulsed light scattering apparatus discussed here) is comparable to that of a conventional ~100 mW cw laser Raman system.

IV. Some Spectroscopic Results

As already indicated above, the present experimental arrangement has features which are not present in cw laser Raman spectrometers and in this section we present some typical results. The large peak power in combination with the short pulse duration of the pulsed laser for instance can be used to populate short-lived excited states of molecules or complexes, and that part of the pulse not used for optical pumping can, within the same pulse duration, serve as the Raman probe.

The degree of population of such an excited state can be determined from a measurement of the transmission of the sample as a function of the intensity of the laser tuned to the frequency of an absorption band of the molecule. For small values of I_L Beer's law is applicable and the transmission remains constant as a function of I_L. If, however,

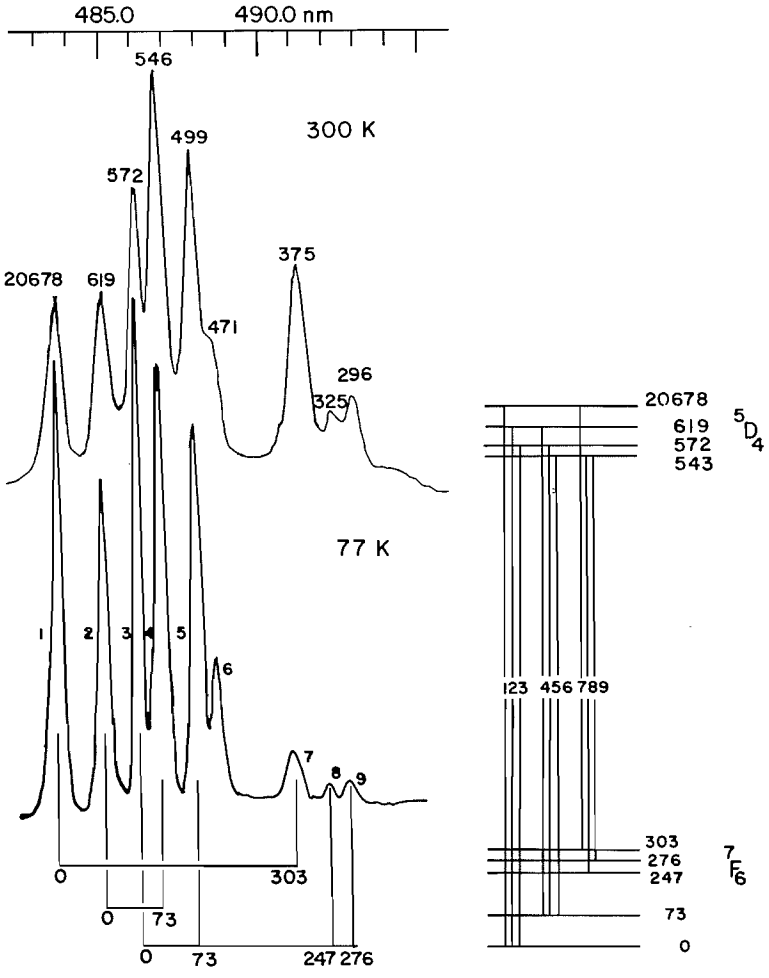


FIG. 12. The absorption spectrum of $TbAl_5O_{12}$ (single crystal) at 300 K and 77 K showing the $^5D_4 \leftarrow {}^7F_6$ transition. The energy level diagram for $^5D_4$ and $^7F_6$ is deduced from the frequency and intensity spectrum.

Can. J. Chem. Downloaded from www.nrcresearchpress.com by 210.87.254.42 on 09/05/12
For personal use only.

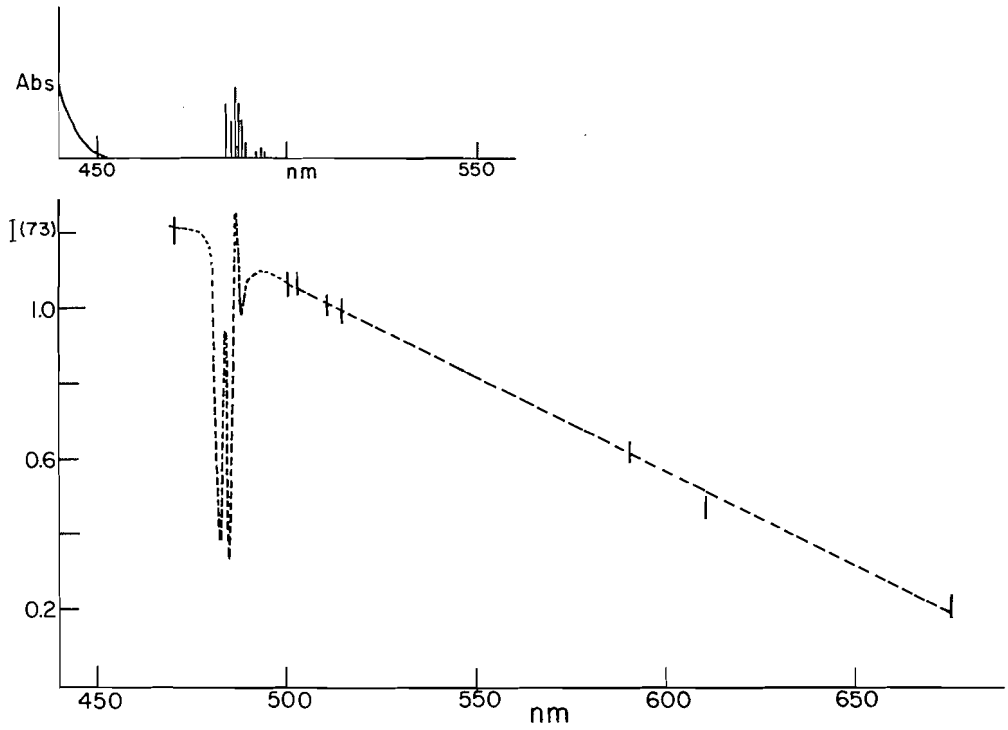


FIG. 13. Resonance enhancement/reduction profile of the intensity for the electronic Raman shift at 73 cm^{-1} of $TbAl_5O_{12}$. Measurements in the range of 483.0–490.0 nm were carried out with an interval of 0.2 nm. The reduction of the Raman intensity is due to interference effects arising from contributions of electric dipole matrix elements of opposite sign in the expression for an element of the electronic Raman scattering tensor.

some population occurs of an excited state then the value of the transmission changes because of depopulation of the ground state. Also, the possibility should not be excluded that another transition originates in the populated excited state and, depending on the cross section of this transition, we find that the value of the transmission increases or decreases if compared to that for low I_L. If conditions of population saturation of the excited state are approached for increasing values of I_L then T too approaches a constant value and such a behaviour was observed for the complex $Cr(byp)_3(ClO_4)_3$ in H_2O (see Fig. 5). A detailed analysis of the absorption process reveals that the $^4T_2$ state of $[Cr(bpy)_3]^{3+}$ is populated and not ^2E (which is at $\sim 13\,400\ cm^{-1}$ and $E_{^4T_2} > E_{^2E}$). The estimated lifetime of the $^4T_2$ state is ~ 10 ps and thus cannot be Raman probed with cw lasers due to power limitations (20). Part of the Raman spectrum $^4T_2$: $Cr(bpy)_3{}^{3+}$ and that of $^4A_2$: $Cr(bpy)_3{}^{3+}$ is shown in Fig. 6. We note a marked increase in the width of the Raman bands of $^4T_2$: $Cr(byp)_3{}^{3+}$ versus those of $^4A_2$: $Cr(bpy)_3{}^{3+}$. The energy of the optical pump at 457.9 nm, which produces population of $^4T_2$, is not in resonance with the 0–0 electronic transition, nor with that of the first vibronic side band of a normal mode. The actual experimental situation is that where the energy of the pump is in resonance with vibrational states having at least $v = 6$ for some of the normal modes in $^4T_2$ and population of the vibrational levels with $v < 0$ of $^4T_2$ is achieved (Fig. 7) via vibration relaxation. Due to the rapid rise time of ~ 2.3 ns (leading edge) of the laser pulse, it could be possible to detect Raman scattering from the excited vibrational levels even if the relaxation time of the cascading process is in the picosecond region. In that case some population would occur of the excited vibrational levels and of relevance here too, from the point of view of experimental observation of Raman scattering from levels with $v \neq 0$, is the fact that the intensity of $I_v(Q)$ of a vibrational Raman process originating in a level labelled with the quantum number v is related to the intensity of a similar process $I_0(Q)$ originating in the level with $v = 0$ by

$$I_v(Q) = (v + 1)I_0(Q)$$

In addition, as a result of the effect of anharmonicity we find that the shift of the Raman band due to the transition originating in higher v levels is smaller than that of the transition originating in $v = 0$. Many of the observed bands of $^4T_2$: $Cr(bpy)_3{}^{3+}$ show a

Can. J. Chem. Downloaded from www.nrcresearchpress.com by 210.87.254.42 on 09/05/12
For personal use only.

Can. J. Chem. Downloaded from www.nrcresearchpress.com by 210.87.254.42 on 09/05/12
For personal use only.

broadening but (see Fig. 8) not a well resolved spectrum towards lower shift values. In Fig. 9 we show recordings of the Raman band centered at $\sim 1040\ cm^{-1}$ of $^4T_2$: $Cr(bpy)_3^{3+}$ under different conditions of the position of the center of the aperture of the boxcar in real time so that in effect the edge, center, and tailing edge of the 3.2 ns long pulse were isolated. In the situation where the aperture is fixed to isolate the leading edge, the overall intensity of the Raman band could contain contributions of transitions originating in the top of the well. On the other hand, contribution to the intensity from transitions in the bottom of the well should occur if the aperture is adjusted to isolate the tailing end of the pulse. Assuming a symmetrical shape for the laser pulse we anticipate for reasons given above that the overall intensity of the Raman band for the former should be stronger than for the latter if the cascading process takes place. The results displayed in Fig. 10 reveal the presence of an intensity enhancing process during the rise time of the laser pulse and are taken as evidence that the band contour of the Raman shifts for $^4T_2$: $Cr(bpy)_3^{3+}$ is mainly due to the cascading (vibrational relaxation) process at the picosecond time scale, the details of which shall be published elsewhere.

We now turn our attention to some other results where advantage has been taken of real time resolution and tunability of the pulsed laser. The Raman spectrum shown in Fig. 11 is that of a single crystal of terbium aluminum garnet and the shift at $\sim 80\ cm^{-1}$ is due to an electronic Raman effect of the crystal field components of the split $^7F_6$ ground manifold (21). It is noted that the $80\ cm^{-1}$ shift is well isolated from the Rayleigh time.

Using the tunability of the system, spectra were also recorded with $481.0 < \lambda_L < 495.0$. Absorptions due to $^5D_4 \leftarrow {}^7F_6$ transitions of Tb^{3+} are shown in Fig. 12 and the exciting radiation is seen to cover the regions where absorption takes place. Conditions are met for the occurrence of either pre or resonance electronic Raman scattering and the results shown in Fig. 13 demonstrate their effects on the intensity enhancements or reduction of the electronics Raman shift. The intensity behaviour can be traced back to the occurrence of electric dipole matrix elements of opposite signs in the well known expression from element $\alpha_{\rho\sigma}$ of the scattering tensor. It is also seen that under rigorous resonance conditions the intensity enhancements or reductions are small on account of the weak ocillator strength of the Laporte forbidden $^5D_4$–$^7F_6$ transitions shown in Fig. 12.

Probably the most interesting aspect of a resonance Raman process is its time dependent behaviour with respect to the non resonance case.

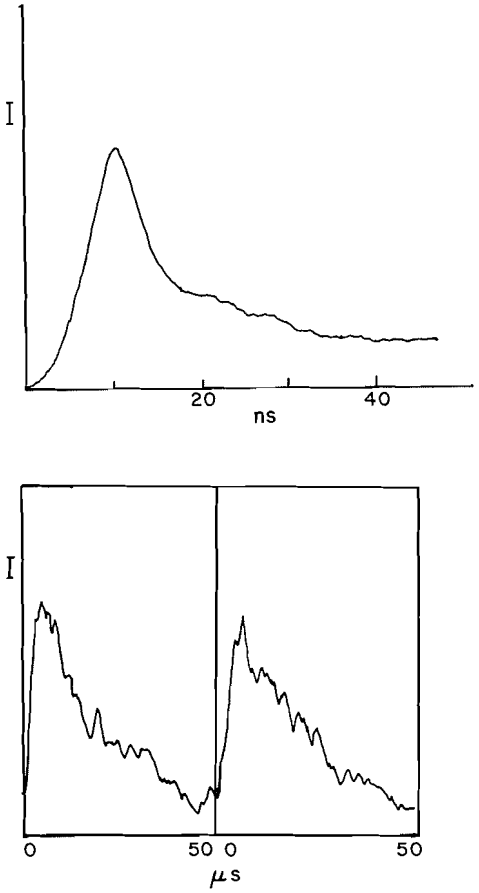


FIG. 14. Raman pulse in real time due to a resonance enhanced electronic light scattering effect with a shift of 73 cm^{-1} of $TbAl_5O_{12}$. The exciting wavelength $\lambda_L = 494.9$ nm is 0.1 nm removed from the position of an absorption band of $TbAl_5O_{12}$ (see Fig. 11). Clearly visible at the 50 ns scale of the boxcar (top) is the tailing end of the Raman pulse, while the decay itself becomes fully visible at the 50 μs scale. A lifetime of $\tau = 31.5\ \mu s$ is determined from the decay which value is in good agreement with the lifetime $\tau = 33.5 \pm 0.1\ \mu s$ (determined from fluorescence transitions) of the resonating excited state at 20 619 cm^{-1} (see Fig. 11) of $TbAl_5O_{12}$.

From the data shown in Fig. 13, it can be seen that for $\lambda_L = 485.0$ nm the maximum contribution due to resonance scattering to the overall intensity is $\sim 50\%$. Given a lifetime of the resonating electronic state longer than the duration of the laser pulse, the effect of such a lifetime on the pulse due to resonance Raman scattering would be visible if this pulse is displayed in real time. In this particular case the Raman pulse displayed in real time should show a decay pattern having its origin located at half the peak height of the pulse (22, 23). The results for the 73 cm^{-1} electronic Raman shift given in Fig. 14 are in good agreement with the predicted pulse shape. Like the results of $Cr(bpy)_3^{3+}$, those of TbA1G shall also be discussed in greater detail

elsewhere, they are used in the present work to demonstrate the capability of the present system to probe effects which occur at the pico and microsecond time scale.

V. Acknowledgements

The authors wish to thank Dr. L. G. van Uitert of Bell Labs, Murray Hill and Dr. C. H. Langford of Carleton University for samples used in the investigations. One of us (J.A.K.) acknowledges in particular the financial support provided by the Natural Sciences and Engineering Research Council of Canada to build the pulsed laser Raman apparatus.

1. R. B. Srivastava, N. W. Schuyler, L. R. Dosser, F. J. Purcell, and C. H. Atkinson. Chem. Phys. Lett. **56**, 595 (1978).
2. W. Werncke, H. J. Weigmann, J. Parold, A. Lau, K. Lenz, and M. Pfeiffen. Chem. Phys. Lett. **61**, 105 (1979).
3. L. R. Dosser, J. B. Pallix, G. H. Atkinson, H. C. Wang, G. Levin, and M. Szwarc. Chem. Phys. Lett. **62**, 555 (1979).
4. Y. Oka and T. Kushida. J. Phys. Soc. Jpn. **33**, 1372 (1972).
5. P. P. Yaney. J. Opt. Soc. Am. **62**, 1297 (1972).
6. J. J. Levatier, R. L. Sandstrom, and S. C. Lin. J. Appl. Phys. **44**, 3273 (1973).
7. M. I. Bell and R. N. Tyte. Appl. Opt. **13**, 1610 (1974).
8. P. Valat and H. Tourbez. J. Raman Spectrosc. **8**, 139 (1979).
9. F. E. Lytle. Anal. Chem. **46**, 545A (1974).
10. F. E. Lytle. Anal. Chem. **46**, 817A (1974).
11. Z. Gulari and B. Chu. Rev. Sci. Instrum. **48**, 1560 (1978).
12. R. S. Neltzer and R. M. Wood. Appl. Opt. **16**, 1432 (1977).
13. T. Imasaka, T. Ogawa, and N. Ishibashi. Anal. Chem. **51**, 502 (1979).
14. J. M. Harris and F. E. Lytle. Rev. Sci. Instrum. **48**, 1463 (1977).
15. K. G. Spears, L. E. Cramer, and L. D. Hoffland. Rev. Sci. Instrum. **49**, 255 (1978).
16. M. Gustavsson, H. Lundberg, L. Nilsson, and S. Svanberg. J. Opt. Soc. Am. **69**, 984 (1979).
17. J. M. Harris, R. W. Christman, F. E. Lytle, and R. S. Tobias. Anal. Chem. **48**, 1937 (1976).
18. A. Szabo. Opt. Commun. **12**, 366 (1974).
19. M. Asano, D. Mongeau, D. Nicollin, R. Sasseville, and J. A. Koningstein. J. Chem. Phys. Lett. **65**, 293 (1979).
20. B. Halperin and J. A. Koningstein. J. Chem. Phys. **69**, 3302 (1978).
21. J. A. Koningstein and G. Schaack. Phys. Rev. **2**, 1242 (1970).
22. J. Behringer. Raman Spectrosc. **2**, 275 (1974).
23. D. L. Rousseau and P. F. William. J. Chem. Phys. **64**, 3519 (1976).

Can. J. Chem. Downloaded from www.nrcresearchpress.com by 210.87.254.42 on 09/05/12
For personal use only.

Tricyclic aromatic ketones by cycliacylation of carboxylic acid derivatives of indan, tetralin, and benzosuberane

M. ELAINE ISABELLE, ROBERT H. WIGHTMAN,[1] HAJRO W. AVDOVICH,[2] AND DAVID E. LAYCOCK[2]

Department of Chemistry, Carleton University, Ottawa, Ont., Canada K1S 5B6

Received April 1, 1980

M. ELAINE ISABELLE, ROBERT H. WIGHTMAN, HAJRO W. AVDOVICH, and DAVID E. LAYCOCK. Can. J. Chem. **58**, 1344 (1980).

The synthesis of a homologous series of new carboxylic acids substituted in the α-position of indan, tetralin, and benzosuberane is accomplished using an efficient general procedure. Cycliacylation of these acids and their corresponding β-isomers produces a complete series of tricyclic aromatic ketones.

M. ELAINE ISABELLE, ROBERT H. WIGHTMAN, HAJRO W. AVDOVICH et DAVID E. LAYCOCK. Can. J. Chem. **58**, 1344 (1980).

Faisant appel à une méthode générale efficace, on a synthétisé une série homologue de nouveaux acides carboxyliques substitués en position α de l'indane, de la tétraline et du benzosubérane. La cycloacylation de ces acides et de leurs isomères β correspondants produit une série complète de cétones tricycliques aromatiques.

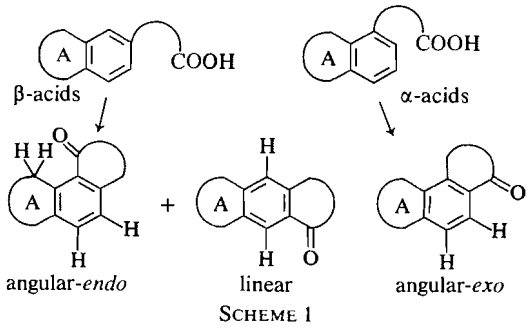
[Traduit par le journal]

Introduction

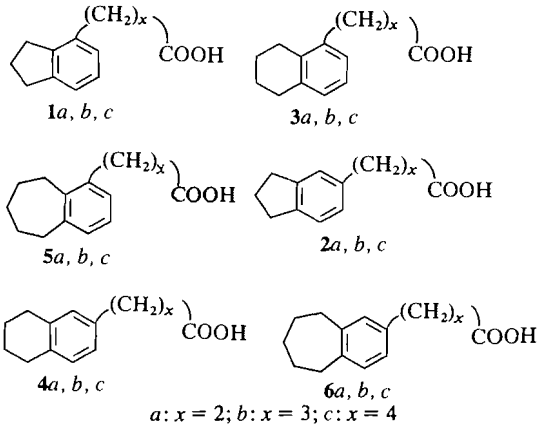
The intramolecular cycliacylation of certain bicyclic acids is a general route for the preparation of a variety of tricyclic ketones with varying acyclic ring sizes and positioning of the carbonyl group as outlined in Scheme 1.

Such tricyclic ketones are potential precursors of the corresponding tricyclic aromatic hydrocarbons (1) or of other more unsaturated species (2). Such compounds could also be useful models for probing conformational effects on the central aromatic ring or anisotropic effects of the carbonyl group.

Intramolecular acylations have been regularly reported in the literature for various simple (3) or substituted carbocyclic (4) and heterocyclic (5) ring systems. Although the β-substituted acids can, in principle, cyclize in two directions to produce a linear[3] or angular-*endo*[3] ketone (6), the predominant linear isomer was often the only product reported (7). Preference for linear formation has been ascribed to "steric effects" (8) despite the fact that in one case complete angular formation has been noted (9).



SCHEME 1



Previous syntheses of the β-substituted acids have exploited the fact that *ortho*-disubstituted benzenes acylate predominantly in the β-position. Thus a propanoylation/Willgerodt sequence (10) or malonic ester condensation on the chloromethyl derivative (9) have been employed for syntheses of propanoic acids of the type **2***a*, **4***a*, **6***a* while acylation with succinic (11) or glutaric (3) anhydride followed by reduction of the keto-acids has been the method of choice for butanoic acids of the type **2***b*, **4***b*, **6***b* or pentanoic acids of the type **2***c*, **4***c*, **6***c*. Only two α-substituted acids have been reported using rather fortuitous **3***a* (12) or lengthy **1***a* (13) sequences.

In this paper we wish to report a short general sequence for preparing the nine pairs of isomeric acids, **1***a*–*c* – **6***a*–*c*, formally derivable from indan,

[1]Author to whom correspondence should be addressed.

[2]Taken in part from the reports submitted by H.W.A. (1975) and D.E.L. (1974) as partial requirements for the B.Sc. (Honours Chemistry) from Carleton University.

[3]We have used the term linear to represent ketones of the type **8**, **11**, **14**, angular-*endo* for compounds **7**, **10**, **13**, and angular-*exo* for **9**, **12**, **15**.

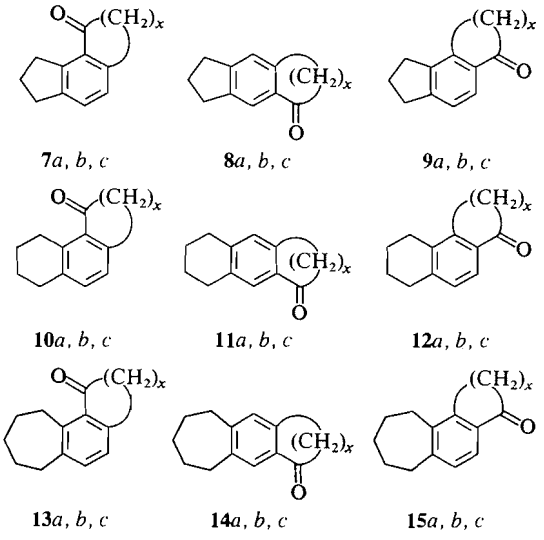
0008-4042/80/131344-06$01.00/0

©1980 National Research Council of Canada/Conseil national de recherches du Canada

Can. J. Chem. Downloaded from www.nrcresearchpress.com by 210.87.254.5 on 09/05/12
For personal use only.

Can. J. Chem. Downloaded from www.nrcresearchpress.com by 210.87.254.5 on 09/05/12
For personal use only.

tetralin, and benzosuberane. The synthesis follows from our recently developed preparative methods (14) for α-substituted (as well as β-substituted) derivatives of these bicyclic hydrocarbons. We also report the cyclization products, the tricyclic ketones **7***a–c* – **15***a–c* which represent all variations of 5, 6, and 7 membered acyclic rings outlined in Scheme 1 and permit, for the first time, direct spectral comparison of these compounds.



7*a, b, c* **8***a, b, c* **9***a, b, c*

10*a, b, c* **11***a, b, c* **12***a, b, c*

13*a, b, c* **14***a, b, c* **15***a, b, c*

a: $x = 2$; *b*: $x = 3$; *c*: $x = 4$

Results and Discussion

*The Bicyclic Acids, 1*a–c – *6*a–c

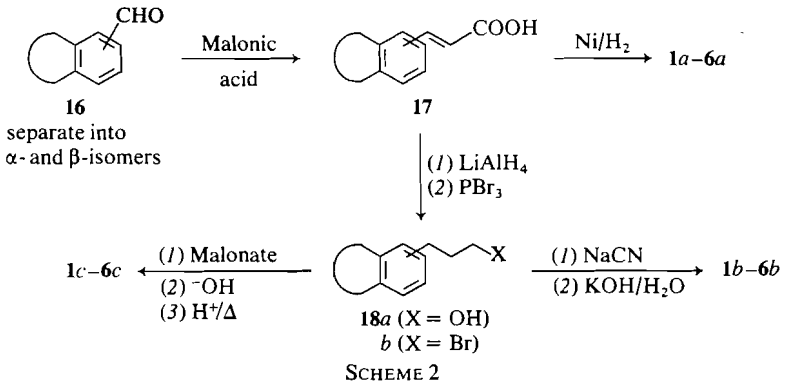
The sequence is outlined in Scheme 2. All acids were synthesized from the corresponding acrylic acids, **17**, which are directly available from the aldehydes, **16**. The aldehydes are quite amenable to separation of α- and β-isomers and readily derivable from the corresponding hydrocarbons. The acrylic acids could then be converted by rather conventional procedures to acids with any desired length of side chain. We have found all steps in the sequence to be clean and of high yield (80–90%) except the final decarboxylation (40–70%). All intermediates were nicely characterizable by ir and ^{1}H nmr.

*The Tricyclic Ketones, 7*a–c – *15*a–c

Scattered reports in the literature propose a variety of conditions which effect such cycliacylations (15) to the tricyclic ketones. The sole variation to this approach involves β-acylation with 3-chloropropanoyl chloride followed by cyclialkylation to produce angular-*exo*[3] ketones **9***a* (10, 16) and **12***a* (17).

Treatment of the acid chloride with $SnCl_4$ apparently maximizes formation of the angular-*endo* isomer from the β-acids (9). By using these conditions, which do not permit equilibration of the two isomers, and glc analytical techniques we were able to complete a comprehensive study of the formation of tricyclic ketones of the type **7***a–c* – **15***a–c*. In general the crude cyclization products were quite clean, any impurities being minor ones as judged by glc. Reaction mixtures could be resolved by preparative layer or short column (18) chromatography. The products from cyclizations of **6***b* and **6***c* were completely resolved by hplc but none of the minor components exhibited spectral characteristics (ir, nmr) expected for the angular-*endo* isomers, **13***b* or **13***c*, respectively. In most cases, the linear isomer predominated and overall yields were lower for cyclization products from the pentanoic acids. These results are summarized in Table 1 together with the ^{1}H nmr pattern for the aromatic protons of the ketones, the most diagnostic structural information.

The lack of detection of the benzosuberane-derived ketones **13***b*, **13***c* together with the rather dramatic differences in linear/angular-*endo* ratios



SCHEME 2

Can. J. Chem. Downloaded from www.nrcresearchpress.com by 210.87.254.5 on 09/05/12
For personal use only.

TABLE 1. Cyclization products of bicyclic acids

Acid	Ketone(s) (crude yield, %)	$\frac{\text{Linear}}{\text{Angular}}$ ratio (values from ref. 8)	^{1}H nmr of Ar*H* (δ)
1*a*	9*a*(73)		7.6(d), 7.2(d)
2*a*	8*a* + 7*a*(71)	$\frac{72}{28}\left(\frac{79}{21}\right)$	7.6(s), 7.3(s) 7.4(d), 7.2(d)
1*b*	9*b*(81)		7.9(d), 7.1(d)
2*b*	8*b* + 7*b*(78)	$\frac{79}{21}\left(\frac{81}{19}\right)$	7.9(s), 7.1(s) 7.3(d), 7.1(d)
1*c*	9*c*(80)		7.6(d), 7.2(d)
2*c*	8*c* + 7*c*(79)	$\frac{91}{9}\left(\frac{93}{7}\right)$	7.6(s), 7.1(s)
3*a*	12*a*(75)		7.5(d), 7.1(d)
4*a*	11*a* + 10*a*(82)	$\frac{25}{75}\left(\frac{34}{66}\right)$	7.4(s), 7.1(s) 7.5(d), 7.1(d)
3*b*	12*b*(82)		7.8(d), 7.0(d)
4*b*	11*b* + 10*b*(82)	$\frac{65}{35}\left(\frac{90}{10}\right)$	7.7(s), 6.9(s)
3*c*	12*c*(44; 87 in 3h)		7.3(d), 7.0(d)
4*c*	11*c* + 10*c*(51)	$\frac{90}{10}\left(\frac{100}{0}\right)$	7.4(s), 6.8(s) 7.0(d), 6.8(s)
5*a*	15*a*(71)		7.5(d), 7.1(d)
6*a*	14*a* + 13*a*(35; 82 in 20h)	$\frac{44}{56}$	7.5(s), 7.2(s) 7.3(d), 7.2(d)
5*b*	15*b*(71)		7.8(d), 7.0(d)
6*b*	14*b*(78) 13*b*	$\frac{100}{0}$	7.7(s), 7.0(s)
5*c*	15*c*(33; 51 in 22h)		7.4(d), 7.0(d)
6*c*	14*c* (46; 78 in 24h) 13*c*	$\frac{100}{0}$	7.5(s), 6.9(s)

induced by merely changing the cyclization conditions would indicate that simple steric arguments are not adequate to explain direction of cyclization. Perhaps the size of ring A has a varying effect on the electron densities of the benzene ring carbons or previous conditions may have permitted linear/angular equilibration (19). As intimated previously (8), an interesting ^{1}H nmr anisotropic effect of the carbonyl group on the nearest benzylic protons of ring A allows differentiation of linear and angular-*endo* isomers. We have found this trend to be less distinguishable as the size of the acyclic rings increases. From such a comprehensive series of ketones we find the *J* values and chemical shifts for the aromatic protons to be more diagnostic.

We hope to be able to prepare the missing ketones by a totally different route (20) and investigate in more detail (*i*) possible factors in the cyclization process and (*ii*) the conformational implications of more detailed spectral analyses of effects of the carbonyl group or its derivatives.

Experimental

General Details

Melting points were obtained on a Buchi SMP-20 melting range apparatus. Infrared spectra in CS_2 (ν_{max} in cm^{-1}) were recorded on a Perkin Elmer 237B spectrophotometer. Ultraviolet spectra [λ_{max} in nm (ε)] were obtained in 95% EtOH on a Perkin Elmer-Coleman-124 spectrophotometer. Proton magnetic resonance (^{1}H nmr) spectra were recorded on a Varian T-60 (60 MHz) instrument; all values are recorded in ppm (δ) with reference to TMS. All ^{1}H nmr were taken in $CDCl_3$ with 1% TMS. Band shape is indicated by s(singlet), d(doublet), t(triplet), m(multiplet), b(broad). Thin or preparative layer chromatography was performed using silica gel G (0.25 mm layers or 2.0 mm respectively) on glass plates (Merck). Analytical glc data were obtained on: (*i*) a Hewlett Packard F&M 402 instrument using a ¼ in. × 6 ft column, oven temperatures of 150–200°C, and flow rate of nitrogen at 70 mL/min or (*ii*) a Perkin Elmer 990 using a ⅛ in. × 12 ft column, temperatures of 160–180°C, and argon flow rate 25 mL/min. Columns were packed with 3% OV210 on Chromosorb W, 100–120 mesh. Microanalyses were obtained from Spang Microanalytical Laboratory, MI, U.S.A.

*Preparation of the Bicyclic Acids, 1*a–c – *6*a–c

All of these compounds exhibited ir bands at 3300–2700 (—OH), 1720 (C=O) typical of carboxylic acids. Additionally

Can. J. Chem. Downloaded from www.nrcresearchpress.com by 210.87.254.5 on 09/05/12
For personal use only.

their ^{1}H nmr spectra displayed a typical pattern consisting of absorptions centred at 11.5–9.0 (disappears with D_2O, —COO*H*), ~7.0 (aromatic *H*), 2.7(benzylic —CH_2— plus —CH_2—COOH) and ~1.8 (other —CH_2—).

Analytical samples could be obtained by crystallization from petroleum ether, sublimation at 0.01 Torr, or isolation from preparative layer plates.

*The Propanoic Acids, 1*a–*6*a

The corresponding acrylic acid **17**(14) was reduced using Raney nickel alloy (Al:Ni = 1:1) in hot aqueous NaOH as outlined by Cook *et al.* (21). Yield of crude product, of sufficient purity for further reaction, was always 85–90%.

1*a*, mp 113–114°C (lit. (13) mp 113–114°C); ^{1}H nmr: 10.7 (1H, bs), 7.1 (3H, m), 2.8 (8H, m), 2.0 (2H, m). **2***a*, mp 84–85°C (lit. (8) mp 85–86°C, lit. (10) mp 83°C); ^{1}H nmr: 8.8 (1H, bs), 7.1 (3H, m), 2.8 (8H, m), 2.1 (2H, m). **3***a*, mp 135–136°C (lit. (12) mp 136–137°C); ^{1}H nmr: 9.9 (1H, bs), 7.0 (3H, s), 2.7 (8H, m), 1.7 (4H, m). **4***a*, mp 82–83°C (lit. (22) mp 81–82°C, lit. (8) mp 78°C, lit. (23) mp 82°C, lit. (24) mp 70–71°C); ^{1}H nmr: 11.1 (1H, bs), 7.0 (3H, s), 2.7 (8H, m), 1.8 (4H, m). **5***a*, mp 84–85°C; ^{1}H nmr: 11.4 (1H, bs), 7.0 (3H, s), 2.8 (8H, m), 1.7 (6H, m); *Anal.* calcd. for $C_{14}H_{18}O_2$: C 77.03, H 8.31; found: C 76.77, H 8.12. **6***a*, mp 99–100°C (lit. (25) mp 102–103°C); ^{1}H nmr: 11.4 (1H, bs), 7.0 (3H, s), 2.8 (8H, m), 1.7 (6H, m).

The acrylic acid **17**(X mol) could be reduced to the corresponding saturated alcohol **18***a* by reduction with $LiAlH_4$(X mol) in anhydrous ether (26). We have found it most convenient to introduce the acid gradually via a Soxhlet extractor and to continue reflux of the ether for 20–24 h. A normal workup would produce 80–90% yields of neutral material, which proved to be the alcohol, in sufficient purity to continue. These compounds were nicely characterized by certain spectral data, notably ir (hydroxyl at 3500, no carbonyl at ~1720) and ^{1}H nmr (3 aromatic *H* at ~7.0, —CH_2—CH_2—OH as a 2H, t centred at ~3.7, and 1 O*H* exchanging with D_2O at ~2.3).

The alcohol **18***a* (X mol) was readily converted to the bromide **18***b* using PBr_3 (0.5 X mol) in benzene (8). After workup the bromide was obtained in 80–90% yield and of sufficient purity to continue. Again the intermediates were easily characterized by selected absorptions in the ir (no hydroxyl bands) with ^{1}H nmr (3 aromatic protons, ~7.1 and —CH_2—CH_2—Br, 2H, t, ~3.4).

*The Butanoic Acids, 1*b–*6*b

The approach outlined by Patwardhan (8) was employed (see also ref. 4). The bromide **18***b* was converted to the corresponding nitrile using KCN in refluxing methanol. Yields were routinely ≥90% of a product judged sufficiently clean by spectral data, e.g. ir ~2250(—CN) and ^{1}H nmr: ~3.0 (2H, t, —CH_2—CH_2—CN), to proceed. Hydrolysis using KOH in refluxing aqueous ethylene glycol produced an acidic product in ≥85% yield.

1*b*, mp 81–83°C; ^{1}H nmr: 10.7 (1H, bs), 7.1 (3H, m), 2.5 (8H, m), 1.9 (4H, m). *Anal.* calcd. for $C_{13}H_{16}O_2$: C 76.44, H 7.89; found: C 76.78, H 7.78. **2***b*, mp 54–55°C (lit. (27) mp 55°C, lit. (28) mp 56°C); ^{1}H nmr: 9.6 (1H, bs), 7.2 (3H, m), 2.9 (8H, m), 2.0 (4H, m). **3***b*, mp 94–95°C; ^{1}H nmr: 9.5 (1H, bs), 7.0 (3H, bs), 2.7 (8H, m), 1.8 (6H, m). *Anal.* calcd. for $C_{14}H_{18}O_2$: C 77.02, H 8.25; found: C 77.25, H 8.29. **4***b*, mp 47–49°C (lit. (23) mp 47–49°C, lit. (8) mp 44–45°C); ^{1}H nmr: 10.9 (1H, bs), 7.0 (3H, m), 2.6 (8H, m), 1.8 (6H, m). **5***b*, mp 55°C; ^{1}H nmr: 10.9 (1H, bs), 7.0 (3H, s), 2.6 (8H, m), 1.7 (8H, m). *Anal.* calcd. for $C_{15}H_{20}O_2$: C 77.55, H 8.68; found: C 77.67, H 8.66. **6***b*, mp 88°C; ^{1}H nmr: 8.5 (1H, bs), 7.0 (3H, m), 2.6 (8H, m), 1.6 (8H, m). *Anal.* calcd. for $C_{15}H_{20}O_2$: C 77.55, H 8.68; found: C 77.90, H 8.40.

*The Pentanoic Acids, 1*c–*6*c

Sodium hydride (X mol, as a 55% mineral dispersion) was freed of mineral oil by rinsing with petroleum ether and decanting (2×), then suspended in dry benzene–DMF (4:1 v/v). Diethyl malonate (X mol) in anhydrous benzene was added dropwise at room temperature, then stirred until evolution of hydrogen was complete (~30 min). This solution was cooled in an ice-bath and the appropriate bromide **18***b* (1.05 X mol) in dry DMF was added dropwise so that the temperature of the reaction mixture never exceeded 15°C. This mixture was stirred at room temperature overnight by which time an aliquot in water gave a neutral pH and the condensation was considered complete. Workup yielded a viscous oil constituting 80–90% mass recovery. Hydrolysis and decarboxylation using a variety of conditions (4, 8, 29) produced an acidic product in yields of 25–60% based on starting bromide.

1*c*, mp 59°C; ^{1}H nmr: 10.7 (1H, bs), 7.1 (3H, m), 3.1–1.4 (14H, m). *Anal.* calcd. for $C_{14}H_{18}O_2$: C 77.03, H 8.31; found: C 76.57, H 8.08. **2***c*, mp 64–65°C (lit. (7) mp 70–71°C), ^{1}H nmr: 10.6 (1H, bs), 7.0 (3H, m), 3.1–1.5 (14H, m). **3***c*, mp 91°C; ^{1}H nmr: 10.8 (1H, bs), 7.0 (3H, m), 2.7 (8H, m), 1.8 (8H, m). *Anal.* calcd. for $C_{15}H_{20}O_2$: C 77.70, H 8.25; found: C 77.62, H 8.44. **4***c*, mp 54–55°C (lit. (11) mp 57–58°C, lit. (8) mp 54–55°C); ^{1}H nmr: 10.9 (1H, bs), 7.0 (3H, m), 2.6 (8H, m), 1.8 (8H, m). **5***c*, amorphous solid, ^{1}H nmr: 10.8 (1H, bs), 7.0 (3H, m), 2.6 (8H, m), 1.6 (10H, m). *Anal.* calcd. for $C_{16}H_{22}O_2$: C 78.01, H 9.00; found: C 78.01, H 9.12. **6***c*, mp 62–64°C (lit. (3) mp 63°C); ^{1}H nmr: 11.5 (1H, bs), 7.0 (3H, m), 2.6 (8H, m), 1.7 (10H, m).

*Preparation of the Tricyclic Ketones, 7*a–c – *15*a–c

The following general procedure, modified from that reported by Arnold and Rondestvedt (9), was employed for all cyclizations. The acid (2.0 mmol) was dissolved in dry benzene (5–10 mL) and to this solution was added PCl_5 (2.2 mmol). The flask was stoppered and the contents magnetically stirred at room temperature until the PCl_5 had dissolved (~30 min). This was taken as indication that the acid chloride was now formed *in situ*. The flask was immersed in an ice-bath and the contents chilled to 0°C at which time $SnCl_4$ (4.0 mmol) was added. The dark coloured reaction mixture was stirred for a further 30 min at 0°C, then for 90 min at room temperature. Yields of cyclized material could be increased if necessary by extending the reaction period at room temperature with no change in the linear/angular ratio, see Table 1 for several examples. The reaction mixture was poured onto ice, rendered acidic, extracted with ether (3×), and the combined organics washed with 5% aqueous NaOH (2×) to remove any unreacted acid (could be recovered). After drying and removing solvent the neutral products could be analyzed by tlc (petroleum ether – benzene 1:1 v/v) or glc. Purification was achieved by silica-gel column chromatography, crystallization (petroleum ether), sublimation, or preparative layer chromatography for separation of linear and angular isomers.

Solvent Variation

Cyclization of the β-acids, **2***a–c*, **4***a–c*, **6***a–c* usually resulted in formation of both linear **8***a–c*, **11***a–c*, **14***a–c* or angular-*endo* compounds **7***a–c*, **10***a–c*, **13***a–c* as easily determined by glc. We have found no difference in linear/angular ratios from **4***a* and **4***b* when the cyclizing medium was nitrobenzene (9) or benzene and therefore have used the latter solvent exclusively. All ratios summarized in Table 1 represent our standard conditions (*vide supra*) and are obviously quite different from other reports, e.g. ref. 8.

Equilibration Studies

No equilibration rearrangements between linear and angular isomer pairs, e.g. **7***b*/**8***b* or **10***b*/**11***b* could be detected by glc using standard cyclization conditions; i.e. $SnCl_4$ (2 equiv.) in benzene for 5 h at room temperature.

Characterization of Ketones

Isolated yields, linear/angular isomer ratios, and selected ^{1}H nmr data are available in Table 1. Additional, unavailable data

Can. J. Chem. Downloaded from www.nrcresearchpress.com by 210.87.254.5 on 09/05/12
For personal use only.

for the tricyclic ketones is as follows. The uv bands are typical for phenones, the ir bands correspond to C=O stretch for conjugated ketones and aromatic C—H bending, respectively, and the ^{1}H nmr spectra show absorptions centred at ~7–8 (aromatic *H*), ~2.7–3.0 (benzylic —C*H*$_2$— and —C*H*$_2$—CO—) and ~1.8 (other —C*H*$_2$—).

7*a*, mp 89–90°C (lit. (30) mp 85°C); ir: 1720, 805; uv: 250 (11 600); ^{1}H nmr: 7.4 (1H, d, J = 8), 7.2 (1H, d, J = 8), 2.9 (8H, m), 2.2 (2H, m). **7***b*, amorphous solid (lit. (8) bp 130°C/2 Torr); ir: 1680, 805; uv: 253 (14 900); ^{1}H nmr: 7.3 (1H, d, J = 8), 7.1 (1H, d, J = 8); 3.3 (2H, t, benzylic —C*H*$_2$— *peri* to C=O), 2.8 (6H, m), 2.1 (4H, m). **7***c*, glass; ir: 1690, 820; uv: 252 (7 300); ^{1}H nmr: 7.2 (1H, d, J = 8), 7.0 (1H, d, J = 8), 2.8 (8H, m), 1.9 (6H, m). *Exact Mass* calcd. for $C_{14}H_{16}O$: 200.1201; found (high resolution ms): 200.1238.

8*a*, mp 75–76°C (lit. (10) mp 80–81°C); ir: 1722, 875; uv: 255 (7 500); ^{1}H nmr: 7.6 (1H, s), 7.3 (1H, s), 2.8 (8H, m), 2.2 (2H, m). **8***b*, mp 38°C (lit. (8) mp 36°C); ir: 1690, 840; uv: 261 (11 600); ^{1}H nmr: 7.9 (1H, s), 7.1 (1H, s), 2.8 (8H, m), 2.1 (4H, m). **8***c*, mp 39°C (lit. (7) bp ~208°C/16 Torr); ir: 1685, 885; uv: 259 (12 500); ^{1}H nmr: 7.6 (1H, s), 7.1 (1H, s), 2.9 (8H, m), 2.0 (6H, m). *Exact Mass* calcd. for $C_{14}H_{16}O$: 200.1201; found (high resolution ms): 200.1178.

9*a*, mp 108°C (lit. (13) mp 108–109°C); ir: 1710, 800; uv: 261 (13 700); ^{1}H nmr: 7.6 (1H, d, J = 8), 7.2 (1H, d, J = 8), 2.9 (8H, m), 2.2 (2H, m). **9***b*, mp 41°C; ir: 1680, 825; uv: 263 (15 500); ^{1}H nmr: 7.9 (1H, d, J = 8), 7.1 (1H, d, J = 8), 2.8 (8H, m), 2.2 (4H, m). *Anal.* calcd. for $C_{13}H_{14}O$: C 83.87, H 7.52; found: C 83.84, H 7.53. **9***c*, oil, bp ~180°C/0.1 Torr; ir: 1675, 829; uv: 258 (9 500); ^{1}H nmr: 7.6 (1H, d, J = 8), 7.2 (1H, d, J = 8), 2.9 (8H, m), 2.0 (6H, m). *Exact Mass* calcd. for $C_{14}H_{16}O$: 200.1201; found (high resolution ms): 200.1172.

10*a*, mp 45°C (lit. (9) mp 46°C, lit. (30) mp 53°C); ir: 1710, 830; uv: 252 (12 200); ^{1}H nmr: 7.5 (1H, d, J = 8), 7.1 (1H, d, J = 8), 2.8 (8H, m), 1.8 (4H, m). **10***b*, mp 37°C (lit. (6) mp 40°C); ir: 1680, 810; uv: 257 (10 000); ^{1}H nmr: 7.1 (1H, d, J = 8), 6.9 (1H, d, J = 8), 2.6 (8H, m), 1.9 (6H, m). **10***c*, glass; ir: 1690, 805; uv: 254 (4 200); ^{1}H nmr: 7.0 (1H, d, J = 8), 6.8 (1H, d, J = 8), 2.6 (8H, m). *Anal.* calcd. for $C_{15}H_{18}O$: C 84.07, H 8.47; found: C 83.96, H 8.43.

11*a*, mp 58°C (lit. (30) mp 56°C); ir: 1701, 865; uv: 255 (14 000); ^{1}H nmr: 7.4 (1H, s), 7.1 (1H, s), 2.8 (8H, m), 1.8 (4H, m). **11***b*, mp 46°C (lit. (6) mp 47°C); ir: 1685, 860; uv: 262 (13 800); ^{1}H nmr: 7.7 (1H, s), 6.9 (1H, s), 2.7 (8H, m), 1.9 (6H, m). **11***c*, mp 51–52°C; ir: 1670, 870; uv: 260 (12 500); ^{1}H nmr: 7.4 (1H, s), 6.8 (1H, s), 2.7 (8H, m), 1.8 (8H, m). *Anal.* calcd. for $C_{15}H_{18}O$: C 84.07, H 8.47; found: C 84.12, H 8.53.

12*a*, mp 58°C (lit. (12) mp 63–64°C); ir: 1710, 805; uv: 261 (8 500); ^{1}H nmr: 7.5 (1H, d, J = 8), 7.1 (1H, d, J = 8), 2.7 (8H, m), 1.8 (4H, m). **12***b*, mp 81°C; ir: 1685, 825; uv: 264 (13 800); ^{1}H nmr: 7.8 (1H, d, J = 8), 7.0 (1H, d, J = 8), 2.6 (8H, m), 1.9 (6H, m). *Anal.* calcd. for $C_{14}H_{16}O$: C 83.96, H 8.05; found: C 83.93, H 7.94. **12***c*, mp 51–52°C; ir: 1675, 820; uv: 258 (11 200); ^{1}H nmr: 7.3 (1H, d, J = 8), 7.0 (1H, d, J = 8), 2.7 (8H, m), 1.8 (8H, m). *Anal.* calcd. for $C_{15}H_{18}O$: C 84.07, H 8.47; found: C 84.16, H 8.52.

13*a*, mp 59°C (lit. (25) mp 63°C); ir: 1700, 840, 825, 810; uv: 250 (10 760); ^{1}H nmr: 7.3 (1H, d, J = 8), 7.2 (1H, d, J = 8), 3.5 (2H, m, benzylic —C*H*$_2$— *peri* to C=O), 2.8 (6H, m), 1.7 (6H, m).

14*a*, mp 115°C (lit. (25) mp 116–117°C); ir: 1710, 885; uv: 255 (14 600); ^{1}H nmr: 7.5 (1H, s), 7.2 (1H, s), 2.8 (8H, m), 1.7 (6H, m). **14***b*, amorphous solid; ir: 1680, 835; uv: 260 (8 214); ^{1}H nmr: 7.7 (1H, s), 7.0 (1H, s), 2.8 (8H, m), 1.7 (8H, m). *Anal.* calcd. for $C_{15}H_{18}O$: C 84.07, H 8.47; found: C 84.06, H 8.39. **14***c*, mp 92–93°C (lit. (3) mp 92°C); ir: 1670, 855; uv: 258 (6 440); ^{1}H nmr: 7.5 (1H, s), 6.9 (1H, s), 2.8 (8H, m), 1.7 (10H, m).

15*a*, mp 106–107°C; ir: 1700, 810; uv: 260 (11 260); ^{1}H nmr: 7.5 (1H, d, J = 8), 7.1 (1H, d, J = 8), 2.8 (8H, m), 1.7 (6H, m). *Anal.* calcd. for $C_{14}H_{16}O$: C 83.96, H 8.05; found: C 84.37, H 8.07. **15***b*, mp 61°C; ir: 1680, 825; uv: 262 (12 420); ^{1}H nmr: 7.8 (1H, d, J = 8), 7.0 (1H, d, J = 8), 2.6 (8H, m), 1.6 (8H, m). *Anal.* calcd. for $C_{15}H_{18}O$: C 84.07, H 8.47; found: C 83.99, H 8.49. **15***c*, amorphous solid; ir: 1675, 815; uv: 260 (4 460); ^{1}H nmr: 7.4 (1H, d, J = 8), 7.0 (1H, d, J = 8), 2.8 (8H, m), 1.7 (10H, m). *Anal.* calcd. for $C_{16}H_{20}O$: C 84.16, H 8.83; found: C 84.42, H 8.71.

Acknowledgements

Much of the financial support for this project derived from the National Research Council of Canada and some from the President's Research Fund, Carleton University. The continued assistance of Mr. G. K. Diedrich is greatly appreciated as was the work of Mr. J. Ounsworth for the final characterization of some products. Thanks also to Professor D. McLean, Department of Chemistry, McMaster University for obtaining the high resolution mass spectra.

1. R. H. Wightman, R. J. Wain, and D. H. Lake. Can. J. Chem. **49**, 1360 (1971).
2. (*a*) Y. Fujise, H. Saito, and S. Ito. Tetrahedron Lett. 1176 (1976); (*b*) S. A. Patwardhan and S. Dev. Tetrahedron, **28**, 1075 (1972).
3. R. Legros and P. Cagniant. C. R. Acad. Sci. **252**, 2733 (1961).
4. M. S. Newman and J. O. Landers. J. Org. Chem. **42**, 2556 (1977).
5. (*a*) H. Grunhaus, M. Paiter, and S. Stof. J. Heterocycl. Chem. **13**, 116 (1976); (*b*) I. W. Mathison, W. E. Solomons, and R. H. Jones. J. Org. Chem. **39**, 2852 (1974).
6. M. Crawford and V. R. Supanekar. J. Chem. Soc. C, 2252 (1966).
7. A. D. Campbell and S. N. Slater. J. Chem. Soc. 4353 (1952).
8. S. Patwardhan. Ind. J. Chem. **7**, 105 (1969).
9. R. T. Arnold and E. Rondestvedt. J. Am. Chem. Soc. **68**, 2176 (1946).
10. R. T. Arnold and E. Rondestvedt. J. Am. Chem. Soc. **67**, 1265 (1945).
11. L. F. Fieser, M. T. Leffler, *et al.* J. Am. Chem. Soc. **70**, 3197 (1948).
12. R. T. Arnold and R. Barnes. J. Am. Chem. Soc. **65**, 2393 (1943).
13. H. Rapoport and G. Smolinsky. J. Am. Chem. Soc. **82**, 1171 (1960).
14. R. H. Wightman, D. E. Laycock, and H. W. Avdovich. J. Org. Chem. **43**, 2167 (1978).
15. W. S. Johnson. Organic reactions. Vol. 2. *Edited by* R. Adams. J. Wiley and Sons, NY. 1944. Chapt. 4. p. 114.
16. R. B. Woodward and T. R. Hoge. J. Am. Chem. Soc. **99**, 8007 (1977).
17. A. Rahman and J. C. Podesta. An. Quim. **69**, 521 (1973).
18. B. J. Hunt and W. Rigby. Chem. Ind. London, 1868 (1967).
19. I. Agranat and Y-S. Shih. J. Chem. Educ. **53**, 488 (1976).
20. A. S. Onishchenko. Diene synthesis. Printed by S. Monson, Jerusalem, for Israel Program for Scientific Translations Ltd. 1964. p. 417.

21. J. W. COOK, R. PHILLIP, and A. R. SOMMERVILLE. J. Chem. Soc. 164 (1948).
22. M. S. AHMAD and G. BADDELEY. J. Chem. Soc. 2520 (1961).
23. M. S. NEWMAN and H. V. ZAHM. J. Am. Chem. Soc. **65**, 1097 (1943).
24. A. RAHMAN and M. C. TORRE. Chem. Ind. London, 446 (1968).
25. R. GRANGER, H. ORZALESI, and A. MURATELLE. C. R. Acad. Sci. **255**, 720 (1962).
26. L. F. FIESER and M. FIESER. Reagents for organic synthesis. Vol. I. J. Wiley and Sons, NY. 1967. p. 592.
27. L. F. FIESER and A. M. SELIGMAN. J. Am. Chem. Soc. **59**, 883 (1937).
28. S. C. SEN-GUPTA. J. Ind. Chem. Soc. **16**, 89 (1939).
29. B. M. TROST, H. C. ARNDT, P. E. STREGE, and T. R. VERHOEVEN. Tetrahedron Lett. 3477 (1976).
30. R. GRANGER, H. ORZALESI, and A. MURATELLE. C. R. Acad. Sci. **252**, 1971 (1961).

Can. J. Chem. Downloaded from www.nrcresearchpress.com by 210.87.254.5 on 09/05/12
For personal use only.

Errata: Axial dissymmetry induced magnetic nonequivalence in the ^{13}C nuclear magnetic resonance spectra of allenes

PIERRE L. BEAULIEU, VERONIQUE M. MORISSET, AND DENNIS G. GARRATT

and

A new synthesis of 2,10,11-trioxatricyclo[4.4.4.0.^{1,6}]tetradecane

NORMAND BEAULIEU AND PIERRE DESLONGCHAMPS

(Ref.: Can. J. Chem. **58**, 875, 928 (1980))

The page numbers for these two papers were interchanged in the Contents of the May 1, 1980 issue. The page number should be 928 for the article by Pierre L. Beaulieu, Veronique M. Morisset, and Dennis G. Garratt and 875 for the article by Normand Beaulieu and Pierre Deslongchamps.

As well, the page number in the Author Index should be 928 for Beaulieu, P. L., Morisset, V. M., and Garratt, D. G. and 875 for Beaulieu, N. and Deslongchamps, P.

Reactions of thiyl radicals. XIII. Photochemically induced exchange reactions of liquid alkyl disulfides

DINESH GUPTA AND ARTHUR R. KNIGHT[1]

Department of Chemistry and Chemical Engineering, University of Saskatchewan, Saskatoon, Sask., Canada S7N 0W0

Received January 3, 1980

DINESH GUPTA and ARTHUR R. KNIGHT. Can. J. Chem. **58**, 1350 (1980).

The liquid phase photolysis of some 35 liquid alkyl disulfide mixtures has been studied. The corresponding unsymmetrical disulfide is the only significant product of the reaction and the system attains a photo-equilibrium state at longer exposure times. Product formation is completely eliminated by the addition of nitric oxide.

Quantum yields have been redetermined for the methyl disulfide – ethyl disulfide system using four different light sources. Initial rates have been measured for each of the 35 combinations and have been shown to be a function of total molecular weight of the disulfide mixture and to be strongly influenced by steric factors. These effects are most pronounced for mixtures wherein the exchange reaction between thiyl radical and a symmetrical disulfide is important as indicated by quantum yields above unity. Combinations of isodisulfides give rise to anomalously high rates.

DINESH GUPTA et ARTHUR R. KNIGHT. Can. J. Chem. **58**, 1350 (1980).

On a étudié la photolyse en phase liquide de 35 mélanges de disulfures d'alkyles à l'état liquide. Le disulfure asymétrique correspondant est le seul produit important de la réaction et le système atteint un état d'équilibre photochimique à des temps d'exposition plus longs. L'addition d'oxyde nitrique élimine complètement la formation des produits.

On a déterminé de nouveau les rendements quantiques du système disulfure de méthyle – disulfure d'éthyle en utilisant quatre sources différentes de lumière. On a mesuré les vitesses initiales pour chacune des 35 combinaisons; on a montré qu'elles dépendent du poids moléculaire total du mélange de disulfure et que des facteurs stériques les influencent fortement. Ces effets sont plus prononcés dans les cas de mélanges où la réaction d'échange entre le radical thiyle et le disulfure symétrique est importante tel qu'indiqué par les rendements quantiques du système déjà mentionné. Les combinaisons d'isodisulfures conduisent à des vitesses anormalement grandes.

[Traduit par le journal]

Introduction

The liquid phase photolysis of mixtures of disulfides and of disulfide–thiol mixtures have been investigated previously by several workers (1–6) and in this laboratory (7, 8).

When mixtures of alkyl disulfides are photolysed in the 250–300 nm region, the corresponding unsymmetrical disulfide is formed rapidly with high quantum yield. On prolonged irradiation the system generally attains a photo-equilibrium with the equilibrium constant for the process

[1] $RSSR + R'SSR' \rightleftharpoons 2\,RSSR'$

having a value of 4.

As a continuation of our investigations in this area we have studied and report here on the photolysis of mixtures of C_2 through C_{10} alkyl disulfides in condensed phase to determine the influence of molecular weight and structure on the initial rate of the exchange reaction. Some additional measurements of quantum yields have been made and the effect of added nitric oxide has been examined.

Experimental

All photolyses were carried out at room temperature with degassed samples. For most initial rate studies the light source was a Vycor 7910 filtered Hanovia 306-20 medium pressure mercury lamp. The combination of cut-off filter, lamp output, and disulfide absorption confined significant absorption to the 230–360 nm region, with the predominant absorption being the strong self-reversed emission around 250 nm. When a low pressure Hanovia 68745 Hg-lamp was used, the absorption was confined essentially to the 253.7 nm line. In the actinometric experiments, the low pressure Hg-lamp, a Zeiss LX501 high pressure xenon lamp and Zeiss M401 1d or Bausch and Lomb 780 TD monochromator combination, or a Spectra-Physics Model 185 He–Cd laser with output at 325 nm were also employed. Quantum yield measurements were carried out with the lamp–cell assembly mounted on a optical bench with a quartz lens system which provided an essentially uniform parallel incident light beam.

Disulfide samples were obtained commercially and purified where required by low pressure distillation or prep-scale gc. Purities were verified by gc or mass spectrometric analysis. Product analysis was by thermal conductivity or flame ionization gc using tricresylphosphate or Apiezon-M columns.

Light intensities were determined using a modified potassium ferrioxalate method (9–11).

For initial rate studies 200 nm^3 samples were irradiated in a 6 mm od quartz tube. For actinometric experiments, the cell was a 1.0 cm square quartz tube with a 2.0 μm^3 sample size.

Results

The attainment of photochemical equilibrium in three representative disulfide mixtures of different proportions was followed using both the medium and low pressure Hg-lamp light sources. The results are summarized in Table 1.

[1]To whom all correspondence should be addressed.

0008-4042/80/131350-05$01.00/0

©1980 National Research Council of Canada/Conseil national de recherches du Canada

Can. J. Chem. Downloaded from www.nrcresearchpress.com by 210.87.254.40 on 09/05/12
For personal use only.

TABLE 1. Equilibrium constants for photolysed disulfide mixtures

Reactants	Mol% composition	Equilibrium constant K^a	Equilibrium constant K^b
$CH_3SSCH_3/C_2H_5SSC_2H_5$	50/50	4.0 ± 0.2	3.7 ± 0.2
	20/80	4.0 ± 0.2	—
	80/20	4.1 ± 0.2	—
$CH_3SSCH_3/n\text{-}C_3H_7SSC_3H_7$	50/50	4.3 ± 0.3	4.2 ± 0.1
	80/20	3.9 ± 0.3	—
$C_2H_5SSC_2H_5/n\text{-}C_3H_7SSC_3H_7$	50/50	4.0 ± 0.4	3.7 ± 0.2
	20/80	2.8 ± 0.5	—
	80/20	3.6 ± 0.7	—

[a]Medium pressure Hg-lamp.
[b]Low pressure Hg-lamp.

With one exception the values observed are close to the statistically expected value of 4.0. Although the 20% ethyl disulfide/80% *n*-propyl disulfide system was carried to what appeared to be a constant composition, it may be that prolonged irradiation is required to attain the equilibrium concentration of the $C_2H_5SSC_3H_7$ product. For these systems the equilibrium state is approached with a rate that varies considerably from mixture to mixture, with the equilibrium state being attained after a period of 1 to 3 h.

The main body of experiments involved the determination of the initial rates in disulfide combinations, photolysed as equimolar pure liquid mixtures by the medium pressure Hg-lamp. In all systems examined the mol% of the unsymmetrical disulfide formed generally increased linearly with exposure time up to ca. 10–15% product.

The initial rate data for straight chain disulfide mixtures from methyl disulfide to pentyl disulfide are shown in Table 2. Here, as with other initial rate data to be tabulated below, the rates were obtained from a least-squares treatment of mol% vs. exposure time. Standard deviations were between 4 and 6%. The initial rate of mixed disulfide formation is lowest for the dibutyl disulfide – dipentyl disulfide systems. The only significant product of these systems is the mixed disulfide. For longer irradiation times with the higher molecular weight mixtures small amounts of other products (<5%) were observed, but were not identified.

Ten additional combinations were studied to compare initial rates in $n\text{-}C_3H_7SSC_3H_7$–RSSR and $i\text{-}C_3H_7SSC_3H_7$–RSSR mixtures. The data are presented, along with the appropriate rates from Table 2 for comparison, in Table 3.

The change from *n*-propyl disulfide to isopropyl disulfide as the second component of the mixture results in a significant decrease in the rate of product formation. The remarkable exception to this trend is the ten-fold increase for the iso–iso combination.

TABLE 2. Initial rates of mixed disulfide formation for straight chain dialkyl disulfides

(RSSR + R'SSR')	Initial mixed disulfide yields, μmol min^{-1} R' = C_2H_5	*n*-C_3H_7	*n*-C_4H_9	*n*-C_5H_{11}
R = CH_3	14.8	13.9	1.44	0.58
C_2H_5	—	71.1	1.01	0.45
n-C_3H_7	—	—	0.84	0.37
n-C_4H_9	—	—	—	0.23

TABLE 3. Initial rates of mixed disulfide formation for propyl disulfide – RSSR mixtures

Disulfide RSSR	Mixed disulfide yields, μmol min^{-1} R' = *n*-C_3H_7	iso-C_3H_7
R = CH_3	13.9[a]	3.0
C_2H_5	71.1[a]	21.6
n-C_4H_9	0.84[a]	0.55
iso-C_4H_9	0.85	8.3
sec-C_4H_9	11.9	4.7
n-C_5H_{11}	0.37[a]	0.14
iso-C_5H_{11}	0.57	5.9

[a]Data from Table 2.

The butyl disulfide – RSSR systems provide an opportunity to examine steric effects over a potentially broader range. Table 4 lists the initial rates for 15 such combinations, again along with 7 rates from Tables 2 and 3 for convenience in comparing values. Two systems could not be studied because of the difficulties in separating reactant and product disulfides.

The additional iso–iso combination included here, 1-$C_5H_{11}SSC_5H_{11}$ – 1-$C_4H_9SSC_4H_9$, shows the even more pronounced rate in rate compared to the analogous *n*–iso system. The trend to lower

Can. J. Chem. Downloaded from www.nrcresearchpress.com by 210.87.254.40 on 09/05/12
For personal use only.

Can. J. Chem. Downloaded from www.nrcresearchpress.com by 210.87.254.40 on 09/05/12
For personal use only.

TABLE 4. Initial rates of mixed disulfide formation for dibutyl disulfide – RSSR mixtures

Disulfide RSSR	Mixed disulfide yields, μmol min^{-1}			
	R′ = *n*-C_4H_9	iso-C_4H_9	*sec*-C_4H_9	*tert*-C_4H_9
R = CH_3	1.44[a]	1.44	2.7	0.13
C_2H_5	1.01[a]	0.89	13.2	0.08
n-C_3H_7	0.84[a]	0.85[b]	11.9[b]	—
iso-C_3H_7	0.55[b]	8.3	4.7	—
n-C_5H_{11}	0.23[a]	0.23	0.13	0.04
iso-C_5H_{11}	0.29	20.6	0.18	0.05

[a]Data from Table 2.
[b]Data from Table 3.

rates with higher molecular weight is again a general characteristic. The lowest rates are observed for the mixtures containing *tert*-butyl disulfide.

In addition to the rates listed in the tables, two other combination were studied, methyl disulfide – isopentyl disulfide and ethyl disulfide – isopentyl disulfide for which the initial rates, in μmol min^{-1}, were 0.71 and 0.61 respectively.

Equimolar mixtures of methyl disulfide and ethyl disulfide were photolysed with three different light sources and apparent initial quantum yield of methylethyl disulfide formation determined as follows: $\phi' = 21.4 \pm 1.9$ (low pressure Hg-lamp, $I_a = 1.28 \pm 0.1$ μEinstein min^{-1}), 20.7 ± 1.8 (medium pressure Hg-lamp, $I_a = 0.81 \pm 0.5$ μEinstein min^{-1} and 24.4 ± 2.2 (325 nm laser, $I_a = 0.16 \pm 0.01$ μEinstein min^{-1}). The values obtained, however, are only apparent quantum yields because of the lack of identity of reactant and actinometer absorption characteristics.

One of the difference factors that can be accommodated, however, is that of concentration. Using 0.762 *M* solution of methyl disulfide – ethyl disulfide in cyclohexane which has the same absorption at 254 nm as the ferrioxalate actinometer, an apparent quantum yield of 15.8 ± 1.0 was found using the low pressure Hg-lamp.

Thus, despite the various uncertainties associated with these data, the quantum yield is evidently on the order of magnitude of 20. On that basis, and if the methyl disulfide – ethyl disulfide system is used as an internal actinometer in this system, disulfide mixtures irradiated with the low pressure lamp and which have initial rates less than 0.75 μmol min^{-1} represent systems with quantum yields less than unity.

The apparent initial quantum yields are evidently independent of both wavelength and, over the very limited range examined, intensity. All wavelengths studied involve excitation in the same absorption band of the disulfides centered at ca. 250 nm and extending to ca. 350 nm. This is consistent with the expectation that in condensed phase the net result of the primary process occurring in this absorption envelope is the production of thermalized RS species.

In previous investigation in this laboratory (7), appreciably higher quantum yields were found. We believe that some of this difference is due to the incorporation into the present experiments of the recently identified (10, 11) modifications and precautions required for accurate light intensity determinations. A more significant factor, however, may be that very small disulfide sample volumes were used in the previous work and the thermal blanks, which in the present systems are insignificant compared to the photochemical reaction in the much larger sample sizes used, may in those experiments, have made a much larger contribution to the total observed yields than was allowed for.

Finally, to establish definitively that the exchange reaction is exclusively free radical in nature, several experiments were conducted in which methyl disulfide – ethyl disulfide mixtures that had been saturated with nitric oxide were photolysed. No mixed disulfide products could be detected in any of these experiments.

Discussion

The general mechanistic features of these disulfide systems are well established. Photolysis leads to S—S bond rupture and the RS radicals formed either recombine, or participate in the exchange reaction with parent disulfide molecules. If a single disulfide is formed, recombination is the only significant reaction and no products can be observed at moderate exposure times.[2]

The overall mechanism which is consistent with the gross features of the photoreaction is as follows:

$$[2a] \quad RSSR + h\nu \leftrightarrows 2\,RS$$

$$[2b] \quad R'SSR' + h\nu \leftrightarrows 2\,R'S$$

$$[3a] \quad R'S + RSSR \rightarrow RSSR' + RS$$

$$[3b] \quad RS + R'SSR' \rightarrow RSSR' + R'S$$

$$[4] \quad RS + R'S \rightarrow RSSR'$$

When the concentration of RSSR′ attains significant levels, its photolysis leads to the observed photo-equilibrium.

$$[2c] \quad RSSR' + h\nu \leftrightarrows RS + R'S$$

The absence of any non-disulfide products and the attainment of the same equilibrium distribution,

[2]Some product formation has been noted (12) for very long exposures in similar systems, but none can be detected from C_2 to C_{10} disulfide mixtures at the exposure times studied here.

Can. J. Chem. Downloaded from www.nrcresearchpress.com by 210.87.254.40 on 09/05/12
For personal use only.

independent of proportion of starting material, along with the previously reported (7) attainment of an equilibrium with $K = 4.0$ beginning with 98% $CH_3SSC_2H_5$, all attest to the validity of this representation of the system.

If k_t represents the average value of k_4 and the rate constants for the reverse of reactions [2*a*] and [2*b*]; k_p, the average of k_{3a} and k_{3b}; and [D], the total disulfide concentration in an equimolar mixture, the mechanism predicts the following expression for the quantum yield of methylethyl disulfide formation

$$[5] \quad \phi_{RSSR'} = [D]k_p(1/I_a k_t)^{1/2}$$

The relative contributions of reactions [3] and [4] to RSSR′ formation will be reflected in quantum yields in the following way. To the extent that reaction [3] is the principal source of RSSR′, the observed quantum yields will be in excess of unity. On the other hand, the more important is reaction [4], and the reverse of [2*a*] and [2*b*] taking place in the bulk of the reaction mixture, the lower will be observed ϕ values. Superimposed on this effect will be the influence of cage recombination of the initially formed thiyl radicals in process [2]. The effective value of k_t will thus be influenced by two different types of RS combinations.

Thus in systems with small quantum yields, the observed variations in rates must be due primarily to alterations in the contributions of reactions [2] and [4].

The observed initial rates listed in Table 2 show that for the straight chain disulfide mixtures yields are in approximately inverse proportion of total molecular weight. The one remarkable exception to this trend is the ethyl disulfide – *n*-propyl disulfide mixture. There is no obvious explanation for this observation.[3]

Three other sets of data for comparison can be extracted from the Tables 2–4, to examine the effect of total molecular weight of the mixture of RSSR′ rates; namely *sec*-butyl disulfide – RSSR, *n*-butyl disulfide – RSSR, and *tert*-butyl disulfide – RSSR, where RSSR represents the various straight chain disulfides whose indicated mixtures could be studied. With again one exception, the CS_3SSCH_3 – *sec*-butyl disulfide mixture, the rates are approximately linearly dependent on total molecular weight. The variation observed, however, is much smaller when the RSSR component is changed from CH_3SSCH_3 to *n*-$C_5H_{11}SSC_5H_{11}$ in the *tert*-butyl disulfide – RSSR mixtures (Table 4). In all of those mixtures, the quantum yields of mixed disulfide formation would be less than ca. 0.2. It would appear therefore that in a system where the exchange reaction [3] is not significant, the effect of molecular weight, essentially thiyl radical size, is relatively minor.

The effect of branching can be illustrated by a comparison of the *n*-propyl disulfide vs. isopropyl disulfide mixtures rates reported in Table 3. Excluding the iso–iso combinations to be discussed below, the observed initial rates are always lower for the mixture containing the isodisulfide. The effect appears to be a general one in that it is observed in mixtures with quantum yields both above and below unity. By contrast, in the butyl systems, the data in Table 4 show relatively little diminuition of rate in changing from an *n*-butyl to an isobutyl disulfide mixture component, although again the iso–iso combinations show much higher yields. The reduced sensitivity of rate of radical reactions for butyl disulfide systems compared to their propyl analogues is consistent with the observations of Pryor and Platt (13) in a study of the reactions of phenyl radicals with propyl and butyl disulfides. As observed here, the sensitivity to steric factors was significantly diminished in the isobutyl systems.

Comparing the rates for the *n*-pentyl disulfide – RSSR and isopenyl disulfide mixtures shows that the latter are slightly higher, iso–iso combinations excepted, and the general trend to lower rates with higher total molecular weight is also apparent. The quantum yields here, however, are mostly less than unity. Thus the steric effect related factors which give rise to a decrease in rate in going from *n*- to isodisulfides are more significant when quantum yields exceed unity (propyl systems) or are near unity (butyl systems) and are evidently counterbalanced by other effects when exchange reactions is diminished in importance as evidenced by quantum yields of less than unity.

The systems containing *tert*-butyl disulfide all exhibit very low rates with quantum yields less than ca. 0.2. Here evidently steric effects are the determining factor. They would presumably both militate against radical diffusion, increasing the probability of cage recombination, and render the RS–disulfide exchange less facile.

Finally, the perplexing behaviour of the iso–iso combinations requires comment. Without exception the observed rate for every iso–iso mixture studied is anomalously high both in terms of its value relative to the appropriate *n*-isomers but absolutely in comparison to all systems studied. The iso–iso combinations for C_3- and C_4-disulfides are

[3]To ensure that the inordinately high rate was not the result of an experimental artifact, the rates for these mixtures were redetermined using American Petroleum Institute Standard samples, confirming the initially observed very large values.

about 10 times larger than the corresponding *n*–iso systems; for C_4–C_5 the factor is about 70. Indeed the isobutyl disulfide – isopentyl disulfide combination shows an initial rate greater than that of the reference methyl disulfide ethyl disulfide system. Since the exchange reaction [3] is almost certainly more efficient when CH_3S radicals attack RSSR than the analogous process with iso-C_5H_9S and iso-C_4H_9S the effect must have its origin in reactions [2] and [4].

Further investigation is evidently required to elucidate this aspect of the system. A study is now being initiated in which the photochemical systems studied here will be used to prepare various unsymmetrical disulfides, such as, for example, iso-C_3H_7SS (*n*-C_3H_7), which can be co-photolysed with symmetrical and other unsymmetrical disulfides, so that the precise effect of these steric factors can be elucidated in the greater amount of detail that will evidently be necessary to understand fully the evident complexities in these systems.

Acknowledgements

The authors gratefully acknowledge the financial support of this work by the National Research Council of Canada and the Natural Sciences and Engineering Research Council of Canada.

1. B. MILLIGAN, D. E. RIVETT, and W. E. SAVIGE. Aust. J. Chem. **16**, 1020 (1963).
2. M. KLEIMAN. U.S.P. 2,474,849; Chem. Abstr. **44**, 6539 (1950).
3. S. F. BIRCH, T. V. CULLUM, and R. A. DEAN. J. Inst. Perbol. **39**, 206 (1953).
4. L. HARALDSON, C. J. OLANDER, S. SUNNER, and E. VARDE. Acta Chem. Scand. **14**, 1509 (1960).
5. C. J. OLANDER and S. SUNNER. Pure Appl. Chem. **2**, 117 (1961).
6. B. NEANDER and S. SUNNER. J. Am. Chem. Soc. **94**, 3576 (1972).
7. K. SAYAMOL and A. R. KNIGHT. Can. J. Chem. **46**, 999 (1968).
8. D. D. CARLSON and A. R. KNIGHT. Can. J. Chem. **51**, 1410 (1973).
9. D. G. HATCHARD and C. A. PARKER. Proc. R. Soc. A**235**, 518 (1956).
10. W. D. BOWMAN and J. N. DEMES. J. Phys. Chem. **80**, 2434 (1976).
11. D. E. NICODEM, M. L. P. F. CABRAL, and J. C. N. FERGERIRA. Mol. Photochem. **8**, 213 (1977).
12. R. G. BUTTERY and R. M. SEIFERT. Agri. Food Chem. **25**, 434 (1977).
13. W. A. PRYOR and P. K. PLATT. J. Am. Chem. Soc. **85**, 1496 (1963).

Can. J. Chem. Downloaded from www.nrcresearchpress.com by 210.87.254.40 on 09/05/12
For personal use only.

Infrared spectra of the ammonium ion in crystals. Part IX. Ammonium tetraphenylborate, $NH_4B(C_6H_5)_4$: crystal structure at room temperature and at 120 K, and evidence of hydrogen bonding[1,2]

WOLFGANG J. WESTERHAUS AND OSVALD KNOP
Department of Chemistry, Dalhousie University, Halifax, N.S., Canada B3H 4J3
AND
MICHAEL FALK
Atlantic Regional Laboratory, National Research Council of Canada, Halifax, N.S., Canada B3H 3Z1
Received February 8, 1980

WOLFGANG J. WESTERHAUS, OSVALD KNOP, and MICHAEL FALK. Can. J. Chem. **58**, 1355 (1980).

A determination of the crystal structure of ammonium tetraphenylborate (ATPB) at 120 K shows that the ammonium ion in this crystal, at a site of symmetry D_{2d}, is oriented in a way consistent with the expectation from a simple model based on Coulombic interaction. Infrared spectra of the isotopic ammonium ions obtained between 10 K and room temperature indicate that the effect of the tetraphenylborate anion on the strength of the N—H bond (as measured by the stretching frequency) is small and independent of temperature, and that the distortion of the ammonium ion from T_d symmetry is slight. From the combined evidence it is concluded that the ammonium ion in ATPB must be regarded as hydrogen-bonded, but the potential field due to the four phenyl rings surrounding the ammonium ion offers little resistance to the bending (and probably also to the librational) motion of the ion.

WOLFGANG J. WESTERHAUS, OSVALD KNOP et MICHAEL FALK. Can. J. Chem. **58**, 1355 (1980).

Une détermination de la structure cristalline de tétraphénylborate d'ammonium (ATPB) à 120 K montre que l'ion ammonium dans ce cristal, au site de symétrie D_{2d}, est orienté d'une manière conforme à celle prévue à partir d'un modèle simple basé sur une interaction coulombienne. Les spectres infrarouge des ions ammonium isotopiques obtenus entre 10 K et la température ambiante indiquent que l'effet de l'anion tétraphénylborate sur la force de la liaison N—H (telle que mesurée par la fréquence de valence) est faible et indépendant de la température et que la distorsion de l'ion ammonium par rapport à la symétrie T_d est faible. L'ensemble de ces preuves permet la conclusion que l'ion ammonium dans l'ATPB doit être considéré comme lié par des liaisons hydrogène, mais le potentiel dû aux quatre cycles phényl entourant l'ion ammonium offre peu de résistance au mouvement de déformation de l'ion (et probablement aussi au mouvement de libration).

[Traduit par le journal]

Introduction

The recent renewal of interest (2, 3) in the title compound (ATPB) has been prompted by the remarks of Nakamoto *et al.* (4) in a paper dealing with stretching frequencies as a function of distance in hydrogen bonds. These authors quote the results of Bonham, who found the ir "non-hydrogen-bonded" NH stretching frequencies for various salts of the $(NEt_nH_{4-n})B(C_6H_5)_4$ type to lie near 3100 cm^{-1}, and they compare these frequencies to the corresponding frequencies in other ammonium salts (e.g. in NH_4Cl, 3110 cm^{-1}) "where hydrogen bonding is probably not an important factor". They note that these frequencies are rather low for hydrogen-bonding interactions as weak as those in N^+—H···Cl^- bonds and suggest that the low frequencies found in such bonds "arise only partly from hydrogen bonding". Consequently charge and coordination effects must be taken into account. The implication for ATPB thus appears to be that (*i*) the hydrogen bonding in this crystal is very weak and (*ii*) the NH stretching frequency is unexpectedly low (i.e. it appears to correspond to a stronger hydrogen bond than the trends observed in other crystals containing N—H···X bonds would warrant), and that for reasons other than hydrogen-bonding interactions. In the present paper we examine new evidence bearing on these two points. Here, as elsewhere in this series, the term "hydrogen bonding" shall include all factors which restrict rotation of the ammonium ion to torsional oscillations.

In Parts IV and VI (2, 3) we reported the isolated ND stretching and bending frequencies of the NH_3D^+ probe ion in ATPB at 90 K. The stretching frequency $\nu_1(NH_3D^+)$, 2364 cm^{-1}, is significantly above the corresponding frequency in NH_4Cl, 2289 cm^{-1}, but similar to the isolated ND stretching frequencies in $(NH_4)_2PbCl_6$ and $(NH_4)_2TeCl_6$, in which crystals hydrogen bonding is judged to be weak but not absent. The position of ATPB in a $\nu_1(NH_3D^+)$ vs. N···X distance plot (X = F, Cl, Br, I; Fig. 1 of ref. 3) is uncertain, for we do not know what constitutes the appropriate N···X distance in this crystal, but in the $\nu_{4bc}(NH_3D^+)$ vs. $\nu_1(NH_3D^+)$

[1]For Part VIII, see ref. 1.
[2]NRCC No. 18224.

0008-4042/80/131355-10$01.00/0
©1980 National Research Council of Canada/Conseil national de recherches du Canada

Can. J. Chem. Downloaded from www.nrcresearchpress.com by 210.87.254.5 on 09/05/12
For personal use only.

Can. J. Chem. Downloaded from www.nrcresearchpress.com by 210.87.254.5 on 09/05/12
For personal use only.

plot (Fig. 3 of ref. 3) the ATPB point falls in a region characteristic of weak hydrogen bonding and high C.N. The ν_{4bc} frequency of ATPB at 90 K is in fact lower than any ν_{4bc} (90 K) frequency observed in an ammonium halide to date. The ν_1 frequency is higher than our estimate of the 'free-ion' ν_1 frequency in simple and complex ammonium halides.[3] This we have ascribed (3) to a state of compression of the ammonium ion in the structure, which is dominated by electrostatic forces; this explanation in a way implies the suggestion of Nakamoto *et al.* that coordination effects are important. The K (5, 6) and Rb (7, 8) tetraphenylborates have been reported to be isostructural with ATPB (disregarding the ammonium hydrogens), and the unit-cell dimensions of the Rb salt (7–9) are practically indistinguishable from those of ATPB. From this it is evident that the non-uniform charge distribution on the ammonium ion and the hydrogen-bonding ability of NH_4^+ do not play a structure-determining role in this crystal at room temperature, which supports the above implication (*i*).

Clearly the increase in ν_1 from the 'free-ion' value[3] due to the compression ('volume') effect could overwhelm any ν_1 lowering that might result from a vestigial hydrogen-bonding interaction. This raises the interesting question of the whereabouts of the ammonium hydrogens in the crystal and the nature of the hydrogen-bonding interaction in a situation where a single ionic charge is spread over an assembly of a number of atoms. Considering the spatial dilution of the anionic charge, there seems to be *a priori* no reason why reorientation of the ammonium ion should not approximate to a very weakly hindered 'free' rotation, unless interaction between the ammonium hydrogen and the charge in the π systems of the benzene rings is significant. If it is, there ought to be a reasonable chance of finding the ammonium hydrogens localized in regions of space corresponding to the hydrogen-bonding geometry between reorientations.

A determination of the room-temperature crystal structure of ATPB by photographic methods (7) did not provide any indication of where the ammonium hydrogens might be located. We therefore set out to redetermine the room-temperature structure from diffractometer intensities and supplement it by a companion determination at low temperature, in the hope that the information so obtained would go some way toward resolving the problem. At the same time we extended the ir study of the NH_3D^+ probe ion in ATPB to include the effect of temperature between 10 and 293 K on the spectrum of this ion as well as on certain bands of the NH_4^+ and ND_4^+ spectra.

[3]We do not know to what extent the 'free-ion' ν_1 frequency estimated for ammonium halides (3) is applicable to ATPB, ammonium halides being so far the only group of ammonium compounds for which such a frequency is available, but it is our present belief that the use of this estimate represents the situation in ATPB essentially correctly.

Structure Determination

Needle-shaped crystals of ATPB (fw = 337.28) precipitated on mixing aqueous solutions of equimolar amounts of the commercial Na salt and NH_4Cl at room temperature. Recrystallization from a 1:1 mixture of water and acetone yielded small stout prisms well suited for diffraction experiments.

Weissenberg photographs at room temperature indicated a body-centred tetragonal unit cell. This is consistent with the space groups $I\bar{4}m\underline{2}$ and $I\bar{4}2m$ considered as likely in ref. 9 and with $I\bar{4}2m$ resulting from the structure determination of ref. 7. The crystallographic data are presented in Table 1. No evidence of crystallographic transition between 10 K and room temperature was found in the ir spectra of ATPB, deuterated or undeuterated, in accord with the unchanged crystallographic symmetry observed at 120 K (see below) and with the heat capacity measurements between 20 and 298 K (Staveley and Davies, cited in ref. 7).

Crystal Structure at Room Temperature

Intensities from a 0.2 × 0.2 × 0.36 mm³ crystal were measured on a Picker FACS-1 diffractometer with an ω–2θ scan ($4° \leq 2\theta \leq 120°$; minimum base width, 2.0°) using Cu Kα radiation. Of the 245 independent reflections 198 had $I > 3\sigma(I)$; these were used in the structure determination. The data were reduced to a standard scale by a routine procedure and corrected for Lorentz and polarization factors but not for absorption ($\mu_{Cu} = 4.05\ cm^{-1}$). Four reflections (110, 002, 004, 006) which were obvi-

TABLE 1. Unit-cell dimensions of $NH_4B(C_6H_5)_4$ ($I\bar{4}2m$, No. 121; $Z = 2$) at room temperature and at 120(10) K

	Value			
			This work	
Parameter	Ref. 9	Ref. 7	R.T.*	120 K†
a, Å	11.24(2)	11.25	11.229(5)	11.176(4)
c, Å	8.08(2)	8.07	8.060(8)	8.032(4)
V, Å³	1021(7)	1021	1016.3(2)	1003.2(2)
d_x, g/cm³	1.097	1.097	1.102	1.117
d_{obs}, g/cm³	1.093	1.09		

*Refined from the diffractometer settings of 12 general single-crystal reflections with $2\theta > 60°$.
†Refined from the diffractometer settings of 25 reflections with $2\theta > 40°$ using a different crystal and instrument (see text).

TABLE 2. Positional and thermal parameters of $NH_4B(C_6H_5)_4$ at room temperature and at 120(10) K*

Atom		S	x	y	z	u_{11}	u_{22}	u_{33}	u_{12}	u_{13}	u_{23}
B	2(*a*)	$\bar{4}2m$	0	0	0	25(3)	25(3)	35(7)	0	0	0
			0	0	0	21(3)	21(3)	22(4)	0	0	0
N	2(*b*)	$\bar{4}2m$	0	0	5000	48(3)	48(3)	36(5)	0	0	0
			0	0	5000	30(3)	30(3)	13(4)	0	0	0
C(1)	8(*i*)	*m*	813(3)	813(3)	1255(6)	32(2)	32(2)	29(3)	−1(2)	3(1)	3(1)
			816(3)	816(3)	1272(6)	25(2)	25(2)	11(2)	−5(2)	1(2)	1(2)
C(2)	16(*j*)	1	408(4)	1894(4)	1924(5)	42(2)	40(2)	36(2)	−4(2)	6(2)	−6(2)
			403(3)	1900(3)	1921(5)	25(2)	28(2)	18(2)	−3(2)	3(2)	1(2)
C(3)	16(*j*)	1	1020(4)	2505(4)	3139(6)	63(2)	45(2)	45(3)	−11(2)	2(2)	−10(2)
			1018(3)	2529(3)	3167(5)	36(2)	29(2)	16(2)	−8(2)	2(2)	−3(2)
C(4)	8(*i*)	*m*	2067(4)	2067(4)	3755(8)	63(2)	63(2)	37(3)	−33(4)	−8(2)	−8(2)
			2075(3)	2075(3)	3785(7)	38(2)	38(2)	12(2)	−15(3)	−4(2)	−4(2)
H(2)	16(*j*)	1	−361(39)	2170(38)	1639(61)	48(12)†					
			−379(28)	2188(29)	1614(38)	16(5)†					
H(3)	16(*j*)	1	651(36)	3283(43)	3548(64)	68(14)†					
			707(33)	3336(33)	3543(42)	48(6)†					
H(4)	8(*i*)	*m*	2488(42)	2488(42)	4607(88)	66(18)†					
			2535(39)	2535(39)	4553(54)	52(6)†					
H(5)	8(*i*)	*m*	604(36)‡	604(36)‡	4705(54)‡	87(6)‡					

*Numbering of atoms as in ref. 6; associated C and H atoms bear the same number. *S*, site symmetry. Upper line, room temperature; lower line, 120 K. The positional parameters have been multiplied by 10^4 and the thermal parameters by 10^3. The anisotropic temperature factor is defined as $T = u_{11}a^{*2}h^2 + 2u_{12}a^*b^*hk + \ldots$.
†Isotropic temperature factor.
‡At 120 K, see text.

ously affected by extinction were omitted from the calculations. Scattering factors for neutral atoms were taken from ref. 10.

The positional parameters of the non-hydrogen atoms in the K salt (6), with N replacing K, were used as starting parameters for a full-matrix least-squares refinement in $I\bar{4}2m$, initially with isotropic temperature factors. The phenyl hydrogens (but not the ammonium hydrogens) were located on a difference Fourier map when the conventional *R* was 0.11. With anisotropic temperature factors for all non-hydrogen atoms *R* converged to 0.047. A difference Fourier map at this stage showed four symmetry-related regions of higher density at approximately 1 Å from the N atom. Fixing the ammonium hydrogens in these positions and taking 0.08 Å^2 as their isotropic temperature factors resulted in $R = 0.040$ and $R_w = 0.041$.[4] A refinement of the positional parameters of all the atoms, including the ammonium hydrogens, converged but yielded very short N—H distances (0.63 Å) and large esd's.

The final values of the positional and thermal parameters are listed in Table 2. The positional parameters differ only slightly from those obtained by Webster (7) using an overall isotropic temperature factor. The geometry of the tetraphenylborate ion is practically indistinguishable from the geometry of the ion in the K salt (6), the differences between the interatomic distances being within one or at most two standard deviations, and similarly for the bond angles.

Crystal Structure at Low Temperature

For the structure determination from low-temperature intensities a larger crystal (0.25 × 0.25 × 0.7 mm^3) and an Enraf-Nonius CAD-4 diffractometer fitted with a cold-gas-flow cryogenic device were used. The crystal was enclosed in a glass capillary. The unit-cell dimensions at 120(10) K are shown in Table 1. The intensity collection at this temperature using Mo Kα radiation (μ_{Mo} = 0.32 cm^{-1}) gave 293 independent reflections with $I > 2\sigma(I)$. All but two were used in the refinement; the 110 and 002 reflections suffered from extinction and were omitted.

A refinement starting from the room-temperature parameter values (excluding the ammonium hydrogens) brought the *R* value down to 0.052. A difference Fourier map at this stage showed four symmetry-related peaks at 0.97 Å from the N atom. Including hydrogens with positional parameters corresponding to these maxima reduced *R* to 0.044 and R_w to 0.041 and gave reasonable esd's for both the positional and thermal parameters of these

[4]Weighting schemes of the type $w^{-1} = \sigma^2|F_o| + k|F_o|^2$ (σ = individual esd calculated from diffractometer counting statistics) were used in all refinements.

Can. J. Chem. Downloaded from www.nrcresearchpress.com by 210.87.254.5 on 09/05/12
For personal use only.

TABLE 3. Interatomic distances (Å) and bond angles (deg) in the tetraphenylborate anion in ATPB at 120(10) K*

Bond	Distance (Å)	Bonds	Angle (deg)
B—C(1)	1.645(7)	C(1)—B—C(1′)	103.2(8)
		C(1)—B—C(1″)	112.7(9)
C(1)—C(2)	1.397(8)		
C(2)—C(3)	1.403(9)	C(2)—C(1)—C(2′)	115.7(9)
C(3)—C)4)	1.378(8)	C(1)—C(2)—C(3)	122.6(13)
		C(2)—C(3)—C(4)	119.5(16)
C(1)—C(3)	2.456(8)	C(3)—C(4)—C(3′)	120.1(10)
C(2)—C(2′)	2.366(7)		
C(2)—C(4)	2.402(10)		
C(3)—C(3′)	2.388(7)		
C(1)—C(4)	2.834(7)		
C(2)—C(3′)	2.760(8)		

*Coordinate transformations: C(1′), $(-x, -y, z)$; C(1″), $(y, -x, -z)$; C(2′) and C(3′), (y, x, z). The sum of the C—B—C bond angles is 657(2)°, corresponding to a mean of 109.5(9)°. The sum of the internal C—C—C bond angles in the phenyl ring is 720(3)°, corresponding to a mean of 120.0(14)°.

atoms, comparable to those of the phenyl hydrogens. The final parameter values are compared in Table 2 with those from the room-temperature determination. Interatomic distances and bond angles in the tetraphenylborate anion calculated from these values are listed in Table 3.

Discussion

A projection of the contents of a unit cell of ATPB on (001) is practically identical with the projection for the K salt in Fig. 1 of ref. 6. The ammonium ion, at a site of symmetry D_{2d}, is inside a cage formed by two pairs of phenyl rings, each pair belonging to a different anion; the two pairs are rotated by 90° relative to each other into a tetrahedral configuration. The electron density distribution corresponding to the ammonium hydrogens is illustrated in Fig. 1. The difference Fourier map obtained with the 120 K data shows clearly the regions of excess electron density associated tetrahedrally with the N atom. The local maxima (labelled H(5) in Table 2) are at 0.98 Å from N and their radius vectors from N point into the phenyl rings, the nearest carbon being C(4) at 2.44 Å and the farthest C(1) at 2.78 Å. The maxima form with the N atom an angle of 152° with the S_4 axis as bisector, and 93° with a twofold axis parallel to (001) as bisector.

The nearest N—H vector of an undistorted NH_4^+ tetrahedron in this orientation would form an angle of ~80° with the C(1)—C(4) line, whilst the radius vector corresponding to H(5) forms an angle of ~60°, i.e. H(5) is closer to C(4) and so presumably closer to the effective location of one-quarter of the anionic charge. It thus appears that the location of the maxima, which does not coincide with the positions of the ammonium hydrogens required by undistorted tetrahedral geometry, is determined by the dynamic behaviour of the ammonium ion.

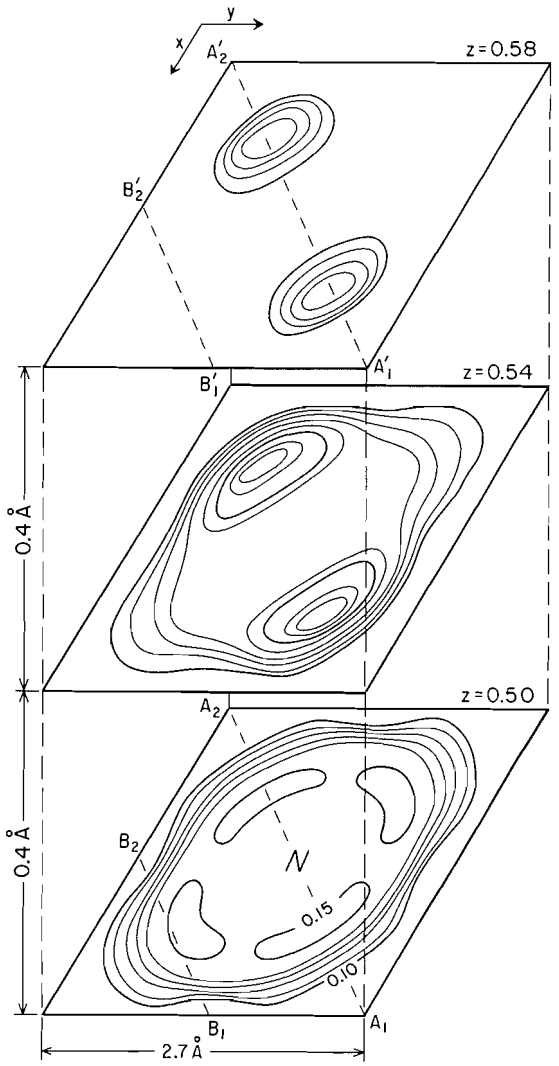


FIG. 1. Difference Fourier map of ATPB at 120 K. Axonometric presentation of sections parallel to (001) showing the 0.01 e/Å^3 contours around the B atom at $(0, 0, \frac{1}{2})$. The $z = 0.46$ and 0.42 sections (not shown) are obtained from the $z = 0.54$ and 0.58 sections respectively through operations of D_{2d} at the $(0, 0, \frac{1}{2})$ site. The outermost contour in each section corresponds to 0.10 e/Å^3.

At room temperature maxima attributable to the ammonium hydrogens are much more diffuse and no meaningful statement can be made about the most probable positions of these atoms.

The question of what constitutes hydrogen bonding apart, the observed orientation of the NH_4^+ ion in ATPB may be viewed simply as a consequence of the nonuniform charge distribution

Can. J. Chem. Downloaded from www.nrcresearchpress.com by 210.87.254.5 on 09/05/12
For personal use only.

Can. J. Chem. Downloaded from www.nrcresearchpress.com by 210.87.254.5 on 09/05/12
For personal use only.

on both ions. Webster (7), without specifying details of the calculation, makes the following statement: "It is calculated that the electrostatic potential energy is lowest when the H atoms of the ammonium ion point towards the centres of the benzene rings. After rotation of the ion through 90° about the *c*-axis, the potential energy is considerably greater and likely to prevent free rotation. When rotated in a direction perpendicular to the *c*-axis, the ion passes through several positions of varying maximum and minimum energy, so that the true nature of the oscillation of the ion is probably complicated." Limited point-charge calculations, with charges of equal magnitude and having the appropriate signs placed on the ammonium hydrogens and the C(4) atoms, confirm Webster's finding (Fig. 2); results of the same type are obtained when the negative charges are on the C(1) instead of the C(4) carbons. It may be significant that rotation about the S_4 axis of the ammonium ion (Fig. 2*A*) is more restrictive than the rotations about axes perpendicular to S_4 (Figs. 2*B*, *C*), for this difference is consistent with what is seen in the Fourier map.

Calculation of the corresponding variation of the Coulombic energy with angle of rotation for other types of reorientation of a rigid NH_4^+ ion, e.g. rotation about a threefold axis, was not attempted. Whilst calculation of the potential energy variation over the entire sphere of rotation would admittedly be instructive, the model underlying the results shown in Fig. 2 is too simplistic to warrant a more extensive effort in that direction. It seems unlikely that a potential minimum lower than that for $\alpha = 45°$ would be found, and the latter should be considered to be the global minimum in the absence of a proof to the contrary.

Infrared Spectroscopy

Partially deuterated ATPB samples were prepared by recrystallization from H_2O–D_2O–acetone mixtures of the appropriate D content. The sample crystals were finely ground and mulled with hydrocarbon or fluorocarbon oil. The mulls were sandwiched between KBr or CaF_2 plates. Details of the ir spectrometer will be found in ref. 11.

The NH_3D^+ probe ion spectrum was studied with samples containing 0.5% D, effectively corresponding to infinite dilution. The highest deuteration obtained, ca. 95% D, was adequate for a study of ND_4^+ and NHD_3^+ bands. However, as the concentration of the latter ion in this sample was not sufficiently low to qualify as isotopic isolation, only the NH stretching frequency of NHD_3^+ is reported. The principal bands of the isotopic ammonium ions observed between 4000 and 1000 cm^{-1} are listed in Table 4.

NH_3D^+ Absorptions

At 10 K the ND stretching fundamental ν_1 and the ND bending fundamental ν_{4bc} (for notation, see ref. 3 and preceding papers in this series) give rise to sharp single bands with halfwidths (= full width at half height) of only 3–4 cm^{-1} (Fig. 3). At higher temperatures both bands broaden and the integrated intensity of ν_1 diminishes, whilst that of ν_{4bc} remains nearly constant. The frequencies shift very little: between 10 K and room temperature ν_1 has shifted by only $-1.6(6)$ cm^{-1} and ν_{4bc} by only $+1.5(6)$ cm^{-1}, while their halfwidths have increased to 11–14 cm^{-1}. The changes of the observed band parameters are gradual (Fig. 4).

NH_4^+ and ND_4^+ Absorptions

A consequence of the large separation of the ammonium ions in the crystal, $d(N\cdots N) \sim 8$ Å, is a relatively weak vibrational coupling between neighbouring ions, with the result that the features observed in the NH_3D^+ probe spectrum are replicated with considerable fidelity in the NH_4^+ and ND_4^+ spectra.

The ir-active fundamental $\nu_3(NH_4^+)$ gives rise, at 10 K, to one main absorption peak and three smaller peaks (Fig. 5); corresponding four maxima appear in the ND_4^+ spectrum. The H/D frequency ratios are about 1.33. This precludes the possibility that some of the bands are due to combinations of ν_3 or ν_1 with translational or collective lattice modes, as such combinations would be expected to yield lower ratios. At higher temperatures the three smaller peaks rapidly lose intensity, and above about 100 K only one symmetric $\nu_3(NH_4^+)$, or $\nu_3(ND_4^+)$, fundamental is observed (Fig. 5). The ir-active bending fundamentals $\nu_4(NH_4^+)$ and $\nu_4(ND_4^+)$, as well as the corresponding overtones $2\nu_4(NH_4^+)$ and $2\nu_4(ND_4^+)$, give rise to only one band each, even at 10 K.

We have examined with special interest the 1600–1700 cm^{-1} region in the spectrum of undeuterated ATPB, where the combination mode $\nu_4 + \nu_6$ involving the librational mode $\nu_6(NH_4^+)$ may occur. At 10 K three sharp bands were observed, at 1712.6, 1686.3, and 1608.5 cm^{-1}. Their intensities diminished rapidly with increasing temperature and the bands were no longer evident above 100 K (Fig. 6). On deuteration the bands disappeared but similar bands emerged in the ND_4^+ spectrum between 1200 and 1250 cm^{-1}. Whilst the exact correspondence of the NH_4^+ and ND_4^+ features is uncertain (the H/D frquency ratios vary from 1.33 to 1.38

Can. J. Chem. Downloaded from www.nrcresearchpress.com by 210.87.254.5 on 09/05/12
For personal use only.

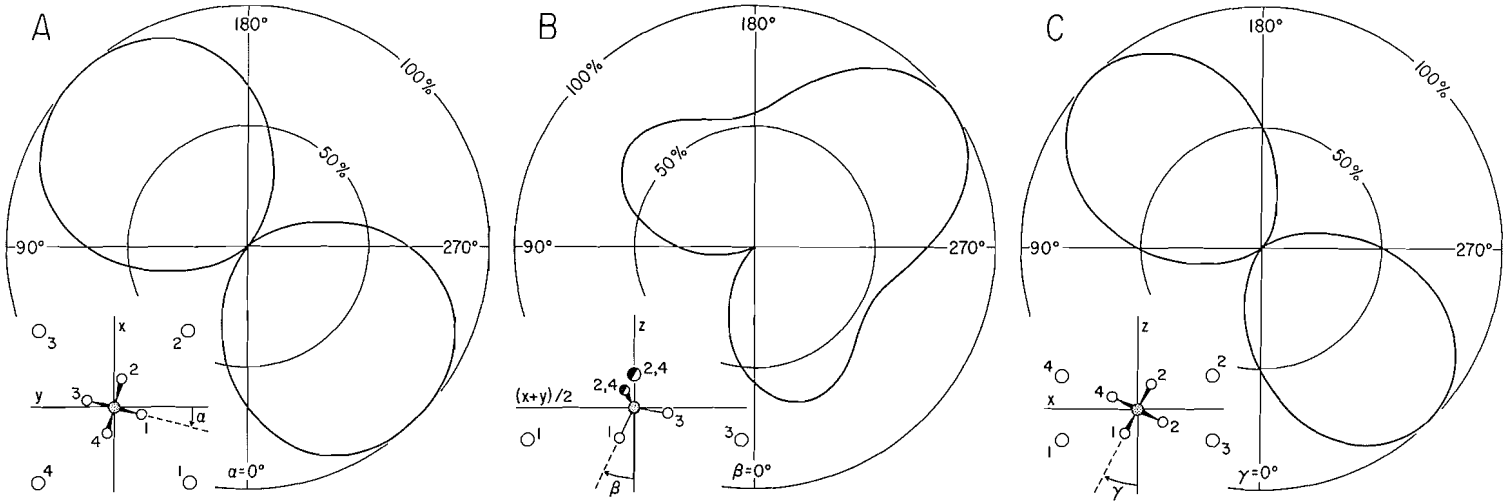


FIG. 2. Variation of the Coulombic interaction energy with the angle of rotation of a rigid NH_4^+ tetrahedron in ATPB. Point charges of equal magnitude are placed on the ammonium hydrogens (positive) and on the C(4) atoms of the anion (negative). (*A*) Rotation about the S_4 axis of the ammonium ion (coincident with *z*). (*B*) Rotation about a line bisecting *x* and *y*. (*C*) Rotation about a C_2 axis of the ammonium ion (coincident with *y*). The values plotted as functions of the angle of rotation represent percentages of the difference between the maximum and the minimum value of the Coulombic energy resulting from the calculation. The minimum value, which corresponds to the most symmetric static orientation of the ammonium ion ($\alpha = 45°$, as found by experiment), is believed to be the global minimum for this model.

TABLE 4. Selected frequencies (cm^{-1}) of the ammonium ion in the ir spectrum of $NH_4B(C_6H_5)_4$*

Mode	NH_4^+ 10 K	NH_4^+ 293 K	ND_4^+ 10 K	ND_4^+ 293 K	H/D frequency ratio 10 K	H/D frequency ratio 293 K
ν_3	3284.5(5)	†	2454.0(20)	†	1.338	
	3232.1(5)	†	2437.0(10)	†	1.326	
	3217.7(5)	3216.5(10)	2412.0(5)	2411.8(10)	1.334	1.334
	3208.7(5)	†	2404.5(20)	†	1.335	
$2\nu_4$	2770.9(3)	2774.0(10)	2106.0(2)	2104.5(8)	1.316	1.318
$\nu_4 + \nu_6$	1712.6(10)	†	1242.0(20)	†	1.379?	
	1686.3(10)	†	1218.0(20)	†	1.382?	
	1608.5(10)	†	1207.0(30)	†	1.332	
ν_4	1389.6(3)	1391.4(5)	1056.2(2)	1055.3(6)	1.316	1.336

Mode	NHD_3^+ probe ion 10 K	NHD_3^+ probe ion 293 K	NH_3D^+ probe ion 10 K	NH_3D^+ probe ion 293 K	H/D frequency ratio 10 K	H/D frequency ratio 293 K
ν_1 (isol.str.)	3156.5(10)	3155.5(15)	2363.6(3)	2362.0(6)	1.335	1.336
ν_4 (isol.bend.)			1232.3(3)‡	1234.3(6)‡		

*The precision of the peak-frequency determination (in parentheses) depends on band shape and intensity. The accuracy of the frequency scale is about ±1 cm^{-1}.
†Intensity rapidly decreases with increasing temperature. Band not observable above about 100 K.
‡This is the ν_{4bc} frequency.

(Table 3)) a strong argument in support of the assignment of these bands to $\nu_4 + \nu_6$ is that no other NH_4^+ absorption occurs in this region except for the bending fundamental $\nu_2(NH_4^+)$. That fundamental, however, is ir-inactive under the D_{2d} site symmetry and has been observed only in a few cases of extreme distortion of the ammonium tetrahedron (cf. ref. 11).

Deductions from the Spectra

(*a*) For $\nu_{4bc}(NH_3D^+)$ the D_{2d} site symmetry of the ammonium ion requires a 1:1 doublet (12). Only a single sharp band is observed down to 10 K, which implies that the symmetry of the ion is effectively T_d, as concluded previously (2). For $\nu_4(NH_4^+)$, $\nu_4(ND_4^+)$, $2\nu_4(NH_4^+)$, and $2\nu_4(ND_4^+)$ two ir-active components are expected under D_{2d}, but only a single band is observed in each case, again implying that the symmetry of the ion is effectively T_d.[5] One may conclude that hydrogen bonding is either very weak or absent; more correctly, there is no indication of hydrogen-bonding interactions that would exert an appreciable distorting force on the ion.

(*b*) For $\nu_1(NH_3D^+)$ a single band is expected for both T_d and D_{2d} symmetry (12). The observed singlet therefore provides no information as to whether or not the ammonium ion is distorted. For $\nu_3(NH_4^+)$ and $\nu_3(ND_4^+)$ a doublet is expected under the D_{2d} site group as opposed to a singlet under T_d. The single band observed above 100 K is consistent with the absence of appreciable distortion from T_d, but the emergence of additional bands on further cooling appears to indicate that some distortion may be present. However, the number of the observed features is larger than expected for a simple distortion. The origin of the small additional bands thus remains uncertain and no firm deduction can be made.

(*c*) As pointed out above, the frequency of the $\nu_{4bc}(NH_3D^+)$ absorption, 1234 cm^{-1}, is the lowest on record. The 293 K frequency of $\nu_4(NH_4^+)$, 1391 cm^{-1}, is lower than all but one of the 35 $\nu_4(NH_4^+)$ frequencies reported for an assortment of ammonium salts at room temperature by Waddington (13) and by Dunsmuir and Lane (14); the only lower frequency is that of $(NH_4)_2ReI_6$, 1388 cm^{-1}. The $2\nu_4(NH_4^+)$ frequency, 2774 cm^{-1}, again is the lowest of the 29 $2\nu_4$ values reported in refs. 13 and 14. These very low frequency values indicate that the potential field due to the four phenyl rings offers little resistance to the bending motion of the ammonium ion, hence hydrogen bonding must be very weak or absent.

(*d*) In contrast, the value of the $\nu_3(NH_4^+)$ frequency is not exceptional. The reported values vary from 3100 to 3300 cm^{-1}, with 14 values higher and 20 values lower than the frequency for ATPB,

[5]The $2\nu_4/\nu_4$ frequency ratio is independent of temperature and isotopic substitution: the average for the values listed in Table 4 is 1.9940(2).

Can. J. Chem. Downloaded from www.nrcresearchpress.com by 210.87.254.5 on 09/05/12
For personal use only.

Can. J. Chem. Downloaded from www.nrcresearchpress.com by 210.87.254.5 on 09/05/12
For personal use only.

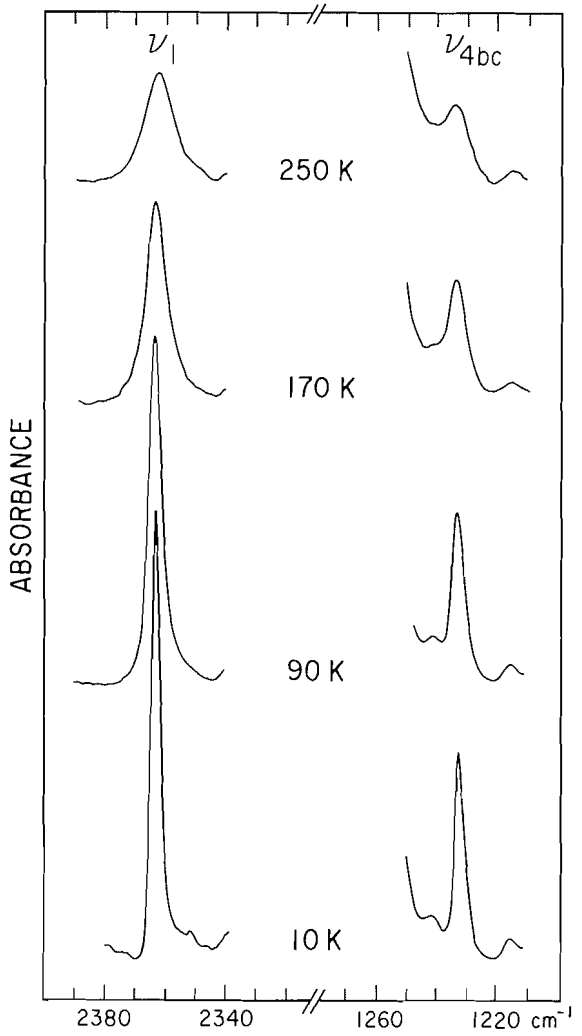


FIG. 3. The regions of the ND stretching fundamental $\nu_1(NH_3D^+)$ and the ND bending fundamental $\nu_{4bc}(NH_3D^+)$ in the ir spectrum of ATPB (0.5% D) at different temperatures.

3216 cm^{-1}. Likewise, the $\nu_1(NH_3D^+)$ frequency is not exceptional for an ammonium ion involved in weak hydrogen bonding. In the plot of $\nu_1(NH_3D^+)$ vs. $\nu_{4bc}(NH_3D^+)$ (Fig. 3 of ref. 3), the point for ATPB falls below the points for cubic $(NH_4)_2MCl_6$ and $(NH_4)_2MBr_6$. This indicates that, by comparison, the hydrogen-bonding interaction in ATPB, as measured by the ν_1 frequency, is very weak but still evident.

(*e*) The bending and stretching frequencies of ATPB remain nearly stationary with temperature between 10 and 293 K. This is a situation analogous to that in $(NH_4)_2SnCl_6$ and $(NH_4)_2PtBr_6$ (11) and is a manifestation of the weakness of hydrogen bonding.

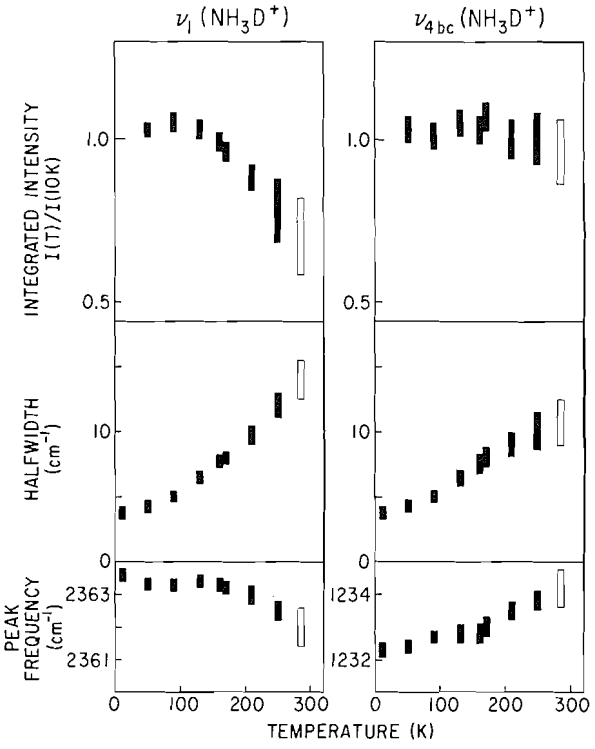


FIG. 4. Effect of temperature on band parameters of $\nu_1(NH_3D^+)$ and $\nu_{4bc}(NH_3D^+)$ of ATPB (0.5% D). The open rectangles denote values at 293 K obtained by extrapolation. The integrated intensities are normalized to the respective 10 K values.

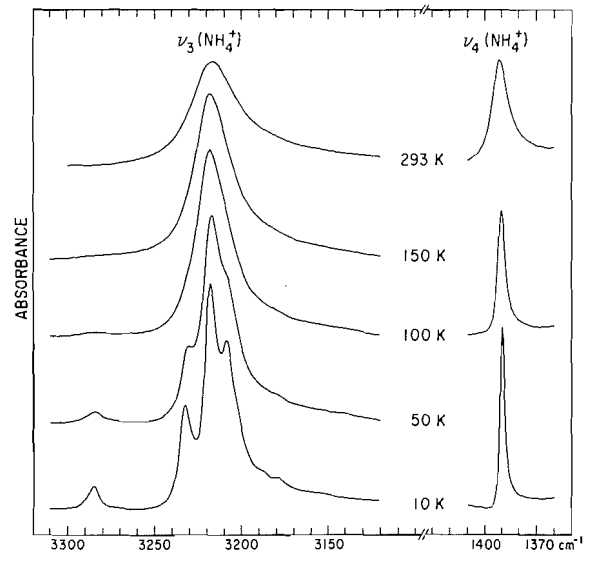


FIG. 5. The regions of the stretching fundamental $\nu_3(NH_4^+)$ and the bending fundamental $\nu_4(NH_4^+)$ in the spectrum of undeuterated ATPB at different temperatures.

Can. J. Chem. Downloaded from www.nrcresearchpress.com by 210.87.254.5 on 09/05/12
For personal use only.

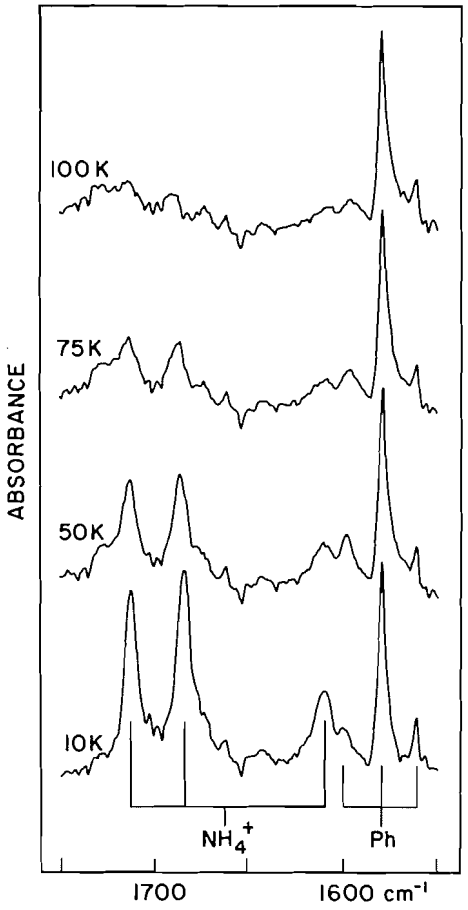


FIG. 6. The region of the combination mode $\nu_4 + \nu_6$ of NH_4^+ in the spectrum of undeuterated ATPB at different temperatures. The bands marked Ph are due to vibrations of the phenyl groups of the anions.

(*f*) In contrast to the band frequencies, which remain almost unchanged, the integrated intensity of the stretching vibrations is appreciably lowered when the temperature is increased above 150 K. The bending vibrations do not undergo such weakening. These observations indicate that the stretching modes have an increased intensity at low temperatures, implying the presence of at least some weak hydrogen bonding.

(*g*) The absorptions due to both the stretching and bending modes of NH_3D^+, NH_4^+, and ND_4^+ gradually broaden as the temperature increases. Studies of other ammonium salts (refs. 1 and 11 and results to be published) seem to indicate that such broadening occurs independently of the strength of hydrogen bonding and cannot serve as its indicator.

(*h*) Some of the evidence under *a* to *g* supports the existence of weak but significant hydrogen bonding (*d*, *f*), some of it indicates the absence of hydrogen bonding (*a*, *c*, *e*), and some of it is indeterminate (*b*, *g*). However, the occurrence of the bands clearly due to the combination $\nu_4 + \nu_6$ (involving the librational mode ν_6) in the low-temperature spectra of both NH_4^+ and ND_4^+ can be taken, following Waddington (13), as unequivocal evidence of the presence of weak hydrogen bonding at least at low temperatures. From the fact that these bands diminish rapidly with increasing temperature and are not observable above 100 K we may estimate the strength of the hydrogen bonding in ATPB relative to that in other ammonium compounds. In the spectrum of $(NH_4)_2SnCl_6$ the $\nu_4 + \nu_6$ bands disappear somewhere between 22 and 80 K (3), whilst those in the spectrum of NH_4ClO_4 disappear at about 150 K (results to be published). The strength of the hydrogen bonding in ATPB is thus intermediate between these two cases.

Conclusions

The picture that emerges on combining the crystallographic and spectroscopic evidence is then as follows. The ammonium ion in ATPB is at a site of symmetry D_{2d} from 10 K to room temperature, but its distortion from T_d symmetry is slight, in fact insufficient to produce an observable splitting of the ν_4, $2\nu_4$, and ν_{4bc} absorptions. The interaction which exists between the charges on the ammonium hydrogens and those residing in the π systems of the anion is strong enough to prevent the ammonium ion from rotating freely, but as the very low value of the $\nu_{4bc}(NH_3D^+)$ frequency indicates, the shape and magnitude of the potential barrier permit rotational displacements of the N—H bonds of appreciable amplitude even at 120 K, at least in some directions. The effect of the anion on the strength of the N—H bond, as measured by the values of the $\nu_1(NH_3D^+)$ and $\nu_3(NH_4^+)$ stretching frequencies, is small, comparable to that in the weakly hydrogen-bonded ammonium ions in $(NH_4)_2MCl_6$ and $(NH_4)_2MBr_6$, and practically unaffected by changes of temperature. We conclude that hydrogen-bonding interactions (i.e. the totality of factors which reduce free rotation of the ammonium ion to torsional oscillations) are present in ATPB, certainly at 120 K and below, and that the ir–spectroscopic manifestations of these interactions are consistent with their weakness.

Acknowledgments

We wish to thank Dr. T. S. Cameron for making available the cold-gas-flow cryogenic device and for his active interest in the execution of the X-ray

study. A research grant from the National Research Council of Canada to one of us (O.K.) is acknowledged.

1. O. KNOP, W. J. WESTERHAUS, and M. FALK. Can. J. Chem. **58**, 867 (1980).
2. I. A. OXTON, O. KNOP, and M. FALK. J. Mol. Struct. **37**, 69 (1977).
3. O. KNOP, I. A. OXTON, and M. FALK. Can. J. Chem. **57**, 404 (1979); **57**, 2003 (1979).
4. K. NAKAMOTO, M. MARGOSHES, and R. E. RUNDLE. J. Am. Chem. Soc. **77**, 6480 (1955).
5. J. OZOLS, I. TETERE, S. VIMBA, and A. IEVIŅŠ. Latvijas PSR Zinat. Akad. Vestis, kim. ser., No. 5, 517 (1975); Chem. Abstr. **84**, 52461e (1976).
6. K. HOFFMANN and E. WEISS. J. Organomet. Chem. **67**, 221 (1974).
7. M. S. WEBSTER. D.Phil. thesis. Oxford University, Oxford, England. 1956.
8. J. OZOLS, S. VIMBA, and A. IEVIŅŠ. Latvijas PSR Zinat. Akad. Vest., No. 4, 93 (1961); Chem. Abstr. **56**, 8109a (1962).
9. S. ARNOTT and S. C. ABRAHAMS. Acta Crystallogr. **11**, 449 (1958).
10. D. T. CROMER and J. B. MANN. Acta Crystallogr. A **24**, 321 (1968).
11. O. KNOP, W. J. WESTERHAUS, and M. FALK. Can. J. Chem. **58**, 270 (1980).
12. I. A. OXTON, O. KNOP, and M. FALK. J. Phys. Chem. **80**, 1212 (1976).
13. T. C. WADDINGTON. J. Chem. Soc. 4340 (1958).
14. J. T. R. DUNSMUIR and A. P. LANE. Spectrochim. Acta, A **28**, 45 (1972).

Can. J. Chem. Downloaded from www.nrcresearchpress.com by 210.87.254.5 on 09/05/12
For personal use only.

Revision of the structures of partially acylated derivatives of aldose diethyl dithioacetals

T. Bruce Grindley[1] and Rathy Ponnampalam

Department of Chemistry, Dalhousie University, Halifax, N.S., Canada B3H 4J3

Received December 28, 1979

T. Bruce Grindley and Rathy Ponnampalam. Can. J. Chem. **58**, 1365 (1980).

^{1}H nuclear magnetic resonance spectroscopy is used to correct the structures of most of the known partially acylated derivatives of aldose diethyl dithioacetals which contain more than one acyl group. Previous work had suggested that the hydroxyl group on carbon-2 was the least readily acylated secondary hydroxyl group; current work indicates that it is among the most readily acylated. Evidence is presented which shows that the preferential methylation of aldose diethyl dithioacetals at O-2 is caused by the presence of the sulfur atoms.

T. Bruce Grindley et Rathy Ponnampalam. Can. J. Chem. **58**, 1365 (1980).

La spectroscopie de rmn ^{1}H est utilisée pour corriger la structure de la plupart des dérivés connus, partiellement acylés, des diéthyl dithioacétals d'aldose contenant plus d'un groupe acyle. Des travaux antérieurs ont suggéré que le groupe hydroxyle sur le carbone 2 était le groupe secondaire le moins facilement acylé. Le présent travail indique que ce groupe est un des plus facilement acylés et on y démontre aussi que la méthylation préférentielle des diéthyl dithioacétals d'aldose à la position O-2 est due à la présence d'atomes de soufre.

Can. J. Chem. Downloaded from www.nrcresearchpress.com by 210.87.254.40 on 09/05/12
For personal use only.

There has been considerable interest in the selective acylation of carbohydrates in the last few years (1). This activity has been directed at evaluating the relative reactivities of the various hydroxyl groups and also at generating useful synthetic intermediates. Although little systematic attention has been given to the partial acylation of aldose diethyl dithioacetals, a number of partially acylated derivatives have been synthesized (2–7). It is well established that acylation can be performed selectively at the terminal primary hydroxyl position (2). In addition, a number of derivatives which are more fully substituted have been prepared in fair to good yields (3–7). With one exception (7), the structures of these derivatives were considered to have the acyl groups on the terminal hydroxyl group and then progressively up the carbon skeleton. For instance, the tri-*O*-benzoyl derivative of D-galactose diethyl dithioacetal was considered to be the 4,5,6-tri-*O*-benzoyl derivative (6). One of these derivatives, the tetrabenzoyl derivative of D-glucose diethyl dithioacetal, has been the subject of a number of reports (9–11) and it has been considered an important enough intermediate for its preparation to be included in *Methods in Carbohydrate Chemistry* (12). The structures of these derivatives were established by chemical methods of which the most important involved initially treating the partially acylated derivative with silver oxide and methyl iodide. Since migration of acyl groups is known to occur under these conditions (1), we considered the structures of the derivatives established in this way to be uncertain. In this publication, we revise the structures of four of the five known derivatives of this type.

Results

Structural Assignment

Structural assignments for this series of compounds were made from the ^{1}H nmr spectra by using the well-known observation (13) that conversion of an hydroxyl group to an acetate causes the signal for a geminal secondary proton to appear 1.0–1.2 ppm downfield from its position in the unsubstituted derivative. The effect of a benzoate group is similar. Since the number of acyl groups present in each derivative was already known, the above observation allowed totally unambiguous structural determination after the individual signals in the ^{1}H nmr spectra had been assigned to specific protons.

2,4,5,6-Tetra-O-benzoyl-D-glucose Diethyl Dithioacetal (1) and its Derivatives

A single tetrabenzoyl derivative (**1**) of D-glucose diethyl dithioacetal had been previously prepared both under Schotten–Baumann conditions (3, 12) (51% yield) and with benzoyl chloride in pyridine (9) (20% yield). To assign its structure, compound **1** had been methylated (14) with silver oxide and methyl iodide to give a monomethyl derivative, which, after debenzoylation and treatment with phenylhydrazine and acid, gave a methoxyl-free osazone. On this basis, compound **1** was assumed to be 3,4,5,6-tetra-*O*-benzoyl-D-glucose diethyl dithioacetal. The tetrabenzoyl derivative synthesized in the current work has nearly identical physical constants as the derivative obtained ear-

[1]Author to whom correspondence should be addressed.

0008-4042/80/131365-07$01.00/0

©1980 National Research Council of Canada/Conseil national de recherches du Canada

Can. J. Chem. Downloaded from www.nrcresearchpress.com by 210.87.254.40 on 09/05/12
For personal use only.

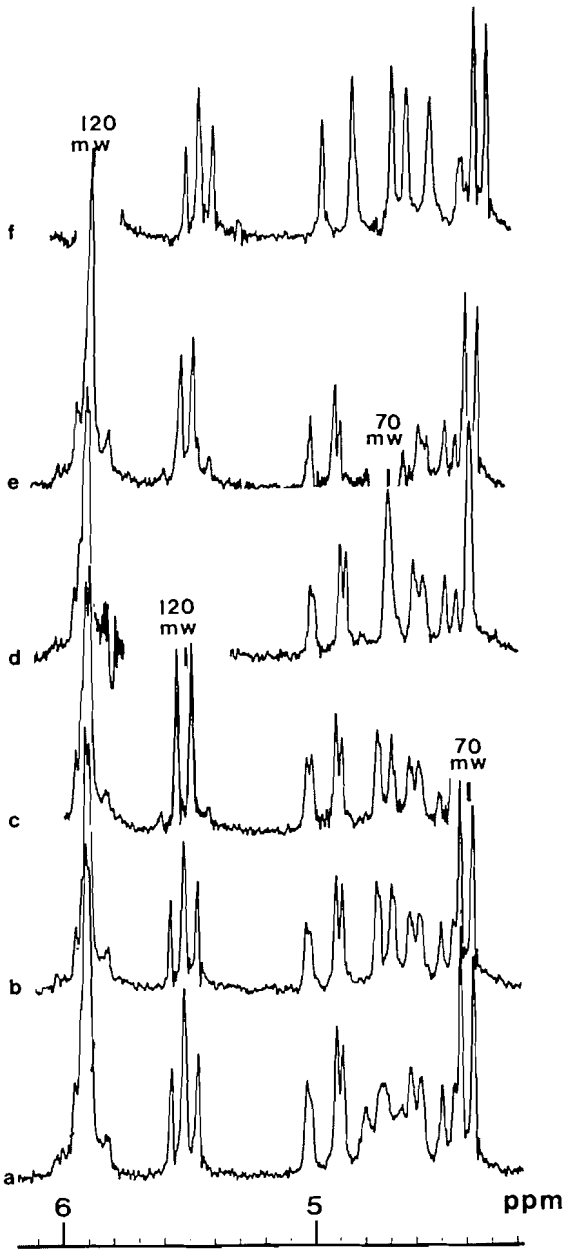


FIG. 1. Partial ^1H nmr spectra at 100 MHz of 2,4,5,6-tetra-*O*-benzoyl-D-glucose diethyl dithioacetal (**1**) in chloroform-*d* under various conditions: (*a*) normal spectrum; (*b*) after exchange with water-d_2; (*c*)–(*f*) decoupling experiments on the exchanged sample using the power indicated.

lier (3, 9, 12). In the nmr spectrum of **1** at 100 MHz in chloroform-*d*, the signals for the individual skeletal protons could be assigned easily by exchange with water-d_2 and by a series of selective homonuclear decoupling experiments. The definitive experiments are shown in Fig. 1. The chemical shifts and coupling constants were obtained by iterative fitting of the signals for H-2, H-3, H-4, H-5, H-6, and H-6′ in the spectra after exchange using a locally modified version of the computer program LAOCN-4A (15). The ^1H nmr spectral parameters are reported in Tables 1 and 2. The signals for H-2, H-4, and H-5 are distinctly further downfield ($\geq$ 0.8 ppm) than that of H-3. In addition, the signal for H-3 shows coupling to a proton which is removed by exchange with water-d_2. Thus, this compound must be 2,4,5,6-tetra-*O*-benzoyl-D-glucose diethyl dithioacetal.

Methylation of **1** with silver oxide and methyl iodide in dioxane gave a monomethyl derivative (**2**), in 58% yield, with identical physical properties to that obtained earlier (14). In the nmr spectrum at 100 MHz of **2** in chloroform-*d*, all signals could be assigned unambiguously by means of a series of decoupling experiments starting with the distinctive doublet for H-1. The signal for H-2 was a quartet at δ 3.83, more than 1.97 ppm upfield of any of the signals for the secondary protons (see Table 1). Thus, this compound was 3,4,5,6-tetra-*O*-benzoyl-2-*O*-methyl-D-glucose diethyl dithioacetal and a benzoyl group had migrated during the methylation step.

Treatment of 2,4,5,6-tetra-*O*-benzoyl-D-glucose diethyl dithioacetal (**1**) with mercuric chloride in absolute methanol in the presence of cadmium carbonate gave the dimethyl acetal (**3**) in 39% yield. All signals in the ^1H nmr spectrum of **3** in

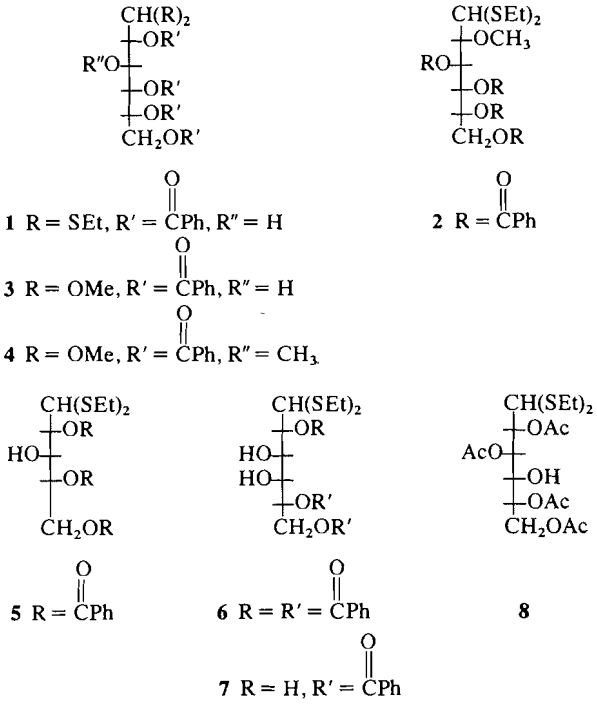


TABLE 1. ^{1}H nuclear magnetic resonance chemical shift data

	Chemical shifts (ppm)[a]										
									$(SEt)_2$ or $(OMe)_2$ groups		
Compound	H-1	H-2	H-3	H-4	H-5	H-6	H-6′	OH	CH_2	CH_3	OMe
1[b]	4.38	5.51	4.71	5.87	5.91	4.54	4.94	2.87	2.54, 2.76	1.13, 1.27	—
2[b]	4.38	3.83	6.29	6.14	5.81	4.65	5.02	—	2.67, 2.82	1.22, 1.28	3.51
3[c]	4.69	5.37	4.50	5.86	5.92	4.56	4.92	3.18	— —	3.37, 3.39	—
4[b]	4.61	5.75	4.19	5.96	5.71	4.66	4.80	—	— —	3.41, 3.42	3.58
5[b]	4.32	5.54	4.74	5.67	—	4.64[d]	4.76[d]	2.88	2.61, 2.74	1.17, 1.20	—
6[c]	4.38	5.47	4.24	3.71	5.76	4.67	4.78	3.63 (OH-3), 3.60 (OH-4)	2.67, 2.67	1.17, 1.20	—
7[b]	4.05	3.89	3.99	4.12	5.79	4.67	4.74	3.43 (OH-2), 3.16, 3.07	2.64, 2.64	1.22, 1.18	—
8[b]	4.08	5.53	5.48	4.04	4.92	4.28	4.47	3.39	2.67, 2.79	1.26, 1.32	—

[a]Downfield from internal TMS in chloroform-*d*.
[b]From spectra at 100 MHz.
[c]From spectra at 250 MHz.
[d]H-5 and H-5′
[e]From spectra at 79.6 MHz.

chloroform-*d* at 250 MHz were assigned to specific protons using decoupling and exchange with water-d_2. Examination of the chemical shifts of the proton signals (see Table 1) showed that the product **3** was 2,4,5,6-tetra-*O*-benzoyl-D-glucose dimethyl acetal. Methylation of **3** under the same conditions as **1** yielded a mixture which was shown by high pressure liquid chromatography to consist of one major component plus a number (>4) of minor components. The major product was separated (48% yield) by preparative high pressure liquid chromatography and was shown by ^{1}H nmr spectroscopy as previously (see Tables 1 and 2) to be 2,4,5,6-tetra-*O*-benzoyl-3-*O*-methyl-D-glucose dimethyl acetal (**4**).

2,4,5-Tri-O-benzoyl-D-xylose Diethyl Dithioacetal (5)

A tribenzoyl derivative (**5**) of D-xylose diethyl dithioacetal had been previously prepared in 29% yield under Schotten–Baumann conditions (4). The same compound was prepared here under both Schotten–Baumann conditions and in better yield (52%) with benzoyl chloride in pyridine. As previously, the ^{1}H nmr spectrum of this compound could be used for structural assignment. The signals for two secondary protons, H-2 and H-4, were considerably downfield of that of the third (H-3). The signal for H-3 also showed coupling to an OH proton. Thus this derivative is 2,4,5-tri-*O*-benzoyl-D-xylose diethyl dithioacetal. The structure of this compound had previously been considered to be 3,4,5-tri-*O*-benzoyl-D-xylose diethyl dithioacetal by analogy with the structure of the glucose derivative (**1**) and by its conversion to crystalline 3,4,5-tri-*O*-benzoyl-D-xylose phenylosazone in 1% yield. This latter process was performed in three steps: conversion to the dimethyl acetal, hydrolysis of this acetal with acid, then conversion to the osazone in a refluxing mixture of acetic acid and phenylhydrazine. The rearrangement may have occurred in either of the last two steps since migrations of benzoyl groups in acid (1) or in the presence of amine bases (16) are well established.

2,5,6-Tri-O-benzoyl-D-galactose Diethyl Dithioacetal (6)

A tribenzoyl derivative (**6**) of D-galactose diethyl dithioacetal had been prepared (5) in 30% yield under Schotten–Baumann conditions and in 52% yield with benzoyl chloride in pyridine. In the present work, a single compound was also prepared in similar yields under these conditions but the compound prepared had a slightly lower mp (153–154°C vs. 160–163°C (5)) and a more negative rotation ($[\alpha]_D^{24.5}$ −10.3° vs. +1.7° (5)). Some difficulty was experienced in recrystallizing this compound since it slowly decomposed in ethanol to a dibenzoyl derivative (**7**) which was separately synthesized from galactose diethyl dithioacetal (see later). It seems unlikely that the sample prepared here is different from that prepared earlier (5) since similar yields were obtained under both sets of reaction conditions. The nmr spectrum of **6** in chloroform-*d* at 80 MHz (see Fig. 2) was analyzed as previously. The low-field chemical shifts of the signals for the secondary protons H-2 and H-5 (see Table 1) indicated that the compound was 2,5,6-tri-*O*-benzoyl-D-galactose diethyl dithioacetal (**6**).

The previous method of structural assignment for compound **6** involved conversion of **6** successively to the dimethylacetal and its di-*O*-methyl

Can. J. Chem. Downloaded from www.nrcresearchpress.com by 210.87.254.40 on 09/05/12
For personal use only.

Can. J. Chem. Downloaded from www.nrcresearchpress.com by 210.87.254.40 on 09/05/12
For personal use only.

TABLE 2. Coupling constants

Compound	Coupling constants (Hz)[a]							
	$J_{1,2}$	$J_{2,3}$	$J_{3,4}$	$J_{4,5}$	$J_{5,6}$	$J_{5,6'}$	$J_{6,6'}$	$J_{H,OH}$
1	5.0	5.7	1.2	7.4	5.2	2.5	−12.4	9.1
2	4.3	6.9	3.0	7.0	5.4	2.9	−12.5	—
3	5.2	2.8	2.7	6.1	6.3	2.9	−12.2	8.0
4	4.8	6.2	3.8	5.1	6.0	3.0	−12.2	—
5	6.2	4.5	4.4	—	6.3[b]	4.2[b]	−11.8[b]	9.0
6	9.3	1.3	9.7	1.7	7.8	4.7	−11.7	5.5 (OH-3), 5.8 (OH-4)
7	9.0	0.6	9.0	1.6	7.0	4.5	−11.7	2.8 (OH-2), 8.5, 8.5
8	3.4	7.9	1.7	9.2	4.6	2.5	−12.4	8.9

[a]In chloroform-*d*.
[b]For the xylose derivative, $J_{4,5}J_{4,5'}$ and $J_{5,5'}$.

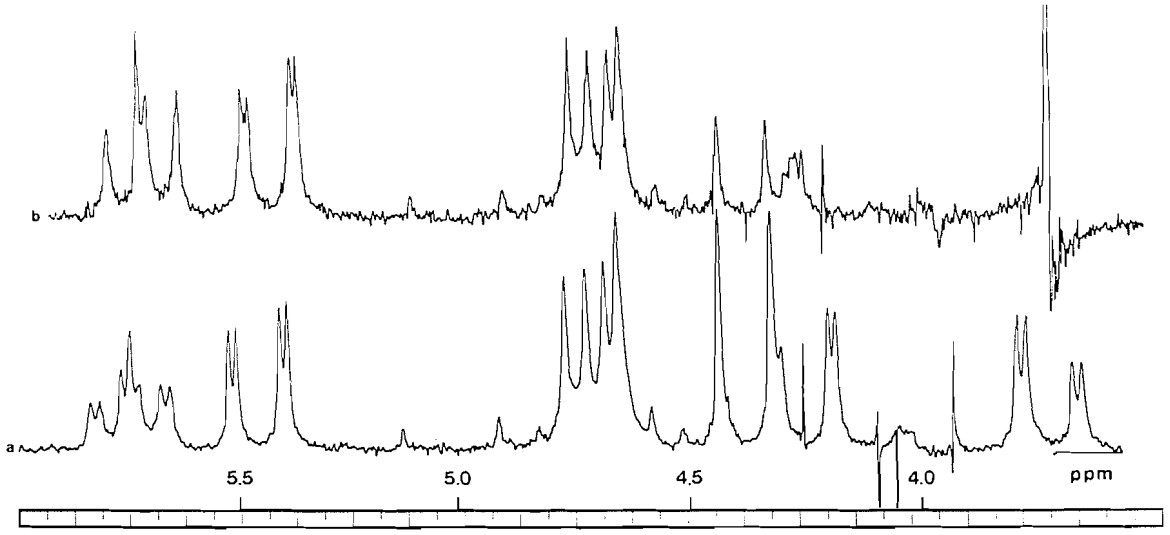


FIG. 2. Partial ^{1}H nmr spectra at 80 MHz of 2,5,6-tri-*O*-benzoyl-D-galactose diethyl dithioacetal (**6**) in chloroform-*d* after exchange with water-d_2 under the following conditions: (*a*) no decoupling; (*b*) decoupling at position indicated by the line which has been cut off.

derivative. Then two hydrolysis steps gave a dimethylgalactose derivative whose rotation was compared with that of authentic 2,3-di-*O*-methyl-D-galactose. All of these compounds derived from **6** were syrups. In addition, the di-*O*-methyl galactose derivative was converted to a mono-*O*-methyl phenylosazone which was shown to be 3-*O*-methyl-D-galactose phenylosazone by comparison of melting points and by a mixed melting point experiment. Unlike the structural proofs used for the earlier compounds, there is no obvious flaw in this method. However, since the nmr evidence presented here is absolutely unambiguous, at some point the previous method of structural proof must have gone astray.

Treatment of D-galactose diethyl dithioacetal with benzoyl chloride (2.2 equiv.) in pyridine yielded 5,6-di-*O*-benzoyl-D-galactose diethyl dithioacetal (**7**) in 77% yield. The structure of this compound was established by ^{1}H nmr spectroscopy as previously (see Tables 1 and 2).

2,3,5,6-Tetra-O-acetyl-D-glucose Diethyl Dithioacetal (8)

A tetra-*O*-acetyl derivative (**8**) of D-glucose diethyl dithioacetal had been prepared from D-glucose diethyl dithioacetal by treatment with acetic anhydride and sodium acetate (6). The same compound was also produced by detritylation of 2,3,4,5-tetra-*O*-acetyl-6-*O*-triphenylmethyl-D-glucose diethyl dithioacetal (**9**) and by mercaptalation of 2,3,4,6-tetra-*O*-acetyl-β-D-glucopyranose with ethanethiol and zinc chloride (17). The sample studied in the current work was initially obtained from chromatography of the mixture resulting from detritylation of **9**. Once seed crystals were obtained, the product from the acetylation of D-glucose diethyl dithioacetal also crystallized.

Can. J. Chem. Downloaded from www.nrcresearchpress.com by 210.87.254.40 on 09/05/12
For personal use only.

Examination of the products obtained from both reactions by tlc showed a very complex mixture in which the crystalline product obtained was the most prominent. In contrast, the products of partial benzoylations were relatively simple with the single product obtained being predominant in all cases. It had previously been shown (6) that this compound (**8**), on methylation with silver oxide and methyl iodide, gave 2-*O*-methyl-3,4,5,6-tetra-*O*-acetyl-D-glucose diethyl dithioacetal. It was recognized at that time (6) that this evidence did not constitute proof of structure. However, it was later considered (8, 18) that the most likely structure was 3,4,5,6-tetra-*O*-acetyl-D-glucose diethyl dithioacetal. Analysis of the ^{1}H nmr spectrum at 100 Hz of **8** in chloroform-*d* as previously with the aid of decoupling experiments unambiguously showed that this product was 2,3,5,6-tetra-*O*-acetyl-D-glucose diethyl dithioacetal (**8**).

Discussion

From the above structural assignments, it is apparent that the 2-hydroxyl group of aldose diethyl dithioacetals is one of the most likely secondary hydroxyl groups to be acylated. Under Schotten–Baumann conditions (i.e. in $CHCl_3$ and NaOH), pure 5,6-di-*O*-benzoyl-D-galactose diethyl dithioacetal (**7**) quickly rearranged to a mixture in which the starting material is most prominent as monitored by tlc. When compound **7** was placed in dry pyridine containing pyridine hydrochloride, compound **7** was stable as indicated by tlc although the reaction mixture from which **7** had been isolated had contained small amounts of other products. Thus reaction under Schotten–Baumann conditions is probably under thermodynamic control whereas that with benzoyl chloride in pyridine is under kinetic control. Since the same major products are produced under both types of reaction conditions, it would appear that the factors which determine the stability of the products are similar to those which determine the rates of reaction and vice versa. However, the factors determining these stabilities are obviously complex and further discussion of selective acylation at this time would be premature.

It is well known that the predominant product of monomethylation of aldose diethyl dithioacetals is the 2-*O*-methyl ether (1, 19). In the current work it has been shown that partially acylated aldose diethyl dithioacetals rearrange on methylation under Purdie's conditions to give the 2-*O*-methyl ether as the predominant product. However, methylation of 2,4,5,6-tetra-*O*-benzoyl-D-glucose dimethyl acetal yields the product of direct methylation at O-3. Hence, it is probably the sulfur atoms of the diethyl dithioacetal group which cause selective methylation at O-2.

The actual role that sulfur plays is somewhat uncertain. Wander and Horton (8) have suggested sulfur participation during the methylation step. Haines (1) has suggested methylation on sulfur followed by an intramolecular nucleophilic displacement. These mechanisms are similar and both involve an intramolecular nucleophilic displacement at a tetrahedral carbon atom in a five-membered ring, a process which has been described as 5-Endo-Tet by Baldwin (20). Because of the geometric requirements of the transition state, such processes are very unfavourable (20). Lemieux (18) has suggested that the solid silver oxide in the methylation reaction mixture adsorbs the sulfur atoms of the diethyl dithioacetal and hence brings the adjacent 2-OH group in close contact with adsorbed methyl iodide. This suggestion seems most reasonable at this time.

Experimental

Melting points were determined by using a Reichert melting point apparatus and are uncorrected. Optical rotations were measured with a Perkin-Elmer 141 automatic polarimeter at 23 ± 3°. The ^{1}H nmr spectra were recorded at 79.6, 100, or 250 MHz on Varian CFT-20, Varian HA-100, or Bruker WM-250 nmr spectrometers in chloroform-*d* with tetramethylsilane as an internal standard. Selective homonuclear decoupling on the CFT-20 and HA-100 spectrometers was performed using Wavetek Model 171 frequency synthesizers. Coupling constants and chemical shifts were determined by using the computer program LAOCN-4A (15) to iteratively simulate those parts of the spectrum which were second order for the spectra of all compounds except **3**. The signals for at least five of the protons were simulated in each case. The 7 spin system of the skeletal protons of **3** was iteratively simulated using the program resident in the WM-250 spectrometer. Thin layer chromatography was performed on 0.25-mm thick Brinkmann silica gel G/uv-254 glass plates cut to be approximately 7 cm long. Plates were developed by spraying with 2% ceric sulfate solution in *M* sulfuric acid and then heating the plates for a few min at 150°C. Eluent systems used were: *A*, 2:1 (v/v) petroleum ether (30–80°C) – ethyl acetate; *B*, 3:1 (v/v) petroleum ether (30–80°C) – ethyl acetate; *C*, 1:1 (v/v) petroleum ether (30–80°C) – ethyl acetate; *D*, 5:1 (v/v) petroleum ether (65–110°C) – ethyl acetate; and *E*, 19:1 (v/v), chloroform–methanol. High pressure liquid chromatography was performed on a Waters analytical liquid chromatograph. Physical constants of compounds prepared by literature methods are listed in Table 3. Elemental analyses were determined by the Microanalysis Laboratory, Toronto and by the Canadian Microanalytical Service, Vancouver, B.C.

2,4,5,6-Tetra-O-benzoyl-D-glucose Dimethyl Acetal (3)

Dried 2,4,5,6-tetra-*O*-benzoyl-D-glucose diethyl dithioacetal (1.0 g, 1.4 m*M*) was dissolved in absolute methanol (15 mL) in which dry cadmium carbonate (1.32 g, 7.7 m*M*) was suspended and the mixture was refluxed at an oil bath temperature of 72°C. A solution of mercuric chloride (2.09 g, 7.7 m*M*) in absolute methanol (10 mL) was added in portions with vigorous mechanical stirring. The mixture was refluxed for 4 h with occasional

TABLE 3. Physical properties of compounds prepared by literature methods

Compound	Melting points (°C) Present work	Melting points (°C) Lit.	Optical rotations Present work	Optical rotations Lit.	Reference
1	165–167	166–168	+22.8	+23.5	12
2	87–88	88–89	+64.6	+64.5	10
5	137.5–139	138–140	−2.5	+6.0	4
6	153–154	161–162	−10.3	+1.7	5
8	117–118	117–118	−24.6	−25	18

addition of small amounts of cadmium carbonate. The mixture was filtered into a flask containing cadmium carbonate (0.5 g) and the filtrate was evaporated to dryness under reduced pressure. The residue was extracted several times with chloroform (4 × 25 mL). The combined chloroform extracts were washed with saturated potassium iodide solution (3 × 25 mL), then with water (3 × 50 mL), and dried over anhydrous magnesium sulfate. The chloroform solution was filtered and the filtrate was evaporated under reduced pressure to a white solid which was recrystallized from methanol; yield 0.35 g (38.5%); mp 139–141°C; R_f 0.44 (solvent *A*); $[\alpha]_D^{25.0}$ +48.9 (*c* 0.55, in chloroform); ^{1}H nmr (HA-100) δ: 7.24–7.44, 7.82–8.00 (m, Ph protons). *Anal.* calcd. for $C_{36}H_{34}O_{11}$: C 67.28, H 5.33; found: C 67.17, H 5.21.

2,4,5,6-Tetra-O-benzoyl-3-O-methyl-D-glucose Dimethyl Acetal (4)

Dried compound **3** (0.266 g, 0.4 m*M*) was stirred at room temperature in dry dioxane (1.4 mL). Methyl iodide (2.6 mL), freshly prepared silver oxide (0.26 g), and Drierite (0.3 g) were added and the stirring was continued for 24 h. The silver salts were collected and washed with methanol. The filtrate was evaporated to a syrup which was purified by high pressure liquid chromatography using a Vydac 10 μm silica gel column (24 cm × 0.76 cm) using solvent *D* as eluant. The syrupy product was homogeneous on hplc, yield 0.13 g (48%); $[\alpha]_D^{22}$ −7.4 (*c* 0.7, in chloroform); ^{1}H nmr (HA-100) δ: 7.26–7.50, 7.88–8.02 (2m, Ph protons). *Anal.* calcd. for $C_{37}H_{36}O_{11}$: C 67.67, H 5.53; found: C 67.97, H 5.48.

2,4,5-Tri-O-benzoyl-D-xylose Diethyl Dithioacetal (5)

A solution of dried D-xylose diethyl dithioacetal (2 g, 7.8 m*M*) in dry pyridine (10 mL) was cooled to 0°C. Benzoyl chloride (2.9 mL, 3.5 g, 3.2 equiv.) was added in 3 equal portions at 5 min intervals. The reaction mixture was stirred at 0°C for 1 h, then overnight at room temperature. The reaction mixture was taken up in methylene chloride (30 mL), and the resulting solution was washed with 1 *N* hydrochloric acid (0°C, 2 × 30 mL), water (30 mL), a saturated sodium bicarbonate solution (30 mL) and water (30 mL), and then dried over anhydrous magnesium sulfate. The solution was concentrated to a yellow syrup which solidified on standing. Recrystallization from ethanol–water gave 2.3 g (52%) of compound **5** with physical constants as in Table 3. The crystals were homogeneous on tlc in solvent *A* (R_f 0.71).

5,6-Di-O-benzoyl-D-galactose Diethyl Dithioacetal (7)

A solution of dried D-galactose diethyl dithioacetal (3.0 g, 10 m*M*) in pyridine (15 mL) was stirred for 15 min at 0°C. Benzoyl chloride (2.68 mL, 2.2 equiv.) was added to the solution in small portions over 15 min. The solution was stirred 1 h at 0°C, then a further 12 h at room temperature. The reaction mixture was taken up in methylene chloride (50 mL) and the resulting solution was washed with ice cold 1 *N* hydrochloric acid solutions (3 × 35 mL), water (40 mL), saturated sodium bicarbonate (30 mL) and water (50 mL), dried over magnesium sulfate, and concentrated to dryness. The resulting amorphous solid was recrystallized twice from chloroform – petroleum ether 1:1, yield 3.72 g (77.5%); R_f 0.70 (solvent *C*); mp 148–149°C; $[\alpha]_D^{24.5}$ +55.8° (*c* 1.15, in chloroform); ^{1}H nmr (HA-100) δ: 1.18, 1.22 (2t, J = 7.5 Hz, 6H, 2-SCH$_2$CH_3); 2.64 (q, J = 7.5 Hz, 4H, 2-SCH_2CH$_3$); 7.34–7.54, 7.92–8.14 (m, 10H, 2-OBz). *Anal.* calcd. for $C_{24}H_{30}S_2O_7$: C 58.28, H 6.11, S 12.96; found: C 58.18, H 6.13, S 13.15.

Equilibration Experiments

Compound **7** (200 mg) in chloroform (2 mL) was mechanically stirred at 0°C. A 2 *N* sodium hydroxide solution (5 mL) was added and the reaction followed by tlc with solvent *E* as eluant. Compound **7** had R_f 0.44 and components with R_f's 0.38, 0.35, and 0.33 had appeared after 5 min. Of these, the component with R_f 0.35 gave the most intense spot. The intensities of these spots varied with time but the one from **7** was always the most intense. Equilibrium was reached at ~30 to 45 min. At this time, of the minor components, the one with R_f 0.38 was most intense but that at R_f 0.33 had disappeared.

Compound **7** (200 mg, 0.4 m*M*) in pyridine (5 mL) containing pyridine hydrochloride (100 mg, 0.87 m*M*) was stirred for 2 days. Thin layer chromatography (solvent *E*) indicated that only the starting material was present.

Acknowledgements

T.B.G. is grateful to the Natural Sciences and Engineering Research Council of Canada for support in the form of a grant. We thank Mr. John van Ingen of the Atlantic Regional Laboratories of the National Research Council of Canada for recording HA-100 spectra, Dr. Charles Rodgers of Bruker Canada for recording a WM-250 spectrum and performing an iterative simulation, and Brian Ross for technical assistance.

1. A. H. HAINES. Adv. Carbohydr. Chem. Biochem. **33**, 11 (1976).
2. H. ZINNER and K. WESSELY. Chem. Ber. **90**, 516 (1957); H. ZINNER, W. BOCK, and H.-P. KLOCKING. Chem. Ber. **92**, 1307 (1959).
3. P. BRIGL and H. MUHLSCHLEGEL. Ber. **63**, 1551 (1930).
4. M. L. WOLFROM and W. VON BEBENBURG. J. Am. Chem. Soc. **81**, 5705 (1959).
5. H. N. BOLLIGER and D. M. SCHMID. Helv. Chim. Acta, **37**, 888 (1954).
6. R. U. LEMIEUX and H. F. BAUER. Can. J. Chem. **32**, 362 (1954).
7. G. REMBARZ. Chem. Ber. **95**, 830 (1962).
8. J. H. WANDER and D. HORTON. Adv. Carbohydr. Chem. Biochem. **32**, 16 (1976).
9. H. R. BOLLIGER and D. M. SCHMID. Helv. Chim. Acta, **34**, 1597 (1951); **34**, 1671 (1951).

Can. J. Chem. Downloaded from www.nrcresearchpress.com by 210.87.254.40 on 09/05/12
For personal use only.

10. P. BRIGL and R. SCHINLE. Ber. **65**, 1890 (1932).
11. D. HORTON, L. G. MAGBANUA, and J. M. J. TRONCHET. Chem. Ind. B, 1718 (1966); B. BERRANG and D. HORTON. Chem. Commun. 1038 (1970).
12. H. R. BOLLIGER and D. M. SCHMID. Methods Carbohydr. Chem. **1**, 186 (1962).
13. L. D. HALL. Adv. Carbohydr. Chem. **19**, 83 (1964).
14. P. BRIGL and R. SCHINLE. Ber. **63**, 2884 (1930).
15. J. A. MUSSO. NMR-LAOCN-4A. Quantum chemistry program exchange. Program 232.
16. A. ZEZEROVICH, E. G. GROS, J. F. SPROVIERO, and V. DEULOFEU. Carbohydr. Res. **4**, 1 (1967); A. B. ZANLUNGO, J. O. DEFERRARI, and R. A. CADENAS. Carbohydr. Res. **10**, 403 (1969).
17. M. L. WOLFROM, S. W. WAISBROT, D. I. WEISBLOT, and A. THOMPSON. J. Am. Chem. Soc. **66**, 2063 (1944).
18. R. U. LEMIEUX. *In* Molecular rearrangements. *Edited by* P. de Mayo. Interscience, New York, NY. 1964. pp 766–768.
19. P. E. PAPADAKIS. J. Am. Chem. Soc. **52**, 2147 (1930); **52**, 3465 (1930); T. LIESER and E. LECKZYCK. Ann. **511**, 137 (1934); G. G. S. DUTTON and K. YATES. Can. J. Chem. **36**, 550 (1958); G. G. S. DUTTON and Y. TANAKA. Can. J. Chem. **39**, 1797 (1961); **40**, 1146 (1962); **41**, 2500 (1963).
20. J. E. BALDWIN. J. Chem. Soc. Chem. Commun. 735 (1976).

Can. J. Chem. Downloaded from www.nrcresearchpress.com by 210.87.254.40 on 09/05/12
For personal use only.

Amide hydrogen bonding in organic medium

J. N. SPENCER,[1] ROBERT C. GARRETT, FRED J. MAYER, JOHANNA E. MERKLE, CARLA R. POWELL, MAI T. TRAN, AND SCOTT K. BERGER

Lebanon Valley College, Annville, PA 17003, U.S.A.

Received February 12, 1980

J. N. SPENCER, ROBERT C. GARRETT, FRED J. MAYER, JOHANNA E. MERKLE, CARLA R. POWELL, MAI T. TRAN, and SCOTT K. BERGER. Can. J. Chem. **58**, 1372 (1980).

Thermodynamic parameters for the self-association of *N*-methylformamide and *N*-methylacetamide in CCl_4 solvent have been determined by infrared spectroscopy. The pure base calorimetric method was used to determine the enthalpy of hydrogen bond complex formation of *N*-methylformamide and *N*-methylacetamide with *N*,*N*-dimethylformamide, *N*,*N*-dimethylacetamide, ethyl acetate, and dioxane. Comparison of the calorimetric and spectroscopic results show that the dimers of *N*-methylformamide and *N*-methylacetamide are linear with hydrogen bond enthalpies of -2.9 and -3.9 kcal mol^{-1} respectively. The carbonyl group of *N*-methylacetamide was found to be a better proton acceptor than the carbonyl of *N*-methylformamide in agreement with theoretical predictions. *N*-methylacetamide was found to be a better proton donor than *N*-methylformamide in disagreement with theoretical predictions. The dimer self-association constants appear to be larger than previously reported.

J. N. SPENCER, ROBERT C. GARRETT, FRED J. MAYER, JOHANNA E. MERKLE, CARLA R. POWELL, MAI T. TRAN et SCOTT K. BERGER. Can. J. Chem. **58**, 1372 (1980).

On a déterminé, par spectroscopie infrarouge, les paramètres thermodynamiques de l'auto-association du *N*-méthylformamide et du *N*-méthylacétamide dans le CCl_4 comme solvant. On a utilisé la méthode rigoureuse de base de la calorimétrie pour déterminer l'enthalpie de la liaison hydrogène lors de la formation des complexes du *N*-méthylformamide et du *N*-méthylacétamide avec le *N*,*N*-diméthylformamide, *N*,*N*-diméthylacétamide, l'acétate d'éthyle et le dioxanne. La comparaison des résultats calorimétriques et spectroscopiques montre que les dimères du *N*-méthylformamide et du *N*-méthylacétamide sont linéaires avec des enthalpies respectives pour la liaison hydrogène de -2.9 et -3.9 kcal mol^{-1}. On a trouvé que le groupe carbonyle du *N*-méthylacétamide est un meilleur accepteur de proton que le groupe carbonyle du *N*-méthylformamide ce qui est en accord avec les prévisions théoriques. On a trouvé contrairement aux prévisions théoriques que le *N*-méthylacétamide est un meilleur donneur de proton que le *N*-méthylformamide. Les constantes d'auto-association du dimère semblent être plus grandes que celles indiquées antérieurements.

[Traduit par le journal]

Introduction

The interpeptide hydrogen bond linkage, N—H···O=C, found in the interior of proteins is generally considered to be in an "organic like" environment. Thus measurements of the enthalpy of formation of analog amide compounds in organic medium have been used to provide estimates of the stability of the interpeptide hydrogen bond in proteins. *N*-methylacetamide (NMA) is the most frequently used analog compound for the peptide unit in proteins. The self-association of NMA in CCl_4 solvent has been studied by various means but considerable disagreement still exists concerning the thermodynamic parameters for this hydrogen bond. Reported equilibrium constants for the dimer of NMA in CCl_4 range from 1 to about 50 (1–7). The hydrogen bond enthalpy has been variously given as -3.7 to -5.4 kcal mol^{-1} (1–7).

Several theoretical studies of the amide group (8–12) have been carried out on the analog compounds, formamide, *N*-methylformamide (NMF), acetamide, and *N*-methylacetamide (NMA). The effect of methyl substitution on the stabilization energies of complexes involving these analog compounds has been of considerable concern (8, 12). Experimental enthalpies of dimerization of NMF and NMA are needed to provide further insight into the relative hydrogen bonding ability of these amides. This paper reports on spectroscopic and calorimetric studies of the hydrogen bonding of NMF and NMA with various proton acceptors. Because of the uncertainty about the degree of polymerization and the importance of linear and cyclic structures, previous results for the thermodynamic parameters for self-association of these amides show considerable differences. The combination of the spectroscopic and calorimetric studies of this work, used independently of each other, remove some of these uncertainties and should provide more reliable estimates of the difference in hydrogen bonding ability of NMF and NMA and of the magnitude of the thermodynamic functions for the N—H···O=C hydrogen bond in organic medium.

Experimental

The calculation of thermodynamic data from spectroscopic data has previously been described (13). Equilibrium constants were determined at 15 and 30°C in CCl_4 for the self-association of NMF and NMA by the method of Liddel and Becker (14). The free N—H stretching frequency at 3475 cm^{-1} for NMA and

[1]Author to whom correspondence may be addressed.

0008-4042/80/131372-04$01.00/0

©1980 National Research Council of Canada/Conseil national de recherches du Canada

Can. J. Chem. Downloaded from www.nrcresearchpress.com by 210.87.254.5 on 09/05/12
For personal use only.

TABLE 1. Enthalpies of solution (kcal mol^{-1})

Solute	Solvent				
	CCl_4	DMA	DMF	EtOAc	Dioxane
NMF	+3.89±0.13	−0.25±0.03	−0.02±0.02	+1.11±0.06	
DMF	+0.85±0.04	−0.10±0.04	+0.00	+0.32±0.02	
NMA[a]	+4.48±0.08	+0.04±0.04	+0.32±0.03	+1.47±0.15	+1.64±0.02
DMA[a]	+0.40±0.09	+0.00	+0.01±0.01	+0.27±0.03	+0.44±0.02

[a]Enthalpies of solution in all solvents determined at 30°C. For NMF and DMF the solution enthalpies were determined at 25°C. Error reported is the standard deviation of a single measurement for those systems showing no concentration dependence; for those systems exhibiting a concentration dependence the uncertainty is the error in the least squares extrapolation to infinite dilution.

3467 cm^{-1} for NMF was monitored and a plot of absorbance divided by initial concentration vs. initial concentration was made to find the limiting slope and intercept from which the equilibrium constants were calculated. The Beckman Acta M IV spectrophotometer with a NIR sensitivity setting of 10× was used to record spectra of the amides down to concentrations of less than 10^{-3} M. The limiting slope was found over the concentration range of about 8×10^{-3} M − 1×10^{-3} M. Overlap of the free and complex band was observed for both self-associated complexes. A correction for the overlap was made by symmetric reflection of the bands. Frequency shifts were determined by extrapolation of a plot of frequency shift vs. concentration to infinite dilution.

The calorimetric method of analysis and the calorimeter have been previously described (15, 16). The pure base calorimetric method was used for all calorimetrically determined enthalpies reported in this work. This method was developed for systems of the type studied here, i.e., systems with low formation constants and small enthalpy changes (17). According to the pure base method, if a small quantity of hydrogen bonding acid is injected into the pure base as solvent, two contributions to the heat observed are involved, the heat due to hydrogen bonding and that heat term which might occur if there were no hydrogen bonding. If a proper model compound is chosen the hydrogen bonding heat term can be isolated. A reference solvent is chosen to correct for enthalpies of solution of the acid and model compound. The enthalpy of hydrogen bond formation, ΔH^{f}_{HB}, can then be calculated from

$$[1] \quad \Delta H^{f}_{HB} = (\Delta H^{A}_{S} - \Delta H^{M}_{S})_{base} - (\Delta H^{A}_{S} - \Delta H^{M}_{S})_{ref}$$

where ΔH_S is the enthalpy of solution and A and M refer to acid and model compound respectively. Thus if the enthalpy of hydrogen bond formation between NMA and DMF is desired, it is only necessary to determine the enthalpy of solution of NMA and its model compound, DMA, in DMF and in the reference solvent which was CCl_4 for all systems in this study. Equation [1] is then used to calculate ΔH^{f}_{HB} and the resulting ΔH^{f}_{HB} is corrected according to procedures already given (16). Millimole quantities of acid were injected in 200 mL of solvent for all systems. In those cases where a concentration dependence of ΔH_S was observed, extrapolation to infinite dilution was made. All enthalpies of solution of NMA and DMA were made at 30°C so that the more easily handled liquid NMA could be injected into the solvent. All other enthalpies of solution were determined at 25°C.

Aldrich 99% NMA and NMF were distilled under nitrogen atmosphere. Aldrich Gold Label DMA was stored over molecular sieves and distilled under nitrogen. The purifications of other reagents have been previously given (15). All sample preparation was carried out in a dry box.

Results and Discussion

The enthalpies of solution at infinite dilution for NMF and NMA in the various solvents of this study are given in Table 1. These enthalpies and eq. [1] were used to calculate the uncorrected pure base enthalpies of hydrogen bond formation given in Table 2. The pure base enthalpies corrected for differences in enthalpies of solution between acid and model compound as outlined previously (16) are also given in Table 2.

The equilibrium constants, frequency shifts, enthalpy, and entropy changes calculated from the spectroscopic data are given in Table 3. The agreement between the spectroscopically determined enthalpy changes for the self-association of NMF and NMA and the calorimetrically determined enthalpy changes for NMF–DMF and NMA–DMA complexes is quite good considering the difficulty of making spectral measurements on such weak complexes. The Liddel–Becker method (14) of calculation of equilibrium constants from spectral data is sensitive to scatter in data points. The estimated uncertainty in the enthalpy change calculated from spectral data for the NMF and NMA dimer formation is about 1 kcal mol^{-1} and the equilibrium constants are uncertain to about 10%.

The calorimetrically determined enthalpy

TABLE 2. Corrected and uncorrected enthalpies for hydrogen bonded complexes determined by the pure base method

Complex	$-\Delta H$ (kcal mol^{-1})	
	Uncorrected	Corrected[a]
NMF–DMA	3.19±0.24	3.1
NMA–DMA	4.04±0.21	3.9
NMF–DMF	3.06±0.19	2.9
NMA–DMF	3.77±0.21	3.6
NMF–EtOAc	2.25±0.25	2.3
NMA–EtOAc	2.88±0.35	2.9
NMA–dioxane	2.88±0.21	2.7

[a]Corrected according to the analysis given in ref. 16.

Can. J. Chem. Downloaded from www.nrcresearchpress.com by 210.87.254.5 on 09/05/12
For personal use only.

TABLE 3. Spectroscopic thermodynamic functions for the self-association of NMF and NMA

	K_{15}[a]	K_{30}[a]	$-\Delta H$ (kcal mol^{-1})	$-\Delta S$ (cal deg^{-1} mol^{-1})	$\Delta\nu$ (cm^{-1})
NMF	25.9	20.6	2.9	3.6	71
NMA	24.5	18.5	3.5	5.8	107

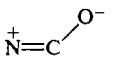
[a]Estimated error in K is ±10%.

changes for the NMF–DMF and NMA–DMA complexes clearly refer to the formation of a single N—H···O=C hydrogen bond. Because of the agreement between the calorimetric enthalpies and the self-association enthalpies for NMF and NMA determined spectroscopically it seems most reasonable to infer that the NMA and NMF dimers are linear and not cyclic.

Several investigators have reported self-association constants of less than 10 for NMA in CCl_4. However, a self-associated complex band is clearly defined at concentrations below 3×10^{-3} *M*. For self-association constants much less than about 20, the molar absorptivity of the complex would have to be quite large to permit observation of this band. From the self-association constants reported in this work the molar absorptivity of the NMA self-associated complex can be calculated to be about 140 which is reasonable compared to the monomer molar absorptivity of about 100. If the self-association constant were 10 the complex absorptivity would have to be greater than 300 for the complex band to be observed at concentrations as low as those used in this work.

The difference between the NMF dimer enthalpy and the NMA dimer enthalpy determined spectroscopically and the difference determined calorimetrically for the NMF–DMF and NMA–DMA complexes are approximately the same and show that NMA forms a stronger hydrogen bonded dimer than NMF. The frequency shifts also support this contention.

Theoretical studies by Johansson *et al.* (9) predict that the amide resonance form



should cause the amide C=O to be a 2.9 kcal mol^{-1} better proton acceptor than an aldehyde C=O. Similar resonance structures can be drawn for ethyl acetate but because the nitrogen is less electronegative than oxygen, the nitrogen of the amide linkage can better accommodate the positive charge than the ester oxygen. The corrected data in Table 2 show that the amide carbonyl is a better proton acceptor than the ethyl acetate carbonyl and illustrate the importance of the amide resonance effect.

Johansson *et al.* (9) predict the amide N—H to be a 2.8 kcal mol^{-1} better proton donor than the amine N—H. No consistent data are available for a non-aromatic amine but comparison with *N*-methylaniline can be made. Previously reported pure base enthalpies (15) for the hydrogen bonded complexes of *N*-methylaniline with ethyl acetate and DMF corrected according to ref. 16 are −1.6 and −2.3 kcal mol^{-1} respectively. The NMF complexes with ethyl acetate and DMF have hydrogen bond enthalpies of −2.3 and −2.9 kcal mol^{-1} respectively, which indicates that the NMF N—H is a 0.6–0.7 kcal mol^{-1} better proton donor than the amine N—H. The NMA complexes with DMF and ethyl acetate show that the N—H of NMA is a 1.3 kcal mol^{-1} better proton donor than the amine N—H.

Del Bene's (12) *ab initio* SCF calculations on the effects of methyl substituents on amide hydrogen bonding predict that NMF should be a better proton donor than NMA and that the carbonyl of NMA should be a better proton acceptor than the carbonyl of NMF. If the hydrogen bond enthalpies of the complexes of NMA and NMF with the same proton acceptor are compared it may be seen from Table 2 that NMA is a stronger proton donor and that the difference in enthalpy between the NMF and NMA complexes is approximately constant at 0.7 kcal mol^{-1} with NMA being the better proton donor in all cases. The enthalpy of complex formation of NMF with DMA is 0.2 kcal mol^{-1} larger than with DMF. Similarly the NMA complex enthalpy with DMA is 0.3 kcal mol^{-1} stronger than with the DMF complex. Del Bene's calculations (12) show that methyl substitution at the nitrogen does not alter electron density at the oxygen of amides so that if DMA and DMF can be taken as representative of the carbonyl in NMF and DMF, the predictions that the NMA carbonyl should be a better proton acceptor than the NMF carbonyl are borne out.

The enthalpy change for the DMA–dioxane complex is included in Table 2 to provide an estimate of the differences in proton accepting ability

Can. J. Chem. Downloaded from www.nrcresearchpress.com by 210.87.254.5 on 09/05/12
For personal use only.

of a carbonyl oxygen and an oxygen in an ether like linkage. The amide carbonyl is a considerably better proton acceptor but the ethyl acetate carbonyl is approximately the same in proton accepting ability as the dioxane oxygen.

The calculations of Del Bene (12) and Johansson *et al.* (9) predict that methyl substitution can cause an increase in electron density about the N—H and carbonyl groups. Del Bene's results show that methyl substitution affects the electron density at the N—H proton substantially the same whether the methyl substituent is bonded to the carbon or nitrogen. Thus methyl substitution at the carbon is primarily responsible for the increased basicity of the amide carbonyl but should have little effect on the N—H proton donating ability. The results of this study are in agreement with the predicted increase in carbonyl basicity due to carbon methyl substitution but disagree with the predictions concerning the proton donating ability of the N—H. Because the experimental work was carried out in condensed medium solvation effects may be important. Unpublished data from this laboratory show that specific solvation interactions may occur at the nitrogen of amides. Methyl substitution at the carbon of an amide may provide steric hindrance to the approach of a solvent molecule and thus account for the increased donating ability of NMA over NMF.

The best enthalpy changes for the self-association of the dimers of NMF and NMA are -2.9 and -3.9 kcal mol^{-1} respectively. Of the 1 kcal mol^{-1} difference in enthalpy of formation between these two dimers about 0.7 kcal mol^{-1} can be attributed to the better proton donating ability of NMA and about 0.3 kcal mol^{-1} to the better proton accepting ability of the NMA carbonyl.

Acknowledgments

Acknowledgment is made to the donors of the Petroleum Research Fund, administered by the American Chemical Society, for support of this research. The authors also acknowledge John Welkie, a Project SEED student, for his assistance in many phases of this work.

1. G. C. Kresheck and I. M. Klotz. Biochemistry, **8**, 8 (1969).
2. I. M. Klotz and J. S. Granzen. J. Am. Chem. Soc. **84**, 3461 (1962).
3. K. R. Znaskar and C. N. R. Rao. Biochim. Biophys. Acta, **136**, 561 (1967).
4. H. Lowenstein, H. Lassen, and Aa. Hridt. Acta Chem. Scand. **24**, 13 (1970).
5. R. D. Grigsby, S. D. Christian, and H. E. Affsprung. J. Phys. Chem. **72**, 2465 (1968).
6. M. Lindheimer, G. Etienne, and B. Brun. J. Chim. Phys. **71**, 135 (1974).
7. L. L. Graham and C. Y. Chang. J. Phys. Chem. **75**, 776 (1971).
8. A. Johansson and P. A. Kollman. J. Am. Chem. Soc. **94**, 6196 (1972).
9. A. Johansson, P. Kollman, S. Rothenberg, and J. McKelvey. J. Am. Chem. Soc. **96**, 3794 (1974).
10. T. Ottersen. J. Mol. Struct. **26**, 365 (1975).
11. T. Ottersen and H. H. Jensen. J. Mol. Struct. **26**, 355 (1975); **26**, 375 (1975).
12. J. Del Bene. J. Am. Chem. Soc. **100**, 1387 (1978).
13. J. N. Spencer, J. R. Sweigart, M. E. Brown, R. L. Bensing, T. L. Hassinger, W. Kelly, D. L. Housel, G. W. Reisinger, D. S. Reifsnyder, J. E. Gleim, and J. C. Peiper. J. Phys. Chem. **81**, 2237 (1977).
14. U. Liddel and E. D. Becker. Spectrochim. Acta, **10**, 70 (1957).
15. J. N. Spencer, J. E. Gleim, M. L. Hackman, C. H. Blevins, and R. C. Garrett. J. Phys. Chem. **82**, 563 (1978).
16. J. N. Spencer, J. E. Gleim, C. H. Blevins, R. C. Garrett, and F. J. Mayer. J. Phys. Chem. **83**, 1249 (1979).
17. E. M. Arnett, E. J. Mitchell, and T. S. S. R. Murty. J. Am. Chem. Soc. **96**, 3875 (1974).

Can. J. Chem. Downloaded from www.nrcresearchpress.com by 210.87.254.5 on 09/05/12
For personal use only.

The conformations of tartaric acids in aqueous solution studied by ^1H and ^{13}C nuclear magnetic resonance

JOSÉ ASCENSO

Centro de Química Estrutural, Instituto Superior Técnico, Lisboa, Portugal

AND

VICTOR M. S. GIL

Centro de Química de Coimbra and Department of Chemistry, University of Aveiro, Portugal

Received October 24, 1979

JOSÉ ASCENSO and VICTOR M. S. GIL. Can. J. Chem. **58**, 1376 (1980).

Vicinal H—H and C—H coupling constants are reported for (+)-tartaric acid and *meso*-tartaric acid at various pH values and used in a discussion of the conformation of these molecules. This is found not to change much with pH. For the *meso* form, in particular, the most favoured conformer is determined not so much by the possibility of internal OH···OOC hydrogen bonding but, at least in part, by stabilization of polar conformations in a solvent (H_2O) of high dielectric constant.

JOSÉ ASCENSO et VICTOR M. S. GIL. Can. J. Chem. **58**, 1376 (1980).

On rapporte les constantes de couplage vicinal H—H et C—H des acides (+)-tartarique et *méso*-tartarique à différents pH; on les utilise pour discuter de la conformation de ces molécules et on a trouvé que celles-ci ne varient pas appréciablement avec le pH. Dans le cas de la forme *méso* en particulier, le conformère le plus favorisé est déterminé non pas tant par la possibilité d'une liaison hydrogène intramoléculaire OH....OOC mais du moins en partie par la stabilisation des conformations polaires par H_2O un solvant de forte constante diélectrique.

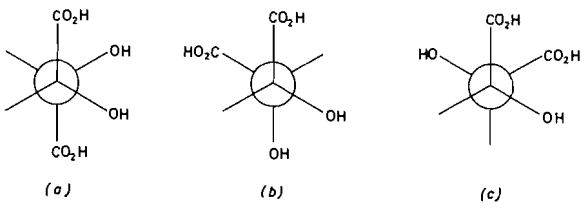
[Traduit par le journal]

Introduction

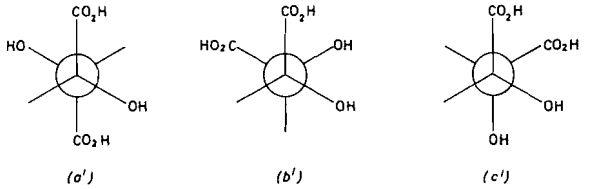
During an nmr study of rotational isomerism and metal complexation of simple carboxylic acids in aqueous solutions, the need was felt to know the conformations of active and *meso*-tartaric acids as free ligands at various pH values.

Such conformations are known for the solid state (1, 2). Regarding solutions, the work of Hargreaves and Richardson (3) on the changes of the rotatory power of (+)-tartaric acid presents an interpretation partly based on conformational changes with temperature, solvent, and concentration, it being assumed that the most stable conformation in solution is essentially the same as that of the crystal. For the optically inactive *meso*-tartaric acid in solution, no report of any conformation study was found.

In solution and at room temperature, there is rapid internal rotation of the molecules around the HC—CH bond. An approximate way of approaching rotational isomerism often used is to regard the mean molecular conformation as an weighted average of the conformations of the three staggered rotational isomers. For (+)-tartaric acid, these are as follows:



whereas for meso-tartaric acid they are:



(*b'*) and (*c'*) being enantiomers.

Since vicinal $^1H—^1H$ ($^3J_{HH}$) and $^{13}C—^1H$ ($^3J_{CH}$) spin coupling constants depend on the dihedral angles, we have obtained those coupling constants for various pH values and related them to the conformation of the tartaric acids in a manner similar to that previously used in related systems.

Experimental

The spectra were run on JEOL PS-100, Varian XL-100, and Varian HA-100 spectrometers, at the temperature of the probes (~30°C) except when otherwise specified. D_2O solutions were used throughout; for ^1H and ^{13}C studies the concentration was, respectively, 0.5 *M* and 2 *M*. The pH was adjusted with NaOD and $(CH_3)_4NOH$. The pH* values quoted are the direct pH-meter readings. Gated irradiation of protons was used to observe nOe in ^{13}C spectra without decoupling.

Results and Discussion

Since, because of symmetry, the normal (C)—^1H spectra of both tartaric and *meso*-tartaric acids consist of just one line, use had to be made of the (^{13}C)—^1H satellites to get $^3J_{HH}$. The values are shown in Table 1.

0008-4042/80/131376-04$01.00/0

©1980 National Research Council of Canada/Conseil national de recherches du Canada

Can. J. Chem. Downloaded from www.nrcresearchpress.com by 210.87.254.5 on 09/05/12
For personal use only.

Can. J. Chem. Downloaded from www.nrcresearchpress.com by 210.87.254.5 on 09/05/12
For personal use only.

TABLE 1. $^3J_{HH}$ values (Hz) for tartaric acids

L(+) Tartaric		*Meso*-Tartaric	
pH*	*J*	pH*	*J*
1.6	2.30±0.05	1.4	2.6
2.5	2.25	2.4	2.6
3.5	2.15	3.7	2.6
4.5	1.80	4.5	2.7
5.5	1.75	5.5	3.0
6.5	1.70	6.5	3.1
7.2	1.70	7.5	3.0
8.4	1.65	9.3	3.0
9.6	1.85	12.6	3.1
10.5	1.80		
11.5	1.75		
12.5	1.80		

Irrespective of the degree of ionization, the *J* values for tartaric acid are typical of an essentially *gauche* coupling constant. This is in accordance with the reasonable assumption that (*a*), which is approximately the conformation in the solid state (1), is the most stable conformer in solution; this arrangement provides, simultaneously, the least repulsion of the carboxylic groups and a possibility of intramolecular OH···CO_2H hydrogen bonds (3). However, a possible contribution of (*c*) cannot be ruled out. The weight of (*a*) is expected to increase upon ionization of the CO_2H groups (due to stronger repulsion of the CO_2^- groups). The observed decrease of J_{HH} is consistent with the expectation; in fact, due to the orientation dependence of substituent effects on $^3J_{HH}$, the OH and CO_2H (or CO_2^-) groups should make $^3J_{HH}$ less for (*a*) than for (*c*) (ref. 4, see also below).

The arguments of least repulsion of carboxylic groups and establishment of intramolecular hydrogen bonds would lead one to expect (*a'*) to be the most favoured conformation for *meso*-tartaric acid in solution. However, the $^3J_{HH}$ values presented in Table 1 are again typical of *gauche* coupling. This shows that the conformations are essentially (*b'*) and (*c'*). It is noted that these are the conformations in any of the crystal forms of *meso*-tartaric acid, stabilized by intermolecular rather than intramolecular hydrogen bonds (2). The ionization of the acid should increase the weight of (*a'*) leading now to an increase of $^3J_{HH}$; this is observed but the effect is small. It is clear that even when the CO_2H groups are fully (and the OH partially) ionized, (*b'*) and (*c'*) are much more stable than (*a'*).

The ^{13}C nmr signal for the carboxylic groups of both acids is the X part of an AA'X spectrum, where A and A' are the CH hydrogen atoms. Figure 1 shows such signals for tartaric acid (pH* = 0.9) and *meso*-tartaric acid (pH* = 0.9).

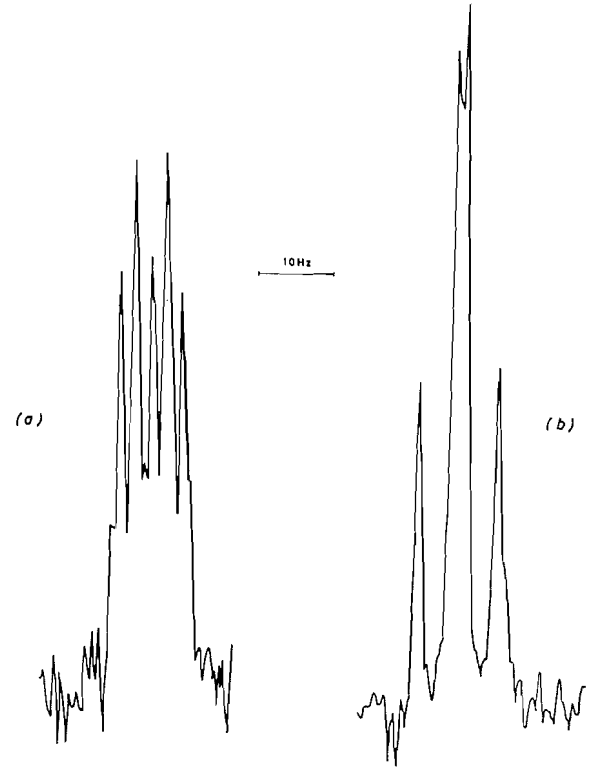


FIG. 1. Carboxylic ^{13}C signal for (*a*) *L*(+) tartaric acid and (*b*) *meso*-tartaric acid (2 *M* solutions in D_2O, pH* = 0.9).

As the X-combination lines are clearly detected and easily assigned on intensity grounds, the analysis of the X spectra gives the values of the vicinal and geminal $^{13}CO_2H—^1H$ coupling constants as pairs (it is not possible to distinguish between J_{AX} and $J_{A'X}$). The analysis immediately shows that these coupling constants have opposite signs, the geminal being almost certainly the negative one. Whenever the magnitudes of $^2J_{^{13}CO_2H—H}$ and $^3J_{^{13}CO_2H—H}$ are appreciably different, the assignments are made by comparison with similar related systems (5) as far as ^2J is concerned, and by recognizing that ^2J for tartaric and *meso*-tartaric acids should be about the same. The various coupling constants are shown in Table 2.

It is thus found that the vicinal $^{13}CO_2H—^1H$ coupling constant in (+)-tartaric acid, for any pH, is typical of a *gauche* orientation of the coupled nuclei (5). This shows that between conformations (*a*) and (*c*), (*a*) is by far the more stable; if it were (*c*) where such orientation is *trans*, the ^3J value should be of the order of 7 Hz (ref. 5, see also below).

Can. J. Chem. Downloaded from www.nrcresearchpress.com by 210.87.254.5 on 09/05/12
For personal use only.

TABLE 2. $^3J_{^{13}CO_2H-^1H}$ and $^2J_{^{13}CO_2H-^1H}$ values (Hz) for tartaric acids

L(+) Tartaric			*Meso*-Tartaric		
pH*	^3J	^2J	pH*	^3J	^2J
0.9	1.0	−5.2	0.9	3.7	−5.1
1.4	1.0	−5.0	3.8	3.9	−4.4
3.5	1.1	−4.8		4.4	or −3.9
5.1	1.3	−4.5	6.9	3.6	−4.3
8.0	1.3	−4.4		4.3	or −3.6
11.4	0.7	−3.9	12.3	3.6	−4.6
				4.6	or −3.6

The vicinal $^{13}CO_2H-^1H$ coupling constant in *meso*-tartaric acid, for any pH, is intermediate between *gauche* and *trans* values, in accordance with the dominant contributions of conformations (*b'*) and (*c'*).

In Table 3 the magnitudes of the geminal $^{13}CH-C^1H$ coupling constant are also recorded. The difference observed for both acids is noteworthy. This must be attributed mainly to the dependence of the $^{13}CH-C^1H$ coupling constant on the orientation of the substituent OH group bonded to ^{13}C, with respect to ^1H. It is expected that $^2J_{CH}$ should increase if the substituent is *trans* to ^1H and decrease if it is *gauche* (6). Accordingly, $^2J_{CH}$ should be larger in tartaric acid (mainly conformation (*a*), *trans* situation) than in *meso*-tartaric acid (mainly conformations (*b'*) and (*c'*), an equal mixture of *trans* and *gauche* arrangements). This is observed if, as is likely, the values for *meso*-tartaric acid are negative.

If, and in spite of the limitations of the method, we attribute reasonable values to the vicinal H—H and C—H coupling constants of the staggered conformers, we can obtain the approximate weight of the conformations (*a*), (*b*), (*c*) and (*a'*), (*b'*), (*c'*).

As far as the $^3J_{HH}$ values are concerned, we take essentially the approach previously used for malic acid (7), coupled with the assumption that, since the effect of an individual substituent is reduced when another similar substituent is present, the total effect of the 4 substituents is in between $\frac{1}{2}$ and $\frac{3}{4}$ of the sum of the individual effects. The various *J*-values would then be as follows: $^3J_{HH}^{(a)} = 1.9 \pm 0.9$, $^3J_{HH}^{(b)} = 13.3 \pm 1.5$, $^3J_{HH}^{(c)} = 3.6 \pm 0.6$, $^3J_{HH}^{(a')} = 13.3 \pm 1.5$, $^3J_{HH}^{(b')} = 2.7 \pm 0.7$, $^3J_{HH}^{(c')} = 2.7 \pm 0.7$.

Regarding the vicinal C—H coupling constants, we base our estimates on the work of Feeney and co-workers (5) on the conformation of amino acids and allowing for the replacement of NH_2 by OH, the presence of a second CO_2H group and the dependence of $^3J_{CH}$ on the orientation of the substituents (6). We thus have the following tentative values: $^3J_{CH}^{(a)} = 1.0 \pm 0.5$, $^3J_{CH}^{(b)} = 1.5 \pm 0.5$, $^3J_{CH}^{(c)} = 6.5 \pm 1.0$, $^3J_{CH}^{(a')} = 2.5 \pm 0.5$, $^3J_{CH}^{(b')}$; $^3J_{CH}^{(c')}$ *gauche* $= 0.5 \pm 0.5$, *trans* $= 6.5 \pm 1.0$.

It is clear that in view of the values shown in Tables 1 and 2, the uncertainties quoted above can lead to appreciable errors. However, we will proceed with the following calculations.

If it is assumed that the tartrate ion exists almost exclusively in conformation (*a*), then, from Table 1, $^3J_{HH}^{(a)} \simeq 1.7$ and from Table 2, $^3J_{CH}^{(a)} \simeq 0.7$. By using $^3J_{HH}^{(b)} = 13.3$, $^3J_{HH}^{(c)} = 3.6$ and $^3J_{CH}^{(b)} = 1.5$, $^3J_{CH}^{(c)} = 6.5$ we obtain the following weights for tartaric acid at pH* = 1.6: $a = 0.91$, $b = 0.04$, $c = 0.05$.

For *meso*-tartaric acid, because of degeneracy of (*b'*) and (*c'*), the J_{HH} or the J_{CH} values alone enable the calculation of the various weights. According to the values above for the three rotamers and those in Tables 1 and 2, we have $2.0 \leq {}^3J_{HH}^{(b')} = {}^3J_{HH}^{(c')} \leq 2.6$ and $2 \times 3.7 \leq J_{CH}^{(b')}(gauche) + {}^3J_{CH}^{(b')}(trans) \leq 8.5$. By then using $^3J_{HH}^{(a')} = 13.3$ and $^3J_{CH}^{(a')} = 2.5$ we obtain, separately (for pH* = 0.9): $a' = 0.03 \mp 0.03$, $b' = c' = 0.48 \pm 0.02$, and $a' = 0.16 \mp 0.16$, $b' = c' = 0.42 \pm 0.08$.

As already mentioned, the finding that conformation (*b'*) (or (*c'*)) is much more stable than (*a'*) is somewhat surprising, although this is the molecular conformation of *meso*-tartaric acid in the solid state (2). To find out whether self-association through intermolecular hydrogen bonding is sufficiently important in aqueous solution to explain the preference for conformation (*b'*) instead of (*a'*), we have obtained the J_{HH} values for 5 *M* and 0.1 *M* solutions of tartaric and *meso*-tartaric acids as well as for solutions at 80°C. Within experimental error (less than ±0.1 Hz) no changes were detected.

An important difference between (*a'*) and (*b'*) is that the former has no electric dipole moment whereas (*b'*) and (*c'*) will have an appreciable di-

TABLE 3. $^2J_{^{13}CH-C^1H}$ values (Hz) for tartaric acids

pH*	*L*(+) Tartaric	*Meso*-Tartaric
0.9	—	4.1
1.4	1.65	—
2.2	1.3	—
2.5	—	3.9
3.5	1.3	3.7
3.8	—	3.5
5.1	1.3	3.2
6.9	—	3.4
8.0	0.7	—
10.0	—	3.4
12.3	0.7	3.4

pole moment. In a solvent of high dielectric constant such as water, these latter conformations will therefore be more stabilized. In tartaric acid the lowest energy conformation (*a*) is also that corresponding most likely to a higher dipole moment. However, in order to assess the importance of this effect as well as specific hydrogen bonding to the H_2O molecules, studies in other solvents are needed. These will be the object of a future paper.

Acknowledgements

Part of this work was presented at the 1978 Meeting of the Portuguese Chemical Society. It is a joint contribution of the Centro de Investigação Química de Coimbra and Centro de Química Estrutural de Lisboa supported by the Instituto Nacional de Investigação Científica.

V.M.S.G. thanks the National Institute for Medical Research, London for the use of a Varian XL-100 spectrometer. Thanks are also due to Drs. J. Feeney and A. V. Xavier and Professor Gillard for helpful discussions.

1. C. A. BEEVERS and F. STERN. Nature, **162**, 854 (1948); C. A. BEEVERS and W. HUGHES. Proc. R. Soc. Sect. A, **177**, 251 (1941).
2. G. A. BOOTSMA and J. C. SCHOONE. Acta Crystallogr. **22**, 522 (1967).
3. M. K. HARGREAVES and P. J. RICHARDSON. J. Chem. Soc. 2260 (1957).
4. R. J. ABRAHAM and G. GATTI. J. Chem. Soc. B, 961 (1969), and references therein.
5. P. E. HANSEN, J. FEENEY, and G. C. K. ROBERTS. J. Magn. Reson. **17**, 249 (1975).
6. D. F. EWING. *In* Annu. Rep. NMR Spectrosc. Vol. 6A. *Edited by* E. F. Mooney. Academic Press, New York. 1975, and references therein.
7. J. S. MARIANO and V. M. S. GIL. Mol. Phys. **17**, 313 (1969).

Can. J. Chem. Downloaded from www.nrcresearchpress.com by 210.87.254.5 on 09/05/12
For personal use only.

Use of ^{13}C in biosynthetic studies. The labeling pattern in dihydrofusarubin enriched from [^{13}C]- and [^{13}C, ^{2}H]acetate in cultures of *Fusarium solani*[1]

ITSUO KUROBANE AND LEO C. VINING
Department of Biology, Dalhousie University, Halifax, N.S., Canada B3H 4J1
AND
A. GAVIN MCINNES AND JOHN A. WALTER
Atlantic Regional Laboratory, National Research Council of Canada, Halifax, N.S., Canada B3H 3Z1

Received December 31, 1979

ITSUO KUROBANE, LEO C. VINING, A. GAVIN MCINNES, and JOHN A. WALTER. Can. J. Chem. **58**, 1380 (1980).

The pattern of ^{13}C and ^{2}H incorporation from [1-^{13}C]-, [2-^{13}C]-, [1-$^{13}C_{0;1;1}$,2-$^{13}C_{1;0;1}$]-, and [2-$^{13}C_{0;1}$,2-$^{2}H_{3;3}$]acetate into dihydrofusarubin **1**, produced by cultures of *Fusarium solani*, has been determined by ^{13}C and ^{2}H nmr of the derivatives anhydrofusarubin **3** and anhydrofusarubin diacetate **4**. The results show that **1** is biosynthesized from seven uniformly-incorporated acetate units with C-3, C-11 originating from the "starter" unit. They strongly suggest that linear head-to-tail condensation of an acetate and six malonate units forms a single-chain heptaketide intermediate. The evidence also suggests that, during conversion of [^{13}C, ^{2}H]-labeled acetyl-CoA to malonyl-CoA, ^{2}H is transferred to biotin carboxyl carrier protein where it does not exchange rapidly with the medium and is available for conversion of endogenous malonyl-CoA to [^{2}H]-enriched acetyl-CoA.

ITSUO KUROBANE, LEO C. VINING, A. GAVIN MCINNES et JOHN A. WALTER. Can. J. Chem. **58**, 1380 (1980).

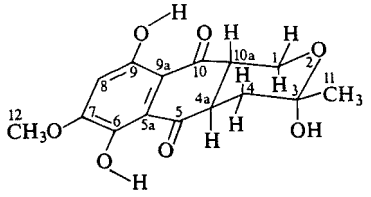
Faisant appel à la rmn du ^{13}C et du ^{2}H des dérivés de l'anhydrofusarubine **3** et du diacétate d'anhydrofusarubine **4**, on a déterminé le schéma d'incorporation du ^{13}C et du ^{2}H présents dans des acétates [^{13}C-1]-, [^{13}C-2]-, [^{13}C-$1_{0;1;1}$,^{13}C-$2_{1;0;1}$] et [^{13}C-$2_{0;1}$,^{2}H-$2_{3;3}$]- dans le dihydrofusarubine **1** qui est produit par des cultures de *Fusarium solani*. Les résultats indiquent que la biosynthèse du composé **1** se fait à partir de sept unités acétate incorporées uniformément avec les C-3, C-11 provenant de l'unité de départ. Ils suggèrent fortement que la condensation linéaire tête-queue d'un acétate et de 6 unités de malonate forme un intermédiaire heptacéture à chaîne droite. Les preuves suggèrent également que pendant la transformation du CoA-acétyle marqué au [^{13}C,^{2}H] en CoA-malonyle, le ^{2}H est transféré au carbonyle de la biotine de la protéine porteuse où il ne s'échange pas rapidement avec le milieu et où il est disponible pour la transformation du CoA-malonyle endogène en CoA-acétyle enrichi en [^{2}H].

[Traduit par le journal]

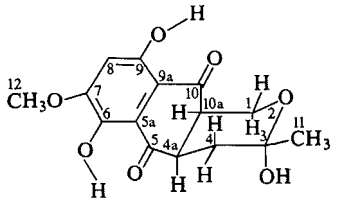
Introduction

We have shown recently (1) that *Fusarium solani* produces two diastereoisomeric 4a, 10a-dihydrofusarubins **1***a* and **1***b* which are non-enzymically oxidized by air to fusarubin (oxyjavanicin) **2** (2–6) when the culture medium becomes alkaline. Javanicin (3), norjavanicin (6), bostrycoidin (7), and (+)-solaniol (8) have also been isolated from this *Fusarium* species.

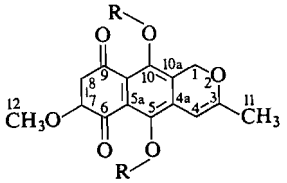
Biosynthetic studies of javanicin (3-acetonyl-5,8 - dihydroxy-6-methoxy-2-methyl-1,4-naphthoquinone) using [1-^{14}C]acetate, [2-^{14}C]malonate, and [Me-^{14}C]methionine (9) suggested that the methoxyl group is formed exclusively from methionine and the remaining carbons from acetate and malonate. The methyl group attached to the napthoquinone ring is derived from C-1 of acetate by reduction. Because of the similarity of their structures, a common progenitor has been considered for **2**, bostrycoidin, (+)-solaniol, and javanicin (8, 10). We have found that javanicin and the dihydrofusarubins are produced by *F. solani* early in the fermentation, norjavanicin appearing as a minor product at a later stage along with **2** during



1*a*



1*b*



3 R = H
4 R = $COCH_3$

[1]NRCC No. 18294.

0008-4042/80/131380-06$01.00/0
©1980 National Research Council of Canada/Conseil national de recherches du Canada

Can. J. Chem. Downloaded from www.nrcresearchpress.com by 210.87.254.6 on 09/05/12
For personal use only.

Can. J. Chem. Downloaded from www.nrcresearchpress.com by 210.87.254.6 on 09/05/12
For personal use only.

the alkaline oxidation of **1**. Full details of these experiments will be published elsewhere (11).

We report here a possible biosynthetic pathway for **1**, established by ^{13}C and ^{2}H nmr spectroscopy of anhydrofusarubin **3** and its acetate derivative **4** enriched with [1-^{13}C]-, [2-^{13}C]-, and [1-$^{13}C_{0;1;1}$,2-$^{13}C_{1;0;1}$]acetate, and of **4** enriched with [2-$^{13}C_{0;1}$,2-$^{2}H_{3;3}$]acetate.

Materials and Methods

Production and Isolation of Fusarubin (2)

Fusarium solani f. sp. *cucurbitae* race 2 S-199, obtained from Professor P. E. Nelson, Department of Plant Pathology, Fusarium Research Center, College of Agriculture, Pennsylvania State University, was maintained on potato-dextrose agar slants. A spore suspension (2.5 mL), adjusted in concentration to OD 0.25 at 640 nm, was used to inoculate each 50 mL of fermentation medium. The medium consisted of maltose (20 g), ammonium tartrate (4.6 g), KH_2PO_4 (1 g), $MgSO_4 \cdot 7H_2O$ (0.5 g), $FeSO_4 \cdot 7H_2O$ (0.01 g), salt solution (10 mL), and mineral solution (10 mL) per liter. The salt solution contained 1% (w/v) each of NaCl and $CaCl_2$; the mineral solution contained (mg L^{-1}) $ZnSO_4 \cdot 7H_2O$ (880), $CuSO_4 \cdot 5H_2O$ (40), $MnSO_4$ (6), H_3BO_3 (6), and $(NH_4)_6Mo_7O_{24} \cdot 4H_2O$ (4). Fermentation was carried out in 250 mL Erlenmeyer flasks for 6 days at 25°C with shaking at 220 rpm. The mycelium was removed by filtration, and fusarubin was extracted with ethyl acetate at pH 3 from the filtrate. After ethyl acetate was removed by evaporation *in vacuo*, the residue was washed with petroleum ether (bp 30–60°C), then crystallized once from ethyl acetate – ethanol (2:1). The average yield was 180 mg per liter.

Fusarubin (**2**): mp 184–185°C, red needles from ethyl acetate – ethanol (2:1); λ_{max} (95% ethanol): 225, 302, 470, 495, and 532 nm (log ε 4.49, 3.94, 3.82, 3.88, and 3.70); ν_{max} (KBr): 3460 (m, free OH), 3405 (m, H-bonded OH), 1595 (s, H-bonded C=O) cm^{-1}; ^{1}H nmr (pyridine-d_5) δ: 1.78 (s, 3H, H-11), 2.82 and 3.26 (AB, 2H, ^{2}J = 18 Hz, H-4), 3.75 (s, 3H, H-12), 5.11 and 5.22 (AB, 2H, ^{2}J = 18 Hz, H-1), 6.38 (s, 1H, H-8), and 13.3–13.5 (bs, 5, 10-OH); ms *m/e*: 306, 288, 273, 259, 245, 217.

Formation and Purification of Anhydrofusarubin (3)

A glacial acetic acid solution of once-crystallized fusarubin was kept for 2 days at 45°C. Cold water was added to the solution and the resultant precipitate of anhydrofusarubin was collected by filtration, washed with water, dissolved in $CHCl_3$, and purified by column chromatography on silicic acid using a mixture of benzene – ethyl acetate (12:1) for elution. The product was dissolved in $CHCl_3$ and washed twice with a 1 m*M* aqueous solution of ethylene diamine tetraacetic acid (EDTA) for ^{13}C nmr analysis.

Anhydrofusarubin (**3**): mp 190–191°C, violet prisms from $CHCl_3$; λ_{max} (95% ethanol): 236.5, 290, 348, and 540 nm (log ε 4.25, 4.22, 3.56, and 3.84); ν_{max} (KBr): 3430 (m, H-bonded OH), 1595 (s, H-bonded C=O) cm^{-1}; ^{1}H nmr ($C^{2}HCl_3$) δ: 2.01 (d, 3H, ^{4}J = 1.0 Hz, H-11), 3.91 (s, 3H, H-12), 5.19 (s, 2H, H-1), 5.96 (q, 1H, ^{4}J = 1.0 Hz, H-4), 6.15 (s, 1H, H-8), 12.57 and 12.97 (s, 5, 10-OH); ms *m/e*: 288, 273, 245, 217.

Acetylation of Anhydrofusarubin

Purified anhydrofusarubin was dissolved in 2 mL of pyridine and 2 mL of acetic anhydride, then kept for 8 h at 45°C. Cold water was added to the reaction mixture and the precipitate of anhydrofusarubin diacetate **4** was collected by filtration, washed with water, dissolved in $CHCl_3$, and washed twice with 1 m*M* EDTA solution for ^{13}C nmr analysis.

Anhydrofusarubin Diacetate (**4**): mp 186–187°C, orange needles from $CHCl_3$; λ_{max} (95% ethanol): 217, 285, and 455 nm (log ε 4.33, 4.20, and 3.59); ν_{max} (KBr): 1755 (s, aliphatic C=O), 1575 (s, H-bonded C=O) cm^{-1}; ^{1}H nmr ($C^{2}HCl_3$) δ: 1.96 (d, 3H, ^{4}J = 1.0 Hz, H-11), 2.43 (s, 3H) and 2.46 (s, 6H), (14, 16-CH_3), 3.81 (s, 3H, H-12), 5.11 (s, 2H, H-1); 5.68 (q, 1H, ^{4}J = 1.0 Hz, H-4), and 5.91 (s, 1H, H-8); ms *m/e*: 372, 330, 288, 273, 245, 217.

Labeled Precursors

Sodium [1-^{14}C]acetate was obtained from New England Nuclear Corporation, Boston, MA. Sodium [1-^{13}C]-, [2-^{13}C]-, and [1-$^{13}C_{0;1;1}$,2-$^{13}C_{1;0;1}$]acetate (all 90% ^{13}C) were supplied by Merck Sharp and Dohme Canada Ltd., Pointe Claire, P.Q. Sodium [2-$^{13}C_{0;1}$,2-$^{2}H_{3;3}$]acetate (90% ^{13}C; >95% ^{2}H) was prepared by dissolving sodium [2-^{13}C]acetate (90% ^{13}C; 37.1 mmol) in sodium deuteroxide solution (7.42 mmol sodium in 22.5 mL $^{2}H_2O$ (99.7% ^{2}H)) and heating in a sealed stainless steel tube for 20 h at 137°C to exchange protons for deuterons (12). This exchange process was repeated four times, resulting in a high deuterium content (>95%) as determined by ^{1}H and ^{13}C nmr analyses. Note that [1-$^{13}C_{0;1;1}$,2-$^{13}C_{1;0;1}$]acetate has been called [1,2-^{13}C]acetate in our previous publications e.g. ref. 13.

Feeding with [1-^{14}C]Acetate

Each 500 mL volume of *F. solani* culture received a supplement of 205 mg of sodium acetate containing 10 μCi of [1-^{14}C]acetate at 1, 1.5, 1.75, 2, 2.5, or 3 days after inoculation. The cultures were harvested at 6 days, and the ^{14}C-labeled fusarubin was isolated, converted to anhydrofusarubin, and purified as described above.

Feeding with [1-^{13}C]-, [2-^{13}C]-, [1-$^{13}C_{0;1;1}$,2-$^{13}C_{1;0;1}$]-, and [2-$^{13}C_{0;1}$,2-$^{2}H_{3;3}$]Acetate

Each 1-litre volume of *F. solani* culture was supplemented with 510 mg of precursor, 40 to 42 h after inoculation. The cultures were harvested at 6 days and the ^{13}C-enriched fusarubin was isolated and converted to anhydrofusarubin diacetate.

Analytical Instruments

Mass spectra were obtained with a Dupont/CEC 21-491 mass spectrometer, uv spectra with a Unicam SP 8000 recording spectrophotometer, and infrared spectra with a Perkin-Elmer 521 grating infrared spectrometer, using samples compressed in KBr pellets. Radioactivity was measured with a Nuclear Chicago ISOCAP/300 scintillation counter. Proton nmr spectra were recorded with a Varian HA-100 continuous-wave spectrometer; conditions were: frequency 100 MHz, sweep rate 2 Hz s^{-1}, radiofrequency field 0.5 mG, filter bandwidth 2 Hz, temperature 30°C, internal lock to $(CH_3)_4$ Si, 5 mm sample tubes. The 25.16 MHz ^{13}C and 15.36 MHz ^{2}H nmr spectra were obtained with a Varian XL-100/15 Fourier-transform nmr spectrometer, at 29°C and using 5 mm diameter sample tubes. For decoupling ^{1}H at 100 MHz, $\gamma H_2/2\pi$ was ca. 3500 Hz with broadband irradiation by 0° to 180° phase modulation at 150 MHz; for decoupling ^{2}H at 15.36 MHz, $\gamma H_2/2\pi$ was ca. 310 Hz, phase modulation frequency 40 Hz. The other conditions for each experiment follow in the sequence: nucleus observed, spectral width, acquisition time, number of data points, flip angle, time constant for weighting free induction decay, amount of sample, solvent, nucleus used for lock, nuclei decoupled: **4** at natural abundance, ^{13}C, 5120 Hz, 1.6 s, 16384, 19° or 30° if high-resolution (hr) spectrum with 1.6 s delay between data acquisition periods, −1.6 s, 83 mg in 0.5 mL $C^{2}HCl_3$, ^{2}H, ^{1}H (switched off during acquisition time for hr spectrum); **3** at natural abundance, ex [1-^{13}C]acetate and ex [2-^{13}C]acetate, ^{13}C, 5120 Hz, 0.8 s (1.6 s for hr with 1.6 s delay between acquisitions), 8192 (16384 for hr), 18° (30° for hr), −0.4 s, ca. 100 mg washed with EDTA, ca.

Can. J. Chem. Downloaded from www.nrcresearchpress.com by 210.87.254.6 on 09/05/12
For personal use only.

3.5 mL C^2HCl_3, ^2H, ^1H; **3** and **4** ex [1-$^{13}C_{0;1;1}$,2-$^{13}C_{1;0;1}$]acetate, ^{13}C, 5120 Hz, 3.2 s, 32768, 40°, −1.6 s, 56 mg in 0.6 mL C^2HCl_3 (**3**) or 120 mg in ca. 1.0 mL $C^2H_2Cl_2$ (**4**), ^2H, ^1H (switched off during acquisition for hr); **4** ex [2-$^{13}C_{0;1}$,2-$^2H_{3;3}$]acetate, ^{13}C, 5120 Hz, 3.2 s, 32768, 25°, −1.6 s, 87 mg in 0.5 mL C^2HCl_3/C_6F_6 4:1, ^{19}F, ^1H, and ^2H, also with relaxation reagent $Cr(acac)_3$ (1.5 mg) added to 0.3 mL solvent (C^2HCl_3/C_6F_6 = 5:1), same conditions except flip angle 54°, delay between data acquisition periods 7 s with ^1H decoupling field off during delay, time constant for weighting −0.4 s; **4** ex [2-$^{13}C_{0;1}$,2-$^2H_{3;3}$]acetate, ^2H, 500 Hz, 2.0 s, 2000, 90°, −0.8 s, 87 mg in 0.5 mL C^2HCl_3/C_6F_6 4:1, ^{19}F, ^1H.

Results

Incorporation of [1-^{14}C]Acetate

A preliminary experiment showed a much higher specific incorporation of ^{14}C into anhydrofusarubin when [1-^{14}C]acetate was fed on the second day of fermentation at a concentration in the culture of 5 m*M* rather than 2 m*M*. Subsequently the same precursor, at 5 m*M* concentration, was fed at times varying between 1 and 3 days from inoculation. After 6 days [^{14}C]-labeled **2** was isolated and converted to **3**. The specific incorporation of radioactivity (Fig. 1) was highest when the precursor was added 40 to 42 h after incoulation, when the pH of the culture was at a minimum.

Since **1** is converted non-enzymically to **2** in the cultures of *F. solani* under alkaline oxidative conditions, the incorporation of acetate should correlate with the production of **1** rather than **2**. Production of **1** could be detected after 12 h of fermentation and increased rapidly up to 2 days, after which its concentration decreased and **2** began to accumulate in the culture (Fig. 2). This evidence indicates clearly that **1** is being converted to **2** after 2 days when the pH of the culture rises, and is consistent with acetate being initially incorporated into **1**.

Assignment of ^{13}C Resonances

The assignment of ^{13}C resonances in the spectra of **3** and **4** was based on chemical shift trends, multiplicities, and J_{CH} values from high resolution (hr) spectra, and ^{13}C—^{13}C coupling information from spectra of **3** and **4** labeled from [1-$^{13}C_{0;1;1}$,2-$^{13}C_{1;0;1}$]acetate. Resonances of carbons bonded to hydrogen were easily recognized through their distinctive multiplicities and long-range ^{13}C—^1H couplings (Table 1): C-1 a triplet ($^1J_{CH}$ to 1-H_2), C-4 a doublet of quartets ($^1J_{CH}$ to 4-H, $^3J_{CH}$ to 11-H_3), C-8 a doublet ($^1J_{CH}$ to 8-H), C-11 a quartet of doublets ($^1J_{CH}$ to 11-H_3, $^3J_{CH}$ to 4-H), and C-12 a quartet ($^1J_{CH}$ to 12-H_3), the latter resonance being at lower field than that of C-11. Matching of ^{13}C—^{13}C coupling constants (Table 1) enabled identification of the resonances of C-10a, C-3, and C-4a. Carbon-8 is ^{13}C—^{13}C coupled to the carbon resonating at lowest field, which must be C-9, since this carbon and C-6 are expected to be the most deshielded.

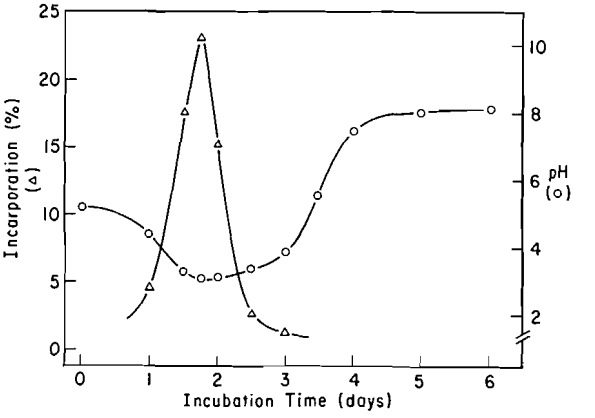


FIG. 1. Incorporation (%) of [1-^{14}C]acetate into dihydrofusarubins (△) and culture pH during fermentation (○).

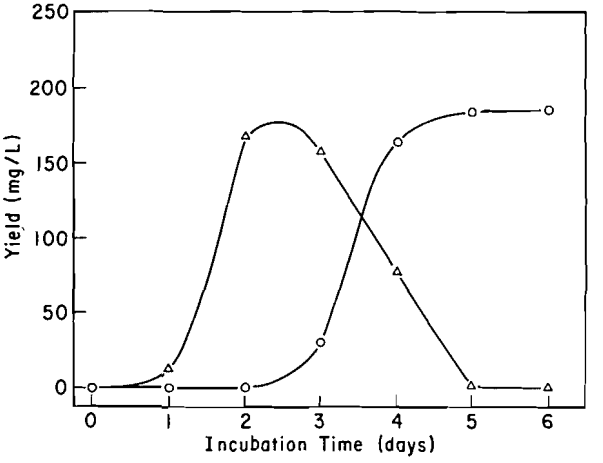


FIG. 2. Production of dihydrofusarubins (△) and fusarubin (○).

Carbon-6 is thereby identified, and the carbon to which it is ^{13}C—^{13}C coupled must be C-7 as its resonance in the hr spectrum shows a quartet characteristic of a carbon bearing a methoxyl group. Of the four remaining carbons, those bonded to oxygen will be less shielded than C-5a and C-9a, and the last is identifiable since its resonance is a doublet in the hr spectrum of **4** ($^3J_{CH}$ to 8-H) while that of C-5a is a singlet (both these resonances, and those of C-6 and C-9, show a small ^{13}C—^1H coupling to the hydroxyl hydrogens in the hr spectrum of **3**). Although the resonance for C-5 of **3** is chemically shifted upfield from that of C-10 by only 1.2 Hz, the two signals were easily distinguished because the former was a doublet ($^3J_{CH}$ to 4-H) in the hr spectrum whereas the other was a triplet ($^3J_{CH}$ to 1-H_2).

Enrichment with [1-^{13}C]- and [2-^{13}C]Acetate

The most favourable conditions determined from feeding experiments with radioactive acetate were used to incorporate [1-^{13}C]- and [2-^{13}C]acetate.

Can. J. Chem. Downloaded from www.nrcresearchpress.com by 210.87.254.6 on 09/05/12
For personal use only.

TABLE 1. Anhydrofusarubin and anhydrofusarubin diacetate: ^{13}C chemical shifts, J_{CH}, and enrichments, intensity ratios, and $^{1}J_{CC}$ resulting from incorporation of [^{13}C] and [^{13}C,^{2}H] acetate labels

					Enrichment (% above natural abundance) and intensity ratios for acetate labels							$^{1}J_{CC}$(Hz)	$^{1}J_{CC}$(Hz)
	δ_c*		$^{1}J_{CH}$ and $^{n}J_{CH}$ (Hz), $n \geq 2$†		1-^{13}C‡	2-^{13}C‡	2-$^{13}C_{0;1}$, 2-$^{2}H_{3;3}$	1-$^{13}C_{0;1;1}$, 2-$^{13}C_{1;0;1}$		1-$^{13}C_{0;1;1}$, 2-$^{13}C_{1;0;1}$		1-$^{13}C_{0;1;1}$, 2-$^{13}C_{1;0;1}$	
Carbon	3	4	3	4	3	3	4	3	4	3, $I_m/(I_d+I_m)$	4, $I_m/(I_d+I_m)$	3	4
C-11	20.08	20.05	qd ^{1}J 128.6 ^{3}J 2.7	qd ^{1}J 128.7 ^{3}J 3.1		1.6	3.0	7.2	6.7	—	—	51.6 51.6	51.5 51.5
C-3	161.51	160.95	m	dq ^{2}J 6.6, ^{2}J 5.0	2.3			5.3	5.1	0.38	0.45	51.6	51.5
C-4	94.54	94.16	dq ^{1}J 171.3 ^{3}J 4.4	dq ^{1}J 164.9 ^{3}J 4.0		1.8	3.4	7.4	6.6	0.44	0.40	55.3 55.2	56.5 56.4
C-4a	132.85	133.33	m	t ^{3}J 3.1	2.1			5.4	7.2	0.49±0.10‖	0.49±0.15‖	55.1	56.3
C-5	157.50	139.89	d ^{3}J 2.7±0.7	d ^{3}J 3.2		1.6	3.3	**	**	0.45	0.43	65.6 65.5	74.5 74.5
C-5a	110.79	123.03	d ^{3}J 4.6	s	1.7			7.9	7.3±3	‖	‖	65.3	74±2
C-6	177.75	178.53	dd ^{3}J 6.7, ^{4}J 1.2	d ^{3}J 7.9		1.6	2.7	6.4±3	5.8	0.37	0.38	61.6 61.4	61±1 60.0
C-7	159.92	158.86	dq ^{2}J 6.5, ^{3}J 4.1	dq ^{2}J, ^{3}J 3.7	2.2			6.6	6.0±2.4	**	0.40	61.3	60.0
C-8	109.84	110.20	d ^{1}J 164.0	d ^{1}J 164.9		1.7	3.1	6.0	5.7	**	0.38¶	59.4 59.5	58.4 58.4
C-9	182.83	182.66	dd ^{2}J, ^{4}J 2.5	d ^{2}J 2.0	1.9			**	6.9	0.39	0.39	59.6	58.4
C-9a	107.86	120.81	dd ^{3}J, ^{3}J 5.0±0.5	d ^{3}J 4.2		2.3	3.1	7.9±2	5.6±2.3	‖	‖	65.6 65.6	75±2 74±2
C-10	157.50	142.44	t ^{3}J 2.7±0.7	m	2.0			**	**	0.45	0.40	65.6	73±2
C-10a	122.62	127.24	bdt ^{3}J, ^{2}J 4.5	dt ^{3}J, ^{2}J 4.3±0.2		1.8	3.0	5.9	5.8	0.58±0.10‖	0.44±0.20‖	45.3 45.3	46.0 46.0
C-1	62.89	63.26	t ^{1}J 151.0	t ^{1}J 150.7	2.1			7.9	6.9±3		—	45.3	46.0
C-12	56.64	56.41	q ^{1}J 146.6	q ^{1}J 146.7									
			Average ± S.D.		2.0±0.2	1.8±0.3	3.1±0.3	6.7±1.0	6.3±0.7	0.41±0.04‖	0.40±0.02‖		
	Typical error except where shown		±0.6 Hz	±0.6 Hz	±0.6	±0.6	±1.0	±1.4	±1.5	±0.06	±0.07	±0.3 Hz	±0.3 Hz

*In ppm (±0.05) referred to $(CH_3)_4Si$. Resonances of acetyl carbons of 4 are: δ_c 20.87, q, $^{1}J_{CH}$ 130.3 Hz (both methyl carbons); δ_c 168.85, 168.95, q, $^{2}J_{CH}$ 7.1 Hz (carbonyl carbons).
†Abbreviations: s = singlet, d = doublet, t = triplet, q = quartet, m = broad multiplet.
‡Calculated from integrated resonance intensities (see text and ref. 13).
§Calculated from I_c, I_d, and I_m of resonance of other carbon in ^{13}C—^{13}C pair (see text and ref. 13). Multiplets were simulated and the total intensity estimated from components that were resolved.
‖I_m could not be accurately measured for these carbons which may be adjacent to three (or fewer) ^{13}C atoms. If the level of incorporation is uniform, $I_m/(I_{d_1} + I_m)$ for these carbons should be ca. $2p/(p + 1) = 0.58$ where p is the average $I_m/(I_{d_1} + I_m)$ for all other labeled carbons shown at foot of column.
¶Satellites of the C-8 resonance showed an additional splitting due to a coupling ($^{2}J_{CC}$ = 13.5 Hz) to C-9a, for which $I_m/(I_d + I_m) = 0.40 \pm 0.04$.
**Not measurable due to overlap of resonances or poor signal/noise.

Can. J. Chem. Downloaded from www.nrcresearchpress.com by 210.87.254.6 on 09/05/12
For personal use only.

Carbon-13 enriched **2** was isolated and converted to **3**. The distribution of ^{13}C label was calculated, as described previously (13), by comparing integrated resonance intensities in ^{13}C nmr spectra of natural-abundance and enriched samples of **3**, using identical experimental conditions. Samples were washed with EDTA in order to remove residual paramagnetic impurities which might affect resonance intensities. The results (Table 1) show ca. 2.0% enrichment from [1-^{13}C]acetate at C-1, C-3, C-4a, C-5a, C-7, C-9, and C-10, and ca. 1.8% enrichment from [2-^{13}C]acetate at C-4, C-5, C-6, C-8, C-9a, C-10a, and C-11.

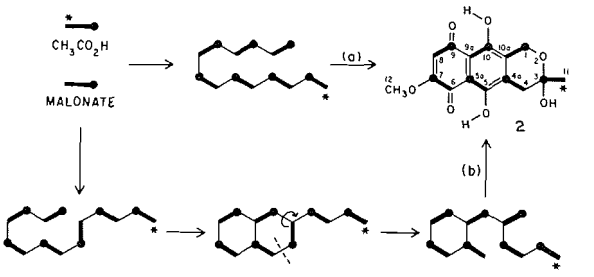
Enrichment with [1-$^{13}C_{0;1;1}$,2-$^{13}C_{1;0;1}$]Acetate

Using the same enrichment methods, **2** was labeled from 90% ^{13}C-enriched [1-$^{13}C_{0;1;1}$,2-$^{13}C_{1;0;1}$]acetate and converted to **3** and **4**. The ^{13}C nmr spectra of these samples showed, in addition to the singlet resonances (integrated intenseity I_c), satellite doublet signals (integrated intensity I_{d_1}) due to ^{13}C—^{13}C spin–spin coupling where intact doubly ^{13}C-labeled units had been incorporated. Seven pairs of covalently-bonded ^{13}C—^{13}C atoms were identified by matching coupling constants (Table 1). This information, together with the enrichment pattern from [1-^{13}C]- and [2-^{13}C]acetate, established the biosynthetic origin of **1** from seven acetate units arranged as in Scheme 1. The presence of multiplets (integrated intensity I_m), arising from the incorporation of more than one ^{13}C atom adjacent to a particular ^{13}C atom, established that the labeled precursor had been incorporated at high concentration (average $I_m/(I_m + I_{d_1})$ = probability of ^{13}C adjacent to a ^{13}C—^{13}C unit = 0.40 ± 0.03) with subsequent dilution by material at natural ^{13}C abundance to an average ^{13}C enrichment $E = 6.5 \pm 0.7\%$ (Table 1). The latter figure was calculated from I_{d_1}, I_m, and I_c for the resonance of the ^{13}C—^{13}C coupled partner of the carbon under consideration, using formula [3] of ref. 13 and solving for $E(\%) = 100\,px\,C^{P}_{13,13}$ since the approximation $px \ll 1$ does not apply in this case. Symbols are defined in ref. 13.

Enrichment with [2-$^{13}C_{0;1}$,2-$^{2}H_{3;3}$]Acetate

The most favourable conditions for incorporating ^{14}C-labeled acetate into **2** were used once again for trideuteroacetate (90% ^{13}C, >95% ^{2}H at C-2). The isotopically enriched **2** was converted to **4** for ^{2}H and ^{13}C nmr analysis.

The only signals observed in the ^{2}H nmr spectrum of ^{13}C,^{2}H-enriched **4** were those at $\delta_{^2H}$ 1.93, which arise from a deuteromethyl group. These consisted of a singlet resonance due to ^{2}H bonded to ^{12}C and a doublet ($^{1}J_{^{13}C^{2}H}$ = 20.5 Hz) for ^{2}H attached to ^{13}C. The singlet–doublet ratio I_c/I_d was



SCHEME 1

ca. 1/4.5 and this unexpected result requires that ^{2}H from the precursor (I_c/I_d = 1/9) has exchanged with ^{1}H bonded to ^{12}C in the endogenous acetate pool before incorporation into the metabolite (see Discussion for possible explanation).

Three isotopically chemically shifted resonances upfield of the C-11 $^{13}C^{1}H_3$ signal were also present in the ^{13}C nmr spectrum obtained with simultaneous [^{1}H,^{2}H]-broadband decoupling. Signal collapse, due to an increase in multiplicity when the ^{2}H-decoupling field was removed, confirmed that these resonances arose from $^{13}C^{1}H_2{}^{2}H$, $^{13}C^{1}H^{2}H_2$, and $^{13}C^{2}H_3$ species. After the ^{13}C natural abundance contribution to the $^{13}C^{1}H_3$ resonance had been subtracted, their distribution was found to be: $^{13}C^{1}H_3$, 8 ± 5%; $^{13}C^{1}H_2{}^{2}H$, 33 ± 5% at $\Delta\delta_c$ 0.24 ppm; $^{13}C^{1}H^{2}H_2$, 39 ± 5% at $\Delta\delta_c$ 0.49 ppm; $^{13}C^{2}H_3$, 20 ± 5% at $\Delta\delta_c$ 0.73 ppm. The estimated error in measuring the isotope chemical shift $\Delta\delta_c$ was ±0.02 ppm. No other resonances due to carbon bearing deuterium were observed. Resonances for C-4, C-11 ($^{2}J_{CC}$ = 6.3 ± 0.5 Hz) and C-8, C-9a ($^{2}J_{CC}$ = 13.5 + 1.0 Hz) were accompanied by satellites arising from two-bond ^{13}C—^{13}C coupling, and the average intensity ratio $I_d/(I_d + I_c)$ = 53 ± 3% for these signals indicated once again that the labeled precursor was incorporated at a high concentration, the enriched metabolite being diluted subsequently with natural abundance material. Some of the resonances for the other enriched carbons had similar satellites but their intensities were not measurable because the $^{2}J_{CC}$'s were small.

Discussion

The results of the enrichment experiments with [1-^{13}C]-, [2-^{13}C]-, and [1-$^{13}C_{0;1;1}$,2-$^{13}C_{1;0;1}$]acetate show that **1** is biosynthesized from seven acetate units, although they do not establish which of several possible biosynthetic routes leads to the final arrangement. Scheme 1 shows two examples. Nevertheless it is noteworthy that overall ^{13}C enrichments in all experiments were uniform within error, favouring a single heptaketide intermediate for **1** since two ketide intermediates (14) would probably be diluted to different extents with

Can. J. Chem. Downloaded from www.nrcresearchpress.com by 210.87.254.6 on 09/05/12
For personal use only.

natural-abundance material. Formation from one polyketide molecule (15), followed by ring scission, is also possible (Scheme 1, route (b)).

The study with [2-$^{13}C_{0;1}$,2-$^{2}H_{3;3}$]acetate established the presence of $^{13}C^{1}H_3$, $^{13}C^{1}H_2{}^{2}H$, $^{13}C^{1}H^{2}H_2$, and $^{13}C^{2}H_3$ species in the ratio 8% : 33% : 39% : 20% (±5%) at position-11. This represents a 57 ± 5% ^{2}H content at this site, which is considerably less than the >95% ^{2}H of the precursor methyl group. In the latter > 86% of the ^{13}C-labeled methyl groups will have been present as $^{13}C^{2}H_3$. Considerable exchange between ^{1}H and ^{2}H must have occurred during incorporation of the precursor, probably as a result of equilibration between acetate and malonate (16). We have suggested above that ^{2}H is transferred from [2-$^{13}C_{0;1}$,2-$^{2}H_{3;3}$]acetate to ^{12}C in the endogenous acetate pool. This would require that ^{2}H transferred to biotin carboxyl carrier protein (17) during conversion of isotopically labeled acetyl-CoA to malonyl-CoA not exchange rapidly with the hydrogens in water but be available to form ^{2}H-enriched acetyl-CoA from endogenous malonyl-CoA. This being so, the reaction in *F. solani* takes place in a hydrophobic environment. The presence of residual $^{13}C^{2}H_3$ in the metabolite, together with the observation that C-3 is derived from the carboxyl group of acetate, demonstrates that C-11 and C-3 originate from the "starter" acetate unit which initiates formation of the polyketide chain. However, our experiments did not show the increased ^{13}C-enrichment at C-11 that has been associated with "starter" groups in some previous studies (15). Lack of ^{2}H at other sites, and particularly at C-4, is noteworthy. It seems unlikely that this can be accounted for by exchange of methylene protons in malonyl thioesters. This, under physiological conditions, is slow on the time-scale of fatty acid (18, 19), and probably also of polyketide, biosynthesis. A more likely reason for the absence of ^{2}H in ring carbons of **1** is that the hydrogens of water exchange with those in the activated methylene groups of a growing poly-β-ketomethylene chain. This type of exchange occurs rapidly with β-ketoacyl thioesters (19). In concluding that the dihydrofusarubins are probably formed by linear head-to-tail condensation of an acetate and six malonate units to form a single-chain heptaketide intermediate, we are influenced primarily by other examples of polyketide-derived metabolites where there is stronger evidence for biosynthesis via a single chain.

Measurements of $I_m/(I_{d_1} + I_m)$ for resonances in the spectra of **3** and **4** (Table 1) indicate that the ^{13}C-enrichment at the time of incorporation of [1-$^{13}C_{0;1;1}$,2-$^{13}C_{1;0;1}$]acetate is ca. 40%. Intensities of satellites arising from two-bond ^{13}C—^{13}C coupling in the spectrum of **4** enriched with [2-$^{13}C_{0;1}$,2-$^{2}H_{3;3}$]acetate permitted comparable ^{13}C-enrichments to be calculated from $I_d/(I_d + I_c)$ for C-4 and C-9a. Since these enrichments were relatively uniform, it follows that the heptaketide precursor of **1** is formed within a short time, during which the precursor is not heavily diluted by unlabeled molecules arising from metabolism of the main carbon source. The low overall ^{13}C enrichment in these experiments is readily explained. Before the feeding with [1-$^{13}C_{0;1;1}$,2-$^{13}C_{1;0;1}$]acetate, 70% of the normal total yield of **1** had been produced (Fig. 2) and supplementation with acetate reduced production to about 80% of the normal yield. Consequently only 1/8th of the total sample is produced after feeding. Since 40% of that is formed from [^{13}C]acetate, the final ^{13}C enrichment is ca. 1/8 × 40% = 5%, in reasonable agreement with the measured average (6.5%, Table 1).

Acknowledgements

The authors wish to thank Professor P. E. Nelson for supplying cultures of *Fusarium solani* and Caren Mofford, Margaret Flack, and John van Ingen for technical assistance.

1. I. KUROBANE, L. C. VINING, A. G. MCINNES, and D. G. SMITH. Can. J. Chem. **56**, 1593 (1978).
2. G. P. ARSENAULT. Can. J. Chem. **43**, 2423 (1965).
3. H. R. V. ARNSTEIN and A. H. COOK. J. Chem. Soc. 1021 (1947); H. R. V. ARNSTEIN, A. H. COOK, and M. S. LACEY. Nature, **157**, 333 (1946).
4. H. W. RUELIUS and A. GAUHE. Ann. **569**, 38 (1950); **570**, 121 (1951).
5. E. HARDEGGER, K. STEINER, E. WIDMER, and A. PFIFFNER. Helv. Chim. Acta, **47**, 2027 (1964).
6. W. S. CHILTON. J. Org. Chem. **33**, 4299 (1968).
7. G. P. ARSENAULT. Tetrahedron Lett. 4033 (1965).
8. G. P. ARSENAULT. Tetrahedron, **24**, 4745 (1968).
9. S. GATENBECK and R. BENTLEY. Biochem. J. **94**, 478 (1965).
10. W. B. WHALLEY. Chem. Ind. 131 (1958).
11. I. KUROBANE, L. C. VINING, and A. G. MCINNES. To be published.
12. J. G. ATKINSON, J. J. CSAKVARY, G. T. HERBERT, and R. S. STUART. J. Am. Chem. Soc. **90**, 498 (1968).
13. J. L. C. WRIGHT, L. C. VINING, A. G. MCINNES, D. G. SMITH, and J. A. WALTER. Can. J. Biochem. **55**, 678 (1977).
14. Z. VANĚK and M. SOUCEK. Folia Microbiol. Prague, **7**, 762 (1962).
15. W. B. TURNER. Fungal metabolites. Academic Press, New York, NY. 1971.
16. C. GREGOLIN, E. RYDER, and M. D. LANE. J. Biochem. **243**, 4227 (1968).
17. J. RÉTEY and F. LYNEN. Biochem. Z. **342**, 256 (1965).
18. B. SEDGWICK, J. W. CORNFORTH, S. J. FRENCH, R. T. GRAY, E. KELSTRUP, and P. WILLADSEN. Eur. J. Biochem. **75**, 481 (1977).
19. K.-I. ARNSTADT, G. SCHINDLBECK, and F. LYNEN. Eur. J. Biochem. **55**, 561 (1975).

Osmotic and activity coefficients in dilute potassium chloride solutions at 25°C

CHAI-FU PAN

Department of Chemistry, Alabama State University, Montgomery, AL 36101, U.S.A.

Received January 28, 1980

CHAI-FU PAN. Can. J. Chem. **58**, 1386 (1980).

Osmotic and activity coefficients of dilute aqueous potassium chloride solutions are calculated from the simplified forms of the Stokes and Robinson equation. The hydration parameters in these equations are obtained from the vapor pressure data measured at higher concentration regions and the ion-size parameter is chosen as the sum of the crystallographic radii of the cation and anion of the electrolyte. The results are very satisfactory in comparison with existing data.

CHAI-FU PAN. Can. J. Chem. **58**, 1386 (1980).

A partir de la forme simplifié de l'équation de Stokes et Robinson, on a calculé les coefficients osmotiques et ceux d'activité de solutions aqueuses diluées de chlorure de potassium. On a obtenu les paramètres d'hydradation de ces équations à partir des données de pression de vapeur mesurée à plus forte concentration et on a choisi comme paramètre de dimension de l'ion la somme des rayons cristallographiques du cation et de l'anion de l'électrolyte. Les résultats sont très satisfaisants si on les compare aux données existantes.

[Traduit par le journal]

Can. J. Chem. Downloaded from www.nrcresearchpress.com by 210.87.254.6 on 09/05/12
For personal use only.

The osmotic and activity coefficients in dilute electrolyte solutions may be calculated from the simplified forms of the Stokes–Robinson equation when the required parameters in these equations are available (1, 2). The ion-size parameter $\mathring{a}$ may be chosen as the sum of the crystallographic radii of the cation and anion of the electrolyte, and the corresponding value for the hydration number h is obtained from vapor pressure data (3). For example, for potassium chloride solutions, $\mathring{a} = 3.14$ Å and $h = 6.5$. The calculated values of h in dilute regions decrease with increasing concentration. This is attributed to the factors other than hydration to cause the deviations from the Debye–Hückel law (4, 5). Osmotic and activity coefficients in the regions are thus obtained when the values of h are available. The application of the method is demonstrated in this short article.

Calculations and Results

By assuming a linear relationship in the plot of h vs. m (3), where $h = 5.548$ when $m = 0.1$ and $h = 6.500$ when m approaches zero, an equation is obtained, i.e., $h = -9.520m + 6.500$. Values of h at different concentrations are calculated from the equation. They are shown in Table 1.

The mean molal activity coefficients of KCl in the concentration range up to 0.1 m are calculated from the following equation (2)

$$[1] \quad \ln \gamma_{\pm} = \frac{K_1 m^{1/2}}{1 + K_2 m^{1/2}} + 0.036(h - 1)m$$

in which $K_1 = -1.17604$ and $K_2 = 0.328618\mathring{a}$.

The molal osmotic coefficients are related to the activity coefficients by the Gibbs–Duhem equation. One convenient form is

$$[2] \quad \phi = 1 + \frac{1}{m}\int_0^m m \, \mathrm{d} \ln \gamma_{\pm}$$

Recall that h is a linear function of m in the regions, it takes the form

$$[3] \quad h = \alpha m + \beta$$

where $\alpha = -9.520$ and $\beta = 6.500$.

By substituting [1] and [3] into [2], we obtain

TABLE 1. Osmotic and activity coefficients in dilute aqueous potassium chloride solutions at 25°C

			$\gamma_{\pm}$		
m	h	ϕ	Eq. [1]	Ref. 6	Ref. 7
0.001	6.490	0.9883	0.9648	0.965	0.9648
0.002	6.481	0.9838	0.9513	0.951	0.951
0.003	6.471	0.9805	0.9414	—	—
0.004	6.462	0.9778	0.9333	—	—
0.005	6.452	0.9755	0.9263	0.927	—
0.006	6.443	0.9735	0.9202	—	—
0.007	6.433	0.9717	0.9147	—	—
0.008	6.424	0.9701	0.9096	—	—
0.009	6.414	0.9686	0.9050	—	—
0.01	6.405	0.9672	0.9006	0.901	0.901
0.02	6.310	0.9568	0.8682	0.869	0.868
0.03	6.214	0.9498	0.8460	—	0.846
0.04	6.119	0.9446	0.8289	—	0.829
0.05	6.024	0.9404	0.8150	0.816	0.816
0.06	5.929	0.9369	0.8031	—	0.804
0.07	5.834	0.9339	0.7928	—	0.794
0.08	5.738	0.9313	0.7836	—	0.785
0.09	5.643	0.9290	0.7754	—	0.777
0.1	5.548	0.9269	0.7680	0.768	0.769

0008-4042/80/131386-02$01.00/0

©1980 National Research Council of Canada/Conseil national de recherches du Canada

$$[4]\quad \phi = 1 + \frac{K_1}{K_2{}^3 m}[(1 + K_2 m^{1/2}) - 2\ln(1 + K_2 m^{1/2}) - (1 + K_2 m^{1/2})^{-1}] + 0.018(\beta - 1)m + 0.024\alpha m^2$$

Values of ϕ at different concentrations are calculated from the above equation. The calculated values of $\gamma_\pm$ and ϕ are collected in Table 1. In comparison with the existing data compiled by Hamer and Wu (6) and Lewis and Randall (7), the results are very satisfactory (see Table 1).

Discussion

The hydration number of an electrolyte ought to be independent of concentration in dilute solutions for which there are a lot of water molecules present for every ion in solution. The value of h in Table 1 decreases with increasing concentration; this is due to factors other than hydration. If all other factors are negligible, the value of h at 0.1 m should be nearly 6.5, for there are still more than 250 water molecules per ion; where $h = 5.548$ at 0.1 m may be considered as an "adjusted value" of the hydration number; it is a parameter only. Consequently, the net effect of all other factors put together lowers the value of h about 15% at 0.1 m. They have greater effects in more concentrated regions.

1. C. PAN. Can. J. Chem. **54**, 9 (1976).
2. C. PAN. J. Chem. Eng. Data, **22**, 234 (1977).
3. C. PAN. J. Phys. Chem. **82**, 2699 (1978).
4. F. VASLOW. *In* Water and aqueous solutions: structure, thermodynamics, and transport processes. *Edited by* R. A. Horne. Wiley-Interscience, New York. 1972. Chapt. 12.
5. J. C. JASAIAH. J. Solution Chem. **2**, 301 (1973).
6. W. J. HAMER and Y. C. WU. J. Phys. Chem. Ref. Data, **1**, 1047 (1972).
7. G. N. LEWIS and M. RANDALL. Thermodynamics. *Revised by* K. S. Pitzer and L. Brewer. 2nd ed. McGraw-Hill, New York. 1961. p. 643.

Can. J. Chem. Downloaded from www.nrcresearchpress.com by 210.87.254.6 on 09/05/12
For personal use only.

Canadian Journal of Chemistry

Published by
THE NATIONAL RESEARCH COUNCIL OF CANADA

Journal canadien de chimie

Publié par
LE CONSEIL NATIONAL DE RECHERCHES DU CANADA

Volume 58 Number 14 July 15, 1980 Volume 58 numéro 14 15 juillet 1980

Can. J. Chem. Downloaded from www.nrcresearchpress.com by 210.87.254.40 on 09/05/12
For personal use only.

The synthesis of oligoribonucleotides VI.[1] The synthesis of a hexadecamer by a block condensation approach

KELVIN K. OGILVIE AND MONA J. NEMER

Department of Chemistry, McGill University, Montreal, P.Q., Canada H3A 2K6

Received December 28, 1979

KELVIN K. OGILVIE and MONA J. NEMER. Can. J. Chem. **58**, 1389 (1980).

The synthesis of the 5′-monomethoxytrityl-2′-*tert*-butyldimethylsilyl-3′-levulinylribonucleosides **4** of the four major bases involved in the phosphite procedure for the synthesis of oligoribonucleotides is described along with the 2′,3′-isomeric derivatives **6**. This report describes a total protection system for nucleotide units which allows for the block condensation procedure to be used for the synthesis of long chains. The procedure is illustrated by the synthesis of a hexadecauridylic acid.

KELVIN K. OGILVIE et MONA J. NEMER. Can. J. Chem. **58**, 1389 (1980).

On décrit la synthèse des monométhoxy-5′ *tert*-butyldiméthylsilyl-2′ lévulinyl-3′ ribonucléosides **4** des quatre bases principales impliquées dans le procédé du phosphite pour la synthèse des oligoribonucléotides ainsi que les dérivés isomères 2′,3′ **6**. Cette publication décrit un système de protection totale des unités nucléotides qui permet la synthèse de longues chaînes. On illustre la méthode en synthétisant l'acide hexadécauridylique.

[Traduit par le journal]

Introduction

Our current research program is directed toward the development of a practical method for the synthesis of oligoribonucleotides. We have been presenting (1–5) the major aspects of our method which involves two important features: (*1*) the use of the *tert*-butyldimethylsilyl (TBDMS) group to protect the 2′-position of ribonucleosides, and (*2*) the use of the phosphite coupling reagents to join the nucleoside units together. The overall approach is outlined schematically in Scheme 1. The major advantages of our method include speed and efficiency. The silylated nucleoside units **1** and **2** can be obtained rapidly and in large quantity. The phosphite procedure allows units **1** and **2** to be coupled together in 30–90 min using very simple techniques.

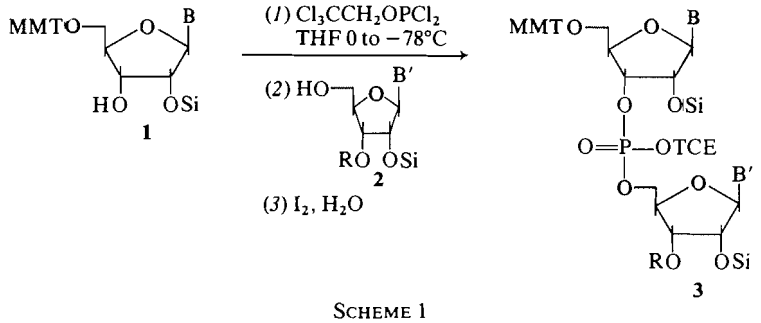
We have previously described in detail the synthesis of all levels of silylated ribonucleosides and the general procedures for the synthesis of nucleotides up to the tetranucleotide stage (2, 3, 5). We have also described (4) the synthesis, by single unit addition, of the heptanucleotide GCAACCA corresponding to the 3′-terminus of the $tRNA^{fMet}$ from *E. coli*. This latter sequence represents the longest ribonucleotide chain assembled by a stepwise route and yields at each stage ranged from 87 to 50% and total condensation times never exceeded 2 h 45 min.

In the present manuscript we wish to describe the extension of our procedures to include block condensations. Such a development is necessary in order to attempt the synthesis of very long chains such as the sequence of nucleotides in a transfer RNA. Others have succeeded in coupling ribonucleotide blocks using different procedures. For example, Ikehara and co-workers have recently (6) coupled a trimer and a tetramer using triisopropylbenzenesulfonyl chloride (TPS) to give a 30% yield (spectrophotometrically determined) after a reaction process that involved 72 h. Werstiuk and Neilson (7) have succeeded in coupling a tetramer and a pentamer to give a nonamer in 50% yield. The condensing agent was mesitylenesulfonyl triazolide (MS-TRI) and a total of 16 days was

[1]This article also constitutes Part XI in a series on silyl protecting groups in nucleoside and nucleotide chemistry. For the previous article in both series see ref. 4.

0008-4042/80/141389-09$01.00/0

©1980 National Research Council of Canada/Conseil national de recherches du Canada



SCHEME 1

required to couple the two units together. van Boom and Burgers added a tetramer to a decamer (4:1 ratio) using triisopropylbenzenesulfonyl-4-nitroimidazolide (TPS-NI) and a 3.5 day reaction (8). The yield was 58%. Wiewiorowski and co-workers (9) combined a trimer and a tetramer in a 58% yield using triisopropylbenzenesulfonyl tetrazolide (TPS-TET) as condensing agent in a 3 h reaction (preceded by a 6–8 h requirement for preparation of the reagents in a form suitable for coupling).

The current article describes the synthesis of the key molecules **2** (R = $CH_3COCH_2CH_2CO$— = Lv) for all the common ribonucleosides and the synthesis of the di, tetra, octa, and hexadecauridylic acids via a block condensation procedure. We believe the hexadecauridylic acid represents the longest reported ribonucleotide synthesized by purely chemical means. As a result, this synthesis clearly demonstrates the success of the methods used. Furthermore, no condensation required more than 90 min to join two blocks together and the ratio of the blocks being coupled was 1 to 0.8 even at the hexadeca stage. Yields ranged from 85% for the synthesis of the dimer **3** (B = Ur, R = Lv), 76% for the tetramer **10***a*, 76% for the octamer **12***a* to 51% for the hexadecamer **13***a*. These yields and times compare favorably with other reported block condensation procedures as discussed above.

Discussion

The general procedure for the synthesis of any ribonucleotide by the phosphite procedure is outlined in Scheme 1 for the synthesis of the dinucleotide **3**. Compound **3** is the smallest nucleotide unit to serve for block condensations. In order to be able to couple preformed blocks together any unit such as **3** must be capable of being extended from either the 3′- or 5′-ends. Thus the choice of the group R is critical to this procedure and we have found the levulinyl group (Lv) to be completely compatible with our system. This group was introduced to carbohydrates by Guthrie and Lucas (10) and extended to nucleosides by Hassner *et al.* (11). van Boom and Burgers (8, 12) have shown the utility of the levulinyl group for 5′-protection in conjunction with the procedures their group has developed for the synthesis of oligoribonucleotides.

The fully protected nucleoside derivatives **4** were obtained in greater than 90% yields (Table 1) within 6 h by treating compounds **1** with levulinic acid and dicyclohexylcarbodiimide (DCC) in dioxane (Scheme 2). Isomerization of the silyl group did not occur during this reaction. This was verified by the preparation of the isomeric compounds **6** from the 3′,5′-diprotected nucleosides **5**. It is interesting to note that with the adenosine derivative **1***b* no levulination occurred at the exocyclic amino group. In fact an attempt to produce *N*-acylation was marginally successful: 2′,3′,5′-tri-TBDMS adenosine (2) was only 10% acylated at the 6-amino group when treated with a 3-fold excess of levulinic acid and DCC.

The 5′-methoxytrityl group can be removed from **4** and **5** using 80% acetic acid at either room temperature for 15 h or at 90°C for 30 min. Yields on detritylation were 80–90%. In preparative conversions of **1** to **2** there is no need to isolate compound **4**.

The isomeric pair **4** and **6** as well as the pair **2** and **7** have different chromatographic properties and are easily distinguished (Table 1). Their nmr spectra are also clearly different. The chemical shift of the H-1′ signal is greatest in all cases for the isomer having the levulinyl group in the 2′-position. This trend corresponds to the general observation made several years ago by Reese and co-workers (13) who also noted that $J_{1',2'}$ is greater for the 3′-isomer than for the 2′-isomer. For the levulinated nucleosides described in this paper $J_{1',2'}$ is greater when the levulinyl group is on the 3′-position for A and G derivatives or on the 2′-position for C and U derivatives. It is also interesting that the magnitude of the coupling constants is greater for the purine derivatives than for the

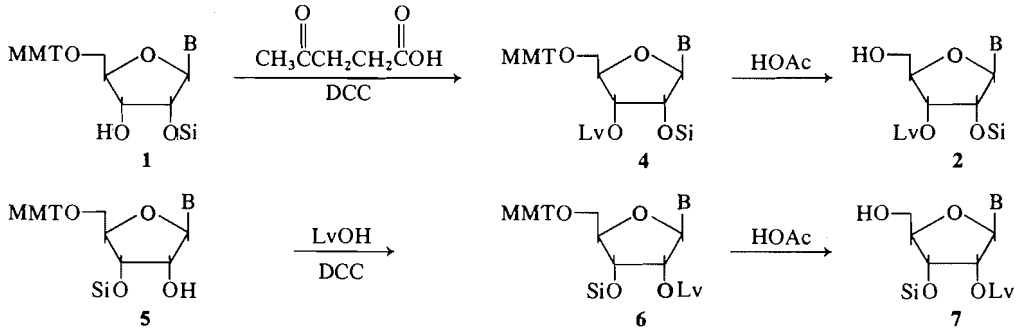
Can. J. Chem. Downloaded from www.nrcresearchpress.com by 210.87.254.40 on 09/05/12
For personal use only.

Can. J. Chem. Downloaded from www.nrcresearchpress.com by 210.87.254.40 on 09/05/12
For personal use only.

TABLE 1. Properties of nucleoside derivatives

Compound	Yield(%)	Melting point(°C)	R_f*	λ_{max}^{EtOH}(nm)	δ(†)CH_3—Si	δ $(CH_3)_3C$	δ CH_3C(=O)	δ H − 1′(d, $J_{1',2'}$(Hz))
MMT-U^{Si}_{Lv} **4***a*	93	79–81	0.50,[a] 0.86,[b] 0.79[c]	260	0.21	1.0	2.33	6.06 (4)
MMT-U^{Lv}_{Si} **6***a*	95	88–92	0.45,[a] 0.69,[b] 0.56[c]	260	−0.01, 0.05	0.86	2.20	6.13 (5)
MMT-A^{Si}_{Lv} **4***b*	94	80–85	0.29,[b] 0.66[c]	258	−0.43, −0.2	0.53	1.98	5.76 (7)
MMT-A^{Lv}_{Si} **6***b*	96	89–105	0.08,[b] 0.56[c]	258	−0.21, 0.03	0.83	1.96	6.10 (6)
MMT-$C^{Bz}{}^{Si}_{Lv}$ **4***c*	91	78–82	0.27,[a] 0.78,[b] 0.77[c]	304, 261	−0.01, 0.08	0.60	2.05	5.85 (3.1)
MMT-$C^{Bz}{}^{Lv}_{Si}$ **6***c*	93	100–104	0.04,[a] 0.40,[b] 0.54[c]	304, 260	−0.16, −0.06	0.37	2.06	6.06 (5)
MMT-$G^{Bz}{}^{Si}_{Lv}$ **4***d*	92	101–105	0.67,[b] 0.61[c]	294, 264, 256	−0.46, 0.08	0.70	2.08	5.65 (7)
MMT-$G^{Bz}{}^{Lv}_{Si}$ **6***d*	89	112–115	0.56,[b] 0.54[c]	294, 264, 256	−0.38, −0.06	0.70	1.98	5.83 (5.5)
U^{Si}_{Lv} **2***a*	81	170–173	0.47,[b] 0.36[c]	259	0.13	0.86	2.23	5.9 (5)
U^{Lv}_{Si} **7***a*	76	178–184	0.41,[b] 0.32[c]	259	0.15, 0.25	0.91	2.16	6.05 (6)
A^{Si}_{Lv} **2***b*	83	158–162	0.20[d](2×), 0.47[c]	258	−0.13, −0.43	0.70	2.20	5.70 (8)
A^{Lv}_{Si} **7***b*	89	170–172	0.13[d](2×), 0.35[c]	258	0.05	0.90	2.10	5.95 (6)
$C^{Bz}{}^{Si}_{Lv}$ **2***c*	85	160–163	0.52,[b] 0.37[c]	302, 260	0.06	0.86	2.08	5.50 (3.1)
$C^{Bz}{}^{Lv}_{Si}$ **7***c*	90	170–175	0.39,[b] 0.26[c]	302, 260	0.12	0.93	2.10	5.80 (4)
$G^{Bz}{}^{Si}_{Lv}$ **2***d*	84	192–196	0.40,[c] 0.53[d](2×)	293, 263, 256	−0.22, −0.45	0.59	2.12	5.60 (8)
$G^{Bz}{}^{Lv}_{Si}$ **7***d*	85	200–203	0.40,[c] 0.47[d](2×)	293, 264, 256	−0.02	0.71	2.01	5.80 (6)

*The tlc data from Brinkman Polygram Sil G/UV254 plastic sheets. Solvents: *a*, ether; *b*, ethyl acetate; *c*, chloroform–ethanol (9:1); *d*, ethyl acetate – chloroform–ethanol (1:0.9:0.1).
†Chemical shift data recorded relative to TMS, in ppm.



MMT = monomethoxytrityl
Si = TBDMS = *tert*-butyldimethylsilyl
Lv = levulinyl
DCC = dicyclohexylcarbodiimide

Series: *a*, *b*, *c*, *d*

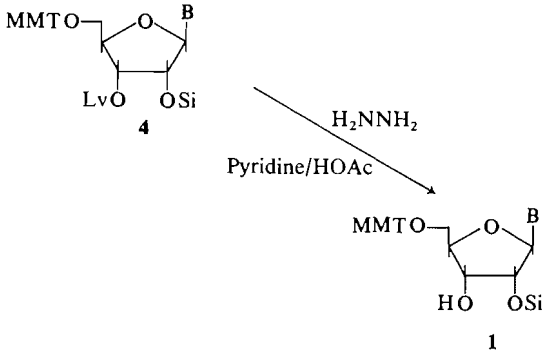
B: Ur = Uracil; Ad = Adenine; C^{Bz} = N-benzoylcytosine; B^{Bz} = N-benzoylguanosine

SCHEME 2

pyrimidine derivatives. This trend is also true for the silyl derivatives that we have previously reported (2, 3).

Nucleosides having a 5′-methoxytrityl group and a 2′ or 3′-TBDMS group show interesting chemical shifts for the methyl and *tert*-butyl protons of the TBDMS group. For pyrimidine nucleosides (C, U), the 3′-TBDMS protons are significantly shielded relative to the 2′-TBDMS isomer. For purines (A, G) the trend is just the reverse (2, 3). The same observation is made for the compounds reported in this manuscript which also contain a levulinyl group. Thus in MMT-U^{Si}_{Lv} and MMT-$C^{Bz}{}^{Lv}_{Si}$ the 3′-TBDMS protons are shielded relative to their 2′-TBDMS isomers **4***a* and **4***c* while the reverse is true for MMTA^{Si}_{Lv} and MMT-$G^{Bz}{}^{Lv}_{Si}$. For the untritylated compounds **2** and **7**, the 3′-TBDMS protons (**7***a–d*) all have greater chemical shifts than the 2′-TBDMS isomer (**2***a–d*).

Compounds **6** and **7** are not only useful in confirming the structure of **4** and **2** but are obvi-



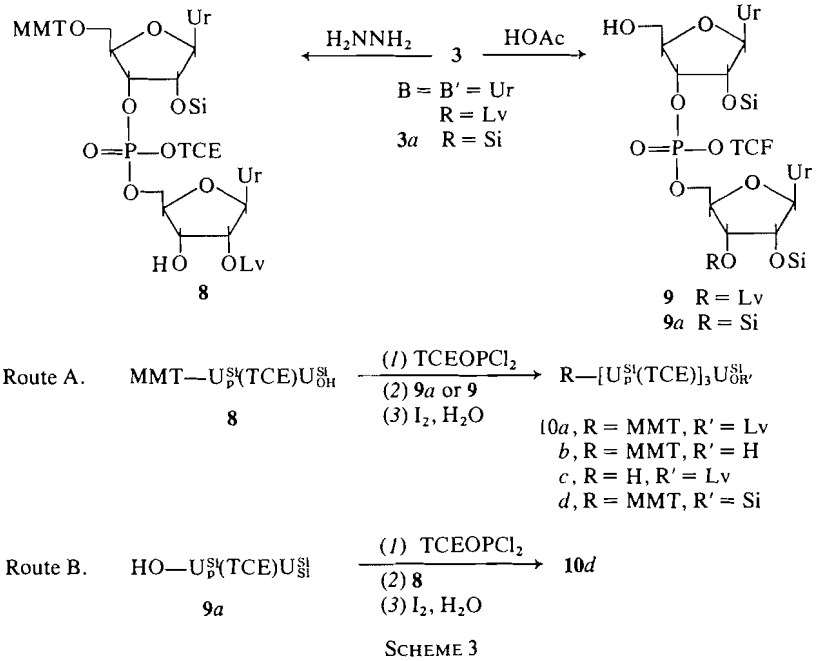
ously useful in the synthesis of 2′–5′ linked ribonucleotides. With the observation of the production of 2′–5′ linked oligoadenylates during the interferon process (14) it has become essential to be able to synthesize such linkages. We have reported the synthesis of a trinucleotide of adenosine possessing 2′–5′ linkages (15) and the development of compounds **6** and **7** will permit the rapid synthesis of any desired sequence involving 2′–5′ linkages.

The levulinyl group is removed rapidly from the fully protected nucleosides. Reactions using pyridine – acetic acid – hydrazine result in complete cleavage of the levulinyl group in less than five minutes. These conditions do not affect *N*-protecting groups nor do they cause isomerization of silyl groups (e.g. in **1**). Using the normal ratio of hydrazine (10 equiv.) with **1***a* resulted in detectable isomerization of the silyl group only after 2 h of stirring. Using 50 equiv. of hydrazine resulted in detectable isomerization after 2 h and led to 30% isomerization after 17 h. Since removal of the levulinyl group requires 5 min or less, there is obviously no problem with isomerization during the conversion of **4** to **1** and none has been detected. Furthermore, these conditions do not affect benzoyl groups on the amino groups of cytidine and guanosine.

Nucleotide Synthesis and Block Condensations

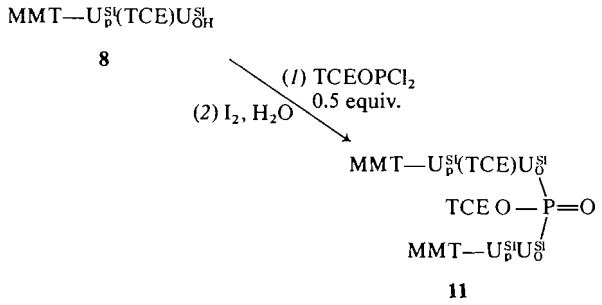
The utility of the above described combination of protecting groups was tested through the synthesis of oligonucleotides of uridine. The dinucleotide **3** (B = B′ = Ur, R = Lv) was prepared on numerous occasions by the phosphite coupling reaction using **1***a* and **2***a*. Yields ranged from 75 to 86% on reaction scales involving from 300 mg up to 7 g of **1***a*. Compound **3** provided the key intermediate for testing the phosphite procedure in block condensations (Scheme 3).

Treatment of **3** with hydrazine gave **8** in over 90% yield while treatment of **3** with acetic acid gave **9** in greater than 85% yield. In an attempt to determine the best conditions for block condensations, compounds **8** and **9***a* were condensed by two different routes to produce the tetranucleotide **10***d*. Route A (Scheme 3) is the route we have normally used (2–4) and involves phosphorylation at the 3′-hydroxyl (of **8**) followed by coupling to the 5′-hydroxyl (of **9***a*). The alternate procedure, Route B, involves phosphorylation first at the 5′-hydroxyl (of **9***a*) followed by coupling to the 3′-hydroxyl (of **8**). We found that Route A gave consistently better yields than Route B. Further we have found that in



SCHEME 3

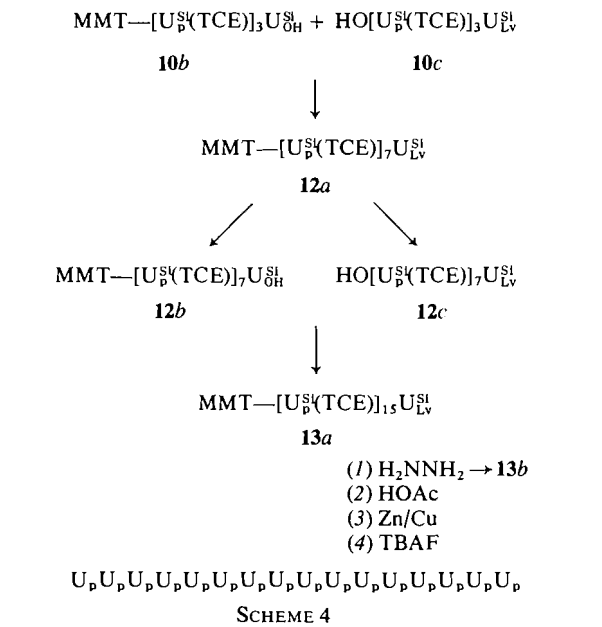
Can. J. Chem. Downloaded from www.nrcresearchpress.com by 210.87.254.40 on 09/05/12
For personal use only.



block condensations better yields are obtained in reactions conducted at 0°C than in those conducted at −78°C.

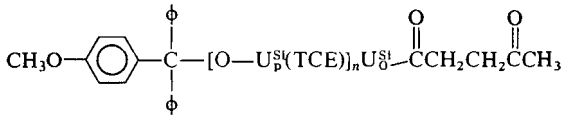
One of the side reactions in the synthesis of short nucleotides via the Route A approach is the formation of 3′–3′ linked nucleotides (2–4). While this seldom represents a separation problem we felt it to be essential to determine the probability of 3′–3′ coupling in block condensations. Consequently an attempt was made to determine the maximum amount of 3′–3′ linked tetramer that could be formed from compound **8**. Compound **8** was treated with 0.5 equiv. of phosphodichloridite at 0°C for 1 h. After work-up, starting material **8** was recovered to the extent of 46%. Compound **11** was obtained in only 10% yield and a large amount of material (presumably phosphorylated **8**) remained at the origin on tlc. The compound **11** was clearly distinguishable from the correct tetranucleotide **10***a*.

Compound **10***a* was converted into the two tetranucleotide units **10***b* and **10***c* which were condensed to form the octamer **12***a* (Scheme 4) in 76% yield. Repeating the hydrazine and acetic acid deprotections on **12***a* gave the units **12***b* and **12***c* which were condensed to produce the fully protected hexadecamer **13***a* in 51% yield. The noteworthy features of this sequence include: (*1*) total reactions times for condensing any two blocks was kept at 90 min, and (*2*) the ratio of 5′-protected unit (e.g. **12***b*) to 5′-unprotected unit (e.g. **12***c*) remained at 1:0.8 throughout the series. Yields and properties of nucleotide units are collected in Tables 2 and 5.



SCHEME 4

While the above results clearly demonstrate the compatibility of this group of protecting groups and their suitability for block extension of chains, there is one additional feature that is very useful. Both the methoxytrityl and levulinyl groups contain an isolated methyl group. Since the methoxytrityl and levulinyl groups occur at opposite ends of the



growing chain, and since the methyl resonances occur at different chemical shifts in the nmr (typically δ 3.85 ppm for CH_3O— and δ 2.26 ppm for CH_3C—) the appearance of these two signals confirms a successful coupling of two units in the correct fashion. Only the formation of a 3′–5′ bridge between two units can result in a molecule possessing both signals. They therefore serve as internal labels. Thus in the condensation of **12***b* and **12***c* to form the hexadecamer, only the desired product **13***a* could contain singlets corresponding to the CH_3O— and CH_3C— groupings. These singlets are easily observed even on small quantities of large molecules such as **13***a*. The disappearance of one of these signals also serves to establish the removal of one or the other of the protecting groups during a deprotection step.

The oligomers **10**, **12**, and **13** were deprotected to the free nucleotides which were completely degraded by pancreatic ribonuclease to uridine 3′-phosphate and uridine in the correct ratios. The sequence for deprotection consists of (*1*) removal of the levulinyl group (hydrazine, 5 min), (2) removal of the methoxytrityl group (80% HOAc, 20–30 min, 80–90°C), (*3*) removal of the trichloroethyl group (Zn/Cu in DMF at 55°C for 8–13 h), and (*4*) removal of the silyl protecting groups with TBAF. In previous reports we had isolated the nucleotidic material after the Zn/Cu

Can. J. Chem. Downloaded from www.nrcresearchpress.com by 210.87.254.40 on 09/05/12
For personal use only.

TABLE 2. Summary of block condensation experiments*

Entry†	Units	Route	Temperature (°C)	Product	Yield(%)
1	**8** and **9***a*	A	−78	**3**(R = Si)	51
2	**8** and **9***a*	A	0	**3**(R = Si)	76
3	**8** and **9***a*	B	−78	**3**(R = Si)	38
4	**8** and **9***a*	B	0	**3**(R = Si)	54
5	**1***a* and **2***a*	A	−78	**3**(R = Lv)	79
6	**8** and **9**	A	0	**10***a*	75
7	**10***b* and **10***c*	A	0	**12***a*	73
8	**12***b* and **12***c*	A	0	**13***a*	51

*Experiments were conducted as described in the Experimental under the general procedure.
†Entries 1–4 were all conducted on the same scale. Entry 5 represents an average over six separate preparations ranging in scale from 300 mg to 7.0 g of **1***a*. Entry 6 represents an average over five preparations ranging from 250 mg to 3.0 g of **8**. Entry 7 represents an average over three condensations ranging from 190 to 420 mg of **10***b*.

treatment by paper chromatography. This procedure had worked well for short nucleotides but as chain length increased so did the difficulty in eliminating salts. We have found that this problem is nicely resolved by applying the products of step (*3*) to pre-adsorbant Analtech silica gel plates. These plates were developed in chloroform–methanol solvents and under these conditions the oligonucleotide separates cleanly as a tight band and the salts remain at the origin.

Conclusion

In this manuscript we have detailed a procedure for the synthesis of oligoribonucleotides using a block condensation approach. This manuscript in conjunction with our previous detailed reports (2–4) completes the basic development of a protection group – condensation procedure that permits the synthesis of oligoribonucleotides on a large scale. The procedure is rapid and the reaction mixtures are clean relative to any of the alternative procedures for oligonucleotide synthesis. We believe that the series of procedures we have developed, and in particular the use of the *tert*-butyldimethylsilyl protecting group, allow, for the first time, the synthesis of oligoribonucleotides at least as rapidly as oligodeoxynucleotides. We will further explore the limits of this procedure through an attempt to synthesize by chemical procedures the sequence of nucleotides corresponding to that of the transfer RNA^{fMet} from *E. coli*.

Experimental

General Methods

All general procedures and techniques including chromatography, uv, nmr, mass spectrometry, elemental analyses, melting points, electrophoresis, and enzyme assays are as previously described (2) with the following exceptions.

Thin layer chromatographic data (R_f values) are recorded from Brinkman Polygram SIL G UV 254 analytical sheets. High pressure liquid chromatography results of enzyme degradations were obtained on a Spectrophysics SP 8000 microprocessor based hplc unit using a Brownlee Labs anion exchange column AX10A (4.1 × 250 mm, 10 micron particles) and an acetonitrile–ammonium phosphate gradient. The nmr measurements were made on a Varian T60 spectrometer.

All starting nucleosides **1***a–d* and **5***a–d* were prepared as previously described (2, 3). The preparation of the TBAF reagent has been previously described (2).

Levulination of Compounds 1 and 5. The Preparation of the Fully Protected Nucleosides 4 and 6

The preparation of both series of compounds **4** and **6** followed the same general procedure. Compound **1** or **5** was dissolved in dry dioxane (10 mL/mmol) and 1.5–2 equivalents of levulinic acid, 3–4 equivalents of dicyclohexylcarbodiimide, and 10 mg/mmol of **1** or **5** of 4-dimethylaminopyridine were added. The solution was stirred at room temperature from 6–13 h although tlc indicated that all reactions were over in 6 h. The solution was filtered from dicyclohexylurea and extracted with 10% sodium bicarbonate in water. The organic layer was concentrated at reduced pressure and the residue was applied to thick layer plates. Solvents used for development of the plates are listed in Table 3. Yields and properties of the products **4**(*a–d*) and **6**(*a–d*) are listed in Table 1.

Preparation of Compounds 2 and 7

These series of compounds were obtained by treating compounds **4** or **6** respectively with 80% acetic acid (10 mL/mmol) at 80–90°C for 20–30 min. Solvents were removed at reduced pressure and the residue was applied to tlc plates developed in the solvents recorded in Table 3. The properties of compounds **2***a–d* and **7***a–d* are collected in Table 1. This same procedure was used for the removal of the methoxytrityl group from nucleotides.

General Procedure for the Removal of the Levulinyl Group

This procedure was general for the removal of the levulinyl group from nucleosides and nucleotides. The compound was dissolved in pyridine (1 mL/mmol) and 10 equiv. of 0.5 *M* hydrazine hydrate in pyridine – acetic acid (3:2) were added. After 5 min, 2,4-pentanedione (10 equiv.) was added with cooling. Solvents were removed by coevaporation with pyridine and the residue was dissolved in chloroform which was washed with water. The organic layer was concentrated and triturated with petroleum ether. Products were isolated by tlc. For oligonucleotides the isolated yields of the compounds **8**, **10***b*, and **12***b* were 92–94, 92–95, and 92–94% respectively. Solvents used for isolating **8**, **10***b*, and **12***b* on tlc are listed in Table 4.

Tests for Isomerization of TBDMS in the Presence of Hydrazine

5′-*O*-Monomethoxytrityl-2′-*O*-TBDMS uridine (**1***a*) was dissolved in two different concentrations of hydrazine hydrate and

Can. J. Chem. Downloaded from www.nrcresearchpress.com by 210.87.254.40 on 09/05/12
For personal use only.

TABLE 3. Solvents used for the isolation of compounds **4**, **6**, **2**, and **7** by thick layer chromatography*

Compound isolated	Solvent used	Number of developments
4*a*	Ether–hexane (3:1)	2
4*b*, **4***c*, **6***a*	Ether	1–2
4*d*, **6***d*	Ether–chloroform (1:1)	2
6*b*, **2***b*, **7***b*	Ethyl acetate – chloroform–ethanol (1:0.9:0.1)	2
6*c*	Ether – ethyl acetate (1:1)	1
2*a*, **2***c*, **7***a*, **7***c*	Ether–chloroform–ethanol (2.5:0.9:0.1)	1–2
2*d*, **7***d*	Ether–chloroform–ethanol (1:0.9:0.1)	2

*On DSF-5 silica gel (Terrochem).

TABLE 4. Solvents used for the isolation of nucleotides by thick layer chromatography

Compound	Solvent	Developments
3, **8**	Ether	1–2
9, **10***a*, **10***b*	Ether–chloroform–ethanol (2.5:0.9:0.1)	2
10*c*, **12***c*, **12***b*, **12***c*	Ethyl acetate – chloroform–ethanol (1:0.9:1)	1–2
13*a*	Ether – ethyl acetate – chloroform–ethanol (1:1:0.9:0.1)	2
11	Chloroform–ethanol–ether (0.9:0.1:5)	1

the solutions were monitored by tlc. At the times indicated the composition of the solution was determined from preparative tlc plates developed in ether–hexane (3:1). (*1*) Compound **1***a* (189 mg, 0.3 mmol) was treated with 10 equivalents (3 mL) of hydrazine hydrate solution as per the above general procedure. Thin layer chromatography gave the first indication of isomerization (trace presence of **5***a*) after 2½ h. The degree of isomerization had reached 10% after 6 h. (*2*) The above test was repeated except that 50 equivalents of hydrazine hydrate (15 mL) solution was added. Isomerization was detectable after 2 h and had reached 30% after 17 h.

General Procedure for Nucleotide Condensations

This procedure is essentially as has been previously described (2–4). In the current reactions a ratio of 1:0.8 of 3′-unblocked to 5′-unblocked units has been used. The procedure is illustrated by example experiments for each of the blocks synthesized. Solvents used in isolating products by thick layer chromatography are listed in Table 4.

Synthesis of MMT-U_p^{Si}(TCE)U_{Lv}^{Si} (3, B = B′ = Ur, R = Lv)

Compound **3** was prepared several times at different scales of reactions. As an example, compound **1***a* (300 mg, 0.47 mmol) in THF (0.65 mL) was added dropwise to a solution of THF (0.5 mL) containing 78 μL (0.52 mmol) of trichloroethyldichlorophosphite and 0.28 mL (2 mmol) of collidine maintained at −78°C. After a total of 10 min at −78°C compound **2***a* (172 mg, 0.38 mmol) in THF (1 mL) was added and the reaction mixture was stirred for 30 min at −78°C and allowed to warm up to room temperature (total 30 min). Iodine (228 mg, 0.88 mmol) in 3 mL of THF–H_2O (2:1) was added and the solution stirred for 5 min. The solvents were removed at reduced pressure and the residue was dissolved in $CHCl_3$ (50 mL) which was extracted with water (40 mL), 5% $NaHSO_3$ (10 mL), and finally with water. Products were isolated by tlc.

Synthesis of the Tetranucleotide MMT-U_p^{Si}(TCE)U_p^{Si}(TCE)U_{Si}^{Si}(10d)

Route A

(*1*) Compound **8** (200 mg, 0.17 mmol) in THF (0.5 mL) was added dropwise to a solution of THF (0.2 mL) containing $TCEOPCl_2$ (27 μL, 0.17 mmol) and collidine (0.1 mL, 0.9 mmol) maintained at −78°C. After a total of 15 min the second component, compound **9***a* (140 mg, 0.135 mmol) in THF (1 mL) was added and stirring was continued for 30 min and allowed to warm to room temperature. Iodine (90 mg, 0.3 mmol) in THF–H_2O (2:1, 1.5 mL) was added and after 5 min the reaction was worked up in the usual fashion. Results of all these condensations are recorded in Table 2.

(*2*) The above reaction was repeated except that the temperature was raised from −78°C to 0°C.

Route B

(*1*) Compound **9***a* (175 mg, 0.17 mmol) in THF (0.8 mL) was added dropwise to a solution of THF (0.1 mL) containing $TCEOPCl_2$ (27 μL, 0.183 mmol) and collidine (0.1 mL, 0.9 mmol) maintained at 0°C. After 15 min, compound **8** (160 mg, 0.135 mmol) in THF (0.5 mL) was added and stirring was continued for 30 min at 0°C followed by warming to room temperature for 15 min. The reaction was treated with iodine and worked up as in the usual fashion.

(*2*) The above reaction was repeated at −78°C.

Synthesis of the 3′–3′ Linked Tetramer, 11

Compound **8** (250 mg, 0.21 mmol) in THF (0.5 mL) was added to a solution of THF (0.3 mL) containing collidine (0.1 mL) and $TCEOPCl_2$ (16 μL, 0.11 mmol) maintained at 0°C. The solution was stirred at 0°C for a total of 1 h followed by warming to room temperature for an additional hour. The reaction mixture was treated with iodine and worked up in the usual fashion (Table 4 for tlc solvents). The desired product, **11**, was obtained in a 10% yield (32 mg) along with 112 mg (45%) of the starting material **8**. Properties of compound **11** are collected in Table 5.

Synthesis of the Octanucleotide MMT-[U_p^{Si}(TCE)]$_7U_{Lv}^{Si}$ (10a)

The general procedure was followed. As an example, compound **10***b* (210 mg, 0.092 mmol) in THF (0.5 mL) was added dropwise to a solution of THF (0.2 mL) containing collidine (0.09 mL) and $TCEOPCl_2$ (16.5 μL, 0.1 mmol) maintained at 0°C. The solution was stirred for a total of 15 min at 0°C where-

Can. J. Chem. Downloaded from www.nrcresearchpress.com by 210.87.254.40 on 09/05/12
For personal use only.

TABLE 5. Properties of protected nucleotides

Compound	Melting point (°C)	λ_{max}^{EtOH}	R_f*			Nuclear magnetic resonance	
			a	*b*	*c*	δ CH_3O(ppm)	δ $CH_3C(=O)$—(ppm)
3	114–118	260	0.76	0.60	0.32	3.90	2.30
8	99–103	261	0.81	0.52	0.33	3.90	—
9	104–109	261	0.45	0.40	0.09	—	2.30
10*a*	128–132	261	0.86	0.49	0.20	3.86	2.26
10*b*	120–124	261	0.80	0.49	0.29	3.86	—
10*c*	150–155	260	0.56	0.42	0.06	—	2.26
11	115–120	261	0.90	0.85	0.56	3.88	—
12*a*	146–150	260	0.93	0.42	0.20	3.85	2.26
12*b*	142–147	260	0.93	0.40	0.16	3.85	—
12*c*	175–179	259	0.50	0.37	0.04	—	2.26
13*a*	163–168	260	0.87	0.50	0.18	3.74	2.17

*Solvents: *a*, ethyl acetate; *b*, chloroform–ethanol (9:1); *c*, ether–chloroform–ethanol (2.5:0.9:0.1).

upon compound **10***c* (150 mg, 0.072 mmol) in THF (0.35 mL) was added and the solution was stirred at 0°C for 30 min followed by warming to room temperature (30 min). The solution was treated with iodine (50 mg, 0.18 mmol) in THF–H_2O (2:1, 1.5 mol) for 5 min and worked up in the usual manner. The yield of **10***a* in this reaction was 76%. Yields and properties are collected in Tables 2, 4, and 5.

*Synthesis of the Hexadecamer MMT-[U_p^{Si}(TCE)]$_{15}U_{Lp}^{Si}$ (**13**a)*

Compound **12***b* (45 mg, 0.01 mmol) in THF (0.3 mL) was added dropwise to a solution of THF (0.1 mL) containing collidine (6.4 μL, 0.045 mmol) and $TCEOPCl_2$ (1.8 μL, 0.012 mmol) at 0°C. The solution was stirred at 0°C for 20 min whereupon compound **12***c* (30 mg, 0.006 mmol) in THF (0.3 mL) was added and stirring was continued at 0°C for 30 min. The solution was allowed to warm up to room temperature for a total of 30 min. Iodine (10 mg, 0.04 mmol) in THF–H_2O (2:1, 0.6 mL) was added and after 5 min the products were isolated in the usual fashion. From this experiment compound **13***a* was obtained in 36% yield. Results and properties are collected in Tables 2, 4, and 5. On a slightly larger scale reaction starting with 75 mg (0.016 mmol) of **12***b*, the yield of **13***a* was 51%.

Complete Deprotection of Oligonucleotides

The first step in complete deprotection was removal of the levulinyl group as previously described. The product of this reaction, without further purification, was subjected to 80% HOAc at 80–90°C during 20–30 min. Reactions were easily followed by tlc using chloroform–ethanol. (9:1). Solvents were removed at reduced pressure and the last traces of acetic acid were removed by coevaporation with ethanol. The residue was dissolved in DMF (0.4 mL/10 mg of starting nucleotide) and 50 mg of freshly prepared Zn/Cu reagent was added and the reaction was stirred at 55°C for 8–13 h. Again the course of the reaction could be followed by tlc using chloroform–ethanol (9:1). The crude mixture was applied directly to a pre-absorbent Analtech silica gel plate (250 micron, 20 × 20 cm, No. 3251, silica gel GH). The plate was developed first in ether and then in chloroform–methanol (4:1). The nucleotide band ($R_f \sim 0.3$–0.6) was eluted with methanol. The solvent was removed at reduced pressure and the product was precipitated from acetone with hexane. The solid was stirred for 1.5 h with TBAF. The solution was passed through a Dowex 50W–X8 (Na^+ form) ion exchange column. The eluant was collected, concentrated, and applied to Whatmann 3MM paper developed in solvent F. Only one nucleotide band was obtained in each case. The product was eluted with water and collected by lyophilization. Yields were 80–90% determined spectrophotometrically. Properties of the deprotected oligonucleotides are collected in Table 6. Each nucleotide was treated with pancreatic ribonuclease and was degraded to 3′-uridylic acid and uridine in the expected ratios as shown in Table 6.

TABLE 6. Properties of oligonucleotides

Compound	*R_f^F	†R_m^{Tp}	Enzyme degradation‡ Up/U
UpU	0.50	0.64	1.09/1.0
UpUpUpU	0.36	0.80	3.12/1.0
$Up(Up)_6U$	0.13	0.85	6.75/1.0
$Up(Up)_{14}U$	0.03	0.92	15.7/1.0

*Solvent F (2): *n*-propanol – concentrated ammonium hydroxide – water (55:10:35).
†Triethylammonium bicarbonate buffer (0.05 *M*, pH 7.5), R_m^{Tp} = electrophoretic mobility relative to Tp (see ref. 2).
‡Ribonuclease degradations were conducted as previously described (2). Degradation products were characterized and quantitated both by hplc (see general methods) and by paper chromatography (2). The only products detected by both techniques were Up and U. No other nucleosidic or nucleotidic material was detected. All starting material was completely degraded.

Acknowledgements

We gratefully acknowledge financial support from the Natural Sciences and Engineering Research Council of Canada, the Quebec Education Ministry, and ens Biological Ltd. We are also indebted to Richard Pon who carried out the hplc analyses of enzyme digests of oligonucleotides, and to Dr. William (Bill) H. Dawson who recorded numerous nmr spectra of both nucleosides and nucleotides.

1. K. K. OGILVIE, N. THERIAULT, and K. SADANA. J. Am. Chem. Soc. **99**, 7741 (1977).
2. K. K. OGILVIE, S. L. BEAUCAGE, A. L. SCHIFMAN, N. Y. THERIAULT, and K. L. SADANA. Can. J. Chem. **56**, 2768 (1978).

Can. J. Chem. Downloaded from www.nrcresearchpress.com by 210.87.254.40 on 09/05/12
For personal use only.

3. K. K. OGILVIE, A. L. SCHIFMAN, and C. L. PENNEY. Can. J. Chem. **57**, 2230 (1979).
4. K. K. OGILVIE and N. Y. THERIAULT. Can. J. Chem. **57**, 3140 (1979).
5. K. K. OGILVIE, K. L. SADANA, E. A. THOMPSON, M. A. QUILLIAM, and J. B. WESTMORE. Tetrahedron Lett. 2861 (1974).
6. E. OHTSUKA, S. TANAKA, and M. IKEHARA. J. Am. Chem. Soc. **100**, 8210 (1978).
7. E. S. WERSTIUK and T. NEILSON. Can. J. Chem. **54**, 2689 (1976).
8. J. H. VAN BOOM and P. M. J. BURGERS. Recl. Trav. Chim. Pays-Bas, **97**, 73 (1978).
9. R. W. ADAMIAK, E. BIALA, K. GRZESKOWIAK, R. KIERZEK, A. KRASZEWSKI, W. T. MARKIEWICA, J. OKUPNIAK, J. STANWINSKI, and M. WIEWIOROWSKI. Nucleic Acids Res. **5**, 1889 (1978).
10. D. GUTHRIE and T. J. LUCAS. Carbohydr. Res. **33**, 391 (1974).
11. A. HASSNER, G. STRAND, M. RUBINSTEIN, and A. PATCHORNIK. J. Am. Chem. Soc. **97**, 1614 (1975).
12. J. H. VAN BOOM and P. M. J. BURGERS. Tetrahedron Lett. 4875 (1976).
13. H. P. M. FROMAGEOT, B. E. GRIFFIN, C. B. REESE, J. E. SULSTON, and D. R. TRENTHAM. Tetrahedron, **22**, 705 (1966).
14. B. R. G. WILLIAMS and I. M. KERR. Nature, **276**, 88 (1978).
15. K. K. OGILVIE and N.Y. THERIAULT. Tetrahedron Lett. 2111 (1979).

Can. J. Chem. Downloaded from www.nrcresearchpress.com by 210.87.254.40 on 09/05/12
For personal use only.

The synthesis and reactions of 2,11-diselena[3,3]metacyclophanes. An investigation of the selenoxide elimination route to metacyclophane-1,8-dienes

REGINALD H. MITCHELL

Department of Chemistry, University of Victoria, Victoria, B.C., Canada V8W 2Y2

Received February 11, 1980

Can. J. Chem. Downloaded from www.nrcresearchpress.com by 210.87.254.5 on 09/05/12
For personal use only.

REGINALD H. MITCHELL. Can. J. Chem. **58**, 1398 (1980).

2,11-Diselena[3,3]metacyclophane and its 9,18-dimethyl derivative are prepared in ca. 7% yield from Na_2Se and xylylene bromide. Wittig rearrangement and benzyne induced Stevens rearrangement gave the ring contracted [2,2]metacyclophane derivative. Attempted selenoxide elimination to produce metacyclophane-diene failed. The ^{1}Hmr spectra of the selenametacyclophane indicate that the *syn*-conformer is the more stable. A general synthesis of aryl-alkenes in an 80% yield starting from benzyl phenyl selenide, alkylation with an alkyl halide, and then selenoxide elimination is given.

REGINALD H. MITCHELL. Can. J. Chem. **58**, 1398 (1980).

On a préparé le diséléna-2,11[3,3] métacyclophane et son dérivé diméthylé en positions 9 et 18 avec un rendement d'environ 7% à partir du Na_2Se et du bromure de xylylène. Les transpositions successives de Wittig et de Stevens induites par le benzyne ont conduit à la formation du dérivé cyclique contracté: [2.2] métacyclophane. Une tentative d'éliminer le sélénoxyde en vue d'obtenir le métacyclophane diène a échoué. Les spectres rmn du ^{1}H du sélénamétacyclophane indiquent que le conformère *syn* est le plus stable. On présente une synthèse générale d'aryl-alcènes qui procède avec un rendement de 80% impliquant une alkylation en partant du séléniure de benzyle et de phényle et d'un halogénure d'alkyle et une élimination de sélénoxyde.

[Traduit par le journal]

Introduction

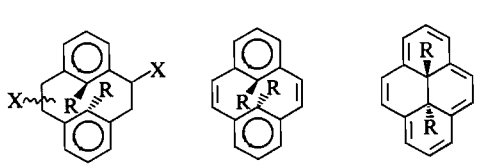
Dithiacyclophanes[1] have attracted much attention in recent years both because of their interesting fluxional properties (1) and because of their ready conversion into both the cyclophanes themselves (2) and into many novel derived polycyclic aromatic compounds (3). However, until our initial report (4), the analagous diselenaphanes were unknown.

There was some considerable incentive to investigate the properties of such compounds because of the early reports (5) on the ease of the selenoxide elimination relative to the well known, but relatively high temperature, sulfoxide elimination. This was pertinent in that conversion of cyclophane **1***Da* into the cyclophane-diene **2***a* could not be achieved in very good yield (6).

We had previously discovered (7) that cyclophane **1***Fb* undergoes Hofmann elimination readily to give diene **2***b* and dihydropyrene **3***b* in excellent yield (>80%) under a variety of base–solvent conditions. The yield of **2***a*, however, from the corresponding **1***Fa* was much poorer (<40%); a competing Stevens rearrangement to give **1***Ha* occurred (6). In other related systems the yields were much worse (8). At the start of this work the sulfoxide elimination had not been reported for these systems, but subsequently Otsubo and Boekelheide (9) have shown that sulfoxides **1***Kb* and **1***Ka* give dihydropyrene **3***b* (34%) and pyrene **4** (37%) respectively on pyrolysis under vacuum. The internal hydrogen substituents of the initially formed **3***a* were evidently lost at the temperature of the pyrolysis. Indeed it has been shown (6) that such hydrogens undergo migration out of the centre of the ring at temperatures above 60°C, and hence the possibility that the selenoxide **1***La* or **1***Na* might undergo elimination at room temperature to give **2***a* was very attractive. We thus decided to investigate the synthesis and reactions of 2,11-diselena[3,3]metacyclophane **5***Aa* and its 9,18-dimethyl derivative **5***Ab*.

Numbering of Compounds

Where a single letter *a* or *b* follows a number, the *a* refers to the series with internal hydrogen atoms, the *b* to the series with internal $-CH_3$ groups. Where two letters follow a number the first capital letter relates to the substituent X or Y in the formulae below and the second small letter to the —H, or $-CH_3$ series.



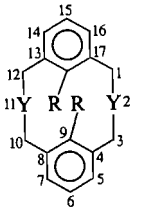
1 **2** **3**

[1]For the nomenclature system used in these compounds see F. Vögtle and P. Neumann. Tetrahedron, **26**, 5847 (1970).

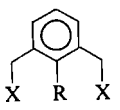
0008-4042/80/141398-09$01.00/0

©1980 National Research Council of Canada/Conseil national de recherches du Canada

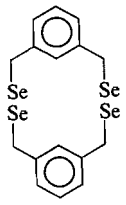
Can. J. Chem. Downloaded from www.nrcresearchpress.com by 210.87.254.5 on 09/05/12
For personal use only.



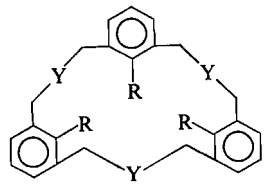
5



6



7



8

Substituents					
	X		Y		R
A	Br	*A*	Se	*a*	H
B	SH	*B*	S	*b*	CH_3
C	SeH	*C*	^+SeMe		
D	SMe	*D*	^+SMe		
E	SeMe				
F	$^+SMe_2$				
G	$^+SeMe_2$				
H	CH_2SMe				
I	SeCN				
J	Sϕ				
K	SOϕ				
L	SeOMe				
M	Seϕ				
N	SeOϕ				

Syntheses

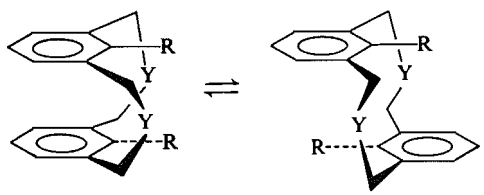
The analogous thiacyclophanes, **5***Ba* and **5***Bb* are best prepared (3, 10) by slowly adding an equimolar solution of bromide **6***A* and thiol **6***B* to dilute potassium hydroxide in 90% aqueous ethanol. Unfortunately selenols are not nearly as easy to prepare and handle as the corresponding thiols (11), and when prepared readily oxidize to diselenides. Solutions containing the selenol **6***Ca* could be generated from the selenocyanate **6***Ia* (12) or from bromide **6***Aa* and NaSeH using the method of Klayman and Griffin (13), and in the presence of excess bromide **6***Aa* form some of the desired selenaphane **5***Aa*, along with tetraselenaphane **7** (12), polymer, and other products. Pure **5***Aa* is, however, difficult to separate from this mixture.

A similar result was obtained when Na_2Se was used in aqueous or ethanolic solvent with bromide **6***Aa*, a procedure which works reasonably well (6) with Na_2S. The best method to prepare the selenaphane **5***Aa* proved to be addition of anhydrous Na_2Se (Alfa) to a solution of *m*-xylylene dibromide **6***Aa* in dry DMF, DMSO, or HMPT (hexamethylphosphoric triamide) under nitrogen. After chromatography on silica gel, 2,11-diselena-[3,3]metacyclophane **5***Aa* was thus obtained in an average 7% yield as pale yellow crystals, mp 121–122°C. There was also obtained 8% of the cyclic trimer **8***Aa*, mp 130–132°C. The identity of these was established by analysis and mass spectrometry, where **5***Aa* gave a molecular ion at *m/e* 368 (97%) with a correct (14) isotope pattern for two Se atoms per molecule, and showed fragment peaks corresponding to loss of one (23%) and two (100%) Se atoms. The trimer **8***Aa* gave a weak molecular ion at *m/e* 552 with correct isotope pattern for three Se atoms per molecule.

A similar reaction between bromide **6***Ab* and Na_2Se gave 7% yield of the dimethylselenaphane **5***Ab*, mp 185–187°C, and the trimer (~5%) **8***Ab*, mp 186°C, again identified by their mass spectra (molecular ions at *m/e* 396 and 594 respectively, with correct Se isotope patterns).

Nuclear Magnetic Resonance Spectra

Despite much previous interest (1) in the conformational equilibrium between the *syn*- and *anti*-isomers of various 2,11-dithia[3,3]-metacyclophanes, the preference for the *syn*-conformer for the parent **5***Ba* has only recently (15) been established by X-ray crystallography in the solid state and by nuclear magnetic resonance spectroscopy in solution. The dimethyl compound **5***Bb* on the other hand exists as discrete *syn*- and *anti*-conformers which are not interconvertible and can be readily distinguished by ^{1}Hmr spectroscopy (6). The *anti*-conformer of **5***Bb* has the internal $-CH_3$ hydrogens at δ 1.30 shielded by the adjacent benzene ring with the aryl hydrogens normal at δ 7.0–7.4. *Syn*-**5***Bb* on the other hand shows the aryl hydrogens shielded by the adjacent ring at δ 6.66 and the $-CH_3$ hydrogens normal for a toluene at δ 2.54. This assignment has been confirmed by X-ray data (16). The conformer of selenaphane **5***Ab* that is isolated shows ^{1}Hmr peaks for the aryl hydrogens at δ 6.97 and for the $-CH_3$ hydrogens at δ 1.77 and



syn-5 *anti*-5

Can. J. Chem. Downloaded from www.nrcresearchpress.com by 210.87.254.5 on 09/05/12
For personal use only.

thus by comparison to the thiacyclophane series is clearly the *anti*-conformer.

The $-CH_3$ hydrogens, however, are 0.47 ppm less shielded in the selenaphane than in the thiaphane. Similarly the selena-trimer **8***Ab* shows its $-CH_3$ hydrogens at δ 2.05, 0.25 ppm less shielded than those of the thia-trimer **8***Bb* at δ 1.80 (6). This reduction of shielding in the selenaphane series is probably a reflection of the longer C—Se bond lengths, 198 pm (17), relative to those of C—S, 182 pm (18), which allow the $-CH_3$ hydrogens to take up a position further away from the opposite benzene ring in the selenaphanes than in the thiaphanes, rather than an electronegativity effect which is minimal (19) and cannot be observed for the methylene bridge hydrogens.

The ^{1}Hmr spectrum for the parent selenaphane **5***Aa* shows the aryl hydrogens at δ 7.04 with the internal hydrogens at δ 6.46 and the bridge protons at δ 3.78. In the thiaphane **5***Ba* these are at δ 6.91, 6.82, and 3.71 respectively. The latter compound is thought to undergo a rapid conformational equilibrium with the *syn*-conformer being preponderant (>90%) (15). If this is the case for selenaphane **5***Aa* the proportion of *anti*-conformer present must be higher in order to yield an average chemical shift of δ 6.46 for the internal hydrogens. Since the difference in chemical shifts between the selena-trimer **8***Aa* and the thia-trimer **8***Ba* is <0.1 ppm for all protons, the chemical shifts for all protons of the *syn*-conformers of **5***Aa* and **5***Ba* might also be expected to be similar, and for the aryl hydrogens to be close to δ 7. For the *anti*-conformer of **5***Aa* the case is not so clear. For *anti*-thiaphane **5***Ba*, the shielded internal hydrogen has been estimated (15) to have (if it could be observed) a chemical shift of ca. δ 5. Considering the Se vs. S size argument that was made above for the dimethyl compounds **5***Ab* and **5***Bb*, the chemical shift of the internal hydrogen of selenaphane **5***Aa* should be greater (i.e. less shielded) than that estimated for **5***Ba*. We have previously reported (4) the variable temperature ^{1}Hmr spectrum of **5***Aa* and have shown that the signal due to the internal hydrogens collapses into the baseline at ca. −96°C. At that time we observed at ca. −110°C a small signal (ca. 0.8H) at δ 4.5 which we assigned to a shielded internal proton of an *anti*-conformer of **5***Aa*. Unfortunately we have not been able to repeat this observation. The probe of our spectrometer was at that time cracked (unknown to us) and we now do not know if the observed peak was real or an artefact of the spectrometer or experiment. It should be pointed out that at that temperature, much of the dissolved material has precipitated out and the solution is on the verge of freezing. We now observe a small peak (ca. 0.6H) at δ 6.0 at ca. −110° to −115°C both on a 90 MHz and 60 MHz instrument (see Fig. 1), which is not a spinning side band, which we were not able to see previously. The sample of **5***Aa* used is identical to the previous samples in all other respects. Examination of molecular models of **5***a* and **5***b* indicates immediately the considerably lower steric demand of an —H than of a $-CH_3$. The models of *anti*-**5***Aa* and **5***Ba* are considerably less stepped than those of the methyl derivatives **5***Ab* and **5***Bb* (see Fig. 2), and hence a chemical shift of δ 6 for the internal hydrogen of *anti*-**5***Aa* is not unreasonable.[2]

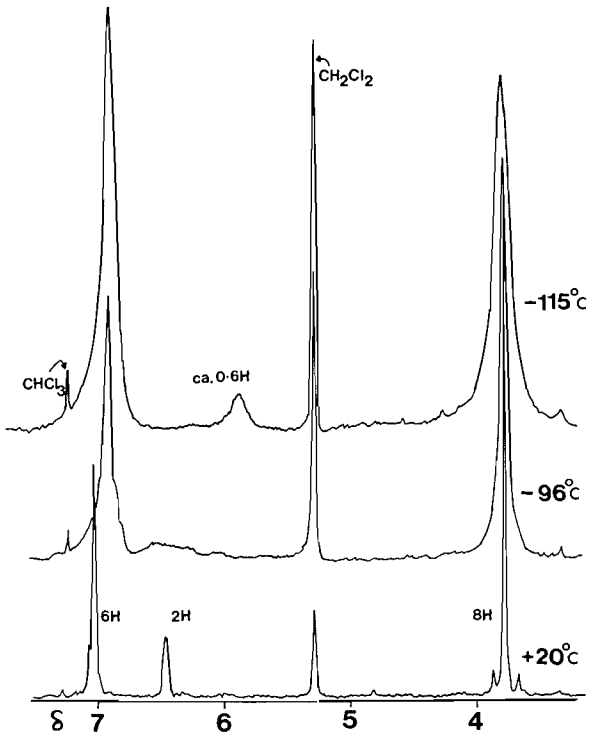


FIG. 1. The ^{1}Hmr spectrum (90 MHz) of **5***Aa* at +20°C, −96°C, and ca. −115°C in $CDCl_3$–CD_2Cl_2 (1:3).

Without being certain as to the exact chemical shift of the internal hydrogens of *anti*-**5***Aa* it is not possible to calculate exactly the relative contributions of the *syn*- and *anti*-conformers. If the δ 6 peak is definitely due to *anti*-**5***Aa*, then from the position of the fast exchanging peak at room temperature of δ 6.5, the relative contributions of *syn*:*anti* would be ca. 1:1. If the previously observed peak at δ 4.5 is correct, the contributions of *syn*:*anti* would be about 4:1. In either case, and together with the

[2]Since many conformers of *anti*-**5***Aa* are possible, which vary depending on the relative orientation of the methylene bridges and selenium atoms, it is possible that now a different conformer than previously is being frozen out.

Can. J. Chem. Downloaded from www.nrcresearchpress.com by 210.87.254.5 on 09/05/12
For personal use only.

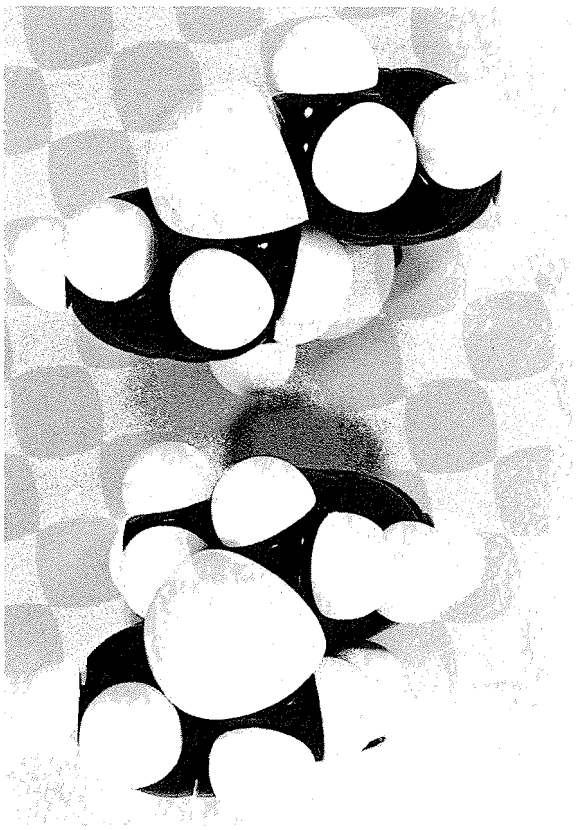


FIG. 2. CPK Models of anti-cyclophanes **5***Ba* (top) and **5***Bb* (bottom).

information that the integrated peak areas for the δ 4.5 peak were 0.8H[3] and for the δ 6 peak 0.6H,[3] we can conclude that as in the case of thiacyclophane **5***Ba*, the *syn*-conformer seems to be preferred. We hope to verify this by X-ray measurements, and also gain some insight as to why *anti*-selenaphane **5***Aa* may be a greater contributor to the *syn–anti* equilibrium than *anti*-thiaphane **5***Ba*. When an ^{1}Hmr sample of selenaphane **5***Aa* is heated (in hexachlorobutadiene) the chemical shift[4] of the internal hydrogens increases from δ 6.32 to δ 6.47, somewhat more than the 0.03 ppm observed for **5***Ba* (15). This possibly indicates a larger change in the position of the *syn–anti* equilibrium in this case than for the thiacyclophanes (which are nearly pure *syn*), consistent with the shift data discussed above. Pertinent also is that the chemical shifts[4] of the dimethyl derivative **5***Ab* over the same temperature range in the same solvent are almost invariant (< ±0.02 ppm). The internal —CH_3 hydrogen signal remains sharp over the range −40°C to +160°C indicating no major conformational change is taking place. The signal for the —CH_2— bridge protons is sharper at −30°C and at +150°C than it is at 60°C when it has partially collapsed into the baseline (Supplementary Figure deposited[4]) indicating that these protons are undergoing a conformational change, possibly a bridge wobble. No significant change[4] is observed in the ^{1}Hmr spectrum of the trimer **8***Aa* over the temperature range +35°C to −110°C.

The ^{13}Cmr spectrum is shown in Table 1 in comparison to several related cyclophanes. The internal aryl carbons (A) are strongly deshielded in the known *anti*-cyclophanes **10** and **11** (1*f*) by about 6–8 ppm from their position in *m*-xylene. In the *syn*-cyclophanes, **5***Ba* and **9**, this is much reduced to 2–3 ppm. Clearly selenaphane, **5***Aa*, most closely resembles the *syn*-series in this respect, consistent with the ^{1}Hmr data. Considering the closeness in chemical shift of the methylene protons of **5***A* and **5***B*, it is somewhat surprising that the chemical shift of the methylene bridge carbons (E) of the selenaphane **5***Aa* are at 9.9 ppm higher field than those of the thiaphane **5***Ba*. The $^1J_{(^{13}C—^{77}Se)}$ coupling constant can be determined from the small side bands to this peak and in **5***Aa* is 65.3 Hz. The $^1J_{(^{13}C—H)}$ coupling constants can be readily determined from the gated spectra and are given in Table 1. Our assignments from these spectra are consistent with those of the thiaphane **5***Ba* (1*f*).

Reactions

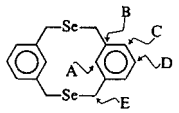
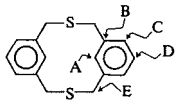
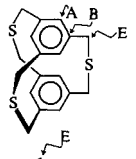
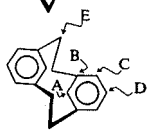
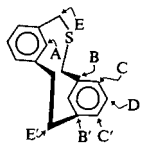
The initial route (7,6) from **5***Bb* to **3***b* involved a Stevens rearrangement of the sulphonium salt **5***Db* to give **1***Db*. While the selenaphane **5***Aa* could be readily methylated with dimethoxycarbonium fluoroborate (20) to give the bis-selenonium salt **5***Ca* in 62% yield, the salt, on attempted rearrangement with either potassium *tert*-butoxide or sodium hydride in tetrahydrofuran (THF), failed to give **1***Ea*, but rather the molecule cleaved to give an oily product, which by ^{1}Hmr contained αα′-bis(methylseleno)-*m*-xylene **6***Ea*. Cleavage of the C—Se bond by strong bases such as butyl lithium was first discovered by Gilman (20) and has been extensively studied by Seebach and Peleties (21) and Krief and co-workers (22) and subsequently avoided by ourselves (23) as well as others (24) by use of lithium dialkylamides when deprotonation of a selenide was required. We were, however, somewhat surprised that easy cleavage occurred with poorer nucleophiles such as *tert*-butoxide and hydride. At that time, no alternative to the Stevens

[3]Average of five spectra. Entirely *anti*-conformer would yield a 2H integration value.

[4]A complete set of data is available, at a nominal charge, from the Depository of Unpublished Data, CISTI, National Research Council of Canada, Ottawa, Ont., Canada K1A 0S2.

Can. J. Chem. Downloaded from www.nrcresearchpress.com by 210.87.254.5 on 09/05/12
For personal use only.

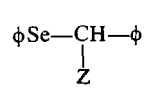
TABLE 1. ^{13}Cmr data[a] for selected cyclophanes

		A	B	C	D	E	Reference
5*Aa*		131.4 (157.4)[b]	137.6 —	127.0 (156.6)	128.6 (159.3)	27.8 (141.2)	This work
5*Ba*		131.6 (157.0)	136.8 —	126.8 (158.4)	128.2 (160.0)	37.7 (138.2)	1*f*, 15 This work
9		130.4	137.2			3.87	15
10		136.3	138.6	125.1	128.6	41.4	1*f*
11		134.3	134.7 139.6	126.5 126.8	128.6	39.0 35.2	1*f*

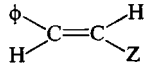
[a]In ppm downfield from Me_4Si, $CDCl_3$.
[b]Values for $^1J_{^{13}C-H}$ are given in parentheses, in Hz.

rearrangement was known. We thus decided that it might be possible to synthesize the desired cyclophane **1***Ea* by an alternate route. It occurred to us then that the selenide function might not only be used in the elimination step but also to build up the carbon skeleton. Since Sharpless *et al.* (25) had been able to alkylate the anion of $\phi SeCH_2CO_2Et$ with alkyl halides, it seemed reasonable to expect that $\phi SeCH_2\phi$, **12**, would behave similarly.[5]

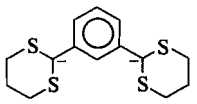
Benzyl phenyl selenide, **12**, was prepared in essentially quantitative yield by reaction of benzyl bromide with NaSeϕ (prepared from ϕSeSeϕ and $NaBH_4$ (13)) in refluxing ethanol, as white plates, mp 32–33°C. This could be benzylated by treatment with lithium di-isopropylamide at 0°C in dry THF, followed by more benzyl bromide, and gave an 87% yield of the selenide **12***a*. The latter on treatment with 30% H_2O_2 in THF at room temperature gave a quantitative yield of *trans*-stilbene **13***a*. There was no need to isolate the intermediate selenide, **12***a*, and the whole sequence could be effected easily in one pot. Thus reaction of the anion of **12** with benzyl bromide, ethyl bromide, and methyl iodide respectively followed by H_2O_2 gave **13***a* (81%), **13***b* (80%), and **13***c* (76%). Subsequently many similar reactions have been reported by others and the whole area has been covered by an excellent review (26). Hylton and Boekelheide (27) had shown that it was possible to alkylate the dianion **14** with *m*-xylylene dibromide



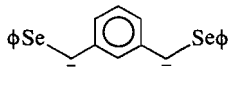
12 Z = H
12*a* Z = $CH_2\phi$
12*b* Z = CH_2CH_3
12*c* Z = CH_3



13*a* Z = ϕ
13*b* Z = CH_3
13*c* Z = H



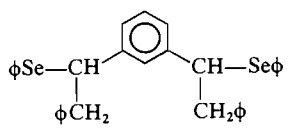
14



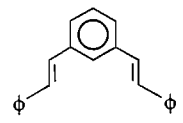
15

6*Aa*, hence we anticipated no problem with similar alkylation of **15** provided that the dianion could be generated. α,α′-Bis(phenylseleno)-*m*-xylene **6***Ma* was obtained in 91% yield as colourless plates mp 41–42°C from *m*-xylylene bromide and NaSeϕ. Treatment with lithium di-isopropylamide and then D_2O indicated that a dianion had formed (^{1}Hmr, ms analysis). That this was the desired dianion **15**, and

[5]Preliminary report: ref. 23.



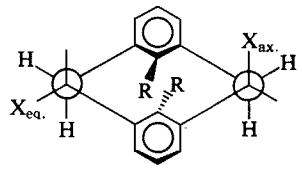
16



17

that this could be bis-alkylated, was shown by addition of benzyl bromide to give the selenide **16**, which showed a molecular ion at *m/e* 598 and gave in its ^{1}Hmr spectrum the 24 aryl hydrogens at δ 6.4–7.8, the 2 methine hydrogens as a triplet at δ 4.39, and the 4 methylene hydrogens as a doublet at δ 3.19. Further treatment of **16** with H_2O_2 at room temperature in THF gave a quantitative yield of *trans-m*-distyryl benzene, **17**, mp 169–170°C (lit. (28) mp 169.5–170°C). When a solution of the dianion **15** (bright yellow) was added dropwise to THF at the same rate as a solution of the bromide **6***Aa*, the colour of the anion was immediately discharged. Chromatography of the reaction mixture yielded only a few mg of the desired cyclophane **1***Ma*, recognised by comparison to an authentic sample prepared by a different route (described below). The major products of this reaction appeared to be higher linear oligomers on the basis of mass spectroscopy. Although this route had failed to yield **1***Ma* in any great yield, it led us to the realisation that it should be possible to generate the dianion of **5** by treatment with a strong base, and that such a dianion might undergo a (Wittig) rearrangement analogous to the Stevens rearrangement of sulphonium salts. Such rearrangement of **5***B* and a number of related compounds to **1***D* occurred (10) smoothly with either butyl lithium or lithium diisopropylamide. When the latter was added to selenaphane **5***Aa*, rearrangement occurred rapidly and after addition of MeI, cyclophane **1***Ea* was obtained as a waxy, foul smelling solid. Its structure was confirmed by the molecular ion at *m/e* 396 in its mass spectrum and by its ^{1}Hmr spectrum which showed the 6 aryl hydrogens at δ 7.5–6.9, the internal hydrogens at δ 5.10 and δ 5.50, and the —$SeCH_3$ hydrogens at δ 1.92 with the remaining hydrogens as a multiplet at δ 4.1–2.0, very similar to the spectrum observed for the analogous **1***Da*. However, after conversion of this product to the selenoxide, no spontaneous elimination occurred, either at room temperature, at 80°C, or on stirring with anhydrous $MgSO_4$. We considered at this time whether this might be due to the fact that we were attempting the elimination of MeSeOH, whereas nearly all the previous literature examples had eliminated φSeOH. We thus decided that the elimination should be tried on the phenyl selenoxide **1***Na*. Attempted generation of selenide **1***Ma* from **1***Fa* by treatment with NaSeφ failed; however, at that time Otsubo and Boekelheide (9) reported the benzyne induced Stevens rearrangement of **5***Ba* to give **1***Ja*, and subsequent thermolysis of its sulfoxide, **1***Ka* to give pyrene in 37% yield.

Reaction of selenaphane **5***Aa* with benzyne (generated from anthranilic acid and butyl nitrite) gave, after chromatography, 75% of the desired cyclophane **1***Ma*, mp 189–191°C. Its structure was readily confirmed by analysis, molecular ion at *m/e* 520, and ^{1}Hmr spectrum. Similarly the dimethyl cyclophane **5***Ab* gave **1***Mb*, in which the characteristic internal —CH_3 signals in the ^{1}Hmr spectrum could be clearly seen at δ 0.9 and 1.2. However, when **1***Ma* was stirred with H_2O_2 in THF at room temperature, only a very low yield of pyrene was obtained. No dihydropyrene **3***b* was obtained from **1***Mb*. Clearly the selenoxide elimination in the cyclophanes **1** is a much less facile elimination than in alicyclic examples. Fragmentation of selenoxides is a *syn* elimination process (25). Attainment of the *syn*-conformation of **1** may be difficult in the case of the cyclophanes because of the rigidity of the molecule caused by the strain in these systems (1*a*, 29). On examination of models, it does not much matter whether the substituents X in **1** are in the axial or equatorial positions as shown, since rotation about the C—C bridge bond, to bring X *syn* with H, thrusts one benzene ring into the other in either case. That this may be less serious when R = H, may be the reason why some pyrene was isolated from **1***Na*, yet no **3***b* from **1***Nb* when R = CH_3. Presumably this barrier can be overcome by going to high temperatures, as is the case in the sulfoxide pyrolysis (9), but then the method offers no advantage since the selenium compounds are significantly less accessible.



SCHEME 1. Newman projection of an isomer of **1**.

Experimental

All melting points were determined on a Kofler hot stage and are uncorrected. The ^{1}Hmr spectra were determined in $CDCl_3$ (unless otherwise stated) on a Perkin-Elmer R12A (60 MHz) or R32 (90 MHz) spectrometer and are reported in ppm downfield from tetramethylsilane as internal standard. The ^{13}Cmr spectra were determined in $CDCl_3$ on a Nicolet TT-14 Fourier transform spectrometer operating at 15.1 MHz. Mass spectra were determined on a Hitachi-Perkin-Elmer RMU-7 or Finnigan 3300 mass spectrometer at 70 eV. Microanalyses were performed by this department. All evaporations were carried out under reduced

Can. J. Chem. Downloaded from www.nrcresearchpress.com by 210.87.254.5 on 09/05/12
For personal use only.

Can. J. Chem. Downloaded from www.nrcresearchpress.com by 210.87.254.5 on 09/05/12
For personal use only.

pressure on a rotary evaporator at ca. 40°C. Extracts were dried with anhydrous sodium sulfate.

*2,11-Diselena[3,3]metacyclophane, 5*Aa

A solution of *m*-xylylene dibromide, **6***Aa*, (10.6 g, 40 mmol) in dry N_2-purged DMF (50 mL) was added under N_2 at room temperature in one portion to a well stirred solution of anhydrous Na_2Se (Alfa, 6.0 g, 48 mmol) in dry DMF (100 mL). After 12 h, the solvent was removed under vacuum, and water and dichloromethane were added. The organic layer was washed well with water, dried, and evaporated. The residue was chromatographed on silica gel (200 g) using pentane–benzene (or CH_2Cl_2) (85:15) as eluant to yield firstly the dimer, ~520 mg (7.1%) as pale yellow crystals from ethanol or cyclohexane, mp 121–122°C; ^{1}Hmr (90 MHz) δ: 7.04 (bs, 6H, ArH), 6.46 (bs, 2H, internal ArH), and 3.78 (s, 8H, —CH_2—); ms, molecular ion at *m/e* 368 ($C_{16}H_{16}{}^{80}Se_2$) with correct isotope pattern for Se_2 (14). *Anal.* calcd. for $C_{16}H_{16}Se_2$: C 52.48, H 4.40; found: C 52.16, H 4.47.

Eluted next was the cyclic trimer, 2,11,19-triselena-[3,3,3]metacyclophane, **8***Aa*, 600 mg (8%), as pale yellow crystals from cyclohexane, mp 130–132°C; ^{1}Hmr (90 MHz) δ: 7.20 (s, 9h, ArH), 7.06 (bs, 3H, internal ArH), and 3.60 (s, 12H, —CH_2—); ms, molecular ion at *m/e* 552 (correct isotope pattern for Se_3). *Anal.* calcd. for $C_{24}H_{24}Se_3$: C 52.48, H 4.40; found: C 52.37, H 4.36. Essentially the same results were obtained when either dimethyl sulphoxide or hexamethylphosphorictriamide were used as solvents.

*Stevens Rearrangement of Selenide 5*Aa

*(a) Bis-selenonium Salt 5*Ca

A solution of the selenide **5***Aa* (800 mg, 2.18 mmol) in CH_2Cl_2 (10 mL) was added to a stirred suspension of dimethoxycarbonium fluoroborate (20) (6.1 mmol) in CH_2Cl_2 (10 mL) under N_2 at −30°C. The mixture was stirred without further cooling for 4 h, when ethyl acetate was added. The mixture was stirred with ethyl acetate until a clean precipitate of bis-salt **5***Ca* formed, which was collected by filtration and dried to yield 767 mg (62%) of powder, dec. ~200°C. *Anal.* calcd. for $C_{18}H_{18}B_2Se_2F_8$: C 38.20, H 3.21; found: C 38.46, H 3.46.

(b) Rearrangement

Potassium *tert*-butoxide (148 mg, 1.33 mmol) was added under N_2 to a stirred suspension of the bis-salt from (*a*) above (250 mg, 0.44 mmol) in dry THF (10 mL). After 15 min, H_2O, aqueous HCl, and CH_2Cl_2 were added, and the organic layer was washed, dried, and evaporated. The residual oil gave ^{1}Hmr (60 MHz) δ: 7.1 (bs, 4H, ArH), 3.62 (s, 4H, Ar*CH*$_2$Se—), and 1.83 (s, 6H, —$SeCH_3$) which indicated its structure to be αα′-bis(methylseleno)-*m*-xylene, **6***Ea*.

*Wittig Rearrangement of Selenide 5*Aa

(a) Using Lithium Diisopropylamide

A solution of *i*-Pr_2NLi (1.1 mmol, prepared from *n*-BuLi and *i*-Pr_2NH) in dry THF (5 mL) was added under N_2 at 0°C to a solution of the diselenide **5***Aa* (183 mg, 0.50 mmol) in dry THF (10 mL). After ca. 2 min, methyl iodide was added until the dark green-brown colour was just discharged. Water, CH_2Cl_2, and aqueous HCl were then added, and the organic layer was washed, dried, and evaporated. The residue was chromatographed on silica gel (140 g) using pentane–benzene (4:1) as eluant to yield firstly mixed isomers of cyclophane **1***Ea*, 95 mg (48%) as a waxy, foul smelling solid; ^{1}Hmr (90 MHz) δ: 7.5–6.9 (m, 6H, ArH), 5.50 and 5.10 (bs, ~1H each, internal ArH), 4.1–2.0 (m, 6H, —CH—CH_2—), and 1.92 (s, 6H, —$SeCH_3$); ms, molecular ion at *m/e* 396 (correct isotope pattern).

When this product was dissolved in THF (60 mL) and 30% H_2O_2 (6 mL) was added, the mixture first became cloudy and then clarified. Thin layer chromatography indicated no cyclophane diene **2***a* or pyrene to be present. This result was not changed on stirring with anhydrous $MgSO_4$ for 24 h or on reflux for 4 h.

(b) Using Benzyne

A solution of anthranilic acid (250 mg) in dry THF (5 mL) was added dropwise over 1 h to a refluxing solution of selenide **5***Aa* (127 mg, 0.35 mmol) and butyl nitrite (500 mg) in dry THF (20 mL) under N_2. After heating under reflux for a further hour, the reaction mixture was cooled and H_2O, aqueous HCl, and CH_2Cl_2 were added. The organic layer was washed, dried, and evaporated. The residue was chromatographed on silica gel (35 g) using pentane–benzene (7:3) as eluant to yield crystalline product **1***Ma*, 136 mg (75%) as white crystals from cyclohexane, mp 189–191°C; ^{1}Hmr (60 MHz) δ: 7.8–6.5 (m, ~16H, ArH), 5.7–5.2 (m, ~2H, internal ArH), and 5.0–2.0 (m, ~6H, —CH—CH_2—); ms, molecular ion at *m/e* 520 (correct isotope pattern). *Anal.* calcd. for $C_{28}H_{24}Se_2$: C 64.87, H 4.67; found: C 64.61, H 4.58.

Oxidation and Elimination

The selenide **1***Ma* from (*b*) above (130 mg) was stirred at room temperature in THF (15 mL) with 30% H_2O_2 (5 mL) for 50 h. The products were extracted into ether and chromatographed on silica gel to yield 1 mg (2%) of pyrene, identified by tlc, uv, and ^{1}Hmr comparison to an authentic sample.

*9,18-Dimethyl-2,11-diselena[3,3]metacyclophane, 5*Ab

From 2,6-bis(bromomethyl)toluene **6***Ab* (6) (11.1 g) and Na_2Se (6.0 g) in DMF as described above for **5***Aa*, there was obtained after chromatography, firstly 555 mg (7%) of dimer **5***Ab*, as very pale yellow crystals from cyclohexane, mp 185–187°C; ^{1}Hmr (90 MHz) δ: 6.97 (s, 6H, ArH), 3.69 (s, 8H, —CH_2—), and 1.77 (s, 6H, —$ArCH_3$); ms, correct molecular ion and isotope pattern for $C_{18}H_{20}Se_2$ at *m/e* 396.

Eluted next was the cyclic trimer (9,17,26-trimethyl-2,11,19-triselena[3,3,3]metacyclophane) **8***Ab*, mp ~186°C from benzene; ^{1}Hmr (60 MHz) δ: 7.00 (s, 9H, ArH), 3.67 (s, 12H, —CH_2—), and 2.05 (s, 9H, $ArCH_3$); ms, correct molecular ion for $C_{27}H_{30}Se_3$ at *m/e* 594.

*Wittig Rearrangement and Attempted Elimination of 5*Ab

From the dimer **5***Ab* (300 mg) and benzyne (excess) as described above for **5***Aa*, there was obtained 525 mg of oily residue, which contained the mixed cyclophane isomers **1***Mb* as indicated by ^{1}Hmr (60 MHz) δ: 7.7–6.9 (m, ArH), 4.0 and 3.7 (t, —*CH*—CH_2—), 2.3–1.7 (m, —CH—*CH*$_2$), and 1.2 and 0.9 (s, internal —CH_3). When these were stirred at room temperature or heated under reflux with 30% H_2O_2 in THF solution, no dimethyldihydropyrene **3***b* could be detected.

Benzyl Phenyl Selenide, 12

Sodium borohydride (3.87 g, 102 mmol) was added in batches to a solution of diphenyl diselenide (15.6 g, 50 mmol) in absolute ethanol (250 mL). Benzyl bromide (17.1 g, 100 mmol) in benzene (50 mL) was then added to the resultant colourless solution of NaSeφ. After refluxing for 2 h, the reaction mixture was cooled and evaporated. The residue was extracted with water and ether, and the organic layer washed, dried, and evaporated to yield quantitatively the product **12**, as an oil, which solidifies on standing and gives white plates from ethanol, mp 32–33°C; ^{1}Hmr (90 MHz) δ: 7.5–6.8 (m, 10H, ArH) and 4.00 (s, 2H, —CH_2—); ms, molecular ion (correct isotope pattern) at *m/e* 248. *Anal.* calcd. for $C_{13}H_{12}Se$: C 63.16, H 4.89; found: C 62.87, H 4.92.

Can. J. Chem. Downloaded from www.nrcresearchpress.com by 210.87.254.5 on 09/05/12
For personal use only.

Benzylation of Benzyl Phenyl Selenide to Give **12**a

A solution of selenide **12** (4.94 g, 20 mmol) in dry THF (20 mL) was added dropwise under N_2 at 0°C to a solution of *i*-Pr_2NLi (20 mmol, prepared from *n*-BuLi and *i*-Pr_2NH) in dry THF (30 mL). Benzyl bromide (3.42 g, 20 mmol) in dry THF (10 mL) was then added dropwise to the dark green reaction mixture at 0°C, which was immediately decolorized. Ether, water, and aqueous HCl were then added, and the organic layer was washed, dried, and evaporated. Chromatography of the residual oil on silica gel (140 g) using pentane as eluant gave the pure product **12***a*, 5.87 g (87%) as a colourless oil; ^{1}Hmr (60 MHz) δ: 7.5–6.8 (m, 15H, ArH), 4.43 (t, J = 8 Hz, 1H, —C*H*—CH_2), and 3.26 (d, J = 8 Hz, 2H, —CH—C*H*$_2$—); ms, molecular ion (correct isotope pattern) at *m/e* 338. *Anal.* calcd. for $C_{20}H_{18}Se$: C 71.21, H 5.38; found: C 70.89, H 5.25.

Oxidation and Elimination to Stilbene

30% H_2O_2 (20 mL) was added to a solution of the selenide **12***a* in THF (100 mL) at room temperature. The reaction mixture was then either stirred at room temperature for 18 h, or in the presence of anhydrous $MgSO_4$ for 4 h, or refluxed for 2 h. In each case the yield of *trans*-stilbene (identical mp, ^{1}Hmr, tlc to an authentic sample) isolated after extraction into ether was quantitative.

General Procedure for in-situ *Alkylation, Oxidation, and Elimination to Yield* trans-*Alkenes*

The selenide **12** (10 mmol) in dry THF (10 mL) was added dropwise under N_2 at 0°C to a soln of *i*-Pr_2NLi (10 mmol) in dry THF (15 mL), followed by the halide (10 mmol), also dropwise in dry THF (5 mL). After 10 min, THF (50 mL) and 30% H_2O_2 (20 mL) were added. The reaction was stirred for 12 h and then ether, water, and aqueous HCl were added. The organic layer was washed, dried, and evaporated (or fractionally distilled) to yield virtually pure product, identical to authentic samples. (See text for yields.)

α,α′-*Bis(phenylseleno)*-m-*xylene* **6**Ma

From diphenyl diselenide (15.6 g, 50 mmol), $NaBH_4$ (3.87 g, 100 mmol), and *m*-xylylene dibromide **6***Aa* (13.2 g, 50 mmol), using the procedure described above for benzyl phenyl selenide **12**, there was obtained 18.8 g (91%) of product **6***Ma*, as colourless plates from ethanol–benzene, mp 41–42°C; ^{1}Hmr (60 MHz) δ: 7.6–6.9 (m, 14H, ArH) and 3.99 (s, 4H, —CH_2—); ms, molecular ion at *m/e* 418 ($^{80}Se_2$, correct isotope pattern). *Anal.* calcd. for $C_{20}H_{18}Se_2$: C 57.70, H 4.36; found: C 57.39, H 4.41.

Bis-benzylation of **6**Ma

From the selenide **6***Ma* (2.5 g, 6 mmol), *i*-Pr_2NLi (12 mmol), and benzyl bromide (12 mmol) in dry THF (35 mL), using the procedure described above for **12**, there was obtained a 90% yield of product **16**, as an oil; ^{1}Hmr (90 MHz) δ: 7.8–6.4 (m, 24H, ArH), 4.39 (t, J = 8 Hz, 2H, —C*H*—CH_2—), and 3.19 (d, J = 8 Hz, 4H, —CH—C*H*$_2$—); ms, molecular ion at *m/e* 598 ($^{80}Se_2$, correct isotope pattern). *Anal.* calcd. for $C_{34}H_{30}Se_2$: C 68.46, H 5.07; found: C 68.84, H 5.13

Oxidative elimination using H_2O_2–THF as described above gave an essentially quantitative yield of *m*-distyrylbenzene, **17**, mp 169–170°C (lit. (28) mp 169.5–170°C); ^{1}Hmr (60 MHz) δ: 7.2–7.7 (m, 14H, ArH) and 7.11 (s, 4H, —CH=CH—).

Cycloalkylation of **6**Ma *with* m-*Xylylene Dibromide,* **6**Aa*; Cyclophane* **1**Ma

A solution of dianion **15** in dry THF (50 mL) was prepared in a needle valve dropping funnel from selenide **6***Ma* (6 mmol) and *i*-Pr_2NLi (12 mmol), and was added dropwise over 2 h at the same rate as a solution of *m*-xylylene dibromide **6***Aa* (6 mmol) in dry THF (50 mL) was added from a second funnel, to vigorously stirred dry THF (50 mL) under N_2. The strong colour of the dianion was decolorized by the bromide on each drop. After 12 h the solvents were evaporated, and water, aqueous HCl, and CH_2Cl_2 were added. The organic layer was washed, dried, and evaporated. The residue was chromatographed on silica gel and yielded a few mg of the product **1***Ma*, recognised by tlc and ^{1}Hmr comparison to that obtained above. Several products were also obtained which on the basis of ms/^{1}Hmr were probably linear tri, tetra, and polymer.

Acknowledgements

I thank the National Research Council of Canada[6] and the University of Victoria for support of this investigation, and Mr. Blaine Hawkins for the illustrative photography.

1. (*a*) T. Sato, M. Wakabayashi, M. Kainosho, and K. Hata. Tetrahedron Lett. 4185 (1968); Tetrahedron, **27**, 2737 (1971); (*b*) F. Vögtle and L. Schunder. Chem. Ber. **102**, 2677 (1969); (*c*) F. Vögtle, R. Schäfer, L. Schunder, and P. Neumann. Ann. **734**, 102 (1970); (*d*) F. Vögtle and P. Neumann. Tetrahedron, **26**, 5299 (1970); (*e*) F. Vögtle, W. Wieder, and H. Förster. Tetrahedron Lett. 4361 (1974); (*f*) T. Takemura and T. Sato. Can. J. Chem. **54**, 3412 (1976).
2. F. Vögtle and P. Neumann. Synthesis, 85 (1973); V. Boekelheide, D. I. Reingold, and M. Tuttle. Chem. Commun. 406 (1973); J. Bruhin and W. Jenny. Tetrahedron Lett. 1215 (1973); T. Umemoto, T. Otsubo, and S. Misumi. Tetrahedron Lett. 1573 (1974).
3. R. H. Mitchell. Heterocycles, **11**, 563 (1978).
4. R. H. Mitchell. Tetrahedron Lett. 1363 (1975).
5. K. B. Sharpless, M. W. Young, and R. F. Lauer. Tetrahedron Lett. 1979 (1973); D. L. J. Clive. Chem. Commun. 695 (1973); H. J. Reich, I. L. Reich, and J. M. Renga. J. Am. Chem. Soc. **95**, 5813 (1973).
6. R. H. Mitchell and V. Boekelheide. J. Am. Chem. Soc. **96**, 1547 (1974).
7. R. H. Mitchell and V. Boekelheide. Tetrahedron Lett. 1197 (1970).
8. J. R. Davy and J. A. Reiss. Tetrahedron Lett. 3639 (1972); P. J. Jessup and J. A. Reiss. Aust. J. Chem. **30**, 843 (1977).
9. T. Otsubo and V. Boekelheide. Tetrahedron Lett. 3881 (1975).
10. R. H. Mitchell, T. Otsubo, and V. Boekelheide. Tetrahedron Lett. 219 (1975).
11. D. L. Klayman. *In* Organic selenium compounds: their chemistry and biology. *Edited by* D. L. Klayman and W. H. H. Gunther. Wiley-Interscience, New York, NY. 1973. Chapt. IV.
12. R. H. Mitchell. Can. J. Chem. **54**, 238 (1976).
13. D. L. Klayman and T. S. Griffin. J. Am. Chem. Soc. **95**, 197 (1973).
14. L. B. Agenäs. *In* Organic selenium compounds: their chemistry and biology. *Edited by* D. L. Klayman and W. H. H. Gunther. Wiley-Interscience, New York, NY. 1973. Chapt. XV.
15. W. Anker, G. W. Bushnell, and R. H. Mitchell. Can. J. Chem. **57**, 3080 (1979).

[6]Now called Natural Sciences and Engineering Research Council of Canada.

16. B. R. DAVIS and I. BERNAL. J. Chem. Soc. B, 2307 (1971).
17. I. L. KARLE and J. KARLE. *In* Organic selenium compounds: their chemistry and biology. *Edited by* D. L. Klayman and W. H. H. Gunther. Wiley-Interscience, New York, NY. 1973. Chapt. XV.
18. O. KENNARD. *In* Handbook of chemistry and physics. 56th ed. *Edited by* R. C. Weast. CRC Press, Cleveland, OH. 1975. F211.
19. A. J. GORDON and R. A. FORD (*Editors*). The chemist's companion. John Wiley and Sons, New York, NY. 1972. p. 82.
20. H. GILMAN and F. J. WEBB. J. Am. Chem. Soc. **71**, 4062 (1949).
21. D. SEEBACH and N. PELETIES. Angew. Chem. Int. Ed. Engl. **8**, 450 (1969); Chem. Ber. **105**, 511 (1972).
22. W. DUMONT, P. BAYET, and A. KRIEF. Angew. Chem. Int. Ed. Engl. **13**, 804 (1974).
23. R. H. MITCHELL. J. Chem. Soc. Chem. Commun. 990 (1974).
24. H. J. REICH, F. CHOW, and S. K. SHAH. J. Am. Chem. Soc. **101**, 6638 (1979).
25. K. B. SHARPLESS, R. F. LAUER, and A. Y. TERANISHI. J. Am. Chem. Soc. **95**, 6137 (1973).
26. D. L. J. CLIVE. Tetrahedron, **34**, 1049 (1978).
27. T. HYLTON and V. BOEKELHEIDE. J. Am. Chem. Soc. **90**, 6887 (1968).
28. E. R. BLOUT and V. W. EAGER. J. Am. Chem. Soc. **67**, 1315 (1945).
29. E. LANGER and H. LEHNER. Tetrahedron Lett. 1357 (1974); C. GLOTZMANN, E. HASLINGER, E. LANGER, and H. LEHNER. Monatsh. **106**, 187 (1975).

Can. J. Chem. Downloaded from www.nrcresearchpress.com by 210.87.254.5 on 09/05/12
For personal use only.

Complex fluoroanions in solution. XI. Complexes of silicon, germanium, and titanium tetrafluorides with simple anions[1]

S. BROWNSTEIN

Division of Chemistry, National Research Council of Canada, Ottawa, Ont., Canada K1A 0R9

Received February 22, 1980

S. BROWNSTEIN. Can. J. Chem. **58**, 1407 (1980).

A fluorine-bridged silicon fluoroanion and many hexa-co-ordinate germanium and titanium fluoroanions have been identified in solution via fluorine magnetic resonance. A generalized shceme is used to correlate all fluorine chemical shift data for hexa-co-ordinate fluorine containing species.

S. BROWNSTEIN. Can. J. Chem. **58**, 1407 (1980).

Nous avons identifié en solution, à l'aide de la resonance magnétique nucleaire de fluor, un fluoroanion du silicium ponté par une atome de fluor ainsi que plusiers fluoroanions du germanium et du titane hexa coordonnés. On utilise un schéma général pour mettre en corrélation toutes les donnés concernant le déplacement chimique de fluors pour les espéces hexa coordonnées contenant du fluor.

Introduction

Complexes of SiF_4 have been reported with some organic bases (1) and with the anions of a few dibasic organic acids (2). A complex was observed with trifluoroacetate (3) but not with fluorosulfate nor trifluoromethanesulfonate anions (4). In the present study the reaction of SiF_4 with a wide range of anions was investigated. Although fluorine bridged complex fluoroanions have been identified with tin and titanium they have not been observed for silicon (5).

There have been more extensive studies of GeF_4 complexes, including complexes with neutral oxygen- and nitrogen-containing organic compounds (1, 6), the anions of some carboxyllic acids (2), and SCN^- and OCN^- (7, 8). Complexes of SnF_4 have been thoroughly studied (9). Homopolymeric fluoroanions of titanium have been described (5), as well as heterospecies with partially oxygenated molybdenum and tungsten species (10). Complexes with the ligands SCN^- and OCN^- have been described (11), as well as with trifluoroacetate, fluorosulfate, and trifluoromethanesulfonate (3, 4). The purpose of the present article is to identify new fluorine bridged complex fluoroanions and to correlate the fluorine chemical shifts of all hexa-co-ordinate fluoride species, regardless of central atom.

Some of the anions employed in this study are potentially bidentate. As an example acetate ion has been shown, by X-ray diffraction studies, to co-ordinate with a central atom via one (12) or both (13) of its oxygen atoms. It does not appear that infrared frequency shifts are adequate to unambiguously decide between the two kinds of co-ordination (14).

Experimental

Fluorine resonance spectra were obtained at 94.18 MHz on a "Varian Associates" XL-100A spectrometer coupled with a "Nicolet Instruments" TT100A Fourier Transform unit. Spectral widths of 20 kHz were accumulated in 16K of memory using an rf pulse of 5 μs (45°). Normally 1000 transients were accumulated and averaged. Chemical shifts are reported in ppm with respect to internal $CFCl_3$ as zero and with shifts to high field considered negative. Samples were prepared with great care to exclude moisture using standard vacuum line and dry box techniques. Infrared spectra were recorded with potassium bromide pellets on a "Beckman Acculab 4" spectrometer.

Silicon and germanium tetrafluorides were employed directly from the cylinders. Titanium tetrafluoride was vacuum sublimed immediately before use. The tetramethyl ammonium salts were employed as previously described (15). Sulfur dioxide, methylene chloride, and acetonitrile were used as solvents (15).

Results and Discussion

Silicon tetrafluoride does not complex with bromide, chloride, perchlorate, fluorosulfate, nor trifluoromethanesulfonate anions. It forms 1:1 complexes with trifluoroacetate, acetate, thiophenolate, chlorate, formate, nitrite, nitrate, azide, cyanide, and thiocyanate ions. The chemical shifts and spin coupling constants for these complexes are listed in Table 1. The values reported are for sulfur dioxide solutions at −75°C unless otherwise noted. In every case except one, to be discussed further in this presentation, change in the ratio of anion-to-SiF_4 from 1:1 to 4:1 has no effect on the chemical shift measured for the complex. Therefore it is safe to assume that formation of the 1:1 complex is essentially complete with stoichiometric quantities of reactants and that no further complex formation occurs. Only a single fluorine resonance line is observed for each of the complexes so it is not possible to assign their stereochemistry. A pentagonal bipyramid with the ligand binding at only one location seems most likely since such structures are often fluxional.

[1]NRCC No. 18310.

0008-4042/80/141407-05$01.00/0

©1980 National Research Council of Canada/Conseil national de recherches du Canada

Can. J. Chem. Downloaded from www.nrcresearchpress.com by 210.87.254.6 on 09/05/12
For personal use only.

Can. J. Chem. Downloaded from www.nrcresearchpress.com by 210.87.254.6 on 09/05/12
For personal use only.

TABLE 1. Chemical shifts and spin coupling constants of complexed SiF_4 anions

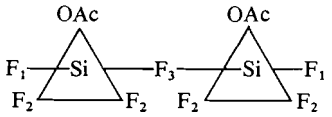
Species	δ_F	J_{Si-F}
SiF_4	−158.8	172
SiF_6^{2-}	−125.0	110
$SiF_4CF_3COO^-$	−124.9	92
$SiF_4CH_3COO^-$	−120.8	155
$SiF_4SC_6H_5^-$	−125.5	
$SiF_4ClO_3^-$	−135.7[a]	
SiF_4OOCH^-	−117.8	
$SiF_4NO_2^-$	−136.5[a]	150
$SiF_4NO_3^-$	−142.3[a]	
$SiF_4N_3^-$	−136.0[a]	132
SiF_4CN^-	−130.1	105
SiF_4SCN^-	−148.7	

[a]In CH_2Cl_2 as solvent.

In the case of acetate ion, if there is more than one equivalent of SiF_4 the fluorine resonance spectra of the solutions may be interpreted according to reaction [1].

[1] $5SiF_4 + 4OAc^- \rightleftharpoons 2[Si_2F_7(OAc)_2]^- + SiF_6^{2-}$

The species $Si_2F_7(OAc)_2^-$ is assigned the structure **I** in terms of the relationships of its fluorine



I

atoms. Similar results would be obtained if the acetate group were bidentate and attached as to give two octahedra joined at a corner. Its fluorine magnetic resonance spectrum is shown in Fig. 1.

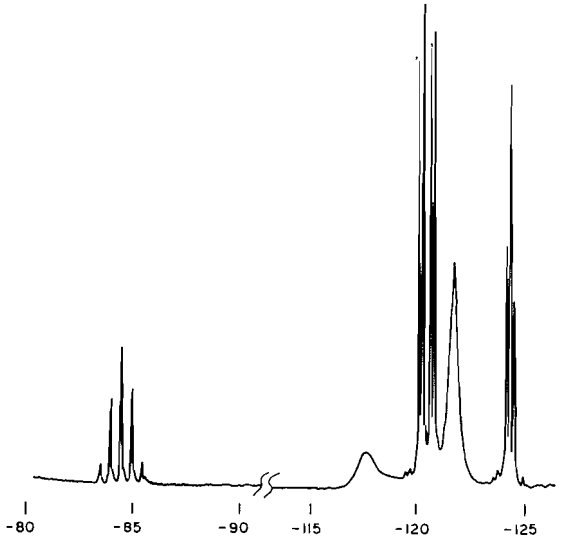
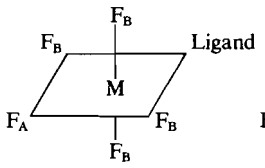


FIG. 1. The fluorine resonance spectrum of a sulfur dioxide solution of tetramethylammonium acetate and 1.20 equivalents of SiF_4 at −70°C.

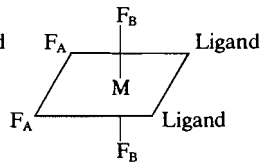
The fluorine resonance parameters of **I** are: $\delta_1 = -128.1$, $\delta_2 = -123.9$, $\delta_3 = -84.6$; $J_{1-2} = 18$ Hz, $J_{1-3} = 0$ Hz, $J_{2-3} = 52$ Hz; $J_{Si-F_1} = 120$ Hz; $J_{Si-F_2} = 120$ Hz; and were obtained by a first-order analysis. The broadened lines at −120.8 and −125.4 are from the 1:1 complex and SiF_6^{2-}. They are broadened by rapid exchange with a small quantity of unreacted SiF_4 since reaction [1] does not quite go to completion.

When 1.5 equivalents of SiF_4 are used the line from the 1:1 complex is no longer observed and the broad line which is the averaged signal of SiF_6^{2-} and SiF_4 is shifted towards the position of free SiF_4 at higher field. In Table 2 are shown the area ratios and chemical shift to be expected if reaction [1] proceeds to completion, and also the experimental values. When a solution containing more than one equivalent of SiF_4 for each acetate is evaporated to dryness under vacuum the resultant solid is SiF_4-OAc^- according to its infrared spectrum and fluorine resonance spectrum. Additional lines are sometimes observed with the other anions but it was not possible to sufficiently slow down exchange reactions to assign the lines.

Complexes of GeF_4 with various simple anions frequently disproportionate to give, amongst other products, complex anions of structure **II**.

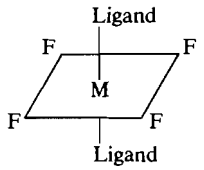


II

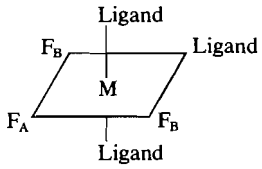


III

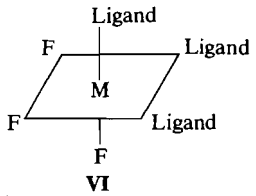
Chemical shifts and spin coupling constants for this species with a variety of ligands are listed in Table 3. The 2:1 adduct of structure **III** is the most commonly observed species. Fluorine resonance parameters for this species are listed in Table 4. Three other species which can sometimes be positively identified have structures **IV**, **V**, and **VI**.



IV



V



VI

TABLE 2. Fluorine resonance parameters for the system OAc^- and SiF_4

	Area of SiF_6^{2-} + SiF_4 / Area of SiF_4OAc^-		Area of SiF_6^{2-} + SiF_4 / Area of fluorine-2		$\delta(SiF_6^{2-} + SiF_4)$	
$[SiF_4]/[OAc^-]$	Experimental	Theoretical	Experimental	Theoretical	Experimental	Theoretical
1.20	3.0	3.0	0.96	0.75	−125.4	−125.0
1.50	∞	∞	1.37	1.25	−132	−138

TABLE 3. Fluorine resonance parameters for germanium fluoroanions of structure **II**

Ligand	δ_A [calcd]	δ_B [calcd]	J_{A-B}
NO_3^-	−130.8[−129.8]	−118.6[−120.3]	52
SCN^-	−129.0[−126.9]	−109.5[−110.5]	48.3
SCN^- [a]	−124.6[−126.9]	−109.8[−110.5]	44
OCN^- [b]	−129.5[−128.5]	−118.0[−117.4]	48
N_3^-	−121.8[−122.6]	−110.2[−113.2]	43.6
NO_2^-	−125.7[−126.2]	−117.9[−118.9]	48.5
CN^-	−121.8[−121.8]	−99.7[−103.3]	38.8

[a]Reference 7.
[b]Reference 8.

TABLE 4. Fluorine resonance parameters for germanium fluoroanions of structure **III**

Ligand	δ_A [calcd]	δ_B [calcd]	J_{A-B}
NO_3^-	−126.4[−127.4]	−121.3[−117.9]	64.1
SCN^-	−115.9[−114.7]	−97.4[−98.3]	50.7
SCN^- [a]	−111.7[−114.7]	−98.5[−98.3]	46
OCN^- [b]	−122.0[−123.2]	−110.5[−112.1]	60
N_3^-	−112.9[−113.1]	−105.5[−103.7]	52.6
NO_2^-	−122.9[−112.4]	−117.4[−115.1]	57
CN^-	−103.7[−102.4]	−91.0[−83.9]	36.8
CF_3COO^-	−122.3[−121.9]	−111.9[−111.1]	57.1
$CF_3SO_3^-$	−126.5[−125.3]	−103.6[−105.1]	69.0
FSO_3^-	−130.9[−131.5]	−110.5[−112.6]	72.5

[a]Reference 7.
[b]Reference 8.

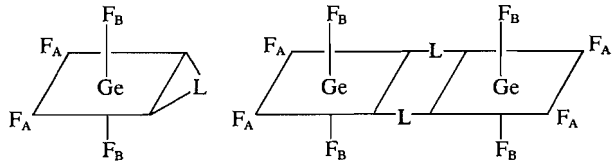
TABLE 5. Fluorine resonance parameters for germanium fluoroanions of structures **IV**, **V**, **VI**, and **VIII**

Structure	Ligand	δ_A [calcd]	δ_B [calcd]	J_{A-B}
IV	SCN^-	−99.3[−98.3]		
IV	SCN^- [a]	−98.5[−98.3]		
IV	OCN^- [b]	−113.3[−112.1]		
IV	N_3^-	−108.2[−103.7]		
IV	CN^-	−84.2[−83.9]		
IV	CF_3COO^-	−110.5[−111.1]		
IV	$CF_3SO_3^-$	−106.3[−105.1]		
IV	FSO_3^-	−112.9[−111.7]		
V	SCN^-	−102.5[−102.5]	−87.9[−86.1]	48.7
V	SCN^- [a]		−88.6[−86.1]	50
V	OCN^- [b]		−105.5[−106.8]	
V	$CF_3SO_3^-$	−114.5[−116.5]	−96.7[−96.3]	85.8
VI	SCN^-	−101.8[−102.5]		
VI	SCN^- [a]	−98.5[−102.5]		
VIII	N_3^-	−131.7	−104.2	70.8
VIII	NO_2^-	−141.2	−121.3	82.4

[a]Reference 7.
[b]Reference 8.

Their fluorine resonance parameters are listed in Table 5.

The spectrum of a representative sample is shown in Fig. 2 along with the assignments. If there are less than two equivalents of anion for each GeF_4 one observes rapid fluorine exchange between the various environments and it is not possible to further interpret the spectra. Two exceptions to the preceding statement are samples with a 1:1 ratio of GeF_4 and the anions nitrite or azide. In both these cases one gets a pair of triplets with different chemical shifts and spin coupling constants than those found in samples containing two equivalents of the anion. The symmetry required by the fluorine resonance spectra is obtained with structures **VII** and **VIII** or a trigonal bipyramid with the ligand in



VII **VIII**

an equatorial position. The latter seems least likely since it would probably be fluxional. Although the bent nitrite ion could be accommodated in either **VII** or **VIII** the linear azide ion would probably require structure **VIII**. It was found impossible to obtain pure 2:1 and 1:1 complexes of structures **III** and **VIII**, uncontaminated by the other adducts, in order to compare and further characterize the 1:1 complex. Therefore the assignment of structure **VIII** to these species must be considered tentative. Their fluorine resonance parameters are listed in Table 5.

Complexes of SnF_4 with simple anions have been reported in considerable detail (9). A scheme was devised to fit the chemical shift data for the tin fluoro complexes to the equation

$$[2] \quad \delta F = pC + qT$$

where δF is the chemical shift difference from MF_6^{2-} and p and q are the number of substituents *cis* and *trans* to the fluorine atom whose shift is calculated. This scheme also works with germanium as central atom and values for C and T are listed in Table 6. Calculated values of the chemical

Can. J. Chem. Downloaded from www.nrcresearchpress.com by 210.87.254.6 on 09/05/12
For personal use only.

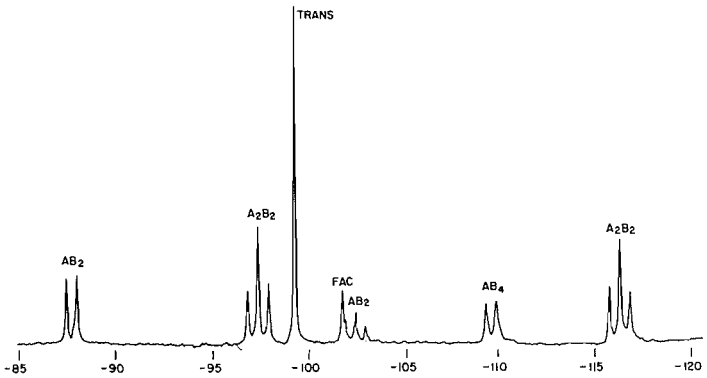


FIG. 2. The fluorine resonance spectrum of a methylene chloride solution of tetrabutylammonium thiocyanate and GeF_4 at −90°C.

TABLE 6. Substituent constants for calculations of chemical shifts for fluorogermanium and fluorotitanium ions

	Germanium		Titanium	
Substituent	*C*	*T*	*C*	*T*
ClO_4^-			54.2	−10.7
NO_3^-	2.4	−7.1		
SCN^-	12.2	−4.2	53.3	−5.7
OCN^-	5.3	−5.8		
N_3^-	9.5	0.1	28	6
NO_2^-	3.8	−3.5		
CN^-	19.4	0.9		
CF_3COO^-	5.8	−5.0	42.5	−4.3
$CF_3SO_3^-$	8.8	−11.4		
FSO_3^-	5.5	−14.3		

TABLE 7. Experimental and calculated fluorine resonance parameters for some species $TiF_4A_2^{2-}$

Substituent	Structure	Fluorine A	Fluorine B	J_{A-B}
CF_3COO^-	**III**	145.2[145]	180.3[192]	38.2
CF_3COO^-	**IV**	203.4[192]		
SCN^-	**III**	154.6[155]	207.7[214]	39.0
SCN^-	**IV**	230.6[214]		
N_3^-	**III**	140.8	163.0	35.4
ClO_4^-	**III**	150.5	215.4	34.6

shifts are also given in Tables 3–5. These results will be discussed in conjunction with those for titanium.

Stannous fluoride, plumbous fluoride and lead tetrafluoride do not appear to give soluble complexes under the conditions of this study. Titanium tetrafluoride gives *cis* and *trans* disubstituted hexafluoroanions of structures **III** and **IV** with CF_3COO^-, SCN^-, and N_3^-. Their chemical shifts are listed in Table 7 and the derived *C* and *T* values in Table 6. It should be noted that the principal lines in the fluorine resonance spectra of the reaction products of TiF_4 with tetramethylammonium and tetrabutylammonium thiocyanate in SO_2 and CH_3CN as solvents are different than those reported for the reaction between di-*n*-propylammonium hexafluorotitanate and tetrabutylammonium hexathiocyanato-*N*-titanate (11). It is assumed that under the somewhat different experimental conditions of this study sulfur–titanium rather than nitrogen–titanium bonding is being observed. Very weak lines from the nitrogen bonded species are also observed in this study. Because of the possibility for binding via nitrogen versus oxygen or sulfur for OCN^- and SCN^-, it is possible that the numbers associated with the entries for these anions might sometimes not refer to effectively the same species.

Condensed species with at least two TiF_4 units joined by fluorine bridges were also observed in the fluorine resonance spectra. Although their spectra could be fitted with plausible structures and parameters the assignments are too tentative to report.

TiF_4 is insoluble in sulfur dioxide but is brought into solution by complexing with the anions listed in Table 7. TiF_4 dissolves in acetonitrile and remains in solution upon addition of a considerable excess of methylene chloride or sulfur dioxide. The two triplets of structure **III** with acetonitrile as ligand (δ = 154.3 and 162.5, J = 34.9) are clearly resolved at −80°C in sulfur dioxide as solvent. Fluorine resonance lines, attributed to polymeric species, are the only ones observed in methylene chloride as solvent. It is possible by prior dissolution in acetonitrile to produce the perchlorate complex of structure **III** in sulfur dioxide as solvent. Only polymeric species are observed in methylene chloride as solvent. Nitrite, nitrate, and chlorate ions appear to react with TiF_4 in sulfur dioxide as solvent. Only polymeric species are observed when they are brought into solution in methylene chloride with the aid of acetonitrile.

Zirconium and hafnium tetrafluorides could not be brought into solution under the conditions used in these studies.

In addition to correlating fluorine chemical shifts

Can. J. Chem. Downloaded from www.nrcresearchpress.com by 210.87.254.6 on 09/05/12
For personal use only.

TABLE 8. $C - T$ values for some ligands and central elements

Ligand	$C - T$			
	Phosphorus[a]	Germanium	Tin[b]	Titanium
Br^-			23.7	
Cl^-	49.3		17.8	
CN^-	27.7	18.5	14.5	
$CF_3SO_3^-$	26.3	20.2	9.1	
FSO_3^-	22.5	19.8	7.8	
ClO_4^-	21.8			65
SCN^-	20.7	16.4	10.4	59
OCN^-		11.1	5.5	20[c]
CF_3COO^-	14.8	10.8	7.5	47
NO_3^-		9.5		
N_3^-	12.5	9.4	5.0	22
NO_2^-	11.4	7.3		
CH_3COO^-	5.3	4.0	2.6	25[d]

[a] From ref. 13.
[b] From ref. 9.
[c] From ref. 11.
[d] From ref. 2.

for hexa-co-ordinate fluorine substituted species eq. [2] can also be used to correlate observations for different ligands and different central elements. If the ligands are ordered according to the value $C - T$ for a given central element, the same order is maintained for other hexa-co-ordinate elements (16). This has been demonstrated for Group V (16), and is illustrated for Group IV in Table 8. Of the 36 values listed only 5 are out of order and 3 of these involve SCN^- or OCN^-. However, as previously noted, the bonding mode of SCN^- in the complexes is not always clear.

1. E. L. MUETTERTIES. J. Am. Chem. Soc. **82**, 1082 (1960).
2. P. A. W. DEAN and D. F. EVANS. J. Chem. Soc. A, 2569 (1970).
3. S. BROWNSTEIN. Can. J. Chem. **56**, 343 (1978).
4. S. BROWNSTEIN, J. BORNAIS, and G. LATREMOUILLE. Can. J. Chem. **56**, 1419 (1978).
5. P. A. W. DEAN. Can. J. Chem. **51**, 4024 (1973).
6. A. D. ADLEY, D. F. R. GILSON, and M. ONYSZCHUCK. Chem. Commun. 813 (1968).
7. YU. A. BUSLAEV, V. O. GEL'MBOL'DT, and S. P. PETROSYANTS. Dokl. Akad. Nauk SSSR, **236**, 880 (1977).
8. YU. A. BUSLAEV, V. O. GEL'MBOL'DT, and S. P. PETROSYANTS. Dokl. Akad. Nauk SSSR, **236**, 1127 (1977).
9. P. A. W. DEAN and D. F. EVANS. J. Chem. Soc. A, 1154 (1968).
10. J. SALA-PALA and J. E. GUERCHAIS. J. Chem. Res. M, 3074 (1978).
11. P. A. W. DEAN and B. J. FERGUSON. Can. J. Chem. **52**, 667 (1974).
12. V. AMIRTHALINGAM and V. M. PADMANALHAN. Acta Crystallogr. **11**, 896 (1958).
13. J. H. TALBOT. Acta Crystallogr. **6**, 720 (1953).
14. K. NAKAMOTO. Infrared spectra of inorganic and coordination compounds. 2nd ed. Wiley, New York. 1978. p. 222.
15. S. BROWNSTEIN and G. L. LATREMOUILLE. Can. J. Chem. **56**, 2764 (1978).
16. P. J. CHEVRIER and S. BROWNSTEIN. J. Inorg. Nucl. Chem. In press.

Can. J. Chem. Downloaded from www.nrcresearchpress.com by 210.87.254.6 on 09/05/12
For personal use only.

Potentiometric properties of trialkylammonium ion-exchangers

MICHEL GÉRIN AND JAMES FRESCO[1]

Department of Chemistry, McGill University, Montreal, P.Q., Canada H3A 2K6

Received February 4, 1980

MICHEL GÉRIN and JAMES FRESCO. Can. J. Chem. **58**, 1412 (1980).

The potentiometric behaviour of nitrobenzene solutions of 21 trialkylammonium salts employed as membrane material has been investigated. Deviations from ideal Nernst response curves for chloride, bromide, iodide, and perchlorate sensors were explicable on the basis of partition and hydrolysis of the ion exchangers. Interference coefficients for the anion selective electrochemical sensor tridodecylammonium perchlorate could be related to the ion-exchange constant of the salt.

MICHEL GÉRIN et JAMES FRESCO. Can. J. Chem. **58**, 1412 (1980).

On a étudié les propriétés potentiométriques des solutions de 21 sels de trialkylammonium utilisés comme matériaux de membrane dans le nitrobenzène. On a expliqué les déviations de la réponse idéale Nernstienne pour ces senseurs aux ions chlorure, bromure, iodure et perchlorate à partir de la partition et de l'hydrolyse des échangeurs ioniques. Un rapport pourrait être établi entre les cœfficients d'interférence du senseur électrochimique au perchlorate de tridodécylammonium et la constante d'échange ionique de ce sel.

Can. J. Chem. Downloaded from www.nrcresearchpress.com by 210.87.254.40 on 09/05/12
For personal use only.

Introduction

Interest in the use of liquid ion exchangers in anion-selective electrochemical sensors has resulted in the examination of a variety of organic salt–solvent combinations as active membrane materials (1). Certain high molecular weight quaternary ammonium salts, in particular, have been successfully applied as exchangers in several studies (2–12). Development of satisfactory electrochemical sensors for ions such as sulphate, chromate, and carbonate has not matched the rapid progress in measurements of other divalent and univalent ions. Membrane electrodes based on trioctylamine and trilaurylamine sulphates in nitrobenzene, however, have been reported to be reversible to sulphate ion over a certain concentration range (13).

Limits of detection and ion selectivity of the electrochemical sensors are generally a focus of most investigations. In a number of cases these properties have been linked to physico-chemical constants of the liquid ion exchangers. The results of previous studies of the partition constants, hydrolysis constants, and ion exchange constants of trialkylammonium salts (14–16) have suggested that these salts may be considered model compounds for testing the effect of molecular structure on the response of anionic electrochemical sensors.

Experimental

Chemicals and Solutions

The preparation of nitrobenzene saturated aqueous solutions of potassium halides and soidum perchlorate has been described (16). Trialkylammonium salts and their 0.1 *M* solutions in nitrobenzene were also prepared as previously described (14, 15).

[1]To whom all correspondence should be addressed.

Experimental Cell

The electrochemical cell was designed to provide maximum flexibility and rapidity of use. Suggested by a design of Eisenman (10) it consisted of a Teflon block divided in two parts connected to each other through a machined key. Each block contained a drilled-out compartment that could be filled with an aqueous solution. The two blocks and compartments were separated by a liquid ion exchanger compartment. Three Teflon O-rings sandwiched two Millipore filter membranes and could be positioned to separate the two compartments. The central space in between the two filters could be filled with liquid ion exchanger.

Two 4 cm long pieces of polyethylene "spaghetti tubing" were inserted in the top part of the central O-ring through fine holes. These allowed the injection of liquid ion exchanger by a syringe in the central space in between the two filters. The aqueous cylindrical compartments were ca. eight cm long with a one cm diameter. The O-rings (Millipore XX3001201) were of 1 cm internal diameter. Reference electrodes (1 *M* calomel electrodes Fisher 13-639-51) contacted the solutions on each side of the membrane through holes drilled in the block.

Several types of filters were tested for the central liquid ion exchanger compartment. Millipore Solvinert filters (UGHP01300) were found to be adequate to retain the nitrobenzene ion exchanger solutions. These filters are described by the manufacturer as solvent resistant hydrophobic filters of 0.25 μ pore size. They were found to swell slightly in nitrobenzene and were adjusted in the compartment after pre-soaking in the organic solutions. The volume of the exchanger compartment was approximately 150 mm^3.

The electrochemical cell was placed in a constant temperature environment. This consisted of a double-walled lucite box through the lid of which reference electrodes could be lowered. The temperature was maintained at 25°C by circulation of water.

Measurements of the potential were performed by a calibrated Accumet Expanded Scale Research pH-meter (model 320) in the expanded mV mode. The potentiometric error was estimated at ±0.2 to 0.3 mV.

Procedure

For each salt tested as a liquid ion exchanger a potential response curve was obtained. First the membranes, after soaking 1 min in the organic liquid, were placed in between the O-rings. The block thus formed was positioned in the cell using

0008-4042/80/141412-06$01.00/0

©1980 National Research Council of Canada/Conseil national de recherches du Canada

Can. J. Chem. Downloaded from www.nrcresearchpress.com by 210.87.254.40 on 09/05/12
For personal use only.

an external centering device. The two blocks were tightened in order to support the exchanger compartment. The 0.1 *M* liquid exchanger was introduced. One of the aqueous compartments was filled with a 0.1 *M* solution of MX, where M is an alkali metal ion and X is the anion of the salt used as exchanger (e.g. $NaClO_4$ for the tridodecylammonium perchlorate, $TLAHClO_4$, exchanger). In the other compartment a series of MX solutions were tested consecutively. Concentration levels usually were 10^{-1} *M*, 10^{-2} *M*, 10^{-3} *M*, and 10^{-4} *M*. In the perchlorate series intermediate concentrations were also tested. For interference measurements the solutions tested were decimolar in KI, KBr, or KCl and contained a range of perchlorate concentrations from 10^{-4} to 10^{-1} *M*.

Solutions were removed from the compartments by drainage through a plug situated on the side of each block. Compartments were refilled from the holes provided on the top of the blocks. Reproducibility was checked by testing duplicate solutions first from dilute to concentrated then in the reverse order. All organic solutions were decimolar (within 5%) in ion exchanger except the TLAHCl solution which was 0.06 *M* and saturated.

The notation TPRAH, TBAH, TPTH, THAH, TOAH, and TLAH denotes tripropylammonium, tributylammonium, tripentylammonium, trihexylammonium, trioctylammonium, and tridodecylammonium, respectively.

Results

The response curves of the electrochemical cell for the four series of salts, perchlorates, iodides, bromides, and chlorides studied appear in Fig. 1. In Fig. 2 the response curve of the $TLAHClO_4$-based electrode in the presence of anion interferences is presented. In these figures the potential *E* is plotted against the log reciprocal of the anion activity. The value for *E* was corrected for the small potential obtained when the two aqueous compartments of the cell contained identical 0.1 *M* MX solution. The anion activity was calculated from the concentration employing the Debye–Hückel equation. In Fig. 1 the straight lines extended by short dashes were calculated from the Nernst equation.

Solutions of pure water tested in the electrode were not recorded since they gave drifty, unstable, and nonreproducible potentials. Generally the response times increased with increasing dilution of the test solutions. Solutions in the range 3×10^{-4} *M* to 10^{-4} *M* frequently required 10–15 min to achieve a stable value. Other more concentrated solutions reached a stable reading within a few minutes. Reproducibility varied with the concentration level and the exchanger tested. High molecular weight ammonium salts usually gave reproducible potentials while low molecular weight exchangers were poorly reproducible. Vertical bars extend to a value of one standard deviation above and below each plotted point.

Potential values obtained for the low molecular weight salts $TPRAHClO_4$, TPRAHI, TBAHI, TBAHBr, and TPTAHBr were stable for a few minutes after which the potential drifted continuously to lower values. For the salts TPRAHBr, TBAHCl, and TPRAHCl no stable value could be recorded. In the case of the $TLAHClO_4$ electrode, response times were found to be longer when interfering ions were present especially at low concentrations of the main ion.

Discussion

Response Curves

High molecular weight ammonium salts in each series usually gave more Nernstian response curves than their low molecular weight homologues. In general the order of increasing deviation from an ideal Nernstian response curve was $ClO_4^- < I^- < Br^- < Cl^-$. Over the range of concentration studied all curves showed deviation from the theoretical slope at low concentrations. These deviations were assignable to contamination of the test aqueous phase by anion migration from the contiguous ion exchanger (1, 10).

Two processes can be examined as the basis for deviations from the ideal Nernst slope. One is the partition of the organic ammonium salt from nitrobenzene into water and the other, hydrolysis of the ion exchanger.

The extent of solubilization of the ion exchanger in an aqueous phase by partition is a function of the K_p value corresponding to the equilibrium

$$\overline{R_3NHX} \rightleftarrows R_3NH^+ + X^-$$

These constants have been measured for various exchangers (15) and were of increasing magnitude in the order

$$TPTAHI < THAHCl < TBAHClO_4 < TPTAHBr < TBAHI < TPRAHClO_4, TPTAHCl < TBAHBr < TPRAHI$$

considering only those salts with K_p values greater than 10^{-4}.

If the deviation from Nernstian slope is due in large part to solubilization, this deviation would follow the same order as K_p (12). For an activity level of 0.01 the order of increasing deviation is (see Fig. 1)

$$TPTAHI\ (\text{no deviation}) < THAHCl, TBAHClO_4 < TBAHI < TPTAHBr < TPRAHClO_4, TPTAHCl, TBAHBr < TPRAHI$$

This is essentially the same order as that of K_p values. No deviation is found for TPTAHI and other salts of higher molecular weight in each series. Thus deviations from the theoretical slope at this concentration level arise from the process of solubilization of the exchanger by partition into the aqueous phase.

Can. J. Chem. Downloaded from www.nrcresearchpress.com by 210.87.254.40 on 09/05/12
For personal use only.

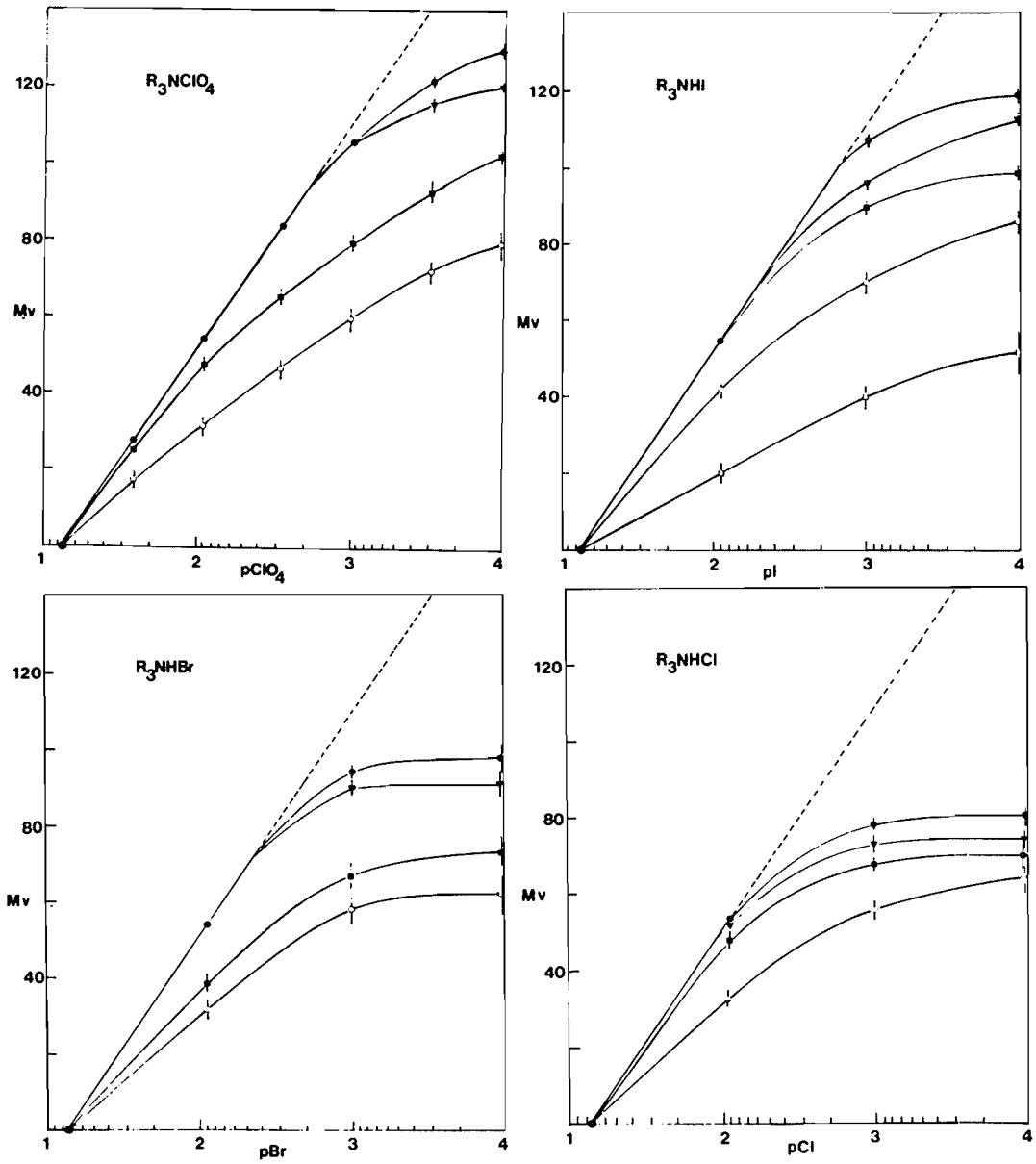


FIG. 1. Response curves of electrodes employing trialkylammonium salts R_3NHX as liquid anion exchangers. ●: $TLAHClO_4$, $TOAHClO_4$, $THAHClO_4$, TLAHI, TOAHI, TLAHBr, TOAHBr, TLAHCl; ▼: $TPTAHClO_4$, THAHI, THAHBr, TOAHCl; ■: $TBAHClO_4$, TPTAHI, TPTAHBr, THAHCl; ○: $TPRAHClO_4$, TBAHI, TBAHBr, TPTAHCl; □: TPRAHI.

It is of interest to compare deviations from Nernst-type behaviour, ΔE_{ex}, at this activity level with those predictable from the theory of Kamo, Hazemoto, and Kobatake (17). The theory relates the potential, E, of a liquid membrane electrode to the partition and dissociation constants of the organic ion exchanger according to

$$E^0 - (RT/F) \ln [(c \sqrt{c^2 + A_x})/2]$$

where c represents the initial anion concentration of the test solution and

$$A_x = 4K_p\bar{c}_{sx}$$

The partition coefficient of the ion exchanger is K_p and $\bar{c}_{sx}$ or $\overline{[R_3NHX]}$ represents the concentration of the undissociated ion exchanger in the membrane. An expression for the deviation from the theoretical slope is easily obtained in the form

$$\Delta E = (RT/F) \ln [(1 + \sqrt{1 + A_x/c^2})/2]$$

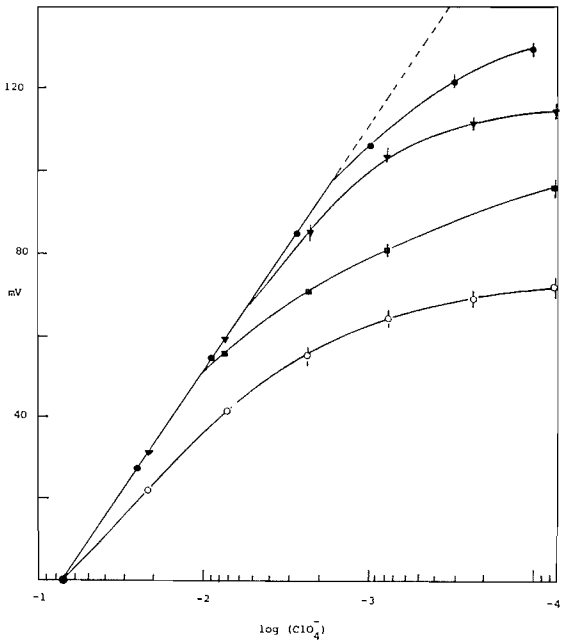


FIG. 2. Response curves of the $TLAHClO_4$ electrode in the presence of extraneous ions. ●: no extraneous salt; ▽: 0.1 *M* potassium chloride; ■: 0.1 *M* potassium bromide; ○: 0.1 *M* potassium iodide.

Theoretical values, ΔE, were calculated for c equals 0.01 and $\bar{c}_{sx}$ equals 0.1 for all the salts studied. These results and the corresponding observed values appear in Table 1. Exchanger dissociation in nitrobenzene was ignored since it is less than 15% for the most extreme case. The 21 ion exchangers could be distributed among three groups according to the data presented in Table 1.

Calculated and experimental deviations are negligibly small for all ion-exchangers with K_p values below 10^{-4}. These include the long chain salts beginning with $TPTAHClO_4$ for the perchlorate series and THAHI, THAHBr, and TOAHCl respectively for the other series. Ion exchangers with intermediate partition coefficients

$$\sim 10^{-4} < K_p < 2 \times 10^{-3}$$

show comparatively small but significant emf deviations. Fair agreement exists between calculated and experimental values for the four salts, $TBAHClO_4$, TPTAHI, TPTAHBr, and THAHCl, comprising this group.

Large deviations exist for ion exchangers with K_p values higher than $\sim 2 \times 10^{-3}$. Calculated ΔE values are considerably greater than the corresponding experimental values. In these cases ΔE has been overestimated by unaccounted loss of ion exchangers to the aqueous test solution through partition.

TABLE 1. Comparison of deviation from ideal Nernst-type response for trialkylammonium ion exchangers

Exchangers*	$K_p(15)$	ΔE, mV	ΔE_{ex}, mV
$TPRAHClO_4$	2.5×10^{-2}	44	23±3
$TBAHClO_4$	8.2×10^{-4}	11	7±3
$TPTAHClO_4$	1.6×10^{-3}	<1	1±1
R'_3NHClO_4	$<10^{-6}$	<1	<1
TPRAHI	2.1×10^{-1}	70	35±3
TBAHI	5.4×10^{-3}	27	13±3
TPTAHI	1.2×10^{-4}	3	1±1
THAHI	2.1×10^{-6}	<1	<1
R'_3NHI	$<10^{-7}$	<1	<1
TBAHBr	1.2×10^{-1}	62	23±3
TPTAHBr	2.1×10^{-3}	18	15±3
THAHBr	3.5×10^{-5}	1	1±1
R'_3NHBr	$<10^{-6}$	<1	<1
TPTAHCl	2.2×10^{-2}	42	22±3
THAHCl	4.4×10^{-4}	7	6±2
TOAHCl	7.1×10^{-7}	<1	2±2
R'_3NHCl	$<10^{-8}$	<1	<1

*R′ denotes the higher members of the series.

When deviations at low concentration levels are analysed (10^{-3}–10^{-4} *M* ion concentration), partition alone would not be sufficient to explain the trends. Response curves for the salts $TLAHClO_4$, $TOAHClO_4$, and $THAHClO_4$ were indistinguishable. The same behaviour was observed for TLAHI and TOAHI, also TLAHBr and TOAHBr. These salts are, however, expected to have different aqueous partition constants. It was also noted that the extent of deviation increases in the order

$$ClO_4^- < I^- < Br^- < Cl^-$$

This is the order expected if this deviation was based on hydrolysis of these high molecular weight salts. Two-phase hydrolysis constants (16) for R_3NHX were shown to increase from perchlorate to chloride and were independent of carbon chain length beyond C_4. Thus the high molecular weight salts cited which have very low partition constants would, however, hydrolyze to the same extent within each series and to a different extent from series to series. This would explain the observed trends.

At all concentrations a combination of the aforementioned effects is undoubtedly largely responsible for the observed behaviour of the electrodes.

Reproducibility, drift and response time are better understood if the reactions mentioned are considered. Occurrence of important partition or hydrolysis is expected to create drift and worsen the reproducibility by changing the composition of the ion exchanger phase. The constant drift encountered in the TPRAHCl, TBAHCl, TPRAHI sys-

Can. J. Chem. Downloaded from www.nrcresearchpress.com by 210.87.254.40 on 09/05/12
For personal use only.

Can. J. Chem. Downloaded from www.nrcresearchpress.com by 210.87.254.40 on 09/05/12
For personal use only.

tems can be assigned to their comparatively large K_p values which will favour depletion of the organic phase of ion exchanger immediately after introduction of the aqueous phases. For the higher molecular weight salts partition is less important. Since hydrolysis or partition are repressed at high aqueous concentration levels, no drift is observed and reproducibility is of the same order as the potentiometric error.

Selectivity

The $TLAHClO_4$ system was chosen for selectivity studies since it represented the exchanger having the most Nernstian response and the best reproducibility. From the plots in Fig. 2 the effect of extraneous halide ions could be assessed. Qualitatively the iodide anion appears to have the most influence on the potential of the perchlorate electrode since the response curve in the presence of a constant level of iodide (0.1 *M*) deviated most from the interference-free perchlorate response curve. Bromide interfered less than iodide, while chloride gave the least interference. The trend in anion interference parallels the trend in the corresponding ion exchange constants (16). The selectivity constant K_{S12} is easily related to ΔE, the difference in mV between the theoretical Nernstian interference-free potential and the actual recorded potential in the presence of interference, according to

$$K_{S12} = a_1 (10^{\Delta E/59} - 1)/a_2$$

The activities of main and interfering monovalent anions are a_1 and a_2 respectively (18, 19).

Values of K_{S12} for the $TLAHClO_4$ electrode were computed at different perchlorate activity levels in the presence of the halide ions. These values varied with the activity level in agreement with previous studies of other ion selective electrodes (20). The average value corresponding to activity levels below 2×10^{-3} was used since in this activity range the response of the electrode was Nernstian. The selectivity constants K_{S12} were ClO_4^-/I^-, ~0.1; ClO_4^-/Br^-, ~0.03; and ClO_4^-/Cl^-, ~0.005. These values are approximate and should be considered as empirical parameters (1) describing interference under specified experimental conditions. Interference clearly increases from Cl^- to Br^- to I^-.

Several authors have attempted to correlate electrochemical selectivity constants with ion exchange constants (5, 8, 10, 12, 21). James *et al.* (8) studied the interference properties of electrodes using tetrahexylammonium iodide dissolved in various organic alcohols as liquid anion exchangers. They found a good correlation between

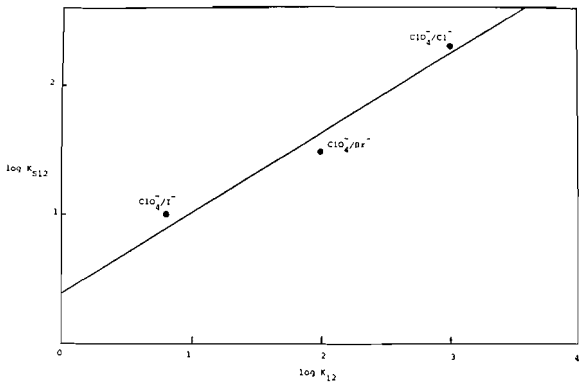


FIG. 3. Comparison of ion-exchange constants, K_{12}, and selectivity constants, K_{S12} for tridodecylammonium perchlorate.

selectivity constants and ion exchange constants in this system. Scibona *et al.* (5) and Fabiani (9) used tetraheptylammonium salts dissolved in various solvents. Applying theoretical equations developed by Eisenman *et al.* (21) they related semiquantitatively interference constants to ion-exchange constants, dissociation constants, and the mobility of the anions in the organic phase. Eisenman (10, 21) mentioned a membrane made of dodecylamine dissolved in nitrobenzene which in an electrochemical cell was selective for I^- in the presence of Br^- and Cl^-. In a more detailed study on di-2-ethylhexyl phosphoric acid in *n*-amyl alcohol, theoretical equations (21) predicted the order of selectivities; however, the agreement was only qualitative.

For the trialkylammonium salts no theoretical equation is available which could relate the interference response curves to the chemical properties of the ion exchanger. The system does not fall in the category of a completely dissociated ion exchanger nor a strongly associated one (~15% of the ion exchanger is ionized). However, a correlation was found between K_{S12} and K_{12} values. In Fig. 3 a plot of log K_{S12} vs. log K_{12} is presented. Values of ion-exchange constants K_{12} were obtained from Table 2 in ref. 16. The slope of the plot is ca. 0.6. A similar correlation with a slope of ca. 0.5 was observed by Bäck and Sandblom (12) with tetraalkylammonium salts in methylene chloride. James *et al.* (8) observed the same phenomenon but with a slope close to one.

The selectivity constants obtained for the tridodecylammonium perchlorate exchanger are of the same order of magnitude as values tabulated by Koryta (22) for other liquid anion exchangers.

Acknowledgement

Financial support by the National Research Council of Canada is gratefully acknowledged.

1. J. W. Ross. *In* Ion selective electrodes. *Edited by* R. A. Durst. N.B.S. Special Publication 314. 1969. Chapt. 2.
2. C. J. Coetzee and H. Freiser. Anal. Chem. **41**, 1128 (1969).
3. M. Matsui and H. Freiser. Anal. Lett. **3**, 161 (1970).
4. P. R. Danesi, G. Scibona, and B. Scuppa. Anal. Chem. **43**, 1893 (1971).
5. P. R. Danesi, F. Salvemini, G. Scibona, and B. Scuppa. J. Phys. Chem. **75**, 554 (1971).
6. S. G. Back. Anal. Lett. **4**, 793 (1971).
7. N. Ishibahi and H. Kohara. Anal. Lett. **4**, 785 (1971).
8. M. J. James, G. P. Carmack, and H. Freiser. Anal. Chem. **44**, 853 (1972).
9. C. Fabiani. Anal. Chem. **48**, 865 (1976).
10. G. Eisenman. Anal. Chem. **40**, 311 (1968).
11. G. Scibona, M. Magini, B. Scuppa, A. Castagnola, and C. Fabiani. Anal. Chem. **49**, 212 (1977).
12. S. Bäck and J. Sandblom. Anal. Chem. **45**, 1680 (1973).
13. E. A. Materova, Z. S. Alagova, and G. R. Mamadieva. Vestn. Leningr. Univ. Fiz. Chim. 147 (1974).
14. M. Gérin and J. Fresco. Anal. Chim. Acta, **97**, 155 (1978).
15. M. Gérin and J. Fresco. Anal. Chim. Acta, **97**, 165 (1978).
16. M. Gérin and J. Fresco. To be published.
17. N. Kamo, N. Hazemoto, and Y. Kobatake. Talanta, **24**, 111 (1977).
18. G. J. Moody and J. D. R. Thomas. Talanta, **19**, 623 (1972).
19. K. Srinivasan and G. A. Rechnitz. Anal. Chem. **41**, 1203 (1969).
20. R. P. Buck. Anal. Chim. Acta, **73**, 321 (1974).
21. G. Eisenman. *In* Ion selective electrodes. *Edited by* R. A. Durst. N.B.S. Special Publication 314. 1969. Chapt. 1.
22. J. Koryta. Ion-selective electrodes, Cambridge Univ. Press. 1975. Chapt. 6.

Can. J. Chem. Downloaded from www.nrcresearchpress.com by 210.87.254.40 on 09/05/12
For personal use only.

Octahedral–tetrahedral equilibria in aqueous cobalt(II) solutions at high temperatures

THOMAS WILSON SWADDLE[1] AND LEONARD FABES

Department of Chemistry, University of Calgary, Calgary, Alta., Canada T2N 1N4

Received February 27, 1980

THOMAS WILSON SWADDLE and LEONARD FABES. Can. J. Chem. **58**, 1418 (1980).

Evidence is presented to indicate that aqueous Co^{2+} exists as the hexaaquo-ion in equilibrium with minor amounts (upper limits 0.08% at 298 K, 7% at 625 K, at 16–25 MPa) of tetraaquocobalt(II), with $\Delta H \sim +17$ kJ mol^{-1}. The single visible absorption band of the supposed $Co(H_2O)_4^{2+}$ has maxima at 552 nm and 486 nm in the intensity ratio 2:1. Hydrogen sulfate ion (up to 0.5 *M* at least) does not complex Co^{2+}(aq) detectably in acidic media, 290–625 K, and sulfuric acid therefore holds promise as a non-complexing strong monobasic acid for high-temperature aqueous studies. In water containing 2.0 *M* or more Cl^-, the tetrahedral form of cobalt(II) is $CoCl_4^{2-}$, ΔH for the octahedral → tetrahedral equilibrium being +62 kJ mol^{-1}; for $CoBr_4^{2-}$, the corresponding ΔH is +70 kJ mol^{-1}, the greater endothermicity accounting entirely for the lower stability relative to $CoCl_4^{2-}$.

THOMAS WILSON SWADDLE et LEONARD FABES. Can. J. Chem. **58**, 1418 (1980).

Dans cet article, on montre que le Co^{2+} en milieu aqueux existe sous forme de l'ion hexahydraté en équilibre avec de petites quantités de tétraquocobalt(II) (limite supérieure: 0.08% à 298 K et 7% à 625 K à 16–25 MPa; $\Delta H \sim +17$ kJ mol^{-1}). L'unique bande d'absorption dans le visible pour l'ion proposé $Co(H_2O)_4^{2+}$ possède un maximum à 552 nm et un à 486 nm dans un rapport d'intensité 2:1. L'ion HSO_4^- ne complexe pas de façon détectable le Co^{2+}(aq) en milieu acide (jusqu'à 0.5 *M* tout au moins, de 290 à 625 K), et ainsi l'acide sulfurique est très prometteur comme acide fort monobasique non-complexant pour les études à haute température dans l'eau. En solution aqueuse 2 *M* ou plus en Cl^-, la forme tétrahédrique du cobalt(II) est $CoCl_4^{2-}$, et le ΔH de l'équilibre octahédrique–tétrahédrique est de +62 kJ mol^{-1}. Pour $CoBr_4^{2-}$, la valeur correspondante de ΔH est +70 kJ mol^{-1}, la relativement faible stabilité du $CoBr_4^{2-}$ par rapport au $CoCl_4^{2-}$ étant due entièrement à la différence des ΔH.

Introduction

The chemistry of cobalt(II) in water at elevated temperatures has attracted attention because of the spectacular thermochromism exhibited when halide ions are present (1–3), and because of its relevance to the understanding of the mechanism of ^{60}Co transport in the heat transfer systems of water-cooled nuclear reactors (4, 5). The present study was therefore undertaken to evaluate visible-region spectrophotometry as a quantitative tool for the study of the high-temperature aqueous chemistry of cobalt(II). In effect, this required the design of a corrosion-resistant optical cell serviceable to at least 30 MPa at 650 K, the identification of the complex species present and the detailed analysis of the temperature dependence of their spectra, and the demonstration of the "inertness" of the supporting electrolytes used.

Several optical cells for high-temperature aqueous studies have been described (1, 3, 6–13). The cell described below has the advantage of simplicity of construction at the expense of permitting contact between the solution sample and the structural metal, but by fabricating the cell body out of titanium – 0.2% palladium alloy corrosive interactions are minimal, even at high chloride concentrations. This alloy is attacked by trifluoromethanesulfonic acid, however, and so this acid and its salts could not be used as noncomplexing supporting electrolytes in place of the usual perchloric acid and perchlorates, which, though intrinsically surprisingly stable kinetically in water at high temperatures, can be catalytically decomposed to a significant extent when transition metal ions are present (14, 15). We have therefore investigated HSO_4^- as a non-complexing supporting anion, as it is isoelectronic with ClO_4^- and has not been reported to form complexes of any significant thermodynamic stability with metal ions in aqueous solution at near-ambient temperatures. The basicity of SO_4^{2-} rises markedly with increasing temperature, so that at 570 K and above sulfuric acid is effectively monobasic (16); thus, in these experiments, free SO_4^{2-} was effectively eliminated simply by having a small stoichiometric excess of H^+ over total sulfate.

Special interest in the spectrum of the aqueous hexaaquocobalt(II) ion was stimulated by the suggestion of Swift and Connick (17, 18) that some tetrahedral $Co(H_2O)_4^{2+}$ might also be present at elevated temperatures. Subsequent work by Fiat *et al.* (19, 20) indicated that the ^{17}O-nmr data (which originally had led Swift and Connick to postulate the existence of $Co(H_2O)_4^{2+}$) are in fact consistent within the experimental uncertainty with the exclusive existence of the hexaaquo-species over the temperature range 263–456 K at least. This did not completely settle the issue, however, since observations of the visible spectrum (17) and temperature-jump relaxation kinetics (18) of

[1]To whom all correspondence should be addressed.

0008-4042/80/141418-09$01.00/0

©1980 National Research Council of Canada/Conseil national de recherches du Canada

Can. J. Chem. Downloaded from www.nrcresearchpress.com by 210.87.254.42 on 09/05/12
For personal use only.

Can. J. Chem. Downloaded from www.nrcresearchpress.com by 210.87.254.42 on 09/05/12
For personal use only.

aquocobalt(II) solutions, made by Swift and Connick in support of their proposal, then remained unexplained. We now present evidence that Swift and Connick were correct, and that the observations of Fiat *et al.* (19, 20) can be accommodated.

Experimental

All chemicals were Baker Analyzed or Fisher Certified reagents. Distilled water was passed through Barnstead deionizer and organic removal cartridges before use.

The spectrophotometer cell (path length 3.42 cm) is shown in Fig. 1. The cell body and K-cross-section seals are of ATL-40 Ti – 0.2% Pd alloy (Atlas Titanium Ltd.), but the end plates, bolts, and pressure connection gland nuts are of type 316 stainless steel. The lower pressure connection facilitates filling, etc., but is not necessary. A prototype using screw-in end-plugs rather than bolted closures was unsuccessful because residual torque on the windows often led to their fracture, usually in the cooling portion of a temperature cycle. Attempts to use commercial K-seals of gold-plated Inconel were unsuccessful, as the smallest penetration of the plating resulted in catastrophic galvanic corrosion of the nickel alloy by the hot salt solutions. The Ti – 0.2% Pd alloy showed excellent corrosion resistance, however, and etching of the sapphire windows (3, 10) was slow enough to be accommodated quite economically by their periodic replacement. Nevertheless, only those sets of spectra which were accurately reproducible in the cooling part of the temperature cycle were accepted; such discrepancies as occasionally occurred were generally attributable to leaks rather than corrosion. The temperature of the cell was measured (±0.25 K) with two thermocouples inserted in 5 cm wells (not shown) drilled parallel to the optical axis, with reference to junctions at 273.2 K. The response of the thermocouples was checked periodically against Fisher T421 Ther-Metric fusion point standards.

The solution samples were permitted to expand into an overflow chamber (Fig. 2), where a free piston loosely separated the liquid phase from the pressurizing fluid (high-pressure argon) to minimize distillation of the solvent. All parts shown with single cross-hatching in Fig. 2 were Ti – 0.2% Pd, so that solutions contacted only titanium alloy and sapphire; the bottom closure nut and all further high-pressure connections were of type 316 stainless steel.

The optical cell is heated with the furnace shown in Fig. 3. Each interlocking half contains an electrical winding of 5 m of 21 AWG chromel-A wire, and a sheath of copper coils to allow cooling water to be circulated in a countercurrent fashion to protect the spectrophotometer from thermal damage. The shells are of aluminum, and the insulation is Sauereisen No. 1 cement. Temperatures can be held constant to within 0.5 K using simply a rheostat or variable transformer in conjunction with a voltage regulator. A heating jacket was also provided for the overflow vessel, but this is unnecessary, particularly if this vessel can be placed lower than the sample cavity in the optical cell to eliminate convective exchange of solution.

The optical cell and its furnace were designed to fit inside the sample compartment of a Cary Model 15 spectrophotometer, although most of the measurements reported here were made with a Model 17H instrument which has a large open sample compartment and excellent baseline stability. Neutral density filters were used as desired to help balance the sample and reference beams, and spectra were referred to baselines obtained in blank runs.

Throughout this article, the symbol M means mol dm^{-3} as measured at 293 K and 0.1 MPa, i.e., it represents a temperature- and pressure-independent concentration scale based on the conditions of preparation of the solutions by volume as a standard state. This is more convenient than the mol kg^{-1} scale where mixed-electrolyte solutions are involved. Corrections for the linear expansion of the cell (9.0×10^{-6} K^{-1}) were generally smaller than the uncertainty in the absorbance measurements and were ignored.

Results

Cobalt(II) Sulfate in Dilute Aqueous Sulfuric Acid

The dependence of the visible absorption spectrum of a typical cobalt(II) sulfate solution in dilute sulfuric acid on temperature T is shown in Fig. 4, just as obtained from the spectrometer. The measured absorbance A must be corrected (A_{corr}) for the thermal expansion of the solutions, which, for these dilute systems, can be equated to the interpolated thermal expansion of water at the appropriate pressures (21). Where necessary, spectra were also corrected for a low intensity absorption which developed to a maximum at ~730 nm, as the temperature rose, while an even weaker absorption around 800 nm decreased concomitantly; this phenomenon appeared in all solutions including plain water, and probably derived from vibrational overtones of H_2O (in which case $\varepsilon_{H_2O} \sim 3 \times 10^{-4}$ M^{-1} cm^{-1} at 730 nm around 500 K, cf. Bell and Krohn (22)).

So long as a sufficient excess of H^+ was present to convert in principle all SO_4^{2-} to HSO_4^- and to suppress the hydrolysis of Co^{2+}(aq) (5), the spectra were quantitatively reproducible to ±2% in molar absorbance ε (= $A_{corr}/3.42[Co]$, M^{-1} cm^{-1}) and ±0.2% in wavelength λ or wavenumber $\bar{\nu}$, for a given temperature and pressure. No significant dependence on the stoichiometric $[H^+]$ or $[SO_4^{2-}]$ could be detected, over the temperature (290–625 K) and concentration (0.1–0.5 M H_2SO_4 or H_2SO_4/$NaHSO_4$) ranges investigated. Thus, *neither complexing by HSO_4^- nor hydrolysis of Co^{2+}(aq) were detectable under these conditions.*

If, however, the stoichiometric $[H^+]$ was *less* than the stoichiometric $[SO_4^{2-}]$, anomalously large red shifts were seen above 400 K, evidently because of hydrolysis of Co^{2+} in the HSO_4^-–SO_4^{2-} buffer; a solid, probably $CoSO_4 \cdot H_2O$ (23), was often precipitated, e.g. above 525 K when $[CoSO_4] = 0.0317$ M and $[H_2SO_4] = 0.0099$ M, and in any case spectral changes occurred which were not reversible over the temperature cycle.

The vastly predominant form of Co^{2+}(aq) in the solutions containing excess stoichiometric H^+ over sulfate was undoubtedly $Co(H_2O)_6^{2+}$, at least near 300 K (17–20), and the absorption band corres-

Can. J. Chem. Downloaded from www.nrcresearchpress.com by 210.87.254.42 on 09/05/12
For personal use only.

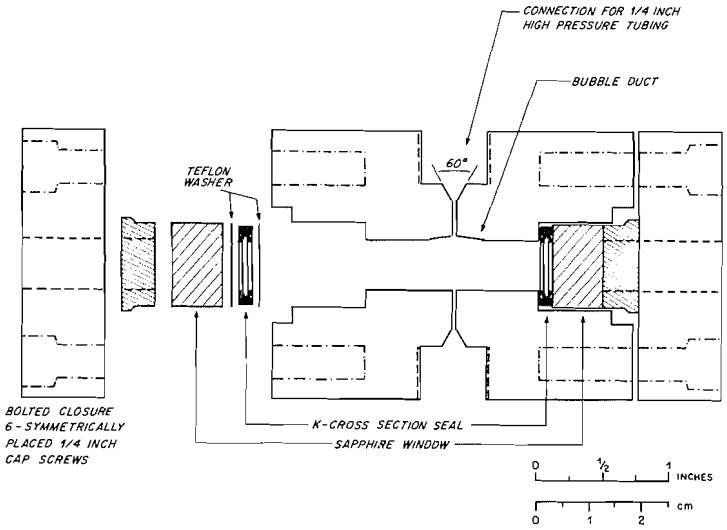


FIG. 1. Pressurizable optical cell.

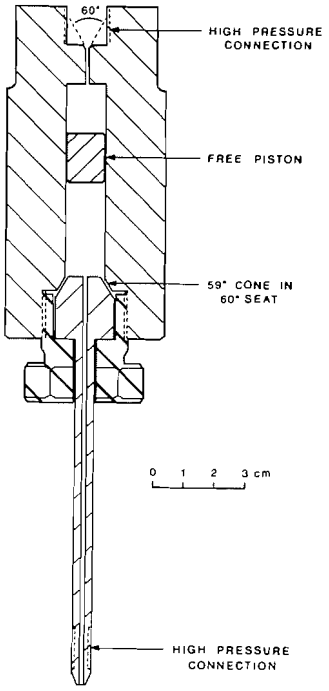


FIG. 2. Expansion chamber.

ponds to the Laporte-forbidden $^4T_{1g}(P) \leftarrow {}^4T_{1g}(F)$ transition (with some admixture of spin-forbidden excitations to states derived from ^2G and ^2H terms of Co^{2+}) (ref. 24, pp. 318–324). This band should therefore derive essentially all its oscillator strength f

$$[1] \quad f = 4.315 \times 10^{-9} \int_0^\infty \varepsilon_{\bar{\nu}}\, d\bar{\nu} \quad (\bar{\nu} \text{ in } cm^{-1})$$

from vibronic coupling, in which case the temperature dependence of f would be expected (25) to follow the equation

$$[2] \quad f = \sum_i C_i \coth (h\nu_i/2kT)$$

where ν_i is the ith normal vibrational mode contributing to vibronic coupling and C_i is a proportionality constant. For $Co(H_2O)_6^{2+}$, the relevant modes are ν_3, ν_4, and ν_6, but ν_6 is inactive and only ν_3 is seen (364 cm^{-1}) (26), possibly because ν_4 lies close; in any event, the hyperbolic cotangent terms are not very sensitive to the choice of ν_i for $\bar{\nu}_i <$ 400 cm^{-1} when $T >$ 300 K, and one can take the ν_3 term alone to obtain

$$[3] \quad f = C \coth (262/T)$$

In fact, the measured whole-band f values increase much more rapidly with rising T than eq. [3] predicts, and even faster again than allowed by the simplified equation

$$[4] \quad f = f_0(1 + \exp (200/T))$$

used by Holmes and McClure (27) to describe the low-temperature behavior of f in solid $CoSO_4 \cdot 7H_2O$. This sharply T-dependent excess oscillator strength might be interpretable in terms of changes in the solvent effect on f as the aqueous medium expands thermally, but the various attempts (28–33) to account for such solvent effects theoretically have either been overly simplistic or led to expressions containing too many parameters, and in any case have dealt only with fully-allowed transitions, primarily in non-polar solvents. These treatments do, however, suggest that a relevant variable is the square of the refractive index of the

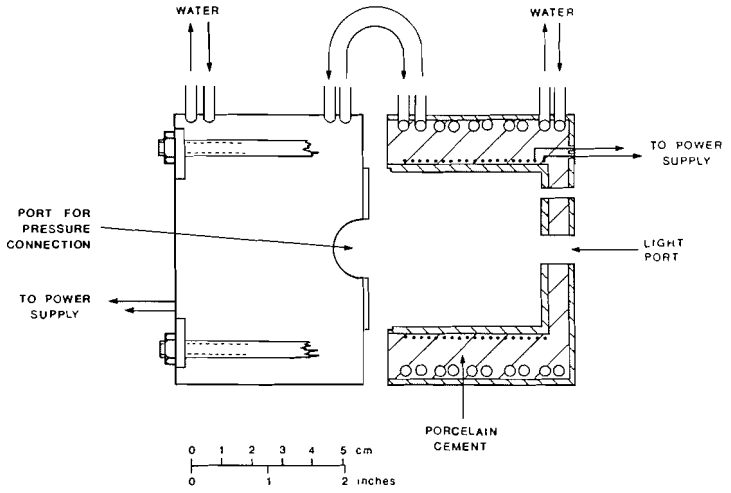


FIG. 3. Furnace for optical cell.

solvent, which in turn suggests that eq. [3] needs to be supplemented with some function of the square of the solution density ρ (34). Bayliss's work (30) links the variation of f with that of the wavenumber $\bar{\nu}_{max}$ of the band maximum, as observed here (empirically, $10^5 f \sim 0.0159\ (20054 - \bar{\nu}_{max})$ for $\bar{\nu}_{max}$ in cm^{-1}), while Robertson and King's suggestion, that pressure (i.e., solvent density) effects on f act through influencing the *populations* of the various solvation spheres around a dissolved absorber, provides a further link with the proposal which follows.

Correction of the spectra of Fig. 4 for expansion, followed by subtraction of the 291 K spectrum, yields the difference spectra of Fig. 5.[2] The striking constancy of the wavelengths (552 ± 2 and 486 ± 1 nm) and relative intensities (1:0.5) of the principal features of these difference spectra over the range of 128 K confirms Swift and Connick's interpretation of their single, lower-temperature difference spectrum (17) as evidence for the presence of a new aquocobalt species at elevated temperatures. The band shape is as expected for the $^4T_1(P) \leftarrow {}^4A_2$ transition of tetrahedral cobalt(II) (see below) at low resolution. Furthermore, taking $Dq = 920$ and $B = 825\ cm^{-1}$ for $Co(H_2O)_6^{2+}$ (ref. 24, pp. 318–324) and, after Smith (35), setting $Dq(T_d)$ to ~0.48 $Dq(O_h)$, we calculate (ref. 24, p. 182) that the $^4T_1(P) \leftarrow {}^4A_2$ maximum of $Co(H_2O)_4^{2+}$ should occur at 17990 cm^{-1} or 556 nm, very close to that observed.

[2]Strictly, the 291 K band should be corrected according to eq. [3] to each of the other four temperatures, but the absorption at 291 K near the maximum of the difference spectra is small and so this correction cannot materially affect the essential features revealed in Fig. 5. Conversely, the extrapolated contribution to the 291 K spectrum of the species having the absorption maximum at 552 nm can be neglected in this context.

In addition, experience with nitratoaquochromium(III) ion (37) suggests that the ligand-field spectrum of $Co(H_2O)_4^{2+}$ should be very similar to that of $Co(NO_3)_4^{2-}$, for which the $^4T_1(P) \leftarrow {}^4A_2$ maximum occurs at 535 nm with $Dq = 466\ cm^{-1}$ and $B = 855\ cm^{-1}$ (38), so lending support to the foregoing estimate and its implicit assumption that $B(T_d) \sim B(O_h)$. It is, therefore, very likely that the excess oscillator strength over that predicted by eq. [3] is indeed due to small amounts of tetraaquocobalt(II) formed in an endothermic equilibrium

$$[5] \quad Co(H_2O)_6^{2+} \rightleftharpoons Co(H_2O)_4^{2+} + 2H_2O$$

whence, taking the activity of solvent water with respect to the 298 K, 0.1 MPa reference state to be given by the relative density $\rho_r (= \rho_{T,P}/\rho_{293,0.1})$, and assuming equal activity coefficients for the hexa- and tetra-aquo ions, we have

$$[6] \quad [Co(H_2O)_4^{2+}]/[Co(H_2O)_6^{2+}] = \rho_r^{-2} \exp(\Delta S/R - \Delta H/RT)$$

$$[7] \quad f = f_{O_h}[Co(H_2O)_6^{2+}]/[Co_{total}] + f_{T_d}[Co(H_2O)_4^{2+}]/[Co_{total}] \approx f_{O_h} + f_{T_d}[Co(H_2O)_4^{2+}]/[Co(H_2O)_6^{2+}]$$

Combination of eqs. [3], [6], and [7] then gives

$$[8] \quad f = C \coth(262/T) + D\rho_r^{-2} \exp(-\Delta H/RT)$$

where

$$[9] \quad D = f_{T_d} \exp(\Delta S/R)$$

and a non-linear least-squares regression gave an excellent fit of a set of 19 data points for $[CoSO_4] = 0.0336\ M$, $[H_2SO_4] = 0.0990\ M$, and $P = 16$ MPa to eq. [7] over the entire range 298–614 K with $C =$

Can. J. Chem. Downloaded from www.nrcresearchpress.com by 210.87.254.42 on 09/05/12
For personal use only.

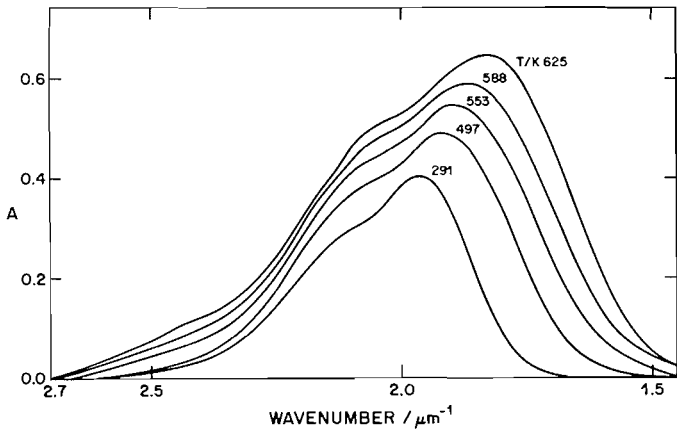


FIG. 4. Spectra of 0.0238 *M* $CoSO_4$ in 0.478 *M* H_2SO_4 at 25 MPa, uncorrected for thermal expansion of solution. Optical path length 3.42 cm.

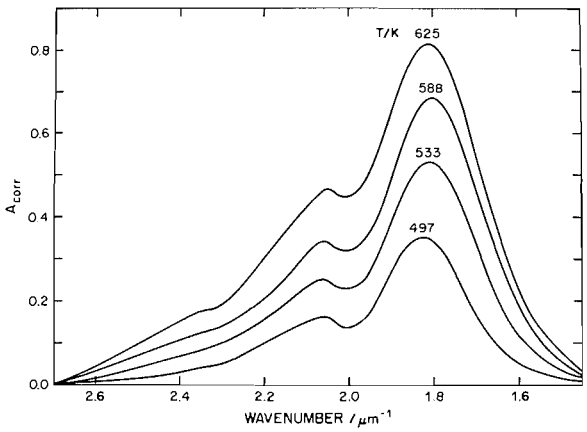


FIG. 5. Difference spectra from Fig. 4, after correction for thermal expansion of solution.

$(5.20 \pm 0.15) \times 10^{-5}\ M^{-1}\ cm^{-2}$, $D = (132 \pm 51) \times 10^{-5}\ M^{-1}\ cm^{-2}$, and the enthalpy of reaction $\Delta H = +16.6 \pm 2.0\ kJ\ mol^{-1}$ (uncertainties are standard deviations).

A plot of eq. [8] with these parameters is shown in Fig. 6, together with the calculated contributions to f of the octahedral and tetrahedral aquocomplexes. The actual concentrations of tetraaquocobalt(II) present cannot be calculated unless f_{T_d} is known; values of 3×10^{-3} to 8×10^{-3} are typical of tetrahedral cobalt(II) (ref. 24, pp. 318–324), but, as argued above, tetranitratocobaltate(II), with the f value of 1.94×10^{-3} for the $^4T_1(P) \leftarrow {}^4A_2$ maximum (38), is probably a better analogue for $Co(OH_2)_4^{2+}$. In that case, about 0.08% of the total aquocobalt(II) is present as $Co(OH_2)_4^{2+}$ at 298 K and ~7% at 625 K,[3] and $\Delta S \sim$

[3]These percentages may at least be taken as upper limits, as the f value chosen for $Co(OH_2)_4^{2+}$ is the lowest of those for tetrahedral cobalt(II) that have appeared in the literature. Similarly, the ΔS cited is the most positive likely value.

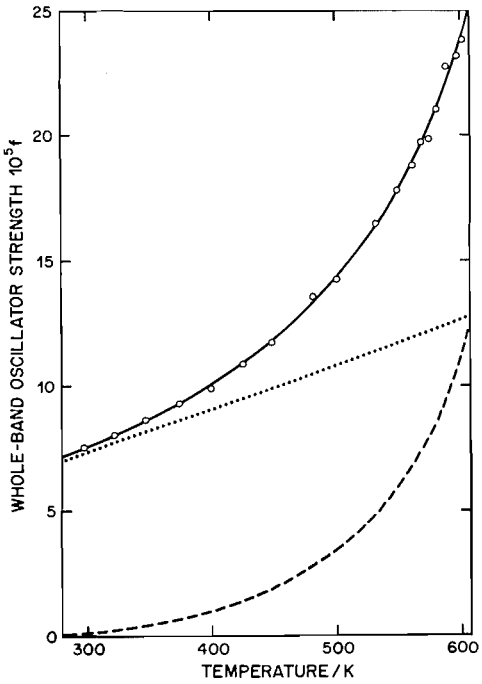


FIG. 6. Temperature dependence of expansion-corrected oscillator strength of 510 nm band of 0.0336 *M* $CoSO_4$ in 0.0990 *M* H_2SO_4 at 16 MPa. Solid curve: eq. [8] with parameters given in text. Dotted curve: estimated contribution of $Co(H_2O)_6^{2+}$ (eq. [3]). Dashed curve: estimated contribution of $Co(H_2O)_4^{2+}$.

$-3\ J\ K^{-1}\ mol^{-1}$. Thus, although the lower-temperature $Co(H_2O)_4^{2+}$ levels are low enough to escape detection by the method of Fiat *et al.* (19, 20), enough $Co(H_2O)_4^{2+}$ is present in aquocobalt(II) solutions to provide a dissociative pathway (D mechanism) for solvent exchange and net substitution in $Co(H_2O)_6^{2+}$. These results also suggest that an endothermic equilibrium similar to eq. [5] may be responsible for the high-temperature broadening of the Raman spectrum of aqueous

Can. J. Chem. Downloaded from www.nrcresearchpress.com by 210.87.254.42 on 09/05/12
For personal use only.

Can. J. Chem. Downloaded from www.nrcresearchpress.com by 210.87.254.42 on 09/05/12
For personal use only.

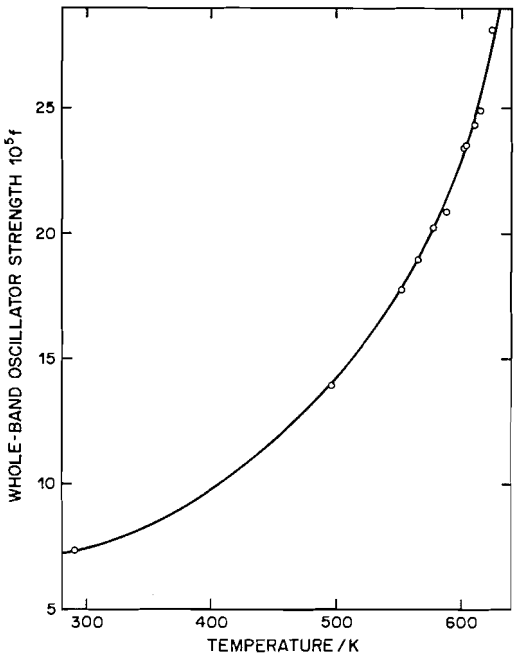


FIG. 7. Temperature dependence of oscillator strength of 510 nm band of 0.0238 *M* $CoSO_4$ in 0.478 *M* H_2SO_4 at 25 MPa. Curve represents eq. [8] with parameters for 0.099 *M* H_2So_4 (see text).

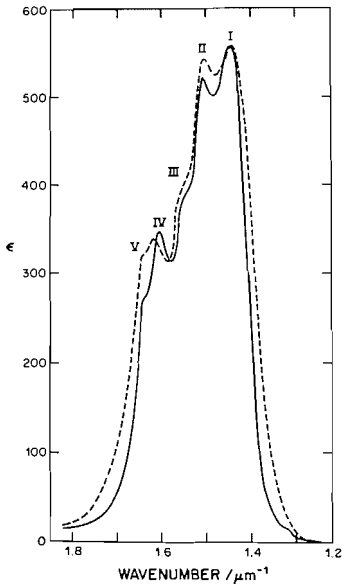


FIG. 8. Expansion-corrected spectra of 5.78 × 10^{-4} *M* $CoSO_4$ in 9.83 *M* LiCl with 1.8 × 10^{-3} *M* HCl at 24 MPa. Solid curve: 346 K. Broken curve: 534 K.

$Mg(H_2O)_6^{2+}$ (ionic radius 72 pm, cf. 73 pm for Co^{2+} (39)), as reported by Irish *et al.* (40); these authors favored an alternative explanation, but did not discount this possibility.

Figure 7 shows that the above parameters for $[H_2SO_4]$ = 0.099 *M* fit the data for $[H_2SO_4]$ = 0.478 *M* equally well (and to a higher upper temperature), so confirming that complexing by SO_4^{2-} or HSO_4^- is negligible and hydrolysis of Co^{2+}(aq) is completely suppressed. Similar results were obtained with other dilute acidic hydrogen sulfate media. This clearly demonstrates the potential usefulness of hydrogen sulfates as "inert" supporting electrolytes for high temperature aqueous chemistry.

Cobalt(II) in Excess Aqueous Chloride

The salient features of the spectra of cobalt(II) chloro-complexes in high temperature aqueous media have been well documented by Lüdemann *et al.* (1–3), while work by Bjerrum *et al.* (41, 42), Krauss and Lehmann (43), and Zeltmann *et al.* (44) has provided a more detailed understanding of these systems at temperatures below 360 K. It is now clear that, contrary to earlier reports suggesting that $CoCl_3OH_2^-$ was the major tetrahedral cobalt(II) species in aqueous chloride media (45), the tetrachlorocobaltate is the only important four-coordinate species in concentrated (~10 *M*) aqueous halide media (3, 41, 42, 44, 46). In more dilute solutions, $Co(H_2O)_4Cl_2^0$ may well be important at near-ambient temperatures (43, 47) and di- and tri-chloro aquocobalt complexes at high temperatures (1, 2).

The present study confirms that the only important tetrahedral Co species in 10 *M* aqueous LiCl at elevated temperatures is $CoCl_4^{2-}$. The spectra of such solutions had the shape and wavelengths characteristic of $CoCl_4^{2-}$ even at 293 K, and intensified with rising temperature, without significant shifts of maxima wavelengths, to reach an almost temperature-independent expansion-corrected intensity at ~ 340 K. Figure 8 shows spectra of $CoCl_4^{2-}$ in 9.8 *M* (52.3%, ρ^{293} = 1.213 g cm^{-3}) LiCl at 346 and 534 K, with expansion corrections based on Maksimova's (48) equation

$$[10] \quad \rho_r = (\rho_{H_2O}{}^T + 0.314)/(\rho_{H_2O}{}^{293} + 0.314)$$

The intensities of the features II and V are somewhat *T*-dependent (ε_{II} actually exceeds ε_I slightly, above about 550 K) and the wholeband oscillator strength rises 20% from 5.06 × 10^{-3} to 6.08 × 10^{-3} M^{-1} cm^{-2}, primarily because of a slight broadening over this 188 K range, but the striking constancy of ε_I (556 ± 7 M^{-1} cm^{-1}) and λ_I (692 ± 1 nm) contrasts with the aquocobalt(II) case considered above and lends itself to quantitative estimation of $CoCl_4^{2-}$ where this is the only tetrahedral halo-species present. The relative insensitivity of this nominally Laporte-forbidden $^4T_1(P) \leftarrow {}^4A_2$

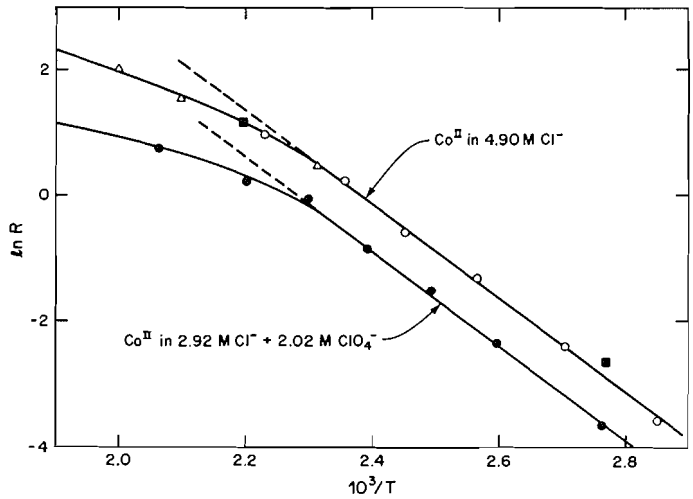


FIG. 9. Temperature dependence of tetrahedral–octahedral ratio R for $CoCl_2$ at 25 MPa in (upper curve) 4.80 M NaCl + 0.098 M HCl and (lower curve) 2.92 M NaCl + 2.024 M $NaClO_4$ + 0.43 mM HCl. $CoCl_2$ concentrations are 0.16 (triangles), 0.32 (squares), 1.32 (filled circles), and 1.60 (open circles) mM.

band of $CoCl_4^{2-}$ to temperature arises because it gains intensity through electronic, rather than vibronic, interactions of Co^{2+} with its ligands (49).

In acidified NaCl solutions, 2.0–5.0 M, the high-temperature densities of which were estimated by the method of Khaibullin and Borisov (36), $CoCl_4^{2-}$ was shown to be the only important absorbing species in the 700 nm region, so that one can use the apparent molar absorbance ε_I^* at 697 nm to measure the ratio R of $CoCl_4^{2-}$ to non-tetrahedral Co species.

$$[11] \quad R = [CoCl_4^{2-}]/[\text{Co(octahedral)}] = \varepsilon_I^*/(\varepsilon_I - \varepsilon_I^*)$$

The equilibrium constant K for the reaction

$$[12] \quad Co(H_2O)_{6-n}Cl_n^{(2-n)+} + (4-n)Cl^- \rightleftharpoons CoCl_4^{2-} + (6-n)H_2O$$

would be given by

$$[13] \quad K = a_{CoCl_4^{2-}} \cdot a_{H_2O}^{(6-n)}/(a_{Cl^-}^{(4-n)} \cdot a_{CoCl_n})$$

or, at constant ionic strength,

$$[14] \quad K' = R a_{H_2O}^{(6-n)}/[Cl^-]^{(4-n)} = \exp(\Delta S/R - \Delta H/RT)$$

Unfortunately, n is not known (but is scarcely likely to be zero at these halide concentrations and high temperatures, a_{H_2O} cannot be set to unity, and there is doubt concerning the validity of the ionic strength principle at these high concentrations and temperatures. Nevertheless, Fig. 9 shows that, at a given $[Cl^-]$, a plot of ln R vs. $1/T$ is linear up to about 50% completion of reaction with the same slope, corresponding to $\Delta H = +62 \pm 2$ kJ mol^{-1} for $[Cl^-]$ = 2.9, 4.0 (not shown), and 4.9 M at ionic strength 4.9 M. Krauss and Lehmann (43) report $\Delta H \sim$ 46 kJ mol^{-1} for the cobalt(II)–chloride octahedral–tetrahedral equilibrium over a smaller (75 K) range of temperatures. At a given temperature, R is dependent on $[Cl^-]$ to the power of about 1.5 at this ionic strength; this does not warrant detailed consideration, for the reasons given above, but suggests that $n = 2$, i.e., that the equilibrium observed is

$$[15] \quad Co(H_2O)_4Cl_2^0 + 2Cl^- \rightleftharpoons CoCl_4^{2-} + 4H_2O$$

This is not unreasonable for conditions of moderate $[Cl^-]$ and elevated temperature, which favor neutral species by virtue of the lowered dielectric constant (see also Krauss and Lehmann's evidence for $Co(H_2O)_4Cl_2^0$ (43)).

For acidic NaCl solutions with $[Cl^-]$ less than about 0.1 M but 2 to 5 × $[Co^{II}]$, broad, rather featureless bands with markedly *temperature-dependent* maxima were observed near 650 nm at elevated temperatures; these were attributed to mixtures of $CoCl_2(OH_2)_2^0$ and $CoCl_3(OH_2)^-$, the spectra being quite distinct from that of $CoCl_4^{2-}$ or any octahedral species, but no further information could be extracted. Similarly, at chloride-to-cobalt ratios of less than unity ($[Cl^-] \sim 0.03$ M or less), shifts and intensifications of the octahedral (510 nm) band showed that $Co(H_2O)_5Cl^+$ was probably important at elevated temperatures, but this was not pursued in detail.

Can. J. Chem. Downloaded from www.nrcresearchpress.com by 210.87.254.42 on 09/05/12
For personal use only.

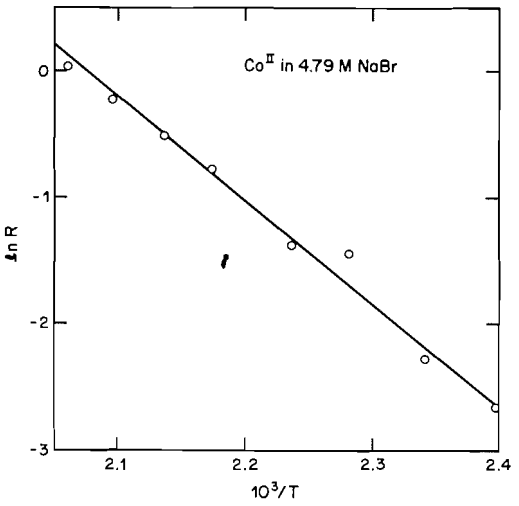


FIG. 10. Temperature dependence of tetrahedral–octahedral ratio for $CoSO_4$ (1.6 m*M*) in 4.79 *M* NaBr with 1.6 m*M* HBr at 24 MPa.

Cobalt in Excess Aqueous Bromide

The visible spectrum of 1.0 m*M* cobalt(II) sulfate in 9.0 *M* HBr shows a band with four well-defined maxima at 723, 697, 664, and 640 nm which reach temperature-independent expansion-corrected molar absorbances of 724, 720, 430, and 330 M^{-1} cm^{-1} respectively as the temperature is increased beyond 345 K. These data evidently characterize $CoBr_4^{2-}$. The same spectrum develops in solutions of cobalt(II) in aqueous NaBr (4.79 *M*, 36.2%, ρ^{293} = 1.364 g cm^{-3}) containing 1.0 m*M* HBr, as the temperature is raised. As with $CoCl_4^{2-}$, we can determine the ratio *R* of $CoBr_4^{2-}$ to octahedral cobalt(II) from the expansion-corrected (47) molar absorbance at 723 or 697 nm, and Fig. 10 shows that ln *R* is in effect a linear function of $1/T$ at least as far as $R \sim 1$, giving $\Delta H = +70 \pm 3$ kJ mol^{-1} for the octahedral → tetrahedral reaction.

The dependence of *R* on $[Br^-]$ was not studied, partly because of doubts regarding the validity of calculations made without direct knowledge of the activity coefficients involved (cf. $CoCl_4^{2-}$) but also because of the lower stability of $CoBr_4^{2-}$ relative to $CoCl_4^{2-}$. At 450 K, for example, $R = 0.30$ for 4.8 *M* NaBr and 3.0 for 4.9 *M* NaCl; the difference amounts to 8 kJ mol^{-1} in free energy, and is completely accounted for by the difference in ΔH.

Acknowledgement

We thank Atomic Energy of Canada, Ltd., for support of this work under contract.

1. H.-D. LÜDEMANN and E. U. FRANCK. Ber. Bunsenges. Phys. Chem. **71**, 455 (1967).
2. H.-D. LÜDEMANN and E. U. FRANCK. Ber. Bunsenges. Phys. Chem. **72**, 514 (1968).
3. H.-D. LÜDEMANN and W. A. J. MAHON. High Temp. High Press. **1**, 215 (1969).
4. M. TOMLINSON. Chem. Can. 21 (October 1974).
5. G. GIASSON and P. H. TEWARI. Can. J. Chem. **56**, 435 (1978).
6. W. C. WAGGENER. Rev. Sci. Instrum. **30**, 788 (1959).
7. W. C. WAGGENER and A. M. TRIPP. Rev. Sci. Instrum. **30**, 677 (1959).
8. E. PETERS and J. J. BYERLEY. Rev. Sci. Instrum. **34**, 819 (1963).
9. T. R. GRIFFITHS, F. LEE, and R. H. WIJAYANAYAKE. J. Sci. Instrum. **44**, 876 (1967).
10. W. C. WAGGENER, A. J. WEINBERGER, and R. W. STOUGHTON. Appl. Spectrosc. **22**, 545 (1968).
11. W. GIGGENBACH. J. Phys. E, **4**, 148 (1971).
12. R. D. ALEXANDER, A. W. L. DUDENEY, and R. J. IRVING. J. Phys. E, **7**, 522 (1974).
13. R. D. ALEXANDER, D. H. BUISSON, A. W. L. DUDENEY, and R. J. IRVING. J. Chem. Soc. Faraday Trans. I, **74**, 1081 (1978).
14. L. FABES and T. W. SWADDLE. Can. J. Chem. **53**, 3053 (1975).
15. M. P. HENDERSON, V. I. MIASEK, and T. W. SWADDLE. Can. J. Chem. **49**, 317 (1971).
16. A. S. QUIST, W. L. MARSHALL, and H. R. JOLLEY. J. Phys. Chem. **69**, 2726 (1965).
17. T. J. SWIFT and R. E. CONNICK. J. Chem. Phys. **37**, 307 (1962).
18. T. J. SWIFT. Inorg. Chem. **3**, 526 (1964).
19. A. M. CHMELNICK and D. FIAT. J. Chem. Phys. **47**, 3986 (1967).
20. D. FIAT, Z. LUZ, and B. L. SILVER. J. Chem. Phys. **49**, 1376 (1968).
21. G. C. KENNEDY and W. T. HOLSER. Handbook of physical constants. *Edited by* S. P. Clark, Jr. Memoir 97, Geological Society of America. New York. 1966. Section 16.
22. J. T. BELL and N. A. KROHN. J. Phys. Chem. **74**, 4006 (1970).
23. P.-C. KONG, T. W. SWADDLE, and P. BAYLISS. Can. J. Chem. **49**, 2442 (1971).
24. A. B. P. LEVER. Inorganic electronic spectroscopy. Elsevier Publishing Co., New York. 1968.
25. C. J. BALLHAUSEN. Introduction to ligand field theory. McGraw-Hill Book Co., Inc., Toronto. 1962. pp. 187–188.
26. D. M. ADAMS. Metal–ligand and related vibrations. Edward Arnold, Ltd., London. 1967. p. 256.
27. O. G. HOLMES and D. S. MCCLURE. J. Chem. Phys. **26**, 1686 (1957).
28. N. Q. CHAKO. J. Chem. Phys. **2**, 644 (1934).
29. L. E. JACOBS and J. R. PLATT. J. Chem. Phys. **16**, 1137 (1948).
30. N. S. BAYLISS. J. Chem. Phys. **18**, 292 (1950).
31. E. G. MCRAE. J. Phys. Chem. **61**, 562 (1957).
32. W. W. ROBERTSON and A. D. KING, JR. J. Chem. Phys. **34**, 1511 (1961).
33. S. F. ADDULNUR. J. Chem. Phys. **58**, 4175 (1973).
34. Y. B. ZELDOVICH, S. B. KORMER, M. V. SINITSYN, and K. B. YUSHKO. Dokl. Akad. Nauk SSSR, **138**, 1333 (1961); Sov. Phys. Dokl. **6**, 494 (1961).
35. D. W. SMITH. J. Inorg. Nucl. Chem. **34**, 3930 (1972).
36. I. KH. KHAIBULLIN and N. M. BORISOV. Russ. J. Phys. Chem. **39**, 361 (1965).
37. T. W. SWADDLE. J. Am. Chem. Soc. **89**, 4338 (1967).
38. F. A. COTTON and T. G. DUNNE. J. Am. Chem. Soc. **84**, 2013 (1962).

Can. J. Chem. Downloaded from www.nrcresearchpress.com by 210.87.254.42 on 09/05/12
For personal use only.

39. R. D. SHANNON and C. T. PREWITT. Acta Crystallogr. B**25**, 925 (1969); B**26**, 1046 (1970).
40. J. T. BULMER, D. E. IRISH, and L. ÖDBERG. Can. J. Chem. **53**, 3806 (1975).
41. J. BJERRUM, A. S. HALONIN, and L. H. SKIBSTED. Acta Chem. Scand. A**29**, 326 (1975).
42. L. H. SKIBSTED and J. BJERRUM. Acta Chem. Scand. A**32**, 429 (1978).
43. U. KRAUSS and G. LEHMANN. Ber. Bunsenges. Phys. Chem. **76**, 1066 (1972).
44. A. H. ZELTMANN, N. A. MATWIYOFF, and L. O. MORGAN. J. Phys. Chem. **72**, 121 (1968).
45. F. A. COTTON, D. M. L. GOODGAME, and M. GOODGAME. J. Am. Chem. Soc. **83**, 4690 (1961).
46. J. M. SMITHSON and R. J. P. WILLIAMS. J. Chem. Soc. 457 (1958).
47. A. YAMAGASHI, T. MASUI, and F. WATANABE. J. Phys. Chem. **84**, 34 (1980).
48. I. N. MAKSIMOVA. Russ. J. Phys. Chem. **39**, 296 (1965).
49. R. GALE, R. E. GODFREY, S. F. MASON, R. D. PEACOCK, and B. STEWART. J. Chem. Soc. Chem. Commun. 329 (1975).

Can. J. Chem. Downloaded from www.nrcresearchpress.com by 210.87.254.42 on 09/05/12
For personal use only.

Total synthesis of 3,17β-dihydroxy-6-oxaestra-1,3,5(10),7-tetraen and related miroestrol analogues

JOHN A. FINDLAY AND PAUL MEBE[1]

Chemistry Department, University of New Brunswick, Fredericton, N.B., Canada E3B 5A3

AND (IN PART)

MICHAEL D. STERN AND M. L. GIVNER

Ayerst Research Laboratories, P.O. Box 6115, Montreal, P.Q., Canada H3C 3J1

Received February 15, 1980

JOHN A. FINDLAY, PAUL MEBE, MICHAEL D. STERN, and M. L. GIVNER. Can. J. Chem. **58**, 1427 (1980).

3,17β-Dihydroxy-6-oxaestra-1,3,5(10),7-tetraen and related steroidal compounds have been synthesized in high yield via condensation of 7-methoxy-4-vinyl coumarin and 2-methyl-1,3-pentanedione. The approximate uterotrophic activity of the synthetic compounds relative to 17β-estradiol has been determined.

JOHN A. FINDLAY, PAUL MEBE, MICHAEL D. STERN et M. L. GIVNER. Can. J. Chem. **58**, 1427 (1980).

On a synthétisé avec des rendements élevés les dihydroxy-3,17β oxa-6 estra tétraène-1,3,5(10),7 ainsi que des stéroides apparentés en faisant appel à la condensation de la méthoxy-7 vinyl-4 coumarin sur la méthyl-2 pentanedione-1,3. On a déterminé l'activité utérotrophique approximative des produits synthétiques par rapport à celle de l'estradiol-17β.

[Traduit par le journal]

Can. J. Chem. Downloaded from www.nrcresearchpress.com by 210.87.254.5 on 09/05/12
For personal use only.

While miroestrol **1**, one of the most potent naturally occurring estrogens discovered (1), has been the subject of two synthetic studies (2) no successful synthesis has been reported to date. Since the compound possesses the 6-oxa-7-ene feature we considered it of interest to synthesize some steroidal analogues possessing this novel B ring enol ether function for pharmacological evaluation. This paper reports an efficient total synthesis of 3,17β-dihydroxy-6-oxaestra-1,3,5(10),7-tetraen, **10***c*, and related compounds.

Our synthesis contains a variant of the Torgov approach (3) involving a Michael type addition of 2-methyl-1,3-cyclopentanedione on the key intermediate 7-methoxy-4-vinyl coumarin **4** leading to the tetracyclic 3-methoxy-6-oxaestra-1,3,5(10),8(9),15-pentaen-7,17-dione, **6**, which by further functional group manipulation gave the prototype target compound **10***a* in 24% overall yield from *m*-methoxyphenol, **2**.

The vinyl coumarin **4** was prepared by condensing *m*-methoxyphenol **2** with ethyl-4-chloroacetoacetate in the presence of concentrated H_2SO_4 to give 7-methoxy-4-chloromethyl coumarin **3***a* which was readily transformed into the triphenylphosphonium salt **3***b*. The latter underwent Wittig condensation with aqueous formaldehyde in the presence of Na_2CO_3 to provide crystalline 7-methoxy-4-vinylcoumarin, **4** in 68% overall yield from **2**.

Compound **4** can also be prepared by oxidation of 7-methoxy-4-methyl coumarin with SeO_2 in refluxing diglyme/benzene to 7-methoxy-4-formyl coumarin which after reduction to the corresponding alcohol, displacement with bromide ion, and triphenylphosphonium salt formation provided **3***c* and an alternate route to **4** in a 50% overall yield. Attempted direct conversion of 7-methoxy-4-formyl coumarin to **4** via Wittig reaction under a variety of conditions was unsuccessful (4).

Condensation of **4** with 2-methyl-1,3-cyclopentanedione in acetonitrile containing KF and 18-crown-6, under N_2, gave the seco steroid **5** in 68% yield. Cyclization of the latter to the α,β-unsaturated ketone **6** was achieved in 80% yield by refluxing with *p*-toluenesulfonic acid in benzene. The ^1H nmr spectrum of **6** shows two sets of double doublets, one at δ 6.20 ($J = 5$ Hz, $J = 2$ Hz) and the other at δ 7.80 ($J = 5$ Hz, $J = 3$ Hz) assigned to C(15)H and C(16)H and constituting an AMX system with C(14)H.

Chemical corroboration of the location of the double bond between C(15) and C(16) is derived from the bromination of **11***a* to **11***b* and the dehydrobromination of **11***b* to give a single product, identical to **6**. The cyclopentanone **11***a* can be obtained by sodium borohydride reduction of **6** to the alcohol **11***c* followed by oxidation with CrO_3/H_2SO_4 or by catalytic hydrogenation of **6**.

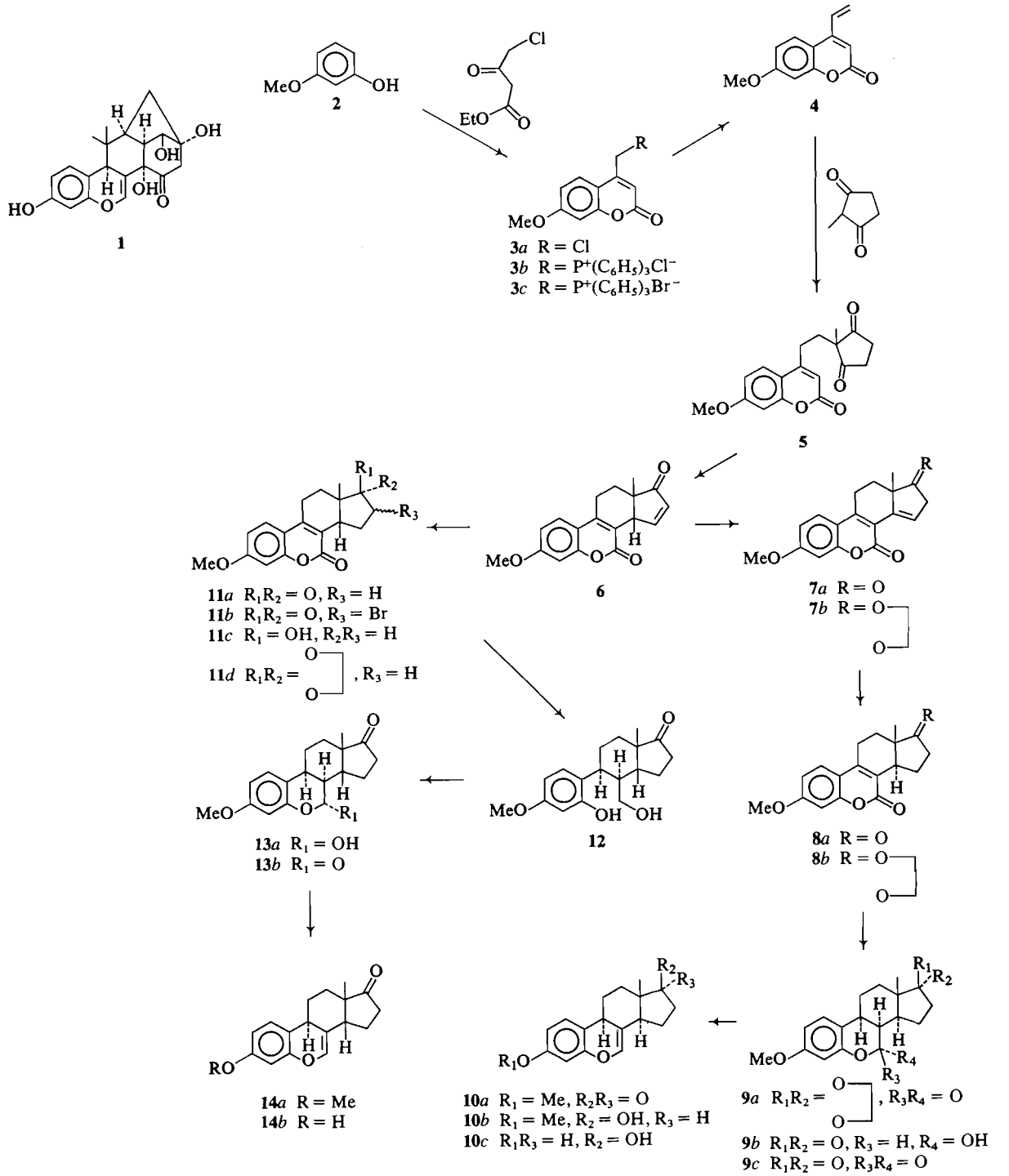
The C/D ring junction in **6** was shown to be *cis* via the following sequence: ketalization gave **7***b* (96% yield) whose ^1H nmr spectrum features a multiplet at δ 6.92 due to the olefinic C(15)H. Deketalization

[1]Present address: Chemistry Department, University of Zimbabwe, Salisbury, Zimbabwe.

0008-4042/80/141427-08$01.00/0

©1980 National Research Council of Canada/Conseil national de recherches du Canada

Can. J. Chem. Downloaded from www.nrcresearchpress.com by 210.87.254.5 on 09/05/12
For personal use only.



afforded the β,γ-unsaturated ketone **7***a* (96% yield) which on hydrogenation using 10% Pd/C in benzene gave the single tetraenone **8***a* in 93% yield, different from the isomer **11***a* obtainable by direct catalytic reduction of **6**. The *trans* C/D ring junction stereochemistry of **8***a* was confirmed by X-ray studies (5) on the reduction product **9***a* of its ketal **8***b* (*vide infra*). Development of the trans C/D ring junction via the H_2/Pd/C/benzene reducing medium has been successfully employed in similar steroidal systems (6).

Direct confirmation of the *cis* C/D ring junction in

TABLE 1. Uterotropic activity of miroestrol analogues

Compound (racemic)	No.	Uterotrophic activity relative to 17β-estradiol
8α-3-Methoxy-7-hydroxy-6-oxaestra-1,3,5(10)trien-17-one	**9***b*	Inactive
8α-3-Methoxy-6-oxaestra-1,3,5(10)-trien-7,17-dione	**9***c*	Slightly active
3-Methoxy-6-oxaestra-1,3,5(10),7-tetraen-17-one	**10***a*	Slightly active
3-Methoxy-6-oxaestra-1,3,5(10),7-tetraen-17β-ol	**10***b*	Slightly active
3-Hydroxy-6-oxaestra-1,3,5(10),7-tetraen-17β-ol	**10***c*	Quite active, but less than 17β-estradiol
14β-3-Methoxy-6-oxaestra-1,3,5(10),7-tetraen-17-one	**14***a*	Inactive

6 and **11***a* comes from X-ray diffraction studies (7) on the hemi-acetal ketone **13***a*, obtained by $Na_2Cr_2O_7$/DMSO oxidation of the major Li/NH_3 reduction product **12** of **11***d*, which revealed the existence of the *cis–anti–cis* ring junction stereochemistry for **13***a*. The ethylene ketal of dione **13***b* was also obtained (17%) in the reduction of **11***d* by Li/NH_3.

Compound **14***a* was obtained in quantitative yield from **13***a* by dehydration with *p*-toluenesulfonic acid in refluxing benzene while **14***b* was available directly from **13***a* in 85% yield by treatment with boron tribromide in dichloromethane at 0°C.

With the stereochemistry of the C/D ring junction now under rigorous control, the α,β-unsaturated lactone ketal **8***b* was transformed into the saturated lactone ketal **9***a* in 93% yield by means of Li/NH_3. Further reduction with one equivalent of diisobutylaluminum hydride at −70°C followed by acidic work up gave the crystalline hemi-acetal ketone **9***b* (85% yield). The ^{1}H nmr spectrum of the latter shows a doublet at δ 5.60 (J = 9 Hz) indicative of a *trans* diaxial relationship of C(7)H/C(8)H.

The keto lactone **9***c* was prepared in quantitative yield by deketalization of **9***a* using *p*-toluenesulfonic acid in acetone.

Dehydration of **9***b* using *p*-toluenesulfonic acid–benzene gave a quantitative yield of the 6-oxa-7-ene steroid **10***a* whose ^{1}H nmr spectrum displays a signal at δ 6.23 for the vinylic C(7)H. Infrared absorptions at 1730 and 1685 cm^{-1} attest to the presence of five-membered ketone and vinyl ether functionalities. 17β-Hydroxy-3-methoxy-6-oxaestra-1,3,5(10)7-tetraen, **10***b*, was obtained from **10***a* in quantitative yield by reduction with sodium borohydride in benzene/methanol. The ^{1}H nmr spectrum displays a signal at δ 3.80 (t, J = 8 Hz) characteristic (8) of the α configuration for C(17)H. Demethylation of **10***b* to 3,17β-dihydroxy-6-oxaestra-1,3,5(10),7-tetraen, **10***c*, was accomplished in 68% yield by heating it at 180–190°C with CH_3MgI. Attempted demethylation of **10***b* using boron tribromide led to intractable mixtures.

The racemic compounds **9***b*, **9***c*, **10***a*, **10***b*, **10***c*, and **14***a* prepared by this route have been tested for uterotrophic activity using the procedure of Rubin *et al.* (9) with minor modification and the results are contained in Table 1. Compound **10***c* was the most potent of the series but less active than 17β-estradiol. Herr *et al.* (10) have shown that the Δ^7-estrogens are more active than those which are saturated in ring B. The results indicate that formation of 6-cyclo-ether analogues of Δ^7-estrogens results in a decrease of uterotrophic activity.

Experimental

Melting points were determined on a Kofler hot stage apparatus and are uncorrected. Mass spectra were obtained with an Hitachi-Perkin-Elmer RMU-6D spectrometer. The ^{1}H nmr spectra were recorded in $CDCl_3$ with a Varian T-60 instrument employing tetramethylsilane as internal standard. Line positions are reported in ppm from this standard. The ir spectra were recorded with a Perkin-Elmer 457 grating infrared spectrophotometer.

7-Methoxy-4-chloromethylcoumarin, 3a from 2

Concentrated H_2SO_4 (200 mL) in a two necked 1-L round bottom flask fitted with dropping funnel and thermometer was cooled below 10°C and a mixture of *m*-methoxyphenol (10 g, 81 mmol) and ethyl 4-chloroacetoacetate (13.15 g, 85 mmol) was slowly added to the stirred solution maintaining the temperature below 15°C. The mixture was then stirred at room temperature for 15 h and the reaction mixture poured into ice/water (800 mL) with vigorous stirring. The precipitated product was filtered off and washed with water to neutrality and then treated with aqueous 5% NaOH (80 mL) to remove phenolic impurities. The residue was washed with water (3 × 50 mL) affording white crystalline 7-methoxy-4-chloromethylcoumarin **3***a* (17.02 g, 94%). Recrystallization from ethanol gave analytically pure material mp 195°C. *Anal.* calcd. for $C_{11}H_9O_3Cl$: C 58.79, H 4.01; found: C 58.48, H 4.30. The mass spectrum *m/e* 226 (32, M + 2), 224 (100, M^+), 196 (43, M − CO), 189 (26, M − Cl), 161 (36). The ^{1}H nmr spectrum δ_{TMS} ($CDCl_3$): 3.90 (s, 3H, CH_3O), 4.63 (s, 2H, $ClCH_2$—), 6.40 (s, 1H, C(3)H), 6.80–7.67 (m, 3H, aromatic). The ir spectrum ν_{max} (KBr): 1725 (carbonyl), 1610 (aromatic), 1400, 1357, 1294, 1269, 1219, 1144, 1061, 1030, 1000, 880, 859, 831 cm^{-1}.

((7-Methoxy-2-oxo-2H-1-benzopyran-4-yl)methyl)triphenylphosphonium Bromide 3c

A mixture of 7-methoxy-4-bromomethylcoumarin (**4**) (0.25 g, 0.93 mmol) and triphenylphosphine (0.24 g, 0.95 mmol) was suspended in dry acetonitrile (15 mL). The mixture was stirred and refluxed under N_2 and the suspended mixture dissolved after 30 min. Refluxing was continued for 18 h, during which

Can. J. Chem. Downloaded from www.nrcresearchpress.com by 210.87.254.5 on 09/05/12
For personal use only.

Can. J. Chem. Downloaded from www.nrcresearchpress.com by 210.87.254.5 on 09/05/12
For personal use only.

time the white phosphonium salt precipitated. The mixture was cooled, filtered, and the salt **3***c* was washed several times with boiling benzene, then dried *in vacuo*, affording pure product (0.44 g, 90%) mp 272–274°C. The product was also obtained (79%) when benzene was used instead of acetonitrile as reaction solvent.

*((7-Methoxy-2-oxo-2*H*-1-benzopyran-4-yl)methyl)triphenylphosphonium Chloride* **3***b*

The phosphonium chloride salt **3***b* was prepared in 82% yield from chloromethylcoumarin **3***a* and excess triphenylphosphine in acetonitrile as previously described for the phosphonium bromide salt **3***c*. The salt, a white powder, was dried *in vacuo* and melted at 266–268°C.

7-Methoxy-4-vinylcoumarin **4** *from* **3***c*

(*a*) The triphenylphosphonium bromide **3***c* (0.61 g, 1.14 mmol) was suspended in 37% formaldehyde (2.2 mL). A solution of 15% Na_2CO_3 (1.5 mL) was added intermittently by a dropping funnel. Each subsequent addition was made after the orange-yellow color of the phosphorane formed had disappeared. When the addition of the base was complete, the mixture was stirred at room temperature for 2 h. The suspended white crystalline product containing triphenylphosphine oxide by-product was extracted three times with ether (100, 50, and 30 mL). The ethereal layer was dried (anhydrous Na_2SO_4) and evaporated. The white residue obtained was chromatographically purified on a short column of silica gel. Elution with ethyl acetate – cyclohexane (2:5) gave pure white crystalline vinylcoumarin **4** (0.20 g, 98%), mp 98°C. Attempts to recrystallize this compound in several solvents were unsuccessful.

Anal. calcd. for $C_{12}H_{10}O_3$: C 71.30, H 4.95; found: C 70.80, H 5.07. The mass spectrum *m/e*: 202 (100, M^+), 174 (78, $M - CO$), 159 (62, $M - CO - CH_3$). The ^1H nmr spectrum δ_{TMS} ($CDCl_3$): 3.90 (s, 3H, CH_3O—), 5.63–6.12 (m, 2H, vinylic), 6.30 (s, 1H, C(3)H), 6.43–7.71 (complex m, 4H, aromatic and vinylic). The ir spectrum ν_{max} (KBr): 1720 (C=O), 1610, 1500, 1155, 861, 814 cm^{-1}.

(*b*) Vinylcoumarin **4** was synthesized as described above in 91% yield from phosphonium chloride salt **3***b* instead of phosphonium bromide salt **3***c*.

3-Methoxy-8,14-seco-6-oxaestra-1,3,5(10),8-tetraen-7,14,17-trione **5** *from* **4**

To a stirred solution of 18-crown-6 (80 mg) in acetonitrile (15 mL) was added KF (310 mg) and the mixture was dried by heating *in vacuo* at 135°C for 1.5 h. Vinylcoumarin **4** (1.73 g, 8.56 mmol) and 2-methylcyclopentane-1,3-dione (1.10 g, 9.81 mmol) were then added to the stirred mixture. The mixture was refluxed under N_2 and the suspended material dissolved. The mixture was refluxed overnight and the resulting white precipitate containing excess diketone reagent was removed by filtration while the reaction mixture was hot. The precipitate was washed with acetonitrile (2 × 10 mL). The filtrate and the washings were combined and acetonitrile was evaporated under reduced pressure. The residue was dissolved in chloroform (100 mL) and washed with 5% $NaHCO_3$ (2 × 20 mL) to remove excess cyclopentanedione. The organic layer was worked up in the usual manner. The pale orange residue was purified by chromatography on silica gel (100 g). Elution with ethyl acetate – cyclohexane (1:2) furnished the pale orange crystalline seco-steroid **5** (1.83 g, 68%). An analytical sample recrystallized from ethyl acetate had mp 128°C.

Anal. calcd. for $C_{18}H_{18}O_5$: C 68.80, H 5.73; found: C 68.14, H 5.66. The mass spectrum *m/e*: 314 (100, M^+), 277 (17), 203 (64, M – H – methylcyclopentanedione), 202 (67, M – methylcyclopentanedione), 190 (29), 174 (36). The ^1H nmr spectrum δ_{TMS} ($CDCl_3$): 1.23 (s, 3H, CH_3—), 1.85–2.30 (m, 2H, C(12)H), 2.40–2.73 (m, 2H, C(13)H), 2.90 (s, 2H, C(15)H and C(16)H), 3.90 (s, 3H, CH_3O—), 6.07 (s, 1H, C(8)H), 6.79–7.98 (m, 2H, aromatic C(2)H and C(4)H), 7.53 (d, J = 8 Hz, 1H, aromatic C(1)H). The ir spectrum ν_{max} (KBr): 1718 (broad, lactone, ketone, C=O), 1612, 1429 cm^{-1}.

*14*β*-3-Methoxy-6-oxaestra-1,3,5(10),8,15-pentaen-7,17-dione* **6** *from* **5**

The secosteroid **5** (2.24 g, 7.13 mmol) was suspended in dry benzene (20 mL) and *p*-toluenesulfonic acid monohydrate (430 mg) was added to the mixture. The mixture was stirred and refluxed under N_2 for 15 h. Water was removed azeotropically employing a Dean–Stark trap filled with Linde molecular sieves, type 5A. The resulting reddish brown mixture was cooled and diluted with benzene (20 mL). The mixture was then washed with 5% $NaHCO_3$ (2 × 20 mL) to remove *p*-toluenesulfonic acid. The organic layer after drying (anhydrous Na_2SO_4) and evaporation gave a reddish brown residue which was chromatographed on a silica gel (100 g) column and elution with ethyl acetate – cyclohexane (2:5) afforded **6** (1.69 g, 80%), mp 143–145°C (recrystallized from ethyl acetate). An analytical sample was homogeneous on tlc and proved to be sensitive to light and moist air resulting in a bright purple color.

Anal. calcd. for $C_{18}H_{16}O_4$: C 72.97, H 5.40; found: C 72.61, H 5.40. The mass spectrum *m/e*: 296 (100, M^+), 281 (13, $M - CH_3$), 269 (12), 268 (76, M – CO), 253 (21). The ^1H nmr spectrum δ_{TMS} ($CDCl_3$): 12.7 (s, 3H, CH_3—), 1.40–3.33 (complex m, 6H), 3.90 (s, 3H, CH_3O—) 6.20 (q, 1H, J = 5 Hz, J = 2 Hz, C(15)H), 6.90 (m, 2H, aromatic C(2)H and C(4)H), 7.48 (d, J = 8 Hz, 1H, aromatic C(1)H), 7.80 (q, 1H, J = 5 Hz, J = 3 Hz, C(16)H). The ir spectrum ν_{max} (KBr): 1730 (shoulder, ketone C=O), 1710 (broad, lactone C=O), 1615, 1520, 1460 cm^{-1}.

3-Methoxy-6-oxaestra-1,3,5(10),8,14-pentaen-7-oxo-17-ethylene acetal **7***b* *from* **6**

To a solution of tetracyclic pentaene **6** (1 g, 3.38 mmol) in benzene (50 mL) was added ethylene glycol (3 mL) and *p*-toluenesulfonic acid (30 mg). The solution was refluxed (while water was removed azeotropically) for 4 h and then cooled to room temperature. The solution was diluted with benzene (50 mL) and the organic layer was evaporated to give the ketal **7***b* in 96% yield, homogeneous on tlc. An analytical sample was recrystallized from ethyl acetate (mp 168°C).

Anal. calcd. for $C_{20}H_{20}O_5$: C 70.59, H 5.88; found: C 70.70, H 5.92. The ^1H nmr spectrum δ_{TMS} ($CDCl_3$): 1.06 (s, 3H, CH_3—), 1.50–3.26 (complex m, 6H), 3.86 (s, 3H, CH_3O—), 4.00 (s, 4H, —OCH_2CH_2O—), 6.92 (m, 1H, C(15)H), 6.84 (m, 2H, aromatic C(2)H and C(4)H), 7.43 (d, J = 8 Hz, 1H, aromatic C(1)H). The ir spectrum ν_{max} (KBr): 1725 (lactone C=O), 1620, 1600 (aromatic), 1300, 1160, 1030, 885, 850, 810 cm^{-1}. The uv spectrum (95% EtOH) λ_{max} nm (ε_{max}): 221 (22 422), 250 (13 918), 350 (25 773).

3-Methoxy-6-oxaestra-1,3,5(10),8,14-pentaen-7,17-dione **7**a

A solution of the tetracyclic ketal **7***b* (1 g, 2.94 mmol) in acetone (30 mL) was treated with a catalytic amount of *p*-toluenesulfonic acid monohydrate. The solution was stirred overnight at room temperature. Most of the product precipitated out of the solution and this fraction was filtered out and washed with 5% $NaHCO_3$ and water to give a pure product **7***a*. The filtrate was concentrated and diluted with benzene (50 mL). The organic layer was washed with 5% $NaHCO_3$ (20 mL) and water. The dried organic layer was evaporated to give a crude residue which was purified on silica gel column and eluted with *n*-hexane – ethyl acetate (1:1). The two fractions were combined to give a total yield of the pentaendione **7***a* (0.835 g, 96%). An analytical sample was recrystallized in acetone – petroleum ether (2:1) to give light orange crystals (mp 212°C dec.).

Can. J. Chem. Downloaded from www.nrcresearchpress.com by 210.87.254.5 on 09/05/12
For personal use only.

The mass spectrum *m/e*: 296 (65, M^+), 269 (19, $M^+ - CH_2{=}CH$), 268 (100, $M^+ - CO$), 267 (12), 253 (26), 240 (13), 239 (13). The ^1H nmr spectrum δ_{TMS} ($CDCl_3$): 1.17 (s, 3H, CH_3—), 1.44–3.33 (complex m, 6H), 3.90 (s, 3H, CH_3O—), 6.90 (multiplet, 2H, aromatic C(2)H and C(4)H), 7.03 (t, J = 2 Hz, 1H, C(15)H), 7.60 (d, J = 8 Hz, 1H, aromatic C(1)H). The ir spectrum ν_{max} (KBr): 1746 (ketone C=O), 1710 (α,β-unsaturated lactone C=O), 1625, 1610, 1595 (aromatic), 1460, 1450, 1400, 1290, 1260, 1210, 1170, 1140, 1030, 830, 820 cm^{-1}. The uv spectrum (95% EtOH) λ_{max} nm (ε_{max}): 216 (18 179), 247 (8 848), 350 (18 179).

3-Methoxy-6-oxaestra-1,3,5(10),8-tetraen-7,17-dione **8**a *from* **7**a

A suspension of 10% palladium on charcoal (50 mg) in sulfur-free benzene (10 mL) was degassed and saturated with H_2. To this catalyst mixture was added a purplish solution of the tetracyclic pentaen **7***a* (100 mg, 0.34 mmol) in benzene (15 mL). The mixture was vigorously stirred and hydrogenation was stopped after about 7 mL of H_2 (required to saturate one double bond) was absorbed. The catalyst was filtered and the clear solution evaporated to dryness to give pure tetraen dione **8***a* (0.094 g, 93%). An analytical sample was recrystallized from benzene to afford white crystals, mp 223–225°C.

Anal. calcd. for $C_{18}H_{18}O_4$: C 72.48, H 6.04; found: C 72.70, H 6.09. The mass spectrum *m/e*: 299 (15, M + 1), 298 (100, M^+), 270 (19, $M^+ - CO$), 255 (50), 243 (39), 242 (55), 241 (44), 229 (28), 227 (20). The ^1H nmr spectrum δ_{TMS} ($CDCl_3$): 0.90 (s, 3H, CH_3O—), 6.90 (m, 2H, aromatic C(2)H and C(4)H), 7.50 (d, J = 8 Hz, 1H, aromatic C(1)H). The ir spectrum ν_{max} (KBr): 1735 (ketone C=O), 1720 (lactone C=O), 1620, 1610 (aromatic), 1510, 1450, 1395, 1295, 1275, 1260, 1230, 1215, 1185 cm^{-1}. The uv spectrum (95% EtOH) λ_{max} nm (ε_{max}): 225 (11 569), 328 (14 204).

3-Methoxy-6-oxaestra-1,3,5(10),8-tetraen-7-oxo-17-ethylene Acetal **8**b *from* **8**a

The tetracyclic ketone **8***a* was ketalized as described in the procedure for compound **7***b* to give the ketal **8***b* in 88% yield. Analytical sample was recrystallized in acetone to give white crystals, mp 184°C. The ^1H nmr spectrum δ_{TMS} ($CDCl_3$): 0.87 (s, 3H, CH_3—), 1.50–3.23 (complex m, 9H), 3.87 (s, 3H, CH_3O—), 3.95 (s, 4H, —OCH_2CH_2O—), 6.42 (m, 2H, aromatic C(2)H and C(4)H), 7.47 (d, J = 8 Hz, 1H, aromatic C(1)H). The ir spectrum ν_{max} (KBr): 1710 (broad lactone C=O), 1610, 1385, 1320, 1300, 1285, 1200, 1160 (broad), 1070 (broad), 970, 855, 810, 790, 780 cm^{-1}. The mass spectrum *m/e*: 342 (17, M^+), 298 (98, $M^+ - CH_2CH_2O$—), 283 (18, $M^+ - CH_2CH_2O + CH_3$), 270 (21, $M^+ - CH_2CH_2O - CO$), 256 (42), 255 (20), 243 (88), 242 (100), 241 (93), 227 (47), 226 (25).

8α-3-Methoxy-6-oxaestra-1,3,5(10)-trien-7-oxo-17-ethylene Acetal **9**a *from* **8**b

Into dry liquid ammonia (300 mL) was added lithium (45 mg), cut into small pieces. The deep blue solution thus formed was stirred vigorously with a magnetic stirrer for 10 min and a suspension of ketalized tetraen **8***b* (1 g, 2.92 mmol) in anhydrous ether (75 mL) was quickly added. The mixture was vigorously stirred for an additional 30 min and quenched with dry NH_4Cl (500 mg) carefully. The ammonia condenser was removed and ammonia allowed to evaporate in a stream of nitrogen. The residual ammonia and ether were evaporated under reduced pressure. The white residue was treated with 5% NaOH solution (25 mL) to remove over-reduced phenolic material. The mixture was stirred, filtered, and washed with water several times and dried. The white crystalline triene **9***a* (0.94 g, 93%) was recrystallized from benzene to give white needles, mp 164°C.

Anal. calcd. for $C_{20}H_{24}O_5$: C 69.76, H 6.97; found: C 69.36, H 6.82. The mass spectrum *m/e*: 344 (88, M^+), 259 (18), 258 (100), 256 (21), 190 (18), 177 (27), 139 (54). The ^1H nmr spectrum δ_{TMS} ($CDCl_3$): 1.00 (s, 3H, CH_3—), 1.33–3.00 (complex m, 11H), 3.80 (s, 3H, CH_3O—), 3.90 (s, 4H, OCH_2CH_2O), 6.63 (m, 2H, aromatic C(2)H and C(4)H), 7.70 (d, J = 8 Hz, 1H, aromatic C(1)H). The ir spectrum ν_{max} (KBr): 1770 (lactone C=O), 1630, 1600 (aromatic), 1515, 1460, 1285, 1240, 1170, 1150 (broad), 1040, 985, 850 cm^{-1}.

8α-3-Methoxy-6-oxaestra-1,3,5(10)-trien-7,17-dione **9**c

The tetracyclic ketal **9***a* was deketalized by stirring in acetone with a catalytic amount of *p*-toluenesulfonic acid monohydrate overnight to give a quantitative yield of the tetracyclic dione **9***c*. An analytical sample was recrystallized from benzene to give white crystals, mp 171°C.

The mass spectrum *m/e*: 301 (20, M + 1), 300 (100, M^+), 229 (18), 216 (14), 215 (12), 177 (27), 176 (20), 163 (24), 150 (38), 148 (20), 137 (31), 124 (20). The ^1H nmr spectrum δ_{TMS} ($CDCl_3$): 1.00 (s, 3H, CH_3—), 1.33–3.23 (complex m, 11H), 3.80 (s, 3H, CH_3O—), 6.60–6.80 (m, 2H, aromatic C(2)H and C(4)H), 7.10 (d, J = 8 Hz, 1H, aromatic C(1)H). The ir spectrum ν_{max} (KBr): 1770 (lactone C=O), 1730 (ketone C=O), 1620, 1590 (aromatic), 1510 (broad), 1450, 1430, 1360, 1330, 1278, 1240, 1201, 1170, 1130 (broad), 1055, 1035, 975, 876, 835 cm^{-1}. The uv spectrum (95% EtOH) λ_{max} nm (ε_{max}): 220 (11 491), 280 (2 771), 285 (2 608).

8α-3-Methoxy-7-hydroxy-6-oxaestra-1,3,5(10)-trien-17-one **9**b *from* **9**a

Into an oven dried pear-shaped flask was added the ethylene ketal lactone **9***a* (0.1 g, 0.29 mmol) and dry toluene (5 mL). The solution was cooled to −70°C and a 1 *M* diisobutylaluminium hydride solution (0.3 mL) was added from a syringe through a septum. The reaction mixture was stirred for 20 min at −70°C and then quenched with methanol (0.5 mL). The mixture was allowed to warm to 0°C and cold 5% HCl (20 mL) was added. The product was extracted twice with chloroform (30 ml, 25 ml) and the organic layer was washed with water twice and dried with $MgSO_4$. Evaporation of the solvent left white crystals which were subsequently deketalized as before affording pure white tetracyclic hemiacetal **9***b* in 85% yield. Recrystallization in ethyl acetate – *n*-hexane (2:1) afforded white needles melting at 175°C.

Anal. calcd. for $C_{18}H_{22}O_4$: C 71.52, H 7.28; found: C 71.56, H 7.30. The mass spectrum *m/e*: 302 (45, M^+), 164 (15), 163 (93), 161 (19), 150 (100), 137 (33). The ^1H nmr spectrum δ_{TMS} ($CDCl_3$): 1.07 (s, 3H, CH_3—), 1.40–3.00 (complex m, 11H), 3.87 (s, 3H, CH_3O—), 5.60 (t, J = 6 Hz, 1H, C(7)H; D_2O added, d, J = 9 Hz), 6.43 (m, 2H, aromatic C(2)H and C(4)H), 6.60 (d, J = 7 Hz, 1H, C(7)OH), 7.00 (d, J = 8 Hz, 1H, aromatic C(1)H). The ir spectrum ν_{max} (KBr): 3420 (OH), 1730 (ketone C=O), 1620, 1590, 1510, 1460, 1450, 1340, 1275, 1200, 1180, 1160, 1124, 1040, 1000, 935, 830 cm^{-1}.

3-Methoxy-6-oxaestra-1,3,5(10),7-tetraen-17-one **10**a *from* **9**b

To a solution of the tetracyclic hemiacetal **9***b* (0.1 g, 0.33 mmol) in benzene (15 mL) was added *p*-toluenesulfonic acid monohydride (30 mg). The mixture was refluxed azeotropically under nitrogen for 1 h. The mixture was cooled to room temperature and diluted with benzene (30 mL). It was washed with 5% $NaHCO_3$ (20 mL), with water, and then dried. Evaporation of the solvent gave a pure white crystalline tetracyclic vinyl ether **10***a* in quantitative yield. A sample was recrystallized from ethyl acetate – *n*-hexane (1:1) giving white crystals, mp 175°C.

Anal. calcd. for $C_{18}H_{20}O_3$: C 76.05, H 7.04; found: C 75.93, H 7.14. The mass spectrum *m/e*: 284 (100, M^+), 269 (9, $M^+ - CH_3$), 256 (35, $M^+ - CO$), 255 (39), 241 (67), 228 (34), 227 (26), 213 (22), 188 (23), 187 (40), 160 (27). The ^1H nmr spectrum δ_{TMS} ($CDCl_3$):

Can. J. Chem. Downloaded from www.nrcresearchpress.com by 210.87.254.5 on 09/05/12
For personal use only.

0.87 (s, 3H, CH_3—), 1.23–2.70 (complex m, 9H), 3.23 (broad m, 1H, benzylic), 3.80 (s, 3H, CH_3O—), 6.23 (t, J = 2 Hz, 1H, C(7)H), 6.60 (m, 2H, aromatic C(2)H and C(4)H), 7.05 (d, J = 8 Hz, 1H, aromatic C(1)H). The ir spectrum ν_{max} (KBr): 1730 (ketone C=O), 1685 (medium, vinyl ether O—CH=C), 1615, 1575, 1500, 1440, 1250, 1240, 1210, 1205, 1175, 1150, 1125, 1040, 935, 860, 830 cm^{-1}. The uv spectrum (95% EtOH) λ_{max} nm (ε_{max}): 225 (11 410), 250 (5 167), 290 (4 629).

3-Methoxy-6-oxaestra-1,3,5(10),7-tetraen-17β-ol ***10b*** *from* ***10a***

To a solution of the tetracyclic ketone **10*a*** (0.412 g, 1.45 mmol) in benzene (15 mL) was added methanol (15 mL). The solution was cooled in an ice-water bath and sodium borohydride (100 mg) was added at once. The mixture was stirred for 5 min and gradually allowed to warm to room temperature. After 45 min the mixture was poured into ice-cold 5% HCl solution (20 mL) and the product was extracted with benzene and the organic layer washed twice with water and dried with $MgSO_4$. Evaporation of the solvent left a white crystalline alcohol **10*b*** (96% yield), pure by ^1H nmr spectrum. A sample was recrystallized from ethyl acetate – *n*-hexane (2:1) to give white crystals melting at 124°C.

Anal. calcd. for $C_{18}H_{22}O_3$: C 75.52, H 7.69; found: C 75.96, H 7.56. The mass spectrum *m/e*: 286 (100, M^+), 257 (50), 241 (49), 187 (82), 161 (48), 137 (25). The ^1H nmr spectrum δ_{TMS} ($CDCl_3$): 0.73 (s, 3H, CH_3—), 1.20–2.50 (complex m, 10H), 3.17 (broad m, 1H, benzylic), 3.80 (s, 3H, CH_3O—), 3.80 (t, 1H, C(17)H), 6.10 (t, J = 2 Hz, 1H, C(7)H), 6.33–6.60 (m, 2H, aromatic C(2)H and C(4)H), 7.00 (d, J = 8 Hz, 1H, aromatic C(1)H). The ir spectrum ν_{max} (KBr): 3420 (broad, OH), 1700 (weak, vinyl ether O—CH=C), 1620, 1585 (aromatic), 1510, 1450, 1210, 1200, 1180, 1135, 1040, 940, 865, 840 cm^{-1}.

3-8Hydroxy-6-oxaestra-1,3,5(10),7-tetraen-17β-ol ***10c*** *from* ***10b***

To methylmagnesium iodide (1.59 mmol) in anhydrous ether (20 mL) was added methyl ether **10*b*** (0.228 g, 0.80 mmol) under nitrogen. The mixture was stirred and ether was removed with a stream of nitrogen. The solid mixture was heated at 180–190°C for 3 h. The mixture was cooled to room temperature and hydrolysed with ice-cold 5% HCl (25 mL). The product was extracted with chloroform (20 mL × 4) and the organic layer was washed several times and dried with $MgSO_4$. Evaporation of the solvent left a crude brown residue which was purified by silica gel preparative tlc (using ethyl acetate – *n*-hexane (1:1)) to give yellowish crystals of the diol **10*c*** (0.148 g, 68%). An analytical sample was recrystallized from 95% ethanol to give white needles, mp 196–201°C (dec.).

The mass spectrum *m/e*: 272 (95, M^+), 243 (48, M^+ – CHO), 227 (35), 173 (100), 147 (52), 123 (24). The ^1H nmr spectrum δ_{TMS} ($CDCl_3$–DMSO-d_6, two drops): 0.73 (s, 3H, CH_3—), 1.00–3.33 (complex m, 9H), 3.33 (broad m, 1H, benzylic C(9)H), 3.80 (broad m, 1H, C(17)OH), 6.10 (broad s, 1H, C(7)H), 6.33–6.60 (m, 2H, aromatic C(2)H and C(4)H), 7.00 (d, J = 8 Hz, 1H, aromatic C(1)H), 8.70 (s, 1H, phenolic OH). The ir spectrum ν_{max} (KBr): 3410 (OH), 3240 (broad, phenolic OH), 1700 (weak, vinyl ether O—CH=C), 1620 (aromatic), 1510, 1460, 1350, 1260, 1180 (sharp), 1135, 1050 cm^{-1}.

14β-3-Methoxy-6-oxaestra-1,3,5(10),8-tetraen-7,17-dione ***11a*** *from* ***6***

Into a 100 mL round-bottomed flask was added 10% Pd/C (100 mg) and dry benzene (15 mL). The mixture was degassed by pumping at reduced pressure and prehydrogenated. A solution of the tetracyclic pentaene **6** (200 mg, 0.68 mmol) in dry benzene (915 mL) was added at once to the catalyst–benzene mixture in a hydrogen atmosphere. The mixture was stirred until one equivalent of hydrogen was absorbed (~15 min). The catalyst was filtered and removal of benzene under reduced pressure gave white crystalline tetracyclic tetraen **11*a*** (200 mg, 98%). An analytical sample, crystallized from benzene–cyclohexane (1:1), had mp 156–159°C.

Anal. calcd. for $C_{18}H_{18}O_4$: C 72.48, H 6.04; found: C 72.11, H 6.06. The mass spectrum *m/e*: 298 (100, M^+), 283 (15, M – CH_3), 270 (16, M – CO), 255 (17), 244 (50), 243 (50), 242 (38), 227 (38). The ^1H nmr spectrum δ_{TMS} ($CDCl_3$): 1.10 (s, 3H, CH_3—), 1.39–3.32 (complex m, 9H), 3.90 (s, 3H, CH_3O—), 6.83–7.00 (m, 2H, aromatic C(2)H and C(4)H), 7.50 (d, J = 8 Hz, 1H, aromatic C(1)H). The ir spectrum ν_{max} (KBr): 1730 (shoulder ketone C=O), 1701 (lactone C=O) cm^{-1}.

14β-3-Methoxy-6-oxaestra-1,3,5(10),8-tetraen-7,17-dione ***11a***

The chromic acid solution (prepared by dissolving CrO_3 (5.298 g) in 10 mL water and then adding H_2SO_4 (5 mL)) was added to a cooled (20°C) solution of the tetracyclic alcohol **11*c*** (0.5 g, 1.67 mmol) in acetone (15 mL). The oxidizing solution (1 mL) was added dropwise, so that the temperature of the reaction mixture did not exceed 35°C. The addition was stopped when the orange color of the oxidizing solution persisted. The mixture was stirred for 30 min and excess oxidant was destroyed with isopropyl alcohol (1/2 mL). The liquid was decanted and the green salts washed with acetone (30 mL) twice. To the combined washings was added $NaHCO_3$ until the solution was neutral. The mixture was filtered and the filtrate evaporated under reduced pressure. The residue was dissolved in $CHCl_3$ (50 mL) and washed with water, saturated sodium chloride solution, and dried with $MgSO_4$. Evaporation of the solution left a residue which was recrystallized to give white crystals of the ketone **11*a*** (0.408 g) in 82% yield, identical with material obtained by catalytic reduction of **6**.

The uv spectrum (95% EtOH) λ_{max} nm (ε_{max}): 222 (11 455), 323 (20 124).

14β-3-Methoxy-16-bromo-6-oxaestra-1,3,5(10),8-tetraen-7,17-dione ***11b***

A solution of the tetracyclic ketone **11*a*** (0.469 g, 1.57 mmol) in dry THF (15 mL) cooled in an ice-water bath was stirred and bromine (0.25 g) in methylene chloride (5 mL) was added dropwise, keeping the temperature of the reaction mixture below 10°C. The yellow mixture was then stirred for 1 h and the reaction was found to be complete on tlc. The mixture was treated with 10 mL of 5% $NaHCO_3$ and then cold water (50 mL) was added. The product was extracted twice with methylene chloride (100 mL, 50 mL). The combined organic layer was washed once with water and dried. Evaporation of the solvent left yellowish crystals which after column purification gave the bromide **11*b*** (0.49 g, 79%). A sample was recrystallized from benzene to give light yellow crystals melting at 222°C.

Anal. calcd. for $C_{18}H_{17}O_4Br$: C 57.29, H 4.51; found: C 57.15, H 4.56. The ^1H nmr spectrum δ_{TMS} (DMSO-d_6): 1.23 (s, 3H, CH_3—), 1.50–3.30 (complex m, 8H), 3.90 (s, 3H, CH_3O—), 4.73 (m, 1H, C(16)H), 7.00 (m, 2H, aromatic C(2)H and C(4)H), 7.73 (d, J = 10 Hz, 1H, aromatic C(1)H). The ir spectrum ν_{max} (KBr): 1750 (ketone C=O), 1710 (α,β-unsaturated lactone C=O), 1610 (aromatic), 1405, 1280, 1212, 1165, 1100, 1045, 838 cm^{-1}. The mass spectrum *m/e*: 378 (83, M + 2), 376 (83, M^+), 298 (49, M + 2 – HBr), 297 (49, M^+ – Br), 244 (56), 243 (100), 242 (65), 241 (35), 227 (39).

14β-3-Methoxy-6-oxaestra-1,3,5(10),8,15-pentaen-7,17-dione ***6*** *from* ***11b***

A solution of the tetracyclic bromoketone **11*b*** (0.147 g, 0.39 mmol) in dimethylformamide (5 mL) was added to a stirred hot (150°C) suspension of magnesium oxide (0.05 g) in dimethylformamide (20 mL). The mixture was stirred at 150°C for 30 min under nitrogen atmosphere. The red solution was cooled to room temperature and ice-cold 5% HCl (20 mL) was added

Can. J. Chem. Downloaded from www.nrcresearchpress.com by 210.87.254.5 on 09/05/12
For personal use only.

and the product extracted with benzene (25 mL) three times. The combined organic layer was washed with 5% $NaHCO_3$ and finally with water and dried. The red solution was decolorized by adding a pinch of activated carbon. Evaporation of the solvent left a purplish residue which after purification on preparative tlc gave the tetracyclic pentaen **6** (0.87 g, 76%) identical with material prepared directly from **5** as previously described.

14β-3-Methoxy-6-oxaestra-1,3,5(10),8-tetraen-7-oxo-17-ol **11***c*

To the solution of the tetracyclic ketone **6** (4.91 g, 16.6 mmol) in benzene (55 mL) was added methanol (55 mL). The solution was cooled in an ice-water bath and sodium borohydride (2.23 g, 55.60 mmol) was added at once. The mixture was stirred for 5 min and the ice-water bath was replaced by a water bath and allowed to warm to room temperature. The yellow mixture was stirred for 2 h and neutralized with ice-cold 5% HCl. The solvent was evaporated under reduced pressure to 1/3 of the original volume. The residue was diluted with ether (150 mL) and washed with water twice. The ethereal layer was dried (anhydrous $MgSO_4$). Evaporation of the solvent gave a quantitative yield of yellow crystalline product **11***c*. Recrystallization in benzene–cyclohexane (1 : 1) gave white crystals, mp 99–101°C.

Anal. calcd. for $C_{18}H_{20}O_4$: C 72.60, H 6.67; found: C 72.90, H 6.64. The mass spectrum *m/e*: 300 (100, M^+), 282 (27, $M^+ - H_2O$), 267 (52, $M^+ - (CH_3$ and $H_2O)$), 243 (72), 241 (40), 240 (21), 227 (19). The ^1H nmr spectrum δ_{TMS} ($CDCl_3$): 1.07 (s, 3H, CH_3—), 1.83 (s, 1H, —OH), 1.40–3.00 (complex m, 9H), 3.90 (s, 3H, CH_3O—), 4.10 (t, J = 8 Hz, 1H, 17αH), 6.82–7.00 (m, 2H, aromatic C(2)H and C(4)H), 7.53 (d, J = 8 Hz, 1H, aromatic C(1)H). The ir spectrum ν_{max} (KBr): 3320 (broad OH), 1710 (lactone C=O), 1615 (aromatic), 1520, 1285, 1170, 840, 685 cm^{-1}.

14β-3-Methoxy-6-oxaestra-1,3,5(10),8-tetraen-7-oxo-17-ethylene Acetal **11***d*

To a solution of the tetraen dione **11***a* (200 mg, 0.67 mmol) in dry benzene (20 mL) was added ethylene glycol (2 mL), and a catalytic amount of *p*-toluenesulfonic acid monohydrate. The mixture was refluxed for 2.5 h and water was removed with aid of a Dean–Stark trap. The mixture was then washed with 5% $NaHCO_3$ (2 × 15 mL) and worked up in the usual manner. The residue was concentrated in benzene (5 mL) and filtered without suction through silica gel (10 g). The adsorbent was washed with ethyl acetate (50 mL) and the combined washings were evaporated under reduced pressure to give a white crystalline ketal **11***d* (210 mg, 95%), homogeneous on tlc.

The ^1H nmr spectrum δ_{TMS}: 0.97 (s, 3H, CH_3—), 1.59–3.18 (complex m, 9H), 3.93 (s, 3H, CH_3O—), 3.98 (s, 4H, OCH_2CH_2O), 6.78–7.56 (m, 3H, aromatic). The ir spectrum ν_{max} (KBr): 1710 (C=O), 1610, 1281, 1199 cm^{-1}.

14β-3-Methoxy-5,7-dihydroxy-5,6-seco-6-oxaestra-1,3,5(10)-trien-17-one **12** *from* **11***d*

Into a two-necked 1 litre round-bottomed flask ammonia (600 mL) was condensed using a Dewar condenser. Excess lithium (619 mg, 88.42 mmol), cut into small pieces, was added against a countercurrent of N_2. The resulting deep blue solution was stirred vigorously for 15 min. Tetracyclic tetraen **11***d* (7.56 g, 22.11 mmol) was added at once from a dropping funnel under N_2 atmosphere. The blue mixture was stirred for another 30 min and then quenched with excess ammonium chloride (5 g). Ammonia was allowed to evaporate in a stream of N_2 and a white residue was obtained. Residual ammonia was removed under reduced pressure. The residue was treated with 5% NaOH (180 mL) and stirred to dissolve the phenolic product. The undissolved material was filtered and washed with water until the washings were not basic, affording the ethylene ketal of **13***b* (1.39 g, 17%), *vide infra*. The basic layer was washed with ether (2 × 30 mL) and after acidification, the product was extracted with ether (3 × 30 mL). After the usual work up, the residue was deketalized to afford a less soluble tricyclic ketone **12** (5.29 g, 79%). An analytical sample recrystallized in acetone melted at 226–228°C.

Anal. calcd. for $C_{18}H_{24}O_4$: C 71.05, H 7.89; found: C 70.93, H 7.64. The mass spectrum *m/e*: 304 (100, M^+), 286 (7, $M - H_2O$), 164 (26), 163 (61), 150 (64), 137 (25). The ^1H nmr spectrum δ_{TMS} ($CDCl_3$ + DMSO-d_6): 1.20 (s, 3H, CH_3—), 1.33–3.58 (complex m, 14H), 3.73 (s, 3H, CH_3O—), 6.21–7.00 (m, 3H, aromatic), 8.90 (s, 1H, phenolic —OH). The ir spectrum ν_{max} (KBr): 3420–3100 (broad —OH), 1720 (C=O), 1614, 1520 cm^{-1}.

8α,14β-3-Methoxy-6-oxaestra-1,3,5(10)-trien-7,17-dione **13**b

The ketal of **13***b*, the minor product of Na/NH_3 reduction of **11***d*, was deketalized by dissolving it in acetone (20 mL) and adding a catalytic amount of *p*-toluenesulfonic acid. The solution was stirred at room temperature overnight. Acetone was evaporated and the pinkish residue, in a minimum amount of benzene, was filtered without suction and washed with ethyl acetate to afford white crystalline tetracyclic ketone **13***b* in 90% yield. An analytical sample recrystallized from benzene melted at 204°C.

Anal. calcd. for $C_{18}H_{20}O_4$: C 72.00, H 6.66; found: C 72.05, H 6.65. The mass spectrum *m/e*: 300 (100, M^+), 204 (43), 203 (97), 202 (84), 174 (52). The ^1H nmr spectrum δ_{TMS} ($CDCl_3$): 1.19 (s, 3H, CH_3—), 1.33–3.21 (complex m, 11H), 3.80 (s, 3H, CH_3O—), 6.60–6.76 (m, 2H, aromatic C(2)H and C(4)H), 7.10 (d, J = 8 Hz, 1H, aromatic C(1)H). The ir spectrum ν_{max} (KBr): 1771 (lactone C=O), 1732 (ketone C=O), 1630, 1596 cm^{-1}.

8α,14β-3-Methoxy-7-hydroxy-6-oxaestra-1,3,5(10)-trien-17-one **13**a *from* **12**

To a stirred solution of $Na_2Cr_2O_7 \cdot 2H_2O$ (2.60 g, 8.82 mmol) in dimethylsulfoxide (25 mL) was added the tricyclic dihydroxytriene **12** (4.10 g, 13.5 mmol) in dimethylsulfoxide (2 mL). Concentrated H_2SO_4 (5 mL) was added slowly keeping the temperature below 70°C. The mixture was cooled, poured into crushed ice-water mixture, and extracted with chloroform (2 × 50 mL). The organic layer was washed with 5% NaOH (2 × 20 mL) and water (3 × 30 mL). The usual work up afforded a brown residue which was purified via a column of silica gel (125 g). Elution with ethyl acetate – cyclohexane (2:5) gave pure white crystalline hemiacetal **13***a* (3.50 g, 86%), mp 192°C (recrystallized from ethyl acetate).

Anal. calcd. for $C_{18}H_{22}O_4$: C 71.52, H 7.28; found: C 71.69, H 7.29. The mass spectrum *m/e*: 302 (64, M^+), 163 (100), 150 (77), 137 (30), 124 (91). The ^1H nmr spectrum δ_{TMS} ($CDCl_3$): 0.97 (s, 3H, CH_3—), 1.32–3.33 (complex m, 11H), 3.59 (d, J = 4.4 Hz, 1H, —OH), 3.80 (s, 3H, CH_3O—), 5.53 (t, J = 4 Hz, 1H, —OCHO—), 6.40–6.63 (m, 2H, aromatic C(2)H and C(4)H), 7.10 (d, J = 8 Hz, 1H, aromatic C(1)H). The ir spectrum ν_{max} (KBr): 3370 (OH), 1715 (C=O), 1612, 1575, 1504 cm^{-1}.

14β-3-Methoxy-6-oxaestra-1,3,5(10),7-tetraen-17-one **14**a *from* **13**b

A solution of the tetracyclic hemiacetal **13***b* (120 mg, 3.97 mmol) in dry benzene (10 mL) was treated with a catalytic amount of *p*-toluenesulfonic acid monohydrate (50 mg). The solution was refluxed for 1 h and water was removed azeotropically with a Dean–Stark trap. The mixture was cooled and diluted with benzene (20 mL), washed with 5% $NaHCO_3$ (30 mL) and water (2 × 20 mL). The usual work up afforded a pure oily vinyl ether **14***a* in quantitative yield. An analytical sample was crystallized from cyclohexane to give white crystals, mp 76–85°C.

Anal. calcd. for $C_{18}H_{20}O_3$: C 76.06, H 7.04; found: C 76.10, H 6.98. The mass spectrum *m/e*: 284 (62, M^+), 269 (22, $M - CH_3$),

188 (55), 187 (90), 86 (23), 85 (67), 84 (38), 83 (100). The ^{1}H nmr spectrum δ_{TMS} ($CDCl_3$): 1.10 (s, 3H, CH_3—), 1.32–3.50 (complex m, 10H), 3.77 (s, 3H, CH_3O—), 6.40–6.72 (m, 3H, aromatic and vinylic), 7.07 (d, J = 8 Hz, aromatic at C(1)H). The ir spectrum ν_{max} (KBr): 1735 (C=O), 1680 (C=C—O), 1620, 1580 cm^{-1}.

3-Hydroxy-6-oxaestra-1,3,5(10),7-tetraen-17-one ***14****b from* ***14****a and from* ***13***

(*a*) To an ice-water cooled solution of boron tribromide (0.72 mL, 7.47 mmol) in dry dichloromethane under N_2 (3 mL) was added slowly a solution of methyl ether **14***a* (753 mg, 2.49 mmol) in dry dichloromethane (6 mL) via a syringe. The mixture was stirred at 0°C for an hour and a yellow precipitate was observed to form. The yellow mixture was further stirred at room temperature for another hour and then quenched with ether (10 mL) and water (5 mL). The mixture was extracted with ether and the ether layer was washed with 5% sodium hydroxide solution to extract the phenolic product. After acidification of the basic aqueous layer and extraction with ether, the dried organic layer on evaporation gave a crude product. Crystallization from ethyl acetate afforded the product **14***b* (412 mg), plus mother liquors which upon chromatography on silica gave additional 103 mg of product. The total yield was 615 mg (92%), mp 160–164°C.

(*b*) In one step the hemiacetal **13***a* (502 mg, 1.66 mmol) was demethylated and dehydrated as described above (*a*) to afford **14***b* (369 mg, 85%).

Anal. calcd. for $C_{17}H_{18}O_3$: C 75.56, H 6.67; found: C 75.52, H 6.69. The mass spectrum *m/e*: 270 (68, M^+), 255 (28, $M-15$), 213 (10), 174 (72), 173 (100). The ^{1}H nmr spectrum δ_{TMS} ($CDCl_3$): 1.10 (s, 3H, CH_3—), 1.32–3.50 (complex m, 10H), 3.5 (complex m, 1H, benzylic), 6.38–6.70 (m, 4H, aromatic C(2)H and C(4)H, vinylic C(7)H and phenolic), 7.00 (d, J = 8 Hz, 1H, aromatic C(1)H). The ir spectrum ν_{max} (KBr): 3380 (broad, OH), 1720 (C=O), 1680 (O—C=C), 1620 and 1595 cm^{-1} (aromatic).

Determination of Uterotrophic Activity of ***9****b,* ***9****c,* ***10****a,* ***10****b,* ***10****c, and* ***14****a*

Immature 21-day old Sprague–Dawley rats weighing 30–40 g were obtained from Canadian Breeding Laboratories, St. Constant, Quebec. The animals were housed in an air-conditioned room 24 to 25°C, 45 to 50% humidity, and given Purina Chow and water *ad libitum*. Test substances (0.01–10 μg per rat) were administered subcutaneously in 0.2 mL sesame oil. Control animals received vehicle only. The work was divided into four experiments, each with control group and three groups receiving fixed amounts of 17β-estradiol (0.02, 0.1, 0.5 μg per rat) as standard.

The rats (10 per group) received three daily injections, and were sacrificed by cervical dislocation 24 h after the last injection. The uteri were excised free of fat and mesentery blotted and weighed to the nearest milligram on a torsion balance.

Acknowledgements

Financial support from the National Research Council of Canada is gratefully acknowledged. Thanks are due to J. J. Krepinsky who directed our attention to miroestrol and assisted in the preliminary phases of this study and to D. C. Neil Swindells for pursuing X-ray studies of two intermediates. The technical assistance of Mrs. Muriel Savary-Langlois in the determination of uterotrophic activity is gratefully acknowledged.

1. (*a*) N. E. Taylor, D. C. Hodgkin, and J. S. Rollett. J. Chem. Soc. 3685 (1960); (*b*) D. G. Bounds and G. S. Pope. J. Chem. Soc. 3696 (1960); (*c*) H. E. H. Jones and G. S. Pope. J. Endocrinol. **22**, 303 (1961); (*d*) H. E. H. Jones, H. B. Waynforth, and G. S. Pope. J. Endocrinol. **22**, 293 (1961); (*e*) G. K. Benson, A. T. Cowie, and Z. D. Hosking. J. Endocrinol. **21**, 401 (1961).
2. (*a*) M. Weigele. Ph.D. Thesis, University of Wisconsin (1965); (*b*) M. Miyano and C. R. Dorn. J. Org. Chem. **37**, 259 (1972).
3. S. N. Ananchenko and I. V. Torgov. Tetrahedron Lett. 1553 (1963).
4. P. Mebe. Ph.D. Thesis, University of New Brunswick (1978).
5. P. S. White and D. C. N. Swindells. Acta Crystallogr. Sect. B, **36**, 491 (1980).
6. C. G. Pitt, A. E. Friedman, D. Rector, and M. C. Wani. Tetrahedron, **31**, 2369 (1969).
7. P. S. White and D. C. N. Swindells. Acta Crystallogr. Sect. B, **36**, 489 (1980).
8. N. S. Bhacca and D. H. Williams. Applications of NMR spectroscopy in organic chemistry. Holden-Day, Inc., San Francisco. 1964. p. 77.
9. B. L. Rubin, A. S. Dorfman, L. Black, and R. I. Dorfman. Endocrinology, **49**, 429 (1951).
10. F. Herr, C. Revesz, A. J. Manson, and J. B. Jewell. *In* Chemical and biological aspects of steroid conjugation. *Edited by* S. Bernstein and S. Solomon. Springer-Verlag, New York. 1970. pp. 368–408.

Can. J. Chem. Downloaded from www.nrcresearchpress.com by 210.87.254.5 on 09/05/12
For personal use only.

Azole derivatives of metals. VI. Binuclear platinum(II) derivatives having both μ-pyrazolato-*N*,*N*′ and methoxy or chloride as bridging groups

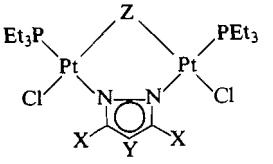
FLAVIO BONATI, HOWARD C. CLARK, and CHUN S. WONG

Guelph–Waterloo Centre for Graduate Work in Chemistry, Guelph Campus, University of Guelph, Guelph, Ont., Canada N1G2W1

Received August 22, 1979[1]

FLAVIO BONATI, HOWARD C. CLARK, and CHUN S. WONG. Can. J. Chem. **58**, 1435 (1980).

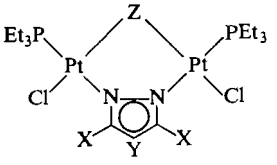
Binuclear platinum(II) complexes of the type



where X = H, CH_3, Y = H, Br, Z = Cl, OCH_3, are synthesized by the reaction of $Pt_2Cl_4(PEt_3)_2$ with the pyrazole and sodium hydroxide in methanol. The nature of the product depends on the amount of sodium hydroxide used.

FLAVIO BONATI, HOWARD C. CLARK et CHUN S. WONG. Can. J. Chem. **58**, 1435 (1980).

En faisant réagir du $Pt_2Cl_4(PEt_3)_2$ avec le pyrazole et l'hydroxyde de sodium dans le méthanol, on a synthétisé des complexes binucléaires du platine(II) du type



où X = H, CH_3, Y = H, Br, Z = Cl, OCH_3. La nature du produit dépend de la quantité d'hydroxyde de sodium utilisée.

[Traduit par le journal]

Introduction

While a pyrazole (*P*zH) is only a monodentate ligand, a pyrazolate anion (Pz^-) can be either monodentate or exobidentate (1, 2).[2] In the last case, two (or more) coordination centers are generally bridged by μ-pyrazolato-*N*,*N*′ groups: e.g. one, or two, or three such groups in the cases of $[Au(pz)]_3$ (3) and $[h^5\text{-}C_5H_5Ni(pz)]_2$ (4), or $[R_2Ga(pz)]_2$ (5) and metal(II) bispyrazolylborates (1), or octahedral metal(II) trispyrazolylborates (1) and $[EtB(\mu\text{-pz-}N,N')_3BEt]BF_4$ (6), respectively.

In pursuing our interest in pyrazolato-bridged compounds (7) and in platinum chemistry (8), we now show that two coordination centers (here Pt(II)) can be simultaneously bridged by a pyrazolato-*N*,*N*′ together with a chloride- or methoxy-groups and that the resulting, asymmetric, five-membered ring Pt-N-N-Pt-Z (Z = Cl or O) is stable.

Results and Discussion

The reaction between bis(triethylphosphine)-dichloro(μ-dichloro) diplatinum, **I**, and one mole of pyrazole in methanol gives different products according to the quantity of alkali present. If only one mole of sodium hydroxide is employed, a binuclear complex, **II**, in which chloride and exobidentate pyrazolato-*N*,*N*′ ligands bridge the two platinum atoms, is obtained (Scheme 1).

Upon treatment of **II** with a second mole of sodium hydroxide in methanol, another binuclear complex, **V**, in which the two metal atoms are bridged by a methoxy and an exobidentate pyrazolato-*N*,*N*′ ligand, is obtained. The same type of compound can be obtained directly by allowing **I** to react with one equivalent of pyrazole dissolved in two equivalents of methanolic sodium hydroxide.

The reaction was found to follow the same courses even when more sterically demanding pyrazoles were employed, such as 3,5-Me_2pzH (9), or an azole with a different basicity, such as 3,5-Me_2-4-BrpzH. Both ligands give the corresponding compounds **III** and **VI**, or **IV** and **VII**, respectively,

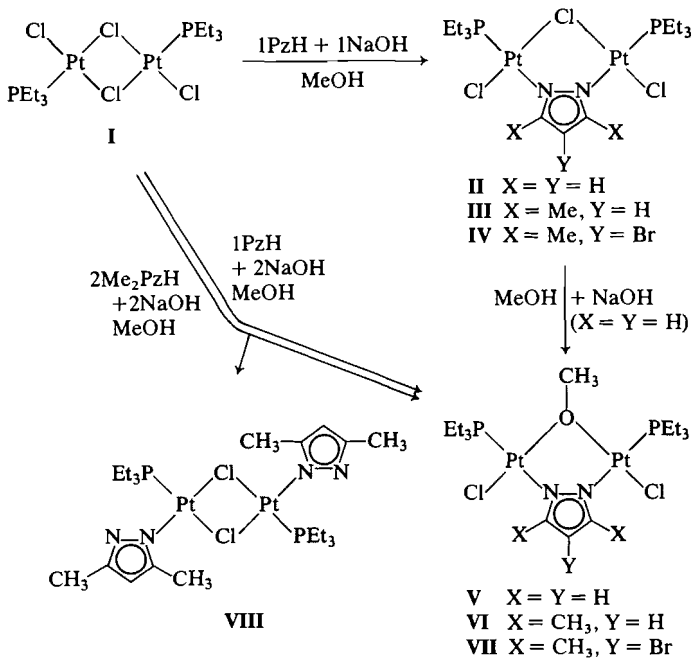
[1]Revision received March 27, 1980.

[2]PzH means $C_3H_4N_2$, i.e. unsubstituted pyrazole, while 3,5-Me_2pzH or 3,5-Me_2-4-Br-pzH mean the pyrazole molecule having the indicated substituents at the designated ring position; a generical pyrazole is indicated by *P*zH.

0008-4042/80/141435-04$01.00/0

©1980 National Research Council of Canada/Conseil national de recherches du Canada

Can. J. Chem. Downloaded from www.nrcresearchpress.com by 210.87.254.42 on 09/05/12
For personal use only.



SCHEME 1

TABLE 1. Analytical and other data

	Analysis								
	C		H		N		Cl*		Decomposition
Compound	Found	Calcd	Found	Calcd	Found	Calcd	Found	Calcd	point (°C)
II	22.68	22.52	4.38	4.16			14.22	13.30	173–175
III	24.85	24.66	4.73	4.53			13.87	12.85	166–169
IV	22.47	22.51	4.08	4.00	3.04	3.09			156–157
V	24.00	24.16	4.69	4.56			10.42	9.41	181–184
VI	26.27	26.20	4.89	4.85	3.36	3.42	9.94	8.61	185–186
VII	23.44	23.96	4.23	4.36	3.06	3.10			172–175
VIII	29.71	29.85	5.19	4.97	6.03	6.32			< 180, m196

*Cl analysis was carried out on very small sample, the results are invariably high.

characterized through analyses (Table 1) and through infrared and nmr spectroscopic data (Table 2). The isolation of derivatives of 3,5-Me_2-4-Br-PzH proves that the bonding to platinum may take place only through the 1-position of the ring, in this case the only unsubstituted one.

When two moles of 3,5-Me_2PzH and of sodium hydroxide were employed, besides **VI**, another binuclear compound was isolated from the mother liquor and identified as **VIII** through analytical and spectral data.

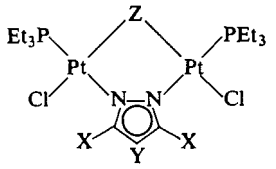
The ^{31}P and ^{1}H nmr spectra (Table 2) show the required resonances, the assignment of which is helped by the coupling to ^{195}Pt (33% abundance; spin = 1/2). Thus, in the case of the methoxy bridged compounds a 1:8:16:8:1 pattern is expected for the protons in the Pt—OMe—Pt system owing to the presence of molecules having two (11.36%) or one (44.68%) ^{195}Pt nucleus together with molecules (43.95%) having no nmr-active platinum isotope. Such a pattern is indeed observed in the spectrum of **V**, although the two weakest signals were detected with some difficulty; ^{3}J(Pt—H) being 46–48 Hz in these cases.

The same pattern is expected for the 4-CH signal of the heterocyclic ring in all the Pt(μ-Pz-*N*,*N'*)Pt system. Nevertheless, only a broadening of the pertinent signal is observed because ^{4}J(Pt—H) is one order of magnitude smaller than ^{3}J; in addition the signal is weak because only one proton is involved.

When the azolato is connected to only one

Can. J. Chem. Downloaded from www.nrcresearchpress.com by 210.87.254.42 on 09/05/12
For personal use only.

TABLE 2. Nuclear magnetic resonance[a] data for



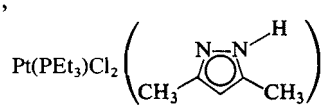
Compound				$^{31}P\{^1H\}$			^1H						
							X			Y		Z	
No.	X	Y	Z	Solvent	δ	^1J(Pt—P)	Solvent	δ	^4J(PtH)	δ	^4J(PtH)	δ	^3J(PtH)
II	H	H	Cl	CH_2Cl_2	−1.84	3086	$CDCl_3$	8.22	[b]	6.28	[b]	—	—
III	Me	H	Cl	CH_2Cl_2	−2.36	3197	CD_2Cl_2	2.54	3.2	5.82	[b]	—	—
IV	Me	Br	Cl	CH_2Cl_2	−1.90	3263	CH_2Cl_2	2.44	3.4	—	—	—	—
V	H	H	OCH_3	CH_2Cl_2	0.67	3501	$CDCl_3$	7.94s	[b]	6.33	[b]	3.59q[c]	46
VI	Me	H	OCH_3	CH_2Cl_2	−1.01	3477	$CDCl_3$	2.47	3	5.81	[b]	2.98q[c]	48
VII	Me	Br	OCH_3	CH_2Cl_2	−1.07	3537	CD_2Cl_2	2.48	[b]	—	—	3.01q[c]	48
VIII	See Scheme			$CDCl_3$	1.61	3363	$CDCl_3$	2.20 2.34	8.3 —	5.97	17		

[a]Nuclear magnetic resonance spectra were recorded on a Brüker instrument operating at 24.88 or 60 MHz for ^{31}P or ^1H respectively; s = singlet; q = 1:8:18:8:1 quintet (see text).
[b]Coupling undetected due to broadness of signal.
[c]See text.

platinum atom (i.e. is monodentate) no such pattern is observed, but just the expected two satellites, as for the 4-CH protons of the 3,5-Me_2Pz^- group in compound **VIII**.

The ^{31}P nmr spectra show a singlet flanked by two ^{195}Pt satellites with ^1J(PtP) = 3.0 to 3.5 kHz, and in one case, **I**, a value of 29.3 Hz is also observed for ^3J(PtP). The singlet pattern implies that the two phosphines are equivalent, i.e. they have the same *trans* ligand. Further, in the ^1H nmr spectra of **V**, **VI**, and **VIII**, the $-OCH_3$ groups exhibit no P—H coupling; the phosphines are therefore *trans* (10) to the exobidentate–pyrazolato bridge (as shown in Scheme 1).

Finally, the reaction of **I** with 3,5-dimethylpyrazole in the absence of added alkali was investigated by ^1H nmr spectroscopy. Immediately after mixing in $CDCl_3$, the methyl singlet due to the ligand was replaced by two equally intense resonances at δ2.52 and 2.23. The high field resonance appeared as a singlet, while the low field one exhibited ^{195}Pt satellites with ^4J(Pt—H) = 4 Hz. The coupling with the ^{195}Pt nuclei is probably also felt by the 4-CH proton, which produces a broad singlet at δ5.95. All these data suggest a monodentate pyrazole ligand, bonded through the 2-N atom,



The colour of the solution is yellow, suggesting *trans* geometry of the two chlorides. This is also consistent with the observed formation of *trans* products in the bridge splitting reaction of the dimer, **I**, with amines (11).

The above results confirm that a pyrazolato group may be either a monodentate or an exobidentate ligand. In the former case, the mode of attachment is the same as that found in $(Ph_2PCH_2)_2Pt(pz)_2$ (12); in the latter case the heterocyclic anion may be accompanied by a second and different bridging group either Cl or OCH_3, affording the stable, homobinuclear complexes, **II–VII** having a novel type of arrangement of ligands.

Experimental

$Pt_2(PEt_3)_2Cl_4$ was prepared according to the literature method (13). ^1H nmr spectra was recorded on a varian A60 spectrometer. ^{31}P nmr spectra were recorded in a Brüker PW60 and were ^1H decoupled; the chemical shifts are relative to 85% H_3PO_4. Infrared spectra were obtained on a Beckmann IR12 instrument. Elemental analyses were performed by Midwest Microlab Ltd., Indianapolis, IN. The substituted pyrazoles were prepared by the method of Morgan and Ackermann (14).

Preparation of VI

4-Bromo-3,5-dimethylpyrazole (88 mg, 0.5 m*M*) was dissolved in 0.5 mL of 1 *N* 90% acqueous methanolic NaOH (0.5 m*M*). The resulting solution was then added to a suspension of 384 mg (0.5 m*M*) of $Pt_2(PEt_3)_2Cl_4$ in 10 mL methanol. The reaction mixture was stirred magnetically for 3 h. The creamy yellow precipitate was filtered, washed with methanol, water, methanol, and ether. Recrystallization from CH_2Cl_2/ethanol afforded yellow needles 397 mg (87%).

The methods of preparation of **II** and **IV** are similar. Both compounds are recrystallized from CH_2Cl_2/aqueous ethanol (yield: **II**, 74%; **IV**, 63%).

Can. J. Chem. Downloaded from www.nrcresearchpress.com by 210.87.254.42 on 09/05/12
For personal use only.

Preparation of VII

(*A*) To a suspension of (0.14 m*M*) 115 mg of **VI** in 2 mL of methanol was added 0.15 mL of 1 *N* NaOH. After stirring for 24 h, the yellow solid was filtered and washed with methanol, water, methanol, and ether. The complex was recrystallized from CH_2Cl_2/ethanol. Yield 70 mg (60%).

(*B*) Alternatively, **III**, **V**, **VII** can be prepared directly from $Pt_2(PEt_3)_2Cl_4$ as follows: a solution of 3,5-dimethylpyrazole (9.6 mg, 0.1 m*M*) in 0.2 mL 1 *M* aqueous methanolic NaOH (0.2 m*M*) was added to a suspension of 76.8 mg of $Pt_2(PEt_3)_2Cl_4$ (0.1 m*M*) in 2 mL of MeOH. After stirring for 24 h, the yellow solid was filtered, washed with methanol, H_2O, methanol, and ether. Recrystallization from CH_2Cl_2/ethanol afforded crystals of **III**, 55 mg (66%).

Compound VIII

To a methanol suspension (10 mL) of the compound **I** (223.5 mg, 0.29 mmol), 3,5-Me_2pzH (58.4 mg; 0.61 mmol) and sodium hydroxide (1 mL of a 90% methanolic solution, 0.614 *M* diluted to 5 mL with methanol) were added, whereupon a yellow solution formed. After overnight standing, yellow crystals of **VI** (73 mg) were filtered off, and the solution was evaporated to dryness, leaving an oily residue which solidified upon standing under ether. The solid was dissolved in warm methanol (8 mL) and the compound **VIII** (34.3 mg) crystallized upon slow evaporation to a volume of 2 mL.

Acknowledgments

The continued financial support of the Natural Sciences and Engineering Research Council of Canada (to H.C.C.) is gratefully acknowledged. One of us (F.B.) thanks the Department of Chemistry of the University of Guelph for the hospitality which allowed him to carry out this work.

1. S. Trofimenko. Chem. Rev. **72**, 497 (1972).
2. A. G. Shaver. J. Organomet. Chem. Library, **3**, 157 (1977).
3. F. Bonati, G. Minghetti, and G. Banditelli. J. Chem. Soc. Chem. Commun. 88 (1973).
4. A. B. Blake, D. F. Ewing, J. E. Hamlin, and J. M. Lockyer. J. Chem. Soc. Dalton Trans. 1897 (1977).
5. A. Arduini and A. Storr. J. Chem. Soc. Dalton Trans. 503 (1974).
6. E. M. Holt, S. L. Holt, K. J. Watson, and B. Olsen. Cryst. Struct. Commun. **7**, 613 (1978).
7. F. Bonati and H. C. Clark. Can. J. Chem. **56**, 2513 (1978).
8. G. Minghetti, G. Banditelli, and F. Bonati. J. Chem. Soc. Dalton Trans. In press; H. C. Clark, A. B. Goel, and C. S. Wong. J. Organomet. Chem. In press.
9. G. Minghetti, G. Banditelli, and F. Bonati. Chem. Ind. 123 (1973).
10. H. C. Clark, T. G. Appleton, and L. E. Manzer. Coord. Chem. Rev. **10**, 335 (1973).
11. J. Chatt and F. G. Mann. J. Chem. Soc. 1622 (1939); J. Chatt and L. M. Venanzi. J. Chem. Soc. 2445 (1957); J. Chatt and L. M. Venanzi. J. Chem. Soc. 3858 (1955).
12. A. L. Bandini, G. Banditelli, F. Bonati, and G. Minghetti. Can. J. Chem. **57**, 3237 (1979).
13. J. Chatt and L. M. Venanzi. J. Chem. Soc. 7533 (1965).
14. E. T. Morgan and I. Ackermann. J. Chem. Soc. 1303 (1923).

Can. J. Chem. Downloaded from www.nrcresearchpress.com by 210.87.254.42 on 09/05/12
For personal use only.

Metal binding to N(9), N(7), and N(3) of adenine. Crystal structure of μ-(adeninato-*N*3,*N*7,*N*9)tris(methylmercury(II)) perchlorate

JOSEPH HUBERT AND ANDRÉ L. BEAUCHAMP

Département de Chimie, Université de Montréal, C.P. 6210, Succ. A., Montréal (Qué.), Canada H3C 3V1

Received December 31, 1979

JOSEPH HUBERT and ANDRÉ L. BEAUCHAMP. Can. J. Chem. **58**, 1439 (1980).

The title compound belongs to space group $P\bar{1}$ with the following cell parameters: $a = 6.304$, $b = 11.925$, $c = 25.946$ Å, $\alpha = 85.76$, $\beta = 89.78$, $\gamma = 83.57°$, and $Z = 4$. The structure was solved by the heavy-atom method and refined on 2570 nonzero reflections to an R factor of 0.044. In the two crystallographically independent $[Adeninato(CH_3Hg)_3]^{2+}$ ions, methylmercury groups are linearly bonded to N(3), N(7), and N(9) of a deprotonated adenine ring, forming Hg—N bonds of normal lengths (ave. 2.08 Å) for two-coordinated mercury. One half of the complex cations are associated in a dimeric unit by a pair of strong N(6)—H(6) ···N(1) hydrogen bonds, while the others are packed as individual species in the crystal. The structure is stabilized by a number of contacts between mercury and perchlorate oxygens.

JOSEPH HUBERT et ANDRÉ L. BEAUCHAMP. Can. J. Chem. **58**, 1439 (1980).

Le composé appartient au groupe d'espace $P\bar{1}$ et possède les constantes réticulaires suivantes: $a = 6.304$, $b = 11.925$, $c = 25.946$ Å, $\alpha = 85.76$, $\beta = 89.78$, $\gamma = 83.57°$ et $Z = 4$. La structure a été résolue par la méthode de l'atome lourd et l'affinement effectué au moyen de 2570 réflexions d'intensité non nulle a convergé jusqu'à $R = 0.044$. Les deux ions complexes $[Adéninato(CH_3Hg)_3]^{2+}$ cristallographiquement indépendants possèdent des groupes méthylmercure à coordination linéaire liés aux atomes N(3), N(7) et N(9) d'une molécule d'adénine déprotonée. Les liaisons Hg—N sont de longueur normale (moy. 2.08 Å) pour un mercure bicoordonné. La moitié des cations complexes sont associés en dimères au moyen d'une paire de liaisons hydrogène fortes N(6)—H(6)···N(1), tandis que les autres s'empilent individuellement dans le cristal. Plusieurs contacts entre le mercure et les atomes d'oxygène des ions perchlorates contribuent à la stabilisation du cristal.

Introduction

Donor basicity in polydentate ligands is affected by metal coordination somewhere else in the molecule. Purines are quite sensitive to such effects because their donor atoms are interconnected by a fluid system of π-electrons. Detailed knowledge of those effects is required to understand the interaction of nucleic acids with metallic species like platinum anticancer drugs, since metal binding at one position is likely to change the ability of other portions of the ligand to form hydrogen bonds, accept more metal atoms, and so on. Direct information of that sort on series of related compounds is still missing.

That problem is investigated using the CH_3Hg^+ ion, a uniligating Lewis acid in which the linear coordination of mercury leads to minimal steric hindrance. The interdependence of donor sites has already been mentioned for adenosine (1) and clear evidence has recently been provided by X-ray work on 9-methyladenine (MAd) complexes. Indeed, the N(1),N(6)-bonded $[(CH_3Hg)_2(MAd—H)]^+$ species is isolated from acidic solutions (2), even though mercury has to displace an amino hydrogen that does not spontaneously dissociate even at high pH. Substitution of that hydrogen is probably facilitated by simultaneous coordination of another CH_3Hg^+ group to position N(1), which was found to be attacked first by mercury (3). Unsubstituted adenine reacts differently because the acidic H(9) proton is readily displaced by CH_3Hg^+. Neutral adenine (HAd) and the neutral CH_3HgAd complex, in which the N(9) sites are occupied by H and CH_3Hg respectively, clearly show changes in the basic character of the remaining nitrogen atoms: adenine accepts the extra proton at N(1) (4), whereas CH_3HgAd accepts a second CH_3Hg^+ group at N(7) (2).

The title compound contains three CH_3Hg^+ groups per ligand. The corresponding protonic species (H_3Ad^{2+}) has hydrogen atoms attached to N(1), N(7), and N(9) (5), but from the above discussion, it is clear that the coordination sites cannot be predicted from the corresponding protonic compound. Inasmuch as no reliable information could be extracted from the vibrational spectra (6) and no other 3:1 complexes had been reported, a crystallographic investigation was undertaken to determine the pattern of site occupancy.

Experimental

Crystal Data

$C_8H_{13}Cl_2Hg_3N_5O_8$ fw = 979.9

Triclinic, space group $P\bar{1}$, $a = 6.304(7)$, $b = 11.925(4)$, $c = 25.946(4)$ Å, $\alpha = 85.76(2)$, $\beta = 89.78(5)$, $\gamma = 83.57(6)°$, $V = 1933$ Å^3, $Z = 4$ formula units per cell, $D_c = 3.362$ g cm^{-3}, $\mu(MoK\alpha) = 240.5$ cm^{-1}, $\lambda(MoK\bar{\alpha}) = 0.71068$ Å, $t = 23°C$.

Crystallographic Measurements

Crystals suitable for X-ray work were obtained directly from

0008-4042/80/141439-05$01.00/0

©1980 National Research Council of Canada/Conseil national de recherches du Canada

Can. J. Chem. Downloaded from www.nrcresearchpress.com by 210.87.254.5 on 09/05/12
For personal use only.

Can. J. Chem. Downloaded from www.nrcresearchpress.com by 210.87.254.5 on 09/05/12
For personal use only.

the reaction mixture as described elsewhere (6). The specimen used had the following distances between the indicated pairs of faces: 0.06 mm (001 and 00$\bar{1}$), 0.14 mm (010 and 0$\bar{1}$0), and 0.17 mm (100 and $\bar{1}$00).

A set of precession and cone axis photographs indicated a triclinic Laue symmetry (space groups $P1$ or $P\bar{1}$) and provided starting cell parameters. According to the estimated density, that cell would contain four formula units, that is, two independent formulas per asymmetric unit in $P\bar{1}$. Such cases have to be carefully checked in order to make sure that the crystal does not belong to a space group of higher symmetry. The triclinic cell is believed to be correct for the following reasons:

(*i*) The set of orientation photographs taken at 10° intervals around the dial axis of the precession camera failed to reveal any symmetry.

(*ii*) A cell with the same dimensions was deduced by the autoindexing routine of the ENRAF-NONIUS CAD4 software from two independent samples of 25 centred reflections found by the SEARCH routine procedure.

(*iii*) The cell provided by the CAD4 software (Reduced cell, type I (7)) has only one apparently specialized Niggli element ($S_{13} = ac \cos\beta \sim 0$) as a consequence of the β angle being close to 90°. A greater specialization of the Niggli elements is necessary to lead to higher symmetry (7). The same conclusion is reached by using TRACER II (8), a computer program working with the slightly different Delauney cell.

(*iv*) Oscillation photographs were recorded with the crystal mounted on the CAD4 diffractometer by placing a Polaroid cassette behind the beam catcher. With a real axis along the vertical direction (z axis) of the instrument, the crystal was allowed to oscillate ±13° about ω and pictures were taken (45 min exposures) about two median ω positions for each of the three axes. The photographs showed the expected layer line separations, but no symmetry. If either *a* or *c* actually belonged to a cell of higher symmetry, the mirror of the Laue group would introduce a top–bottom mirror symmetry in the oscillation photograph.

(*v*) The solved structure (see below) shows that one half of the complex cations form hydrogen-bonded dimeric groups, whereas the others are packed individually. Those strikingly different, but chemically reasonable, packing modes confirm that the two formula units are crystallographically independent and could not belong to a cell of higher symmetry, where they would have to become symmetrically equivalent.

Intensity measurements were collected using the $\omega/2\theta$ scan technique. A fixed slit of 3.0 mm was used and the scan range (ω) was $(0.90 + 0.35 \tan\theta)°$ extended 25% on each side for background. Scan speed S between 6.7 and 0.67 deg min^{-1} was automatically selected to make $I/\sigma(I) = 100$, but a maximum scan time of 120 s was imposed. Prescans at 6.7° min^{-1} were done and all the weak reflections ($I/\sigma(I) < 1$) were not remeasured at low speed. Their F_o and $\sigma(F_o)$ values were taken from the prescan counts. Three standard reflections were monitored as a check on instrument and crystal stability. They showed random fluctuations within ±4% about their respective means. Crystal orientation was checked every 100 reflections by recentering three reflections. Misorientation was always <0.1° and no crystal recentering was done.

A total of 4989 independent reflections (hkl, $\bar{h}kl$, $h\bar{k}l$, and $\bar{h}\bar{k}l$, $2\theta \leq 45°$) were measured using Enraf–Nonius option FLAT, a procedure to measure intensity at the ψ angle where absorption is minimum for a plate-like crystal. Net intensity I was obtained from $I = (P - B/0.50)S$, where P is the total scan count and B is the total background count measured during one half of scanning time. The standard deviation was calculated from $\sigma(I) = (P + B/0.25)S^2 + (0.02I)^2$. A set of 2570 reflections with $I/\sigma(I) \geq 3$ was retained for structure determination. The crystal was highly absorbing and an absorption correction was applied (Gaussian integration, grid 8 × 8 × 8). For most of the measurements, the transmission factors ranged from 0.15 to 0.30. For the six $h00$ and three more reflections, diffractometer geometry allowed measurement only at the most unfavorable ψ position. Their transmission coefficients were < 0.02 and they were arbitrarily assigned zero weight. The data were finally corrected for Lorentz and polarization effects.

Resolution of the Structure

The structure was solved by the heavy-atom method. In space group $P\bar{1}$, there are six crystallographically independent Hg atoms, two of which were first located from a Patterson synthesis. The four remaining Hg atoms were visible on a Fourier map. All nonhydrogen atoms were finally located from a subsequent Fourier map phased on the six Hg atoms. Full-matrix least-squares refinement of positional and isotropic thermal parameters with unit weights converged to $R = \Sigma||F_o| - |F_c||/\Sigma|F_o| = 0.098$. The Hg atoms were then anisotropically refined and the R factor reduced to 0.059. At this point, the structure was essentially correct and refinement was continued by using block-diagonal least-squares to save computer time. The hydrogen atoms on C(2), C(8), and the N(6) amino group of each ring were then fixed at their calculated positions (C(N)—H = 0.95 Å, sp^2 hybridization) with isotropic temperature factors B of 6.0 Å^2 (U = 0.076 Å^2). Hydrogen parameters were not refined, but the coordinates were recalculated after each cycle. The methyl hydrogens were not found. In the last cycles of refinement, individual weights $w = 1/\sigma(F)^2$ were used for each reflection. Anisotropic refinement of all nonhydrogen atoms converged to $R = 0.044$ and $R_w = [\Sigma w(|F_o| - |F_c|)^2/\Sigma w|F_o|^2]^{1/2} = 0.051$. The goodness-of-fit ratio was 1.52. There were no indications in the final ΔF map that the space group might be $P1$ instead of $P\bar{1}$. The map showed a general background ≤0.8 e/Å^3, except for a few peaks of 1.1–1.8 e/Å^3 within 1.1 Å from Hg.

The refined coordinates are listed in Table 1. Lists of structure factors and temperature factors are available upon request.[1] The scattering curves were those of Cromer and Waber (9), except for hydrogen (10). Anomalous scattering coefficients $\Delta f'$ and $\Delta f''$ for Hg and Cl were taken from Cromer (11).

Description of the Structure

In the 2:1 complex, imidazolic nitrogen atoms N(7) and N(9) are occupied by CH_3Hg groups (2). This first example of a 3:1 adenine complex shows that the third binding site is N(3). In all known N(3)-bonded compounds, the ligand is bridging via N(9) and N(3) and the species that most closely resemble the present situation are the dimeric cations $[Cu_2(HAd)_4Cl_2]^{2+}$ (12) and $[Cu_2(HAd)_4(H_2O)_2]^{4+}$ (13) in which N(7) is protonated. However, other cases of N(3),N(9)-bridging are known in which N(1) and N(7) are either both free (14) or both protonated (15, 16).

Interatomic distances and bond angles are schematically represented in Fig. 1. Unless otherwise stated, they correspond to average values

[1]The supplementary material includes lists of observed and calculated structure factors, anisotropic temperature factors of nonhydrogen atoms, coordinates of hydrogen atoms, individual interatomic distances and bond angles, and details of best-plane calculations. Complete set of data is available, at a nominal charge, from the Depository of Unpublished Data, CISTI, National Research Council of Canada, Ottawa, Ont., Canada K1A 0S2.

Can. J. Chem. Downloaded from www.nrcresearchpress.com by 210.87.254.5 on 09/05/12
For personal use only.

TABLE 1. Refined fractional coordinates of nonhydrogen atoms ($\times 10^3$, Hg $\times 10^4$)

Atom	x	y	z
Hg(13)	4277(2)	1958(1)	−1521(1)
Hg(17)	309(2)	3020(1)	1106(1)
Hg(19)	−177(2)	3499(1)	−1272(1)
Hg(23)	3969(2)	2122(1)	3261(1)
Hg(27)	−1731(2)	2943(1)	5745(1)
Hg(29)	148(2)	623(1)	3699(1)
Cl(1)	−271(13)	107(6)	−1514(4)
Cl(2)	4792(13)	5126(7)	−949(4)
Cl(3)	4214(14)	884(8)	5820(5)
Cl(4)	1057(15)	5852(8)	6740(4)
O(11)	−22(6)	−45(3)	−105(1)
O(12)	171(4)	−23(2)	−174(1)
O(13)	−187(4)	−11(3)	−185(2)
O(14)	−62(7)	120(2)	−143(2)
O(21)	318(4)	550(2)	−60(1)
O(22)	549(5)	609(2)	−123(1)
O(23)	404(4)	443(2)	−132(1)
O(24)	643(6)	448(4)	−65(2)
O(31)	280(5)	30(3)	556(2)
O(32)	295(5)	188(2)	601(1)
O(33)	587(6)	118(3)	552(2)
O(34)	517(6)	24(3)	623(2)
O(41)	146(4)	702(2)	669(1)
O(42)	102(4)	545(2)	624(1)
O(43)	259(5)	518(3)	702(1)
O(44)	−102(4)	584(2)	694(1)
N(11)	639(4)	113(2)	5(1)
C(12)	593(5)	127(2)	−47(1)
N(13)	438(4)	182(2)	−72(1)
C(13)	411(6)	204(3)	−229(2)
C(14)	286(5)	231(2)	−41(1)
C(15)	302(4)	219(2)	10(1)
C(16)	492(5)	164(3)	38(2)
N(16)	535(4)	145(2)	87(1)
N(17)	122(4)	280(2)	35(1)
C(17)	−49(7)	317(3)	187(1)
C(18)	14(5)	323(3)	−8(1)
N(19)	101(3)	294(2)	−53(1)
C(19)	−124(5)	395(3)	−201(2)
N(21)	426(4)	404(2)	457(1)
C(22)	446(5)	347(3)	418(1)
N(23)	342(3)	264(2)	401(1)
C(23)	466(6)	157(4)	256(2)
C(24)	186(5)	242(2)	436(2)
C(25)	140(4)	299(2)	478(1)
C(26)	271(5)	382(2)	491(1)
N(26)	255(4)	440(2)	531(1)
N(27)	−40(4)	252(2)	505(1)
C(27)	−294(6)	342(3)	646(2)
C(28)	−85(5)	179(3)	473(2)
N(29)	40(4)	165(2)	432(1)
C(29)	2(4)	−38(2)	306(1)

over the two independent complex cations.[2] Mercury exhibits the expected linear two-coordination within experimental error (C—Hg—N = 177(1)°).

[2]The conventional one-digit numbering scheme is used to discuss features common to both independent complex cations in the cell. Whenever reference is made to a specific cation, symbols N(11), C(12) ... (cation No. 1) or N(21), C(22) ... (cation No. 2) are used.

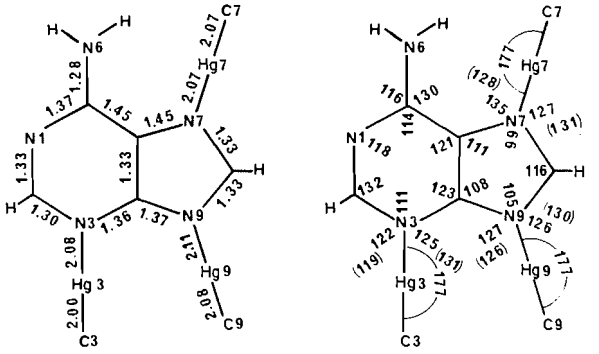


FIG. 1. Average interatomic distances and bond angles in [Adeninato(CH_3Hg)$_3$](ClO_4)$_2$. The two values for C—N—Hg angles refer to cation No. 1 (unparenthesized) and cation No. 2 (parenthesized), respectively. The standard deviations on bond lengths are 0.04–0.05 Å, except for Hg—N(C), 0.02–0.04 Å, and on bond angles, 3°, except for C—Hg—N, 1°.

All three nitrogen atoms bind the metal equally strongly with a normal average Hg—N bond length (2.08(3) Å) (17). The Hg—CH_3 distances (ave. 2.05(4) Å) also agree with previous studies (17).

Because electron density is largely concentrated in a few mercury atoms, the light atom portion of the structure is defined with limited accuracy. Corresponding distances and angles in the two independent cations are equal within experimental errors. The average results given in Fig. 1 agree with 2σ with the normal geometry of the ligand (18).[1] Both adenine rings are planar within 0.05 Å (1.5σ) and the amino groups do not significantly deviate from their respective planes.[1] The greater out-of-plane bending of the CH_3Hg group as a whole (Hg–plane distance = 0.07–0.35 Å) is undoubtedly due to molecular packing.

The four perchlorate ions have the expected tetrahedral geometry. The O—Cl—O angles range from 105 to 116° (σ = 2°, ave. 109°). The Cl—O bonds lengths are spread between 1.33 and 1.47 Å (σ = 0.03 Å) with a normal average value of 1.40 Å.

Packing efficiency is achieved by parallel positioning of the flat complex cations (Fig. 2). However, in contrast with free ligands and a number of complexes, adenine rings are not in direct contact. Two different packing patterns can be recognized. In layers parallel to *ab* at z = 1/2, complex cations (black atoms) form centrosymmetric "dimers" via a pair of strong N(26)—H(26)···N(21) hydrogen bonds: N(26)···N(21) = 2.92(4) Å, C(26)—N(26)—N(21) = 117(2)°, C(22)—N(21)—N(26) = 116(2)°. In layers at z = 0, the cations (white atoms) pack as individual units and their amino groups form only weak hydrogen bonds with a perchlorate ion: N(16)···O(12) = 3.10(4) Å, C(16)—N(16)—O(12) = 149(2)°, Cl(1)—O(12)—N(16) = 107(2)°. An

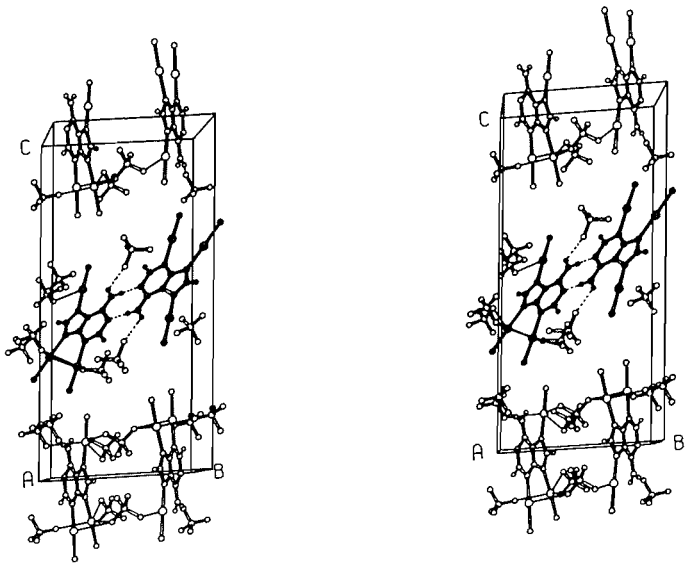


FIG. 2. Stereoscopic projection of the molecular packing in [Adeninato$(CH_3Hg)_3$]$(ClO_4)_2$. Mercury and chlorine atoms are represented by larger spheres of arbitrary sizes. Dotted lines represent H-bonds, and Hg—O contacts are shown as thin bonds. The two independent complex cations are shown with white (No. 1) and black atoms (No. 2), respectively.

important contribution to crystal stabilization results from mercury–perchlorate interactions. Contacts commonly exist between linearly coordinated mercury and extra donors in the equatorial plane. Such contacts may be moderately strong with halogeno–mercury compounds, for instance, but they tend to be much weaker with CH_3Hg groups. In fact, only three Hg···O contacts are found to be shorter than 2.9 Å, the sum of the admitted van der Waals radii of mercury (1.5 Å) (19) and oxygen (1.4 Å) (20). However, Grdenic (19) suggests that a radius as high as 1.73 Å can be used for mercury if very weak interactions are taken into account. There are 11 more Hg—O contacts in the 2.9–3.1 Å interval and they are all located within ±15° from the equatorial plane (Fig. 2). Although those interactions are individually weak, they probably have a determining effect on molecular packing.

Discussion

The most significant characteristic of the present crystal structure is the apparent absence of affinity of N(1) for mercury. Indeed, the latter site is the first to react with CH_3Hg^+ in adenosine (21) and 9-methyladenine (3) and the first to protonate in neutral adenine and the above derivatives (1, 4). Because of the availability of N(9) for coordination, adenine was expected to differ in reactivity from its N(9)-substituted analogues. Nevertheless, it was not anticipated that N(1) would become the worst heterocyclic nitrogen donor, poorer than N(3).

The lack of reactivity of N(3) in N(9)-substituted adenines is mainly due to steric hindrance (see ref. 3, Fig. 3). Replacement of bulky N(9)-alkyl or -ribosyl by either copper (12–15), silver (16) or as the present case, mercury leaves enough space for a second metal atom to bind to N(3) without experiencing appreciable strain. The Hg(3)—Hg(9) distances (3.270(2) and 3.310(2) Å) are slightly lower than the long contacts in solid mercury (3.47 Å) (19), but the lack of Hg–Hg repulsion is evidenced from the nearly equal Hg—N—C angle pairs for each CH_3Hg group bonded to N(3) or N(9).

Even if the presence of CH_3Hg instead of a bulkier group at N(9) makes N(3) sterically more available, it must be remembered that N(1) is not hindered either. Hence, steric hindrance alone cannot explain that N(3) reacts better than N(1). We have proposed (2) that the replacement of H(9) by a less electronegative Hg atom should spread more electron density into the ligand, increasing the basicity of other nitrogen donors. Assuming that such a basicity enhancement should be more pronounced for nitrogen atoms closer to N(9), we were able to explain that the second CH_3Hg^+ ion was bound to N(7) instead of N(1) in the 2:1 complex. Inasmuch as N(7) and N(3) are separated from N(9) by the same number of bonds and, according to theoretical work by Pullman and co-workers (22), there should be only small differences in electrostatic potential at N(3) and N(1) in the free neutral ligand, the basicity enhancement experienced by N(3)

Can. J. Chem. Downloaded from www.nrcresearchpress.com by 210.87.254.5 on 09/05/12
For personal use only.

could be sufficient to make it a better binding position than N(1).

1. L. G. MARZILLI. Prog. Inorg. Chem. **23**, 255 (1977).
2. L. PRIZANT, M. J. OLIVIER, R. RIVEST, and A. L. BEAUCHAMP. J. Am. Chem. Soc. **101**, 2765 (1979).
3. M. J. OLIVIER and A. L. BEAUCHAMP. Inorg. Chem. **19**, 1064 (1980).
4. D. J. HODGSON. Prog. Inorg. Chem. **23**, 211 (1977).
5. T. J. KISTENMACHER and T. SHIGEMATSU. Acta Crystallogr. B**30**, 1528 (1974); R. F. BRYAN and K. TOMITA. Acta Crystallogr. **15**, 1179 (1962).
6. L. PRIZANT, R. RIVEST, and A. L. BEAUCHAMP. To be published.
7. International tables for X-ray crystallography. Kynoch Press, Birmingham. Vol. I. 1969. p. 530.
8. S. L. LAWTON and R. A. JACOBSON. The reduced cell and its crystallographic applications. U.S. Atomic Energy Commission, Report IS-1141. 1965.
9. D. T. CROMER and J. T. WABER. Acta Crystallogr. **18**, 104 (1965).
10. R. F. STEWART, E. R. DAVIDSON, and W. T. SIMPSON. J. Chem. Phys. **42**, 3175 (1965).
11. D. T. CROMER. Acta Crystallogr. **18**, 17 (1965).
12. P. DEMEESTER and A. C. SKAPSKI. J. Chem. Soc. A, 2167 (1971).
13. A. TERZIS, A. L. BEAUCHAMP, and R. RIVEST. Inorg. Chem. **12**, 1166 (1973).
14. E. SLETTEN. Acta Crystallogr. B**25**, 1480 (1969).
15. P. DEMEESTER and D. M. L. GOODGAME. J. Chem. Soc. Dalton Trans. 2400 (1972).
16. C. GAGNON, J. HUBERT, R. RIVEST, and A. L. BEAUCHAMP. Inorg. Chem. **16**, 2469 (1977).
17. A. J. CANTY, N. CHAICHIT, B. M. GATEHOUSE, and A. MARKER. Acta Crystallogr. B**34**, 3229 (1978) and references therein.
18. D. VOET and A. RICH. Prog. Nucl. Acid Res. Molec. Biol. **10**, 183 (1970).
19. D. GRDENIC. Q. Rev. **19**, 303 (1965).
20. F. A. COTTON and G. WILKINSON. Advanced inorganic chemistry. Interscience, New York. 1972. p. 120.
21. S. MANSY and R. S. TOBIAS. J. Am. Chem. Soc. **96**, 6874 (1974).
22. R. BONACCORSI, A. PULLMAN, E. SCROCCO, and J. TOMASI. Theor. Chim. Acta, **24**, 51 (1972); **36**, 339 (1975).

Can. J. Chem. Downloaded from www.nrcresearchpress.com by 210.87.254.5 on 09/05/12
For personal use only.

The crystal structure of the neuroleptic agent (±)-deoxybutaclamol and its significance for the topography of the central dopamine receptor[1]

S. FORTIER AND M. PRZYBYLSKA

Division of Biological Sciences, National Research Council of Canada, Ottawa, Ont., Canada K1A 0R6

AND

L. G. HUMBER

Chemistry Department, Ayerst Laboratories, Montreal, P.Q., Canada H3C 3J1

Received February 6, 1980

S. FORTIER, M. PRZYBYLSKA, and L. G. HUMBER. Can. J. Chem. **58**, 1444 (1980).

(±)-Deoxybutaclamol, $C_{25}H_{31}N$, crystallizes in space group $P2_1/a$ with cell dimensions: a = 16.626(3), b = 10.646(2), c = 11.278(3) Å, β = 90.47(4)°. The structure was solved by direct methods using the QTAN program. The coordinates were refined by block-diagonal least-squares calculations to R = 0.052 for 3147 observed reflections.

The structure of (±)-deoxybutaclamol was found to be very similar to that of equipotent (±)-butaclamol and is in agreement with that assigned on the basis of chemical, spectral, crystallographic, and pharmacological studies. This confirmation validates the coordinates of a lipophilic accessory binding site in a proposed model of the central dopamine receptor.

S. FORTIER, M. PRZYBYLSKA, et L. G. HUMBER. Can. J. Chem. **58**, 1444 (1980).

Le (±)-désoxybutaclamol, $C_{25}H_{31}N$, cristallise dans le groupe d'espace $P2_1/a$ et les dimensions de la maille sont: a = 16.626(3), b = 10.646(2), c = 11.278(3) Å, β = 90.47(4)°. On a résolu la structure par des méthodes directes en faisant appel au programme QTAN. On a affiné les coordonnées par la méthode des moindres carrés (blocs diagonaux) jusqu'à une valeur de R = 0.052 pour 3147 réflexions observées.

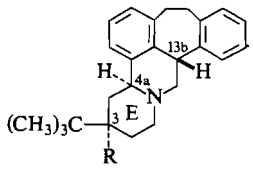
On a trouvé que la structure du (±)-désoxybutaclamol est très semblable à celle du (±)-butaclamol de puissance semblable et qu'elle est en accord avec celle attribuée en se basant sur des études chimiques spectrales, cristallographiques et pharmacologiques. Cette confirmation rend valable les coordonnées d'un site récepteur accessoire lipophile dans un modèle proposé du récepteur central de la dopamine.

[Traduit par le journal]

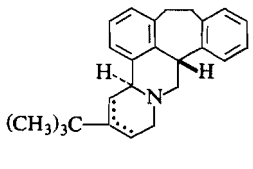
Introduction

Recent studies have shown that (±)-butaclamol, **1**, (1) is a clinically active antipsychotic agent in man (2–7), and in animals exhibits a psychopharmacological profile typical of antipsychotic agents (8). These effects of antipsychotic agents are believed to be mediated via the blockade, in the brain, of the receptors for the endogenous neurotransmitter dopamine (for a review of the dopamine hypothesis of schizophrenia, see ref. 9).

(±)-Butaclamol has been demonstrated to be a high-affinity dopamine receptor antagonist (10, 11), and its ability to bind to the dopamine receptor has been ascribed to the presence in its semirigid benzocycloheptapyridoisoquinoline nucleus of an extended phenylethylamine pharmacophore (12), the nitrogen atom and phenyl ring of which bind to primary binding sites on the receptor macromolecule (13, 14). It was suggested (12) that the hydroxyl and *tert*-butyl groups of (±)-butaclamol contribute to the affinity between ligand and receptor through binding to accessory binding sites on the receptor macromolecule. Further studies, however, have demonstrated (13) that the hydroxyl group does not contribute to binding affinity since (±)-deoxybutaclamol, **2**, was found to be virtually equipotent to (±)-butaclamol using *in vivo* (13) and *in vitro* (15) models of dopamine receptor blockade. In contrast, the presence of the *tert*-butyl or other similar lipophilic group at the 3-position of the benzocycloheptapyridoisoquinoline nucleus was found to be critical for dopamine receptor antagonist activity (13).



1 (R = OH)
2 (R = H)



3

This necessity for the presence of a lipophilic group confirmed the existence of a lipophilic accessory binding site and has led to the proposal (13, 14) of a model of the dopamine receptor which incorporates primary as well as accessory binding sites. The coordinates of the lipophilic accessory binding site were assigned with the assumptions that the *tert*-butyl group at position-3 of (±)-deoxybutaclamol, **2**, was attached equatorially, that ring

[1]NRCC No. 18303.

0008-4042/80/141444-05$01.00/0

©1980 National Research Council of Canada/Conseil national de recherches du Canada

Can. J. Chem. Downloaded from www.nrcresearchpress.com by 210.87.254.6 on 09/05/12
For personal use only.

Can. J. Chem. Downloaded from www.nrcresearchpress.com by 210.87.254.6 on 09/05/12
For personal use only.

E assumed a chair conformation, and, that the molecule possessed a 4a,13b-*trans* relative configuration.

While the latter assumption was verified by proton magnetic resonance spectral evidence (13), there remained uncertainties with respect to the first two. These uncertainties existed since in the synthesis of (±)-deoxybutaclamol by the catalytic reduction of the olefin mixture **3** with platinum oxide as catalyst, apart from a 34% yield of (±)-deoxybutaclamol, there was also obtained a 30% yield of an isomeric compound (mass spectrum and elemental analysis) which retained a 4a,13b-*trans* relative configuration (pmr spectrum) (13).

On the basis of equipotency between (±)-butaclamol and (±)-deoxybutaclamol (13, 15), and the absence of activity with the isomer, (±)-deoxybutaclamol was assigned a structure with an equatorial *tert*-butyl configuration and a ring E-chair conformation, similar to that observed in the crystal structure of (±)-butaclamol (16).

Since the validity of the coordinates for the lipophilic accessory binding site in the proposed model of the dopamine receptor are critically dependent on the correctness of the above configurational and conformational assignments, we have undertaken a crystal structure analysis of (±)-deoxybutaclamol.

Experimental

(±)-Deoxybutaclamol hydrochloride was converted to the free base which was crystallized from 2-propanol and had mp 110–113°C. The crystal data of (±)-deoxybutaclamol are as follows:

$C_{25}H_{31}N$ fw = 345.5
Monoclinic, $P2_1/a$, a = 16.626(3), b = 10.646(2), c = 11.278(3) Å, β = 90.47(4)°, V = 1996.1 Å^3, Z = 4, ρ_o = 1.150 (by flotation at 24°C), ρ_c = 1.150 g cm^{-3}, Cu Kα(λ(α_1) = 1.54050, λ(α_2) = 1.54434 Å).

The space group was established from precession films. The data were measured on an automatic Picker diffractometer with Ni-filtered Cu radiation using an almost spherical crystal of diameter 0.61 mm. The unit cell parameters were derived from the angular settings of five high-order axial reflections (2θ = 80–111°) and their equivalents. The intensities were measured by the θ–2θ scan procedure at 3.5° take-off angle and with 2θ scanning speed of 2° min^{-1}. The backgrounds were recorded for 20 s with a stationary counter at the start and end of each scan. The intensities of two standard reflections were examined at regular intervals for scaling. Of the 3396 non-equivalent reflections ($2\theta_{max}$ = 130°), 3147 (93%) had significant net counts and were considered observed. Net intensities were corrected for Lorentz and polarization effects, but not for absorption (μ(Cu) = 4.59 cm^{-1}).

The structure was solved by direct methods using the program QTAN (17). An E map computed from the solution with the most negative NQEST figure of merit (18) showed two images of the molecule, each with 24 out of the 26 non-hydrogen atoms, and translated by about 1.5 Å from one another along the y axis (19). Averaging the y coordinates gave the correct structure. The hydrogen atoms were located from a difference map computed at a later stage.

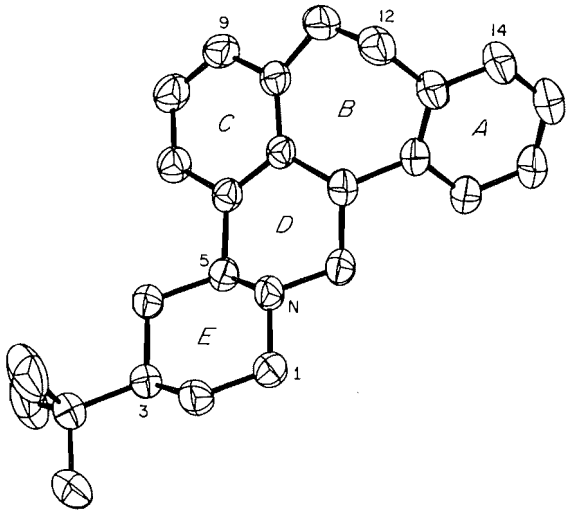


FIG. 1. The molecular structure of deoxybutaclamol with 50% probability thermal ellipsoids.

Refinement was carried out by block-diagonal least-squares with only the observed reflections, minimizing $\Sigma w(|F_o| - |F_d|)^2$ with weights $w = 1/[\sigma^2(F) + 0.002\,F^2]$, where $\sigma(F)$ is the esd in the observed amplitude based on counting statistics.

Anisotropic thermal parameters were used for C and N atoms, but H atoms were treated isotropically. Three hydrogen atoms of the butyl group (H(23, 3), H(24, 3), and H(25, 1)) did not refine well, resulting in unacceptably long C—H bond lengths and consequently they were included at the fixed positions deduced from molecular geometry.

All the reflections with highest net counts were corrected for extinction and three planes which suffered from multiple diffraction (724, 152, and $\bar{7}82$) were excluded from the final stages of refinement.

All calculations were carried out with the NRCC crystallographic computer programs by Ahmed, Hall, Pippy, and Huber (20). The scattering factor curves were those of Hanson, Herman, Lea, and Skillman (21) for C and N; and of Stewart, Davidson, and Simpson (22) for H. The refinement converged to R = 0.052 and Rw = 0.100 for the 3147 observed reflections and the mean and maximum shifts/esd were 0.16 and 0.90, respectively. The refined atomic coordinates are presented in Table 1.[2] A final difference map revealed no significant peaks, as the values were within −0.22 and 0.20 e Å^{-3}.

Results and Discussion

A view of one of the two enantiomorphs of (±)-deoxybutaclamol present in the crystal structure, drawn by ORTEP program (23), is shown in Fig. 1.

[2]Tables of observed and calculated structure factor amplitudes and of temperature factors are available, at a nominal charge, from the Depository of Unpublished Data, CISTI, National Research Council of Canada, Ottawa, Ont., Canada K1A 0S2.

Can. J. Chem. Downloaded from www.nrcresearchpress.com by 210.87.254.6 on 09/05/12
For personal use only.

TABLE 1. Final fractional coordinates with esd's in parentheses ($\times 10^4$ for C, N; and $\times 10^3$ for H) and equivalent isotropic temperature factors (Å^2)

Atom	X	Y	Z	B
N(1)	4951(1)	−191(1)	7035(1)	3.5
C(1)	4977(1)	−1565(1)	6978(1)	4.3
C(2)	5825(1)	−2042(1)	7181(2)	4.2
C(3)	6129(1)	−1644(1)	8399(1)	3.5
C(4)	6054(1)	−211(1)	8492(1)	3.5
C(5)	5202(1)	250(1)	8211(1)	3.1
C(6)	5120(1)	1675(1)	8281(1)	3.0
C(7)	5524(1)	2302(1)	9193(1)	3.7
C(8)	5510(1)	3591(1)	9272(1)	4.3
C(9)	5109(1)	4266(1)	8418(1)	4.1
C(10)	4692(1)	3695(1)	7493(1)	3.4
C(11)	4334(1)	4602(1)	6587(2)	4.5
C(12)	3943(1)	4084(1)	5472(1)	4.5
C(13)	3209(1)	3337(1)	5778(1)	3.8
C(14)	2440(1)	3818(2)	5575(1)	4.7
C(15)	1765(1)	3177(2)	5949(2)	4.9
C(16)	1854(1)	2059(1)	6535(1)	4.4
C(17)	2617(1)	1558(1)	6733(1)	3.7
C(18)	3303(1)	2187(1)	6360(1)	3.3
C(19)	4150(1)	1656(1)	6536(1)	3.3
C(20)	4137(1)	259(1)	6815(1)	4.0
C(21)	4660(1)	2370(1)	7452(1)	3.0
C(22)	6975(1)	−2145(1)	8755(2)	4.3
C(23)	7136(1)	−1861(2)	10066(2)	7.0
C(24)	7639(1)	−1548(3)	8037(3)	8.1
C(25)	7007(1)	−3560(2)	8592(3)	7.9
H(1,1)	477(1)	−181(1)	620(1)	3.7(0.3)
H(1,2)	458(1)	−198(1)	759(2)	5.2(0.4)
H(2,1)	619(1)	−168(1)	650(1)	3.8(0.3)
H(2,2)	584(1)	−301(2)	706(2)	6.0(0.5)
H(3)	577(1)	−206(1)	900(2)	4.2(0.4)
H(4,1)	643(1)	19(2)	793(2)	4.8(0.4)
H(4,2)	621(1)	7(1)	930(2)	4.4(0.4)
H(5)	482(1)	−11(1)	879(1)	3.1(0.3)
H(7)	579(1)	183(1)	978(2)	3.6(0.3)
H(8)	576(1)	397(1)	994(2)	4.8(0.4)
H(9)	511(1)	519(1)	844(1)	4.1(0.4)
H(11,1)	395(1)	514(2)	701(2)	5.3(0.4)
H(11,2)	474(1)	520(2)	636(2)	5.6(0.4)
H(12,1)	378(1)	479(1)	494(1)	4.1(0.3)
H(12,2)	436(1)	356(2)	503(1)	4.0(0.3)
H(14)	235(1)	464(2)	518(2)	5.8(0.4)
H(15)	123(1)	352(2)	586(2)	5.8(0.4)
H(16)	137(1)	161(2)	677(2)	5.2(0.4)
H(17)	266(1)	72(1)	713(1)	3.7(0.3)
H(19)	441(1)	170(1)	576(1)	4.3(0.4)
H(20,1)	392(1)	−19(1)	612(2)	4.7(0.4)
H(20,2)	378(1)	6(2)	750(2)	5.0(0.4)
H(23,1)	763(1)	−226(2)	1042(2)	7.2(0.5)
H(23,2)	720(2)	−88(3)	1015(3)	12.4(1.0)
H(23,3)	663(0)	−216(0)	1056(0)	11.0(0.0)
H(24,1)	815(1)	−187(2)	827(2)	7.6(0.6)
H(24,2)	752(1)	−171(2)	717(2)	8.4(0.6)
H(24,3)	765(0)	−56(0)	820(0)	11.0(0.0)
H(25,1)	691(0)	−379(0)	767(0)	11.0(0.0)
H(25,2)	756(2)	−384(2)	886(3)	9.5(0.7)
H(25,3)	655(2)	−387(2)	903(3)	9.7(0.7)

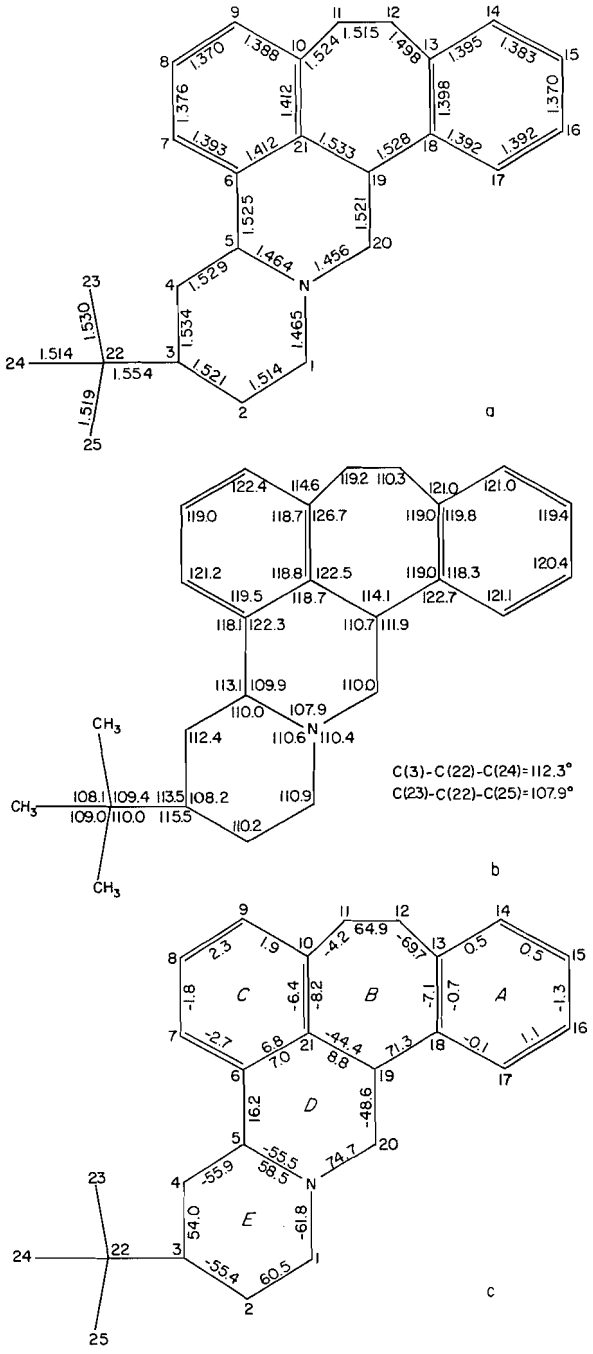


FIG. 2. (*a*) Bond lengths (Å); the esd's are ≤0.003 Å. (*b*) Valency angles (deg); the esd is 0.2°. (*c*) Endocyclic torsion angles (deg); the esd is 0.4°.

Its stereochemistry is very similar to that of (±)-butaclamol hydrobromide and the more accurately determined (+)-dexclamol hydrobromide (16). The rings D and E are *trans*-fused: in Fig. 1 the H atom attached to C(5) is directed downwards and

TABLE 2. Mean planes

(*a*) Parameters for the planes $lX + mY + nZ = p$, where X, Y, Z are orthogonal coordinates in Å

Ring	l	m	n	p
A	−0.0403	−0.4809	−0.8758	−7.6237
B(1)	0.8589	−0.0744	−0.5067	2.0736
B(2)	−0.0126	−0.4323	−0.9017	−7.5097
C	0.8208	0.0313	−0.5704	1.6267
D	0.7699	0.0717	−0.6341	0.7322
E	0.7445	0.5188	−0.4202	2.6357

(*b*) Atomic displacements (Å), esd = 0.002 Å

Atom	Displacement from A	Atom	Displacement from B(1)	Atom	Displacement from C	Atom	Displacement from D	Atom	Displacement from E
C(13)	−0.005	C(10)	−0.007	C(6)	0.026	C(5)	0.015	C(2)	−0.005
C(14)	0.000	C(11)	−0.065	C(7)	0.004	C(6)	−0.031	C(3)	0.005
C(15)	0.005	C(12)	0.062	C(8)	−0.022	C(19)	−0.014	C(5)	−0.005
C(16)	−0.007	C(19)	−0.065	C(9)	0.009	C(21)	0.031	N	0.005
C(17)	0.003	C(21)	0.075	C(10)	0.022	C(20)*	−0.340	C(1)*	−0.693
C(18)	0.003	C(12)	Displacement	C(21)	−0.039	N*	0.509	C(4)*	0.659
C(12)*	−0.134	C(13)	from B(2)	C(11)*	0.153				
C(19)*	0.044	C(18)	−0.015	C(19)*	−0.162				
C(20)*	0.484	C(19)	0.032	C(5)*	0.136				
N*	0.442		−0.032	N*	0.543				
			0.015						

*Identifies atoms not included in the mean plane calculation.

the lone pair of electrons of N is pointing up. The *tert*-butyl group is attached equatorially.

Bond lengths and angles are presented in Fig. 2(*a* and *b*). The mean value of 1.525 Å for C(sp^3)—C(sp^3) bonds came close to that for C(sp^3)—C(sp^2) bonds (1.522 Å). This overall slight shortening for C—C single bonds is comparable to that found in (+)-isobutaclamol hydrobromide (24), where C(sp^3)—C(sp^3) bonds gave the mean of 1.527 Å. The longest bond is C(3)—C(22) (1.554 Å), an expected result due to the substitution by the large *tert*-butyl group. The mean value for C(sp^2)—C(sp^2) bonds is 1.390 Å and the mean of C—N bonds is 1.462 Å, which is in agreement with the value for the C to three-covalent N distance. The C—H are in the range 0.94–1.08 Å (mean = 1.00 and esd = 0.03 Å). The valency angles have normal values with the exception of three endocyclic angles in the cycloheptane ring. The values for C(21)—C(10)—C(11), C(10)—C(11)—C(12), and C(18)—C(19)—C(21) are considerably larger than normal (126.7, 119.2, and 114.1°). They agree with the corresponding angles in (+)-dexclamol hydrobromide (16) which are 129, 118, and 112°, respectively.

The angles at the attachment of the *tert*-butyl group are also abnormally large (113.5 and 115.5.°). Since some of the hydrogen atoms attached to C(24) and C(25) make short intermolecular contacts with hydrogen atoms of neighbouring molecules, these increases may be caused by the crystal packing.

The C—C—H and H—C—H angles vary from 101.9 to 122.8° and give the average 110.9°.

Endocyclic torsion angles are shown in Fig. 2(*c*) and mean plane calculations in Table 2. Ring A is almost planar with $\chi^2 = 47.2$, but ring C is not, showing large atomic displacements up to 0.039 Å. The dihedral angle between their mean planes is 63.2°.

Ring E has a regular chair conformation, but ring D is a half-chair with C(20) and N distances of −0.34 and 0.51 Å from the plane of the other four atoms of the ring. The cycloheptane ring B is of V shape, folded along C(12)···C(19) line. The displacements of the atoms from the mean planes of the two portions of the ring B are given in Table 2. The dihedral angle between them is 61.4°. Atoms H(12, 2) and H(19) exhibit a flagpole-bowsprit interaction between them, being separated by 2.15 Å.

The molecules are separated by normal van der Waals contacts. There are no C···H distances below 2.89 Å and the shortest H···H contact is H(12, 2) to H(2, 2) of 2.45 Å.

In summary, (±)-deoxybutaclamol possesses a molecular structure in agreement with that as-

Can. J. Chem. Downloaded from www.nrcresearchpress.com by 210.87.254.6 on 09/05/12
For personal use only.

signed previously and this finding validates the coordinates of a lipophilic accessory binding site in a proposed model of the central dopamine receptor.

Acknowledgements

The authors wish to thank Mrs. M. E. Pippy and Mrs. H. M. Sheppard for their assistance with the computations.

1. F. T. BRUDERLEIN, L. G. HUMBER, and K. VOITH. J. Med. Chem. **18**, 185 (1975).
2. D. H. MIELKE, D. M. GALLANT, T. OELSNER, C. M. KESSLER, W. K. TOMLINSON, and G. H. COHEN. Dis. Nerv. Syst. **36**, 7 (1975).
3. L. E. HOLLISTER, K. L. DAVIS, and P. A. BERGER. Psychopharmacol. Commun. **1**, 493 (1975).
4. J. M. GALLART-CAPDEVILA. Arch. Neurobiol. **38**, 545 (1975).
5. F. IMAZ, T. A. BAN, and H. E. LEHMANN. Psychopharmacol. Bull. **12**, 31 (1976).
6. M. L. CLARK, A. PAREDES, J. P. COSTILOE, and F. WOOD. J. Clin. Pharmacol. **17**, 529 (1977).
7. M. L. CLARK, J. P. COSTILOE, F. WOOD, A. PAREDES, and G. FULKERSON. Dis. Nerv. Syst. **38**, 943 (1977).
8. K. VOITH and F. HERR. Psychopharmacologia, **42**, 11 (1975).
9. S. SNYDER. Am. J. Psychiat. **133**, 197 (1976).
10. P. SEEMAN, M. CHAU-WONG, J. TEDESCO, and K. WONG. Proc. Natl. Acad. Sci. U.S.A. **72**, 4376 (1975).
11. D. R. BURT, S. ENNA, I. CREESE, and S. H. SNYDER. Proc. Natl. Acad. Sci. U.S.A. **72**, 4655 (1975).
12. L. G. HUMBER, F. T. BRUDERLEIN, and K. VOITH. Mol. Pharmacol. **11**, 833 (1975).
13. L. G. HUMBER, F. T. BRUDERLEIN, A. H. PHILIPP, M. GÖTZ, and K. VOITH. J. Med. Chem. **22**, 761 (1979).
14. A. H. PHILIPP, L. G. HUMBER, and K. VOITH. J. Med. Chem. **22**, 768 (1979).
15. W. LIPPMANN and T. A. PUGSLEY. Private communication.
16. P. H. BIRD, F. T. BRUDERLEIN, and L. G. HUMBER. Can. J. Chem. **54**, 2715 (1976).
17. D. A. LANGS and G. T. DE TITTA. Acta Crystallogr. **A31**, S16, Abstract 02.2-14 (1975).
18. G. T. DE TITTA, J. W. EDMONDS, D. A. LANGS, and H. HAUPTMAN. Acta Crystallogr. **A31**, 472 (1975).
19. C. S. HUBER. Acta Crystallogr. **B31**, 108 (1975).
20. F. R. AHMED, S. R. HALL, M. E. PIPPY, and C. P. HUBER. NRC Crystallographic Programs for the IBM 360 System, Accession Nos. 133–147, J. Appl. Crystallogr. **6**, 309 (1973).
21. H. P. HANSON, F. HERMAN, J. D. LEA, and S. SKILLMAN. Acta Crystallogr. **17**, 1040 (1964).
22. R. F. STEWART, E. R. DAVIDSON, and W. T. SIMPSON. J. Chem. Phys. **42**, 3175 (1965).
23. C. K. JOHNSON. ORTEP, Report ORNL-3794, revised. Oak Ridge National Laboratory, Tennessee. 1965.
24. F. R. AHMED and M. PRZYBYLSKA. Acta Crystallogr. **B35**, 2169 (1979).

Can. J. Chem. Downloaded from www.nrcresearchpress.com by 210.87.254.6 on 09/05/12
For personal use only.

Aromatic fluorination with xenon difluoride: L-3,4-dihydroxy-6-fluoro-phenylalanine

GUNTER FIRNAU,[1] RAMAN CHIRAKAL, SUDESH SOOD, AND STEPHEN GARNETT

Department of Nuclear Medicine, McMaster University Medical Centre Division, Chedoke–McMaster Hospital, M.P.O. Box 2000, Hamilton, Ont., Canada L8N 3Z5

Received March 10, 1980

GUNTER FIRNAU, RAMAN CHIRAKAL, SUDESH SOOD, and STEPHEN GARNETT. Can. J. Chem. **58**, 1449 (1980).

L-3-Methoxy-4-hydroxyphenylalanine was fluorinated directly with XeF_2 in CH_2Cl_2 at −60°C *in vacuo*. After hydrolysis with 48% aqueous HBr, L-6-fluorodopa was obtained. The yield, based on XeF_2, was 25%. This reaction might be applied when chiral biomolecules are to be tagged with fluorine-18.

GUNTER FIRNAU, RAMAN CHIRAKAL, SUDESH SOOD et STEPHEN GARNETT. Can. J. Chem. **58**, 1449 (1980).

Le produit de la réaction de L-3-methoxy-4-hydroxyphenylalanine avec le difluorure de xénon en chlorure de methylène sous vide à −60°C a été hydrolisé par le l'acide bromique aqueux (48%) pour produire exclusivement du L-6-fluorodopa. Le rendement de cette réaction est de l'ordre de 25% (basé sur XeF_2). Cette réaction pourrait être utilisée lors du marquage de molecules biochimiques chirales avec du fluor-18.

Can. J. Chem. Downloaded from www.nrcresearchpress.com by 210.87.254.42 on 09/05/12
For personal use only.

The radioactive tracer DL[^{18}F]3,4- dihydroxy-5-fluorophenylalanine (DL[^{18}F]-5-fluorodopa) has enabled us to make novel measurements of intracerebral dopamine metabolism, non-invasively in primates, by means of simple gamma ray detectors placed over the head (1). The synthesis of DL-5-fluorodopa is cumbersome (2) and, from a biological point of view, the L-stereoisomer would be much preferred. In this communication we describe a simple and rapid fluorination with xenon difluoride that yields the unique molecule L-6-fluorodopa. This procedure could be adapted to make the ^{18}F labelled analogue.

The direct fluorination of L-dopa with XeF_2 is not possible. XeF_2 oxidizes the catechol in L-dopa to *o*-quinone. Further, fluorinations with XeF_2 are reported to proceed best in methylene chloride (3) but L-dopa does not dissolve in it. Because L-3-methoxy-4-hydroxyphenylalanine ethyl ester is soluble in methylene chloride and it is not oxidized, it was reacted with XeF_2 in methylene chloride at −60°C *in vacuo* and the reaction products hydrolysed immediately with 48% HBr. The reaction mixture was chromatographed by reversed phase hplc and 6-fluorodopa was the only fluorinated product. The 6-fluorodopa was identified by ms and ^{19}Fmr.

In order to prove that 6-fluorodopa was the L-enantiomer, it was used as a substrate for the stereospecific L-amino acid decarboxylase (E.C.4.1.1.26). This enzyme is known to decarboxylate 5-fluorodopa (4) and a wide variety of other aromatic amino acids. The product of the enzymatic reaction of 6-fluorodopa was isolated by reversed phase hplc and shown to be 6-fluorodopamine.

Fluorinations with XeF_2 usually yield isomeric mixtures of fluoroaromatics (3). Only one of the three possible fluorodopa isomers was detected from our synthesis. The exclusive fluorination of dopa in the 6-position is in accord with the suggested electrophilic character of the reaction (3). This mild fluorination reaction may be applicable to other fragile and chiral biomolecules, such as L-hydroxytryptophan.

Experimental

Preparation of L-3-Methoxy-4-hydroxyphenylalanine Ethyl Ester

L-3-Methoxytyrosine (7.83 g, 40 mmol, SIGMA Chemical Company) was suspended in absolute ethanol (150 mL) and HCl gas was passed through for 30 min. The reaction mixture was kept at room temperature overnight before the ethanol was evaporated. The remainder was twice redissolved in water (50 mL each) and evaporated. Recrystallizations from methanol–ether gave 10 g L-3-methoxy-4-hydroxyphenylalanine ethyl ester hydrochloride. This hydrochloride (9.7 g, 35 mmol), dissolved in 15 mL of water, was neutralized with 1.4 g sodium hydroxide. The neutralized solution was extracted three times with hot ethyl acetate. The combined extracts were dried over anhydrous Na_2SO_4. Evaporation of ethyl acetate left 7.0 g of white crystals, yield 73%, based on L-3-methoxy-4-hydroxyphenylalanine, mp 93–94°C, uncorrected. *Anal.* calcd. for $C_{12}H_{17}NO_4$ (239.3): C 60.23, H 7.18, N 5.85; found: C 60.22, H 7.14, N 5.83 (Microanalysis Laboratories, A. B. Gygli, Toronto).

Preparation of L-6-Fluorodopa

A solution of 17 mg (0.1 mmol) xenon difluoride (PCR, Research, Inc.) in 2 mL methylene chloride was placed in a Kel-F tube and frozen with liquid nitrogen. The pressure in the tube was reduced to about 10 μm Hg. Anhydrous hydrogen fluoride (10 μL) and a solution of 71 mg (0.3 mmol) L-3-methoxy-4-hydroxyphenylalanine ethyl ester in 1 mL methylene chloride was added. The Kel-F tube was warmed up to −60°C. The

[1]Author to whom correspondence may be addressed.

0008-4042/80/141449-02$01.00/0

©1980 National Research Council of Canada/Conseil national de recherches du Canada

colour of the reaction mixture changed from green to yellow-brown over a period of 10 min. The methylene chloride was evaporated at room temperature *in vacuo*. To the yellow remainder 10 mL of 48% hydrobromic acid was added. The hydrolysis mixture was treated at 140°C for 15 min while hydrogen gas was passed through. The hydrobromic acid was removed by evaporation *in vacuo*. The dry residue was twice redissolved in water and evaporated. Finally, the residue was dissolved in 5 mL water. This solution was chromatographed in aliquots with hplc (column: μBondapak™/C-18, 7.8 mm × 300 mm; mobile phase: 0.1% acetic acid in water at 2 mL/min; detector: uv at 280 nm). The fluorodopa fraction was collected and the solvent evaporated. Yield 5.4 mg or 25% based on XeF_2; $^{19}Fmr(D_2O)$ δ: 36.4 (s) ppm downfield from hexafluorobenzene, measured with a Bruker WH 90 FT nmr spectrometer at 84.66 MHz at 25°C. In comparison, 6-fluorodopamine has a chemical shift of 37 ppm downfield from hexafluorobenzene (6). Gas chromatography – mass spectroscopy: the trimethylsilyl derivative of 6-fluorodopa was prepared (7). The gas chromatograph (Varian 2700) was fitted with a 1800 mm × 2 mm column (1.5% OV-17 on Chromosorb W, 80–100 mesh). The operating conditions were: injector at 305°C, column at 270°C, interface and Watson–Biemann separator at 300°C, flow rate 50 mL of He/min. The mass spectrograph was a Varian Mat CH7, which was operated with an ionization voltage of 70 eV, and an emission current of 300 μA. The ion source was maintained at 300°C. The observed mass fragments at 218 and 219 are typical for trimethylsilylated amino acids (8). Those at 197 and 285 are consistent with the structure of a fluorinated bistrimethylsilylated methyl catechol cation (7). The uv absorption: λ_{max}: 284 nm in 0.1% acetic acid.

Proof that the L-*Stereoisomer of 6-Fluorodopa had been Produced*

L-Amino acid decarboxylase was prepared from rabbit kidney cortex by the method of Lancaster and Sourkes (5) and purified up to the $(NH_4)_2SO_4$ fractionation. A chromatographically pure sample of 6-fluorodopa, derived from the XeF_2 reaction, was incubated for 2 h with the decarboxylase. The enzyme reaction was terminated by addition of 5% phosphotungstic acid in 2 *N* HCl and then heated at 100°C for 1 min. After the precipitated proteins had been removed by centrifugation, an aliquot of that solution was chromatographed with hplc (column: μBondapak™/C-18, 7.8 mm × 300 mm; mobile phase: 0.05 *M* NaH_2PO_4 buffer pH 3.5 at 2.0 mL/min; detector: uv at 280 nm). The presence of 6-fluorodopamine was confirmed by spiking with the authentic material. During the enzymatic reaction the amount of 6-fluorodopa was reduced by 90%. The appropriateness of the enzymatic assay was established by showing that under the above conditions (4) authentic L-dopa and L-5-fluorodopa were completely converted to dopamine and 5-fluorodopamine, respectively.

Acknowledgements

We thank Dr. R. J. Gillespie, Department of Chemistry, for constructive discussions on this subject.

This research was supported by grants from the Natural Sciences and Engineering Research Council of Canada, the Medical Research Council of Canada, and the Ontario Mental Health Foundation.

1. E. S. GARNETT, G. FIRNAU, C. NAHMIAS, S. SOOD, and L. BELBECK. Am. J. Physiol. **238**, R 318 (1980).
2. G. FIRNAU, C. NAHMIAS, and E. S. GARNETT. J. Med. Chem. **16**, 416 (1973).
3. R. FILLER. Isr. J. Chem. **17**, 71 (1978), and references therein.
4. G. FIRNAU, E. S. GARNETT, T. L. SOURKES, and K. MISSALA. Experientia (Basel), **31**, 1254 (1975).
5. G. A. LANCASTER and T. L. SOURKES. Can. J. Biochem. **50**, 791 (1972).
6. K. KIRK. J. Org. Chem. **41**, 2373 (1976).
7. N. NARASIMACHARI and P. VOUROS. Anal. Biochem. **45**, 154 (1972).
8. W. J. A. VANDEN HEUVEL and J. L. SMITH. J. Chromatogr. Sci. **8**, 567 (1970).

Can. J. Chem. Downloaded from www.nrcresearchpress.com by 210.87.254.42 on 09/05/12
For personal use only.

Déshydratation des diols-1,2 α,β-éthyléniques IV:[1] rôle de la stéréomutation des carbocations allyliques α-hydroxylés sur l'orientation des réactions observées

GILBERT DANA ET JOSYANE GHARBI-BENAROUS

Laboratoire de Stéréochimie Réactionnelle, Université Pierre et Marie Curie, 4 Place Jussieu, 75230 Paris, France

ET

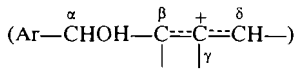
SA LE THI THUAN

Laboratoire de Chimie des Hétérocycles, Université Pierre et Marie Curie, 4 Place Jussieu, 75230 Paris, France

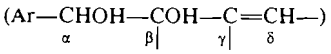
Reçu le 27 août 1979

GILBERT DANA, JOSYANE GHARBI-BENAROUS et SA LE THI THUAN. Can. J. Chem. **58**, 1451 (1980).

L'évolution du carbocation allylique hydroxylé du type *C*



issus des diols du type *A*

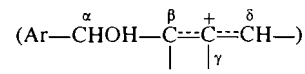


peut se dérouler suivant cinq processus: trois attaques nucléophiles, (en β ou en δ, par une molécule du solvant ou en δ par l'hydroxyle intramoléculaire), une réaction de dégradation, et la transposition pinacolique.

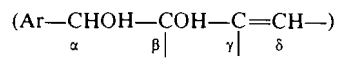
Les attaques nucléophiles sur le pôle δ aussi bien intramoléculaires (formation de dihydrofurannes) que par une molécule de solvant (formation de cétone de type *B*), sont des processus très sélectifs qui s'excluent mutuellement dans le cas d'un substituant unique en β, γ, ou δ. Pour les carbocations disubstitués en γ et en δ, la sélectivité est moindre et on obtient des mélanges différents de ces deux types de produits, suivant l'encombrement des substituants. On a pu ainsi analyser le rôle des différents facteurs stériques qui régissent l'équilibre de stéréomutation du carbocation allylique et par là, déterminent l'orientation de la déshydratation.

GILBERT DANA, JOSYANE GHARBI-BENAROUS, and SA LE THI THUAN. Can. J. Chem. **58**, 1451 (1980).

The allylic carbocations



formed during the dehydration of diols of type *A*



are found to react by five different processes: three nucleophilic attacks (by solvent at the β or δ positions, or by the intramolecular hydroxyl group at δ), a degradation reaction between C_α and C_β and the classical pinacol rearrangement.

Nucleophilic attack at the carbon δ is a very efficient reaction and sometimes (for monosubstituted substrates in β, γ or δ) gives quasi-exclusive products: a ketone for the reaction with H_2O in δ or a 2,5-dihydrofuran product for the intramolecular reaction.

In the case of γ and δ disubstituted carbocations, the selectivity is less and we show that it is possible to analyze the different steric effects commanding the stereomutation equilibrium of the allylic carbocation and so determining the orientation in the dehydration.

Introduction

L'étude de la réactivité des carbocations allyliques α-hydroxylés du type *C*, issus des diols-1,2 du type *A*, effectuée dans trois précédents mémoires (1, 2, 3) a permis de mettre en évidence cinq réactions possibles bien distinctes (schéma 1). Ces réactions, observées de façon souvent sélective pour des carbocations non-substitués ($R_\alpha = R_\beta = R_\gamma = R_\delta = H$) ou monosubstitués par un méthyle dans l'une des trois positions β, γ ou δ, sont les suivantes.[2]

(*a*) Une attaque nucléophile du solvant en δ conduisant à une cétone (cétone *B*) et observée essentiellement dans le cas des diols Ar—CHOH—CHOH—CH=CH—CH_3 (diols **1**) et Ar—CMeOH—CHOH—CH=CH—CH_3 (diols **2**) ($R_\delta = CH_3$) (1, 4).

[1]Précédent mémoire de la série, réf. 3.

[2]La numérotation des différents diols fait suite à celle utilisée pour les premiers mémoires (1, 2, 3).

0008-4042/80/141451-12$01.00/0

©1980 National Research Council of Canada/Conseil national de recherches du Canada

Can. J. Chem. Downloaded from www.nrcresearchpress.com by 210.87.254.6 on 09/05/12
For personal use only.

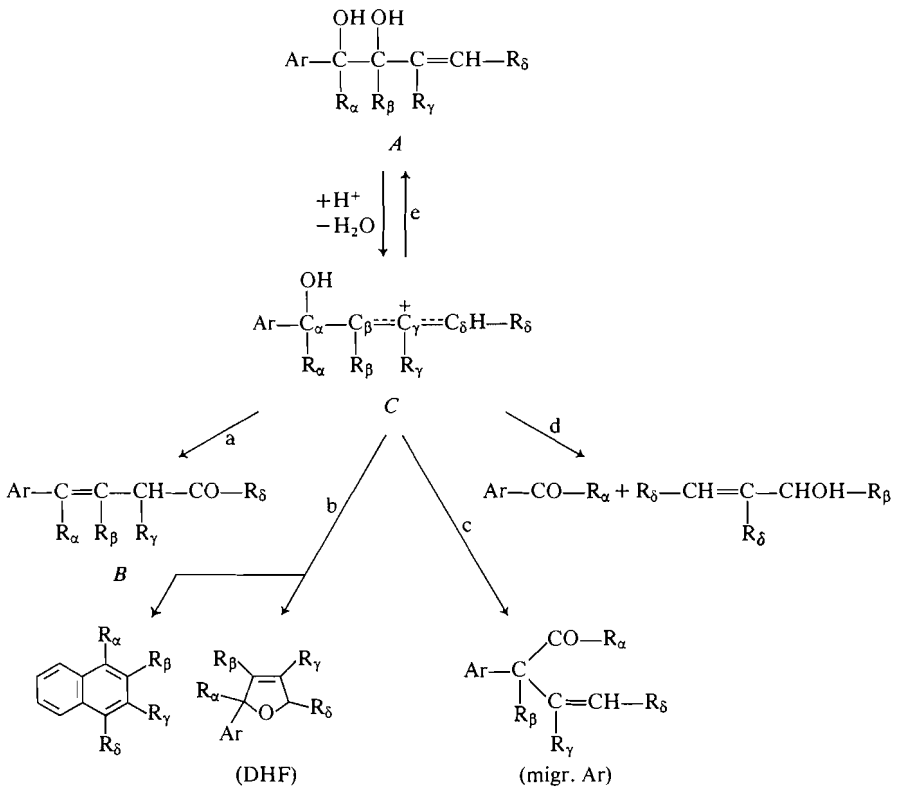


SCHÉMA 1. Les cinq évolutions observées du carbocation allylique *C*

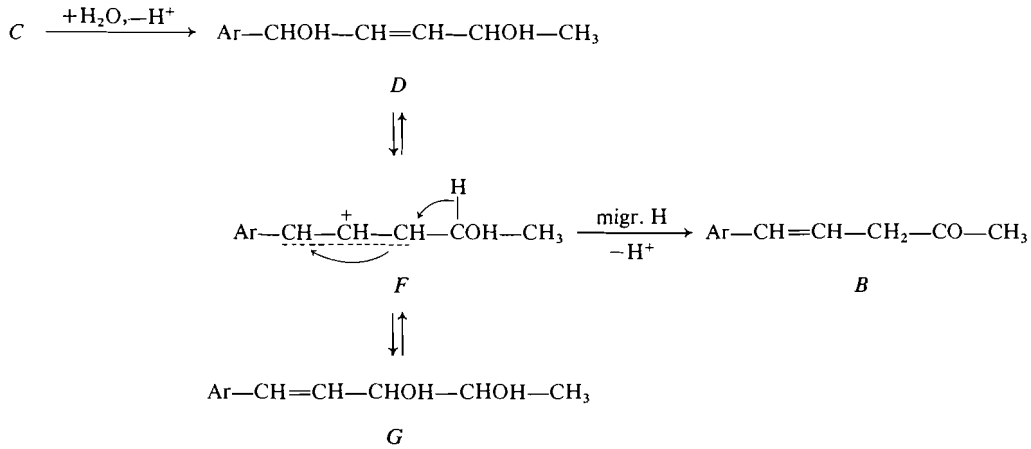
Cette formation de la cétone de type *B* est donc finalement le résultat de la transposition pinacolique (migr. H) du carbocation *F* et apparaît effectivement (1, 4) sous sa forme carbonyle non conjugué.

(*b*) Une attaque nucléophile intramoléculaire de l'hydroxyle en α sur le carbone δ (cyclisation en dihydrofuranne et éventuellement transformation en naphtalène), observée essentiellement dans le cas des diols Ar—CHOH—CMeOH—CH=CH_2 (diols **4**) ($R_\beta = CH_3$) (2, 5).

(*c*) La transposition pinacolique (tp), plus ou moins observée dans tous les cas, mais surtout importante pour les diols Ar—CHOH—CHOH—CH=CH_2 (diols **3**) ($R_\alpha = R_\beta = R_\gamma = H$) (2).

(*d*) Une réaction de dégradation (6) (coupure de la liaison C_α—C_β) observée essentiellement avec les diols Ar—CHOH—CHOH—CMe=CH_2 (diols **5**) ($R_\gamma = CH_3$) (3).

(*e*) Une attaque nucléophile du solvant en β (retour interne (7)), réaction inverse de l'ionisation du diol de départ et matérialisée par l'établissement



Can. J. Chem. Downloaded from www.nrcresearchpress.com by 210.87.254.6 on 09/05/12
For personal use only.

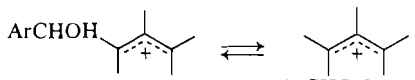
Can. J. Chem. Downloaded from www.nrcresearchpress.com by 210.87.254.6 on 09/05/12
For personal use only.

rapide d'un équilibre *érythro–thréo* de ce diol. Cette réaction est observée uniquement lorsque $R_\beta = CH_3$ (diols **4**) (8).

L'influence des substituants donneurs ou attracteurs du noyau aromatique sur la (ou les) réaction(s) observée(s) nous a permis chaque fois d'interpréter l'évolution du système. Toutefois, le caractère quasi-exclusif des différentes réactions interdisait d'apprécier l'importance relative des différents facteurs (électroniques ou stériques) dûs à la présence du méthyle dans les différentes positions envisagées.

Dans le présent mémoire, nous nous proposons d'étudier les réactions observables lorsque les carbocations portent deux substituants en γ et en δ, dont les effets spécifiques sont, dans une certaine mesure antagonistes. L'effet des différents substituants étant plus nuancé, les réactions observées sont moins sélectives et la comparaison des différents facteurs devient possible.

Nous introduirons alors quelques uns des résultats antérieurs dans la discussion générale en vue d'illustrer notamment le rôle de la configuration du carbocation allylique résultant de l'équilibre de stéréomutation (9).

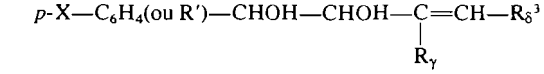


Forme ArCHOH *exo* Forme ArCHOH *endo*

Résultats

Déshydratation des diols γ-δ disubstitués (schémas 2, 3 et tableau 1)

La déshydratation est effectuée dans les mêmes conditions que pour les séries précédentes (1, 2, 3) dans l'acide sulfurique normal (entraînement à la vapeur d'eau), sur le mélange équimolaire des diols *érythro* et *thréo*. Seuls apparaissent des produits de déshydratation sans perte de carbone. Trois types de substances sont identifiés.[4]



6: $R_\gamma = R_\delta = CH_3$ *b* X = H, *c* X = CH_3, *d* X = OCH_3 et *e* R' = C_2H_5
7: $R_\gamma = CH_3$, $R_\delta = C_2H_5$ *b* X = H, *c* X = CH_3
8: $R_\gamma = C_2H_5$, $R_\delta = CH_3$ *c* X = CH_3
9: $R_\gamma = C_2H_5$, $R_\delta = C_3H_7$ *e* R' = C_2H_5

[3]Voir note 2. Les lettres *a*, *b*, *c* ... désignant le substituant X du groupe aromatique (*e* désigne le remplacement du groupe aromatique entier par le reste saturé éthyle) sont également repris des mémoires précédents et ont la même signification pour les neuf séries de diols.

[4]Les dérivés des diols sont désignés par un numéro dont le premier chiffre désigne le diol de départ (1 à 9) et le deuxième chiffre, le type du dérivé.

(*a*) *La cétone du type* B ***(62, 72, 82 ou 92)*** sous sa forme conjuguée ou non conjuguée (isomère *E* unique). En ce qui concerne la réaction de formation de ces cétones *B*, elles apparaissent dans ces séries, généralement sous forme d'un mélange (quasi)équilibré; dans le cas des cétones **62***b* ⇄ **62′***b*, le mélange obtenu dans la réaction a, en fait, la même composition que le mélange équilibré (équilibration de chacun des isomères, conjugué et non conjugué dans les conditions de la déshydratation, par l'acide sulfurique normal à reflux). Toutefois en l'absence du groupe aromatique (pour les diols **6***e* ou **9***e*, R' = C_2H_5) la forme non conjugée **62′***e* ou **92′***e* domine dans le mélange réactionnel (tableau 1 et schéma 3) alors qu'elle est presque absente à l'équilibre.

(*b*) *Les produits de cyclisation, dihydrofurannes* cis *et* trans *(**63**, **73** ou **83**) ou naphtalènes (**64**, **74** ou **84**) (tableau 1)*

Ces dérivés cyclisés, observés déjà de façon importante pour la série de diols **4** ($R_\beta = CH_3$, $R_\gamma = R_\delta = H$) (2), apparaissent dans les trois séries des diols **6**, **7** et **8**, surtout sous forme de dérivés dihydro-2,5 furanniques, alors que les dérivés naphtaléniques ne constituent que des traces détectables par cpv (ou par rmn après enrichissement).

(*c*) *Un aldéhyde de transposition pinacolique (**61**, **71** ou **81**)* résultant de la migration du groupe aryle sur le carbocation allylique (formes *Z* ou *E* conjuguées, schéma 2, tableau 1). Dans le cas du diol **9***e* (schéma 3) ne comportant pas de groupe aromatique, on observe la migration d'un hydrogène (cétones **96***e* et **96′***e* 14%) plutôt que celle de C_2H_5 (cétones **91***e*, 5%), moins favorable.

Discussion

Etude des attaques nucléophiles en δ

(A) Rôle des facteurs électroniques

Il est intéressant de noter pour les quatre séries de diols étudiés dans ce mémoire, que les produits de coupure cessent d'être observés (malgré la présence du méthyle en γ (3)) et que la transposition pinacolique diminue chaque fois au profit d'une attaque nucléophile en δ, soit intermoléculaire (formation des cétones *B*) soit intramoléculaire (produits cyclisés). La polarité du carbone δ se prête donc bien à ce type d'attaque, ce qui confirme les prévisions que l'on pouvait faire à partir des charges totales ($\sigma + \pi$) calculées pour des substrats analogues comportant ou pas un méthyle en γ ou en δ. Nous avons vu (3) en effet qu'un méthyle en γ polarise négativement le carbone δ d'environ 9 à 12 $\times 10^{-3}$ unités de charge et constitue donc un substituant défavorable aux attaques nucléophiles en δ. En revanche, un méthyle en δ, polarise positivement ce carbone δ de 23 à 25 $\times 10^{-3}$ unités de charge

Can. J. Chem. Downloaded from www.nrcresearchpress.com by 210.87.254.6 on 09/05/12
For personal use only.

TABLEAU 1. Bilan des déshydratations des diols **6**, **7** et **8**[a]

Ar = p-XC_6H_4 ou R′ = C_2H_5	Séries de diols						
	6*e*	**6***b*	**6***c*	**6***d*	**7***b*	**7***c*	**8***c*
	R′ = C_2H_5	X = H	X = CH_3	X = OCH_3	X = H	X = CH_3	X = CH_3
Transposition pinacolique							
Aldéhydes Z	tr.	7	30	80	20	26	25
Aldéhydes E	—	—	10%	35%	10%	13%	—
			20	45%	10%	13%	—
Cétones *B*							
conj.	100	63	50	20	52	30	40
conj.	30%	33%	26%	10%	26%	15%	20%
non conj.	70%	30%	24%	10%	26%	15%	20%
Cyclisation							
DHF	0	30	20	tr.	28	44	35
Naphtalène	0	30% tr.	15% 5%	—	25% 3%	40% 4%	32% 3%

[a]Les pourcentages sont calculés par rapport au total des produits de déshydratation.

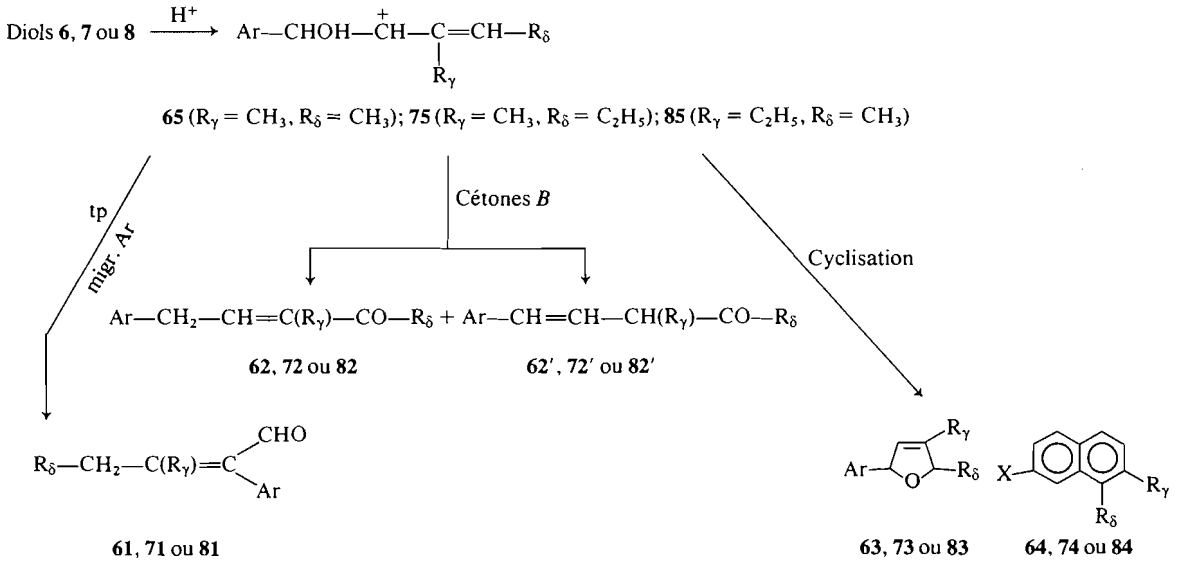


SCHÉMA 2. Produits de déshydratation des diols **6**, **7** et **8**. N.B. Le premier chiffre du numéro de chaque substance désigne le diol de départ. Le deuxième chiffre indique la nature du produit (cf. notes 2–4).

et constitue donc un substituant très favorable aux attaques nucléophiles en δ. Ces effets apparaissent de manière très claire pour les diols **1** ou **2** (R_γ = H, R_δ = CH_3) qui donnent de façon privilégiée les cétones *B* (1), et pour les diols **5** (R_γ = CH_3, R_δ = H) qui évoluent vers des réactions de coupure (3). Les valeurs des charges indiquées montrent que l'influence favorable du méthyle en δ est plus importante que l'influence défavorable du méthyle en γ; aussi pour les diols **6** à **9** on n'observe pas de coupure mais seulement des attaques nucléophiles en δ. D'ailleurs le calcul des charges totales (σ + π) montre bien qu'il y a additivité des effets de méthyles en γ et δ puisqu'en présence des deux substituants R_γ = R_δ = CH_3, on trouve une polarisation positive de 15 à 13 × 10^{-3} unités de charge sur le carbone δ.[5]

Il n'est donc pas étonnant d'observer pour les diols disubstitués en γ et δ que les produits de coupure ne se forment pas. Il en est de même pour le retour interne. En effet, la charge partielle positive, relativement faible sur le pôle β du carbocation semble aussi insuffisante pour qu'on observe la fixation d'un hydroxyle du solvant sur ce pôle. L'attaque nucléophile en β se trouve masquée (10) par les attaques nucléophiles en δ, plus rapides, en

[5]Y. L. Pascal, communication personnelle. Calculs effectués par la méthode IEHT sur IBM 3600. Nous remercions vivement l'auteur qui a mis à notre disposition les résultats obtenus au cours de ses travaux.

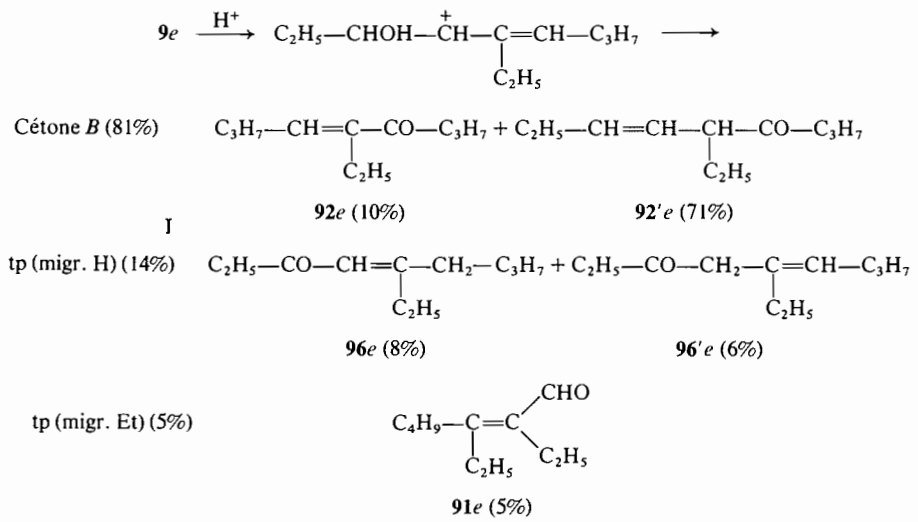


SCHÉMA 3. Produits de déshydratation du diol **9***e*. Pour la désignation des substances, cf. note schéma 2.

raison de la différence des charges partielles sur les deux extrémités du carbocation.

Un problème intéressant dans le cas de ces diols, est la compétition entre la réaction inter ou intramoléculaire. Dans cette compétition, la configuration du carbocation allylique joue un rôle déterminant.

(B) Rôle des effets stériques

On sait que les substrats allyliques subissent une solvolyse 10^4 à 10^5 fois plus rapide que les substrats saturés de même classe (11). Cette accélération résulte de l'assistance du doublet π au départ du groupe partant. Il est donc probable que l'ionisation du diol conduit directement à l'une des formes délocalisées C_1, C_2, C_3 ou C_4 (schéma 4).

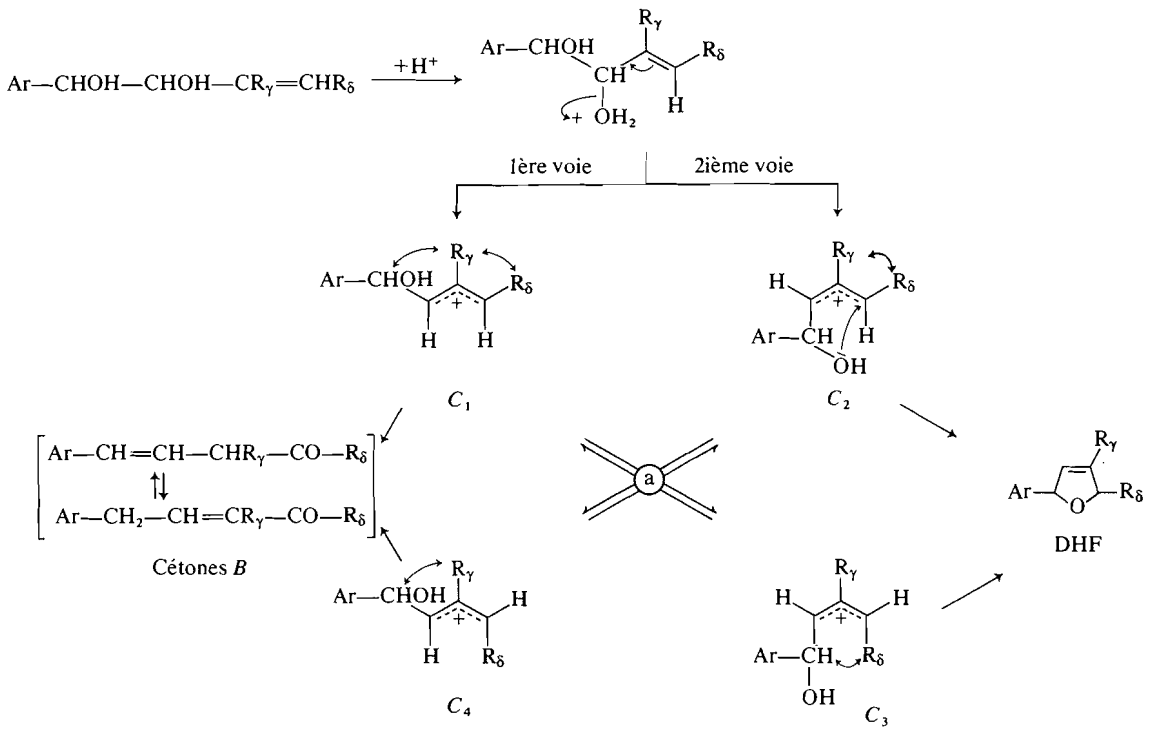
Bien que les doubles liaisons trisubstituées des α-diols aient dans des cas analogues et pour une petite partie la configuration *Z* (12), on peut admettre une configuration majoritairement *E* de la double liaison des diols **6**, **7**, **8** et **9**. Il en résulte que, seules deux formes isomères C_1 ou C_2 semblent devoir prendre naissance directement par ionisation. Les deux autres formes isomères C_3 et C_4 résultent des précédentes par stéréomutation (schéma 4). Des calculs effectués dans des cas plus simples semblent indiquer que cette stéréomutation est possible par deux voies différentes (9) suivant que $R_\gamma = CH_3$ (passage par un ion cyclopropylium avec fermeture et ouverture disrotatoires, schéma 4) ou que $R_\gamma = H$ (passage par un carbocation à double liaison localisée, schéma 5).

On peut noter sur le schéma 4 que les formes C_2 et C_3 dans lesquelles le groupe ArCHOH occupe une position *endo*, peuvent *a priori* conduire indifféremment aux cétones *B* par attaque d'une molécule de solvant H_2O sur le pôle δ, ou aux dérivés dihydrofuranniques par attaque de l'hydroxyle en α bien placé, sur le carbone δ. En revanche les formes C_1 et C_4 (groupe ArCHOH *exo*) ne peuvent, en absence de stéréomutation, conduire qu'aux cétones *B*. Mais comme nous allons le voir, en fait, chaque fois que les effets stériques sont favorables à la forme C_1 ou C_4, la formation des cétones *B* est accrue, alors qu'elle peut éventuellement disparaître lorsque ce sont les formes C_2 ou C_3 qui sont favorisées (cas des diols **4**, $R_\beta = CH_3$, schéma 5). Tout se passe comme si les formes C_2 et C_3 capables d'évoluer aussi bien vers les cétones *B* que vers les dérivés dihydrofuranniques, donnent de préférence ces derniers. On comprend d'ailleurs aisément que dans ce cas, les facteurs entropiques soient plus favorables à la réaction intramoléculaire qu'intermoléculaire, et cela d'autant plus que des interactions de stabilisation entre l'hydroxyle et le site cationique du type solvatation de l'ion (13) favorisent une géométrie moléculaire (ArCHOH *endo*) qui préfigure l'attaque nucléophile et y conduit donc de façon très naturelle.

De plus, il est probable que dans cette configuration le noyau benzénique puisse aussi interagir favorablement avec la charge +, électrophile, par formation d'un complexe du type π. Le fait est qu'en l'absence de groupe aryle ($R' = C_2H_5$, **6***e*, **9***e*, schéma 6) cette configuration C_2 ne semble pas intervenir.

Ces interactions stabilisatrices sont d'ailleurs en compétition avec les interactions stériques qui poussent au contraire le groupe ArCHOH volumineux, à se placer, comme nous le verrons dans le cas des diols **1**, en position *exo*. De telles interac-

Can. J. Chem. Downloaded from www.nrcresearchpress.com by 210.87.254.6 on 09/05/12
For personal use only.



Formes C_1 et C_4 ArCHOH en position *exo*

Formes C_2 et C_3: ArCHOH en position *endo*

SCHÉMA 4

Equilibre de stéréomutation des carbocations allyliques Ar—CHOH—$\overset{+}{C}$H—$\overset{+}{C}$R$_\gamma$—CHR$_\delta$

65 R$_\gamma$ = R$_\delta$ = CH$_3$; **75** R$_\gamma$ = CH$_3$, R$_\delta$ = C$_2$H$_5$; **85** R$_\gamma$ = C$_2$H$_5$, R$_\delta$ = CH$_3$; **95** R$_\gamma$ = C$_2$H$_5$, R$_\delta$ = C$_3$H$_7$.

(a): Inversion simultanée de deux extrémités du carbocation dans l'hypothèse du passage par un ion cyclopropylium (ref. 9) (fermeture et ouverture disrotatoire) si R$_\gamma$ = CH$_3$($C_1 \rightleftarrows C_3$ et $C_2 \rightleftarrows C_4$) ou passage par un carbocation localisé si R$_\gamma$ = H ($C_1 \rightleftarrows C_4$ et $C_3 \rightleftarrows C_2$). .

tions stabilisatrices n'interviennent pas pour le groupe R$_\delta$ lorsqu'il occupe la position *endo*, stériquement très gênée, et nous verrons que, sauf interaction stérique R$_\gamma$ ↔ R$_\delta$ exceptionnellement

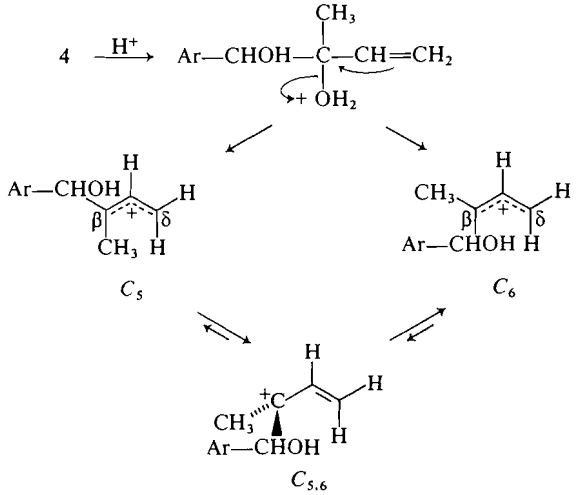


SCHÉMA 5. Stéréomutation du carbocation allylique très dissymétrique (primaire–tertiaire) issu du diol **4**.

importante (R$_\gamma$ = Et, R$_\delta$ = Pr), R$_\delta$ reste de préférence en position *exo* (formes C_1 ou C_2). Il a bien été observé qu'un méthyle (14*a*) ou un phényle seul (14*b*) occupent de préférence la position *exo*.

Nous admettrons donc (et les résultats suivants le confirment) que les cétones *B* se forment essentiellement à partir des seuls carbocations C_1 (ou C_4) alors que C_2 (et C_3) sont les précurseurs des dérivés cyclisés. En fait, pour la formation des cétones *B*, il existe entre ce carbocation allylique C_1 et la cétone *B*, un autre intermédiaire obligatoire *D*, qui est un γ-diol éthylénique (1), dont l'ionisation elle-même va conduire à un nouveau carbocation allylique *F* (voir Introduction et schéma 7).

D'après la configuration du carbocation précurseur C_1 ce γ-diol *D* a obligatoirement la configuration *E*. Il apparait donc que ce diol évolue en raison de cette configuration vers la cétone *B*. De tels exemples de sélectivité sont connus (4*a*, 15).

En ce qui concerne les dérivés dihydrofuranniques, il est possible également que l'on passe par l'intermédiaire d'un γ diol éthylénique. En raison de la structure de son précurseur C_2, ce

Can. J. Chem. Downloaded from www.nrcresearchpress.com by 210.87.254.6 on 09/05/12
For personal use only.

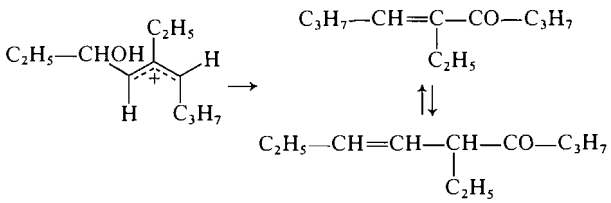


SCHÉMA 6. Rôle de la configuration C_4 en l'absence du groupe aromatique et pour un diol très encombré (diol **9***e*).

diol *D'* isomère du précédent *D*, doit avoir la configuration *Z*.

La déshydratation de tels diols conduit généralement à des mélanges de dérivés dihydrofuranniques et de cétones (16). Les réactions sont alors peu sélectives et souvent même les cétones prédominent (17). Ceci ne correspond pas aux observations dans notre cas. En effet, l'examen des résultats observés pour les diols de la série **4**, montre que dans le cas où la formation des dérivés dihydrofuranniques est privilégiée, il ne se forme pas de produits *B*. Il apparaît donc légitime d'admettre la cyclisation directe du carbocation C_2 en DHF.

Nous allons montrer que l'évolution du taux de cyclisation par rapport à la somme des attaques

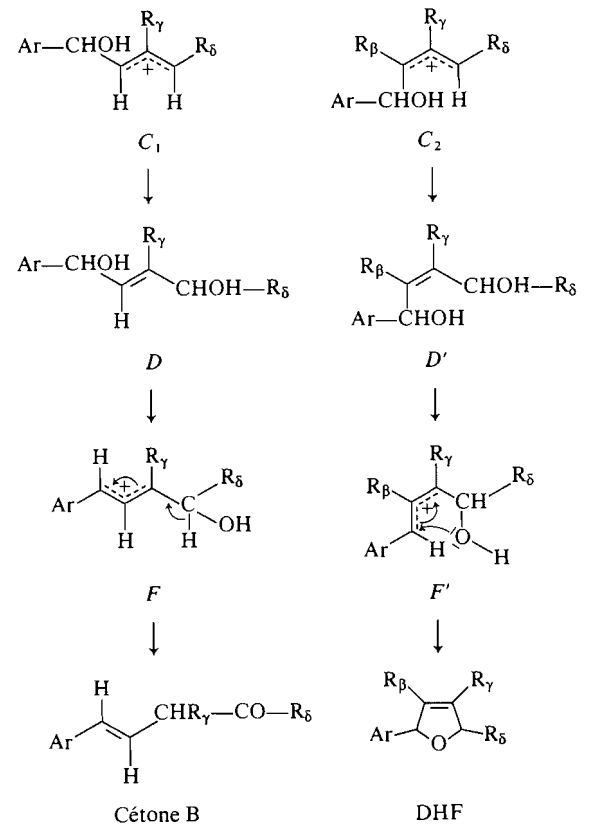


SCHÉMA 7. Importance de la stéréochimie des γ-diols intermédiaires éventuels.

nucléophiles en δ (produits cyclisés + cétones *B*), dans les diverses séries de diols étudiés, est en bon accord avec l'attribution des cations précurseurs des cétones *B* et des dihydrofurannes.

(a) Rôle de R_γ

On peut noter d'abord que pour $R_\delta = CH_3$, plus R_γ est gros, plus il favorise la réaction de cyclisation, en déplaçant l'équilibre de stéréomutation de C_1 vers C_2. Dans ces cas (avec $R_\delta = CH_3$), les interactions stériques $R_\delta \leftrightarrow R_\gamma$ restent en effet modérées et nous pouvons négliger le rôle des configurations C_3 ou C_4. L'examen des résultats du tableau 2 montre, en effet, que pour Ar donné (Ar = *p*-CH_3—C_6H_4) le taux de cyclisation augmente progressivement pour $R_\gamma = H$, CH_3 ou C_2H_5. Ainsi dans le cas des diols **1** ($R_\delta = CH_3$, $R_\gamma = H$), le carbocation allylique peut prendre naissance sous deux formes délocalisées C_1 ou C_2 (schéma 4). En l'absence du méthyle central R_γ, l'isomère C_1 est plus stable que C_2 (les effets stériques favorables à la forme ArCHOH *exo* étant plus importants que les interactions de stabilisation de la forme ArCHOH *endo*) et la première voie, conduisant directement à la cétone *B* devient le processus privilégié (taux de cyclisation du diol **1***c*: 13%).

En revanche pour le diol **6***c* ($R_\gamma = R_\delta = CH_3$), la présence d'un méthyle en γ, déplace l'équilibre de stéréomutation vers la forme C_2 apte à se cycliser (schéma 4) et sur les 70% de produits résultant des attaques nucléophiles en δ, on trouve 20% de produits dihydrofuranniques (soit un taux de cyclisation de 29%). De la même façon, pour le diol correspondant de la série **8** (diol **8***c*: $R_\gamma = C_2H_5$, $R_\delta = CH_3$), la présence de l'éthyle en γ rend la forme C_2 encore plus abondante et on trouve pour ce même taux, 46% (tableau 2).

Sur l'effet stérique de R_γ, on peut conclure qu'en présence d'un substituant en cette position, la réaction intramoléculaire, quand elle est possible (polarisation + en C_δ, $R_\delta \neq H$), est toujours privilégiée. Plus R_γ est gros, plus la formation du cation précurseur des dérivés cyclisés est favorisée par les facteurs stériques et on observe un accroissement du rendement de ces derniers par rapport aux cétones *B*.

(b) Rôle de R_δ

Si dans le diol **6** ($R_\gamma = CH_3$, $R_\delta = CH_3$), on remplace le méthyle en δ par un éthyle: diol **7** ($R_\gamma = CH_3$, $R_\delta = C_2H_5$) on favorise la formation des dérivés cyclisés au détriment des cétones *B*. Ainsi pour Ar = *p*-CH_3—C_6H_4, diol **7***c*, le taux de cyclisation atteint la valeur de 60% au lieu de 29% pour le diol **6***c* (tableau 2).

On a donc favorisé C_2 au détriment de C_1 (schéma 4), R_δ étant plus encombrant, l'effet

Can. J. Chem. Downloaded from www.nrcresearchpress.com by 210.87.254.6 on 09/05/12
For personal use only.

TABLEAU 2. Comparaison générale de l'orientation des déshydratations et des taux de cyclisation dans les attaques nucléophiles en fonction de l'encombrement stérique du carbocation allylique (cas Ar = p-CH_3—C_6H_4)

	Présence d'un substituant en δ (R_β = H)					Absence d'un substituant en δ		
Série de diols	Diol **1***c*	Diol **6***c*	Diol **8***c*	Diol **7***c*	Diol **9***e*[a]	Diol **4***c*	Diol **5***c*	Diol **3***c*
Position des substituants	R_γ = H	R_γ = CH_3	R_γ = C_2H_5	R_γ = CH_3	R_γ = C_2H_5	R_γ = H	R_γ = CH_3	R_γ = H
						R_β = CH_3	R_β = H	R_β = H
	R_δ = CH_3	R_δ = CH_3	R_δ = CH_3	R_δ = C_2H_5	R_δ = C_3H_7	R_δ = H	R_δ = H	R_δ = H
Transposition pinacolique	37%	30%	25%	26%	19%	47%	65%	100%
Attaque nucléophile en δ	(63)	(70)	(75)	(74)	(81)	(53)	(0)	(0)
Cétone *B*	55	50	40	30	81			
Cyclisation	8	20	35	44	0	53		
Taux de cyclisation[b]	13%	29%	46%	60%	0%	100%	—	—
Coupure							35	

La totalité des produits de déshydratation récupérés représente environ 80% du diol consommé.
[a]Le diol 9*c*, avec Ar = CH_3—C_6H_4, a été déshydraté, mais le mélange obtenu, n'a pu être analysé avec assez de précision (mélange complexe de substances peu volatiles).
[b]Taux de cyclisation = $\frac{\text{Cyclisation}}{\text{Cétones } B + \text{Cyclisation}} \times 100$ (par rapport au total des attaques nucléophiles en δ).

"d'arc-boutant" qu'il exerce sur le méthyle central en γ va en fait aggraver l'interaction de ce dernier avec le groupe ArCHOH *exo* dans la forme C_1 au profit de C_2. Le rôle de cet effet "d'arc-boutant" de R_δ dans l'équilibre de stéréomutation apparaît même très important puisqu'il semble aussi efficace de remplacer méthyle par éthyle en δ (diols **6** et **7**, 29 à 60%) que de remplacer H par méthyle en γ (diols **1** et **6**, 13 à 29%).

(c) Effet stérique croissant de R_γ et R_δ

Dans le cas du diol **9** (R_γ = C_2H_5, R_δ = C_3H_7), on augmente simultanément la grosseur des substituants en γ et en δ. On crée alors une telle compression stérique que la forme C_4 apparaît comme la seule forme possible stable et ainsi comme le seul précurseur privilégié des cétones du type *B* (schéma 6).

Cet effet de compression stérique excessif dans le diol **9***e* explique donc l'apparition des produits *B* en grande quantité (81%) alors que les dérivés cyclisés sont absents, leurs ions précurseurs C_2 ou C_3 étant improbables. En conclusion, les résultats observés montrent qu'en augmentant à la fois et de manière trop importante, l'encombrement stérique des substituants R_γ central et R_δ, on favorise la formation exclusive des cétones *B*, alors qu'en augmentant seulement R_γ, on favorise la cyclisation.

(d) Retour sur le rôle de R_β

Cette importance de la configuration du carbocation allylique dans l'orientation des réactions observées permet de comprendre certains résultats antérieurement décrits. Aussi, dans le cas des diols de la série **4** (R_β = CH_3, R_γ = R_δ = H) (2), il y avait formation de dérivés cyclisés sans trace de cétones *B* (**4***c*, 53% de cyclisation) (tableau 2).

Dans ce cas, il n'existe que deux ions stéréoisomères C_5 et C_6 (schéma 5), se transformant l'un en l'autre par l'intermédiaire de la forme localisée $C_{5,6}$ puisque R_γ = H. On peut d'ailleurs noter que ces diols **4** sont les seuls pour lesquels nous avons observé l'existence d'une réaction d'isomérisation *érythro–thréo* (retour interne) au cours de la déshydratation. Cette possibilité de réversibilité de l'ionisation du diol, est liée à la polarité + importante sur le pôle β tertiaire. Peut être le retour se produit-il justement lors du passage du carbocation par sa forme localisée $C_{5,6}$ (9*a*).

Entre ces deux ions C_5 et C_6, les facteurs stériques qui différencient les formes Me_β ou ArCHOH en position *exo* sont minimisés par rapport au cas H_β ou ArCHOH *exo*. Seules les interactions stabilisatrices, spécifiques à ArCHOH sont bien différentes entre les deux isomères. Ces interactions sont favorables à la forme C_6 (précurseur des dihydrofurannes) qui apparaît donc seule jouer un rôle dans les attaques nucléophiles (polarisation + trop faible en δ pour donner lieu à une attaque du solvant comme dans le cas des diols **3**, R_α = R_β = R_γ = R_δ = H qui ne donnent lieu qu'à la transposition pinacolique).

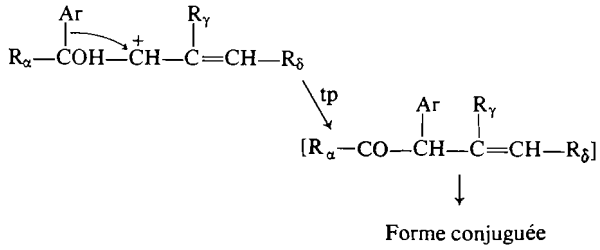
La discussion sur l'équilibre de stéréomutation permet donc d'interpréter les résultats observés en ce qui concerne la compétition entre la formation des cétones *B* et celle de dérivés cyclisés. La compétition entre la transposition pinacolique et l'ensemble de ces attaques nucléophiles en δ résulte elle, de l'intervention de facteurs stériques et électroniques plus classiques.

Etude de la transposition pinacolique (tp). Importance des facteurs stériques

Nous avons montré dans le 1er mémoire (1) que par un effet de décompression au cours de la trans-

Can. J. Chem. Downloaded from www.nrcresearchpress.com by 210.87.254.6 on 09/05/12
For personal use only.

position, un groupe méthyle en R_α accélére la migration du groupe aromatique:



L'effet inverse dû à R_γ peut être mis en évidence dans la présente étude. Remarquons que pour le diol **6***d* (X = OCH_3), on observe 20% de cétones *B* (tableau 1). Le carbocation allylique existe donc bien, malgré la grande stabilisation du carbocation concurrent en α (due à la présence du groupe anisyle). Cependant ce carbocation allylique est loin d'évoluer exclusivement dans le sens de la migration du groupe anisyle pourtant si mobile. En fait la présence d'un substituant méthyle en γ introduit un accroissement de la compression stérique dans la molécule au cours de la transposition, et ralentit la migration au profit des attaques nucléophiles en δ. Cette diminution de la transposition pinacolique est régulière lorsque R_γ augmente de volume. On peut suivre cette évolution dans le tableau 2 pour R_δ = CH_3 dans le cas du groupe migrant Ar = *p*-CH_3—C_6H_4 (**1***c*, R_γ = H, tp = 37%; **6***c*, R_γ = CH_3, tp = 30%; **8***c*, R_γ = C_2H_5, tp = 25%).

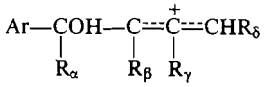
Nous avons aperçu le même effet défavorable à la transposition pinacolique et trouvé les mêmes évolutions lorsque le substituant encombrant se trouve sur le carbone γ (**3***c*, R_γ = H, tp = 100%; **5***c*, R_γ = CH_3, tp = 65 à 75%) ou sur le carbone β lui-même (**3***c*, R_β = H, tp = 100%; **4***c*, R_β = CH_3, tp = 47% seulement).

Evidemment cet effet stérique se superpose à l'effet électronique classique de X sur l'aptitude migratrice du groupe Ar.

Il convient de rappeler toutefois que dans le cas des diols bisecondaires, l'aldéhyde de transposition pinacolique peut provenir soit du carbocation allylique avec migration du groupe Ar, soit du carbocation benzylique avec migration du groupe éthylénique. Donc les valeurs signalées constituent la limite supérieure du taux de transposition dans l'évolution du carbocation allylique.

Conclusion

La configuration du carbocation allylique α-hydroxylé de formule générale



apparaît comme un facteur déterminant dans l'orientation de la déshydratation des diols 1,2 α-β éthyléniques correspondants.

Cette configuration est très sensible à l'effet stérique des substituants, qui peut s'exercer soit directement, soit par effet "d' arc-boutant", pour modifier l'équilibre de stéréomutation et probablement, par là, la configuration *Z* ou *E* du γ-diol intermédiaire, notamment en ce qui concerne la formation de cétones du type *B*. Des effets stériques plus classiques interviennent aussi (effets de compression ou de décompression) au cours de la transposition pinacolique.

Toutefois, les effets électroniques des substituants sont loin d'être négligeables et il s'y ajoute probablement des interactions à distance de la lacune électronique du carbocation avec le groupe hydroxyle et avec le groupe aromatique.

De la conjugaison de ces différents effets résultent les modifications spectaculaires observées dans l'orientation de la déshydratation entre les cinq schémas réactionnels mis en évidence.

Partie expérimentale

La préparation et la déshydratation dans H_2SO_4 normal des diols ont été réalisées selon la méthode exposée dans la réf. 1. Les rendements obtenus pour la déshydratation sont toujours voisins de 75%. On détermine la composition des mélanges de produits transposés, par rmn dans le distillat brut après avoir purifié les différents produits par chromatographie en phase vapeur (cpv) sur colonne de XF 1150 et établi les structures par voie spectroscopique. Les analyses ont été effectuées sur les échantillons chromatographiés, après une rapide distillation sous vide. (Laboratoire de Microanalyse du Centre de Spectrochimie de Paris-Centre.)

Les spectres rmn ont été réalisés sur appareil Varian-A60, (solution $CDCl_3$, δ en ppm par rapport au TMS, référence interne). Les mêmes solutions ont été utilisées pour les spectres ir (spectrographe Perkin-Elmer, modèle 357, étalonnage par film de polystyrène).

Les spectres d'absorption uv sont enregistrés (appareil Varian modèle 635) en solution dans l'éthanol à 95%.

1. Déshydratation des diols 6: Ar (ou R')—CHOH—CHOH—C(CH_3)=$CHCH_3$

1. Déshydratation du diol **6e** *(R' = éthyle)*

La réduction par le Zn et l'acide acétique du mélange acroléine et aldéhyde tiglique, donne le *méthyl-3 heptadiène-2,6 diol-4,5* (18) (pé 122°C/0.02 Torr) dont la semi-hydrogénation (Ni de Raney dans l'alcool) permet d'obtenir le *méthyl-3 heptène-2 diol-4,5*, **6a** (18).

La déshydratation de ce diol conduit aux deux cétones *B* isomères:

la E-*méthyl-3 heptène-3 one-2*, **62e** (isomère conjugué prédominant). Sa configuration *E* et sa conformation transoïde sont déterminées par utilisation des chélates de terres rares en rmn. On observe en effet que ΔvMe(3) > ΔvH(4) > ΔvCH$_2$(5) (tableau 3); ir: 1665 cm^{-1}; rmn δ(ppm): 2.20 (s, H1), 1.70 (d, *J* = 1.2 Hz, Me 3), 6.56 (H4), 2.23 (q, *J* = 7 Hz, H5), 1.50 (H6), 0.97 (t, *J* = 7 Hz, H7).

la *méthyl-3 heptène-4 one-2*, **62'e**, ir: 1715 cm^{-1}; rmn δ (ppm): 2.03 (s, H1), 3.06 (quintuplet, H3), 1.08 (d, *J* = 6.5 Hz, Me 3), 5.1–5.9 (m, H4, H5), 2.06 (quintuplet, H6), 1.00 (t, *J* = 6.5 Hz, H7).

Can. J. Chem. Downloaded from www.nrcresearchpress.com by 210.87.254.6 on 09/05/12
For personal use only.

Can. J. Chem. Downloaded from www.nrcresearchpress.com by 210.87.254.6 on 09/05/12
For personal use only.

TABLEAU 3. Détermination de la configuration *Z* ou *E* des dérivés du diol **6** par rmn en présence des complexe $Eu(fod)_3$

Composé no.	Déplacement chimique ν_0 en Hz (à 60 MHz) en l'absence de complexe et $\Delta\nu$ variation[a] du déplacement chimique pour [complexe]/[soluté] = 0.5					
		$CH_3(1)$	$CH_3(3)$	H(4)	$CH_2(5)$	$CH_2(6)$	$CH_3(7)$
62*e*	ν_0	132	102	394	134	90	58
	$\Delta\nu$	420	300	240	135	80	55
		CHO	Ar	$CH_3(3)$	$CH_2(4)$	$CH_3(5)$	
61*b E*	ν_0	578	416	139	129	61	
	$\Delta\nu$	487	140	118	92	58	
61*b Z*	ν_0	578	415	111	166	75	
	$\Delta\nu$	420	122	80	103	54	
61*c E*	ν_0	578	418	139	129	61	
	$\Delta\nu$	490	168	120	97	59	
61*c Z*	ν_0	569	418	111	166	75	
	$\Delta\nu$	371	120	75	92	48	
		$CH_3(1)$	$CH_3(3)$	H(4)	$CH_2(5)$	Ar	
62*b*	ν_0	133	111	401	217	433	
	$\Delta\nu$	285	230	170	94	26	
62*c*	ν_0	136	113	406	213	427	
	$\Delta\nu$	275	226	167	90	14	

[a]L'incertitude sur les déterminations de $\Delta\nu$ est de l'ordre de 5%.

2. Déshydratation des diols **6**b, **6**c *et* **6**d *(Ar = p-X—C_6H_4)*

(a) Aldéhydes **61** *(transposition pinacolique).* La configuration *Z* ou *E* de ces aldéhydes et leur conformation transoïde ont été établies par l'utilisation des chélates de terres rares en rmn (tableau 3). On note en effet pour les $\Delta\nu Ar > CH_3(3) > CH_2(4)$ pour les isomères *E* et $Ar > CH_2(4) > CH_3(3)$ pour les isomères *Z*. Nous avons obtenu les liquides jaune clair suivants; les analyses sont effectuees sur des mélanges d'isomères *Z* et *E*.

Le *méthyl-3 phényl-2 pentène-2 al (61*b), *isomère* Z; ir: 1665 cm^{-1}; rmn δ(ppm): 10.11 (s, H1), 1.81 (s, H3), 2.75 (q, H4), 1.25 (t, *J* = 7 Hz, H5). *Isomère* E; ir: 1670 cm^{-1}; rmn δ(ppm): 10.11 (s, H1), 2.30 (s, H3), 2.10 (q, H4), 1.01 (t, *J* = 7 Hz, H5). *Anal.* calc. pour $C_{12}H_{14}O$: C 82.72, H 8.10; trouvé: C 82.85, H 7.89.

Le *méthyl-3 paratolyl-2 pentène-2 al (61*c), *isomere* Z; ir: 1660 cm^{-1}; rmn δ(ppm): 9.63 (s, H1), 1.85 (s, H3), 2.77 (q, H4), 1.25 (t, *J* = 7 Hz, H5). *Isomère* E; ir: 1665 cm^{-1}; rmn δ(ppm): 9.63 (s, H1), 2.31 (s, H3), 2.15 (q, H4), 1.02 (t, *J* = 7 Hz, H5). *Anal.* calc. pour $C_{13}H_{16}O$: C 82.93, H 8.57; trouvé: C 82.78, H 8.62.

Le *méthyl-3 paraanisyl-2 pentène-2 al (61*d), *isomère* Z; ir: 1670 cm^{-1}; rmn δ(ppm): 9.48 (s, H1), 1.85 (s, H3), 2.76 (q, H4), 1.25 (t, *J* = 7 Hz, H5). *Isomère* E; ir: 1675 cm^{-1}; rmn δ(ppm): 9.63 (s, H1), 2.31 (s, H3), 2.15 (q, H4), 1.02 (t, *J* = 7 Hz, H5). *Anal.* calc. pour $C_{13}H_{16}O_2$: C 76.44, H 7.90; trouvé: C 76.59, H 7.66.

(b) Cétones **62** *(cétones du type* B). Un isomère est prédominant. Sa configuration *E* et sa conformation transoïde sont établies par utilisation des chélates de terre rares en rmn (tableau 3). On observe en effet l'ordre suivant de déplacement des protons: $CH_3(1) > CH_3(3) > H(4) > CH_2(5) > Ar$. Nous avons ainsi obtenu les liquides suivants.

Le *méthyl-3 phényl-5 pentène-3 one-2 (62*b), ir: 1675 et 1635 cm^{-1}; uv: 236 nm (ε = 12 440); rmn δ(ppm): 2.21 (s, H1), 1.85 (Me 3), 6.69 (*J* = 7 et 1.2 Hz, H4), 3.61 (d, H5). *Anal.* calc. pour $C_{12}H_{14}O$: C 82.72, H 8.10; trouvé: C 82.63, H 8.29.

Le *méthyl-3 paratolyl-5 pentène-3 one-2 (62*c), ir: 1670 et 1635 cm^{-1}; uv: 239 nm (ε = 12 660) (inflexion); rmn δ(ppm): 2.26 (s, H1), 1.88 (Me 3), 6.76 (*J* = 7 et 1.2 Hz, H4), 3.55 (d, H5). *Anal.* calc. pour $C_{13}H_{16}O$: C 82.93, H 8.57; trouvé: C 82.81, H 8.75.

Le *méthyl-3 paraanisyl-5 pentène-3 one-2 (62*d), ir: 1670 et 1635 cm^{-1}; uv: 234 nm (ε = 12 000); rmn δ(ppm): 2.21 (s, H1), 1.83 (Me 3), 6.70 (*J* = 7 et 1.2 Hz, H4), 3.50 (d, H5). *Anal.* calc. pour $C_{13}H_{16}O_2$: C 76.44, H 7.90; trouvé: C 76.31, H 7.97.

(c) Cétones 62' (cétones du type B). Nous avons obtenu les isomères suivants.

Le *méthyl-3 phényl-5 pentène-4 one-2 (62'*b), ir: 1720 et 1625 cm^{-1}; uv: 243 nm (ε = 11 140); rmn δ(ppm): 2.09 (s, H1), 1.22 (d, *J* = 7 Hz, Me 3), 3.26 (H3), 6.02 (dd, *J* = 16 et 7 Hz, H4), 6.51 (d, *J* = 16 Hz, H5). *Anal.* calc. pour $C_{12}H_{14}O$: C 82.72, H 8.10; trouvé: C 82.75, H 8.04.

Le *méthyl-3 paratolyl-5 pentène-4 one-2 (62'*c), ir: 1730 et 1625 cm^{-1}; uv: 255 nm (ε = 16 300); rmn δ(ppm): 2.16 (s, H1), 1.25 (d, *J* = 7 Hz, Me 3), 3.35 (H3), 6.11 (dd, *J* = 16 et 7 Hz, H4), 6.56 (d, *J* = 16 Hz, H5). *Anal.* calc. pour $C_{13}H_{16}O$: C 82.93, H 8.57; trouvé: C 82.98, H 8.51.

Le *méthyl-3 paraanisyl-5 pentène-4 one-2 (62'*d), ir: 1720 et 1635 cm^{-1}; uv: 248 nm (ε = 10 950); rmn δ(ppm): 2.10 (s, H1), 1.2 (d, *J* = 7 Hz, Me 3), 3.23 (H3), 5.93 (dd, *J* = 16 et 7 Hz, H4), 6.45 (d, *J* = 16 Hz, H5). *Anal.* calc. pour $C_{13}H_{16}O_2$: C 76.44, H 7.90; trouvé: C 76.29, H 7.95.

(d) Dihydro-2,5 furanne (63)

Le *diméthyl-4,5 phényl-2 dihydro-2,5 furanne (63*b), ir: 1660 cm^{-1}; uv: 307 nm (ε = 1780) et 290 nm (ε = 2660); rmn δ(ppm): 5.4–5.7 (m, H2, H3), 1.75 (m, Me 4), 4.8 (m, H5), 1.28 (d, Me 5, 45% *cis*) et 1.32 (d, Me 5, 55% *trans*). *Anal.* calc. pour $C_{12}H_{14}O$: C 82.72, H 8.10; trouvé: C 82.90, H 8.05.

Can. J. Chem. Downloaded from www.nrcresearchpress.com by 210.87.254.6 on 09/05/12
For personal use only.

Le *diméthyl-4,5 paratolyl-2 dihydro-2,5 furanne (63c)*, ir: 1665 cm^{-1}; uv: 255 nm (ε = 3090); rmn δ(ppm): 5.35–5.85 (m, H2, H3), 1.75 (m, Me 4), 4.88 (m, H5), 1.31 (d, Me 5, 45% *cis*) et 1.35 (d, Me 5, 55% *trans*). *Anal.* calc. pour $C_{13}H_{16}O$: C 82.93, H 8.57; trouvé: C 82.77, H 8.59.

(e) Naphtalènes 64

Le *diméthyl-1,2 naphtalène-(64b)*, le *triméthyl-1,2,7 naphtalène (64c)* et le *diméthyl-1,2 méthoxy-7 naphtalène (64d)*.

Ces produits sont identifiés par leurs propriétés spectroscopiques (19, 20).

II. Déshydratation des diols 7:

p-*X*—C_6H_4—*CHOH—CHOH—C*(CH_3)=*CH—*CH_2—CH_3

1. Aldéhyde 71 (transposition pinacolique)

On obtient deux isomères *Z* et *E* pour l'aldéhyde **71**; leur configuration a été attribuée par analogie avec les déplacements chimiques des protons des aldéhydes **61**. Les analyses sont effectuées sur des mélanges d'isomères *Z* et *E*.

Le *méthyl-3 phényl-2 hexène-2 al (71b)*, *isomère* Z; ir: 1665 cm^{-1}; rmn δ(ppm): 10.25 (s, H1), 1.80 (s, Me 3), 2.73 (t, *J* = 7 Hz, H4), 1.65 (H5), 1.02 (t, *J* = 7 Hz, H6). *Isomère* E; ir: 1670 cm^{-1}; rmn δ(ppm): 10.25 (s, H1), 2.30 (s, Me 3), 2.10 (t, *J* = 7 Hz, H4), 1.50 (H5), 0.80 (t, *J* = 7 Hz, H6). *Anal.* calc. pour $C_{13}H_{16}O$: C 82.93, H 8.57; trouvé: C 83.10, H 8.48.

Le *méthyl-3 paratolyl-2 hexène-2 al (71c)*, *isomère* Z; ir: 1660 cm^{-1}; rmn δ(ppm): 10.25 (s, H1), 1.81 (s, Me 3), 2.80 (t, *J* = 7 Hz, H4), 1.66 (H5), 1.03 (t, *J* = 7 Hz, H6). *Isomère* E; ir: 1660 cm^{-1}; rmn δ(ppm): 10.25 (s, H1), 2.28 (s, Me 3), 2.13 (t, *J* = 7 Hz, H4), 1.50 (H5), 0.82 (t, *J* = 7 Hz, H6). *Anal.* calc. pour $C_{14}H_{18}O$: C 83.12, H 8.97; trouvé: C 83.33, H 8.81.

2. Cétones 72E et 72' trans *(cétones du type* B*)*

La *méthyl-4 phényl-6 hexène-4 one-3 (72b)*, ir: 1670 cm^{-1}; rmn δ(ppm): 1.08 (H1), 2.52 (H2), 1.90 (Me 4), 6.75 (tq, *J* = 7 et 1.2 Hz, H5), 3.53 (d, H6). *Anal.* calc. pour $C_{13}H_{16}O$: C 82.93, H 8.57; trouvé: C 82.80, H 8.61.

La *méthyl-4 phényl-6 hexène-5 one-3 (72'b)*, ir: 1715 cm^{-1}; rmn δ(ppm): 1.03 (H1), 2.54 (H2), 3.35 (H4), 1.23 (d, Me 4), 6.12 (dd, *J* = 16 et 7 Hz, H5), 6.55 (d, *J* = 16 Hz, H6). *Anal.* calc. pour $C_{13}H_{16}O$: C 82.93, H 8.57; trouvé: C 83.07, H 8.69.

La *méthyl-4 paratolyl-6 hexène-4 one-3 (72c)*, ir: 1665 cm^{-1}; rmn δ(ppm): 1.08 (H1), 2.53 (H2), 1.91 (Me 4), 6.75 (tq, *J* = 7 et 1.2 Hz, H5), 3.53 (d, H6). *Anal.* calc. pour $C_{14}H_{18}O$: C 83.12, H 8.97; trouvé: C 82.95, H 8.83.

La *méthyl-4 paratolyl-6 hexène-5 one-3 (72'c)*, ir: 1710 cm^{-1}; rmn δ(ppm): 1.05 (H1), 2.57 (H2), 3.36 (H4), 1.26 (Me 4), 6.10 (dd, *J* = 16 et 7 Hz, H5), 6.55 (d, *J* = 16 Hz, H6). *Anal.* calc. pour $C_{14}H_{18}O$: C 83.12, H 8.97; trouvé: C 83.20, H 8.78.

3. Dihydro-2,5 furanne (73)

L'*éthyl-5 méthyl-4 phényl-2 dihydro-2,5 furanne (73b)*, rmn δ(ppm): 5.5–5.8 (H2, H3), 1.71 (Me 4), 4.75 (H5), 1.51 et 0.95 (50% *cis*, CH_2CH_3) et 1.63 et 0.97 (50% *trans*, CH_2CH_3).

L'*éthyl-5 méthyl-4 paratolyl-2 dihydro-2,5 furanne (73c)*, rmn δ(ppm): 5.4–5.8 (H2, H3), 1.71 (Me 4), 4.75 (H5), 1.48 et 0.95 (CH_2CH_3, 50% *cis*) et 1.60 et 0.97 (CH_2CH_3, 50% *trans*). *Anal.* calc. pour $C_{14}H_{18}O$: C 83.12, H 8.97; trouvé: C 83.25, H 8.76.

4. Naphtalènes (74) (22, 23)

L'*éthyl-1 méthyl-2 naphtalène (74b)* et l'*éthyl-1 diméthyl-2,7 naphtalène (74c)*

III. Déshydratation du paratolyl-1 éthyl-3 penténe-3 diol-1,2 (8c)

Nous avons d'abord préparé le *trans*-éthyl-2 butène-2-al par crotonisation de l'éthanal et du butanal par la soude normale.

Dans un ballon de 2 L à 0°C muni d'un agitateur rodé, d'un réfrigérant, d'un thermomètre et d'une ampoule à brome, on met 520 cm^3 de NaOH (*N*). On verse par l'ampoule les deux aldéhydes (10 mol de butanal et 10 mol d'éthanal fraîchement distillés) préalablement refroidis vers −30°C.

La réaction est exothermique et il faut maintenir la température du ballon au dessous de 40°C.

Lorsque la température redescend vers 20°C, on arrête l'agitation, décante, extrait à l'éther et lave à l'eau jusqu'à neutralité. On sèche, on sépare par distillation une fraction de 400 g (pé 110–150°C/1 Torr) que l'on redistille à la colonne à bande tournante, pour séparer le *trans* éthyl-2 butène-2-al (300 g pur, pé 135°C/1 Torr); rmn δ(ppm): 0.96 (t, Me) et 2 (d, Me), 2.20 (CH_2), 6.6 (CH=C), 9.41 (s, $CH_{(ald)}$).

Le diol **8***c* a été obtenu par réduction du *trans*-éthyl-2 butène-2-al avec le paratolylaldéhyde par la poudre de zinc et l'acide acétique.

Par déshydratation, on obtient l'*éthyl-3 paratolyl-2 pentène-2 al (81c)*, ir: 1685 cm^{-1}; rmn δ(ppm): 10.2 (s, H1), 1.96 et 2.66 (CH_2), 0.96 et 1.20 (Me). *Anal.* calc. pour $C_{14}H_{18}O$: C 83.12, H 8.97; trouvé: C 83.24, H 8.74.

E-*éthyl-3 paratolyl-5 pentène-3 one-2 (82c)*, ir: 1665 et 1630 cm^{-1}; rmn δ(ppm): 2.23 (s, H1), 6.68 (tt, *J* = 7 et 1.3 Hz, H4), 3.51 (d, *J* = 7 Hz, H5), 2.25 et 0.93 (CH_2CH_3). *Anal.* calc. pour $C_{14}H_{18}O$: C 83.12, H 8.97; trouvé: C 83.29, H 8.85.

L'*éthyl-3 paratolyl-5 pentène-4 one-2 (82'c)*, ir: 1705 et 1630 cm^{-1}; rmn δ(ppm): 2.13 (s, H1), 3.06 (q, H3), 5.96 (dd, *J* = 16 et 7 Hz, H4), 6.49 (d, H5), 1.6 et 0.85 (CH_2CH_3). *Anal.* calc. pour $C_{14}H_{18}O$: C 83.12, H 8.97; trouvé: C 83.09, H 9.03.

L'*éthyl-3 méthyl-2 paratolyl-5 dihydro-2,5 furanne (83c)*, rmn δ(ppm): 4.83 (H2), 5.3 à 5.7 (H4, H5), 1.25 (d, Me 2, *cis*), 1.31 (d, Me 2, *trans*), 2.0 et 1.05 (CH_2CH_3). *Anal.* calc. pour $C_{14}H_{18}O$: C 83.12, H 8.97; trouvé: C 83.32, H 8.84.

L'*éthyl-2 diméthyl-1,7 naphtalène (84c)*. Il ne constitue qu'une trace détectable par cpv et identifié par rmn après enrichissement par comparaison avec les produits décrits (20, 21).

IV. Déshydratation de l'éthyl-5 nonène-5 diol-3,4 (9e)

Par réduction des deux aldéhydes, acroléine et éthyl-2 hexène-2 al, nous avons obtenu l'*éthyl-5 nonadiène-1,5 diol-3,4* (18), pé 132°C/0.01 Torr. Nous avons réalisé une semi-hydrogénation de ce diol en présence de Ni de Raney pour obtenir ainsi l'*éthyl-5 nonène-5 diol-3,4* (**9***e*, pé 128°C/0.007 Torr). La déshydratation de ce diol conduit aux produits suivants.

1. Produits de transposition pinacolique

Le *diéthyl-2,3 heptène-2 al (91e)*, 5%, détectable sur cpv et identifié (après enrichissement) par ir et rmn (δ: 9.3 (s, CHO))ppm.

L'*éthyl-5 nonène-4 one-2 (96e)*, ir: 1680 cm^{-1}; rmn δ(ppm): 2.40 (q, H2), 5.98 (t, *J* = 1.2 Hz, H4).

L'*éthyl-5 nonène-5 one-3 (96'e)* E, ir: 1715 cm^{-1}; rmn δ(ppm): 2.5 (q, *J* = 6.5 Hz, $CH_2$2), 3.03 (s, $CH_2$4), 6.55 (t, *J* = 7 Hz, H6).

La configuration *E* de cet isomère est démontrée par la règle d'additivité des déplacements chimiques (21), δ H6 (E_{calc}) = 6.55; δ H6 (Z_{calc}) = 6.26 ppm.

2. Cétones du type B

L'*éthyl-5 nonène-5 one-4 (92e)* E (attribution par analogie avec la cétone **62***e*), ir: 1670 cm^{-1}; rmn δ(ppm): 6.4 (tt, *J* = 7 et 1.2 Hz, H6).

L'*éthyl-5 nonène-6 one-4, (92'e)*, isomère *E* prédominant, ir: 1710 cm^{-1}; rmn δ(ppm): 2.42 (t, *J* = 7 Hz, $CH_2$3), 2.83 (q, *J* = 7 Hz, H5), 5.26 (2d, H6), et 5.63 (2t, H7): partie AB d'un système $ABMX_2$ analysable à 80 MHz, *J* (H6, H7) = 16 Hz; ^{13}C rmn: 11.74(CH_3), 13.83(2CH_3), 17.20($CH_2$2), 24.39(CH_2, Et), 25.67 (CH_2 8), 43.42 (CH_2 3), 58.44 (CH 5), 127.26 (CH 7), 135.90 (CH 6), 212 (CO 4) ppm.

1. G. Dana, Sa Le Thi Thuan et J. Gharbi-Benarous. Bull. Soc. Chim. Fr. 1676 (1973).

2. G. DANA, SA LE THI THUAN et J. GHARBI-BENAROUS. Bull. Soc. Chim. Fr. 2089 (1974).
3. G. DANA, SA LE THI THUAN et J. GHARBI-BENAROUS. Bull. Soc. Chim. Fr. 2063 (1976).
4. (*a*) C. PREVOST. Bull. Soc. Chim. Fr. 218 (1944); (*b*) C. PREVOST et H. ROBERT. Bull. Soc. Chim. Fr. 225 (1944); (*c*) J. WIEMANN et H. DANECHPEJOUH. C. R. Acad. Sci. Ser. C, **266**, 1165 (1968); (*d*) J. BENAROUS, SA LE THI THUAN et G. DANA. Bull. Soc. Chim. Fr. 3261 (1971).
5. (*a*) J. CHUCHE et J. WIEMANN, Bull. Soc. Chim. Fr. 1497 (1968); (*b*) J. P. GIRAULT, P. SCRIBE et G. DANA. Bull. Soc. Chim. Fr. 2279 (1971).
6. SA LE THI THUAN et J. WIEMANN. Bull. Soc. Chim. Fr. 4622 (1968).
7. (*a*) W. G. YOUNG, S. WINSTEIN et H. L. GOERING. J. Am. Chem. Soc. **73**, 1958 (1951); (*b*) P. B. D. DE LA MARE et C. A. VERNON, J. Chem. Soc. 2504 (1954); (*c*) H. L. GOERING et E. F. SILVERSMITH. J. Am. Chem. Soc. **77**, 6249 (1955).
8. J. GHARBI-BENAROUS. Thèse, Paris (1975).
9. (*a*) L. RADOM, P. C. HARIHARAN, J. A. POPLE et P.v. R. SCHLEYER. J. Am. Chem. Soc. **95**, 6531 (1973); (*b*) L. RADOM, J. A. POPLE et P.v. R. SCHLEYER. J. Am. Chem. Soc. **95**, 8193 (1973).
10. T. W. BENTLEY, S. H. LIGGERO, M. A. IMHOFF et P.v. R. SCHLEYER. J. Am. Chem. Soc. **96**, 1970 (1974).
11. J. B. HENDRICKSON, D. J. CRAM et G. S. HAMMOND. Organic chemistry. 3ième éd. McGraw Hill, New York. 1970. p. 399.
12. SA LE THI THUAN et J. WIEMANN. Bull. Soc. Chim. Fr. 1861 (1972).
13. R. BRESLOW, S. GARRATT, L. KAPLAN et D. LAFOLLETTE. J. Am. Chem. Soc. **90**, 4051 (1968); **90**, 4056 (1968).
14. (*a*) P.v. R. SCHLEYER, T. M. SU, M. SAUNDERS et J. C. ROSENFELD. J. Am. Chem. Soc. **91**, 5174 (1969); (*b*) J. A. OLAH et R. J. SPEAR. J. Am. Chem. Soc. **97**, 1539 (1975).
15. (*a*) N. LOZAC'H. Bull. Soc. Chim. Fr. 286 (1949); (*b*) H. MORRISON et S. R. KUROWSKY. Chem. Commun. 1098 (1967).
16. (*a*) A. VALETTE. C. R. Acad. Sci. **223**, 907 (1946); (*b*) R. E. WERNER et W. B. REYNOLDS. J. Am. Chem. Soc. **69**, 633 (1947).
17. (*a*) M. GOUGE. Ann. Chim. 648 (1951); 704 (1951); (*b*) H. B. SING. Diss. Abstr. **34**, 202 (1973).
18. H. DANECHPEJOUH. Thèse, Paris (1973).
19. (*a*) W. HUECKEL, C. M. JENNEWEIN, M. WARTINI et J. WOLFERING. Ann. Chem. **686**, 51 (1965); (*b*) F. F. H. YEW, R. J. KURLAND et B. J. MAIR. Anal. Chem. **36**, 843 (1964); **38**, 231 (1966); (*c*) N. K. WILSON et J. B. STOTHERS. J. Magn. Reson. **15**, 31 (1974).
20. (*a*) J. J. MAYER et J. DUSWALT. J. Chem. Eng. Data, **18**, 337 (1973); Anal. Chem. **42**, 1789 (1970); (*b*) R. B. CARLIN et K. S. KRISHMAN. J. Org. Chem. **35**, 3368 (1970); (*c*) S. WINSTEIN et R. F. HECK. J. Org. Chem. **37**, 825 (1972).
21. U. E. MATTER, C. PASCUAL, E. PRETSCH, A. PROSS, W. SIMON et S. STERNHELL. Tetrahedron, **25**, 691 (1969).

Can. J. Chem. Downloaded from www.nrcresearchpress.com by 210.87.254.6 on 09/05/12
For personal use only.

The distribution of trialkylphosphates between dodecane and water[1]

NORMAN H. SAGERT AND WOON LEE

Research Chemistry Branch, Atomic Energy of Canada Research Company, Whiteshell Nuclear Research Establishment, Pinawa, Man., Canada R0E 1L0

Received February 27, 1980

Can. J. Chem. Downloaded from www.nrcresearchpress.com by 210.87.254.6 on 09/05/12
For personal use only.

NORMAN H. SAGERT and WOON LEE. Can. J. Chem. **58**, 1463 (1980).

The distribution of the four lower trialkylphosphates, triethyl, trimethyl, tripropyl, and tributylphosphates, between dodecane and water has been measured as a function of temperature between 293.15 K and 313.15 K, and as a function of trialkylphosphate concentration at concentrations below 0.1 mol/dm^3. From these results, the thermodynamic functions associated with the transfer of each of these trialkylphosphates from water to dodecane were calculated. With the exception of trimethylphosphate, free energies of transfer changed by −3.5 kJ/mol for each methylene group added to the solute. The enthalpies of transfer for all the trialkylphosphates were in the range of 26 to 30 kJ/mol, so that most of the differences in the free energies of transfer arise from entropic differences.

Dimerization constants for the trialkylphosphates in dodecane were consistent with those available in the literature.

NORMAN H. SAGERT et WOON LEE. Can. J. Chem. **58**, 1463 (1980).

On a mesuré la distribution des 4 trialkylphosphates inférieurs, triéthyl-, triméthyl-, tripropyl- et tributylphosphates, entre le dodécane et l'eau, en fonction de la température entre 293.15 et 313.15 K et en fonction de la concentration de trialkylphosphate pour des concentrations inférieurs à 0.1 mol/dm^3. A partir de ces résultats, on a calculé les fonctions thermodynamiques associées au transfert de chacun de ces trialkylphosphates de l'eau au docécane. A l'exception du cas du triméthylphosphate, l'addition d'un groupe méthylénique au soluté provoque une variation de −3.5 kJ/mol dans l'énergie libre de transfert. Les enthalpies de transfert de tous les trialkylphosphates sont de l'ordre de 26 à 30 kJ/mol de telle sorte que la plupart des différences des énergies libres de transfert proviennent de différences entropiques.

Les constantes de dimérisation des trialkylphosphates dans le dodécane sont en accord avec celles rapportées dans la littérature.

[Traduit par le journal]

Introduction

Tributylphosphate has been widely used in extraction processes for separating the components of irradiated nuclear fuel (1). As part of a program to study the interfacial properties relevant to such solvent extraction systems, we have studied the adsorption of trimethylphosphate (TMP), triethylphosphate (TEP), tripropylphosphate (TPP), and tributylphosphate (TBP) (2) at the dodecane–water interface. In order to interpret these adsorption results, it is necessary to have a good thermodynamic description of the process in which solute is transferred from the aqueous phase to the organic phase. The thermodynamics of this transfer process may then be compared with the thermodynamics of adsorption from the organic phase or from the aqueous phase to the interface.

Unfortunately, good thermodynamic descriptions of the transfer processes are not available. Distribution ratios for TBP and TPP are known at room temperature (3, 4). If the enthalpies of solution of these solutes in both dodecane and water were known, complete thermodynamic descriptions of the transfer processes could be obtained. However, the enthalpy of solution of TBP in water has not been measured because TBP is not very soluble in water (5, 6). Enthalpies of solution of TBP have been measured in hexane and dodecane (7) and enthalpies of solution of TPP are available for water (6), and *i*-octane (8). The distribution ratios of TEP and TMP between water and dodecane have not been measured. For both solutes good calorimetric data on enthalpies of solution in water (5) are available but little is known about their enthalpies of solution in alkanes. The only data available are for TEP in *i*-octane (8).

It therefore seemed appropriate to make a complete study of the distribution ratios of the four lower trialkylphosphates at solute concentrations low enough that the ratios can be extrapolated to infinite dilution with some confidence. Free energies of transfer can then be calculated, and from their variation with temperature, enthalpies and entropies of transfer can be calculated, albeit with less precision than from direct calorimetric measurements.

Although the primary purpose of this work is to examine the thermodynamics of transfer, an analysis of the data should give some information on the state of aggregation of trialkylphosphates in the dodecane.

Experimental

Vials containing 5.0 cm^3 dodecane, 5.0 cm^3 water, and varying amounts of one of the trialkylphosphates were prepared as previously described (2) and were shaken for at least 40 h in a thermostatted water bath. Temperatures of the water bath were

[1]AECL No. 6858.

0008-4042/80/141463-05$01.00/0

©1980 National Research Council of Canada/Conseil national de recherches du Canada

Can. J. Chem. Downloaded from www.nrcresearchpress.com by 210.87.254.6 on 09/05/12
For personal use only.

controlled to ±0.1 K. Samples were withdrawn for analysis while keeping the vials thermostatted. Analyses were done by gas chromatography on a Varian model 1800 gas chromatograph fitted with hydrogen flame detectors and on-column injectors. The sample size was 1 mm³. For TEP analyses a 2 m × 3 mm column of 80–100 mesh Poropak P was used at 493 K. For analyses of the other trialkylphosphates, a 3 m × 3 mm column of 3% nitrile silicone gum XE50 on Chromosorb G was used at 493 K.

The sources and purification of dodecane and water have been described (2). The TMP, TEP, and TPP were purchased from Aldrich, and the source and preliminary purification of TBP have been described (2). The trialkylphosphates were further purified by distillation at reduced pressure using a spinning band distillation column. They were stored over activated molecular sieve 4A.

Results and Discussion

Distribution ratios were measured at 293.15 K, 298.15 K, 303.15 K, 308.15 K, and 313.15 K for TMP, TEP, TPP, and TBP distribution between dodecane and water. The TEP and TMP concentration ranges were 0 to 0.1 mol/dm³ in the aqueous phases and TPP and TBP concentration ranges were 0 to 0.1 mol/dm³ in the dodecane. Results[2] for TEP are shown in Fig. 1, where the distribution ratio, D, is defined as (molarity of TEP in the dodecane)/(molarity of TEP in the water). Consideration of the chromatographic techniques used would allow error estimates of ±2% at higher concentrations rising to ±10% at lower concentrations for values of D. The distribution ratios increase very slightly with increasing TEP concentration in the water, but can easily be extrapolated back to zero molarity to give the distribution coefficient K_D.

Table 1 lists all the measured distribution coefficients, K_D, and these are valid to within ±5%. Table 1 also includes mole fraction distribution coefficients K_D^X since it is usual to express results in terms of mole fractions and to employ mole fraction standard states for calculations involving thermodynamics of transfer (9, 10, 11). These have the advantage that the reference base is temperature independent so that enthalpies are equivalent to those measured calorimetrically (12). Since K_D and K_D^X refer to infinite dilution conditions, they are related by eq. [1]

$$[1] \quad K_D^X/K_D = V^{0,\beta}/V^{0,\alpha}$$

where $V^{0,\alpha}$ and $V^{0,\beta}$ are the molar volumes of water and dodecane respectively.

Following Aveyard and Mitchell (9), the standard free energies of transfer of the trialkylphosphates from water to dodecane can be calculated

[2]All the measured distribution ratios are available, at a nominal charge, from the Depository of Unpublished Data, CISTI, National Research Council of Canada, Ottawa, Ont., Canada K1A 0S2.

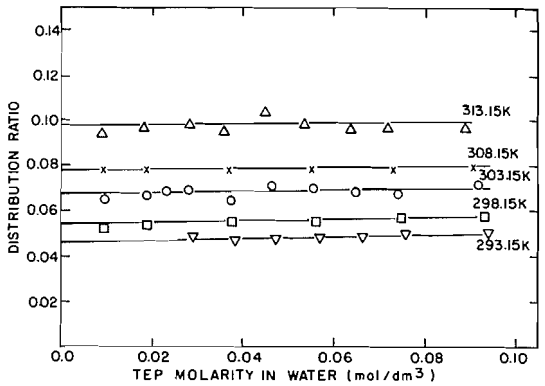


FIG. 1. Distribution ratios, D, for TEP plotted against TEP molarity in the aqueous phase at the five indicated temperatures.

from the value of K_D^X. If the trialkylphosphate is designated as component 1, the aqueous phase called the α phase, and the dodecane phase the β phase, then chemical potentials of solute 1 in the two phases are given by [2] and [3],

$$[2] \quad \mu_1^{\alpha} = \mu_1^{\theta,\alpha} + RT \ln f_1^{\alpha} X_1^{\alpha}$$

$$[3] \quad \mu_1^{\beta} = \mu_1^{\theta,\beta} + RT \ln f_1^{\beta} X_1^{\beta}$$

in which $\mu_1^{\theta,\alpha}$ and $\mu_1^{\theta,\beta}$ are the standard chemical potentials, f_1^{α} and f_1^{β} are the activity coefficients, and X_1^{α} and X_1^{β} are the mole fractions of 1 in the α and β phase respectively. The activity coefficients are chosen to become unity as the mole fractions approach zero. Thus, at infinite dilution, the standard free energy of transfer from water to dodecane is given by eq. [4],

$$[4] \quad \mu_1^{\theta,\beta} - \mu_1^{\theta,\alpha} = \Delta_{\alpha}^{\beta}\bar{G}_1^{\theta} = -RT \ln K_D^X$$

provided the standard state is chosen to be the hypothetical standard state of unit solute mole fraction with unit activity coefficient.

The standard enthalpy of transfer may then be calculated from the temperature variation of the standard free energy of transfer using eq. [5].

$$[5] \quad \Delta_{\alpha}^{\beta}\bar{H}_1^{\theta} = \partial(\Delta_{\alpha}^{\beta}\bar{G}_1^{\theta}/T)/\partial(1/T)$$

Figure 2 shows a plot of $\Delta_{\alpha}^{\beta}\bar{G}_1^{\theta}/T$ against $1/T$ for the solute TEP. Over the small range of temperature investigated, a reasonably linear relationship is obtained, indicating a constant enthalpy of transfer over this range. Values for the standard entropies of transfer may then be calculated easily, and Table 2 lists all the free energies, enthalpies, and entropies of transfer for the four solutes studied. The errors in the enthalpies are at least ± 1 kJ/mol from random deviations and may be as high as ±2 kJ/mol if undetected systematic deviations occur.

As has been noted for many other systems (9, 10), the standard free energies of transfer for these

TABLE 1. Distribution ratios at infinite dilution for trialkylphosphate–water–dodecane systems. The transfer of trialkylphosphates is defined as from water to dodecane

	TMP		TEP		TPP		TBP	
T(K)	10^3K_D	$K_D{}^x$	K_D	$K_D{}^x$	K_D	$K_D{}^x$	K_D	$K_D{}^x$
293.15	2.41	0.030	0.046	0.581	—	—	204	2570
294.15	—	—	—	—	3.66	46.2	—	—
298.15	2.98	0.0377	0.054	0.675	4.06	51.4	252	3190
303.15	3.51	0.044	0.067_5	0.857	4.85	61.6	290	3670
308.15	4.26	0.054	0.078	0.993	5.81	74.0	350	4460
313.15	5.13	0.0655	0.098	1.25	6.94	88.6	410	5240

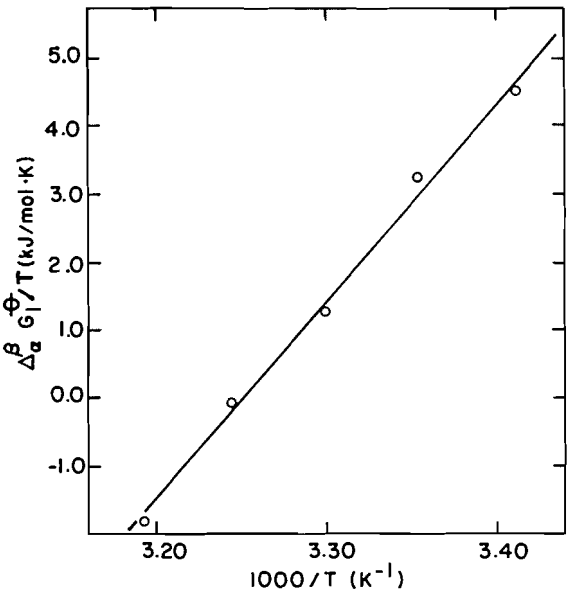


FIG. 2. Enthalpy of transfer plot of the standard free energy of transfer divided by the temperature plotted against reciprocal temperature. These results are for TEP and the slope corresponds to 29.5 kJ/mol.

TABLE 2. Standard free energies, entropies, and enthalpies of transfer of trialkylphosphates from water to dodecane

Solute	$\Delta_\alpha^\beta \bar{G}_1{}^\theta$ (kJ/mol)	$\Delta_\alpha^\beta \bar{H}_1{}^\theta$ (kJ/mol)	$\Delta_\alpha^\beta \bar{S}_1{}^\theta$ (J/mol·K)
TMP	8.1_3±0.4	29.0±1.0	69.9±2.0
TEP	0.97±.05	29.5±1.0	95.7±3.0
TPP	−9.76±0.5	26.6±1.2	121.8±3.7
TBP	−20.0±0.9	26.8±1.2	157.2±4.7

trialkylphosphates are a linear function of the number of methylene groups in the molecule. The free energies are shown in Fig. 3 as a function of the number of carbon atoms in the solute. Also shown is the result for TPP in *n*-hexane at 298.15 K given by Dyrssen and Petković (4) as well as the value for TBP in dodecane given by Marcus (3). The results

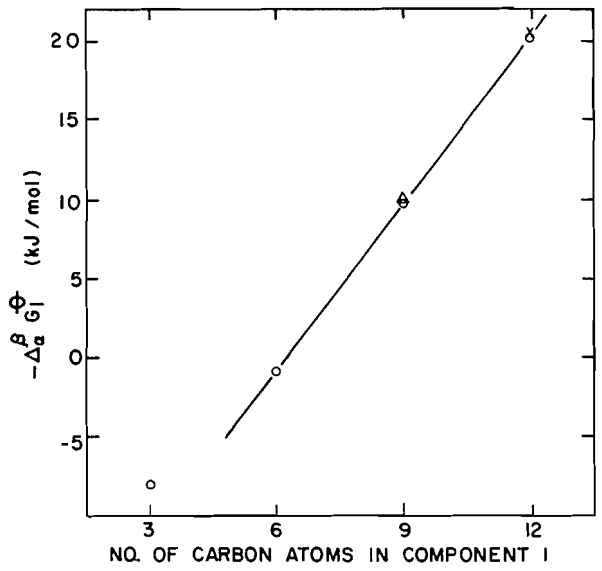


FIG. 3. Variation of standard free energy of transfer with number of carbon atoms in trialkylphosphate solute. The circles (O) refer to this work, the triangle (Δ) to ref. 4, and the cross (×) to ref. 3. The line has a slope of 3.5 kJ/mol per CH_2 unit.

of Aveyard and Mitchell (9) show that, for alcohols at least, the chain length of the hydrocarbon used as the organic phase does not greatly affect the standard free energies of transfer. Our results, when compared to those of Dyrssen and Petković (4), suggest that this is the case for the trialkylphosphates as well.

The solid line in Fig. 3 has a slope corresponding to −3.5 kJ/mol per CH_2 group. This value is almost in the middle of the range, −3.56 ± 0.1 kJ/mol per CH_2 group, quoted by Tanford (11) as expected for transfer of a large variety of organic solutes from water to hydrocarbons. The constancy of this value is one of the bases for the postulate of the "hydrophobic effect" (10). The standard free energy of transfer of TMP is not on the line, but it is reasonable to expect the addition of the first methylene group to the chains to be somewhat anomalous (13).

Can. J. Chem. Downloaded from www.nrcresearchpress.com by 210.87.254.6 on 09/05/12
For personal use only.

Can. J. Chem. Downloaded from www.nrcresearchpress.com by 210.87.254.6 on 09/05/12
For personal use only.

In contrast to the standard free energies of transfer, the standard enthalpies of transfer do not show a large variation with chain length, although there appears to be some lowering with increased chain length. Similar behaviour has been observed for alcohols (14). Thus the changes in the standard free energies of transfer result largely from changes in the standard entropies of transfer (Table 2). The enthalpies of solution are very large and negative, implying a distinct enthalpic preference for the water phase. Since these are much larger than the enthalpies of transfer of the pure hydrocarbons from water to hydrocarbons (10), the phosphate group is probably responsible for most of the enthalpic effects. A similar suggestion has been made for the OH groups in alcohols (9).

For some solutes, our standard enthalpies of transfer may be compared with direct calorimetric measurements, since the enthalpy of transfer from water to hydrocarbon will be equal to the enthalpy of solution in the hydrocarbon minus that in the water (8, 14). Kertes *et al.* (7) give 7.4 kJ/mol and 7.2 kJ/mol for the enthalpies of solution of TBP in dodecane and hexane respectively, and Rytting *et al.* (8) give 7.6 and 10.8 kJ/mol for the enthalpies of solution of TPP and TEP respectively in *i*-octane. Kertes and Tsimering (5) found enthalpies of solution in water to be −21.2 and −25.2 kJ/mol for TMP and TEP respectively, while, earlier, Lindenbaum *et al.* (6) had found enthalpies of solution in water of −21.1 and −22.6 kJ/mol for TEP and TPP. Thus, if the enthalpies of solution in *i*-octane can be taken as applicable to dodecane, then from Kertes *et al.* the enthalpy of transfer should be 35.9 kJ/mol for TEP whereas, from Lindenbaum *et al.*, it should be 32.0 kJ/mol for TEP and 30.3 kJ for TPP. Our results, which are 29.5 kJ/mol for TEP and 26.6 kJ/mol for TPP are rather lower than these calorimetric results.

A number of reasons may be considered for our lower results. First of all, strictly speaking the systems are not the same since our experiments measure the thermodynamics of transfer from mutually saturated phases, whereas the calorimetric experiments measured the thermodynamics of solution into pure solvents. It is unlikely that the small solubility of dodecane in water is very important. However, water solubility in dodecane is known to be altered by TBP, with one mole of TBP carrying along one mole of water into the organic phase (3). A loose complex has been proposed (3, 15). Thus water solubility in the dodecane could well result in lower enthalpies of transfer, which perhaps may be more accurately thought of as enthalpies of transfer for trialkylphosphate–water complexes. Secondly, we have used enthalpies of solution in *i*-octane because none were available for dodecane, although the differences should be small. Thirdly, for the calorimetry, agreement between reputable workers is none too good and is outside estimated error limits. Thus, if error limits, including our own, are much larger than estimated, much of the disagreement may be illusory.

There do not seem to be any reliable data on enthalpies of solution of TMP in dodecane, probably because of the low limiting solubility. However, if an enthalpy of solution of about 12 kJ/mol is inferred from the TEP and TPP data, then the enthalpies of solution measured by Kertes *et al.* (5) and Lindenbaum *et al.* (6) yield enthalpies of transfer of 34 kJ/mol and 24 kJ/mol respectively. Our value of 29.0 is thus exactly midway between these estimates. If our results really are expected to be lower than the calorimetric results as outlined in the above paragraph, our value of 29.0 kJ/mol for an enthalpy of transfer supports the higher estimate of the enthalpy of solution obtained by Kertes and Tsimering (5). No calorimetric data on the enthalpies of solution of TBP in water are available because of the low solubility of TBP in water (5, 16).

Generally one would expect some finite change in heat capacity to be associated with the transfer of these trialkylphosphates (10). However, with the large experimental error and the small temperature range examined, it is perhaps not surprising that there is no curvature in the plot of $\Delta_{\alpha}^{\beta}\bar{G}^{\theta}/T$ against $1/T$ (Fig. 2), and thus no observable change in heat capacity.

Finally, we would like to see if our data can be used to say anything about the aggregation of trialkylphosphate molecules in dodecane. In principle, the slopes of the lines in Fig. 1 can be used to determine the extent of association in the dodecane. Following Woolley *et al.* (12), the general association reaction is written as eq. [6]

$$[6] \quad nP \overset{K_n}{\rightleftharpoons} P_n$$

if monomer is the predominant species in the aqueous phase. The distribution ratio D has been defined as the total trialkylphosphate molarity in the dodecane divided by that in the aqueous phase. This quantity D is the ratio plotted in Fig. 1. The distribution coefficient K_D is defined at infinite dilution and thus represents the ratio of trialkylphosphate monomers in the dodecane to trialkylphosphate in the aqueous phase.

Dimers are thought to be the predominant associated trialkylphosphate species in alkane solvents, and it is not usually necessary to consider

higher degrees of association (4, 8, 17). Thus, from eq. [6] we obtain eq. [7]

$$[7] \quad D = K_D + 2K_2K_D^2[\mathrm{TAP}]_{aq}.$$

where K_2 is, of course, the equilibrium constant for dimerization as given in eq. [6]. Our experiments were not planned for the purpose of obtaining K_2 and were limited to low concentrations. For the two lower trialkylphosphates with low K_D's, our slopes in plots like Fig. 1 are not significantly different from zero. This is consistent with a K_2 of 0.7 for TEP in hexane as observed by Petković (17) since any observable slope in our plots would imply a very much higher value for K_2.

The situation is somewhat better for TPP and TBP. Here, for TPP we obtain an estimate for K_2 of 1.3 at 294.15 K and 1.5 at 298.15 K. This can be compared with 1.2 at 295.15 K in hexane as measured by Dyrssen and Petković (4) using solvent extraction techniques. Similarly, for TBP, we obtain 2.0 to be compared with 2.9 by Petković (18) in hexane and 2.6 and 2.5 by the same author (17) in dodecane and cyclohexane respectively. In view of the small concentration range used in this work, all that can be said is that our dimerization constants are not inconsistent with those found in the literature.

Acknowledgements

We thank Professor A. S. Kertes for access to work in press and for his interest in this work. Professor L. G. Hepler is also thanked for his interest and helpful comments. We thank our colleagues at WNRE for useful aid and discussions.

1. Y. Marcus and A. S. Kertes. Ion exchange and solvent extraction of metal complexes. John Wiley, New York. 1969. p. 650.
2. N. H. Sagert, W. Lee, and M. J. Quinn. Can. J. Chem. **57**, 1218 (1979).
3. Y. Marcus. Critical evaluation of some equilibrium constants involving organophosphorus extractants. Butterworths, London. 1974. pp. 27–33.
4. D. Dyrssen and D. Petković. J. Inorg. Nucl. Chem. **27**, 1381 (1965).
5. A. S. Kertes and L. Tsimering. J. Phys. Chem. **81**, 120 (1977).
6. S. Lindenbaum, D. Stevenson, and J. H. Rytting. J. Solution Chem. **4**, 893 (1975).
7. A. S. Kertes, L. Tsimering, and F. Grauer. J. Inorg. Nucl. Chem. **38**, 867 (1976).
8. J. H. Rytting, A. Goldkamp, and S. Lindenbaum. J. Solution Chem. **4**, 1005 (1975).
9. R. Aveyard and R. W. Mitchell. Trans. Faraday Soc. **65**, 2645 (1969).
10. C. Tanford. The hydrophobic effect: formation of micelles and biological membranes. John Wiley, New York. 1973. pp. 4–15.
11. C. Tanford. J. Phys. Chem. **83**, 1802 (1979).
12. E. M. Woolley, J. G. Travers, B. P. Erno, and L. G. Hepler. J. Phys. Chem. **75**, 3591 (1971).
13. C. Tanford. Science, **200**, 1012 (1978).
14. A. S. Kertes and W. C. Lai. Colloids Surf. **1**, 197 (1980).
15. J. W. Roddy. J. Inorg. Nucl. Chem. **40**, 1787 (1978).
16. K. Alcock, S. S. Grimley, T. V. Healy, J. Kennedy, and H. A. C. McKay. Trans. Faraday Soc. **52**, 39 (1956).
17. D. M. Petković. J. Inorg. Nucl. Chem. **30**, 603 (1968).
18. D. M. Petković. Solvent extraction chemistry. *Edited by* D. Dyrssen, J. O. Liljenzin, and J. Rydberg. North Holland, Amsterdam. 1967. pp. 305–308.

Can. J. Chem. Downloaded from www.nrcresearchpress.com by 210.87.254.6 on 09/05/12
For personal use only.

Thermodynamics of molecular interactions between nitromethane and aromatic hydrocarbons

RAM K. NIGAM,[1] PREM P. SINGH,[1] RUCHI MISHRA, AND MOHAN SINGH
Department of Chemistry, Maharshi Dayanand University, Rohtak- 124001, Haryana, India
Received March 26, 1979[2]

RAM K. NIGAM, PREM P. SINGH, RUCHI MISHRA, and MOHAN SINGH. Can. J. Chem. 58, 1468 (1980).

Excess volumes of mixing V^E, excess enthalpies H^E, and excess Gibbs free energies of mixing G^E, of binary mixtures of nitromethane with aromatic hydrocarbons have been measured at 303.15 and 313.15 K. The V^E, H^E, and G^E data, which are positive throughout the entire range of concentrations, have been examined with Winnick's theory. The calculated V^E, H^E, and G^E values compare reasonably well with the corresponding experimental values. The theory also correctly predicts the influence of temperature on these excess functions.

RAM K. NIGAM, PREM P. SINGH, RUCHI MISHRA et MOHAN SINGH. Can. J. Chem. 58, 1468 (1980).

On a mesuré à 303.15 et à 313.15 K les volumes de mélange en excès, V^E, les enthalpies en excès, H^E, et les énergies libres de Gibbs de mélange en excès, G^E, de mélanges binaires formés de nitrométhane et d'hydrocarbures aromatiques. On a examiné à l'aide de la théorie de Winnick les données de V^E, H^E et G^E qui ont des valeurs positives dans tout l'intervalle de concentration utilisée. Les valeurs calculées de V^E, H^E et G^E se comparent raisonnablement bien aux valeurs expérimentales. La théorie prédit également d'une façon précise l'influence de la température sur ces fonctions d'excès.

[Traduit par le journal]

Introduction

Renon *et al.* (1), following Prigogine (2), have proposed a semi-empirical partition function for simple liquids based on a three parameter theory of corresponding states. Winnick and Prausnitz (3) have recently extended this partition function to mixtures using Scott's two fluid theory (4) and have tested the resulting expressions for the excess thermodynamic functions against the corresponding experimental data for some polar–polar and polar–non-polar mixtures. It would, therefore, be interesting to see if the V^E, H^E, and G^E data of the binary mixtures of nitromethane with aromatic hydrocarbons can aptly be described by this theory.

Experimental

Analytical grade benzene, toluene, *o*-, *m*-, and *p*-xylenes were purified as described earlier (5) while nitromethane (B.D.H., A.R. Grade) was purified as suggested by Saunders and Spaull (6). The purity of the final samples was checked by measuring their density at 298.15 ± 0.01 K which agreed to within ±0.00005 g/cm³ with the corresponding literature values (refs. 7–10, ref. 28, p. 165).

Excess volumes of mixing were measured as a function of composition using the direct dilatometric method (11). The temperature of the thermostatic bath was controlled to ±0.01 K. The uncertainty in experimental V^E values is about 0.5%.

Heats of mixing measurements were made in an adiabatic calorimeter which has been described elsewhere (12). The time was recorded by an electronic timer (type 701 SR.No.010, Systronic, Ahmedabad, India) which could read to ±0.0001 s. The temperature variations of the thermostatic bath were found to be within ±0.01 K. The uncertainty in H^E values is about 1.1%.

Vapour pressures of these mixtures were determined by a static method described previously (13). The apparatus was placed in a water thermostat which in turn was placed in another water thermostat. The temperature of the outer thermostat was controlled to ±0.01 K and the temperature drift in the inner thermostat was found to be less than ±0.003 K. The mercury heights in the manometer were read by a cathetometer which could read to ±0.001 cm. All vapour pressure measurements were reproducible to better than ±0.02 Torr.

Our measured vapour pressures of aromatic hydrocarbons and nitromethane at 303.15 K compare to within 0.3% with that obtained from the corresponding data (refs. 14–17, ref. 28, pp. 143, 577) reported for these compounds at various temperatures.

Results

The experimental V^E, H^E, and G^E data for binary mixtures of nitromethane with benzene, toluene, *o*-xylene, *p*-xylene, and *m*-xylene at 303.15 and 313.15 K as function of composition are recorded in Tables 1 to 3.[3]

V^E data were fitted to the equation

$$[1]\quad V^E/x_1(1-x_1)\ \text{cm}^3\ \text{mol}^{-1} = [V_0 + V_1(2x_1 - 1) + V_2(2x_1 - 1)^2]$$

while H^E data were fitted to the equation

$$[2]\quad H^E/x_1(1-x_1)\ \text{J mol}^{-1} = [h_0 + h_1(2x_1 - 1) + h_2(2x_1 - 1)^2]$$

where V_0, V_1, V_2, h_0, h_1, and h_2 are adjustable parameters of [1] and [2] respectively and x_1 is the mole fraction of nitromethane. These parameters were evaluated by fitting $V^E/x_1(1 - x_1)$ and $H^E/x_1(1 - x_1)$ to [1] and [2] respectively by the method of least squares and are recorded along

[1]Authors to whom correspondence should be addressed.
[2]Revision received April 14, 1980.

[3]Complete set of data may be obtained, at a nominal charge, from the Depository of Unpublished Data, CISTI, National Research Council of Canada, Ottawa, Ont., Canada K1A 0S2.

0008-4042/80/141468-05$01.00/0
©1980 National Research Council of Canada/Conseil national de recherches du Canada

Can. J. Chem. Downloaded from www.nrcresearchpress.com by 210.87.254.6 on 09/05/12
For personal use only.

TABLE 1. Parameters of eqs. [1], [2], and [3] along with the standard deviation $\sigma(V^E)$ and $\sigma(H^E)$ for the various systems at 303.15 and 313.15 K

Parameters	Value				
	Nitromethane + benzene	Nitromethane + toluene	Nitromethane + *p*-xylene	Nitromethane + *o*-xylene	Nitromethane + *m*-xylene
			303.15 K		
V_0	0.828	0.635	0.900	0.973	1.092
V_1	0.361	0.246	0.545	0.648	0.291
V_2	−0.159	0.085	0.035	0.385	0.290
h_0	4593	4824	5504	5562	5598
h_1	1282	1115	2926	2577	908
h_2	6001	3285	2926	2577	2822
G_0	0.9632	1.1345	1.1547	1.1687	1.1839
G_1	−0.6876	0.9218	0.8972	0.8889	0.9618
G_2	0.3749	1.0348	0.9065	0.9170	1.0038
$\sigma(V^E)$ cm^3 mol^{-1}	0.0034	0.0034	0.0063	0.0035	0.0038
$\sigma(H^E)$ J mol^{-1}	6.3	6.4	6.6	5.0	6.2
			313.15 K		
V_0	0.709	0.629	0.976	1.049	1.177
V_1	0.289	0.468	0.425	0.452	0.574
V_2	0.256	−0.131	0.278	0.929	0.250
h_0	3667	4008	4664	4649	4727
h_1	762	−185	−597	641	309
h_2	187	780	−719	492	−1417
G_0	0.8831	1.0530	1.1015	1.1306	1.1147
G_1	−0.5934	−0.8928	−0.8263	−0.7964	−0.8469
G_2	0.2243	1.0017	0.8775	0.9064	0.9169
$\sigma(V^E)$ cm^3 mol^{-1}	0.0041	0.0041	0.0043	0.0024	0.0042
$\sigma(H^E)$ J mol^{-1}	6.1	4.5	4.5	5.5	4.1

with the standard deviations, $\sigma(V^E)$ and $\sigma(H^E)$, of the molar excess volumes and molar excess enthalpies respectively in Table 1.

The vapour pressure data for these mixtures at 303.15 and 313.15 K were used to evaluate the molar excess Gibbs free energies of mixing, G^E, by Barker's method (18). The form of the function used for G^E, following Redlich and Kister (19), is

$$[3] \quad G^E/RT = x_1(1 - x_1)[G_0 + G_1(2x_1 - 1) + G_2(2x_1 - 1)^2]$$

where G_0, G_1, and G_2 are adjustable parameters. These parameters are recorded in Table 1. All calculations were made on an I.B.M. 1620 computer. The second virial coefficient of benzene was taken from literature (20) while those for nitromethane, toluene, *o*-xylene, *p*-xylene, and *m*-xylene were calculated from Berthelot's equation (21); the necessary critical constant data were taken from the literature (22).

Discussion

Suri (23) has determined the V^E values for benzene + nitromethane mixtures at 298.15 and 303.15 K. While our V^E values at 303.15 K for this mixture are more positive in the concentration range $0 < x_1 < 0.53$ (the values differ by as much as 0.035 cm^3 mol^{-1} at $x_1 = 0.3$), they are more negative (maximum difference being 0.025 cm^3 mol^{-1} at $x_1 = 0.7$) in the rest of the nitromethane concentration range. Again Brown and Fock (24) have determined the H^E values of benzene + nitromethane mixtures at 318.15 K. Assuming that H^E varies linearly with temperature in the temperature range 303.15–318.15 K, our H^E values at 318.15 K agree to within ±10 J mol^{-1} with those reported by Brown and Fock (24). The same, however, is not true of the G^E data reported (25) for this mixture at 318.15 K (our extrapolated G^E values at 318.15 K are more negative by as much as 250 J mol^{-1} at $x_1 = 0.6$ from those reported by Brown and Smith (25)). We are unaware of any V^E, H^E, and G^E data at 303.15 or 313.15 K with which to compare our results for the remaining binary mixtures. The H^E values for the various mixtures as evaluated from the corresponding G^E values did not agree with the corresponding experimental H^E values. This is consistent with the earlier observation (21, 26) regarding the evaluation of H^E data from the corresponding G^E data. Further V^E, H^E, and G^E values

Can. J. Chem. Downloaded from www.nrcresearchpress.com by 210.87.254.6 on 09/05/12
For personal use only.

Can. J. Chem. Downloaded from www.nrcresearchpress.com by 210.87.254.6 on 09/05/12
For personal use only.

are positive throughout the entire concentration range for all the mixtures studied here. Again while V^E data vary in the order

toluene < benzene < *p*-xylene < *o*-xylene < *m*-xylene

H^E and G^E data follow the sequence

benzene < toluene < *p*-xylene < *m*-xylene ≈ *o*-xylene

At the simplest qualitative level the V^E data can be explained if it is assumed that these mixtures are characterised by (*a*) steric repulsion and (*b*) dipole – induced dipole interactions between the components of these mixtures. Such a scheme of molecular interactions would suggest that, compared to benzene, the electron-rich end of the toluene moiety would interact strongly with electron deficient $-CH_3$ end of the nitromethane moiety so that V^E values for nitromethane + toluene mixtures should be less positive than that for nitromethane + benzene mixtures. The experimental V^E data support this conjecture. For nitromethane + xylene mixtures the dipole – induced dipole interactions would be of the same order of magnitude as that for nitromethane + toluene mixtures but the steric repulsion between nitromethane on the one hand and the two bulky CH_3 substituents in xylenes on the other would increase considerably. This would require that the V^E values for xylenes + nitromethane mixtures should be more positive than that for benzene + nitromethane mixtures. The experimental V^E data lend further support to this conjecture. Further within the xylenes the steric repulsion between the nitromethane and xylenes would vary in the order

p-xylene < *o*-xylene < *m*-xylene

so that V^E values for *p*-xylene + nitromethane mixtures should be less positive than that for *o*-xylene + nitromethane or *m*-xylene + nitromethane mixtures. This has, in fact, been observed.

The enthalpic effect on the other hand is the cumulative sum of the contribution due to interactions (*a*) (which are always endothermic) and (*b*) (which are exothermic) mentioned above. Our H^E data suggest that the contribution due to the factor (*a*) always outweighs those due to factor (*b*) for the mixtures studied here so that the H^E values should vary in the order

benzene < toluene < *p*-xylene < *m*-xylene < *o*-xylene

The present study thus suggests that binary mixtures of nitromethane with aromatic hydrocarbons are characterised by dipole – induced dipole interactions and that steric repulsion also plays an important part.

We next examined our V^E, H^E, and G^E data for Winnick theory (26). Based on a configurational partition function (27) of a pure liquid suggested by cell theory, Winnick (26) expressed the configurational partition function for a polar–non-polar mixture of mole fraction x_1 by the expression

$$[4]\quad Q_m = \frac{\prod_{i=1}^{2} \{[V_{im}^*(\tilde{V}_{im}^{1/3} - 1)^{3C_i} J(\tilde{T}_{im})]^{N_i} \exp(-x_i E_{im}/kT)\}}{N_i!}$$

where

$$[5]\quad E_{im} = -[(U_{im}^*/\tilde{V}_{im}) + M_{im}]$$

$$[6]\quad M_{im} = \sum_{i=1}^{2} p_j M_{ij}$$

$$[7]\quad M_{ij} = m_{im}'\mu_1^2\left(\frac{\varepsilon - 1}{\varepsilon + 2}\right) V_2^*/(V_{12}^*)^2$$

and

$$[8]\quad V_{12}^* = N_A\xi[\tfrac{1}{2}(\sigma_{1m} + \sigma_{2m})^3]$$

All the quantities in eqs. [4] to [8] have the same significance as suggested by Winnick and Prausnitz (3, 26). V^E, G^E, and H^E, according to this theory, were calculated from the following expressions

$$[9]\quad V^E = V_m - \sum_{i=1}^{2} x_i V_i = \sum_{i=1}^{2} (x_i \tilde{V}_{im} V_{im}^*) - \sum_{i=1}^{2} x_i V_i$$

$$[10]\quad A^E \approx G^E = A_m - \sum_{i=1}^{2} x_i A_i - RT \sum_{i=1}^{2} x_i \ln x_i$$

and

$$[11]\quad U^E \approx H^E = U_m - \sum_{i=1}^{2} x_i U_i$$

with

$$[12]\quad U_{mi} = RT^2 \ln Q_{mi}$$

and

$$[13]\quad A_{mi} = -kT \ln Q_{mi}$$

$$[14]\quad J(\tilde{T}) = \exp\left[-28.025 \exp\left(-\frac{4.84}{\tilde{T}_i}\right) - \frac{2.320}{\tilde{T}_i} + \zeta\right]$$

In order to evaluate V^E, H^E, and G^E according to the Winnick theory (26), we evaluated the various parameters in the following manner: the reduced

Can. J. Chem. Downloaded from www.nrcresearchpress.com by 210.87.254.6 on 09/05/12
For personal use only.

TABLE 2. Parameters for pure components at 303.15 and 313.15 K

Components	V^*/cm^3 mol^{-1}	V/cm^3 mol^{-1}	$\sigma \times 10^8$/cm	$E \times 10^{21}$/J mol^{-1}
		303.15 K		
Nitromethane	48.21	56.12	5.11	6.32
Benzene	69.14	89.94	4.84	6.03
Toluene	83.70	107.38	5.18	6.32
p-Xylene	103.52	124.60	5.56	6.38
o-Xylene	100.20	121.14	5.50	6.53
m-Xylene	101.85	124.04	5.53	6.42
		313.15 K		
Nitromethane	48.33	56.76	5.11	6.32
Benzene	69.58	90.87	4.84	6.03
Toluene	84.07	108.49	5.18	6.31
p-Xylene	103.98	125.81	5.56	6.38
o-Xylene	101.08	122.99	5.50	6.53
m-Xylene	102.81	125.17	5.53	6.42

TABLE 3. Comparison of H^E, G^E, and V^E values calculated according to Winnick theory with the corresponding experimental values for three mole fraction $x_1 = 0.3, 0.5$, and 0.7 at 303.15 and 313.15 K

Temperature (K)	Mole fraction of nitromethane (x_1)	H^E/J mol^{-1}		G^E/J mol^{-1}		V^E/cm^3 mol^{-1}	
		Calcd	Expt	Calcd	Expt	Calcd	Expt
	Nitromethane (A) + benzene (B), $m_{12}' = -2.34 \times 10^7$ D						
303.15	0.3	679	877	567	687	0.073	0.138
	0.5	1231	1148	467	601	0.378	0.207
	0.7	894	1092	541	396	0.180	0.199
313.15	0.3	647	712	712	632	0.069	0.133
	0.5	965	915	490	574	0.293	0.177
	0.7	723	840	694	372	0.174	0.189
	Nitromethane (A) + toluene (B), $m_{12}' = -3.51 \times 10^7$ D						
303.15	0.3	983	1113	828	874	0.225	0.116
	0.5	1327	1205	591	739	0.358	0.159
	0.7	1014	1113	358	513	0.193	0.156
313.15	0.3	923	803	778	858	0.156	0.080
	0.5	1055	1002	534	685	0.195	0.157
	0.7	968	859	325	486	0.149	0.166
	Nitromethane (A) + *p*-xylene (B), $m_{12}' = -4.98 \times 10^7$ D						
303.15	0.3	969	1149	835	877	0.297	0.144
	0.5	1373	1375	626	727	0.385	0.225
	0.7	1230	1358	365	497	0.130	0.236
313.15	0.3	900	905	799	859	0.218	0.178
	0.5	1177	1166	603	716	0.339	0.243
	0.7	1038	1005	357	507	0.213	0.249
	Nitromethane (A) + *o*-xylene (B), $m_{12}' = -4.76 \times 10^7$ D						
303.15	0.3	1204	1228	848	915	0.185	0.169
	0.5	1313	1390	638	745	0.248	0.243
	0.7	1273	1280	373	507	0.170	0.278
313.15	0.3	1115	938	810	892	0.344	0.212
	0.5	1215	1162	615	741	0.384	0.262
	0.7	1024	1013	370	524	0.255	0.289
	Nitromethane (A) + *m*-xylene (B), $m_{12}' = -4.91 \times 10^7$ D						
303.15	0.3	1255	1194	841	884	0.175	0.214
	0.5	1343	1399	628	732	0.409	0.273
	0.7	1216	1346	368	513	0.135	0.263
313. 15	0.3	1115	938	810	892	0.344	0.213
	0.5	1213	1162	615	741	0.384	0.262
	0.7	1024	1013	370	524	0.255	0.289

Can. J. Chem. Downloaded from www.nrcresearchpress.com by 210.87.254.6 on 09/05/12
For personal use only.

volume of the component i in the mixture was evaluated by solving the expression

[15] $\tilde{V}_{im}^{4/3} = 9.008(\tilde{V}_{im}^{1/3} - 1)/\tilde{T}_{im}$

where

[16] $T_{im}^* = (aU^*)_{im}/(ak)_i RC_i$

while the characteristic volume of the components i in the mixture, V_{im}^*, was evaluated from the equation

[17] $V_{im}^* = N_A \xi \sigma_{im}^3$

where N_A is Avogadro's number, K is a constant having a value of 9.008, and ξ is the packing factor which is assumed to have the same values in pure components and also in mixtures. Further, U_{im}^* and σ_{im} for the component i in the mixture were calculated using the relations

[18] $U_{im}^* = \frac{1}{2} N_A S_{im} E_{im}$

[19] $\sigma_{im} = \Sigma p_j \sigma_{ij}$

where

[20] $$S_{im} = S_i \sigma_{im}^2 \Big/ \sum_{i=1}^{2} p_j \sigma_{jm}^2$$

[21] $$P_j = x_j \sigma_j^d \Big/ \sum_{j=1}^{2} x_i \sigma_{ij}^d$$

[22] $$E_{im} = \sum_{j=1}^{2} p_j (E_{ii} \cdot E_{jj})^{1/2} (1 - K_{ij})$$

[23] $\sigma_{ij} = \frac{1}{2}(\sigma_{ii} + \sigma_{jj})$

and K_{ij} in [22] is a parameter that takes into account the deviation of E_{ij} from the geometric mean of E_{ii} and E_{jj} and for the present investigations has been assumed to be zero. The choice of S_i in eq. [18] is not critical and for the present analysis we have taken $S_1 = 8$ for hydrocarbons and 6 for nitromethane. The parameter m_{12}' which is the only one not predetermined in [7] was assumed to be independent of temperature, and was evaluated in the manner suggested by Winnick (26). Its value is listed in Table 3. All other parameters are given in Table 2 while V^E, H^E, and G^E values for all the binary mixtures studied here at $x_1 = 0.3$, 0.5, and 0.7 are given in Table 3. An examination of Table 3 reveals that the theoretical V^E, H^E, and G^E values compare reasonably well with the corresponding experimental values. The theory also correctly predicts the influence of temperature on these excess thermodynamic functions of these binary mixtures.

Acknowledgement

R.M. and M.S. wish to thank the U.G.C., Delhi, India for the award of Research Scholarships.

1. H. Renon, C. A. Eckert, and J. M. Prausnitz. Ind. Eng. Chem. Fundam. **6**, 52 (1967); **7**, 335 (1968).
2. I. Prigogine. The molecular theory of solutions. North Holland, Amsterdam. 1957.
3. J. Winnick and J. M. Prausnitz. Chem. Eng. J. **2**, 241 (1971).
4. R. L. Scott. J. Chem. Phys. **25**, 193 (1956).
5. R. K. Nigam and B. S. Mahl. Indian J. Chem. **77**, 2081 (1973).
6. D. F. Saunders and A. J. B. Spaull. Z. Phys. Chem. Neue Folge, Bd. **28**, S. 332 (1961).
7. A. V. Few and J. W. Smith. J. Chem. Soc. London, 753 (1949).
8. A. F. Forziati, A. R. Glasgow, Jr., C. B. Willingham, and F. D. Rossini. J. Res. Natl. Bur. Stand. **36**, 129 (1946).
9. H. Perkin. J. Chem. Soc. London, 267 (1900).
10. J. W. Sears and E. H. Hopke. J. Am. Chem. Soc. **71**, 1632 (1949); **71**, 2575 (1949).
11. R. K. Nigam and P. P. Singh. Trans. Faraday Soc. **65**, 950 (1969).
12. R. K. Nigam and B. S. Mahl. Trans. Faraday Soc. **68**, 1508 (1972).
13. R. K. Nigam and B. S. Mahl. Indian J. Chem. **9**, 1250 (1971).
14. E. R. Smith. J. Res. Natl. Bur. Stand. **26**, 129 (1941).
15. C. B. Willingham, W. J. Taylor, J. M. Pignocco, and F. D. Rossini. J. Res. Natl. Bur. Stand. **35**, 219 (1945).
16. K. S. Pitzer and D. W. Scott. J. Am. Chem. Soc. **40**, 345 (1948).
17. N. I. Joukovsky. Bull. Soc. Chim. Phys. Belg. **43**, 397 (1934).
18. J. A. Barker. Aust. J. Chem. **6**, 207 (1953).
19. O. Redlich and A. I. Kister. Ind. Eng. Chem. **40**, 345 (1948).
20. P. W. Allen, D. H. Everett, and M. F. Penney. Proc. R. Soc. A, **212**, 149 (1952).
21. G. Scatchard and L. B. Ticknor. J. Am. Chem. Soc. **74**, 3724 (1952).
22. R. C. Reid and T. S. Sherwood. The properties of gases and liquids. McGraw Hill Book Co., NY. 1958. pp. 515, 583.
23. S. K. Suri. Indian J. Chem. **12**, 620 (1956).
24. I. Brown and W. Fock. Aust. J. Chem. **9**, 180 (1956).
25. I. Brown and F. Smith. Aust. J. Chem. **8**, 501 (1955).
26. J. Winnick. Ind. Eng. Chem. Fundam. **12**, 203 (1973).
27. J. Winnick and J. M. Prausnitz. Chem. Eng. J. **2**, 233 (1971).
28. J. Timmermans. Physico-chemical constants for pure organic compounds. Elsevier, Amsterdam. 1950.

Mössbauer study of the reduction of α-Fe_2O_3 in hydrogen

DIMITAR G. KLISSURSKI AND IVAN G. MITOV

Institute of General and Inorganic Chemistry, Bulgarian Academy of Sciences, Sofia 1113, Bulgaria

AND

TRIFON TOMOV

Institute for Nuclear Research and Nuclear Energy, Bulgarian Academy of Sciences, Sofia 1113, Bulgaria

Received November 2, 1979

DIMITAR G. KLISSURSKI, IVAN G. MITOV, and TRIFON TOMOV. Can. J. Chem. 58, 1473 (1980).

The kinetics and mechanism of reduction of α-Fe_2O_3 by hydrogen has been studied by a static circulation method in the temperature range 220–350°C. It has been established that the reaction order with respect to the hydrogen pressure is 0.86 ± 0.07 and the activation energy of the process is 17.9 ± 0.7 kcal/mol. The kinetic results and the Mössbauer spectra of specimens reduced to different degrees have shown no accumulation of wüstite phase during the reaction.

DIMITAR G. KLISSURSKI, IVAN G. MITOV et TRIFON TOMOV. Can. J. Chem. 58, 1473 (1980).

On a étudié la cinétique et le mécanisme de la réduction du α-Fe_2O_3 par l'hydrogène par la méthode de circulation statique dans l'intervalle de température 220–350°C. On a établi que l'ordre de la réaction, en fonction de la pression d'hydrogène, est de 0.86 ± 0.07 et que l'énergie d'activation de la réaction est de 17.9 ± 0.7 kcal mol^{-1}. Les résultats cinétiques et les spectres Mössbauer de quelques échantillons réduits à des degrés différents ont montré qu'il n'y a pas d'accumulation de wüstite pendant la réaction.

[Traduit par le journal]

Introduction

The kinetics and mechanism of reduction of α-Fe_2O_3 (hematite) with hydrogen have been the subject of a number of studies (1–9). However, in many cases the effects of internal and external diffusion on the kinetic data have not been eliminated. In addition, there are contradictions in the conclusions on the basic stages of reduction (1, 2, 6–9).

The present paper aimed at studying the reduction of α-Fe_2O_3 at relatively low temperatures using a static-circulation method.

Experimental

The α-Fe_2O_3 used for the kinetic investigations was prepared by thermal decomposition of ferric hydroxide in air at 400°C followed by calcination for 5 h at 800°C. The ferric hydroxide was precipitated at pH 9 from solutions of $Fe(NO_3)_3 \cdot 9H_2O$ and NH_4OH. The specific surface area of the specimen as measured and calculated according to the BET method using low-temperature adsorption of krypton was $0.29\ m^2\ g^{-1}$. The phase identity of the initial α-Fe_2O_3 was confirmed by X-ray phase analysis and Mössbauer spectroscopy. The reduction was carried out with an all-glass static-circulation system (1) which enabled us to make measurements at a constant pressure or at a constant volume of hydrogen. Most of the measurements were carried out at constant pressure of hydrogen during the reduction. In order to establish the conditions under which the results are influenced neither by internal nor by external diffusion, we first studied the effect of the sample grain size and the speed of hydrogen circulation on the rate of reduction. Sample fractions with grain sizes of 0.100–0.125 mm were chosen and used in the kinetic measurements.

Immediately before the measurements the samples were heated for 2 h under vacuum. The water vapour formed during the reduction was frozen by a trap cooled with liquid nitrogen. The amount of hydrogen consumed during the reduction at a constant pressure was measured volumetrically by a mercury-filled gas burette. The rate of reduction R was calculated by graphic differentiation of the kinetic curves. For determination of the reduction rate at different pressures of hydrogen (R^1) the reciprocical time needed for 3% degree of reduction of the samples was also taken.

Results and Discussion

The temperature dependence of the deduction rate is shown in Arrhenius coordinates in Fig. 1. The calculated activation energy of the process was found to be 17.9 ± 0.7 kcal/mol. This value is close to the values obtained by other authors (1, 4). Boreskov (4) and Rostovtsev *et al.* (1) have found the values of 21.0 kcal/mol and 17.7 kcal/mol, respectively.

The dependence of the rate of the reduction process on the hydrogen pressure is shown in Fig. 2. The calculated order of the reduction reaction with respect to the hydrogen pressure was 0.86 ± 0.07. In studies on the initial stage of the reduction of

0008-4042/80/141473-03$01.00/0

©1980 National Research Council of Canada/Conseil national de recherches du Canada

Can. J. Chem. Downloaded from www.nrcresearchpress.com by 210.87.254.40 on 09/05/12
For personal use only.

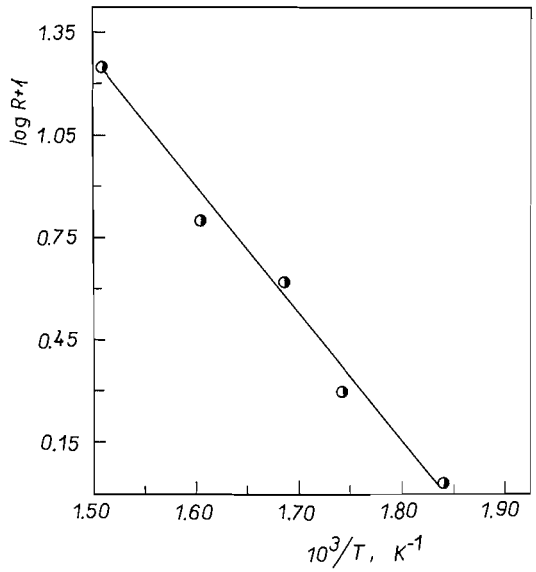


FIG. 1. Temperature dependence of the rate of reduction R, mL H_2/min (NTP); P_{H_2} = 80 Torr; α-Fe_2O_3, 0.200 g.

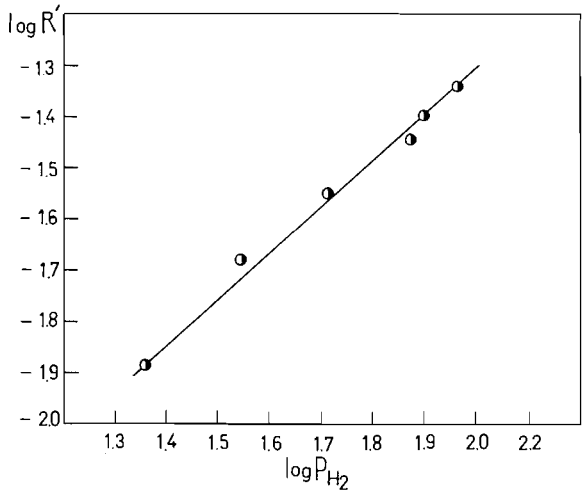


FIG. 2. Dependence of the rate of reduction R^1 on the hydrogen pressure (Torr) ($R^1 = 1/\tau_{0.03}$; where 0.03 is the time for reaching a reduction degree α = 3%); T = 300°C; α-Fe_2O_3, 0.200 g.

α-Fe_2O_3 Boreskov (4) have found a value very close to that established in the present work.

A number of previous studies showed that when α-Fe_2O_3 is reduced to iron, it successively passes into magnetite (Fe_3O_4) and then to wüstite (FeO). As a rule these phase transitions are accompanied by changes in the rate of reduction. The curves of reduction rate vs. reduction degree show characteristic minima at reduction degrees of 11% and 33%, which correspond to the iron/oxygen atomic ratio in magnetite (1:1.33) and wüstite (1:1).

As is evident from Fig. 3, the characteristic minimum for a reduction degree of 11% is clearly expressed under our experimental conditions.

Figure 4 (curve 2) shows the Mössbauer spectrum of an α-Fe_2O_3 sample reduced to 11%. As can be seen, the basic component is magnetite. Traces of α-Fe_2O_3 are also discernible. The spectrum obtained corresponds to non-stoichiometric magnetite ($Fe_{3-v}O_4$). The value of v can be determined from the ratio of the areas of lines A and B (Fig. 4).

According to Topsöe (10):

$$v = \frac{2 - S_B/S_A}{6 + 5(S_B/S_A)}$$

where S_A and S_B are the areas of lines A and B.

For samples of α-Fe_2O_3 reduced to 11% and 33%, v = 0.06 and 0.09, respectively. This enables one to determine the degrees of reduction. The calculated values are 10% and 35%. They are in good agreement with the data for the degrees of reduction calculated on the basis of volumetric measurements.

It is worth noting that at a reduction degree of 33%, there is no pronounced minimum in the curves of reduction rate vs. reduction degree. As was already pointed out, this minimum is associated with the appearance of the wüstite phase. The possibility of wüstite formation with reduction proceeding under our experimental conditions has not been clarified by previous investigations. According to the phase diagram of the iron–oxygen system, wüstite may exist as a stable phase only at temperatures higher than the point of eutectoid transition (570°C). Below this point the wüstite should decompose to magnetite and iron, i.e. the reduction process should take place without formation of wüstite phase. However, as was already pointed out, the available experimental data are very contradictory. Romanov *et al.* (6) have observed the formation of wüstite phase at 520°C whereas Rostovtsev and co-workers (1, 2) described the appearance of wüstite at temperatures of 400°C as well.

Our investigations showed that the Mössbauer spectrum of α-Fe_2O_3 reduced to 33% (Fig. 4, curve 3) corresponded to the spectra of α-Fe and of the magnetite phase (Fe_3O_4) with traces of α-Fe_2O_3. This indicates that under our experimental conditions no accumulation of the wüstite phase is observed, i.e. the reduction of magnetite to α-Fe proceeds without a pronounced phase transition to wüstite.

Some of the contradictory results of previous investigations on the reduction of α-Fe_2O_3 with hydrogen can be connected with the great differ-

Can. J. Chem. Downloaded from www.nrcresearchpress.com by 210.87.254.40 on 09/05/12
For personal use only.

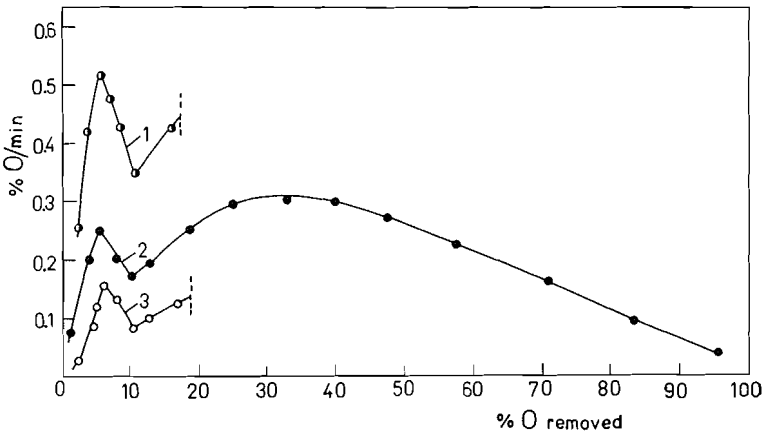


FIG. 3. Dependence of the reduction rate, in % O removed per min, on the degree of reduction, in % O removed.

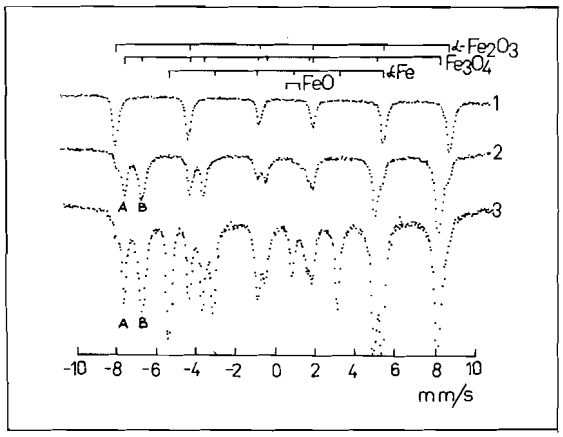


FIG. 4. Mössbauer spectra of: (*1*) α-Fe_2O_3; (*2*) α-Fe_2O_3 reduced to a degree of 11%; (*3*) α-Fe_2O_3 reduced to α = 33%.

ence between the experimental conditions. Our results are in good agreement with the results of the thermodynamic studies of the Fe–O system. This implies that at temperatures below the eutectoid transition point of 570°C, the probability of the formation and accumulation of a wüstite phase during the reduction process would strongly decrease.

1. S. T. ROSTOVTSEV and A-P. EM. Dokl. Akad. Nauk SSSR, **93**, 131 (1953); **93**, 329 (1953).
2. V. G. BEL'CHENKO, V. K. SIMONOV, and S. T. ROSTOVTSEV. Izv. Vuz. Chernaya Metallurgia (Russ), **9**, 9 (1969).
3. S. KH. EGUBAEV, S. A. ROTOZHINA, D. A. KUZNETSOVA, and E. I. ZUBOVA. Zh. Prikl. Khim. **39**, 20 (1966).
4. G. K. BORESKOV. Kinet. Katal. **11**, 374 (1970).
5. U. COLOMBO, F. GAZZARINI, and G. LANZAVECHHIA. Mater. Sci. Eng. **2**, 125 (1967).
6. V. P. ROMANOV, P. A. TATSIENKO, L. F. CHECHERSKAYA, G. P. BASANTSEV, and V. D. CHECHERSKII. Inorg. Mater. USSR, Engl. Transl. **7**, 396 (1971).
7. V. P. ROMANOV, L. F. CHECHERSKAYA, and P. A. TATSIENKO. Phys. Status Solidi, a, **15**, 721 (1973).
8. M. J. GRAHAM, D. A. CHANNING, G. A. SWALLOW, and R. D. JONES. J. Mater. Sci. **10**, 1175 (1975).
9. R. P. WISWANATH and B. WISWANATAN. Trans. Jpn. Inst. Met. **18**, No 3, 149 (1977).
10. H. TOPSÖE. Ph.D. Thesis. Stanford University. 1972.

Can. J. Chem. Downloaded from www.nrcresearchpress.com by 210.87.254.40 on 09/05/12
For personal use only.

Mercury(II) and cadmium(II) halide complexes of tertiary phosphine sulfides and selenides

SAMUEL O. GRIM,[1] EDWARD D. WALTON,[2] AND LARRY C. SATEK

Department of Chemistry, University of Maryland, College Park, MD 20742, U.S.A. and Department of Chemistry, City of London Polytechnic, 31 Jewry Street, London EC3N 2EY, U.K.

Received November 19, 1979

Can. J. Chem. Downloaded from www.nrcresearchpress.com by 210.87.254.42 on 09/05/12
For personal use only.

SAMUEL O. GRIM, EDWARD D. WALTON, and LARRY C. SATEK. Can. J. Chem. **58**, 1476 (1980).

Phosphorus-31 nmr data are reported for tri-*n*-butylphosphine selenide complexes of mercury(II) and cadmium halides and for some miscellaneous complexes of tertiary phosphine sulfides and selenides with the same metal halides. The ligands in the complexes are labile in solution at room temperature but the exchange can be "frozen out" in certain cases at reduced temperature. Selenium-77–phosphorus-31 coupling constants are less in the complexes than in the free ligands and $^1J_{PSe}$ decreases in each observable case with decreasing temperature. Two bond mercury-199–phosphorus-31 coupling is observed in some of the cooled solutions of the complexes.

SAMUEL O. GRIM, EDWARD D. WALTON et LARRY C. SATEK. Can. J. Chem. **58**, 1476 (1980).

On présente les données de la rmn du ^{31}P des complexes du séléniure de tri-*n*-butylphosphine avec les halogénures de mercure(II) et de cadmium ainsi que celles obtenues pour des complexes divers de sulfures de phosphines tertiaires avec les mêmes halogénures métalliques. Les ligands de ces complexes sont labiles en solution, à la température ambiante, mais l'échange peut être bloqué dans certains cas à des températures plus basses. Les constantes de couplage sélénium-77–phosphore-31 sont plus faibles dans les complexes que dans les ligands libres et la valeur de $^1J_{PSe}$ décroît avec la température dans tous les cas où l'on peut faire des observations. Dans les cas de certaines solutions refroidies de complexes on observe le couplage ^{199}Hg–^{31}P à travers deux liaisons.

[Traduit par le journal]

The research activity in phosphine selenide coordination chemistry has not been nearly as exhaustive as that of phosphine oxides and sulfides (1). However, since selenium has an nmr-active isotope (^{77}Se, 7.58%, $I = 1/2$) of reasonable abundance, a new dimension for examining the properties of the phosphorus–selenium bond is available (2, 3), which is important because of the continuing interest in the nature of the phosphorus chalcogen bond (4, 5). We report here the results of an nmr (^{31}P) study on the complexes of some tertiary phosphine selenide and sulfide complexes with mercury(II) and cadmium(II) halides. A preliminary communication of this work has already appeared (6). In spite of the fact that these coordination complexes are very simple addition compounds, many of them have not been previously reported and characterized.

Results and Discussion

Tertiary phosphine selenides are prepared by reaction of a tertiary phosphine with potassium selenocyanate in acetonitrile (7) or perhaps more conveniently by the reaction of red elemental selenium and the tertiary phosphine in refluxing toluene (8). Triphenylphosphine selenide reacts with mercuric halides to produce primarily the 1:1 molar adduct, i.e., $(Ph_3PSe)_2Hg_2X_4$, even when 3:1 (ligand:Hg) reaction ratios are used. These compounds are not very soluble in common organic solvents and thus were not investigated further. However, tri-*n*-butylphosphine selenide reacts with mercury(II) and cadmium halides in a 2:1 molar ratio to produce the six pure compounds, $(n\text{-}Bu_3PSe)_2MX_2$, where M is Hg or Cd, and X is Cl, Br, or I, in good isolated yield. The 2:1 adducts with $n\text{-}Bu_3PSe$ even form preferentially if the ligand:metal ratio is 1:1. In addition, several miscellaneous compounds, including $(n\text{-}BuPh_2PSe)_2Hg_2I_4$, $(n\text{-}Bu_2PhPSe)_2HgCl_2$, $(n\text{-}Bu_2PhPSe)_2HgI_2$, $(n\text{-}Bu_2PhPSe)_2HgBr_2$, $(n\text{-}Bu_2PhPSe)_2CdI_2$, $(Ph_3PSe)_2Hg_2Br_4$, and $(Ph_3PSe)_2Hg_2I_4$ were prepared. Phosphorus-31 nmr data for the soluble phosphine selenide complexes and also two phosphine sulfide complexes, viz., $(n\text{-}Bu_3PS)_2HgCl_2$ and $(n\text{-}Bu_3PS)_2HgBr_2$, are given in Table 1. The observations from these data are: (*a*) at room temperature, the phosphine sulfide and phosphine selenide ligands in solutions of L_2HgX_2 and L_2CdX_2 are labile, i.e., they exchange rapidly on the nmr time scale. This is demonstrated by the results shown in Fig. 1. For $(n\text{-}Bu_3PSe)_2HgI_2$ in concentrated CH_2Cl_2 solution at room temperature, J_{PSe} is 584 Hz and δ_P is 42.7 ppm. The free

[1]Sir John Cass's Foundation Senior Research Fellow, 1979–1980. To whom all correspondence should be addressed at the University of Maryland.

[2]Graduate Research Fellow, National Organization for the Professional Advancement of Black Chemists and Chemical Engineers, 1976–1977.

0008-4042/80/141476-04$01.00/0

©1980 National Research Council of Canada/Conseil national de recherches du Canada

Can. J. Chem. Downloaded from www.nrcresearchpress.com by 210.87.254.42 on 09/05/12
For personal use only.

TABLE 1. Phosphorus-31 nmr data for L_2MX_2, where L is a tertiary phosphine sulfide or selenide, M is Hg or Cd, and X is Cl, Br, or I[a]

Compound	T(°C)	δ_P (ppm)	$^1J_{PSe}$ (Hz)	$^2J_{PM}$
$(n\text{-}Bu_3PSe)_2HgCl_2$	33	45.1	551	—
	−12	45.4	539	—
	−45	45.5	535	—
	−55	—[b]	526	157
	−65	—	525	157
	−96	—	524	159
$(n\text{-}Bu_3PSe)_2HgBr_2$	33	44.3	560	—
	0	44.8	554	—
	−29	45.0	546	—
	−57	—[b]	539	—
	−68	—	538	122
	−75	—	536	132
	−87	—	535	141
$(n\text{-}Bu_3PSe)_2HgI_2$	33	42.9	583	—
	−97	—[b]	554±5	—
$(n\text{-}Bu_3PSe)_2CdCl_2$	33	42.5	564	—
	−59	—[b]	544	—
	−85	—	530	—
$(n\text{-}Bu_3PSe)_2CdBr_2$	33	42.3	569	—
	−62	—[b]	543	—
	−72	—	542	40
$(n\text{-}Bu_3PSe)_2CdI_2$	33	41.8	572	—
	−72	—[b]	548	—
$(n\text{-}Bu_2PhPSe)_2HgCl_2$	33	43.5	555	—
$(n\text{-}Bu_2PhPSe)_2HgBr_2$	33	42.5	575	—
	−29	43.2	563	—
$(n\text{-}Bu_2PhPSe)_2HgI_2$	33	40.0	613	—
$(n\text{-}Bu_2PhPSe)_2CdI_2$	33	40.8	591	—
	0	41.2	588	—
	−30	41.5	577	—
	−57	—[b]	574	—
	−68	—	567	—
	−75	—	565	—
$(Ph_3PSe)_2CdBr_2$	33	34.6	696	—
$(BuPh_2PSe)_2Hg_2I_4$	33	37.4	586	—
$(n\text{-}Bu_3PS)_2HgCl_2$	33	57.3	—	—
	−57	—	—	—
	−68	—	—	116
	−75	—	—	122
	−88	—	—	125
$(n\text{-}Bu_3PS)_2HgBr_2$	33	56.3	—	—
	−75	—	—	—
	−87	—	—	~103±8

[a]Temperatures are accurate to ±3°; δ_P's to ±0.01 ppm; J's to ±2 Hz unless otherwise indicated.
[b]The reference (85% H_3PO_4) freezes so that accurate δ's are not recorded.

ligand values are 693 Hz and 37.0 ppm, respectively. As excess n-Bu_3PSe is added to the solution of complex only one phosphorus resonance (with ^{77}Se satellites) is observed, but J_{PSe} increases and δ_P decreases to reflect the weighted average of the complexed and free ligand values in the equilibrium:

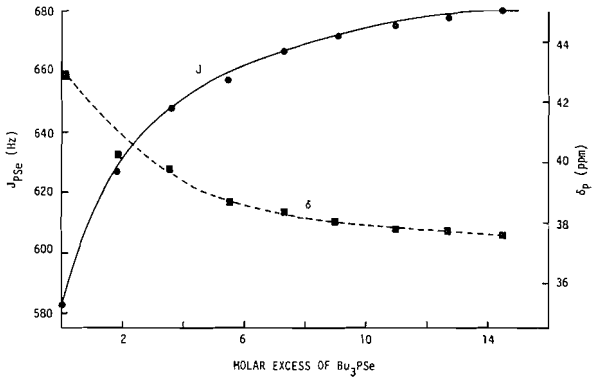


FIG. 1. The variation of $^1J_{PSe}$ (●, left ordinate, solid line) and δ_P (■, right ordinate, dashed line) with the excess moles of ligand in a solution of $(n\text{-}Bu_3PSe)_2HgI_2$.

[1] $n\text{-}Bu_3PSe^* + (n\text{-}Bu_3PSe)_2HgI_2 \rightleftarrows (n\text{-}Bu_3PSe)(n\text{-}Bu_3PSe^*)HgI_2 + n\text{-}Bu_3PSe$

Previous studies which have noted the lability of ligands by ^{31}P nmr measurements include phosphine complexes of cadmium (9) and mercury(II) (10–14) and phosphine oxide complexes of zinc, cadmium, and mercury(II) salts (15). (*b*) J_{PSe} decreases upon complexation, and the magnitude of the decrease is greatest for the most acidic of the mercury Lewis acids, i.e., $HgCl_2$ (ΔJ = 142 Hz) > $HgBr_2$ (ΔJ = 133 Hz) > HgI_2 (ΔJ = 110 Hz). The trend is the same for the CdX_2 compounds, but the differences among the compounds is not as great as for the mercury compounds. (*c*) The ligand exchange rate decreases with decreasing temperature, so that some of the complexes become "frozen out" on the nmr time scale. This is demonstrated by the appearance of two separate ^{31}P resonances (one due to ligand and one due to complex) when excess n-Bu_3PSe is added to a solution of $(n\text{-}Bu_3PSe)_2HgBr_2$ in CH_2Cl_2–$CDCl_3$ at −89°C. In the mercury series, the HgI_2 complexes are most labile and the $HgCl_2$ the least, as indicated by the temperature at which the exchange is slow on the nmr time scale. The $(n\text{-}Bu_3PSe)_2HgCl_2$ exchange is frozen out at about −50°C, the $HgBr_2$ complex at about −70°C, and the experimental conditions were not reached to stop the ligand exchange in the HgI_2 complex. In the cadmium series, crystallization of the complexes at reduced temperature hampered similar experiments but the $(n\text{-}Bu_3PSe)_2CdBr_2$ exchange was "stopped" at about −70°C also. By comparison, the corresponding phosphine sulfide complexes, i.e., $(n\text{-}Bu_3PS)_2HgCl_2$ and $(n\text{-}Bu_3PS)_2HgBr_2$ became inert at about −65°C and −87°C, respectively, roughly 15° lower in temper-

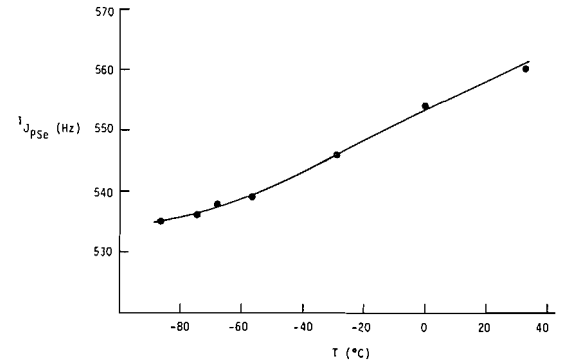


FIG. 2. The variation of $^1J_{PSe}$ with temperature in a solution of $(n\text{-}Bu_3PSe)_2HgBr_2$.

ature than the selenide analogues. (*d*) As the temperature is decreased, J_{PSe} decreases also. The rate of change of J_{PSe} is shown graphically for $(n\text{-}Bu_3PSe)_2HgBr_2$ in Fig. 2. It can be seen that J_{PSe} approaches a minimum value, which is presumably that of the non-exchanging complex. Possible rationalization for the decrease of J_{PSe} with decreasing temperature include: a decrease in the equilibrium constant, $K_{[2]}$, of a dissociation equilibrium such as represented in eq. [2]

[2] $(n\text{-}Bu_3PSe)_2HgBr_2 \rightleftarrows (n\text{-}Bu_3PSe)HgBr_2 + n\text{-}Bu_3PSe$

a weakening of the P—Se bond due to the strengthening of the Hg—Se bond; and hybridization changes at Se which would change the *s*-character of the P—Se bond. A dilution study (from 0.4 *M* to 0.04 *M* in five steps) of $(n\text{-}Bu_3PSe)_2HgBr_2$ in CH_2Cl_2 at ambient temperature resulted in an approximate increase in J_{PSe} of only about 2 Hz over this ten-fold concentration range. Although it is difficult to predict what J_{PSe} would be in the tricoordinated species of eq. [2], if it is assumed to be approximately the same as in the tetracoordinated species, then a change in J_{PSe} of the experimentally observed magnitude upon a ten-fold dilution would result only if $K_{[2]} < 10^{-4}$. If $K_{[2]}$ is this small (4.9% dissociation for the 0.04 *M* case and 1.6% dissociation for the 0.4 *M* case), a further decrease of $K_{[2]}$ at reduced temperature would not produce the observed changes in the magnitude of J_{PSe} upon cooling. Therefore, the correct explanation for the decrease of J_{PSe} in $(n\text{-}Bu_3PSe)_2HgBr_2$ with decreasing temperature is not clear from these data. (*e*) At low temperatures, two bond mercury-199–phosphorus-31 coupling is observed in the complexes $(n\text{-}Bu_3PSe)_2HgCl_2$, $(n\text{-}Bu_3PSe)_2HgBr_2$, $(n\text{-}Bu_3PS)_2HgCl_2$, and $(n\text{-}Bu_3PS)_2HgBr_2$. The values are, respectively, 157 Hz, 141 Hz, 115 Hz, and 103 Hz, i.e., coupling through selenium is greater than through sulphur. Weak satellites appear in the spectrum of $(n\text{-}Bu_3PS)_2CdBr_2$ at −70°C which we believe are due to two bond coupling of cadmium-111 and cadmium-113 to phosphorus, with $^2J_{CdP}$ equal to 40 Hz. This value and corresponding $^2J_{HgP}$ value give a reduced coupling constant (16) ratio $^2K_{CdP}/^2K_{HgP}$ of 0.27 which is close to the range expected (0.28–0.36) for analogous compounds of mercury and cadmium (9).

The J_{PSe} values in the free ligands, $n\text{-}Bu_3PSe$, $n\text{-}Bu_2PhPSe$, $n\text{-}BuPh_2PSe$, and Ph_3PSe vary in the manner (693, 715, 730, and 740 Hz, respectively) expected based on the electron drawing ability of the organic substituents. This was also the same order reported earlier (3) for the $Et_nPh_{3-n}PSe$ compounds.

In summary, we have shown that a study of phosphorus–selenium coupling constants in complexes of phosphine selenide ligands adds an interesting new dimension to the investigation of phosphorus chalcogen bonds.

Experimental

Phosphorus-31 nmr spectra were obtained with a Varian XL-100 Fourier Transform spectrometer equipped with a Nicolet Multi-Observe Nuclei Accessory (MONA) unit operating at 40.5 MHz using broad band proton decoupling. Samples were contained in spinning 10 mm tubes with a mixture of CH_2Cl_2:$CDCl_3$ (1:1 or 2:1) as the solvent system with a 1 mm capillary tube containing 85% H_3PO_4 as reference concentrically inserted in the sample tube. Deuterium in the solvent provided the frequency lock. Temperatures were determined by inserting a pentane thermometer directly into the solutions before and after each measurement.

Microanalyses were performed by Dr. F. Kasler of the University of Maryland.

$n\text{-}Bu_3P$ (Aldrich) and Ph_3P (M and T Chemicals) were used as supplied commercially. $n\text{-}Bu_2PhP$ and $n\text{-}BuPh_2P$ were prepared by *n*-butyl Grignard reaction with $PhPCl_2$(Aldrich) and Ph_2PCl (Aldrich), respectively (17). Tertiary phosphine sulfides were prepared by direct reaction of S with the phosphine in refluxing toluene. Tertiary phosphine selenides were prepared from the phosphine and KSeCN in CH_3CN (7) or by direct reaction of elemental red Se with the phosphine in refluxing toluene (8). ^{31}P nmr data are: Ph_3PSe, δ 36.9 ppm, J_{PSe} 740 Hz (lit. (3) δ36.1, J_{PSe} 738); $n\text{-}BuPh_2PSe$, δ 34.6, J_{PSe} 730; $n\text{-}Bu_2PhPSe$, δ 37.6, J_{PSe} 715; $n\text{-}Bu_3PSe$, δ 37.0, J_{PSe} 693.

(n-Bu$_3$PS)$_2$HgCl$_2$. Mercuric chloride (1.36 g, 5 mmol) in 50 mL of EtOH was added to 2.34 g (10 mmol) of Bu_3PS in 50 mL of EtOH. The volume was reduced to 25 mL by rotary evaporation and the solution was cooled, whereupon 3.1 g (83%) of crystals were formed. The product, mp 79–81°C, was recrystallized from EtOH. *Anal.* calcd. for $C_{24}H_{54}Cl_2HgP_2S_2$: C 38.94, H 7.35; found: C 39.07, H 7.55.

(n-Bu$_3$PS)$_2$HgBr$_2$ was prepared in a similar manner and was recrystallized from CH_2Cl_2/EtOH. The product, mp 75–76°C, was produced in 63% yield. *Anal.* calcd. for $C_{24}H_{54}Br_2HgP_2S_2$: C 34.77, H 6.56; found: C 34.67, H 6.82.

(n-Bu$_3$PSe)$_2$HgI$_2$. To a solution of HgI_2 (1.74 g, 3.8 mmol) in 300 mL of EtOH was added 2.20 g (7.8 mmol) of $n\text{-}Bu_3PSe$ in 10 mL of EtOH. The solution was concentrated by evaporation at room temperature by a stream of N_2 until crystals, mp 68.5–70°C, 3.1 g (80%) formed. *Anal.* calcd. for $C_{24}H_{54}HgI_2P_2Se_2$: C 28.35, H 5.35; found: C 28.21, H 5.57.

Can. J. Chem. Downloaded from www.nrcresearchpress.com by 210.87.254.42 on 09/05/12
For personal use only.

Can. J. Chem. Downloaded from www.nrcresearchpress.com by 210.87.254.42 on 09/05/12
For personal use only.

Similarly prepared were (n-$Bu_3PSe)_2HgBr_2$, mp 84–85°C, 80%. *Anal.* calcd. for $C_{24}H_{54}Br_2HgP_2Se_2$: C 31.23, H 5.90; found: C 31.13, H 5.65, (n-$Bu_3PSe)_2HgCl_2$, mp 91–92°C, 87%. *Anal.* calcd. for $C_{24}H_{54}Cl_2HgP_2Se_2$: C 34.56, H 6.53; found: C 34.82, H 6.78. (n-$Bu_3PSe)_2CdCl_2$, mp 76–77°C, 74%. *Anal.* calcd. for $C_{24}H_{54}CdCl_2P_2Se_2$: C 38.65, H 7.30; found: C 38.42, H 7.30. (n-$Bu_3PSe)_2CdBr_2$, mp 68–69°C, 70%. *Anal.* calcd. for $C_{24}H_{54}Br_2CdP_2Se_2$: C 34.53, H 6.52; found: C 34.50, H 6.80. (n-$Bu_3PSe)_2CdI_2$, mp 68–69°C, 79%. *Anal.* calcd. for $C_{24}H_{54}CdI_2P_2Se_2$: C 31.04, H 5.86; found: C 31.01, H 6.05. (n-$Bu_2PhPSe)_2HgI_2$, mp 98–100°C, 88%. *Anal.* calcd. for $C_{28}H_{46}HgI_2P_2Se_2$: C 31.82, H 4.39; found: C 31.83, H 4.74. (n-$BuPh_2PSe)_2Hg_2I_4$, mp 97–99°C, was prepared in a similar manner but with 1:1 (ligand:mercury) stoichiometry, in 90% yield. *Anal.* calcd. for $C_{32}H_{38}Hg_2I_4P_2Se_2$: C 24.78, H 2.47; found: C 25.07, H 2.77. ($Ph_3PSe)_2Hg_2I_4$ was prepared in a similar manner. *Anal.* calcd. for $C_{36}H_{30}Hg_2I_4P_2Se_2$: C 27.17, H 1.90; found: C 27.11, H 1.73. ($Ph_3PSe)_2Hg_2Br_4$ was prepared similarly. *Anal.* calcd. for $C_{36}H_{30}Br_4Hg_2P_2Se_2$: C 30.81, H 2.15; found: C 30.83, H 2.21.

(n-$Bu_3PSe)_2HgI_2$ *with excess* n-Bu_3PSe. To a solution of 1.0 g (0.99 mmol) of (n-$Bu_3PSe)_2HgI_2$ in 3 mL of CH_2Cl_2 were added 0.5 g (1.81 mmol) aliquots of n-Bu_3PSe. The ^{31}P nmr spectrum was recorded after each aliquot of excess ligand was added. The data given are: the aliquot number, total g of excess ligand, total mmol of excess ligand, J_{PSe}, and δ_P, 0, 0, 0, 584, 42.7; 1, 0.5, 1.8, 627, 40.2; 2, 1.0, 3.6, 649, 39.9; 3, 1.5, 5.4, 658, 38.7; 4, 2.0, 7.2, 666, 38.4; 5, 2.5, 9.1, 671, 38.1; 6, 3.0, 10.9, 675, 37.9; and 6, 3.5, 12.7, 678, 37.8. These data are plotted in Fig. 1.

Acknowledgements

We are grateful to the National Science Foundation for support of this work (Grant No. CHE78-09536) and for funds for the purchase of nmr equipment (Grant No. GP43155). We also wish to thank Dr. Ian J. Colquhoun and Dr. William McFarlane, City of London Polytechnic, for carrying out the nmr dilution experiment on (n-$Bu_3PSe)_2HgBr_2$ and for helpful discussions.

1. N. M. KARAYANNIS, C. M. MIKULSKI, and L. L. PYTLEWSKI. Inorg. Chim. Acta Rev. **5**, 69 (1977).
2. W. MCFARLANE and D. S. RYCROFT. J. Chem. Soc. Dalton Trans. 2162 (1973).
3. W. J. STEC, A. OKRUSZEK, B. UZNANSKI, and J. MICHALSKI. Phosphorus, **2**, 97 (1972).
4. J. A. MILLER. *In* Organophosphorus chemistry. Vol. 7. The Chemical Society, London. 1976. Chapt. 4.
5. R. R. CARLSON and D. W. MEEK. Inorg. Chem. **13**, 1741 (1974).
6. S. O. GRIM, E. D. WALTON, and L. C. SATEK. Inorg. Chim. Acta, **27**, L115 (1978).
7. P. NICPON and D. W. MEEK. Inorg. Synth. **10**, 157 (1967).
8. L. MAIER. *In* Organic phosphorus compounds. Vol. 4. *Edited by* G. M. Kosolapoff and L. Maier. Wiley-Interscience, New York. 1972. Chapt. 7.
9. B. E. MANN. Inorg. Nucl. Chem. Lett. 7, 595 (1971).
10. R. G. GOEL, W. P. HENRY, and W. O. OGINI. Can. J. Chem. **57**, 762 (1979).
11. E. C. ALYEA, S. A. DIAS, R. G. GOEL, W. O. OGINI, P. PILON, and D. W. MEEK. Inorg. Chem. **17**, 1697 (1978).
12. T. ALLMAN, R. G. GOEL, and P. PILON. Can. J. Chem. **57**, 91 (1979).
13. S. O. GRIM and D. P. SHAH. Inorg. Nucl. Chem. Lett. **14**, 105 (1978).
14. S. O. GRIM, D. P. SHAH, C. K. HAAS, J. M. RESSNER, and P. H. SMITH. Inorg. Chim. Acta, **36**, 139 (1979).
15. S. O. GRIM and L. C. SATEK. J. Coord. Chem. **6**, 39 (1976).
16. W. MCFARLANE. Q. Rev. **23**, 187 (1969).
17. L. MAIER. *In* Organic phosphorus compounds. Vol. 1. *Edited by* G. M. Kosolapoff and L. Maier. Wiley-Interscience, New York. 1972. Chapt. 1.

Influence de la température sur les constantes B.E.T. de dissolution de l'eau dans un mélange fondu [$AgNO_3$ + $TlNO_3$]

MARIE-CHRISTINE ABRAHAM ET MAURICE ABRAHAM[1]

Département de Chimie, Université de Montréal, C.P. 6210, Succursale A, Montréal (Qué.), Canada H3C 3V1

ET

JAMES SANGSTER

Département de Génie Chimique, Ecole Polytechnique, C.P. 6079, Succursale A, Montréal (Qué.), Canada H3C 3A7

Reçu le 20 février 1980

MARIE-CHRISTINE ABRAHAM, MAURICE ABRAHAM et JAMES SANGSTER. Can. J. Chem. **58**, 1480 (1980).

Nous avons étudié l'influence de la température sur les constantes B.E.T. de dissolution de l'eau dans un mélange fondu [$AgNO_3$ + $TlNO_3$], contenant $AgNO_3$ à la fraction molaire 0.515, dans l'intervalle de température 85–110°C, pour des fractions molaires d'eau comprises entre 0 et 0.5 environ. Ces constantes B.E.T. sont: r: rapport molaire des sites d'adsorption aux sels; ΔE: différence entre l'énergie molaire d'adsorption de l'eau sur un site disponible dans les sels fondus et l'énergie molaire de condensation de l'eau.

Nous avons observé, dans ce travail, que l'influence de la température peut se résumer dans les énoncés des deux propriétés suivantes: (*1*) r est une fonction linéaire croissante de la température; (*2*) le produit $r\Delta E$ est sensiblement indépendant de la température.

MARIE-CHRISTINE ABRAHAM, MAURICE ABRAHAM, and JAMES SANGSTER. Can. J. Chem. **58**, 1480 (1980).

The temperature dependence of the B.E.T. constants for water dissolved in the melt (0.515 $AgNO_3$ + 0.485 $TlNO_3$) has been studied in the range 85–110°C at water mole fractions between 0 and 0.5. The B.E.T. constants are: r: the mole ratio of adsorption sites to salt; ΔE: the difference between the molar energy of adsorption of water on an available site in the melt and the molar energy of liquefaction of water.

It was found in this work that (*1*) r increases linearly with temperature and (*2*) the product $r\Delta E$ is perceptibly independent of temperature.

Introduction

Au cours de travaux récents (1–5) nous avons mesuré les pressions de vapeur d'eau de quelques mélanges eau–nitrates fondus pouvant contenir de l'eau à toute concentration à des températures relativement basses, au voisinage de 100°C et à des pressions inférieures à celle de l'atmosphère. Nous avons alors trouvé que la théorie B.E.T. adaptée aux solutions d'électrolytes forts (6, 7) permet de prévoir l'existence de certaines propriétés des solutions d'eau dans les sels fondus. Par exemple, nous avons montré que les constantes B.E.T. de dissolution de l'eau suivent des règles d'additivité quand on fait varier la concentration d'un des constituants des mélanges de nitrates fondus, dans certaines limites, suivant les cas. Après avoir ainsi étudié en particulier l'influence du facteur concentration, nous poursuivons en examinant l'influence de la température sur les constantes B.E.T. de dissolution de l'eau relative à un mélange ($AgNO_3$ + $TlNO_3$) de composition eutectique.

Résultats expérimentaux

La méthode de mesure des pressions de vapeur et la détermination des activités ont été décrits dans un travail précédent (1). La fraction molaire de $AgNO_3$ dans le mélange de sels fondus anhydres a été fixée à 0.515. Les mesures ont été faites à 87, 93 et 105°C. A ces températures, le deuxième coefficient du viriel pour la vapeur d'eau a respectivement pour valeurs: −525, −492 et −435 cm^3/mol. Les valeurs correspondantes de la fugacité sont: 463.62, 581.31 et 891.1 Torr. Le même système ayant été étudié auparavant à 98.5 et 111°C (2, 3), les données expérimentales ainsi réunies ont permis de tirer des conclusions quant à l'influence de la température sur la pression de vapeur d'eau et des paramètres thermodynamiques utiles qui lui sont reliés. Les valeurs mesurées de la pression p ainsi que les valeurs correspondantes de la fugacité f, de l'activité a et du coefficient d'activité γ sont disponibles ailleurs.[2]

Discussion

Les isothermes et les constantes B.E.T.

L'équation B.E.T. adaptée aux solutions d'électrolytes (7) s'écrit

$$[1] \quad \frac{a_e(1 - x_e)}{x_e(1 - a_e)} = \frac{1}{cr} + \frac{c - 1}{cr} a_e$$

où a_e *et* x_e = activité et fraction molaire de l'eau; r = rapport molaire des sites d'adsorption aux sels; c est donnée approximativement par l'expression

$$[2] \quad c = \exp(-\Delta E/RT)$$

avec $\Delta E = E - E_L$.

[1]Personne à qui adresser la correspondance.

[2]On peut obtenir les données mises en dépôt, à un prix nominal, en s'adressant au Dépôt de données non publiées, ICIST, Conseil national de recherches du Canada, Ottawa (Ont.), Canada K1A 0S2.

0008-4042/80/141480-04$01.00/0

©1980 National Research Council of Canada/Conseil national de recherches du Canada

Can. J. Chem. Downloaded from www.nrcresearchpress.com by 210.87.254.40 on 09/05/12
For personal use only.

Can. J. Chem. Downloaded from www.nrcresearchpress.com by 210.87.254.40 on 09/05/12
For personal use only.

Dans [2], E et E_L ont les significations suivantes: E = énergie molaire d'adsorption de l'eau sur un site disponible dans le sel fondu; E_L = énergie molaire de condensation de l'eau.

A l'aide des valeurs de x_e et a_e la fonction

$$f(a_e) = \frac{a_e(1 - x_e)}{x_e(1 - a_e)}$$

est représentée graphiquement. Les droites isothermes de la fig. 1 sont ainsi obtenues, dans l'intervalle $0 < a_e < 0.7$, par la méthode des moindres carrés, avec un coefficient de corrélation supérieur à 0.999. En appliquant les éqs [1] et [2], l'ordonnée à l'origine et la pente des isothermes donnent les valeurs des constantes c, r et ΔE groupées dans le tableau 1, qui contient également celles obtenues antérieurement (2, 3). L'examen de ce tableau montre qu'une élévation de température augmente r et diminue c ainsi que $-\Delta E$. La dernière colonne du tableau montre que r augmente et $-\Delta E$ diminue de manière à fixer le produit $-r\Delta E$ pratiquement indépendant de la température, dans l'intervalle étudié. D'où la relation:

[3] $r\Delta E \cong -0.155$ kcal mol^{-1}

Sur la fig. 2 sont représentés r et $-r\Delta E$ en fonction de la température. r apparaît comme droite. Son équation, en utilisant les températures en Kelvin, est:

[4] $r = 2.38 \times 10^{-3}T - 0.401$

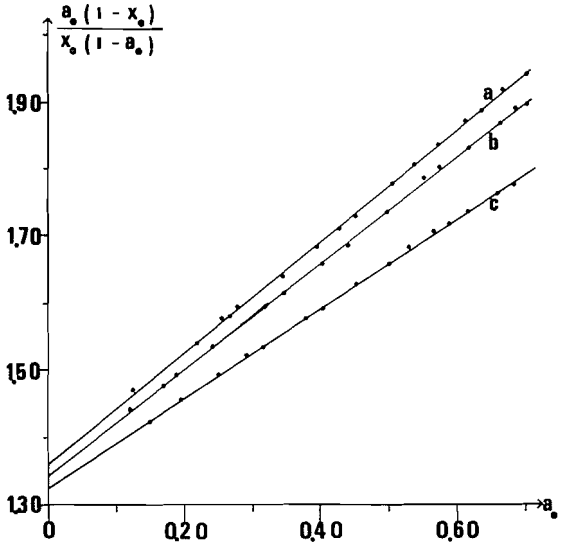


FIG. 1. Les isothermes B.E.T. de dissolution de l'eau dans le mélange de sels fondus [$AgNO_3$ + $TlNO_3$] contenant $AgNO_3$ à la fraction molaire 0.515, à 87.0°C (*a*), 93.0°C (*b*) et 105.0°C (*c*).

TABLEAU 1. Les constantes B.E.T. pour le système [$AgNO_3$ + $TlNO_3$ + H_2O] à cinq températures. Fraction molaire de $AgNO_3$ dans le mélange de sels fondus: 0.515

θ (°C)	r	c	$-\Delta E$ (kcal/mol d'eau)	$-r\Delta E$ (kcal/mol de sel)
87.0[a]	0.456	1.61	0.342	0.156
93.0[a]	0.469	1.59	0.335	0.157
98.5[b]	0.486	1.54	0.317	0.154
105.0[a]	0.502	1.50	0.307	0.154
111.0[c]	0.511	1.49	0.305	0.156

[a]Cette étude.
[b]Référence 2.
[c]Référence 3.

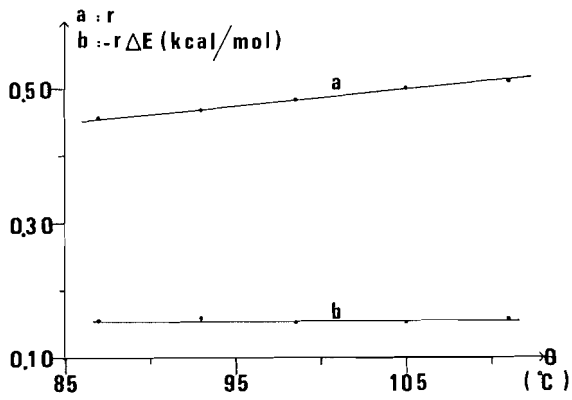


FIG. 2. Les expressions B.E.T. "r" et "$r\Delta E$" en fonction de la température, relatives aux solutions d'eau dans le mélange de sels fondus [$AgNO_3$ + $TlNO_3$] contenant $AgNO_3$ à la fraction molaire 0.515.

Les grandeurs molaires d'excès de l'eau à dilution infinie dans les sels fondus

Ces paramètres peuvent être calculés par les relations suivantes:

[5] $\Delta\mu_e^\infty = RT \ln \gamma^\infty$

[6] $\Delta s_e^\infty = -\frac{\partial}{\partial T}(RT \ln \gamma^\infty)$

[7] $\Delta h^\infty = \Delta\mu_e^\infty + T\Delta s_e^\infty$

γ^∞, $\Delta\mu_e^\infty$, Δs_e^∞ et Δh^∞ coefficient d'activité, enthalpie libre molaire d'excès, entropie molaire d'excès et enthalpie de transfert de l'eau à dilution infinie dans les sels fondus.

γ^∞ s'exprime en fonction des constantes B.E.T. (8) par:

[8] $\gamma^\infty = 1/cr$

Les relations [5]–[8] et [2] donnent:

[9] $\Delta\mu_e^\infty = \Delta E - RT \ln r$

[10] $\Delta s_e^\infty = \frac{RT}{r}\frac{\partial r}{\partial T} + R \ln r - \frac{\partial \Delta E}{\partial T}$

Can. J. Chem. Downloaded from www.nrcresearchpress.com by 210.87.254.40 on 09/05/12
For personal use only.

$$[11] \quad \Delta h^{\infty} = \Delta E - T\frac{\partial \Delta E}{\partial T} + \frac{RT^2}{r}\frac{\partial r}{\partial T}$$

Le tableau 2 donne les valeurs de $\Delta\mu_e^{\infty}$, Δs_e^{∞} et Δh^{∞} calculées par les relations [3], [4], [9], [10] et [11].

La constante rigoureuse de la loi de Henry

Cette constante K_H^{∞} s'exprime en fonction du coefficient d'activité de l'eau à dilution infinie dans les sels fondus γ^{∞}, et de la fugacité de l'eau pure f_0 par la relation suivante:

$$[12] \quad K_H^{\infty} = \gamma^{\infty} f_0$$

Les valeurs de γ^{∞}, f_0 et K_H^{∞} aux températures étudiées sont données dans le tableau 3. La température influence dans le même sens f_0 et K_H^{∞}. Elle influence en sens contraire γ^{∞} et K_H^{∞}. Le sens de variation de f_0 avec la température impose celui de K_H^{∞}. Ceci provient de la petitesse relative de l'enthalpie de transfert de l'eau de la phase eau pure à la phase sels fondus contenant une quantité infiniment petite d'eau. En effet, la relation [12] donne:

$$[13] \quad \frac{\partial \ln K_H^{\infty}}{\partial(1/T)} = \frac{\partial \ln \gamma^{\infty}}{\partial(1/T)} + \frac{\partial \ln f_0}{\partial(1/T)}$$

Or, on a les relations ci-dessous [14]–[16]

$$[14] \quad \frac{\partial \ln \gamma^{\infty}}{\partial(1/T)} = \frac{\Delta h^{\infty}}{R}$$

TABLEAU 2. Grandeurs molaires d'excès de l'eau à dilution infinie dans le mélange fondu [$AgNO_3$ + $TlNO_3$] en fonction de la température. Fraction molaire de $AgNO_3$ dans le mélange fondu: 0.515

θ (°C)	$\Delta\mu_e^{\infty}$ (kcal/mol)	Δh^{∞} (kcal/mol)	Δs_e^{∞} (u.e.)
87.0	0.22	0.36	0.4
93.0	0.23	0.41	0.5
98.5	0.22	0.44	0.6
105.0	0.21	0.48	0.7
111.0	0.21	0.52	0.8

TABLEAU 3. Influence de la température sur la constante de la loi de Henry K_H^{∞} de dissolution de la vapeur d'eau dans le mélange de sels fondus [$AgNO_3$ + $TlNO_3$] contenant $AgNO_3$ à la fraction molaire 0.515

θ (°C)	f_0 (atm)	$\gamma^{\infty}(=1/cr)$	K_H^{∞} (atm)
87.0[a]	0.610	1.36	0.83
93.0[a]	0.765	1.34	1.02
98.5[b]	0.934	1.34	1.25
105.0[a]	1.172	1.33	1.55
111.0[c]	1.434	1.31	1.88

[a]Cette étude.
[b]Référence 2.
[c]Référence 3.

$$[15] \quad \frac{\partial \ln f_0}{\partial(1/T)} = \frac{-\Delta H_v^0}{R}$$

où ΔH_v^0 est l'enthalpie molaire de vaporisation de l'eau pure.

$$[16] \quad \Delta H_v^{\infty} = \Delta H_v^0 - \Delta h^{\infty}$$

où ΔH_v^{∞} est l'enthalpie molaire de vaporisation de l'eau à dilution infinie dans les sels fondus. Des relations [13]–[16], on obtient la relation [17].

$$[17] \quad \frac{\partial \ln K_H^{\infty}}{\partial(1/T)} = -\frac{\Delta H_v^{\infty}}{R}$$

La pente de la droite $\ln K_H^{\infty} = f(1/T)$ représentée à la fig. 3 est imposée par la valeur moyenne de ΔH_v^{∞} qui est 9.4 kcal/mol. Elle est proche de la valeur moyenne de ΔH_v^0 dans le même intervalle de température: 9.8 kcal/mol.

Le coefficient d'activité de l'eau

La fig. 4 ne reproduit les résultats que pour les deux températures extrêmes étudiées afin d'en faciliter l'examen. Essentiellement on constate que la courbe représentative de la fonction $\gamma_e = f(a_e)$ passe par un maximum. L'élévation de température abaisse la courbe en l'aplatissant. Le tableau 4 donne

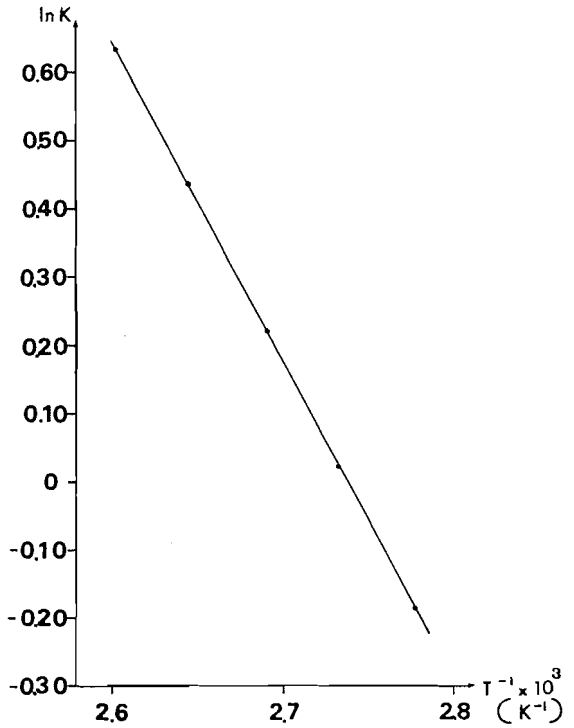


FIG. 3. Influence de la température sur la constante de la loi de Henry de dissolution de l'eau dans le mélange de sels fondus [$AgNO_3$ + $TlNO_3$] contenant $AgNO_3$ à la fraction molaire 0.515.

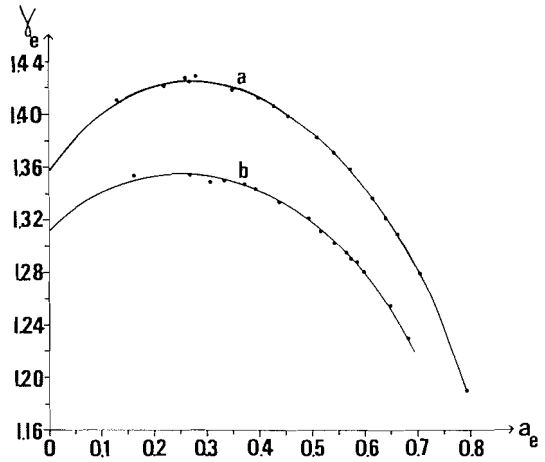


FIG. 4. Le coefficient d'activité de l'eau en fonction de son activité dans le système [$AgNO_3$ + $TlNO_3$ + H_2O] pour une fraction molaire 0.515 de $AgNO_3$ dans le mélange fondu [$AgNO_3$ + $TlNO_3$] à 87.0°C (*a*) et 111.0°C (*b*).

le maximum γ_m et l'activité correspondante a_m, en fonction de la température, calculés par les formules [18] et [19] établies précédemment (9)

$$[18] \quad \gamma_m = \frac{(c - 2 + cr)^2}{4cr(c - 1)} + \frac{1}{cr}$$

$$[19] \quad a_m = \frac{c - 2 + cr}{2(c - 1)}$$

On voit que a_m est comprise dans l'intervalle de validité de l'éq. [1] et que γ_m diminue quand la température augmente. On a aussi (3) la relation [20].

$$[20] \quad \frac{d^2\gamma_e}{da_e^2} = -\frac{2(c - 1)}{cr}$$

TABLEAU 4. Le coefficient d'activité maximum de l'eau γ_m, l'activité correspondante a_m et la dérivée seconde $d^2\gamma/da^2$ en fonction de la température. Solutions d'eau dans le mélange de sels fondus [$AgNO_3$ + $TlNO_3$] contenant $AgNO_3$ à la fraction molaire 0.515

θ (°C)	γ_m	a_m	$-d^2\gamma/da^2$
87.0	1.43	0.28	1.66
93.0	1.41	0.28	1.58
98.5	1.39	0.27	1.44
105.0	1.37	0.25	1.33
111.0	1.36	0.26	1.29

Or, comme l'indique le tableau 4, la valeur absolue de $d^2\gamma_e/da_e^2$ diminue en restant plus grande que un, quand la température augmente.

Les relations [18]–[20] issues du modèle B.E.T. expliquent bien les caractéristiques principales des courbes $\gamma_e = f(a_e)$ à l'aide de deux paramètres expérimentaux dont les définitions sont simples.

1. M. C. TRUDELLE, M. ABRAHAM et J. SANGSTER. Can. J. Chem. **55**, 1713 (1977).
2. J. SANGSTER, M. C. ABRAHAM et M. ABRAHAM. Can. J. Chem. **56**, 348 (1978).
3. M. C. ABRAHAM, M. ABRAHAM et J. SANGSTER. J. Chim. Phys. **76**, 125 (1979).
4. J. SANGSTER, M. C. ABRAHAM et M. ABRAHAM. J. Chem. Thermodyn. **11**, 619 (1979).
5. M. C. ABRAHAM, M. ABRAHAM et J. SANGSTER. J. Solution Chem. **8**, 647 (1979).
6. S. BRUNAUER, P. M. EMMETT et E. TELLER. J. Am. Chem. Soc. **60**, 309 (1938).
7. R. H. STOKES et R. A. ROBINSON. J. Am. Chem. Soc. **70**, 1870 (1948).
8. H. BRAUNSTEIN et J. BRAUNSTEIN. J. Chem. Thermodyn. **3**, 419 (1971).
9. M. C. ABRAHAM, M. ABRAHAM et J. SANGSTER. Can. J. Chem. **56**, 635 (1978).

Can. J. Chem. Downloaded from www.nrcresearchpress.com by 210.87.254.40 on 09/05/12
For personal use only.

Some studies on the solvolysis of 1-chloro-1-alkyl cycloalkanes

K. RANGANAYAKULU,[1] M. VASUMATHI DEVI, R. BALAJI RAO, AND K. RAJESWARI

Department of Chemistry, Banaras Hindu University, Varanasi - 221 005, India

and

Department of Chemistry, University of Calgary, Calgary, Alta., Canada T6G 2G2

Received March 20, 1979[2]

K. RANGANAYAKULU, M. VASUMATHI DEVI, R. BALAJI RAO, and K. RAJESWARI. Can. J. Chem. **58**, 1484 (1980).

The effect of the bulk of the sidechain on the rate of solvolysis of 1-alkyl cyclopentyl, cyclohexyl, and cycloheptyl chlorides has been studied. With the exception of the *t*-butyl systems, the ratio of solvolysis rates for the three ring systems falls in a given series. The slower rate of solvolysis in the six-membered ring system may be due to an extra activation energy contribution caused by the conversion of a neutral chair form to the twist boat or half chair conformation, prior to the actual solvolysis. In the case of five- and seven-membered ring systems the formation of an intermediate carbonium ion is sterically favoured (I-strain or eclipsing interaction) consistent with earlier findings. The faster rate of solvolysis of 1-*t*-butylcycloalkyl chlorides is likely due to a rearrangement reaction where alkyl participation enhances the rate of solvolysis.

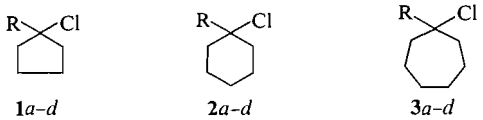
K. RANGANAYAKULU, M. VASUMATHI DEVI, R. BALAJI RAO et K. RAJESWARI. Can. J. Chem. **58**, 1484 (1980).

On a étudié l'effet de l'encombrement de la chaîne latérale sur la vitesse de solvolyse des chlorures d'alkyl-1 cyclopentyle, cyclohexyle et cycloheptyle. A l'exception des systèmes *tert*-butyle, le rapport des vitesses de solvolyse des trois systèmes cycliques correspond à une série donnée. Le fait que la vitesse de solvolyse est plus lente dans les cycles à 6 chaînons peut être due à une contribution supplémentaire de l'énergie d'activation provoquée par l'interconversion d'une forme chaise neutre en une forme bateau-croisée ou demi-chaise avant la solvolyse. Dans le cas des systèmes cycliques à 5 et 7 chaînons, la formation d'un carbocation intermédiaire est favorisée par des facteurs stériques (tension-I ou interaction éclipsée) en accord avec les résultats obtenus antérieurement. Le fait que la vitesse de solvolyse des chlorures de *tert*-butyl-1 cycloalkyle soit plus grande est probablement due à une réaction de transposition où la participation du groupe alkyle augmente la vitesse de solvolyse.

[Traduit par le journal]

Introduction

The solvolyses rates of various ring halides have been extensively studied (1–5). A 125-fold increase in the rate of solvolysis of **1***a* relative to **2***a* has been attributed to relief in steric strain in the transition state of the chloride **1***a* and an increase in steric strain in the transition state of the chloride **2***a*. Since strain effects could originate from the ring as well as the sidechain, we have studied the effect of the bulk of the sidechain on the rate of solvolysis of 1-alkyl cyclopentyl **1***a–d*, cyclohexyl **2***a–d*, and cycloheptyl chlorides **3***a–d*.



1*a–d* **2***a–d* **3***a–d*

a, R = Me; *c*, R = *i*-Pr
b, R = Et; *d*, R = *t*-Bu

Experimental

All the compounds used in this study were prepared using procedures reported in the literature (5–10). All solvolysis experiments were carried out in 80% aqueous ethanol at 30°C. The rate constants for compounds **1***a–c*, **2***a–c*, and **3***a–c* were measured using the procedure adopted by Brown *et al.* (11). The rate constants for compounds **1***d*, **2***d*, and **3***d* were measured using an automatic capacitance bridge with a digital control unit (type 1673A, General Radio Company, Concord, MA, U.S.A.).

Product analysis in each case was done by carrying out the solvolysis reaction in water. The chloride (500 mg) was added to 10 cm^3 of water and allowed to stir at room temperature for 3 days. The reaction mixture was extracted with pentane (4 × 30 mL) and dried over anhydrous magnesium sulphate. The solvent was removed using a fractionating column (24 in.) and the residue was analysed by nmr spectroscopy and glc. The residue in the case of Me, Et, and *i*-Pr substituted compounds was found to be a mixture of unrearranged alkene and alcohol by nmr analysis.

In the case of *t*-butyl systems the residue in each case appeared to contain more than two products and these were separated by preparative glc on a Varian Aerograph model 90-P with a 3/8 in. × 6 ft, 10% SE-30 on 60/80 chromosorb P column. A column temperature of 125°C was used to separate products of **1***d* and **2***d* and a temperature of 135°C was used in case of **3***d*. Each glc separated fraction was analysed by its nmr spectrum (obtained on a Varian XL-200 spectrometer) in $CDCl_3$ using tetramethylsilane as the internal standard. The nmr spectra were consistent with the structures proposed and the chemical shifts of the characteristic peaks are reported (on the product structures) in ppm (δ) downfield from TMS. The peaks reported are sharp singlets unless otherwise mentioned and integrate well for the number of protons. The results are given in detail subsequently.

Results and Discussion

The results of the solvolyses experiments are given in Table 1. The solvolysis data for 3-chloro-3-alkylpentanes have also been included for com-

[1]To whom all correspondence should be addressed.
[2]Revision received March 10, 1980.

0008-4042/80/141484-06$01.00/0
©1980 National Research Council of Canada/Conseil national de recherches du Canada

Can. J. Chem. Downloaded from www.nrcresearchpress.com by 210.87.254.42 on 09/05/12
For personal use only.

Can. J. Chem. Downloaded from www.nrcresearchpress.com by 210.87.254.42 on 09/05/12
For personal use only.

TABLE 1. Rate constants for the solvolysis of 1-chloro-1-alkyl cycloalkanes in 80% aqueous ethanol

Compound	Rate constant (10^5 k, 30°C), s^{-1}			
	Me	Et	*i*-Pr	*t*-Bu
1-Chloro-1-alkyl cyclopentane	88.05	81.38	40.83	246
1-Chloro-1-alkyl cyclohexane	1.30	1.22	1.0	4.27
1-Chloro-1-alkyl cycloheptane	81.94	76.66	35.55	542.7
3-Chloro-3-alkylpentane[a]	2.38	2.75	1.83	44.44

[a]From ref. 11.

TABLE 2. Rate ratios for the solvolyses of 1-chloro-1-alkyl cycloalkanes

Ratio	Value			
	Methyl	Ethyl	*i*-Propyl	*t*-Butyl
$\frac{\text{5-membered}}{\text{6-membered}}$	67.70	66.70	40.83	57.61
$\frac{\text{7-membered}}{\text{6-membered}}$	63.03	62.83	35.55	127.09

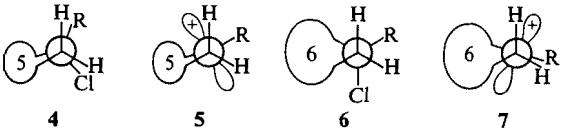
parison purposes (11). The kinetics show first order behaviour in all the cases studied. The rate ratios for the solvolyses of five-, six-, and seven-membered ring compounds are given in Table 2.

The rate of solvolysis in any given ring system where the R sidechain is changed could be affected by one or more of the following factors:

(*i*) In going from the reactant to the transition state leading to the carbonium ion intermediate, there should be a decrease in the eclipsing interaction in the case of the five-membered ring system, **4** → **5**, whereas in the case of the six-membered ring system, **6** → **7**, there should be an increase (I-strain) (12). This will have the effect of increasing the rate with increase in the bulk of the 1-alkyl group in the five-membered ring system, and correspondingly decreasing the rate in the six-membered ring system. However, the near constancy of the relative rates of the five- and the six-membered ring systems in going from the methyl to the *t*-butyl sidechain suggests that this is not an important contributing factor in causing the basic differences in solvolysis rates between these two ring systems.

(*ii*) In the case of the five-membered ring system, there are four α-hydrogens (ring) in a favourable orientation for hyperconjugative stabilization, see **5**, while in the case of the six-membered ring system there are only two such hydrogens, **7** (13). This latter statement assumes that the solvolysis reaction in the six-membered ring system proceeds via a chair conformation in the transition state. Brown *et al.* (14) have made a detailed study of the solvolyses of 1-aryl-1-cycloalkyl and 1-aryl-1-alkylcarbinyl 3,5-dinitrobenzoates. Their results reveal a close similarity in the ρ^+ values for methyl, isopropyl, cyclobutyl, and cyclohexyl groups indicating no significant difference in the electronic contributions to an electron deficient centre. However, the ρ^+ values for cyclopentyl and cycloheptyl groups are considerably less negative and this has been attributed to a combination of I-strain and superior hyperconjugative contributions by the cyclopentyl group, and to I-strain alone in the case of the cycloheptyl group. β-Deuterium isotope effects involving ring hydrogens are known for the solvolysis of both cyclopentyl (2,2,5,5-d_4) tosylate (15*a*) and cyclohexyl (2,2,6,6-d_4) tosylate (15*b*), $k_H/k_D = 2.06$ and 2.34, respectively. This isotope effect implies that hyperconjugative stabilization is more important in the cyclohexyl case so that this hyperconjugative argument can hardly explain the faster rate of solvolysis found for the cyclopentyl system.

(*iii*) Conformational preference for hyperconjugative participation by the C—H hydrogens of the alkyl group in the five- and seven-membered ring systems. From electron spin resonance results and from the observation of secondary β-deuterium isotope effects in bridgehead systems (16), one can show that hyperconjugation is dependent on the angle (θ) between the "*p*" orbital on the trigonal carbon and the neighboring C—H bond (Fig. 1). If indeed this is the reason for the observed difference in solvolysis rates of five- and six-membered ring compounds, then there should be a large difference



4 **5** **6** **7**

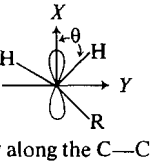
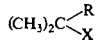


FIG. 1. View along the C—C bond (*z*).

TABLE 3. Rate ratios for the solvolysis of 1-methyl- and 1-methyl-d_3 cycloalkyl chlorides in 80% aqueous ethanol

Compound	T (°C)	k_{CH_3}/k_{CD_3}	k_{CH_3}/k_H	Reference
	35 25	1.21 1.25	27 600	17
	60	1.21	22 800	17
	—	1.33	10^6	17
	20 55.6	2.419 2.086	—	18

in the isotope effect of the 1-CD_3-cycloalkyl substituted compounds. The Me-d_3 isotope effects for the solvolysis of methylcyclopentyl chloride and methylcyclohexyl chloride are given in Table 3. Since the isotope effects are temperature dependent, one can assign a rough value of 1.3 for k_{CH_3}/k_{CD_3} at 25°C for methyl cyclohexyl chloride. Thus, it can be concluded that the 1-alkyl group stabilises the intermediate carbonium ion better in a six-membered ring system than in the five-membered ring. Therefore, this factor also seems not to be responsible for the observed rate differences in the solvolysis of five- and six-membered ring compounds.

(*iv*) An increase in Baeyer strain in the formation of a five-membered ring cation (109° to 115°) compared to a six-membered ring cation (109° to 120°). This effect is likely to reverse the rates of solvolysis of five- and six-membered ring systems from the observed results, and therefore may not be the significant factor in changing the rates of solvolysis in different ring systems.

(*v*) Decreasing solvation in all the ring systems with increase in the bulk of the alkyl group.

To summarize, the regular decrease in the solvolysis rates of all the three ring systems with the increase in the bulk of the alkyl group suggests relief of eclipsing interactions in the chloride, differential hyperconjugative participation of the β-hydrogens of the ring or of the 1-alkyl sidechain, and Baeyer strain are not the major contributing factors accounting for the differences in solvolysis rates of the different ring systems. However, in a given series **1***a–c*, **2***a–c*, and **3***a–c* the results could very well be explained by considering hyperconjugative participation of β-hydrogens of the 1-alkyl group, in addition to solvation effects.

Solvolysis of *t*-Butyl Systems

The *t*-butyl chlorides **1***d*, **2***d*, and **3***d* all solvolyse much faster than the methyl systems **1***a*, **2***a*, and **3***a*. Obviously some new factor must be involved here and as a first step we have carried out a product analysis. For the product study, the solvolysis of **1***d*, **2***d*, **3***d* was carried out in water in order to simplify the nature of the products, specifically to avoid the formation of ethers which will only complicate the analysis. In each case both the nmr (200 MHz) and glc analyses showed the presence of rearranged products.

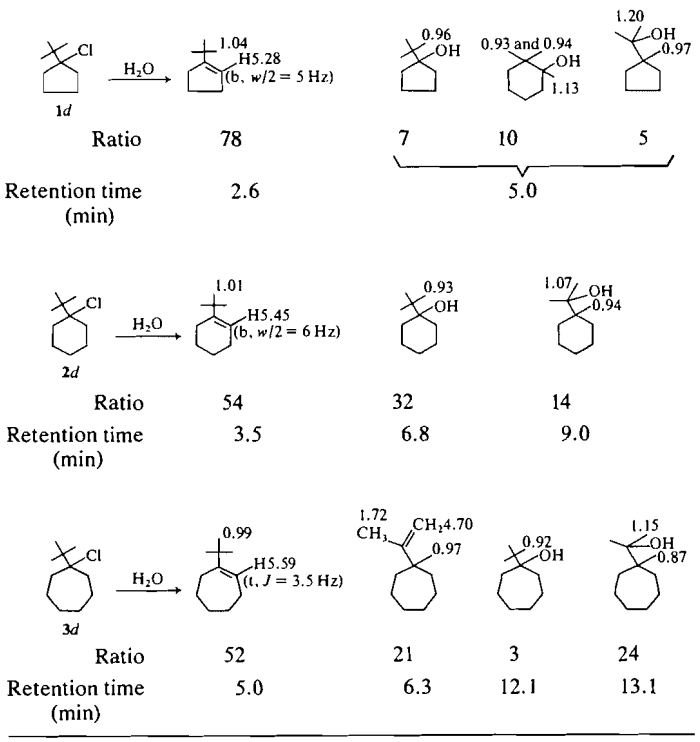
The products from the chloride **1***d* could not be separated in glc under the conditions used. The first fraction contained the unrearranged alkene but the second fraction consisted of a mixture of three alcohols, 1-*t*-butylcyclopentanol, 1,2,2-trimethylcyclohexanol, and 2-(1-methylcyclopentyl)-2-propanol. The identity of these alcohols was confirmed by synthesizing these, 1-*t*-butylcyclopentanol and 1,2,2-trimethylcyclohexanol according to the literature procedures (10, 18*a*) and 2-(1-methylcyclopentyl)-2-propanol by adding methyllithium to 1-acetyl-1-methylcyclopentane (kindly supplied by Dr. T. S. Sorensen). The nmr spectrum of the mixture of these authentic alcohols matched well with that of the second fraction.

In the case of the chlorides **2***d* and **3***d* the solvolysis products could be separated well under the glc conditions used and the products could be easily identified.

The ratios of each of the products, the chemical shifts of the characteristic proton signals, and the retention times are given in Table 4. Recovery experiments have also been carried out for the solvolysis of the Me, Et, and *i*-propyl compounds and these show no rearranged products. The faster rate of solvolysis in the *t*-butyl compounds can therefore be correlated with the appearance of rearrangement products. Brown *et al.* (10) have studied the rate of solvolysis of 1-*t*-butylcycloalkylcarbinyl *p*-nitrobenzoates and the results are as follows: cyclopentyl, $k_1 = 0.236\ s^{-1}$, cyclohexyl, $k_1 = 7.35 \times 10^{-3}\ s^{-1}$, cycloheptyl, $k_1 = 1.15\ s^{-1}$. The corre-

Can. J. Chem. Downloaded from www.nrcresearchpress.com by 210.87.254.42 on 09/05/12
For personal use only.

TABLE 4. Solvolyses of 1*d*, 2*d*, and 3*d*



sponding ratios, $k_{t\text{-butyl}}/k_{\text{methyl}}$, are 112, 134, and 273. Using the chlorides the corresponding ratios are $k_{t\text{-butyl}}/k_{\text{methyl}} = 2.8$, 3.28, and 6.62. In the *p*-nitrobenzoates there is a large rate difference between the methyl and *t*-butyl substituents and this has been atrributed by Brown *et al.* (10) to the relief of steric strain in going to the transition state. On first glance these results seem to be different from those obtained by us using 1-*t*-butylcycloalkyl chlorides. However, the F-strain involving ionisation of *p*-nitrobenzoates is larger than for the corresponding chlorides (19) and therefore the chlorides appear to be better for studies of structural effects in which large F-strain factors should be avoided (10). Also, introduction of two or three bulky groups at a tertiary center can result in far larger rate enhancements (20). However, the significant factor is that the relative reactivities of five-, six-, and seven-membered ring compounds are not very different, irrespective of the leaving group. Thus:

$$(k_5(t\text{-Bu})/k_6(t\text{-Bu}))_{Cl} = 57.67$$

$$(k_5(t\text{-Bu})/k_6(t\text{-Bu}))_{OPNB} = 32.10$$

$$(k_7(t\text{-Bu})/k_6(t\text{-Bu}))_{Cl} = 127.09$$

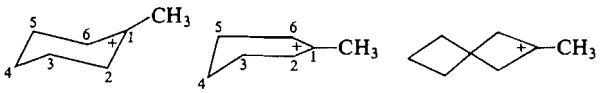
$$(k_7(t\text{-Bu})/k_6(t\text{-Bu}))_{OPNB} = 156.46$$

It seems to us that the dramatic rate increase in *t*-butyl substituted cycloalkyl chlorides is not primarily of F-strain origin because: (*a*) the chlorides are much less susceptible to this factor as shown above and (*b*) there should be a steady progression from R = Me to R = *t*-butyl, if this phenomenon is involved. It has been suggested that methyl participation in *t*-butyl substituted systems enhances the rate of solvolysis (21). Our results are consistent with this argument although it is somewhat peculiar that in the cyclopentyl and cyclohexyl series the rearranged products only account for 15% and 14% respectively of the total. Thus the participation does not involve the complete breaking of the methyl carbon bond in the solvolysis transition state.

Solvolysis Rate Comparisons Between the Three Ring Systems

Up to now we have discussed two phenomena: a slight rate decrease in all the three rings in going from Me to *i*-Pr; secondly, the fairly large increase in all cases with the *t*-butyl substitutent. Neither of these factors relates directly to the question of why the six-membered ring system solvolyses slower than its counterparts. We have previously suggested that eclipsing interactions are not of primary importance in causing the rapid rate in the five-

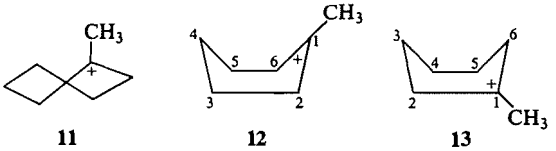
Can. J. Chem. Downloaded from www.nrcresearchpress.com by 210.87.254.42 on 09/05/12
For personal use only.



8 9 10

membered ring system, since a rate increase would have been expected with increasing bulk. This relief of eclipsing interactions is the usual argument given, e.g. work of Brown (5, 10), for this rate increase and this could still be possible if compensating factors were at work, i.e. a large rate decrease on going from methyl to isopropyl due to solvation and/or hyperconjugation effects, balanced by a smaller increase caused by the eclipsing relief. The rate increase in the seven-membered case seems to fit Brown's I-strain concept. One possibility for the cyclohexyl system could be that the solvolysis might not involve the chair form and in this case the large rate decrease predicted on going from Me to *i*-Pr would not necessarily apply, i.e. development of eclipsing interactions in a chair cation intermediate **8**. In the case of the six-membered cation several conformations, **8–13**, could be considered. Taking steric factors alone into consideration, the carbonium ion intermediate in the six-membered ring system is more crowded than the neutral molecule. Recently Sorensen *et al.* (22) have shown that the twist boat form of methylcyclohexyl cation **10** is more stable (ca. 500 cal/mol) than the chair form **8**, although there is a rapid equilibration of the two conformers even at low temperatures. With an increase in the bulk of the 1-alkyl group it is likely that the equilibrium would be shifted even more towards the half chair or the twist boat form since there is a smaller eclipsing interaction of the alkyl group with C_2-hydrogens. In the ground state chlorides, the difference in energy between the chair form and the half chair or twist boat form will be even higher (ca. 3–4 kcal/mol). Although the chair conformation is undoubtedly the ground state for the chlorides, the eclipsing interaction in the chair cation may make it more economical for the molecule to solvolyse via a twist boat ground state as long as the energy gain through forming a better cation transition state is enough to counter-balance the energy differences between the neutral chair and the twist boat chlorides. In any case, the solvolysis rate would be slower than in the other two ring systems since it is a matter of deciding between the best of two bad situations.

In some ways the conformational argument involving a twist boat transition state seems better, since this fits with the small rate decrease observed in going from methyl to isopropyl, and it should be noted that some solvolysis data on secondary cyclohexyl systems have already been rationalised by involving a non-chair conformation transition state (15*a*, 23).



11 12 13

Acknowledgements

We wish to thank the University Grants Commission, India, for providing financial assistance to one of us (M.V.D.) and to Professors T.S. Sorensen and R. E. Robertson, Department of Chemistry, University of Calgary, for providing some laboratory facilities and for useful discussions.

1. A. P. Krapcho and D. E. Horn. Tetrahedron Lett. 6107 (1966).
2. H. C. Brown and F. J. Chloupek. J. Am. Chem. Soc. **85**, 2322 (1963).
3. G. Le Ny. Compt. Rend. **251**, 1526 (1960).
4. H. C. Brown, R. S. Fletcher, and R. B. Johannesen. J. Am. Chem. Soc. **73**, 212 (1951).
5. H. C. Brown and M. Borkowski. J. Am. Chem. Soc. **74**, 1894 (1952).
6. R. Ya. Levina and N. N. Mezentsova. Fiz. Khim. **11**, No. 1, 205 (1956).
7. A. F. Aliev, F. A. Mamedov. I. G. Ismailzade, and S. D. Mekhtiev. Azerb. Khim. Zh. **6**, 73 (1961).
8. G. S. Skinner and F. P. Florentine, Jr. J. Am. Chem. Soc. **76**, 3200 (1954).
9. L. Schmerling. J. Am. Chem. Soc. **69**, 1121 (1947).
10. E. N. Peters and H. C. Brown. J. Am. Chem. Soc. **97**, 2892 (1975).
11. H. C. Brown and R. S. Fletcher. J. Am. Chem. Soc. **71**, 1845 (1949).
12. H. C. Brown, J. H. Brewster, and H. Shechter. J. Am. Chem. Soc. **76**, 467 (1954).
13. T. S. Sorensen. J. Am. Chem. Soc. **91**, 6398 (1969).
14. (*a*) H. C. Brown, M. Ravindranathan, and M. M. Rho. J. Am. Chem. Soc. **98**, 4216 (1976); (*b*) H. C. Brown, C. G. Rao, and M. Ravindranathan. J. Am. Chem. Soc. **99**, 7663 (1977).
15. (*a*) W. H. Saunders, Jr. and K. T. Finley. J. Am. Chem. Soc. **87**, 1384 (1965); (*b*) A. Streitwieser, Jr., R. H. Jagow, R. C. Fahey, and S. Suziki. J. Am. Chem. Soc. **80**, 2326 (1958).
16. (*a*) J. F. Gibson, D. J. E. Ingram, M. E. Townsend, and M. C. R. Symons. Trans. Faraday Soc. **53**, 914 (1957); (*b*) W. Gordy and C. G. McCormick. J. Am. Chem. Soc. **78**, 3243 (1956); (*c*) M. C. R. Symons. J. Chem. Soc. 277 (1959); (*d*) G. A. Olah, C. U. Pittman, Jr., and M. C. R. Symons. Carbonium ions. Vol. I. *Edited by* G. A. Olah and P.v.R. Schleyer. Interscience Publishers, John Wiley and Sons, New York. 1968. p. 216; (*e*) V. J. Shiner, Jr. and J. S. Humphrey, Jr. J. Am. Chem. Soc. **85**, 2416 (1963); (*f*) H. Maskill. J. Chem. Soc. Perkin II, 1889 (1976); (*g*) V. J. Shiner, Jr. and J. G. Jewett. J. Am. Chem. Soc. **87**, 1382 (1965).

Can. J. Chem. Downloaded from www.nrcresearchpress.com by 210.87.254.42 on 09/05/12
For personal use only.

17. K. L. SERVIS, S. BORČIČ, and D. E. SUNKO. Tetrahedron, **24**, 1247 (1968).
18. (*a*) L. HAKKA, A. QUEEN, and R. E. ROBERTSON. J. Am. Chem. Soc. **87**, 161 (1965); (*b*) T. TSUJI, I. MORITANI, S. NISHIDA, and G. TADOKORO. Bull. Chem. Soc. Jpn. **40**, 2344 (1967).
19. J. SLUTSKY, R. C. BINGHAM, P.v.R. SCHLEYER, W. C. DICKASON, and H. C. BROWN. J. Am. Chem. Soc. **96**, 1969 (1974).
20. (*a*) P. D. BARTLETT and M. STILES. J. Am. Chem. Soc. **77**, 2806 (1955); (*b*) P. D. BARTLETT and M. S. SWAIN. J. Am. Chem. Soc. **77**, 2801 (1955); (*c*) P. D. BARTLETT and T. T. TIDWELL. J. Am. Chem. Soc. **90**, 6621 (1968); (*d*) T. T. TIDWELL. J. Org. Chem. **39**, 3533 (1974).
21. P. D. BARTLETT. J. Chem. Educ. **30**, 22 (1953).
22. R. P. KIRCHEN and T. S. SORENSEN. J. Am. Chem. Soc. **100**, 1487 (1978).
23. (*a*) V. J. SHINER, JR. and J. G. JEWETT. J. Am. Chem. Soc. **87**, 1382 (1965); **87**, 1383 (1965); (*b*) J. E. NORDLANDER, J. M. BLANK, and S. P. JINDAL. Tetrahedron Lett. 3477 (1969).

Can. J. Chem. Downloaded from www.nrcresearchpress.com by 210.87.254.42 on 09/05/12
For personal use only.

Cation mobilities in liquid and supercritical C_1–C_4 hydrocarbons

NORMAN GEE AND GORDON R. FREEMAN

Chemistry Department, University of Alberta, Edmonton, Alta., Canada T6G 2G2

Received February 18, 1980

NORMAN GEE and GORDON R. FREEMAN. Can. J. Chem. **58**, 1490 (1980).

The relationship between ion mobility and liquid viscosity is commonly expressed as $\mu \propto \eta^{-m}$. In hydrocarbons the value of m tends to be near 1.0 at $\eta > 5$ mP, $m > 1.0$ at $\sim 5 < \eta < 1$ mP, and $m < 1.0$ at $\eta < 0.5$ mP. Thus there is a maximum in a plot of $\mu\eta$ against η^{-1} and Walden's rule ($m = 1.0$) is only a rough approximation. The decrease of $\mu\eta$ as the critical region is approached is accompanied by an increase in the ratio of diffusion coefficients $D_{\text{molec}}/D_{\text{ion}}$. Ion mobilities in the liquids well below their normal boiling points are chiefly controlled by the fluidity. At higher temperatures and concomitant lower liquid densities and viscosities $\mu\eta$ first increases, due to an increasing ion mean free path, then decreases as the critical region is approached, due to the increasing liquid compressibility and consequent electrostriction about the ion.

NORMAN GEE et GORDON R. FREEMAN. Can. J. Chem. **58**, 1490 (1980).

On exprime communément la relation entre la mobilité de l'ion et la viscosité du liquide par $\mu \propto \eta^{-m}$. Dans les hydrocarbures, la valeur de m tend vers 1.0 à $\eta > 5$ mP, $m > 1.0$ à $\sim 5 < \eta < 1$ mP et $m < 1.0$ à $\eta < 0.5$ mP. Ainsi il existe un maximum dans la courbe $\mu\eta$ en fonction de η^{-1} et la règle de Walden ($m = 1.0$) n'est qu'une grossière approximation. Lorsqu'on s'approche de la région critique, la diminution de $\mu\eta$ s'accompagne d'une augmentation du rapport des coefficients de diffusion $D_{\text{molécule}}/D_{\text{ion}}$. Les mobilités ioniques dans les liquides à des températures bien au-dessous de leur point d'ébullition sont principalement contrôlées par la fluidité. A des températures plus élevées et à des viscosités et des densités concomitantes plus faibles, $\mu\eta$ décroît d'abord, grâce à une augmentation du libre parcours moyen de l'ion, puis diminue lorsqu'on s'approche de la région critique par suite de l'augmentation de la compressibilité du liquide et d'une électrostriction conséquente autour de l'ion.

[Traduit par le journal]

Introduction

Ion mobilities μ in liquid hydrocarbons are often compared with the viscosity η, since by Walden's rule $\mu\eta$ should be constant and independent of temperature (1–9). In general this is not true. Earlier results, which were restricted to temperatures near or below the normal boiling points of the measured liquids, indicate that $\mu\eta$ increases with temperature in many systems (1, 2). This is equivalent to saying that μ varies as η^{-m}, $m > 1.0$ (6–9). Recent development of high pressure conductance cells has allowed mobility measurements over the entire liquid range at temperatures up to the critical (7–9). The effects of molecular structure and temperature on $\mu\eta$ are now examined by measurements of μ in eight small hydrocarbons (the C_1 to C_4 alkanes and alkenes, with the exceptions of the butenes). Ion mobilities in the butenes have been reported (7), but measured liquid viscosities are not available for three of the isomers and are only reported for temperatures below 239 K in 1-butene. The butenes are therefore not included in the present discussion.

Experimental

Purification of methane and ethane samples is described in ref. 10, and of propane, propene, and cyclopropane in ref. 11. The remaining samples were all Phillips Research Grade of > 99.90% purity. Further purification of ethene was effected by holding the liquid on KOH pellets overnight at 195 K and subsequent treatment as for ethane. The butanes were purified at room temperature in the same vacuum line described in refs. 10 and 11, except that Davison 4A Molecular Sieves were used instead of Davison 3A and a sodium–potassium alloy was used instead of potassium mirrors.

The conductance cells were described in refs. 8 and 9, the cooling system in ref. 6 and the heating system in ref. 9.

Mobilities were measured by a time-of-flight method (6). Electrons were swept from the liquids by the electric field, so there was no interference from anions. The liquids were under their vapor pressure.

Viscosities for the compounds were taken from ref. 12, except for isobutane and cyclopropane. Values were only used for temperature ranges where experimental data exist. For isobutane, ref. 12 did not give experimental results over the entire liquid range. A composite of the results in refs. 13 and 14 was used instead. The data in Fig. 1 of ref. 13*d* are incorrect; Figs. 4 and 5 should be used. For cyclopropane no liquid viscosities to our knowledge have been measured. At $T < 300$ K values have been estimated by the method of Morris (15).

Results

The ion mobilities μ are plotted against the temperature in Fig. 1. Increasing the temperature towards the critical region leads to a monotonic increase of the mobility for all the compounds except cyclopropane. The cyclopropane curve exhibits a small maximum at ~393 K (~5 K below the critical temperature). The ion mobilities in all of the present hydrocarbons at ~1 K above T_c are in the range $(4.9 \pm 0.6) \times 10^{-3}$ cm²/V s, except in methane, where it is 7.8×10^{-3} cm²/V s.

Figure 2 shows the product of the ion mobility and the fluid viscosity, $\mu\eta$, plotted against η^{-1}. Figure 2A includes the present results except those for propene, cyclopropane, and isobutane. The mobilities in *n*-hexane are from ref. 8 and the vis-

0008-4042/80/141490-05$01.00/0

©1980 National Research Council of Canada/Conseil national de recherches du Canada

Can. J. Chem. Downloaded from www.nrcresearchpress.com by 210.87.254.42 on 09/05/12
For personal use only.

Can. J. Chem. Downloaded from www.nrcresearchpress.com by 210.87.254.42 on 09/05/12
For personal use only.

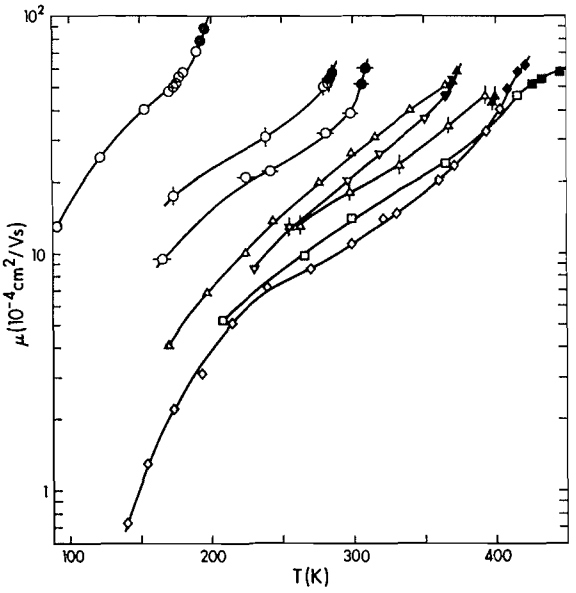


FIG. 1. Mobility μ plotted against temperature. Liquids: methane, O; ethane, —O—; ethene, ○; propane, △; propene, ▽; cyclopropane, ▲; *n*-butane, □; isobutane, ◇. Closed symbols represent supercritical fluids at the critical densities.

cosities are from ref. 14. Figure 2*B* includes the isobutane and propene results, plus *n*-pentane mobilities from ref. 9 and viscosities from ref. 14. Results are only shown for ranges where experimental viscosity values are available. The value of m in $\mu \propto \eta^{-m}$ tends to be approximately 1.0 at $\eta^{-1} < 200\ P^{-1}$, while at $\eta^{-1} > 200\ P^{-1}$ m can either > 1.0 or < 1.0. As the critical region is approached ($\eta^{-1} > 2000\ P^{-1}$) we always observe $m < 1.0$ (Fig. 2). It has previously been found that in many $C_{n\geq 5}$ hydrocarbons below their normal boiling points, in the range $40 < \eta^{-1} < 400\ P^{-1}$, the value of m is > 1.0 (1, 9).

There is a distinct maximum in the μη plots for

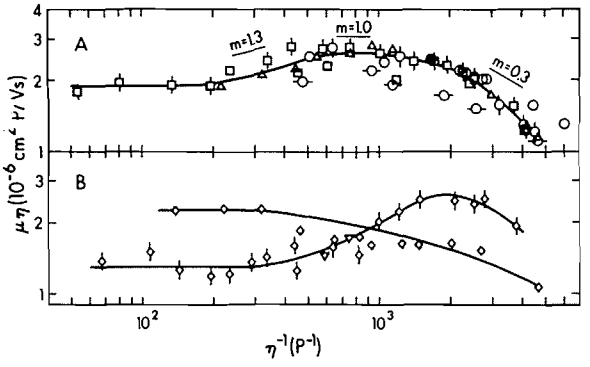


FIG. 2. Plot of μη against the inverse viscosity η^{-1}. The symbols are the same as in Fig. 1, with the addition of *n*-pentane (◇, ref. 9) and *n*-hexane (□, ref. 8). The dashed lines and values of m illustrate $\mu \propto \eta^{-m}$.

propane, *n*-pentane, and *n*-hexane (Fig. 2). The possibility of a maximum for the other liquids cannot be ruled out.

The mobility in cyclopropane is plotted against T^{-1} in Fig. 3. The dashed line represents $E_\mu = 4.6$ kJ/mol. Although no experimental viscosity data are available for cyclopropane, from Fig. 2 it can be expected that the value of m will be much closer to 1 than to 2. Hence we conclude that $E_\eta \approx 4$–5 kJ/mol for liquid cyclopropane well away from the critical region. The values of η for cyclopropane given in ref. 16 were estimated by the method of Souders and they yield a value of E_η that is too small (2.3 kJ/mol). The method of Morris is

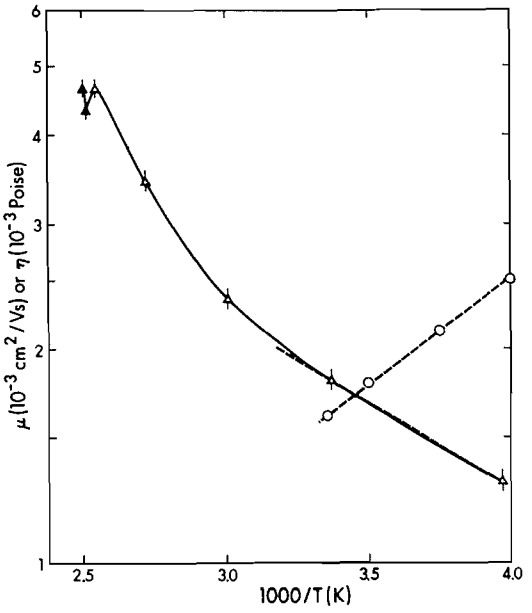


FIG. 3. Arrhenius plots of mobility and viscosity for cyclopropane. Mobilities: liquid, △; supercritical fluid at critical density, ▲. The viscosities (O) were estimated by the method of Morris (15). The dashed lines were used to estimate the values of E_μ and E_η given in the text.

recommended for small cyclic compounds (15), and it gives $E_\eta = 5.7$ kJ/mol for cyclopropane at the temperatures in question (Fig. 3), in satisfactory agreement with the estimate based upon the cation mobilities.

It should be mentioned that the viscosities of a number of liquids given in ref. 16 were estimated by the method of Souders, and these should not be used. The viscosity values are probably accurate to within 25% (not the 3–5% stated), but the activation energies might be wrong by a factor of 2. The method of van Velzen is recommended for open chain hydrocarbons (15).

Can. J. Chem. Downloaded from www.nrcresearchpress.com by 210.87.254.42 on 09/05/12
For personal use only.

Discussion

The plot of cation mobility against temperature contains a small dip in the critical region for cyclopropane, but not for the other hydrocarbons (Fig. 1). In earlier work a dip was also noticed only for cyclic hydrocarbons (8, 17). In all the other systems there is a monotonic increase of cation mobility with temperature. The reason for the difference in behavior is not known. The dip in cation mobility is not related to the much larger decrease in electron mobility in the high temperature portion of the liquid range of spherelike and globular hydrocarbons (7, 9, 10, 18, 19). The latter has been attributed to the break up of a conduction band, which participates in the transport of the electrons (9, 20) but not of the ions. The extent of electrostriction about the ions should be similar in all the hydrocarbon critical fluids, so it is unclear why the cyclic hydrocarbons display slightly different behavior.

It should be mentioned that the very large fluctuations in density that are characteristic of the critical fluid have correlation lengths much greater than the electron or ion interaction distances, so the mobilities of electrons and ions in the critical fluid are not much different from those in the adjacent fluids on either side of the critical region.

While Walden's rule is not generally true in detail (Fig. 2), all of the present results can be represented to within a factor of two by the approximation:

$$[1] \quad \mu\eta \approx 2 \times 10^{-6}\ \text{cm}^2\ \text{P/V s}$$

It is surprising that the same approximation applies to within a factor of two to cation mobilities in widely differing liquids (1, 21), from viscous paraffin oils (21), through C_{16} (21) to C_1 alkanes, to liquid nitrogen (22), hydrogen (23), argon (22, 24), neon (25), helium (26, 27) and even ammonia (calculated from data in refs. 22 and 28). Although any particular solvent has been measured over a relatively small range of viscosities (21), approximation [1] is valid in the extensive zone $0.2 < \eta^{-1} < 40\,000\ \text{P}^{-1}$.

Stokes' law, or some treatment from which Stokes' law is recoverable, is the more usual starting point for examination of ion mobilities (24, 29–35). An early attempt to connect liquid and gas behavior, that is, to account for the effect of changing the fluid density, involves modification of Stokes' law to (29, 30):

$$[2] \quad \mu\eta = \frac{e}{6\pi r}\left(1 + \frac{c\lambda}{r}\right)$$

where r is the ion radius, λ is the mean free path, and c a constant. The 6π indicates that the medium "wets" the ion (perfect stick). If the ion moves through the fluid by pushing molecules out of its path, the factor 6π would be 4π (perfect slip).

It may be mentioned that the semihydrodynamic equation used successfully to explain the mobility of electrons (large-bubble state) in dense helium gas at low temperatures (ref. 36 and subsequent work on electrons in dense helium gas) corresponds to eq. [2] with $c = 3/2$ and λ given by:

$$[3] \quad \lambda = 3\eta/\rho\bar{v}$$

where ρ is the density in g/cm^3 and $\bar{v}$ is the mean speed of the Maxwellian distribution of molecular velocities. However, [2] with [3] was not used for the electron bubble state in liquid helium (37) and is unsuitable for the liquid state in general. The attempt to use this semihydrodynamic equation to describe the mobility of electrons in the localized state in liquid hydrocarbons (38) is inappropriate. A reason in addition to those given previously (39) is the following. Equation [3] applies to dilute gases. At higher densities λ is smaller than indicated by [3] (40). The use of realistic values for ionic or electron bubble radii in liquids, with λ from [3], always gives $(c\lambda/r) \gg 1$. Thus [3] leads to $\mu\eta$ that are much too large for ions or localized electrons in liquids.

In dense liquids one has $(c\lambda/r) < 1$ and Stokes' law is a reasonable approximation of [2]. This is the situation at low values of η^{-1} (Fig. 2). The value of η^{-1} was increased experimentally by heating the liquid under its vapor pressure. This also decreased the liquid density and thereby increased λ. When $(c\lambda/r)$ approaches unity eq. [2] indicates that $\mu\eta$ should increase above that expected from Stokes' law, in qualitative agreement with the results at $\eta^{-1} > 200\ \text{P}^{-1}$ (Fig. 2). However, the subsequent decrease of $\mu\eta$ at $\eta^{-1} > 10^3\ \text{P}^{-1}$ must have a different cause, because one might expect λ to continue to increase with decreasing density.

The charged ion interacts more strongly with neighboring molecules than would a neutral particle (31–35, 41). There are two main sources of friction in addition to that expected from a hard core (Stokes' law). One is the electrostriction of the solvent about the ion (34, 35, 41), which increases the local density and thereby the local viscosity. This effect occurs in both nonpolar and polar solvents and increases with increasing compressibility of the liquid. The other is the interaction between the ion charge and the electric dipoles of the solvent molecules, which produces a drag on the translational motion of the ion (31, 33). This effect increases with increasing solvent dipole moment (or dielectric constant) and decreasing ion radius.

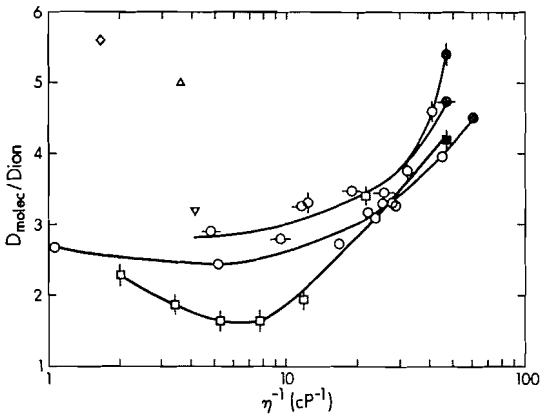


FIG. 4. Ratio of diffusion coefficients D_{molec}/D_{ion} plotted against the inverse viscosity. Methane, O; ethane, —O—; ethene, ○; *n*-hexane, □, ref. 8. The closed symbols represent ratios for molecules in the critical fluid and ions in the gas at the critical density and 1–2 K above T_c. The ratios for the noble liquids are for a pressure of 15 atm, ref. 24: argon, △; krypton, ▽; xenon, ◇. The argon viscosity value is from ref. 46, and those for krypton and xenon are from ref. 47. The viscosity increases by ~2% on going from 1 to 15 atm (46*b*).

The behavior of the ion can be compared with that of the neutral solvent molecules through the ratio of their diffusion coefficients D.

$$[4] \quad D_{molec}/D_{ion} = eD_{molec}/\mu kT$$

where e is the number of protonic charges on the ion, $k = 8.6 \times 10^{-5}$ eV/K is Boltzmann's constant, and T is the absolute temperature. In the noble liquids argon, krypton, and xenon at 15 atm pressure and temperatures slightly above their normal boiling points, the ratio D_{molec}/D_{ion} has values from 3.2 to 5.6 (24, 35). The values were accounted for by assuming that the ions were dimeric (the hard core radius of M_2^+ is greater than that of M^+), and considering the effect of the ion–molecule polarization interaction upon the local density (electrostriction).

Self diffusion coefficients have been measured up to the critical point in methane (42), ethane (43, 44), and ethene (45). The ratio D_{molec}/D_{ion} is plotted against η^{-1} in Fig. 4 for these liquids and for *n*-hexane (8). The ratio has values of 2–3 in the liquids at or below their normal boiling points ($\eta^{-1} \leq 800$ P^{-1}), but they increase to 4–5 in the near critical fluids. The ratios in the hydrocarbons are lower than those in the noble liquids at the same value of η^{-1} (Fig. 4 and refs. 46 and 47). This may imply that the relative effect of electrostriction is smaller when the molecule and ions are larger and more complex, or that the ions are smaller than solvent dimers, or both.

The earlier suggestion that the cation in liquid ethane drags with it a solvent shell comprised of eleven additional ethane molecules (4) is not correct. Furthermore, the values of $\mu\eta$ in the earlier work were 35% lower than the present values at the same η^{-1}; the sample treatment (4) might have generated olefins which could form relatively large (multimeric) cations.

The fact that $\mu\eta$ for radiolytic ions is relatively insensitive to the molar volume of the hydrocarbon (Fig. 2 and ref. 1) may be attributed to a smaller role of electrostriction when the ions and solvent molecules are larger.

The value of D_{molec}/D_{ion} is also increased by the presence of a permanent dipole moment on the molecules (17), which contributes to the drag on the ion. The value of the ratio for the nonpolar benzene is 2.0 ± 0.1 at temperatures from 290 to 550 K (17, 48), while in the polar toluene (dipole moment = 0.4–0.6 D in the liquid phase, ref. 49) the ratio is 3.8 ± 0.2 over the temperature range 180 to 380 K (17, 48*c*, 50).

The decrease of $\mu\eta$ and increase of D_{molec}/D_{ion} at high η^{-1} (Figs. 2 and 4, respectively) are attributed to increased electrostriction in the high temperature liquids. The extent of electrostriction increases with the liquid compressibility (41). As the critical region is approached the compressibility increases rapidly.

In summary, ion mobilities in liquid hydrocarbons well below their normal boiling points are chiefly controlled by the fluidity. The value of $\mu\eta$ is not very sensitive to the size of the hydrocarbon molecule, and hence of the ion in these radiolytic systems. This is attributed to a smaller relative effect of electrostriction when the ions and molecules are larger. At higher temperatures and concomitant lower densities $\mu\eta$ first increases due to an increasing mean free path of the ion, then decreases as the critical region is approached, due to the increasing liquid compressibility and consequent electrostriction about the ion.

Acknowledgement

We would like to thank the staff of the Radiation Research Center for aid with the electronics.

1. I. ADAMCZEWSKI. Ionization, conductivity, and breakdown in dielectric liquids. Taylor and Francis Ltd., London. 1969. Chapt. 12.
2. T. J. GALLAGHER. Simple dielectric liquids. Clarendon Press, Oxford. 1975. Chapt. 1.
3. G. BAKALE and W. F. SCHMIDT. Z. Naturforsch. **28a**, 511 (1973).
4. W. F. SCHMIDT, G. BAKALE, and U. SOWADA. J. Chem. Phys. **61**, 5275 (1974).
5. P. H. TEWARI and G. R. FREEMAN. J. Chem. Phys. **49**, 4394 (1968).

Can. J. Chem. Downloaded from www.nrcresearchpress.com by 210.87.254.42 on 09/05/12
For personal use only.

Can. J. Chem. Downloaded from www.nrcresearchpress.com by 210.87.254.42 on 09/05/12
For personal use only.

6. J.-P. DODELET and G. R. FREEMAN. Can. J. Chem. **53**, 1263 (1975).
7. J.-P. DODELET and G. R. FREEMAN. Can. J. Chem. **55**, 2893 (1977).
8. S. S.-S. HUANG and G. R. FREEMAN. J. Chem. Phys. **50**, 1538 (1979).
9. J.-P. DODELET and G. R. FREEMAN. Can. J. Chem. **55**, 2264 (1977).
10. N. GEE and G. R. FREEMAN. Chem. Phys. Lett. **60**, 439 (1979).
11. N. GEE and G. R. FREEMAN. Rad. Phys. Chem. **15**, 267 (1980).
12. Y. S. TOULOUKIAN, S. C. SAXENA, and P. HESTERMANS. Viscosity, thermophysical properties of matter. Vol. 11. IFI/Plenum, New York. 1975.
13. (*a*) B. H. SAGE, W. D. YALE, and W. N. LACEY. Ind. Eng. Chem. **31**, 223 (1939); (*b*) M. R. LIPKIN, J. A. DAVISON, and S. S. KURTZ, JR. Ind. Eng. Chem. **34**, 976 (1942); (*c*) API tables, selected values of physical and thermodynamic properties of hydrocarbons and related compounds. Vol. II. Am. Petrol. Inst. Res. Project 44, Thermodynamic Res. Center, Texas A and M University, College Station, TX; (*d*) M. H. GONZALEZ and A. L. LEE. J. Chem. Eng. Data, **11**, 357 (1966).
14. N. B. VARGAFTIK. Tables on the thermophysical properties of liquids and gases. 2nd ed. J. Wiley, Halsted Press. 1975.
15. R. C. REID, J. M. PRAUSNITZ, and T. K. SHERWOOD. The properties of gases and liquids. 3rd ed. McGraw-Hill. 1977.
16. R. W. GALLANT. Physical properties of hydrocarbons. Vols. 1 and 2. Gulf Publ. Co. Houston, TX. 1968.
17. S. S.-S. HUANG and G. R. FREEMAN. J. Chem. Phys. **72**, 1989 (1980).
18. J. M. L. ENGELS and A. J. M. VAN KIMMENADE. Chem. Phys. Lett. **48**, 451 (1977).
19. I. GYÖRGY and G. R. FREEMAN. J. Chem. Phys. **70**, 4769 (1979).
20. J. LEKNER and A. R. BISHOP. Phil. Mag. **27**, 297 (1973).
21. I. ADAMCZEWSKI and B. JACHYM. Acta Phys. Pol. **30**, 767 (1966) and references therein.
22. B. L. HENSON. Phys. Rev. **135**, A1002 (1964).
23. N. ZESSOULES, J. BRINKERHOFF, and A. THOMAS. J. Appl. Phys. **34**, 2010 (1963).
24. H. T. DAVIS, S. A. RICE, and L. MEYER. J. Chem. Phys. **37**, 947 (1962).
25. R. J. LOVELAND, P. G. LECOMBER, and W. E. SPEAR. Phys. Lett. **39A**, 225 (1972).
26. R. L. WILLIAMS. Can. J. Phys. **35**, 134 (1957).
27. L. MEYER, H. T. DAVIS, S. A. RICE, and R. J. DONNELLY. Phys. Rev. **126**, 1927 (1962).
28. D. S. BURNS. Adv. Chem. Ser. **50**, 82 (1965).
29. E. CUNNINGHAM. Proc. R. Soc. London, a**83**, 357 (1910).
30. J. J. THOMSON and G. P. THOMSON. Conduction of electricity through gases. Vol. 1. 3rd ed. Cambridge University Press. 1928.
31. D. F. EVANS, T. TOMINAGA, J. B. HUBBARD, and P. G. WOLYNES. J. Phys. Chem. **83**, 2669 (1978) and references therein.
32. M. BORN. Z. Phys. **1**, 221 (1920).
33. R. M. FUOSS. Proc. Natl. Acad. U.S.A. **45**, 807 (1959).
34. K. R. ATKINS. Phys. Rev. **116**, 1339 (1959).
35. S. A. RICE and P. GRAY. The statistical mechanics of simple liquids. Interscience Publ., New York. 1965.
36. J. L. LEVINE and T. M. SANDERS, JR. Phys. Rev. Lett. **8**, 159 (1962); Phys. Rev. **154**, 138 (1967).
37. J. JORTNER, N. R. KESTNER, S. A. RICE, and M. H. COHEN. J. Chem. Phys. **43**, 2614 (1965).
38. YU. A. BERLIN, L. NYIKOS, and R. SCHILLER. J. Chem. Phys. **69**, 2401 (1978).
39. G. R. FREEMAN. J. Chem. Phys. **71**, 564 (1979).
40. J. JEANS. The dynamic theory of gases. 4th ed. Cambridge University Press. 1925. Chapt. XI.
41. S. D. HAMANN. *In* High pressure physics and chemistry. Vol. 2. *Edited by* R. C. Bradley. Academic Press, London. 1963. pp. 146, 147.
42. P. H. OOSTING and N. J. TRAPPENIERS. Physica, **51**, 418 (1971).
43. J. V. GAVEN, W. H. STOCKMAYER, and J. S. WAUGH. J. Chem. Phys. **37**, 1188 (1962).
44. J. D. NOBLE and M. BLOOM. Phys. Rev. Lett. **14**, 250 (1965).
45. H. HAMANN, H. RICHTERING, and U. ZUCKER. Ber. Bunsenges. Phys. Chem. **70**, 1084 (1966).
46. (*a*) W. M. HAYNES. Physica, **67**, 440 (1973); (*b*) A. DE BOCK, W. GREVENDONK, and W. HERREMAN. Physica, **37**, 227 (1967).
47. W. HERREMAN. Cryogenics, **17**, 415 (1977).
48. (*a*) R. E. RATHBUN and A. L. BABB. J. Phys. Chem. **65**, 1072 (1961); (*b*) R. HAUSSER, G. MAIER, and F. NOACK. Z. Naturforsch. **21**, 1410 (1966); (*c*) G. M. PANCHENKOV, N. N. BORISENKO, and V. V. ERCHENKOV. Russ. J. Phys. Chem. **44**, 1633 (1970).
49. A. L. MCCLELLAN. Tables of experimental dipole moments. Freeman, San Francisco. 1963. p. 251.
50. D. E. O'REILLY and E. M. PETERSON. J. Chem. Phys. **56**, 2262 (1972).

An infrared study of water in perfluorosulfonate (Nafion) membranes[1]

MICHAEL FALK

Atlantic Regional Laboratory, National Research Council of Canada, Halifax, N.S., Canada B3H 3Z1

Received February 21, 1980

Can. J. Chem. Downloaded from www.nrcresearchpress.com by 210.87.254.40 on 09/05/12
For personal use only.

MICHAEL FALK. Can. J. Chem. **58**, 1495 (1980).

We have studied the infrared spectra of H_2O, D_2O, and HDO in hydrated Nafion membranes in the sodium form. The spectrum of isotopically isolated HDO exhibits two distinct absorption bands in the OH stretching region and similarly in the OD stretching region. These bands have been taken to correspond to two distinct environments of the OH groups in Nafion, identified as O—H···O and O—H···CF_2. It appears that a substantial proportion of water molecules have an OH group (or occasionally both OH groups) exposed to the fluorocarbon environment. This implies that the hydrated ion clusters are either much smaller than previously estimated or, more likely, are non-spherical in shape with frequent local intrusions of the fluorocarbon phase. Water in Nafion is much less strongly hydrogen-bonded than water in aqueous salt solutions at the same temperature and may be expected to have distinct physical properties.

MICHAEL FALK. Can. J. Chem. **58**, 1495 (1980).

Nous avons étudié les spectres infrarouge de H_2O, D_2O et HDO dans des membranes hydratées de Nafion sous forme de sel de sodium. Le spectre du HDO isotopiquement isolé montre deux bandes distinctes d'absorption dans la région de vibration de valence OH et de même dans la région de valence OD. On admet que ces bandes correspondent à deux environnements distincts des groupements OH dans le Nafion, identifiés comme étant: O—H···O et O—H···CF_2. Il semble qu'une proportion appréciable des molécules d'eau ont un groupement OH (ou occasionnellement les deux groupements OH) exposés à l'environnement du fluorocarbone. Ceci indique que les groupes d'ions hydratés sont ou bien plus petits que prévu ou, plus probablement, possèdent une forme non sphérique avec de fréquentes intrusions locales de la phase fluorocarbone. L'eau dans le Nafion a des liaisons hydrogène moins fortes que celles de l'eau dans les solutions salines à la même température et on doit s'attendre à lui trouver des propriétés physiques différentes.

[Traduit par le journal]

Infrared spectroscopy can be an effective tool in the investigation of water dispersed in other media. As a part of a program of spectroscopic studies on water in different molecular environments, we have investigated water in hydrated Nafion membranes. Nafion is a perfluorosulfonate resin developed by the Plastics Department of du Pont (1). This polymer consists of a perfluorinated polyethylene backbone with pendant side-chains terminating with —$SO_3^-M^+$ groups, where M^+ is an exchangeable cation. The incidence and length of the side-chains is variable within limits and Nafion membranes used in electrochemical applications usually have equivalent weights of 1100 to 1500 per —$SO_3^-M^+$ group. Nafion membranes are used extensively as separators in electrolytic cells, their industrial importance being due to their exceptional chemical, thermal, and mechanical stability, combined with high permeability to cations (2).

The mechanism of cation transport, which holds the key to the membranes' performance, is not yet well understood, largely because of the lack of knowledge about the detailed microstructure of hydrated Nafion. Hydrated membranes of equivalent weight 1200, in the sodium form, contain up to 21% of water by weight or 18 H_2O per —$SO_3^-Na^+$ pair, the exact amount of water depending on pretreatment and on the thermal history of the sample (1). Studies of low-angle X-ray scattering and of other physical properties by Yeo and Eisenberg (3), Gierke (4), and others (5), as well as analogy with other ionomers (6), suggest that hydrated Nafion is a two-phase system, consisting of hydrated clusters of ions embedded in the surrounding fluorocarbon medium. Observed Bragg spacings are taken to indicate that the hydrated clusters are about 50 Å apart. Assuming that they are spherical in shape, and considering the volume changes occurring during the hydration process, Gierke estimated that the clusters are about 40 Å in diameter (4). Apart from this rough estimate of size, little is known to-date about the geometry of these hydrated ion clusters or about the state of water within them.

Some structural deductions may be made *a priori*. In the hydrated sodium form of Nafion there is sufficient water to complete the coordination of the sodium ion (which requires six H_2O) and of the polymer-bound sulfonate ion (which also requires about six H_2O), especially as water molecules may be shared between the cation and the anion. The ion pairs —$SO_3^-Na^+$ can therefore be expected to be fully surrounded by water, with the individual ions separated most of the time. This is indeed confirmed by the infrared study of the stretching vibrations of the —SO_3^- ion in Nafion by Mauritz and Lowry (7) and by the sodium-23 nmr study by

[1]NRCC No. 18318.

0008-4042/80/141495-07$01.00/0

©1980 National Research Council of Canada/Conseil national de recherches du Canada

Can. J. Chem. Downloaded from www.nrcresearchpress.com by 210.87.254.40 on 09/05/12
For personal use only.

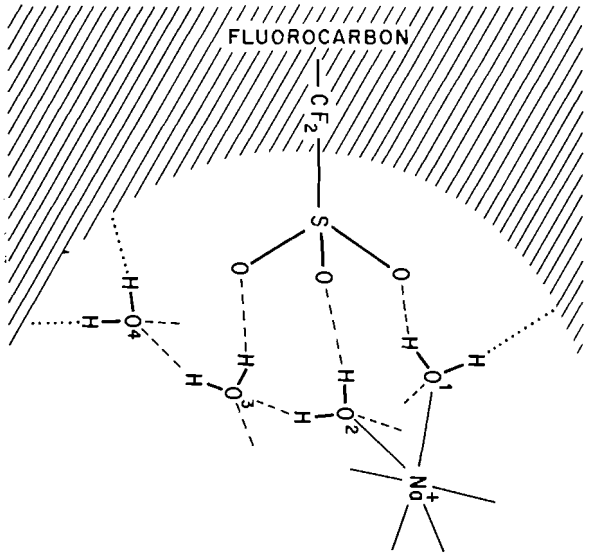


FIG. 1. Hydrogen-bonded (---) and non-hydrogen-bonded (···) interactions of water molecules in a portion of a hydrated ion cluster in Nafion.

Komoroski and Mauritz (8). The lone pairs of electrons on the water molecules within the clusters may interact either with a sodium ion or with an OH group of another water molecule. Similarly, the OH groups may interact either with an oxygen atom of an anion or with the oxygen of another water molecule (Fig. 1). Because of electrostatic repulsion, the periphery of the cluster is not likely to be completely lined with $—SO_3^-$ ions, so that some peripheral water molecules may find themselves in direct contact with the fluorocarbon phase. This would lead to the occurrence of a certain proportion of non-hydrogen-bonded OH groups, which should be detected and, in principle, quantitatively estimated by infrared spectroscopy.

Infrared spectra of Nafion have already been reported by Mauritz and Lowry (7), by Lopez *et al.* (9), and by Heitner-Wirguin (10), but these authors did not concern themselves in detail with the absorption bands due to water. Lopez *et al.* did not comment on the presence of a high-frequency shoulder in their spectra of H_2O in Nafion (Fig. 1 of ref. 9), while Heitner-Wirguin simply assigned such high-frequency shoulders to "free H_2O" (Table 3 of ref. 10), without any discussion of the structural implications of such an assignment. The present investigation deals specifically with the bands due to OH and OD stretching of the isotopic molecules H_2O, D_2O, and HDO, and those due to the bending fundamental of H_2O in the sodium form of Nafion (a similar study of other cationic forms will be presented separately). Special attention has been paid to the spectral profiles of the stretching bands of isotopically isolated HDO, which are most directly interpretable structurally (11, 12).

Experimental

Homogeneous Nafion films bearing product designations 125 (equivalent weight 1200, thickness 127 μm) and 142 E (equivalent weight 1400, thickness 51 μm) were obtained from the Plastics Department, E. I. du Pont de Nemours and Co. These films were supplied in the protonated form. Prior to use they were submitted to a standard pre-treatment (1) by boiling in distilled water for 30 min. They were then converted to the sodium form by immersion in 1 *N* NaCl solution for 1 h or more, rinsed, and dried over sulfuric acid.

The films were mounted in an infrared cell with silver chloride windows. The cell formed a part of a hygrostatic system in which moist air was continuously circulated, keeping the sample temperature at about 30°C and maintaining a constant relative humidity (rh) level and D/H ratio. The infrared absorption of the H_2O/D_2O vapor in the sample cell was compensated by a matched reference cell. A low rh level of about 3% was maintained with concentrated sulfuric acid. Higher levels of rh were obtained with saturated solutions in H_2O/D_2O of one of the following salts: $MgCl_2$ (about 33% rh), $NaNO_2$ (about 66% rh), or KBr (about 84% rh). High value of rh, approaching 100%, was maintained with an appropriate mixture of neat H_2O and D_2O. The films which have been equilibrated at 100% rh will be referred to as "hydrated", though their water content (found for Nafion 125 to be about 9% H_2O by weight) was substantially lower than that of fully hydrated Nafion as reported in ref. 1.

The spectra were recorded on a model 180 Perkin-Elmer spectrophotometer. The thickness of Nafion films was suitable for the study of the OH stretching fundamental of HDO when the films were about 90–95% deuterated, and for the study of the OD stretching fundamental of HDO when they were about 10% deuterated. The much more intense H_2O stretching fundamental in undeuterated films could only be studied at lower water contents, up to about 84% rh in Nafion 142 E and up to about 33% rh in the thicker films of Nafion 125. In recording the spectra in the region of the OD stretching fundamental, the absorption of dry Nafion due to overtones of the CF stretching vibrations was compensated by a matching dry film of undeuterated Nafion, placed in the reference beam outside of the hygrostatic system. In the regions of the OH stretching and HOH bending fundamentals, dry Nafion has no appreciable absorption bands and there was no need for compensation. The regions of the D_2O and HDO bending fundamentals were too strongly obscured by Nafion absorption to yield useful spectra.

Results and Band Assignments

HDO Stretching

Figure 2 shows the region of the OH stretching fundamental in the infrared spectrum of HDO in fully hydrated films of Nafion 125 and 142 E. The spectral profiles are very nearly the same, indicating that the state of water in Nafion does not change appreciably with the sulfonate content. The same conclusion was derived from the observations on the other water bands investigated.

The infrared spectrum of HDO in liquid water has a single broad OH stretching band, with a maximum, at 30°C, near 3404 cm^{-1} (13). Spectra of HDO in aqueous salt solutions (13) and those of

Can. J. Chem. Downloaded from www.nrcresearchpress.com by 210.87.254.40 on 09/05/12
For personal use only.

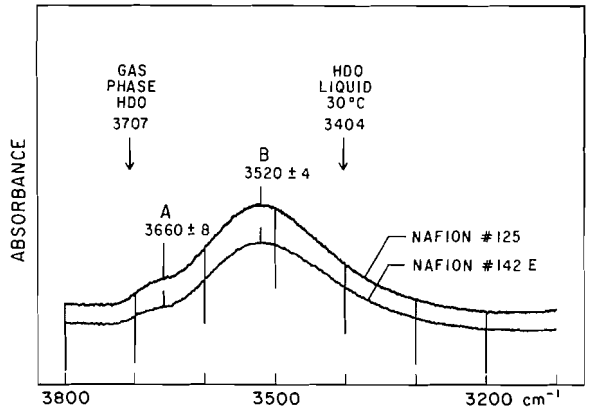


FIG. 2. The OH stretching region of HDO in the spectrum of two fully hydrated Nafion films (100% rh; 5% H, 95% D).

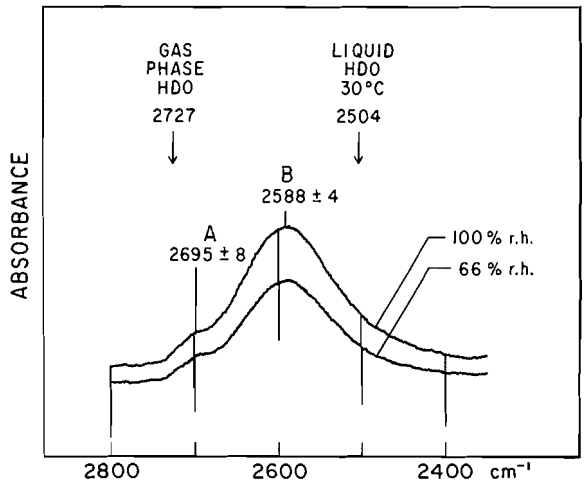


FIG. 3. The OD stretching region of HDO in the spectrum of Nafion 125 at two degrees of hydration (90% H, 10% D).

HDO in hydrophilic polymers such as nucleic acids (14) resemble the spectrum of the pure liquid at the corresponding temperature. In sharp contrast, the spectrum of HDO in hydrated Nafion consists of *two bands*, marked A and B in Fig. 2, whose frequencies, 3660 and 3520 cm^{-1}, are *much higher* than those of HDO in liquid water. Apparently OH groups in hydrated Nafion occur in two distinct types of surroundings, which we shall refer to as A and B, pending further discussion below.

Figure 3 shows the corresponding OD stretching absorption of HDO in Nafion 142 E at two water contents. The upper spectrum corresponds to fully hydrated Nafion and is analogous to the OH stretching spectra in Fig. 2. The OH/OD frequency ratios are $(3660 \pm 8)/(2695 \pm 8) = 1.358 \pm 0.005$ for band A, and $(3520 \pm 4)/(2588 \pm 4) = 1.360 \pm 0.003$ for band B, the same within experimental error as the ratio for HDO in the gas phase, 3707.5/2726.7 = 1.360 (15).

The lower spectrum in Fig. 3 shows that upon partial dehydration of Nafion small changes occur in the band shape. These changes are consistent with the frequencies of bands A and B remaining unchanged, and the ratio of the intensity of band A relative to band B increasing slightly upon dehydration. Similar observations were made for Nafion 125 and for the OH stretching band of HDO.

Structural Identification of Bands A and B

The main band in the spectrum of HDO in Nafion, labelled B, is clearly associated with those OH (or OD) groups of water in Nafion which form hydrogen bonds. Two types of hydrogen bonds are possible, water···water and water···sulfonate (Fig. 1). The occurrence of only one band with no resolved sub-structure indicates that these two possible types of O—H···O bonds are of similar average strength. Similarly, there is no spectroscopic distinction between the stretching frequencies of those water molecules which are interacting through their lone electron pairs with the sodium ions (H_2O^1 and H_2O^2 in Fig. 1) and those which only interact with other water molecules (H_2O^3 and H_2O^4 in Fig. 1). The situation is not unlike that observed in the spectra of HDO in salt solutions, discussed in ref. 13. The large shift of band B to high frequency with respect to the liquid-phase value (cf. Figs. 2 and 3) shows that the mean strength of hydrogen bonds is substantially lower than in liquid water.

The smaller band, labelled A, is at a frequency sufficiently close to that of gas-phase HDO (cf. Figs. 2 and 3) that is must be considered due to OH groups not involved in O—H···O hydrogen bonding. We believe that this band originates in the OH groups exposed to the fluorocarbon environment. The frequencies of HDO in monomeric water dissolved in perfluorinated solvents may be deduced from the data in refs. 16 and 17 to be about 3680 cm^{-1} for OH stretch and about 2705 cm^{-1} for OD stretch. The slightly lower observed frequencies of band A in Nafion (3660 cm^{-1} for OH stretch and 2695 cm^{-1} for OD stretch) are what would be expected for water molecules on the periphery of the flurocarbon medium, with one or both OH groups exposed to the flurocarbon, but also engaging in some water–water and water–ion interactions (cf. Fig. 1).

H_2O and D_2O Stretching

Figure 4 shows the OH stretching region of the spectrum of H_2O in undeuterated Nafion 142 E at different hydrations. Four distinct bands are re-

Can. J. Chem. Downloaded from www.nrcresearchpress.com by 210.87.254.40 on 09/05/12
For personal use only.

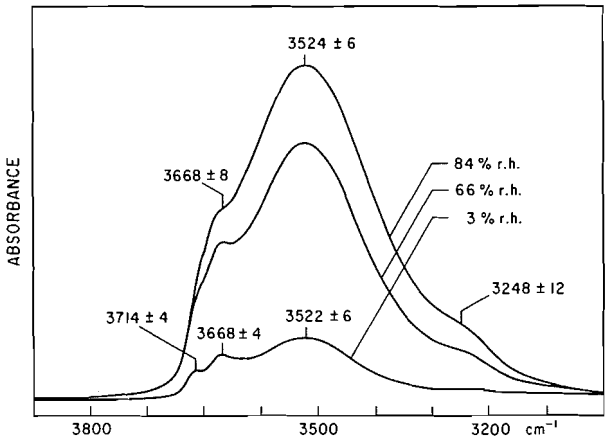


FIG. 4. The OH stretching region of H_2O in the spectrum of undeuterated Nafion 142 E at three degrees of hydration.

solved at low hydrations, three of them being still detectable at 84% rh. Figure 5 shows the corresponding OD stretching region of D_2O in the same Nafion sample in a nearly fully deuterated state. The D_2O features do not exactly correspond to the H_2O features of Fig. 4. For D_2O five distinct bands are evident at low hydrations and four at higher hydrations. The assignment of these H_2O and D_2O absorption bands, as well as their correspondence to the HDO bands A and B, require the following analysis.

If, as has been concluded from the HDO spectrum, OH groups in Nafion occur in two types of spectroscopically distinct surroundings, A and B, which differ widely as to the strength of hydrogen bonding, then the corresponding H_2O spectrum should consist of a superposition of contributions from two stretching fundamentals, ν_1 and ν_3, of H_2O molecules in each of three distinct types of

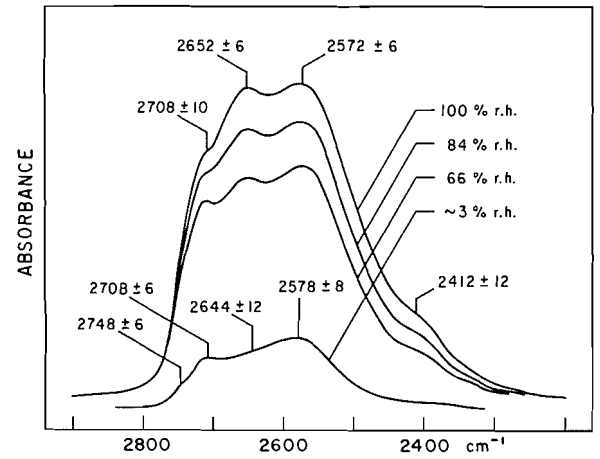


FIG. 5. The OD stretching region of D_2O in the spectrum of Nafion 142 E at four degrees of hydration (about 5% H, 95% D).

surroundings: A···HOH···A, A···HOH···B, and B···HOH···B. For brevity we shall refer to them as AA, AB, and BB. In addition, the lower-frequency portion of the OH stretching region of the H_2O spectrum may also contain a contribution from the overtone $2\nu_2$ of the HOH bending vibration, at about $2 \times 1630 = 3260\ cm^{-1}$. This overtone may complicate the observed spectrum by entering into Fermi resonance with the lower-frequency H_2O stretching fundamental, ν_1, resulting in intensity redistribution and frequency shifts (17). An analogous situation may be expected to occur for D_2O.

Schiffer *et al.* (18) have established a correlation between stretching frequencies of HDO and the

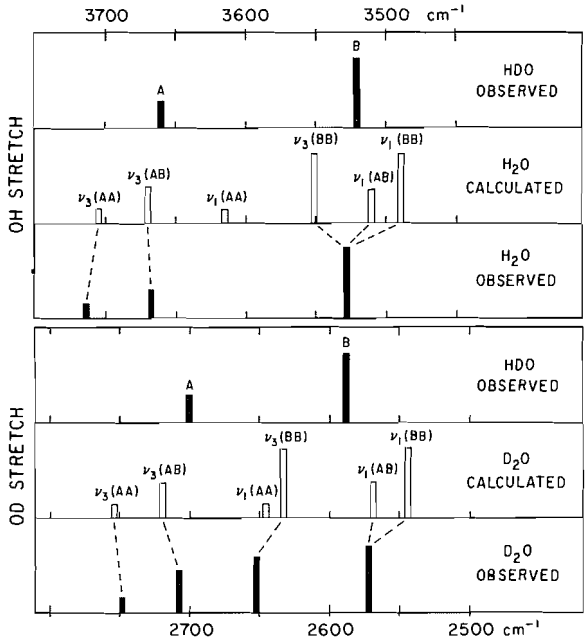


FIG. 6. Comparison of the observed stretching frequencies of H_2O and D_2O in Nafion with those calculated from the corresponding HDO frequencies.

corresponding frequencies of H_2O and D_2O. Using eqs. [1], [2], [15], and [16] in ref. 18, and the observed values of HDO frequencies, we have calculated the ν_1 and ν_3 frequencies of the H_2O and D_2O molecules of type AA, BB, and AB in Nafion. These calculated frequencies, which must be considered first-order approximations, since they neglect Fermi resonance with $2\nu_2$ and the coupling of like vibrations on neighboring molecules, are shown schematically in Fig. 6.

The observed H_2O spectrum (Fig. 4) shows a broad band at about $3248\ cm^{-1}$, which clearly corresponds to the $2\nu_2$ overtone, allowing for a small downward shift due to Fermi resonance. The remaining three observed features, at 3714, 3668, and

Can. J. Chem. Downloaded from www.nrcresearchpress.com by 210.87.254.40 on 09/05/12
For personal use only.

3524 cm^{-1}, are then assigned to the ν_1 and ν_3 fundamentals of AA, AB, and BB molecules as shown by broken lines in the upper part of Fig. 6. Apparently the bands due to ν_3(BB), ν_1(AB), and ν_1(BB) overlap into a single unresolved band, while ν_1(AA) is too weak to be observed in the midst of other, more intense absorptions. As may be expected from the HDO spectrum, most of the intensity arises from absorptions due to molecules of type BB, with a smaller contribution from AB, and a very small but observable contribution from AA.

Similarly, the observed D_2O spectrum (Fig. 5) shows a band at about 2412 cm^{-1}, which is due to the $2\nu_2$ overtone. This leaves four features which are then assigned to the partly superposed ν_1 and ν_3 fundamentals of the three types of D_2O molecules, as shown by broken lines in the lower part of Fig. 6. The reason for one more band being resolved in the D_2O spectrum than in the H_2O spectrum is the larger separation between the ν_1 and ν_3 fundamentals in molecules of type BB. As a result, D_2O and H_2O spectra present a different appearance in the stretching region. As before, the observation of the D_2O band at 2748 cm^{-1} shows the non-negligible occurrence of water molecules of type AA, at least at lower hydrations.

H_2O Bending

Figure 7 shows the region of the HOH bending fundamental in the spectrum of undeuterated Nafion at different degrees of hydration. Only one band is resolved in all cases, its maximum shifting slightly from about 1625 cm^{-1} in nearly dry Nafion to 1630 cm^{-1} in the fully hydrated material. The halfwidth varies from about 40 cm^{-1} to about 60 cm^{-1} with increasing hydration.

We interpret the single band as an unresolved envelope resulting from the superposition of bands due to HOH bending of the different types of water molecules. In general, increased hydrogen bonding increases the HOH bending frequency, hence the frequencies of molecules AA, AB, and BB may be expected to increase in that order. The observed small increase in frequency and bandwidth with increasing hydration may therefore reflect a minor increase in the relative proportions of the more strongly hydrogen-bonded molecules BB with respect to those of types AB and AA.

Discussion

Fraction of OH Groups Exposed to the Fluorocarbon Environment

The ratio of areas of bands A and B of HDO in Nafion should in principle provide a measure of the relative proportions of O—H···CF_2 and O—H···O

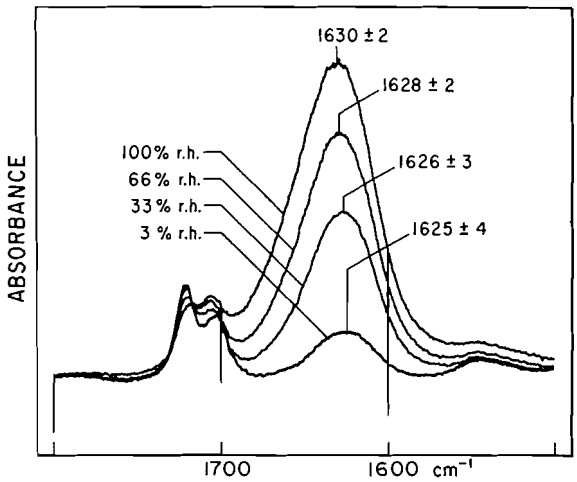


FIG. 7. The HOH bending region in the spectrum of undeuterated Nafion 142 E at four degrees of hydration. The small bands at 1545, 1705, and 1722 cm^{-1} are absorptions of dry Nafion.

environments. Unfortunately, a quantitative estimation is not possible but nevertheless a useful order-of-magnitude estimate can be made.

The individual areas of bands A and B are difficult to determine accurately because of severe overlap and uncertain profiles of the component bands. The best possible estimate is that bands A and B have an area ratio of the order of 1:13. In order to calculate the actual ratio of OH groups in the two environments, we have to allow for the well-known increase of the infrared absorptivity of OH (or OD) oscillators with hydrogen bonding. Glew and Rath found that the integrated absorptivity of the OH stretching fundamental is proportional to the frequency shift from the gas-phase frequency (16). Irregularities in such behavior are sometimes found (19), but assuming that the linear relation of Glew and Rath holds, we estimate that the OH groups giving rise to band B at 3520 cm^{-1} (2580 cm^{-1} for OD) probably absorb four times more intensely than those which give rise to band A at 3660 cm^{-1} (2695 cm^{-1} for OD). This means that the ratio of OH groups in OH···CF_2 environments to those in OH···O environments is of the order of 4:13. In other words, a fraction 4/(13 + 4) or roughly one quarter of all OH groups do not participate in OH···O bonding.

Geometry of the Hydrated Ion Clusters

We have deduced a rather surprising fact that a high proportion of water molecules in Nafion are exposed to the fluorocarbon medium, with somewhere of the order of a quarter of all OH groups so exposed. This finding has important implications for the size and shape of the hydrated ion clusters.

Can. J. Chem. Downloaded from www.nrcresearchpress.com by 210.87.254.40 on 09/05/12
For personal use only.

We must first of all assert that most of the water in hydrated Nafion is indeed in the clusters and is not dispersed in the fluorocarbon medium at the molecular level. Three observations point strongly to this being the case. Firstly, the solubility of water in the fluorocarbon medium may be expected to be very low. We have been unable to detect water spectroscopically in Teflon sheets thoroughly soaked in water (20). Secondly, the OH stretching frequencies of band A of HDO as well as the stretching frequencies of H_2O and D_2O assigned to ν_3(AA), are lower by 10–20 cm^{-1} than the frequencies reported for H_2O (16, 17) or calculated for D_2O for monomeric water molecules completely surrounded by liquid fluorocarbon. Thirdly, in the spectrum of Nafion at higher hydrations the relative intensity of bands assigned to ν_3(AA) of H_2O and D_2O is very small, showing that water molecules in $CF_2\cdots HOH\cdots CF_2$ environments are uncommon relative to those in $CF_2\cdots HOH\cdots O$ environments. Hence it is possible to conclude that most of the $OH\cdots CF_2$ interactions occur at the interface between the aqueous regions and the non-polar fluorocarbon phase, and not totally within the fluorocarbon phase. This implies a high surface-to-volume ratio for the hydrated clusters and points either to their small size or to a highly non-spherical shape.

If we assume that the clusters are approximately spherical, and are sharply defined from the surrounding phase, then the high surface-to-volume ratio requires that they have an average diameter of the order of 12 Å. This is much smaller than Gierke's estimate of 40 Å, (4) even after allowing for some diminution of cluster size with lowering of water content.[2]

If the clusters are indeed 30–40 Å in diameter, then the present results imply large-scale deviations from spherical geometry. The picture that emerges is that of the aqueous phase forming irregularly shaped bodies with numerous interconnections and local intrusions of the fluorocarbon phase. The side-chains, which due to their ether links are much less hydrophobic than the main fluorocarbon chain, are most likely to form such intrusions.

State of Water in Nafion

Our results indicate not only that a sizable fraction of OH groups of water in Nafion are exposed to the fluorocarbon medium and thus do not participate in hydrogen bonding, but also that those OH groups which do participate in the hydrogen bonding, do so weakly. Using the well-known linear relation between the lowering of the OH stretching frequency from the gas-phase value and the strength of the hydrogen bond, due to Badger and Bauer (21), the average strength of the remaining hydrogen bonds of water in Nafion can be estimated as about 62% of the value for liquid water at the same temperature: $(3707 - 3520)/(3707 - 3404) = (2727 - 2588)/(2727 - 2504) = 0.62$.

The cooperativity of hydrogen bonding between water molecules has been recognized long ago (22) and has been stressed again recently (23). Single water molecules are poor hydrogen-bond donors and acceptors, and the strength of hydrogen bonding increases rapidly with the size of the water cluster (24). Water in cellulose acetate membranes has recently been found to be relatively weakly hydrogen-bonded, which has been explained by the small average size of the clusters of water molecules in that medium (25). Judging from the OH or OD stretching frequencies of water in Nafion, hydrogen bonding in this medium appears to be even weaker than in cellulose acetate. This appears to be due not so much to the small size of the water clusters, as to the incompleteness of the hydrogen bonding in the aqueous phase, caused by what must be very frequent local intrusions of the fluorocarbon phase. In any event, it is clear that water in Nafion is in a state quite distinct from the liquid phase and may be expected to have physical properties widely different from those of bulk water or aqueous solutions.

Conclusions

1. Infrared spectra indicate that hydrogen bonding of water in fully hydrated Nafion is considerably weaker than in liquid water at the same temperature.

2. A substantial proportion of water molecules have one OH (or occasionally both OH groups) exposed to the fluorocarbon environment.

3. The hydrated ion clusters are either much smaller than previously estimated or, more likely, are highly non-spherical in shape with frequent local intrusions of the fluorocarbon phase.

4. Water absorbed in Nafion appears to be in a state quite unlike the liquid phase and may be expected to have physical properties widely different from those of water in aqueous solutions of electrolytes.

[2]Gierke's more recent results lead to the cluster diameter of about 30 Å for sodium Nafion of 1200 equivalent weight and a water content of 9% by weight, corresponding to the "hydrated" films used in the present study. I wish to thank Dr. Gierke for communicating these results to me prior to publication.

1. W. G. F. Grot, G. E. Munn, and P. N. Walmsey. Paper presented to the 141st National Meeting of the Electrochemical Society, Houston, TX, May 1972.

2. W. G. F. GROT. Chem. Inorg. Technol. **50**, 299 (1978).
3. S. C. YEO and A. EISENBERG. J. Appl. Polymer Sci. **21**, 875 (1977).
4. T. D. GIERKE. Paper presented at the 152nd National Meeting of the Electrochemical Society, Atlanta, GA, October 1977.
5. A. J. HOPFINGER, K. A. MAURITZ, and C. J. HORA. Paper presented at the 152nd National Meeting of the Electrochemical Society, Atlanta, GA, October 1977.
6. A. EISENBERG. Pure Appl. Chem. **46**, 171 (1976).
7. K. A. MAURITZ and S. R. LOWRY. Paper presented at the 152nd National Meeting of the Electrochemical Society, Atlanta, GA, October 1977.
8. R. A. KOMOROSKI and K. A. MAURITZ. J. Am. Chem. Soc. **100**, 7487 (1978).
9. M. LOPEZ, B. KIPLING, and H. L. YEAGER. Anal. Chem. **48**, 1120 (1976).
10. C. HEITNER-WIRGUIN. Polymer, **20**, 371 (1979).
11. M. FALK and T. A. FORD. Can. J. Chem. **44**, 1699 (1966).
12. M. FALK and O. KNOP. *In* Water: a comprehensive treatise. Vol. 2. *Edited by* F. Franks. Plenum Press, New York. 1973. Chapt. 2.
13. H. R. WYSS and M. FALK. Can. J. Chem. **48**, 607 (1970).
14. M. FALK, A. G. POOLE, and C. G. GOYMOUR. Can. J. Chem. **48**, 1536 (1970).
15. W. S. BENEDICT, N. GAILAR, and E. K. PLYLER. J. Chem. Phys. **24**, 1139 (1956).
16. D. N. GLEW and N. S. RATH. Can. J. Chem. **49**, 837 (1971).
17. J. R. SCHERER. *In* Advances in infrared and Raman spectroscopy. *Edited by* R. J. H. Clark and R. E. Hester. Vol. 5. Heyden and Son, London. 1978. Chapt. 3.
18. J. SCHIFFER, M. INTENZO, P. HAYWARD, and C. CALABRESE. J. Chem. Phys. **64**, 3014 (1976).
19. M. FALK and M. J. WOJCIK. Spectrochim. Acta, **35A**, 1117 (1979).
20. M. FALK and P. F. SETO. Unpublished results.
21. G. C. PIMENTEL and A. L. MCCLELLAN. The hydrogen bond. W. H. Freeman and Company, San Francisco. 1960. p. 83.
22. H. S. FRANK and W.-Y. WEN. Discuss. Faraday Soc. **24**, 133 (1957).
23. P. BARNES, J. L. FINNEY. J. D. NICHOLAS, and J. E. QUINN. Nature, **282**, 459 (1980).
24. D. HANKINS, J. W. MOSKOWITZ, and F. H. STILLINGER. J. Chem. Phys. **53**, 4544 (1970).
25. C. TOPRAK, J. N. AGAR, and M. FALK. J. Chem. Soc. Faraday Trans. I, **75**, 803 (1979).

Can. J. Chem. Downloaded from www.nrcresearchpress.com by 210.87.254.40 on 09/05/12
For personal use only.

Canadian Journal of Chemistry
Published by
THE NATIONAL RESEARCH COUNCIL OF CANADA

Journal canadien de chimie
Publié par
LE CONSEIL NATIONAL DE RECHERCHES DU CANADA

Volume 58 Number 15 August 1, 1980 Volume 58 numéro 15 1 août 1980

Can. J. Chem. Downloaded from www.nrcresearchpress.com by 210.87.254.5 on 09/05/12
For personal use only.

Etude en rmn ^{13}C de bicyclo[4,*n*,0]alcanones-3 *trans* α-substitués. Influence de la nature et de l'orientation du substituant sur le déplacement chimique du ^{13}C du carbonyle

PIERRE METZGER, ELIETTE CASADEVALL ET ANDRÉ CASADEVALL
Ecole Nationale Supérieure de Chimie de Paris, Laboratoire de Chimie Organique Physique, ERA CNRS 685, 11 Rue Pierre et Marie Curie, F 75231 Paris, France

ET

MARIE-JOSÉ POUET
Ecole Nationale Supérieure de Chimie de Paris, Laboratoire de Spectrographie, ERA CNRS 390, 11 rue Pierre et Marie Curie, F 75231 Paris, France

Reçu le 9 janvier 1980

PIERRE METZGER, ELIETTE CASADEVALL, ANDRÉ CASADEVALL et MARIE-JOSÉ POUET. Can. J. Chem. **58**, 1503 (1980).

Les spectres rmn ^{13}C de 31 bicyclo[4,*n*,0]alcanones-3, à jonction de cycle *trans*, α substituées, αα′ et αα disubstituées ont été déterminés. Les effets des substituants sont analysés en fonction de leur nature électronique, de leur configuration axiale ou équatoriale et du degré de déformation du cycle portant la fonction carbonyle. L'influence du substituant sur le déplacement chimique du $^{13}C{=}O$ est discutée sur la base de l'existence de formes de résonance du carbonyle, et des interactions de non liaison entre C=O et X. Comme les spectroscopies ir et uv, la rmn ^{13}C s'avère un bon outil pour déterminer la configuration d'un substituant en α du C=O dans les systèmes figés.

PIERRE METZGER, ELIETTE CASADEVALL, ANDRÉ CASADEVALL, and MARIE-JOSÉ POUET. Can. J. Chem. **58**, 1503 (1980).

The ^{13}C nmr spectra of α, αα, and αα′ substituted *trans-fused* bicyclo[4,*n*,0]alkan-3 ones, are described. Substituent effects are discussed in terms of their electron withdrawing character, axial or equatorial configuration, and cyclohexane deformation. $^{13}C{=}O$ chemical shifts are shown to be based on the polarization of π bond and on C=O/X non-bonded interactions. As in ir and uv spectroscopy, ^{13}C nmr is a convenient method for detecting an α substituent configuration in fixed ring ketones.

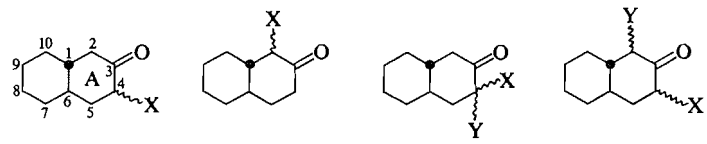
Les déplacements chimiques des carbones d'une molécule sont des données qui traduisent à la fois la géométrie moléculaire et l'environnement électronique. Au premier titre la rmn ^{13}C, tout comme la rmn ^{1}H qu'elle complète efficacement, a été utilisée pour résoudre des problèmes d'analyse conformationnelle de cyclanones et de leurs dérivés substitués (1, 2). Au second titre, l'influence du carbonyle sur les déplacements chimiques des autres carbones du cycle a été étudiée (3). Toutefois, la variation du déplacement chimique du $^{13}C{=}O$ en fonction de la nature électronique du substituant et de sa configuration axiale ou équatoriale, a été jusqu'ici peu explorée (4). C'est pourquoi il nous a paru intéressant de rapporter et de comparer les données rmn ^{13}C relatives à une série de 31 bicyclo[4,*n*,0]alcanones-3, α substituées, à jonction de cycle *trans*, avec $n = 4$, 3 ou 2 (Schéma 1 et Tableaux 1, 2, 3) et de dégager les relations qu'une telle comparaison peut mettre en évidence.

L'emploi d'un système figé permettant de distinguer plus aisément les effets électroniques, nous avons déterminé dans un premier temps, l'influence de la nature des substituants et de leur orientation axiale ou équatoriale sur le déplacement chimique des ^{13}C de la molécule, dans le cas de la bicyclo[4,4,0]décanone-3 *trans* avec X-4 = H, CH_3, OCH_3, $OCOCH_3$, C_6H_5, Br, Cl, F, NO_2, CN, $CO_2C_2H_5$ et C≡CH (composés **1** à **12** du Tableau 1). Cette étude a été étendue à quelques dérivés disubstitués -4,4 et -2,4 (composés **13** à **16**, du Tableau 2).[1]

Le système décanique à jonction *trans* étant un

[1]Bien qu'une nomenclature analogue à celle des cycles A et B des stéroïdes soit plus couramment utilisée pour la série décalinique, nous avons préféré utiliser une numérotation homogène pour les trois séries.

0008-4042/80/151503-09$01.00/0
©1980 National Research Council of Canada/Conseil national de recherches du Canada



1 à 12 **17 et 18** **13 et 14** **15 et 16**

Bicyclo[4,4,0]décanones-3 *trans*



19 et 20 **21 et 22**

Bicyclo[4,3,0]nonanones-3 *trans* Bicyclo[4,2.0]octanones-3 *trans*

SCHÉMA I

système cyclohexanique non déformé, il était par ailleurs intéressant de connaître l'influence d'une déformation géométrique du cycle sur les effets des substituants. Pour cela nous disposions de dérivés bicyclononaniques et bicyclooctaniques *trans* (composés **20** à **23** du Tableau 3 et Schéma 1). On sait en effet que la tension qui résulte d'une jonction 1–2 *trans* entraîne une déformation du cycle A qui est d'autant plus grande que le cycle qui lui est joint est plus petit (5, 6). Cette déformation qui se manifeste par un applatissement du cycle A au niveau du dièdre en *para* de la jonction, se traduit en particulier par la perte du caractère purement axial ou équatorial des liaisons *exocycliques* des carbones C_3 et C_4 délimitant ce dièdre.

Déplacements chimiques ^{13}C

Les carbones primaires, secondaires, tertiaires ou quaternaires ont été identifiés à l'aide de la méthode d'off-resonance. Selon les cas, un échange proton–deutérium en α' et (ou) en α du C=O, ou une irradiation sélective des protons H-2 et H-4 ont permis de différencier les carbones 2 et 4. Par ailleurs les effets γ d'un substituant axial d'une part, β et γ du deutérium (7) d'autre part, ont aidé à l'attribution des signaux correspondants aux carbones situés en β et γ du substituant. La caractérisation des signaux des ^{13}C en position 7, 8, 9 et 10 pour les composés décaniques, 7, 8 et 9 pour les composés nonaniques, 7 et 8 pour les composés octaniques a été réalisée sur la base de l'atténuation des effets δ, ε et ζ du substituant et des effets β du cycle A.

Les effets des substituants sur le déplacement chimique des différents carbones sont portés dans le Tableau 1 pour les dérivés monosubstitués de la bicyclo[4,4,0]décanone-3 *trans*, dans le Tableau 2 pour les dérivés disubstitués. Dans la Tableau 3 est établie une comparaison des déplacements chimiques ^{13}C des cétones appartenant aux trois séries bicycliques ainsi que de ceux de leurs dérivés chlorés.

Enfin dans le Tableau 4 nous mentionnons à titre indicatif le déplacement chimique des carbones 3 et 4 des cétones spontanément énolisables dans le solvant utilisé et de leurs énols respectifs: cyano-4*e*, nitro-4*e* et carbethoxy-4*e* bicyclo[4,4,0]-décanones-3 *trans*. Les autres carbones des formes énoliques n'ont pu être identifiés avec certitude, en raison même de l'existence de l'équilibre céto–énolique (environ 80:20). Si les $\delta^{13}C$ énoliques sont conformes à ce qui a déjà été observé (8), il faut noter que les signaux des $^{13}C_4$ des dérivés cyano et carbéthoxy se situent à des champs relativement forts pour des carbones de type sp^2.

Discussion des effets de substituants sur le déplacement chimique des carbones sp^3

(A) Bicyclo[4,4,0]décanones-3 trans *substituées en position-4*

1. Effet α C_4

La nature inductive de l'effet α se manifeste par la variation des valeurs des $\delta^{13}C_{\alpha X} - \delta^{13}C_{\alpha H}$ qui suit sensiblement l'échelle d'électronégativité des substituants (Tableau 5), avec cependant deux exceptions, déjà relevées pour les systèmes cyclohexaniques (10), celles des groupements C≡N et C≡C—H.

La comparaison des résultats figurant dans le Tableau 1, à ceux rapportés dans la littérature pour les cyclohexanes monosubstitués (10, 11) montre, comme cela a été antérieurement souligné (2), que la présence du carbonyle entraîne un affaiblissement de l'effet α.

Can. J. Chem. Downloaded from www.nrcresearchpress.com by 210.87.254.5 on 09/05/12
For personal use only.

Can. J. Chem. Downloaded from www.nrcresearchpress.com by 210.87.254.5 on 09/05/12
For personal use only.

TABLEAU 1. Effets des substituants sur le déplacement chimique des ^{13}C* de la bicyclo[4,4,0]décanone-3 *trans*

	δC_1	$\gamma' C_2$	βC_3	αC_4	βC_5	γC_6	δC_7	εC_8	ζC_9	εC_{10}	Autres carbones†
1 H†	43,67	48,67	208,78	41,63	34,06	42,23	33,34	(26,78)	(26,73)	34,76	
2*a* CH_3	−0,07	−3,81	3,65	3,23	6,23	−5,60	0,25	0,06	−0,01	−0,28	17,73
2*e* CH_3	0,97	0,03	1,22	3,26	9,39	0,45	−0,20	−0,09	−0,07	−0,25	14,63
3*a* OCH_3	1,01	−3,81	1,09	42,72	6,27	−5,66	−0,23	−0,05	−0,04	−0,22	56,67
3*e* OCH_3	0,61	−0,94	−1,54	42,26	7,27	−0,90	−0,35	−0,34	−0,16	−0,58	57,74
4*a* $OCOCH_3$	0,53	−3,40	−3,45	35,38	5,01	−5,13	−0,35	−0,14	−0,16	−0,28	169,39(CO); 20,42(CH_3)
4*e* $OCOCH_3$	0,33	−1,68	−6,03	34,60	5,53	−1,51	−0,37	−0,38	−0,18	−0,65	169,61(CO); 20,26(CH_3)
5*a* C_6H_5	0,41	−2,20	0,81	12,91	3,05	4,45	0,06	−0,13	−0,15	−0,52	139,21(C_1'); 129,15(*o*) 127,42(*m*); 126,95(*p*)
5*e* C_6H_5	0,84	0,43	−1,49	15,65	8,69	0,66	−0,26	−0,06	−0,04	−0,23	140,01(C_1'); 129,33(*o*) 128,36(*m*); 126,89(*p*)
6*a* Br	−0,11	−5,95	−6,07	10,63	7,71	−5,71	−0,82	−0,29	−0,21	−0,69	
6*e* Br	0,06	−1,06	−9,35	14,74	12,24	1,41	−0,76	−0,46	−0,34	−0,74	
7*a* Cl	0,12	−5,66	−5,66	19,57	7,67	−6,27	−0,76	−0,24	−0,16	−0,58	
7*e* Cl	0,08	−0,89	−8,65	22,39	11,38	0,31	−0,71	−0,46	−0,31	−0,76	
8*a* F	0,89	−3,58	−3,34	52,08	6,28	−5,79	−0,48	−0,17	−0,15	−0,34	
8*e* F	0,04	−1,84	−5,61	50,74	6,71	−1,99	−0,41	−0,42	−0,22	−0,75	
9*e* CN	−0,19	−1,18	−9,17	−0,10	4,24	1,06	−0,89	−0,29	−0,29	−0,52	117,16
10*e* NO_2	−0,30	−1,48	−10,63	50,53	3,90	−2,23	−0,72	−0,46	−0,39	−0,82	
11*e* $CO_2C_2H_5$			−4,30	15,79							172,77(CO); 60,47(CH_2) 14,40(CH_3)
12*a* C≡C—H	0,72	−3,91	−3,96	1,75	5,73	−4,29	−0,57	−0,17	−0,10	−0,36	82,93(C_1'); 74,04(C_2')

*En ppm, par rapport à X = H.
†Déplacements chimiques par rapport au TMS.

Can. J. Chem. Downloaded from www.nrcresearchpress.com by 210.87.254.5 on 09/05/12
For personal use only.

TABLEAU 2. Déplacements chimiques des ^{13}C des dérivés disubstitués de la bicyclo[4,4,0]décanone-3 *trans*

		C_1	C_2	C_3	C_4	C_5	C_6	C_7	C_8	C_9	C_{10}
13 CH_3-4*e*, Cl-4*a*	obs.	44,09	43,67	203,15	70,88	49,70	38,30	32,60	(26,49)	(26,13)	34,00
	calc.	44,80	43,00	204,30	64,50	51,10	36,40	32,40	26,50	26,00	33,90
14 CH_3-4*a*, Cl-4*e*	obs.	43,66	45,29	202,62	74,08	51,74	40,16	32,83	(26,43)	(25,96)	33,85
	calc.	43,80	44,00	203,80	67,30	51,70	36,50	32,90	26,40	25,90	33,70
15 Cl-2*e*, CH_3-4*e*	obs.	52,32	70,82	202,03	44,44	42,90	42,30	33,11	(26,43)	(25,77)	32,40
	calc.	52,81	70,70	201,39	44,07	43,16	43,13	33,14	26,24	25,70	32,50
16 Br-2*e*, Br-4*e*	obs.	51,49	62,52	191,88	53,70	45,59	43,73	33,84	(26,25)	(25,71)	32,75
	calc.	52,14	64,26	190,28	55,60	46,54	44,96	32,95	26,08	25,66	32,67

TABLEAU 3. Déplacements chimiques ^{13}C pour les bicyclo[4,*n*,0]décanones-3 *trans** et incréments pour leurs dérivés chlorés† en position 4

Composés	Système bicyclique et nature de X	δC_1	γC_2	βC_3	αC_4	βC_5	γC_6	δC_7	εC_8	C_9‡	εC_{10}
1	$n = 4$, H	43,67	48,67	208,78	41,63	34,06	42,23	33,34	(26,78)	(26,23)	34,76
7*a*	$n = 4$, Cl *a*	0,12	−5,66	−5,66	19,57	7,67	−6,27	−0,76	−0,24	−0,16	−0,58
7*e*	$n = 4$, Cl *e*	0,08	−0,89	−8,65	22,39	11,38	0,31	−0,71	−0,46	−0,31	−0,76
19	$n = 3$, H	47,44	47,44	209,26	40,92	32,03	45,64	29,98	23,79	30,48	
20*a*	$n = 3$, Cl *a*	0,01	−5,17	−6,10	19,55	6,25	−6,41	−0,17	−0,30	1,05	
20*e*	$n = 3$, Cl *e*	0,17	−1,50	−8,52	23,53	9,62	0,19	−0,12	0,26	0,85	
21	$n = 2$, H	42,47	48,68	207,65	41,70	30,66	43,55	27,73	28,09		
22*a*	$n = 2$, Cl *a*	−0,04	−4,46	−7,12	20,41	8,97	−5,77	−0,46	0,07		
22*e*	$n = 2$, Cl *e*	0,24	−0,49	−8,34	23,20	12,53	−0,84	−0,58	−0,25		

*$\delta^{13}C$ par rapport au TMS.
†$\delta^{13}C$ par rapport à X = H.
‡Effets sur C_9: ζ pour **1**, 7*a* et 7*e*, ε pour **19**, **20***a* et **20***e*.

Can. J. Chem. Downloaded from www.nrcresearchpress.com by 210.87.254.5 on 09/05/12
For personal use only.

TABLEAU 4. Déplacements chimiques des carbones 3 et 4 des formes énoliques des cyano, nitro et carbéthoxy-4*e* bicyclo[4,4,0]-décanones-3 *trans*, en ppm par rapport au TMS

X		C_3	C_4
CN	enol.	165,46	81,19
	Δ*	−34,15	39,66
NO_2	enol.	171,18	124,26
	Δ	−29,97	32,07
$CO_2C_2H_5$	enol.	172,07	97,21
	Δ	−32,41	39,79

*$\Delta = \delta^{13}C_{enol} - \delta^{13}C_{cétone}$.

Une autre observation, bien que n'ayant pas de lien direct avec l'effet α, découle de cette comparaison. En considérant que l'adjonction d'un cycle en C_6 au cyclohexane ne modifie que très peu le déplacement chimique des carbones situés en *para* de la jonction de cycle nouvellement formée, ce qui est le cas lorsque X = H, on peut calculer pour chaque substituant X un effet du carbonyle en β du substituant (effet βC=O) sur le carbone α portant le substituant:

$$\beta C{=}O = \delta^{13}C_4 - \delta^{13}C_{\alpha\ (cyclohexane\ monosubstitué)}$$

Les valeurs ainsi obtenues permettent de mesurer l'importance des interactions intramoléculaires C=O/X ressenties par le carbone α. Les valeurs de βC=O rassemblées dans le Tableau 6 montrent que les composés se classent suivant deux catégories par rapport à la cétone non substituée: (*1*) les composés dont le carbone α ne ressent pas plus de perturbation que lorsqu'il existe une interaction C=O/H. Il s'agit en particulier des composés à $CH_3(e)$, CN(*e*), et C≡C—H (*a*); (*2*) ceux dont le carbone α ressent une perturbation plus ou moins grande suivant le substituant, perturbation qui est nominalement supérieure ou inférieure à celle observée pour une interaction C=O/H.

TABLEAU 5. Variation de l'effet α du substituant en fonction de son électronégativité pour les bicyclo[4,4,0]décanones-3 substituées en position-4

X	Electronégativité (9)	$\delta^{13}C_X - \delta^{13}C_H$ X axial	X équatorial
H	2,28	0	
CH_3	2,3	3,23	3,26
Br	2,80	10,63	14,74
C_6H_5	3,0	12,91	15,65
$CO_2C_2H_5$			15,79
Cl	3,03	19,57	22,39
CN	3,3		−0,10
C≡C—H	3,3	1,75	
$OCOCH_3$		35,38	34,60
NO_2	3,4		50,53
OCH_3	3,7	42,72	42,26
F	3,95	52,08	50,74

TABLEAU 6. Effets du C=O sur le carbone α de bicyclo[4,4,0]-décanones-3 substitués en position-4

X	Effet $\beta_{C=O}$
H	14,7
$CH_3(a)$	17,8
C≡C—H(*a*)	14,8
C≡N (*e*)	13,8
CH_3 (*e*)	12,3
OCH_3 (*a*)	9,7
OAc (*a*)	7,7
NO_2 (*e*)	7,2
F (*a*)	5,7
Br (*e*)	4,4
Cl (*e*)	4,4
OCH_3 (*e*)	4,0
OAc (*e*)	2,7
Cl (*a*)	1,9
F (*e*)	0,9
Br (*a*)	−2,1

Il est intéressant de noter que pour un substituant X, le maximum de perturbation enregistrée sur C_α intervient pour celui des deux épimères (axial ou équatorial) qui est thermodynamiquement le plus stable. Il a été montré dans le cas des halogèno cétones (12), que la stabilisation des isomères à F(*e*), Cl(*a*) et Br(*a*) par rapport à leurs épimères respectifs provient d'une plus grande interaction orbitalaire entre les paires d'électrons libres de l'halogène et les orbitales

$$\sigma^*\left(\begin{array}{c} (X)\quad (O) \\ \diagdown\ \diagup\!\!\diagup \\ C\text{—}C \end{array}\right) \text{ ou } \pi^*(C{=}O)$$

Nous verrons plus loin que ces mêmes interactions peuvent permettre d'interpréter l'influence de l'halogène sur les déplacements chimiques $^{13}C{=}O$ relatifs, des halogéno-cétones épimères.

2. Effet β C_5

Tous les substituants ont un effet de déblindage sur le C_5, en général amplifié par rapport à l'effet de champ électrique $\langle E^2 \rangle$ observé en série cyclohexanique (13). Mis à part le cas des halogènes (2), il ne semble pas y avoir de lien entre l'intensité de cet effet et l'encombrement du substituant.

3. Effets γ

Dans tous les cas les effets γ des substituants axiaux produisent un blindage des signaux des carbones considérés ; cependant quelques différences apparaissent selon que le carbone est séparé de

TABLEAU 7. Influence de l'isomérie de position-2*e* et -4*e*, sur les effets Δ des substituants dans le cas des chloro et bromo bicyclo-[4,4,0]décanones-3 *trans* ($\Delta = \delta^{13}C_{\text{cétone halogénée}} - \delta^{13}C_{\text{cétone}}$)

	X-2	αC_2	βC_3	βC_1	$\gamma' C_4$	γC_6	γC_{10}	δC_5	δC_7	δC_9	εC_8
17	Cl-2*e*	21,98	−8,61	8,17	−0,82	0,45	−2,31	−0,29	−0,10	−0,46	−0,45
18	Br-2*e*	16,65	−9,15	8,41	−0,77	1,32	−1,35	0,24	0,37	−0,23	−0,24
	X-4	αC_4	βC_3	βC_5	$\gamma' C_2$	γC_6	δC_7	δC_1	εC_8	εC_{10}	ζC_9
7*e*	Cl-4*e*	22,39	−8,65	11,38	−0,89	−0,14	−0,71	0,18	−0,46	−0,76	−0,31
6*e*	Br-4*e*	14,74	−9,35	12,24	−1,06	1,41	−0,76	0,06	−0,46	−0,74	−0,34

celui portant le substituant par C=O (γ') ou non (γ). On peut noter qu'en valeur absolue $|\gamma C_6| > |\gamma' C_2|$, et que $\gamma' C_2$ est plus sensible à la nature du substituant que γC_6:

$$-5{,}70 < \gamma C_6 < -4{,}45 \quad -5{,}95 < \gamma' C_2 < -2{,}20$$

A l'inverse, les effets γ des substituants équatoriaux sont nettement moins marqués: (*1*) effet de déblindage faible ou nul dans le cas de CH_3 et C_6H_5 sur C_2 et C_6, et de Br et CN sur C_6, et (*2*) effet de blindage faible dans tous les autres cas.

4. Effets δ, ε *et* ζ

Ces effets sont peu importants comparativement aux autres effets et à leurs analogues déterminés en série cyclohexanique (10). Néanmoins les tendances suivantes sont relevées : effet de déblindage sur $\delta' C_1$; effet de blindage sur δC_7; effet de blindage sur $\varepsilon' C_{10}$ et εC_8, avec $|\varepsilon' C_{10}| > |\varepsilon C_8|$; effet de blindage faible sur le carbone ζC_9.

(B) Bicyclo[4,4,0]décanones-3 trans αα *et* αα' *disubstituées*

Les déplacement chimiques des dérivés αα et αα' disubstitués de la bicyclo[4,4,0]décanone-3 *trans* sont rapportés dans le Tableau 2. Les valeurs expérimentales sont comparées aux valeurs calculées à partir des incréments des dérivés monosubstitués en position-4 pour les dérivés αα, en position-4 et -2 pour les dérivés αα'. A ce titre les incréments des chloro-2*e* et -4*e* et bromo-2*e* et -4*e* bicyclo[4,4,0]décanones-3 *trans* sont rapportés dans le Tableau 7. On peut y noter pour chaque halogène une assez bonne concordance entre les valeurs d'incréments des deux isomères de position avec cependant trois déviations, celles: des effets α sur les carbones C_2 et C_4, des effets γ sur les carbones C_{10} et C_7, et des effects β sur les carbones C_1 et C_5. Ces déviations résultent pour les deux premières de l'interaction 1–3 de type diaxial entre X-2*e* et H-10*e*, interaction qui n'a pas son équivalent pour les isomères X-4*e*. Pour la troisième de ces déviations, elle trouve vraisemblablement son origine dans la différence de degré de substitution entre les carbones C_1 (tertiaire) et C_5 (secondaire). Revenons maintenant aux dérivés disubstitués **13** à **16** (Tableau 2); pour ces quatre composés un bon accord n'est observé entre valeurs calculées et expérimentales que pour le composé **15** (chloro-2*e* méthyl-4*e*). Dans les autres cas on n'observe pas d'additivité des incréments pour les carbones C_1 à C_7 du composé **16** (dibromo-2*e*, 4*e*) et C_2, C_3, C_6 et surtout C_4 des composés **13** et **14** (méthyl-4*e* chloro-4*a* et méthyl-4*a* chloro-4*e*). Ce manque de concordance peut être imputé à des déformations moléculaires provenant pour **16** de l'interaction stérique $H_{10e}/Br_{2e}/O_3/Br_{4e}$ qui doit être plus importante que $H_{10e}/Cl_{2e}/O_3/(CH_3)_{4e}$, dans le cas de **15**, et pour **13** et **14**, d'une disubstitution sur le même atome de carbone, comme cela a déjà été observé dans le cas de *gem* diméthyl ou dichloro substitution (1*c* et références citées). Les interactions de type dipole–dipole introduites par la disubstitution (14) et orbitalaires, à travers les liaisons pour le dérivé dibromé **16** (15), sont aussi susceptibles de rendre compte de la non-additivité des incréments.

(C) Influence de la déformation du cycle

Les déplacements chimiques $\delta^{13}C$ pour les bicyclo[4,4,0]alcanones-3 *trans* et les valeurs de $\Delta\delta^{13}C$ pour leurs dérivés α chlorés (chlore axial et équatorial) sont rassemblés dans le Tableau 3. A partir de ces données, il est difficile de définir une tendance générale de variation des déplacements chimiques en fonction de la déformation de cycle, comme dans le cas analogue des benzo[1,2 : 4,5]dicycloalcènes (16). Cependant si on limite la discussion aux carbones sp^3 C_2 et C_4, on peut noter que l'effet γ du chlore axial d'une part et la différence $^{Cl}\Delta$ = effet $\alpha_{eq.}$ − effet $\alpha_{ax.}$ diminuent lorsque la déformation du cycle A croît. Ces deux résultats sont en accord avec la perte de caractère axial ou équatorial du substituant sur le cycle en C_6 résultant de la modification des angles de torsion $X_4C_4C_3O$ (Tableau 8) lorsque le nombre d'atomes de carbone du cycle joint diminue (5, 6, 17).

Can. J. Chem. Downloaded from www.nrcresearchpress.com by 210.87.254.5 on 09/05/12
For personal use only.

Can. J. Chem. Downloaded from www.nrcresearchpress.com by 210.87.254.5 on 09/05/12
For personal use only.

TABLEAU 8. Valeurs des angles de torsion des chloro-4 bicyclo[4,*n*,0]alcanones-3 *trans**

	Valeur de *n*		
Angles de torsion	4†	3‡	2†
$X_{4e}C_4C_3 = 0$	2°9	4°3	8°4
$X_{4a}C_4C_3 = 0$	117°1	115°6	110°2

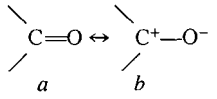
*C. Cabestaing, travaux non publiés.
†A partir de structure déterminées aux rayons X.
‡Par calcul d'optimisation.

Effets des substituants sur le déplacement chimique du $^{13}C{=}O$

L'examen des déplacements chimiques des $^{13}C{=}O$ rapportés dans les Tableaux 1, 2 et 3 permet de mettre en évidence plusieurs résultats: (*1*) la substitution d'un hydrogène en α du C=O par un atome ou un groupement électroattracteur se traduit par un blindage du $^{13}C{=}O$, généralement d'autant plus important que le pouvoir inductif du substituant est plus élevé. Inversement un groupe tel que CH_3, provoque un déblindage du $^{13}C{=}O$. Les déplacements chimiques extrêmes sont séparés de 14 ppm; (*2*) Pour un même substituant attracteur d'électron, une orientation équatoriale a un effet de blindage supérieur à celui d'une orientation axiale; (*3*) Une déformation de cycle croissante tend à diminuer l'écart $\Delta\beta C_3$ défini dans le Tableau 9.

Si l'effet de blindage d'un $^{13}C{=}O$ par les substituants électroattracteurs est relativement bien connu (réf. 4, voir aussi réf. 3, p. 279) par contre l'effet de l'orientation axiale ou équatoriale dans le cas de composés cycliques l'est beaucoup moins. Pour rendre compte de ces résultats deux interprétations basées l'une sur la polarisation de la double liaison C=O l'autre sur les interactions de non liaison C=O/X, sont envisageables.

Considérons en premier lieu les deux formes de résonance, *a* et *b*, généralement admises pour les cétones (19)



Ces deux formes contribuent à la distribution électronique totale autour du carbonyle, dont dépend le $\delta^{13}C{=}O$. Un atome d'halogène par ses électrons non partagés, en apportant une contribution électronique à l'environnement immédiat du carbonyle tendra à contrebalancer l'effet de la forme *b* et l'on observera un blindage du carbonyle pour les cétones halogénées par rapport aux cétones non substituées. Cette participation des électrons non partagés de l'halogène à la densité électronique sur le carbonyle, dépendra directement, pour des cétones de structure figée, des orientations relatives des liaisons C=O et C—X, une déviation à la coplanéarité ayant pour effet de réduire les interactions de résonance. Ceci se traduira par un blindage du $^{13}C{=}O$ plus important pour l'épimère à halogène équatorial que pour celui à halogène axial.

TABLEAU 9. $\Delta\beta C_3$ = effet $\beta_{eq.}$ − effet $\beta_{ax.}$, cas des chloro-4 bicyclo[4,*n*,0]alcanones-3 *trans*

n	4	3	2
$\Delta\beta C_3$	−3,01	−2,42	−1,22

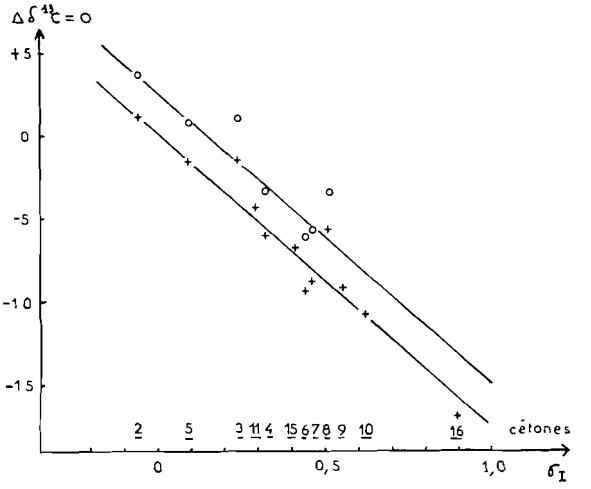


FIG. 1. Relations linéaires entre $\Delta\delta^{13}C{=}O$ et σ_I; ○: X axial, +: X équatorial.

L'existence de deux corrélations linéaires et parallèles, une pour chaque série d'épimères, entre le blindage de $^{13}C{=}O$ et les paramètres d'énergie libre σ_I des substituants[2] (Fig. 1) vient d'appuyer cette interprétation. (Ce même type de corrélation a précédemment été observée (*4c*) avec les dérivés du camphre substitués en position-4.) Il faut noter cependant deux exceptions: avec OCH_3 et F, les $^{13}C{=}O$ sont moins blindés que ne laissent prévoir les valeurs de σ_I. L'appartenance à cette corrélation des composés αα′ disubstitués, en tenant compte des valeurs de σ_I de chaque substituant montre que si une modification structurale par rapport aux dérivés monosubstitués existe, elle doit être très peu importante. Par contre les composés αα disubstitués, en raison de la double orientation de leurs substituants ne se situent sur aucune des deux droites.

La théorie des orbitales offre une autre méthode plus quantitative, méthode déjà utilisée par d'autres auteurs (*1d*, 2, 22), pour interpréter le blindage

[2] Les valeurs de σ_I sont celles indiquées dans la littérature (19), sauf pour $OCOCH_3$ (20), CN et $CO_2C_2H_5$ (21).

Can. J. Chem. Downloaded from www.nrcresearchpress.com by 210.87.254.5 on 09/05/12
For personal use only.

du $^{13}C{=}O$ par les substituants électroattracteurs sur la base d'interactions orbitalaires entre atomes non liés. Dans le cas des halogénocétones il a été montré que l'un des facteurs régissant la stabilité relative de deux épimères est lié à la grandeur des interactions orbitalaires qui existent entre les groupes non liés C=O et X (12).

$$c \quad n_X/\sigma^*(C{-}C)$$
$$\quad\quad\quad

*Nitro-4*e *bicyclo[4,4,0]décanone-3* trans, ***10***e

La réaction du nitrate d'amyle sur la bicyclo[4,4,0]-décanone-3 *trans* en présence de tertiobutylate de potassium selon une méthode déjà décrite (29) conduit essentiellement (>95%) au composé **10***e*, pf 81°C; ir (CCl_4) ν C=O:1735 cm^{-1}; ν C=C (énol): 1620 cm^{-1}; ν C—NO_2: 1560 cm^{-1}; rmn H (CCl_4) δ_{H_3}:5,23 ppm, quadruplet $J_{AX} + J_{BX} = 18{,}5$ Hz; $\delta_{OH_{énol}}$: 13,70 ppm.

*Carbéthoxy-4*e *bicyclo[4,4,0]décanone-3* trans, ***11***e

La méthode de synthèse employée (30) conduit aux isomères carbéthoxy-4*e* et carbéthoxy-2*e* dans les proportions 85:15. Des essais de séparation sur colonne de silice s'étant avérés infructueux c'est le mélange d'isomères qui a été utilisé. ir (CCl_4) ν C=O:1712 cm^{-1}; ν C=O (ester):1737 cm^{-1}; ν C=O (ester, forme énolique):1652 cm^{-1}; ν C=C (énol): 1610 cm^{-1}; rmn H (CCl_4) $\delta_{O—CH_2—CH_3}$:4,18 ppm, $J = 7$ Hz; $\delta_{O—CH_2—CH_3}$:1,27 ppm, $J = 7$ Hz; $\delta_{OH_{énol}}$:12,03 ppm.

*Dibromo-2*e,*4*e *bicyclo[4,4,0]décanone-3* trans, ***16***

Ce composé est obtenu par addition de 2 équivalents de brome sur la bicyclo[4,4,0]décanone-3 *trans* en solution dans l'acide acétique. Après décoloration du milieu réactionnel et extraction usuelle, le dérivé diéquatorial est isolé des autres isomères par cristallisation dans l'hexane, pf 133°C; ir (CCl_4) ν C=O:1755 cm^{-1}; rmn H (CCl_4) δ_{H_2}:4,41 ppm, $J = 11$ Hz; δ_{H_4}:4,71 ppm, $J_{AX} + J_{BX} = 18$ Hz.

1. (*a*) J. B. Stothers et C. T. Tan. Can. J. Chem. **52**, 308 (1974); (*b*) S. H. Grover, D. H. Marr, J. B. Stothers et C. T. Tan. Can. J. Chem. **53**, 1351 (1975); (*c*) M. F. Grenier Loustalot, P. Iratçabal, A. Forchioni et F. Metras. Org. Magn. Reson. **8**, 544 (1976); (*d*) J. Reise, C. Piccinni Leopardi, J. P. Zahra, B. Waegell et J. Fournier. Org. Magn. Reson. **9**, 512 (1977).
2. R. Jantzen, M. Tordeux, G. De Villardi et C. Chachaty. Org. Magn. Reson. **8**, 183 (1976).
3. J. B. Stothers. ^{13}C nmr spectroscopy. Academic Press, New York. 1972. p. 173 et suivantes.
4. (*a*) G. E. Maciel. J. Chem. Phys. **42**, 2776 (1965); (*b*) O. A. Gansow, D. A. Schexnayder et B. Y. Kimura. J. Am. Chem. Soc. **94**, 3406 (1972); (*c*) D. G. Morris et A. M. Murray. J. Chem. Soc. Perkin Trans. II, 1579 (1976); (*d*) F. C. Brown et D. G. Morris. J. Chem. Soc. Perkin Trans. II, 125 (1977); (*e*) F. C. Brown, D. G. Morris et A. M. Murray. Tetrahedron, **34**, 1845 (1978).
5. E. Casadevall, C. Largeau, P. Moreau et M. Bouisset. Tetrahedron, **29**, 1865 (1973).
6. B. L. Barnett et R. E. Davis. Acta Crystallogr. Sect. B, **26**, 326 (1970).
7. A. P. Tulloch. Can. J. Chem. **55**, 1135 (1977).
8. (*a*) J. H. Billman, S. A. Sojka et P. R. Taylor. J. Chem. Soc. Perkin Trans. II, 2034 (1972); (*b*) N. N. Shapet'ko, S. S. Berestova, G. M. Lukovkin et Y. S. Bogachev. Org. Magn. Reson. **7**, 237 (1975).
9. P. R. Wells. Progress in physical organic chemistry. Vol. 6. Interscience Publishers, John Wiley, New York, NY. 1968. p. 127.
10. H. J. Schneider et V. Hoppen. J. Org. Chem. **43**, 3866 (1978).
11. O. A. Subbotin et N. M. Sergeyev. J. Am. Chem. Soc. **97**, 1080 (1975); J. Chem. Soc. Chem. Commun. 141 (1976).
12. (*a*) O. Eisenstein, N. Trong Anh, A. Devaquet, J. Cantacuzene et L. Salem. Tetrahedron, **30**, 1717 (1974); (*b*) M. Loudet, F. Metras, J. Petrissans et G. Pfister-Guillouzo. J. Mol. Struct. **29**, 263 (1975).
13. H. J. Schneider et W. Freitag. J. Am. Chem. Soc. **99**, 8363 (1977).
14. H. J. Schneider, G. Becker, W. Freitag et V. Hoppen. J. Chem. Res. S, 14 (1979).
15. H. Duddeck. Tetrahedron, **34**, 247 (1978).
16. R. P. Thummel et W. Nutakul. J. Org. Chem. **43**, 3170 (1978).
17. P. Metzger, A. Casadevall et E. Casadevall. Tetrahedron Lett. 2027 (1973).
18. E. L. Eliel, N. L. Allinger, S. J. Angyal et G. A. Morrison. Conformational analysis. John Wiley, Inc., New York, NY. 1965. p. 462.
19. S. Ehrenson. Progress in physical organic chemistry. Vol. 2. Interscience Publishers, John Wiley, New York, NY. 1964. pp. 232 et 242.
20. R. W. Taft, E. Price, I. R. Fox, I. C. Lewis, K. K. Anderson et G. T. Davis. J. Am. Chem. Soc. **85**, 709 (1963).
21. L. P. Hammett. Physical organic chemistry. 2ème éd. McGraw Hill, New York, NY. 1970. p. 384.
22. H. Duddeck et P. Wolff. Org. Magn. Reson. **9**, 528 (1977).
23. R. S. Brown. Can. J. Chem. **54**, 5206 (1976); M. Tan Phan Viet, J. Lessard et J. K. Saunders. Tetrahedron Lett. 317 (1979).
24. L. Mion, A. Casadevall et E. Casadevall. Bull. Soc. Chim. Fr. 2950 (1968).
25. L. Mion, A. Casadevall et E. Casadevall. Bull. Soc. Chim. Fr. 3199 (1969).
26. L. Mion, A. Casadevall et E. Casadevall. Bull. Soc. Chim. Fr. 984 (1970).
27. P. Metzger, E. Casadevall et A. Casadevall. J. Chem. Res. S, 257 (1977); M, 2853 (1977).
28. J. C. Jallageas, A. Casadevall et E. Casadevall. Bull. Soc. Chim. Fr. 4321 (1969).
29. R. E. Schaub, W. Fulmor et M. J. Weiss. Tetrahedron, **20**, 273 (1964).
30. E. J. Corey, R. B. Mitra et H. Uda. J. Am. Chem. Soc. **86**, 485 (1964).

Can. J. Chem. Downloaded from www.nrcresearchpress.com by 210.87.254.5 on 09/05/12
For personal use only.

Viscosities of glycine and DL-alanine in water acetonitrile mixtures between 25 and 40°C

NIBARAN C. DEY AND BIRENDRA K. SAIKIA
Regional Research Laboratory, Jorhat, Assam, India
AND
INAMUL HAQUE
Dibrugarh University, Dibrugarh, Assam, India

Received July 25, 1979[1]

NIBARAN C. DEY, BIRENDRA K. SAIKIA, and INAMUL HAQUE. Can. J. Chem. **58**, 1512 (1980).

The relative viscosities and densities of glycine in 5%, 10%, 15%, and 20% w/w acetonitrile–water mixtures at 25, 30, 35, and 40°C and of DL-alanine in water, 5%, 15%, and 20% w/w acetonitrile water mixtures at 30 and 40°C have been determined. The viscosity *B* coefficients have been found to increase with increase in concentration of acetonitrile and also with the increase of temperature in both cases.

The limiting apparent molar volumes and limiting value of effective flow volumes have also been calculated.

NIBARAN C. DEY, BIRENDRA K. SAIKIA et INAMUL HAQUE. Can. J. Chem. **58**, 1512 (1980).

On a déterminé les viscosités et les densités relatives de la glycine dans des mélanges d'acétonitrile–eau à 5, 10, 15 et 20% (w/w), à 25, 30, 35 et 40°C et celle de la DL-alanine dans des mélanges d'acétonitrile–eau à 5, 15 et 20% (w/w), à 30 et 40°C. On a trouvé que les coefficients de viscosité *B* dans les deux cas augmentent avec la concentration de l'acétonitrile et également avec la température.

On a également calculé les volumes molaires apparents limites et la valeur limite des volumes d'écoulement effectif.

[Traduit par le journal]

Viscosity measurement provides valuable information about the size and state of solvation of molecules in solution (1). Such measurements on dipolar ions, particularly of the amino acids, have been carried out by a number of workers (2–5), namely, in aqueous solutions. However, the work has not been extended to nonaqueous or mixed aqueous solvents. The temperature effect on the solvation has also not been extensively studied. The present work reports viscosity and density measurements between 25 and 40°C in aqueous acetonitrile solutions of glycine and DL-alanine.

Experimental

Glycine and DL-alanine (A.R. Grade) were purified and dried by usual methods and stored in a desiccator over P_2O_5. Acetonitrile (reagent grade) was dried over anhydrous copper sulfate for several days with frequent agitation. It was doubly distilled each time collecting only the middle fraction. Its refractive index, density, and viscosity compared well with the literature values (6). Doubly distilled water was used for making up solutions. All the solutions were prepared by weight and vacuum correction was made for each weight.

Viscosity was measured with a Cannon Fenske direct flow viscometer having a viscosity constant of about 0.003 at 25°C. The kinetic energy correction term was found to fall in the region of experimental error for the solutions under study and, therefore, was neglected. Flow time measurement was repeated for each solution until three successive measurements agreed to within ±0.02%. Loading error was minimised by using capillary head pipette.

All the viscosity and density measurements were carried out in a thermostatic water bath, the temperature of which was kept constant to within ±0.01°C.

[1]Revision received March 30, 1980.

Results and Discussion

The relative viscosity η_r was calculated by using the equation (1)

$$[1] \quad \eta_r = (\eta/\eta_0) = (\rho t/\rho_0 t_0)$$

where η, ρ, "t" represent the viscosity, density, and flow time respectively of the solution and η_0, ρ_0, and "t_0" refer to those of the solvent.

Experimental values of relative viscosity were fitted into eq. [2] by the method of least squares.

$$[2] \quad \eta_r = (\eta/\eta_0) = 1 + BC + DC^2$$

The constant B measures the size and shape effect of the solute as well as structural modification, induced by solute solvent interaction, and is the major contributor to relative viscosity in eq. [2]. The constant D is relatively small in magnitude and its significance is not clearly understood (5). The contribution of D in the relative viscosity for the concentrations under study is small and, therefore, could not be evaluated with sufficient precision for a comparative study. In general, the values of D for glycine in water–acetonitrile solution lie between 0.015 to 0.03 and for DL-alanine between 0.03 to 0.07, for the concentration and temperature ranges covered in the present study.

In order to compare our results with those of others (5), we determined the density and viscosity of glycine in water at 25°C. The overall reproducibility in the individual viscosity measurement was found to be better than 0.1%. Figure 1 shows the

0008-4042/80/151512-04$01.00/0
©1980 National Research Council of Canada/Conseil national de recherches du Canada

Can. J. Chem. Downloaded from www.nrcresearchpress.com by 210.87.254.105 on 09/05/12
For personal use only.

Can. J. Chem. Downloaded from www.nrcresearchpress.com by 210.87.254.105 on 09/05/12
For personal use only.

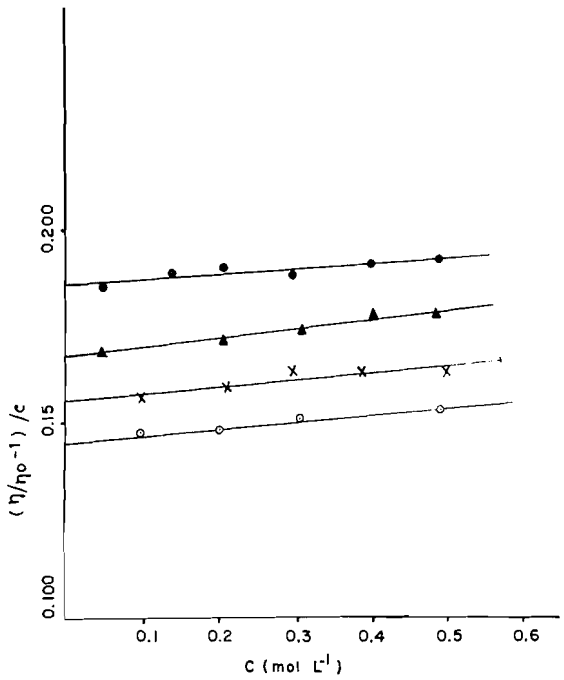


FIG. 1. Variation of B and D coefficients of eq. [2] for glycine with acetonitrile concentration; 5% AN, ⊙; 10% AN, ×; 15% AN, ▲; 20% AN, ●.

variation of B and D constants with concentration of glycine in different water–acetonitrile mixtures at 25°C.

The B value[2] of glycine increases with the increase in temperature up to 35°C in all the solvent compositions. Since (dB/dT) is positive for a structure-breaking solute (7–9), we easily classify glycine as a structure breaker in water–acetonitrile solvent mixtures. In structured solvents, a solute with or without a primary solvation sheath can apparently affect the degree of "structure" of solvent molecules at relatively large distances. Tyrrell and Kennerley (4) proposed that in aqueous solution, glycine has a primary solvation shell and that the solvated solute is a net structure breaker. Devine and Lowe (5) classified glycine as a net structure breaker in aqueous solution assuming that the electrostrictive solvation of NH_3^+ and CO_2^- varies little with temperature. This assumption is likely to be valid at relatively lower temperature. We observed a negative (dB/dT) at 40°C for 15% and 20% acetonitrile solutions and this might be a result of decrease in solvation.

For DL-alanine we observe a negative (dB/dT) in pure water. At 5% acetonitrile solution, (dB/dT) is insignificant and at higher acetonitrile concentration (dB/dT) is positive. Devine and Lowe (5) from a study of the viscosity of aqueous β-alanine concluded that β-alanine is a structure breaker. Phang (10) has proposed that DL-alanine is a structure breaker in aqueous dimethylformamide solution. Mason *et al.* (2), however, classified both α-alanine and β-alanine as structure makers from a study of differential entropies of dilution and the differential activation energy for viscous flow. The controversy seems to arise from the hydrophobic structure stabilization by the apolar groups and the structure breaking by NH_3^+ and CO_2^- groups, the net effect of which might vary under experimental conditions. It has been shown (5) that the contribution per CH_2 group of the aminoacids towards viscosity B coefficient (ΔB) in water at 25°C is 0.084 $dm^3\ mol^{-1}$, instead of the hydrodynamically predicted value of 0.038. This implies that CH_2 groups lead to stabilization of water structure. In glycine the hydrophobic stabilization effect is overcompensated by structure breaking. In case of DL-alanine in pure water structure stabilization is higher and we observe a negative (dB/dT). In aqueous acetonitrile solution the hydrophobic stabilization is less effective and we observe a positive (dB/dT) at higher acetonitrile concentration as a result of net structure-breaking effect.

The B value of glycine increases with increase in acetonitrile concentration. In aqueous solution the B value of glycine at 25°C as given by Devine and Lowe (5) is 0.143 ± 0.002. The corresponding value at 20% acetonitrile solution is 0.187. For DL-alanine also, the B value increases with increase in acetonitrile concentration. The B value of DL-alanine at 30°C is 0.241 and 0.261 in pure water and 20% acetonitrile solution, respectively. In view of the opposite nature of glycine and DL-alanine in pure water, this increase in B value in aqueous acetonitrile solution cannot alone be due to disruption of water structure by acetonitrile. The solutes might, therefore, be solvated by acetonitrile. Since positive (dB/dT) was observed as discussed above, acetonitrile must be strongly attached to the solutes. Zana *et al.* (11) have recently shown that electrostriction of ions in acetonitrile is larger than in water. The steep increase of B value between 15% and 20% acetonitrile solution must be con-

[2]The experimental values of density, relative viscosity, and the B coefficient values for glycine in 5%, 10%, 15%, and 20% acetonitrile solutions at 25°C, 30°C, 35°C, and 40°C; for DL-alanine in water, 5%, 15%, and 20% acetonitrile solutions at 30°C and 40°C and the density and viscosity of mixed solvents are available, at a nominal charge, from the Depository of Unpublished Data, CISTI, National Research Council of Canada, Ottawa, Ont., Canada K1A 0S2.

TABLE 1. Limiting apparent molar volume ϕ_v^0 ($cm^3\ mol^{-1}$) and B/ϕ_v^0 (cm^{-3}) values for glycine in aqueous acetonitrile solution

Solvent composition	25°C		30°C		35°C		40°C	
	ϕ_v^0	$10^3B/\phi_v^0$	ϕ_v^0	$10^3B/\phi_v^0$	ϕ_v^0	$10^3B/\phi_v^0$	ϕ_v^0	$10^3B/\phi_v^0$
Pure water*	42.9	3.33						
5% acetonitrile	43.0	3.37	43.7	3.37	43.5	3.47	44.0	3.52
10% acetonitrile	42.9	3.65	43.2	3.71	43.2	3.81	43.4	3.83
15% acetonitrile	42.2	3.95	42.3	4.21	42.2	4.25	42.3	4.10
20% acetonitrile	42.0	4.44	42.0	4.51	42.7	4.76	42.9	4.36

*From ref. 5.

nected, at least partially, with water-structure breaking by acetonitrile. Gorbunov *et al.* (12) found from ir spectroscopic study that the hydrogen bond of H_2O molecules becomes weaker in the presence of acetonitrile.

In both the solutes, the B coefficient increases more rapidly with increase in acetonitrile concentration than in the case of aqueous dimethylformamide solution (10). The graphically obtained B values of glycine for 0.05 mole fraction of acetonitrile and dimethylformamide in aqueous solution is found to be 0.157 and 0.152 respectively. This higher B value in acetonitrile solution might be connected with stronger solvation by acetonitrile.

The apparent molar volumes (ϕ_v) were calculated from the experimental density data. The limiting apparent molar volumes (ϕ_v^0) were then calculated by the method of least squares from the equation.

$$[3]\quad \phi_v = \phi_v^0 + AC$$

where A is a constant and C is the molarity. The values of ϕ_v^0 at 25°C are close to those reported in water (2, 5) and aqueous dimethylformamide solution (10). Within experimental error ϕ_v^0 varies little. A small increase is observed with rise in temperature. The values of ϕ_v^0 and B/ϕ_v^0 are shown in Tables 1 and 2.

In order to treat the aminoacids as suspension of rigid particles, we made use of the Vand (13) equation, as modified by Eagland and Pilling (14), shown in eq. [4],

$$[4]\quad C/[\log \eta/\eta_0] = 2.303/2.5V_h - 2.303QC/2.5$$

where Q is a particle interaction coefficient and V_h is the effective flow volume. V_h includes that part of the solvent molecules which are immobilized inside the cavities of the solute molecules. It will also include the solvent molecules in a primary solvation layer for a solvated species. A plot of $C/(\log \eta/\eta_0)$ against C should be linear with a slope of $2.303Q/2.5$ and an intercept of $2.303/2.5V_h$ when $C \rightarrow 0$. This effective flow volume as $C \rightarrow 0$ is

TABLE 2. Limiting apparent molar volume ϕ_v^0 ($cm^3\ mol^{-1}$) and B/ϕ_v^0 (cm^{-3}) values for DL-alanine in aqueous acetonitrile solution

Solvent composition	30°C		40°C	
	ϕ_v^0	$10^3B/\phi_v^0$	ϕ_v^0	$10^3B/\phi_v^0$
Pure water	61.0	3.95	61.7	3.77
5% acetonitrile	59.9	4.12	60.1	4.08
15% acetonitrile	60.0	4.19	60.2	4.33
20% acetonitrile	60.5	4.31	60.7	4.45

termed as the "limiting value of effective flow volume" (V_h^0). For spherical suspension it has been shown by Eagland and Pilling (14) that

$$[5]\quad B = 2.5V_h^0$$

The variation of V_h^0 with temperature and acetonitrile concentration for glycine and DL-alanine is shown[3] in Fig. 2. It was found that V_h^0 obtained from eq. [4] also satisfied eq. [5], within experimental error. Therefore, the spherical approximation is valid for both glycine and DL-alanine.

The large value of the ratio B/ϕ_v^0 as shown in Tables 1 and 2 and also the large value of V_h^0 compared to ϕ_v^0 undoubtedly suggest primary solvation of glycine and DL-alanine. As seen in Fig. 2, V_h^0 is larger in mixed solvent than in pure water. Further increase in V_h^0 with increase in acetonitrile concentration is more significant in case of glycine than in DL-alanine. The steep increase in V_h^0 between 15% and 20% acetonitrile is quite distinguishable. It is interesting to note that the solvent viscosity decreases at this concentration. We conclude that at this concentration acetonitrile is capable of quickly destroying the prevailing "water structure" in the mixed solvent.

Hereby we conclude that acetonitrile breaks water strucuture, particularly at concentrations above 15%. Glycine and DL-alanine, which are normally solvated in aqueous solution, are also sol-

[3]Values of V_h^0 of glycine in water at 25°C and 35°C are obtained from ref. 2.

Can. J. Chem. Downloaded from www.nrcresearchpress.com by 210.87.254.105 on 09/05/12
For personal use only.

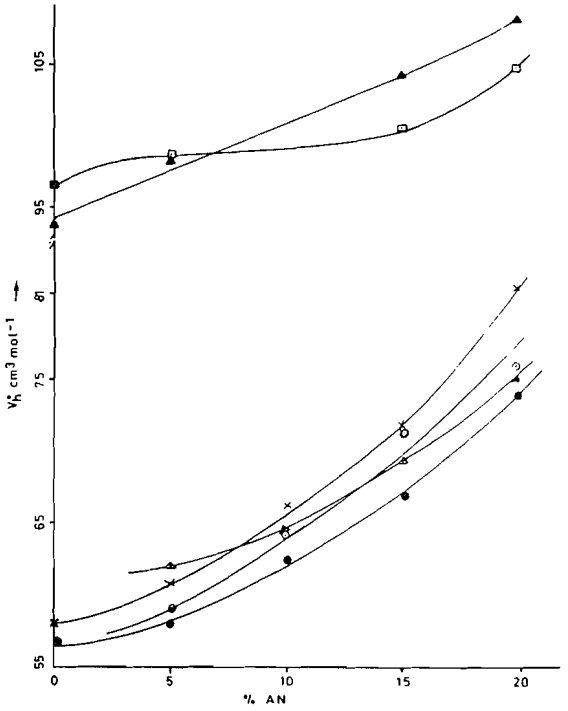


FIG. 2. Limiting value of "effective flow volume" as a function of AN concentration and temperature for glycine at 25°C, ●; 30°C, ⊙; 35°C, ×; 40°C, △; and DL-alanine at 30°C, ⊡ and 40°C, ▲.

vated by acetonitrile in aqueous acetonitrile solution. Both glycine and DL-alanine behave as net structure breakers in aqueous acetonitrile solution and this behaviour is the result of long range structure breaking beyond the structure forming solvation zone. Assumption of rigid spherical suspension is valid for both solvated glycine and DL-alanine.

Acknowledgements

We thank Dr. G. Thyagarajan, Director, Regional Research Laboratory, Jorhat, for his encouragement and permission to publish this paper. We also thank Mr. P. G. Rao for programming the calculations.

1. R. H. STOKES and R. MILLS. Viscosity of electrolytes and related properties. Pergamon, London. 1965.
2. L. S. MASON, P. M. KAMPMEYER, and A. L. ROBINSON. J. Am. Chem. Soc. **74**, 1287 (1952).
3. J. N. TSANGARIS and R. B. MARTIN. Arch. Biochem. Biophys. **112**, 267 (1965).
4. H. J. V. TYRRELL and M. KENNERLEY. J. Chem. Soc. A, 2724 (1968).
5. W. DEVINE and B. M. LOWE. J. Chem. Soc. A, 2113 (1971).
6. C. MARSDEN and S. MANN. Solvents guide. 2nd ed. Interscience, New York. 1963. p. 16.
7. R. W. GURNEY. Ionic processes in solution. McGraw Hill, New York. 1953. Chapts. 9 and 10.
8. H. S. FRANK and M. W. EVANS. J. Chem. Phys. **13**, 507 (1948).
9. H. S. FRANK and W. Y. WEN. Discuss. Faraday Soc. **24**, 133 (1957).
10. S. PHANG. Aust. J. Chem. **30**, 1605 (1977).
11. R. ZANA, G. PERRON, and J. E. DESNOYERS. J. Soln. Chem. **8**(10), 729 (1979).
12. B. Z. GORBUNOV and YU. I. NABERUKHIN. Zh. Strukt. Khim. **16**, 816 (1975).
13. V. VAND. J. Phys. Chem. **52**, 277 (1948).
14. D. EAGLAND and G. PILLING. J. Phys. Chem. **76**, 1902 (1972).

Can. J. Chem. Downloaded from www.nrcresearchpress.com by 210.87.254.105 on 09/05/12
For personal use only.

Specific decomposition rate constants in unimolecular reactions[1]

HUW O. PRITCHARD AND GALINA M. DIKER
Centre for Research in Experimental Space Science, York University, Downsview, Ont., Canada M3J 1P3
AND
ANDREW W. YAU
Herzberg Institute of Astrophysics, National Research Council of Canada, Ottawa, Ont., Canada K1A 0R6
Received January 11, 1980

HUW O. PRITCHARD, GALINA M. DIKER, and ANDREW W. YAU. Can. J. Chem. 58, 1516 (1980).

The original treatment of unimolecular reactions given by Polanyi and Wigner in 1928 is recast in quantum terms. It is found that very simple and natural choices for the oscillation which is assumed to cause reaction lead to good predictions of the specific reaction rate constant $k(E)$, and also the overall rate of reaction: nitrous oxide, carbon dioxide, methyl isocyanide, trideuteriomethyl isocyanide, ethyl isocyanide, ethyl chloride, cyclopropane, cyclobutane, and ethane are treated as illustrations.

HUW O. PRITCHARD, GALINA M. DIKER et ANDREW W. YAU. Can. J. Chem. 58, 1516 (1980).

Le travail original de Polanyi et Wigner (1928) sur les réactions unimoléculaires est revu en termes quantiques. Un choix naturel et simple de l'oscillation qui cause présumément la réaction fournit de bonnes prédictions pour les constantes de vitesse spécifiques de réaction $k(E)$ aussi bien que la vitesse globale de réaction. Comme examples, on utilise l'oxide nitreux, l'oxide carbonique, l'isocyanure de méthyle, l'isocyanure de trideutérométhyle, l'isocyanure d'éthyle, le chlorure d'éthyle, le cyclopropane, le cyclobutane et l'éthane.

[Traduit par le journal]

Introduction

In 1928, Polanyi and Wigner proposed the first molecular-dynamic picture of a unimolecular reaction (1). They imagined the molecule to consist of n atoms of essentially equal mass, held together by roughly equally strong forces; they then analysed in simple terms the vibrational motions of such a collection of atoms and concluded that an amount of energy greater than ε would be concentrated in a particular bond approximately $\nu e^{-\varepsilon/kT}$ times per second, where ν is the fastest vibrational frequency in the molecule, and $\varepsilon \gg kT$. Thus, if ε is identified as the critical energy required for dissociation or for transformation to another species (we shall use E_{crit} for this quantity in our reformulation), then it follows naturally that the rate constant for the reaction is, in its simplest form,

$$[1] \quad k \simeq \nu e^{-\varepsilon/kT}$$

This expression applies only if the critical energy ε is assumed to be confined in one linear dimension, but Polanyi and Wigner also derived formulae applicable to the cases where ε was assumed to be concentrated in either two or three linear dimensions, the latter yielding the rate constant expression

$$[2] \quad k \simeq \frac{2\nu\varepsilon}{kT} e^{-\varepsilon/kT}$$

This primitive treatment of molecular vibration was developed extensively by Slater (2) in a slightly different form, but nevertheless one which was foreseen by Polanyi and Wigner in their original discussion: he defined a critical coordinate, and attempted to calculate the mean frequency with which, in an oscillating molecule, this coordinate would exceed a certain length, and reaction was assumed to have taken place at this point. Using a harmonic-oscillator model for cyclopropane, Slater calculated the shape of the fall-off curve for the isomerisation to propylene (3) simultaneously with and independently of (ref. 2, p. 181) our measurements (5) on this reaction, and his theory was received with tremendous enthusiasm as the result of the remarkable agreement between his predictions and the experiment. Later, however, as Slater tried to extend his approach to anharmonic oscillators and to quantised oscillators (ref. 2, Chapt. 10), and because of insuperable difficulties relating to degeneracy changes upon partial isotopic substitution of highly symmetrical molecules, e.g., *cyclo*-C_3H_6 and *cyclo*-$C_3H_4D_2$, or CH_3NC and CH_2DNC (7), the theory has fallen into disrepute. This, taken together with other unsuccessful attempts based upon eq. [2] to account for high frequency factors (8, 9), seems an unfitting fate for such an attractive concept.

In this paper, we present a quantum formulation for the approximate rate of decomposition of a vibrationally excited molecule, based upon the origi-

[1]NRCC No. 18312.

0008-4042/80/151516-11$01.00/0
©1980 National Research Council of Canada/Conseil national de recherches du Canada

Can. J. Chem. Downloaded from www.nrcresearchpress.com by 210.87.254.40 on 09/05/12
For personal use only.

Can. J. Chem. Downloaded from www.nrcresearchpress.com by 210.87.254.40 on 09/05/12
For personal use only.

nal concept of Polanyi and Wigner (1), and we show, within the limitations of the available spectroscopic data and our understanding of the nature of molecular vibrations, that acceptable results can be obtained.

Basic Formulation

We begin by regarding the molecule as a collection of s independent oscillators and rigid rotors, with a set of vibration–rotation states $i = \{n_1, n_2, n_3, \cdots, n_s\}$ at energies

$$[3] \quad E_i = \sum_{j=1}^{s} \varepsilon_j(n_j)$$

where $\varepsilon_j(n_j)$ is the energy associated with the jth oscillator/rotor in the quantum state n_j. We then attempt to represent the reaction process by the motion of a particular oscillator, r, and assume that reaction can occur if more energy than the critical energy of the reaction, E_{crit}, is found in this oscillator, i.e.

$$[4] \quad \varepsilon_r \geq E_{crit}$$

Furthermore, we assume, in the spirit of Polanyi and Wigner (1), that if a molecule finds itself in a state in which it has more energy than E_{crit} in oscillator r, it will decompose within the vibrational period of that oscillator: for either a harmonic or a Morse oscillator, this is

$$[5] \quad \tau = (2c\nu_r)^{-1} \text{ seconds}$$

where c is the velocity of light and ν_r is the vibrational frequency of the oscillator r in wavenumber units.

If we now denote the state density of the molecule at energy E by $\rho_s(E)$ and the corresponding state density of a *hypothetical submolecule* with oscillator r removed by $\rho^r_{s-1}(E)$, then the fraction of states at E that decompose to products with time constant τ^{-1} is

$$[6a] \quad \alpha_1(E) = \Sigma \rho^r_{s-1}[E - \varepsilon_r(n_r)]/\rho_s(E)$$

where the summation is over n_r for which $E_{crit} \leq \varepsilon_r(n_r) \leq E$; in the quantity $\rho^r_{s-1}(E)$, the subscript $s-1$ refers to the remaining $(s-1)$ oscillators in the hypothetical submolecule when the oscillator r has been removed. The specific rate constant is then

$$[7a] \quad k_1(E) = 2c\nu_r\alpha_1(E)$$

Equations [6a] and [7a] are based on the postulate that the critical energy is localised in one oscillator, and are thus the quantum analogue of eq. [1]. In a more complex molecule where we may envisage the critical energy to be shared between m of the s oscillators, eq. [6a] is generalised to

$$[6b] \quad \alpha_m(E) = \Sigma \rho^{r_1 r_2 \cdots r_m}_{s-m}(E - \varepsilon_R) g_m(\varepsilon_R)/\rho_s(E)$$

where $\rho^{r_1 r_2 \cdots r_m}_{s-m}(E)$ is the state density of the hypothetical submolecule with the oscillators $r_1, r_2, \cdots, r_m$ removed,

$$\varepsilon_R = \varepsilon_{r_1}(n_{r_1}) + \varepsilon_{r_2}(n_{r_2}) + \ldots \varepsilon_{r_m}(n_{r_m})$$

is the energy in the reactive oscillators $r_1, r_2, \cdots, r_m$ in the state $\{n_{r_1}, n_{r_2}, \ldots, n_{r_m}\}$, $g_m(\varepsilon_R)$ is the state degeneracy of the group of m interesting oscillators at energy ε_R, and the summation is over all values of n_r for which $E_{crit} \leq \varepsilon_R \leq E$. The average lifetime of these states is, following Polanyi and Wigner (1), that of the oscillator with the highest frequency, viz. $|\nu_r|_{max}$, whence [7a] is generalised to

$$[7b] \quad k_m(E) = 2c|\nu_r|_{max}\alpha_m(E)$$

The computation of $k(E)$ using eqs. [6] and [7] requires as input parameters the relevant vibration–rotation constants of the molecule and the critical energy of the reaction. Since, except for the simplest of molecules, we have no *a priori* knowledge of E_{crit}, we will use the observed infinite-pressure activation energy, E_∞, as the critical energy, E_{crit}. In addition, for the sake of logical consistency, we adjust the chosen value of ν_r (or else $|\nu_r|_{min}$, the smallest of the group of m frequencies) very slightly to ensure that there is a reactive level *exactly* at E_{crit}; typically, this adjustment amounts only to a few percent of the value of ν_r (or $|\nu_r|_{min}$). We will proceed to examine the behaviour of eqs. [6] and [7] in considerable detail for two test cases, the thermal isomerisations of methyl isocyanide and of cyclopropane, and thereafter will present more briefly applications to other reactions, and discussions of various points which arise in respect of the formulation and of the results.

Some Preliminaries

In the discussion which follows, we will always compare our synthetic $k(E)$ function with those derived for the same molecular model using the Slater–Forst and RRKM procedures; moreover, with a single exception noted below, we will always regard the molecule as a collection of rigid rotating Morse oscillators. Thus, before tests of eqs. [6] and [7] can be made, it is necessary to describe the nature of such tests.

(i) Slater–Forst Procedure

We take as the target against which to compare our synthetic $k(E)$ function, the empirical specific rate function $k(E)$ derived from the experimental

Can. J. Chem. Downloaded from www.nrcresearchpress.com by 210.87.254.40 on 09/05/12
For personal use only.

rate law by the Slater–Forst procedure (10, 11), i.e.

$$[8] \quad \bar{k}(E) = A_\infty \rho(E - E_\infty)/\rho(E)$$

where E_∞ and A_∞ are respectively the infinite-pressure activation energy and frequency factor: we have given detailed arguments (12) why [8] should provide a reasonable estimate for the specific rate function, and more recently, we have made detailed numerical tests of its accuracy (13).

The specific rate function $\bar{k}(E)$ given by eq. [8] is not entirely unique, but depends slightly upon the assumed molecular model, as is shown in Fig. 1 for methyl isocyanide. Of the three curves shown, the topmost one assumes that the molecular oscillations are harmonic, whereas the bottom one assumes that they are Morse oscillators with the anharmonicity factors we estimated previously (12): we have concluded since that those empirical anharmonicity factors were much too severe, and we have evolved a new empirical scheme (which is described in the Appendix), based upon the assumed dissociation behaviour of the oscillator in question; this scheme will be used throughout this paper, and the resulting $\bar{k}(E)$ function for methyl isocyanide lies between the other two curves.

(ii) RRKM Calculations

The RRKM specific rate functions $k^*(E)$ shown for comparison in the following sections are computed by a relatively simple procedure, roughly equivalent in its degree of sophistication to our model described by eqs. [6] and [7]: $k^*(E)$ is calculated using eq. [6.20] of ref. 7, assuming no adiabatic rotations; the program used was essentially that supplied by Holbrook (ref. 7, p. 149), but modified for Morse oscillators, and with the sums and densities of states calculated by our own techniques (15). The calculations of $k(E)$, $\bar{k}(E)$, and $k^*(E)$ are always mutually consistent in the sense that they use the same set of frequencies, anharmonicities, and rotational constants for the molecule in question; likewise, all calculations use the same value of E_∞, and the same value of A_∞ is used in the Slater–Forst procedure and in the RRKM frequency adjustment. In the latter case, after the choice of the reaction coordinate (which is usually taken to be one of the frequencies chosen as ν_r), the two lowest frequencies remaining in the molecule were always adjusted to achieve the matching with the entropy of activation: the results for $k^*(E)$, of course, are insensitive to the choice of reaction coordinate (cf. Fig. 3 below) provided the assumed activated complex has the required entropy.

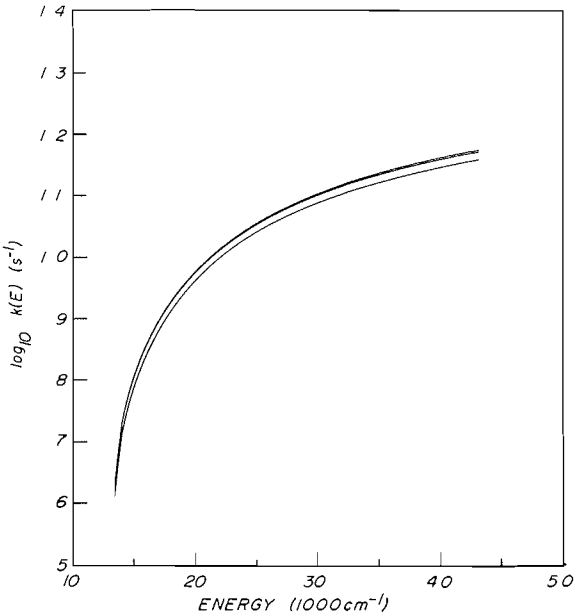


FIG. 1. Comparison of three empirical $\bar{k}(E)$ functions for methyl isocyanide, which are, in order: topmost curve, harmonic oscillators; middle curve, Morse oscillators with anharmonicities defined by eq. [A1]; bottom curve, Morse oscillators with anharmonicities from ref. 12.

(iii) The Overall Rate Constant

As is shown in Fig. 1, the numerical magnitudes of $\bar{k}(E)$, and also $k^*(E)$, are model-dependent and as can be seen in subsequent diagrams, $\bar{k}(E)$ and $k^*(E)$ can often be markedly different although they always correspond to the same value of the rate constant at the RRKM fitting temperature. Thus, whilst our primary aim in this work has been to compare the synthetic $k(E)$ function with the empirical $\bar{k}(E)$ function, a complete test of the synthetic $k(E)$ function requires that it also give acceptable values for the overall activation energy and frequency factor. Consequently, for each synthetic $k(E)$ function, (and also for each empirical $\bar{k}(E)$ function), we have always reconstructed the overall rate constant for the reaction using

$$[9] \quad k_\infty(T) = [Q(T)]^{-1} \int_0^\infty \rho(E) k(E)\, e^{-E/RT}\, dE$$

where $Q(T)$ is the reactant partition function, and compared the synthetic overall rate constant with the observed value. We also examined the derived Arrhenius parameters A_∞ and E_∞ for constancy with temperature. In the case of the $\bar{k}(E)$ function, this simply served as a check on the correctness and consistency of the partition functions and densities of states used in the calculations. On the other hand, using the synthetic $k(E)$ functions there were small, and real, variations of up to 0.2 or 0.3 kcal mol^{-1} in E_∞ and up to about ±30% in A_∞ over

Can. J. Chem. Downloaded from www.nrcresearchpress.com by 210.87.254.40 on 09/05/12
For personal use only.

a temperature range of a factor of two in T. Consequently, to complete the test of each model calculation, the computed values of A_∞ and E_∞ in the appropriate experimental temperature range are listed in the caption of each diagram, along with the observed values, the latter in italics.

Methyl Isocyanide

There have been several theoretical studies of the potential energy surface for the transition between methyl isocyanide and methyl cyanide (16–18), and it is clear that if one had to postulate a single vibrational mode which, if sufficiently excited, would lead to reaction, one would naturally choose the C—N—C bending mode $\nu_8 = 263\ cm^{-1}$ (19). Figure 2 shows the result of the application of eqs. [6*a*] and [7*a*] for this model, with $\nu_8 = 263\ cm^{-1}$ adjusted slightly to $\nu_r = 267\ cm^{-1}$ to ensure that a reactive level occurs exactly at the value of the critical energy. Also shown on the same diagram are the RRKM $k^*(E)$ function and the empirical $\bar{k}(E)$ function, and the agreement with the latter is remarkable; likewise, the agreement of the overall rate constant with experiment, as documented in the legend to the diagram, is excellent.

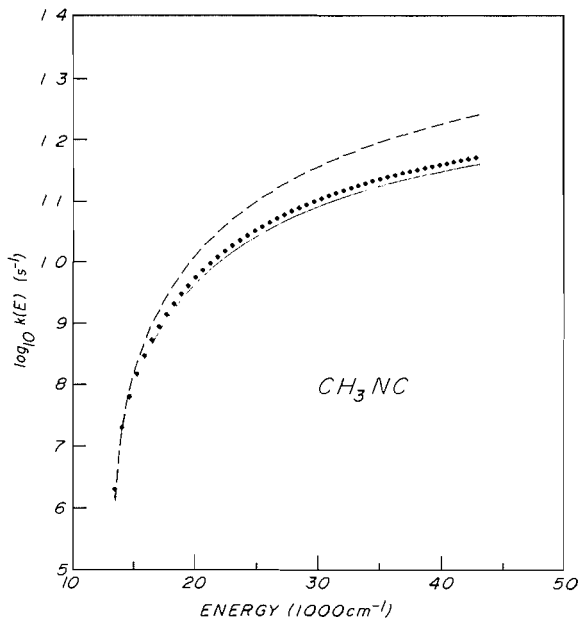


FIG. 2. Comparison of synthetic $k(E)$, empirical $\bar{k}(E)$, and RRKM $k^*(E)$ functions for methyl isocyanide using anharmonicities defined by eq. [A1]: solid line, $k(E)$ using $\nu_r = 263\ cm^{-1}$; individual points, $\bar{k}(E)$; dashed line, $k^*(E)$. The rate constants calculated from $k(E)$ using eq. [9] give the following Arrhenius parameters: $E_\infty = 38.2$ (*38.2*) kcal mol^{-1}, $A_\infty = 1.9$ (*2.2*) $\times 10^{13}\ s^{-1}$ at 500 K.

Sensitivity of the Computed Results to the Nature of the Assumed Model

As we noted above, and showed in Fig. 1, the computed values of $\bar{k}(E)$ depend very slightly upon the oscillator model assumed for the reacting molecule, but nevertheless, any of these functions will reproduce the observed rate constant when substituted in eq. [9]; likewise, the $k^*(E)$ function calculated by the RRKM prescription, although significantly different from $\bar{k}(E)$, still corresponds to the same value of the rate constant at the matching temperature.[2] Inspection of eqs. [6*a*] and [7*a*], however, shows that our synthetic $k(E)$, and the derived overall rate constant, should be quite sensitive to the choice of the reactive oscillator ν_r, and the nature of this sensitivity is shown in Fig. 3*a*. In this diagram, [6*a*] and [7*a*] were applied to the rotating *harmonic*-oscillator model of methyl isocyanide and ν_r was considered to be, in turn, $\nu_8 = 263$, $\nu_4 = 945$, $\nu_3 = 1429$, $\nu_2 = 2166$, and $\nu_1 = 2966\ cm^{-1}$. Most of the sensitivity of $k(E)$ to ν_r arises in eq. [7*a*] and, in fact, for harmonic oscillators $k(E)$ is directly proportional (to within about 3 or 4%) to ν_r at any value of E: thus, the computed overall rate constant is also approximately proportional to ν_r, with $A_\infty \simeq (1.9 \times 10^{13}) \times (\nu_r/267)\ s^{-1}$ in this case; this proportionality does not hold, however, as we shall see below for strongly anharmonic oscillators.

In contrast, Fig. 3*b* shows the RRKM results for $k^*(E)$ where, in turn, each of the five frequencies treated as ν_r in Fig. 3*a* is regarded as the critical reaction coordinate; this figure again demonstrates the now well-known insensitivity of the RRKM $k^*(E)$ function to the choice of reaction coordinate, which arises through the frequency adjustment procedure to match the experimental A-factor (12). Thus, we see that the present formulation, using eqs. [6] and [7], has the *potential* for making predictions, whereas the RRKM method does not possess this capability.

[2]The RRKM $k^*(E)$ functions are always lower than the empirical $\bar{k}(E)$ functions at low energy: this is because the threshold occurs at an energy E_0 which is lower than E_∞ in RRKM theory (eq. [6.5] of ref. 7), so that eq. [9] will only give the same value of $k_\infty(T)$ at the matching temperature if the mean value of $k^*(E)$ is below the mean value of $\bar{k}(E)$ in the significant energy range. The magnitudes of these differences viz. between E_0 and E_∞, or between $k^*(E)$ and $\bar{k}(E)$, become more marked the greater is the required extent of the frequency adjustment in the RRKM entropy matching procedure (cf. eq. [6.4] of ref. 7): thus, if there is a large frequency adjustment (as in Figs. 4, 6, and 10), $k^*(E)$ will always be below $\bar{k}(E)$ in the useful energy range, but if there is only a small frequency adjustment (as in Figs. 2, 7, 8, and 9) $k^*(E)$ will cross $\bar{k}(E)$ at high energy because it has a slightly smaller curvature, corresponding to the fact that the RRKM k_∞ increases with increasing temperature more quickly than strict Arrhenius (12).

Can. J. Chem. Downloaded from www.nrcresearchpress.com by 210.87.254.40 on 09/05/12
For personal use only.

Cyclopropane

A property of eq. [6*a*] is that if the critical energy and critical frequency ν_r are held constant, but the complexity of the molecule is increased, the ratio of active to passive states decreases somewhat; thus, it is clear that if the critical energy is considered to be localised in only one oscillator, one will not compute frequency factors much in excess of 2×10^{14} s^{-1}, the value obtained for methyl isocyanide using the asymmetric C—H stretch $\nu_1 = 2966$ cm^{-1} for ν_r, as in Fig. 3*a*. However, if the critical energy does not have to be localised in one degree of freedom but can be distributed in some other way then, as Polanyi and Wigner recognised, frequency factors greater than 10^{15} s^{-1} are possible, via eq. [2]; our quantum reformulation of this concept is embodied in eqs. [6*b*] and [7*b*], and we will now demonstrate their application to the cyclopropane isomerisation reaction.

According to calculations by Jug (20), the reaction coordinate in the isomerisation of cyclopropane to propylene can be visualised as a superposition of the torsional vibration ν_3 and an asymmetric stretch ν_{6b}, where these are the normal modes of vibration of a simplified model of cyclopropane, i.e. X_3Y_3 and the notation is that of Herzberg (21). Extending, and being guided by, this idea, we show in Fig. 4 the results of a series of calculations for cyclopropane. We chose two normal vibrations of cyclopropane, $\nu_3 = 1188$ cm^{-1}, the ring stretch, and $\nu_6 = 3103$ cm^{-1}, an asymmetric CH_2 stretch (19) to represent the critical motion in this reaction. The lowest two synthetic curves show that localisation of the critical energy in either one of these oscillators cannot generate the high observed reaction rate for this molecule. However, if we allow the critical energy to be shared *in any fashion* between these two oscillators of frequency 1188 and 3103 cm^{-1}, and accept Polanyi and Wigner's suggestion (1) that the lifetime for this complex oscillator is simply the lifetime of the oscillator having the higher frequency, then agreement with the empirical $k(E)$ is remarkable; also, the computed frequency factor of 1.4×10^{15} s^{-1} is in excellent agreement with experiment.

Although, as noted above, the present procedure provides us with the potential for exploring different "reaction co-ordinates" in a way which is not possible using the RRKM procedure, our choice in Fig. 4 for the reaction co-ordinate for cyclopropane is not unique. We notice that Jug's picture (20) of the reaction process also includes some rotational motion of one of the CH_2 groups: thus if we had chosen to share the critical energy between the ring stretch ν_3 at 1188 cm^{-1} with *one or other* of the degenerate pair of CH_2 twists, also at 1188 cm^{-1} (19), we would have calculated a synthetic $k(E)$ function only slightly below our first choice, as shown in Fig. 4, and with a frequency factor[3] of 1.6×10^{15} s^{-1}. However, were we to share the energy equally among all three oscillators of frequency 1188 cm^{-1}, the calculated $k(E)$ function would be about an order of magnitude larger than the result of sharing between two.

Non-adiabatic Reactions

The use of eq. [5] to give the rate of disruption of an oscillator involves the assumption that the process is an adiabatic one and, in general, we do not know whether this is or is not the case. The dissociation of CO_2 into CO+O is, however, clearly a non-adiabatic reaction and so it is interesting at this juncture to examine the application of eqs. [6] and [7] to this reaction. The molecule has two stretching modes, a symmetric one ν_1 leading to simultaneous dissociation of both C—O bonds, and an asymmetric one ν_3 which will lead to dissociation into O and CO; it also has a pair of bending modes ν_2 which, for the time being (see Appendix), are treated as being harmonic. Moreover, it appears from our recent calculations (22) that both in N_2O and CO_2, the transmission efficiency for curve crossing is about 1 in every 100 oscillations: the results presented in Fig. 5 assume therefore that ν_3 is the critical oscillator ($\nu_r = \nu_3 = 2349$ cm^{-1}) and that a transmission coefficient $\kappa = 0.01$ is included in eq. [5] to take rough account of the non-adiabatic problem. The agreement is reasonable, as also it is for N_2O using again ν_3 as the critical frequency ($\nu_r = \nu_3 = 2283$ cm^{-1}) and the same value of 0.01 for the transmission coefficient.

For the remainder of the paper, we will assume that the reactions we consider are adiabatic processes, although in general we have no way of knowing whether or not this is strictly true: thus, it should be kept in mind that we are always in danger of overestimating the rate constant through the neglect of a non-adiabatic transmission coefficient κ in eqs. [5]–[7].

Other Molecules

In this section, we will inspect briefly the extent to which eqs. [6] and [7] are successful in reproducing the specific rate functions and observed rate constants for the usual selection of other test-case thermal unimolecular reactions.

Cyclobutane

We proceed here by analogy with the treatment

[3]Although the lower $k(E)$ function gives the higher A-factor, there is no inconsistency since it also gives a slightly higher activation energy, see legend to Fig. 4.

Can. J. Chem. Downloaded from www.nrcresearchpress.com by 210.87.254.40 on 09/05/12
For personal use only.

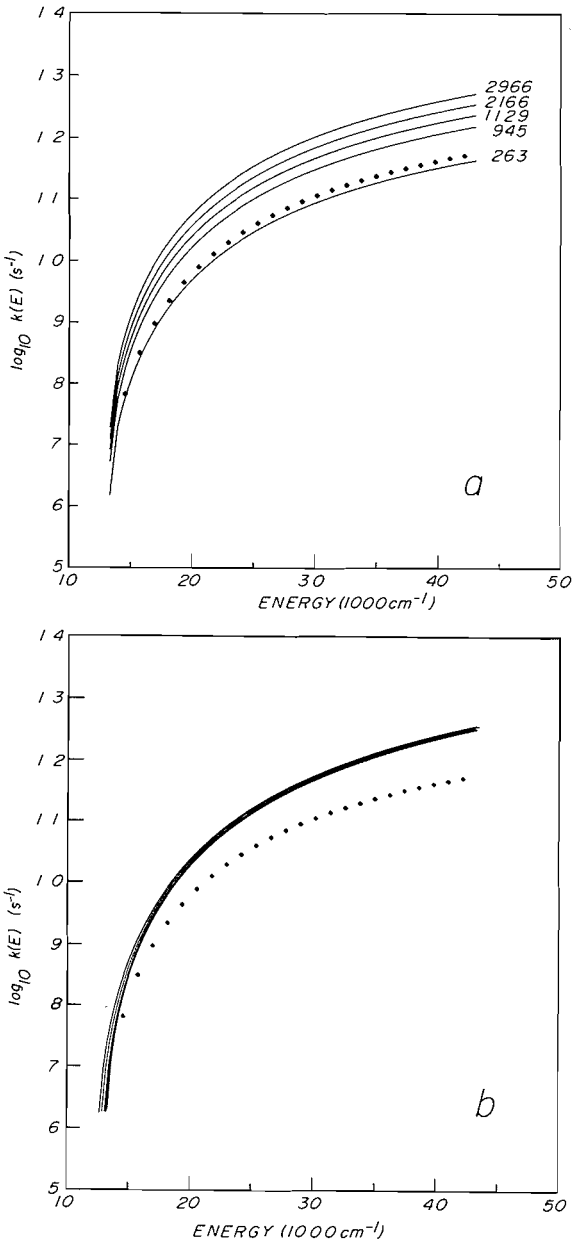


FIG. 3. (*a*) Comparison of five synthetic rate functions calculated according to eq. [7*a*] for methyl isocyanide, in the harmonic-oscillator approximation; the lines are labelled by the value of the frequency, in cm^{-1}, chosen for ν_r. (*b*) Five RRKM $k^*(E)$ functions using, in turn, the same five frequencies for the reaction co-ordinate. On both diagrams, the individual points represent the empirical $\bar{k}(E)$ function calculated according to eq. [8], also in the harmonic-oscillator approximation.

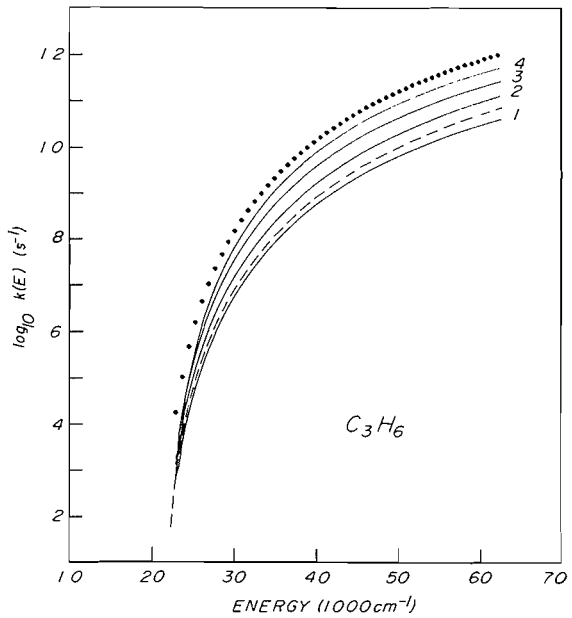


FIG. 4. Comparison of four synthetic $k(E)$ functions (solid lines) with the empirical $\bar{k}(E)$ function (points) and the RRKM $k^*(E)$ function (dashed line) for cyclopropane. Curves 1 and 2 use eq. [7*a*] with ν_r = 1188 and 3103 cm^{-1} respectively; curves 3 and 4 use eq. [7*b*] and share 1188 (g = 1) with 1188 (g = 2) and 1188 (g = 1) with 3103 (g = 1) cm^{-1} respectively. The rate constants calculated from the synthetic functions using eq. [9] give the following Arrhenius parameters (in order 1, 2, 3, 4): E_∞ = 65.5, 65.5, 67.2, 66.0 (*65.6*) kcal mol^{-1}, A_∞ = 0.07, 0.19, 1.6, 1.4 (*1.9*) × 10^{15} s^{-1} respectively, at 700 K.

of cyclopropane we gave above: the concentration of the critical energy in any single skeletal motion (having frequencies in the range 200–1000 cm^{-1}) gives rather low rates, and so we assume that the critical energy needs to be shared between two oscillational modes. Inspection of the normal modes of vibration of cyclobutane (23) shows that there is a pair having B_{1g} symmetry which form a natural choice for the reaction co-ordinate: one is the ring deformation ν_9 at 926 cm^{-1} in which the C_1—C_2 and C_3—C_4 lengths extend simultaneously while the C_2—C_3 and C_4—C_1 lengths decrease; the other is the CH_2 wagging ν_8 at 1219 cm^{-1} which simultaneously moves the H_2 pairs towards (and away from) the line of the C—C bonds, as required by the end of the dissociation process. Figure 6 compares the computed $k(E)$ function based on this assumption with the empirical $\bar{k}(E)$ and RRKM $k^*(E)$ functions: the computed rate constants are about a factor of 3.5 too high when compared with the experimental values between 700 and 800 K.

Ethyl Chloride

Figure 7 shows the results of choosing the critical coordinate to be one of the C—C—Cl deformation ν_{11} = 336 cm^{-1}, the C—Cl stretch ν_{10} = 671 cm^{-1} or the CH_3 degenerate stretch ν_2 = 2946 cm^{-1} (19). The choice of the C—Cl stretch ν_{10} gives almost exact agreement for the $k(E)$ function with the calculated rate constant some 20–25% below the ob-

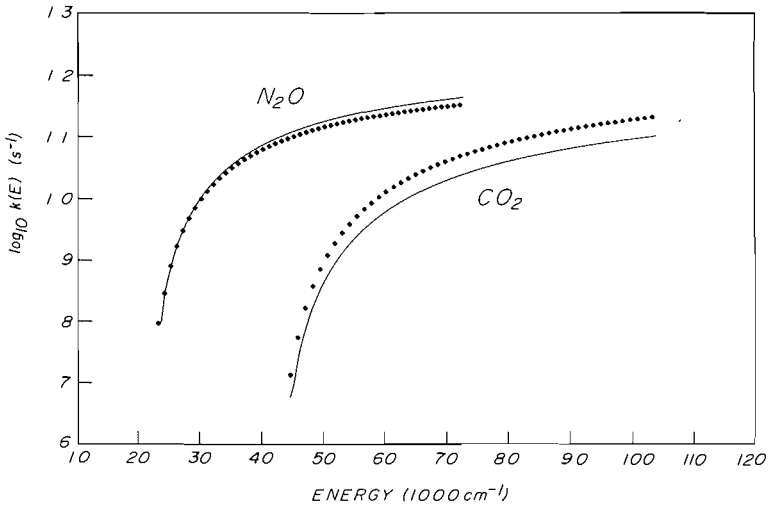


FIG. 5. Comparison of synthetic and empirical rate functions for carbon dioxide and nitrous oxide. The rate constants calculated from the synthetic functions using eq. [9] give the following Arrhenius parameters: CO_2, $E_\infty = 124\,(127)$ kcal mol^{-1}, $A_\infty = 1.2\,(2.0) \times 10^{12}$ s^{-1} at 3000 K; N_2O, $E_\infty = 66\,(66)$ kcal mol^{-1}, $A_\infty = 1.9\,(1.5) \times 10^{12}$ s^{-1} at 2000 K.

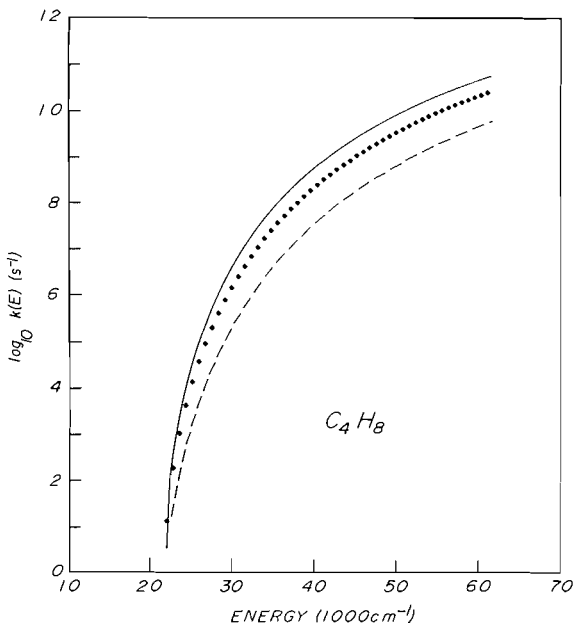


FIG. 6. Comparison of synthetic, empirical, and RRKM rate functions for cyclobutane. The rate constants calculated from the synthetic rate function according to eq. [9] give the following Arrhenius parameters: $E_\infty = 62.9\,(62.5)$ kcal mol^{-1}, $A_\infty = 16\,(3.7) \times 10^{14}$ s^{-1} at 700 K.

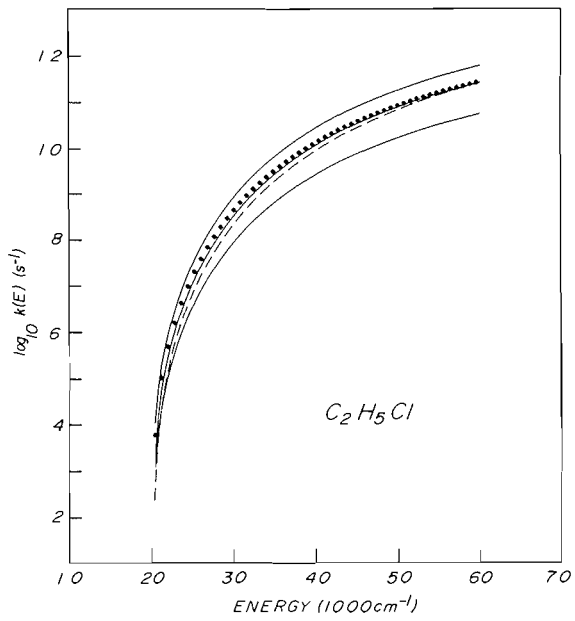


FIG. 7. Comparison of three synthetic rate functions, calculated according to eq. [7*a*] with the empirical and RRKM rate functions for ethyl chloride: the synthetic functions, from top to bottom, use $\nu_r = 2946$, 676, and 336 cm^{-1} respectively, and using eq. [9], give rise to the following Arrhenius parameters: $E_\infty = 58.4$, 58.6, 58.4 (*58.4*) kcal mol^{-1}, $A_\infty = 2.0$, 0.9, 0.2 (*1.1*) $\times 10^{14}$ s^{-1} at 600 K.

served values. In this calculation, the synthetic $k(E)$ curves do not fall exactly into a sequence as happens in Fig. 3*a*: this is because $\nu_{11} = 336$ cm^{-1} is treated as being harmonic, whereas $\nu_{10} = 676$ is assigned an anharmonicity $x_e = 0.006$ and $\nu_2 = 2946$ cm^{-1} has $x_e = 0.018$; in fact, were we to imagine that any one of $\nu_4 = 1463$ cm^{-1} (CH_3 degenerate deformation) or $\nu_5 = 1448$ cm^{-1} (scissors) or $\nu_{14} = 1448$ cm^{-1} (CH_3 degenerate deformation) (19), all treated as harmonic in our empirical assignment of anharmonicity, was the critical oscillator, the computed $k(E)$ function would be indistinguishable on

Can. J. Chem. Downloaded from www.nrcresearchpress.com by 210.87.254.40 on 09/05/12
For personal use only.

Can. J. Chem. Downloaded from www.nrcresearchpress.com by 210.87.254.40 on 09/05/12
For personal use only.

the scale of the diagram from the one shown for $\nu_{10} = 676\,cm^{-1}$, $x_e = 0.006$. Thus, although Fig. 1 shows that the deduction of the Slater–Forst $\bar{k}(E)$ function is relatively insensitive to the anharmonicities chosen for the various oscillators in the molecule, our computed $k(E)$ function is sensitive to the anharmonicity chosen for the critical oscillator itself; the reason for this is quite clear on inspection of eq. [6*a*], since the spacings of the $\varepsilon_r(n_r)$ depend strongly upon the value of x_e in the reactive region.

Ethyl Isocyanide

Ethyl isocyanide possesses two bending frequencies, cf., ethyl cyanide (19), $\nu_{13} = 226\,cm^{-1}$ and $\nu_{20} = 270\,cm^{-1}$ (24). Figure 8 shows the empirical $\bar{k}(E)$ function, the RRKM $k^{\ddagger}(E)$ function and two synthetic $k(E)$ functions, one for a single oscillator ($\nu_r = \nu_{13} = 226\,cm^{-1}$) and the other for which the critical energy is shared between the two bending motions: the latter is rather better.

Trideuteriomethyl Isocyanide

Figure 9 shows the results for CD_3NC analogous to the calculations presented for CH_3NC in Fig. 2: considering the excellent agreement with experiment for CH_3NC, the results shown in Fig. 9 for CD_3NC are somewhat disappointing, but nevertheless the predicted rate is well within a factor of 3 of the correct result.

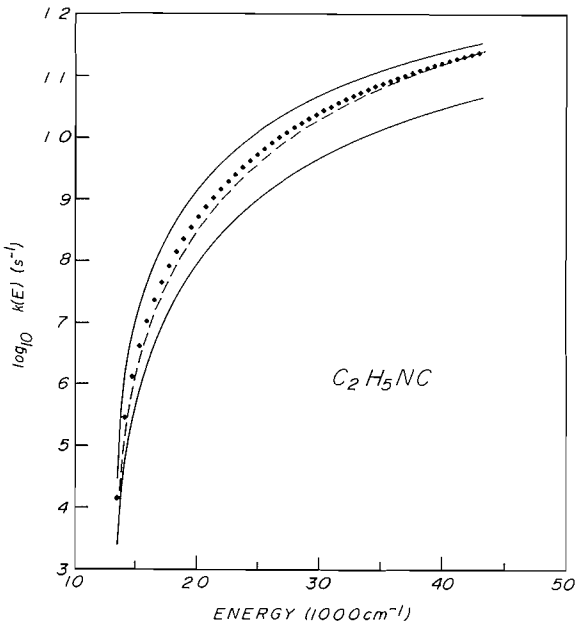


FIG. 8. Comparison of two synthetic rate functions with the empirical and RRKM rate functions for ethyl isocyanide: the lower synthetic function uses eq. [7*a*] and one bending frequency, the upper one uses eq. [7*b*] and both bending frequencies. The rate constants calculated from these synthetic rate functions according to eq. [9] give the following Arrhenius parameters: $E_\infty = 38.3, 38.1$ (*38.4*) kcal mol^{-1}, $A_\infty = 1.5, 31$ (*7.8*) $\times 10^{13}\,s^{-1}$ at 500 K.

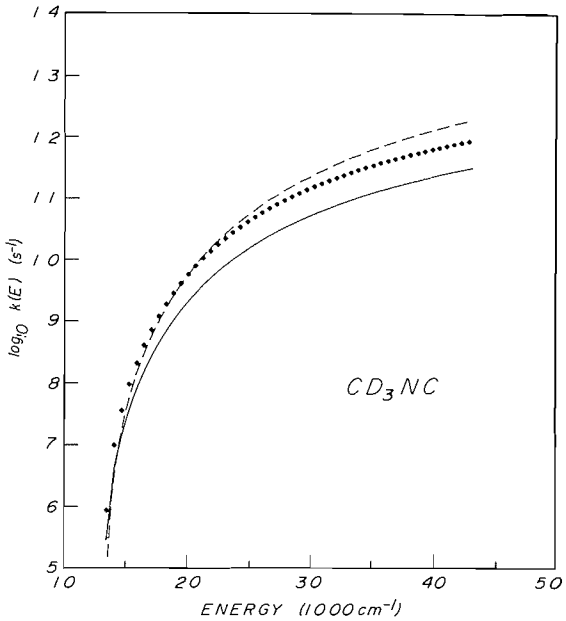


FIG. 9. Comparison of synthetic, empirical, and RRKM rate functions for trideuteriomethyl isocyanide. The rate constants calculated from the synthetic rate function according to eq. [9] give the following Arrhenius parameters: $E_\infty = 38.5$ (*38.5*) kcal mol^{-1}, $A_\infty = 1.7$, (*4.5*) $\times 10^{13}\,s^{-1}$ at 500 K.

Ethane

The ethane molecule possesses 6 singly degenerate and 6 doubly degenerate normal modes of vibration (ref. 21, p. 115). The ethane decomposition also has a very high frequency factor (26) of about $6.3 \times 10^{16}\,s^{-1}$, so it is clear that $m > 1$ in eq. [6*b*]. Examination of the normal-mode diagrams shows that there are only three of them which lead to any significant extension and contraction of the C—C bond, namely $\nu_1 = 2954\,cm^{-1}$ (CH_3 symmetric stretch), $\nu_2 = 1388\,cm^{-1}$ (CH_3 symmetric deformation), and $\nu_3 = 995\,cm^{-1}$ (C—C stretch) (19). Sharing of the critical energy of reaction between these three degrees of freedom yields a synthetic $k(E)$ function remarkably close to the empirical one, with the rate constant only about a factor of 3 too low.

Discussion

In this paper, we have taken the original concept of Polanyi and Wigner and reformulated it in discrete or quantised form.[4] As a result, we have

[4]As such, this reformulation is probably the nearest attainable approach to the quantum (anharmonic) form of the Slater theory, which so eluded Noel Slater, and others, over the years.

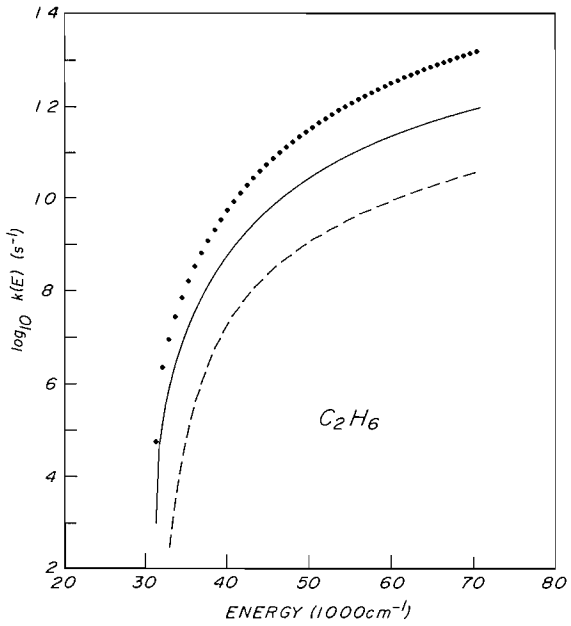


FIG. 10. Comparison of synthetic, empirical, and RRKM rate functions for ethane. The rate constants calculated from the synthetic rate function according to eq. [9] give the following Arrhenius parameters: 89.8 (*89.2*) kcal mol^{-1}, $A_\infty = 2.7$ (*6.3*) $\times$ 10^{16} s^{-1} at 900 K.

found that the rate of the unimolecular disruption of a rotationally and vibrationally excited molecule can be calculated with reasonable accuracy (usually within a factor of 3 or 4) by a very simple procedure. One first identifies the type of vibrational motion which, if carried to its limit, will result in the required reaction process. For simple molecules, it appears that this is always a simple process, and can be represented as the concentration of the critical energy in a *single* oscillator; for more complicated molecules it appears that, in general, the critical energy can be shared among two or perhaps three oscillators, and the choice of such oscillators is not very difficult in certain cases, e.g. cyclobutane, or possibly ethane. Then one enumerates the states of the molecule which have more than the critical energy localised in the critical oscillator(s) and assigns to them a mean lifetime which is simply half the vibrational period of the fastest critical oscillator: the remainder of the states are treated as being passive, and the synthetic $k(E)$ function is just the product of the mean decay rate constant for an active state with the ratio of the number of active to passive states.

It would be wise not to read too much physical significance into the apparent success of this simple model at this early stage, for several reasons. First, each state is treated as being discrete and infinitely narrow, whereas in reality each level is broadened from a number of causes, and in fact each level is overlapped by many of its neighbours: we intend to address this problem in a later publication.

Second, we have used a normal-mode representation of the internal motions of the molecule, whereas at these moderately high levels of excitation, a local-mode representation may be more appropriate: we are assuming here, of course, that the normal-mode and local-mode representations are commensurable in the sense that either will give us about the same densities of passive and active states in the given energy region. Hence, the mapping of the normal modes into the local modes would be a prerequisite for the proper choice of the critical oscillator for each reaction. It is clear, however, that the actual disruption process is often going to be representable by the concentration of the critical energy into a single local mode: as examples, we have in this paper the cases of methyl isocyanide and ethyl chloride: the latter result is rather surprising in view of the amount of effort which has been expended in the past trying to formulate the nature of the transition state[5] in such four-centre reactions! For such cases, the principal requirement is a knowledge of the frequency of the local mode leading to reaction[6]. For more complicated molecules, the critical energy can be shared between two, or perhaps even three vibrational degrees of freedom, and by using (not illogical) combinations of such oscillations, it is fairly easy to generate acceptable $k(E)$ functions and rate constants: this sharing of the critical energy among two or more oscillators leads directly to the prediction of "high" frequency factors (1, 8, 9, 27).

Third, our knowledge of the energy-level density in any molecule must be very imperfect because, in general, we have very scant knowledge of anharmonicities and of rotation–vibration interaction constants, both of which affect the level densities

[5]We always have to keep in mind, of course, that a curve-crossing may be involved, and that we are really dealing with a more complex (and therefore faster) process moderated by a non-adiabatic transmission factor κ.

[6]In this context, the apparent discrepancy noted above between the success of the method for methyl isocyanide and for its isotopic variant becomes explicable. In methyl isocyanide, we have assumed equally spaced harmonic levels of the 263 cm^{-1} oscillation in evaluating eq. [6*a*], whereas, above threshold, this oscillation must degenerate into a rotation with *increasing* level spacings as the energy increases. Likewise, in the deuteriated molecule, the analogous bending at 249 cm^{-1} also degenerates into a rotation, but because of the increased effective moment of inertia for this rotation, the level spacings will be closer than for the normal molecule. Thus, in the final analysis, the $k(E)$ function for the heavier molecule will not be a factor of three below that for the normal molecule, as we find here using our normal-mode approximations; similar considerations might apply also to ethyl isocyanide.

Can. J. Chem. Downloaded from www.nrcresearchpress.com by 210.87.254.40 on 09/05/12
For personal use only.

Can. J. Chem. Downloaded from www.nrcresearchpress.com by 210.87.254.40 on 09/05/12
For personal use only.

significantly. We have tried to allow for the former in a very empirical manner, but have ignored completely the problem of rotation–vibration interaction, although we have allowed for the density of rotational states at all stages in the formulation: this is analogous to the approximations we have made previously in treating the dissociations of CO_2 and N_2O, both at high (22) and low (4) pressures, but it is clear, especially in the former case, that the neglect of rotation–vibration interaction has an adverse effect on the quality of the computed rate constants; there is, of course, no *a priori* reason why one should not consider the critical energy to be shared between rotation and vibration, but we have not explored the behaviour of such calculations.

In conclusion, we believe that the present approach has a number of favourable qualities. It is simple in concept, and simple to use: moreover, for simple molecules (fewer than 5 or 6 atoms, say) there usually appears to be a fairly unambiguous choice of critical oscillator which causes eqs. [6] and [7] to give results within a factor of about 3 of the empirical Slater–Forst $\bar{k}(E)$ function. For such molecules, it is now becoming possible to compute, *ab initio*, potential surfaces of "chemical accuracy" from which all the required molecular parameters, i.e. potential barrier, vibration frequencies, moments of inertia, and so on can be derived: thus, a true *ab initio* calculation of a unimolecular rate constant becomes a possibility. For more complicated molecules, this approach gives hope that we will be able eventually to distinguish between alternative pathways in a manner which is not possible with the RRKM method: this is because we do not have to adjust the frequencies of the molecule to match the observed frequency factor, but rather we take the natural frequencies as best we can determine them, and by the appropriate choice of a reaction co-ordinate are led to the unambiguous calculation of the frequency factor. Thus, this approach has considerably greater predictive potential when one is interested in the rates of reactions for which no measurements are possible at infinite pressure; however, before true predictions can be made for reactions in general, a period of exploration is required in which we examine, for a series of reaction types, the correspondence between the structure of the molecule and the nature of the appropriate reaction co-ordinate.

1. M. POLANYI and E. WIGNER. Z. Phys. Chem. **139**, 439 (1928).
2. N. B. SLATER. Theory of unimolecular reactions. Methuen, London. 1959.
3. N. B. SLATER. Proc. R. Soc. London A, **218**, 224 (1953).
4. A. W. YAU and H. O. PRITCHARD. Can. J. Chem. **57**, 1723 (1979).
5. H. O. PRITCHARD, R. G. SOWDEN, and A. F. TROTMAN-DICKENSON. Proc. R. Soc. London A, **217**, 563 (1953).
6. J. CHAO, R. C. WILHOIT, and B. J. ZWOLINSKI. J. Phys. Chem. Ref. Data, **2**, 427 (1973).
7. P. J. ROBINSON and K. A. HOLBROOK. Unimolecular reactions. John Wiley, London. 1972.
8. H. O. PRITCHARD. Recl. Trav. Chim. Pays-Bas, **74**, 745 (1955).
9. H. O. PRITCHARD. J. Chem. Phys. **25**, 267 (1956).
10. N. B. SLATER. Proc. Leeds Philos. Lit. Soc. Sci. Sect. **6**, 259 (1955).
11. W. FORST. J. Phys. Chem. **76**, 342 (1972).
12. A. W. YAU and H. O. PRITCHARD. Can. J. Chem. **56**, 1389 (1978).
13. A. W. YAU and H. O. PRITCHARD. Can. J. Chem. **57**, 2458 (1979).
14. S. J. CYVIN. Spectrochim. Acta, **16**, 1022 (1960).
15. A. W. YAU and H. O. PRITCHARD. Can. J. Chem. **55**, 992 (1977).
16. G. W. VAN DINE and R. HOFFMANN. J. Am. Chem. Soc. **90**, 3227 (1968).
17. M. J. S. DEWAR and M. C. KOHN. J. Am. Chem. Soc. **94**, 2704 (1972).
18. J. B. MOFFAT and K. F. TANG. Theor. Chim. Acta, **32**, 171 (1974).
19. T. SHIMANOUCHI. Tables of molecular vibrational frequencies. NSRDS-NBS 39, Washington, DC. 1972.
20. K. JUG. Theor. Chim. Acta, **42**, 303 (1976).
21. G. HERZBERG. Infrared and Raman spectra. Van Nostrand, New York, NY. 1945. p. 91.
22. A. W. YAU and H. O. PRITCHARD. Can. J. Chem. **57**, 1731 (1979).
23. R. C. LORD and I. NAKAGAWA. J. Chem. Phys. **39**, 2951 (1963).
24. K. M. MALONEY and B. S. RABINOVITCH. J. Phys. Chem. **73**, 1652 (1969).
25. G. HERZBERG. Diatomic molecules. Van Nostrand, New York, NY. 1950. p. 100.
26. A. B. TRENWITH. J. Chem. Soc. Faraday Trans. I, **75**, 614 (1979).
27. D. CLARK and H. O. PRITCHARD. J. Chem. Soc. 2136 (1956).

Appendix
Anharmonicities and Other Molecular Constants

In general, the calculations reported in this paper use the same set of molecular and reaction rate constants as we used previously, viz. Tables 2 and 3 of ref. 12; ethane was not considered in that paper, but the vibration frequencies (19), moments of inertia (6), the barrier to internal rotation (6) and the rate parameters (26) are taken from recent reliable sources. However, the anharmonicities we used previously are rather unsatisfactory for the present application. In that work (12) we examined the variation in density of states for methyl isocyanide and for cyclopropane as a function of the anharmonicity chosen for certain oscillators, and from the extent of that variation, it became clear that the choice of anharmonicities would have only a moderate effect on the derived $\bar{k}(E)$ function,

essentially since eq. [8] contains a ratio of terms which are changed in the same sense by changes in anharmonicity. Based on Cyvin's treatment of cyclopropane (14), we had recommended some empirical anharmonicity factors for use in these calculations (12) but these anharmonicities are, in general, too large: for example, the bending frequency of 263 cm^{-1} in methyl isocyanide would "dissociate" before the critical energy of 13 361 cm^{-1} is reached, making the application of eq. [6*a*] impossible. These large anharmonicities, although acceptable for general statistical calculations, are unreasonable for molecular-dynamic applications. Consequently, we have adopted an empirical method of assigning anharmonicity factors based upon the nature of the vibration in question and its estimated dissociation limit. We assign an effective dissociation limit D_i to each vibration: for example, the C—C stretch in ethane would have $D_i \simeq 90$ kcal mol^{-1}, the symmetric stretch of a CH_3 group would have $D_i \simeq 300$ kcal mol^{-1} and the asymmetric stretch of the same group about 100 kcal mol^{-1}; all bending or deformation degrees of freedom, which cannot be assigned a dissociation energy in this simple way, were assumed to be harmonic. To simplify the procedure even more, it matters very little what effective dissociation energy D_i is assigned to an oscillator once $D_i > 2E_{crit}$; consequently, all anharmonic oscillators were given a number N_i in the range $1 \leq N_i \leq 2$ where $N_i = D_i/E_{crit}$ for $D_i \leq 2E_{crit}$ or $N_i = 2$ for $D_i > 2E_{crit}$, and the anharmonicity factor was then calculated according to the standard Morse-oscillator equation (25).

$$[A1] \quad \omega_e x_e = \omega_e^2/4N_i E_{crit}$$

The only exception to the use of this recipe was in the case of N_2O, where reliable values for the anharmonicities exist, cf. Table 1 of ref. 4.

Can. J. Chem. Downloaded from www.nrcresearchpress.com by 210.87.254.40 on 09/05/12
For personal use only.

Effect of *t*-butanol on the structural propensities of alkali halides in water

NERIYANURI MANOHARA MURTHY AND SARASWATULA VENKATA SUBRAHMANYAM

Department of Physics, SVU Autonomous Post-Graduate Centre, Anantapur 515 003, India

Received July 11, 1979[1]

NERIYANURI MANOHARA MURTHY and SARASWATULA VENKATA SUBRAHMANYAM. Can. J. Chem. **58**, 1527 (1980).

The effect of NaCl, KCl, RbCl, KBr, and KI on the temperature corresponding to the sound velocity maximum (TSVM) of aqueous *t*-butanol has been studied. The structural contribution to the shift in the TSVM of aqueous *t*-butanol by the addition of alkali halides was found to be in the order NaCl > KCl > RbCl and KCl > KBr > KI, thereby indicating that $Na^+ > K^+ > Rb^+$ and $Cl^- > Br^- > I^-$ in disrupting the hydrogen-bonded structure of water. The results also indicate an enhancement in the structure-breaking characteristic of both cations and anions in the presence of *t*-butanol. However, the order is the reverse of that found for pure water, i.e. $Rb^+ > K^+ > Na^+$ and $I^- > Br^- > Cl^-$. The results have been explained on the basis of hydrophobic–hydrophilic interactions prevalent in the ternary systems.

NERIYANURI MANOHARA MURTHY et SARASWATULA VENKATA SUBRAHMANYAM. Can. J. Chem. **58**, 1527 (1980).

On a étudié l'effet des sels suivants NaCl, KCl, RbCl, KBr et KI sur la température correspondant à la vitesse maximale du son (VMS) dans des solutions aqueuses de *tert*-butanol. On a trouvé que la contribution structurale au déplacement de la VSM du *tert*-butanol aqueux par l'addition d'halogénures de métaux alcalins varie dans l'ordre NaCl > KCl > RbCl et KCl > KBr > KI indiquant ainsi que la destruction des liaisons hydrogènes dans l'eau se fait dans l'ordre: $Na^+ > K^+ > Rb^+$ et $Cl^- > Br^- > I^-$. Les résultats indiquent également une augmentation caractéristique dans la dislocation de la structure pour les cations et les anions en présence du *tert*-butanol. Cependant l'ordre est l'inverse de celui trouvé pour l'eau pure soit $Rb^+ > K^+ > Na^+$ et $I^- > Br^- > Cl^-$. On a expliqué les résultats en fonction des interactions hydrophobe–hydrophyle qui existent finalement dans les systèmes tertiaires.

[Traduit par le journal]

Introduction

The viscosity *B*-coefficient (1), activation energy of viscous flow (2), compressibility data (3, 4), and the data on the structural contribution to the shift in the temperature of sound velocity maximum in water (5) for alkali halides indicate a structure-ordering effect for Li^+ and Na^+ and a structure-breaking effect for Rb^+ and K^+. Li^+ was found to be more effective than Na^+ in structure-making, i.e. enhancement of long range order in water, and Rb^+ was found to be more effective than K^+ in structure-breaking, i.e. disruption of the hydrogen-bonded structure of water. For anions the structure-breaking effect was found to be in the order $I^- > Br^- > Cl^-$.

Conductivity measurements by Broadwater and Kay (6) on KCl, CsCl, LiBr, KBr, Me_4NBr, Bu_4NBr, and Me_4NI in aqueous mixtures containing *t*-butanol at 25°C indicate that the structural effects of cations and anions are modified significantly in the presence of *t*-butanol. Structure-breaking ions were found to be more effective and this effect was found to be maximum around 10 mol% of *t*-butanol, the concentration at which maximum enhancement of water structure by *t*-butanol is believed to take place. It was also observed that the order found in the structure-breaking power of both cations and anions to be reverse of the order found for the same ions in pure water.

The behaviour of water + *t*-butanol system has been extensively studied from different angles, particularly in the water-rich region in view of the highly hydrophobic character of *t*-butanol. The various studies (7–21) indicate an enhancement in the hydrogen-bonded structure of water by *t*-butanol when present in small amounts. The maximum in the hydrophobic interactions between *t*-butanol and water molecules occurs in the region 3 to 8 mol% of *t*-butanol as evidenced by the existence of extrema in many of the physical properties. But, Hepler (22) points out that there is no unambiguous numerical measure of structure-making or -breaking by a solute. However, since a shift in the equilibrium between the hydrogen-bonded bulk form and non-hydrogen-bonded dense form of water is accompanied by a volume change, one can take the partial molar volume of the solute to provide a rough measure of the effect of that solute on the structure of water (23). The minimum in ϕ_v occurs at 25°C near 0.04 mole fraction of *t*-butanol (12), the concentration at which most of the properties (9, 13, 18) exhibit maxima or minima.

The strength of the hydrophobic interaction of *t*-butanol is sensitive to temperature. The sharp minimum in the hydroxyl-proton chemical shift (16) as a function of concentration of *t*-butanol in aqueous *t*-butanol rapidly diminishes on heating, being entirely lost in the region of 67°C. The minimum in ϕ_v versus X_2 and the maximum in ϕ_c versus X_2 (X_2 is the mole fraction of *t*-butanol) are more pronounced in the water-rich region of aqueous *t*-

[1]Revision received December 11, 1979.

0008-4042/80/151527-06$01.00/0

©1980 National Research Council of Canada/Conseil national de recherches du Canada

Can. J. Chem. Downloaded from www.nrcresearchpress.com by 210.87.254.105 on 09/05/12
For personal use only.

Can. J. Chem. Downloaded from www.nrcresearchpress.com by 210.87.254.105 on 09/05/12
For personal use only.

butanol (12), reflecting promotion of ordered structure of water, which shift to lower concentrations as the temperature is increased (the minimum in ϕ_v and maximum in ϕ_c versus X_2 occur around $X_2 \simeq 0.02$ at 55°C).

Our earlier studies on the effect of isomeric butanols on the temperature of adiabatic compressibility minimum (24) and sound velocity maximum (25) indicate *t*-butanol to promote the hydrogen-bonded structure of water. These studies indicate maximum enhancement in the structure of water to occur around $X_2 \simeq 0.0193$ and 0.0046, respectively. It may be noted that the compressibility and velocity studies are confined to 64 and 74°C respectively.

Studies on the effect of electrolytes on the solution structure of aqueous *t*-butanol have been made extensively (26–30) by measuring the thermodynamic functions such as free energies, enthalpies, entropies, heat capacities, and volumes, and evaluating the corresponding transfer functions of the concerned solutes from water to water + *t*-butanol. The large concentration dependence of the transfer functions observed in the water-rich region has been explained in terms of the solute–solute interactions between the reference solute and the cosolvent taking into account the ordered structure of the aqueous *t*-butanol.

In order to understand the influence of alkali halides on the solution structure of aqueous *t*-butanol in the water-rich region through ultrasonic velocity measurements and also to see whether the findings of Broadwater and Kay (6) regarding the structure-breakings power of anions and cations still persist even at high temperatures, we have taken up the study of the effect of alkali halides on the temperature of sound velocity maximum (TSVM) of water and the results are reported here.

Experimental

Triply distilled degassed water was used to prepare stock solution of aqueous *t*-butanol. The mole fraction of *t*-butanol in the stock solution is 0.0046, the concentration at which maximum enhancement of water structure is supposed to occur as revealed from TSVM studies. Each time about 1 L solution was prepared by weighing the samples using a triple beam balance. This stock solution was used to prepare solutions of desired concentration of the electrolytes under study, namely AR grade NaCl, KCl, RbCl, KBr, and KI.

Ultrasonic velocity in the ternary system (electrolyte + aqueous *t*-butanol) was determined with an accuracy of ±0.003% using a single crystal variable path interferometer working at 3 MHz, the details of which are discussed elsewhere (24), over a range of 5°C on either side of TSVM at an interval of 2 to 3°C.

Results

The experimentally determined ultrasonic velocity data at different temperatures in the ternary solutions (water + *t*-butanol + electrolyte) at different concentrations of electrolytes have been used, after effecting diffraction correction (31), to determine the temperature of the sound velocity maximum in the ternary solution. In all cases, since the shape of the velocity temperature curves are similar to that of aqueous *t*-butanol and also to that of pure water, a transparent template of the velocity–temperature curve of pure water itself was used to fix the TSVM of the ternary solution and the accuracy in fixing TSVM is ±0.2°C. Typical results are shown graphically in Fig. 1 and the values of TSVM obtained at different concentrations of electrolytes in the ternary solutions are given in Table 1.

Discussion

The shift in the temperature corresponding to the sound velocity maximum in the solution of aqueous *t*-butanol caused by the addition of an electrolyte is given by

$$[1] \quad \Delta T' = T_{\text{ternary sol.}} - T_{\text{binary sol.}}$$

$\Delta T'$ may be thought of as arising due to two effects, namely, dilution effect and structural effect. The dilution effect is always negative while the structural effect may be positive or negative depending on the change in the solution structure towards

TABLE 1. $T'_{exp.}$, $T'_{id.}$, and $[\Delta T'_{str.}]_{exp.}$ at different concentrations of alkali halides in the ternary solution

Weight fraction w	$T'_{exp.}$ (°C)	$T'_{id.}$ (°C)	$\Delta T'$ (°C)	$[\Delta T'_{str.}]_{exp.}$ (°C)
NaCl				
0.0100	68.8	72.6	−4.1	−3.8
0.0204	66.8	72.3	−6.1	−5.5
0.0296	64.9	71.9	−8.0	−7.0
0.0402	63.9	71.5	−9.0	−7.6
KCl				
0.0129	71.1	72.7	−1.8	−1.6
0.0234	69.7	72.5	−3.2	−2.8
0.0330	67.7	72.3	−5.2	−4.6
0.0482	66.2	72.0	−6.7	−5.8
RbCl				
0.0114	71.8	72.8	−1.1	−1.0
0.0285	70.1	72.6	−2.8	−2.5
0.0450	68.5	72.4	−4.4	−3.9
KBr				
0.0125	71.4	72.9	−1.5	−1.5
0.0229	70.1	72.9	−2.8	−2.8
0.0339	68.8	72.8	−4.1	−4.0
0.0480	67.7	72.7	−5.2	−5.0
KI				
0.0116	71.9	72.9	−1.0	−1.0
0.0243	70.4	72.7	−2.5	−2.3
0.0343	69.9	72.6	−3.0	−2.7
0.0474	68.8	72.5	−4.1	−3.7

Can. J. Chem. Downloaded from www.nrcresearchpress.com by 210.87.254.105 on 09/05/12
For personal use only.

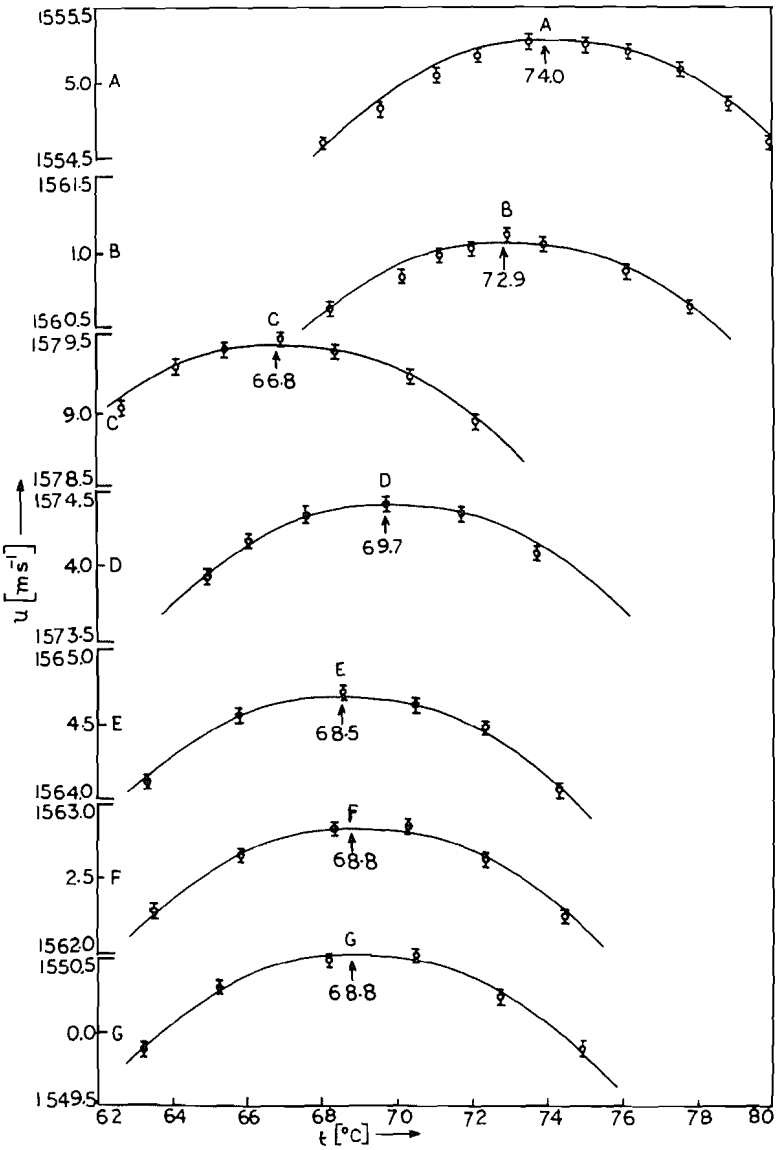


FIG. 1. Ultrasonic velocity versus temperature in aqueous *t*-butanol at different concentrations of electrolytes. *A*, pure water; *B*, $w = 0.0000$ aqueous *t*-butanol, $X_2 = 0.0046$; *C*, water + *t*-butanol + NaCl, $w = 0.0204$; *D*, water + *t*-butanol + KCl, $w = 0.0234$; *E*, water + *t*-butanol + RbCl, $w = 0.0450$; *F*, water + *t*-butanol + KBr, $w = 0.0339$; *G*, water + *t*-butanol + KI, $w = 0.0474$.

more order or less order owing to the interaction of the electrolyte with water molecules. It is necessary to separate these two effects to delineate the structural propensities of different ions. The effect of dilution in lowering the TSVM of aqueous *t*-butanol can be obtained by considering the expressions representing the temperature dependence of sound velocity in aqueous *t*-butanol and in the solute (electrolyte).

The velocity in aqueous *t*-butanol in which the mole fraction of *t*-butanol is 0.0046 conforms to the relation

$$[2] \quad u_{12} = 1561.02 - 0.0196[73.0 - t]^2$$

where t represents the temperature in °C. The velocity in the solute can be written as

$$[3] \quad u_2 = u_2^0 - \alpha_u t$$

where u_2^0 is the velocity at 0°C and α_u represents the temperature coefficient of sound velocity.

Considering the internal energy U of a mixture is additive on mole fraction basis (32), we can write

$$[4] \quad U = (1 - x)U_1 + xU_2$$

Can. J. Chem. Downloaded from www.nrcresearchpress.com by 210.87.254.105 on 09/05/12
For personal use only.

where U_1 and U_2 are the internal energies of the components 1 and 2 respectively and x represents the mole fraction of component 2 in the mixture. Differentiating eq. [4] with respect to volume (V) at constant entropy (S) and using the relation

$$[5] \quad \left[\frac{\partial^2 U}{\partial V^2}\right]_S = \frac{u^2 M}{V^2}$$

where u and M represent the ultrasonic velocity in the liquid and molecular weight of the liquid respectively, we get

$$[6] \quad u^2 = \frac{(1-x)M_1}{\bar{M}} u_1^2 + \frac{xM_2}{\bar{M}} u_2^2$$

In the above equation $\bar{M}$ represents the molecular weight of the mixture given by

$$[7] \quad \bar{M} = (1-x)M_1 + xM_2$$

Equation [6] can be rewritten as

$$[8] \quad u^2 = (1-w)u_1^2 + wu_2^2$$

where w represents the weight fraction of the second component in the solution.

Equation [8] has been applied by Kudriavtsev (32) to calculate the sound velocities in aqueous solutions of electrolytes. The same relation has also been utilized (5, 33) to obtain an expression for the ideal shift in the temperature of sound velocity maximum in water due to the addition of an electrolyte.

In view of the fact that in the water-rich region aqueous t-butanol behaves as pure water, in respect of velocity–temperature profile, we can use the following relation to represent the velocity in the ternary solution containing an electrolyte

$$[9] \quad u^2 = wu_2^2 + (1-w)u_{12}^2$$

where w represents the weight fraction of the electrolyte in the ternary solution. Substituting eqs. [2] and [3] in eq. [9] and differentiating the resulting equation with respect to temperature and using the condition $du/dt = 0$ at $t =$ TSVM of the solution, we get

$$[10] \quad [1561.02 - 0.0196(73.0 - T')^2] \times 0.0392(73.0 - T') = -\frac{w}{(1-w)} \times [(u_2^0 - \alpha_u T')\alpha_u]$$

where T' represents the TSVM in the ternary solution. The term within the square bracket on the left hand side of eq. [10] represents the velocity in aqueous t-butanol at the TSVM of the ternary solution and can be replaced by 1561.02 ms^{-1} provided T' does not differ from 73.0°C appreciably which is true. Hence

$$[11] \quad T' = T'_{id.} = \frac{4467 - bu_2^0\alpha_u}{61.2 - b\alpha_u^2}$$

Here $T'_{id.}$ represents the ideal value of TSVM when no structural changes are involved and $b = w/(1-w)$. The structural contribution to the shift in TSVM can be written as

$$[12] \quad [\Delta T'_{str.}]_{exp.} = T'_{exp.} - T'_{id.}$$

In order to evaluate the structural contribution to the shift in TSVM we have to calculate $T'_{id.}$. As per eq. [11] we need α_u and u_2^0 in the solute. Since the solutes used are solid electrolytes which have cubic structure, we have three velocities associated with sound wave propagation, namely, one longitudinal and two torsional. The problem now is which one of these velocities we have to take to evaluate u_2^0 and α_u that may be used in eq. [11] to obtain $T'_{id.}$. Since there is no reason to prefer any one of these velocities we may use the mean velocity $\bar{u}_m$ for u_2 in the electrolyte given by the following relation

$$[13] \quad u_2 = \bar{u}_m = \frac{1}{3}\left[\frac{2}{\bar{u}_s^3} + \frac{1}{\bar{u}_l^3}\right]^{-1/3}$$

where $\bar{u}_l$ and $\bar{u}_s$ represent the longitudinal and torsional wave velocities in the polycrystalline aggregates of the electrolytes. Indeed to evaluate the Debye characteristic temperature of polycrystalline samples the average velocity normally used is the one given by eq. [13] and we feel our preference to use $\bar{u}_m$ instead of any one of the u_l or u_s to evaluate $T'_{id.}$ is reasonable. The values of u_2^0 and α_u calculated using the elastic constants and their temperature dependence (34–36) for the electrolytes under study are given in Table 2.

The observed shift $\Delta T'$ and the values of the structural contribution to the shift in TSVM, $[\Delta T'_{str.}]_{exp.}$, evaluated using eqs. [1] and [11] and [12] respectively at different concentrations of NaCl, KCl, RbCl, KBr, and KI are presented in Table 1 along with $T'_{exp.}$ and $T'_{id.}$ values. Since weight fraction of the electrolyte is involved in the evaluation of the ideal shift and hence the structural shift, it is more appropriate to see how the structural shifts change with weight fraction of the electrolyte in the ternary solution rather than the molality or volume fraction and there by delineate the structural propensities of individual ions. In view of this the values of $[\Delta T'_{str.}]_{exp.}$ for NaCl, KCl, and RbCl and KCl, KBr, and KI as a function of weight fraction are represented graphically in Figs. 2 and 3, respectively. The values of the structural contribution to the shift in TSVM of water, $[\Delta T_{str.}]_{exp.}$,

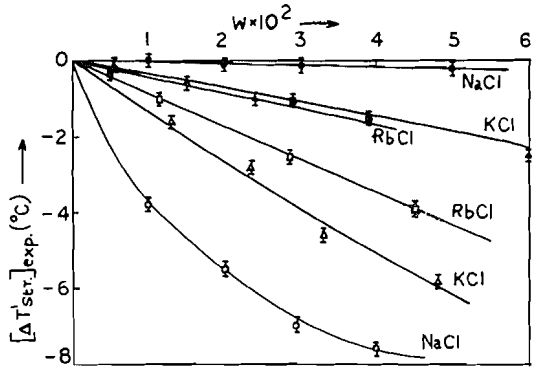


FIG. 2. $[\Delta T'_{str.}]_{exp.}$ versus weight fraction w of NaCl, KCl, and RbCl in aqueous t-butanol. ●, ■, ▲ correspond to pure water.

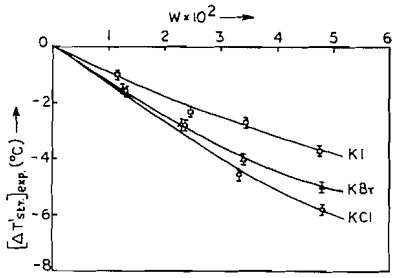


FIG. 3. $[\Delta T'_{str.}]_{exp.}$ versus weight fraction w of KCl, KBr, and KI in aqueous t-butanol.

as a function of weight fraction of NaCl, KCl, and RbCl available in literature (5) are also included in Fig. 2. An examination of the data presented in Fig. 2 indicates that the values of $[\Delta T'_{str.}]_{exp.}$ for NaCl, KCl, and RbCl are negative and also greater than $[\Delta T_{str.}]_{exp.}$, indicating that the structure-breaking efficiency of these solutes gets enhanced in the presence of t-butanol. The values of $[\Delta T'_{str.}]_{exp.}$ and $[\Delta T_{str.}]_{exp.}$ are accurate to ±0.2°C. Within the limits of experimental error we clearly see that at any given concentration $[\Delta T'_{str.}]_{exp.}$ for NaCl > KCl > RbCl, indicating that in the presence of t-butanol the structure-breaking efficiency of $Na^+ > K^+ > Rb^+$ whereas in pure water the TSVM studies indicate that the structure-breaking efficiency of $Rb^+ \geq K^+ > Na^+$. The viscosity B-coefficient for Na^+, K^+, and Rb^+ respectively are +0.086, −0.007, and −0.029, indicating that the structure-breaking efficiency of these ions are in the order $Rb^+ > K^+ > Na^+$ (1).

From Fig. 3 we notice that within the limits of experimental error the values of $[\Delta T'_{str.}]_{exp.}$ for KCl ≥ KBr > KI up to $w \simeq 0.025$. But as the concentration of the solute increases ($w > 0.025$) we definitely see that at any given concentration $[\Delta T'_{str.}]_{exp.}$ for KCl > KBr > KI. From these observations we may conclude that in general the structure-breaking efficiency of $Cl^- > Br^- > I^-$ in the presence of t-butanol. In pure water the structure-breaking efficiency of these ions are in the order $I^- > Br^- > Cl^-$ as revealed from TSVM studies on halides of lithium (5) and viscosity data. The viscosity B-coefficient for Cl^-, Br^-, and I^- respectively are −0.007, −0.032, and −0.080 (1).

The results of the present study are in line with the observation made by Broadwater and Kay (6). This indicates that the interactions responsible for enhancement in the structure-breaking nature of both cations and anions such as hydrophobic–hydrophilic interactions between cosolvent and the solute and dehydration of the ions due to the presence of t-butanol persist even at high temperatures. The collapse of the three dimensional structure of the solution readily due to the addition of hydrophilic solutes may be related to the strong solute–water, cosolvent–water, and solute–cosolvent structural interactions (30, 37). It is also worthwhile to note that the enhancement in the hydrophobic interactions of n-Am_4NBr, Bu_4NBr, and $NaBPh_4$ at 30°C around $X_2 \simeq 0.03$ to 0.04 of t-butanol has been attributed to a mechanism of mutual enhancement of water structure by both the hydrophobic solutes (38). Hence it may be inferred that t-butanol enhances the hydrophilic or hydrophobic interactions respectively of structure-breaking or structure-making solutes in aqueous ternary systems when present in small amounts at which the binary cosolvent structure is more ordered than pure water.

TABLE 2. Sound velocities and temperature coefficient of velocity in polycrystaline alkali halides

Alkali halide	u_2^0 (ms^{-1})	α_u ($ms^{-1}\,°C^{-1}$)	Reference
NaCl	2910	0.74	34
KCl	2449	0.50	35
RbCl	1853	0.46	36
KBr	1334	0.24	36
KI	1538	0.44	36

Acknowledgements

The authors thank the referees and Professor J. E. Desnoyers for valuable comments.

1. R. W. GURNEY. Ionic processes in solution. McGraw Hill, New York. 1953.
2. E. R. NIGHTINGALE, JR. *In* Chemical physics of ionic solutions. *Edited by* B. E. Conway and R. G. Barradas. John Wiley, New York. 1966.
3. S. V. SUBRAHMANYAM. Acustica, **13**, 111 (1963).
4. R. E. GIBSON and J. F. KINCAID. J. Am. Chem. Soc. **59**, 580 (1937).

Can. J. Chem. Downloaded from www.nrcresearchpress.com by 210.87.254.105 on 09/05/12
For personal use only.

5. S. V. SUBRAHMANYAM and C. V. RAGHAVAN. Acustica, **28**, 215 (1973).
6. T. L. BROADWATER and R. L. KAY. J. Phys. Chem. **74**, 3802 (1970).
7. C. J. BURTON. J. Acoust. Soc. Am. **20**, 186 (1948).
8. E. K. BAUMGARTNER and G. T. ATKINSON. J. Phys. Chem. **75**, 2336 (1971).
9. M. J. BLANDAMER, D. E. CLARKE, N. J. HIDDEN, and M. C. R. SYMONS. Trans. Faraday Soc. **64**, 2691 (1968).
10. K. TAMURA, M. MAEKAWA, and T. YASUNAGA. J. Phys. Chem. **81**, 2122 (1977).
11. T. STONE and R. E. PARTINEN. J. Chem. Phys. **45**, 2407 (1967).
12. C. DE VISSER, G. PERRON, and J. E. DESNOYERS. Can. J. Chem. **55**, 856 (1977).
13. M. J. BLANDAMER and O. J. WADDINGTON. J. Phys. Chem. **74**, 2569 (1970).
14. G. L. BERTRAND and L. E. SMITH. J. Phys. Chem. **74**, 4171 (1970).
15. G. WADA and S. UMEDA. Bull. Chem. Soc. Jpn. **35**, 646 (1962).
16. B. KINGSTON and M. C. R. SYMONS. J. Chem. Soc. Faraday II, **69**, 978 (1973).
17. D. OAKENFULL and D. E. FENWICK. J. Chem. Soc. Faraday I, **75**, 636 (1979).
18. R. K. MOHANTY, T. S. SHARMA, S. SUBRAMANIAN, and J. C. AHLUWALIA. Trans. Faraday Soc. **67**, 305 (1971).
19. E. R. ROBERTSON and S. E. SUGAMORI. Can. J. Chem. **50**, 1353 (1972).
20. F. FRANKS and D. J. G. IVES. Q. Rev. **20**, 1 (1966).
21. E. M. ARNETT and D. R. MCKELVEY. J. Am. Chem. Soc. **87**, 1393 (1965).
22. L. G. HEPLER. Can. J. Chem. **47**, 4613 (1969).
23. F. FRANKS and D. S. REID. *In* Water: a comprehensive treatise. Vol. 2. *Edited by* F. Franks. Plenum, New York. 1973. p. 482.
24. S. V. SUBRAHMANYAM and N. MANOHARA MURTHY. J. Sol. Chem. **4**, 347 (1975).
25. N. MANOHARA MURTHY and S. V. SUBRAHMANYAM. Bull. Chem. Soc. Jpn. **50**, 2589 (1977).
26. G. PERRON, D. JOLY, J. E. DESNOYERS, L. AVEDIKIAN, and J. P. MOREL. Can. J. Chem. **56**, 552 (1978).
27. J. E. DESNOYERS, G. PERRON, L. AVEDIKIAN, and J. P. MOREL. J. Soc. Chem. **5**, 631 (1976).
28. L. AVEDIKIAN, G. PERRON, and J. E. DESNOYERS. J. Sol. Chem. **4**, 331 (1975).
29. N. DOLLET and J. JUILLARD. J. Sol. Chem. **5**, 77 (1976).
30. J. E. DESNOYERS, O. KIYOHARA, G. PERRON, and L. AVEDIKIAN. Adv. Chem. Ser. No. 155, 274 (1976).
31. S. V. SUBRAHMANYAM, V. HYDERKHAN, and C. V. RAGHAVAN. J. Acoust. Soc. Am. **46**, 272 (1969).
32. B. B. KUDRIAVTSEV. Sov. Phys. Acoustics, **2**, 36 (1956); **2**, 172 (1956).
33. C. V. RAGHAVAN. Ph.D. Thesis. S. V. University, Tirupati, India. 1970.
34. L. HUNTER and S. SIEGEL. Phys. Rev. **61**, 84 (1942).
35. S. V. SUBRAHMANYAM. Proc. Indian Acad. Sci. **47**, 25 (1958).
36. S. HAÜSSEL. Z. Phys. **159**, 223 (1960).
37. C. DE VISSER, G. PERRON, and J. E. DESNOYERS. J. Am. Chem. Soc. **99**, 5894 (1977).
38. R. K. MOHANTY, S. SUNDAR, and J. C. AHLUWALIA. J. Phys. Chem. **76**, 2577 (1972).

Can. J. Chem. Downloaded from www.nrcresearchpress.com by 210.87.254.105 on 09/05/12
For personal use only.

A type II aqueous cholesteric lyomesophase

MAHMUT ACIMIS[1] AND LEONARD W. REEVES[2]

Department of Chemistry, University of Waterloo, Waterloo, Ont., Canada N2L 3G1

Received January 15, 1979[3]

MAHMUT ACIMIS and LEONARD W. REEVES. Can. J. Chem. **58**, 1533 (1980).

The lyotropic liquid crystals formed by optically active detergents, water, and electrolyte have been investigated near and above the water-rich limit of the lamellar mesophase by using nuclear magnetic resonance, relative density observations, and polarized microscopy. The racemic mixture of α-alanine decyl ester forms a lamellar phase, a disc-micelle type II phase (which may co-exist in equilibrium), followed by an isotropic material as the water content increases. The resolved *d* or *l* detergent also forms a lamellar mesophase which may coexist with a type II disc-micelle system; however, as water content increases a transition occurs to a cholesteric lyotropic mesophase which itself passes over to an isotropic phase at the highest water contents studied. The range of existence, as a function of water content, for these intermediate type II DM and cholesteric phases is very narrow. The screw axis of the cholesteric mesophase aligns parallel to the magnetic field. A tentative structure of the cholesteric phase based on disc micelles distorted into a partial helix is suggested.

MAHMUT ACIMIS et LEONARD W. REEVES. Can. J. Chem. **58**, 1533 (1980).

Opérant dans la zone située tout près et au-dessus de la limite riche en eau de la mésophase lamellaire et faisant appel à la rmn, à des observations de densité relative et à la microscopie polarisée, on a étudié les cristaux liquides lyotropes formés par les détergents optiquement actifs, l'eau et un électrolyte. Le mélange racémique de l'ester décyclique de l'α alanine forme une phase lamellaire, une phase disque-micelle de type II (qui peut coexister en équilibre) qui est suivie d'un produit isotrope lorsque la teneur en eau augmente. Le détergent résolu (*d* ou *l*) forme également une mésophase lamellaire qui peut coexister avec un système disque-micelle de type II; cependant lorsque la teneur en eau augmente, il se produit une transition en une mésophase cholestérique lyotrope qui elle-même se transforme en une phase isotrope pour la plus haute teneur en eau étudiée. Le domaine d'existence, en fonction de la teneur en eau, de ces intermédiaires de type II DM et des phases cholestériques est très étroit. L'axe sans fin de la mésophase cholestérique s'aligne parallèlement au champ magnétique. On suggère une structure non définitive pour la phase cholestérique basée sur les disques micellaires déformés en une hélice partielle.

[Traduit par le journal]

Introduction

Lawson and Flautt (1) discovered lyotropic liquid crystals that spontaneously align in the static magnetic fields used for nuclear magnetic resonance (nmr) studies. These uniaxial fluids may be prepared using chemical variations, either with positive (type I) or negative (type II) diamagnetic anisotropy (2). We have investigated the effect of chemical changes in the composition of such systems, and a recent overview article summarizes the results of these extensive studies (3). The type II lyomesophases can have the infinite lamellar structure, in which case they are not spontaneously aligned by magnetic fields, or they can be nematic[4] with a disc bilayer structure of finite micelles with orientational order only (3, 13). The possibility of preparing an aqueous chiral lyotropic mesophase has been one of our continuing investigations since the aligning mesophases attracted our attention some ten years ago (3). The biological membrane bilayer is made up of optically active amphiphiles (4, 12).

Two previous co-workers (5, 6) have studied the effect of optically active amphiphile components as guests in these mesophases. Radley and Saupe (7) used the decylammonium chloride – cholesterol system (9) in order to investigate an induced twisted structure by optical methods. In their quantitative study of the induced twist in a type II DM lyomesophase, the chemical system was ex-

[1]Present address: Cukurova Üniversitesi, Faculty of Basic Sciences, P.K. 171, Adana, Turkey.

[2]Author to whom correspondence should be addressed.

[3]Revision received November 27, 1979.

[4]Footnote added in proof. While this article was in press, an article by Charvolin *et al.*, J. Phys. Lett. **40**, 587 (1979), has appeared on the low angle X-ray diffraction of a type II DM mesophase. These authors conclude that this mesophase is nematic with disc-micelles. The Laue camera, used by these workers, obscures the observation of the inner diffraction reported by Lia Q. do Amaral (13) using full low angle X-ray diffraction apparatus. Furthermore, the experimental conditions of Charvolin *et al.* with respect to sample thickness, so important in the detection of residual magnetic orientation, are not stated. More recently, Lia Q. do Amaral and co-workers (Mol. Cryst. Liq. Cryst. Lett., in press) have seriously questioned the use of the word "nematic" for these intermediate mesophases. The outer sharp maxima have been assigned as a Bragg diffraction arising from regions of positionally ordered disc-micelles. We feel that the notation Type II DM and Type I CM mesophases accommodates the lack of nematic behaviour (19) and avoids the necessity of implying nematic structures. Our notation (19) also accommodates the formation of Type II CM and Type I DM mesophases, which have yet to be experimentally realised. The reversal of the diamagnetic anisotropy sign for the amphiphiles in constituent micelles is a chemically accessible variable and we can expect reports on these predicted mesophases in the future.

0008-4042/80/151533-09$01.00/0

©1980 National Research Council of Canada/Conseil national de recherches du Canada

Can. J. Chem. Downloaded from www.nrcresearchpress.com by 210.87.254.105 on 09/05/12
For personal use only.

Can. J. Chem. Downloaded from www.nrcresearchpress.com by 210.87.254.105 on 09/05/12
For personal use only.

tended to include brucine sulphate and tartaric acid guests (7). Tracey and Diehl (8) prepared a mesophase similar to that of Flautt and Lawson (1) but with optically active sodium decyl-2-sulphate as a guest amphiphile.

There is no report on aqueous lyotropic mesophases that exhibit polymorphism with chiral amphiphiles, however, two non-aqueous systems (10, 11, 14) have been investigated. These liquid crystalline systems are not related to the aqueous bilayer micelle structures in any simple way (12).

The present study is directed toward the first synthesis of cholesteric aqueous lyotropic systems which are related to the type II DM systems, but prepared with a pure optically resolved amphiphile. The results will show that true cholesteric phases can be prepared as well as their nematic[4] racemate. A polymorphism of liquid crystalline forms occurs because the transition to the cholesteric state requires a critical water content.

The paper is divided into two parts, first the nmr study of the cholesteric mesophases and their nematic[4] racemate at higher water content, and secondly, a polarized microscopic investigation with parallel nmr studies at lower water contents to illustrate the relationship and polymorphism of the mesophases formed with chiral detergents.

Experimental

Materials

α-Alanine hydrochloride decylester (α-ADE) was synthesized in the following manner. HCl gas was passed into 31.5 g (~0.2 mol) *n*-decanol in a 3-necked flask at a temperature of 60–65°C and agitated by a bar magnet. After 10 min, 5 g (~0.056 mol) α-alanine was poured into the flask (Aldrich Chemical Co.), and solution of the solid took place over a 2 h period. At this point the stream of HCl gas was stopped and the reaction mixture stored overnight at room temperature. The next day, the excess HCl was removed by reducing the pressure with a water pump; crude α-ADE crystallized out and was filtered from excess *n*-decanol. The crude product was recrystallized three times from ethylacetate and dried several hours in a vacuum oven (15 Torr) at 50°C to give an 80% or better yield. The purified α-ADE gave the following physical constants. L-alanine hydrochloride decylester (*l*-ADE), mp 105°C; $[\alpha]_{578}^{24}$ −6.8° (*c* 2.1, H_2O), *d*-alanine hydrochloride decylester (*d*-ADE), mp 105°C; $[\alpha]_{578}^{24}$ +6.8° (*c* 2.1, H_2O); the racemic mixture (d*l*-ADE), mp 73°C. The rotation angles were measured on a Carl Zeiss 340740 polarimeter.

Compositions of Mesophases with α-ADE

The racemic mixture and separate enantiomers of the *d*- and *l*-alanine hydrochloride decylester were used respectively to form type II DM and cholesteric lyomesophases with the following composition:

	α-ADE's	Na_2SO_4	D_2O
Weight %	50.955	5.095	43.949
Moles	1.000	0.187	11.450

The ingredients were weighed in test-tubes, which were sealed in order to prevent evaporation and homogenized by warming on a water bath with intervening periods of centrifugation through small constrictions in the tube. It was found that α-alanine hydrochloride decylesters (α-ADE's) form different mesophases, dependent on water content. This polymorphism was independent of the sign of the chirality. The range of stability of the different mesophases on changing the water content is given below. By keeping the moles of the α-ADE's and Na_2SO_4 constant as above, we use the term "Moles of water per one mole of amphiphile, MWPA" to describe the composition of mixtures.

(*i*) Lamellar phases of all the α-ADE's exist at and below 10.600 MWPA. (*ii*) Co-existent lamellar and type II DM mesophases exist between 10.700 and 11.250 MWPA. (*iii*) Cholesteric mesophases of the chiral α-ADE's and a type II DM mesophase of the racemic mixture exist between 11.300 and 11.850 MWPA. At 12.000 MWPA an anisotropic and an isotropic phase coexist, providing the temperature is less than 30°C. All these phases are liquid crystalline at 0°C.

Nuclear Magnetic Resonance Measurements

The deuterium nmr of D_2O in the liquid crystals was performed in a Bruker SXP 60 pulse spectrometer, with a high resolution probe at 9.21 MHz as described previously (3). The probe temperature was 27 ± 1°C, and microscopic studies were made at the same ambient temperature. Na-23 nmr spectra were measured at 15.781 MHz. Both nuclei measured can be observed with good signals at less than 20 pulses.

Preparation of the Microscope Slides

The preparation of the microscope slides was achieved by using a Teflon spacer allowing 0.05 mm sample thickness between the slide and coverglass.

Results

Types of Mesophases Formed

Lamellar Phases

At low water contents, 10.600 MWPA, the *l*-, *d*-, and *dl*-alanine hydrochloride decylesters form lamellar phases. The nmr samples of these lamellar phases did not spontaneously align in the magnetic field at room temperature. The sealed nmr sample tubes were heated above the isotropic point ~85°C and then allowed to cool in the magnetic field to the probe temperature. This manner of aligning lamellar phases has been used previously by Tiddy *et al.* (21). For the aligned samples, the D_2O signals were a doublet of splitting 1010 ± 30 Hz for all three α-ADE's if the same concentrations were used and they were assigned as type II behaviour ($\Delta\chi < 0$) (15). These nmr samples were investigated in the polarizing microscope. The three mesophase samples of α-ADE's exhibited approximately the same texture as shown in Plate 1. This texture was assigned by Rosevear (18) as "Coarse mosaic texture" of the neat phase (Fig. 4 in ref. 18).

Coexistent Lamellar and Type II DM Phases

In the range 10.700–11.250 MWPA the three α-ADE's form two coexistent phases. In this region of coexistence both phases became aligned after a

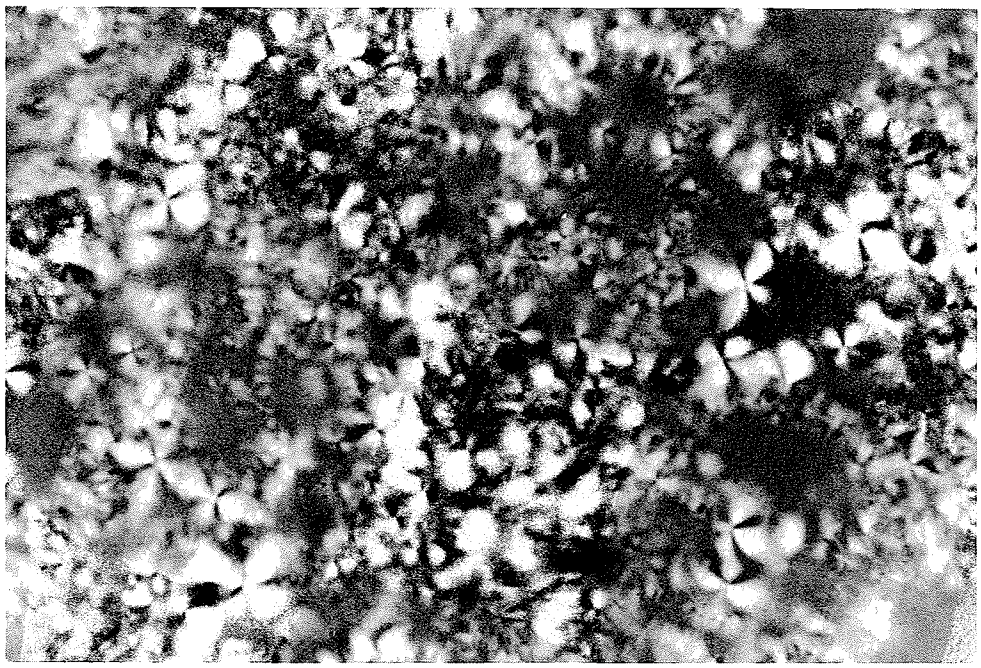


PLATE 1. A coarse mosaic texture of lamellar phases formed by α-alanine hydrochloride decylesters. Crossed polarizers. Magnification 400 ×.

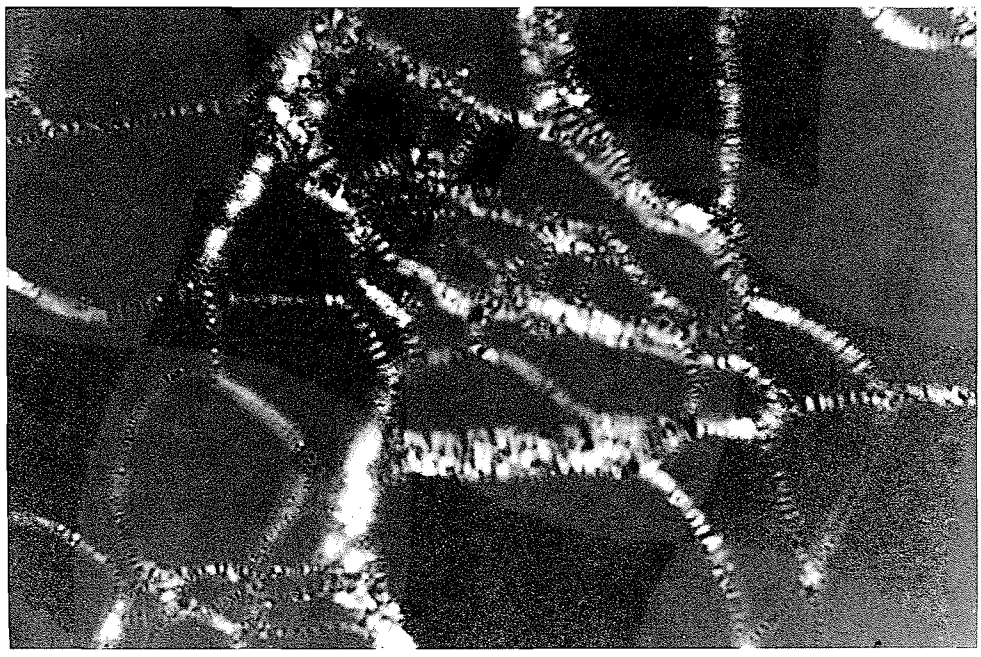


PLATE 2. Two phase region formed by α-alanine hydrochloride decylesters. The texture shown in the photomicrograph pertains to a lamellar phase whereas the black areas contained "threaded" texture as in Plate 3 which appears dark, since, after a few minutes, it aligned perpendicular to microscope slide glass surface.

Can. J. Chem. Downloaded from www.nrcresearchpress.com by 210.87.254.105 on 09/05/12
For personal use only.

Can. J. Chem. Downloaded from www.nrcresearchpress.com by 210.87.254.105 on 09/05/12
For personal use only.

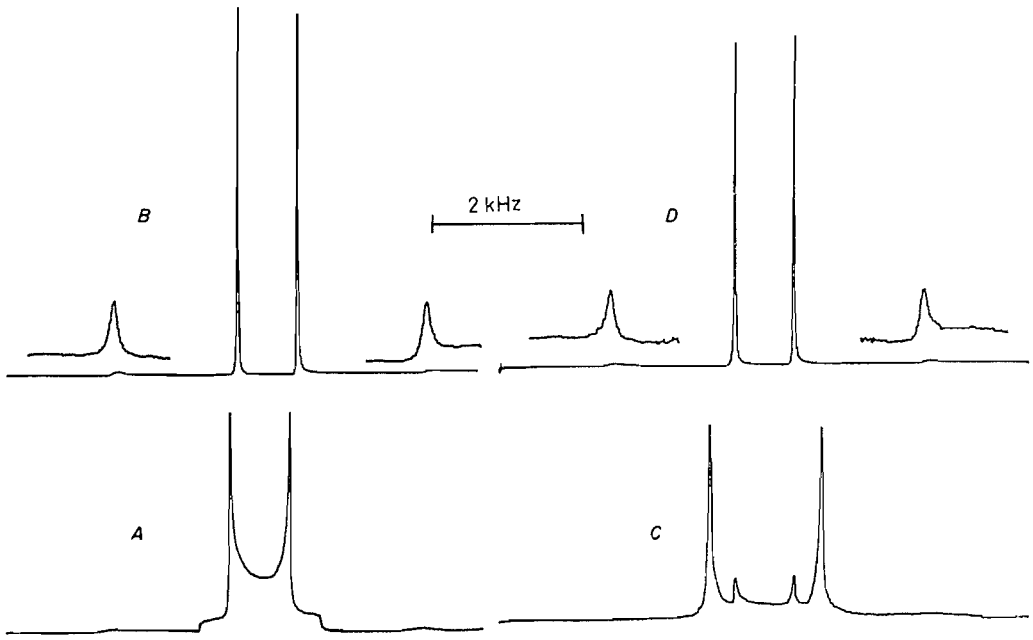


FIG. 1. Deuterium nuclear magnetic resonance spectra of D_2O in α-alaninehydrochloride decylester mesophases. *A*. Compensated mesophase immediately on immersion in the magnetic field. *B*. Spectrum taken a few minutes later after alignment in the field without spinning. *C*. Spectrum after a $\pi/2$ rotation of the nmr sample tube to rotate the perpendicular plane into the field. *D*. During spinning of the sample tube. Amplified peaks above the spectra are assigned to the $-ND_3^+$ group.

few hours at room temperature. The D_2O signals consisted of two doublets of 930 ± 10 Hz for the outer peaks and 770 ± 10 Hz for the inner peaks if 11.120 MWPA were used. Accordingly, the outer doublet can be attributed to a lamellar phase which has the lower density, and the inner doublet to a type II DM phase. Microscopic investigations confirmed the existence of two phases (Plate 2). The texture in Plate 2 shows some resemblance to Figs. 14, 15, and 16 in ref. 18. These textures were assigned by Rosevear (18) as "Additional textures of neat phase". We have assigned the black parts in Plate 2 to the type II DM phase (19). The type II DM phase aligns in a few minutes perpendicular to the microscope glass surface; it is viewed along the optic axis, and thus appears dark through crossed polarizers, i.e. the phase has an isotropic plane perpendicular to this direction.

Type II DM Phase and Cholesteric Phases

Between 11.300 and 11.850 MWPA the racemic mixture of α-ADE forms a type II disc micelle DM mesophase, and the enantiomers form cholesteric phases with opposite helicity. The pitch of the screw axis of these cholesteric phases depends on the water content. A quantitative study of this subject is in progress. In the case of the type II DM phases the mean size of the disc probably becomes smaller at higher water content.

Nuclear Magnetic Resonance Studies of the Mesophases Formed

Mesophases Formed from the Racemic Mixture of α-ADE

The racemic mixture of α-ADE forms lamellar mesophases at lower water contents, which are characterized by the photomicrograph studies, as well as having the property of lower density and higher quadrupole splitting for the deuterium magnetic resonance signal of D_2O in the system than the mesophase, which occurs in coexistence at higher water contents. The mesophase occurring at the higher water contents investigated is characterized by the property of rapid alignment in the magnetic field, higher density, and lower quadrupole splitting for the D_2O. This mesophase is also type II $\Delta\chi < 0$ in diamagnetic properties and is clearly identifiable with the previously assigned type II DM phase (15). Figure 1 shows the deuterium magnetic resonance signals for the intermediate type II DM mesophases with differing alignment procedures. The figure reproduces exactly the behaviour previously observed (15). In Fig. 1*A*, the initial spectrum on placing the sample in the magnetic field is typical for random orientation of the directors in having the powder pattern form for 3 dimensions. After a short time, in the neighborhood of a few minutes, the directors align in a plane perpendicular to the magnetic field and a

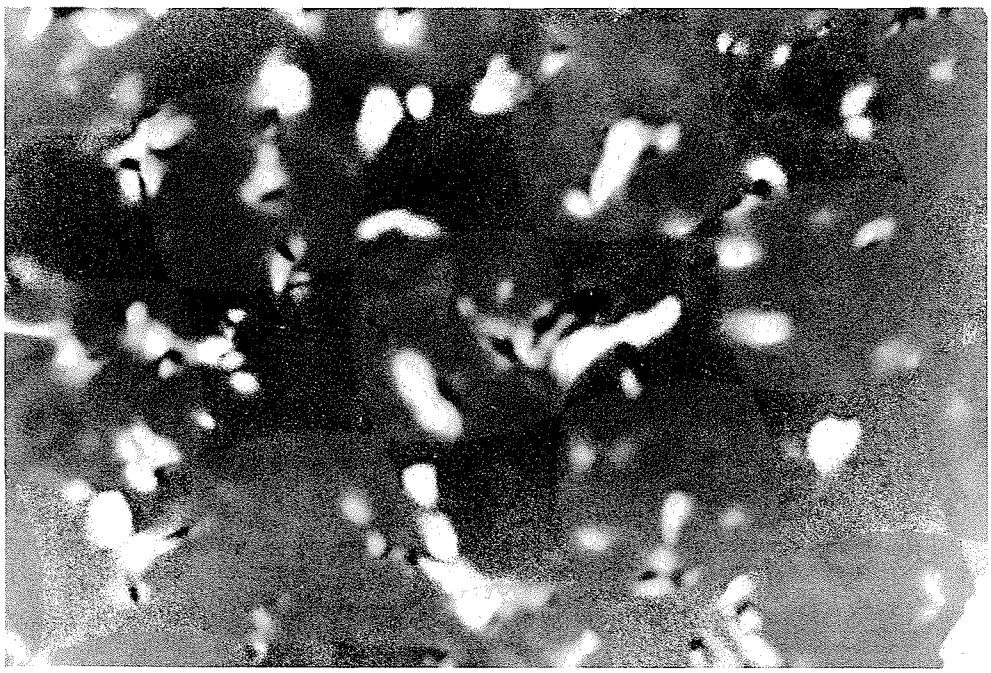


PLATE 3. "Threaded" or "Schlieren" texture of type II (DM) phase formed by *dl*-alanine hydrochloride decylester. This texture disappears in a few minutes. Crossed polarizers. Magnification 100 ×.

sharp doublet is observed, which is equal to the doublet splitting in the powder pattern (2). If the distribution of directors in this perpendicular plane is monitored by rotating the sample tube by 90° (Fig. 1*C*) so that the perpendicular plane is turned into the magnetic field, the spectrum indicates an unsymmetrical distribution of directors in this plane. Such behaviour has been described previously for the type II DM mesophases. If sample spinning is set in motion, the directors rapidly align along the spinning axis of the tube (15) (Fig. 1*D*).

It is interesting to note that separate signals for the more highly ordered $-ND_3^+$ group in the amino-acid residue are clearly resolved, and for Figs. 1*B* and *D* they have been amplified above the recorded spectrum. These amino-acid residues are located at the bilayer interface with the aqueous compartment and are thus more highly ordered than the D_2O. Table 1 includes details of all quadrupole splittings measured.

The results of microscopic investigations of the type II DM phases prepared from the racemic mixture are shown in Plate 3. The texture of type II DM (19) with a negative diamagnetic anisotropy is nematic-like and shows "threaded" or "schlieren" texture (Plate 3) (1, 20). This texture is not stable because of the tendency of the director to align perpendicular to the microscope slide glass surface. This alignment occurs in a few minutes if such microscope samples are placed in the magnetic field

TABLE 1. Mesophases derived from α-alanine-hydrochloride decylesters[a]

Signal	*dl*-ADE	*l*-ADE	*d*-ADE
D_2O	776 ± 10	683 ± 10	780 ± 10
$-ND_3^+$	4090 ± 40	3700 ± 40	4150 ± 40
Na-23	6425 ± 40	6180 ± 40	6950 ± 40

[a]Nuclear quadrupole splittings for cholesteric and compensated mesophases at 30 ± 1°C measured in Hz.

(14.1 kG), with the direction of the aligning magnetic field parallel to the surface of the microscope slide glass. (The optic axis of the type II DM phase aligns perpendicular to the magnetic field direction.)

Mesophases Derived from l-*ADE and* d-*ADE*

The cholesteric mesophases which occur at higher water contents with optically resolved α-ADE's are significantly different in their behaviour in the magnetic field. In Figs. 2*A* and 3*A*, the powder diagram for the *l*-ADE and *d*-ADE mesophases obtained on first immersion in the magnetic field are the same as the compensated type II DM phase. The alignment of the cholesteric liquid crystals is slow compared to the compensated phase, and the final alignment never becomes as homogeneous. In Figs. 2*B* and 3*B* the doublet of the quadrupole splitting for D_2O is on the order of 30 Hz in half width for each peak after 5 h alignment time. For the compensated type II DM mesophase, corresponding

Can. J. Chem. Downloaded from www.nrcresearchpress.com by 210.87.254.105 on 09/05/12
For personal use only.

Can. J. Chem. Downloaded from www.nrcresearchpress.com by 210.87.254.105 on 09/05/12
For personal use only.

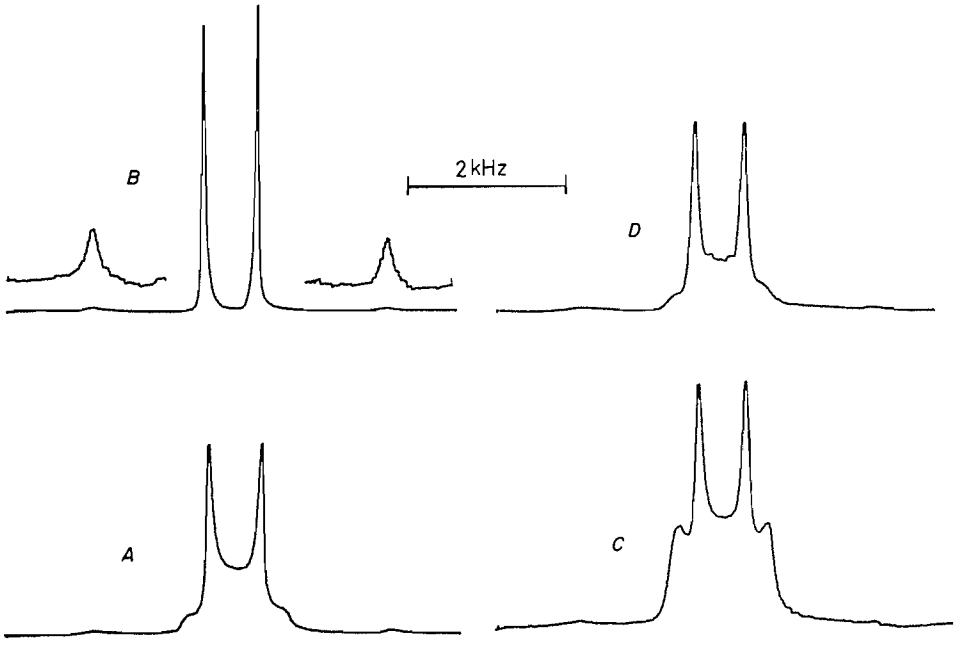


FIG. 2. *A*, *B*, *C*, and *D* are corresponding spectra (as in Fig. 1) for the cholesteric *l*-alanine ester mesophase. Orientation time is on the order of 5 h in these cases.

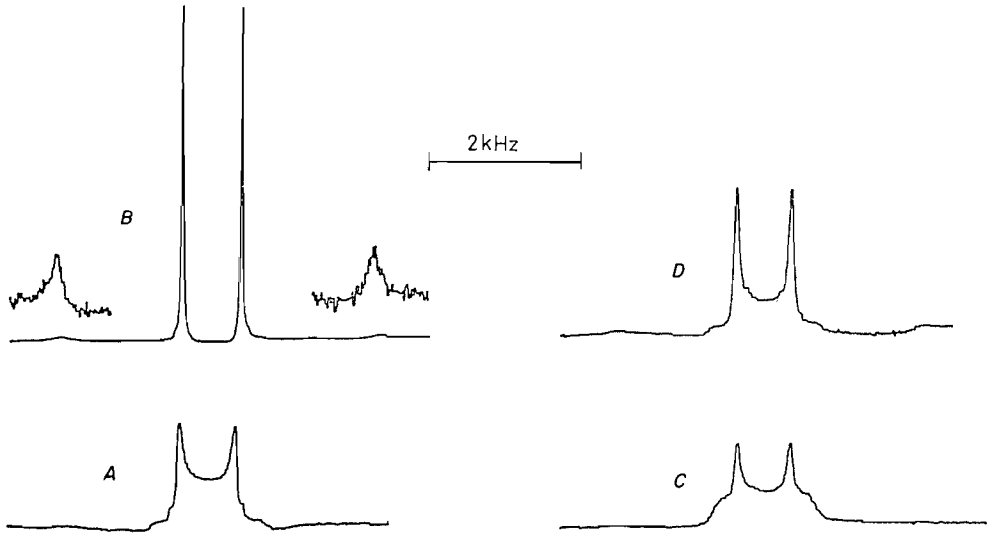


FIG. 3. *A*, *B*, *C*, and *D* corresponding spectra (as in Fig. 1) for the *d*-alanine ester cholesteric mesophase, alignment time 5 h.

peaks are on the order 10 Hz in half width for stationary samples in 8 mm nmr tubes. The experiment which monitors the director distribution in a perpendicular plane to the magnetic field (Figs. 2*C* and 3*C*) gives a quite different result compared to the compensated type II DM mesophase. The director distribution after rotating the nmr tube by $\pi/2$ is much more uniform than the compensated nematic phase and resembles the true 2-dimensional powder pattern spectrum with the plane in the magnetic field (Fig. 4, ref. 15). Figures 2*D* and 3*D* are a clear contrast to the behaviour of the compensated nematic mesophase. On spinning the sample tube there is no alignment along the tube axis of the director, instead the random distribution in the perpendicular plane (yz) to the magnetic field

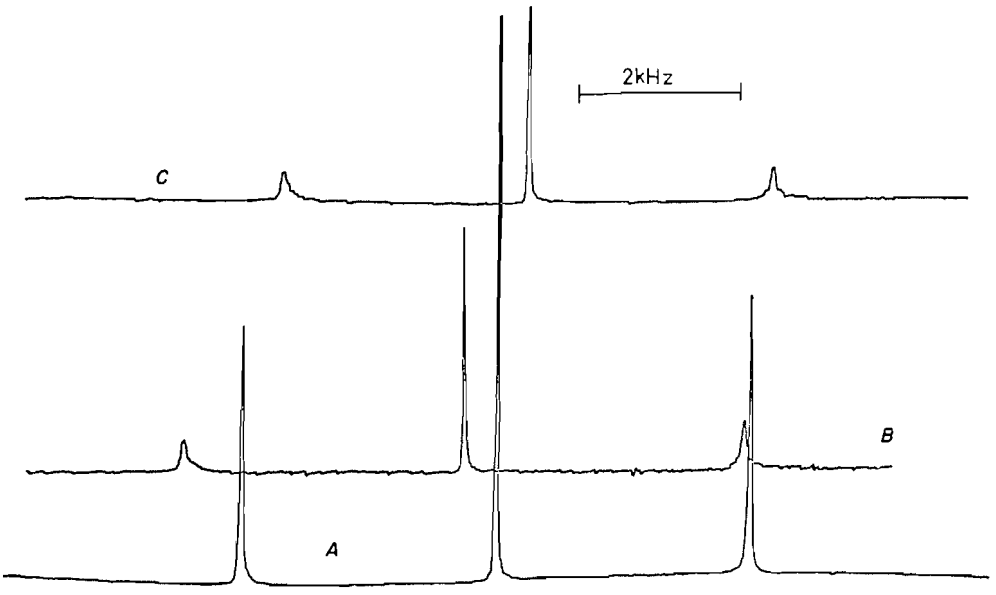


FIG. 4. Sodium nuclear magnetic resonance spectra; *A* for the aligned compensated type II mesophases; *B* the cholesteric *d*-alanine ester mesophase; and *C* the *l*-alanine ester mesophase.

(z direction) is rotated about the y axis to give an effective 3-dimensional random distribution of directors. This reproduces a typical powder spectrum like series *A* of the figures; however, unlike the type II DM mesophases, subsequent alignment under the spinning constraint never occurs. The additional signals in Figs. 2*B* and 3*B* are assigned to the $-ND_3^+$ group of the amino-acid residues in the head groups as before.

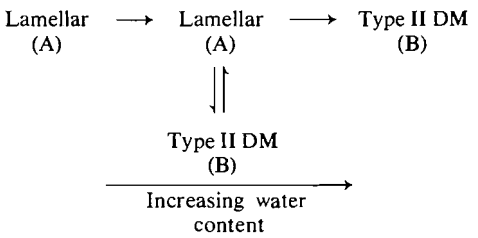
The sodium-23 nmr spectra of non-spinning samples for liquid crystals prepared from *dl*-ADE in a compensated mesophase are shown as Fig. 4*A*, the *d*-ADE mesophase as spectrum 4*B*, and the *l*-ADE mesophase as spectrum 4*C*. The samples were allowed to align for 5 h in the case of the cholesteric liquid crystals. The broadening of the satellites in Figs. 4*B* and 4*C* show the distribution of alignment of the directors in the cholesteric mesophase (16). The separation of the quadrupole splittings for sodium are all listed in Table 1.

The results of polarizing microscope studies of *l*- and *d*-alanine hydrochloride decylester mesophases are shown in Plates 4(*a*) and 4(*b*). Plate 4(*a*) shows non-aligned cholesteric bands, after the microscope sample was equilibrated for 2 h. The ordering in the magnetic field produces a regular direction of the screw axis along the magnetic field as in Plate 4(*b*).

Discussion

The mixtures of water, α-ADE's, and sodium sulphate studied in this work evidently embrace a series of mesophases of distinctly different structure. The two investigative tools, polarized microscopy and deuterium nmr, are not sufficient to determine the structure of these liquid crystals, but they are sufficient together to distinguish between different mesophases and identify some previously known phases. The relative density of the mesophases is an important piece of corroborative evidence, because water being more dense than the inner core of hydrophobic chains, the more water-rich of two coexisting phases becomes the lower layer in a two phase system. In view of the evidence presented in the Experimental, we conclude that there is a regular progression in the polymorphism of the mesophase, which differs for resolved *l*- or *d*-α-ADE and racemic α-ADE. This progression can be separately considered, as (I) for racemic α-ADE and (II) for *l*- or *d*-α-ADE as below. The mesophase with the lowest water content is stated first.

(I) Racemic α-ADE



The type II DM mesophase is composed of disc-

Can. J. Chem. Downloaded from www.nrcresearchpress.com by 210.87.254.105 on 09/05/12
For personal use only.

Can. J. Chem. Downloaded from www.nrcresearchpress.com by 210.87.254.105 on 09/05/12
For personal use only.

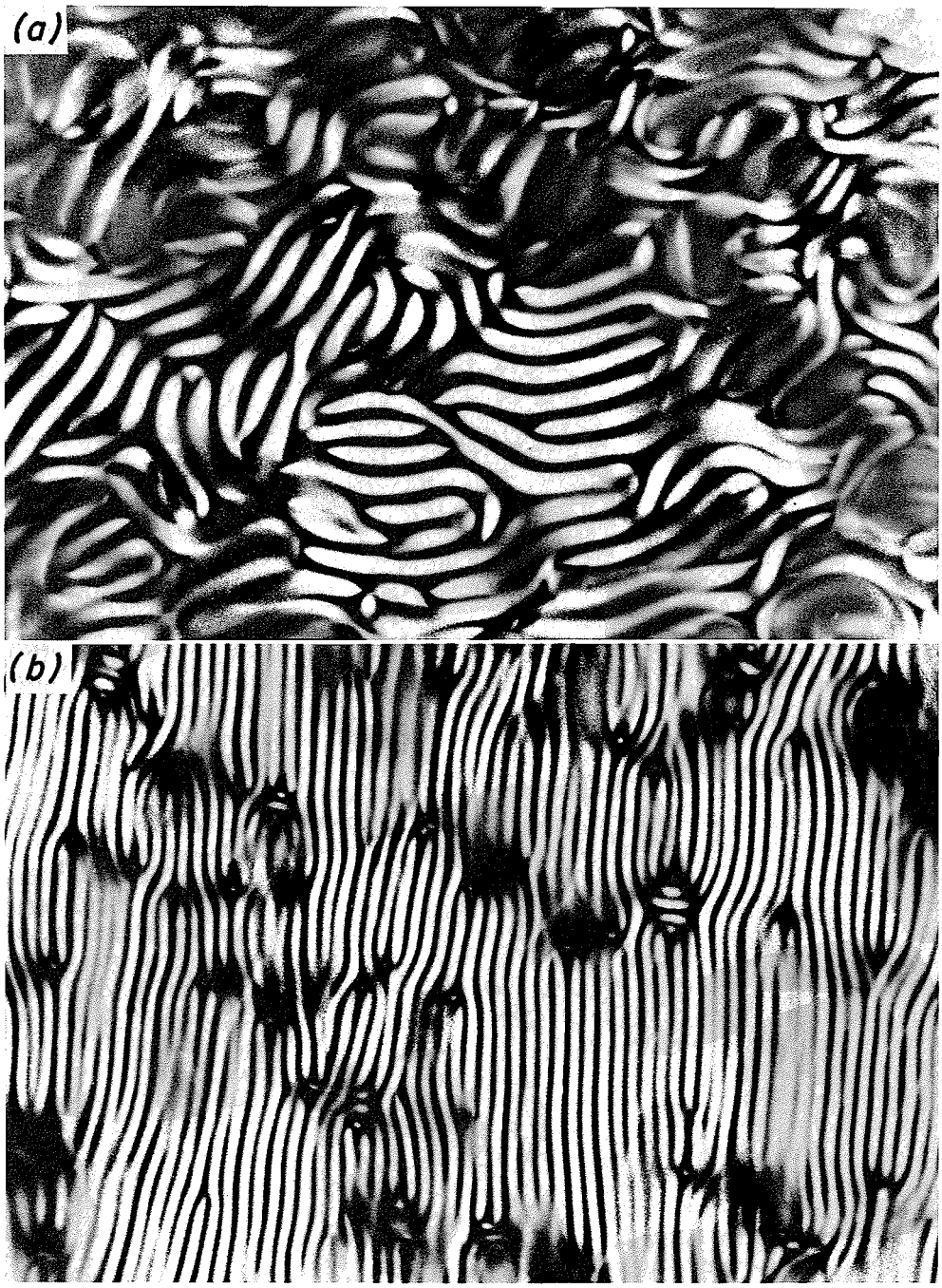
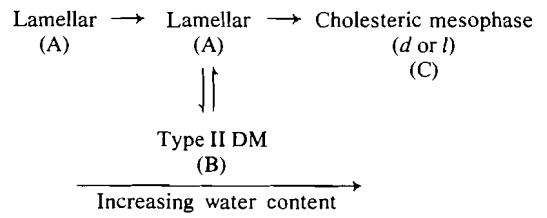


PLATE 4. (*a*) Non-aligned cholesteric texture. The mesophase was equilibrated two hours on the microscope slide. (*b*) Aligned cholesteric texture. The above microscope sample was placed two hours in the 14.1 kG magnetic field. The direction of the magnetic field was parallel to the surface of the microscope slide glass from left to right. Crossed polarizers. Magnification 100 ×.

like bilayer micelles of finite size disposed with long range orientational, but little[4] long range positional order (13, 15).

(II) *l* or *d* α-ADE



The nmr and microscopic evidence does not distinguish between the lamellar (A) phases in I and II nor the type II DM mesophases in I and II, but we assume that these phases have the same structure in both cases. Three different mesophase structures are encountered, the third type is a cholesteric type mesophase. The compensated type II DM mesophase has negative diamagnetic anisotropy (2, 22) and thus the derived cholesteric phase, prepared using the resolved detergent, has a screw or helical axis, which is parallel to the magnetic field direction (17). The directors are arranged in each successive plane perpendicular to the screw axis with regular angular displacement and thus although still close to being perpendicular to the field direction they are fanned out evenly in their projections on this perpendicular plane. The even distribution of the directors in this perpendicular plane has been demonstrated (Figs. 2*C* and 3*C*) by rotating this plane into the magnetic field and observing the two dimensional powder pattern. Plates 4(*a*) and 4(*b*) confirm the twisted structure and the texture illustrates the fact that the screw axis is parallel to the applied magnetic field direction. This cholesteric mesophase, because it is prepared using a single optically active amphiphile and can be prepared with opposite helical forms as well as in the compensated *d*/*l* mixture, represents the *first* report of the aqueous lyotropic analogue of the thermotropic cholesteric liquid crystal. The quantitative study of the effect of water content on unbalanced mixtures of *d* and *l* forms and impurities on the pitch of the screw axis is in progress. The origin of the cholesteric behaviour is an interesting question. A good postulate for the structure can be made by considering the relationship to the type II DM mesophase. In the one case where the structure has been determined by low angle X-ray diffraction (13) the type II DM mesophase has been shown to consist of large disc micelles of bilayer thickness, disposed without long range positional order but retaining orientational order.[4]

It is reasonable to assume that at a critical water content, i.e. at a critical average inter-micelle distance, the inter-micelle forces fall off sufficiently to allow a helical type distortion of the disc-shape to occur because of more efficient packing of the optically active head groups within the micelle units of the structure. The packing of these micelles can lead to a helical structure of the mesophase and thus typical cholesteric properties.

Acknowledgement

L.W.R. would like to thank the National Research Council of Canada for their support of this work.

1. K. D. LAWSON and T. J. FLAUTT. J. Am. Chem. Soc. **89**, 5490 (1967).
2. K. RADLEY, L. W. REEVES, and A. S. TRACEY. J. Phys. Chem. **80**, 174 (1976).
3. F. FUJIWARA, L. W. REEVES, M. SUZUKI, and J. A. VANIN. Solution chemistry of surfactants. Proceedings of National Colloid Symposium, Knoxville, TN. June, 1978. *Edited by* K. Mittal. Plenum Press. 1979.
4. L. L. M. VAN DEENEN. The molecular basis of membrane function. *Edited by* D. C. Tosteson. Prentice-Hall, New Jersey. 1969. p. 47.
5. K. RADLEY and L. W. REEVES. Can J. Chem. **53**, 2998 (1975).
6. L. W. REEVES and A. S. TRACEY. J. Am. Chem. Soc. **96**, 365 (1974).
7. K. RADLEY and A. SAUPE. Mol. Phys. **35**, 1405 (1978).
8. A. S. TRACEY and P. DIEHL. FEBS Lett. **59**, 131 (1975).
9. F. Y. FUJIWARA and L. W. REEVES. J. Am. Chem. Soc. **98**, 6790 (1976).
10. F. F. KNAPP and H. J. NICHOLAS. Mol. Cryst. Liq. Cryst. **6**, 319 (1970).
11. F. D. SAEVA and G. R. OLIN. J. Am. Chem. Soc. **95**, 7882 (1973).
12. V. LUZATTI. *In* Biological membranes. *Edited by* D. Chapman. Academic Press, New York. 1968.
13. L. Q. DO AMARAL, C. PIMENTAL, M. R. TAVARES, and J. A. VANIN. J. Chem. Phys. **71**, 2940 (1979).
14. C. ROBINSON. Mol. Cryst. Liq. Cryst. **1**, 467 (1966).
15. F. Y. FUJIWARA and L. W. REEVES. Can. J. Chem. **56**, 2178 (1978).
16. N. KAMEZAWA. J. Magn. Reson. **21**, 211 (1976); **27**, 325 (1977).
17. F. SACKMANN, S. MEIBOOM, L. C. SNYDER, A. E. MEIXNER, and R. E. DIETZ. J. Am. Chem. Soc. **90**, 3567 (1968).
18. F. B. ROSEVEAR. J. Am. Oil Chem. Soc. **31**, 628 (1954).
19. F. Y. FUJIWARA and L. W. REEVES. J. Phys. Chem. **84**, 653 (1980).
20. P. J. BLACK, K. D. LAWSON, and T. J. FLAUTT. Mol. Cryst. Liq. Cryst. **7**, 201 (1969).
21. G. J. T. TIDDY, J. B. HAYTER, A. M. HECHT, and J. W. WHITE. Ber. Bunsenges. **78**, 961 (1974).
22. L. POHL, R. EIDENSCHINK, J. KRAUSE, and G. WEBER. Phys. Lett. A, **65**, 169 (1978).

Can. J. Chem. Downloaded from www.nrcresearchpress.com by 210.87.254.105 on 09/05/12
For personal use only.

Disc micelles in type II DM phases: short chains in long chain host bilayers

MAHMUT ACIMIS[1] AND LEONARD W. REEVES[2]
Department of Chemistry, University of Waterloo, Waterloo, Ont., Canada N2L 3G1
Received December 13, 1979

MAHMUT ACIMIS and LEONARD W. REEVES. Can. J. Chem. **58**, 1542 (1980).

Host bilayers of the large disc shaped micelles in type II DM phases have been prepared with two detergents having a 16 carbon chain. Studies of small quantities of 10 carbon guest amphiphiles have been made using deuterium magnetic resonance. The host bilayer solution is only slightly perturbed by changes in simple counter and co-ions. The only major change in host chain order profiles is obtained when its pyridinium head groups are changed for *N*-trimethyl head groups. The guest chain motions near the non-polar chain terminus are considerably more restricted than in bilayers prepared from hosts of shorter chain length conforming closely to the guest chain length. The small changes observed in motion behaviour of the chains as a function of simple counter and co-ions can be a standard to test the effect of specific complexing agents on guest chain motions in the present system.

MAHMUT ACIMIS et LEONARD W. REEVES. Can. J. Chem. **58**, 1542 (1980).

On a préparé des doubles couches pouvant servir de cages aux micelles ayant la forme de disque dans des phases DM de type II en utilisant deux détergents ayant une chaîne à 16 atomes de carbone. On a étudié des petites quantités d'amphiphiles susceptibles d'être encagées à 10 atomes de carbone en utilisant la rmn du ^2H. La solution réceptrice à double couches est légèrement perturbée par les changements dans les ions simples opposés et les ions simples de même signe. On obtient le seul changement important dans l'ordre de la chaîne réceptrice lorsque ses têtes de groupe pyridinium sont remplacées par des têtes de groupe *N*-triméthyle. Les mouvements de la chaîne encagée près du bout de chaîne non polaire sont considérablement plus restreints que dans les doubles couches préparées à partir des récepteurs à chaîne plus courte se rapprochant de très près de la longueur de chaîne encagée. Les petits changements observés dans le comportement des chaînes en fonction des ions simples opposés et des ions simples de mêmes signes peuvent servir de référence pour vérifier l'effet des agents complexants spécifiques sur les mouvements de la chaîne encagée dans le présent système.

[Traduit par le journal]

Introduction

Intermediate phases in aqueous lyotropic systems (1, 2) are formed when a hexagonal or lamellar structure is diluted with water and a quantity of electrolyte is added (3, 4). These phases align spontaneously in an applied magnetic field and for type II DM ($\Delta\chi < 0$) systems the constituent disc-micelles align with the normal to their interfaces perpendicular to the applied field (5, 6). The structure of one type II DM mesophase has been determined by low-angle X-ray diffraction methods (7). The micelles are of bilayer thickness and the dimension of their planar extent in the case studied (7) is in excess of 1000 Å.

The present study is designed to investigate the following aspects of the bilayer of the constituent micelles in the Type II DM phase. (*a*) The degree of order profiles of guest amphiphiles of short length (10 segments) in a disc bilayer micelle of longer chain amphiphiles (16 segments). (*b*) The variation of chemistry of the polar or ionic head group in the guests to include cationic, anionic, and neutral groups. (*c*) The study of two 16 carbon chain host systems with *N*-trimethyl and pyridinium head groups. (*d*) The variation of the chemical identity of simple counter and co-ions. We have recently completed a rather thorough study of the reverse case where the host bilayer is prepared from amphiphiles of short chain length compared to the guests (6).

Experimental

Materials

1-Hexadecylpyridinium chloride and 1-hexadecyltrimethylammonium bromide were purchased from J. T. Baker Co., and purified by recrystallization, hexadecylpyridinium chloride from cyclohexane–ethanol and hexadecyltrimethylammonium bromide from ethyl acetate.

1-Hexadecyltrimethylammonium chloride and 1-hexadecyltrimethylammonium nitrate were synthesized by converting 1-hexadecyltrimethylammonium bromide to 1-hexadecyltrimethylammonium hydroxide by treatments with silver oxide (Ag_2O) in methanol (8). After filtering the precipitated AgBr, the 1-hexadecyltrimethylammonium hydroxide was neutralized by appropriate acids.

All perdeuteriated compounds were made from potassium salts of fatty acids according to a variation of the procedure of Dinh-Nguyen *et al.* (9) in a steel bomb. Perdeuteriated 1-decanol, sodium 1-decylsulfate, 1-decylammonium chloride, 1-hexadecylpyridinium chloride, 1-hexadecyltrimethylammonium chloride, 1-hexadecyltrimethylammonium bromide, and 1-hexadecyltrimethylammonium nitrate were made from the appropriate perdeuteriated potassium salts of the fatty acids. The deuteriated fatty acid salts were converted to fatty acids and these were reacted to give acid chlorides by means of thionyl chloride ($SOCl_2$). The acid chlorides were then reduced with lithium aluminum deuteride ($LiAlD_4$) to the appropriate perdeuteriated alcohols (10).

[1]Present address: Cukurova Üniversitesi, Temel Bilimler Fakultesi, Kimya Bölümü, Köprüköyü, Adana, Turkey.

[2]Author to whom correspondence should be addressed.

0008-4042/80/151542-08$01.00/0
©1980 National Research Council of Canada/Conseil national de recherches du Canada

Can. J. Chem. Downloaded from www.nrcresearchpress.com by 210.87.254.42 on 09/05/12
For personal use only.

TABLE 1. Compositions of systems studied[a]

Mesophase A			Mesophase B		
Compounds	Weight %	Moles	Compounds	Weight %	Moles
HDTACl system					
HDTACl	29.60	1.000	HDTACl	29.33	1.000
NaDS	2.56	0.100	DACl	2.22	0.115
NaCl	3.23	0.598	NaCl	3.00	0.558
1-Decanol	5.61	0.383	1-Decanol	6.85	0.472
H_2O	59.00	35.430	H_2O	58.60	35.514
HDTABr system					
HDTABr	27.28	1.000	HDTABr	29.19	1.000
NaDS	2.62	0.129	DACl	2.41	0.143
NaBr	2.83	0.382	NaBr	3.07	0.372
1-Decanol	2.67	0.234	1-Decanol	5.01	0.394
H_2O	65.60	50.565	H_2O	60.32	41.827
$HDTANO_3$ system					
$HDTANO_3$	34.55	1.000	$HDTANO_3$	34.03	1.000
NaDS	2.51	0.091	DACl	2.37	0.125
$NaNO_3$	2.29	0.270	$NaNO_3$	2.29	0.274
1-Decanol	3.50	0.222	1-Decanol	4.75	0.306
H_2O	57.15	31.850	H_2O	56.56	32.000
HDPCl system					
HDPCl	28.36	1.000	HDPCl	32.66	1.000
NaDS	2.73	0.112	DACl	1.93	0.095
NaCl	2.26	0.544	NaCl	3.99	0.710
1-Decanol	3.63	0.275	1-Decanol	5.72	0.376
H_2O	62.72	41.758	H_2O	55.70	32.210

[a]Composition of studied systems are given in weight percent and moles. Abbreviations of the components are listed in Experimental.

Perdeuteriated Sodium 1-Decylsulfate

Perdeuteriated 1-decanol was converted to sodium 1-decylsulfate using chlorosulfuric acid and subsequent neutralization with NaOH.

Perdeuteriated 1-Decylammonium Chloride

Perdeuteriated 1-decanol was converted to decylamine as previously described (11). The prepared amine was then neutralized by hydrochloric acid.

Perdeuteriated Hexadecyl Compounds

Perdeuteriated 1-hexadecyltrimethylammonium chloride, bromide, and nitrate were synthesized from 1-perdeuteriated hexadecyliodide with aqueous trimethylamine (25–30%). Perdeuteriated hexadecyliodide was made from perdeuteriated hexadecylalcohol (12). The prepared perdeuteriated 1-hexadecyltrimethylammonium iodide was converted to perdeuteriated 1-hexadecyltrimethylammonium hydroxide by means of silver oxide (Ag_2O) as described above. The perdeuteriated 1-hexadecyltrimethyl hydroxide was then neutralized by appropriate acids. Perdeuteriated 1-hexadecylpyridinium chloride was synthesized from perdeuteriated 1-hexadecyl iodide and pyridine. 1-Hexadecylpyridinium iodide was converted to the chloride by means of silver oxide and subsequent neutralization with hydrochloric acid. The purity of the compounds was checked by thin layer chromatography and sometimes by proton nmr as well.

Composition of the Mesophases

All samples were prepared by weighing the required amounts of the components into test tubes. In order to keep the contents of the mesophases constant, the tubes were sealed, and the samples homogenized by warming on a water bath and centrifuging. The homogenized samples were opened and poured into 10 mm nmr tubes. The compositions are given in moles (host detergent normalized to one mole) and weight percent (Table 1). The given moles and percentage of sodium 1-decylsulfate and 1-decylammonium chloride originate from deuteriated molecules, assuming a 90% deuteriation. The water used contained 0.1% D_2O. In order to avoid long repetitions, some abbreviations of the compounds are introduced.

1-Hexadecyltrimethylammonium chloride, HDTACl
1-Hexadecyltrimethylammonium bromide, HDTABr
1-Hexadecyltrimethylammonium nitrate, $HDTANO_3$
1-Hexadecylpyridinium chloride, HDPCl
} Hosts

Sodium-1-decylsuphate, NaDS
1-Decanol, Dec.
1-Decylammonium chloride, DaCl
} Guests

All nmr spectra were determined at 9.1 MHz on a Bruker SXP pulse nmr spectrometer using an external proton water lock. The ambient temperature was 32 ± 1°C. Spectral widths on the order of 20–30 kHz were used, and approximately 5 000 to 60 000 transients were required.

Results

Systems Studied

In this study the host mesophase is based on the hexadecylhydrocarbon chain while the guests are 1-decylsulphate, 1-decylammonium, and 1-decanol, these being respectively negative, positive, and no net charge on the head group. The

Can. J. Chem. Downloaded from www.nrcresearchpress.com by 210.87.254.42 on 09/05/12
For personal use only.

Can. J. Chem. Downloaded from www.nrcresearchpress.com by 210.87.254.42 on 09/05/12
For personal use only.

host head group has been varied between trimethylammonium and pyridinium, the first with chloride, bromide, and nitrate counter ions and the second with only chloride counter ions. In this systematic manner, the chemical changes at the interface can be studied for both changes in the order of the water and the totally deuteriated hydrocarbon chains of the guests and hosts.

The study for comparison of three guests in type II DM bilayers was made in two steps. Mesophases labelled "A" contain both the NaDS guest and small amounts of 1-decanol. However, since replacement of the same mol% of 1-decylsulphate in the mesophase by 1-decylammonium ion provoked a phase change, a set of mesophases labelled "B" contain the 1-decylammonium ion with slightly different mole percentages of 1-decanol, in order to preserve the type II nematic mesophase. The effects on the hosts were monitored by including some perdeuteriated host detergent in each mesophase. The deuterium quadrupole splittings measured for the 0.1% D_2O in H_2O were always very low in the range 20–50 Hz. This is entirely consistent with the recent studies from this laboratory on mixed bilayers with carboxylate and pyridinium or trimethylammonium head groups (8). It is evident that the strong hydration of carboxylate groups at the interface imposes a strong ordering effect on the interface water, but the more shielded positive charges and lack of donor or acceptor sites for hydrogen bonding for the $-N(CH_3)_3^+$ and pyridinium head groups leads to transfer of little ordering effect to the water at the interface (8). The host mesophases here all fall into the latter class.

Deuterium Magnetic Resonance Studies

The use of the residual deuterium quadrupole splittings to measure degrees of order along C—D bonds in the hydrocarbon chains of liquid crystals has already been adequately described in the literature (14–17). The measurements reported here consist of determining and assigning the quadrupole splittings of specifically deuteriated chains, both for hosts and guests. This quadrupole splitting is proportional to the degree of order along the C—D bonds. Since the proportionality is always the same, we use the quadrupole splitting directly as a measure of the degrees of order.

Mesophases A

The deuterium quadrupole splittings for mesophases A may be obtained from the supplementary data[3] and are plotted in Figs. 1 to 4 against the carbon number of the respective $-CD_2-$ group in the hydrocarbon chains. An undesirable transition to an isotropic phase predicated some small variations from the A mesophases in the mole fraction of components which make up the B mesophases (Table 1). These small differences are not important as we shall show in the discussion.

Mesophases A with the host HDTA were prepared with different counter ions, Cl^-, Br^-, and NO_3^-. The plateau of uniform order extends to the carbon 9 segment, followed by a rapidly decreasing quadrupole splitting for segments 10 to 16. The chloride counter ion does affect the order of the segment of carbon 1 in this mesophase, the degree of order being displaced above the plateau. For mesophases containing HDPCl the uniform degree of order extends to the 10th carbon (Fig. 4).

Some general observations are possible with respect to the relative degrees of order of hosts and guests in the same bilayer solution of mesophases A. The 1-decylsulphate has a short plateau of uniform order of 4 carbon segments, which lies above the corresponding host segments in all mesophases while the same region for 1-decanol segments always lies well below that of the host. There are differences in the magnitude of this relative ordering which depend primarily on the identity of the counter ion. Changes in the absolute values of de-

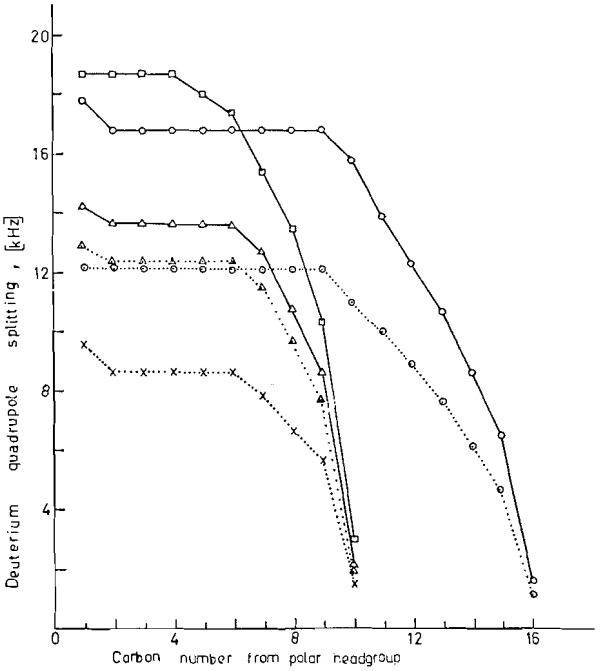


FIG. 1. H^2 quadrupole splittings are plotted versus corresponding carbon numbers for 1-hexadecyltrimethylammonium chloride, HDTACl-d_{33} host bilayers. Mesophases A: the host, ○; guests, NaDS-d_{21}, □, and 1-decanol-d_{22}, △. Mesophases B: the host, ⊙; guests, DACl-d_{21}, ×, and 1-decanol-d_{22}, ⧋.

[3]Tables of supplementary data are available for a nominal fee from the Depository of Unpublished Data, CISTI, National Research Council of Canada, Ottawa, Ont., Canada K1A 0S2.

Can. J. Chem. Downloaded from www.nrcresearchpress.com by 210.87.254.42 on 09/05/12
For personal use only.

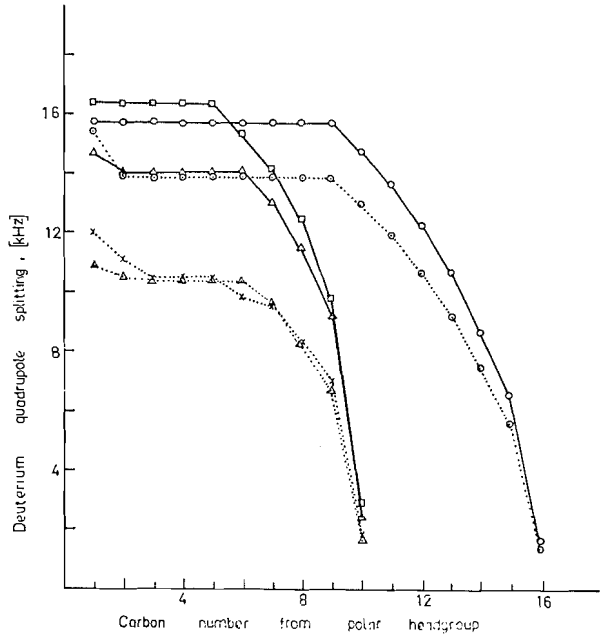


FIG. 2. Legend as in Fig. 1 except that the host is 1-hexadecyltrimethylammonium bromide, HDTABr-d_{33}.

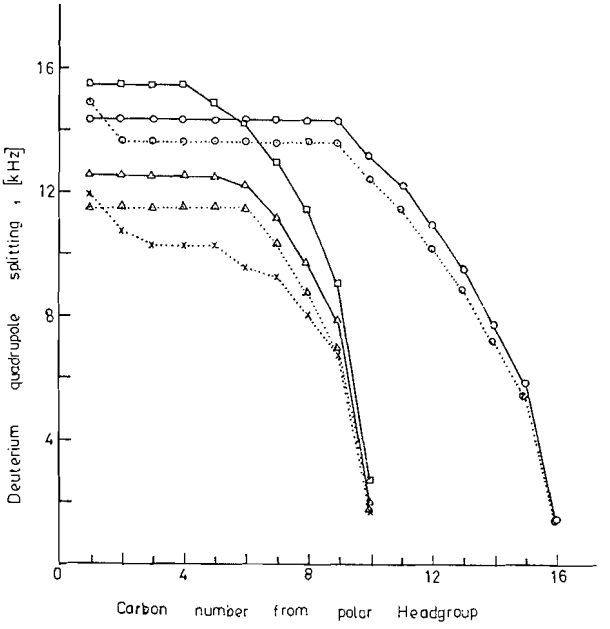


FIG. 3. Host is 1-hexadecyltrimethylammonium nitrate, HDTANO_3-d_{33}, otherwise as in Fig. 1.

grees of order, that affect all components of the bilayer solution of the extended micelle, can be associated with the overall changes in motion of the micelle as a body (6). On the other hand, relative changes in the motion of host and guest in different mesophases must derive from changes in the bilayer solution of amphiphiles which make up the

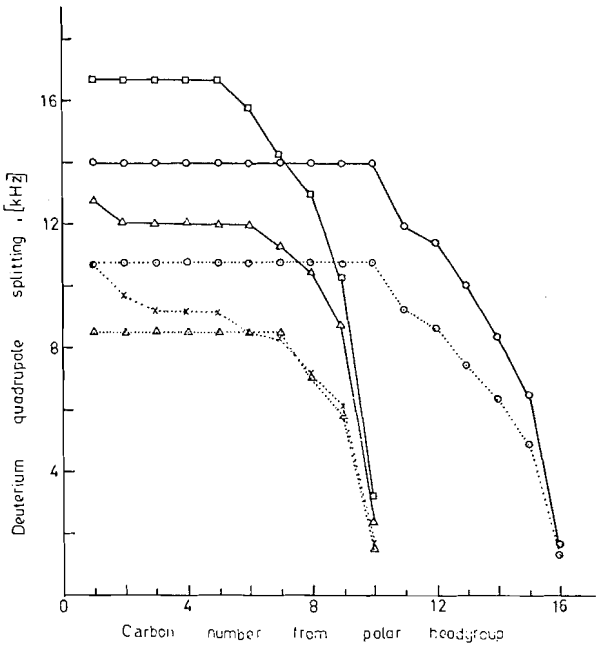


FIG. 4. Host is 1-hexadecylpyridinium chloride, HDPCl-d_{33}, otherwise as in Fig. 1.

micelle. The magnitudes of plateau degrees of order for HDTA ion segments decrease slightly for the three mesophases A with the effect for $Cl^- > Br^- > NO_3^-$ counter ions (Figs. 1–3). They correspond to 16.8 kHz, 15.8 kHz, and 14.5 kHz, respectively, in terms of quadrupole splittings.

Mesophases B

These liquid crystals contain the neutral guest amphiphiles, 1-decanol, and the cation, 1-decylammonium.

With a cationic guest amphiphile for series B the plateau of order in the host HDTA is always lower than in series A with an anionic guest, but the difference depends on the choice of the small counter and co-ion. The difference is large with Cl^- and smaller with Br^- and NO_3^-. This change in absolute order can be accounted for by assuming that mean micelle diameter is in general smaller with the cationic guest allowing larger amplitude motions of the micelle as a body. The same decrease in plateau order of the host on changing the nature of the guest is seen in Fig. 4 where results on HDPCl are summarized. The 1-decylammonium ion segments do not in general have a well developed plateau of uniform order, but they always appear of lower order than the host.

Discussion

General Consideration of Degrees of Order

The degree of order along a C—D bond may be

written as a product of the different angular contributions about different axes (11, 13). For the type II mesophases studied here, the disc-shaped micelles of bilayer thickness have a symmetry axis normal to the disc, which oscillates about the director, i.e., optic axis of the uniaxial liquid crystal. The optic axis in the aligned type II mesophases is disposed in a perpendicular direction to the applied magnetic field. The experimental degree of order for —CD_2— segment i in mesophase α is therefore written:

$$[1] \quad S^{\alpha}_{\text{expt}(i)} = S^{\alpha}_{\text{mo}(i)} \cdot S^{\alpha}_{\text{co}(i)} \cdot S^{\alpha}_{k/j(i)} \cdot S^{\alpha}_{\text{dif}(i)} \cdot 1/2(3\cos^2\Omega - 1)$$

where $S^{\alpha}_{\text{expt}(i)}$ = experimentally measured degree of order in mesophase α. $S^{\alpha}_{\text{mo}(i)}$ = contribution to the measured degree of order from oscillation of the normal to the disc micelle, about the director or optic axis of the mesophase. $S^{\alpha}_{\text{co}(i)}$ = contribution of the oscillation of the pseudo-rigid hydrocarbon chain as a unit about the normal to the micelle interface. The separation of internal motions of the chain from the motions of the pseudo-rigid chain is a reasonable and common assumption. $S^{\alpha}_{\text{dif}(i)}$ = contribution from diffusive motions of the pseudo-rigid chain in the micelle bilayer. Normally in the present situation only diffusive motion around the edge of the finite bilayer disc can make a contribution. This term therefore does vary with the size of the disc micelle as does $S^{\alpha}_{\text{mo}(i)}$, but if we assume the disc micelle is very large compared to its thickness (7), the diffusion term becomes very small and $S^{\alpha}_{\text{dif}(i)} \simeq 1$. $S^{\alpha}_{k/j(i)}$ = contributions derived from internal motions of the chain. $\Omega = 90°$, the angle between the mesophase director and the magnetic field. Thus [1] may be shortened to:

$$[2] \quad S^{\alpha}_{\text{expt}(i)} = -1/2\, S^{\alpha}_{\text{mo}(i)} \cdot S^{\alpha}_{\text{co}(i)} \cdot S^{\alpha}_{k/j(i)}$$

For the same mesophase α, it is clear that since $S^{\alpha}_{\text{mo}(i)}$ and $S^{\alpha}_{\text{co}(i)}$ are rigid chain motions, they are the same for all segments with the same chain and therefore:

$$[3] \quad S^{\alpha}_{\text{expt}(i)}/S^{\alpha}_{\text{expt}(j)} = S^{\alpha}_{k/j(i)}/S^{\alpha}_{k/j(j)}$$

The relative contributions to the internal motions at segments i and j in the same chain are directly comparable in the ratio profile by eq. [3]. These ratio profiles are known to be independent of water content of mesophases within the variations possible for type II aligning mesophases (6, 11). This reasonable experimental result is explicable in terms of changes in micelle size and water thickness but not of internal packing of amphiphiles in disc micelles, within the limits that these are large enough to make negligible the small proportion of amphiphiles at the disc edges (6). Table 2 lists the quadrupole splitting ratios as in eq. [3] where segment i is arbitrary and segment j is the terminal methyl segment.

If there is no change in the averaged segmental motion of a given amphiphile in two different mesophases, we should obtain an experimental result according to [4], where α and β denote mesophase change for the same amphiphile:

$$[4] \quad S^{\alpha}_{k/j(i)}/S^{\alpha}_{k/j(j)} = S^{\beta}_{k/j(i)}/S^{\beta}_{k/j(j)}$$

The only differences in the composition of mesophases listed in Table 1 are associated with the counter ions and the nature of a minor guest. It is instructive to examine the quadrupole splitting ratios in [4] as the mesophases are altered. The differences in ratios [4] from phase to phase for the hexadecyltrimethylammonium segments are small, e.g., the ratios of the plateau order to the terminal methyl degree of order are 10.59, 9.85, 9.90, 10.74, 10.31, and 10.13 (Table 2). This is a much smaller range than the parent quadrupole splittings, which vary widely for a given segment in different mesophases. The variation in the ratios of the host segments from mesophase to mesophase does indicate some very minor changes in the kink/jog motions and thus of packing of the host amphiphile in the bilayer. Both the change of counter and co-ion and the small quantity of guest appear to be factors in these small changes of the bilayer solvent.

The ratios of quadrupole splittings for the hexadecylpyridinium ion are quite distinct from the hexadecyltrimethylammonium[3] confirming that the chemical effect of prime importance is the change of identity of the polar head group. On the other hand for mesophase A and B in this system, the ratios as defined in eq. [4] are the same within experimental error.[3] The change of the minor amount of guest between 1-decylsulphate and 1-decylammonium, with conservation of the chloride counter ion, has absolutely no effect on the chain motions of this host.

These interesting quantitative results on the degree of order profile of the host amphiphile chain segments assure us that the bilayer solvent chain motions are almost unchanged, although the micelle size may change from mesophase to mesophase. With this fact in mind we can pass on to discuss the dilute solutes in this host bilayer.

Concentrating now on the changes, if any, in the motion of the 1-decanol guest or solute chain as the mesophase is altered with respect to counter ion and other guest, we see from Table 2 that within the mesophases containing HDTA ions the variations in ratios are small. These small variations in ratios

Can. J. Chem. Downloaded from www.nrcresearchpress.com by 210.87.254.42 on 09/05/12
For personal use only.

Can. J. Chem. Downloaded from www.nrcresearchpress.com by 210.87.254.42 on 09/05/12
For personal use only.

TABLE 2. Quadrupole splitting ratios of mesophases A and B[a]

Mesophases A				Mesophases B			
HDTACl-d_{33}	HDTABr-d_{33}	HDTANO$_3$-d_{33}	HDPCl-d_{33}	HDTACl-d_{33}	HDTABr-d_{33}	HDTANO$_3$-d_{33}	HDPCl-d_{33}
11.21 (1)	9.85 (1–9)	9.90 (1–9)	8.25 (1–10)	10.74 (1–9)	11.45 (1)	11.03 (1)	8.29 (1–10)
10.59 (2–9)	—	—	—	—	10.31 (2–9)	10.13 (2–9)	—
9.48 (10)	9.25 (10)	9.12 (10)	—	9.76 (10)	9.66 (10)	9.23 (10)	—
8.77 (11)	8.57 (11)	8.49 (11)	7.08 (11)	8.89 (11)	8.88 (11)	8.55 (11)	7.10 (11)
7.74 (12)	7.69 (12)	7.59 (12)	6.74 (12)	7.90 (12)	7.93 (12)	7.60 (12)	6.65 (12)
6.72 (13)	6.69 (13)	6.62 (13)	5.95 (13)	6.78 (13)	6.82 (13)	6.62 (13)	5.74 (13)
5.41 (14)	5.41 (14)	5.37 (14)	4.94 (14)	5.45 (14)	5.53 (14)	5.36 (14)	4.93 (14)
4.09 (15)	4.10 (15)	4.07 (15)	3.81 (15)	4.14 (15)	4.13 (15)	4.07 (15)	3.78 (15)
1.00 (16)	1.00 (16)	1.00 (16)	1.00 (16)	1.00 (16)	1.00 (16)	1.00 (16)	1.00 (16)
1-Decanol-d_{22}	1-Decanol-d_{22}	1-Decanol-d_{22}	1-Decanol-d_{22}	1-Decanol-d_{22}	1-Decanol-d_{22}	1-Decanol-d_{22}	1-Decanol-d_{22}
6.51 (1)	6.25 (1)	6.43 (1–5)	5.40 (1)	6.73 (1)	6.54 (1)	6.70 (1–6)	5.46 (1–7)
6.25 (2–6)	5.93 (2–6)	6.23 (6)	5.08 (2–6)	6.43 (2–6)	6.30 (2–6)	—	—
5.83 (7)	5.53 (7)	5.75 (7)	4.77 (7)	6.00 (7)	5.86 (7)	6.02 (7)	—
4.96 (8)	4.89 (8)	4.96 (8)	4.43 (8)	5.03 (8)	4.98 (8)	5.09 (8)	4.56 (8)
3.97 (9)	3.94 (9)	4.03 (9)	3.70 (9)	4.01 (9)	3.99 (9)	4.08 (9)	3.73 (9)
1.00 (10)	1.00 (10)	1.00 (10)	1.00 (10)	1.00 (10)	1.00 (10)	1.00 (10)	1.00 (10)
NaDS-d_{21}	NaDS-d_{21}	NaDS-d_{21}	NaDS-d_{21}	DACl-d_{21}	DACl-d_{21}	DACl-d_{21}	DACl-d_{21}
6.14 (1–4)	5.71 (1–5)	5.74 (1–4)	5.14 (1–5)	6.62 (1)	6.62 (1)	7.20 (1	6.60 (1)
5.90 (5)	—	5.51 (5)	—	5.97 (2–6)	6.13 (2)	6.47 (2)	6.02 (2)
5.70 (6)	5.35 (6)	5.29 (6)	4.85 (6)	—	5.80 (3–5)	6.19 (3–5)	5.69 (3–5)
5.06 (7)	4.93 (7)	4.81 (7)	4.46 (7)	—	5.46 (6)	5.77 (6)	5.26 (6)
4.41 (8)	4.34 (8)	4.25 (8)	4.01 (8)	5.42 (7)	5.29 (7)	5.57 (7)	5.15 (7)
3.39 (9)	3.42 (9)	3.37 (9)	3.17 (9)	4.63 (8)	4.62 (8)	4.82 (8)	4.47 (8)
1.00 (10)	1.00 (10)	1.00 (10)	1.00 (10)	3.90 (9)	3.92 (9)	4.07 (9)	3.83 (9)
				1.00 (10)	1.00 (10)	1.00 (10)	1.00 (10)

[a]The components of each system are arranged vertically so that the hosts and guests in all mesophases can be directly compared by moving from left to right. The ratios were calculated according to eq. [3] using the measured quadrupole splittings. The ratios are normalized to the quadrupole splitting of the terminal methyl group, which splitting includes the effect of methyl group rotations. The carbon number in the chains is placed in parentheses after each ratio, e.g. 9.90 (1–9) means ratio constant for carbon segments 1–9 at a value 9.90.

Can. J. Chem. Downloaded from www.nrcresearchpress.com by 210.87.254.42 on 09/05/12
For personal use only.

cannot be associated specifically with counter ion change or the nature of other guest. A large change in the 1-decanol ratios occurs, when this amphiphile is transferred to a bilayer whose solvent detergent is HDPCl. The kink/jog motion of 1-decanol is thus altered a great deal in this process, showing us that the internal packing of the micelle unit changes near this decanol guest. The primary cause is evidently the specific effect of change in the host amphiphile.

The 1-decylsulphate ion is somewhat sensitive to the change in counter ion to a minor degree in mesophases A, but the ratios for a given segment do not vary more than 10% in changing the counter ion. The guest 1-decylammonium ion behaves in a similar fashion.

Comparison with Prior Studies of Counter Ion Effects

A simple substitution in the sodium counter ion of a type I (cylindrical micelle) mesophase by 5% cesium ion with the composition otherwise unchanged is sufficient to change the liquid crystal to a type II (disc-micelle) mesophase (3). It is reasonable to investigate therefore any influence of the counter ion on the bilayer solutions of constituent micelles. Fujiwara and Reeves (11) have shown that the quadrupole coupling ratios are somewhat affected by the change Cl^-, BF_4^-, and F^- as counter ions in mesophases based on the decylammonium ion (See Table 1, ref. 11). These 1-decylammonium phases are now known to be type II disc-micelles (DM) with orientational but no positional order (6). A study of the methyl-substituted ammonium counter and co-ions and their effect on quadrupole splitting ratios for the 1-decylsulphate chain in a type II DM mesophase showed that, in this case, the balance between methyl groups, which are non polar, and hydrogen bonding N—H bonds does affect the ratios in a systematic manner (14).

The present study is the first which attempts to investigate the whole motion profiles of guests and hosts in a disc-micelle nematic phase as a function of counter ion. Very minor changes in the motions of the bilayer solution have been found as a result of those counter and co-ion changes for simple hydrophilic negative ions. This rather remarkable result provides us with a standard so that real chemical interface interactions, such as complexing of a metal ion, can be safely embarked upon in this system. A polar or ionic head group of a guest solute in the bilayer can be changed in the formation of a complex without affecting the host amphiphiles simply from a careful choice of the chemistry. Such studies are now in progress.

The Aspects of Mis-fit Guest Chains

The host bilayers correspond to 16 carbon chain lengths while the guests have 10 hydrocarbon segments. There is a considerable increase in motional freedom (fall off in degrees of order) of the short guest chains within the region carbons 1–9 of the host of high uniform order (Figs. 1–4). Superficially at least, the guest chains appear to have a motion profile similar to one for a 10-segment half-bilayer (11, 14).

The region of carbon segments 6–10 for the guests exemplifies motions which therefore are to a first approximation not determined by the host bilayer. Similar results have been reported recently by Charvolin and Mely (15) for bilayers of fatty acids in non-aligned lamellar mesophases.

Comparison with 10-segment half-bilayers is possible using our previously published data (11, 14). The ratio of deuterium quadrupole splittings in aligned mesophases of 1-decylammonium chloride (11) for plateau to penultimate $—CD_2—$ segment is about 1.9, while decylammonium guests in the present studies have a corresponding ratio of the order of 1.51 for all host bilayers (Figs. 1–4). This is a significant change and corresponds to a less flexible chain (closer to a rigid all *trans* chain) in the present cases. The fall in degrees of order towards the bilayer centre is known to be determined by an increasing probability of single *gauche* rotations (16, 17). For 1-decylsulphate chains in aligned mesophases of this amphiphile, the ratio of plateau to penultimate $—CD_2$-quadrupole splittings is also $\sim$1.90 but the 1-decylsulphate guests in the present systems studies have ratios 1.80 in Fig. 1; 1.67 in Fig. 2; 1.70 in Fig. 3; and 1.62 in Fig. 4. The higher probability of all *trans* segments for a short misfit chain near its non-polar terminus is clearly demonstrated. 1-Decanol is a major component of the type II mesophase based on 1-decylsulphate; and it shows in this 10-segment half-bilayer the ratio 1.8 (14). The 1-decanol guests in mesophases A and B of the present series show the same ratio between 1.57 and 1.64 depending on the particular system. There is, in all cases of the misfit short chains studied here, a higher probability of extended all *trans*-arrangements or lower probability of single *gauche* rotations in host bilayers of 16 carbon segments in length.

Acknowledgements

The financial support of the National Research Council of Canada in operating grants to LWR is gratefully acknowledged. We wish to thank M. M. Tracey for synthesizing some of the perdeuteriated compounds.

1. F. Y. FUJIWARA, L. W. REEVES, M. SUZUKI, and J. A. VANIN. "Overview paper." *In* Solution chemistry of surfactants. Proceedings of National Colloid Symposium, Knoxville, TN. June, 1978. *Edited by* K. Mittal. Plenum Press. 1979.
2. V. LUZZATI. Biological membranes. *Edited by* D. Chapman. Academic Press, New York. 1968.
3. K. RADLEY, L. W. REEVES, and A. S. TRACEY. J. Phys. Chem. **80**, 174 (1976).
4. D. M. CHEN, F. Y. FUJIWARA, and L. W. REEVES. Can. J. Chem. **55**, 2396 (1977).
5. F. Y. FUJIWARA and L. W. REEVES. Can. J. Chem. **56**, 2178 (1978).
6. B. J. FORREST, F. Y. FUJIWARA, and L. W. REEVES. J. Phys. Chem. **84**, 662 (1980).
7. LIA Q. DO AMARAL, C. PIMENTEL, M. R. TAVARES, and J. A. VANIN. J. Chem. Phys. **71**, 2940 (1979).
8. L. W. REEVES, A. S. TRACEY, and M. M. TRACEY. Can. J. Chem. **57**, 747 (1979).
9. NG. DINH-NGUYEN, A. RAAL, and E. STENHAGEN. Chem. Scr. **2**, 171 (1972).
10. R. F. NYSTROM and W. G. BROWN. J. Am. Chem. Soc. **69**, 1197 (1947).
11. F. Y. FUJIWARA and L. W. REEVES. J. Am. Chem. Soc. **98**, 6790 (1976).
12. Org. Synthesis, Vol. 2, p. 322, John Wiley and Sons, Inc., New York. 1969.
13. P. DIEHL and C. L. KHETRAPAL. NMR basic principles and progress. Vol. 1. *Edited by* P. Diehl, E. Fluck, and R. Kosfeld. Springer-Verlag, New York. 1969. p. 1.
14. L. W. REEVES and A. S. TRACEY. J. Am. Chem. Soc. **97**, 5729 (1975).
15. J. CHARVOLIN and B. MELY. Mol. Cryst. Liq. Cryst. Lett. **41**, 209 (1978).
16. J. SEELIG and W. NIEDERBERGER. Biochemistry, **13**, 1585 (1974).
17. A. SEELIG and J. SEELIG. Biochemistry, **13**, 4839 (1974).

Can. J. Chem. Downloaded from www.nrcresearchpress.com by 210.87.254.42 on 09/05/12
For personal use only.

An investigation of the dilute solutions of lauric acid and laurate ion in cationic and anionic bilayers of disc micelles

F. Y. FUJIWARA[1] AND L. W. REEVES[2]

Department of Chemistry, University of Waterloo, Waterloo, Ont., Canada N2L 3G1 and Institute de Quimica, Universidade de Sao Paulo, Caixa Postal 20780, Sao Paulo, Brazil

Received January 10, 1980

F. Y. FUJIWARA and L. W. REEVES. Can. J. Chem. **58**, 1550 (1980).

Type II DM mesophases with disc-shaped micelles have been synthesized from decylammonium chloride and sodium decylsulphate – decanol amphiphiles with added water and electrolyte. Small amounts of guest amphiphiles have been added in the form of lauric acid or laurate ion. Specific and perdeuterated amphiphiles have been prepared and included in small quantities in the mesophases. The deuterium magnetic resonance spectra of the magnetically aligned phases has been studied and quadrupole splitting doublets assigned to all segments of both host and guest hydrocarbon chains. The mesophases have been diluted with water over the stable range of type II DM behaviour at 34 ± 0.2°C.

The quadrupole splittings of all hydrocarbon chain segments, which reflect the degrees of order along C—D bonds in these segments, are accurately reproduced at all water contents by a knowledge of one quadrupole splitting in the chain and a simple proportionality constant which is derived for each segment of the chain. This further extends the previous results for host chains to those of guest chains studied here. The absolute degrees of order of chain segments are greatly influenced by water content because motion of the constituent disc micelles depends on the volume of interstitial water and they also vary in size as water is added. The packing in the bilayer solution of the disc micelles of the amphiphiles is therefore not a function of the interstitial water content in so far as the detailed *trans/gauche* motions of the hydrocarbon chains are not affected by changes in water content.

The lauric acid-d_{23} chain in the decylammonium chloride bilayer has the same degree of order along the D—D axis and the C—D bond, confirming that the motion of the pseudo rigid chain in the bilayer is cylindrically symmetric. The degree of order profiles of hosts and guests are all quite distinct indicating that chemical identity of the head group and its anchoring in the interface is the main determinant of the motion profiles.

F. Y. FUJIWARA et L. W. REEVES. Can. J. Chem. **58**, 1550 (1980).

On a synthétisé des mésophases DM de type II ayant des micelles en forme de disques à partir des composés amphiphiles: chlorure de décylammonium et décylsulfate de sodium – décanol en présence d'eau et d'un électrolyte. On a ajouté des petites quantités d'amphiphiles susceptibles d'être encagées sous forme d'acide laurique ou d'ions laurate. On a préparé des composés amphiphiles spécifiques et perdeutérés et on les a introduit en petites quantités dans les mésophases. On a étudié les spectres de rmn du ^{2}H des phases magnétiques alignées et on a identifié le dédoublement quadrupolaire des doublets de toutes les portions des chaînes hydrocarbonées des récepteurs et des molécules encagées. On a dilué les mésophases avec de l'eau dans le domaine de comportement stable du DM de type II à 34 ± 0.2°C.

On a reproduit avec précision les dédoublements quadrupolaires de toutes les portions de chaîne hydrocarbonées qui réflètent le degré de l'ordre le long des liaisons C—D de ces fragments pour toutes les teneurs en eau à partir de la connaissance d'un dédoublement quadrupolaire dans la chaîne et d'une constante simple de proportionnalité qui est déduite pour chaque segment des chaînes. Ceci permet d'étendre les résultats antérieurs pour les chaînes réceptrices aux chaînes encagées étudiées ici. Les dégrés absolus de l'ordre des segments de chaînes sont grandement influencés par la teneur en eau parce que le mouvement des micelles constituantes en forme de disque dépend du volume d'eau interstitielle et leur taille varie lorsqu'on ajoute de l'eau. Le tassement dans la solution à double couche des micelles en forme de disques des amphiphiles n'est toutefois par une fonction de la teneur en eau interstitielle dans la mesure où les mouvements détaillés *trans/gauche* des chaînes hydrocarbonées ne sont pas affectées par les variations de la teneur en eau.

La chaîne d'acide laurique d_{23} dans la double couche de chlorure de décylammonium a le même degré d'ordre le long de l'axe D—D et de la liaison C—D confirmant ainsi que le mouvement de la chaîne pseudo rigide dans la double couche est cylindriquement symétrique. Les profils du degré d'ordre des molécules réceptrices et des molécules encagées sont tout à fait distincts, indiquant par là que l'identité chimique du groupe de tête et de son point d'attache à l'interface détermine principalement le profil du mouvement.

[Traduit par le journal]

Introduction

Lyotropic mesophases, obtained by diluting the hexagonal or lamellar phases with water and adding small amounts of electrolyte, are nematic in character (1). The type II DM liquid crystal is derived from the lamellar phase and has finite bilayer disc-like micelles disposed with orientational long range order, but little positional order of their centres of gravity (2). The present study is confined to this type of mesophase. Recently a variety of investigations, using deuterium magnetic resonance, have sought to probe several aspects of the hydrocarbon chain segment order profiles in the micelles as a function of chemical change (3, 4). The first major study of degrees of order profiles in

[1]Present address: Instituto de Quimica, Universidade Estadual de Campinas, UNICAMP, Campinas, Brazil.

[2]Author to whom correspondence should be addressed. Visiting Professor Universidade de Sao Paulo since 1967.

0008-4042/80/151550-08$01.00/0

©1980 National Research Council of Canada/Conseil national de recherches du Canada

Can. J. Chem. Downloaded from www.nrcresearchpress.com by 210.87.254.42 on 09/05/12
For personal use only.

Can. J. Chem. Downloaded from www.nrcresearchpress.com by 210.87.254.42 on 09/05/12
For personal use only.

Type II DM lyotropic systems[3] (5) utilized specific deuteriation techniques to assign the —CD_2— resonances to specific segments in decanol and decyl sulphate ions. The principal conclusion of this first detailed study was that degrees of order profiles are a function primarily of the polar or ionic head group identity.

Carboxylic acids and carboxylates labelled at the α position and of chain length 2–16 were then studied as guests in the nematic type II sodium decyl sulphate – decanol–water–Na_2SO_4 system (6). Apart from some water dispersion of shorter chain carboxylates, the degree of order of the —αCD_2— position increased linearly with the carbon chain length (6) but no further increase in degree of order of the —αCD_2— accompanied chain lengths beyond the half-bilayer distance. A nematic type II DM mesophase composed of hexadecylpyridinium and hexadecyltrimethylammonium ions can be prepared in all proportions of the two amphiphiles and deuteriated decanol can be added in small amounts (7). The segmental order profiles of both host amphiphiles are remarkably insensitive to the mole fraction of each amphiphile in the micelle. Decanol, however, in the 16-carbon host bilayer, is noticeably affected near the non-polar terminus, where single *gauche* rotations are less probable than in host bilayers of shorter chain length (7) Studies of complete order profiles of guest and host have been completed for cases where the guest chain exceeds the host chain in length (4). Several types of behaviour have been noted depending on the chemistry of the interface (4). Phospholipid chains included in 16-carbon chain host bilayers differ only to a small extent in order profile from the homogeneous lipid bilayers prepared as membrane models (8, 9, 10). For butyric acid and butyrate ion guests the assignment of quadrupole splittings for the three segments has been made (11). In the form of butyric acid the all-*trans* form predominates to 63% (11). The systematic study of short chain length guests in longer chain host bilayers further confirmed that in all cases investigated the probability of single *gauche* rotations near the non-polar terminus of the guest chain are less probable than in host bilayers composed of amphiphiles with shorter chain lengths (12).

The purpose of the present study is (*a*) to further verify and statistically test the simple proportionality between degrees of order for different —CD_2— segments in the guest chains as water content is varied (1); (*b*) to obtain a measure of the degree of order along the D—D axis of a —CD_2— group and compare it to the value obtained from deuterium quadrupole splitting along the C—D bond; (*c*) to study, qualitatively at least, the degree of order profile of an acid amphiphile and its conjugate base in both cationic and anionic host bilayers, i.e., to probe the anchoring as a function of changes in interface chemistry.

[3]Notation Type II DM assigned in ref. 1 at a later date.

Experimental

The chemical syntheses of the specifically and massively deuteriated amphiphiles used in this study have been described clearly in other papers (1, 13) in which references are located to original methods and those adopted by us. A complete set of references is appended to a recent overview article (3).

The nuclear magnetic resonance (nmr) methods are standard. Deuterium nmr was observed using a Varian XL-100 spectrometer with Gyrocode option. Very good signal to noise was obtained from the low concentrations of deuteriated hydrocarbon chains with about 20–50 000 transients. Spectrometer settings were always optimized for each case by considerable previous experience.

In order to relieve the congestion of signals, which occurs when both host and guest chains are deuteriated in the same mesophase, the host chain segments were deuteriated in one system and the guests in another but the composition of both phases was the same. The care in permuting specifically deuteriated chains of the host in equivalent mesophases allows unequivocal assignment of the quadrupole doublets to specific segments (5, 15). The results for lauric acid-d_{23} and laurate ion-d_{23} in type II DM mesophases prepared originally by Lawson and Flautt (16) have been discussed previously (4) in another context, but the results for the same guests in mesophases of decylammonium chloride (17) are presented here for the first time. The compositions of mesophases are given in Table 1 in order that others may reproduce these rather difficult systems. Purification procedures can be found in our previously published work (see ref. 3 for a list of references). Experimental temperature of nmr observations was 34°C.

Results

The deuterium magnetic resonance spectra of sodium laurate-d_{23} and lauric acid-d_{23} have been discussed previously (1) in the context of a set of experiments designed to study the effect of a lengthening chain on degree of order profiles in SDS–decanol mesophases. The other acids and carboxylates of the same head group chemistry had longer chains as in myristic, palmitic, and stearic acids (1). These results are important in this new context, where a common carboxylate and carboxylic acid, laurate and lauric acid are used as small concentrations of guests in two host mesophases, one based on the cationic detergent decylammonium and the other based on the anionic detergent decyl sulphate (with a small amount of decanol). In the present case all amphiphiles have approximately the same chain length. The results

Can. J. Chem. Downloaded from www.nrcresearchpress.com by 210.87.254.42 on 09/05/12
For personal use only.

TABLE 1. Composition of mesophases used in this study

(*a*) Lauric acid in SDS (11) mesophase

Standard phase (D7):	Mol%
H_2O (pH ~ 2, 0.1% D_2O)	92.02
Lauric acid-d_{23}	0.12
Decanol	1.40
Sodium decylsulphate (SDS)	5.44
Sodium sulphate	1.04

Diluted phases: D7, as above, D7-1, 92.62 mol% water; D7-2, 93.10 mol% H_2O; D7-3, 93.54 mol% H_2O; D7-4, 93.95 mol% H_2O.

The diluted phases were merely obtained by adding water to the standard D7 mesophase so as to achieve the overall mol% water in the diluted mesophases. This procedure applies to the other entries below for other systems.

Standard phase (D6):	Mol%
H_2O (pH ~ 2, 0.1% D_2O)	92.00
Lauric acid	0.12
Decanol	1.39
SDS (17.45% 3, 3, 4, 4-d_4)	5.43
Na_2SO_4	1.06

Diluted phases: D6-1, 92.71 mol% H_2O; D6-2, 93.18 mol% H_2O; D6-3, 93.59 mol% H_2O; and D6-4, 93.97 mol% H_2O.

Standard phase (D30):	Mol%
H_2O (pH ~ 2, 0.1% D_2O)	92.01
Lauric acid	0.12
Decanol	1.40
SDS (10.04% 1, 1, 9, 9, 10, 10, 10-d_7, 9.6% 22-d_2)	5.44
Na_2SO_4	1.04

Standard phase (D32):	Mol%
H_2O (pH ~ 2, 0.1% D_2O)	92.00
Lauric acid	0.12
Decanol	1.40
SDS (9.3% 1, 1, 9, 9, 10, 10, 10-d_7, 9.7% 3, 3, 4, 4-d_4)	5.44
Na_2SO_4	1.04

Diluted phases: D32-1, 92.6 mol% H_2O; D32-2, 93.09 mol% H_2O; D32-3, 93.54 mol% H_2O; D32-4, 93.93 mol% H_2O.

(*b*) Lauric acid in decylammonium chloride mesophase

Standard phase (D5):	Mol%
H_2O (pH ~ 2, 0.1% D_2O)	91.906
Lauric acid-d_{23}	0.140
Decylammonium chloride	5.854
Sodium chloride	2.100

Diluted phases: D5-1, 92.23 mol% H_2O; D5-2, 92.58 mol% H_2O; D5-3, 92.89 mol% H_2O; and D5-4, 93.07 mol% H_2O.

Standard phase (D4):	Mol%
H_2O (pH ~ 2, 0.1% D_2O)	91.917
Decylammonium chloride (3.2% 2, 2-d_2, 5.1% 1, 1, 9, 9, 10, 10, 10-d_7)	5.846
Sodium chloride	2.097
Lauric acid	0.140

Diluted phases: D4-1, 92.24 mol% H_2O; D4-2, 92.6 mol% H_2O; D4-3, 92.93 mol% H_2O; D4-4, 93.15 mol% H_2O.

Standard phase (D15):	Mol%
H_2O (pH ~ 2, 0.1% D_2O)	91.92
Lauric acid	0.140
Decylammonium chloride (31.3% 2, 2, 3, 3-d_4, 4.2% 1, 1, 9, 9, 10, 10, 10-d_7)	5.84
Sodium chloride	2.10

Diluted phases: D15-1, 92.29 mol% H_2O; D15-2, 92.63 mol% H_2O; D15-3, 93.09 mol% H_2O.

TABLE 1 (*Concluded*)

Standard phase (D16):	Mol%
H_2O (pH ~ 2, 0.1% D_2O)	91.92
Lauric acid	0.140
Decylammonium chloride (25.12% 3, 3, 4, 4-d_4 7.17% 1, 1, 9, 9, 10, 10, 10-d_7)	5.83
Sodium chloride	2.11

Diluted phases: D16-1, 92.3 mol% H_2O; D16-2, 92.63 mol% H_2O; D16-3, 92.95 mol% H_2O.

(*c*) Sodium laurate in SDS mesophases

Standard phase (D10):	Mol%
H_2O (pH ~ 12, 0.1% D_2O)	91.73
Sodium laurate-d_{23}	0.13
Decanol	1.44
Sodium decylsulphate	5.63
Sodium sulphate	1.07

Diluted phases: D10-1, 92.35 mol% H_2O; D10-2, 92.91 mol% H_2O; D10-3, 93.59 mol% H_2O.

Standard phase (D8):	Mol%
H_2O (pH ~ 12, 0.1% D_2O)	91.77
Sodium laurate	0.13
Sodium decylsulphate (52.3% 3, 3, 4, 4-d_4)	5.59
Sodium sulphate	1.07

Diluted phases: D8-1, 92.41 mol% H_2O; D8-2, 92.99 mol% H_2O; D8-3, 93.60 mol% H_2O.

Standard phase (D31):	Mol%
H_2O (pH ~ 10, 0.1% D_2O)	91.80
Decanol	1.43
Sodium laurate	0.13
Sodium decylsulphate (15.1% 1, 1, 9, 9, 10, 10, 10-d_7 6.2% 2, 2-d_2)	5.57
Sodium sulphate	1.06

Standard phase (D33):	Mol%
H_2O (pH ~ 10, 0.1% D_2O)	91.74
Decanol	1.44
Sodium laurate	0.13
Sodium decylsulphate (14.8% 1, 1, 9, 9, 10, 10, 10-d_7)	5.62
Sodium sulphate	1.07

(*d*) Sodium laurate in decylammonium chloride mesophases

Standard phase (D22):	Mol%
H_2O (pH ~ 10, 0.1% D_2O)	92.49
Sodium laurate-d_{23}	0.08
Decylamine	0.18
Decylammonium chloride	5.34
Sodium chloride	1.91

Diluted phases: D22-1, 92.81 mol% H_2O; D22-2, 93.12 mol% H_2O; D22-3, 93.4 mol% H_2O; D22-4, 93.56 mol% H_2O.

Standard phase (D21):	Mol%
H_2O (pH ~ 10, 0.1% D_2O)	92.49
Sodium laurate	0.08
Decylamine	0.18
Decylammonium chloride (17.2% 1, 1, 9, 9, 10, 10, 10-d_7, 16.8% 2, 2-d_2)	5.34
Sodium chloride	1.91

Diluted phases: D21-1, 92.81 mol% H_2O; D21-2, 93.12 mol% H_2O; D21-3, 93.43 mol% H_2O; D21-4, 93.65 mol% H_2O.

Can. J. Chem. Downloaded from www.nrcresearchpress.com by 210.87.254.42 on 09/05/12
For personal use only.

pertinent to the cationic amphiphile type II DM system have not been previously reported.

Lauric Acid-d_{23} *in Decylammonium Chloride Mesophases*

The deuterium quadrupole splittings measured for each segment in the standard and diluted mesophases (see Table 1) decrease for both guest and host as water is added within the stable existence of the type II DM mesophase system. The curves of degree of order of C—D bonds in segments (1) are very similar to those published before (1, 3, 15). For the host segments (16) we have shown that the decrease is at first linear with water concentration, but afterwards falls off much more steeply, until the mixture undergoes a phase separation to form two layers with the lower layer isotropic in properties (15). In the coexistence region of the type II DM and the isotropic phase the deuterium splittings of the host do not depend on overall water content.

The strict proportionality between deuterium quadrupole splittings, which we have previously reported for this host mesophase (15), as the water content is varied, has been confirmed during the present study for both guests and hosts. Figure 1 illustrates that segmental order ratios (3) for the guest are independent of water concentration in the phase. The degrees of order of DOH measured from the doublet splitting in the water are linear with the splitting for the αCD_2 group of the chain. The intercept for zero splitting in the water occurs at about +750 Hz for the αCD_2 group splitting. The spectrum of lauric acid-d_{23} is shown as Fig. 2 for the standard mesophase. It shows resolution of each segment and in the first few segments the dipole–dipole coupling effect between the two deuterium nuclei in each —CD_2— group. Such dipole–dipole coupling lends itself to the determination of the degree of order of the D—D axis in the —CD_2— group. The analysis of two spin 1 particles in the nmr spectra of oriented species was published some time ago (18). Assuming the two spins are equivalent and thus scalar coupling is zero, each quadrupole doublet component is split into 3 resolvable transitions (18) of significant intensity. One splitting between the three peaks is four times the dipole–dipole coupling and the other twice (18). The dipole–dipole coupling is given by:

$$[1] \quad D_{12} = -2829/r_{12}^3 S_{12}$$

where D_{12} is the dipole–dipole coupling constant; −2829 is a factor of nuclear constants designed to express the result of D_{12} in Hz; r_{12} is the distance between deuterium nuclei in Å; S_{12} is the degree of order of the internuclear axis. Taking r_{12} = 1.8 Å, we obtain D_{12} = 485 S_{12}. Assuming the nuclear quadrupole coupling constant for the C—D bond to be 170 kHz and that the asymmetry parameter η = 0, we can express the degree of order along the C—D bond in the segment as:

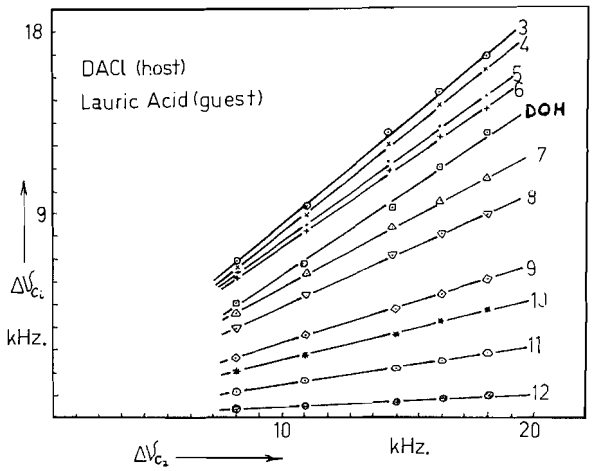


FIG. 1. Deuterium quadrupole splittings of an arbitrary segment $\Delta\nu_{C_i}$, denoted by the value of i placed against each line at the right, and the use of different distinguishing symbols for each set of points, plotted against the quadrupole splitting in the segment of carbon 2 of the chains, denoted as $\Delta\nu_{C2}$. The values of $\Delta\nu_{Ci}$ and $\Delta\nu_{C2}$ are strictly proportional and independent of the water content of the type II DM mesophases. The data corresponds to the mesophases D5 to D5-4 of Table 1. The quadrupole splittings of the water (DOH) are also included as square points ⊡ and the line so marked at the right hand side.

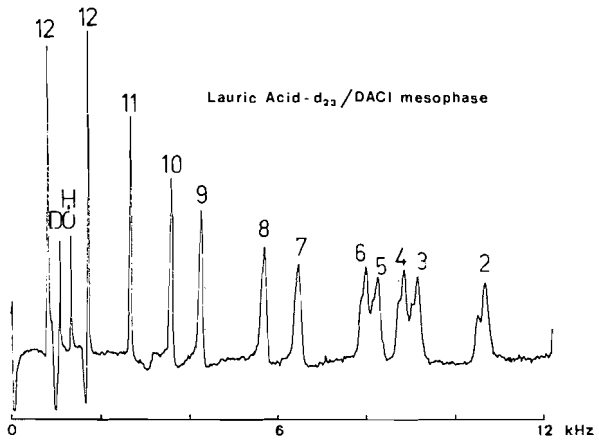


FIG. 2. Deuterium spectrum of sample D5. Spectral width 12341 Hz; aquisition time 0.1 s; pulse width 40 μs; number of transients 21 676. All eleven —CD_2— segments of lauric acid-d_{23} are resolved separately in increasing segment number from the right. The DOH doublet appears as the second and third peaks from the left. The spectrum is symmetric about this point. The left hand doublet components are not observed. On the right hand side of the half spectrum, resolution of dipole–dipole splittings between segmental —CD_2— deuteriums is seen.

Can. J. Chem. Downloaded from www.nrcresearchpress.com by 210.87.254.42 on 09/05/12
For personal use only.

[2] $\Delta\gamma_Q = 255\, S_{CD}$

where $\Delta\gamma_Q$ is the quadrupole splitting in kHz.

The simultaneous measurement of degrees of order S_{CD} along the C—D bond and S_{12} along the DD axis from the same spectrum enables us to compare degrees of order in different perpendicular directions to the axis of the pseudo-extended chain. It is assumed in the pseudo-rigid chain model of packing of amphiphiles in bilayers, that the anisotropic motion of the chain is cylindrically symmetric (19), i.e. all directions perpendicular to the pseudo-extended chain axis are equivalent. These spectra are therefore an important test of this point. The low and high field components of the quadrupole doublets have been used to determine an average for four independent values $S_{12} = S_{DD}$ from each spectrum. The comparisons are: (*a*) segment at carbon 2, αCD_2, $S_{CD} = 0.158$, $S_{DD} = 0.168$; (*b*) segment 3, $S_{CD} = 0.124$, $S_{DD} = 0.130$; (*c*) segment 4, $S_{CD} = 0.120$, $S_{DD} = 0.118$; (*d*) segment 5, $S_{CD} = 0.110$, $S_{DD} = 0.118$; (*e*) segment 6, $S_{CD} = 0.106$, $S_{DD} = 0.106$.

The error in the value of S_{DD} is large because of the small value of the dipole–dipole coupling. The best estimate of this error is ± 0.01 in the value S_{DD}. Having taken this into account it is clear that the degrees of order in the two directions are, within this error, the same.

The quadrupole splittings for the standard D5 mesophase (Table 1) were observed to be: 2, 19.01 {1} kHz; 3, 15.91 {1}; 4, 15.32 {1}; 5, 14.13 {1}; 6, 13.57 {1}; 7, 10.52 {1}; 8, 8.954 {5}; 9, 6.066 {5}; 10, 4.712 {5}; 11, 2.859 {5}; 12, 0.908 {5}. The first number is the segment corresponding to the carbon number in the chain, the values are all in kilo-Hertz and the bracketed numbers after the splittings are the random error in the last significant figure. Thus the entry 4. 15.32 {1} means that for the —CD_2— segment at carbon number 4 in standard mesophase D5 (see Table 1) the deuterium quadrupole splitting is 15.32 kHz with a random error ± 0.01 kHz. The quadrupole splittings in all mesophases of the D5 series can be reproduced by giving one value of the splitting in the chain for each diluted mesophase of D5-1–D5-4 and the slopes of the proportionality in Fig. 1. The values for splittings of the αCD_2 positions (segment at carbon 2) are the following for designated diluted phases (Table 1); D5-1, 16.99 {1}; D5-2, 14.75 {1}; D5-3, 11.14 {2}; D5-4, 8.10 {5}. The mean proportionality constants are expressed as $\Delta\nu_{C_x}/\Delta\nu_{C2}$, (the splitting of the xth segment divided by that of carbon 2) are: $x = 3$, 0.8442; $x = 4$, 0.8107; $x = 5$, 0.7521; $x = 6$, 0.7242; $x = 7$, 0.5610; $x = 8$, 0.4808; $x = 9$, 0.3239; $x = 10$, 0.2481; $x = 11$, 0.1477; $x = 12$, 0.0464.

In order to clearly illustrate this way of presenting the data in its most compact form, the quadrupole splitting of carbon segment 4 for mesophase D5-2 is computed and compared to the experimental value measured. The required splitting is evidently $(\Delta\nu_{C4}/\Delta\nu_{C2}) \times \Delta\nu_{C2} = 0.8107 \times 14.75 = 11.96$ kHz which compares to the measured value 11.98 kHz.

The same procedure can be used to describe the array of quadrupole splittings for the host chains. Taking the series D4, D15, and D16 together the proportionality ratios in decylammonium chains can be averaged for all determinations. The ratio computed is again that for arbitrary segment C_x divided by that for the first carbon: Values $\Delta\nu_{C_x}/\Delta\nu_{C1}$ are: $x = 2$, 0.9180; $x = 3$, 0.9040; $x = 4$, 0.8743; $x = 8$, 0.6358; $x = 9$, 0.5194; and $x = 10$, 0.1216. The single quadrupole couplings which will facilitate the computation of all others in the diluted mesophases are: D4, 16.11 {2}; D4-1, 14.07 {2}; D4-2, 11.72 {2}; D4-3, 7.98 {5} for the first carbon segment in kHz with errors in the last significant figures in brackets. For the D15 series values are: D15, 16.08 {2}; D15-1, 14.22 {2}; D15-3, 6.49 {5}, again for the first carbon CD_2 segment in kHz. For the D16 series, D16, 16.76 {2}; D16-1, 14.35 {2}; D16-2, 12.12 {2}; and D16-3, 9.03 {2}.

The complete array of data on quadrupole couplings for the lauric acid guest, decylammonium chloride host, can be reconstructed from the compact listings above, for the corresponding compositions given in Table 1.

An important feature of the quadrupole coupling ratios in a pseudo-extended chain is the ratio of splittings in the terminal —CD_2CD_3 segment. If the chain were really rigid and extended the ratio should be 3 (5, 15, 20). For the case of guest lauric acid chains, the value is 3.183, and for the host decylammonium chloride the value is 4.271, these being averages for all mesophases in this section.

The quadrupole splittings of the water (DOH) are somewhat lower than in mesophases based on decylsulphate ions (1, 5) but still much higher than mesophases prepared with head groups —$N(CH_3)_3^+$ and pyridinium (14). The values measured are: D5, 251 {2}; D5-1, 221 {2}; D5-2, 185 {2}; D5-3, 135 {2}; D5-4, 100 {5} partly isotropic; D4, 250 {2}; D4-1, 217 {2}; D4-2, 180 {2}; D4-3, 121 {2}; D15, 241 {2}; D15-1, 206 {2}; and D15-3, 92 {2} partly isotropic. The splittings are given in Hertz and errors in the last significant figure in brackets.

Sodium Laurate -d_{23} in Decylammonium Chloride Mesophases

The plateau of uniform degree of order is rather

Can. J. Chem. Downloaded from www.nrcresearchpress.com by 210.87.254.42 on 09/05/12
For personal use only.

well developed for laurate ion in decylammonium chloride, consequently Fig. 3 contains the quadrupole splittings of position 8 plotted against all other arbitrary segments where overlap of peaks did not occur. The variable is the usual chemical one of water content over the stable range of type II DM mesophases. Simple proportionality of order among —CD_2— segments is once again illustrated by the results in the figure.

The D22 series of the Experimental embraces the following deuterium quadrupole splittings for the segment 8 of the chain: D22, 13.87 {2}; D22-1. 12.63 {2}; D22-2. 10.96 {2}; D22-3. 8.80 {2}; and D22-4. 6.84 {5} partly isotropic. The following ratios obtained $\Delta\nu_{Cx}/\Delta\nu_{C8}$ facilitate the generation of all quadrupole splittings measured for the guest in the D22 series: $x = 1$, 1.428; $x = 3$, 4, 1.383; $x = 5$, 1.331; $x = 6$, 1.265; $x = 7$, 1.142; $x = 9$, 0.8029; $x = 10$, 0.6097; $x = 11$, 0.4041; and $x = 12$, 0.0897. The quadrupole splittings are in kHz.

The deuterium quadrupole splittings for the host may be generated from the following similar data for the αCD_2 splittings in kHz from the D21 series of the Experimental (Table 1): D21, 15.81 {2}; D21-1, 13.82 {2}; D21-2, 11.64 {2}; D21-3, 8.49 {2}; and D21-4, 6.69 {5} partly isotropic. The ratios of quadrupole couplings expressed as $\Delta\nu_{Cx}/\Delta\nu_{C1}$ for the decylammonium chain are: $x = 2$, 0.9306; $x = 8$, 0.6452; $x = 9$, 0.5223; and $x = 10$, 0.1223.

The ratios of the degrees of order for segments of the host chain are slightly different from values obtained with the lauric acid guest. The differences are of the order of 1%. This can be ascribed to the presence of a small amount of decylamine added in the mesophases containing sodium laurate. The agreement is satisfactory enough to regard the bilayer matrix unchanged as far as the guest is concerned. Ratios of splittings in the —CD_2CD_3 terminal fragments are: 4.27 for the host decylammonium chain and 4.58 for the guest laurate chains.

The data for lauric acid and laurate ion in host micelle bilayers of decylsulphate–decanol have been previously presented (1).

Comparison of Complete Order Profiles of Guests and Hosts in Standard Mesophases

The quadrupole splittings for host and guest segments in standard mesophases prepared here and presented previously (1) have been plotted against segment numbers in Fig. 4. In the case of decylsulphate and decylammonium chloride carbon 1 is plotted with the segment number 2 in order to compensate for the first carbon in the carboxyl moieties being in the head group —CO_2— or —COOH.

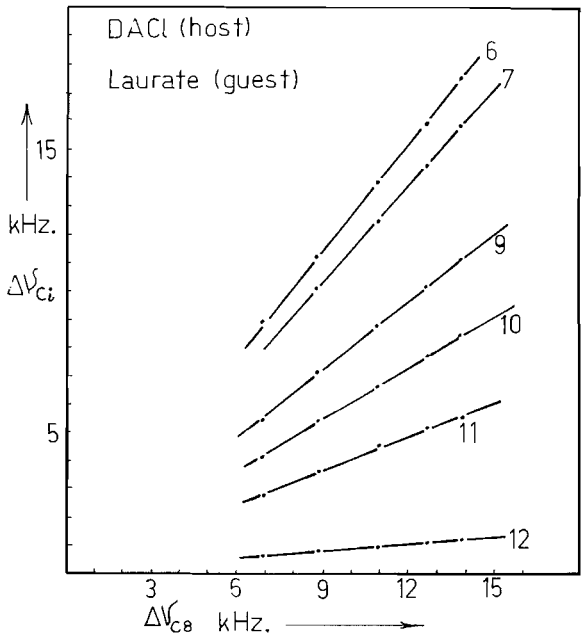


FIG. 3. Deuterium quadrupole splittings of arbitrary segment $\Delta\nu_{C_i}$ versus quadrupole splittings for the 8th segment $\Delta\nu_{C8}$ in perdeuteriated hydrocarbon chains of the laurate ion guests in a type II DM mesophase based on decylammonium chloride. Samples D22 to D22-4 in Table 1.

Discussion

Interpretation of Constant Ratios of Order in Segments

According to the recent low angle X-ray diffraction studies of Queiroz do Amaral and co-workers (2) the type II DM mesophase is a collection of disc-like micelles of diameter greater than 1000 Å and of bilayer thickness. The uniaxial properties of the fluid depend on the long range orientational order of these discs, but absence of positional order.[4] The aligned mesophases in a spinning nmr tube perpendicular to the magnetic field achieve a unique alignment along the axis of the spinning tube (13). The configuration for the present nmr experiments and all those for type II mesophases similarly aligned previously (3) is such that the planes of the discs are in the axis of the magnetic field direction and the normal to the flat faces is oriented along the axis of the nmr tube. This is diagrammatically pictured in the figure of a previous article (4). The micelle size is large enough to make negligible the influence of amphiphiles, which complete the edge of the disc.

If the degree of order measured for segments in

[4]Some positional ordering occurs, dependent on the nature and size of the sample tube. L. Q. do Amaral (Mol. Cryst. Liq. Cryst. Lett., in press).

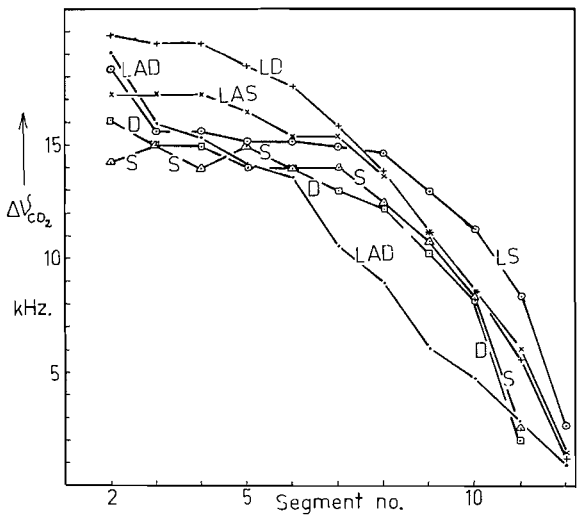


FIG. 4. A direct graphical comparison of quadrupole splittings in $—CD_2—$ segments (proportional to degrees of order along C—D bonds) in guests and hosts for the systems lauric acid and laurate ion guests in a micelle layer of decylsulphate–decanol, and the same guests in a bilayer of decylammonium ion – decylamine. The order profiles for the host bilayers are also plotted. The points correspond to the standard mesophases, the compositions of which are listed in Table 1. The profiles may be identified by both the type of point used and entries on each line, where distinction might be difficult. Temperature of experiments 34.0 ± 0.1°C. All mesophases type II DM. + Laurate ion in decylammonium mesophase (LD); ● lauric acid in decylammonium mesophase (LAD); ⊙ laurate ion in SDS/decanol mesophase (LS); × lauric acid in SDS/decanol mesophase (LAS); ⊡ profile of decylsulphate host chains (S); △ profile of decylammonium host chains (D). The segment numbers correspond to carbon number in the chain for guests and for the host chain segment 2 is the first carbon in the chain.

the same chain is separated into intra and extra chain contributions (1, 21) we may write:

$$[3] \quad (So)_n = (St/g)_n \cdot S_c$$

$(So)_n$ is the observed degree of order in the nth segment. $(St/g)_n$ is the intra chain contribution and S_c the contribution arising from the motion of the pseudo-rigid chain as a whole. A ratio for two segments in the same chain gives:

$$[4] \quad (So)_n/(So)_m = (St/g)_n/(St/g)_m$$

The intra chain contributions arise only because of the *trans/gauche* rotations along the chain (19). Since the ratio $(So)_n/(So)_m$ has been shown to be invariant it follows that the *trans/gauche* motions along the chain are not altered as water is added. The conclusion drawn is that the internal packing of the host and guest amphiphiles in the micelle does not change as the system is diluted with water. The lower degrees of order, measured as water dilutes the orientationally ordered micelles, owe their origin to larger amplitude movements of the micelle mostly deriving from changes in size of the micelle as more water is added (21). The results presented here do show very small differences in degrees of order of decylammonium chains between series D4, D15 and D6, and D21 but this is easily accounted for by the exchange process involving added decylamine in series D21. The guests are amphiphiles added in dilute solution in the micelle; the *trans/gauche* motions along these chains are also invariant to water content.

Motions Perpendicular to Pseudo-extended Chain Axes

The data presented in the Results, with respect to the lauric acid-d_{23} guest in the decylammonium chloride mesophase, show that for all perpendicular directions to the extended chain the degrees of order are the same. Cylindrical symmetry of motion about the long axis of the chain is a very useful assumption which is now justified by the present results. The uniaxial properties depend on long range orientational order of the rather large flat discs of the micelles.

Comments on Comparisons of Guest and Host Order

The plateau region of uniform degree of order in segments is not well developed for 10 or 12 carbon segment chains; this is especially the case for lauric acid guests in decylammonium bilayers (Fig. 4). The guest amphiphiles are either neutral at the polar head or negative. Oppositely charged head interactions occur for laurate guests in decylammonium chloride bilayers. The higher degree of order of the first five segments of this guest probably arises because of Coulombic attractions which induce a firmer anchoring at the guest head group site. On the other hand the segments 3–5 for laurate in decylsulphate–decanol bilayers have lower order than other guests. In so far as the absolute degrees of order carry the component of micelle motion which may differ from host to host, comparison of degrees of order of guest between host bilayers is not a reliable procedure. The main conclusion available is that the intrachain motions are peculiar to each guest and host amphiphile. This reflects the different anchoring of the head groups in the interface of the bilayer and confirms our earlier work in this respect on other systems (3). The individuality of these anchorings and profiles of order requires that studies on real membrane systems be aimed toward the behaviour of given lipids, to characterize their motion profiles, rather than designing experiments in the false hope that the motion profile of one lipid can be informative of the situation of the other lipids (8).

Can. J. Chem. Downloaded from www.nrcresearchpress.com by 210.87.254.42 on 09/05/12
For personal use only.

The lauric acid in decylammonium bilayers and laurate ion in decylsulphate–decanol bilayers are marked by a considerably higher order of the first $—CD_2—$ group over subsequent ones. The participation of this segment in the *trans/gauche* rotations of the carbon–carbon bonds is thus inhibited by head group anchoring.

With respect to the ratio of degrees of order in the $—CD_2CD_3$ terminal segments, treated in the manner reported before (20), the single *gauche* rotation about the last CD_2—CD_2 bond in the chain is more probable the higher the value of the ratio $\Delta\nu_{CD_2}/\Delta\nu_{CD_3}$. In decylammonium chains this ratio is 4.27, for guest laurate 4.58, for guest lauric acid in decylsulphate–decanol 4.29. These single *gauche* rotations are less probable in the other cases, ratios being 3.18 for lauric acid in decylammonium bilayers and 3.25 for decylsulphate chains. The participation of chain segments in terminal single *gauche* rotations is most highly developed for the lauric acid in decylammonium bilayers. This profile has no plateau of uniform order and the larger decreases in order per segment occur from carbon number 6 on.

Acknowledgments

This work was supported by the National Research Council of Canada (NRCC) in operating grants to L.W.R. The work in Brazil was assisted by the Banco Nacional de Desenvolvemento Economico (BNDE), and the NRCC/Conselho Nacional de Pesquisas exchange program, Canada/Brazil.

1. F. Y. Fujiwara and L. W. Reeves. J. Phys. Chem. **84**, 653 (1980).
2. L. Q. do Amaral, C. Pimentel, M. R. Tavares, and J. A. Vanin. J. Chem. Phys. **71**, 2940 (1979).
3. F. Y. Fujiwara, L. W. Reeves, M. Suzuki, and J. A. Vanin. *In* Solution chemistry of surfactants. Vol. 1. Proceedings of National Colloid Symposium, Knoxville, TN. 1978. Plenum Press. 1979. p. 63.
4. B. J. Forrest, F. Y. Fujiwara, and L. W. Reeves. J. Phys. Chem. **84**, 662 (1980).
5. L. W. Reeves and A. S. Tracey. J. Am. Chem. Soc. **97**, 5729 (1975).
6. D. M. Chen, F. Y. Fujiwara, and L. W. Reeves. Can. J. Chem. **55**, 2404 (1977).
7. L. W. Reeves, A. S. Tracey, and M. M. Tracey. Can. J. Chem. **57**, 747 (1979).
8. B. J. Forrest and L. W. Reeves. Chem. Phys. Lipids, **24**, 183 (1979).
9. G. W. Stockton, C. F. Polnaszek, A. P. Tulloch, F. Hasan, and I. C. P. Smith. Biochemistry, **15**, 954 (1976).
10. I. C. P. Smith, G. W. Stockton, A. P. Tulloch, C. F. Polnaszek, and K. G. Johnson. J. Colloid Interface Sci. **58**, 439 (1977).
11. B. J. Forrest, L. Hecker, and L. W. Reeves. Mol. Cryst. Liq. Cryst. **58**, 223 (1980).
12. M. Acimis and L. W. Reeves. Can. J. Chem. **58**, 1542 (1980).
13. F. Y. Fujiwara and L. W. Reeves. Can. J. Chem. **56**, 2178 (1978).
14. Y. Lee, L. W. Reeves, and A. S. Tracey. Can. J. Chem. **58**, 110 (1980).
15. F. Y. Fujiwara and L. W. Reeves. J. Am. Chem. Soc. **98**, 6790 (1976).
16. K. D. Lawson and T. J. Flautt. J. Am. Chem. Soc. **89**, 5489 (1967).
17. L. W. Reeves, A. S. Tracey, and M. M. Tracey. J. Am. Chem. Soc. **95**, 3799 (1973).
18. A. Saupe and J. Nehring. J. Chem. Phys. **47**, 5459 (1967).
19. S. Marcelja. Nature, **241**, 451 (1973); Biochim. Biophys. Acta, **367**, 165 (1974).
20. F. Y. Fujiwara, L. W. Reeves, A. S. Tracey, and L. A. Wilson. J. Am. Chem. Soc. **96**, 5249 (1974).
21. B. J. Forrest and L. W. Reeves. Mol. Cryst. Liq. Cryst. **58**, 233 (1980).

Can. J. Chem. Downloaded from www.nrcresearchpress.com by 210.87.254.42 on 09/05/12
For personal use only.

Extraction of Zn(II) and Cd(II) with anthranilic acid in the presence of nitrogen-containing organic bases

BINA JAIN, J. M. SINGH, R. N. GOYAL, AND S. N. TANDON
Department of Chemistry, University of Roorkee, Roorkee-247672, India

Received October 11, 1979[1]

BINA JAIN, J. M. SINGH, R. N. GOYAL, and S. N. TANDON. Can. J. Chem. **58**, 1558 (1980).

Zinc and cadmium anthranilates do not extract into non-polar solvents alone in the pH range 4.5–6.5. But their extraction is synergistically enhanced in presence of N bases, apparently by displacement of coordinated water. The synergistic effect varies with the bases in the order β-picoline > pyridine > quinoline. The values of extraction constants suggest that cadmium forms more stable complexes than zinc.

BINA JAIN, J. M. SINGH, R. N. GOYAL et S. N. TANDON. Can. J. Chem. **58**, 1558 (1980).

Dans l'intervalle de pH 4,5 à 6,5, les anthranilates de zinc et de cadmium ne peuvent être extraits à l'aide de solvants non-polaires seuls. Mais leur extraction est activée synergétiquement en présence des bases azotées, apparemment par déplacement d'eau coordonnée. L'effet synergétique varie avec les bases dans l'ordre: β-picoline > pyridine > quinoléine. Les valeurs des constantes d'extractions suggèrent que le cadmium forme des complexes plus stables que ceux du zinc.

[Traduit par le journal]

Introduction

Anthranilic acid is known to be a good complexing agent and has found extensive applications as an analytical reagent. Some studies have also been reported on the use of anthranilic acid for the extraction of metals in oxygenated solvents. Harvey *et al.* (1) studied the extraction of Pu(IV) anthranilate into amyl acetate and reported the effect of pH on extraction. Hök (2) carried out extraction studies of some lanthanides using anthranilic acid and proposed their separations. Dinsel and Sweet (4) separated Fe(II) from Fe(III) using their extraction in the presence of anthranilic acid and determined the latter spectrophotometrically. Schweitzer and Howe (6) extracted Co(II) from anthranilic acid solution into different oxygenated solvents and reported $pH_{0.5}$ and maximum log D values. Sheyanova and Boyarkina (8) investigated the extraction of Co(II), Ni(II), Zn(II), and Cd(II) anthranilates and reported the pH values for their maximum extraction.

On the other hand, the anthranilates of some metals show poor extraction in non-polar solvents like chloroform (3) and benzene. However, the addition of neutral donors like heterocyclic nitrogen-containing organic bases to such systems increases the extraction significantly. The present article reports the extraction of Zn(II) and Cd(II) anthranilates into benzene in the presence of nitrogen-containing organic bases like pyridine, picolines, and quinoline. To the best knowledge of the authors it is the first report of a successful extraction of metal anthranilates into a non-polar solvent. The extracting species have been identified and the extraction constants calculated. On the basis of extraction data, the stability of the mixed complexes of zinc and cadmium has been computed. The study also gives an idea about the relative effectiveness of different bases as synergists. No attempts have been made to utilize the system for proposing separations. However, the investigations offer an entirely new system for achieving separations of metals as anthranilates.

Experimental

Reagents

The metal ion solutions were prepared by dissolving analytical grade sulphates of zinc and cadmium in doubly distilled water. The solutions were standardized by EDTA titrations. The nitrogen-containing organic bases pyridine, picolines, and quinoline were also of analytical grade. Freshly prepared aqueous solution of anthranilic acid (AR) was used throughout the investigation. ^{65}Zn and ^{115m}Cd isotopes of specific activity 321 mC/g Zn and 17 mC/g Cd were procured from Bhabha Atomic Research Centre, Bombay, India, and used for distribution studies. At around 55% extraction a precision of ±1% in the case of zinc and ±2% in the case of cadmium was obtained.

Analytical Procedure

In each set equal volumes of aqueous (1.0×10^{-4} M Zn(II) or Cd(II) and 0.04 M anthranilic acid or any other concentration) and organic phase (benzene) were shaken at room temperature 30 ± 2°C for half an hour which was found sufficient for complete equilibration. The pH of the aqueous phase was adjusted with perchloric acid or sodium hydroxide. After equilibration the two phases were separated and pH of the aqueous phase was determined. Suitable aliquots of each phase were pipetted out and counted using a well-type NaI(Tl) scintillation counter for ^{65}Zn and a G.M. counter for ^{115m}Cd. The pH range for the extraction of Zn(II) and Cd(II) lies between 4.5 and 6.5. The optimum concentration with regard to the bases are 0.25, 0.50, and 2.0 M for β-picoline, pyridine, and quinoline, respectively, for maximum extraction at an overall anthranilic acid concentration of

[1]Revision received April 9, 1980.

0008-4042/80/151558-04$01.00/0
©1980 National Research Council of Canada/Conseil national de recherches du Canada

Can. J. Chem. Downloaded from www.nrcresearchpress.com by 210.87.254.40 on 09/05/12
For personal use only.

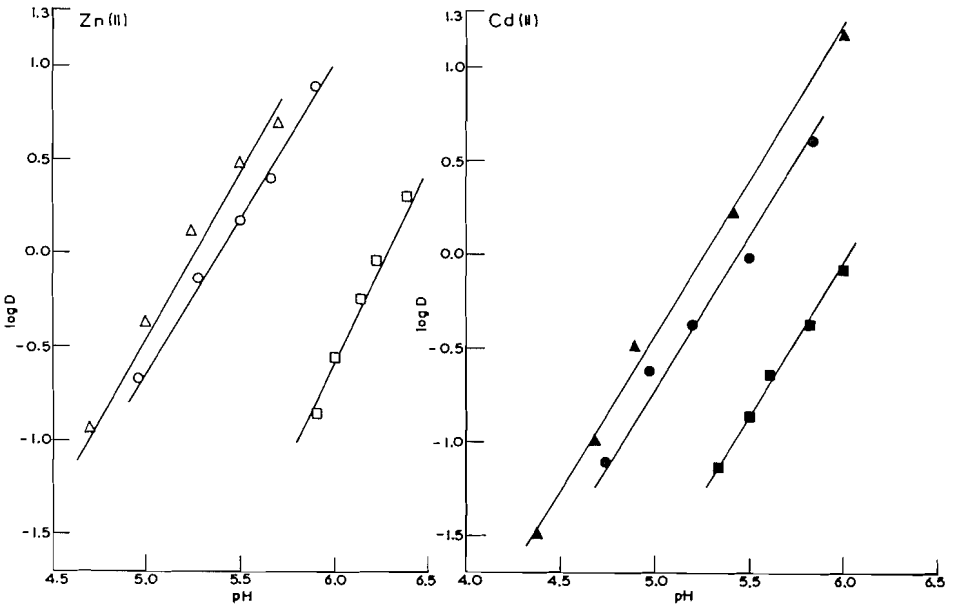


FIG. 1. Effect of pH on the extraction of Zn(II) and Cd(II) complexes with anthranilic acid (4×10^{-2} *M*) in presence of nitrogen-containing organic bases: ○, ●, pyridine, 0.35 *M*; △, ▲, β-picoline, 0.25 *M*; □, ■, quinoline; 2.0 *M*.

0.04 *M*. The ionic strength of aqueous phase was maintained constant (0.1 *M*) by adding sodium perchlorate.

Results and Discussion

The zinc and cadmium anthranilates in benzene alone show poor extraction (< 5%) over the pH range studied (4.5–6.5). But the addition of neutral donors like pyridine, picolines, and quinoline has a striking effect on the extraction and metal gets extracted to the extend of 80–90%. Obviously, this happens by the replacement of water molecules from the coordination sphere of the metal, rendering the species less hydrophilic, thereby enhancing its extraction into benzene.

For the extraction of Zn(II) and Cd(II) anthranilates into benzene in the presence of organic bases plots were drawn for log *D* vs. equilibrium pH of aqueous phase (Fig. 1) and log *D* vs. log of anthranilic acid concentration (Fig. 2). The straight lines with slope near 2 were obtained suggesting the release of two protons and the utilization of two acid molecules per metal atom. In order to find the ratio of metal-to-base, log *D* was plotted against log $[B]_{total}$ (Fig. 3). The straight lines with a slope of unity in the case of zinc and with a slope value near two for cadmium were obtained. Thus, the extracting species may be represented as $[Zn(anthra)_2 \cdot B \cdot H_2O]$ and $[Cd(anthra)_2 \cdot 2B]$ assuming the coordination number of zinc and cadmium to be four. It has been observed that out of the different nitrogen-containing organic bases used α-picoline is unable to enhance extraction. This may be explained on the basis of poor basicity of α-picoline; the steric factor may also play a role.

Tandon *et al.* (9, 10) studied the extraction of zinc and cadmium salicylates in the presence of some organic bases and reported similar species.

The reaction for mixed complex formation can be represented as

$$M_{aq}^{2+} + 2H_2A_{aq} + nB_{aq} \rightleftharpoons [M(HA)_2 \cdot nB]_{org} + 2H_{aq}^{+}$$

where M^{2+} represents Zn^{2+} or Cd^{2+} and H_2A stands for anthranilic acid. The equilibrium constant for extraction will be given by equation

$$K_{ex} = \frac{[M(HA)_2 \cdot nB]_{org}[H^+]_{aq}^2}{[M^{2+}]_{aq}[H_2A]_{aq}^2[B]_{aq}^n}$$

Hence

$$[1] \quad \log D = \log K_{ex} + 2 \log [H_2A]_{aq} + n \log [B]_{aq} + 2\,pH$$

where

$$D = \frac{[M(HA)_2 \cdot nB]_{org}}{[M^{2+}]_{aq}}$$

Mass balance for the base is given by the expression

$$[B]_{total} = [B]_{org} + [B]_{aq} + [BH^+]_{aq} + n[M(HA)_2 \cdot nB]_{org}$$

Can. J. Chem. Downloaded from www.nrcresearchpress.com by 210.87.254.40 on 09/05/12
For personal use only.

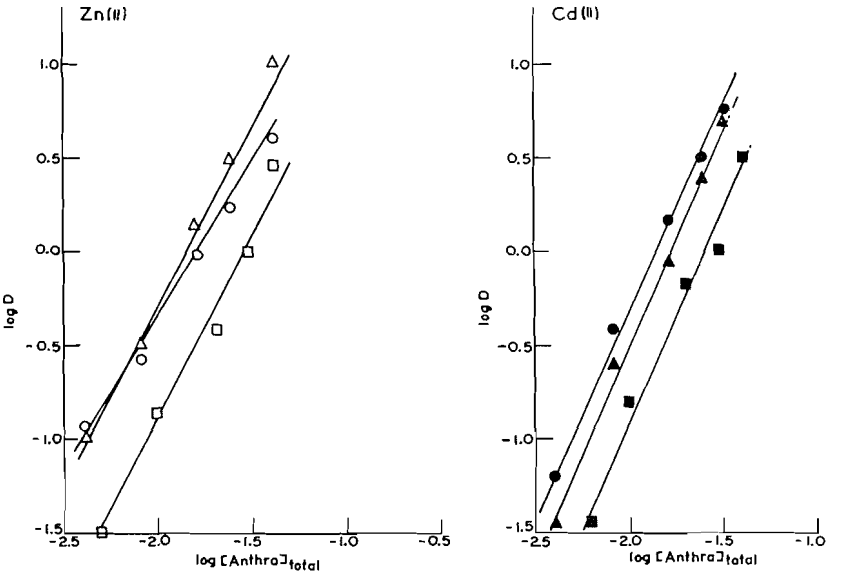


FIG. 2. Variation of distribution ratio for Zn(II) and Cd(II) as a function of anthranilic acid concentration at constant pH and base concentration: ○, pyridine, 0.35 *M*, pH = 6.3; △, β-picoline, 0.25 *M*, pH = 5.8; □, quinoline, 2.0 *M*, pH = 6.5; ●, pyridine, 0.35 *M*, pH = 6.3; ▲, β-picoline, 0.25 *M*, pH = 6.2; ■, quinoline, 2.0 *M*, pH = 6.4.

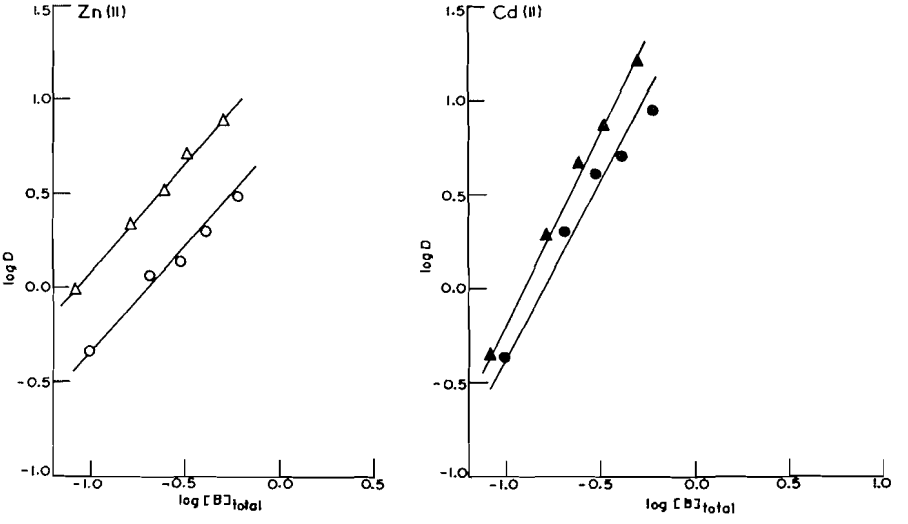


FIG. 3. Variation of distribution ratio as a function of base concentration at constant pH and anthranilic acid concentration (4×10^{-2} *M*): ○, pyridine, pH = 6.44; △, β-picoline, pH = 6.50; ●, pyridine, pH = 6.50; ▲, β-picoline, pH = 6.32.

Hence

$$[2] \quad [B]_{aq} = \frac{[B]_{total} - n[M(HA)_2 \cdot nB]_{org}}{\{P_B + 1 + [H^+]/K_{BH^+}\}}$$

where P_B and K_{BH^+} are the partition coefficient and ionisation constant respectively of BH^+ of the base. The average values of partition coefficient for pyridine and β-picoline are 1.95 and 1.85 respectively (10). K_{BH^+} values were taken from the literature (5, 7). Equilibrium concentration of base $[B]_{aq}$ was calculated using eq. [2]. Plot of log *D* vs. log $[B]_{aq}$ (Fig. 4) gave straight lines with a slope value of 1 in the case of zinc and 2 in the case of cadmium. These values again confirm the presence of one base molecule in zinc complex and two in cadmium complex.

The extraction constant (K_{ex}) is computed using eq. [1]. Values of extraction constant show that cadmium forms more stable complex with anthranilic acid than zinc. The results for pyridine and β-picoline are given in Tables 1 and 2. The data for quinoline are not given as in view of its distribution (5) being highly in favour of organic phase ($P_B >$

Can. J. Chem. Downloaded from www.nrcresearchpress.com by 210.87.254.40 on 09/05/12
For personal use only.

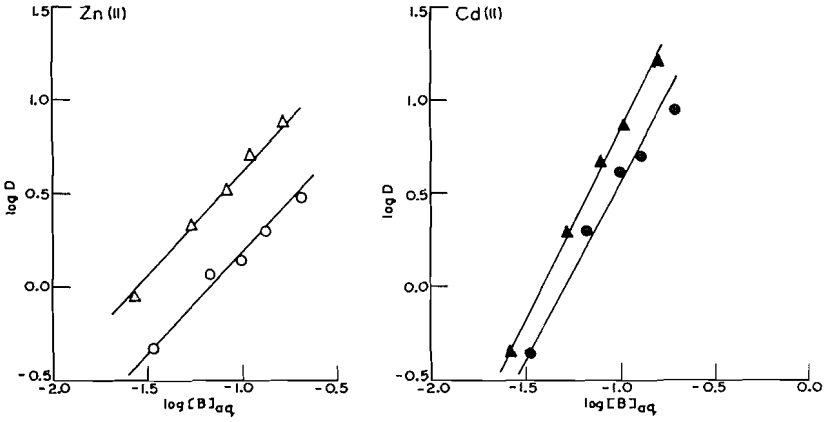


FIG. 4. Plots of log D vs. log $[B]_{aq}$ at constant pH and anthranilic acid concentration (4.0×10^{-2} M). ○, pyridine, pH = 6.44; △, β-picoline, pH = 6.50; ●, pyridine, pH = 6.50; ▲, β-picoline, pH = 6.32.

TABLE 1. Variation of $[B]_{aq}$ for Zn(II) at constant $[\text{anthranilic acid}]_{total}$ and pH

$\log [B]_{total}$	$\log D$	$\log [B]_{aq}$	$\log K_{ex}$	Mean of $\log K_{ex}$
(*a*) Pyridine				
$[\text{anthranilic acid}]_{total} = 0.04$ M and pH = 6.44				
−1.000	−0.332	−1.477	−8.94	
−0.699	0.074	−1.176	−8.83	
−0.522	0.143	−1.000	−8.94	−8.90
−0.397	0.305	−0.875	−8.90	
−0.221	0.482	−0.699	−8.90	
(*b*) β-Picoline				
$[\text{anthranilic acid}]_{total} = 0.04$ M and pH = 6.50				
−1.088	−0.029	−1.572	−8.65	
−0.787	0.332	−1.270	−8.60	
−0.611	0.500	−1.087	−8.61	−8.59
−0.486	0.700	−0.961	−8.54	
−0.309	0.880	−0.785	−8.54	

TABLE 2. Variation of $[B]_{aq}$ for Cd(II) at constant $[\text{anthranilic acid}]_{total}$ and pH

$\log [B]_{total}$	$\log D$	$\log [B]_{aq}$	$\log K_{ex}$	Mean of $\log K_{ex}$
(*a*) Pyridine				
$[\text{anthranilic acid}]_{total} = 0.04$ M and pH = 6.5				
−1.000	−0.363	−1.483	−7.60	
−0.699	0.306	−1.182	−7.53	
−0.522	0.626	−1.005	−7.56	−7.65
−0.397	0.702	−0.880	−7.74	
−0.221	0.956	−0.704	−7.84	
(*b*) β-Picoline				
$[\text{anthranilic acid}]_{total} = 0.04$ M and pH = 6.32				
−1.088	−0.365	−1.586	−7.03	
−0.787	0.289	−1.284	−6.98	
−0.611	0.674	−1.101	−6.96	−7.00
−0.486	0.866	−0.975	−7.02	
−0.309	1.206	−0.799	−7.04	

100) as compared to other bases, it is likely that a mixed complex is formed in the organic phase in this case.

The extraction data reveal that the effectiveness of the bases as synergists follows the sequence β-picoline > pyridine > quinoline, the concentrations required for a particular extraction (%) are in the reverse order. The stability of the complexes of β-picoline is higher than those of pyridine. A similar sequence of stability of complexes has been observed in other systems, also in consideration of both the strength of the base and steric factors (9, 10).

The infrared spectra give the usual peaks of anthranilate ion and bases, and no conclusive information is obtained from them.

Acknowledgement

Financial assistance of Council of Scientific and Industrial Research, New Delhi, India is gratefully acknowledged.

1. B. G. HARVEY, H. G. HEAL, A. G. MADDOCK, and E. L. ROWLEY. J. Chem. Soc. 1010 (1947).
2. B. H. BERNSTROM. Svensk Tidskr. **68**(11), 34 (1956).
3. G. K. SCHWEITZER and D. R. RANDOLPH. Anal. Chim. Acta, **26**, 567 (1962).
4. D. L. DINSEL and T. R. SWEET. Anal. Chem. **35**, 2077 (1963).
5. H. M. N. H. IRVING and N. S. AL-NIAMI. J. Inorg. Nucl. Chem. **27**, 1671 (1965).
6. G. K. SCHWEITZER and L. H. HOWE. Anal. Chim. Acta, **37**(3), 316 (1967).
7. H. AKAIWA and H. KAWAMOTO. J. Inorg. Nucl. Chem. **29**, 1345 (1967).
8. F. R. SHEYANOVA and V. U. BOYARKINA. Tr. Khim. Khim. Tekhnol. **2**, 213 (1970).
9. J. M. SINGH, O. V. SINGH, and S. N. TANDON. Ind. J. Chem. **16A**, 1083 (1978).
10. J. M. SINGH and S. N. TANDON. Can. J. Chem. **56**, 2922 (1978).

Can. J. Chem. Downloaded from www.nrcresearchpress.com by 210.87.254.40 on 09/05/12
For personal use only.

Electrical conductivities of molten zinc chloride – lithium chloride mixtures between 320 and 450°C

SLIMANE BENHENDA[1] AND JEAN-BAPTISTE LESOURD

Laboratoire de Dynamique et de Thermophysique des Fluides, Université de Provence, Centre de Saint-Jérôme, 13397 Marseille Cedex 4, France

Received January 2, 1980

SLIMANE BENHENDA and JEAN-BAPTISTE LESOURD. Can. J. Chem. **58**, 1562 (1980).

Specific conductivities of $ZnCl_2$–LiCl liquid mixtures have been determined in the 320–450°C temperature interval and in the 0–0.54 LiCl mole fraction interval. They were found to increase steadily with both temperature and LiCl mole fraction, which was shown to be related to an increasing ionic character of the melt.

SILMANE BENHENDA et JEAN-BAPTISTE LESOURD. Can. J. Chem. **58**, 1562 (1980).

Les conductivités spécifiques des mélanges $ZnCl_2$–LiCl liquides ont été déterminées dans l'intervalle de temperature 320–450°C et dans l'intervalle 0–0,54 des fractions molaires de LiCl. On a observé une forte croissance de celles-ci à la fois avec la température et la fraction molaire de LiCl; la discussion montre que cette propriété est à rapprocher du caractère ionique croissant du liquide.

Can. J. Chem. Downloaded from www.nrcresearchpress.com by 210.87.254.5 on 09/05/12
For personal use only.

Introduction

Thermodynamic measurements in the $ZnCl_2$–LiCl liquid mixtures have been the object of several studies (1–6). In a previous work (7) we attempted to determine the internal transport numbers of the Zn^{2+} and Li^+ ions in these melts.

But no conductivity data concerning the $ZnCl_2$–LiCl liquid system have been reported, to our knowledge. It was therefore found desirable to investigate the latter data; the results of this investigation are the object of the present paper.

$ZnCl_2$-containing melts seem to be interesting owing to their peculiar structure which is characterized by partially covalent Zn—Cl bonds. Furthermore, high temperature electrochemical cells have recently been studied in view of possible applications (8, 9).

Experimental

The method used was a modification of the four-electrode method described previously (10).

Conductivity cell

The conductivity cell was made of Pyrex glass and such that the resistance of the melt be as high as possible. The useful part of the cell was a U-shaped tube (inner diameter: 1.5 mm; total length: 30 mm). Cells were calibrated with 0.1 *N* and 1 *N* KCl standard solutions at 20°C, and this was cross-checked with a 1 *N* NaCl solution at 20°C. Typical cell constants were of the order of 120 cm^{-1}.

Electrodes

Electrodes were made of platinum wire (0.5 mm in diameter, as supplied by Compagnie des Métaux Précieux, France) connected to pure silver leads (1 mm in diameter, as supplied by Compagnie des Métaux Précieux, France). All connections were made in the central hot part of the cell in order to avoid thermocouple effects. The leads were introduced in silica tubes for the sake of insulation.

Apparatus

The measuring circuit was composed of:

(*i*) A sine wave generator, with which a preliminary test was carried out at variable frequencies; it was thus ascertained that the effect of frequency was negligible above 1000 Hz. All other measurements were performed at 1500 Hz.

(*ii*) An insulator stepdown transformer, which protected the measuring circuit against any external noise.

(*iii*) A calibrated, variable R_0 resistor.

(*iv*) A recording millivoltmeter (M. E. C. I., France, equipment built under a Leeds and Northrup licence), selecting successively every one of six channels in the course of a 30-second cycle. The potentials across R_0 and the unknown R_x resistance, after rectification and amplification (rectifying probe and amplifier supplied by Lemouzy, France), were connected to the first two channels. A change over relay, triggered by the channel-switching device, connected alternately the potentials across R_0 and R_x to the meter. This ensured that both potentials were rectified and amplified rigorously in the same way, and were thus strictly comparable. Two other channels were used for recording the emf's of two calibrated Pt–(Pt – 10% Rh) thermocouple which served for the determination of the melt temperature. The last two channels were short-circuited for zero potential calibration.

(*v*) The cell was maintained at the desired temperature by an electric tube furnace supplied with a temperature control unit, as described previously (11).

Procedure

Mixtures were prepared and purified as previously (4, 12). Measurements were carried out at constant composition and the temperature varied in the course of a given run. All temperatures given were stable within ± 1°C for at least 30 min.

For the determination of R_x, the potentials across R_x and R_0 were set equal, whence, the impedance of the measuring circuit being very large, $R_x = R_0$ at equilibrium of the bridge, achieved by adjustment of R_0.

Miscellaneous

All calculations were carried out on the University of Provence PDP 11/45 computer. Equations given were fitted by using a non-linear least-squares regression method.

[1]Present address: Institut de Physique, Université d'Oran, La Sénia, Algeria.

0008-4042/80/151562-04$01.00/0

©1980 National Research Council of Canada/Conseil national de recherches du Canada

Can. J. Chem. Downloaded from www.nrcresearchpress.com by 210.87.254.5 on 09/05/12
For personal use only.

Results[2]

The specific conductivities (σ) of $ZnCl_2$–LiCl liquid mixtures may be represented satisfactorily as a function of temperature (T) at constant composition by an equation of the form

$$\sigma = a + bT + cT^2 + dT^3$$

σ in Ω^{-1} cm^{-1}; T in K. The values of a, b, c, and d as functions of LiCl mole fraction (x_{LiCl}) are given in Table 1. Figures 1 and 2 give the variation of σ against temperature.

These data may be compared with previous data at only one point: $x_{LiCl} = 0$, i.e. pure $ZnCl_2$, for which several previous studies are available (13–20). In Fig. 1, we have compared our results with some of these previous results. Our data appear to fall between the other ones, but closer to the values resulting from the compilation of Janz *et al.* (18) and the work of Doucet *et al.* (20) than to the less recent values of Biltz and Klemm (13).

The standard deviation on our data in pure $ZnCl_2$ with respect to the adjusted polynomial is about $1.5 \times 10^{-4}\ \Omega^{-1}$ cm^{-1}. From this, the possible relative error on our data in the middle of the range investigated is about 2.5% (at 377°C), with the hypothesis of a normal distribution of errors and within a 95% confidence level. This is consistent with experimental errors due to temperature fluctuations of ±1°C, and to the instrumental error. It is, however, higher than in similar measurements with typically ionic melts such as fused KNO_3. But the standard deviation given by Janz (19) (about $0.003\ \Omega^{-1}$ cm^{-1} between 700 and 900 K) leads to a relative error of the same order of magnitude as ours. It is clear that this error, due to peculiar experimental difficulties encountered with this system, is large enough to account for differences between our data and, say, those given by Janz *et al.* (18). At higher x_{LiCl} mole fractions, these difficulties appear less acute, and the relative errors calculated as above are much lower, and more in line with those observed in similar experiments with typically ionic molten salts. For instance, for $x_{LiCl} = 0.218$, the standard deviation is $1.625 \times 10^{-4}\ \Omega^{-1}$ cm^{-1}, which corresponds to a relative error of 0.3% at 350°C.

At 400°C, the specific conductivities of $ZnCl_2$–LiCl liquid mixtures may be represented by the equation

$$\sigma = 3.6676\, x_{LiCl}^3 + 0.590\, x_{LiCl} + 0.02$$

where σ is in Ω^{-1} cm^{-1}. Extrapolating to $x_{LiCl} = 1$, one obtains $\sigma = 4.28\ \Omega^{-1}$ cm^{-1}, whereas the extrapolated value, at 400°C, for the specific conductivity of molten LiCl is $\sigma = 4.43\ \Omega^{-1}$ cm^{-1}, according to Janz *et al.* (18). The relative difference is about 3%. If one considers the value of the relative error encountered here, and the fact that the extrapolated value of 4.43 refers to a metastable liquid, LiCl being normally a solid at 400°C, such an agreement may be considered as quite satisfactory.

If v_m stands for the molar volume of the system, one can also from our data calculate molar conductivities for $ZnCl_2$–LiCl liquid systems, as defined by the equation: $\Lambda = \sigma v_m$. This calculation was carried out using the density data of Bloom and Weeks (5), and those of Markov and Volkov (6). At 400°C, Λ was represented by the following equation:

$$\Lambda = 87.316\, x_{LiCl}^2 + 17.046\, x_{LiCl} + 1.15$$

with σ in Ω^{-1} cm^2 mol^{-1}.

TABLE 1. Coefficients a, b, c, and d of equation expressing σ as a function of T at various x_{LiCl} values*

x_{LiCl}	a	$b \times 10^2$	$c \times 10^5$	$d \times 10^8$
0.0	−3.1504	1.5355	−2.516	1.388
0.066	0.95537	−0.33978	0.30351	—
0.089	1.0271	−0.38062	0.35558	—
0.108	1.6002	−0.57325	0.51851	—
0.160	1.0545	−0.42616	0.43241	—
0.218	1.0546	−0.43847	0.46169	—
0.283	−0.99582	0.18472	—	—
0.365	−1.0934	0.21943	—	—
0.433	−1.6097	0.33041	—	—
0.540	−1.6075	0.37135	—	—

*Coefficient d is zero for $x_{LiCl} > 0$; coefficients c and d are zero for $x_{LiCl} > 0.218$, which amounts to linear behaviour.

Discussion

It appears that σ increases steadily with both temperature and LiCl mole fraction, and of course the same is true of Λ. Such a behaviour was expected, since pure $ZnCl_2$ is known for its partially covalent structure; its conductivity is, therefore, much lower than the conductivities of typically ionic molten salts (such as alkali nitrates) at the same temperature. However, upon heating, $ZnCl_2$ progressively shifts to an ionic structure, whereby its conductivity is considerably increased. Another piece of evidence for this behaviour is the convexity of the σ vs. temperature curves, as the latter are convex for melts with a low LiCl content. This means that these curves lie above any of their tangents, and, consequently, that σ increases much faster with temperature than in the case of typically

[2]The detail of the data is available as supplementary material, at a nominal charge, from the Depository of Unpublished Data, CISTI, National Research Council of Canada, Ottawa, Ont., Canada K1A 0S2.

Can. J. Chem. Downloaded from www.nrcresearchpress.com by 210.87.254.5 on 09/05/12
For personal use only.

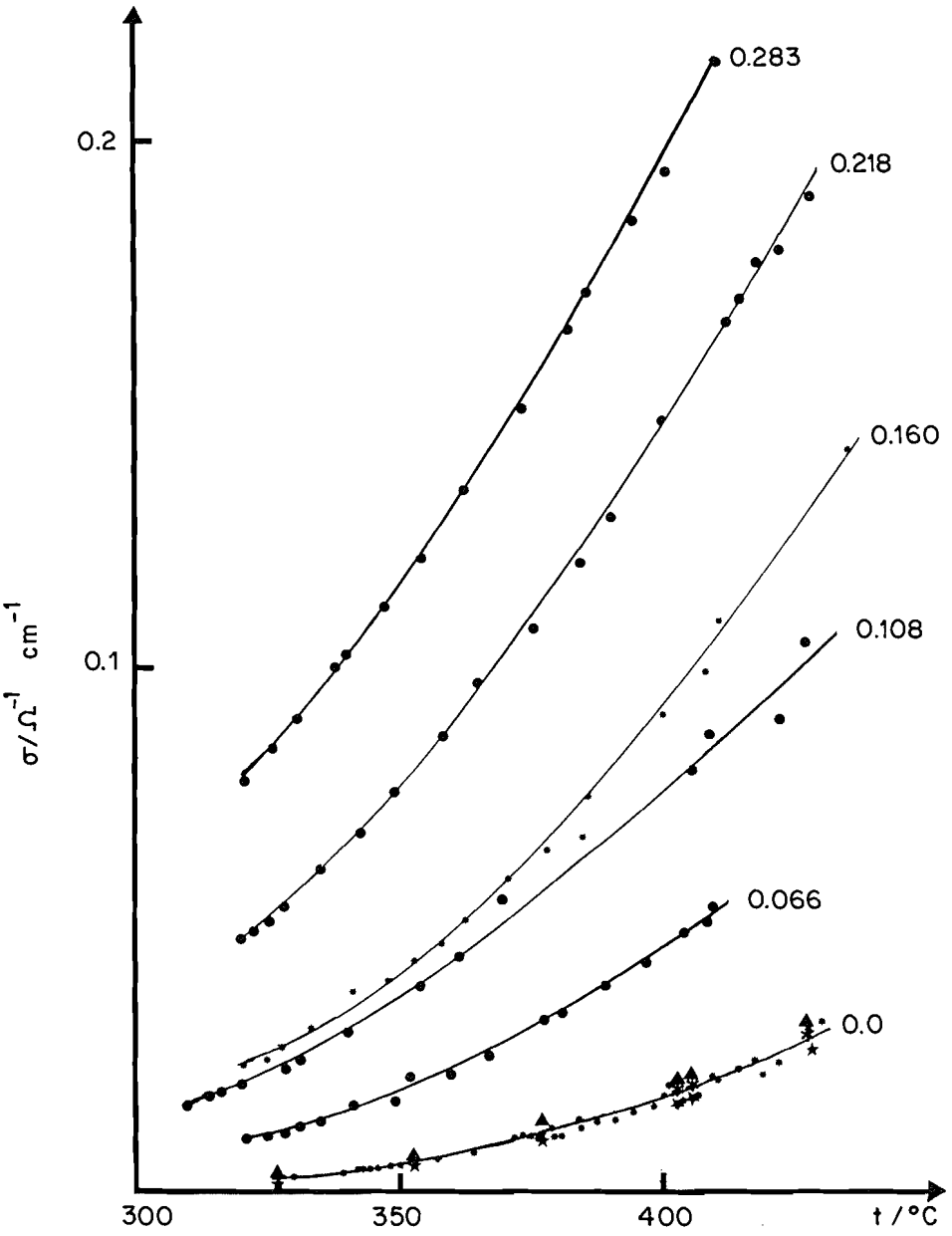


FIG. 1. Variation of $\sigma(\Omega^{-1}\,cm^{-1})$ against t (°C) ($0 \leq x_{LiCl} \leq 0.283$). Symbols: ∗ and ●: our data; ★: after ref. 13; ▲: after ref. 18; ∗: after ref. 20. Values of x_{LiCl} are given on various graphs.

ionic melts, for which σ generally exhibits a nearly linear behaviour on a 100°C temperature interval. Such a linear behaviour is observed, for example, in the case of the specific conductivities of molten $LiNO_3$ and $NaNO_3$ (21). We also observe this linear variation of σ against T here for melts with relatively high mole fractions ($x_{LiCl} > 0.25$). In these melts, the concentration in Li^+ ions (which are unable to enter in covalent bonds with neighbouring Cl^- ions) is large enough for the conductivity to behave as in a typically ionic liquid.

At constant temperature, one also encounters a strong increase in conductivity as the $ZnCl_2$–LiCl systems become more ionic upon LiCl addition.

Conclusion

Our conductivity measurements in $ZnCl_2$–LiCl liquid systems yield significant new experimental

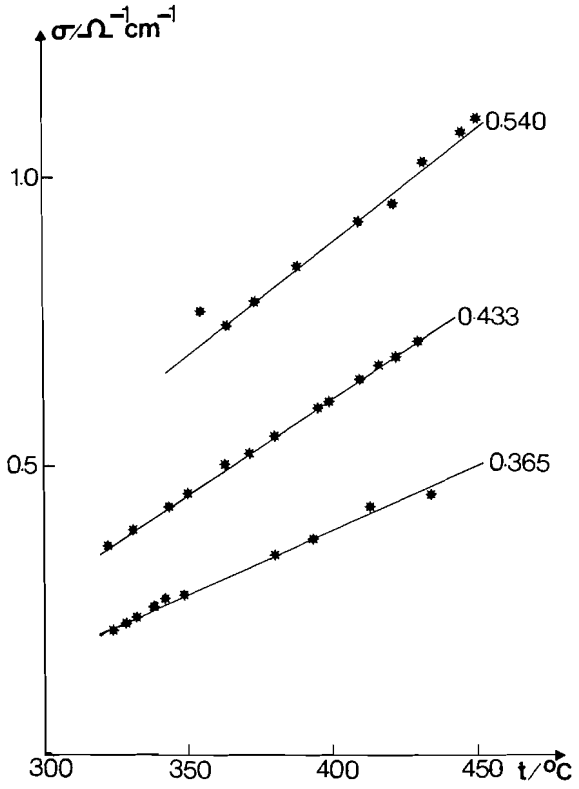


FIG. 2. Variation of $\sigma(\Omega^{-1}\ cm^{-1})$ against t (°C) ($x_{LiCl} \geq 0.365$). Values of x_{LiCl} are given on various graphs.

data which are interesting in that the mixtures shift progressively from a partially covalent structure to an ionic structure upon increasing temperature and LiCl mole fraction.

In the future, it might be desirable to extend the present study to higher temperatures (above 450°C) and to other transport phenomena such as shear viscosity and heat conductivity.

Furthermore, although some interesting spectroscopic data have been published about both pure $ZnCl_2$ (22–25) and $ZnCl_2$-containing melts (26–28), a complete understanding of the structure of these systems has not yet been reached. The molecular dynamics study of Rahman *et al.* (29) for BeF_2–LiF melts (BeF_2 being characterized, in the liquid state, by a covalent structure) indicates that computer simulation would perhaps be of interest for the study of the structure of $ZnCl_2$-containing melts.

Acknowledgements

The authors wish to thank Dr. A. D. Pelton (Ecole Polytechnique, Montréal, P.Q., Canada) for helpful discussion of the data given in this paper.

1. G. N. PAPATHEODOROU and O. J. KLEPPA. Z. Anorg. Allg. Chem. **401**, 132 (1973).
2. S. V. VOLKOV and R. A. LAZORENKO. Ukr. Khim. Zh. **34**, 528 (1968).
3. B. F. MARKOV and S. V. VOLKOV. Ukr. Khim. Zh. **30**, 341 (1964).
4. S. BENHENDA and J.-B. LESOURD. J. Chim. Phys. **74**, 1042 (1977).
5. H. BLOOM and I. A. WEEKS. Trans. Faraday Soc. **67**, 1410 (1971).
6. B. F. MARKOV and S. V. VOLKOV. Ukr. Khim. Zh. **29**, 945 (1963).
7. S. BENHENDA and J.-B. LESOURD. Rev. Chim. Minérale. **15**, 40 (1978).
8. S. VON WINBUSH and A. F. SAMMELS. J. Electrochem. Soc. **123**, 650 (1976).
9. R. J. HANS and J. J. EGAN. Communication, International Symposium on Molten Salts, Washington D.C., U.S.A., May, 1976.
10. M. BIZOUARD, P. CERISIER and B. DE GASQUET. Revue Générale de l'Electricité. **77**, 697 (1968).
11. J.-B. LESOURD, C. VALLET and Y. DOUCET. J. Electroanal. Chem. **48**, 99 (1973).
12. J.-B. LESOURD, Y. ROCCA-SERRA and Y. DOUCET. J. Chem. Thermodyn. **9**, 333 (1977).
13. W. BILTZ and W. KLEMM. Z. Phys. Chem. **110**, 318 (1924).
14. F. R. DUKE and R. A. FLEMING. J. Electrochem. Soc. **104**, 251 (1957).
15. J. O'M. BOCKRIS, E. H. CROOK, H. BLOOM and N. E. RICHARDS. Proc. R. Soc. (London). A, **255**, 558 (1960).
16. J. D. MCKENZIE and W. K. MURPHY. J. Chem. Phys. **33**, 366 (1960).
17. L. F. GRANTHAM and S. J. YOSIM. J. Chem. Phys. **45**, 1192 (1966).
18. G. J. JANZ, F. W. DAMPIER, G. R. LAKSHMINARAYANAN, P. K. LORENZ, and R. P. T. THOMKINS. Molten salts. Vol. I. Electrical conductance, density and viscosity data. National Bureau of Standards Document NSRDS – NBS 15. U.S. Government Printing Office, Washington D.C., U.S.A. 1968.
19. G. J. JANZ. Molten salts handbook. Academic Press, New York. 1967. p. 292.
20. Y. DOUCET, J.-P. CHAREYRE, R. SANTINI, and A. TETE. C. R. Acad. Sc. Paris. B, **273**, 339 (1971).
21. Y. DOUCET and M. BIZOUARD. Bull. Soc. Chim. Fr. 1570 (1959).
22. W. BUES. Z. Anorg. Allg. Chem. **279**, 104 (1955).
23. D. E. IRISH and T. F. YOUNG. J. Chem. Phys. **43**, 1765 (1965).
24. J. R. MOYER, J. C. EVANS and G. Y.-S. LO. J. Electrochem. Soc. **113**, 158 (1966).
25. R. B. ELLIS. J. Electrochem. Soc. **113**, 485 (1966).
26. D. M. GRUEN and R. L. MCBETH. Appl. Chem. **6**, 23 (1963).
27. G. P. SMITH, C. R. BOSTON and J. BRYNESTAD. J. Chem. Phys. **45**, 829 (1966).
28. C. A. ANGELL and D. M. GRUEN. J. Am. Chem. Soc. **88**, 5192 (1966).
29. A. RAHMAN, R. H. FOWLER and A. H. NARTEN. J. Chem. Phys. **57**, 3010 (1972).

Can. J. Chem. Downloaded from www.nrcresearchpress.com by 210.87.254.5 on 09/05/12
For personal use only.

Complexes of substituted benzothiazoles. 2. Copper(II) complexes of the 'tripod' ligand tris(2-benzothiazolylmethyl)amine

LAURENCE K. THOMPSON[1]

Department of Chemistry, Memorial University of Newfoundland, St. John's, Nfld., Canada A1B 3X7

AND

RICHARD G. BALL AND JAMES TROTTER

Department of Chemistry, University of British Columbia, 2075 Wesbrook Mall, Vancouver, B.C., Canada V6T 1W5

Received February 25, 1980

LAURENCE K. THOMPSON, RICHARD G. BALL, and JAMES TROTTER. Can. J. Chem. **58**, 1566 (1980).

A series of copper(II) complexes of the title ligand are reported which exhibit both five-coordinate trigonal bipyramidal and pseudo-octahedral stereochemistries. Mixed stereochemistry complexes $[Cu(NTBT)X]_2[CuX_4]$ (X = Cl, Br), $[Cu(NTBT)Br]_2[Cu_2Br_6]\cdot CH_3CN$, and the complexes $[Cu(NTBT)Cl]BPh_4(CH_3CN)_2\cdot\frac{1}{2}H_2O$, $[Cu(NTBT)(NO_3)]NO_3\cdot\frac{1}{2}H_2O$, contain trigonal bipyramidal cations while six-coordinate structures are implicated in the systems $[Cu(NTBT)Br_2]\cdot H_2O$ and $[Cu(NTBT)(H_2O)_2](ClO_4)_2\cdot MeOH\cdot H_2O$. The molecular structure of $[Cu(NTBT)(NO_3)]NO_3\cdot\frac{1}{2}H_2O$ has been determined by single crystal X-ray diffractometry. The crystal is monoclinic and belongs to the space group $C2/c$ with $Z = 8$, $a = 24.254(3)$, $b = 14.107(2)$, $c = 16.329(2)$ Å and $\beta = 105.94(1)°$. The complex adopts a distorted trigonal bipyramidal structure (no axial symmetry) with the ligand coordinating in a 'tripod' fashion as an N_4 donor. The fifth ligand is a monodentate nitrate. The mean Cu—N distance is 2.07(3)Å and the Cu—O distance is 1.938(3) Å. A second nitrate oxygen atom is close to the copper centre (Cu—O distance 2.783(4) Å) and may represent a weakly bound sixth ligand. Both infrared and electronic spectral data support the presence of a sixth ligand.

LAURENCE K. THOMPSON, RICHARD G. BALL et JAMES TROTTER. Can. J. Chem. **58**, 1566 (1980).

On a préparé une série de complexes de cuivre(II) avec le ligand mentionné dans le titre; ils se présentent sous des stéréochimies pentacoordonnées à la fois trigonale bipyramidale et pseudo-octaédriques. Les complexes à stéréochimie mixte: $[Cu(NTBT)X]_2[CuX_4]$ (X = Cl, Br), $[Cu(NTBT)Br]_2[Cu_2Br_6]\cdot CH_3CN$ et les complexes $[Cu(NTBT)Cl]BPh_4(CH_3CN)_2\cdot\frac{1}{2}H_2O$, $[Cu(NTBT)(NO_3)]NO_3\cdot\frac{1}{2}H_2O$ contiennent des cations trigonaux bipyramidaux tandis que des structures hexacoordonnées sont impliquées dans les systèmes $[Cu(NTBT)Br_2]\cdot H_2O$ et $[Cu(NTBT)(H_2O)_2](ClO_4)_2\cdot MeOH\cdot H_2O$. On a déterminé la structure moléculaire du $[Cu(NTBT)(NO_3)]NO_3\cdot\frac{1}{2}H_2O$ par diffraction de rayons-X sur un monocristal. Le cristal est monoclinique et appartient au groupe d'espace $C2/c$ avec $Z = 8$, $a = 24.254(3)$, $b = 14.107(2)$, $c = 16.329(2)$ Å et $\beta = 105.94(1)°$. Le complexe adopte une structure déformée trigonale bipyramidale (pas d'axe de symétrie) avec le ligand coordonnée en un "trépied" comme un donneur de N_4. Le 5^e ligand est un nitrate monodentate. La distance moyenne Cu—N est de 2.07(3) Å et la distance Cu—O est de 1.938(3) Å. Un second atome d'oxygène du nitrate est près du centre du cuivre (distance Cu—O 2.783(4) Å) et peut représenter un sixième ligand faiblement lié. Les données spectrales électronique et infrarouge militent en faveur de la présence d'un sixième ligand.

[Traduit par le journal]

Introduction

The coordination chemistry of polyfunctional 'tripod' ligands with just nitrogen donors has received modest attention in recent years. However, for the most part, the ligands studied have been polyamines (1–5). We have recently studied the tetradentate 'tripod' ligand tris(2-benzimidazylmethyl)amine (NTB), which forms predominantly trigonal bipyramidal complexes with cobalt, copper, and zinc salts (6–8). In these systems the three pendant benzimidazole groups coordinate to the metal ion in the equatorial triangular plane. Electron spin resonance spectra of the copper complexes in frozen glass are characteristic of trigonal bipyramidal species with $g_{||} < g_{\perp}$ and low values of $A_{||}$. Similar spectra are observed for copper complexes of trenMe, trenEt (9, 10).

The coordination chemistry of monodentate and bidentate benzothiazoles has shown that in almost all cases involving complexes with first row transition metal ions (M = Fe, Co, Ni, Cu, Zn) the benzothiazole group is N-bonded (11–20). In the present study we have investigated copper complexes of the tris-benzothiazole, tripod, ligand tris(2-benzothiazolylmethyl)amine (NTBT) (Fig. 1) which is the benzothiazole analogue of NTB. This is the first report of coordination complexes of a

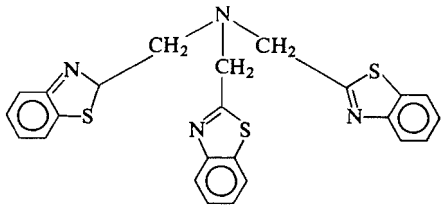


FIG. 1. NTBT.

[1]To whom all correspondence should be addressed.

0008-4042/80/151566-11$01.00/0

©1980 National Research Council of Canada/Conseil national de recherches du Canada

Can. J. Chem. Downloaded from www.nrcresearchpress.com by 210.87.254.42 on 09/05/12
For personal use only.

Can. J. Chem. Downloaded from www.nrcresearchpress.com by 210.87.254.42 on 09/05/12
For personal use only.

tris-benzothiazole ligand of this sort. In all cases NTBT appears to behave as an N_4 donor, similar to NTB, and forms both trigonal bipyramidal and pseudo-octahedral complexes. An X-ray structure confirms the molecular identity of NTBT itself (the ligand has not been previously reported) and the distorted trigonal bipyramidal nature of the nitrate complex $[Cu(NTBT)(NO_3)]NO_3 \cdot \frac{1}{2}H_2O$.

Experimental

Electronic spectra were recorded on a Cary 17 spectrometer, infrared spectra were obtained with a Perkin-Elmer model 283 spectrometer, and electron spin resonance spectra were recorded at −196°C on Varian E-3 and Jeolco ME-3X X-band spectrometers, the magnetic field strength being calibrated with an nmr probe or with Mn(II) in MgO powder. Magnetic susceptibilities were obtained at room temperature by the Faraday method with a Cahn model #7600 Faraday Magnetic Susceptibility system, coupled to a Cahn gram electrobalance and conductance data were obtained with a General Radio Company bridge with impedance comparator and a constant temperature bath adjusted to 25°C. Microanalyses were carried out in part by Canadian Microanalytical Service, Vancouver and by Atlantic Microlab, Inc., Atlanta, GA. Metal analyses were determined by Atomic Absorption with a Varian techtron AA-5, after digestion of the samples in concentrated HNO_3 or aqua-regia.

Tris(2-benzothiazolylmethyl)amine (NTBT)

Nitrilotriacetonitrile (15.0 g, 0.112 mol) and *o*-aminobenzenethiol (42.0 g, 0.336 mol) were mixed and heated slowly up to 190–200°C. At around 100°C an initial reaction occurs with frothing and rapid evolution of ammonia gas. The reaction mixture was maintained at 190–200°C for 7 h during which time ammonia gas was evolved. The product was cooled and the solid extracted into dichloromethane and refluxed with decolourizing charcoal. The solution was filtered and reduced in volume to give buff coloured crystals (28.0 g, 54.6%). Recrystallization was effected from dichloromethane and the product dried under vacuum (mp 191–192°C. Some preliminary softening occurred around 150–155°C, prior to melting, which could be associated with a phase change). *Anal.* calcd. for $C_{24}H_{18}N_4S_3$: C 62.9, H 3.93, N 12.2; found: C 62.7, H 4.00, N 12.2. Infrared spectrum (Nujol mull) 1626, 1596 (νCN) cm^{-1}; nmr ($CDCl_3$) (σ(relative intensity)) 7.94(28), 7.45(28) (complex multiplets, aromatic CH), 4.38(28) (CH_2); mass spectrum, major mass peaks (*m/e* (relative intensities)) 458(2)P, 324(2), 310(100), 283(15), 175(12), 149(78), 148(80), 137(3), 121(4), 108(8), 104(12).

Copper Complexes of NTBT

*$[Cu(NTBT)X]_2[CuX_4]$ (X = Cl, Br) (**I**, **II**)*

NTBT (0.75 g, 0.0016 mol) was dissolved in dichloromethane (50 mL) and excess $CuBr_2$ (3.0 g, 0.013 mol) dissolved in methanol (150 mL). The solutions were warmed and mixed. Dark purple – black crystals formed after a few minutes, which were filtered, washed with methanol and dichloromethane and dried. The product was recrystallized from nitromethane and dried under vacuum.

The chloro-complex was prepared as a lime–green powder by refluxing NTBT with about 10 equiv. of $CuCl_2 \cdot 2H_2O$ in methanol for 4 h. The complex was filtered, washed with methanol and dichloromethane, and dried under vacuum. The mixed solvent method described above did not work consistently for the chloro-complex.

*$[Cu(NTBT)Cl]BPh_4 \cdot (CH_3CN)_2 \cdot \frac{1}{2}H_2O$ (**III**)*

NTBT (0.80 g, 0.0017 mol) and $NaBPh_4$ (0.61 g, 0.0018 mol) were dissolved in acetonitrile (125 mL). $CuCl_2 \cdot 2H_2O$ (0.30 g, 0.0018 mol) was dissolved in CH_3CN (50 mL) and the hot solutions mixed. After standing for 2 h a dirty white precipitate (identified as NaCl) was filtered off and the volume of the green filtrate reduced by half. Golden orange crystals formed, which were filtered, washed, with acetonitrile, and dried under vacuum.

*$[Cu(NTBT)Br]_2[Cu_2Br_6] \cdot CH_3CN$ (buff–brown, **IV**),*
*$[Cu(NTBT)Br_2] \cdot H_2O$ (lime–green, **V**)*

NTBT (0.75 g, 0.0016 mol) was dissolved in dichloromethane (75 mL). $CuBr_2$ (0.37 g, 0.0017 mol) was dissolved in hot methanol (15 mL) and filtered into the NTBT solution. A green coloured solution formed which deposited yellow–green crystals on cooling. The product was recrystallized from acetonitrile to give lime–green crystals which were filtered off, washed with acetonitrile, and dried under vacuum. This product was shown to be $[Cu(NTBT)Br_2] \cdot H_2O$ (**V**).

Attempts to produce $[Cu(NTB)Br]BPh_4$ by a similar route to that used for the analogous chloro-complex were largely unsuccessful (on one occasion golden brown crystals were obtained whose ir and electronic spectra suggested the formation of a tetraphenylborate analogue). In a typical reaction NTBT (0.80 g, 0.0017 mol) and $NaBPh_4$ (0.61 g, 0.0018 mol) were dissolved in hot acetonitrile (125 mL) and $CuBr_2$ (0.40 g, 0.0018 mol) dissolved in hot acetonitrile (50 mL). The two were mixed and stirred at room temperature for 15 min with the formation of a khaki–green solution (no precipitate formed), which was filtered and allowed to stand. Buff–brown crystals formed and were filtered off, washed with acetonitrile, ether, and dried under vacuum (0.5 g). This product was shown to be $[Cu(NTBT)Br]_2[Cu_2Br_6] \cdot CH_3CN$ (**IV**). On standing, the mother liquor deposited lime–green crystals, which were recrystallized from acetonitrile and dried under vacuum. This product was shown to be the same as the lime–green complex **V**. Reduction in volume of the mother liquor produced unreacted $NaBPh_4$.

A further attempt to produce $[Cu(NTBT)Br]BPh_4$, by reacting $[Cu(NTBT)Br]_2[CuBr_4]$ with two equivalents of $NaBPh_4$ in acetonitrile, failed. Buff–brown crystals of **IV** were produced initially followed by lime–green crystals (**V**) from the mother liquor. The attempted isolation of $[Cu(NTBT)Br]^+$ as the tetrafluoroborate or hexafluorophosphate salt also failed.

*$[Cu(NTBT)(NO_3)]NO_3 \cdot \frac{1}{2}H_2O$ (**VI**),*
*$[Cu(NTBT)(H_2O)_2](ClO_4)_2 \cdot H_2O \cdot MeOH$ (**VII**)*

NTBT (0.8 g, 0.0017 mol) was dissolved in dichloromethane (50 mL) and $Cu(NO_3)_2 \cdot 3H_2O$ (0.45 g, 0.0019 mol) dissolved in methanol (50 mL) and the hot solutions mixed. The resulting green solution was heated to remove most of the dichloromethane and allowed to cool. A small quantity of buff crystals was removed by filtration and the green solution reduced in volume by heating on a steam bath to induce crystallization. Bright green crystals formed on standing. Recrystallization was effected from methanol and the product filtered, washed with methanol/ether (50/50), and dried under vacuum.

The perchlorate complex was produced similarly and recrystallized from methanol/TEOF.

Analytical data for the copper complexes are given in Table 1.

*Crystallographic Data for $[Cu(NTBT)(NO_3)]NO_3 \cdot \frac{1}{2}H_2O$ (**VI**)*

Preliminary photographic examination showed the crystals to be monoclinic. The systematic absences, $h + k$ odd for *hkl* and *l* odd for *h0l* indicated the space group to be either *C*2/*c* or *Cc*. As

TABLE I. Analytical and other data

Compound	Colour	Found C	Found H	Found N	Found M	Calcd. C	Calcd. H	Calcd. N	Calcd. M
I, $[Cu(NTBT)Cl]_2[CuCl_4]$	Lime–green	43.6	2.49	8.39	14.0	43.6	2.72	8.48	14.4
II, $[Cu(NTBT)Br]_2[CuBr_4]$	Purple–black	36.5	2.31	7.14	11.5	36.3	2.27	7.06	12.0
III, $[Cu(NTBT)Cl]BPh_4 \cdot (CH_3CN)_2 \cdot \frac{1}{2}H_2O$	Orange–yellow	64.7	4.65	8.65	6.3	64.5	4.65	8.69	6.4
IV, $[Cu(NTBT)Br]_2[Cu_2Br_6] \cdot CH_3CN$	Buff–brown	32.8	2.12	6.52	13.6	32.4	2.11	6.81	13.7
V, $[Cu(NTBT)Br_2] \cdot H_2O$	Lime–green	41.0	2.48	7.99	8.8	41.2	2.86	8.01	9.1
VI, $[Cu(NTBT)(NO_3)]NO_3 \cdot \frac{1}{2}H_2O$	Green	44.2	2.90	12.8	9.4	44.0	2.90	12.8	9.7
VII, $[Cu(NTBT)(H_2O)_2](ClO_4)_2 \cdot MeOH \cdot H_2O$	Green	37.4	3.02	6.99	8.1	37.2	3.47	6.94	7.9

the measured density indicated eight formula units per unit cell the centric space group $C2/c$ was chosen and this choice was confirmed by successful refinement of the structure.

The crystal chosen for data collection was mounted in a non-specific orientation on an Enraf-Nonius CAD-4 diffractometer. The unit cell constants and an orientation matrix were determined from a least-squares fit of 25 carefully centered reflections having $22 < 2\theta < 44°$. The crystal data are:

$C_{24}H_{18}CuN_6O_6S_3 \cdot \frac{1}{2}H_2O$ fw = 655.196

Monoclinic, $a = 24.254(3)$, $b = 14.107(2)$, $c = 16.329(2)$ Å, $\beta = 105.94(1)°$, $V = 5372.2$ Å^3, $Z = 8$ (22°C, MoKα, $\lambda = 0.71073$ Å); $\mu = 10.32$ cm^{-1}, $D_o = 1.637(2)$ g cm^{-3} (by flotation in CH_2Cl_2 and $CHBr_3$), $D_c = 1.62$ g cm^{-3}.

The experimental conditions for data collection and reduction were: MoKα radiation (graphite monochromator); ω–2θ scan with a range of $(0.5 + 0.347 \tan\theta)°$, extended 25% on either side for backgrounds; variable scan speed of 0.7 to 10.1 deg min^{-1} to give $I/\sigma(I) \geq 20$; $\sigma(I) = \{\text{Int} + 4(\text{BGL} + \text{BGH}) + (0.04I)^2\}^{1/2}$; 6367 data measured to $2\theta = 55°$ for $\pm h,k,l$; three reflections were monitored every hour of exposure time for intensity fluctuations and three reflections were recentered every 100 reflections to monitor crystal orientation.

Of the 6367 reflections measured, 3614 had $F > 3\sigma(F)$ and these were used in the structure solution and refinement.

Structure Solution and Refinement[2]

The positional parameters of the Cu atom were determined from a three-dimensional Patterson synthesis and the remaining non-hydrogen atoms were found using three iterations of the usual combination of least-squares refinement and difference Fourier synthesis.

Refinement of atomic parameters was carried out using full-matrix least-squares techniques on F, minimizing the function $\Sigma w(|F_o| - |F_c|)^2$, where $|F_o|$ and $|F_c|$ are the observed and calculated structure factor amplitudes, respectively. The weighting factor w is given by $w = 4F_o^2/\sigma^2(F_o^2)$. The neutral atom scattering factors for all atoms were calculated from the analytical expression for the scattering factor curves (21). The f' and f'' components of anomalous dispersion were those of Cromer and Liberman (22) and were included in the calculations for the Cu and S atoms.

Refinement of all non-hydrogen atoms of the cation and anion, with anisotropic thermal ellipsoids, resulted in agreement factors of $R_1 = \Sigma(||F_o| - |F_c||)/\Sigma F_o = 0.081$ and $R_2 = (\Sigma w(|F_o| - |F_c|)^2/\Sigma w(F_o)^2)^{1/2} = 0.124$. A difference Fourier synthesis revealed 18 peaks corresponding to the H atoms in the cation and a peak at the special position $0y\frac{1}{4}$ which was assigned to the oxygen of a water molecule. In addition to these peaks there was evidence of disorder in the anion. A disorder model was constructed which had one nitrate (population of 0.85) refined anisotropically and a second nitrate, rotated, and slightly displaced from the first (population of 0.15), refined isotropically. Once the second nitrate had refined to its optimum position it was left fixed in subsequent refinement cycles.

The water molecule also appeared to be disordered among several orientations. This disorder could not be adequately defined nor could the hydrogen atom positions be determined, so only the oxygen atom corresponding to the most populated orientation was included in the refinement.

Refinement of the H atoms proceeded satisfactorily except for HC(14) and HC(23) which shifted to unrealistic positions. As a result these two were put in at their calculated positions (C—H 0.95 Å, C sp^2 geometry) and not refined in the last cycles.

In the final cycle 430 variables were refined using 3614 observations to final agreement factors of $R_1 = 0.044$ and $R_2 = 0.060$. The error in an observation of unit weight was 1.62e and the largest parameter shift was 0.8 times its estimated standard deviation. The largest peak in a difference Fourier, calculated from the final structure factors, with an electron density of 0.27 e Å^{-3} and located at (0.025, 0.226, 0.354) was not deemed chemically significant.

The final atomic positional and thermal parameters are given in Tables 2 and 3 while the list of observed and calculated structure factors is presented in Table 4.[3]

Results and Discussion

Characterization of the Ligand

In a previous paper (6) we reported the synthesis of the 'tripod' ligand tris(2-benzimidazylmethyl)amine by the high temperature condensation of nitrilotriacetonitrile with *o*-phenylenediamine. Extension of this reaction to the thermal fusion of nitrilotriacetonitrile and *o*-aminobenzenethiol led to the formation of the trisbenzothiazole analogue, tris(2-benzothiazolylmethyl)amine (NTBT, Fig. 1). This compound, which has not been previously reported in the literature, is characterized by elemental analysis, infrared, nmr, and mass spectral data (see Experimental). In the nmr spectrum a single methylene resonance occurs at 4.38 ppm and two complex multiplets at 7.45 and

[2]The computer programs used include local modifications of the following: full-matrix least-squares, ORFLS by W. R. Busing, K.O. Martin, and H. A. Levy; Patterson and Fourier syntheses, FORDAP by A. Zalkin, functions and errors, ORFFE by W. R. Busing, K. O. Martin, and H. A. Levy; crystal structure illustrations, ORTEP II by C. K. Johnson.

[3]The structure factor table is available, at a nominal charge, from the Depository of Unpublished Data, CISTI, National Research Council of Canada, Ottawa, Ont., Canada K1A 0S2.

Can. J. Chem. Downloaded from www.nrcresearchpress.com by 210.87.254.42 on 09/05/12
For personal use only.

TABLE 2. Atomic positional and anisotropic thermal parameters*

Atom	x	y	z	U_{11}	U_{22}	U_{33}	U_{12}	U_{13}	U_{23}
Cu	1582.4 (2)	2263.0 (4)	2084.4 (3)	37.2 (3)	38.2 (3)	40.0 (3)	5.7 (2)	11.4 (2)	0.1 (2)
S(1)	1324 (1)	4168 (1)	4134 (1)	69 (1)	52 (1)	48 (1)	9 (1)	15 (1)	−13 (1)
S(2)	2304 (1)	4041 (1)	386 (1)	62 (1)	60 (1)	62 (1)	7 (1)	26 (1)	22 (1)
S(3)	−294 (1)	1950 (1)	967 (2)	34 (1)	85 (1)	283 (3)	−3 (1)	4 (1)	−16 (2)
N(1)	1148 (1)	3512 (2)	1705 (2)	34 (2)	43 (2)	44 (2)	5 (2)	9 (2)	−3 (2)
N(2)	1632 (1)	2816 (2)	3310 (2)	43 (2)	41 (2)	40 (2)	5 (2)	14 (2)	−1 (2)
C(1)	1449 (2)	3689 (3)	3236 (3)	41 (2)	43 (2)	44 (2)	−1 (2)	9 (2)	−9 (2)
C(2)	1563 (2)	3126 (3)	4688 (3)	41 (2)	59 (3)	42 (2)	−5 (2)	12 (2)	−7 (2)
C(3)	1709 (2)	2472 (3)	4130 (3)	34 (2)	48 (2)	37 (2)	−1 (2)	12 (2)	−4 (2)
C(4)	1902 (2)	1568 (4)	4419 (3)	59 (3)	51 (3)	45 (3)	2 (2)	19 (2)	1 (2)
C(5)	1942 (2)	1354 (4)	5255 (3)	69 (3)	56 (3)	54 (3)	3 (3)	22 (3)	11 (3)
C(6)	1799 (2)	2013 (4)	5795 (3)	69 (4)	82 (4)	41 (3)	−5 (3)	20 (3)	5 (3)
C(7)	1607 (2)	2891 (4)	5526 (3)	59 (3)	75 (4)	46 (3)	2 (3)	17 (2)	−14 (3)
C(8)	1352 (2)	4201 (3)	2412 (3)	49 (3)	41 (2)	49 (3)	4 (2)	13 (2)	−2 (2)
N(3)	2149 (1)	2910 (2)	1537 (2)	39 (2)	41 (2)	38 (2)	3 (1)	11 (1)	1 (2)
C(9)	1898 (2)	3566 (3)	996 (3)	46 (2)	42 (2)	39 (2)	3 (2)	13 (2)	5 (2)
C(10)	2863 (2)	3292 (3)	877 (3)	49 (3)	51 (3)	54 (3)	0 (2)	20 (2)	3 (2)
C(11)	2707 (2)	2735 (3)	1491 (3)	37 (2)	43 (2)	45 (2)	1 (2)	12 (2)	−2 (2)
C(12)	3099 (2)	2103 (3)	1987 (3)	44 (2)	47 (3)	53 (3)	0 (2)	11 (2)	0 (2)
C(13)	3626 (2)	2007 (4)	1841 (4)	44 (3)	60 (3)	75 (4)	7 (2)	16 (3)	−1 (3)
C(14)	3772 (2)	2533 (4)	1209 (4)	44 (3)	80 (4)	93 (4)	7 (3)	30 (3)	−7 (3)
C(15)	3404 (3)	3185 (5)	734 (4)	62 (4)	82 (4)	80 (4)	−8 (3)	40 (3)	7 (4)
C(16)	1289 (2)	3836 (4)	921 (3)	49 (3)	48 (3)	46 (3)	11 (2)	9 (2)	3 (2)
N(4)	776 (2)	1682 (3)	1682 (3)	39 (2)	53 (2)	108 (4)	−1 (2)	19 (2)	5 (2)
C(17)	388 (2)	2335 (4)	1423 (4)	35 (2)	62 (3)	87 (4)	−1 (2)	15 (2)	3 (3)
C(18)	−46 (3)	801 (5)	1131 (9)	56 (4)	78 (5)	347 (16)	−21 (4)	43 (7)	−12 (7)
C(19)	540 (3)	771 (4)	1549 (6)	49 (3)	56 (4)	221 (9)	−6 (3)	41 (5)	8 (5)
C(20)	817 (3)	−76 (6)	1745 (9)	74 (5)	68 (5)	340 (16)	−6 (4)	81 (7)	29 (7)
C(21)	511 (5)	−900 (7)	1523 (14)	91 (7)	65 (5)	580 (32)	−15 (5)	99 (11)	24 (11)
C(22)	−74 (5)	−860 (8)	1031 (17)	96 (8)	83 (7)	831 (50)	−49 (7)	128 (16)	−64 (15)
C(23)	−356 (4)	−36 (8)	889 (17)	63 (5)	97 (7)	916 (48)	−37 (6)	84 (14)	−83 (16)
C(24)	520 (2)	3350 (4)	1544 (4)	35 (2)	57 (3)	56 (3)	9 (2)	7 (2)	−5 (3)
N(5)	2093 (2)	571 (3)	1906 (3)	47 (2)	41 (2)	83 (3)	3 (2)	16 (2)	−13 (2)
O(1)	2011 (1)	1118 (2)	2493 (2)	58 (2)	40 (2)	51 (2)	12 (1)	12 (1)	1 (1)
O(2)	2347 (2)	−177 (3)	2131 (3)	74 (3)	53 (2)	128 (4)	25 (2)	6 (2)	−18 (2)
O(3)	1903 (2)	811 (3)	1156 (3)	128 (4)	62 (2)	58 (2)	1 (2)	37 (2)	−10 (2)
N(6)	4715 (2)	1104 (4)	4240 (3)	67 (3)	78 (4)	53 (3)	−6 (3)	17 (3)	−11 (3)
O(4)	4349 (2)	842 (4)	3627 (3)	84 (4)	118 (4)	69 (3)	−17 (3)	−2 (3)	−33 (3)
O(5)	4564 (3)	894 (5)	4912 (4)	100 (4)	177 (6)	86 (4)	−1 (4)	27 (3)	1 (4)
O(6)	5152 (3)	1441 (6)	4289 (5)	70 (4)	261 (9)	151 (6)	−77 (5)	−13 (4)	110 (7)
O(7)	0	5039 (5)	2500	176 (7)	82 (4)	137 (6)	0	113 (6)	0

*Estimated standard deviations in this and other tables are given in parentheses and correspond to the least significant digits. The positional parameters are $\times 10^4$ and the thermal parameters are $\times 10^3$. $U_{ij} = B_{ij}/(2\pi^2 a^*_i a^*_j)$ Å^2. The thermal ellipsoid is given by $\exp\{-(B_{11}h^2 + B_{22}k^2 + B_{33}l^2 + 2B_{12}hk + 2B_{13}hl + 2B_{23}kl)\}$.

TABLE 3. Positional ($\times 10^3$) and isotropic thermal ($\times 10^2$) parameters

Atom	x	y	z	U	Atom	x	y	z	U
N(6)′	479	121	413	7	O(4)′	484	177	470	4
O(5)′	509	128	368	14	O(6)′	443	69	404	7
HC(4)	197 (2)	112 (4)	398 (3)	8 (2)	HC(5)	205 (3)	80 (4)	542 (4)	9 (2)
HC(6)	184 (2)	181 (4)	628 (3)	6 (2)	HC(7)	149 (2)	331 (4)	588 (3)	6 (1)
HC(12)	299 (2)	171 (3)	240 (3)	5 (1)	HC(13)	389 (2)	146 (4)	226 (3)	7 (2)
HC(14)	414	244	112	8	HC(15)	346 (2)	355 (3)	38 (3)	5 (1)
HC(20)	124 (2)	−11 (4)	201 (3)	6 (2)	HC(21)	70 (4)	−146 (8)	156 (6)	17 (4)
HC(22)	−21 (4)	−130 (7)	92 (6)	17 (4)	HC(23)	−74	0	52	20
H1C(8)	108 (2)	474 (3)	237 (2)	4 (1)	H2C(8)	166 (2)	441 (3)	240 (3)	5 (1)
H1C(16)	123 (2)	442 (4)	92 (3)	6 (2)	H2C(16)	104 (2)	352 (3)	46 (3)	5 (1)
H1C(24)	36 (2)	367 (4)	112 (3)	7 (2)	H2C(24)	41 (2)	348 (3)	203 (3)	6 (1)

Can. J. Chem. Downloaded from www.nrcresearchpress.com by 210.87.254.42 on 09/05/12
For personal use only.

TABLE 5. Electronic spectra (cm^{-1})*

Compound	*d–d*	Other
I, $[Cu(NTBT)Cl]_2[CuCl_4]$	*a* [13200]9800 *b* [12300]9800	24400 ($CuCl_4^{2-}$,CT)
II, $[Cu(NTBT)Br]_2[CuBr_4]$	*a* [12300]9200 *b* [11400]10200 *c* [11400]10000	18500,16100($CuBr_4^{2-}$,CT) 16900 15800 ($Cu_2Br_6^{2-}$,CT)
III, $[Cu(NTBT)Cl]BPh_4 \cdot (CH_3CN)_2 \cdot \frac{1}{2}H_2O$	*a* [12400]9250 *b* [12500]9500†	
IV, $[Cu(NTBT)Br]_2[Cu_2Br_6] \cdot CH_3CN$	*a* [12300]9100 *b* 9400 *c* 10500	13900
V, $[Cu(NTBT)Br_2] \cdot H_2O$	*a* 10900 *b* {11400}(270),10300(280) *c* 10700(320)	
VI, $[Cu(NTBT)(NO_3)]NO_3 \cdot \frac{1}{2}H_2O$	*a* 11800[9100] *b* 12600(135)	
VII, $[Cu(NTBT)(H_2O)_2](ClO_4)_2 \cdot MeOH \cdot H_2O$	*a* 15000,9500 *b* [14100](99),11800(112)	
$K_2[Cu_2Br_6]$	*a* 13200[11400] *b* [10800](127),9200(133)	23600(1520),15800(1060)(CT)

*Labels mean the following: *a*, mull transmittance spectrum (room temperature); *b*, solution in nitromethane; *c*, solution in acetonitrile; [ ] shoulder, ( ) molar extinction coefficient.
†Solution decomposes on standing.

7.94 ppm, typical of 2-substituted benzothiazoles. X-ray crystallography confirms the molecular identity of NTBT in the complex $[Cu(NTBT)(NO_3)]\ NO_3 \cdot \frac{1}{2}H_2O$.

Characterization of the Complexes

Ligand Field and Electron Spin Resonance Spectra

The mixed stereochemistry complexes $[Cu(NTBT)X]_2[CuX_4]$ (X = Cl, Br) (**I**, **II**) have solid state electronic spectra which comprise *d–d* bands associated with trigonal bypyramidal copper centres, $[Cu(NTBT)X]^+$ (1, 4, 7, 8), and also charge transfer absorptions associated with the tetrahalogenocuprate anions (23) (Table 5). *d–d* bands associated with these anions could not be clearly discerned in the solid state spectra, but would probably occur below 9000 cm^{-1} (24). The chloro-complex $[Cu(NTBT)Cl](BPh_4) \cdot (CH_3CN)_2 \cdot \frac{1}{2}H_2O$ (**III**) exhibits a solid state spectrum similar to compound **I**, associated with the trigonal bipyramidal cation $[Cu(NTBT)Cl]^+$.

Many attempts to synthesize the analogous bromide complex, $[Cu(NTBT)Br](BPh_4)$, were unsuccessful. In the reaction between copper bromide, NTBT, and sodium tetraphenylborate in acetonitrile two products were obtained. Initially a buff–brown crystalline solid (**IV**) was obtained followed by lime–green crystals (**V**). The buff–brown product (**IV**) has a major absorption at 9100 cm^{-1} with a shoulder at 12 300 cm^{-1} in its solid spectrum, suggesting the presence of the cation $[Cu(NTBT)Br]^+$. No other *d–d* or charge transfer absorptions were apparent in the spectrum below 25 000 cm^{-1}. The lime–green product (**V**) exhibits just one major absorption in the solid state at 10 900 cm^{-1}. The absence of a high energy shoulder in this case probably signals the presence of a six-coordinate species. A neutral derivative involving two coordinated bromine atoms is supported by other data. Reaction of $[Cu(NTBT)Br]_2[CuBr_4]$ (**II**) with sodium tetraphenylborate in acetonitrile led to the same mixture of products.

Compound **IV** appears to contain the five-coordinate cation $[Cu(NTBT)Br]^+$, but must also have a metal-containing anion (Table 1). A clue as to the identity of this anion comes from the solution spectrum of $[Cu(NTBT)Br]_2[CuBr_4]$ (**II**) in acetonitrile. This compound has a dark purple – black colour in the solid state but dissolves in acetonitrile to give a green solution. The electronic spectrum of this solution (Fig. 2*A*) has a *d–d* absorption at 10 000 cm^{-1}, with a high energy shoulder at 11 400 cm^{-1}, and an intense charge transfer band at 15 800 cm^{-1}. No absorptions due to $[CuBr_4]^{2-}$ are observed. The charge transfer absorption at 15 800 cm^{-1} corresponds very closely with an equivalent band observed for $[Cu_2Br_6]^{2-}$ in solution in glacial acetic acid (24) and in acetonitrile (Table 5). It is suggested that $[Cu(NTBT)Br]_2[CuBr_4]$ is undergoing an equilibrium disproportionation in acetonitrile according to the following

Can. J. Chem. Downloaded from www.nrcresearchpress.com by 210.87.254.42 on 09/05/12
For personal use only.

Can. J. Chem. Downloaded from www.nrcresearchpress.com by 210.87.254.42 on 09/05/12
For personal use only.

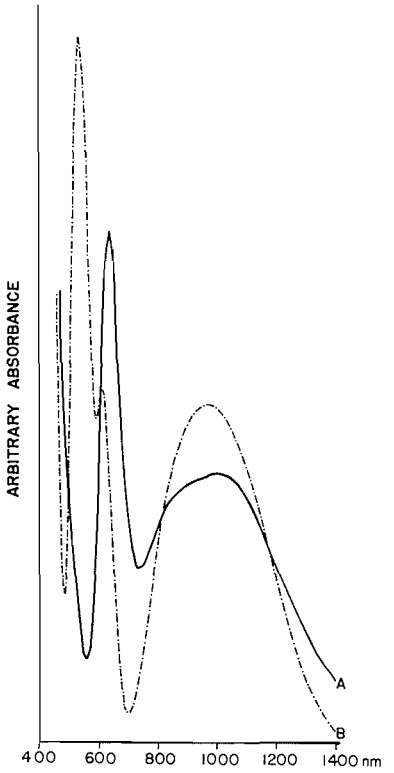


FIG. 2. Electronic spectrum of $[Cu(NTBT)Br]_2[CuBr_4]$ (*A*) in acetonitrile; (*B*) with added Br^-.

equation:

$$2[Cu(NTBT)Br]_2[CuBr_4] \quad \text{(purple)} \rightleftharpoons[CH_3CN] [Cu(NTBT)Br_2] + 2[Cu(NTBT)Br]^+ + [Cu_2Br_6]^{2-} \quad \text{(green)}$$

Addition of bromide ion to the green solution causes an immediate colour change to purple and a concomitant change in the spectrum (Fig. 2*B*) revealing the loss of $[Cu_2Br_6]^{2-}$ and the appearance of charge transfer bands associated with $[CuBr_4]^{2-}$. The absorption envelope around 10 000 cm^{-1}, which must contain components associated with $[Cu(NTBT)Br]^+$, $[Cu(NTBT)Br_2]$, and $[Cu_2Br_6]^{2-}$ increases in intensity on addition of bromide, with the loss of the shoulder at 11 400 cm^{-1}, and on further addition of bromide approaches the absorption energy associated with $[Cu(NTBT)Br_2]\cdot H_2O$. Addition of excess bromide causes enhancement of the bands associated with $[CuBr_4]^{2-}$ and a weakening of the absorption around 10 000 cm^{-1} indicating displacement of NTBT. A similar situation is observed in nitromethane.

The mixture of products (**IV** and **V**) obtained in these reactions in acetonitrile can be explained by the above equation. The lime-green crystalline product (**V**) is identified as $[Cu(NTBT)Br_2]\cdot H_2O$, a neutral six-coordinate species while compound **IV** is identified as $[Cu(NTBT)Br]_2[Cu_2Br_6]\cdot CH_3CN$. Since no charge transfer band is observed for $[Cu_2Br_6]^{2-}$ in the solid state (24) (Table 5) it is no surprise that only *d–d* bands are observed in the solid state spectrum of this compound.

The solution spectra of compound **IV** do not exhibit any charge transfer bands attributable to $[Cu_2Br_6]^{2-}$ in either acetonitrile or nitromethane. In acetonitrile the only absorption is a symmetrical single band at 10 500 cm^{-1}, corresponding almost exactly with the spectrum of $[Cu(NTBT)Br_2]\cdot H_2O$ (**V**) and it is perhaps no coincidence that this species is obtained as the sole product on recrystallization of $[Cu(NTBT)Br]_2[Cu_2Br_6]$ from acetonitrile. Although no spectral evidence exists for the presence of $[Cu_2Br_6]^{2-}$ in a nitromethane solution of **IV**, the band at 13 900 cm^{-1} is perhaps indicative of a partially solvated species derived from $[Cu_2Br_6]^{2-}$. On addition of bromide ion this band and the absorption at 9 400 cm^{-1}, due to $[Cu(NTBT)Br]^+$, rapidly coalesce with the formation of a single absorption at 10 600 cm^{-1}, followed by the appearance of charge transfer bands due to $[CuBr_4]^{2-}$.

Solution spectra of $[Cu(NTBT)Cl]_2[CuCl_4]$ (**I**) in acetonitrile and nitromethane exhibit bands attributable to $[Cu(NTBT)Cl]^+$ but no charge transfer bands are observed which can be associated with $[CuCl_4]^{2-}$ or $[Cu_2Cl_6]^{2-}$ (24). Presumably the major components in these solutions are [Cu(NTBT)Cl]Cl and solvated $CuCl_2$.

The solid state spectrum of the nitrate complex **VI** exhibits a major absorption at 11 800 cm^{-1} with a low energy shoulder, perhaps more typical of a six-coordinate derivative. X-ray structural data (see Discussion) indicate a highly distorted five-coordinate structure in which the close approach of a second oxygen atom from the coordinated nitrate group can possibly be considered as a weakly bound sixth ligand. In solution in nitromethane a single absorption is observed at 12 600 cm^{-1}, associated with a 1:1 electrolyte (see conductance discussion). A six-coordinate solution species with, e.g., a CuN_4O_2 chromophore would be expected to absorb at somewhat higher energy and so the nitromethane solution species is assumed to be $[Cu(NTBT)(NO_3)]^+$.

The solid state spectrum of the perchlorate complex reveals two quite widely separated bands at 15 000 and 9 500 cm^{-1}. The high energy absorption and the large separation of the two components

TABLE 6. Electron spin resonance data*

Compound		⟨g⟩	$g_{\|}$	$g_{\perp}$	$\|A_{\perp}\|$†	$g(\Delta M=2)$
I, $[Cu(NTBT)Cl]_2[CuCl_4]$	*a*	2.15				
	b	2.129				4.00
II, $[Cu(NTBT)Br]_2[CuBr_4]$	*a*	2.13				
	b	2.121				3.97
III, $[Cu(NTBT)Cl]BPh_4 \cdot (CH_3CN)_2 \cdot \frac{1}{2}H_2O$	*a*		2.22	2.12		
	b			2.191	63	
IV, $[Cu(NTBT)Br]_2[Cu_2Br_6] \cdot CH_3CN$	*a*		2.21	2.05		
	b	2.136				3.99
V, $[Cu(NTBT)Br_2] \cdot H_2O$	*a*		2.20	2.04		
	b	2.137				
	c			2.23	120	
VI, $[Cu(NTBT)(NO_3)]NO_3 \cdot \frac{1}{2}H_2O$	*a*	2.10				
	b			2.250	120	
VII, $[Cu(NTBT)(H_2O)_2](ClO_4)_2 \cdot MeOH \cdot H_2O$	*a*		2.24	2.12		
	b‡			2.250	120	

*Labels mean the following: *a*, powder spectrum (room temperature); *b*, frozen nitromethane glass (77 K); *c*, frozen methanol glass (77 K).
†Hyperfine coupling constants in units 10^{-4} cm^{-1}
‡$g_{\|} = 1.94$, $A_{\|} = 68 \times 10^{-4}$ cm^{-1} (estimated).

suggests a six-coordinate solid state structure (25) involving two coordinated water molecules. In nitromethane an absorption at 11 800 cm^{-1} with a high energy shoulder is indicative of a trigonal bipyramidal solution species involving either coordinated water or solvent.

In all the systems studied *d–d* absorptions associated with five- or six-coordinate complexes are comparable in energy with those observed for copper complexes of NTB (7, 8), in which the tripod ligand acts as an N_4 donor. This, combined with the absence of any absorption which could be associated with Cu–S interactions, suggests that NTBT is acting as a nitrogen donor in all cases. Confirmation of this, of course, is evident from the X-ray structure of $[Cu(NTBT)(NO_3)]NO_3 \cdot \frac{1}{2}H_2O$.

The 'tripod' ligand tris(2-benzimidazylmethyl)amine (NTB), which is structurally similar to NTBT, forms copper complexes with both five-coordinate trigonal bipyramidal and pseudo-octahedral stereochemistries (7, 8). Powder esr spectra recorded at X-band frequency and ambient temperature for the pseudo-octahedral systems in general exhibit three *g* values, while only one signal is observed in the powder spectra of the five-coordinate derivatives. In frozen methanol glass (77 K) all the copper/NTB complexes exhibit spectra typical of trigonal bipyramidal species in which $g_{\|} < g_{\perp}$ and low values of $A_{\|}$ are observed (7, 9, 10).

Broad isotropic resonances are observed in the powder spectra of the mixed stereochemistry complexes $[Cu(NTBT)X]_2[CuX_4]$ (X = Cl, Br) (**I**, **II**) and also in the case of the nitrate complex $[Cu(NTBT)(NO_3)]NO_3 \cdot \frac{1}{2}H_2O$ (Table 6). The bromo-complex $[Cu(NTBT)Br]_2[Cu_2Br_6] \cdot CH_3CN$ has one major resonance at $g = 2.16$ with a weak additional feature at $g = 2.06$ which distinguishes this system from bromo-complex **II**. It is clear that in these systems intermolecular interactions are responsible for the exchange broadening apparent in the spectra. For the remaining complexes $g_{\|}$ and $g_{\perp}$ have been estimated, but again exchange broadening gives spectra which provide little definitive structural information.

In frozen glass at 77 K the esr spectra of some of these complexes are much more informative. The chloro-complex **III** has a typical trigonal bipyramidal spectrum in the $\perp$ region with a very low value of the hyperfine coupling constant (63×10^{-4} cm^{-1}) (Fig. 3). The lowest value previously reported for a trigonal bipyramidal system of this sort was for $[Cu(Et_6tren)Cl]Cl$ ($A_{\perp} = 79 \times 10^{-4}$ cm^{-1}) (9). No clearly defined features appear in the parallel region of the spectrum. A similar situation exists in the cases of the nitrate and perchlorate complexes (**VI**, **VII**). Typical trigonal bipyramidal features are observed in the $\perp$ region of the spectra with much larger values of $A_{\perp}$. Very weak features occur in the parallel region and only in the case of the perchlorate complex could an estimate of $g_{\|}$ and $A_{\|}$ be made. The close similarity between the spectra of these two systems suggests structurally similar species in the frozen glass.

The six-coordinate bromo-complex $[Cu(NTBT)Br_2] \cdot H_2O$ (**V**) exhibits a broad single

Can. J. Chem. Downloaded from www.nrcresearchpress.com by 210.87.254.42 on 09/05/12
For personal use only.

Can. J. Chem. Downloaded from www.nrcresearchpress.com by 210.87.254.42 on 09/05/12
For personal use only.

resonance in nitromethane at 77 K but in methanol the spectrum resembles that of a trigonal bipyramidal species. Copper hyperfine features are observed only in the $\perp$ region of the spectrum and it appears that in methanol at 77 K dissociation occurs to produce a five-coordinate species, possibly $[Cu(NTBT)Br]^+$. The complexes $[Cu(NTBT)X]_2[CuX_4]$ (X = Cl, Br) (**I**, **II**) exhibit essentially broad single resonances in nitromethane at 77 K with weak copper hyperfine splitting on the low field side of the resonance, suggesting the presence of a five-coordinate species. The weakness of these features prevented an estimate of g and A. It is evident that exchange effects in the glass are responsible for these largely structureless spectra. A similar situation is observed in the case of the complex $[Cu(NTBT)Br]_2[Cu_2Br_6]\cdot CH_3CN$ (**IV**). An examination of the half field region reveals signals at $g \simeq 4$ for compounds **I**, **II**, and **IV** suggesting the presence of spin-coupled dimeric species in all cases. For compound **IV** the antiferromagnetically coupled anion $[Cu_2Br_6]^{2-}$ could be responsible for the $g \simeq 4$ signal while in compound **II** it has already been shown that $[Cu_2Br_6]^{2-}$ is present in nitromethane. While it is not obvious from the room temperature electronic spectrum of $[Cu(NTBT)Cl]_2[CuCl_4]$ (**I**) in nitromethane that, e.g., $[Cu_2Cl_6]^{2-}$ is present, the appearance of a $g \simeq 4$ signal in the frozen glass esr spectrum does suggest the presence of an antiferromagnetically coupled species like $[Cu_2Cl_6]^{2-}$.

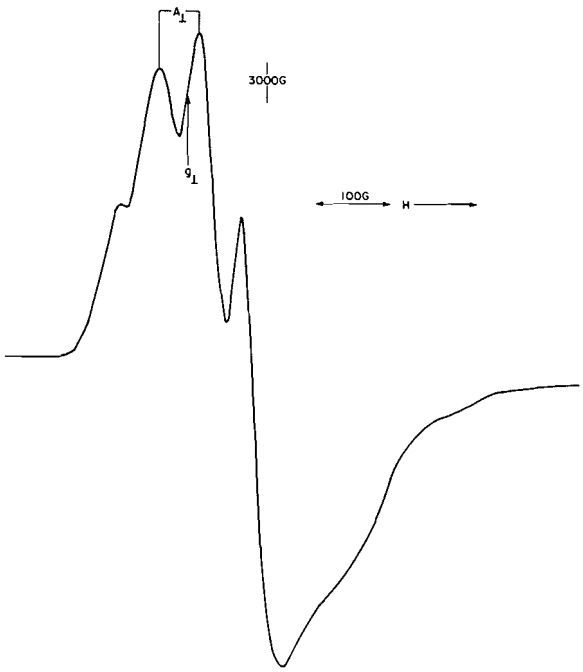


FIG. 3. Electron spin resonance spectrum (X-band) of frozen solution of $[Cu(NTBT)Cl]BPh_4\cdot(CH_3CN)_2\cdot\frac{1}{2}H_2O$ in nitromethane at 77 K.

Infrared Spectra

A comparison of compounds **I**–**V** allows the assignment of bands associated with metal–halogen and metal–nitrogen stretching (Table 7). Single absorptions are observed for ν(M—X) in the trigonal bipyramidal cations $[Cu(NTBT)X]^+$ (X = Cl, Br) while in the case of the pseudo-octahedral complex $[Cu(NTBT)Br_2]\cdot H_2O$ (**V**) two bands associated with Cu—Br stretching can be observed, consistent with a *cis*-structure. Absorptions at 272 (**I**) and 220 cm^{-1} (**II**) are assigned to Cu—X stretching in $[CuCl_4]^{2-}$ and $[CuBr_4]^{2-}$ respectively (26, 27), while for **IV** two absorptions at 240 (sh) and 225 cm^{-1} are associated with Cu—Br stretching in $[Cu_2Br_6]^{2-}$ (24).

Combination bands ($\nu_1 + \nu_4$) due to nitrate absorptions in **VI** occur at 1755, 1736, and 1719 cm^{-1}. The band at 1736 cm^{-1} can be associated with ionic nitrate while the other two bands are due to a coordinated nitrate group. The separation of these two bands is usually a reasonable indication of the bonding mode of such a group (28) and a difference of 36 cm^{-1} is large enough to suggest a bidentate nitrate. In this case, however, X-ray data formally define the coordinated nitrate as monodentate but weak involvement of a second nitrate oxygen to the copper centre is suggested from infrared data. In the perchlorate complex (**VII**) the ν_3 perchlorate absorption appears as a broad strong single band indicating the presence of ionic perchlorate and weak absorptions at 3580 and 3460 cm^{-1} are associated with coordinated water.

The complex $[Cu(NTBT)Cl]BPh_4(CH_3CN)_2\cdot\frac{1}{2}H_2O$ (**III**) has doublet absorptions at 2248, 2260 and 2290, 2300 cm^{-1} which are associated with lattice bound acetonitrile. No evidence exists for coordinated acetonitrile. Similar, but very weak, absorptions are found in the bromo-complex **IV** (29).

Magnetism and Conductance

Magnetic moments (Table 8) for compounds **I**–**III**, **V**–**VII** are normal for Cu(II) complexes of this sort. However, the moment associated with $[Cu(NTBT)Br]_2[Cu_2Br_6]\cdot CH_3CN$ falls below the spin only value at room temperature and is consistent with the presence of the antiferromagnetically coupled anion $[Cu_2Br_6]^{2-}$ (30). The room temperature moment of $KCuBr_3$ lies below the spin only value ($\mu_{eff(295\ K)} = 1.52$ BM) and so would be responsible for reducing the net moment of compound **IV**.

Conductance data are reported for several com-

TABLE 7. Infrared data (cm^{-1})

Compound	ν(CuX)	ν(CuN)	Other
I, $[Cu(NTBT)Cl]_2[CuCl_4]$	292 272($CuCl_4^{2-}$)	321	
II, $[Cu(NTBT)Br]_2[CuBr_4]$	256 220($CuBr_4^{2-}$)	312	
III, $[Cu(NTBT)Cl]BPh_4 \cdot (CH_3CN)_2 \cdot \frac{1}{2}H_2O$	309	325	2300,2290,2260,2248(CH_3CN)
IV, $[Cu(NTBT)Br]_2[Cu_2Br_6] \cdot CH_3CN$	255 240sh,225($Cu_2Br_6^{2-}$)	314	
V, $[Cu(NTBT)Br_2] \cdot H_2O$	248sh,241	326	
VI, $[Cu(NTBT)(NO_3)]NO_3 \cdot \frac{1}{2}H_2O$		326	311,ν(CuO) 1755,1736,1719($\nu_1 + \nu_4, NO_3^-$)
VII, $[Cu(NTBT)(H_2O)_2](ClO_4)_2 \cdot MeOH \cdot H_2O$		325	1100(ν_3, ClO_4^-)

TABLE 8. Magnetic moment and conductance data

Compound	μ(BM) (room temperature)	$\Lambda_M(MeNO_2)$ (Ω^{-1} mol^{-1} cm^2)
I, $[Cu(NTBT)Cl]_2[CuCl_4]$	1.90	
II, $[Cu(NTBT)Br]_2[CuBr_4]$	1.94	
III, $[Cu(NTBT)Cl]BPh_4 \cdot (CH_3CN)_2 \cdot \frac{1}{2}H_2O$	1.75	40
IV, $[Cu(NTBT)Br]_2[Cu_2Br_6] \cdot CH_3CN$	1.62	
V, $[Cu(NTBT)Br_2] \cdot H_2O$	1.84	36
VI, $[Cu(NTBT)(NO_3)]NO_3 \cdot \frac{1}{2}H_2O$	1.83	73
VII, $[Cu(NTBT)(H_2O)_2](ClO_4)_2 \cdot MeOH \cdot H_2O$	1.79	130

pounds (Table 8). $[Cu(NTBT)(H_2O)_2](ClO_4)_2 \cdot H_2O \cdot MeOH$ (**VII**) behaves as a 1:2 electrolyte in nitromethane. The lime-green neutral complex $[Cu(NTBT)Br_2] \cdot H_2O$ (**V**) has a low conductance, although it is largely undissociated. The low value associated with $[Cu(NTBT)Cl]BPh_4 \cdot (CH_3CN)_2 \cdot \frac{1}{2}H_2O$ (**III**) is consistent with a 1:1 electrolyte involving the large tetraphenylborate anion (31) and $[Cu(NTBT)(NO_3)]NO_3 \cdot \frac{1}{2}H_2O$ (**VI**) appears to be a 1:1 electrolyte also in nitromethane.

Structure Description

A perspective view of the cation, including the atom numbering scheme, is shown in Fig. 4. The Cu atom is coordinated to the four N atoms of NTBT and to an oxygen atom (O(1)) of one of the nitrate anions to form a distorted trigonal bipyramidal structure, with N(1) and O(1) axial. The ligand NTBT coordinates to the Cu atom in a tripod fashion similar to that observed in a series of Cu–tren and Cu–trenMe complexes (2, 3, 32, 33), and Cu–NTB complexes (7, 8). The 'backbone' of the NTBT ligand is a close structural analogue to tren, trenMe, and NTB and it is not surprising that a similar coordinating geometry should be adopted in the Cu complexes of these ligands.

The distortion from a regular trigonal bipyramid in the copper coordination polyhedron occurs in two ways. The bond angles N(1)—Cu—N(2), N(1)—Cu—N(3), and N(1)—Cu—N(4) are all less than 84°, indicating a tetrahedral distortion with the copper atom displaced below the equatorial plane. This sort of distortion is common in other systems

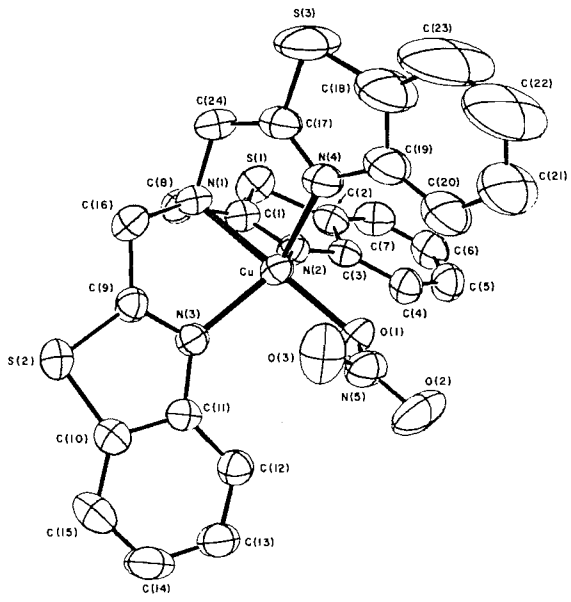


FIG. 4. Perspective view of the cation showing the atom numbering scheme. The atoms are represented by 50% probability thermal ellipsoids and the hydrogens have been omitted for clarity.

Can. J. Chem. Downloaded from www.nrcresearchpress.com by 210.87.254.42 on 09/05/12
For personal use only.

Can. J. Chem. Downloaded from www.nrcresearchpress.com by 210.87.254.42 on 09/05/12
For personal use only.

TABLE 9. Selected interatomic distances and angles

(*a*) Coordination sphere and anion

Atoms	Distance (Å)	Atoms	Angle (deg)
Cu—N(1)	2.059(3)	N(1)—Cu—N(2)	82.0(1)
Cu—N(2)	2.120(3)	N(1)—Cu—N(3)	80.6(1)
Cu—N(3)	2.048(3)	N(1)—Cu—N(4)	83.2(1)
Cu—N(4)	2.056(4)	N(2)—Cu—N(3)	112.2(1)
Cu—O(1)	1.938(3)	N(2)—Cu—N(4)	104.5(2)
Cu—O(3)	2.783(4)	N(3)—Cu—N(4)	137.0(2)
		O(1)—Cu—N(1)	177.2(1)
N(5)—O(1)	1.288(5)	O(1)—Cu—N(2)	95.5(1)
N(5)—O(2)	1.227(5)	O(1)—Cu—N(3)	99.3(1)
N(5)—O(3)	1.232(5)	O(1)—Cu—N(4)	98.7(1)
		O(1)—Cu—O(3)	51.0(1)
N(6)—O(4)	1.199(6)	Cu—N(1)—C(8)	107.0(2)
N(6)—O(5)	1.284(7)	Cu—N(1)—C(16)	107.6(3)
N(6)—O(6)	1.145(7)	Cu—N(1)—C(24)	109.7(3)
N(6)—N(6)'*	0.324(6)	O(1)—N(5)—O(2)	117.4(5)
N(6)'—O(4)'	1.199	O(1)—N(5)—O(3)	118.9(4)
N(6)'—O(5)'	1.173	O(2)—N(5)—O(3)	123.7(5)
N(6)'—O(6)'	1.111	Cu—N(3)/O(1)—O(3)	63.9(2)
O(3)—N(3)	3.051(5)	Cu—N(4)/O(1)—O(3)	75.9(2)
O(3)—C(11)	3.300(6)		
O(3)—C(12)	3.379(6)		
O(3)—N(4)	3.318(6)		
O(3)—C(19)	3.535(7)		
O(3)—C(20)	3.289(9)		

*The primed atoms are those of the disordered anion not refined in the final cycles.

(*b*) Within NTBT ligand

Atoms	Distance (Å)	Atoms	Distance (Å)	Atoms	Distance (Å)
N(1)—C(8)	1.487(6)	N(1)—C(16)	1.485(6)	N(1)—C(24)	1.491(6)
N(2)—C(3)	1.389(5)	N(3)—C(11)	1.397(5)	N(4)—C(19)	1.399(7)
S(1)—C(2)	1.740(5)	S(2)—C(10)	1.732(5)	S(3)—C(18)	1.724(8)
C(1)—S(1)	1.717(4)	C(9)—S(2)	1.719(4)	C(17)—S(3)	1.706(5)
C(1)—N(2)	1.302(5)	C(9)—N(3)	1.308(5)	C(17)—N(4)	1.301(6)
C(1)—C(8)	1.488(6)	C(9)—C(16)	1.498(6)	C(17)—C(24)	1.469(8)

Atoms	Angle (deg)	Atoms	Angle (deg)	Atoms	Angle (deg)
N(1)—C(8)—C(1)	108.6(4)	N(1)—C(16)—C(9)	107.8(4)	N(1)—C(24)—C(17)	110.3(4)
C(1)—S(1)—C(2)	90.0(2)	C(9)—S(2)—C(10)	89.6(2)	C(17)—S(3)—C(18)	88.6(3)
S(1)—C(1)—N(2)	115.4(3)	S(2)—C(9)—N(3)	115.6(3)	S(3)—C(17)—N(4)	116.4(4)
C(1)—N(2)—C(3)	111.8(3)	C(9)—N(3)—C(11)	111.5(4)	C(17)—N(4)—C(19)	111.8(4)

involving tren and trenMe (2, 3, 32, 33). Also the ligand does not possess C_3 crystallographic symmetry and is bent back with a large equatorial angle N(3)—Cu—N(4) of 137°. The other two equatorial angles are, as a consequence, significantly less than 120°. Although in the tren complex, [Cu(tren)NCS]NCS, a large equatorial angle of 130° is observed (2), angles closer to 120° are observed in other tren complexes, e.g., $[Cu_2(tren)_2X_2](BPh_4)_2$ (X = Cl, NCO, CN) (32, 33). In the case of the complex [Cu(trenMe)Br]Br (3) the ligand exhibits C_3 crystallographic symmetry, perhaps indicating the presence of a steric constraint due to the bulk of the N-methyl groups.

The Cu—N distances in $[Cu(NTBT)(NO_3)]\text{-}NO_3\cdot\frac{1}{2}H_2O$ (Table 9) range from 2.048(3) to 2.120(3) Å and do not differ significantly from the mean value of 2.07(3) Å. These distances are comparable to the Cu—N distances observed in the tren and trenMe complexes (2, 3, 32, 33) and are representative of normal Cu—N bond lengths.

The internal geometry of the NTBT ligand shows no unusual features, with the bond distances and angles of the benzothiazole rings similar to values

Can. J. Chem. Downloaded from www.nrcresearchpress.com by 210.87.254.42 on 09/05/12
For personal use only.

determined in a crystal structure of a Cu complex of another ligand containing these groups (34). The mean distances and angles within the phenyl rings are: for C(2)—C(7), 1.38(2) Å, 120(2)°; for C(10)—C(15), 1.39(2) Å, 120(1)°; for C(18)—C(23), 1.38(3) Å, 120(1)°. The C—H distances range from 0.7(1) to 1.10(5) Å with appropriate geometries for sp^2 and sp^3 C atoms.

When bonding to a single metal atom a nitrate group may behave as a unidentate ligand or a symmetrical or unsymmetrical bidentate ligand. In a review of metal–nitrate bonding (35) it is suggested that the nitrate is to be considered unidentate if the difference in the two closest metal–oxygen distances exceeds 0.7 Å. In the present complex the difference between Cu—O(1) and Cu—O(3) is 0.84(5) Å. While this exceeds the limit suggested by Addison *et al.* (35) it is not unambiguous, from the structural information, that the nitrate is unidentate.

One of the major distortion features of the structure is the large equatorial angle N(3)—Cu—N(4) of 137°. Oxygen atom O(3) is within 3.3 Å of N(3) and N(4) with N(3) and N(4) lying 1.82 and 1.98 Å respectively on opposite sides of the mean plane of Cu—O(1)—O(2)—O(3)—N(5). The nitrate plane therefore approximately bisects the N(3)—Cu—N(4) angle, being somewhat closer to N(3). If this structural perturbation can be considered to be the result of a close approach of oxygen O(3) to the copper centre, then a decision as to whether it should be considered a ligand may be difficult to make on the basis of X-ray data alone. According to Addison *et al.* (35) a decrease in the Cu—O(3) separation of only 0.14 Å would qualify the nitrate as a bidentate ligand. It is evident that the bending back of the N(3)—Cu—N(4) framework could be carried to a logical conclusion in which the N(3)—Cu—N(4) angle approached 180° and resulted in a pseudo-octahedral species. Under these circumstances the ambiguous structural results may be clarified by examining the spectroscopic properties of the complex. In this case there is evidence, *vide supra*, that the nitrate is acting as a pseudo-bidentate ligand, with a weak interaction from O(3), making the Cu complex almost six-coordinate.

The nitrate anions and the water molecule may be involved in a weak hydrogen bonding network, with the closest distances of approach being 2.57 Å between O(7) and O(4) and 2.96 Å between O(7) and O(5)′.

Acknowledgments

We thank the Natural Sciences and Engineering Research Council of Canada for financial support of this work and the University of British Columbia Computing Centre for assistance.

1. M. Ciampolini and N. Nardi. Inorg. Chem. **5**, 41 (1966).
2. P. C. Jain and E. C. Lingafelter. J. Am. Chem. Soc. **89**, 724 (1967).
3. M. Di Vaira and P. L. Orioli. Acta Crystallogr. Sect. B, **24**, 595 (1968).
4. G. Albertin, E. Bordignon, and A. A. Orio. Inorg. Chem. **14**, 1411 (1975).
5. R. Barbucci and A. Mastroianni. Inorg. Chim. Acta, **27**, 109 (1978).
6. L. K. Thompson, B. S. Ramaswamy, and E. A. Seymour. Can. J. Chem. **55**, 878 (1977).
7. L. K. Thompson, B. S. Ramaswamy, and R. D. Dawe. Can. J. Chem. **56**, 1311 (1978).
8. A. W. Addison, J. Reedijk, and L. K. Thompson. Unpublished work.
9. R. Barbucci and M. J. M. Campbell. Inorg. Chim. Acta, **15**, L15 (1975).
10. R. Barbucci, A. Bencini, and D. Gatteschi. Inorg. Chem. **16**, 2117 (1977).
11. M. Goodgame and M. J. Weeks. J. Chem. Soc. A, 1156 (1966).
12. R. A. Ford, G. Halkyard, and A. E. Underhill. Inorg. Nucl. Chem. Lett. **4**, 507 (1968).
13. E. J. Duff, M. N. Hughes, and K. J. Rutt. J. Chem. Soc. A, 2354 (1968).
14. N. N. Y. Chan, M. Goodgame, and M. J. Weeks. J. Chem. Soc. A, 2499 (1968).
15. E. J. Duff, M. N. Hughes, and K. J. Rutt. J. Chem. Soc. A, 2101 (1969).
16. M. J. M. Campbell, D. W. Card, and R. Grzeskowiak. Inorg. Nucl. Chem. Lett. **5**, 39 (1969).
17. M. J. M. Campbell, D. W. Card, R. Grzeskowiak, and M. Goldstein. J. Chem. Soc. A, 672 (1970).
18. S. E. Livingston and J. D. Nolan. J. Chem. Soc. Dalton, 218 (1972).
19. D. R. Lorenz, T. M. Barbara, and J. R. Wasson. Inorg. Nucl. Chem. Lett. **12**, 65 (1976).
20. J. C. T. Rendell and L. K. Thompson. Can. J. Chem. **57**, 1 (1979).
21. International Tables for X-ray Crystallography. Vol. IV. The Kynoch Press, Birmingham, England. 1974. p. 99.
22. D. T. Cromer and D. Liberman. J. Chem. Phys. **53**, 1891 (1970).
23. B. D. Bird and P. Day. J. Chem. Phys. **49**, 392 (1968).
24. R. A. Howald and D. P. Keeton. Spectrochim. Acta, **22**, 1211 (1966).
25. E. D. McKenzie. J. Chem. Soc. A, 3095 (1970).
26. A. Sabatini and L. Sacconi. J. Am. Chem. Soc. **86**, 17 (1964).
27. D. M. Adams and P. J. Lock. J. Chem. Soc. A, 620 (1967).
28. A. B. P. Lever, E. Mantovani, and B. S. Ramaswamy. Can. J. Chem. **49**, 1957 (1971).
29. R. A. Walton. Spectrochim. Acta, **21**, 1795 (1965).
30. M. Inoue, M. Kishita, and M. Kubo. Inorg. Chem. **6**, 900 (1967).
31. W. J. Geary. Coord. Chem. Rev. **7**, 81 (1971).
32. D. M. Duggan and D. N. Hendrickson. Inorg. Chem. **13**, 1911 (1974).
33. E. J. Laskowski, D. M. Duggan, and D. N. Hendrickson. Inorg. Chem. **14**, 2449 (1975).
34. R. G. Ball and J. Trotter. Can. J. Chem. **57**, 1368 (1979).
35. C. E. Addison, N. Logan, S. C. Wallwork, and C. D. Garner. Q. Rev. Chem. Soc. **25**, 289 (1971).

A high-field proton magnetic resonance and nuclear Overhauser effect study of prostaglandin E_2[1]

GEORGE KOTOVYCH,[2] GERDY H. M. AARTS, AND GLEN BIGAM
Department of Chemistry, University of Alberta, Edmonton, Alta., Canada T6G 2G2

Received February 18, 1980

GEORGE KOTOVYCH, GERDY H. M. AARTS, and GLEN BIGAM. Can. J. Chem. **58**, 1577 (1980).

The proton magnetic resonance (^{1}H nmr) spectrum of prostaglandin E_2 (PGE_2) in $CDCl_3$ at 400 MHz has been completely analyzed utilizing homonuclear double resonance, inversion recovery, and nOe difference experiments. The nOe difference experiments are used to assign points of configuration, namely the H-10β and the H-10α proton resonances. A spectral analysis shows that the two protons at C-3 and the two protons at C-4 are nonequivalent, indicating a hindered rotation of the chain. This is possibly due to the hairpin conformation of PGE_2 in solution.

GEORGE KOTOVYCH, GERDY H. M. AARTS et GLEN BIGAM. Can. J. Chem. **58**, 1577 (1980).

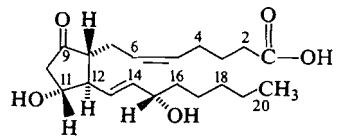
On a analysé en détail le spectre de résonance magnétique du ^{1}H de la prostaglandine E_2 (PGE_2) dans le $CDCl_3$ à 400 MHz, en utilisant la double résonance homonucléaire, l'inversion de recouvrement et les expériences de différence d'effet Overhauser nucléaire (eOn). On a utilisé les expériences de différence de eOn pour établir la configuration en certaines positions de la molécule, par exemple les résonances du H-10β et du H-10α. L'analyse spectrale révèle que les deux protons en C-3 et en C-4 ne sont pas équivalents, indiquant ainsi que la rotation de la chaîne n'est pas libre. Ceci est probablement dû à une conformation en épingle à cheveux du PGE_2 en solution.

[Traduit par le journal]

Introduction

The prostaglandins, fatty acids with a wide range of biological activities, are being extensively studied from a structure–activity viewpoint (1–6). Many of the prostaglandins are characterized by a hairpin-like structure (5), which can be seen from the structural formula for prostaglandin E_2 (PGE_2). X-ray studies on a variety of prostaglandins including PGE_2 (8) have been carried out (P. Crabbé, ref. 2, pages 315–319; 7, and references therein), but since structure and activity are intimately related, the solution conformation may also be important.

One approach to the study of solution conformation involves nuclear Overhauser enhancement (nOe) experiments (9) which give information on molecular geometry. We have therefore undertaken a 400 MHz proton magnetic resonance study of PGE_2. The high-field instrument was required in order to separate the various resonances arising from the presence of a large number of similar protons in the molecule. A complete assignment of the resonances is achieved mainly by means of selective decoupling experiments. The nOe difference experiments are used to confirm several proton assignments. This technique was previously applied to gain information concerning the spatial structures of the basic pancreatic trypsin inhibitor (10), for spectral assignments in lysozyme (11), and in the study of the dependence of the homonuclear nOe, at two frequencies, on the correlation time (12). We have applied this technique in the study of vitamins D_2 and D_3 (13) and prostacyclin (14). Proton nOe difference experiments have the distinct advantage in that one experiment picks out all of the protons that are in close proximity to the irradiated proton even if these proton resonances are hidden by other multiplets.



In previous studies, the chemical shifts of prostaglandin A_2 methyl ester in the presence and absence of a lanthanide ion shift reagent have been measured in $CDCl_3$ at 100 MHz (15). Most of the protons could be assigned but H-3, H-18, and H-19 could only be assigned in the presence of the shift reagent. H-8, H-16, and H-17 could not be assigned. The nonequivalence of H-16 and 16* or H-7 and 7* could not be observed. Proton chemical shifts for prostaglandin $F_{2\alpha}$ in phosphate buffer were assigned at 270 MHz using decoupling techniques (16), but the chemical shift of the protons at C-3 and the nonequivalence of the protons at C-7 and C-16 were also not observed. Conover and Fried (16) analyzed the proton–proton coupling constants for the five-membered ring in terms of the Karplus curve (17, 18) and the analysis indicates a

[1]This is paper No. 5 in a series of high-field nmr studies on prostaglandins and vitamins. Paper No. 4 is ref. 13 and paper No. 3 is ref. 14.

[2]Formerly Kotowycz.

0008-4042/80/151577-07$01.00/0
©1980 National Research Council of Canada/Conseil national de recherches du Canada

Can. J. Chem. Downloaded from www.nrcresearchpress.com by 210.87.254.6 on 09/05/12
For personal use only.

Can. J. Chem. Downloaded from www.nrcresearchpress.com by 210.87.254.6 on 09/05/12
For personal use only.

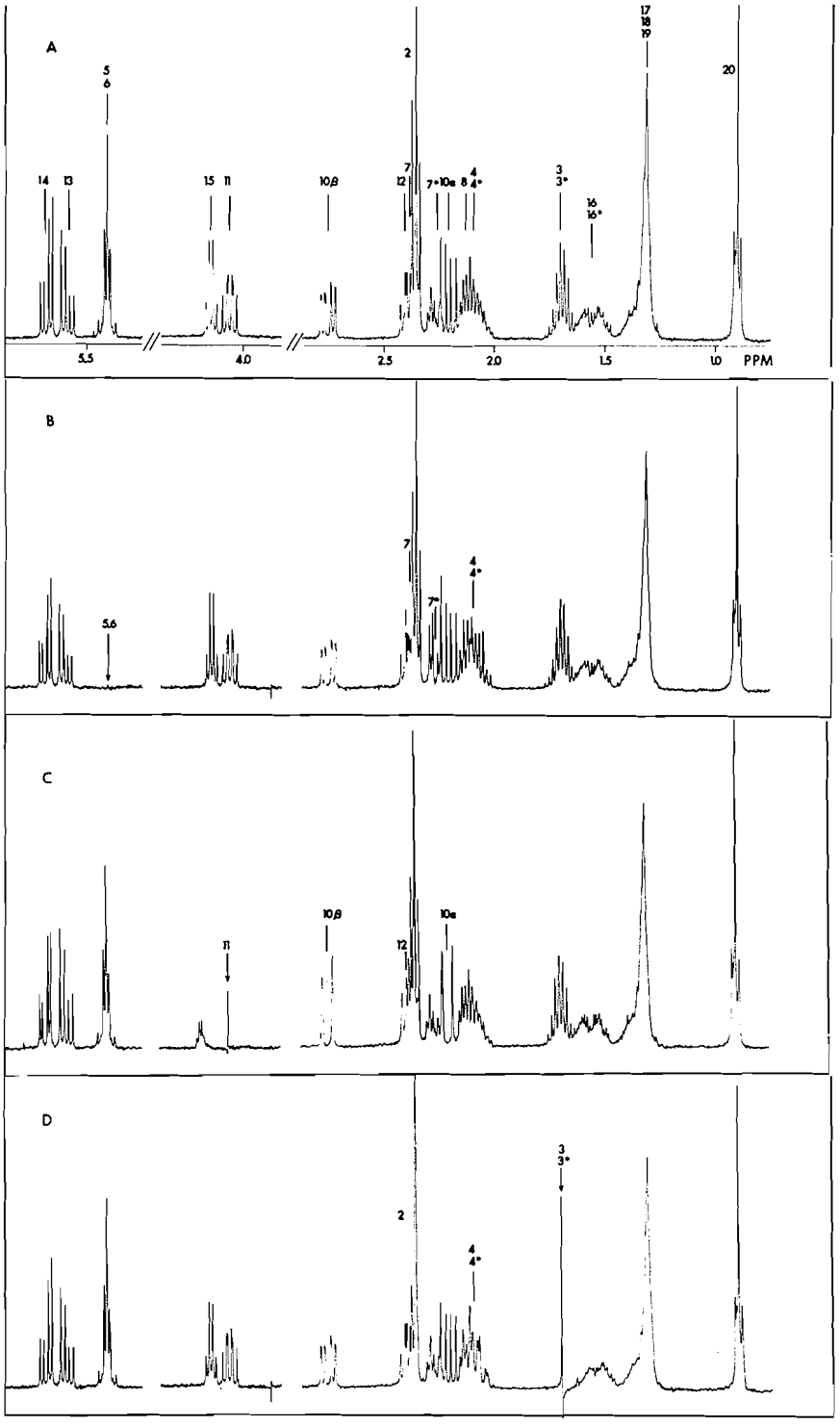


FIG. 1. (A) The 400 MHz proton magnetic resonance spectrum of PGE_2 in $CDCl_3$ at 297 K. The proton resonances are assigned as discussed in the text. (B) Results of the homonuclear decoupling experiment in which the H-5 and H-6 multiplet is irradiated. In (C), the multiplet corresponding to H-11 is irradiated whereas in (D), the H-3 multiplet is irradiated. The protons affected by the decoupling experiments are indicated in spectra 1B to 1D.

Can. J. Chem. Downloaded from www.nrcresearchpress.com by 210.87.254.6 on 09/05/12
For personal use only.

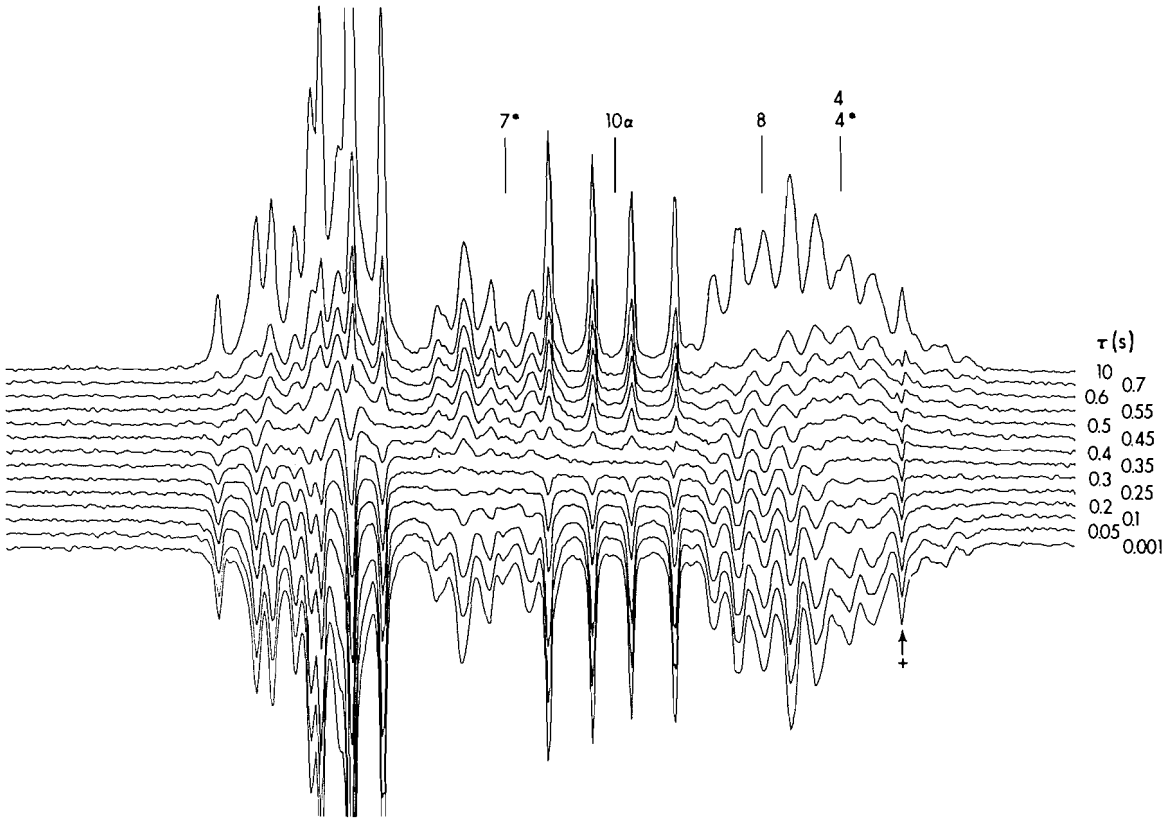


FIG. 2. The 180°—τ—90° inversion recovery spectra of PGE_2 in $CDCl_3$ at 297 K obtained at 400 MHz. The + indicates an instrumental artifact.

favored half-chair conformation for the ring which causes the maximum number of substituents of this ring to be pseudo-equatorial. Only the hydroxyl group at C-9 is in the pseudo-axial orientation.

In the present study, a complete, unambiguous assignment of the proton magnetic resonance spectrum of PGE_2 is obtained. The nOe difference experiments verify the assignment of the H-10α and H-10β resonances. Exact chemical shifts for some of the overlapping multiplets are obtained with the aid of inversion recovery measurements (19, 20). A spectral analysis shows that the protons at C-3 and C-4 are nonequivalent.

Materials and Methods

Prostaglandin E_2 was obtained from Sigma Chemical Co., St. Louis, MO, U.S.A. The samples were prepared in $CDCl_3$, 99.8% deuterated, obtained from SCI-Graphics at a concentration of 2 mg per 0.35 cc. The $CDCl_3$ was purified by treating it with Al_2O_3 (B.D.H. Chemicals Ltd.) and then vacuum degassing it several times before transferring it *in vacuo* into the nmr tube containing the solid prostaglandin, which was then sealed. All glassware was extensively cleaned to eliminate paramagnetic impurities following procedures previously reported (21).

The proton magnetic resonance spectra were obtained at 297 K on a Bruker WH-400/DS nmr spectrometer (400 MHz) operating in the pulsed Fourier transform mode using the Bruker Aspect 2000 computer, 16K data points, and a pulse width of 5 μs. The deuterium resonance of the solvent $CDCl_3$ was used as the lock signal. The homonuclear decoupling experiments were also performed in the pulse mode and these experiments allowed the assignment of all proton resonances in the molecule following standard procedures (22–24). The chemical shifts and coupling constants were calculated from normal spectra (except for H-2, 3, 3*, 4, 4*), obtained using 32K data points and expanded to a sweep width of 2 Hz/cm. Specific examples of some of the decoupling experiments are now summarized. The complete 400 MHz spectrum of PGE_2 is shown in Fig. 1A. Irradiation of H-5 and H-6 indicates the chemical shifts of H-7 and 7*, and H-4 and 4* (Fig. 1B). Upon irradiating H-11 (Fig. 1C), the H-10β and H-10α multiplets collapsed into doublets and were assigned, as was the multiplet for H-12. Upon irradiating H-13, the H-12 multiplet simplified and the centre of the multiplet could be determined. In Fig. 1D, the H-3 and 3* multiplet was irradiated, indicating the chemical shift of H-2 and H-4. Finally, irradiation of H-15 gives the position of the H-16 and 16* multiplets.

The chemical shifts, especially for the overlapping multiplets, can be confirmed by the inversion recovery experiments. In Fig. 2, for a time interval of 0.35 s between the 180° and the 90° pulses, the H-4 multiplet is nulled, whereas an excellent, but inverted spectrum is observed for H-8, confirming the chemical shift for this proton. As well, inversion recovery experiments were repeated with simultaneous decoupling of the protons at C-5 and C-6. Using a τ value of 0.57 s, an excellent spectrum is obtained for the two C-4 protons, which are nonequivalent. This

Can. J. Chem. Downloaded from www.nrcresearchpress.com by 210.87.254.6 on 09/05/12
For personal use only.

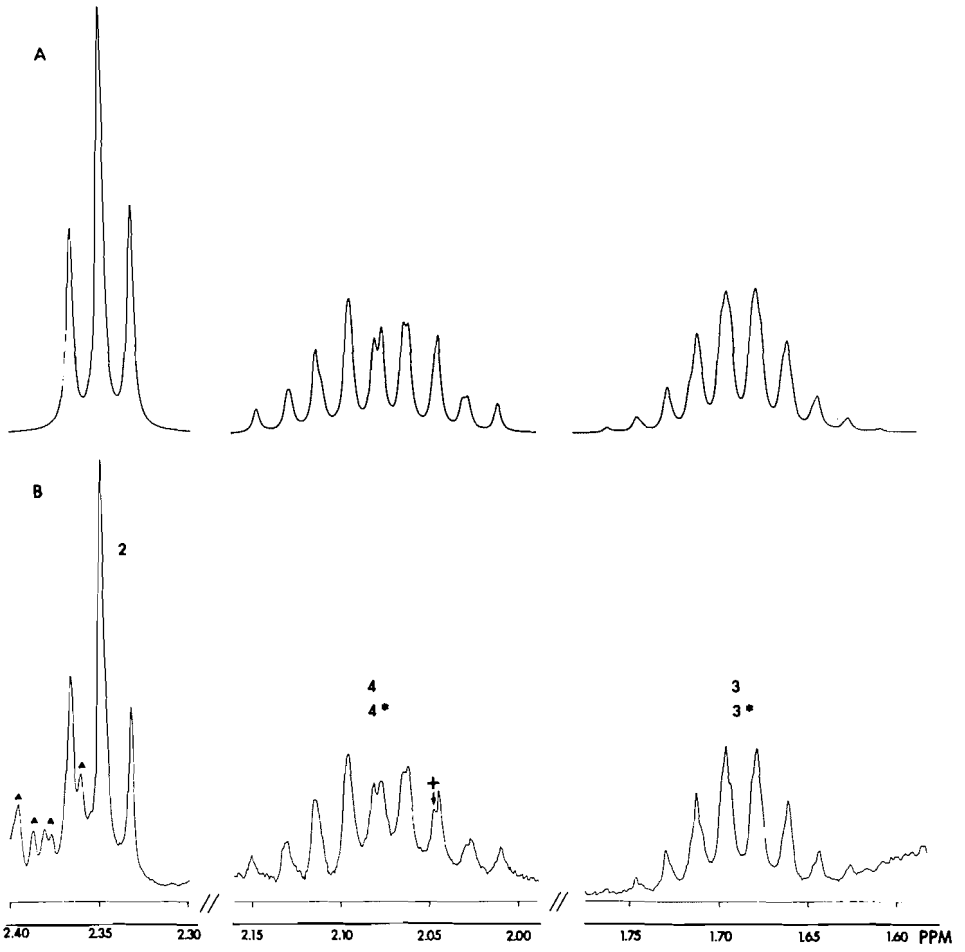


FIG. 3. (A) Simulated spectrum for the H-2, H-4*, 4, and the H-3*, 3 protons from low to high field, respectively. A line width at half height of 1.7 Hz was used. (B) The observed spectra for these protons, obtained with simultaneous decoupling of H-5 and H-6. The spectrum for H-4 and 4* was obtained from the 180°—τ—90° inversion recovery experiment ($\tau = 0.57$ s) also while irradiating H-5 and H-6. The delay time was 10.0 s; 32K data points were used to obtain maximum resolution. The + indicates an experimental artifact, seen in Fig. 2. The ▲ indicates peaks corresponding to protons 7 and 12.

was shown by a computer simulation of an $ABMNX_2$ system, where A and B refer to H-4 and 4*, M and N refer to H-3 and 3*, and X_2 refers to the two C-2 protons. The simulated spectrum is shown in Fig. 3A whereas the observed spectrum is shown in Fig. 3B. The observed spectrum for H-3 and 3* as well as for H-2 was obtained with simultaneous decoupling of the protons at C-5 and C-6. Considering the fact that the H-2 multiplet partially overlaps the H-7 multiplet, that the H-3 and 3* multiplet partially overlaps the H-16 and 16* multiplet, and the fact that the H-4 and 4* multiplet is obtained from an inversion recovery experiment, the agreement between the calculated and experimental spectra is very good. A computer iteration was not attempted but the shifts and coupling constants were varied to obtain a good visual match between the calculated and the observed spectra. 32K data points were used to obtain the best experimental spectrum and the computer analysis was carried out using the Bruker software package.

The results of the nOe difference experiments, carried out in the standard manner (10, 12) are shown in Fig. 4. 16K data points were used for these experiments, a pulse width of 10.7 μs (90° pulse) and a delay time of 6 s.

Results and Discussion

The complete proton magnetic resonance spectrum of prostaglandin E_2 is shown in Fig. 1. The assignments corresponding to the individual protons are indicated on the spectrum. The calculated chemical shifts in ppm and coupling constants in Hz are given in Table 1. These were obtained from the regular, coupled spectra as well as from the inversion recovery experiments. With the exception of the data for protons 2, 3 and 3*, and 4 and 4*, the chemical shifts and coupling constants are reported to first order, and error limits of ±0.01 ppm (±4 Hz) for the chemical shifts and ±0.2 Hz for the coupling constants are reported. However, for many of the protons these error limits are considerably smaller.

The nOe difference experiments in Fig. 4 make use of the fact that only those protons in close

Can. J. Chem. Downloaded from www.nrcresearchpress.com by 210.87.254.6 on 09/05/12
For personal use only.

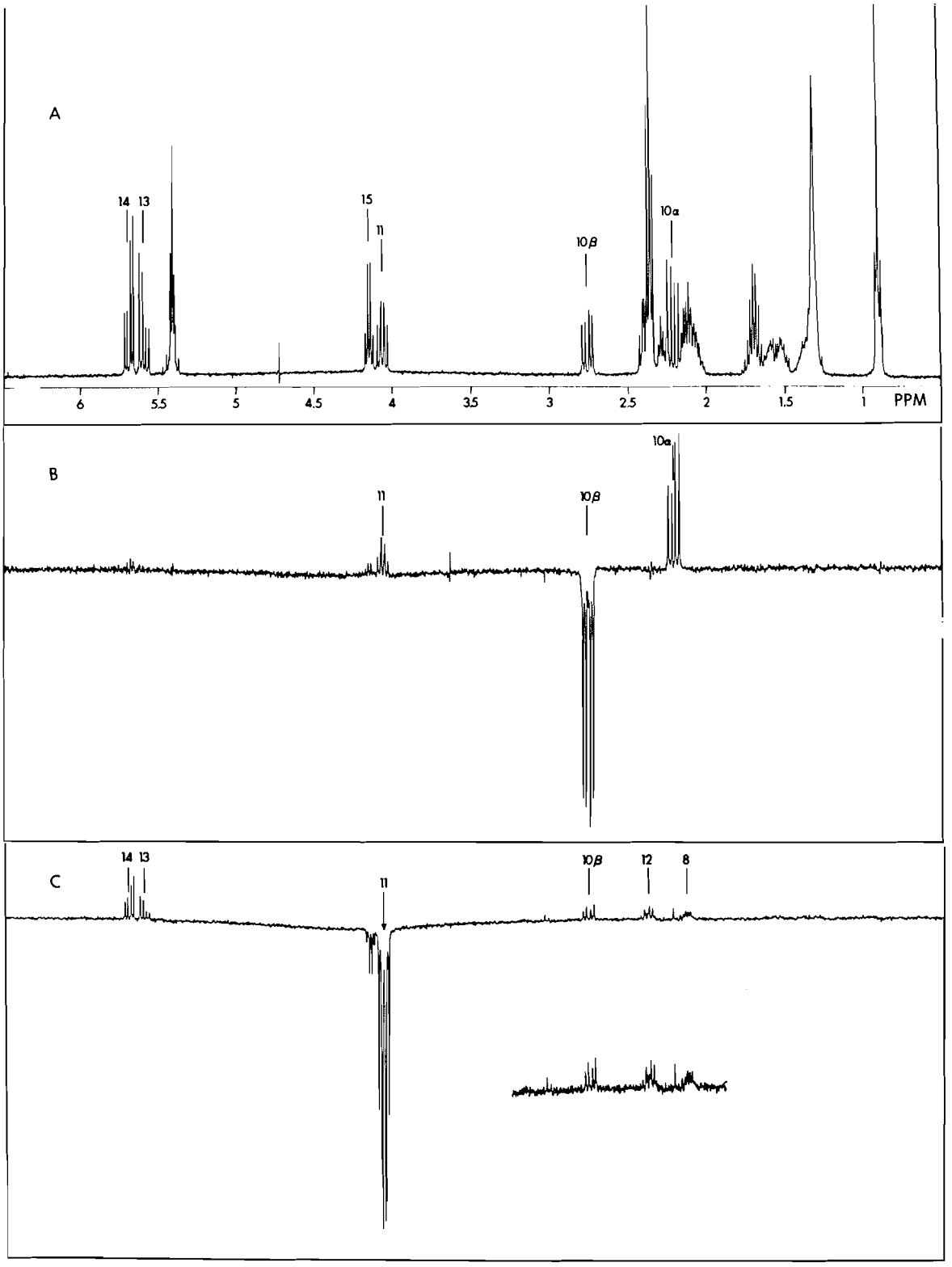


FIG. 4. Results of the difference nOe experiments performed at 400 MHz at 297 K. The normal spectrum is seen in A. In B, H-10β is saturated, and in C, H-11 is saturated.

Can. J. Chem. Downloaded from www.nrcresearchpress.com by 210.87.254.6 on 09/05/12
For personal use only.

TABLE 1. Chemical shifts and coupling constants for PGE_2 in $CDCl_3$ at 297 K[a]

Proton	Chemical shifts (ppm)	Coupling constants (Hz)
A. From the simulated spectrum with H-5 and H-6 decoupled		
2	2.35	$J(gem) = -14.3$
		$J(2—3) = 6.88$
		$J(2—3^*) = 6.88$
3	1.66	$J(3—3^*) = -13.5$
		$J(3—4) = 8.2$
		$J(3—4^*) = 6.5$
3*	1.70	$J(3^*—4) = 6.5$
		$J(3^*—4^*) = 8.2$
4	2.05	$J(4—4^*) = -13.5$
4*	2.11	
B. From the normal spectra		
5, 6	5.41	
7	2.38	$J(7—7^*) = 14.8$[b]
		$J(7—8) = 5.8$[b]
7*	2.27	$J(6—7^*) = 5.8$[b]
		$J(7^*—8) = 5.8$[b]
8	2.13	$J(8—12) = 11.6$
		$J(8—10\beta) = 1.2$
10α	2.21	$J(10\alpha—10\beta) = 18.35$
		$J(10\alpha—11) = 9.8$
10β	2.75	$J(10\beta—11) = 7.4$
11	4.06	$J(11—12) = 8.55$
12	2.40	$J(12—13) = 8.3$
13	5.59	$J(13—14) = 15.3$
14	5.69	$J(14—15) = 6.6$
15	4.14	$J(15—16) = J(15—16^*) = 6.6$
16, 16*	1.53, 1.59	
17, 18, 19	1.31	
20	0.90	$J(19—20) = 6.7$

[a]The chemical shifts, with respect to TMS, and the coupling constants are calculated to first order except for H-2, H-3 and 3*, and H-4 and H-4* where those parameters were obtained from the simulated spectrum. The conditions for the experimental spectra are in the Fig. 3 legend.
[b]The H-7 and H-7* multiplets cannot be analyzed to first order due to virtual coupling arising from the nearly equivalent shifts for H-5 and H-6. Therefore measured splittings are reported, and where relevant, averaged with the splitting obtained for the H-8 multiplet from the inversion recovery spectra.

physical proximity to the irradiated proton will be observed, even if these proton resonances are hidden by other multiplets. Resonances corresponding to protons further removed from the irradiated protons will not be observed. As seen in Fig. 4B, upon saturation of the H-10β multiplet (and inversion, since a difference experiment is carried out), the H-10α proton experiences a very large nOe, as it is nearest the H-10β proton. An nOe is also observed for H-11 which is β to the ring. This shows that the low-field H-10 multiplet corresponds to H-10β. The assignment of H-10β to low field of the H-10α multiplet was confirmed by an nOe experiment in which H-11 is saturated (Fig. 4C) and an nOe is observed for the other protons that are β to the ring, namely H-10β and H-8β. An enhancement was not observed for H-10α. Protons H-12, H-13, and H-14 also experience an nOe. The H-10β multiplet has also been assigned to low field of the H-10α multiplet in prostacyclin (14) and this assignment is consistent with the torsion angle dependence of chemical shifts due to OH groups in pentacyclic systems (25). Previously for $PGF_{2\alpha}$, H-10α was assigned to low field of H-10β (16).

Additional nOe difference experiments on a sample containing a drop of D_2O were carried out to check for the effect of irradiation of the broad OH resonance which appears between ~2.5 and 5.5 ppm. Similar results to those seen in Figs. 4B and 4C were obtained, and the very small peaks at 5.6 and 4.14 ppm, observed in Fig. 4B, are not seen. The presence of the OH signal does not affect the conclusions reached from the nOe difference experiments.

The nonequivalence of H-7, 7* and H-16 and 16* is expected as they are bonded to a carbon next to an asymmetric centre, but the nonequivalence of protons 3, 3* and 4, 4* is most interesting. This may arise from hindered rotation of the α-chain, possibly due to the hairpin conformation of PGE_2. In fact, Anderson and Ramwell (5) in discussing prostaglandin conformations, suggest "that the major change in conformation in transport from lipid to aqueous media is the restriction of free rotation of the carboxyl side chain, which is consistent with the hairpin model". We suggest that the nonequivalence of H-3, 3* and H-4, 4* is due to this restriction of free rotation.

In summary, high field nmr double resonance, inversion recovery, and nOe difference experiments have allowed the assignment of the complete spectrum of prostaglandin E_2. The protons at C-3 and C-4 are nonequivalent, indicating a hindered rotation of the α-chain, possibly due to the hairpin conformation of PGE_2.

Acknowledgements

The authors thank Dr. T. T. Nakashima for valuable discussions, and the Natural Sciences and Engineering Research Council of Canada and the University of Alberta for generous financial assistance. We also thank the Natural Sciences and Engineering Research Council of Canada for a grant towards the purchase of the Bruker WH-400/DS nmr spectrometer.

1. P. W. RAMWELL (*Editor*). The prostaglandins. Vol. I. Plenum Press, New York. 1973.
2. P. CRABBÉ (*Editor*). Prostaglandin research. Academic Press, New York. 1977.
3. B. SAMUELSSON, P. W. RAMWELL, and R. PAOLETTI (*Editors*). Advances in prostaglandin and thromboxane research. Vols. 6–8. Raven Press, New York. 1980.

4. N. H. ANDERSEN, P. W. RAMWELL, E. M. K. LEOVEY, and M. JOHNSON. *In* Advances in prostaglandin and thromboxane research. Vol. I. *Edited by* B. Samuelsson and R. Paoletti. Raven Press, New York. 1976. p. 271.
5. N. H. ANDERSEN and P. W. RAMWELL. Arch. Intern. Med. **133**, 30 (1974).
6. J. JARABAK and J. FRIED. Prostaglandins, **18**, 241 (1979).
7. G. T. DETITTA, D. A. LANGS, and J. W. EDMONDS. Biochemistry, **18**, 3387 (1979).
8. J. W. EDMONDS and W. L. DUAX. Prostaglandins, **5**, 275 (1974).
9. J. H. NOGGLE and R. E. SCHIRMER. The nuclear Overhauser effect. Academic Press, New York. 1971. Chapt. 3.
10. R. RICHARZ and K. WÜTHRICH. J. Magn. Reson. **30**, 147 (1978).
11. G. E. CHAPMAN, B. D. ABERCROMBIE. P. D. CARY, and E. M. BRADBURY. J. Magn. Reson. **31**, 459 (1978).
12. J. D. GLICKSON, S. L. GORDON, T. P. PITNER, D. G. AGRESTI, and R. WALTER. Biochemistry, **15**, 5721 (1976).
13. G. KOTOVYCH, G. M. M. AARTS, and K. BOCK. Can. J. Chem. **58**, 1206 (1980).
14. G. KOTOVYCH, G. H. M. AARTS, T. T. NAKASHIMA, and G. BIGAM. Can. J. Chem. **58**, 974 (1980).
15. G. A. GARCIA, E. DIAZ, and P. CRABBÉ. Chem. Ind. (London), 585 (1973).
16. W. W. CONOVER and J. FRIED. Proc. Natl. Acad. Sci. U.S.A. **71**, 2157 (1974).
17. M. KARPLUS. J. Chem. Phys. **30**, 11 (1959).
18. M. KARPLUS. J. Am. Chem. Soc. **85**, 2870 (1963).
19. R. L. VOLD, J. S. WAUGH, M. P. KLEIN, and D. E. PHELPS. J. Chem. Phys. **48**, 3831 (1968).
20. T. C. FARRAR and E. D. BECKER. Pulse and Fourier transform NMR. Academic Press, New York. 1971 pp. 20–22.
21. Y. THERIAULT, Y. MORIO, and G. KOTOWYCZ. Can. J. Biochem. **57**, 165 (1979).
22. R. FREEMAN. Mol. Phys. **4**, 385 (1961).
23. R. FREEMAN and W. A. ANDERSON. J. Chem. Phys. **37**, 2053 (1962).
24. G. KOTOWYCZ and T. SCHAEFER. Can. J. Chem. **44**, 2743 (1966).
25. M. ANTEUNIS and D. DANNEELS. Org. Magn. Reson. **7**, 345 (1975).

Can. J. Chem. Downloaded from www.nrcresearchpress.com by 210.87.254.6 on 09/05/12
For personal use only.

The enthalpy of solution of NaI, NaCl, $NaClO_4$, and urea in water–tetrahydrofuran mixtures at 298.15 K

STEFANIA TANIEWSKA-OSIŃSKA, BOŻENA PIESTRZYŃSKA, AND ROMAN ŁOGWINIENKO

Department of Physical Chemistry, Institute of Chemistry, University of Łódź, 18 Nowotki Street, Poland

Received September 13, 1979[1]

STEFANIA TANIEWSKI-OSIŃSKA, BOŻENA PIESTRZYŃSKA, and ROMAN ŁOGWINIENKO. Can. J. Chem. **58**, 1584 (1980).

The integral enthalpy of solution of NaI, NaCl, $NaClO_4$, and urea was measured in the concentration range 0.01–0.5 mol/kg in mixtures of water and 2.5, 5, 7.5, 10, and 20 mol% of tetrahydrofuran at 298.15 K.

STEFANIA TANIEWSKA-OSIŃSKA, BOŻENA PIESTRZYŃSKA, et ROMAN ŁOGWINIENKO. Can. J. Chem. **58**, 1584 (1980).

On a mesurée l'enthalpie integrale de dissolution de NaI, NaCl, $NaClO_4$ et de l'urée dans l'intervalle des concentrations 0.01–0.5 mol/kg dans les mélanges contenant de l'eau et de 2.5, 5, 7.5, 10, et 20 mol % de tetrahydrofuranne à la temperature de 298.15 K.

Introduction

The addition of a small amount of monohydric alcohol to water causes the occurrence of the maximum of solution enthalpy for electrolytes and urea. So far, alcohols have constituted the only known group behaving like that. The examinations of urea solutions in water + THF which were carried out by Treiner and Tzias (1) have suggested to us a possibility of observing similar changes in the enthalpies of solution of inorganic salts in H_2O + THF mixtures. The chosen electrolytes are NaI, NaCl, and $NaClO_4$. The common cation of these salts permitted to investigate the influence of iodide, chloride, and perchlorate anions on the structure of the mixed solvent. Non-electrolyte, urea, was chosen for the examination to allow us a comparison of the results obtained with the data contained in the literature.

Materials

$NaClO_4 \cdot xH_2O$ "puriss" produced by Merck, BRD, was dried at 90°C. NaI "puriss" produced by POCh Gliwice, Poland, was crystallized from an acetone–water mixture and dried under vacuum at 60°C (2). NaCl "puriss" and urea "puriss" produced by POCh Gliwice, Poland, was crystallized from twice distilled water and dried under vacuum at 100°C and 70°C respectively (2, 3).

Tetrahydrofuran "pure" produced by POCh Gliwice, Poland, was used. Peroxides were removed from it by shaking THF with $FeSO_4$ and then left over sodium hydroxide for 10 days, then distilled from above sodium (1) and distilled each time before use. Impurities together with water content in THF was estimated using a gas chromatograph by "Perkin–Elmer–Hitachi" and it did not exceed 0.02%. The estimation of water content in THF by Karl Fisher's method gave similar results.

Relative index, n_D = 1.4047 of THF is in reasonable agreement with literature data n_D = 1.4051 (4), 1.4048 (5).

Aqueous solutions of THF were prepared by weight. Twice distilled water was used.

Apparatus

The enthalpy of solution was measured using an "isoperibol" calorimeter. A glass calorimetric vessel with a capacity of approximately 200 cm^3 was provided with a glass stirrer and a calorimeter heater made from constantan wire (R = 25). The stirrer ended with a funnel to attach a thin-walled ampoule containing the investigated substance. The ampoule was broken against the bottom of the calorimeter. The calorimeter temperature was measured by a 16-junction thermocouple system connected to a DC nanovoltmeter type 252 produced by "Unipan". The temperature sensitivity was 5×10^{-5} deg.

Results and Discussion

The values of enthalpy of solution for NaI, NaCl, $NaClO_4$, and urea in THF + H_2O mixtures are presented in Figs. 1, 2, 3, 4 respectively. The measured enthalpies of solution of salts were extrapolated to zero concentration by the method used by Criss and Cobble (6). The dielectric constants and densities necessary for the calculations were taken from the literature (7, 8). The values for compositions used in this work were interpolated graphically. Since in the literature there were no data on the temperature dependence of dielectric constants the derivatives dD/dT corresponding to the examined compositions of the mixed solvent were determined graphically from the data of Bury *et al.* (7). The accuracy of interpolation $dD/dT = f(x)$ introduces an error into the enthalpy values, which does not exceed 4 J. The solution enthalpies of urea were extrapolated graphically. The obtained heats of solution at infinite dilution of the investigated electrolytes and urea in THF–H_2O mixtures are presented in Table 1 and in Fig. 5.

The standard integral enthalpy of solution of urea in water determined by us is 15.39 kJ mol^{-1} whereas the data of Malec and Sarnowski (9) 15.41 kJ mol^{-1}; Łogwinienko (10), 15.49 kJ mol^{-1}; de Visser *et al.* (11), 15.28 kJ mol^{-1}; Schrier *et al.* (12), 15.29 kJ mol^{-1}; Desnoyers *et al.* (13), 15.30 kJ mol^{-1}; Egon and Luff (14), 15.31 kJ mol^{-1}; and Bury *et al.* (15), 15.32 kJ mol^{-1}.

Our value for ΔH^0 of NaCl in water is 3.79 kJ

[1]Revision received April 25, 1980.

0008-4042/80/151584-05$01.00/0

©1980 National Research Council of Canada/Conseil national de recherches du Canada

Can. J. Chem. Downloaded from www.nrcresearchpress.com by 210.87.254.40 on 09/05/12
For personal use only.

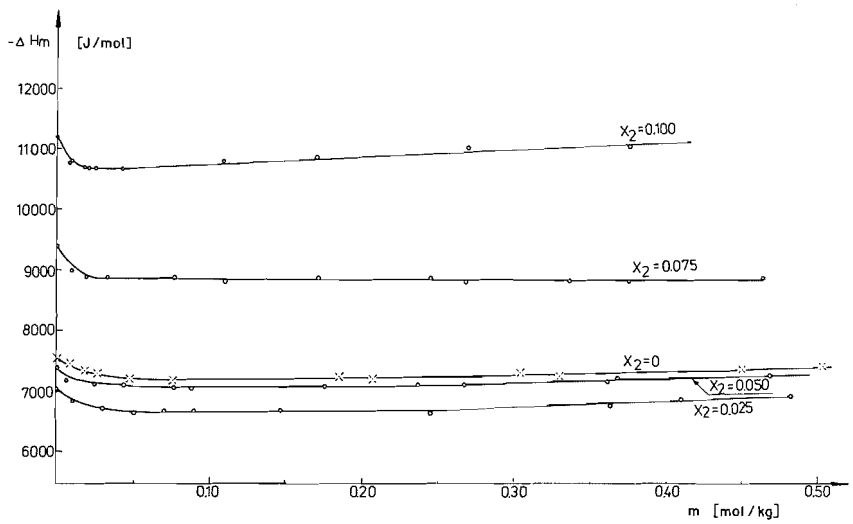


FIG. 1. Enthalpies of solution ΔH_m of NaI in THF + H_2O mixtures at 298.15 K; x_2 = mole fraction of THF.

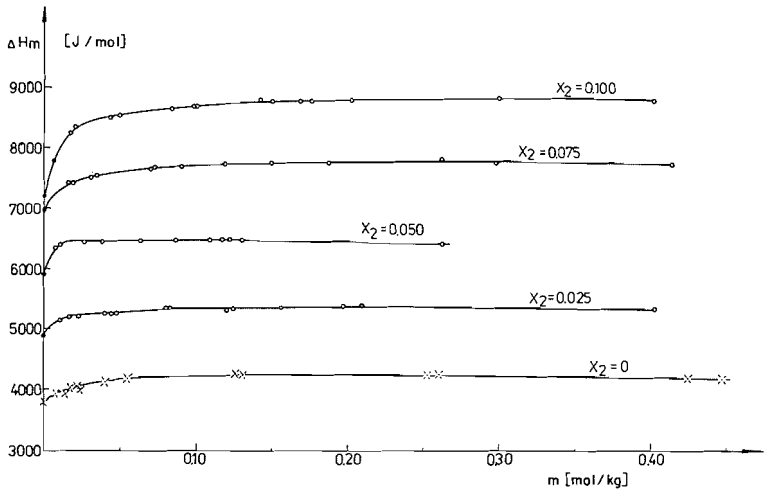


FIG. 2. Enthalpies of solution ΔH_m of NaCl in THF + H_2O mixtures at 298.15 K; x_2 = mole fraction of THF.

mol^{-1} whereas the literature values vary from 3.80 to 3.88 kJ mol^{-1} (6, 7, 16, 17). For ΔH^0 of NaI we obtained 7.54 kJ mol^{-1}, the literature values range from 7.58 to 7.79 kJ mol^{-1} (18–20). The standard ΔH^0 for $NaClO_4$ from our measurements is 14.57 kJ mol^{-1}. According to Lange and Martin (21), it amounts to 14.49 kJ mol^{-1}.

The heat of solution of NaCl and urea in H_2O + THF mixtures was also determined by Bury *et al.* (7, 15) and their data are also shown in Fig. 5. The reasons for disagreement between our data for urea and those of the above-mentioned authors are obscure.

Within the range of 0.035–0.045 mole fraction of THF the maximum of solution enthalpy for NaI, $NaClO_4$, and urea occurs. It is for the first time that in this work maxima of ΔH^0 within the water rich range have been observed for electrolytes in water–organic system not containing monohydric alcohol. It seems interesting that ΔH^0 maximum does not occur in NaCl solutions while in salt solutions in water–alcohol mixtures it occurs for all salts investigated up to now. Since the salts chosen have common cations we can compare the maxima of solution enthalpy regarding the relation between the anion size and the height of the observed maximum. As it is seen in Fig. 5 the height of maximum grows with increasing anion radius.

Dollet and Juillard (22, 23) examined the effect of substituents of benzoate ion on the transfer en-

Can. J. Chem. Downloaded from www.nrcresearchpress.com by 210.87.254.40 on 09/05/12
For personal use only.

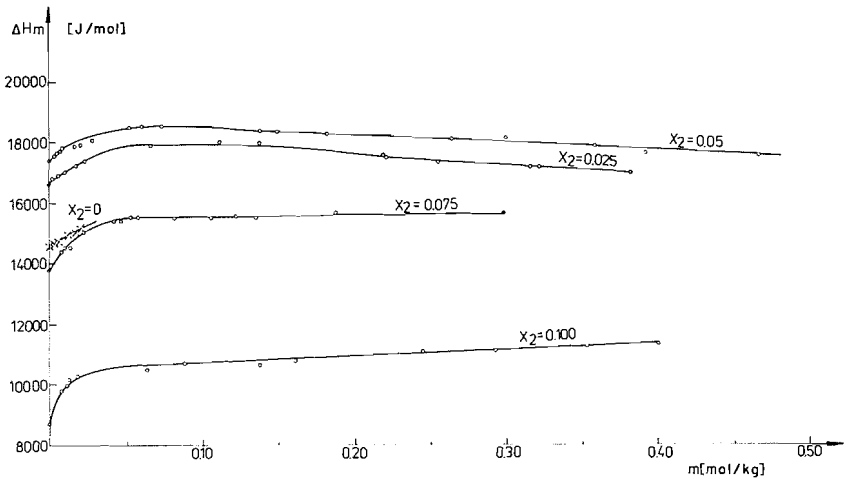


FIG. 3. Enthalpies of solution ΔH_m of $NaClO_4$ in THF + H_2O mixtures at 298.15 K; x_2 = mole fraction of THF.

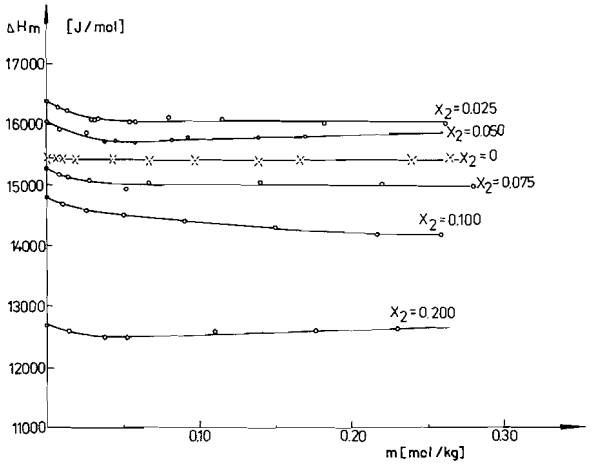


FIG. 4. Enthalpies of solution ΔH_m of urea in THF + H_2O mixtures at 298.15 K; x_2 = mole fraction of THF.

thalpy from water to water–*tert*-butanol mixtures. These authors observed the growth of the enthalpy maximum height with the substituent size. We have not found in the literature such observation in case of inorganic salt solutions, including electrolytes used in this work, in water–alcohol mixtures.

The maximum of the solution enthalpy of urea occurs due to the relatively large dimension of its molecule, half of the longest diameter, calculated according to the method of Kitaigorodsky (24) is 2.9 Å. The dimension of the urea molecule is smaller than the sum of the radii of the electrolytes exhibiting extrema, investigated in this work, and therefore the height of the maximum shown by the urea is smaller than the others.

It follows that the height of the maximum of solution enthalpy is affected only by the volume of the molecule solved and not by the presence or absence of the charges of ions.

The similarity of THF to alcohols arising from the observed maximum of the solution enthalpies of electrolytes in mixed solvents suggests that in the investigated system we deal with water structure ordering by small additions of THF. This is the reason why the lack of maximum for NaCl solutions is not clear. However, the values of entropy of transfer of NaCl from water to water + THF mixtures presented by Bury *et al.* (7) show a minimum.

Considering the fact that the entropy changes reflect the structure changes in the best way (19, 25), it can be assumed that NaCl behaviour does not differ from that of other solutes.

In many previous works (26–31), the conclusion on ordering and disordering effect of organic substances on water was drawn from the occurrence of maxima of the solution enthalpy of salts. It follows from the above that such reasoning may be misleading and the determination of entropy seems necessary as a criterion of structure changes.

Analogous course of mixing enthalpy of alcohols with water at 25°C, especially that of *n*-propanol (32) and of THF with water (33) reinforce the assumption about ordering effect of THF on water.

Kiyohara *et al.* (8) has observed a distinct maximum of partial molal excess thermal expansivity corresponding to 0.06 mol% of THF in water. The authors think that the physical sense of this extremum is not clear.

The analysis of nuclear magnetic relaxation times carried out by Goldammer and Hertz (34) has led to the conclusion that within the range of small THF content H_2O–H_2O interaction strengthens while THF–H_2O interaction can be neglected as

Can. J. Chem. Downloaded from www.nrcresearchpress.com by 210.87.254.40 on 09/05/12
For personal use only.

Can. J. Chem. Downloaded from www.nrcresearchpress.com by 210.87.254.40 on 09/05/12
For personal use only.

TABLE 1. Standard enthalpies of solution of some solutes in THF + H_2O mixtures at 298.15 K

X_{THF} (mole fraction)	ΔH^0 (Joule/mol)			
	NaI	NaCl	$NaClO_4$	Urea
0.000	7536	3789	15570	15390
0.025	7055	4899	16664	16349
0.050	7411	5903	17375	16035
0.075	9378	6950	13816	15270
0.100	11178	7201	8688	14800
0.200				12686

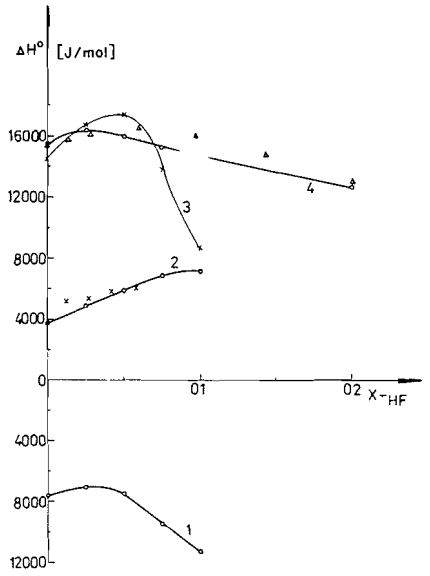


FIG. 5. Standard enthalpies of solution ΔH^0 of some solutes in THF + H_2O mixtures as a function of the mole fraction of THF at 298.15 K. *1*, NaI–THF + H_2O; *2*, NaCl–THF + H_2O; × NaCl–THF + H_2O (7); *3*, $NaClO_4$–THF + H_2O; *4*, urea–THF + H_2O; △ urea–THF + H_2O (1).

weak. This view speaks for the ordering effect of THF on water structure.

Analysing the physico-chemical properties of THF + H_2O mixtures, nmr spectra (35) and the shift of the temperature of maximum density of water affected by addition of THF, as well as the argon solubility data in THF + H_2O mixture (36), Kessler *et al.* (37) have come to the same conclusion as ours about water structure ordering by THF.

Extremum on curve $v = f(x)$ (38) (where v is the ultrasound velocity) corresponds, according to the authors, to the concentration 5 mol% at which the ordering of solvent is greatest but it is explained by the formation of clathrates with water by THF (one THF molecule – 17 water molecules).

Recently Iwasaki and Fujiyama (39) express their opinion on the existence of clathrates of THF in water and Gough (40) has the opposite opinion.

The extremes of solution enthalpy observed permit us to infer that the H_2O–H_2O interaction is amplified in the immediate vicinity of THF molecules, which are the guests of the II type clathrate-like cages.

1. C. TREINER and P. TZIAS. J. Sol. Chem. **4**, 471 (1975).
2. J. SUPNIEWSKI. Preparatyka nieorganiczna, PWN Warsaw. 1958.
3. S. SUBRAMANIAN *et al.* J. Phys. Chem. **75**, 815 (1971).
4. I. MATOUS, I. P. NOVAK, I. SOBR, and I. PICK. Collect. Czech. Chem. Commun. **37**, 2653 (1972).
5. R. SINGER, H. ARM, and H. DAENIKER. Helv. Chim. Acta, **52**, 2347 (1969).
6. C. M. CRISS and J. W. COBBLE. J. Am. Chem. Soc. **83**, 3223 (1961).
7. R. BURY, A. MAYAFFRE, and M. CHEMLA. J. Chim. Phys. **73**, 935 (1976).
8. O. KIYOHARA, D. J. D'ARCY, and G. C. BENSON. Can. J. Chem. **56**, 2803 (1978).
9. I. MALEC and M. SARNOWSKI. Rocz. Chem. **45**, 1369 (1971).
10. R. ŁOGWINIENKO. Thesis, Univ. Łódź, Poland. 1972.
11. C. DE VISSER, H. J. M. GRÜNBAUER, and G. SOMSEN. Z. Phys. Chem. N.F. **97**, 69 (1975).
12. M. Y. SCHRIER, P. J. TURNER, and E. E. SCHRIER. J. Phys. Chem. **79**, 1391 (1975).
13. J. E. DESNOYERS, G. PERRON, L. AVEDIKIAN, and J. P. MOREL. J. Sol. Chem. **5**, 631 (1976).
14. E. P. EGON and B. B. LUFF. J. Chem. Eng. Data, **11**, 192 (1966).
15. R. BURY, A. MAYAFFRE, and M. CHEMLA. J. Chim. Phys. **74**, 745 (1977).
16. L. V. COULTER. J. Phys. Chem. **57**, 553 (1953).
17. V. B. PARKER. Thermal properties of aqueous uni-univalent electrolytes. Natl. Stand. Ref. Data, N.B.S. 2, 1965.
18. D. FEAKINS, B. C. SMITH, and L. THAKUR. J. Chem. Soc. A. Inorg. Phys. Theoret. **6**, 714 (1966).
19. K. P. MISHCHENKO and G. M. POLTORATSKII. Problems of thermodynamics and structure of aqueous and non-aqueous electrolyte solutions. Plenum Publishing Corporation, New York. 1972.
20. E. M. ARNETT and D. R. MCKELVEY. J. Am. Chem. Soc. **88**, 2598 (1966).
21. E. LANGE and W. MARTIN. Z. Phys. Chem. **180**, 233 (1937).
22. N. DOLLET and J. JUILLARD. IUPAC, IV International Symposium on Solute–Solute–Solvent Interactions, Vienna. 1978. p. 39.
23. N. DOLLET and J. JUILLARD. J. Sol. Chem. **5**, 77 (1976).
24. A. I. KITAIGORODSKY. Krystaly molekularne, PWN, Warsaw. 1976. p. 28.
25. H. S. FRANK and A. L. ROBINSON. J. Chem. Phys. **8**, 933 (1940).
26. G. A. KRESTOV, Termodynamika yonnykh procesov v rastvorakh. *Edited by* Khimiya, Leningrad. 1973.
27. G. NEMETHY. Ann. I st. Super. Sanita, **6**, 487 (1970).
28. O. YA. SAMOILOV. Zhur. Struct. Khim. **7**, 175 (1964).
29. M. N. BUSLAEVA and O. YA. SAMOILOV. Zhur. Struct. Khim. **4**, 502 (1963).
30. W. A. MIKHAILOV and L. U. PONOMAREVA. Zhur. Struct. Khim. **9**, 12 (1968).

31. G. NEMETHY and H. A. SCHERAGA. J. Phys. Chem. **66**, 1773 (1962).
32. R. SIGNER, H. ARM, and H. DAENIKER. Helv. Chim. Acta, **52**, 2347 (1969).
33. J. ERVA. Suom. Komistil. B**28**, 131 (1955).
34. E. V. GOLDAMMER and H. G. HERTZ. J. Phys. Chem. **74**, 3734 (1970).
35. A. T. MISHUSTIN, A. I. PODKOVYRIN, YU. M. KESSLER. The I-th All-Union Conference on Solvation and Complex Formation in Solutions, Ivanovo. 1977. p. 75.
36. YU. M. KESSLER. *et al.* The I-th All-Union Conference on Solvation and Complex Formation in Solutions, Ivanovo, 1977. pp. 13, 14.
37. YU. M. KESSLER, V. D. GROUBA, V. F. STOLYPIN, and M. S. DOBROLYUBOVA. IUPAC IV International Symposium on Solute–Solute–Solvent Interactions, Vienna. 1978. p. 165.
38. E. K. BAUMGARTNER and G. ATKINSON. J. Phys. Chem. **75**, 2336 (1971).
39. K. IWASAKI and T. FUJIYAMA. J. Phys. Chem. **81**, 1908 (1977).
40. S. R. GOUGH. J. Sol. Chem. **8**, 371 (1979).

Can. J. Chem. Downloaded from www.nrcresearchpress.com by 210.87.254.40 on 09/05/12
For personal use only.

Alkoxylation of 2,3-dialkylindoles utilizing iodosobenzene diacetate[1]

DENNIS V. C. AWANG[2] AND ANDRÉ VINCENT

Health and Welfare Canada, Drug Research Laboratories, Sir Frederick Banting Research Centre, Tunney's Pasture, Ottawa, Canada K1A 0L2

Received November 19, 1979

DENNIS V. C. AWANG and ANDRÉ VINCENT. Can. J. Chem. **58**, 1589 (1980).

Iodosobenzene diacetate has been employed in the development of a simple procedure for the production of 3-alkoxyindolenines from 2,3-disubstituted indoles, by treatment of the indoles with the reagent in alcoholic solvent.

Primary and secondary alkoxy functions have been incorporated at the β-site of 2,3-dimethylindole but the reaction with *tert*-butanol leads to other complex products. Good yields of 9-*n*-alkoxy-9*H*-reserpines have been realised but no reaction is observed in secondary alcohols.

DENNIS V. C. AWANG et ANDRÉ VINCENT. Can. J. Chem. **58**, 1589 (1980).

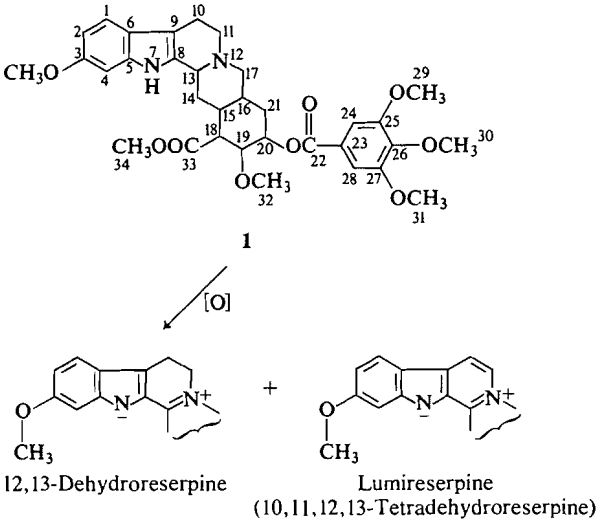
On a utilisé le diacétate de l'iodosobenzène dans la mise au point d'une méthode simple de production des alkoxy-3 indolénines impliquant le traitement d'indoles disubstitués en positions 2 et 3 par le réactif dans un solvant alcoolique.

On a incorporé les fonctions alkoxy primaire et secondaire au niveau du site β du diméthyl-2,3 indole mais la réaction avec l'alcool *tert*-butylique conduit à d'autres produits complexes. On a obtenu d'excellents rendements en *n*-alkoxy-9 réserpines 9*H* mais on n'a pas observé de réaction avec les alcools secondaires.

[Traduit par le journal]

The indole alkaloid reserpine (**1**) is oxidized in good yield by lead tetraacetate in acetic acid, generating predominantly 12,13-dehydroreserpine (**2**) or "lumireserpine" (**3**) depending on the molar ratio of reagent to substrate (1) (Scheme 1). Ajmalicine (2), 3-epi-α-yohimbine (3), and deserpidinediol (4) have similarly been converted to their tetradehydro derivatives. However, it has been reported (5) that reserpine could be converted in good yield (72%) to the corresponding acetoxyindolenine by treatment with lead tetraacetate *in cold methylene chloride solution*; also the indole dihydrocorynantheine was converted in 25% yield to the acetoxyindolenine upon treatment with lead tetraacetate *in benzene solution* (6). Reaction of reserpine with lead tetraacetate in methanol solution produced, following chromatography (5), roughly 10% of crude product from which the corresponding methoxyindolenine was obtained by recrystallization. The yields of acetoxy, benzoyloxy, and bromobenzoyloxy derivatives were variable.

The mechanisms of these reactions have not been elucidated and the stereochemistry of the substituted indolenines has not been determined; the latter authors (5), on the basis of the universally recognized proclivity of indoles towards *electrophilic* attack at the β-position, suggest an intermediate **4** which then suffers *nucleophilic* attack by



1 → **2** + **3**

SCHEME 1

acetic acid at the same site, a seemingly unlikely sequence (Scheme 2).[3]

In the present study, it has been found that iodosobenzene diacetate (IBD), less reactive than lead tetraacetate but a much more conveniently utilized reagent, effects similar oxidation of reserpine in acetic acid, but can also be employed in a simple procedure for introduction of primary alkoxy substituents at the β-position.

[1]Presented in part at the 176th National Meeting of the American Chemical Society, Miami Beach, Florida, September 11–17, 1978.

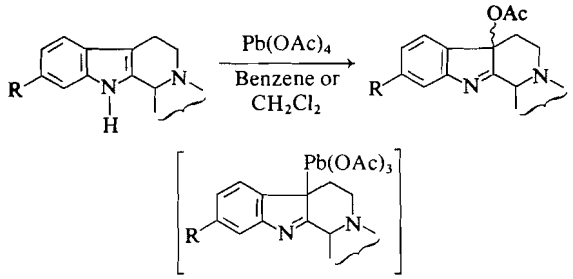
[2]Author to whom correspondence may be addressed.

[3]Examples of introduction of a nucleophile at this site are extremely rare; only two such reactions have been hitherto identified in the literature, namely, the silver ion assisted displacement of iodide by acetate (7), and intramolecular substitution by oxygen at the β-carbon of *N*-benzenesulfonylindoles (8).

0008-4042/80/151589-03$01.00/0

©1980 National Research Council of Canada/Conseil national de recherches du Canada

Can. J. Chem. Downloaded from www.nrcresearchpress.com by 210.87.254.42 on 09/05/12
For personal use only.



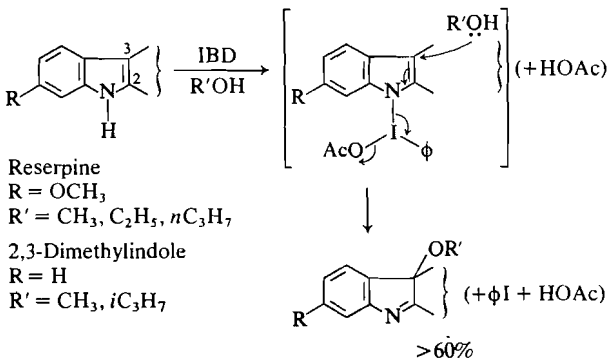
4

SCHEME 2

Alkoxyindolenines have been derived in good yield and quality from reactions of reserpine with IBD in methanol, ethanol, and *n*-propanol solvent at room temperature, but upon treatment with IBD in solvent *i*-propanol the only reaction products generated, after several hours, were 3,4-dehydroreserpine and lumireserpine, in trace amounts.

It seems reasonable to conclude from the above data that the reactions of indole compounds with IBD and lead tetracarboxylates to produce substituted indolenines involve initial condensation reactions to form reactive *N*-substituted intermediates (9), which then undergo nucleophilic attack at the indole β-position (Scheme 3). In inert solvents such as benzene and methylene chloride, attack occurs by the liberated carboxylic acid, whereas solvent gains ascendancy when reactions are performed in alcoholic medium. The effectiveness of IBD and lead tetraacetate in oxidizing reserpine and related alkaloids to their dehydro derivatives in acetic acid medium likely reflects a more polar transition state for such reactions, which would therefore be promoted in the more polar acidic solvent.

2,3-Dimethylindole gives good yields of 3-alkoxy-2,3-dimethylindolenines upon reaction with IBD in methanol and *i*-propanol; tlc examination of the product of reaction with IBD in *tert*-butanol



SCHEME 3

indicates a gross mixture of compounds which have not been investigated further. The success of the *i*-propanol reaction (which fails with reserpine) is attributed to reduced steric hindrance to approach by the alcohol at the β-indole site of the 2,3-dimethylindole iodoso complex, as compared to relatively severe 1,3-diaxial interactions with the C-10 and C-13 hydrogens of reserpine.

The reactions of indoles, unsubstituted at the α- and/or β-carbons, are not as straightforward. In the case of indole itself, refractory high-molecular weight products are formed, whereas less-efficient and obviously more complex reactions result from monosubstituted substrates. 2-Methylindole and 3-methylindole, upon treatment with IBD in methanol, both give rise to at least four products as indicated by tlc; these gross mixtures were not investigated further on account of their apparent preparative inutility.

No contamination by epimers could be detected in the alkoxyindolenine products derived from the reaction of reserpine with IBD in methanol, ethanol, and *n*-propanol. The ir, ^{1}H nmr, and ^{13}C nmr spectra of 9-methoxy-9*H*-reserpine[4] are identical with those of the product of methanolysis of 9-chloro-9*H*-reserpine (**5**), the singular product of reaction of reserpine with *tert*-butyl hypochlorite. Steric considerations indicate the latter compound to be the 9β-compound resulting from attack by *tert*-butyl hypochlorite upon the less hindered face of the indole. Moreover, the identity of the methoxy product from IBD–methanol with the product of solvolysis of **5** suggests that methanol attack *beta* to indole nitrogen, upon both the IBD intermediate and the carbonium ion (undoubtedly easily generated at such an allylic–benzylic site), also takes place from the same less crowded side.

Further work on the chemistry of indolenine derivatives of indole alkaloids is in progress and should further elucidate the sterochemistry of their formation and transformations.

Experimental

General

Melting points are uncorrected. The ^{1}H and ^{13}C nmr spectra of reserpine and its derivatives were obtained on Varian A-60A and CFT-20 spectrometers respectively, using Me_4Si as internal standard. The ^{1}H and ^{13}C spectra of 2,3-dimethylindole products were recorded on a Bruker Spectrospin 80 MHz–20.1 MHz instrument. Elemental analyses were carried out by Mr. Hector Séguin of the National Research Council of Canada's Microanalytical Laboratory, Ottawa, Ontario.

[4]The numbering system is that employed by Wehrli (10) in recently published ^{13}C studies. The older system utilized by Levin, Lallemand, and Roberts (11) in their ^{13}C work originates from the indole nitrogen and would designate such compounds as C-7 substituted indolenines.

Can. J. Chem. Downloaded from www.nrcresearchpress.com by 210.87.254.42 on 09/05/12
For personal use only.

Can. J. Chem. Downloaded from www.nrcresearchpress.com by 210.87.254.42 on 09/05/12
For personal use only.

Materials

Reserpine, 2-methylindole, 3-methylindole, and 2,3-dimethylindole were all commercially obtained and their purity checked by tlc prior to use.

General Alkoxylation Procedure for Reserpine

To a solution of 500 mg (0.082 mol) of reserpine in 80 mL of the alcohol, was added in one portion 250 mg (0.082 mol) of IBD in 20 mL of the alcohol and the mixture stirred in the dark for ½h. The precipitated solid[5] was filtered, washed with cold methanol, and dried under vacuum. The product of methanol reaction had mp C_2H_5OH 231–232°C (lit. (5) (9-methoxy-9*H*-reserpine) mp from CH_2Cl_2–ether 233–235°C); ^1H nmr ($CDCl_3$) δ: 2.78[6] (s, 3H, C9–OCH_3); ^{13}C nmr ($CHCl_3$): 181.0[6] (C=N); ms (70 eV) *m/e*: 638 (parent). 9-Ethoxy-9*H*-reserpine had mp C_2H_5OH 234–236°C; ^{13}C nmr ($CHCl_3$):182.96 (C=N); ms (70 eV) *m/e*: 652 (M).

9-*n*-Propoxy-9*H*-reserpine had mp C_2H_5OH 239–241°C; ^{13}C nmr ($CHCl_3$):182.98 (C=N); ms (70 eV) *m/e*: 666 (parent).

3-Methoxy-2,3-dimethylindolenine

To a magnetically stirred solution of 249 mg (0.0017 mol) of 2,3-dimethylindole in 30 mL of methanol, cooled in an ice-bath and under nitrogen, was added dropwise 554 mg (0.0017 mol) of IBD dissolved in 10 mL of the same solvent, also ice-cooled over a period of 15 min. The resulting solution was stirred for a further 30 min, at the end of which it was diluted with 80 mL water and extracted with 3 × 60 mL portions of benzene. Preparative tlc on 1000 μ silica gel GF coated glass plates (Analtech) using benzene–ether–methanol 7:2:0.5 yielded 195 mg (35%) of light yellow oil which showed one spot on tlc using similar 250 μ plates. The product had ^1H nmr ($CDCl_3$) δ:1.45 (s, 3H, CH_3), 2.25 (s, 3H, =C—CH_3), 2.85 (s, 3H, OCH_3), 7.37 (m, 4H, aryl); ^{13}C nmr ($CHCl_3$) δ:183.2 (C2), 152.1 (C8), 136.1 (C9), 128.1, 124.3, 121.2, 118.8 (C4, 5, 6, 7), 87.4 (C3), 51.2 (OCH_3), 21.0 (C3, CH_3), 13.5 (C2, CH_3); ms (70 eV) *m/e*:175 (M).

3-Isopropoxy-2,3-dimethylindolenine

To a magnetically stirred solution of 451 mg (0.0031 mol) of 2,3-dimethylindole in 135 mL of isopropanol under nitrogen at room temperature was added in one portion 1.00 g (0.0031 mol) of IBD. The resulting solution was stirred at room temperature and monitored by tlc. After 45 min, at which time tlc of the solution indicated no appreciable reduction in the amount of residual starting material, solvent was evaporated and the major product (of lowest R_f save for minor secondary products) was isolated by preparative tlc. A yield of 114.5 mg of light brown solid was obtained which had ^1H nmr ($CDCl_3$) δ: 0.92 (d, 3H, $CHCH_3$, J = 6 Hz), 1.03 (d, 3H, $CHCH_3$), 1.43 (s, 3H, CH_3), 2.30 (s, 3H, =C—CH_3), 3.07 (m, 1H, OCH), 7.21 (m, 4H, aryl); ^{13}C nmr ($CHCl_3$) δ:186.2 (C=N), 153.8 (C8), 139.3 (C9), 129.7, 125.9, 123.5, 120.6 (C4, 5, 6, 7), 88.4 (C3), 68.9 (OCH), 24.5 ($CH(CH_3)$),[7] 23.7 (C3, $CH(CH_3)$),[7] 15.5 (C2); ms (70 eV) *m/e*: 203 (M), 160, 144, 117, 105, 91.

Satisfactory elemental analyses were obtained for all products.

Acknowledgements

The authors acknowledge the assistance of Drs. I. C. P. Smith and R. Des Lauriers of the National Research Council of Canada and Dr. A. By, Dr. G. A. Neville, and Mssrs. H. Avdovich, D. Legault, and J.-C. Ethier of the Drug Research Laboratories of Health and Welfare Canada, Ottawa.

1. G. E. WRIGHT and T. Y. TANG. J. Pharm. Sci. **61**, 299 (1972).
2. F. L. WEISENBORN, M. MOORE, and P. A. DIASSI. Chem. Ind. (London), 375 (1954).
3. F. E. BADER, D. F. DICKEL, R. A. LUCAS, and E. SCHITTLER. J. Am. Chem. Soc. **77**, 3547 (1955).
4. H. B. MACPHILLAMY, C. F. HEUBNER, E. SCHITTLER, A. F. ST. ANDRE, and P. R. ULSHAFER. J. Am. Chem. Soc. **77**, 4335 (1955).
5. N. FINCH, C. W. GEMENDEN, I. H.-C. HSU, and W. I. TAYLOR. J. Am. Chem. Soc. **85**, 1520 (1963).
6. L. J. DOLBY and S. SAKAI. Tetrahedron, **23**, 1 (1967).
7. R. D. ARNOLD, W. M. NUTTER, and W. L. STEPP. J. Org. Chem. **24**, 117 (1959).
8. M. M. COOPER, G. J. HIGNETT, R. F. NEWTON, J. A. JOULE, and (in part) M. HARRIS and J. D. HINCHLEY. J. Chem. Soc. Chem. Commun. 432 (1977).
9. K. H. PAUSACKER. J. Chem. Soc. 1989 (1953).
10. F. W. WEHRLI. Adv. Mol. Relaxation Processes, **6**, 139 (1974).
11. R. H. LEVIN, J-Y. LALLEMAND, and J. D. ROBERTS. J. Org. Chem. **38**, 1983 (1973).

[5]9-Propoxy-9*H*-reserpine was not precipitated readily and the reaction mixture was diluted with water and refrigerated in order to induce crystallization. The respective yields of precipitated solid, homogeneous by tlc analysis, were 76, 45, and 36% for methoxy-, ethoxy-, and *n*-propoxy derivatives, respectively.

[6]These chemical shifts are characteristic of fully substituted benzylic methoxyl protons and indolenine carbon, respectively. Complete details of a reinvestigation of the ^1H nmr and ^{13}C nmr spectra of reserpine and deserpidine, as well as elucidation of the spectra of a variety of their derivatives, will appear shortly.

[7]The accidental equivalence of the chemical shift of one of the isopropyl carbons with that of the methyl carbon attached to C3 was established by selective on-resonance decoupling.

Electron spin resonance study of spin-trapped azide radicals in aqueous solutions[1,2]

WALTER KREMERS AND AJIT SINGH[3]

Medical Biophysics Branch, Whiteshell Nuclear Research Establishment, Atomic Energy of Canada Limited (Research Company), Pinawa, Man., Canada R0E 1L0

Received March 17, 1980

WALTER KREMERS and AJIT SINGH. Can. J. Chem. **58**, 1592 (1980).

Organic spin traps have been used to study the formation of azide radicals during the reaction of azide anions with hydroxyl radicals. The azide radicals have been successfully trapped with three spin traps: 5,5-dimethylpyrroline-1-oxide (DMPO), phenyl-*N-tert*-butyl nitrone (PBN), and 4-pyridyl-*N-tert*-butyl nitrone (PyBN). The azide radicals produced from ^{15}N sodium azide have also been trapped. The hyperfine splittings of the resulting radicals have been determined.

WALTER KREMERS et AJIT SINGH. Can. J. Chem. **58**, 1592 (1980).

On a utilisé des pièges à spin organique pour étudier la formation des radicaux azotures lors de la réaction des anions azotures avec les radicaux hydroxyles. On a piégé avec succès les radicaux azotures à l'aide de trois pièges à spin: le diméthyl-5,5 pyrroline oxyde-1 (DMPO), la phényl-N-*tert*-butyl nitrone (PBN) et la pyridyl-4-*N-tert*-butyl nitrone (PyBN). On a également piégé les radicaux azotures produits à partir de l'azoture de sodium marqué au ^{15}N. On a déterminé les couplages hyperfins des radicaux qui en résultent.

[Traduit par le journal]

Introduction

It has been suggested that azide anions react with hydroxyl radicals to generate $N_3^{\cdot}$ radicals [1] (1–5).

[1] $N_{3aq}^- + {}^{\cdot}OH \rightarrow N_3^{\cdot} + OH_{aq}^-$

The reaction continues to be studied by pulse radiolysis (6, 7). However, results on the formation of $N_3^{\cdot}$ radical by this reaction using the electron spin resonance (esr) technique have not been reported in the literature.[4] We described in this paper our work on the study of reaction [1] by the esr technique. Photolysis of azido cobalt(III) complexes also produces $N_3^{\cdot}$ radicals, which have been trapped with phenyl-*N-tert*-butyl nitrone (PBN) (8). The esr spectrum of the PBN–$N_3^{\cdot}$ adduct obtained by us agrees with that obtained by Rehorek *et al.* (8).

Experimental

5,5-Dimethylpyrroline-1-oxide (DMPO) and phenyl-*N-tert*-butyl nitrone (PBN) (Aldrich), 4-pyridyl-*N-tert*-butyl nitrone (PyBN) (Spin Trap Producers, Guelph, Ontario) and 100% ^{15}N-labelled sodium azide (Stohler Isotope Chemicals) were used as obtained. Other chemicals used were laboratory reagent quality or better; triple distilled water was used for all the experiments.

Electron spin resonance experiments were performed on a Varian V4500 spectrometer. Solutions containing a spin trap and sodium azide were deaerated and saturated with N_2O to increase the yield of $^{\cdot}OH$ (9) and irradiated with 3 MeV electrons from a nominally 4 MeV Van de Graaff accelerator, to a dose of ~4 Gy. The irradiated solution was then quickly transferred (within minutes) to the esr spectrometer cell and a spectrum recorded on a Nicolet 1074 signal averager. The esr spectrum of the DMPO–N_3 adduct was also obtained by *in situ* radiolysis. The equipment and the techniques used are essentially those described by Sargent and co-workers (10).

Hydroxyl radicals were also generated by the action of uv light on 1% hydrogen peroxide solutions (11). A 150 W Xenon arc lamp (Oriel) was used for irradiations, at a distance of 45 cm from the esr cell. Several spectra were normally accumulated during each photolysis run. In the case of PBN–N_3 adduct, the solution was found to be rather unstable so spectra were accumulated from several successive runs.

Results and Discussion

PBN

Photolysis of a 1% solution of H_2O_2 in the presence of PBN (5×10^{-2} mol dm^{-3}) and sodium azide (0.1 mol dm^{-3}) gives an esr spectrum consisting of a triplet of quartets (1:2:2:1) with the hyperfine splitting constants (hfsc) given in Table 1. This spectrum is identical to that reported by Rehorek *et al.* (8) and identified as the spin-trapped azide radical. In the absence of sodium azide, the PBN–OH adduct is obtained (Table 1).

PyBN

Photolysis of H_2O_2 (1%) in the presence of PyBN (5×10^{-2} mol dm^{-3}) and sodium azide (0.1 mol dm^{-3}) also gives an esr spectrum (Fig. 1*b*) consisting of a triplet of quartets with the hyperfine splitting constants (hfsc) given in Table 1. The simulation of this spectrum was computed with a

[1] AECL No. 6864.

[2] The work described in this paper was presented at the International Conference on ESR of Organic and Bio-organic Radicals, University of York, March 1980.

[3] To whom all correspondence should be addressed.

[4] A spectrum attributable to DMPO–N_3 adduct has been seen by Dr. G. R. Buettner (personal communication, 1979). Results similar to our own are being reported by Dr. E. G. Janzen and co-workers in an accompanying paper in this issue.

0008-4042/80/151592-04$01.00/0

©1980 National Research Council of Canada/Conseil national de recherches du Canada

Can. J. Chem. Downloaded from www.nrcresearchpress.com by 210.87.254.42 on 09/05/12
For personal use only.

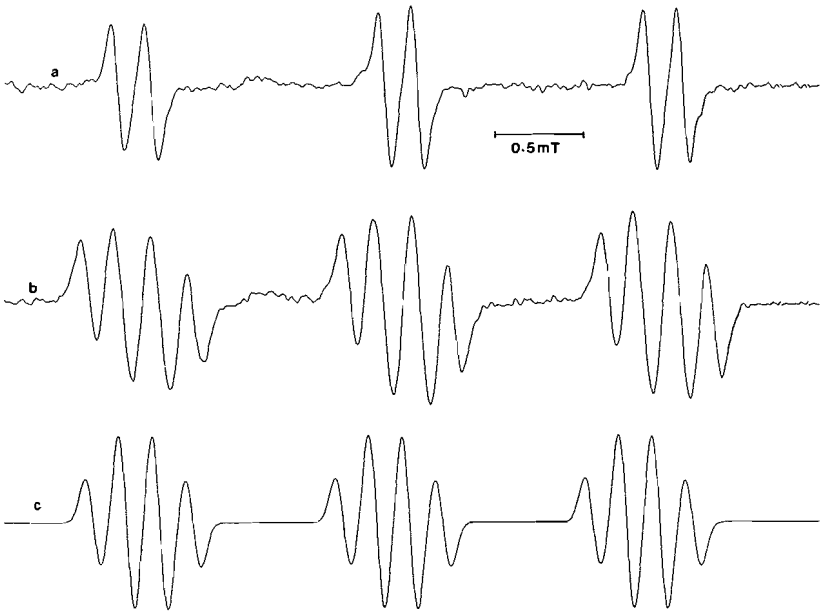


FIG. 1. Photolysis of 1% aqueous H_2O_2 in the presence of PyBN (5×10^{-2} mol dm^{-3}); esr spectra of spin-trapped ·OH and N_3· radicals. (*a*) No additive, (*b*) NaN_3 (5×10^{-2} mol dm^{-3}), (*c*) computer simulation of PyBN$\dot{}$–N_3 adduct.

TABLE 1. Hyperfine splitting constants for the ·OH and N_3· spin adducts

Spin trap	·OH mT	N_3· mT
DMPO	$\alpha_H = 1.49$ $\alpha_N = 1.49$	$\alpha_H = 1.47$ $\alpha_{N1} = 1.47$ $\alpha_{N2} = 0.30$
PBN	$\alpha_H = 0.27$ $\alpha_N = 1.56$	$\alpha_H = 0.206$ $\alpha_{N1} = 1.505$ $\alpha_{N2} = 0.206$
PyBN	$\alpha_H = 0.19$ $\alpha_N = 1.50$	$\alpha_H = 0.195$ $\alpha_{N1} = 1.468$ $\alpha_{N2} = 0.195$

*$\alpha_{N1}(^{14}N) = 1.47$, $\alpha_{N2}(^{15}N) = 0.45$, and $\alpha_H = 1.47$, for the ^{15}N-labelled N_3· trapped with DMPO.

peak-to-peak linewidth of 0.92 G (0.092 mT) and is shown in Fig. 1*c*. The spectrum and hfsc for PyBN$\dot{}$–OH adduct are given in Fig. 1*a* and Table 1.

DMPO

With DMPO as the spin trap, we have obtained a series of esr spectra which show first the formation of the DMPO$\dot{}$–OH adduct (10, 12) (1% H_2O_2; DMPO, 5×10^{-2} mol dm^{-3}) (Fig. 2*a* and Table 1) and then its gradual replacement by the DMPO$\dot{}$–N_3 adduct as the concentration of sodium azide in the solution is increased to 5×10^{-2} mol dm^{-3} (Fig. 2*b–e* and Table 1). The esr spectrum of the DMPO$\dot{}$–N_3 adduct consists of a quartet of triplets; it is shown in Fig. 2*e* and the hfsc's are listed in Table 1. The quartet of triplets (1:1:1:2:2:2:2:2:2:1:1:1) is a result of overlap of the hfsc of the proton and the nitroxyl nitrogen, with further splitting by the azide nitrogen. The slight asymmetry of the spectum can be explained by a very small contribution of the DMPO$\dot{}$–OH adduct (Fig. 2*a*) to the DMPO$\dot{}$–N_3 spectrum (Fig. 2*e*). Simulation of this spectrum was computed with a peak-to-peak line width of 1.2 G (0.12 mT) and is shown in Fig. 2*f*. Comparative runs in H_2O vs. D_2O solutions gave identical esr spectra of the DMPO$\dot{}$–N_3 adduct.

Reaction of Fenton's reagent (ferrous ammonium sulfate and hydrogen peroxide), which is a known source of hydroxyl radicals [2] (13, 14 and references therein),

[2] $Fe_{aq}^{2+} + H_2O_2 \rightarrow Fe_{aq}^{3+} + \cdot OH + OH_{aq}^-$

with sodium azide, in the presence of DMPO gives an esr spectrum identical to that in Fig. 2*e*.

In situ radiolysis of an N_2O-saturated aqueous solution of sodium azide (0.1 mol dm^{-3}) and DMPO (5×10^{-2} mol dm^{-3}) produced an esr spectrum identical to that of Fig. 2*e*. This spectrum also consists of spectra of electrons trapped in the walls of the quartz cell and of DMPO$\dot{}$–H adduct (10).

Variation of sodium azide concentration, from 10^{-3} mol dm^{-3} up to 1 mol dm^{-3} did not change the shape of the observed spectrum of the DMPO$\dot{}$–N_3 adduct. The intensity of the peaks plateaued at ~5

Can. J. Chem. Downloaded from www.nrcresearchpress.com by 210.87.254.42 on 09/05/12
For personal use only.

Can. J. Chem. Downloaded from www.nrcresearchpress.com by 210.87.254.42 on 09/05/12
For personal use only.

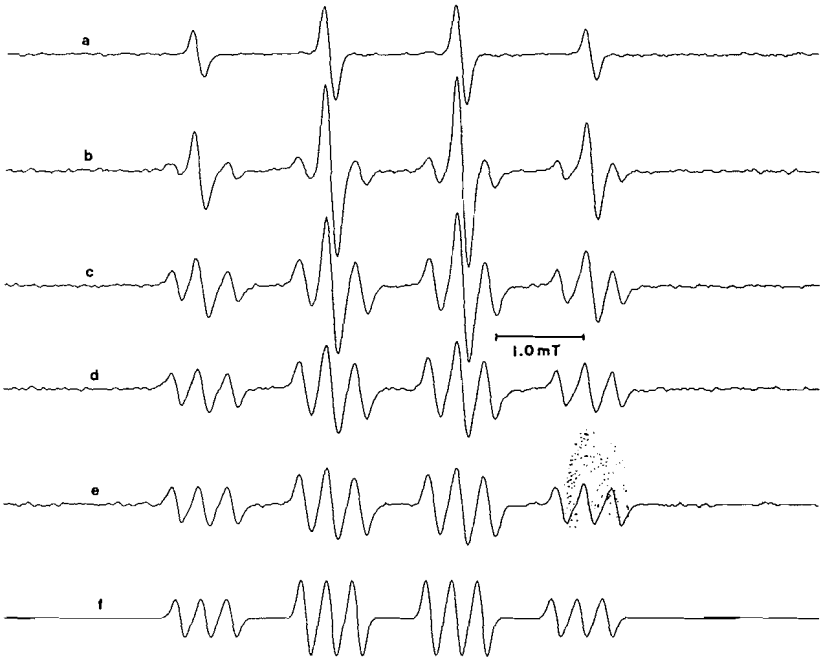


FIG. 2. Photolysis of 1% aqueous H_2O_2 in the presence of DMPO (5×10^{-2} mol dm^{-3}); esr spectra of spin-trapped $^{\cdot}OH$ and $N_3^{\cdot}$ radicals. (*a*) No additive, (*b*) NaN_3 (1×10^{-3} mol dm^{-3}), (*c*) NaN_3 (5×10^{-3} mol dm^{-3}), (*d*) NaN_3 (1×10^{-2} mol dm^{-3}), (*e*) NaN_3 (5×10^{-2} mol dm^{-3}), (*f*) computer simulation of DMPO$\dot{}$–N_3 adduct.

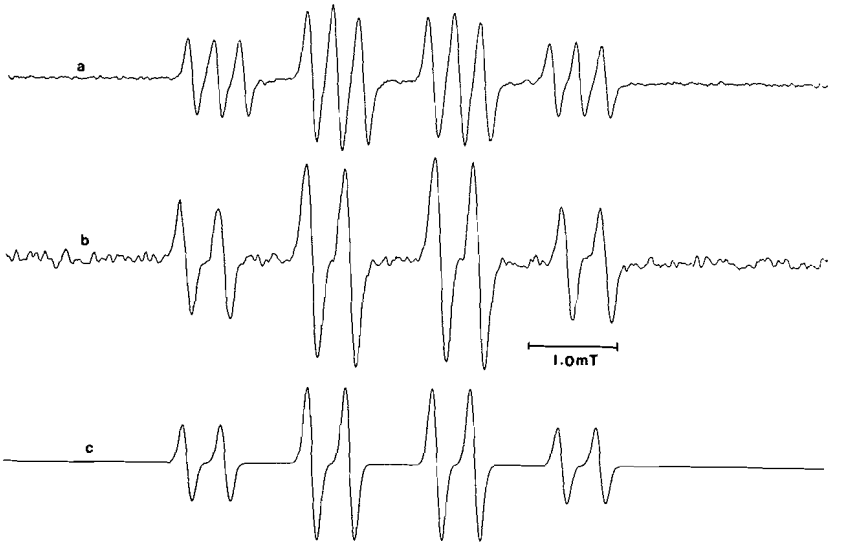


FIG. 3. Photolysis of 1% aqueous H_2O_2 in the presence of DMPO; esr spectra of spin-trapped ^{14}N and ^{15}N azide radicals. (*a*) NaN_3 (^{14}N, natural abundance) (5×10^{-2} mol dm^{-3}), (*b*) NaN_3 (^{15}N, 100%) (5×10^{-2} mol dm^{-3}), (*c*) computer simulation of DMPO$\dot{}$–(^{15}N)N_3 adduct.

$\times 10^{-2}$ mol dm^{-3}. It has been suggested that $N_3^{\cdot}$ adds on to the azide anion [3] (5) and recent pulse radiolysis work (7) strongly supports this suggestion.

[3] $N_3^{\cdot} + N_{3aq}^{-} \rightarrow (N_3)_{2aq}^{\cdot -}$

Thus at the higher concentrations of sodium azide, reaction [3] would compete with trappings of $N_3^{\cdot}$. The lack of any effect of sodium azide concentration suggests that the esr spectra of the DMPO$\dot{}$–N_3 and DMPO$\dot{}$–$(N_3)_{2aq}^{-}$ are identical. The possibility that $(N_3)_{2aq}^{\cdot -}$ is not trapped is ruled out by the fact that at 1 mol dm^{-3} concentration of sodium azide, where most of the $N_3^{\cdot}$ should exist as $(N_3)_{2aq}^{-\cdot}$ (7),

there is no reduction in the intensity of the DMPO̊–N_3 spectrum as compared to that at $\sim 5 \times 10^{-2}$ mol dm^{-3}.

In our work no secondary splittings due to the other two nitrogens (of N_3·) have been observed. Rehorek *et al.* (9) did observe these with nitrosodurene as a spin trap in methanol solutions. We plan to extend our work with the use of this spin trap.

^{15}N-labelled Azide Radical

The nuclear spin of ^{14}N is 1, which gives rise to the triplets observed in our spectra (15). The nuclear spin of ^{15}N is only 1/2; therefore, the spectra derived from ^{15}N-labelled azide radicals should consist of doublets instead of triplets (15). This was indeed observed. The spectrum of the DMPO̊–$^{15}N_3$ adduct (derived from 100% ^{15}N-labelled sodium azide) consists of a quartet of doublets (Fig. 3*b*, Table 1). The simulated spectrum (Fig. 3*c*) is computed with a peak-to-peak linewidth of 1.2 G (0.12 mT). The spectrum of the ^{14}N (natural abundance) DMPO̊–N_3 is shown in Fig. 3*a*, for comparison.

Untrapped N_3·

It has not been possible to observe the esr spectrum of N_3· in steady-state work. This is attributable to its short half-life (10^{-5}–10^{-6} s) (7).

Conclusion

Our work confirms that N_3· is formed in reaction of ·OH radicals with azide anions. The esr spectra of spin-trapped N_3· and $(N_3)_{2aq}^{-}$·, with DMPO, appear to be indistinguishable. The expected change in the number of peaks is seen in going from trapped ^{14}N azide radical (natural abundance) to the 100% ^{15}N-labelled one.

Acknowledgements

We wish to thank Dr. F. P. Sargent for helpful advice during this work, and Dr. E. G. Janzen for helpful discussion and for a preprint of his paper describing work on azide radicals.

1. P. Kelly and M. Smith. J. Chem. Soc. 1479 (1961); 1487 (1961).
2. A. Treinin and E. Hayon. J. Chem. Phys. **50**, 538 (1969).
3. F. Barat, B. Hickel, and J. Sutton. Chem. Commun. 125 (1969).
4. E. Hayon and M. Simic. J. Am. Chem. Soc. **92**, 7486 (1970).
5. I. Kraljić. *In* Proceedings of the Third Tihany Symposium on Radiation Chemistry. *Edited by* J. Dobo and P. Hedvig. Akadémiai Kiado, Budapest. 1972. p. 1405.
6. E. J. Land and W. A. Prütz. Int. J. Radiat. Biol. **32**, 203 (1977).
7. A. Singh, G. W. Koroll, and R. B. Cundall. To be published.
8. D. Rehorek, P. Thomas, and H. Hennig. Inorg. Chim. Acta, **32**, L1 (1979).
9. I. G. Draganić and Z. D. Draganić. The radiation chemistry of water. Academic Press, New York. 1971.
10. (*a*) F. P. Sargent and M. G. Bailey. Can. J. Chem. **51**, 3211 (1973); (*b*) F. P. Sargent and E. M. Gardy. Can. J. Chem. **54**, 275 (1976).
11. J. G. Calvert and J. N. Pitts, Jr. Photochemistry. John Wiley and Sons, Inc. New York. 1967. p. 202.
12. E. G. Janzen. *In* Free radicals in biology. Vol. 4. *Edited by* W. A. Pryor. Academic Press, New York. 1980. p. 115.
13. C. Walling. Acc. Chem. Res. **8**, 125 (1975).
14. A. Singh. Photochem. Photobiol. **28**, 429 (1978).
15. H. M. Swartz, J. R. Bolton, and D. C. Borg. Biological applications of electron spin resonance. Wiley-Interscience, New York. 1972.

Can. J. Chem. Downloaded from www.nrcresearchpress.com by 210.87.254.42 on 09/05/12
For personal use only.

Can. J. Chem. Downloaded from www.nrcresearchpress.com by 210.87.254.105 on 09/05/12
For personal use only.

Spin trapping azidyl (N_3·), cyanatyl (OCN·), cyanyl (·CN) radicals, and chlorine atom (Cl·)

EDWARD G. JANZEN, HENRY J. STRONKS, DALE E. NUTTER, JR., AND EDWARD R. DAVIS
Department of Chemistry, Guelph–Waterloo Centre for Graduate Work in Chemistry, University of Guelph, Guelph, Ont., N1G 2W1 and Department of Chemistry, The University of Georgia, Athens, GA 30602, U.S.A.

HENRY N. BLOUNT
Brown Chemical Laboratory, The University of Delaware, Newark, DE 19711, U.S.A.

AND

J. LEE POYER AND PAUL B. MCCAY
Oklahoma Medical Research Foundation, Biomembrane Research Laboratory, Oklahoma City, OK 73104, U.S.A.

Received March 3, 1980

EDWARD G. JANZEN, HENRY J. STRONKS, DALE E. NUTTER, JR., EDWARD R. DAVIS, HENRY N. BLOUNT, J. LEE POYER, and PAUL B. MCCAY. Can. J. Chem. **58**, 1596 (1980).

Azidyl, cyanatyl, and cyanyl radicals and chlorine atoms have been detected by spin trapping using α-phenyl *N-tert*-butyl nitrone (PBN) in the monoelectronic electrooxidations of azide, cyanate, cyanide, and chloride. Azidyl and cyanatyl radicals were also detected with PBN in the persulfate oxidations of azide and cyanate. Azidyl radicals could be detected in the reaction of azide with hydroxyl radicals in the presence of PBN.

EDWARD G. JANZEN, HENRY J. STRONKS, DALE E. NUTTER, JR., EDWARD R. DAVIS, HENRY N. BLOUNT, J. LEE POYER et PAUL B. MCCAY. Can. J. Chem. **58**, 1596 (1980).

On a décelé lors de l'électrooxydation monoélectronique de l'azoture, du cyanate, du cyanure et du chlorure des radicaux azotyle, cyanatyle et cyanyle et des atomes de chlore en piégeant des spins grâce à l'α-phényl *N-tert*-butyl nitrone (PBN). On a également pu déceler la présence des radicaux azotyle et cyanatyle lors de l'oxydation par les persulfate de l'azote et du cyanate. On a aussi mis en évidence la présence des radicaux azotyles lors de la réaction de l'azoture avec les radicaux hydroxyles en présence de PBN.
[Traduit par le journal]

Introduction

A recent paper by Rehorek, Thomas, and Hennig (1) which reports the detection of azidyl radicals in the photolysis of $K_3[Co(CN)_5N_3]$ and $[Co(NH_3)_5N_3]Cl_2$ in aqueous and methanolic solutions prompts us to communicate some preliminary results of the spin trapping chemistry observed in the one electron oxidations of azide ion and other pseudohalides in the presence of PBN. Because the reaction of hydroxyl and sulfatyl radicals with pseudohalides is very fast (2–4), both Fenton's reagent and persulfate were used in an attempt to produce the neutral radicals from the corresponding pseudohalides. Also, electrochemical oxidations were performed at potentials where the spin trap was electroinactive (5):

$$X^- - e^-(HO\cdot \text{ or } SO_4^{\cdot-} \text{ or electrochemical}) \longrightarrow X\cdot$$

where X = N_3, OCN, CN, Cl.

Experimental

Three different methods of oxidations were employed. All concentrations stated are final concentrations.

Reactions with Persulfate

Solutions of 1 *M* alkali metal pseudohalides containing 0.05 *M* PBN were mixed with 0.01 *M* $Na_2S_2O_8$ or $(NH_4)_2S_2O_8$ both previously outgassed with N_2 (10–15 min) and immediately monitored by esr. Conrol experiments (e.g. PbO_2 + NaN_3) indicated that spin adduct formation was not due to addition followed by oxidation. Photolysis experiments were performed with a medium pressure Hg arc which irradiated the quartz cell directly in the esr cavity.

Reactions with Fenton's Reagent

PBN (0.1 *M*) was added to a stock solution of 2×10^{-5} *M* $FeCl_3$ and 8×10^{-4} *M* adenosine diphosphate (ADP) shortly before performing the experiment and mixed with 0.1 *M* NaN_3 and 5×10^{-2} *M* H_2O_2 both previously outgassed with N_2. Control experiments gave no signal in the absence of any one component except for a weak signal when H_2O_2 and NaN_3 were mixed with PBN alone. This signal could be eliminated by the addition of EDTA.[1]

Apparatus

A description and figure showing the mixing chambers and esr cell arrangement have been published (6). For the electrolysis experiments a Varian E-256 cell was used.

[1]Trace metal ion impurities in water may catalyze the decomposition of H_2O_2 producing hydroxyl radicals. Complexation of these metal ions with EDTA appears to eliminate this problem.

0008-4042/80/151596-03$01.00/0
©1980 National Research Council of Canada/Conseil national de recherches du Canada

Can. J. Chem. Downloaded from www.nrcresearchpress.com by 210.87.254.105 on 09/05/12
For personal use only.

Electrochemical Oxidations

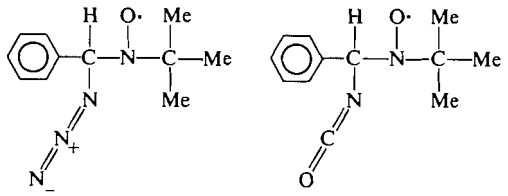
In situ electrochemical oxidations were carried out at a platinum gauze electrode in CH_3CN (AN)/0.10 *M* tetraethylammonium perchlorate solutions at potentials where substrate alone was oxidized (5). Sources of and purification procedures for AN and tetraethylammonium perchlorate have already been reported (7). Tetraethyl- or tetra-*n*-butylammonium (TEA or TBA) salts (TEA ClO_4, TEA CN, TBA N_3, TBA Cl, TEA NCO) were either commercially available or were prepared by standard methods (8). All potentials are reported relative to the aqueous saturation calomel electrode (sce).

Electron Spin Resonance

Three different Varian spectrometers were used in this work: V4502 (Georgia), E-9 (Oklahoma), and E-104 (Guelph). Hyperfine splitting constants (hfsc) were obtained by calibrating with Fremy's salt or stable "spin label" nitroxyl in solution.

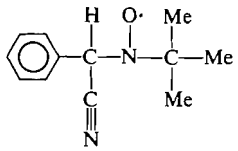
Results

A spectrum consisting of a triplet of 1:2:2:1 quartets ($a_\beta^N = a_\beta^H$) is found when azide ions are oxidized electrochemically at 0.08 V in AN, by Fenton's reagent in H_2O, or upon photolysis in H_2O in the presence of PBN (see Table 1 for hfsc's). This spectrum is assigned to the adduct of the azidyl radical (**I**) and is in agreement with the results reported by Rehorek and co-workers (1).



I

II



III

Although the presence of splitting from a β-nitrogen is consistent with this assignment the spectrum does not give information about the nature of the remaining atoms in the group which was the radical. That this spectrum is not due to the amino adduct has been shown in independent experiments (9).

With persulfate three additional nitroxyl-type triplets are detected: $a_N = 13.03$ G due to Fremy's salt, $^-SO_3—\overset{O\cdot}{N}—SO_3^-$; $a_N = 17.03$ G due to $Me_3C—\overset{O\cdot}{N}—CMe_3$; $a_N = 14.58$ G perhaps due to $Me_3C—\overset{O\cdot}{N}—SO_3^-$. Fremy's salt is detected with 1 *M* NaN_3 plus 0.01 *M* $(NH_4)_2S_2O_8$ alone. The reaction between 0.1 *M* $Me_3C—N{=}O$, 0.1 *M* $(NH_4)_2S_2O_8$, and 1 *M* NaN_3 in H_2O produces the 13.0 G triplet, the 14.58 G triplet, and later the 17.03 G triplet. Much later (2 days) a 12.06 G triplet is found.

Photolysis or the persulfate oxidation of aqueous solutions of cyanate containing PBN produces a poorly resolved triplet of 1:1:1, 1:1:1 multiplets. A more well-resolved spectrum in which each multiplet becomes a doublet of triplets is obtained by electrooxidation of 0.90 V in AN. This spectrum is assigned to spin adduct **II** where the nitrogen atom of the cyanatyl group is bonded to an α-carbon of spin trap.

The electrochemical oxidation of cyanide produces a spin adduct spectrum only in the presence of high concentrations of PBN (~3.6 *M*). The assignment of this spectrum to the cyanyl radical adduct (**III**) is based on an independent spin trapping experiment:

$$Me_3COOC\overset{O}{\overset{\|}{C}}\overset{O}{\overset{\|}{C}}OOCMe_3 \longrightarrow 2Me_3CO\cdot + 2CO_2$$

$$Me_3CO\cdot + PhCH_2CN \longrightarrow Me_3COH + Ph\dot{C}HCN$$

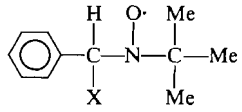
$$Ph\dot{C}HCN + Me_3CN{=}O \longrightarrow PhCH(CN)\overset{O\cdot}{N}CMe_3$$

The spectra obtained (see Table 1 for hfsc's) are in good agreement with an earlier report by Forester and Hepburn (10): $a_N = 15.2$, $a_\beta^H = 2.4$ G from NaCN/HCl in H_2O/C_2H_5OH. However, two recent publications have assigned the following hfsc's to **III**: $a_N = 14.4$, $a_\beta^H = 5.5$, $a_\gamma^N = 1.2$ G (11) and $a_N = 14.6$, $a_\beta^H = 4.9$, $a_\gamma^N = 1.6$ G (12). Further experiments are planned to confirm this assignment.

The chlorine atom adduct is detectable in the electrochemical oxidation of chloride in the presence of PBN in AN. The assignment of the spin adduct is obvious from the relative large Cl-35, Cl-37 hfsc observed. The same spectrum can be obtained by photolysis of CCl_4 (see Table 1) or reaction with *tert*-butyl hypochlorite (13).

Electrooxidations of thiocyanate and bromide in the presence of PBN have produced triplets of doublets but the assignments are not clear at this time. Spin trapping experiments with PBN in the electrooxidation of selenocyanate have been unsuccessful to date.

TABLE 1. Hyperfine splitting constants of PBN spin adducts[a]



—X_3	Conditions	a_{NO}^N	a_β^H	a_β^N
—N_3	0.1 *M* NaN_3, 0.1 *M* PBN, $FeCl_3/H_2O_2$/ADP, H_2O[b]	14.9	2.1	2.1
—N_3	1 *M* NaN_3, 0.05 *M* PBN, 0.01 *M* $Na_2S_2O_8$, H_2O[c]	14.91	2.25	2.25
—N_3	1 *M* NaN_3, 0.05 *M* PBN, *hν*, H_2O	14.9	2.1	2.1
—N_3	$K_3[Co(CN)_5N_3]$, *hν*, H_2O[d]	15.01	2.01	2.01
—N_3	0.004 *M* TBA N_3, 0.05 *M* PBN, +0.08 V, CH_3CN	14.06	1.89	1.89
—NCO	1 *M* KOCN, 0.05 *M* PBN, 0.01 *M* $Na_2S_2O_8$, H_2O	15.91	3.21	1.89
—NCO	1 *M* KOCN, 0.05 *M* PBN, *hν*, H_2O	15.76	3.26	1.81
—NCO	0.005 *M* TEA OCN, 0.05 *M* PBN, +0.90 V, CH_3CN	15.09	3.15	1.84
—CN	0.001 *M* TEA CN, 3.6 *M* PBN, +0.85 V, CH_3CN	15.04	1.98	—
—CN	$C_6H_5CH_2CN$, Me_3C—N=O, DBPO, C_6H_6	14.96	1.94	—
—Cl	0.002 *M* TBA Cl, 0.08 *M* PBN, +0.95 V, CH_3CN	12.27	0.82	6.20[e] 5.12[g]
—Cl	Me_3COCl, 0.1 *M* PBN, C_6H_6[f]	12.12	0.75	6.05[e] 4.88[g]
—Cl	CCl_4, 0.1 *M* PBN, *hν*, CCl_4	12.22	0.8	6.08[e] 5.0[g]

[a]All experiments at room temperature; all hyperfine splitting constants in G; all potentials vs. sce.
[b]See text for concentrations.
[c]Other triplet spectra detected; see text.
[d]Reference 1.
[e]Cl-35 hfsc.
[f]Concentrations unknown, ref. 13.
[g]Cl-37 hfsc.

Acknowledgements

This work is being supported by the Natural Sciences and Engineering Research Council of Canada and Grant #AM08397 from the National Institutes of Health, USPHS. Grateful acknowledgement is hereby made.

1. D. REHOREK, P. THOMAS, and H. HENNIG. Inorg. Chim. Acta, **32**, L1 (1979); D. REHOREK and H. HENNIG. Z. Chem. **19**, 263 (1979).
2. E. HAYON and M. SIMIC. J. Am. Chem. Soc. **92**, 7486 (1970).
3. E. J. LAND and W. A. PRÜTZ. Int. J. Radiat. Biol. **32**, 203 (1977).
4. O. P. CHAWLA and R. W. FESSENDEN. J. Phys. Chem. **79**, 2693 (1975).
5. G. L. MCINTIRE, H. N. BLOUNT, H. J. STRONKS, R. V. SHETTY, and E. G. JANZEN. J. Phys. Chem. **84**, 916 (1980).
6. G. A. RUSSELL, E. G. JANZEN, and E. T. STROM. J. Am. Chem. Soc. **86**, 1807 (1964).
7. D. T. SHANG and H. N. BLOUNT. J. Electroanal. Chem. **54**, 305 (1974); J. F. EVANS and H. N. BLOUNT. Anal. Lett. **7**, 445 (1974).
8. J. F. EVANS. Ph.D. Dissertation, The University of Delaware. 1977.
9. E. G. JANZEN and E. R. DAVIS. To be published.
10. A. R. FORRESTER and S. P. HEPBURN. J. Chem. Soc. C, 701 (1971).
11. S. W. MAO and L. KEVAN. J. Phys. Chem. **80**, 2330 (1976).
12. D. REHOREK, J. SALVETTER, A. HANTSCHMANN, H. HENNIG, Z. STASICKA, and A. CHODKOWSKA. Inorg. Chim. Acta, **37**, L471 (1979).
13. E. G. JANZEN, B. R. KNAUER, L. T. WILLIAMS, and W. B. HARRISON. J. Phys. Chem. **74**, 3025 (1970).

Can. J. Chem. Downloaded from www.nrcresearchpress.com by 210.87.254.105 on 09/05/12
For personal use only.

The mild rhodium(I), and phase transfer catalyzed, dehydrogenation of benzylic alcohols

HOWARD ALPER,[1] KHALED HACHEM, AND SANDRO GAMBAROTTA
Department of Chemistry, University of Ottawa, Ottawa, Ont., Canada K1N 9B4

Received April 7, 1980

This paper is dedicated to Prof. Raymond U. Lemieux on the occasion of his 60th birthday

HOWARD ALPER, KHALED HACHEM, and SANDRO GAMBAROTTA. Can. J. Chem. **58**, 1599 (1980).

Benzylic alcohols can be dehydrogenated to carbonyl compounds by phase transfer catalyzed reaction (8 *M* NaOH, benzene, and $PhCH_2N(C_2H_5)_3^+Cl^-$ as the catalyst) in the presence of catalytic amounts of chlorodicarbonylrhodium(I) dimer. Evidence is presented for the intermediacy of *ortho*-metalated complexes in these reactions.

HOWARD ALPER, KHALED HACHEM et SANDRO GAMBAROTTA. Can. J. Chem. **58**, 1599 (1980).

Les alcools benzyliques peuvent être déshydrogénés en composés carbonylés par une réaction catalysée de transfert de phase (NaOH 8 *M*, benzène et $PhCH_2N(C_2H_5)_3^+Cl^-$ comme catalyseur) en présence de quantités catalytiques de dimère du chlorodicarbonylrhodium (I). On apporte les preuves de la présence de complexes orthométallés intermédiaires au cours de ces réactions.
[Traduit par le journal]

Can. J. Chem. Downloaded from www.nrcresearchpress.com by 210.87.254.42 on 09/05/12
For personal use only.

Phase transfer catalysis has recently become an important method for effecting reactions catalyzed by organometallic compounds (1). Examples include the cobalt carbonyl catalyzed carbonylation of dienes or trienes to unsaturated ketones (2), the palladium(II) catalyzed addition of benzene to α,β-unsaturated ketones (3), and the nickel(0) catalyzed cyanation of aryl halides (4). We now wish to demonstrate that phase transfer catalysis can be applied to the dehydrogenation of alcohols by rhodium(I) catalysts.

Treatment of a benzene solution of an alcohol (**1**) with a catalytic amount of chlorodicarbonylrhodium(I) dimer (**2**) ((25–100) : 1 mole ratio of **1**:**2**), sodium hydroxide (8 *M*), and benzyltriethylammonium chloride as the phase transfer catalyst, for 4 h at 55°C, or 18–30 h at room temperature, affords the dehydrogenated carbonyl compound (**3**). Reasonable yields (Table 1) of ketones were obtained from a variety of benzylic alcohols. Ethers were formed as by-products in two cases, with recovered alcohol as the only other organic species. Interestingly, primary alcohols were significantly less reactive than secondary alcohols. For example, 2-naphthalenemethanol was converted to 2-naphthaldehyde in 42% yield, and a small amount of naphthalene was also isolated. In addition, 1-adamantanemethanol and 3β-cholestanol failed to react under these conditions. One can take advantage of this difference in reactivity by selectively dehydrogenating a secondary alcohol in the presence of a primary one (e.g. 1-phenyl-1,3-propanediol).

$$\underset{\mathbf{1}}{R_2CHOH} \xrightarrow[PhCH_2N(C_2H_5)_3^+Cl^-]{[Rh(CO)_2Cl]_2\ (\mathbf{2})} \underset{\mathbf{3}}{R_2C{=}O}$$

C_6H_6, 8 *M* NaOH

Other rhodium(I) complexes could be used as catalysts, including chlorotris(triphenylphosphine)-rhodium(I) ($(Ph_3P)_3RHCl$, Wilkinson's catalyst), and chlorocarbonylbis(triphenylphosphine)rhodium(I) ($(Ph_3P)_2Rh(CO)Cl$), but conversions were significantly lower and the work-up of these reactions was not as simple as with $(Rh(CO)_2Cl)_2$. The same observations were noted when dichlorotris(triphenylphosphine)ruthenium ($RuCl_2(PPh_3)_3$) was employed as the catalyst.

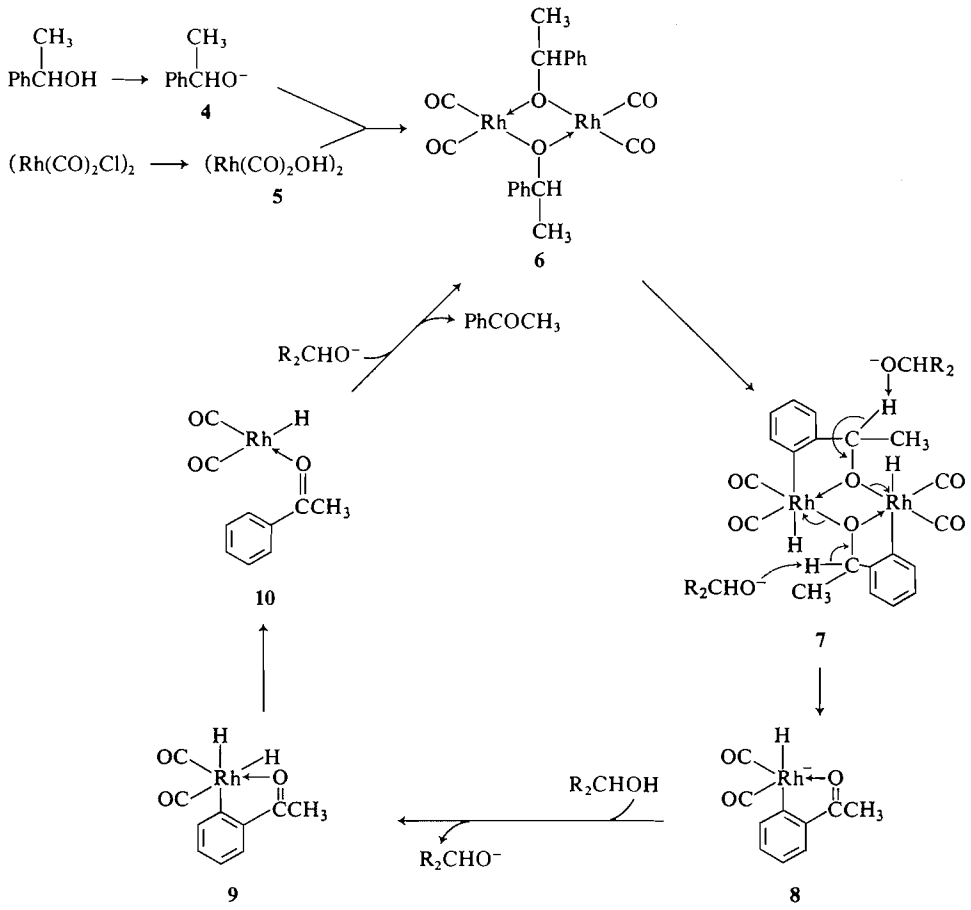
Another useful phase transfer catalyst for the dehydrogenation reaction is Aliquat 336 (tricaprylmethylammonium chloride). Carbonyl compounds were also formed when the reaction was effected in the absence of a phase transfer catalyst (i.e. as a two-phase reaction), but with reduced product yields. No reaction occurred in the absence of both the phase transfer and rhodium(I) catalysts, or in the absence of only the latter.

A possible mechanism for the phase transfer catalyzed dehydrogenation of alcohols, catalyzed by complex **2**, is outlined in the catalytic cycle in Scheme 1 (illustrated with 1-phenylethanol). It is likely that the quarternary ammonium hydroxide, generated by hydroxide ion displacement of the chloride ion of the phase transfer catalyst in the aqueous phase, serves two functions in the overall process: (*1*) formation of the alkoxide **4**, and (*2*) displacement of the bridging chloride ligand of $(Rh(CO)_2Cl)_2$ to give **5**. These reactions likely

[1]Author to whom correspondence may be addressed. E. W. R. Steacie Fellow, 1980–1982.

0008-4042/80/151599-03$01.00/0
©1980 National Research Council of Canada/Conseil national de recherches du Canada

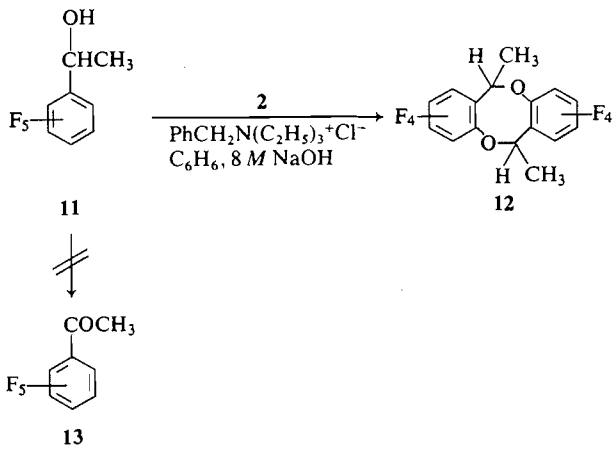
Can. J. Chem. Downloaded from www.nrcresearchpress.com by 210.87.254.42 on 09/05/12
For personal use only.



SCHEME 1

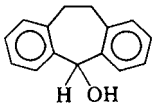
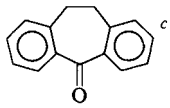
occur in the organic phase, and the phase transfer catalyzed substitution of hydroxo for chloride bridges has previously been described for several platinum complexes (5). Addition of the alkoxide to **5** would afford **6**, which by hydrogen transfer from an *ortho*-substituted carbon to each rhodium atom would give the rhodium(III) complex **7**. Carbon–hydrogen bond cleavage of **7** by alkoxide ion would generate **8**. Protonation of the latter would afford **9**, which is convertible to the rhodium(I) complex **10**. Acetophenone would then be formed by alkoxide ion displacement, regenerating **6**.

Solid evidence for the intermediacy of *ortho*-metalated complexes (6,7) in this reaction was obtained by the use of 1-pentafluorophenylethanol (**11**) as the substrate. Treatment of **11** with a catalytic amount of $(Rh(CO)_2Cl)_2$, under identical conditions to those described for 1-phenylethanol, gave the *ortho*-disubstituted compound **12** in 70% yield,[2] but no ketone (**13**). There is precedence for the removal of fluorine during *ortho*-metalation (8,9). The fluorine analog of **7** likely undergoes reductive elimination to give **12**, rather than conversion to the fluorinated derivative of **8**. The required formation of an *ortho*-metalated intermediate in the dehydrogenation reaction accounts for the failure to ob-



[2]Infrared spectra ($CHCl_3$) ν (OH): absent; ^1H nmr ($CDCl_3$) δ: 1.75 (d, CH_3), 5.63 (m,CH); ^{13}C nmr ($CDCl_3$) δ: 20.16 (CH_3), 74.05 (CH); ms *m/e*: 384 (M^+). *Anal.* calcd. for $C_{16}H_8O_2F_8$: C 50.01, H 2.10; found: C 50.17, H 2.13.

TABLE 1. Yields of carbonyl compounds obtained by phase transfer catalyzed dehydrogenation with **2**

Alcohol	Product[a]	Yield, %
2-Methylbenzhydrol	2-Methylbenzophenone	62
1-Phenylethanol	Acetophenone	78 (97)[e]
1-Ferrocenylethanol	Acetylferrocene[b]	81
1-*p*-Methoxyphenylethanol	*p*-Methoxyacetophenone	57
		64
2-Naphthalenemethanol	2-Naphthaldehyde[d]	42
$PhCH(OH)CH_2CH_2OH$	$PhCOCH_2CH_2OH$	46

[a] The structures of the products were characterized by comparison of physical data with those for authentic samples.
[b] $(C_5H_5FeC_5H_4CHCH_3)_2O$ was also formed in 6–7% yield.
[c] The ether $(C_{15}H_{13})_2O$ was isolated in 10% yield.
[d] Naphthalene was a low yield by-product (< 5%).
[e] Yield by gas chromatography.

serve dehydrogenation with simple alcohols such as 3β-cholestanol.

It is noteworthy that transfer hydrogenation was not observed when the dehydrogenation of 1-phenylethanol was effected in the presence of either cyclohexene or 1-decene, implying that hydrogen gas is not evolved during the reaction.[3] Finally, the dehydrogenation reaction is inhibited by the use of a carbon monoxide rather than a nitrogen atmosphere. This may be a consequence of the addition of carbon monoxide to each rhodium of **6** to give an 18-electron ligand complex, from which *ortho*-metalation would be unlikely to occur.

The following general procedure was used: a mixture of the alcohol, **1** (5.0 mmol), and **2** (0.05–0.20 mmol) in benzene (20–25 mL), 8 *M* NaOH (15–20 mL), and benzyltriethylammonium chloride (0.5–2.0 mmol) were stirred at room temperature (18–30 h) or at 55°C (4 h); the reaction was followed by thin-layer chromatography. The layers were separated, and the organic phase was dried ($MgSO_4$ or Na_2SO_4) and then concentrated to give the carbonyl compound. Further purification, if necessary, was effected by column chromatography, recrystallization, or distillation.

Acknowledgements

We are grateful to Imperial Oil Limited, and to the Natural Sciences and Engineering Research Council of Canada for support of this research.

[3] We are grateful to the referees for suggesting this experiment.

1. H. ALPER. Adv. Organometal. Chem. In Press.
2. H. ALPER and J. K. CURRIE. Tetrahedron Lett. 2665 (1979).
3. S. CACCHI, F. LA TORRE, and D. MISITI. Tetrahedron Lett. 4591 (1979).
4. L. CASSAR, M. FOA, F. MONTANARI, and G. P. MARINELLI. J. Organometal. Chem. **173**, 335 (1979).
5. M. E. FAKLEY and A. PIDCOCK. J. Chem. Soc. Dalton Trans. 1444 (1977).
6. M. I. BRUCE. Angew. Chem. Int. Ed. Engl. **16**, 73 (1977).
7. I. OMAE. Coord. Chem. Rev. **28**, 97 (1979).
8. M. I. BRUCE, R. C. F. GARDNER, and F. G. A. STONE. J. Chem. Soc. Dalton Trans. 81 (1976).
9. M. I. BRUCE, B. L. GOODALL, G. L. SHEPPARD, and F. G. A. STONE. J. Chem. Soc. Dalton Trans. 591 (1975).

Homoenolization of 3,3,6,6-tetramethylbicyclo[2.2.1]heptane-2,5-dione. Rearrangement to 1,3,3-trimethylbicyclo[2.2.1]octane-2,5-dione via a novel β-homoenolate switch

NICK HENRY WERSTIUK AND SHAHIN YEROUSHALMI
Department of Chemistry, McMaster University, Hamilton, Ont., Canada L8S 4M1

Received May 7, 1980

NICK HENRY WERSTIUK and SHAHIN YEROUSHALMI. Can. J. Chem. **58**, 1601 (1980).

Treatment of 3,3,6,6-tetramethylbicyclo[2.2.1]heptane-2,5-dione (**1**) with $K^+\bar{O}t$Bu in *t*-BuOH at 175°C results in rearrangement to 1,3,3-trimethylbicyclo[2.2.2]octane-2,5-dione (**3***a*) vai a novel β-homoenolate switch.

NICK HENRY WERSTIUK et SHAHIN YEROUSHALMI. Can. J. Chem. **58**, 1601 (1980).

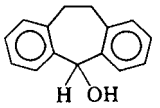
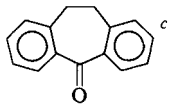
La tétraméthyl-3,3,6,6 bicyclo[2.2.1]heptane dione-2,5 (**1**), traitée par du K^+OtBu^- dans *t*-BuOH à 175°C, se transpose en triméthyl-1,3,3 bicyclo[2.2.1] octanedione-2,5 (**3***a*) en passant par un nouveau β-homoénolate.

[Traduit par le journal]

0008-4042/80/151601-03$01.00/0
© 1980 National Research Council of Canada/Conseil national de recherches du Canada

Can. J. Chem. Downloaded from www.nrcresearchpress.com by 210.87.254.42 on 09/05/12
For personal use only.

TABLE 1. Yields of carbonyl compounds obtained by phase transfer catalyzed dehydrogenation with **2**

Alcohol	Product[a]	Yield, %
2-Methylbenzhydrol	2-Methylbenzophenone	62
1-Phenylethanol	Acetophenone	78 (97)[c]
1-Ferrocenylethanol	Acetylferrocene[b]	81
1-*p*-Methoxyphenylethanol	*p*-Methoxyacetophenone	57
		64
2-Naphthalenemethanol	2-Naphthaldehyde[d]	42
$PhCH(OH)CH_2CH_2OH$	$PhCOCH_2CH_2OH$	46

[a] The structures of the products were characterized by comparison of physical data with those for authentic samples.
[b] $(C_5H_5FeC_5H_4CHCH_3)_2O$ was also formed in 6–7% yield.
[c] The ether $(C_{13}H_{13})_2O$ was isolated in 10% yield.
[d] Naphthalene was a low yield by-product (< 5%).
[e] Yield by gas chromatography.

serve dehydrogenation with simple alcohols such as 3β-cholestanol.

It is noteworthy that transfer hydrogenation was not observed when the dehydrogenation of 1-phenylethanol was effected in the presence of either cyclohexene or 1-decene, implying that hydrogen gas is not evolved during the reaction.[3] Finally, the dehydrogenation reaction is inhibited by the use of a carbon monoxide rather than a nitrogen atmosphere. This may be a consequence of the addition of carbon monoxide to each rhodium of **6** to give an 18-electron ligand complex, from which *ortho*-metalation would be unlikely to occur.

The following general procedure was used: a mixture of the alcohol, **1** (5.0 mmol), and **2** (0.05–0.20 mmol) in benzene (20–25 mL), 8 *M* NaOH (15–20 mL), and benzyltriethylammonium chloride (0.5–2.0 mmol) were stirred at room temperature (18–30 h) or at 55°C (4 h); the reaction was followed by thin-layer chromatography. The layers were separated, and the organic phase was dried ($MgSO_4$ or Na_2SO_4) and then concentrated to give the carbonyl compound. Further purification, if necessary, was effected by column chromatography, recrystallization, or distillation.

Acknowledgements

We are grateful to Imperial Oil Limited, and to the Natural Sciences and Engineering Research Council of Canada for support of this research.

[3] We are grateful to the referees for suggesting this experiment.

1. H. ALPER. Adv. Organometal. Chem. In Press.
2. H. ALPER and J. K. CURRIE. Tetrahedron Lett. 2665 (1979).
3. S. CACCHI, F. LA TORRE, and D. MISITI. Tetrahedron Lett. 4591 (1979).
4. L. CASSAR, M. FOA, F. MONTANARI, and G. P. MARINELLI. J. Organometal. Chem. **173**, 335 (1979).
5. M. E. FAKLEY and A. PIDCOCK. J. Chem. Soc. Dalton Trans. 1444 (1977).
6. M. I. BRUCE. Angew. Chem. Int. Ed. Engl. **16**, 73 (1977).
7. I. OMAE. Coord. Chem. Rev. **28**, 97 (1979).
8. M. I. BRUCE, R. C. F. GARDNER, and F. G. A. STONE. J. Chem. Soc. Dalton Trans. 81 (1976).
9. M. I. BRUCE, B. L. GOODALL, G. L. SHEPPARD, and F. G. A. STONE. J. Chem. Soc. Dalton Trans. 591 (1975).

Homoenolization of 3,3,6,6-tetramethylbicyclo[2.2.1]heptane-2,5-dione. Rearrangement to 1,3,3-trimethylbicyclo[2.2.1]octane-2,5-dione via a novel β-homoenolate switch

NICK HENRY WERSTIUK AND SHAHIN YEROUSHALMI
Department of Chemistry, McMaster University, Hamilton, Ont., Canada L8S 4M1

Received May 7, 1980

NICK HENRY WERSTIUK and SHAHIN YEROUSHALMI. Can. J. Chem. **58**, 1601 (1980).

Treatment of 3,3,6,6-tetramethylbicyclo[2.2.1]heptane-2,5-dione (**1**) with $K^+\bar{O}t$Bu in *t*-BuOH at 175°C results in rearrangement to 1,3,3-trimethylbicyclo[2.2.2]octane-2,5-dione (**3***a*) vai a novel β-homoenolate switch.

NICK HENRY WERSTIUK et SHAHIN YEROUSHALMI. Can. J. Chem. **58**, 1601 (1980).

La tétraméthyl-3,3,6,6 bicyclo[2.2.1]heptane dione-2,5 (**1**), traitée par du K^+OtBu^- dans *t*-BuOH à 175°C, se transpose en triméthyl-1,3,3 bicyclo[2.2.1] octanedione-2,5 (**3***a*) en passant par un nouveau β-homoénolate.

[Traduit par le journal]

0008-4042/80/151601-03$01.00/0
© 1980 National Research Council of Canada/Conseil national de recherches du Canada

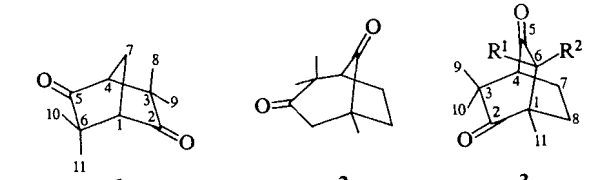
Can. J. Chem. Downloaded from www.nrcresearchpress.com by 210.87.254.6 on 09/05/12
For personal use only.

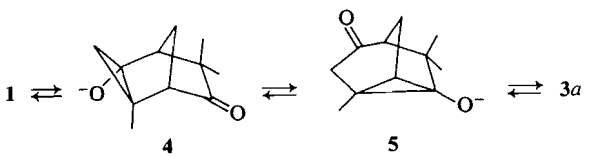
Can. J. Chem. Downloaded from www.nrcresearchpress.com by 210.87.254.6 on 09/05/12
For personal use only.

There are chronicled in the literature (1–16) a number of reports on base-catalyzed homoenolization of polycyclic monoketones. While several groups have quantified the rates of homoenolization and established propensities for rearrangement of monoketones, the homoenolization and rearrangement of polycyclic polyketones where remote C—H bonds are activated by two or more carbonyl groups have not been studied.

Our interest in the enolization of bicyclic diketones (17,18) led us to study the $K^+\bar{O}tBu$ catalyzed H–D exchange of 3,3,6,6-tetramethylbicyclo[2.2.1]heptane-2,5-dione (**1**) to establish whether or not bishomoenolization occurs at C-7. We reported previously that **1** undergoes unusually rapid H–D exchange at C-7 and the bridgeheads (19). We found also that **1** rearranges to an isomeric diketone via conversion of a methyl into a methylene. From ^1H nmr and ^{13}C nmr spectroscopic data and simple mechanistic considerations we speculated at that time that the isomeric diketone was **2**. We now report that **1**, in fact, rearranges to 1,3,3-trimethylbicyclo[2.2.2]-octane-2,5-dione (**3***a*)[1] via a novel β-homoenolate switch.

Table 1 lists a representative selection of isomerization studies of **3***a*. To establish conclusively the structure of the rearrangement product we converted it into the dibromide and determined the X-ray crystallographic structure (20). That the structure of the dibromide is **3***b* establishes 1,3,3-trimethylbicyclo[2.2.2]octane-2,5-dione (**3***a*) as the rearrangement product. The formation of **3***a* is readily accounted for by a mechanism which involves a β-enolization of a methyl group of **1** to yield homoenolate **4**. Homoenolate **4** undergoes a novel β-enolate switch to homoenolate **5** (Scheme 1) that homoketonizes to **3***a*.[2] As far as we are aware this is only the second report of rearrangement that occurs via a homoenolate switch. Reusch and co-workers have shown that 6-methyl-5-hydroxytricyclo [4.4.0.0][1,5]decan- 9-one (**6**)[3] and several derivatives undergo rearrangement in base via a homoenolate switch (21,22). We plan to study other polycyclic diones to establish the generality and synthetic utility of the rearrangement.





SCHEME 1

TABLE 1. K^+-OtBu catalyzed isomerization of 3,3,6,6-tetramethylbicyclo[2.2.1]heptane-2,5-dione (**1**) in *tert*-butyl alcohol at 175°C

Concentration **1** (*M*)	Reaction time (h)	Concentration base (*M*)	Conversion* to **3***a* (%)
0.40	78.5	1.03	34
0.40	98	1.16	44
0.38	102	1.15	63

*The combined recovery of **1** and **3***a* generally was 70–85% after correction for preparative glpc collection efficiency.

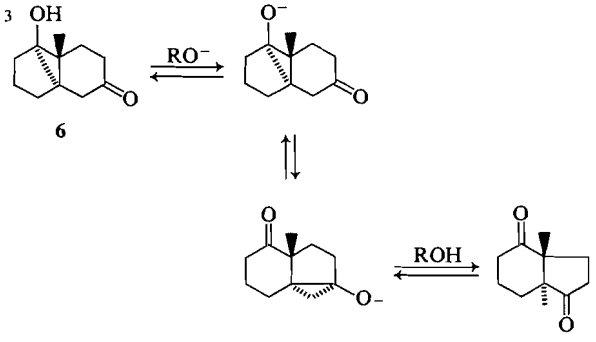
Acknowledgments

We thank the Natural Sciences and Engineering Research Council of Canada for financial support and the Ministry of Science and Higher Education of Iran for awarding a scholarship to S.Y.

1. A. NICKON and J. L. LAMBERT. J. Am. Chem. Soc. **84**, 4604 (1962).
2. A. NICKON, J. L. LAMBERT, and J. E. OLIVER. J. Am. Chem. Soc. **88**, 2787 (1966).
3. A. NICKON, H. KWASNIK, T. SWARTZ, R. O. WILLIAMS, and J. B. DIGIORGIO. J. Am. Chem. Soc. **87**, 1615 (1965).
4. R. HOWE and S. WINSTEIN. J. Am. Chem. Soc. **87**, 915 (1965).
5. T. FAKUNAGA. J. Am. Chem. Soc. **87**, 916 (1965).
6. R. M. COATES and J. P. CHEN. Chem. Commun. 1481 (1970).
7. K. W. TURNBULL, S. J. GOULD, and D. ARIGONI. Chem. Commun. 597 (1972).
8. D. H. HUNTER, A. L. JOHNSON, J. B. STOTHERS, A. NIC-

[1]Compound **3***a* has a mp of 48–50°C, a carbonyl absorption at 1725 cm^{-2} ($CDCl_3$), and three methyls at δ 1.17, 1.04, and 1.01 in the ^1H nmr spectrum. The ^{13}C chemical shifts (CCl_4) and off-resonance multiplicities are: C-2, 217.6(s); C-5, 211.8(s); C-4, 56.4(d); C-3, 46.2(s); C-6, 46.1(t); C-1, 44.5(s); C-8, 29.8(t); C-9, 24.9(q); C-10, 22.9(q); C-11, 19.4(q); C-7, 18.8(t).

[2]By heating **3***a* under homoenolization conditions, we established, as expected, that the **1** ⇄ **3***a* equilibrium lies in favour of **3***a*. Less than 1% of **1** is formed from **3***a*.



KON, J. L. LAMBERT, and D. F. COVEY. J. Am. Chem. Soc. **94**, 8582 (1972).
9. J. B. STOTHERS and C. T. TAN. J. Chem. Soc. Chem. Commun. 738 (1974).
10. A. L. JOHNSON, N. W. PETERSEN, M. B. RAMPERSAD, and J. B. STOTHERS. Can. J. Chem. **52**, 4143 (1974).
11. A. J. JOHNSON, J. B. STOTHERS, and C. T. TAN. Can. J. Chem. **53**, 212 (1975).
12. D. M. HUDYMA, J. B. STOTHERS, and C. T. TAN. Org. Magn. Reson. 614 (1974).
13. A. NICKON, D. F. COVEY, C. D. PANDIT, and J. T. FRANK. Tetrahedron Lett. 3681 (1975).
14. A. NICKON, J. L. LAMBERT, J. E. OLIVER, D. F. COVEY, and J. MORGAN. J. Am. Chem. Soc. **98**, 2593 (1976).
15. A. R. CHENG, J. B. STOTHERS, and C. T. TAN. Can. J. Chem. **55**, 447 (1977).
16. A. K. CHENG and J. B. STOTHERS. Can. J. Chem. **55**, 4184 (1977).
17. N. H. WERSTIUK and R. TAILLEFER. Can. J. Chem. **48**, 3966 (1970).
18. N. H. WERSTIUK, R. TAILLEFER, and S. BANERJEE. Can. J. Chem. **56**, 1148 (1978).
19. N. H. WERSTIUK. Can. J. Chem. **53**, 2211 (1975).
20. C. J. L. LOCK, R. FAGGIANI, N. H. WERSTIUK, and S. YEROUSHALMI. J. Org. Chem. In press.
21. W. REUSCH, K. GRIMM, J. E. KAROGLAN, J. MARTIN, K. P. SUBRAHAMANIAN, P. S. VENKATARAMANI, and J. D. YORDY. J. Am. Chem. Soc. **99**, 1958 (1977).
22. J. D. YORDY and W. REUSCH. J. Am. Chem. Soc. **99**, 1965 (1977).

Homoenolization of 1,3,3-trimethylbicyclo[2.2.2]octane-2,5-dione. Unusually rapid H–D exchange of a bridgehead methyl

NICK HENRY WERSTIUK AND SHAHIN YEROUSHALMI

Department of Chemistry, McMaster University, Hamilton, Ont., Canada L8S 4M1

Received May 7, 1980

NICK WERSTIUK and SHAHIN YEROUSHALMI. Can. J. Chem. **58**, 1603 (1980).

The title compound **2***a* undergoes unusually rapid H–D exchange at the bridgehead methyl at a rate 5300 times faster than exchange of the bridgehead methyl of 1,3,3-trimethylbicyclo[2.2.1]heptan-2-one (fenchone). From the isotopic composition of partially deuterated **2***a*, we deduce that exchange occurs via an isomer, in equilibrium with **2***a*, which contains an active methylene derived from the bridgehead methyl.

NICK HENRY WERSTIUK et SHAHIN YEROUSHALMI. Can. J. Chem. **58**, 1603 (1980).

Le composé mentionné dans le titre subit un échange H–D au niveau du méthyle en tête de pont à une vitesse 5300 fois plus rapide que l'échange au niveau du méthyle en tête de pont de la triméthyl-1,3,3 bicyclo[2.2.1] heptanone-2 (fenchone). A partir de la composition isotopique du composé **2***a* partiellement deutéré, nous en déduisons que l'échange se produit par l'intermédiaire d'un isomère, en équilibre avec **2***a*, qui contient un méthylène activé provenant du méthyle en tête de pont.

[Traduit par le journal]

Over the past decade there has been a steady increase in the number of publications dealing with the homoenolization of polycyclic monoketones (1–16). Substantial progress has been made as regards the factors which control the rate of homoenolization and the rearrangement of polycyclic monoketones via homoenolate anions. However, there were no reports of studies of homoenolization of polycyclic polyketones prior to our report of the homoenolization and rearrangement of 3,3,6,6-tetramethylbicyclo[2.2.1]heptane-2,5-dione (**1**). We found that **1** rearranges to 1,3,3-trimethylbicyclo[2.2.2]octane-2,5-dione (**2**) via a novel homoenolate switch (17). We found also that one of the methyl groups of **2** underwent unusually rapid H–D exchange under the conditions (~1 *M* $K^+\bar{O}t$Bu/*t*-BuOD, 175°C) used to homoenolize and rearrange **1**. In this communication we report on a preliminary study of the homoenolization of **2**. We present evidence that it is the bridgehead methyl of **2** that undergoes rapid exchange. Equally surprising is the unusual mechanism of H–D exchange which must involve conversion of the bridgehead methyl into an active methylene of an isomer which is in equilibrium with **2**.

Table 1 lists a representative selection of homoenolization experiments that illustrate the degree of deuterium incorporation of **2** as a function of base concentration, temperature, and reaction time. Equilibration of the hydrogens α to the carbonyl with the deuterium pool, as expected, occurs readily with the incorporation of 1.5–1.6 atoms of deuterium (entry 3). Additional deuterium is incorporated into **2** predominately by rapid exchange of

0008-4042/80/151603-03$01.00/0

© 1980 National Research Council of Canada/Conseil national de recherches du Canada

Can. J. Chem. Downloaded from www.nrcresearchpress.com by 210.87.254.6 on 09/05/12
For personal use only.

KON, J. L. LAMBERT, and D. F. COVEY. J. Am. Chem. Soc. **94**, 8582 (1972).
9. J. B. STOTHERS and C. T. TAN. J. Chem. Soc. Chem. Commun. 738 (1974).
10. A. L. JOHNSON, N. W. PETERSEN, M. B. RAMPERSAD, and J. B. STOTHERS. Can. J. Chem. **52**, 4143 (1974).
11. A. J. JOHNSON, J. B. STOTHERS, and C. T. TAN. Can. J. Chem. **53**, 212 (1975).
12. D. M. HUDYMA, J. B. STOTHERS, and C. T. TAN. Org. Magn. Reson. 614 (1974).
13. A. NICKON, D. F. COVEY, C. D. PANDIT, and J. T. FRANK. Tetrahedron Lett. 3681 (1975).
14. A. NICKON, J. L. LAMBERT, J. E. OLIVER, D. F. COVEY, and J. MORGAN. J. Am. Chem. Soc. **98**, 2593 (1976).
15. A. R. CHENG, J. B. STOTHERS, and C. T. TAN. Can. J. Chem. **55**, 447 (1977).
16. A. K. CHENG and J. B. STOTHERS. Can. J. Chem. **55**, 4184 (1977).
17. N. H. WERSTIUK and R. TAILLEFER. Can. J. Chem. **48**, 3966 (1970).
18. N. H. WERSTIUK, R. TAILLEFER, and S. BANERJEE. Can. J. Chem. **56**, 1148 (1978).
19. N. H. WERSTIUK. Can. J. Chem. **53**, 2211 (1975).
20. C. J. L. LOCK, R. FAGGIANI, N. H. WERSTIUK, and S. YEROUSHALMI. J. Org. Chem. In press.
21. W. REUSCH, K. GRIMM, J. E. KAROGLAN, J. MARTIN, K. P. SUBRAHAMANIAN, P. S. VENKATARAMANI, and J. D. YORDY. J. Am. Chem. Soc. **99**, 1958 (1977).
22. J. D. YORDY and W. REUSCH. J. Am. Chem. Soc. **99**, 1965 (1977).

Can. J. Chem. Downloaded from www.nrcresearchpress.com by 210.87.254.42 on 09/05/12
For personal use only.

Homoenolization of 1,3,3-trimethylbicyclo[2.2.2]octane-2,5-dione. Unusually rapid H–D exchange of a bridgehead methyl

NICK HENRY WERSTIUK AND SHAHIN YEROUSHALMI
Department of Chemistry, McMaster University, Hamilton, Ont., Canada L8S 4M1

Received May 7, 1980

NICK WERSTIUK and SHAHIN YEROUSHALMI. Can. J. Chem. **58**, 1603 (1980).

The title compound **2***a* undergoes unusually rapid H–D exchange at the bridgehead methyl at a rate 5300 times faster than exchange of the bridgehead methyl of 1,3,3-trimethylbicyclo[2.2.1]heptan-2-one (fenchone). From the isotopic composition of partially deuterated **2***a*, we deduce that exchange occurs via an isomer, in equilibrium with **2***a*, which contains an active methylene derived from the bridgehead methyl.

NICK HENRY WERSTIUK et SHAHIN YEROUSHALMI. Can. J. Chem. **58**, 1603 (1980).

Le composé mentionné dans le titre subit un échange H–D au niveau du méthyle en tête de pont à une vitesse 5300 fois plus rapide que l'échange au niveau du méthyle en tête de pont de la triméthyl-1,3,3 bicyclo[2.2.1] heptanone-2 (fenchone). A partir de la composition isotopique du composé **2***a* partiellement deutéré, nous en déduisons que l'échange se produit par l'intermédiaire d'un isomère, en équilibre avec **2***a*, qui contient un méthylène activé provenant du méthyle en tête de pont.

[Traduit par le journal]

Over the past decade there has been a steady increase in the number of publications dealing with the homoenolization of polycyclic monoketones (1–16). Substantial progress has been made as regards the factors which control the rate of homoenolization and the rearrangement of polycyclic monoketones via homoenolate anions. However, there were no reports of studies of homoenolization of polycyclic polyketones prior to our report of the homoenolization and rearrangement of 3,3,6,6-tetramethylbicyclo[2.2.1]heptane-2,5-dione (**1**). We found that **1** rearranges to 1,3,3-trimethylbicyclo[2.2.2]octane-2,5-dione (**2**) via a novel homoenolate switch (17). We found also that one of the methyl groups of **2** underwent unusually rapid H–D exchange under the conditions (~1 *M* $K^+\bar{O}t$Bu/*t*-BuOD, 175°C) used to homoenolize and rearrange **1**. In this communication we report on a preliminary study of the homoenolization of **2**. We present evidence that it is the bridgehead methyl of **2** that undergoes rapid exchange. Equally surprising is the unusual mechanism of H–D exchange which must involve conversion of the bridgehead methyl into an active methylene of an isomer which is in equilibrium with **2**.

Table 1 lists a representative selection of homoenolization experiments that illustrate the degree of deuterium incorporation of **2** as a function of base concentration, temperature, and reaction time. Equilibration of the hydrogens α to the carbonyl with the deuterium pool, as expected, occurs readily with the incorporation of 1.5–1.6 atoms of deuterium (entry 3). Additional deuterium is incorporated into **2** predominately by rapid exchange of

0008-4042/80/151603-03$01.00/0
© 1980 National Research Council of Canada/Conseil national de recherches du Canada

Can. J. Chem. Downloaded from www.nrcresearchpress.com by 210.87.254.42 on 09/05/12
For personal use only.

TABLE 1. H–D Exchange of 1,3,3-trimethylbicyclo[2.2.2]octane-2,5-dione in $K^+\bar{O}t$Bu/*t*-BuOD

Entry	Concentration (*M*) **2***a*[a]	Concentration (*M*) base	Temperature °C	Reaction time (h)	Excess *d* per molecule[b] (*d* in methyl)
1	0.15	1.14	175	55	5.86 (2.31)[c]
2	0.12	1.05	150	4	4.10 (2.63)[c]
3	0.13	1.05	100	5	1.68 (0.13)[d]
4	0.11	1.03	100	25	2.01 (0.51)[d]
5	0.11	1.08	100	75	2.78 (1.06)[d]

[a]Recoveries of **2***a* were in the 80–90% range.
[b]Determined mass spectrometrically at low voltage (10–15 eV).
[c]Determined by ^{2}H nmr spectroscopy in the presence of Eu(fod)$_3$.
[d]Determined by ^{2}H nmr in the absence of Eu(fod)$_3$.

the bridgehead methyl. In fact, from a one-point kinetic analysis we find that the methyl of **2** exchanges 5300 times faster than the bridgehead methyl of fenchone (11). Although homoenolization occurs most readily at the bridgehead methyl, deuterium is also incorporated at C-7 and C-8 as is indicated by the data in entry 1. This conclusion is also supported by the ^{2}H nmr spectrum of deuterated **2** isolated from the reaction described in entry 1.

That a methyl undergoes exchange is established by the absence of a methyl signal at σ 1.04 in the ^{1}H nmr spectrum of deuterated **2***a* isolated from the experiment described in entry 1. That it is the bridgehead methyl that undergoes rapid exchange is supported by the following evidence. Irradiation of the C-3 methyls of **2***a* containing 4.9 excess deuterium atoms yielded an increase of 10.5% and 12.6% (average of three determinations) in the signal due to H-4. The nOe's (18) establish that the C-3 methyls must flank H-4. Also, that the ^{13}C signal due to C-1 of deuterated **2***b* obtained from a highly deuterated sample of **2***a* (6.5 excess deuterium atoms per molecule) was absent, an indication of a long relaxation time, establishes that C-1 must be attached to carbon atoms which bear oxygen, bromine, or deuterium as indicated in **3**. Furthermore, the signal at 19.4 ppm of the ^{13}C spectrum of **2***a* that we assign with certainty to the bridgehead methyl,[1] essentially disappears on deuteration.

Equally interesting is the fact that deuterium is incorporated into **2***a* in an unusual fashion. The expected sequence of exchange

$$d_0 \xrightarrow{k_1} d_1 \xrightarrow{k_2} d_2 \xrightarrow{k_2} d_3 \xrightarrow{k_3} d_4 \xrightarrow{k_4} k_5$$

where

$$k_1 \sim k_2 \gg k_3 \sim k_4 \sim k_5$$

would lead to a build up and then a gradual decrease of d_3 and d_4 species as conversion to **2***a*-d_5 occurs. However, it is clear from the distribution of deuterated species (Fig. 1) that there is a slow conversion of **2***a*-d_2 to **2***a*-d_3 and then a fast conversion of **2***a*-d_3 to **2***a*-d_5. That is,

$$k_1 \sim k_2 \gg k_3 < k_4 \sim k_5$$

Even in the case where there is minimal exchange of the methyl (entry 3) it is clear that **2***a*-d_3 must be converted rapidly to **2***a*-d_5 (Fig. 1). When the peak intensities of **2***a* isolated from the experiment listed in entry 5 are corrected for $M + 1$ and $M + 2$ contributions, **2***a* is a composite of 2.4% d_0, 14.7% d_1, 43.7% d_2, 4.1% d_3, 12.5% d_4, 22.5% d_5, and $< 1\%$ d_6 species. These results suggest that exchange of the bridgehead methyl must occur predominately via an isomer which is in equilibrium with **2***a*[2] and the isomer probably has an active methylene group that is derived from the

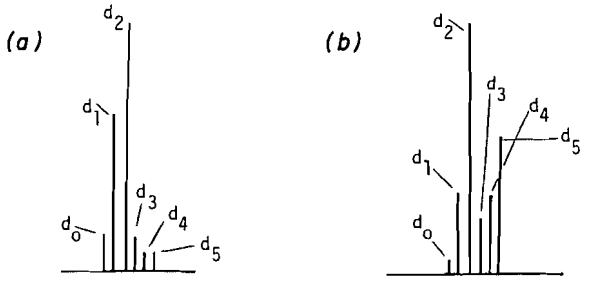
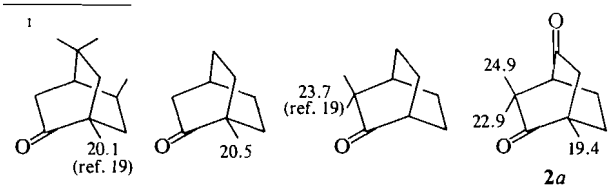
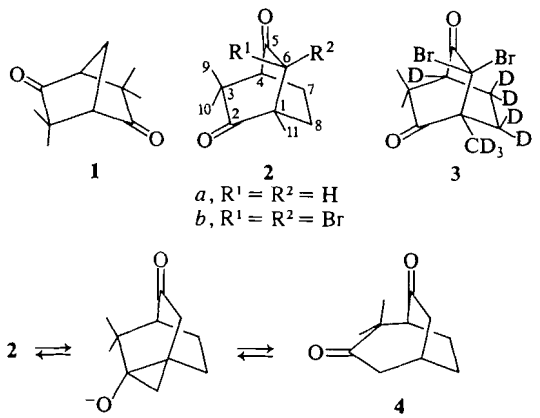


FIG. 1. (*a*) Molecular ion of deuterated **2**a from entry 3; (*b*) molecular ion of deuterated **2**a from entry 5.



We thank Professor C. Djerassi for providing us with a sample of 1-methylbicyclo[2.2.2]octan-2-one.

[2]The isomer which undergoes fast exchange must be present in a small amount because we cannot detect (< 1%) any other major components. If **4** is in fact the isomer of **2***a*, it must homoenolize rapidly as well.



SCHEME 1

bridgehead methyl. A possible candidate is 2,2-dimethylbicyclo[3.2.2]nonane-3,7-dione (**4**) (Scheme 1). We are currently investigating the homoenolization of other methylated bicyclo-[2.2.2]octanones and bicyclo[3.2.2]octanediones to establish the reason for the facile homoenolizations.

Acknowledgements

We thank the Natural Sciences and Engineering Research Council of Canada for financial support and the Ministry of Science and Higher Education of Iran for awarding a scholarship to S.Y.

1. A. NICKON and J. L. LAMBERT. J. Am. Chem. Soc. **84**, 4604 (1962).
2. A. NICKON, J. L. LAMBERT, and J. E. OLIVER. J. Am. Chem. Soc. **88**, 2787 (1966).
3. A. NICKON, H. KWASNIK, T. SWARTZ, R. O. WILLIAMS, and J. B. DIGIORGIO. J. Am. Chem. Soc. **87**, 1615 (1965).
4. R. HOWE and S. WINSTEIN. J. Am. Chem. Soc. **87**, 915 (1965).
5. T. FUKUNAGA. J. Am. Chem. Soc. **87**, 916 (1965).
6. R. M. COATES and J. P. CHEN. Chem. Commun. 1481 (1970).
7. K. W. TURNBULL, S. J. GOULD, and D. ARIGONI. Chem. Commun. 597 (1972).
8. D. H. HUNTER, A. L. JOHNSON, J. B. STOTHERS, A. NICKON, J. L. LAMBERT, and D. F. COVEY. J. Am. Chem. Soc. **94**, 8582 (1972).
9. J. B. STOTHERS and C. T. TAN. J. Chem. Soc. Chem. Commun. 738 (1974).
10. A. L. JOHNSON, N. W. PETERSEN, M. B. RAMPERSAD, and J. B. STOTHERS. Can. J. Chem. **52**, 4143 (1974).
11. A. J. JOHNSON, J. B. STOTHERS, and C. T. TAN. Can. J. Chem. **53**, 212 (1975).
12. D. M. HUDYMA, J. B. STOTHERS, and C. T. TAN. Org. Magn. Reson. 614 (1974).
13. A. NICKON, D. F. COVEY, C. D. PANDIT, and J. T. FRANK. Tetrahedron Lett. 3681 (1975).
14. A. NICKON, J. L. LAMBERT, J. E. OLIVER, D. F. COVEY, and J. MORGAN. J. Am. Chem. Soc. **98**, 2593 (1976).
15. A. R. CHENG, J. B. STOTHERS, and C. T. TAN. Can. J. Chem. **55**, 447 (1977).
16. A. K. CHENG and J. B. STOTHERS. Can. J. Chem. **55**, 4184 (1977).
17. N. H. WERSTIUK and S. YEROUSHALMI. Can. J. Chem. **58**, 1601 (1980).
18. R. A. BELL and J. K. SAUNDERS. *In* Topics in stereochemistry. Vol. 7. *Edited by* E. L. Eliel and N. L. Allinger. Wiley Interscience, New York. 1973. Chapt. 1.
19. K. R. STEPHENS, J. B. STOTHERS, and C. T. TAN. *In* Mass spectrometry and nmr spectroscopy in pesticide chemistry. *Edited by* R. Hagrice and F. J. Biros. Plenum Press, New York. 1974. pp 179–196.

A highly asymmetric synthesis of the *O*-2-isocephem class of β-lactam antibiotics

SHEILA M. TENNESON AND BERNARD BELLEAU

Department of Chemistry, McGill University, Montreal, P.Q., Canada H3A 2K6

Received May 5, 1980

This paper is dedicated to Prof. Raymond U. Lemieux on the occasion of his 60th birthday

SHEILA M. TENNESON and BERNARD BELLEAU. Can. J. Chem. **58**, 1605 (1980).

Starting from D-threonine, an asymmetric synthesis of the dextrorotatory bioactive enantiomer of 3-methyl-7-phenylacetamido-*O*-2-isocephem was accomplished. The key step, where asymmetric cycloaddition of azidoacetyl chloride to the cinnamylidene Schiff base of protected D-threonine is induced, generates the desired *cis*-β-lactam in 90% optical yield. The absolute configuration of the final product was confirmed by comparing its antimicrobial activity with that of its corresponding racemate.

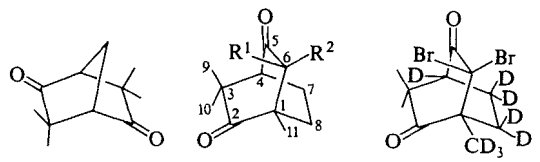
SHEILA M. TENNESON et BERNARD BELLEAU. Can. J. Chem. **58**, 1605 (1980).

En partant de la D-thréonine, on a réalisé une synthèse asymétrique de l'énantiomère dextrogyre biologiquement actif du méthyl-3 phénylacétamido-7 *O*-isocéphème-2. L'étape principale implique la cycloaddition asymétrique du chlorure d'azidoacétyle sur la base de Schiff de la cinnamaldéhyde avec la D-thréonine protégée et elle engendre la β-lactame *cis* désirée avec un rendement optique de 90%. On a confirmé la configuration absolue du produit final en comparant son activité antimicrobienne à celle du racémate correspondant. [Traduit par le journal]

0008-4042/80/151605-03$01.00/0

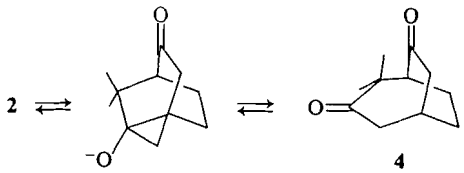
©1980 National Research Council of Canada/Conseil national de recherches du Canada

Can. J. Chem. Downloaded from www.nrcresearchpress.com by 210.87.254.42 on 09/05/12
For personal use only.



1 2 3

a, $R^1 = R^2 = H$
b, $R^1 = R^2 = Br$



4

SCHEME 1

bridgehead methyl. A possible candidate is 2,2-dimethylbicyclo[3.2.2]nonane-3,7-dione (**4**) (Scheme 1). We are currently investigating the homoenolization of other methylated bicyclo-[2.2.2]octanones and bicyclo[3.2.2]octanediones to establish the reason for the facile homoenolizations.

Acknowledgements

We thank the Natural Sciences and Engineering Research Council of Canada for financial support and the Ministry of Science and Higher Education of Iran for awarding a scholarship to S.Y.

1. A. NICKON and J. L. LAMBERT. J. Am. Chem. Soc. **84**, 4604 (1962).
2. A. NICKON, J. L. LAMBERT, and J. E. OLIVER. J. Am. Chem. Soc. **88**, 2787 (1966).
3. A. NICKON, H. KWASNIK, T. SWARTZ, R. O. WILLIAMS, and J. B. DIGIORGIO. J. Am. Chem. Soc. **87**, 1615 (1965).
4. R. HOWE and S. WINSTEIN. J. Am. Chem. Soc. **87**, 915 (1965).
5. T. FUKUNAGA. J. Am. Chem. Soc. **87**, 916 (1965).
6. R. M. COATES and J. P. CHEN. Chem. Commun. 1481 (1970).
7. K. W. TURNBULL, S. J. GOULD, and D. ARIGONI. Chem. Commun. 597 (1972).
8. D. H. HUNTER, A. L. JOHNSON, J. B. STOTHERS, A. NICKON, J. L. LAMBERT, and D. F. COVEY. J. Am. Chem. Soc. **94**, 8582 (1972).
9. J. B. STOTHERS and C. T. TAN. J. Chem. Soc. Chem. Commun. 738 (1974).
10. A. L. JOHNSON, N. W. PETERSEN, M. B. RAMPERSAD, and J. B. STOTHERS. Can. J. Chem. **52**, 4143 (1974).
11. A. J. JOHNSON, J. B. STOTHERS, and C. T. TAN. Can. J. Chem. **53**, 212 (1975).
12. D. M. HUDYMA, J. B. STOTHERS, and C. T. TAN. Org. Magn. Reson. 614 (1974).
13. A. NICKON, D. F. COVEY, C. D. PANDIT, and J. T. FRANK. Tetrahedron Lett. 3681 (1975).
14. A. NICKON, J. L. LAMBERT, J. E. OLIVER, D. F. COVEY, and J. MORGAN. J. Am. Chem. Soc. **98**, 2593 (1976).
15. A. R. CHENG, J. B. STOTHERS, and C. T. TAN. Can. J. Chem. **55**, 447 (1977).
16. A. K. CHENG and J. B. STOTHERS. Can. J. Chem. **55**, 4184 (1977).
17. N. H. WERSTIUK and S. YEROUSHALMI. Can. J. Chem. **58**, 1601 (1980).
18. R. A. BELL and J. K. SAUNDERS. *In* Topics in stereochemistry. Vol. 7. *Edited by* E. L. Eliel and N. L. Allinger. Wiley Interscience, New York. 1973. Chapt. 1.
19. K. R. STEPHENS, J. B. STOTHERS, and C. T. TAN. *In* Mass spectrometry and nmr spectroscopy in pesticide chemistry. *Edited by* R. Hagrice and F. J. Biros. Plenum Press, New York. 1974. pp 179–196.

A highly asymmetric synthesis of the *O*-2-isocephem class of β-lactam antibiotics

SHEILA M. TENNESON AND BERNARD BELLEAU

Department of Chemistry, McGill University, Montreal, P.Q., Canada H3A 2K6

Received May 5, 1980

This paper is dedicated to Prof. Raymond U. Lemieux on the occasion of his 60th birthday

SHEILA M. TENNESON and BERNARD BELLEAU. Can. J. Chem. **58**, 1605 (1980).

Starting from D-threonine, an asymmetric synthesis of the dextrorotatory bioactive enantiomer of 3-methyl-7-phenylacetamido-*O*-2-isocephem was accomplished. The key step, where asymmetric cycloaddition of azidoacetyl chloride to the cinnamylidene Schiff base of protected D-threonine is induced, generates the desired *cis*-β-lactam in 90% optical yield. The absolute configuration of the final product was confirmed by comparing its antimicrobial activity with that of its corresponding racemate.

SHEILA M. TENNESON et BERNARD BELLEAU. Can. J. Chem. **58**, 1605 (1980).

En partant de la D-thréonine, on a réalisé une synthèse asymétrique de l'énantiomère dextrogyre biologiquement actif du méthyl-3 phénylacétamido-7 *O*-isocéphème-2. L'étape principale implique la cycloaddition asymétrique du chlorure d'azidoacétyle sur la base de Schiff de la cinnamaldéhyde avec la D-thréonine protégée et elle engendre la β-lactame *cis* désirée avec un rendement optique de 90%. On a confirmé la configuration absolue du produit final en comparant son activité antimicrobienne à celle du racémate correspondant. [Traduit par le journal]

0008-4042/80/151605-03$01.00/0

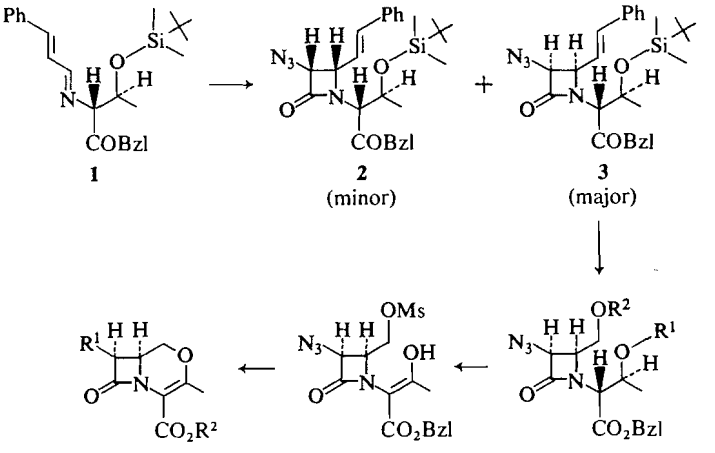
©1980 National Research Council of Canada/Conseil national de recherches du Canada

Can. J. Chem. Downloaded from www.nrcresearchpress.com by 210.87.254.105 on 09/05/12
For personal use only.

Can. J. Chem. Downloaded from www.nrcresearchpress.com by 210.87.254.105 on 09/05/12
For personal use only.

Efficient and stereospecific syntheses of isocephems and the analogous *O*- and *N*-2-isocephems were recently reported by the Bristol Canada group (1). The *O*-2-isocephems in particular constitute a new class of β-lactam antibiotics whose effectiveness against some common pathogenic bacteria compare favorably with analogous cephalosporins currently in use. As is the case of all β-lactam antibiotics, antibacterial activity of a prototype *O*-2-isocephem was associated exclusively with one of the enantiomers (dextrorotatory) of the synthetic racemix mixture (1*f*). A single key step of the synthesis, the cycloaddition of azidoacetyl chloride to a cinnamylidene Schiff base introduces simultaneously the only two asymmetric centers appearing in the final product. However, only one racemate is obtained owing to the exclusive *cis*-stereospecificity of the cycloaddition. For obvious reasons of economics, a synthetic process leading mainly to the bioactive enantiomer from inexpensive starting materials became an important goal. Such an asymmetric process demands that the steric course of the cycloaddition be sensitive to chirality effects about an appropriate α-aminoester Schiff base. Although the chiral α-carbon of an aminoacid Schiff base is not proximal to the reacting aldimine carbon, preliminary observations by the Bristol group some time ago[1] strongly indicated that asymmetric cycloaddition was induced in some degree using a protected L-threonine Schiff base as the reaction partner. However, similar experiments by Just and Liak (2), but with a protected L-serine cinnamylidene Schiff base, led only to racemic material and thus could not yield any information on the possibility of asymmetric induction during the cycloaddition. This provided an additional incentive to reexamine, but in detail, the use of a protected enantiomer of a threonine Schiff base as a potential inducer of asymmetry. Mechanistic considerations allowed the prediction that, for the bioactive enantiomer of the end-product to be obtained, the D-isomer of threonine should be used as staring material. Thus, starting from D-threonine benzyl ester, the synthesis of optically pure (+)-3-methyl-7-phenyl-acetamido-*O*-2-isocephem of *cis*-configuration was accomplished as shown in Scheme 1.

Silylation (3) of D-Thr-ObzL·Hcl (4) (mp 126.5–127.5°C; $[\alpha]_D^{23}$ +10.1 (*c* 4.5, MeOh) in HMPT with *tert*-butyldimethylsilyl chloride gave the *O*-silyl ether[2] which was converted to Schiff base **1** on reaction with cinnamaldehyde (1*a*). The crude Schiff base plus triethylamine (1.3 equiv.) in dry CH_2Cl_2 was treated at −10°C with azidoacetyl chloride (1.2 equiv.) according to published procedures (1) to give β-lactams **2** and **3** (60% from D-Thr-ObzL·HCl), the azidoacetyl amide of protected threonine (~ 30%), and small amounts of unidentified material. The β-lactam fraction was submitted to hplc (Spherisorb, Si 100, 10 μm; MeOh–EtOAc–hexane (0.1:5:95)) to give pure **3** ($[\alpha]_D^{23}$ −150 (*c* 2.5, hexane)) and **2** ($[\alpha]_D^{23}$ +80 (*c*



SCHEME 1

[1]B. Belleau, J. L. Douglas, and D. E. Horning, unpublished results.

[2]For all substances the spectra (ir, pmr, and ms) were in agreement with the assigned structures. Satisfactory microanalyses were obtained for key products. All rotations are for $CHCl_3$ solution unless stated otherwise.

Can. J. Chem. Downloaded from www.nrcresearchpress.com by 210.87.254.105 on 09/05/12
For personal use only.

1.5, hexane)) in a ratio of 9:1. That both **3** and **2** had *cis*-stereochemistry was inferred from their respective 200 MHz pmr spectra ($CDCl_3$)(**3**: $\delta = 4.90$ (d, $J = 5.3$ Hz, 1H, H-3) and 4.92 (dd, $J = 5.3$ and 8.8 Hz, 1H, H-4) ppm; **2**: $\delta = 4.89$ (d, $J = 5.2$ Hz, 1H, H-3) and 4.80 (dd, $J = 5.2$ and 8.8 Hz, 1H, H-4) ppm). Hence, the cycloaddition reaction proceeds asymmetrically to give a *cis* β-lactam in 90% optical yield.

The major β-lactam **3** was submitted to ozonolysis (CH_2Cl_2–MeOH, 9:1) at −70°C followed by reductive workup with $NaBH_4$–Alox (5) to give **4** (90%, $[\alpha]_D^{23}$ −158 (*c* 3.7)). Mesylation (6), then hydrolysis of the silyl ether with 95% TFA afforded alcohol mesylate **6** (85% from **4**, mp 100–101°C, $[\alpha]_D^{23}$ −112 (*c* 3) which on oxidation with Jones' reagent (7) (1.1 equiv.) at 15–20°C gave the enol mesylate **7** (1*b*) plus unreacted **6** which was recycled.[3] Without further purification, **7** was treated with triethylamine in refluxing CH_2Cl_2 (2.5 h) to give *O*-2-isocephem derivative **8** (1*b*) ($[\alpha]_D^{23}$ −22 (*c* 2.4)). Hydrogenation of **8** over Pt gave the amine **9** (1*b*) which was coupled with phenylacetic acid using EEDQ (8) to give the ester amide **10** (65% from **8**) ($[\alpha]_D^{23}$ +154 (*c* 0.6)). Hydrogenolysis (10% Pd/C) of **10** in EtOH–Thf (10:7) gave the *O*-2-isocephem acid **11**, (mp 95–105°C (dec.); $[\alpha]_D^{23}$ +155 (*c* 1, acetone)).

The respective *in vitro* antimicrobial activity (expressed as MIC's) of **11** and its corresponding racemate BC-L30 (9) against 5 typical strains of bacteria were as follows: *Streptococcus pneumoniae*, 0.25 and 0.5; *Streptococcus pyrogenes*, 0.5 and 0.5; *Staphylococcus aureus*, 0.5 and 1.0; *Escherichia coli*, 32 and 125; *Proteus mirabilis*, 8 and 16. These results establish the absolute configuration of **11** and its precursors. It appears to be the first time that a highly asymmetric cycloaddition on a Schiff base has been developed successfully for the production of the bioactive enantiomer of a β-lactam antibiotic. The mechanistic implications of this asymmetric cycloaddition, as well as other pertinent applications of this approach, will be described later.

[3]The oxidation was monitored by tlc and stopped at about 50% at which point side reactions became significant.

Acknowledgements

Financial support from Bristol Laboratories of Canada and the Natural Sciences and Engineering Research Council of Canada is gratefully acknowledged. Thanks are also due to J. Honek for the 200 MHz nmr measurements, B. Compton for suggestions on the use of hplc, Dr. J. Douglas and D. Horning for valuable preliminary experiments, and to M. Misiek for the microbiological data.

1. (*a*) T. W. Doyle, B. Belleau, B.-Y. Luh, C. F. Ferrari, and M. P. Cunningham. Can. J. Chem. **55**, 468 (1977); (*b*) T. W. Doyle, B. Belleau, B.-Y. Luh, T. T. Conway, M. Menard, J. L. Douglas, D. T.-W. Chu, G. Lim, L. R. Morris, P. Rivest, and M. Casey. Can. J. Chem. **55**, 484 (1977); (*c*) T. W. Doyle, B.-Y. Luh, and A. Martel. Can. J. Chem. **55**, 2700 (1977); (*d*) T. W. Doyle, A. Martel, and B.-Y. Luh. Can. J. Chem. **55**, 2708 (1977); (*e*) T. W. Doyle. Can. J. Chem. **55**, 2714 (1977); (*f*) T. W. Doyle, B.-Y. Luh, D. T.-W. Chu, and B. Belleau. Can. J. Chem. **55**, 2719 (1977); (*g*) T. W. Doyle, J. L. Douglas, B. Belleau, J. Meunier, and B.-Y. Luh. Can. J. Chem. **55**, 2873 (1977); (*h*) T. T. Conway, G. Lim, J. L. Douglas, M. Menard, T. W. Doyle, P. Rivest, D. Norning, L. R. Morris, and D. Cimon. Can J. Chem. **56**, 1335 (1978); (*i*) J. L. Douglas, D. E. Norning, and T. T. Conway. Can. J. Chem. **56**, 2879 (1978); (*j*) T. W. Doyle, T. T. Conway, M. Casey, and G. Lim. Can. J. Chem. **57**, 222 (1979); (*k*) T. W. Doyle, T. T. Conway, G. Lim, and B.-Y. Luh. Can. J. Chem. **57**, 227 (1979); (*l*) A. Martel, T. W. Doyle, and B.-Y. Luh. Can. J. Chem. **57**, 614 (1979).
2. G. Just and T.-J. Liak. Can. J. Chem. **56**, 211 (1978).
3. E. J. Corey and A. Venkateswarlu. J. Am. Chem. Soc. **94**, 6190 (1972).
4. (*a*) E. Schnabel, H. Klostermeyer, and H. Berndt. Justus Liebigs Ann. Chem. **749**, 90 (1971); (*b*) J. D. Cipera and R. V. V. Nicholls. Chem. Ind. 16 (1955); (*c*) N. Ono, T. Yamada, T. Saito, K. Tanaka, and A. Kaji. Bull. Chem. Soc. Jpn. **51**, 2401 (1978).
5. E. Santaniello, F. Ponti, and R. Manzocchi. Synthesis, 891 (1978).
6. R. K. Crossland and K. L. Servis. J. Org. Chem. **35**, 3195 (1970).
7. (*a*) K. Bowden, I. M. Heilbron, E. R. H. Jones, and B. C. L. Weedon. J. Chem. Soc. 39 (1946); (*b*) R. H. Mueller and R. M. DiPardo. J. Org. Chem. **42**, 3210 (1977).
8. B. Bellau and G. Malek. J. Am. Chem. Soc. **90**, 1651 (1968).
9. T. W. Doyle, J. L. Douglas, B. Belleau, T. T. Conway, C. Ferrari, D. E. Horning, G. Lim, B.-Y. Luh, A. Martel, M. Menard, and L. R. Morris. Can. J. Chem. Submitted.

Canadian Journal of Chemistry
Published by
THE NATIONAL RESEARCH COUNCIL OF CANADA

Journal canadien de chimie
Publié par
LE CONSEIL NATIONAL DE RECHERCHES DU CANADA

Volume 58 Number 16 August 15, 1980 Volume 58 numéro 16 15 août 1980

Can. J. Chem. Downloaded from www.nrcresearchpress.com by 210.87.254.42 on 09/05/12
For personal use only.

N,N-Dimethylpicramide–methoxide ion interactions: 1:1 and 2:1 σ-complex formation

ERWIN BUNCEL,[1] MASASHI HAMAGUCHI,[2] AND ALBERT R. NORRIS[1]
Department of Chemistry, Queen's University, Kingston, Ont., Canada K7L 3N6
Received January 21, 1980

ERWIN BUNCEL, MASASHI HAMAGUCHI, and ALBERT R. NORRIS. Can. J. Chem. **58**, 1609 (1980).

The interactions of *N,N*-dimethylpicramide (DMP) with methoxide ion in dimethylsulfoxide–methanol media have been investigated spectrophotometrically at 25.0°C. Both the 1:1 and 2:1 σ-complexes of DMP and methoxide ion have been observed under the various reaction conditions employed. However, dimethylsulfoxide has been found to preferentially stabilize the 1:1 σ-complex relative to the 2:1 σ-complex. As a consequence, at low base concentrations in dimethylsulfoxide–methanol solutions rich in dimethylsulfoxide (i.e. 95/5, v/v, DMSO/MeOH), the 1:1 σ-complex can be formed in the absence of any 2:1 σ-complex. This observation has been used to obtain, for the first time, values of the absorption maxima and molar absorptivities at the absorption maxima of both the 1:1 and 2:1 σ-complexes.

ERWIN BUNCEL, MASASHI HAMAGUCHI et ALBERT R. NORRIS. Can. J. Chem. **58**, 1609 (1980).

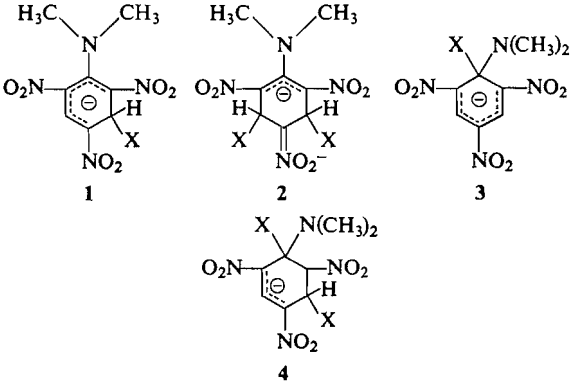
On a étudié par spectrophotométrie à 25°C les interactions du *N,N*-diméthylpicramide (DMP) avec l'ion méthylate dans un milieu de diméthylsulfoxyde–méthanol. On a observé les deux complexes σ 1:1 et 2:1 du DMP avec l'ion méthylate dans les différentes conditions de réaction utilisées. Cependant on a trouvé que le diméthylsulfoxyde stabilise préférentiellement le complexe σ 1:1 par rapport au complexe σ 2:1. En conséquence, à de faibles concentrations de base dans les solutions de diméthylsulfoxyde–méthanol riches en diméthylsulfoxyde (i.e. 95/5, v/v DMSO/MeOH), le complexe σ 1:1 peut être formé en l'absence de tout complexe 2:1. On a utilisé cette observation en vue d'obtenir pour la première fois les valeurs d'absorption maximale et les absorptivités molaires à l'absorption maximale des deux complexes σ 1:1 et 2:1.

[Traduit par le journal]

Introduction

Investigations of several different types have been carried out on the reversible reactions of *N,N*-dimethylpicramide (DMP) with hydroxide ion (1, 2) and sulfite ion (3–5) in water and water–dimethylsulfoxide mixtures and with methoxide ion in methanol and methanol–dimethylsulfoxide mixtures (6–8).

^{1}H nmr studies (2, 4, 5, 7, 8) indicate that, in the solvents employed, at mole ratios of base-to-DMP less than one, all three bases add at C-3 (or C-5) to form 1:1 σ-complexes such as **1** (X = OH, OCH_3, SO_3^-). At mole ratios of base-to-DMP greater than 1, 2:1 σ-complexes such as **2** are observed (X = OH, OCH_3, SO_3^-). In no instance was there evidence for the formation of a C-1 adduct, **3** (X = OH, OCH_3, SO_3^-), or the formation of 2:1 σ-complexes involving addition of the base at both the C-1 and C-3 (or C-5) positions to yield complexes such as **4** (X = OH, OCH_3, SO_3^-).



However, although complexes of DMP such as **3** have not yet been reported, comparable species are known in systems closely related to *N*-methylpi-

[1]To whom all correspondence should be addressed.
[2]Permanent address: Department of Chemistry, College of General Education, Osaka University, Osaka 560, Japan.

0008-4042/80/161609-06$01.00/0
©1980 National Research Council of Canada/Conseil national de recherches du Canada

Can. J. Chem. Downloaded from www.nrcresearchpress.com by 210.87.254.42 on 09/05/12
For personal use only.

cramide (9). Transient intermediates of structure type **3** have been reported in the reactions of picryl ethers with aliphatic amines (10).

While ultraviolet–visible studies clearly indicate a marked difference in the absorption spectra of complexes such as **1** and **2** (X = OH, OCH_3, SO_3^-) (1, 3–5), particularly in those cases in which X = OH and OCH_3, only in the case of **1** and **2** with X = SO_3^- have both the band shapes and molar absorptivity values (ε) at the absorption maxima (λ_{max}) been reported for both the 1:1 and 2:1 complexes (3–5).

We report here on our studies of the reaction of DMP with methoxide ion in dimethylsulfoxide–methanol (95/5, v/v) as solvent. Under our reaction conditions the stability constants which characterize the formation of the 1:1 and 2:1 σ-complexes are sufficiently different that good absorption data can be obtained for each complex.

Results and Discussion

In the wavelength region 200–900 nm, *N,N*-dimethylpicramide (DMP) in mixed dimethylsulfoxide–methanol (DMSO–MeOH, 95/5, v/v) as solvent exhibits a single, broad absorption band which displays a maximum at 383 nm ($\varepsilon_{383} = 1.41 \times 10^4\ M^{-1}\ cm^{-1}$).

The addition of progressively larger amounts of sodium methoxide in DMSO–MeOH solution (95/5, v/v) to a DMSO–MeOH (95/5, v/v) solution of fixed DMP concentration ($3.18 \times 10^{-4}\ M$) resulted in the simultaneous disappearance of the absorption band due to DMP and the appearance of a new absorption band possessing absorption maxima at 402 and 474 nm. Solutions containing only DMP and this new absorbing species, Q, were characterized by an isosbestic point at 370 nm (Fig. 1). The reaction of DMP to yield Q occurred well within the time required to mix the two solutions and record the absorption spectrum of the resulting mixture (<20 s). Conversion of DMP to Q was dependent on the mole ratio of $NaOCH_3$ to DMP and was essentially complete at a mole ratio of $NaOCH_3$ to DMP of 1.36. The addition of excess trifluoracetic acid (CF_3COOH) to the reaction mixtures rapidly and quantitatively converted Q to DMP.

If species Q is the result of a 1:1 interaction of DMP and CH_3O^-, we can write

[1] $\mathrm{DMP} + \mathrm{CH_3O^-} \rightleftharpoons \mathrm{Q}$

and

[2] $K_1 = [\mathrm{Q}]/[\mathrm{CH_3O^-}][\mathrm{DMP}]$

where [Q], [CH_3O^-], and [DMP] represent the equilibrium concentrations of Q, CH_3O^-, and DMP, respectively.

For a 1.00 cm cell the absorbance, A, at a specified wavelength is given by

[3] $A = \varepsilon_Q[\mathrm{Q}] + \varepsilon_{DMP}[\mathrm{DMP}]$

where ε_Q and ε_{DMP} are the molar absorptivities, in $M^{-1}\ cm^{-1}$, of species Q and DMP, respectively. At any given wavelength, ε_Q can be evaluated from the limiting absorbance value ($A_{limiting}$) in a plot of absorbance versus [CH_3O^-] under conditions of [CH_3O^-]/[DMP] $\simeq$ 1.1 to 1.4. Values of ε_Q, determined in this manner at selected wavelengths, are given in Table 1 together with values of ε_{DMP} at the same wavelengths.

Employing the material balance equations

[4] $[\mathrm{DMP}]_0 = [\mathrm{Q}] + [\mathrm{DMP}]$

and

[5] $[\mathrm{CH_3O^-}]_0 = [\mathrm{CH_3O^-}] + [\mathrm{Q}]$

where $[DPM]_0$ and $[CH_3O^-]_0$ represent total concentrations of DMP and CH_3O^- in solution, absorbance data collected at a given wavelength and values of ε_Q and ε_{DMP} at that wavelength one can, with the aid of eq. [3], evaluate [Q], [DMP], [CH_3O^-] and hence calculate K_1. From absorbance data collected at 402 nm, over the range of base concentrations in which DMP was being converted to Q, a mean K_1 of $1.4 \pm 0.4 \times 10^3\ M^{-1}$ at 25.0°C was obtained. Treatment in the same manner of absorbance data recorded at 444 and 474 nm yielded values of K_1 of comparable magnitude to that just quoted. The agreement among the values of K_1 calculated using absorbance data collected at the three wavelengths confirms the validity of eqs. [5], [4], and [3] and the 1:1 stoichiometry of species Q.

Quite independent of the wavelengths at which absorbances were recorded, the values of K_1, calculated in the manner described above, were found to increase slightly with increasing concentration of sodium methoxide in solution. This behavior was observed both when the reactions were carried out under conditions of varying ionic strength (0.50×10^{-4} to $9.00 \times 10^{-4}\ M$) and under conditions of a constant ionic strength of 0.20 M maintained with $(C_2H_5)_4NClO_4$.

Since the ^1H nmr studies (2, 7, 8) establish that the product formed as a result of the 1:1 interaction of CH_3O^- and DMP in both MeOH and DMSO–MeOH mixtures is **1** (X = OCH_3), and our value of λ_{max} for species Q (402 nm) agrees well with the λ_{max} value previously reported for the 1:1

Can. J. Chem. Downloaded from www.nrcresearchpress.com by 210.87.254.42 on 09/05/12
For personal use only.

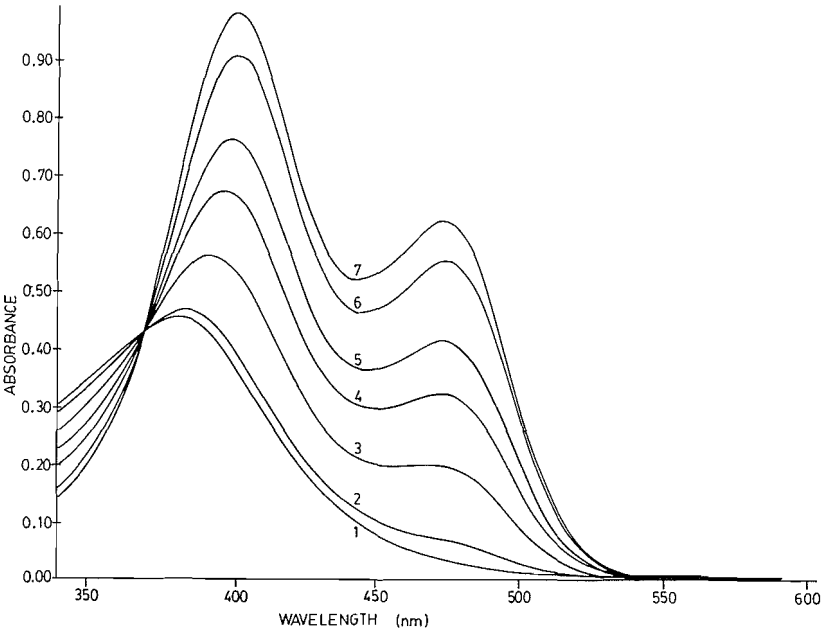
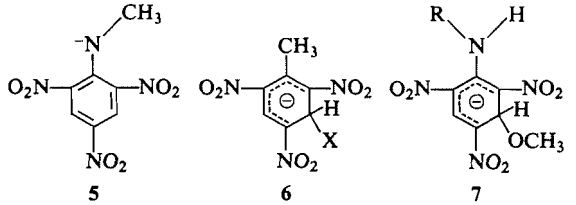


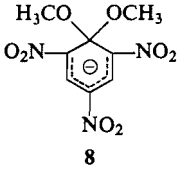
FIG. 1. Absorption spectra of dimethylsulfoxide–methanol solutions (95/5, v/v) 3.18×10^{-4} *M* in *N,N*-dimethylpicramide with $[NaOCH_3]_0$ (*M*) equal to: *1*, 0; *2*, 0.51×10^{-4}; *3*, 1.33×10^{-4}; *4*, 2.20×10^{-4}; *5*, 2.97×10^{-4}; *6*, 3.55×10^{-4}; *7*, 4.34×10^{-4}.

TABLE 1. Molar absorptivities, ε, at selected wavelengths for DMP and species Q and R in DMSO–MeOH (95/5, v/v) at 25.0°C

	ε (M^{-1} cm^{-1}) at the indicated λ (nm)			
Compound	384	402	430	474
DMP	1.41×10^4	1.08×10^4	0.52×10^4	0.06×10^4
Q	2.20×10^4	3.07×10^4	1.90×10^4	1.94×10^4
R	0.95×10^4	1.76×10^4	2.93×10^4	0.44×10^4

adduct in methanol (400 nm) (6), we can fairly confidently assign Q as having structure **1** (X = OCH_3). The similarities in the shapes of the absorption bands and the values of ε at λ_{max} of Q (complex **1**, X = OCH_3) and complex **6** (11)





lends support to our argument. Further, complex **7** (R = *i*-Pr) has been reported to possess a λ_{max} at 405 nm in methanol, although no mention is made by the authors (12) of either the value of ε at this wavelength or of a longer wavelength maximum associated with this species. Since complex **8** has a uv–visible absorption pattern and values of ε at λ_{max} very similar to those reported above for Q (13), our assignment of structure **1** rather than structure **3** to Q rests very heavily on the results of the ^1H nmr studies which show that species such as **3** are not formed in detectable concentrations in either methanol or methanol–dimethylsulfoxide mixtures (2, 4, 7, 8). That there are limitations associated with using only the shapes of absorption bands and values of ε at λ_{max} to differentiate the structures of related complexes in solution is further illustrated by the observation that the 1:1 σ-complexes **1** (X = OCH_3 in methanol as solvent) and **1** (X = SO_3^- in water or water–dimethylsulfoxide) have quite different band shapes and values of ε at λ_{max} (3, 4, 6).

The equilibrium constant for the formation of the 1:1 σ-complex **1** (X = OCH_3) in DMSO–MeOH (95/5, v/v) is substantially larger (1.4×10^3 M^{-1}) in this solvent than it is in methanol (7 M^{-1}) (1). Similar large increases in the values of *K* as a result of increasing the DMSO content of DMSO–MeOH mixtures have been noted in the formation reactions leading to **9** (X = CH_3O, C_2H_5S, and C_6H_5S) and a variety of related σ-complexes (14–17). The trend in *K* values is attributed primarily to a less effective solvation of methoxide ion by DMSO than by methanol; anionic σ-complex and the starting

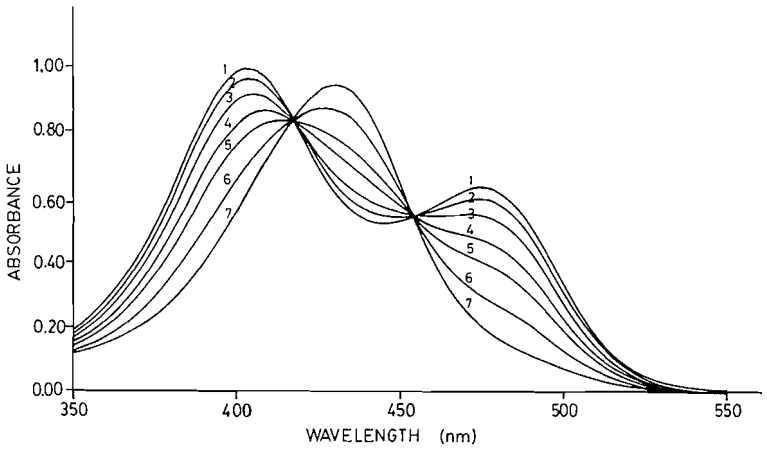
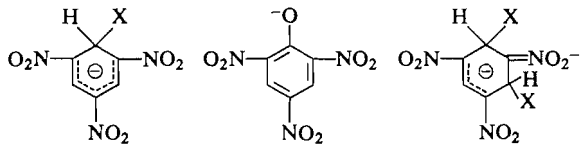


FIG. 2. Absorption spectra of dimethylsulfoxide–methanol solutions (95/5, v/v) 3.21×10^{-4} *M* in *N,N*-dimethylpicramide with $[NaOCH_3]_0$ (*M*) equal to: *1*, 4.34×10^{-4}; *2*, 16.3×10^{-4}; *3*, 28.7×10^{-4}; *4*, 46.7×10^{-4}; *5*, 62.6×10^{-4}; *6*, 99.8×10^{-4}; *7*, 153.0×10^{-4}.

nitroaromatic compound are considered to possess comparable solvation properties. Our lower ratio of *K* values (~200), as compared to values of 4×10^4 and 10^8 in other systems, may indicate that **1** (X = OCH_3) is far less effectively solvated by DMSO than is DMP. This is perhaps not surprising in view of the rather bulky nature of the dimethylamino group in the molecule.



The addition of NaOMe to solutions of fixed DMP concentration, beyond the mole ratio of CH_3O^- to DMP of 1.4, resulted in the disappearance of species Q and the appearance of a new species, R, characterized by a single absorption maximum at 430 nm ($\varepsilon = 2.93 \times 10^4\ M^{-1}\ cm^{-1}$). The spectra of solutions containing only species Q and R were characterized by isosbestic points at 417 and 454 nm (Fig. 2). Conversion of Q to R was effected within the time required to mix and record the spectrum of each solution (<20 s) at 25.0°C. Within minutes of mixing, the reaction of Q to yield R could be quantitatively reversed upon the addition of excess CF_3COOH. However, additional very slow spectral changes were noted in these solutions and, within 1 or 2 days of conversion of Q to R, complete recovery of DMP as a result of acidification of the solutions was not achieved. Similar observations of a very slow secondary reaction have been made by Gold and Rochester (1) in connection with the reaction of DMP and CH_3O^- in methanol. We find that the resulting spectra of the solutions are *not* consistent with the presence of either **8** or **10** in solution (18) and the reaction product(s) is (are), as yet, unidentified.

If species R is formed as a result of a 1:1 interaction of Q and CH_3O^- we have

[6] $Q + CH_3O^- \rightleftharpoons R$

and

[7] $K_2 = [R]/[Q][CH_3O^-]$

Employing absorbance data recorded at 402 nm and the arguments and procedures described earlier, a value of $K_2 = 1.4 \pm 0.2 \times 10^2\ M^{-1}$ was evaluated.[3] Values of K_2 of comparable magnitude were obtained from absorbance data collected at 430 and 474 nm. The invariance in the values of K_2, evaluated using the absorbance data obtained at the three wavelengths, offers strong support for the formulation of R as a species resulting from a 1:1 interaction of Q and CH_3O^-.

We note that the values of K_2 calculated using eq. [7] are not constant but increase slightly with increasing concentration of $NaOCH_3$. However, for the same range of $NaOCH_3$ concentrations, the variation in K_2 is significantly smaller than is the variation in K_1. This is somewhat surprising in the light of Crampton's observation that in the reaction

[3]Alternatively the experimental data could be treated using the Benesi–Hildebrand (19) equation in the form

[8] $\{A - \varepsilon_Q[Q]_0\}^{-1} = \{K(\varepsilon_Q - \varepsilon_R)[MeO^-]_0[Q]_0\}^{-1} + \{(\varepsilon_Q - \varepsilon_R)[Q]_0\}^{-1}$

The slope and intercept of the linear graph of the left-hand side of this equation versus $[MeO^-]_0^{-1}$ yielded values of *K* and ε_R in good agreement with those obtained using the procedure noted previously. Values of ε_R at selected wavelengths are listed in Table 1.

Can. J. Chem. Downloaded from www.nrcresearchpress.com by 210.87.254.42 on 09/05/12
For personal use only.

TABLE 2. Absorption data for some complexes of type **2**

X	Solvent	$\lambda_{max}(\varepsilon)$	Reference
HO	H_2O	410 nm (2.16×10^4 M^{-1} cm^{-1})	1
SO_3^-	H_2O	417 nm (2.0×10^4 M^{-1} cm^{-1})	3
CH_3O	MeOH	423 nm	6
CH_3O	DMSO–MeOH (95/5, v/v)	430 nm (2.93×10^4 M^{-1} cm^{-1})	This work

Can. J. Chem. Downloaded from www.nrcresearchpress.com by 210.87.254.42 on 09/05/12
For personal use only.

of sulfite ion and DMP in water, the formation constant for the 2:1 σ-complex was more susceptible to ionic strength effects than the formation constant of the 1:1 σ-complex (4). Perhaps, though, the systems are not comparable because of the differences in both charge types and the solvents employed in the two studies.

The ratio K_2/K_1 of $\sim10^{-2}$ for the reactions of DMP and CH_3O^- in our solvent system may be compared to the corresponding ratio of ~2 for the DMP–sulfite ion interactions in water (3, 4) and a value of $K_2/K_1 \gg 1$ for the DMP–hydroxide ion interactions in water (1). The results are completely in accord with earlier suggestions that, in the DMSO/MeOH solvent system, solvation of the diadduct by DMSO is far less favorable than is solvation of the monoadduct (4, 16). In contrast, solvation of the diadduct in water is comparable energetically to solvation of the monoadduct, irrespective of whether X = OH or SO_3^-.

Combining our mean values of K_1 and K_2 for the interactions of DMP and methoxide ion in DMSO/MeOH (95/5, v/v) we obtain a K for the overall reaction

[9] $\mathrm{DMP} + 2CH_3O^- \rightleftharpoons \mathrm{R}$

of 1.96×10^5 M^{-2} at 25.0°C. While Gold and Rochester (6) have also postulated the formation of the 2:1 σ-complex, **R**, in pure methanol, the K value they report (26 M^{-3} at 25.0°C) is formulated in terms of the apparent reaction

[10] $\mathrm{DMP} + 3CH_3O^- \rightleftharpoons \mathrm{R}$

and, as such, cannot be compared directly to our value of 1.96×10^5 M^{-2}. Based on the K_2/K_1 values quoted above, a ratio of K_2/K_1 for the DMP–CH_3O^- interaction in methanol of <1 might, however, be anticipated. Given that K_1 for the interaction is 6 M^{-1} at 25.0°C (12) a predicted value of $K_2 < 6$ M^{-1} is obtained. This then places an upper limit of <3.6 M^{-2} on the K for the overall reaction of DMP and $2CH_3O^-$ to yield R in methanol. On going from methanol as solvent to 95/5, v/v, DMSO–MeOH as solvent the increase in K_2 ($>10^5$) is clearly much larger than the increase in K_1 (~200).

In light of the ^1H nmr results, which show that 2:1 σ-complexes of DMP with HO^-, CH_3O^-, and SO_3^- possess structure **2** in solution, and the similarities in the ultraviolet–visible spectral characteristics of **2** (X = HO or SO_3^-) and species R, we propose structure **2** (X = CH_3O) for the 2:1 species, **R**, formed by the interaction of DMP and CH_3O^- in DMSO–MeOH.[4] Relevant spectral data are given in Table 2. We note that a number of 2:1 σ-complexes of TNB **11** (X = HO^-, SO_3^-, $C_2H_5S^-$, CH_3O^-) are also characterized by a single absorption maximum in the visible region and ε values, at λ_{max}, of magnitude $2.5 \pm 0.5 \times 10^4$ M^{-1} cm^{-1}.

Experimental

N,N-Dimethylpicramide was prepared by adding an excess of dimethylamine in ethanol to a 5% solution of 1-chloro-2,4,6-trinitrobenzene in ethanol and evaporating the resulting solution to dryness. The solution formed by extraction of the residue with acetone was filtered to remove the insoluble dimethylammonium chloride and evaporated to dryness. The resulting solid was recrystallized to constant melting point from absolute alcohol. After drying *in vacuo* over phosphorus(V) pentoxide, the product had a melting point of 138°C; lit. (21) 138°C. Sodium methoxide solutions were prepared by dissolving clean sodium in Analar methanol under nitrogen and were titrated with standard acid using phenolphthalein as an indicator. Dimethylsulfoxide (DMSO) was dried over calcium hydride and fractionated under reduced pressure, the middle fraction being collected. Eastman tetraethylammonium perchlorate was dried to constant weight *in vacuo* over phosphorus(V) pentoxide. Reagent grade trifluoroacetic acid was used as received.

Stock solutions of *N,N*-dimethylpicramide in DMSO, DABCO in DMSO, $(C_2H_5)_4NClO_4$ in DMSO, and $NaOCH_3$ in methanol were made up under nitrogen in a drybox and were protected from light. Solutions used in the equilibrium studies were also prepared in the drybox by adding appropriate volumes of the stock solutions to a known volume of DMSO. After thorough mixing, a portion of the solution was transferred to a clean dry spectrophotometric cell and the cell and its contents then placed in the spectrophotometer.

[4]A referee has suggested that simultaneously with the uv–visible study, one should also obtain ^1H nmr spectra on the same solutions, using pulse FT techniques. While in principle this may be possible, the observed slow decomposition of the dianionic species over the time period required to accumulate the necessary spectra, on solutions ca. 10^{-4} M, is likely to lead to ambiguous results. In a previous study we were able to obtain uv–visible, ir, and nmr spectral results on solutions having approximately equal concentrations and the results of all three techniques could consistently be interpreted as arising from the particular σ-complex species (20).

Optical measurements were carried out on a Beckman Acta IV spectrophotometer using matched silica cells of 1.0 mm and 5.0 mm path length. The temperature in the cells was maintained constant at 25.0 ± 0.1°C by circulating water from a constant temperature bath through a specially designed cell holder in the spectrophotometer.

Acknowledgment

Financial support of this research by the Natural Sciences and Engineering Research Council of Canada is acknowledged.

1. V. GOLD and C. H. ROCHESTER. J. Chem. Soc. 1727 (1964).
2. M. R. CRAMPTON and V. GOLD. J. Chem. Soc. Chem. Commun. 256 (1965).
3. E. BUNCEL, A. R. NORRIS, K. E. RUSSELL, and P. E. SHERIDAN. Can. J. Chem. **52**, 25 (1974).
4. M. R. CRAMPTON. J. Chem. Soc. 1341 (1967).
5. M. R. CRAMPTON and M. J. WILLISON. J. Chem. Soc. Perkin II, 160 (1976).
6. V. GOLD and C. H. ROCHESTER. J. Chem. Soc. 1697 (1964).
7. M. R. CRAMPTON and V. GOLD. Proc. Chem. Soc. 298 (1964); J. Chem. Soc. B, 893 (1966).
8. K. L. SERVIS. J. Am. Chem. Soc. **87**, 5495 (1965); **89**, 1508 (1967).
9. E. BERGMAN, N. R. MCFARLANE, and J. J. K. BOULTON. J. Chem. Soc. Chem. Commun. 511 (1970); J. J. K. BOULTON and N. R. MCFARLANE. J. Chem. Soc. B, 925 (1971); J. J. K. BOULTON, P. J. JEWESS, and N. R. MCFARLANE. J. Chem. Soc. B, 928 (1971).
10. C. A. FYFE, S. W. H. DAMJI, and A. KOLL. J. Am. Chem. Soc. **101**, 951 (1979).
11. C. A. FYFE, C. D. MALKIEWICH, S. W. H. DAMJI, and A. R. NORRIS. J. Am. Chem. Soc. **98**, 6983 (1976).
12. M. R. CRAMPTON and B. GIBSON. J. Chem. Soc. Perkin II. In press.
13. E. BUNCEL, A. R. NORRIS, and K. E. RUSSELL. Q. Rev. Chem. Soc. **22**, 123 (1968).
14. M. R. CRAMPTON. J. Chem. Soc. B, 1208 (1968).
15. M. J. STRAUSS. Chem. Rev. **70**, 667 (1970) and references therein.
16. (*a*) F. TERRIER, A-P. CHATROUSSE, and R. SCHAAL. J. Org. Chem. **37**, 3010 (1972); (*b*) F. TERRIER and F. MILOT. Bull. Soc. Chim. Fr. 1743 (1970).
17. J. W. LARSEN, K. AMIN, and J. H. FENDLER. J. Am. Chem. Soc. **93**, 2910 (1971).
18. V. GOLD and C. H. ROCHESTER. J. Chem. Soc. 1687 (1964).
19. H. A. BENESI and J. H. HILDEBRAND. J. Am. Chem. Soc. **71**, 2703 (1949).
20. A. R. NORRIS. J. Org. Chem. **34**, 1486 (1969).
21. J. R. A. POLLOCK and R. STEVENS (*Editors*). Dictionary of organic compounds. 4th ed. Eyre and Spottiswoode, Ltd., London. 1965.

Can. J. Chem. Downloaded from www.nrcresearchpress.com by 210.87.254.42 on 09/05/12
For personal use only.

N-Methylpicramide–methoxide ion interactions: proton abstraction versus σ-complex formation

ERWIN BUNCEL,[1] MASASHI HAMAGUCHI,[2] AND ALBERT R. NORRIS[1]

Department of Chemistry, Queen's University, Kingston, Ont., Canada K7L 3N6

Received January 21, 1980

ERWIN BUNCEL, MASASHI HAMAGUCHI, and ALBERT R. NORRIS. Can. J. Chem. **58**, 1615 (1980).

The interactions of *N*-methylpicramide (NMP) with methoxide ion in dimethylsulfoxide–methanol media and with 1,4-diazabicyclooctane in dimethylsulfoxide have been investigated spectrophotometrically at 25.0°C. Dimethylsulfoxide has been found to stabilize the conjugate base of NMP, formed via loss of hydrogen ion from the methylamino group, with respect to the anionic σ-complex generated via addition of methoxide ion to a ring carbon position. As a result, methanol–dimethylsulfoxide solutions rich in dimethylsulfoxide (i.e., 95/5, v/v, DMSO/MeOH) contain the conjugate base of NMP as the sole product of the 1:1 interaction of NMP and methoxide ion. At mole ratios of methoxide ion to NMP > 1 a second interaction results, yielding a dianion formed via addition of methoxide ion to one of the H-bearing ring carbon atoms of the conjugate base. Values of absorption maxima and molar absorptivities at the absorption maxima for the conjugate base of NMP and the dianion are reported here for the first time.

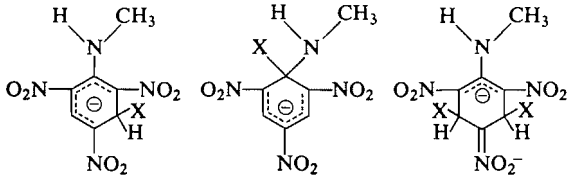
ERWIN BUNCEL, MASASHI HAMAGUCHI et ALBERT R. NORRIS. Can. J. Chem. **58**, 1615 (1980).

On a étudié par spectrophotométrie à 25°C les interactions du *N*-méthylpicramide (NMP) avec l'ion méthylate dans une solution de diméthylsulfoxyde–méthanol et également les interactions avec le diaza-1,4 bicyclooctane dans le diméthylsulfoxyde. On a trouvé que le diméthylsulfoxyde stabilise la base conjuguée du NMP formée par l'intermédiaire d'une élimination d'ion hydrogène du groupe méthylamino, par rapport au complexe σ anionique produit par l'addition de l'ion méthylate sur un carbone du cycle. En conséquence, les solutions de méthanoldiméthylsulfoxyde riches en diméthylsulfoxyde (i.e. 95/5 v/v DMSO/MeOH contiennent la base conjuguée du NMP comme produit unique de l'interaction 1:1 entre le NMP et l'ion méthylate. Pour des rapports molaires ion méthylate/NMP > 1, il en résulte une deuxième interaction conduisant à un dianion qui se forme par l'addition de l'ion méthylate sur l'un des atomes de carbone du cycle de la base conjuguée lié à un hydrogène. On présente pour la première fois les valeurs d'absorption maximale et les absorptivités molaires pour une absorption maximale de la base conjugée du NMP et du dianion.

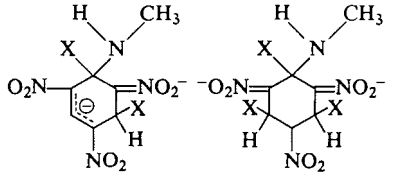
[Traduit par le journal]

Introduction

The interaction of *N*-methylpicramide (NMP) with base X^- can, in principle, lead to a variety of products. Thus, 1:1, 2:1, and 3:1 σ-complexes may be formed by the attachment of 1, 2, or 3 base ions to a variety of ring carbon centres to yield complexes **1–5**.

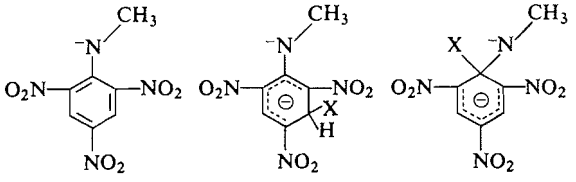


1 **2** **3**

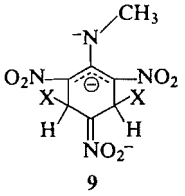


4 **5**

In addition, the conjugate base of NMP, **6**, may be formed via the loss of a proton from the methylamino group and this anion may, in turn, add further base to form the additional complexes **7–9**.



6 **7** **8**



9

Previous studies (1–5) have established the existence, in solution, of species such as **1** (X = CH_3O, SO_3^-), **3** (X = CH_3O, SO_3^-), **6**, and **7** (X = HO, CH_3O). With X^- = HO^- and CH_3O^-, both the types of complexes formed and the equilibrium constants for the formation of a particular type of complex were found to depend strongly on the properties of the solvents used in the respective studies (3–6). While complexes such as **2** (X = CH_3O) have not been reported, comparable species

[1]To whom all correspondence should be addressed.

[2]Permanent address: Department of Chemistry, College of General Education, Osaka University, Osaka 560, Japan.

0008-4042/80/161615-06$01.00/0

©1980 National Research Council of Canada/Conseil national de recherches du Canada

Can. J. Chem. Downloaded from www.nrcresearchpress.com by 210.87.254.6 on 09/05/12
For personal use only.

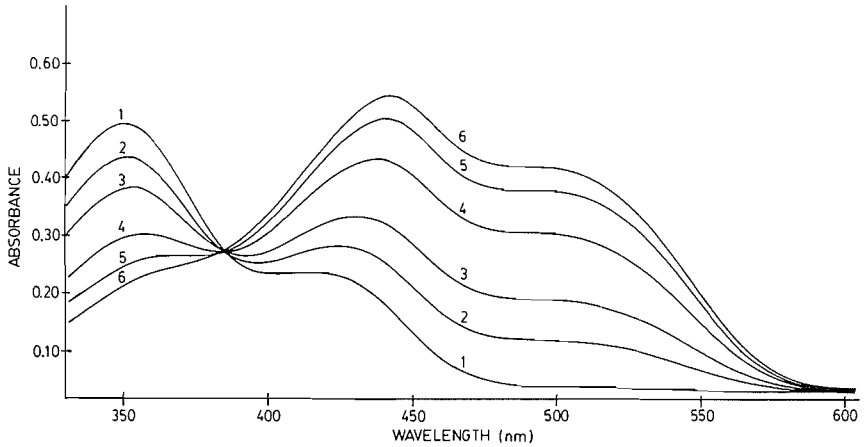


FIG. 1. Initial absorption spectra of *N*-methylpicramide in dimethylsulfoxide/methanol (95/5, v/v) containing various concentrations of sodium methoxide. [OMe^-] (*M*): , 0; *2*, 0.61×10^{-4}; *3*, 1.26×10^{-4}; *4*, 2.22×10^{-4}; *5*, 3.00×10^{-4}; *6*, 3.57×10^{-4}. [*N*-Methylpicramide] = 3.05×10^{-4} *M*; 10 cm cell; 25.0°C.

are known in systems closely related to NMP (7). Transient intermediates with structures analogous to **2** have also been observed in the reactions of picryl ethers with aliphatic amines (8, 9).

While species of types **1**, **3** and **7** (X = HO, CH_3O, SO_3^-), and **6** are fully characterized in terms of their ^1H nmr properties (1–4), they are less well characterized in terms of their ultraviolet–visible absorption properties, particularly in those cases in which X = HO and CH_3O (6). The reason for this is that, with these bases, the solvents utilized in the studies were such that the solutions invariably contained mixtures of the various σ-complexes and the conjugate base of NMP.

In this work we report on the interactions of NMP with 1,4-diazabicyclooctane (DABCO) in dimethylsulfoxide (DMSO) and also with methoxide ion in dimethylsulfoxide–methanol (95/5, v/v). The ultraviolet–visible spectra of species **6** and **7** (X = CH_3O) are reported here for the first time.

Results and Discussion

N-Methylpicramide (NMP) in a medium of dimethylsulfoxide–methanol (DMSO/MeOH, 95/5, v/v) exhibits a broad absorption band which displays an absorption maximum at 350 nm ($\varepsilon = 1.54 \times 10^4\ M^{-1}\ cm^{-1}$) and a shoulder with mid-point at 410 nm ($\varepsilon = 0.67 \times 10^4\ M^{-1}\ cm^{-1}$).

The addition of progressively larger amounts of sodium methoxide (NaOMe) to solutions of fixed concentration of NMP (3.00×10^{-4} *M*) lead to the simultaneous disappearance of the absorption maximum due to NMP and the appearance of a new absorption band possessing an absorption maximum at 442 nm and a shoulder with mid-point at 494 nm (Fig. 1). Formation of this second absorbing species, Y, was complete within the time required to mix the stock solutions of NaOMe and NMP and record the spectrum of the resulting mixture (<20 s). The extent of conversion of NMP to absorbing species Y was dependent on the concentration of NaOMe in solution; conversion was essentially complete with the addition of approximately 1.1 molar equivalents of NaOMe to the system. Throughout the course of the conversion of NMP to Y the solutions displayed a single isosbestic point at 385 nm (Fig. 1). The species whose absorption maximum occurred at 442 nm was stable for several days at room temperature. Over these periods of time addition of excess trifluoroacetic acid (CF_3COOH) rapidly and quantitatively converted this species to NMP.

The reaction of NMP with DABCO in pure, dry DMSO also resulted in the conversion of NMP to species Y as evidenced by the generation of a final spectrum identical to that obtained with $NaOCH_3$ above. Associated with the conversion of NMP to Y in pure DMSO is an isosbestic point at 388 nm. Formation of species Y again occurred within the time required to mix the stock solutions of the two reagents and record the spectrum of the resulting solution and the reaction to form Y was completely and rapidly reversed on the addition of excess CF_3COOH to the system. Complete conversion of NMP to species Y required the addition of more than 1 molar equivalent of DABCO to the system. Under identical experimental conditions, *N,N*-dimethylpicramide (*N,N*-DMP, 3.00×10^{-4} *M*) plus excess DABCO in pure, dry DMSO yielded no

Can. J. Chem. Downloaded from www.nrcresearchpress.com by 210.87.254.6 on 09/05/12
For personal use only.

Can. J. Chem. Downloaded from www.nrcresearchpress.com by 210.87.254.6 on 09/05/12
For personal use only.

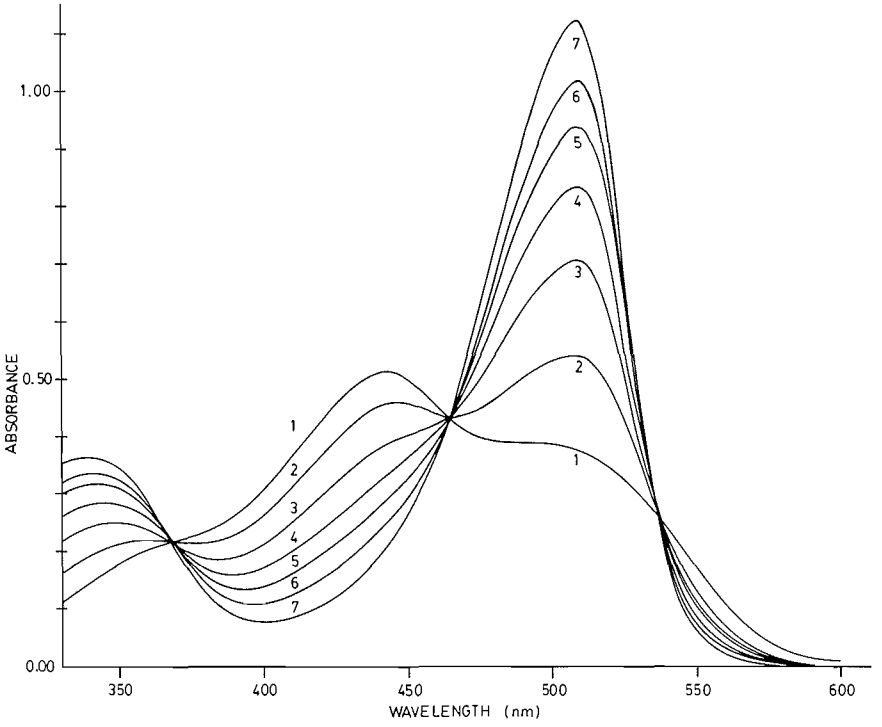


FIG. 2. Initial absorption spectra of *N*-methylpicramide in dimethylsulfoxide/methanol (95/5, v/v) containing various concentrations of sodium methoxide. [OMe^-] (*M*): *1*, 3.57×10^{-4}; *2*, 4.47×10^{-4}; *3*, 7.11×10^{-4}; *4*, 1.15×10^{-3}; *5*, 1.70×10^{-3}; *6*, 2.12×10^{-3}; *7*, 3.10×10^{-3}. [*N*-Methylpicramide] = 3.04×10^{-4} *M*; 0.10 cm cell; 25.0°C.

evidence of any reaction in solution, i.e. the spectrum due to *N,N*-DMP remained unchanged using DABCO concentrations of up to ~1 *M*.

Solutions of fixed NMP concentration (3.00×10^{-4} *M*) containing >1.1 molar equivalents of NaOMe underwent additional spectral changes as the concentration of NaOMe was increased. At concentrations of $MeO^- \sim 3.0 \times 10^{-2}$ *M*, the second sequence of spectral changes was essentially complete and a species possessing absorption maxima at 508 ($\varepsilon = 4.00 \times 10^4\ M^{-1}\ cm^{-1}$) and 335 nm ($\varepsilon = 1.23 \times 10^4\ M^{-1}\ cm^{-1}$) was observed (species Z). The spectra of solutions containing both Y and Z were characterized by isosbestic points at 366, 464, and 532 nm (Fig. 2). Conversion of Y to Z was rapid at room temperature ($t_{1/2} < 20$ s). At any fixed concentration of NaOMe, at room temperature, the concentration of Z decreased very slowly with time; $t_{1/2}$ for this decomposition was of the order of 1 day. However, within short periods of time (< 10 min after preparation) Z was converted quantitatively to Y (and, in the limit, to NMP) by the addition of appropriate amounts of CF_3COOH.

In pure, dry DMSO, even at DABCO concentrations up to the level of 1 *M*, there was no evidence for the formation of species Z from species Y. (The spectrum of Y was completely unaffected by the addition of DABCO up to this level of concentration.)

At fixed concentrations of NMP equal to 3.00×10^{-4} *M* and concentrations of $MeO^- > 3 \times 10^{-2}$ *M* the absorbance at 508 nm decreased in magnitude with increasing concentration of base. However, these decreases were not completely reversible upon the immediate addition of acid to the solution and the interaction of NMP and MeO^- under these conditions was therefore not studied quantitatively.

If species Y is the result of a 1:1 interaction of NMP and MeO^-, we can write

[1] $\text{NMP} + \text{MeO}^- \rightleftarrows \text{Y}$

and

[2] $K_1 = [\text{Y}]/[\text{NMP}][\text{MeO}^-]$

For a 0.10 cm cell, the absorbance, *A*, at a specified wavelength is given by

[3] $A = \{\varepsilon_Y[\text{Y}] + \varepsilon_{NMP}[\text{NMP}]\}0.10$

where ε_Y and ε_{NMP} are the molar absorptivities, in $M^{-1}\ cm^{-1}$, of species Y and NMP, respectively. At any given wavelength ε_Y can be evaluated from the

TABLE 1. Values of molar absorptivities, ε, at selected wavelengths for *N*-methylpicramide, species Y and species Z; 95/5 (v/v) dimethylsulfoxide/methanol solvent; $T = 25.0°C$

	ε (M^{-1} cm^{-1}) at λ (nm)				
Compound	335	350	420	442	508
NMP	1.33×10^4	1.54×10^4	0.67×10^4	0.46×10^4	0
Species Y	0.41×10^4	0.59×10^4	1.42×10^4	1.71×10^4	1.29×10^4
Species Z	1.22×10^4	1.11×10^4	0.24×10^4	0.56×10^4	4.00×10^4

limiting absorbance value (A_{limiting}) in a plot of absorbance versus [MeO$^-$]. Values of ε_{NMP} and ε_Y at selected wavelengths are given in Table 1.

In addition, we have the material balance equations

[4] $[NMP]_{Stoich} = [Y] + [NMP]$

and

[5] $[MeO^-]_{Stoich} = [OMe^-] + [Y]$

where $[NMP]_{Stoich}$ and $[MeO^-]_{Stoich}$ represent total concentrations of DMP and CH_3O^-, respectively, in solution.

Employing $\varepsilon_{NMP} = 0.46 \times 10^4\ M^{-1}\ cm^{-1}$ and $\varepsilon_Y = 1.71 \times 10^4\ M^{-1}\ cm^{-1}$ at 442 nm and absorbance data recorded at 442 nm, we can evaluate K_1, over the range of base concentrations in which NMP is being converted to Y, as $2 \pm 1 \times 10^5\ M^{-1}$. Treatment, in the same fashion, of absorbance data recorded at 464 and 500 nm yields K_1 values of comparable magnitude. The agreement among the values of K_1, calculated using absorbance data collected at the three wavelengths, confirms the validity of eq. [2] and 1:1 stoichiometry of species Y.

For solutions of fixed total concentration of NMP equal to $3.03 \times 10^{-4}\ M$, the values of K_1, determined using eq. [2], were found to increase by a factor of approximately four as the total base concentration in solution varied from $3.75 \times 10^{-5}\ M$ to $19.0 \times 10^{-5}\ M$. It seems unlikely that the variation in K_1 is due to an ionic strength effect because a comparable increase in K_1 values was observed when the experiments were carried out under conditions in which the base concentration varied from $3.75 \times 10^{-5}\ M$ to $20.0 \times 10^{-5}\ M$ but the ionic strength was maintained constant at $0.20\ M$ with added $(C_2H_5)_4NClO_4$.

If species Y also results from a 1:1 interaction of NMP and DABCO according to the equation

[6] $NMP + DABCO \rightleftarrows DABCOH^+ + Y$

we have

[7] $K_1' = [DABCOH^+][Y]/[NMP][DABCO]$

Utilizing absorbance data recorded at 442 nm and the values of ε_{NMP} and ε_Y at 442 nm quoted above, we find a constant value for K_1', over the entire range of DABCO concentrations employed, of 9.5×10^{-3}.

If complex Z is formed as a result of a 1:1 interaction of Y and MeO$^-$ we have

[8] $Y + MeO^- \rightleftarrows Z$

and

[9] $K_2 = [Z]/[Y][MeO^-]$

Using the arguments and procedures described above, the following parameters were obtained: $\varepsilon_Z = 4.00 \times 10^4\ M^{-1}\ cm^{-1}$ (508 nm), $\varepsilon_Y = 1.29 \times 10^4\ M^{-1}\ cm^{-1}$ (508 nm), and $K_2 = 1.5 \pm 0.2 \times 10^3\ M^{-1}$, over the range of base concentrations employed in these studies.

Although calculated values of K_2 showed a tendency to increase with increasing concentration of $NaOCH_3$ in solution, this tendency was much less marked than in the case of the K_1 values. Comparable variations in K_2 values were observed when the studies of the conversion of Y to Z were carried out in solutions whose ionic strength was maintained constant at $0.20\ M$ with added $(C_2H_5)_4NClO_4$ and in solutions in which the ionic strength was allowed to vary from $0.00032\ M$ to $0.0050\ M$.

It seems probable that the decrease in absorbance at 508 nm at concentrations of $MeO^- > 3 \times 10^{-2}\ M$ is due to both a 1:1 interaction of Z and MeO$^-$ and a slow decomposition of NMP. 3:1 σ-complexes such as **5** (X = CH_3O) have been observed in pure methanol and it has been noted that the stabilities of such complexes decrease markedly as the DMSO content of the solvent mixture increases (5, 6, 10).

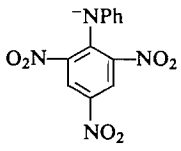
The structure of the 1:1 complex Y is quite readily deduced by considering the results obtained from the reactions of NMP and DABCO in pure, dry DMSO and of NMP with MeO$^-$ in DMSO/MeOH. Thus, the observation that DABCO, which cannot form σ-complexes of any type (11), reacts with NMP to yield Y firmly establishes that Y is the anion **6**. The fact that the species generated by the reaction of NMP with 1 molar equivalent of MeO$^-$ in DMSO/MeOH has absorption properties identical to those of the species

Can. J. Chem. Downloaded from www.nrcresearchpress.com by 210.87.254.6 on 09/05/12
For personal use only.

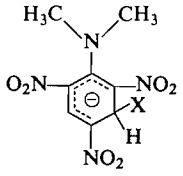
Can. J. Chem. Downloaded from www.nrcresearchpress.com by 210.87.254.6 on 09/05/12
For personal use only.

generated in pure, dry DMSO establishes that the anion **6** is also the exclusive species formed under these reaction conditions.

In agreement with this conclusion we note that Crampton and Gibson (12) have reported a λ_{max} of 435 nm for **10** which is the sole species formed in the reaction of MeO^- with *N*-phenylpicramide in methanol. Also in agreement with the above con-

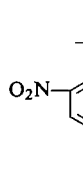


10

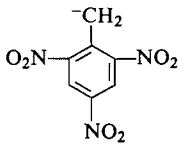


11

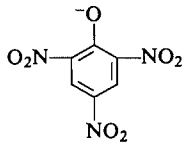
clusion is the general dissimilarity of the spectrum of Y (**6**) and the spectra of species such as **1** (X = OCH_3, SO_3^-, OH) and **11** (X = OCH_3, SO_3^-) (λ_{max} for X = OCH_3 species ~400 nm, $\varepsilon_{400} \simeq 3.2 \times 10^4\ M^{-1}\ cm^{-1}$). We note in passing the rather comparable shapes of the ultraviolet–visible absorption bands and values of ε at λ_{max} of the three closely related ions **6**, **12**, and **13** (13, 14).



6



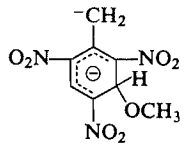
12



13

Parameter	Value		
	6	**12**	**13**
λ_{max} (nm)	442	520	360
$\varepsilon_{\lambda_{max}}$ ($M^{-1}\ cm^{-1}$)	1.71×10^4	1.7×10^4	1.5×10^4

The exclusive formation of **6** under our reaction conditions is in accord with Crampton and Gibson's observations that, for a given *N*-alkylpicramide, the fraction of starting material converted to the conjugate base increases as the DMSO content of the solvent increases. Specifically for NMP they found this fraction to be 0.60 in pure MeOH and 0.90 in DMSO/MeOH (87/13, v/v) (12). Similar observations have been made by Fyfe *et al.* in connection with the reactions of 2,4,6-trinitrotoluene and methoxide ion to form **12** and **14** in DMSO/MeOH mixtures (15).

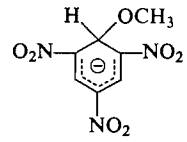


14

That increasing proportion of DMSO in the solvent will favor conjugate base formation over methoxide ion addition is to be expected since in reaction [10]

[10] $\mathbf{1} \rightleftharpoons \mathbf{6} + MeOH$

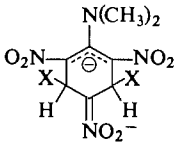
the two complexes differ by 1 molecule of MeOH. In addition, solvation of **6** by DMSO is probably more effective than solvation of **1** by this solvent.



15

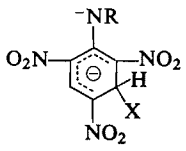
Alternatively, one would expect that MeOH would less effectively solvate **1** than **6**.

A K_1 value of $20\ M^{-1}$ for the formation of **6** in pure methanol at 25.0°C has been reported (12). Our value of K for the same process in DMSO/MeOH (95/5, v/v) is $2 \pm 1 \times 10^5\ M^{-1}$ at 25.0°C. Similar large increases in K, as the result of increasing the DMSO content of DMSO–MeOH solvent systems, have been observed previously in the reactions of 1,3,5-trinitrobenzene with methoxide ion to form σ-complex **15** and in a number of related σ-complex forming reactions (16, 17). Preferential solvation by DMSO of the anion **15** as compared to CH_3O^- is considered to be the main factor leading to an increase in K as the proportion of DMSO in the solvent mixture increases (16, 17).



16

Since under the experimental conditions in which the 1:1 interaction predominates the exclusive 1:1 interaction product is **6**, it seems reasonable to assign the 1:2 adduct, species Z, as **7**. Support for this formulation comes from the observation that the spectral characteristics of the 2:1 adduct **16** (λ_{max} = 480 nm, $\varepsilon = 2.9 \times 10^4\ M^{-1}\ cm^{-1}$) are quite different from those of species Z. In addition, Z and complex **14** have very similar ultraviolet–visible absorption bands and ε values at λ_{max}. Crampton and Gibson (12) have reported λ_{max} values of 480 nm for a series of 2:1 adducts **17**



17

where X = OCH_3 and R = H, CH_3, i-C_3H_7, n-C_4H_9, t-C_4H_9, and C_6H_5 but make no mention of a second absorption maximum at wavelengths between 350 and 480 nm, or the magnitudes of the ε values at 480 nm.

Experimental

N-Methylpicramide was prepared by adding an excess of methylamine in ethanol to a 5% solution of 1-chloro-2,4,6-trinitrobenzene in ethanol and evaporating the resulting solution to dryness. The solution formed by extraction of the residue with acetone was filtered to remove the insoluble methylammonium chloride and evaporated to dryness. The resulting solid was recrystallized to constant melting point from absolute alcohol. After drying *in vacuo* over phosphorus(V) pentoxide, the product had a melting point 114–115°C; lit. (18) 115°C. Sodium methoxide solutions were prepared by dissolving clean sodium in Analar methanol under nitrogen and were titrated with standard acid using phenolphthalein as an indicator. Dimethylsulfoxide (DMSO) was dried over calcium hydride and fractionated under reduced pressure, the middle fraction being collected. DABCO was recrystallized twice from benzene and dried *in vacuo*. The resulting material was mixed with an equal amount of barium oxide and sublimed twice to yield white crystals, mp 157°C. Eastman tetraethylammonium perchlorate was dried to constant weight *in vacuo* over phosphorus(V) pentoxide. Reagent grade trifluoroacetic acid was used as received.

Stock solutions of *N*-methylpicramide in DMSO, DABCO in DMSO, $(C_2H_5)_4NClO_4$ in DMSO, and $NaOCH_3$ in methanol were made up under nitrogen in a drybox and were protected from light. Solutions used in the equilibrium studies were also prepared in the drybox by adding appropriate volumes of the stock solutions to a known volume of DMSO. After thorough mixing, a portion of the solution was transferred to a clean dry spectrophotometric cell and the cell and its contents then placed in the spectrophotometer.

Optical measurements were carried out on a Beckman Acta IV spectrophotometer using matched silica cells of 1.0 mm and 5.0 mm path length. The temperature in the cells was maintained constant at 25.0 ± 0.1°C by circulating water from a constant temperature bath through a specially designed cell holder in the spectrophotometer.

Acknowledgment

Financial support of this research by the Natural Sciences and Engineering Research Council of Canada is gratefully acknowledged. We thank Dr. M. R. Crampton for communicating results prior to publication.

1. M. R. Crampton and V. Gold. Proc. Chem. Soc. 298 (1964); J. Chem. Soc. B, 893 (1966).
2. K. L. Servis. J. Am. Chem. Soc. **87**, 5495 (1965); **89**, 1508 (1967).
3. M. R. Crampton. J. Chem. Soc. B, 1341 (1967).
4. E. Buncel, A. R. Norris, K. E. Russell, and P. E. Sheridan. Can. J. Chem. **52**, 25 (1974).
5. M. R. Crampton and M. J. Willison. J. Chem. Soc. Perkin II, 160 (1976).
6. V. Gold and C. H. Rochester. J. Chem. Soc. 1697 (1964).
7. (*a*) E. Bergman, N. R. McFarlane, and J. J. K. Boulton. J. Chem. Soc. Chem. Commun. 511 (1970); (*b*) J. J. K. Boulton and N. R. McFarlane. J. Chem. Soc. B, 225 (1971); (*c*) J. J. K. Boulton, P. J. Jewess, and N. R. McFarlane. J. Chem. Soc. B, 928 (1971).
8. L. B. Clapp, H. Lacey, G. G. Beckwith, R. M. Srivastava, and N. Muhammad. J. Org. Chem. **23**, 4262 (1968).
9. C. A. Fyfe, S. W. H. Damji, and A. Koll. J. Am. Chem. Soc. **101**, 957 (1979).
10. F. Terrier. Ann. Chim. 153 (1969).
11. E. Buncel and W. Eggimann. J. Am. Chem. Soc. **99**, 5958 (1977).
12. M. R. Crampton and B. Gibson. J. Chem. Soc. Perkin II. In press.
13. E. Buncel, A. R. Norris, K. E. Russell, and R. Tucker. J. Am. Chem. Soc. **94**, 1646 (1972).
14. V. Gold and C. H. Rochester. J. Chem. Soc. 1722 (1964).
15. C. A. Fyfe, C. D. Malkiewich, S. W. H. Damji, and A. R. Norris. J. Am. Chem. Soc. **98**, 6983 (1976).
16. M. J. Strauss. Chem. Rev. **70**, 667 (1970).
17. E. Buncel and H. Wilson. Adv. Phys. Org. Chem. **14**, 133 (1977).
18. J. Glazer, E. D. Hughes, C. K. Ingold, A. T. James, G. T. James, and E. Roberts. J. Chem. Soc. 2674 (1950).

Can. J. Chem. Downloaded from www.nrcresearchpress.com by 210.87.254.6 on 09/05/12
For personal use only.

A wavelength specific photo-electric detector

R. STEPHENS

Trace Analysis Research Centre, Department of Chemistry, Dalhousie University, Halifax, N.S., Canada

Received January 17, 1980

R. STEPHENS. Can. J. Chem. **58**, 1621 (1980).

A photo-electric detector is described which is capable of showing selectivity towards atomic resonance radiation. Details are given of the construction of such a device suitable for use with the mercury 253.7 nm line. A possible mechanism for the operation of the detector is considered. Its spectral selectivity is illustrated by an examination of the atomic absorption signals obtained with a partially reversed line source.

R. STEPHENS. Can. J. Chem. **58**, 1621 (1980).

On décrit un détecteur photoélectrique capable d'être sélectif vis à vis la radiation de résonance atomique. On fournit les détails concernant la construction d'un tel appareil convenant à une utilisation dans la région de la raie du mercure à 253.7 nm. On considère un mécanisme possible d'utilisation du détecteur. La sélectivité spectrale est illustrée par un examen des signaux d'absorption atomique obtenus à l'aide d'une source de raies partiellement inversée.

[Traduit par le journal]

Can. J. Chem. Downloaded from www.nrcresearchpress.com by 210.87.254.5 on 09/05/12
For personal use only.

Introduction

Recent work has shown the opto-galvanic effect to offer an ingenious and effective technique for the detection of low concentrations of atomic species, by the measurement of vapour phase ionisation currents produced under laser illumination (1–7). A natural question which arises from this work is whether the inverse process is also feasible; that is, can lower intensities of resonance radiation usefully be detected by the measurement of ionisation currents in atomic vapours of higher concentration? Such a detector would be of interest in analytical atomic spectroscopy in that it could provide a device with unusually high optical resolution, a large optical aperture, and automatic tolerance to stray light. It would also bring considerable simplification to the design of equipment intended for the measurement of resonance radiation.

At the present time there is no device available with all of these properties. The nearest approach is probably the resonance monochromator–photomultiplier combination described by Walsh and co-workers (8–11), which measures resonance fluorescence from a sputtered vapour. Even here, however, the functions of spectral isolation and photo-electric detection are carried out by separate instruments, which reduces both tolerance to stray light and the effective aperture of the system (since only a small fraction of fluorescent radiation can be collected).

This paper describes the construction and behaviour of a wavelength specific detector based on the opto-galvanic effect. For reasons of technical convenience the present device was designed for the detection of the mercury 253.7 nm line.

Experimental

Mercury was chosen as a suitable test element because high vapour pressures can be obtained readily and controllably, because intense discharge emission sources are available, and because the photon energy of the 253.7 nm line is sufficiently high to cause ionisation quite easily under the correct conditions.

Mercury vapour shows no useful ionisation upon irradiation by a resonance discharge source. Accordingly it was necessary to add an ionisation agent to the system. Potassium vapour was selected for this purpose, since its ionisation potential (4.3 eV) is just below that of a 253.7 nm photon (4.9 eV). It is of interest to record that sodium (ionisation potential = 5.1 eV) vapour can be used in place of potassium, although the resulting signals are smaller.

The source used in all the present experiments was an Oriel C-73-14 penlight discharge lamp. This gave sufficient intensity to examine the behaviour of the detector over a range of conditions. An ordinary mercury hollow cathode lamp driven at 2 or 3 mA also gave satisfactory signals provided all detector parameters were set reasonably close to the optimum.

Figures 1 and 2 show respectively the detector design used and the associated measuring apparatus. The detector was permanently attached to a vacuum line; no attempt was made to build a sealed system. Mercury vapour was supplied continuously at room temperature from (solid) zinc–mercury amalgam. Potassium was contained in a copper jacket, surrounded by an external heater. Constantin wire was welded to the bottom of the jacket to provide a thermocouple junction. The thermocouple readings were used to determine the vapour pressure of potassium in the jacket, and hence in the cell volume immediately above it. Ionisation was detected by two copper electrodes located over the exit of the potassium furnace. The electrodes were connected to a 0–300 V dc supply via a 10 MΩ load resistor. The signal developed across the resistor was ac coupled to a FET input pre-amplifier mounted directly on the end of the detector. Both the pre-amplifier and the detector (except for its front window) were covered by aluminum foil to provide electrical screening. An argon supply was available at the front of the detector, to sweep excess mercury vapour from the system, and also to permit the effect of inert gas pressure to be examined.

Construction of several detectors of this general type showed that their performance was not particularly affected by the extent of vacuum de-gassing of cell walls, electrodes, etc. (pre-

0008-4042/80/161621-06$01.00/0

©1980 National Research Council of Canada/Conseil national de recherches du Canada

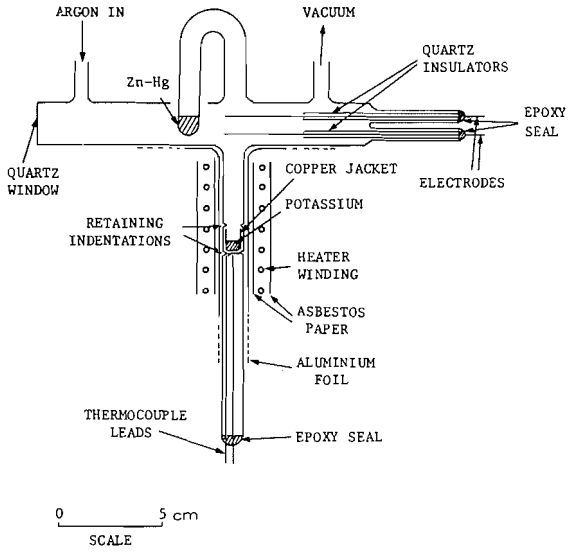


FIG. 1. Schematic diagram of the detector.

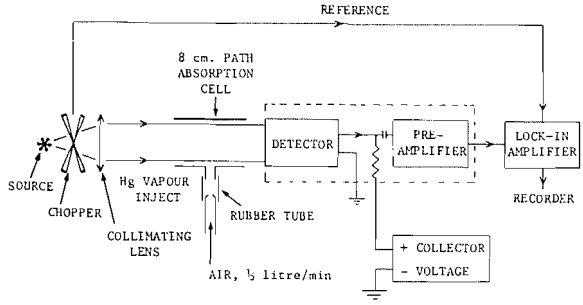


FIG. 2. Layout of the detector and associated equipment.

sumably because the potassium vapour acts as an effective getter in the ionisation region). However, it was essential to thoroughly melt and de-gas the potassium before use. This operation is most easily accomplished by initially introducing a piece of the metal into the copper jacket, then heating it under a few Torr of argon. This procedure minimizes migration of solid metal up the furnace walls.

It was found that careful design was necessary to avoid detection of spurious signals. Two causes of such signals were observed. The first occurred if solid potassium migrated onto either the electrodes or onto the glass walls surrounding them. The glass was effectively at ground potential, and could pass enough leakage current to enable the system to act as an ordinary vacuum photodiode. The second effect was observed in the event of the glass around the ionisation region becoming hot, in which case it showed photoconductivity. The detector design shown in Fig. 1 eliminated both of these processes quite effectively: however, as an added precaution the detector was operated under normal laboratory lighting throughout this work. Because both of the above effects show a wide spectral response, unlike the resonance response of present interest, their onset then was automatically signalled by a rapid increase of detector noise, followed by amplifier saturation. This mode of use also illustrates the tolerance of the detector towards stray light, mentioned previously. An additional effect that was observed even during proper operation of the detector was the existence of a dc background current. This was not easy to measure quantitatively, but it appeared to be of the same order of magnitude as the peak photo-current. The behaviour of this dc background was not examined here; nor was it included in any of the present measurements.

During operation the collector voltage (Fig. 2) and potassium furnace temperature were set to their required values, and a few millilitres of argon were allowed to enter the detector. The resulting signal form is shown in Fig. 3. An initial sharp rise occurs as mercury vapour is swept from the front of the detector, permitting more radiation to reach the ionisation region. Further argon flow then sweeps potassium and mercury vapours out of the ionisation region, and the signal falls to zero. When the argon flow stops the signal rises to a maximum as potassium and mercury vapours return, and finally falls again as mercury once more causes attenuation of the radiation reaching the ionisation region by re-diffusing to the front of the detector. The following measurements were all made on the signal peak observed after an injection of argon. Unless otherwise stated the detector remained continuously connected to the vacuum line, and therefore operated at the minimum pump pressure (about 0.2 Torr). When data were required at higher pressures the vacuum line was shut off and the detector filled with argon to a pressure somewhat beyond the required value. The line was then momentarily re-connected, to drop the pressure to the required value and simultaneously to sweep away excess mercury, and the reading was measured as described above.

Results and Discussion

The response characteristics of the device are shown in Figs. 4–6. Figure 4 shows the dependence of signal on the collector voltage applied to the detector electrodes. The initial rise of the signal from zero is consistent with an increasing efficiency of electron collection with increasing voltage. However, the curve shows no tendency to reach a plateau, which suggests that some degree of signal amplification may occur at higher voltages due to secondary electron production by collisional ionisation. The plot terminates at 270 V due to initiation of a continuous discharge.

Figure 5 shows the signal dependence on argon pressure. The signals are inversly proportional to argon pressure (slopes of both curves are −1.2)

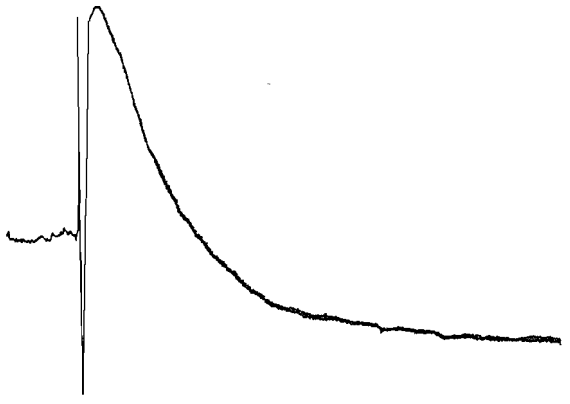


FIG. 3. Signal output with time observed after an injection of argon.

Can. J. Chem. Downloaded from www.nrcresearchpress.com by 210.87.254.5 on 09/05/12
For personal use only.

Can. J. Chem. Downloaded from www.nrcresearchpress.com by 210.87.254.5 on 09/05/12
For personal use only.

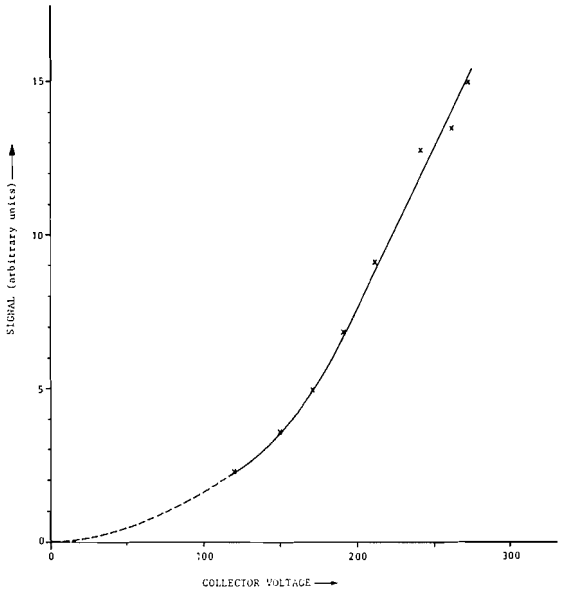


FIG. 4. Signal vs. voltage at an argon pressure of 0.2 Torr. Readings were taken up to the plasma ionisation limit.

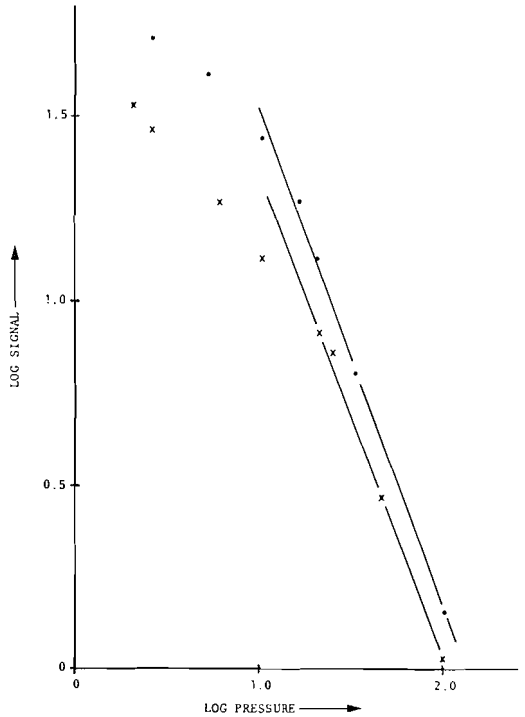


FIG. 5. log signal vs. log argon pressure (Torr).

except at low pressures, where the slope is reduced.

Figure 6 shows signal variations with the temperature of the potassium furnace. All readings were separated by a 3 min time interval for thermal equilibration. This interval was chosen as a compromise between thermal hysteresis (which is apparent in the results) and the need to minimize long term drift in the system. The results show an initial exponential increase, but appear to approach a maximum at about 600 K.

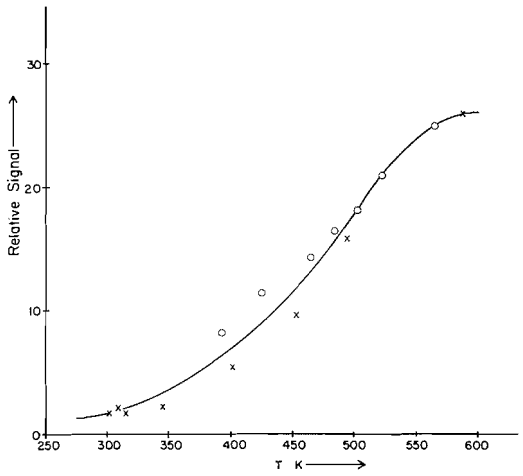


FIG. 6. Signal vs. potassium furnace temperature. Symbols ×, ○ represent respectively data taken with temperature increased from ambient, and that taken with temperature decreased from 600 K.

Comparison of the detector output with that of a conventional spectrometer showed (*a*) that the detector output was linearly dependent on source intensity (using neutral density filters); (*b*) that under optimum conditions the detector gave a p-p ac output of 60 mV across 3.9 MΩ. The source output measured by the spectrometer corresponded to an intensity of 8×10^{11} photons s^{-1}, about one third of which could be absorbed in a volume of saturated mercury vapour equivalent to the ionisation region in the detector. Hence it was estimated that the detector gave an output of about one electron for three photons absorbed in the ionisation region, or one electron for eight incident photons. This "quantum efficiency" is encouragingly high, being of the order of that given by a vacuum photodiode. There seems little doubt that it could be further improved upon by improved detector design.

Mechanism of the Detector

The behaviour described above can be accounted for as follows. Electrons are produced by collision between excited mercury and ground state potassium atoms. The state of the former ($^3P_1$ or metastable $^3P_0$) is not specified. Competition exists for the electrons between the applied electric field and vapour phase K^+ ions. The latter are produced according to the Saha equation (12) which, it is felt, will be displaced towards higher K^+ concentrations by the applied field. This arises because the field,

Can. J. Chem. Downloaded from www.nrcresearchpress.com by 210.87.254.5 on 09/05/12
For personal use only.

being close to the limit set by plasma formation, will transport electrons very effectively and quite irrespective of whether those electrons are produced thermally (as a dc background current) or by photo-ionisation (the signal or interest). These processes are described quantitatively below.

[1] $Hg + h\nu \underset{k_{-1}}{\overset{k_1}{\rightleftharpoons}} Hg^*$

[2] $Hg^* + K \underset{k_{-2}}{\overset{k_2}{\rightleftharpoons}} Hg + K^+ + e^-$

[3] $Ar + K^+ + e^- \underset{k_{-3}}{\overset{k_3}{\rightleftharpoons}} Ar + K$

The reaction $2K \rightleftharpoons K_2$ is not included in this scheme. The equilibrium position of the reaction is reported to be well to the left (13), and the present results can be accounted for reasonably well without it.

Putting i_- as the current flow from the negative (ground) electrode and i_+ as the current flow to the positive electrode,

$$d[e^-]/dt = k_2[Hg^*][K] + k_{-3}[Ar][K] - k_{-2}[Hg][K^+][e^-] - k_3[Ar][K^+][e^-] + (i_- - i_+)$$

Under steady state conditions $d[e^-]/dt = 0$ and $i_+ = i_-$. Therefore provided the charge separation induced by the spatial separation of i_+ and i_- causes no major perturbation, and that no significant charge storage occurs in the device,

[4] $$k_2[Hg^*][K] + k_{-3}[Ar][K] - k_{-2}[Hg][K^+][e^-] - k_3[Ar][K^+][e^-] = 0$$

Putting I as the incident light intensity and again considering steady state conditions, eqs. [1] and [2] give

$$d[Hg^*]/dt = k_1 I[Hg] + k_{-2}[Hg][K^+][e^-] - k_{-1}[Hg^*] - k_2[Hg^*][K] = 0$$

$\therefore$

[5] $$[Hg^*] = (k_1 I + k_{-2}[K^+][e^-])[Hg]/(k_{-1} + k_2[K])$$

Equilibrium of eq. [3] requires

[6] $$k_3/k_{-3} = [K]/[K^+][e^-]$$

Charge balance requires

[7] $$[K^+] = [e^-]$$

Substitution of eqs. [5]–[7] into [4] leads to

$$[e^-]\left\{1 - \frac{k_2 k_{-2}[K][Hg]}{(k_{-1} + k_2[K])(k_{-2}[Hg] + k_3[Ar])}\right\} = \left(\frac{k_3[K]}{k_{-3}}\right)^{1/2} \frac{k_1 k_2 I[Hg]/(k_{-1} + k_2[K]) + k_{-3}[Ar]}{k_{-2}[Hg] + k_3[Ar]}$$

Assuming that the observed signal is proportional to $[e^-]$, and recognising that the output of the synchronous amplifier represents only the term containing I, this rather cumbersome expression can be re-cast as

$$S\left\{1 - \frac{k_2 k_{-2}[K][Hg]}{(k_{-1} + k_2[K])(k_{-2}[Hg] + k_3[Ar])}\right\} = \left(\frac{k_3[K]}{k_{-3}}\right)^{1/2} \frac{k_1 k_2 I[Hg]}{(k_{-1} + k_2[K])(k_{-2}[Hg] + k_3[Ar])}$$

where S is the output signal of the amplifier; i.e.

[8] $$S = \frac{k_1 k_2 (k_3/k_{-3})^{1/2} I[Hg][K]^{1/2}}{k_{-1}k_{-2}[Hg] + k_{-1}k_3[Ar] + k_2 k_3[K][Ar]}$$

Under the present conditions, [Hg] is constant. Assuming [K] and [Ar] respectively to be proportional to the pressures P_K and P_{Ar} determined in the potassium furnace and in the vacuum line (eq. [8]) now gives:

[9] $$S = IP_K^{1/2}/(a + bP_{Ar} + cP_{Ar}P_K)$$

where a, b, and c are constants.

Equation [9] can account for most of the results found here. Thus linearity on I and inverse proportionality to P_{Ar} at high argon pressures (P_K fixed) are self-evident, with a plateau in the log S vs. log P_{Ar} curve (Fig. 5) being reached when $a \sim (b + cP_K)P_{Ar}$. The signal dependence on potassium vapour pressure has the form $S \propto P_K^{1/2}(A + P_K)$, where A is a constant. Qualitatively this accounts for the behaviour observed in Fig. 6. Thus at low temperature the signal is approximately proportional to $P_K^{1/2}$, which leads to the initial exponential rise of the curve, while at higher temperatures a maximum is reached when P_K and A are equal. However, quantitative agreement is less satisfactory. Figure 7 shows a plot of log S vs. log $P_K^{1/2}/(A + P_K)$ for the data from Fig. 6, using a value of $A = 0.5$ (corresponding to the position of the maximum

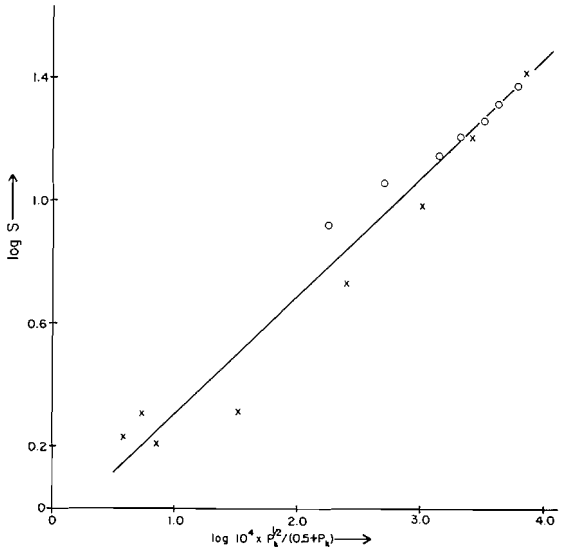


FIG. 7. Observed signals and potassium vapour pressure fitted to eq. [9]. Values of P_K were determined from the equation $\log_{10} P_{mm} = 7.45 - 4450/T$. Numerical constants in this equation are from the centre of a range given in ref. 13.

in the curve of Fig. 6, judged from the available data). Although the linearity of the curve is as expected, the value of the slope is closer to one third than to unity. One possible reason that can be suggested for this behaviour might be that, with the present cell design, potassium vapour pressure in the ionisation region where the photo-current originates is not in fact linearly related to the vapour pressure within the furnace, in contradiction to the assumption which connects eqs. [8] and [9].

Analytical Applicability of the Detector

From the viewpoint of the analytical spectroscopist the most interesting property of the present device is its optical selectivity. Thus the detector is expected to respond only to radiation that can be absorbed in the ionisation region, and to ignore all other incident frequencies. This property has been observed experimentally, as illustrated in Fig. 8. Figure 8(*a*) shows absorption signals caused by the injection of 1 mL of saturated mercury vapour into the absorption cell (Fig. 2). A 1 cm path sealed cell containing saturated mercury vapour was then inserted into the optical path. By selectively absorbing at the centre of the source emission profile this procedure caused in effect a large and reproducible broadening of the source emission line. The amplifier gain was then increased, to restore the output signal to its original value, and 1 mL of mercury vapour again injected into the absorption cell. The resulting signal is shown in Fig 8(*b*). Comparison of Fig. 8 (*a*) and (*b*) shows little difference between the two, as expected for a detector which is behaving selectively towards resonance radiation. For comparison the same procedure was carried out with the same source, etc., and using a conventional Varian-Techtron AA5 as the detection system. The resulting signals are shown in Fig. 8 (*c*) and (*d*). Again predictably, a marked difference is now observed.

The data in Fig. 8 (*a*), (*b*) were obtained after equilibration of mercury vapour had occurred, some minutes after an injection of argon, in order to obtain a flat baseline and hence to simplify comparison of repetitive results. This equilibration slightly biases the signals in Fig. 8 (*a*), (*b*) towards the observed condition of mutual agreement, because atomic absorption is already occurring in the detector ahead of the ionisation region even before the second cell is introduced. However, it is clear from the magnitudes of the signals in Fig. 8 that

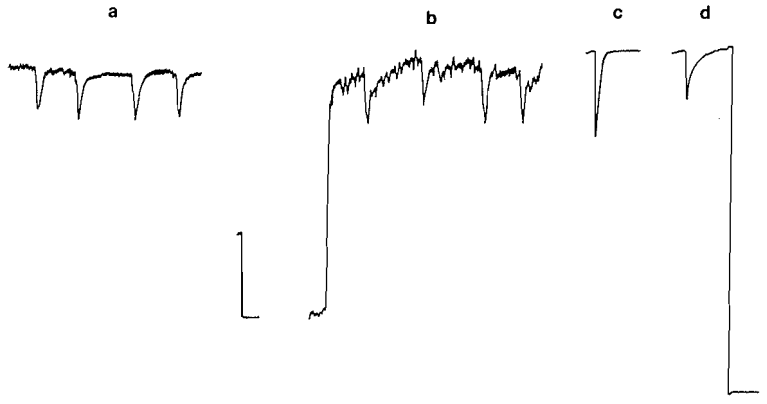


FIG. 8. (*a*) Absorption signal due to injection of 1 mL of mercury vapour into the absorption cell shown in Fig. 2. The ripple observed on the baseline is a beat frequency between the chopper and the rectified 60 Hz frequency of the fluorescent room lights. The latter show a measurable output at 253.7 nm. (*b*) Procedure in (*a*), repeated after placing a sealed absorption cell in front of the source. (*c*), (*d*) Procedure in (*a*) and (*b*) repeated on a conventional Varian-Techtron AA5 spectrometer.

Can. J. Chem. Downloaded from www.nrcresearchpress.com by 210.87.254.5 on 09/05/12
For personal use only.

such a bias does not affect either the nature or the validity of the preceding discussion.

Conclusions

The present results are considered to demonstrate the feasibility of obtaining selective detection of resonance radiation with a useful degree of optical sensitivity. The suggested detector mechanism involves ionisation of potassium vapour, both thermally and by collision with photo-excited mercury atoms. The K^+ population arising from thermal ionisation appears to act as an electron "buffer", by competing with the external electric field for the available electrons. The effect is thought to be enhanced due to electron loss to the external field in the form of a dc background current. This is not a useful process, since the existence of such a background automatically reduces the signal-to-noise ratio of the detector; for this reason the temperature in the ionisation region should be kept as low as possible.

The presence of argon is found to reduce signal magnitudes. It appears likely that other rare gases would show a similar effect. This does not represent a problem in the present apparatus, in which argon pressure can be reduced to zero if required. However, the effect is likely to be important if metal vapours are to be generated by sputtering rather than by thermal volatilisation, since a compromise would become necessary between the low gas pressure required to obtain a maximum signal and the finite value required to maintain a sputtering discharge.

The detector shows optical properties which include high resolving power, large aperture, good quantum efficiency, automatic tolerance towards stray light, and optical simplicity. This combination is felt to be of particular interest in the area of analytical atomic spectroscopy; an area where instrumental design problems involving some need for one or more of the above characteristics are encountered quite routinely at the present time.

Acknowledgement

The author is indebted to the Natural Sciences and Engineering Research Council of Canada for support of this work.

1. R. B. Green, R. A. Keller, G. G. Luther, P. K. Schenck, and J. C. Travis. Appl. Phys. Lett. **29**, 727 (1976).
2. R. B. Green, R. A. Keller, G. G. Luther, P. K. Schenck, and J. C. Travis. J. Am. Chem. Soc. **98**, 8517 (1976).
3. G. C. Turk, J. C. Travis, J. R. DeVoe, and T. C. O'Haver. Anal. Chem. **50**, 817 (1978).
4. K. C. Smyth and P. K. Schenck. Chem. Phys. Lett. **55**, 466 (1978).
5. E. F. Zalewski, R. A. Keller, and R. Engleman, Jr. J. Chem. Phys. **70**, 1015 (1979).
6. J. C. Travis, P. K. Schenck, G. C. Turk, and W. G. Mallard. Anal. Chem. **51**, 1516 (1979).
7. G. C. Turk, J. C. Travis, J. R. DeVoe, and T. C. O'Haver. Anal. Chem. **51**, 1891 (1979).
8. B. J. Russell and A. Walsh. Spectrochim. Acta, **15**, 883 (1959).
9. J. V. Sullivan and A. Walsh. Spectrochim. Acta, **22**, 1843 (1966).
10. J. A. Bowman. Anal. Chim. Acta, **37**, 465 (1967).
11. J. V. Sullivan and A. Walsh. Appl. Opt. **7**, 1271 (1968).
12. A. G. Gaydon and H. G. Wolfhard. Flames, their structure, radiation and temperature. 3rd ed. Chapman and Hall, London. 1970. Chapt. XIII.
13. A. N. Nesmeianov. Vapour pressure of the elements. *Edited by* J. I. Carasso. Academic Press, New York. 1963.

Can. J. Chem. Downloaded from www.nrcresearchpress.com by 210.87.254.5 on 09/05/12
For personal use only.

A ^{31}P nuclear magnetic resonance spectroscopic study of some 2:1, 3:1, and 4:1 complexes of phosphine sulfides and selenides with cadmium(II), including some complexes with mixed ligands[1]

PHILIP A. W. DEAN[2] AND LIJANA POLENSEK

Department of Chemistry, University of Western Ontario, London, Ont., Canada N6A 5B7

Received April 1, 1980

Can. J. Chem. Downloaded from www.nrcresearchpress.com by 210.87.254.40 on 09/05/12
For personal use only.

PHILIP A. W. DEAN and LIJANA POLENSEK. Can. J. Chem. **58**, 1627 (1980).

Using low-temperature ^{31}P nmr, many new complexes formed between divalent cadmium (as $Cd(SbF_6)_2$) and monodentate phosphine chalcogenides in liquid SO_2 have been characterized. A 4:1 (L:M) complex is formed with Bu^t_3PS and, possibly, Bu^t_3PSe. 4:1 and 3:1 complexes are formed with Ph_3PE, $(o\text{-}C_6H_4Me)Ph_2PE$, $(p\text{-}C_6H_4Me)_3PE$, and $(C_6H_{11})_3PE$ (E = S or Se) as well as $(o\text{-}C_6H_4Me)_2PhPSe$, while 4:1, 3:1 and 2:1 complexes occur for $(o\text{-}C_6H_4Me)_3PE$ (E = S or Se), and, probably, $(o\text{-}C_6H_4Me)_2PhPS$. In addition, all the mixed ligand complexes in the series

$[Cd(SeP(C_6H_{11})_3)_n(SP(C_6H_{11})_3)_{4-n}]^{2+}$, $[Cd(SeP(C_6H_{11})_3)_n(SP(C_6H_{11})_3)_{3-n}]^{2+}$, and $[Cd(SeP(o\text{-}C_6H_4Me)_3)_n(SP(o\text{-}C_6H_4Me)_3)_{3-n}]^{2+}$

have been identified.

Trends in the ^{31}P nmr data are discussed.

PHILIP A. W. DEAN et LIJANA POLENSEK. Can. J. Chem. **58**, 1627 (1980).

On a caractérisé plusieurs nouveaux complexes entre le cadmium bivalent (sous forme de $Cd(SbF_6)_2$) et les chalcogénures de phosphine monodentates dans le SO_2 liquide en utilisant la rmn du ^{31}P à basse température. Un complexe du type 4:1 (L:M) se forme avec Bu^t_3PS et peut être avec Bu^t_3PSe. Des complexes du type 4:1 et 3:1 se forment avec Ph_3PE, $(o\text{-}C_6H_4Me)Ph_2PE$, $(p\text{-}C_6H_4Me)_3PE$ et $(C_6H_{11})_3PE$ (E = S ou Se) aussi bien qu'avec $(o\text{-}C_6H_4Me)_2PhPSe$, tandis que des complexes du type 4:1, 3:1 et 2:1 se forment avec $(o\text{-}C_6H_4Me)_3PE$ (E = S ou Se) et, probablement, $(o\text{-}C_6H_4Me)_2PhPS$. De plus, on a identifié tous les complexes de ligands mixtes dans les séries $[Cd(SeP(C_6H_{11})_3)_n(SP(C_6H_{11})_3)_{4-n}]^{2+}$, $[Cd(SeP(C_6H_{11})_3)_n(SP(C_6H_{11})_3)_{3-n}]^{2+}$, $[Cd(SeP(o\text{-}C_6H_4Me)_3)_n(SP(o\text{-}C_6H_4Me)_3)_{3-n}]^{2+}$.

On discute des tendances qui se manifestent dans les données de la rmn du ^{31}P.

[Traduit par le journal]

Introduction

A recent paper (1) has described the characterization, mainly by reduced temperature ^{31}P nmr, of a representative range of cadmium(II) complexes with monodentate, bidentate, and tridentate, or potentially tridentate, phosphine oxides, sulfides, and selenides. With the oxygen donors, the maximum coordination number was found to be six, while both the sulfur and the selenium donors gave a maximum coordination number of four. The ligands $Ph_2P(E)(CH_2)_2P(E)Ph(CH_2)_2P(E)Ph_2$ (E = S or Se) gave complexes in which only three Group VI donor atoms were bound to the metal, but with the monodentate ligands Ph_3PE (E = S or Se) only the 4:1 complexes, $[Cd(EPPh_3)_4]^{2+}$, were fully characterized, though the exchange-averaged ^{31}P nmr spectra of the system Ph_3PSe–$Cd(SbF_6)_2$–SO_2 at low Ph_3PSe/Cd ratios suggested the occurrence of lower coordinate species.

For our future ^{113}Cd nmr studies, it seemed particularly desirable that this earlier work with the triphenylphosphine chalcogenides should be extended to a wider range of phosphine chalcogenides and that the lower coordinate species should be completely characterized if possible. In this way, systematic variation of both the number and the type of donor groups about cadmium would become accessible. With these goals, in the present work we have used ^{31}P nmr to examine the systems R_3PS–$Cd(SbF_6)_2$–SO_2 and R_3PSe–$Cd(SbF_6)_2$–SO_2 (R_3 = Ph_3, $(o\text{-}C_6H_4Me)_3$, $(o\text{-}C_6H_4Me)_2Ph$, $(o\text{-}C_6H_4Me)Ph_2$, $(p\text{-}C_6H_4Me)_3$, Et_3, $(C_6H_{11})_3$, or Bu^t_3), as well as some systems likely to yield complexes with mixed ligands. Among the latter, $(o\text{-}C_6H_4Me)_3PS$–$(o\text{-}C_6H_4Me)_3PSe$–$Cd(SbF_6)_2$–SO_2 and $(C_6H_{11})_3PS$–$(C_6H_{11})_3PSe$–$Cd(SbF_6)_2$–SO_2 were studied in most detail.

Other than our previous paper (1), we could find only one other report dealing with the ^{31}P nmr spectra of cadmium complexes of phosphine chalcogenides (2):[3] in that report, the slow-exchange ^{31}P nmr spectrum of $CdCl_2(SePPh_3)_2$ in $CDCl_3$ at an unspecified temperature was presented, showing a 7 Hz reduction in $|^1J(^{31}P—^{77}Se)|$ on complexation and a value of 10.5 Hz for $|^2J(^{111/113}Cd—^{31}P)|$. In addition, there have been several studies of cadmium(II)–phosphine chalcogenide complexes in the solid state (e.g. refs. 3–6).

[1]No reprints available.

[2]To whom correspondence should be addressed.

[3]This reference escaped the literature search made as part of ref. 1, but should have been included there.

0008-4042/80/161627-06$01.00/0

©1980 National Research Council of Canada/Conseil national de recherches du Canada

Can. J. Chem. Downloaded from www.nrcresearchpress.com by 210.87.254.40 on 09/05/12
For personal use only.

TABLE 1. ^{31}P nmr spectral parameters of some 4:1 complexes of phosphine selenides with cadmium(II), $Cd(SePR_3)_4^{2+}$, in liquid SO_2

R_3 in $SePR_3$[a]	T (K)	δ_P[b] (ppm)	$\Delta\delta_P$[c] (ppm)	$\lvert{}^1J(^{31}P—^{77}Se)\rvert$ (Hz)	$\Delta^1J(^{31}P—^{77}Se)$[d] (Hz)	$\lvert{}^2J(^{111/113}Cd—^{31}P)\rvert$ (Hz)
Ph_3[e]	209	30.7	−2.4	585	−70	48
$Ph_2(o\text{-tol})$	209	29.8	−0.6	583	−69	53
$Ph(o\text{-tol})_2$	209	29.3	1.7	583	−54	58
$(o\text{-tol})_3$[f]	196	29.8	2.8	~590	~−36	≳63
$(p\text{-tol})_3$	209	29.5	−2.3	576	−65	48
$(chx)_3$	209	61.4	−0.9	552	−25	57
$(Bu^t)_3$[g]	196	93.1	1.0	536	−55	~80

[a]o-tol = $o\text{-}C_6H_4Me$; p-tol = $p\text{-}C_6H_4Me$; chx = C_6H_{11}.
[b]Relative to external $OP(OMe)_3$ in $(CD_3)_2CO$; shifts to increasing frequency are taken as positive: $\delta_{OP(OMe)_3}(ext) = \delta_{H_3PO_4}(ext) - 1.7$ ppm.
[c]$\delta_{complex} - \delta_{free}$.
[d]$\lvert{}^1J(P—Se)\rvert_{complex} - \lvert{}^1J(P—Se)\rvert_{free}$.
[e]From ref. 1.
[f]This spectrum was incompletely resolved (see text).
[g]See text.

Results and Discussion

Complexes of a Single Ligand

In all of the systems studied, rapid intermolecular exchange occurs for all L/M ratios at ambient probe temperature. However, at reduced temperature, slow exchange spectra could be obtained for most of the systems at some values of L/M.

When L/M ≳ 3, the behaviour of the systems R_3PS–$Cd(SbF_6)_2$–SO_2 (R_3 = Ph_3, $(o\text{-}C_6H_4Me)_3$, $(o\text{-}C_6H_4Me)_2Ph$, $(o\text{-}C_6H_4Me)Ph_2$, $(p\text{-}C_6H_4Me)_3$, or $(C_6H_{11})_3$), and R_3PSe–$Cd(SbF_6)_2$–SO_2 (R_3 = Ph_3, $(o\text{-}C_6H_4Me)_2Ph$, $(o\text{-}C_6H_4Me)Ph_2$, $(p\text{-}C_6H_4Me)_3$, or $(C_6H_{11})_3$) is very similar. When L/M > 4, the systems behave as described earlier (1) for Ph_3PS and Ph_3PSe as ligands: the yellow colour of the free ligand – SO_2 charge transfer complex is visible, and the low temperature ^{31}P nmr spectra show a free ligand signal together with a signal with $^{111/113}Cd$ satellites, which, by integral analysis, is readily assigned to a 4:1 complex. The ^{31}P nmr spectral parameters of the 4:1 complexes of R_3PSe and R_3PS are given in Tables 1 and 2, respectively. At L/M ≃ 4 neither the yellow colour of the ligand–SO_2 complex nor the nmr signal of the free ligand is evident. The spectrum shows just the signal of the 4:1 complex. As L/M is decreased further, a new signal, with $^{111/113}Cd$ satellites, grows relative to that of the 4:1 complex, becoming dominant at L/M ≃ 3. Integral analysis in the range 4 > L/M > 3 confirms that this second signal is from a 3:1 complex. Details of the ^{31}P nmr spectra of the 3:1 complexes of R_3PSe and R_3PS are summarized in Tables 3 and 4, respectively.

The behaviour of the $(o\text{-}C_6H_4Me)_3PSe$-containing system is similar to that just described, except that when L/M ≳ 4, the spectra show some broadening, characteristic of slow intermolecular exchange, even at 196 K, the lowest accessible temperature. The value of $\lvert{}^2J(^{111/113}Cd—^{31}P)\rvert$ given in Table 1 for $[Cd(SeP(o\text{-tol})_3)_4]^{2+}$ should therefore be regarded as the minimum value.

TABLE 2. ^{31}P nmr spectral parameters of some 4:1 complexes of phosphine sulfides with cadmium(II), $Cd(SPR_3)_4^{2+}$, in liquid SO_2

R_3 in SPR_3[a]	T (K)	δ_P[b] (ppm)	$\Delta\delta_P$[c] (ppm)	$\lvert{}^2J(^{111/113}Cd—^{31}P)\rvert$ (Hz)
Ph_3[d]	209	40.6	−0.4	37
$Ph_2(o\text{-tol})$	196	41.0	1.0	42
$Ph(o\text{-tol})_2$	209	42.6	3.0	47
$(o\text{-tol})_3$	209	44.2	5.2	51
$(p\text{-tol})_3$	209	39.9	−0.3	34
$(chx)_3$	209	65.0	0.4	48
$(Bu^t)_3$[e]	196	89.7	1.2	73

[a]o-tol = $o\text{-}C_6H_4Me$; p-tol = $p\text{-}C_6H_4Me$; chx = C_6H_{11}.
[b]Relative to external $OP(OMe)_3$ in $(CD_3)_2CO$; shifts to increasing frequency are taken as positive: $\delta_{OP(OMe)_3}(ext) = \delta_{H_3PO_4}(ext) - 1.7$ ppm.
[c]$\delta_{complex} - \delta_{free}$.
[d]From ref. 1.
[e]See text.

The ligand Bu^t_3PS gives a 4:1 complex at L/M ≳ 4 as described above, but a second signal ($\delta_{OP(OMe)_3}$ ≈ 86.5 ppm), occurring when L/M < 4, had no cadmium satellites and so could not be attributed with certainty to $[Cd(SPBu^t_3)_3]^{2+}$.[4] Similarly, only one obvious cadmium-containing species $[Cd(SePBu^t_3)_n]^{2+}$ was identified with Bu^t_3PSe as ligand. In the system Bu^t_3PSe–$Cd(SbF_6)_2$–SO_2 the bright yellow colour of $Bu^t_3PSe{\cdot}SO_2$ persists to L/M ≈ 2.5, when at 196 K the broad spectrum shows partially-resolved cadmium satellites.[5] The odd behaviour of this system precluded direct determination of the number of ligands, but our prejudice is for n = 4, as in $Cd(SPBu^t_3)_4^{2+}$: neither $\lvert{}^2J(^{111/113}Cd—^{31}P)\rvert$ nor $\Delta^1J(^{31}P—^{77}Se)$ seem large

[4]This signal is not from a decomposition product: it collapses with the signal from $[Cd(SPBu^t_3)_4]^{2+}$ at ambient probe temperature.

[5]The decrease of 62 Hz in $\lvert{}^1J(^{31}P—^{77}Se)\rvert$ on changing from CH_2Cl_2 to SO_2 as solvent at 313 K indicates adduct formation (7).

TABLE 3. ^{31}P nmr spectral parameters of some 3:1 complexes of phosphine selenides with cadmium(II), $Cd(SePR_3)_3^{2+}$, in liquid SO_2

R_3 in $SePR_3$[a]	T (K)	δ_P[b] (ppm)	$\Delta\delta_P$[c] (ppm)	$\lvert^1J(^{31}P—^{77}Se)\rvert$ (Hz)	$\Delta^1J(^{31}P—^{77}Se)$[d] (Hz)	$\lvert^2J(^{111/113}Cd—^{31}P)\rvert$ (Hz)
Ph_3	196	32.0	−1.1	542	−84	58
$Ph_2(o\text{-tol})$	209	30.3	−0.1	543	−110	61
$Ph(o\text{-tol})_2$	196	29.2	1.7	540	−97	63
$(o\text{-tol})_3$	196	28.0	0.9	529	−97	67
$(p\text{-tol})_3$	209	30.5	−1.3	533	−109	57
$(chx)_3$	209	63.6	1.3	513	−64	61

[a] o-tol = o-C_6H_4Me; p-tol = p-C_6H_4Me; chx = C_6H_{11}.
[b] Relative to external $OP(OMe)_3$ in $(CD_3)_2CO$; shifts to increasing frequency are taken as positive; $\delta_{OP(OMe)_3}(ext) = \delta_{H_3PO_4}(ext) - 1.7$ ppm.
[c] $\delta_{complex} - \delta_{free}$.
[d] $|^1J(P—Se)|_{complex} - |^1J(P—Se)|_{free}$.

TABLE 4. ^{31}P nmr spectral parameters of some 3:1 complexes of phosphine sulfides with cadmium(II), $Cd(SPR_3)_3^{2+}$, in liquid SO_2

R_3 in SPR_3[a]	T (K)	δ_P[b] (ppm)	$\Delta\delta_P$[c] (ppm)	$\lvert^2J(^{111/113}Cd—^{31}P)\rvert$ (Hz)
Ph_3	209	42.2	1.2	43
$Ph_2(o\text{-tol})$	196	41.6	1.6	48
$Ph(o\text{-tol})_2$	209	42.1	2.5	51
$(o\text{-tol})_3$	196	42.1	3.2	54
$(p\text{-tol})_3$	209	41.2	1.0	44
$(chx)_3$	209	65.8	1.2	54

[a] o-tol = o-C_6H_4Me; p-tol = p-C_6H_4Me; chx = C_6H_{11}.
[b] Relative to external $OP(OMe)_3$ in $(CD_3)_2CO$; shifts to increasing frequency are taken as positive; $\delta_{OP(OMe)_3}(ext) = \delta_{H_3PO_4}(ext) - 1.7$ ppm.
[c] $\delta_{complex} - \delta_{free}$.

enough, by comparison with possible analogues, for $n = 3$. Possibly the electron-rich Bu^t_3PSe is very strongly solvated, so the equilibrium

$$Cd^{2+}(solv) + SePBu^t_3(solv) \rightleftarrows [Cd(SePBu^t_3)_{4(?)}]^{2+}$$

is driven to the right only in the presence of a significant excess of Cd^{2+}.

Blanching of the colour of $Et_3PSe{\cdot}SO_2$ when $L/M \lesssim 4$, together with a reduction in $|^1J(^{31}P—^{77}Se)|$ in the cadmium-containing solutions, shows that Cd(II)–$SePEt_3$ complexes do form, but we were unable to stop rapid intermolecular exchange in either ligand-rich or metal-rich mixtures. $SPEt_3$ complexes were also labile, though in the ligand-rich systems the region of intermediate exchange was reached at 196 K, suggesting that for $[Cd(SPEt_3)_4]^{2+}$, $\delta_{OP(OMe)_3} \approx 63.4$ ppm ($\Delta\delta_P \approx 9.8$ ppm).

When L/M is decreased below three, an exchange-averaged spectrum is observed for systems containing Ph_3PSe or Ph_3PS, as noted earlier (1); systems containing $(p\text{-}C_6H_4Me)_3PSe$ and $(p\text{-}C_6H_4Me)_3PS$ behave similarly. However, the 3:1 spectrum persists to at least L/M = 2.5 when L = $(C_6H_{11})PS$, $(C_6H_{11})_3PSe$, $(o\text{-}C_6H_4Me)Ph_2PS$, $(o\text{-}C_6H_4Me)Ph_2PSe$, or $(o\text{-}C_6H_4Me)_2PhPSe$, though in all these cases a collapsed spectrum is observed by the time L/M = 1.5 is reached.

For all the selenides mentioned so far, $|^1J(^{31}P—^{77}Se)|$ is less in the collapsed spectrum than in the 3:1 complex, suggesting the occurrence of lower coordinate species as already noted (1). The resolved spectrum of the lower coordinate species is observed down to at least L/M = 1.5 when L is $(o\text{-}C_6H_4Me)_2PhPS$, $(o\text{-}C_6H_4Me)_3PS$, or $(o\text{-}C_6H_4Me)_3PSe$. For the first of these three, the new signal is shielded by 0.1_2 ppm relative to the signal of the 3:1 complex but no $^{111/113}Cd$ satellites were observed with certainty due to signal overlap. The full spectra of what we presume to be 2:1 complexes are observed for $(o\text{-}C_6H_4Me)_3PS$ and $(o\text{-}C_6H_4Me)_3PSe$. Details of the ^{31}P nmr spectra of these two 2:1 species are given in Table 5, and again it can be seen, by comparison with the data in Tables 2 and 4, that the shifts of the 2:1 complexes are very close to those of the corresponding 3:1 complexes.

Several noteworthy trends are exhibited by the data in Tables 1–5. The data in Tables 1, 3, and 5 show that for the same ligand, $|^1J(^{31}P—^{77}Se)|$ decreases as the number of coordinated phosphine selenides decreases. Grim and co-workers (8) have observed that in HgX_2 complexes of Bu^n_3PSe, $|^1J(^{31}P—^{77}Se)|$ decreases as the Lewis acidity of the acceptor increases. Our results are consistent with such an explanation, for the order of Lewis acidity will be $Cd(SePR_3)^{2+} > Cd(SePR_3)_2^{2+} > Cd(SePR_3)_3^{2+}$. Even in the 4:1 complexes, where the Lewis acidity of the metal centre is lowest, the change in $|^1J(^{31}P—^{77}Se)|$ on complexation is much larger than that observed in $CdCl_2(SePPh_3)_2$ (2).

In the 4:1 complexes of the triarylphosphine selenides (Table 1), the values of $|^1J(^{31}P—^{77}Se)|$ fall within a small range, in contrast to the corresponding couplings in the free ligands which are influenced by steric factors (9). Apparently in the 4:1 complexes there is little variation in the nature of the P—Se linkages. In view of this, the variation of $|^2J(^{111/113}Cd—^{31}P)|$ with different degrees of o-

Can. J. Chem. Downloaded from www.nrcresearchpress.com by 210.87.254.40 on 09/05/12
For personal use only.

TABLE 5. ^{31}P nmr spectral parameters of $[Cd(SP(o\text{-}C_6H_4Me)_3)_2]^{2+}$ and $[Cd(SeP(o\text{-}C_6H_4Me)_3)_2]^{2+}$ in liquid SO_2 at 196 K

Parameter	Value	
	$[Cd(SP(o\text{-tol})_3)_2]^{2+}$	$[Cd(SeP(o\text{-tol})_3)_2]^{2+}$
δ_P(ppm)[a]	42.1	28.2
$\Delta\delta_P$(ppm)[b]	3.2	1.1
$\lvert^2J(^{111/113}Cd—^{31}P)\rvert$(Hz)	70	83
$\lvert^1J(^{31}P—^{77}Se)\rvert$(Hz)	—	505

[a]Relative to external $OP(OMe)_3$ in $(CD_3)_2CO$; shifts to increasing frequency are taken as positive; $\delta_{OP(OMe)_3}(ext) = \delta_{H_3PO_4}(ext) - 1.7$ ppm.
[b]$\delta_{complex} - \delta_{free}$.

TABLE 6. ^{31}P nmr spectral parameters of the 4:1 mixed ligand complexes $[Cd(SeP(chx)_3)_n(SP(chx)_3)_{4-n}]^{2+}$ in liquid SO_2 at 209 K[a]

	$SeP(chx)_3$			$SP(chx)_3$	
n	δ_P[b] (ppm)	$\lvert^1J(^{31}P—^{77}Se)\rvert$ (Hz)	$\lvert^2J(^{111/113}Cd—^{31}P)\rvert$ (Hz)	δ_P[b] (ppm)	$\lvert^2J(^{111/113}Cd—^{31}P)\rvert$ (Hz)
(Free ligands)	(62.2_9)	(577)		(64.5_2)	
0				64.9_5	$48._0$
1	61.9_3	541	$56._7$	64.8_1	$49._0$
2	61.7_8	545	$57._1$	65.5_9	$49._7$
3	61.6_1	548	$56._8$	64.3_5	$51._2$
4	61.4_4	552	$57._2$		

[a]chx = C_6H_{11}.
[b]Relative to external $OP(OMe)_3$ in $(CD_3)_2CO$; shifts to increasing frequency are taken as positive; $\delta_{OP(OMe)_3}(ext) = \delta_{H_3PO_4}(ext) - 1.7$ ppm.

methylation, shown also by the data in Tables 2–4, is surprising. However, the similarities of the data for corresponding complexes of Ph_3PE and $(p\text{-}C_6H_4Me)_3PE$ suggests that electronic effects on $^2J(^{111/113}Cd—^{31}P)$ are not important. Accordingly, it seems that $|^2J(^{111/113}Cd—^{31}P)|$ increases with increasing steric crowding between ligands, a suggestion supported by the relatively large two-bond couplings found in $(C_6H_{11})_3PE$ complexes and the very large couplings found in complexes of the sterically demanding $Bu^t{}_3PE$.

For both the sulfides and the selenides, it is found that for the same ligand, $|^2J(^{111/113}Cd—^{31}P)|$ increases as the number of ligands bonded decreases. For example, in the most complete series, those involving $(o\text{-}C_6H_4Me)_3PE$, ^2J is $\gtrsim$ 63, 67, and 83 Hz for E = Se, and 51, 54, and 70 Hz, for E = S, as n = 4, 3, and 2, respectively, in $[Cd(EP(o\text{-}C_6H_4Me)_3)_n]^{2+}$. These changes probably reflect changes in the hybridization of cadmium from approximately sp^3 in the 4:1 complexes, through approximately sp^2 in the 3:1 complexes towards approximately sp in the 2:1 complexes. However, two other effects may attenuate the two-fold reduction in ^2J expected to occur between the 4:1 and 2:1 complexes: firstly, there may be coordination, albeit weak, of either SO_2 or SbF_6^-, or both, and this coordination may divert "s" character from the Cd—E linkage and hence decrease $|^2J|$, and secondly, there should be release of steric crowding on reduction of the number of ligands coordinated, and our results suggest that this also leads to a decrease in $|^2J|$.

Complexes of Mixed Ligands

In their reduced temperature ^{31}P nmr spectra, most of the mixed ligand systems tried (both R_3PSe/R_3PS and $R_3PE/R_3'PE$ mixtures), gave evidence for the formation of complexes with mixed ligands. The complexes

$$[Cd(SeP(C_6H_{11})_3)_n(SP(C_6H_{11})_3)_{4-n}]^{2+}$$

$$[Cd(SeP(C_6H_{11})_3)_n(SP(C_6H_{11})_3)_{3-n}]^{2+}$$

and

$$[Cd(SeP(o\text{-}C_6H_4Me)_3)_n(SP(o\text{-}C_6H_4Me)_3)_{3-n}]^{2+}$$

provided the most useful combination of solubility and spectral resolution and therefore were studied in detail (Tables 6–8). The data for these complexes clearly establish the $CdSe_nS_{4-n}$ and $CdSe_nS_{3-n}$ kernels,[6] which we intend to study by ^{113}Cd nmr in the near future. In terms of the ^{31}P nmr spectra, perhaps the most noteworthy feature of the various spectra is the low sensitivity of the ^{31}P chemical shift and various coupling constants to replacement of R_3PSe by R_3PS, or vice-versa.

[6]Kernels of mixed Group VIA atoms are not widely known for cadmium (10).

Can. J. Chem. Downloaded from www.nrcresearchpress.com by 210.87.254.40 on 09/05/12
For personal use only.

TABLE 7. ^{31}P nmr spectral parameters of the 3:1 mixed ligand complexes $[Cd(SeP(chx)_3)_n(SP(chx)_3)_{3-n}]^{2+}$ in liquid SO_2 at 209 K[a]

	$SeP(chx)_3$			$SP(chx)_3$	
n	δ_P[b] (ppm)	$\lvert^1J(^{31}P—^{77}Se)\rvert$ (Hz)	$\lvert^2J(^{111/113}Cd—^{31}P)\rvert$ (Hz)	δ_P[b] (ppm)	$\lvert^2J(^{111/113}Cd—^{31}P)\rvert$ (Hz)
(Free ligands)	(62.2_9)	(577)		(64.5_2)	
0				65.8_4	54
1	63.7_9	502	~64	65.7_4	~54
2	63.6_7	~510	~62	65.6_2	51
3	63.5_9	513	61		

[a]chx = C_6H_{11}.
[b]Relative to external $OP(OMe)_3$ in $(CD_3)_2CO$; shifts to increasing frequency are taken as positive; $\delta_{OP(OMe)_3}(ext) = \delta_{H_3PO_4}(ext) - 1.7$ ppm.

TABLE 8. ^{31}P nmr spectral parameters of the 3:1 mixed ligand complexes $[Cd(SeP(o\text{-tol})_3)_n(SP(o\text{-tol})_3)_{3-n}]^{2+}$ in liquid SO_2 at 209 K[a]

	$SeP(o\text{-tol})_3$			$SP(o\text{-tol})_3$	
n	δ_P[b] (ppm)	$\lvert^1J(^{31}P—^{77}Se)\rvert$ (Hz)	$\lvert^2J(^{111/113}Cd—^{31}P)\rvert$ (Hz)	δ_P[b] (ppm)	$\lvert^2J(^{111/113}Cd—^{31}P)\rvert$ (Hz)
(Free ligands)	(26.9_8)	(629)		(39.0_1)	
0				42.1_3	55
1	28.2_8	530	71	41.9_7	53
2	28.1_1	533	70	41.9_1	~50
3	27.9_6	529	67		

[a]o-tol = o-C_6H_4Me.
[b]Relative to external $OP(OMe)_3$ in $(CD_3)_2CO$; shifts to increasing frequency are taken as positive; $\delta_{OP(OMe)_3}(ext) = \delta_{H_3PO_4}(ext) - 1.7$ ppm.

Experimental

Materials

Triethylphosphine (PCR, Inc.), and tris(*t*-butyl)phosphine, tris(*o*-tolyl)phosphine, tris(*p*-tolyl)phosphine, bis(*o*-tolyl)-phenylphosphine, and *o*-tolyldiphenylphosphine (all from Strem Chemicals, Inc.) showed no significant impurities by ^{31}P nmr (11*a*, 12), and were used as received, as was the CS_2 adduct of tricyclohexylphosphine (Strem). Triphenylphosphine (Eastman Kodak Co.) was recrystallized from ethanol. $Cd(SbF_6)_2$ was prepared as described earlier (13).

Phosphine Sulfides and Selenides

Ph_3PS, Et_3PSe, $(C_6H_{11})_3PSe$, Ph_3PSe, $(o\text{-}C_6H_4Me)_3PSe$, and $(p\text{-}C_6H_4Me_3)PSe$ were prepared during prior studies (1, 7). The other sulfides and selenides were prepared analogously by reflux of the phosphine[7] with sulfur or selenium in benzene under nitrogen. Most of these compounds are known (11*b*), but Bu^t_3PSe, $(o\text{-}C_6H_4Me)_2PhPSe$, and $(o\text{-}C_6H_4Me)Ph_2PSe$ appear to be new compounds. The properties of the three compounds are:

Bu^t_3PSe: mp(uncorr.) 221–222°C (from Bu^nOH); exact mass calcd. for $C_{12}H_{27}PSe$: 282.1016; found (high resolution ms): 282.1015; ^{31}P nmr (CH_2Cl_2; 313 K): $\delta_{OP(OMe)_3}$ = 90.0 ppm; $\lvert^1J(^{31}P—^{77}Se)\rvert$ = 692 Hz.

$(o\text{-}C_6H_4Me)_2PhPSe$: mp(uncorr.) 161–162°C (from Bu^nOH); exact mass calcd. for $C_{20}H_{19}PSe$: 370.0389, found (high resolution ms): 370.0386; ^{31}P nmr (CH_2Cl_2; 313 K): $\delta_{OP(OMe)_3}$ = 26.2 ppm; $\lvert^1J(^{31}P—^{77}Se)\rvert$ = 719 Hz.

$(o\text{-}C_6H_4Me)Ph_2PSe$: mp(uncorr.) 149–150°C (from Bu^nOH); exact mass calcd. for $C_{19}H_{17}PSe$: 356.0233; found (high resolution ms): 356.0233; ^{31}P nmr (CH_2Cl_2; 313 K): $\delta_{OP(OMe)_3}$ = 28.8 ppm; $\lvert^1J(^{31}P—^{77}Se)\rvert$ = 732 Hz.

[7]$(C_6H_{11})_3P{\cdot}CS_2$ in the preparation of $(C_6H_{11})_3PS$.

Preparation of Nuclear Magnetic Resonance Samples

Samples containing one ligand were prepared in 10 mm od tubes as reported earlier (1). The ligand mixtures for preparation of complexes with two different ligands were made by mixing known amounts of methylene chloride solutions of the separate ligands in the 10 mm nmr tube, followed by removal of the solvent by evaporation under nitrogen, with final drying *in vacuo*. $Cd(SbF_6)_2$ was added in the glove box as before. For a given mixed ligand system, several different ratios of the two ligands were used to assist signal assignment.

^{31}P-{^1H} Nuclear Magnetic Resonance Spectra

The spectra were measured as reported in preceding publications (1, 7). The digital resolution was 0.3 Hz, but the natural broadness of the observed lines certainly leads to larger errors in line positions than is implied by this. We estimate that we can measure chemical shifts and values of $\lvert^2J(^{111/113}Cd—^{31}P)\rvert$ to ±1 Hz (0.025 ppm). $\lvert^1J(^{31}P—^{77}Se)\rvert$ probably has a maximum error of ±2 Hz.

Mass Spectra

High resolution mass spectra were obtained using a Varian MAT-311A spectrometer.

Acknowledgements

We wish to thank Mr. Doug Hairsine of this Department for measurement of the mass spectra, and both the Academic Development Fund of the University of Western Ontario and the Natural Sciences and Engineering Research Council of Canada for financial support.

1. P. A. W. DEAN and M. K. HUGHES. Can. J. Chem. **58**, 180 (1980).

Can. J. Chem. Downloaded from www.nrcresearchpress.com by 210.87.254.40 on 09/05/12
For personal use only.

2. C. GLIDEWELL and E. J. LESLIE. J. Chem. Soc. Dalton Trans. 527 (1977).
3. P. NIPCON and D. W. MEEK. Chem. Commun. 398 (1966).
4. G. EASTLAND, JR. Inorg. Nucl. Chem. Lett. **11**, 373 (1975).
5. S. S. SANDHU and T. SINGH. Indian J. Chem. **15A**, 831 (1977).
6. F. G. MOERS, P. W. W. M. MÜSKENS, and J. FRANCOT. J. Inorg. Nucl. Chem. **41**, 759 (1979).
7. P. A. W. DEAN. Can. J. Chem. **57**, 754 (1979).
8. S. O. GRIM, E. D. WALTON, and L. C. SATEK. Inorg. Chim. Acta, **27**, L115 (1978).
9. R. P. PINNELL, C. A. MEGERLE, S. L. MANNATT, and P. A. KROON. J. Am. Chem. Soc. **95**, 977 (1973).
10. D. G. TUCK. Rev. Inorg. Chem. To be published.
11. L. MAIER. *In* Organic phosphorus compounds. *Edited by* G. M. Kosolapoff and L. Maier. Wiley-Interscience, New York. 1972. (*a*) Vol. 1. Chapt. 1, and references therein; (*b*) Vol. 4. Chapt. 7, and references therein.
12. S. O. GRIM and A. W. YANKOWSKY. Phosphorus Sulfur, **3**, 191 (1977).
13. L. C. DAMUDE and P. A. W. DEAN. J. Organomet. Chem. **168**, 123 (1979).

Can. J. Chem. Downloaded from www.nrcresearchpress.com by 210.87.254.40 on 09/05/12
For personal use only.

Structure and conformation of the hydrochloride of pseudoisocytidine, an antileukemic *C*-nucleoside[1]

GEORGE I. BIRNBAUM[2]

Division of Biological Sciences, National Research Council of Canada, Ottawa, Ont., Canada K1A 0R6

AND

KYOICHI A. WATANABE AND JACK J. FOX

Laboratory of Organic Chemistry, Memorial Sloan-Kettering Cancer Center, Sloan-Kettering Institute, Sloan-Kettering Division of Graduate School of Medical Sciences, Cornell University, New York, NY 10021, U.S.A.

Received March 10, 1980

GEORGE I. BIRNBAUM, KYOICHI A. WATANABE, and JACK J. FOX. Can. J. Chem. **58**, 1633 (1980).

The three-dimensional structure of pseudoisocytidine hydrochloride was determined by X-ray crystallography. The crystals belong to the triclinic space group $P\bar{1}$ and the cell dimensions are $a = 6.623(2)$, $b = 8.053(2)$, $c = 6.201(2)$ Å, $\alpha = 108.35(2)$, $\beta = 101.36(2)$, $\gamma = 93.54(2)°$. Intensity data were measured with a diffractometer and the structure was solved by a combination of heavy-atom and direct methods. Least-squares refinement, which included hydrogen atoms, converged at $R = 0.040$. The conformation about the glycosyl bond is *anti* ($\chi_{CC} = 21.6°$), the pucker of the furanose ring is C(1′)*exo*, and the conformation of the $-CH_2OH$ side chain is *gauche–trans* (t). An examination of bond lengths indicates that of the three main resonance forms of the isocytosine cation the fully conjugated one contributes more to the structure than the cross-conjugated one. Bond angles in the sugar ring reflect its rare conformation.

GEORGE I. BIRNBAUM, KYOICHI A. WATANABE et JACK J. FOX. Can. J. Chem. **58**, 1633 (1980).

On a déterminé la structure tridimensionnelle du chlorhydrate de pseudoisocytidine par diffraction de rayons-X. Les cristaux appartiennent au groupe spatial triclinique $P\bar{1}$ et les dimensions de la maille sont: $a = 6.623(2)$, $b = 8.053(2)$, $c = 6.201(2)$ Å, $\alpha = 108.35(2)$ $\beta = 101.36(2)$, $\gamma = 93.54(2)°$. On a mesuré les données d'intensité à l'aide d'un diffractomètre et on a résolu la structure à l'aide d'une combinaison de la méthode d'atome lourd et des méthodes directes. L'affinement des paramètres atomiques, qui inclut les atomes d'hydrogène, a été effectué par moindres carrés. L'indice final R est égal à 0.040. La conformation autour de la liaison glycosyle est *anti* ($\chi_{CC} = 21.6°$), le plissement du cycle furannose est C(1′)*exo* et la conformation de la chaîne latérale CH_2OH est *gauche-trans* (t). Un examen des longueurs de liaison indique que parmi les trois formes principales de résonance du cation isocytosine, la forme complètement conjuguée contribue plus à la structure que la forme où la conjugaison est opposée. Les angles de liaison dans le cycle furannose reflètent sa conformation rare.

[Traduit par le journal]

Among many naturally occurring nucleosides, a group of compounds, *C*-nucleosides, possess a unique structural feature in which the aglycon and sugar moieties are linked through a carbon-to-carbon (C—C) bond rather than the C—N glycosyl linkage. Most of these *C*-nucleosides are antibiotics, and many exhibit some anticancer and antiviral activities (1, 2). Recently, Chu *et al.* (3) synthesized a pyrimidine *C*-nucleoside, pseudoisocytidine, which was subsequently shown to be active in vitro and in vivo against various lines of mouse leukemia which are resistant to arabinosylcytosine (ara-C) (4).

The mechanism by which these substances act, whether as a result of being incorporated in DNA or RNA or by inhibiting cell activity at another stage of the cell growth, depends very much on their structure and conformation. Consequently, the solution conformations of pyrazomycin (5), formycin (6), and its analogs (7) have been studied in detail by nmr techniques. In addition, crystal structure determinations have been carried out for formycin monohydrate (8), formycin hydrobromide (9), 2-methylformycin (10), formycin B (11), oxoformycin B (11), showdomycin (12), α-pseudouridine (13), and pyrazomycin (14), but no details have been published about pyrazomycin. We now present the crystal structure of pseudoisocytidine hydrochloride, the first *C*-nucleoside with an isocytosine base to be so studied.

Experimental

Pseudoisocytidine hydrochloride was prepared as described by Hirota *et al.* (15). In order to obtain large crystals for the present study, the compound (200 mg) was dissolved in hot, concentrated hydrochloric acid (10 mL) and the solution diluted with hot ethanol (20 mL). The mixture was cooled slowly to room temperature, and the deposited crystals were filtered. The ^1H nmr spectrum of these crystals in D_2O was identical with that reported (3) for pseudoisocytidine hydrochloride, indicating that no *net* isomerization had occurred during the recrystallization procedure. All attempts to obtain large crystals from other solvent systems (e.g. MeOH, EtOH, MeOH–H_2O, EtOH–H_2O, etc.) were unsatisfactory. The colorless prisms belong to the triclinic space group $P\bar{1}$. A crystal fragment measuring 0.22 × 0.25 × 0.25 mm was mounted on a Picker four-circle diffractometer; it provided the following data:

[1]NRCC No. 18351.

[2]To whom all correspondence should be addressed.

0008-4042/80/161633-06$01.00/0

©1980 National Research Council of Canada/Conseil national de recherches du Canada

Can. J. Chem. Downloaded from www.nrcresearchpress.com by 210.87.254.105 on 09/05/12
For personal use only.

Can. J. Chem. Downloaded from www.nrcresearchpress.com by 210.87.254.105 on 09/05/12
For personal use only.

$C_9H_{13}N_3O_5 \cdot HCl$ fw = 279.7

Triclinic, a = 6.623(2), b = 8.053(2), c = 6.201(2) Å, α = 108.35(2), β = 101.36(2), γ = 93.54(2)°, V = 305.0 Å^3, D_x = 1.52, D_m = 1.53 g cm^{-3} (flotation in bromobenzene–iodobenzene), Z = 1 (21°C; CuKα_1, λ = 1.54056; CuKα_2, λ = 1.54439 Å), F(000) = 146, μ (MoKα) = 3.3 cm^{-1}.

Intensities were measured with Nb-filtered MoKα radiation, using the moving-crystal/moving-counter method ($\theta/2\theta$ scan). Reflections with net counts < 100 or < 5% of background were categorized as unobserved. There were 1399 unique reflections with 2θ < 55° of which 1328 (95%) had intensities above threshold values. The intensities were corrected for Lorentz and polarization factors; absorption corrections were unnecessary.

A Fourier map, calculated with phases from the chloride ion at the origin, was not interpretable owing to the introduction of a false center of symmetry. However, two high peaks with a reasonable interatomic distance between them were selected, in addition to the chloride ion, as a partial structure. The positions of the 15 other nonhydrogen atoms were obtained after several cycles of tangent refinement (16). The structure was refined by block-diagonal least-squares with anisotropic temperature parameters. All hydrogen atoms were located on a difference Fourier map and refined with isotropic temperature parameters. The scattering factors were taken from the International tables for X-ray crystallography (17) and the chloride curve was corrected for anomalous dispersion. Throughout the refinement the function $\Sigma w(|F_o| - |F_c|)^2$ was minimized and a factor of 0.8 applied to all shifts. The following weighting scheme was used during the final stages: $w = |F_o|/4.8$ for $|F_o| \leq 4.8$ and $w = 4.8/|F_o|$ for $|F_o| > 4.8$. This scheme made the average values of $w(\Delta F^2)$ independent of $|F_o|$ and $\sin^2\theta$. The thermal vibration of O(3′) was found to be rather high perpendicular to the C(3′)—O(3′) bond. However, examination of a difference map showed no evidence of static disorder. After the final cycle the average parameter shift equalled 0.14σ and the largest 0.53σ. The conventional residual index R is 0.040 and the weighted index R' is 0.046. A final difference Fourier map was featureless. The coordinates are listed in Table 1; lists of anisotropic temperature parameters and of observed and calculated structure factors are available.[3] The overall conformation and the atomic numbering scheme are shown in Fig. 1.

TABLE 1. Final atomic parameters and their standard deviations

(*A*) Nonhydrogen atoms[a]

Atom	*x*	*y*	*z*
N(1)	5042(4)	755(3)	4400(5)
C(2)	3600(5)	985(4)	5653(5)
N(2)	3065(5)	−229(4)	6521(6)
N(3)	2702(4)	2474(4)	5963(4)
C(4)	3218(4)	3830(4)	5106(5)
O(4)	2333(4)	5129(3)	5535(5)
C(5)	4799(4)	3503(4)	3756(5)
C(6)	5619(5)	1985(4)	3451(6)
C(1′)	5506(4)	4846(4)	2756(5)
O(1′)	6435(4)	3978(3)	879(4)
C(2′)	7249(5)	6272(4)	4403(5)
O(2′)	6451(4)	7618(3)	5970(4)
C(3′)	8236(5)	6908(4)	2699(7)
O(3′)	7310(7)	8362(4)	2389(7)
C(4′)	7726(5)	5302(4)	468(5)
C(5′)	9663(5)	4566(5)	−111(6)
O(5′)	9250(4)	2982(4)	−2072(4)
Cl^-	0(0)	0(0)	0(0)

(*B*) Hydrogen atoms[b]

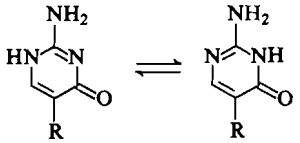
Atom	*x*	*y*	*z*	*B*
H(1)	563(7)	−29(6)	407(7)	2.8(0.7)
H1(N2)	385(9)	−112(8)	636(10)	5.8(1.2)
H2(N2)	198(9)	5(8)	744(11)	5.4(1.2)
H(3)	147(7)	251(7)	678(9)	4.1(0.9)
H(6)	657(6)	164(6)	265(7)	3.1(0.9)
H(1′)	437(5)	545(4)	220(5)	1.0(0.5)
H(2′)	830(6)	571(5)	528(6)	2.3(0.7)
H(O2′)	763(6)	819(5)	706(7)	2.9(0.8)
H(3′)	966(7)	719(6)	342(8)	4.2(1.0)
H(O3′)	796(8)	876(7)	167(9)	5.3(1.1)
H(4′)	690(6)	566(5)	−86(7)	2.9(0.8)
H(5′)	1040(6)	427(6)	125(8)	3.2(0.9)
H(5″)	1044(8)	545(7)	−47(9)	5.0(1.1)
H(O5′)	896(8)	212(7)	−147(9)	4.7(1.1)

[a]All coordinates were multiplied by 10^4.
[b]All coordinates were multiplied by 10^3.

Results and Discussion

Isocytosine Moiety

Pseudoisocytidine (**1***a*) differs from cytidine in two respects: the ribose ring is attached to C(5) rather than to N(1) and the functions at C(2) and C(4) are interchanged. Both **1***a* and isocytosine (**1***b*) can exist in the two main tautomeric forms shown below.

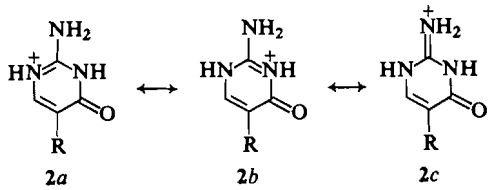


1*a*: R = β-D-ribofuranosyl
1*b*: R = H

[3]These tables may be obtained, at a nominal charge, from the Depository of Unpublished Data, CISTI, National Research Council of Canada, Ottawa, Ont., Canada K1A 0S2.

In aqueous solution the two tautomers of **1***b* coexist in comparable amounts (18) and in the X-ray analysis of **1***b* both tautomers were found in the asymmetric unit (19). The ^{1}H nmr spectra of **1***b* and its cation have been studied by Wagner and von Philipsborn (20).

Protonation of the different tautomers of the isocytosine base (**1**) results in a common cation (**2**), present in our structure, for which three main resonance forms can be written.



2*a* **2***b* **2***c*

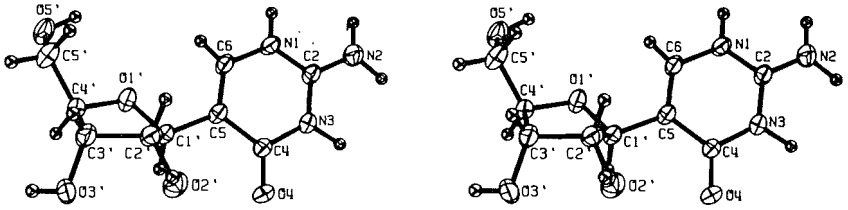


FIG. 1. Stereoscopic view of pseudoisocytidine hydrochloride; the ellipsoids include 50% probability.

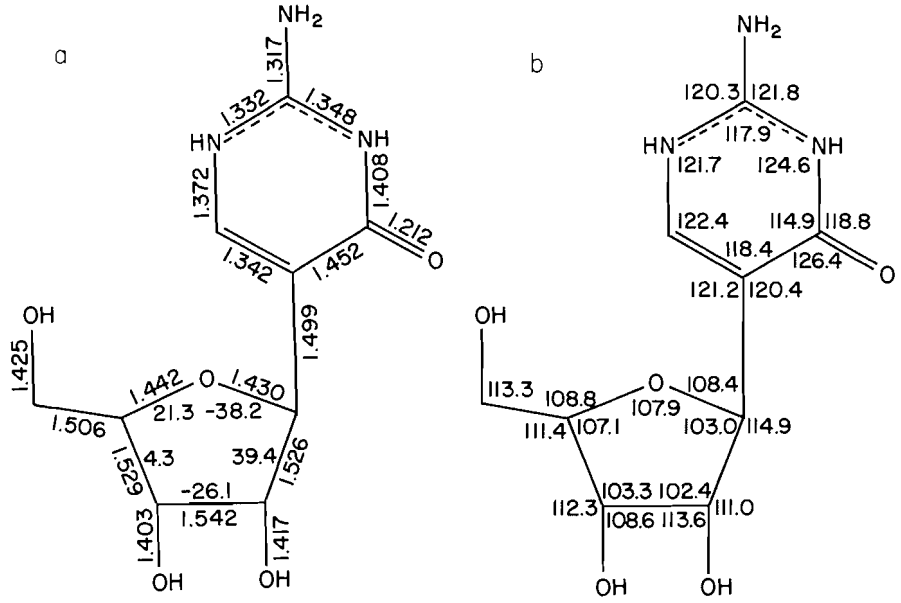


FIG. 2. Molecular geometry: (*a*) bond lengths and ribose ring torsion angles; esd's are 0.004–0.005 Å and 0.4°, respectively; (*b*) bond angles; esd's are 0.3°.

It is of interest to examine the contributions of these forms to the structure of the cation. This can be done by comparing the bond lengths in this structure (Fig. 2) with those in isocytosine (19) as well as in unprotonated and protonated cytosines (21–23). The exocyclic C—N bond in isocytosine (1.324(3) Å) is 0.010(3) Å shorter than the analogous C(4)—N(4) bond in cytosine, indicating more double bond character. When cytosine is protonated, this bond length decreases by 0.021 Å to 1.313 Å (21), suggesting a strong delocalization of the unshared electron pair from N(4) to N(3). Roberts and his colleagues arrived at the same conclusion on the basis of ^{15}N nmr spectroscopy (24). These observations agree with the previously determined energy barrier of ~15 kcal/mol which restricts the rotation about the exocyclic C—N bond in cytosine derivatives (25). Protonation of isocytosine decreases the length of C(2)—N(2) by only 0.007 Å; thus, there is relatively less delocalization of electrons into the ring in this system. However, we found this bond length (1.317 Å) to be very similar to the analogous bond lengths in protonated cytosines (21). Consequently, the contribution of the imino resonance from **2***c* must be similar in protonated cytosine and isocytosine systems. The relative contributions of the two other resonance forms (**2***a* and **2***b*) can be assessed by comparing the bond lengths N(1)—C(2) and C(2)—N(3). The latter is approximately equal to the analogous N(3)—C(4) bond lengths in protonated cytosines (21, 23). On the other hand, N(1)—C(2) has the same length as the more localized C=N bonds in unprotonated cytosine (26) and isocytosine (19). On the basis of these comparisons, and the relative lengths of these bonds, it appears that N(1)—C(2) has more double bond character than C(2)—N(3), i.e. **2***a* contributes more than **2***b*. This may be explained by the fact that **2***a* is fully conjugated, whereas there is unfavorable cross-conjugation in **2***b*.

The effects of protonation of cytosine and its

Can. J. Chem. Downloaded from www.nrcresearchpress.com by 210.87.254.105 on 09/05/12
For personal use only.

Can. J. Chem. Downloaded from www.nrcresearchpress.com by 210.87.254.105 on 09/05/12
For personal use only.

derivatives on bond angles are well established. Protonation occurs at N(3) and causes the endocyclic bond angle at that atom to increase by 4–5°, while the angles at the adjacent atoms C(2) and C(4) drecrease by the same amount (21–23). When we compare the geometry of our structure (Fig. 2) with that of isocytosine (19), we see the same changes of the bond angles in the ring. In fact, taking into account the interchange of functions at C(2) and C(4), the angles we found are in excellent agreement with the average values calculated from 12 protonated cytosine derivatives (22). There is, however, a difference in the exocyclic angles at the carbonyl carbon atom. In protonated cytosines N(1)—C(2)—O(2) is no more than 2.5° larger than N(3)—C(2)—O(2). On the other hand, in our structure C(5)—C(4)—O(4) is 7.6° larger than N(3)—C(4)—O(4). Exactly the same angles were found in isocytosine protonated at N(3) (19). This significant difference appears to be a peculiarity of the isocytosine system.

The six atoms of the pyrimidine ring are coplanar (Table 2) and the exocyclic amino group is in the same plane. However, O(4) and C(1′) are displaced from this plane, a phenomenon which is not unusual (27–29).

TABLE 2. Least-squares planes and deviations of atoms from them[a]

Plane 1[b]		Plane 2[b]	
Atom	Δ, Å[c]	Atom	Δ, Å[c]
N(1)	−0.003	C(2′)	−0.015
C(2)	−0.006	C(3′)	0.030
N(3)	0.009	C(4′)	−0.025
C(4)	−0.006	O(1′)	0.009
C(5)	−0.003	C(1′)*	0.571
C(6)	0.009	C(5)*	0.181
N(2)*	−0.005	C(5′)*	−1.294
O(4)*	−0.017		
C(1′)*	−0.029		

[a]Atoms marked with an asterisk were not included in the calculation of the plane..
[b]Plane 1: $0.5210X + 0.1803Y + 0.8343Z - 3.4888 = 0$. Plane 2: $0.8121X - 0.5033Y + 0.2954Z - 1.8520 = 0$.
[c]Esd's are 0.003 Å.

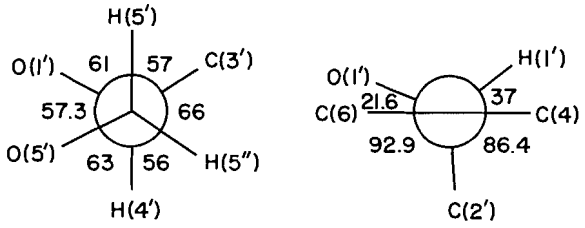


FIG. 3. Newman projections along C(4′)—C(5′) and C(5)—C(1′).

Ribose Moiety

The ribose ring adopts the rather unusual C(1′) *exo* conformation ($_1E$), the puckering at C(1′) displacing that atom by 0.571 Å (Table 2). The conformational parameters (30) $P = 130.3°$ and $\tau_m = 40.4°$ indicate that it is outside the usual ranges $P = 0$–36 and 144–180°. We have recently determined several nucleoside structures with unusual conformations of the deoxyribose ring (28, 29, 31), providing additional evidence of a relatively lower energy barrier between the C(2′)*endo* and C(3′)*endo* conformation of these rings (32–35). We have also shown that these conformations (O(1′)*endo*, C(1′)*exo*, C(1′)*exo*—C(2′)*endo*) very likely exist in solution as well, since this assumption results in a better agreement with observed J_{HH} coupling constants than the usual assumption of a C(2′)*endo* ⇄ C(3′)*endo* equilibrium. Thus, it appears probable that the C(1′)*exo* conformation which we found in the present crystal structure also contributes to the equilibrium population in solution. A study of the conformation of pseudoisocytidine in solution is now underway.

The ribose ring is attached to C(5) and the torsion angle about the glycosyl bond, C(6)—C(5)—C(1′)—O(1′), is 21.6° (Fig. 3), corresponding to the *anti* conformation (36). In pyrimidine *N*-nucleosides this is the more stable conformation, and it is almost always found in crystal structures unless a bulky substituent at C(6) imposes a *syn* conformation (29). The length of the C—C glycosyl bond (1.499 Å) is in very good agreement with values found in other *C*-nucleosides (8–13). It is interesting to note that C(4′)—O(1′) is just barely longer than C(1′)—O(1′) instead of by 0.03–0.05 Å. This reflects the fact that, in the present structure, C(1′) is bonded to only one electronegative atom (37). Other bond distances are normal and require no comments.

Bond angles in the furanose rings of nucleosides are known to depend on the conformation of the ring and, in the case of exocyclic angles, on the —OH substituent: whether "down" (ribose) or "up" (lyxose (38), xylose (39), or arabinose (27, 37)). Sundaralingam published average values for ribose and arabinose rings in the common C(2′)*endo* and C(3′)*endo* conformations (37). However, data on unusual sugars and/or conformations are relatively scarce. In a recently published statistical analysis of furanose bond angles in 110 ribo-, deoxyribo-, and arabino-nucleosides (40) there were no structures with the phase angle of pseudorotation (P) in the range 92–137°. Inclusion of such conformations will facilitate future analyses which are of great value in the interpretation of electron density maps of nucleic acids. The following observations can be made regarding the

TABLE 3. Distances and angles for hydrogen bonds

Bonds	Distances, Å			Angles, deg	
	$D\cdots A$	$H\cdots A$	$H\cdots A_{corr}$	D—H$\cdots A$	H—$D\cdots A$
N(1)—H···O(3′)[a]	2.666	1.85	1.76	146	23
N(2)—H(1)···O(2′)[a]	2.926	2.07	1.94	158	16
N(2)—H(2)···Cl⁻[b]	3.214	2.26	2.19	161	13
N(3)—H···O(5′)[c]	2.788	1.77	1.77	166	9
O(2′)—H···Cl⁻[d]	3.092	2.19	2.13	167	9
O(3′)—H···Cl⁻[e]	3.015	2.22	2.05	174	4
O(5′)—H···Cl⁻[f]	3.083	2.26	2.21	150	22

[a] At $x, -1+y, z$.
[b] At $x, y, 1+z$.
[c] At $-1+x, y, 1+z$.
[d] At $1+x, 1+y, 1+z$.
[e] At $1+x, 1+y, z$.
[f] At $1+x, y, z$.

present structure (Fig. 2). The smallest endocyclic angle is, as usual in ribosides, at C(2′), but the angles at the puckered atom C(1′), as well as at C(3′), are not significantly larger. In fact, the angle at C(1′) is significantly smaller than 104.7°, the value which Westhof and Sundaralingam (41) recently derived for ribonucleosides in C(1′)*exo* conformation. However, these values were obtained on the basis of insufficient data from unusual ring conformations. The present structure analysis should therefore serve to improve the correlation between the bond angles and *P*. A similar situation was encountered in the structure of 5-hydroxymethyl-2′-deoxyuridine (hm⁵dU) where the deoxyribose ring also adopts a C(1′)*exo* conformation (28). The largest ring angle is, again as usual, at O(1′), but it is about 2° smaller than normal, reflecting the unusual ring pucker (40, 41). The difference between the smallest and largest ring angles is 5.5° in this structure and 5.0° in hm⁵dU; in C(2′)*endo* and in C(3′)*endo* ribosides that difference is about 9° (41).

There are also some unusual exocyclic bond angles. The two adjacent angles C(2′)—C(3′)—O(3′) and C(4′)—C(3′)—O(3′) are normally identical (37, 40), but sometimes the latter is much smaller (31, 42). In this structure, and in hm⁵dU (28), the reverse is true, indicating a possible correlation between these angles and the C(1′)*exo* ring conformation. The C(4′)—C(5′)—O(5′) angle (113.3°) is considerably larger than normal, but there is no obvious explanation for this distortion.

The conformation of the —CH_2OH side chain is *gauche–trans* (Fig. 3). Although not as common as *gauche–gauche* (g^+), this conformation (t) is not unusual. A correlation between the conformations of the side chain and of the sugar ring has been the subject of many studies. On the basis of crystal structures, Sundaralingam found the g^+ conformation to be the most preferred, regardless of the puckering of the sugar (43). A more recent and exhaustive survey found no correlation between the conformations of the side chain and the ring (40). On the other hand, from a survey of nmr data such a correlation for pyrimidine nucleosides and their 3′-monophosphates in *anti* conformation was postulated by Hruska (44) and was later described more quantitatively by Davies (45). However, the nmr data have always been interpreted by assuming a C(2′)*endo* ⇄ C(3′)*endo* equilibrium. As more unusual sugar puckers are being found, such correlations may have to be revised.

Hydrogen Bonding

There are seven protons capable of hydrogen bonding and all seven participate in such bonds. Details of the geometry are given in Table 3. As commonly observed in X-ray analyses, most O—H and N—H bonds appear shorter than their real values of 0.97 and 1.04 Å, respectively, which are obtained from neutron diffraction studies. By expanding the covalent bond lengths in the direction of the bond up to their real values, one obtains corrected H···*A* distances that express more accurately the strength of the hydrogen bond (46). Thus, it can be seen that one N—H···O, one N—H···Cl⁻, and one O—H···Cl⁻ bond are relatively weak (23). It should be noted that there are no hydrogen bonds between the pyrimidine bases. Also, the bases are not stacked, the shortest intermolecular distance between them being N(2)···O(4) 3.578 Å. Apart from the hydrogen bonds there are no intermolecular distances shorter than the sum of van der Waals radii.

Acknowledgments

All crystallographic computations were carried out with programs written by Ahmed *et al.* (47). Figure 1 was drawn with the ORTEP program of Johnson (48).

Can. J. Chem. Downloaded from www.nrcresearchpress.com by 210.87.254.105 on 09/05/12
For personal use only.

1. E. De Clercq and P. F. Torrence. J. Carbohydr. Nucleosides Nucleotides, **5**, 187 (1978).
2. R. J. Suhadolnik. Prog. Nucleic Acid Res. Mol. Biol. **22**, 193 (1979).
3. C. K. Chu, K. A. Watanabe, and J. J. Fox. J. Heterocycl. Chem. **12**, 817 (1975); C. K. Chu, I. Wempen, K. A. Watanabe, and J. J. Fox. J. Org. Chem. **41**, 2793 (1976).
4. J. H. Burchenal, K. Ciovacco, K. Kalaher, T. O'Toole, R. Kiefner, M. D. Dowling, C. K. Chu, K. A. Watanabe, I. Wempen, and J. J. Fox. Cancer Res. **36**, 1520 (1976).
5. J. M. Neumann, J. Borrel, J. M. Thiéry, W. Guschlbauer, and S. Tran-Dinh. Biochim. Biophys. Acta, **479**, 427 (1977).
6. H.-D. Lüdemann and E. Westhof. Z. Naturforsch. C, **32**, 528 (1977).
7. S. Tran-Dinh, J. M. Neumann, J. M. Thiéry, T. Huynh-Dinh, J. Igolen, and W. Guschlbauer. J. Am. Chem. Soc. **99**, 3267 (1977).
8. P. Prusiner, T. F. Brennan, and M. Sundaralingam. Biochemistry, **12**, 1196 (1973).
9. G. Koyama, H. Umezawa, and Y. Iitaka. Acta Crystallogr. Sect. B, **30**, 1511 (1974).
10. J. Abola, M. J. Sims, D. J. Abraham, A. F. Lewis, and L. B. Townsend. J. Med. Chem. **17**, 62 (1974).
11. G. Koyama, H. Nakamura, H. Umezawa, and Y. Iitaka. Acta Crystallogr. Sect. B, **32**, 813 (1976).
12. Y. Tsukuda and H. Koyama. J. Chem. Soc. B, 1709 (1970).
13. D. C. Rohrer and M. Sundaralingam. J. Am. Chem. Soc. **92**, 4950 (1970).
14. N. D. Jones and M. O. Chaney. Acta Crystallogr. Sect. A **28**, S48 (1972).
15. K. Hirota, K. A. Watanabe, and J. J. Fox. J. Org. Chem. **43**, 1193 (1978).
16. J. Karle. Crystallographic computing. *Edited by* F. R. Ahmed. Munksgaard, Copenhagen. 1970. pp. 37–40.
17. J. A. Ibers and W. C. Hamilton (*Editors*). International tables for X-ray crystallography. Vol. IV, Kynoch Press, Birmingham, England. 1974.
18. C. Hélène and P. Douzou. C.R. Acad. Sci. **259**, 4387 (1964).
19. B. D. Sharma and J. F. McConnell. Acta Crystallogr. **19**, 797 (1965).
20. R. Wagner and W. von Philipsborn. Helv. Chim. Acta, **53**, 299 (1970).
21. N. S. Mandel. Acta Crystallogr. Sect. B, **33**, 1079 (1977).
22. A. H. J. Wang, J. R. Barrio, and I. C. Paul. J. Am. Chem. Soc. **98**, 7401 (1976).
23. G. I. Birnbaum, T. Kulikowski, and D. Shugar. Can. J. Biochem. **57**, 308 (1979).
24. V. Markowski, G. R. Sullivan, and J. D. Roberts. J. Am. Chem. Soc. **99**, 714 (1977).
25. R. R. Shoup, H. T. Miles, and E. D. Becker. J. Phys. Chem. **76**, 64 (1972).
26. R. J. McClure and B. M. Craven. Acta Crystallogr. Sect. B, **29**, 1234 (1973).
27. G. I. Birnbaum, E. Darzynkiewicz, and D. Shugar. J. Am. Chem. Soc. **97**, 5904 (1975).
28. G. I. Birnbaum, R. Deslauriers, T.-S. Lin, G. T. Shiau, and W. H. Prusoff. J. Am. Chem. Soc. **102**, 4236 (1980).
29. G. I. Birnbaum, F. E. Hruska, and W. P. Niemczura. J. Am. Chem. Soc. In press.
30. C. Altona and M. Sundaralingam. J. Am. Chem. Soc. **94**, 8205 (1972).
31. G. I. Birnbaum, T.-S. Lin, G. T. Shiau, and W. H. Prusoff. J. Am. Chem. Soc. **101**, 3353 (1979).
32. D. M. Cheng and R. H. Sarma. J. Am. Chem. Soc. **99**, 7333 (1977).
33. A. L. George, F. E. Hruska, K. K. Ogilvie, and A. Holy. Can. J. Chem. **56**, 1170 (1978).
34. M. A. Viswamitra, O. Kennard, P. G. Jones, G. M. Sheldrick, S. Salisbury, L. Falvello, and Z. Shakked. Nature, London, **273**, 687 (1978).
35. M. Levitt and A. Warshel. J. Am. Chem. Soc. **100**, 2607 (1978).
36. J. Donohue and K. N. Trueblood. J. Mol. Biol. **2**, 363 (1960).
37. M. Sundaralingam. Ann. N.Y. Acad. Sci. **255**, 3 (1975).
38. I. Ekiel, E. Darzynkiewicz, G. I. Birnbaum, and D. Shugar. J. Am. Chem. Soc. **101**, 4724 (1979).
39. G. I. Birnbaum, J. Giziewicz, C. P. Huber, and D. Shugar. J. Am. Chem. Soc. **98**, 4640 (1976).
40. P. Murray-Rust and S. Motherwell. Acta Crystallogr. Sect. B, **34**, 2534 (1978).
41. E. Westhof and M. Sundaralingam. J. Am. Chem. Soc. **102**, 1493 (1980).
42. G. I. Birnbaum and D. Shugar. Biochim. Biophys. Acta, **517**, 500 (1978).
43. M. Sundaralingam. Jerusalem Symp. Quantum Chem. Biochem. **5**, 417 (1973).
44. F. E. Hruska. Jerusalem Symp. Quantum Chem. Biochem. **5**, 345 (1973).
45. D. B. Davies. Jerusalem Symp. Quantum Chem. Biochem. **11**, 71 (1978).
46. G. A. Jeffrey and S. Takagi. Acta Crystallogr. Sect. B, **33**, 738 (1977).
47. F. R. Ahmed, S. R. Hall, M. E. Pippy, and C. P. Huber. J. Appl. Crystallogr. **6**, 309 (1973).
48. C. K. Johnson. ORTEP Report ORNL-3794. 2nd revision. Oak Ridge National Laboratory, Oak Ridge, TN. 1970.

Can. J. Chem. Downloaded from www.nrcresearchpress.com by 210.87.254.105 on 09/05/12
For personal use only.

Thermolysis of alkylated 2-cyclohexenones and related monoterpenoid ketones

GORDON L. LANGE, VINCENT A. PEREIRA, AND MICHAEL WEEDLE

Guelph–Waterloo Centre for Graduate Work in Chemistry, Department of Chemistry, University of Guelph, Guelph, Ont., Canada N1G 2W1

Received January 16, 1980

GORDON L. LANGE, VINCENT A. PEREIRA, and MICHAEL WEEDLE. Can. J. Chem. **58**, 1639 (1980).

2-Cyclohexenone and three methylated cyclohexenones were thermolyzed at 400°C for 20 hours to give conversions to products in the range 11 to 45%. When three monoterpenes containing the cyclohexenone moiety were thermolyzed under the same conditions the conversions were over 75%. The major products formed were alkylated benzenes, alkylated phenols, and double bond isomers of the starting enones. Mechanisms are proposed to account for these products.

GORDON L. LANGE, VINCENT A. PEREIRA et MICHAEL WEEDLE. Can. J. Chem. **58**, 1639 (1980).

La cyclohexènone-2 et les trois méthyl-cyclohexènones thermolysées à 400°C pendant 20 heures conduisent aux produits de conversion dans la proportion de 11 à 45%. La thermolyse de trois monoterpènes contenant le noyau cyclohexènone dans les mêmes conditions conduit à des conversions avec des rendements supérieurs à 75%. Les produits principaux sont les benzènes et les phénols alkylés et les isomères de position des énones de départ. On propose un mécanisme qui tient compte de ces produits.

[Traduit par le journal]

Introduction

We wish to report our studies on the vapor phase thermolysis at 400°C of three methylated cyclohexenones and four monoterpenoid ketones. Our interest in this area of research was stimulated by an earlier investigation (1), in which the thermolysis of the monoterpene (+)-dihydrocarvone (**1**) yielded not only the desired (+)-camphor (**2**) but also significant amounts of toluene (**3**) and *m*-xylene (**4**) (Scheme 1). It was proposed that a retro-Diels–Alder reaction of the enol tautomer of **5** yielded cyclohexenones **6** and **7** which were then transformed to the aromatic hydrocarbons **3** and **4**, respectively. As a result of this investigation we felt two questions deserved closer scrutiny: (*i*) is the cyclohexenone → substituted benzene conversion a general thermal reaction? (*ii*) are aromatic hydrocarbons also formed on the thermolysis of other monoterpenoid ketones? This paper will outline the research that we have conducted to answer these questions.

Experimental

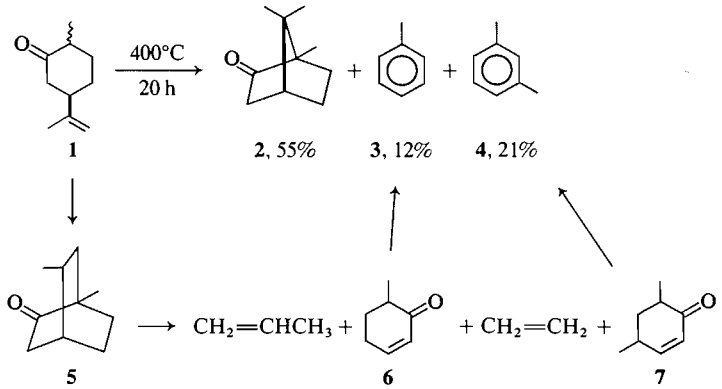
Instrumentation

Infrared (ir) spectra were recorded on a Beckman AccuLab 6 spectrophotometer, ultraviolet (uv) spectra on a Beckman Model 24 spectrophotometer with 95% ethanol as solvent, proton nuclear magnetic resonance (nmr) spectra on a Varian A-60A spectrometer with TMS (δ = 0.0) as internal standard, and mass spectra on a VG Micromass 7070F spectrometer coupled to a gas chromatography unit (gc–ms) equipped with a 6 ft × 0.25 in. 20% Carbowax 20 M column.

Gas chromatographic (gc) analyses were performed on an Aerograph Autoprep Model A-700 using the following columns: column A, 9 ft × 0.25 in. 20% Carbowax 20 M; column B, 6 ft × 0.125 in. 8% GE SF 96 silicone; column C, 6 ft × 0.125 in. 20% diethylene glycol succinate. In the analysis of the thermolysis products reported in Table 1 the areas of all peaks on the gc tracings were determined by triangulation and the areas were not corrected for differences in the thermal response of the detector. Each of the entries given in Table 1 is an average of at least two runs.

Thermolyses and Product Identification

Compounds **8**, **9**, **10**, **11**, **12**, and **15** were commercially available while **13** was prepared by acid treatment of camphor (2) and **14** was prepared by homogeneous catalytic hydrogenation of carvone (3). These compounds were purified by fractional dis-



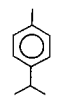
SCHEME 1

0008-4042/80/161639-06$01.00/0

©1980 National Research Council of Canada/Conseil national de recherches du Canada

Can. J. Chem. Downloaded from www.nrcresearchpress.com by 210.87.254.6 on 09/05/12
For personal use only.

TABLE 1. Thermolysis results (conditions: 400°C for 20 hours)

Experiment No.	Ketone substrate	Surface area	% Conversion	% yield of products[a]								
												Others
1	 8	Normal	18	4								14[b]
2	 9	Normal	11		3				4			
3	 10	Normal	38		8			2		8		7[c]
4		Large	44		12			6		10		6[c]
5	 11	Normal	45			28				14	3	
6	 12	Normal	84		5	6	14	3	3	16	5	7[d], 11[e]
7		Large	95		12	10	9	8	7	28	5	12[c]
8	 13	Normal	74		2	1	10		25			8[f], 10[g], 2[h]
9		Large	98		6	4	7		41			20[g], 5[h]
10	 14	Normal	77			1	5		49			16[i]
11	 15	Normal	28[j]									23[k], 5[l]
12		Large	65[j]									61[k], 4[l]

[a]In some of the analyses the total of the product yields does not equal the percentage conversion because all the peaks have not been identified.
[b]3-Cyclohexenone. In a previous study (1) this compound was not reported as it apparently isomerized to 8 prior to or during gc analysis.
[c]3-Methyl-3-cyclohexenone (18).
[d]3-Methyl-2-cyclohexenone (10).
[e]2-Ethyl-5-methylphenol (24).
[f]Carvotanacetone (14).
[g]3-Isopropylphenol.
[h]5-Isopropyl-2-methylphenol.
[i]Carvenone (13).
[j]The ratio of the two epimers of 15 in the starting material was 2.0:1 while the ratio after the thermolysis was 1.6:1.
[k]3-Methylcyclohexanone.
[l]2-Ethylidene-5-methylcyclohexanone (25).

tillation or preparative gc immediately prior to reaction and the sample size was 0.40 g for each run. The thermolyses were conducted at 400 ± 2°C for 20 h in a 650-mL evacuated (< 0.02 Torr) Pyrex reactor similar to that previously described (4). In some runs the surface area of the reaction was increased by a factor of ten (Table 1, large surface area) by filling the reactor with pieces of glass tubing (7 mm long × 6 mm od). The products were distilled into a cold finger cooled in liquid nitrogen and then analyzed by gc. The crude distillation recoveries were always high as very little tar formation was evident in any of the runs. The gc peaks were identified by coincident retention times with known samples on two or three columns, by the peak enhancement method, by gc–ms analysis, and in many instances by preparative gc collection and spectral analysis. Components more volatile than benzene were not analyzed but normally these were a relatively small percentage of the total products. The phenolic products had retention times longer than the starting enone and were routinely collected by preparative gc (column A) and their spectral data compared with authentic samples. In addition, the following compounds were collected and their spectra determined.

Experiment 1 3-Cyclohexenone was eluted before 2-cyclohexenone and its ir and nmr spectra were the same as those previously reported (5).

Experiment 3 3-Methyl-3-cyclohexenone was eluted before 3-methyl-2-cyclohexenone and its ir and nmr spectra were the same as those previously reported (5).

Experiments 6 and 7 (*a*) *m*-Xylene was collected and its ir spectrum determined to clearly establish that other xylene isomers were not present; (*b*) 2-ethyl-5-methylphenol eluted between *m*-cresol and 3,5-dimethylphenol and exhibited the following spectral data: nmr (CCl_4) δ: 1.2 (3H, t), 2.3 (3H, s), 2.6 (2H, quartet), 4.3 (1H, br s), 6.4–7.1 (3H, m); mass spectrum *m/e*: 136 (M^+).

Experiments 8 and 9 The collected sample of 5-isopropyl-2-methylphenol was identical to a sample prepared by treatment of carvone with $RhCl_3 \cdot 3H_2O$ (6).

Experiments 11 and 12 (*a*) The 3-methylcyclohexanone peak exhibited spectral properties identical to an authentic sample: (*b*) 2-ethylidene-5-methylcyclohexanone (**25**) eluted after menthone (**15**) but before a sample of pulegone (2-isopropylidene-5-methylcyclohexanone) which was added for

Can. J. Chem. Downloaded from www.nrcresearchpress.com by 210.87.254.6 on 09/05/12
For personal use only.

Can. J. Chem. Downloaded from www.nrcresearchpress.com by 210.87.254.6 on 09/05/12
For personal use only.

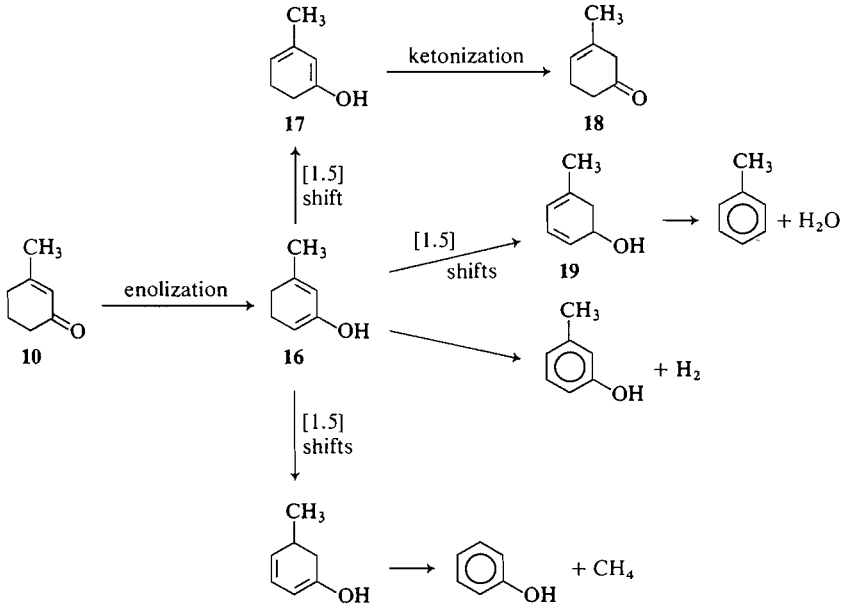
purposes of comparison. Compound **25** exhibited the following spectral data: uv λ_{max}: 244 nm; ir (CCl_4):1695, 1625 cm^{-1}; nmr (CCl_4) δ: 1.0 (3H, d), 1.7 (3H, d), 1.6–2.6 (7H, m), 6.6 (1H, m). These data are consistent with the reported data for the related compounds 2-ethylidene-6-methylcyclohexanone (7) and the available pulegone.

Results and Discussion

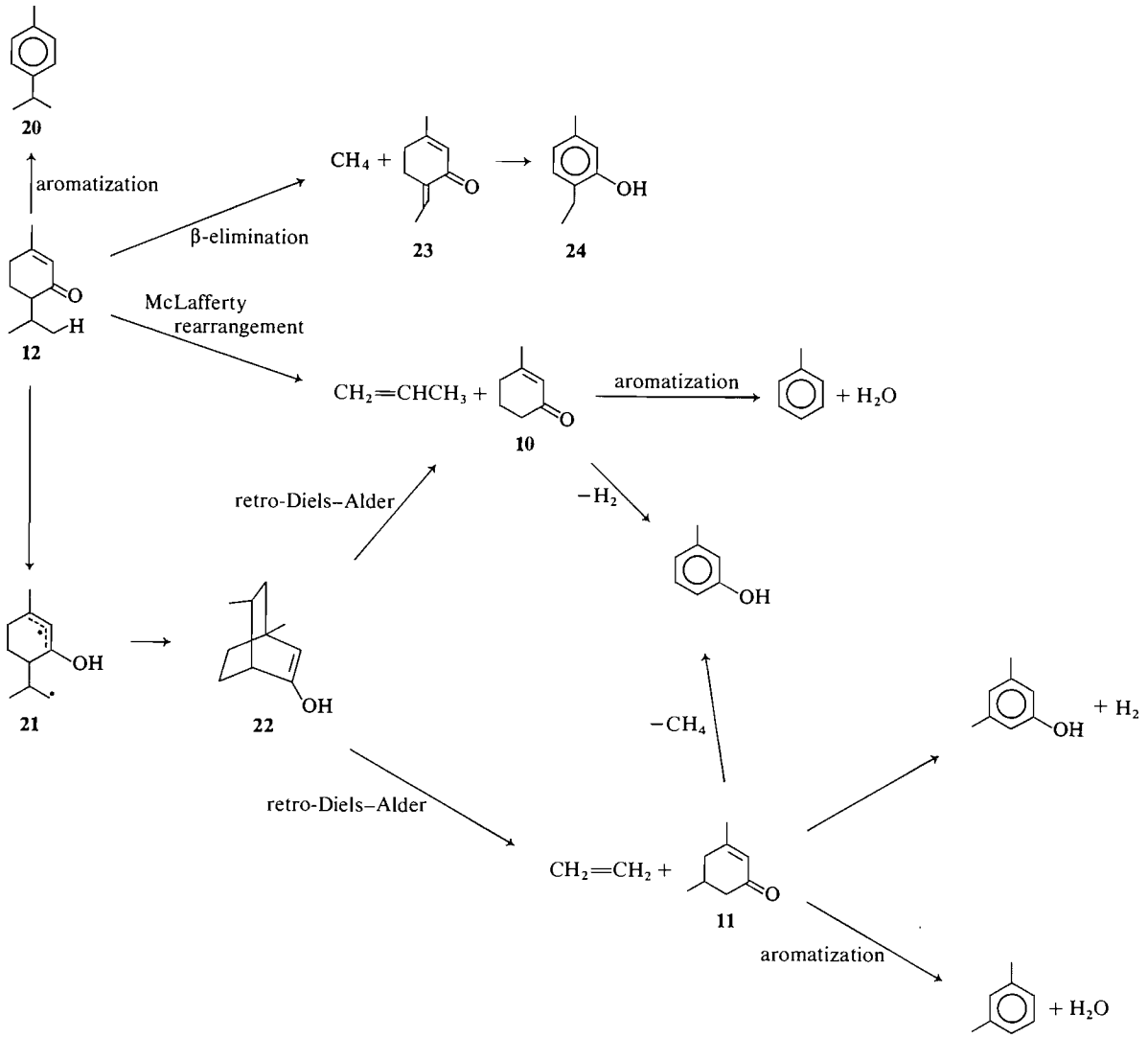
In the initial stages of our investigation, we examined the thermolysis of a number of methylated 2-cyclohexenones (**8–11**) to determine the effect of the position and of the number of substituents on the percentage conversion and the product composition (Table 1, Experiments 1–5). All thermolyses described were conducted in the vapor phase at 400°C for 20 h. The percentage conversions varied from 11 to 45% for these enones and the percentage of aromatization to a substituted benzene (e.g. 3-methyl-2-cyclohexene (**10**) → toluene) varied from 3 to 28%. Using either of these criteria of reaction, it appears that methyl substituents facilitate the conversions although the position of the substituents is also important (e.g. Experiment 2 vs. 3). Experiments 3 and 4 indicate that a ten-fold increase in the surface area within the reaction flask enhances the conversion slightly.

Scheme 2 outlines mechanisms to account for the products (Table 1, Experiments 3 and 4) formed by thermolysis of 3-methyl-2-cyclohexenone (**10**). Similar mechanisms would account for the products obtained from **8**, **9**, and **11**. Enolization of the enone is an essential step in almost all the transformations described and may be either a thermal or a catalyzed reaction on the glass surface of the reaction flask. Intermediate **16**, formed by enolization of **10**, may undergo the four possible reactions indicated in Scheme 2 to give the products isolated. First, a [1.5] sigmatropic hydrogen shift yields enol **17**, which then tautomerizes to give the unconjugated ketone **18**. Spangler and Hennis (8) have shown that these [1.5] shifts readily occur with 1,3-cyclohexadienes above 325°C. In the thermolysis of 2-cyclohexenone (**8**) the major product was also the unconjugated isomer (Experiment 1). In Scheme 2, the second pathway from **16** involves several [1.5] hydrogen shifts to give **19** which readily dehydrates to yield toluene. The driving force behind this aromatization sequence is presumably the formation of the stable benzene ring. Similarly, in the thermolysis of 3,5-dimethyl-2-cyclohexenone (**11**) the major product was *m*-xylene, formed by this aromatization process. The final two pathways from **16** involve elimination of a molecule of hydrogen or methane to give *m*-cresol or phenol, respectively. The very volatile products in these reactions were not analyzed so we have no direct evidence for the formation of products such as methane. In a similar manner, thermolysis of **11** yielded 3,5-dimethylphenol and *m*-cresol after loss of hydrogen or methane, respectively, while **9** yielded *o*-cresol and hydrogen.

Experiments 1 to 5 provided a better understanding of the types of processes to be expected upon thermolysis of methyl-substituted cyclohexenones. Next we proceeded to the thermolysis of more complex cyclohexenones, namely, the naturally occurring monoterpenes piperitone



SCHEME 2



SCHEME 3

(**12**), carvenone (**13**), and carvotanacetone (**14**). One striking feature of these reactions (Experiments 6–10) was the much higher conversions (>70%) which were attained. Evidently the isopropyl group of the monoterpenes enhances the reactivity of enones in these thermal transformations.

Scheme 3 outlines a number of pathways to explain the formation of the seven major components detected in the thermolysis of piperitone (**12**). Similar transformations will explain most of the products obtained from **13** and **14**. In this scheme, the enolization and [1.5] shifts are not shown in detail, but it is clear that *p*-cymene (**20**) is formed from **12** by the aromatization reaction discussed previously. A McLafferty-type rearrangement (9) is possible when an isopropyl group is on a carbon *alpha* to the carbonyl group. This fragmentation with **12** yields propene and **10**, which then gives toluene upon aromatization. Compound **10** also may be converted to *m*-cresol by loss of hydrogen. A pathway for the formation of *m*-xylene from **12** is not obvious but it should be emphasized at this point that the *meta* isomer is not formed by isomerization of either the *ortho* or *para* isomer. Thermolysis of either *o*- or *p*-xylene under the usual reaction conditions gave complete recovery of the starting material with no evidence of isomerization. We suggest that a primary hydrogen of the isopropyl group in **12** is transferred to the carbonyl group to give the allylic biradical **21**, which then cyclizes to form the bicyclo[2.2.2] system **22**.

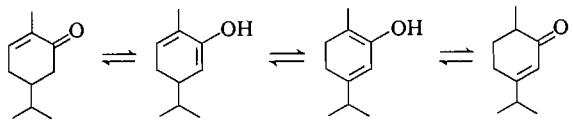
Can. J. Chem. Downloaded from www.nrcresearchpress.com by 210.87.254.6 on 09/05/12
For personal use only.

Can. J. Chem. Downloaded from www.nrcresearchpress.com by 210.87.254.6 on 09/05/12
For personal use only.

Retro-Diels–Alder fragmentation of **22** gives either propene and **10** or ethene and **11**. As observed in Experiment 5, **11** yields *m*-xylene, *m*-cresol, and 2,4-dimethylphenol, which are three of the products also formed from **12**. Retro-Diels–Alder reactions of bicyclo[2.2.2] systems previously were shown to occur under these reaction conditions (1).

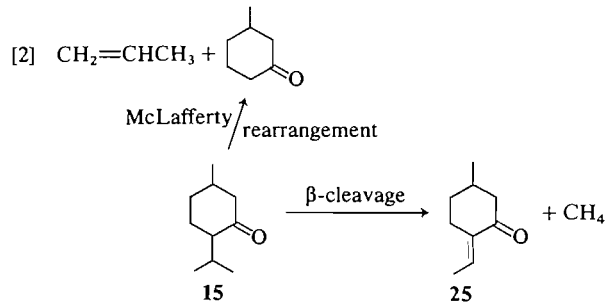
The last pathway in Scheme 3 accounts for the formation of 2-ethyl-5-methylphenol (**24**) from piperitone (**12**). Judging from a limited number of examples, it appears that alkyl substituents at the 5-position in 2-cyclohexenones (i.e. *beta* to the carbonyl group) are most readily eliminated under our thermolysis conditions. For example, β-elimination of the methyl group of **11** yielded *m*-cresol (Experiment 5), which was one of the major products in that reaction. Likewise, elimination of a β-methyl group (along with an α-hydrogen) from **12** gives **23** (Scheme 3), which isomerizes to **24**. In the thermolysis of carvotanacetone (**14**), β-elimination of the isopropyl group gives the major product, *o*-cresol. The driving force in these reactions is presumably the formation of the new conjugated enone and ultimately the aromatic ring.

The double bond in the starting enone may isomerize from one side of the carbonyl group to the other via the enol and [1.5] sigmatropic shifts. For example, thermolysis of carvotanacetone (**14**) yields some carvenone (**13**) or thermolysis of **13** gives **14** (eq. [1]). Thus, the major product obtained in Experiments. 8 and 9 was *o*-cresol, formed by isomerization of **13** to **14** followed by β-elimination of the isopropyl group.

[1] 

14 **13**

To this point in our investigation, the only systems examined were substituted cyclohex*enones*. For purposes of comparison we thought it would be of interest to determine the products obtained from thermolysis of a naturally occurring cyclohex*anone*, namely the common monoterpene menthone (**15**). Experiments 11 and 12 indicated that the larger surface area increased the percentage conversion quite substantially but in both instances the major product was 3-methylcyclohexanone, formed by a McLafferty-type rearrangement as discussed earlier for piperitone (**12**). The other product formed in this thermolysis is proposed to be 2-ethylidene-5-methylcyclohexanone (**25**) (eq. [2]), on the basis of the spectral

[2] 

15 **25**

information reported in the Experimental. Compound **25** is formed by β-cleavage of one of the methyl groups of the isopropyl substituent. The menthone used in this study was a 2:1 mixture of the two epimers (actually menthone and isomenthone). Analysis of the menthone recovered after the thermolysis indicated the epimer ratio was 1.6:1. At a temperature of 400°C it would be expected that the equilibrium would be shifted towards the less stable epimer (10) and upon distillation of the products from the thermolysis flask the new equilibrium mixture would effectively be "trapped".

Summary and Conclusions

As a result of these studies it is possible to make several generalizations concerning the type of products to be anticipated upon thermolysis of substituted cyclohexenones. (*i*) At 400°C these enones readily undergo [1.5] sigmatropic hydrogen shifts via their enol tautomer to yield double bond isomers which may be isolated or be involved in further transformations. (*ii*) All of the cyclohexenones yielded varying amounts of substituted benzenes and thus this aromatization reaction is common to these systems. (*iii*) The enone may lose either a molecule of hydrogen or a simple alkane (e.g. methane or propane) to give a phenol. (*iv*) An alkyl group at the 5-position of a 2-cyclohexenone appears to be eliminated most readily in a so-called β-cleavage process. (*v*) Some transformations are more complex (e.g. **12** → *m*-xylene) and it is necessary to postulate an intermediate bicyclo[2.2.2] system, which then undergoes a retro-Diels–Alder reaction to give a new cyclohexenone and an alkene.

In conclusion, the thermal transformations of a variety of substituted cyclohexenones, including monoterpenoids, may be rationalized on the basis of a limited number of mechanistic pathways. These investigations may provide a better understanding of more complex thermal processes such as the conversion of terpenoids to aromatic hydrocarbons during the formation of petroleum (11) and other biomass conversions.

Acknowledgement

The authors acknowledge the financial assistance of the National Research Council of Canada.

1. J. M. CONIA and G. L. LANGE. J. Org. Chem. **43**, 564 (1978).
2. P. SINGH. J. Org. Chem. **36**, 3334 (1971).
3. R. E. IRELAND and P. BEY. Org. Synth. **53**, 63 (1973).
4. J. M. CONIA and P. LE PERCHEC. Synthesis, 1 (1975).
5. D. S. NOYCE and M. EVETT. J. Org. Chem. **37**, 394 (1972).
6. P. A. GRIECO and N. MARINOVIC. Tetrahedron Lett. 2545 (1978).
7. R. E. IRELAND and P. W. SCHIESS. J. Org. Chem. **28**, 6 (1963).
8. (*a*) C. W. SPANGLER and R. P. HENNIS. J. Org. Chem. **36**, 917 (1971); (*b*) C. W. SPANGLER. Chem. Rev. **76**, 187 (1976).
9. H. BUDZIKIEWICZ, C. DJERASSI, and D. H. WILLIAMS. Mass spectrometry of organic compounds. Holden-Day, San Francisco, CA. 1967. p. 147.
10. R. O. C. NORMAN. Principles of organic synthesis. 2nd ed. Chapman and Hall, London. 1978. p. 9.
11. B. J. MAIR. Geochim. Cosmochim. Acta, **28**, 1303 (1964).

Can. J. Chem. Downloaded from www.nrcresearchpress.com by 210.87.254.6 on 09/05/12
For personal use only.

Formation of furofurans from tetraacetylethylene. Molecular and crystal structure of a spiro[furan-2(5*H*),2′(3′*H*)-furo[2,3-*b*]furan]

GIORGIO ADEMBRI AND DONATO DONATI
Istituto di Chimica Organica, Piano dei Mantellini, 44, Siena, Italy

RENZO CINI
Istituto di Chimica Generale, Piano dei Mantellini, 44, Siena, Italy

AND

RODOLFO NESI AND MIRELLA SCOTTON[1]
Centro di Studio del C.N.R. sulla Chimica et la struttura dei composti eterociclici, c/o Instituto di Chimica Organica, Via G. Capponi, 9 Firenze, Italy

Received February 14, 1980

GIORGIO ADEMBRI, DONATO DONATI, RENZO CINI, RODOLFO NESI, and MIRELLA SCOTTON. Can. J. Chem. **58**, 1645 (1980).

Dimerization of tetraacetylethylene (TAE) **1** has led to a spiro[furan-2(5*H*),2′(3′*H*)-furo[2,3-*b*]furan], whose structure was established by X-ray analysis. The trend of TAE to furan ring closure was confirmed by the reaction with ethyl vinyl ether, where the first product of the reaction, the pyran adduct **8**, smoothly rearranged to a furo[2,3-*b*]furan derivative **9**.

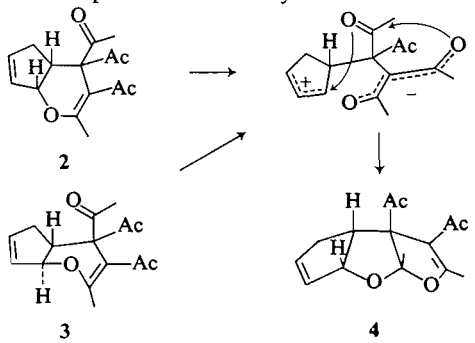
GIORGIO ADEMBRI, DONATO DONATI, RENZO CINI, RODOLFO NESI et MIRELLA SCOTTON. Can. J. Chem. **58**, 1645 (1980).

La dimérisation du tétra-acétyléthylène (TAE) **1** conduit au dérivé spiro[furan-2(5*H*),2′(3′*H*)-furo[2,3-*b*]furanne] dont on a établi la structure par analyse aux rayons-X. On a confirmé la tendance du TAE à se transformer en un cycle furanne par la réaction avec l'éther éthylvinyle, où le premier produit de la réaction, l'adduit pyranne **8**, se transpose facilement en un dérivé furo[2,3-*b*] furanne **9**.

[Traduit par le journal]

Tetraacetylethylene (TAE) **1**, a conjugated system with a highly activated double bond, reacted with nucleophiles, electrophiles, and dienes to give homocycles, heterocycles, and cycloadducts respectively (1, 2). The cycloadducts obtained from cyclopentadiene easily converted into furan derivatives through a rearrangement which was promoted by steric hindrance and by the presence of an oxygen atom suitably placed with respect to an electron-deficient carbon atom. Thus, the *cis*-cyclopenta[*b*]pyran **2**, obtained from TAE and cyclopentadiene through a sigmatropic[3.3] rearrangement, and the *trans*-isomer **3** convert into the more stable cyclopenta[*d*]furo[2,3-*b*]furan **4** (3, 4).

Our interest in studying the reactivity of TAE led us to attempt some other cycloaddition reactions.



SCHEME 1

We found that they were sometimes slow or did not take place at all, for instance with butadiene, anthracene, hexachlorocyclopentadiene, diphenylfulvene. We attributed this behavior to the lack of planarity of TAE as follows from ir and Raman spectra (1). In all cases we isolated compound **5**, a dimer of TAE. The dimer **5** was prepared in 80% yield by refluxing TAE in an inert solvent, such as benzene, for 28 h. The ir spectrum showed a sharp band at 3420 cm^{-1} (OH), three bands at 1715, 1700, and 1685 cm^{-1} (CO groups), and a very strong band at 1605 cm^{-1}, which was indicative of a conjugated —CO—C=C—O— system (5, 6), confirmed by the uv absorption at 266 nm. The second maximum at 220 nm suggested the presence of a conjugated Ac—C=C—Ac system (7). The ^1H nmr spectrum, in deuterioacetone, displayed a singlet (1H) at δ5.85 for the OH group (the signal disappeared on deuteration) and two mutually coupled doublets (1H each, J = 14 Hz) at δ 3.36 and 2.15 attributable to methylene protons. There were also six singlets due to seven methyl groups; whereas five resonated at δ 2.36, 2.31, 2.15, and 2.04 (integral ratio 6:3:3:3), the other two showed a remarkable upfield shift (δ 1.56 and 1.47).

[1]Author to whom correspondence should be addressed.

0008-4042/80/161645-06$01.00/0
©1980 National Research Council of Canada/Conseil national de recherches du Canada

TABLE 1. Positional parameters ($\times 10^4$), thermal parameters[a] ($Å^2 \times 10^3$), and estimated standard deviations for the atoms of tetraacetylethylene dimer

Atom	x/a	y/b	z/c	U_{11}	U_{22}	U_{33}	U_{12}	U_{13}	U_{23}
O(1)	9325(3)	9937(7)	6773(4)	54(4)	49(5)	33(4)	−15(3)	9(3)	−6(3)
O(1′)	8394(3)	388(7)	7777(5)	36(4)	29(4)	51(4)	3(3)	3(3)	−6(3)
O(6′)	7741(3)	9193(8)	6469(5)	47(4)	45(4)	48(4)	10(3)	−9(3)	0(4)
O(7)	1112(3)	2009(10)	8205(8)	33(4)	89(6)	236(11)	0(4)	−11(5)	−52(7)
O(10)	9832(3)	2015(8)	119(5)	73(5)	67(5)	55(5)	6(4)	−20(4)	−21(4)
O(13)	8164(4)	5889(11)	9243(6)	137(7)	122(8)	47(5)	−72(6)	−21(5)	21(5)
O(16)	9100(3)	4605(8)	6768(5)	70(5)	47(4)	55(4)	15(4)	−2(4)	−3(4)
O(22)	9964(3)	2106(8)	6063(5)	85(5)	35(5)	61(5)	4(4)	32(4)	2(4)

Atom	x/a	y/b	z/c	U	Atom	x/a	y/b	z/c	U
C(2)	9056(4)	9786(11)	7816(7)	33(2)	C(9)	462(5)	4422(15)	8502(9)	76(4)
C(3)	9489(4)	942(11)	8479(7)	35(2)	C(11)	9374(4)	1422(12)	9589(8)	44(3)
C(3′)	9019(4)	7924(12)	8152(7)	37(2)	C(12)	8737(5)	1306(14)	122(9)	78(4)
C(3′a)	8363(4)	7331(12)	7628(7)	37(2)	C(14)	8041(5)	5932(13)	8314(9)	53(3)
C(4)	6(4)	1478(11)	7924(7)	36(2)	C(15)	7551(5)	4739(13)	7848(8)	65(3)
C(4′)	8408(4)	6872(11)	6461(7)	36(2)	C(17)	8816(4)	5458(13)	6099(8)	43(3)
C(5)	9949(4)	816(13)	6811(8)	47(3)	C(18)	8919(5)	5058(14)	4961(9)	68(3)
C(5′)	8055(4)	7986(13)	5881(7)	44(3)	C(19)	7906(4)	8193(13)	4742(8)	59(3)
C(6′a)	7955(4)	9034(13)	7582(7)	41(3)	C(20)	7350(4)	9256(13)	8276(8)	59(3)
C(8)	569(5)	2578(13)	8219(8)	55(3)	C(21)	501(5)	9545(14)	6511(8)	65(3)

Atom[b]	x/a	y/b	z/c	Atom[b]	x/a	y/b	z/c
H(22)	9679	3227	6565	H(181)	9040	5985	4726
H(3′1)	8947	7906	9031	H(182)	9023	3493	4854
H(3′2)	9385	7361	7707	H(183)	8473	4626	4451
H(91)	419	4903	7740	H(191)	7926	9572	4432
H(92)	9977	4577	8735	H(192)	8398	7757	4353
H(93)	375	4566	9298	H(193)	7541	7121	4449
H(121)	8620	140	200	H(201)	7130	9646	7949
H(122)	8460	236	9830	H(202)	7156	8749	7782
H(123)	8422	986	9657	H(203)	7564	9179	9132
H(151)	7292	5480	7235	H(211)	540	8838	7030
H(152)	7726	3772	7453	H(212)	349	9000	5722

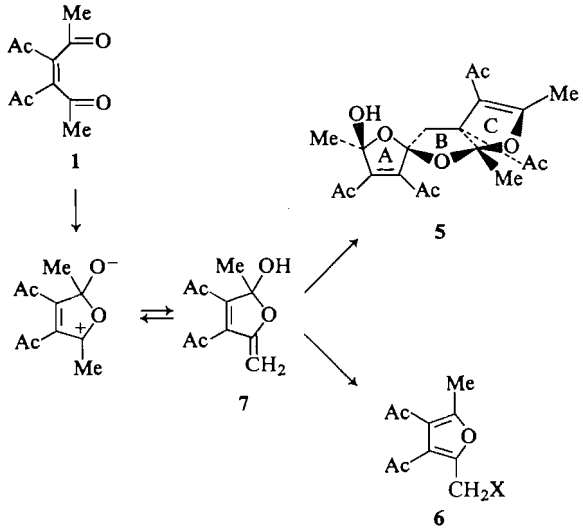
[a] Anisotropic thermal factors are of the form: $\exp(-2\pi^2(\sum_{i=j} h_i h_j a_i^* a_j^* U_{ij}))$.
[b] Isotropic thermal factor for hydrogen atoms was fixed to $U = 0.06$ Å^2.

The evidence presented above was not sufficient to choose among the variety of structures possible for compound **5**, keeping in mind the trend of TAE to furan ring closure which involves the introduction of several chiral centers. Consequently an X-ray structure determination was undertaken which established that it had the (2*R**,3′a*R**,5*R**,6′a*R**)3,3′a,4,4′-tetraacetyl-5-hydroxy-5,5′,6′a-trimethylspiro[furan-2(5*H*),2′(3′*H*)-furo[2,3-*b*]-furan] structure.

Details of the crystallographic analysis are reported in the Experimental.

A possible mechanism pathway would involve the dimerization of an intermediate such as **7** which could account for the stereochemistry of the dimer **5**. The same furan **7** could be invoked for the formation of 3,4-diacetyl-2-halomethyl-5-methylfuran **6** from TAE and concentrated haloacids (1).

TAE reacted with ethyl vinyl ether, an activated



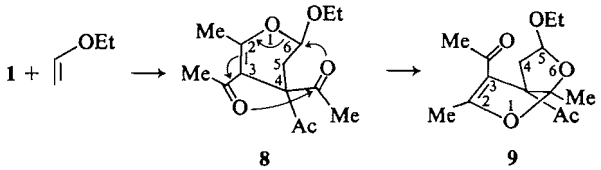
SCHEME 2

TABLE 2. Bond lengths (Å) and angles (deg) with estimated standard deviations in parentheses (bond lengths and angles involving hydrogen atoms are not reported)

a) Bond	Length (Å)	Bond	Length (Å)
O(22)—C(5)	1.383(10)	C(19)—C(5′)	1.479(12)
O(1)—C(5)	1.442(10)	C(4′)—C(5′)	1.342(11)
C(4)—C(5)	1.504(12)	C(17)—C(4′)	1.456(11)
O(1)—C(2)	1.438(10)	C(20)—C(6′a)	1.527(11)
O(1′)—C(2)	1.425(9)	C(21)—C(5)	1.547(12)
C(3′)—C(2)	1.518(11)	C(8)—C(4)	1.476(11)
C(3)—C(2)	1.510(11)	C(11)—C(3)	1.475(12)
C(3)—C(4)	1.334(10)	O(13)—C(14)	1.200(11)
C(3′a)—C(14)	1.544(12)	C(15)—C(14)	1.482(12)
C(3′)—C(3′a)	1.554(11)	O(10)—C(11)	1.233(9)
C(4′)—C(3′a)	1.523(11)	C(12)—C(11)	1.468(12)
C(6′a)—C(3′a)	1.567(11)	O(7)—C(8)	1.189(10)
O(1′)—C(6′a)	1.403(10)	C(9)—C(8)	1.501(14)
O(6′)—C(6′a)	1.476(10)	O(16)—C(17)	1.219(9)
O(6′)—C(5′)	1.364(10)	C(18)—C(17)	1.491(13)

b) Bond angle	Degrees	Bond angle	Degrees
C(15)—C(14)—O(13)	120.3(10)	C(2)—O(1′)—C(6′a)	110.8(6)
C(3′a)—C(14)—O(13)	119.1(9)	C(5′)—O(6′)—C(6′a)	109.2(7)
C(3′a)—C(14)—C(15)	120.5(9)	C(4′)—C(3′a)—C(3′)	115.2(7)
C(12)—C(11)—O(10)	115.9(9)	C(4′)—C(3′a)—C(14)	114.1(8)
C(3)—C(11)—O(10)	119.3(8)	C(6′a)—C(3′a)—C(3′)	102.3(7)
C(3)—C(11)—C(12)	124.8(9)	C(6′a)—C(3′a)—C(14)	113.3(7)
C(9)—C(8)—O(7)	119.9(10)	C(6′a)—C(3′a)—C(4′)	101.6(7)
C(4)—C(8)—O(7)	119.7(10)	C(14)—C(3′a)—C(3′)	109.6(7)
C(4)—C(8)—C(9)	120.4(9)	C(21)—C(5)—O(22)	106.2(8)
C(18)—C(17)—O(16)	119.2(9)	C(21)—C(5)—O(1)	108.9(8)
C(4′)—C(17)—O(16)	117.5(9)	C(4)—C(5)—O(22)	112.9(8)
C(4′)—C(17)—C(18)	123.3(9)	C(4)—C(5)—O(1)	104.8(7)
C(4)—C(3)—C(11)	123.6(8)	C(4)—C(5)—C(21)	113.7(8)
C(2)—C(3)—C(11)	125.8(8)	O(1)—C(5)—O(22)	110.3(7)
C(2)—C(3)—C(4)	110.5(8)	O(6′)—C(6′a)—O(1′)	106.6(7)
C(3)—C(4)—C(8)	131.3(9)	C(20)—C(6′a)—O(1′)	109.1(8)
C(5)—C(4)—C(8)	119.3(8)	C(20)—C(6′a)—O(6′)	107.9(7)
C(5)—C(4)—C(3)	109.4(8)	C(3′a)—C(6′a)—O(1′)	107.4(6)
C(3′a)—C(4′)—C(17)	121.6(8)	C(3′a)—C(6′a)—O(6′)	104.9(7)
C(5′)—C(4′)—C(17)	128.4(9)	C(3′a)—C(6′a)—C(20)	120.2(8)
C(5′)—C(4′)—C(3′a)	110.0(8)	O(1′)—C(2)—O(1)	107.8(7)
C(19)—C(5′)—O(6′)	111.3(8)	C(3′)—C(2)—O(1)	110.9(7)
C(4′)—C(5′)—O(6′)	113.5(8)	C(3′)—C(2)—O(1′)	106.1(7)
C(4′)—C(5′)—C(19)	135.1(10)	C(3)—C(2)—O(1)	103.8(7)
C(2)—O(1)—C(5)	110.3(6)	C(3)—C(2)—O(1′)	111.5(7)
C(2)—C(3′)—C(3′a)	102.1(7)	C(3)—C(2)—C(3′)	116.5(8)

electron-rich olefin, through an 1,4-dipolar addition to give 3,4,4-triacetyl-6-ethoxy-2-methyl-5,6-dihydro-4*H*-pyran **8** whose structure followed from spectral data. The presence of a —CO—C=C—O— system was revealed by the most intense band in the ir spectrum at 1620 cm^{-1} and confirmed by uv absorption at 259 nm. The ^1H nmr spectrum in deuteriochloroform showed four three-proton singlets at δ 2.11, 2.17, 2.31, and 2.45 for the methyl groups (the three signals at highest field partially overlapped a multiplet (2H) attributable to the methylene ring protons) and a doublet of doublets (1H, $J_{5',6}$ = 2.3 Hz, $J_{5'',6}$ = 4.0 Hz) at δ 5.08, which was assigned to the H-6 proton (this multiplet collapsed to a singlet by irradiation at 2.17). The spectrum also exhibited a triplet (3H), at δ 1.17 and a 16-component pattern (2H) centered at δ 3.68



8 9

SCHEME 3

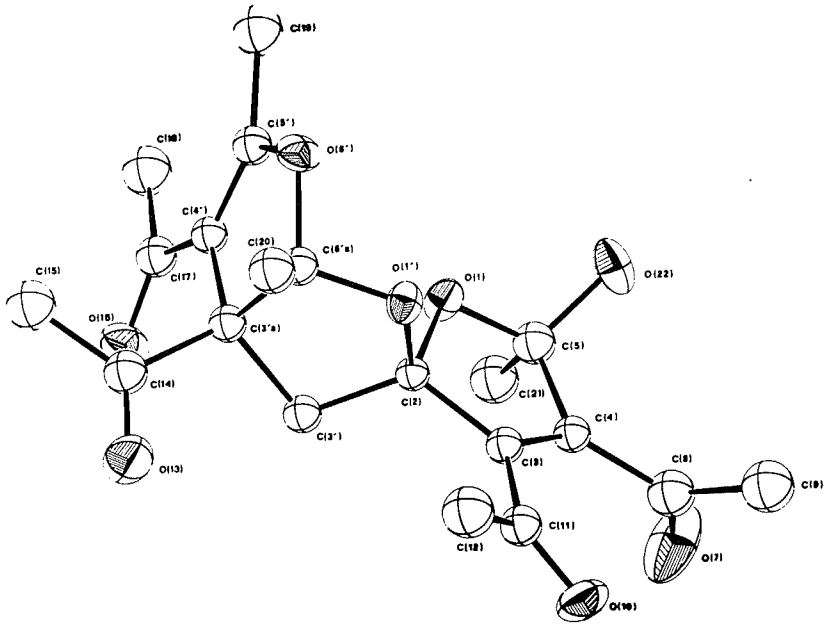


FIG. 1. ORTEP drawing of the molecule with 30% probability thermal ellipsoids and atom labelling system used in the crystallographic analysis.

for the ABX_3 system (J_{AB} = 9.5 Hz, $J_{AX} = J_{BX}$ = 7.0 Hz) of the O—CH_2—CH_3 group, according to the diastereotopic methylene protons (8, 9).

The pyran **8** was unstable and, both in the solid state and faster in solution, it rearranged intramolecularly to a compound, mp 65–67°C, which we assigned the structure of 3,3a-diacetyl-5-ethoxy-2,6a-dimethyl-*cis*,3a,4,5,6a-tetra-hydrofuro[2,3-*b*]furan **9** on the basis of spectral evidence and by analogy with foregoing cases. Both ir and uv spectra supported the presence of the same conjugated system as in isomer **8**. The same signals of the ABX_3 system (J_{AB} = 9.5 Hz, $J_{AX} = J_{BX}$ = 7.0 Hz) were also present in the ^{1}H nmr spectrum of this isomer at δ 1.2 (3H) and 3.67 (2H) respectively, whereas the H-5 and the methylene ring protons gave rise to three doublets of doublets (1H) at δ 5.16, 2.84, and 2.25 ($J_{4',4''}$ = 14.0 Hz, $J_{4',5}$ = 5.2 Hz, $J_{4'',5}$ = 6.3 Hz). The multiplet at highest field was partially obscured by three singlets (3H) at δ 1.32, 1.28, and 1.15 attributable to the methyl protons; as reported for compounds **4** and **5** the resonance of the methyl group at 6a position (δ 1.46) showed a remarkable upfield shift.

Experimental

Infrared spectra were measured for dispersions in potassium bromide with a Perkin-Elmer 457 spectrometer and uv spectra for solutions in methanol with a Cary 14 recording spectrophotometer. The ^{1}H nmr spectra were recorded with a Perkin-Elmer R 32; chemical shifts are reported in ppm downfield from tetramethylsilane as internal reference and coupling constants in Hz and are discussed in the Introduction. Molecular weight of compound **5** was determined with a Hitachi Perkin-Elmer 115 Apparatus.

(2R,3'aR*,5R*,6'aR*)3,3'a,4,4'-Tetraacetyl-5-hydroxy-5,5',6'a-trimethylspiro-[furan-2(5H),2'(3'H)-furo[2,3-b]furan]* **5**

TAE (0.4 g) was refluxed in benzene (2 mL) for 28 h. Evaporation of the solvent followed by crystallization of the resulting syrup with water gave the dimer **5** as colorless prisms, mp 144–146°C, (0.32 g, 80%); uv λ_{max} (log ε): 220(3.72) and 266 (3.96) nm; ir ν_{max}: 3420, 1715, 1700, 1685, 1645, 1605 cm^{-1}. *Anal.* calcd. for $C_{20}H_{24}O_8$: C 61.22, H 6.16, Mol. Wt. 392; found: C 61.48, H 6.14, Mol. Wt. 384.

TABLE 3. Selected intramolecular non-bond distances <3.5 Å

Atom pairs	Distance (Å)
O(1)---C(5')	3.191
O(1)---C(3'a)	3.027
O(1)---C(6'a)	3.054
O(1)---C(4')	3.055
C(19)---C(18)	3.207
O(16)---C(14)	3.098
O(13)---C(3')	2.736
C(15)---C(4')	2.990
C(20)---C(14)	2.951
C(21)---C(8)	3.210
O(10)---C(9)	3.066
O(1')---C(12)	3.127
O(1')---C(11)	3.129
C(8)---C(11)	3.127
O(10)---C(8)	2.877
O(1')---C(12)	3.127

TABLE 4. Least-squares plane equations referred to the crystallographic axes, with deviations (Å) of the atoms from the planes and angles (deg) between planes

Plane	Eq: $PX + QY + RZ - S = 0$				Atom	Deviation from plane	Angle between planes
	P	Q	R	S			
A	10.4883	−6.4276	2.9314	5.4404	O(1)	−0.062	A—B 85.2
					C(2)	0.059	
					C(3)	−0.036	
					C(4)	−0.001	
					C(5)	0.039	
B	−4.8292	0.2209	12.3171	5.6603	O(1')	0.095	B—C 73.6
					C(2)	−0.190	
					C(3')	0.200	
					C(3'a)	−0.141	
					C(6'a)	0.037	
C	16.5192	4.4607	−1.4528	16.0084	O(6')	−0.060	A—C 85.7
					C(6'a)	0.061	
					C(3'a)	−0.032	
					C(4')	0.008	
					C(5')	0.006	
					C(19)	0.017	

3,4,4-Triacetyl-6-ethoxy-2-methyl-5,6-dihydro-4H-pyran **8**

TAE (0.8 g) was refluxed with ethyl vinyl ether (6 mL) for 28 h. The excess of the reagent was evaporated and the residue triturated with a little ether gave on filtration the pyran **8**, (0.88 g, 80%), mp 70–72°C (from light petroleum bp 40–70°C); uv λ_{max} (log ε): 259 (4.01) nm; ir ν_{max}: 1710, 1700, 1650, 1620 cm^{-1}. *Anal.* calcd. for $C_{14}H_{20}O_5$: C 62.67, H 7.51; found: C 62.83, H 7.52.

Preparative tlc of the ether solution (with ether as eluent) gave, in order of mobility, another crop of the pyran **8** (20 mg) and the dimer **5** (30 mg) (identical mp and ir spectrum with material obtained as above).

Isomerization of the Pyran **8**

The pyran **8** was not very stable and set aside in ether for a few days isomerized into 3,3a-diacetyl-5-ethoxy-2,6a-dimethyl-*cis*-3a,4,5,6a-tetrahydrofuro[2,3-*b*]furan **9**, mp 65–67°C, (from light petroleum bp 40–70°C); uv λ_{max} (log ε): 265 (4.08) nm); ir ν_{max}: 1710, 1615 cm^{-1}. *Anal.* calcd. for $C_{14}H_{20}O_5$: C 62.67, H 7.51; found: C 62.95, H 7.49.

Crystal Data of Compound **5**

$C_{20}H_{24}O_8$ fw = 392.4

Monoclinic, a = 20.30 (2), b = 7.80(1), c = 12.66(1) Å, β = 90.64(4)°, V = 2004.5 $Å^3$, ρ_c = 1.30 $g.cm^{-3}$, Z = 4, $F(000)$ = 832.0 (20°C, Mo-Kα, λ = 0.7107 Å), μ(Mo-Kα) = 1.08 cm^{-1}. Space group $P2_1/a$ from systematic absences $h0l$ for $h = 2n + 1$, $0k0$ for $k = 2n + 1$.

An irregular prism-shaped fragment of dimension ca. 0.2 × 0.25 × 0.15 mm^3 was mounted on a Philips automated diffractometer (graphite monochromator, Mo-Kα radiation). Cell constants were determined by least-squares treatment of angles of 25 reflections. The reflections were collected within $2\theta < 50°$ by ω-2θ step-scan at a scan speed of 0.04° s^{-1} and a scanwidth of 1.60° in ω. Background counts were measured at either end of the scan for 20 s. Two standard reflections monitored periodically showed no significant variation. After correction for Lorentz and polarization effects, 801 reflections with $I > 2\sigma(I)$ were considered observed and used in the structure solution and refinement. Absorption corrections were not applied.

Structure Analysis

The structure was solved by use of automatic centrosymmetric direct methods of the SHELX (1976) program system (10). Most of the non-hydrogen atoms were located in the E map, the remainder by Fourier maps of electron density. Two cycles of full matrix least-squares refinement with unit weight and isotropic temperature factors reduced R to 0.10. Two cycles of least-squares refinement with anisotropic temperature factors for all the oxygen atoms reduced the R factor to 0.081. The weighting scheme used was $w = (\sigma^2(F_0) + 0.005\ F_0^2)^{-1}$ where $\sigma(F_0)$ is the individual estimated standard deviation for each reflection from diffractometer counting statistics. A difference Fourier synthesis calculated at this point showed fifteen hydrogen atoms. These atoms were introduced in the calculation without further refinement of their position, with a temperature factor U of 0.06 $Å^2$. One additional least-squares cycle on non-hydrogen atom parameters gave an R factor of 0.056. At this stage a second difference Fourier synthesis showed seven new hydrogen atoms which were introduced in the final refinement. Three least-squares cycles gave the final disagreement indices R and R_w of 0.050 and 0.053 respectively. Final positional and thermal parameters with the estimated standard deviations are listed in Table 1. Observed and calculated structure factors have been placed in the Depository of Unpublished Data.[2]

Description of the Structure

The ORTEP (11) drawing in Fig. 1 shows clearly the spiran system between a furan ring and a *cis*-fused furo[2, 3-*b*]furan system in the molecular structure of compound **5**.

Table 2 reports bond lengths and angles in the molecule, Table 3 the shortest significant intramolecular distances, and Table 4 equations of best least-squares planes through the rings and the angles between them. The rings A and C are essentially planar; evident puckering is present in ring B with the C(3') atom projecting (0.50 Å) out of the plane of the four other atoms.

[2]These tables are available, at a nominal charge, from the Depository of Unpublished Data, CISTI, National Research Council of Canada, Ottawa, Ont., Canada K1A 0S2.

The most interesting feature in this molecule is the conjugated system O(16) = C(17)—C(4') = C(5')—O(6') in the ring C, which had been expected on the basis of the uv and ir spectra and by analogy with compound **4** (4). The conjugation is the driving force for the coplanarity of the acetyl group O(16)—C(17)—C(18) with the ring plane (about 5.7° between the two planes) and consequently, owing to the strong steric hindrance between the acetyl and the methyl group C(19), the angles C(17)—C(4')—C(5') and C(19)—C(5')—C(4') widen to 128.4° and 135.1° respectively.

The steric hindrance between the two acetyl groups O(10)—C(11)—C(12) and O(7)—C(8)—C(9) of the A ring is apparently more important than the conjugation and forces them out of coplanarity (17.8° and 67.0° respectively between the acetyl planes and the ring plane).

Acknowledgements

The authors wish to thank Prof. Mammi for the use of a diffractometer at the Istituto di Chimica Organica dell'Università di Padova. Financial support by Consiglio Nazionale delle Ricerche of Italy is gratefully acknowledged.

1. G. ADEMBRI, F. DE SIO, R. NESI, and M. SCOTTON. J. Chem. Soc. C, 1536 (1970).
2. G. ADEMBRI, R. NESI, and M. SCOTTON. Chim. Ind. Milan, **57**, 782 (1975).
3. G. ADEMBRI, R. NESI, and M. SCOTTON. Tetrahedron Lett. 3961 (1977).
4. G. ADEMBRI, R. CINI, P. L. ORIOLI, R. NESI, and M. SCOTTON. J. Chem. Soc. Perkin Trans. II, 903 (1979).
5. A. ROEDIG, J. HILBERTH, and H. A. RENK. Ann. 2251 (1975).
6. P. BRAVO, C. TICOZZI, and D. MOGGI. Heterocycles, **4**, 1755 (1976).
7. J. LEVISALLES. Bull. Soc. Chim. Fr. 997 (1957).
8. G. DESIMONI, M. J. COOK, and G. TACCONI. Gazz. Chim. Ital. **100**, 208 (1970).
9. W. FRIEDRICHSEN. Ann. 1545 (1975).
10. G. M. SHELDRICK. SHELX program system. University Chemical Laboratory, Lensfield Road, Cambridge, England.
11. C. K. JOHNSON. ORTEP. A Fortran thermal ellipsoid plot program for crystal structure illustration. Oak Ridge National Laboratory, Oak Ridge, Tennessee. 1971.

An X-ray crystallographic, Raman, and infrared spectral study of crystalline potassium uranyl carbonate, $K_4UO_2(CO_3)_3$

ANTHONY ANDERSON

Department of Physics, University of Waterloo, Waterloo, Ont., Canada N2L 3G1

AND

CHUNG CHIEH, DONALD E. IRISH, AND JAMES P. K. TONG

Department of Chemistry, Guelph–Waterloo Centre for Graduate Work in Chemistry, Waterloo Campus, University of Waterloo, Waterloo, Ont., Canada N2L 3G1

Received January 18, 1980

ANTHONY ANDERSON, CHUNG CHIEH, DONALD E. IRISH, and JAMES P. K. TONG. Can. J. Chem. **58**, 1651 (1980).

X-ray diffraction studies have revealed that $K_4UO_2(CO_3)_3$ is isostructural with $(NH_4)_4UO_2(CO_3)_3$; the crystal is monoclinic with a = 10.247(3), b = 9.202(2), c = 12.226(3) Å, β = 95.11(2)°, Z = 4, and space group $C2/c$. Three carbonate anions are arranged in bidentate fashion in the equatorial plane of UO_2^{2+}; one of these occupies a C_2 site and the other two occupy C_1 sites. All carbonates are significantly distorted from D_{3h} symmetry. The binding of carbonates to uranyl is strong and thus the lattice can be considered to be composed of $[UO_2(CO_3)_3]^{4-}$ anions and K^+ cations. The Raman and infrared spectra exhibit fewer lines than predicted for such a crystal. Tentative assignments are suggested for the more prominent bands of the constituent polyatomic species.

ANTHONY ANDERSON, CHUNG CHIEH, DONALD E. IRISH et JAMES P. K. TONG. Can. J. Chem. **58**, 1651 (1980).

Des études de diffraction de rayons-X révèlent que le $K_4UO_2(CO_3)_3$ a la même structure que le $(NH_4)UO_2(CO_3)$. Le cristal est monoclinique et appartient au groupe d'espace $C2/c$ avec a = 10.247(3), b = 9.202(2), c = 12.226(3) Å, β = 95.11(2)°, Z = 4. Les trois anions carbonates sont disposés de façon bidentate dans le plan équatorial de UO_2^{2+}; l'un d'eux est en position C_2 et les deux autres en position C_1. Tous les carbonates sont déformés de façon significative par rapport à une symétrie D_{3h}. La liaison carbonate-uranyle est forte et on peut alors considérer que le réseau est constitué d'anions $[UO_2(CO_3)_3]^{4-}$ et de cations K^+. Les spectres Raman et infrarouges montrent moins de raies que celles attendues pour ce genre de cristal. On a identifié provisoirement les bandes principales des constituants des espèces polyatomiques.

[Traduit par le journal]

Introduction

It is well known that in aqueous solution carbonate anions bind strongly to uranyl cations (1). Because the resulting complexes are very stable and interference from hydrolytic species is considerable it has been difficult to obtain accurate stability constants (2). The species $[UO_2(CO_3)_3]^{4-}$ is considered to predominate at 298 K when the carbonate ion is in large stoichiometric excess (2), although it carries the relatively uncommon four negative charges. This species is also known to occur in the crystalline state. Thus its structure has been reported for $(NH_4)_4UO_2(CO_3)_3$ (3). In this paper we report the structure of the complex as it is found in the potassium salt. Raman and infrared spectra, each measured at two temperatures, are also presented and assignments are proposed for the major bands.

Experimental

Sample Preparation

Uranyl carbonate (0.3 g) was dissolved in 60 mL of aqueous potassium carbonate solution containing an excess of the salt. Following dissolution by heating over a steam bath, filtration, and evaporation to about 16 mL, bright pale yellow crystals formed when left overnight at room temperature (298 K). The crystals were washed with cold water to free them from excess potassium carbonate and recrystallized. A yield of 90% (with respect to uranyl carbonate) was achieved.

X-ray Crystallography

Preliminary X-ray photographic studies indicated that the possible space groups of the crystal were $C2/c$ and Cc. The unit cell constants were found to be similar to those of tetraammonium uranyltricarbonate (3). Crystal data are as follows:

$C_3K_4O_{11}U$ fw = 606.4

Monoclinic, a = 10.247(3), b = 9.202(2), c = 12.226(3) Å, β = 95.11(2)°, V = 1148.2(6) Å^3, ρ_o = 3.5 (by liquid displacement), Z = 4, ρ_c = 3.507, μ(Mo-Kα) = 148 cm^{-1}, λ(Mo-K$\bar{\alpha}$) = 0.71069 Å, space group $C2/c$ (C_{2h}^6, No. 15).

The single crystal used for intensity measurements was cubic with ca. 0.08 mm edges. It was mounted on a Syntex $P2_1$ diffractometer and monochromatic (by graphite crystal) Mo-K$\bar{\alpha}$ radiation was used. Among 1693 independent reflections ($2\theta \leq 55°$), 1621 had net intensities greater than $\sigma(I)$; however, all reflections were included in the structural analysis. Lorentz and polarization factors were applied to derive the structure amplitudes. No absorption correction was made (μR = 0.6).

Because $K_4UO_2(CO_3)_3$ and $(NH_4)_4UO_2(CO_3)_3$, whose space group is $C2/c$, have similar cell constants, they were assumed to be isostructural. The K^+ ions were placed on NH_4^+ ion sites. This assumption was proven to be correct by the subsequent successful refinement. Atomic scattering factors for U, K, C, and O from Cromer and Waber (4) with anomalous dispersion corrections (5) for U and K were used. At the final stage, a weighting function $w^{-1} = 80 - F_o + 0.011F_o^2$ was introduced and the final R ($= \Sigma(|F_o| - |F_c|)/\Sigma|F_o|$) and R_w($= (\Sigma w(|F_o| - |F_c|)^2/\Sigma wF_o^2)^{1/2}$) were 0.038 and 0.045 respectively. This

0008-4042/80/161651-08$01.00/0

©1980 National Research Council of Canada/Conseil national de recherches du Canada

Can. J. Chem. Downloaded from www.nrcresearchpress.com by 210.87.254.5 on 09/05/12
For personal use only.

Can. J. Chem. Downloaded from www.nrcresearchpress.com by 210.87.254.5 on 09/05/12
For personal use only.

TABLE 1. Final atomic parameters (esd's) (0, 0, 0 and 1/2, 1/2, 0) $\pm \mid x, y, z; x, \bar{y}, 1/2 + z \mid \times 10^{-4}$

Atom	x	y	z	U*
U	5000	6945.1(4)	2500	12(1)
K(1)	6837(2)	3458(2)	3469(1)	15(2)
K(2)	6023(2)	8198(2)	5440(1)	15(1)
O(1)	5430(6)	9298(6)	1699(5)	16(3)
O(2)	6039(5)	6785(6)	789(4)	15(2)
O(3)	5651(6)	4738(6)	1611(4)	15(2)
O(4)	5000	11432(8)	2500	17(6)
O(5)	7013(6)	4739(7)	278(5)	17(5)
O(6)	6618(5)	6959(6)	3210(5)	16(2)
C(1)	6272(7)	5373(8)	859(6)	20(1)
C(2)	5000	10068(12)	2500	21(3)

*U is the average of the root-mean-square displacements (10^{-2} Å) and the values in parentheses are standard deviations from the average, $[\Sigma U_i^2 - (\Sigma U_i)^2/3]/2$; where $i = 1, 2$, and 3.

weighting scheme gave uniform average values of $w(|F_o| - |F_c|)^2$ over ranges of $|F_o|$.

On the final cycle of least-squares, the mean and maximum parameter shifts corresponded to 0.10σ and 0.72σ respectively. A final difference Fourier map showed no features of chemical significance. The final atomic parameters are given in Table 1.[1]

Raman and Infrared Spectroscopy

For the Raman spectra, polycrystalline samples were sealed in Pyrex glass melting point capillaries and placed at the focus of the 514.5 nm beam of a Spectra-Physics 165 argon ion laser. Light scattered at 90° was analyzed by a Jarrell-Ash 25-100 1.0 m double Czerny-Turner monochromator, equipped with an S.S.R. model 1105/1120 photon-counting system. Spectral resolutions of 1.5 to 3 cm^{-1} were used. For low temperature studies, the capillaries were placed in a simple double-walled glass cryostat and cooled by a controlled flow of nitrogen gas which passed through a copper coil immersed in liquid nitrogen. Temperatures were measured by a copper–constantan thermocouple in contact with the capillary.

Far infrared spectra were recorded with a Fourier Transform Spectrophotometer (Beckman RIIC 620), equipped with a 6 μm Mylar beam divider, quartz enveloped mercury lamp source, and germanium bolometer detector operating at 4 K. Digitized interferogram signals were transformed by a Data General (Nova 2) mini-computer, with a spectral resolution of 2.5 cm^{-1}. A thin layer of finely ground sample was sandwiched between two 3 mm sheets of polyethylene, and mounted on the cold finger of a simple glass cryostat. Spectra were recorded at ambient (~300 K) and low (~90 K) temperatures. Room temperature spectra were also obtained from Nujol mull samples on a polyethylene substrate.

Mid infrared spectra were recorded on three conventional grating spectrometers, Perkin Elmer 180, Beckman IR 12 and IR 9 using spectral resolutions of 1 to 2.5 cm^{-1}.

A variety of sampling techniques was used: mulls with Nujol or halocarbon grease were deposited on sodium chloride or silver bromide plates; dry powders were placed in contact with the KRS-5 prism of a Wilks model 9 multiple internal reflectance (MIR) attachment; and a thin layer of powder was sandwiched between silver bromide plates for transmission spectra. In the last case, the sample was also mounted in a cryostat and cooled to 83 K.

[1]Tables of structure factors and anisotropic thermal parameters are available from the Depository of Unpublished Data, CISTI, National Research Council of Canada, Ottawa, Ont., Canada K1A 0S2.

Generally, the frequencies of sharp lines from room temperature samples agree to within ±2 cm^{-1} for all spectra. In a few cases the peak frequencies and band shapes of strong broad absorptions depend somewhat on the sampling technique used, and a weighted mean frequency was deduced for assignment purposes. In no case is the uncertainty greater than 5 cm^{-1}.

Results and Discussion

Crystal Structure

The structure consists of K^+ and $[UO_2(CO_3)_3]^{4-}$ ions. Atoms O(4), C(2), and U are located on a crystallographic two-fold axis; the other two carbonates are related to each other by a C_2 operation. Bond lengths and angles are incorporated with the ORTEP drawing, Fig. 1; the atomic numbering follows the scheme used for $(NH_4)_4UO_3(CO_3)_3$ (3) except that the labels for C(1) and C(2) are interchanged such that C(1) and C(2) are on C_1 and C_2 sites respectively.

The carbonates are bidentate with a mean U—O(carbonate) bond length of 2.430(5) Å. The U—O(uranyl) distance is 1.802(6) Å. This value is similar to that found in $(NH_4)_4UO_2(CO_3)_3$ (1.79(1) Å) and appears to be longer than that reported for UO_2CO_3 (1.67(9) Å) (6). Two types of C—O dis-

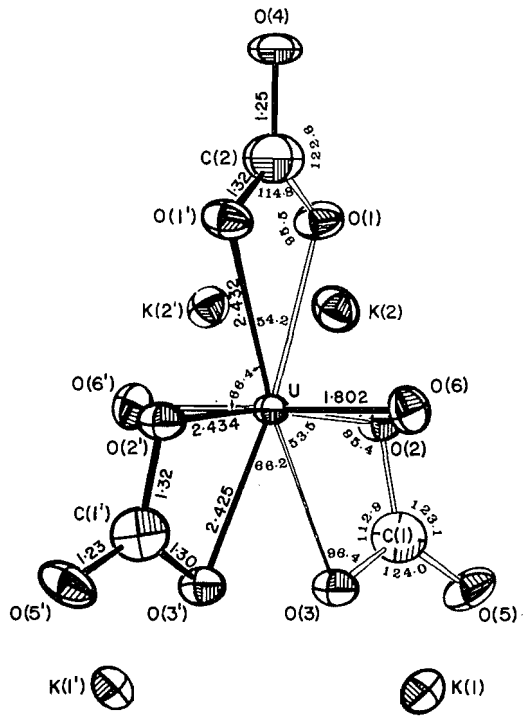


FIG. 1. Bond lengths and angles for the anion $UO_2(CO_3)_3^{4-}$. The anion has a 2-fold axis. Additional angles (deg) are: O(6)UO(1), 89.8; O(6)UO(1'), 89.5; O(6)UO(2), 87.7; O(6)UO(2'), 92.3; O(6)UO(3), 86.8; O(6)UO(3'), 93.9. Standard deviations: σ(U—O), 0.006 Å; σ(C—O), 0.01 Å; σ(OUO), 0.2°; σ(OCO), 0.3°; σ(COU), 0.2°.

TABLE 2. Least-squares planes

(*a*) Equations of the form $lX + mY + nZ = d$ where X, Y, and Z refer to the a, b, and c^* directions

Plane	Atoms	l	m	n	d (Å)
1	U C(1) C(2) O(1) ··· O(5)	0.7761	0.0275	0.6301	5.72
2	U C(1) C(2)	0.8035	0	0.5953	5.71
3	U C(2) O(1) O(4)	0.8790	0	0.4754	5.72
4	C(1) O(2) O(3) O(5)	0.7140	0.1757	0.6778	6.10

(*b*) Interplanar angles

Planes	Angle (deg)
2–3	8.4
2–4	12.3
3–4	18.2

tance are observed: a mean C—O (uncoordinated) equal to 1.24(1) Å and a mean C—O (coordinated) equal to 1.31(1) Å. From the standard deviations, the difference between the two types of OCO angle is significant; when only one oxygen atom is coordinated the mean OCO angle is 123.2(7)°. A smaller mean value, 113.9(1.3)°, is observed when both oxygens are coordinated. There is little difference between equivalent OUO angles: thus O(1)UO(2) and O(3)UO(3′) are equal (66.3(2)°) and O(1)UO(1′) and O(2)UO(3) are equal (53.7(4)°). For angles involving one uranyl oxygen, O(6), the OUO angles are given in the legend for Fig. 1. The two extreme values are 86.8(2)° and 93.9(2)° for O(6)UO(3) and O(6)UO(3′) respectively. The U—O(6) bond is not normal to the C(1)UC(2) plane but is inclined at an angle of 82.1(2)°; however, the C(2)UO(6) angle is 89.6(2)° and the O(6)UO(6′) angle is 179.2(2)°.

In order to determine the planarity of the atoms in the equatorial plane of the anionic species, four least-squares planes were calculated and are presented in Table 2. Giving equal weight to atoms, U, C(1), C(2), O(1), . . . O(5), the equation for plane *1* does not lead to a value of zero for coefficient m. Even though the number of atoms has been restricted to those designated above, the deviation from planarity is not insignificant; the three largest displacements from the plane are: U, 0.13 Å; O(2), −0.21 Å; and O(5), 0.16 Å whereas other atoms deviate less than 0.04 Å. Plane *2* passes through U and the centers of the carbonate ions, C(1) and C(2). The oxygen atoms of the carbonates are displaced from this plane by the following values: O(1), −0.16 Å; O(2), −0.24 Å; O(3), −0.03 Å; O(4), 0.00 Å; O(5), 0.24 Å. The carbonate centered on C(2), plane *3*, is planar as required by symmetry whereas the maximum displacement from the plane of the carbonate situated on the C_1 site, plane *4*, is 0.005 Å. The two planes, *3* and *4*, defined by the carbonates tilt slightly from the plane defined by UC(1)C(2), angles being 8.4 and 12.3°, Table 2. Thus the deviations of atoms in $U(CO_3)_3$ from planes *1* and *2* and the significant orientational differences between the carbonates centered on C(1) and C(2) indicate that the anion, $UO_2(CO_3)_3^{4-}$ does not have D_{3h} or D_3 symmetry. Additional evidence leading to this conclusion has already been given in the previous paragraph.

The packing of K^+ and $UO_2(CO_3)_3^{4-}$ ions, looking from the c^* direction is shown in Fig. 2. Because of the large anion, it is very difficult to define the number of K^+ ions around each anion and vice versa. Since the shortest K···C distance is 3.23 Å, we choose to list all K···O distances less than 3.30 Å in Table 3. The shortest of these is 2.673(7) Å (K(2)···O(5^6)). It is worthwhile noting that there are 8 oxygen atoms within 3.20 Å around K(2) and 9 around K(1). These interionic contacts correspond well with those of $(NH_4)_4UO_2(CO_3)_3$ (3) indicating that hydrogen bonding does not influence the crystal structure of the latter.

Vibrational Spectra

The Raman and infrared spectra are illustrated in Fig. 3 and tabulated in Table 4. An analysis of the vibrational spectra could start from the premise that within the lattice there are potassium cations and $[UO_2(CO_3)_3]^{4-}$ anions. In a first approximation the latter could be considered to have D_{3h} symmetry. From group theoretical considerations the species and activities of the normal modes would be $5A_1'(R) + 3A_2'(ia) + 9E'(R, ir) + A_1''(ia) + 4A_2''(ir) + 4E''(R)$. From the crystal structure it is clear that the anionic species departs significantly from D_{3h} and has in fact been reduced to C_2 symmetry. For this case 39 modes with frequencies coincident in

Can. J. Chem. Downloaded from www.nrcresearchpress.com by 210.87.254.5 on 09/05/12
For personal use only.

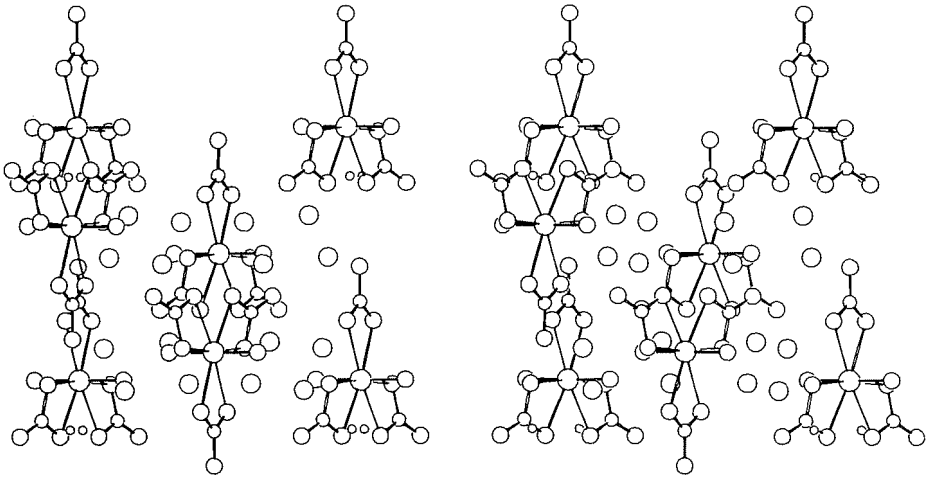


FIG. 2. Packing of ions in $K_4UO_2(CO_3)_3$ viewed from the c^* direction. The a and b axes are horizontal and vertical respectively on the page.

TABLE 3. Interionic distances*

From K(1) to	Distance (Å)	From K(2) to	Distance (Å)
O(1[1])	2.930(7)	O(1[3])	3.064(6)
O(2[1])	2.753(6)	O(2[3])	2.801(6)
O(2[2])	3.030(6)	O(3[2])	3.097(6)
O(3)	2.745(6)	O(4[5])	2.834(2)
O(3[3])	2.802(6)	O(5[6])	2.673(7)
O(4[4])	2.833(6)	O(5[2])	2.899(7)
O(5[2])	2.758(7)	O(6)	3.066(6)
O(6)	3.243(6)	O(6[7])	2.807(6)
O(6[1])	3.033(6)		

*Superscripts refer to equivalent positions: [1], $1.5 - x, y - 0.5, 0.5 - z$; [2], $x, 1 - y, 0.5 + z$; [3], $1 - x, y, 0.5 - z$; [4], $x, y - 1, z$; [5], $1 - x, -y, 1 - z$; [6], $1.5 - x, 0.5 + y, 0.5 - z$; [7], $1.5 - x, 1.5 - y, 1 - z$.

infrared and Raman spectra are predicted. The anion occupies a site of C_2 symmetry so no further complication arises from site splitting. There are two anions per primitive unit cell and the unit cell group is C_{2h}. Because of the centre of symmetry each band will be split by correlation field coupling into a Raman active component (A_g or B_g) and a noncoincident infrared active component (A_u or B_u).

Although the spectra are rich, the number of predicted lines was not observed and the complexity precludes a complete assignment. Instead a simpler approach has been taken. The primitive cell contains two approximately linear ($D_{\infty h}$) UO_2^{2+} cations on C_2 sites, 2 distorted (from D_{3h} to C_{2v}) CO_3^{2-} ions on C_2 sites, 4 distorted (from D_{3h} to approximately C_{2v}) CO_3^{2-} ions on C_1 sites, and $8K^+$ ions on C_1 sites. The vibrations of the polyatomic species can be assigned by analogy to similar groupings in other crystals or solutions and the crystal field splittings can be considered as perturbations.

For the uranyl ion (7) the symmetric UO_2^{2+} stretching vibration clearly occurs as a very strong sharp Raman band at 806 cm^{-1}. The infrared counterpart, forbidden under $D_{\infty h}$, is probably too weak to detect; the weak infrared bands in the 840–860 cm^{-1} region probably have a frequency too high to be considered to arise from correlation field coupling. The low value of the symmetric stretch suggests strong binding of carbonate to uranium. In aqueous perchlorate solution the band occurs at 872 cm^{-1}; replacement of water molecules by ligands such as nitrate and chloride lowers the frequency significantly (8). On the other hand for solid UO_2CO_3, we have observed a higher Raman frequency, equal to 884 cm^{-1}, consistent with a reported shorter U—O bond length (6).

The antisymmetric stretching vibration of UO_2^{2+} is clearly the intense infrared band at 882 cm^{-1}; there is no detectable Raman intensity and thus $D_{\infty h}$ selection rules hold. These two modes can be considered pure, involving little or no mixing (9). On the other hand the v_2 deformation mode, nominally expected in the 200 cm^{-1} region, involves changes in the oxygen–uranium–carbonate angles and thus is strongly coupled with low frequency external modes of the carbonate ions (9). No single frequency can be assigned and discussion is left until the lattice modes are considered.

The carbonate ions on the C_2 sites (designated C(2) after the carbon atom numbering) have C_{2v} symmetry and will vibrate largely independently of each other because of the orientations and distances involved. The carbonate ions on C_1 sites (designated C(1)) have C_1 symmetry (slightly distorted from C_{2v}). The two of these associated with a given uranyl ion will couple strongly and thus give rise to twice as many modes as C(2). For example,

Can. J. Chem. Downloaded from www.nrcresearchpress.com by 210.87.254.5 on 09/05/12
For personal use only.

Can. J. Chem. Downloaded from www.nrcresearchpress.com by 210.87.254.5 on 09/05/12
For personal use only.

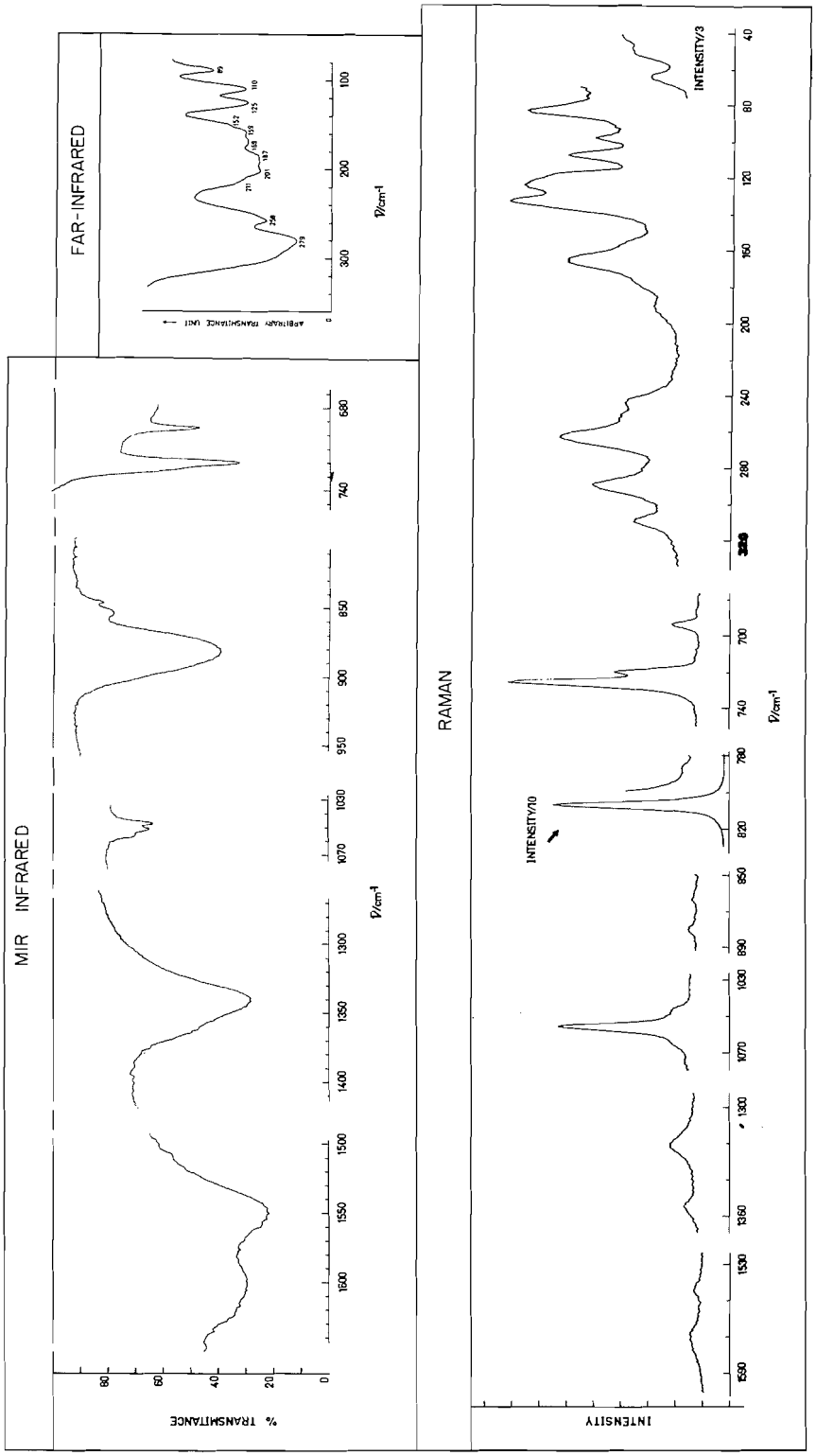


FIG. 3. Raman, multiple internal reflectance (MIR) infrared, and Fourier transform (FT) far-ir spectra of $K_4UO_2(CO_3)_3$.

TABLE 4. Raman and infrared frequencies (cm^{-1}) and assignments of $K_4UO_2(CO_3)_3$*

Raman				Infrared						Assignments
140 K		300 K		90 K		300 K		MIR		
51	w	48	w							Translations (including K)
59	vw									
68	vw	63	m							
75	w, sh	74	w, sh							
84	m	82	m							
92	vvw	91	vvw	92	m, sp	89	m, sp			
99	w	96	w							
109	m	106	m	112	s, sp	110	s, sp			UO_2^{2+} librations
		119	sh	118	sh					
123	sh									
127	m, sp	123	m, br							
135	s	132	m	130	s, sp	125	s, sp			
157	w, sh	154	sh	157	sh	152	sh			CO_3^{2-} librations
166, 170	db, m	165	m	164	s, sp	159	s, br			
				176	s, sp	169	s, br			
182	w, sp	176	sh	188	w, sh					
196	w	191	w	197	s, sp	187	s, br			
				210	s, sp	201	s, br			
				220	sh	211	sh			
				233	w ?					
244	w	241	m							UO_2^{2+} deformations
253, 259	sh, db	249, 251	w, db							
				255	sh	251	sh			
265	s, sp	262	s, sp	264	m, sp	258	m			
292	m, sp	288	m, sp	285	vs, br	279	vs, br			
				300	sh	297	sh			
311	m, sp	307	m, sp							
696	w, sp	693	w	695	m, sp	694	m, sp	694	m, sp	CO_3^{2-} deformations
721	w, sp	719	w			719	s, sp	720	s, sp	
728	m, sp	725	m, sp	724	s, sp			724	sh	
		785	vw							
809	vs, sp	806	vs, sp							UO_2^{2+} stretch
				841	vw					CO_3^{2-} out-of-plane C(1) deformations C(2)
		863	vw	849	vw	847	w, sp	847	sh	
		879	vw	858	w	855	w, sp	855	sh	
				893	s, br	882	s, br	882	s, br	UO_2^{2+} antisymmetric stretch
1046	w	1046	w, sh	1046	w, sh	1045	m, sp	1046.5	m	CO_3^{2-} stretch C(2)
				1052	m	1049	m, sp	1050.5	m	CO_3^{2-} stretch C(1)
1057	m, sp	1055	m	1055	sh	1054	sh	1055	m	
		1065	w, sh							
1323	w	1320	w			1338	m, br	1340	m, br	CO_3^{2-} antisymmetric stretching region
1356	vw	1354	vw	1354†	s, br	1358	sh	1360	sh	
				1517	vw ?			1509	w, sh	
				1538	vw ?					
1545	vw	1543	vw	1561	m, br	1550	m, br	1550	s, br	
1573	w	1569	w	1608	m, br	1600	m, br	1600	m, br	
				1630	sh	1620	sh			Overtones
						1674	w, sh			
				1715	vw	1710	vw			

*w, weak; m, medium; s, strong; v, very; sh, shoulder; sp, sharp; br, broad; db, doublet.
†Possible doublet.

Can. J. Chem. Downloaded from www.nrcresearchpress.com by 210.87.254.5 on 09/05/12
For personal use only.

Can. J. Chem. Downloaded from www.nrcresearchpress.com by 210.87.254.5 on 09/05/12
For personal use only.

considering the symmetric CO_3^{2-} stretching vibration, C(2) will generate A_g(R) and A_u(ir) whereas C(1) will generate A_g(R) + B_g(R) + A_u(ir) + B_u(ir). Assignments for these two classes of carbonate anions can be made starting from a D_{3h} model of an unperturbed carbonate anion. Such an anion would generate the following spectrum: $\nu_1(A_1')$ Raman active, symmetric stretch at about 1090 cm^{-1}; $\nu_2(A_2'')$ infrared-active, out-of-plane deformation at about 860 cm^{-1}; $\nu_3(E')$ and $\nu_4(E')$ both ir- and Raman-active antisymmetric stretching and bending modes at about 1400 and 700 cm^{-1} respectively (10). On changing to C_{2v} or C_1 symmetry the degeneracies of ν_3 and ν_4 are lifted and all modes are both Raman and infrared active and coincident. However, because of the centre of symmetry of the C_{2h} factor group which governs the selection rules for the correlation field coupling, the Raman and infrared bands may be slightly separated. One other guide to the assignments is the population ratio of 1:2 for the carbonates on C_2 and C_1 sites which should be reflected in the relative intensities.

Thus we assign 1046 (R,A_g) and 1045 (ir,A_u) to ν_1 of C(2); 1055 (R,A_g), 1065 (R,B_g), 1050 (ir,A_u), and 1055 (ir,B_u) to ν_1 of C(1). The higher frequency Raman and infrared lines are assigned to antisymmetric stretching modes: 1543 (R,A_g), 1600 (ir,A_u) and 1354 (R,B_g), 1360 (ir,B_u) are assigned to ν_3 of C(2); 1569 (R,A_g), 1550 (ir,A_u) and 1320 (R,B_g), 1340 (ir,B_u) are assigned to ν_3 of C(1). These bands are broad and the coupling of the C(1) ions is not resolved.

The weak Raman intensity of 879 cm^{-1} and the more intense infrared band at 855 cm^{-1} are probably the out-of-plane deformation (ν_2) of C(2) and similarly 863 and 847 cm^{-1} apply to C(1).

For the ν_4 deformation three Raman lines and three infrared lines are observed. Two possibilities occur. If site splitting is significant Raman bands at 719 and 693 with corresponding infrared bands at 724 and 694 can be assigned to C(2), based on the intensities. This indicates a site splitting of 26 cm^{-1} and a correlation field coupling of 2 to 5 cm^{-1}. For C(1) the Raman modes are 725 and 693 cm^{-1}, and the infrared modes are 720 and 694 cm^{-1}. The alternative scheme is to assign the 693, 694 cm^{-1} pair to A_g and A_u of C(2) and the 725, 724 and the 719, 720 pairs to A_g, A_u and B_g, B_u modes of two coupled carbonate anions for which the splitting due to loss of degeneracy of E' is too small to detect. (For distorted nitrates in solution the splitting of ν_4 is frequently not detectable even when ν_3 is split by 50 to 100 cm^{-1} (11).) In view of the 188 and 250 cm^{-1} splits in the ν_3 region the former analysis of ν_4 seems more probable, although the latter cannot be excluded. The frequencies and tentative assignments are summarized in Table 4.

With this approach to the assignments the uranyl–carbonate stretching and deformation modes will be classified as external modes. Analysis reveals that there will be 45 translatory modes, 22 librational modes, and 3 acoustic modes. Of the 22 librational modes, 11 are Raman-active ($5A_g$ and $6B_g$) and 11 are noncoincident infrared-active modes ($5A_u$ and $6B_u$).

The uranyl ion is nonpolar and therefore its librational modes are not expected to give intense infrared absorption; on the other hand the carbonate ions in their distorted form possess a dipole and hence their librations (except those about the dipole axis) will give moderate infrared absorption. All modes are mixed because of the low site symmetry and thus unique assignments are impossible. Furthermore the deformation of UO_2^{2+} (which involves a dipole change and hence appreciable infrared activity) is accompanied by motions of the carbonate ions and that internal mode cannot be uniquely designated (9). However, it is reasonable to attribute the grouping of bands from 240 to 320 cm^{-1} largely to motions involving uranyl deformation, bands from 150 to 240 cm^{-1} to carbonate librations and bands from 100 to 150 cm^{-1} to uranyl librations since the moment of inertia of UO_2^{2+} is larger than that of the carbonates. Translatory modes are expected to occur at low frequencies, some probably below the range of detection, because virtually all atoms including the massive uranium are involved in the motions. The representation of these translatory modes is $11A_g + 13B_g + 10A_u + 11B_u$, but only 7 peaks (6 Raman and 1 infrared) were observed.

Conclusions

The structure and vibrations of solid potassium uranyl carbonate have been studied by X-ray, Raman, and infrared techniques. A group theoretical analysis, based on the observed symmetries of the polyatomic ions (some of which are distorted from their free form), and those of their lattice sites and the monoclinic unit cell, has been applied in an attempt to assign the observed spectroscopic features. However, because of the low symmetry and subsequent mixing between modes, it is possible to categorize only the major features of the complex spectra. Spectroscopic confirmation is obtained for certain structural features such as the rather long U—O bond and the presence of distorted CO_3^{2-} ions on two types of sites.

Acknowledgements

This work was supported by grants from the Natural Sciences and Engineering Research Council of Canada and from a contract with Atomic Energy of Canada Limited, WNRE, Pinawa. The authors express thanks to Dr. R. Lemire for providing the uranyl carbonate and for helpful discussions.

1. D. LANGMUIR. Geochim. Cosmochim. Acta, **42**, 547 (1978).
2. S. Ó. CINNÉIDE, J. P. SCANLAN, and M. J. HYNES. J. Inorg. Nucl. Chem. **37**, 1013 (1975).
3. R. GRAZIANI, G. BOMBIERI, and E. FORSELLINI. J. Chem. Soc. Dalton, 2059 (1972).
4. D. T. CROMER and J. T. WABER. Acta Crystallogr. **18**, 104 (1965).
5. D. T. CROMER. Acta Crystallogr. **18**, 17 (1965).
6. D. T. CROMER and P. E. HARPER. Acta Crystallogr. **8**, 847 (1955).
7. L. H. JONES. Spectrochim. Acta, **10**, 395 (1958).
8. D. E. IRISH and J. P. K. TONG. Unpublished work.
9. YU. YA. KHARITONOV and N. A. KNYAZEVA. Russ. J. Inorg. Chem. **11**, 1458 (1966).
10. M. H. BROOKER and J. B. BATES. J. Chem. Phys. **54**, 4788 (1971).
11. D. E. IRISH and M. H. BROOKER. *In* Advances in infrared and Raman spectroscopy. Vol. 2. *Edited by* R. J. H. Clark and R. E. Hester. Heyden, London. 1976. p. 280.

Can. J. Chem. Downloaded from www.nrcresearchpress.com by 210.87.254.5 on 09/05/12
For personal use only.

Ultraviolet photoelectron spectra of 2-norbornanone, 2,5-norbornanedione, their alkyl derivatives and thio-analogues. An investigation of transannular interactions by photoelectron spectroscopy

DAVID C. FROST AND NICHOLAS P. C. WESTWOOD

Department of Chemistry, 2036 Main Mall, University Campus, Vancouver, B.C., Canada V6T 1Y6

AND

NICK H. WERSTIUK

Department of Chemistry, McMaster University, Hamilton, Ont., Canada L8S 4M1

Received February 4, 1980

DAVID C. FROST, NICHOLAS P. C. WESTWOOD, and NICK H. WERSTIUK. Can. J. Chem. **58**, 1659 (1980).

HeI photoelectron spectra are reported for a series of methyl-substituted monoketones and diketones based on 2-norbornanone. The effect of methyl substitution, and the inductive effect of a second carbonyl group has been studied. The diketones show a small separation between the two ketone moieties due to a through-bond interaction. Replacement with a thiocarbonyl group permits a comparison of the relative C=S and C=O interactions. The relative merits of the semi-empirical HAM/3 and CNDO/2 methods for such molecules are assessed.

DAVID C. FROST, NICHOLAS P. C. WESTWOOD et NICK H. WERSTIUK. Can. J. Chem. **58**, 1659 (1980).

On rapporte les spectres photoélectroniques HeI d'une série de monocétones et de dicétones portant un substituant méthyle et dérivées de la norbornanone-2. On a étudié l'effet du substituant méthyle ainsi que l'effet inductif d'un second groupe carbonyle. Les dicétones montrent une faible séparation entre les deux fonctions cétones par suite d'une interaction à travers la liaison. Le remplacement par un groupe thiocarbonyle permet de comparer les interactions relatives C=S et C=O. On évalue les mérites relatifs des méthodes semi-empiriques de HAM/3 et de CNDO/2 pour ce type de molécules.

[Traduit par le journal]

Introduction

Carbonyl compounds provide a rich fund of information for the photoelectron (PE) spectroscopist (1, 2) since the carbonyl group exhibits a distinctive oxygen non-bonding type orbital which acts as a probe for electronic interactions within a molecule. We use the term "non-bonding" loosely here, since it is well established that considerable delocalization into the adjacent σ framework can occur.

A number of carbonyls and dicarbonyls have been investigated by ultraviolet photoelectron spectroscopy (UPS) (1, 2), although few γ-dicarbonyls have been studied except for benzoquinone and its substituted derivatives (3–6). For most dicarbonyl compounds, interest arises in the mechanism of the interaction between the two carbonyl groups, and whether it occurs through-space or through-bond (2, 3, 7–9). A typical case, particularly germane to the compounds studied in this work, is 1,4-cyclohexanedione which can exist in three conformations: boat (C_{2v}), chair (C_{2h}), and skew (or twist) (D_2). The twist configuration appears to be preferred (10), with a splitting of 0.15–0.2 eV between the n_- and n_+ oxygen lone pair combinations (2, 3) (see refs. 2 and 3 for the notation employed here).

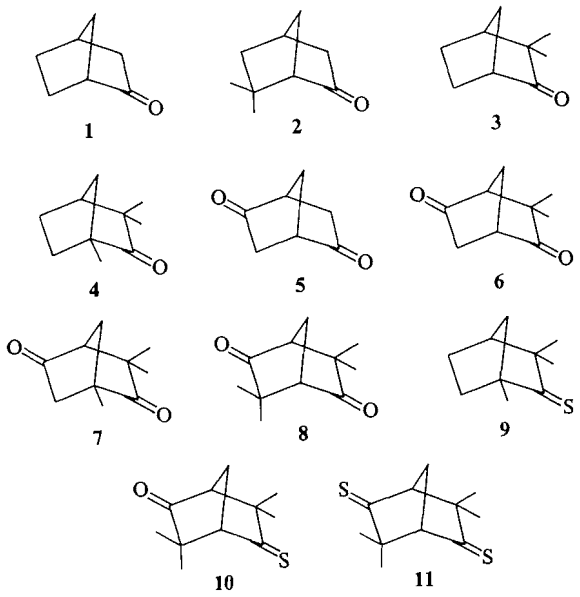
Our interest in the bonding in the diones, ketothione, and dithione studied here stems from our systematic study of the base-catalyzed hydrogen isotope exchange of the substrates (11–13). In addition, the parent unsubstituted compound, norbornane, has been previously investigated by UPS and shows broad bands above 10 eV (14). The ketones and diketones investigated here are expected to have non-bonding orbitals primarily (although not entirely) localized on the C=O group, thereby showing a distinct, relatively sharp, ionization potential (IP) at less than 10 eV, well separated from those IP's belonging to the σ framework. We shall see later that interaction with the σ framework does occur to some extent.

The monosubstituted ketones in question are: 2-norbornanone (**1**); 6,6-dimethyl-2-norbornanone (**2**); 3,3-dimethyl-2-norbornanone (**3**), and 1,3,3-trimethyl-2-norbornanone (**4**). The diones are 2,5-norbornanedione (**5**); 3,3-dimethyl-2,5-norbornanedione (**6**); 1,3,3-trimethyl-2,5-norbornanedione (**7**), and 3,3,6,6,-tetramethyl-2,5-norbornanedione (**8**). Also studied were 1,3,3-trimethyl-2-norbornanethione (thiofenchone) (**9**); 3,3,6,6-tetramethyl-5-oxo-2-norbornanethione (**10**), and 3,3,6,6-tetramethyl-2,5-norbornanedithione (**11**). The series of monosubstituted ketones (**1–4**) thus provide an indication of the effect of successive alkylation upon the carbonyl lone pair ionization

0008-4042/80/161659-07$01.00/0

©1980 National Research Council of Canada/Conseil national de recherches du Canada

Can. J. Chem. Downloaded from www.nrcresearchpress.com by 210.87.254.42 on 09/05/12
For personal use only.



energy. Addition of a second carbonyl group (**5–8**) provides a measure of the inductive effect of such a γ-carbonyl group, and the extent of interaction between the two groups. Finally, the thio-analogues (**9–11**) indicate if replacement of oxygen by sulphur alters the extent of interaction. Furthermore, the C=S π type orbital is no longer overlapped by the σ type orbitals (as in the case of the C=O compounds) and therefore provides additional information upon the interaction of the two C=S groups.

Experimental

Monoketones **2** and **3** were prepared via published procedures (15, 16), as were diones **5** and **7** (17, 18). **6** was prepared by oxidizing campheniyl acetate (19), hydrolyzing the ketoacetate, and oxidizing the ketol. Dione **8** was prepared by methylating **5** (11). The thio analogues **9**, **10**, and **11** were synthesized by heating **4** and **8** at reflux temperature in a P_2S_5 saturated solution of xylene. Each compound was carefully purified by preparative glpc before recording the photoelectron spectrum.

HeI photoelectron spectra were obtained on a PE spectrometer as previously described (20). Spectra were calibrated using the known IP's of CH_3I, N_2, and Ar. Although the resolution in these experiments is 35–40 meV, there is some vibrational structure unresolved on several of the first IP's. All quoted IP's are vertical IP's (band maxima).

Semiempirical calculations were performed with the standard CNDO/2 method (21), and the more recent HAM/3 method (22) which we have found to perform with good reliability in the prediction of IP's of organic molecules. Since the HAM/3 method uses a transition state concept and avoids problems associated with Koopmans' theorem (23), we prefer this method. Thus IP's for all ketones and diketones have been calculated using this procedure. HAM/3 is only parameterized for first row elements, and so calculations on the thio-compounds were performed using CNDO/2. Identical CNDO/2 calculations were also performed on all the ketones and diketones so that a direct comparison with the HAM/3 method could be made.

Results and Discussion

The HeI photoelectron spectra of compounds **1–11** are shown in Figs. 1 and 2. Values for the first few distinct IP's, and σ_{onset} are given in Tables 1–3, together with any associated vibrational structure and the full width at half maximum (fwhm) of the first band. Also included are the IP's calculated using the HAM/3 and CNDO/2 semiempirical methods. The HAM/3 results can be directly compared, however the CNDO/2 results (assuming the validity of Koopmans' theorem (23)) have been uniformly shifted by 3 eV to concur with the HAM/3 results and the experimental values.

Monoketones

IP's for 2-norbornanone (**1**) have been reported previously (24, 25), but no spectrum provided. This is shown in Fig. 1(*a*). There are some discrepancies in the values for the first vertical IP (9.17 eV (this work), 9.14 eV (25), and 8.94 eV (24)), probably due to difficulties in locating the adiabatic and vertical IP's (approximately the same intensity). This molecule provides the starting point for the methyl-substituted derivatives (**2–4**).

The interesting feature of these molecules is the absolute position of the first IP, and its corresponding fwhm, since these values provide a measure of the interaction of the methyl substituent with the carbonyl non-bonding orbital. Thus, this IP, as usual, shifts to lower bonding energy with increasing methyl substitution (particularly if methylation occurs adjacent to the C=O group), it becomes broader losing its sharp, non-bonding envelope and in some cases shows partially resolvable vibrational structure, typically between 750 and 1250 cm^{-1} (Table 1). These features are indicative of appreciable delocalization of the non-bonding orbital, and are followed by a decrease in the σ IP upon methyl substitution.

To assess these effects, we have performed semiempirical HAM/3 calculations (22) for norbornane (see ref. 14 for PE spectrum) and the monoketones **1–4**. The first two IP's obtained by the HAM/3 and CNDO/2 calculations are listed in Table 1. Geometries were based on that of norbornane (26, 27), with a C=O bond length of 1.24 Å and C—C(H-3) bond lengths of 1.53 Å. The C=O bond was constrained in the plane of C-1, C-2, and C-3, with the overall molecular framework kept symmetrical upon methyl substitution. This standard structure gave good agreement with the experimental IP's of all the monoketones using the HAM/3 method and no empirical shifting was necessary (compare CNDO/2). Therefore these geometries were used as a basis for the structures of the diketones.

Can. J. Chem. Downloaded from www.nrcresearchpress.com by 210.87.254.42 on 09/05/12
For personal use only.

Can. J. Chem. Downloaded from www.nrcresearchpress.com by 210.87.254.42 on 09/05/12
For personal use only.

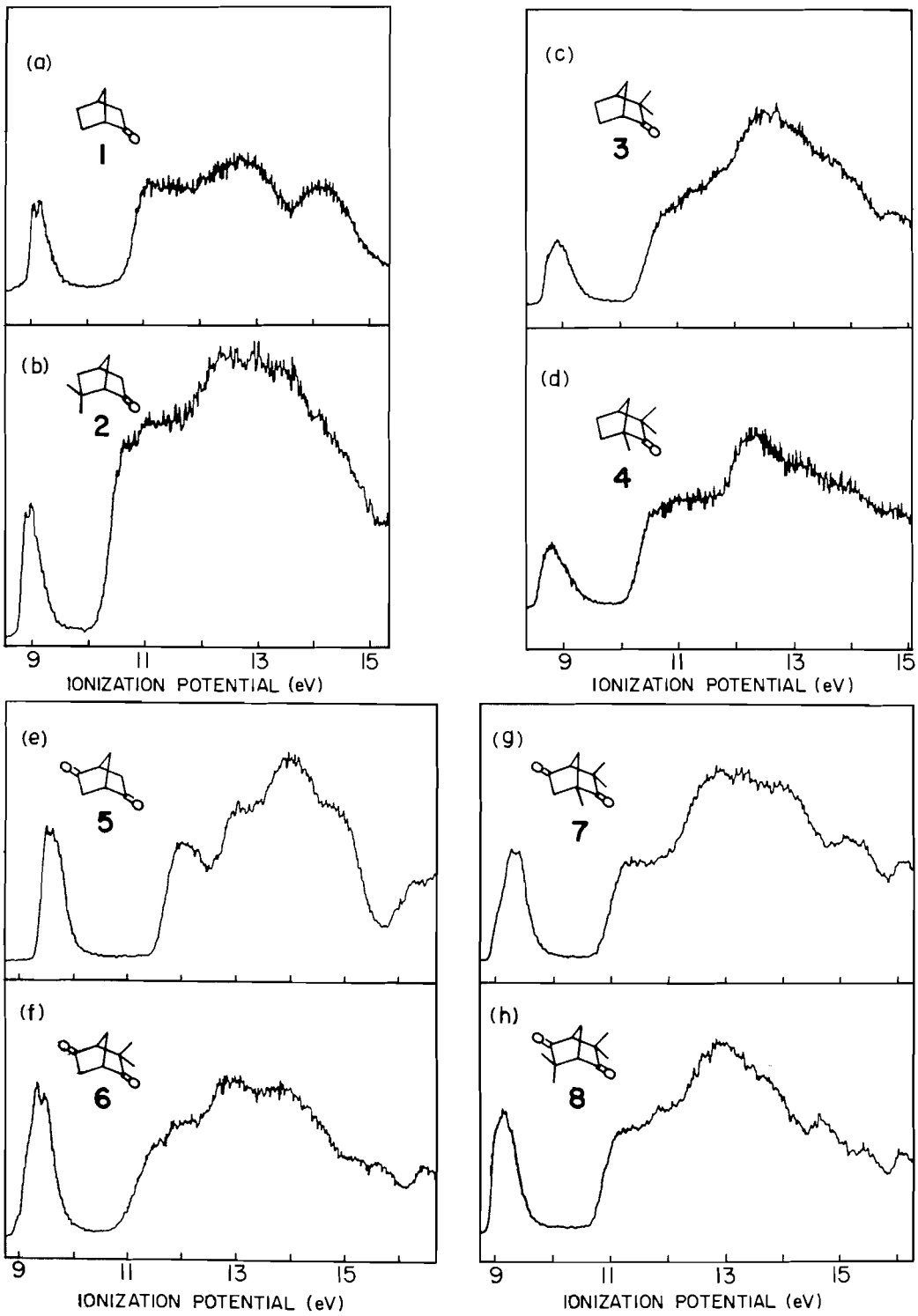


FIG. 1. (*a*), HeI photoelectron spectrum of **1**; (*b*), **2**; (*c*), **3**; (*d*), **4**; (*e*), **5**; (*f*), **6**; (*g*), **7**; and (*h*), **8**.

Can. J. Chem. Downloaded from www.nrcresearchpress.com by 210.87.254.42 on 09/05/12
For personal use only.

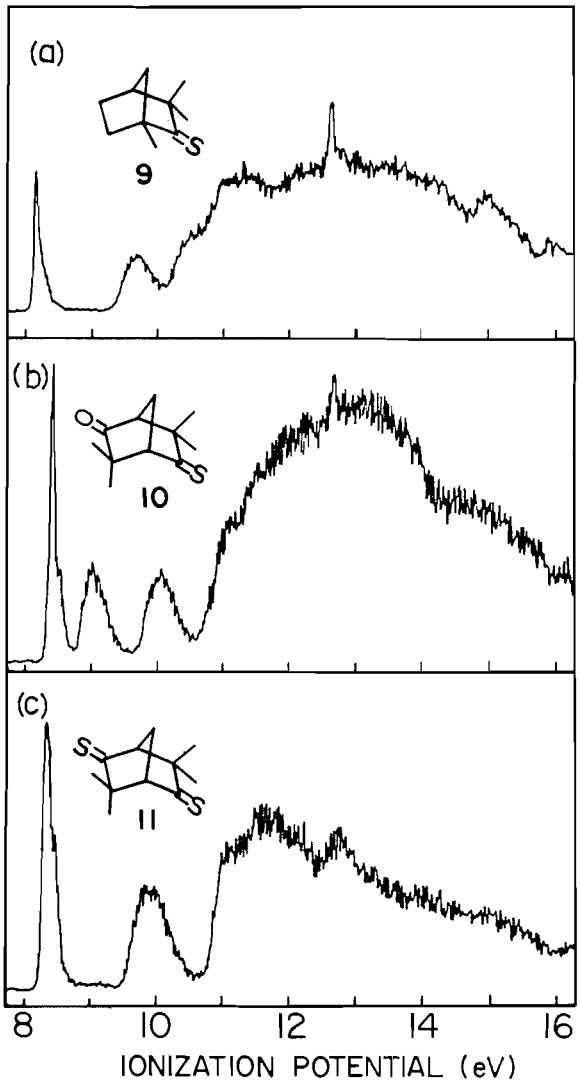


FIG. 2. (*a*), HeI photoelectron spectrum of **9**; (*b*), **10**; and (*c*), **11**.

The second IP in **1** (maximum 11.1 eV) is mainly due to a C 2*p* orbital localized on C-7. This orbital corresponds to the highest occupied molecular orbital (HOMO) of norbornane (experimental IP, 10.7 eV (14), calculated IP, 10.64 eV (HAM/3)) inductively shifted to higher binding energy. The carbonyl π type orbital in **1** is predicted at 12.3 eV, and so is masked by the σ structure. The corresponding HAM/3 calculations for **2**, **3**, and **4** parallel the observed shift of the first IP to lower binding energy, and indicate a decreased oxygen 2*p* contribution confirming the further delocalization of the non-bonding orbital. The CNDO/2 calculations reproduce this shift and delocalization trend.

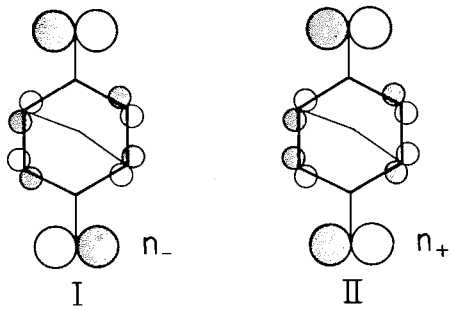
The first IP of **1** (9.17 eV) is 0.11 eV less than that of the non-bridged analogue, cyclopentanone (ca. 9.28 eV) (24, 28–30), but of a similar magnitude to that of cyclohexanone (ca. 9.15 eV) (29, 30). Bridging cyclohexanone, to give **1**, therefore has little effect upon the first IP and indeed, similar vibrational structure obtains for both cyclohexanone and **1**. However, the σ structure in cyclohexanone (vertical, 11.4 eV) is shifted to ca. 11.1 eV upon bridging. This is not surprising since the calculations indicate this orbital in **1** to be primarily C 2*p* in character and localized on C-7.

Diketones

Two main effects are observed when a second carbonyl group is introduced into **1** at C-5 giving the diketone **5**. Firstly, the vertical IP increases to 9.55 eV (average of n_- and n_+), and secondly, the two carbonyl groups interact to give a small but measurable splitting.

The observed stabilization of 0.38 eV arises from the inductive effect of introducing a second carbonyl group into the ring system. For the cyclohexanone, 1,4-cyclohexanedione molecules, Houk *et al.* (31) determine a value of 0.59 eV as the inductive shift of a second carbonyl group. This shift is thus larger than that found here for the bridged compounds **1** and **5**, indicative of a mediating influence by the bridge methylene group.

The observed splitting between the two oxygen non-bonding orbitals of **5** (0.16 eV) is due to a through-bond interaction (7, 8), i.e. a mixing of the n_0 orbitals with the skeletal σ orbitals. The two HOMO's can be represented by I and II, which show the phasing of the oxygen 2*p* orbitals and the σ ring orbitals as the molecule is viewed from above C-7.



The experimental magnitude of this splitting is partly confused by the presence of some partly resolved vibrational structure, but to all intents and purposes is identical to the first band of 1,4-cyclohexanedione. In both cases the coupling of the ring *p* orbitals with the carbonyl groups is poor, resulting in a small n_-/n_+ separation. However, the similarity of the two bands indicates that 1,4-cyclo-

TABLE 1. Experimental and calculated IP's of the monoketones

Compound	Experimental: First IP (eV)[a] structure (cm^{-1})	Fwhm (eV)[b]	σ_{onset} (eV)[c]	σ_{max} (eV)[c]	Calculated: HAM/3 IP's[d] First	HAM/3 IP's[d] Second	CNDO/2 IP's[d] First	CNDO/2 IP's[d] Second
1	9.17 (1000 ± 60, 510 ± 60)	0.36	10.5	11.1	9.13 n	11.04 σ	9.59 n	11.48 σ
2	9.00 (780 ± 60)[e]	0.37	10.2	10.7	8.98	10.99	9.25	11.05
3	8.89 (840 ± 60)[e]	0.49	10.1	10.8	8.99	10.87	8.94	10.80
4	8.80 (1225 ± 80)	0.52	10.1	10.6	8.97	10.85	8.60	10.62

[a]Vertical IP, ±0.02 eV.
[b]Full width at half maximum.
[c]±0.1 eV.
[d]HAM/3 not scaled, CNDO/2 uniformly shifted by 3 eV.
[e]Plus other unresolved structure.

TABLE 2. Experimental and calculated IP's of the diketones

Compound	Experimental: First and second IP's (eV)[a] (structure, cm^{-1})	σ_{onset} (eV)[b]	σ_{max} (eV)[b]	Calculated: HAM/3 IP's[c] First	HAM/3 IP's[c] Second	HAM/3 IP's[c] Third	CNDO/2[c] IP's First	CNDO/2[c] IP's Second	CNDO/2[c] IP's Third
5	9.47 9.63	11.5	11.9	9.40 n_-	9.46 n_+	11.52 σ	9.72 n_-	10.22 n_+	12.12 σ
6	9.30 9.45	10.7	11.5	9.23	9.29	11.36	9.14	9.79	11.51
7	9.24 9.39	10.8	11.4	9.16	9.26	11.33	8.82	9.71	11.35
8	9.00 9.08	10.6	11.2	9.15	9.18	11.26	8.80	9.32	11.15

[a]Vertical IP, ±0.02 eV. Some IP's show partially resolved structure.
[b]±0.1 eV.
[c]HAM/3 not scaled, CNDO/2 uniformly shifted by 3 eV.

hexanedione does exist predominately in one conformation (probably twist), since **5** is effectively locked into a similar configuration. Although the separation is small, compared, for example, to the planar *p*-benzoquinone and methyl derivatives (Δn = 0.3–0.5 eV), we prefer the assignment IP(n_-) < IP(n_+), since in II (n_+), the σ ring orbital has fewer nodes, and is subsequently more stabilized than in I (n_-). This also follows the generalization (2, 32) that the HOMO ordering should be IP(n_-) < IP(n_+) for any through-bond interaction over an odd number of intervening bonds when the carbonyl groups are coaxial.

The calculated values for the first two IP's of diones **5–8** are listed in Table 2. The ordering is confirmed by both the HAM/3 and the (shifted) CNDO/2 calculations with the splitting predicted by HAM/3 in excellent agreement with the experimental diketone n_-/n_+ separation. The CNDO/2 splitting is larger. Both the idealized geometry used here, and the X-ray geometry (33) give O---O distances of 5.21 and 4.92 Å respectively, indicating a negligible through-space overlap. The HAM/3 calculations predict the C=O π type orbitals at 12.0 and 12.5 eV, thus lying under the σ type orbitals and not observed on the spectra.

Substitution of the simple diketone **5** with methyl groups gives the unsymmetrical diketones **6** and **7**, and correspondingly, the Franck–Condon envelopes and fwhm's of the first bands reflect this asymmetry (Fig. 1 (*f*) and (*g*)). All IP's are decreased (Table 2) and the separation between n_- and n_+ is slightly increased since these two semilocalized orbitals are non-degenerate in zeroth order. HAM/3 gives reasonable values for the splitting in **6** and **7**, whereas CNDO/2 shows a wider margin between the n_- and n_+ orbitals.

The symmetric diketone **8** is substituted with four methyl groups, and so relative to **5** the mean of the n_-/n_+ IP's has decreased by 0.51 eV. This shift

Can. J. Chem. Downloaded from www.nrcresearchpress.com by 210.87.254.42 on 09/05/12
For personal use only.

Can. J. Chem. Downloaded from www.nrcresearchpress.com by 210.87.254.42 on 09/05/12
For personal use only.

TABLE 3. Experimental and calculated IP's of the thiones

Compound	IP (eV)[a]	Structure (cm^{-1})	CNDO/2[b]
9	8.13	1050 ± 60	8.01
	9.69		8.69
	(10.1 σ_{onset})		
	10.5 σ_{max}		10.32
10	8.44	$890 + 60$	8.23
	9.05	910 ± 80	8.69
	10.06		9.39
	(10.6 σ_{onset})		
	11.2 σ_{max}		10.55
11	8.35	$\left[\begin{matrix}370 \pm 60 \\ 1160 \pm 60\end{matrix}\right]$[c]	8.16
	8.35		8.32
	9.87		8.70
	10.04		9.07
	(10.8 σ_{onset})		
	11.2 σ_{max}		10.57

[a]First vertical IP, ±0.02 eV; higher IP's and σ structure ±0.05 and ±0.1 eV, respectively.
[b]Scaled by 3 eV.
[c]See text.

is parallelled by the calculations (Table 2), which also predict a small decrease in the splitting.

Thioketones

IP's for thiofenchone, **9**, have been reported before (34), with the well separated sulphur non-bonding and sulphur π type orbitals measured at 8.1 and 9.6 eV, respectively. The spectrum is shown in Fig. 2(*a*) and we agree with the numerical values (Table 3) and with the vibrational structure ($1050 \pm 60\ cm^{-1}$) observed on the first band. The CNDO/2 calculations (shifted by the usual 3 eV) confirm this ordering although the n and π orbitals are placed closer together than the experimental values.

The ketothione **10**, with one oxygen and one sulphur atom, shows three bands below 10.5 eV. The first sharp band at 8.44 eV can easily be assigned to the sulphur non-bonding orbital (structure $= 890 \pm 60\ cm^{-1}$), with the IP inductively increased by the oxygen relative to the value in thiofenchone (**9**). The next IP at 9.05 eV shows some structure ($910 \pm 80\ cm^{-1}$), and the third IP at 10.06 eV is unresolved. From the separation between the S non-bonding and C=S π orbital in thiofenchone, and the position of the O non-bonding orbital in **8**, we assign the ordering of these three bands in **10** as S non-bonding, O non-bonding, and C=S π. The CNDO/2 calculations show extensive mixing between the second and third orbitals, albeit weighting the second orbital with more C=S π character.

If the remaining oxygen atom in **10** is replaced with a sulphur atom, we obtain the tetramethyldithione **11** which gives only two IP's below 10.5 eV. These are relatively more intense (with respect to the σ structure) than the corresponding two bands of thiofenchone (**9**). Each band may therefore be assigned to two orbitals the first with a maximum at 8.35 eV, to both the n_- and n_+ sulphur non-bonding orbitals. A precise value for the separation cannot be measured but the fwhm is much larger than the corresponding band in **10** (or even **9**). Some structure can be measured, viz. 370 ± 60 and $1160 \pm 60\ cm^{-1}$, but it is impossible to tell if part of this may result from the n_-/n_+ splitting. The second, broader band is centred at 9.95 eV and in this case shows a resolvable separation (0.17 eV) into two peaks. These correspond to the two C=S π orbitals, which in the oxygen analogue were masked by the σ structure. The increased separation of these two π orbitals compared to the n orbitals is followed by the CNDO/2 calculations (Table 3), viz. calculated $\Delta n_-/n_+ = 0.16$ eV, $\Delta \pi_-/\pi_+ = 0.37$ eV. It thus appears that the separation of the π orbitals in such thiocarbonyl compounds provides a more sensitive test of the interaction of these functional groups compared to the separation of the n orbitals. This is particularly true for the S non-bonding orbitals (which show no measurable splitting) since the through-bond interaction here will be quite small, as the S 3*p* orbitals are energetically far removed from the σ type orbitals and therefore do not overlap as efficiently. In fact the sharp nature of these S non-bonding orbitals illustrates that they are indeed more non-bonding than their oxygen counterparts.

Summary

UPS has been used to determine the carbonyl non-bonding energies in a series of 2-norbornanones and 2,5-norbornanediones. A reduction in binding energy with increasing methylation is observed, whereas introduction of a second carbonyl group inductively increases the IP. Additionally, there is a small (< 0.16 eV) n_-/n_+ separation in the diketones, arising from a through-bond interaction. Replacement of O by S indicates a reduced n_-/n_+ interaction, but permits observation of a larger π_-/π_+ separation. These results are supported by semiempirical (HAM/3 and CNDO/2) calculations; the former may be used without any scaling.

Acknowledgements

N.H.W. thanks Professors D. C. Frost, C. A. McDowell, and their colleagues for the hospitality afforded during the course of a sabbatical leave at the University of British Columbia. We thank C. A. McDowell for his interest in this work, E. Lindholm (Stockholm) for making the HAM/3 programme available to us, and D. P. Chong for

adapting it to our computer. This work was supported by grants from the Natural Sciences and Engineering Research Council of Canada.

1. J. L. MEEKS, H. J. MARIA, P. BRINT, and S. P. MCGLYNN. Chem. Rev. **75**, 603 (1975).
2. D. DOUGHERTY, P. BRINT, and S. P. MCGLYNN. J. Am. Chem. Soc. **100**, 5597 (1978).
3. D. O. COWAN, R. GLEITER, J. A. HASHMALL, E. HEILBRONNER and V. HORNUNG. Angew. Chem. Int. Ed. **10**, 401 (1971).
4. T. KOBAYASHI. J. Electron Spectrosc. Relat. Phenom. **7**, 349 (1975).
5. G. LAUER, W. SCHÄFER, and A. SCHWEIG. Chem. Phys. Lett. **33**, 312 (1975).
6. D. DOUGHERTY and S. P. MCGLYNN. J. Am. Chem. Soc. **99**, 3234 (1977).
7. R. HOFFMANN. Acc. Chem. Res. **4**, 1 (1971).
8. W. HUG, J. KUHN, K. J. SEIBOLD, H. LABHART, and G. WAGNIÈRE. Helv. Chim. Acta, **54**, 1451 (1971).
9. R. GLEITER. Angew. Chem. Int. Ed. **13**, 696 (1974).
10. P. DOWD, T. DYKE, and W. KLEMPERER. J. Am. Chem. Soc. **92**, 6327 (1970).
11. N. H. WERSTIUK. Can. J. Chem. **53**, 2211 (1975).
12. N. H. WERSTIUK, R. TAILLEFER, and S. BANERJEE. Can. J. Chem. **56**, 1140 (1978).
13. N. H. WERSTIUK, R. TAILLEFER, and S. BANERJEE. Can. J. Chem. **56**, 1148 (1978).
14. P. BISCHOF, J. A. HASHMALL, E. HEILBRONNER, and V. HORNUNG. Helv. Chim. Acta, **52**, 1745 (1969).
15. M. DONALDSON. Doctoral Dissertation, Princeton, N.J. 1968.
16. P. S. BAILEY. Chem. Ber. **88**, 795 (1955).
17. J. MEINWALD, J. K. CRANDALL, and P. G. GASSMAN. Tetrahedron, **18**, 815 (1962).
18. D. E. BAYS, G. W. CANNON, and R. C. COOKSON. J. Chem. Soc. B, 885 (1966).
19. J. MEINWALD, P. G. GASSMAN, and J. G. HURST. J. Am. Chem. Soc. **84**, 3722 (1962).
20. D. C. FROST, S. T. LEE, C. A. MCDOWELL, and N. P. C. WESTWOOD. J. Electron Spectrosc. Relat. Phenom. **12**, 95 (1977).
21. J. A. POPLE and D. L. BEVERIDGE. Approximate molecular orbital theory. McGraw Hill, New York. 1970.
22. L. ASBRINK, C. FRIDH, and E. LINDHOLM. Chem. Phys. Lett. **52**, 69 (1977).
23. T. KOOPMANS. Physica, **1**, 104 (1933).
24. D. CHADWICK, D. C. FROST, and L. WEILER. J. Am. Chem. Soc. **93**, 4962 (1971).
25. G. HENTRICH, E. GUNKEL, and M. KLESSINGER. J. Mol. Struct. **21**, 231 (1974).
26. J. F. CHIANG, C. F. WILCOX, and S. H. BAUER. J. Am. Chem. Soc. **90**, 3149 (1968).
27. A. YOKOZEKU and K. KUCHITSU. Bull. Chem. Soc. Jpn. **44**, 2356 (1971).
28. D. CHADWICK, D. C. FROST, and L. WEILER. J. Am. Chem. Soc. **93**, 4320 (1971).
29. D. CHADWICK, D. C. FROST, and L. WEILER. Tetrahedron Lett. **47**, 4543 (1971).
30. B. J. COCKSEY, J. H. D. ELAND, and C. J. DANBY. J. Chem. Soc. B, 790 (1971).
31. K. N. HOUK, L. P. DAVIS, G. R. NEWKOME, R. E. DUKE, and R. V. NAUMAN. J. Am. Chem. Soc. **95**, 8364 (1973).
32. R. HOFFMANN, A. IMAMURA, and W. J. HEHRE. J. Am. Chem. Soc. **90**, 1499 (1968).
33. R. FAGGIANI, N. H. WERSTIUK, and S. Y. YEROUSHALMI. Acta Crystallogr. In press.
34. C. GUIMON, D. GONBEAU, G. PFISTER-GUILLOUZO, L. ÅSBRINK, and J. SANDSTRÖM. J. Electron Spectrosc. Relat. Phenom. **4**, 49 (1974).

Can. J. Chem. Downloaded from www.nrcresearchpress.com by 210.87.254.42 on 09/05/12
For personal use only.

The formation and reactions of aromatic dimer cations in a high pressure photoionization source

JOHN A. STONE AND MARGARET S. LIN

Department of Chemistry, Queen's University, Kingston, Ont., Canada K7L 3N6

Received December 31, 1979

JOHN A. STONE and MARGARET S. LIN. Can. J. Chem. **58**, 1666 (1980).

Aromatic dimer cations (M_2^+) have been generated for a series of aromatic compounds in a high pressure photoionization source. Relative third order rate constants for formation of M_2^+ have been obtained for benzene (1.0), benzene-d_6 (2.7), toluene (0.8), *o*-xylene (1.5), *p*-xylene (0.7), fluorobenzene (0.3), *m*-fluorotoluene (0.5), *m*-chlorotoluene (0.7), *p*-chlorotoluene (0.5), and *o*-methoxytoluene (0.4). These values are consistent with and supplement previous data for such systems. Reagent ion monitoring has been used to determine the relative rates of reaction of both M_2^+ and the monomer ions, M^+, with a series of (mainly) aromatic compounds (X). Reaction of $C_6H_6^+$ is by charge transfer to compounds of lower ionization potential than C_6H_6. $(C_6H_6)_2^+$ reacts only by charge transfer, if the ionization potential of X is more than 0.5 eV lower than that of benzene. When the difference is smaller, mixed dimer cations are observed which are probably formed in a switching reaction $(C_6H_6)_2^+ + X \rightarrow (C_6H_6 \cdot X)^+ + C_6H_6$.

JOHN A. STONE et MARGARET S. LIN. Can. J. Chem. **58**, 1666 (1980).

Dans une source d'ionisation photochimique à haute pression, on a produit les cations aromatiques dimères (M_2^+) d'une série de composés aromatiques. On a obtenu les constantes de vitesse relative d'ordre 3 de la formation de M_2^+ du benzène (1.0), du benzène-d_6 (2.7), du toluène (0.8), des *o*- (1.5) et *p*-xylène (0.7), du fluorobenzène (0.3), du *m*-fluorotoluène (0.5), des *m*- (0.7) et *p*- (0.5) chlorotoluènes et du *o*-méthoxytoluène (0.4). Ces valeurs sont non seulement conformes aux donnés antérieures obtenues pour ce genre de systèmes (5) mais aussi elles en constituent un complément. On a utilisé le contrôle du réactif ionique pour déterminer les vitesses relatives de la réaction des ions dimères M_2^+ et monomères M^+ avec une série de composés (principalement) aromatiques (X). La réaction de $C_6H_6^+$ a lieu par transfert de charge aux composés ayant un potentiel d'ionisation plus faible que celui du C_6H_6. L'ion dimère $(C_6H_6)_2^+$ réagit seulement par transfert de charge si le potentiel d'ionisation de X est inférieur de plus de 0.5 eV à celui du benzène. Quand la différence est plus faible, on observe des cations dimères mixtes qui sont probablement formés par une réaction d'exchange: $(C_6H_6)_2^+ + X \rightarrow (C_6H_6 \cdot X)^+ + C_6H_6$.

[Traduit par le journal]

Introduction

The dimer cation of benzene $(C_6H_6)_2^+$ has been studied in the gas phase (1–5) and has been observed as an intermediate species in the radiolysis of benzene (6). Thermochemical determinations yielded a binding energy for this "sandwich" shaped complex of 17 kcal mol^{-1}, which is ~6 kcal mol^{-1} greater than that calculated for a purely electrostatic interaction (7). The observation that the binding energy for mixed dimers, e.g. $(C_6H_6 \cdot C_6H_5CH_3)^+$ is always less than for the symmetric dimer led to the suggestion that additional binding in $(C_6H_6)_2^+$ is obtained by electron delocalization, a contribution to the total binding energy that will be at a maximum for symmetric dimers. In mixed dimers containing benzene the binding energy decreases smoothly from the 17 kcal mol^{-1} for $(C_6H_6)_2^+$ to a minimum value of ~10 kcal mol^{-1} as the difference in ionization potential between benzene and the second aromatic constituent increases.

The stabilization of aromatic cations by dimer formation obviously has implications for the photochemistry and radiation chemistry of aromatics in the gaseous, liquid, and solid states. The reactions of such ions have received little attention. Important reactions of the dimer cations in such systems will be charge transfer to species of lower ionization potential and possibly exchange reactions of the form

[1] $(B_1 \cdot B_2)^+ + B_3 \rightarrow (B_1 \cdot B_3)^+ + B_2$

We report a study of the reactivity of some dimeric cations with a variety of neutrals, mainly aromatics and substituted aromatics, employing the technique of reactant ion monitoring (RIM) (8). The relative rates and the products of reaction have been determined. The third order relative rates of formation of some dimer cations have also been determined.

Experimental

The measurements were made using the high pressure instrument described previously (9) but with a new photoionization source (Fig. 1). The source was constructed from a cylindrical piece of stainless steel, 1.5 cm in diameter and 15 cm long. The cylinder is attached directly to a flange of the vacuum housing and is run at ground potential. The ionization chamber, a cavity of volume ~2 cm^3, has LiF windows and a circular ion exit 0.5 mm in diameter. The source may be heated by cartridge heaters embedded in blind holes drilled from outside the vacuum chamber. All gas connections to the chamber are of 1/8 in. OD stainless steel tubing. In the RIM mode a flow system is employed to prevent degradation of resolution in GC/MS work.

Reagent gas is led from a heated oven to the ion source via a

0008-4042/80/161666-07$01.00/0

©1980 National Research Council of Canada/Conseil national de recherches du Canada

Can. J. Chem. Downloaded from www.nrcresearchpress.com by 210.87.254.105 on 09/05/12
For personal use only.

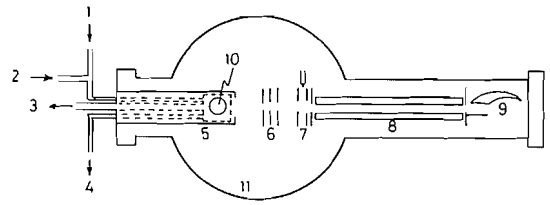


FIG. 1. Sketch of the instrument: *1*, inlet from gas chromatograph; *2*, inlet from heated reservoir; *3*, connection to capacitance manometer; *4*, connection to 1 in. diffusion pump; *5*, photoionization source; *6*, Einsel lens; *7*, electron impact ion source; *8*, quadrupole; *9*, continuous dynode electron multiplier; *10*, LiF window; *11*, vacuum housing leading to 6 in. diffusion pump.

heated Granville-Phillips variable leak valve. Between this leak valve and the ion source is a "T" connector which leads to a gas chromatograph via a Nupro fine metering valve. The chromatographic column effluent is split by a "T" connection inside the column oven, about 25% going to the ion source and 75% to a flame ionization detector. The internal volume of the tube connecting this "T" to the metering valve is only 40 μL which leads to practically simultaneous responses of flame ionization detector and mass spectrometer. All gas lines leading to the photoionization source are heated to ~100°C with heating tapes but for most experiments the ion source was operated at ambient temperature (25 ± 2°C). Cartridge heaters embedded in the ion source block allow operation at temperatures up to 200°C.

The 6 ft × 1/8 in. chromatographic columns contained 10% OV-1 or OV-11 on Chromosorb W. The column temperature was programmed from ambient temperature to 200°C. The benzene was J. T. Baker Ultrex (99.99%) and the toluene was Fisher Certified A.C.S. grade. All other chemicals were of the highest purity available. Solutions for the 1 μL chromatograph injections contained cyclohexane, cyclopentane, or *n*-hexane as solvents with solute concentrations in the range 10^{-2}–10^{-1} *M*.

Chromatographic and ion current signals were recorded simultaneously on a two channel, strip chart recorder. Peak area measurements for the ion current were made using a Nicolet 1170 signal processor.

Results and Discussion

The ionization potential of benzene is 9.24 eV (10) and the first electronic excited state of the ion is 2.25 eV higher (10) so that only ground state $C_6H_6^+$ will be formed initially by the krypton resonance radiation (10.03 eV (86%) and 10.64 eV (14%)). Up to 1.4 eV of vibrational excitation can be initially present but this excess energy will be rapidly degraded by collision and by bimolecular resonance charge transfer. The same relaxation processes will prevail for the other aromatics employed.

Third Order Relative Rate Constants

The initial experiments (non-RIM) were to obtain the relative rates of disappearance of the molecular ions in the pure reactants. In agreement with Sieck and Gorden (5), who also used a photoionization source, the only reaction of the molecular cation (M^+) observed in any single component system is the formation of the dimeric cation (M_2^+) in a third order process. A typical result is shown in Fig. 2 for C_6D_6. The decay of $C_6D_6^+$ is accompanied by a symmetrical increase in $(C_6D_6)_2^+$. Rate constant data are obtained from plots of $\log i_{M^+}/(i_{M^+} + i_{M_2^+})$ versus (pressure)^2, where i_{M^+} and $i_{M_2^+}$ are the ion currents due to monomeric and dimeric ions respectively at the same pressure. These plots are linear for decreases of up to 20% in the fractional yield of the molecular ion. The equation for such a line is $\ln i_{M^+}/(i_{M^+} + i_{M_2^+}) = -k[M]^2\tau$ where k is the rate constant for the reaction

[2] $M^+ + 2M \rightarrow M_2^+ + M$

τ is the average residence time for M^+ in the source and is not easily calculable since the ion path lengths are not well defined. However, relative rate constants are readily obtained from the relative slopes of such plots, a correction being made for the different residence times. Molecular flow is assumed so that $\tau_1/\tau_2 = (M_1/M_2)^{1/2}$ where M is the molecular weight. Reproducibility is ~± 10% and each of the results shown is the average of two or more determinations. The relative rate constants obtained are compared in Table 1 with those reported by Sieck and Gorden (5). (Their absolute value for $C_6H_6^+$ is 1.9×10^{-25} cm^6 molecule^{-2} s^{-1} compared with the value of 1.2×10^{-25} cm^6 molecule^{-2} s^{-1} of Anicich and Bowers (4).) The two sets of relative values are in good agreement and the observation of the high rate constant for $C_6D_6^+$ relative to that for $C_6H_6^+$ is confirmed. With the exception of *o*-xylene, substituents on the aromatic ring lead to a lowering of the rate constant, this being particularly noticeable for fluorobenzene. The rates of formation of these dimer cations are in

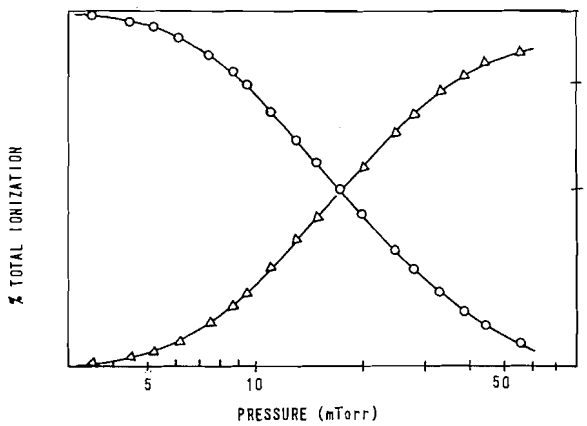


FIG. 2. The relative yields of $C_6D_6^+$ (○) and $(C_6D_6)_2^+$ (Δ) as functions of benzene-d_6 pressure.

Can. J. Chem. Downloaded from www.nrcresearchpress.com by 210.87.254.105 on 09/05/12
For personal use only.

Can. J. Chem. Downloaded from www.nrcresearchpress.com by 210.87.254.105 on 09/05/12
For personal use only.

TABLE 1. Third order rate constants relative to that of benzene for the dimerization reaction $M^+ + 2M \rightarrow M_2^+ + M$

Compound M	$k_{M^+}/k_{C_6H_6^+}$ This work	$k_{M^+}/k_{C_6H_6^+}$ Sieck and Gorden[a]	ΔH^0 (kcal mol^{-1})[b]	K^0 (atm^{-1})[b]
Benzene	1.0	1.0	−17.0	2.8×10^6
Benzene-d_6	2.3	2.7	[c]	[c]
Toluene	0.8	1.0	−16.0	1.9×10^5
o-Xylene	1.5	1.7	[c]	[c]
p-Xylene	0.7	0.7	−15.6	1.8×10^4
Fluorobenzene	0.3	0.2	−14.1	6.9×10^3
m-Fluorotoluene	0.5	[c]	[c]	[c]
m-Chlorotoluene	0.7	[c]	[c]	[c]
p-Chlorotoluene	0.5	[c]	[c]	[c]
o-Methoxytoluene	0.4	[c]	[c]	[c]

[a]Reference 5.
[b]ΔH^0 and K for the equilibrium $M^+ + M \rightleftharpoons 2M^+$ from ref. 7.
[c]Not determined.

the same order as their stabilities measured by the enthalpy for dissociation of M_2^+, as shown in Table 1. Equilibrium constants K for the reaction

$$[2a] \quad M^+ + 2M \underset{k_r}{\overset{k_f}{\rightleftharpoons}} M_2^+ + M$$

determined by Meot-Ner *et al.* (7) are also shown in Table 1. If $K = k_f/k_r$, then it is apparent that the rate constant for the reverse reaction, k_r, increases much more rapidly with change of binding energy of M_2^+ than does the forward rate constant. Unfortunately there is no thermodynamic data for *o*-xylene, which has a very high value for k_f.

At pressures beyond the range shown in Fig. 2, ions appear which may be associated with impurities and their intensities increase with increasing pressure. The nature of these ions depends on the particular compound being studied and sometimes on the compounds just previously used in the instrument. The ions all arise from aromatic impurities of lower ionization potential than the compound under study, and may be the impurity molecular ion or a mixed dimer cation containing both the impurity and the compound under study. The relative yields of these products will be discussed later. In the low pressure region, where relative rate constants are determined, impurity peaks are not significant.

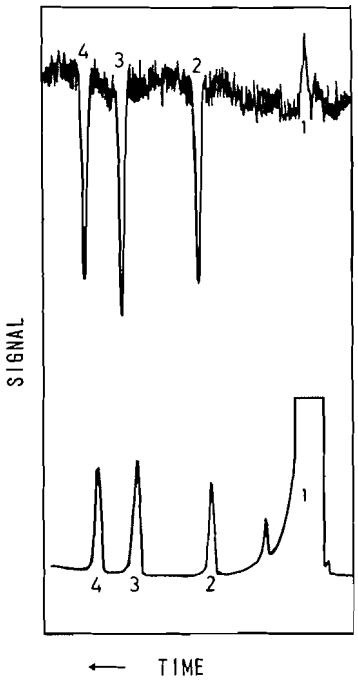


FIG. 3. Gas chromatogram (lower trace) and $(C_6H_6)_2^+$ ion current (upper trace). (*1*) *n*-hexane solvent, (*2*) toluene, (*3*) *o*-xylene, (*4*) mesitylene. The peaks in the upper trace correspond to about 15% decreases in the total ion intensity. Benzene pressure ~0.15 Torr, roughly 5×10^{-8} mol of each aromatic injected into the chromatograph.

Reagent Ion Monitoring (RIM)

The technique of reagent ion monitoring has been described in detail (8). Figure 3 shows the results obtained using $(C_6H_6)_2^+$ as the reagent ion. A steady flow of benzene from the heated reservoir gives a constant partial pressure (~0.15 Torr) in the ion source. Helium flowing at a constant rate from the chromatograph, gives a constant total pressure of ~0.8 Torr. Under these conditions the dominant ion is $(C_6H_6)_2^+$. The steady signal due to this ion is monitored. Components emerging from the chromatograph, which can react with $(C_6H_6)_2^+$, cause a decrease in the signal which generates an inverted "peak" similar to, and contemporaneous with, the chromatographic peak. It was ascertained in separate experiments that there is no mass dis-

Can. J. Chem. Downloaded from www.nrcresearchpress.com by 210.87.254.105 on 09/05/12
For personal use only.

crimination in the gc/ms interface. Both the gc trace and that for the $(C_6H_6)_2^+$ ion current shown in Fig. 3 result from the injection into the chromatograph of 1 μL of a solution approximately 10^{-2} *M* in each of toluene, *o*-xylene, and mesitylene. The solvent, *n*-hexane, causes a slight increase in the $(C_6H_6)_2^+$ signal due to charge transfer from *n*-$C_6H_{14}^+$ formed by direct photoionization. Since the concentrations of the other constituents of the mixture are about 10^3 times less than that of the solvent, their direct photoionization is not of consequence. This was proved in a separate experiment in the absence of benzene when no ions, other than those from the solvent, were detected for compounds eluting from the chromatographic column.

The ratio of rate constants, k_1/k_2, for the reactions of compounds **1** and **2** with $(C_6H_6)_2^+$, is given by (11)

$$\frac{k_1}{k_2} = \frac{A_1}{A_2} \cdot \frac{X_2}{X_1} \cdot \left(\frac{M_2}{M_1}\right)^{1/2}$$

where A_1 and A_2 are the peak areas for compounds **1** and **2** respectively, obtained from the monitored reagent ion trace, and X_1/X_2 is the molar ratio of **1** and **2** in the chromatographic sample.

Figure 4 shows the RIM peak areas for *o*-xylene and mesitylene relative to that of toluene as functions of the amount of material injected into the chromatograph. The relative rate constant ratios computed as above are $k_{o\text{-xylene}}/k_{\text{toluene}} = 0.95$ and $k_{\text{mesitylene}}/k_{\text{toluene}} = 0.94$. As seen from Fig. 3, the low intensity of the ion signal causes some uncertainty in the base line and reproducibility of results is usually of the order of ±8%. Within this error limit, all three compounds have the same rate constant for reaction with $(C_6H_6)_2^+$. Figure 5*a* shows the rate constants relative to that of mesitylene for a series of compounds. The values are plotted against the ionization potentials of the compounds, which range from well above that of benzene (9.24 eV) to well below. For comparison, Fig. 5*b* shows the relative rates of reaction for many of the same compounds with $C_6H_6^+$. This ion was monitored under conditions where the concentration of $(C_6H_6)_2^+$ was small; the benzene pressure was lowered to ~30 mTorr and the ion source temperature was raised to ~120°C.

The shapes of the curves in Fig. 5 *a* and *b* are similar to those reported previously for the reaction of $C_6H_6^+$ (12, 13). For the low concentrations of reagents employed in the ion source no reaction is observed for compounds with ionization potentials above a well defined threshold. Below this threshold value the relative rate of reaction rises rapidly and soon attains a value which is little different for all the compounds. The threshold for $C_6H_6^+$ is very close to the ionization potential of benzene (9.24 eV) but that for $(C_6H_6)_2^+$ is about 0.2 eV lower. This difference, and kinetic considerations detailed below, show that these compounds are indeed reacting at high benzene pressure with $(C_6H_6)_2^+$, and not its precursor, $C_6H_6^+$.

If X is a reactive compound eluted from the

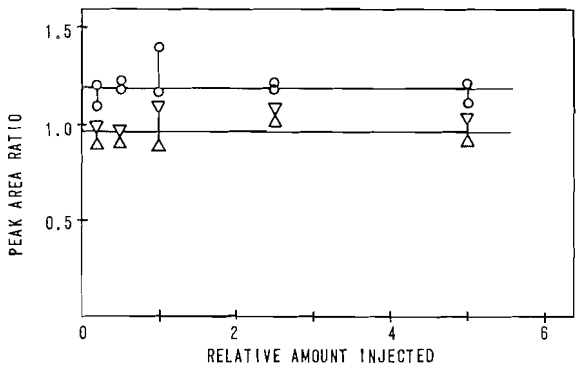


FIG. 4. RIM peak areas relative to those for toluene for *o*-xylene (△) and mesitylene (○) as functions of the amount of material injected into the chromatograph. Approximately equal concentrations of aromatics, with the maximum amount of each injected ~2 × 10^{-7} mol. Points show reproducibility of two separate runs.

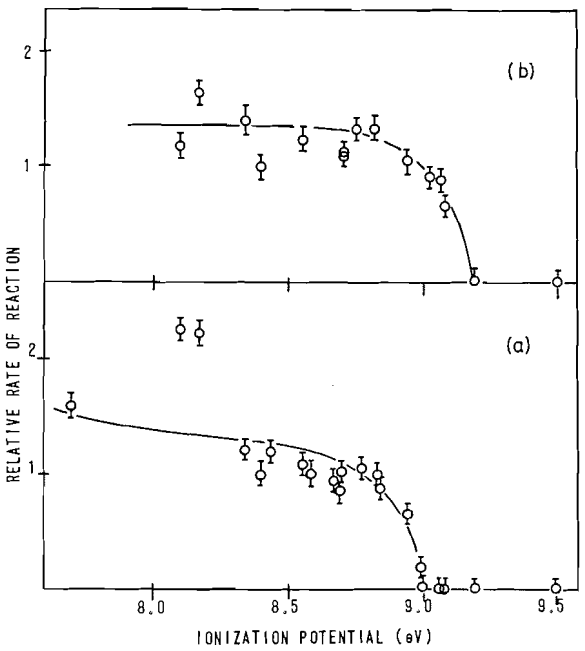


FIG. 5. (*a*) The relative rates of reaction of various compounds with $(C_6H_6)_2^+$; (*b*) the relative rates of reaction of various compounds with $C_6H_6^+$. The rate of reaction with mesitylene is taken as unity. Benzene pressure ~0.15 Torr.

Can. J. Chem. Downloaded from www.nrcresearchpress.com by 210.87.254.105 on 09/05/12
For personal use only.

chromatograph, then the competing reactions are

[3] $C_6H_6^+ + C_6H_6 \xrightarrow{M} (C_6H_6)_2^+$

[4] $C_6H_6^+ + X \xrightarrow{M} (C_6H_6 \cdot X)^+$

[5] $C_6H_6^+ + X \rightarrow$ Products

[6] $(C_6H_6)_2^+ + X \rightarrow$ Products

The rate constant for **3** is large ($\sim 2 \times 10^{-25}$ cm^6 molecule^{-2} s^{-1} (5)) and there is no reason for that for **4** to be any larger. The very small concentration of X relative to that of C_6H_6 ensures that reaction [4] does not compete effectively with reaction [3]. If a maximum rate constant equal to the Langevin collision rate constant ($\sim 1 \times 10^{-9}$ cm^3 molecule^{-1} s^{-1}) is assigned to reaction [5], then the rate of reaction [3] relative to that of [5] is $2 \times 10^{-25}[C_6H_6]^2/1 \times 10^{-9}[X]$. At 0.1 Torr, $[C_6H_6]$ is 3×10^{15} molecules cm^{-3} and [X] is less than 0.1% of this value. The bimolecular reaction rate is therefore at least a factor of 100 less than the termolecular rate. The only reaction of X that need be considered at high benzene concentration is reaction [6].

Figures 6 and 7 show the results of similar experiments carried out with toluene and *m*-fluorotoluene. For toluene the threshold for reaction of $(C_6H_5CH_3)_2^+$ is about 0.1 eV lower than that for $(C_6H_5CH_3)^+$ whereas the thresholds for $(m\text{-}C_6H_4FCH_3)_2^+$ and $(m\text{-}C_6H_4FCH_3)^+$ are not experimentally distinguishable.

Reaction Products

The signal averager was employed to scan continuously the complete mass range (*m/e* 1–400) as each chromatographic peak was eluted. The ion signals due to products were not of sufficient intensity for quantitative determinations but accurate mass identifications could be made. The product observed for the reaction of all compounds with $C_6H_6^+$ i.e. at low benzene concentration, was the molecular ion, X^+, formed by charge transfer. Reaction with $(C_6H_6)_2^+$ leads to more than one product as shown in Table 2. The products are predominantly the molecular ion (X^+) and the mixed dimer $(C_6H_6 \cdot X)^+$. For every compound that reacts with $(C_6H_6)_2^+$, except bromobenzene which is very weakly reactive, the molecular ion is observed. It is the predominant product for all compounds except those with ionization potentials very close to the threshold for which the mixed dimer predominates. Since the ions suffer many potentially reactive collisions before leaving the ion source, the nature of the products observed does not necessarily show directly the products of the initial reaction with $(C_6H_6)_2^+$.

Sieck and Gorden (5) suggest that the initial

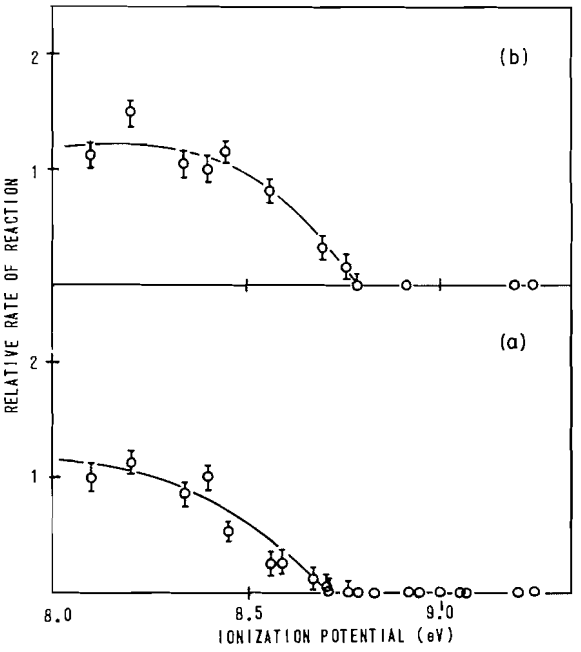


FIG. 6. (*a*) The relative rates of reaction of various compounds with $(C_6H_5CH_3)_2^+$; (*b*) the relative rates of reaction of various compounds with $C_6H_5CH_3^+$. The rate of reaction with mesitylene is taken as unity. Toluene pressure ~0.15 Torr.

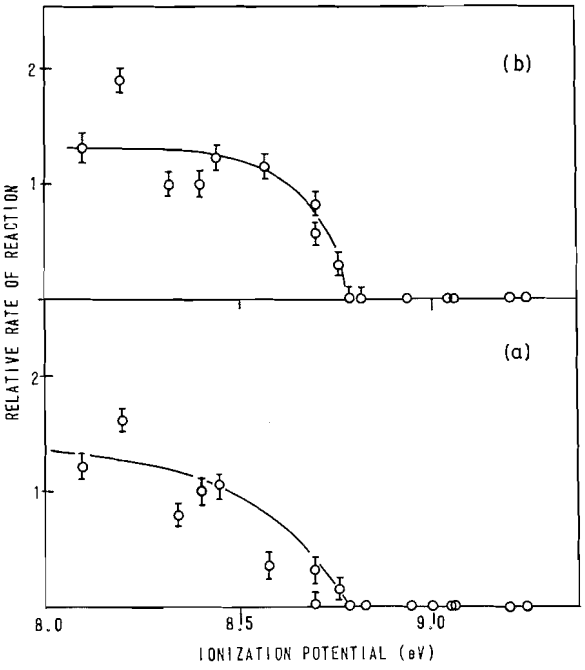


FIG. 7. (*a*) The relative rates of reaction of various compounds with $(m\text{-}CH_3C_6H_4F)_2^+$; (*b*) the relative rates of reaction of various compounds with $m\text{-}CH_3C_6H_4F^+$. The rate of reaction with mesitylene is taken as unity. *m*-Fluorotoluene pressure ~0.15 Torr.

TABLE 2. Products of the reaction of compound X with $(C_6H_6)_2^+$

Compound X	IP (eV)	Δ(IP)[a]	X^+	$(C_6H_6 \cdot X)^+$	Other ions (*m/e*)
1, Cyclohexane	9.81	+0.57	—	—	
2, Benzaldehyde	9.51	+0.27	—	—	
3, 1-Hexene	9.45	+0.21	—	—	
4, Benzene	9.24	0.00	—	—	
5, Fluorobenzene	9.19	−0.05	—	—	
6, Chlorobenzene	9.07	−0.17	—	—	
7, 1,2-Dichlorobenzene	9.06	−0.18	—	—	
8, Cyclopentene	9.01	−0.23	*b*	*b*	
9, Bromobenzene	8.95	−0.29	—	*c,d*	
10, Cyclohexene	8.95	−0.29	*c*	*c,d*	
11, *m*-Fluorotoluene	8.92	−0.32	*c*	*c,d*	
12, *m*-Chlorotoluene	8.83	−0.41	*c,d*	*c*	
13, Toluene	8.82	−0.42	*c,d*	*c*	
14, *p*-Fluorotoluene	8.79	−0.45	*c,d*	*c*	
15, Ethylbenzene	8.76	−0.48	*c,d*	*c*	
16, *p*-Chlorotoluene	8.69	−0.55	*c*	—	
17, Butylbenzene	8.69	−0.55	*c*	—	
18, Iodobenzene	8.69	−0.55	*c*	—	
19, 2-Methyl-2-butene	8.67	−0.57	*c,d*	*c*	128,147
20, *cis*-1,3-Pentadiene	8.59	−0.65	*c,d*	*c*	
21, *o*-Xylene	8.56	−0.68	*c*	—	
22, *p*-Xylene	8.44	−0.80	*c*	—	
23, Mesitylene	8.40	−0.84	*c*	—	
24, 2,3-Dihydropyran	8.34	−0.90	*c,d*	*c*	X_2^+,141
25, Anisole	8.20	−1.04	*c*	—	
26, 2-Methoxytoluene	8.10	−1.14	*c*	—	
27, Aniline	7.70	−1.54	*b*	*b*	

[a]Ionization potential with respect to benzene from ref. 10.
[b]Not determined.
[c]Product ion observed.
[d]Largest product ion peak.

reaction in benzene containing a very small amount of toluene, is the charge transfer reaction

[7] $(C_6H_6)_2^+ + C_6H_5CH_3 \rightarrow 2C_6H_6 + C_6H_5CH_3^+$

The suggestion is based on the observation that in benzene containing very small traces of toluene as impurity, the major initial impurity peak is $C_6H_5CH_3^+$ and not $(C_6H_6 \cdot C_6H_5CH_3)^+$. We have made a similar observation at benzene pressures of ~50 mTorr. However, Meot-Ner *et al.* (7) estimate a recombination energy of 8.55 eV for $(C_6H_6)_2^+$ so that reaction [7] is endothermic by ~6 kcal (IP($C_6H_5CH_3$) = 8.82 eV).

At the threshold potential of Fig. 5*a* only the mixed dimer ion is observed for C_6H_5Br. We suggest that for compounds of ionization potential given by this point, the switching reaction [8] is thermoneutral and for compounds of lower ionization potential it is exothermic.

$$[8]\quad X + (C_6H_6)_2^+ \xrightarrow{\Delta H_1} (C_6H_6 \cdot X)^+ + C_6H_6$$
$$\Delta H_2 \downarrow \qquad\qquad \uparrow \Delta H_4$$
$$[9]\quad X + C_6H_6^+ + C_6H_6 \xrightarrow{\Delta H_3} X^+ + 2C_6H_6$$

At the threshold $\Delta H_1 = 0$, i.e. $-\Delta H_3 = (\Delta H_2 + \Delta H_4)$. ΔH_3, the difference at the threshold in ionization potential between benzene and X, is (9.24 − 9.05) eV = 4.6 kcal mol^{-1} (see Fig. 5). $\Delta H_2 + \Delta H_4$ is the difference in binding energy between $(C_6H_6 \cdot X)^+$ and $(C_6H_6)_2^+$. This is entirely consistent with the results of Meot-Ner *et al.* (7) who give a value of ~4 kcal mol^{-1} for $(\Delta H_2 + \Delta H_4)$ when Δ(IP) is −5 kcal mol^{-1}. The switching mechanism is therefore energetically feasible.

As Δ(IP) increases ΔH_4 decreases (7) and reaches a limiting value of ~10 kcal mol^{-1}, corresponding to non-resonance stabilized binding. At the same time the possibility arises for competition between reaction [8] and the charge transfer reaction analogous to reaction [7]. The present results can only give a measure of the difference in binding energies $(\Delta H_2 + \Delta H_4)$ for the two dimer cations and not their absolute values. Meot-Ner *et al.* (7) obtain $\Delta G^0 = -4.6 \pm 1.5$ kcal mol^{-1} for the equilibrium

$$[10]\quad C_6H_5CH_3^+ + C_6H_6 \overset{M}{\rightleftharpoons} (C_6H_5CH_3 \cdot C_6H_6)^+$$

Therefore $K = 2.1 \times 10^3$ atm^{-1}, i.e. $[BT^+]/[T^+] = [(C_6H_5CH_3 \cdot C_6H_6)^+]/[C_6H_5CH_3^+)] = 2.1 \times 10^3 P_{C_6H_6}$. If the pressure of benzene is 0.15 Torr then $[BT^+]/[T^+] = 0.4$. If the actual value of ΔG^0 is

Can. J. Chem. Downloaded from www.nrcresearchpress.com by 210.87.254.105 on 09/05/12
For personal use only.

Can. J. Chem. Downloaded from www.nrcresearchpress.com by 210.87.254.105 on 09/05/12
For personal use only.

smaller but still within the assigned error limit then $[BT^+]/[T^+]$ can be as low as 0.05. The observation that when a very small concentration of toluene is present in benzene, then most of the toluene containing ions are T^+ rather than BT^+, is not inconsistent with the thermodynamic data of ref. 7 or the present results. A switching reaction produces $(C_6H_6 \cdot C_6H_5CH_3)^+$ which subsequently dissociates.

The difference between the thresholds for monomer and dimer cations is large for benzene, less for toluene, and not distinguishable from zero for *m*-fluorotoluene. At threshold for $(CH_3C_6H_4F)_2^+$, ΔH_5 is zero.

$$[11]\quad (CH_3C_6H_4F)_2^+ + X \xrightarrow{\Delta H_5} (CH_3C_6H_4F \cdot X)^+ + CH_3C_6H_4F$$
$$\downarrow \Delta H_6 \qquad\qquad \uparrow \Delta H_8$$
$$[12]\quad CH_3C_6H_4F^+ + CH_3C_6H_4F + X \xrightarrow{\Delta H_7} 2CH_3C_6H_4F + X^+$$

Then $-\Delta H_7 = \Delta H_6 + \Delta H_8$. Since $\Delta H_7 = \Delta(IP)$, the difference between $IP(CH_3C_6H_4F)$ and IP(X), the binding energies of $(CH_3C_6H_4F)_2^+$ and $(CH_3C_6H_4F \cdot X)^+$ are the same. The binding energy for *m*-fluorotoluene has not been measured but it will most probably be of the order of 12–14 kcal mol^{-1} as found for other halogenated aromatics (7). There can therefore be little stabilization of the dimer from electron delocalization and it follows that there can be only a small numerical difference between ΔH_6 and ΔH_8. The thresholds for the monomer and dimer cations are therefore close together. The difference between the thresholds for toluene is intermediate between that for benzene and that for *m*-fluorotoluene. This is consistent with the binding energy of the toluene dimer cation (16.0 kcal mol^{-1}) being lower than that of the benzene dimer (17.0 kcal mol^{-1}) (7) but higher than that of the *m*-fluorotoluene dimer.

The curves of Figs. 5–7 show that when the ionization potential of the compounds eluted from the gas chromatograph are well away from threshold, the relative rate constants tend to be comparable. This behaviour has been found for the benzene ion (8, 12) and also for charge transfer in gaseous alkane mixtures (14). In this latter case the reaction probability for collision was found to approach unity for $\Delta(IP) \sim 0.3$ eV. By analogy we suggest that the same is true in the present system. At the moment the precision of our relative rate constants is not sufficient for comparison of experimental and theoretical values. We hope that this situation may be changed by the improvements presently in hand to increase the signal-to-noise ratio by raising the efficiency of ion transmission. The only relative rate constant which is consistently anomalous is the one for the reaction of anisole with all the six ions studied. Since the final product of reaction, the anisole molecular ion, is no different in nature to those for other compounds of similar ionization potential, we do not at the moment understand this anomaly which is too large to be explained by the ADO theory.

Experiments with $C_6H_6^+$ led to suggestions that this ion is a useful reagent ion for chemical ionization mass spectrometry when operating in the RIM mode (8, 12). It can be used to discriminate between molecules according to their ionization potentials. The present results show that even greater versatility is available with benzene since $(C_6H_6)_2^+$ may also be used in a source operated at low temperature. Indeed a whole range of useful reagent ions is available if all the substituted benzenes are considered.

Acknowledgement

The authors thank the National Research Council of Canada for financial assistance.

1. A. HENGLEIN. Z. Naturforsch. A, **17**, 44 (1962).
2. F. H. FIELD, P. HAMLET, and W. F. LIBBY. J. Am. Chem. Soc. **89**, 6035 (1967).
3. S. WEXLER and L. G. POBO. J. Phys. Chem. **74**, 257 (1970).
4. V. G. ANACICH and M. T. BOWERS. J. Am. Chem. Soc. **96**, 1279 (1974).
5. L. W. SIECK and R. GORDEN, JR. Int. J. Mass Spectrom. Ion Phys. **19**, 269 (1976).
6. O. EDLUND, P-O. KINELL, A. LUND, and A. SHIMIZU. J. Chem. Phys. **46**, 3679 (1967).
7. M. MEOT-NER, P. HAMLET, E. P. HUNTER, and F. H. FIELD. J. Am. Chem. Soc. **100**, 5466 (1978).
8. F. HATCH and B. MUNSON. J. Phys. Chem. **82**, 2362 (1978).
9. J. E. KRONBERG and J. A. STONE. Int. J. Mass Spectrom. Ion Phys. **24**, 323 (1977).
10. H. M. ROSENSTOCK, K. DRAXL, B. W. STEINER, and J. T. HERRON. J. Phys. Chem. Ref. Data, **6**, 1 (1977); Supplement No. 1.
11. C. W. POLLEY, JR. Paper FC14, presented at the 26th Conference on Mass Spectrometry, St. Louis. 1978. p. 519.
12. S. C. SUBBA-RAO and C. FENSELAU. Anal. Chem. **50**, 511 (1978).
13. B. MUNSON and C. W. POLLEY, JR. Paper FC15, presented at the 26th Conference on Mass Spectrometry, St. Louis. 1978. p. 552.
14. S. G. LIAS, P. AUSLOOS, and Z. HORVATH. Int. J. Chem. Kinet. VIII, 725 (1976).

The electrochemical synthesis of organometallic halides of titanium, zirconium, and hafnium

FAROUQ F. SAID AND DENNIS G. TUCK

Department of Chemistry, University of Windsor, Windsor, Ont., Canada N9B 3P4

Received February 18, 1980

FAROUQ F. SAID and DENNIS G. TUCK. Can. J. Chem. **58**, 1673 (1980).

The electrochemical oxidation of titanium, zirconium, or hafnium (= M) in a cell containing an organic halide RX results in the formation of an organometallic halide of the metal concerned. These compounds are conveniently isolated as adducts of acetonitrile or 2,2′-bipyridine (bipy) also present in the electrolyte phase. The products most commonly isolated are the $R_2MX_2 \cdot L_2$ ($L = CH_3CN$ or $\frac{1}{2}$bipy), but other species were obtained in certain cases. Possible reasons for these findings are discussed.

FAROUQ F. SAID et DENNIS G. TUCK. Can. J. Chem. **58**, 1673 (1980).

L'oxydation électrochimique du titane, du zirconium ou de l'hafnium (= M) dans une cellule contenant un halogénure organique RX conduit à la formation d'un halogénure organométallique du métal concerné. Ces composés peuvent être isolés d'une façon convenable sous la forme de produits d'addition avec l'acétonitrile ou de la bipyridine-2,2′ (bipy) qui sont également présents dans la phase électrolytique. Les produits les plus communéments isolés sont le $R_2MX_2 \cdot L_2$ ($L = CH_3CN$ ou $\frac{1}{2}$bipy) mais dans certains cas on a obtenu d'autres espèces. On discute des causes probables qui expliquent ces résultats.

[Traduit par le journal]

Can. J. Chem. Downloaded from www.nrcresearchpress.com by 210.87.254.40 on 09/05/12
For personal use only.

Introduction

The use of the direct electrochemical oxidation of metals in non-aqueous media has proven to be an effective route for the synthesis of organometallic halides of a number of main group metals (1). Less is known about the efficacy of such direct syntheses for transition metals, although the production of RMX adducts for M = Ni and Pd has been reported (2). We now describe the application of electrochemical methods in the direct synthesis of organohalides of titanium, zirconium, and hafnium. The oxidation of these metals to the corresponding tetrachlorides or tetrabromides, which were conveniently stabilized and handled as neutral adducts or anionic complexes, has already demonstrated the potential of the method for these elements (3).

The organometallic compounds of the Group IVA elements have been the subject of a number of reviews (4, 5). The standard preparative routes for the organometallic halides involve reaction of the appropriate halide with organolithium compounds, Grignard reagents, or zinc and aluminum alkyls. The stability of the resultant compounds apparently depends on the number and nature of the organic groups involved, on the particular halide, and on the presence of coordinating ligands. In view of this last consideration, we have carried out the electrochemical oxidation in the presence of a coordinating solvent (acetonitrile) and/or the ligand 2,2′-bipyridine in order to stabilize the products of the electrochemical oxidation.

Experimental

Materials, Analysis, Spectroscopic Methods

In all these respects, the experimental techniques were essentially identical to those described earlier (3).

Preparative Procedures

The general electrochemical techniques were as in previous work (6), with the metal to be oxidized forming the anode of a simple cell, which was sealed so that this and all other operations were performed under dry nitrogen. The total volume of the solution phase was 15–40 cm^3, comprised as follows: ethyl bromide, phenyl chloride, phenyl bromide, benzyl chloride, benzyl bromide: 20 cm^3 RX + 20 cm^3 acetonitrile (+ 2 cm^3 methanol in the case of Zr, or Hf, with benzyl bromide); benzyl iodide: 0.7 g RX + 40 cm^3 acetonitrile; phenyl iodide: 15 cm^3 RX + 15 cm^3 acetonitrile + 2 cm^3 methanol; methyl iodide: 20 cm^3 RX + 2 cm^3 methanol. Approximately 20 mg of tetraethylammonium halide was added in each experiment; in the preparation of 2,2′-bipyridine adducts, 0.5 g of this ligand was also added.

Table 1 gives the initial current for each system for an applied voltage of 50 V, the length of time of the electrolysis and the weight of metal dissolved from the anode. The method of isolation of the product depended on the individual circumstances as determined experimentally. For derivatives of benzyl chloride, bromide, and iodide, ethyl bromide, methyl iodide (with zirconium), and phenyl iodide, the products were those which precipitated from the solution phase as the electrolysis proceeded. The remainder was obtained from the solution by evaporation of solvent (phenyl bromide/titanium) or by the addition of benzene (phenyl bromide/zirconium), acetonitrile (methyl iodide/zirconium), or by acetonitrile followed by diethyl ether (methyl iodide/titanium). Table 1 also notes certain systems for which no identifiable product could be obtained. The overall yield of product was typically ca. 50%, based on the quantity of metal dissolved.

Electrolysis in which ethyl bromide was the parent organic halide provides typical examples of the preparation of R_2MX_2 adducts of zirconium and hafnium, and details of the procedures are given below. With titanium, detailed investigations showed that two products could be isolated from the electrolyte phase. Analytical results for all the compounds obtained in this work are listed in Tables 2 and 3.

Preparation of $(C_2H_5)_2MBr \cdot 2CH_3CN$ (M = Zr, Hf)

These electrochemical oxidations were amongst the fastest observed in this work. Almost immediately after beginning the electrolysis, a colorless crystalline solid deposited on the anode

0008-4042/80/161673-05$01.00/0

©1980 National Research Council of Canada/Conseil national de recherches du Canada

Can. J. Chem. Downloaded from www.nrcresearchpress.com by 210.87.254.40 on 09/05/12
For personal use only.

TABLE 1. Electrochemical oxidation of titanium, zirconium, and hafnium in presence of alkyl and anyl halides: experimental conditions

Systems[a,b]	Metals	Initial current (mA)	Time of electrolysis (h)	Metal dissolved (mg)
C_2H_5Br/CH_3CN	Ti	30	5	102
	Zr	25	3	103
	Hf	15	2	94
C_2H_5Br/bipy	Ti	30	1.5	25
	Zr	50	1.5	104
	Hf	20	8.5	114
$C_6H_5CH_2Cl/CH_3CN$	Ti[d]	25	18	140
	Zr[d]	25	18	330
	Hf	25	20	220
$C_6H_5CH_2Cl$/bipy	Ti	40	5.5	59
	Zr	40	2.5	132
	Hf	25	5.5	196
$C_6H_5CH_2Br$/bipy	Ti	50	3.0	97
	Zr	20	14.5	69
	Hf	25	3.0	129
$C_6H_5CH_2I$/bipy	Ti	25	3	20
	Zr	50	5.5	[c]
	Hf	25	3	24
C_6H_5Cl/CH_3CN	Ti	10	40	40
	Zr	15	14	145
	Hf	10	16	143
C_6H_5Br/CH_3CN	Ti	15	14	37
	Zr	80	5	258
	Hf[d]	40	4	211
C_6H_5I/CH_3CN	Ti	20	48	30
	Zr	10	13	45
	Hf[d]	10	[c]	67
CH_3I/bipy	Ti	10	4	51
	Zr	40	10	180
	Hf	30	12	55

[a]For solution composition, see text.
[b]bipy = 2,2′-bipyridine.
[c]Not recorded.
[d]No identifiable compound could be isolated from this system.

surface, and subsequently settled on the bottom of the cell. This material was collected and dried *in vacuo*.

Preparation of $(C_2H_5)_2TiBr_2 \cdot 2CH_3CN$

When titanium metal was electrolyzed in a solution consisting of 10 cm³ C_2H_5Br, 20 cm³ CH_3CN, and 30 mg $(C_2H_5)_4NBr$, at a constant current of 30 mA (25 V), it appeared that two products were being formed. After the first few minutes of electrolysis, a yellow colour began to appear around the anode, and the colour of the solution progressively changed to brown. After about 45 min, a green solid started to deposit in the cell; this was collected and dried *in vacuo* (found: Ti 13.1, Br 44.0). When the filtrate was treated with diethyl ether, a brown solid precipitated (found: Ti 14.3, Br 45.4). We believe that the brown solid is indeed $(C_2H_5)_2TiBr_2 \cdot 2CH_3CN$ (cf. Table 2), whilst the green material may be a mixture of this and some reduction product (cf. bipy case below).

Preparation of $(C_2H_5)_2MBr \cdot bipy$ ($M = Zr, Hf$)

A pink colouration was observed around the anode at the beginning of the electrolysis, but this persisted for only a short time. A yellow solid subsequently began to deposit on the anode surface and in the bottom of the cell, and the overall colour of the solution progressively changed to yellow. At the end of the electrolysis the yellow solid was collected by filtration and dried *in vacuo*.

Electrochemical Preparation of $(C_2H_5)TiBr_2 \cdot 2bipy$ and $(C_2H_5)_2TiBr_2 \cdot bipy$

Titanium was electrolyzed in conditions similar to those above, and again two different compounds were seen to form, one green and the other brown. The brown compound which precipitated was collected, and identified as $(C_2H_5)_2TiBr_2 \cdot bipy$ (see Table 2). The green material which was precipitated by adding diethyl either to the filtrate analyzed as $(C_2H_5)TiBr_2 \cdot 2bipy$ (found: Ti 8.6, Br 28.9; calcd.: Ti 8.7, Br 29.1).

Characterization of Products

Each isolated substance was analyzed for metal and halogen, and in addition, infrared and nmr spectroscopy were used to confirm the presence of the appropriate donor ligand and organic group bonded to the metal. The proton nmr spectra, given in Table 4, call for little comment other than that they confirm the presence of the appropriate structural units.

The infrared spectra of the 2,2′-bipyridine adducts showed the spectral features associated with bidentate coordination of this ligand (7). The $\nu(C{\equiv}N)$ vibrations of the acetonitrile adducts are listed in Table 5. The values are similar to those reported for the MX_4 adducts (3), and show little dependence on R or X. The presence of the doublet indicates that the acetonitrile ligands have *cis* stereochemistry. We were not able to study the far infrared spectra of the compounds to establish the stereochemistry of these molecules.

Results and Discussion

General

As with previous electrochemical synthesis, the experiments show that the method is a simple and inexpensive route to a variety of organometallic halides. The method appears to be a general one, although there are certain systems (see Table 1) from which no reaction product could be isolated, even though significant quantities of metal dissolved. We attempted the preparation of anionic complexes by electrolysis of the metal in the presence of organic halide and excess (i.e. approximately 1 g) tetraalkyl ammonium halide, but obtained only on the salt of the corresponding anionic inorganic halogeno complex (cf. ref. 3).

The compounds obtained are sensitive to hydrolysis, but otherwise stable under nitrogen over some days. The presence of the complexing ligand during the preparative process, coupled with the immediate precipitation which occurs in many cases, is no doubt responsible for stabilizing the compounds, particularly against those processes arising from intermolecular interactions which are prevented by increasing the coordination number of the metal. Previous authors have shown that the thermal stabilities of benzyl zirconium iodides are improved by coordination with 2,2′-bipyridine (8); despite this approach, some of the results in Table 2 suggest that some decomposition may have occurred.

TABLE 2. Analytical results for adducts of diorganohalides of titanium, zirconium, and hafnium

Compound	Colour	Found (%)		Calculated (%)	
		Metal	Halogen	Metal	Halogen
$(C_2H_5)_2TiBr_2 \cdot 2CH_3CN$	Brown	14.3	45.4	13.8	45.8
$(C_2H_5)_2ZrBr_2 \cdot 2CH_3CN$	Colourless	23.9	40.6	23.3	40.9
$(C_2H_5)_2HfBr_2 \cdot 2CH_3CN$	Colourless	37.2	33.3	37.2	33.5
$(C_2H_5)_2TiBr_2 \cdot$ bipy	Brown	11.5	37.1	11.4	37.8
$(C_2H_5)_2ZrBr_2 \cdot$ bipy	Yellow	19.6	34.6	19.6	34.4
$(C_2H_5)_2HfBr_2 \cdot$ bipy	Yellow	32.0	29.2	32.3	29.0
$(C_6H_5CH_2)_2HfCl_2 \cdot 2CH_3CN$	Pale yellow	33.8	13.8	34.7	13.7
$(C_6H_5CH_2)_2TiCl_2 \cdot$ bipy	Dark brown	10.7	15.5	10.5	15.4
$(C_6H_5CH_2)_2ZrCl_2 \cdot$ bipy	Pink	18.9	14.1	18.2	14.0
$(C_6H_5CH_2)_2HfCl_2 \cdot$ bipy	Pink	30.1	11.9	30.4	12.0
$(C_6H_5CH_2)_2TiBr_2 \cdot$ bipy	Brown	10.0	35.9	10.6	35.2
$(C_6H_5CH_2)_2ZrBr_2 \cdot$ bipy	Pink	15.5	27.8	15.5	27.2
$(C_6H_5CH_2)_2HfBr_2 \cdot$ bipy	Pink	26.5	24.0	26.3	23.7
$(C_6H_5CH_2)_2TiI_2 \cdot$ bipy[a]	Dark brown	6.7	37.8	7.5	39.7
$(C_6H_5CH_2)_2ZrI_2 \cdot$ bipy	Dark brown	13.0	37.3	13.3	37.1
$(C_6H_5CH_2)_2HfI_2 \cdot$ bipy	Dark brown	22.1	32.5	23.1	33.0
$(C_6H_5)_2TiCl_2 \cdot 2CH_3CN$	Pale yellow	13.6	19.8	13.6	19.8
$(C_6H_5)_2ZrCl_2 \cdot 2CH_3CN$	Colourless	23.1	17.1	22.9	17.6
$(C_6H_5)_2HfCl_2 \cdot 2CH_3CN$	Colourless	36.5	14.4	36.8	14.5
$(C_6H_5)_2TiBr_2$[b]	Yellow–brown	13.5	44.5	13.3	44.2
$(C_6H_5)_2ZrBr_2$[b]	Colourless	22.0	39.2	22.5	39.5

[a]This compound proved extremely hard to dissolve for analysis.
[b]Compound isolated in uncomplexed form despite presence of CH_3CN.

TABLE 3. Analytical results for trimethyliodo and triphenyliodo compounds of titanium, zirconium, and hafnium

Compound	Colour	Found (%)		Calculated (%)	
		Metal	Halogen	Metal	Halogen
$(CH_3)_3TiI \cdot$ bipy	Yellow	12.7	34.1	12.8	33.8
$(CH_3)_3ZrI \cdot$ bipy	Yellow	21.8	30.3	21.7	30.3
$(CH_3)_3HfI \cdot$ bipy	Yellow	35.6	25.1	35.2	25.0
$(C_6H_5)_3TiI$	Brown	11.0	30.9	11.8	31.3
$(C_6H_5)_3ZrI$	Yellow	20.0	27.8	20.3	28.3

Reaction Pathway

The present work offers both interesting parallels and significant differences with that on the electrochemical synthesis of diorganotin(IV) dihalides (6). The most obvious point is that while with tin the products were invariably adducts of the R_2MX_2 compounds, the present experiments yield adducts of R_2MX_2, or adducts of R_3MX, or uncomplexed R_3MX, depending on R and X. We believe that the explanation is similar to that which we have given elsewhere (9) in terms of the electrochemical synthesis of organoindium(III) halides, namely anodic oxidation of the metal to a low oxidation state, followed by reaction with excess organic halide, followed by either complexation and precipitation or rearrangement reactions in solution.

In all our electrochemical work using organic halides, we have based the explanation on the first step of cathodic reduction (1).

[1] $RX + e \rightarrow R + X^-$

Migration of X^- to the anode is then followed by

[2] $X^- + M \rightarrow MX + e$

[3] $MX + RX \rightarrow RMX + X$

This sequence of reactions [2] and [3] can lead to a current efficiency (defined as moles of metal dissolved per Faraday) greater than unity, and non-integral. Examples of this have been found for tin (6) and cadmium (10), while for indium (9) reaction [3] is replaced by the formation of the indium(III) compound R_2MX. Attempts to measure the current efficiency were confounded by the formation of solids which adhered to the surface of the electrode; typical values were in the range 0.3–0.4 mol F^{-1}, which is higher than the value of 0.25 expected for Faradaic behaviour, but which gives no insight into the details of the electrode reactions. Evidence

Can. J. Chem. Downloaded from www.nrcresearchpress.com by 210.87.254.40 on 09/05/12
For personal use only.

Can. J. Chem. Downloaded from www.nrcresearchpress.com by 210.87.254.40 on 09/05/12
For personal use only.

TABLE 4. Proton nmr spectra of adducts of some organometallic halides of titanium, zirconium, and hafnium in perdeuteromethanol (in ppm, from TMS)

Compound	R	Neutral ligand
$(C_6H_5CH_2)_2HfCl_2 \cdot 2CH_3CN$[a]	1.30 (CH_2)	2.2
	7.4 (C_6H_5)	
$(C_6H_5CH_2)_2TiCl_2 \cdot bipy$	1.25 (CH_2)	7.75–9.5[b]
$(C_6H_5CH_2)_2ZrCl_2 \cdot bipy$	1.25 (CH_2)	7.38–9.0[b]
	1.45 (CH_2)[c]	7.9 –9.1[b]
$(C_6H_5CH_2)_2HfCl_2 \cdot bipy$	1.1 (CH_2)	7.4 –9.0[b]
	1.5 (CH_2)[c]	8.0 –9.25[b]
$(C_6H_5CH_2)_2TiBr_2 \cdot bipy$	1.9 (CH_2)	7.0 –9.0[b]
$(C_6H_5CH_2)_2ZrBr_2 \cdot bipy$	2.0 (CH_2)	7.25–9.0[b]
$(C_6H_5CH_2)_2HfBr_2 \cdot bipy$	2.0 (CH_2)	7.3 –9.0[b]
$(C_6H_5)_2ZrCl_2 \cdot 2CH_3CN$	7.25	2.0
$(C_6H_5)_2HfCl_2 \cdot 2CH_3CN$	7.35	2.0
$(C_6H_5)_2TiBr_2$	7.3	—
$(C_6H_5)_2ZrBr_2$	7.35	—
$(C_6H_5)_3TiI$	7.2–7.9	—
$(C_6H_5)_3ZrI$	6.6–7.6	—

[a]Although not well characterized analytically, the presumed zirconium analogue gave an essentially identical nmr spectrum.
[b]No attempt made to distinguish the overlapping benzyl and 2,2′-bipyridine resonances in this region.
[c]Spectrum in d_6-dimethylsulphoxide.

TABLE 5. Infrared absorptions of acetonitrile adducts of organo group IVA halides[a]

Compound	ν(C≡N)
$(C_6H_5)_2TiCl_2 \cdot 2CH_3CN$	2280, 2310
$(C_6H_5)_2ZrCl_2 \cdot 2CH_3CN$	2300[b]
$(C_6H_5)_2HfCl_2 \cdot 2CH_3CN$	2280, 2305
$(C_2H_5)_2TiBr_2 \cdot 2CH_3CN$	2300, 2351
$(C_2H_5)_2ZrBr_2 \cdot 2CH_3CN$	2295, 2312
$(C_2H_5)_2HfBr_2 \cdot 2CH_3CN$	2290, 2305

[a]Frequencies in cm^{-1}; samples run as Nujol mulls between potassium bromide plates.
[b]Broad band, not resolved.

for the oxidative insertion of $(C_5H_5)_2Ti(CO)_2$ into the C—X bond of alkyl halides lends some support to the proposed reaction [4].

In the case of tin, it was suggested that the reaction

[4] $RMX + RX \rightarrow R_2MX_2$

followed by *in situ* complexation lead to the precipitation of $R_2MX_2 \cdot L_2$, whose insolubility prevented the redistribution reactions which otherwise result in R_2MX, RMX_3, etc. The importance of redistribution reaction in the present work is shown by the fact that when the product precipitates during the electrolysis, the products are generally the adducts $R_2MX_2 \cdot 2CH_3CN$ or $R_2MX_2 \cdot bipy$. The exceptions to this rule are $(C_6H_5)_3TiI$ and $(C_6H_5)_3ZrI$, which precipitated slowly as sticky solids during the electrolysis. There may be steric reasons why these compounds fail to complex with acetonitrile, and the slight solubility in this solvent may account for the formation of the triorganohalide by a redistribution reaction of $(C_6H_5)_2MI_2$. Similar arguments probably apply in the case of CH_3I/M systems, where adducts of the $(CH_3)_3MI$ species are formed with 2,2′-bipyridine; with hafnium, precipitation of the product occurs slowly during the electrolysis, whereas with titanium and zirconium addition of solvent(s) was required for precipitation. Here again, steric effects may mitigate against the stability of R_2MI_2 compounds, although in fairness one must note the formation of such species with $R = C_6H_5CH_2$.

One further piece of experimental evidence supports the proposed redistribution reactions. When zirconium was oxidized in the presence of phenyl iodide, the formation of iodine was observed, and subsequent analysis (thiosulphate titration) showed that 0.35 mmol I_2 was generated, and that 0.37 mmol Zr had dissolved. These results are compatible with the formation of $(C_6H_5)_3ZrI$ by either

[5] $C_6H_5ZrI + 2C_6H_5I \rightarrow (C_6H_5)_3ZrI + I_2$

or

[6] $(C_6H_5)_2ZrI_2 + C_6H_5I \rightarrow (C_6H_5)_3ZrI + I_2$

We have no reason to prefer one reaction over the other at the present time.

The final point about the solution chemistry which follows the electrochemical oxidation is that for titanium we observed some reduction of the M(IV) compounds. The synthesis was carried out in an undivided cell and reduction of solution species therefore is always a possibility, although clearly this cannot occur when the product precipitates. The evidence for this reduction is ambiguous for $Ti/C_2H_5Br/CH_3CN$ (cf. Experimental), but much better based for $Ti/C_2H_5Br/bipy$. Polarographic evidence (12, 13) for the reduction of $(C_5H_5)_2TiCl_2$ to give green $(C_5H_5)_2TiCl$ is in keeping with these observations.

In general then, the experimental results on the electrochemical preparation of organometallic halides of titanium, zirconium, and hafnium are in keeping both with the known properties of these elements, and with earlier work on direct electrochemical synthesis.

Acknowledgement

This work was supported by Operating Grants from the Natural Sciences and Engineering Research Council of Canada.

1. D. G. TUCK. Pure Appl. Chem. **51**, 2005 (1979).
2. J. J. HABEEB and D. G. TUCK. J. Organomet. Chem. **139**, C17 (1977).
3. J. J. HABEEB, F. F. SAID, and D. G. TUCK. Can. J. Chem. **55**, 3882 (1977).

4. R. J. H. CLARK. The chemistry of titanium, zirconium and hafnium. Pergamon Press, New York. 1975.
5. P. C. WAILES, R. S. P. COUTTS and H. WEIGOLD. Organometallic chemistry of titanium, zirconium and hafnium. Academic Press, New York. 1974.
6. J. J. HABEEB and D. G. TUCK. J. Organomet. Chem. **134**, 363 (1977).
7. A. A. SCHILT and R. C. TAYLOR. J. Inorg. Nucl. Chem. **9**, 211 (1959).
8. K. H. THIELE, E. KOHLIER, and B. ALDER. J. Organomet. Chem. **50**, 153 (1973).
9. J. J. HABEEB, F. F. SAID, and D. G. TUCK. J. Organomet. Chem. **190**, 325 (1980).
10. J. J. HABEEB and D. G. TUCK. J. Organomet. Chem. **146**, 213 (1978).
11. C. FLORIANI and G. FACHINETTI. Chem. Commun. 790 (1972).
12. R. E. DESSY, R. B. KING, and M. WALDROP. J. Am. Chem. Soc. **88**, 5112 (1966).
13. S. P. GUBIN and S. A. SMIRNOVA. J. Organomet. Chem. **20**, 229 (1969); **20**, 241 (1969).

Can. J. Chem. Downloaded from www.nrcresearchpress.com by 210.87.254.40 on 09/05/12
For personal use only.

Erratum: A ^{13}Cmr study of 2′-deoxynucleotides in the *syn* and *anti* conformation

WALTER P. NIEMCZURA AND FRANK E. HRUSKA

Department of Chemistry, University of Manitoba, Winnipeg, Man., Canada R3T 2N2

(Ref.: Can. J. Chem. **58**, 472 (1980))

Received May 5, 1980

On page 475, line 18, the sentence should read: This range comprises adjoining segments of the $g^-(\phi')$ domain (centered at $-60°$) and the $t(\phi')$ domain (centered at $-180°$).

Can. J. Chem. Downloaded from www.nrcresearchpress.com by 210.87.254.40 on 09/05/12
For personal use only.

Fourier transform carbon-13 spin–lattice relaxation study of motion of cyclic hydrocarbons

DAVID E. AXELSON[1] AND CLIVE E. HOLLOWAY

Department of Chemistry, York University, 4700 Keele Street, Downsview, Ont., Canada M3J 1P3

Received July 30, 1979[2]

DAVID E. AXELSON and CLIVE E. HOLLOWAY. Can. J. Chem. **58**, 1679 (1980).

The molecular dynamics in solution for a series of cyclic and bicyclic hydrocarbon derivatives has been investigated by C-13 pulsed Fourier Transform nuclear magnetic resonance spin–lattice relaxation experiments. Molecular motion has been analysed in terms of an anisotropic rotational diffusion model, and an attempt has been made to assess the effects of structure on the observed rotational diffusion constants. Errors in the diffusion constants are discussed, and some of the other problems inherent in the use of these parameters to obtain structural information are outlined.

DAVID E. AXELSON et CLIVE E. HOLLOWAY. Can. J. Chem. **58**, 1679 (1980).

On a étudié la dynamique moléculaire d'une série d'hydrocarbures cycliques et bicycliques en solution en faisant appel à des expériences de relaxation spin–réseau par RMN du ^{13}C opérant par transformation de Fourier à impulsion. On a analysé le mouvement moléculaire en fonction d'un modèle de diffusion d'anisotropie rotationnelle et on a essayé d'évaluer les effets de structure sur les constantes de diffusion rotationnelle observées. On discute des erreurs sur les constantes de diffusion et on souligne quelques autres problèmes inhérents à l'utilisation de ces paramètres en vue d'obtenir des informations sur la structure.

[Traduit par le journal]

Introduction

Carbon-13 spin–lattice relaxation times (T_1) have been widely used to investigate details of molecular motion in solution (1). A major contribution to T_1 of a carbon-13 nucleus in an organic molecule arises from dipolar interactions with protons (T_1^{dd}). Under conditions of rapid molecular reorientation, and in the extreme narrowing limit of the ^{13}C resonances signal, the T_1^{dd} contribution is given by eq. [1], where τ_c is the correlation time for rotational motion and r_{CH} is the carbon–proton internuclear distance.

$$[1] \quad (T_1^{dd})^{-1} = \hbar^2 \gamma_C^2 \gamma_H^2 \sum_i r_{CH_i}^{-6} \tau_c$$

A molecule which is not spherically symmetric will probably undergo anisotropic rotation as it moves around in the magnetic field and eq. [1] will not be directly applicable. The anisotropy of rotation can arise because of inertial differences and because the ellipsoidal shape of the molecule causes differences in the barriers to diffusional motion about the rotation axes in solution. With relatively simple molecules the observed T_1^{dd} values are often interpreted qualitatively in terms of the geometry and assumed axes of rotation of the molecule. Thus carbons with unusually short T_1^{dd} values relative to similar carbons in the molecule are assumed to have their relevant C—H internuclear vectors lying on or close to the axis of fastest molecular rotation. This simple treatment can lead to misinterpretation of the observed relaxation data and may obscure useful dynamic and structural information.

When there are enough unique carbon–hydrogen vectors present in a molecule more detailed calculations (2) for anisotropic motion can be carried out. If a diffusion model can be assumed for molecular reorientation, the motion can be described by a rotational diffusion tensor analogous to the moment of inertia tensor for a free molecule (2–5). The intramolecular contributions to T_1^{dd} are then related to the elements of the diagonalized rotational diffusion tensor. For a structurally rigid molecule the three rotational diffusion constants, R_1, R_2, and R_3, indicate the relative rates of rotation about their respective axes. However, internal motions can also affect T_1^{dd} if the maximum in the frequency distribution of such modes lies in the region of the ^{13}C Larmor precession frequency. The analysis of the motion in terms of anisotropic rotational diffusion may then be misleading unless the effect of the internal motions can be factored out. The effect of internal or segmental motions is seen as an increase in T_1 for spinning methyl groups and for the carbons of flexible long chain substituents. These effects are usually analysed relative to the overall molecular motion as defined by a rigid part of the same molecule. In cyclic systems, such as those investigated here, the internal motions are ring flexing modes which involve the entire molecule and their effects are not readily separ-

[1]Present address: Research Centre, Research Division, Dupont Canada Inc., P.O. Box 5000, Kingston, Ont., Canada.

[2]Revision received April 16, 1980.

0008-4042/80/161679-08$01.00/0

©1980 National Research Council of Canada/Conseil national de recherches du Canada

Can. J. Chem. Downloaded from www.nrcresearchpress.com by 210.87.254.5 on 09/05/12
For personal use only.

Can. J. Chem. Downloaded from www.nrcresearchpress.com by 210.87.254.5 on 09/05/12
For personal use only.

able from rotational diffusion. Altering the rigidity of the ring system without changing the overall molecular shape can result in different relative values of R_1, R_2, and R_3 in a series of closely related derivatives. An attempt has been made to discern such effects in this study.

Calculation of the diffusion constants depends explicitly on molecular structure through the direction cosines of the relevant C—H vectors. It should therefore be possible to obtain structural information by determining the rotational diffusion tensor elements for various geometries, and using these to calculate T_1^{dd} values to compare with the observed values. In the exomethylene bicyclic systems there is evidence (6) that the methylene groups are skewed. Here an attempt has been made to assess the sensitivity of the motional analysis to minor modifications of this type.

We have also investigated the effect of errors in T_1^{dd} on the calculated rotational diffusion constants. Because each T_1^{dd} depends on the relative orientation of particular C—H vectors some motions may have little or no effect on a given T_1^{dd}. Conversely an error in any T_1^{dd} can affect each of the three R_i values quite differently. The degree to which the propagation of such errors interferes with the interpretation of molecular motion from T_1 data is discussed.

Experimental

Preparative methods for the less common derivatives examined are available in the literature (6, 7). Solutions for nmr were prepared in $CDCl_3$ and sealed in tubes. Samples were not degassed unless otherwise noted. Spectra were obtained on a Varian CFT 20 spectrometer with an 8 mm variable temperature probe (ambient temperature 37°C) and an 8K 620L-100 computer. All spectra were obtained under noise modulated proton decoupling conditions.

The T_1 data were obtained using the full inversion-recovery pulse sequence (8) for very short values, the progressive saturation technique (9) for longer values, and the intensity ratio approximation of this technique for very long values (10). The observed T_1 values were determined from a linear least-squares fit (11, 12) of intensity data to eq. [2],

$$[2] \quad \ln (M_\infty - M_\tau) = -\tau/T_1$$

where M_∞ is the equilibrium magnetisation, M_τ is the magnetisation at time τ, and τ is the pulse delay time.

Each T_1 value was measured at least three times and the estimated precision varies from ±5% for the shorter to ±10% for the longer values.

Nuclear Overhauser enhancements (nOe) were measured in the gated decoupling mode (13, 14) and repeated several times for each sample. The results have an estimated precision of from ±10% for a full nOe ($\eta = 2.0$) to ±14% for $\eta = 1$. The dipolar contribution to T_1 is given (15) by eq. [3].

$$[3] \quad \eta = 1.987\,(T_1^{dd})^{-1}/(T_1)\ \text{observed}))^{-1}$$

The error in T_1^{dd} becomes 14.5% ($\eta = 2.0$) for the least precise (longest) T_1 value. Since most of the T_1 values measured in this study at ambient temperatures are relatively short, with all the corresponding nOe values being 2.0 ± 10%, the T_1^{dd} precision probably lies closer to 11.5% in these cases. Because only T_1^{dd} is relevant to the motional analysis this is the value tabulated and referred to in the text. Where results from other studies are used, the relevant T_1(observed) and nOe values may be obtained from the appropriate references.

The analysis of the T_1^{dd} values was performed by a computer programme based on the equations of Woessner (2) for anisotropic rotational diffusion. The input to this programme is T_1^{dd} and the associated direction cosines of the relevant C—H vectors referred to a coordinate system which diagonalizes the moment of inertia tensor (*vide infra*). Starting values for the rotational diffusion constants (R_i) are also entered, a suitable choice of values being obtained by assuming isotropic reorientation.

Theory

(*i*) *The Choice of Principal Diffusion Axes (3, 5, 16)*

The orientation of the diffusion tensor principal axis system is the resultant of a number of forces acting on the system, reflecting the overall shape of the molecule and possible intermolecular interactions. Choosing the orientation is always difficult but can be simplified to some extent.

To a first approximation the principal axes of the moment of inertia tensor are the same as those of the diffusion tensor. This implies that overall molecular geometry is the primary factor involved in determining rotational diffusion constants, and this can only be true in the absence of polar groups and heavy atoms. Polar groups may also generate an electric dipole moment which can affect molecular motions (17). The overall symmetry of the system should be fairly high since it may not otherwise be possible to diagonalize the diffusion tensor (5, 16). At least three geometrically unique C—H vectors are necessary to determine the diffusion constants. It is important to recognize that the centre of the diffusion axes system cannot be located since the angles which appear in the equations for anisotropic rotational diffusion arise from a rotational transformation. Translational shifts of the centre of the diffusion axis coordinate system do not affect the relaxation times.

(*ii*) *Tests of the Applicability of the Diffusion Equation*

There are a number of criteria which can be used to test for the applicability of the small-angle rotational diffusion model for a particular axis of reorientation (17). The χ test proposed by Wallach and Huntress (18) compares the experimental correlation times (τ_c) with the theoretical reorientation time of a free gas molecule (τ_f),

$$\chi_i = \tau_{c_i}/\tau_{f_i} = (5/18D_i)(kT/I_i)^{1/2}$$

where I_i is the moment of inertia about axis i, and D_i

Can. J. Chem. Downloaded from www.nrcresearchpress.com by 210.87.254.5 on 09/05/12
For personal use only.

the diffusion constant. If the former is much larger than the latter, the molecule is quite rigidly held relative to its neighbours and the reorientation process is characterized by a random walk of small angle steps. Conversely, if the molecule is rotating about an axis with a substantial angular momentum, the reorientation is said to be in the inertial limit. Such behaviour can sometimes lead to a spin rotation contribution (19) to T_1. Gillen and Noggle (17) have suggested the arbitrary distinction that for $\chi < 3$ the molecule is in the inertial limit, and for $\chi > 5$ it is in the diffusion region, and this is also used as guide in the present study. Values for I_i were obtained by a computer reconstruction of the molecule, from known X-ray data if possible or extrapolations from the data for similar compounds, and subsequent determination of the moment of inertia tensor.

(iii) Errors in Calculated Rotational Diffusion Constants

As pointed out in a recent communication (20), errors in T_1^{dd} can be greatly magnified in computed R_i values. Because of the dependence of T_1^{dd} on the relative orientations of the C—H vectors, some motions may have little effect on an observed T_1. Conversely, errors in T_1^{dd} are not necessarily transmitted equally in the three dimensions of R_i. There will also be an interdependence between the three axes such that positive errors along one axis require negative errors along another to maintain a calculated T_1^{dd} within the experimental error limit. However, in a study such as this, it is the ordering of the R_i values that is important. In each case we have allowed the computer programme to sample a range of R_i values, calculate the corresponding T_1^{dd} values and estimate a standard deviation. Although the variation of R_i values was found to be large, in cases where anisotropic reorientation was evident the axis of fastest rotation can be identified unambiguously. The ordering of the other two R_i values cannot always be determined, however. The errors in R_i do place a severe limit on the sensitivity of the analysis to structural changes. Consequently, the interpretation of such data in terms of conformational details should be viewed with extreme caution in most cases. A typical set of R_i values and their associated T_1^{dd} values are shown in Table 1 for compound **5** (see Fig. 2).

It has been suggested (20) that all C—H interactions out to 2.5 Å should be taken into account in the calculation of R_i values. We have investigated this for each of the monocyclic derivatives by including all intramolecular C—H interactions. We found no significant differences in the calculated R_i values from those obtained using only bonded C—H interactions. A representative bicyclic system (**3**, Fig. 2) was similarly investigated, with particular reference to the skewing of the exomethylene groups. No significant differences were observed. This result is probably largely due to the relatively few non-bonded C—H interactions closer than 2.5 Å in the molecules studied here.

TABLE 1. Rotational diffusion constants and calculated dipolar relaxation time for compound **5**

			Calculated T_1^{dd} values (s)			
R_1*	R_2*	R_3*	$C_{1,4}$	$C_{5,6,7,8}$	$C_{9,10}$	σ† (s)
350	1500	350	9.78	10.06	6.48	0.46
450	1300	250	9.69	9.48	6.44	0.57
450	1500	250	9.70	10.22	6.61	0.43
550	1500	150	9.45	10.23	6.62	0.52
650	1300	150	10.60	10.07	7.18	0.51
750	1300	50	10.04	9.86	7.03	0.11
750	1500	50	10.17	10.68	7.24	0.60

*In 10^8 rad s^{-1}.
†Standard deviation of calculated T_1^{dd} from observed values (Table 3).

Results and Discussion

(i) Monocyclic Systems

Experimental and calculated ^{13}C T_1^{dd} values and corresponding rotational diffusion constants (R_i) for some simple ring systems are given in Table 2. The definition of the principal diffusion axes used here and the numbering scheme are shown in Fig. 1. In all of these molecules the moments of inertia are in the order $I_1 > I_2 > I_3$.

Pure methylcyclohexane and methoxycyclohexane behave very similarly, R_1 being the fastest diffusion constant, followed by R_3, with R_2 being the smallest. The calculated rotational diffusion constants are insensitive to the conformational geometry of the substituted ring, both axial and equatorial conformations giving indistinguishable results within the error limits of the calculations. Dilution of methylcyclohexane in $CDCl_3$ changes the diffusion constants towards less anisotropic reorientation, R_1 decreasing and R_2 and R_3 increasing. The short value of T_1^{dd} for the C-4 carbon in each of these compounds has been previously assumed to be due to the close alignment of the

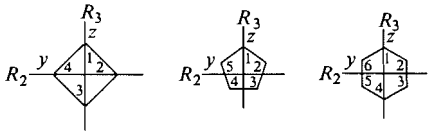


FIG. 1. Orientation of principal axes of diffusion in monosubstituted cyclic hydrocarbons: R_1 and x axis perpendicular to page; substituent at carbon 1.

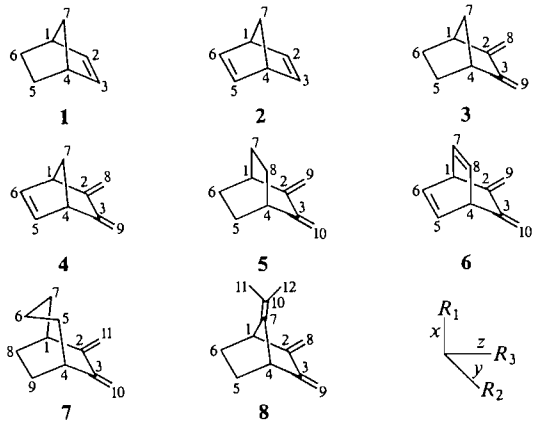


FIG. 2. Numbering scheme and orientation of principal axes of diffusion in bicyclic hydrocarbons.

C—H vector with the fastest axis of rotation (21). The present analysis shows this to be incorrect, as the T_1 difference between C-4 and C-2 or 3 must arise from a difference between the two slower axes of rotation, R_2 and R_3. This small difference may reflect differences in the moments of inertia (I_3 = 122 amu Å^2; I_2 = 414 amu Å^2). However, the slower motion about the y-axis (R_2) can also be due to the fact that this motion moves both the ring and the substituent, thereby sweeping out a greater volume. Similarly, the fastest motion (R_1) involves the axis with the highest moment of inertia, and this is best rationalized in terms of minimal disturbance of neighbouring molecules during this rotation. Application of the χ test shows that R_1 is near the inertial limit while R_2 and R_3 are essentially diffusion controlled (e.g. for methoxycyclohexane χ_1 = 1.7; χ_2 = 8.8; χ_3 = 5.4). The dominance of R_1 over R_2 and R_3 in planar or near planar ring systems seems to be fairly general in the absence of other complicating factors, for example in pyridine (22) and mesitylene (23).

The very short T_1 values for cyclohexanol reflect increased molecular association via hydrogen bonding. The ordering of the diffusion constants is also different, with R_3 the fastest. Qualitatively this is what one would expect for a hydrogen-bonded dimer. Quantitative conclusions about the motion of cyclohexanol are clouded by the probability that in such associated systems the principal diffusion axes and principal inertial axes are no longer aligned, and also the effect of the electric dipole moment in a molecule of this size has not been properly delineated. Dilution decreases the degree of self association and the ordering of the R_i values becomes similar to the other two derivatives. The closer resemblance between dilute cyclohexanol and methoxycyclohexane, rather than methylcyclohexane, may reflect the effect of the dipole moment.

The five membered ring of cyclopentene shows an appreciable contribution from spin-rotation to the T_1 values of the ethylenic carbons (16). Calculation of the motional characteristics from the T_1^{dd} contribution (Table 2) reveals fastest motion about the y-axis (R_2) followed closely by R_3 and R_1. The χ test is less than four in each case, suggesting at least partial inertial control of rotation. Grant and co-workers (16) have suggested that internal puckering vibrations also contribute substantially to the motions. Grandjean and co-workers (24) consider that the R_i values are essentially isotropic since previous calculations have ignored the shorter length of the olefinic C—H bond. While both considerations are valid, it should be emphasized that as inertial control becomes important the premises upon which the diffusion equations are based become increasingly inadequate.

Methylcyclopentane resembles methylcyclohexane in its rotational diffusion ($R_1 \gg R_3 > R_2$), while methoxycyclopentane and cyclopentanol differ in the relative ordering of R_2 and R_3. The χ test for methoxycyclopentane indicates that R_1 and R_2 are in the inertial limit (χ = 0.7 and 1.3 respectively) while R_3 is not (χ = 4.6). In all of these cases contributions to T_1^{dd} from ring flipping are possible, there being other evidence for large amplitude motions of this type in small rings (25–28). The T_1^{dd} values in cyclopentanol, compared to the other five membered ring derivatives, indicate considerable molecular association. It is interesting to note that changing from methyl to the more polar methoxy substituent substantially alters R_1 and R_3. The former is effectively perpendicular to the averaged dipole of the freely rotating methoxy group while the latter is colinear with the dipole. Introduction of hydrogen-bonding, with cyclopentanol, causes a major change in R_2 and a change in R_1, both of which are perpendicular to the direction of the interaction. As noted above, in such a case the principal axes of the diffusion tensor and the inertia tensor may no longer be aligned.

The fastest rotation in methylcyclobutane (R_3) appears to be governed by inertial considerations. The hydrogen-bonded neat cyclobutanol has very short T_1^{dd} values, characteristic of self-association, which give an ordering of rotation diffusion constants of $R_1 \gg R_2 > R_3$. A close similarity with cyclopentanol is noted, suggesting that internal puckering modes, if important, are similar in both ring systems. Dilution decreases the effect of hydrogen-bonding, and R_1 decreases while R_3 and R_2 both increase. Similar R_i values are noted for chlorocyclobutane, which does not associate ap-

Can. J. Chem. Downloaded from www.nrcresearchpress.com by 210.87.254.5 on 09/05/12
For personal use only.

Can. J. Chem. Downloaded from www.nrcresearchpress.com by 210.87.254.5 on 09/05/12
For personal use only.

precisely but does have a net electric dipole like cyclobutanol. Increasing the mass of the substituent while retaining the electric dipole, with bromocyclobutane, causes a reordering of the rates of rotational diffusion to $R_3 > R_2 > R_1$, which is in the inverse order of the moments of inertia. The complex interplay of effects upon which T_1^{dd} and R_i depend is effectively demonstrated by this series of related substituted cyclobutanes. It must be remembered that the defined orientation of the diffusion tensor principal axes in terms of the moment of inertia principal axes is a simplification which becomes invalid if either is subject to large perturbations. The presence of heavy atoms will perturb the latter and self-association and an electric dipole moment will perturb the former. Thus discussion of T_1^{dd} and R_i in terms of such effects is, at best, qualitative using the present approach. Similarly, the effect of other accompanying changes, structural or internal vibrational, for example, becomes impossible to specify.

(ii) Bicyclic Hydrocarbons

Experimental T_1^{dd} values and calculated R_i values are shown in Table 3 for a series of bicyclic hydrocarbons. Recalculated T_1^{dd} values have been omitted for clarity since the variations observed are similar to those shown in Table 2, and one derivative has been listed in detail in Table 1. The principal diffusion axes and numbering scheme for these derivatives are shown in Fig. 2. The moments of inertia are in the order $I_1 > I_2 > I_3$ for all of these derivatives.

Norbornane, norbornene, and norbornadiene have been previously investigated (16, 13, 29) and provide a convenient basis for comparison of the other bicyclic derivatives in this work. Differences in NT_1^{dd} are relatively small in these compounds and close to the experimental error. Concentration effects were found to be small for both T_1 and diffusion constants, and for norbornene increasing temperature causes a monotonic increase in T_1 for all carbons. If the spin–rotation mechanism were important in this temperature range, a levelling off of T_1 would be expected, such as observed for camphor (30) (above 315 K) and norbornadiene (28) (above 330 K). Under the conditions in this study the rotational diffusion constants for norbornene were in the order $R_3 > R_2 > R_1$, which is the inverse order of the moments of inertia. For the room temperature data, the χ test indicates inertial control for R_3 ($\chi = 1.5$) and R_2 ($\chi = 3.1$) and diffusion control for R_1 ($\chi = 8.5$). Assuming an Arrhenius temperature dependence for R_i, the energy barrier to rotation about the x and y axes is 9.2 kJ mol^{-1} (R_1 and R_2) and 10.5 kJ mol^{-1} for the z axis (R_3). These

TABLE 2. C-13 dipolar relaxation times and calculated rotational diffusion constants for some monosubstituted cyclic hydrocarbons

Compound		T_1^{dd}* (s)					R_i (10^{10} rad s^{-1})			Conditions
		C_1	C_2	C_3	C_4	CH_3	R_1	R_2	R_3	
Methylcyclohexane	(1)	14.1 (14.4)	10.9 (11.0)	11.0 (11.0)	10.0 (10.1)		48±12	3±2	8±3	Neat 35°C, ref. 19
	(2)	21.7 (21.9)	13.7 (13.9)	14.0 (13.9)	12.7 (12.9)	11.6	19±2	6±1	13±0.6	5 *M* $CDCl_3$ degsd. 35°C, ref. 19
Methoxycyclohexane		13.4	8.2	8.4	7.4	11.6	12±4	2.5±1.5	7.5±2.5	Neat 35°C, ref. 21
Cyclohexanol	(1)	0.72 (0.79)	0.59 (0.52)	0.60 (0.52)	0.32 (0.39)		0.6±0.1	0.1	0.8±0.2	Neat 35°C, ref. 21
	(2)	11.5 (11.6)	7.4 (7.4)	7.6 (7.4)	5.6 (5.6)		11±4	<2	10±2	0.4 *M* CCl_4/C_3D_6O, ref. 21
Cyclopentene		59.4 (58.2)	32.5 (32.2)	33.0 (33.9)			17±4	29±7	21±5	Reference 16
Methylcyclopentane		37.5 (38.4)	31.5 (32.0)	31.7 (30.1)	—	17.6	95±28	16	24±19	5 *M* $CDCl_3$, 30°C, ref. 19
Methoxycyclopentane		23.4 (24.8)	17.3 (17.1)	19.4 (17.6)	—	15.2	36±5	20±4	<1	Neat liquid, ref. 21
Cyclopentanol		2.5 (2.7)	4.1 (4.3)	3.3 (2.8)	—	—	19±2	2±1	<1	Neat liquid, ref. 21
Cyclobutanol	(1)	3.2 (3.5)	3.1 (3.4)	4.3 (3.9)			18±2	<3	<2	Neat 35°C, ref. 21
	(2)	12.4 (12.6)	10.7 (10.8)	11.6 (11.6)			48±9	<8	<5	0.4 *M* CCl_4/acetone
	(3)	21.8 (22.4)	13.9 (13.9)	12.7 (12.7)			20±6	6±4	10±4	0.2 *M* CCl_4/acetone
Methylcyclobutane		52.2 (56.8)	33.7 (38.1)	23.6 (26.8)		36.1	25±3	<4	61±15	5 *M* $CDCl_3$, 30°C, ref. 19
Chlorocyclobutane		28.6 (28.5)	19.3 (19.4)	19.4 (17.3)			39±5	11±2	9±2	0.4 *M* CCl_4/acetone, ref. 21
Bromocyclobutane		33.0 (32.6)	15.0 (15.3)	14.6 (14.7)			6±3	11±4	16±7	0.4 *M* CCl_4/acetone, ref. 21

*Values in parentheses are calculated from R_i values.

Can. J. Chem. Downloaded from www.nrcresearchpress.com by 210.87.254.5 on 09/05/12
For personal use only.

TABLE 3. C-13 dipolar relaxation times and calculated rotational diffusion constants for bicyclic hydrocarbons

Compound	Conditions	T_1^{dd} (s)										R_i (10^{10} rad s^{-1})		
		$C_{1,4}$	$C_{2,3}$	C_5	C_6	C_7	C_8	C_9	C_{10}	C_{11}	C_{12}	R_1	R_2	R_3
Norbornene	253 K	12.3	10.3	7.3	7.3	6.9	—	—	—	—	—	2.4±1.2	5.6±0.8	6.4±1.6
	315 K	32.8	25.9	16.7	16.7	15.6	—	—	—	—	—	6±3	10±2	20±7
	328 K	38.5	33.9	20.4	20.4	19.0	—	—	—	—	—	7±4	15±2	25±9
Norbornadiene		30.1	23.0	23.0	23.0	15.0	—	—	—	—	—	3±1	11±2	25±6
3		11.4	—	5.4	5.4	5.3	6.5	6.5	—	—	—	8±2	3.5±0.5	1.8±0.9
4	233 K	2.0	—	2.1	2.1	1.2	1.0	1.0	—	—	—	1.3±0.6	0.6±0.1	0.4±0.1
	256 K	4.1	—	3.4	3.4	1.9	2.2	2.2	—	—	—	4.0±0.6	0.9±0.2	0.3±0.1
	308 K	12.8	—	10.9	10.9	5.7	6.5	6.5	—	—	—	12.5±2	3.4±0.8	0.6±0.2
5	Neat	9.9	—	9.9	9.9	9.9	9.9	7.1	7.1	—	—	5.5±2	14±1	2±1
6	3.5 *M* $CDCl_3$ 308 K	9.0	—	7.0	7.0	7.0	7.0	4.8	4.8	—	—	10±5	1.6±1	1.4±0.8
	292 K	8.2	—	6.3	6.3	6.3	6.3	4.1	4.1	—	—	6±3	1.4±0.8	1.4±0.4
	275 K	5.7	—	3.9	3.9	3.9	3.9	2.8	2.8	—	—	3.9±1.2	0.6±0.3	1.3±0.3
7	$CDCl_3$	8.8	—	3.2	2.7	3.2	3.7	3.7	3.5	3.5	—	6.4±2	0.3±0.2	2.0±1
8	1.8 *M* $CDCl_3$	7.4	—	2.3	2.3	—	3.6	3.6	—	7.3	7.3	10.2±2	0.8±0.2	0.8±0.2

values are similar to those reported by Sato and co-workers (29) for norbornadiene (10.5 kJ mol^{-1}) and slightly higher than the value reported (30) for a $CDCl_3$ solution. However, there is some discrepancy with these proton studies which report the motion of norbornadiene as isotropic at 25°C with $R = 7 \times 10^{10}$ s^{-1}. By contrast, data for the structurally similar norbornane (16) also indicates anisotropic motion, and a small observed anisotropy is not unexpected if the ellipticity factor ε is considered. This is the ratio of the maximum separation of atoms along axes perpendicular to the given rotation axis. The greater the value of ε, the slower the motion about that axis. Thus the axis of R_1, with the largest moment of inertia (183 amu Å^3) has an intermediate ε and the R_2 axis (I_2 = 145 amu Å^3) has the highest ε. Such opposing effects would tend to partially cancel out and minimize the net anisotropy of reorientation, making it more difficult to detect by a technique subject to quite large errors.

The derivatives **3** to **8** (Fig. 2) all contain exomethylene groups attached to a bicyclic skeleton. The immediate effect in **3** and **4** is a marked increase in the inertial anisotropy with I_1 increasing by a greater factor than I_2 greater than I_3. Subsequent changes, **5** to **8**, tend to decrease the inertial anisotropy again. The behaviour of **3** (2,3-dimethylene bicyclo(2.2.1)heptane) and **4** (2,3-dimethylene bicyclo(2.2.1)hept-5-ene) are quite different from the norbornane systems, as shown by the data in Table 3. The rotational diffusion constants for **3** do not correlate with moments of inertia, and the χ tests indicate that inertial effects are minimal for R_2 (χ = 8.6) and R_3(χ = 32.6), but may be important for R_1 (χ = 2.6). There is a similarity to the six membered ring systems in that the largest diffusion constant represents motion about an axis that appears to sweep out the least volume of solvent. The ε values for the three axes correlate with this effect, and a similar behaviour has been noted before (16) in the elongated molecule of *trans*-decalin. A low temperature study on **4** reveals a large change in R_1 and R_2 with temperature while R_3 changes only slightly. Steric, inertial, and electric dipole terms may be considered responsible for this observation. The relevant ellipticities relate to steric effects and should be more important for R_2 and R_3 than R_1. Inertial effects should give the order $R_3 > R_2 > R_1$, and a similar order is anticipated for the small electric dipole contribution aligned with the z axis. The χ test indicates that R_1 changes from diffusion (χ = 16) at low temperature to inertial (χ = 2) control at room temperature, R_2 moves in this direction also (χ = 39 to χ = 8) whereas R_3 remains under diffusional control (χ = 73 to χ = 56). The resulting nature of

Can. J. Chem. Downloaded from www.nrcresearchpress.com by 210.87.254.5 on 09/05/12
For personal use only.

the motion at any temperature thus represents a compromise between greater steric hindrance about the z axis and the less favourable inertial and electric dipole effects about the x axis. A similar trend has been found for *N,N*-dimethylformamide (5) in which steric and electric dipole effects compete, and in which there is also a marked shift of the principal diffusion tensor axes away from the principal inertial axes due to the large electric dipole. The present case is an interesting example involving a molecule with no large electric dipole moment, suggesting that such non-Arrhenius behaviour may be more common than hitherto believed.

Calculation of the diffusion constants depends explicitly on the molecular structure through the direction cosines of the relevant C—H vectors. Structural changes are therefore only detectable if there is a significant rotational shift of C—H vectors. In compounds **3** and **4** the orientation of the exomethylene groups may be skewed due to internal steric interactions of the inner C—H bonds. Compound **3** was used to estimate the variation in calculated diffusion constants on rotating the *sp* carbon bond angles between 114° and 130°. No significant changes in the diffusion constants were found.

Compound **5** (2,3-dimethylene bicyclo(2.2.2)-octane) illustrates another problem in delineating trends. The pure liquid has rotational diffusion constants in the order $R_2 > R_1 > R_3$ in contrast to the heptane analogue **3**. Bicyclo(2.2.2)octane itself exhibits a similar anisotropy with $R_{\|}(R_2) = 17 \pm 4 \times 10^{10}$ rad s^{-1} and $R_{\perp}(R_1, R_3) = 9 \pm 2 \times 10^{10}$ rad s^{-1}. Compound **6** (2,2-dimethylene bicyclo(2.2.2)octa-5,7-diene), however, was found to be similar to the heptane analogue **4** with $R_1 > R_2 > R_3$.

Explanation of the preferred axes of rotation in **5** and **6** is not straightforward. Considerations of ellipticity do not explain the differences between **5** and **6**, and in neither case do the R_i values relate inversely to the moments of inertia (e.g. for **6**, $I_1 = 386$; $I_2 = 337$; and $I_3 = 228$ amu Å^2). The parallel between compounds **4** and **6** was found to extend over a similar temperature range with a large change in R_1 and almost no change in R_3.

Compound **7** (2,3-dimethylene bicyclo(3.2.2)-nonane) introduces a further minor change in the bicyclo skeleton with little overall effect on the diffusional behaviour of the molecule. The ordering of the rotational diffusion constants is $R_1 > R_3 > R_2$ which correlates with the ellipticities ($\varepsilon_1 = 1.16$, $\varepsilon_2 = 1.42$, $\varepsilon_3 = 1.22$).

Compound **8** (2,3-dimethylene-7-isopropylidene bicyclo(2.2.1)heptane) is structurally different along the axis of R_1, and again the ordering of the diffusional constants essentially follows that of the ellipticities; ($\varepsilon_1 = 1.07$, $\varepsilon_3 = 1.15$, $\varepsilon_2 = 1.24$). Despite the structural modification, the relative magnitudes of the diffusion constants are similar to those of the related bicyclic systems **3** and **4**.

The structural change from the norbornyl skeleton to the exomethylene derivatives **3** and **4** causes a marked change in the rotational diffusion behaviour of the molecule. By contrast, the more flexible bicyclo(2.2.2)octane skeleton when similarly modified to give compound **5** shows considerably less change in diffusional behaviour. Also, while the norbornyl derivatives **3** and **4** are similar in behaviour, there is a substantial change in rotational behaviour between **5** and **6**. It is known (31–33) that bicyclo(2.2.2)octane and its derivatives undergo relatively large amplitude internal oscillations which can effect T_1^{dd}. Calculations (32) on the parent hydrocarbon indicate a barrier of 420 J mol^{-1} and a root-mean-square amplitude of 12° for twisting about the D_{3h} symmetry axis. Such a motional contribution to T_1^{dd} may overshadow the changes wrought by introduction of exomethylene groups to give compound **5**. Damping these oscillations by the introduction of double bonds in the ring, compound **6**, then gives the expected changes so that compounds **4** and **6** resemble each other. Going in the direction of increasing ring flexibility, compound **7**, also appears to have a similar effect on the R_i values, perhaps indicating that the flexing motions are now too facile and occurring too rapidly to affect T_1^{dd} under the present experimental conditions.

Conclusions

The errors introduced into the rotation diffusion constants from experimental errors of the relaxation times are often disturbingly large. These errors do not generally permit elucidation of effects other than major structural changes in a series of compounds. In addition, use of variable temperature T_1^{dd} data directly to estimate energy barriers to diffusional reorientation can also be misleading in view of the possible non-Arrhenius behaviour noted for the calculated R_i values. Large amplitude internal motions also contribute to T_1^{dd} and hence possibly affect R_i values. Dilution, temperature and viscosity changes can alter the relative contributions to T_1^{dd} of internal motions and rotational diffusion, and change the relative importance of electric dipole, inertial, and steric effects in the latter. Consequently, comparisons from one study to another can be risky unless all these effects can be taken into account. A recent study on 1-substituted adamantanes (34) has specifically looked at solvent effects.

However, we believe that in molecules where substantial anisotropic reorientation is occurring it is usually possible to identify the fastest axis of rotation. This axis is not always the one that might be picked intuitively from considerations of the molecular structure, or even from the observed T_1 values. Thus the calculations are of obvious value in such cases. The observed relative rates of rotational diffusion can, in many cases be correlated in a qualitative sense with either inertial effects or ellipticities. The former are most important in smaller molecules and are characterized by low values in the χ test and, in the extreme, spin rotation contributions to the observed relaxation rate.

Acknowledgements

The authors wish to thank Dr. D. N. Butler and Dr. R. A. Snow for supplying the bicyclic compounds, and the Natural Sciences and Engineering Research Council of Canada for financial support.

1. E. Breitmaier, K. H. Spohn, and S. Berger. Angew. Chem. Int. Ed. **14**, 144 (1975).
2. D. E. Woessner. J. Chem. Phys. **37**, 647 (1962).
3. G. C. Levy and I. R. Peat. J. Magn. Res. **18**, 500 (1975).
4. L. D. Favro. Phys. Rev. **119**, 53 (1960).
5. W. T. Huntress Jr. Adv. Magn. Res. **41**, 1 (1970).
6. D. N. Butler and R. A. Snow. Can. J. Chem. **50**, 795 (1972).
7. R. A. Snow, Ph.D. Thesis, York University. 1976.
8. R. L. Vold, J. S. Waugh, M. P. Klein, and D. E. Phelps. J. Chem. Phys. **48**, 3831 (1968).
9. R. Freeman and H. D. W. Hill. J. Chem. Phys. **54**, 3367 (1971).
10. R. Freeman, H. D. W. Hill, and R. Kaptein. J. Magn. Res. **7**, 82 (1972).
11. P. R. Bevington. Data reduction and error analysis for the physical sciences. McGraw-Hill, New York. 1969.
12. D. L. Fontaine, D. K. Ross, and B. Ternai. J. Magn. Reson. **18**, 276 (1975).
13. S. J. Opella, D. J. Nelson, and O. Jardetzky. J. Chem. Phys. **64**, 2533 (1976).
14. O. A. Gansow and W. Schittenhelm. J. Am. Chem. Soc. **93**, 4294 (1971).
15. J. R. Lyerla and G. C. Levy. Topics in carbon-13 nmr spectroscopy. Vol. 1. Wiley Interscience. 1974. Chapt. 3.
16. D. M. Grant, R. J. Pugmire, E. P. Black, and K. A. Christensen. J. Am. Chem. Soc. **95**, 8465 (1973).
17. K. T. Gillen and J. H. Noggle. J. Chem. Phys. **53**, 801 (1970).
18. D. Wallach and W. T. Huntress Jr. J. Chem. Phys. **50**, 1219 (1969).
19. S. Berger, F. R. Kreissl, D. M. Grant, and J. D. Roberts. J. Am. Chem. Soc. **97**, 1805 (1975).
20. P. Stilbs and M. E. Moseley. J. Magn. Reson. **33**, 209 (1979).
21. (*a*) G. C. Levy, R. A. Komoroski, and R. E. Echols. Org. Magn. Reson. **7**, 172 (1975); (*b*) R. A. Komoroski and G. C. Levy. J. Phys. Chem. **80**, 2410 (1976).
22. L. H. Scharpen. J. Chem. Phys. **48**, 3552 (1968).
23. D. R. Bauer, G. R. Alms, J. I. Brauman, and R. Pecora. J. Chem. Phys. **61**, 225 (1974).
24. J. Grandjean and P. Laszlo. Mol. Phys. **30**, 413 (1975).
25. W. J. Adams, H. J. Geise, and L. S. Bartell. J. Am. Chem. Soc. **92**, 5013 (1970).
26. L. A. Carreira, G. J. Jiang, W. B. Person, and J. N. Willis, Jr. J. Chem. Phys. **56**, 1440 (1972).
27. (*a*) J. R. Dwig and D. W. Wertz. J. Chem. Phys. **49**, 2118 (1968); (*b*) A. Almenningen, H. M. Seip, and T. Willadsen. Acta Chem. Scand. **23**, 2748 (1969); (*c*) H. J. Geise, W. J. Adams, and L. S. Bartell. Tetrahedron, **25**, 3045 (1969).
28. R. DesLauriers and I. C. P. Smith. Topics in carbon-13 nmr spectroscopy. Vol. 2. *Edited by* G. C. Levy, Wiley Interscience. 1975. Chapt. 1.
29. K. Sato and A. Nishioki. J. Magn. Reson. **6**, 231 (1972).
30. J. Grandjean and P. Laszlo. Mol. Phys. **25**, 695 (1973).
31. E. Hirota. J. Mol. Spectrosc. **38**, 367 (1971).
32. A. Yokozeki, K. Kuchitsu, and Y. Morino. Bull. Chem. Soc. Jpn. **43**, 2017 (1970).
33. O. Ermer and J. D. Dunitz. Chem. Commun. 567 (1968); O. Ermer and J. D. Dunitz. Helv. Chim. Acta, **52**, 1861 (1969).
34. H. Beierbeck, R. Martino, and J. K. Saunders. Can. J. Chem. **57**, 1224 (1979).

Can. J. Chem. Downloaded from www.nrcresearchpress.com by 210.87.254.5 on 09/05/12
For personal use only.

Modification of HAM/3 excitation energies for $\pi\pi^*$ transitions of linear molecules

DELANO P. CHONG[1]

Department of Chemistry, 2545 The Mall, University of Hawaii at Manoa, Honolulu, HI 96822, U.S.A. and NASA-Ames Research Center, Moffett Field, CA 94035, U.S.A.

Received March 6, 1980

DELANO P. CHONG. Can. J. Chem. **58**, 1687 (1980).

The excitation energies calculated by the HAM/3 procedure for $\pi\pi^*$ transitions in linear molecules can be internally inconsistent by as much as ± 0.6 eV. In the recent study by Åsbrink *et al.*, the problem was avoided by adopting Recknagel's expressions and requiring the proper average $\pi\pi^*$ excitation energy. In this paper, we trace the small inconsistency back to its origin in HAM/3 theory and derive the analytical expression for the energy correction as well as Recknagel's formulas. Numerical examples studied include all seven linear molecules investigated by Åsbrink *et al.* The explicit expression for the correction enables us to perform meaningful configuration-interaction calculations on the excited states, as illustrated by the carbon suboxide molecule.

DELANO P. CHONG. Can. J. Chem. **58**, 1687 (1980).

Les énergies d'excitations des transitions $\pi\pi^*$ calculées par la technique HAM/3 pour les molécules linéaires peuvent contenir des erreurs internes pouvant aller jusqu'à $\pm$ 0.6 eV. Dans une étude récente, Åsbrink *et al.* ont contourné le problème en adoptant des expressions de Recknagel et en faisant appel à une moyenne appropriée de l'énergie d'excitation $\pi\pi^*$. Dans cet article nous avons retrouvé la cause des ces erreurs dans la théorie HAM/3 et nous déduisons l'expression analytique pour la correction de l'énergie ainsi que pour les formules de Recknagel. Les exemples numériques étudiés comprennent toutes les sept molécules linéaires étudiées par Åsbrink *et al.* L'expression explicite de la correction nous permet d'effectuer des calculs significatifs d'interaction de configuration des états excités tel qu'illustré par la molécule de sous-oxyde de carbone.

[Traduit par le journal]

1. Introduction

In a recent paper (1), Åsbrink *et al.* applied their new semi-empirical HAM/3 molecular orbital method (2) to calculate valence excitation energies of linear molecules. If they had used HAM/3 formalism throughout, the result would have shown that the two components of the $\pi\pi^*$ $^1\Delta$ state are split (by as much as 1.2 eV), as are those of $^3\Delta$. However, Åsbrink *et al.* (1) avoided the difficulty by adopting Recknagel's expression (3, 4) and by equating the average $\pi\pi^*$ excitation energy to the difference in HAM/3 orbital energies. Consequently, their numerical results are not affected by the present analysis.

In this paper, we first point out the origin of the deficiency in the HAM/3 procedure. Then, we obtain an explicit expression for the correction to HAM/3 excitation energies for $\pi\pi^*$ transitions of linear molecules. After the correction, Recknagel's formulas are recovered. Numerical results for the correction are confirmed for all seven linear molecules studied by Åsbrink *et al.* (1).

With the correction, it is now meaningful to perform configuration-interaction (CI) calculations to improve on the Recknagel energies. Numerical results of such calculations are reported for C_3O_2 in Section 3.

[1]Permanent address: Department of Chemistry, University of British Columbia, 2075 Wesbrook Place, Vancouver, B.C., Canada V6T 1W5.

2. The Correction

To keep the notation simple, we shall consider a linear molecule belonging to the $C_{\infty v}$ point group. Appropriate subscripts u or g should be added for linear molecules with $D_{\infty h}$ symmetry. The degenerate π orbitals of interest are denoted by x and y and the π^* orbitals by X and Y. Following Åsbrink *et al.*, we define the electron repulsion integrals: $a = 2(\mathrm{xy}|\mathrm{XY})$, $b = 2(\mathrm{xY}|\mathrm{xY}) = 2(\mathrm{yX}|\mathrm{yX})$, $2c = K + \bar{K}$, $K = (\mathrm{xX}|\mathrm{xX}) = (\mathrm{yY}|\mathrm{yY})$, and $\bar{K} = (\mathrm{xX}|\mathrm{yY})$. The relative signs of the molecular orbitals are arbitrary and affect the signs of a and $\bar{K}$. To be consistent with Recknagel's expressions (3), we choose a to be positive so that if a computed value of a is negative, we would change the signs of a and $\bar{K}$ simultaneously ($\bar{K}$ may end up to be negative). Also we shall follow Åsbrink *et al.* (1) in using state symbols for excitation energies although it is not a standard practice.

The origin of the deficiency of HAM/3 theory when applied to $\pi\pi^*$ transitions of linear molecules lies in the fact that the average of the singlet and triplet excitation energies is given by $\Delta\varepsilon$ whether the transition is $\mathrm{x} \rightarrow \mathrm{X}$ or $\mathrm{x} \rightarrow \mathrm{Y}$, in contrast to standard Hartree–Fock theory (5).

The deficiency can be corrected in the following manner. Let the average of the singlet and triplet excitation energies be given by $\Delta\varepsilon + \delta$ for $\mathrm{x} \rightarrow \mathrm{X}$ or $\mathrm{y} \rightarrow \mathrm{Y}$ transition and $\Delta\varepsilon - \delta$ for $\mathrm{x} \rightarrow \mathrm{Y}$ or $\mathrm{y} \rightarrow \mathrm{X}$. Then, it can be shown that, when we do a simple 2

0008-4042/80/161687-04$01.00/0

©1980 National Research Council of Canada/Conseil national de recherches du Canada

Can. J. Chem. Downloaded from www.nrcresearchpress.com by 210.87.254.40 on 09/05/12
For personal use only.

Can. J. Chem. Downloaded from www.nrcresearchpress.com by 210.87.254.40 on 09/05/12
For personal use only.

× 2 configuration-interaction calculation on the degenerate transitions, we get

$$[1] \quad K - b/2 = c = \bar{K} + b/2$$

$$[2] \quad \delta = c/2 - a/2$$

and recover Recknagel's expressions (3) which were used by Åsbrink *et al.* (1)

$$\begin{aligned} {}^1\Sigma^+ &= C - a + 4c \\ {}^1\Delta &= C + 2b \\ {}^{1,3}\Sigma^- &= C + a \\ {}^3\Delta &= C \\ {}^3\Sigma^+ &= C - a \end{aligned} \quad [3]$$

where

$$C = \Delta\varepsilon - b/2 - c/2$$

As noted by Åsbrink *et al.*, the INDO-like approximation formula for the repulsion integrals in HAM/3 makes $a = b$ for linear molecules. Consequently, eq. [2] can also be written as

$$[4] \quad \delta = K/2 - 3b/4$$

For the seven linear molecules[2] studied by Åsbrink *et al.* (1), the shift δ ranges from −0.0012 eV for $1\pi_u \rightarrow 2\pi_g$ of C_2N_2 to 0.6079 eV for $2\pi \rightarrow 3\pi$ of N_2O.

The $1e_{1g}(\pi)$ to $1e_{2u}(\pi^*)$ transition of benzene presents a similar situation. If one considers the $1a_2$, $2b_1$, $2a_2$, and $3b_1$ π-molecular orbitals (in C_{2v} representation) of benzene as the analogs of the x, y, X, and Y orbitals of linear molecules respectively, then the counterparts of the molecular levels ${}^1\Sigma^+$, ${}^1\Delta$, ${}^{1,3}\Sigma^-$, ${}^3\Delta$, and ${}^3\Sigma^+$ are ${}^1B_{1u}$, ${}^1E_{1u}$, ${}^{1,3}B_{2u}$, ${}^3E_{1u}$, and ${}^3B_{1u}$, respectively. However, the integral a for benzene is 0.4946 eV (according to HAM/3) compared to $b = 1.4533$ eV. In other words, eq. [4] is not valid for benzene and the δ-correction must be obtained from eq. [2]. For benzene, the δ-correction is found to be −0.0972 eV.

With the explicit expression for the δ-correction, it is now meaningful to perform CI calculations on the excited states. The carbon suboxide molecule is studied as an example.

3. Carbon Suboxide

The electronic structure of C_3O_2 has been the subject of a number of studies (7–16). The absorption spectrum (7–11) between 4–11 eV has been reviewed by Roebber (11). However, the peaks between 13 and 19 eV (10) remain unassigned. It is our hope that HAM/3 calculations can increase our understanding of the absorption spectrum.

The uv and X-ray photoelectron spectra have also been studied (12–14). There remains, however, a disagreement (at the same laboratory) on the ordering of the third to the fifth ionization potentials. The results of HAM/3 calculations are presented in Table 1, together with the experimental results and values from other calculations. It is not surprising that the HAM/3 results are very good (17).[3] As Table 1 shows, the HAM/3 results favor the ordering of Gelius *et al.* (13). On the other hand, C_3O_2 is one of 80 molecules used in the parametrization process (18), and there may be an inherent bias because that assignment was used in the parametrization procedure.

The absorption spectrum is not completely understood. Roebber (11) assigned the three bands between 4 and 8 eV based on effect of temperature and pressure, the Herzberg–Teller theory of vibrationally induced electronic transitions, and on INDO molecular orbital calculations. Figure 1 shows a composite spectrum from the studies of various workers (7, 10, 11). The energy scale is not linear and the absorption scale is not uniform. The first band at 4.67 eV (7) was assigned to the ${}^1\Sigma_u^-$ and ${}^1\Delta_u$ states arising from $2\pi_u$ to $2\pi_g$ excitation, both states calculated to be 3.71 eV above the ${}^1\Sigma_g^+$ ground state by the INDO method (11). The second band at 6.96 eV (10, 11) was first assigned to ${}^1\Sigma_u^+(2\pi_u \rightarrow 2\pi_g)$ (10), but was then changed to ${}^1\Sigma_g^-(2\pi_u \rightarrow 3\pi_u)$ and ${}^1\Delta_g(2\pi_u \rightarrow 3\pi_u)$ (11). This band can also be interpreted as the $n = 3$ member of first Rydberg series (δ = 1.00) as pointed out by Robin (19). The intensive ($f = 1.5$) band at 7.82 eV (10, 11) was assigned to the combination of ${}^1\Sigma_u^+(2\pi_u \rightarrow 2\pi_g)$ and ${}^1\Pi_u(2\pi_u \rightarrow 3s$ Rydberg). The 8–11 eV region was assigned (10) to $2\pi_u \rightarrow ns$ Rydberg series with either upper-state vibrations or a second Rydberg series. There remains some uncertainty and some unassigned peaks at higher energies, because of diffuseness of the bands and the unreliability of the INDO results.

The numerical results from HAM/3 are summarized in Table 2. There are two sets of unoccupied π* molecular orbitals $2\pi_g$ and $3\pi_u$. The molecular states arising from the one-electron transitions from $2\pi_u$, $1\pi_g$, and $1\pi_u$ to $2\pi_g$ are labelled as A, B, and C respectively, while those from $2\pi_u$, $1\pi_g$, and $1\pi_u$ to $3\pi_u$ are denoted by D, E, and F respectively in Table 2. While the results from HAM/3 are by no means definitive, they offer interesting alternatives to the INDO interpretations. There is little doubt concerning the assignment of

[2]The equilibrium geometry of all of the molecules studied in this paper has been taken from Hellwege's compilation (6).

[3]In ref. 17, the two consecutive entries at −0.30 and −0.30 in the column headed by HAM/3 in Table 1 should read −0.15 and −0.45, respectively.

TABLE 1. Vertical ionization potentials (in eV) of C_3O_2

MO	HAM/3	Experiment PES (12)	Experiment Ref. 14	Experiment XPS (13)	CNDO/2 (15)	INDO (11)	Xα (16)	*Ab initio* (13)
$2\pi_u$	10.9	10.7	10.75	10.8	12.42	9.57	13.5	11.1
$1\pi_g$	15.2	14.8	14.8	15.0*	20.09	16.2	16.9	17.7
$1\pi_u$	15.8	15.9	17.5	16.0*	24.93	17.6	17.4	18.7
$5\sigma_u$	17.3	17.0	15.8	17.3*		15.7	20.4	20.3
$6\sigma_g$	17.3	17.3	17.0	17.5*		17.1	20.6	20.6
$4\sigma_u$	20.7	19		21.9		23.9	24.0	26.1
$5\sigma_g$	25.5			25.6		33.6	25.8	30.7
$3\sigma_u$	35.8			35.5		47.1	32.4	41.8
$4\sigma_g$	36.0			35.5		46.7	32.7	41.8
C_2K	289.2			291.5			306.0	307.3
C_1K	292.2			294.9			309.4	312.3
OK	538.1			539.7			536.4	562.6

*Best fit.

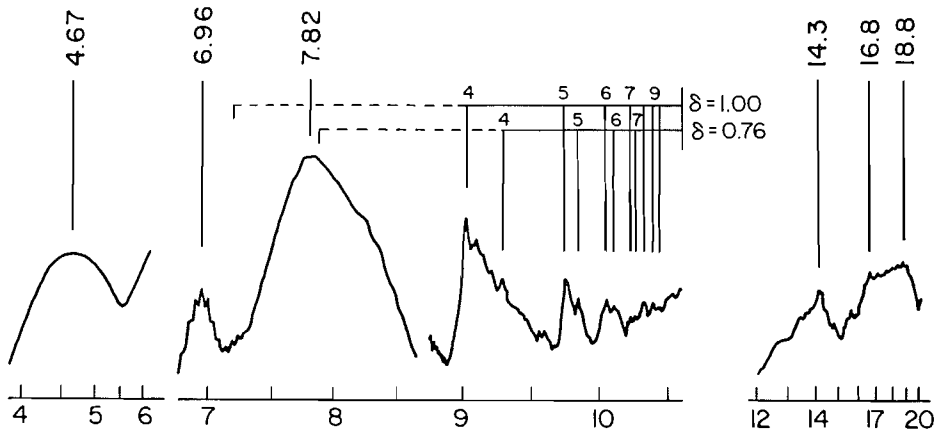


FIG. 1. Composite absorption spectrum of C_3O_2, taken from the studies of refs. 7, 10, and 11.

the 4.67 and 7.82 eV bands, although HAM/3 does poorly on those excitation energies, even after CI. The other results are quite different from INDO: (*a*) If the $^1\Sigma_g^-$ and $^1\Delta_g$ states are responsible for the 6.96 eV band they would seem to come from transition (B) $1\pi_g \rightarrow 2\pi_g$, rather than from (D) $2\pi_u \rightarrow 3\pi_u$, which was indicated by the INDO results. According to HAM/3, the latter states are about 9.8 eV above the $^1\Sigma_g^+$ ground state. (*b*) The assignment of the Rydberg region to one main series with upper-state vibrations was preferred (10) because the bands at 74.4 kK (9.22 eV) and 77.2 kK (9.57 eV) could not be fitted into any Rydberg series. The HAM/3 results offer some possible excited states for the alternative interpretation. There are two states with non-zero oscillator strengths at 10.5 and 10.6 eV according to HAM/3. (*c*) Between 14 and 19 eV there are four allowed transitions with *f*-value ranging from 0.006 to 0.45 which may contribute to the unassigned bands in that region.

4. Discussion

The preceding section shows that HAM/3 provides very good ionization potentials for C_3O_2, but the calculated excitation energies even after CI are not as accurate as those of other linear molecules (1). Leaving the example of carbon suboxide, let us examine the general performance of the semi-empirical HAM/3 molecular orbital method. Although the most frequent applications of HAM/3 have been the calculations of (*a*) vertical ionization potentials, (*b*) excitation energies, (*c*) electron affinities, and (*d*) anion excitations, the method has also been applied (see ref. 20) to (*e*) shake-up satellites in valence-electron photoelectron spectra, (*f*) core-electron binding energies in ESCA, (*g*) doubly charged cations, (*h*) core-electron excitation spectra, (*i*) X-ray emission spectra, and (*j*) shake-up satellites in core-electron ESCA. It can be seen that HAM/3 can be useful for a wide range of problems. Moreover, after some initial criticism

Can. J. Chem. Downloaded from www.nrcresearchpress.com by 210.87.254.40 on 09/05/12
For personal use only.

TABLE 2. Results of HAM/3 singlet excitation energies (in eV) and *f*-values in parentheses, compared with the observed values and Roebber's assignments (11)

State*	Singlet excitation energy			
	w/o CI	CI	Obs. (7, 10, 11)	INDO state†
Σ_u^-(A)	3.84	3.74(0)	4.67(0.002)	3.71 Σ_u^-(A)
Δ_u(A)	4.01	3.89(0)		3.71 Δ_u(A)
				5.70 $\Pi_u(2\pi_u \rightarrow 7\sigma_g)$
Σ_g^-(B)	8.60	7.53(0)	6.96(0.08)	5.92 Σ_g^-(D)
Δ_g(B)	8.93	7.91(0)		5.92 Δ_g(D)
Σ_u^+(A)	9.08	8.63(4.1)	7.82(1.5)	7.16 Σ_u^+(A)
Σ_g^-(D)	9.19	9.66(0)		
Σ_u^-(C)	9.23	8.55(0)		
Δ_g(D)	9.47	10.00(0)		
Δ_u(C)	9.53	9.01(0)		
Σ_u^+(C)	10.77	10.55(1.4)		
Σ_g^+(B)	10.84	9.81(0)		
$\Pi_u(5\sigma_u \rightarrow 2\pi_g)$	11.14	10.50(0.10)		9.17 $\Pi_u(5\sigma_u \rightarrow 2\pi_g)$
$\Pi_g(6\sigma_g \rightarrow 2\pi_g)$	11.23	10.56(0)		
Σ_g^+(D)	11.99	12.50(0)		8.76 Σ_g^+(D)
Σ_u^-(E)	13.77	14.58(0)		
Δ_u(E)	13.92	14.55(0)		
Σ_g^-(F)	14.36	14.97(0)		
Σ_u^+(E)	14.47	14.86(0.14)		
Δ_g(F)	14.55	15.04(0)		
$\Pi_u(4\sigma_u \rightarrow 2\pi_g)$	14.67	14.53(0.45)		
Σ_g^+(F)	14.73	15.10(0)		
$\Pi_g(5\sigma_g \rightarrow 3\pi_u)$	15.99	16.62(0)		
$\Pi_u(6\sigma_g \rightarrow 3\pi_u)$	16.07	16.79(0.006)		
$\Pi_u(2\pi_u \rightarrow 7\sigma_g)$	18.85	18.81(0.02)		
$\Pi_g(5\sigma_g \rightarrow 2\pi_g)$	19.34	18.87(0)		
etc.				

*See text for the $\pi\pi^*$ transitions A to F.
†Reference 11.

(21), a firmer theoretical basis of the HAM model has gradually emerged (22, 23). Because the cost of a HAM calculation is about the same as CNDO, it would be a powerful research tool when the extension (24) to molecules containing elements up to Br is completed.

Acknowledgements

The author is grateful to Professor E. Lindholm for suggesting the problem, to Dr. L. Åsbrink for helpful correspondence, to Professor R. G. Inskeep for his hospitality, and to the National Aeronautics and Space Adminstration for a NASA-ASEE Summer Faculty Fellowship.

1. L. ÅSBRINK, C. FRIDH, and E. LINDHOLM. Chem. Phys. **27**, 159 (1978); **27**, 169 (1978).
2. L. ÅSBRINK, C. FRIDH, and E. LINDHOLM. Chem. Phys. Lett. **52**, 63 (1977); **52**, 69 (1977); **52**, 72 (1977).
3. A. RECKNAGEL. Z. Phys. **87**, 375 (1934).
4. C. W. SCHERR. J. Chem. Phys. **23**, 569 (1955).
5. C. C. J. ROOTHAAN. Rev. Mod. Phys. **23**, 69 (1951).
6. K. H. HELLWEGE and LANDOLT -BÖRNSTEIN. Numerical data and functional relationships in science and technology, New Series, Group II, Vol. 7. Springer-Verlag, Berlin. 1976.
7. K. D. BAYES. J. Am. Chem. Soc. **84**, 4077 (1962).
8. S. BELL, T. S. VARADRARJAN, A. D. WALSH, P. A. WARSOP, J. LEE, and L. SUTCLIFFE. J. Mol. Spectrosc. **21**, 42 (1966).
9. H. H. KIM and J. L. ROEBBER. J. Chem. Phys. **44**, 1709 (1966).
10. J. L. ROEBBER, L. C. LARRABEE, and R. E. HUFFMAN. J. Chem. Phys. **46**, 4594 (1967).
11. J. L. ROEBBER. J. Chem. Phys. **54**, 4001 (1971).
12. C. BAKER and D. W. TURNER. Chem. Commun. 400 (1968).
13. U. GELIUS, C. J. ALLAN, D. A. ALLISON, H. SIEGBAHN, and K. SIEGBAHN. Chem. Phys. Lett. **11**, 224 (1971).
14. J. W. RABALAIS, T. BERGMARK, L. O. WERME, L. KARLSSON, M. HUSSAIN, and K. SIEGBAHN. *In* Electron spectroscopy. *Edited by* D. A. Shirley. North-Holland, Amsterdam. 1972. pp. 425*ff*.
15. J. F. OLSEN and L. BURNELLE. J. Phys. Chem. **73**, 2298 (1969).
16. J. W. D. CONNOLLY, H. SIEGBAHN, U. GELIUS, and C. NORDLING. J. Chem. Phys. **58**, 4265 (1973).
17. D. P. CHONG. Theor. Chim. Acta, **51**, 55 (1979).
18. E. LINDHOLM and L. ÅSBRINK. Personal communication.
19. M. B. ROBIN. Higher excited states of polyatomic molecules. Vol. 2. Academic Press, New York. 1975. pp. 205–208.
20. D. P. CHONG. To be published.
21. S. DE BRUIJN. Chem. Phys. Lett. **52**, 76 (1977); Theor. Chim. Acta, **50**, 313 (1979).
22. L. ÅSBRINK, C. FRIDH, E. LINDHOLM, and S. DE BRUIJN. Chem. Phys. Lett. **66**, 441 (1979).
23. L. ÅSBRINK, C. FRIDH, E. LINDHOLM, S. DE BRUIJN, and D. P. CHONG. Phys. Scripta. In press.
24. L. ÅSBRINK, C. FRIDH, and E. LINDHOLM. Personal communication.

Can. J. Chem. Downloaded from www.nrcresearchpress.com by 210.87.254.40 on 09/05/12
For personal use only.

Kinetic studies of the reactions of 4-nitrobenzofuroxan with cyanide ion and isopropoxide ion in isopropanol

MICHAEL E. MOIR AND ALBERT R. NORRIS[1]

Department of Chemistry, Queen's University, Kingston, Ont., Canada K7L 3N6

Received February 4, 1980

MICHAEL E. MOIR and ALBERT R. NORRIS. Can. J. Chem. **58**, 1691 (1980).

Kinetic studies of the reactions in isopropanol of 4-nitrobenzofuroxan with cyanide ion and isopropoxide ion have been carried out over the temperature range 15.0 to 35.0°C. For both bases, the first species identifiable using stopped-flow reaction techniques is postulated to be a C-7 σ-complex of 4-nitrobenzofuroxan and base. Specific rate constants and activation parameters for the formation of these σ-complexes are compared to corresponding data relating to the formation of cyanide ion and isopropoxide ion — σ-complexes of 1,3,5-trinitrobenzene in isopropanol.

MICHAEL E. MOIR et ALBERT R. NORRIS. Can. J. Chem. **58**, 1691 (1980).

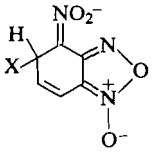
On a effectué des études cinétiques relatives à la réaction du nitro-4 benzofuranne avec l'ion cyanure et l'ion isopropylate dans l'alcool isopropylique dans l'intervalle de température 15–35°C. Sur la base des techniques de réaction à flux stoppé on suppose dans les deux cas que la première espèce identifiable est un complexe σ entre le C-7 du nitro-4 benzofuranne et la base. On a comparé les constantes de vitesse spécifique et les paramètres d'activation de la formation de ces complexes σ aux données correspondantes se rapportant à la formation des complexes σ entre l'ion cyanure ainsi que l'ion isopropylate avec le trinitro-1,3,5 benzène dans l'alcool isopropylique.

[Traduit par le journal]

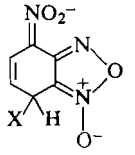
Introduction

The discovery (1) that certain benzofuroxan and benzofurazan derivatives act as powerful inhibitors of nucleic acid and protein biosynthesis in many types of animal cells has generated considerable interest in these classes of compounds (2–10). Especially noteworthy has been the observation that 4-nitrobenzofuroxan exhibits a toxic effect on the metabolism of leukocites in vitro (2), suggesting thereby the possibility that such compounds may act as potential antileukemic and immunosuppressive drugs. Since 4-nitrobenzofuroxan readily formed Meisenheimer type σ-complexes with nucleophiles and since drug action was abolished by preincubation with aliphatic thiols, it was concluded (2) that drug action was related to σ-complex formation of 4-nitrobenzofuroxan with intracellular thiol groups (9–11).

Previous studies (12, 13) of the interaction of 4-nitrobenzofuroxan and methoxide ion in methanol and methanol–dimethylsulfoxide mixtures have shown that both a kinetically controlled C-5 σ-complex, **1** (X = OCH_3), and a thermodynamically controlled C-7 σ-complex, **2** (X = OCH_3), are formed rapidly at 25.0°C. Slow reactions following the formation of these σ-complexes were shown to result in the generation of 7-hydroxy-4-nitrobenzofurazan, **3** (as the anion), and the 7,7′-dimethoxy-4-nitrobenzofurazan σ-complex, **4** (X = OCH_3) (12). Possible reaction pathways for the formation of these secondary products



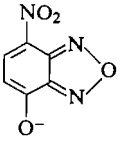
1



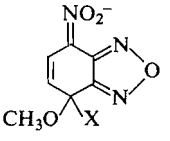
2

via the σ-complexes and the implications of these observations as regards to the proposed mode of drug action of this compound have been presented (12).

As part of a comprehensive study designed to obtain kinetic and thermodynamic data relating to σ-complex formation reactions in these systems



3



4

and to establish the generality of the combined deoxygenation of the *N*-oxide function and substitution of the aromatic hydrogen at C-7 by nucleophiles, we have investigated the reactions of 4-nitrobenzofuroxan with cyanide ion and isopropoxide ion in isopropanol. We report here the results of our kinetic studies.

Results and Discussion

Above 250 nm the ultraviolet–visible absorption spectrum of 4-nitrobenzofuroxan (4NBFO), in isopropanol as solvent, displays a single broad ab-

[1]To whom all correspondence should be addressed.

0008-4042/80/161691-06$01.00/0

©1980 National Research Council of Canada/Conseil national de recherches du Canada

Can. J. Chem. Downloaded from www.nrcresearchpress.com by 210.87.254.6 on 09/05/12
For personal use only.

Can. J. Chem. Downloaded from www.nrcresearchpress.com by 210.87.254.6 on 09/05/12
For personal use only.

sorption band with absorption maximum at 408 nm ($\varepsilon = 8.50 \pm 0.05 \times 10^3\ M^{-1}\ cm^{-1}$).

The addition of progressively larger amounts of sodium isopropoxide (Na *i*-PrO) to solutions containing a fixed concentration of 4NBFO ($5.00 \times 10^{-4}\ M$) leads to a decrease in the absorption at 408 nm and the simultaneous appearance of two new absorption bands possessing absorption maxima at 338 and 275 nm. These two absorption bands were ascribed to the presence of a single new species, Y, in solution. Formation of Y was complete within the time required to mix the stock solutions of 4NBFO and Na *i*-PrO and record the spectrum of the resulting mixture (< 20 s). The extent of conversion of 4NBFO to Y was dependent on the concentration of *i*-PrO^- ion in solution; at 25.0°C the conversion was essentially complete after the addition of 10.5 molar equivalents of Na *i*-PrO to the system. Based on the formation of one molecule of Y per molecule of 4NBFO reacted, the molar absorptivity (ε) of Y at 338 nm was $1.30 \pm 0.05 \times 10^4\ M^{-1}\ cm^{-1}$. Throughout the course of the conversion of 4NBFO to Y, the spectra of the solutions displayed an isosbestic point at 372 nm.

Species Y was not stable for long periods of time at room temperature. Within several minutes of its formation, the addition of excess trifluoroacetic acid (CF_3COOH) to the solution rapidly and quantitatively regenerated 4NBFO. However, over a period of hours, Y apparently underwent additional reactions as indicated by the observations that the absorbances due to Y at 275 and 338 nm decreased in intensity and a new band (centered at 455 nm) slowly appeared in the visible region. The addition of excess CF_3COOH to solutions allowed to stand for a few hours at room temperature did not result in the complete regeneration of 4NBFO. Over still longer periods of time, the spectral changes observed in the reaction of 4NBFO and *i*-PrO^- ion in isopropanol closely paralleled those observed previously in the reactions of 4NBFO and methoxide ion in both methanol and methanol–dimethylsulfoxide mixtures (12).

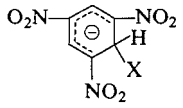
For the reversible formation of species Y according to the equation

$$[1] \qquad 4NBFO + i\text{-}PrO^- \underset{k_{-1}}{\overset{k_1}{\rightleftharpoons}} Y$$

carried out under reaction conditions such that $[i\text{-}PrO^-]_0 \gg [4NBFO]_0$ ($[\ ]_0$ represents the total initial concentration), the k_{obs} obtained from the slope of the $\ln(A_\infty - A_t)$ or $\ln(A_t - A_\infty)$ versus time plots is related to the specific rate constants k_1 and k_{-1} and the $[i\text{-}PrO^-]_0$ as shown in eq: [2].

$$[2] \qquad k_{obs} = k_1[i\text{-}PrO^-]_0 + k_{-1}$$

At any given $[i\text{-}PrO^-]_0$ and temperature, k_{obs} values calculated using absorbance data recorded at 408 nm (disappearance of 4NBFO, $\ln(A_t - A_\infty)$ versus time plots) or absorbance data recorded at 338 nm or 275 nm (appearance of species Y, $\ln(A_\infty - A_t)$ versus time plots) were, within experimental error, equal. At a fixed temperature, plots of k_{obs} versus $[i\text{-}PrO^-]_0$ were strictly linear up to a $[i\text{-}PrO^-]_0$ of $3.2 \times 10^{-3}\ M$. Typical data are shown in Fig. 1 for the reactions of 4NBFO and *i*-PrO^- at 15.0, 25.0, and 35.0°C. The linearity of the k_{obs} versus $[i\text{-}PrO^-]_0$ plots strongly suggests that ion-pairing effects are not a problem at the concentrations of base employed in these studies. A similar absence of ion-pairing effects was noted previously in our studies of the reaction of 1,3,5-trinitrobenzene and isopropoxide ion to form σ-complex **5** (X = *i*-PrO) in isopropanol (14).



5

The slopes (k_1) and intercepts (k_{-1}) of the k_{obs} versus $[i\text{-}PrO^-]_0$ plots for the reaction of 4NBFO and *i*-PrO^- ion at 15.0, 25.0, and 35.0°C are given in Table 1. Values of K (k_1/k_{-1}) for the formation of Y are calculated to be 1.96×10^3, 2.43×10^3, and $3.01 \times 10^3\ M^{-1}$ at 15.0, 25.0, and 35.0°C, respectively. The magnitude of the calculated K at 25.0°C is completely in accord with the experimental observation that formation of Y is essentially complete at a $[i\text{-}PrO^-]_0/[4NBFO]_0$ ratio > 10.5. Plots of $\ln(k_1/T)$ versus $1/T$ and $\ln(k_{-1}/T)$ versus $1/T$ yielded the values of the activation parameters $\Delta H_1\dagger$, $\Delta S_1\dagger$, $\Delta H_{-1}\dagger$, and $\Delta S_{-1}\dagger$, respectively, listed in Table 2.

The reaction of 4NBFO and cyanide ion in isopropanol proceeded in two distinct fast steps sufficiently different in rate to enable a separate study of each step under available reaction conditions. The sequence of spectral changes described below was independent of whether the source of CN^- ions was ϕ_4AsCN, KCN plus an equimolar amount of 18-crown-6 or $(C_2H_5)_4NCN$.

The first stage in the reaction was, in many respects, similar to the fast reaction between 4NBFO and *i*-PrO^- described above. Thus, for solutions containing a fixed concentration of 4NBFO ($5.00 \times 10^{-4}\ M$), the addition of progressively larger amounts of ϕ_4AsCN leads to the disappearance of the absorption band at 408 nm and the simultaneous appearance of a new absorption band with absorption maximum at 340 nm. (A new absorption band with λ_{max} at 275 nm was not observed in these studies due to strong absorption of ϕ_4AsCN in this

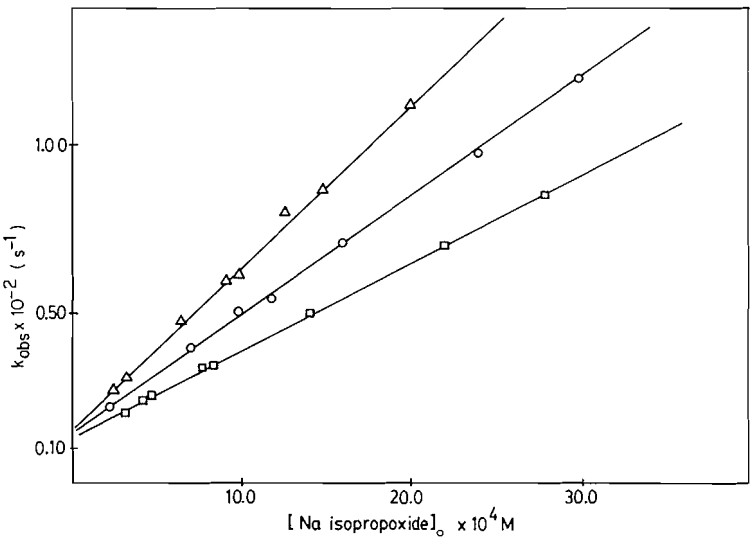


FIG. 1. Plot of k_{obs} versus concentration of isopropoxide ion for the σ-complex formation reactions between 4-nitrobenzofuroxan and isopropoxide ion in isopropanol at 15.0 (□), 25.0 (○), and 35.0°C (△).

TABLE 1. Specific rate constants for the reactions of 4-nitrobenzofuroxan with isopropoxide ion and cyanide ion in isopropanol[a]

	k_1 (M^{-1} s^{-1})		k_{-1} (s^{-1})	
T (°C)	*i*-PrO$^-$	CN$^-$	*i*-PrO$^-$	CN$^-$
15.0	2.55×10^4	1.60×10^2	13.0	—
25.0	3.53×10^4	2.74×10^2	14.5	—
35.0	4.81×10^4	4.60×10^2	16.0	—

[a] k_1 and k_{-1} values obtained from the slopes and intercepts of the k_{obs} versus $[base]_o$ plots. In the 4-nitrobenzofuroxan – cyanide ion system only points at low $[CN^-]_o$ were used to evaluate k_1.

region). Formation of the species absorbing at 340 nm was again rapid, i.e. complete within the time required to mix the reagents and record the spectrum of the resulting solution. The extent of conversion of 4NBFO to the new absorbing species was dependent on the concentration of CN^- ion in solution with conversion being essentially complete upon the addition of 1.1 molar equivalents of ϕ_4AsCN to the solution. Based on a 1:1 conversion of 4NBFO to the new absorbing species the molar absorptivity (ε) of the new species at 340 nm was $1.30 \pm 0.05 \times 10^4$ M^{-1} cm^{-1}. Throughout the course of the conversion of 4NBFO to this new species, the uv–visible spectra of the solutions displayed an isosbestic point at 373 nm. Within several seconds of the complete conversion of 4NBFO to the species whose λ_{max} occurred at 340 nm, the addition of excess CF_3COOH or *p*-toluenesulphonic acid (PTSA) to the solution resulted in the rapid, quantitative regeneration of 4NBFO.

Following closely on the heels of this initial, fast, reaction was a somewhat slower (though still fast) reaction that led to a decrease in the absorption at 340 nm and the appearance of a new, very broad absorption band in the visible whose λ_{max} occurred at 540 nm. Associated with this second reaction was a color change of the solutions from colorless to purple. Based on the formation of one mole of this colored species per mole of 4NBFO reacted, the molar absorptivity (ε) of this colored species at 540 nm was 8.80×10^3 M^{-1} cm^{-1}. Once the absorbance at 540 nm was fully developed, the addition of excess CF_3COOH or TPSA to the solutions rapidly discharged the purple color of the solutions but did not quantitatively regenerate 4NBFO. The species whose absorption maximum occurred at 540 nm was also unstable at room temperature as evidenced by the fact that the absorption maximum of a solution containing this species slowly shifted to shorter wavelengths. The final product(s) of this reaction has (have) not yet been identified.

In the kinetic studies described below ϕ_4AsCN, KCN plus an equimolar amount of 18-crown-6 and $(C_2H_5)_4NCN$ were all utilized as sources of cyanide ion. The majority of the studies were carried out using ϕ_4AsCN.

At any given temperature and $[CN^-]_0$, k_{obs} values for the first reaction, calculated using absorbance data recorded at 408 nm (disappearance of 4NBFO) and absorbance data recorded at 340 nm (appearance of the new absorbing species) were, within experimental error, equal. For a specified $[CN^-]_0$, k_{obs} values were, within experimental error, independent of the source of the cyanide ion and, in runs using ϕ_4AsCN as a source of cyanide ion, independent of the total ionic strength of the solu-

Can. J. Chem. Downloaded from www.nrcresearchpress.com by 210.87.254.6 on 09/05/12
For personal use only.

TABLE 2. Kinetic and thermodynamic parameters for the formation of some σ-complexes of 4-nitrobenzofuroxan and 1,3,5-trinitrobenzene in isopropanol at 25.0°C[a]

Parameter	Value			
	2 (X = *i*-PrO)	**2** (X = CN)	**5** (X = *i*-PrO)[b]	**5** (X = CN)[c]
k_1 (M^{-1} s^{-1})	3.53×10^4	2.74×10^2	9.67×10^4	2.45×10^3
k_{-1} (s^{-1})	14.5	<0.01	1.7	0.048
k_1/k_{-1} (M^{-1})	2.43×10^3	$>2.74 \times 10^4$	5.6×10^4	5.1×10^4
$\Delta H_1\dagger$ (kJ mol^{-1})	20.9 ± 2.1	36.8 ± 2.5	24.3 ± 1.7	49.0 ± 2.1
$\Delta S_1\dagger$ (J mol^{-1} K^{-1})	-87.4 ± 4.6	-75.7 ± 6.7	-49.0 ± 5.9	-5.0 ± 5.9
$\Delta H_{-1}\dagger$ (kJ mol^{-1})	5.14 ± 3.3	—	66.9 ± 4.2	78.7 ± 5.4
$\Delta S_{-1}\dagger$ (J mol^{-1} K^{-1})	-205 ± 18	—	-8.4 ± 15.0	11.7 ± 14.2

[a]Error limits for $\Delta H\dagger$ values are based on the maximum and minimum slopes obtained in plots of log (k/T) versus $1/T$. Errors in $\Delta S\dagger$ are based on the maximum and minimum intercepts obtained, at $1/T = 0$, in plots of log (k/T) versus $1/T$.
[b]Data from ref. 14.
[c]Data from ref. 15.

tion up to a $\mu = 5.02 \times 10^{-3}$ M (μ maintained constant with ϕ_4AsNO_2). Plots of k_{obs} versus $[CN^-]_0$ were linear at low concentrations of CN^- ion but curved slightly upwards at higher concentrations of CN^- ion. This curvature seemed to become more pronounced the higher the temperature. Similar observations relating to the dependence of k_{obs} on $[CN^-]_0$ have been noted previously in connection with the reactions of cyanide ion with 1,3,5-trinitrobenzene and 2,4,6-trinitrotoluene in isopropanol (15).

The slopes (k_1) of the k_{obs} versus $[CN^-]_0$ plots (obtained at low concentrations of cyanide ion) for the reactions of 4NBFO and CN^- at 15.0, 25.0, and 35.0°C are listed in Table 1. Values of the intercepts in the k_{obs} versus $[CN^-]_0$ plots were too small to permit an accurate evaluation of k_{-1} values at these temperatures. Based on an estimated value of K at 25.0°C of $>10^5$ M^{-1}, k_{-1} can be estimated to be $<10^{-3}$ at 25.0°C. A plot of $\ln(k_1/T)$ versus $1/T$ yielded the activation parameters $\Delta H_1\dagger$ and $\Delta S_1\dagger$ listed in Table 2.

At a given temperature and $[CN^-]_0$, k_{obs} values for the slow reaction, calculated using absorbance data recorded at 540 nm, were found to be independent of the source of the CN^- ion and, in runs utilizing ϕ_4AsCN as a source of CN^- ion, unaffected by changing the ionic strength up to a maximum μ of 5.02×10^{-3} M. Plots of k_{obs} for the slow reaction versus $[CN^-]_0$ were found to be strictly linear over the entire range of CN^- concentrations employed (5.02×10^{-3} M). The slopes (k_1^{slow}) of the k_{obs} versus $[CN^-]_0$ plots were 5.3×10^1, 1.09×10^2, and 2.25×10^2 M^{-1} s^{-1} at 15.0, 25.0, and 35.0°C, respectively. A plot of $\ln(k_1^{slow}/T)$ versus $1/T$ yielded values of $\Delta H_1\dagger$ and $\Delta S_1\dagger$ for the slow reaction of 53.1 ± 2.1 kJ mol^{-1} and -36.0 ± 5.9 J mol^{-1} K^{-1}, respectively.

Based on our previous ^1H nmr and uv–visible spectroscopic studies of the 4NBFO – methoxide ion reaction in methanol and methanol–dimethylsulfoxide mixtures (12), the species formed rapidly and reversibly as a result of the interactions of 4NBFO with *i*-PrO^- ion (λ_{max} 338 nm) and CN^- ion (λ_{max} 340 nm) in isopropanol are formulated as the σ-complexes **2** (X = *i*-PrO and CN), respectively. We have obtained no kinetic or spectroscopic evidence to suggest the formation of a C-5 σ-complex **1** (X = *i*-PrO or CN) in either system. However, in each case, a complex of this type could be formed more rapidly ($t_{1/2} < 1$ ms) and at low concentrations prior to the formation of the corresponding C-7 σ-complex and not be detected under our experimental conditions. We note that a species possessing a λ_{max} at 335 nm is also formed rapidly in the reaction of 4NBFO and sulfite ion in either water (at pH 8.5) or ethanol. On the addition of excess TFA acid or PTSA this species is rapidly and quantitatively converted to 4NBFO (16).

The markedly different spectra associated with the final reaction mixtures in the 4NBFO – cyanide ion and 4NBFO – isopropoxide ion interactions clearly indicate that different reaction products are formed in the two systems. We note that the final spectra observed in the reactions of 4NBFO and CN^- ion in isopropanol are very similar to the spectra generated in the initial, rapid, reversible reactions of cyanide ion and 4-nitrobenzofurazan in polar, aprotic solvents (17). The stoichiometries and structures of the colored species giving rise to these spectra have yet to be established.

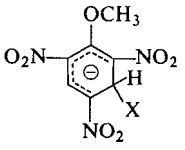
It is of interest to compare the specific rate constants and activation parameters for the formation of σ-complexes **2** (X = *i*-PrO) and **5** (X = *i*-PrO) and **2** (X = CN) and **5** (X = CN) in isopropanol. The specific rate constant for the formation of **2** (X =

Can. J. Chem. Downloaded from www.nrcresearchpress.com by 210.87.254.6 on 09/05/12
For personal use only.

Can. J. Chem. Downloaded from www.nrcresearchpress.com by 210.87.254.6 on 09/05/12
For personal use only.

i-PrO) at 25.0°C is approximately one-third the specific rate constant for the formation of **5** (X = *i*-PrO) at 25.0°C. Since values of $\Delta H_1\dagger$ for the two reactions are comparable, the difference in k_1 values is related primarily to a difference in values of $\Delta S_1\dagger$. The more negative value of $\Delta S_1\dagger$ observed in the formation of **2** (X = *i*-PrO) suggests that ordering of solvent in going from reactants to the activated complex associated with formation of σ-complex is greater in the 4NBFO–*i*-PrO^- reaction than in the TNB–*i*-PrO^- reaction. Since desolvation of *i*-PrO^- is expected to be comparable in both reactions, the implication of the difference in $\Delta S_1\dagger$ values is that σ-complex **2** (X = *i*-PrO) is itself more strongly solvated than σ-complex **5** (X = *i*-PrO). Some support for this suggestion comes from a consideration of comparable data relating to the formation of **2** (X = CN) and **5** (X = CN). In this case k_1 for formation of **2** (X = CN) at 25.0°C is approximately one-tenth the k_1 for formation of **5** (X = CN) at this temperature. Although $\Delta H_1\dagger$ for the formation of **2** (X = CN) is somewhat less than $\Delta H_1\dagger$ for the formation of **5** (X = CN), this factor is outweighed by the $\Delta S_1\dagger$ value for the formation of **2** (X = CN) being far more negative than the $\Delta S_1\dagger$ for the formation of **5** (X = CN). Again, if one accepts that desolvation of the anion should proceed to comparable extents in both reactions, more extensive solvation of the activated complex leading to **2** (X = CN), than the activated complex leading to **5** (X = CN) is indicated. Further discussion of solvent effects clearly requires knowledge concerning enthalpies of solution of both TNB and 4NBFO in isopropanol.

Comparisons of the available kinetic data (15) suggest that, in terms of solvational changes, **2** (X = CN) and **6** (X = CN) might be far more comparable systems than **2** (X = CN) and **5** (X = CN). Unfortunately, no data are yet available for the formation of **6** (X = *i*-PrO) in isopropanol.



6

The curvature in the k_{obs} versus $[CN^-]_0$ plots observed in 1,3,5-trinitrobenzene–CN^- and 2,4,6-trinitrotoluene–CN^- ion interactions was ascribed to the operation of a weak stabilizing effect associated with the interaction of ϕ_4As^+ with the nitro groups or with the π-electron system of the substrate in the activated complex (15). A similar explanation might be invoked to explain the slight curvature in the k_{obs} versus $[CN^-]_0$ plots observed for the fast reaction between 4NBFO and CN^- ion. However, the observation that at a given $[CN^-]_0$, ϕ_4AsCN, KCN plus 18-crown-6 and $(C_2H_5)_4NCN$ all yield the same k_{obs} suggests that ϕ_4As^+, the 18-crown-6-K^+ complex and $(C_2H_5)_4N^+$ are all equally effective in stabilizing the activated complex for σ-complex formation. This seems rather unlikely in view of the rather different charge densities associated with these three cations. Further detailed studies of cation effects on the rates of reaction of CN^- ion with 4NBFO and the solubility of 4NBFO in isopropanol as a function of the concentration of ϕ_4AsCN and related salts are planned in order to shed more light on the reasons for the observed dependence of k_{obs} on cation concentration.

Experimental

Reagents

4-Nitrobenzofuroxan was prepared as described by Ghosh (3) (method B), mp 143°C.

Tetraphenylarsonium cyanide was prepared as previously described (18) and dried to constant weight *in vacuo* over phosphorus(V) pentoxide. Tetraphenylarsonium nitrite was prepared in a similar fashion but using sodium nitrite in place of sodium cyanide in both the initial preparation and the recrystallization procedures. After two recrystallizations the compound was dried to constant weight *in vacuo* over phosphorus(V) pentoxide.

Tetraethylammonium cyanide was prepared according to the method outlined by Andreades and Zahnow (19). After two recrystallizations from acetonitrile the compound was dried to constant weight *in vacuo* over phosphorus(V) pentoxide.

18-Crown-6 was used as received from PCR Research Chemicals, Inc.

All other reagents used in the study were A.R. grade or better.

Fisher Certified ACS isopropanol was normally dried by refluxing over Linde 4 Å Molecular Sieve overnight and then distilled under a dry nitrogen atmosphere. Only the middle portion of the distillate was retained. No discernible differences in rate constants were observed in those instances in which the preliminary drying of the isopropanol was effected according to Vogel's procedure (20).

Stock solutions of sodium isopropoxide were prepared by adding freshly cut sodium metal, pre-washed in dry isopropanol, to pure solvent maintained in an atmosphere of dry nitrogen. Solutions thus prepared were stored under nitrogen and standardized immediately before use by titration with 0.100 *M* HCl to the phenolphthalein end point. Stock solutions of sodium isopropoxide were usually 0.05 to 0.10 *M* in concentration. Solutions of lower concentration were prepared by dilution.

Stock solutions of 4-nitrobenzofuroxan and the various cyanide ion-containing salts were prepared by dissolving weighed quantities of each reagent in a known volume of isopropanol. Solutions of lower concentrations, used in the kinetic and equilibrium studies, were prepared by dilution.

Instruments

Ultraviolet–visible absorption spectra were obtained using Cary 14 and Unicam SP-1700 spectrophotometers and matched silica cells of 1.0 cm path length. The sample compartments of both spectrophotometers were kept at a constant temperature by circulating water from a constant temperature water bath through specially designed cell holders.

Kinetic measurements were carried out on a Durrum–Gibson stopped-flow spectrophotometer. A closed circuit temperature control system utilizing an Ultra Kryomat TK30D constant temperature bath kept the temperature in the valve-block, drive syringes and observation cell constant to within ±0.1°C. A stopped-flow cell of 2.0 cm path length and minimum "dead time" of 2 ms was used in all the kinetic runs.

Procedure

All kinetic runs were carried out with base in large excess over 4NBFO. Concentrations of 4NBFO varied from 1.0×10^{-5} to 7.0×10^{-5} *M*. Concentrations of *i*-PrO^- varied from 6.0×10^{-4} to 60.0×10^{-4} while concentrations of CN^- ion varied from 3.0×10^{-4} to 50.0×10^{-4} *M*. The ionic strength of the reaction mixtures was not maintained constant except as indicated.

Changes in concentration of 4NBFO were followed by means of the absorbance at 408 nm. Pseudo-first-order rate constants (k_{obs}) were obtained from the slopes of the $\ln(A_t - A_\infty)$ versus time plots where A_∞ and A_t refer to absorbances at times infinity and t respectively. Plots were normally linear to approximately 80% completion of the reaction. Individual k_{obs} values were reproducible to ±3% in the reaction of 4NBFO and isopropoxide ion and to ±5% in the reaction of 4NBFO and cyanide ion. Changes in concentration of σ-complex were followed by means of the absorbances at 338 and 275 nm (4NBFO–isopropoxide) and 340 (4NBFO–CN^-). In these cases pseudo-first-order rate constants were obtained from the slopes of $\ln(A_\infty - A_t)$ versus time plots.

Acknowledgments

We gratefully acknowledge financial support of this research by the Natural Sciences and Engineering Research Council of Canada and the Atkinson Foundation. We are indebted to Siegfried Prager and Stuart Fergusson for help in obtaining some of the experimental data.

1. P. B. GHOSH and M. W. WHITEHOUSE. J. Med. Chem. **11**, 305 (1968).
2. M. W. WHITEHOUSE and P. B. GHOSH. Biochem. Pharmacol. **17**, 158 (1979).
3. P. B. GHOSH. J. Chem. Soc. B, 334 (1968).
4. P. B. GHOSH and M. W. WHITEHOUSE. J. Med. Chem. **11**, 158 (1969).
5. P. B. GHOSH, B. TERNAI, and M. W. WHITEHOUSE. J. Med. Chem. **15**, 255 (1972).
6. D. DAL MONTE, E. SANDRI, and W. CERÉ. Ann. Chim. Rome, **60**, 801 (1970).
7. D. DAL MONTE, E. SANDRI, L. DI NUNNO, S. FLORIO, and P. E. TODESCO. Chim. Ind. Milan, **53**, 940 (1971).
8. L. DI NUNNO, S. FLORIO, and P. E. TODESCO. J. Chem. Soc. Perkin Trans. II, 1469 (1975).
9. F. TERRIER, F. MILLOT, and W. P. NORRIS. Bull. Soc. Chim. Fr. 551 (1975).
10. F. TERRIER, F. MILLOT, and W. P. NORRIS. J. Am. Chem. Soc. **98**, 5883 (1976).
11. W. P. NORRIS and J. OSMUNDSEN. J. Org. Chem. **30**, 2407 (1965).
12. E. BUNCEL, N. CHUAQUI-OFFERMANNS, and A. R. NORRIS. J. Chem. Soc. Perkin Trans. I, 415 (1977).
13. F. TERRIER, F. MILLOT, A. P. CHATROUSSE, M. J. POUET, and M. P. SIMONNIN. Org. Magn. Reson. **8**, 56 (1976).
14. L. H. GAN and A. R. NORRIS. Can. J. Chem. **49**, 2490 (1971).
15. L. H. GAN and A. R. NORRIS. Can. J. Chem. **52**, 8 (1974).
16. M. MOIR and A. R. NORRIS. To be published.
17. E. MCINTYRE and A. R. NORRIS. To be published.
18. E. BUNCEL, A. R. NORRIS, K. E. RUSSELL, and W. PROUDLOCK. Can. J. Chem. **47**, 4129 (1969).
19. S. ANDREADES and E. W. ZAHNOW. J. Am. Chem. Soc. **91**, 4181 (1969).
20. A. I. VOGEL. Practical organic chemistry. 3rd ed. Longman, London. 1956.

Can. J. Chem. Downloaded from www.nrcresearchpress.com by 210.87.254.6 on 09/05/12
For personal use only.

Solution properties of the molten hydrates of zinc nitrate

SURENDER KUMAR JAIN[1] AND REITA TAMAMUSHI
The Institute of Physical and Chemical Research, Wako-shi, Saitama – 351, Japan

Received November 15, 1979

SURENDER KUMAR JAIN and REITA TAMAMUSHI. Can. J. Chem. **58**, 1697 (1980).

Density, conductivity, viscosity, refractive index, and surface tension of the molten $Zn(NO_3)_2 \cdot xH_2O$ ($2 \leq x \leq 6$) systems have been measured as a function of temperature. Both conductivity and fluidity exhibit a non-Arrhenius temperature dependence for all the compositions and have been described in terms of three parameter equations

$$Y(\Lambda, \phi) = A_Y T^{-1/2} \exp[-B_Y/(T - T_{0,Y})]$$
$$Y(\Lambda, \phi) = A_Y' \exp[-B_Y'/(V - V_{0,Y})]$$

based on the free volume model. The parameters $A_Y, A_Y', B_Y, B_Y', T_{0,Y}$, and $V_{0,Y}$ are the constants characteristic of the medium. The composition dependence of these parameters has been discussed. The temperature dependence of the Walden's product could be satisfactorily described by the equation

$$\Lambda\eta^p = \text{constant}$$

where p equals the ratio E_Λ/E_ϕ; E_Λ and E_ϕ being the apparent activation energy for the conductance and the viscous flow respectively. The molar polarisations (P_{LL}) computed using the Lorenz–Lorentz equation showed a slight temperature variation (< 0.2%) over the range 40–70°C. Thermal expansivity (α) and the ratio α/α_{GD} for the systems show a continuous fall with the decrease in the water content of the medium; the changes becoming more marked at $x < 4$. The surface tension – composition isotherms show a maximum near $x = 4$. The results are consistent with the change of configuration from octahedral to tetrahedral around Zn^{2+}, the increased covalent character in the Zn^{2+}—ONO_2^- bond and the water molecule acting as a bridging ligand in the melts containing less than 4 moles of water per mole of the salt.

SURENDER KUMAR JAIN et REITA TAMAMUSHI. Can. J. Chem. **58**, 1697 (1980).

On a mesuré en fonction de la température, la densité, la conductivité, la viscosité, l'indice de réfraction et la tension superficielle des systèmes $Zn(NO_3)_2 \cdot H_2O$ ($2 \leq x \leq 6$) à l'état fondu. La relation entre la conductivité et la fluidité d'une part et la température d'autre part ne correspond pas à la théorie d'Arrhénius pour toutes les compositions et on les a décrit selon des équations à trois paramètres basées sur le modèle de volume libre

$$Y(\Lambda, \phi) = A_Y T^{-1/2} \exp[-B_Y/(T - T_{0,Y})]$$
$$Y(\Lambda, \phi) = A_Y' \exp[-B_Y'/(V - V_{0,Y})]$$

Les paramètres $A_Y, A_Y', B_Y, B_Y', T_{0,Y}$ et $V_{0,Y}$ sont des constantes caractéristiques du milieu. On discute de l'effet de la composition sur ces paramètres. L'effet de la température sur les produits de Walden pourrait être décrit de façon satisfaisante par l'équation

$$\Lambda\eta^p = \text{constant}$$

où $p = E_\Lambda/E_\phi$; E_Λ et E_ϕ étant respectivement l'énergie d'activation apparente de la conductance et de l'écoulement visqueux. Les polarisations molaires (P_{LL}) calculées en utilisant l'équation de Lorenz–Lorentz indiquent une légère variation de la température (<0.2%) dans l'intervalle de 40–70°C. La dilatation thermique (α) et le rapport α/α_{GD} des systèmes diminuent continuellement avec la teneur en eau du milieu; les variations deviennent plus importantes pour $x < 4$. La tension superficielle isotherme de composition montre un maximum près de $x = 4$. Les résultats sont en accord avec un changement de configuration allant de octaédrique à tétraédrique autour de Zn^{2+}, l'augmentation du caractère covalent de la liaison Zn^{2+}—ONO_2^- et la molécule d'eau agissant comme ligand en position de pont dans les sels fondus contenant moins de 4 moles d'eau par mole de sel.

[Traduit par le journal]

Introduction

In the past few years the investigation of physico-chemical properties of the hydrated melts has attracted a good deal of attention. Of particular interest are the studies (1–9) of hydrated melts containing multivalent cations, such as Ca^{2+} and Mg^{2+}. Recently, Jain (10–15) has reported some physico-chemical measurements on a number of the molten hydrated nitrates of the metals belonging to the 3*d* series of transition elements. These studies were carried out at concentrations where sufficient water was present to fill the first or even the second (partially) coordination sphere of the cations. Solution properties of such systems at very low water content, insufficient even to fill the first coordination sphere where competitive solvation of cations and anions and the interionic interactions are expected to greatly influence the solution properties, have not been investigated. The solubility studies (16–18) indicate that the zinc nitrate – water system can be very conveniently studied up to

[1]JSPS Visiting Scientist (June 1978 – May 1979). On leave from Hindu College, University of Delhi, Delhi-110007, India.

0008-4042/80/161697-07$01.00/0
©1980 National Research Council of Canada/Conseil national de recherches du Canada

Can. J. Chem. Downloaded from www.nrcresearchpress.com by 210.87.254.105 on 09/05/12
For personal use only.

≃82% (by weight) of the salt concentration. Recently, the vibrational spectral studies of zinc nitrate – water system up to such high salt concentrations have been reported by Sze and Irish (19). For our interest in the solution properties at such high concentrations, we present some physico-chemical properties of this system with a view to see if there existed some correlation between the solution properties and the spectral studies.

Experimental

Material

Analytical grade (Wako Chemical Ind., Japan) hexahydrate of zinc nitrate was used in the study. The hexahydrate salt was fused in an airtight flask, maintained slightly above its melting temperature for a few hours, and then filtered through glass filter (porosity G-3). The filtered melt was then kept at ≃60°C for 2–3 h for maturing. On analysis the water content of the melt was found to correspond to a stoichiometry 6.01 ± 0.03. The melts with lower water contents were prepared by removing a calculated amount of water from the weighed quantity of the hexahydrate melts by continuous evacuation at ≃50°C. All the melts were transparent in the molten state.

Measurements

Densities were measured by measuring the volume of a known amount of the melt by using a precalibrated densitometer. The densitometer design, its calibration, and the measuring technique were similar to those reported earlier (9). The reported results are estimated to be accurate to ±0.1%.

Viscosities were measured with Ubbelohde type viscometers calibrated with aqueous solution of glycerol. The viscometer constants were 0.2352 and 0.08196 cP s^{-1} (1 cP = 10^{-3} N m^{-2} s). Inherent accuracy of these values is estimated to be better than ±0.5%.

The conductivity of the melts was measured by employing the four-electrode cell method. The details about the circuit design and the operational usefulness of this method have been described earlier (20). The cell resistance was observed to be independent of frequency over the range 10–1600 Hz. The reported results correspond to the measurements made at 1 kHz. The expected accuracy of the results is ±0.3%.

The refractive indices were measured on an Abbe type (Erma, Tokyo) refractometer, whose prisms were maintained at the highest (70°C) temperature by circulating water from a constant temperature bath through the prism compartments. A drop of the melt was directly placed onto the lower prism and the prisms were immediately clamped into the position and the measurement was made. The measurements were continued on the descending temperature scale at an interval of 10 deg, until the crystallization. The values were reproducible to ±0.0002.

The surface tensions were measured by the differential capillary rise method, as described earlier (11). The reported values are estimated to be accurate to ±0.5%.

The density, viscosity, and the conductivity measurements were carried out simultaneously in the same constant temperature bath (capacity 20 dm^3) and the temperatures were controlled and measured to ±0.1°C.

All measurements reported here were begun at high temperature and carried out downwards. At each temperature the constancy of the cell resistance for ≃10 min was taken as proof for the thermal equilibrium between the melt and the bath liquid. Reproducibility of results in heating and cooling cycles was taken as evidence that there was no appreciable loss of water during experiment.

Results and Discussion

Concentration Units

For the present results the compositions are expressed in terms of the water:salt mole ratios, designated as x. The normality (N) unit, which defines the concentration of electrostatic charge in equivalents per litre of the solution, has also been used for the interpretation of the present results. The normalities (at 60°C) corresponding to each x value are shown in Table 1.

Density and Equivalent Volume

The densities (ρ) and equivalent volumes (V_e) of the molten $Zn(NO_3)_2 \cdot xH_2O$ system corresponding to x ranging from 2.02 to 6.01 varied linearly with temperature and could be satisfactorily described by the equations

$$[1] \qquad \rho(\text{g cm}^{-3}) = a - bt(^\circ\text{C})$$

$$[2] \qquad V_e(\text{cm}^3 \text{ equiv.}^{-1}) = A + Bt(^\circ\text{C})$$

respectively. The coefficients a, b, A, and B are presented in Table 1. The present value of 82.4 cm^3 equiv.$^{-1}$ for V_e (at $x = 6.01$ and at 50°C) compares well with the value 82.0 cm^3 equiv.$^{-1}$, for $x = 6.00$, reported earlier (11). The density and equivalent volume at any temperature varied systematically with the changes in the water-to-salt mole ratio, and could be described by a second degree polynomial in x. The coefficients of the least-squares equations are presented in Table 2. The expansivities (α) expressed as

$$[3] \qquad \alpha = (1/V_e)\,(dV_e/dT)_p$$

show a regular decrease with the decrease in the water content of the medium; the decrease being more marked at water-to-salt mole ratios less than 4. This may be due to an increase in the electrostriction of the melt arising out of the increased effective electrostatic charge concentration (N) in the medium. Alternatively, because the total ligand concentration ($H_2O + NO_3^-$) is insufficient to allow a six coordination at these concentrations, this effect thus may be due to a configurational change from octahedral to tetrahedral coordination around Zn^{2+} ion. The spectral studies of Sze and Irish (19) on the zinc nitrate – water systems appear to support the latter possibility.

Conductivity and Fluidity

The conductivities and fluidities of the molten $Zn(NO_3)_2 \cdot xH_2O$ systems exhibited a non-Arrhenius temperature dependence and could be adequately described in terms of the equation

$$[4] \qquad Y(\Lambda, \phi) = A_Y T^{-1/2} \exp\left[-B_Y/(T - T_{0,Y})\right]$$

Can. J. Chem. Downloaded from www.nrcresearchpress.com by 210.87.254.105 on 09/05/12
For personal use only.

TABLE 1. Density/equivalent volume – temperature equations for the molten $Zn(NO_3)_2 \cdot xH_2O$ systems

x	N^a (equiv. dm^{-3})	Data points	Temperature range (°C)	ρ(g cm^{-3}) = $a - bt$(° C)			V_e(cm^3 equiv.$^{-1}$) = $A + Bt$(°C)			$10^4\alpha^a$ (deg^{-1})
				a	10^4b	10^3SE	A	10^2B	10^2SE	
6.01	12.06	9	26–67	1.8622	11.25	0.08	79.86	5.11	0.8	6.16
5.02	13.41	10	24–69	1.9469	11.65	0.18	71.82	4.55	0.9	6.10
4.06	14.87	9	30–70	2.0226	11.69	0.33	64.85	3.98	0.9	5.91
3.07	16.78	9	32–70	2.1238	11.67	0.16	57.58	3.35	0.3	5.62
2.02	18.94	3	59–71	2.2029	10.66	0.17	51.22	2.63	0.3	4.98

[a]For 60°C.

TABLE 2. Density/equivalent volume – composition isotherms for $Zn(NO_3)_2 \cdot xH_2O$ melts

T (°C)	Data points	x	ρ(g cm^{-3}) = $a - bx + cx^2$				V_e(cm^3 equiv.$^{-1}$) = $A + Bx + Cx^2$			
			a	10^2b	10^3c	10^3SE	A	B	$10C$	SE
70.0	5	2–6	2.3249	9.90	1.46	4.5	41.01	5.36	2.83	0.13
50.0	5	2–6	2.3408	9.54	1.04	4.6	40.78	5.21	2.87	0.13
30.0	4	3–6	2.4405	12.90	4.56	3.2	38.49	5.96	1.94	0.11

TABLE 3. Parameters of eqs. [4] and [6] for the conductivity – temperature/molar volume data of the $Zn(NO_3)_2 \cdot xH_2O$ melts

x	Data points	Temperature range (°C)	$\Lambda = A_\Lambda T^{-1/2} \exp[-590/(T - T_{0,\Lambda})]$			T_g (K)	$\Lambda = A_\Lambda \exp[-B_\Lambda'/(V - V_{0,\Lambda})]$				$V_{0,\Lambda(extr)}$ (cm^3 mol^{-1})
			A_Λ (S cm^2 equiv.$^{-1}$)	$T_{0,\Lambda}$ (K)	SE		A_Λ' (S cm^2 equiv.$^{-1}$)	B_Λ' (cm^3 mol^{-1})	$V_{0,\Lambda}$ (cm^3 mol^{-1})	SE	
6.01	9	26–67	5931.1	178.5	0.08	197	116.9	36.05	152.96	0.5	150.05
5.02	10	24–69	5328.1	188.7	0.05	205	87.2	30.09	138.65	0.09	135.95
4.06	9	30–70	4645.9	196.0	0.03	213	79.7	27.54	125.70	0.08	123.56
3.07	9	32–70	3718.0	204.9	0.01	—	113.2	31.77	111.26	0.04	110.58
2.02	5	46–71	3048.8	214.8	0.01	—	3171	80.16	95.50	0.06	99.37

based on the free volume model of Cohen and Turnbull (21) or the cooperative rearrangement theory of Adam and Gibbs (22). The terms A_Y, B_Y, and $T_{0,Y}$ are constants characteristic of the system. The parameter $T_{0,Y}$ has been interpreted as theoretical glass transition temperature and its thermodynamic nature has been discussed by Cohen and Turnbull (21), Adam and Gibbs (22), and Angell and Rao (23). The exponential coefficient B_Y according to Adam and Gibbs (22) is expressed as

$$[5] \qquad B_Y = N_L \Delta\mu S_c^*/R\Delta C_p$$

where N_L is Avogadro's number, S_c^* is the minimum configurational entropy per particle required for a mass transporting rearrangement, $\Delta\mu$ is a free-energy barrier opposing the rearrangements, and ΔC_p is the change in heat capacity of the liquid at the glass transition. In view of the suggestion that the changes in $\Delta\mu$ from system to system may be offset, at least partially, by parallel changes in ΔC_p, it appears reasonable to consider B_Y to be composition independent. This empirical rule has been found to hold good for a large variety of the molten salt systems and concentrated electrolyte solutions (1, 3, 14, 15, 24–28). However, for $Ca(NO_3)_2 + H_2O$ system (29, 30) the parameter B_Y has been observed to vary systematically with composition. The present data accordingly were fitted into eq. [4] with all three parameters (A_Y, B_Y, and $T_{0,Y}$) as adjustable parameters. This method of data analysis did not give any meaningful composition dependence of these parameters. This might be due to the limited amount of the present data, and a strong interdependence of these parameters. It is probable that some clear and meaningful composition dependence of B_Y in the present system might become evident if extensive measurements are made with a sufficiently high precision. Under the circumstances, the present conductivity and fluidity data were fitted into [4], at near universal values of B_Λ (= 590 K) and B_ϕ (= 675 K). The best fit parameters are presented in Tables 3 and 4. For each process, the parameter $T_{0,Y}$ has a similar composition dependence and differs by ≃1 K in their absolute value. The experimental glass transition temperatures (T_g's) for some compositions were

Can. J. Chem. Downloaded from www.nrcresearchpress.com by 210.87.254.105 on 09/05/12
For personal use only.

Can. J. Chem. Downloaded from www.nrcresearchpress.com by 210.87.254.105 on 09/05/12
For personal use only.

TABLE 4. Parameters of eqs. [4] and [6] for the fluidity – temperature/molar volume data of the $Zn(NO_3)_2 \cdot xH_2O$ melts

x	Data points	Temperature range (°C)	$\phi(P^{-1}) = A_\phi T^{-1/2} \exp[-675/(T - T_{0,\phi})]$			$\phi(P^{-1}) = A_\phi' \exp[-B_\phi'/(V - V_{0,\phi})]$				$V_{0,\phi(\text{extr})}$ ($cm^3\,mol^{-1}$)
			A_ϕ (P^{-1})	$T_{0,\phi}$ (K)	10SE	A_ϕ' (P^{-1})	B_ϕ' ($cm^3\,mol^{-1}$)	$V_{0,\phi}$ ($cm^3\,mol^{-1}$)	10SE ($cm^3\,mol^{-1}$)	
6.01	9	26–67	17133	179.7	0.05	637.5	60.60	150.74	0.05	150.17
5.02	9	28–69	14939	189.1	0.09	604.6	56.22	136.27	0.07	135.99
4.06	9	30–70	12993	196.6	0.05	455.8	46.61	124.11	0.03	123.61
3.07	6	45–70	10341	205.1	0.05	545.8	46.15	110.36	0.04	110.60
2.02	5	46–71	8261	213.7	0.05	—	—	—	—	—

estimated from the work of Angell and Sare (31) and are included in Table 3. Somewhat lower values for $T_{0,Y}$'s relative to T_g' are expected because of the long relaxation times encountered in the measurement of the latter quantity. A similar composition dependence of $T_{0,Y}$'s and T_g's confirms the belief that both are governed by similar forces; the electrostatic charge concentration being the most important (31). Figure 1 shows the variation of $T_{0,Y}$ and T_g with the normality (N) of the melt. The curvature in $T_{0,Y}$ vs. N plot can be interpreted as due to the increased penetration of the NO_3^- ion into the coordination sphere of the hydrated zinc ion, thereby resulting in a partial neutralization of the cationic charge and hence the effective electrostatic charge concentration. The presence of the bands at 750 and 760 cm^{-1} and the intensity analyses of the 950–1150 and 1150–1600 cm^{-1} regions in the Raman spectra (19) of the $Zn(NO_3)_2 \cdot xH_2O$ melts at low water content ($x < 4$) also indicate the increased interactions of the NO_3^- with Zn^{2+} at these concentrations.

The parameters A_Λ and A_ϕ show a regular decrease with a decrease in the water content of the medium. Obviously, the variations are in the reverse directions to that predicted by theory (21). Similar composition dependence of A_Λ's and A_ϕ's has also been observed earlier (14, 15, 32). The possibility that A_Y varies inversely with the rigidity of the medium (15) appears to be rather more convincing in light of the present results. However, the suggestion (32) that this discrepancy between

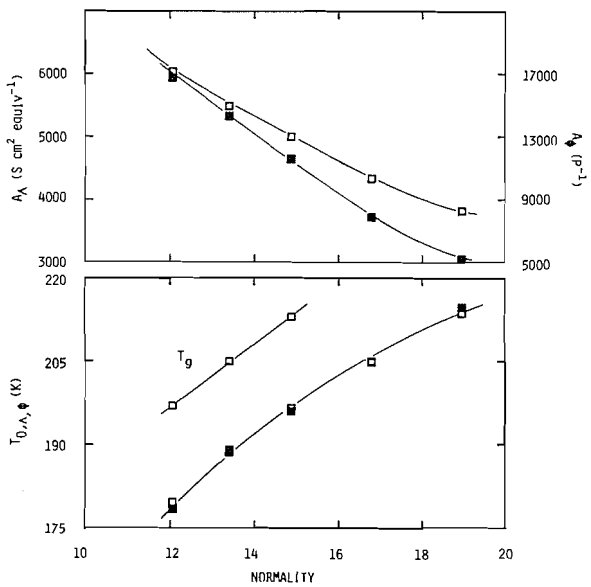


FIG. 1. The plots showing the variation of the parameters $T_{0,\Lambda}$ (■), $T_{0,\phi}$ (□), T_g, A_Λ (■), and A_ϕ (□) with the normality (N, at 60°C) for $Zn(NO_3)_2 \cdot xH_2O$ melts.

Can. J. Chem. Downloaded from www.nrcresearchpress.com by 210.87.254.105 on 09/05/12
For personal use only.

the theory and experiment regarding the composition dependence of the pre-exponential coefficient (A_Y) may be related to the differences in the lability of water or nitrate ion in the coordination sphere of the cation also appears reasonable for the present system.

The Doolittle equation (33) in the form

[6] $$Y(\Lambda, \phi) = A_Y' \exp[-B_Y'/(V - V_{0,Y})]$$

has been found successful in describing the free volume (hence temperature) dependence of the transport properties (Λ and ϕ) of the present system. The terms A_Y' and B_Y' are empirical parameters, V is the molar volume at the temperature of property Y, and $V_{0,Y}$ is the intrinsic volume, i.e., the molar volume at the ideal glass transition temperature. The computed $V_{0,Y}$'s for the two processes (Tables 3 and 4) are almost equal and vary in the same fashion with composition. Like other systems (15, 27) here too, the intrinsic volumes are found to be nearly equal to the molar volumes at $T_{0,Y}$, obtained by extrapolation of the equation

[7] $$V(\text{cm}^3\ \text{mol}^{-1}) = \alpha + \beta(T - 273.15)$$

This is consistent with the view (21) that it is the region above $T_{0,Y}$ (K) and not 0 (K) which is of significance to the transport processes in such liquids.

A typical variation of Λ and ϕ (at 70°C) is shown as a function of normality (N) in Fig. 2. For the same change in concentration, the fluidity changes more rapidly than the conductivity. These variations in the magnitude of the transport properties are consistent with the changes postulated above. Low fluidities of the melts containing low water content ($x < 4$) may also arise owing to water molecules acting as bridging ligands at these concentrations. The intensity analysis of the Raman bands in the region 950–1150 cm^{-1} for $Zn(NO_3)_2 \cdot xH_2O$ melts of these concentrations led Sze and Irish (19) to postulate such a possibility at higher concentrations.

The log $\Lambda(\phi)$ vs. $1/N$ plots were curved. An attempt to describe the present results in terms of the equations (3)

[8] $$Y_T(\Lambda, \phi) = A_Y'' \exp[-B_Y''/(N_{0,Y} - N)]$$

yielded a value of ≃44 equiv. dm^{-3} for $N_{0,Y}$ (at 60°C), the limiting concentration at which $T_{0,Y}$ (K) equals the isothermal temperature, T (K). This value obviously is very high when compared with the charge concentration of ≃24.7 equiv. dm^{-3} in the anhydrous melt containing $KNO_3 + Ca(NO_3)_2$ (55:45), for which a value of 330 K (= 57°C) for T_0 has been reported (25).

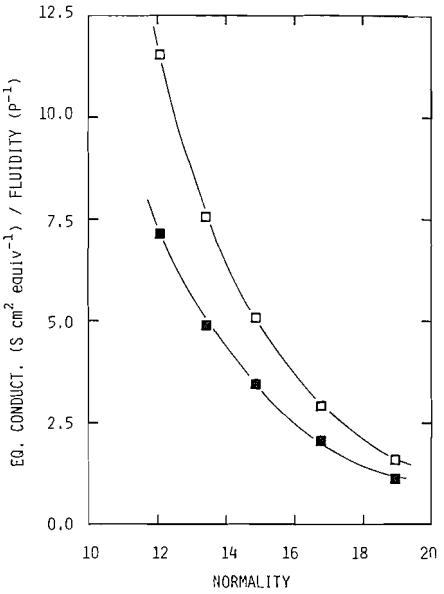


FIG. 2. Variations in the conductivity (■) and fluidity (□) values with the normality for the $Zn(NO_3)_2 \cdot xH_2O$ melts at 70°C.

The temperature dependence of Walden's product ($\Lambda\eta$) has been satisfactorily described by the equation (34)

[9] $$\Lambda\eta^p = \text{constant}$$

The computed parameters for the present system are recorded in Table 5. The value of p, which remains fairly constant at 0.87 ± 0.02, equals the average value of the ratio E_Λ/E_ϕ; E_Λ and E_ϕ being the apparent activation energy for the conductance and the viscous flow respectively.

Refractive Index

The refractive index (n) for all the compositions varied linearly with temperature. The n–t (°C) equations are presented in Table 6. The refractive index – x isotherms could be adequately described by a second degree polynomial in x. The corresponding equations are given in Table 7.

The molar polarisations at 60 and 40°C were calculated using the Lorenz–Lorentz equation

[10] $$P_{LL}(\text{cm}^3\ \text{mol}^{-1}) = [(n^2 - 1)/(n^2 + 2)]V$$

TABLE 5. Parameters of the equation $\Lambda\eta^p$ = constant (K) for Walden's product data of the $Zn(NO_3)_2 \cdot xH_2O$ melts

x	Data points	Temperature range (°C)	$\log\Lambda = \log K - p\log\eta$		
			$\log K$	p	10^2SE
6.01	9	26–67	1.654	0.85	0.5
5.02	9	28–69	1.647	0.85	0.5
4.06	9	30–70	1.650	0.86	0.4
3.07	6	45–70	1.629	0.86	0.2
2.02	5	46–71	1.654	0.89	0.7

TABLE 6. Refractive index – temperature equations and the molar polarisations for the $Zn(NO_3)_2 \cdot xH_2O$ melts[a]

x	Data points	Temperature range (°C)	$n = p - qt$ (°C) p	10^4q	10^4SE	P_{LL} (cm^3 mol^{-1}) 60°C	40°C	$10^4\alpha_{LL}$ (deg^{-1})	$10^4\alpha_{GD}$ (deg^{-1})	α/α_{GD}
6.01	5	30–70	1.4703	2.77	0.3	44.89	44.80	5.27	6.10	1.01
5.02	5	30–70	1.4810	2.86	0.6	41.13	41.06	5.31	6.17	0.99
4.06	5	30–70	1.4889	2.86	0.6	37.64	37.58	5.20	6.06	0.97
3.07	4	40–70	1.4990	2.95	0.9	33.93	33.90	5.23	6.13	0.91
2.02	2	60–70	1.5075	2.90	—	30.53	—	5.03	5.92	0.84

[a]Reported α's correspond to 60°C.

TABLE 7. Refractive index/molar polarisation – composition isotherms for the $Zn(NO_3)_2 \cdot xH_2O$ melts

x	Data points	Temperature (°C)	$n = a - bx - cx^2$ a	10^3b	10^4c	10^4SE	P_{LL}(cm^3 mol^{-1}) $= A + Bx + Cx^2$ A	B	10^2C	SE
2–6	5	60.0	1.5066	7.84	1.55	3.2	24.12	3.00	7.68	0.06
3–6	4	40.0	1.5125	7.75	1.81	4.2	22.85	3.56	1.55	0.03

in which V is the molar volume. The calculated values are included in Table 6. The molar polarisation – composition (x) isotherms are given in Table 7. The P_{LL} values show a slight (< 0.2%) variation over the range 40–60°C. A systematic decrease in the temperature coefficient of P_{LL} with decreasing x values is worth noting. As a first approximation if this variation of P_{LL} with temperature is ignored, the expansivities of these melts may be calculated from the temperature coefficient of the refractive index and the differential forms of the Gladstone–Dale and the Lorenz–Lorentz equations, through the expressions (35)

$$[11] \quad \alpha_{GD} = [1/(n-1)]dn/dT$$

$$[12] \quad \alpha_{LL} = [6n/(n^2-1)(n^2+2)]dn/dT$$

The computed values of α_{GD} and α_{LL} are included in Table 6; α_{LL} always being smaller than α_{GD}. The ratio α/α_{GD} continues to decrease with the decrease in the water content of the medium. The values lower than 1 for the ratio α/α_{GD} are interpreted as a reflection of the increased covalent character in the Zn^{2+}–NO_3^- bonding. The appearance of 285 cm^{-1} Raman band in the spectra of zinc nitrate – water melts, below $x = 4$, has been ascribed by Sze and Irish (19) to the increased covalent character in the Zn^{2+}–ONO_2^- bond.

Surface Tension

The surface tension (σ) – temperature data were fitted into the equation

$$[13] \quad \sigma \text{ (mN m}^{-1}) = p - qt(°C)$$

The coefficients p and q are given in Table 8. The composition dependence of surface tension at 40 and 60°C is shown in Fig. 3. The corresponding

TABLE 8. Surface tension – temperature equations for the $Zn(NO_3)_2 \cdot xH_2O$ melts

x	Data points	Temperature range (°C)	σ(mN m^{-1}) $= p - qt$(°C) p	$10q$	SE
6.01	2	40–60	93.80	1.08	—
5.02	3	40–70	98.47	1.76	0.4
4.06	3	50–70	100.98	1.91	0.04
3.07	3	50–70	95.78	1.11	0.1
2.02	2	60–70	93.60	0.94	—

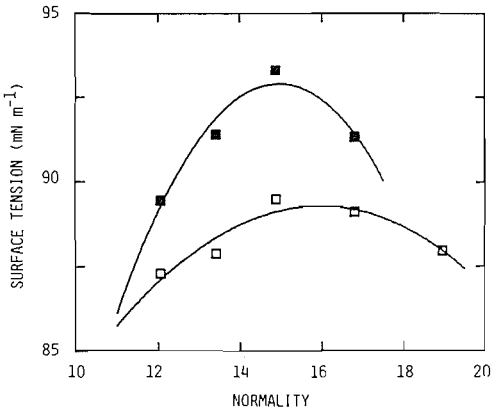


FIG. 3. Variation of the surface tension values with the normality for the $Zn(NO_3)_2 \cdot xH_2O$ melts; 60°C (□) and 40°C (■).

equations are tabulated in Table 9. The initial increase in the surface tension values may be seen as the effect of increased electrostatic charge concentration in the medium. The decrease in the σ values at concentrations corresponding to x below 4, in the light of above observations, is certainly a reflection of the increased covalent character in the zinc – nitrate ion bonding. The existence of maxima

Can. J. Chem. Downloaded from www.nrcresearchpress.com by 210.87.254.105 on 09/05/12
For personal use only.

TABLE 9. Surface tension – composition isotherms for the $Zn(NO_3)_2 \cdot xH_2O$ melts

x	Data points	T (°C)	$\sigma(mN\ m^{-1}) = a + bx - cx^2$ a	b	c	SE
2–6	5	60.0	83.77	2.92	0.39	0.3
3–6	4	40.0	75.06	8.50	1.02	0.4

near $x = 4$ may thus arise out of the counterbalancing nature of the two effects.

Acknowledgments

The authors wish to thank Dr. Katsuo Takahashi for the construction of the apparatus for the conductivity measurements and for many helpful discussions during the progress of the work. One of us (S.K.J.) wishes to acknowledge with pleasure the financial support extended to him by the Japan Society for the Promotion of Science.

1. C. A. ANGELL. J. Electrochem. Soc. **112**, 1224 (1965).
2. C. A. ANGELL. J. Phys. Chem. **69**, 2137 (1965).
3. C. A. ANGELL. J. Phys. Chem. **70**, 3988 (1966).
4. J. BRAUNSTEIN, L. ORR, and W. MACDONALD. J. Chem. Eng. Data, **12**, 415 (1967).
5. C. A. ANGELL and D. M. GRUEN. J. Am. Chem. Soc. **88**, 5192 (1966).
6. J. BRAUNSTEIN, A. R. ALVAREZ-FUNES, and H. BRAUNSTEIN. J. Phys. Chem. **70**, 2734 (1966).
7. C. T. MOYNIHAN. J. Phys. Chem. **70**, 3399 (1966).
8. C. T. MOYNIHAN and A. FRATIELLO. J. Am. Chem. Soc. **89**, 5546 (1967).
9. S. K. JAIN. J. Chem. Eng. Data, **18**, 397 (1973).
10. S. K. JAIN. J. Chem. Eng. Data, **22**, 383 (1977).
11. S. K. JAIN. J. Chem. Eng. Data, **23**, 170 (1978).
12. S. K. JAIN. J. Chem. Eng. Data, **23**, 216 (1978).
13. S. K. JAIN. J. Chem. Eng. Data, **23**, 266 (1978).
14. S. K. JAIN. J. Phys. Chem. **82**, 1272 (1978).
15. S. K. JAIN and R. TAMAMUSHI. Sci. Papers IPCR (Japan), In press.
16. W. W. EWING, J. J. MCGOVERN, and G. E. MATHEWS. J. Am. Chem. Soc. **55**, 4827 (1933).
17. W. W. EWING, A. J. RICARDS, W. J. TAYLOR, JR., and D. W. WINKLER. J. Am. Chem. Soc. **55**, 4830 (1933).
18. A. SIEVERTS and W. PETZOLD. Z. Anorg. Allgem. Chem. **212**, 49 (1933).
19. Y.-K. SZE and D. E. IRISH. J. Soln. Chem. **7**, 395 (1978).
20. R. TAMAMUSHI and K. TAKAHASHI. J. Electroanal. Chem. **50**, 277 (1974).
21. M. H. COHEN and D. TURNBULL. J. Chem. Phys. **31**, 1164 (1959).
22. G. ADAM and J. H. GIBBS. J. Chem. Phys. **43**, 139 (1965).
23. C. A. ANGELL and K. J. RAO. J. Chem. Phys. **57**, 470 (1972).
24. C. A. ANGELL. J. Phys. Chem. **68**, 1917 (1964).
25. C. A. ANGELL. J. Phys. Chem. **70**, 2793 (1966).
26. C. A. ANGELL. J. Chem. Phys. **46**, 4673 (1967).
27. N. ISLAM and K. ISMAIL. J. Phys. Chem. **79**, 2180 (1975).
28. N. ISLAM and K. ISMAIL. J. Phys. Chem. **80**, 1929 (1976).
29. C. A. ANGELL and R. D. BRESSEL. J. Phys. Chem. **76**, 3244 (1972).
30. J. H. AMBRUS, C. T. MOYNIHAN, and P. B. MACEDO. J. Electrochem. Soc. **119**, 192 (1972).
31. C. A. ANGELL and E. J. SARE. J. Chem. Phys. **52**, 1058 (1970).
32. C. T. MOYNIHAN, C. R. SMALLEY, C. A. ANGELL, and E. J. SARE. J. Phys. Chem. **73**, 2287 (1969).
33. A. K. DOOLITTLE. J. Appl. Phys. **22**, 1471 (1951).
34. R. A. ROBINSON and R. H. STOKES. Electrolyte solutions. 2nd ed. Butterworths, London. 1959.
35. K. J. RAO, D. B. HELPHREY, and C. A. ANGELL. Phys. Chem. Glasses, **14**, 26 (1973).

Can. J. Chem. Downloaded from www.nrcresearchpress.com by 210.87.254.105 on 09/05/12
For personal use only.

Acid-catalyzed solvolysis: unusually rapid solvolysis of 3-fluoronortricyclene in $CD_3COOD - 0.1\ M\ D_2SO_4$

NICK HENRY WERSTIUK AND GEORGE TIMMINS

Department of Chemistry, McMaster University, Hamilton, Ont., Canada L8S 4M1

Received February 1, 1980

NICK HENRY WERSTIUK and GEORGE TIMMINS. Can. J. Chem. **58**, 1704 (1980).

3-Fluoronortricyclene (**1***a*) undergoes unusually facile solvolysis in $CD_3COOD - 0.1\ M\ D_2SO_4$ at 67°C and yields 3-acetoxynortricyclene-d_3 (**1***d*) which ring-opens to a mixture of deuterated norbornyl diacetates. This result contrasts with the behaviour of 3-chloro- (**1***b*) and 3-bromonortricyclene (**1***c*) that undergo cleavage of the three-membered ring in $CD_3COOD - 0.1\ M\ D_2SO_4$. The estimated rate accelaration for solvolysis of alkyl fluorides in acid media is 10^7-10^8.

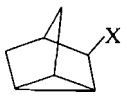
NICK HENRY WERSTIUK et GEORGE TIMMINS. Can. J. Chem. **58**, 1704 (1980).

Le fluoro-3 nortricyclène (**1***a*) se solvolyse avec une facilité surprenante dans le $CD_3COOD - D_2SO_4 - 0.1\ M$, à 67°C et conduit à l'acétoxy-3 nortricyclène-d_3 (**1***d*) qui subit une ouverture du cycle avec formation d'un mélange de diacétates de norbornyles deutérés. Ce résultat est contraire au comportement des chloro-3 (**1***b*) et bromo-3 (**1***e*) nortricyclène qui subissent une ouverture du cycle à 3 chaînons dans le $CD_3COOD - D_2SO_4 - 0.1\ M$. La vitesse d'accélération des fluorures d'alkyles en milieu acide est évaluée à 10^7-10^8.

[Traduit par le journal]

Introduction

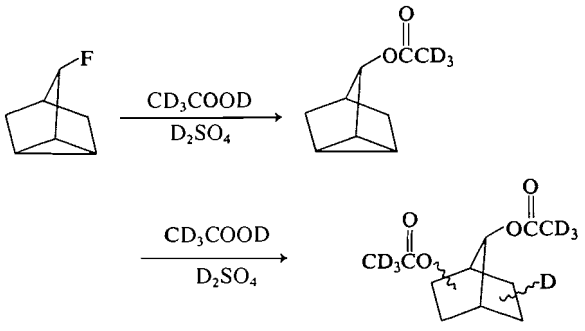
Although chloride and bromide are considered to be good leaving groups, in CD_3COOD containing D_2SO_4 (0.1 *M*), 3-chloro- (**1***b*) and 3-bromonortricyclene (**1***c*) ring-open, producing mainly *syn*- and *anti*-7-halo-2-*exo*-acetoxynorbornanes; no products due to solvolysis are detected (1). To complete our study of the effect of an electron-withdrawing group at C7 on the magnitude of the solvolytic γ-KIE of norbornyl sulfonates (1), we attempted to prepare 6-deuterated *syn*- and *anti*-7-fluoro-*exo*-2-norborneols — the brosylate precursors — by ring-opening 3-fluoronortricyclene (**1***a*). In contrast to the behaviour of **1***b* and **1***c* in acid medium, 3-fluoronortricyclene (**1***a*) undergoes rapid solvolysis followed by slow ring-opening of the 3-acetoxynortricyclene (**1***d*) (Scheme 1).



1*a*, X = F
b, X = Cl
c, X = Br
d, X = OAc

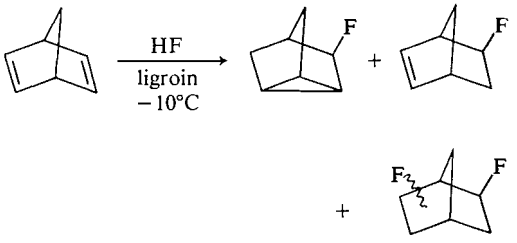
Results

For the ring-opening study we prepared **1***a* by addition of hydrogen fluoride to norbornadiene (Scheme 2). Side-reaction products, fluoronorbornene and difluoronorbornanes, were converted to norbornadiene by elimination with potassium *tert*-butoxide in DMSO, and solid **1***a* was isolated by sublimation and purified by preparative glpc. Its pmr spectrum (Fig. 1*a*) is consistent with the proposed structure ($^2J^{H,F} = 60$ Hz).



SCHEME 1

In CD_3COOD containing D_2SO_4, 3-chloro- and 3-bromonortricyclene ring-open, yielding halonorbornyl acetates with no detectable solvolysis products being formed (**1**). In contrast with this, **1***a* undergoes rapid solvolysis followed by a much slower ring-opening of **1***d* (Fig. 1*b*). This sequence of events is indicated in the pmr spectra illustrated in Fig. 1 *c* to *h*. The decreasing intensity of the doublet of **1***a* centered at δ 4.75 indicates almost



SCHEME 2

0008-4042/80/161704-05$01.00/0

©1980 National Research Council of Canada/Conseil national de recherches du Canada

Can. J. Chem. Downloaded from www.nrcresearchpress.com by 210.87.254.6 on 09/05/12
For personal use only.

Can. J. Chem. Downloaded from www.nrcresearchpress.com by 210.87.254.6 on 09/05/12
For personal use only.

complete solvolysis after 2.04×10^4 s (Fig. 1*d*, *e*) with formation of **1***d*. The ring-opening of **1***d* that yields a mixture of four diacetates, as determined by analytical glpc, is monitored by the decrease in the peak at δ 1.7 in the pmr spectra shown in Fig. 1*f* to *h*. The pmr data also provided a rough measure of the solvolytic rate constant ($k \sim 6.5 \times 10^{-5}$ s^{-1} at 67°C) for **1***a*. This value is much higher than the values for 3-chloro- and 3-bromonortricyclene derived from published work (15, 16) (chloride, $k_1 \sim 0.33 \times 10^{-7}$ s^{-1} at 65°C, bromide, $k_1 \sim 2.1 \times 10^{-7}$ s^{-1} at 65°C).[1]

Discussion

The resistance of alkyl fluorides to displacement under alkaline conditions has been noted for many years (2–5, 12). In ethanolic sodium ethoxide primary alkyl fluorides undergo mainly substitution at rates which are 10^3–10^4 times slower than the corresponding bromides (5). Under the same conditions, secondary and tertiary fluorides react at rates which are 10^5–10^6 times slower than the corresponding bromides and produce predominately elimination products (5). This low reactivity of alkyl fluorides toward nucleophilic substitution is a reflection of the strength of the carbon–fluorine bond compared to carbon–bromine or carbon–chlorine bonds.

Although the rate of solvolysis of alkyl chlorides is usually not affected by the addition of acid (7, 8) exceptions have been noted in the case of chloroethers (9, 10) and the reaction of trityl chloride with phenol (11). With respect to alkyl fluorides, however, several workers (3, 6, 12–14) have discovered enhanced rates in the presence of acid. Berstein and Miller (4) observed that the rate of reaction of substituted benzyl fluorides in 70% aqueous ethanol containing various concentrations of hydrochloric acid was dependent on the initial concentration of acid. Addition of 0.1 *N* HCl resulted in slight rate increases; percent reaction after 10 h in the presence of 0.93 *N* HCl was approximately the same as after 120 h in the presence of an equal volume of 0.1 *N* HCl. Similar results were obtained by Chapman and Levy (6) for the solvolysis of *tert*-butyl and *tert*-amyl fluorides in aqueous ethanol containing hydrochloric acid. The latter authors also observed autocatalysis in initially neutral solutions or those with relatively high initial concentrations of alkyl fluoride (ratio of fluoride-to-HCl greater than 100). The autocatalytic effect was sufficient to produce apparent zero-order kinetics in some cases. Hydrolysis of benzoyl fluoride in aqueous acetone is also catalysed by acid (14). That alkyl fluorides undergo substitution much slower than alkyl chlorides or bromides in neutral or alkaline medium (*vide supra*) and **1***a* solvolyzes approximately 3×10^2 faster than **1***c* *establishes a rate acceleration of 10^7–10^8 for solvolysis of alkyl fluorides in acid media.*

Several authors have made suggestions about the nature of the rate-determining step and transition state involved in this acid-catalysed reaction. Bevan and Hudson (14) concluded that water was not strongly involved in the transition state of the rate-determining step. Likewise Swain and Spalding (13) suggested that a species similar to **2** with

$$RCH_2\overset{+}{F}H$$
2

water only loosely bound must be involved and that the rate-determining step may be

$$RCH_2\overset{+}{F}H \rightarrow R\overset{+}{C}H_2 + HF$$

The results of the solvolysis of **1***a* therefore confirm previous experimental observations of a large rate increase due to catalysis in acid media and allow us to estimate that the rate acceleration is in the order of 10^7–10^8. The reactivity of alkyl fluorides towards nucleophilic displacement appears to be controlled by two factors: in the absence of acid the strong fluorine–carbon bond results in slow rates of reaction relative to the corresponding alkyl chlorides and bromides whereas protonation (or hydrogen bonding) of fluorine results in relatively fast reaction rates in acid media.

Experimental

*Preparation of 3-Fluoronortricyclene (***1a***)*

Norbornadiene (25.2 g) was dissolved in purified ligroin (375 mL) contained in a 500 mL polyethylene bottle fitted with a stir-bar, a $CaCl_2$ drying tube, and a polyethylene inlet tube. The mixture was cooled in an ice–salt bath and HF (7.5 g) was bubbled into the solution over a period of 1 h. The black solution was stirred for 1 h and carefully poured onto 500 mL of ice–water containing K_2CO_3 (42 g). The organic layer was separated, washed with aqueous bicarbonate (2 × 50 mL) and water (2 × 50 mL), and dried. After the solution was treated with decolourizing carbon the solvent was removed by distillation through a 12 in. glass helicies column. Analytical glpc analysis of the residue (37.2 g) on a 1/8 in. × 10 ft 5% SE 30 column at 60°C established that three major products (>85%) were present in a ratio 2:2:1. To a solution of $K^+\bar{O}tBu$ (57.5 g) in DMSO (550 mL)

[1]Converted from data (15, 16) for the solvolysis rates in 80% EtOH – H_2O using the Winstein–Grunwald linear free energy relationship, $\log k/k_0 = mY$, with $Y = -1.64$ for 100% acetic acid. The rate comparison is necessarily approximate since the rate data for **1***a* is for fully deuterated acetic acid containing D_2SO_4. Temperature corrections were made assuming a rate doubling for each 10°C change.

Can. J. Chem. Downloaded from www.nrcresearchpress.com by 210.87.254.6 on 09/05/12
For personal use only.

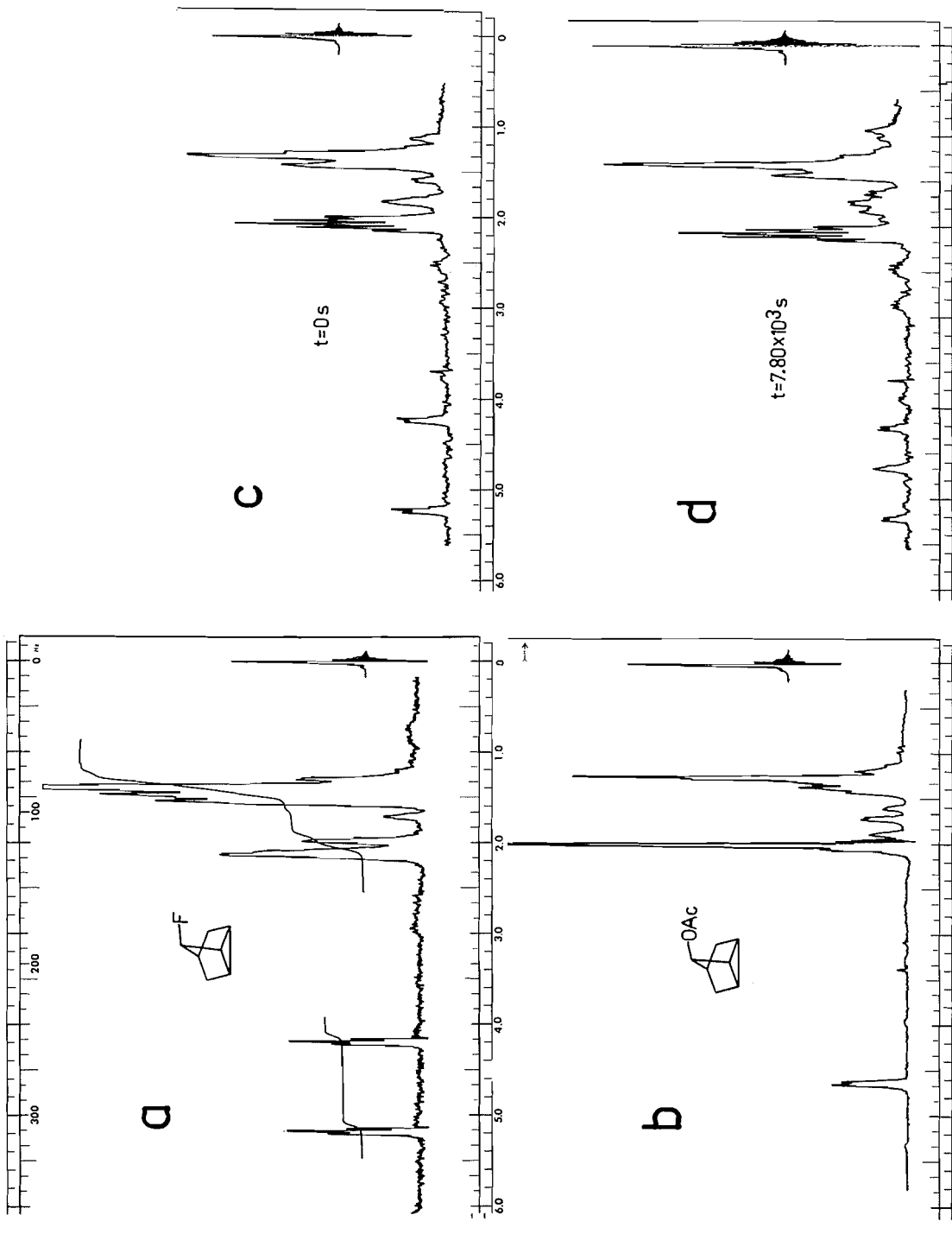


FIG. 1. (*a*), 60 MHz spectrum (CS_2) of 3-fluoronortricyclene; (*b*), 60 MHz spectrum (CD_3COOD) of 3-acetoxynortricyclene; (*c*)–(*h*), 60 MHz spectra used to monitor reaction of 3-fluoronortricyclene in 0.1 *M* D_2SO_4 – CD_3COOD at 67°C.

Can. J. Chem. Downloaded from www.nrcresearchpress.com by 210.87.254.6 on 09/05/12
For personal use only.

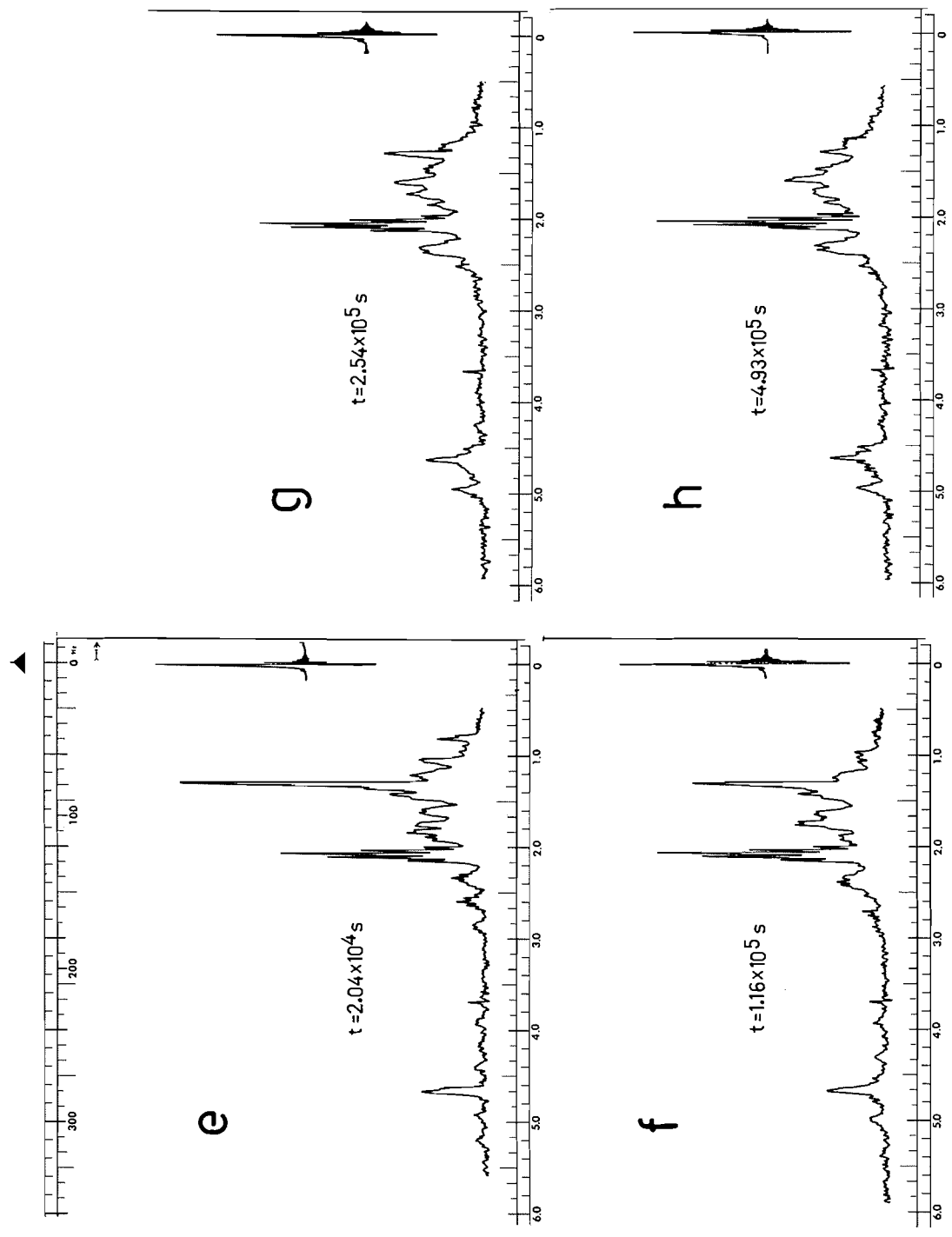


FIG. 1 (*Concluded*)

were added 31.7 g of the reaction mixture. The solution was stirred for 2.5 h at 80°C, water was added (1 L), and the mixture was extracted with ether (3 × 500 mL). The combined ether extracts were washed with water (2 × 300 mL), saturated aqueous NaCl (300 mL), and dried. Analytical glpc analysis on a 1/8 in. × 10 ft SE-30 column at 60°C showed that the peaks due to first and third major products had disappeared while the second product remained unchanged. The ether and most of the *tert*-BuOH were removed by distillation and the crude **1***a* was isolated from the tarry residue by sublimation. Solid **1***a* (0.94 g) was isolated from the sublimate by preparative glpc on a 1/4 in. × 12 ft 20% SE-30 column at 125°C; nmr (CS_2, 60 MHz) δ 4.75 (dt, 1H, J = 60 Hz, H-3), 2.3–1.9 (broad m, 2H, H-4 and H-7 *syn* to C—F), 1.8–1.1 (nortricyclyl envelope); ir (CS_2): 3075, 3000, 2950, 2875, 1348, 1360, 1308, 1288, 1134, 1063, 1040, 945, 907, 813, 802, 699.

D_2SO_4-catalyzed Ring-opening of 3-Fluoronortricyclene in CH_3COOD

3-Fluoronortricyclene (0.11 g) was dissolved in CH_3COOD (1 mL) that contained D_2SO_4 (0.02 g) and the solution was heated for 20 h at 85°C. The reaction mixture was poured onto saturated $NaHCO_3$ solution and the mixture was extracted with ether (3 × 25 mL). The combined ether extracts were washed with water (2 × 10 mL), dried, and the solvent was evaporated.

Analysis of the residue (0.13 g) by analytical glpc on a 1/8 in. × 10 ft FFAP column at 180°C established that four major products (>90%) were present in a ratio of 1:8:3:10; nmr (CH_3COOD, 60 MHz) δ 4.8 (broad m due to several peaks, —CHOAc), 2.5 (broad m, H-1 and H-4), 2.10 (broad s with shoulder, CH_3COO—), 2.2–1.1 (norbornyl envelope); ms M^+ *m/e* 213 $C_{11}H_{15}DO_4$ (deuterated norbornyl diacetates).

Kinetics of D_2SO_4-catalyzed Ring-opening of 3-Fluoronortricyclene in CD_3COOD

3-Fluoronortricyclene (0.022 g) was disolved in 1 mL of CD_3COOD that contained D_2SO_4 (0.010 g). The solution was transferred into an nmr tube, the tube was heated at 67 ± 3°C and 60 MHz pmr spectra were recorded at appropriate intervals. The spectra (Fig. 1) clearly indicated that **1***a*, after 5 h 40 min, was almost completely converted to 3-nortricyclyl acetate-d_3. After 137 h the conversion to deuterated norbornyl diacetates was essentially complete.

The approximate rate constant was determined by cutting and weighing the peaks for 3-H of 3-fluoro- and 3-acetoxynortricyclane. First-order kinetics were assumed and the rate constant ($k \sim 6.5 \times 10^{-5}\ s^{-1}$) was determined from the average of three weighings from each of two kinetic runs.

Acknowledgement

We thank the Natural Sciences and Engineering Research Council of Canada for financial support.

1. F. P. Cappelli, G. Timmins, and N. H. Werstiuk. Can. J. Chem. **50**, 2163 (1972).
2. F. W. Hoffman. J. Org. Chem. **15**, 425 (1950).
3. K. A. Cooper and E. D. Hughes. J. Chem. Soc. 1183 (1937).
4. J. Bernstein and Wm. T. Miller. J. Am. Chem. Soc. **70**, 3600 (1948).
5. N. B. Chapman and J. L. Levy. J. Chem. Soc. 1673 (1952).
6. N. B. Chapman and J. L. Levy. J. Chem. Soc. 1677 (1952).
7. S. C. J. Olivier and G. Berger. Recl. Trav. Chim. **41**, 637 (1922).
8. S. C. J. Olivier and A. Ph. Weber. Recl. Trav. Chim. **53**, 869 (1934).
9. H. Bohme. Ber. **74B**, 248 (1941).
10. R. Leimer and P. Salomaa. Acta Chem. Scand. **1**, 353 (1947).
11. H. Hart and F. A. Cassis. J. Am. Chem. Soc. **76**, 1634 (1954).
12. C. G. Swain, T. E. C. Knees, and A. MacLachlan. J. Am. Chem. Soc. **82**, 6101 (1960).
13. C. G. Swain and E. T. Spalding. J. Am. Chem. Soc. **82**, 6104 (1960).
14. C. W. L. Bevan and R. F. Hudson. J. Chem. Soc. 2187 (1953).
15. J. D. Roberts, W. Bennett, and R. Armstrong. J. Am. Chem. Soc. **72**, 3329 (1950).
16. J. D. Roberts and W. Bennett. J. Am. Chem. Soc. **76**, 4623 (1954).

Can. J. Chem. Downloaded from www.nrcresearchpress.com by 210.87.254.6 on 09/05/12
For personal use only.

Stereochemistry of acid-catalyzed cleavage of 3-chloro- and 3-bromonortricyclene in deuterated medium. Evidence for edge protonation of nortricyclenes

NICK HENRY WERSTIUK, GEORGE TIMMINS, AND FRANK PETER CAPPELLI
McMaster University, Hamilton, Ont., Canada L8S 4M1

Received December 5, 1979

NICK HENRY WERSTIUK, GEORGE TIMMINS, and FRANK PETER CAPPELLI. Can. J. Chem. **58**, 1709 (1980).

Cleavage of 3-chloronortricyclene (**4***c*) and 3-bromonortricyclene (**4***d*) occurs faster than solvolysis in D_2SO_4–DOAc at 70–75°C and yields *syn*-7-, *anti*-7-, *exo*-5-, and *endo*-5-halo-*exo*-2-norbornyl acetates as products. That the 7-chloroacetates comprise 70% of the reaction mixture, that 30% of the 5-chloro-*exo*-2-norbornyl acetates which comprised 28% of the reaction mixture are derived via rearrangement of the *syn*-7- and *anti*-7-chloronorbornyl cations, and that the deuterium at C-6 is at least 90% stereochemically pure *endo* is evidence that cleavage of the bond farthest removed from the electron withdrawing halogen is preferred 5:1 over the other bonds of the three-membered ring. The stereochemistry of the ring-opening is rationalized on the basis of cleavage via edge-deuteronation with formation of classical halocations as intermediates. The location of deuterium in the 5-halo-*exo*-norbornyl acetates is used to define the pathways whereby the 5-haloacetates are formed. This study also establishes that C-6 *endo* deuterated 7-chloro- and 7-bromo-*exo*-2-norbornyl brosylates can be synthesized from the corresponding 3-halonortricyclenes.

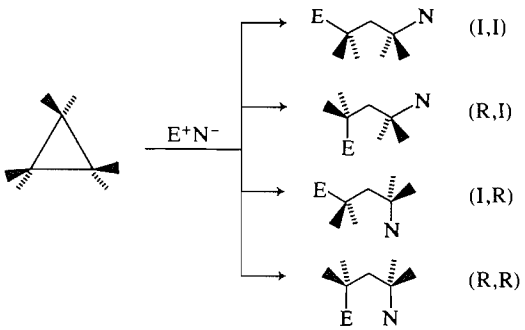
NICK HENRY WERSTIUK, GEORGE TIMMINS et FRANK PETER CAPPELLI. Can. J. Chem. **58**, 1709 (1980).

Le clivage des chloro-3 et bromo-3 nortricyclènes (**4***c*) et (**4***d*) se produit plus rapidement que la solvolyse dans le mélange D_2SO_4–DOAc à 70–75°C et conduit aux acétates des halogèno-7-*syn*, 7-*anti*, 5-*exo* et 5-*endo* norbornyles-2-*exo*. Le fait que (*a*) les acétates des chloro-7 norbornyles constituent 70% du mélange réactionnel, (*b*) 30% des acétates des chloro-5 norbornyles-2-*exo*, qui constituent 28% du mélange réactionnel, proviennent de la transposition des cations chloro-7 *syn* et 7-*anti* norbornyles et (*c*) le deutérium en C-6 est au moins à 90% *endo* montre que le clivage de la liaison la plus éloignée de l'halogène électro-attracteur se fait préférentiellement et environ 5 fois plus rapidement que les autres liaisons du cycle à trois chaînons. On rationnalise la stéréochimie de l'ouverture du cycle en se basant sur une rupture par l'intermédiaire d'une deutération par l'arête avec formation d'halogènes cationiques comme intermédiaire. On utilise la position du deutérium dans les acétates des halogènes-5 *exo* norbornyles pour définir les voies de formation des acétates des halogènes-5. Cette étude établit également que les brosylates des chloro-7 et bromo-7 C-6 *endo* norbornyles-2 *exo* peuvent être synthétisés à partir des halogènes-3 nortricyclènes correspondants.

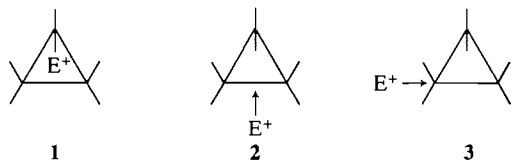
[Traduit par le journal]

Introduction

Over the past two decades the mechanistic details of the electrophilic cleavage of cyclopropanes have been elucidated by stereochemical and product studies. Generally, electrophilic cleavage occurs to yield products with either retention (R) or inversion (I) at the carbon atoms of the C—C bond which is cleaved by the electrophile (1–6). In general attempts have been made to establish how



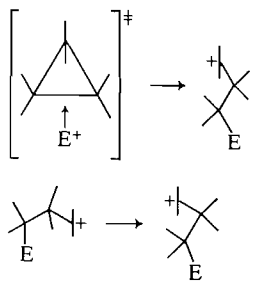
substituents borne by a cyclopropane and the nature of the electrophile control the mechanism of the ring-opening. While a proton (deuteron) can attack cyclopropane face-wise, edge-wise, or



1 2 3

corner-wise as depicted in **1**, **2**, and **3**, respectively, face-wise attack does not occur because face-protonated cyclopropane is a high energy species (7, 8). Edge-wise attack can formally lead to open cations,[1] an edge-protonated cyclopropane, or a

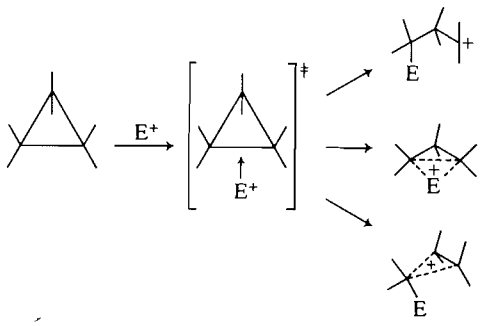
[1]While retention of configuration is indicated in the above diagram, it is conceivable that the C—C bond adjacent to the bond being attacked by the electrophile is cleaved. It is also possible that the first formed ion undergoes a 1,2-alkyl shift and thereby yields products of ring-opening by inversion.



0008-4042/80/161709-16$01.00/0
©1980 National Research Council of Canada/Conseil national de recherches du Canada

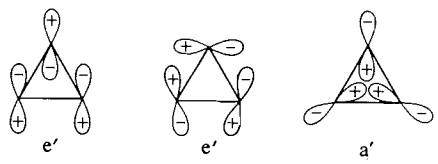
Can. J. Chem. Downloaded from www.nrcresearchpress.com by 210.87.254.40 on 09/05/12
For personal use only.

Can. J. Chem. Downloaded from www.nrcresearchpress.com by 210.87.254.40 on 09/05/12
For personal use only.

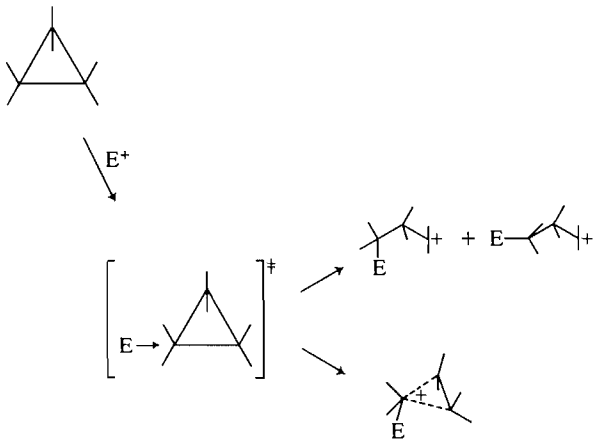


corner protonated cyclopropane which is formed by a proton-slide (9) to the corner after initial edge-approach.

Edge-wise attack is expected to be the preferred mode of cleavage because the majority of the polarizable electron density is located between the carbon atoms of the strained σ bonds. In the Walsh model, the degenerate e′ π type HOMO's of cyclopropane and nortricyclene (10) that are expected to bind with the incoming electrophile, contain four electrons and the a_1' MO, which is considerably lower in energy, contains two electrons.



It is clear from the MO's of cyclopropane documented by Jorgensen and Salem (11) that there is significant electron density at the corners in both the e′ and a_1' orbitals so that corner bonding of the electrophile with both types of MO's is possible.



It is not possible to predict the stereochemistry of such cleavage should it occur. It is possible, however, that cleavage occurs with both retention or inversion of configuration to yield classical cations. It is also possible that a corner-substituted cyclopropane that reacts to yield products of both retention and inversion of configuration is involved as an intermediate. From an electron density map of cyclopropane it is clear that there is less electron density localized at the corners than at the centres of the strained σ bonds. On this basis edge-wise attack would be preferred. This conclusion is in accord with LCAO SCF MO calculations of the electrostatic potential energy experienced by a positive charge as it interacts with the electrons and nuclei of cyclopropane (12).

The electrophilic cleavage of three-membered rings has been the subject of a number of reviews and as Cristol *et al.* (13) have stated " ... it is clear that inversion or retention of configuration by the nucleophile or electrophile may attend electrophilic addition to cyclopropanes and that no single mechanism can accommodate all data". It appears, however, that in most cases a proton (deuteron) cleaves a cyclopropane with retention of configuration. Of the studies involving a proton (deuteron) as the electrophile, investigations of the ring-opening of nortricyclene and several derivatives have generated considerable interest because the results relate to the long-standing norbornyl cation problem (14). Nickon and Hammons (15) and Hammons and co-workers (16) studied the D_2SO_4-catalysed acetolysis of nortricyclene (**4***a*) and 1-methylnortricyclene (**5**), respectively, and concluded that corner-protonated (deuterated) nortricyclenes **6** and **7**, the non-classical cations, were involved as intermediates.

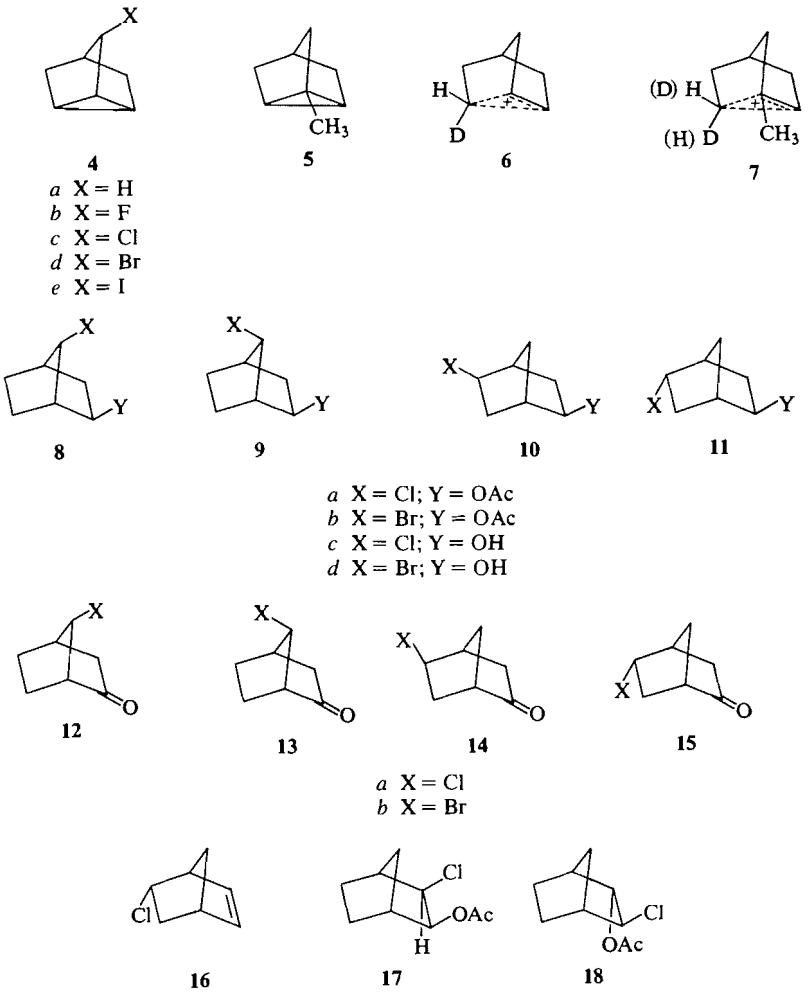
Our interest in the non-classical ion problem (17, 18), and in the stereochemistry of 1,3-elimination in norbornyl systems (19), the reverse of protonation of nortricyclenes, led us to study the D_2SO_4-catalyzed ring-opening of the 3-halonortricyclenes **4***b–e*. We wished to determine whether the halonortricyclenes were ring-opened by edge or corner protonation and to prepare specifically C-6 deuterated *syn*- and *anti*-7-halo-*exo*-2-norbornyl brosylates which we required for a study of the effect of an electron withdrawing group on the unusually large γ-kinetic isotope effects (KIE's) observed in the solvolysis of *exo*-norbornyl sulfonate esters (2). In the following papers we expand on the preliminary reports of our work (17, 20).

Results

Identification of Products

Treatment of 3-chloronortricyclene (**4***c*) and 3-bromonortricyclene (**4***d*) with 0.1 *M* H_2SO_4–HOAc at 70 ± 2°C, respectively, yielded the *syn*-7-halo-

Can. J. Chem. Downloaded from www.nrcresearchpress.com by 210.87.254.40 on 09/05/12
For personal use only.



4
a X = H
b X = F
c X = Cl
d X = Br
e X = I

5 **6** **7**

8 **9** **10** **11**

a X = Cl; Y = OAc
b X = Br; Y = OAc
c X = Cl; Y = OH
d X = Br; Y = OH

12 **13** **14** **15**

a X = Cl
b X = Br

16 **17** **18**

exo-2-norbornyl acetates **8***a* and **8***b*, the *anti*-7-halo-*exo*-2-norbornyl acetates **9***a* and **9***b*, the *exo*-5-halo-*exo*-2-norbornyl acetates **10***a* and **10***b*, and the *endo*-5-halo-*exo*-2-norbornyl acetates **11***a* and **11***b*. Solvolysis (< 5%) of the nortricyclenes did not compete with ring-opening. The fluoride **4***b*, however, underwent unusually fast solvolysis, as documented in a following paper, and yielded nortricyclyl acetate that was slowly converted into diacetates. Iodide **4***e* liberated iodine and yielded two major products which we assumed were the corresponding 7-iodoacetates. However, the study of **4***e* was abandoned after several preliminary experiments.

Since the chloroacetates **8***a*, **10***a*, and **11***a* had virtually identical glpc retention times, the following procedure was used to establish that four major products were formed. The *anti*-acetate **9**a was isolated from the reaction mixture by preparative glpc and reduced to **9***c*. The remaining acetates were reduced to the chlorohydrins **8***c*, **10***c*, and **11***c* by LAH, and the *syn*-7-chlorohydrin **8***c*, that has a shorter retention time than other chlorohydrins, was isolated by preparative glpc. Chromic acid oxidation of the mixture of chlorohydrins obtained by LAH reduction of the total reaction mixture yielded the chloro-2-norbornanones **12***a* (26 ± 1%), **13***a* (44 ± 2%), **14***a* (14 ± 1%), **15***a* (14 ± 1%), and 2 ± 1% of two unidentified products. A sample of **9**a was prepared by acetylation of an authentic sample of **9***c* (21) and its ir and ^{1}H nmr spectra were identical to the spectra of **9***a* obtained from the ring-opening. A sample of *exo*-5-chloroketone **14***a* was prepared via the reaction of nortricyclanone with anhydrous HCl in CCl_4. Its ^{1}H nmr spectrum was identical to the spectrum of **14***a* obtained by chromic acid oxidation of the chlorohydrin mixture. To prepare an authentic sample of the *endo*-5-chloroketone **15***a*, *endo*-5-chloro-2-norbornene was hydroborated and the resulting mixture of

Can. J. Chem. Downloaded from www.nrcresearchpress.com by 210.87.254.40 on 09/05/12
For personal use only.

TABLE 1. Deuterium content of halo-2-norbornanones

Halonorbornanone	Composition*			Excess d per molecule
	% d_0	% d_1	% d_2	
Syn-7-chloro-	3.33 ± 0.02	95.01 ± 0.21	1.67 ± 0.24	0.985 ± 0.002
Anti-7-chloro-	3.81 ± 0.01	95.04 ± 0.18	1.15 ± 0.18	0.976 ± 0.004
Exo-5-chloro-	9.84 ± 0.25	89.41 ± 0.59	0.67 ± 0.88	0.910 ± 0.015
Endo-5-chloro-	12.87 ± 0.01	84.65 ± 0.01	2.47 ± 0.01	0.894 ± 0.002
Syn-7-bromo-	4.27 ± 0.18	94.03 ± 0.42	1.71 ± 0.24	0.967 ± 0.005
Anti-7-bromo-	5.63 ± 0.12	92.48 ± 0.28	1.40 ± 0.20	0.977 ± 0.007
Exo-5-bromo-	15.24 ± 0.34	81.04 ± 0.31	2.25 ± 0.08	0.867 ± 0.022
Endo-5-bromo-	10.47 ± 0.56	86.54 ± 0.40	2.99 ± 0.67	0.914 ± 0.033

*Determined at low voltage (10–15 eV). Average of at least five determinations. The deviations are the standard deviations.

endo-5-chloro-*exo*-2- and *endo*-5-chloro-*exo*-3-norbornanols was oxidized to the chloroketones. The ^{1}H nmr spectrum of **15***a* isolated from a mixture of **15***a* (42%) and *endo*-6-chloro-2-norbornanone (58%) by preparative glpc was identical to the spectrum of **15***a* that was obtained by chromic acid oxidation of the chlorohydrin mixture (*vide supra*). To establish whether the isomeric 3-chloro-*exo*-2-norbornyl acetates **17** and **18** were significant products of the ring-opening, we prepared *exo*-3-chloro-2-norbornanone and *endo*-3-chloro-2-norbornanone (22, 23) and compared their glpc retention times with the retention times of the chloroketones. From the analysis we estimate that the 3-chloroacetates were formed in not more than 2% yield. By reducing the mixture of chloroacetates with Na in 2-propanol and analyzing the product by analytical glpc, we established an upper limit of 1% for the yield of *endo*-acetates. We checked the stability of the acetates **8***a*, **9***a*, **11***a*, **17**, and **18** under the reaction conditions by heating the compounds in 0.1 *M* H_2SO_4–HOAc at 70°C for 500 h. Compounds **8***a*, **9***a*, **11***a*, **17**, and **18** underwent 12 ± 1%, <3%, 15 ± 1%, <3%, and <2% rearrangement, respectively. Compound **8***a* rearranged to **9***a* and **11***a* rearranged to **10***a*. Acetates **17** and **18** used in the isomerization experiments were prepared by acetylation of the corresponding chlorohydrins that were obtained via a published route (22).

The products of the acid-catalyzed ring-opening of 3-bromonortricyclene, **8***b*, **9***b*, **10***b*, and **11***b*, were also characterized and their yields established basically by the procedure which we used to identify the products of the ring-opening of **4***b*. The relative yields of the bromoacetates **8***b*, **9***b*, **10***b*, and **11***b* were similar to the yields of the corresponding chloroacetates. The *syn*- and *anti*-7-bromo-*exo*-2-norbornyl acetates were converted to the corresponding bromoketones, **12***b* and **13***b*, and the bromoketones were identified as their 2,4-dinitrophenylhydrazones. An authentic sample of *exo*-5-bromo-2-norbornanone (**14***b*) was prepared by the addition of HBr to nortricyclanone and *endo*-5-bromo-2-norbornanone (**15***b*) was identified by the fact that its ^{1}H nmr spectrum was essentially identical to the spectrum of the corresponding chloroketone **15***a*.

Stereochemistry of Ring-opening: Cleavage in Deuterated Medium

To determine the stereochemistry of the electrophilic cleavage, **4***c* and **4***d* were ring-opened in deuterated medium. Since an extended reaction period (500 h) was required for **4***c* at 70°C, we avoided dilution of the deuterium pool by methyl exchange of CH_3COOD by carrying out the ring-opening in CD_3COOD. In CH_3COOD at 75 ± 1°C the ring-opening of **4***d* was essentially complete after 77 h. The haloacetates were converted to the corresponding ketones and the ketones were analyzed for deuterium mass spectrometrically (Table 1). To determine the deuterium distribution in the chloroacetates, the 2-norbornanols derived from the chloroketones were subjected to a lanthanide shift reagent (LSR) study. The ^{1}H nmr spectra of the natural abundance and deuterated *exo*-2- and *endo*-2-norbornanols are given in Figs. 1*a–f*. The LAH reduction of *syn*-chloroketone **12***a-d* gave predominately *exo*-2-norbornanol-*d* and reduction of **13***a-d* and **15***a-d* gave 85% of *endo*-2-norbornanol-*d* and 15% of *exo*-2-norbornanol-*d*. Surprisingly, **14***a-d* yielded predominately *exo*-2-norbornanol-*d*. Since hydride attacks the carbonyl group of **14***a-d* from the *exo* face to yield the *endo*-alkoxide and direct displacement of the chlorine by hydride is slow, solvolysis of the *exo*-5-chloro-*endo*-alkoxide must yield a pair of rapidly-equilibrating norbornyl cations that are trapped by hydride according to their equilibrium populations. Each norbornanol was carefully purified by preparative glpc before the ^{1}H nmr analysis was carried out.

The signal at δ 14.9 of the spectrum of *endo*-2-norbornanol (Fig. 1*a*) is clearly due to *endo*-6-H. That the signal at δ 6.9 of the spectrum of *exo*-2-

TABLE 2. Deuterium distribution in chloroacetates*

Deuterated acetate	C1	C2	C3		C6		Total *d* by ^{1}H nmr
			Exo	*Endo*	*Exo*	*Endo*	
Syn-7-	—	—	—	—	—	0.90 ± 0.05	0.90 ± 0.05
Anti-7-	—	—	—	—	—	0.90 ± 0.05	0.90 ± 0.05
Exo-5-	0.10 ± 0.02	0.08 ± 0.01†	0.25 ± 0.03	0.25 ± 0.03	0.20 ± 0.03	0.15 ± 0.02	1.03 ± 0.15
Endo-5-	0.10 ± 0.02	0.08 ± 0.01†	—	—	0.55 ± 0.05	0.35 ± 0.04	1.08 ± 0.12

*Limit of detectability is estimated to be 0.05 *d*.
†Determined by mass spectrometry as described in the text.

Can. J. Chem. Downloaded from www.nrcresearchpress.com by 210.87.254.40 on 09/05/12
For personal use only.

norbornanol (Fig. 1*d*) is due to *endo*-6-H was corroborated by a critical examination of the non-shifted 100 MHz spectra of **8***a*, **8***a-d*, and *syn*-7-chloro-*exo*-2-norbornanol-*exo*,*exo*-5,6-d_2 in the region of δ 1.5–2.8 where the *endo*-5-H and *endo*-6-H resonances appear. Since a decrease in the signal intensity corresponding to one proton is observed at the high field end of the spectrum of **8***a-d*, the deuterium must be located *endo* at C-6. The deuterated norbornanols were complexed with $Eu(thd)_3$ and the deuterium distribution was established by subtracting the integral for a proton at a specific site from the integral for a proton at a site bearing only natural abundance deuterium (*anti*-7-H and H-4 of *exo*-2-norbornanol-*d* and *anti*-7-H, *exo*-5-H and *endo*-5-H of *endo*-2-norbornanol-*d*). Figure 1*b* illustrates the shifted spectrum of deuterated *endo*-norbornanol obtained by LAH reduction of deuterated *anti*-7-chloro-2-norbornanone and Fig. 1*c* illustrates the spectrum of the deuterated *endo*-norbornanol derived from deuterated *endo*-5-chloro-2-norbornanone. Figure 1*e* shows the spectrum of deuterated *exo*-2-norbornanol obtained from *syn*-7-chloro-2-norbornanone and Fig. 1*f* is the spectrum of the deuterated *exo*-norbornanol obtained from deuterated *exo*-5-chloro-2-norbornanone. Since the accuracy of the integration is not better than ±5%, the error quoted is the sum of the errors in the specific-site and standard integrals. The deuterium content at C-2 was taken as the difference between the average deuterium content of the 7-chloroketones and the deuterium content of the appropriate 5-chloroketone (Table 1). The results of the ^{1}H nmr analysis are listed in Table 2. The deuterium content established by ^{1}H nmr considering the errors involved, compares favourably with the deuterium content determined by mass spectrometry. Thus, it is clear that the deuterium at C-6 of the 7-chloroacetates is at least 90% stereochemically pure *endo*.

The LSR analyses were not carried out in the case of the bromoketones. Instead, the ir fingerprint regions of the deuterated *exo*-2-norbornanols obtained from **8***d-d* and **9***d-d* were compared with the fingerprint regions of authentic samples[2] of *exo*-2-norbornanol-*exo*-6-*d* and *exo*-2-norbornanol-*endo*-6-*d*. From the spectra shown in Figs. 2*a–d*, it is clear that the deuterium in the 7-bromoacetates is at least 90% stereochemically pure *endo*. To corroborate this assignment we compared the spectra of **9***b* and **9***b-d* in the region of δ 1.2 where the *endo* proton resonances appear. That there was a decrease in intensity of the signal corresponding to approximately one proton indicates that the deuterium is located predominately *endo* at C-6. Since the 5-bromoketones contain less deuterium than the 7-bromoketones (Table 1) the deuterium distribution in the 5-bromoacetates must by similar to the deuterium distribution in the 5-chloroacetates.

Discussion

That the deuterium at C-6 of the *syn*-7- and *anti*-7-haloacetates **19***a*, **19***b*, **20***a*, and **20***b* is at least 90% stereochemically pure *endo*, in our view, establishes that the ring-opening occurs predominately by edge-deuteration of the bond farthest removed from the electron withdrawing halogen (Scheme 1). Although D^+ attacks the three-membered ring edge-wise, the question arises whether classical (Path a, Scheme 1) or non-classical (Path b, Scheme 1) intermediates are formed. In our view, classical[3] rather than non-classical cations are involved simply because participation of the C1—C6 bond should lead to development of positive charge at C-1 that is adjacent to the carbon bearing the electron withdrawing halogen.[4] It seems to us reasonable that this would

[2]We thank Professor A. Nickon for copies of the ir spectra of the deuterated *exo*-norbornanols.

[3]Since in our view (18) the norbornyl cation is a classical species, the 5- and 7-halonorbornyl cations are represented in that form in this and subsequent papers.

[4]Although Goering and Degani (24) suggest that non-classical 7-chlorocations are involved as intermediates in the acetolysis of 7-chloro-*exo*-2-norbornyl tosylates, they state that the low yield (≃ 2%) of 3-chloro-2-norbornyl acetates ... "is probably due to the low cationic character at C-1 because of the inductive effect of the adjacent chlorine atom."

Can. J. Chem. Downloaded from www.nrcresearchpress.com by 210.87.254.40 on 09/05/12
For personal use only.

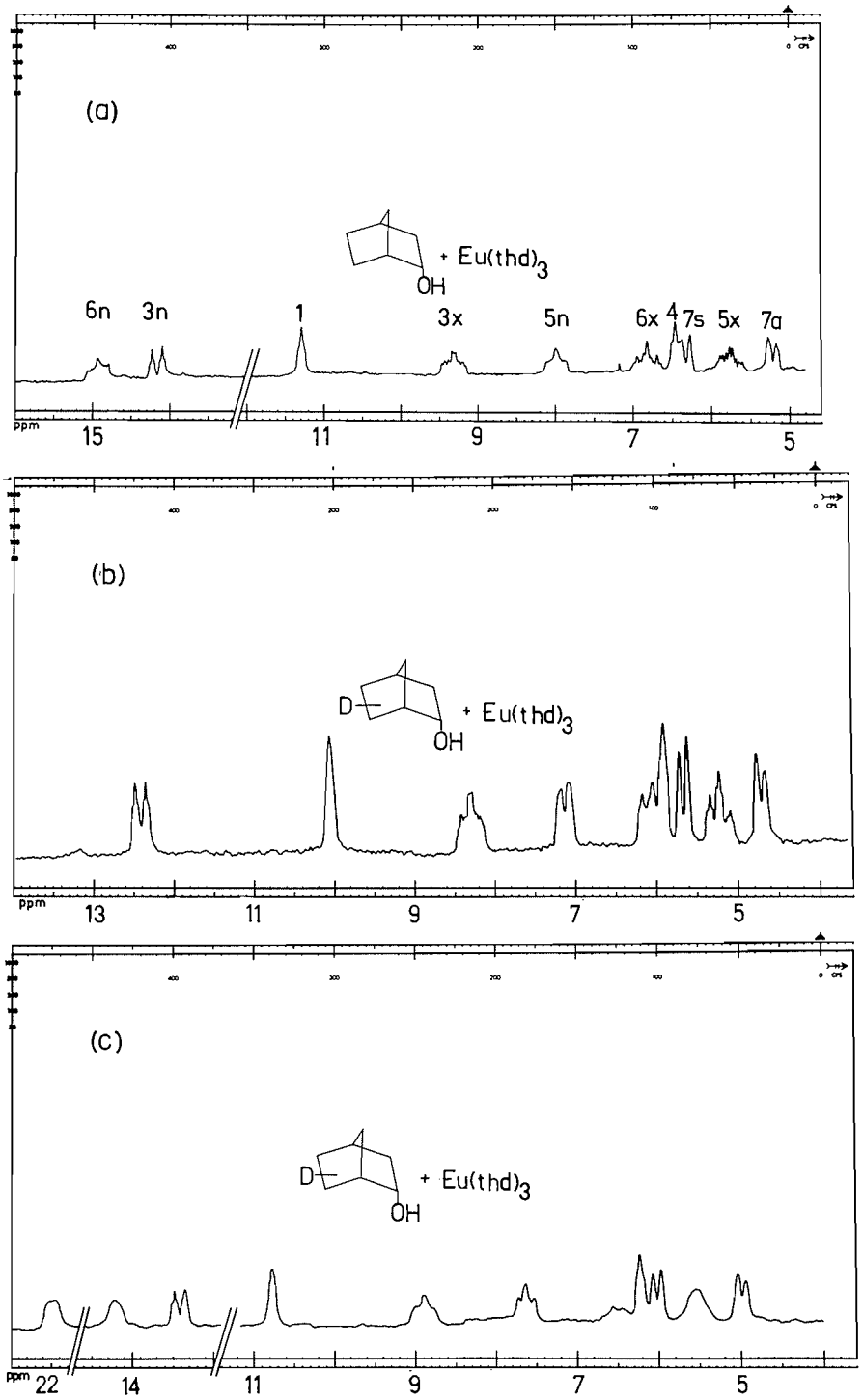


FIG. 1. (*a*) The 100 MHz ^{1}H nmr spectrum (CCl_4) of *endo*-2-norbornanol complexed with $Eu(thd)_3$; (*b*) 100 MHz ^{1}H nmr spectrum of deuterated *endo*-2-norbornanol derived from **13***a-d* complexed with $Eu(thd)_3$; (*c*) 100 MHz ^{1}H nmr spectrum (CCl_4) of deuterated *endo*-2-norbornanol derived from **15***a-d* complexed with $Eu(thd)_3$; (*d*) 100 MHz ^{1}H nmr spectrum (CCl_4) of *exo*-2-norbornanol in the presence of $Eu(thd)_3$; (*e*) 100 MHz ^{1}H nmr spectrum (CCl_4) of deuterated *exo*-2-norbornanol derived from **12***a-d* complexed with $Eu(thd)_3$; (*f*) 100 MHz ^{1}H nmr spectrum (CCl_4) of deuterated *exo*-2-norbornanol derived from **14***a-d* complexed with $Eu(thd)_3$.

Can. J. Chem. Downloaded from www.nrcresearchpress.com by 210.87.254.40 on 09/05/12
For personal use only.

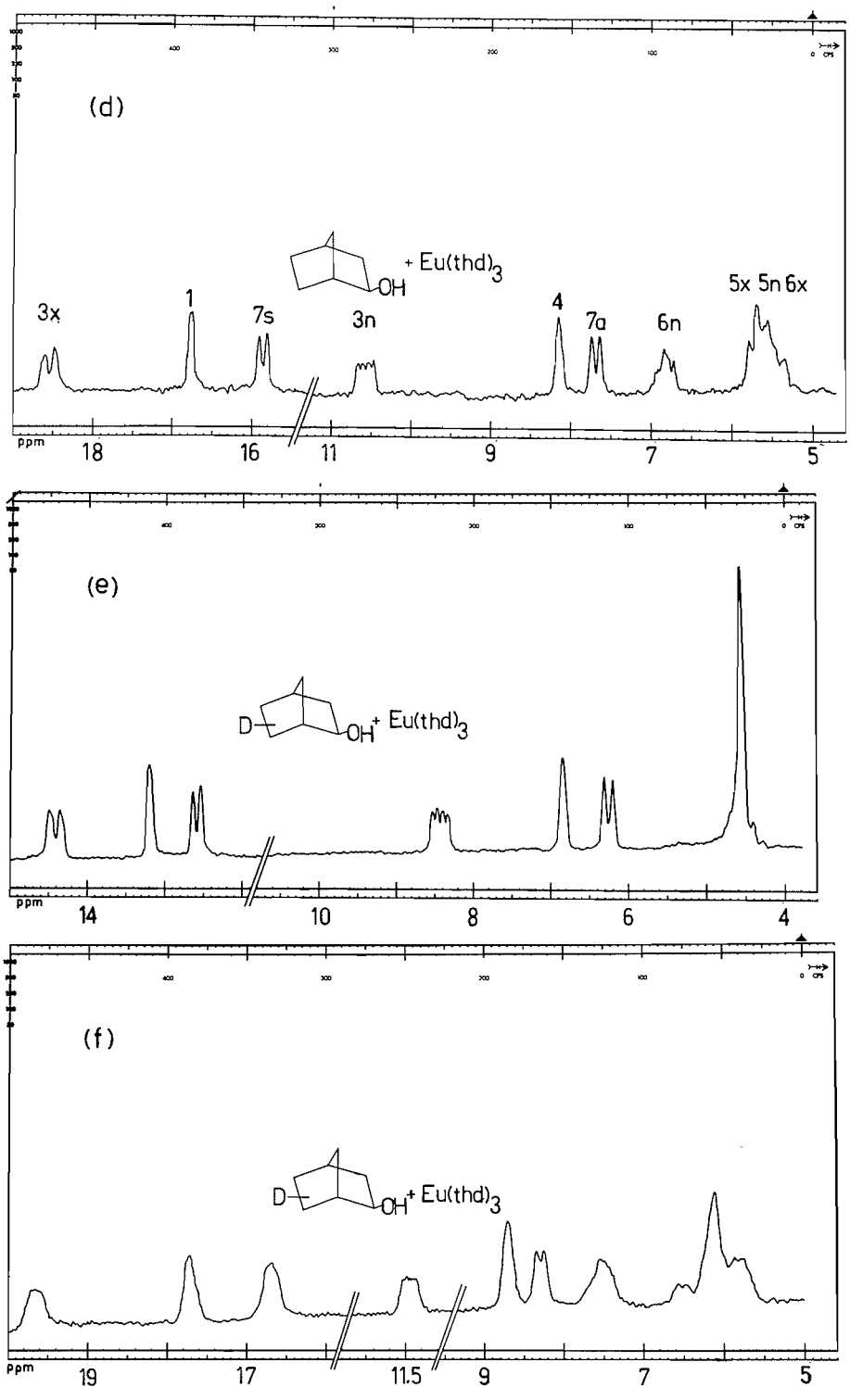


FIG. 1 (*concluded*).

Can. J. Chem. Downloaded from www.nrcresearchpress.com by 210.87.254.40 on 09/05/12
For personal use only.

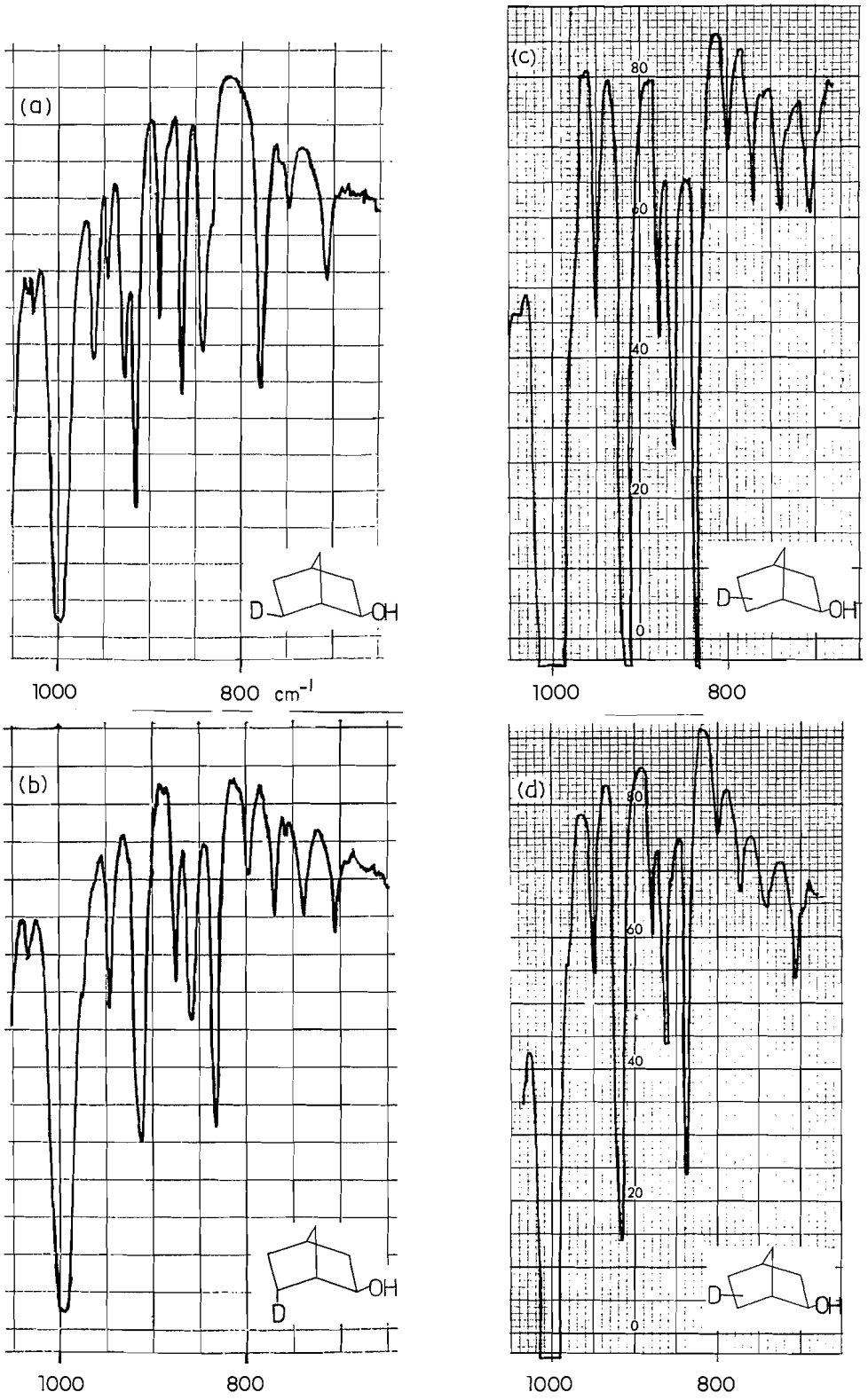
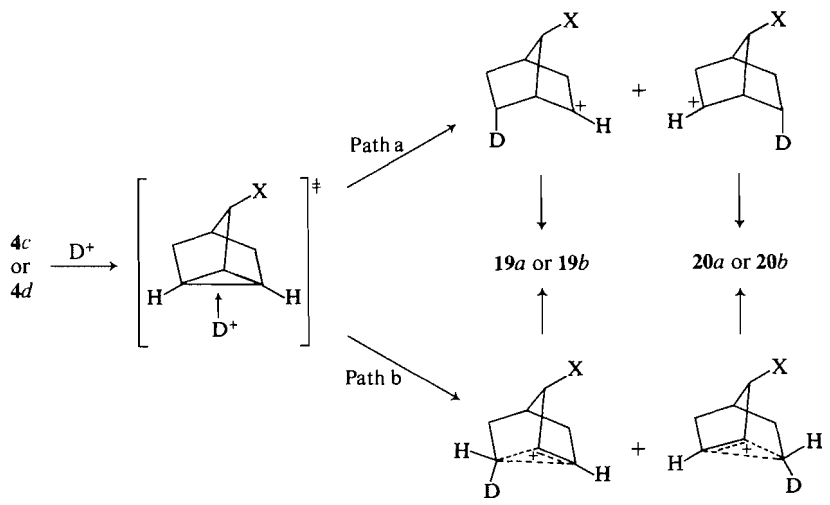
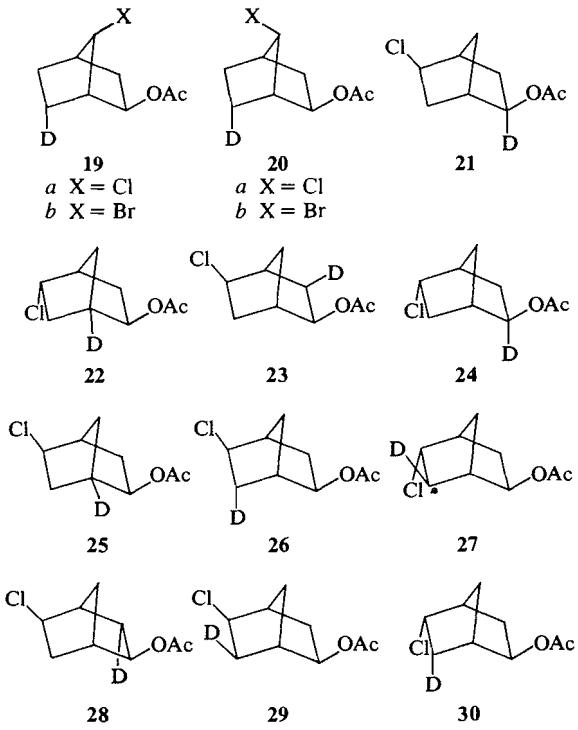


FIG. 2. (*a*) Partial ir spectrum (CS_2) of *exo*-2-norbornanol-6-*exo*-*d*; (*b*) partial ir spectrum (CS_2) of *exo*-2-norbornanol-6-*endo*-*d*; (*c*) partial ir spectrum (CS_2) of deuterated *exo*-2-norbornanol derived from **8***d*-*d*; (*d*) partial ir spectrum (CS_2) of deuterated *exo*-2-norbornanol derived from **9***d*-*d*.



SCHEME 1

lead to a destabilization of the cation. That *exo*-3-chloro-*exo*-2-norbornyl tosylate is 250 times less reactive solvolytically than the 7-chloro tosylate supports our view. Thus ring-opening of **4***c* and **4***b* occurs predominately by deuteronation of the most basic C—C bond. The stereochemistry of the ring-opening is nicely accounted for on the basis of cleavage via edge-deuteronation with retention of configuration at C-6 and inversion of configuration at C-2 (Path a, Scheme 1). Although we consider that classical 7-halonorbornyl cations are the important intermediates, an edge deuteronated nortricyclene is a possible intermediate as well.

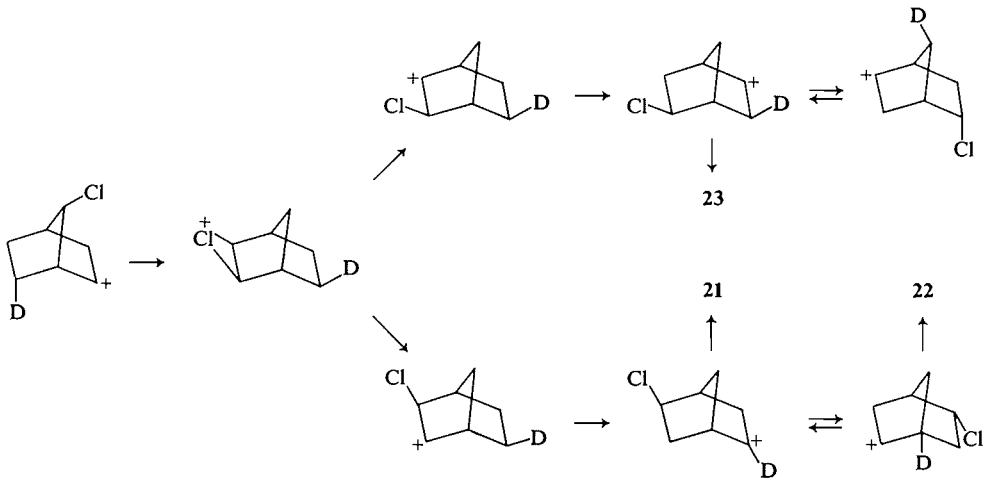


The pathways whereby the *syn*-7- and *anti*-7-halonorbornyl cations are converted to the 5-halonorbornyl cations are defined by the deuterium distribution in 5-chloronorbornyl acetates. Since **21** ($0.10 \pm 0.02 \times 14\%$) and **22** ($0.08 \pm 0.01 \times 14\%$) are formed, a 1,2-alkyl shift, a 6,2 hydride shift, and a 1,2-alkyl shift must occur in sequence to a minor extent to generate the cations that are the precursors of **21** and **22**. Since **23** ($0.25 \pm 0.03 \times 14\%$) is formed also, an *exo* chloronium ion (Scheme 2) is implicated as an intermediate. That we did not detect significant amounts of deuterium at C-7 of the *endo*-5-chloroacetate may be due to the fact that the *exo*-5-chlorocation is more stable than the *endo* isomer and that the integration method is inaccurate at low deuterium incorporations (< 0.05 *d*).

The presence of **24** ($0.08 \pm 0.01 \times 14\%$) and **25** ($0.10 \pm 0.02 \times 14\%$) indicates that the deuterated *anti*-7-chloronorbornyl cation rearranges, as depicted in Scheme 3, to the cations that are precursors of **24** and **25**. Since deuterium is not detected at C-3 of the *endo*-5-chloroacetate and at C-7 of the *exo*-5-chloroacetate, the *endo*-chloronium ion, as expected, is not an important intermediate.

Based on our analysis, the *exo*-5- and *endo*-5-chloroacetates formed by rearrangement of the *syn*-7- and *anti*-7-halocations comprise $8.5 \pm 1.7\%$ ($1.4 \pm 0.3\% + 1.1 \pm 0.2\% + 3.5 \pm 0.4\% + 1.1 \pm 0.2\% + 1.4 \pm 0.3\%$) of the reaction mixture. This result is nicely in accord with the work of Goering and Degani (24) which established that the *exo*-5- and *endo*-5-chloroacetates, in total, comprise 15.2% and 12.3% of the reaction products of the acetolysis of the *syn*-7- and *anti*-7-chloro-*exo*-2-norbornyl tosylates, respectively. Thus approxi-

Can. J. Chem. Downloaded from www.nrcresearchpress.com by 210.87.254.40 on 09/05/12
For personal use only.



SCHEME 2

SCHEME 3

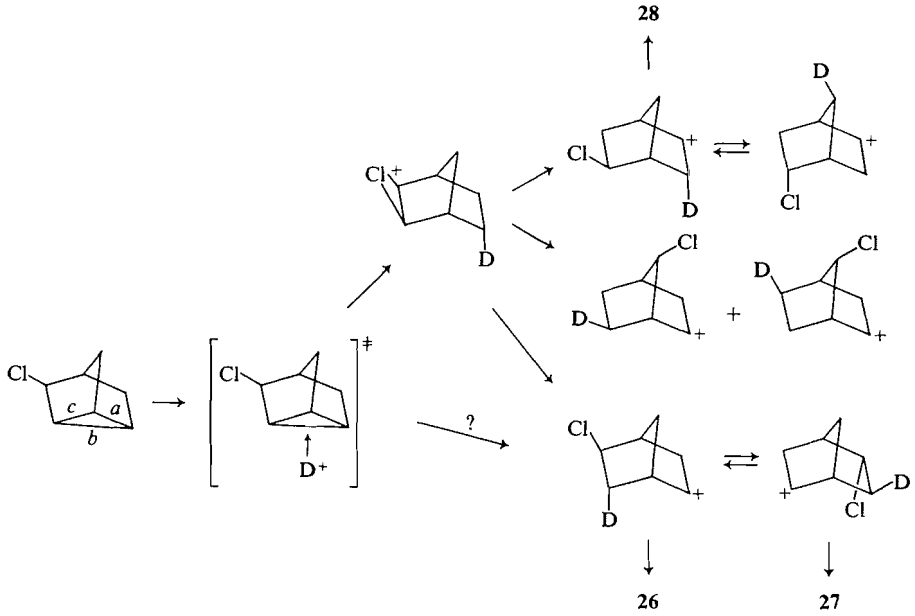
mately ((70% + 8.5%) × 0.9) or 71% of the chloroacetates result from edge-deuteronation of the bond farthest removed from the electron withdrawing chlorine atom. If deuteronation of the other two bonds is assumed to be equally likely, then deuteronation of the most basic bond is preferred by (71/29 × 2) or 5:1 over the other bonds. Since the *exo*-5- and *endo*-5-chloroacetates are formed in greater yield (28%) when **4***c* is ring-opened in acetic acid, the other bonds of the three-membered ring also must be cleaved. Here too, the deuterium distributions in the 5-chloroacetates define the mechanistic details. Edge-deuteration of bond *b* leads to several cations (Scheme 4) and, in fact, can introduce *exo*-deuterium at C-6 of the *syn*-7-chloroacetate. Chloroacetates **26** (0.15 ± 0.02 × 14%) and **27** (0.55 ± 0.05 × 14%) are formed directly by deuteronation of bond *b*. The formation of **28** (0.25 ± 0.03 × 14%) implicates an *exo* chloronium ion (Scheme 4) as an intermediate that possibly leads to a *syn*-7-chloronorbornyl cation with *exo* deuterium at C-6. That bond *c* is cleaved by edge-wise attack (Scheme 5) is indicated by the formation of acetate **29** (0.20 ± 0.04 × 14%). It is also possible that a small amount of the *anti*-7-chloronorbornyl cation with *exo* deuterium at C-6 is formed as well (Scheme 5).

Conclusions

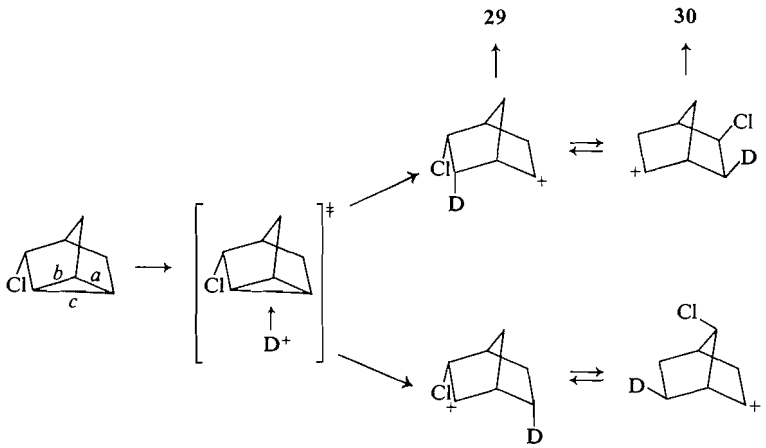
We have established that the D_2SO_4-catalyzed ring-opening of 3-chloro- and 3-bromonortricyclene occurs faster than solvolysis in acetic acid and that the deuterium at C-6 of the major products is at least 90% stereochemically pure *endo*. Clearly

Can. J. Chem. Downloaded from www.nrcresearchpress.com by 210.87.254.40 on 09/05/12
For personal use only.

Can. J. Chem. Downloaded from www.nrcresearchpress.com by 210.87.254.40 on 09/05/12
For personal use only.



SCHEME 4



SCHEME 5

then, edge-deuteronation of the bond farthest removed from the chlorine is preferred over deuteronation of the other bonds by 5:1. Because the electronegativities of bromine and chlorine are comparable, we observe a similar preference for deuteronation of 3-bromonortricyclene. The small effect of the halogens on the regiochemistry is in keeping with the results of other studies which have established that substituent effects on the electrophilic cleavage of three-membered rings are usually small (6).

By determining the distribution of deuterium in the 5-chloroacetates we have elucidated the mechanisms of formation of the minor products as well.

Furthermore, this work has established that the ring-opening of **4***c* and **4***d* in deuterated medium, followed by LAH reduction of the acetates and a brosylation, is a viable route to C-6 *endo* deuterated *syn*-7-chloro-, *anti*-7-chloro-, *syn*-7-bromo-, and *anti*-7-bromo-*exo*-2-norbornyl brosylates. A study of the effect of an electron withdrawing group located at C-7 on the solvolytic γ-KIE's of *exo*-2-norbornyl sulfonate esters can now be realized.

Experimental

General

Proton magnetic resonance spectra were recorded on Varian T-60, A-60, and HA-100 spectrometers with tetramethylsilane (TMS) as the internal standard. Samples were dissolved in either carbon tetrachloride or carbon disulfide. Chemical shifts are expressed in parts per million downfield from internal tetramethylsilane. Infrared spectra were recorded on Perkin Elmer 337 and Beckman IR-5 infrared spectrometers and the samples were dissolved in carbon tetrachloride or carbon disulfide. Ab-

Can. J. Chem. Downloaded from www.nrcresearchpress.com by 210.87.254.40 on 09/05/12
For personal use only.

sorption frequencies were calibrated with polystyrene film and are expressed in reciprocal centimeters (cm^{-1}). For brevity, the notation cm^{-1} is omitted. Mass spectra were taken on a Hitachi-Perkin-Elmer RMU-6A spectrometer at 80 eV. Deuterium assay analyses were performed at 10 to 15 eV and are expressed as atoms of deuterium per molecule in excess of natural abundance deuterium. Analytical gas liquid partition chromatography was performed on a Varian Aerograph Model 204B dual column analytical gas chromatograph equipped with dual flame ionization detectors using helium as the carrier gas. The gas flow rate was usually 20–30 mL/min. Preparative gas liquid partition chromatography was carried out on a Varian Aerograph Model A-90-P gas chromatograph with a thermal conductivity detector and a helium flow rate of 50–60 mL/min. Spinning band distillations were performed on a Nester–Faust auto-annular Teflon spinning band distillation column. Melting points were recorded on a Kofler hot-stage apparatus and are uncorrected. Boiling points are also uncorrected.

All organic solutions were dried with either anhydrous sodium sulfate or magnesium sulfate.

*Sulfuric Acid-catalyzed Cleavage of 3-Chloronortricyclene (**4c**) in Acetic Acid*

3-Chloronortricyclene prepared by the method of Roberts *et al.* (21) (10.13 g, 79 mmol), sulfuric acid (1.31 g), and 150 mL of acetic acid (distilled from acetic anhydride) were mixed in a 250 mL flask fitted with a calcium chloride drying tube. The flask was placed in an oil bath maintained at 70 ± 3°C and the mixture was stirred magnetically. The reaction was monitored by glpc and after 120 h it was estimated to be >97% complete. Three-quarters of the reaction mixture was neutralized by slow addition to a saturated sodium bicarbonate solution and the products were extracted into ether (3 × 150 mL). The ethereal extracts were washed with water (75 mL), saturated bicarbonate solution (75 mL), and water (75 mL). After the solution was dried and the solvent was removed, there remained 10.9 g (98%) of chloroacetates. The glpc analysis on a 1/8 in. × 10 ft 10% Carbowax column at 180°C showed three products, and only the product with the shortest retention time (7 min) was resolved from the others. It was isolated by preparative glpc on a 10 ft × 1/4 in. 15% Carbowax column maintained at 175°C and identified as *anti*-7-chloro-*exo*-2-norbornyl acetate (**9a**) by comparison of its spectral data to those of an authentic sample.

Lithium Aluminum Hydride Reduction of Chloroacetates

Into a 125 mL three-necked flask fitted with a condenser, a calcium chloride drying tube, an adding funnel, and a magnetic stirrer was placed a slurry of lithium aluminum hydride (1.92 g, 51 mmol) in dry ether (55 mL). The mixture of chloroacetates (4.46 g, 24 mmol) was dissolved in dry ether (10 mL) and slowly added to the slurry. After the mixture was refluxed for 4 h, the reaction flask was cooled in ice and excess hydride was carefully destroyed by the dropwise addition of water. The white precipitate was filtered off, the filtrate was acidified with hydrochloric acid (10%, 20 mL), and the ethereal layer was separated. The aqueous layer was extracted with ether (2 × 75 mL) and the combined ethereal layers were washed with water (50 mL), dried, and concentrated to yield 3.3 g (94%) of foul-smelling chlorohydrins. The glpc analysis on a 10 ft × 1/8 in. 10% Carbowax column at 178°C revealed at least three products with only the product of shortest retention time (5 min) being resolved from the others. This product was isolated by preparative glpc on a 1/4 in. × 10 ft. 15% Carbowax column at 175°C and identified as *syn*-7-chloro-*exo*-2-norbornanol (**4c**) by comparison of its spectra to those from an authentic sample (19).

Oxidation of Chlorohydrins

The oxidizing agent (24) was prepared in the following manner. Sodium dichromate (10 g) was dissolved in water (20 mL) and sulfuric acid (7.5 mL) was added. For each millimole of alcohol to be oxidized, 0.5 mL of solution was used.

To a solution of the mixture of chlorohydrins (0.20 g, 1.4 mmol) in ether (5 mL, pre-treated with oxidizing agent) in a 50 mL flask equipped with a condenser and magnetic stirrer, the oxidizing agent (0.8 mL) was slowly added. After the solution was vigorously stirred for 6.5 h, the ethereal layer was separated and the aqueous layer was extracted with ether (5 × 20 mL). The combined ethereal layers were washed with saturated bicarbonate (2 × 15 mL), water (2 × 20 mL), and then dried. Analytical glpc on 1/8 in. × 10 ft 10% Carbowax and 1/8 in. × 10 ft 20% Ucon Polar columns at 190°C and 180°C, respectively, showed three products that were isolated by preparative glpc on a 1/4 in. × 10 ft 15% Carbowax column at 170°C. The product with shortest retention time was *anti*-7-chloro-2-norbornanone (**13a**); ir (CS_2): 1760 (C=O); nmr (CCl_4, 60 MHz) δ: 4.2 (s with fine structure, 1H, *syn*-7-H), 2.6 (broad s, 2H, H-1 and H-4), 2.5–1.5 (m, 6H, norbornyl envelope). The product of intermediate retention time (15 min) was *exo*-5-chloro-2-norbornanone (**12a**) and the product of longest retention time (19 min) was *endo*-5-chloro-2-norbornanone (**15a**). Chloroketones **12a** and **15a** were identified by comparison of their ir and nmr spectra to those obtained from authentic samples.

In a separate experiment, a small portion of the chlorohydrin mixture which was obtained from the chloroacetates by reduction was oxidized and the reaction mixture was analyzed by analytical glpc on a 1/8 in. × 10 ft 15% Carbowax column at 190°C. Compounds **13a** (44 ± 2%), **14a** (14 ± 1%), **12a** (26 ± 1%), and **15a** (14 ± 1%) were identified as the products.

Reduction of the Chlorohydrins by Sodium in 2-Propanol

To a magnetically stirred 2-propanol (50 mL, reagent grade) solution of the chlorohydrins (0.75 g, 5.2 mmol), small pieces of sodium metal (1.0 g, 43 mmol) were added at a sufficient rate to maintain the heated solution at reflux. After the sodium completely dissolved, the solution was refluxed for 3.0 h and the brown solid that formed when the mixture was cooled was dissolved in water (50 mL). The aqueous solution was extracted with pentane (4 × 70 mL) and the combined pentane extracts were washed with dilute hydrochloric acid (10%, 40 mL), water (2 × 40 mL), dried, and concentrated to yield 0.45 g (78%) of a white solid. Analytical glpc on 1/8 in. × 10 ft 10% Carbowax column at 130°C showed one major product (>95%) that was isolated by preparative glpc on a 1/4 in. × 10 ft 15% Carbowax column at 140°C. Its spectral properties were shown to be identical to those of *exo*-2-norbornanol; ir (CS_2): 3600 (free OH), 3600–3200 (hydrogen bonded OH); nmr (CCl_4, 60 MHz) δ:3.6 (d, 1H, *endo*-2-H), 2.2 (broad s, 1H, bridgehead), 2.0 (broad s, 1H, bridgehead), 1.9–0.7 (m, 9H, norbornyl envelope and OH). Another product (<5%) of slightly longer retention time than *exo*-2-norbornanol was not identified.

From an analysis on a 1/8 in. × 10 ft 10% FFAP column at 105°C that involved tracing and weighing the peaks, the ratio of *exo*-2-norbornanol to *endo*-2-norbornanol was 98 ± 1: 2 ± 1.

Preparation of Syn- *and* Anti-*7-chloro-exo-2-norbornanols*

The *syn*- and *anti*-7-chloro-*exo*-2-norbornanols were prepared by the addition of hypochlorous acid to norbornene according to the procedure of Roberts *et al.* (21) and purified by preparative glpc on a 1/4 in. × 10 ft 15% Carbowax column at 160°C. *Syn*-7-chloro-*exo*-2-norbornanol (**8c**) had the following properties: mp 87–91°C (lit. (18) mp 89–90°C); ir (CCl_4): 3590 (OH); nmr (CS_2, 100 MHz) δ:3.86 (m, 1H, *anti*-7-H), 3.60 (broad quintet, 1H, J = 6 Hz, *endo*-2-H), 2.25 (m, 2H, H-1 and H-4), 1.88 (m, 3H, *exo*-3-H, *endo*-3-H and -OH), 1.53 (m, 2H, *exo*-5-H and *exo*-6-H), 1.10 (m, 2H, *endo*-5-H and *endo*-6-H).

Anti-7-chloro-*exo*-2-norbornanol (**9c**) exhibited the following spectra: ir (CCl_4): 3620 (free OH), 3650–3200 (hydrogen bonded OH); nmr (CCl_4, 100 MHz): δ:4.19 (broad s with fine structure,

Can. J. Chem. Downloaded from www.nrcresearchpress.com by 210.87.254.40 on 09/05/12
For personal use only.

1H, *syn*-7-H), 3.75 (d of d, 1H, J = 7.5 and 2.5 Hz, *endo*-2-H), 2.69 (broad s, 1H, OH), 2.26 and 2.14 (broad s, each 1H, bridgeheads), 2.00–1.67 (m, 3H, *exo*-3-H, *exo*-5-H and *exo*-6-H), 1.40 (broad d, 1H, J = 15 Hz, *endo*-3-H), 1.10 (m, 2H, *endo*-5-H and *endo*-6-H).

Exo-*3-chloro-2-norbornanone*

2-Norbornanone (11.7 g, 0.11 mol) was treated with sulfuryl chloride (15.0 g, 0.11 mol) in carbon tetrachloride (20 mL) at 25°C for 195 h (20). The major product, *exo*-3-chloro-2-norbornanone, was purified by preparative glpc on a 1/4 in. × 10 ft 15% Carbowax column at 168°C and exhibited the infrared absorptions previously reported (20); nmr (CS_2, 60 MHz) δ:3.5 (d, 1H, J = 3 Hz, *endo*-3-H), 2.6 (broad s, 2H, H-1 and H-4), 2.4–1.3 (m, 6H, norbornyl envelope).

Endo-*3-chloro-2-norbornanone*

Exo-3-chloro-2-norbornanone (0.64 g) was isomerized to the *endo* isomer in a refluxing aqueous solution (60 mL) of lithium carbonate (1.7 g).

Exo-*5-chloro-2-norbornanone* (***14***a)

Nortricyclanone (0.37 g, 3.4 mmol) was dissolved in carbon tetrachloride (25 mL) in a 50 mL round bottom flask fitted with a condenser and a magnetic stirrer. While the solution was heated to 70 ± 5°C in an oil bath, anhydrous hydrogen chloride was bubbled through the solution for 67 h. The mixture was neutralized with saturated sodium bicarbonate and the aqueous solution was extracted with carbon tetrachloride (4 × 55 mL). The combined extracts were washed with saturated bicarbonate (40 mL), water (3 × 25 mL), dried, and the organic solvent was removed by distillation through a 15 cm glass-helices column. Analysis of the residue by glpc on a 1/8 in. × 10 ft 10% Carbowax column at 185°C revealed one product.

Hydroboration of Endo-*5-chloronorbornene* (***16***)

Into a 250 mL flask fitted with a magnetic stirrer and a pressure equalizing funnel were placed **16** (192 g, 15.0 mmol) dissolved in tetrahydrofuran (40 mL, freshly distilled), and sodium borohydride (1.21 g, 31.8 mmol). After the flask was purged for 10 min with nitrogen, boron trifluoride etherate (6.5 g, 46 mmol, freshly distilled) in tetrahydrofuran (20 mL) was slowly added to the stirred solution containing olefin. After the addition was complete, the mixture was stirred for 1.5 h at room temperature. The funnel was replaced with a condenser, water was added to the mixture until hydrogen was no longer evolved, and sodium hydroxide (10%, 30 mL) was added. Hydrogen peroxide (30%, 6 mL) was slowly added to maintain a reflux and the solution was stirred for 3 h. The mixture was extracted with ether (3 × 80 mL), the extracts were washed with dilute hydrochloric acid (10%, 10 mL), water (2 × 20 mL), dried, and concentrated to yield a white solid (1.3 g, 59%). The two chlorohydrins, *endo*-5-chloro-*exo*-3-norbornanol and *endo*-6-chloro-*exo*-2-norbornanol, could not be separated by preparative glpc on a 1/4 in. × 10 ft 10% Carbowax column maintained at 180°C.

Endo-*5-chloro-2-norbornanone* (***15***a)

The mixture of chlorohydrins was oxidized as previously described to a mixture of chloroketones. Each chloroketone was purified by preparative glpc on a 1/4 in. × 10 ft 15% Carbowax column maintained at 170°C. The ketone of shortest retention time (17 min) was *endo*-5-chloro-2-norbornanone (42%); ir (CS_2): 1750 (C=O), 1310, 1280, 1260, 1180, 1150, 1075, 1060, 960, 940, 915, 890, 865, 770, 695, 675; nmr (CS_2, 100 MHz) δ: 4.30 (m, 1H, *exo*-5-H), 2.80–1.30 (m, 8H, norbornyl envelope). The ketone of longest retention time (23 min) was *endo*-6-chloro-2-norbornanone; ir (CS_2): 1760 (C=O), 1300, 1280, 1260, 1230, 1190, 1150(s), 1120, 1070(s), 1030, 970, 945, 925, 885, 865, 765, 735, 640; nmr (CS_2, 100 MHz) δ: 4.30 (m, 1H, *exo*-6-H), 2.70–1.40 (m, 8H, norbornyl envelope).

Exo-*2-chloro*-exo-*2-norbornyl* tert-*Butyl Ether and* Endo-*3-chloro*-exo-*2-norbornyl* tert-*Butyl Ether*

The *tert*-butyl ethers were prepared by the treatment of norbornene with *tert*-butyl hypochlorite (20). The *endo*-3-chloroether was isolated by preparative glpc on a 1/4 in. × 10 ft 15% FFAP column at 155°C; ir (neat): 1120 and 1075 (C—O); nmr (CCl_4, 60 MHz) δ: 3.8 (m, 1H, *exo*-3-H), 3.2 (t, 1H, *endo*-2-H), 1.2 (s, 9H, —$C(CH_3)_3$), 2.3–1.0 (m, 8H, norbornyl envelope). Similarly, the *exo*-3-chloroether was isolated by preparative glpc; ir (neat): 1090 (C—O); nmr (CCl_4, 60 MHz) δ: 3.8 (dd, 1H, J = 6 Hz and 1 Hz, *endo*-3-H), 3.5 (dd, 1H, J = 6 Hz and 1 Hz, *endo*-2-H), 1.2 (s, 9H, —$C(CH_3)_3$), 2.4–0.9 (m, 8H, norbornyl envelope).

Exo-*3-chloro*-exo-*2-norbornanol and* Endo-*3-chloro*-exo-*2-norbornanol*

The chlorohydrins were prepared according to the literature method (22) by treating the corresponding *tert*-butyl ethers with anhydrous hydrogen chloride. The nmr spectra of the chlorohydrins were identical to the reported spectra.

Exo-*3-chloro*-exo-*2-norbornyl Acetate and* Endo-*3-chloro*-exo-*2-norbornyl Acetate*

The chlorohydrins were acetylated by acetic anhydride in pyridine. Analytical glpc on a 1/8 in. × 10 ft. 10% Carbowax column at 190°C revealed that each acetate was >97% pure.

Endo-*5-chloro*-exo-*2-norbornyl Acetate* (***11***a)

Acetylation of a mixture of *endo*-5-chloro-*exo*-2-norbornanol and *endo*-6-chloro-*exo*-2-norbornanol prepared previously (*vide supra*) gave a mixture of the chloroacetates. *Endo*-5-chloro-*exo*-2-norbornyl acetate contaminated with 18% of the *endo*-6-isomer was isolated by preparative glpc on a 1/4 in. × 10 ft 15% Carbowax column at 175°C.

Stability of Chloroacetates

In a typical control reaction, 0.15 g of the chloroacetate was dissolved in acetic acid (5 mL) containing 0.10 M sulfuric acid and heated at 70 ± 5°C in an oil bath for 500 h. The extent of isomerization was monitored by analytical glpc on a 1/8 in. × 10 ft 15% Carbowax column programmed between 150 and 185°C and the following results were obtained. *Syn*-7-chloro-*exo*-2-norbornyl acetate underwent 12 ± 1% isomerization to *anti*-7-chloro-*exo*-2-norbornyl acetate, *endo*-5-chloro-*exo*-2-norbornyl acetate underwent 15 ± 1% isomerization to *exo*-5-chloro-*exo*-2-norbornyl acetate, *exo*-3-chloro-*exo*-2-norbornyl acetate, *endo*-3-chloro-*exo*-2-norbornyl acetate, and *anti*-7-chloro-*exo*-2-norbornyl acetate each underwent <3% rearrangement.

Deuterosulfuric Acid Catalyzed Cleavage of 3-Chloronortricyclene

3-Chloronortricyclene (18.5 g, 145 mmol) was dissolved in 80 mL of a mixture of acetic acid-d_4 (Merck, Sharp and Dohme of Canada Ltd., 99.5 at.% d) and 0.82 g of sulfuric acid-d_2 (Merck, Sharp and Dohme) in a 250 mL flask fitted with a calcium chloride drying tube. The mixture was heated in an oil bath at 70 ± 3°C for 504 h. Sodium acetate-d_3 (1.7 g) was added to the mixture and acetic acid-d_4 (55 mL) was removed by distillation under reduced pressure (5–7 Torr). The remaining solution was neutralized with saturated sodium bicarbonate and extracted with ether. After the extracts were washed with water and dried, evaporation of solvent left 26.5 g (95%) of deuterated chloroacetates.

Reduction of Deuterated Chloroacetates

The deuterated chloroacetate mixture (17.6 g, 92 mmol) was dissolved in dry ether (20 mL) and reduced by lithium aluminum hydride (1.89 g, 50 mmol) as previously described (*vide supra*). After workup, 12.7 g (94%) of deuterated chlorohydrins were obtained.

Can. J. Chem. Downloaded from www.nrcresearchpress.com by 210.87.254.40 on 09/05/12
For personal use only.

Oxidation of the Deuterated Chlorohydrins

The deuterated chlorohydrins from the previous reaction (12.7 g, 86 mmol) were oxidized by the method previously described (44 mL oxidizing agent) and 12.0 g (97%) of the deuterated chloroketones were isolated. Each chloroketone was isolated by preparative glpc on a 1/4 in. × 10 ft 15% Ucon Polar column at 130°C and the deuterium was assayed by mass spectrometry; *anti*-7-chloro-2-norbornanone was a composite of 3.81 ± 0.01% d_0, 95.04 ± 0.18% d_1, 1.15 ± 0.18% d_2 species (0.976 ± 0.004 excess d per molecule) and *syn*-7-chloro-2-norbornanone was a composite 3.33 ± 0.02% d_0, 95.01 ± 0.21% d_1, 1.67 ± 0.24% d_2 species (0.985 ± 0.002 excess d per molecule); *exo*-5-chloro-2-norbornanone was a composite of 9.84 ± 0.25% d_0, 89.41 ± 0.59% d_1 and 0.67 ± 0.88% d_2 species (0.910 ± 0.015 excess d per molecule); *endo*-5-chloro-2-norbornanone was a composite of 12.87 ± 0.01% d_0, 84.65 ± 0.01% d_1, and 2.47 ± 0.01% d_2 species (0.894 ± 0.002 excess d per molecule).

Determination of the Deuterium Distribution

The deuterated chloroketones that had been previously separated by preparative glpc on a 1/4 in. × 10 ft 15% Ucon Polar column at 130°C were individually reduced by lithium aluminum hydride to a mixture of *exo*- and *endo*-2-norbornanol. In a typical reaction, the deuterated chloroketone (0.10 g) in ether (15 mL) was reduced by lithium aluminum hydride to the deuterated 2-norbornanols after a 15-day reflux. Whereas reduction of deuterated *anti*-7-chloro-2-norbornanone and *endo*-5-chloro-2-norbornanone gave *endo*-2-norbornanol-*d* as the major product and the *exo*-alcohol as the minor product, reduction of deuterated *syn*-7-chloro-2-norbornanone and *exo*-5-chloro-2-norbornanone gave *exo*-2-norbornanol-*d* as the major product. In each case about 0.020 g of the major isomer that was isolated by preparative glpc on a 1/4 in. × 10 ft 15% Carbowax column at 110°C was dissolved in CCl_4 (1 mL) solution of $Eu(thd)_3$ (0.030 g) and the pmr spectrum was recorded. The combined mass spectral and nmr data (Figs. 1*a–g*) established that >90% of deuterium in the *syn*-7- and *anti*-7-chloro-*exo*-2-norbornyl acetates was situated at C-6 with at least 90% *endo* stereochemical purity. The deuterium in *exo*-5-chloro-*exo*-2-norbornyl acetate was located at C-1 (0.10 ± 0.05), *endo* at C-2 (0.10 ± 0.05), *exo* at C-3 (0.20 ± 0.05), *endo* at C-3 (0.20 ± 0.05), *endo* at C-6 (0.20 ± 0.05), and the deuterium in *endo*-5-chloro-*exo*-2-norbornyl acetate was located at C-1 (0.10 ± 0.05), *endo* at C-2 (0.55 ± 0.05), and *endo* at C-6 (0.25 ± 0.05).

Check for Deuterium Loss During Preparative Gas–Liquid Partition Chromatography

A sample of *anti*-7-chloro-2-norbornanone that was collected by preparative glpc on a 1/4 in. × 10 ft Ucon Polar column at 130°C was analyzed for deuterium mass spectrometrically and was found to contain 0.95 excess deuterium atoms per molecule. Reinjection of a small portion of the chloroketone followed by a mass spectrometric analysis established that the deuterium content was 0.96 excess deuterium atoms per molecule.

Similarly, deuterated *exo*-5-chloro-2-norbornanone was tested for deuterium loss during isolation by preparative glpc. After a single injection and collection the norbornanone contained 0.90 excess d per molecule. After a reinjection and collection the ketone was found to contain 0.90 excess d per molecule.

Check for Deuterium Loss During Oxidation

Anti-7-chloro-2-norbornanone-*endo*-6-*d* (0.010 g, 0.95 excess d per molecule) in ether (3 mL, pretreated with oxidizing agent) and oxidizing agent (*vide supra*) (2 mL) were vigorously stirred together for 3.5 h at room temperature. The reaction was worked up and the product was isolated by preparative glpc on a 1/4 in. × 10 ft 15% Ucon Polar column at 140°C. Mass spectral analysis established that the ketone contained 0.96 excess d per molecule and this was identical within experimental error, to the deuterium content of the starting ketone.

Deuterated *exo*-5-chloro-2-norbornanone (0.90 excess d per molecule) that contained deuterium *exo* at C-3 was subjected to the chromic acid oxidation reaction conditions and the deuterium was assayed by mass spectrometry. Within experimental error, the deuterium content was identical to the deuterium content of the starting material (0.90 excess d per molecule).

Sulfuric Acid Catalyzed Cleavage of 3-Bromonortricyclene

Freshly distilled 3-bromonortricyclene (5.00 g) was dissolved in glacial acetic acid (75 mL) that contained concentrated H_2SO_4 (0.74 g, 0.10 *M*) and the solution was heated at 74 ± 2°C for 30 h. The cooled solution was carefully poured onto a saturated sodium bicarbonate solution contained in a 2 L beaker and the aqueous layer was extracted with ether (4 × 80 mL). The combined extracts were dried and the ether was removed to yield 6.47 g of an oil. Analytical glpc analysis on a 1/8 in. × 10 ft 10% Carbowax column at 210°C showed three peaks in a ratio of 4:54:42, the first peak being starting material. The major products were separated by preparative glpc on a 1/4 in. × 10 ft 20% DEGS column at 195°C. Seven fractions were collected with fractions 4 and 6 corresponding to the centre cuts of the main product peaks; fraction 4 was **9***b*; nmr (CS_2, 60 MHz) δ: 4.52 (q, 1H, J = 8, 3.5 Hz, H-2), 4.05 (m, 1H, *syn*-7-H), 2.3–1.0 (norbornyl envelope), 1.88 (s, 3H, CH_3CO—); fraction 6; nmr (CS_2, 60 MHz) δ: 4.5 (q, 1H, *endo*-2-H), 4.80 (m, 1H, *anti*-7-H), 2.5–1.1 (norbornyl envelope), 1.85 (s, 3H, CH_3CO—).

LAH Reduction of Fraction 4

The bromoacetate **9***b* (0.81 g) that was collected by preparative glpc was dissolved in dry ether (50 mL) and LAH was added in portions to the refluxing solution until reduction was complete as indicated by analytical glpc analysis on a 1/8 in. × 10 ft 10% Carbowax column at 210°C. The excess LAH was quenched with wet ether and water (1 mL) and the salts were filtered off and washed with additional ether (3 × 15 mL). The ether solution was dried and the solvent was removed on the rotary evaporator to yield 0.55 g of a viscous oil. Analytical glpc analysis on a 1/8 in. × 10 ft 10% Carbowax column at 210°C indicated that the bromohydrin **9***d* was approximately 85% pure.

LAH Reduction of Fraction 6

The bromoacetate (0.43 g) that was collected by preparative glpc was dissolved in dry ether (25 mL) and LAH was added in portions to the refluxing solution until reduction was complete. The excess LAH was quenched with wet ether and water (1 mL) and the filtered salts were washed with additional ether (3 × 10 mL). After the solution was dried, the solvent was removed on the rotary evaporator to yield 0.15 g of viscous oil. Analytical glpc analysis on a 1/8 in. × 10 ft 10% Carbowax column at 210°C established that four major products were present in a ratio of 32:43:11:9. Two minor products, of longer retention time, comprised a total of 6% of the mixture. The retention time of the first component was identical to retention time of *exo*-2-norbornanol.

LAH Reduction of Bromoacetates

An ether solution (25 mL) of a mixture of bromoacetates (9.35 g) obtained from a large scale ring-opening of 15.0 g 3-bromonortricyclene was added dropwise to a vigorously stirred slurry of LAH (0.87 g) in dry ether (75 mL). After the addition was complete the solution was refluxed for 2 h and the excess LAH was quenched with wet ether. The filtered salts were washed with ether (3 × 10 mL), the ether layer was dried, and the solvent was evaporated to yield 7.06 g of a viscous oil. Analytical glpc analysis on a 1/8 in. × 10 ft 10% Carbowax column at 210°C established the presence of five major products

Can. J. Chem. Downloaded from www.nrcresearchpress.com by 210.87.254.40 on 09/05/12
For personal use only.

and the approximate relative yields were 7:27:3:11:51 in order of increasing retention time. The peaks due to the last three products overlapped considerably. The first peak had a retention time which was identical to the retention time of *exo*-2-norbornanol. The major components that comprised 27% and 51% of the reaction mixture, respectively, were isolated by preparative glpc on a 1/4 in. × 5 ft 15% Carbowax column at 175°C. From 6.17 g of reaction mixture 0.97 g of the 27% component and 1.34 g of the 51% component were isolated after the collected samples were reinjected and recollected. Analytical glpc analysis on a 1/8 in. × 10 ft 10% Carbowax column at 210°C established that both samples were >90% pure; *syn*-7-bromo-*exo*-2-norbornanol (**8***b*); nmr (CS_2, 60 MHz) δ: 3.86 (m, 1H, *anti*-7-H), 3.67 (m, 1H, *endo*-2-H), 2.35 (bs, 3H, H-1, H-4, and —OH), 2.1–1.0 (norbornyl envelope, 6H). *Anti*-7-bromo-*exo*-2-norbornanol (**9***b*); nmr (CS_2, 60 MHz) δ: 4.12 (m, 1H, *syn*-7-H), 3.70 (dd, 1H, *endo*-2-H), 3.63 (s, 1H, —OH), 2.3–0.9 (8H, norbornyl envelope).

Oxidation of Syn-*7-bromo*-exo-*2-norbornanol*

The *syn*-bromohydrin (**8***b*) (0.79 g) was dissolved in preoxidized ether (2.5 mL) and the solution was vigorously stirred for 3 h in the presence of 2.5 mL of Brown's reagent. Water was added (4 mL) and the mixture was extracted with ether (4 × 10 mL). The combined ether extracts were washed with saturated $NaHCO_3$ solution, water (10 mL), and dried. Evaporation of the solvent gave 0.69 g of a viscous liquid. The *syn*-7-bromoketone (**12***b*) (0.33 g, >90% pure) was isolated by preparative glpc on a 1/4 in. × 5 ft 15% Carbowax column at 165°C; ir (neat): 2970, 2880, 1752, 1402, 1302, 1080, 1045, 950, 808, 742; nmr (CS_2, 60 MHz) δ: 4.14 (m, 1H, *anti*-7-H), 2.8–1.3 (8H, norbornyl envelope). The 2,4-DNP that was recrystallized from 95% EtOH – ethyl acetate and chromatographed over neutral alumina had a mp 202.5–203.5°C (lit. (25) mp 201.5–202.5°C).

Oxidation of Anti-*7-bromo*-exo-*2-norbornanol*

The *anti*-bromohydrin (0.88 g) was dissolved in preoxidized ether (2.5 mL) and the solution was vigorously stirred for 5 h in the presence of 2.8 mL of Brown's reagent. Water was added (4 mL) and the aqueous layer was extracted with additional portions of ether (4 × 10 mL). The combined extracts were washed with saturated $NaHCO_3$ solution, water (2 × 10 mL), and dried. Evaporation of the solvent gave 0.62 g of a viscous oil. In addition to *anti*-7-bromo-2-norbornanone (55%) there were three other components (20:10:14) of longer retention times. The *anti*-7-bromo-2-norbornanone (0.10 g) was isolated by preparative glpc on a 1/4 in. × 5 ft 15% Carbowax column at 170°C; ir (neat): 2960, 2870, 1752, 1400, 1267, 1242, 1122, 1075, 922, 788, 730; nmr (CS_2, 60 MHz) δ: 4.18 (m, 1H, *syn*-7-H) 2.8–1.3 (8H, norbornyl envelope). The 2,4-DNP was recrystallized from 95% EtOH and had a mp 153–155.5°C (lit (26) mp 151.5–152.5°C).

Preparation of Acetic Acid-O-d

To 146.0 g of freshly distilled acetic anhydride was added 28.6 g of D_2O (99.77%). After the solution stood overnight at ambient temperature, it was stirred at 70°C for 1 h. The ^1H nmr analysis established that the CH_3COOD was 99% isotopically pure and that there remained 2% of acetic anhydride.

D_2SO_4 Catalyzed Ring-Opening of 3-Bromonortricyclene

3-Bromonortricyclene (20.0 g, freshly distilled) was dissolved in CH_3COOD (300 mL) that contained 3.0 g of D_2SO_4 and the solution was heated at 75 ± 2°C for 77 h. Analytical glpc on a 1/8 in. × 10 ft 10% Carbowax column at 185°C indicated that the reaction was 95% complete. Two-thirds of the reaction mixture was removed and poured onto a saturated solution of $NaHCO_3$ in a 3 L beaker. The aqueous layer was extracted with ether (4 × 100 mL), the combined ether layers were dried, and the solvent was evaporated to yield 15.5 g of a mixture of bromoacetates. Analytical glpc analysis on the Carbowax column at 125°C showed by the presence of a shoulder on the peak of longest retention time that there were at least three components. The products from a portion (2.0 g) of the reaction mixture were separated on a 1/4 in. × 10 ft 15% Carbowax glass column at 170°C into two fractions. To minimize isomerization a glass tube was also inserted into the injection port of the glpc. The first fraction (0.89 g) consisted of deuterated *anti*-7-bromo-*exo*-2-norbornyl acetate and the second (0.77 g) was a composite of deuterated *syn*-7-bromo-*exo*-2-norbornyl acetate and the other two acetates. *Anti*-7-bromo-*exo*-2-norbornyl acetate-*d*; nmr (CS_2, 100 MHz) δ: 4.56 (dd, 1H, *endo*-2-H), 4.10 (m, 1H, *syn*-7-H), 2.33 (bm, 2H, H-1 and H-4), 2.1–1.1 (5H, norbornyl envelope), 1.93 (s, 3H, CH_3CO—).

LAH Reduction of Anti-*7-bromo-2*-exo-*norbornyl Acetate*-d

The *anti*-bromoacetate-*d* (1.05 g) was dissolved in dry ether (10 mL), and added to a stirred slurry of LAH (0.11 g) in ether (10 mL). The mixture was stirred at reflux for 4 h and the excess LAH was quenched by the addition of ether saturated with water (10 mL) and water (1 mL). The filtered salts were washed with ether (3 × 10 mL), the ether solution was dried, and the solvent was evaporated to yield 0.69 g of a viscous oil that was shown by analytical glpc on a 1/8 in. × 10 ft 10% Carbowax column at 200°C to be composed of 94% of one component. The main component, *anti*-7-bromo-*exo*-2-norbornanol-*d* (0.46 g, >95% pure) was isolated by preparative glpc on a 1/4 in. × 10 ft 15% Carbowax glass column at 180°C; mp 52–55°C; nmr (CS_2, 100 MHz) δ: 4.20 (narrow m, 1H, *syn*-7-H), 3.73 (dd, 1H, J = 7 and 3 Hz, *endo*-2-H), 2.28 (bm, 1H, bridgehead), 2.15 (m, 1H, bridgehead), 2.1–1.0 (5H, norbornyl envelope), 1.72 (s, 1H, —OH).

LAH Reduction of a Mixture of Syn-*7-bromo*-exo-*2-norbornyl Acetate*-d *and Other Acetates*

Run 1. A portion of fraction 2 (0.99 g) that was predominately *syn*-7-bromo-*exo*-2-norbornyl acetate-*d* was dissolved in dry ether (10 mL) and added to a LAH (0.10 g) slurry in ether. The excess LAH was destroyed by the addition of wet ether (10 mL) and water (1 mL). The filtered salts were washed with ether (2 × 10 mL), the combined ether extracts were dried, and the solvent was evaporated to yield 0.84 g of a viscous oil. Analytical glpc on a 1/8 in. × 10 ft 10% Carbowax column at 200°C showed that three products, in order of increasing retention time, were present in a ratio of 55:19:26. The products were separated by preparative glpc on a 1/4 in. × 10 ft 15% Carbowax glass column at 150°C. *Syn*-7-bromo-*exo*-2-norbornanol-*d* (0.20 g), the product of shortest retention time had a mp 43.5–45.5°C (lit (25) mp 40–43°C); nmr (CS_2, 100 MHz) δ: 3.87 (narrow m, 1H, *anti*-7-H), 3.67 (m, 1H, *endo*-2-H), 2.38 (bm, 2H, H-1 and H-4), 2.06 (s, 1H, —OH), 2.10–1.0 (5H, norbornyl envelope).

Run 2. Additional bromoacetate mixture (1.65 g) was reduced and the three products were collected in two fractions. One fraction was *syn*-7-bromo-*exo*-2-norbornanol-*d* and the other consisted of the two products of longer retention time.

Oxidation of Bromohydrins and Mass Spectrometric Analysis of Deuterated Bromoketones

The *syn*-bromohydrin (0.23 g) isolated from Run 2 was dissolved in preoxidized ether (1.5 mL) and the mixture was stirred for 6 h in the presence of 1 mL of Brown's reagent. Water was added (5 mL), the mixture was extracted with ether (3 × 5 mL), the combined ether extracts were washed with aqueous $NaHCO_3$ (2 × 5 mL), and dried. The solvent was removed on a rotary evaporator to yield 0.19 g of a viscous oil that was shown by analytical glpc to be composed essentially of a single component (>95%). The bromoketone was purified by preparative glpc on a 1/4 in. × 10 ft 15% Carbowax glass column at 165°C; ms *m/e*:

Can. J. Chem. Downloaded from www.nrcresearchpress.com by 210.87.254.40 on 09/05/12
For personal use only.

189 (M^+); 4.27 ± 0.18% d_0, 94.03 ± 0.42% d_1, 1.71 ± 0.24% d_2 (0.967 ± 0.005 excess d per molecule).

The *anti*-bromohydrin (0.084 g) isolated from the reduction of bromoacetates was dissolved in preoxidized ether (0.5 mL) and treated with Brown's reagent (0.4 mL). After the usual work-up and preparative glpc on a 1/4 in. × 10 ft 15% Carbowax glass column at 160°C, a pure sample of the *anti*-bromoketone was isolated; ms *m/e*: 189 (M^+); 5.63 ± 0.12% d_0, 92.48 ± 0.28% d_1, 1.90 ± 0.20% d_2 (0.977 ± 0.007 excess d per molecule).

The second fraction (0.20 g) isolated from Run 2 was dissolved in preoxidized ether (1.5 mL) and stirred for 5 h in the presence of 0.5 mL of Brown's reagent. Work-up yielded 0.15 g of a viscous oil that was shown by analytical glpc to be comprised mainly of two components which were 47% and 34%, respectively, of the mixture. The bromoketones were separated by preparative glpc on a 1/4 in. × 10 ft 15% Carbowax glass column at 160°C. Compound **14**; nmr (CS_2, 100 MHz) δ: 4.10 (bt, 1H, *endo*-5-H), 2.80 (bm, 1H, H-4), 2.45 (m, 1H, H-1), 2.3–1.6 (norbornyl envelope); ms *m/e*: 189 (M^+); 15.24 ± 0.34% d_0, 81.04 ± 1.31% d_1, 2.25 ± 0.08% d_2 (0.867 ± 0.022 excess d per molecule). Compound **15**; nmr (CS_2, 100 MHz) δ: 2.53 (dd, 1H, J = 8 and 4 Hz, *exo*-3-H), 2.33 (bm, 1H, 1H, H-1), 2.15–1.5 (norbornyl envelope); ms *m/e*: 189 (M^+); 10.47 ± 0.56% d_0, 86.54 ± 0.40% d_1, 2.99 ± 0.67% d_2 (0.914 ± 0.033 excess d per molecule).

HBr-catalyzed Ring-opening of Nortricyclanone

Anhydrous HBr that was passed through concentrated H_2SO_4 was slowly bubbled through a magnetically stirred solution of nortricyclanone (0.28 g) in CCl_4 (15 mL) maintained at 70 ± 2°C. After 20 h the mixture was washed with water (10 mL), saturated aqueous $NaHCO_3$ (2 × 15 mL), aqueous $Na_2S_2O_7$ (10 mL), and dried. After the solution was treated once with Norit, the solvent was removd on the rotary evaporator to yield 0.32 g of a viscous oil. *Exo*-5-bromo-2-norbornanone that comprised >95% of the reaction mixture was isolated by preparative glpc on a 1/4 in. × 10 ft 15% Carbowax column at 175°C; nmr (CS_2, 100 MHz) δ: 4.12 (td, 1H, *endo*-5-H), 2.84 (m, 1H, H-4), 2.47 (m, 1H, H-1), 2.4–1.6 (norbornyl envelope).

Determination of the Deuterium Distribution

The *syn*-7-bromohydrin-*d* (0.090 g, >90% pure) was dissolved in 2-propanol (6 mL) and sodium (0.2 g) was added in small portions to the solution that was maintained at reflux. After a 2 h reflux most of the 2-propanol was removed by distillation, water was added (2 mL), the solution was extracted with ether (3 × 10 mL), and the combined ether extracts were dried. After one treatment with Norit the ether was removed on a rotary evaporator to yield a viscous oil. Analytical glpc on a 1/8 in. × 10 ft 10% Carbowax column at 150°C established that product was *exo*-2-norbornanol-*d* (>95%). A pure sample of the *exo*-2-norbornanol-6-*endo*-*d* was isolated by preparative glpc on a 1/4 in. × 5 ft 15% Carbowax column at 80°C; ir (CS_2): 948, 915, 878, 860, 835, 798, 770, 740, 705 (Fig. 2*c*). There was no significant absorption at 960, 890, and 780 that would indicate the presence of *exo*-2-norbornanol-6-*exo*-*d* (Fig. 2*a*).

The *anti*-bromohydrin-*d* (0.93 g) was dissolved in 2-propanol (50 mL) and sodium (1.0 g) was added in small portions to the solution. After a 2 h reflux the reaction mixture was worked up and the *exo*-2-norbornanol-6-*endo*-*d* was isolated by preparative glpc from the oily solid that remained after the solvent was evaporated; ir (CS_2): 948, 915, 878, 835, 798, 770, 740, 705 (Fig. 2*a*). There was no significant absorption at 960, 890, and 780 that would indicate the presence of a significant amount (>10%) of *exo*-2-norbornanol-6-*exo*-*d* (Fig. 2*a*).

Acknowledgement

We thank the Natural Sciences and Engineering Research Council of Canada for financial assistance.

1. C. H. DePuy. Acc. Chem. Res. **1**, 33 (1968).
2. C. J. Collins. Chem. Rev. **69**, 543 (1969).
3. C. C. Lee. Progr. Phys. Org. Chem. **7**, 129 (1970).
4. J. L. Fry and G. J. Karabatsos. *In* Carbonium Ions. Vol. 2. *Edited by* G. A. Olah and P. von R. Schleyer. Wiley-Interscience, New York, NY. 1970. Chapt. 4.
5. M. Saunders, P. Vogel, E. L. Hagen, and R. Rosenfeld. Acc. Chem. Res. **53**, 6 (1973).
6. C. H. DePuy. Fortschr. Chem. Forsch. **40**, 73 (1973).
7. J. E. Williams, R. Sustmann, L. C. Allen and P. v. R. Schleyer. J. Am. Chem. Soc. **91**, 1037 (1969).
8. R. Sustmann, J. E. Williams, M. J. S. Dewar, L. C. A. Chen, and P. v. R. Schleyer. J. Am. Chem. Soc. **91**, 5350 (1969).
9. C. H. DePuy, P. C. Funfschilling, A. H. Andrist, and J. M. Olson. J. Am. Chem. Soc. **99**, 6297 (1977).
10. E. Haselbach, E. Heilbronner, H. Musso, and A. Schmelzer. Helv. Chim. Acta, **55**, 302 (1972).
11. W. L. Jorgensen and L. Salem. The organic chemist's book of orbitals. Academic Press. New York, NY. 1973.
12. R. Bonaccorsi, E. Scrocco, and J. Tomasi. J. Chem. Phys. **52**, 5270 (1970).
13. S. J. Cristol, W. Y. Lim, and A. R. Dahl. J. Am. Chem. Soc. **92**, 4013 (1970).
14. H. C. Brown. *In* The non-classical ion problem. Plenum Publishing Corp., New York, NY. 1977.
15. A. Nickon and J. H. Hammons. J. Am. Chem. Soc. **86**, 3322 (1964).
16. J. H. Hammons, E. K. Probasco, L. H. Sanders, and E. J. Whalen. J. Org. Chem. **33**, 4493 (1968).
17. N. H. Werstiuk, G. Timmins, and F. P. Cappelli. Can. J. Chem. **51**, 3473 (1973).
18. S. Banerjee and N. H. Werstiuk. Can. J. Chem. **54**, 678 (1976).
19. N. H. Werstiuk. Can. J. Chem. **53**, 26 (1975).
20. N. H. Werstiuk, G. Timmins, and F. P. Cappelli. Can. J. Chem. **50**, 2163 (1972).
21. J. D. Roberts, F. O. Johnson, and R. A. Carboni. J. Am. Chem. Soc. **76**, 5692 (1954).
22. E. Tobler, D. E. Battin, and D. J. Foster. J. Org. Chem. **29**, 2834 (1964).
23. R. N. McDonald and T. E. Tabor. J. Org. Chem. **33**, 2934 (1968).
24. H. L. Goering and M. J. Degani. J. Am. Chem. Soc. **91**, 4506 (1969).
25. H. C. Brown and C. P. Garg. J. Am. Chem. Soc. **83**, 2952 (1961).
26. L. H. Zalkow and A. C. Oehlschlager. J. Org. Chem. **29**, 1625 (1964).

Stereochemistry of acid-catalyzed cleavage of 7-chloro-1-methylnortricyclene in deuterated medium; evidence for edge protonation of nortricyclenes

NICK HENRY WERSTIUK AND FRANK PETER CAPPELLI

Department of Chemistry, McMaster University, Hamilton, Ont., Canada L8S 4M1

Received December 5, 1979

NICK HENRY WERSTIUK and FRANK PETER CAPPELLI. Can. J. Chem. **58**, 1725 (1980).

Cleavage of 7-chloro-1-methylnortricyclene (**1***e*) in D_2SO_4–DOAc yields deuterated *syn*-7-chloro-1-methyl-*exo*-2-norbornyl acetate (**3***a-d*) (1.04 excess *d* per molecule) and deuterated *anti*-7-chloro-1-methyl-*exo*-2-norbornyl acetate (**3***b-d*) (1.28 excess *d* per molecule) as the kinetic products. ^1H and ^2H nuclear magnetic resonance spectroscopic analysis of the corresponding alcohols complexed with $Eu(fod)_3$ shows that deuterium is located *endo* at C-6 and in the methyl group of the *syn*-7-chloroacetate, *endo* at C-6 and C-2, at C-7, and in the methyl group of the *anti*-7-chloroacetate. That the deuterium at C-6 of both acetates is 80-90% stereochemically pure *endo*, in our view, establishes that the bond farthest removed from the electron-withdrawing chlorine is preferentially cleaved via edge deuteronation.

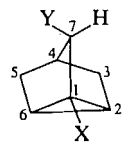
NICK HENRY WERSTIUK et FRANK PETER CAPPELLI. Can. J. Chem. **58**, 1725 (1980).

Les produits cinétiques du clivage du chloro-7-méthyl-1 nortricyclène (**1***e*) dans le mélange de D_2SO_4–DOAc sont les suivants: les acétates du chloro-7 *syn* méthyl-1 norbornyle-2 *exo* (**3***a–d*) deutérés (1.04 de *d* en excès par molécule) et les acétates du chloro-7 *anti* méthyl-1 norbornyle-2 *exo* (**3***b–d*) deutérés (1.28 de *d* en excès par molécule). L'analyse par spectroscopie de rmn du ^1H et du ^2H des alcools correspondants complexés avec $Eu(thd)_3$ révèle que le deutérium est situé en position *endo* du C-6 et dans le groupe méthyle de l'acétate du chloro-7 *syn* est en position *endo* des carbones-2,6 et 7 dans le groupe méthyle de l'acétate du chloro-7 *anti*. Le fait que 80 à 90% du deutérium en C-6 des deux acétates soit sous la forme *endo*, prouve, à notre avis, que la liaison la plus éloignée du chlore électro-attracteur est scindée préférentiellement par l'intermédiaire d'une deutération par l'arête.

[Traduit par le journal]

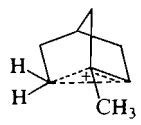
Introduction

Over the past two decades the mechanisms of electrophilic cleavage of cyclopropanes have been probed by stereochemical studies. To determine the structures of transition states and intermediates involved in the ring-openings and to establish how substituents and the nature of the electrophile affect transition state structure is the usual objective of researchers (1–6). Although an electrophile can attack face-wise, edge-wise, or corner-wise, all results obtained have been interpreted on the basis of edge protonation or corner protonation because face-protonated cyclopropane is a high-energy species (7, 8). While inversion or retention may attend attack by an electrophile, a proton, in most cases, cleaves a three-membered ring with retention of configuration at the carbon bearing the proton. Studies involving the protonation of nortricyclene and several of its derivatives have generated considerable interest because the results relate to the long-standing norbornyl cation problem (9). From a study of the cleavage of nortricyclene (**1***a*) Nickon and Hammons (10) concluded that the cleavage of the three-membered ring yields the non-classical norbornyl cation. However, the results of our study (11) of 3-chloronortricyclene (**1***b*) and 3-bromonortricyclene (**1***c*) as documented in the preceding paper, point to ring cleavage via edge protonation (deuteronation) as the major reaction pathway and the classical *syn* and *anti*-7-halo-2-norbornyl cations are formed. In our view nortricyclene (**1***a*) also undergoes ring-opening via edge-wise attack and a rapidly-equilibrating norbornyl cation is formed. To determine quantitatively the stereochemistry of the ring opening of 1-methylnortricyclene (**1***d*) and to identify the kinetic products, Hammons *et al.* (12) studied the D^+ catalyzed ring-opening of **1***d*. They established that *endo*-2-methyl-*exo*-2-norbornyl acetate, in fact, is the kinetic product and that cleavage of the C1—C2 and C1—C6 bonds occurs with 62 ± 3% retention and 38 ± 3% inversion of configuration. The results were discussed on the basis of an intermediate non-classical 1-methylnorbornyl cation (**2**).

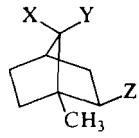


1

a X = Y = H
b X = H, Y = Cl
c X = H, Y = Br
d X = CH_3, Y = H
e X = CH_3, Y = Cl



2



3

a X = H, Y = Cl, Z = OAc
b X = Cl, Y = H, Z = OAc
c X = H, Y = Cl, Z = OH
d X = Cl, Y = H, Z = OH

To extend our studies of the electrophilic cleavage of 3-halonortricyclenes and to determine whether 1-methylnortricyclene undergoes cleavage via non-selective, statistical, edge-wise proton-

0008-4042/80/161725-13$01.00/0

©1980 National Research Council of Canada/Conseil national de recherches du Canada

Can. J. Chem. Downloaded from www.nrcresearchpress.com by 210.87.254.5 on 09/05/12
For personal use only.

Can. J. Chem. Downloaded from www.nrcresearchpress.com by 210.87.254.5 on 09/05/12
For personal use only.

ation of the two different cyclopropane bonds to form classical cations rather than a non-classical ion we prepared 7-chloro-1-methylnortricyclene (**1***e*) and carried out the ring-opening in non-deuterated and deuterated medium. We were also interested in preparing specifically C-6 deuterated 1-methyl-*exo*-2- and 7-chloro-1-methyl-*exo*-2-norbornyl brosylates that we required to extend our study of the unusually large γ-KIE's observed for solvolysis of *exo*-norbornyl sulfonate esters (13, 14). The results of our study of the acid-catalyzed ring-opening of 7-chloro-1-methylnortricyclene are documented in this publication.

Results

Synthesis of 7-Chloro-1-methylnortricyclene (1e)

A Diels–Alder reaction between methylcyclopentadiene and ethene yielded a mixture of 1-methyl- and 2-methyl-2-norbornenes. Their spectral characteristics were identical to those published previously (15). Chlorination of 2-methyl-2-norbornene in CH_2Cl_2, in the presence of pyridine, gave previously unknown **1***e*. The ir and nmr spectra of **1***e* were consistent with the proposed structure.

Ring-opening in H_2SO_4–CH_3COOH; Identification of Products

When **1***e* was heated in 0.1 *M* H_2SO_4 – CH_3COOH at 62 ± 2°C for 105 h, it was converted into *syn*-7-chloro-1-methyl-*exo*-2-norbornyl acetate (**3***a*) (24%) and *anti*-7-chloro-1-methyl-*exo*-2-norbornyl acetate (**3***b*) (71%). We established, by analytical glpc, that the relative yields of the products did not change during the reaction and that the products did not rearrange in the injection block of the gas chromatograph. The analysis also showed that there were two very minor products, each < 2%, in the region of the chloroacetates and three very minor products, each < 2%, close in retention time to starting material. The minor components, which may have been tertiary acetates and isomeric alkenes (*vide infra*), were not isolated because they were present in very small amounts.

That there is a one-proton resonance at δ 4.50 in the ^1H nmr spectrum of **3***a* and a one-proton resonance at δ 4.55 in the spectrum of **3***b*, identified the products as secondary acetates. The chemical shifts of the *anti*-7-proton (δ 3.51) of **3***a* and the *syn*-7-proton (δ 3.77) of **3***b* are in agreement with assigned structures because a proton at C-7 *syn* to an *exo* acetoxyl group is deshielded relative to *anti*-proton by about 0.2–0.3 ppm (11, 16).

Reduction of the mixture of chloroacetates by sodium in 2-propanol gave 1-methyl-2-norbornanol (96%) and 4% of an unidentified product. From an analytical glpc analysis we established that < 5% of the *endo* alcohol was present. When the mixture of chloroacetates was reduced by LAH a mixture of the *syn*-7-chloro-1-methyl-*exo*-2-norbornanol (**3***c*) (22%) and *anti*-7-chloro-1-methyl-*exo*-2-norbornanol (**3***d*) (78%) was obtained. Analytical glpc analysis showed that **3***c* and **3***d* comprised > 95% of the reaction mixture. That **3***c* was the minor component (22%) was corroborated by the fact that its retention time, due to internal hydrogen bonding, was considerably shorter than the retention time of **3***d*.[1]

Cleavage in D_2SO_4–CD_3COOD; Determination of the Stereochemistry of Ring-opening

Compound **1***e* was ring-opened in 0.1 *M* D_2SO_4 – CD_3COOD (65 ± 2°C, 60 h) and yielded 27% of **3***a-d* and 73% of **3***b-d*. The acetates were reduced by LAH in ether, the deuterated chlorohydrins were isolated by preparative glpc, and a small portion of each chlorohydrin was oxidized to the corresponding chloroketone by Brown's reagent. The chloroketones, after being purified by preparative glpc, were assayed for deuterium mass spectrometrically. As in the case of the deuteronation of 1-methylnortricyclene the acetates contained greater than one deuterium atom per molecule (Table 1). To establish the location of the deuterium the ^1H nmr spectra of the chlorohydrins were obtained in the absence and presence of the lanthanide shift reagent Eu(fod)$_3$. To provide a check for the ^1H nmr analysis we also obtained ^2H nmr spectra of the deuterated chlorohydrins in the presence of Eu(fod)$_3$. In the ^1H nmr spectrum of the non-deuterated *syn*-chlorohydrin **3***c* given in Fig. 1*a*, it is interesting to note that the resonance due to *endo*-2-H, unlike the resonance of the *anti*-chlorohydrin **3***d* (Fig. 1*c*), is a broad multiplet. We believe that the coupling of *endo*-2-H to —O—H is observed in this case because internal hydrogen bonding to the chlorine reduces the rate of exchange of the —O—H. The spectrum of the deuterated *syn*-chlorohydrin **3***c-d* is given in Fig. 1*b* and the spectra of **3***c* and **3***c-d* complexed with Eu(fod)$_3$ are given in Figs. 2*a* and 2*b*, respectively. Assignment of the signals at δ 16.7 (*endo*-2-H), 10.7 (*exo*-3-H), 7.7 (CH_3—), 7.1 (*anti*-7-H), 6.1 (*endo*-3-H), and 5.1 (H-4) in Fig. 2*a* is straightforward. That the signal at δ 3.7 is due to the *endo*-proton at C-6 is established from a comparison of the non-shifted spectra of **3***c* (Fig. 1*a*) and **3***c-d*

[1]This behaviour parallels the behaviour of the *syn*-7- and *anti*-7-chloro-*exo*-2-norbornanols (11) on a Carbowax column.

TABLE 1. Deuterium content of *syn*-7- and *anti*-7-chloro-1-methyl-2-norbornanones

Ketone	Composition*				Excess *d* per molecule
	d_0	d_1	d_2	d_3	
syn-7-Chloro	3.72±0.42	86.19±0.86	9.09±0.27	—	1.044±0.016
anti-7-Chloro	5.24±0.14	65.95±0.47	22.10±0.18	5.98±0.22	1.281±0.007

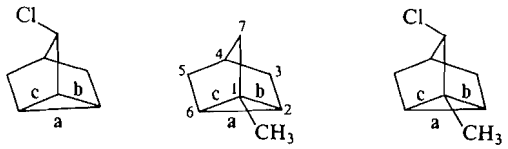
*Mass spectrometric analyses were carried out at low voltage (10–15 eV). Averages of five determinations. Deviations are the standard deviations.

(Fig. 1*b*). Since *endo* protons at C-5 and C-6 of norbornanes generally appear at higher field (≃1 ppm) than *exo* protons (17,18) it is clear from the reduction of the signal intensity in the high field region, δ 1.1–1.2, of **3***c*-*d* (Fig. 1*b*) that the deuterium is located at an *endo* position. Since there is no viable mechanism for introducing *endo* deuterium at C-5, the deuterium must be located *endo* at C-6. While it is clear from the shifted spectrum of **3***c*-*d* (Fig. 2*b*) that most of the deuterium is located *endo* at C-6, we established by integration that deuterium was located in the methyl group as well.

The ^{1}H nmr spectra of the *anti*-chlorohydrins **3***d* and **3***d*-*d* are given in Figs. 1*c* and 1*d*, respectively. The spectrum of *anti*-chlorohydrin **3***d* complexed with Eu(fod)$_3$ is given in Fig. 2*c*. Here too, the assignment of the signals at δ 17.9 (*endo*-2-H), 12.9 (*exo*-3-H), 12.3 (*syn*-7-H), 7.4 (CH_3—), 7.0 (*endo*-3-H), and 5.1 (H-4) is straightforward. That the signal at δ 4.5 is due to the *endo*-proton at C-6 and that the deuterium in **3***d*-*d* is located predominantly at this position is established from a comparison of the spectra of **3***d* and **3***d*-*d* and from an inspection of the shifted spectrum of the deuterated *anti*-chlorohydrin **3***d*-*d* (Fig. 2*d*). As in the case of the *syn*-chlorohydrin, it is clear from a careful inspection of the high field regions (δ 0.7–1.0) of the spectra of **3***d* and **3***d*-*d* (Figs. 1*c* and 1*d*) that there is a significant reduction of the signal intensity in the spectrum of the latter. This is consistent with deuterium being located *endo* at C-6. While it is clear from the shifted spectrum of **3***d*-*d* (Fig. 2*d*) that the deuterium is located predominately *endo* at C-6, we established by integration that deuterium was also located at C-2, C-7, and in the methyl group. That the ^{1}H nmr integrals are a good measure of the deuterium distribution is confirmed by the ^{2}H nmr spectra of the deuterated *syn*- and *anti*-chlorohydrins obtained in the presence of Eu(fod)$_3$ (Figs. 3*a* and 3*b*). The deuterium distributions in the chloroacetates, as determined by ^{1}H and ^{2}H nmr are listed in Table 2. It should be noted that the deuterium content of **3***d*-*d* established by mass spectrometric assay of the corresponding ketone is slightly less than the actual deuterium content because the deuterium located at C-2 (Table 2) is lost during oxidation.

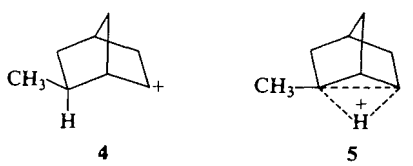
Discussion and Conclusions

In the preceding paper we showed that the deuterium at C-6 of the major products *syn*-7- and *anti*-7-chloro-*exo*-2-norbornyl acetates of ring-opening of 3-chloronortricyclene (**1***b*) is 85–90% stereochemically pure *endo* and thereby established that edge deuteronation of bond **a** of **1***b* is preferred over edge deuteronation of bonds **b** and **c** by 5:1. Hammons *et al.* (12) in a related study established that 1-methylnortricyclene (**1***d*) is ring-opened with 62 ± 3% retention and 38 ± 3% inversion of configuration and interpreted the results on the basis of a mechanism which involved formation of a non-classical 2-methylnorbornyl cation.



1*b* **1***d* **1***e*

In our view the ratio of 1.6:1, in favour of retention, is near the ratio which would be observed if bonds **a** and **b** of **1***d* are cleaved simply on the basis of a statistical edge-wise attack of D^+. This, of course, is possible only if the directing effect of the methyl group is small. That a methyl group enhances the rate of a 6,2-hydride shift in the 6-methyl-2-norbornyl cation **4** only by a factor between 5 and 15 (19) (the transition states for the hydride shift and ring-opening of **1***d*, both depicted by **5**, should be similar with respect to charge distribution) establishes that the directing effect of methyl in the ring-opening should be small.



4 **5**

To quantitatively establish the effect of a methyl group on the cleavage of **1***b*, we determined the rate

Can. J. Chem. Downloaded from www.nrcresearchpress.com by 210.87.254.5 on 09/05/12
For personal use only.

Can. J. Chem. Downloaded from www.nrcresearchpress.com by 210.87.254.5 on 09/05/12
For personal use only.

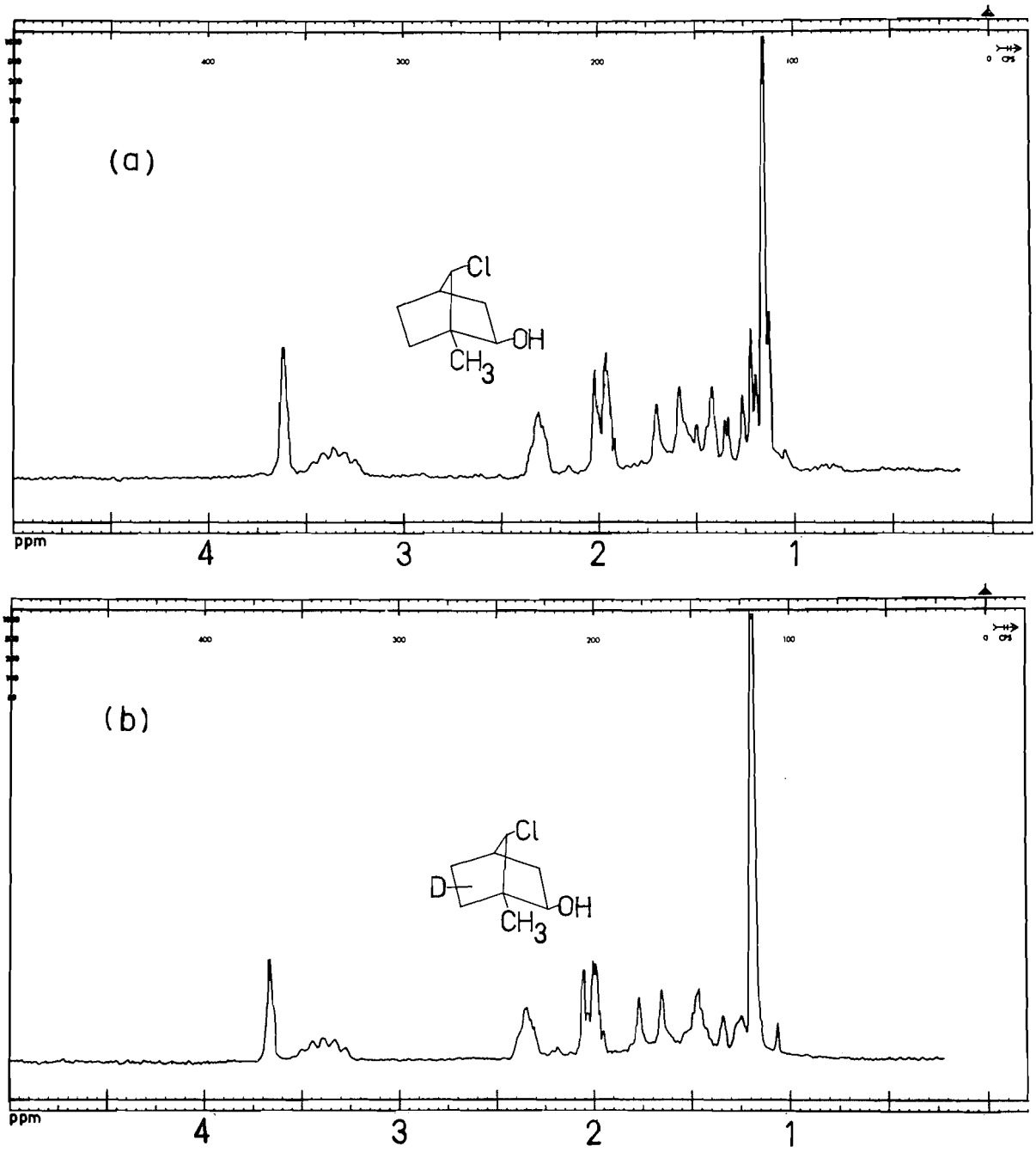


FIG. 1. (*a*) 100 MHz (CS_2) ^1H nmr spectrum of *syn*-7-chloro-1-methyl-*exo*-2-norbornanol; (*b*) *syn*-7-chloro-1-methyl-*exo*-2-norbornanol-*d*; (*c*) *anti*-7-chloro-1-methyl-*exo*-2-norbornanol; (*d*) *anti*-7-chloro-1-methyl-*exo*-2-norbornanol-*d*.

constants for ring opening of **1***b* and **1***e* in 0.1 *M* H_2SO_4 – CH_3COOH at 70°C (see Experimental). That a small rate acceleration of 3.9 is observed upon introduction of a methyl group is in accord with our view that the methyl group *does not control* the regiochemistry of the initial protonation (deuteronation) of nortricyclenes.

That phenylcyclopropane is 7.8 times less reactive than cyclopropane (20) provides further support that cation stabilizers borne by the cyclopropane do not significantly stabilize the transition state. In the case of 1-methylnortricyclene a small rate-retarding steric effect (1) of the methyl could mask a small preference for addition to the C1—C2

Can. J. Chem. Downloaded from www.nrcresearchpress.com by 210.87.254.5 on 09/05/12
For personal use only.

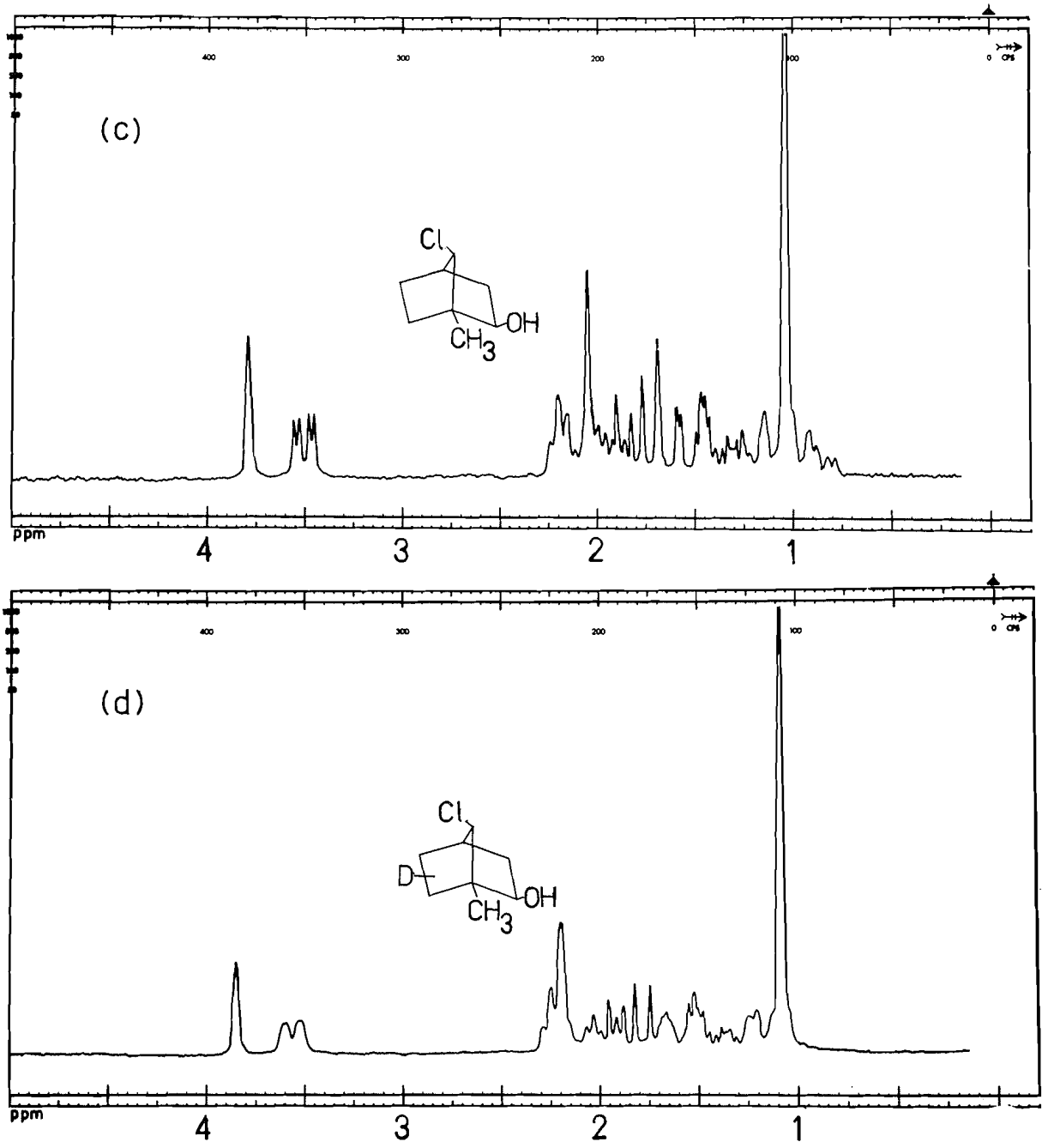


FIG. 1 (*concluded*)

and C1—C6 bonds so that protonation, and of course the stereochemical outcome of the reaction, would be controlled basically by the statistical factor. If this is indeed the case, then deuteronation (Scheme 1) of bond **a** of 7-chloro-1-methylnortricyclene, as in the case for 3-chloronortricyclene, should be preferred over deuteronation of bonds **b** and **c** by about 5:1. Since cations **6** and **7** are the initial intermediates, the stereochemistry of the cleavage should be similar to the stereochemistry of the ring-opening of 3-chloronortricyclene (11). From the data listed in Table 2 it is clear that this is indeed the case because the deuterium at C-6 of the 7-chloro-1-methyl-*exo*-2-norbornyl acetates is 80–90% stereochemically pure *endo*.

Clearly then, our studies have established that

Can. J. Chem. Downloaded from www.nrcresearchpress.com by 210.87.254.5 on 09/05/12
For personal use only.

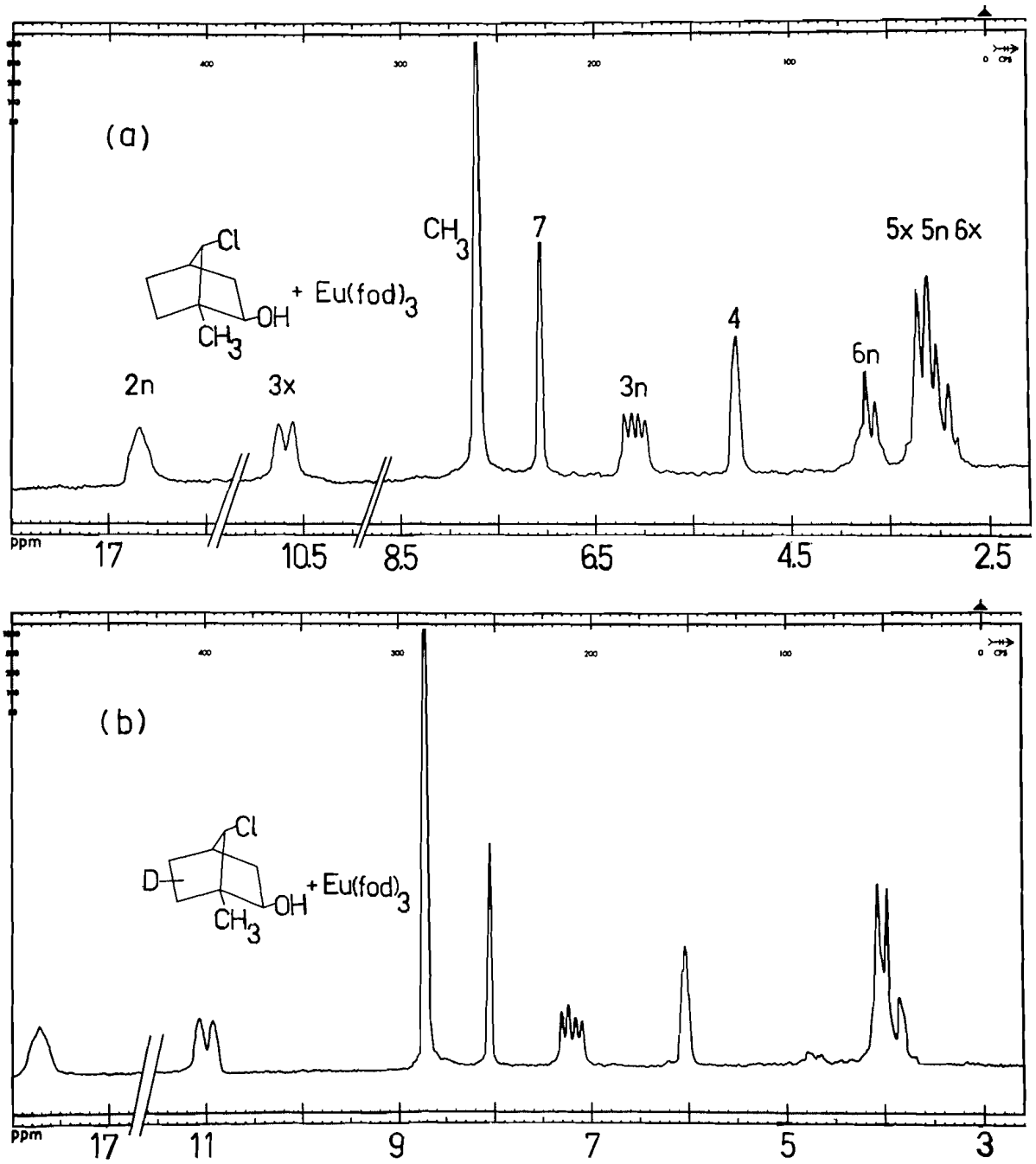


FIG. 2. (*a*) 100 MHz (CCl_4) ^1H nmr spectrum of *syn*-7-chloro-1-methyl-*exo*-2-norbornanol complexed with $Eu(fod)_3$; (*b*) *syn*-7-chloro-1-methyl-*exo*-2-norbornanol-*d* complexed with $Eu(fod)_3$; (*c*) *anti*-7-chloro-1-methyl-*exo*-2-norbornanol complexed with $Eu(fod)_3$; (*d*) *anti*-7-chloro-1-methyl-*exo*-2-norbornanol-*d* complexed with $Eu(fod)_3$.

there exists a common mechanism for the acid-catalyzed ring-opening of nortricyclene, 1-methylnortricyclene, and their halo-derivatives **1***b* and **1***e*.

That deuterium is located at C-7 and in the methyl group of the chloroacetates indicates that formation of the isomeric chloroalkenes **10**, **11**, **12**, **17**, **18**, and **19** attends the ring-opening. Possible routes to the chloroalkenes are listed in Schemes 1 and 2. The appearance of minor components which had glpc retention times very close to **1***e* is consistent with this requirement. The deuterated 2-

Can. J. Chem. Downloaded from www.nrcresearchpress.com by 210.87.254.5 on 09/05/12
For personal use only.

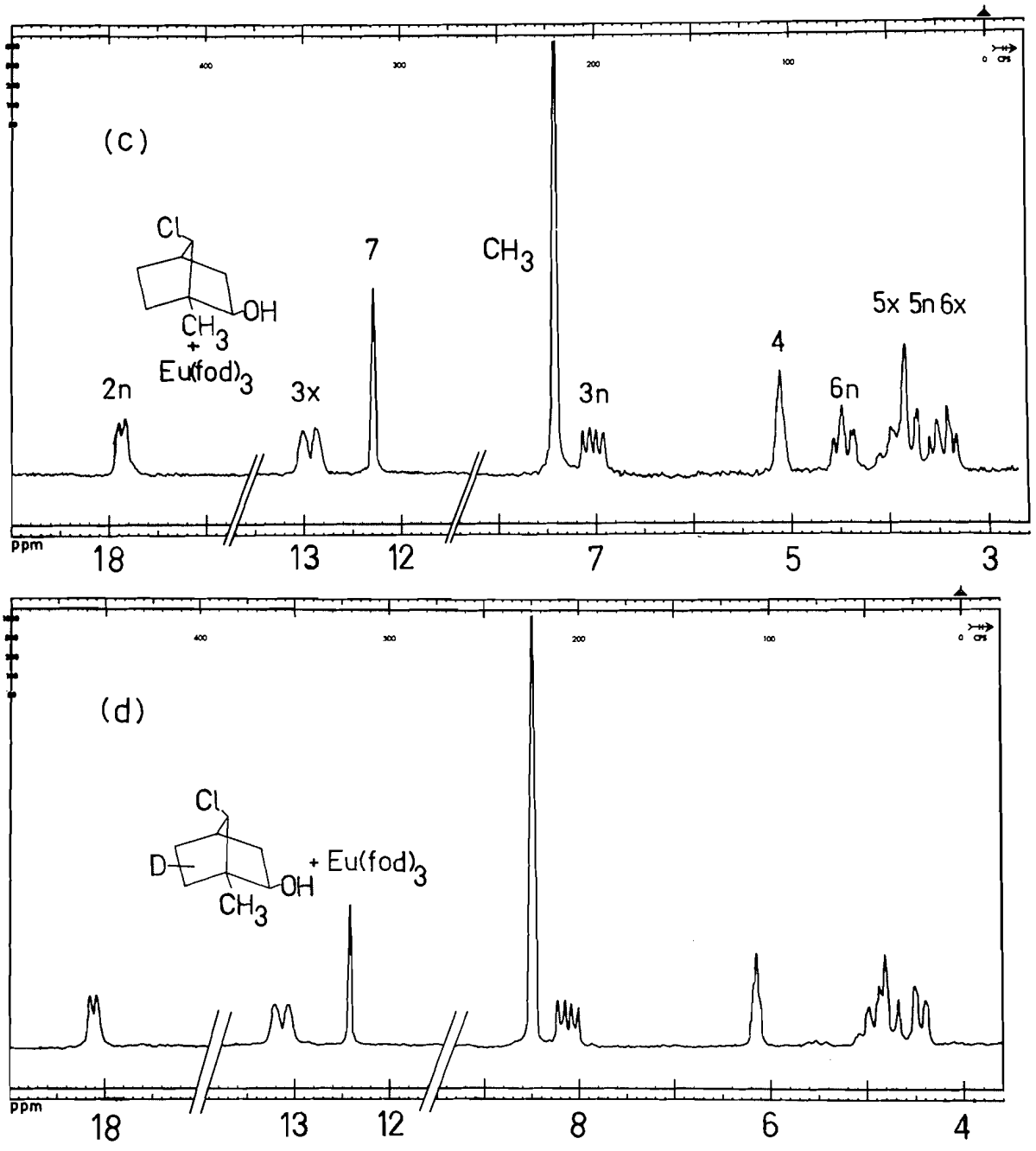


FIG. 2 (*concluded*)

chloro-3-methyl-2-norbornenes, **11** and/or **18**, are mandatory intermediates and it is clear that deuterium is incorporated at C-7 only in the *anti*-7-chloroacetate because deuteronation of **11** and/or **18** occurs predominately from the *exo* face (Scheme 3). While the chloroalkenes **10**, **11**, **12**, **17**, **18**, and **19** can be generated by deuteronation of bonds **a**, **b**, and **c** (Schemes 1 and 2), the deuterium distribution in the products and stereochemical outcome of the reaction points to their formation predominantly via deuteronation of bonds **b** and **c**. If, as we postulate, bonds **a**, **b**, and **c** of **1***e* are deuteronated with the same selectivities as bonds **a**, **b**, and **c** of **1***b* (11), then approximately 20% of the ring-opening of **1***e* should occur via cleavage of bonds **b** and **c**. Our claim that ring-opening of **1***e* occurs via deuteronation of bonds **b** and **c** to the same extent as in 3-chloronortricyclene is sup-

Can. J. Chem. Downloaded from www.nrcresearchpress.com by 210.87.254.5 on 09/05/12
For personal use only.

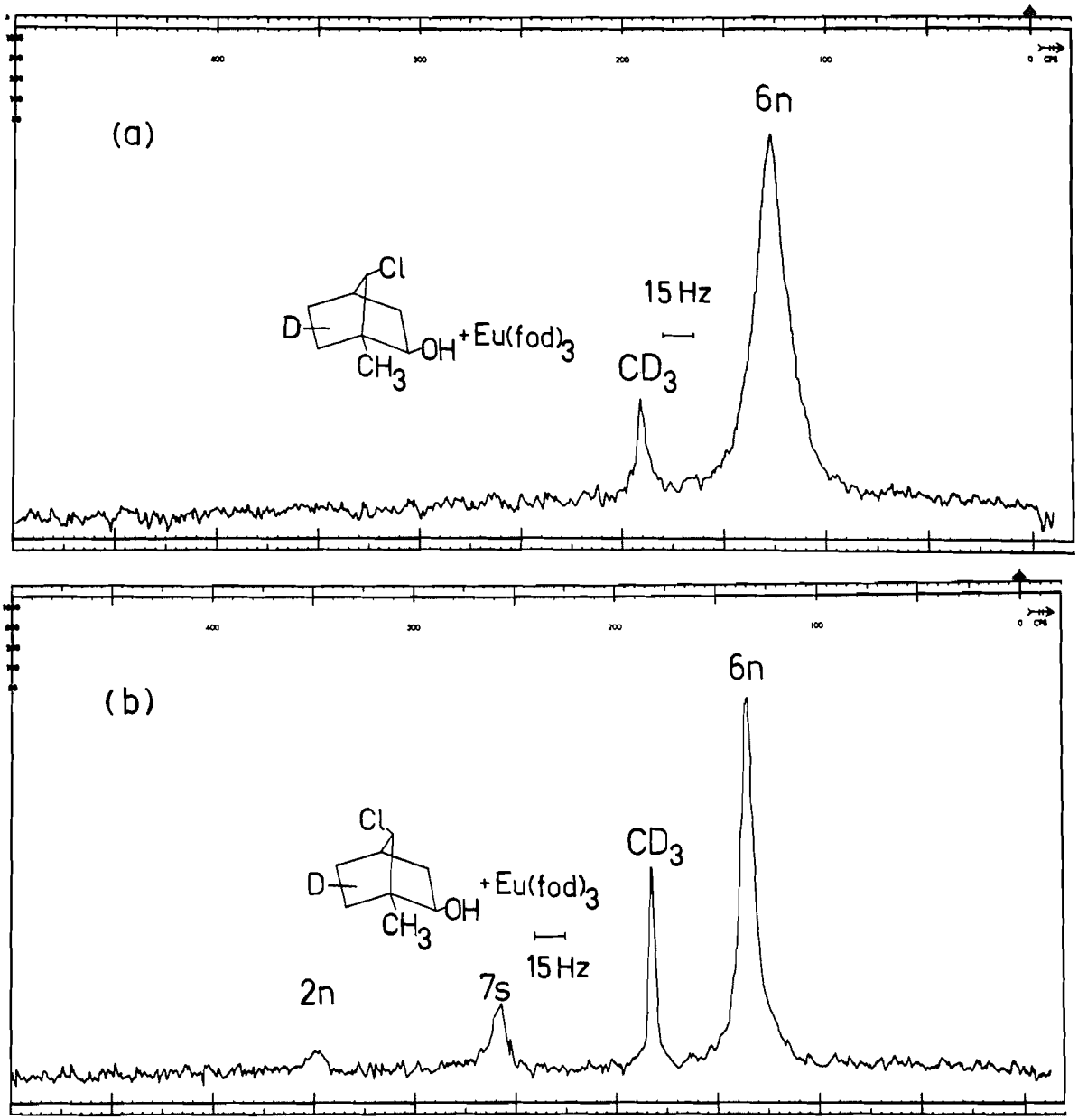


FIG. 3. (*a*) 15.4 MHz (CCl_4) ^2H nmr spectrum of *syn*-7-chloro-1-methyl-*exo*-2-norbornanol-*d* complexed with $Eu(fod)_3$; (*b*) *anti*-7-chloro-*exo*-2-norbornanol-*d* complexed with $Eu(fod)_3$.

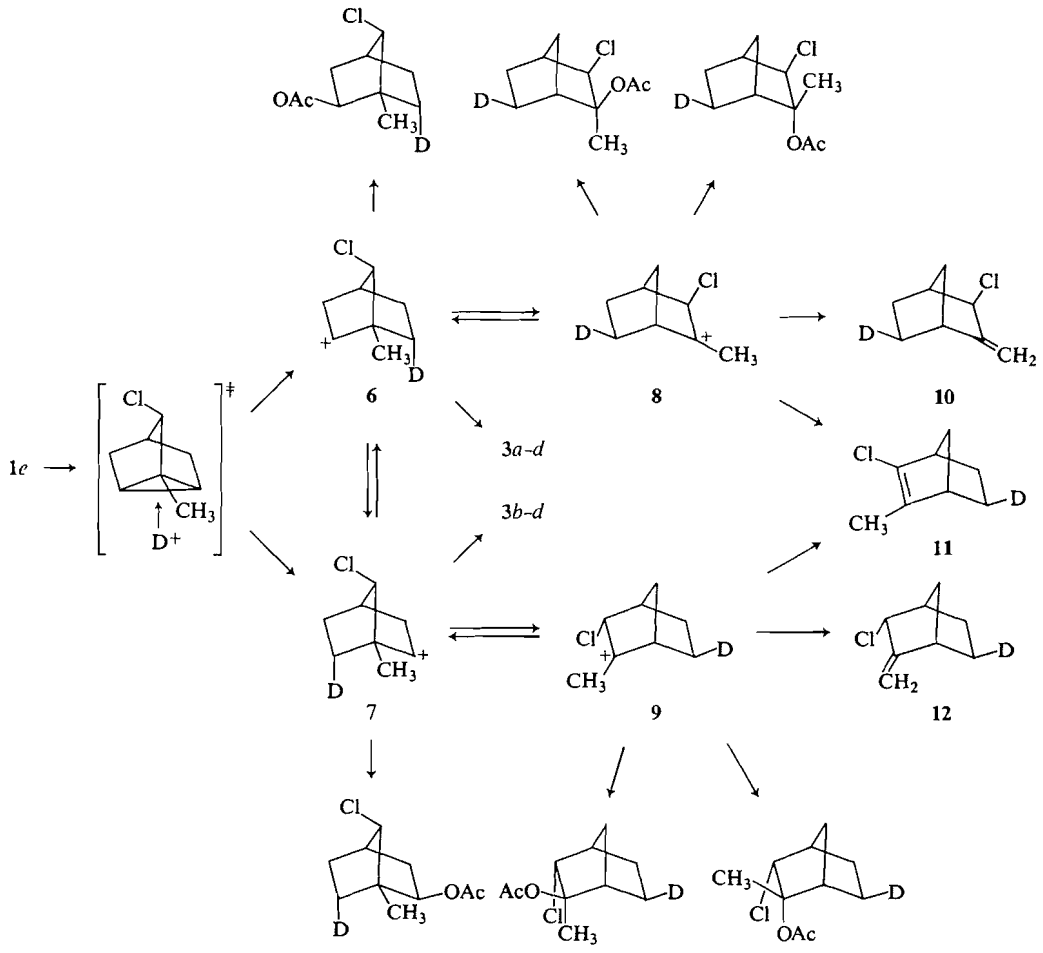
ported by an analysis based on the stereochemical purity of the deuterium at C-6 of the 7-chloroacetates. Since edge deuteronation of bonds **b** and **c** (Scheme 2) eventually leads to *syn*-7- and *anti*-7-chloroacetates with deuterium located *exo* at C-6, the amount of *exo* deuterium should be a measure of the extent of protonation of bonds **b** and **c**. From the ^1H nmr and ^2H nmr analyses it is clear that approximately 10–20% of the deuterium is *exo* at C-6 and this result supports our proposal.

That deuterium is located at C-2 of **3***d*-*d* indicates that bond **b** of **1***e* is edge deuteronated to yield cation **15** that in turn leads, via an alkyl shift and a hydride shift, to *anti*-7-chloro-1-methyl-*exo*-2-norbornylacetate-*endo*-2-*d* (Scheme 4). It is interesting to note that there is no deuterium at C-2 of the *syn*-7-chloroacetate, and we suggest two reasons for this result. If deuteronation of bond **c** occurs to yield cation **16** that rearranges via a 1,2-alkyl shift (Scheme 5), perhaps the 6,2-hydride shift

TABLE 2. Distribution of deuterium in 7-chloro-1-methyl-*exo*-2-norbornyl acetates

Substrate	Method	CH_3	H-2	*endo*-6-H	H-7	*d* by ^1H nmr
3*a*-*d*	Pmr*	0.05±0.17		0.89±0.06		0.94±0.21
	Dmr†	0.09±0.10		0.96±0.10‡		
3*d*-*d*	Pmr*	0.10±0.07	0.15±0.10	0.94±0.07	0.13±0.09	1.37±0.33
	Dmr†	0.22±0.02	0.05±0.01	0.88±0.09‡	0.14±0.02	

*The errors are the sum of errors (±5%) in the integral at the labelled site and in a standard one proton integral derived as an average of the H-4, *endo*-3-H, and *exo*-3-H integrals with an assumed error of ±5% in each.
†The peaks were traced, cut out, and weighed. An error of ±10% is assumed in this analysis and the deuterium content at each site is related to the total deuterium content determined by mass spectrometry.
‡These values correspond to *endo* and *exo* deuterium at C-6.



SCHEME 1

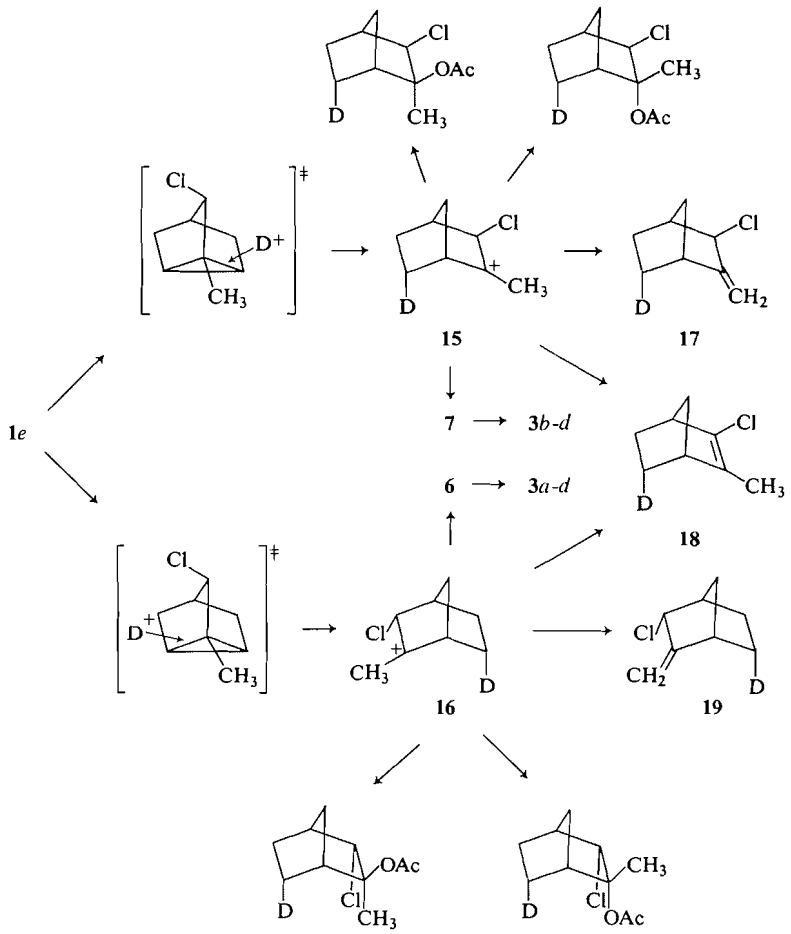
required to convert the *anti*-7-chlorocation to the *syn*-7-chlorocation does not compete with reaction with solvent. This, however, seems an unreasonable expectation because the *anti* to *syn* conversion via a hydride shift competes with solvent capture in the acetolysis of *anti*-7-chloro-*exo*-2-norbornyl tosylate (16). Perhaps bond **c** of **1***e* is sterically hindered by the chloro and methyl groups to the point where ring-opening occurs predominately by cleavage of bonds **a** and **b**.

As far as exchange of the methyl group is concerned, 3-chloro-2-methylenenorbornanes **12** and/or **19** must be involved as intermediates (Schemes 1 and 2).

It is interesting to note that in this case the secondary acetates are the kinetic products rather than the tertiary acetates which are the kinetic products of the ring-opening of 1-methylnortricyclene (**1***d*). This must be a consequence of the fact that the $-I$ effect of the chlorine outweighs the small $+I$ effect

Can. J. Chem. Downloaded from www.nrcresearchpress.com by 210.87.254.5 on 09/05/12
For personal use only.

Can. J. Chem. Downloaded from www.nrcresearchpress.com by 210.87.254.5 on 09/05/12
For personal use only.



SCHEME 2

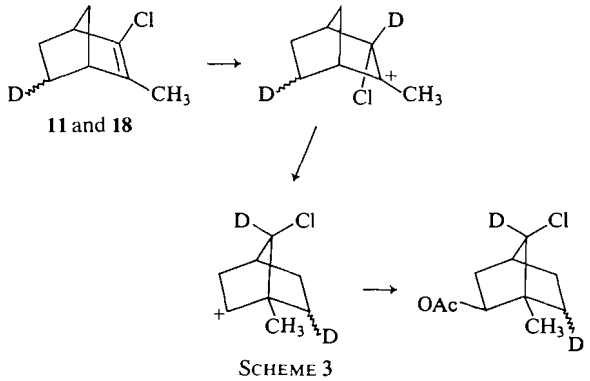
of the methyl group and thereby directs the ring-opening via bond *a*.

Experimental

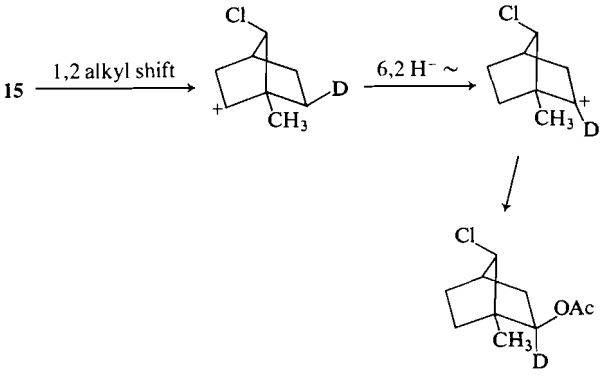
General

Proton magnetic resonance (pmr) spectra were recorded on Varian T-60, A-60, and HA-100 spectrometers with tetramethylsilane (TMS) as the internal standard. Samples were dissolved in either carbon tetrachloride or carbon disulfide. Deuterium magnetic resonance (dmr) spectra were recorded on a Varian model XL-100 spectrometer. Chemical shifts are expressed in parts per million downfield from internal tetramethylsilane. Infrared spectra were recorded on Perkin Elmer 337 and Beckman IR-5 infrared spectrometers and the samples were dissolved in carbon tetrachloride or carbon disulfide. Absorption frequencies were calibrated with a polystyrene film and are expressed in reciprocal centimeters (cm^{-1}). For brevity, the notation cm^{-1} is excluded. Mass spectra were taken on a Hitachi Perkin Elmer RMU-6A spectrometer at 80 eV. Deuterium assay analyses were performed at 10 to 15 eV and are expressed as atoms of deuterium per molecule in excess of natural abundance deuterium. Analytical gas liquid partition chromatography was performed on a Varian Aerograph Model 204B dual column analytical gas chromatograph equipped with dual flame ionization detectors using helium as the carrier gas. The gas flow rate was usually 20–30 mL/min. Preparative gas liquid partition chromatography was carried out on a Varian Aerograph Model A-90-P gas chromatograph with a thermal conductivity detector and a helium flow rate of 50–60 mL/min. Spinning band distillations were performed on a Nester–Faust auto annular 30 in Teflon spinning band distillation column. Melting points were recorded on a Kofler hot-stage apparatus and are uncorrected. Boiling points are also uncorrected.

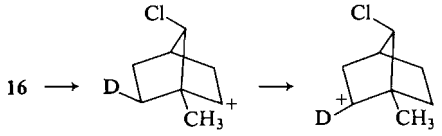
All organic solutions were dried with either anhydrous sodium sulfate or magnesium sulfate.



SCHEME 3



SCHEME 4



SCHEME 5

2-Methyl-2-norbornene

In a typical run, ethylene (800 psi) and methylcyclopentadiene dimer (125 g) were reacted at 200°C for 12 h in a Monel pressure apparatus (Parr Model 4914) fitted with a glass liner. The reaction vessel was cooled to room temperature and the excess ethylene was released. The reaction mixtures of eight runs were combined, filtered, and distilled through a 30 cm vacuum-jacketed Vigreux column. The fraction boiling between 110 and 120°C was collected and redistilled at atmospheric pressure through the Nester–Faust spinning-band column. After a forerun of 5 g was collected, the first fraction (100 g, head temperature 80–120°C), 1-methyl-2-norbornene was collected; ^{1}H nmr (CCl_4, 100 MHz) δ: 5.98 (quartet, 1H, J = 5.0 and 2.5 Hz, H-3), 5.75 (d, 1H, J = 5.0 Hz, H-2), 2.78 (broad s, 1H, H-4), 1.37 (s, 3H, —CH_3), 1.90–0.95 (m, 6H, norbornyl envelope). The second fraction (50 g, head temperature 105°C) was a mixture of 1- and 2-methyl-2-norbornenes; ir (neat): 3060 (olefinic C—H); ^{1}H nmr (CCl_4, 100 MHz) δ: 5.48 (broad s, 1H, H-3), 2.75, and 2.58 (broad s, each 1H, bridgeheads), 1.74 (d, 3H, J = 1.5 Hz, —CH_3), 1.74–0.85 (m, 6H, norbornyl envelope).

Chlorination of 2-Methyl-2-norbornene

2-Methyl-2-norbornene (110 g, 1.02 mol) was dissolved in methylene chloride (500 mL) and pyridine (105 mL) in a three-necked flask fitted with a mechanical stirrer and gas inlet and outlet tubes. The flask was cooled in an ice bath and chlorine gas that was first passed through concentrated sulfuric acid was bubbled into the stirred solution until the mixture turned yellow permanently. After the solution reached room temperature it was washed with water (150 mL), dilute hydrochloric acid (10%, 2 × 200 mL), saturated bicarbonate solution (2 × 200 mL), and water (2 × 200 mL). The organic layer was dried, concentrated, and the yellow oil (150 g) that remained was analyzed by analytical glpc on a 1/8 in. × 10 ft, 5% SE-30 column at 140°C. The major component (35%) of a total of at least seven products had the shortest retention time. Separation of the tricyclic compound was attempted by fractional distillation through a 30 cm glass column packed with glass helices and wrapped several times with aluminum foil. During the early stages of the distillation a white substance solidified in the column and caused the forerun to become cloudy. The first fraction consisted of 30.0 g of a colorless liquid, bp 35–40°C (20–25 Torr), which was shown by analytical glpc on a 1/8 in. × 10 ft, 10% Carbowax column (190°C) and nmr spectroscopy to be >96% pure. This compound was labile on a 5% SE-30 column at 100°C when the injector and detector block temperatures were high (>200°C). The second fraction was 47 g of a clear yellow liquid; bp 80–90°C (20–25 Torr); ^{1}H nmr (CCl_4, 60 MHz) δ: 4.1 and 3.3 (AB quartet, J = 11 Hz), 3.9 (m, 1H), 2.3–1.2 (m, 7H). After the second fraction was collected, a yellow solid collected in the condenser and the distillation was stopped. No further attempts were made to separate the compounds remaining in the pot.

The first fraction (30 g) was further purified by spinning-band distillation under reduced pressure (80 ± 2 Torr) with a head temperature of 51°C and a pot temperature of 56°C. After 2 mL of forerun, three separate fractions were collected and each was estimated by analytical glpc on a 1/8 in. × 10 ft, 5% SE-30 column at 100°C to be at least 97% pure. The fractions were combined to yield 18.0 g of 7-chloro-1-methylnortricyclene (**1***e*); ir (neat): 3075 and 3010 (cyclopropyl C—H), 1455, 1445, 1310, 1295, 1240, 925, 905, 850, 800, 775; ^{1}H nmr (CCl_4, 100 MHz) δ: 3.65 (d, 1H, J = 1.5 Hz, H—C—Cl), 2.12 and 1.4 (AB pattern, each 1H, J = 10.5 Hz, protons at C-7), 2.03 (broad s, 1H, H-4), 1.40 (m, 2H, protons at C-5), 1.23 (s, 3H, —CH_3), 1.04 (s, 2H, H-1 and H-6).

Cleavage of 7-Chloro-1-methylnortricyclene in Acid Medium

7-Chloro-1-methylnortricyclene (5.47 g, 39 mmol) was dissolved in 75 mL of 0.1 M H_2SO_4 – CH_3COOH and the mixture was heated to 62 ± 2°C under an atmosphere of nitrogen in an oil bath. The progress of the reaction was monitored by analytical glpc on a 1/8 in. × 10 ft, 15% Carbowax column at 180°C and was estimated to be >93% complete after 105 h. The excess acid was quenched with saturated sodium bicarbonate solution and the products were extracted into ether (3 × 350 mL). The combined extracts were washed with water (4 × 100 mL), dried, and concentrated to yield 7.7 g (97%) of chloroacetates. Analytical glpc on a 1/8 in. × 10 ft, 15% Carbowax column at 180°C showed two products in a ratio of 24:76 which did not change through the course of the reaction. To check for decomposition and/or rearrangement of the reaction products during analysis by gas chromatography, the injector and detector block temperatures were altered. There was no significant change of the product ratio as the injector (215 to 130°C), detector (225 to 140°C), and column temperatures (180 to 150°C) were varied.

The two products were isolated by preparative glpc on a 1/4 in. × 10 ft, 15% FFAP column at 150°C and the compound of shortest retention time (13 min) was identified as *anti*-7-chloro-1-methyl-*exo*-2-norbornyl acetate (**3***a*); ir (CS_2): 1740 (C=O), 1380, 1235(s), 1060, 1025, 860(s), 695; ^{1}H nmr (CS_2, 100 MHz) δ: 4.55 (d of d, 1H, J = 8.0 and 3.0, *endo*-2-H), 3.77 (broad s, 1H, *syn*-7-H), 1.89 (s, 3H, —OAc), 0.97 (s, 3H, —CH_3) 2.25–1.00 (m, 7H, norbornyl envelope); ms (70 eV) *m/e* (relative intensity): 202(2), 160(4), 142(11), 124(25), 109(22), 80(100). The compound of longest retention time (15 min) was *syn*-7-chloro-1-methyl-*exo*-2-norbornyl acetate; ir (CS_2): 1740 (C=O), 1375, 1240, 1065, 1030, 860, 695; ^{1}H nmr (CS_2, 100 MHz) δ: 4.51 (t with fine structure, 1H, J = 6 Hz, *endo*-2-H), 3.51 (broad s, 1H, *anti*-7-H), 2.22 (broad s, 1H, H-4), 1.87 (s, 3H, —OAc), 1.02 (s, 3H, —CH_3), 2.02–0.95 (m, 6H, norbornyl envelope); ms (79 eV) *m/e* (relative intensity): 142(10), 107(91), 81(75), 80(100). The molecular ion at *m/e* 202 was discernable only at an ionizing voltage of 10–15 eV.

LAH Reduction of Chloroacetates

To a slurry of lithium aluminum hydride (0.95 g, 25 mmol) and dry ether (50 mL) in a 125 mL flask fitted with a reflux condenser, a calcium chloride drying tube, and a magnetic stirrer, were slowly added 3.28 g (16 mmol) of the mixture of

Can. J. Chem. Downloaded from www.nrcresearchpress.com by 210.87.254.5 on 09/05/12
For personal use only.

Can. J. Chem. Downloaded from www.nrcresearchpress.com by 210.87.254.5 on 09/05/12
For personal use only.

chloroacetates dissolved in dry ether (20 mL). The mixture was refluxed for 3.0 h and cooled. The excess hydride was carefully destroyed with water (3 mL) and the products were extracted into ether (3 × 100 mL). After the ethereal extracts were washed with water (1 × 50 mL), dried, and concentrated, an oily residue (2.5 g, 97%) with a foul odour was obtained. Analytical glpc on a 1/8 in. × 10 ft, 15% Carbowax column at 180°C revealed two products in a ratio of 22:78 which were separable by preparative glpc on a 1/4 in. × 10 ft, 15% FFAP column at 170°C. The product of shortest retention time was collected as a white waxy solid and was identified as *syn*-7-chloro-1-methyl-*exo*-2-norbornanol; ir (CS_2): 3600(OH), 1305, 1265, 1210, 1145, 1095, 1080, 1030, 1015, 980, 940, 860, 830, 805, 770; ^1H nmr (CS_2, 100 MHz, Fig. 1*a*) δ: 3.62 (broad s with fine structure, 1H, *anti*-7-H), 3.35 (broad quintet, 1H, *endo*-2-H), 2.31 (broad s, 1H, H-4), 1.16 (s, 3H, $—CH_3$), 2.03–1.05 (m, 7H, norbornyl envelope and OH). *Anal.* calcd. for $C_8H_{13}OCl$: C 59.81, H 8.10, Cl 22.12; found: C 59.63, H 8.02, Cl 22.28.

The compound of longest retention time was collected as a white waxy solid and identified as *anti*-7-chloro-1-methyl-*exo*-2-norbornanol; ir (CS_2): 3625 (free OH), 3700–3250 (hydrogen bonded OH), 1340, 1310, 1290, 1270, 1235, 1195, 1075, 1005, 965, 905, 840, 740; ^1H nmr (CS_2, 100 MHz, Fig. 1*c*) δ: 3.81 (broad s, 1H, J = 8.0 and 3.0 Hz, *endo*-2-H), 1.05 (s, 3H, $—CH_3$), 2.25–0.75 (m, 7H, norbornyl envelope and OH). *Anal.* calcd. for $C_8H_{13}OCl$: C 59.81, H 8.10, Cl 22.12; found: C 59.68, H 8.13, Cl 21.96.

The *syn*-7-chlorohydrin (0.030 g) was complexed with 0.114 g of $Eu(fod)_3$ in carbon tetrachloride (0.5 mL); ^1H nmr (100 MHz, Fig. 2*a*) δ: 16.7 (broad s, 1H, *endo*-2H), 10.7 (d, 1H, J = 14 Hz, *exo*-3-H), 7.7 (s, 3H, $—CH_3$), 7.1 (s, 1H, *anti*-7-H), 6.1 (dd, 1H, J = 14 and 7 Hz, *endo*-3-H), 5.1 (broad s, 1H, H-4), 3.70 (m, 1H, *endo*-6-H), 3.30–2.80 (m, 3H, *exo*-5-H, *exo*-6-H, and *endo*-5-H).

Similarly, the *anti*-7-chlorohydrin (0.44 g) was complexed with 0.208 g of $Eu(fod)_3$ in carbon tetrachloride (0.5 mL); ^1H nmr (100 MHz, Fig. 2*c*) δ: 17.9 (d, 1H, J = 7 Hz, *endo*-2-H), 12.9 (d, 1H, J = 14 Hz, *exo*-3-H), 12.3 (s, 1H, *syn*-7-H), 7.4 (s, 3H, $—CH_3$), 7.0 (dd, 1H, J = 14 and 7 Hz, *endo*-3-H), 5.1 (broad s, 1H, H-4), 4.5 (t with fine structure, 1H, J = 8 Hz, *endo*-6-H), 4.10–3.25 (m, 3H, *exo*-5-H, *exo*-6-H, and *endo*-5-H).

Oxidation of Chlorohydrins

A mixture (3.0 g) of the chlorohydrins was oxidized by Brown's reagent (21) to a mixture of chloroketones in 95% yield. Analytical glpc on 1/8 in. × 10 ft, 15% Carbowax column at 165°C showed two products in a ratio of 23:77 that were separated by preparative glpc on a 1/4 in. × 10 ft, 15% FFAP column at 140°C. The product of shortest retention time was identified as *anti*-7-chloro-1-methyl-2-norbornanone; ir (CS_2): 1760 (C=O), 1305, 1280, 1090, 1055(s), 1005, 975, 905, 855(s), 800, 740, 615; ^1H nmr (CS_2, 100 MHz) δ: 3.75 (s with fine structure, 1H, *syn*-7-H), 2.58 (m, 1H, H-4), 1.04 (s, 3H, $—CH_3$), 2.35–1.15 (m, 6H, norbornyl envelope); ms (70 eV) *m/e* (relative intensity): M^+ 158(6), 114(12), 81(100). The product of longest retention time was *syn*-7-chloro-1-methyl-2-norbornanone; ir (CS_2): 1760 (C=O), 1340, 1315, 1300, 1265, 1240, 1165, 1130, 1065, 1030, 965, 950, 930, 895, 875, 865, 835, 790, 760; ^1H nmr (CS_2, 100 MHz) δ: 3.98 (m, 1H, *anti*-7-H), 1.06 (s, 3H, $—CH_3$), 2.65–1.45 (m, 7H, norbornyl evelope); ms (70 eV) *m/e*: M^+ 158.

Reduction of Chloroacetates by Sodium in 2-Propanol

The mixture of chloroacetates (0.5 g) was reduced by sodium in 2-propanol as described in the preceding paper (11). Analytical glpc on a 1/8 in. × 10 ft, Carbowax column at 150°C revealed one major product (>95%) that was isolated by preparative glpc on a 1/4 in. × 10 ft, 15% FFAP column at 130°C. It was shown to be 1-methyl-*exo*-2-norbornanol by comparison of its pmr and ir spectra to those of an authentic sample.

Cleavage of 7-Chloro-1-methylnortricyclene in D_2SO_4–CD_3COOD

Into a three-necked flask fitted with a condenser and a calcium chloride drying tube were placed 50 mL of acetic acid-d_4 (Merck, Sharp and Dohme of Canada Ltd., 99.5 at.% *d*) and sulfuric acid-d_2 (0.516 g). Nitrogen gas was slowly bubbled through the solution that was heated to 65 ± 2°C in an oil bath. 7-Chloro-1-methylnortricyclene (2.99 g, 21 mmol) was added to the flask, the mixture was magnetically stirred, and the progress of the reaction was monitored by analytical glpc on a 1/8 in. × 10 ft, 15% Carbowax column at 175°C. After 60 h, the reaction was neutralized with saturated aqueous sodium bicarbonate and the products were extracted into ether. The extracts were washed with water, dried, and concentrated to yield 7.1 g (91%) of deuterated chloroacetates.

LAH Reduction of Deuterated Chloroacetates

The deuterated chloroacetate mixture (4.0 g, 19 mmol) was reduced with lithium aluminum hydride (0.84 g, 22 mmol), as previously described, to 3.0 g (97%) of a mixture of *anti*-7-chloro-1-methyl-*exo*-2-norbornanol-*d* and *syn*-7-chloro-1-methyl-*exo*-2-norbornanol-*d*. The deuterated chlorohydrins were separated by preparative glpc on a 1/4 in. × 10 ft, 25% GE XF-1150 column at 170°C, *syn*-7-chloro-1-methyl-*exo*-2-norbornanol-*d* (0.045 g) was complexed with $Eu(fod)_3$ (0.215 g) in carbon tetrachloride (0.5 mL) and its spectrum recorded. Analysis of the integrals (average of 5) established that deuterium was located in the methyl group (0.05 ± 0.17) and *endo* at C-6 (0.89 ± 0.06). Analysis of this sample by ^2H nmr (Fig. 3*a*) showed that deuterium was located in the methyl group (0.09 ± 0.01) and at C-6 (0.96 ± 0.04).

From the ^1H nmr spectrum of *anti*-7-chloro-1-methyl-*exo*-2-norbornanol-*d* (0.034 g) complexed with 0.192 g of $Eu(fod)_3$ in carbon tetrachloride (0.5 mL) (Fig. 2*d*) the following deuterium distribution was determined: CH_3, 0.10 ± 0.07; *endo*-2-H, 0.15 ± 0.10; *endo*-6-H, 0.94 ± 0.07; H-7, 0.13 ± 0.09. Analysis by ^2H nmr (Fig. 3*b*) gave the following results: CH_3, 0.22 ± 0.02; *endo*-2-H, 0.05 ± 0.01; H-6, 0.88 ± 0.09; H-7, 0.14 ± 0.02.

Oxidation of Deuterated Chlorohydrins

A mixture of *anti*-7-chloro-1-methyl-*exo*-2-norbornanol-*d* and 1-methyl-*syn*-7-chloro-*exo*-2-norbornanol-*d* was oxidized to a mixture of the corresponding chloroketones. After work-up, each ketone was isolated by preparative glpc on a 1/4 in. × 10 ft, 25% GE XF-1150 column at 157°C and assayed for deuterium mass spectrometrically. The deuterated *syn*-7-chloroketone was a composite of 4% d_0, 87% d_1, 9% d_2 species (1.05 excess *d* per molecule) and the *anti*-7-chloroketone was a composite of 5% d_0, 67% d_1, 22% d_2, 6% d_3 species (1.29 excess *d* per molecule).

Kinetic Measurements

In a typical run 0.16 mmol of each nortricyclene and *cis*-decalin, which was used as the internal standard, were dissolved in 0.1 *M* H_2SO_4 – CH_3COOD (10 mL) in a 25 mL round-bottom flask sealed with a serum cap. The mixture was placed in a Haake constant temperature bath maintained at 70.0 ± 0.1°C and after a 15 min equilibration period aliquots (0.4 mL) were withdrawn two at a time at approximately 1.5 h intervals over a period of 25 h. When the aliquots were withdrawn, ether (2 mL) was added and the acid was neutralized by $NaHCO_3$.

Each aliquot was analyzed three times by analytical glpc using a 4 mm × 2 m 3% OV-1 column maintained initially at a temperature of 65°C. After the nortricyclenes and the *cis*-decalin exited, the oven temperature was increased rapidly to 200°C to remove the higher boiling acetates. Peak areas were determined with a Varian Aerograph Model 485 electronic integrator. The pseudo-first-order rate constants were calculated by a least-squares evaluation of a plot of log (peak area nortricyclene/peak

area *cis*-decalin) vs. time. The correlation coefficients were greater than 0.996 and the average error was ±10%. The second order rate constants are 1.96×10^{-4} and 7.59×10^{-4} M^{-1} s^{-1} for **1***b and* **1***e*, respectively.

Acknowledgements

We thank the Natural Sciences and Engineering Research Council of Canada for financial support. We thank Mr. Julius Fulop, holder of a McMaster University Highschool Studentship, for carrying out the kinetic study.

1. C. H. DePuy. Acc. Chem. Res. **1**, 33 (1968).
2. C. J. Collins. Chem. Rev. **69**, 543 (1969).
3. C. C. Lee. Prog. Phys. Org. Chem. **7**, 129 (1970).
4. J. L. Fry and G. J. Karabatsos. *In* Carbonium ions. Vol. 2. *Edited by* G. A. Olah and P. von R. Schleyer. Wiley-Interscience, New York, NY. 1970. Chapt. 4.
5. M. Saunders, P. Vogel, E. L. Hagen, and J. Rosenfeld. Acc. Chem. Res. **6**, 53 (1973).
6. C. H. DePuy. Fortschr. Chem. Forsch. **40**, 73 (1973).
7. J. E. Williams, R. Sustmann, L. C. Allen, and P. von R. Schleyer. J. Am. Chem. Soc. **91**, 1037 (1969).
8. R. Sustmann, J. F. Williams, M. J. S. Dewar, L. C. A. Chen, and P. von R. Schleyer. J. Am. Chem. Soc. **91**, 5350 (1969).
9. H. C. Brown. *In* The non-classical ion problem. Plenum Publishing Corp., New York, NY. 1977.
10. A. Nickon and J. J. Hammons. J. Am. Chem. Soc. **86**, 3322 (1964).
11. N. H. Werstiuk, G. Timmins, and F. P. Cappelli. Can. J. Chem. **58**, 1709 (1980).
12. J. H. Hammons, E. K. Probasco, L. A. Sanders, and E. J. Whalen. J. Org. Chem. **33**, 4493 (1968).
13. B. L. Murr, A. Nickon, J. D. Swartz, and N. H. Werstiuk. J. Am. Chem. Soc. **89**, 1730 (1967).
14. J. M. Jerkunica, S. Borčič, and D. E. Sunko. J. Am. Chem. Soc. **89**, 1732 (1967).
15. C. K. Alden and D. I. Davies. J. Chem. Soc. C, 709 (1968).
16. H. L. Goering and M. J. Degani. J. Am. Chem. Soc. **91**, 4506 (1969).
17. E. W. C. Wong and C. C. Lee. Can. J. Chem. **42**, 1245 (1964).
18. P. Laszlo and P. von R. Schleyer. J. Am. Chem. Soc. **86**, 1171 (1964).
19. J. A. Berson, R. C. Bergman, J. H. Hammons, and A. W. McRowe. J. Am. Chem. Soc. **89**, 2581 (1967).
20. M. A. McKinney and E. L. So. J. Org. Chem. **37**, 2818 (1972).
21. H. C. Brown and C. P. Garg. J. Am. Chem. Soc. **83**, 2952 (1961).

Can. J. Chem. Downloaded from www.nrcresearchpress.com by 210.87.254.5 on 09/05/12
For personal use only.

Solvolysis of specifically deuterated 7-chloro- and 7-bromo-*exo*-2-norbornyl brosylates; unusually large γ-kinetic isotope effects in the absence of σ-participation

NICK HENRY WERSTIUK, GEORGE TIMMINS, AND FRANK PETER CAPPELLI
Department of Chemistry, McMaster University, Hamilton, Ont., Canada L8S 4M1

Received December 5, 1979

NICK HENRY WERSTIUK, GEORGE TIMMINS, and FRANK PETER CAPPELLI. Can. J. Chem. **58**, 1738 (1980).

A series of specifically deuterated *syn*-7-chloro-, *anti*-7-chloro-, *syn*-7-bromo-, and *anti*-7-bromo-*exo*-2-norbornyl brosylates have been prepared and solvolyzed in NaOAc-buffered 80:20 EtOH–H_2O. For solvolysis at 25°C the γ-kinetic isotope effects (KIE's) for *syn*-7-chloro-*exo*-2-norbornyl brosylate-*endo*-6-*d* (**1***e*), *anti*-7-chloro-*exo*-2-norbornyl brosylate-*endo*-6-*d* (**2***c*), *syn*-7-bromo-*exo*-2-norbornyl brosylate-*endo*-6-*d* (**1***f*), *anti*-7-bromo-*exo*-2-norbornyl brosylate-*endo*-6-*d* (**2***d*), *syn*-7-chloro-*exo*-2-norbornyl brosylate-*exo*,*exo*-5,6-d_2 (**1***g*), *anti*-7-chloro-*exo*-2-norbornyl brosylate-*exo*,*exo*-5,6-d_2 (**2***e*) are 1.125 ± 0.007, 1.128 ± 0.005, 1.063 ± 0.008, 1.149 ± 0.020, 1.119 ± 0.011, and 1.115 ± 0.013, respectively. There is no detectable γ-kinetic isotope effect for solvolysis of *anti*-7-chloro-*endo*-2-norbornyl brosylate-*endo*-6-*d* (**3***a*) and the β-KIE for *anti*-7-chloro-*exo*-2-norbornyl brosylate-*exo*-3-*d* (**4***a*) is 1.111 ± 0.011. From a consideration of the possible sources of the unusually large secondary KIE's, we conclude that the *exo*-6-*d* and *endo*-6-*d* γ-KIE's likely are derived from a combination of effects rather than from participation of the C1—C6 bond in the ionization step.

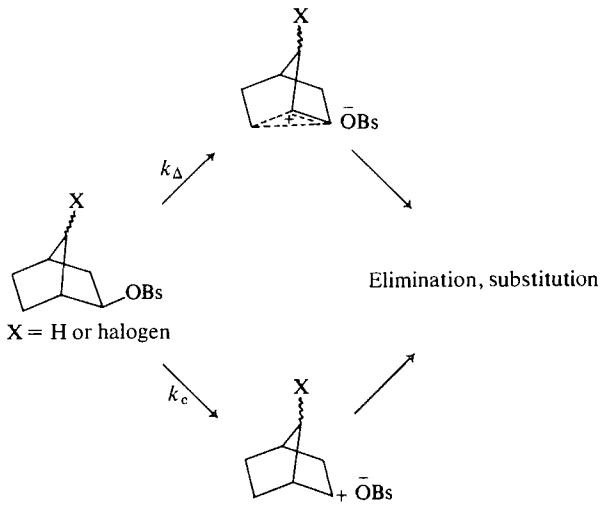
NICK HENRY WERSTIUK, GEORGE TIMMINS et FRANK PETER CAPPELLI. Can. J. Chem. **58**, 1738 (1980).

On a préparé et solvolysé, dans une solution tampon de AcONa 80:20 EtOH–H_2O, les brosylates norbornyl-2-*exo* deutérés de façon spécifique des chloro-7 *syn*, chloro-7 *anti*, bromo-7 *syn* et bromo-7 *anti*. Les effets isotopiques cinétiques γ (EIC) de la solvolyse à 25°C sont respectivement de: 1,125 ± 0,007, 1,128 ± 0,005, 1,063 ± 0,008, 1,149 ± 0,020, 1,119 ± 0,011 et 1,115 ± 0,013 pour les brosylates des chloro-7 *syn* norbornyl-2-*exo* *d*-6-*endo* (**1***e*), chloro-7 *anti* *d*-6-*endo* (**2***c*), bromo-7 *syn* *d*-6-*endo* (**1***f*), bromo-7 *anti* *d*-6-*endo* (**2***d*), chloro-7 *syn* d_2-5,6-*exo*,*exo* (**1***g*) norbornyl-2 *exo*, chloro-7 *anti* d_2-5,6-*exo*,*exo* (**2***e*) norbornyl-2 *exo*. Il n'y a pas d'effet isotopique cinétique γ apparent pour la solvolyse du brosylate du chloro-7 *anti* *d*-6-*endo* norbornyl-2 *endo* (**3***a*) et l'effet isotopique cinétique β du brosylate de chloro-7 *anti* *d*-3-*exo* norbornyl-2 *exo* (**4***a*) est égale à 1,111 ± 0,011. A partir d'une considération des sources probables des effets isotopiques cinétiques secondaires anormalement élevés, nous concluons que les EIC-γ des brosylates *d*-6 *exo* et *d*-6 *endo* proviennent probablement d'une combinaison d'effets plutôt que d'une participation de la liaison C1—C6 à l'étape d'ionisation.

[Traduit par le journal]

Introduction

γ-Kinetic hydrogen isotope effects (KIE's) have been used to probe the nature of transition states and intermediates generated solvolytically (1). Murr and Jerkunica and their co-workers (2, 3) observed unusually large γ-KIE's for solvolysis of *exo*-2-norbornyl brosylate-*exo*-6-*d* (**1***a*) and *exo*-2-norbornyl brosylate-*endo*-6-*d* (**1***b*), and interpreted the results on the basis of an assisted ionization. Our interest in detailing the mechanisms of acid-catalyzed ring opening of nortricyclenes (4) and in the non-classical ion problem (5), led us to determine the γ-KIE's for norbornyl substrates bearing an electron withdrawing group at C-7 to establish more accurately the source of the γ-KIE's. Since the large γ-KIE's are supposedly derived from participation of the C1—C6 bond (2, 3) we reasoned that introduction of a strongly electron withdrawing group at C-7 should reduce the contribution of the k_Δ process (Scheme 1) and thereby reduce the γ-KIE. Since our studies (4, 6) of the ring-opening of 3-halonortricyclenes provided us with ample stocks of *syn*-7-chloro-*exo*-2-norbornanol-*endo*-6-*d* (**1***c*), *syn*-7-bromo-*exo*-2-norbornanol-*endo*-6-*d* (**1***d*), *anti*-7-chloro-*exo*-2-norbornanol-*endo*-6-*d* (**2***a*), and *anti*-7-bromo-*exo*-2-norbornanol-*endo*-6-*d* (**2***b*), it was a simple matter to prepare the corresponding brosylates **1***e*, **1***f*, **2***c*, and **2***d* and determine the solvolytic γ-KIE's.



SCHEME 1

0008-4042/80/161738-13$01.00/0
©1980 National Research Council of Canada/Conseil national de recherches du Canada

Can. J. Chem. Downloaded from www.nrcresearchpress.com by 210.87.254.6 on 09/05/12
For personal use only.

TABLE 1. Hydrogen isotope effects for solvolysis of norbornyl brosylates

Deuterated brosylate	Excess $d^{a,b}$ per molecule	k_H/k_D[a,e,f,g]	(k_H/k_D) 25°C[h]
Syn-7-chloro-*exo*-2-*endo*-6-*d* (**1***e*)	0.985±0.002	1.115±0.007	1.125±0.007
Anti-7-chloro-*exo*-2-*endo*-6-*d* (**2***c*)	0.976±0.004	1.114±0.005	1.120±0.005
Syn-7-bromo-*exo*-2-*endo*-6-*d* (**1***f*)	0.967±0.005	1.055±0.008	1.063±0.008
Anti-7-bromo-*exo*-2-*endo*-6-*d* (**2***d*)	0.977±0.007	1.132±0.020	1.149±0.020
Syn-7-chloro-*exo*-2-*exo*,*exo*-5,6-d_2 (**1***g*)	1.847±0.015	1.109±0.011	1.119±0.011
Anti-7-chloro-*exo*-2-*exo*,*exo*-5,6-d_2 (**2***e*)	1.849±0.002[c]	1.134±0.013	1.150±0.013
Anti-7-chloro-*endo*-2-*endo*-6-*d* (**3***a*)	0.976±0.004	0.983±0.030	1.021±0.030
Anti-7-chloro-*exo*-2-*exo*-3-*d* (**4***a*)	0.936±0.003	1.100±0.011	1.111±0.011
Exo-2-*exo*-6-*d* (**1***a*)		1.09 ±0.01[i]	
Exo-2-*endo*-6-*d* (**1***b*)		1.11 ±0.01[i]	
Endo-2-*exo*-6-*d*		1.00 ±0.02[i]	
Endo-2-*endo*-6-*d*		0.97 ±0.01[i]	

[a]Determined mass spectrometrically at low voltage (10–15 eV). Average of five determinations. Deviations are the standard deviations.
[b]Obtained by analysis of the corresponding ketones.
[c]Obtained by analysis of *anti*-7-chloronorbornene-*exo*,*exo*-5,6-d_2.
[d]The halobrosylates were solvolyzed in 80:20 volume percent ethanol–water buffered by 0.040 *M* sodium acetate.
[e]Average of at least three runs. Deviations are the standard deviations.
[f]Corrected for incomplete deuteration according to the method of Schepple *et al.* (51).
[g]For a discussion of the temperatures at which the solvolyses were carried out see the Experimental. The cell compartment temperatures were 50°, 60.0°, 60.0°, 60.0°, 57.8°, 51.1°, and 57.8°C for **1***e*, **2***c*, **1***f*, **1***g*, **2***e* and **4***a*, respectively. The external bath temperature for **3***a* was 80.0°C.
[h]Isotope effect at 25°C evaluated using the equation $RT/n \ln (k_H/k_D) = \Delta(\Delta F)$ (ref. 12).
[i]See ref. 2.

To complete the study and to establish a point of comparison with the parent *exo*-brosylates, **1***a* and **1***b*, we prepared *syn*-7-chloro-*exo*-2-norbornyl brosylate-*exo*,*exo*-5,6-d_2 (**1***g*), *anti*-7-chloro-*exo*-2-norbornyl brosylate-*exo*,*exo*-5,6-d_2 (**2***e*), *anti*-7-chloro-*endo*-2-norbornyl brosylate-*endo*-6-*d* (**3***a*), *anti*-7-chloro-*exo*-2-norbornyl brosylate-*exo*-3-*d* (**4***a*), and determined the KIE's in buffered (0.04 *M* NaOAc) 80:20 EtOH–H_2O.

Surprisingly, we find the γ-KIE's for 7-halo-*exo*-brosylates **1***e*, **1***g*, **2***c*, **2***d*, and **2***e* to be slightly larger than the γ-KIE's for the parent *exo* substrates and the γ-KIE for *syn*-7-bromo-*exo*-brosylate **1***f* is less than the KIE for brosylate **1***b* (Table 1). Also, as in the case of *endo*-2-norbornyl tosylate, the γ-KIE for *anti*-7-chloro-*endo*-2-brosylate **3***a* is negligibly small. In this paper we expand on a preliminary account of our work (7) and give a detailed interpretation of the results.

Results

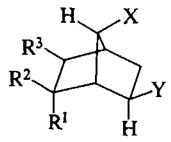
Preparation of Substrates

The chloro and bromobrosylates **1***e*, **1***f*, **2***c*, and **2***d* were prepared from the corresponding deuterated chlorohydrins and bromohydrins **1***c*, **1***d*, **2***a*, and **2***b* that were obtained via acid-catalyzed ring-opening of 3-chloro- and 3-bromonortricyclene (6). That the deuterium in **1***c*, **1***d*, **2***a*, and **2***b* was at least 90% stereochemically pure *endo* at C-6 was established by nmr and ir spectroscopy. The non-deuterated chlorohydrins were synthesized by the method of Roberts *et al.* (8) and the bromohydrins were prepared from bromoacetates obtained by the acid-catalyzed ring opening of 3-bromonortricyclene (6). To prepare *syn*-7-chloro-*exo*-2-norbornyl brosylate-*exo*,*exo*-5,6-d_2 (**1***g*), we converted norbornene-*endo*,*endo*-5,6-d_2 (9) into deuterated chlorohydrin **1***h* and brosylated the chlorohydrin. The synthesis of *anti*-7-chloro-*exo*-2-norbornyl brosylate-*exo*,*exo*-5,6-d_2 (**2***e*) began with a $LiAlD_4$ reduction of acetoxynorbornadiene (10) that yielded *anti*-7-norbornenol-*exo*,*exo*-5,6-d_2 (**5***a*). Conversion of the dideuterated norbornenol to *anti*-7-chloronorbornene-*exo*,*exo*-5,6-d_2 (**5***b*) (11), followed by hydroboration and brosylation, gave **2***e*. That the deuterium was at least 90% stereochemically pure *exo* was established by ^1H nmr. To prepare the chlorohydrins **3***b* and **3***d*, the precursors of the deuterated and nondeuterated *endo*-2-brosylates **3***a* and **3***c*, chloroketones **6***a* and **6***b* were reduced by lithium tri-*tert*-butoxyaluminum hydride to a 92:8 mixture of the *endo*- and *exo*-chlorohydrins, and the *endo*-chlorohydrin was isolated by preparative glpc. *Anti*-7-chloro-*exo*-2-norbornanol-*exo*-3-*d* (**4***b*), the precursor of brosylate **4***a*, was prepared by deuteroboration of *anti*-7-norbornenyl chloride. To insure that the deuterium was located specifically *exo* at C-3, a ^1H nmr study using $Eu(fod)_3$ was carried out as described in the Experimental. The deuterium content of each brosylate, based on the analysis of the corresponding ketone, is listed in Table 1.

Kinetic Measurements

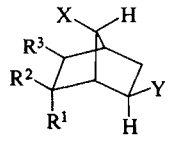
Simultaneous solvolyses of deuterated and non-

Can. J. Chem. Downloaded from www.nrcresearchpress.com by 210.87.254.6 on 09/05/12
For personal use only.



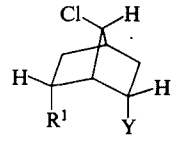
1

a $R^1 = R^3 = X = H, R^2 = D, Y = OBs$
b $R^1 = D, R^2 = R^3 = X = H, Y = OBs$
c $R^1 = D, R^2 = R^3 = H, X = Cl, Y = OH$
d $R^1 = D, R^2 = R^3 = H, X = Br, Y = OH$
e $R^1 = D, R^2 = R^3 = H, X = Cl, Y = OBs$
f $R^1 = D, R^2 = R^3 = H, X = Br, Y = OBs$
g $R^1 = H, R^2 = R^3 = D, X = Cl, Y = OBs$
h $R^1 = H, R^2 = R^3 = D, X = Cl, Y = OH$
i $R^1 = R^2 = R^3 = H, X = Cl, Y = OBs$
j $R^1 = R^2 = R^3 = H, X = Br, Y = OBs$



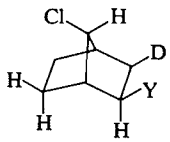
2

a $R^1 = D, R^2 = R^3 = H, X = Cl, Y = OH$
b $R^1 = D, R^2 = R^3 = H, X = Br, Y = OH$
c $R^1 = D, R^2 = R^3 = H, X = Cl, Y = OBs$
d $R^1 = D, R^2 = R^3 = H, X = Br, Y = OBs$
e $R^1 = H, R^2 = R^3 = D, X = Cl, Y = OBs$
f $R^1 = H, R^2 = R^3 = D, X = Cl, Y = OH$
g $R^1 = R^2 = R^3 = H, X = Cl, Y = OBs$
h $R^1 = R^2 = R^3 = H, X = Br, Y = OBs$



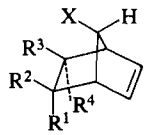
3

a $R^1 = D, Y = OBs$
b $R^1 = D, Y = OH$
c $R^1 = H, Y = OBs$
d $R^1 = H, Y = OH$



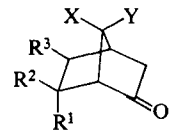
4

a Y = OBs
b Y = OH



5

a $R^1 = R^4 = H, R^2 = R^3 = D, X = OH$
b $R^1 = R^4 = H, R^2 = R^3 = D, X = Cl$



6

a $R^1 = D, X = Cl, Y = H$
b $R^1 = H, X = Cl, Y = H$
c $R^1 = D, X = H, Y = Cl$
d $R^1 = H, R^2 = R^3 = D, X = H, Y = Cl$
e $R^1 = D, R^2 = R^3 = H, X = Cl, Y = H$
f $R^1 = R_2 = R_3 = H, X = Cl, Y = H$
g $R^1 = D, R^2 = R^3 = H, X = Cl, Y = H$
h $R^1 = D, R^2 = R^3 = H, X = H, Y = Br$
i $R^1 = D, R^2 = R^3 = H, X = Br, Y = H$

deuterated brosylates were carried out in 80:20 (volume percent) EtOH–H_2O buffered by 0.04 *M* sodium acetate in a temperature-controlled cell compartment of a Cary Model 14 ultraviolet spectrophotometer. First-order rate constants and the standard deviations for the *exo*-brosylate solvolyses were calculated from sets of $-\ln(A_t - A_\infty)$ and time data by means of a linear least-squares analysis. Since A_∞ for *endo*-brosylates **3***a* and **3***c* could not be determined because of long half-lives, first-order rate constants were determined by computer-fitting the absorbance and time data to an exponential curve of the form $A_t = Be^{-kt} + C$. To check the accuracy of the curve fitting procedure the experimental values of A_t for solvolysis of the *exo*-brosylates were similarly fitted to the exponential curve. Since the A_∞'s and the rate constants obtained by curve-fitting the data for *exo* solvolyses were in excellent agreement with those obtained directly, we are confident that the *endo* rate constants obtained by the curve-fitting method are also accurate. Representative first-order plots for the simultaneous solvolysis of the pairs of brosylates **1***i* and **1***i*, **1***e* and **1***i*, and **2***d* and **2***h* are given in Figs. 1(*a*), 1(*b*), and 1(*c*), respectively. The isotope effects are listed in Table 1 and Table 2 lists the relative percent yields of the products of solvolysis of the 7-chloro- and 7-bromo-*exo*-2-brosylates. Because the extended reaction time led to decomposition of products we were unable to obtain an accurate product analysis for the *endo*-brosylates **3***a* and **3***c*.[1]

Discussion

Solvolysis of a norbornyl sulfonate ester is describable by a modified Winstein ion pair scheme (Scheme 2) which includes the possibility for a 1,2-alkyl shift ((k_R^I) or hydride shift (k_{HS}^I) at the intimate ion pair (IIP) stage. If nonclassical rather than classical ions are intermediates the scheme is simplified somewhat because species IV and VI generated by a 1,2-alkyl shift need not be considered. While internal return ($k_{-1} \neq 0$) occurs when *exo*-norbornyl substrates are solvolyzed, external return does not occur ($k_{-2} = 0$) and substitution takes place at the solvent separated ion pair (SSIP) stage

[1]Gassman and Hornback (13) found that 3-chloronortricyclene (7%), *syn*-7-chloro-*exo*-2-norbornyl acetate (11%), *anti*-7-chloro-*exo*-2-norbornyl acetate (69%), and *exo*-5-chloro-*exo*-2-norbornyl acetate (8%) are the major products of acetolysis of *anti*-7-chloro-*endo*-2-norbornyl tosylate after 10% reaction.

Can. J. Chem. Downloaded from www.nrcresearchpress.com by 210.87.254.6 on 09/05/12
For personal use only.

Can. J. Chem. Downloaded from www.nrcresearchpress.com by 210.87.254.6 on 09/05/12
For personal use only.

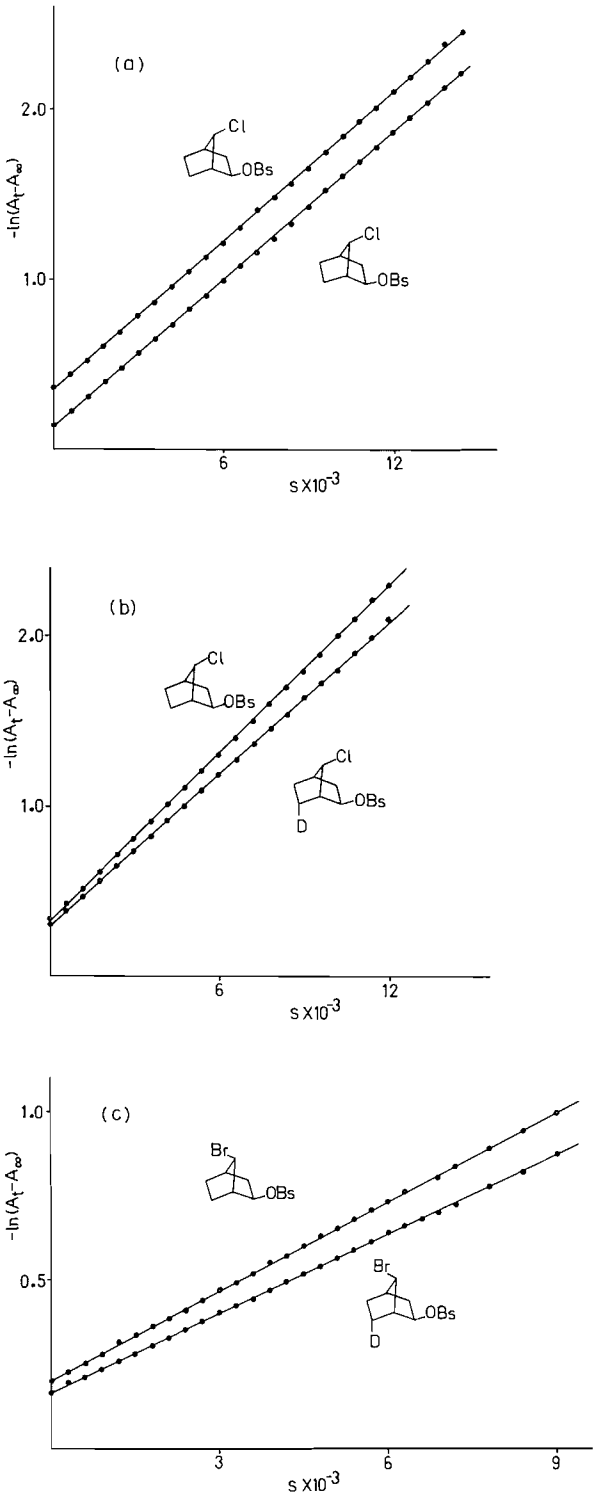


FIG. 1. (*a*) First-order plots of the simultaneous solvolysis of *syn*-7-chloro-*exo*-2-norbornyl brosylate. (b) *Syn*-7-chloro-*exo*-2-norbornyl brosylate and *syn*-7-chloro-*exo*-2-norbornyl brosylate-6-*endo*-*d*. (c) *Anti*-7-bromo-*exo*-2-norbornyl brosylate and *anti*-7-bromo-*exo*-2-norbornyl brosylate-6-*endo*-*d*.

(14). External return does not occur when *endo* substrates are solvolyzed, and, since racemic *exo* products are formed (15), substitution also occurs predominately at the SSIP stage. It is clear then that the destruction of IIP's is rate determining in norbornyl solvolyses and in order to interpret the unusually large γ-deuterium isotope effects observed for the solvolysis of *exo*-norbornyl and 7-halo-*exo*-norbornyl brosylates it is imperative to establish which processes contribute to the rate-determining destruction of IIP's and to establish whether or not hydrogen isotope effects on the processes contribute to the observed KIE's. To that end, the following questions must be addressed. Since halonortricyclenes are significant products (Table 2) of the solvolysis of 7-halonorbornyl substrates, is elimination (k_E^1) from the IIP rate determining? Does participation of the *endo* hydrogen at C-6 occur during ionization? Does a rate determining hydride shift (k_{HS}^1) occur at the IIP stage to form a separated ion pair which is instantaneously scavenged by solvent? And, finally, if the γ-KIE is solely due to a change in C—H force constants as a result of participation of the C1—C6 bond, is the partition isotope effect (PIE), $(k_{1H}/k_{-1D})/(k_{2H}/k_{-2D})$ significant (16)?

Elimination

While a number of recent reports have documented the correlation between rate-determining 1,2-elimination and β-KIE's (17–24), up to the present there have been no reports of comparable studies involving bicyclic systems which yield cyclopropanes by 1,3-elimination. Where 1,2-elimination at the IIP stage is considered to be one of the rate-controlling steps, unusually large β-KIE's are associated with substantial yields of alkene. Also the variation of the β-KIE correlates with the amount of elimination which is usually controlled by solvent nucleophilicity (22). In general, elimination occurs at the IIP stage when a proton is abstracted by an adjacent fairly basic leaving group in non-nucleophilic polar solvents (24). On the other hand, when elimination occurs from SSIP's there is no correlation between the β-KIE's and the extent of elimination. Such is the case when 7-methyl-7-norbornyl tosylate[2] (22) and *tert*-butyl chloride[3] (18, 25, 26) are solvolyzed. In the former case (22) the authors suggested that

[2]Isotope effects (k_H/k_{D_3}) of 1.94, 1.84, 2.10, and 2.00 were observed in HOAc (78% elim), 80% EtOH–H_2O (65%), 97% TFE–H_2O (62%), and 80% TFE–H_2O (51%) respectively.

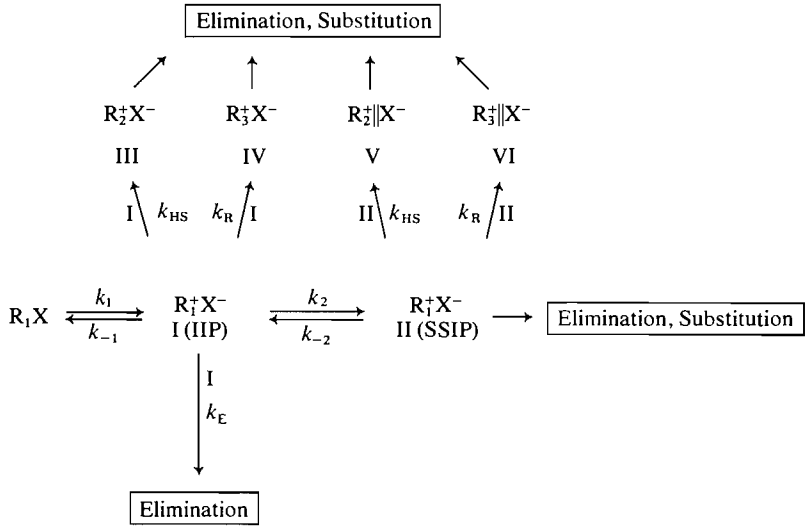
[3]Isotope effects $(k_H/k_{D_3})^{\frac{1}{3}}$ of 1.378, 1.356, 1.33, 1.34, 1.34, 1.35, and 1.32 were observed in 70% TFE–H_2O (17%) and 54% EtOH–H_2O (8.3%), 63% HOAc–H_2O (13.2%), 48% 2-propanol–H_2O (8.1%), 51% pyridine–H_2O (12.8%), and 29% HOAc–HCOOH (11.8%), respectively.

Can. J. Chem. Downloaded from www.nrcresearchpress.com by 210.87.254.6 on 09/05/12
For personal use only.

TABLE 2. Relative percent yields of solvolysis products[a]

Brosylate	Δ	*Syn*-OEt	*Anti*-OEt	*Syn*-OH	*Anti*-OH	Other
Syn-7-chloro-*exo*-2- (**1***i*)[b]	30	24	11	23	8	4
Syn-7-chloro-*exo*-2-*endo*-6-*d* (**1***e*)	20	31	10	30	8	1
Anti-7-chloro-*exo*-2- (**2***g*)[b]	21	5	36	4	29	5
Anti-7-chloro-*exo*-2-*endo*-6-*d* (**2***c*)	13	4	40	3	33	7
Syn-2-bromo-*exo*-2- (**1***i*)	25	37	12	22	1	3
Syn-7-bromo-*exo*-2-*endo*-6-*d* (**1***f*)	18	39	10	28	2	4
Anti-7-bromo-*exo*-2- (**2***h*)	10	9	48	5	20	8
Anti-7-bromo-*exo*-2-*endo*-6-*d* (**2***d*)	7	8	56	5	16	7
Syn-7-chloro-*exo*-2- (**1***i*)[b]	35	21	11	19	11	3
Syn-7-chloro-*exo*-2-*exo*,*exo*-5,6-d_2 (**1***g*)	20	27	11	25	17	0
Anti-7-chloro-*exo*-2- (**2***g*)[b]	20	7	39	5	23	6
Anti-7-chloro-*exo*-2-*exo*,*exo*-5,6-d_2 (**2***e*)	22	6	38	4	23	7
Anti-7-chloro-*exo*-2- (**2***g*)[b]	19	7	40	5	22	7
Anti-7-chloro-*exo*-2-*exo*-3-*d* (**4***a*)	28	7	36	5	18	6

[a]The relative percent yields were determined by electronic integration of peak areas and are averages of at least four determinations. The average error was ±10%.
[b]Since the product ratios were determined for different runs, the results give an indication of the reproducibility of the experiments.



SCHEME 2

elimination from the IIP was not significant because the tosylate anion is a weak base.

Since solvolysis of a 7-halonorbornyl brosylate yields a weakly basic anion remote from the *exo* and *endo* hydrogens at C-6, the proximity effect that facilitates 1,2-elimination at the IIP stage is not important in norbornyl solvolyses unless there is movement of the anion at the IIP stage. That *syn*-7-chloro-*exo*-2-norbornyl tosylate isomerizes appreciably to the *anti*-tosylate during acetolysis (27) shows that the tosylate anion is mobile at the IIP stage in acetic acid. In our case, however, that there is no detectable curvature of the *syn*-halobrosylate rate plots (Figs. 1(*a*) and (*b*)) establishes that there is no build-up of the least reactive *anti*-halobrosylates during solvolysis. Hence, movement of the brosylate anion does not occur in 80:20 EtOH–H_2O that is more nucleophilic than HOAc.

It may be argued that acetate ion, present at a concentration of 0.04 *M*, acts as a base. However, since Winstein *et al.* (28) determined that nortricyclene is only a minor product (5%) of solvolysis of *exo*-norbornyl tosylate in acetic acid containing 0.1 *M* KOAc, 0.04 *M* acetate is not expected to promote elimination at the IIP stage in a nucleophilic solvent such as 80:20 EtOH–H_2O.

That there is no correlation between the γ-KIE's and the extent of 1,3-elimination from the *syn*- and *anti*-halobrosylates (Table 3) is characteristic of the tertiary systems (*vide supra*) where elimination oc-

Can. J. Chem. Downloaded from www.nrcresearchpress.com by 210.87.254.6 on 09/05/12
For personal use only.

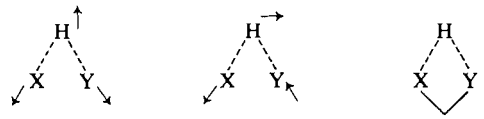
TABLE 3. γ-KIE's and relative percent yields of halonortricyclenes

Brosylates	γ-KIE	Relative % yield of halonortricyclenes: Non-deuterated brosylate	Relative % yield of halonortricyclenes: Deuterated brosylate
1*i*, **1***e*	1.115±0.007	35	20
2*g*, **2***c*	1.114±0.005	21	13
1*j*, **2***f*	1.055±0.008	25	18
2*h*, **2***d*	1.132±0.020	10	7

curs predominantly at the SSIP stage. That 1,3-elimination of a proton occurs at the SSIP stage and therefore is not rate determining is also supported by the fact that the γ-KIE's for *exo* and *endo* deuterium at C-6 are identical. If, in fact, rate determining elimination was the major source of the γ-KIE's, since the *endo* hydrogen (deuterium) is lost preferentially (Table 4) with an isotope effect of 1.5–1.8,[4,5] the γ-KIE's for the *endo* deuterated 7-halo-*exo*-brosylates **1***e*, **1***f*, **2***c*, and **2***d* should be greater than KIE's of **1***g* and **2***e* because the latter effects would only be related to an α-effect of less than 1.2. Furthermore, acetolysis of *anti*-7-chloro-*endo*-2-norbornyl tosylate (13), for which we expect the γ-KIE to be negligibly small based on our results for **3***a*, yields 3-chloronortricyclene (7%) as a major product (13).

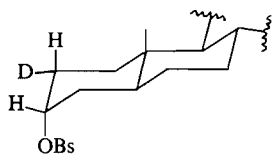
Hydrogen Participation

Participation of the *endo* hydrogen at C-6 in the ionization step is also a possibility because the edge-protonated nortricyclene may approach the classical or bridged ions in stability.[6] Although there are no documented examples of 1,3-hydrogen participation, 1,2-participation seems well established and manifests unusually large solvolytic β-KIE's (32–35) which are considered to be small primary KIE's. The β-KIE's are small primary KIE's for two reasons. The transition states are not linear and bond cleavage at the migration origin is compensated by bond formation at the migration terminus. According to O'Ferrall's (36) model for 1,2-hydrogen participation, both the symmetric *I*($v_R^{\ddagger}$) and asymmetric *II* ($v_L^{\ddagger}$) modes are sensitive to the isotopic mass of the migrating group but quite insensitive to transition state asymmetry, unlike $v_R^{\ddagger}$ and $v_L^{\ddagger}$ for linear transition states. Since the isotope effects for E-1 1,2-elimination, 1,2-hydride shifts, and 1,2-hydrogen participation all fall in the same range (1), the transition states for these processes must be similar in structure. That the isotope effects for E-1 1,3-elimination (29, 32) fall in



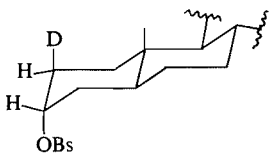
I($v_R^{\ddagger}$) II($v_L^{\ddagger}$) III

the range of the isotope effects for 1,2-elimination strongly indicates that 1,3-processes involving transition states or intermediates of the type III are describable on the same basis as 1,2-processes.[7] Therefore, we expect an isotope effect of 1.5–2 for 1,3 (6,2)-hydrogen participation. As in the case of rate-determining 1,3-elimination (*vide supra*) if there is no 1,3-hyperconjugative stabilization of the developing norbornyl cation by the *exo*-C—H bond at C-6, the solvolytic *endo* γ-KIE should be larger than the *exo* γ-KIE because the latter effect would be related only to an α-effect of less than 1.2. That 1,2-elimination and 1,2-hydrogen participation exhibit β-KIE's which are of the α-type has been established by Tarle *et al.* (33) who determined the solvolytic β-KIE's for the 3-α-cholestanyl brosylates **13** and **14**. The large β-KIE exhibited by **14** is due to 1,2-hydrogen participation and rate determining 1,2-elimination. The KIE observed for **13** results from an α-type effect on the two processes and a hyperconjugative component.



k_H/k_D = 1.130±0.019

13



k_H/k_D = 1.599±0.013

14

[4]We assume here that there is no selective homohyperconjugative stabilization of the *exo*-transition state by the *exo*-C—H bond at C-6.

[5]Since the elimination isotope effect (k_H/k_D) is defined by the ratio

$$\left(\frac{\%\Delta}{\%\text{ other products}}\right)_H \Big/ \left(\frac{\%\Delta}{\%\text{ other products}}\right)_D$$

(29) the elimination KIE's are 1.78, 1.71, 1.58, and 1.52 for the *syn*-7-chloro, *anti*-7-chloro, *syn*-7-bromo, and *anti*-7-bromo-*exo*-2-brosylates, respectively.

[6]It has been established that the activation energy for 6,2-hydride shift in the norbornyl system is 5.9 kcal per mole (31). Thus for the edge protonated species to be a significant intermediate, a stabilization of approximately 6 kcal must result from C—H participation in the 7-halo systems.

[7]It is also possible that 1,3 (6,2)-elimination and 6,2-shifts occur basically from a classical ion via very similar transition states. That 1,3 (6,2)-elimination occurs in preference to 1,2 (3,2)-elimination, that 6,2-hydride shifts occur more readily than 3,2-shifts, that loss of an *endo* hydrogen is preferred, and that the stereochemistry of the 6,2-shift is *endo–endo*, provide support for such a hypothesis in the case of the norbornyl system.

Can. J. Chem. Downloaded from www.nrcresearchpress.com by 210.87.254.6 on 09/05/12
For personal use only.

TABLE 4. Deuterium content of halonortricyclenes and fractional percent deuterium losses

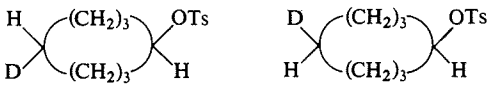
Halobrosylate (excess d per molecule)	Halonortricyclene[a] $\%d_0$	$\%d_1$	$\%d_2$	Excess d per molecule	Fractional % deuterium loss
1*e* (0.98)	78[c]	22	0	0.22	77.6
2*c* (0.97)	77	23	0	0.23	76.3
1*f* (0.97)	62	38	0	0.38	59.8
2*d* (0.97)	68	31	1	0.33	64.8
1*g* (1.85)	7	9	84	1.77	3.9
2*e* (1.82)	7	4	89	1.81	0.5

[a]The halonortricyclenes were isolated from large scale solvolyses (0.2–1 g) in 35–50 mL of solvent.
[b]Rounded to the nearest 0.01 d.
[c]Rounded to the nearest unit.

Since the γ-KIE's for the 7-chlorobrosylates **1***e*, **1***g*, **2***c*, and **2***e* are much less than 1.5 and they are identical within experimental error, a k_Δ process involving the *endo* hydrogen at C-6 cannot be the sole source of the solvolytic γ-KIE's. In this respect it is interesting to note that Parker and Watt (38) have established that the KIE's for solvolysis of 5-deuterated cyclooctyl tosylates **15** and **16** depend on the orientation of the deuterium relative to the leaving group (see also ref. 37). A 1,5-hydride shift occurs during solvolysis and a *trans*-1,5-shift is preferred over a *cis*-1,5-shift by 10:1. Based on the assumption that the participation isotope effect should be in the range of 1.5–3.0 they interpreted the results on the basis of a 50–20% fractional involvement of a k_Δ process involving the *trans* hydrogen.[8] It is conceivable that a fraction of the solvolysis of the 7-halo-*exo*-2-brosylates **1***e*, **1***f*, **1***g*, **2***c*, **2***e*, and **2***d* also occurs by participation of the *endo* hydrogen at C-6. It is interesting to note that the isotope effect for **16**, related to an α-effect, is less than the primary KIE for hydrogen participation in the case of **15**.

6,2-Hydride Shifts

As is shown in Table 2 the halohydrins and ethers formed via a 6,2-hydride shift constitute 10–20% of the solvolysis products. This result indicates that 6,2-shifts occur to the same extent as in the solvolysis of other *exo*-norbornyl substrates (29, 30, 39–41). If classical (**16**) or non-classical (**17**) intermediates are involved and a 6,2-hydride shift occurs at the IIP stage to yield an ion pair which reacts at a diffusion controlled rate with solvent, a primary KIE, estimated to be around 1.5, could contribute to the observed KIE (Scheme 3). As in the case of 1,3 (6,2)-elimination and 1,3 (6,2)-hydrogen participation (*vide supra*) it is difficult to account for the *exo* isotope effect on that basis unless selective homohyperconjugative stabilization of the *exo* transition state by the *exo*-C—H bond also occurs during ionization.

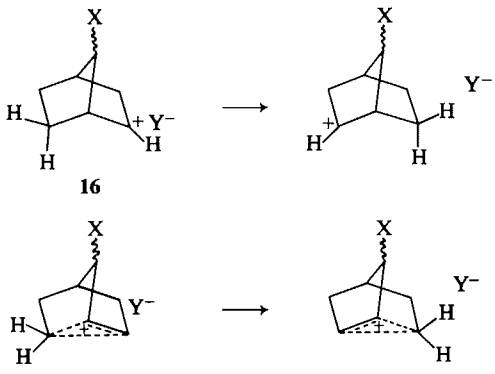


$k_H/k_D = 1.124 \pm 0.008$ **15**

$k_H/k_D = 1.044 \pm 0.010$ **16**

Ionization Isotope Effect

That *exo*-2-norbornyl brosylates and tosylates solvolyses are characterized by unusually large γ-KIE's[9] has been taken as evidence that solvolysis is assisted (2, 3). If solvolysis of an *exo* substrate indeed leads to a non-classical cation, then alkyl migration isotope effects should serve as good models for the solvolytic γ-KIE because the bonding in the non-classical ion (**20**) and the transition



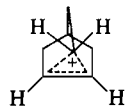
SCHEME 3

[8]An attractive alternative source of the KIE's not discussed by Parker (38) involves a rate determining 1,5-hydride shift at the IIP stage to form a separated ion pair that reacts at a diffusion controlled rate with solvent. The KIE's for the 1,5-shift would be similar to the KIE's for the k_Δ process.

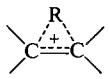
[9]While Murr *et al.* (2) have reported that the KIE's for solvolysis of the 6-*exo*-*d* and 6-*endo*-*d*-*exo*-brosylates are identical within experimental error in 80:20 ethanol–water (1.09 ± 0.03 and 1.11 ± 0.01) and in acetic acid (1.09 ± 0.01 and 1.11 ± 0.01), Jerkunica *et al.* (3) have reported that the *exo* KIE (1.149 ± 0.016) is somewhat larger than the *endo* KIE in acetic acid (1.097 ± 0.011). The source of this difference is not obvious.

Can. J. Chem. Downloaded from www.nrcresearchpress.com by 210.87.254.6 on 09/05/12
For personal use only.

states for alkyl migration (**21**) should be similar. The results of several important studies which bear on this point have been published recently. Shubert and LeFevre (42) established that the migrational isotope effect for acid-catalyzed rearrangement of 1,1-diphenyl-2-methyl-1,2-propanediol (**22**) is 1.064 per deuterium and Vitullo and Logue (43) reported that the migrational KIE for acid-catalyzed rearrangement of 4,4-dimethylcyclohexadiene (**23**) is 1.077 per deuterium. Also, Winnik *et al.* (44) showed that the KIE for benzyl migration in the Baeyer–Villiger oxidation of 1-phenyl-2-propanone is 1.034 per deuteron and suggested that the transition state for migration was product-like. In our view it is reasonable to assume that the average

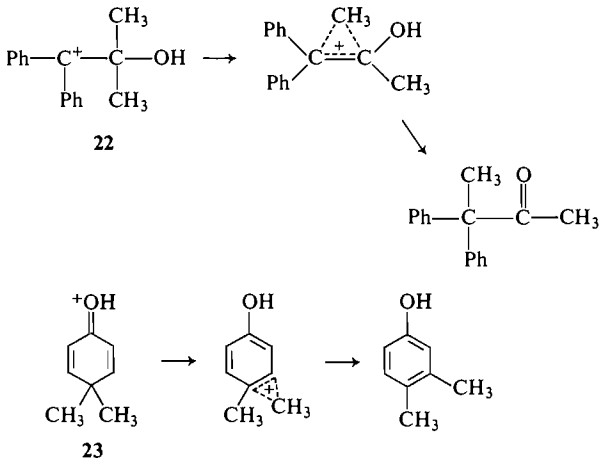


20



21

of the methyl migrational KIE's (1.07) is a good measure of the maximum KIE because the methyl group should be approximately half-transferred in both transition states. Since maximum change of C—H force constants at C-6 of the norbornonium ion is achieved when the ion is fully formed and the transition state of its formation lies approximately midway between substrate and the ion, a γ-KIE much less than 1.07 of perhaps 1.02–1.04 per deuterium would be expected for assisted solvolysis. Clearly, the γ-KIE's observed for **1***e*, **1***f*, **1***g*, **2***c*, **2***d*, and **2***e* are not in accord with this ex-



22

23

pectation. Furthermore, the halogen at C-7 would reduce the contribution of a k_Δ pathway (Scheme 1), should such a process be involved in *exo* solvolysis, because charge would develop at C-1. Although Goering and Degani (27) suggest that nonclassical ions are involved as intermediates in the acetolysis of 7-chloro-*exo*-2-norbornyl tosylates, they state that the low yield (~2%) of 3-chloro-2-norbornyl acetates is probably due to the low cationic character at C-1 because of the inductive effect of the adjacent chlorine atom. Consequently, if the γ-KIE's are derived from γ-participation, the KIE's for **1***e*, **1***f*, **1***g*, **2***c*, and **2***e* should be smaller than the KIE's for **1***a* and **1***b*. Again, this expectation is not borne out by our experiments. That charge development at C-1 would result in a destabilization of the 7-halocations is supported by the work of Goering and Degani (27) who showed that the 7-chloronorbornyl tosylates are 250 times more reactive solvolytically than *exo*-3-chloro-*exo*-2-norbornyl tosylate.

It is interesting to note that the β-KIE for solvolysis of *anti*-7-chloro-*exo*-2-norbornyl brosylate-*exo*-3-*d* (**4***e*), within experimental error, is identical to the β-KIE for solvolysis of *exo*-2-norbornyl brosylate-*exo*-3-*d* (KIE = 1.11 ± 0.01) in 80:20 EtOH–H_2O (45). This provides support for our view that the 7-halo-*exo*-2- and *exo*-2-norbornyl brosylates solvolyse by similar mechanisms.

Conclusions

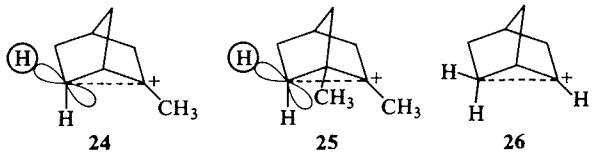
It appears from our analysis, that 1,3 (6,2)-elimination and/or 6,2-hydride shifts at the IIP stage and *endo*-hydrogen participation individually or in combination, cannot account for the large γ-KIE's observed for the solvolysis of 7-halo-*exo*-2-norbornyl brosylates. From an analysis based on methyl migrational KIE's and the fact that the halogen at C-7 should reduce the contribution of a k_Δ process, it is clear also that the unusually large γ-KIE's observed for **1***e*, **1***f*, **1***g*, **2***c*, **2***d*, and **2***e* cannot be derived from participation of the C1—C6 bond.

In our view there are two possible sources of the large γ-KIE's. It is conceivable that the isotope effects are equal within experimental error because of a fortuitous combination of isotope effects derived from several sources. While the *exo* isotope effect may be a combination of a primary isotope effect due to 1,3 (6,2)-participation of the *exo*-C—H bond and an α-effect derived from 1,3 (6,2)-elimination and/or a 6,2-hydride shift at the IIP stage, the *endo* KIE can result from 1,3 (6,2)-elimination and/or a 6,2-shift at the IIP stage. With respect to 1,3-participation of the *exo*-C—H bond, Olah and co-workers (31, 46) found that the *exo* proton at C-6 of the norbornyl cations **25** and **26** is deshielded and stated that a 1,3 (6,2)-interaction was responsible for the effect. Since participation of the *exo*-C—H bond in the ionization step and 1,3

Can. J. Chem. Downloaded from www.nrcresearchpress.com by 210.87.254.6 on 09/05/12
For personal use only.

(6,2)-elimination and/or 6,2-shifts at the IIP stage can occur only when *exo* substrates are solvolyzed, our hypothesis is consistent with the γ-KIE's observed for the *exo*- and *endo*-brosylates.

A 1,3 carbon interaction, as described recently by Bauld *et al.* (47), is a possible alternative source of the unusually large γ-KIE's. Such an interaction between C-2 and C-6 in the norbornyl cation, as represented by **26**, would very nicely account for



24 **25** **26**

the observed KIE's because the *exo-d* and *endo-d* effects would be expected to be identical and independent of the substituent at C-7. That the 1,3 (6,2)-carbon interaction is predicted to be most pronounced for ionization of an *exo* substrate (47) is in keeping with the fact that the *exo* KIE's are larger than the *endo* KIE's. It is possible that the interaction between the *syn* groups in the bromobrosylate 1*f* distorts the 2.2.1-system, reduces the degree of 6,2-carbon interaction in the transition state, and thereby lowers the γ-KIE.

Experimental

General

Nuclear magnetic resonance spectra were recorded on Varian T-60, A-60, and HA-100 spectrometers with tetramethylsilane (TMS) as the internal standard. Samples were dissolved in either carbon tetrachloride or carbon disulfide and chemical shifts are expressed in parts per million downfield from internal tetramethylsilane. Infrared spectra were recorded on Perkin Elmer 337 and Beckman IR-5 infrared spectrometers and the samples were dissolved in carbon tetrachloride or carbon disulfide. Spectra were calibrated with a polystyrene thin film and peak positions are expressed in cm^{-1}. Ultraviolet spectra were recorded on a Cary spectrophotometer Model 14. Mass spectra were recorded on a Hitachi-Perkin-Elmer RMU-6A spectrometer at 80 eV and deuterium assays were performed at 10–15 eV. Analytical gas liquid partition chromatograms (glpc's) were obtained on a Varian Aerograph Model 204B dual column analytical gas chromatograph equipped with dual flame ionization detectors using helium as the carrier gas. The helium flow rate was usually 20–30 mL/min. Product ratios were determined by an Aerograph Model 485 electronic digital integrator. Preparative gas liquid partition chromatography was carried out on a Varian Aerograph Model A-90-P gas chromatograph equipped with a thermal conductivity detector at a helium flow rate of 50–60 mL/min. Melting points were recorded on a Kofler hot-stage apparatus and are uncorrected. Boiling points are also uncorrected. Pentane was stirred vigorously over fuming sulfuric acid, washed with sodium bicarbonate solution, dried, and distilled. Dry ether refers to ether that was distilled from lithium aluminum hydride. Pyridine was refluxed over barium oxide for 48 h and distilled. All solutions were dried with either anhydrous sodium sulfate or magnesium sulfate. Microanalyses were performed by Galbraith Laboratories, Inc., Knoxville, TN.

Preparation of Brosylates

In a typical brosylation reaction, the chlorohydrin or bromohydrin was dissolved in dry pyridine and the solution was cooled in an ice bath. A 10–20% mole excess of freshly recrystallized brosyl chloride (mp 73–74°C), recrystallized from petroleum ether (30–60°C), was slowly added to the ice-cold solution of chlorohydrin which was placed in the refrigerator at 0°C for at least one week. The brosylation of the *syn*-bromohydrin required two weeks. The product was isolated in the following manner. Several small pieces of ice were added to the solution and the reaction vessel was allowed to warm to room temperature. After the ice had melted, the solution was diluted with water and extracted with chloroform. The combined extracts were washed successively with cold water, cold dilute hydrochloric acid, saturated bicarbonate solution, cold water, and dried. After the solvent was removed under reduced pressure, the solid or oil which remained was decolorized with carbon and then recrystallized from a suitable solvent system. Crude yields of 80–95% were usually obtained.

Deuterium Assay

Since both the deuterated halohydrins and their corresponding halobrosylates gave weak parent ions when analyzed by mass spectrometry, the determination of deuterium content of these compounds by this method was not reliable. Therefore, we determined the deuterium content mass spectrometrically by analyzing the corresponding deuterated haloketones which were obtained by oxidation of the deuterated halohydrins.

Syn-*7-chloro*-exo-*2-norbornyl Brosylate (1i)*

The brosylate was recrystallized from pentane–ether and had the following characteristics: mp 112–113°C; ir (CS_2): 1375, 1350, 1315, 1190, 1100, 1075, 1040, 1020, 970, 940, 895, 875, 825, 775, 750, 640, 620, 600, 550; nmr (CS_2, 100 MHz) δ: 7.63 (m, 4H, arom), 4.50 (m, 1H, *endo*-2-H), 3.76 (broad s with fine structure, 1H, *anti*-7-H), 2.43 and 2.28 (broad s, each 1H, bridgeheads), 2.20–1.10 (m, 6H, norbornyl envelope). *Anal.* calcd. for $C_{13}H_{14}SO_3Br$: C 42.69, H 3.83; found: C 42.57, H 3.84.

Syn-*7-chloro*-exo-*2-norbornanol*-endo-6-d *(1c)*

The deuterated chlorohydrin was prepared by LAH reduction of *syn*-7-chloro-*exo*-2-norbornyl trideuteroacetate-*endo*-6-*d* that was obtained from the electrophilic cleavage of 3-chloronortricyclene in deuterated medium (6). A small sample of the chlorohydrin was oxidized to **6***c* and deuterium was assayed mass spectrometrically: 3.33 ± 0.02% d_0, 95.01 ± 0.21% d_1, 1.67 ± 0.24% d_2; 0.985 ± 0.002 excess deuterium atoms per molecule.

Syn-*7-chloro*-exo-*2-norbornyl Brosylate*-endo-6-d *(1e)*

The brosylate **1***e* had the following properties: mp 112–112.5°C; ir (CS_2): 1360, 1300, 1190(s), 1100, 1070, 1040, 1015, 970, 935, 890, 820, 775(s), 635, 610, 595, 550; nmr (CCl_4, 100 MHz) δ: 7.68 (m, 4H, arom), 4.60 (m, 1H, *endo*-2-H), 3.79 (broad s, 1H, *anti*-7-H), 2.50 and 2.30 (broad s, each 1H, bridgeheads), 2.20–1.05 (m, 5H, norbornyl envelope).

Norbornene-exo,exo-*5,5*-d_2

Norbornadiene (50.0 g, 0.54 mol) was dissolved in methanol (75 mL), 3 g of palladium on powdered charcoal (10% catalyst) were added and the mixture was treated with deuterium gas (13.2 L, 0.54 mol, 700 Torr) (48). A similar run was performed and the solutions were combined and filtered. Water (300 mL) was added and the products were extracted into pentane (3 × 300 mL). After the extracts were washed with water (2 × 50 mL) and dried, the organic solvent was removed by distillation through a 70 cm glass column filled with glass helices. Short path distillation of the products into a flask cooled by Dry Ice yielded 100 g of waxy solid. Analytical glpc on 1/8 in. × 10 ft 5% SE-30

Can. J. Chem. Downloaded from www.nrcresearchpress.com by 210.87.254.6 on 09/05/12
For personal use only.

column at 60°C showed that the reaction mixture consisted of 12% norbornadiene, 71% norbornene-*exo*,*exo*-5,6-d_2, and 17% norbornane-d_4.

Syn-7-exo-*2-dibromonorbornane*-endo,endo-*5,6*-d_2

To 100 g of the mixture, dissolved in methylene chloride (300 mL) and pyridine (70 mL) and cooled in an ice-water bath, was slowly added bromine (161 g, 1.0 mol) in methylene chloride (50 mL) over a period of three hours. After the addition was complete, the organic layer was washed with dilute sodium thiosulfate solution (2 × 100 mL), water (2 × 100 mL), dilute hydrochloric acid (10%, 2 × 70 mL), saturated sodium bicarbonate solution (100 mL), and water (2 × 100 mL). The organic layer was dried and methylene chloride was removed by distillation through a 30 cm glass column filled with glass helices. Distillation of the pot residue through a 30 cm vacuum jacketed Vigreux column afforded 24 g of deuterated 3-bromonortricyclene and 53.2 g of *syn*-7-*exo*-2-dibromonorbornane-*endo*,*endo*-5,6-d_2; bp 80–85°C/0.7 Torr (lit. (49) bp 70–74°C/0.25–0.30 Torr). Redistillation of the fraction afforded 42.0 g of dibromide of bp 80–83°C/0.7 Torr; nmr (CCl_4, 100 MHz) δ: 3.90 (m, 2H, *anti*-7-H and *endo*-2-H), 2.70–2.10 (m, 4H, *exo*-3-H, *endo*-3-H, H-1 and H-4), 1.65 (broad s, 2H, *exo*-5-H and *exo*-6-H). It was noted that isomerization of the dibromide occurred during analysis by glpc if the injector and detector block temperatures were kept above 160°C.

Syn-7-*bromonorbornene*-endo,endo-*5,6*-d_2

Syn-7-*exo*-2-dibromonorbornane-*endo*,*endo*-5,6-d_2 (35.6 g, 139 mmol) was dissolved in a saturated solution of potassium *tert*-butoxide in *tert*-butanol (1 *M*, 350 mL) and the mixture was refluxed for 33 h on a steam bath. The brown solution was poured into water (350 mL) and extracted with pentane (3 × 300 mL). After the extracts were washed with water (150 mL), dilute hydrochloric acid (10%, 100 mL), saturated sodium bicarbonate solution (100 mL), water (2 × 100 mL), and dried, pentane was removed by distillation through a 30 cm Vigreux column. The brown oily residue which remained was vacuum distilled to yield 17.0 g (70%) of *syn*-7-bromonorbornene-*endo*,*endo*-5,6-d_2 of bp 67–68°C/20 Torr; nmr (CCl_4, 100 MHz) δ: 5.95 (s with fine structure, 2H, H-2 and H-3), 3.79 (s, 1H, *anti*-7-H), 2.95 (m, 2H, H-1 and H-4), 1.72 (broad s, 2H, *exo*-5-H and *exo*-6-H), 1.10 (m, 0.08H, *endo*-5-H and *endo*-6-H). The integrals showed that the deuterium at C-5 and C-6 was at least 90% stereochemically pure *endo*.

Norbornene-endo,endo-*5,6*-d_2

Syn-7-bromonorbornene-*endo*,*endo*-5,6-d_2 (17.0 g, 97 mmol) and tri-*n*-butyl tin hydride (85.9 g, 0.30 mol) were sealed in a thick walled glass tube under vacuum. After being heated over a steam bath for 36 h, the tube was opened and its contents were poured into a 250 mL three necked flask which was connected to three gas dispersion bottles. The first bottle was empty, the second contained water, and the third contained sodium hydroxide pellets. The flask was heated gently with a heat gun and nitrogen gas was bubbled directly through the reaction mixture. At the outlet of the three gas dispersion bottles, 7.0 g (75%) of norbornene-*endo*,*endo*-5,6-d_2 were collected in a receiver cooled by Dry Ice. Its nmr spectrum was identical to the spectrum reported previously (9); nmr (CCl_4, 100 MHz) δ: 5.90 (t, 2H, H-2 and H-3), 2.80 (m, 2H, H-1, and H-4), 1.55 (broad s with fine structure, 2H, *exo*-5-H and *exo*-6-H), 1.31 and 1.04 (d with fine structure, 1H each, J = 8 Hz, *syn*-7-H and *anti*-7-H). Deuterium was assayed mass spectrometrically (1.90 excess deuterium atoms per molecule).

Syn-7-*chloro*-exo-*2-norbornanol*-exo,exo-*5,6*-d_2 *(1h)*

Hypochlorous acid prepared from hydrochloric acid (10%, 10 mL) and sodium hypochlorite (40 mL) was vigorously stirred with norbornene-*endo*, *endo*-5,6-d_2 (0.74 g, 8.0 mmol) at 0°C for 24 h. (8). Deuterated 3-chloronortricyclene and *syn*-7-chloro-*exo*-2-norbornanol-*exo*,*exo*-5,6-d_2 (**1***h*), the major products, were isolated by preparative glpc on a 1/4 in. × 10 ft 15% FAPP column at 150°C. Deuterium in 3-chloronortricyclene was assayed mass spectrometrically: 5% d_0, 35% d_1, 61% d_2 species; 1.57 excess *d* per molecule: **1***h*; nmr (CS_2, 100 MHz) δ: 3.85 (m, 1H, *anti*-7-H), 3.62 (broad m, 1H, *endo*-2-H), 2.30 (d, 1H, H-4), 2.25 (broad s, 1H, H-1), 2.00 (broad s, 1H, —OH), 1.90 (m, 2H, *exo*-3-H and *endo*-3-H), 1.11 (broad s with fine structure, 2H, *endo*-5-H and *endo*-6-H). The chloroketone **6***d* obtained from **1***h* by oxidation was assayed for deuterium mass spectrometrically; 4.67 ± 0.18% d_0, 5.99 ± 0.02% d_1, 89.40 ± 0.48% d_2 species, 1.847 ± 0.015 excess deuterium atoms per molecule.

Syn-7-*chloro*-exo-*2-norbornyl Brosylate*-exo,exo-*5,6*-d_2 *(1g)*

Syn-7-chloro-*exo*-2-norbornyl brosylate-*exo*,*exo*-5,6-d_2 prepared from **1***h* had a mp 112–113°C; nmr (CCl_4, 100 MHz) δ: 7.64 (m, 4H, arom), 4.52 (m, 1H, *endo*-2-H), 3.75 (broad s with fine structure, 1H, *anti*-7-H), 2.43 and 2.26 (broad s, each 1H, bridgeheads), 2.15–1.70 (m, 2H, *exo*-3-H), 1.15 (s, 2H, *endo*-5-H and *endo*-6-H).

Anti-7-*chloro*-exo-*2-norbornanol*

Anti-7-chloro-*exo*-2-norbornanol was prepared by treatment of norbornene with hypochlorous acid as reported by Roberts *et al.* (8), by LAH reduction of *anti*-7-chloro-*exo*-2-norbornyl acetate that was obtained from electrophilic (CH_3CO_2H, H_2SO_4) cleavage of 3-chloronortricyclene (6), and by hydroboration of *anti*-7-chloronorbornene (11) that was prepared from *anti*-7-norbornenol.

Hydroboration of anti-7-*chloronorbornene*

Anti-7-chloronorbornene was hydroborated and the organoborane was treated with alkaline hydrogen peroxide according to the published procedure (27) to give a 95% yield of *anti*-7-chloro-*exo*-2-norbornanol. The product was shown to be homogeneous by analytical glpc on a 1/8 in. × 10 ft 3% GE-XF1150 column at 155°C.

Anti-7-*chloro*-exo-*2-norbornyl Brosylate (2g)*

Anti-7-chloro-*exo*-2-norbornyl brosylate recrystallized from 1:2 ether – petroleum ether (30–60°C) had a mp 69.5–71.0°C; ir (CS_2): 1375, 1190(s), 1180, 1100, 1075, 1065, 1015, 970, 940, 920, 890, 870, 825, 780, 605, 550; nmr (CCl_4, 11 MHz) δ: 7.75 (m, 4H, arom), 4.47 (m, 1H, *endo*-2-H), 4.16 (broad s, 1H, *syn*-7-H), 2.42 and 2.30 (broad s, each 1H, bridgeheads), 2.05–1.60 and 1.20 (m, 6H, norbornyl envelope). *Anal.* calcd. for $C_{13}H_{14}SO_3Br$: C 42.69, H 3.83; found: C 42.72, H 3.88.

Anti-7-*chloro*-exo-*2-norbornanol*-endo-*6*-d *(2a)*

Anti-7-chloro-*exo*-2-norbornyl trideuteroacetate-*endo*-6-*d* obtained by electrophilic cleavage of 3-chloronortricyclene in deuterated medium (6) was reduced by LAH in ether to *anti*-7-chloro-*exo*-2-norbornanol-*endo*-6-*d* (**2***a*); ir (CS_2): 3600, 1310, 1280, 1265, 1225, 1085, 1070, 1030, 995, 940, 910, 870, 850, 815, 805, 785, 700; nmr (CCl_4, 100 MHz) δ: 4.18 (s with fine structure, 1H, *syn*-7-H), 3.75 (dd, 1H, J = 7.5 and 2.5 Hz, *endo*-2-H), 2.23 and 2.11 (broad s, each 1H, bridgeheads), 2.00–1.00 (m, 6H, norbornyl envelope and —OH). A small sample of the chlorohydrin was oxidized to chloroketone **6***e* and deuterium was assayed mass spectrometrically; 3.81 ± 0.01% d_0, 95.04 ± 0.18% d_1, 1.15 ± 0.18% d_2 species; 0.976 ± 0.004 excess deuterium atoms per molecule.

Anti-7-*chloro*-exo-*2-norbornyl Brosylate*-endo-*6*-d *(2c)*

The deuterated chlorobrosylate had a mp 71–72°C; ir (CS_2): 1320, 1310, 1190(s), 1100, 1070, 1055, 1015, 980, 965, 935, 915, 890, 870(s), 825, 790, 740, 700, 640, 625, 605, 550; nmr (CCl_4, 100 MHz) δ: 7.76 (s, 4H, arom), 4.46 (m, 1H, *endo*-2-H), 4.15 (s,

Can. J. Chem. Downloaded from www.nrcresearchpress.com by 210.87.254.6 on 09/05/12
For personal use only.

1H, *syn*-7-H), 2.40 and 2.30 (broad s, each 1H, bridgeheads), 2.00–1.79 and 1.15 (m, 5H, norbornyl envelope).

Anti-*7-norbornenol*-exo,exo-*5,6*-d_2 (*5a*)

7-Acetoxynorbornadiene (20 g, 0.13 mol) was reduced by LAD (6.0 g, 0.14 mol) in dry ether (125 mL) under an atmosphere of nitrogen. After 4.5 h at room temperature a paste of sodium sulfate (dried at 150°C for 3 days) and deuterium oxide was carefully added to the reaction mixture until gas was no longer evolved. The mixture was stirred overnight (13 h) and then the inorganic salts were filtered off. The ethereal layer was separated and the aqueous phase was extracted with ether (3 × 50 mL). After the combined organic layers were washed with water, solvent was removed by distillation through a 30 cm glass column filled with glass helices to yield *anti*-7-norbornenol-*exo*,*exo*-5,6-d_2 (48, 50).

Anti-*7-chloronorbornene*-exo,exo-*5,6*-d_2 (*5b*)

Anti-7-chloronorbornene-*exo*,*exo*-5,6-d_2 was prepared in 50% yield by treatment of *anti*-7-norbornenol-*exo*,*exo*-5,6-d_2 with thionyl chloride according to the literature method (11); nmr (CCl_4, 100 Mz) δ: 6.00 (t, 2H, J = 2 Hz, H-2 and H-3), 3.67 (s with fine structure, 1H, *syn*-7-H), 2.70 (m, 2H, H-1 and H-4), 2.00 (m, 0.12 H, *exo*-5-H and *exo*-6-H), 0.98 (s, 2H, *endo*-5-H and *endo*-6-H). Integration showed that deuterium at C5 and C6 was at least 90% stereochemically pure *exo*. Deuterium was assayed mass spectrometrically: 7.36 ± 0.02% d_0, 3.40 ± 0.33% d_1, 89.40 ± 0.43% d_2 species; 1.849 ± 0.002 excess deuterium atoms per molecule.

Anti-*7-chloro*-exo-*2-norbornanol*-exo,exo-*5,6*-d_2 (*2f*)

Hydroboration of *anti*-7-chloronorbornene-*exo*,*exo*-5,6-d_2 (*5b*) with subsequent oxidation by alkaline hydrogen peroxide (27) gave 90% of *anti*-7-chloro-*exo*-2-norbornanol-*exo*,*exo*-5,6-d_2 (*2f*) that was purified by preparative glpc on a 1/4 in. × 10 ft 25% GE XF-1150 column at 180°C; nmr (CCl_4, 100 MHz) δ: 4.16 (broad s with fine structure, 1H, *syn*-7-H), 3.75 (dd, 1H, J = 7 and 3 Hz, *endo*-2-H), 2.24 (d, 1H, J = 4 Hz, H-4), 2.11 (broad s, 1H, H-1), 2.06 (s, 1H, —OH), 1.75 (dd, 1H, J = 7 and 13 Hz, *endo*-3-H), 1.40 (d of d, 1H, J = 3 and 13 Hz, *exo*-3-H), 1.05 (broad s, 2H, *endo*-5-H and *endo*-6-H).

Anti-*7-chloro*-exo-*2-norbornyl Brosylate*-exo,exo-*5,6*-d_2 (*2e*)

Anti-7-chloro-*exo*-2-norbornyl brosylate-*exo*,*exo*-5,6-d_2 recrystallized from 1:2 ether – petroleum ether (30–60°C) had a mp 69–70°C; nmr (CCl_4, 100 MHz) δ: 7.65 (s, 4H, arom), 4.45 (dd, 1H, J = 4 and 6 Hz, *endo*-2-H), 4.10 (broad s with fine structure, 1H, *syn*-7-H), 2.39 (broad s, 1H, H-1), 2.27 (m, 1H, H-4), 1.75 (m, 2H, *exo*-3-H and *endo*-3-H), 1.11 (s, 2H, *endo*-5-H and *endo*-6-H).

Anti-*7-chloro*-exo-*2-norbornanol*-exo-*3*-d (*4b*)

Into a three necked flask fitted with a magnetic stirrer, condenser, addition funnel, drying tube, and nitrogen inlet were placed *anti*-7-chloronorbornene (3.0 g, 16 mmol), diglyme (7 mL, distilled from lithium aluminum hydride) and sodium borodeuteride (0.34 g, 8 mmol). Freshly distilled boron trifluoride etherate (1.4 g, 10 mmol) dissolved in diglyme (6 mL) was slowly added to the flask at room temperature and then the mixture was stirred for 3 h. Water (20 mL) was added to the reaction mixture followed by sodium hydroxide (3 *N*, 7 mL) and hydrogen peroxide (33%, 7 mL). After the solution was stirred for 14 h, it was extracted with ether (4 × 30 mL), the combined ether extracts were washed with water (3 × 20 mL), and dried. A 90% yield (2.1 g) of *anti*-7-chloro-*exo*-2-norbornanol-*exo*-3-*d* (*4b*) was obtained; nmr (CCl_4, 100 MHz) δ: 4.19 (broad s, 1H, *syn*-7-H), 3.77 (d, 1H, J = 7 Hz, *endo*-2-H), 2.60 (broad s, 1H, —OH), 2.26 and 2.14 (broad s, each 1H, bridgeheads), 2.05–1.70 and 1.10 (m, norbornyl envelope).

The position of deuterium was verified by complexation of non-deuterated and deuterated chlorohydrins with $Eu(fod)_3$. When 0.134 g of $Eu(fod)_3$ was complexed with 0.034 g of *anti*-7-chloro-*exo*-2-norbornanol in carbon tetrachloride (0.5 mL), most of the proton resonances were separated from each other: nmr (CCl_4, 100 MHz) δ: 16.90 (d, 1H, J = 7 Hz, *endo*-2-H), 12.40 (s, 1H, *syn*-7-H), 1084 (broad d with fine structure, 1H, J = 4 Hz, *exo*-3-H), 10.25 (broad s, 1H, H-1), 6.38 (dd, 1H, J = 7 and 14 Hz, *endo*-3-H), 5.10 (broad s, 1H, H-4), 3.80–3.00 (m, 4H, H-5 and H-6). Complexation of *anti*-7-chloro-*exo*-2-norbornanol-*exo*-3-*d* (0.037 g) with $Eu(fod)_3$ (0.160 g) in carbon tetrachloride (0.5 mL, mole ratio LSR/alcohol = 0.61) and subsequent analysis by nmr spectroscopy revealed that the *exo* proton (σ 11.20) at C-3 was absent; nmr (CCl_4, 100 MHz) δ: 17.90 (d, 1H, J = 7 Hz, *endo*-2-H), 12.90 (s, 1H, *syn*-7-H), 10.80 (broad s, 1H, H-1), 6.60 (d, 1H, J = 7 Hz, *endo*-3-H), 5.17 (broad s, 1H, H-4), 4.00–3.00 (m, 4H, H-5 and H-6). The resonance due to *endo*-3-H (δ: 6.60) appeared as a doublet due to loss of geminal coupling with *exo*-3-H.

A small sample of *4b* was oxidized to *anti*-7-chloro-2-norbornanone-*exo*-3-*d* and the deuterium was assayed mass spectrometrically: 6.58 ± 0.01% d_0, 93.52 ± 0.21% d_1, 0.10 ± 0.23% d_2 species; 0.936 ± 0.003 excess deuterium per molecule.

Anti-*7-chloro*-exo-*2-norbornyl Brosylate*-exo-*3*-d (*4a*)

The deuterated chlorobrosylate had the following properties: mp 70–71°C; nmr (CCl_4, 100 MHz) δ: 7.70 (s, 4H, arom), 4.45 (d, 1H, J = 7 Hz, *endo*-2-H), 4.13 (broad s, 1H, *syn*-7-H), 2.41 and 2.29 (broad s, each 1H, bridgeheads), 2.15–1.80 (m, 3H, *exo*-5-H, *exo*-6-H, and *endo*-3-H), 1.15 (m, 2H, *endo*-5-H, and *endo*-6-H).

Anti-*7-chloro-2-norbornanone* (*6f*)

The chloroketone *6a* was obtained via electrophilic (CH_3CO_2H, H_2SO_4) cleavage of 3-chloronortricyclene as previously reported (6).

Lithium Tri-tert-*butoxyaluminum Hydride Reduction of* Anti-*7-chloro-2-norbornanone*

Anti-7-chloro-2-norbornanone (0.61 g, 4 mmol) in tetrahydrofuran (20 mL) was added to a stirred solution of lithium tri-*tert*-butoxyaluminum hydride (1.3 g, 5 mmol) in tetrahydrofuran (15 mL). The yellow solution was refluxed and after 7.5 h it was estimated by analytical glpc that the reaction was >95% complete. Water (50 mL) and dilute hydrochloric acid (10%, 20 mL) were added to the reaction mixture and the products were extracted into ether (4 × 50 mL). The combined ethereal extracts were washed with water (50 mL), saturated bicarbonate solution (50 mL), water (50 mL), and dried. Evaporation of solvent under reduced pressure left a white solid (0.56 g). Analytical glpc analysis on a 1/8 in. × 10 ft 3% GE XF-1150 column at 155°C revealed that *anti*-7-chloro-*endo*-2-norbornanol (92%) and *anti*-7-chloro-*exo*-2-norbornanol (8%) were present. A pure sample of *anti*-7-chloro-*endo*-2-norbornanol (*3d*) had a mp 83–84°C (lit. (49) mp 84–86°C); nmr (CCl_4, 100 MHz) δ: 4.00 (quintet with fine structure, 1H, *exo*-2-H), 3.70 (broad s with fine structure, 1H, *syn*-7-H), 2.83 (s, 1H, —OH), 2.25–0.85 (m, 8H, norbornyl envelope).

Anti-*7-chloro*-endo-*2-norbornyl Brosylate* (*3c*)

The chlorobrosylate purified by recrystallization from ether – petroleum ether 30–60°C (1:2) had a mp 49–51°C; nmr (CCl_4, 100 MHz) δ: 7.70 (m, 4H, arom), 4.75 (quintet with fine structure, 1H, *exo*-2-H), 3.80 (broad s, 1H, *syn*-7-H), 2.50–1.20 (m, 8H, norbornyl envelope). *Anal.* calcd. for $C_{13}H_{14}SO_3Br$: C 42.69, H 3.83; found: C 42.83, H 3.79.

Anti-*7-chloro-2-norbornanone*-endo-*6*-d (*6g*)

The deuterated chloroketone *6g* was prepared from the corre-

Can. J. Chem. Downloaded from www.nrcresearchpress.com by 210.87.254.6 on 09/05/12
For personal use only.

sponding acetate which was obtained via electrophilic (CD_3CO_2D–D_2SO_4) cleavage of 3-chloronortricyclene as previously reported (6). Mass spectrometric analysis established that the sample contained 0.976 ± 0.004 excess deuterium atoms per molecule.

Lithium Tri-tert-*butoxaluminum Hydride Reduction of* Anti-*7-chloro-2-norbornanone*-endo-*6*-d

The deuterated chloroketone (0.50 g) was reduced to the chlorohydrin by the method previously described. A pure sample of *anti*-7-chloro-*endo*-2-norbornanol-*endo*-6-d was isolated by preparative glpc on a 1/4 in. × 10 ft 25% GE XF-1150 column at 160°C; nmr (CCl_4, 100 MHz) δ: 4.00 (multiplet, 1H, *exo*-2-H), 3.70 (broad s with fine structure, 1H, *syn*-7-H), 2.52 (s, 1H, —OH), 2.20–0.85 (m, 7H, norbornyl envelope).

Anti-*7-chloro*-endo-*2-norbornyl Brosylate*-endo-*6*-d *(3a)*

The chlorobrosylate had a mp 48–50°C; nmr (CCl_4, 100 MHz) δ: 7.70 (m, 4H, arom), 4.75 (quintet with fine structure, 1H, *exo*-2-H), 3.80 (s, 1H, *syn*-7-H), 2.50–1.25 (m, 7H, norbornyl envelope).

Syn-*7-bromo*-exo-*2-norbornyl Brosylate (1j)*

Syn-7-bromohydrin (0.18 g, 90% pure) obtained via the acid-catalyzed ring-opening of 3-bromonortricyclene (6) was converted to 0.086 g of brosylate that exhibited a mp of 122–123°C after three recrystallizations from ether; nmr (CS_2, 100 MHz) δ: 7.63 (narrow m, 4H, arom), 4.48 (dd with fine structure, 1H, *endo*-2-H), 3.73 (narrow m, 1H, *anti*-7-H), 2.46 (broad m, 1H, H-1), 2.28 (broad m overlapped norbornyl envelope, H-4), 2.3–1.0 (norbornyl envelope).

Syn-*7-bromo*-exo-*2-norbornanol-6*-endo-d *(1d)*

The deuterated bromohydrin was prepared by LAH reduction of *syn*-7-bromo-*exo*-2-norbornyl acetate-6-*endo-d* that was obtained by electrophilic cleavage of 3-bromonortricyclene in deuterated medium (6). A small sample of the bromohydrin was oxidized to ***6h*** and deuterium was assayed mass spectrometrically: 4.27 ± 0.18% d_0, 94.03 ± 0.42% d_1, 1.71 ± 0.24% d_2 species; 0.967 ± 0.005 excess deuterium atoms per molecule.

Syn-*7-bromo*-exo-*2-norbornyl Brosylate-6*-endo-d *(1f)*

Deuterated *syn*-bromohydrin (0.90 g) (6) was converted into 0.096 g of brosylate of mp 123–124°C after three recrystallizations from pentane–ether. Its nmr (CS_2, 100 MHz) was similar to that of **1*j*** (*vide supra*), the only differences being a simplification of the norbornyl envelope from σ 2.3–0.10 and a significant decrease in intensity of the signal in the region of σ 1.1.

Anti-*7-bromo*-exo-*2-norbornyl Brosylate (2h)*

The bromohydrin (0.14 g) obtained via the acid catalyzed ring-opening of 3-bromonortricyclene (6) was converted into 0.076 g of brosylate that exhibited a mp of 76–77°C after three recrystallizations from pentane–ether; nmr (CS_2, 100 MHz) δ: 7.65 (sharp s, 4H, arom), 4.39 (dd, 1H, *endo*-2-H), 4.03 (sharp m, 1H, *syn*-7-H), 2.26 (broad m, 2H, H-1 and H-4), 3.1–0.9 (norbornyl envelope).

Anti-*7-bromo*-exo-*2-norbornanol-6*-endo-d *(2b)*

The deuterated bromohydrin was prepared by LAH reduction of *anti*-7-bromo-*exo*-2-norbornyl acetate-6-*endo-d* that was obtained by electrophilic cleavage of 3-bromonortricyclene in deuterated medium (6). A small sample was oxidized to ***6i*** and deuterium was assayed mass spectrometrically: 5.63 ± 0.12% d_0, 92.48–0.28% d_1, 1.90 ± 0.20% d_2 species; 0.977 ± 0.007 excess deuterium atoms per molecule.

Anti-*7-bromo*-exo-*2-norbornyl Brosylate-6*-endo-d *(2h)*

Anti-7-bromo-*exo*-2-norbornanol-*endo*-6-*d* (0.065 g) was converted into 0.057 g of brosylate that exhibited a mp of 75–76°C after three recrystallizations from pentane–ether; nmr (CS_2, 100 MHz) δ: 7.65 (sharp s, 4H, arom), 4.40 (dd, 1H, *endo*-2-H), 4.05 (sharp m, 1H, *syn*-7-H), 2.28 (broad m, 2H, H-1 and H-4), 2.1–1.0 (norbornyl envelope). Its nmr spectrum was similar to that of the non-deuterated brosylate, the major difference being a reduction of the signal at σ 1.1.

Kinetic Measurements

Solvolyses were carried out in 80:20 EtOH–H_2O containing 0.04 *M* sodium acetate. Water was refluxed in potassium permanganate for several hours and distilled five times and ethanol was purified by two distillations. An ultraviolet spectrum of the solvent mixture did not reveal any interfering absorptions. Solvolysis isotope effects were obtained by simultaneously observing the solvolysis of the non-deuterated and deuterated substrates spectrophotometrically in a Cary Model 14 spectrophotometer. By circulating water from a Haake Model NBe bath through the temperature controlled cell compartment, the desired temperature and temperature control were achieved during the kinetic runs. At the start of a kinetic run several Pasteur pipettes, each wrapped with aluminum foil, and three sample cells were placed in the cell compartment to equilibrate with the temperature of the cell compartment for at least 10 h. Before a solvolysis run was initiated, the appropriate brosylates were purified by recrystallization and kept under a vacuum at room temperature for 0.5 h. The brosylates (2–3 mg) were weighed into 2 mL volumetric flasks that were then equilibrated in the water bath for 0.5 h. Solvent (2 mL) that also was equilibrated to the bath temperature was rapidly transferred into two volumetric flasks containing the brosylates, the flasks were vigorously shaken in order to ensure complete solution, and allowed to equilibrate in the water bath for 5 min. Each solution was rapidly transferred, with insulated Pasteur pipettes, into a 1.00 cm cell in the compartment of the spectrophotometer. After 10 min, readings were taken at an absorbance maximum initially at 5 min intervals by running the pen and chart paper from 10 s before to 10 s after the minute. As the rate decreased readings were taken at 10 min intervals and then at 20 min intervals. The cells were switched simply by shutting off the recorder and manually manipulating the cell carriage. The slit controls were shut off during a run to avoid fluctuations. Absorbance readings were taken for at least three half-lives. A check of the zero reading on the instrument after the infinity reading (10 half-lives) generally revealed a negligible baseline drift of less than ±0.003 of an absorbance unit. The rate data which usually consisted of 20–30 sets of data points were subjected to a least-squares analysis to evaluate the slopes and standard deviation in the slopes. Changes in absorbance as a function of time were monitored for *anti*-7-chlorobrosylate at 276 nm and for *syn*-7-chlorobrosylate at 260 nm. The *syn*- and *anti*-7-bromobrosylates were monitored at 260 and 266 nm, respectively. Kinetic runs with deuterated material were performed only after control runs with two non-deuterated brosylates showed that a ratio of the rate constants between 0.99 ± 0.01 to 1.01 ± 0.01 was routinely obtainable. Corrections due to incomplete deuteration were usually small because of the high degree of deuterium incorporation in the compounds. The kinetic runs for non-deuterated and deuterated *syn*-7-chloro-*exo*-2-norbornyl brosylate were carried out at a cell temperature in the region of 50°C. Half-lives were generally in the order of 50–60 minutes. For *anti*-7-chloro-*exo*-2-norbornyl brosylates, the solvolyses were performed at 60°C and the half-lives were around 35–40 min. The kinetic procedure for *anti*-7-chloro- *endo*-2-norbornyl brosylate was slightly different from that described above. Water at 80°C was circulated through cell holders and the cell compartment was maintained at 71°C with water from a second Haake Model NBe circulating bath. Absorbance readings at 266 nm were taken as a function of time for about 36 h at approximately 4–6 h intervals and 9–10

points were used to determine the first-order rate constants. Since the half-life of the solvolytic reaction was about 12 h, A_∞ and the rate constant were calculated from the (A_t, t) readings by curve-fitting routine which fitted the data to an equation of the form $A_t = Be^{-k}$. To check the accuracy of this method, all the solvolytic data for *anti*- and *syn*-7-chloro-*exo*-2-norbornyl brosylates were analyzed by this method and A_∞ and k were calculated. Excellent agreement between fitted and experimental values and ratio constants was noted. The rate constants and standard deviations, for representative runs of *exo*-brosylate, along with the cell compartment temperatures, are as follows: **1***i*, $1.645 \pm 0.005 \times 10^{-4}$ s^{-1}; **1***e*, $1.498 \pm 0.005 \times 10^{-4}$ s^{-1} (50.0°C); **2***g*, $3.427 \pm 0.004 \times 10^{-4}$ s^{-1}; **2***c*, $3.077 \pm 0.005 \times 10^{-4}$ s^{-1} (60.0°C); **1***j*, $5.738 \pm 0.017 \times 10^{-4}$ s^{-1}; **1***f*, $5.452 \pm 0.016 \times 10^{-4}$ s^{-1} (60.0°C); **2***h*, $3.050 \pm 0.004 \times 10^{-4}$ s^{-1}; **2***d*, $2.733 \pm 0.003 \times 10^{-4}$ s^{-1} (60.0°C); **2***g*, $2.875 \pm 0.003 \times 10^{-4}$ s^{-1}; **4***a*, $2.627 \pm 0.004 \times 10^{-4}$ s^{-1} (57.8°C). Rate constants of $1.497 \pm 0.020 \times 10^{-5}$ s^{-1} and $1.567 \pm 0.020 \times 10^{-5}$ s^{-1} (80.0°C) were obtained for a typical simultaneous solvolysis of the *endo*-brosylates **3***a* and **3***c*, respectively. While the temperature of the bath was set in the range 50–60°C and controlled to better than ±0.05°C, the temperature within the cell compartment was several degrees lower than the bath. That the temperature control was adequate is seen from the quality of the rate data (Figs. 1(*a*), (*b*), and (*c*)).

Acknowledgement

We thank the Natural Sciences and Engineering Research Council of Canada for financial support.

1. S. E. Schepple. Chem. Rev. **72**, 511 (1972).
2. B. L. Murr, A. Nickon, T. D. Swartz, and N. H. Werstiuk. J. Am. Chem. Soc. **89**, 1730 (1967).
3. J. M. Jerkunica, S. Borčić, and D. E. Sunko. J. Am. Chem. Soc. **89**, 1732 (1967).
4. F. P. Cappelli, G. Timmins, and N. H. Werstiuk. Can. J. Chem. **50**, 2163 (1972).
5. N. H. Werstiuk, R. Taillefer, and S. Banerjee. Can. J. Chem. **56**, 1148 (1978).
6. N. H. Werstiuk, and F. P. Cappelli. Can. J. Chem. **58**, 1725 (1980).
7. N. H. Werstiuk, G. Timmins, and F. P. Cappelli. Can. J. Chem. **51**, 3473 (1973).
8. J. D. Roberts, F. O. Johnson, and R. A. Carboni. J. Am. Chem. Soc. **76**, 5692 (1973).
9. N. H. Werstiuk. Can. J. Chem. **48**, 2310 (1970).
10. B. Franzus and E. I. Snyder. J. Am. Chem. Soc. **87**, 3423 (1965).
11. H. Tanida and Y. Hata. J. Org. Chem. **30**, 977 (1965).
12. R. R. Johnson and E. S. Lewis. Proc. Chem. Soc. 52, (1958).
13. P. G. Gassman and J. M. Hornback. J. Am. Chem. Soc. **44**, 7010 (1972).
14. S. Winstein and D. Trifan. J. Am. Chem. Soc. **74**, 1154 (1952).
15. S. Winstein and D. Trifan. J. Am. Chem. Soc. **74**, 1147 (1952).
16. B. L. Murr and J. A. Conkling. J. Am. Chem. Soc. **92**, 3462 (1970).
17. S. G. Smith and D. J. W. Coon. J. Org. Chem. **34**, 3127 (1969).
18. V. J. Shiner, Jr., W. Dowd, R. D. Fisher, S. R. Hartshorn, M. A. Kessick, L. Milakofsky and M. W. Rapp. J. Am. Chem. Soc. **91**, 4836 (1969).
19. H. Humski. Croat. Chem. Acta, **42**, 501 (1970).
20. J. A. Cramer and J. G. Jewett. J. Am. Chem. Soc. **94**, 1377 (1971).
21. K. Humski, V. Sendijarevic, and V. J. Shiner, Jr. J. Am. Chem. Soc. **95**, 7722 (1973).
22. R. D. Fisher, R. C. Sieb, V. J. Shiner, I. Szele, M. Tomic, and D. E. Sunko. J. Am. Chem. Soc. **97**, 2408 (1975).
23. D. Kovačević, B. Goričnik and Z. Majerski. J. Org. Chem. **43**, 4008 (1978).
24. R. C. Seib, V. J. Shiner, Jr., V. Sendijarevic, and K. Humski. J. Am. Chem. Soc. **100**, 8133 (1978).
25. G. J. Frisone and E. R. Thornton. J. Am. Chem. Soc. **86**, 1900 (1964).
26. G. J. Frisone and E. R. Thornton. J. Am. Chem. Soc. **90**, 1211 (1968).
27. H. L. Goering and M. J. Degani. J. Am. Chem. Soc. **91**, 4506 (1969).
28. S. Winstein, E. Clippinger, R. Howe, and E. Vogelfanger. J. Am. Chem. Soc. **87**, 376 (1965).
29. N. H. Werstiuk. Can. J. Chem. **53**, 26 (1975).
30. J. A. Berson, R. C. Bergamn, J. A. Hammons, and A. W. McRowe. J. Am. Chem. Soc. **89**, 2581 (1967).
31. G. A. Olah, A. M. White, J. R. DeMember, A. Commeyras, and C. Y. Lui. J. Am. Chem. Soc. **92**, 4627 (1970).
32. S. Winstein and J. Takahashi. Tetrahedron, 316 (1958).
33. M. Tarle, S. Borčić, and D. E. Sunko. J. Org. Chem. **40**, 2949 (1975).
34. V. J. Shiner, Jr. and J. G. Jewett. J. Am. Chem. Soc. **87**, 1382 (1965).
35. M. Tichy, J. Hapala, and J. Sicher. Tetrahedron Lett. 373 (1969).
36. R. A. More O'Ferrall. J. Chem. Soc. B, 785 (1970).
37. A. Nickon and N. H. Werstiuk. J. Am. Chem. Soc. **89**, 3914 (1967).
38. W. Parker and C. I. F. Watt. J. Chem. Soc. Perkin Trans. II, 1647 (1975).
39. J. D. Roberts, C. C. Lee, and W. H. Saunders, Jr. J. Am. Chem. Soc. **76**, 4501 (1954).
40. A. Colter, E. C. Friedrich, N. J. Holness, and S. Winstein. J. Am. Chem. Soc. **87**, 378 (1965).
41. J. B. Stothers, C. T. Tan, A. Nickon, F. Huang, R. Sridhar, and R. Weglein. J. Am. Chem. Soc. **94**, 8581 (1972).
42. W. M. Schubert and P. H. LeFevre J. Am. Chem. Soc. **94**, 1639 (1972).
43. V. P. Vitullo and E. A. Logue. J. Am. Chem. Soc. **98**, 5906 (1976).
44. M. A. Winnik, V. Stoute, and P. Fitzgerald. J. Am. Chem. Soc. **96**, 1977 (1974).
45. B. L. Murr and J. A. Conkling. J. Am. Chem. Soc. **92**, 3464 (1970).
46. G. Olah, J. R. DeMember, C. Y. Lui, and R. D. Porter. J. Am. Chem. Soc. **93**, 1442 (1971).
47. N. L. Bauld, J. Cessac, and R. L. Holloway. J. Am. Chem. Soc. **99**, 8140 (1977).
48. B. Franzus and J. H. Surridge. J. Org. Chem. **33**, 1288 (1968).
49. H. Kwart and L. Kaplan. J. Am. Chem. Soc. **76**, 4072 (1954).
50. P. R. Story. J. Org. Chem. **26**, 287 (1961).
51. S. E. Schepple, P. L. Grizzle, and D. W. Miller. J. Am. Chem. Soc. **97**, 6165 (1975).

Can. J. Chem. Downloaded from www.nrcresearchpress.com by 210.87.254.6 on 09/05/12
For personal use only.

Synthesis of 4-deoxydaunosamine and 4-deoxyristosamine[1]

HANS H. BAER AND HANNA R. HANNA
Department of Chemistry, University of Ottawa, Ottawa, Ont., Canada K1N 9B4

Received April 2, 1980

HANS H. BAER and HANNA R. HANNA. Can. J. Chem. **58**, 1751 (1980).

Treatment of methyl 3,6-dideoxy-2,4-di-*O*-methylsulfonyl-3-nitro-α-L-glucopyranoside (**2**) with sodium acetate and acetic acid in acetone gave methyl 4-*O*-acetyl-2,3,6-trideoxy-3-nitro-α-L-*erythro*-hex-2-enopyranoside (**3**) as a kinetic product, and the 2-*O*-acetyl-3,4,6-trideoxy-3-nitro-α-L-*threo*-hex-3-eno isomer **4** as the thermodynamically preferred product. Treatment of **2** or **4** with sodium borohydride produced a separable mixture of methyl 2,3,4,6-tetradeoxy-3-nitro-α-L-*threo*-hexopyranoside (**5**) and its α-L-*erythro* epimer (**6**), the latter being convertible into the former by base-catalyzed epimerization. Acid hydrolysis of **5** and **6** afforded the corresponding free nitro sugars **7** and **8**. Catalytic hydrogenation of **5** led to the corresponding amino glycoside, isolated as the acetate **9** or hydrochloride **10**; similarly, **6** gave the epimeric amine which was isolated as its acetate **14** or picrate **15**. *N*-Trifluoroacetylation of **9** provided the *N*-trifluoroacetyl glycoside **12** which was hydrolyzed to give a 49% yield (overall from **2**) of 2,3,4,6-tetradeoxy-3-trifluoroacetamido-L-*threo*-hexose (4-deoxy-*N*-trifluoroacetyldaunosamine, **13**). Analogously, **14** afforded the epimeric *N*-trifluoroacetyl glycoside **17** which was hydrolyzed to give a 28% overall yield of 2,3,4,6-tetradeoxy-3-trifluoroacetamido-L-*erythro*-hexose (4-deoxy-*N*-trifluoroacetylristosamine, **18**).

HANS H. BAER et HANNA R. HANNA. Can. J. Chem. **58**, 1751 (1980).

Le méthyl-3,6-didesoxy-2,4-di-*O*-méthylsulfonyl-3-nitro α-L-glucopyranoside (**2**) traité par l'acétate de sodium et l'acide acétique dans l'acétone donne le méthyl-4-*O*-acétyl-2,3,6-tridésoxy-3-nitro-α-L-*érythro* hex-2-ène pyrannoside (**3**) comme produit cinétique et l'isomère 2-*O*-acétyl-3,4,6-tridésoxy-3-nitro-α-L-*thréo*-hex-3-ène (**4**) comme produit thermodynamique. Les composés **2** ou **4**, traités par le borohydrure de sodium, conduisent à un mélange dont on peut séparer le méthyl-2,3,4,6-tétradésoxy-3-nitro-α-L-*thréo*-hexopyranoside (**5**) et son épimère α-L-*érythro* (**6**); ce dernier peut être transformé en composé *thréo* par épimérisation en présence d'une base. L'hydrolyse acide de **5** et de **6** conduit aux sucres nitro libres **7** et **8**. L'hydrogénation catalytique de **5** conduit à l'aminoglucoside correspondant que l'on a isolé sous forme d'acétate **9** ou de chlorhydrate **10**. D'une manière analogue, le composé **6** donne l'amine épimère que l'on a isolé sous forme d'acétate **14** ou de picrate **15**. La *N*-trifluoroacétylation du composé **9** fournit le *N*-trifluoroacétylglycoside **12** qui par hydrolyse donne avec un rendement de 49% (à partir de **2**) le 2,3,4,6-tétradésoxy-3-trifluoroacétamido-L-*thréo* hexose (4-désoxy-*N*-trifluoroacétylduanosamine, **13**). De la même manière, le composé **14** conduit au *N*-trifluoroacétylglycoside épimère **17** qui par hydrolyse conduit avec un rendement global de 28% au 2,3,4,6-tétradésoxy-3-trifluoroacétamido-L-*érythro* hexose (4-désoxy-*N*-trifluoroacétylristosamine, **18**).

[Traduit par le journal]

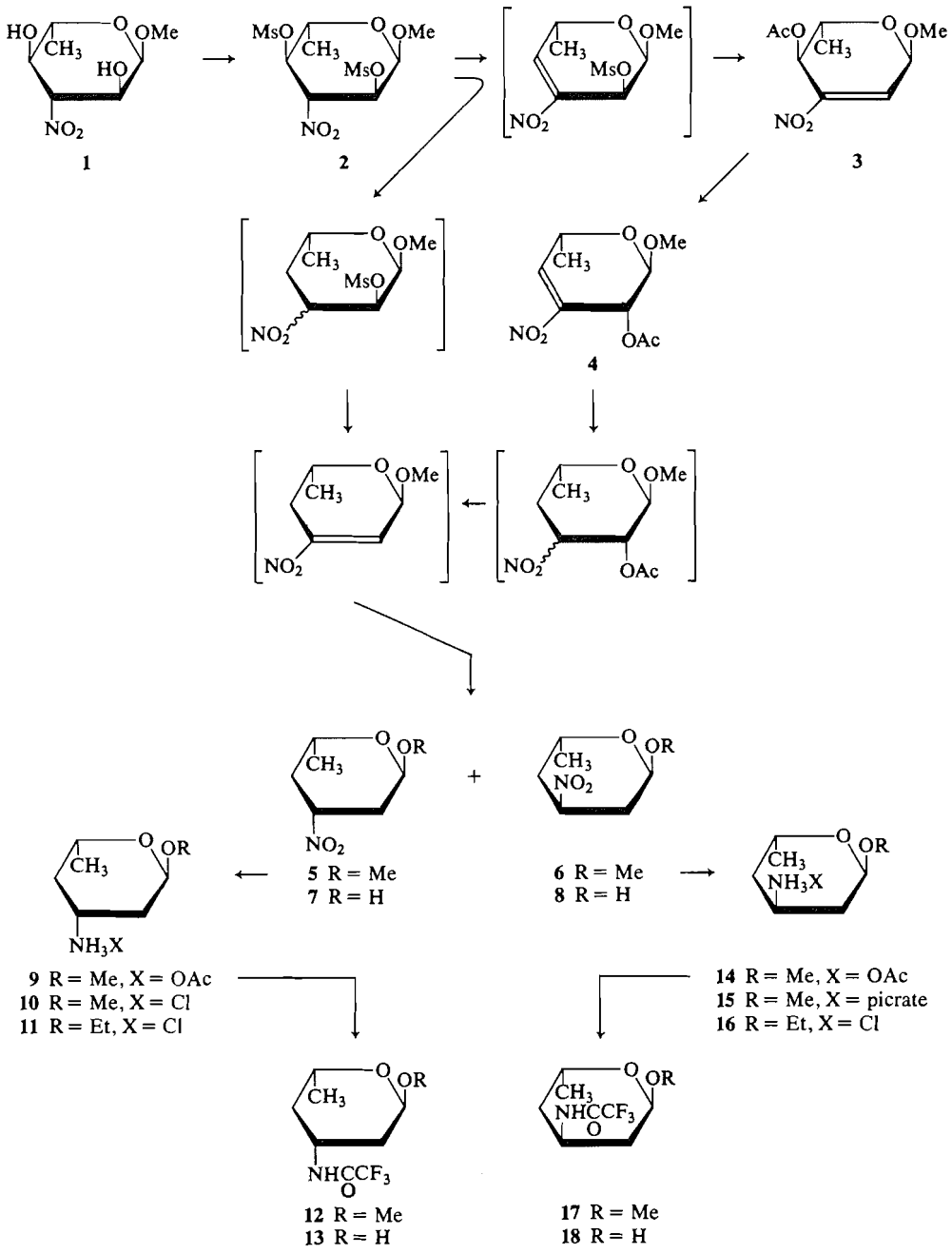
The amino sugars daunosamine (3-amino-2,3,6-trideoxy-L-*lyxo*-hexose) and ristosamine (its L-*ribo* isomer) are objects of much interest in medicinal chemistry. The former constitutes the sugar moiety of the anthracycline glycosides daunorubicin and adriamycin, which are effective therapeutic agents against a broad spectrum of human tumors (1), and the latter is a component of the antibiotic, ristomycin-A, isolated from *Proactinomyces fructiferi* (2). Intensive and promising efforts are currently directed in several laboratories towards the development of semisynthetic, modified analogs of daunorubicin and adriamycin which might display increased efficacy or lower cardiopathogenicity, a cumulative, dose-related side-effect (3) that curtails the administration of the natural drugs. To this end, a large variety of analogs modified in the sugar portion have been synthesized and, in part, evaluated pharmacologically (4–10). Among the substitutes for daunosamine whose attachment to the anthracyclinone aglycons showed promise in early screening were 4-deoxydaunosamine (6) and ristosamine (7); the D-enantiomer of ristosamine also gave an active glycoside (10). These developments motivated the search for new and convenient synthetic approaches to these and similar amino sugars. Of particular advantage are designs furnishing the desired amino sugars in a form suitable for subsequent linking to aglycons, e.g., as *N*-trifluoroacetyl derivatives. Continuing our program (11, 12) in the area of preparative chemistry of nitrogenous, polydeoxy sugars, we have recently announced (13) the synthesis of various derivatives of 3-amino-2,3,4,6-tetradeoxy-L-*threo*-hexose (4-deoxydaunosamine) and its L-*erythro* isomer (4-deoxyristosamine); the present article records full experimental details together with some additional, appertaining results.

4-Deoxy-*N*-trifluoroacetyldaunosamine (**13**) has been prepared previously in a four-step reaction sequence from methyl *N*-trifluoroacetyldaunosaminide which, in turn, had been elaborated from natural daunorubicin (5, 6). It would doubtless be possible to produce it similarly from synthetic

[1]The essential results of this work were first disclosed at the 62nd Canadian Chemical Conference, Vancouver, B.C., June, 1979. For a preliminary communication, see ref. 13.

0008-4042/80/161751-08$01.00/0
©1980 National Research Council of Canada/Conseil national de recherches du Canada

Can. J. Chem. Downloaded from www.nrcresearchpress.com by 210.87.254.6 on 09/05/12
For personal use only.



daunosamine for which there is now available a practical method of preparation starting from methyl α-D-mannopyranoside and comprising 9 steps (14). A multistep, achiral synthesis of racemic, 4-deoxy-D,L-daunosamine has also been achieved (15). The main feature of our alternative approach is the use of nitro sugars as intermediates; it leads to **13** and, in parallel, to the isomer **18**, with six steps being required for each from readily available methyl α-L-rhamnopyranoside.

The starting point was methyl 3,6-dideoxy-3-nitro-α-L-glucopyranoside (**1**), a key intermediate used in previous amino sugar syntheses (11, 16, 17); it is conveniently prepared in crystalline form, in about 40% yield, from methyl α-L-rhamnopyranoside by the nitromethane cyclization method. The glycoside **1** was converted into its 2,4-dimesylate **2** (yield, 80%) as already described for the D-enantiomer (12*a*). Introduction of the required deoxy functions in the positions 2 and 4 was

Can. J. Chem. Downloaded from www.nrcresearchpress.com by 210.87.254.6 on 09/05/12
For personal use only.

Can. J. Chem. Downloaded from www.nrcresearchpress.com by 210.87.254.6 on 09/05/12
For personal use only.

then achieved, either in a stepwise sequence or in a single operation. For the former mode, **2** was treated with sodium acetate and acetic acid in acetone solution, in order to produce the 2-O-acetyl-3-enoside **4** according to the procedure first applied (12*d*) in the D-series. As expected, this was successful. However, it was discovered in the present work, through the use of a different solvent for monitoring the reaction by tlc, that under the conditions previously specified (namely, after 10 min of heating at reflux temperature), an additional product was actually present in the reaction mixture. It disappeared when the reaction time was extended to 1 h, and pure crystalline **4** was then isolated in 70% yield. To investigate the nature of the intermediary compound, the reaction was performed at room temperature, at which the rate was conveniently slow. The intermediary product was then seen to arise first, and it could be isolated in crystalline form upon work-up of the reaction mixture after 2 h, at the time of incipient appearance of **4**. It proved to be the known, isomeric 4-*O*-acetyl-2-enoside **3** by comparison of its nmr spectrum and optical rotation with reported data (11*b*). When crystalline **3** was resubjected to the aforementioned reaction conditions, it was completely converted into **4**.

The discovery of **3** as a kinetic intermediate between **2** and **4** provides an interesting supplement to our earlier discussion (12*d*) of the elimination–addition mechanism proposed for this reaction. We had considered two possible pathways without expressing a preference. One of them was assumed to lead, via a 4-*O*-mesyl-2-enoside, to **4** directly, while the other one was formulated to give, via the isomeric 2-*O*-mesyl-3-enoside, an intermediary 4-*O*-acetyl-2-enoside which would then rearrange to **4**. The actual occurrence of **3** as such an intermediate can now be taken as evidence for the second alternative.[2] It is thought that this pathway is favored for electronic reasons. An initial elimination of mesylate anion in **2** should preferentially occur from position 4, rather than from position 2 where the inductive effect of the neighboring anomeric center renders anion departure more difficult (11*b*).

Reduction of **4** with sodium borohydride followed by acidification gave, in up to 90% yield, a mixture of methyl 2,3,4,6-tetradeoxy-3-nitro-α-L-*threo*-hexopyranoside (**5**) and its α-L-*erythro* isomer (**6**). The ratio of **5** to **6**, visually estimated by tlc as approximately 1:2 or 2:3, did not appear to change materially with variations in reaction temperature (−30 to +25°C) or solvent (ethanol, methanol, or *tert*-butanol). A similar mixture was obtained, more conveniently and in nearly quantitative yield, by treatment of the dimesylate **2** with sodium borohydride in dichloromethane–ethanol (1.5 h at 25°C). Whereas part of the preponderant isomer **6** crystallized directly from the acidified reaction mixture, the bulk of the products had to be separated by column chromatography on silica gel, whereby it was essential to maintain the medium lightly acidic throughout the operation. Pure **5** and crystalline **6** were thus isolated in yields of 26 and 56%, respectively. Compound **6** was thermodynamically unstable and tended to epimerize to **5** in neutral to slightly basic medium. This conversion, occurring for example in methanolic solution in the presence of silica gel and a trace of triethylamine, could be readily monitored by tlc; after 6 h, only a trace of **6** was left. By making preparative use of this epimerization, pure **5** could be isolated, after chromatography, in a yield of 71% based on **2**.

The formation and interconversion of **5** and **6** must involve the nitronate anion common to the two epimers. Evidently, protonation leads to **6** as the kinetically favored product. The nmr spectrum of **6** is consistent with the normal chair conformation having an axial nitro group. Although a limited distortion cannot be ruled out, any significant deviation (e.g., adoption of a skew form) should have manifested itself clearly in the ring-proton coupling pattern. Since axial-nitro epimers are rarely encountered in sugar nitronate protonation (see refs. 18 for discussions), **6** provided a surprise, not so much in that it was formed in the present case but in that it was sufficiently stable for isolation.

Although not required for the planned amino sugar synthesis, the free nitro sugars **7** and **8** were prepared from their respective glycosides **5** and **6**. Whereas the hydrolysis of **5** was performed under customary conditions using hot, 0.5 *M* aqueous sulfuric acid (1.5 h), that of **6** was achieved best at room temperature by treating the compound for 2 h with moist chloroform saturated with hydrogen chloride. Hydrolyses with hot, aqueous sulfuric or acetic acids resulted in considerable degrees of decomposition and gave poor yields of **8**. The 2,3,4,6-tetradeoxy-3-nitro-L-hexoses crystallized in the form of upward-mutarotating α-anomers.

Apart from the fact that reduction of **5** followed by *N*-acylation and hydrolysis led to the known

[2]We had tentatively formulated (12*d*) as a then hypothetical intermediate, the 4-epimer of (D) **3**, for reasons of its advantage in conformational energy (absence of $A^{(1,2)}$ strain). However, the less-stable **3** which has now been found as a kinetic product makes the facile rearrangement to **4** an even more plausible event. Incidentally, **3** cannot have arisen from a 4-*O*-mesyl-2-enoside precursor by an S_N2 displacement, in view of the retention of the C-4 configuration. Had the 4-epimer been found, such a displacement might have been invoked as an alternative to the elimination–addition sequences which we advocate.

Can. J. Chem. Downloaded from www.nrcresearchpress.com by 210.87.254.6 on 09/05/12
For personal use only.

amino sugar **13** (see below), the configurational assignment of **5** and **6** was readily derived from nmr spectra (100 MHz in $CDCl_3$). Thus, the nitromethine proton (H-3) in the equatorial-nitro glycoside **5** gave a low-field, symmetrical triplet of triplets whose spacings of 12 and 4.5 Hz indicated diaxial relations with H-2a and H-4a and axial–equatorial relations with H-2e and H-4e. These splittings were mirrored in the well-separated, highfield signals of H-2a (a symmetrical triplet of doublets) and H-4a (a quartet) showing, respectively, additional coupling with H-1 (3.5 Hz) and H-5 (12 Hz) as well as geminal coupling (12–13 Hz). Spacings found in the well-separated multiplets for H-5 (a sextet of doublets) and H-2e and H-4e (partially overlapping) accorded therewith. The spectrum of the free sugar **7** showed almost the same features except for some reasonably expected differences in chemical shifts and, of course, for the absence of a methoxyl resonance. By contrast, the glycoside **6** displayed for its (equatorial) H-3 proton a narrow multiplet containing only small vicinal couplings. Deshielding of H-3 was somewhat weaker, and that of H-5 was slightly stronger, than in the epimer **5**. The clearly separated signals for H-2a (an octet) and H-4a (a septet) reflected the small vicinal couplings with H-3 (5.5 and 4.5 Hz) in addition to 14.5–15 Hz geminal couplings and 3.7 and 11.5 Hz couplings with H-1 and H-5, respectively. The free sugar **8** gave a less well resolved spectrum (taken in dimethyl sulfoxide-d_6 because of insufficient solubility in chloroform). However, the character of the clear signals for H-3 (a narrow multiplet) and H-4a (a septet as in **6**) corroborated the assignment.

Platinum-catalyzed hydrogenation of the nitro glycoside **5** furnished methyl 3-amino-2,3,4,6-tetradeoxy-α-L-*threo*-hexopyranoside, isolated in >90% yields either as the acetate salt **9** or the hydrochloride **10** (both crystalline). When **9** was treated for 5 min at room temperature, with chloroform saturated with hydrogen chloride and containing 0.75% of ethanol,[3] it was converted in high yield into the corresponding ethyl glycoside hydrochloride **11**. Next, the salt **9** was quantitatively *N*-trifluoroacetylated in the presence of triethylamine, to give crystalline methyl 4-deoxy-*N*-trifluoroacetyl-α-daunosaminide (**12**) which was hydrolyzed with 3.5 *M* acetic acid, affording in 94% yield the crystalline 2,3,4,6-tetradeoxy-3-trifluoroacetamindo-α-L-*threo*-hexose (**13**). The overall yield in the sequence **1** → **2** → **5** → **9** → **12** → **13** was 49%, based on isolated pure intermediates.

An analogous sequence of reactions was performed in the 3-epimeric, L-*erythro* series. Thus, catalytic hydrogenation of **6** in the presence of acetic acid gave methyl 3-amino-2,3,4,6-tetradeoxy-α-L-*erythro*-hexopyranoside acetate (**14**) in virtually quantitative yield. Although crystallizable, **14** was both hygroscopic and rather volatile, subliming *in vacuo*; it was characterized by its nmr spectrum but, for elemental analysis, it was first converted into the highly crystalline picrate **15**. The ethyl aminoglycoside hydrochloride **16** was obtained from **14** exactly like **11** from **9**. *N*-Trifluoroacetylation of **14** provided in 92% yield methyl 4-deoxy-*N*-trifluoroacetyl-α-ristosaminide (**17**) as a chromatographically pure, volatile syrup that was characterized spectroscopically and hydrolyzed with acetic acid to afford crystalline 2,3,4,6-tetradeoxy-3-trifluoroacetamido-α-L-*erythro*-hexose (**18**). The overall yield in the sequence **1** → **2** → **6** → **14** → **17** → **18** was 28%.

Experimental

For general procedures and instrumental techniques, see previous articles from this laboratory (18). The nmr data refer to 100-MHz spectra of solutions in chloroform-*d* (unless otherwise specified) containing tetramethylsilane as an internal standard. Splittings were measured in expanded spectra, usually of 250 Hz sweep width. All new compounds gave infrared spectra consistent with the assigned structures. Optical rotations were recorded at room temperature. The following solvent mixtures (v/v) were used for tlc: 1:2 ethyl acetate – chloroform (*A*); 1:2 methanol–chloroform (*B*); ethyl acetate – petroleum ether in the proportions 1:1 (*C*), 1:2 (*D*), 1:3 (*E*), and 1:4 (*F*); and 1:6 ethyl acetate – hexane (*G*). Petroleum ether refers to the fraction of bp 30–60°C.

Methyl 3,6-Dideoxy-3-nitro-α-L-glucopyranoside (1)

The preparation of **1** from methyl α-L-rhamnopyranoside as originally performed by us (17) yielded 26% of the product by direct crystallization plus ca. 14% by column chromatography of the mother liquor. A minor modification of the procedure, employed later on (12*c*) in the D-series, gave 35% of product by crystallization, processing of the mother liquor being dispensed with. For the present work, we routinely prepared the mixture of stereoisomeric nitro glycosides as previously described and applied the whole, crude mixture (from 25 g of methyl α-L-rhamnopyranoside) to a column containing 800 g of silica gel (packed by suspending the gel in chloroform). Elution with 4:1 chloroform – ethyl acetate produced syrupy L-*manno* isomer followed by a mixture of the L-*gluco* and L-*galacto* isomers. This mixture was passed through a second column of the same size, which was eluted with 1:1 ethyl acetate – hexane to give pure **1** (11.9 g, 41%) melting at 141–143°C as recorded (17), followed by a small amount of the L-*galacto* isomer, mp 155–156°C (lit. (17) mp 154–157°C). A procedural variant involved omission of the first-mentioned column. The slow-moving L-*galacto* isomer was separated, by one chromatography using 1:1 ethyl acetate – hexane, from jointly emerging L-*manno* isomer and **1**, and the latter was then obtained pure in good yield by crystallization from chloroform.

Methyl 3,6-Dideoxy-2,4-di-O-methylsulfonyl-3-nitro-α-L-glucopyranoside (2)

A solution of **1** (2.0 g) in dichloromethane (100 mL; dried over molecular sieve) containing freshly distilled methanesulfonyl chloride (2.6 mL) was cooled to −40°C, and a solution of

[3]Ordinary, ethanol-stabilized, chloroform was used.

Can. J. Chem. Downloaded from www.nrcresearchpress.com by 210.87.254.6 on 09/05/12
For personal use only.

triethylamine (3.4 mL; dried over and distilled from CaH_2) in dry dichloromethane (20 mL) was then added dropwise over a period of 10 min. (Pilot experiments had shown that, at this point, all of **1** ($R_f \sim 0.2$) had disappeared and a strong spot of **2** ($R_f \sim 0.6$) was visible together with a weak, faster spot ($R_f \sim 0.8$; tlc with solvent *A*) which presumably represented an elimination product.) The reaction was immediately quenched by the addition of methanol (40 mL) at −40°C before the mixture was allowed to assume room temperature. Solvent evaporation gave a residue that was taken up in a small amount of ethyl acetate whereby the main part of crystalline triethylammonium chloride remained undissolved. The solution was filtered by suction through a 2-cm layer of silica gel (prewashed with ethyl acetate) which removed remnant salt; the filter cake was washed with ethyl acetate followed by petroleum ether. The filtrate was evaporated and coevaporated with several portions of added 1-propanol. Finally, the residue was dissolved in a minimal amount of hot 1-propanol from which **2** crystallized upon slow cooling to room temperature. The yield was 2.82 g (80%); mp 133–134°C, $[\alpha]_D$ −122.9° (*c* 1, chloroform). The ir and nmr spectra were identical with those of the D-enantiomer for which was found (12*a*) mp 132–132.5°C and $[\alpha]_D$ + 110.5°.

*Methyl 4-O-Acetyl-2,3,6-trideoxy-3-nitro-*α*-*L*-*erythro*-hex-2-enopyranoside (3) and Methyl 2-O-Acetyl-3,4,6-trideoxy-3-nitro-*α*-*L*-*threo*-hex-3-enopyranoside (4)*

The dimesylate **2** (1.0 g) and anydrous sodium acetate (0.5 g) were stirred at room temperature in acetone (25 mL) containing glacial acetic acid (0.5 mL). Monitoring by tlc (solvent *E*) revealed the concurrent consumption of **2** (R_f 0.15) and appearance of **3** (R_f 0.5) as a single product. After 2 h, traces of a second product, namely **4** (R_f 0.45) began to appear. (The spots of **3** and **4** were clearly separated provided the quantity of mixture applied to the plate was not too large.) The reaction was stopped at this point by the addition of ether (10 mL), which precipitated sodium acetate, and evaporation of the filtrate therefrom, followed by azeotropic removal of acetic acid with added toluene. The residue was extracted three times with boiling hexane. The extracts were evaporated giving a material that yielded nearly pure **3** (210 mg, 33%) by crystallization from absolute ethanol at −70°C. Recrystallized once from hot hexane (with slow cooling and storage of the solution at room tmperature), **3** formed long needles (180 mg), mp 87°C and $[\alpha]_D$ +97.3° (*c* 1.3, chloroform). The data recorded (11*b*) for **3** obtained in a different way were mp 81–81.5°C and $[\alpha]_D$ +99.3° (chloroform); the nmr spectrum of the present sample agreed with the published one (11*b*) in every detail.

For the preparation of **4**, a solution of **2** (1.0 g) and anhydrous sodium acetate (1.0 g) in acetone (25 mL) containing glacial acetic acid (1 mL) was boiled under reflux. Thin layer chromatography with solvent *E* indicated the disappearance of **2** and the occurrence of **3** and **4** early on; the intensity of **3** (R_f 0.5) subsequently diminished and, after 1 h, **4** (R_f 0.45) remained as the sole detectable product. The reaction mixture was processed as described above except that the residue obtained after removal of the acetic acid was passed through a small tube (disposable pipet) filled with silica gel, by means of solvent *C*. After solvent evaporation, **4** crystallized from a minimal amount of absolute ethanol on storage at −27°C; yield, 0.45 g (70%), mp 81–82°C, $[\alpha]_D$ −162.6° (*c* 1.5, chloroform). Literature (11*b*) mp 81–81.5°C and $[\alpha]_D$ −165°, and for the D-enantiomer, lit. (12*d*) mp 81–82°C and $[\alpha]_D$ +163°. The nmr spectrum was identical with the published (11*b*) spectrum of **4**.

*Methyl 2,3,4,6-Tetradeoxy-3-nitro-*α*-*L*-threo-hexopyranoside (5) and L-erythro Isomer 6*

Preparation from 4

Sodium borohydride (500 mg) was added to a solution of **4** (500 mg) in absolute ethanol (50 mL) which was stirred at +5°C. After 15 min methanol (15 mL) and an acidic cation exchange resin were added. The deionized solution was evaporated to give a residue from which several portions of methanol were evaporated to remove boric acid. The syrupy product was dissolved in ethyl acetate, treated with activated charcoal, and recovered after filtration through Celite and solvent removal. The dried syrup (350 mg, 92%) was a mixture of **5** (R_f 0.42) and **6** (R_f 0.28), with the latter predominating (tlc with solvent *F*; droplets of acetic acid were applied with the sample spots at the starting line of the plates).

Preparation from 2

Sodium borohydride (1.0 g) followed by absolute ethanol (30 mL) was added at room temperature to a stirred solution of **2** (1.0 g) in dichloromethane (100 mL). An exothermic reaction ensued, causing some refluxing of solvent. Monitoring by tlc as just described indicated complete consumption of **2** after 1–1.5 h and the formation of **5** and **6** in proportions similar to those above. The reaction mixture was then cooled (5–10°C), acidified to pH 4 by slow addition of glacial acetic acid, and filtered through a layer of Celite (prewashed with acetic acid followed by dichloromethane). Evaporation of the filtrate gave a white residue that was extracted several times with warm petroleum ether. The combined extracts were freed from acetic acid by coevaporation with toluene, and the remaining syrup was freed from residual toluene by short drying in an oil pump vacuum at room temperature. The product was then redissolved in petroleum ether, a small amount of insoluble material being filtered off. It was determined in one experiment that 470 mg (97.5%) of **5** + **6** was present at that stage.

Separation

The mixture of **5** and **6** (from 1.0 g of **2**) contained in a minimum volume of petroleum ether deposited long needles of **6** (153 mg) upon storage overnight at −27°C. The mother liquor was chromatographed on silica gel (20 g). The column was prepared by first soaking the gel in a mixture of acetic acid and dichloromethane for 2 h and then washing the packed column with hexane (50 mL). Irrigation with a mixture of petroleum ether (400 parts), benzene (100 parts), ethyl acetate (50 parts), and acetic acid (1.2 parts) gave homogeneous but syrupy **5** (126 mg, 26%) and crystalline **6** (115 mg, 56% when added to the previous crystals). The two isomers gave well-resolved ir spectra (ν_{max} 1550 cm^{-1}, strong, NO_2) which were very similar in character but showed significant differences in band positions and intensities in the fingerprint region.

Compound **5** showed $[\alpha]_D$ −139° (*c* 1.3, chloroform); nmr δ: 4.90 (dd, $J_{1,2e}$ = 2, $J_{1,2a}$ = 3.5 Hz, H-1), 4.84 (tt, partially overlapping H-1, $J_{2a,3} = J_{3,4a}$ = 12 Hz, $J_{2e,3} = J_{3,4e}$ = 4.5 Hz, H-3), 3.90 (12 lines, $J_{4e,5}$ = 2, $J_{4a,5}$ = 12, $J_{5,6}$ = 6.3 Hz, H-5), 3.34 (s, 3H, OMe), 2.43–2.18 (m, 2H, H-2e and H-4e), 2.01 (octet, $J_{1,2a}$ = 3.5, $J_{2a,3}$ = 12, $J_{2a,e}$ = 13 Hz, H-2a), 1.70 (q, $J_{3,4a} = J_{4a,5} = J_{4a,e}$ = 12 Hz, H-4a), 1.23 (d, 3H, *J* = 6.3 Hz, H-6).

Compound **6** showed mp 43°C, $[\alpha]_D$ −145° (*c* 1.1, chloroform); nmr δ: 4.73 (narrow m, $J_{1,2a}$ = 3.5, $J_{1,2e}$ = 2, $J_{1,4e}$ = 0.8 Hz, H-1), 4.49 (m, 16 lines; $J_{2e,3}$ = 2.7, $J_{2a,3}$ = 5.5, $J_{3,4e}$ = 3.3, $J_{3,4a}$ = 4.5 Hz, H-3), 4.19 (m, 12 lines; $J_{4e,5}$ = 2.5, $J_{4a,5}$ = 11.5, $J_{5,6}$ = 6.5 Hz, H-5), 3.27 (s, 3H, OMe), 2.72 (d sx, $J_{2a,e}$ = 15, $J_{1,2e}$ = 2, $J_{2e,3}$ = 2.7, $J_{2e,4e}$ = 1.2 Hz, H-2e), 2.52 (dm, with low-field m partially overlapping upfield sx of H-2e; $J_{4a,e}$ = 14.5, and *J* = 0.8, 1.2, 2.5, and 3.3 Hz, H-4e), 2.09 (dq, $J_{2a,e}$ = 15, $J_{1,2a}$ = 3.5, $J_{2a,3}$ = 5.5 Hz, H-2a), 1.61 (dq, $J_{4a,e}$ = 14.5, $J_{3,4a}$ = 4.5, $J_{4a,5}$ = 11.5, H-4a), 1.22 (d, 3H, *J* = 6.5 Hz, *C*—Me). *Anal.* calcd. for $C_7H_{13}NO_4$ (175.2): C 47.99, H 7.48, N 8.00; found: C 48.00, H 7.32, N 8.10. The crystals were volatile; they sublimed when being kept overnight in an oil-pump vacuum at room temperature.

Similar yields of **5** and **6** could be obtained by chromatography of their whole mixture (without prior partial crystallization of **6**), in which case a correspondingly larger proportion of silica gel

Can. J. Chem. Downloaded from www.nrcresearchpress.com by 210.87.254.6 on 09/05/12
For personal use only.

(30–35 g) had to be used. However, when a mixture of **5** and **6** (350 mg) was chromatographed on silica gel (35 g) which had *not* been pretreated with acetic acid, and elution was performed with solvent *G* instead of the aforementioned slightly acidic solvent, there was obtained pure **5** (202 mg) followed by mixed fractions totalling 103 mg, and no pure **6** emerged. It appeared that the slower-moving **6** was continuously being isomerized on the way through the column. To verify this, a sample of such a mixture (from 50 mg of **2**) was dissolved in methanol (5 mL) and stirred with silica gel (1 g) in the presence of a few drops of triethylamine. The isomerization was monitored by tlc (solvent *F*). After 10 min, the spot intensities were reversed, and after 6 h, only a trace of **6** remained visible.

Accordingly, for the preparation of **5** in optimum yield, the dimesylate **2** (500 mg) was treated with sodium borohydride as described before. After acidification and filtration through Celite, the reaction mixture was evaporated and an ethereal solution (50 mL) of the crude product was washed with cold, saturated $NaHCO_3$ solution (3×) and water (2×), dried over $MgSO_4$, and evaporated to give a ~2:3 mixture of **5** and **6** (214 mg, 89%). This was stirred for 3 h at room temperature with silica gel (1 g) in methanol (5 mL) containing triethylamine (10 drops). Upon removal of the gel and solvent, the isomerized material was purified by passage through a column of silica gel (15 g) by means of solvent *G*. There was obtained 170 mg (70.5%) of pure **5** followed by a small fraction (27 mg) containing **5** and **6**.

*2,3,4,6-Tetradeoxy-3-nitro-α-*L*-*threo*-hexose (**7**)*

A solution of **5** (200 mg) in tetrahydrofuran (2 mL) and 0.5 *M* sulfuric acid (20 mL) were heated on a steam bath for 90 min. The tlc (solvent *E*) then indicated **5** to be absent and showed a single, mobile spot (R_f 0.2) together with an immobile spot. The cooled hydrolyzate was extracted several times with ethyl acetate, and the combined extracts were washed several times with small volumes of aqueous $NaHCO_3$ solution and once with water. Drying ($MgSO_4$) and evaporation of the organic solution gave a yellow syrup that was purified by redissolution in ethyl acetate and treatment with activated charcoal followed by filtration through a small quantity of silica gel. The product was then recovered as a chromatographically homogeneous solid (112 mg, 61%) that formed colorless crystals from ethyl acetate – petroleum ether; mp 117–118°C, $[\alpha]_D$ −96° (3 min) → −76.3° (21 h, final; *c* 1, chloroform) and −39.8° (8 min) → −36.0° (20 and 120 min; *c* 1, water). Nuclear magnetic resonance δ: 5.48 (narrow m; d after D_2O exchange; $J_{1,2e} = 2$, $J_{1,2a} = 3.5$ Hz, H-1), 4.94 (tt, $J_{2a,3} = J_{3,4a} = 12$, $J_{2e,3} = 4.5$, $J_{3,4e} = 4$ Hz, H-3), 4.19 (m, 16 lines; $J_{4a,5} = 11.5$, $J_{5,6} = 6.5$, $J_{4e,5} = 2$ Hz, H-5), 2.95 (t, $J \sim 2.7$ Hz, removable by D_2O exchange, OH), 2.42 (d sx, $J_{2a,e} = 13$, $J_{1,2e} = J_{2e,4e} = 2$, $J_{2e,3} = 4.5$ Hz, H-2e), 2.35 (d of quintets partially overlapping the H-2e multiplet, $J_{4a,e} = 13$, $J_{4e,5} = J_{2e,4e} = 2$, $J_{3,4e} = 4$ Hz, J-4e), 2.03 (o, $J_{2a,e} = 13$, $J_{2a,3} = 12$, $J_{1,2a} = 3.5$ Hz, H-2a), 1.74 (q, with center lines broadened; $J_{4a,5} = 11.5$, $J_{3,4a} = 12$, $J_{4a,e} = 13$ Hz, H-4a), 1.25 (d, 3H, $J = 6.5$ Hz, *C*—Me). *Anal.* calcd. for $C_6H_{11}NO_4$ (161.2): C 44.72, H 6.88, N 8.69; found : C 44.75, H 6.93, N 8.54.

*2,3,4,6-Tetradeoxy-3-nitro-α-*L*-erythro-*hexose (**8**)*

A mixture of glycoside **6** (100 mg) and ethanol-free chloroform (10 mL) saturated with gaseous hydrogen chloride was stirred at room temperature for 2 h, with the addition of a few drops of water. Evaporation then gave a solid (89 mg, 97%) that was recrystallized from hot ethanol with addition of ethyl acetate, to give colorless **8** (70 mg, 76%), mp 141.5–142°C; $[\alpha]_D$ −59.6° (5 min) → −46.2° (15 min) → −23.0° (45 min) → +3.2° (17 h, const; *c* 1, methanol). The sugar was sparingly soluble in cold water; nmr in $(CD_3)_2SO$ δ: 6.07 (m, removable with D_2O, OH), 5.06 (narrow m, H-1), 4.70 (narrow m, H-3), 4.27 (broad m, H-5), 2.5–1.9 (unresolved m, 3H), 1.55 (septet, $J = 4.5$, 11, and 15 Hz, H-4a), 1.12 (d, $J = 6.5$ Hz, *C*—Me). *Anal.* calcd. for $C_6H_{11}NO_4$ (161.2): C 44.72, H 6.88, N 8.69; found: C 44.49, H 7.01, N 8.55.

*Methyl 3-Amino-2,3,4,6-tetradeoxy-α-*L*-threo-*hexopyranoside Acetate (**9**)*

Platinum dioxide catalyst (500 mg) was prehydrogenated in glacial acetic acid (30 mL), and a solution of **5** (500 mg) in absolute ethanol (20 mL) was added. The hydrogenation was performed for 10 h at ambient temperature and pressure. Thereafter, tlc indicated complete reaction of **5** (R_f 0.5 in solvent *F* or ~ 0.8 in solvent *B*) and the presence of **9** (R_f 0 and ~ 0.2, respectively). The filtered solution was evaporated, with azeotropic removal of acetic acid by addition of toluene. The remaining syrup gave crystals, mp 108°C (with prior sintering), from dichloromethane – ethyl acetate – petroleum ether, but these were found to contain 5% of ash (by combustion analysis). An ethyl acetate solution of the product was treated with charcoal, filtered through a layer of Celite, and evaporated to give pure **9** (540 mg, 92%), mp 115–116°C, $[\alpha]_D$ −115° (*c* 1.3, chloroform); nmr δ: 8.20 (s, 3H, $\overset{+}{N}H_3$), 4.79 (narrow m, H-1), 3.85 (broad m, H-3), 3.45 (broad m, H-5), 3.31 (s, 3H, OCH_3), 1.95 (s, 3H, AcO^-, superposed on unresolved m for H-2e and H-4e in the 2.2–1.9 region), 1.61 (sx containing 1 small and 2 large splittings, H-2a), 1.31 (q, $J \approx 12$ Hz, H-4a), 1.20 (d, 3H, $J = 6.5$ Hz, *C*—Me). *Anal.* calcd. for $C_9H_{19}NO_4$ (205.3): C 52.66, H 9.33, N 6.82; found: C 52.81, H 9.28, N 6.76.

*Methyl 3-Amino-2,3,4,6-tetradeoxy-α-*L*-threo-*hexopyranoside Hydrochloride (**10**)*

Compound **5** (100 mg, 0.57 mmol) in 95% ethanol (7 mL) was added to platinum dioxide catalyst (100 mg) that had been prehydrogenated in a mixture of ethanol (2 mL), water (0.4 mL), and *N* hydrochloric acid (0.6 mL). Complete hydrogenation at ambient temperature and pressure required 24 h. Removal of the catalyst and solvent gave a solid which was dried *in vacuo* and then washed with ethyl acetate, dissolved in ethanol, treated with charcoal, and recovered by evaporation of the solution. The colorless material then crystallized from ethanol – ethyl acetate and showed mp 175°C (dec.), raised to 182–183°C by recrystallization from methanol – ethyl acetate. The yield of pure **10** was 98 mg (94.5%), R_f 0.5 (tlc with solvent *B*), $[\alpha]_D$ −108.3° (*c* 1, water); nmr in $(CD_3)_2SO$ δ: 8.43 (s, 3H, $\overset{+}{N}H_3$), 4.79 (narrow m, H-1), 3.74 (broad m, H-3), ~3.4 (broad m, H-5), 3.24 (s, 3H, OCH_3), 2.2–1.9 (unresolved m, 2H, H-2e and H-4e), 1.63 (sx, $J = 3.5$ and 2 × 12.5 Hz, H-2a), 1.31 (q, $J = 3 \times 12$ Hz, H-4a), 1.13 (d, 3H, $J = 6.5$ Hz, *C*—Me). *Anal.* calcd. for $C_7H_{16}ClNO_2$ (181.7): C 46.28, H 8.88, N 7.71; found: C 46.36, H 9.06, N 7.53.

A sample of the acetate **9** (27 mg) was dissolved in 1% methanolic hydrogen chloride (10 mL). Evaporation gave crystalline **10** (23 mg, 96%), mp 182–183°C after recrystallization from methanol – ethyl acetate.

*Ethyl 3-Amino-2,3,4,6-tetradeoxy-α-*L*-threo-*hexopyranoside Hydrochloride (**11**)*

Compound **9** (100 mg) was dissolved in chloroform (10 mL) that contained 0.75% of ethanol as a stabilizer and that had been saturated with hydrogen chloride. After 5 min the solution was evaporated and the residue was recrystallized from chloroform and a few drops of ethanol by slow addition of ethyl acetate. The yield of **11** was 80 mg (84%); mp 190–192°C (dec.), $[\alpha]_D$ −94° (*c* 0.7, water). Nuclear magnetic resonance ($CDCl_3$ + CD_3OD) δ: 4.94 (narrow m, H-1), 4.0–3.4 (unresolved m, 4H, H-3, H-5, and ethyl CH_2), 2.35–2.0 (unresolved m, 2H, H-2e and H-4e), 1.80 (sx, $J = 3.5$ and 2 × 12 Hz, H-2a), 1.50 (q, $J = 3 \times 12$ Hz, H-4a), 1.21 (d, $J = 6.5$ Hz, *C*—Me), 1.18 (t, 3H, $J = 7$ Hz, ethyl CH_3).

Can. J. Chem. Downloaded from www.nrcresearchpress.com by 210.87.254.6 on 09/05/12
For personal use only.

Anal. calcd. for $C_8H_{18}ClNO_2$ (195.7): C 49.10, H 9.27, N 7.16; found: C 48.84, H 9.56, N 6.91.

*Methyl 2,3,4,6-Tetradeoxy-3-trifluoroacetamido-α-*L*-threo-hexopyranoside (12)*

To a cooled (−30°C) solution of **9** (300 mg) in spectroscopy-grade chloroform (14 mL) was added dry triethylamine (1 mL) followed by trifluoroacetic anhydride (1.5 mL) which was introduced dropwise while the temperature was allowed to rise to −20°C. Shortly thereafter, tlc (solvent *D*) indicated **12** (R_f 0.4) as the sole product. Water (10 mL) was added at −20°C and, after some stirring, the separated aqueous phase was extracted three times with chloroform. The combined organic phase and extract was washed with sodium bicarbonate solution followed by water, dried ($MgSO_4$), and evaporated to give a solid residue (365 mg). Recrystallization from ethyl acetate – petroleum ether gave long, colorless needles of **12** (350 mg, 99%), mp 123–123.5°C, $[\alpha]_D$ −128.8° (*c* 0.7, chloroform); nmr δ: 6.26 (broad signal, NH), 4.83 (narrow m, H-1), 4.37 (11 peaks, sx of overlapping t; $J_{2e,3} = J_{3,4e} = 4$, $J_{3,NH} = 8$, $J_{2a,3} = J_{3,4a} = 12$ Hz, H-3), 3.94 (16 lines, q of dd; $J_{4e,5} = 2$, $J_{4a,5} = 12$, $J_{5,6} = 6.3$ Hz, H-5), 3.34 (s, 3H, OCH_3), 2.2–1.9 (m, 2H, ill-resolved), 1.52 (sx with broadened center peaks; $J_{1,2a} = 3.5$, $J_{2a,3} = 12$, $J_{2a,e} = 13$ Hz, H-2a), 1.195 (d, 3H, $J = 6.3$ Hz for *C*—Me, superposed on q, 1H, $J = 3 \times 12$ Hz, H-4a). *Anal.* calcd. for $C_9H_{14}F_3NO_3$ (241.2): C 44.82, H 5.85, N 5.81; found: C 44.59, H 5.94, N 5.68.

*2,3,4,6-Tetradeoxy-3-trifluoroacetamido-*L*-threo-hexose (13)*

The glycoside **12** (160 mg) was hydrolyzed with 3.5 *M* acetic acid (16 mL) at 90°C for 2.5 h, after which tlc (solvent *D*) indicated complete conversion of **12** (R_f 0.4) into **13** (R_f 0.15). The hydrolyzate was diluted with water and extracted five times with chloroform. The extract was washed five times with small amounts of cold sodium bicarbonate solution and then once with water, dried ($MgSO_4$), and evaporated. The solid residue was crystallized from ethyl acetate – petroleum ether to give **13** (141 mg, 94%), mp 166–167°C; ms *m/e*: 227 (M^+), 210 (weak, $M^+ - OH$), and 209 (strong, $M^+ - H_2O$); $[\alpha]_D$ −85° (initial, extrapolated) → −80° (5 min) → −74° (15 min) → −57° (80 min) → −48° (4 h) → −47° (20 h, *c* 0.18, chloroform), and −26.4° (4 min) → −24.6° (2 h, final, *c* 0.5, water); lit. (6) mp 159–160°C, $[\alpha]_D$ −80° (*c* 0.1 in chloroform; no mutarotation recorded). Nuclear magnetic resonance in $(CD_3)_2SO$ δ: 9.2 (broad, NH), 6.49 (d, 0.15H, $J = 6.5$ Hz, OHβ), 6.12 (dd, 0.85H, $J = 1$ and 4 Hz, OHα), 5.18 (broad s, $W_H = 6$ Hz, H-1e; intensity slightly less than 1H but supplemented by a weak signal for H-1a at 4.60), 4.4–3.8 (m, 2H, H-3 and H-5), 1.9–1.4 (m, 3H, H-2e, H-4e, and H-2a), 1.20 (q, $J = 3 \times 12$ Hz, H-4a), 1.06 (d, 3H, $J = 6$ Hz, *C*—Me), in good agreement with the reported (6) data. Upon addition of D_2O, the NH and OH signals disappeared and, because of progressive mutarotation, the signal for H-1a (dd, $J = 2$ and 8.5 Hz) grew in intensity and a second *C*—Me doublet became visible at δ 1.12. *Anal.* calcd. for $C_8H_{12}F_3NO_3$ (227.2): C 42.29, H 5.32, N 6.17; found: C 42.42, H 5.17, N 5.97.

*Methyl 3-Amino-2,3,4,6-tetradeoxy-α-*L*-erythro-hexopyranoside Acetate (14) and Picrate (15)*

The nitro glycoside **6** (430 mg) was hydrogenated catalytically in acetic acid – ethanol as described for **5**. The reaction was complete after 6 h as indicated by tlc (solvents *F* and *B*), and processing was performed as for **9**. The crude product was briefly dried *in vacuo* at 25°C (prolonged drying results in losses owing to sublimation), then dissolved in ethyl acetate and filtered through Celite. Careful addition of petroleum ether to the concentrated solution followed by storage at −27°C produced colorless, hygroscopic crystals (**14**) which were rapidly dried *in vacuo* after decanting the mother liquor; yield, 500 mg (99%). Thorough drying for analysis was impractical because of the volatility of the compound; nmr δ: 7.28 (broad signal, $\overset{+}{N}H_3$, removable by D_2O exchange), 4.82 (narrow m, H-1), 4.06 (broad m, H-5), 3.52 (narrower m, H-3), 3.32 (s, 3H, OCH_3), 1.96 (s, 3H, AcO^-), 2.1–1.4 (unresolved m), 1.21 (d, 3H, $J = 6$ Hz, *C*—Me).

Concentrated solutions of **14** and picric acid, both in benzene, were mixed and cooled to ~+6°C. Yellow, crystalline **15** precipitated in nearly quantitative yield. Isolated and washed with ether, it had mp 163–164°C (dec.), raised to 164–165°C (dec.) by recrystallization from benzene–ether; $[\alpha]_D$ −59.2° (*c* 1.4, methanol); nmr in $(CD_3)_2CO$ δ: 8.67 (s, 2H, arom.), 4.89 (narrow m, H-1), 4.24 (broad m, 12 lines, H-5), 3.94 (narrow m, H-3), 3.35 (s, 3H, OCH_3), 1.75 (o, $J_{3,4a} = 4.5$, $J_{4a,5} = 12$, $J_{4a,e} = 15$ Hz, H-4a), 1.20 (d, 3H, $J = 6.3$ Hz, *C*—Me). The remaining ring proton signals were obscured by solvent signals. *Anal.* calcd. for $C_{13}H_{18}N_4O_9$ (374.3): C 41.71, H 4.85, N 14.97; found: C 41.74, H 4.75, N 14.86.

*Ethyl 3-Amino-2,3,4,6-tetradeoxy-α-*L*-erythro-hexopyranoside Hydrochloride (16)*

Obtained from the acetate **14** (150 mg) exactly as described for the preparation of **11** from **9**, compound **16** (122 mg, 86%) was recrystallized from chloroform – ethyl acetate; mp 141–142°C (dec.), $[\alpha]_D$ −84.6° (*c* 0.7, water); nmr δ: 8.47 (broad, removed by D_2O exchange, $\overset{+}{N}H_3$), 4.96 (narrow m, H-1), 4.11 (broad m, H-5), 3.85 (m, H-3), 3.5 (m, 2H, ethyl CH_2), 2.4–2.0 (m, 2H, unresolved, H-2e and H-4e), 1.86 (dt, $J = J' = 3.5$, $J_{gem} = 15$ Hz, H-2a), 1.63 (septet, $J = 4$, $J' = 12$, $J_{gem} = 15.5$ Hz, H-4a), 1.27 (t, 3H, $J = 7$ Hz, ethyl CH_3), 1.21 (d, 2H, $J = 6.3$ Hz, *C*—Me). *Anal.* calcd. for $C_8H_{18}ClNO_2$ (195.7): C 49.10, H 9.27, N 7.16; found: C 48.88, H 9.56, N 6.91.

*Methyl 2,3,4,6-Tetradeoxy-3-trifluoroacetamido-α-*L*-erythro-hexopyranoside (17)*

The glycoside acetate **14** (120 mg) in chloroform (7 mL) was treated with triethylamine (1 mL) and trifluoroacetic anhydride (0.5 mL) as described for the preparation of **12** from **9**, at an initial temperature of −30°C, rising to 0°C by the end of the addition. Completion of the reaction was verified by tlc (solvent *E*). The mixture was cooled again (−10°C) before the reaction was quenched by the addition of water (10 mL). Work-up as described for **12** gave **17** as a yellow syrup that was purified by passage through a small column of silica gel (8 g), with 1:5 ethyl acetate – petroleum ether as the eluent. There was obtained **17** (130 mg, 92%) as a colorless, chromatographically homogeneous syrup, R_f 0.3 (tlc with solvent *E*), $[\alpha]_D$ −4.3° (*c* 2.1, chloroform); nmr δ: 8.0 (broad, NH), 4.84 (broad s, $W_H = 6$ Hz, H-1), 4.29 (m, H-3), 3.94 (broad m, H-5), 3.40 (s, 3H, OCH_3), 2.1–1.8 (m, 3H, unresolved), 1.50 (septet, $J = 3.5$, $J' = 11.5$, $J_{gem} = 15$ Hz, H-4a), 1.19 (d, 3H, $J = 6.5$ Hz, *C*—Me). The compound was volatile *in vacuo* so as to render drying for analysis impractical.

*2,3,4,6-Tetradeoxy-3-trifluoroacetamido-*L*-erythro-hexose (18)*

Glycoside **17** (300 mg) was hydrolyzed for 2.5 h with 3.5 *M* acetic acid (40 mL) at 90°C. Complete hydrolysis of **17** (R_f 0.6) to **18** (R_f 0.5) was indicated by tlc (solvent *D*). Processing as described for **13** gave **18** (200 mg, 70%) as colorless crystals from ethyl acetate – petroleum ether; mp 112–113°C, $[\alpha]_D$ +28.9° (*c* 1.5, chloroform) and +10° (*c* 1.3, water); ms *m/e*: 227 (M^+), 210 (weak, $M^+ - OH$), and 209 (strong, $M^+ - H_2O$). Nuclear magnetic resonance δ: 8.3 (broad, removable by D_2O exchange, NH), 5.43 (narrow m, $W_H = 7$ Hz, contracting to t with $W_H = 5$ Hz after D_2O exchange, H-1), 4.3 (m, 2H, H-3 and -5), 3.82 (narrow t, $J = 2$ Hz, removable by D_2O exchange, OH), 2.1–1.7 (m, 3H, unresolved), 1.52 (septet, $J_{3,4a} = 3.5$, $J_{4a,5} = 11.5$, $J_{4a,e}$

= 14.5 Hz, H-4a), 1.20 (d, 3H, J = 6.5 Hz, C—Me). *Anal.* calcd. for $C_8H_{12}F_3NO_3$ (227.2): C 42.29, H 5.32, N 6.17; found: C 41.98, H 5.58, N 5.95.

Acknowledgment

This work was supported financially by the Natural Sciences and Engineering Research Council of Canada.

1. S. K. CARTER. J. Natl. Cancer Inst. **55**, 1265 (1975); A. DIMARCO, F. ARCAMONE, and F. ZUNINO. *In* Antibiotics. Vol. III. *Edited by* J. W. Corcoran and F. E. Hahn. Springer-Verlag, New York. 1975. pp. 101–128.
2. G. F. GAUZE, E. S. KUDRINA, R. S. UKHOLINA, and G. V. GAVRILINA. Antibiotiki, **8**, 387 (1963); N. N. LOMAKINA, I. A. SPIRIDONOVA, R. BOGNÁR, M. PUSKAS, and F. SZTARICSKAI. Antibiotiki, **13**, 975 (1968); R. BOGNÁR, F. SZTARICSKAI, M. E. MUNK, and J. TAMAS, J. Org. Chem. **39**, 2971 (1974).
3. M. GHIONE. Cancer Chemother. Pharmacol. **1**, 5 (1978).
4. A. BARGIOTTI, G. CASSINELLI, G. FRANCHI, B. GIOIA, E. LAZZARI, S. REDAELLI, A. VIGEVANI, and F. ARCAMONE. Carbohydr. Res. **58**, 353 (1977).
5. F. ARCAMONE, S. PENCO, A. VIGEVANI, S. REDAELLI, G. FRANCHI, A. DIMARCO, A. CASAZZA, T. DASDIA, F. FORMELLI, A. NECCO, and C. SORANZO. J. Med. Chem. **18**, 703 (1975).
6. F. ARCAMONE, S. PENCO, S. REDAELLI, and S. HANESSIAN. J. Med. Chem. **19**, 1424 (1976).
7. F. ARCAMONE, A. BARGIOTTI, G. CASSINELLI, S. PENCO, and S. HANESSIAN. Carbohydr. Res. **46**, C3 (1976).
8. H. S. EL KHADEM and D. L. SWARTZ. Carbohydr. Res. **65**, C1 (1978).
9. E.-F. FUCHS, D. HORTON, W. WECKERLE, and B. WINTER. J. Antibiot. **32**, 229 (1979); J. Med. Chem. **22**, 406 (1979).
10. D. HORTON, R. G. NICKOL, W. WECKERLE, and E. WINTER-MIHALY. Carbohydr. Res. **76**, 269 (1979).
11. H. H. BAER and C.-W. CHIU. (*a*) Carbohydr. Res. **31**, 347 (1973); (*b*) Can J. Chem. **52**, 111 (1974); (*c*) Can. J. Chem. **52**, 122 (1974).
12. H. H. BAER and F. F. Z. GEORGES. (*a*) J. Org Chem. **41**, 3474 (1976); (*b*) Carbohydr. Res. **55**, 253 (1977); (*c*) Can. J. Chem. **55**, 1100 (1977); (*d*) Can. J. Chem. **55**, 1348 (1977).
13. H. H. BAER and H. R. HANNA. Carbohydr. Res. **77**, C12 (1979).
14. D. HORTON and W. WECKERLE. Carbohydr. Res. **44**, 227 (1975).
15. H.-K. HUNG, H.-Y. LAM, W. NIEMCZURA, M.-C. WANG, and C.-M. WONG. Can. J. Chem. **56**, 638 (1978).
16. A. C. RICHARDSON and K. A. MCLAUGHLAN. J. Chem. Soc. 2499 (1962); K. Čapek, J. Šteffková, and J. Jarý. Collect. Czech. Chem. Commun. **31**, 1854 (1966).
17. H. H. BAER and K. Čapek. Can. J. Chem. **47**, 99 (1969).
18. (*a*) H. H. BAER. Adv. Carbohydr. Chem. Biochem. **24**, 67 (1969); (*b*) H. H. BAER and J. KOVÁŘ. Can. J. Chem. **49**, 1940 (1971); (*c*) J. KOVÁŘ, K. ČAPEK, and H. H. BAER. Can. J. Chem. **49**, 3960 (1971); H. H. BAER, C. B. MADUMELU, Z. S. HANNA, and P. G POTVIN. Carbohydr. Res. **76**, 141 (1979).

Can. J. Chem. Downloaded from www.nrcresearchpress.com by 210.87.254.6 on 09/05/12
For personal use only.

The solvolysis of the *p*-toluenesulphonate and methanesulphonate of cholesta-1,5-diene-3β-ol

PARIS E. GEORGHIOU[1] AND MARGARET A. MACDIARMID
Department of Chemistry, Memorial University of Newfoundland, St. John's, Nfld., Canada A1B 3X7

Received August 20, 1979[2]

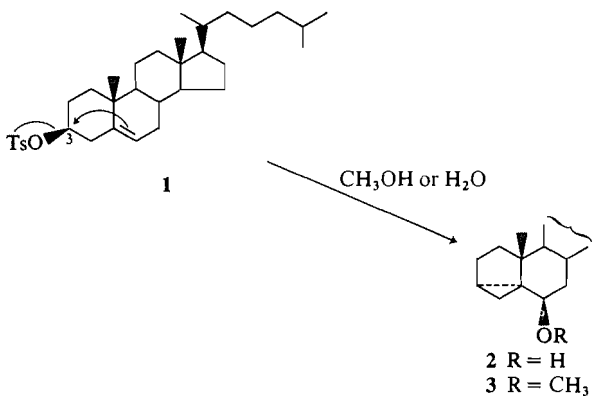
PARIS E. GEORGHIOU and MARGARET A. MACDIARMID. Can. J. Chem. **58**, 1759 (1980).

In situ preparations of 3β-tosyloxycholesta-1,5-diene and 3β-mesyloxycholesta-1,5-diene were subjected to methanolysis and hydrolysis. The products obtained were those of nucleophilic displacement with inversion at C3, as well as the epimers formed with retention of stereochemistry. No cyclized products could be isolated.

PARIS E. GEORGHIOU et MARGARET A. MACDIARMID. Can. J. Chem. **58**, 1759 (1980).

Nous décrivons la préparation *in situ* du tosylate et du mésylate de cholesta-1,5-diene-3β-ol. Le méthanolyse et l'hydrolyse en milieu acétonique aqueux de ces deux composés conduit à la formation aussi bien des produits avec inversion que des produits avec retention de configuration en position 3. On n'a pas observé expérimentalement la formation d'un produit de cyclisation.

Baldwin recently proposed a set of simple empirical rules (1) to predict the relative facility of different ring closures. According to the these rules, both 3-*exo*–*tet* and 3-*exo*–*trig* ring closures leading to the formation of three-membered rings are favoured processes. The well-known "*i*-cholesteryl" solvolytic rearrangement (2) of cholesteryl tosylate **1** to form the C3—C5 bicyclo ring A steroids **2** or **3** is an example of the former type. Here, the breaking of the C3–oxygen bond of the tosylate **1** is exocyclic to the 3-membered ring formed in the reaction and the geometry of C3 is tetrahedral (see Scheme 1):

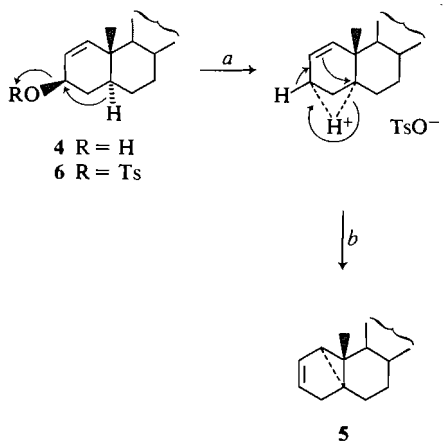


SCHEME 1

There are no simple examples of the 3-*exo*–*trig* ring closure resulting in the formation of a three-membered carbon ring in steroids.[3]

It appeared to us that cholesta-1,5-diene-3β-ol, **7** could serve to ascertain whether or not a preference is exhibited for one type of three-membered ring formation over the other. In principle, the C1—C5 bicyclo ring A-type compound[4] **8** could be formed via a 3-*exo*–*trig* ring closure with concommitant elimination. On the other hand, the *i*-cholesteryl-type product **9** could be formed via the 3-*exo*–*tet* mode (see Scheme 2):

formation of 1α,5-cyclo-5α-cholest-2-ene, **5**. A mechanism was proposed which involved a 1,3-transannular hydrogen shift in the tosylate **6** which is too unstable to be isolated. The second step in the rearrangement (step (*b*)) could be regarded as an example of a 3-*exo*–*trig* ring closure in which C5 is an incipient carbonium ion which could be considered to be approximately trigonal:

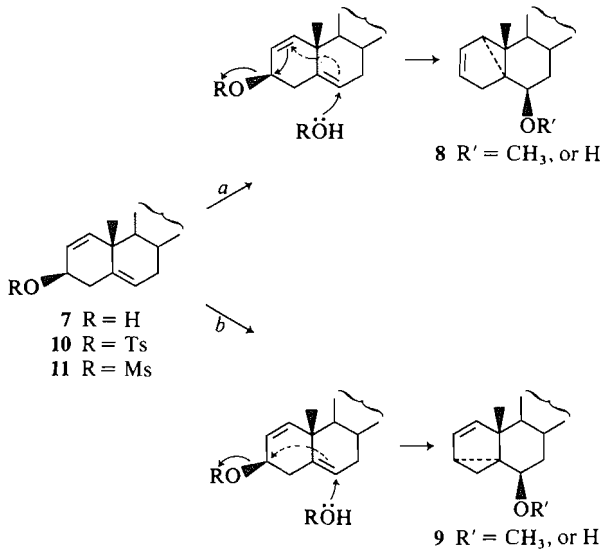


[1]Author to whom correspondence should be addressed.
[2]Revision received May 12, 1980.
[3]Laing and Sykes (3) however, have reported that the attempted tosylation of 5α-cholest-1-en-3β-ol, **4**, resulted in the

[4]The preparation of another C1—C5 bicyclo ring A steroid, 1α,5-cyclo-5α-cholestan-3β-ol-6-one in which ring B is functionalized has been reported by Laing and Sykes (4). These results, however, could not be duplicated (see ref. 5).

0008-4042/80/161759-04$01.00/0
©1980 National Research Council of Canada/Conseil national de recherches du Canada

Can. J. Chem. Downloaded from www.nrcresearchpress.com by 210.87.254.105 on 09/05/12
For personal use only.



SCHEME 2

Thus, the preparation of the tosylate, **10**, or the mesylate, **11**, could provide the means for the solvolytic pathways envisioned by paths (*a*) or (*b*) depicted in Scheme 2. The dienol **7** was prepared by the method of Kaneko *et al.* (6). It was, however, unstable in pyridine, and underwent a rapid, irreversible rearrangement as evidenced by ^{1}Hmr spectroscopy. Thus, since the conventional method (7) could not be employed, the tosylate, **10**, and mesylate, **11**, were formed by using stoichiometric amounts of *n*-butyllithium as the base, hexamethylphosphoric triamide (HMPA), and an excess of the appropriate sulphonyl chloride at low temperatures. The resulting products, however, could not be isolated; upon concentration of the organic solutions used to extract the steroidal compounds from the reaction mixture the products decomposed spontaneously and rapidly. It was therefore necessary to use the preparations containing the sulphonates **10** or **11** *in situ*, without further attempts at their isolation. Thus, the crude reaction mixtures were quenched by their addition to the respective solvolytic media. Typically, one-half of a tosylation mixture was removed by use of a syringe and methanolysed in potassium acetate-buffered 80% methanol–chloroform; the second half and hydrolysed in potassium acetate–buffered 80% acetone–water (2). The products were monitored, isolated, and characterized in the usual manner.

Methanolysis

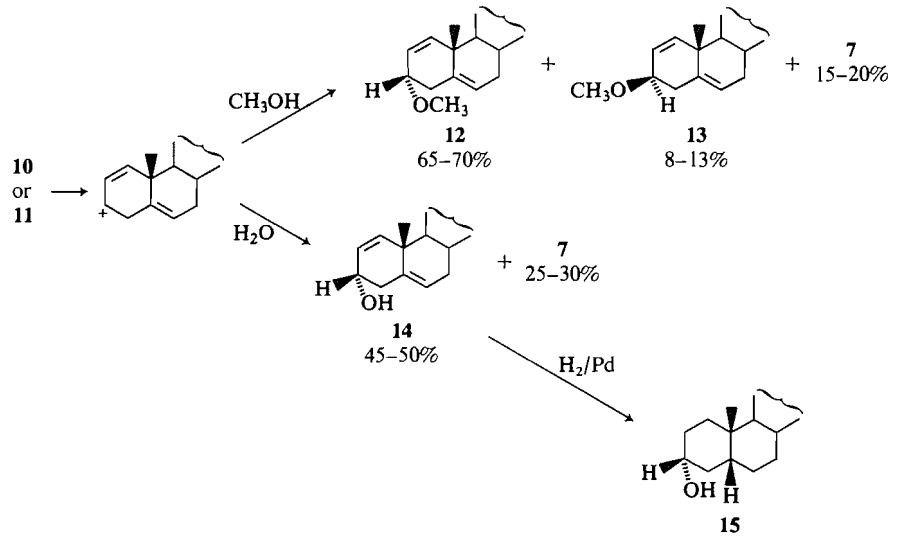
The products (and their yields) obtained by the methanolysis of the sulphates **10** and **11** were identical. A non-polar component (65–70%) and a second, more polar component (15–20%), were isolated by preparative layer chromatography (plc). The latter was shown to be identical to the starting dienol **7**. The balance of material consisted of several minor components (each < 1%) which could not be identified. Spectroscopy revealed that the non-polar component consisted of a mixture which was further separated by high pressure liquid chromatography (hplc). Two products were isolated in pure form. The major product had spectral characteristics consistent with the structure for 3α-methoxycholesta-1,5-diene, **12**. High resolution ^{1}Hmr and spin-decoupling experiments of the minor compound showed this to be the 3β-methoxy compound **13**. The latter was confirmed by its preparation directly from the dienol **7** under conditions which would ensure no epimerization of the C3 position, namely by using *n*-butyllithium, HMPA, and methyl iodide. The methyl ether thus produced was analysed by hplc and it consisted of a single component with no trace of the more strongly retained epimer. Thus, the formation of the β-methoxide **13** does not merely result from the presence of the corresponding amount of epimer as an impurity in the starting dienol **7**.

Hydrolysis

The hydrolyses of the two sulphonates **10** and **11** afforded identical products and yields, a similar observation to that made in the methanolyses described above. Again, two major components could be detected and isolated by plc. The less polar compound constituted only 45–50% of the total yield of recovered products and the second, more polar compound, which was identical with the starting material **7**, comprised 25–30%. These yields were obtained consistently. Thus, the methanolyses, which were conducted in parallel with one-half of the same tosylate and mesylate preparations afforded approximately 10% less of the dienol **7**. It can be concluded that approximately 10% of the *in situ*-formed tosylate or mesylate was hydrolysed by a pathway which leads to retention of configuration to produce **7**. In the methanolysis of course, the equivalent reaction leads to the formation of the 3β-methoxy compound **13**. Presumably, the tosylation or mesylation was only of the order of 80–85% complete, so that the plc work-up of crude typical sulphonation reaction mixtures affords approximately 20–15% of the unreacted dienol **7**.

The major product of the hydrolysis is the C3 epimer of **7**, namely cholesta-1,5-dien-3α-ol, **14**, which was confirmed by its hydrogenation to produce a compound which was identical in all respects to 5β-cholestan-3α-ol ("epicoprastanol"), **15**. Scheme 3 summarizes these results:

Can. J. Chem. Downloaded from www.nrcresearchpress.com by 210.87.254.105 on 09/05/12
For personal use only.



SCHEME 3

Discussion

We were unable to detect either the C3—C5, or the C1—C5 cyclized products **8** or **9**. Thus we cannot make any unambiguous conclusions on the question of the competitive modes of ring closure, on the basis of these experiments.

In order to establish whether or not the presence of HMPA in the crude tosylate (or mesylate) preparations affects the pathway of the subsequent solvolyses, the solvolytic procedure described above was repeated using cholesteryl tosylate **1** prepared in an identical manner. We observed results comparable to those of Kosower and Winstein (2), and obtained 3,5-cyclocholestan-6β-ol, **2**, and 3,5-cyclocholestan-6β-yl methyl ether, **3**, from the *in situ* preparations of **1**.

The products which we observed during this study can most easily be accounted for in terms of an S_N1-type substitution involving a carbocationic intermediate **18**. We were unable to isolate any of the allylic-rearrangement products but we cannot exclude the likely possibility that allylic stabilization of the C3 carbonium ion by the C1—C2 double bond does occur. The high inversion-to-retention product ratio can be accounted for by a shielding of the β-face of the steroid to the nucleophile by the leaving group, and by the steric effect due to the C19-methyl group.

Experimental

All reactions were carried out under argon. Melting points were determined on a Fisher–Johns melting point (hot stage) apparatus. Infrared spectra were recorded on a Perkin–Elmer 237B grating ir spectrophotometer, in carbon tetrachloride solutions. Proton magnetic resonance spectra were recorded with a Varian Model A-60 60 MHz, or a Bruker WP-80 80 MHz instrument in deuteriochloroform solutions. Ultraviolet spectra were recorded on a Perkin–Elmer 202 uv–vis spectrophotometer in hexane solutions. Baker silicic acid was used for column chromatography. Merck silica gel PF 254-366 was used for preparative layer chromatography (plc) using 20 × 20 cm plates of 1.0 mm thickness. High-pressure liquid chromatography (hplc) was performed on an Altex Model 312 liquid chromatographic system.

Cholesta-1,5-diene-3β-ol (7)

The dienol **7** was prepared by the method of Kaneko *et al.* (6). An improvement to this procedure was found to be one in which cholesta-1,5-diene-3-one was purified by chromatography on silicic acid prior to its reduction to **7**.

In situ *Preparations of Cholesta-1,5- diene-3β-tosylate (10)*

A solution of the dienol **7** (384 mg, 1 mmol) in freshly distilled tetrahydrofurane (4.0 mL) was prepared in a dry 10-mL reaction flask fitted with a rubber septum, a stirring bar, and an argon inlet needle. To this solution was added distilled hexamethylphosphoric triamide (0.35 mL) and a small amount (1–2 mg) of triphenylmethane. The solution was cooled to −40°C and treated with *n*-butyllithium (~0.25 mL of 2.2 *M* solution in hexane) added dropwise with the help of a syringe. The resulting pink solution was then warmed to 0°C and to this was added *p*-toluenesulphonyl chloride (380 mg, 2.0 mmol) which had been freshly purified by Pelletier's method (8). The pink colour immediately disappeared.

When this mixture was worked up in the usual manner by pouring into ice-cold water, extracting with ether, followed by washing the ether extracts with cold freshly prepared 5% aqueous sodium bicarbonate, the resultant colorless oil obtained upon concentration of the ether extract rapidly decolorized, indicating decomposition. The crude reaction mixtures were therefore used directly in the subsequent methanolysis and hydrolysis.

In situ *Preparations of Cholesta-1,5-diene-3β-mesylate (11)*

The crude mesylate preparations used in the methanolysis and hydrolysis of **11** were prepared exactly as described for **10** except that freshly distilled methanesulphonyl chloride was used.

Methanolysis of in situ *Preparations of (10) and (11)*

In a typical methanolysis, an aliquot estimated to contain approximately 1.0 mmol of **10** (or **11**) was removed from the crude tosylation (or mesylation) preparation described above. This was added directly with the help of a syringe into a mixture

Can. J. Chem. Downloaded from www.nrcresearchpress.com by 210.87.254.105 on 09/05/12
For personal use only.

Can. J. Chem. Downloaded from www.nrcresearchpress.com by 210.87.254.105 on 09/05/12
For personal use only.

containing anhydrous potassium acetate (392 mg, 4 mmol), anhydrous methanol (4.0 mL), and chloroform (4.0 mL). After stirring for 10 min at room temperature, a precipitate formed. At this point tlc indicated that the reaction was complete but the mixtures were usually worked up after 1 h. The solvent was removed under vacuum. The residue was dissolved in ether (10 mL), washed with three portions (1.0 mL) of aqueous phosphate pH 7.0 buffer, dried over anhydrous magnesium sulphate, and concentrated to dryness. The residue (300 mg) was chromatographed on plc plates using a benzene 8 – ether 1 mixture as the solvent system. Ultraviolet light examination of the developed plates revealed several compounds which were separated and analysed spectroscopically. The total yield of material recovered from the plc plates was 297 mg. A band of R_f 0.9 consisted of 15 mg of a compound whose spectra are characteristic of *n*-butyltosylate. The band at R_f 0.75 consisted of 200 mg (75%) of a mixture of **12** containing approximately 10% of its epimer, **13**. The only other band containing a significant amount, 35 mg (13%), of product had R_f 0.25 and was identical in its spectral and chromatographic features to **5**.

The mixture consisting of **12** and **13** was separated on hplc using a Partisil-10 9 mm id column and 10% hexane – 90% dichloromethane as the solvent. Two major products were eluted and collected. The less polar compound was 3α-methoxycholesta-1,5-diene **12**, mp 81°C, from methanol; ir ν_{max}: 2950, 1080 cm^{-1}; uv λ_{max} (ε): 208 (32000) nm; ^{1}Hmr δ: 0.68 (s, methyl at C(18)), 0.83 (s, methyl at C(19)), 2.40 (m, two protons at C(4) spin-coupled to proton at C(3)), 3.34 (s, methyl of methoxy group at C(3)), 3.69 (m, proton at C(3) spin-coupled to protons at C(4) and C(2)), 5.40 (m, proton at C(6)), 5.73 (d of d, B portion of an AB-type system due to proton at C(2), which is spin-coupled (J = 10 Hz) to proton at C(1), also (J = 5 Hz) to proton at C(3) and by long-range coupling to a proton at C(4)), and 6.02 (d, A portion of an AB-type system due to proton at C(1), which shows only spin-coupling to proton at C(2)); ms *m/e*: 398 (M^+), 383 ($M^+ - CH_3$), 366 ($M^+ - CH_3OH$), 351 (383 – CH_3), 285 ($M^+ - C_8H_{17}$), 253 (285 – C_8H_{17}), 211 ($M^+ - C_{11}H_{22}$, CH_3OH). *Anal.* calcd. for $C_{28}H_{46}O$: C 84.36, H 11.63; found: C 84.10, H 11.42. The other compound was 3β- methoxycholesta-1,5-diene **13**, mp 65.5°C from methanol; ν_{max}: 2950, 1085 cm^{-1}; uv λ_{max}: 210 nm; ^{1}Hmr δ: 0.70 (s, methyl at C(18)), 0.83 (s, methyl at C(19)), 2.50 (m, two protons at C(4)), 3.38 (s, methyl of methoxy group at C(3)), 3.80 (m, proton at C(3) spin-coupled to protons at C(4), C(1), and C(2)), 5.43 (m, proton at C(6)), 5.58 (d of t, B portion of an AB-type system due to proton at C(2), which is spin-coupled (J = 10 Hz) to proton at C(1), also (J = 0.5 Hz) to protons at C(3) and a proton at C(4)), and 5.82 (d of d, A portion of the AB-type system due to proton at C(1) which is spin-coupled to C(2) and has long-range (J = 1.0 Hz) spin coupling with proton at C(3); ms *m/e*: 398 (M^+), 383 ($M^+ - CH_3$), 366 ($M^+ - CH_3OH$), 351 (383 – CH_3), 285 ($M^+ - C_8H_{17}$), 253 (285 – C_8H_{17}), 211 ($M^+ - C_{11}H_{22}$, CH_3OH). *Anal.* calcd. for $C_{28}H_{46}O$: C 84.36, H 11.63; found: C 84.18, H 11.52%.

Hydrolysis of in situ *Preparations of (10) and (11)*

In a typical hydrolysis, an aliquot estimated to contain approximately 1.0 mmol of **10** (or **11**) was removed from the crude tosylation (or mesylation) preparation described above. This was added directly with the help of a syringe into a solution containing potassium acetate (393 mg, 4 mmol), 2.0 mL water, and 8.0 mL acetone. The mixture was stirred overnight before work-up. The mixture was concentrated under vacuum. The residue was dissolved in ether (10 mL), washed with three portions (1.0 mL) of aqueous phosphate pH 7.0 buffer, dried over magnesium sulphate, and concentrated to dryness. The residue (360 mg) was chromatographed on plc plates using a benzene 8 – ether 1 mixture as the solvent system. Several compounds could be detected by ultraviolet light and these were separated and analysed spectroscopically. The total yield of material recovered from the plc plates was 290 mg. The major band R_f 0.40 consisted of 155 mg (54%) of cholesta-1,5-dien-3α-ol **14**, mp 51–52°C from aqueous acetone; ir ν_{max}: 3560, 3350, 2940, 1030 cm^{-1}; ^{1}Hmr δ: 0.75 (s, methyl at C(18)), 0.86 (s, methyl at C(19)), 2.70 (m, two protons at C(4) spin-coupled to proton at C(3)), 4.10 (m, proton at C(3) spin-coupled to protons at C(4) and C(2)), 5.53 (m, proton at C(6)), 5.76 (d of d, B portion of an AB-type system due to proton at C(2) which is spin-coupled (J = 10 Hz) to proton at C(1), also (J = 5 Hz) to proton at C(3) and by long-range coupling to a proton at C(4)), and 5.96 (d, A portion of an AB-type system due to proton at C(1), which shows only spin-coupling to proton at C(2)); ms *m/e*: 384 (M^+), 383, 369 ($M^+ - CH_3$), 366 ($M^+ - H_2O$), 355 ($M^+ - C_2H_5$), 351 ($M^+ - CH_3$, H_2O), 271 ($M^+ - C_8H_{17}$). *Anal.* calcd. for $C_{27}H_{44}O$: C 84.31, H 11.53; found: C 84.15, H 11.48%.

The other major band, R_f 0.25, consisted of 70 mg (24%) of **7**.

3β-Methoxycholesta-1,5-diene (13)

A solution of **7** (40 mg) in freshly distilled tetrahydrofurane (10 mL) was prepared in a 5-mL reaction flask fitted with a rubber septum and an argon inlet needle. To this solution was added distilled hexamethylphosphoric triamide (0.04 mL) and a small amount (< 1 mg) of triphenylmethane. The solution was cooled to −40°C and treated with a few drops of *n*-butyllithium (2.2 *M* solution in hexane) with the help of a syringe until a pink colour formed. After a few minutes' standing, a few drops of methyl idodide was added to the pink solution, again with the help of a syringe. The resultant light yellow solution was warmed to room temperature and then concentrated under vacuum. The plc purification of the crude residue obtained afforded **13** which was identical in all respects with **13** obtained in the methanolysis of **10** and **11**.

Hydrogenation of Cholesta-1,5-dien-3α-ol (14)

A mixture consisting of **14** (22 mg) glacial acetic acid (5 mL) and platinum oxide (3 mg) was hydrogenated at atmospheric pressure. Even though tlc indicated that starting material was still present, the reaction was worked up after 2 h. The catalyst was filtered off and the acetic acid removed under vacuum. The residue was chromatographed on plc using the benzene 8 – ether 1 solvent system. A band was isolated consisting of 9.3 mg (78% of reacted material) of a compound identical in all respects with 5β-cholestan- 3α-ol, **15**.

Acknowledgements

The authors wish to thank the Department of Chemistry of Memorial University of Newfoundland for their technical and financial support and also the Natural Sciences and Engineering Research Council of Canada for its financial support. In particular, Professor A. R. Stein is thanked for his useful suggestions and comments.

1. J. E. Baldwin. J. Chem. Soc. Chem. Commun. 734 (1976).
2. E. M. Kosower and S. Winstein. J. Am. Chem. Soc. **78**, 4347 (1956), and references cited therein.
3. S. B. Laing and P. J. Sykes. J. Chem. Soc. C, 653 (1968).
4. S. B. Laing and P. J. Sykes. J. Chem. Soc. C, 937 (1968).
5. P. E. Georghiou and G. Just. J. Chem. Soc. Perkin Trans. I, 70 (1973).
6. D. Kaneko, S. Yamada, A. Sugimoto, Y. Eguchi, M. Ishikawa, T. Suda, M. Suzuki, S. Kakuta, and S. Sasaki. Steroids, **23**, 75 (1974).
7. L. F. Fieser and M. Fieser. Reagents for organic synthesis. J. Wiley and Sons, Inc. 1967. p. 1180.
8. S. W. Pelletier. Chem. Ind. 1034 (1953).

Canadian Journal of Chemistry
Published by
THE NATIONAL RESEARCH COUNCIL OF CANADA

Journal canadien de chimie
Publié par
LE CONSEIL NATIONAL DE RECHERCHES DU CANADA

Volume 58 Number 17 September 1, 1980

Volume 58 numéro 17 1 septembre 1980

Can. J. Chem. Downloaded from www.nrcresearchpress.com by 210.87.254.40 on 09/05/12
For personal use only.

Kinetics of the magnetite–maghemite–hematite transformation, with special reference to hydrothermal systems

THOMAS WILSON SWADDLE[1] AND PHILLIP OLTMANN
Department of Chemistry, The University of Calgary, Calgary, Alta., Canada T2N 1N4

Received January 23, 1980

THOMAS WILSON SWADDLE and PHILLIP OLTMANN. Can. J. Chem. **58**, 1763 (1980).

Maghemite, prepared in the usual way (but with exclusion of silica, e.g., from glassware) by precipitation of non-stoichiometric magnetite $Fe_{3-x}O_{4-x}$ in aqueous MOH (M = Na, K) followed by air oxidation, picks up moisture from the air to reach the limiting composition $M_\delta H_{1-\delta}Fe_5O_8$, where $\delta \sim 0.02$–0.03 for fresh material, but changes under hydrothermal conditions because of ion exchange. Despite the role of absorbed moisture in stabilizing maghemite, formation of the latter from $Fe_{3-x}O_{4-x}$ is markedly retarded, and its decomposition to α-Fe_2O_3 greatly accelerated, under hydrothermal conditions relative to the rates of the corresponding reactions of the dry solids. The rate of hydrothermal decomposition of maghemite is strongly retarded by silica. Over the range 160–187°C at least, silica-free maghemite decomposes in water according to the empirical equation $-\ln(1-\alpha) = (kt)^n$, where α is the fractional extent of decomposition, and $n \sim 2.5$ for neutral water (with $k = 1.3 \times 10^{-5}$ s^{-1} at 160°C and 3.1×10^{-5} s^{-1} at 175°C) but approaches unity, without major effects on the overall time-scale of reaction, at high [MOH]. The mechanistic significance of these and previous results are considered; the hydrothermal conversion of maghemite to hematite evidently proceeds by a dissolution–reprecipitation sequence.

THOMAS WILSON SWADDLE et PHILLIP OLTMANN. Can. J. Chem. **58**, 1763 (1980).

La maghémite, préparée de manière habituelle (mais avec élimination de la silice par exemple celle de la verrerie) par précipitation de la magnétite non stoechiométrique $Fe_{3-x}O_{4-x}$ dans du MOH aqueux (M = Na, K) suivie d'une oxydation à l'air, absorbe l'humidité de l'air pour atteindre une composition limite de $M_\delta H_{1-\delta}Fe_5O_8$ où $\delta \sim 0.02$–0.03 pour le produit frais, mais il se produit des changements dans des conditions hydrothermiques par suite de l'échange d'ions. En dépit du rôle de l'humidité absorbée en tant que stabilisatrice de la maghemite, la formation de cette dernière à partir de $Fe_{3-x}O_{4-x}$ est fortement retardée et sa décomposition en Fe_2O_3 α est grandement accélérée dans des conditions hydrothermiques s'apparentant aux vitesses des réactions correspondantes des solides secs. La vitesse de décomposition hydrothermique de la maghémite est fortement retardée par la silice. Au moins dans l'intervalle de 160–187°C, la maghémite dépourvue de silice se décompose dans l'eau selon l'équation empirique $\ln(1-\alpha) = (kt)^n$, où α est le degré fracitonnel de décomposition et $n \sim 2.5$ pour l'eau neutre (avec $k = 1.3 \times 10^{-5}$ s^{-1} à 160°C et 3.1×10^{-5} s^{-1} à 175°C) mais s'approche de l'unité sans effet appréciable sur le temps global de réaction à forte concentration de MOH. On considère la signification du point de vue du mécanisme de ces résultats et des résultats antérieures; la conversion hydrothermique de la maghémite en hématite se fait évidemment selon la séquence dissolution–reprécipitation.

[Traduit par le journal]

Introduction

The cubic iron(III) oxide maghemite ("γ-Fe_2O_3"), although thermodynamically unstable with respect to hematite (α-Fe_2O_3) and not usually considered a common mineral, does occur widely in terrestrial (notably highly-weathered tropical) soils (1, 2), has been reported to be an important secondary mineral in certain subvolcanic hydrothermal breccia bodies (3), appears to be a major constituent of the sands of Mars (4, 5), and has even been said to be the substance responsible for the visible absorption spectrum of interstellar matter (6), though the last seems improbable (7).

Maghemite forms in nature either through the oxidation of magnetite (Fe_3O_4) if this is sufficiently finely-divided (3, 8–15), through the oxidation at ambient temperatures of aqueous iron(II) via precipitated "green rusts" under conditions of limited O_2 supply (i.e., slow reaction) (16, 17), and possibly through dehydration of lepidocrocite (γ-FeO(OH)) (1, 18–20) although a redox cycle may be involved in this last case (1, 21). Whatever the mechanism, it appears that the presence of water is necessary for the formation of maghemite, natural or synthetic (7,

[1]To whom correspondence should be addressed.

0008-4042/80/171763-10$01.00/0
©1980 National Research Council of Canada/Conseil national de recherches du Canada

Can. J. Chem. Downloaded from www.nrcresearchpress.com by 210.87.254.40 on 09/05/12
For personal use only.

11, 22, 23), probably because the cation vacancies in the pseudo-spinel lattice can be stabilized by the occupation of some or all of the vacant octahedral cation sites by H^+ up to the limiting composition HFe_5O_8, i.e., $5Fe_2O_3 \cdot H_2O$ (24, 25), and indeed virtually all samples of maghemite seem to contain some bound water (11, 22–25). Yet, in spite of this, it has been shown (20, 26, 27) that water also facilitates the conversion of maghemite to α-Fe_2O_3.

A major objective of the present study was therefore to elucidate the kinetic factors governing the metastability of maghemite in aqueous (in effect, hydrothermal) environments. This has relevance to the understanding of the corrosion of ferrous metals in high-temperature aqueous environments; a film of maghemite is known to form in the anodic oxidation of iron in water at room temperature (28) and in the aqueous corrosion of pearlitic steel at pH 6.2–6.8 over the temperature range 20–287°C (29), as well as in the "dry" oxidation of iron by (moist) air near 20°C (30, 31). Maghemite may, in fact, be more common as a corrosion product than is generally appreciated, since the X-ray diffraction pattern of the poorly-crystalline material is difficult to distinguish from that of magnetite (30); this may have relevance, for example, to the characterization of the finely-divided corrosion products ("crud") formed in the heat-transfer systems of water-cooled nuclear power reactors, especially if there exists the possibility of an excursion to oxidizing conditions. In any event, we wish to stress once again (32) that the possible formation and persistence of metastable intermediates such as maghemite must be taken into account when making thermodynamically-based predictions about the outcome of hydrothermal reactions, since these substances could well be the actual reactive species governing the mechanism and course of reaction.

Experimental

Characterization of Materials

Solids in general were characterized by their powder X-ray diffraction (XRD) patterns in comparison with those in the JCPDS files. Elemental analyses, where required, were carried out on solutions of the solids in a small excess of 8–12 *M* HCl (*M* = mol dm^{-3} at 294 K and 89 kPa). Iron(II) was determined by titration with chromate(VI), and iron(III) both gravimetrically as tris(8-hydroxyquinolinato) iron(III) and volumetrically with chromate(VI) after $SnCl_2$ reduction, with good agreement (±0.2%) (33). The sodium and potassium contents of iron compounds were determined (±2%) by flame emission analysis, using a Varian Techtron Model 1200 spectrophotometer and KNO_3 and CsCl as the respective ionization suppressants.

Specific surface areas (SSA) were determined (±2 $m^2 g^{-1}$) by the BET(N_2) method with a Micromeritics Model 2200 High-Speed Surface Area Analyzer, degassing the samples for 40 min at 180 ± 10°C under dry N_2.

Preparation of Materials

Except where the use of glassware is specifically indicated, the maghemite samples and reaction media referred to below were "silica-free", i.e., they were prepared using polyethylene or other non-siliceous laboratory ware exclusively. Fresh Fisher Certified analytical grade reagents were used; KOH was supplied in plastic bottles, and was therefore preferred over NaOH, which came in glass jars. Distilled water was passed through Barnstead deionizer and organic removal cartridges before use.

Magnetite

Finely-particulate "magnetite", conveniently described as a non-stoichiometric solid solution, $x\gamma$-$Fe_2O_3 \cdot (1 - x)Fe_3O_4$ or $Fe_{3-x}O_{4-x}$ exclusive of absorbed water, was typically prepared by slowly adding 1500 cm^3 of a solution of iron(II) sulfate (0.14 *M*) and iron(III) ammonium sulfate (0.28 *M*) to 500 cm^3 fresh aqueous KOH (6.4 *M*), maintained at 90–95°C with vigorous stirring throughout the addition. The black precipitate was filtered, washed thoroughly with water until the filtrate was neutral and then with acetone, air-dried, and powdered. This material was typically found to contain 14.5% iron(II) (cf. 24.1% for stoichiometric Fe_3O_4), i.e., x in $Fe_{3-x}O_{4-x}$ was 0.49, ignoring the small absorbed water content. Removal of O_2 from the reaction mixture by purging with N_2 increased the iron(II) content only marginally (to 15.1%), since most of the loss of iron(II) probably resulted from the spontaneous decomposition of $Fe(OH)_2$ (34, 35). The XRD patterns contained no reflections other than those of $Fe_{3-x}O_{4-x}$; in particular, no iron silicates were detectable even when the preparation was done in glassware (contrast the formation of nickel talc in $Ni(OH)_2$ preparations (32)). The specific surface area (SSA) of samples so prepared was typically 75 $m^2 g^{-1}$; larger SSA's (to 120 $m^2 g^{-1}$) were obtainable by more rapid mixing of the reagents and allowing the temperature to fall accordingly, while very slow mixing produced an SSA of about 45 $m^2 g^{-1}$.

Well-crystallized (SSA < 0.1 $m^2 g^{-1}$), stoichiometric magnetite was made by hydrothermal decomposition of FeNTA·H_2O (36). Yields of some 90% were obtained in 50–80 h at 240°C with initial concentrations Fe(III) ~ 0.1 *M*, NaOH ~ 0.3 *M*. With [FeNTA] ~ 0.2 *M*, well-crystallized $FeCO_3$ was also precipitated, while at 185–190°C the product was α-Fe_2O_3.

Maghemite

Finely-particulate magnetite was completely converted to maghemite by heating in air for 15 min at 180°C. At room temperature, the product picked up moisture rapidly from the air until a constant weight was reached. No crystalline phases other than maghemite could be detected by XRD in this final product, even after heating for a further 72 h in air at 180°C. A sample (**A**) of specific surface 72 $m^2 g^{-1}$, used in most of the kinetic experiments described below, analyzed as follows: Fe^{3+}, 68.0 ± 0.2%; Fe^{2+}, < 0.005; H_2O (weight loss on heating to 800°C), 2.1 ± 0.1; K^+, 0.279 ± 0.005; Na^+, < 0.005; SO_4^{2-}, undetectable. *Anal.* calcd. for $(K_{0.029}H_{0.971})Fe_5O_8$: Fe^{3+} 68.2, H_2O 2.20, K^+ 0.277.

A sample (**B**) of maghemite (SSA 76 $m^2 g^{-1}$) prepared using NaOH in place of KOH analyzed similarly to **A** but with 0.103 ± 0.002% Na^+ and no detectable K^+; this corresponds to $(Na_{0.020}H_{0.980})Fe_5O_8$.

On going from $Fe_{3-x}O_{4-x}$ to maghemite, the attainable saturation magnetization (see below) increased by about 7%, but there was no significant change in the SSA.

In our hands, attempts to prepare maghemite by the method of Rao *et al.* (37) involving thermal decomposition of $FeC_2O_4 \cdot 2H_2O$ gave products which contained 50–80% α-Fe_2O_3 (XRD) and up to 1.7% iron(II), as well as maghemite.

Kinetics of the Hydrothermal Conversion of Maghemite to α-Fe_2O_3

Typically, 0.500 ± 0.003 g maghemite was mixed with water

Can. J. Chem. Downloaded from www.nrcresearchpress.com by 210.87.254.40 on 09/05/12
For personal use only.

or aqueous alkali[2] (usually 5.0 or 10.0 cm^3) in PTFE-lined autoclaves (small capacity of stainless steel (38), larger of titanium (35)), sealed under nitrogen or air as required, and thermostatted to ±0.2 K in a preheated forced-convection oven (38). The autoclaves were withdrawn and quenched in cold water after selected times t_{oven} in the furnace; the effective reaction time t_{corr} was taken to be $t_{oven} - 0.7$ h, as previously established and verified by extrapolation in those cases exhibiting "first order" kinetics (see below). The solid contents were filtered, washed with water and then acetone, then air-dried.

The percentage of maghemite in these products was estimated from the apparent percentage weight increase Δw experienced by small samples in a Faraday magnetic susceptibility apparatus (cf. ref. 39) under conditions of linear dependence of Δw on applied field, i.e., of saturation magnetization. Calibration with $HgCo(NCS)_4$ indicated the product of field and field gradient, held constant according to a gaussmeter for all samples in a given kinetic run, to be typically about 3×10^3 g cm^{-2} s^{-2}, giving Δw of about 26% for freshly-prepared maghemite, as against 0.03% for the feebly ferromagnetic product, α-Fe_2O_3. It was established, using prepared mixtures of maghemite and α-Fe_2O_3, that Δw was essentially proportional (±2%) to the percentage of maghemite, once this had been equilibrated with the hydrothermal medium (see below). The magnetization of hydrothermally-treated maghemite just before the onset of conversion to hematite in a kinetic run was taken to represent 100% maghemite; in most cases, the Δw value for $t_{oven} = 0.5$ h sufficed.

Results

(*i*) The aerial oxidation of magnetite to maghemite proceeded more rapidly in the "dry" state than under hydrothermal conditions. The oxidation of $Fe_{3-x}O_{4-x}$ (SSA ~ 75 m^2 g^{-1}) at 180°C was complete in 15 min without change in SSA (cf. refs. 14 and 40), and the product remained unchanged over a further 72 h at this temperature, whether prepared with exclusion of silica or not. By contrast, oxidation of $Fe_{3-x}O_{4-x}$ by excess air under hydrothermal conditions (1.0 *M* alkali or neutral) at 180°C was incomplete after several hours, in which time conversion of maghemite to α-Fe_2O_3 would have been important (e.g., 99% complete in 12 h in water, if silica-free).

(*ii*) Coarsely-crystalline, stoichiometric Fe_3O_4 underwent "dry" oxidation in (moist) air slowly and directly to α-Fe_2O_3, whereas finely-particulate $Fe_{3-x}O_{4-x}$ oxidized rapidly to maghemite first. Well-crystallized magnetite (SSA < 0.1 m^2 g^{-1}, particle size 10–100 μm (36)) gave only 2% α-Fe_2O_3 after 24 h at 260°C, according to chemical analysis and XRD; the small-angle reflections characteristic of maghemite were entirely absent. Under these conditions, a sample of genuine maghemite (SSA 72 m^2 g^{-1}) decomposed only to the extent of 5% α-Fe_2O_3; at 400°C, 50% α-Fe_2O_3 resulted after 24 h, and 95% after 4 days. Thus, had maghemite been the initial product of oxidation of the well-crystallized Fe_3O_4 at 260°C, it would surely have been detected.

(*iii*) Freshly-prepared silica-free maghemite picked up moisture from the air, reaching constant weight within a few hours. This material contained significant amounts of alkali metal ion M^+ from the MOH used in making $Fe_{3-x}O_{4-x}$, despite washing this last until the filtrate was neutral, and analyzed as $(H_{1-\delta}M_\delta)Fe_5O_8$, within experimental uncertainty, with δ typically 0.02 (material **B**, M = Na) to 0.03 (material **A**, M = K). Hydrothermal treatment at ~175°C in pure water decreased the M^+ content slightly, e.g., from 0.28 to 0.22% K in **A**, before decomposition to α-Fe_2O_3 was detectable, and this was accompanied by an increase of ~5% in the apparent SSA (measured *after drying* at 180°C; see Table 1) as well as an increase of 11–13% in the saturation magnetization attainable in the Faraday measurements. Samples of $Fe_{3-x}O_{4-x}$ also showed an augmentation in the attainable saturation magnetization on hydrothermal treatment, the increase being roughly proportional to x.

Treatment of $H_{1-\delta}M_\delta Fe_5O_8$ with aqueous MOH (0.1–1.0 *M*) at ~175°C, on the other hand, increased δ markedly (e.g., from 0.28 to 0.82% K^+ for **A** in 1.0 *M* KOH) before detectable α-Fe_2O_3 formation, and the attainable saturation magnetization *decreased* by 7% (0.1 *M* KOH) to 12% (1.0 *M* KOH) simultaneously. Treatment of $H_{1-\delta}M_\delta Fe_5O_8$ with aqueous M′OH at ~175°C led to the replacement of most of the M by M′, as well as an overall increase in the alkali metal ion content; thus, after $t_{oven} = 0.5$ h with the oven at 175°C, the K^+ content of substance **A** in 1 *M* NaOH fell from 0.28 to 0.047%, while the Na^+ content rose from < 0.005% to 0.32%.

The amount of moisture driven off from $H_{1-\delta}M_\delta Fe_5O_8$ at 180°C under dry nitrogen was close to that released on total decomposition to α-Fe_2O_3 in air at 800°C (2.1%), especially when δ was relatively large (Table 1), suggesting that small residual amounts of H^+ *or* M^+ are intricately involved in maintaining the spinel structure (cf. refs. 24, 25). Larger percentages of moisture (to ~5% for SSA ~ 120 m^2 g^{-1}) were recovered at 180°C from hydrothermally-treated maghemite which had been prepared using glassware; these percentages correlated roughly with surface area, and probably reflected contamination by silica.

(*iv*) The presence of silica retarded the hydrothermal decomposition of maghemite. Maghemite, made from $Fe_{3-x}O_{4-x}$ prepared with ~1.5 h exposure to boiling KOH in Pyrex glassware, was only 7% converted to α-Fe_2O_3 after 3 h in water at 187°C, whereas for silica-free maghemite the conversion to hematite was over 97% complete under

[2]Throughout this paper, concentration data refer to the original solutions at 294 K and 89 kPa, rather than hydrothermal conditions. Increases in concentration due to the generation of the saturated vapor pressure were in no case more than 0.3%.

Can. J. Chem. Downloaded from www.nrcresearchpress.com by 210.87.254.40 on 09/05/12
For personal use only.

TABLE 1. Correlation between the extent of hydrothermal conversion of silica-free maghemite (material A) to hematite and the specific surface and adsorbed moisture of the solid phases

T (°C)	Medium	t_{oven} (h)	% maghemite[a]	Specific surface[b] ($m^2 g^{-1}$)	Water loss, 180°C ($mg g^{-1}$)
170.6	Water	2.0	100	74	
		4.0	98	70	
		6.0	90	69	
		8.0	76	59	
		10.0	58	43	
		13.5	27	22	
		16.0	12	12	
		22.0	1.5	5	
		28.0	0.4	3	
174.2	1.0 *M* KOH	0.5	100	75	20
		1.0	94	75	22
		2.0	92	75	22
		3.0	80	66	20
		5.0	62	51	14
		7.0	44	37	10
		9.0	28	24	8
		12.0	19	14	5
		17.8	5	4	1
		22.0	2	<1	<1
179.1	Water	0.5	100	74	16
		0.8	100	73	15
		1.0	100	73	17
		2.0	100	74	18
		3.0	94	72	18
		4.0	83	65	15
		6.0	60	46	9
		8.0	21	20	4
		12.0	2.3	$\lesssim 2$	—

[a]Experimental Δw values.
[b]Originally 71.5 $m^2 g^{-1}$.

TABLE 2. Effect of contaminants on the extent of hydrothermal decomposition of maghemite at 174.8°C

Preparation of maghemite	Reaction medium	Time t_{oven} (h)	% maghemite remaining	Added solids per g maghemite	Specific surface ($m^2 g^{-1}$) Initial	Specific surface ($m^2 g^{-1}$) After t_{oven}
Glassware	Water	21	100	—	118	113
		91	96	—		116
Silica-free	Water	19	<0.1[a]	—	75	~ 2[b]
	1.0 *M* KOH	19	2	—		$\lesssim 0.1$
			93	20 mg SiO_2		49
			94	{20 mg SiO_2 + 20 mg α-Fe_2O_3}		74

[a]Calculated from data in Table 3.
[b]Typical value.

the same conditions. Table 2 gives data which confirm this effect and show unambiguously that the deliberate introduction of reagent-grade SiO_2 into the maghemite–hematite reaction mixture had similar results.

(*v*) The *nature* of the hydrothermal decomposition products of maghemite, also, depended to some extent upon the presence or absence of silica and the composition and temperature of the reaction medium. Silica-free maghemite was converted exclusively to α-Fe_2O_3 in both plain water and 1.0 *M* KOH or NaOH at all temperatures (150–190°C). Hematite was again the sole product in plain water when maghemite prepared in glassware was used, but in strongly alkaline solutions α-FeO(OH) (goethite) was also formed, and was the exclusive product in 1 *M* NaOH at 150–166°C. The product distribution was then also

Can. J. Chem. Downloaded from www.nrcresearchpress.com by 210.87.254.40 on 09/05/12
For personal use only.

sensitive to the cation present; after 116 h at 174.8°C in 1 *M* MOH, maghemite prepared in glassware decomposed to the extent of 59% giving α-Fe_2O_3 and a trace of α-FeO(OH) when M was Na, and 90% giving α-FeO(OH) and a trace of α-Fe_2O_3 when M was K (silica-free maghemite decomposed to α-Fe_2O_3 completely and exclusively in all control experiments).

(*vi*) Neither the original maghemite nor its decomposition product, hematite, showed any decreases in surface area on hydrothermal treatment in water or 1 *M* NaOH that could be attributed to a significant degree of Ostwald ripening (crystal growth by dissolution and reprecipitation of the same phase) on the time-scale of the hydrothermal kinetic experiments, according to BET–SSA measurements and the scanning electron microscope (SEM). Thus, the decline in SSA accompanying the disappearance of maghemite, exemplified in Table 1, was a direct consequence of reaction to form relatively large crystals of hematite, growth of which effectively ceased on depletion of the maghemite nutrient. The small *increase* noted above in the apparent SSA of maghemite on initial exposure to hydrothermal environments probably reflected surface roughening by hydration followed by drying at 180°C in the BET procedure.

The final product in plain water was red hematite of SSA about 2 $m^2 g^{-1}$ (cf. 40–120 $m^2 g^{-1}$ for the original maghemite); a sample of SSA 5 $m^2 g^{-1}$ in which 4% unreacted maghemite remained was seen under the SEM to consist mainly of α-Fe_2O_3 rhombohedra of size 0.3 μm in general and in no case greater than 1.0 μm. In 1.0 *M* KOH, the hematite product was purple–brown to metallic grey, the SSA was not measurable ($\lesssim$ 0.1 $m^2 g^{-1}$) with the apparatus available, and the SEM showed it to consist mainly of well-crystallized tables up to 5 μm across and about 1 μm thick, morphologically similar to the larger hematite crystals prepared hydrothermally by Laudise and co-workers (41).

Maghemite (substance **A**, 72 $m^2 g^{-1}$), heated for 1 h at 800°C in air, decomposed to hematite of SSA 5 $m^2 g^{-1}$.

(*vii*) The decay curves of maghemite, defined by Δw, were sigmoidal in plain water but approached exponential at high alkali concentrations (Table 1 and Fig. 1). These curves can be generally represented to within the experimental uncertainty by the equation

$$[1] \quad -\ln(1-\alpha) = (kt_{corr})^n$$

where α is the molar fractional extent of reaction at the effective reaction time t_{corr} (so that % maghemite = $100(1 - \alpha)$), n is a constant determining

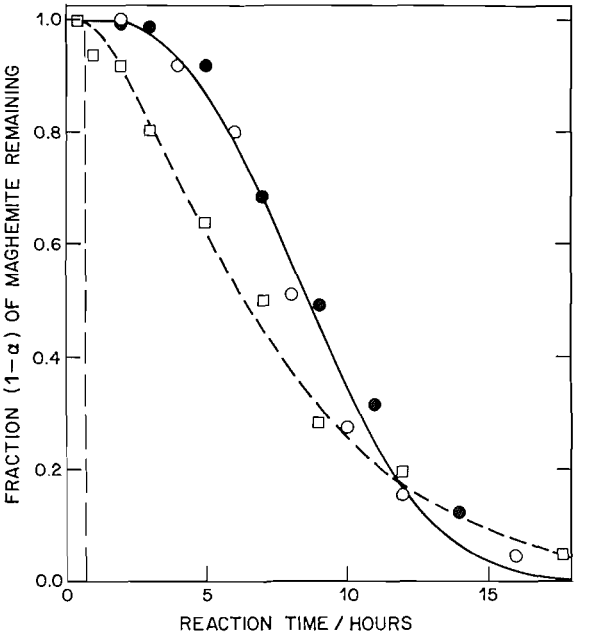


FIG. 1. Hydrothermal conversion of silica-free maghemite (preparation **A**) to hematite at 174.5 ± 0.3°C. Open circles: plain water. Filled circles: plain water, 20 mg α-Fe_2O_3 per g maghemite added. Squares: 1.05 *M* KOH. Vertical broken line: effective zero reaction time. Curves: fit of data to eq. [1].

curve shape (exponential if $n = 1$, sigmoidal if $n > 1$), and k is a time-scaling constant. Equation [1] resembles those developed by Avrami (42), Erofeyev (43), and others (44, 45) for phase transformations in homogeneous solids, but similar equations describe some chemical dissolution processes involving metal oxides (46) and, indeed, a variety of non-chemical phenomena (Weibull–Kao statistics) (47, 48). We emphasize that our choice of eq. [1] was made on purely empirical grounds, without reference to any mechanistic model, and accordingly no special interpretation should be attached to the shape and scaling parameters, n and k.

Table 3 summarizes the kinetics of the hydrothermal transformation of silica-free maghemite to hematite according to eq. [1], based on Δw measurements; SSA and moisture content data (Table 1) and estimates of the relative amounts of maghemite and hematite by XRD were less precise than Δw, but confirmed these results semi-quantitatively at least. These reaction rates were independent of the age of the maghemite sample (up to 1 year), the presence of O_2 or CO_2 in the autoclaves, the nature of M^+ in the MOH used in the preparation and in the reaction mixture, the relative amounts of the solid and liquid phases (the latter was always at least 10-fold greater by weight), and the dimensions and structural metal of the autoclaves. After comple-

Can. J. Chem. Downloaded from www.nrcresearchpress.com by 210.87.254.40 on 09/05/12
For personal use only.

TABLE 3. Representation of the kinetics of the hydrothermal conversion of silica-free maghemite (material **A**) to hematite in terms of eq. [1][a]

[KOH] (M)	T (°C)	M	$10^5 k$ (s^{-1})	r (no. of data)
None	187.2	2.24 ± 0.18	20.2 ± 1.4	0.982(8)
	179.1	2.59 ± 0.12	4.2 ± 0.3	0.997(5)
	174.7	2.64 ± 0.17	3.1 ± 0.4	0.992(7)
	170.6	2.80 ± 0.08	2.33 ± 0.15	0.998(7)
	160.6	2.45 ± 0.10	1.36 ± 0.16	0.998(7)
1.0×10^{-3}	174.3	2.40 ± 0.24	2.7 ± 0.6	0.986(5)
1.0×10^{-2}	174.7	2.37 ± 0.16	5.7 ± 0.7	0.991(6)
1.0×10^{-1}	174.3	1.70 ± 0.07	3.1 ± 0.3	0.993(9)
1.0	174.2	1.35 ± 0.03	3.8 ± 0.2	0.999(8)
1.0×10^{-1}	187.2	1.34 ± 0.06	8.9 ± 0.4	0.997(4)
1.0	187.2	1.69 ± 0.09	9.7 ± 0.5	0.997(4)

[a]From magnetization (Δw) data; r is the coefficient of correlation, and $\pm$ indicates standard deviation. Specific surface of starting material 72 $m^2 g^{-1}$ in all cases.

tion of the reactions in plain water, the liquid phase was neutral or slightly alkaline.

Early experiments using maghemite prepared in glassware showed, in general, a similar conformity to eq. [1], e.g., at 178°C, $n = 1.8$ with $k = 4.3 \times 10^{-5}$ s^{-1} for 0.01 M NaOH, and $n = 1.0$ with $k = 2.7 \times 10^{-5}$ s^{-1} for 0.10 M NaOH, confirming the general effect of $[OH^-]$ upon n seen in Table 3; the possibility of silica contamination, however, excludes these data from the table.

(*viii*) "Seeding" the reaction mixture with α-Fe_2O_3 up to the same amount as maghemite did *not* accelerate the conversion of maghemite to hematite, regardless of the presence or absence of alkali or of silica (Table 2 and Fig. 1). An apparent slight *retarding* effect of added hematite is too small to be significant.

(*ix*) The rate of the hydrothermal conversion of maghemite to hematite was somewhat greater the larger the SSA of the starting material (A_0), as Table 4 shows for silica-free maghemite in water. These data, on fitting to eq. [1] with n fixed at 2.24, give $k = 1.7 \times 10^{-4}$ s^{-1} for $A_0 = 46$ $m^2 g^{-1}$ and $k = 2.0 \times 10^{-4}$ s^{-1} for $A_0 = 75$ $m^2 g^{-1}$. In an early experiment, good fits to eq. [1] were obtained with $n = 1.00$ (cf. "first order" homogeneous reaction kinetics) for maghemite samples of $A_0 = 85$ and 120 $m^2 g^{-1}$ in 0.1 M NaOH at 178°C, giving $k = 2.7 \times 10^{-5}$ and 6.4×10^{-5} s^{-1} respectively; these samples were, however, prepared using glassware. The important point is that the effect of SSA was quite small below, say, 80 $m^2 g^{-1}$, so that it was possible to obtain reproducible kinetics from one batch of maghemite to another so long as the SSA's were roughly similar.

(*x*) "Maghemite" made from ferrous oxalate (37) had a relatively low SSA (32 $m^2 g^{-1}$) yet showed a rapid decline in Δw on hydrothermal treatment, e.g., even at 95°C, $k \sim 4 \times 10^{-5}$ s^{-1} with $n \sim 1.0$ in eq. [1]. This material, however, contained 0.7% iron(II) in addition to some 50% α-Fe_2O_3; since the latter has been shown not to affect the hydrothermal conversion rate of pure maghemite to hematite, it appears that iron(II) may catalyze the reaction. For all other maghemite preparations used in these kinetic studies, however, the iron(II) content was known to be much less than 0.01% and was probably less than 0.001%.

TABLE 4. Effect of initial surface area A_0 on the kinetics of hydrothermal conversion of silica-free maghemite to hematite in water at 187.5°C

t_{oven} (h)	% γ observed ($A_0 = 46$ $m^2 g^{-1}$)	% γ calculated[a] ($A_0 = 75$ $m^2 g^{-1}$)
0.5	100	100
1.0	90	97
2.0	53	42
2.5	28	16
3.0	11	4

[a]Interpolated from data of Table 2.

Discussion

The analytical data and the observations (*iii*) support the suggestion of Braun (24) that maghemite, as prepared and used in this study, is better represented as HFe_5O_8, rather than in the traditional way as "γ-Fe_2O_3", but they also show that the protons which fill the octahedral cation vacancies of the pseudo-spinel Fe_2O_3 structure (24, 25) are to some extent exchangeable with Na^+ and K^+. These respective ions will therefore be present in maghemite derived from magnetite prepared by precipitation of iron(II)–(III) mixtures with hot aqueous NaOH or KOH, since this magnetite is not stoichiometric Fe_3O_4 but rather a solid solution of Fe_3O_4 in maghemite, represented above as $Fe_{3-x}O_{4-x}$ but in fact containing moisture (and hence protons in cation sites) roughly in proportion to x. Alkali-metal ferrites with the spinel ($LiFe_5O_8$, $NaFe_5O_8$) (24, 49) or other (KFe_5O_8) (49, 50) structures, or of the "β-alumina" type $(1 + y)M_2O \cdot 11Fe_2O_3$ (M = Na, K) which retains some elements of the spinel structure (51–56), are well known, as are some mixed-alkali-metal analogues (51, 57). The maghemite samples $H_{1-\delta}M_\delta Fe_5O_8$ prepared in this study contained far less alkali metal ion than these ferrites, since δ was always less than 0.1, but we note that the saturation magnetization of maghemite decreased as δ increased, in accordance with the lack of ferromagnetism at room temperature in ferrites such as KFe_5O_8, KFe_7O_{11}, and $KFe_{11}O_{17}$ (50, 52).

Can. J. Chem. Downloaded from www.nrcresearchpress.com by 210.87.254.40 on 09/05/12
For personal use only.

The mechanism of oxidation of "dry" magnetite by air has been the subject of controversy (9–13), but it seems that the presence of water is necessary for maghemite production, otherwise hematite is formed (9, 11, 22–25). This applies whether or not α-Fe_2O_3 nuclei are present (13, 23). The present study (results (*iii*)) suggests that uptake of water from the gas phase by magnetite is associated with non-stoichiometry in the latter ($Fe_{3-x}O_{4-x}$, $0 < x \leq 1$), presumably because the protons of the water can be accommodated in the cation vacancies, concomitantly stabilizing the spinel structure (22–25, 58); thus, coarsely crystalline, *stoichiometric* Fe_3O_4 oxidizes to α-Fe_2O_3 even when prepared by a "wet" method (36) (results (*ii*)). Since the finely-particulate magnetite which results from conventional "wet" methods is invariably non-stoichiometric, and indeed since surface oxidation of any very finely powdered magnetite can lead to significant overall departures from stoichiometry, the well-established correlation (9–15) between magnetite particle size and oxidation product can be recast in terms of the capacity of the non-stoichiometric solid for water uptake.

The oxidation of magnetite evidently involves the migration of Fe^{3+} ions outwards toward newly-formed O^{2-} at the crystal surface (40). The oxidation should therefore proceed relatively quickly to maghemite if sufficient water protons are present to preserve the spinel structure during oxidation, but *not* so many as to *eliminate* the cation vacancies, through which the Fe^{3+} ions can diffuse with relative ease. If this picture is correct, the aerial oxidation of $Fe_{3-x}O_{4-x}$ in hydrothermal conditions should still yield maghemite, but at a much *slower rate* than in air alone, because cation vacancies will be almost immediately eliminated by the large excess of water. This is indeed the case (result (*i*)); thus, paradoxically, although water is necessary for the production of maghemite, a superabundance of water suppresses the rate of the process dramatically.

A further paradox is that the presence of liquid water accelerates the subsequent decomposition of maghemite to hematite, despite the importance of water in enabling maghemite to exist.

The hydrothermal decomposition of maghemite occurs in a temperature regime some 170°C cooler than does the "dry" transformation to hematite, as may be seen by comparing Tables 1 and 2 with Feitknecht and Mannweiler's Fig. 2 (59) (which refers to a maghemite preparation "1" closely similar in particle size to our preparations **A** and **B**). The SEM showed that the reaction in plain water gave nicely-formed rhombohedra of α-Fe_2O_3, much larger (~300 nm length) and better shaped than either the parent maghemite crystals or hematite formed by the decomposition of the dry solid in air at higher temperatures, as exemplified by Feitknecht and Mannweiler's Fig. 6 (59). Thus, although increases in crystallite size and decreases in SSA are observed in the conversion of "dry" maghemite to hematite as well as in the hydrothermal reaction, the mechanisms of reaction are evidently different, a topotactic particle-to-particle chain reaction being likely in the former (59) and a dissolution–reprecipitation process involving discrete particles in the latter. Alkaline hydrothermal media produced still larger, clean-facetted tables of hematite, characteristic of growth from hydrothermal solution (41).

The kinetics of the hydrothermal decomposition of maghemite in plain water (results (*vii*)) differed from those of the "dry" reaction in being much faster and in the sigmoidal, as opposed to roughly exponential, shape of the plots of extent of reaction vs. time (Fig. 1, compare refs. 58 and 59). Again, markedly different reaction mechanisms are indicated. The Avrami–Erofeyev type of relationship (eq. [1]), which describes the sigmoidal curves, empirically, is commonly associated with reactions occurring in initially homogeneous solid phases (42–45), although Kabai (46) applied it to the kinetics of dissolution of metal oxides in aqueous acids with the conclusion that values of n greater than unity were associated with physical disintegration of the solid oxide (increase in SSA); neither situation, however, seems relevant in the present context.

The observation (*viii*), that seeding with α-Fe_2O_3 does *not* accelerate the hydrothermal transformation of maghemite, eliminates hematite nucleation and the availability of hematite surfaces for growth as rate-determining factors. Furthermore, the absence of any evidence for hydrothermal ripening of either maghemite or hematite on the time-scale of these kinetic experiments (results (*vi*)) argues against any rapid dissolution–reprecipitation pre-equilibrium, or reversibility of the precipitation of α-Fe_2O_3, as mechanistically significant processes. The most feasible remaining mechanistic model, therefore, is one in which both the dissolution of maghemite and a subsequent solution-phase step leading to the precipitation of α-Fe_2O_3 are slow and irreversible. The latter process may require a pre-existing α-Fe_2O_3 surface or surrogate, but the *extent* of this may not be rate determining if the concentration of iron(III) in solution is very low (as seems likely). Reactions [2] and [3] seem reasonable models; the aqueous form of iron(III) is taken

Can. J. Chem. Downloaded from www.nrcresearchpress.com by 210.87.254.40 on 09/05/12
For personal use only.

to be the neutral hydroxo-species in accordance with the predominance of cation hydrolysis under hydrothermal conditions (35) and the absence of any significant effect of low concentrations of alkali.

[2] $2HFe_5O_8(s) + 14H_2O(l) \rightarrow 10Fe(OH)_3(aq)$

[3] $10Fe(OH)_3(aq) \rightarrow 5\alpha\text{-}Fe_2O_3(s) + 15H_2O(l)$

Taking reaction [3] to be first-order in iron(III) its rate will be limited at first by the slow build-up of $[Fe(OH)_3]$ from zero; then, after a relatively rapid main phase, the diminished surface of maghemite remaining will limit the dissolution rate (we note that SSA does affect the reaction rate somewhat — observation (*ix*)), leading to a sigmoidal plot of α against time. Assuming, by analogy with $Ni(OH)_3^-(aq)$ (32), that $Fe(OH)_4^-(aq)$ becomes the important iron(III) species in water at high pH and elevated temperatures, we can anticipate that high $[OH^-]$ will speed up the supply of iron(III) to the solution phase but, by the same token, slow the precipitation step by permitting higher [Fe(III)] to remain in solution. This will lead to an approach to exponential kinetics ($n = 1$ in eq. [1]) which are faster than the corresponding sigmoidal kinetics in the earlier stages but slower later; this is indeed observed (Fig. 1), and the larger, better-formed $\alpha\text{-}Fe_2O_3$ crystals obtained in 1 *M* alkali also suggest higher iron(III) levels in solution and slower precipitation.

[4] $2HFe_5O_8(s) + 10OH^-(aq) + 14H_2O(l) \rightleftharpoons 10Fe(OH)_4^-(aq)$

[5] $10Fe(OH)_4^-(aq) \rightarrow 5\alpha\text{-}Fe_2O_3(s) + 10OH^-(aq) + 15H_2O(l)$

Since maghemite exhibits ion-exchanging properties, the solid that reacts in aqueous KOH is not, strictly speaking, chemically the same as that in aqueous NaOH or in plain water. Fortunately, the rate of formation of hematite from maghemite was found to be the same in 1 *M* NaOH as in 1 *M* KOH, so that it is permissible to write eqs. [4] and [5] simply in terms of HFe_5O_8 and OH^-.

The above facts and proposed mechanisms contrast with those for the superficially similar alkaline hydrothermal conversion of $Ni(OH)_2$ to NiO (32), in which the reaction corresponding to [4] is rapid and reversible (giving rise to Ostwald ripening of $Ni(OH)_2$), the rate of the step analogous to [5] is completely controlled by the available area of NiO (leading to a dependence of α on t_{corr}^3), and neutral-pH pathways analogous to [2] and [3] are undetectable.

The dramatic retardation of the hydrothermal decomposition of maghemite by silica (results (*iv*), (*v*)) has obvious implications relating to the survival of maghemite in nature, where it is usually accompanied by quartz (2), and to laboratory practice in investigating iron oxides. Any explanation of the effect needs to accommodate the facts that, when silica is present and the pH is high, goethite may form in place of hematite when the alkali cation present in solution is K^+ but is itself suppressed, leaving hematite as the major product in the long term, when the cation is Na^+. Four distinct modes of involvement of silica can readily be visualized, but each presents problems.

(*a*) Iron(III) becomes complexed by silicate species in solution, so retarding steps [3] and [5]. Thermodynamic data on the weak complexing of Fe^{3+} by $Si(OH)_4$ at 25°C and low pH are available (60) but are inapplicable to high temperatures and neutral or alkaline solutions because of hydrolysis and polymerization. Even if the complexing power of low levels of dissolved silicate could be shown to be sufficient to reduce the iron(III) concentration markedly, however, this alone would not explain why goethite may form instead of hematite in some circumstances but not in others. Many polybasic anions (61) including silicate (62, 63) are known to inhibit the somewhat analogous aqueous conversion of iron(III) hydroxide gels to α-FeO(OH), but there is no correlation of this effect with iron(III) complex stability constants, again suggesting that inhibition by such potential complexing agents occurs elsewhere than in the solution phase.

(*b*) Silica impregnates or coats the maghemite with a dissolution-resistant iron(III) silicate, so suppressing steps [2] and [4]. Chemisorption of this kind has been demonstrated for other iron(III) oxide – hydroxide materials by infrared spectroscopy, although, just as in the present study, XRD patterns gave no indication of this (17, 63). Highly resistant coatings of acmite, $NaFeSi_2O_6$, form readily in hydrothermal media containing NaOH, iron(III), and silica, but no potassium analogue is known (64); this suggests a connection with the fact that goethite formation, though favored by high concentrations of KOH (cf. decomposition of ferrihydrite (65)), is itself suppressed by NaOH. It is, however, difficult to see why the identity of the final product should be determined by suppression of step [4] rather than by influencing [5]; goethite was never obtained when silica was absent.

(*c*) Decomposition via dissolution is stopped by silica as in (*b*), but slow solid-phase reactions continue (cf. Schwertmann (61)). Neither direct measurement (results (*i*)) nor extrapolation of rate data (58, 59) indicate any significant solid-state decomposition of maghemite at ~180°C on the time-scale of our experiments, but it is conceded that "dry"

Can. J. Chem. Downloaded from www.nrcresearchpress.com by 210.87.254.40 on 09/05/12
For personal use only.

decompositions involve a different (partially dehydrated) kind of maghemite from that present in the hydrothermal systems.

(*d*) Silica eliminates the nuclei or coats the growth surfaces of the product, possibly by acmite formation. Such an interaction would presumably affect goethite differently from the less reactive hematite, and would also explain the cation effect as in (*b*). Unfortunately, the evidence of seeding experiments (results (*viii*), Fig. 1, and Table 2) indicated in every case that nucleation and product surface availability were *not* rate-controlling in hematite formation, although they might have been in the production of goethite (65, 66). The possibility remains that these factors may come to be rate-controlling if they are drastically reduced by interaction with silica; a small quantity of silica could conceivably deactivate large areas of product growth surface or large numbers of nuclei.

Some light may be shed on this mechanistic problem by comparing the characteristics of the hydrothermal transformation of maghemite ("γ-Fe_2O_3") with those reported by Schwertmann and Taylor (66) for the conversion of lepidocrocite (γ-FeO(OH)) to goethite in aqueous alkali at 20–80°C. In common with the Fe_2O_3 system, the FeO(OH) conversion occurs via solution rather than topotactically, is faster for smaller particles, follows various kinds of rate equations (including sigmoidal and quasi-exponential) depending on [KOH] and temperature, and is suppressed by silicate. On the other hand, the Ostwald ripening of FeO(OH) in the presence of silicate, the marked accelerating effect of KOH, and the facilitation of reaction by seeding differentiate the FeO(OH) system from the Fe_2O_3. Schwertmann and Taylor (66) argue persuasively that silicate affects the γ-FeO(OH) reaction by inhibiting nucleation of goethite. We therefore suggest that silica together with Na^+ affects the production of goethite from maghemite by suppressing its nucleation, but that silica affects the more important reaction, α-Fe_2O_3 formation, through some other process, probably similar to (*b*) above.

Finally, we note that agitation had no significant effect on the rate of reaction of γ-FeO(OH) (66). The same was taken to be true of the maghemite reaction, since diffusional processes are rapid in hydrothermal systems, but we were unable to check this assumption for lack of PTFE-lined, non-magnetic stirred autoclaves with precise temperature control.

Acknowledgements

We thank Dr. A. E. Oldershaw for SEM photographs, Mrs. D. Johnson for XRD patterns, Drs. P. Bayliss and H. L. Yeager for technical advice, and the Natural Sciences and Engineering Research Council of Canada for financial assistance.

1. U. SCHWERTMANN. Fortschr. Miner. **46**, 274 (1968).
2. R. M. TAYLOR and U. SCHWERTMANN. Clay Miner. **10**, 289 (1974).
3. E. I. NIKITINA, V. I. SOTNIKOV, A. A. PROSKURYAKOV, D. K. ARCHIPENKO, and L. M. KRIVOPUTSKAYA. Miner. Paragenezisy Miner. Gidroterm. Mestorozhd. 61 (1974); Chem. Abstr. **83**, 100844 (1975).
4. P. TOULMIN III, A. K. BAIRD, B. C. CLARK III, K. KEIL, H. R. ROSE, JR., R. P. CHRISTIAN, P. H. EVANS, and W. C. KELLIHER. J. Geophys. Res. **82**, 4625 (1977).
5. A. O. FULLER and R. B. HARGREAVES. Icarus, **34**, 614 (1978).
6. D. R. HUFFMANN. Astrophys. J. **161**, 1157 (1970).
7. P. G. MANNING. Chem. Soc. Rev. **5**, 233 (1976).
8. E. Z. BASTA. Econ. Geol. **54**, 698 (1959).
9. W. FEITKNECHT and H. W. LEHMANN. Helv. Chim. Acta, **42**, 2035 (1959).
10. U. COLOMBO, F. GAZZARRINI, G. LANZAVECCHIA, and G. SIRONI. Science, **147**, 1033 (1965).
11. T. ELDER. J. Appl. Phys. **36**, 1012 (1965).
12. K. J. GALLAGHER, W. FEITKNECHT, and U. MANNWEILER. Nature, **217**, 1118 (1968).
13. W. FEITKNECHT and K. J. GALLAGHER. Nature, **228**, 548 (1970).
14. K. HANEDA and A. H. MORRISH. J. Phys. **38**, C1-321 (1977).
15. B. GILLOT, A. ROUSSET, and G. DUPRE. J. Solid State Chem. **25**, 263 (1978).
16. R. M. TAYLOR and U. SCHWERTMANN. Clay Miner. **10**, 299 (1974).
17. U. SCHWERTMANN and H. THALMANN. Clay Miner. **11**, 189 (1976).
18. V. I. BAGIN. Izv. Akad. Nauk S.S.S.R., Fiz. Zemli, 104 (1967); Chem. Abstr. **67**, 48439k (1967).
19. J. D. BERNAL, D. R. DASGUPTA, and A. L. MACKAY. Nature, **180**, 645 (1957).
20. R. GIOVANOLI and R. BRÜTSCH. Thermochim. Acta, **13**, 15 (1975).
21. H. W. VAN DER MAREL. J. Sedimentol. Petrol. **21**, 12 (1951).
22. I. DAVID and A. J. E. WELCH. Trans. Faraday Soc. **52**, 1642 (1956).
23. H. P. JOHNSON and R. T. MERRILL. J. Geophys. Res. **77**, 334 (1972).
24. P. B. BRAUN. Nature, **170**, 1123 (1952).
25. A. AHARONI, E. H. FREI, and M. SCHIEBER. J. Phys. Chem. Solids, **23**, 545 (1962).
26. M. A. GHEITH. Am. J. Sci. **250**, 677 (1952).
27. J. L. KULP and A. F. TRITES. Am. Miner. **36**, 23 (1951).
28. M. NAGAYAMA and M. COHEN. J. Electrochem. Soc. **109**, 781 (1962); **110**, 670 (1963).
29. K. A. NESMEYANOVA, V. I. KASATKIN, V. A. GASHENKO, and V. G. KASATKINA. Teploenergetika (Moscow), 54 (1976); Chem. Abstr. **84**, 183175n (1976).
30. D. E. DAVIES and U. R. EVANS. J. Chem. Soc. 4373 (1956).
31. U. R. EVANS. The corrosion and oxidation of metals. First supplementary volume. Edward Arnold, Ltd., London. 1968. pp. 25, 26.
32. T. W. SWADDLE and T. C. T. WONG. Can. J. Chem. **56**, 363 (1978).
33. A. I. VOGEL. A textbook of quantitative inorganic analysis. 3rd ed. Longmans, London. 1961.

34. G. N. SCHRAUZER and T. D. GUTH. J. Am. Chem. Soc. **98**, 3508 (1976).
35. T. W. SWADDLE, J. H. LIPTON, G. GUASTALLA, and P. BAYLISS. Can. J. Chem. **49**, 2433 (1971).
36. M. BOOY and T. W. SWADDLE. Can. J. Chem. **56**, 402 (1978).
37. V. RAO, A. L. SHASHIMOHAN, and A. B. BISWAS. J. Mater. Sci. **9**, 430 (1974).
38. M. BOOY and T. W. SWADDLE. Can. J. Chem. **55**, 1762 (1977).
39. N. A. VASYUTINSKII. Izv. Akad. Nauk S.S.S.R. Met. Gorn. Delo, 39 (1963); Chem. Abstr. **59**, 12511e (1963).
40. P. S. SIDHU, R. J. GILKES, and A. M. POSNER. J. Inorg. Nucl. Chem. **39**, 1953 (1977).
41. E. D. KOLB, A. J. CAPORASO, and R. A. LAUDISE. J. Cryst. Growth, **19**, 242 (1973).
42. M. AVRAMI. J. Chem. Phys. **7**, 1103 (1939); **8**, 212 (1940).
43. B. V. EROFEYEV. Compt. Rend. Acad. Sci. U.R.S.S. **52**, 511 (1946).
44. D. TURNBULL. Solid State Phys. **3**, 225 (1956).
45. A. R. ALLNATT and P. W. M. JACOBS. Can. J. Chem. **46**, 111 (1968).
46. J. KABAI. Acta Chim. (Budapest), **78**, 57 (1973).
47. W. WEIBULL. J. Appl. Mech. **18**, 293 (1951).
48. J. H. K. KAO. Technometrics, **1**, 389 (1959).
49. E. LICHTNER and G. SZALEK. Z. Anorg. Allgem. Chem. **360**, 151 (1968).
50. C. J. M. ROOYMANS, C. LANGEREIS, and J. A. SCHULKES. Solid State Commun. **3**, 85 (1965).
51. K. O. HEVER. J. Electrochem. Soc. **115**, 826 (1965).
52. W. L. ROTH. U.S. Patent No. 3,284,359 (Nov. 8, 1966).
53. W. L. ROTH and R. J. ROMANCZUK. J. Electrochem. Soc. **116**, 975 (1969).
54. B. C. H. STEELE. MTP Intern. Rev. Sci., Inorg. Chem., Ser. 1, Vol. 10. Butterworths, London. 1972. pp. 137–139.
55. G. J. DUDLEY and B. C. H. STEELE. J. Solid State Chem. **21**, 1 (1977); J. Mater. Sci. **13**, 1267 (1968).
56. G. C. FARRINGTON and J. L. BRIANT. Science, **204**, 1371 (1979).
57. M. LENGLET. Rev. Chim. Miner. **5**, 1169 (1968).
58. F. E. DEBOER and P. W. SELWOOD. J. Am. Chem. Soc. **76**, 3365 (1954).
59. W. FEITKNECHT and U. MANNWEILER. Helv. Chim. Acta, **50**, 571 (1967).
60. L. L. OLSON and C. R. O'MELIA. J. Inorg. Nucl. Chem. **35**, 1977 (1973).
61. U. SCHWERTMANN. Geoderma, **3**, 207 (1969).
62. W. SCHELLMANN. Chem. Erde, **20**, 104 (1959).
63. A. J. HERBILLON and J. TRAN VINH AN. J. Soil Sci. **20**, 233 (1969).
64. R. A. LAUDISE. Prog. Inorg. Chem. **3**, 1 (1962).
65. D. G. LEWIS and U. SCHWERTMANN. Clays Clay Miner. **27**, 195 (1979).
66. U. SCHWERTMANN and R. M. TAYLOR. Clays Clay Miner. **20**, 150 (1972); **20**, 159 (1972).

Can. J. Chem. Downloaded from www.nrcresearchpress.com by 210.87.254.40 on 09/05/12
For personal use only.

Kinetics and mechanism of the oxidation of tris(4,7-dihydroxy-1,10-phenanthroline)-iron(II) by molecular oxygen

FLORA T. T. NG[1] AND PATRICK M. HENRY

Guelph–Waterloo Centre for Graduate Work in Chemistry, University of Guelph, Guelph, Ont., Canada N1G 2W1

Received August 15, 1979[2]

Can. J. Chem. Downloaded from www.nrcresearchpress.com by 210.87.254.105 on 09/05/12
For personal use only.

FLORA T. T. NG and PATRICK M. HENRY. Can. J. Chem. **58**, 1773 (1980).

The reaction of $(OHP)_3Fe(II)$ (OHP = 4,7-dihydroxy-1,10-phenanthroline) with oxygen in aqueous 0.1 *N* NaOH solution takes place according to the stoichiometry:

$$4\,(OHP)_3Fe(II) + 2H_2O + O_2 \rightarrow 4(OHP)_3Fe(III) + 4OH^-$$

This stoichiometry holds whether $(OHP)_3Fe(II)$ or O_2 is in excess. The rate law over a wide range of $(OHP)_3Fe(II)$ and O_2 concentrations at 0.1 *N* NaOH has the form:

$$-\tfrac{1}{4}[(OHP)_3Fe(II)]/dt = -d[O_2]/dt = k_2[(OHP)_3Fe(II)][O_2]$$

A notable feature of this oxidation is that *free* HO_2^- is not produced as an intermediate. A plausible mechanism involving *bound* superoxide or peroxide as intermediates is proposed. Due to the redox nature of the OHP ligand and the low potential of the $(OHP)_3Fe(II)$ complex, a 4 electron transfer from one $(OHP)_3Fe(II)$ to one O_2 to give a Fe(IV) species with an oxidized ligand is a distinct possibility. The rate–pH profile is consistent with the protonation of $(OHP)_3Fe(II)$ ($pK_a \approx 9.4$) to give a more reactive species.

FLORA T. T. NG et PATRICK M. HENRY. Can. J. Chem. **58**, 1773 (1980).

La réaction du $(OHP)_3Fe(II)$ (OHP = dihydroxy-4,7 phénanthroline-1,10) avec l'oxygène dans une solution aqueuse de NaOH 0,1 *N* se fait selon la stoechiométrie:

$$4\,(OHP)_3Fe(II) + 2H_2O + O_2 \rightarrow 4(OHP)_3Fe(III) + 4OH^-$$

Cette stoechiométrie est valable même lorsque $(OHP)_3Fe(II)$ et O_2 sont en excès. Sur une large échelle de concentration de $(OHP)_3Fe(II)$ et de O_2 dans le NaOH 0,1 *N*, la loi de la vitesse a la forme:

$$-\tfrac{1}{4}[(OHP)_3Fe(II)]/dt = -d[O_2]/dt = k_2[(OHP)_3Fe(II)][O_2]$$

Le fait important de cette oxydation est l'absence de l'intermédiaire HO_2^- libre. On propose un mécanisme plausible impliquant comme intermédiaire un superoxyde ou un peroxyde lié. Compte tenu de la nature redox du ligand OHP et du faible potentiel du complexe de $(OHP)_3Fe(II)$, on peut considérer une autre possibilité faisant intervenir un transfert de 4 électrons d'un $(OHP)_3Fe(II)$ à un O_2 conduisant à l'espèce Fe(IV) avec un ligand oxydé. Le profil de la vitesse vs. le pH est en accord avec la protonation de $(OHP)_3Fe(II)$, ($pK_a \approx 9.4$) qui conduit à des espèces plus réactives.

[Traduit par le journal]

Introduction

The interaction of dioxygen with iron has aroused considerable interest in recent years both because of the importance of such interactions in biological systems such as hemoproteins and oxidases (1–5) as well as in the reduction of oxygen for fuel cell applications (6). A fundamental understanding of the reaction of dioxygen with iron complexes would help elucidate similar processses in biological systems.

A number of workers have reported the oxidation of Fe(II) species by O_2 in aqueous solution (7–14). In general two types of kinetic behaviour are observed: first order in [oxygen] and second order in [Fe(II)] or an anion promoted reaction which is first order in [oxygen] and first order in [Fe(II)]. The former must proceed by the interaction of two atoms of Fe^{2+} with O_2 [1]–[3],

[1] $Fe^{2+} + O_2 \rightleftharpoons Fe^{2+}O_2$

[2] $Fe^{2+}O_2 + Fe^{2+} \rightarrow Fe^{2+}O_2Fe^{2+}$

[3] $Fe^{2+}O_2Fe^{2+} + 2H^+ \rightarrow 2Fe^{3+} + H_2O_2$

while the second is postulated to involve formation of superoxide in the rate limiting step [4], [5]

[4] $Fe^{2+}O_2 + X^- \xrightarrow{\text{slow}} FeX^{2+} + O_2^-$

[5] $Fe^{2+} + O_2^- + 2H^+ \xrightarrow{\text{fast}} Fe^{3+} + H_2O_2$

although it has been pointed out that iron(IV) rather than O_2^- could be an intermediate in the second mechanism [6].

[6] $X^- + Fe^{2+}O_2 + 2H^+ \rightarrow FeX^{3+} + H_2O_2$

In all mechanisms it is assumed that the hydrogen peroxide formed reacts rapidly with more Fe^{2+} to complete the reduction to water.

[1]Present address: Department of Chemical Engineering, University of Waterloo, Waterloo, Ont., Canada N2L 3G1.

[2]Revision received April 29, 1980.

0008-4042/80/171773-07$01.00/0

©1980 National Research Council of Canada/Conseil national de recherches du Canada

Can. J. Chem. Downloaded from www.nrcresearchpress.com by 210.87.254.105 on 09/05/12
For personal use only.

TABLE 1. Stoichiometry of the oxidation of 4,7-dihydroxy-1,10-phenanthroline, $(OHP)_3Fe(II)$, by molecular oxygen at 25°C using either an oxygen electrode or gas uptake apparatus[a]

$[(OHP)_3Fe(II)]$ (mol × 10^6)	Initial $[O_2]$ (ppm)	Final $[O_2]$ (ppm)	O_2 consumed In ppm	O_2 consumed In mol × 10^6	$\frac{(OHP)_3Fe(II)}{O_2}$
Oxygen electrode runs					
10.0	8.3	5.3	3.0	2.82	3.5
10.0	24.8	21.5	3.3	3.14	3.2
14.0	8.3	4.2	4.1	3.90	3.6
16.2	11.0	6.5	4.5	4.28	3.8
16.2	8.0	3.5	4.5	4.28	3.8
19.8	8.1	2.5	5.6	5.33	3.2
30.0	20.4	12.2	8.2	7.81	3.8
Gas uptake					
125				35	3.6
125				30	4.2
125				28	4.5
				Ave.	3.7

[a]Volume of solution = 30.5 mL.

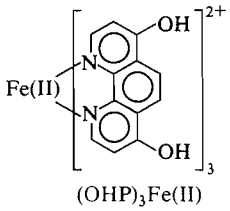
[7] $H_2O_2 + 2Fe^{2+} + 2H^+ \rightarrow 2Fe^{3+} + 2H_2O$

Of interest in regard to possible Fe(IV) intermediates is the work of Hammond and Wu (15) who studied the reaction of Fe(II) chloride species with O_2 in non-aqueous solvents. Their results were consistent with a $4e^-$ reduction of O_2 by $2Fe^{2+}$ [8].

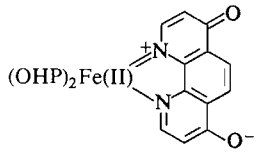
[8] $2FeCl_2 + O_2 \rightarrow Cl_2FeOOFeCl_2 \rightarrow 2Cl_2FeO$

Collman and co-workers (6) have synthesized bridged porphyrin rings for the purpose of preparing binuclear iron(II) porphyrins which would cause a similar $4e^-$ reduction of O_2 by formation of two Fe(IV) species. Iron(IV) porphyrins have been characterized (16–18).

Tris(4,7-dihydroxy-1,10-phenanthroline)iron(II), $(OHP)_3Fe(II)$, reacts so rapidly with O_2 in alkaline aqueous solution that it has been used as a reagent for determination of dissolved oxygen (19). The mechanism of this oxidation is of interest for several reasons. First the oxidation very likely proceeds by a mechanism not involving direct interaction of O_2 with the Fe(II) atom since the Fe(II) is coordinately saturated. To our knowledge no reactions of Fe(II) with O_2 in which O_2 does not enter the primary Fe(II) coordination sphere have been reported. However, outersphere oxidations of ruthenium(II) amines (20, 21) and hexacyanochromium(II) have been reported (22). Secondly the reduction potential of this complex is so low (−0.06 V in basic media (23)) that Fe(IV) species become likely intermediates. Finally the ligand is formally analogous to hydroquinone and should itself be capable of donating two electrons to O_2:

[9] 

$(OHP)_3Fe(II)$

$\xrightarrow{-2H^+}$ 

+ $2e^-$

1

This paper describes a kinetic study of the reaction of $(OHP)_3Fe(II)$ with O_2 in aqueous basic medium.

Results

(a) Stoichiometry and Products

A solution of $(OHP)_3Fe(II)$ in 0.1 *N* NaOH is rose red with an absorption maximum at 520 nm ($\varepsilon = 1.48 \times 10^4$). As reported by Poe and Diehl (19) passage of air or oxygen through the solution resulted in a blackish grey solution with absorption maxima at 750 nm ($\varepsilon = 1.6 \times 10^3$), 650 nm (broad, $\varepsilon = 1.6 \times 10^3$), and 520 nm ($\varepsilon = 3.3 \times 10^3$). The colour of $(OHP)_3Fe(II)$ could not be restored by passage of argon or nitrogen through the solution but the addition of ascorbic acid or sodium dithionite as reducing agents under an O_2 free atmosphere did give a rose red solution with a spectrum quantitatively the same as the starting $(OHP)_3Fe(II)$ solution.

By adding O_2 gradually to a solution of $(OHP)_3Fe(II)$, Poe and Diehl (19) found that the

Can. J. Chem. Downloaded from www.nrcresearchpress.com by 210.87.254.105 on 09/05/12
For personal use only.

overall stoichiometry of the reaction was 4-$(OHP)_3Fe(II)$'s per O_2 consumed. To determine if H_2O_2 is an intermediate in the reaction we have independently measured the stoichiometry when O_2 is in excess. For this purpose we used both a constant pressure gas uptake apparatus (24) and an oxygen electrode. The results are listed in Table 1. Within experimental error the data are consistent with the stoichiometry shown below:

$$[10] \quad 4(OHP)_3Fe(II) + O_2 + 2H_2O \rightarrow 4(OHP)_3Fe(III) + 4OH^-$$

Hydrogen peroxide was not detected by the standard KI /starch indicator method.

(b) Kinetics of Reaction of $(OHP)_3Fe(II)$ with Molecular Oxygen

The oxidation kinetics were measured under pseudo first order conditions using either O_2 or $(OHP)_3Fe(II)$ in excess. Most runs were followed spectrophotometrically using a stopped-flow reactor but a few with $(OHP)_3Fe(II)$ in excess were followed by metering the O_2 concentration with an oxygen electrode. All kinetic runs obeyed good pseudo first order kinetics. As expected from the stoichiometry given by [10] the values of the pseudo first order rate constant, k_{obs}, obtained when O_2 was in excess were about four times those when $(OHP)_3Fe(II)$ was in excess. The data, which are listed in Tables 2 and 3, are consistent only with the rate expression given by [11]

$$[11] \quad -\frac{1}{4}\frac{d[(OHP)_3Fe(II)]}{dt} = \frac{-d[O_2]}{dt} = k_2[(OHP)_3Fe(II)][O_2]$$

where k_2 has a value of $114 \pm 11\ M^{-1}\ s^{-1}$ at 25°C. Addition of excess OHP ligand did not affect the value of k_2.

Rates were measured over the temperature range of 25–45°C (Table 4). Values of $\Delta H^{\ddagger} = 14.8 \pm 0.6$ kcal/mol and $\Delta S^{\ddagger} = 0.8 \pm 2$ eu were calculated from the data.

To determine the effect of pH on rate the kinetics were studied over the pH range 8–13. Data could not be obtained at lower pH because of the instability of $(OHP)_3Fe(II)$ at pH $\leq$ 8 (25). A plot of k_2 versus pH is shown in Fig. 1. The value of k_2 is practically constant between the pH range of 10–13. The value of k_2 increases rapidly in the region 9.75–9.0 and levels off again. The midpoint of the curve is at about pH = 9.4.

(c) Reaction of $(OHP)_3Fe(II)$ with HO_2^-

The approximate rate of reaction of hydrogen peroxide in 0.1 *M* NaOH with $(OHP)_3Fe(II)$ at 25°C was determined using peroxide in excess. Since the K_a of H_2O_2 in H_2O at 25°C is 2.4×10^{-12} (26) the peroxide will exist as HO_2^- under these conditions. Pseudo first order kinetics were observed. At $[(OHP)_3Fe(II)] = 5 \times 10^{-5}\ M$ in 0.1 *M* NaOH the $t_{1/2}$ was 50 s at $5 \times 10^{-4}\ M$ $[HO_2^-]$ and 4 s at $5 \times 10^{-3}\ M$ $[HO_2^-]$. Thus the rate expression is of the form given by [12] with a value of approximately $14\ M^{-1}\ s^{-1}$ for k_2'.

TABLE 2. Kinetic data for the oxidation of $(OHP)_3Fe(II)$ by molecular oxygen at 25°C and 0.1 *N* NaOH obtained by spectrometric techniques[a]

$[(OHP)_3Fe(II)]$ ($M \times 10^6$)	$[O_2]$[b] ($M \times 10^4$)	k_{obs} ($s^{-1} \times 10^2$)	k_2 ($M^{-1}\ s^{-1}$)
3.2	2.0	8.7	109
4.1	2.0	8.0	100
4.7	2.0	7.8	98
100	5.0	23	115
100	0.1	1.25	125
140	0.1	1.6	110
500	1.0	6.6	131
1000	1.0	12.6	125
100	5.0	23	115[c]
100	2.5	11.3	113
100	4.0	17	106
100	1.7	8.1	119
50	5.0	21.6	108

[a]Since the k_2 is defined by the rate expression given by [11]: when $(OHP)_3Fe(II)$ is in excess, $k_2 = k_{obs}/[(OHP)_3Fe(II)]$; when $[O_2]$ is in excess, $k_2 = k_{obs}/4[O_2]$.
[b]Solubility of O_2 was obtained from ref. 43.
[c]Also $3 \times 10^{-4}\ M$ in excess OHP.

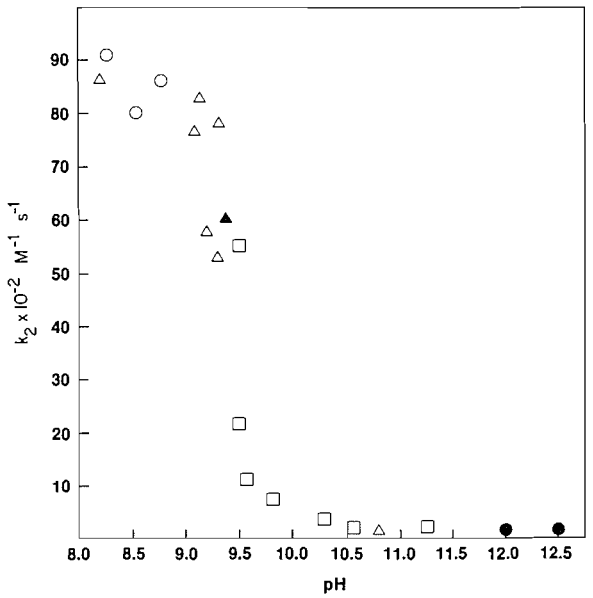


FIG. 1. Oxidation of $(OHP)_3Fe(II)$ by oxygen at 25°C. Variation of k_2 (see [11]) with pH. ●, pH adjusted by addition of NaOH; △, NH_4Cl/NH_4OH buffer; ○, tris/$HClO_4$ buffer; □, glycine/NaOH buffer; ▲, pH obtained by mixing $(OHP)_3Fe(II)$ in ca. 0.1 *M* NaOH solution with ca. 0.1 *M* HCl solution saturated with O_2 in a stopped flow spectrophotometer. The final pH of the resulting solution was measured.

TABLE 3. Kinetic data for the oxidation of $(OHP)_3Fe(II)$ by molecular oxygen at 25°C and 0.1 *N* NaOH obtained by the oxygen electrode techniques

$[(OHP)_3Fe(II)]$ ($M \times 10^4$)	$[O_2]$ ($M \times 10^5$)	$d[O_2]/dt$ ($M\ s^{-1} \times 10^6$)	k_{obs} ($s^{-1} \times 10^2$)	k_2 ($M^{-1}\ s^{-1}$)
1.0	39.4	5.0		127
2.5	6.0		3.13	127
3.3	41.5	15.6		114[a]
5.0	6.2	5.75		115

[a]Also 3.3×10^{-3} *M* in excess OHP.

TABLE 4. Variation of k_2 with temperature[a]

Temperature (K)	k_2 ($M^{-1}\ s^{-1}$)
298	114
308	274
317.5	555

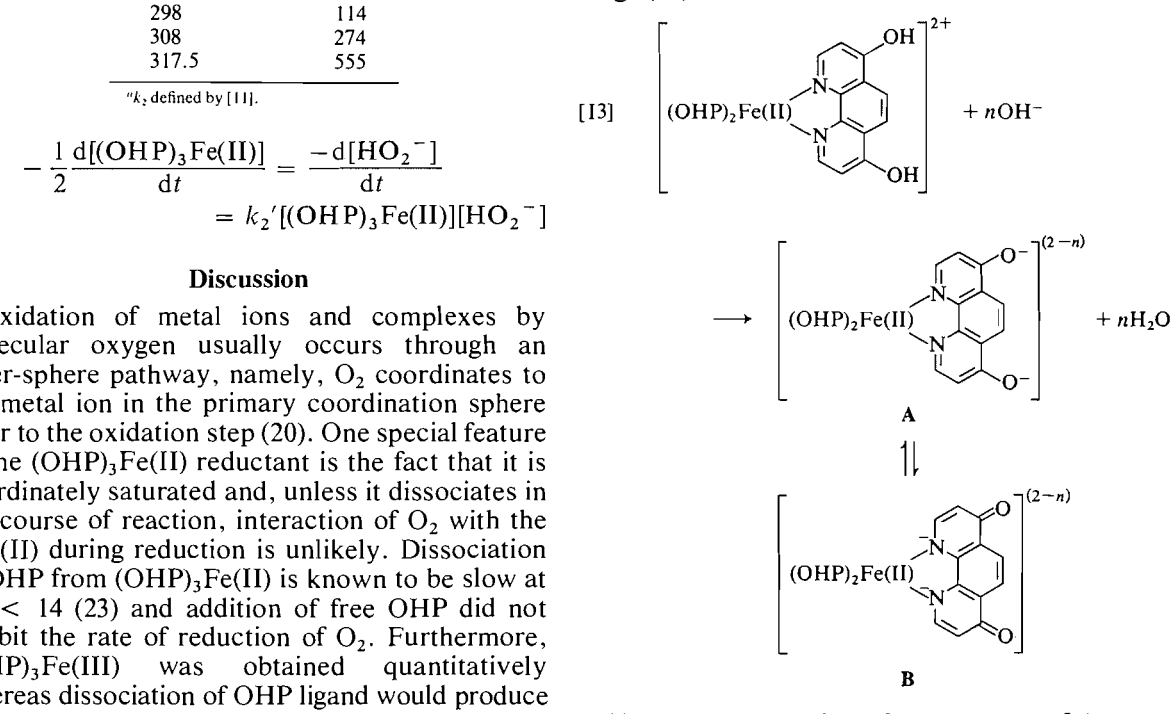
[a]k_2 defined by [11].

$$[12] \quad -\frac{1}{2}\frac{d[(OHP)_3Fe(II)]}{dt} = \frac{-d[HO_2^-]}{dt} = k_2'[(OHP)_3Fe(II)][HO_2^-]$$

Discussion

Oxidation of metal ions and complexes by molecular oxygen usually occurs through an inner-sphere pathway, namely, O_2 coordinates to the metal ion in the primary coordination sphere prior to the oxidation step (20). One special feature of the $(OHP)_3Fe(II)$ reductant is the fact that it is coordinately saturated and, unless it dissociates in the course of reaction, interaction of O_2 with the iron(II) during reduction is unlikely. Dissociation of OHP from $(OHP)_3Fe(II)$ is known to be slow at pH < 14 (23) and addition of free OHP did not inhibit the rate of reduction of O_2. Furthermore, $(OHP)_3Fe(III)$ was obtained quantitatively whereas dissociation of OHP ligand would produce Fe(III) hydroxyl species as final products (23). The value of $\Delta S^{\neq} = 0.8 \pm 2$ eu also suggests that no OHP dissociation occurs in the rate determining step. Thus oxidation of $(OHP)_3Fe(II)$ by O_2 very likely occurs via a path without direct coordination of O_2 to $(OHP)_3Fe(II)$ in the primary coordination sphere; however, a 7 coordinate intermediate could not be ruled out. A seven coordinate dioxygen adduct of Fe(II) with a binuclear structure bridged by a singlet dioxygen has been reported (27).

The exact state of $(OHP)_3Fe(II)$ in basic solution is not known for certain but all or most of the six protons must be removed by equilibria such as [13] where the deprotonated ligand can exist in either the **A** or **B** forms. Recent studies with a Ru(II)–OHP complex indicate that form **B** is important for the deprotonated ligand (28). The value of E_0 for $(OHP)_3Fe(II)$ does not change from pH 10 to 13 suggesting only one species is present in this range (23).

[13] 

Since the protonation of one or more of the oxygens in $(OHP)_3Fe(II)$ could profoundly affect the electron transfer capability of the ligand, a rate–pH study was undertaken. The rate–pH profile shown in Fig. 1 resembles a pH titration curve with a pK_a of ca. 9.4 strongly suggesting that one of the phenoxide anions is being protonated to give a species which is about 80 times more reactive. Of course as mentioned earlier, the state of protonation of the $(OHP)_3Fe(II)$ under the reaction conditions is not known but it is probably close to being completely deprotonated. The value of 9.4 for pK_a is reasonable for one of the six protonation equilibria; $Ru(II)(OHP)(2,2\text{-bipyridine})_2$ has a pK_a of 10.1 for the loss of both protons (28).

Can. J. Chem. Downloaded from www.nrcresearchpress.com by 210.87.254.105 on 09/05/12
For personal use only.

Can. J. Chem. Downloaded from www.nrcresearchpress.com by 210.87.254.105 on 09/05/12
For personal use only.

The proton acceleration could also result from stabilization of intermediate species by protonation. Kurimura and co-workers (14) found in the reduction of O_2 by iron(II) chelated with ligands such as EDTA the protonated chelate ring reacted about 30 times faster than the unprotonated chelate. This was attributed to stabilization of O_2^- by formation of O_2H. However, the acid dissociation constant of O_2H is 5×10^{-5} (29) so this stabilization would not occur under the basic conditions of the present study if O_2^- existed as a true intermediate. However, there would be no conflict with the experimental result if O_2^- is associated with the $(OHP)_3Fe(II)$ complex (see later discussion).

The rate expression given by [11] eliminates mechanisms such as given by [1]–[3] involving the interaction of $2(OHP)_3Fe(II)$ with one O_2 in the rate limiting step, but is consistent with an initial one electron transfer from one $(OHP)_3Fe(II)$ to one O_2 giving O_2^- [14].

$$[14] \quad (OHP)_3Fe(II) + O_2 \underset{k_{-2}}{\overset{k_2}{\rightleftharpoons}} (OHP)_3Fe(III) + O_2^-$$

$$[15] \quad O_2^- + (OHP)_3Fe(II) \xrightarrow[k_3,\ H^+]{\text{fast}} (OHP)_3Fe(III) + HO_2^-$$

Thus using an E_0 value of 0.06 for $(OHP)_3Fe(II)$–$(OHP)_3Fe(III)$ potential and a value of -0.563 for the O_2–O_2^- potential (30) an equilibrium constant of 3×10^{-9} can be calculated for [14]. This value combined with an experimental k_2 value of 114 M^{-1} s^{-1} gives a value of 3.8×10^{10} M^{-1} s^{-1} for k_{-2} which is greater than or equal to the diffusion controlled rate constant. Since good first order kinetics were observed for over 90% of reaction, a k_3 value greater than k_{-2} is required. Thus on the basis of the k_{-2} and k_3 values as calculated from the literature values of redox potential, a mechanism involving production of *free* superoxide in a one electron transfer step does not appear likely. An alternative would involve a two electron transfer to produce Fe(IV) and peroxide intermediates [16].

$$[16] \quad (OHP)_3Fe(II) + O_2 \xrightarrow{H^+} (OHP)_3Fe(IV) + HO_2^-$$

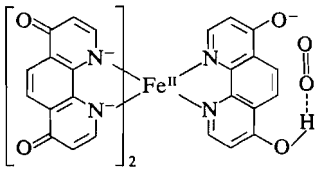
However, there is a piece of experimental evidence which argues against the production of a free HO_2^- intermediate as written in [15] and [16]. In most studies on Fe(II) oxidation, the peroxide formed would react rapidly with more Fe(II) via [7] to give the observed stoichiometry of 4 Fe(II) per O_2. In the present system the rate of reaction of $(OHP)_3Fe(II)$ with O_2 is 8 times faster than its reaction with HO_2^-. Thus in the runs using excess O_2 the observed stoichiometry should be 2 rather than the 4 observed.[3] Furthermore, it is of interest to note the oxidation of bipyridyl and phenanthroline complexes of Fe(II) with H_2O_2 has been reported to occur via a ligand dissociation mechanism (31). The conclusion from our experimental result is that HO_2^- is not produced as a *free* intermediate, but rather is oxidized to OH^- before it escapes from the solvent cage. Two electron transfer within the solvent cage has been suggested in the oxidation of Fe(II) (EDTA) complex by H_2O_2 (32).

To account for the kinetic data and the fact that no free HO_2^- was produced, a mechanism involving bound superoxide [17] or peroxide intermediates [18] are proposed.

$$[17] \quad (OHP)_3Fe(II) + O_2 \rightleftharpoons (OHP)_3Fe(III)O_2^-$$

$$[18] \quad (OHP)_3Fe(II) + O_2 \rightleftharpoons (OHP)_3Fe(IV)O_2^{2-}$$

Formulations of bound superoxide or peroxide as $(OHP)_3Fe(III)O_2^-$ or $(OHP)_3Fe(IV)O_2^{2-}$ respectively do not necessarily imply direct bonding of O_2 to Fe(II). Furthermore, the $\Delta S^{\neq}$ value of 0.8 $\pm$ 2 eu suggests that a seven coordinate intermediate is not formed in the rate determining step. An attractive possiblity is the association of O_2 with $(OHP)_3Fe(II)$ via the π system of the phenanthroline ring. Donor and acceptor type interaction between O_2 and the porphyrin ring has been proposed in the O_2 binding to solid hemes (33). Thus, electron transfer could occur through the π-system of the phenanthroline ring in a manner analogous to that suggested for electron transfer through porphyrin or polypyridyl rings in several systems (18, 34–37). The effect of H^+ on rate could be interpreted as stabilization of bound O_2 and/or its reduction intermediates via possibly hydrogen bonding with the OH group on the phenanthroline ring as represented in **2**. Stabilization of O_2 via hydrogen bonding has been proposed by Pauling in oxyhaemoglobin (38)



2

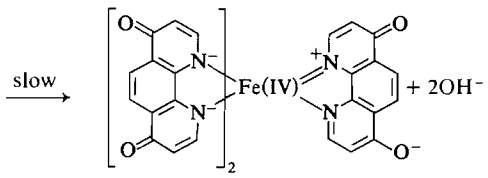
If the rate determining step is as indicated in [17], an interesting possibility arises in that multielectron transfer from $Fe(III)(OHP)_3$ to bound O_2^- could occur within the solvent cage of the inter-

[3]Of course if $(OHP)_3Fe(II)$ is in excess the observed stoichiometry would be 4 since HO_2^- would eventually be able to react with the excess $(OHP)_3Fe(II)$.

Can. J. Chem. Downloaded from www.nrcresearchpress.com by 210.87.254.105 on 09/05/12
For personal use only.

mediate $[(OHP)_3Fe(III)O_2^-]$ species. Enzymatic reduction of O_2 to H_2O is thought to take place by multielectron transfer steps (39). A simultaneous reversible 2 electron transfer at the same potential on a bis(1,3,5-triketonato) dicopper(II) has been reported (40). Multielectron transfer in the present system seems reasonable since OHP is an organic redox system (see [9]). Also Fe(IV) species could be involved since the negative charge of the OHP ligand would stabilize this oxidation state of iron. In the limit, a 4 electron reduction of O_2 would be accomplished within the lifetime of $[(OHP)_3Fe(III)O_2^-]$ to produce a highly oxidized Fe species, **3**, as shown in [19] and [20].

[19] $(OHP)_3Fe(II) + O_2$



3

[20] $\mathbf{3} + 3(OHP)_3Fe(II) \xrightarrow{fast} 4(OHP)_3Fe(III)$

The nature of **3** is speculative and an intermediate involving Fe(II) and 2 oxidized ligands is also feasible. In **3**, the high positive charge at the metal center is largely neutralized by **B** forms of the other anionic ligands. As mentioned earlier for a Ru(II) complex of OHP the **B** forms are of considerable importance in deprotonated ligands (28). One might argue that **3** is produced from four 1 electron transfer steps, a sequence of two 2 electron transfer steps or a direct 4 electron step. On the basis of the results presently available, one cannot distinguish between these possibilities. However, a four electron reduction of O_2 by one metal center within the lifetime of the solvent cage (regardless of the detailed electron transfer step) is a distinct possibility.

Experimental

Materials

4,7-Dihydroxy-1,10-phenanthroline and ferrous sulfate were purchased from G. Frederick Smith. Oxygen and argon were obtained from Canadian Oxygen Limited. All other chemicals were of reagent grade.

Tris(4,7-dihydroxy-1,10-phenanthroline)iron(II) was prepared *in situ* by adding a 1:3 molar ratio of $FeSO_4 \cdot 7H_2O$ in H_2O to 4,7-dihydroxy-1,10-phenanthroline dissolved in NaOH in the absence of oxygen. Such solutions were prepared as needed since air had to be rigorously excluded.

Kinetic Studies

Kinetic studies were carried out on a Durrum stopped-flow spectrophotometer with gas-tight syringes or a Cary 118 spectrophotometer. Standard gas-tight syringe techniques were used to transfer air sensitive solutions which were degassed with argon. The reactions were carried out under pseudo first order conditions with either O_2 or $(OHP)_3Fe(II)$ in excess. The rates were followed by measuring either the decrease of the iron(II) species at 510 nm or the increase of the iron(III) species at 750 nm. Good pseudo first order kinetics were observed for most runs and the pseudo first order rate constants were obtained from a plot of $\log (OD_\infty - OD_t)$ against time.

A few experiments were performed by monitoring the O_2 concentration using a Beckman oxygen meter equipped with an oxygen electrode. A thermostated cell with an air tight stopper was used to house the electrode system. The oxygen meter was connected to a strip chart recorder. A measured amount of $(OHP)_3Fe(II)$ was added to a solution of known $[O_2]$ in the cell and the kinetics followed by decrease in $[O_2]$ with time.

The study of the variation of rate with pH was carried out using the Durrum stopped-flow spectrophotometer. At pH's of 12 or above the $(OHP)_3Fe(II)$ in solutions of the desired hydroxide concentration was mixed with solutions of the same hydroxide concentration saturated with O_2. Most of the runs at lower pH were made using buffer solutions. Stock solutions of 5×10^{-3} *M* $(OHP)_3Fe(II)$ were made up in 0.1 *M* NaOH and aliquots of the stock solution were added to an argon degassed buffer solution (ca. 0.4 mL of stock $(OHP)_3Fe(II)$ solution to ca. 10 mL of buffer solution). The rates of oxidation were obtained from the increase in OD at 750 nm with time. In all runs the ionic strength was maintained at 0.1 *M* by addition of $NaClO_4$.

Buffers used were NH_4Cl/NH_4OH, glycine/NaOH (41*a*) and tris(hydroxymethyl)aminoethane hydrochloride (tris)/$HClO_4$ (41*b*). The concentration of glycine and tris were kept at 0.01 *M*.

Stoichiometry

The stoichiometry of the oxidation was obtained using a Beckman oxygen meter and electrode or a constant pressure gas uptake apparatus described in ref. 24.

The H_2O_2 analysis in oxidized solutions of $(OHP)_3Fe(II)$ was carried out by the KI/starch procedure (42). Since $(OHP)_3Fe(III)$ would interfere with the determination, sulfuric acid was first added to the reaction mixture until the pH was less than 5. This precipitated the $(OHP)_3Fe(III)$ as a purplish black solid. After filtration the filtrate was treated with a 10% KI solution in 2 *N* H_2SO_4. After standing for a few minutes the solution was titrated with a standard $K_2S_2O_3$ solution (Fisher Scientific) using ca. 0.5 mL of a starch indicator solution to detect the endpoint. There was always a small amount of I_2 produced, but much less than that expected from the stoichiometry of [3] or [5] $(2(OHP)_3Fe(II)/H_2O_2)$. The small amount of oxidant present is very likely Fe(III) (aq) formed from dissociation of $(OHP)_3Fe(III)$ upon addition of H_2SO_4. A typical analysis is given below:

Oxidized $(OHP)_3Fe(II)$ solution (5 mL, 6×10^{-4} *M*) required 2.0 mL of 2.0×10^{-4} *M* $Na_2S_2O_3$ solution to discharge the blue colour. Since 1 mL of 1*M* $Na_2S_2O_3$ is equivalent to 0.017 g of H_2O_2, if I_2 is formed from peroxide, its concentration is given by the following calculation.

$$[H_2O_2] = \frac{2.0 \times (2.0 \times 10^{-4}) \times 0.017}{34 \times 5.0} \times 1000\ M = 4.0 \times 10^{-5}\ M$$

If one H_2O_2 were formed from two $(OHP)_3Fe(II)$ the peroxide concentration would be 3×10^{-4} *M*.

Acknowledgement

The authors thank the Natural Sciences and Engineering Research Council of Canada for financial support.

Can. J. Chem. Downloaded from www.nrcresearchpress.com by 210.87.254.105 on 09/05/12
For personal use only.

1. B. R. JAMES. The porphyrins. Vol. V. Academic Press Inc., New York. 1978. p. 205.
2. J. P. COLLMAN, R. R. GAGNE, C. A. REED, T. R. HALBERT, G. LANG, and W. T. ROBINSON. J. Am. Chem. Soc. **97**, 1427 (1975) and references therein.
3. O. H. W. KAO and J. H. WANG. Biochemistry, **4**, 342 (1965).
4. A. D. GILMOUR and A. MCAULEY. J. Chem. Soc. A, 1006 (1970).
5. G. GREENWOOD and Q. H. GIBSON. J. Biol. Chem. **242**, 1782 (1967).
6. J. P. COLLMAN, C. M. ELLIOTT, T. R. HALBERT, and B. S. TOVROG. Proc. Natl. Acad. Sci. U.S.A. **74**, 18 (1977).
7. M. CHER and N. DAVIDSON. J. Am. Chem. Soc. **77**, 793 (1955).
8. R. E. HUFFMAN and N. DAVIDSON. J. Am. Chem. Soc. **78**, 4836 (1956).
9. P. GEORGE. J. Chem. Soc. 4349 (1954).
10. J. KING and N. DAVIDSON. J. Am. Chem. Soc. **80**, 1542 (1958).
11. B. MACEJEVSKIS, A. VLASOVA, and L. LIEPINA. Latv. PSR Zinat. Akad. Vestis, **12**, 85 (1960).
12. J. WEISS. J. Chim. Phys. **48**, 6 (1951); Experientia, **9**, 61 (1953); Proc. R. Soc. London, A**222**, 124 (1954).
13. Y. KURIMURA and H. KURIYAMA. Bull. Chem. Soc. Jpn. **42**, 2238 (1969).
14. Y. KURIMURA, R. OCHIAI, and N. MATSUURA. Bull. Chem. Soc. Jpn. **41**, 2234 (1968).
15. G. S. HAMMOND and C.-H. S. WU. Adv. Chem. Ser. **77**, 186 (1968).
16. R. H. FELTON, G. C. OWEN, D. DOLPHIN, and J. FAJER. J. Am. Chem. Soc. **93**, 6332 (1971).
17. R. H. FELTON, G. S. OWEN, D. DOLPHIN, A. FORMAN, D. BORG, and J. FAJER. Ann. N.Y. Acad. Sci. **206**, 504 (1973).
18. K. M. KADISH, M. M. MORRISON, L. A. CONSTANT, L. DICKENS, and D. G. DAVIS. J. Am. Chem. Soc. **98**, 8387 (1976).
19. D. P. POE and H. DIEHL. Talanta, **21**, 1065 (1974).
20. J. R. PLADZIEWICZ, T. J. MEYER, J. A. BROOMHEAD, and H. TAUBE. Inorg. Chem. **12**, 639 (1973).
21. D. M. STANBURY, O. HAAS, and H. TAUBE. Inorg. Chem. **19**, 518 (1980).
22. A. HAIM and W. K. WILMARTH. J. Am. Chem. Soc. **83**, 509 (1961).
23. D. P. POE and H. DIEHL. Talanta, **23**, 147 (1976).
24. B. R. JAMES and G. L. REMPEL. Can. J. Chem. **44**, 233 (1966).
25. A. SCHILT, G. F. SMITH, and A. HEIMBUCH. Anal. Chem. **28**, 809 (1956).
26. R. C. WEAST (*Editor*). CRC handbook of chemistry and physics. 51st ed. Chemical Rubber Co., Cleveland. 1971–1972. p. D121.
27. V. MCKEE, S. M. NELSON, and J. NELSON. Chem. Commun. 225 (1976).
28. P. J. GIORDANO, C. R. BOCK, and M. S. WRIGHTON. J. Am. Chem. Soc. **100**, 6960 (1978).
29. G. CZAPSKI and B. H. J. BIELSKI. J. Phys. Chem. **67**, 2180 (1963).
30. G. MILAZZO, S. CAROLI, and V. K. SHARMA. Tables of standard electrode potentials. John Wiley and Sons, Ltd., New York. 1978. p. 228.
31. J. BURGESS and R. H. PRINCE. J. Chem. Soc. 6061 (1965).
32. C. WALLING. Acc. Chem. Res. **8**, 125 (1975).
33. W. H. FUSHMAN, C. H. BARLOW, W. J. WALLACE, and W. S. CAUGHEY. Biochem. Biophys. Res. Commun. **61**, 635 (1974).
34. J. K. YANDELL, D. P. FAY, and N. SUTIN. J. Am. Chem. Soc. **95**, 1131 (1973).
35. P. HAMBRIGHT and E. B. FLEISHER. Inorg. Chem. **4**, 912 (1965).
36. C. E. CASTRO and H. F. DAVIS. J. Am. Chem. Soc. **91**, 5405 (1969).
37. F. T. T. NG and P. M. HENRY. J. Am. Chem. Soc. **98**, 3606 (1976).
38. L. PAULING. Nature, **203**, 182 (1964).
39. J. A. FEE. Struct. Bonding Berlin, **23**, 1 (1975).
40. D. E. FENTON and R. L. LINSTREDT. J. Am. Chem. Soc. **99**, 6367 (1978).
41. D. D. PERRIN. Buffers for pH and metal ion control. Chapman and Hall, London. 1974. (*a*) p. 51; (*b*) p. 46.
42. A. I. VOGEL. A text-book of quantitative inorganic analysis. 3rd ed. Longmans, Green and Co., London. 1961. p. 363.
43. F. LINKE. Solubilities of inorganic and metal organic compounds. Vol. 2. 4th ed. Am. Chem. Soc., Washington, DC. 1965. p. 1229.

Théorie de l'absorption ultrasonore des solutions micellaires d'amphiphiles. Application à l'effet de la force ionique sur la dynamique d'échange d'amphiphiles entre micelles et solution environnante

R. ZANA ET S. YIV

CNRS, Centre de Recherches sur les Macromolécules, 6, rue Boussingault, 67083 Strasbourg-Cedex, France

Reçu le 27 février 1980

R. ZANA et S. YIV. Can. J. Chem. **58**, 1780 (1980).

L'expression de l'absorption ultrasonore associée au processus d'échange d'ions amphiphiles entre micelles et solution environnante a pu être établie par un calcul simple basé sur des hypothèses identiques à celles ayant permis à Aniansson et Wall d'obtenir l'expression du temps de relaxation associé à ce processus. L'expression obtenue étend les possibilités d'études de systèmes micellaires au moyen des méthodes de relaxation ultrasonore. Elle a été utilisée pour l'interprétation quantitative de mesures d'absorption ultrasonore relatives à l'effet de la force ionique sur la dynamique du processus d'échange dans les solutions micellaires de décanoate de potassium.

R. ZANA and S. YIV. Can. J. Chem. **58**, 1780 (1980).

An expression for the amplitude of the ultrasonic relaxation arising from the exchange of amphiphiles between micelles and surrounding solution has been derived on the basis of the same assumptions as used by Aniansson and Wall to obtain the expression of the relaxation time for this process. The derived expression somewhat extends the range of investigation of micellar systems which can be performed by means of the ultrasonic relaxation method. It has been used for the quantitative interpretation of ultrasonic absorption measurements concerning the effect of ionic strength on the dynamics of the exchange process in micellar solutions of potassium decanoate.

I. Introduction

Les solutions micellaires de détergents à chaîne alkyle comportant jusqu'à 12 carbones ont fait l'objet de nombreuses études par absorption ultrasonore (1–15). La plupart d'entre elles (1–10) sont antérieures à la publication de la théorie d'Aniansson et Wall (16) de la dynamique des solutions micellaires et une controverse était apparue en ce qui concerne la nature du processus de relaxation détecté par mesure de l'absorption ultrasonore: équilibre d'ionisation des contreions (1–3, 13) ou équilibre d'échange d'ions amphiphiles entre micelles et solution environnante (4, 5). Il est maintenant généralement accepté, depuis les travaux de Graber et coll. (4, 5) que la seconde attribution est la bonne. On peut donc dire que la méthode de relaxation ultrasonore a la première permis la mise en évidence et l'étude qualitative de la cinétique de l'échange des ions amphiphiles entre micelles et solution (4, 5). Toutefois, aucune interprétation quantitative basée sur le modèle d'Aniansson et Wall (16) n'a été donnée, à ce jour, aux nombreux résultats d'amplitudes de relaxation ultrasonore rapportés dans la littérature. La seule raison en est que le calcul de l'expression de l'absorption ultrasonore d'une solution d'amphiphile due au processus d'échange, basé que un modèle semblable à celui utilisé par Aniansson et Wall (16) pour établir l'expression du temps de relaxation τ_1 associé au processus d'échange, n'avait pas encore été effectué (17)[1]. Cette situation nous semblait d'autant plus regrettable que l'amplitude d'une relaxation ultrasonore ne nécessite pas pour son interprétation de mesures additionnelles, à la différence des amplitudes de relaxation déterminées au moyen des méthodes transitoires de relaxation chimique. Comme nous le verrons plus loin, l'amplitude R d'une relaxation ultrasonore contient des quantités cinétiques (constantes de vitesse) et thermodynamiques (changements de volume et d'enthalpie associé au processus). L'étude de R permet donc de compléter et/ou confirmer les informations obtenues à partir du temps de relaxation.

Ceci nous a conduit à établir l'expression de l'absorption ultrasonore due au processus d'échange d'ions amphiphiles entre micelles et solution environnante, sur la base du mécanisme utilisé par Aniansson et Wall (16) pour établir l'expression du temps de relaxation de ce processus et avec les mêmes hypothèses.

Dans une deuxième étape nous avons étudié l'effet de la force ionique sur la cinétique du processus d'échange par relaxation ultrasonore et interprété les résultats obtenus au moyen des expressions établies

[1]Durant la preparation de ce manuscrit est paru un article de Teubner (17) dans lequel cet auteur calcule l'expression de l'absorption ultrasonore associée au processus d'echange par une methode matricielle. Le résultat obtenu est comme nous le verrons plus loin identique au nôtre.

0008-4042/80/171780-08$01.00/0

©1980 National Research Council of Canada/Conseil national de recherches du Canada

Can. J. Chem. Downloaded from www.nrcresearchpress.com by 210.87.254.105 on 09/05/12
For personal use only.

Can. J. Chem. Downloaded from www.nrcresearchpress.com by 210.87.254.105 on 09/05/12
For personal use only.

pour l'absorption ultrasonore. En effet, en dépit des nombreuses études de solutions micellaires par absorption ultrasonore et plus généralement au moyen des méthodes de relaxation chimique, aucune étude systématique de l'effet de la force ionique sur la cinétique du processus d'échange n'avait été effectuée. On trouve dans la littérature seulement quelques résultats très fragmentaires qui indiquent que, à une concentration en détergent donnée, le temps de relaxation associé au processus d'échange est peu affecté par l'addition de sel (2, 12).

Des considérations expérimentales nous ont guidé dans le choix de l'amphiphile ionique étudié. Rappelons que l'absorption ultrasonore ne permet pas d'étudier les amphiphiles dont la chaîne alkyle comporte plus de 12 atomes de carbone (4). L'équipement disponible au laboratoire qui permet d'explorer les fréquences comprises entre 0,8 et 300 MHz nous a fait choisir le décanoate de potassium pour lequel les temps de relaxation correspondent à des fréquences situées dans ce domaine. Un autre avantage du décanoate de potassium est qu'il a été étudié par Graber et coll. (4) et Yasunaga et coll. (2) en solution aqueuse, en l'absence de sel.

Nous présentons successivement le calcul de l'absorption ultrasonore, la partie expérimentale et la discussion des résultats.

II. Expression de l'absorption ultrasonore associée au processus d'échange d'ions amphiphiles entre micelles et solution environnante

(1) Les hypothèses

On suppose que la formation des micelles est régie par la loi d'action de masse et fait intervenir une série de réactions bimoléculaires:

$$A_1 + A_1 \underset{k_2^-}{\overset{k_2^+}{\rightleftharpoons}} A_2$$

$$[1] \qquad A_2 + A_1 \underset{k_3^-}{\overset{k_3^+}{\rightleftharpoons}} A_3$$

$$\text{----------}$$

$$A_{s-1} + A_1 \underset{k_s^-}{\overset{k_s^+}{\rightleftharpoons}} A_s$$

$$\text{----------}$$

où A_1 représente un amphiphile isolé et A_s une espèce associée comportant s amphiphiles (le caractère ionique des amphiphiles et la présence des contreions ne sont pas explicitement pris en considération).

Comme Aniansson et Wall, on fait l'hypothèse que la courbe de distribution des espèces associées, en fonction du nombre d'association s peut être divisée en 3 parties: une région 1 ($s < s_1$) qui correspond aux monomères et oligomères, une région 2 ($s_1 < s < s_2$) qui est celle des espèces associées présentes dans la solution micellaire à des concentrations extrêmement faibles, et une région 3 ($s > s_2$) qui correspond aux micelles proprement dites.

L'existence de la région 2 impose au système micellaire soumis à une perturbation très rapide de répondre dans un premier temps par un rééquilibrage rapide entre les micelles de la région 3 par des réactions du type [1]. Ces réactions d'échange d'ions amphiphiles entre micelles et solution environnante laissent le nombre de micelles de la région 3 inchangé, c'est-à-dire

$$[2] \qquad \sum A_s = \text{constante} \qquad \text{d'où} \sum \mathrm{d}A_s = 0$$

où les sommes sont prises sur toutes les espèces de la région 3, A_s est la concentration de l'espèces associée A_s.

De plus, on suppose que la distribution des micelles dans la région 3 obéit à une statistique gaussienne (16):

$$[3] \qquad A_s = A_0 \exp - \frac{(s-n)^2}{2\sigma^2}$$

où σ caractérise la largeur de la courbe de distribution, c'est-à-dire la polydispersité des micelles, n étant le nombre d'agrégation moyen des micelles.

Enfin, on suppose que les constantes de vitesse d'association k_s^+ et de dissociation k_s^- constantes et égales à k^+ et k^- dans la région 3. Cette hypothèse réduit le spectre de temps de relaxation relatif au système de réactions [1] à un seul temps de relaxation τ_1 dont l'expression a été donnée par Aniansson et Wall et que nous retrouvons dans le calcul qui suit.

(2) Le calcul

Il s'agit donc de calculer l'absorption ultrasonore associée à toutes les réactions couplées [1] se produisant dans la région 3. L'équation de vitesse relative au monomère s'écrit:

$$[4] \qquad \mathrm{d}A_1/\mathrm{d}t = \sum k^- A_s - \sum k^+ A_{s-1} A_1$$

où les A représentent des concentrations instantanées. Les ondes ultrasonores apportent une perturbation périodique aux valeurs des concentrations et des constantes de vitesse. Pour des ondes de fréquence angulaire $\omega = 2\pi f$ on peut écrire:

$$k^- = \bar{k}^- + \Delta k^- \, \mathrm{e}^{i\omega t}$$

$$k^+ = \bar{k}^+ + \Delta k^+ \, \mathrm{e}^{i\omega t}$$

$$[5] \qquad A_s = \bar{A}_s + \Delta A_s \, \mathrm{e}^{i\omega t} = \bar{A}_s + \xi_s \bar{A}_s \, \mathrm{e}^{i\omega t}$$

$$A_{s-1} = \bar{A}_{s-1} + \Delta A_{s-1} \, \mathrm{e}^{i\omega t}$$

$$= A_{s-1} + \xi_{s-1} \bar{A}_{s-1} \, \mathrm{e}^{i\omega t}$$

$$A_1 = \bar{A}_1 + \Delta A_1 \, \mathrm{e}^{i\omega t} = \bar{A}_1 + \xi_1 \bar{A}_1 \, \mathrm{e}^{i\omega t}$$

Can. J. Chem. Downloaded from www.nrcresearchpress.com by 210.87.254.105 on 09/05/12
For personal use only.

La barre sur un symbole donné indique la valeur à l'équilibre de la quantité correspondante. Les Δ représentent les amplitudes des perturbations. Pour les concentrations nous avons fait usage des quantités ξ_s introduites par Aniansson et données par

[6] $\xi_s = (A_s - \bar{A}_s)/\bar{A}_s$

Si l'on remplace dans [4] les différentes quantités par leurs expressions [5] et que l'on tient compte de la condition d'équilibre

[7] $\bar{k}^+\bar{A}_1\bar{A}_{s-1} = \bar{k}^-\bar{A}_s$

de l'éq. [2] qui devient

[8] $\sum \Delta A_s = \sum \xi_s \bar{A}_s = 0$

et de la définition

[9] $K = k^-/k^+ = A_1A_{s-1}/A_s$

qui conduit à:

[10] $\Delta k^- = K\Delta k^+ + k^+\Delta K$

on obtient l'équation:

[11] $i\omega\xi_1\bar{A}_1 = -\bar{k}^-[\sum \bar{A}_s\xi_{s-1} + \xi_1\sum \bar{A}_s] + \bar{k}^+\Delta K \sum \bar{A}_s$

On transforme le terme entre crochets dans [11] en écrivant (18):

[12] $\bar{A}_s = \bar{A}_{s-1} + \frac{\partial \bar{A}_{s-1}}{\partial s}[s - (s-1)]$

$= \bar{A}_{s-1} + \frac{\partial \bar{A}_{s-1}}{\partial s}$

Pour calculer la dérivée de $\bar{A}_{s-1}$ par rapport à s on utilise l'éq. [3] d'où:

[13] $\sum \frac{\partial \bar{A}_s}{\partial s}\xi_s = -\frac{1}{\sigma^2}\sum s\bar{A}_s\xi_s = \frac{1}{\sigma^2}\xi_1\bar{A}_1$

La dernière égalité dans [13] représente la loi de conservation de la masse. Le terme entre crochets dans [11] s'écrit donc:

[14] $\xi_1\bar{A}_1\left[\frac{\bar{k}^-}{\sigma^2} + \bar{k}^-\frac{\sum \bar{A}_s}{\bar{A}_1}\right] = \xi_1\bar{A}_1/\tau_1$

En effet, la quantité entre crochets dans l'éq. [14] est identique à l'expression donnée par Aniansson et Wall (16) pour l'inverse du temps de relaxation associé au processus d'échange. L'équation [11] devient donc:

[15] $\xi_1\bar{A}_1 = \Delta\bar{A}_1 = \bar{k}^+\Delta K\tau_1 \sum \bar{A}_s/(1 + i\omega\tau_1)$

En outre on sait que:

[16] $\frac{\mathrm{d}\log K}{\mathrm{d}P} = -\frac{\Delta V_0}{\underline{R}T}$

d'où:

$$\Delta K \cong -\frac{\Delta V_0}{\underline{R}T}\bar{K}\Delta P$$

où ΔV_0 est le changement de volume associé à la réaction d'échange d'un ion amphiphile.

La combinaison des eqs [15] et [16] conduit à:

[17] $\frac{\Delta\bar{A}_1}{\Delta P}(1 + i\omega\tau_1) = -\frac{\bar{k}^-\Delta V_0\tau_1\sum\bar{A}_s}{\underline{R}T}$

La partie relaxationnelle (chimique) β_R de la compressibilité du système étudié s'exprime en fonction de $\Delta\bar{A}_1/\Delta P$ (qui est en fait la dérivée du degré d'avancement de la réaction par rapport à la pression) et est de plus reliée à l'absorption par longueur d'onde μ_M à la fréquence angulaire $\omega = 1/\tau_1$ par les relations (19):

[18] $\beta_R = -\Delta V_0\frac{\Delta\bar{A}_1}{\Delta P}(1 + i\omega\tau_1) = \frac{2\mu_M}{\pi d v^2}$

où d est la densité de la solution et v la vitesse de propagation des ondes ultrasonores.

D'autre part, l'équation qui relie μ_M à l'amplitude R de la relaxation ultrasonore s'écrit:

[19] $R = 4\pi\tau_1\mu_M/10^3 v$

où le facteur 10^3 a été introduit parce que les concentrations sont exprimées en mol/L.

L'équation qui donne l'absorption ultrasonore α/f^2 (α = coefficient d'absorption ultrasonore à la fréquence f) s'écrit:

[20] $\frac{\alpha}{f^2} = \frac{R}{1 + 4\pi^2 f^2\tau_1^2}$

où l'expression de R obtenue par combinaison des éqs [17] à [19] s'écrit:

[21] $R = \frac{2\pi^2}{10^3}\frac{dv}{\underline{R}T}\Delta V_0^2\tau_1^2\bar{k}^-\sum\bar{A}_s$

soit, en tenant compte de:

[22] $\sum \bar{A}_s = (C - \bar{A}_1)/n \cong (C - \mathrm{cmc})/n$

et en posant

[23] $a = (C - \bar{A}_1)/\bar{A}_1 \cong (C - \mathrm{cmc})/\mathrm{cmc}$

où C est la concentration de l'amphiphile en mol/L et où la concentration $\bar{A}_1$ du monomère est supposée égale à la concentration micellaire critique dénotée cmc,

Can. J. Chem. Downloaded from www.nrcresearchpress.com by 210.87.254.105 on 09/05/12
For personal use only.

$$[24] \quad R = \frac{2\pi^2}{10^3}\frac{dv}{RT}\Delta V_0{}^2 \text{ cmc } \left(\frac{k^-}{n}\right) a\tau_1{}^2$$

avec

$$[25] \quad \frac{1}{\tau_1} = \frac{k^-}{\sigma^2}\left(1 + \frac{\sigma^2}{n}a\right)$$

L'expression [24] de R est identique à un facteur 2 près, à celle donnée par Teubner (17)[1]. Cet auteur a en fait établi l'expression du coefficient d'absorption de l'énergie transportée par l'onde ultrasonore, qui est deux fois plus grand que le coefficient d'absorption de l'amplitude de l'onde ultrasonore. Les appareillage utilisés en laboratoire mesurent ce dernier coefficient et il convient donc d'utiliser l'expression [24] dans les calculs relatifs à l'interprétation de ces mesures.

On peut facilement montrer par manipulation des éqs [20] et [24] que

(*1*) α/f^2 et R passent par un maximum pour des valeurs a_M et $a_{M,0}$ de a respectivement données par:

$$[26] \quad a_M = \left[\frac{\omega^2 + (\bar{k}^-/\sigma^2)^2}{(\bar{k}/n)^2}\right]^{1/2}$$

et

$$a_{M,0} = \frac{n}{\sigma^2}$$

(*2*) Les variations de α/f^2 et R au voisinage de la cmc ($a = 0$) sont linéaires avec C avec des pentes p et p_0 à la cmc, respectivement données par:

$$[27a] \quad p = 2\pi^2 dv\Delta V_0{}^2(\bar{k}^-/n)/10^3\underline{R}T[(\bar{k}^-/\sigma^2)^2 + \omega^2]$$

$$[27b] \quad p_0 = 2\pi^2 dv\Delta V_0{}^2(\bar{k}^-/n)/10^3\underline{R}T(\bar{k}^-/\sigma^2)^2$$

L'équation [27*a*] donne la possibilité d'obtenir $\bar{k}^-/n$ à partir de la courbe $\alpha/f^2 = f(C)$ à une fréquence donnée lorsque ΔV_0 a été préalablement déterminé. En fait, cette relation permet d'élargir les possibilités d'étude des amphiphiles par absorption ultrasonore, jusqu'ici restreintes aux amphiphiles comportant *moins* de 12 atomes de carbone, à des amphiphiles comportant jusqu'à 13 atomes de carbone dans leur chaîne alkyle. En effet, pour ces derniers on ne peut, avec les appareillages existant au laboratoire, mesurer l'absorption ultrasonore à des fréquences suffisamment basses pour la détermination de τ_1 et ainsi de $\bar{k}^-/n$, à partir des spectres ultrasonores (courbes α/f^2 en fonction de f). Il est par contre possible de déterminer les courbes $\alpha/f^2 = f(C)$ à une fréquence donnée. La pente de cette courbe à C = cmc permet alors d'obtenir $\bar{k}^-/n$, connaissant ΔV_0 et en supposant $(\bar{k}^-/\sigma^2)^2 \ll \omega^2$. La validité de cette approximation peut être contrôlée a posteriori, une fois $\bar{k}^-/n$ calculé. En effet, en prenant $\sigma^2/n = 2$ (ce qui correspond à une valeur maximum de n/σ^2) on peut alors vérifier que

$$(\bar{k}^-/n)^2(n/\sigma^2)^2 \ll \omega^2$$

Si celà n'est pas le cas, il suffit de refaire les mesures en fonction de la concentration à une fréquence plus élevée, de sorte que l'inégalité ci-dessus soit satisfaite.

Dans la suite, $\bar{k}^-$ est écrit k^-, par souci de simplification.

III. Partie expérimentale

(1) Méthodes

Le décanoate de potassium a été préparé par neutralisation stoechiométrique d'acide décanoique (Fluka purissinum) par de la potasse 1 *M* (Titrisol Merck).

Les absorptions ultrasonores ont été mesurées en utilisant un dispositif interferométrique aux fréquences inférieures à 5 MHz et un dispositif impulsionnel aux fréquences plus élevées (4).

Les nombres d'agrégation des micelles de décanoate de potassium en présence de KCl n'étant pas connus nous les avons déterminés en utilisant à cet effet la méthode récemment proposée par Turro et Yekta (20). Cette méthode repose sur la mesure de l'intensité de fluorescence d'une solution micellaire dans laquelle on introduit de faibles quantités d'une sonde de fluorescence et d'un inhibiteur. Ces deux types de molécules se distribuent parmi les micelles selon une statistique de Poisson. On peut alors montrer (20) que la relation suivante existe entre les concentrations c_Q et C_M de l'inhibiteur et des micelles et les intensités de fluorescence I et I_0 en présence et en l'absence d'inhibiteur:

$$[28] \quad I/I_0 = \exp(-c_Q/C_M)$$

avec

$$[29] \quad C_M = \frac{C - \text{cmc}}{n}$$

Comme Turro et Yekta (20) nous avons utilisé le 9-méthylanthracène comme inhibiteur et le [ruthénium tris(bipyridine)]$^{2+}$ comme sonde de fluorescence. Le 9-méthylanthracène utilisé (Aldrich 99%) contenait en fait près de 30% d'impuretés insolubles dans les solutions micellaires. Nous l'avons purifié par recristallisation fractionnée dans l'éthanol. Le [ruthénium tris(bipyridine)]$^{2+}$ était sous forme de sulfate. Nous avons vérifié la bonne marche de l'équipement utilisé et la bonne qualité des produits en reproduisant les expériences de Turro et Yekta sur le dodecylsulfate de sodium dans l'eau (20). Le nombre d'agrégation obtenu dans ces expériences: 62, était égal à celui donné par ces auteurs.

Les mesures ont été effectuées en gardant constantes les concentrations en inhibiteur (10^{-4} *M*) et en sonde de luminescence (2×10^{-4} *M*) et en faisant varier la concentration C en décanoate de potassium. Dans la pratique, ceci est obtenu en mélangeant deux solutions de décanoate de potassium de concentrations différentes mais de même teneur en inhibiteur et en sonde et en mesurant l'intensité de fluorescence à 600 nm. Le tracé de $(\log_e I_0/I)^{-1}$ en fonction de C donne une droite dont la pente fournit le nombre d'agrégation n des micelles. La cmc est la concentration pour laquelle $(\log_e I_0/I)^{-1}$ s'annule. Notons que si cette méthode fournit des valeurs relativement

Can. J. Chem. Downloaded from www.nrcresearchpress.com by 210.87.254.105 on 09/05/12
For personal use only.

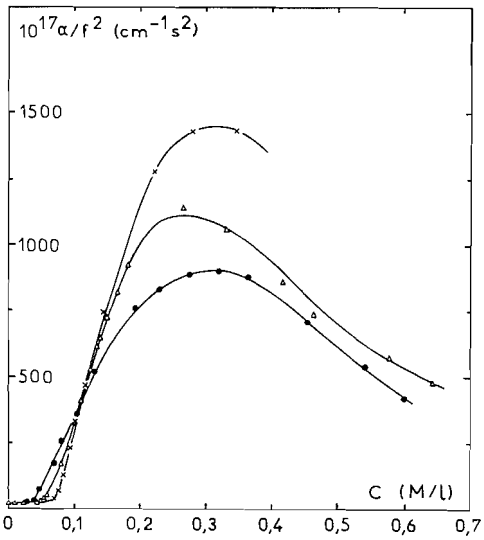


FIG. 1. Variation de l'absorption ultrasonore en fonction de la concentration en décanoate de potassium à 25°C et 2,82 MHz, en présence de 0,1 *M* KCl, (×); 0,25 *M* KCl (△) et 0,5 *M* KCl (●).

TABLEAU 1. Effet de l'addition de KCl sur la cmc du décanoate de potassium à 25°C

C_{KCl} (*M*/L)	cmc (*M*/L)
0	0,1[a]
0,1	0,075
0,25	0,058
0,5	0,040

[a]Valeur déterminée dans la réf. 4.

précises de *n*, les valeurs de cmc sont beaucoup moins précises que celles déterminées par d'autres méthodes, telles la conductivité ou l'absorption ultrasonore.

Nous avons ainsi obtenu en l'absence de KCl, et en présence de 0,1 *M* et 0,5 *M* de KCl les valeurs 32, 38 et 66 pour *n* et les valeurs 0,105 *M*, 0,085 *M* et 0,035 *M* pour la cmc, respectivement.

La valeur $n = 32$ obtenue en l'absence de KCl est en excellent accord avec les valeurs données par Tartar (21) pour des amphiphiles ayant la même chaîne alkyle. Cette valeur est également en bon accord avec celle que l'on peut calculer en supposant une micelle sphérique de rayon égal à celui de la chaîne étirée et ayant une densité égale à celle de la paraffine correspondante (21).

(2) Résultats ultrasonores

Les mesures d'absorption ultrasonore à une fréquence donnée (2,8 MHz) ont été utilisées pour obtenir les valeurs des cmc du décanoate de potassium en présence de KCl (voir fig. 1 et tableau 1). On sait en effet que les courbes $\alpha/f^2 = f$(concentration) présentent une augmentation de pente importante au-delà de la cmc, ce qui permet une détermination précise de cette concentration (4, 5). Les valeurs des cmc obtenues par absorption ultrasonore confirment la validité de la méthode

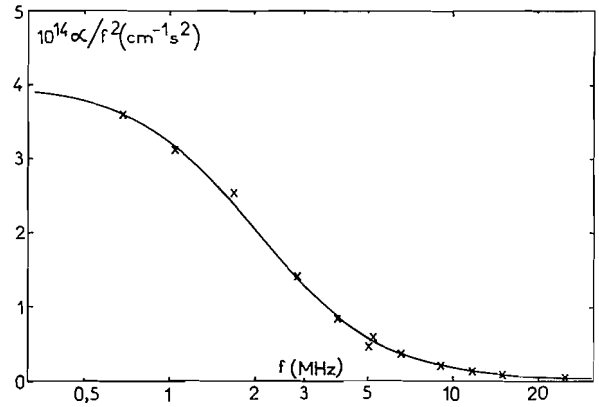


FIG. 2. Spectre ultrasonore d'une solution de décanoate de potassium $C = 0{,}28$ *M*, dans $H_2O - 0{,}1$ *M* KCl.

d'inhibition de fluorescence utilisée dans ce travail pour la détermination des nombres micellaires.

Comme le prévoient les calculs de Shinoda (22), la variation de log cmc en fonction de log (cmc + c_{KCl}) est une droite dont la pente (−0,56) se situe dans le domaine prévu par la théorie (−0,4 à −0,6).

L'absorption ultrasonore de solutions de décanoate de potassium en présence de KCl a été mesurée en fonction de la fréquence. L'équation:

$$[30] \quad \frac{\alpha}{f^2} = \frac{R}{1 + 4\pi^2 f^2 \tau_1^2} + B$$

a été utilisée pour rendre compte des résultats expérimentaux, *B* étant une constante ajustable généralement peu différente de l'absorption du solvant. A cet effet, nous avons adopté une méthode de moindres carrés pondérés, à deux paramètres *R* et τ_1, qui minimise la quantité

$$[31] \quad Q = \sum \left[\left[\left(\frac{\alpha}{f^2}\right)_{exp} - \left(\frac{\alpha}{f^2}\right)_{cal} \right] \Big/ \left(\frac{\alpha}{f^2}\right)_{exp} \right]^2$$

le paramètre *B* ayant été pris égal à 22×10^{-17} cm^{-1} s^2, valeur de α/f^2 pour l'eau et les solutions de KCl utilisées dans ce travail. Dans *Q* la somme est prise sur un nombre de termes égal au nombre de résultats expérimentaux pour chaque solution étudiée. La fig. 2 montre un exemple de spectre ultrasonore: la courbe en trait plein qui obéit à l'éq. [30] est celle qui rend le mieux compte des résultats expérimentaux. Le tableau 2 donne les valeurs de *R* et τ_1 ainsi obtenues pour chaque solution étudiée. Nous avons également fait figurer les valeurs obtenues à partir des résultats de Graber et coll. (4) pour le décanoate de potassium dans l'eau. Ces valeurs diffèrent légèrement de celles publiées (4), ces dernières n'ayant pas été obtenues par une méthode de moindres carrés pondérés mais par une méthode qui minimise la sommes des numérateurs dans l'éq. [31] et met ainsi un poids très grand sur les résultats à basse fréquence qui sont les moins précis.

Dans une deuxième étape l'éq. [25] a été utilisée pour rendre compte des résultats relatifs à τ_1, avec k^-/n et k^-/σ^2 comme paramètres ajustables (voir fig. 3). La méthode de moindres carrés pondérés conduit à des valeurs relativement précises de k^-/n qui représente la pente des droites $1/\tau_1 = f(a)$. Par contre les valeurs obtenues pour k^-/σ^2 (ordonnée à l'origine dans la représentation précédente) peuvent être très imprécises et il convient donc de déterminer cette quantité ou tout autre quantité permettant d'accéder à σ par une autre méthode.

TABLEAU 2. Valeurs de τ_1 et R pour les solutions de décanoate de potassium en présence de KCl, à 25°C

	$C_{KCl} = 0$		$C_{KCl} = 0{,}1\ M$		$C_{KCl} = 0{,}5\ M$		
C (M/L)[a]	$10^7\tau_1$[b]	$10^{17}R$[c]	$10^7\tau_1$[b]	$10^{17}R$[c]	C (M/L)[a]	$10^7\tau_1$[b]	$10^{17}R$[c]
0,16	2,07	9970	1,58	7260	0,07	4,42	12000
0,22	1,16	6000	1,05	5570	0,15	1,47	4290
0,28	0,784	4290	0,777	3980	0,23	0,95	3380
0,35	0,600	3110	0,603	2910	0,32	0,647	2210

[a]Valeurs en mol/L.
[b]Valeurs en s^{-1}.
[c]Valeurs en $cm^{-1}\,s^2$.

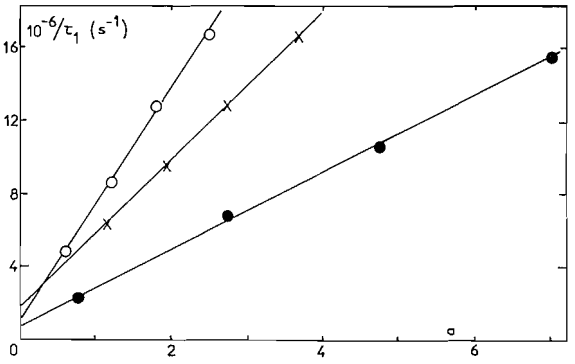


FIG. 3. Solutions de décanoate de potassium à 25°C. Variation de $1/\tau_1$ en fonction de a, en l'absence de KCl (○) et avec 0,1 M KCl (×) et 0,5 M KCl (●). Les droites obéissent l'éq. [25] et ont été obtenues comme indiqué dans le texte.

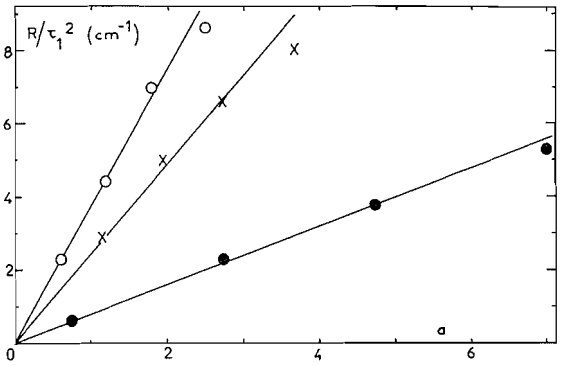


FIG. 4. Solutions de décanoate de potassium à 25°C. Variation de R/τ_1^2 en fonction de a sans KCl (○), avec 0,1 M KCl (×) et 0,5 M KCl (●). Les droites obéissent l'éq. [24] et ont été obtenues comme indiqué dans le texte.

Les valeurs de k^-/n et l'éq. [24] ont ensuite été utilisées pour rendre compte des valeurs de R/τ_1^2 en fonction de a, avec ΔV_0^2 comme seul paramètre ajustable (voir fig. 4).

Dans une dernière étape, les valeurs de ΔV_0 et k^-/n obtenues comme on vient de le dire ont été insérées dans l'éq. [24] où τ_1 a été remplacé par son expression [25] pour rendre compte des valeurs de R, avec σ^2/n comme seul paramètre ajustable (voir fig. 5). Les valeurs de σ^2/n ainsi obtenues sont en excellent accord avec celles calculées en formant le rapport $(k^-/n)/(k^-/\sigma^2)$ à partir des valeurs obtenues plus haut.

Les valeurs de k^-/n, ΔV_0 et σ^2/n obtenues comme on vient de le décrire sont données dans le tableau 3.

Nous avons également fait usage des courbes $\alpha/f^2 = f$(concentration) à fréquence fixe utilisées pour obtenir les cmc. Ces courbes obéissent à l'équation résultant de la combinaison des éqs [20] et [24] et la pente de ces courbes au voisinage de la cmc est donnée par l'éq. [27a]. Nous avons calculé à partir des valeurs de ces pentes, k^-/n en prenant les ΔV_0 de la colonne (d) du tableau 3 et inversement les ΔV_0, en prenant les valeurs de k^-/n de la colonne (a) du tableau 3. On voit que les valeurs de k^-/n obtenues à partir des droites $1/\tau_1 = f(C)$ sont en bon accord avec celles calculées comme il vient d'être décrit. De même les deux séries de valeurs de ΔV_0 sont en bon accord. Notons qu'à la fréquence 2,82 MHz à laquelle ont été réalisées les mesures de $\alpha/f^2 = f(C)$ en présence de KCl, l'éq. [27a] se simplifie car $(k^-/\sigma^2)^2 \ll \omega^2$. En l'absence de KCl, nous avons fait usage des valeurs de $\alpha/f^2 = f(C)$ rapportées par Graber et coll. (4) à 3,37 MHz pour calculer ΔV_0 et k^-/n comme nous venons de le dire.

Les trois dernières colonnes du tableau 3 donnent les valeurs de k^- calculées à partir de k^-/n (colonne (a)) et n, de σ

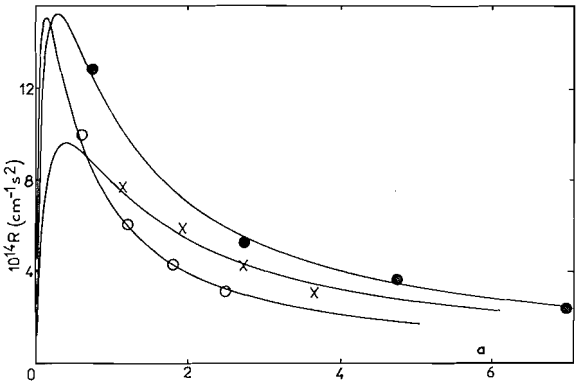


FIG. 5. Solutions de décanoate de potassium à 25°C. Variation de R en fonction de a sans KCl (○), avec 0,1 M KCl (×) et 0,5 M KCl (●). Les courbes obéissent l'éq. [24] et ont été obtenues comme indiqué dans le texte.

calculées à partir de σ^2/n (colonne (a)) et n et k^+, constante de vitesse de la réaction d'association d'un ion amphiphile à une micelle, calculée à partir de la relation (23)

[32] $k^+ = k^-/\text{cmc}$

IV. Discussion des résultats

La variation de k^+ avec la force ionique est dans le sens attendu. En effet, l'addition de sel apporte une

Can. J. Chem. Downloaded from www.nrcresearchpress.com by 210.87.254.105 on 09/05/12
For personal use only.

TABLEAU 3. Valeurs de k^-/n, σ^2/n, ΔV_0, k^-, k^+ et σ obtenues à partir des calculs décrits dans le texte

C_{KCl} (M/L)	cmc (M/L)	n	$10^{-6}(k^-/n)$ (s^{-1}) (a)	(b)	σ^2/n (a)	(c)	ΔV_0 (cm^3/mol) (d)	(e)	$10^{-8}k^-$ (s^{-1}) (f)	$10^{-9}k^+$ (M^{-1} s^{-1}) (g)	σ (h)
0	0,1	32	$6,3_5$	5,5	6,1	6,5	7,0	6,5	2	2	14
0,1	0,075	38	$4,0_4$	3,9	2,2	2,4	8,2	8,1	1,5	2	9
0,25	0,058	—	—	$2,8_5$[i]	—	—	—	—		—	—
0,5	0,04	66	$2,1_3$	1,7	3,1	3,2	8,8	7,8	1,4	3,5	14

[a]Obtenu à partir de $1/\tau_1 = f(a)$.
[b]Calculé à partir de la pente des courbes $\alpha/f^2 = f(C)$ à la cmc, en utilisant les ΔV_0 de la colonne (*d*).
[c]Obtenu à partir des courbes $R = f(a)$, en utilisant les valeurs de ΔV_0 de la colonne (*d*).
[d]Obtenu à partir des courbes $R/\tau_1^2 = f(a)$, en utilisant les valeurs de k^-/n de la colonne (*a*).
[e]Calculé à partir de la pente des courbes $\alpha/f^2 = f(C)$ à la cmc en utilisant les valeurs de k^-/n de la colonne (*a*).
[f]Calculé à partir des valeurs de k^-/n de la colonne (*a*) et de *n*.
[g]Calculé à partir de $k^+ = k^-/\text{cmc}$.
[h]Calculé à partir des valeurs de σ^2/n de la colonne (*a*) et de *n*.
[i]Calculé en supposant $\Delta V_0 = 8,4$ cm^3/mol, sur la base des valeurs de ΔV_0 en présence de KCl.

réduction des répulsions électrostatiques entre ions détergents libres et micelles, d'où une association plus facile de ces ions aux micelles, et des valeurs plus élevées de k^+. Il est intéressant de comparer les valeurs de k^+ du tableau 3 à la valeur $k_d{}^+$ calculée pour une réaction d'association complètement contrôlée par la diffusion, entre deux espèces non chargées, en utilisant à cet effet la relation de Smoluchowski:

$$[33] \quad k_d{}^+ = 4\pi r(D_{mic} + D_{mon})N_A/1000$$

Dans cette équation r représente la distance minimum d'approche ou distance de réaction, N_A est le nombre d'Avogadro, et D_{mic} et D_{mon} les coefficients de diffusion de translation des micelles et des ions détergents libres, respectivement. On prend pour r la longueur de la chaîne alkyle de l'ion décanoate soit 13×10^{-8} cm. En effet, on peut considérer que la collision entre une micelle et un ion détergent libre a lieu lorsque la distance entre la surface micellaire et le groupe chargé de l'ion détergent devient égale à la longueur de la chaîne alkyle. D'autre part, en première approximation D_{mic} peut être négligé devant D_{mon}. Cette dernière quantité a été calculée à partir de la conductivité équivalente limite de l'ion décanoate, en utilisant la relation donnée par Robinson et Stokes (24). On trouve ainsi $D_{mon} = 5,3 \times 10^{-6}$ cm^2 s^{-1}. L'insertion des valeurs de r et D_{mon} dans l'éq. [33] donne:

$$k_d{}^+ = 5,2 \times 10^9 \, M^{-1} \, s^{-1}$$

Cette valeur est proche de celle obtenue pour k^+ à forte force ionique. Elle diffère de la valeur obtenue à faible force ionique par un facteur 2,6, qui semble donc essentiellement dû aux répulsions électrostatiques.

Aniansson et coll. (25) ont donné l'équation suivante:

$$[34] \quad \frac{k^-}{n} = \frac{D_{mon}}{l_b{}^2} \exp(-\varepsilon/kT)$$

l_b est une longueur voisine de 1,265 Å indépendamment de la force ionique et ε représente la variation d'énergie libre associée au transfert d'un amphiphile d'une position dans laquelle sa chaîne alkyle est complètement à l'intérieur de la micelle, à une position où le groupe méthyl terminal est en contact avec la surface de la micelle. Cette expression ne permet pas de prévoir facilement le sens de la variation de cette quantité et donc de k^- avec la force ionique. En effet, à la variation de n se superpose celle de ε qui est la somme de deux contributions de signes opposés: l'une, ε_E d'origine électrostatique et l'autre, ε_H, d'origine hydrophobe. L'augmentation de force ionique se traduit par une diminution de ε_E mais également de ε_H. Le fait que k^- ne diminue que légèrement sous l'effet de la force ionique alors que n est doublé, indique que $e^{-\varepsilon/kT}$ diminue donc que ε augmente. Le terme ε_E diminue donc plus que ε_H en présence de 0,5 M KCl, par rapport à la situation qui prévaut en l'absence de force ionique.

Considérons maintenant les valeurs de ΔV_0 qui est le changement de volume associé au transfert d'un ion amphiphile de la phase aqueuse à la phase micellaire. En l'absence de force ionique le ΔV_0 du décanoate de potassium a été obtenu par mesure des densités (26, 27). La valeur moyenne est 9,5 cm^3/mol. Cette valeur est environ 35% plus grande que celle calculée à partir des résultats de Graber et coll. (4). L'amplitude R de la relaxation ultrasonore étant proportionnelle à $\Delta V_0{}^2$, la différence entre les valeurs obtenues par densité (26, 27) et par absorption ultrasonore correspond à une erreur par un facteur 1,84 sur R. On doit donc conclure que la valeur obtenue à partir des résultats de Graber et coll. (4) est trop faible, en partie peut être en raison d'erreurs dans

Can. J. Chem. Downloaded from www.nrcresearchpress.com by 210.87.254.105 on 09/05/12
For personal use only.

Can. J. Chem. Downloaded from www.nrcresearchpress.com by 210.87.254.105 on 09/05/12
For personal use only.

l'étalonnage des appareils ultrasonores utilisés à l'époque. Les résultats obtenus dans notre travail, c'est-à-dire en présence de force ionique semblent raisonnables sur la base de la différence entre les ΔV_0 pour le décanoate et le nonanoate de sodium (26, 27) et de la variation du ΔV_0 du nonanoate de sodium avec la force ionique (28). Ainsi ce ΔV_0 passe de 9,2 à 7,8 cm^3/mol lorsque la concentration en NaCl passe de 0 à 0,4 M (l'effet de la nature du contreion sur ΔV_0 est très faible). Notons toutefois que les calculs de ΔV_0 ont été faits sur la base d'équations dans lesquelles les activités des solutés ont été remplacées par les concentrations. Cette approximation, valable pour les solutions diluées, ne s'applique plus pour les concentrations auxquelles ont été réalisées les expériences discutées ici et peut donner lieu à d'importantes erreurs, particulièrement dans le cas des résultats relatifs aux mesures effectuées en l'absence de force ionique (29).

Nous terminons cette discussion par les valeurs de σ^2/n. En présence de force ionique, les valeurs obtenues pour cette quantité sont très proches de celles trouvées pour de nombreux autres détergents, les alkylsulfates de sodium 23 par exemple et correspondent à des indices de polydispersité de 1,05 environ. Au contraire, la valeur $\sigma^2/n = 6$ obtenue à partir des résultats de Graber et coll. (4) semble trop élevée. A ce point il convient à nouveau de rappeler que l'erreur sur les valeurs de σ^2/n (et donc sur σ) est importante. Néanmoins, la concordance entre les valeurs de σ^2/n dans les colonnes (*a*) et (*c*) tout comme celles de k^-/n dans les colonnes (*a*) et (*b*) et de ΔV_0 dans les colonnes (*d*) et (*e*) souligne la cohérence des différentes équations utilisées et également des résultats dérivés à partir des valeurs des temps de relaxation et des amplitudes de relaxation qui sont des quantités de nature différente.

Cette conclusion donne une base solide à l'utilisation des équations établies dans ce travail pour l'interprétation des résultats ultrasonores relatifs à d'autres systèmes (30).

1. T. YASUNAGA, H. OGURI et M. MIURA. J. Colloid Interface Sci. **23**, 352 (1967).
2. T. YASUNAGA, S. FUJII et M. MIURA. J. Colloid Interface Sci. **30**, 399 (1969).
3. T. YASUNAGA, S. FUJII et M. MIURA. 6e Int. Cong. Acoustics, Tokyo, 1968, papier J5-8.
4. E. GRABER, J. LANG et R. ZANA. Kolloid Z. Z.Polym. **233**, 470 (1970).
5. E. GRABER et R. ZANA. Kolloid Z. Z. Polym. **233**, 479 (1970).
6. P. SAMS, E. WYN-JONES et J. RASSING. Chem. Phys. Lett. **13**, 233 (1972).
7. J. RASSING, P. SAMS et E. WYN-JONES. J. Chem. Soc. Faraday Trans. II, **69**, 180 (1973).
8. J. RASSING, P. SAMS et E. WYN-JONES. J. Chem. Soc. Faraday Trans. II, **70**, 1247 (1974).
9. J. RASSING and E. WYN-JONES. Chem. Phys. Lett. **21**, 93 (1973).
10. D. ADAIR, V. REINSBOROUGH, N. PLAVAC et J. VALLEAU. Can. J. Chem. **52**, 429 (1974).
11. D. ADAIR, V. REINSBOROUGH, H. TRENHOLM et J. VALLEAU. Can. J. Chem. **54**, 1162 (1976).
12. D. ADAIR, V. REINSBOROUGH et S. ZAMORA. Adv. Mol. Relaxation Processes, **11**, 63 (1977).
13. KUN MOO LEE. Daehan Hwahak Hwoejee (J. Korean Chem. Soc.), **17**, 72 (1973); **20**, 193 (1976).
14. T. TAKEDA. J. Sci. Hiroshima Univ., Ser. A, **40**, 87 (1976).
15. S. DIEKMANN. Ber. Bunsenges. Phys. Chem. **83**, 528 (1979).
16. E. A. G. ANIANSSON et S. WALL. J. Phys. Chem. **78**, 1024 (1974); **79**, 857 (1975).
17. M. TEUBNER. J. Phys. Chem. **83**, 2917 (1979).
18. H. HOFFMANN, R. NAGEL, G. PLATZ et W. ULBRICHT. Colloid Polym. Sci. **254**, 812 (1977).
19. M. MANES. J. Chem. Phys. **21**, 1791 (1953).
20. N. TURRO et A. YEKTA. J. Am. Chem. Soc. **100**, 5951 (1978).
21. H. TARTAR. J. Colloid Interface Sci. **14**, 115 (1959).
22. K. SHINODA. Colloidal surfactants. *Edité par* E. Hutchinson et Van Rysselberghe. Academic Press, New York. 1963. pp. 58–63.
23. E. A. G. ANIANSSON, S. WALL, M. ALMGREN, H. HOFFMANN, I. KIELMANN, W. ULBRICHT, R. ZANA, J. LANG et C. TONDRE. J. Phys. Chem. **80**, 905 (1976).
24. R. ROBINSON et R. STOKES. Electrolyte solutions. Butterworths, London. 2e Edition revisée. 1975. p. 288.
25. E. ANIANSSON, M. ALMGREN et S. WALL. Chemical and biological applications of relaxation spectrometry. D. Reidel Publ. Co., Dordrecht. 1975. p. 239.
26. K. KALE et R. ZANA. J. Colloid Interface Sci. **61**, 312 (1979).
27. E. VIKINGSTAD, A. SKAUGE et H. HOILAND. J. Colloid Interface Sci. **72**, 59 (1979).
28. E. VIKINGSTAD, A. SKAUGE et H. HOILAND. Acta Chem. Scand. **A33**, 235 (1979).
29. J. STUEHR et E. YEAGER. Physical acoustics. Vol. IIA. *Edité par* W. P. Mason. Academic Press, New York. 1963. pp. 381–391.
30. R. ZANA et S. YIV. J. Colloid Interface. Sous presse.

Photo- and thermal isomerization of some 1-methoxyallyl cations

RONALD F. CHILDS[1] AND MARK E. HAGAR

Department of Chemistry, McMaster University, Hamilton, Ont., Canada L8S 4M1

Received February 19, 1980

RONALD F. CHILDS and MARK E. HAGAR. Can. J. Chem. **58**, 1788 (1980).

The 1-methoxy-, 1-methoxy-3-methyl-, and 1-methoxy-2,3-dimethylallyl cations, **2**, **5**, and **9**, were prepared by treatment of the dimethyl acetals of acrolein, crotonaldehyde, and tiglaldehyde, respectively, with FSO_3H. Each of these ions was capable of existing in various stereoisomeric forms. The thermodynamically preferred conformation of **2**, **5**, and **9** all had a C1—O, *E* configuration and **5** and **9** an *E* configuration about the C2—C3 bonds. Irradiation of FSO_3H solutions of these ions at −70°C using 254 nm light caused them to be converted to the other stereoisomers. Relatively efficient photoisomerism about both the C1—O and C2—C3 bonds was observed. The rates of the reverse thermal conversion of the photoproducts to **2**, **5**, and **9** were measured and on the basis of medium and substituent effects it was concluded that thermal isomerism about the C1—O bond takes place by an inversion process while stereomutation about the C2—C3 bond involves the addition of base to C3.

RONALD F. CHILDS et MARK E. HAGAR. Can. J. Chem. **58**, 1788 (1980).

On a préparé les cations allyliques: méthoxy-1, méthoxy-1 méthyl-3 et méthoxy-1 diméthyl-2,3 (**2**, **5** et **9**) en traitant respectivement les acétals diméthylés de l'acroléine, de la crotonaldéhyde et de la tiglaldéhyde par du FSO_3H. Chacun de ces isomères peut exister sous différentes formes stéréoisomères. La conformation thermodynamique préférée par **2**, **5** et **9** est celle où tous les trois ont une configuration *E* en C1—O et dans le cas de **5** et de **9** une configuration *E* autour des liaisons C2—C3. Par irradiation à 254 nm ces ions et solution dans le FSO_3H se transforment en d'autres stéréoisomères. On a observé une isomérisation photochimique relativement efficace autour des deux liaisons C1—O et C2—C3. On a mesuré les vitesses de transformation thermique inverse de ces produits photochimiques en **2**, **5** et **9** en fonction du milieu et des effets de substituants et on a conclu que l'isomérisation thermique autour de la liaison C1—O se fait par inversion tandis que la stéréomutation autour de C2—C3 implique l'addition d'une base à C3.

[Traduit par le journal]

There have been several reports over the past few years on the photoreactions of protonated unsaturated carbonyl compounds (1, 2).[2] Frequently these cationic systems have been found to undergo photoisomerizations which are very similar to those encountered with the corresponding neutral compounds. A case in point, which forms the substance of this present paper, concerns the α,β-unsaturated carbonyl compounds. These, when irradiated in conventional solvents (3) or as protonated species in super acid media (2), undergo stereomutation about the carbon–carbon double bond. Protonated carbonyl compounds, however, have an additional mode of photoisomerization available which is not open to the neutral compounds, namely isomerization about the carbon–oxygen double bond. This potential photoreaction has not been detected with any of the protonated carbonyl compounds so far investigated.

Stereoisomerism about the carbon–oxygen bond of protonated carbonyl compounds is well established (4). In general, protonation of a carbonyl compound leads to a thermodynamic equilibrium mixture of the two possible stereoisomers. Interconversion of the two stereoisomers is facile and a variety of mechanisms have been suggested to account for this stereomutation. Exchange of the proton on oxygen with the acid pool is one of the more frequently encountered pathways for these isomerizations (5).

In order to eliminate the possibility of exchange reactions taking place with the acid medium and thus rendering potential photoisomerizations about the carbon–oxygen bond undetectable, it was decided to work with the corresponding *O*-methyl derivatives. We report here the preparation, photoisomerism, and thermal rearrangements of several 1-methoxyallyl cations. A preliminary account of part of this work has appeared (6).

Results

Preparation of Cations

1-Methoxyallyl cations were prepared by the protonation and cleavage in FSO_3H of the dimethyl acetals of several unsaturated aldehydes. In order to get clean solutions of these ions, it was found best to extract the acetal from Freon 11 into the acid at −78°C. The pale yellow solutions prepared by this route were stable for long periods and showed no discoloration when left at room temperature for several hours. Indeed a convenient way of removing the Freon was to purge the solutions with an

[1]Author to whom correspondence may be addressed.

[2]For a review see R. F. Childs. Rev. Chem. Intermed. In press.

0008-4042/80/171788-07$01.00/0

©1980 National Research Council of Canada/Conseil national de recherches du Canada

Can. J. Chem. Downloaded from www.nrcresearchpress.com by 210.87.254.5 on 09/05/12
For personal use only.

Can. J. Chem. Downloaded from www.nrcresearchpress.com by 210.87.254.5 on 09/05/12
For personal use only.

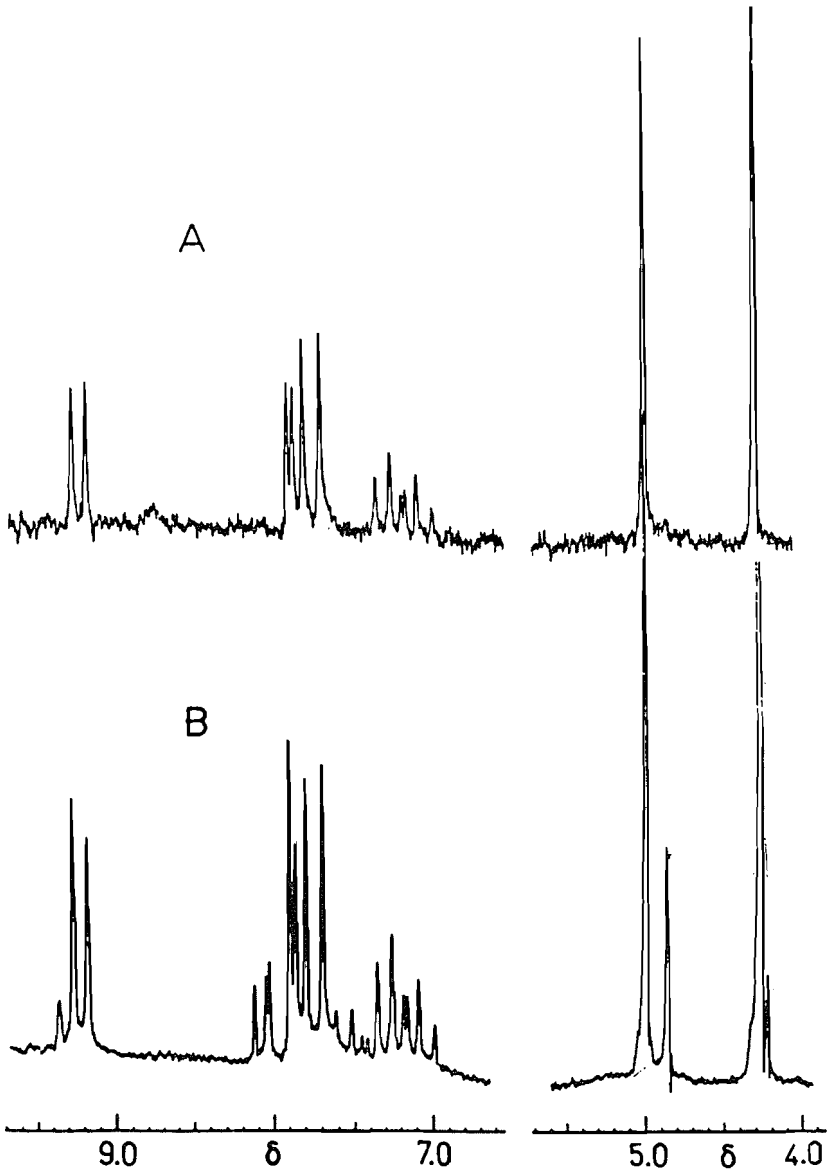


FIG. 1. ^{1}H nmr spectrum of **2**. A, prior to irradiation; B, after irradiation.

argon stream at room temperature. Protonated methanol (7), exhibiting a methyl resonance at ca. δ 4.25, was also present in the solutions. This did not interfere with any of the subsequent studies, although it was noted that thermally induced reactions of $CH_3OH_2^+$ occurred when the samples were kept at high temperatures.

Solution of acrolein dimethyl acetal, **1**, in FSO_3H gave **2**. The identity of this ion was evident from its ^{1}H nmr spectrum (Fig. 1A, Table 1) which was very similar to that of protonated acrolein (8). Neglecting stereoisomerism about the C1—C2 bond of **2**, which is expected to have a very low barrier to rotation (9), there are two possible isomers of the 1-methoxyallyl cation. It was clear from the nmr spectrum of the cation derived from **1** that one of the two possible isomers predominated. On the basis of the known steric preferences for protonated enals (4), the C1—O, *E* configuration was assigned to **2**.

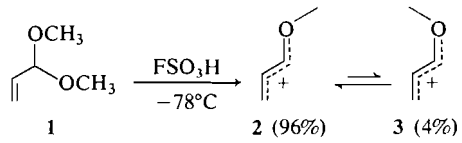
As will be shown later, the C1—O, *Z* isomer **3** can be prepared and knowing its nmr spectrum it

Can. J. Chem. Downloaded from www.nrcresearchpress.com by 210.87.254.5 on 09/05/12
For personal use only.

TABLE 1. ^{1}H chemical shifts of acetals and cations

	Chemical shifts (ppm)[a]					Coupling constants (Hz)		
	H1	H2	H3	H4	OCH_3	$J_{1,2}$	$J_{2,3}$	$J_{3,4}$
1	4.78 dt	5.80 ddd	5.2–5.5 m	—	3.30 s	3.5	10, 17.5	—
2	9.21 d	7.16 m	7.83 d, 7.76 d	—	5.01 s	9	10, 16.5	—
3	9.30 d	7.43 m	8.06 d, 7.96 d	—	4.87 s	10	10, 16	—
4	4.72 d	5.44 dd	5.83 dq	1.75 d	3.30 s	5	17	6
5	8.96 d	6.99 dd	8.54 dq	2.55 d	4.84 s	9	15	7
6	9.50 d	6.91 t	8.45 dq	2.60 d	4.89 s	10	10.5	7
7	9.06 d	7.40	8.7[b]	2.65	4.68 s	8	—	—
12	9.56 d	7.4[b]	8.7[b]	2.7[b]	4.70 s	10.5	—	—
8	4.43 s	1.58 s[c]	5.60 q	1.64 d	3.25 s	—	—	7
9	8.85 s	2.03 s[c]	8.29 q	2.49 d	4.84 s	—	—	7.5
10	9.48 s	2.07 s[c]	8.24 q	2.53 q	4.90 s	—	—	7.5

[a]All shifts relative to TMS for acetals or $(CH_3)N^+BF_4^-$ taken as δ 3.1 for cations; d = doublet, m = multiplet, q = quartet, s = singlet, t = triplet.
[b]Peak obscured by resonances of other cations and exact chemical shift uncertain.
[c]C2 methyl resonance.

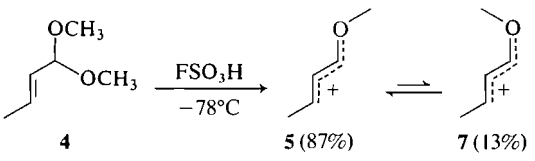


1 **2** (96%) **3** (4%)

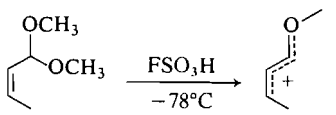
was possible to detect a small amount (4%) of **3** in equilibrium with **2**. This low concentration of **3** was observed in all samples of **2** that were prepared, even when the acid solutions were kept at temperatures well above those required for the thermal interconversion of **2** and **3**.

Extraction of **4** into FSO_3H led to the formation of predominantly one cation which was identified as **5**. The ^{1}H nmr spectrum of **5** (Fig. 2A) was very similar to that of the corresponding protonated aldehyde (2). It was clear that low concentrations of additional cations were present. Warming the solution to room temperature for several hours caused one of the minor cations to isomerize to **5**. This ion, which is characterized by a doublet resonance at δ 9.50 (Fig. 2A), was identified as **6**. (Evidence to support this will be presented later.) It would appear that **6** arises from protonation of small amounts of the dimethyl acetal of *cis*-crotonaldehyde formed during the synthesis of **1**.

The other minor isomer present was identified as



4 **5** (87%) **7** (13%)

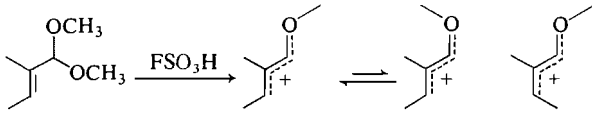


6

7, the C1—O bond isomer of **5**, *vide infra*. The ratio of **5** to **7** was found to be 87 to 13 at −20°C.

Treatment of tiglaldehyde acetal **8** with FSO_3H gave very largely **9** together with a small amount of **10** (ca. 10%). Again it would seem that this minor isomer results from a *cis* impurity in the starting acetal. When the acid samples were held at 50°C the minor isomer reverted to **9**. No evidence for the presence of **11**, the C1—O *Z* isomer of **9**, could be detected either on the initial protonation or after the sample had stood at room temperature for a while.

The uv spectra of the cations **2**, **5**, and **9** were obtained at room temperature in concentrated H_2SO_4 and are summarized in Table 2. In each case the ions exhibited an intense absorption in the neighbourhood of 250 nm.



8 **9** **11** **10**

Photoisomerizations of the cations were carried out at low temperature (−70°C) using 254 nm light. Reactions were followed by low temperature ^{1}H nmr assay directly on the irradiated acid solutions. Degassing the samples prior to irradiation appeared to make no difference to the products observed.

Irradiation of a FSO_3H solution of **2** led to the formation of a new cation. The nmr spectrum of the resulting mixture (Fig. 1B) clearly showed that the product was closely related to **2**. Three vinyl resonances were present which had a very similar coupling pattern to that of **2**. In addition the new cation had an *O*-methyl group resonance at δ 4.87. On this basis the photoproduct was assigned the structure **3**. A similar photoisomerization was observed when **2** was irradiated in FSO_3H/SbF_5 (3:1) at low temperatures.

Can. J. Chem. Downloaded from www.nrcresearchpress.com by 210.87.254.5 on 09/05/12
For personal use only.

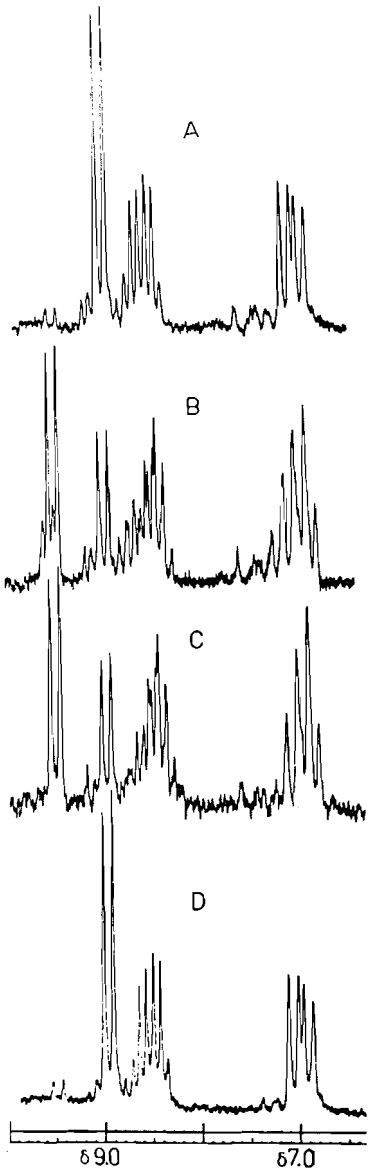


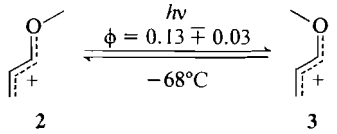
FIG. 2. Part of the ^{1}H nmr spectrum of **5**. A, prior to irradiation; B, after irradiation, sample kept at −50°C; C, after warming sample to −20°C; D, after warming to 38°C.

A photostationary state was set up between **2** and **3** consisting of 73% **2** and 27% **3** at −70°C. The quantum efficiency of the conversion of **2** to **3** was measured at −68°C using a relative method. A quantum yield of 0.13 ∓ 0.03 was found with FSO_3H as the acid medium. It was not possible to measure the quantum efficiency of the reverse reaction as we have been unable to generate a mixture of **2** and **3** which contained an excess of the latter ion.

On warming the acid solutions containing **2** and **3** to −20°C, a clean rearrangement of the latter ion to **2** was observed. The rate constants for this first order reaction were measured in FSO_3H and FSO_3H/SbF_5 media and are given in Table 3.

TABLE 2. Ultraviolet spectra of cations in H_2SO_4

Cation	λ_{max} (nm)	log ε
2	234	3.97
5	255.5	4.28
9	268.5	4.30



2 **3**

Irradiation of a cation mixture containing mostly **5**, as illustrated in Fig. 2A, or a mixture consisting of only **5** and **7**, led to the formation of a complex mixture of ions, Fig. 2B. On the basis of the results obtained with **2** above and protonated crotonaldehyde previously (2), it was expected that photoisomerization about both the C,C and C,O double bonds of **5** could take place to give a mixture of four isomers. Examination of the downfield region of the ^{1}H nmr spectrum of the mixture showed four doublets to be present. These doublet resonances were in a typical position for the C1-proton signals of the 1-methoxyallyl cations (Fig. 2B).

The system could be partially simplified by warming the FSO_3H solution to −20°C when two of the cations largely reverted to the other two (Fig. 2C). One of the two remaining ions was the starting cation **5**, while the other appeared to be **6**. Evidence for this latter assignment comes from the magnitude of the coupling constant between the two protons on the C2—C3 bond, J = 10.5 Hz. This coupling constant is very similar to that found for protonated *cis*-crotonaldehyde and is indicative of the C2—C3 bond of **6** having a *Z* configuration. When the acid solutions were warmed above room temperature, **6** was found to isomerize back to **5** (Fig. 2D).

With isomerism about the C2—C3 bond of **6** occurring at room temperature and above, then the reactions taking place at −20°C must have been stereomutations about the C1—O bonds. This means that **6** would be expected to have the more stable *E*-conformation about the C1—O bond and that the other two isomers seen initially at low temperatures would correspond to the C1—O *Z* isomers of **5** and **6**. One of these isomers is in thermal equilibrium with **5** in the final solution and

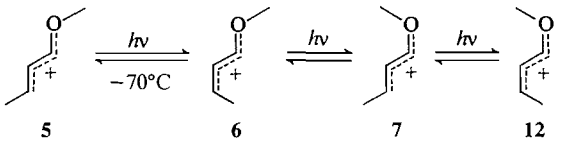
Can. J. Chem. Downloaded from www.nrcresearchpress.com by 210.87.254.5 on 09/05/12
For personal use only.

TABLE 3. Rate data for isomerizations

Reaction	Temperature (°C)	Medium	k (s^{-1})	$\Delta G^{\ddagger}$ (kcal/mol)
3 → **2**	−20	FSO_3H	$(1.1 \mp 0.1) \times 10^{-4}$	19.2
3 → **2**	−20	FSO_3H/SbF_5	$(2.8 \mp 0.4) \times 10^{-5}$	19.9
12 → **6**	−20	FSO_3H	$(6.0 \mp 0.6) \times 10^{-4}$	18.4
12 → **6**	−20	FSO_3H/SbF_5	$(4.0 \mp 1.0) \times 10^{-4}$	18.6
6 → **5**	+38	FSO_3H	$(4.4 \mp 0.3) \times 10^{-4}$	22.9
6 → **5**	+50	FSO_3H/SbF_5	$(4.0 \mp 0.3) \times 10^{-6}$	26.8
10 → **9**	+50	FSO_3H	$(5.4 \mp 0.3) \times 10^{-5}$	25.2

TABLE 4. Changes in composition on irradiation of **5**

	Composition (%)			
	5	**6**	**7**	**12**
Initial	82	8	10	0
After irradiation	31	49	7	13
After heating to −20°C	32	62	5	0
After heating to 38°C	87	0	13	0



5 **6** **7** **12**

was given the structure **7**. The other, by process of elimination, must be **12**. A summary of the composition changes as a function of irradiation and heating cycles is given in Table 4. The rate constants for the isomerizations are given in Table 3.

Measurement of the quantum yields associated with the various reactions taking place on irradiation of **5** was complicated by our inability to obtain pure samples of all the possible isomers. The only value obtained with any degree of confidence was that of the conversion of **5** to **6**, $\Phi = 0.24 \mp 0.05$ at −68°C in FSO_3H.

In contrast to the complex situation encountered with **5**, irradiation of **9** led to the production of only one new cation. The photoproduct was stable at room temperature and only underwent a slow isomerization to **9** when heated to 50°C. The high temperature required for this rearrangement indicated that the photoproduct was **10**, the C2—C3 isomer of **9**. No evidence for the presence of any additional isomers of **9** and **10** could be detected even when the ^1H nmr spectra of the solutions were recorded at −70°C immediately after irradiation.

Discussion

The results described above for **2**, **5**, and **9** clearly indicate that photoinduced stereomutations can occur about both the C1—O and C2—C3 partial bonds of these cations. Both of these processes have relatively high quantum yields suggesting that twisting about these bonds constitutes the major relaxation pathway for the excited states involved. In this regard the photochemical behaviour of these cations is more similar to that of a diene than that of the corresponding neutral carbonyl compounds (10).

One of the issues that has been investigated with the photoisomerizations of dienes is whether rotation about both double bonds can take place on a single excitation. A similar question can be raised with the 1-methoxyallyl cations. In this present work, however, it has not been possible to obtain sufficient quantum yield data or relative rates of initial isomerizations to answer this point.

Two-bond isomerizations would be expected only if triplet states of the 1-methoxyallyl cations were involved in these photoisomerizations. This would seem unlikely under the conditions used and most probably singlet π,π^* states are involved. Certainly such singlet states would be the lowest energy states available under the direct irradiation conditions used in this work (11). Intersystem crossing to the triplet manifold would be expected to be relatively inefficient, just as has been found for the simple dienes (10). Further evidence to support the suggestion that singlet states are involved in these reactions comes from the absence of any effect when oxygen is present. Assuming a singlet state to be involved, then perhaps the best way of viewing the reactions of these cations is for the initial excitation to give a planar diradical cation which can undergo rotation about either the C1—O or C2—C3 bonds. For isomerization about the C,C bond, the best representation of the structure when the C2—C3 bond is twisted through 90° would be one with the positive charge very largely localized on C3 (12).

Thermal Isomerizations

As can be seen from the data in Table 3, there is a marked contrast in the effect of medium change (FSO_3H, FSO_3H/SbF_5) on the rate of

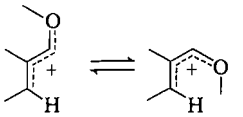
Can. J. Chem. Downloaded from www.nrcresearchpress.com by 210.87.254.5 on 09/05/12
For personal use only.

stereoisomerism about the C2—C3 and C1—O bonds of the various cations. The large decrease in rate constant observed on addition of SbF_5 to the FSO_3H in the case of the conversion of **6** to **5** parallels that found for the corresponding protonated aldehyde isomerization (2) and indicates that this particular reaction proceeds by the specific interaction of base (FSO_3^-) with C3 during the isomerization (13).

On the other hand, stereomutation about the C1—O bond cannot involve such a base addition pathway. As can be seen by the data in Table 3, the rate constants for these reactions are almost medium independent. Moreover, the effect of introduction of a methyl group at C3 (cf. **3** → **2** with **7** → **5**) is also very small, indicating that there is no major change in charge distribution during the isomerization about the C1—O bond. Rather it would seem that this stereomutation involves an inversion at oxygen (14, 15, 16). The isoelectronic aldimines and ketimines undergo a similar inversion at nitrogen (15, 17).

The situation of the *O*-methyl cations derived from tiglaldehyde merit special mention in that no evidence was found for isomerism about the C1—O bond of these cations. The difference between the tiglaldehyde based systems and the other 1-methoxyallyl cations is the presence of the methyl group on C2. This will result in substantially increased steric interactions when the C1—O bond is in the *Z* configuration. If cation **11** were to adopt what seems to be the usually preferred C1—C2, *E* conformation, then a severe steric interaction between the methyl groups on C2 and the oxygen would result. The magnitude of this steric strain in the directly comparable allyl cations has been found to be of the order of 6 kcal/mol (18). On the other hand, if **11** were to adopt the C1—C2, *Z* configuration, then a severe interaction between the methyl group on oxygen and the C3 proton would result.

This steric strain associated with the *O*-methyl group interactions will have the effect of raising the ground state energy of the C1—O, *Z* isomers in the tiglaldehyde based systems. Consequently, in the equilibrium studies, it is not surprising that **11** was not detected in the presence of **9**. Moreover, this steric strain would also be reflected in a reduced barrier to the thermal isomerization of **11** to **9**. It would appear in the case of the photoisomerization of **9** that the reverse thermal isomerization of **11** to **9** could be considerably faster than the rate of its formation in the photochemical step and as a consequence, even if formed photochemically, remain undetected.



11 **11**

Experimental

General

The ^1H nmr spectra were recorded on Varian HA 100 and EM 390 spectrometers. All rate measurements were carried out on the former instrument with the probe temperatures being measured with an iron–constantan thermocouple. The uv spectra were obtained on a Cary 14 spectrometer. Preparative gas chromatography was performed on an Aerograph A-90-P3 instrument using a 10 ft × 1/4 in. column packed with 15% SE30 on Chromosorb W. FSO_3H was purified by distillation, purging the distillate with dry nitrogen and a further distillation. The acid so obtained had no absorption in the uv region at wavelengths greater than 235 mm.

Acetals

A procedure similar to that described by Van Allen (18) was used in all cases. The aldehyde (3.6×10^{-2} mol), trimethyl orthoformate (4.0 mL), anhydrous methanol (1.6 mL), and NH_4NO_3 (0.14 g) were stirred at room temperature for 5 h. The reaction mixture was filtered, treated with Na_2CO_3 (0.18 g) and distilled from bulb to bulb. Final purification of the acetals was carried out by preparative gas chromatography using a column temperature of 110°C. Acrolein dimethylacetal, **1** (19), retention time 2 min; crotonaldehyde dimethyl acetal, **4**, (20), retention time 2.3 min; tiglaldehyde acetal, **8** (21), retention time 3.5 min. With the latter two compounds no evidence of the presence of small amounts of the corresponding *cis*-isomers could be detected in their ^1H nmr spectra (Table 1).

Protonations

The acetal (10–20 mg) was weighed into a nmr tube and Freon 11 (0.25 mL) added in such a way that all the acetal was washed to the bottom of the tube. The tube was cooled in Dry Ice/acetone and cold FSO_3H (0.5 mL) added. Mixing of the two layers was carried out with a glass rod. For recording the ^1H nmr spectra at low temperature, it was not necessary to remove the Freon 11. For the photochemical experiments the Freon 11 was removed by purging the solution with argon at room temperature.

Irradiations

All photoisomerizations were carried out using 10 low pressure mercury lamps (Southern New England Ultraviolet Co. RPR 2537A) arranged in a circle around a partially silvered quartz Dewar. The Dewar was cooled to −70°C with a FTS FC2084P1 refrigeration unit. The samples were contained in 5 mm quartz nmr tubes which were sealed with regular plastic caps. In most cases the samples were not degassed. Reactions were monitored by low temperature ^1H nmr. Quantum yield measurements were carried out using a relative method with the photoinduced conversion of protonated *trans*-pent-3-en-2-one to the *cis*-isomer serving as the reference actinometer. The apparatus and techniques used have been reported separately (22).

Rate Measurements

These were carried out by monitoring the change in relative concentration of the various cationic species present in a given solution by ^1H nmr as a function of time. The temperature of the probe was measured before and after each kinetic run. The

relative concentrations were estimated by using peak heights of appropriate resonance of the cations.

Acknowledgement

The financial support of the National Sciences and Engineering Research Council of Canada is gratefully acknowledged.

1. R. F. CHILDS and C. V. ROGERSON. J. Am. Chem. Soc. **100**, 649 (1978); K. E. HINE and R. F. CHILDS. J. Chem. Soc. Chem. Commun. 145 (1972); D. G. CORNELL and N. FILIPESCU. J. Org. Chem. **42**, 3331 (1971); J. W. PAVLIK and R. J. PASTERIS. J. Am. Chem. Soc. **96**, 6107 (1974); R. NOYORI, Y. OHNISHI, and M. KATO. J. Am. Chem. Soc. **94**, 5105 (1972); J. W. PAVLIK, D. R. BOLIN, K. C. BRADFORD, and W. G. ANDERSON. J. Am. Chem. Soc. **99**, 2816 (1977).
2. R. F. CHILDS, E. F. LUND, A. G. MARSHALL, A. G. MORRISEY, and C. V. ROGERSON. J. Am. Chem. Soc. **98**, 5924 (1976).
3. A. DEFLANDRE, A. LHEUREUX, F. RIOUAL, and J. LEMAIRE. Can. J. Chem. **54**, 2127 (1976); H. MORRISON and O. RODRIQUEZ. J. Photochem. **3**, 471 (1974/5); P. BORRELL and J. D. HOLMES. J. Photochem. **1**, 433 (1972/3); R. S. TOLBERG and J. N. PITTS, JR. J. Am. Chem. Soc. **80**, 1304 (1958).
4. G. A. OLAH, A. M. WHITE, and D. H. O'BRIEN. Carbonium ions. Vol. IV. *Edited by* G. A. Olah and P. v. R. Schleyer. Wiley–Interscience, New York. 1973. p. 1697.
5. H. HOGEVEEN. Recl. Trav. Chim. Pays-Bas, **86**, 696 (1967); D. M. BROUWER. Recl. Trav. Chim. Pays-Bas, **86**, 879 (1967).
6. R. F. CHILDS and M. E. HAGER. J. Am. Chem. Soc. **101**, 1052 (1979).
7. G. A. OLAH, J. SOMMER, and E. NAMANWORTH. J. Am. Chem. Soc. **89**, 3576 (1967).
8. D. M. BROUWER. Tetrahedron Lett. 453 (1968); G. A. OLAH, Y. HALPERN, Y. K. MO, and G. LIANG. J. Am. Chem. Soc. **94**, 3554 (1972).
9. J. BARTHELEMY, R. JOST, and J. SOMMER. Org. Magn. Reson. **11**, 443 (1978).
10. J. SALTIEL, J. D. D'AGOSTINO, E. D. MEGARITY, L. METTS, K. R. NEUBERGER, M. WRIGHTON, and O. C. ZAFIRIOV. Organic photochemistry. Vol. III. *Edited by* O. C. Chapman. M. Dekker, Inc., New York. 1973. p. 1.
11. G. J. BREALY and M. KASHA. J. Am. Chem. Soc. **77**, 4462 (1955); R. RUSAKOWICZ, G. W. BYERS, and P. A. LEERMAKERS. J. Am. Chem. Soc. **93**, 3263 (1971).
12. L. SALEM and P. BRUCKMANN. Nature, **258**, 526 (1975).
13. N. C. DENO, R. C. HADDON, and E. N. NOWAK. J. Am. Chem. Soc. **92**, 6691 (1970).
14. H. KALINOUSKI and H. KESSLER. Topics in stereochemistry. Vol. 7. *Edited by* N. L. Allinger and E. L. Eliel. Interscience, New York. 1973. p. 295.
15. P. ROS. J. Chem. Phys. **49**, 4902 (1969); F. BERNARDI, I. CSIZMADIA, H. B. SCHLEGEL, and S. WOLFE. Can. J. Chem. **53**, 1144 (1975); P. v. R. SCHLEYER and E. D. JEMMIS. J. Chem. Soc. Chem. Commun. 190 (1978); R. K. LUSTGARTEN, M. BROOKHART, and S. WINSTEIN. Tetrahedron Lett. 141 (1971).
16. C. G. MCCARTY. Chemistry of the carbon–nitrogen double bond. *Edited by* S. Patai. Interscience, New York. 1970. p. 363.
17. P. v. R. SCHLEYER, T. M. SU, M. SAUNDERS, and J. C. ROSENFELD. J. Am. Chem. Soc. **91**, 5174 (1969); N. L. ALLINGER and J. H. SIEFERT. J. Am. Chem. Soc. **97**, 752 (1975).
18. J. A. VAN ALLEN. Org. Synth. Coll. Vol. IV. *Edited by* N. Rabjohn. Wiley, New York. 1963. p. 21.
19. B. HELFERICH and J. HAUSEN. Ber. **57**, 795 (1924).
20. I. N. NAZAROV, S. M. MAKIN, B. K. KRUPTSOV, and V. A. MIRANOV. J. Gen. Chem. USSR, **29**, 111 (1959).
21. A. WOHL and FR. MEMBER. Ber. **47**, 3346 (1914).
22. R. F. CHILDS. Submitted to J. Org. Chem.

Can. J. Chem. Downloaded from www.nrcresearchpress.com by 210.87.254.5 on 09/05/12
For personal use only.

The partial molal volume of two nickel chelate complexes

Y. K. SZE
Whiteshell Nuclear Research Establishment, Atomic Energy of Canada Ltd., Pinawa, Man., Canada R0E 1L0

AND

W. A. E. MCBRYDE
Department of Chemistry, University of Waterloo, Waterloo, Ont., Canada N2L 3G1

Received September 5, 1979[1]

Y. K. SZE and W. A. E. MCBRYDE. Can. J. Chem. **58**, 1795 (1980).

Partial molal volumes have been determined for the nickel(II) complexes of ethylenediaminetetraacetic acid (*mono* complex) and methyliminodiacetic acid (*bis* complex). The formation of these is accompanied by appreciable increases in volume, greater in the case of the second ligand. The observations are discussed in terms of reduced electrostriction of water by the complexes, and the different volume increases are accounted for by structural features of the complexes which are partially confirmed by spectral measurements.

Y. K. SZE et W. A. E. MCBRYDE. Can. J. Chem. **58**, 1795 (1980).

On a déterminé les volumes molaires partiels des complexes entre le nickel(II) et les acides éthylènediaminetétraacétique (complexe simple) et méthyliminodiacétique (complexe double). La formation de ces composés s'accompagne d'une augmentation importante de volume et elle est plus élevée dans le cas du deuxième ligand. On discute de ces observations en fonction d'un électrostriction réduite de l'eau par ces complexes et on attribue les différentes augmentations de volume à des caractéristiques structurales des complexes que les mesures spectrales confirment.

[Traduit par le journal]

Introduction

This investigation was prompted by the idea that volume changes which occur during formation of metal complexes might provide some evidence concerning the accompanying uptake or exclusion of solvent molecules. The concept of solvent exclusion has proved to be of some value in accounting for changes in stability constants observed as a result of changes in solvent composition (1, 2). The apparent molal volume of a solute at infinite dilution, obtained from measurements of the densities of solutions of graded concentrations, can be conventionally divided into partial molal volumes of ions, and from the latter, volume changes that accompany formation of a given complex may be derived. However, the interpretation of such volume changes appears to be limited to systems where the formation of complex from the reactants appears to be essentially complete.

We have selected for initial study the complexes of nickel(II) formed by ethylenediaminetetraacetic acid (EDTA) and methyliminodiacetic acid (MIDA), the molecule of the latter being very close to half that of the former. These ligands yield very stable complexes with nickel(II), the *bis* complex of the latter being of the same charge as the *mono* complex of the former. The essential difference between the two complexes is the absence of one chelate ring in the methyliminodiacetate case.

Experimental

Preparation of Solutions

Five series of solutions were studied, the preparation of which is described as follows.

Series 1. $Na_2NiEDTA \cdot 2NaClO_4$

A stock solution was prepared by refluxing NiO (Baker Analyzed) with $HClO_4$ (Baker Analyzed) for 24 h. Disodium EDTA dihydrate (Baker Analyzed) and NaOH (Baker analytical concentrate) in amounts slightly less than stoichiometric for $Na_2NiEDTA \cdot 2NaClO_4$ were added and refluxing continued. A small amount of NiO remaining undissolved was removed by filtration through a tared sintered-glass crucible. Its mass was determined to be about 0.5% of the NiO taken, and the concentration of the solution calculated from the mass of NiO actually dissolved. More Na_2EDTA, NaOH, and $HClO_4$ were added to provide the exact stoichiometry represented by the above formula. When cooled, the solution was transferred to a volumetric flask, diluted to the mark, and stored at a temperature close to 25°C. More dilute solutions were prepared by weighing portions of the stock solution and mixing with water in a volumetric flask.

Series 2. $K_2NiEDTA \cdot 2KNO_3$

This solution was prepared by direct weighing from $Ni(NO_3)_2 \cdot 6H_2O$ (BDH Analar, dried over anhydrous $CaSO_4$), EDTA (Baker Analyzed), and KOH (BDH concentrated volumetric solution).

Series 3. $Na_2Ni(MIDA)_2 \cdot 2NaClO_4$

Prepared from stoichiometric proportions of $Ni(NO_3)_2 \cdot 6H_2O$, methyliminodiacetic acid (Aldrich Analyzed 99%), and NaOH.

[1]Revision received May 17, 1980.

0008-4042/80/171795-04$01.00/0

©1980 National Research Council of Canada/Conseil national de recherches du Canada

Can. J. Chem. Downloaded from www.nrcresearchpress.com by 210.87.254.5 on 09/05/12
For personal use only.

Can. J. Chem. Downloaded from www.nrcresearchpress.com by 210.87.254.5 on 09/05/12
For personal use only.

Series 4. $Na_4EDTA \cdot 2NaOH$

Prepared from stoichiometric proportions of $Na_2EDTA \cdot 2H_2O$ and NaOH.

Series 5. $Na_2MIDA \cdot NaOH$

Prepared from stoichiometric proportions of methyliminodiacetic acid and NaOH.

Density Measurements

Densities of the solutions were measured by a vibration-tube flow densimeter (Sodev Model 0.1 D) under flow conditions (0.1 cm^3 min^{-1} for liquid and ca. 3 cm^3 min^{-1} for nitrogen). The resonance period of the vibrating tube was measured with a Hewlett Packard digital electronic counter (Model 5245 L). The densimeter was calibrated several times during each run with dried, filtered nitrogen gas, preheated to 25 ± 0.01°C, and with filtered, deionized, distilled, and degassed water (3). The consistency of the densimeter was checked with absolute methanol (Baker Photrex Reagent).

The temperature of the vibrating tube in the densimeter was maintained by water pumped through insulated tubing from a precision thermostat. The temperature of the water in the latter was controlled by a precision controller (Tronac Inc., Model PTC-1000) equipped with anticipating and proportioning devices and an integrator circuit to minimize temperature fluctuation. Cooling water for the precision thermostat was supplied from an auxiliary thermostat maintained at 24.5 ± 0.05°C through brass coils immersed in the former.

The temperature of the precision thermostat was set at 25°C by means of a thermometer with 0.1°C subdivisions and calibrated against an NBS-certified master. A Beckmann differential thermometer (0.01°C subdivisions) was used to note variation in temperature of the bath (to 0.0002°C). The latter was also monitored with a probe consisting of a thermistor in series with a metal-film resistor forming one arm of a Wheatstone bridge circuit. Alternatively the ratio of the resistances of the thermistor and the metal-film resistor was measured with a Hewlett Packard ratiometer. In either arrangement the output of the circuit was connected to a recorder the signal of which indicated that the temperature was contolled to within 0.0001°C during each day and rarely varied by more than 0.0002°C between days.

Densities (ρ) are related to the resonance period (τ) of the vibrating tube by the equation

$$\rho = A + B\tau^2$$

in which A and B are constants found by measuring the densities of two pure fluids, nitrogen gas and water.

Apparent molal volume, ϕ_v, was calculated by the equation

$$\phi_v = 1000(\rho^0 - \rho)/C\rho^0 + M_2/\rho^0$$

in which ρ is the density of the solution/g cm^{-3}, ρ^0 is the density of pure water/g cm^{-3}, C is the concentration of the solution/mmol cm^{-3} or mol dm^{-3}, and M_2 is the molar mass of the solute.

Spectroscopic Measurements

Visible spectra were recorded with a Cary 118 spectrophotometer at 25°C and in 1-cm cells.

Results and Discussion

Molar Volumes

Values found for ϕ_v are shown plotted against $C^{1/2}$ for the five series of solutions in Figs. 1 and 2. The plots in general support Redlich and Rosenfeld's equation (4). Only in the $Na_2NiEDTA \cdot 2NaClO_4$ series is some curvature apparent. By extrapolation to infinite dilution the partial molal volumes, $\bar{V}_2^0$, of the solute are obtained. The $\bar{V}_2^0$ values for $K_2NiEDTA \cdot 2KNO_3$ and $Na_2NiEDTA \cdot 2NaClO_4$ are (258.8 ± 0.5) cm^3 mol^{-1} and (242.9 ± 0.7) cm^3 mol^{-1} respectively. These two systems have $NiEDTA^{2-}$ as a common constituent. The difference in the $\bar{V}_2^0$ values for the two systems, namely 15.9 cm^3 mol^{-1}, can be accounted for in terms of the other constituents in the solutions. From the literature, $\bar{V}_2^0(KNO_3)$ = 38.0 cm^3 mol^{-1} (5), $\bar{V}_2^0(NaClO_4)$ = 42.9 cm^3 mol^{-1} (6), $\bar{V}_2^0(KClO_4)$ = 55.2 cm^3 mol^{-1} (7). Hence

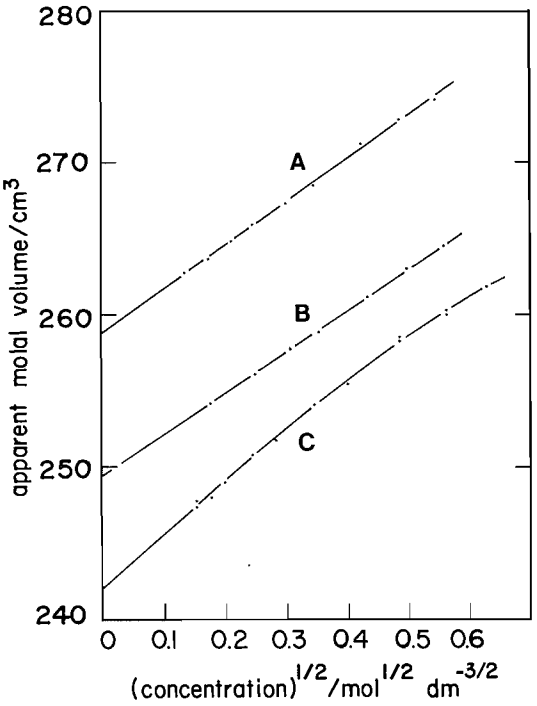


FIG. 1. Apparent molal volumes in aqueous solution. *A*, $K_2NiEDTA \cdot 2KNO_3$; *B*, $Na_2Ni(MIDA)_2 \cdot 2NaClO_4$; *C*, $Na_2NiEDTA \cdot 2NaClO_4$.

[1] $$\bar{V}_2^0(K^+) - \bar{V}_2^0(Na^+) = \bar{V}_2^0(KClO_4) - \bar{V}_2^0(NaClO_4) = 55.2 - 42.9 = 12.3 \text{ cm}^3 \text{ mol}^{-1}$$

[2] $$\bar{V}_2^0(KNO_3) - \bar{V}_2^0(NaClO_4) = 38.0 - 42.9 = -4.9 \text{ cm}^3 \text{ mol}^{-1}$$

From [1] and [2]

$$\bar{V}_2^0(K_2NiEDTA \cdot 2KNO_3) - \bar{V}_2^0(Na_2NiEDTA \cdot 2NaClO_4) = 2 \times (12.3 - 4.9) = 14.8 \text{ cm}^3 \text{ mol}^{-1}$$

This value is sufficiently close to the experimentally measured value, 15.9 cm^3 mol^{-1}, to support the supposition that the partial molal volume of the constituent, $NiEDTA^{2-}$, is independent of background ions in the solution.

Can. J. Chem. Downloaded from www.nrcresearchpress.com by 210.87.254.5 on 09/05/12
For personal use only.

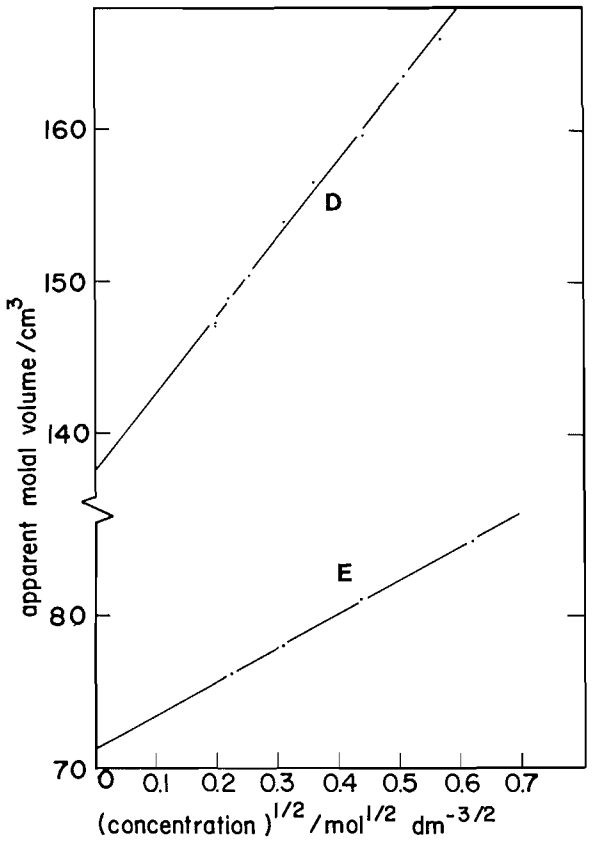


FIG. 2. Apparent molal volumes in aqueous solution. *D*, $Na_4EDTA \cdot 2NaOH$; *E*, $Na_2MIDA \cdot NaOH$.

TABLE 1. Apparent and partial molal volumes

Solution	$\bar{V}_2^0$/cm³
$Na_2NiEDTA \cdot 2NaClO_4$	242.9±0.7
$NiEDTA^{2-}$	170.3±0.7[a]
$Na_2Ni(MIDA)_2 \cdot 2NaClO_4$	249.2±0.3
$Ni(MIDA)_2^{2-}$	176.6±0.3[a]
$Na_4EDTA \cdot 2NaOH$	137.6±0.9
$EDTA^{4-}$	174.4±0.9[a]
$Na_2MIDA \cdot NaOH$	71.1±0.2
$MIDA^{2-}$	89.5±0.2[a]
Ni^{2+}	−29.4[a]

[a]The partial molal volumes of ions were calculated using the results of this study and values of conventional partial molal volume of ions at 25°C (ref. 9*b*) corrected using Zana and Yeager's value for H^+, $\bar{V}^0(H^+) = -5.4$ at 25°C (ref. 9*b*, p. 542 and ref. 8).

In Table 1 are summarized the $\bar{V}_2^0$ values for $Na_2NiEDTA \cdot 2NaClO_4$, $Na_2Ni(MIDA)_2 \cdot 2NaClO_4$, $Na_4EDTA \cdot 2NaOH$, and $Na_2MIDA \cdot NaOH$ together with those of some other ions of interest. These latter values were calculated with the aid of $\bar{V}_2^0$(ion) values based on Zana and Yeager's method for $\bar{V}_2^0(H^+)$ (8); this method is regarded as more reliable than others because it leads to better internal consistency among derived values of $\bar{V}_2^0$(ion) (9–12).

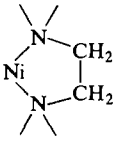
The following can be obtained from Table 1:

1. Reactions represented by

Ni^{2+}	+ $EDTA^{4-}$	→ $NiEDTA^{2-}$	$\Delta\bar{V}^0$
−29.4	174.2	170.3	+25.5 cm³ mol⁻¹
Ni^{2+}	+ $2MIDA^{2-}$	→ $Ni(MIDA)_2^{2-}$	
−29.4	2 × 89.6	176.6	+26.8 cm³ mol⁻¹

show considerable increase in volume. This may be attributed in part to a neutralization effect, and also to the fact that in the product the charge is distributed inside the complex entity with little interaction with water. These two factors lead to a significant decrease in electrostriction, with a consequent increase in volume (9).

2. The partial molal volume of $Ni(MIDA)_2^{2-}$ (176.6 cm³ mol⁻¹) is larger than that of $NiEDTA^{2-}$ (170.3 cm³ mol⁻¹). This difference in volume is believed to be statistically significant, and may be interpreted as follows: (*a*) The packing in the five-membered ring in $NiEDTA^{2-}$ should require less space than that required for $Ni(MIDA)_2^{2-}$ where



this ring is lacking. (*b*) In $NiEDTA^{2-}$ the nitrogen donor atoms are *cis* to one another, whereas in $Ni(MIDA)_2^{2-}$ the *trans* isomers are the likely configurations (see discussion of spectral observations). The consequent larger over-all dipole moment in the case of $NiEDTA^{2-}$ would cause a larger electrostriction of solvent, and may be responsible for its smaller volume. (*c*) The additional chelate effect (13) in $NiEDTA^{2-}$ results in stronger metal–ligand interactions with shorter Ni—O and Ni—N distances compared to those in $Ni(MIDA)_2^{2-}$.

Spectroscopy

In both $NiEDTA^{2-}$ and $Ni(MIDA)_2^{2-}$ there are two N and four O donor atoms, and therefore the complexes must be of lower symmetry than octahedral. These two elements are, however, close to one another in the spectrochemical series, and so to a good approximation the complexes can be treated as having a pseudo-octahedral geometry to which the rule of average environment can be applied (ref. 14, pp. 98, 103, 104). This is especially true for spectra of solutions at room temperature which is the case in the present study.

Can. J. Chem. Downloaded from www.nrcresearchpress.com by 210.87.254.5 on 09/05/12
For personal use only.

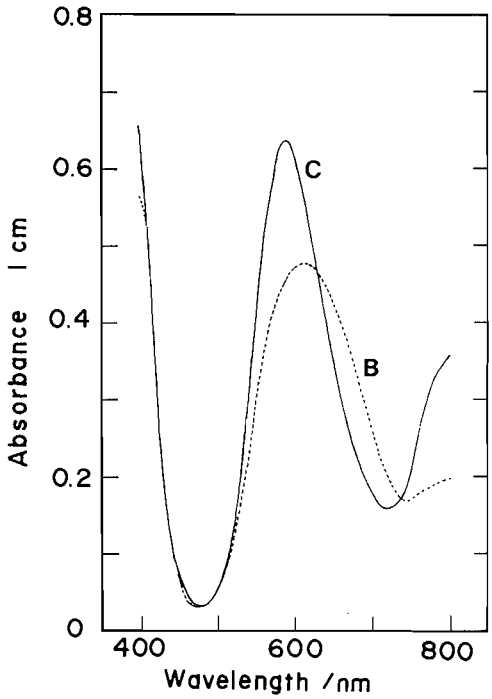


FIG. 3. Visible spectra of complexes in aqueous solution. *C*, $Na_2NiEDTA \cdot 2NaClO_4$, 0.080 mol dm^{-3}; *B*, $Na_2Ni(MIDA)_2 \cdot 2NaClO_4$, 0.094 mol dm^{-3}.

Our results show that within the range studied (up to 0.16 mol dm^{-3} $Na_2NiEDTA \cdot 2NaClO_4$ and 0.125 mol dm^{-3} $Na_2Ni(MIDA)_2 \cdot 2NaClO_4$) the absorbance, integrated from 730 nm to 470 nm (Fig. 3), is directly proportional to concentration for both systems. Also there is no change in band shape with concentration. These findings suggest that there are no shifts in equilibrium as concentration changes. In Fig. 3 the actual spectra for representative solutions of the two systems are shown. The absorbances and band positions are typical for a nickel complex with an octahedral field (15). The peaks at 588 nm and 610 nm for the $Na_2NiEDTA \cdot 2NaClO_4$ and $Na_2Ni(MIDA)_2 \cdot 2NaClO_4$ solutions respectively can be attributed to the $^3A_{2g} \rightarrow {}^3T_{1g}(F)$ transition of $NiEDTA^{2-}$ and $Ni(MIDA)_2^{2-}$. These positions lie between those for nickel complexes with six O donors (e.g., ca. 700 nm for $Ni(H_2O)_6^{2+}$) and those with six N donors (e.g., ca. 550 nm for $Ni(en)_3^{2+}$) (16). The solutions containing $NiEDTA^{2-}$ have higher molar peak absorbance (see Fig. 3) as well as greater integrated molar absorbance (1010 vs. 820 in units of absorbance × nm). This observation can be attributed (ref. 14. pp. 105, 106) to the lower symmetry for the $NiEDTA^{2-}$ complex as discussed previously.

The shorter wavelength for the peak observed for solutions containing $NiEDTA^{2-}$ compared to those containing $Ni(MIDA)_2^{2-}$ confirms that EDTA interacts more strongly with Ni than MIDA does. Such a shift can also be caused by ligands lying toward the stronger end of the spectrochemical series (15), but since the donor atoms are the same in the two systems, we attribute the shift to the additional chelate effect in EDTA. This interpretation is in accord with conclusions reached from a study of a large number of complexes of nickel with multidentate amines (ref. 14, pp. 105, 106, ref. 16).

Conclusions

(*1*) Complex formation in the two examples studied was accompanied by a considerable increase in molar volume which has been attributed to diminished electrostriction of solvent.

(*2*) The chelate effect, which has been established from stability constants of complexes, is also evident in the present study of partial molar volumes and spectra of $NiEDTA^{2-}$ and $Ni(MIDA)_2^{2-}$. The generality of these conclusions will require examination of other appropriate systems of complexes.

1. K. K. MUI, W. A. E. MCBRYDE, and E. NIEBOER. Can. J. Chem. **52**, 2512 (1973).
2. S. H. MEHDI, D. A. BRISBIN, and W. A. E. MCBRYDE. J. Soln. Chem. **4**, 497 (1975).
3. G. S. KELL. J. Chem. Eng. Data, **12**, 66 (1967).
4. O. REDLICH and P. ROSENFELD. Z. Elektrochem. **37**, 705 (1931); Z. Phys. Chem. A**155**, 61 (1931).
5. L. A. DUNN. Trans. Faraday Soc. **62**, 2348 (1966).
6. H. E. WIRTH and F. N. COLLIER, JR. J. Am. Chem. Soc. **72**, 5292 (1950).
7. E. GLNECKAUF. Trans. Faraday Soc. **61**, 914 (1965); P. MUKERJEE. J. Phys. Chem. **65**, 740 (1961); **65**, 744 (1961).
8. R. ZANA and E. YEAGER. J. Phys. Chem. **70**, 954 (1966); **71**, 521 (1967); **71**, 4241 (1967).
9. (*a*) F. J. MILLERO. Chem. Rev. **71**, 168 (1971); (*b*) F. J. MILLERO. *In* Water and aqueous solutions: structure, thermodynamics and transport processes. *Edited by* R. A. Horne. Wiley-Interscience, New York. 1972. Chapt. 13.
10. M. SAKURAI, T. KOMATSU, and T. NAKAGAWA. Bull. Chem. Soc. Jpn. **48**, 3491 (1975).
11. M. SAKURAI. Bull. Chem. Soc. Jpn. **46**, 1596 (1973).
12. H. HOILAND. J. Chem. Soc. Faraday Trans. I, **71**, 797 (1975).
13. S. CHABEREK and A. E. MARTELL. Organic sequestering agents. Wiley-Interscience. 1959. p. 140.
14. C. R. HARE. *In* Spectroscopy and structure of metal chelate compounds. *Edited by* K. Nakamoto and P. J. McCarthy. Wiley-Interscience, New York. 1968.
15. F. A. COTTON and G. WILKINSON. Advanced inorganic chemistry. 2nd ed. Wiley-Interscience, New York. pp. 881, 882.
16. C. K. JORGENSEN. Acta Chem. Scand. **10**, 887 (1956).

Oxidation products of arachidonic acid II. The synthesis of methyl 8*R*,9*S*,11*R*-trihydroxy-5*Z*,12*E*,14*Z*-eicosatrienoate

GEORGE JUST AND CORINNE LUTHE[1]

Department of Chemistry, McGill University, 801 Sherbrooke Street West, Montreal, P.Q., Canada H3A 2K6

Received December 17, 1979

This paper is dedicated to the memory of Dr. Leo Marion

GEORGE JUST and CORINNE LUTHE. Can. J. Chem. **58**, 1799 (1980).

A stereospecific total synthesis of the title compound, **37**, starting from diacetone glucose (**9**), is described. Key intermediates in the synthesis are 3-deoxy-5,6-anhydro-1,2-*O*-isopropylidene-glucofuranose (**15**), obtained in 55% yield from **9**, and methyl 8-*tert*-butyldiphenylsilyl-9,11-*O*-isopropylidene-8*R*,9*S*,11*R*-trihydroxy-12-oxo-dodeca-5*Z*-enoate (**33**), an important intermediate in the synthesis of other oxidation products of arachidonic acid.

GEORGE JUST et CORINNE LUTHE. Can. J. Chem. **58**, 1799 (1980).

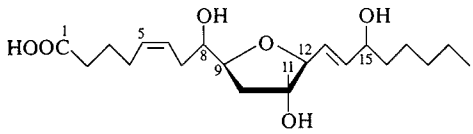
On décrit une synthèse totale stéréospécifique du composé mentionné dans le titre en partant du glucose diacétone (**9**). Les intermédiaires principaux de la synthèse sont: le déoxy-3 anhydro-5,6 *O*-isopropylidène-1,2 glucofurannose (**15**) obtenu avec un rendement de 55% à partir de **9** et le *tert*-butyldiphénylsilyl-8 *O*-isopropylidène-9,11 trihydroxy-8*R*,9*S*,11*R* oxo-12 dodécène-5*Z* oate de méthyle (**33**) un intermédiaire important dans la synthèse d'autres produits d'oxydation de l'acide arachidonique.

[Traduit par le journal]

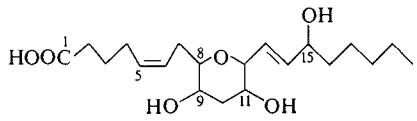
A few years ago, Pace-Asciak and Wolfe (1) reported the isolation of compounds **1** and **2** and of 5,6-dihydro-**1** from the enzymatic conversion of tritiated arachidonic acid by sheep seminal vesicles. An apparently identical tetrahydrofuran of type **1** was recently isolated by Axelrod and co-workers from incubation of the same substrate with soy-bean lipoxygenase II (2). The structure of these compounds was determined from gc–ms data and a limited number of degradation studies. Their stereochemistry is at present unknown.

Pace-Asciak and Wolfe reported that **1** and **2** were synthesized along with prostaglandins (PGE_2). Axelrod and co-workers demonstrated that prostaglandin-like material was synthesized along with **1** (2*b*), and that two molecules of O_2 were incorporated per molecule of arachidonic acid during its soy-bean lipoxygenase II induced oxidation. These results have to be treated with some caution, since **1** made up only 10% of total oxidation product of arachidonic acid.

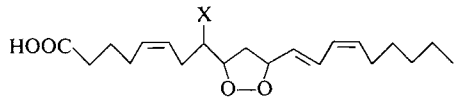
Based on these data, the biosynthetic pathway postulated by Pace-Asciak and Wolfe (1*b*), and the assumption that a stereochemically similar enzyme-site is responsible for both the formation of prostaglandin and **1** or **2**, the following biosynthetic pathway may be postulated. Removal of the 13-pro-*S* hydrogen of arachidonic acid (**6**) and reaction of the radical thus formed with O_2 leads to the formation of hypothetical intermediate **7**, either directly or via a hydroperoxide, which either cyclizes to form PGG_2 (3) (conventional PG-synthesis), or, due to some change of the enzyme-cavity, traps oxygen to give hydroperoxy-peroxide **3**. This or a related product may be envisaged to cyclize in a free radical manner (with further uptake of a molecule of O_2), or, if the oxygenation data are correct, in an ionic manner as depicted in Scheme 1. The polarization of the O—O bond into O^+ and



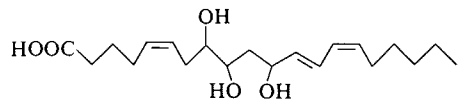
1



2



3 X = OOH
4 X = OH



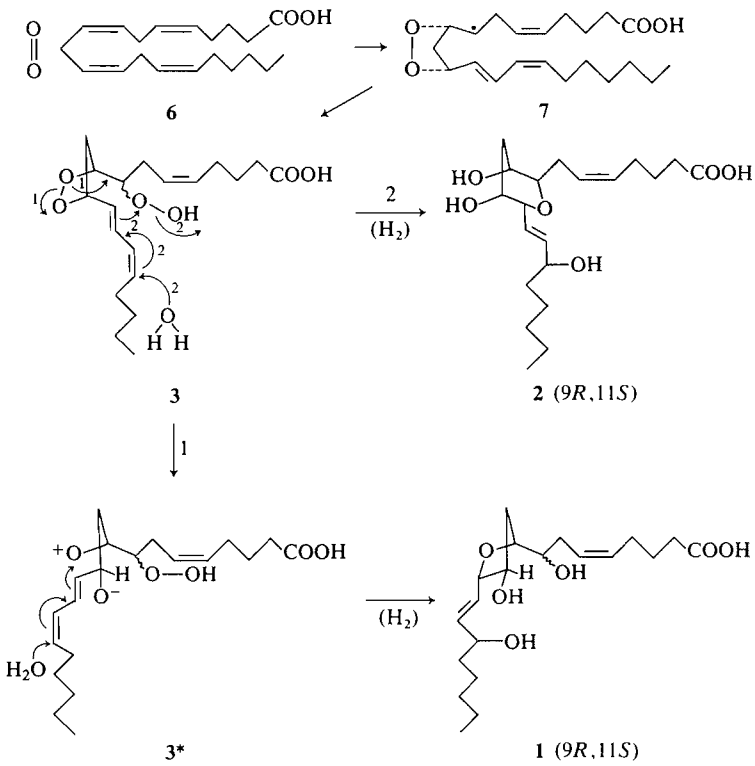
5

[1]Holder of a National Research Council of Canada Scholarship, 1977–1979, and a scholarship of the Ministry of Education of the Province of Quebec, 1977–1980.

0008-4042/80/171799-07$01.00/0

©1980 National Research Council of Canada/Conseil national de recherches du Canada

Can. J. Chem. Downloaded from www.nrcresearchpress.com by 210.87.254.5 on 09/05/12
For personal use only.



SCHEME 1

O^- is, of course, only a formalism not implying a free cationic species.

Nucleophilic attack (arrows labelled 2) of the olefinic linkage on the hydroperoxy oxygen, followed by hydration of the intermediate allylic carbonium ion, results in the formation of **2** after reduction of the peroxide. For the formation of **1**, a polarization of the peroxy linkage (see arrows labelled 1), followed by a 120° rotation of the C(10)—C(11) bond, leads to intermediate **3*** similar to the one postulated in the conversion of PGH_2 to PGI_2. Cyclization, hydration, and reduction of the hydroperoxide to an alcohol group then gives tetrahydrofuran **1**.

Whatever the mechanism of these rearrangements, this hypothesis predicts that the absolute stereochemistry of the oxygen atoms attached to C(9) and C(11) in **1** and **2** would be the same as those of the 4 and 2 positions of glucose.

On the other hand, one may envisage that the C(1)—C(9) chain of arachidonic acid (**6**) folds in the opposite manner, giving **1** and **2** in which the stereochemistry at C(9) and C(11) would be identical to those of the 4 and 2 positions of galactose. The double bond at C(5) and C(13) may be assumed to be identical to that of arachidonate derived prostaglandins, ie 5-*Z* and 13-*E*.

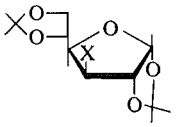
The peroxyhydroperoxide **3**, and its corresponding reduction products **4** and **5** have never been isolated. We hypothesize that this may be due to their instability, and propose to synthesize compounds **1**–**5** in a stereospecific manner, making use of the biosynthetic hypothesis described above to guide us in the selection of the most likely target molecules.

Since **1** and **2** contain five chiral centers (32 stereoisomers), and **3**, **4**, and **5** only three (8 stereoisomers), we propose to synthesize in the first instance triol **5** and attempt to detect its presence in the soy-bean lipoxygenase or sheep seminal vesicle induced oxidation of arachidonic acid. Positive identification of triol **5** would ascertain the stereochemistry of three of the five chiral centers in **1** and **2**.

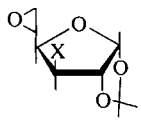
As our first synthetic goal, we chose to prepare from the readily available diacetone glucose **9** compounds of the type **33**, convenient precursors to metabolites **1**–**5**.

The key steps in its synthesis from diacetone glucose **9** are its efficient transformation to the known epoxide **15** (4), previously obtained by a somewhat cumbersome procedure, attachment of the side-chain and transformation of the 1,2-acetonide into a free aldehyde. An important

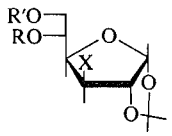
Can. J. Chem. Downloaded from www.nrcresearchpress.com by 210.87.254.5 on 09/05/12
For personal use only.



9 X = OH
10 X = OCSSMe
11 X = H



12 X = OH
13 X = OCSSMe
14 X = OAc
15 X = H



10 RR′ = CMe_2, X = OCSSMe
16 R = R′ = H, X = OCSSMe
17 R = R′ = Ac, X = OCSSMe
18 R = R′ = Ac, X = H
19 R = R′ = H, X = H
20 R = H, R′ = Ts, X = H
21 R = R′ = Ts, X = H

further consideration is that the hydroxy groups at C(8) and C(9) of **33** be clearly differentiated, since tetrahydrofuran **1** and -pyran **2** differ only in the attachment of these two hydroxyl groups to C(12) of **33**.

In the first series of experiments, xanthate **10** (11) was submitted to the action of tributyltin hydride (5) according to the procedure of Barton and McCombie (6). The 3-deoxyglucose **11** (7) thus obtained could not be separated cleanly from tributyltin derivatives by distillation. However, when triphenyltin hydride (8), obtained by $LiAlH_4$ reduction of triphenyltin chloride (5), was used instead of tributyltin hydride, the deoxysugar **11**, bp 74–75°C, 0.3 Torr, could be prepared and isolated in large quantities without chromatography. Whereas the partial hydrolysis of the 5,6-acetonide poses no problems in diacetone glucose derivatives functionalized at C(3), a clean partial hydrolysis of **11** could not be effected.

We next prepared xanthate **13** from the readily available epoxyalcohol **12** (9) and treated it with triphenyltin hydride. Comparison of the reaction product with authentic deoxyepoxide **15** indicated that less than 20% of **15** had been formed.

Epoxide **15** was obtained in good yield upon photolysis of acetate **14** of alcohol **12** (9) in aqueous HMPA using the method of Pete and Portella (10), but scaling up of the reaction gave very erratic results.

Deoxyepoxide **15** was eventually obtained in 55% yield, based on diacetone glucose, when the following procedure was used.

Xanthate **10** (11), made by an adaptation of a procedure described by Barton and McCombie (6), was hydrolysed to diol xanthate **16** with methanolic sulphuric acid, being careful to avoid any base in the workup as it resulted in the formation of poorly defined mixtures. Acetylation gave **17**, which was reduced with tributyltin hydride (6) in toluene. Evaporation gave semi-crystalline deoxydiacetate **18**, which was hydrolyzed with methanolic sodium methoxide to the deoxydiol **19**. Tosylation of crude **19** with one equivalent of *p*-toluenesulphonyl chloride – pyridine in chloroform gave monotosylate **20**, contaminated with 10–15% each of ditosylate **21** and diol **19**. Treatment with aqueous methanolic potassium hydroxide, followed by distillation, gave deoxyepoxide **15**. Treatment of **15** with the dilithium salt of 5-hexynoic acid (12) in HMPA gave in 57% yield acetylenic acid **22**, which was isolated either as its crystalline methyl ester **23**, mp 41–42°C, after treatment with diazomethane, or as its methyl ester methyl ether **24** by direct alkylation of the reaction mixture with excess methyl iodide. Hydroxy ester **23** was further characterized as its acetate **25**.

Alcohol **23**, methyl ether **24**, and acetate **25** were all three cleanly hydrogenated to the corresponding *Z*-olefins **26**, **27**, and **28**, using Brown's P-2 nickel-boride catalyst (13). Only one isomer was formed, as established by gc–ms and ^{13}C nmr. The geometry of the double-bond generated was assigned the *Z*-configuration, based mainly on analogy (13).

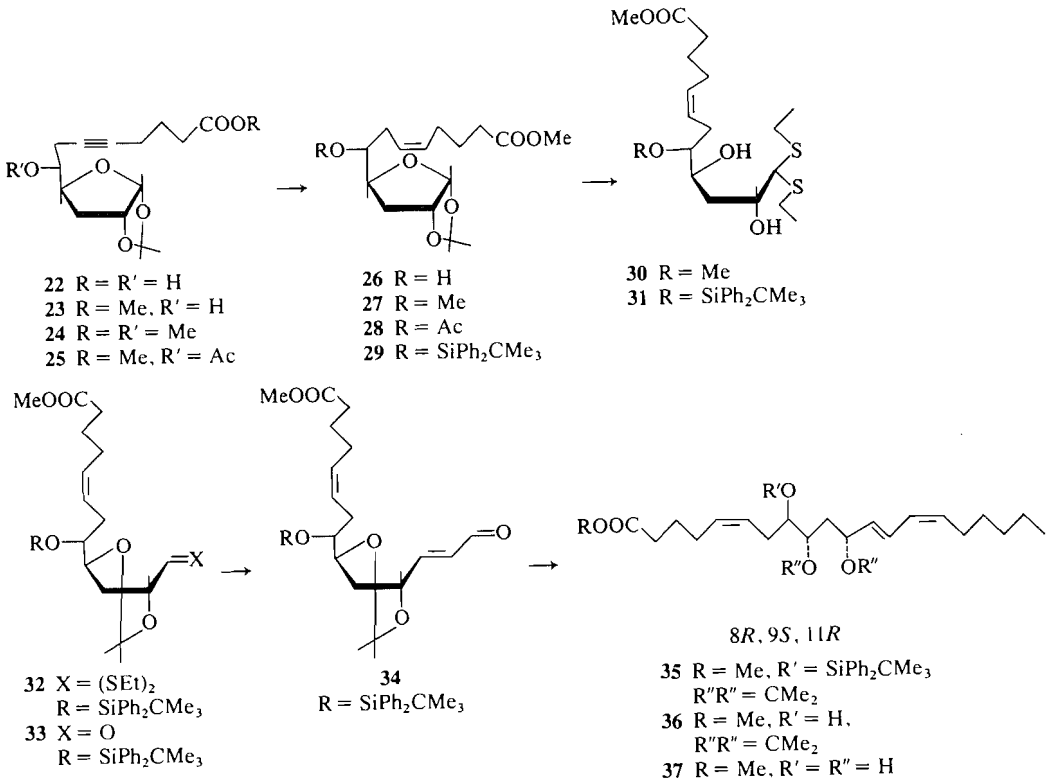
Alcohol **26** was transformed to its *tert*-butyldiphenylsilyl ether **29** (14), which is relatively acid- and base-stable, and can be removed in the presence of most other protecting groups.

Treatment of methyl ether **27** or silyl ether **29** with ethanethiol–$ZnCl_2$ at −10°C gave directly diol thioacetals **30** and **31**. The latter was transformed to its stable oily isopropylidene derivative **32**. Hydrolysis transformed the thioacetal to the corresponding unstable aldehyde **33**, which was converted to the unstable *E*-α,β-unsaturated aldehyde **34** by means of formylmethylenetriphenylphosphorane (15). Its ^1H nmr and ^{13}C nmr spectra clearly indicated the *E*-configuration of the newly established double-bond and attested to its purity (>95%). Reaction of **34** with triphenylhexylphosphorane gave two isomeric olefins in a ratio of approximately 9:1, as established by gc–ms, hplc, and ^{13}C nmr.

The major isomer was assigned structure **35**, based on the knowledge that unstabilized phosphoranes give *Z*-olefins as a major product. The minor component is therefore the 14-*E* isomer of **35** (14-*E*-**35**).

Reaction of **35** contaminated with 14-*E*-**35** with

Can. J. Chem. Downloaded from www.nrcresearchpress.com by 210.87.254.5 on 09/05/12
For personal use only.



tetra-*n*-butylammonium fluoride in boiling tetrahydrofuran gave **36** contaminated with 10–15% of its 14-*E* isomer. Mild acid hydrolysis of crude **36** gave triol ester **37**, which would be cleanly separated from its 14-*E* isomer by flash-chromatography (16).

Experimental

General

Melting points were determined on a Gallenkamp block and are uncorrected. Mass spectra (ms) were obtained on a HP 5984 mass spectrometer or on a LKB-9000 mass spectrometer at 70 eV. Infrared (ir) spectra were obtained on a Perkin Elmer 297 spectrophotometer. Proton and carbon-13 magnetic resonance spectra were recorded on Varian T-60, T-60A, and on Brucker FT 90 spectrometers.

Xanthate of 1,2:5,6-Di-O-isopropylidene-α-D-glucofuranose (10)

The xanthate was prepared according to a slight modification of a procedure outlined by Barton and McCombie (6). To a stirred suspension of sodium hydride (8 g (50% oil dispersion), 0.17 mol) in 500 mL dry tetrahydrofuran (10°C, N_2) was added carbon disulfide (22.8 g, 0.30 mol), methyl iodide (28.4 g, 0.20 mol), imidazole (20 mg), and diacetone glucose (**9**) (26 g, 0.10 mol). The reaction was complete instantaneously; the excess sodium hydride was destroyed with glacial acetic acid. The solvents were removed *in vacuo*, and the residue extracted with ether (3 × 500 mL), washed with aqueous $NaHCO_3$ (2 × 50 mL) and water (3 × 50 mL), and dried over $MgSO_4$. Removal of the ether *in vacuo* yielded the pure xanthate **10**, mp 58–59°C (lit. (11) mp 60°C), quantitatively; nmr ($CDCl_3$) δ: 1.35 (s, 6H, CMe_2), 1.43 (s, 3H, CH_3), 1.55 (s, 3H, CH_3), 2.60 (s, 3H, S—CH_3), 3.93–4.40 (m, 4H, C(4)H, C(5)H, C(6)H), 4.66 (d, 1H, J = 4 Hz, C(2)H), 5.85–5.97 (m, 2H, C(1)H, C(3)H).

Xanthate of 1,2-O-isopropylidene-α-D-glucofuranose (16)

Xanthate **10** (35 g, 0.1 mol) was dissolved in a mixture of MeOH (575 mL), concentrated H_2SO_4 (14 mL), and H_2O (75 mL) and stirred at room temperature for 5 h to effect complete hydrolysis. Aqueous saturated sodium chloride solution was then added and the methanol was evaporated at 40°C *in vacuo*; the residue was extracted with CH_2Cl_2 (2 × 500 mL), washed with saturated salt solution until the aqueous layer was no longer acidic, and dried over $MgSO_4$. Evaporation of the solvent gave quantitatively oily xanthate **16**, which was used without purification in the next step. Nuclear magnetic resonance ($CDCl_3$) δ: 1.33 (s, 3H, CH_3), 1.53 (s, 3H, CH_3), 2.60 (s, 3H, S—CH_3), 2.75–3.25 (m, 2H, C(6)H), 3.60–4.15 (m, 3H, C(5)H, $(OH)_2$), 4.20–4.45 (m, 1H, C(4)H), 4.66 (d, 1H, $J_{1,2}$ = 4Hz, C(2)H), 5.93 (d, 1H, $J_{1,2}$ = 4 Hz, C(1)H), 6.03 (d, 1H, $J_{3,4}$ = 3 Hz, C(3)H).

Xanthate of 1,2-O-isopropylidene-5,6-di-O-acetyl-α-D-glucofuranose (17)

A solution of crude diol **16** (31 g, 0.1 mol) in anhydrous ether (800 mL) containing dry acetic anhydride (38 mL, 0.4 mol) and 4-dimethylaminopyridine (1.22 g) was stirred at room temperature for 1.5 h. The ether was then evaporated *in vacuo* and excess reagents were removed by azeotroping with toluene. The residue was extracted with ether (3 × 500 mL), washed with 1% HCl (2 × 50 mL), H_2O (3 × 50 mL), and dried over $MgSO_4$. Removal of the solvent yielded the xanthate diacetate quantitatively, which was used without purification in the next step; nmr ($CDCl_3$) δ: 1.34 (s, 3H, CH_3), 1.57 (s, 3H, CH_3), 2.00 (s, 3H, $COCH_3$), 2.08 (s, 3H, $COCH_3$), 2.60 (s, 3H, SCH_3), 3.97–4.80

Can. J. Chem. Downloaded from www.nrcresearchpress.com by 210.87.254.5 on 09/05/12
For personal use only.

Can. J. Chem. Downloaded from www.nrcresearchpress.com by 210.87.254.5 on 09/05/12
For personal use only.

(m, 3H, C(4)H, C(6)H), 4.64 (d, 1H, $J_{1,2}$ = 4 Hz, C(2)H), 5.10–5.43 (m, 1H, C(5)H), 5.97 (d, 1H, $J_{1,2}$ = 4 Hz, C(1)H), 6.08 (d, 1H, $J_{3,4}$ = 3 Hz, C(3)H).

1,2-O-isopropylidene-3-deoxy-5,6-di-O-acetyl-α-D-ribohexofuranose (18)

To tributyltin hydride (48 mL) in dry refluxing toluene (800 mL), under a N_2 atmosphere, was added over 1 h the crude diacetate xanthate **17** (35 g, 0.1 mol) in toluene (800 mL). The solution was refluxed for 16 h to effect complete reduction of the xanthate functionality. The toluene was then removed at reduced pressure. The deoxyfuranose **18** either crystallized out spontaneously, or had to be heated with ether–hexane to induce crystallization. Filtration gave **18**, contaminated with tributyltin by-products, which was used as such in the subsequent hydrolysis; nmr ($CDCl_3$) δ: 1.30 (s, 3H, CH_3), 1.50 (s, 3H, CH_3), 1.57–2.33 (m, 2H, C(3)H), 2.03 (s, 3H, $COCH_3$), 2.07 (s, 3H, $COCH_3$), 3.88–4.55 (m, 3H, C(4)H, C(6)H), 4.72 (dd, 1H, $J_{1,2} \sim J_{2,3}$ = 4 Hz, C(2)H), 5.00–5.26 (m, 1H, C(5)H), 5.76 (d, 1H, $J_{1,2}$ = 4 Hz, C(1)H); $[\alpha]_D^{23}$ +18.4° (*c* 5.75 in $CHCl_3$).

1,2-O-isopropylidene-3-deoxy-α-D-ribohexofuranose (19)

Crude deoxy-diacetate **18** (25 g) in 280 mL dry 0.02 *M* methanolic sodium methoxide was maintained at room temperature for 2 h and then neutralized with acidic resin (AM-120 H^+). Removal of the resin, followed by evaporation of the methanol, gave the diol **19**, mp 81–82°C, (lit. (4) mp 80–81°C) in quantitative yield. It was used as such in the next step; nmr ($CDCl_3$, D_2O) δ: 1.32 (s, 3H, CH_3), 1.50 (s, 3H, CH_3), 1.60–2.30 (m, 2H, C(3)H), 3.40–4.40 (m, 4H, C(4)H, C(5)H, C(6)H), 4.70–4.83 (dd, 1H, $J_{1,2} \sim J_{2,3}$ = 4 Hz, C(2)H), 5.81 (d, 1H, $J_{1,2}$ = 4 Hz, C(1)H).

1,2-O-isopropylidene-3-deoxy-6-O-p-toluenesulfonyl-α-D-ribohexofuranose (20) (4)

To the deoxy-diol **19** (17.4 g, 86 mmol, crude from previous reaction) and *p*-toluenesulfonyl chloride (16.40 g, 86 mmol) in 225 mL $CHCl_3$ (freshly distilled from P_2O_5) at −50°C under N_2 was added dropwise dry pyridine (19 mL) in 20 mL $CHCl_3$; the solution was maintained at −50°C for 3 h, and at room temperature for 20 h. The product was extracted with CH_2Cl_2 (2 × 700 mL), washed with cold 1% HCl till the washings were acidic, and then with H_2O (4 × 100 mL). The CH_2Cl_2 extracts were dried over $MgSO_4$, and evaporation of the solvent yielded a mixture of mono- and di-tosylate **20** and **21** (~9:1), which was used without purification in the subsequent epoxidation step. A sample of pure **20** was obtained by chromatography; nmr ($CDCl_3$, D_2O) δ: 1.27 (s, 3H, CH_3), 1.46 (s, 3H, CH_3), 1.65–2.28 (m, 2H, C(3)H), 2.42 (s, 3H, C_6H_4—CH_3), 3.82–4.30 (m, 4H, C(4)H, C(5)H, C(6)H), 4.69 (dd, 1H, $J_{1,2} \sim J_{2,3}$ = 4 Hz, C(2)H), 5.71 (d, 1H, *J* = 4 Hz, C(1)H), 7.55 (4H, AB_q, δ_{AB} = 0.45, *J* = 8 Hz).

5,6-Anhydro-3-deoxy-1,2-isopropylidene-α-D-ribohexofuranose (15) (5)

The mixture of mono- and di-tosylates (25.9 g, crude from previous reaction) in MeOH (300 mL)/H_2O (60 mL) was cooled in an ice bath; the ice bath was then removed and approximately 1 equiv. aqueous KOH (1.17 *N*) was added dropwise till the pH of the solution remained basic; the reaction mixture was neutralized with acidic resin (AM-120 H^+) and the MeOH was evaporated at reduced pressure (<40°C). The residue was extracted with ether (3 × 750 mL); the ether fractions were washed with saturated salt solution (3 × 50 mL), dried over $MgSO_4$, and evaporated to give an oil which was distilled (110°C/0.3 Torr; Kugelrohr) to give the 5,6-anhydro-sugar (10.2 g, 55% yield from diacetone glucose), slightly contaminated with tri-butyltin by-products. The epoxide was used without further purification in the subsequent step; nmr ($CDCl_3$) δ: 1.33 (s, 3H, CH_3), 1.44–2.30 (m, 2H, C(3)H), 1.50 (s, 3H, CH_3), 2.53–2.89 (m, 2H, C(6)H), 3.05–3.23 (m, 1H, C(5)H), 4.05–4.36 (m, 1H, C(4)H), 4.75 (dd, 1H, $J_{1,2} \sim J_{2,3}$ = 4 Hz, C(2)H), 5.81 (d, 1H, $J_{1,2}$ = 4 Hz, C(1)H).

Acid 22 and Methyl Ester 23

To 5-hexynoic acid (12) (1.9 g, 17 mmol) in 20 mL dry HMPA in an argon atmosphere at 5°C was added dropwise *n*-BuLi (21.1 mL, 33.8 mmol). The colorless solution became bright orange. The epoxide **15** (1.57 g, 8.45 mmol) in 10 mL HMPA was added dropwise, the ice bath removed (precipitation of the dianion may otherwise occur), and the reaction mixture was stirred at room temperature for 20 h. Acetic acid (0.97 mL, 17 mmol) was then added and the solvents were removed by Kugelrohr distillation (110°C/0.1 Torr). The residue was stirred and shaken in 1 *N* aqueous HCl – ether, and was then extracted with ether (3 × 400 mL); the ether extracts were washed with saturated salt solution (10 × 30 mL), dried over $MgSO_4$, and evaporated to yield oily **22** which was methylated with ethereal diazomethane; excess methyl hexynoate was removed at 60°C/0.1 Torr, and the residual oil was purified by flash chromatography (petroleum ether (30–60°C) – ethyl acetate, 4.6:4.0) to yield 1.5 g (57% yield) of crystalline **23**, mp 41–42°C. Infrared ($CHCl_3$): 1735 (C=O), 3480 (OH) cm^{-1}; nmr ($CDCl_3$) δ (glucose numbering): 1.31 (s, 3H, CH_3), 1.48 (s, 3H, CH_3), 1.54–2.58 (m, 10H, C(3)H, C(6)H, $CH_2CH_2CH_2$), 3.08 (br s, 1H, OH, exchangeable with D_2O), 3.66 (s, 3H, CO_2CH_3), 3.68–4.47 (m, 2H, C(4)H, C(5)H), 4.74 (dd, 1H, $J_{1,2} \sim J_{2,3}$ = 4 Hz, C(2)H), 5.78 (d, 1H, $J_{1,2}$ = 4 Hz, C(1)H). ms (70 eV) *m/e*: 297 (*M* − 15), 173 (*M* − (CH_2—C≡C—$(CH_2)_3$—CO_2Me)), 169 (HO—CH—CH_2C≡C—$(CH_2)_3$—CO_2Me), 143 (*M* − 169); $[\alpha]_D^{23}$ −16.5° (*c* 2.75 in $CHCl_3$); *Anal.* calcd. for $C_{16}H_{24}O_6$: C 61.54, H 7.69; found: C 61.77, H 7.50.

When the reaction was scaled up by a factor of two, problems with precipitation of reactants were encountered.

Methyl Ether 24

The reaction conditions were identical to those used for the formation of the alcohol methyl ester **23**, except that excess methyl iodide was used to quench the reaction instead of acetic acid. The reaction mixture was then stirred at 65°C for 2 h, and after the addition of 300 mL H_2O, it was extracted with ether (3 × 500 mL); the extracts were washed with H_2O (4 × 50 mL), dried over $MgSO_4$, and evaporated to give methyl ether **24** contaminated with 10% alcohol **23** and methyl 5-heptynoate. The latter was removed at 60°C/0.2 Torr and the product was then further purified by flash chromatography (petroleum ether (30–60°C) – ethyl acetate, 3:2) to give pure **24** (1.6 g, 58% yield). The proportions of **23** and **24** tended to fluctuate, depending on humidity and other variables which are not understood. Infrared ($CHCl_3$): 1737 (C=O), absence of OH at 3480 cm^{-1}; nmr ($CDCl_3$) δ (glucose numbering): 1.32 (s, 3H, CH_3), 1.49 (s, 3H, CH_3), 1.50–2.60 (m, 10H, C(3)H, C(6)H, $CH_2CH_2CH_2$), 3.30–3.70 (m, 1H, C(5)H), 3.44 (s, 3H, OCH_3), 3.65 (s, 3H, CO_2CH_3), 4.16–4.48 (m, 1H, C(4)H), 4.71 (dd, 1H, $J_{1,2} \sim J_{2,3}$ = 4 Hz, C(2)H), 5.77 (d, 1H, $J_{1,2}$ = 4 Hz, C(1)H): ms *m/e*: 326 (M^+), 311 (*M* − CH_3), 143 (*M* − MeOCHCH$_2$—CH≡CH$(CH_2)_3$COOMe); $[\alpha]_D^{23}$ −26.2° (*c* 2.55 in $CHCl_3$).

Acetate 25

A solution of **23** (0.93 g, 3 mmol), 4-dimethylaminopyridine (0.036 g, 0.3 mmol), and acetic anhydride (0.56 mL, 6 mmol) in anhydrous ether (25 mL) was stirred at room temperature for 1.5 h. The excess reagents were azeotroped off with toluene at 40°C, and the residue was extracted with ether (3 × 350 mL); the extracts were washed with cold 1% HCl (3 × 20 mL), H_2O (5 × 20 mL), dried over $MgSO_4$, and evaporated *in vacuo* to give the

Can. J. Chem. Downloaded from www.nrcresearchpress.com by 210.87.254.5 on 09/05/12
For personal use only.

acetate **25** in quantitative yield; nmr ($CDCl_3$) δ (glucose numbering): 1.23–2.61 (m, 10H, C(3)H, C(6)H, $CH_2CH_2CH_2$), 1.32 (s, 3H, CH_3), 1.50 (s, 3H, CH_3), 2.07 (s, 3H, $COCH_3$), 3.64 (s, 3H, CO_2CH_3), 4.15–4.53 (m, 1H, C(4)H), 4.70 (dd, 1H, $J_{1,2} \sim J_{2,3}$ = 4 Hz, C(2)H), 5.01 (dt, 1H, $J_{5,6} \sim J_{5,4}$ = 6 Hz, C(5)H), 5.76 (d, 1H, $J_{1,2}$ = 4 Hz, C(1)H).

Reduction of 23, 24, and 25 to Z-olefins 26, 27, and 28

To nickel acetate (0.76 g, 3 mmol) in a three-neck flask equipped with a septum was added 5 mL of 95% ethanol. The flask was connected to the hydrogenation apparatus and was flushed with hydrogen. The catalyst was produced by injecting 4.5 mL of a 0.5 *M* solution of sodium borohydride in 95% ethanol to the rapidly stirred solution of nickel acetate. The reaction vessel was reflushed with hydrogen and ethylene diamine (0.3 mL) was added. Hydrogenation was then initiated by introducing the acetylenic alcohol **23** (3.29 g, 10.5 mmol), in 15 mL ethanol, via the septum. Hydrogen uptake was quantitative within an hour and then virtually ceased. The reaction mixture was filtered through Celite, the ethanol was removed under reduced pressure, and the residue was extracted with ether (2 × 350 mL). The combined ether extracts were washed with H_2O (3 × 40 mL), dried over $MgSO_4$, and evaporated *in vacuo* to give the olefinic alcohol **26** in quantitative yield. Nuclear magnetic resonance ($CDCl_3$) δ (glucose numbering): 1.24–2.47 (m, 10H, C(3)H, C(6)H, $CH_2CH_2CH_2$), 1.30 (s, 3H, CH_3), 1.49 (s, 3H, CH_3), ~3.6–4.2 (br s, 1H, OH, exchangeable with D_2O), 3.60–4.36 (m, 2H, C(4)H, C(5)H), 3.63 (s, 3H, CO_2CH_3), 4.60–4.80 (m, 1H, C(2)H), 5.33–5.56 (m, 2H, *Z*—CH=CH), 5.75 (d, 1H, $J_{1,2}$ = 4 Hz, C(1)H). The ^{13}C nmr spectrum indicated the presence of one major isomer; ^{13}C nmr ($CDCl_3$) δ: 173.93 (CO_2Me), 131.48 (C=C), 125.76 (C=C), 111.15, 105.27, 80.50, 70.58, 66.32, 51.38, 33.31, 31.90, 30.83, 26.73, 26.62, 26.08, 24.62. This was confirmed by gc–ms of **26**-*O*-trimethylsilyl ether, which indicated the presence of <3% of a minor impurity, possibly the *trans*-isomer, having approximately the same retention time; ms *m/e*: 371 ($M - CH_3$), 245 ($M - CH_2CH{=}CH(CH_2)_3COOCH_3$), 243 ($Me_3SiOCHCH_2CH{=}CH(CH_2)_3COOCH_3$), 143 ($M - 243$); $[\alpha]_D^{23}$ − 5.51 (*c* 4.05 in $CHCl_3$).

Acetate 28 was obtained from **25** using the same conditions. Its spectral data were similar to those of **25** except for the presence of the olefinic protons at 5.23–5.48 (m, 2H); ms *m/e*: 356 (M^+).

Methyl ether 27 was obtained from **24**, using ~35% of the catalyst used in the reduction of **23**. Its ^1H nmr spectrum was similar to that of **24** except for the olefinic protons at 5.47 ppm (m, 2H).

tert-*Butyldiphenylsilyl Ether 29*

To the alcohol **26** (3 g, 9.5 mmol) in dry dimethylformamide (6 mL) under N_2 was added *tert*-butylchlorodiphenylsilane (2.87 g, 10.5 mmol) and imidazole (1.42 g, 20.9 mmol); the reaction mixture was then stirred at 78°C for 17 h to effect complete silylation. Water (100 mL) was added and the product was extracted with ether (3 × 350 mL); the combined ether extracts were washed with H_2O (3 × 40 mL), dried over $MgSO_4$, and evaporated to afford the silylated alcohol, as a pale yellow oil, in quantitative yield. Infrared 1740 (COOMe) cm^{-1}; nmr (glucose numbering) ($CDCl_3$) δ: 1.07 (s, 9H, $SiCMe_3$), 1.24–2.40 (m, 10H, C(3)H, C(6)H, $CH_2CH_2CH_2$), 1.27 (s, 3H, CH_3), 1.44 (s, 3H, CH_3), 3.59 (s, 3H, CO_2CH_3), 3.87–4.36 (m, 2H, C(4)H, C(5)H), 4.54–4.73 (m, 1H, C(2)H), 5.13–5.37 (m, 2H, HC=CH), 5.56 (d, 1H, $J_{1,2}$ = 4 Hz, C(1)H), 7.13–7.80 (m, 10H, $SiPh_2$). The ^{13}C nmr spectrum was consistent with the structure proposed; $[\alpha]_D^{23}$ −25.1° (*c* 5.25 in $CHCl_3$).

*Methyl 8*R-tert-*butyldiphenylsilyloxy-9*S,*11*R-*dihydroxy-9,11-O-isopropylidene-12,12-di(ethylthio)dodeca-5*Z-*enoate (32) from 29 and 30 from 27*

To the silylated alcohol **29** (1.5 g, 2.7 mmol) in ethanethiol (3 mL) at −10°C was added anhydrous zinc chloride (1.4 g, 10.3 mmol). After one hour at −10°C, the excess ethanethiol was removed at −10°C *in vacuo*. The foamy residue was dissolved in ethyl acetate (50 mL) and aqueous $NaHCO_3$ (10 mL) was added; the precipitate which formed was filtered off and the filtrate was extracted with ethyl acetate (3 × 400 mL); the ethyl acetate extracts were washed with saturated salt solution (3 × 50 mL), dried over $MgSO_4$, and evaporated to give the thioacetal **31** in quantitative yield. Its nmr spectrum was consistent with the structure proposed; **30** was obtained from **27** in the same way.

To an acetone (100 mL) solution of thioacetal **31** (2.5 g, 4 mmol) obtained in this manner was added dimethoxypropane (5 mL) and *p*-toluenesulfonic acid (catalytic). After 1 h at room temperature the acetone was removed at reduced pressure and the residue extracted with ethyl acetate (3 × 400 mL); the ethyl acetate extracts were washed with aqueous $NaHCO_3$ (3 × 30 mL), saturated salt solution (3 × 30 mL), dried over $MgSO_4$, and evaporated to give the isopropylidene thioacetal **32** as a pale yellow oil, in quantitative yield. Infrared: 1737 (COOMe) cm^{-1}; nmr ($CDCl_3$) δ: 1.08 (s, 9H, Si—CMe_3), 1.10–2.92 (m, 16H, $5CH_2$, $2CH_3$), 1.34 (s, 6H, CMe_2), 2.70 (q, 4H, *J* = 7 Hz, $2SCH_2CH_3$), 3.60 (s, 3H, CO_2CH_3), 3.60–4.20 (m, 4H, H—CS, H—C—O), 5.19–5.44 (m, 2H, *Z*-HC=CH), 7.17–7.84 (m, 10H, $SiPh_2$); ms *m/e* (70 eV): 584 ($M^+ - CH_2C(OMe)OH$), 135 ($CH(SEt)_2$, 100%); *Anal.* calcd. for $C_{36}H_{54}O_5S_2Si$: C 65.65, H 8.21, S 9.73; found: C 65.69, H 7.96, S 9.49; $[\alpha]_D^{23}$ −29.4° (*c* 2.85 in $CHCl_3$).

*Methyl 8*R-tert-*butyldiphenylsilyloxy-9*S,*11*R-*dihydroxy-9,11-O-isopropylidene-12-oxo-dodeca-5*Z-*enoate (33)*

To the dithioacetal **32** (5.5 g, 8.4 mmol) in acetone–water (300 mL/30 mL) was added mercuric oxide (15 g, 69 mmol), and mercuric chloride (6.22 g, 23 mmol); the heterogeneous reaction mixture was stirred at room temperature for 8 h, and was then filtered into aqueous $NaHCO_3$ (100 mL); the filtrate was refiltered, the acetone removed *in vacuo*, and the residue extracted with CH_2Cl_2 (2 × 300 mL); the extracts were washed with aqueous KI (2 × 50 mL), saturated salt solution (3 × 50 mL), dried with $MgSO_4$, and evaporated to give in quantitative yield the oily, somewhat unstable aldehyde, in part as a hydrate; nmr ($CDCl_3$) δ: 0.90–2.40 (m, 10H, $5CH_2$), 1.07 (s, 9H, $SiCMe_3$), 1.37 (s, 3H, CH_3), 1.41 (s, 3H, CH_3), 3.60 (s, 3H, CO_2CH_3), 3.60–4.00 (m, 2H, C(8)H, C(9)H), 4.04–4.36 (m, 1H, C(11)H, 5.17–5.40 (m, 2H, HC=CH), 7.09–7.80 (m, 10H, $SiPh_2$), 9.53 (s, 0.8H, CHO).

*Methyl 8*R-tert-*butyldiphenylsilyloxy-9*S,*11*R-*dihydroxy-9,11-O-isopropylidene-14-oxo-tetradeca-5*Z,*12*E-*dienoate (34)*

To aldehyde **33** (4.34 g, 7.86 mmol) in 25 mL dry dimethylformamide under N_2, was added formylmethylenetriphenylphosphorane (2.4 g, 7.86 mmol) (15). After 20 h stirring at room temperature, water (300 mL) was added to the reaction mixture which was then extracted with ether (3 × 600 mL); the ether extracts were then washed with H_2O (3 × 50 mL), dried over $MgSO_4$, and evaporated to give the α,β unsaturated aldehyde in 90% yield; nmr ($CDCl_3$) δ: 0.96–2.43 (m, 10H, $5CH_2$), 1.09 (s, 9H, $SiCMe_3$), 1.39 (s, 6H, CMe_2), 3.60 (s, 3H, CH_3), 3.60–4.00 (m, 2H, C(8)H, C(9)H), 4.33–4.72 (m, 1H, C(11)H),

Can. J. Chem. Downloaded from www.nrcresearchpress.com by 210.87.254.5 on 09/05/12
For personal use only.

5.20–5.44 (m, 2H, *Z*-CH=CH), 6.42 (AB q, 2H, $J_{12,13}$ = 16 Hz, $J_{13,14}$ = 6.5 Hz, $J_{11,13}$ = 1 Hz, $J_{11,12}$ = 4 Hz, OCH(11)—*CH*(12)=*CH*(13)—CH(14)O), 7.15–7.77 (m, 10H, $SiPh_2$), 9.47 (d, 1H, $J_{13,14}$ = 6.5 Hz, CHO).

*Methyl 8*R-tert-*butyldiphenylsilyloxy-9*S,*11*R-*dihydroxy-9,11*-O-*isopropylidene-eicosa-5*Z,*12*E,*14*Z-*trienoate (35)*

To *n*-hexyltriphenylphosphonium bromide (2.8 g, 6.6 mmol) in dry THF (15 mL) under argon at room temperature was rapidly added *n*-BuLi (5.1 mmol). The reaction mixture turned red immediately; it was stirred for 10 min, cooled to −78°C, and then aldehyde **34** (2.7 g, 4.7 mmol, in 10 mL THF) was added slowly via syringe. The reaction was over immediately and was warmed up rapidly by immersion into a room temperature water bath. The reaction mixture was quenched with H_2O, the THF removed *in vacuo*, and the residue extracted with hexanes (3 × 350 mL); the extracts were washed with H_2O (4 × 50 mL), dried over $MgSO_4$, and evaporated to give the desired 14-*Z* olefin **35**, as an oil, in 80% yield. A separation of the minor 14-*E* impurity was not carried out at this stage of the synthesis, since the peaks overlapped in hplc; nmr ($CDCl_3$) δ: 0.68–2.48 (m, 21H, $9CH_2$, $1CH_3$), 1.09 (s, 9H, $SiCMe_3$), 1.38 (s, 6H, CMe_2), 3.60 (s, 3H, $COOCH_3$), 3.60–3.93 (m, 2H, C(8)H, C(9)H), 4.13–4.53 (m, 1H, C(11)H), 5.17–6.70 (m, 6H, olefinic H's), 7.17–7.82 (m, 10H, $SiPh_2$); $[\alpha]_D^{23}$ −10.9° (*c* 3.60 in $CHCl_3$); *Anal.* calcd. for $C_{40}H_{58}SiO_5$: C 74.30, H 8.98; found: C 73.99, H 9.01.

*Methyl 8*R,9S,*11*R-*trihydroxy-9,11*-O-*isopropylidene-eicosa-5*Z,*12*E,*14*Z-*trienoate (36)*

A mixture of **35** (0.67 g, 1.04 mmol) and tetra-*n*-butyl ammonium fluoride (1.9 mmol) was stirred in dry tetrahydrofuran (11 mL) at 60°C under a nitrogen atmosphere for 4 h; the tetrahydrofuran was removed *in vacuo* and the residue was extracted with ether (3 × 350 mL), washed with H_2O (3 × 30 mL), and dried over $MgSO_4$ to give a quantitative yield of **36**, contaminated with diphenyl-*tert*-butyl silanol; the latter was removed by flash chromatography (petroleum ether – ethyl acetate, 4.3:1.0); nmr ($CDCl_3/D_2O$) δ: 0.68–2.46 (m, 21H, $9CH_2$, $1CH_3$), 1.42 (s, 3H, CH_3), 1.46 (s, 3H, CH_3), 3.39–3.98 (m, 2H, C(8)H, C(9)H), 3.63 (s, 3H, CO_2CH_3), 4.15–4.55 (m, 1H, C(11)H), 5.13–6.69 (6H, olefinic H's). The gc–ms analysis of a trimethyl silylated sample showed the presence of a minor component (~10–15%) with slightly longer retention time (14*E* isomer of **36**), and **36**. Both spectra were nearly superimposable; ms *m/e*: 480 (M^+), 243 ($Me_3SiOCH—CH_2CH=CH(CH_2)_3COOMe$). Its ^{13}C nmr confirmed the presence of a minor isomer; $[\alpha]_D^{23}$ +7.19° (*c* 2.60 in $CHCl_3$). The isomer could be cleanly separated by hplc (petroleum ether (30–60°C) – ethyl acetate, 8.5:1).

*Methyl 8*R,9S,*11*R-*trihydroxy-5*Z,*12*E,*14*Z-*eicosatrienoate (37)*

Alcohol **36** (0.41 g, 1 mmol) in 8 mL methanol and 2 mL 0.1 *N* aqueous HCl was stirred at room temperature for 1 h to effect complete hydrolysis. The solution was neutralized with basic resin (IR-45 OH), and the solvents removed *in vacuo*; the residue was redissolved in ether and dried over $MgSO_4$. Evaporation of the solvent gave triol **37**, as a mixture of 14*E* and *Z* isomers, in quantitative yield. The two olefins were separated by flash chromatography (petroleum ether – ethyl acetate, 3:4). Infrared (neat) 1735 (C=O), 3400 (OH) cm^{-1}; ^1H nmr ($CDCl_3$) δ: 0.67–2.50 (m, 21H, $9CH_2$, $1CH_3$), 3.17–4.00 (m, 4H, C(8)H, C(9)H, two OH (exchangeable with D_2O)), 3.63 (s, 3H, CO_2CH_3), 4.20–4.60 (m, 1H, C(11)H), 5.18–6.68 (m, 6H, olefinic H's); ^{13}C nmr (acetone-d_6) δ: 174.10 (CO_2Me), 137.69, (C=C), 132.41 (C=C), 130.79 (C=C), 129.17 (C=C), 128.47 (C=C), 125.29 (C=C), 75.28, 74.74, 72.31, 51.49, 40.10, 33.74, 32.12, 31.53, 30.07, 28.24, 27.27, 25.54, 23.11, 14.26; ms *m/e* of tristrimethylsilyl ether: 584 (M), 243 ($Me_3SiOCHCH_2CH=CH(CH_2)_3COOCH_3$), $[\alpha]_D^{23}$ +5.81° (*c* 3.10 in $CHCl_3$); *Anal.* calcd. for $C_{21}H_{36}O_5$: C 68.48, H 9.78; found: C 68.39, H 9.77.

The ^{13}C-spectrum showed 6 olefinic C's, indicating the presence of one isomer only.

Acknowledgements

We wish to thank the Natural Sciences and Engineering Research Council of Canada for financial support.

1. (*a*) C. PACE-ASCIAK. Biochemistry, **10**, 3664 (1971); (*b*) C. PACE-ASCIAK and L. S. WOLFE. Chem. Commun. 1234 (1970); (*c*) C. PACE-ASCIAK and L. S. WOLFE. Chem. Commun. 1235 (1970).
2. (*a*) G. BILD, S. G. BHAT, C. S. RAMADOSS, B. AXELROD, and C. SWEELEY. Biochem. Biophys. Res. Commun. **81**, 486 (1978); (*b*) G. BILD, S. G. BHAT, C. S. RAMADOSS, and B. AXELROD. J. Biol. Chem. **253**, 21 (1978).
3. M. HAMBERG and B. SAMUELSON. J. Biol. Chem. **242**, 5336 (1967).
4. P. SZABO and L. SZABO. J. Chem. Soc. 5139 (1964).
5. L. GHOSEZ, R. MONTAIGNE, A. ROUSSEL, H. VANLIERDE, and P. MOLLET. Tetrahedron, **27**, 615 (1971).
6. H. R. BARTON, and S. W. MCCOMBIE. J. Chem. Soc. Perkin Trans. I, 1574 (1975).
7. E. J. HEDGELEY, W. G. OVEREND, and R. A. C. RENNIE. J. Chem. Soc. 4701 (1963), and references cited therein.
8. G. J. M. VAN DER KERK, J. G. NOLTES, and J. G. A. LUIJTEN. J. Appl. Chem. **7**, 366 (1957).
9. R. L. WHISTLER and M. L. WOLFROM. Methods in carbohydrate chemistry. Vol. II. Academic Press, New York, NY. 1963. p. 190.
10. J. PETE and C. PORTELLA. Synthesis, **11**, 774 (1977).
11. K. FREUDENBERG and A. WOLF. Ber. Dtsch. Chem. Ges. **60**, 232 (1927).
12. H. GILMAN and B. HOLLAND. Synth. Commun. **4**, 199 (1974); G. JUST, C. LUTHE, H. OH, and J. MONTGOMERY. Synth. Commun. **9**, 613 (1979).
13. C. A. BROWN and V. K. AHUJA. J. Chem. Soc. Chem. Commun. 553 (1973).
14. S. HANESSIAN and P. LAVALLÉE. Can. J. Chem. **53**, 2975 (1975).
15. S. TRIPPETT and D. M. WALKER. J. Chem. Soc. 1266 (1961).
16. W. C. STILL, M. KAHN, and A. MITRA. J. Org. Chem. **43**, 2923 (1978).

Mechanism of the formation of quinoline from *N*-methylacetanilide studied using ^{13}C-labeled substrates[1]

EDWARD LEETE

Natural Products Laboratory,[1] School of Chemistry, University of Minnesota, Minneapolis, MN 55455, U.S.A.

Received February 8, 1980

This paper is dedicated to the memory of Dr. Léo Marion[2]

EDWARD LEETE. Can. J. Chem. **58**, 1806 (1980).

Pictet discovered 90 years ago that quinoline and *p*-toluidine were formed on heating *N*-methylacetanilide with zinc chloride. It has now been shown that 6-methylquinoline is also produced in this reaction. It was established by means of ^{13}C nmr that [1-^{13}C-*acetyl*]-*N*-methylacetanilide affords quinoline and its 6-methyl derivative enriched at C-4. [*N*-*methyl*-^{13}C]-*N*-Methylacetanilide yielded [2-^{13}C]quinoline and [2,6-*methyl*-$^{13}C_2$]-6-methylquinoline. *N*-Methylpropionanilide afforded 3-methylquinoline. These results are in accord with a new mechanism for the formation of quinoline, different from the one previously proposed.

EDWARD LEETE. Can. J. Chem. **58**, 1806 (1980).

Il y a de cela 90 ans Pictet a découvert que le chauffage du *N*-méthylacétanilide en présence de chlorure de zinc produisait la quinoléine et la *p*-toluidine. Il est maintenant prouvé qu'il se forme également de la méthyl-6 quinoléine au cours de cette réaction. On a établi, au moyen, de la rmn du ^{13}C, que le [^{13}C-1 *acétyle*]-*N*-méthylacétanilide produit la quinoléine et ses dérivés substitués en position 6 enrichis au niveau du carbone en position 4. Le [*N*-*méthyl*-^{13}C]-*N*-méthylacétanilide produit la [^{13}C-2] quinoléine et la [2,*méthyl*-6 $^{13}C_2$] méthyl-6 quinoléine. Le *N*-méthylpropionanilide conduit à la méthyl-3 quinoléine. Ces résultats sont en accord avec un nouveau mécanisme de formation de la quinoléine, différent de celui proposé antérieurement.

[Traduit par le journal]

Introduction

In 1889 Pictet and Bunzl (1) discovered that *N*-ethylacetanilide (**1**) on heating with zinc chloride yielded a mixture of *p*-ethylaniline and 2-methylquinoline (**3**). Later it was found that *N*-methylacetanilide (**4**) afforded a mixture of *p*-toluidine (**7**) and quinoline (**8**) (2). These reactions have received no further study; indeed a recent review of synthetic methods for preparing quinolines (3) failed to even mention these publications of Pictet. Elderfield (4) discussed these reactions and rationalized them as illustrated in Fig. 1. It was proposed that the ethyl group of **1** migrated to the *ortho*-position under the influence of the zinc chloride to yield *o*-ethylacetanilide (**2**) which then cyclized to 2-methylquinoline. The formation of quinoline from **4** was considered to proceed via *N*-acetyl-*o*-toluidine (**5**) and 2-methylindole (**6**). 2-Methylindole can certainly be formed from **5** (Madelung synthesis) and a small amount of quinoline was obtained by heating 2-methylindole with zinc chloride (5). These obscure reactions of Pictet came to my attention serendipitously when checking the melting point of *N*-methylacetanilide (6). [1-^{13}C]Acetaldehyde was being prepared by the reduction of [1-^{13}C-*acetyl*]-*N*-methylacetanilide with lithium aluminum hydride (7), and the mechanism of the formation of quinoline from **4** seemed worthy of investigation using the ^{13}C-labeled **4**. The location of the excess ^{13}C in the ultimate quinoline could be readily determined by ^{13}C nmr spectroscopy.

Results and Discussion

[1-^{13}C-*acetyl*]-*N*-Methylacetanilide was prepared from *N*-methylaniline hydrochloride and sodium [1-^{13}C]acetate, condensing in aqueous solution in the presence of 1-ethyl-3-(3-dimethylaminopropyl)carbodiimide hydrochloride (8). This amide was heated with zinc chloride at 290°C for 6 h in the presence of air. We confirmed the results of Pictet and obtained a small yield of *p*-toluidine (17%) and quinoline (6.5%) along with some *N*-methylaniline (28%). In addition 6-methylquinoline (4%) was isolated, identical with an authentic specimen (9), and readily separated from quinoline by gas chromatography. The ^{13}C nmr spectra of quinoline and 6-methylquinoline have been previously determined (10–12). An examination of the ^{13}C nmr spectra of the quinoline and 6-methylquinoline derived from [1-^{13}C-*acetyl*]-*N*-methylacetanilide revealed that they

[1]Contribution No. 173 from this laboratory.

[2]I worked with Dr. Marion as a postdoctoral fellow (1951–1954) at the National Research Council of Canada Laboratories, Ottawa. He introduced me to alkaloid chemistry and we collaborated in some of the first investigations on the biosynthesis of hordenine, gramine, and the tropane alkaloids. The present publication is relevant to his scientific accomplishments, since one of his earlier papers was a definitive study of the monomethyl and dimethylquinolines (ref. 17).

0008-4042/80/171806-04$01.00/0

©1980 National Research Council of Canada/Conseil national de recherches du Canada

Can. J. Chem. Downloaded from www.nrcresearchpress.com by 210.87.254.5 on 09/05/12
For personal use only.

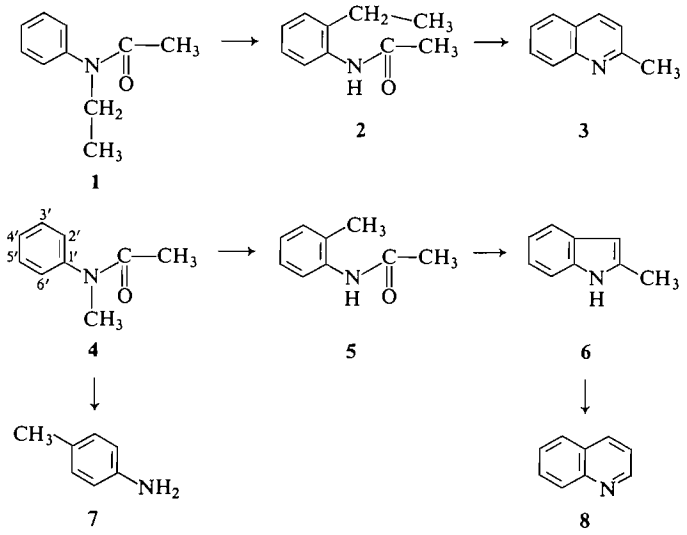


FIG. 1. Reactions discovered by Pictet and their previous rationalization.

were enriched only at C-4. This result is not consistent with the previous rationalization for the formation of quinoline. We thus suggest that quinoline and 6-methylquinoline are formed by the scheme illustrated in Fig. 2. It is proposed that the zinc chloride complex of *N*-methylacetanilide (**9**) serves as a source of acetylium and methyl carbonium ions. Electrophilic attack of *N*-methylaniline with the acetylium ion could yield *o*-acetyl-*N*-methylaniline (**11**) which would yield the imine **13** on dehydrogenation. An aldol condensation then affords 2,3-dihydro-4-quinolone (**15**), a compound having the same oxidation state as quinoline. The latter could thus be formed by enolization, double bond migration, and dehydration. 6-Methylquinoline (**14**) would be formed by an analogous series of reactions from 2-acetyl-4-methyl-*N*-methylaniline (**10**). It seems unlikely that **14** would be formed by reaction of quinoline with methyl carbonium ions, since electrophilic attack of quinoline occurs mainly at the 3, 5, and 8 positions. In a reaction which is considered to involve attack of quinoline with methyl carbonium ions, the main alkylated product was 3-methylquinoline (13). *p*-Toluidine results from electrophilic attack of acetanilide with methyl carbonium ions followed by deacetylation. In this hypothesis the *N*-methyl group of **4** becomes C-2 of quinoline. This was confirmed by carrying out the reaction with [N-*methyl*-^{13}C]-*N*-methylacetanilide. This labeled compound was obtained by reaction of acetanilide with sodium hydride in tetrahydrofuran, followed by addition of [^{13}C]methyl iodide. In a preliminary experiment acetanilide was reacted with butyl lithium followed by [^{13}C]methyl iodide. A mixture of the desired compound and [*N-methyl*-^{13}C, 3-^{13}C-*propionyl*]-*N*-methylpropionanilide (**15**) was obtained, the latter compound being the result of both *N*- and *C*-methylation. The ^{13}C nmr spectrum of this doubly labeled compound was of interest in that a four bond coupling (3.5 Hz) was observed between the highly enriched carbons. Our first thought that this splitting of the enriched positions was due to restricted rotation about the amide bond was rejected when it was found that no such splitting was observed in **15** of natural abundance. The quinoline and 6-methylquinoline derived from [*N-methyl*-^{13}C]-**4** were enriched at C-2, and the latter compound was also enriched at its C-methyl group. Further support for the scheme in Fig. 2 was obtained by heating **15** with zinc chloride. 3-Methylquinoline (**16**) was obtained as expected, together with a small amount of a dimethylquinoline which is probably the 3,6-dimethyl derivative.

Experimental

General

Melting points were determined in glass capillaries and are corrected. The ^{13}C nmr spectra were determined on a Varian XL-100-15 instrument operating at 25.16 MHz interfaced with a VFT-100 Fourier transform system. Chemical shifts are expressed in parts per million from tetramethylsilane (internal reference). Mass spectra were determined on an AEI-MS-30 double beam, double focusing spectrometer.

[*1*-^{13}*C*-acetyl]-N-*Methylacetanilide*, *4*

Sodium [1-^{13}C]acetate (91% ^{13}C, prepared from methyl magnesium iodide and $^{13}CO_2$ (14) (0.83 g, 0.01 mol), *N*-methylaniline

Can. J. Chem. Downloaded from www.nrcresearchpress.com by 210.87.254.5 on 09/05/12
For personal use only.

Can. J. Chem. Downloaded from www.nrcresearchpress.com by 210.87.254.5 on 09/05/12
For personal use only.

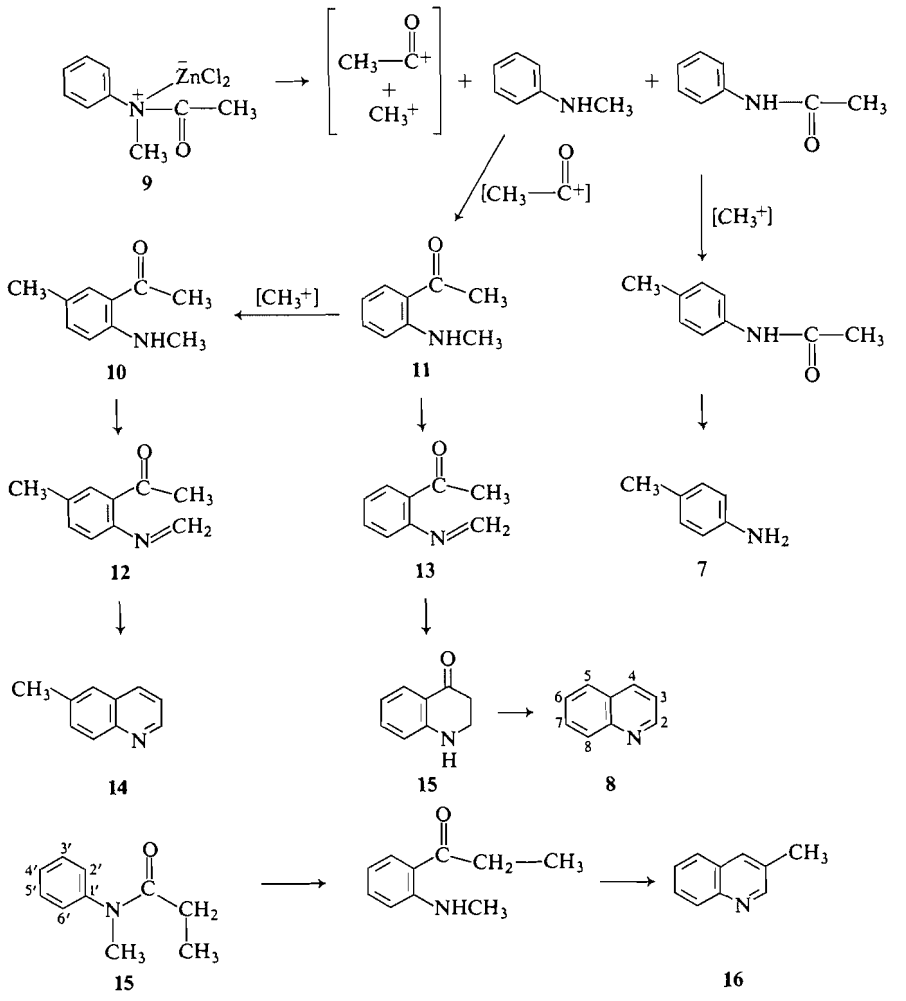


FIG. 2. Proposed mechanism for the formation of quinolines from *N*-acyl-*N*-methylanilines.

hydrochloride (1.6 g, 0.011 mol), and 1-ethyl-3-(3-dimethylaminopropyl)carbodiimide hydrochloride (4 g) were dissolved in water (5 mL). After stirring for a few minutes a white solid separated which was crystallized from hot water affording **4** as colorless plates (1.31 g, 87% yield) mp 101–102°C; ^{13}C nmr ($CDCl_3$) δ: 170.1 (C=O), 146.4 (1'), 129.5 (3',5'), 127.5 (4'), 126.9 (2',6'), 37.0 (NMe), 22.2 (t, $'J$ = 53.3 Hz, CMe). Assignments were made by comparison with the spectrum of acetanilide (15).

[N-methyl-^{13}C]-N-*Methylacetanilide*

A solution of acetanilide (0.675 g, 0.005 mol) in tetrahydrofuran (5 mL) was added to a suspension of sodium hydride (0.26 g, 0.0054 mol, of a 50% suspension in mineral oil which had been washed with benzene by decantation) in tetrahydrofuran (10 mL) at 0°C in an N_2 atmosphere. After stirring for 10 min [^{13}C]methyl iodide (0.31 mL, 0.005 mol, 91% ^{13}C) dissolved in tetrahydrofuran (2 mL) was added during 20 min. The solution was stirred at 20°C for 1 h and then evaporated. The residue was suspended in water and extracted with ether. The residue obtained on evaporation of the dried (Na_2SO_4) extract was subjected to preparative tlc on Silica Gel 60 PF254 (Merck) developing with a mixture of chloroform, ethanol, and concentrated ammonia (100: 5: 0.5). Two main zones corresponding to *N*-methylacetanilide and acetanilide were obtained. Extraction of the upper zone with methanol afforded [*N-methyl*-^{13}C]-*N*-methylacetanilide which was purified by sublimation (90°C, 0.001 Torr) and crystallization from hexane (0.45 g, 60% yield). Its mass spectrum, run along with natural abundance material, indicated ^{13}C enrichment of 90.7%. Two prominent peaks at 106, 107 due to C_6H_5N-CH_3 and $C_6H_5NHCH_3$, respectively, in the unenriched material, were shifted to 107 and 108 in the ^{13}C-labeled compound. Its ^{13}C nmr spectrum was identical with unenriched material except that the signal due to the *N*-methyl group was greatly enhanced. No splitting of the other resonances were observed due to two or three bond couplings.

[N-methyl-^{13}C, 3-^{13}C-propionyl]-N-*Methylpropionanilide*, *15*

Butyllithium (3.0 mL of a 2.34 *M* solution in hexane = 0.0070 mol) was added at 0°C to a solution of acetanilide (0.78 g, 0.0058 mol) in tetrahydrofuran (10 mL) stirred in an N_2 atmosphere. After 5 min [^{13}C]methyl iodide (0.31 mL, 0.005 mol, 91% ^{13}C) was added and the mixture stirred for 3 h at 0°C. The reaction was worked up as described for [*N-methyl*-^{13}C]-*N*-methylacetanilide, and tlc yielded 3 components: *N*-methylpropionanilide (0.27 g) colorless plates from hexane, mp 58–59°C (lit. (16) mp 58.5°C), *N*-methylacetanilide (0.21 g), and acetanilide (0.25 g); ^{13}C nmr ($CDCl_3$) δ: 173.3 (C=O), 144.2 (1'),

129.2 (3′, 5′), 127.4 (4′), 127.1 (2′, 6′), 37.1 (d, ^4J = 3.5 Hz, NMe), 27.3 (t, ^1J = 35 Hz, CH_2), 9.7 (d, ^4J = 3.5 Hz, CMe).

Reaction of N-*Methylacetanilide with Zinc Chloride*

N-Methylacetanilide (0.5 g) was added to anhydrous zinc chloride (4 g) in a 50 mL round bottom flask and the mixture heated with an air condensor in a metal bath at 290°C for 6 h. The dark brown reaction mixture was then cooled, dissolved in 2 *N* hydrochloric acid, and then made strongly basic with NaOH. The mixture was extracted with ether and the dried (Na_2SO_4) extract evaporated to yield a brown oil which was distilled (160°C, 0.001 Torr).[3] The pale yellow oil (0.242 g) was subjected to tlc in Silica Gel 60 PF254. Many discrete zones were observed (by uv light). The compound with the highest R_f was *N*-methylaniline (102 mg), followed by *p*-toluidine (63 mg), and then a zone which had the same R_f as quinoline (47 mg). This material, dissolved in benzene was subjected to glc on an 8 ft × $^1/_4$ in. column of 5% Carbowax 20 M on Chromosorb W (60–80 mesh) at 160°C. With a He flow rate of 60 mL/min, the retention times of benzene, quinoline, and 6-methylquinoline were 4, 25, and 37 min, respectively. The ratio of quinoline to 6-methylquinoline in the reaction mixture was 3:2. The ^{13}C nmr spectra of the quinoline and 6-methylquinoline were essentially the same (± 0.2 ppm) from the previously published and assigned spectra (10–12). The *N*-methylacetanilide labeled with ^{13}C on the carbonyl or *N*-methyl group was reacted in the same way with zinc chloride. However, unenriched quinoline and 6-methylquinoline were added to the "quinoline" fraction from the tlc in order to facilitate their isolation and purification prior to ^{13}C nmr spectroscopy.

Reaction of N-*Methylpropionanilide with Zinc Chloride*

N-Methylpropionanilide (1.0 g) was heated with zinc chloride (8 g) at 290°C for 6 h and the reaction mixture worked up as described in the previous section. The "quinoline" fraction after distillation (160°, 0.001 Torr) yielded a picrate (25 mg), mp 188–189°C identical (mixture mp, ms, ir) with 3-methylquinoline picrate (lit. (17) mp 190°C). The mass spectra of the crude quinoline fraction indicated the presence of a small amount of a dimethylquinoline which was not isolated in a pure state.

Acknowledgements

This investigation was supported by a research grant GM-13246 from the National Institutes of Health, U.S. Public Health Service. I thank the Stable Isotope Resource (SIR) at the Los Alamos Scientific Laboratory (supported by NIH grant RR-00962, Division of Research Resources) for supplying [^{13}C]methyl iodide and barium [^{13}C]carbonate (91% ^{13}C) (used for the synthesis of [1-^{13}C]acetic acid). The ^{13}C nmr spectra were determined by Dr. Robert M. Riddle, and the mass spectra by Dr. Roger Upham, both at the University of Minnesota.

[3]Léo Marion was the one who taught me how to distill small quantities of liquid under reduced pressure using the technique he had learned from Späth in Vienna.

1. A. Pictet and R. Bunzl. Chem. Ber. **22**, 1847 (1889).
2. A. Pictet and J. Fert. Chem. Ber. **23**, 1890 (1890).
3. G. Jones. The chemistry of heterocyclic compounds. Vol. 32. Quinolines, Part I. J. Wiley, New York. 1977. pp. 93–318.
4. R. C. Elderfield. Heterocyclic compounds. Vol. 4. *Edited by* R. C. Elderfield. J. Wiley, New York, 1952. p. 64.
5. E. Fischer and A. Steche. Chem. Ber. **20**, 818 (1887).
6. Dictionary of organic compounds, 4th ed. Oxford University Press. 1965.
7. F. Weygand, G. Eberhardt, H. Linden, F. Schäfer, and I. Eigen. Angew. Chem. **65**, 525 (1953).
8. J. C. Sheehan, P. A. Cruickshank, and G. L. Boshart. J. Org. Chem. **26**, 2525 (1961).
9. Z. H. Skraup. Monatsh. **2**, 139 (1881).
10. R. J. Pugmire, D. M. Grant, M. J. Robins, and R. K. Robins. J. Am. Chem. Soc. **91**, 6381 (1969).
11. J.-A. Su, E. Siew, E. V. Brown, and S. L. Smith. Org. Magn. Reson. **10**, 122 (1977).
12. S. R. Johns, R. I. Willing, P. A. Claret, and A. G. Osborne. Aust. J. Chem. **32**, 761 (1979).
13. G. A. Collins. Brit. Patent No. 845,562 (1960); Chem. Abstr. **55**, 5543 (1961).
14. M. Calvin, C. Heidelberger, J. C. Reid, B. M. Tolbert, and P. F. Yankwich. Isotopic carbon. J. Wiley, New York. 1949. p. 178.
15. J. F. Johnson and W. C. Jankowski. Carbon-13 nmr spectra. Spectrum No. 295. J. Wiley, New York. 1972.
16. L. M. Norton and A. W. Allen. Chem. Ber. **18**, 1995 (1885).
17. R. H. F. Manske, L. Marion, and F. Leger. Can. J. Res. Sect. B, **20**, 133 (1942).

Can. J. Chem. Downloaded from www.nrcresearchpress.com by 210.87.254.5 on 09/05/12
For personal use only.

Synthesis and stereochemistry of hydrogenated 1,1,4,4,7a-pentamethylindenes

ALAN FRANCIS THOMAS, MICHEL OZAINNE, AND RENÉE GUNTZ-DUBINI

Research Laboratories, Firmenich SA, Geneva, Switzerland

Received January 29, 1980

Dédié à la mémoire de Dr. Léo Marion

ALAN FRANCIS THOMAS, MICHEL OZAINNE, and RENÉE GUNTZ-DUBINI. Can. J. Chem. **58**, 1810 (1980).

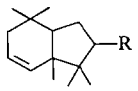
Ease of methylation of hydrogenated 2*H*-inden-2-ones depends on the presence of a double bond in the cyclohexane ring, and occurs readily with compound **20** but not with **10**. Differences of reactivity are also noted in Wittig reactions. Most reactions of the system are highly stereoselective, and the stereochemistry of hydrogenated indenes is discussed.

ALAN FRANCIS THOMAS, MICHEL OZAINNE et RENÉE GUNTZ-DUBINI. Can. J. Chem. **58**, 1810 (1980).

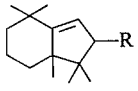
La facilité avec laquelle les indène-2*H* ones-2 hydrogénées sont méthylées dépend de la présence d'une double liaison dans le cycle à six chaînons; ainsi, la méthylation du composé **20** est beaucoup plus facile que celle du composé **10**. On constate également des différences de réactivité lors de la réaction de Wittig. La plupart des réactions de ce système sont hautement stéréosélectives, ce qui nous a permis d'ailleurs d'approfondir notre connaissance de la stéréochimie des indènes hydrogénés.

Introduction

In the course of other work, we had occasion to investigate the stereochemistry of highly substituted hydroindanes. These substances are little known, and in particular, we chose to synthesize the crowded molecules **1** and **2** (where R contains a carbonyl or hydroxyl function to permit complexation with a lanthanide shift reagent), because in such cases, each atom should be readily identifiable by nmr methods.



1

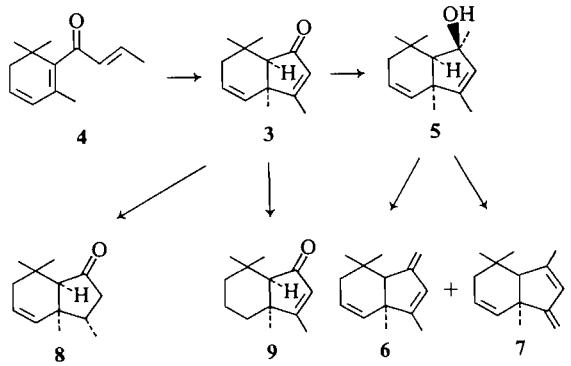


2

Syntheses

Initially, it appeared that the most rapid approach to the pentamethylated structures we had in mind would be by addition of a second methyl group in the β-position of the αβ-unsaturated cyclic ketone **3** obtained (1) from damascenone **4**, using lithium dimethylcuprate. The reaction was very slow, and only the 1,2-Grignard addition product **5** was isolated, together with the two hydrocarbons, **6**, **7**, from the dehydration of **5**. The normal Grignard reaction also works badly with ketone **3**; after 12 h at room temperature in the presence of excess methylmagnesium iodide, 60% of the starting material is recovered unchanged and about 30% is reduced (to the saturated ketone, **8**) without addition. To find out whether a compound with one or both of the double bonds reduced would perform better in organometallic addition reactions, catalytic reduction of **3** was undertaken, but a complex mixture of products was obtained, from which only the dihydroketone **9** could be identified.

We then investigated the methylation of 4,4,7a-trimethyl-1,4,5,6,7,7a-hexahydro-2*H*-inden-2-one **10**. This appears to be a new compound, and is readily made by a modification of the cyclization originally described by Islam and Raphael (2). Various conditions were tried for the introduction of a C_3 chain into 2,2,6-trimethylcyclohexanone at C(6). Using sodium hydride in dimethylformamide and 2,3-dichloropropene, 23% of the methylacetylene **11** was formed, together with a trace of the corresponding allene **12** and the terminal acetylene **13**. The latter was the major product (60%) using sodium amide in toluene and either propargyl chloride (the bromide is much less satisfactory[1]) or 2,3-dichloropropene. One of the reasons for the lower yield in this step is the formation of considerable amounts of a heavier compound, $C_{21}H_{34}O_2$, to which we ascribe the structure **14**, and which would arise from the addition of the terminal acetylene **13** to a second molecule of trimethylcyclohexanone. Using the usual conditions



4 **3** **5** **8** **9** **6** **7**

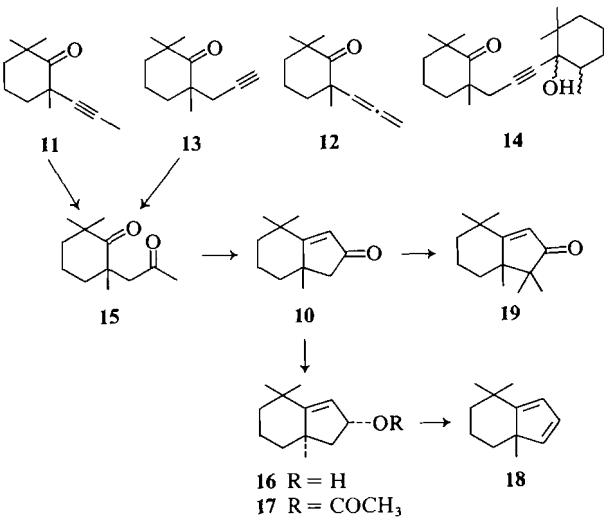
[1]Miller (3) obtained 26% yield in a similar reaction with 2-methylcyclohexanone and propargyl bromide. Certainly the yield would have been much improved if he had used the chloride.

0008-4042/80/171810-11$01.00/0

©1980 National Research Council of Canada/Conseil national de recherches du Canada

Can. J. Chem. Downloaded from www.nrcresearchpress.com by 210.87.254.6 on 09/05/12
For personal use only.

Can. J. Chem. Downloaded from www.nrcresearchpress.com by 210.87.254.6 on 09/05/12
For personal use only.



(acid + Hg^{2+}, see below), we were unable to hydrate the triple bond assumed to be present in **14**, so this was not usable for subsequent steps of the reaction sequence.

Hydration of the acetylenes **11** or **13** using Hg-impregnated Dowex 50 resin gave the diketone **15** in over 80% yield. Many variations for cyclizing conditions of this type of diketone have been described (2, 4), usually with yields of 60–75%, although Yoshikoshi and co-workers have reported higher yields (5). Using catalytic amounts of dry, powdered potassium hydroxide in boiling xylene, the bicyclic ketone **10** was obtained in one hour in 96% yield. Lithium aluminum hydride reduction of **10** gave an alcohol that was > 90% sterically homogeneous. This alcohol is presumably *cis* **16**, assuming approach of the reagent from the side of the molecule opposite to the angular methyl group (for spectral evidence see below). There is little information published about the metal hydride reduction of 7a-methylhexahydro-2-indenones of this type, although Furth *et al.* prepared both isomers of unsubstituted hexahydro-2*H*-inden-2-ol by a different route (6). Such alcohols are very easily dehydrated (cf. (7)) and both **16** and its acetate **17** could not be gas chromatographed, only the diene **18** being recovered.

Methylation of the ketone **10** proceeded very poorly, but a 20% yield of the ketone **19** was obtained, together with a certain amount of *O*-methylated products. Subsequently we were able to prepare **19** more efficiently, although it turned out to be of only limited use.

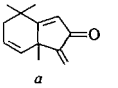
By a similar route to that just described, but starting from 2,6,6-trimethylcyclohex-2-enone (8), we prepared 4,4,7a-trimethyl-1,4,5,7a-tetrahydro-2*H*-inden-2-one **20** in acceptable yield. In this connection, we also prepared the chloroketone **21** in poor yield from 2,6,6-trimethylcyclohex-2-enone and 2,3-dichloroprop-1-ene in the presence of sodium amide in toluene. Lithium aluminum hydride reduction of **21** yielded a mixture of the corresponding stereoisomeric alcohols which should be cyclizable with formic acid according to Lansbury *et al.* (9). We were unable to confirm this, and indeed, it should be noted that Lansbury's cyclization is an unfavored "5-endo-trig" type following Baldwin's postulate (10).

The metal hydride reduction of the ketone **20** proceeded in the same way as for the more saturated ketone **10** (the alcohol **22** and its acetate were again unstable to gas chromatography), but methylation was much easier, 86% of 1,1,4,4,7a-pentamethyl-1,4,5,7a-tetrahydro-2*H*-inden-2-one **23** being isolated.[2] This fact illustrates how reactivity in the cyclopentane part of the molecule can be strongly influenced by unsaturation in the cyclohexane part, hindrance when this is saturated being the cause of the extensive *O*-alkylation of **10**. Catalytic hydrogenation of **23** gave the ketone **19** almost quantitatively by a much more convenient route than the earlier one.

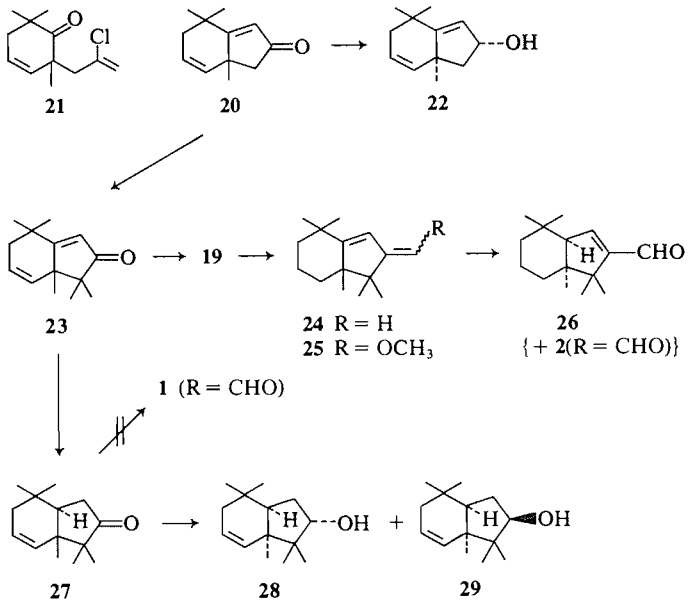
The ketone **19** readily underwent Wittig reactions. After a small-scale reaction with methylenetriphenylphosphorane had been shown to give **24**, a similar reaction using methoxymethyltriphenyl phosphonium chloride in tetrahydrofuran with butyllithium yielded two isomers of the enol ether **25**. Without separating them, these were refluxed with oxalic acid for 2 h, when they were converted to the conjugated aldehyde **26**. No conditions were found to yield more than impure traces of the unconjugated aldehyde **2** (R = CHO). This behavior again contrasts with that of the analog unsaturated in the cyclohexane ring (see below). We believed that it would be difficult to convert **26** to our target molecules **2**, and impossible to convert it to **1**, and so the following approach was adopted.

The conjugated double bond of the unsaturated ketone **23** was readily reduced by lithium in liquid ammonia, yielding a single substance **27**, to which a *cis* configuration was attributed, based on spectral

[2]An attempt to introduce a substituent at C(1) of **20** via the C(1)-methylene compound *a* gave such poor yields that it was abandoned (see Experimental).



a



data (below) of both it and the two alcohols **28**, **29** (and their acetates) obtained from it by lithium aluminum hydride reduction. Furthermore, models show clearly that the 1,3-diaxial interaction between the angular methyl group and one of the methyl groups at C(4) would cause considerable strain in a *trans*-fused system. Compound **27** has a very unreactive carbonyl group. Although we could prepare **28** and **29** and their acetates, we were unable to carry out any form of Wittig reaction, and even methylmagnesium iodide and methyllithium were without action. Sowerby and Coates's method (11) for placing a methylene group at the position of a hindered carbonyl group by addition of the lithium salt of thioanisole followed by benzoylation yielded only the enol benzoate of **27**.

The more unsaturated ketone **23** reacted readily with the ylide from methoxymethyltriphenylphosphonium chloride. Probably two isomers were formed, but after chromatography on silica gel, only the *Z*-isomer **30** was characterized. Hydrolysis of the latter was very slow, 25% of the starting material being recovered after reflux for 30 h with oxalic acid (this recovered material was now a mixture of two isomers visible by gc), but it was also possible to isolate the unconjugated aldehyde **31** in ca. 50% yield, together with a small amount of the conjugated aldehyde **32**. In an attempt to improve the yield from the hydrolysis of the enol ether **30**, aqueous/ethereal perchloric acid was tried, but the only substances isolated from the reaction were the *E*-isomer of **30** (apparently less readily hydrolyzed than the *Z*-isomer[3]) and the ester **33**, easily recognizable from its nmr spectrum, and confirmed by the mass spectrum. This ester presumably arises by oxidation of the aldehyde **31** by the perchloric acid, and esterification by the methanol present. The conjugated aldehyde **32** could be obtained from the unconjugated one **31** by treatment with methanolic potassium hydroxide, and the two aldehydes are readily separable by gc, when **31** has a much shorter retention time on most columns than **32**.

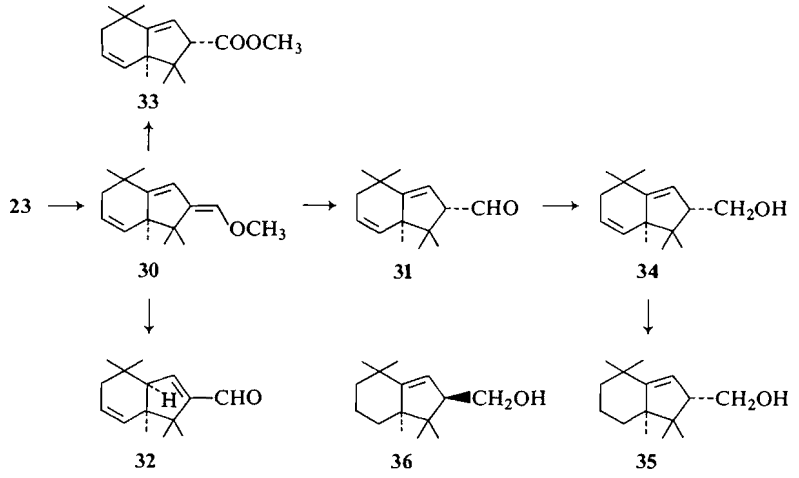
Lithium aluminum hydride reduction of the unconjugated aldehyde **31** gave an alcohol **34**, catalytic hydrogenation of which yielded the alcohol **35**, both **34** and **35** being almost (>98%) stereochemically homogeneous. Metal hydride reduction of the aldehyde **26**, however, yielded the corresponding alcohol together with ca. 12% of a mixture (3:2) of the alcohol **35** and its stereoisomer **36**. This mixture proved to be inseparable on packed gc columns, and even on the capillary column at our disposal, only a single peak was observed.[4]

In order to make compounds of the type **1**, it is necessary to reduce the double bond of the cy-

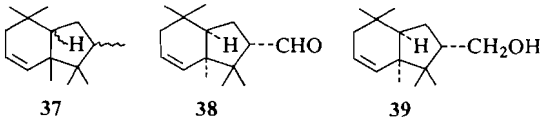
[3]The fact that we isolated the *E*-enol ether after acid hydrolysis of the *Z*-enol ether suggests that protonation is reversible, and the rate-determining step in this case is hydration, unlike certain other examples of enol ether hydrolysis (12).

[4]A referee has pointed out that $LiAlH_4$ in ether is not a normal medium for $\alpha, \beta \leftrightarrows \beta, \gamma$ interconversion of the double bond. We suggest one possible explanation: formation of the enolate with $LiAlH_4$, which undergoes decomposition and reduction on addition of water, leading to both alcohols **35** and **36**.

Can. J. Chem. Downloaded from www.nrcresearchpress.com by 210.87.254.6 on 09/05/12
For personal use only.



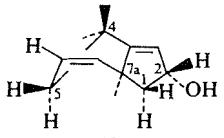
clopentene ring of **31**. Treatment of **31** with lithium in liquid ammonia (in the hope that the double bond would be first displaced, then hydrogenated) left the material unchanged, while similar treatment of the conjugated aldehyde **32** yielded practically exclusively hydrocarbons (apparently the major product was a single isomer of **37**). Catalytic reduction of a mixture of the aldehydes **31** and **32** in ethanolic potassium hydroxide proceeded rapidly until about 0.6 equivalents of hydrogen had been absorbed, at which point unchanged unconjugated aldehyde **31** was recovered from the mixture, together with the aldehyde **38**. Reduction of **38** with lithium aluminum hydride yielded the single, crystalline alcohol **39**.



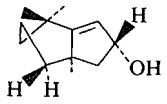
37 **38** **39**

Stereochemistry

The first stereochemical problem concerns the orientation of metal hydride reduction of the indenones **10** and **20**, in which the product is stereochemically almost homogeneous. Models suggest a boat-shaped cyclohexene ring for the ketone **20**, and possibly even for **10**, which avoids a 1,3-diaxial methyl group interaction. Approach from above would thus appear preferred, leading to configuration (and conformation) **22***a* for alcohol **22**. We have been unable to locate any earlier work on the stereochemistry of metal hydride reduction of this kind of system, but it is known that attack on the carbonyl group of 3-substituted cyclopentanones by metal hydrides (13) and Grignard reagents (14) occurs with slight preference from the opposite side of the ring to the substituent. Presumably this tendency will be augmented by the rigidity of the system, and the raising of the "flap" C(1) above the plane of the other four atoms of the cyclopentene ring. After reduction, this C(1) flap will be below the plane of the ring to ease the strain of the new hydroxyl group. This structure **22***a* is



22*a*



16*a*

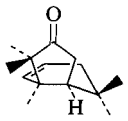
supported by the following spectral evidence. Of the protons at C(1), the ^{1}H nmr spectrum shows for one a signal at 1.49 ppm, and for the other at 2.24. The one at higher field is *cis* to the OH group (because of the much greater shift induced by Eu(fod)$_3$) and is "axial-like", so shifted upfield from what one might normally expect.[5] The protons at C(5) exhibit signals at about 1.96 ppm. They are indistinguishable until Eu(fod)$_3$ is added, when one shifts with $\Delta(\delta) = 0.16$ ppm (arbitrary concentration) at the same time as the other shifts with 0.32 ppm. The former is presumably *trans* to the OH group, and has $J_{5,6} = 6$ Hz, while the other proton at C(5) has $J_{5,6} = 2$ Hz (the geminal coupling, $J_{5,5'}$ is 17 Hz). We must thus place the *cis* C(5) proton nearly at right angles to the vinyl proton at C(6), the other C(5) proton being nearly parallel to C(6)—H. The ^{1}H nmr spectrum of the indenol saturated in the cyclohexane ring **16***a* is so similar to that of **22***a* that the stereochemistry of the cyclopentene ring must be the same. Using the

[5]We have recently reported a similar case of a high upfield shift of a C(4) proton in a cyclopentene (15).

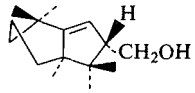
Can. J. Chem. Downloaded from www.nrcresearchpress.com by 210.87.254.6 on 09/05/12
For personal use only.

Can. J. Chem. Downloaded from www.nrcresearchpress.com by 210.87.254.6 on 09/05/12
For personal use only.

$Eu(fod)_3$ shift reagent, it was possible to see that one of the protons at C(7) was responsible for a signal at 1.28 and the other at 1.73 ppm (found by extrapolating back to zero $Eu(fod)_3$ from the methylene group which shifted the most after $C(1)H_2$). Generally, axial protons are at higher field than equatorial protons, and the proton at 1.28 had J = 15, 12, and 4 Hz, consistent with a geminal, a *trans*-diaxial, and an equatorial coupling respectively, while the other proton had J = 15 and about 2 Hz. The axial proton was more strongly shifted by $Eu(fod)_3$ than the equatorial proton ($\Delta(\delta)$ = 0.62 and 0.38), so either the OH group is on the side of the axial proton, or the ring approaches a boat shape. We prefer the latter explanation, as this will relieve the strain of the 1,3-diaxial methyl groups at C(4) and C(7). In **16***a*, $J_{1,2}$ = 6.5 Hz for both the *cis* and *trans* couplings, but in **22***a*, $J_{1\text{-}cis,2}$ = 6 Hz, while $J_{1\text{-}trans,2}$ = 8 Hz, demonstrating again the fact that coupling constants around 5-membered rings are "notoriously uncertain" (16).



27*a*



35*a*

It has been mentioned in the literature without experimental evidence that lithium in liquid ammonia reduction of 7a-methyl-1,4,5,6,7,7a-hexahydro-2*H*-inden-2-one gives 70% of the *cis* ring fused product (17). We ascribe a *cis* ring junction to the product **27***a* of the lithium in liquid ammonia reduction on the unsaturated ketone **23**. Models show this to be the more stable configuration, and some support is provided by the ^{13}C nmr spectra. On comparing the ^{13}C nmr spectrum of the relatively flat **20** and **23** (Table 1), for which there is no ambiguity, with the compounds having a reduced C(3)—C(3a) bond, we find that the signal for C(5) is always lower by about 6 Hz in the latter. These figures can only be accounted for by the presence in the reduced compounds of a nearly axial substituent at C(3a). A consequence of this *cis* configuration for **27***a* is the inaccessibility of the carbonyl group.[6] Metal hydride reduction of this ketone is much less stereoselective than with the others we have mentioned, but there is some preference for approach of the reagent from the *exo* side. Both the ^1H and the ^{13}C nmr spectra of the two alcohols **28** and **29** produced in this reaction lead to the assignment of the *endo* configuration, **29**, to the major product. In this case there is a marked downfield shift of especially C(7)H caused by the proximity of the oxygen atom. In the *exo* alcohol, **28**, the carbinol proton C(2)H is nearly parallel to the C(3a)—C(4) bond, causing a shielding of C(2) in this isomer, and there is also a small γ-effect of the hydroxyl group on C(3a) comparable with the effect in *cis* and *trans* 3-methylcyclopropanol (18).

The single alcohol, **35**, obtained after the Wittig reaction from ketone **23** had a signal (360 MHz ^1H nmr) corresponding to C(2)—H at 2.55 ppm, similar in appearance to the C(2)—H signal of **34**, with coupling constants of 6 and 9 Hz with the two dissimilar protons of the carbinol group; $J_{2,3}$ is very small (about 1 Hz). During the reduction of the conjugated aldehyde **26**, however, the allyl rearrangement that occurs is not stereospecific, and the mixture of **35** and **36** obtained exhibited all the signals of the alcohol **35** obtained by the other route, together with additional ones, notably a signal at 2.21 ppm which, in addition to the couplings of 6 and 9 Hz, had another ($J_{2,3}$) of 2.5 Hz. We assign the compound with the higher field signal for C(2)—H the stereochemistry with C(7a)—methyl and C(2)—H *cis*, the other (major) product being as shown in **35***a*. The lower $J_{2,3}$ coupling constant of the latter reflects the greater deformation of the cyclopentene ring in this case, increasing the dihedral angle between C(2)—H and C(3)—H.

If the deductions about the alcohols **34** and **35** are correct, it follows that the aldehyde **31** must also be *cis*, and probably the ester **33** too.

Experimental

The ^1H and ^{13}C nmr spectra were recorded on a Bruker 90 or a Bruker VH-360 instrument for higher resolution spectra. The 60 MHz ^1H nmr spectra were recorded on a Hitachi-Perkin Elmer R20B instrument. The solvent was always deuterochloroform, and chemical shifts (δ) were measured downfield from tetramethylsilane. Singlets, doublets, etc. are identified by their initial letters; $w_{\frac{1}{2}}$ = width in Hz of signal at half height. Mass spectra (ms) were measured on an Atlas CH 4 mass spectrometer using an inlet temperature of about 150°C, or on a MAT 110 instrument coupled with a capillary column gas chromatograph, both spectrometers using electrons of 70 eV. Results are quoted in *m/e* (% most important fragment) and generally the ten most important fragments are given. The uv spectra were measured on a Unicam SP 700A spectrometer in ethanol, with λ_{max} (ε) in nm. Infrared spectra were obtained on a Perkin Elmer type 125 spectrophotometer. Gas chromatography (gc) was carried out on a Carlo-Erba type GT chromatograph with He as carrier gas.

All compounds are characterized by nmr and ms; elemental analyses were also carried out when it was felt they could contribute useful information.

[6]It should be noted that another conformation besides **27***a* (or a more skewed version of **27***a*) is possible for this compound having the "flap" of the cyclohexene ring that carries the *gem*-dimethyl group (C(4)) upwards, but this would give severe strain between one of the methyl groups at C(1) and the axial methyl group at C(4); furthermore, it is difficult to account for the ^{13}C nmr spectra with this model.

TABLE 1. ^{13}C nuclear magnetic resonance spectra of hydrogenated indenes

	C(1)	C(2)	C(3)	C(3a)	C(4)	C(5)	C(6)	C(7)	C(7a)	Methyl groups					$CH_2(OH)$
20	53.8	206.5	132.9	192.6	35.4	42.3	123.9	125.1	45.4	27.1	28.9	29.1			
23	55.4	213.1	122.1	190.2	35.3	40.9	125.0	129.7	51.9	17.5	27.2	27.6	27.8	29.1	
22	53.8	75.8	124.6	159.3	33.3	41.8	122.5	135.2	47.5	26.8	27.0	28.8			
16	55.1	75.3	124.6	160.3	33.9	41.2*	19.4	41.8*	46.3	27.0	27.6	31.2			
27	53.4	221.4	38.5	47.3	31.6	34.5	124.7	130.8	45.1	17.2	21.6	21.8	29.7	30.5	
28	45.9*	78.5	34.0*	49.7	32.2	33.7*	124.4	132.9	46.9*	16.3	20.8	22.0	29.2	30.1	
29	46.0	81.1	33.9	51.7	31.9	36.8	125.1	135.3	49.4	17.9	22.3	23.9	29.0	29.9	
34	48.5	54.1	119.3	157.0	33.5	41.1	124.3	131.8	52.9	19.9	20.1	20.3	27.8	28.9	62.6
35	47.2	54.1	119.3	157.3	33.6	40.6	19.2	31.0	51.1	20.1	20.9	22.4	29.8	31.5	63.1
39	45.8†	51.1	30.5	48.8	32.3	33.8	125.0	132.7	45.8	18.1	21.1	22.2	29.5	30.2	65.3

*Alternative assignments.
†Doubtful assignment because signal is coincident with C(7a).

Dry, powdered potassium hydroxide is supplied by SUGRO, Basle, Switzerland, and the suspension of sodium amide in toluene is a product of DEGUSSA, Germany.

*1,3,3a,7,7-Pentamethyl-3a,6,7,7a-tetrahydro-1*H*-inden-1-ol, 5*

Into a suspension of cuprous iodide (4.3 g) in dry ether (80 mL) at −10°C was introduced a solution of methyllithium (prepared from 0.7 g Li and 7.1 g methyl iodide). The mixture was cooled to −60°C and 3,3a,7,7-tetramethyl-3a,6,7,7a-tetrahydro-1*H*-inden-1-one (**3**, 0.9 g) in absolute ether (5 mL) was added. After 5 h at 0°C, 55% of the starting material was unchanged (workup by quenching in NH_4Cl solution and ether extraction). The products were purified by gc (SP 1000 column), when the alcohol **5** was separated from the hydrocarbons **6** and **7**. Spectra of the title alcohol, **5**: ^1H nmr (60 MHz) δ: 1.05, 1.18, 1.28, 1.42, 1.69 (each s, CH_3); 5.17 (1H, $w_{\frac{1}{2}}$ = 4 Hz); 5.60 (2H, s + narrow d); ms: 173 (100), 188 ($M-18^{+\cdot}$, 55), 131 (31), 145 (22), 91 and 43 (16), 174, 158, and 41 (12), 132 (11), 191 ($M-15^{+}$, 6).

*3,3a,7,7-Tetramethyl-1-methylene-3a,6,7,7a-tetrahydro-1*H*-indene, 6*

^1H nmr (60 MHz) δ: 0.60 (s), 1.01 (6H, s), 1.75 (3H, d, J = 2 Hz, CH_3), 4.71 (1H) and 4.89 (1H) (each s, C=CH_2), 5.65 and 5.69 (each apparent s, 3H in all); ms: 173 (100), 131 (37), 188 ($M^{+\cdot}$, 26), 174, 145, and 91 (13), 158 and 132 (11).

*3,4,4,7a-Tetramethyl-1-methylene-3a,4,5,7a-tetrahydro-1*H*-indene, 7*

^1H nmr (60 MHz) δ: 0.62 (s), 1.08 (6H, s), 1.92 (3H, broad s) (CH_3); 4.50 and 4.68 (each s, C=CH_2), 5.50–6.0 (3H, m); ms: 173 (100), 188 ($M^{+\cdot}$, 61), 145 (56), 131 (54), 132 (35), 91 (27), 119 (22), 117 (21), 105 (19). This compound (**7**) has a slightly longer retention time on an SP 1000 column than **6**. The distinction between them is based on the shielding of the =CH_2 group by the adjacent methyl group in **7**, and the fact that this methyl group should be lost more easily in the ms of **6** (i.e. *m/e* 173 is a larger proportion of the total ionization in **6** than in **7**).

*3,3a,7,7-Tetramethyl-2,3,3a,6,7,7a-hexahydro-1*H*-inden-1-one, 8.*

3,a,7,7-Tetramethyl-3a,6,7,7a-tetrahydro-1*H*-inden-1-one, **3** (1.9 g, 0.5 equiv.) was added to a Grignard reagent prepared from magnesium (0.48 g) and methyl iodide (2.9 g) in ether. After 12 h at room temperature, the mixture was decomposed with saturated aqueous NH_4Cl solution. The product was extracted in ether and purified by chromatography on silica gel. There were isolated ca. 10% of the hydrocarbons **6** and **7** (but no alcohol **5**, which probably decomposed during chromatography), unchanged starting material (ca. 60%), and the title product. This was purified by gc on SP 1000; ^1H nmr (60 MHz) δ: 1.00 (9H, narrow m), 1.12 (3H, s) (CH_3), 5.67 (s) superimposed on a d (2H); ms: 107 (100), 192 ($M^{+\cdot}$, 43), 122 (42), 177 (19), 91 (15), 41 (14), 83 (13), 123 (11).

*3,3a,7,7-Tetramethyl-3a,4,5,6,7,7a-hexahydro-1*H*-inden-1-one, 9*

A solution of 3,3a,7,7-tetramethyl-3a,6,7,7a-tetrahydro-1*H*-inden-1-one, **3** (1.9 g) in ethanol (190 mL) was shaken in H_2 over a Pd–C (10% Pd) catalyst. The theoretical amount of H_2 was absorbed in 1 h. The mixture was filtered and from the residue, after concentration of the solvent, only the compound with the longest retention time (gc on SP 1000) was isolated from the complex mixture; ^1H nmr (60 MHz) δ: 0.90 (3H, s), 1.18 (6H, s), 1.99 (3H, d, J = 1.5 Hz, CH_3), 5.75 (1H, q, J = 1.5 Hz); ms: 110 (100), 123 (61), 177 (56), 192 ($M^{+\cdot}$, 24), 109 (21), 121 (20), 41 (19), 95 (16), 55 (13), 82 and 111 (11).

2,6,6-Trimethyl-2-(prop-1-ynyl)-cyclohexanone, 11

A suspension of sodium hydride (55% in oil, 33 g) was washed once with hexane, then dimethylformamide (1000 mL) was added. With efficient stirring, 2,2,6-trimethylcyclohexanone[7] (100 g) was added, and the mixture heated at 45–55°C for ca. 20 h, then cooled to 20°C. 2,3-Dichloropropene (95 g) was added over 45 min, during which the temperature rose to 30°C where it was maintained for a further 4.5 h. The mixture was then continuously extracted with pentane, and the pentane solution washed (water, 10% HCl, water, $NaHCO_3$, water), dried, and distilled. After 2,2,6-trimethylcyclohexanone (35 g, bp 40°C/10 Torr), the title product distilled (15 g, bp 100°C/10 Torr). For analysis, 2 g of this fraction was chromatographed on silica gel in hexane–ether (9:1), when 1.5 g was recovered (98% pure by gc on Apiezon). After gc, the substance had the following spectra: ^1H nmr (60 MHz) δ: 1.01, 1.22, 1.35, 1.73 (CH_3); ms: 80 (100), 79 (91), 135 (79), 107 (76), 91 (69), 93 (67), 106 (58), 41 (54), 39 (35)...178 ($M^{+\cdot}$, 8.5). *Anal.* calcd. for $C_{12}H_{18}O$: C 80.85, H 10.18; found: C 81.10, H 10.00. The remaining 2% of this fraction, collected from the Apiezon column just after **11**, was *2,6,6,-trimethyl-2-(propa-1,2-dienyl)-cyclohexanone*, **12**. ^1H nmr (60 MHz) δ: 1.04 (3H), 1.12 (6H, s, CH_3), 4.80 (2H, d, J = 6–7 Hz), 5.20 (1H, d of d, J = 6 and 7 Hz, presumably negative (19)); ms: 122 (100), 109 (80), 108 (61), 121 (40), 79 (36), 41 and 43 (35), 178 ($M^{+\cdot}$, 32), 135 (27), 91 and 107 (26). A much heavier fraction, bp 120–125°C/0.001 Torr, was obtained at the end of the distillation. It was never completely pure but appeared to be mainly 2-(1-(1-hydroxy-2,6,6-trimethylcyclohexyl)-prop-1-yn-3-yl)-2,6,6-trimethylcyclohexanone, **14**. Infrared: 1690, 3550 cm^{-1} (C=O and OH); ^1H nmr (90 MHz)

[7]Prepared by catalytic reduction of 2,6,6-trimethylcyclohex-2-enone (8).

Can. J. Chem. Downloaded from www.nrcresearchpress.com by 210.87.254.6 on 09/05/12
For personal use only.

On p. 1816, the preparation by method A of 2,6,6-trimethyl-2-(prop-2-ynyl)-cyclohexanone, 13, is incorrect. Method B is correct, and leads to 13, which has the spectral properties and microanalysis ascribed to it under method A.

δ: 0.95–1.25 (ca. 18H, m), 2.43 and 2.52 (ca. 2H, each s), no vinyl signals; ms: 82 (100), 55 (98), 69 (97), 41 (90), 42 (75), 83 (63), 57 (56), 75, 95, and 109 (42)...179 (33)...318 ($M^{+\cdot}$, 5). *Anal.* calcd. for $C_{21}H_{34}O_2$: C 79.19, H 10.76; found: C 80.51, H 11.03.

2,6,6-Trimethyl-2-(2-chloroprop-2-enyl)-cyclohex-3-enone, 21

2,6,6-Trimethylcyclohex-2-enone (138 g) and sodium amide (70% in toluene, 55 mL) were heated in toluene (1300 mL) at 85°C for 3.5 h, then for 2 h at reflux. The mixture was cooled to 10°C, and 2,3-dichloroprop-1-ene (114 g) added. After 17 h, the mixture was poured onto ice and extracted with pentane. Distillation of the products after concentration gave a fraction (16%) with bp 50–52°C/0.1 Torr which was practically pure **21**; ^{1}H nmr (60 MHz) δ: 1.12 (3H), 1.28, (6H, CH_3), 2.30 (d, J = 13 Hz, superimposed on another signal), 3.10 (1H, d, J = 13 Hz), 5.08 and 5.20 (each 1H, s), 5.72 (s, superimposed on d, 2H in all); ms: 70 and 109 (100), 93 and 107 (75), 41 (61), 177 (60), 137 (52), 68 (46), 91 (44)...212/214 ($M^{+\cdot}$, 4.5). *Anal.* calcd. for $C_{12}H_{17}ClO$: C 67.75, H 8.05; found: C 67.89, H 8.06. *2,6,6-Trimethyl-2-(prop-1-ynyl)-cyclohex-3-enone* was made either as for compound **11**, or by treatment of the chloro-compound **21** with sodium amide in dimethylformamide at 80°C for 6 h. The product had bp 40–45°C/0.1 Torr; ^{1}H nmr (60 MHz) δ: 1.10, 1.31, 1.35, 1.75 (s, CH_3), 2.30 (2H, apparent d, 2 Hz between signals), 5.71 (2H, s); ms: 91 (100), 133 (55), 106 (53), 105 (49), 41 (27), 39 (22), 70 (14), 77 (13), 161 (12)...176 ($M^{+\cdot}$, 2).

2,6,6-Trimethyl-2-(2-chloroprop-2-enyl)-cyclohex-3-enol

The ketone **21** was reduced with excess lithium aluminum hydride in dry ether. The excess reagent was decomposed with water, the mixture was filtered and concentrated, and the product was not purified further; ^{1}H nmr (60 MHz) δ: 0.96, 1.00, 1.01, 1.08, 1.20 (9H in all, CH_3), 1.91 (2H, d, J = 2.5 Hz), 2.46 and 2.66 (each 1H), 3.40 and 3.62 (1H together, broad s, carbinol H, ratio 6:4 corresponding to two isomers), 5.15 and 5.29 (each 1H, s), 5.53–5.55 (2H); ms: 43 (100), 139 (41), 95 (35), 41 (34), 81, 72, and 55 (21), 57 (19), 39, 59, and 121 (18), 178 (M − $HCl^{+\cdot}$, trace).

2,6,6-Trimethyl-2-(prop-2-ynyl)-cyclohexanone, 13

Method A ERRATA

2,2,6-Trimethylcyclohexanone (7 g) was added during 15 min to a suspension of sodium amide (70% in toluene, 3.2 mL) in toluene (70 mL). The mixture was heated 1.25 h at reflux, then cooled at 20°C while 2,3-dichloropropene (7.8 g) was added over 15 min, maintaining the temperature at 18–20°C. The mixture was kept overnight at 20°C, washed with water, dried, and concentrated. Distillation yielded 3.9 g of **13**, bp 95°C/10 Torr (60%, taking account of 1.8 g of starting material recovered in the top fraction). For analysis, it was purified by gc on OV 17; ^{1}H nmr (60 MHz) δ: 1.10, 1.15, 1.20 (each 3H, s, CH_3), 2.40 (2H, t, J = 2 Hz); ms: 82 (100), 55 (85), 41 (74), 79 (70), 107 (58), 69 and 72 (55), 39 (30), 93 (29)...178 ($M^{+\cdot}$, 24). *Anal.* calcd. for $C_{12}H_{18}O$: C 80.85, H 10.18; found: C 80.80, H 10.27.

Method B

The 2,2,6-trimethylcyclohexanone enolate was prepared as in method A. Propargyl chloride (7.8 g) was added at 20°C. After 18 h stirring at this temperature, the mixture was washed with water, dried, and concentrated. Distillation of the residue yielded 3.8 g of **13**. Use of propargyl bromide gave only 23% yield of **13**.

2,6,6-Trimethyl-2-(prop-2-ynyl)-cyclohex-3-enone was made in the same way as that described for **13** (previous experiment), but starting from 2,6,6-trimethylcyclohex-2-enone (8). It was obtained in 57% yield, bp 47–58°C/0.1 Torr, sufficiently pure for subsequent experiments. For analysis it was purified by gc on OV 17; ^{1}H nmr (60 MHz) δ: 1.12, 1.28, 1.30 (each 3H, s, CH_3), 1.92 (1H, t, J = 3 Hz), 2.20–2.55 (4H, m), 5.6–6.0 with sharp s at 5.83 (2H); ms: 91 (100), 70 (80), 109 (70), 105 (69), 41 and 106 (45), 39, 67, and 92 (33), 161 (31)...176 ($M^{+\cdot}$, 2).

FOR ERRATA SEE at the top of this page, V59 #3 1981 p. 590

2,6,6-Trimethyl-2-(2-oxopropyl)-cyclohexanone, 15

2,6,6-Trimethyl-2-(prop-1-ynyl)-cyclohexanone (10 g) and Hg-impregnated Dowex 50 resin (20) in water (4 mL) and methanol (10 mL) were stirred for 1.3 h. The temperature rose to 32°C, and when it fell again, the mixture was filtered, concentrated, and distilled, bp 50°C/0.001 Torr, to yield 8.1 g (80%) of **15**; ^{1}H nmr (60 MHz) δ: 1.08 (6H, s), 1.14, 2.02 (each 3H, s, CH_3); AB system with A 2.27, B 3.25, $J_{A,B}$ = 18 Hz; ms: 43 (100), 114 (66), 69 (34), 41 (24), 95 (18), 55 (17), 82 (16), 81 (12), 139 (11)...196 ($M^{+\cdot}$, 2.4). *Anal.* calcd. for $C_{12}H_{20}O_2$: C 73.43, H 10.27; found: C 73.54, H 10.40.

2,6,6-Trimethyl-2-(2-oxopropyl)-cyclohex-3-enone was made in the same way from either 2,6,6-trimethyl-2-(prop-1-ynyl)-cyclohex-3-enone or 2,6,6-trimethyl-2-(prop-2-ynyl)-cyclohex-3-enone. The crude product could be distilled, bp 66°C/10 Torr, but generally it was cyclized directly; ^{1}H nmr (60 MHz) δ: 1.15 (6H, s), 1.20, 2.02 (each 3H, s, CH_3), ABX system with A 2.08, B 2.73, X 5.80, $J_{A,B}$ = 17, $J_{A,X}$ = 6, $J_{B,X}$ = 2 Hz; AB system with A 2.53, B 3.28, $J_{A,B}$ = 17 Hz. The vinyl proton (X) of the ABX system is coupled to another vinyl proton at 5.41 (J = 10 Hz); ms: 43 (100), 70 (29), 81 (27), 123 (25), 109 (23), 124 (15), 41 (14), 82 (13), 95 (12)...194 ($M^{+\cdot}$, 7.2).

4,4,7a-Trimethyl-1,4,5,6,7,7a-hexahydro-2H-inden-2-one, 10

A suspension of dry powdered potassium hydroxide (0.5 g) in xylene (40 mL) was heated at reflux with a water separator while 2-(2-oxopropyl)-2,6,6-trimethylcyclohexanone (4 g) was added. After a few minutes, water began to separate, and when this was finished (ca. 1 h), the xylene was washed (water) and concentrated. The residue was distilled, bp 40–45°C/0.01 Torr, to yield 3.5 g (96%) of **10**. Infrared: 1600, 1700 cm^{-1}; ^{1}H nmr (60 MHz) δ: 1.16, 1.21, 1.31 (each 3H, s, CH_3), 2.26 (2H, s), 5.80 (1H, s); ms: 136 (100), 121 (61), 108 (59), 178 ($M^{+\cdot}$, 56), 135 (54), 107 (51), 109 and 122 (44), 163 (43), 41 (41). *Anal.* calcd. for $C_{12}H_{18}O$: C 80.85, H 10.18; found: C 81.01, H 10.15.

4,4,7a-Trimethyl-1,4,5,7a-tetrahydro-2H-inden-2-one, 20 was prepared similarly to **10** from 2-(2-oxopropyl)-2,6,6-trimethylcyclohex-3-enone (72 g) and anhydrous potassium hydroxide (1.1 g, then after 45 min, a further 0.5 g) in xylene (800 mL). After distillation, bp 65–70°C/0.01 Torr, 59.8 g (91%) of **20** was obtained which crystallized on cooling, mp 43–44.5°C; uv λ_{max}: 234 (ε_{max} 14 370); ^{1}H nmr (60 MHz) δ: 1.25, 1.31, 1.39 (CH_3), 2.15 (2H, d, J = 2.5 Hz), 2.38 (2H, s), 5.68 (t, J = 2.5 Hz) and 5.70 (2H together), 5.85 (1 H, s); ms: 133 (100), 161 (99), 176 ($M^{+\cdot}$, 91), 105 (53), 91 (46), 41 (39), 119 and 134 (33), 67 (31), 39 (28). *Anal.* calcd. for $C_{12}H_{16}O$: C 81.77, H 9.15; found: C 81.71, H 9.17.

4,4,7a-Trimethyl-1-methylene-1,2,4,5-tetrahydroinden-2-one, compound *a* in footnote 2. A solution of lithium amide in liquid ammonia (made from 6 g Li in 400 mL ammonia containing 0.3 g of ferric nitrate) was stirred while 4,4,7a-trimethyl-1,4,5,7a-tetrahydro-2*H*-inden-2-one (**20**, 143 g) in dry ether (300 mL) was added. The ammonia was allowed to evaporate overnight, and dry ether (100 mL) was added, then formaldehyde (25 g, made by heating paraformaldehyde, dried over P_2O_5, to 150°C) was passed into the solution in a current of dry nitrogen. The addition lasted 3 h, and the mixture was allowed to stand overnight before pouring onto ice and 10% hydrochloric acid. The products were extracted into pentane, and the organic layers were washed ($NaHCO_3$, water), dried, and concentrated. A sample (1 g) was distilled in a bulb apparatus, bp ≃ 100°C (oven temperature)/0.01 Torr, and gc then indicated ca. 70% unchanged starting material together with ca. 10% of a new substance of longer retention time, which was collected as the

Can. J. Chem. Downloaded from www.nrcresearchpress.com by 210.87.254.6 on 09/05/12
For personal use only.

Can. J. Chem. Downloaded from www.nrcresearchpress.com by 210.87.254.6 on 09/05/12
For personal use only.

product. Larger scale distillation resulted in polymerization; uv λ_{max}: 252 (ε_{max} 3 130); ^{1}H nmr (60 MHz) δ: 1.29, 1.35, 1.46 (CH_3), 2.15 (2H, broad s, C(5)H_2), 5.28 (1H, s), 5.8 (2H, m), 5.93 and 6.11 (each 1H, s); ms: 173 (100), 145 (60), 188 ($M^{+\cdot}$, 55), 130 and 105 (20), 91 (16), 115 and 77 (13), 117 (12). *Anal.* calcd. for $C_{13}H_{16}O$: C 82.93, H 8.56; found: C 83.13, H 8.52.

*1,1,4,4,7a-Pentamethyl-1,4,5,7a-tetrahydro-2*H*-inden-2-one, 23*

A suspension of sodium amide (12 mL, 70% in toluene) in toluene (700 mL) was stirred at reflux while 4,4,7a-trimethyl-1,4,5,7a-tetra hydro-2*H*-inden-2-one (**20**, 35 g) was added dropwise during 0.5 h. After a further 1.5 h at reflux, the mixture was cooled to 12°C and methyl iodide (25 mL) was added rapidly. The temperature rose to 26°C. After stirring for 2 h, the mixture was poured onto ice and the organic layer was washed, dried, and concentrated, yielding 42.4 g of material which appeared (gc) to be nearly homogeneous. The nmr spectrum indicated the presence of 4 CH_3 groups, one of which had δ 0.95 (d, J = 7 Hz) corresponding to a single C(1)—CH_3 group. The whole of this material was then treated again as before (with sodium amide and methyl iodide), and after concentration of the toluene, the residue was distilled to yield 38.4 g (86%) of practically pure **23**, bp 62–65°C/0.001 Torr. For analysis this was purified by gc on SP 1000; ^{1}H nmr (60 MHz) δ: 0.90, 1.05, 1.20, 1.25, 1.31 (CH_3), 2.11 (2H, d, J = 3 Hz, C(5)H_2), 5.61 (1H, s), 5.20 (1H, t, J = 3 Hz), 5.80 (1H, s); ms: 189 (100), 204 ($M^{+\cdot}$, 39), 190 (15), 41 (13), 119 (12), 161 (10). *Anal.* calcd. for $C_{14}H_{20}O$: C 82.30, H 9.87; found: C 81.91, H 9.86.

*1,1,4,4,7a-Pentamethyl-1,4,5,6,7,7a-hexahydro-2*H*-inden-2-one, 19*

A. The foregoing experiment (for **23**) was carried out with ketone **10** (1.5 g), repeating the process as described. The residue was distilled, bp 58–60°C/0.1 Torr, to yield 0.3 g of material containing a number of products. The main one was isolated by gc on silicone oil, and proved to be the title product, mp. 36–36.2°C; uv λ_{max}: 237 (ε_{max} 12 300); ^{1}H nmr (90 MHz) δ: 1.02 (6H), 1.22 (6H), 1.28 (3H, CH_3), 5.82 (1H, s); ms: 191 (100), 137 (64), 136 (60), 206 ($M^{+\cdot}$, 45), 41 (38), 163 (34), 123 (33), 121 and 69 (28), 43 and 149 (24). *Anal.* calcd. for $C_{14}H_{22}O$: C 81.50, H 10.75; found: C 81.72, H 10.70.

Immediately preceding this compound in the gc (silicone oil) was a peak with spectra consistent with *1,4,4,7a-tetramethyl-1,4,5,6,7,7a-hexahydro-2*H*-inden-2-one*: ^{1}H nmr (90 MHz) δ: 1.05 (3H, d, J = 7 Hz), 1.15, 1.21, 1.27 (CH_3), 5.88 (1H, s); ms: 122 (100), 177 (90), 136 (89), 192 ($M^{+\cdot}$, 80), 41 (78), 173 (72), 149 (66), 121 (64), 69 (58), 107 (53). Other by-products were not fully characterized, but often exhibited a signal in the ^{1}H nmr spectrum at δ ≈ 3.8 (OCH_3).

B. The ketone **23** was hydrogenated in ethanol over a palladium on charcoal catalyst (10% Pd). There was quantitative absorption of 1 equivalent of H_2 to give the title compound, **19**, identical with the material described above.

1,1,4,4,7a-Pentamethyl-cis-*1,3,3a,4,5,7a-hexahydro-2*H*-inden-2-one, 27*

Small pieces of lithium (containing 1% of sodium, 4.2 g in all) were dissolved in ammonia (1000 mL). During 40 min, solution of 1,1,4,4,7a-pentamethyl-1,4,5,7a-tetrahydro-2*H*-inden-2-one (**23**, 28 g, 0.14 mol) in *tert*-butanol (12.6 g, 0.17 mol) and dry ether (250 mL) was added. After further stirring for 10 min, solid ammonium chloride (30 g) was added over 10 min, then the ammonia was allowed to evaporate while ether (250 mL) was added. The resulting ethereal solution was poured into water, washed, and concentrated. Distillation of the residue yielded 39.7 g (98%) of practically pure title product; ir: 1735 cm^{-1}; ^{1}H nmr (60 MHz) δ: 0.94, 0.97 (each s, 9H altogether), 1.20, 1.28 (CH_3), 5.52 (2H, s); ms: 121 (100), 206 ($M^{+\cdot}$, 15), 105 (14), 41 and 122 (10).

This compound was recovered unchanged from the following reactions: CH_3MgI in ether, CH_3Li in ether, $(C_6H_5)_3P{=}CHOCH_3$ in toluene or tetrahydrofuran, $(C_6H_5)_3P{=}CH_2$ in toluene or tetrahydrofuran, prepared using either sodium hydride or butyllithium.

Lithium aluminum hydride reductions of 2H*-inden-2-ones* were carried out by adding the ketone (1 g) dropwise to a suspension of lithium aluminum hydride (0.2 g) in dry ether (50 mL). Excess reagent was decomposed by addition of water, and the solution was filtered and concentrated. Acetates were made by acetylation of the crude alcohol in pyridine with acetic anhydride. The following were thus obtained.

*4,4,7a-Trimethyl-1,4,5,6,7,7a-hexahydro-2*H*-inden-2-*cis*-ol, 16*

Spectra were measured on the crude material which decomposed on gc; ^{1}H nmr (360 MHz) δ: 1.05, 1.12, 1.17 (CH_3), ABX system with A 1.45, B 2.24, X 4.89, $J_{A,B}$ = 12, $J_{A,X}$ = 8, $J_{B,X}$ = 6.5 Hz; X is also coupled with C(3)H at 5.35 (J = 1.5 Hz). A weak signal at 5.50 (d, J = 2 Hz, C(3)H) was consistent with the presence of < 10% of the *trans* alcohol; ms: 147 (100), 97 (78), 123 (56), 107 (49), 109 (48), 41 (43), 96 (39), 91 (38), 43 and 119 (37)...180 ($M^{+\cdot}$, 12).

The *acetate* was purified by distillation, bp 58–59°C/0.01 Torr; ^{1}H nmr (60 MHz) δ: 1.09, 1.10, 1.20, 2.03 (CH_3), 2.30 (1H, d of d, J = 6.5 and 12 Hz), 5.38 (1H, d, J = 1.5 Hz), 5.73 (1H, t, J = 6.5 + ca. 1.5 Hz); ms: 147 (100), 43 and 119 (35), 91 (28), 105 (26), 93 (23), 162 (22), 41 (21), 107 and 123 (14)...222 ($M^{+\cdot}$, 2).

*4,4,7a-Trimethyl-1,4,5,7a-tetrahydro-2*H*-inden-2-*cis*-ol, 22*

The crude material was distilled, bp 57–60°C/0.001 Torr, and was then practically pure (thin-layer chromatography) but decomposed on gc; ^{1}H nmr (360 MHz) δ: 1.12, 1.17, 1.20 (CH_3), ABX system with A 1.49, B 2.24, X 4.97, $J_{A,B}$ = 12.5, $J_{A,X}$ = 8, $J_{B,X}$ = 6 Hz, 1.96 (2H, m, see theoretical part), 5.38 (1H, s, C(3)H), 5.47 (1H, d of q, J = 10, 6, and 2.5 Hz, C(6)H), 5.59 (1H, d + further coupling, J = 10 Hz, C(7)H); ms: 145 (100), 163 (97), 121 (63), 105 (50), 122 (46), 41 and 43 (41), 91 (37), 107 (35)...178 ($M^{+\cdot}$, 25). A very weak signal was just visible at δ 5.73 (d, J = 10 Hz) consistent with C(7)H of the *trans* alcohol.

The *acetate* distilled at bp 41°C/0.001 Torr and decomposed on gc; ^{1}H nmr (60 MHz) δ: 1.11, 1.15, 1.22, 2.01 (CH_3), 5.38 (1H, broad s), 5.52 (t, J = 3 Hz) overlapping 5.55 (s, together 2H), 5.80 (1H, t, J = 7 Hz); ms: 145 (100), 43 (23), 105 and 160 (16), 130 and 146 (13), 91 (10)...205 (2.5), 220 ($M^{+\cdot}$, 0.5).

*1,1,4,4,7a-Pentamethyl-2,3,3a,4,5,7a-hexahydro-1*H*-inden-2-ols, 28 and 29*

The crude material from the $LiAlH_4$ reduction exhibited two peaks (gc on Carbowax). Separated by preparative gc, the alcohol with the shorter retention time (55% of the mixture) was the *endo* alcohol **29**, and was liquid at 20°C: ^{1}H nmr (360 MHz) δ: 0.79, 0.93, 0.98, 0.99, 1.02 (CH_3), 1.48 (1H, d of d, J = 7 and 16 Hz, C(3)—*exo*-H), 2.32 (1H, d of d of d, J = 7, 11, and 16 Hz, C(3)—*endo*-H), ABX system with A 1.65, B 2.01, X 5.66, $J_{A,B}$ = 17, $J_{A,X}$ = 6, $J_{B,X}$ = 2 Hz, C(5)CH_2—C(6)H, 1.75 (1H, m, J = 1, 7, and 11 Hz, C(3a)H, 3.50 (1H, d of d, J = 7 and 11 Hz, C(2)H), 5.76 (1H, d of d, J = 1 and 10 Hz, C(7)H); ms: 107 (100), 122 (56), 121 (42), 41 (24), 43, 69, 93 and 105 (15), 91 and 175 (13)...190 (9), ...208 ($M^{+\cdot}$, trace).

The endo-*acetate* was distilled (bulb, bp ≈ 60°C/0.001 Torr); ^{1}H nmr (60 MHz) δ: 0.85, 0.88 (2), 0.99, 1.00, 1.95 (CH_3), 4.71 (1H, d of d, J = 4 and 6.5 Hz), 5.51 (2H, d, J = 2 Hz); ms: 107 (100), 122 (96), 43 (39), 121 (31), 119 (23), 175 and 41 (22), 105 (20), 69 (18)...250 ($M^{+\cdot}$, 4.5).

The alcohol with the longer retention time (45% of the mix-

Can. J. Chem. Downloaded from www.nrcresearchpress.com by 210.87.254.6 on 09/05/12
For personal use only.

ture) was the *exo* alcohol, **28**, and crystallized, mp 77–78°C; ^{1}H nmr (360 MHz) δ: 0.80, 0.86, 0.91, 0.96, 1.01 (CH_3), 1.49 (d of d of d, J = 9, 12, and 13 Hz, C(3)—*endo*-H), 1.86 (d of d of d, J = 5, 9, and 13 Hz, C(3)—*exo*-H), 1.77 (d of d, J = 5 and 12 Hz, C(3a)H, ABX system with A 1.53, B 1.95, X 5.55, $J_{A,B}$ = 17, $J_{A,X}$ = 2, $J_{B,X}$ = 6 Hz, C(5)H_2—C(6)H, 5.44 (d of d, J = 2 and 10 Hz, C(7)H); ms: 107 (100), 122 (54), 121 (43), 41 (29), 43 and 69 (19), 91, 93, and 105 (17), 123 and 128 ($M^{+\cdot}$, 14)...190 (3).

The exo-*acetate* was distilled (bulb, bp ≃ 60°C/0.001 Torr); ^{1}H nmr (60 MHz) δ: 0.83, 0.86, 0.89, 0.98, 1.03, 2.01 (CH_3), 4.70 (1H, m, C(2)H), 5.52 (2H, broad s + m); ms: 122 (100), 107 (99), 43 (40), 121 (28), 41 (25), 119 and 69 (20), 123 (16), 134 (15), 175 and 105 (13)...250 ($M^{+\cdot}$, 4.3).

*3a,7,7-Trimethyl-4,5,6,7-tetrahydro-3a-*H*-indene,* ***18***

Either 4,4,7a-trimethyl-1,4,5,6,7,7a-hexahydro-2*H*-inden-*cis*-2-ol, **16**, or its acetate, **17**, was injected into a gas chromatograph and the single product collected; uv λ_{max}: 256 (ε_{max} 10 500); ^{1}H nmr (60 MHz) δ: 1.08 (6H, s), 1.21 (3H, s, CH_3), 5.90 (1H, t, J = 1 Hz), 6.22 (2H, apparent d, J = 1 Hz); ms: 147 (100), 119 (37), 91 (27), 162 ($M^{+\cdot}$) and 105 (25), 93 (20), 41 and 148 (11), 77 and 133 (10).

*1,1,4,4,7a-Pentamethyl-2-methylene-1,4,5,6,7,7a-hexahydro-*2H*-indene,* ***24*** *(R = H)*

A solution of methyltriphenylphosphonium bromide (1 g) in absolute tetrahydrofuran (10 mL) was treated with butyllithium (1.1 equiv.) in hexane. When solution was complete, the pentamethylindenone (**19**, 0.1 g) was added at 0°C. The mixture was refluxed for 1 h, then poured into water, and the product was isolated in pentane. For analysis it was purified by gc on silicone oil; ^{1}H nmr (90 MHz) δ: 0.97, 1.03, 1.04, 1.16, 1.18 (CH_3), 4.58, 4.77, 5.88 (each 1H, s); ms: 189 (100), 133 (65), 119 (63), 204 ($M^{+\cdot}$, 55), 147 (42), 134 (42), 135 (41), 41 (39).

Attempted Coates Reaction of ***27****: 1,1,4,4,7a-Pentamethyl-3a,4,5,7a-tetrahydro-1*H*-inden-2-yl Benzoate,* ***11***

To a solution of thioanisole (2.8 g) and 1,4-diazabicyclo[2.2.2]octane (2.5 g) in dry tetrahydrofuran (30 mL) at 0°C was added butyllithium (1 equivalent) in hexane during 12 min. The precipitate said to occur here was not observed. A solution of the ketone **27** (4 g) in dry tetrahydrofuran (10 mL) was added at 0°C, the temperature was allowed to rise to 30°C, and the mixture allowed to stand overnight at room temperature. It was then cooled to 0°C and benzoic anhydride (9.9 g) in tetrahydrofuran (20 mL) was added. After standing for 3 h at room temperature, the mixture was stirred with 100 mL of pentane and filtered, the filtrate being directly chromatographed on silica gel in hexane. From the first fractions about 2.3 g of thiosanisole was recovered, then 4.5 g of a mixture which, after rechromatography on silica gel, gave 4 g of material which was distilled (bp ca. 180°C, (oven temperature)/0.001 Torr) and consisted of nearly pure title product. ^{1}H nmr (60 MHz) δ: 1.05, 1.10 (15H, CH_3), 5.50 (2H, broad s), 5.75 (1H, d, J ≃ 1 Hz), 7.2–7.6 (3H, m), 7.95–8.2 (2H, m); ms: 105 (100), 123 (47), 77 (42), 41 (24), 56 (22), 55 (14), 43, 51, and 122 (13)...205 and 220 (1).....234 (trace), 310 ($M^{+\cdot}$, 0). *Anal.* calcd. for $C_{21}H_{26}O_2$: C 81.25, H 8.44; found: C 80.98, H 8.17.

*2(Z)-Methoxymethylene-1,1,4,4,7a-pentamethyl-1,4,5,7a-tetrahydro-2*H*-indene,* ***30***

Butyllithium (8% in hexane, 15 mL) was added to methoxymethyltriphenylphosphonium chloride (7 g) in dry tetrahydrofuran (50 mL) at 0°C. After 30 min, 1,1,4,4,7a-pentamethyl-1,4,5,7a-tetrahydro-2*H*-inden-2-one (**23**, 2 g) was added at −80°C over 10 min. The temperature was allowed to rise to 25°C, then stirring was continued overnight. The mixture was poured into water, and the product isolated in ether. The residue after concentration was chromatographed in hexane over a small column of silica gel (25 g). Concentration of the eluate yielded a single substance (gc on SP 1000) which was purified for analysis by preparative gc; ^{1}H nmr (60 MHz) δ: 0.87, 1.03, 1.15 (2), 1.28, 3.52 (CH_3), 1.91 (2H,d, J = 3 Hz), 5.55 (d, J = 3 Hz) superimposed on 5.58 (s) (together 3H), 5.97 (1H, s). The stereochemistry is attributed on account of the chemical shifts of the C(3)H and CH_3O protons, compared with the other isomer (following experiment). Mass spectra: 217 (100), 107 (45), 232 ($M^{+\cdot}$, 33), 106 (25), 79 (20), 39 and 185 (17), 41 and 218 (16), 43 and 187 (15).

*2(E)-Methoxymethylene-1,1,4,4,7a-pentamethyl-1,4,5,7a-tetrahydro-2*H*-indene and Methyl 1,1,4,4,7a-Pentamethyl-1,4,5,7a-tetrahydro-2*H*-indene-2-carboxylate (*cis*?),* ***33***

A solution of perchloric acid in ether was prepared by shaking aqueous perchloric acid (70%) with ether. To this solution (50 mL of the upper layer) 1,1,4,4,7a-pentamethyl-2(*Z*)-methoxymethylene-1,4,5,7a-tetrahydro-2*H*-indene, (**30**, 1 g), was added. After 15 min, the mixture was washed to neutrality, dried, and concentrated. Purified by gc (SP 1000), the first peak consisted mainly of the *E*-isomer of the starting material with the following spectra; ^{1}H nmr (60 MHz) δ: 0.88, 1.01, 1.03, 1.19, 1.20, 3.61 (CH_3), 1.95 (2H, d, J = 3 Hz), 5.57 (d, J = 3 Hz) superimposed on 5.63 (s, 3H together), 6.01 (1H, s). The main product, purified by gc (Apiezon) from a small amount of the corresponding aldehyde (**31**, described below), was the ester **33**; ^{1}H nmr (60 MHz) δ: 0.66, 1.05, 1.11, 1.16, 1.20, 3.68 (CH_3), 1.93 (2H, d, J = 3 Hz), 3.45 (1H, d, J = Hz, C(2)H), 5.43 (broad s overlapping a multiplet, total 3H); ms: 173 (100), 233 (89), 189 (71), 119 (65), 201 (42), 248 ($M^{+\cdot}$) and 147 (36), 41 (33),133 (32), 159 (29).

*2-Methoxymethylene-1,1,4,4,7a-pentamethyl-1,4,5,6,7,7a-hexahydro-2*H*-indene, 25*

Following the procedure just described (for **30**), the title product was prepared from 1,1,4,4,7a-pentamethyl-1,4,5,6,7,7a-hexahydro-2*H*-inden-2-one (**19**, 3.3 g), methoxymethyltriphenylphosphonium chloride (25.5 g), and butyllithium (9.16% in hexane, 46 mL) in tetrahydrofuran (70 mL), leaving the mixture for 21 h at room temperature. The product was purified by chromatography on silica gel. A sample collected from gc on SP 1000 had ^{1}H nmr (60 MHz) δ: 0.99, 1.02, 1.09, 1.14, 1.20, 3.52 (CH_3, signals from another isomer visible), 5.58 and 5.92. The crude material was used in the next experiment.

*1,1,4,4,7a-Pentamethyl-*cis*-3a,4,5,6,7,7a-hexahydro-1*H*-indene-2-carbaldehyde,* ***26***

The material from the previous experiment (ca. 3g) was heated at reflux for 2 h in dioxan (30 mL), water (30 mL), and oxalic acid (5 g). Gas chromatography showed the reaction to be complete, and the product was then isolated in pentane. Over 90% was the title material, and it was purified by gc (SP 1000); ^{1}H nmr (60 MHz) δ: 0.95 (3H), 1.06 (12H, CH_3), 2.35 (1H, d, J = 2 Hz), 6.81 (1H, d, J = 2 Hz), 9.73 (1H, s); ms: 220 ($M^{+\cdot}$), 123 and 121 (100), 137 and 41 (92), 205 (71), 135 (70), 107 (67), 109 (64), 69 (59). *Anal.* calcd. for $C_{15}H_{24}O$: C 81.76, H 10.98; found: C 80.88, H 10.86. These figures reflect the ready oxidation of the substance in air. Immediately before the gc peak corresponding to this aldehyde, there was a small region from which a mixture of two unconjugated aldehydes was identified. Too little was available for full spectral analysis, but the following were observed: ^{1}H nmr (90 MHz) δ: 2.75 (t, J = 4 Hz) and 3.18 (t, J = 2 Hz), 5.33 (d, J = 4 Hz) and 5.54 (d, J = 2 Hz), 9.70 (d, J = 4 Hz) and 9.80 (d, J = 2 Hz); ms: 191 (100), 69 (46), 135 (43), 121 and 109 (41), 41 (38), 123 (26), 43 (25), 107 (23)...220 ($M^{+\cdot}$, 2); small fragments at *m/e* 235 and 250 indicated the presence of the corresponding methyl ester.

Can. J. Chem. Downloaded from www.nrcresearchpress.com by 210.87.254.6 on 09/05/12
For personal use only.

1,1,2,4,4,7a-Hexamethyl-2,3,3a,4,5,7a-hexahydro-1H-indene, 37

Lithium (0.2 g) in small pieces was added to liquid ammonia (50 mL). After 30 min, 1,1,4,4,7a-pentamethyl-3a,4,5,7a-tetrahydro-1*H*-indene-2-carbaldehyde (**32**, 0.5 g) in *n*-butanol (0.25 mL) and dry ether (10 mL) was added over 10 min. The mixture was stirred for a further 10 min, the solid ammonium chloride was added, followed by ether (20 mL). The ammonia was allowed to evaporate, ice and a little HCl were added, and the mixture was washed to neutrality. Concentration of the solvents left a nearly homogeneous substance (by capillary column on UCON) which had the following spectra: ^{1}H nmr (90 MHz) δ: 0.94, 0.95, 0.98, 1.09, 1.18 (in all 18H, CH_3), 4.51 (s superimposed on d, 2H together); ms: 121 (100), 41 and 105 (20), 206 ($M^{+\cdot}$, 20), 43, 57, 91, 93 (9).

*1,1,4,4,7a-Pentamethyl-1,4,5,7a-tetrahydro-2H-indene-2-*cis*-carbaldehyde, 31, and 1,1,4,4,7a-Pentamethyl-*cis*-3a,4,5,7a-tetrahydro-1H-indene-2-carbaldehyde, 32*

1,1,4,4,7a-Pentamethyl-2(*Z*)-methoxymethylene-1,4,5,7a-tetrahydro-2*H*-indene (**30**, 4.7 g) was heated in dioxan (30 mL) and saturated aqueous oxalic acid (50 mL) in an apparatus fitted with a water separator. After 3 h the dioxan in the separator was removed, then again after 7 h. Refluxing was continued for a total of 30 h, then the mixture was extracted with pentane and the organic phase washed with water to neutrality, dried, and concentrated to yield a residue that consisted of about 25% starting material, now two peaks on gc (1:1, SP 1000 column). The remainder was a mixture of the two title aldehydes which were separated by gc (SP 1000). The spectral properties were, for aldehyde **31**: ^{1}H nmr (60 MHz) δ: 0.79, 1.08, 1.14, 1.20 (2) (CH_3), 1.95 (2H, m, C(5)H_2), 3.32 (1H, t, J = 1.5 Hz, C(2)H), ca. 5.5 (3H, m), 9.81 (1H, d, J = 1.5 Hz); ms: 189 (100), 133 (38), 119 (35), 69 and 41 (28), 190 (24), 147 (23), 105 (20), 175 and 91 (18)...218 ($M^{+\cdot}$, 16).

For aldehyde **32**: ^{1}H nmr (60 MHz) δ: 1.04, 1.06, 1.10, 1.15, 1.21 (CH_3), 1.75 (2H, m), 2.47 (1H, broad s), 6.77 (1H, d, J = 2.5 Hz), 9.70 (1H, s); ms: 121 (100), 41 (50), 203 (42), 147 (39), 107 (36), 105 (35), 119 and 91 (34), 189 and 218 ($M^{+\cdot}$, 31).

Treatment of **31** with methanolic potassium hydroxide at 60°C for 2 h yielded almost exclusively **32**.

*(1,1,4,4,7a-Pentamethyl-1,4,5,7a-tetrahydro-2H-inden-*cis*-2-yl)-methanol, 34*

1,1,4,4,7a-Pentamethyl-1,4,5,7a-tetrahydro-2*H*-indene-2-*cis*-carbaldehyde (**31**, 0.1 g) was reduced as usual with excess lithium aluminum hydride in dry ether. After the usual workup, a small amount was isolated by gc (SP 1000) for analysis, the remainder being reduced catalytically directly (next experiment); ^{1}H nmr (360 MHz) δ: 0.63, 1.04, 1.06, 1.11, 1.15 (CH_3), 1.86 (2H, m, C(5)H) displaced by Eu(fod)$_3$ to respectively, 2.17 (d of d, J = 5 and 17 Hz) and 2.29 (J = 2.5 and 17), 2.73 (1H, d of d of d, J = 6, 9, and 1.5 Hz, C(2)H), 3.56 (d of d, J = 9 and 10.5 Hz), and 3.71 (d of d, J = 6 and 10.5 Hz, carbinol CH_2), 5.27 (s, C(3)H), 5.37 (1H, d of t, J = 10 and 1 Hz, C(7)H), 5.60 (1H, d of t, J = 4, 4, and 10 Hz); ms: 189 (100), 119 (50), 220 ($M^{+\cdot}$, 46), 133 (44), 205 and 55 (41), 41 (38), 145 (35), 187 and 69 (29). *Anal.* calcd. for $C_{15}H_{24}O$: C 81.76, H 10.98; found C 81.76, H 10.80.

*(1,1,4,4,7a-Pentamethyl-1,4,5,6,7,7a-hexahydro-2H-inden-*cis*-2-yl)-methanol, 35*

The crude material (0.09 g) from the previous experiment was shaken in hydrogen over platinum on charcoal (10% Pt) in ethanol (5 mL). Absorption ceased after 35 min, when 90% of the theoretical volume of H_2 was absorbed. Filtration and concentration yielded practically pure **35**, which was purified by gc (on SP 1000). The ^{1}H nmr spectrum showed it to contain < 10% of the *trans* isomer; ^{1}H nmr (360 MHz) δ: 0.70, 0.98, 1.04, 1.09 (2) (CH_3), 1.69 (1H, m, C(6)H), 2.55 (1H, m, J = 1.5, 6, and 8 Hz, C(2)H, 3.56 and 3.69 (each 1H, m, carbinol CH_2), 5.29 (broad s, $w_{\frac{1}{2}}$ = 2.5 Hz, C(3)H); ms: 191 (100), 69 (37), 109 (35), 135 (32), 41 (31), 121 (27), 107 and 55 (49), 43 (21), 207 (18)...222 ($M^{+\cdot}$, 6.5). See also the following experiment.

*(1,1,4,4,7a-Pentamethyl-3a,4,5,6,7,7a-hexahydro-1H-inden-*cis*-2-yl)-methanol*

The aldehyde **26** was reduced as usual with excess lithium aluminum hydride in dry ether. The product consisted of about 88% of the title product (by gc on SP 1000) which was purified by gc from ca. 12% of a peak with shorter retention time. The main product had ^{1}H nmr (60 MHz) δ: 0.79, 0.87, 1.00 (3) (CH_3), 2.18 (1H, $w_{\frac{1}{2}}$ ≃ 5 Hz, C(3a)H), 4.15 (2H, apparent q, w ≃ 5 Hz, carbinol CH_2), 5.61 (1H, d, J = 1 Hz); ms: 109 (100), 207 (82), 191 (78), 121 (71), 41 (66), 69 (48), 189 (42), 135 and 107 (39), 55 (38)....222 ($M^{+\cdot}$, 22). The smaller peak with shorter retention time was repurified by gc on OV 17, and consisted of a mixture (3:2) of the alcohol **35**, described in the foregoing experiment, and what was apparently the *trans* isomer, **36**, identified by the presence of the following signals (360 MHz) δ: 0.92, 0.94, 1.08, 1.12, 1.13 (CH_3), 2.21 (d of d of d, J = 3, 6, and 8 Hz, C(2)H), 5.36 (d, J = 3 Hz, C(3)H).

*1,1,4,4,7a-Pentamethyl-*cis*-2,3,3a,4,5,7a-hexahydro-1H-indene-2-*exo*-carbaldehyde, 38*

A solution of a 6:4 mixture of 1,1,4,4,7a-pentamethyl-1,4,5,7a-tetrahydro-2*H*-indene-2-*cis*-carbaldehyde, **31**, and 1,1,4,4,7a-pentamethyl-*cis*-3a,4,5,7a-tetrahydro-1*H*-indene-2-carbaldehyde, **32** (0.22 g, obtained directly from hydrolysis of the enol ether **30**) in ethanolic potassium hydroxide (20 mL 5% KOH) was hydrogenated over a palladium on charcoal catalyst (10% Pd). After 0.6 equivalents of H_2 were absorbed, the rate of uptake slowed to nearly zero, and the mixture was diluted with water and extracted with pentane. Concentration of the pentane yielded the title product, **38**, together with unchanged **31**. The former was purified by gc on SP 1000, but only a mass spectrum was recorded, the remainder being converted directly to the alcohol (see next experiment); ms: 107 (100), 121 (76), 134 (67), 123 (62), 41 and 122 (55), 93 and 119 (40), 69 (38)...220 ($M^{+\cdot}$, 20).

*(1,1,4,4,7a-Pentamethyl-*cis*-2,3,3a,4,5,7a-hexahydro-1H-inden-2-*exo*-yl)-methanol 39*

The mixture obtained in the foregoing experiment was reduced directly with excess lithium aluminum hydride in dry ether. After workup, the mixture of **34** and **39** was separated by either chromatography on silica gel, or by preparative gc on SP 1000, the title product **39** having the shorter retention time in both cases, and crystallizing on elution, mp 100–102°C; ^{1}H nmr (360 MHz) δ: 0.71, 0.89, 0.92, 0.98, 1.00 (CH_3), 1.52 (d of d, J = 5 and 17 Hz) and 2.01 (broad d, J = 2 and 17 Hz, C(5)H_2), 3.46 (d of d, J = 8.5 and 10.5 Hz) and 3.69 (d of d, J = 5 and 10.5 Hz, carbinol CH_2), 5.46 (d of d, J = 3 and 10 Hz, C(7)H), 5.57 (d of d of d, J = 2, 6, and 10 Hz, C(6)H; ms: 107 (100), 122 (95), 121 and 41 (35), 123 (28), 136 (25), 93 (22), 119 and 69 (15)...189 (3)...222 ($M^{+\cdot}$, 5). *Anal.* calcd. for $C_{15}H_{26}O$: C 81.02, H 11.79; found: C 80.75, H 11.56.

Acknowledgements

We are indebted to Dr. K. H. Schulte-Elte for useful discussions and a sample of compound **3**. Useful suggestions from Dr. G. Ohloff are also gratefully acknowledged. Mr. René Menghetti is thanked for assistance in the preparation of com-

pound *a*. We are grateful to Dr. W. Hoffmann, BASF, Ludwigshafen, for a supply of 2,6,6-trimethylcyclohex-2-enone. Mr. W. Thommen is thanked for meticulous nmr measurements.

1. G. OHLOFF, K. H. SCHULTE-ELTE, and E. DEMOLE. Helv. Chim. Acta, **54**, 2913 (1971); E. DEMOLE and P. ENGGIST. Helv. Chim. Acta, **59**, 1938 (1976).
2. A. M. ISLAM and R. A. RAPHAEL. J. Chem. Soc. 4086 (1952).
3. R. B. MILLER. Synth. Commun. **2**, 267 (1972).
4. R. M. JACOBSON, R. A. RATHS, and J. H. MCDONALD III. J. Org. Chem. **42**, 2545 (1977); D. A. EVANS, C. L. SIMS, and G. C. ANDREWS. J. Am. Chem. Soc. **99**, 5453 (1977).
5. M. MIYASHITA, T. YANAMI, and A. YOSHIKOSHI. J. Am. Chem. Soc. **98**, 4679 (1976).
6. B. FURTH, G. DACCORD, and J. KOSSANYI. Tetrahedron Lett. 4259 (1975).
7. G. SCHMITT and S. ÖZMAN. Chem. Ztg. **100**, 143 (1976).
8. M. BAUMANN and W. HOFFMANN. Ger. Patent No. 2,547,223 (Oct. 22, 1975); M. BAUMANN, W. HOFFMANN, and A. NÜRRENBACH. Justus Liebigs Ann. Chem. 1945 (1979).
9. P. T. LANSBURY, E. J. NIEUHAUS, D. J. SCHARF, and F. R. HILFIKER. J. Am. Chem. Soc. **92**, 5649 (1970).
10. J. E. BALDWIN. J. Chem. Soc. Chem. Commun. 734 (1976).
11. R. L. SOWERBY and R. M. COATES. J. Am. Chem. Soc. **94**, 4758 (1972).
12. Y. CHIANG, A. J. KRESGE, and C. I. YOUNG. Can. J. Chem. **56**, 461 (1978).
13. B. FUCHS and R. G. HABER. Tetrahedron Lett. 1323 (1966); R. G. HABER and B. FUCHS. Tetrahedron Lett. 1447 (1966).
14. J.-C. RICHER and P. BÉLANGER. Can. J. Chem. **44**, 2067 (1966).
15. A. F. THOMAS and M. OZAINNE. Helv. Chim. Acta, **62**, 361 (1979).
16. P. DE CLERCQ, D. VAN HAVER, D. TAVERNIER, and M. VANDEWALLE. Tetrahedron, **30**, 55 (1974).
17. D. CAINE. Org. React. **23**, 104 (1976); R. E. IRELAND, P. A. ARISTOFF, and C. F. HOYNG. J. Org. Chem. **44**, 4318 (1979).
18. M. CHRISTL, H. J. REICH, and J. D. ROBERTS. J. Am. Chem. Soc. **93**, 3463 (1971); R. G. S. RITCHIE, N. CYR, B. KORSCH, H. J. KOCH, and A. S. PERLIN. Can. J. Chem. **53**, 1424 (1975).
19. E. I. SNYDER and J. D. ROBERTS. J. Am. Chem. Soc. **84**, 1582 (1962).
20. R. HEILMAN and R. GLÉNAT. C. R. Acad. Sci. **240**, 2317 (1955).

Can. J. Chem. Downloaded from www.nrcresearchpress.com by 210.87.254.6 on 09/05/12
For personal use only.

The crystal structure of ethyl-*Z*-3-amino-2-benzoyl-2-butenoate and measurement of the barrier to *E*,*Z*-isomerization

GARY D. FALLON, BRYAN M. GATEHOUSE, ALLAN PRING, IAN D. RAE, AND JOSEPHINE A. WEIGOLD

Chemistry Department, Monash University, Wellington Road, Clayton, Victoria, Australia 3168

Received December 31, 1979

This paper is dedicated to the memory of Dr. Léo Marion

GARY D. FALLON, BRYAN M. GATEHOUSE, ALLAN PRING, IAN D. RAE, and JOSEPHINE A. WEIGOLD. Can. J. Chem. **58**, 1821 (1980).

Ethyl-3-amino-2-benzoyl-2-butenoate crystallizes from pentane as either the *E* (mp 82–84°C) or the *Z*-isomer (mp 95.5–96.5°C). The *E* isomer is less stable, and changes spontaneously into the *Z*, which has been identified by X-ray crystallography. The structure is characterised by an N–H/ester CO hydrogen bond and a very long C2—C3 bond (1.39 Å). Nuclear magnetic resonance methods have been used to measure the rate of $Z \rightleftharpoons E$ isomerization at several temperatures, leading to the estimate that the free energy of activation at 268 K is 56 ± 8 kJ.

GARY D. FALLON, BRYAN M. GATEHOUSE, ALLAN PRING, IAN D. RAE et JOSEPHINE A. WEIGOLD. Can. J. Chem. **58**, 1821 (1980).

L'amino-3 benzoyl-2 butène-2 oate d'éthyle cristallise dans le pentane sous la forme *E* (pf 82–84°C) ou sous la forme *Z* (pf 95,5–96,5°C). L'isomère *E* est moins stable et se transforme spontanément en la forme *Z* que l'on a identifiée par cristallographie de rayons-X. La structure est caractérisée par une liaison hydrogène N—H/ester-CO et une liaison C2—C3 (1,39 Å) très longue. On a utilisé la rmn pour mesurer la vitesse d'isomérisation $Z \rightleftharpoons E$ à différentes températures; on évalue l'énergie libre d'activation à 56 ± 8 kJ à 268 K.

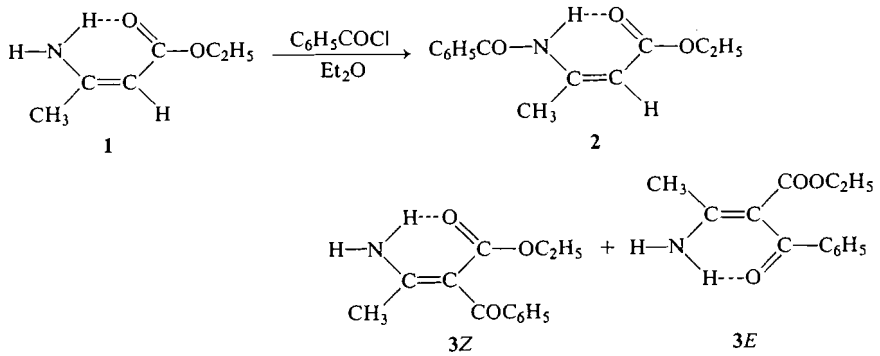
[Traduit par le journal]

Introduction

The benzoylation of ethyl 3-amino-2-butenoate **1** gives approximately equal quantities of *N*- and *C*-acylated products, **2** and **3** respectively, as reported by Buckler *et al.* (1). These authors gave no physical data for their products, but did convert ester **2** to the corresponding carboxylic acid, the melting temperature of which was comparable to that reported by Barker (2). Barker prepared the acid from an ester, mp 95°C, which had been reported much earlier by Benary (3).

Benary, in his work, had isolated *two* benzoyl derivatives from benzoylation of ester **1**, each of which upon mild acid-catalysed hydrolysis yielded a neutral substance which was identified as benzamide (although just how, Benary does not say). Each of the benzoyl compounds was thus classified as an *N*-benzoyl compound. The melting temperatures were 95–96°C and 46–48°C with the latter compound being much the more soluble in organic solvents.

We report here that benzoylation of ester **1** gives *three* products, the *N*-benzoyl **2** with melting temperature 48–48.5°C, and the *C*-benzoyl compounds **3***Z* melting at 95.5–96.5°C and **3***E* at 82–84°C. This last melting temperature is recorded with rapid heating, for with slower heating the crystals of this isomer melt in the range 76–83°C, resolidify, and then melt again at 96–97°C. The infrared spectra of the two isomers are quite different, and our structural assignments are supported by ^1H and ^{13}C nmr spectra at several temperatures, and by X-ray diffraction studies with the **3***Z* isomer. We have also determined the average energy of activation and other thermodynamic parameters for the isomerization $3Z \rightleftharpoons 3E$.



1 2 3Z 3E

0008-4042/80/171821-08$01.00/0

©1980 National Research Council of Canada/Conseil national de recherches du Canada

Can. J. Chem. Downloaded from www.nrcresearchpress.com by 210.87.254.105 on 09/05/12
For personal use only.

Can. J. Chem. Downloaded from www.nrcresearchpress.com by 210.87.254.105 on 09/05/12
For personal use only.

Results

X-Ray Crystallography

The crystal structure is shown in Fig. 1 and consists of the packing of discrete molecules which, besides the normal van der Waals interactions, are held together by an intermolecular hydrogen bond between H(2N) and the ether oxygen, O(3); H(2N)···O(3), 1.88 Å; N···O(3) 2.90 Å. There is also an intramolecular hydrogen bond between H(1N) and the ester carbonyl oxygen, H(1N)···O(1), 1.82 Å; N···O(1)2.66 Å. There are no other unusual intermolecular contacts. (The data are summarized in Tables 1–4.) Fig. 2 indicates the intermolecular hydrogen bond and the labelling scheme of the atoms.

Due to the presence of the intramolecular hydrogen bond between H(1N) and O(1) the atoms C(1)—C(5), N, O(1), O(2) form a nearly coplanar arrangement (Table 4), the maximum deviation being 0.085(3) Å by O(2). The structure is also highly polarized, as depicted in structure **4***Z*, resulting in short C(3)—N and C(2)—C(5) ester distances and a long C(2)—C(3) bond. For comparison, C(2)—C(3) is 1.390(5) Å whereas the "double" bond length in several α,β-unsaturated carbonyl compounds is 1.36(1) Å(4), and C(3)—N is 1.320(4) Å, even shorter than the C—N distance in most amides, 1.333(5) Å(4).

On the other side of the double bond, however, the C(2)—C(5) benzoyl distance is greater than the C(2)—C(1) ester distance, 1.480(4) vs. 1.444(5) Å, and thus more normal (4), and the benzoyl carbonyl is twisted out of the plane of the molecular backbone by 48.5°, with O(3) 0.758(3) Å above the plane (Table 4). There is also a twist of 31.0°, in the opposite sense, about the C_6H_5—CO bond, as is commonly observed in the benzoyl moiety e.g. 26° in benzamide (5).

Nuclear Magnetic Resonance Spectra

The ^{1}H nmr spectrum of the *N*-benzoyl compound **2** shows the expected multiplets for the ethoxy group and the benzoyl moiety, slightly broadened singlets for the methyl (2.55) and vinyl hydrogens (5.05 ppm) and a broad signal for the amide hydrogen.

The spectra of the isomers **3***E* and **3***Z* (Table 5) are quite distinct but it was not possible to deduce structures by consideration of these spectra alone. The hydrogens of the ethoxy groups are shielded in both isomers, but more so in the *Z*-isomer. If we take as standards the values for ethyl acetate (6), then the CH_2 and CH_3 of **3***Z* are shielded by 0.63 and 0.45 ppm respectively, and those of **3***E* by 0.50 and 0.20 ppm.

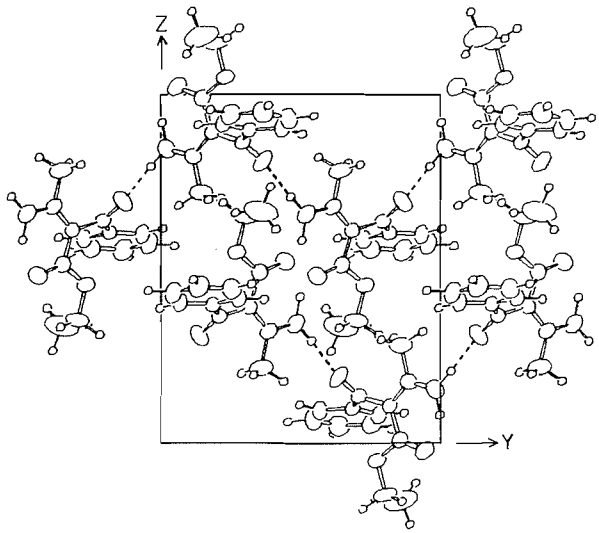


FIG. 1. Unit cell contents projected down a^*. The intermolecular hydrogen bonds are shown with dotted lines. Hydrogen thermal parameters were reduced for clarity.

The NH_2 resonances are the only ones to show appreciable changes with temperature. At low temperatures, they are unusually sharp (width at half-height about 5 Hz) and ^2J is evident as a splitting in each of the NH signals. The observed value, 6 Hz, is comparable to the 4.9 Hz observed for $^2J_{HNH}$ in 2-aminoacetophenone-^{15}N by Wasylishen and Schaefer (7), but approximately twice as large as those for NH_2 in amides (examples and references collected by Wasylishen and Schaefer (7)). The splitting is lost at temperatures above 233 K, and those which are not intramolecularly hydrogen-bonded move upfield at temperatures above 250 K. The assignment of these two types of NH is made on the basis of their chemical shifts i.e., intramolecularly hydrogen-bonded NH resonances at lower field.

In DMSO-d_6 solution, only a single set of signals is observed and it was not possible to cool the solution far enough before crystallization intervened to observe separation of resonances for the individual isomers or even substantial line-broadening.

The ^{13}C nmr assignments (Table 6) have been made by comparison with literature values, including those for 3-amino-2-enones (8) which confirmed the values for C2 and C3. The C2 and ester CO resonances were assigned on the basis that the latter would have the longer relaxation time, being further from any hydrogen atoms, and therefore give a less intense peak in the normal spectrum.

Can. J. Chem. Downloaded from www.nrcresearchpress.com by 210.87.254.105 on 09/05/12
For personal use only.

TABLE 1. Final positional parameters and thermal parameters[a,b]

Atom	x/a	y/b	z/c	U_{11}	U_{22}	U_{33}	U_{23}	U_{13}	U_{12}
C(1)	2567(5)	3523(3)	4896(3)	42(2)	44(2)	48(3)	−1(2)	12(2)	7(2)
C(2)	2067(4)	3174(3)	3914(3)	36(2)	36(2)	39(2)	−2(2)	10(2)	1(2)
C(3)	850(5)	3848(3)	3232(3)	40(2)	50(2)	44(3)	7(2)	15(2)	4(2)
C(4)	342(6)	3577(4)	2188(3)	76(3)	94(4)	43(3)	6(3)	6(3)	20(3)
C(5)	2795(5)	2072(3)	3636(3)	43(2)	41(2)	37(2)	−2(2)	11(2)	−4(2)
C(6)	4728(5)	1844(3)	3975(2)	41(2)	37(2)	38(2)	−2(2)	15(2)	2(2)
C(7)	5936(5)	2766(3)	4171(3)	45(2)	40(2)	58(3)	−2(2)	20(2)	1(2)
C(8)	7744(5)	2517(4)	4420(3)	43(3)	63(3)	72(3)	−6(2)	18(2)	−5(2)
C(9)	8309(6)	1348(4)	4482(3)	48(3)	72(3)	81(4)	9(3)	20(3)	17(3)
C(10)	7115(6)	434(4)	4298(3)	68(3)	48(3)	79(3)	11(2)	25(3)	21(3)
C(11)	5326(5)	672(3)	4029(3)	58(3)	35(2)	64(3)	2(2)	21(2)	5(2)
C(12)	4349(6)	3007(4)	6475(3)	73(3)	96(4)	34(3)	−14(3)	8(2)	6(3)
C(13)	6012(8)	3568(7)	6642(4)	97(5)	197(7)	77(4)	−38(4)	17(4)	−54(5)
N	92(4)	4808(3)	3440(3)	71(3)	55(2)	62(3)	14(2)	22(2)	27(2)
O(1)	2098(4)	4422(2)	5212(2)	86(2)	63(2)	56(2)	−13(2)	12(2)	33(2)
O(2)	3579(3)	2700(2)	5475(2)	63(2)	57(2)	35(2)	−1(1)	10(1)	12(2)
O(3)	1838(4)	1360(2)	3088(2)	56(2)	60(2)	75(2)	−32(2)	2(2)	−9(2)

[a]Anisotropic thermal parameters were of the form
$\exp[-2\pi^2(U_{11}h^2a^{*2} + \ldots + 2U_{23}b^*c^*kl\ldots)]$
[b]Positional parameters × 10^4; thermal parameters (U) × 10^3.

TABLE 2. Hydrogen positional parameters (× 10^3) and thermal parameters (× 10^3)

Atom	x/a	y/b	z/c	B
H(1C4)	146	331	197	176(9)
H(2C4)	−23	437	181	176(9)
H(3C4)	−63	287	203	176(9)
H(C7)	549	368	413	88(7)
H(C8)	869	323	457	88(7)
H(C9)	970	115	467	88(7)
H(C10)	757	−48	436	88(7)
H(C11)	439	−5	386	88(7)
H(1C12)	450	221	689	176(9)
H(2C12)	348	361	668	176(9)
H(1C13)	665	391	734	176(9)
H(2C13)	643	408	613	176(9)
H(3C13)	637	265	661	176(9)
H(1N)	35	497	419	119(13)
H(2N)	−68	537	294	119(13)

Thermodynamic Parameters

When an isomer mixture can be enriched in one isomer, or a single isomer can be generated in solution, and then the system be observed during the approach to equilibrium, it is possible to evaluate a rate constant k, which is the average for the forward and reverse reactions (9, 10). In our case, the equilibrium ratio **3***Z*:**3***E* is 1.1 : 1 and almost invariant with temperature. Thus the forward and reverse rates must be almost equal, so k is a very good approximation to the separate rates and ΔG for the isomerization is calculated to be 0.23 kJ mol^{-1}. The values of k, derived by Gutowsky *et al.*'s method (9) are given in the Experimental for temperatures in the range 243 K to 268 K. The values were used in a graphical solution of the Arrhenius equation (11*a*) which yielded a value of 56 ± 2 kJ mol^{-1} for the activation energy. A similar treatment using the Eyring equation (11*b*, 12) gave $\Delta H^{\ddagger}$ = 61 ± 15 kJ mol^{-1} and $\Delta S^{\ddagger}$ = 17 J deg^{-1} mol^{-1} with a large uncertainty. The calculated value for the free energy of activation, $\Delta G^{\ddagger}$, at 268 K is 56 ± 8 kJ mol^{-1}.

Discussion

The X-ray diffraction results reveal a molecule (**3***Z*) in which the amino group is hydrogen-bonded to, and coplanar with, the ester group while the benzoyl group is twisted out of the plane. There was some expectation that the benzoyl group might be held closer to the plane by conjugation with the amino group i.e., a contribution from canonical structure **4***Z*. The two bases for this expectation are that, first, methyl 3-dimethylamino-2-propenoate is found (13) only in the *E* form **5**, and attempts to prepare the *Z* isomer have been unsuccessful (14). Second, the crystal structure of dimethyl (dimethylaminomethylene)-malonate **6** shows (14) that the dimethylamino group and the *trans* ester group are coplanar. In our case, the hydrogen-bonding interaction in **3***Z* is sufficient to reverse this preference for *trans* over *cis* conjugation.

Two other enamine crystal structures, of compounds **7** and **8**, are relevant to our discussion. In compound **7**, there is *trans* conjugation of nitrogen and carbonyl but also a 25° twist about the tetrasubstituted double bond (15). In compound **8**, the intramolecular hydrogen bonding stabilizes the planar *Z* geometry (16). The critical bond lengths for the conjugated path in these four compounds

Can. J. Chem. Downloaded from www.nrcresearchpress.com by 210.87.254.105 on 09/05/12
For personal use only.

TABLE 3. Intramolecular bonding distances and selected bond angles

	Bonding distances (Å)		Bonding distances (Å)
C(1)—C(2)	1.444(5)	C(12)—C(13)	1.419(6)
C(2)—C(3)	1.390(5)		
C(2)—C(5)	1.480(4)	C(1)—O(1)	1.221(4)
C(3)—C(4)	1.509(5)	C(1)—O(2)	1.348(4)
C(5)—C(6)	1.489(5)	C(5)—O(3)	1.225(4)
C(6)—C(7)	1.383(5)	C(12)—O(2)	1.463(4)
C(7)—C(8)	1.401(5)		
C(8)—C(9)	1.383(5)	C(3)—N	1.320(4)
C(9)—C(10)	1.369(5)		
C(10)—C(11)	1.383(5)		
C(11)—C(6)	1.395(5)		

	Angles (degrees)		Angles (degrees)
O(1)—C(1)—O(2)	121.0(4)	C(1)—O(2)—C(12)	117.8(3)
O(1)—C(1)—C(2)	126.4(3)	O(2)—C(12)—C(13)	110.9(4)
O(2)—C(1)—C(2)	112.4(3)		
C(1)—C(2)—C(3)	120.0(3)	C(7)—C(6)—C(11)	119.4(3)
C(1)—C(2)—C(5)	120.1(3)	C(6)—C(7)—C(8)	119.9(4)
C(3)—C(2)—C(5)	119.8(3)	C(7)—C(8)—C(9)	119.7(4)
N—C(3)—C(4)	114.2(4)	C(8)—C(9)—C(10)	120.5(4)
N—C(3)—C(2)	122.8(4)	C(9)—C(10)—C(11)	120.2(4)
C(2)—C(3)—C(4)	123.0(4)	C(6)—C(11)—C(10)	120.2(4)
C(2)—C(5)—C(6)	120.3(3)		
C(2)—C(5)—O(3)	121.0(3)	C(5)—C(6)—C(7)	121.6(3)
C(6)—C(5)—O(3)	118.6(3)	C(5)—C(6)—C(11)	118.8(3)

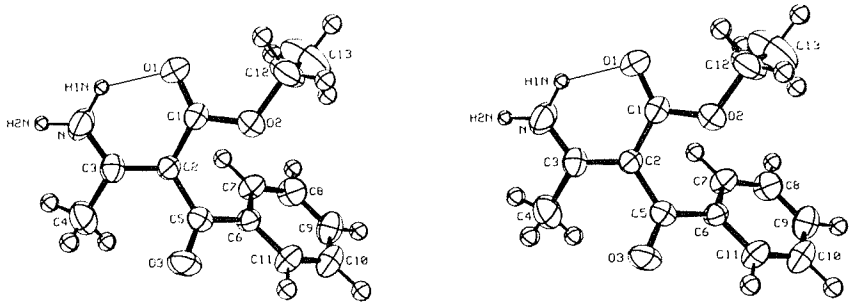


FIG. 2. Molecular structure, showing skeletal numbering. The intramolecular hydrogen bond is shown as a fine line. Hydrogen thermal parameters were reduced for clarity.

TABLE 4. Equation for mean plane and deviations (Å) of atoms from the planes. The plane is represented by an equation of the type $Ax + By + Cz - D = 0$

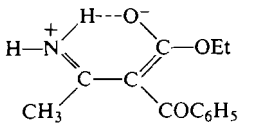
Plane 1	C(1)—C(5),N,O(1),O(2)	
Parameters	Deviations	
A 0.8426	C(1) 0.036(4)	N −0.080(4)
B 0.5277	C(2) 0.024(4)	O(1) 0.083(3)
C 0.1078	C(3) −0.026(4)	O(2) −0.085(3)
D 1.1292	C(4) 0.037(5)	
	C(5) 0.011(4)	O(3) −0.758(3)
		O(6) 0.992(4)

are collected in Table 7, from which it can be seen that crowding in compound **7** has reduced significantly the extent of conjugation. In our compound **3***Z*, the non-conjugated carbonyl is twisted out of the general plane by 49° whereas, in compound **6**, the non-conjugated *cis* carbonyl is twisted through 54°.

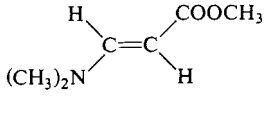
The barrier to rotation about the formal carbon–carbon double bond in compound **3** may also be compared to those observed for other 3-amino-2-enoates, but only values for tertiary amines are available for comparison. Thus, for compound **6**

TABLE 5. ^{1}H Nuclear magnetic resonance spectra for isomers of ethyl 3-amino-2-benzoyl-2-butenoate

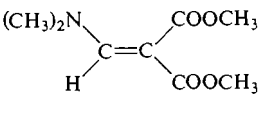
	Chemical shifts (ppm downfield from internal $(CH_3)_4Si$) and coupling constants, J(Hz)		
	Solution in $CDCl_3$ at 233 K		
Assignment	Isomer **3***E*	Isomer **3***Z*	Solution in DMSO-d_6 at 300 K
CH_3CH_2O	0.623	0.747	0.619
CH_3CH_2O	3.769	3.916	3.719
$^3J_{HCCH}$	7.0	7.0	7.0
CH_3—C	2.400	2.214	2.184
Aromatic *m* and *p*	7.43	7.43	7.404
o	7.43	7.80	7.404
NH free	5.997	5.575	8.31
H-bonded	10.860	9.167	10.41
$^2J_{HNH}$	6.0	6.0	—



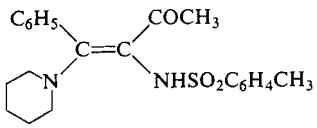
4*Z*



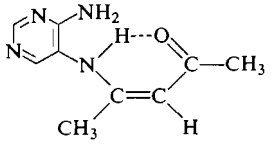
5



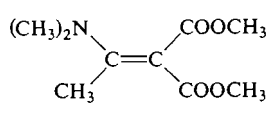
6



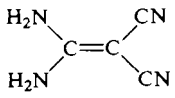
7



8



9



10

$\Delta G^{\ddagger}$ is 65.3 kJ mol^{-1} (at 291–295 K for solution in CH_2Cl_2) (17) but the extra methyl substituent in the amino-ethylidine compound **9** decreases this barrier to ca. 26 kJ mol^{-1}, presumably by destabilizing the planar ground state of the conjugated system (17). The value for **3** is higher than might be expected from these comparisons, and from consideration of the values collected by Jackman (18) for similar systems, and we attribute this to the stabilizing influence of the intramolecular hydrogen bond in **3***E* and **3***Z*.

The shielding of the ethyl group by the benzene ring which is so evident in the ^{1}H nmr spectra of both isomers, but particularly in **3***E*, is not evident in the corresponding ^{13}C nmr spectra and probably arises from rotations about the O—CH_2 and CH_2—CH_3 bonds which bring the hydrogens close to the face of the ring. The relatively large value for $^2J_{HNH}$, for a molecule in which the configuration about nitrogen is planar and in which the nitrogen lone pair is extensively delocalized, is in accord with the predictions, based on MO calculation, of Wasylishen and Schaefer (7). The apparent lowering of the barrier to rotation about C2—C3 for solutions in DMSO-d_6 is to be expected if the transition state is highly polarized and thus better stabilized in the polar solvent than in $CDCl_3$. Similar reductions have been noted for ketene mercaptals which are essentially planar in the ground state (19).

In the ^{13}C spectra, the non-conjugated carbonyl substituent has only a small effect on the chemical shift of C3 for which the observed values are much like those reported (20) for ethyl-*E*-3-dimethylamino-2-butenoate (C2 84.0, C3 160.6 ppm) and *E*-4-dimethylamino-3-penten-2-one (C3 93.7, C4 160.3 ppm). The chemical shifts of the olefinic carbons C2 and C3 in compound **3***Z* also attest to the extensive polarization of the system depicted in structure **4***Z* and discussed above in connection with the bond length and barrier to rotation. The accumulation of positive charge in the C3—N region, and of negative charge at the C2—CO, would result in deshielding of C3 and shielding of C2 as observed. More extreme examples of this kind are described by W. A. Thomas (private communication) including compound **10** for which the C3 resonance is found at 166.1 ppm and C2 at 31.9 ppm, reflecting considerable charge accumulation at C2 as well as the normal shielding effect of the nitrile group on an adjacent carbon (21).

Can. J. Chem. Downloaded from www.nrcresearchpress.com by 210.87.254.105 on 09/05/12
For personal use only.

TABLE 6. ^{13}C Nuclear magnetic resonance spectra for ethyl 3-amino-2-benzoyl-2-butenoate

	Chemical shifts (ppm downfield from internal $(CH_3)_4Si$)		
	$CDCl_3$ solution, 233 K		
Assignment	*Z*-isomer	*E*-isomer	DMSO-d_6 solution, 308 K
CH_3CH_2O	13.00	13.39	13.26
CH_3CH_2O	60.21	59.23	58.65
Ester CO (C1)	170.41	166.97	168.92
C2	100.97	97.96	
C3	169.50	169.50	
CH_3(C4)	22.63	21.98	20.87
Benzoyl CO	194.99	197.07	193.43
Aromatic *ipso*	143.04	141.61	143.11
ortho	128.09	126.01	127.83
meta	128.09	126.01	126.59
para	129.97	131.60	129.78

TABLE 7. Selected bond lengths from X-ray crystal structures (Å)

	Bond lengths				
Compound	N—C	C=C	C1—C2	C=O	Reference
3*Z*	1.320	1.390	1.444	1.225	This work
6	1.337	1.380	1.443	1.223	16
7	1.368	1.374	1.474	1.236	17
8	1.37	1.37	1.41	1.26	18

In isomer **3***Z* the angle between the ring and carbonyl planes is at 31° only slightly larger than that observed in other compounds in which a C_6H_5—CO—C=C group is present (22). A Dreiding model of isomer **3***E*, however, suggests that the steric pressures on the benzoyl group are somewhat larger when the ester group is not constrained by an intramolecular hydrogen bond, and it is reasonable to suppose that the benzene ring will adopt a conformation in which it is roughly orthogonal to the plane of the conjugated and hydrogen-bonded system. Such a configuration would be consistent with our observation that the hydrogens of this ring all have approximately the same chemical shift, since deshielding of the *ortho* hydrogens by the carbonyl would not be significant.

There remains the question of how selective crystallization of one or other isomer may be brought about from a solution containing both **3***E* and **3***Z*. The material obtained from the crude products of benzoylation of enamine **1** was isomer **3***E* which was used successfully to seed the chromatographic column fractions. This material shows the double melting point which signifies its thermal transition to isomer **3***Z*. This crystalline isomer **3***E* spontaneously changes to isomer **3***Z* when left at room temperature, and subsequent recrystallization from pentane always gave **3***Z*. On only one occasion has our subsequent work produced the single isomer **3***E*, and then as a crystalline mass obtained from evaporation of a $CDCl_3$ solution (not strictly a recrystallization). We did commence a crystal structure determination with isomer **3***E* but the crystal changed before the measurements could be completed, and subsequent measurements on some unaltered crystals, which had constituted only a very small fraction of the original material, revealed the *Z*-isomeric structure discussed above. Infrared spectra confirmed that these small crystals were not the same as those which initially constituted the bulk of the material but that, after a time, the crystals were homogeneous in an infrared, but not a morphological sense.

Experimental

General

Infrared spectra were recorded for paraffin mulls on a Jasco IRA-1 grating infrared spectrophotometer. ^1H and ^{13}C nuclear magnetic resonance spectra were recorded on a Bruker WH90 spectrometer operating at 90 and 22.62 MHz respectively. The $CDCl_3$ was shaken with solid Na_2CO_3 immediately prior to use to remove traces of acid which catalysed the isomerization. The probe temperature of the spectrometer was adjusted with a stream of cold nitrogen gas and controlled with a Bruker temperature control unit.

Can. J. Chem. Downloaded from www.nrcresearchpress.com by 210.87.254.105 on 09/05/12
For personal use only.

Can. J. Chem. Downloaded from www.nrcresearchpress.com by 210.87.254.105 on 09/05/12
For personal use only.

Suitable single crystals for X-ray investigation were obtained by recrystallizing the compound from pentane. A crystal of dimensions 0.08 × 0.10 × 0.07 mm was selected for the study. Unit cell parameters were refined by least-squares refinement of 2θ values ($24 < 2\theta < 60$) for 32 reflections measured on a Philips PW1100 automatic diffractometer with graphite monochromated CuKα_1 radiation (λ = 1.54051 Å). Crystal data (at 18°C) are:

$C_{13}H_{15}NO_3$ fw = 233.26
Monoclinic, a = 7.983(4), b = 11.234(7), c = 14.873(8) Å, β = 108.08(9)°, V = 1268.0 Å^3, ρ_o = 1.21(2), Z = 4, ρ_c = 1.22 g·cm^{-3} (20°C, by flotation), $F(000)$ = 496, μ(CuKα_1) = 6.33 cm^{-1}. Space group $P2_1/c$ (No. 14).

A unique data set was collected out to 2θ = 130° by the ω-scan technique. 2153 unique reflections were measured; of those 1314 obeyed the condition $F_o^2 \geq 3\sigma(F_o)^2$ and were used in the subsequent calculations. Three strong reflections, monitored every 2 h, showed no significant variation in intensity over the data collection period.

The data were processed with a program written for the PW1100 diffractometer (23). A value of 0.04 was used for p in the estimation of $\sigma(F_o^2)$. All reflections were corrected for Lorentz polarization and absorption effects, (transmission factors ranged between 0.959 to 0.940), but not extinction. Scattering factors for C°, H°, N°, and O° were corrected for anomalous dispersion (24).

The structure was solved by direct methods. Phases for 241 terms with $|E|$ values greater than 1.20 were determined by application of the tangent formula (25). The best E map gave sites for 16 of the 17 non-hydrogen atoms. A Fourier synthesis revealed the position of the remaining non-hydrogen atom. Full-matrix least-squares refinement in which the non-hydrogen atoms were given anisotropic temperature factors yielded an R index of 0.106. Calculated coordinates for those H atoms bonded to carbon, assuming a C—H bond length of 1.08 Å, were included in the refinement, and the sites of the hydrogens on nitrogen were located by difference Fourier. The H atom positional parameters were not refined; the refined isotropic thermal parameter for the H atoms grouped as alkyl, aryl, and nitrogen hydrogen atoms are listed in Table 2. Refinement converged to give R = 0.067 and $R_w = (\Sigma w||F_o| - |F_c||^2/\Sigma w|F_o|^2)^{1/2}$ = 0.060. The reflections 121, 202, and 104 were considered to be extinction affected and were omitted from the final cycles of the refinement, which converged to give R = 0.060 and R_w = 0.056 for the 1311 observed terms. (R = 0.107 for the total data.)

The direct-method calculations and least-squares refinements were made with the SHELX76 program (26). In the latter, the function minimized was $\Sigma w(|F_o| - |F_c|)^2$ with the terms being weighted according to $w = 1/\sigma^2|F_o|$. Final atomic coordinates and thermal parameters are listed in Table 2. The program ORTEP (27) was used to produce the diagrams. Details of intramolecular distances and angles, and least squares planes are given in Tables 3 and 4. Standard errors are enclosed in parentheses and are in units of the last place of decimals. Structure factors are deposited.[1]

Benzoylation of Ethyl 3-Amino-2-butenoate

The amino ester (12.9 g, 0.10 mol) and triethylamine (10.0 g, 0.10 mol) were boiled under reflux in tetrahydrofuran (200 mL) while benzoyl chloride (14.57 g, 0.105 mol) was added dropwise over 1 h. The solution was boiled for a further 2 h and then cooled and filtered to remove triethylamine hydrochloride. The filtrate was evaporated and the oily residue was recrystallized from pentane (500 mL) to give white crystals, mp 82–84°C (2.92 g). This material dissolved in $CDCl_3$ to give a 1:1 mixture of isomers **3***Z* and **3***E*, but was subsequently shown to be crystalline **3***E*. The mother liquor from the crystallization was evaporated and the remaining oil was dissolved in benzene and chromatographed over alumina. The first fraction (3.07 g) was recrystallized from pentane to give the *N*-benzoyl compound **2**, mp 48–48.5°C. Infrared spectrum ν_{max}: 3200, 1700, 1665 and 1630 cm^{-1}; ^{1}H nmr spectrum: 1.30 (t, J = 8 Hz, 3H), 2.55 (s, 3H), 4.23 (q, J = 8 Hz, 2H), 5.05 (s, 1H), 7.55 (m, 3H), 8.0 (m, 2H), 7.9 (bs, 1H). Subsequent fractions gave an oil (2.80 g) which could be seeded to yield crystalline **3***E*, followed by mixtures eluted with benzene – 5% ethyl acetate and containing ethyl acetoacetate.

Kinetics

The isomer **3***Z* (5.5 mg) was dissolved in $CDCl_3$ (0.50 mL) at 195 K (acetone – solid CO_2) in the nmr tube, which was then inserted into the precooled probe and warmed to the operating temperature for each run. Following Gutowsky (11) the average rate constant, k, was calculated by integration of several pairs of signals, but the best results were obtained with the singlet methyl resonances and these were used in the calculations. The values of k (s^{-1}) at the various temperatures were:
1.25×10^{-4} at 243 K; 2.26×10^{-4} at 248 K; 4.90×10^{-4} at 253 K; 6.08×10^{-4} at 258 K; 5.75×10^{-4} at 263 K; 1.88×10^{-3} at 268 K.

Acknowledgement

We record our appreciation of some discussions with Professor J. Clardy, Cornell University.

1. R. T. Buckler, H. E. Hartzler, and B. M. Phillips. J. Med. Chem. **18**, 509 (1975).
2. C. C. Barker. J. Chem. Soc. 317 (1954).
3. E. Benary. Ber. **42**, 3912 (1909).
4. Interatomic distances supplement. Chemical Society Special Publication No. 18. The Chemical Society, London. 1965.
5. B. R. Penfold and J. C. B. White. Acta Crystallogr. **12**, 130 (1959).
6. High resolution NMR spectra catalog. Spectrum No. 79. Varian Associates, Palo Alto, CA. 1962.
7. R. E. Wasylishen and T. Schaefer. Can. J. Chem. **51**, 3087 (1973).
8. D. Tourwé, G. Van Binst, S. A. G. De Graff, and U. K. Pandit. Org. Magn. Reson. **7**, 433 (1975).
9. H. S. Gutowsky, J. Jonas, and T. H. Siddall III. J. Am. Chem. Soc. **89**, 4300 (1967).
10. H. A. Staab and D. M. Lauer. Chem. Ber. **101**, 864 (1968).
11. S. Glasstone, K. J. Laidler, and H. Eyring. The theory of rate processes. McGraw-Hill, New York. 1941. (*a*) p. 1; (*b*) pp. 195–196.
12. A. A. Frost and R. G. Pearson. Kinetics and mechanism. 2nd ed. Wiley, New York. 1961. p. 100.
13. H. E. A. Kramer and R. Gompper. Z. Phys. Chem. **43**, 292 (1964).
14. U. Shmueli, H. Shanan-Atidi, H. Horwitz, and Y. Shvo. J. Chem. Soc. Perkin Trans. II, 657 (1973).
15. G. D. Andreetti, G. Bocelli, and P. Sgarabolto. J. Chem. Soc. Perkin Trans. II, 876 (1979).
16. J. Silverman and N. F. Yannoni. Acta Crystallogr. **18**, 756 (1965).
17. Y. Shvo and H. Shanan-Atidi. J. Am. Chem. Soc. **91**, 6683 (1969).
18. L. M. Jackman. *In* Dynamic nuclear magnetic resonance

[1]Copies may be obtained, at a nominal charge, from the Depository of Unpublished Data, CISTI, National Research Council of Canada, Ottawa, Ont., Canada K1A 0S2.

spectroscopy. *Edited by* L. M. Jackman and F. A. Cotton. Academic Press, New York. 1975.
19. U. BERG and U. SJÖSTRAND. Org. Magn. Reson. **11**, 555 (1978).
20. S. RAJAPPA and K. NAGARAJAN. J. Chem. Soc. Perkin Trans. II, 912 (1978).
21. G. E. MACIEL. J. Phys. Chem. **69**, 1947 (1965).
22. D. RABINOVITCH and Z. SHAKKED. Acta Crystallogr. Sect. B, **30**, 2829 (1974).
23. J. HORNSTRA and B. STUBBE. PW1100 Data Processing Program. Philips Research Laboratories, Eindhoven. 1972.
24. International tables for X-ray crystallography. Vol. 4. *Edited by* J. A. Ibers and W. C. Hamilton. Kynoch Press, Birmingham, England. pp. 99 and 148.
25. I. L. KARLE and J. KARLE. Acta Crystallogr. **17**, 1356 (1966).
26. G. M. SHELDRICK. SHELX, Program for crystal structure determination. Cambridge, England. 1975.
27. C. K. JOHNSON. ORTEP, Report ORNL-3794. Oak Ridge National Laboratory, Oak Ridge, TN. 1965.

Can. J. Chem. Downloaded from www.nrcresearchpress.com by 210.87.254.105 on 09/05/12
For personal use only.

Studies on the total synthesis of bisindole alkaloids within the voacamine family

JAMES P. KUTNEY,[1] AKIO HORINAKA, ROBERT S. WARD, AND BRIAN R. WORTH

Department of Chemistry, University of British Columbia, 2036 Main Mall, University Campus, Vancouver, B.C., Canada V6T 1Y6

Received February 11, 1980

This paper is dedicated to the memory of Dr. Léo Marion

JAMES P. KUTNEY, AKIO HORINAKA, ROBERT S. WARD, and BRIAN R. WORTH. Can. J. Chem. **58**, 1829 (1980).

The reactions of perivinol (**27**) with voacangine (**3**), and of perivinol with catharanthine (**29**), yield in each case two bisindole alkaloids of the voacamine type. ^1H and ^{13}C nmr data are used to assign structures to these compounds and the general utility of these techniques for determining the position of attachment of the 2-acylindole unit to the Iboga unit in such compounds is discussed. The reaction of dregaminol (**28**) with catharanthine is also reported.

JAMES P. KUTNEY, AKIO HORINAKA, ROBERT S. WARD et BRIAN R. WORTH. Can. J. Chem. **58**, 1829 (1980).

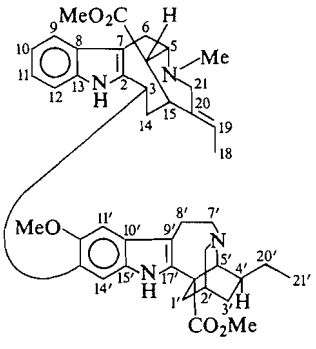
Les réactions du périvinol (**27**) avec la voacangine (**3**) et du périvinol avec la catharanthine (**29**) donnent dans chaque cas deux alcaloides bisindoles du type voacamine. On a utilisé les données de la rmn du ^1H et du ^{13}C pour attribuer les structures de ces composés et on discute de l'utilité générale de ces techniques dans la détermination du point d'attache de l'unité acyl-2 indole à l'unité Iboga dans ces composés. On décrit également la réaction du drégaminol (**28**) avec la catharanthine.

[Traduit par le journal]

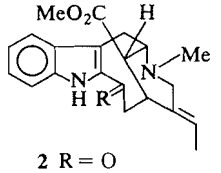
Introduction

The bisindole alkaloids of the voacamine type represent a large family of natural products which has received considerable attention in numerous laboratories (1). The majority of these investigations have concentrated on the isolation and structure elucidation of these systems and on the development of some chemistry concerned with the structural relationships between the various members. Our own recent interests have been concerned with the development of a totally synthetic approach which we hope could be sufficiently versatile to encompass the preparation of a substantial number of alkaloids within this family.

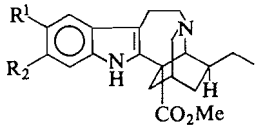
Structural analysis of voacamine (**1**) as the parent member of this series, as well as the more recently isolated alkaloids reveals that they all possess an indole part plausibly derived from a 2-acyl indole unit, for example vobasine (**2**), and an Iboga system, for example voacangine (**3**). Indeed a partial synthesis of voacamine (**1**) and its natural isomer voacamidine (**4**) was first achieved by Büchi and co-workers (2) by heating vobasinol (**5**) and voacangine (**3**) in dilute methanolic hydrogen chloride.



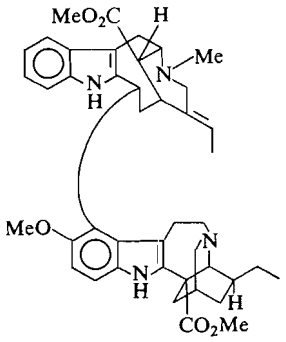
1



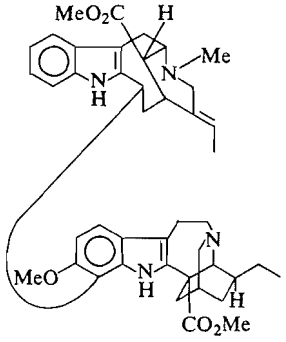
2 R = O
5 R = H, OH



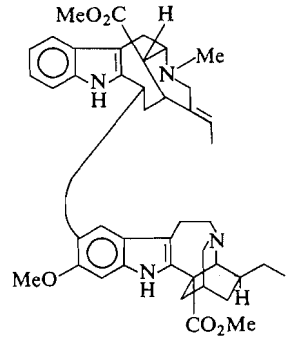
3 R^1 = MeO; R^2 = H
8 R^1 = H; R^2 = OMe



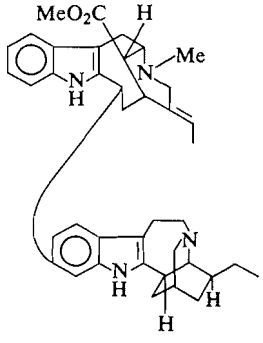
4



6



7



9

[1]Author to whom correspondence may be addressed.

0008-4042/80/171829-10$01.00/0

©1980 National Research Council of Canada/Conseil national de recherches du Canada

Can. J. Chem. Downloaded from www.nrcresearchpress.com by 210.87.254.5 on 09/05/12
For personal use only.

Can. J. Chem. Downloaded from www.nrcresearchpress.com by 210.87.254.5 on 09/05/12
For personal use only.

The bisindole alkaloids conodurine (**6**) and conoduramine (**7**) (3) represent examples where the Iboga unit is isovoacangine (**8**) while tabernamine (**9**) (4) represents the first example in which the aromatic ring of the Iboga unit lacks an oxygen substituent.

The recently isolated tabernaelegantines (5), for example, tabernaelegantines A and C (**10**), contain the dihydrovobasine type unit while the alkaloid accedinisine (**11**) (6) reveals a dimeric structure in which the Iboga unit has been replaced by a normacusine B type skeleton, the latter having been interrelated chemically with the 2-acylindole family (7).

On the basis of these examples it is clear that any versatile synthetic approach to this family of alkaloids must allow the functional variations inherent in these units.

The synthesis of the Iboga unit, as portrayed in tabernamine, has been completed in these and other laboratories (8) so that the introduction of the methoxyl group into the aromatic ring remains as the only synthetic step to be achieved. This problem is presently under study in these laboratories.

A synthetic sequence to the 2-acylindole unit has been recently completed in our laboratories (9) and the approach is sufficiently versatile to allow the extension to the various types of systems noted above.

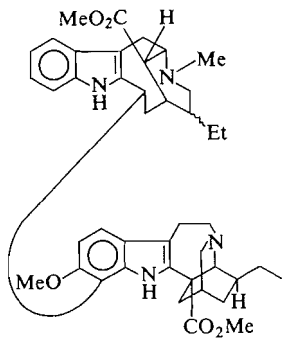
The third phase of our program concerns the further development of a versatile coupling process which would allow the required bisindole system to be derived from the appropriate monomeric units. We wish to report here some of our initial observations concerned with this aspect of the overall study.

As noted above, the coupling of vobasinol (**5**) with voacangine (**3**) does provide an entry into the voacamine family. However, in this instance the methoxyl activation within the voacangine system allows a specific reaction of carbon atoms 11 and 13 generating **1** and **4**. The situation is less clear with indole units lacking such functionality, as would be required in the synthesis of **9** and **11**. Although there are now a number of reported instances in which this type of reaction has been employed (4–7, 10–12), the position of attachment of the 2-acylindole unit to the Iboga system has not in all cases been unequivocally established. It became necessary to provide a more detailed study of this reaction and to determine its general utility with various indole systems.

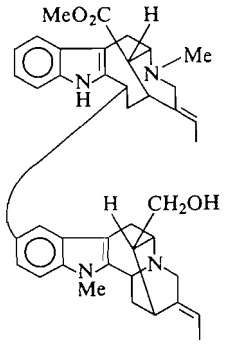
At the outset it was clear that an unambiguous spectroscopic method for direct assignment of the mode of coupling would be highly desirable and we selected ^{1}Hmr and ^{13}Cmr spectroscopy for this purpose. The results presented below amplify the utility of this method.

^{1}H Nuclear Magnetic Resonance Spectra

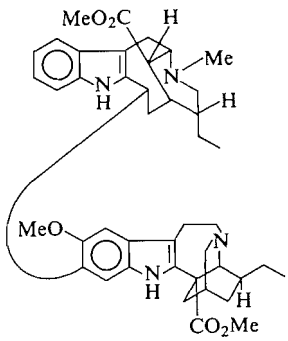
When the aromatic ring of the Iboga unit carries a methoxyl substituent, as in voacamine, the position of attachment of the 2-acyl indole moiety can be readily established on the basis of the ^{1}H nmr spectrum. Thus, the spectrum of voacamine (**1**) contains two one-proton singlets at 6.76 and 6.92 ppm



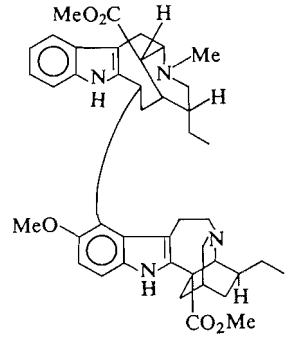
10



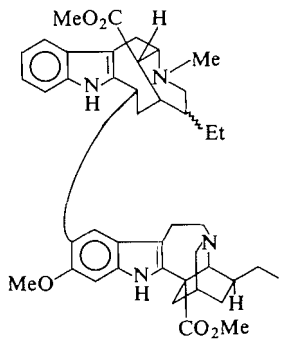
11



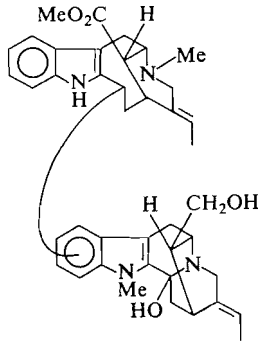
12



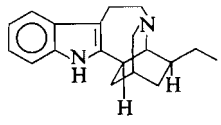
13



14



15



16

TABLE 1. ^{1}H nuclear magnetic resonance spectra of bisindole alkaloids derived from voacangine

	Voacangine **3**	Voacamine[a] **1**	Dihydrovoacamine **12**	Voacamidine[b] **4**	Dihydrovoacamidine **13**
H-11′	6.96 d (2)[c]	6.76 s	6.65 s	—	—
H-13′	6.83 dd (2, 8)	—	—	6.70 d (8.5)	6.76 d (8)
H-14′	7.16 d (8)	6.92 s	6.93 s	7.05 d (8.5)	7.09 d (8)
H-9 to H-12	—	≈7.02 m and 7.50	7.07 and 7.50 m	≈7.02 m and 7.50 d	7.02 and 7.47 m
NH	7.66 br s	7.71 and 7.50	7.76 and 7.46	7.85 and 7.41	7.82 and 7.42
H-3	—	5.2 br d	5.08 br d	5.50 m	5.46 br d
OMe	3.86 s	3.95 s	3.98 s	?	3.77 s
CO_2Me	3.72 s	3.61 s	3.64 s	3.08 s	3.04 s
NMe	—	2.58 s	2.93 s	2.58 s	2.84 s
CO_2Me	—	2.44 s	2.44 s	?	2.42 s

[a]References 2 and 6.
[b]References 3 and 6.
[c]Numbers in parentheses are J values (Hz).

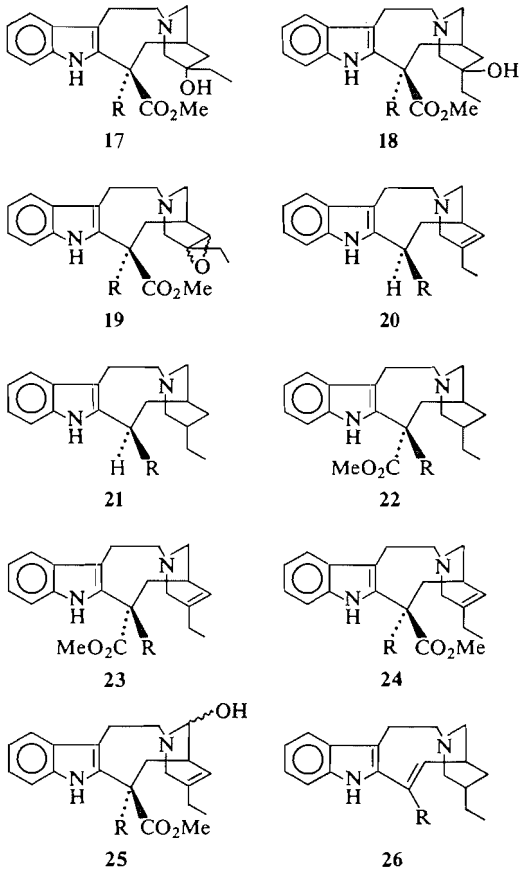
(2, 6), which can be assigned to H-11′ and H-14′. Voacamidine (**4**) on the other hand gives rise to two one-proton doublets (J = 8.5 Hz) at 6.70 and 7.05 ppm (3, 6), which can be assigned to the *ortho* related protons H-13′ and H-14′. Similarly, the spectrum of conodurine (**6**) contains two one-proton doublets (J = 8 Hz) at 7.26 and 6.82 ppm, while the spectrum of conoduramine (**7**) contains two one proton singlets at 6.91 and 6.79 ppm. Other relevant examples are shown in Tables 1 and 2.

If we next consider compounds in which the Iboga unit carries no other substituents on the aromatic ring, as in tabernamine (**9**), then the problem of assigning the correct structures becomes more difficult since the aromatic region of the ^{1}H nmr spectrum is more complex. Tabernamine is in fact the only compound of this type so far reported, although accedinisine (**11**) and accedinine (**15**) (6) are also useful for comparison purposes (cf. capuvosine and capuvosidine (12)). On the basis that, in the unsubstituted monomeric alkaloids, e.g. ibogamine (**16**), H-11 appears well downfield from the other aromatic protons (13, 14) the presence of a low-field doublet at 7.28 ppm in the spectrum of tabernamine (**9**) (4) is taken as evidence that the 2-acyl indole unit is bonded to C-13′ (see Table 3). By the same token, in accedinisine (**11**) the 2-acyl indole unit is assumed to be attached to C-12′ since a low-field singlet is observed at 7.20 ppm which can be assigned to H-11′ (6).

^{13}C *Nuclear Magnetic Resonance Spectra*

Examination of the ^{13}C nmr spectra of alkaloids of the vinblastine type (Table 4) reveals that the carbon atom of the vindoline unit which is directly bonded to the cleavamine unit is shifted downfield by ca. 16.4 ppm relative to its position in the spectrum of vindoline itself (see Fig. 1). Neighbouring carbon atoms are also affected in a reproducible manner by attachment of the cleavamine moiety.

Of more relevance to the present study is the observation of similar shifts in the spectra of tabernaelegantines A–D (5) when compared with the spectrum of isovoacangine (**8**) (Table 5). The ^{13}C nmr spectra therefore provide another approach to the problem of identifying the point of attachment in voacamine type alkaloids, and could be particularly useful in cases where the aromatic ring of the



Can. J. Chem. Downloaded from www.nrcresearchpress.com by 210.87.254.5 on 09/05/12
For personal use only.

TABLE 2. ^{1}H nuclear magnetic resonance spectra of bisindole alkaloids derived from isovoacangine

	Isovoacangine **8**	Conodurine **6**	Tabernaelegantines[a] **10A**	Tabernaelegantines[a] **10C**	Conoduramine **7**	Tabernaelegantines[a] **14B**	Tabernaelegantines[a] **14D**
H-11′	7.35 d (9)[b]	7.26 d (8)	7.24 d (9)	7.26 d (9)	6.91 s		
H-12′	6.78 m	6.28 d (8)	6.83 d (9)	6.84 d (9)	—	—	—
H-14′		—	—	—	6.79 s	6.78 s	6.78 s
H-9 to H-12	—	7.0–7.15 m	6.9–7.2 m	6.9–7.2 m	7.05 m	6.90–7.14 m	6.84–7.14 m
NH	7.65 m	7.56 and 7.68	7.62 and 7.68	7.58 and 7.64	7.54 and 7.63	7.56 and 7.68	7.59 and 7.74
H-3	—	5.30 m	5.29 m	5.27 m	5.13 m	5.06 m	5.04 m
OMe	3.83 s	3.97 s	3.96	3.96	3.97 br s	3.91 br	3.92 br
CO_2Me	3.72 s	3.69 s	3.70	3.70	3.66 s	3.67	3.67
NMe	—	2.68 br s	2.57	2.64	2.64 br s	2.57	2.63
CO_2Me	—	2.51 s	2.48	2.52	2.44 s	2.43	2.44

[a]Reference 5.
[b]Numbers in parentheses are J values (Hz).

TABLE 3. ^{1}H nuclear magnetic resonance spectra of bisindole alkaloids which lack a MeO substituent

	Ibogamine **16**	Tabernamine[a] **9**	Accedinisine[b] **11**	Accedinine[b] **15**
H-11′	7.50 (m, 1H)	7.28 d (8)[c]	7.20 s	
H-12′	7.0–7.3 (m, 3H)	6.88 d (8)	7.14 d (7)	6.92 s
H-13′		7.54 (m, 1H)	7.53 d (5)	7.54 m
H-14′		7.04(m, 4H)	6.90–7.09 (4H)	6.84–7.11 (5H)
H-9 to H-12	—			
NH	7.65 m		7.80	7.54
H-3	—	5.38 m	4.64 d (10)	4.60 d (10)
CO_2Me	—	—	—	—
NMe	—	2.56 s	2.58 s	2.60 s
CO_2Me	—	2.50 s	2.36 s	2.43 s

[a]Reference 4.
[b]Reference 6.
[c]Numbers in parentheses are J values (Hz).

Iboga unit is unsubstituted as for example in tabernamine (**9**).

Chemical Experiments

We have studied the reactions of perivinol (**27**) and dregaminol (**28**) with voacangine (**3**) and catharanthine (**29**), using the HCl/MeOH coupling procedure developed by Büchi *et al.* (2). The reaction of dregaminol with voacangine has been previously shown to yield two products, dihydrovoacamine (**12**) and dihydrovoacamidine (**13**) (2). The reaction of perivinol (**27**) with voacangine (**3**) also gave two products which were separated in small amounts by hplc and which both gave a molecular ion at m/e 690 in their mass spectra (for details see Experimental). The two compounds were identified as *N*-demethylvoacamine (**30**) and *N*-demethylvoacamidine (**31**) on the basis of their 270 MHz ^{1}H nmr spectra (Table 6). Thus, *N*-demethylvoacamine (**30**) exhibits two singlets in the aromatic region of its spectrum at 6.79 and 6.92 ppm which can be assigned to H-11′ and H-14′, whereas *N*-demethylvoacamidine exhibits two doublets (J = 8 Hz) at 6.77 and 7.09 ppm, which can similarly be assigned to H-13′ and H-14′. *N*-Demethylvoacamine has been reported as a natural product, occurring along with voacamine and voacamidine in *Tabernaemontana accedens* (6).

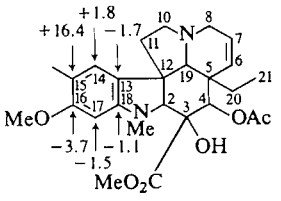
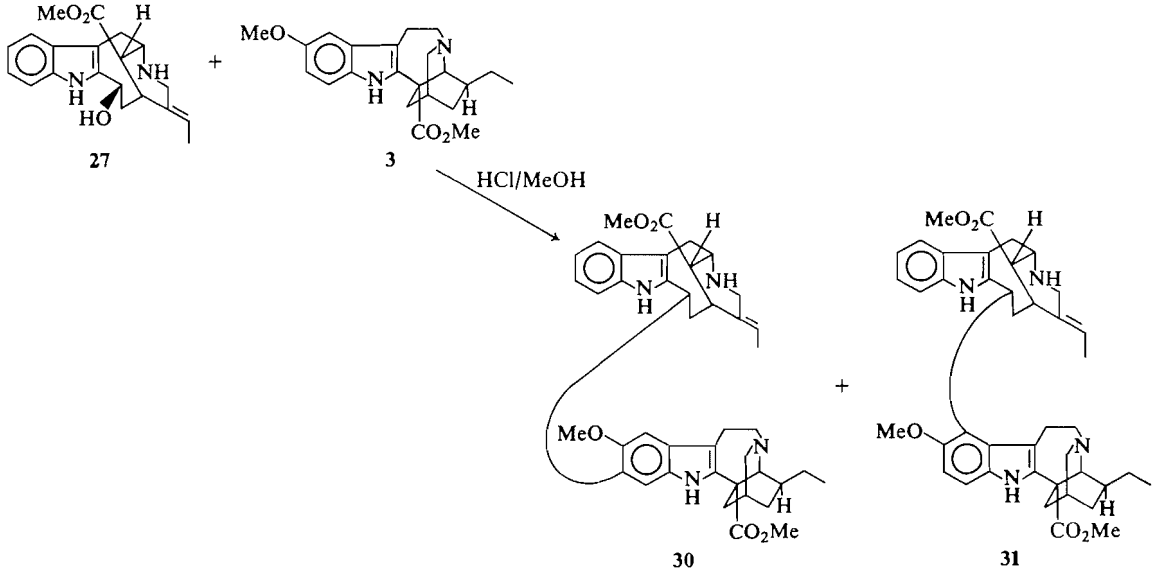


FIG. 1

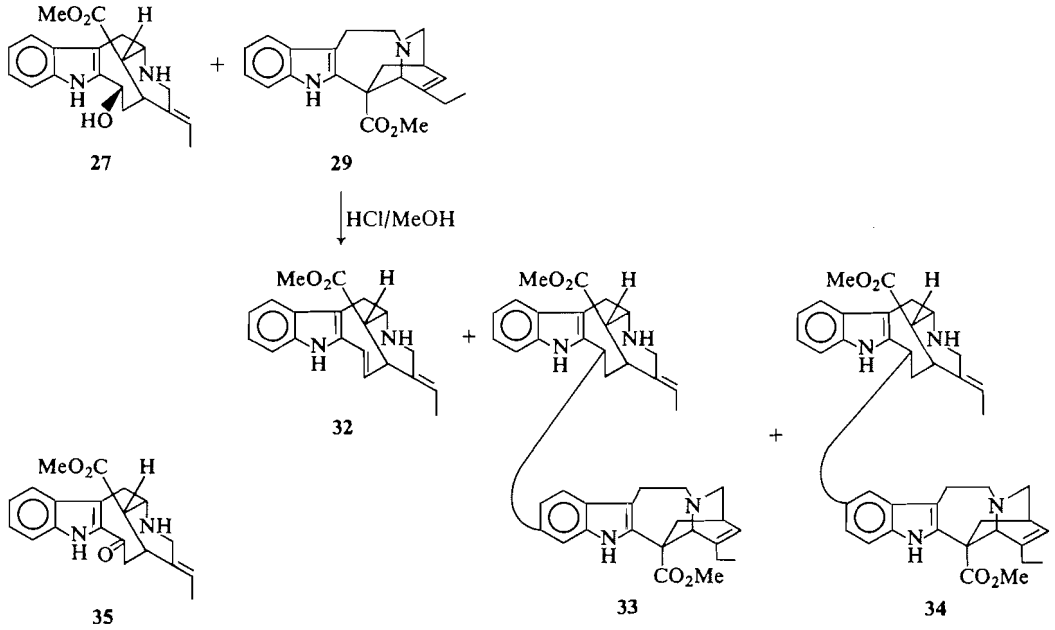
The reaction of perivinol (**27**) with catharanthine (**29**) afforded three products along with large amounts of unreacted catharanthine. The major product (34% yield) was readily identified as the alkene (**32**) formed by dehydration of perivinol (7). The two minor products (7% each) both showed a molecular ion at m/e 658 in their mass spectra and

Can. J. Chem. Downloaded from www.nrcresearchpress.com by 210.87.254.5 on 09/05/12
For personal use only.



exhibited uv spectra similar to that of tabernamine (**9**) (4). Although the ^{1}H nmr spectra of these products were, as expected, more complex than those of the methoxy substituted compounds, their structures could be tentatively assigned on the basis of their aromatic proton signals. Thus the presence of a doublet (J = 8 Hz) at 7.39 ppm in the spectrum of the less polar compound (Table 7), which can be assigned to H-11′ , indicates that both the 11′ and 12′ positions are unsubstituted in this compound. Furthermore, the presence of a singlet at 6.95 ppm indicates that the acyl–indole unit must be attached to C-13′ and the compound is therefore assigned structure **33**. In contrast, the ^{1}H nmr spectrum of the more polar compound showed a low-field singlet at 7.31 ppm, which can be assigned to H-11′, and which therefore indicates that in this case the acyl–indole unit is attached to C-12′. This compound is therefore assigned structure **34**.

These tentative conclusions are supported by an analysis of the ^{13}C nmr spectra of both compounds (Tables 8 and 9). The signal at 139.9 ppm in the spectrum of **33** can be assigned to C-13′ and is therefore shifted downfield by 18.6 ppm relative to its position in the spectrum of catharanthine itself (18). Similarly the signal at 137.6 ppm in the spec-



Can. J. Chem. Downloaded from www.nrcresearchpress.com by 210.87.254.5 on 09/05/12
For personal use only.

Can. J. Chem. Downloaded from www.nrcresearchpress.com by 210.87.254.5 on 09/05/12
For personal use only.

TABLE 4. ^{13}C nuclear magnetic resonance spectra of alkaloids of the vinblastine type

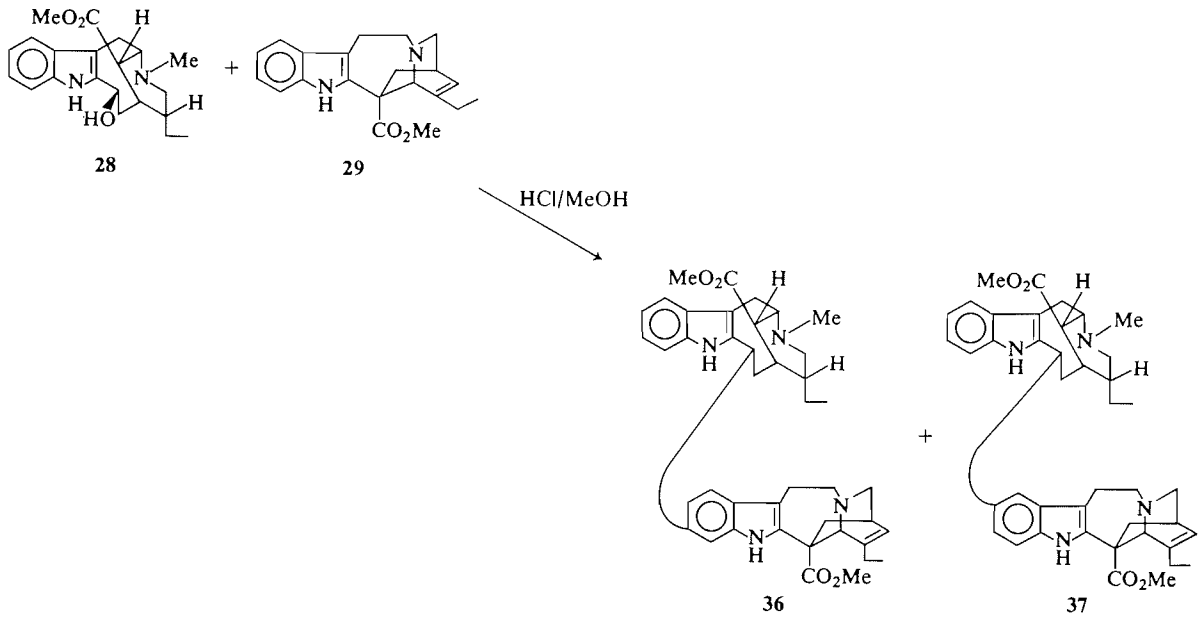
	Vindoline	Vinblastine[a] 17	Leurosidine[a] 18	Leurosine[a] 19	18′α-(15-Vindolyl) cleavamine[b] 20	21[c]	22[c]	23[c]	24[c]	25[c]	26[c]
2	83.2	83.0	83.1	83.1	83.2	83.3	83.0	83.1	83.5	83.3	83.8
3	79.5	79.3	79.5	79.5	79.5	79.9	80.0	79.9	79.8	79.7	80.2
4	76.2	76.1	76.2	76.2	76.2	76.4	76.6	76.5	76.5	76.5	76.8
5	42.8	42.3	42.6	42.6	42.8	42.8	42.9	42.9	42.9	42.8	43.2
6	130.2	129.7	129.7	129.7	130.2	130.6	130.6	130.6	130.1	129.8	130.6
7	123.9	124.3	124.3	124.3	124.0	124.4	124.4	124.6	124.5	123.4	124.4
8	50.9	50.0	50.2	50.2	50.9	50.9	50.9	50.9	50.5	50.3	51.3
10	51.9	50.0	50.2	50.2	52.0	50.9	50.9	50.9	50.5	50.3	52.0
11	43.9	44.3	44.5	44.5	43.9	43.8	43.9	43.8	44.6	44.6	44.1
12	52.6	52.9	53.1	53.1	53.0	53.2	53.3	53.4	53.6	53.3	53.3
13	124.9	122.6 (−1.9)[d]	123.0 (−1.9)	123.0 (−1.9)	122.4 (−2.5)	123.9 (−1.0)	124.4 (−0.5)	124.3 (−0.6)	122.5 (−2.4)	122.9 (−2.0)	123.4 (−1.5)
14	122.4	123.1 (+0.7)	123.4 (+1.0)	123.4 (+1.0)	124.6 (+2.2)	125.7 (+3.3)	126.1 (+3.7)	124.3 (−1.9)	123.2 (+0.8)	123.4 (+1.0)	124.7 (+2.3)
15	104.5	120.4 (+15.9)	120.4 (+15.9)	120.4 (+15.9)	120.2 (+15.7)	121.4 (+16.9)	121.6 (+17.1)	121.4 (+16.9)	121.2 (+16.7)	120.2 (+15.7)	122.0 (+17.5)
16	161.1	157.8 (−3.3)	157.6 (−3.5)	157.6 (−3.5)	157.4 (−3.7)	156.8 (−4.3)	156.3 (−4.8)	156.4 (−4.7)	158.2 (−2.9)	158.1 (−3.0)	158.1 (−3.0)
17	95.6	93.9 (−1.7)	94.0 (−1.6)	94.0 (−1.6)	93.9 (−1.7)	93.7 (−1.9)	94.5 (−1.1)	94.5 (−1.1)	94.3 (−1.3)	94.2 (−1.4)	94.4 (−1.2)
18	153.6	152.5 (−1.1)	152.8 (−0.8)	152.8 (−0.8)	151.7 (−1.9)	151.8 (−1.8)	152.0 (−1.6)	151.9 (−1.7)	153.0 (−0.6)	153.2 (−0.4)	153.1 (−0.5)
19	67.0	65.2	65.5	65.5	66.5			66.0	65.8	65.7	67.3
20	30.6	30.4	30.7	30.7	30.7	30.6	30.8	30.7	30.9	30.9	31.2
21	7.5	8.1	8.3	8.3	7.4	7.7	7.7	7.5	8.4	8.4	8.1
CO_2Me	170.4	170.6	170.7	170.7	170.4	170.8	170.8	170.7	170.9	170.9	171.1
	51.9	51.8	51.9	52.1	51.9	52.1	52.1	52.0	52.1	52.2	52.4
ArOMe	55.1	55.3	55.7	55.7	55.7	55.9	56.1	56.0	55.9	55.0	56.3
NMe	38.0	38.0	38.2	38.2	38.5	38.1	38.3	38.3	38.3	38.2	38.7
Ac	171.7	171.4	171.4	171.4	171.5	171.7	171.6	171.6	171.7	171.7	172.1
	20.8	20.7	21.0	21.0	20.9	21.0	21.1	21.0	21.1	21.1	21.4

[a]Reference 15.
[b]Reference 16.
[c]J. P. Kutney, V. E. Ridaura-Sanz, E. Jahngen, and J. Balsevich. Unpublished results.
[d]Values in parentheses represent the shift from the corresponding value for vindoline.

TABLE 5. ^{13}C nuclear magnetic resonance spectra of tabernaelegantines

	Isovoacangine[a]	Tabernaelegantines[b]			
	8	**10A**	**10C**	**14B**	**14D**
17	136.3	136.3	136.2	135.1	135.5
19	51.4	51.3	51.3	51.6	51.5
7	53.1	53.0	53.0	53.2	53.4
8	22.2	22.1	22.1	22.2	22.0
9	110.0	110.5	110.3	111.1	110.1
10	123.2	124.6(+1.4)[c]	124.5 (+1.3)	122.9 (−0.3)	122.7 (−0.5)
11	119.0	117.1 (−1.9)	117.1 (−1.9)	117.6 (−1.4)	117.3 (−1.7)
12	108.9	105.1 (−3.8)	105.1 (−3.8)	127.9 (+19.0)	126.9 (+18.0)
13	156.5	152.1 (−4.4)	152.1 (−4.4)	153.8 (−2.7)	153.4 (−3.1)
14	94.3	114.9 (+20.6)	115.1 (+20.8)	93.0 (−1.3)	93.2 (−1.1)
15	135.3	135.4 (+0.1)	135.3 0	138.2 (+2.9)	139.0 (+3.7)
2	27.4	27.2	27.1	27.5	27.3
3	32.1	32.0	31.9	32.2	31.8
18	55.1	54.7	54.6	55.2	54.9
1	36.4	35.0	35.1	36.5	36.1
21	11.7	11.6	11.6	11.7	11.7
20	26.7	26.6	26.6	26.8	26.8
4	39.2	38.9	38.9	39.3	39.1
5	57.6	57.6	57.6	57.7	57.6
CO	175.9	174.9	175.0	176.2	175.8
OMe	52.5	52.3	52.3	52.5	52.7
ArOMe	55.7	57.0	56.8	56.0	56.1

[a]Reference 17.
[b]Reference 5.
[c]Values in parentheses represent the shift from the corresponding value for isovoacangine.



trum of **34** can be assigned to C-12′ and is shifted downfield by 18.7 ppm relative to its position in the spectrum of catharanthine (**29**).

The reaction of dregaminol (**28**) with catharanthine (**29**) also gave two dimeric products (M^+ 674) which by analogy with the perivinol–catharanthine reaction are assumed to have structures **36** and **37**. The two compounds were separated by thick layer chromatography but due to the very small amounts of material available were not fully characterized.

Although these preliminary efforts did show the feasibility of coupling various indole units to the voacamine type dimers, the method was obviously not satisfactory for the efficient production of compounds for biological testing. In this light, alternative methods of accomplishing the coupling in-

Can. J. Chem. Downloaded from www.nrcresearchpress.com by 210.87.254.5 on 09/05/12
For personal use only.

TABLE 6. ^{1}H nuclear magnetic resonance spectra of products from perivinol–voacangine reaction

	N-Demethylvoacamine **30**	*N*-Demethylvoacamidine **31**
H-11′	6.79 s	—
H-13′	—	6.77 d (8)[a]
H-14′	6.92 s	7.09 d (8)
H-9 to H-12	7.05 and 7.55 m	7.04 and 7.55 m
NH	7.70 and 7.50	7.77 and 7.44
H-3	5.15 m	5.25 m
OMe	3.95 br s	3.78 s
CO_2Me	3.68 s	3.14 s
CO_2Me	2.50 s	2.48 s

[a]Numbers in parentheses are *J* values (Hz).

cluding the further use of the alkenes such as **32** have come under active investigation. Products derivable by these means will be reported elsewhere.

Experimental

Ultraviolet spectra were recorded on a Cary 15 spectrophotometer. Low resolution mass spectra were recorded on either an Atlas CH-4B or an AEI MS-902 spectrometer. High resolution mass measurements were made on an AEI MS-50 spectrometer. THe ^{1}H nmr spectra were recorded on Varian XL-100 and Nicolet Oxford H-270 instruments; ^{13}C nmr spectra were recorded on a Bruker WP-80 instrument. Chemical shifts are reported as ppm from tetramethylsilane which was used as internal standard. Nuclear magnetic resonance data for compounds **30**–**34** are given in Tables 6–9.

Perivinol (**27**) and dregaminol (**28**) were prepared by sodium borohydride reduction of the corresponding 2-acyl indole alkaloids (2). Dihydrovoacamine (**12**) and dihydrovoacamidine (**13**) were prepared by the method previously described by Büchi *et al.* (2).

Reaction of Voacangine with Perivinol

A mixture of voacangine (20 mg) and perivinol (20 mg) in 1% methanolic hydrogen chloride (4 mL) was heated under reflux for 1½ h in an atmosphere of nitrogen. The reaction mixture was then diluted with water (8 mL) and neutralized with sodium carbonate giving a heavy white precipitate which was extracted with dichloromethane. The residue obtained on evaporation (40 mg) was separated by column chromatography on silica gel to give the two bisindole alkaloids (total yield 26 mg) which were further purified by reverse phase hplc (70% CH_3CN – 30% H_2O) to give N-*demethylvoacamine* (**30**); uv (EtOH) λ_{max}: 220 (27, 922), 284 (10, 578), 292 (10, 488) nm; *m/e*: 704(*M* + 14, 1%), 690(M^+, 1.7%), 538(1), 524(1), 511(1.3), 491(0.7), 463(0.7), 446(0.7), 435(0.7), 429(1.5), 421(1), 407(1), 393(1.5), 379(1), 368(2.5), 355(2.5), 341(1.5), 323(2), 309(2), 295(2), 281(7), 207(7), 149(80), 121(35), 119(94), 117(100%); *Exact Mass* calcd. for $C_{42}H_{50}N_4O_5$: 690.3780; found (ms): 690.3791); and N-*demethylvoacamidine* (**31**); uv(EtOH) λ_{max}: 228 (24, 840), 284 (11, 040), 292 (10, 488) nm; *m/e*: 704(*M* + 14, 2%), 690(M^+, 1.7%), 538(3.5), 524(1.5), 511(0.5), 509(1), 409(1), 393(1), 368(1), 355(1), 350(1.5), 295(1.7), 281(2.5), 207(7), 149(100), 121(25), 119(50), 117(60%); *Exact Mass* calcd. for $C_{42}H_{50}N_4O_5$: 690.3780; found (ms): 690.3784.

Reaction of Catharanthine with Perivinol

A mixture of catharanthine (250 mg) and perivinol (250 mg) in 1% methanolic hydrogen chloride (25 mL) was heated under reflux for 1½ h in an atmosphere of nitrogen. Work-up as described in the previous experiment gave a residue (ca. 500 mg) which was separated by preparative hplc using a stainless steel column (12 in. × 1 in.) packed with Porasil A. Elution with dichloromethane – 2% methanol containing 0.1% triethylamine at a flow-rate of ca. 18 mL/min afforded unreacted catharanthine (210 mg), *3,14-dehydrodeoxoperivine* (**32**) (86 mg); uv(EtOH) λ_{max}: 227 (19, 588), 296 (9, 258) nm; *m/e*: 322.1681(M^+, $C_{20}H_{22}N_2O_2$, 55%), 263.1546(*M* − 59, $C_{18}H_{19}N_2$, 12%), 222.1269 ($C_{16}H_{16}N$, 15%), 221.1202 ($C_{16}H_{15}N$, 23%), 220.1128 ($C_{16}H_{14}N$, 20%), 206.0959 ($C_{15}H_{12}N$, 23%), 194.0956 ($C_{14}H_{12}N$, 11%), 180.0816 ($C_{13}H_{10}H$, 12%), 168.0799 ($C_{12}H_{10}N$, 18%), 167.0729 ($C_{12}H_9N$, 36%), 149.0244 ($C_{11}H_3N$, 15%), 130.0653 ($C_9H_{10}N$, 11%); *3-(13′-catharanthinyl)deoxoperivine* (**33**) (34 mg); uv(EtOH) λ_{max}: 228 (45, 786), 285 (16, 724), 293 (16, 450) nm; *m/e*: 672(*M* + 14, 0.2%), 658(M^+, 0.5%), 644(0.2), 551(1),

TABLE 7. ^{1}H nuclear magnetic resonance spectra of products from perivinol–catharanthine reaction

	Perivinol **27**	Catharanthine **29**	**32**	**33**	**34**
H-11′	—	7.37 d (8)[a]	—	7.39 d (8)	7.31 s
H-12′	—	7.03 m	—	7.05 m	6.9–7.15 m
H-13′	—		—		
H-14′	—	7.14 d (8)	—	6.95 s	
H-9	7.51 d (8)	—	7.52 d (8)	7.54 d (8)	7.55 m
H-10	7.11 m	—	7.10 m	7.05 m	6.9–7.15 m
H-11		—			
H-12	7.27 d	—	7.25 d		
NH	8.40 s	7.72 s	7.97 s	7.57 m	7.45 and 7.6
H-3		—	6.35 dd (3,12)	4.66 d (12)	4.66 d (12)
H-3′	—	5.92 d (4)	—	5.90 br d	5.90 br d.
H-21′	—	1.10 t (7)	—	1.03 t (7)	1.03 t (7)
H-19	5.38 q (6.5)	—	5.51 q (6.5)	5.37 q (6.5)	5.35 q (6.5)
H-18	1.68 dd (2,6.5)	—	1.73 dd (2,6.5)	1.65 dd	1.64 dd
CO_2Me	—	3.71 s	—	3.68 s	3.72 s
CO_2Me	2.39 s	—	2.38 s	2.50 s	2.48 s

[a]Numbers in parentheses are *J* values (Hz).

Can. J. Chem. Downloaded from www.nrcresearchpress.com by 210.87.254.5 on 09/05/12
For personal use only.

TABLE 8. ^{13}C nuclear magnetic resonance spectra of acyl–indole derivatives

	Vobasine[a] **2**	Vobasinol[a] **5**	Perivine **35**	Perivinol **27**	**32**	**33**	**34**
2	133.8	135.4	134.2	135.6	134.8	135.3	136.1
3	189.9	66.8	190.4	67.3	120.9	38.4	38.5
5	57.0	59.4	56.8	53.3	47.4	53.4	53.4
6	20.2	19.6	22.6	24.9	22.6	24.8	25.0
7	119.9	107.3	119.1	108.3	109.9	109.6	109.9
8	128.0	128.7	128.4	129.2	128.2	128.6	129.1
9	120.3	117.6	121.3	117.8	118.4	118.6	118.1
10	119.9	118.6	118.7	118.1	118.9	119.2	119.0
11	126.2	121.4	126.4	122.0	121.9	121.9	121.7
12	111.8	110.0	111.9	110.5	110.6	110.9	110.7
13	136.4	136.7	136.7	137.1	136.3	136.8	137.2
14	42.8	35.5	42.8	35.8	132.8	37.6	37.4
15	30.5	29.2	29.9	30.0	37.1	34.2	34.2
16	46.2	47.1	48.5	50.7	50.4	49.7	49.9
18	12.0	12.2	12.8	12.1	12.3	12.2	12.2
19	120.0	118.6	120.4	119.2	119.4	119.5	119.0
20	135.8	136.5	138.3	139.9	135.5	137.4	137.3
21	51.5	53.9	43.4	44.5	43.6	44.4	44.0
CO	170.9	174.3	172.2	174.8	170.3	171.6	171.4
OMe	50.1	50.3	50.7	50.5	49.8	50.7	49.9
NMe	42.2	42.1	—	—	—	—	—

[a]Reference 19.

TABLE 9. ^{13}C nuclear magnetic resonance spectra of catharanthine derivatives

	Catharanthine **29**	**33**	**34**
17′	136.0	136.1	136.1
19′	52.9	53.1	53.4
7′	49.3	49.4	49.9
8′	21.0	21.4	21.5
9′	110.2	110.6	110.2
10′	128.4	129.7 (+1.3)[a]	129.8 (+1.4)
11′	117.7	117.7 (0)	116.9 (−0.8)
12′	118.9	121.7 (+2.8)	137.6 (+18.7)
13′	121.3	139.9 (+18.6)	117.7 (−3.6)
14′	110.2	110.0 (−0.2)	111.1 (+0.9)
15′	134.7	133.6 (−1.1)	133.9 (−0.8)
2′	30.4	30.8	31.1
3′	123.4	123.5	123.5
18′	55.0	55.5	55.5
1′	38.0	39.3	38.5
21′	10.5	10.7	10.7
20′	25.9	26.2	26.2
4′	148.5	149.3	149.3
5′	61.5	62.0	61.8
CO	173.6	173.9	174.0
OMe	52.0	52.3	52.3

[a]Values in parentheses represent the shift from the corresponding value for catharanthine.

446(0.5), 385(1), 372(2), 368(2.5), 354(14), 352(13), 340(17), 336(17), 323(25), 322(62), 321(34), 237(62), 180(62), 169(62), 168(70), 167(63), 166(64), 156(65), 135(73), 108(77), 107(100), 106(92%); *Exact Mass* calcd. for $C_{41}H_{46}N_4O_4$: 658.3513, found (ms): 658.3531; and *3-(12′-catharanthinyl)deoxoperivine* (**34**) (35 mg); uv(EtOH) λ_{max}: 228 (33, 448), 284 (15, 902), 292 (14, 806) nm; *m/e*: 672(*M* + 14, 0.3%), 658(M^+, 1%), 644(0.7), 551(0.5), 446(0.5), 385(1), 372(1), 368(2), 354(5), 352(7), 340(10), 336(8), 323(15), 322(46), 321(25), 237(18), 180(28), 169(55), 168(63), 167(37), 166(30), 156(35), 135(70), 108(75), 107(100), 106(96%); *Exact Mass* calcd. for $C_{41}H_{46}N_4O_4$: 658.3513; found (ms): 658.3525.

Reaction of Catharanthine with Dregaminol

A mixture of catharanthine (30 mg) and dregaminol (35 mg) in 1% methanolic hydrogen chloride (5 mL) was heated under reflux for 1½ h in an atmosphere of argon. Work-up as described above gave a yellow oil which was separated by preparative tlc to give catharanthine (17 mg) and the two bisindole alkaloids which were further purified by preparative tlc to give *3-(13′-catharanthinyl)deoxodregamine* (**36**) (26 mg); uv(MeOH) λ_{max}: 227 (47, 813), 286 (15, 554), 293 (16, 702) nm; ν_{max}($CHCl_3$): 3465, 3360, 2940, 1720, 1465, 1450, 1440, 1340, 1326, 1290, 1155, 1080, 1050, 985, 900, 880 cm^{-1}; δ ($CDCl_3$): 8.14 (br s, 2H, NH), 7.1–7.6 (m, 7H), 5.00 (dd, 4, 11), 3.38 (s, 3H), 2.77 (s, 3H), 2.48 (s, 3H); *m/e*: 688(*M* + 14, 0.5%), 674(M^+, 2.7%), 565(0.8), 547(0.8), 533(0.8), 492(1), 479(0.8), 387(4), 385(5), 370(18), 354(32), 352(30), 338(100), 323(90%); and *3-(12′-catharanthinyl)deoxodregamine* (**37**) (6 mg); uv(MeOH) λ_{max}: 227(41, 442), 287 (14, 118), 293 (14, 573) nm; *m/e*: 688(*M* + 14, 0.2%), 674(M^+, 3.3%), 493(0.8), 480(1), 383(13), 370(65), 369(85), 367(55), 353(70), 351(55), 339(74), 338(84), 337(88), 336(75), 323(75), 322(84), 321(76), 308(68), 307(63), 306(79), 305(78), 304(74), 293(65), 292(76), 291(62), 290(80), 280(78), 279(80), 278(90), 276(80), 264(65), 252(82), 251(68), 250(65), 248(68), 238(80), 237(75), 235(75), 224(85), 223(85), 222(80), 221(80), 220(70), 219(70), 210(80), 209(90), 208(80), 207(85), 206(80), 205(80), 187(100), 181(100%).

Acknowledgements

Financial aid from the Natural Sciences and Engineering Research Council of Canada is gratefully acknowledged. We are also grateful to the Lilly

Can. J. Chem. Downloaded from www.nrcresearchpress.com by 210.87.254.5 on 09/05/12
For personal use only.

Laboratories, Indianapolis, IN, for generous gifts of perivine and catharanthine and to Dr. U. Renner, Research Laboratories, Ciba-Geigy, Basel for samples of voacangine and various bisindole alkaloids.

1. A. A. GORMAN, M. HESSE, H. SCHMID, P. G. WASER, and W. H. HOPFF. *In* The alkaloids. *Edited by* J. E. Saxton. Specialist Periodical Reports. Vol. 1. The Chemical Society, London. 1971. p. 242.
2. G. BÜCHI, R. E. MANNING, and S. A. MONTI. J. Am. Chem. Soc. **85**, 1893 (1963); **86**, 4631 (1964).
3. U. RENNER and H. FRITZ. Tetrahedron Lett. 283 (1964).
4. D. G. I. KINGSTON, D. B. GERHART, and F. IONESCU. Tetrahedron Lett. 649 (1976).
5. E. BOMBARDELLI, A. BONATI, B. GABETTA, E. M. MARTINELLI, G. MUSTICH, and B. DANIELS. J. Chem. Soc. Perkin Trans. I, 1432 (1976).
6. H. ACHENBACH and E. SCHALLER. Chem. Ber. **109**, 3527 (1976).
7. M. GORMAN and J. SWEENEY. Tetrahedron Lett. 3105 (1964).
8. J. P. KUTNEY. *In* Alkaloids. *Edited by* K. Wiesner. MTP International Review of Science. Series 1. Vol. 9. Butterworths, London. 1973. p. 27.
9. J. P. KUTNEY, G. K. EIGENDORF, H. MATSUE, A. MURAI, K. TANAKA, W. L. SUNG, K. WADA, and B. R. WORTH. J. Am. Chem. Soc. **100**, 938 (1978).
10. J. R. KNOX and J. SLOBBE. Aust. J. Chem. **28**, 1813 (1975).
11. F. PUISIEUX, J.-P. DEVISSAGUET, C. MIET, and J. POISSON. Bull. Soc. Chim. Fr. 251 (1967).
12. I. CHARDON-LORIAUX and H.-P. HUSSON. Tetrahedron Lett. 1845 (1975); I. CHARDON-LORIAUX, M.-M. DEBRAY, and H.-P. HUSSON. Phytochem. **17**, 1605 (1978).
13. P. J. BLACK and M. L. HEFFERNAN. Aust. J. Chem. **18**, 353 (1965).
14. J.-Y. LALLEMAND and T. BERNATH. Bull. Soc. Chim. Fr. 4091 (1970).
15. E. WENKERT, E. W. HAGAMAN, B. LAL, G. E. GUTOWSKI, A. S. KATNER, J. C. MILLER, and N. NEUSS. Helv. Chim. Acta, **58**, 1560 (1975).
16. E. WENKERT, E. W. HAGAMAN, N. KUNESCH, N.-Y. WANG, and B. ZSADON. Helv. Chim. Acta, **59**, 2711 (1976).
17. M. DAMAK, C. POUPAT, and A. AHOND. Tetrahedron Lett. 3531 (1976).
18. E. WENKERT, D. W. COCHRAN, H. E. GOTTLIEB, E. W. HAGAMAN, R. B. FILHO, F. J. A. MATOS, and M. I. L. C. MADRUGA. Helv. Chim. Acta, **59**, 2437 (1976).
19. A. AHOND, A. M. BUI, P. POTIER, E. W. HAGAMAN, and E. WENKERT. J. Org. Chem. **41**, 1878 (1976).

Can. J. Chem. Downloaded from www.nrcresearchpress.com by 210.87.254.5 on 09/05/12
For personal use only.

Direct non-invasive observation of metabolism in living cells by ^{13}C nuclear magnetic resonance spectroscopy

GERARDO BURTON, ROBERT L. BAXTER, J. MARTYN GUNN, PHILIP J. SIDEBOTTOM, PAUL E. FAGERNESS, KOZO SHISHIDO, JOHN Y. LEE, AND A. IAN SCOTT[1]

Departments of Chemistry and Biochemistry, Texas A&M University, College Station, TX 77843, U.S.A.

Received February 12, 1980

This paper is dedicated to the memory of Dr. Léo Marion

GERARDO BURTON, ROBERT L. BAXTER, J. MARTYN GUNN, PHILIP J. SIDEBOTTOM, PAUL E. FAGERNESS, KOZO SHISHIDO, JOHN Y. LEE, and A. IAN SCOTT. Can. J. Chem. **58**, 1839 (1980).

Applications of ^{13}C nmr in following the metabolism and fate of ^{13}C enriched substrates in whole cells are described. Studies on the elaboration of coproporphyrinogens I (**2***a*) and III (**2***b*) from [5-^{13}C]-δ-aminolevulinic acid (**1**) and [11-^{13}C]-porphobilinogen (PBG, **3**), in *Rhodopseudomonas spheroides* and *Propionibacterium shermanii*, respectively, the randomization of ^{13}C from [3-^{13}C]-propionate by *P. shermanii*, the biosynthesis of citrate, gentisalcohol (**4**), and patulin (**5**) from [2-^{13}C]-acetate by *Penicillium urticae*, and the anaerobic metabolism of [1-^{13}C]-glucose in rabbit erythrocytes are reported.

GERARDO BURTON, ROBERT L. BAXTER, J. MARTYN GUNN, PHILIP J. SIDEBOTTOM, PAUL E. FAGERNESS, KOZO SHISHIDO, JOHN Y. LEE et A. IAN SCOTT. Can. J. Chem. **58**, 1839 (1980).

On décrit les applications de la rmn du ^{13}C à l'étude du métabolisme et de l'évolution des substrats enrichis en ^{13}C dans les cellules entières. On décrit les études réalisées (*a*) sur l'élaboration des coproporphyrinogènes I (**2***a*) et III (**2***b*) à partir de l'acide [^{13}C-5]-δ-aminolévulinique (**1**) et du [^{13}C-11]porphobilinogène (PBG, **3**) dans le *Rhodopseudomonas sphéroides* et le *Propionibactérium shermanii* respectivement, (*b*) sur la distribution au hasard du ^{13}C du [^{13}C-3]propionate par le *P. shermanii*, (*c*) sur la biosynthèse du citrate, du gentisalcool (**4**) et de la patuline (**5**) à partir de l'acétate [^{13}C-2] par le *Penicillium urticae* et (*d*) sur le métabolisme anaérobique du [^{13}C-1] glucose dans les érythrocytes du lapin.

[Traduit par le journal]

In the last decade nmr spectroscopy has been developed as an elegant method of studying metabolic processes *in vivo*. The pioneering studies of Moon and Richards in 1973 set the stage for numerous studies using ^{31}P nmr as a non-invasive technique for metabolic studies (1–4 and references cited therein). Although ^{13}C nmr was first used in 1972 (5) as a probe for yeast metabolism, the inherent difficulties of sensitivity and decoupling with ^{13}C delayed the development of the method until quite recently when it was shown independently by Shulman and co-workers (6, 8) and by our group (7) that Cmr spectroscopy is a powerful tool for viewing the metabolic flux of ^{13}C-enriched substrates *in vivo*. In this paper we describe the further development of this technique to study metabolic processes in four organisms, *Rhodopseudomonas spheroides, Propionibacterium shermanii, Penicillium urticae,* and red blood cells (rabbit erythrocytes). The technique has the great advantage of viewing intracellular and extracellular metabolites as they are formed, since the simple experiment of washing the cells and resuspension can be used to check location of the signals. The main problem is that of maintaining field homogeneity, but the examples which follow have all been studied at low field (20 MHz in ^{13}C) in a Varian FT-80 instrument using conventional programming and standard 10 mm tubes. Under these conditions excellent spectra can be recorded. These studies should also be regarded as a preliminary test of a method which will gain its full power at superconducting fields in wide tubes where other problems such as dissipation of heat generated by decoupling have to be solved.

δ-*Aminolevulinic Acid Metabolism in* Rhodopseudomonas spheroides

The ^{13}C nmr spectra of cells of *R. spheroides* immediately following addition of [5-^{13}C]-aminolevulinic acid (**1**) and after a 16 h incubation are shown in Fig. 1. Multiplets observed at 21.9 and 125.0 ppm ($^1J_{^{13}C-^{13}C}$ = 51.5 Hz) are assigned to the *meso* methylene and α-pyrrolic carbons of coproporphyrinogens (copro'gen) I (**2***a*) and III (**2***b*) (1:3), respectively. While the type I isomer presents only two doublets at 125.0 and 21.9 ppm corresponding to the α-pyrrolic and *meso* carbons, copro'gen III has a doublet at 125 ppm for the α-pyrrolic carbons, a doublet at 22.0 ppm corresponding to the α and β *meso* carbons, a triplet at 22.0 ppm for the γ *meso* carbon, and a singlet at 21.9 ppm for the δ *meso* carbon.

Due to the superposition of copro'gen I and III

[1]Author to whom correspondence should be addressed at the Chemistry Department, University of Edinburgh, West Mains Road, Edinburgh, Scotland.

0008-4042/80/171839-08$01.00/0

©1980 National Research Council of Canada/Conseil national de recherches du Canada

Can. J. Chem. Downloaded from www.nrcresearchpress.com by 210.87.254.42 on 09/05/12
For personal use only.

Can. J. Chem. Downloaded from www.nrcresearchpress.com by 210.87.254.42 on 09/05/12
For personal use only.

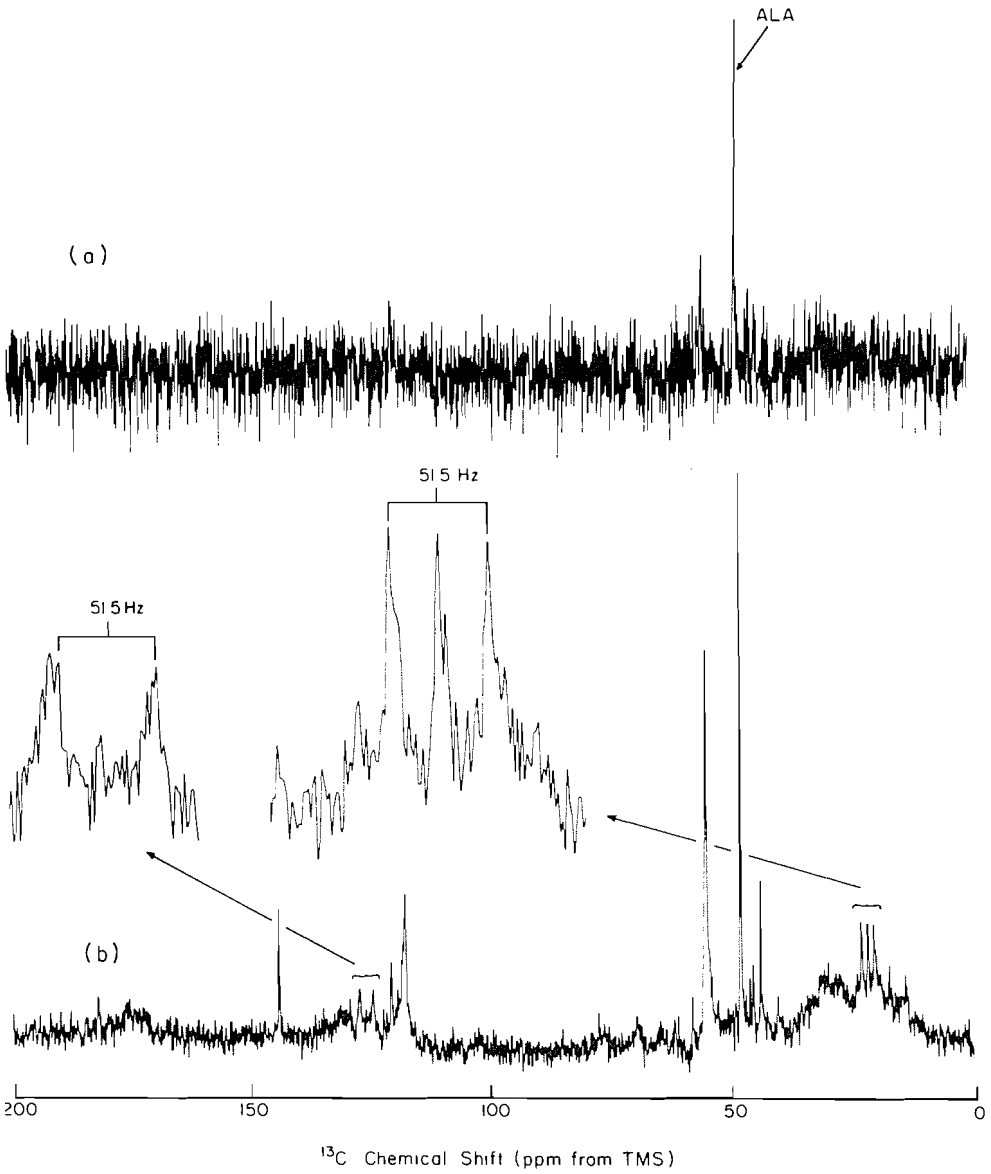
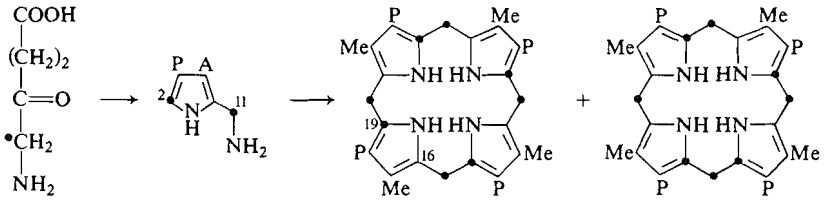


FIG. 1. Spectra of cells of *R. spheroides* (ATCC 17023) fed with [5-^{13}C]-aminolevulinic acid (ALA, 12 μmol). Cells were grown anaerobically under illumination for 17 days in ATCC medium 550, harvested by centrifugation at 13 700 g, washed and suspended in phosphate buffer (100 μ*M*, pH 7.6, ca. 10^9 cells/mL); (*a*) spectrum at 0 h (900 pulses), (*b*) spectrum at 16 h (70 713 pulses).

resonances and the non-quantitative instrumental conditions (dictated by signal-to-noise considerations), it is not possible to determine accurately the relative incorporation of [5-^{13}C]-ALA into each of the *meso* and α-pyrrolic positions by analysis of line intensities (9). However, the close similarity of the observed *meso* carbon multiplet to the intensity pattern calculated for a 1:3 mixture of **2***a* and **2***b* uniformly enriched in the positions shown indicates that the labelled precursors are not significantly diluted by endogenous substrates. Similar spectra were obtained for the supernatant and for washed packed cells showing that isomers were observed both intra- and extra-cellularly.

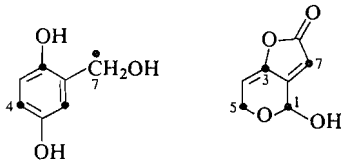
Porphobilinogen and Glucose Metabolism in Propionibacterium shermanii

In a similar experiment, [11-^{13}C]-PBG (**3**) was added to *P. shermanii* cells in a glucose-supplemented phosphate buffer, thus producing copro'gen I (**2***a*) and III (**2***b*) labelled exclusively in the *meso* methylene groups. Porphyrinogen biosynthesis was monitored over a period of 82 h in the nmr tube by observing the decrease in intensity



1 3 (A = CH_2CO_2H) (P = $CH_2CH_2CO_2H$) 2a 2b

•denotes ^{13}C



4 5

of the PBG signal at 35.5 ppm and the complementary increase of the broad signal of copro'gen I and III (δ 22.0 ppm). Representative spectra obtained at 4, 31, and 82 h are shown in Fig. 2. Simultaneously, since non-enriched glucose was periodically added to the medium during the first 24 h, the formation of propionate (CH_3, 10.9; CH_2, 31.2 ppm[2]), acetate (CH_3, 24.0 ppm), and succinate (CH_2, 34.8 ppm) was observed at natural abundance as the glucose concentration decreased. A disaccharide, identified as αα'-trehalose, can be discerned (C-1, 93.9 ppm) as it initially accumulates in the glucose-rich medium and is slowly consumed later by the starved cells. The fact that some trehalose but no propionate, succinate, or acetate is present in the spectrum of the washed cells indicates that the disaccharide is an intracellular component.

A further extension of this experiment was to incubate washed *P. shermanii* cells with [3-^{13}C]-sodium propionate; in this case (Fig. 3) a rapid randomization of the ^{13}C label between positions 2 and 3 of the substrate (31.2 and 10.9 ppm) and C-2 of succinate (34.8 ppm) was observed, indicative of equilibrium in the methylmalonyl pathway.

Polyketide Biosynthesis in Penicillium urticae

An illustration of acetate metabolism was provided by a time course experiment on the mould *P. urticae*. After 30 h of growth [2-^{13}C]-sodium acetate (10 μmol/mL) was added to the medium and a further aliquot was added after an additional 12 h. Spectra obtained on samples of aliquots of the culture at 0, 12, 24, and 36 h after the initial feeding are shown in Fig. 4. After 12 h all of the added [2-^{13}C]-acetate had been metabolized primarily to citrate (46.1 ppm) while within 24 h resonances at 116.7, 116.5, and 60.3 ppm, corresponding to the C-4, C-6, and hydroxymethyl carbon of gentisalcohol (**4**), were in evidence. Following the appearance of these signals, peaks at 111.4, 89.2, and 60.4 ppm assignable to the C-7, C-1, and C-5 of patulin (**5**) were observed (11). Accumulation of intracellular saturated fatty acids was evident from the gradual increase in the characteristic "even carbon" signals at 14.7, 27.9, 30.5, and 32.5 ppm. Concomitant with the decrease of citrate concentration, an increase of the succinate (C-2) signal at 34.2 ppm was observed. In an analogous experiment using [1-^{13}C]-acetate over a shorter time course (48 h), peaks at 117.6 and 177.1 ppm corresponding to C-6 of gentisalcohol and the carbonyl of citric acid were observed, together with a peak at 63.5 ppm which could not be assigned.

Glycolysis in Erythrocytes

Time-elapsed spectra of rabbit erythrocytes fed with [1-^{13}C]-D-glucose under essentially anaerobic conditions are shown in Fig. 5. A gradual increase in intensity of the signal at 20.7 ppm corresponds to accumulation of [3-^{13}C]-lactic acid as the principal end product of anaerobic glycolysis. In a similar experiment with [6-^{13}C]-D-glucose the 20.7 ppm signal was also observed. In both cases a broad peak (A, Fig. 5) is evident at 67.2 ppm. A signal close to this frequency has previously been assigned to C-1 of fructose-1,6-diphosphate (FDP) in *E. coli* cells (6) and to C-3 of 2,3-diphosphoglycerate (DPG) in erythrocytes (12). However, at physiological pH, FDP exhibits resonances at 66.9 and 65.4 ppm for C-1 and C-6, respectively,

[2]Chemical shifts of α and β carbons or carboxylic acids are pH dependent (10). Assignments of such signals are based on identical chemical shifts at the pH of the media and spiking of cell homogenates with authentic compounds.

Can. J. Chem. Downloaded from www.nrcresearchpress.com by 210.87.254.42 on 09/05/12
For personal use only.

Can. J. Chem. Downloaded from www.nrcresearchpress.com by 210.87.254.42 on 09/05/12
For personal use only.

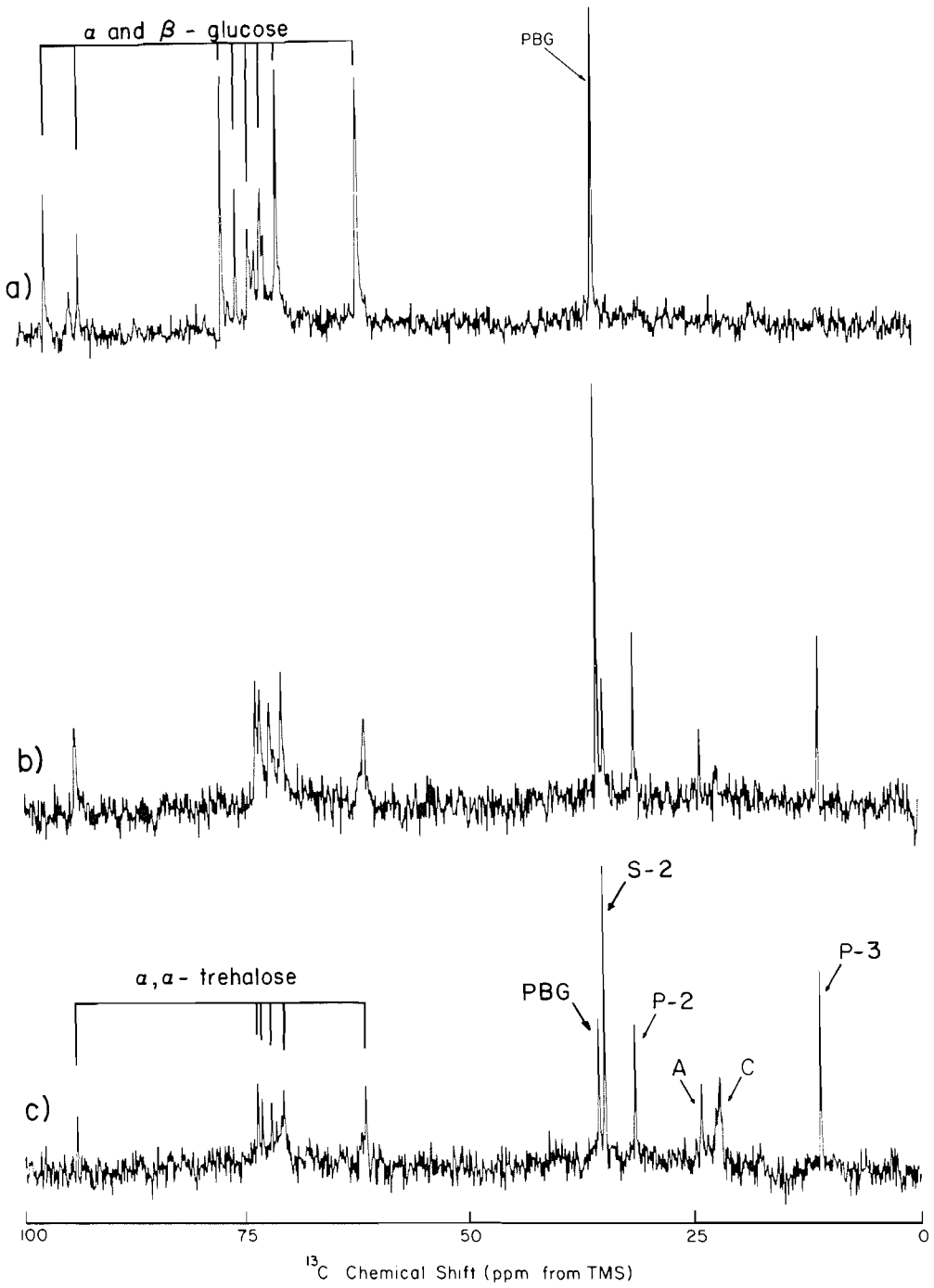


FIG. 2. Metabolism of [11-^{13}C]-porphobilinogen (PBG) by cells of *Propionibacterium shermanii* (ATCC 9614). Cells were grown anaerobically for 17 days, harvested by centrifugation, and incubated at 28°C in phosphate buffer – glucose (pH 7.6). Spectra (15 000 pulses) recorded at (*a*) 4 h, (*b*) 31 h, and (*c*) 82 h after addition of PBG. P-2 and P-3 (C-2 and C-3 of propionate); A (C-2 of acetate); S-2 (C-2 of succinate); C (*meso*-C of coproporphyrinogen I and III).

while the C-3 signal of DPG is an apparent triplet (J_{COP} = 4.5 Hz, J_{CCOP} = 4.5 Hz) at 67.2 ppm. In view of the high concentration of the latter compound in erythrocytes under anaerobic conditions (13), the 67.2 ppm resonance can be assigned to C-3 of DPG. Broadening of the C-3 signal may reflect an increase in reorientational correlation time for DPG due to binding with intracellular deoxyhemoglobin

Can. J. Chem. Downloaded from www.nrcresearchpress.com by 210.87.254.42 on 09/05/12
For personal use only.

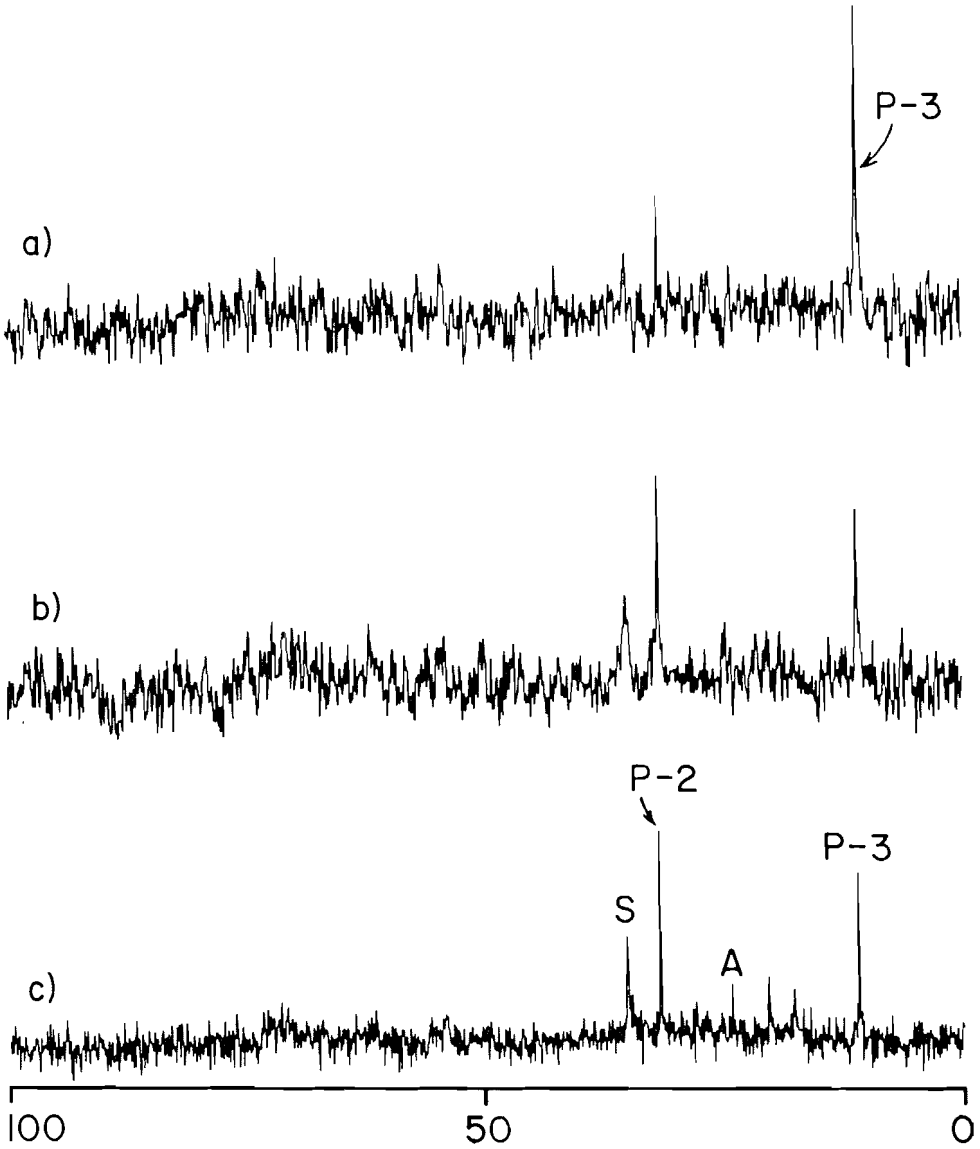


FIG. 3. Metabolism of [3-^{13}C]-propionate by *P. shermanii*. Washed cells suspended in phosphate buffer (100 μ*M*, pH 7.6) containing [3-^{13}C]-propionate (26 μmol). Spectra were recorded at (*a*) 10 min (2 200 pulses), (*b*) 70 min (2 200 pulses), and (*c*) 9 h (9 000 pulses). A (C-2 of acetate); S (C-2 of succinate); P-2, P-3 (C-2, C-3 of propionate).

(13). However, interaction of the 2 and 3 phosphate groups with metal ions may also be responsible for broadening of the resonance. Binding of DPG to deoxyhemoglobin has recently been studied by ^{31}P nmr (14).

The above examples are illustrative of a powerful non-invasive method applicable to detection of metabolic intermediates at concentrations down to approximately 1 μmol/mL of packed cells (10^8–10^{10} cells). It should be emphasized that this technique can provide information which is frequently lost during chemical analysis of disrupted cells. The assignment of chemical shifts in ^{13}C nmr spectroscopy is obviously of paramount importance in this field and the present studies are now being extended to multiply-labelled substrates, e.g., uniformly enriched ^{13}C-glucose, where appropriate homo- and heteronuclear couplings will provide diagnostic evidence for the structures of the intermediates detected.

Experimental

[5-^{13}C]-δ-Aminolevulinic acid (ALA, 86 atom% ^{13}C) was synthesized from K^{13}CN (90 atom% ^{13}C) and ethyl 3-formyl

Can. J. Chem. Downloaded from www.nrcresearchpress.com by 210.87.254.42 on 09/05/12
For personal use only.

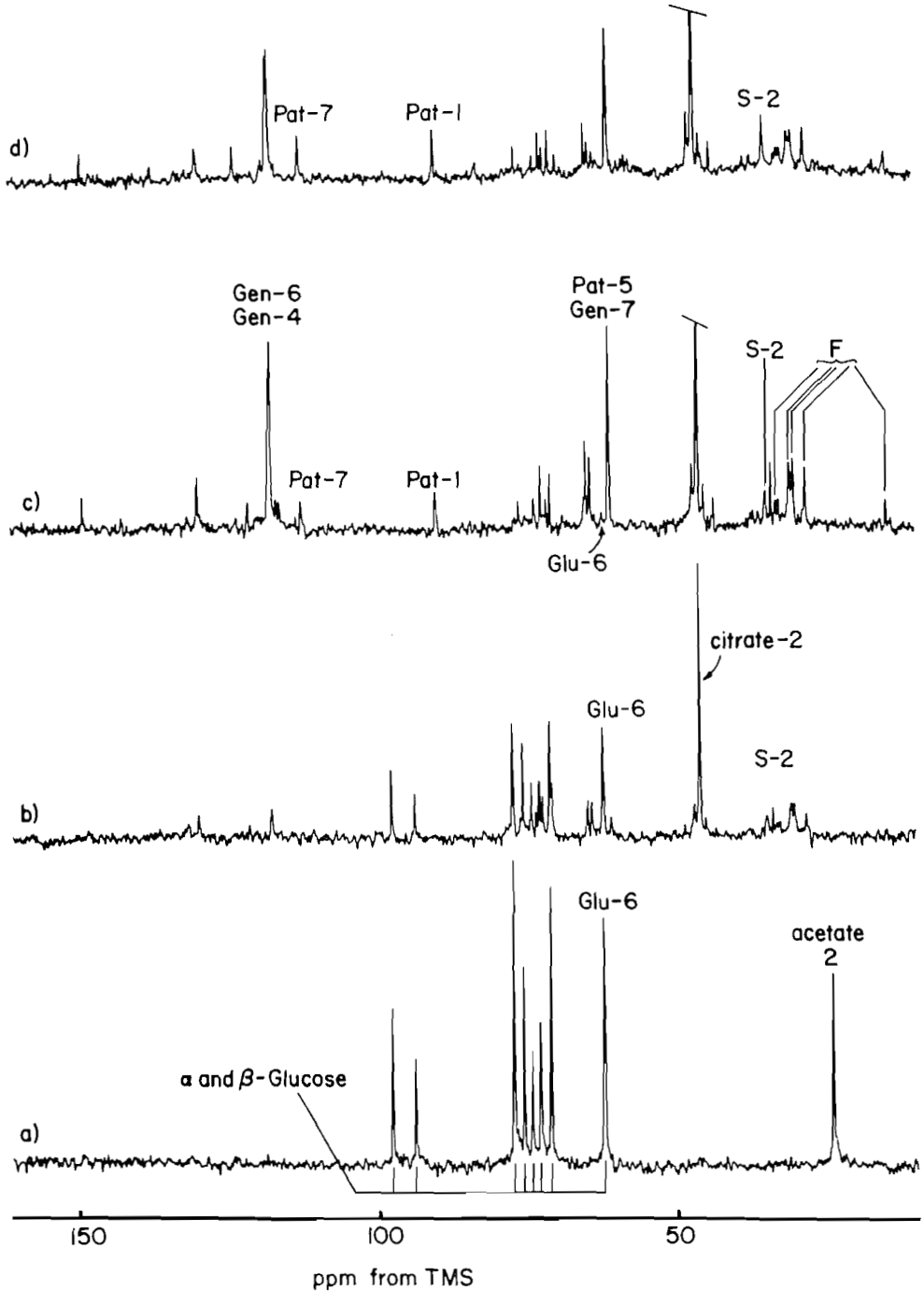


FIG. 4. Metabolism of [2-^{13}C]-acetate by *P. urticae* (NRRL 2159A). Cells were grown aerobically under previously described conditions (13) (pH 4.6) for 30 h and transferred to shake flasks containing medium supplemented with [2-^{13}C]-acetate (10 μ*M*, 90 atom%); additional [2-^{13}C]-acetate added after a further 12 h. Spectra (2 000 pulses) were recorded on aliquots of packed cells at (*a*) 0, (*b*) 12, (*c*) 24, and (*d*) 36 h after feeding. Pat-1, 5, and 7, Gen-4, 6, and 7 and S-2 denote the labelled carbons of patulin (**5**), gentisalcohol (**4**), and succinate, respectively. F denotes the signals assigned to the (even) carbons of cellular fatty acids.

Can. J. Chem. Downloaded from www.nrcresearchpress.com by 210.87.254.42 on 09/05/12
For personal use only.

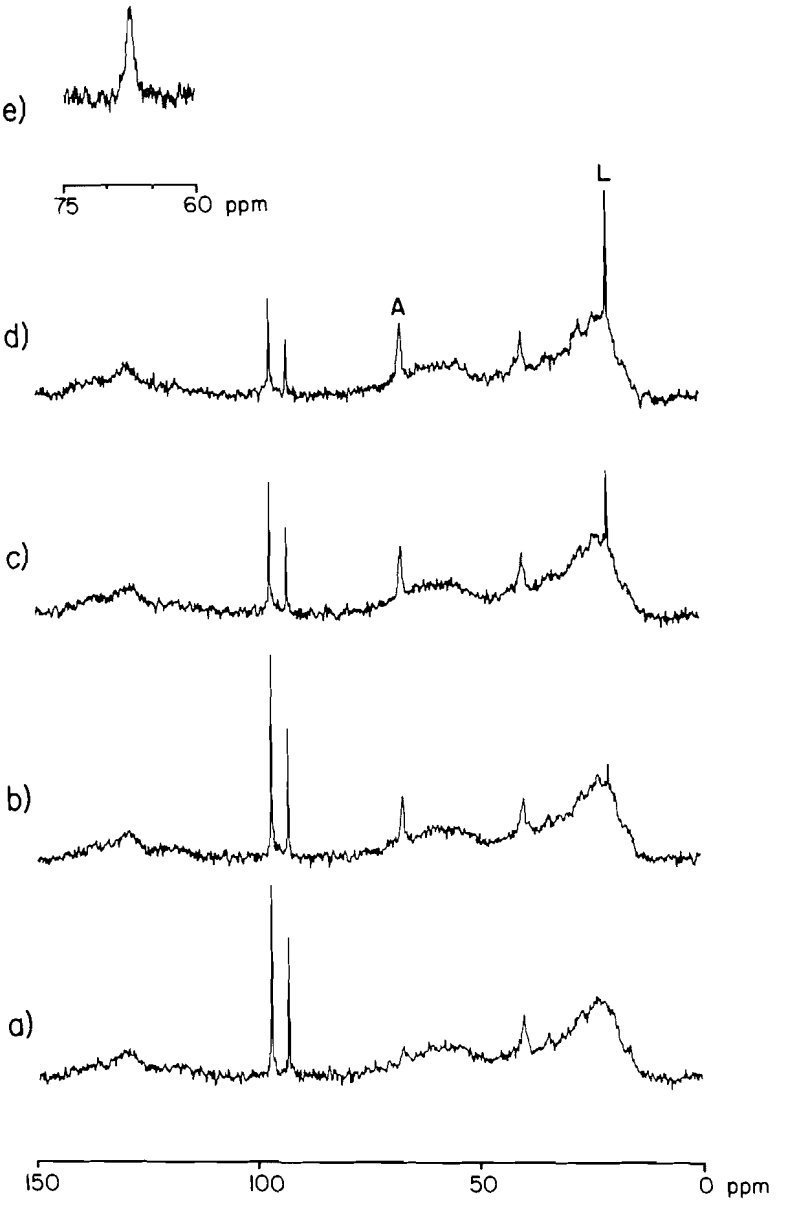


FIG. 5. Time course of [1-^{13}C]-glucose metabolism by rabbit erythrocytes. Cells were separated from whole blood, obtained by heart puncture, by centrifugation at 1 000 g, washed, and suspended in 20 m*M* phosphate – 150 m*M* NaCl buffer, (pH 7.4, ca. 10^8 cells/mL). [1-^{13}C]-Glucose (5 μ*M*) was added as an unequilibrated mixture containing principally the β anomer. Spectra (3 750 pulses, 0.5 s acquisition time, and 1.6 Hz line broadening) at (*a*) 0, (*b*) 4, (*c*) 8, and (*d*) 12 h after feeding, (*e*) higher resolution spectrum of 67.2 ppm peak (10^5 pulses, 0.8 s acquisition time, 0.7 Hz line broadening); A, C-3 of DPG; L, C-3 of lactate.

propionate (15); [11-^{13}C]-porphobilinogen (PBG, 87 atom% ^{13}C) was prepared by a modification of the synthesis of Fuhrhop and Smith (16); [3-^{13}C]-sodium propionate (87 atom% ^{13}C) was prepared from $^{13}CH_3I$ (90 atom% ^{13}C) and diethyl malonate (17); [1-^{13}C]- and [2-^{13}C]-sodium acetate (90 atom% ^{13}C) were purchased from Stohler Isotope Chemicals, Waltham, MA; [1-^{13}C]- and [6-^{13}C]-D-glucose (90 atom% ^{13}C) were kindly provided by Los Alamos Scientific Laboratory. Where appropriate, ^{13}C enrichments of precursors were measured by ^{1}H nmr.

The ^{13}C nmr spectra were obtained at 20 MHz on a Varian FT-80 spectrometer in 10 mm tubes using approximately 1.1 mL of cell suspension containing 10% D_2O as an internal lock. Typically, spectra were run at 28–30°C using 90° pulses, a spectral width of 5 000 Hz, an 8K data table, a 0.8 s pulse repetition rate and ca. 0.7 Hz of line broadening due to exponential weighting of the free induction decay (F.I.D.).

Acknowledgements

Work from this laboratory was supported in part by a grant from the Robert A. Welch Foundation,

N.I.H., and by an instrument grant from the National Science Foundation.

1. M. K. BATTERSBY, P. B. GARLICK, P. J. SEELEY, P. A. SEHR, and G. K. RADDA. *In* Biomolecular structure and function. *Edited by* P. F. Agris. Academic Press, New York. 1978. p. 175.
2. R. G. SHULMAN, G. NAVON, S. OGAWA, T. YAMANE, P. GLYNN, T. R. BROWN, K. UGURBIL, and H. ROTTENBERG. *In* Biomolecular structure and function. *Edited by* P. F. Agris. Academic Press, New York. 1978. p. 195.
3. R. B. MOON and J. H. RICHARDS. J. Biol. Chem. **248**, 7276 (1973).
4. K. UGURBIL, H. HOLMSEN, and R. G. SHULMAN. Proc. Natl. Acad. Sci. USA, **76**, 2227 (1979).
5. R. T. EAKIN, L. O. MORGAN, C. T. GREGG, and N. A. MATWIYOFF. FEBS Lett. **28**, 259 (1972).
6. K. UGURBIL, T. R. BROWN, J. A. DEN HOLLANDER, P. GLYNN, and R. G. SHULMAN. Proc. Natl. Acad. Sci. USA, **75**, 3742 (1978).
7. A. I. SCOTT, G. BURTON, and P. E. FAGERNESS. J. Chem. Soc. Chem. Commun. 199 (1979).
8. S. M. COHEN, S. OGAWA, and R. G. SHULMAN. Proc. Natl. Acad. Sci. USA, **76**, 1603 (1979).
9. R. E. LONDON, V. H. KOLLMAN, and N. A. MATWIYOFF. J. Am. Chem. Soc. **97**, 3565 (1975).
10. J. B. STOTHERS. *In* Carbon-13 nmr spectroscopy. Academic Press, New York. 1972. p. 147.
11. J. SEKIGUCHI and G. M. GAUCHER. Biochemistry, **17**, 1785 (1978).
12. P. STYLES, C. GRATHWOHL, and F. F. BROWN. J. Magn. Reson. **35**, 329 (1979).
13. A. ARNONE. Nature, **237**, 146 (1972).
14. R. K. GUPTA, J. L. BENOVIC, and Z. B. ROSE. J. Biol. Chem. **254**, 8250 (1979).
15. A. R. BATTERSBY, E. HUNT, E. MCDONALD, and J. MORAN. J. Chem. Soc. Perkin Trans. I, 2917 (1973).
16. J.-H. FUHRHOP and K. M. SMITH. *In* Porphyrins and metalloporphyrins. *Edited by* K. M. Smith. Elsevier, Amsterdam. 1975. p. 96.
17. N. WEINER. Org. Synth. Coll. Vol. **II**, 279 (1943).

Can. J. Chem. Downloaded from www.nrcresearchpress.com by 210.87.254.42 on 09/05/12
For personal use only.

Preparation and X-ray crystal structure of (4bα,6β,9β,9aα,10α,13α)-4b,5,6,7,8,9,9a,10,11,12,13,14-dodecahydro-4b-phenyl-6,9:10,13-dimethanodicyclohepta[*a*,*c*]naphthalene

ALAN RICHARD HARRIS, KEITH MILLS, AND MICHAEL MARTIN-SMITH
Chemistry Division, Glaxo Group Research Ltd., Ware, Hertfordshire, SG12 0DJ England
AND
PETER MURRAY-RUST AND JUDITH MURRAY-RUST
Department of Chemistry, University of Stirling, Stirling, FK9 4LA Scotland

Received February 21, 1980

This paper is dedicated to the memory of Dr. Léo Marion

ALAN RICHARD HARRIS, KEITH MILLS, MICHAEL MARTIN-SMITH, PETER MURRAY-RUST, and JUDITH MURRAY-RUST. Can. J. Chem. **58**, 1847 (1980).

The novel hexacyclic title hydrocarbon, formed by an unusual oxidative dimerization of 3-phenylbicyclo[3.2.1]oct-2-ene, has been isolated and its structure elucidated by means of X-ray crystallography. The trivial name 4b-phenylmariontetraene is proposed for the hydrocarbon. Crystals are orthorhombic, *Pbca*; $a = 21.87(2)$, $b = 10.57(2)$, $c = 17.41(2)$ Å from diffractometer measurements (Mo $K\bar{\alpha}$ radiation). $V = 4024.2$ Å^3, $Z = 8$, $D_c = 1.21$ Mg m^{-3}, $F(000) = 1584$, $\mu = 0.34$ cm^{-1}. The structure was solved by direct phasing methods with MULTAN 78 and was refined by weighted full-matrix least-squares procedures to $R = 0.046$ for 2287 observed reflexions.

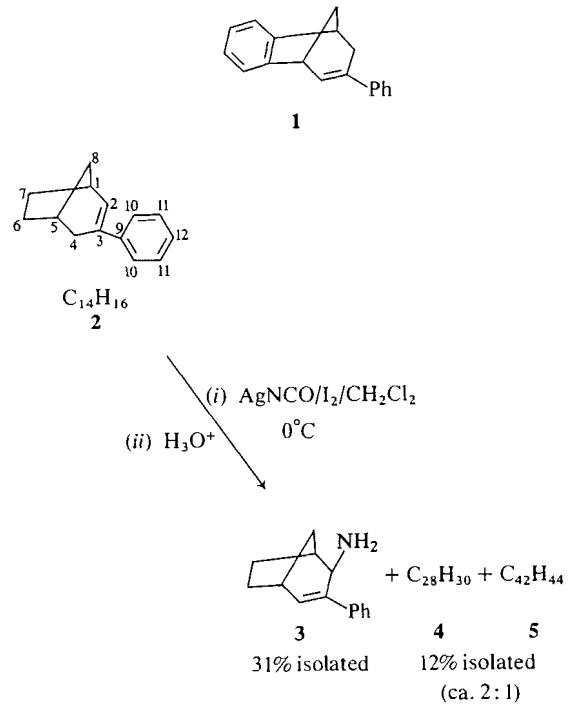
ALAN RICHARD HARRIS, KEITH MILLS, MICHAEL MARTIN-SMITH, PETER MURRAY-RUST et JUDITH MURRAY-RUST. Can. J. Chem. **58**, 1847 (1980).

On a isolé le nouvel hydrocarbure hexacyclique mentionné dans le titre qui se forme par une dimérisation oxydante inhabituelle du phényl-3 bicyclo[3.2.1]octène-2, et on a déterminé sa structure par diffraction de rayons-X. Pour cet hydrocarbure, on propose le nom vulgaire suivant phényl-4b mariontétraène.

A partir des mesures de diffraction (radiation Mo $K\bar{\alpha}$), on a trouvé que les cristaux sont orthorhombiques *Pbca*; $a = 21,87(2)$, $b = 10,57(2)$, $c = 17,41(2)$ Å. $V = 4024,2$ Å^3, $Z = 8$, $D_c = 1,21$ Mg m^{-3}, $F(000) = 1584$, $\mu = 0,34$ cm^{-1}. On a résolu la structure par la méthode des moindres carrés (matrice entière) et on l'a affinée jusqu'à une valeur de $R = 0,046$ pour 2287 réflexions observées.

[Traduit par le journal]

The last twenty-five years have witnessed a fine honing of X-ray crystallographic technique to provide an extremely sharp tool capable of giving rapid elucidation of the full molecular constitutions of crystalline organic compounds of high structural complexity. The economy of time inherent in the method is reflected in the present structural elucidation of an unexpected by-product, a report offered in tribute to Léo Marion's early appreciation (1–5) of the potential of the X-ray method. Reaction of the alkene **2** (6) with a mixture of silver cyanate and iodine, applying the conditions employed by Stoll *et al.* (7) on the related alkene **1**, gave not only the expected allylamine **3** but also two hydrocarbons **4** and **5** shown by mass spectrometry and microanalysis to have the empirical formulae $C_{28}H_{30}$ and $C_{42}H_{44}$ respectively. Application of ^{13}C and ^1H nmr spectroscopy to the lower molecular weight hydrocarbon **4** (isolated in 12% yield) did not permit unequivocal structural assignment. Accordingly an X-ray crystallographic analysis was undertaken on the hydrocarbon **4**, which can be formally viewed as representing a dimerization of **2** with concurrent loss of two hydrogen atoms. The



0008-4042/80/171847-04$01.00/0
©1980 National Research Council of Canada/Conseil national de recherches du Canada

Can. J. Chem. Downloaded from www.nrcresearchpress.com by 210.87.254.105 on 09/05/12
For personal use only.

Can. J. Chem. Downloaded from www.nrcresearchpress.com by 210.87.254.105 on 09/05/12
For personal use only.

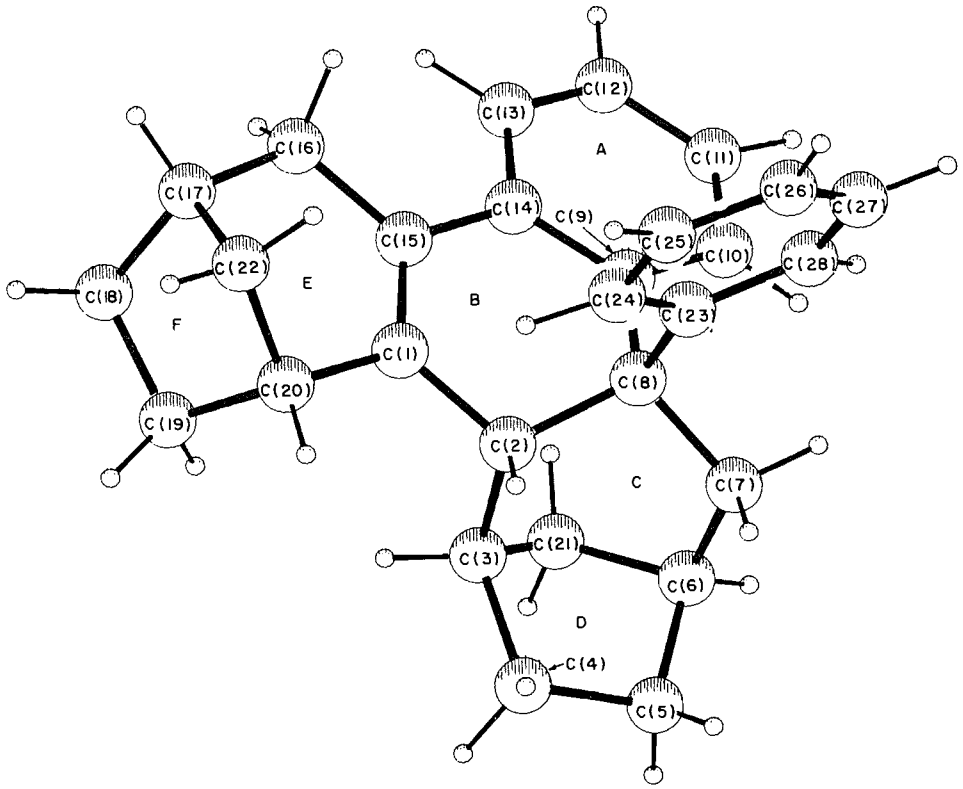
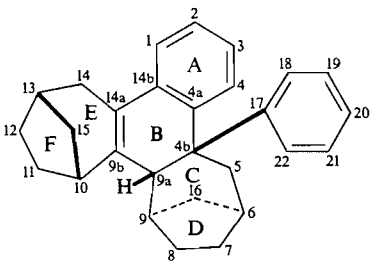


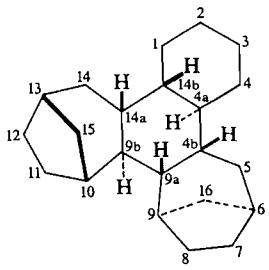
FIG. 1. View of the molecule of the hydrocarbon $C_{28}H_{30}$, **4**, employing the arbitrarily assigned crystallographic numbering. Tables of fractional atomic co-ordinates, bond distances, bond angles, and torsion angles employing this crystallographic numbering system together with lists of structure factors and thermal parameters have been deposited with the Depository of Unpublished Data, CISTI, National Research Council of Canada, Ottawa, Ont., Canada K1A 0S2 and with the Crystallographic Data Centre, Cambridge, England.

result, portrayed in accordance with the initially assigned (arbitrary) X-ray numbering, is shown in Fig. 1, permitting representation of the compound in accordance with Chemical Abstracts convention as **6**, namely



6

(4bα,6β,9β,9aα,10α,13α)-4b,5,6,7,8,9,9a,10,11,12,13,14-dodecahydro-4b-phenyl-6,9:10,13-dimethanodicyclohepta[*a,c*]naphthalene. It is proposed that the trivial name, marionane, be given to the saturated hexacyclic ring system **7** in the stereochemistry shown, thus permitting **6** to be termed 4b-phenylmarion-1,3,4a(14b),9b(14a)-tetraene. The highly bridged ring system present in **6** has not been studied structurally before. The X-ray results as shown in Fig. 1 reveal the conformation of the rings in terms of the crystallographic numbering to be as follows. Rings D and F are both envelopes with flaps at C(21) and C(22) respectively. Ring C is a boat with prows at C(8) and C(21) but flattened and twisted at C(2), C(8). Ring B is an irregular half chair. Ring E is a sofa with almost perfect mirror symmetry and the E/F system has almost perfect local mirror symmetry, the plane



7

Can. J. Chem. Downloaded from www.nrcresearchpress.com by 210.87.254.105 on 09/05/12
For personal use only.

passing through C(15), C(22) and the mid-point of C(18)—C(19). Work directed towards the purification and structural elucidation of the second hydrocarbon by-product, $C_{42}H_{44}$ (corresponding to an oxidized trimer of **2**) and on the mechanism of formation of both the hydrocarbons is in progress and will be reported elsewhere.

Experimental

X-ray Crystallographic Data

On crystallization from toluene–ethanol the hydrocarbon **4** afforded large rhombs. A crystal with dimensions 0.5 × 0.65 × 0.65 mm was used for the study. Systematic absences (from Weissenberg photographs) *hk*0 *h* odd, *h*0*l* *l* odd and 0*kl* *k* odd indicated space group *Pbca*. Crystal data:

$C_{28}H_{30}$ fw = 366

a = 21.87(2), b = 10.57(2), c = 17.41(2) Å, from diffractometer measurements (Mo $K\bar{\alpha}$ radiation) V = 4024.2 Å^3, Z = 8, D_c = 1.21 Mg m^{-3}, F(000) = 1584, μ = 0.34 cm^{-1}.

Data were collected for *h*0-11*l* with θ_{max} = 25° on a Stoe STADI-2 2-circle diffractometer (graphite monochromated Mo $K\bar{\alpha}$ radiation). This gave 3348 data of which 2287 unique reflexions with $I > 3\sigma(I)$ were used in subsequent calculations. Lorentz and polarization corrections (but none for extinction or absorption) were applied and the data scaled by a Wilson plot. The structure was solved by direct phasing methods with MULTAN 78 (8) and the SHELX-76 system of programs (9) was used for refinement calculations. Complex neutral atomic scattering factors were taken from International Tables for X-ray Crystallography (10). Weighted full-matrix least-squares refinement (including isotropic hydrogen atoms) converged at R = 0.046 for 2287 observed reflexions ($R = \Sigma||F_o| - |F_c||/\Sigma|F_o|$); R_w = 0.047 ($R_w = \Sigma(||F_o| - |F_c||\cdot w^{1/2})/\Sigma(|F_o|\cdot w^{1/2})$, $w = 3.81/(\sigma^2(F_o) + 4.6 \times 10^{-4}F_o^2)$. (The weighting scheme parameters were adjusted by the SHELX program (9).) In the final cycle all shifts in parameters were less than their standard deviations.

Preparation of Compounds

Melting points were determined on a Townson and Mercer melting point apparatus and are uncorrected. Proton magnetic resonance spectra were recorded on a Varian Associates EM390 90 MHz spectrometer and ^{13}C spectra were recorded on a Varian Associates XL100 spectrometer. Signal positions are quoted in δ units with TMS or DSS as the internal standard. Gas–liquid chromatography was carried out on a Perkin-Elmer F30 machine. Mass spectra were recorded on a Kratos-AEI MS30 spectrometer. Ultraviolet spectra were recorded on a Perkin-Elmer 402 spectrometer and infrared spectra were recorded on a Perkin-Elmer 357 grating spectrometer.

3-Phenylbicyclo[3,2,1]oct-2-ene **2**

This compound was prepared by a nickel(II) acetylacetonate catalysed coupling reaction (11) between phenyl magnesium bromide and 3-bromo- or 3-chlorobicyclo[3,2,1]oct-2-ene. This method gives a 6–8-fold increase in yield over the literature procedure (6). A solution of phenyl magnesium bromide (prepared from magnesium (9.6 g; 0.4 mol) and bromobenzene (42 mL; 62 g; 0.4 mol)) in ether (150 mL) was added dropwise, with cooling (0°C) under nitrogen, to a stirred mixture of nickel acetylacetonate (0.3 g) and 3-bromobicyclo[3,2,1]oct-2-ene (50 g, 0.267 mol) (12). The mixture was stirred at room temperature for 20 h and then hydrochloric acid (200 mL; 2 *M*) was added dropwise at 0°C. The organic phase was separated and the aqueous phase was extracted with ether (2 × 200 mL). The combined organic solutions were dried ($MgSO_4$) and evaporated *in vacuo*. The residual yellow oil (50 g) was distilled to give the title compound as a colourless oil (45 g; 91%), bp 109–113°C/1.5 Torr (lit. (6) bp 80°C/0.5 Torr); uv λ_{max} (EtOH): 220 (ε 9 200), 253 (12 000), 292 (sh, 500) nm; ir ν_{max} ($CHBr_3$): 1630 cm^{-1} (m, C=C); ^{1}H nmr ($CDCl_3$): 7.70–7.00 (5H, m, aromatic), 6.40 (1H, d, J = 7Hz, —*CH*=CPh—), 2.80–1.00 (10H, m, aliphatic); ^{13}C nmr δ (ppm): 141.3, s(C3); 133.1, s(C9); 131.1, d(C2); 128.1, d and 124.6, d(C10 and C11); 126.5, d(C12); 38.9, t(C4); 35.7, d(C1); 35.3, t(C7 and C8); 33.5, d(C5); 30.5, t(C6).

Reaction of Alkene 2 with a Mixture of Iodine and Silver Cyanate

A solution of the alkene **2** (43 g; 0.23 mol) in dichloromethane (400 mL) at 0°C under nitrogen atmosphere was treated with silver cyanate (13) (43 g; 0.22 mol) and then with iodine (57 g; 0.22 mol) in portions (~5 g) over 1 h. The mixture was stirred at 0°C for 4 h and kept at 0–5°C overnight, filtered, and the filtrate washed with aqueous sodium thiosulphate solution (8%; 250 mL). The solution was dried ($MgSO_4$) and evaporated *in vacuo*. The residual pale yellow oil (45 g) was dissolved in a mixture of acetone (600 mL) and concentrated hydrochloric acid (100 mL), kept at room temperature overnight, and then evaporated *in vacuo*. The residue was partitioned between water (300 mL) and ethyl acetate (400 mL) and some insoluble material (A) was filtered off (see below). The aqueous layer was separated, washed with ethyl acetate (300 mL), and then basified with aqueous sodium hydroxide (2 *M*). The crude basic material was extracted into ethyl acetate (3 × 200 mL). The combined extracts were dried ($MgSO_4$) and evaporated to ca. 200 mL *in vacuo*. The solution was treated with ethereal hydrogen chloride (8%) until no more precipitate formed and the salt was filtered off and crystallized from a mixture of methanol and ethyl acetate to give 3-phenylbicyclo[3,2,1]oct-3-en-*exo*-2-amine, hydrochloride,[1] **3** (14.4 g; 31%) as a white powder mp 249–251°C (dec). Ultraviolet (EtOH) λ_{max}: 244 nm (ε 11 100); ^{1}H nmr (D_2O): 7.65 (5H, br s, aromatic), 6.60 (1H, d, J = 7 Hz, —CH=CPh—), 4.32 (1H, d, J = 3.5 Hz, $>CH—NH_2$), 2.90–1.40 (8H, m, remaining aliphatic). *Anal.* calcd. for $C_{14}H_{17}N{\cdot}HCl$: C 71.33, H 7.69, N 5.95, Cl 15.04; found: C 71.41, H 7.78, N 6.19, Cl 15.23%.

The insoluble material (A) described above was filtered off and crystallized from a mixture of toluene and ethanol to give the hydrocarbon **4** (5 g; 12%) as off-white crystals mp 167–170°C (X-ray sample had mp 167.5–170°C); glc 4 *M* 2% OV-17 column at 280°C, retention time 11.4 min, 98.8% purity. Ultraviolet (cyclohexane) λ_{max}: 221 (ε 21 000), 227 (21 000), 233 (17 500), 283 (9 100) nm; ^{1}H nmr ($CDCl_3$): 7.30–6.80 (9H, m, aromatic), 2.87–0.88 (21H, m, aliphatic); ^{13}C nmr δ(ppm): 150.6, s(C14a); 143.2, s and 142.2, s(C14b and C9b); 134.8, s(C4a); 127.3, d and 126.9, d, (C18, C19, C21, and C22); 126.3, d, 125.9, d, 125.6, d, 125.2, d, and 122.4, d(C1, C2, C3, C4, and C20); 121.8, s(C17); 58.1, d(C9a); 42.7, d and 42.1, d(C9 and C10); 42.4, s(C4b); 39.2, d(C6); 36.7, t, 35.9, t, 35.5, t, 34.1, t, 33.6, t, and 32.6, t(C5, C7, C8, C11, C14, C15, and C16); 32.4, d(C13); 31.3, t(C12) (numbering as in **6**); ms *m/e*: 366 (100%; M^+), 297 (28%; $M - C_5H_9$), 286 (91%; $M - C_6H_8$), 217 (33%; $M - C_{11}H_{17}$). *Anal.* calcd. for $C_{28}H_{30}$: C 91.80, H 8.20; found: C 91.79, H 8.32%.

Acknowledgments

We thank Dr. J. Hunt and his staff of the Analytical Research Department, Glaxo Group Research

[1]The *exo* configuration of the amine function is apparent from the coupling constant of the *endo*-2 proton in the nmr spectrum (12, 14, 15).

(Ware), for the provision of spectral and microanalytical data. We also thank Dr. D. D. MacNicol for providing ^{13}C nmr spectra and Dr. T. J. Cholerton for interpretation. Grateful acknowledgement is made to Dr. D. R. Wilson for helpful discussions. One of us (JM-R) thanks G.G.R. (Ware) Ltd. for financial support.

1. M. PRZYBYLSKA and L. MARION. Can. J. Chem. **34**, 185 (1956).
2. M. PRZYBYLSKA and L. MARION. Can. J. Chem. **35**, 1075 (1957).
3. M. PRZYBYLSKA and L. MARION. Can. J. Chem. **37**, 1116 (1959).
4. M. PRZYBYLSKA and L. MARION. Can. J. Chem. **37**, 1848 (1959).
5. M. PRZYBYLSKA and L. MARION. Can. J. Chem. **39**, 2124 (1961).
6. C. W. JEFFORD and E. HUANG-YEN. Tetrahedron, **23**, 4549 (1967).
7. A. P. STOLL, H. R. LOOSLI, P. NIKLAUS, and T. ZARDINI-TARTAGLIA. Helv. Chim. Acta, **61**, 648 (1978).
8. P. MAIN. MULTAN 78 program for crystal structure solution. University of York, England. 1978.
9. G. M. SHELDRICK. SHELX-76 program for crystal structure determination. University of Cambridge, England. 1976.
10. International tables for X-ray crystallography. Vol. IV. Kynoch Press, Birmingham. 1974. p. 99.
11. R. J. P. CORRIU and J. P. MASSE. Chem. Commun. 144 (1972).
12. W. R. MOORE, W. R. MOSER, and J. E. LAPRADE. J. Org. Chem. **28**, 2200 (1963).
13. C. H. HEATHCOCK and A. HASSNER. Org. Synth. **51**, 112 (1971).
14. C. W. JEFFORD, S. MAHAJAN, J. WASLYN, and B. WAEGELL. J. Am. Chem. Soc. **87**, 2183 (1965).
15. C. W. JEFFORD, B. WAEGELL, and K. RAMEY. J. Am. Chem. Soc. **87**, 2191 (1965).

Can. J. Chem. Downloaded from www.nrcresearchpress.com by 210.87.254.105 on 09/05/12
For personal use only.

Reactions of the Lythraceae alkaloids. Regio and stereoselective methoxylations and hydroxylations of lythrine

I. LANTOS,[1] C. RAZGAITIS, B. LOEV, AND B. DOUGLAS

Research and Development Division, Smith Kline and French Laboratories, P.O. Box 7929, Philadelphia, PA 19101, U.S.A.

Received February 11, 1980

This paper is dedicated to the memory of Dr. Léo Marion

I. LANTOS, C. RAZGAITIS, B. LOEV, and B. DOUGLAS. Can. J. Chem. **58**, 1851 (1980).

Mercuric acetate assisted methoxylations and hydroxylations of lythrine resulted in a regio and stereoselective introduction of the substituent at the benzylic position with *S*-stereochemistry. The compounds obtained are thus epimeric at C13 with the naturally hydroxylated alkaloid lythridine and its derivatives. The implications of the results in planning the total synthesis of lythrine is discussed.

I. LANTOS, C. RAZGAITIS, B. LOEV et B. DOUGLAS. Can. J. Chem. **58**, 1851 (1980).

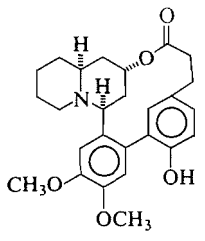
Les méthoxylations et hydroxylations de la lythrine assistées par l'acétate mercurique conduisent à une introduction régiosélective et stéréosélective d'un substituant en position benzylique avec une stéréochimie *S*. Les composés obtenus sont donc épimères au niveau du carbone en position 13 de l'alcaloïde naturel lythridine hydroxylé et de ses dérivés. On discute des implications de ces résultats dans la planification de la synthèse totale de la lythrine.

[Traduit par le journal]

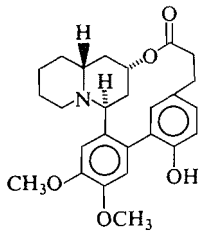
Since their initial isolation (1) alkaloids of the Lythracea plant family have provided a wealth of research opportunities for workers primarily interested in their structural elucidation (2) or total synthesis (3). Structurally, they are classified into five distinct classes (4*a*) depending on the presence of a quinolizidine ring in either the *cis*- or *trans*-configuration or of a piperidinyl moiety and whether these are associated with a biphenyl or diphenyl ether aromatic fragment.

Previous work within our laboratories described the isolation (1*b*), structure elucidation (2*b*), and total synthesis of decinine (**1**) (3*a*), and decamine (**2**) (3*b*), compounds with *trans* and *cis*-quinolizidine configuration respectively, linked to biphenyl moieties. That report, as well as those of others (3*c*), which describe the total synthesis of the analogous diphenyl ether, utilizes methodology appropriate for the synthesis of alkaloids containing a fully saturated methylene chain in the macrocyclic lactone portion. Extension of this basic synthetic scheme to the biosynthetically related lythrine[2] (**3**) and lythridine (**5**), necessitated an investigation into some of the reactions and potential interconversions of these species, and these results are disclosed herein. We anticipated that the previously known conformation of the macrocyclic lactone ring in **3** and **5** (2*b*, *c*) would facilitate the interpretation of the stereochemical course of the reaction.

Mercuric acetate assisted methoxylation (5) of methyl lythrine (**6**) over a period of 48 h resulted in the formation of a single methoxy derivative **7** (Scheme 1). The proton nmr of this newly formed compound suggested that the methoxy substituent entered at the benzylic position. Spectral comparison of **7** with the dimethyl derivative of lythridine (**8**), prepared by MeI/NaH treatment of the natural product **5**, revealed that both compounds exhibited methine proton signals of the ABX spectral pattern, centered within the same range of the spectra at 4.50 ppm (however, while the Hx quartet in the spectrum of **7** derived from splitting by coupling constants of 2 and 6 cps, the corresponding signals



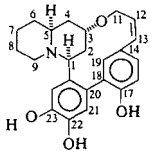
1



2

[1]Author to whom correspondence may be addressed.

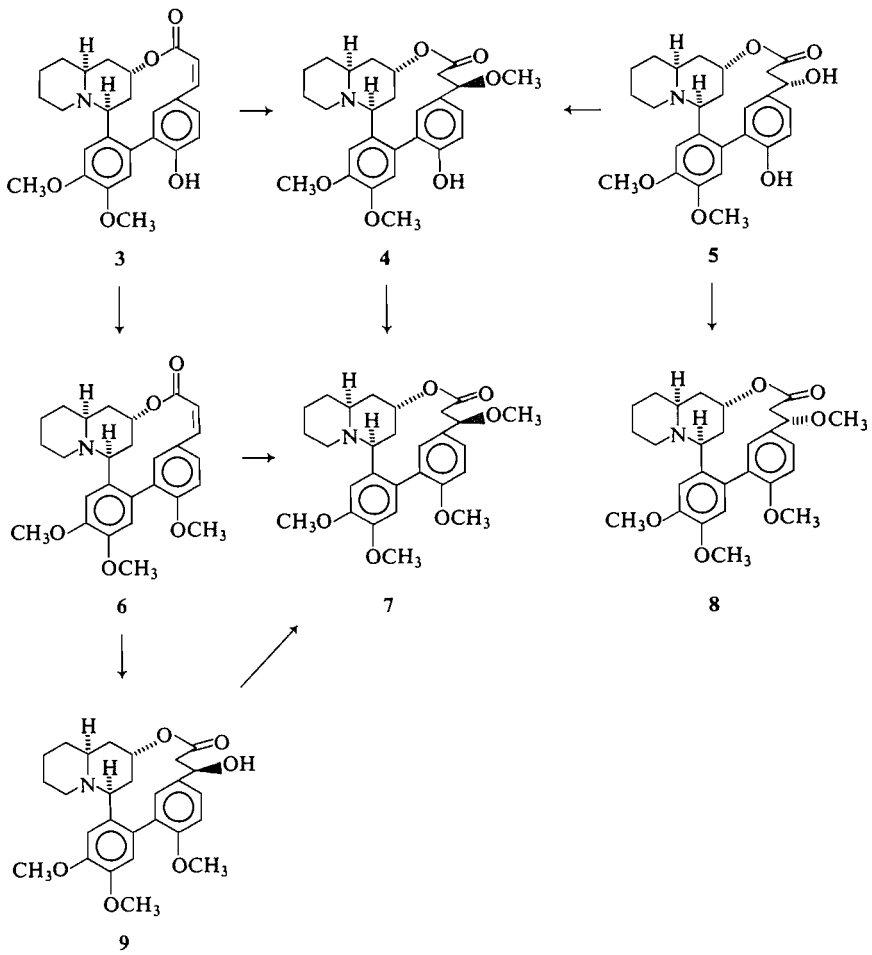
[2]Throughtout the text all alkaloids are referred to by their trivial names in common usage. Systematic names can be derived from the core name *lythran* assigned to the basic structure below with the numbering system according to ref. 6. We have included these Chem. Abstr. names in the Experimental.



0008-4042/80/171851-04$01.00/0

©1980 National Research Council of Canada/Conseil national de recherches du Canada

Can. J. Chem. Downloaded from www.nrcresearchpress.com by 210.87.254.5 on 09/05/12
For personal use only.



SCHEME 1

in the nmr of **8** had splittings of 3 and 10 cps and were thus a much broader pattern). Since no other change could be detected from a spectral comparison of **7** and **8**, the two compounds were assigned epimeric structures at C13. This assignment was unequivocally proven by the series of conversions shown in Scheme 1.

Conversion of lythridine to the *epi*- series took advantage of the solvolytic lability of the secondary benzylic hydroxyl group in its molecule. We had expected that treatment with methanol under strongly acidic conditions would lead to unimolecular displacement resulting in at least partial inversion of this asymmetric centre. We were quite surprised, however, to find that stirring **5** in MeOH·BF_3 at room temperature for 0.5 h resulted in the formation of a single methoxy derivative **4**, in better than 80% yield, which was identical to the methoxy compound obtained from lythrine (**3**) with $Hg(OAc)_2$/MeOH.

The methine proton signals in the spectrum of **4** displayed a pattern typical of **7** with splitting constants of 2 and 5 cps, and the structural relationship with **7** was fully established by methylation with MeI/K_2CO_3. The ease with which transformation 5 → 4 occurred excludes the probability of structural changes taking place other than epimerization at C13 and thus unambiguously supports our structural assignments for **4** and **7**. It is noteworthy that in the above methoxylation no methoxy compound with the natural C13-*R*-stereochemistry was formed.

Hydroxylation of **6** with mercuric acetate in aqueous THF followed the same stereochemical course. A single hydroxy compound (**9**) was isolated which proved to be epimeric with lythridine at C13 through its conversion to the *epi*-dimethyl compound **7**, by MeI/NaH or $CH(OCH_3)_3$·BF_3 (7).

The foregoing results indicate that mercury assisted additions to the α,β-unsaturated lactone of lythrine take place in a fully regio and stereoselective manner. The newly formed substitutent always

Can. J. Chem. Downloaded from www.nrcresearchpress.com by 210.87.254.5 on 09/05/12
For personal use only.

Can. J. Chem. Downloaded from www.nrcresearchpress.com by 210.87.254.5 on 09/05/12
For personal use only.

enters at the benzylic β-position and obtains the *S*-stereochemistry, epimeric to the naturally hydroxylated alkaloids. Furthermore, it is also seen that the benzylic substituent readily undergoes ionization under the influence of Lewis acids, and trapping of the carbonium ion by the solvent always affords the thermodynamically more stable *epi*-substituted products. Our experimental finding that hydroxy compound **9** afforded dimethyl *epi*-lythridine (**7**) via both basic methylation and acid assisted methoxylation further supports this unimolecular methoxylation mechanism.

Oxymercuration studies in the literature (8, 9) suggest a mechanistic course highly dependent on the substitution pattern about the olefin and its geometry. Both *syn* and *anti* additions of the mercurial and nucleophile have been observed. An examination of the molecular geometry of lythrine, based on the X-ray model (2*b*), indicates a rather rigid framework with substantial steric crowding from the pro-*R* face of the double bond. As a stereochemical consequence *direction of mercurial approach* (8) governs the product configuration in analogy with strained ring oxymercuration reactions. The nature of the intermediate seems to be a highly stabilized mercury substituted carbonium ion as previously suggested by Brown and Kawakami (10).

Our results are relevant in the design of a synthetic scheme toward the total synthesis of lythrine and lythridine. We have previously attempted to prepare lythrine (**3**) from the open *cis*-α,β-unsaturated hydroxy acid precursor but this was unsuccessful. Our present work suggests a more accessible intermediate, *epi*-lythridine (**9**), whose preparation requires no stereochemical control at the dihydroxy acid stage because of its much preferred formation in the ring closed macrocycle. We are currently working on methods to transform the *epi*-hydroxy group to the *cis* olefinic linkage of the natural product. The total synthesis of lythridine (**5**), on the other hand, will require a dihydroxy acid precursor with defined stereochemistry together with mild conditions for the cyclization to avoid epimerization of the C13 asymmetric centre.

Experimental

Melting points were determined on a Thomas–Hoover melting point apparatus and are uncorrected. Infrared spectra were recorded on a Perkin–Elmer Infracord spectrophotometer and ^{1}H nmr spectra were obtained on a Varian Associates model T-60 spectrometer. Signal positions are given in δ units with tetramethylsilane as internal standard.

Preparation of 17-Methyllythrine (17,22,23-Trimethoxylythran-11-one, 6)

To a stirred solution of lythrine (47.0 g, 0.108 mol) in 1.4 L of 10% sodium hydroxide and 800 mL of dioxane was added dropwise 140 mL dimethyl sulfate. The reaction was allowed to stir overnight at ambient temperature and the precipitated product was filtered and crystallized from chloroform – petroleum ether (1:1) mixture to afford 34.0 g (72%) of **6**, mp 236–237°C; ir (Nujol): 1694, 1257, 1123, 1030 cm^{-1}; ^{1}H nmr ($CDCl_3$): 7.13 (s, 1H, aromatic), 6.95 (m, 5H, aromatic), 6.84 and 5.82 (AB system, 2H, J = 13 Hz, CH=CH), 5.26 (m, 1H, C*H*—OCO), 3.90, 3.84, and 3.76 (s, 3 × 3H, 3 × CH_3O), 2.8 to 1.3 (m, 14H). *Anal.* calcd. for $C_{17}H_{31}NO_5$: C 72.14, H 6.95, N 3.12; found: C 72.34, H 7.24, N 3.02.

Preparation of 13,17-Dimethyl-13-epilythridine (12,13-Dihydro-13(S),17,22,23-tetramethoxylythran-11-one, 7)

Method A: To a solution of **6** (2.0 g, 4.5 mmol) in 50 mL of methanol was added 4.3 g of mercuric acetate and the solution was stirred at room temperature for 96 h. After cooling the reaction mixture in an icebath, sodium borohydride (0.8 g, 21 mmol) was slowly added and the resulting dark grey suspension was diluted with water to 120 mL. The solution was extracted with chloroform, the organic extract was dried over anhydrous magnesium sulfate, and after filtration was evaporated to an oil which was crystallized by trituration with ether. A yield of 1.2 g (54%) of **7** was obtained by this method, mp 222–223.5°C, ir (Nujol): 1709, 1250, 1197, 1123 cm^{-1}; ^{1}H nmr ($CDCl_3$): 7.1 (s, 1H, aromatic), 7.0 (m, 3H, aromatic), 6.9 (s, 1H, aromatic), 5.1 (br s, 1H, CHOCO), 4.52 (q, 1H, X part of ABX system, J_{AX} = 2 Hz, J_{BX} = 6 Hz, C*H*OCH_3), 3.92, 3.86, 3.76, and 3.35 (s, 4 × 3H, 4 × OCH_3), 3.2–1.1 (m). *Anal.* calcd. for $C_{28}H_{35}NO_6$: C 69.83, H 7.33, N 2.91; found: C 70.02, H 7.24, N 2.92.

Method B: 13-Methyl-*epi*-lythridine (**4**, 1.67 g, 3.5 mmol) was dissolved in a mixture of 50 mL dioxane and 50 mL 10% sodium hydroxide, and dimethyl sulfate (4.5 mL) was added over the period of 15 min. The mixture was allowed to stir overnight and was evaporated at reduced pressure to almost dryness, yielding a glassy residue which was diluted with 50 mL of water and was extracted with methylene chloride (150 mL). The organic extract was dried over anhydrous magnesium sulfate, was filtered, and the filtrate was evaporated to a glass which was triturated with ether and crystallized; 1.15 g of **7** was obtained (67%).

Method C: 17-Methyl-13-*epi*-lythridine (**9**, 2.0 g, 4.3 mmol) was dissolved in 30 mL of dimethylformamide, and sodium hydride (50% oil, 0.2 g, 4.5 mmol) was added. The anion was generated with stirring at room temperature for 0.5 h and methyl iodide (0.7 g, 5 mmol) was added to the suspension. Stirring was continued overnight and the reaction was diluted with water to 100 mL. The product was extracted with ether, the ethereal solution was dried over anhydrous magnesium sulfate, and after filtration the filtrate was evaporated at reduced pressure to a glass. The product (1.8 g, 88%) was obtained crystalline by trituration with ether.

Preparation of 13-Methyl-epi-lythridine (12,13-Dihydro-17-hydroxy-13(S),22,23-trimethoxylythran-11-one, 4)

Method A: To a solution of 2.0 g (4.75 mmol) of lythrine in 50 mL of methanol was added mercuric acetate (4.3 g) and the mixture was stirred at ambient temperaturs for 3 days. The solution was cooled in an ice bath and 1.0 g (26 mmol) of sodium borohydride was slowly added, resulting in a darkly colored mixture which was diluted with water to 120 mL and was extracted with chloroform. Evaporation of the chloroform extract at reduced pressure resulted in a glassy solid which was dissolved in 50 mL of methanol and was saturated with hydrogen sulfide gas. The alcoholic solution was filtered over a Celite bed and was evaporated to yield 2.07 g (98%) of **4**, which was recrystallized from methylene chloride – ether, mp 160–165°C; ir (Nujol): 3448, 1694, 1204, 1123, 1052 cm^{-1}; ^{1}H nmr ($CHCl_3$):

Can. J. Chem. Downloaded from www.nrcresearchpress.com by 210.87.254.5 on 09/05/12
For personal use only.

7.3–7.0 (m, 3H, aromatic), 6.85 (s, 1H, aromatic), 5.05 (br s, 1H, C*H*OCO), 4.45 (q, X part of AB system, 1H, $J_{AX} = 2$ Hz, $J_{BX} = 5$ Hz, $CHOCH_3$), 3.90, 3.82, and 3.30 (s, 3 × 3H, 3 × OCH_3), 3.30–1.2 (m).

Method B: Boron trifluoride etherate (1.35 mL, 11 mmol) was added in one portion to a cooled solution of lythridine (1.3 g, 3 mmol) in 40 mL of methylene chloride followed by the dropwise addition of trimethylorthoformate (0.76 g, 7.2 mmol) over the period of 20 min. Stirring was maintained for an additional 0.5 h and the solution was diluted to 150 mL with methylene chloride. After washing the solution with 2 *N* hydrochloric acid (3 × 50 mL) and 5% sodium carbonate (2 × 50 mL), it was dried over anhydrous sodium sulfate, filtered, and evaporated to an oil at reduced pressure. Trituration of the oily residue with methylene chloride – ether mixture resulted in 0.9 g of the crystalline **4**.

Method C: Lythridine **5** (0.10 g, 0.2 mmol) was added to 2 mL of $BF_3 \cdot 2CH_3OH$ complex and the reaction was allowed to stand at room temperature for 0.5 h. Chloroform (30 mL) was added, and the resultant solution was washed with 5% sodium carbonate (2 × 30 mL) and saturated brine. After drying the solution over anhydrous magnesium sulfate it was filtered and the filtrate was evaporated to a glass at reduced pressure. Trituration with methylene chloride – ether obtained 0.07 g of solid product **4**.

*13,17-Dimethyllythridine (12,13-Dihydro-13(*R*),17,22,23-tetramethoxylythran-11-one, 8)*

To a solution of 0.9 g (2 mmol) of lythridine (**5**) in 20 mL dry tetrahydrofuran was added 0.29 g of sodium hydride (50% oil, 6 mmol) and the suspension was stirred at 0–5°C for 0.5 h. Methyl iodide (2.84 g, 20 mmol) was added to the resulting suspension and stirring continued at ice bath temperature for an additional 5 h. The reaction was diluted with water to 100 mL and was extracted with ether. The organic extract was washed with water, dried over anhydrous $MgSO_4$, and after filtration was evaporated to a glassy residue. Column chromatography of this material on Al_2O_3 with ether solvent yielded 0.3 g of the desired compound ($R_f = 0.62$), mp 138–140°C; ir (Nujol): 1724, 1123, 1052, 1030 cm^{-1}; ^1H nmr ($CDCl_3$): 7.45–6.7 (m, 5H, aromatic), 4.90 (s, 1H, C*H*OCO), 4.5 (q, X part of ABX system, 1H, $J_{AX} = 3$ Hz, $J_{BX} = 10$ Hz, C*H*OCH_3), 3.82, 3.75, 3.67, and 3.35 (s, 4 × 3H, 4 × OCH_3), 3.1–1.2 (m). *Anal.* calcd. for $C_{28}H_{35}NO_6 \cdot 1/2\ H_2O$: C 68.55, H 7.40, N 2.86; found: C 68.57, H 7.50, N 2.76.

*17-Methyl-13-*epi*-lythridine (12,13-Dihydro-17,22,23,-trimethoxy-13(*S*)-hydroxylythran-11-one, 9)*

A solution of **6** (2.0 g, 4.2 mmol) in 50 mL of aqueous (1:1) tetrahydrofuran was treated with 4.6 g (6.3 mmol) of mercuric acetate at room temperature for 96 h. The solution was cooled in an icebath while 1.0 g (30 mmol) of sodium borohydride was slowly added. The product was separated from the metallic mercury precipitate by extraction with chloroform (3 × 40 mL) and the organic extract was dried over anhydrous sodium sulfate. After filtration the chloroform solution was chromatographed on an alumina column using ethyl acetate solvent. After elution of 0.8 g of recovered starting material, 1.2 g (57%) of product **9** ($R_f = 0.2$) was isolated, crystallized from petroleum ether – chloroform, mp 187–188°C; ir (Nujol); 1680, 1250, 1123, 1030 cm^{-1}; ^1H nmr ($CDCl_3$): 7.0–6.7 (m, 5H, aromatic), 4.90 (br s, 1H, CHOCO), 4.2 (br m, 1H, C*H*OH), 3.90, 3.80, and 3.70 (s, 3 × 3H, 3 × OCH_3), 3.15–1.3 (m). *Anal.* calcd. for $C_{27}H_{33}NO_6 \cdot 1/4\ H_2O$: C 68.89, H 7.15, N 2.96; found: C 68.40, H 7.13, N 2.93.

Acknowledgements

The authors are indebted to our Analytical and Physical Section personnel for analytical and physical data. We are also grateful to Dr. B. M. Sutton for his assistance in the preparation of the manuscript.

1. (*a*) J. P. Ferris. J. Org. Chem. **27**, 2985 (1962); (*b*) B. Douglas, J. L. Kirkpatrick, R. R. Raffauf, D. Ribeiro, and J. A. Weisbach. Lloydia, **27**, 25 (1964); (*c*) R. N. Blomster, A. E. Schwarting, and J. M. Bobbitt. Lloydia, **27**, 15 (1964).
2. (*a*) J. P. Ferris. J. Org. Chem. **28**, 817 (1963); J. P. Ferris, R. C. Briner, and C. B. Boyce. J. Am. Chem. Soc. **93**, 2953 (1971); **93**, 2958 (1971); (*b*) D. E. Zacharias, G. A. Jefferey, B. Douglas, J. A. Weisbach, J. L. Kirkpatrick, J. P. Ferris, C. B. Boyce, and R. C. Briner. Experientia, **21**, 247 (1965); (*c*) S. C. Chu, G. A. Jeffrey, B. Douglas, J. L. Kirkpatrick, and J. A. Weisbach. Chem. Ind. (London), 1795 (1966).
3. (*a*) B. Loev, I. Lantos, and H. Van Hoeven. Tetrahedron Lett. 1101 (1974); (*b*) I. Lantos, C. Razgaitis, H. Van Hoeven, and B. Loev. J. Org. Chem. **42**, 228 (1977); (*c*) J. T. Wrobel and W. M. Golebiewsky. Tetrahedron Lett. 4293 (1973); M. Hanaoka, N. Ogawa, and Y. Arata. Tetrahedron Lett. 2355 (1973); Chem. Pharm. Bull. (Japan), **22**, 973 (1974).
4. (*a*) E. Fujita and K. Fuji. *In* International review of science, Organic Chemistry Series Two. Vol. 3. *Edited by* K. Wiesner. Butterworths, London. 1976. pp. 119–159; (*b*) K. Fuji, K. Ichikawa, and E. Fujita. Tetrahedron Lett. 361 (1979).
5. H. C. Brown and M.-H. Rei. J. Am. Chem. Soc. **91**, 5646 (1969); H. C. Brown and P. J. Geoghegan, Jr. J. Org. Chem. **35**, 1844 (1970).
6. P. Horsewood, W. H. Golebiewski, J. T. Wrobel, I. D. Spenser, J. F. Cohen, and F. Comer. Can. J. Chem. **57**, 1615 (1979).
7. R. F. Borch. Chem. Commun. 442 (1968).
8. T. G. Traylor. Acc. Chem. Res. **2**, 152 (1969).
9. R. C. Fahey. The stereochemistry of electrophilic additions to olefins and acetylenes. *In* Topics in stereochemistry. Vol 3. *Edited by* E. L. Eliel and N. L. Allinger. Interscience, New York. 1968.
10. H. C. Brown and J. H. Kawakami. J. Am. Chem. Soc. **95**, 8665 (1973).

(−)-4-Hydroxy-*N*-formylmorphinan-6-one, a versatile intermediate for the synthesis of 3-deoxyopioids

MARIA D. ROZWADOWSKA,[1] FU-LIAN HSU, ARTHUR E. JACOBSON, KENNER C. RICE, AND ARNOLD BROSSI[2]

Medicinal Chemistry Section, National Institute of Arthritis, Metabolism and Digestive Diseases, National Institutes of Health, Bethesda, MD 20205, U.S.A.

Received February 19, 1980

This paper is dedicated to the memory of Dr. Léo Marion

MARIA D. ROZWADOWSKA, FU-LIAN HSU, ARTHUR E. JACOBSON, KENNER C. RICE, and ARNOLD BROSSI. Can. J. Chem. **58**, 1855 (1980).

(−)-4-Hydroxy-*N*-formylmorphinan-6-one (**4**) was prepared in 70% overall yield from ketone **1**, via carbamate **2**, and *N*-formylation of ketone **3**. Bromination of **4** afforded either the 6-ketomorphinan **7** or the ketone **8**, depending on the reaction conditions applied. Both bromo ketones **7** and **8** could be converted by standard reactions into 4,5-epoxy-*N*-methylmorphinan-6-one (**1**). The ketomorphinan **4** emerges from these investigations as a versatile intermediate, well suited for the synthesis of 4-hydroxymorphinans and 3-deoxyopioids.

MARIA D. ROZWADOWSKA, FU-LIAN HSU, ARTHUR E. JACOBSON, KENNER C. RICE et ARNOLD BROSSI. Can. J. Chem. **58**, 1855 (1980).

On a préparé la (−)hydroxy-4 *N*-formylmorphinanone-6 (**4**) avec un rendement global de 70% en transformant la cétone **1** en carbamate **2** suivie de la *N*-formylation de la cétone **3**. La bromation du composé **4** conduit suivant les conditions de réaction soit à la céto-6 morphinane **7** soit à la cétone **8**. Les deux bromocétones **7** et **8** peuvent être transformées en époxy-4,5 *N*-méthylmorphinanone-6 (**1**) en faisant appel à des réactions connues. Sur la base de ces études, la cétomorphinane **4** apparait comme un intermédiaire polyvalent convenant très bien à la synthèse des hydroxy-4 morphinanes et des déoxy-3 opioides.

[Traduit par le journal]

The interesting pharmacological profiles recently reported for several 3-deoxy opioids (1), prepared by chemical deoxygenation of (−)-dihydromorphine, prompted a search for a more versatile route into the 3-deoxy series. In this connection it became apparent that 3-deoxynor derivatives, or precursors which could readily be *N*-deblocked, would offer advantages. In order to study this problem, which is of interest in connection with a total synthesis, and to prepare samples needed for the ultimate comparison with synthetic material, we initiated a program on which we would like to report. All of the compounds prepared were derived from dihydromorphine and therefore possess the absolute configuration expressed in their formulas.

Treatment of 4,5-epoxy-*N*-methylmorphinan-6-one (**1**) (1) with 2,2,2-trichloroethyl chloroformate (2) readily provided carbamate **2** in 92% yield. Reduction of **2** with Zn/NH_4Cl in ethanol (3) smoothly effected the cleavage of the carbamate function with concomitant reductive opening of the oxide bridge, to afford the norketone **3** in 94% yield. On the other hand, when carbamate **2** was treated with zinc in aqueous acetic acid (2), the oxide bridge remained intact and the morphinone **5** was obtained in 87% yield. It is interesting to note that the different activity of the zinc in these media, observed previously by Schöpf and Pfeifer (4) and Beyerman and co-workers (2, 3), determines whether only cleavage of the carbamate function occurs or whether this reduction involves simultaneous opening of the oxygen bridge. *N*-formylation of **3** and **5** with refluxing ethyl formate gave the corresponding *N*-formyl derivatives **4** and **6** in 75% and 85% yield, respectively. Both **4** and **6**, as well as the other *N*-formyl derivatives prepared, showed the existence of pairs of rotamers, as observed in similar cases (5, 6). The two rotamers were visible by nmr and tlc but isolation afforded only one single compound. The measured value of the optical rotation of the *N*-formyl derivatives may depend on the proportion of the individual rotamers. Hydrolysis of **6** with dilute HCl in MeOH afforded the nor compound **5** in quantitative yield. Bromination of **4** with 1.1 mol of bromine in AcOH afforded, as in the *N*-Me series (7), the 1-bromo congener **7** in 56% yield from which **4** was smoothly regenerated by hydrogenolysis with Pd/C in MeOH. Morphines (8) and 4-hydroxymorphinans (7, 9) are believed to brominate first in the 1-position, and successful conversion of compound **7** into the morphine derivative **8** is in agreement with this assumption. The aromatic protons seen as

[1]Visiting scientist from A. Mickiewicz University, 60–780 Poznań, Poland.

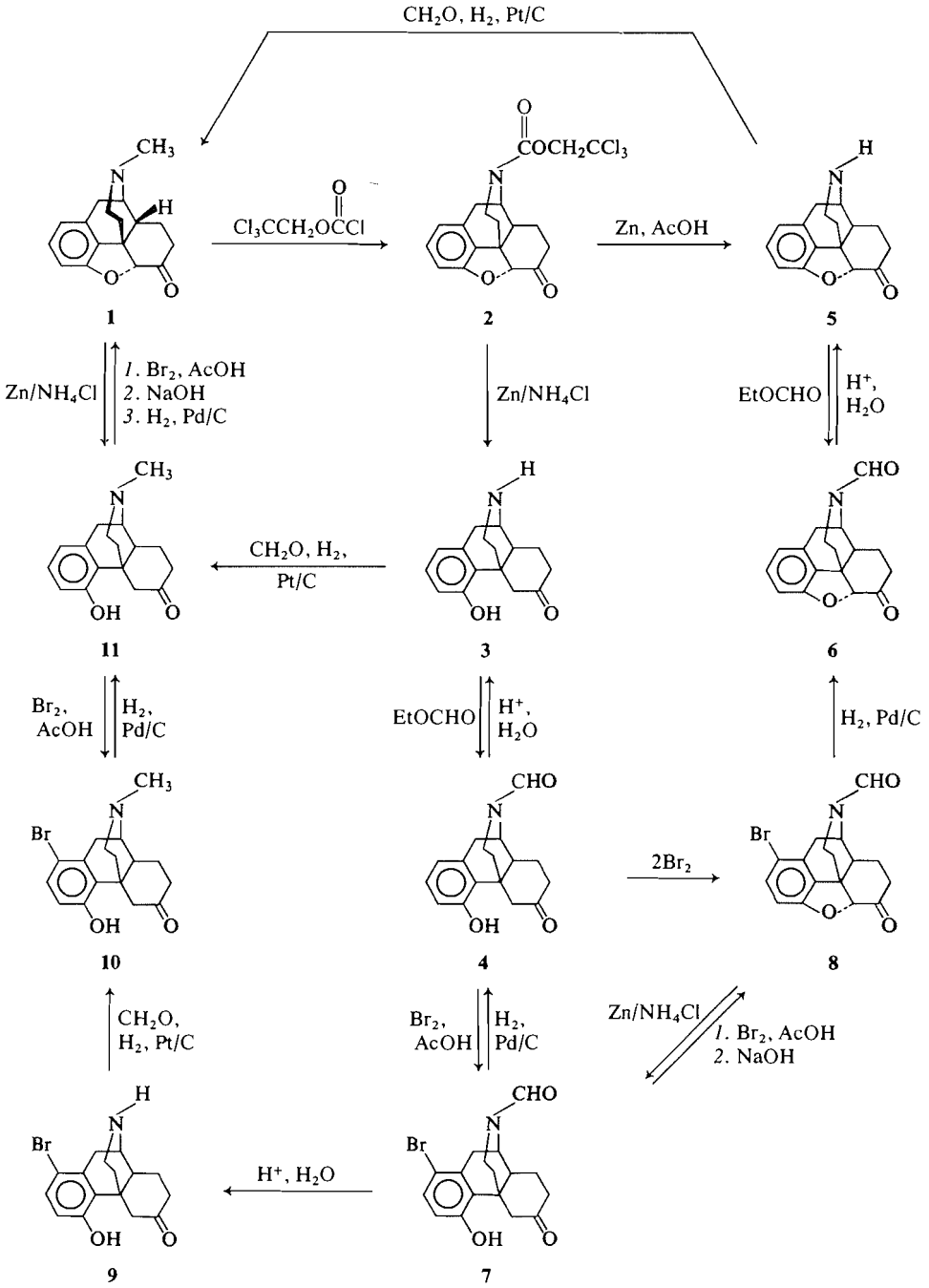
[2]Author to whom correspondence should be addressed.

0008-4042/80/171855-05$01.00/0

©1980 National Research Council of Canada/Conseil national de recherches du Canada

Can. J. Chem. Downloaded from www.nrcresearchpress.com by 210.87.254.42 on 09/05/12
For personal use only.

Can. J. Chem. Downloaded from www.nrcresearchpress.com by 210.87.254.42 on 09/05/12
For personal use only.



doublets at 7.31 and 6.63 ppm do not clearly discriminate between **7** and its 3-bromo isomer.[3] The *N*-substituent seems to have little influence as shown by the formation of **10** (**7** → **9** → **10**) from **11**. Bromination of **4** with 2.2 mol of bromine in AcOH, followed by treatment of the residue with aqueous NaOH, gave the 4,5-epoxy derivative **8** in 85% yield. Precedent for oxide ring closure of this type is found in the conversion of dihydrothebainone to dihydrocodeinone (8, 9, 10).

Reductive cleavage of the oxide bridge of amide **8** to regenerate the 1-bromo derivative **7** was accomplished in 61% yield with Zn/NH_4Cl in ethanol, as in the case of the transformation of **2** to **3**. It is

[3]Details of this ^{13}C nmr study, which was done by C. D. Hufford, School of Pharmacy, University of Mississippi, will be published elsewhere.

Can. J. Chem. Downloaded from www.nrcresearchpress.com by 210.87.254.42 on 09/05/12
For personal use only.

interesting to note that this reduction leaves the 1-bromo substituent intact, as well as the *N*-CHO group. Hydrogenolysis of the bromine in **8** with $Pd/C/H_2$ afforded **6** in 88% yield. Acid hydrolysis of the title compound **4** gave **3** in quantitative yield. Reductive alkylation of **3** with $CH_2O/H_2/Pt/C$ gave the *N*-methyl derivative **11**, isolated as the hydrobromide hemihydrate which could be transformed to bromoketone **10** by treatment with 1.1 mol of bromine in AcOH (50% yield). Regeneration of **11** from **10** by hydrogenolysis ($Pd/C/H_2$) in aqueous AcOH was readily accomplished. Bromination of **11** with 2.5 mol of bromine in AcOH, followed by treatment of the residue with aqueous NaOH and catalytic reduction of the nonphenolic fraction, afforded **1** in 84% yield based on **11**. The norketone **5**, which was obtained by acid hydrolysis of **6** and from **2** as described above, also afforded **1** on reductive alkylation with $Pd/C/CH_2O/H_2$ (78% yield). Reductive cleavage of the oxide bridge in **1** was efficiently effected with Al/Hg (95% yield) (7) or, preferably, with Zn/NH_4Cl reagent in ethanol in similar yield. Furthermore, acid hydrolysis of the 1-bromo derivative **7** afforded the nor base **9** which was reductively alkylated with $Pt/C/H_2/CH_2O$ to **10**. 4,5-Epoxy-*N*-methylmorphinan-6-one (**1**) is best accessible from ketone **4** by either of two sequences: **4** → **6** → **5** → **1** or **4** → **3** → **11** → **1**, both involving three practical operations. We prefer at this moment the former sequence, which seems to give better yields and intermediates which are easier to purify.

The *N*-formyl ketone **4** emerges from these investigations not only as a versatile intermediate for a synthesis of **1** and congeners, but can also be utilized to prepare antinociceptive 4-hydroxymorphinans,[4] and their *N*,*O*-substituted congeners.

Experimental

Melting points (uncorrected) were determined on a Fisher–Johns apparatus. Elemental analyses were performed by the Section on Microanalytical Services and Instrumentation of the laboratory. Infrared spectra were recorded on a Beckman IR 4230 instrument. Optical rotations were measured using a Perkin–Elmer Model 141 polarimeter using the solvents and concentrations specified. Nuclear magnetic resonance spectra were determined using a JOEL JNM-FX 100 spectrometer with TMS as the internal reference. Mass spectra were obtained with a Hitachi Perkin–Elmer RMU-6E spectrometer (70 eV). Thin layer chromatography (tlc) utilized silica gel GF plates from Analtech, Inc., (Newark, DE.), and $CHCl_3$–MeOH–NH_4OH (90:9:1) as the solvent system, unless otherwise stated.

*4,5-Epoxy-*N*-(2,2,2-trichloroethoxycarbonyl)-morphinan-6-one (2)*

To a well stirred mixture of 7.0 g (26 mmol) of **1**, 70 mL of chloroform and 38.0 g (0.38 mol) of anhydrous potassium bicarbonate, 21.6 g (101 mmol) of 2,2,2-trichloroethyl chloroformate was added dropwise during 10 min, under argon. The mixture was refluxed for 3 h, cooled, and 70 mL of water and 60 mL of chloroform were added. The aqueous layer was separated and extracted (2×) with 30 mL of chloroform. The combined organic layers were washed with water, 5% HCl, water, dried, and evaporated. The oily residue was treated with 40 mL of ether, which immediately deposited a crystalline solid. The solid was digested with 100 mL of ether for 15 min under reflux to give 10.3 g (92%) of **2**; mp 206–208°C; $[\alpha]_D^{20}$ −240° (*c* 0.63, $CHCl_3$); ir (KBr): 1710, 1725 (shoulder, CO) cm^{-1}; nmr ($CDCl_3$) δ: 7.12 (1H, m, ArH), 6.76 (2H, m, ArH), 4.80 (2H, m, CH_2), 4.66 (1H, s, C5–H); ms *m/e*: 429 (M^+), 431 ($M^+ + 2$), 433 ($M^+ + 4$). *Anal.* calcd. for $C_{19}H_{18}NO_4Cl_3$ (430.71): C 52.98, H 4.21, N 3.25, Cl 24.69; found: C 53.23, H 4.49, N 3.34, Cl 24.28.

4-Hydroxymorphinan-6-one (3)

(*A*) From **2**. Ammonium chloride (40.7 g, 0.76 mol) was added to a solution of 10.3 g (24 mmol) of carbamate **2** in 400 mL of ethanol, and the mixture was heated to reflux. To this heterogeneous system, zinc powder (6.1 g, 90 mg-at.) was added portionwise during 6 h. A second portion of zinc (6.1 g, 90 mg-at.) was added in one batch and the mixture was refluxed until tlc indicated that **2** had completely reacted (24 h). After cooling, the catalyst was filtered off and washed several times with 95% ethanol until a positive test with Dragendorff reagent was no longer observed.

The combined filtrates were evaporated to dryness, saturated sodium sulfate solution (70 mL) was added, and this slurry was extracted several times (total 800 mL) with chloroform–isopropanol (3:1). The organic extracts were evaporated to dryness and the residue was dissolved in 50 mL of 1% HCl. The acidic solution was washed (2×) with 70 mL of chloroform, then rendered alkaline (pH 9) with concentrated NH_4OH and extracted several times with a total volume of 400 mL of chloroform–isopropanol (3:1). After drying, solvents were removed *in vacuo* to give 6.1 g of an oil, which upon treatment with tetrahydrofuran deposited an off-white crystalline solid (5.8 g, 94%); mp 220°C (dec.); $[\alpha]_D^{20}$ −72° (*c* 0.935, MeOH); ir (KBr): 1710 (CO), 3300 (NH), 3400 (broad, OH) cm^{-1}; nmr (DMSO-d_6) δ: 6.92 (1H, m, ArH), 6.48 (2H, m, ArH); ms *m/e*: 258 ($M^+ + 1$). *Anal.* calcd. for $C_{16}H_{19}NO_2$ (257.33): C 74.68, H 7.44, N 5.44; found: C 74.98, H 7.42, N 5.44.

(*B*) From **4**. A solution of 285 mg (1 mmol) of **4** in 8 mL of methanol which contained 0.8 mL of 37% HCl was refluxed overnight. The methanol was evaporated, 3 mL of 1% HCl added, and the mixture was extracted with 15 mL of chloroform. The aqueous layer was rendered alkaline with concentrated NH_4OH (pH 9) and extracted with chloroform until a negative Dragendorff test was obtained. After drying and removal of the solvent, the remaining foam was treated with tetrahydrofuran, to give 210 mg (82%) of pure **3**.

N-*Formyl-4-hydroxymorphinan-6-one (4)*

(*A*) From **3**. Compound **3** (6.1 g, 23.7 mmol) was refluxed in 600 mL of ethyl formate for 48 h to give *N*-formyl derivative **4** as a solid which was filtered (3.8 g). The filtrate was washed with 1% HCl, water, dried, and concentrated to ca. ¼ of its volume, depositing an additional amount of **4** (1.3 g, 75% overall); mp > 310°C (dec.); $[\alpha]_D^{20}$ −237° (*c* 0.6, AcOH); ir (KBr): 1640 (CO), 1710 (CO), ca. 3100 (broad, OH) cm^{-1}; nmr (DMSO-d_6) δ: 9.42 (1H, s, OH, exchanges with D_2O), 6.90 (1H, m, ArH), 6.55 (2H, m, ArH); ms *m/e*: 285 (M^+). *Anal.* calcd. for $C_{17}H_{19}NO_3$ (285.35): C 71.56, H 6.71, N 4.91; found: C 71.61, H 6.51, N 4.75.

(*B*) From **7**. One hundred and twenty milligrams (0.33 mmol) of **7** in 12 mL of methanol was hydrogenated at 45 psi in the presence of 10% Pd/C catalyst at room temperature, overnight. The catalyst was filtered, washed with methanol, and the filtrate

[4]The antinociceptive activities of the compounds discussed and several of their derivatives will be published elsewhere.

Can. J. Chem. Downloaded from www.nrcresearchpress.com by 210.87.254.42 on 09/05/12
For personal use only.

was concentrated *in vacuo* to half its volume, to give 50 mg of pure **4** (tlc, ms, mp), followed by a second crop of crystals (35 mg, 90% total).

4,5-Epoxymorphinan-6-one (5)

(*A*) From **2**. Compound **2** (4.5 g, 17.5 mmol) was heated to solution in a mixture of 42 mL of 80% acetic acid and 52 mL of glacial acetic acid, cooled to room temperature, and stirred overnight with 2.9 g of powdered zinc (44 mg-at.). Water (4 mL) was added and the zinc filtered. The filtrate was evaporated to a syrup and treated with 20 mL of saturated sodium sulfate and 40 mL of chloroform. The aqueous layer was separated and extracted with chloroform until the Dragendorff test was negative. The combined organic layers were extracted with 2 × 10 mL of 1% HCl and discarded. The aqueous phase was rendered alkaline with concentrated NH_4OH and extracted with chloroform–isopropanol (3:1) until, again, a negative Dragendorff test was obtained. Organic extracts were combined, dried, and evaporated to give a crystalline residue. This was digested with ether, leaving 2.3 g (87%) of crystalline **5**; mp 160–161°C; $[\alpha]_D^{20}$ −273° (*c* 0.99, $CHCl_3$); ir (KBr): 1725 (CO), ca. 3350 (NH) cm^{-1}; nmr ($CDCl_3$) δ: 7.08 (1H, m, ArH), 6.72 (2H, m, ArH), 4.6 (1H, s, C5—H); ms *m/e*: 255 (M^+). *Anal.* calcd. for $C_{16}H_{17}NO_2$ (255): C 75.29, H 6.66, N 5.49; found: C 75.07, H 6.77, N 5.45. Hydrobromide salt, mp 240°C (dec.), $[\alpha]_D^{20}$ −171° (*c* 0.5, CH_3OH). *Anal.* calcd. for $C_{16}H_{17}NO_2 \cdot HBr \cdot \frac{1}{2} H_2O$ (345.24): C 55.66, H 5.55, N 4.06, Br 23.14; found: C 55.33, H 5.78, N 3.79, Br 22.79

(*B*) From **6**. One hundred and twenty-four milligrams (0.5 mmol) of **6** was refluxed with methanol (4 mL) containing 0.4 mL of 37% HCl for 6 h. The solution was concentrated to half volume and left overnight to afford, quantitatively, the hydrochloride salt of mp > 280°C. The base prepared from it in the usual way was identical with that prepared above (mixture mp, ms, tlc using $CHCl_3$–MeOH–NH_4OH (80:18:2)).

4,5-Epoxy-N-formylmorphinan-6-one (6)

(*A*) From **5**. Compound **5** (1.1 g, 4.3 mmol) and 50 mL of ethyl formate were refluxed overnight to give crystalline **6** (0.55 g). Additional amounts of **6** (0.49 g) were recovered from the filtrate, after washing with 1% HCl, drying, and concentration (total yield 85%); mp 246–247°C (after recrystallization from ethyl acetate); $[\alpha]_D^{20}$ −360° (*c* 0.89, $CHCl_3$); ir (film): 1660 (CHO), 1720 (CO) cm^{-1}; nmr ($CDCl_3$) δ: 8.20 and 8.00 (1H, 2s, CHO, signals of two rotamers), 7.12 (1H, m, ArH), 6.86 (2H, m, ArH), 4.64 (1H, s, C5—H); ms *m/e*: 283 (M^+). *Anal.* calcd. for $C_{17}H_{17}NO_3$ (283.33): C 72.07, H 6.05, N 4.94; found: C 72.18, H 6.24, N 4.87.

(*B*) From **8**. A solution of **8** (0.18 g, 0.5 mmol) in AcOH (6 mL) containing 300 mg (3.6 mmol) of sodium acetate and 40 mg of 10% Pd/C was hydrogenated at 50 psi for 18 h, at room temperature. The catalyst was filtered and washed with 20 mL of AcOH. The combined filtrates were evaporated, and the residue partitioned between 2% NaOH and chloroform. The aqueous phase was extracted (2×) with chloroform. The combined organic layers were washed with 1% HCl and brine, dried, and evaporated to give **6** as an oil (0.14 g) which crystallized from methanol (0.125 g, 88%). The material was identical (mp, tlc, ir) with that prepared above.

(*C*) From **4**. The ketone **6** could be prepared from **4** in 62% yield via **7** and **8** without isolation (see below).

1-Bromo-4-hydroxy-N-formylmorphinan-6-one (7)

(*A*) From **4**. To a well stirred solution of **4** (1.14 g, 4 mmol), 44 mL (4.4 mmol) of 0.1 *M* Br_2 in AcOH was introduced dropwise over 1.5 h at room temperature. After an additional 0.5 h, the solvent was evaporated and the residue was partitioned between 1% HCl and chloroform (50 mL). The separated aqueous layer was extracted (2×) with 20 mL of chloroform. The combined organic extracts were treated with 20 mL of 2% NaOH. After 10 min, the separated organic phase was extracted with 10 mL of 2% NaOH. The alkaline extracts were treated with 37% HCl to pH 9, and extracted with chloroform (3 × 50 mL). The combined chloroform extracts were washed with water and dried to give a foam (1.2 g). Crystallization from ethanol gave **7** (820 mg, 56%); mp 286–287°C (dec.); $[\alpha]_D^{20}$ −270° (*c* 0.53, $CHCl_3$); ir (KBr): 1645 (CHO), 1705 (CO), 3250 (broad, OH) cm^{-1}; nmr ($CDCl_3$) δ: 8.40 (1H, s, OH, disappears on treatment with D_2O), 8.22 and 8.06 (1H, 2s, CHO, pair of rotamers), 7.24 (1H, d, *J* = 9 Hz, ArH), 6.68 (1H, d, *J* = 9 Hz, ArH); ms *m/e*: 364 (*M* + 1), 366 (*M* + 3). *Anal.* calcd. for $C_{17}H_{18}BrNO_3$ (364.25): C 56.06, H 4.98, N 3.84, Br 21.94; found: C 56.19, H 5.07, N 3.63, Br 21.69.

(*B*) From **8**. To a refluxing mixture of 130 mg (0.34 mmol) of **8** and 1.7 g (31 mmol) of NH_4Cl in 17 mL of 95% ethanol, two 250 mg (3.8 mg-at.) batches of powdered zinc were added at 1 h intervals. After refluxing 3 h, the mixture was cooled and the catalyst was filtered and washed with anhydrous ethanol. The combined solvent was evaporated to dryness *in vacuo*, saturated Na_2SO_4 (2 mL) was added, and this was extracted with chloroform (25 mL). The organic layer was washed with 1% HCl and brine, dried, and evaporated to give 98 mg of a foam which, after crystallization from ethanol, gave 75 mg (61%) of pure **7** identical with a specimen prepared above (mp, tlc, ir).

1-Bromo-4,5-epoxy-N-formylmorphinan-6-one (8)

(*A*) From **4**. A solution of 0.1 *M* bromine in AcOH (22 mL, 2.2 mmol) was added dropwise during 0.5 h to a solution of **4** (285 mg, 1 mmol) in 10 mL of AcOH at room temperature. After stirring for another 0.5 h the solvent was evaporated and the residue partitioned between 2% NaOH and 20 mL chloroform, after a pH of 11 was sustained. After 5 min the organic phase was separated, the aqueous phase extracted with 10 mL chloroform (2×), the combined organic extracts washed with 1% HCl, brine, dried, and evaporated to give an oil which crystallized from methanol to afford 310 mg (85%) of compound **8**; mp 222–224°C; $[\alpha]_D^{20}$ −313° (*c* 0.53, $CHCl_3$); ir (KBr): 1645 (CHO), 1725 (CO) cm^{-1}; nmr ($CHCl_3$) δ: 8.20 and 9.04 (1H, 2s, CHO, a pair of rotamers), 7.32 (1H, d, *J* = 8 Hz, ArH), 6.72 (1H, d, *J* = 8 Hz, ArH), 4.68 (1H, s, C5—H); ms *m/e*: 362 (M^+ + 1), 364 (M^+ + 3). *Anal.* calcd. for $C_{17}H_{16}BrNO_3$ (362.23): C 56.37, H 4.45, N 3.87, Br 22.06; found: C 56.00, H 4.48, N 3.80, Br 22.34.

(*B*) From **7**. Compound **7** (0.24 g, 0.66 mmol), in 7 mL of AcOH, was brominated with 6.7 mL (0.67 mmol) of 0.1 *M* bromine in AcOH, according to the procedure used for the preparation of **7**, except that extraction was carried out at pH > 11. Recrystallization from methanol gave 0.165 g (69%) of **8**, identical with the material described above (mp, tlc, ir).

4-Hydroxy-N-methylmorphinan-6-one (11)

(*A*) From **3**. A mixture of 257 mg (1 mmol) of **3**, 0.7 mL of aqueous 37% formalin, and 70 mg of 10% Pt/C catalyst, in 15 mL of methanol, was hydrogenated at room temperature, at 40 psi, overnight. The catalyst was filtered, washed with methanol, and the solvent evaporated to dryness. The residue was partitioned between 1% HCl and chloroform and the aqueous layer was rendered alkaline with concentrated NH_4OH and extracted with chloroform–isopropanol (3:1). Drying and evaporation of solvents gave 250 mg of an oil that crystallized from methanol to give 190 mg (70%) of pure **11**, identical with material previously reported. *Anal.* calcd. for $C_{17}H_{21}NO_2$ (271.36): C 75.24, H 7.80, N 5.16; found: C 75.21, H 7.89, N 5.23.

(*B*) From **10**. A mixture of **10** (70 mg, 0.16 mmol), anhydrous NaOAc (124 mg), and 10% Pd/C catalyst (20 mg) in 2 *N* AcOH (5 mL) was hydrogenated at 50 psi at room temperature for 16 h.

Can. J. Chem. Downloaded from www.nrcresearchpress.com by 210.87.254.42 on 09/05/12
For personal use only.

The catalyst was filtered and was washed with 2 *N* AcOH. The solution was adjusted to pH 9–10 with NH_4OH and extracted with chloroform. The combined chloroform extracts were washed with H_2O, dried, and evaporated to give a crude product which was recrystallized from benzene – petroleum ether to afford **11** (40 mg, 91%), identical with material prepared above (tlc, ir, mixture mp).

*1-Bromo-4-hydroxy-*N*-methylmorphinan-6-one (**10**)*

(*A*) From **11**. To a solution of **11** (400 mg, 1.47 mmol) in 15 mL AcOH was added a solution of Br_2 in AcOH (0.1 *M*, 14.7 mL) dropwise at room temperature. The solution was stirred for 10 min and the excess bromine and AcOH evaporated to give a residue which was recrystallized from H_2O to afford **10** (0.25 g, 50%); mp 218–221°C: $[\alpha]_D^{20}$ −43.2° (*c* 0.92, MeOH); ir (KBr): 3300 (OH), 1705 (CO) cm^{-1}; nmr (CD_3OD) δ: 7.31 (1H, d, J = 9.5 Hz, ArH), 6.63 (1H, d, J = 9.5 Hz, ArH), 4.30 (1H, d, J = 14 Hz, C5—H), 2.97 (3H, s, NCH_3); ms *m/e*: 349 (M^+), 351 ($M^+ + 2$). *Anal.* calcd. for $C_{17}H_{20}BrNO_2 \cdot HBr \cdot 0.5\,H_2O$ (440.18): C 46.39, H 5.04, N 3.18, Br 36.31; found: C 46.25, H 5.33, N 2.91, Br 36.43. The free base was prepared in the usual way, mp 222–224°C (MeOH). *Anal.* calcd. for $C_{17}H_{20}BrNO_2$ (350.26): C 58.3, H 5.76, N 4.00, Br 22.81; found: C 58.58, H 5.76, N 4.14, Br 22.61.

(*B*) From **9**. A mixture of 95 mg (0.26 mmol) of **9** · HCl, 0.22 mL of 37% formalin, and 21 mg of 10% Pt/C catalyst, in 10 mL of methanol, was hydrogenated under 40 psi at room temperature overnight. The catalyst was filtered and washed with methanol. The solvent was evaporated and the residue was partitioned between 5 mL of ether and 3 mL of 1% HCl to give a white precipitate. Filtration gave 65 mg of pure **10** · HCl: mp 220°C (dec.). *Anal.* calcd. for $C_{17}H_{20}NO_2Br \cdot HCl \cdot 1.5\,H_2O$ (413.74): C 49.35, H 5.85, N 3.39; found: C 49.27, H 5.53, N 3.49.

*1-Bromo-4-hydroxymorphinan-6-one (**9**)*

A solution of 140 mg (0.38 mmol) of **7** in 4 mL of methanol containing 0.4 mL of 37% HCl was refluxed for 6 h. The solution was then concentrated to half volume and, after standing overnight, gave 110 mg (71%) of crystalline **9** · HCl; mp 280°C (dec.); $[\alpha]_D^{20}$ −19° (*c* 1.25, MeOH); ir (KBr): 1710 (CO), 2400–3600 (broad, OH, NH_2^+) cm^{-1}; nmr (DMSO-d_6) δ: 10.16 (1H, s, NH), 9.5 (2H, broad, NH, OH), 7.3 (1H, d, J = 9 Hz, ArH), 6.7 (1H, d, J = 9 Hz, ArH); ms *m/e*: 335 (M^+), 337 ($M + 2$). *Anal.* calcd. for $C_{16}H_{18}Br \cdot NO_2 \cdot HCl$ (372.70): C 51.56, H 5.14, N 3.76, Cl 9.51, Br 21.44; found: C 51.18, H 5.18, N 3.73, Cl 9.48, Br 21.15.

*4,5-Epoxy-*N*-methylmorphinan-6-one (**1**)*

(*A*) From **5** · HBr. A mixture of the hydrobromide of **5** (0.168 g, 0.5 mmol), 0.42 mL of 37% formalin, and 42 mg of 10% Pt/C, in 10 mL of methanol, was hydrogenated under 45 psi at room temperature for 7 h. The catalyst was filtered and washed with methanol. The methanolic solution was concentrated *in vacuo* and the residue was dissolved in 1% HCl (5 mL). The aqueous solution, after washing with chloroform, was rendered alkaline with concentrated NH_4OH and extracted with chloroform until a negative Dragendorff test was obtained. The combined organic extracts were dried and evaporated to give a solid which after recrystallization from ethyl acetate gave pure **1** (0.1 g, 78%) identical with a reference sample.

(*B*) From **11**. A solution of bromine in AcOH (0.1 *M*, 46 mL, 4.6 mmol) was added dropwise to a solution of **11** (0.5 g, 1.84 mmol) in AcOH (6 mL), stirred for 20 min, and the AcOH then evaporated. The crude brominated product was treated with 0.5 *N* NaOH (5 mL) and chloroform and stirred for 10 min. The $CHCl_3$ layer was separated and the aqueous layer was extracted with $CHCl_3$. The combined chloroform extracts were washed with H_2O, dried, and evaporated to give a solid (240 mg). A part of this material (160 mg) and 10% Pd/C catalyst (40 mg) were suspended in a solution of anhydrous NaOAc (350 mg) in 6 mL of 2 *N* AcOH and hydrogenated at 50 psi for 16 h. The catalyst was filtered and washed with 2 *N* AcOH. The filtrate was adjusted to pH 10 with 6 *N* NaOH and extracted with chloroform. The combined chloroform extracts were washed with H_2O, dried, and evaporated to give a solid which was recrystallized from ethyl acetate to afford **1** (102 mg, 82%), identical with the material prepared above.

Acknowledgments

We would like to thank Dr. Franz Scheidl, head of the Microanalytical Laboratory, Hoffmann–La Roche Inc., Nutley, NJ, U.S.A., for having analyzed several samples described in this paper. The interest of Dr. C. D. Hufford, School of Pharmacy, University of Mississippi, University, MS, in the ^{13}C nmr spectra of several brominated morphinans is gratefully appreciated.

1. J. Reden, M. F. Reich, K. C. Rice, A. E. Jacobson, A. Brossi, R. S. Streaty, and W. A. Klee. J. Med. Chem. **22**, 256 (1979).
2. H. Beyerman, L. van Bommel, L. Maat, and C. Olieman. Recl. Trav. Chim. Pays-Bas, **95**, 312 (1976).
3. C. Olieman, L. Maat, and H. C. Beyerman. Recl. Trav. Chim. Pays-Bas, **95**, 189 (1976).
4. C. Schöpf and T. Pfeifer. Ann. **483**, 157 (1930).
5. K. C. Rice and A. Brossi. J. Org. Chem. **45**, 592 (1980).
6. H. C. Beyerman, E. Burrman, T. S. Lie, and L. Maat. Recl. Trav. Chim. Pays-Bas, **95**, 43 (1976); C. Olieman, L. Maat, K. Waliszewski, and H. C. Beyerman. J. Chromatogr. **133**, 382 (1977).
7. F.-L. Hsu, A. E. Jacobson, K. C. Rice, and A. Brossi. Heterocycles, **13**, 259 (1979).
8. M. Gates and A. Tschudi. J. Am. Chem. Soc. **78**, 1380 (1956).
9. C. Olieman, L. Maat, and H. C. Beyerman. Recl. Trav. Chim. Pays-Bas, **97**, 31 (1978).
10. D. W. Weller and H. Rapoport. J. Med. Chem. **19**, 1171 (1976).

Conversion of stereoisomeric 2-amino-1-carbamoylcyclohexane-5,5-dicarboxylates into 6-amino-3-azabicyclo[3.3.1]nona-2,4-dione-1-carboxylates

VINKO ŠKARIĆ, MIRJANA SEDJAK, VERA TURJAK-ZEBIĆ, AND DJURDJICA ŠKARIĆ

Laboratory of Stereochemistry and Natural Products, Rudjer Bošković Institute, 41001 Zagreb, Croatia, Yugoslavia

Received February 11, 1980

This paper is dedicated to the memory of Dr Léo Marion

VINKO ŠKARIĆ, MIRJANA SEDJAK, VERA TURJAK-ZEBIĆ, and DJURDJICA ŠKARIĆ. Can. J. Chem. **58**, 1860 (1980).

The separation of *cis*- and *trans*-2-amino-*r*-1-carbamoylcyclohexane-5,5-dicarboxylates **2** and **3** as 2-*N*-benzyloxycarbonyl (**15**, **16**) and 2-*N*-benzoyl- (**17**, **18**) derivatives is described. A dipeptide containing suitably protected L-phenylalanine and *cis*-2-amino-1-carbamoylcyclohexane (**2**) was also prepared. Moreover, *cis*- (**17**) and *trans*- (**18**) benzamido isomers were converted into ethyl *t*-6- (**23**) and *c*-6- (**24**) benzamido-*r*-1-carboxylate-3-azabicyclo[3.3.1]nona-2,4-dione, respectively. Similarly, ethyl *c*-6-phthalimido-*r*-1-carboxylate-3-azabicyclo[3.3.1]nona-2,4-dione (**25**) was obtained from diethyl *t*-2-phthalimido-*r*-1-carbamoylcyclohexane-5,5-dicarboxylate (**22**).

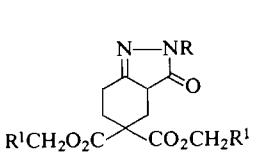
VINKO ŠKARIĆ, MIRJANA SEDJAK, VERA TURJAK-ZEBIĆ et DJURDJICA ŠKARIĆ. Can. J. Chem. **58**, 1860 (1980).

On décrit la séparation des composés amino-2 carbamoyl-1-*r* cyclohexanedicarboxylates-5,5 *cis* et *trans* **2** et **3** sous forme de dérivés *N*-benzyloxycarbonyl-2 (**15**, **16**) et *N*-benzoyl-2 (**17**, **18**). On a également préparé un dipeptide contenant la L-phénylalanine et l'amino-2 carbamoyl-1 cyclohexane *cis* (**2**) convenablement protégés. De plus, on a transformé les isomères benzamido *cis* (**17**) et *trans* (**18**) respectivement en benzamido 6-*t* (**23**) et 6-*c* (**24**) aza-3 bicyclo[3.3.1] nonadione-2,4 carboxylate 1-*r* d-éthyle. D'une façon analogue, on a obtenu le phtalimido 6-*c* aza-3 bicyclo[3.3.1] nonadione-2,4 carboxylate 1-*r* d'éthyle (**25**) à partir du phtalimido 2-*t* carbamoyl 1-*r* cyclohexanedicarboxylate-5,5 d'éthyle (**22**).

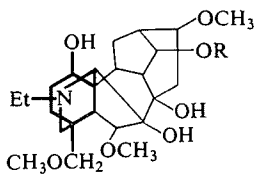
[Traduit par le journal]

Previously, we described the synthesis and properties of all possible positional isomers in the 4,5,6,7- tetrahydro- 3- oxo- 2*H*- indazolecarboxylic acid series (1) as part of our continuing interest in the stereochemical criteria of their reductive ring opening. For instance diethyl 4,5,6,7-tetrahydro-3-oxo-2*H*-indazole-5,5-dicarboxylate **1** was cleaved (2) into a mixture of diethyl *c*-2- (**2**) and *t*-2- (**3**) amino-*r*-1-carbamoylcyclohexane-5,5-dicarboxylate. With these polyfunctional alicyclic isomers on hand, the synthesis of an essential part of delcosine (**4**) and delsoline (**5**) alkaloids[1] (indicated with heavy lines) via the 3-azabicyclo[3.3.1]nonane derivatives (*vide infra*) seemed accessible. However, no precise knowledge has yet been obtained with regard to the separation of isomers **2** and **3**. The present paper deals with 2-*N*-acyl derivatives of the compounds **2** and **3**, most of which have been successfully separated and utilized in several sterically controlled intramolecular cyclizations.

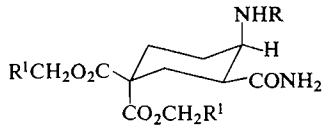
We first showed that compound **1** on treatment with freshly prepared Raney nickel (6) in isopropanol underwent several concomitant reactions. However, a mixture of the desired aminocarbamoylcyclohexanes **2** and **3** was isolated as the main product, showing very close tlc mobilities at



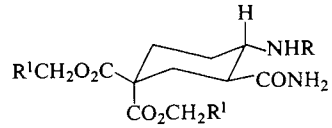
1 R = H, R[1] = CH_3
8 R = Ph, R[1] = CH_3
11 R = R[1] = H



4 R = H
5 R = CH_3



2 R = H, R[1] = CH_3
12 R = R[1] = H
15 R = $PhCH_2$—O—CO, R[1] = CH_3
17 R = Bz, R[1] = CH_3
19 R = Bz, R[1] = H
21 R = L-BOC—Phe, R[1] = CH_3



3 R = H, R[1] = CH_3
7 R = *i*-Pr, R[1] = CH_3
13 R = R[1] = H
16 R = $PhCH_2$—O—CO, R[1] = CH_3
18 R = Bz, R[1] = CH_3
20 R = Bz, R[1] = H

[1]This study was undertaken as a continuation of a memorable scientific association with Dr. Léo Marion at the National Research Council of Canada, 1957–1959, concerning the investigation of delcosine and delsoline alkaloids (3–5), isolated from *Delphinium consolida L.*

0008-4042/80/171860-05$01.00/0

©1980 National Research Council of Canada/Conseil national de recherches du Canada

Can. J. Chem. Downloaded from www.nrcresearchpress.com by 210.87.254.6 on 09/05/12
For personal use only.

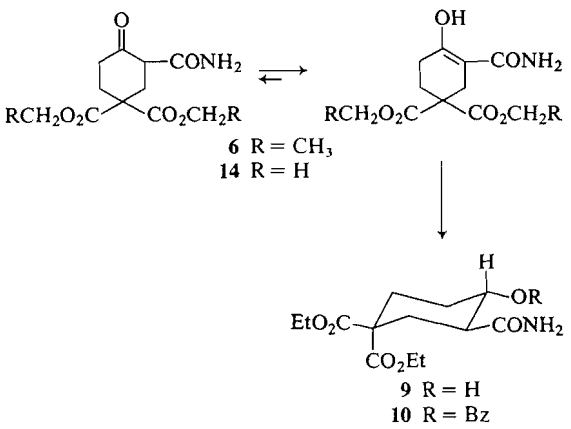
Can. J. Chem. Downloaded from www.nrcresearchpress.com by 210.87.254.6 on 09/05/12
For personal use only.

$R_f \sim 0.11$. Two isolated by-products were identified as diethyl 2-oxo-1-carbamoylcyclohexane-5,5-dicarboxylate (**6**) and diethyl *t*-2-isopropylamino-*r*-1-carbamoylcyclohexane-5,5-dicarboxylate (**7**). The formation of the cyclohexanone **6** can be explained by invoking a partial hydrolysis of an intermediary monocyclic ketimine (7). In other words the Raney nickel hydrogenolysis of compound **1** was preceded by =N–NH— bond rupture.

By simply allowing compound **6** to react with phenylhydrazine in 50% ethanol, 4,5,6,7-tetrahydro-3-oxo-2-phenylindazole-5,5-dicarboxylate (**8**) was easily prepared. The latter was identical with an authentic sample independently prepared from 2-oxo-1,5,5-tricarbethoxycyclohexane (8). It should be mentioned that the ^{1}H nmr spectrum of **6** exhibited a singlet at δ 14.03 suggesting a predominance of enol rather than keto form. A weak multiplet at δ 3.70–3.30 and a weak triplet at 1.30 were assigned to the C(1) and methyl protons of the minor keto tautomer. It is also interesting to note the highly stereoselective hydrogenation of the compound **6** by Raney nickel in isopropanol which gave diethyl *t*-2-hydroxy-*r*-1-carbamoylcyclohexane-5,5-dicarboxylate (7) (**9**) in 97% yield. The latter was characterized as *t*-2-*O*-benzoyl derivative (**10**), showing nmr spectral characteristics consistent with the conformational assignment.

The nmr signals of the C(2) protons of compounds **2** and **3**, obscured by those of methylene protons of the ethyl groups, prompted us to undertake the synthesis of dimethyl 4,5,6,7-tetrahydro-3-oxo-2*H*-indazole-5,5-dicarboxylate (**11**) to be reductively cleaved into a mixture of dimethyl *c*-2- (**12**) and *t*-2- (**13**) amino-*r*-1-carbamoylcyclohexane-5,5-dicarboxylates. Dimethyl 2-oxo-1-carbamoylcyclohexane-5,5-dicarboxylate (**14**) was also isolated as a by-product. The ^{1}H nmr spectrum of **14** exhibited a broad singlet at δ 14.88 attributed to the OH of the preferential enol form.

To obtain pure stereoisomeric cyclohexylamines **2** and **3** the 2-*N*-benzyloxycarbonyl derivatives **15** and **16**, which were prepared and separated successfully, were subjected to deprotection reactions. To our surprise, these reactions under mild hydrogenating conditions gave back a mixture of **2** and **3**. In every case tested, spontaneous isomerization and conformational equilibration of non-derivatized isomers **2** and **3** led to mixtures, thus preventing chromatographic separation of the components. In order to elucidate the conformational properties of the separated isomers **2** and **3**, blocking the 2-amino groups as *N*-benzoyl derivatives **17** and **18** has proven effective, as we already described in the ethyl 3(4)-aminocyclohexanecarboxylate series (9). In this manner dimethyl *c*-2- (**19**) and *t*-2- (**20**) benzamido-*r*-1-carbamoylcyclohexane-5,5-dicarboxylate were also successfully separated.



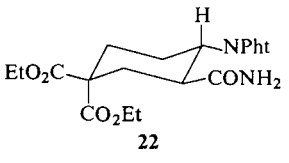
The successful separation of the *N*-acylated isomers described, in which the *trans* were favoured over the *cis* isomers, encouraged us to attempt the preparation of the corresponding aminocyclohexane carboxylic acid peptides. However, condensation of the stereoisomeric cyclohexylamines **2** and **3** with *tert*-butoxycarbonyl-L-phenylalanine *N*-hydroxysuccinimidoester (10) afforded diethyl 2-*N*-(*tert*-butoxycarbonyl-L-phenylalanyl)-*c*-2-amino-*r*-1-carbamoylcyclohexane-5,5-dicarboxylate (**21**) as the only crystalline product, in 33.4% yield. A very specific reaction resulted when a stereoisomeric mixture of compounds **2** and **3** was treated with phthalic anhydride at elevated temperature, affording diethyl *t*-2-phthalimido-*r*-1-carbamoylcyclohexane-5,5-dicarboxylate (**22**) in 68% yield. This could be explained by an epimerization which favours the *trans*-isomer **3** but as yet no precise information has been obtained experimentally to substantiate such transformations.

The nmr spectra support the geometries proposed for the *N*-acylated compounds which exhibited downfield multiplets centred at δ:4.02, ~4.69, and 4.38 for the equatorial protons at C(2) in the *cis* series (**15**, **17**, **19**), and at δ:3.59, ~3.64, ~3.69, and 3.61 for the axial protons at C(2) in the *trans* series (**16**, **18**, **20**, and **22**), respectively. All chemical shifts and pertinent characteristics of the ^{1}H nmr spectra are assembled in the Experimental.

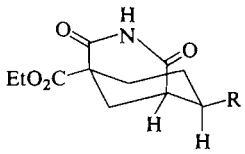
Attention was next directed to the challenging problem of intramolecular cyclizations of the *N*-acylated, polyfunctional, and conformationally

Can. J. Chem. Downloaded from www.nrcresearchpress.com by 210.87.254.6 on 09/05/12
For personal use only.

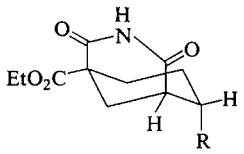
correlated alicyclic compounds. The benzamido derivatives **17** and **18** proved to be the most versatile, being converted at elevated temperature under nitrogen into ethyl *t*-6-benzamido- (**23**) and *c*-6-benzamido- (**24**) *r*-1-carboxylate-3-azabicyclo[3.3.1]nona-2,4-dione, respectively. These stereoselective intramolecular cyclizations establish an axial proton at C(6) in compound **23** and an equatorial one in compound **24**, appearing in the nmr spectra as unresolved multiplets shifted downfield at δ 4.10 and 4.35, respectively.



22



23 R = NHBz



24 R = NHBz
25 R = NPht

The efficient separation of the *t*-2-phthalimido compound (**22**) allowed its cyclization into the ethyl *c*-6-phthalimido-*r*-1-carboxylate-3-azabicyclo-[3.3.1]nona-2,4-dione (**25**). Nuclear magnetic resonance data of the latter revealed the axial conformation of the C(6) proton, as shown by the multiplet at δ:4.77–4.50.

Experimental

Melting points are uncorrected and were determined on a Kofler hot-stage apparatus. The infrared spectra were performed for potassium bromide pellets on a Perkin-Elmer 137 spectrophotomer, ultraviolet spectra for solution in 95% ethanol on a Beckman DU-2-spectrophotometer, and proton magnetic resonance spectra for solutions in deuteriochloroform on a Varian A60 or JEOL JNMC-60HL spectrometer using tetramethylsilane as an internal standard. Mass spectra were determined on a Varian MAT CH7 spectrometer. Column chromatography was performed over silica gel (Merck; 0.08 mm). The silica gel (Merck HF_{254}, type 60) which was used for preparative and thin layer chromatography (20 cm plates) was activated at 110°C for 60 min. The plates were developed in methylene chloride – methanol (95:5) unless otherwise stated and located by exposure to iodine vapour, uv illumination, or ninhydrin spray.

Reductive Cleavage of Diethyl 4,5,6,7-Tetrahydro-3-oxo-2H-indazole-5,5-dicarboxylate (2) (1)

To a solution of indazoledicarboxylate (2) (**1**) (500 mg, 1.75 mmol) in isopropanol (50 mL), Raney nickel (6) (~5 g), previously washed with isopropanol, was added. The mixture was refluxed and stirred for 2.5 h. The catalyst was filtered and washed with hot isopropanol. The filtrate and washings were evaporated to an oil (340 mg) under reduced pressure, dissolved in methylene chloride, and chromatographed on a silica gel (17 g) column. Methylene chloride eluted a fraction, $R_f \sim 0.67$ (95 mg, 19%), identified as diethyl 2-oxo-1-carbamoylcyclohexane-5,5-dicarboxylate (**6**), mp 119–120°C (from methylene chloride – ether – *n*-hexane); uv λ_{max}: 256 nm (log ε 3.79); ir ν_{max}: 3423, 3350, 1749, 1724, 1672, 1638 cm^{-1}; nmr δ: 14.03 (~0.8H, s, OH of predominant enolic form, disappearing in D_2O), 5.78 br (2H, s, $CONH_2$, disappearing in D_2O), 4.22 and 4.19 (4H, 2q, J_{ET} = 7.2 Hz, $2OCH_2$ of enolic and keto form, respectively), 3.70–3.30 (~0.2H, m, H at C(1) of minor keto form), 2.73 br (2H, s, H_2 at C(6)), 1.30 and 1.25 (6H, 2t, J_{ET} = 7.2 Hz, CH_3 of keto and enolic form, respectively); ms *m/e*: 285 (M^+), 240 ($M^+ - 45$), 212 ($M^+ - CO_2Et$). *Anal.* calcd. for $C_{13}H_{19}NO_6$ (285.29): C 54.73, H 6.71, N 4.91; found: C 54.49, H 6.61, N 5.14.

Elution with methylene chloride – methanol (98:2) afforded an unidentified product (14 mg), $R_f \sim 0.54$, mp 165–170°C. Methylene chloride – methanol (95:5) then eluted diethyl *t*-2-isopropylamino-*r*-1-carbamoylcyclohexane-5,5-dicarboxylate (**7**) (33 mg, 6.6%), $R_f \sim 0.22$, mp 117–119°C (from methylene chloride – ether – *n*-hexane); ir ν_{max}: 3390, 1745, 1684, 1631 cm^{-1}; nmr δ: 5.68 br (2H, s, $CONH_2$, disappearing in D_2O), 4.22 and 4.16 (4H, 2q, J_{ET} = 7.1 Hz, $2OCH_2$), ~2.92 (1H, partly obscured m, H_a at C(2)), 1.25 and 1.21 (6H, 2t, J_{ET} = 7.1 Hz, $2CH_3$), 1.04 and 1.0 (6H, 2d, $C(CH_3)_2$); ms *m/e*: 328 (M^+), 313 ($M^+ - 15$), 296 ($M^+ - 32$), 283 ($M^+ - 45$), ($M^+ - 60$). *Anal.* calcd. for $C_{16}H_{28}N_2O_5$ (328.40): C 58.71, H 8.59, N 8.53; found: C 58.44, H 8.45, N 8.37.

Further elution with methylene chloride – methanol (95:5) afforded fractions showing $R_f \sim 0.10$ and 0.11 (180 mg, 35%) identified as a mixture of stereoisomeric diethyl 2-amino-1-carbamoylcyclohexane-5,5-dicarboxylates **2** and **3**.

Diethyl 4,5,6,7-Tetrahydro-3-oxo-2-phenylindazole-5,5-dicarboxylate (8)

A solution of cyclohexanone (**6**) (78 mg, 0.273 mmol) in 50% ethanol (1.05 mL) was treated with phenylhydrazine (30.2 mg, 0.279 mmol) and refluxed for 6 h, cooled, and refrigerated overnight. The crystalline product (74.9 mg, 73%), $R_f \sim 0.66$ (methylene chloride – methanol (9:1)), mp 65–71°C, was identical (mixture mp, and uv and ir spectra) with that obtained previously (8). Nuclear magnetic resonance δ: 10.20–9.90 (~0.9H, m, OH-enolic, disappearing in D_2O), 7.65–7.37 (2H, m, aromatic protons), 7.27–7.00 (3H, m, aromatic protons), 4.12 (4H, q, J_{Et} = 7.0 Hz, $2OCH_2$), 3.70–3.10 (~0.1H, m, H at C(3a) of minor keto form), 2.66 (2H, s, H_2 at C(4)), 1.18 (6H, t, J_{Et} = 7.0 Hz, $2CH_3$).

Stereoselective Reduction of 2-Oxo-1-carbamoylcyclohexane-5,5-dicarboxylate (6)

To a solution of cyclohexanone (**6**) (100 mg, 0.351 mmol) in isopropanol (10 mL) Raney nickel (~1 g) was added. The mixture was stirred and refluxed for 2 h and then filtered. The filtrate was evaporated under reduced pressure to an oil which crystallized from chloroform (98 mg, 97%), identified as the previously prepared diethyl *t*-2-hydroxy-*r*-1-carbamoylcyclohexane-5,5-dicarboxylate (7) (**9**), R_f ~ 0.34, mp 156–157°C. The ir spectra of the samples were superimposable. Nuclear magnetic resonance δ: (in DMSO-d_6): 7.15 br and 6.70 br (2H, 2s, $CONH_2$, disappearing in D_2O), 4.75 (1H, d, OH, disappearing in D_2O), 4.12 and 4.04 (4H, 2q, J_{Et} = 6.8 Hz, $2OCH_2$), 3.69 (1H, obscured m, H_a at C(2)), 1.20 and 1.16 (6H, 2t, J_{Et} = 6.8 Hz, $2CH_3$); ms *m/e*: 288 (M^+). *Anal.* calcd. for $C_{13}H_{21}NO_6$ (287.31): C 54.34, H 7.37, N 4.88; found: C 53.98, H 7.69, N 4.99.

Diethyl t-2-O-benzoyl-r-1-carbamoylcyclohexane-5,5-dicarboxylate (10)

To a solution of cyclohexanol (**9**) (43 mg, 0.149 mmol) in methylene chloride (0.2 mL) and pyridine (2 mL), benzoyl chloride (0.017 mL, 0.149 mmol) was added. The mixture was set aside at room temperature for 48 h and then poured into

Can. J. Chem. Downloaded from www.nrcresearchpress.com by 210.87.254.6 on 09/05/12
For personal use only.

chilled water to be partitioned with methylene chloride. The organic layer was washed with 5% HCl, 5% $NaHCO_3$, and water, and then evaporated under reduced pressure to an oil (35.2 mg, 60%). Preparative tlc ($R_f \sim 0.68$) afforded the product, mp 159–160°C (from methylene chloride – ether – *n*-hexane); uv λ_{max}: 231 nm (log ε 4.13), λ_{min}: 209 nm (log ε 3.46); ir ν_{max}: 3420, 3300, 1753, 1731, 1723, 1679, 1663 cm^{-1}; nmr δ: 8.15–7.82 (2H, m, aromatic protons) 7.62–7.32 (3H, m, aromatic protons), 5.68 br (2H, s, $CONH_2$), 5.42–4.85 (1H, m, H_a at C(2)), 4.25 and 4.17 (4H, 2q, J_{ET} = 7.1 Hz, $2OCH_2$), 1.28 and 1.25 (6H, 2t, J_{Et} = 7.1 Hz, $2CH_3$).

Dimethyl 4,5,6,7-Tetrahydro-3-oxo-2H-indazole-5,5-dicarboxylate (11)

A solution of 4,5,6,7-tetrahydro-3-oxo-2*H*-indazole-5,5-dicarboxylic acid (11) (500 mg, 2.212 mmol) in 3% methanolic hydrochloric acid (50 mL) was heated under reflux for 16 h. The mixture was evaporated to dryness under reduced pressure by azeotropic distillation with anhydrous methanol and then with benzene. The residue dissolved in water was passed through a column of Amberlite IR-4B (10 mL) and evaporated to a crystalline product (375.3 mg, 67%), mp 196–197°C (from methanol–ether – *n*-hexane); uv λ_{max}: 249 nm (log ε 3.44), λ_{min}: 214 nm (log ε 3.11); ir ν_{max}: 3559, 1757, 1739 cm^{-1}; nmr δ (in DMSO-d_6): 11.00–9.00 (2H, m, NH and OH enolic), 3.65 (6H, 2s, $2OCH_3$). *Anal.* calcd. for $C_{11}H_{14}N_2O_5$: C 51.96, H 5.55, N 11.02; found: C 51.99, H 5.59, N 11.08.

Reductive Cleavage of Dimethyl 4,5,6,7-Tetrahydro-3-oxo-2H-indazole-5,5-dicarboxylate (11)

A solution of indazoledicarboxylate (**11**) (500 mg, 1.97 mmol) in isopropanol (50 mL) was treated with Raney nickel (~5 g), heated under reflux for 1.5 h, and worked up as described for compound **1**. An oil (316 mg) was obtained which, dissolved in chloroform, separated into neutral (93 mg) and basic (198 mg) fractions by partitioning with 0.5% sulphuric acid and then with basic solution by $NaHCO_3$ treatment. The preparative tlc and column chromatography of isolated fractions using methylene chloride – methanol (98:2) as eluant afforded a product, $R_f \sim$ 0.63 (32.5 mg, 6.4%), identified as dimethyl 2-oxo-1-carbamoylcyclohexane-5,5-dicarboxylate (**14**), mp 154–156°C (from methylene chloride – ether – *n*-hexane); uv λ_{max}: 254 nm (log ε 3.85); ir ν_{max}: 3484, 3390, 1736, 1718, 1692 cm^{-1}; nmr δ (in DMSO-d_6): 14.88 br (1H, s, OH enolic, disappearing in D_2O), 7.23 (2H, s, $CONH_2$, disappearing in D_2O), 3.65 (6H, s, $2OCH_3$), 3.20–2.80 (1H, m, H at C(1)), 2.64 (2H, s, H_2 at C(6)). *Anal.* calcd. for $C_{11}H_{15}NO_5$: C 51.36, H 5.88, N 5.45; found: C 51.43, H 5.74, N 5.73.

Methylene chloride – methanol (95:5) eluted from the chromatographs of the basic fraction two unidentified products showing $R_f \sim 0.49$ (28 mg) and 0.18 (21 mg). Further elution with the same solvent afforded a product (113 mg, 26%), $R_f \sim 0.10$, identified as a mixture of stereoisomeric dimethyl 2-amino-1-carbamoylcyclohexane-5,5-dicarboxylates **12** and **13**, mp 174–176°C (from methylene chloride – ether – *n*-hexane); ir ν_{max}: 3430, 3360, 1745, 1725, 1665 cm^{-1}; nmr δ: 6.71 and 5.65 br (2H, 2s, $CONH_2$, disappearing in D_2O), 3.75 and 3.68 (6H, 2s, $2OCH_3$), 1.77 (2H, s, NH_2, disappearing in D_2O). *Anal.* calcd. for $C_{11}H_{18}N_2O_5$: C 51.15, H 7.03, N 10.85; found: C 51.34, H 7.34, N 10.60.

Diethyl c-2- *(15) and* t-2- *(16) Amino*-N-*benzyloxycarbonyl*-r-1-*carbamoylcyclohexane-5,5-dicarboxylates*

To a cooled solution (0°C) of stereoisomers **2** and **3** (250 mg, 0.873 mmol) in methylene chloride (15 mL) 50% benzyloxycarbonyl chloride (0.147 mL, 0.437 mmol) solution in toluene was added. The mixture was stirred for 2 min, then treated with triethylamine (0.15 mL, 0.873 mmol). After 10 min a second portion of benzyloxycarbonyl chloride (0.147 mL) was added and stirring continued for an additional 5 min at 0°C and then at room temperature for 1.5 h. Water was added and the product separated by extraction with methylene chloride. The organic layer was dried over sodium sulphate and then evaporated to a mixture of stereoisomeric products (367 mg). Preparative tlc (three developments, acetone as eluant) separated the *cis*-benzyloxycarbonyl derivative **15**, $R_f \sim 0.68$ (59 mg, 16%), mp 122–123°C (from methylene chloride – ether – *n*-hexane); ir ν_{max}: 3405, 3330, 1728, 1690, 1655 cm^{-1}; nmr δ: 7.36 (5H, s, aromatic protons), 5.81 (2H, s, $CONH_2$, disappearing in D_2O), ~5.52 (1H, partly obscured m, NHOCO, disappearing in D_2O), 5.08 (2H, s, CH_2), 4.21 and 4.18 (4H, 2q, J_{Et} = 7.1 Hz, $2OCH_2$), ~4.02 (1H, partly obscured, m, H_e at C(2)), 1.25 and 1.24 (6H, 2t, J_{Et} = 7.1 Hz, $2CH_3$). *Anal.* calcd. for $C_{21}H_{28}N_2O_7$: C59.99, H 6.71, N 6.66; found: C 59.71, H 6.75, N 6.89.

The *trans*-isomer **16**, $R_f \sim 0.65$ (160 mg, 44%) recrystallized from methylene chloride – ether – *n*-hexane, mp 167–168°C; ir ν_{max}: 3440, 3330, 1728, 1685, 1655 cm^{-1}; nmr δ: 7.35 (5H, s, aromatic protons), 6.44 br and 5.99 br (2H, 2s, $CONH_2$, disappearing in D_2O), 6.35–5.38 (1H, m, NHOCO), 5.08 (2H, s, CH_2), 4.24 and 4.17 (4H, 2q, J_{Et} = 7.1 Hz, $2OCH_2$), 3.85–3.34 (1H, m, H_a at C(2)), 1.25 and 1.23 (6H, 2t, J_{Et} = 7.1 Hz, $2CH_3$). *Anal.* calcd. for $C_{21}H_{28}N_2O_7$: C 59.99, H 6.71, N 6.66; found: C 60.18, H 6.51, N 6.33.

Diethyl c-2- *(17) and* t-2- *(18) Benzamido*-r-1-*carbamoylcyclohexane-5,5-dicarboxylates*

To a solution of stereoisomers **2** and **3** (130 mg, 0.454 mmol) in methylene chloride (0.3 mL) and anhydrous pyridine (3.4 mL) benzoyl chloride (0.052 mL, 0.454 mmol) was added, and then stirred at room temperature for 24 h. The work up was as described for compound **10**. A mixture of the stereoisomers was obtained from the organic layer (CH_2Cl_2) in 70% yield (124.3 mg). Preparative tlc (in methylene chloride – ether (9:1), four developments, acetone as eluant) separated the *cis*-stereoisomer **17**, $R_f \sim 0.64$ (23.0 mg, 13%), mp 199–200°C (from methanol–ether – *n*-hexane); uv λ_{max}: 228.5 nm (log ε 3.80), λ_{min}: 212.5 nm (log ε 3.56); ir ν_{max}: 3323, 1735, 1695, 1656 cm^{-1}; nmr δ (in DMSO-d_6): 7.89 (1H, d, J = 6 Hz, NH—CO, disappearing in D_2O), 7.88–7.64 (3H, m, aromatic protons), 7.58–7.27 (2H, m, aromatic protons), 6.80 br (2H, s, $CONH_2$, disappearing in D_2O), ~4.69 (1H, partly obscured m, H_e at C(2)), 4.18 and 4.14 (4H, 2q, J_{Et} = 7.1 Hz, $2OCH_2$), 1.19 and 1.15 (6H, 2t, J_{Et} = 7.1 Hz, $2CH_3$); ms *m/e*: 390 (M^+), 345 ($M^+ - CONH_2$), 317 ($M^+ - CO_2Et$), 300 ($M^+ - CO_2Et - NH_2$). *Anal.* calcd. for $C_{20}H_{26}N_2O_6$ (390.42): C 61.52, H 6.71; found: C 61.40, H 6.88.

The *trans*-isomer **18**, $R_f \sim 0.60$ (51.2 mg, 28%) recrystallized from methanol–ether – *n*-hexane, mp 224–226°C; uv λ_{max}: 228 nm (log ε 4.01), λ_{min}: 212.5 nm (log ε 3.80); ir ν_{max}: 3365, 3290, 1753, 1720, br, 1673, 1640 cm^{-1}; nmr δ (in DMSO-d_6): 8.00 (1H, d, J = 8.3 Hz, NHCO, disappearing in D_2O), 7.92–7.67 (2H, m, aromatic protons), 7.60–7.30 (3H, m, aromatic protons), 6.95 and 6.85 br (2H, s, $CONH_2$, disappearing in D_2O), 4.23 and 4.14 (4H, 2q, J_{Et} = 7.1 Hz, $2OCH_2$), ~3.64 (1H, obscured m, H_a at C(2)), 1.21 and 1.18 (6H, 2t, J_{Et} = 7.1 Hz, $2CH_3$); ms *m/e*: 390 (M^+), 345 ($M^+ - CONH_2$), 317 ($M^+ - CO_2Et$), 300 ($M^+ - CO_2Et - NH_2$). *Anal.* calcd. for $C_{20}H_{26}N_2O_6$: C 61.52, H 6.71, N 7.18; found: C 61.50, H 6.99, N 7.40.

Dimethyl c-2- *(19) and* t-2- *(20) Benzamido*-r-1-*carbamoylcyclohexane-5,5-dicarboxylates*

A solution of stereoisomers **12** and **13** (96.4 mg, 0.373 mmol) in methylene chloride (0.2 mL) and pyridine (3 mL) was treated with benzoylchloride (0.043 mL, 0.373 mmol) and worked up as for compounds **17** and **18**. A crude mixture of stereoisomers was isolated in 73% yield (98 mg). Preparative tlc separated the *cis*-isomer **19**, $R_f \sim 0.53$ (13.1 mg, 13.4%), mp 206–207°C (from

Can. J. Chem. Downloaded from www.nrcresearchpress.com by 210.87.254.6 on 09/05/12
For personal use only.

methylene chloride – ether – *n*-hexane); uv λ_{max}: 227.5 nm (log ε 4.06), λ_{min}: 213 nm (log ε 3.89); ir ν_{max}: 3403, 3268, 3215, 1743, 1726, 1698, 1673 cm^{-1}; nmr δ (in DMSO-d_6): 7.89 (1H, d, J = 7.8 Hz, NHCO), 7.80–7.15 (5H, m, aromatic protons), 6.82 br (2H, s, $CONH_2$), 6.49–4.07 (1H, m, H_e at C(2)), 3.68 and 3.63 (6H, 2s, $2OCH_3$); ms *m/e*: 362 (M^+), 330 ($M^+ - 32$), 303 ($M^+ - 59$), 286 ($M^+ - 76$).

The *trans*-isomer **20**, $R_f \sim 0.51$ (36 mg, 37%) was recrystallized from methylene chloride – ether – *n*-hexane, mp 250–253°C; uv λ_{max}: 228 nm (log ε 3.92), λ_{min}: 213 (log ε 3.71); ir ν_{max}: 3360, 3195, 1745, 1730, 1678, 1665 cm^{-1}; nmr δ (in DMSO-d_6): 8.02 (1H, d, J = 8.8 Hz, NHCO, disappearing in D_2O), 7.88–7.58 (2H, m, aromatic protons), 7.52–7.21 (3H, m, aromatic protons), 6.97 br and 6.85 br (2H, 2s, $CONH_2$, disappearing in D_2O), ~3.9 (1H, obscured m, H_a at C(2)), 3.72 and 3.67 (6H, 2s, $2OCH_3$); ms *m/e*: 362 (M^+), 345 ($M^+ - 17$), 331 ($M^+ - 31$), 317 ($M^+ - 45$). *Anal.* calcd. for $C_{18}H_{32}N_2O_6$ (362.37): C 59.66, H 6.12, N 7.73; found: C 59.85, H 6.17, N 7.89.

Diethyl 2-N-(tert-*butoxycarbonyl*-L-*phenylalanyl*)-c-2-*amino*-r-1-*carbamoylcyclohexane*-5,5-*dicarboxylate* (**21**)

A mixture of stereoisomers **2** and **3** (286 mg, 1 mmol) and *N*-BOC-L-Phe-ONSu (10) (362 mg, 1 mmol) were dissolved in 1,2-dimethoxyethane (5 mL) and stirred at room temperature for 4.5 h. The mixture was then partitioned between water and methylene chloride. The organic layer was dried over $MgSO_4$ and then evaporated to an oil (530 mg). The preparative tlc separated the product (178 mg, 33.4%), $R_f \sim 0.55$, mp 186–187°C (from ethylacetate–ether – *n*-hexane); ir ν_{max}: 3430, 3325, 1738 (sh), 1728, 1687 (br), 1650 (sh) cm^{-1}; nmr δ: 7.23 (5H, s, aromatic protons), 6.65–6.20 (1H, m, PhNH, disappearing in D_2O), 5.90 br and 5.40 br (2H, s, $CONH_2$, disappearing in D_2O), ~4.25 (1H, obscured m, H_e at C(2)), 4.17 and 4.12 (4H, 2q, J_{Et} = 7.0 Hz, $2OCH_2$), 1.37 and 1.35 (6 + 3H, 2s; $C(CH_3)_3$), 1.23 (6H, t, J_{Et} = 7.0 Hz, $2CH_3$). *Anal.* calcd. for $C_{27}H_{39}N_3O_8$: C 60.77, H 7.37, N 7.88; found: C 60.52, H 7.08, N 8.17.

Diethyl t-2-*Phthalimido*-r-1-*carbamoylcyclohexane*-5,5-*dicarboxylate* (**22**)

A mixture of the stereoisomers **2** and **3** (252 mg, 0.882 mmol) and phthalic anhydride (131 mg, 0.882 mmol) was ground in a mortar and then heated at 220–225°C under nitrogen. The product was partitioned between chloroform and 5% $NaHCO_3$. The organic layer was washed with 0.5 mol dm^{-3} H_2SO_4 and water, dried over sodium sulphate, and evaporated to a crude product (320 mg, 87%) which on preparative tlc afforded the product (250 mg, 68%), $R_f \sim 0.59$, mp 208–209°C (from methylene chloride – *n*-hexane); uv λ_{max}: 222 nm (log ε 4.64); ir ν_{max}: 3484, 3268, 1786 sh, 1784, 1709, 1667 cm^{-1}; nmr δ: 7.99–7.51 (4H, m, aromatic protons); 5.62 br (2H, s, $CONH_2$, disappearing in D_2O), 4.30 and 4.20 (4H, 2q, J_{Et} = 7.1 Hz, $2OCH_2$), 3.61 (1H, sx, $J_{2a,1a}$ = 12 Hz, $J_{2a,3a}$ = 12 Hz, $J_{2a,3e}$ = 3.5 Hz, H_a at C(2)), 1.35 and 1.24 (6H, 2t, J_{ET} = 7.1 Hz, $2CH_3$). *Anal.* calcd. for $C_{21}H_{24}N_2O_7$: C 60.56, H 5.81, N 6.73; found: C 60.79, H 5.80, N 6.83.

Ethyl t-6-*Benzamido*-r-1-*carboxylate*-3-*azabicyclo*-[3.3.1]*nona*-2,4-*dione* (**23**)

The *cis*-benzamido compound **17** (46 mg, 0.118 mmol) was heated at 220–230°C under nitrogen for 20 min and then dissolved in methylene chloride and filtered. Preparative tlc afforded the product (31.6 mg, 78%), $R_f \sim 0.77$, mp 191–192°C (from methylene chloride – ether); ir ν_{max}: 3395, 3250, 1738, 1720 sh, 1705, 1645 cm^{-1}; nmr δ (in DMSO-d_6): 11.18 br (1H, s, H at N(3)), 8.24 (1H, d, J = 7.6 Hz, CONH), 8.00–7.70 (2H, m, aromatic protons), 7.67–7.36 (3H, m, aromatic protons), 4.18 (2H, q, J_{Et} = 7.1 Hz, OCH_2), ~4.10 (1H, obscured m, H_a at C(6)), 1.19 (3H, t, J_{Et} = 7.1 Hz, CH_3). *Anal.* calcd. for $C_{18}H_{20}N_2O_5$: C 62.78, H 5.86, N 8.14; found: C 63.01, H 6.16, N 8.29.

Ethyl c-6-*Benzamido*-r-1-*carboxylate*-3-*azabicyclo*-[3.3.1]*nona*-2,4-*dione* (**24**)

The *trans*-benzamido compound **18** (59 mg, 0.151 mmol) was heated at 240–250°C for 20 min, worked up, and purified as described above. The product (31 mg, 60%) crystallized from methylene chloride – ether, mp 217–218°C; ir ν_{max}: 3323, 3223, 1746, 1728, 1696, 1638 cm^{-1}; nmr δ (in DMSO-d_6): 11.21 br (1H, s, H at N(3)), 8.34 (1H, d, J = 7.7 Hz, CONH), 8.09–7.76 (2H, m, aromatic protons), 7.62–7.38 (3H, m, aromatic protons), 4.42–4.28 (1H, obscured m, H_e at C(6)), 4.17 (2H, q, J_{Et} = 7.1 Hz, OCH_2), 1.20 (3H, t, J_{Et} = 7.1 Hz, CH_3). *Anal.* calcd. for $C_{18}H_{20}N_2O_5$: C 62.78, H 5.85, N 8.14; found: C 62.48, H 5.64, N 7.88.

Ethyl c-6-*Phthalimido*-r-1-*carboxylate*-3-*azabicyclo*-[3.3.1]*nona*-2,4-*dione* (**25**)

The *trans*-phthalimido compound **22** (188 mg, 0.452 mmol) was heated at 240–250°C for 20 min. The product (158 mg) was purified on tlc plates, R_f ~0.78. Yield 29.3 mg (17.5%), mp 214–215°C (from methylene chloride – ether); uv λ_{max}: 222 nm (log ε 4.59); ir ν_{max}: 3462, 3250, 1775, 1748, 1728, 1710 cm^{-1}; nmr δ: 8.53–8.20 (1H, m, H at N(3)), 8.06–7.59 (4H, m, aromatic protons), 4.77–4.50 (1H, m, H_e at C(6)), 4.28 (2H, q, J_{Et} = 7.1 Hz, OCH_2). *Anal.* calcd. for $C_{19}H_{18}N_2O_6$: C 61.61, H 4.90, N 7.56; found: C 61.40, H 5.12, N 7.39.

From preparative tlc plates an unidentified product, $R_f \sim 0.83$ (13 mg), separated, mp 165–166°C (from methylene chloride – *n*-hexane).

Acknowledgements

The authors wish to thank Dr. D. Srzić for mass measurements, Mrs. B. Vinković for recording the nmr spectra, and Mrs. A. Poturić for technical assistance.

1. V. Škarić and V. Turjak-Zebić. J. Chem. Soc. Perkin Trans. 1, 2099 (1979).
2. Dj. Škarić, V. Škarić, and V. Turjak-Zebić. Croat. Chem. Acta, **35**, 143 (1963).
3. V. Škarić and L. Marion. Can. J. Chem. **38**, 2433 (1960).
4. V. Škarić and L. Marion. Can. J. Chem. **39**, 1579 (1961).
5. V. Škarić and L. Marion. J. Am. Chem. Soc. **80**, 4434 (1958).
6. R. Mozingo. Org. Synth. Coll. Vol. **III**, 181 (1955).
7. Dj. Škarić, V. Škarić, V. Turjak-Zebić, and Z. Veksli. Croat. Chem. Acta, **34**, 75 (1962).
8. Dj. Škarić, V. Škarić, and V. Turjak-Zebić. Croat. Chem. Acta, **35**, 267 (1963).
9. V. Škarić, M. Kovačević, and Dj. Škarić. J. Chem. Soc. Perkin Trans. 1, 1199 (1976).
10. G. W. Anderson, J. E. Zimmerman, and F. M. Callahan. J. Am. Chem. Soc. **86**, 1839 (1964).
11. V. Turjak-Zebić, Dj. Škarić, and V. Škarić. Croat. Chem. Acta, **41**, 235 (1969).

Tetranortriterpenoids and related compounds. Part 25.[1] Two 3,4-secotirucallane derivatives and 2′-hydroxyrohitukin from the bark of *Guarea cedrata* (Meliaceae)

JOHN A. AKINNIYI, JOSEPH D. CONNOLLY,[2] AND DAVID S. RYCROFT
Department of Chemistry, University of Glasgow, Glasgow G12 8QQ, Scotland
AND
B. LUCAS SONDENGAM AND N. PATIENCE IFEADIKE
Department of Chemistry, University of Yaoundé, Yaoundé, Cameroon
Received February 21, 1980
This paper is dedicated to the memory of Dr. Léo Marion

JOHN A. AKINNIYI, JOSEPH D. CONNOLLY, DAVID S. RYCROFT, B. LUCAS SONDENGAM, and N. PATIENCE IFEADIKE. Can. J. Chem. **58**, 1865 (1980).

Three new compounds, 3,4-secotirucalla-4(28),7,24-trien-3,21-dioic acid **1**, the corresponding 3-monomethyl ester **12**, and 2′-hydroxyrohitukin **13**, have been isolated from the bark of *Guarea cedrata* (Meliaceae). The structures of **1** and **12** were confirmed by correlation with methyl 3-oxotirucalla-8,24-dien-21-oate (methyl isoelemonate) **6**. The ^1H and ^{13}C nmr data are reported.

JOHN A. AKINNIYI, JOSEPH D. CONNOLLY, DAVID S. RYCROFT, B. LUCAS SONDENGAM et N. PATIENCE IFEADIKE. Can. J. Chem. **58**, 1865 (1980).

On a isolé, de l'écorce de *Guarea cedrata* (Méliaceae), trois triterpènoides nouveaux, l'acide 3,4-secotirucalla-4(28),7,24-trièn-3,21-dioique **1**, son ester méthylique **12** et 2′-hydroxyrohitukin **13**. On a confirmé les structures **1** et **12** par une corrélation avec méthyl 3-oxotirucalla-8,24-dièn-21-oate **6**. Les spectres rmn sont présentés.

In a continuation of our investigation (1, 2) of the constituents of the Meliaceae family we have examined the extract of the bark of *Guarea cedrata* and have isolated three new compounds, the ring A secotirucallane derivatives *A* **1** and *B* **12** and 2′-hydroxyrohitukin **13**, whose structures were assigned on the following evidence.

Compound *A* **1**, $C_{30}H_{46}O_4$, has spectroscopic properties consistent with the presence of two carboxyl groups (ir: 3200–2500 (br), 1709 cm^{-1}; δ_C 183.5 and 181.3), an exomethylene (δ_H 4.80 (2H, bs); δ_C 132.4 (s) and 114.1 (t)), and two trisubstituted double bonds (δ_H 5.23 (m, H-7) and 5.09 (bt, H-24); δ_C 123.5 (d, C-24), 147.5 (s, C-25), and 118.0 (d, C-7), 145.8 (s, C-8)). The molecule is therefore tricarbocyclic. In addition there are three tertiary methyls (δ_H 0.81, 0.87, and 0.95) and three vinyl methyls (δ_H 1.55, 1.65, and 1.75). Hydrogenation over palladium/charcoal of the dimethyl ester **2**, obtained by reaction of **1** with diazomethane, afforded the tetrahydroderivative **3** whose ^{13}C nmr spectrum (δ_C 118.3 (d, C-7) and 145.6 (s, C-8)) clearly showed that one of the trisubstituted double bonds was resistant to hydrogenation under normal conditions. On treatment with dry hydrogen chloride in chloroform the tetrahydrodimethyl ester **3** was converted into the isomeric compound **4** with a tetrasubstituted double bond. Under similar conditions the dimethyl ester **2** gave the chlorodiene **5** (δ_C 70.8 (s, C-25), 147.3, 137.6 (both s, C-8 and C-9), 129.8 (s, C-4), 113.8 (t, C-28)). This acid-induced isomerisation of a hindered trisubstituted to a tetrasubstituted double bond is reminiscent of the behaviour of Δ^7 tetracyclic triterpenoids, e.g. odoratol (3), and, taken in conjunction with the above spectroscopic evidence, led us to **1** as a biogenetically acceptable structure for compound *A*. This was confirmed in the following way.

Methyl 3-oxotirucalla-8,24-dien-21-oate **6**, isolated from elemi resin according to the procedure of Halsall and co-workers (4), was hydrogenated over palladium/charcoal to give the non-crystalline 24,25-dihydro-derivative **7**. Baeyer–Villiger oxidation of **7** with peracetic acid afforded a mixture of the lactone **8** and the epoxylactone **9**, separable by preparative tlc. The former was converted into the diene dimethyl ester **11**, via the hydroxy dimethyl ester **10**, by alkaline hydrolysis, methylation, and dehydration with thionyl chloride. Hydrogenation of **11** yielded dimethyl 3,4-secotirucall-8-en-3,21-dioate **4**, identical in all respects with the product of acid isomerisation of dimethyl tetrahydro-*A* **3**. This series of transformations confirmed that compound *A* is 3,4-secotirucalla-4(28),7,24-trien-3,21-dioic acid **1**.

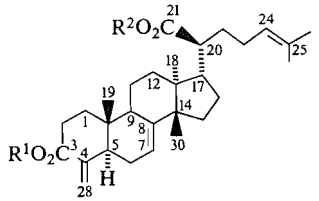
The spectroscopic properties of compound *B* **12**, $C_{31}H_{48}O_4$, (see Experimental) suggested that it is a monomethyl ester of compound *A*. This was readily established by methylation with diazomethane

[1]For Part 24 see ref. 1.
[2]Author to whom correspondence may be addressed.

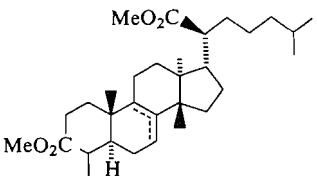
0008-4042/80/171865-04$01.00/0
©1980 National Research Council of Canada/Conseil national de recherches du Canada

Can. J. Chem. Downloaded from www.nrcresearchpress.com by 210.87.254.40 on 09/05/12
For personal use only.

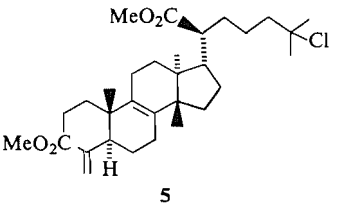
Can. J. Chem. Downloaded from www.nrcresearchpress.com by 210.87.254.40 on 09/05/12
For personal use only.



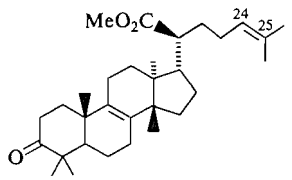
1 $R^1 = R^2 = H$
2 $R^1 = R^2 = Me$
12 $R^1 = Me; R^2 = H$



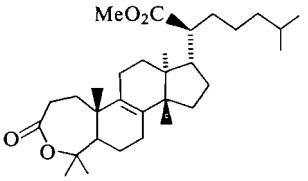
3 Δ^7
4 Δ^8



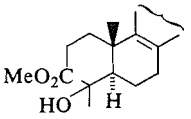
5



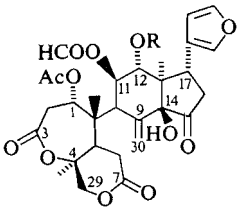
6
7 24,25-Dihydro



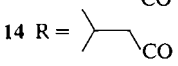
8
9 8α,9α-Epoxide



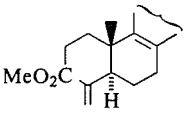
10 as **8**



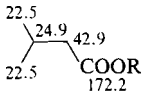
13 R =



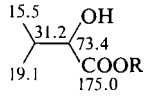
14 R =



11 as **8**



15



16

to give the dimethyl ester **2**. Comparison of the ^{13}C nmr spectra of the three compounds **1**, **2**, and **12** indicated that the free carboxyl group of *B* (δ_C 183.5) is associated with the downfield carboxymethyl group (δ_C 176.4) of the dimethyl ester **2**. It is therefore assigned as the C-21 carboxyl group on the basis of normal ^{13}C substitution rules (5). Thus compound *B* is 3,4-secotirucalla-4(28),7,24-trien-3,21-dioic acid 3-methyl ester **12**.

The third compound from the extract is a new complex tetranortriterpenoid, 2′-hydroxyrohitukin **13**, $C_{34}H_{42}O_{14}$, belonging to the small group of compounds, related to prieurianin and rohitukin **14**, (2), which give broad ^1H nmr spectra at room temperature as a result of conformational processes occurring at an intermediate rate on the nmr time scale. At 60°C the ^1H nmr spectrum of **13** is well resolved and readily revealed the structural features. Thus it has resonances for a β-substituted furan, an acetate, a formate, two hydroxyl groups (δ 5.21 and 2.45, exchangeable with D_2O), 2H-29 (δ 4.17, bs), H-17 (δ 3.98, t, J = 9 Hz), an *exo*-methylene (δ 5.90 and 5.49, both s, 2H-30), H-1 (δ 5.10, m), H-2′ (δ 3.13, d, J = 4 Hz), three tertiary (δ 0.95, 1.73, and 1.78) and two secondary methyl groups (δ 0.83 and 0.65, both d, J = 7 Hz). Decoupling experiments identified the characteristic ring C system involving H-9 (δ 3.76, d, J = 7 Hz), H-11 (δ 5.45, dd, J = 12, 7 Hz) and H-12 (δ 6.13, d, J = 12 Hz). The ^{13}C nmr spectrum (see Experimental) confirmed the presence of the ε- and δ-lactones and the ketol system in ring D. The above data suggested that **13** only differed from rohitukin **14** in the nature of the ester function attached to C-12. This was confirmed by comparison of their ^{13}C nmr spectra which are virtually identical with the exception of the resonances associated with the ester functions. It is apparent that the 3-methylbutanoate **15** (5) of rohitukin has been replaced by a 2-hydroxy-3-methylbutanoate **16** in **13**.

Can. J. Chem. Downloaded from www.nrcresearchpress.com by 210.87.254.40 on 09/05/12
For personal use only.

Experimental

Nuclear magnetic resonance spectra (^1H and ^{13}C) were run at ambient temperature (unless otherwise stated) on a Varian XL-100 spectrometer with VFT-100 accessory, for solutions in deuteriochloroform with tetramethylsilane as internal reference. The ^{13}C assignments are based on chemical shifts, multiplicities in off-resonance decoupled spectra, and comparison with similar compounds (2).

Extraction

Powdered bark (6 kg) of *G. cedrata*, collected in Okonolinga (Cameroon), was extracted with hexane in a Soxhlet. A solid (1.2 g) which separated during the extraction was shown by preparative tlc (benzene – ethyl acetate, 3:1) to be mainly one compound. Crystallization from methanol afforded *2'-hydroxyrohitukin* **13** (0.6 g), mp 231–237°C; ir (CCl_4): 3620, 3440, 1750, 1740 and 1720 cm^{-1}; ^{13}C nmr δ (at 60°C): 206.4 (C-15), 173.3 (C-7), 169.4 (C-3), 169.4 (CH_3COO), 160.3 (HCOO), 143.3 (C-23), 140.9 (C-21), 124.9 (C-20), 110.6 (C-22), 138.9 (C-8), 122.8 (C-30), 81.1 (C-4), 79.4 (C-14), 78.1 (C-29), 75.6 (C-12), 74.9 (C-11), 71.3 (C-1), 51.9 (C-9), 49.8 and 46.3 (C-10 and C-13), 42.7 (C-5), 42.0 (C-16), 37.5 (C-2), 35.4 (C-17), 32.1 (C-6), 23.3, 21.4, 13.0 (C—*Me*), and 21.2 (CH_3COO); ms *m/e*: 614 ($M - 60$). *Anal.* calcd. for $C_{34}H_{42}O_{14} \cdot H_2O$: C 58.95, H 6.35; found: C 58.9, H 6.3. A further crop of solid (0.5 g) was shown by tlc (methylene chloride – methanol, 19:1) to contain a second compound as a major component. Chromatography over silica gel and elution with hexane–ether (19:1) yielded compound *B*, *3,4-secotirucalla-4(28),7,24-trien-3,21-dioic acid 3-methyl ester* **12** (300 mg) mp 190°C (ex methanol), $[\alpha]_D + 11°$ (*c* 0.5, methanol); ir (CCl_4): 3500–2500, 1741, 1703, 1640 cm^{-1}; ^1H nmr δ: 0.78, 0.89 and 0.97 (C—*Me*), 1.75, 1.65 and 1.55 (vinyl Me), 3.62 (CO_2Me), 4.8 (2H, bs, $CH_2{=}C\lesssim$), 5.09 (1H, bt, H-24), and 5.23 (1H, m, H-7); ^{13}C nmr δ: 183.4 (C-21), 174.4 (C-3), 147.3 (C-25), 123.6 (C-24), 145.9 (C-8), 118.3 (C-7), 132.3 (C-4), 113.9 (C-28), 51.4 (CO_2Me), 51.3, 43.3 and 36.8 (s), 50.0, 49.3, 47.5, and 40.6 (d), 33.6, 32.2, 32.0, 30.2, 30.1, 28.1, 27.4, 26.1, and 18.1 (t), and 27.4, 25.7, 22.5, 21.7, 17.6, and 15.8 (q); ms *m/e*: 484. *Anal.* calcd. for $C_{31}H_{48}O_4$: C 76.8, H 10.0; found: C 76.85, H 9.70. Concentration of the hexane extract gave an oily solid which was washed with benzene and chloroform. The solid residue (8 g) was dissolved in methanol–chloroform and adsorbed on a silica gel column. Elution with benzene gave compound *A*, *3,4-secotirucalla-4(28),7,24-trien-3,21-dioic acid* **1** (5.75 g) mp 170°C (ex benzene), $[\alpha]_D + 18°$ (*c* 1.4, methanol); ^{13}C nmr δ: 51.4, 43.3, and 36.4 (s), 50.3, 50.0, 48.8, and 40.7 (d), 33.6, 32.3, 30.5, 30.1, 30.1, 27.2, 27.2, 26.0, and 18.1 (t), 27.0, 25.7, 21.7, 21.4, 17.7, and 16.2 (q); ms *m/e*: 470. *Anal.* calcd. for $C_{30}H_{46}O_4 \cdot H_2O$: C 75.3, H 10.0; found: C 75.0, H 10.3.

Dimethyl 3,4-Secotirucalla-4(28),7,24-trien-3,21-oate 2

Reaction of either compound *A* **1** or compound *B* **12** with diazomethane in methanol followed by purification by preparative tlc yielded the non-crystalline dimethyl ester **2**; ^1H nmr δ: 0.78, 0.83, and 0.94 (C—*Me*), 1.74, 1.64, and 1.53 (vinyl Me), 3.63 (2 × CO_2Me), 4.80 (2H, bs, $CH_2{=}C\lesssim$), 5.05 (1H, bt, H-24), and 5.23 (1H, m, H-7); ^{13}C nmr δ: 176.5 (C-21), 174.3 (C-3), 147.3 (C-25), 123.7 (C-24), 145.9 (C-8), 118.3 (C-7), 132.0 (C-4), 113.9 (C-28), 51.5 and 51.1 (2 × CO_2Me), 51.1, 43.1, and 36.8 (s), 49.8, 49.4, 47.6, and 40.6 (d), 33.8, 32.4, 31.8, 30.2, 30.2, 28.1, 27.4, 26.1, and 17.8 (t), and 27.1, 25.7, 22.4, 21.9, 17.6, and 15.9 (q); ms *m/e*: 498.

Dimethyl 3,4-Secotirucall-7-en-3,21-dioate 3

The dimethyl ester **2** (146 mg) in ethyl acetate solution was hydrogenated over 10% palladium/charcoal until uptake of hydrogen ceased. Normal work-up afforded the non-crystalline *tetrahydrodimethyl ester* **3** (140 mg); ^1H nmr δ: 3.64 (2 × CO_2Me) and 5.26 (1H, m, H-7); ^{13}C nmr δ: 176.6 (C-21), 174.6 (C-3), 145.6 (C-8), 118.3 (C-7), 51.5 and 51.1 (2 × CO_2Me); ms *m/e*: 502.

Dimethyl 3,4-Secotirucall-8-en-3,21-dioate 4

Dry hydrogen chloride gas was bubbled through a chloroform solution of the tetrahydrodimethyl ester **3** (100 mg) for ten minutes and the reaction left for one hour at room temperature. *Dimethyl 3,4-secotirucall-8-en-3,21-dioate* **4** (90 mg), obtained on work-up, was crystallized from ether – light petroleum and had mp 92–94°C; ^1H nmr δ: 3.64 (2 × CO_2Me), no vinyl protons; ms *m/e*: 502. *Anal.* calcd. for $C_{32}H_{54}O_4$: C 76.45, H 10.85; found: C 76.3, H 10.85.

Dimethyl 25-Chloro-3,4-secotirucalla-4(28),8-dien-3,21-dioate 5

On treatment with dry hydrogen chloride gas under the above conditions the dimethyl ester **2** (100 mg) was converted into the *chlorodiene* **5** (87 mg) mp 114–115°C (ex ether – light petroleum); ^1H nmr δ: 0.80, 0.86, 0.90 (C—*Me*), 1.52 (6H, Cl—C*Me*$_2$), 1.73 (vinyl Me), 3.68 (2 × CO_2Me), 4.68 and 4.89 (each 1H, bs, $CH_2{=}C\lesssim$); ms *m/e*: 498 (M – HCl). *Anal.* calcd. for $C_{32}H_{51}O_4Cl$: C 71.85, H 9.55, Cl 6.65; found: C 71.85, H 9.8, Cl 6.7.

Methyl 3-Oxotirucall-8-en-21-oate 7

Methyl 3-oxotirucalla-8,24-dien-21-oate **6** (150 mg) mp 110–113°C, isolated from elemi resin (4), was dissolved in ethyl acetate and hydrogenated over 10% palladium/charcoal. Normal work-up afforded the non-crystalline methyl 3-oxotirucall-8-en-21-oate **7** (130 mg); ^1H nmr δ: 3.66 (CO_2Me); ms *m/e*: 470.

Baeyer–Villiger Oxidation of 7

Acetic anhydride (20 mL) was added dropwise over a period of twenty minutes to a stirred, ice-cold solution of methylene chloride (20 mL) containing hydrogen peroxide (90%, 6 mL) and a drop of concentrated sulphuric acid. Stirring was continued for thirty minutes at room temperature. Excess of this peracetic acid was added dropwise to a stirred, ice-cold solution of the dihydroderivative **7** (130 mg) in dry methylene chloride (20 mL) in the presence of anhydrous disodium hydrogen phosphate (160 mg) and the reaction allowed to stand overnight at room temperature. Analytical tlc of the crude product showed the presence of two products which were separated by preparative tlc (13% ether–benzene). The *lactone* **8** (50 mg) was crystallized from ether – light petroleum and had mp 135–137°C; ^1H nmr δ: 3.66 (CO_2Me); ^{13}C nmr δ: 176.7 (C-21), 174.3 (C-3), 134.2 and 133.5 (C-8 and C-9), 86.0 (C-4), 51.0 (CO_2Me); ms *m/e*: 486. *Anal.* calcd. for $C_{31}H_{50}O_4$: C 76.5, H 10.35; found: C 76.5, H 10.45. The *epoxylactone* **9** (40 mg) was crystallized from ether – light petroleum and had mp 169–170°C; ^1H nmr δ: 3.63 (CO_2Me); ^{13}C nmr δ: 176.6 (C-21), 173.3 (C-3), 85.5 (C-4), 69.6 and 68.8 (C-8 and C-9), 51.5 (CO_2Me); ms *m/e*: 502. *Anal.* calcd. for $C_{31}H_{50}O_5$: C 74.05, H 10.05; found: C 74.25, H 10.0.

Dimethyl 4-Hydroxy-3,4-secotirucall-8-en-3,21-dioate 10

The lactone **8** (50 mg) was refluxed in ethanolic potassium hydroxide solution (5%) for two hours. Acidification with acetic acid, extraction with chloroform, methylation with diazomethane, and purification by preparative tlc (13% ether–benzene) yielded the *hydroxy dimethyl ester* **10** (40 mg) mp 97–98°C (ex ether – light petroleum); ir (CCl_4): 3501 and 1735 cm^{-1}; ^1H nmr δ: 3.66 (2 × CO_2Me); ^{13}C nmr δ: 176.8 (C-21), 176.0 (C-3), 138.5 and 130.8 (C-8 and C-9), 75.3 (C-4), 51.7 and 51.0 (2 × CO_2Me); ms *m/e*: 500 (M – 18). *Anal.* calcd. for $C_{32}H_{54}O_5$: C 74.1, H 10.5; found: C 74.4, H 10.6.

Dimethyl 3,4-Secotirucalla-4(28),8-dien-3,21-dioate 11

An ice-cold solution of the hydroxy dimethyl ester **10** (28 mg) in dry pyridine (3 mL) was treated with thionyl chloride (three drops) and allowed to stand for five minutes. Water was added

and the solution extracted with chloroform. The crude product was purified by preparative tlc (13% ether–benzene) to give the *diene dimethyl ester* **11** (25 mg) mp 105–106°C (ex ether – light petroleum; ^{1}H nmr δ: 4.68 and 4.89 (each 1H, bs, CH_2=C<), 3.66 (2 × CO_2Me), 1.72 (vinyl Me); ms *m/e*: 500. *Anal.* calcd. for $C_{32}H_{52}O_4 \cdot H_2O$: C 74.1, H 10.5; found: C 74.2, H 10.5.

Hydrogenation of 11

The diene dimethyl ester **11** (25 mg) was dissolved in ethyl acetate and hydrogenated over 10% palladium/charcoal as above. Preparative tlc of the crude product and crystallization from ether – light petroleum gave *dimethyl 3,4-secotirucall-8-en-3,21-dioate* **4** (21 mg) mp 92–93°C, identical in all respects (nmr, mass spectrum, mixture mp, and tlc) with the compound obtained by hydrogenation and acid isomerisation of the dimethyl ester **2** derived from compounds *A* **1** and *B* **12**. *Anal.* calcd. for $C_{32}H_{54}O_4$: C 76.45, H 10.85; found: C 76.4, H 11.0.

1. J. D. CONNOLLY and C. LABBÉ. J. Chem. Soc. Perkin Trans. I, 529 (1980).
2. J. D. CONNOLLY, C. LABBÉ, D. S. RYCROFT, D. A. OKORIE, and D. A. H. TAYLOR. J. Chem. Res. (S), 256 (1979); (M), 2858 (1979).
3. J. D. CONNOLLY, K. L. HANDA, R. MCCRINDLE, and K. H. OVERTON. J. Chem. Soc. C, 2230 (1968).
4. G. P. COTTERRELL, T. G. HALSALL, and M. J. WRIGLESWORTH. J. Chem. Soc. C, 739 (1970).
5. P. A. COUPERUS, A. D. H. CLAGUE, and J. P. C. M. VAN DONGEN. Org. Magn. Reson. **11**, 590 (1978).

Can. J. Chem. Downloaded from www.nrcresearchpress.com by 210.87.254.40 on 09/05/12
For personal use only.

The synthesis of daunosaminyl ε-rhodomycinone, daunosaminyl 10-epi-ε-rhodomycinone, daunosaminyl ε-pyrromycinone, and 10-descarbomethoxy-ε-pyrromycin

JOHN M. ESSERY[1] AND TERRENCE W. DOYLE

Research Division, Bristol Laboratories, Division of Bristol-Myers Company, Syracuse, NY 13201, U.S.A.

Received February 6, 1980

This paper is dedicated to the memory of Dr. Léo Marion

JOHN M. ESSERY and TERRENCE W. DOYLE. Can. J. Chem. **58**, 1869 (1980).

The epimerisation at C10 of ε-rhodomycinone by aqueous alkali treatment of its 6,7-acetonide is described. Daunosaminyl ε-rhodomycinone and daunosaminyl 10-epi-ε-rhodomycinone were prepared and compared with regard to their antibacterial properties. Daunosaminyl ε-pyrromycinone and 10-descarbomethoxy-ε-pyrromycin were synthesized and their antitumor properties were compared with some naturally occurring glycosides of ε-pyrromycinone.

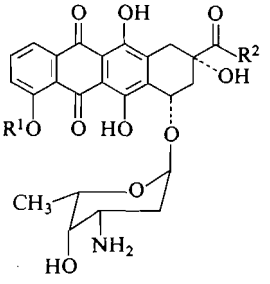
JOHN M. ESSERY et TERRENCE W. DOYLE. Can. J. Chem. **58**, 1869 (1980).

On décrit l'épimérisation, au niveau du carbone en position 10 de l'ε-rhodomycinone, à partir de son acétonide-6,7 sous l'influence d'une solution aqueuse de base. On a préparé la daunosaminyl ε-rhodomycinone et la daunosaminyl épi-10 ε-rhodomycinone et on les a comparé par rapport à leurs propriétés antibactériennes. On a synthétisé la daunosaminyl-ε-pyrromycinone et la descarbométhoxy-10 pyrromycine et on a comparé leurs propriétés anti-tumorales à celles de quelques glycosides de ε-pyrromycinone naturelles.

[Traduit par le journal]

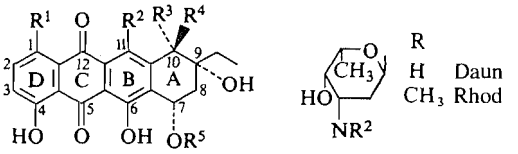
Can. J. Chem. Downloaded from www.nrcresearchpress.com by 210.87.254.105 on 09/05/12
For personal use only.

The chemistry and biology of adriamycin (**1***a*) and the structurally related anthracyclines daunomycin (**1***b*) and carminomycin (**1***c*) have been extensively studied (1). Recently the isolation and characterization of a number of new anthracyclines which have considerable structural and biological differences from the adriamycin class of antitumor agents have been reported (2). Earlier communications from these laboratories have described a number of new agents based on the aglycone ε-



1*a* $R^1 = CH_3$, $R^2 = CH_2OH$
1*b* $R^1 = R^2 = CH_3$
1*c* $R^1 = H$, $R^2 = CH_3$

pyrromycinone (**2***a*) (2*a*–*d*). Oki and co-workers (2*e*–*g*) have reported additional members of this group as well as numerous antitumor agents based on the closely related aglycone aklavinone (**2***b*). Structurally there are a number of differences between the members of the aklavinone–pyrromycinone group and those of the adriamycin group. While the monosaccharides **1***a*–*c* are quite



	R^1	R^2	R^3	R^4	R^5
2*a*	OH	H	H	CO_2CH_3	H
2*b*	H	H	H	CO_2CH_3	H
2*c*	OH	H	H	CO_2CH_3	Rhod
2*d*	H	H	H	CO_2CH_3	Rhod
2*e*	OH	H	H	H	Rhod
2*f*	OH	H	H	CO_2CH_3	Daun
2*g*	H	OH	H	CO_2CH_3	Daun
2*h*	H	OH	CO_2CH_3	H	Daun
2*i*	H	OH	H	CO_2CH_3	H
2*j*	H	OH	CO_2CH_3	H	H

potent antitumor agents, it has been shown that pyrromycin (**2***c*) and aklavin (**2***d*) possess little or no antitumor activity (2*e*, 3). *A priori* a number of reasons may be advanced to explain this lack of activity: (*1*) the substitution of rhodosamine for daunosamine in the glycosides **2***c* and **2***d*; (*2*) the presence of a 10-carbomethoxy group in compounds **2***c* and **2***d*; and (*3*) the different oxygenation pattern in the anthraquinone portion of the molecule.

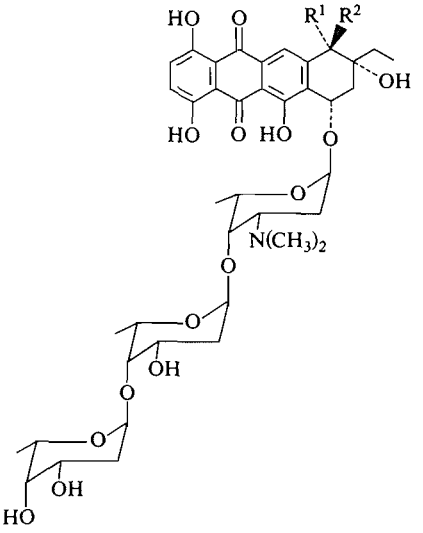
We have shown previously that removal of the 10-carbomethoxy function or epimerization at C10 in marcellomycin (**3***a*) resulted in compounds **3***b* and **3***c*, respectively. These compounds were significantly less active than **3***a* (2*b*, *d*). We would now like to report the syntheses of 10-descarbomethoxy-ε-pyrromycin (**2***e*), daunosaminyl

[1]Author to whom correspondence may be addressed.

0008-4042/80/171869-06$01.00/0

©1980 National Research Council of Canada/Conseil national de recherches du Canada

Can. J. Chem. Downloaded from www.nrcresearchpress.com by 210.87.254.105 on 09/05/12
For personal use only.



3*a* $R^1 = H, R^2 = CO_2CH_3$
3*b* $R^1 = R^2 = H$
3*c* $R^1 = CO_2CH_3, R^2 = H$

ε-pyrromycinone (**2***f*), daunosaminyl ε-rhodomycinone (**2***g*),[2] and daunosaminyl 10-epi-ε-rhodomycinone (**2***h*). We felt that a comparison of the activities of **2***c*, **2***e*, **2***f*, and **2***g* would permit an estimate of whether or not the lack of activity of pyrromycin was due to the amino sugar differences, the presence of the 10-carbomethoxy group, or the anthracycline oxygenation pattern. It has been shown that both ε-pyrromycinone (**2***a*) and ε-rhodomycinone (**2***i*) possess the absolute stereochemistry 7*S*,9*R*,10*R* (5, 6). It was suggested that the preferred conformation of ring A in **2***a* and **2***i* was that shown in partial structure **2***i* (Fig. 1), i.e. with the 10-carbomethoxy group pseudoaxial (5).

While in the pyrromycinone-based anthracyclines epimerization at C10 was readily effected by treatment with 1,5-diazabicyclo[4.3.0]-non-5-ene (DBN) (2*c*), similar attempts with ε-rhodomycinone **2***i* failed completely. In the case of **3***a* the ratio of marcellomycin (**3***a*) to mimimycin (**3***c*) at equilibrium was 77:23. Presumably in the ε-rhodomycinone series the added steric effect of an 11-hydroxyl with the 10-carbomethoxy group in the 10*S* (pseudoequatorial) configuration was sufficient to displace the equilibrium completely towards the naturally occurring 10*R* configuration. In **2***i* the conformation of the A ring holds both the 7-hydroxyl and the 10-carbomethoxy groups in a pseudoaxial position. We suspected that if the 6,7-acetonide (**5***a*) could be formed, ring A would be forced into a conformation resulting in a steric interaction between the carbomethoxy group and the *peri*-phenolic group at C11. This steric strain could be relieved by epimerization at C10 as depicted in Fig. 1. Acid-catalyzed reaction of **2***i* with 2,2-dimethoxypropane gave as expected the 7,9-acetonide (**4**) (5). In the presence of *N*,*N*-dimethylformamide, however, there was obtained a mixture of **4** and the 6,7-acetonide (**5***a*) (Scheme 1) which was readily separated by column chromatography. Epimerization at C10 occurred when a chloroform solution of **5***a* was stirred with dilute aqueous sodium hydroxide to give a roughly 60:40 mixture of **5***a* and **5***b*. The epimer **5***b* was separated by silica gel chromatography and was characterized by the ^1H nmr spectrum. An upfield shift of 0.26 ppm for the resonance due to the C10 proton relative to that of **5***a* and a downfield shift of 0.06 ppm for the carbomethoxy resonance was observed. These are similar to the shifts found for the corresponding resonances in mimimycin (**3***c*) compared to marcellomycin (**3***a*) although in the present case the shift in the carbomethoxy resonance is smaller. Hydrolysis of **5***b* provided 10-epi-ε-rhodomycinone (**2***j*) which crystallized from methanol as red needles of mp 197–198°C. The infrared spectrum of **2***j*, in both the solid state and in solution, was very similar to that of **2***i* with absorptions due to the ester carbonyl at 1725 cm^{-1} and to the hydrogen-bonded quinone carbonyls at 1600 cm^{-1}. The uv–visible spectrum of **2***j* was also similar to that of **2***i* but with an additional absorption at 577 nm. The three phenolic protons gave singlets in the nmr spectrum at 13.5, 12.9, and 11.9 ppm, indicating hydrogen bonding to the quinone carbonyl groups. The signals due to the aromatic, ethyl, and C7 protons had similar chemical shifts to those in **2***i* although the line shape of the signal for the C7 proton was very similar to that seen in **5***b*, indicating a pseudoaxial orientation for this proton. The most notable differences in the spectra of **2***j*

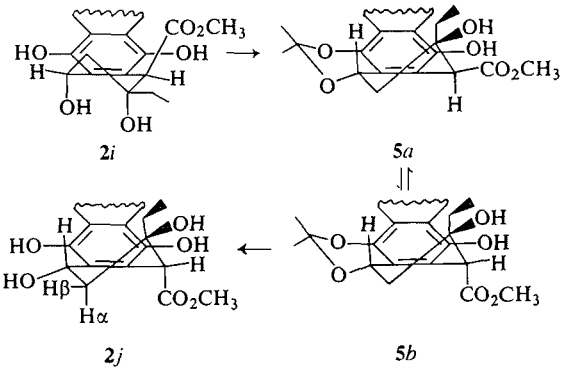
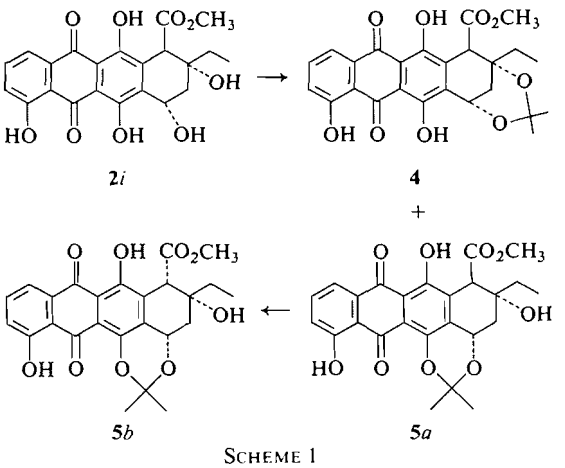


FIG. 1. Conversion of **2***i* to **2***j*.

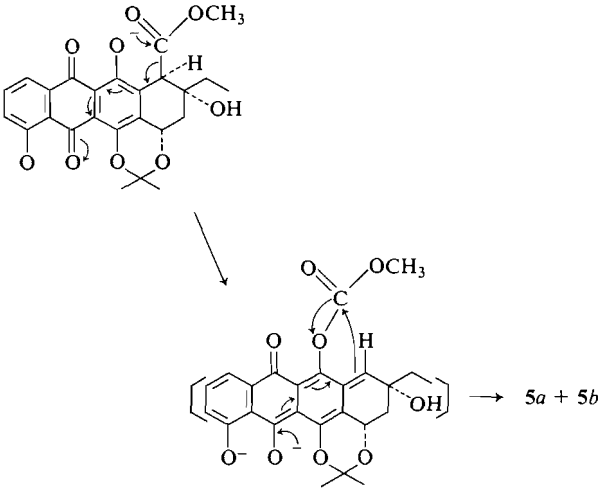
[2]While our work was in progress the synthesis of **2***g* was reported (4).

Can. J. Chem. Downloaded from www.nrcresearchpress.com by 210.87.254.105 on 09/05/12
For personal use only.



SCHEME 1

and **2***i* were the upfield shift of 0.21 ppm of the C10 proton resonance and the change in both chemical shift and coupling constants for the C8 protons, the latter reflecting a change in conformation of the saturated ring. In this case, the carbomethoxy resonance was shifted upfield by 0.04 ppm relative to that in **2***i*. The ^{13}C spectrum of **2***j* was very similar to that of **2***i* (**2***c*) there being only minor differences in most carbon resonances for the A ring. A shift of 1.7 ppm to higher field for the C9 resonance was the greatest shift observed. These properties showed **2***j* to be different from an aglycone, isolated from an unnamed *Streptomyces* species by Bowie and Johnson (7), called θ-rhodomycinone which they suggested was an isomer of ε-rhodomycinone. θ-Rhodomycinone, mp 220°C dec., had carbonyl absorptions at 1712, 1642, and 1622 cm^{-1} and it was postulated that the ester group was equatorial and hydrogen-bonded to the C11 phenolic group. The infrared and nmr spectral evidence clearly indicate that in **2***j* the C11 phenol is bonded to the C12 carbonyl and not to the ester. When the epimerization of **5***a* was carried out in a $CDCl_3$–D_2O–NaOD mixture, it was found by monitoring the course of the reaction via nmr spectra that the C10 proton did not exchange with the deuterium atoms present. This would seem to preclude proton abstraction at C10 as the mechanism for the epimerization, and leads us to postulate participation by the *peri*-phenol anion as follows:[3]



Relief of steric strain in the saturated ring is a consequence of the change in configuration of the ester group from pseudoequatorial (as in **5***a*, Fig. 1) to pseudoaxial, which lessens its interaction with the 9-ethyl and 11-hydroxyl groups. If this mechanism is operating, it would be expected that the corresponding epimerization would not occur with the 6,7-acetonide of ε-pyrromycinone which does not possess the necessary phenol function at C11. Unfortunately we were unable to prepare this compound. Reaction of **2***a* with 2,2-dimethoxypropane in the absence of DMF afforded the 7,9-acetonide **6**, and in the presence of DMF the only isolable products were the 7,9-acetonide and the known η-pyrromycinone (**7**) which resulted by elimination of water from **2***a* (Scheme 2). It was found that neither of the 7,9-acetonides **4** and **6** underwent base-catalyzed epimerization at C10.

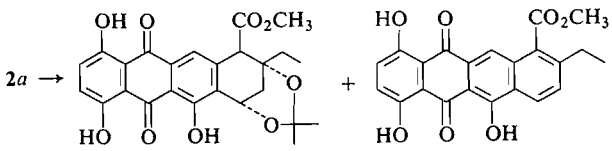
With the appropriate aglycones in hand i.e., **2***a*, **2***i*, and **2***j*, the conversion of these into their daunosamine glycosides was carried out. Following known procedures daunosamine (**8**) was converted to the *O*,*N*-protected bromo-sugar **9** (8) which was condensed with **2***i* to yield **2***g* (after removal of the protecting groups (8)) as its α-anomer. This was shown by the position (δ 5.5) and appearance (broadened singlet of half-band width 6 Hz) of the anomeric proton in the ^1H nmr spec-

TABLE 1. ^{13}C nmr shifts for selected carbons in **2***c* and **2***e*[a]

Carbon	**2***c*	**2***e*
C10	57.4 d	42.9 t
C9	71.8 s	70.0 s
C8	34.2 t	35.0 t
C7	71.1 d	70.8 d
C13	32.3 t	37.3 t
C14	6.7 q	7.4 q

[a]Recorded in $CDCl_3$ at 25.2 MHz. Chemical shifts are relative to internal TMS.

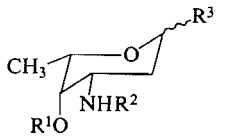
[3]A referee has pointed out that an alternate hypothesis, that of ClO—H proton abstraction followed by redelivery of the proton to the opposite face, may be operative.



6 7

SCHEME 2

trum (9). Similarly 10-epi-ε-rhodomycinone (**2***j*) provided in low yield the α-glycoside **2***h*. For the conversion of ε-pyrromycinone (**2***a*) to its glycoside **2***f* the method of Arcamone *et al.* (10) using the *O*,*N*-bistrifluoroacetyl daunosaminyl chloride **10** was employed. This gave **2***f* in low yield following deprotection.



	R^1	R^2	R^3
8	H	H	OH
9	*p*-$NO_2C_6H_4CO$	$COCF_3$	Br
10	$COCF_3$	$COCF_3$	Cl

The synthesis of 10-descarbomethoxy-ε-pyrromycin (**2***e*) was accomplished using the method of Wiley *et al.* (11). Treatment of **2***c* with aqueous potassium hydroxide gave the crude 10-carboxylic acid which, when allowed to stand in dimethylformamide, decarboxylated to yield **2***e*. The structure of **2***e* was evident from its ^1H and ^{13}C nmr spectra. Thus the loss of signals for the C10 and carbomethoxy protons in **2***c* coupled with the appearance of an AB quartet at δ 1.99 for the C10 protons in **2***e* indicated that the desired conversion had been achieved. In the ^{13}C nmr spectrum the signal for C10 at δ 57.4 in **2***c* disappeared to be replaced by a methylene signal at δ 42.9 in **2***e*. The signals for C13 and C9 also showed significant shifts (Table 1).

Pyrromycin (**2***c*) has been shown previously to be marginally active against L-1210 leukemia (3). Both 10-descarbomethoxy-ε-pyrromycin (**2***e*) and daunosaminyl ε-pyrromycinone (**2***f*) were inactive in L-1210 leukemia and displayed lower antibacterial activity in a plate assay.[4] Previously Smith *et al.* (4) have shown that daunosaminyl ε-rhodomycinone **2***g* was 16-fold less active than **2***c*. This loss in potency parallels that observed in going from marcellomycin (**3***a*) to mimimycin (**3***c*). In the paper describing the synthesis of **2***g* (4) the synthesis and activity of 13-deoxydaunomycin was reported. This compound was less potent (~½) but had comparable activity to **1***b*.

[4]W. T. Bradner and M. Misiek, unpublished results. The plate assay is against *B. subtilis* ATCC 6633.

These results indicate that anthracyclines containing a carbomethoxy function at C10 and an ethyl group at C9 are inactive or marginally active antitumor agents when in the form of monosaccharides containing daunosamine or rhodosamine. For expression of significant activity, the substituent at C7 must be a di- or tri-saccharide, and maximum antitumor activity is associated with 10*R* stereochemistry. The lack of activity of 10-descarbomethoxy-ε-pyrromycin (**2***e*), in contrast to that of 13-deoxydaunomycin, may be a reflection of the deleterious effect of the hydroxyl group at C1.

Experimental

Melting points were determined in open capillary tubes and are uncorrected. Nuclear magnetic resonance spectra were recorded on a Varian HA-100 or XL-100 spectrometer using $CDCl_3$ as solvent (unless otherwise specified) and tetramethylsilane as internal standard. Infrared spectra were recorded as KBr disks on a Beckman IR-2420 and uv–visible spectra on a Beckman Acta III spectrophotometer.

ε-Rhodomycinone-7,9-acetonide (4) and -6,7-Actonide (5a)

A mixture containing 21.4 g of ε-rhodomycinone (**2***i*), 0.7 g of *p*-toluenesulfonic acid monohydrate, 350 mL of 2,2-dimethoxypropane, and 175 mL of dry DMF was heated under reflux with stirring for 17 h. Volatile components were removed under reduced pressure and the residue was triturated with $CHCl_3$ to provide 5.32 g of **4**. Recrystallization from $CHCl_3$ gave an orange solid, 252–253°C; nmr δ:13.47 (s, 1H, OH), 12.86 (s, 1H, OH), 12.26 (s, 1H, OH), 7.94–7.63 (m, 2H, C1—H and C2—H), 7.35 (dd, 1H, C3—H), 5.48 (m, 1H, C7—H), 4.25 (s, 1H, C10—H), 3.79 (s, 3H, CO_2CH_3), 2.42 (m, 2H, C8—H), 1.95–1.50 (m, 5H, CH_2—CH_3 and C—CH_3), 1.27–1.06 (m, 6H, CH_2—CH_3 and C—CH_3). *Anal.* calcd. for $C_{25}H_{24}O_9$: C 64.10, H 5.16; found: C 63.77, H 5.26.

The filtrate from **4** was evaporated and the residue chromatographed on 300 g of silica gel (Mallinckrodt CC-7) using chloroform as the solvent to give 0.44 g of **4** and then 17.7 g of a mixture containing **4** and **5***a*. This mixture was rechromatographed by the dry column technique on deactivated silica gel using $CHCl_3$–MeOH 95:5 as the solvent, and provided 1.70 g of **4** (total yield 7.46 g, 32%), 2.42 g (10%) of **5***a*, and 10.55 g (49%) of ε-rhodomycinone. Compound **5***a*, mp 164–165°C; ir: 1735, 1620 cm^{-1}; uv–visible (EtOH) λ_{max}:476 (ε15 000), 291 (10 800), 251 (sh 21 700), 234 (44 400); nmr δ:13.60 (s, 1H, OH), 13.01 (s, 1H, OH), 7.76–7.46 (m, 2H, C1—H, C2—H), 7.18 (dd obscured by solvent, C3—H), 5.06 (dd, J = 8 Hz, 1H, C7—H), 4.32 (s, 1H, C10—H), 3.71 (s, 3H, CO_2CH_3), 2.59 (dd, J = 8 Hz, 14 Hz, 1H, C8—H), 2.26–1.56 (m, 9H includes C8—H, CH_2CH_3, $C(CH_3)_2$), 1.08 (t, 3H, CH_2—CH_3). *Anal.* calcd. for $C_{25}H_{24}O_9 \cdot 1/4\ H_2O$: C 63.48, H 5.22; found: C 63.56, H 5.34.

10-epi-ε-Rhodomycinone-6,7-acetonide (5b)

A solution of 1.52 g of **5***a* in 75 mL of $CHCl_3$ was stirred for 16 h with 7.5 mL of 2.5% aqueous NaOH. The mixture was diluted with H_2O and acidified with HOAc. The $CHCl_3$ layer was separated, washed (H_2O), dried (Na_2SO_4), and evaporated to give 1.43 g of red foam. This was chromatographed on a dry column of 140 g of deactivated silica gel using $CHCl_3$–EtOAc 9:1 as the developing solvent to provide 228 mg of **5***a*, 450 mg of a mixture of **5***a* and **5***b*, and 600 mg of **5***b* as a red foam. A portion of this was crystallized from ether – Skellysolve B to give a red solid of mp 177–178°C. Infrared: 1740, 1615 cm^{-1}; uv–visible (EtOH) λ_{max}:475 (ε 10 400), 293 (6040), 250 (14 000), 234 (30 600); nmr δ: 7.81–7.50 (m, 2H, C1—H, C2—H), 7.25 (obscured by

Can. J. Chem. Downloaded from www.nrcresearchpress.com by 210.87.254.105 on 09/05/12
For personal use only.

Can. J. Chem. Downloaded from www.nrcresearchpress.com by 210.87.254.105 on 09/05/12
For personal use only.

solvent, C3—H), 5.26 (dd, J = 6 Hz, 11Hz, 1H, C7—H), 4.06 (s, 1H, C10—H), 3.79 (s, 3H, CO_2CH_3), 2.38 (dd, J = 6 Hz, 13 Hz, 1H, C8—H), 1.90–1.54 (m, 9H, includes C8—H, CH_2—CH_3, $C(CH_3)_2$), 1.01 (t, 3H, CH_2—CH_3). *Anal.* calcd. for $C_{25}H_{24}O_9 \cdot H_2O$: C 61.72, H 5.39; found: C 61.88, H 5.23.

10-epi-ε-Rhodomycinone (2j)

A solution of 550 mg of **5***b* in 40 mL of THF and 20 mL of 2 *N* HCl was stirred for 5 h. The solution was diluted with THF and washed with 2 × 10 mL portions of brine. The organic phase was dried (Na_2SO_4) and the solvent removed to give a red solid which was chromatographed on a dry column of deactivated silica gel using $CHCl_3$–MeOH 9:1 as the developing solvent. The major fraction consisted of **2***j* contaminated with traces of **2***i*. A 140 mg sample of pure **2***j* was obtained and recrystallization from methanol gave red needles of mp 197–198°C. Infrared ($CHCl_3$): 1725, 1600 cm^{-1}; uv–visible (EtOH) λ_{max}:577 (ε 9900), 531 (15 600), 495 (10 600), 295 (11 100), 251 (38 000), 234 (46 800); $[\alpha]_{578}^{23}$ +218° (*c* 0.05, THF); nmr δ: 13.48 (s, 1H, OH), 12.88 (s, 1H, OH), 11.87 (s, 1H, OH), 7.84–7.53 (m, 2H, C1—H, C2—H), 7.24 (dd partially obscured by solvent, C3—H), 5.20 (m, 1H, C7—H), 4.02 (s, 1H, C10—H), 3.72 (s, 3H, CO_2CH_3), 3.56 (bs, 1H, OH), 2.36 (dd, 1H, J_1 = 14, J_2 = 6 Hz, C8—Hα), 1.95 (dd, 1H, J_1 = 14, J_2 = 4 Hz, C8—Hβ), 1.68 (m, 2H, CH_2CH_3), 0.98 (t, 3H, J = 7 Hz, CH_2CH_3); ^{13}C nmr (DMSO-d_6):189.6 (C5), 185.5 (C12), 170.39 (CO_2CH_3), 161.1 (C4), 155.2, 155.9 (C6, C11), 138.6 (C12a), 137.0 (C2), 134.7 (C10a), 132.8 (C6a), 124.3 (C1), 118.8 (C3), 115.7 (C4a), 110.4, 110.5 (C11a, C5a), 69.8 (C9), 61.0 (C7), 51.5 (CO_2CH_3), 51.0 (C10), 35.8 (C8), 32.8 (C13), 7.57(C14). *Anal.* calcd. for $C_{22}H_{20}O_9$: C 61.68, H 4.71; found: C 61.32, H 4.86.

Daunosaminyl ε-Rhodomycinone (2g)

To a stirred slurry of 143 mg (0.33 mmol) of ε-rhodomycinone, 500 mg (2.3 mmol) of yellow mercuric oxide, 103 mg (0.35 mmol) of mercuric bromide, and 3 g of powdered 3A molecular sieves in 40 mL of dry THF under reflux was added 0.33 mmol of a solution of the bromo-sugar **9** (prepared according to Acton *et al.* (8)) in 4 mL of THF. After the mixture had been heated for 20 h, an additional 0.33 mmol of **9** was added and after another 7 h another 0.33 mmol of **9** was added. After an additional 16 h under reflux, the mixture was allowed to cool and was filtered and the filtrate (and THF washings) were evaporated to a red foam. This was chromatographed on a dry column of deactivated silica gel to provide 825 mg of a mixture of **2***i* and product. Column chromatography on silica gel using $CHCl_3$–Et_2O 1:1 provided the desired product as the first fraction. Removal of the protecting groups (as in ref. 7) gave 64 mg of red solid. Column chromatography on silica gel with $CHCl_3$ removed impurities and **2***g* was eluted with $CHCl_3$–MeOH 1:1 to afford 32 mg (15%). Infrared: 1730, 1600 cm^{-1}; nmr δ: 7.88–7.56 (m, C1—H, C2—H), 7.26 (dd partially obscured by solvent, C3—H), 6.30 (broad, includes exchangeable protons), 5.50 (bs, peak width at 1/2 height 6 Hz, C1′-H), 5.25 (bs, C7—H), 4.3 (s, C10—H), 4.3–4.06 (m, C5—H), 3.76 (s, CO_2CH_3), 3.54 (bs, C4′—H), 3.18 (b, C3′—H), 2.40–2.24 (m, C8—H), 2.02–1.09 (m, includes C2′—H, CH_2—CH_3, C5′—CH_3, CH_2—CH_3). *Anal.* calcd. for $C_{28}H_{31}NO_{11} \cdot 2H_2O$: C 56.65, H 5.94, N 2.36; found: C 56.51, H 5.87, N 2.46.

Daunosaminyl 10-epi-ε-Rhodomycinone (2h)

Similarly, 143 mg (0.33 mmol) of 10-epi-ε-rhodomycinone (**2***j*) was reacted with 1 mmol of bromo-sugar (**9**) to provide 23 mg (12%) of **2***h*. Infrared: 1730, 1600 cm^{-1}; nmr ($CDCl_3$ + D_2O) δ: 7.95–7.56 (m, 2H, C1—H, C2—H), 7.28 (dd partially obscured by solvent, C3—H), 5.46 (bs, 1H peak width at 1/2 height 6 Hz, C1′—H), 5.14 (bm, 1H, C7—H), 4.22 (s, 1H, C10—H), 3.98 (q, 1H, C5′—H), 3.74 (s, 3H, CO_2CH_3), 3.65–3.32 (m, 2H, C3′—H, C4′—H), 2.6–0.8 (m, includes C8—H, C2′—H, CH_2—CH_3, C5′—CH_3). *Anal.* calcd. for $C_{28}H_{31}NO_{11} \cdot 0.5\ H_2O$: C 59.36, H 5.69, N 2.47; found: C 59.35, H 5.63, N 2.25.

Daunosaminyl ε-Pyrromycinone (2f)

A slurry of 214 mg (0.5 mmol) of ε-pyrromycinone (**2***a*), 428 mg (1.98 mmol) of yellow mercuric oxide, 107 mg (0.30 mmol) of mercuric bromide, and 1.0 g of powdered molecular sieves (3A) in 45 mL of ethanol-free $CHCl_3$ was stirred for 1 h. A solution of 1.2 mmol of the chloro-sugar (**10**, prepared according to Arcamone *et al.* (10)) in 10 mL of $CHCl_3$ was added in two equal portions 22 h apart. After a reaction time of 93 h, the mixture was filtered and the filtrate was evaporated to dryness. The residue was dissolved in 100 mL MeOH and heated under reflux for 30 min. The mixture was filtered and the filtrate evaporated to dryness. The residue was chromatographed on a dry column of deactivated silica gel using $CHCl_3$–MeOH 9:1 as the solvent to provide, as the fast-moving fraction, 15 mg of η-pyrromycinone (**7**), mp 218–220°C. The major fraction was a mixture of the aglycone (**2***a*) and the *N*-protected glycoside, and the latter crystallized from a concentrated solution of this mixture in $CHCl_3$. A solution of 100 mg of this glycoside in 10 mL of THF and 10 mL of 0.1 *N* NaOH was stored at 5°C for 4.5 h. The solution was diluted and the pH adjusted to 8.5. The product was extracted into $CHCl_3$ and the washed (H_2O) and dried (Na_2SO_4) extracts were evaporated to a purple solid which crystallized from ether to give 38 mg (14%) of **2***f*, mp 154–155°C. Infrared: 1735, 1600 cm^{-1}; nmr δ: 7.63 (s, 1H, C11—H), 7.20 (s, 2H, C2—H C3—H), 6.80 (b, 5H, exchangeable protons), 5.46 (s, 1H, peak width at half-height 6 Hz, C1′—H), 5.26 (s, 1H, C7—H), 4.30–4.06 (m, 2H, includes C5′—H, C10—H), 3.76 (s, 3H, CO_2CH_3), 3.50 (m, 1H, C4′—H), 3.15 (b, 1H, C3′—H), 2.70–2.24 (m, 2H, C8—H), 2.0–1.5 (m, 4H, C2′—H, CH_2—CH_3). 1.5–1.0 (m, 6H, C5′—CH_3—CH_2CH_3). *Anal.* calcd. for $C_{28}H_{31}NO_{11} \cdot H_2O$: C 58.43, H 5.78; found: C 58.32, H 5.72.

10-Descarbomethoxypyrromycin (2e)

A solution of 1.17 g (2 mmol) of pyrromycin (**2***c*) in 10 mL of 0.53 *N* potassium hydroxide was let stand 16 h at ~23°C. The solution was diluted with 20 mL of water and the pH was adjusted to 5.9 with 2 *N* hydrochloric acid. The slurry was filtered and the resulting solid washed with water. The combined mother liquors were lyophilized. Both solids (1.113 g) were combined, dissolved in 30 mL of dimethylformamide, and let stand for 18 h. The solvent was removed at reduced pressure and the resulting gum chromatographed on 15 g of silica gel (10% by weight of water added) using chloroform as eluent. Fractions were collected visually and assayed by tlc. In addition to a number of unidentified by-products, there was obtained 83 mg of η-pyrromycinone (**7**) and 642 mg of crude **2***e*. Compound **2***e* was rechromatographed on silica gel (10% by weight of water added) using chloroform–methanol (9:1) as eluent to yield 140 mg of **2***e* mp 188–190°C; ^1H nmr ($CDCl_3$) δ: 7.56 (s, 1H, C11—H), 7.25 (s, 2H, C2—H + C3—H), 5.50 (bs, 1H, C1′—H), 5.20 (bs, 1H, C7—H), 2.5–3.2 (m, 3H, C3′, C4′, C5′H's), 1.99 (AB quartet, 2H, C10—H's), 2.27 (s, 6H, $N(CH_3)_2$), 1.5–2.0 (m, 6H, C8, C13, C2′H's), 1.43 (d, 3H, C5′—CH_3), 1.09 (t, 3H, CH_2CH_3); ^{13}C nmr ($CDCl_3$) δ:190.1 (C5), 185.6 (C12), 161.7 (C6), 158.0, 157.4 (C1, C4), 145.6 (C10a), 132.0 (C6a), 130.7 (C11a), 129.6, 129.4 (C2, C3), 120.7 (C11), 113.5 (C5a), 112.4, 112.1 (C4a, C12a), 100.7 (C1′), 70.8 (C7), 70.0 (C9), 66.5, 65.9 (C4′, C5′), 60.0 (C3′), 42.0 (C10), 41.9 (NMe_2), 37.3 (C13), 35.0 (C8), 28.4 (C2′), 17.0 (C6′), 7.4 (C14). *Anal.* calcd. for $C_{28}H_{33}NO_9 \cdot 3/2\ H_2O$: C 60.64, H 6.50, N 2.53; found: C 59.84, H 6.26, N 2.66.

Acknowledgements

We thank Drs. Bradner and Misiek for biological testing.

1. F. ARCAMONE. *In* Topics in antibiotic chemistry. Vol. 2. *Edited by* P. G. Sammes. Ellis Horwood, Ltd., Chichester, New York, Brisbane, Toronto. 1978. pp. 102–278.
2. (*a*) D. E. NETTLETON, JR., W. T. BRADNER, J. A. BUSH, A. B. COON, J. E. MOSELEY, R. W. MYLLYMAKI, F. A. O'HERRON, R. H. SCHREIBER, and A. L. VULCANO. J. Antibiot. **30**, 525 (1977); (*b*) D. E. NETTLETON, JR., D. M. BALITZ, T. W. DOYLE, W. T. BRADNER, D. L. JOHNSON, F. A. O'HERRON, R. H. SCHREIBER, A. B. COON, J. E. MOSELEY, and R. W. MYLLYMAKI. J. Nat. Prod. In press; (*c*) T. W. DOYLE, D. E. NETTLETON, JR., R. E. GRULICH, D. M. BALITZ, D. L. JOHNSON, and A. L. VULCANO. J. Am. Chem. Soc. **101**, 7041 (1979); (*d*) V. H. DUVERNAY, J. M. ESSERY, T. W. DOYLE, W. T. BRADNER, and S. T. CROOKE. Mol. Pharmacol. **15**, 341 (1979); (*e*) T. OKI. Jpn. J. Antibiot. S, **30**, 70 (1977); (*f*) T. OKI, I. KITAMURA, A. YOSHIMOTO, Y. MATSUZAWA, N. SHIBAMOTO, T. OGASAWARA, T. INUI, A. TAKAMATSU, T. TAKEUCHI, T. MASUDA, M. HAMADA, H. SUDA, M. ISHIZUKA, T. SAWA, and H. UMEZAWA. J. Antibiot. **32**, 791 (1979); (*g*) T. OKI, I. KITAMURA, Y. MATSUZAWA, N. SHIBAMOTO, T. OGASAWARA, A. YOSHIMOTO, T. INUI, H. NAGANAWA, T. TAKEUCHI, and H. UMEZAWA. J. Antibiot. **32**, 801 (1979).
3. W. T. BRADNER and M. MISIEK. J. Antibiot. **30**, 519 (1977).
4. T. H. SMITH, A. N. FUJIWARA, and D. W. HENRY. J. Med. Chem. **21**, 280 (1978).
5. H. BROCKMANN, H. BROCKMANN, JR., and J. NIEMEYER. Tetrahedron Lett. 4719 (1968).
6. H. BROCKMANN, JR. and M. LEGRAND. Tetrahedron, **19**, 395 (1963).
7. J. H. BOWIE and A. W. JOHNSON. J. Chem. Soc. 3927 (1964).
8. E. M. ACTON, A. N. FUJIWARA, and D. W. HENRY. J. Med. Chem. **17**, 659 (1964).
9. F. ARCAMONE, S. PENCO, A. VIGEVANI, S. REDAELLI, and G. FRANCHI. J. Med. Chem. **18**, 703 (1975).
10. F. ARCAMONE, A. DIMARCO, and S. PENCO. Ger. Patent No. 2,510,926 (1974).
11. P. F. WILEY, J. L. JOHNSON, and D. J. HOUSER. J. Antibiot. **30**, 628 (1977).

Can. J. Chem. Downloaded from www.nrcresearchpress.com by 210.87.254.105 on 09/05/12
For personal use only.

^{13}C nuclear magnetic resonance spectroscopy of methylenedioxy group-containing C_{19}-diterpenoid alkaloids and their derivatives

S. WILLIAM PELLETIER, NARESH V. MODY, AND OLIVER D. DAILEY, JR.

Institute for Natural Products Research and Department of Chemistry, University of Georgia, Athens, GA 30602, U.S.A.

Received February 18, 1980

This paper is dedicated to the memory of Dr. Léo Marion

S. WILLIAM PELLETIER, NARESH V. MODY, and OLIVER D. DAILEY, JR. Can. J. Chem. **58**, 1875 (1980).

The natural abundance carbon-13 nmr spectra of some methylenedioxy group-containing C_{19}-diterpenoid alkaloids and their derivatives (dictyocarpine, 14-acetyldictyocarpine, dictyocarpinine, 14-dehydrodictyocarpine, 14-dehydrodictyocarpinine, 6-dehydrodictyocarpinine, 6,14-didehydrodictyocarpinine, deltaline (eldeline), deltamine (eldelidine), 6-dehydrodeltamine, delcorine, 6-acetyldelcorine, and 6-dehydrodelcorine) have been determined. Self-consistent assignments of nearly all the resonances in these compounds have been made with the aid of single-frequency off-resonance proton decoupling techniques, additivity relationships, and the effects induced by certain structural changes. Particular attention is directed towards features of the spectra which are most useful for structure elucidation and identification of the C_{19}-diterpenoid alkaloids.

S. WILLIAM PELLETIER, NARESH V. MODY et OLIVER D. DAILEY, JR. Can. J. Chem. **58**, 1875 (1980).

On a déterminé les spectres rmn du ^{13}C de quelques alcaloides diterpéniques en C-19 contenant des groupes méthylènedioxy et de leurs dérivés (dictyocarpine, acétyl-14 dictyocarpine, dictyocarpinine, déhydro-14 dictyocarpine, déhydro-14 dictyocarpinine, déhydro-6 dictyocarpinine, didéhydro-6,14 dictyocarpinine, deltaline (eldeline), deltamine (eldelidine), déhydro-6 deltamine, delcorine, acétyl-6 delcorine et la déhydro-6 delcorine). On a identifié d'une façon positive presque toutes les résonances de ces composés en utilisant les techniques de découplage hors champs du proton à fréquence unique, les relations d'additivité et les effets induits par certains changements de structure. On a accordé une attention spéciale aux particularités des spectres qui sont les plus utiles à la détermination de la structure et à l'identification des alcaloides diterpéniques en C-19.

[Traduit par le journal]

Can. J. Chem. Downloaded from www.nrcresearchpress.com by 210.87.254.6 on 09/05/12
For personal use only.

Introduction

Plants of *Aconitum*, *Consolida*, and *Delphinium* species are known to elaborate a variety of alkaloids modelled on a C_{19}-skeleton (1). Some of these alkaloids are highly poisonous and exhibit marked biological activity. Recently there has been a great deal of interest in this class of alkaloids because of the wide range of biological activities exhibited by the extracts of *Aconitum* species. The structures of these alkaloids are complex and their determination in early work depended largely on chemical degradation. Because of the low yields of these alkaloids from the plant, such studies were time-consuming and difficult. Structure determination by ^1H nmr analysis is not conclusive or reliable. Although mass spectroscopy has made some contributions to the elucidation of the structures of these alkaloids, this method is not unambiguous in establishing the stereochemistry and position of various substituent groups. The application of ^{13}C nmr spectroscopy to the structure elucidation of the C_{19}-diterpenoid alkaloids was introduced for the first time in 1972 by Jones and Benn (2). Later we reported comprehensive ^{13}C nmr studies of more than sixty aconitine- and lycoctonine-type alkaloids and their derivatives (3–5). While the ^{13}C nmr spectra of these alkaloids have been examined extensively, not a single spectrum for methylenedioxy group-containing diterpenoid alkaloids has been recorded. In this paper, we report for the first time an analysis of the ^{13}C nmr spectra of some rare C_{19}-diterpenoid alkaloids which contain the methylenedioxy and C(10) hydroxy groups. The purpose of this paper is to describe approaches we have used to analyze and interpret the ^{13}C nmr spectra of these alkaloids. Because structure elucidation of these alkaloids is frequently so difficult as to require extensive chemical work or X-ray crystallography, this ^{13}C nmr analysis should be of considerable value in solving structural problems in related systems.

Results and Discussion

The general method for ^{13}C nmr data acquisition and assignment of the carbon resonances for the compounds reported here involved determination of the noise-decoupled and the single-frequency off-resonance decoupled (SFORD) spectra. The signals were assigned with the help of the single-frequency proton off-resonance decoupling technique, application of known chemical shift rules for hydroxyl substitution and acetylation shifts, steric effects, and from comparisons of spectra from compound to compound.

Assignments for Dictyocarpine (1), 14-Acetyldictyocarpine (2), and Dictyocarpinine (3)

During an investigation of the alkaloids of *Delphinium glaucescens*, a plant native to the western

0008-4042/80/171875-05$01.00/0

©1980 National Research Council of Canada/Conseil national de recherches du Canada

TABLE 1. Carbon-13 chemical shifts and assignments for methylenedioxy group-containing lycoctonine-type alkaloids[a]

	1	2[b]	3	4	5	6	7	8	9	10	11	12	13
C(1)	78.7	79.0	79.9	78.2	79.8	77.1	77.1	79.2	80.2	77.0	83.1	83.4	82.7
C(2)	26.4	27.0	26.4	26.0	26.1	26.4	26.2	27.1	27.0	27.0	26.4	26.6	26.5
C(3)	37.6	37.3	36.9	36.3	35.9	37.7	37.3	39.4	38.7	39.2	31.8	31.7	32.2
C(4)	34.0	33.7	33.9	34.2	34.1	35.2	35.2	33.7	33.6	35.2	38.1	38.0	41.8
C(5)	51.8	50.4[c]	51.9	50.5	51.7	56.5	56.5	50.4	51.0	57.2	52.6	51.1	56.5
C(6)	77.2	77.3	77.3	77.1	77.1	217.7	215.6	77.3	77.4	216.7	78.9	78.4	216.7
C(7)	93.0	91.7	93.4	92.7	93.0	91.2	90.6	91.6	92.4	90.2	92.7	92.0	90.4
C(8)	82.9	83.3	82.8	87.1	87.3	82.2	86.2	83.8	83.5	82.8	83.9	83.3	81.5
C(9)	50.4	49.9[c]	51.6	58.1	57.9	53.8	59.6	50.4	51.5	51.2	48.1	48.4	47.8
C(10)	79.9	81.3	80.5	79.4	79.5	79.7	79.0	81.6	82.4	80.3	40.3	40.0	38.6
C(11)	55.1	55.8	55.4	55.2	55.4	51.5	51.6	56.0	56.2	51.7	50.2	50.1	46.1
C(12)	36.5	36.6	36.7	36.3	36.5	37.3	36.1	36.5	36.8	37.7	28.1	28.0	27.7
C(13)	36.6	38.9	36.5	45.4	45.2	36.3	45.2	38.5	37.6	38.3	37.9	38.7	38.7
C(14)	72.8	74.7	72.6	215.0	213.6	71.9	211.2	81.7[c]	81.6	81.3	82.5	81.9[c]	82.4[c]
C(15)	32.9	35.0	33.2	30.9	31.7	32.7	31.1	34.8	34.3	34.0	33.3	33.9	32.9
C(16)	81.2	81.3	81.2	83.9	84.0	81.0	83.4	81.5[c]	81.6	81.0	81.8	81.7[c]	82.3[c]
C(17)	64.4	63.9	64.0	64.9	64.5	63.4	63.8	63.5	63.2	62.6	63.9	64.5	63.0
C(18)	25.5	25.6	25.4	25.4	25.4	24.8	24.6	25.7	25.6	25.0	78.9	78.0	76.8
C(19)	56.9	56.9	57.2	57.0	57.2	57.2	57.0	56.9	57.3	56.5	53.7	53.3	53.4
N—CH_2	50.4	50.4	50.5	50.2	50.6	50.0	50.2	50.2	50.4	50.0	50.7	50.5	50.2
CH_3	14.0	13.9	14.0	14.0	14.0	13.8	13.8	13.8	13.9	13.7	14.0	13.9	13.7
C(I)'[d]	55.6	55.4	55.6	55.6	55.6	55.9	55.7	55.3	55.5	55.7	55.5	55.3	55.9
O—CH_2—O	94.0	93.8	93.4	94.7	94.3	95.8	96.4	93.9	93.3	95.5	92.9	93.5	95.3
C(14)'	—	—	—	—	—	—	—	57.7	57.9	58.1	57.8	57.7	58.1
C(16)'	56.3	56.1	56.3	56.1	56.1	56.5	56.2	56.2	56.2	56.5	56.3	56.2	56.5
C(18)'	—	—	—	—	—	—	—	—	—	—	59.6	59.3	59.2
C(6)—OC=O	170.2	170.0	—	170.2	—	—	—	169.9	—	—	—	170.0	—
CH_3	21.8	21.7	—	21.6	—	—	—	21.8	—	—	—	21.6	—

[a]Chemical shifts in ppm downfield from TMS; solvent is deuteriochloroform.
[b]Chemical shifts for the C(14) acetyl group occur at 171.7 and 21.4 ppm.
[c]These assignments may be interchanged in any vertical column.
[d]Values given for primed carbons refer to chemical shifts for methoxyls.

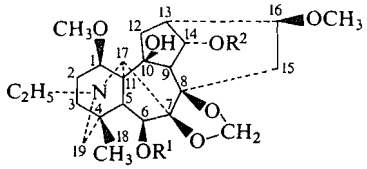
United States, we isolated[1] a known alkaloid, dictyocarpine. Along with dictyocarpine, we also isolated a new alkaloid, dictyocarpinine (**3**), a basic hydrolysis product of dictyocarpine. Dictyocarpine has been reported (6) to occur in *D. dictyocarpum*, a plant native to the Soviet Union. On the basis of extensive degradation work, ^{1}H nmr, and mass spectral data, structure **1** was assigned to dictyocarpine by Yunusov and co-workers (6).

The ^{13}C chemical shifts and assignments for dictyocarpine (**1**), 14-acetyldictyocarpine (**2**), and dictyocarpinine (**3**) are presented in Table 1. The chemical shift assignments for these alkaloids were made by correlation with previously published ^{13}C nmr spectra of the lycoctonine-type alkaloids (4). The presence of the methylenedioxy group in dictyocarpine was confirmed by observing a triplet at 94.0 ppm in the single-frequency off-resonance spectrum. The chemical shift of C(11) in **1** appears at 55.1 ppm, significantly downfield compared with other lycoctonine-type alkaloids such as delcorine (**11**) and lycoctonine (4). This observation suggests that the neighbouring carbon at C(10) is substituted by a hydroxyl group. The presence of the tertiary hydroxy group at C(10) was confirmed by a singlet at 79.9 ppm in the spectrum of dictyocarpine. A quartet at 25.5 ppm and a singlet at 34.0 ppm indicate the presence of the methyl group at C(4). The unusual upfield shift (~3 ppm) of the C(14) hydroxyl group in comparison with other lycoctonine-type alkaloids (e.g. browniine, delcosine) (4) results from the presence of the β-hydroxyl at C(10) in ring C of dictyocarpine. The assignments of the two quaternary carbons at C(8) and C(10) are based on the spectra of delcorine (**11**) and its derivatives. Two singlets at 82.9 and 79.9 ppm are assigned to C(8) and C(10), respectively; the singlet at 79.9 ppm is absent in the specrtrum of delcorine.

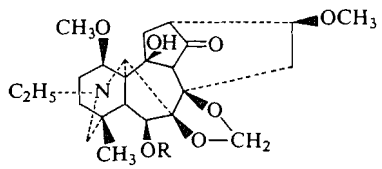
Comparison of the spectrum of dictyocarpine (**1**) with that of dictyocarpinine (**3**) reveals the absence in **3** of chemical shifts due to an acetyl group, some minor changes in the chemical shifts at C(7) and the methylenedioxy carbon, and no change in the chemical shift at C(6). The latter was expected because similar phenomena were observed in other

[1]S. W. Pelletier, O. D. Dailey, Jr., N. V. Mody, and J. D. Olsen. Unpublished results on the alkaloids of *Delphinium glaucescens*.

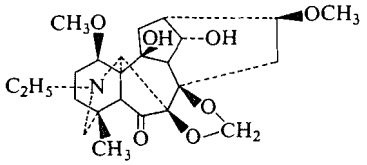
Can. J. Chem. Downloaded from www.nrcresearchpress.com by 210.87.254.6 on 09/05/12
For personal use only.



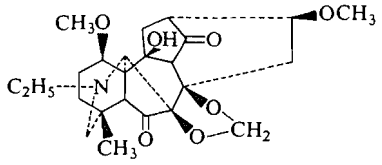
1 R^1 = Ac; R^2 = H Dictyocarpine
2 R^1 = R^2 = Ac
3 R^1 = R^2 = H Dictyocarpinine



4 R = Ac
5 R = H



6



7

C_{19}-diterpenoid alkaloids containing the C(6) β-hydroxyl and acetate groups (7). In contrast, ^{1}H nmr studies showed a profound change in the chemical shifts of the C(6) α proton and methylenedioxy carbon-containing protons between dictyocarpine and dictyocarpinine. Acetylation of the C(14) hydroxy group of **1** shifted the C(14) resonance in **2** downfield (~2 ppm) as a result of the electron withdrawing effect of the acetoxy group relative to the hydroxy group. The ^{13}C nmr spectrum of 14-acetyldictyocarpine (**2**) reveals the presence of two extra signals at 21.4 and 171.7 ppm for an acetyl group at C(14) in comparison with dictyocarpine. All the ^{13}C chemical shifts of dictyocarpine, 14-acetyldictyocarpine, and dictyocarpinine are in agreement with their structures **1**, **2**, and **3**, respectively.

Assignments for 14-Dehydrodictyocarpine (4), 14-Dehydrodictyocarpinine (5), 6-Dehydrodictyocarpinine (6), and 6,14-Didehydrodictyocarpinine (7)

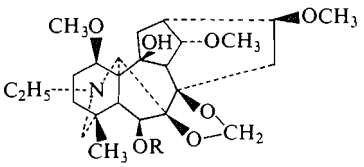
The recent discovery of several C(6) and C(14) keto group-containing lycoctonine-type alkaloids in some *Delphinium* species prompted us to examine the ^{13}C nmr spectra of this type of compound. We have prepared[1] 14-dehydrodictyocarpine (**4**), 14-dehydrodictyocarpinine (**5**), 6-dehydrodictyocarpinine (**6**), and 6,14-didehydrodictyocarpinine (**7**). A downfield singlet at 215.0 ppm in compound **4** indicates the presence of the carbonyl group at the C(14) position. The presence of the carbonyl group at C(14) in **4** moves the chemical shifts at C(8), C(9), C(13), and C(16) significantly downfield in comparison with dictyocarpine. These shifts are a result of the disappearance of the 1,3-diaxial interactions of the C(14) α-hydroxyl group with the C(16) β-methoxyl group and the C(8) oxygen. Comparison of the ^{13}C nmr spectrum of **5** with that of **4** revealed the absence of acetoxy group signals and an unusual upfield shift (1.4 ppm) of the C(14) carbonyl group.

The introduction of a keto group at C(6) in compound **6** results in a number of chemical shift changes. The resonance for C(6) is shifted to the five-membered ring ketone region (217.7 ppm) and the C(5) and C(4) resonances are moved downfield 4.6 and 1.3 ppm, respectively, as expected, relative to dictyocarpinine (**3**). The unusual upfield shifts of C(7) and C(11) in **6** relative to **3** can be explained by the presence of the strained five-membered ring ketone at C(16) (11). Two singlets at 211.2 and 215.6 ppm in compound **7** are assigned to C(14) and C(6) by comparison with compounds **5** and **6**. As a result of the β-effect of the C(6) and C(14) keto groups, the methine resonances at C(5), C(9), and C(13) in compound **7** have moved downfield as expected. The quaternary carbons at C(4), C(7), C(8), and C(11) in **7** are also shifted accordingly in comparison with dictyocarpinine.

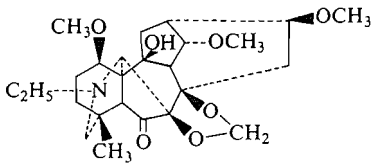
Assignments for Deltaline (8), Deltamine (9), and 6-Dehydrodeltaline (10)

Deltaline, also known as eldeline, was isolated as one of the minor alkaloids of *D. glaucescens*.[1] Previously deltaline had been isolated from several *Delphinium* species and the structure was established (9) as **8** on the basis of chemical correlation with lycoctonine. Compounds **9** and **10** were prepared by standard procedures.[1] The chemical shift assignments for compounds **8** to **10** are made by correlation with the earlier described ^{13}C nmr spectra of dictyocarpine and its derivatives. These data indicate that compounds **8**, **9**, and **10** are similar to **1**, **3**, and **6**, respectively, except for the presence of the methoxyl group at C(14) instead of the

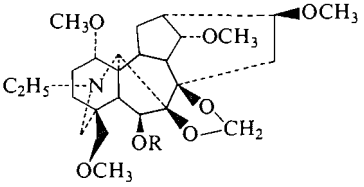
Can. J. Chem. Downloaded from www.nrcresearchpress.com by 210.87.254.6 on 09/05/12
For personal use only.



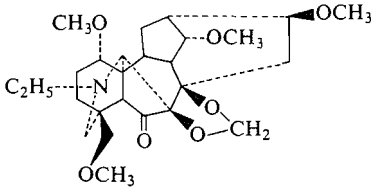
8 R = Ac Deltaline
9 R = H Deltamine



10



11 R = H Delcorine
12 R = Ac



13

hydroxyl group. The presence of the methoxyl group at C(14) in **8** to **10** results in the downfield shifts of C(13) and C(14) relative to compounds **1**, **3**, and **6**, respectively. The ^{13}C chemical shifts of deltaline, deltamine, and 6-dehydrodeltamine are in agreement with their respective structures **8**, **9**, and **10**.

Assignments for Delcorine (11), 6-Acetyldelcorine (12), and 6-Dehydrodelcorine (13)

Delcorine was isolated (10) from *D. corumbosum* by Yunusov and co-workers in 1973. On the basis of extensive chemical reactions and spectral studies, structure **11** was established for delcorine. Recently the isolation of 6-dehydrodelcorine from *D. iliense* was reported (8). Table 1 presents the ^{13}C chemical shifts and assignments for delcorine (**11**), 6-acetyldelcorine (**12**), and 6-dehydrodelcorine (**13**). Comparison of the ^{13}C nmr spectrum of delcorine with that of deltamine (**9**) reveals the absence of chemical shifts due to the C(10) tertiary hydroxyl group and the presence of some new chemical shifts due to the CH_2—O—CH_3 group at C(4). As expected, changes in chemical shifts of quaternary carbons C(4) and C(11), relative to deltamine, are evident. The singlets of C(4) (38.1 ppm) and C(11) (50.2 ppm) were shifted downfield and upfield, respectively, in delcorine. The chemical shifts of the ring A carbons changed also as expected because of the change in stereochemistry of the C(1) methoxyl group. The ^{13}C nmr spectrum of 6-acetyldelcorine indicated the presence of two more signals (21.6 and 170.0 ppm) of the acetoxy group than are present in delcorine. Acetylation of the secondary hydroxyl group at C(6) in **12** showed no substitution effect on the chemical shift of C(6) and very little effect on the neighbouring carbon atoms (ref. 11, pp. 149–150).

The new downfield resonance at 216.7 ppm in 6-dehydrodelcorine (**13**) is a singlet and can be assigned to C(6). The most noticeable changes are the large downfield shifts at C(4), C(5), and the methylenedioxy carbon, and the upfield shifts at C(7), C(8), C(10), and C(11) in compound **13**, relative to delcorine, caused by the presence of a five-membered ring ketone at C(6). All other assignments in the ^{13}C nmr spectra of compounds **11**, **12**, and **13** are in agreement with their structures.

This catalogue of ^{13}C chemical shifts of an important group of alkaloids should assist in the structure elucidation of newly isolated methylenedioxy and C(10) hydroxyl group-containing C_{19}-diterpenoid alkaloids.

Experimental

Carbon-13 nmr spectra were determined at 15.03 MHz in the Fourier mode using a JEOL FX-60 spectrometer in conjunction with a JEC-980 computer. The spectra were obtained at 30°C in deuteriochloroform solutions (which also provided the lock signal) with tetramethylsilane as an internal reference. Samples were contained in precision ground 5 mm od tubes. On the average a 5 μs pulse, corresponding to an approximate tilt angle of 45°, was employed. For the average spectral width of 4000 Hz, the delay between pulses was 2.5 s. Acquisition times averaged 2–24 h over 8K data points for concentrations of the order of 0.05–0.5 *M*. For off-resonance spectra this time was 8–48 h.

Details of the isolation of compounds **1**, **3**, and **8** and of the preparation of compounds **2–7**, **9**, **10**, **12**, and **13** will be reported at a later date.[1]

Acknowledgments

The authors thank Drs. M. S. Yunusov and S. Yu. Yunusov of the Institute of the Chemistry of Plant Substances, Academy of Sciences of the

Can. J. Chem. Downloaded from www.nrcresearchpress.com by 210.87.254.6 on 09/05/12
For personal use only.

Uzbek SSR, Tashkent for samples of delcorine, deltaline, and dictyocarpine.

1. S. W. PELLETIER and N. V. MODY. *In* The alkaloids. Vol. 17. *Edited by* R. H. F. Manske and R. Rodrigo. Academic Press, New York. 1979. Chapt. 1.
2. A. J. JONES and M. H. BENN. Can. J. Chem. **51**, 486 (1973).
3. S. W. PELLETIER and Z. DJARMATI. J. Am. Chem. Soc. **98**, 2626 (1976).
4. S. W. PELLETIER, N. V. MODY, R. S. SAWHNEY, and J. BHATTACHARYYA. Heterocycles, **7**, 327 (1977).
5. S. W. PELLETIER, N. V. MODY, and R. S. SAWHNEY. Can. J. Chem. **57**, 1652 (1979).
6. A. S. NARZULLAEV, M. S. YUNUSOV, and S. YU. YUNUSOV. Khim. Prir. Soedin. **8**, 498 (1972); **9**, 443 (1973).
7. S. W. PELLETIER, N. V. MODY, A. J. JONES, and M. H. BENN. Tetrahedron Lett. 3025 (1976); P. W. CODDING, K. A. KERR, M. H. BENN, A. J. JONES, S. W. PELLETIER, and N. V. MODY. Tetrahedron Lett. 127 (1980).
8. M. G. ZHAMIERASHVILI, V. A. TEL'NOV, M. S. YUNUSOV, and S. YU. YUNUSOV. Khim. Prir. Soedin. **13**, 836 (1977).
9. M. CARMACK, J. P. FERRIS, J. HARVEY, P. L. MAGAT, E. W. MARTIN, and D. W. MAYO. J. Am. Chem. Soc. **80**, 497 (1958).
10. A. S. NARZULLAEV, M. S. YUNUSOV, and S. YU. YUNUSOV. Khim. Prir. Soedin. **9**, 497 (1973).
11. J. B. STOTHERS. *In* Carbon-13 NMR spectroscopy. Academic Press, New York. 1972. pp. 174–175.

Can. J. Chem. Downloaded from www.nrcresearchpress.com by 210.87.254.6 on 09/05/12
For personal use only.

Photocyclization of aryl halides. Part I. 5-(2-Halogenophenyl)-1,3-diphenylpyrazoles; homolytic fission assisted by radical complexation

JAMES GRIMSHAW AND A. PRASANNA DE SILVA

Department of Chemistry, Queen's University, Belfast BT9 5AG, Northern Ireland

Received February 12, 1980

This paper is dedicated to the memory of Dr. Léo Marion

JAMES GRIMSHAW and A. PRASANNA DE SILVA. Can. J. Chem. **58**, 1880 (1980).

The photocyclization of 5-(2-halogenophenyl)-1,3-diphenyl pyrazoles proceeds efficiently with the exclusion of solvent participation hydrogen abstraction reactions. In a given solvent, the quantum yields of cyclization (ϕ) of Cl, Br, and I compounds show no correlation with carbon–halogen bond dissociation energies. In a series of solvents, ϕ varies smoothly with solvent viscosity and is independent of solvent polarity. The ϕ values are independent of triplet quenchers, air, intensity and wavelength of radiation, and reactant concentration. Photocyclization can be triplet sensitized at up to 80% of the direct reaction rate and the reactant triplet energies are about 65 kcal mol^{-1} while D_{C-Br} is 81 and D_{C-Cl} is 95 kcal mol^{-1}. A mechanism of homolytic fission assisted by radical complexation is proposed to accommodate the results. Photocyclization of the H- and MeO-substituted analogues proceeds inefficiently and with ϕ values dependent on solvent polarity. An electrocyclic mechanism is followed in these cases. The assisted homolysis model explains several anomalies in the field of aryl halide photochemistry.

JAMES GRIMSHAW et A. PRASANNA DE SILVA. Can. J. Chem. **58**, 1880 (1980).

La photocyclisation des (halogéno-2 phényl)-5 diphényl-1,3 pyrazoles se fait d'une manière efficace sans participation du solvant et sans élimination d'hydrogène. Dan un solvant donné, les rendements quantiques de cyclisation (ϕ) des composés du chlore, du brome et de l'iode n'indiquent pas de corrélation avec les énergies de dissociation de la liaison carbone–halogène. Dans une série de solvants, les valeurs de ϕ varient légèrement avec la viscosité du solvant et sont indépendantes de sa polarité. Les valeurs de ϕ sont indépendantes des inhibiteurs de triplets, de l'air, de l'intensité et de la longueur d'onde de la radiation et de la concentration des réactifs. La photocyclisation peut être sensibilisée par un triplet jusqu'à 80% de la vitesse de la réaction directe et les énergies des reactifs triplets sont d'environ 65 kcal mol^{-1} tandis que les valeurs de D_{C-Br} et D_{C-Cl} sont respectivement égales à 81 et à 95 kcal mol^{-1}. Pour expliquer ces résultats, on propose un mécanisme de scission homolytique assistée par une complexation radicalaire. La photocyclisation des analogues ayant des substituants H ou MeO n'est pas efficace et dans ces cas les valeurs de ϕ dépendent de la polarité du solvant. Dans ces cas on a un mécanisme électrocyclique. Le modèle d'homolyse assistée explique plusieurs anomalies dans le domaine de la photochimie des halogénures d'aryles.

[Traduit par le journal]

Introduction

The intermolecular photochemical reaction of aryl iodides in benzene to give diphenyls has been known since 1961 (1). The related intramolecular photochemical cyclization of appropriately substituted aryl halides has been used extensively as a synthetic route since the early work of Kupchan and Wormser (2) and of Kharasch and co-workers (3). Reviews devoted to the photochemistry of aryl halides (4) and the photocyclization reaction (5) discuss the early work and the photocyclization reaction continues to be of use in synthesis. As background to the present paper we will cite the synthesis of aporphine alkaloids by this route.

The synthesis of aporphine alkaloids by photocyclization of substrates bearing non-conjugated aromatic rings, e.g. **1** → **2**, proceeds in yields of 15–30% and photochemically induced homolytic cleavage of the carbon–halogen bond is assumed to be the first step (6). Photocyclization of substrates bearing conjugated aromatic rings, e.g. **3** → **5**, proceeds in alcoholic solvents in presence of a base and it has been speculated that these reactions proceed via an electrocyclic reaction and intermediates like **4** (7). There is no mechanistic investigation in the literature of an aryl halide cyclization to support either of these speculations. We have embarked on an examination of the photocyclization process, in view of its considerable value for synthesis, and a preliminary account of this paper has appeared (8).

The fission of a single bond is conceptually one of the simplest chemical reactions and if it occurs in a molecule which can be studied conveniently, a detailed mechanistic understanding can be expected to emerge. The photocyclizations of 5-(2-halogenophenyl)-1,3-diphenylpyrazoles, **6** → **7**, are conveniently studied and the results described here are applicable to improving the yield from other reactions. Compounds **6**, (X = H, OAc, OMe) also gave relevant mechanistic information. Much recent interest has been shown in general aryl halide photochemistry stemming from the presence of aryl chlorides as environmental contaminants and the quantitative information which is available is discussed in the final section dealing with our results and mechanistic discussion.

The pyrazoles **6**, (X = Cl, Br, I, OAc, and OMe)

0008-4042/80/171880-09$01.00/0

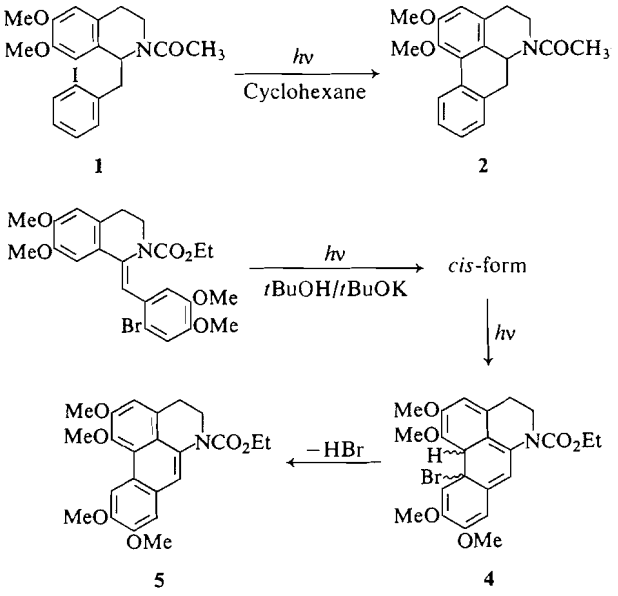
©1980 National Research Council of Canada/Conseil national de recherches du Canada

Can. J. Chem. Downloaded from www.nrcresearchpress.com by 210.87.254.5 on 09/05/12
For personal use only.

TABLE 1. Yields from the direct irradiation of **6** to give **7**

Compound **6**	Irradiation[a] period	Conversion (%) by hplc analysis	Isolated (%) yield of **7**
X = Cl	60 min	82	80
Br	55 min	90	84
I	85 min	88	83
Cl[b]	60 min	77	61
OAc	12.5 h	86	61
OMe	96 h	80	52

[a] 6×10^{-3} *M* solutions in methanol, N_2 atmosphere, PCQ-X1 Hg resonance lamp.
[b] This experiment was performed under air.



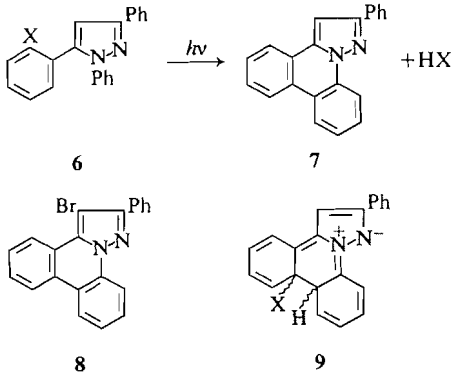
show similar uv, fluorescence, and phosphorescence spectra, and data for the chloro-compound are given in the Experimental. From the fluorescence and phosphorescence spectra in ethanol we can derive the singlet energy, E_S = 84 kcal mol^{-1} and the triplet energy, E_T = 65 kcal mol^{-1}. The ring system in the parent compound **6**, (X = H) can become more planar so that its spectral characteristics are somewhat different from those of the chloro-compound. The intensities of these luminescence phenomena reveal a moderate internal heavy atom effect for the bromo- and iodo-compounds and the phosphorescence lifetime ($\tau_P \sim$ 0.11 s) for **6** (X = H) suggests that the phenomenon is associated with a $^3\pi,\pi^*$ transition rather than a $^3n,\pi^*$ transition which would have a millisecond lifetime (9).

Preparative Photochemistry

The photoreaction **6** → **7** has been described (10). It is very clean when carried out with light of 254 nm wavelength in deoxygenated methanol and hplc monitoring shows the formation of one product **7** only. Checks showed that the monitoring procedure could separate the starting material, **6** (X = H), and **7**. The conversion and isolated yields recorded in Table 1 are limited by mechanical losses during the analytical procedure and isolation respectively. The presence of air does not alter the rate of formation of **7** or the conversion but gives rise to coloured side products. Yields of cyclized product **7** from the acetoxy- and methoxy-compounds are lower due to slower reaction and incomplete conversion.

Cyclization of **6** (X = Cl, Br, or I) could also be sensitized by benzophenone in benzene solution to give fair yields of **7** reported in Table 2. Cyclohexane could also be successfully used as solvent in this sensitized reaction but slow consumption of benzophenone then occurred due to its hydrogen abstraction reaction with solvent molecules. In contrast, cyclization of **6** (X = OAc or OMe) was not sensitized significantly, even prolonged irradiation gave only traces or none of **7** (by hplc) corresponding to maximum sensitized rates of 4% and 1% respectively of the direct reaction rates. Xanthone as sensitizer in methanol also failed to effect any significant cyclization in these two cases.

A second reaction occurred on prolonged sen-



Can. J. Chem. Downloaded from www.nrcresearchpress.com by 210.87.254.5 on 09/05/12
For personal use only.

Can. J. Chem. Downloaded from www.nrcresearchpress.com by 210.87.254.5 on 09/05/12
For personal use only.

TABLE 2. Yields from the benzophenone sensitized irradiation of **6** to give **7**

Compound **6**	Irradiation[a] period (min)	Isolated (%) yield of **7**
X = Cl	100	66
Br	90	77
I	130	69
Cl[b]	60	70

[a]1 to 6 × 10^{-3} *M* solutions of **6** and benzophenone in benzene, nitrogen atmosphere, TQ-150P medium pressure Hg lamp with Pyrex and $BiCl_3$ filters ($\lambda > 350$ nm).
[b]Cyclohexane was used as solvent.

sitized irradiation of **6** (X = Br), particularly using xanthone as sensitizer in methanol, and a new product appeared at the expense of **7**. On the basis of its molecular formula and uv spectrum, the new product appeared to be a bromo-substitution product of **7** and indeed it was readily obtained by bromination of **7**. Simple pyrazoles are readily brominated on the 4-position of the pyrazole ring (e.g. ref. 11) so this product is assigned structure **8**. Its mass spectrum shows an abundant fragment at *m/e* 190 ($C_{14}H_8N$) which is also present in the mass spectrum of **7** and corresponds to the loss of PhCN and either Br or H from the molecular ion by breakup of the pyrazole ring. In the nmr spectrum of **7** the line due to the pyrazole ring proton lies under the aromatic proton envelope. Bromination of **7** causes one aromatic proton resonance to move 0.5 ppm downfield and appear as the X-part of an ABX system, which is consistent with structure **8** for the product, and such long range deshielding effects of a halogen atom are well documented (12).

Oxidative photocyclization of **6** (X = H) failed to yield **7** in any isolable quantity under a variety of conditions, though hplc and uv monitoring revealed the appearance of **7** at a slow but finite rate (Table 5). This rate of appearance is faster by a factor of 5 in methanol than in cyclohexane which is compatible with a dipolar electrocyclic intermediate **9** (X = H). This point will be amplified in connection with **6** (X = OMe). However the subsequent bimolecular oxidation step by O_2 and I_2 is also slow, which means that the overall reaction will be polarity dependent to only a moderate degree.

Excluding the parent heterocycle, in all of the above cyclization experiments no **6** (X = H) could be detected as a product (0.2% conversion could have been detected) at any stage of the reactions. Such side reactions brought about by hydrogen abstraction from the solvent are known to compete with some photocyclizations[1] and are believed to arise because phenyl σ-radicals are reaction intermediates.

The photochemistry of aryl halides in the presence of a dialkylaniline as light absorber has been studied (14). Reaction occurs via an exciplex between the excited dialkylaniline and the aryl halide, with electron transfer from the dialkylaniline to form the aryl halide radical-anion, which decomposes with carbon–halogen bond fission to give the aryl σ-radical and halide ion. Application of this method using diethylaniline as light absorber gave exclusive cyclization from **6** (X = Cl). However, since E_T for diethylaniline (15) is 69 kcal mol^{-1} and is greater than the pyrazole triplet energy, reaction could be due to energy transfer sensitization and electron transfer may not occur in this case.[2]

Photochemical Kinetics
Results and Mechanistic Discussion

The effect of variables on the quantum yield (ϕ) for the formation of **7** from **6** was examined.

Substrate Concentration, Irradiation Intensity

The insensitivity of ϕ (see Table 3) to a twenty-fold change in concentration of **6** (X = Cl, Br, or I) confirms the intramolecular nature of the cyclization at its rate determining stages. All quantum yields are reproducible to a maximum error of ±10% but the figures are dependent on whether apparatus A or B, whose illumination conditions are very different (see Experimental), was used. Moderate changes of irradiation intensity cause

TABLE 3. 254 nm Irradiation of aerated solutions of **6** in methanol to give **7** at 35°C using apparatus B

	ϕ, Group X =		
Concentration (*M*)	Cl	Br	I
4.0×10^{-3}	0.51	0.63	0.35
1.0×10^{-3}	0.52	0.65	0.35
2.0×10^{-4}	0.48	0.59	0.34

TABLE 4. Effect of radiation intensity on ϕ at 354 nm for the conversion of **6** to **7** in methanol under nitrogen at 25°C using apparatus A

	ϕ, Group X =		
Intensity absorbed 10^5 E L^{-1} min^{-1}	Cl	Br	I
9.6	0.53	0.54	0.31
3.2	0.52	0.52	0.32
1.63	0.47	0.48	0.30
0.70	0.51	0.51	0.28

[1]For examples of exclusive hydrogen abstraction in some hydrogen donor solvents see ref. 13.

[2]The fluorescence of diethylaniline is quenched by added **6** (X = Cl), indicating that at least part of the reaction proceeds via singlet quenching by electron transfer.

TABLE 5. 254 nm Irradiation of aerated $4 \times 10^{-3} M$ solutions of **6** to give **7** at 35°C using apparatus A

Solvent	η(35°C)[a] (cP)	Z[b]	φ, Group X = Cl	Br	I	OAc	OMe	H
Hexane	0.28	30.9	0.38	0.45	0.35			
Methanol	0.49	55.5	0.33	0.42	0.27	0.015	0.0032	0.0008[d]
Cyclohexane	0.80	31.2	0.34	0.40	0.21	0.011[c]	<0.0001	
Dioxan	1.0	36.0			0.20			
tert-Butyl alcohol	3.0	43.9	0.21	0.20	0.12	0.009[c]	<0.0001	
Ethane-1,2-diol	12	56.3	0.09	0.09	0.021	0.0042	0.0041	

[a]Interpolated from J. A. Riddick and W. B. Bunger. Organic solvents. 3rd ed. Wiley, New York. 1970.
[b]Solvent polarity parameter (C. Reichardt. Angew. Chem. 18, 98 (1979).
[c]Concurrent formation of a very minor side product.
[d]In the presence of $4 \times 10^{-5} M$ iodine.

TABLE 6. 254 nm Irradiation of $4 \times 10^{-3} M$ solutions of **6** in cyclohexane under N_2 to give **7** using apparatus A. Influence of additives

Additive	Additive conc. (M)	E_T[a] (kcal mol^{-1})	φ, Group X = Cl	Br	I
None			0.32	0.45	0.22
Oxygen		22.5	0.34	0.40	0.21
Piperylene	4.0×10^{-2}	59.2	0.36	0.44	0.21
Benzophenone[b]	1.0×10^{-2}	68.5	0.29	0.33	0.17
Triphenylene[b]	4.0×10^{-3}	66.5	0.21	0.30	0.12
Phenanthrene[b]	6.0×10^{-3}	62.0	−0.02[c]	0.00[c]	0.01[d]

[a]These and other necessary sensitizer data: S. L. Murov. Handbook of photochemistry. Dekker, New York. 1973.
[b]Due to practical considerations involving the uv monitoring of 7, the sensitizer concentrations were such that definite fractions of radiation were directly absorbed by **6**. These were calculated and allowed for to yield the sensitized φ values given. Fractions of radiation absorbed by benzophenone, triphenylene, and phenanthrene were 0.63, 0.74, and 0.67 respectively. The quantum yields of intersystems crossing of the sensitizers were also taken into account.
[c]±0.02.
[d]±0.01.

negligible alteration in φ values (Table 4), and the results from apparatus A or B show only 50% variation in φ even though I_{abs} varies by a factor of 2000.

Substituent X and Solvent

The results are summarized in Table 5. Contrary to expectations based on a simple homolysis mechanism, the three halogen compounds **6** (X = Cl, Br, or I) have comparable φ values in a given solvent even though the bond strengths D_{C-X} vary considerably. However, a further small increase in D_{C-X} for the compounds **6** (X = OAc and OMe) causes a precipitous drop in φ. A further observation is the smooth correlation of φ with solvent viscosity for compounds **6** (X = Cl, Br, I, or OAc) even though the solvents differ widely in polarity. This suggests a reaction involving non-polar intermediates and a step involving an increase in effective volume and/or a separation of radical species (16). In contrast, the φ values for compound **6** (X = OMe) with the highest D_{C-X} show a strong polarity (as opposed to viscosity) sensitivity. Thus a discontinuous change in the photocyclization mechanism occurs at high values of D_{C-X}.

Additives Including Energy-transfer Agents

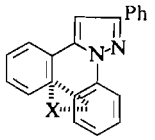
Table 6 gives data for the influence or triplet quenchers on φ. For compounds **6** (X = Cl, Br, or I), φ is unaltered by the presence of low energy triplet quenchers, oxygen or piperylene. Thus the direct reaction proceeds via unquenchable excited states which eliminates T_1 as a possible intermediate state. Evidence given below shows that the T_1 can be quenched. Reactive free radical intermediates such as phenyl σ-radicals which can be diverted from cyclization by reaction with oxygen (17) or alkenes (18) can also be excluded.

The cyclization can be efficiently triplet sensitized and forced to proceed via T_1 even though the direct unsensitized reaction avoids this state. The T_1 state is quenched reversibly by energy-transfer agents as evidenced by the dependence of the value of φ for the sensitized reaction on the sensitizer E_T (19). A further observation is the similarity of the sensitized and unsensitized φ values; the former is 80% of the latter when high energy triplet donors are used, which suggests that these two reaction routes may have some common intermediate states.

Can. J. Chem. Downloaded from www.nrcresearchpress.com by 210.87.254.5 on 09/05/12
For personal use only.

Can. J. Chem. Downloaded from www.nrcresearchpress.com by 210.87.254.5 on 09/05/12
For personal use only.

Another important point to emerge from these results is the fact that the input of 65 kcal mol^{-1} (E_T of **6**) is sufficient to cleave effectively C—Cl, C—Br, and C—I bonds of D_{C-X} 95, 81, and 64 kcal mol^{-1} respectively (20). This rules out a simple homolysis mechanism, at least in the cases of the chloro- and bromo-compounds and shows the presence of some factor which provides a much lower energy path for cyclization. This factor cannot efficiently accommodate the cleavage of C—OAc and C—OMe bonds where the bond strength (21) is approximately 98 kcal mol^{-1}.



10

Because of the solvent effects mentioned previously, this factor is related in some way to simple homolysis. We believe this factor to be a type of anchimeric assistance whereby the l-phenyl ring can, through its π-cloud, complex the developing radical centres in the stretching C—X bond and thus lower the transition state energy for reaction. Halogen atoms are electron deficient species with high electron affinities (22) and their complexation by aromatic molecules is well known from photohalogenation (23) and flash photolysis (24) studies. Such complexation has been considered important in several photochemical problems (25), though these reactions were subsequently reinterpreted along different lines (26). Anchimeric assistance to bond homolysis by radical complexation is not a new concept, having been documented twenty years ago in thermal free radical chemistry by product analysis and activation parameters (27). These principles can be applied to the photochemistry of aryl halides, and the transition state, or intermediate, in the cyclization of **6** will therefore be represented by **10**.

The mechanism affords an explanation why, in a given solvent, the chloro-compound cyclizes faster than the iodo-compound even though $D_{C-Cl} > D_{C-I}$, since the transition state **10** is reached earlier along the reaction coordinate for X = Cl than for X = I due to the higher electron affinity of the chlorine atom (22). Even though D_{C-Cl} is high, only a small fraction of that energy is required to reach the transition state. The moderate efficiency for cyclization of **6** (X = OAc) seems to be the limit of rate enhancement by assistance since ϕ has dropped markedly from the values obtained with the halogen compounds. At a small further increase of D_{C-X} in **6** (X = OMe), the mechanism suffers a discontinuous change.

Cyclization of **6** (X = OMe) would therefore involve relatively high energy reaction intermediates. Coupling this deduction with the solvent polarity effect seen in Table 3 suggests the dipolar intermediate **9** (X = OMe) arising from an electrocyclic reaction as the reaction intermediate. The strong polarity effect is observed because formation of **9** (X = OMe) is probably the rate determining stage and subsequent elimination of methanol is rapid. Attempts to trap this 1,3-dipolar species in the case of **9** (X = H) with dimethyl acetylenedicarboxylate gave inconclusive results due to complications of light absorption by the dipolarophile and the possibilities for formation of 2π + 2π adducts with **9** (X = H) by analogy with reactions of furans (28).

Several examples (29) of photocyclization with loss of the elements of methanol are known and in each of these cases the corresponding oxidative photocyclization of the parent compound (3, 30) can be brought about. Photocyclization with loss of methanol is assumed in the literature to involve an electrocyclic intermediate as for our example but no mechanistic evidence has previously been brought forward to support this view.

Wavelength of Irradiation

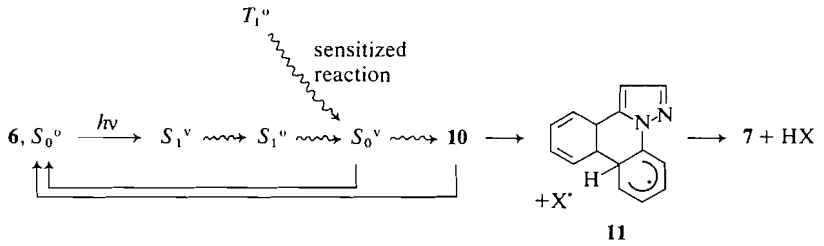
The observed invariance, within experimental error, of ϕ values with irradiation wavelength (Table 7) renders unlikely the possibility of a mechanism of predissociation into a repulsive state involving σ* orbitals from the higher vibrational levels of S_1. This conclusion holds within the range of energies studied which covered the whole absorption band. It is characteristic of such a mechanism that ϕ changes when the molecule is excited to an S_1^v level close to the crossing point into the dissociative state (31).

This conclusion coupled with those reached from the sensitization studies leads to the suggestion that

TABLE 7. Wavelength dependence of ϕ for irradiation of 4×10^{-3} *M* solutions of **6** in aerated methanol to give **7** using apparatus B

	ϕ,[a] Group X =		
Wavelength (nm)	Cl	Br	I
254	0.51	0.63	0.35
265	0.54	0.63	0.36
280	0.63	0.66	0.33
302	0.57	0.63	0.35

[a]A quinine sulphate quantum counter was used to check equal intensity of irradiation, ref. 49.



SCHEME 1

a vibrationally excited ground state is the reactive excited state. The role of S_0^v states in general aryl halide photochemistry has been debated in the literature (32), but we believe that this state can lead to carbon–halogen bond weakening within a single vibrational period. The results from sealed tube thermolyses of **6** (X = Br and OMe) support this idea. The bromo-compound gives a 5% yield of **7** after 48 h at 370°C, whereas the methoxy-compound gives no detectable amounts of **7** after similar treatment. Because the two compounds show this different behaviour, a thermal electrocyclic mechanism is unlikely and we can conclude that assisted homolysis of **6** (X = Br) via transition state **10** is possible at 370°C. In contrast, thermal homolysis of bromobenzene derivatives requires temperatures in excess of 700°C (33).

Further Mechanistic Discussion

The deductions made thus far enable us to propose a reasonable mechanism for the transformation of **6** (X = Cl, Br, or I) to **7** as given in Scheme 1. The species **10** is given the status of a reaction intermediate where the π-donor aromatic ring complexes the halogen atom and possibly also the formed carbon σ-radical. This complexed radical may relax to **6** or proceed to **11**. An alternative view is that species **10** is a transition state which continues along the reaction path to give **11** as a caged radical pair which may either revert to **6** or form a separated radical pair and eventually give **7**.

The lack of correlation between fission rate and bond strength was noted for compounds **6** (X = Cl, Br, I) and a similar phenomenon has been reported for the photoreduction of other aryl halides (34). Comment has also been made in the literature on the homolytic fission of bonds when the excited state energy is less than the bond strength in the cases of some halogeno-biphenyls (35, 36) and naphthalenes (37, 38). This anomaly was explained by assuming intermolecular exciplex formation between an excited and a ground state molecule of the substrate with subsequent electron transfer to give a radical-ion pair and then decomposition of the radical-anion to generate aryl radicals. As a test for this mechanism, the rate of carbon–halogen bond cleavage was enhanced on addition of triethylamine which functioned as an alternative electron donor to the excited aryl halide molecule.

For our particular compounds **6** (X = Cl, Br, or I) the exciplex model is inapplicable on several grounds. First, the quantum yield for this model which involves radical-ion pair formation by complete electron transfer is dependent on the solvent polarity and greatest in polar solvents. Quantitative information on this solvent dependence is available for the photoreduction of 4-chlorobiphenyl in the presence of triethylamine (35). For our halogeno-compounds, ϕ is independent of solvent polarity. Also, ϕ is independent of concentration, so any electron transfer must be intramolecular. The phosphorescence emissions of the halogen compounds are not red shifted nor are they weak with respect to **6** (X = H) as would be expected if a triplet exciplex reaction involving the C—X bond was present under the observation conditions. Geometric restrictions do not allow the sandwich arrangement usually, though not necessarily (39), attained in π,π type exciplexes. Finally, contrary to our observations, radical-anions from iodobenzenes dissociate faster than those from bromo- and chlorobenzenes (40).

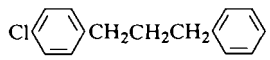
From a general viewpoint, the choice between the electron transfer and the assisted homolysis models may depend on the molecule under consideration. Those molecules with extensive delocalization such as fused aromatic hydrocarbons have redox properties favorable to the electron transfer model and bond fission can occur in spite of their low excited state energies. In contrast benzene systems show a bias towards the homolysis model and their higher excited state energy is a key factor. Proponents of the exciplex, electron transfer model have recently demonstrated that it cannot account for the photoreduction of chlorobenzene and that the compound **12**, which can be demonstrated spectroscopically to form an intramolecular exciplex, has a cleavage rate lower than that for chlorobenzene (41).

Early workers (42) noted a rate enhancement of

Can. J. Chem. Downloaded from www.nrcresearchpress.com by 210.87.254.5 on 09/05/12
For personal use only.

Can. J. Chem. Downloaded from www.nrcresearchpress.com by 210.87.254.5 on 09/05/12
For personal use only.

the photolysis of 4-bromobutyrophenone by potential quenchers, pentene and piperylene, and more recently quantitative measurements have been made for a similar rate enhancement observed with chloronaphthalenes (37, 43). These results



12

(37, 43) have been interpreted in terms of the exciplex, electron transfer model where the added quencher acts as an electron donor. Quenchers of the diene type have polarizable π-clouds and we therefore make the suggestion that rate enhancement can be the result of the assisted homolysis model with intermolecular complexation between the diene and the developing radical centres of the excited aryl halide.

A further anomaly which can be explained on the assisted homolysis model is, for example, the non-identity of the electro- and photoreduction products from **13** (44). Whereas the photogenerated primary product is a type of radical pair, one partner of which is the electron deficient bromine atom, the electro-generated primary product is a radical-anion which decomposes to a phenyl radical and a bromide ion where the electron deficiency is much less. Thus complexation effects would be important in the photochemistry but not in the electrochemistry of **13**, which would therefore lead to different products.

Finally, mention must be made of reactions which lead to halogen atom dependent product distributions, sometimes resulting in high product specificities. An extreme example, which was explained in terms of thermodynamic and kinetic control of strained intermediates, is the photolysis of **14** (45). The product distribution is understandable in terms of a transition state analogous to **10** which is reached early when X = Cl, leading to predominant cyclization, but late for the weak complex from X = I. If the strain energy associated with complexation is large as in this case, this transition state may well be nonexistent for X = I, so that simple homolysis of a weak bond determined by the excited state energy leads to free radical derived products, competing cyclization, and reaction with solvent.

In conclusion we wish to emphasize the importance of homolysis assisted by radical complexation in the photochemistry of aryl halides and are of the opinion that this concept may be relevant to other photochemical systems. Experiments to test the scope and applicability of the assisted fission model are in progress.

Experimental

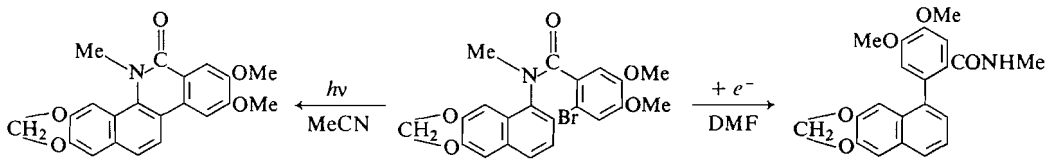
Irradiation Apparatus

It was impractical to use a single irradiation apparatus for photochemical kinetic measurements. Two basic systems were used with modifications, as required, for the study with each variable. Due to the differences between these systems, the results obtained on one cannot be strictly compared with those obtained on the other.

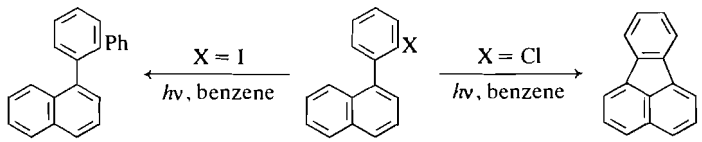
Apparatus A

The light source was a 72 W low pressure mercury arc lamp (PCQ-Xl from Ultra-Violet Products Inc.) consisting of four independent circular units which allowed the insertion of a quartz photolysis tube with its quartz filter jacket along the cylindrical cavity. Homogeneity of the photolyte was attained by magnetic stirring and gas bubbling. The filter (46) was a 0.6 cm path of an aqueous solution of $CoSO_4 \cdot 7H_2O$ (117 g L^{-1}) and $NiSO_4 \cdot 6H_2O$ (333 g L^{-1}) and gave 254 nm irradiation of 94% purity from the above source. After preirradiation for 1 h this filter maintained its transmittance indefinitely. The experimental arrangement was completed by surrounding the lamps with a cylinder and a cone of aluminium which acted as a reflector and helped to maintain a constant photolyte temperature of 35 ± 2°C. Light flux was determined by uranyl oxalate actinometry (47) (0.01 *M* in UO_2^{2+} and 0.05 *M* in $C_2O_4^{2-}$) before and after the kinetic runs. Apparent intensities (flux/photolyte volume) of ca. 4×10^{-4} E L^{-1} min^{-1} were obtained.

The data in Table 4 were obtained using a single lamp of the PCQ-Xl source with interposed gauze cylinders varying in



13



14

Can. J. Chem. Downloaded from www.nrcresearchpress.com by 210.87.254.5 on 09/05/12
For personal use only.

number and mesh size. The photolyte temperature was 25 ± 3°C and ferrioxalate actinometry (48) was necessary.

Apparatus B

The output of a 125 W medium pressure mercury arc lamp (Phillips) was focussed onto the entrance slit of a monochromator using a quartz lens. The photolyte was contained in a 1 cm square quartz cell which could be reproducibly repositioned. The intensity was monitored before and after kinetic runs by (*a*) a quantum counter (49) constructed from a 1 cm quartz cell containing quinine sulphate (4 g L^{-1}) in *N*-sulphuric acid, the output falling on a photomultiplier tube, and (*b*) ferrioxalate actinometry. The irradiation intensities at different wavelengths were equalized to about 1×10^{-7} E L^{-1} min^{-1} by adjusting the monochromator slit width. There was no facility for stirring the photolyte but reactions were slow enough (low I_{abs}) for diffusion to prevent the establishment of concentration gradients.

Quantum Yields

These were calculated from measurements on the appearance rate of the product **7** at low conversions for optically dense solutions of **6**, and actinometry. With apparatus A, the large photolyte volume (100 mL) permitted withdrawal of aliquots and the construction of concentration–time profiles from which the initial gradient, constant up to 15% conversion, was obtained. With apparatus B, the total photolyte volume was analysed after 1% conversion. Large rate reductions result at high conversions due to screening and quenching by the more conjugated product.

All data are reproducible within the limits of error, ±10% except where otherwise stated.

The ultraviolet absorption of **7** shows sharp vibronic bands at long wavelengths where **6** has negligible absorption. The longest wavelength band was used to follow the appearance of **7**. Though **7** may be first formed as the hydrohalide salt, atmospheric moisture causes hydrolysis to the free base. Solutions of **7** in methanol show no change in uv spectrum when made $10^{-3}M$ in hydrochloric acid.

Preparation of Pyrazoles (6)

These were prepared from the chalcone and phenylhydrazine and then oxidation of the pyrazoline with lead-(iv) acetate (10). The following pyrazoles are new and were crystallized from ethanol: 5-(2-methoxyphenyl)-1,3-diphenylpyrazole, mp 142–143°C; *Anal.* calcd. ($C_{22}H_{18}N_2O$): C 81.0, H 5.6, N 8.6%; found: C 81.2, H 5.6, N 8.4; 5-(2-acetoxyphenyl)-1,3-diphenylpyrazole, mp 98–100°C; *Anal.* calcd. ($C_{23}H_{18}N_2O_2$): C 78.0, H 5.3, N 7.9%; found: C 78.0, H 5.3, N 8.0; 5-(2-iodophenyl)-1,3-diphenylpyrazole, mp 116–117°C; *Anal.* calcd. ($C_{21}H_{15}IN_2$): C 59.7, H 3.6, N 6.6%; found: C 59.8, H 3.6, N 6.7.

5-(2-Chlorophenyl)-1,3-diphenylpyrazole in cyclohexane showed λ_{max}: 259 nm (ε 26 000) and in ethanol at 80 K fluorescence λ_{max}: 343 nm, phosphorescence λ_{max}: 446 nm. 1,3,5-Triphenylpyrazole in cyclohexane showed λ_{max}: 255 nm (ε 31 000) and in ethanol at 80 K fluorescence λ_{max}: 347 nm, phosphorescence λ_{max}: 463 nm.

Preparative Photochemistry

Conversion of 6 to 7

The pyrazole **6** (0.66 mmol) in methanol (100 mL) was irradiated with the PCQ-X1 lamp under nitrogen until tlc or hplc monitoring indicated absence of **6**. The photolyte was then evaporated and the residue recrystallized from ethanol to yield **7**, mp 152–154°C with a solid phase change at 140–142°C (lit. (10) mp 151–153°C); ms *m/e*: M^+ 294 (100%), 293 (20%), 190 (16, $M - H - PhCN$), 147 (10, M^{2+}). For hplc analysis (Spectraphysics SP 3500 instrument) aliquots were evaporated, dissolved in benzene, and injected on a 250 mm column of Spherisorb silica (S5 W) eluted with dichloromethane–cyclohexane (2:1, by volume), flow rate 0.8 mL min^{-1}, uv monitoring at 260 nm. Thin layer chromatography was carried out on silica plates with the same solvent system. No **6** (X = H) was detected by hplc and the system could separate this from all the starting pyrazoles.

Benzophenone Sensitized Conversions

Radiation with $\lambda > 350$ nm, not absorbed by **6**, was obtained by filtering the output from a 150 W medium pressure mercury arc (TQ-150, Hanau) through a 0.2 cm path of Pyrex glass and 0.5 cm path of $2.5 \times 10^{-3}M$ bismuth chloride in $6M$ hydrochloric acid (50). The filtered source was immersed in a solution (100 mL) of 1 to $6 \times 10^{-3}M$ pyrazole **6** and an equimolar amount of benzophenone in benzene under nitrogen. When tlc indicated complete reaction, the mixture was evaporated and crystallized from ethanol to yield **7**, mp 152–154°C.

Xanthone Sensitized Conversion of 6 (X = Br) to 7

The bromopyrazole (125 mg, 0.3 mmol) and xanthone (130 mg, 0.6 mmol) in methanol (500 mL) was irradiated as in the previous paragraph for 10 min, after which tlc showed signs of commencement of consecutive reactions. The mixture was made alkaline by addition of triethylamine (1 mL) and evaporated to yield a solid which was subjected to preparative tlc (silica, elution with dichloromethane–cyclohexane 2:1 by volume) to give, after crystallization from methanol, **7** as needles (58 mg, 58%), mp. 152–153°C.

Upon repetition of the experiment with an irradiation time of 30 min, tlc showed the disappearance of **7** with the formation of **8**. The photolyte was evaporated to dryness and chromatographed on a silica column with the above eluant to retain the xanthone. Elution and then crystallization from benzene – light petroleum (bp 40–60°C) afforded *3-bromo-2-phenylpyrazolo[1,5-f] phenanthridine* as needles (80 mg, 64%), mp 176–178°C; ms *m/e*: M^+ 374 and 372 (100%), 294 (20), 293 (35, $M^+ - Br$), 292 (28), 190 (65, $M^+ - Br - PhCN$). *Anal.* calcd. ($C_{21}H_{13}BrN_2$): C 67.6, H 3.5, N 7.5%; found: C 67.6, H 3.7, N 7.3.

Compound **7** (30 mg, 0.1 mmol) in refluxing methanol (10 mL) was treated dropwise with bromine (16 mg, 0.1 mmol) in methanol (5 mL) with instant decolorization. A colorless solid precipitated on cooling and crystallized from benzene – light petroleum to give **8** (23 mg), mp and mixture mp 176–178°C.

Photolysis of 6 (X = Cl) in Presence of Diethylaniline

A solution of the chloropyrazole (110 mg, 0.33 mmol), diethyl aniline (500 mg, 3.3 mmol), and triethylamine (330 mg, 3.3 mmol) in methanol (150 mL) was irradiated under nitrogen with radiation of $\lambda > 300$ nm obtained by filtering the TQ-150 lamp emission through 0.2 cm Pyrex glass. The hplc monitoring showed no detectable **6** (X = H) at any stage and formation of **7** was rapid. After 30 min irradiation the photolyte was evaporated, the residue dissolved in benzene, washed with hydrochloric acid and water, dried ($MgSO_4$), and evaporated to yield **7**, needles from ethanol, mp 153–154°C (55 mg, 56%).

Thermolysis of 6 (X = Br and OMe)

The bromopyrazole (250 mg) in a sealed tube was kept at 370°C for 48 h. The resulting black mass was dissolved in chloroform, filtered through a short silica column, and chromatographed on silica plates with chloroform elution to yield **7** (10 mg, 5%) as needles, mp 151–153°C. No reaction of **6** (X = Br) occurred at 180°C. An identical experiment with **6** (X = OMe) (100 mg) at 370°C gave no evidence for the formation of **7** by tlc or uv spectroscopy.

Can. J. Chem. Downloaded from www.nrcresearchpress.com by 210.87.254.5 on 09/05/12
For personal use only.

Acknowledgement

One of us (A.P. de S.) thanks the Queen's University of Belfast for financial support.

1. W. WOLF and N. KHARASCH. J. Org. Chem. **26**, 283 (1961); N. KHARASCH and L. GÖTTLICH. Angew. Chem. **74**, 651 (1962).
2. S. M. KUPCHAN and H. C. WORMSER. J. Org. Chem. **30**, 3792 (1965).
3. B. S. THYAGARAJAN, N. KHARASCH, H. B. LEWIS, and W. WOLF. J. Chem. Soc. Chem. Commun. 614 (1967).
4. R. K. SHARMA and N. KHARASCH. Angew. Chem. Int. Ed. Engl. **7**, 36 (1968); P. G. SAMMES. *In* Chemistry of the carbon–halogen bond. *Edited by* S. Patai. Wiley, New York. 1972. p. 747.
5. T. KAMETANI and K. FUKUMOTO. Acc. Chem. Res. **5**, 212 (1972).
6. S. M. KUPCHAN and R. M. KANOJIA. Tetrahedron Lett. 5353 (1966); J. L. NEUMEYER, K. H. OH, K. K. WEINHARDT, and B. R. NEUSTADT. J. Org. Chem. **34**, 3786 (1969); S. M. KUPCHAN, J. L. MONIOT, R. M. KANOJIA, and J. B. O'BRIEN. J. Org. Chem. **36**, 2413 (1971).
7. M. P. CAVA, M. J. MITCHELL, S. C. HAVLICEK, A. LINDERT, and R. J. SPANGLER. J. Org. Chem. **35**, 175 (1970); M. P. CAVA, P. STERN, and K. WAKISAKA. Tetrahedron, **29**, 2245 (1973); M. P. CAVA and S. S. LIBSCH. J. Org. Chem. **39**, 577 (1974); L. CLEAVER, S. NIMGIRAWATH, E. RICHIE, and W. C. TAYLOR. Aust. J. Chem. **29**, 2003 (1976).
8. J. GRIMSHAW and A. P. DE SILVA. Chem. Commun. 193 (1979).
9. M. KASHA. Radiat. Res. Suppl. **2**, 243 (1960).
10. W. J. BEGLEY, J. GRIMSHAW, and J. TROCHA-GRIMSHAW. J. Chem. Soc. Perkin Trans. I, 2633 (1974).
11. E. G. BRAIN and I. L. FINAR. J. Chem. Soc. 2435 (1958).
12. A. HUITRIC, W. C. CLARKE, K. LEIGH, and D. C. STAIFF. J. Org. Chem. **27**, 715 (1962); R. C. FORT, G. W. H. CHEESEMAN, and E. C. TAYLOR. J. Org. Chem. **29**, 2440 (1964).
13. W. CARRUTHERS and N. EVANS. J. Chem. Soc. Perkin Trans. I, 1523 (1974); P. W. JEFFS, J. F. HANSEN, and G. A. BRINE. J. Org. Chem. **40**, 2883 (1975).
14. T. TOSA, C. PAC, and H. SAKURAI. Tetrahedron Lett. 3635 (1969); Bull. Chem. Soc. Jpn. **45**, 1169 (1972); T. LATOWSKI. Z. Naturforsch. Teil A, **23**, 1127 (1968); M. GRODOWSKI and T. LATOWSKI. Tetrahedron, **30**, 767 (1974); O. M. SOLOVEICHIK, V. L. IVANOV, and M. G. KUZ'MIN. Zh. Org. Khim. **12**, 859 (1976).
15. R. S. DAVIDSON and M. SANTHANAM. J. Chem. Soc. B, 1151 (1971).
16. D. GEGIOU, K. A. MUSZKAT, and E. FISCHER. J. Am. Chem. Soc. **90**, 12 (1968); D. BOOTH and R. M. NOYES. J. Am. Chem. Soc. **82**, 1868 (1960); W. A. PRYOR and K. SMITH. J. Am. Chem. Soc. **92**, 5403 (1970).
17. G. A. RUSSELL and R. F. BRIDGER. J. Am. Chem. Soc. **85**, 3765 (1963).
18. C. WALLING. Free radicals in solution. Wiley, New York. 1957. Chapt. 3.
19. P. S. ENGEL and B. M. MONROE. Adv. Photochem. **8**, 245 (1971); K. SANDROS. Acta Chem. Scand. **18**, 2355 (1964).
20. K. W. EGGER and A. T. COCKS. *In* Chemistry of the carbon–halogen bond. Part 2. *Edited by* S. Patai. Wiley, New York. 1973. p. 677.
21. R. C. WEAST (*Editor*). Handbook of chemistry and physics. CRC Press. 56th ed. 1975. F 231.
22. R. S. BERRY and C. W. REIMANN. J. Chem. Phys. **38**, 1540 (1963).
23. G. A. RUSSELL. J. Am. Chem. Soc. **79**, 2977 (1957); **80**, 4987 (1958).
24. S. J. RAND and R. L. STRONG. J. Am. Chem. Soc. **82**, 5 (1960); R. L. STRONG, S. J. RAND, and J. A. BRITT. J. Am. Chem. Soc. **82**, 5053 (1960); J. A. GROVER and G. PORTER. Proc. Roy. Soc. Ser. A, **262**, 476 (1961); R. E. BÜHLER. Helv. Chim. Acta, **51**, 1558 (1968).
25. M. A. FOX, W. C. NICHOLS, and D. M. LEMAL. J. Am. Chem. Soc. **95**, 8164 (1973); B. MILLIGAN, R. L. BRADOW, J. E. ROSE, H. F. HUBBERT, and A. ROE. J. Am. Chem. Soc. **84**, 158 (1962).
26. D. R. ARNOLD and P. C. WONG. J. Am. Chem. Soc. **99**, 3361 (1977); J. T. ECHOLS, V. T. C. HUANG, C. S. PARRISH, J. E. ROSE, and B. MILLIGAN. J. Am. Chem. Soc. **89**, 4081 (1967).
27. T. W. KOENIG and J. C. MARTIN. J. Org. Chem. **29**, 1520 (1964) and previous papers; D. B. DENNEY, R. L. ELLSWORTH, and D. Z. DENNEY. J. Am. Chem. Soc. **86**, 1116 (1964).
28. H. M. ROSENBERG and P. SERVE. J. Org. Chem. **33**, 1653 (1968).
29. Y. KANAOKA and K. ITOH. J. Chem. Soc. Chem. Commun. 647 (1973); R. G. F. GILES and M. V. SARGENT. J. Chem. Soc. Chem. Commun. 215 (1974); G. R. LENZ. J. Org. Chem. **39**, 2839 (1974); J. A. ELIX and D. R. MURPHY. Aust. J. Chem. **28**, 1559 (1975).
30. C. S. WOOD and F. B. MALLORY. J. Org. Chem. **29**, 3373 (1964); K. P. ZELLER and H. PETERSEN. Synthesis, 532 (1975).
31. N. J. TURRO, V. RAMAMURTHY, W. CHERRY, and W. FARNETH. Chem. Rev. **78**, 125 (1978).
32. E. J. BAUM and J. N. PITTS. J. Phys. Chem. **70**, 2066 (1966); G. E. ROBINSON and J. M. VERNON. J. Chem. Soc. C, 3363 (1971).
33. M. SZWARC and D. WILLIAMS. J. Chem. Phys. **20**, 1171 (1952).
34. J. T. PINHEY and B. D. G. RIGBY. Tetrahedron Lett. 1267 (1969).
35. M. OHASHI, K. TSUJIMOTO, and K. SEKI. J. Chem. Soc. Chem. Commun. 384 (1973).
36. N. J. BUNCE, S. SAFE, and L. O. RUZO. J. Chem. Soc. Perkin Trans. I, 1607 (1975).
37. L. O. RUZO, N. J. BUNCE, and S. SAFE. Can. J. Chem. **53**, 688 (1975).
38. N. J. BUNCE, P. PILON, L. O. RUZO, and D. J. STURCH. J. Org. Chem. **41**, 3023 (1976).
39. G. N. TAYLOR, E. A. CHANDROSS, and A. H. SCHIEBEL. J. Am. Chem. Soc. **96**, 2693 (1974); T. OKADA, T. FRYITA, M. KUBOTA, S. MASAKI, N. MATAGA, R. IDE, Y. SAKATA, and S. MISUMI. Chem. Phys. Lett. **14**, 563 (1972).
40. C. P. ANDRIEUX, C. BLOCMAN, J. M. DUMAS-BOUCHIAT, and J. M. SAVÉANT. J. Am. Chem. Soc. **101**, 3431 (1979).
41. N. J. BUNCE and L. RAVANAL. J. Am. Chem. Soc. **99**, 4150 (1977).
42. E. J. BAUM and J. N. PITTS. J. Phys. Chem. **70**, 2066 (1966).
43. L. O. RUZO and N. J. BUNCE. Tetrahedron Lett. 511 (1975).
44. W. J. BEGLEY and J. GRIMSHAW. J. Chem. Soc. Perkin Trans. I, 2324 (1977).
45. W. A. HENDERSON, R. LOPRESTI, and A. ZWEIG. J. Am. Chem. Soc. **91**, 6049 (1969).
46. J. G. CALVERT and J. N. PITTS. Photochemistry. Wiley, New York. 1966. p. 729.
47. W. G. LEIGHTON and G. S. FORBES. J. Am. Chem. Soc. **52**, 3139 (1930).
48. C. G. HATCHARD and C. A. PARKER. Proc. Roy. Soc. Ser. A, **235**, 518 (1956).
49. W. H. MELHUISH. J. Opt. Soc. Am. **52**, 1256 (1962).
50. H. E. ZIMMERMAN. Mol. Photochem. **3**, 281 (1971).

Can. J. Chem. Downloaded from www.nrcresearchpress.com by 210.87.254.40 on 09/05/12
For personal use only.

A stereospecific synthesis of napelline

SAT PAUL SETHI, KARNAIL S. ATWAL, RINALDO M. MARINI-BETTOLO, THOMAS Y. R. TSAI, AND KAREL WIESNER

Natural Products Research Center, University of New Brunswick, Fredericton, N.B., Canada E3B 5A3

Received January 31, 1980

This paper is dedicated to the memory of Dr. Léo Marion

SAT PAUL SETHI, KARNAIL S. ATWAL, RINALDO M. MARINI-BETTOLO, THOMAS Y. R. TSAI, and KAREL WIESNER. Can. J. Chem. **58**, 1889 (1980).

A simple and stereospecific synthesis of the triketolactam **15** is described. This compound has been previously converted to napelline **I**. The key step of the synthesis is the rearrangement of the "denudatine" intermediate **11** to the napelline derivative **12**. The denudatine skeleton was constructed by a stereospecific diene addition between the *o*-quinone acetal **4** and benzyl vinyl ether. It is expected that this last process will be capable of general application in the synthesis of complex compounds.

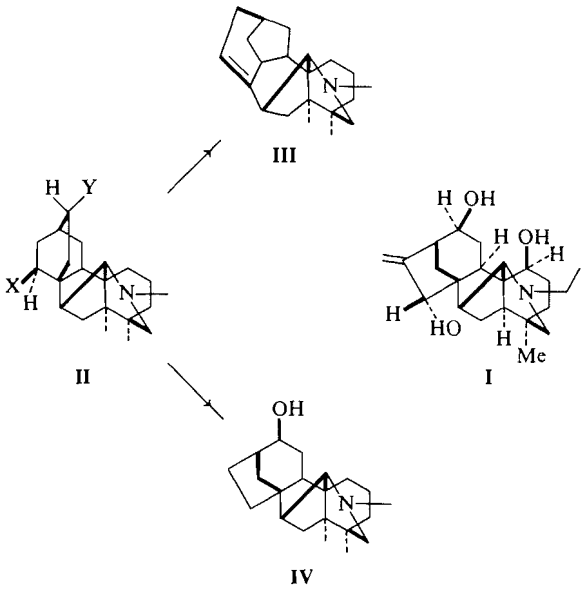
SAT PAUL SETHI, KARNAIL S. ATWAL, RINALDO M. MARINI-BETTOLO, THOMAS Y. R. TSAI et KAREL WIESNER. Can. J. Chem. **58**, 1889 (1980).

On décrit une synthèse simple et stéréospécifique du tricétolactame **15**. On a transformé antérieurement ce composé en napelline **I**. L'étape clef de cette synthèse est la transposition de l'intermédiaire "dénudatine" **11** en un dérivé de la napelline **12**. On a réalisé le squelette de la dénudatine par une addition stéréospécifique, de type diènique entre l'acétal de *o*-quinone et l'éther benzylvinylique. On espère que ce dernier procédé pourra être appliqué d'une façon générale à la synthèse de composés complexes.

[Traduit par le journal]

Several years ago we reported a stereoselective synthesis of the hexacyclic aconite alkaloid napelline **I** (1).

We now wish to disclose a very much more efficient stereospecific and simple construction of the same compound based on our "fourth generation methods" which we have developed for the synthesis of delphinine-type alkaloids (2). Both the delphinine and the napelline system may be built by basically the same strategy which is illustrated by the formulae **II**, **III**, and **IV**.



Ejection of the leaving group X from the "denudatine" structure **II** followed by rearrangement and deprotonation yields a "pyrodelphinine"-type intermediate **III**. Alternatively, the napelline derivative **IV** may be obtained by ejection of the leaving group Y followed by rearrangement and capture of a nucleophile. An exploration of this strategy on model compounds has been published (3).

The starting material was the aromatic intermediate **1** (mp 138–140°C) (4) which was synthesized exactly as the analogous derivative used previously in the construction of 13-desoxydelphonine (2).[1]

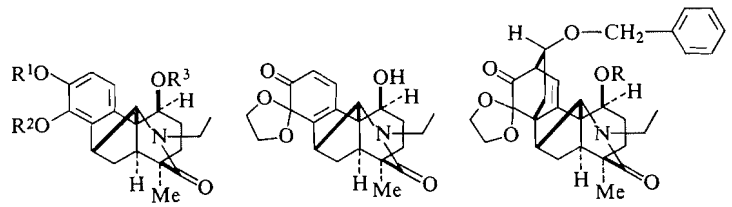
Lithium borohydride reduction of compound **1** yielded the alcohol **2** (mp 104–105°C). This material was heated with 6 *N* HCl to 50°C for 1 h and the product **3** (mp 121.5–122.5°C) was purified by

[1]All compounds gave a molecular ion in mass spectrometry and all spectral data were compatible with the structures assigned to them. All crystalline compounds gave acceptable elemental analyses.

0008-4042/80/171889-03$01.00/0

©1980 National Research Council of Canada/Conseil national de recherches du Canada

Can. J. Chem. Downloaded from www.nrcresearchpress.com by 210.87.254.40 on 09/05/12
For personal use only.



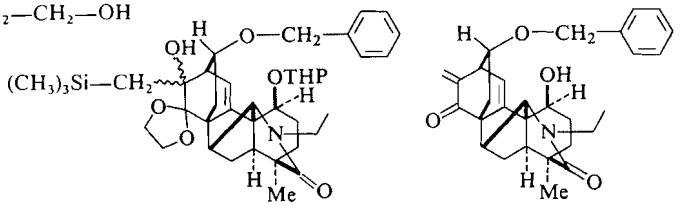
1 $R^1 = -CH_2-O-CH_3$
$R^2 = -CH_2-CO_2CH_3$
R^3 = THP

2 $R^1 = -CH_2-O-CH_3$
$R^2 = -CH_2-CH_2-OH$
R^3 = THP

3 R^1, R^3 = H
$R^2 = -CH_2-CH_2-OH$

4

5 R = H
6 R = THP



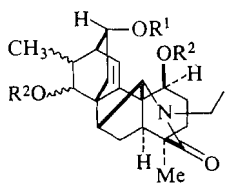
7

8

chromatography and crystallization. The yields of all these operations were practically quantitative.

A suspension of $CaCO_3$ in a solution of the phenol **3** in THF was cooled to 0°C and $Tl(NO_3)_3$ was added. The mixture was stirred for 15 min, poured into saturated aqueous bicarbonate, and extracted with $CHCl_3$. The *o*-quinone acetal **4** (mp 204–205°C) was purified by crystallization from $CHCl_3$–ether and it was obtained in a yield of 95%; uv (EtOH) λ_{max}: 245, 294 nm ($\log \varepsilon$ = 4.2, 3.5); ir ($CHCl_3$): 3670 (OH), 1685 (CO), 1635 (CON) cm^{-1}; ^1H nmr ($CDCl_3$) τ: 2.33, 4.30 (2d, J = 10 Hz, 1H each, vinylic H), 5.80 (m, 4H, $-O-CH_2-CH_2-O$). The masked quinone **4** was heated with an excess of benzyl vinyl ether in CH_2Cl_2 to 40°C for 24 h. The adduct **5** (mp 192–193°C) was purified by chromatography and crystallization and it was obtained in a yield of 94%;[2] ir ($CHCl_3$): 3650 (OH), 1740 (CO), 1635 (CON) cm^{-1}; ^1H nmr ($CDCl_3$) τ: 2.70 (s, 5H, aromatic H), 3.77 (d, J = 6 Hz, 1H, olefinic H), 5.57 (m, 2H, benzylic, 1H, C*H*OH), 5.93 (m, 4H, $-O-CH_2-CH_2-O$).

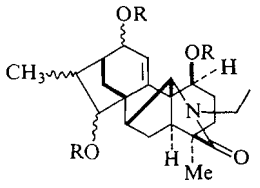
The adduct **5** was converted quantitatively to the oily tetrahydropyranyl derivative **6** by treatment with dihydropyran and pyridinium *p*-toluenesulfonate in CH_2Cl_2. Treatment of compound **6** with trimethyl silyl methyl magnesium chloride in dry THF (cf. ref. 3) at 80°C for 12 h gave the two epimeric alcohols **7** in a yield of 84%. This material was immediately without separation heated in a mixture of 70% $HClO_4$ and THF to 60°C for 2 h. The α,β-unsaturated ketone **8** (mp 170–172°C) was obtained in a yield of 85% after crystallization from ether–hexane; uv (EtOH) λ_{max}: 217 nm ($\log \varepsilon$ = 4.3); ir ($CHCl_3$): 3640 (OH), 1710 (CO), 1635 (CON, $>C=CH_2$) cm^{-1}; ^1H nmr ($CDCl_3$) τ: 2.67 (s, 5H, aromatic H), 3.43 (d, J = 6 Hz, 1H, endocyclic



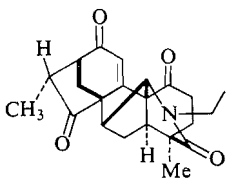
9 $R^1 = -CH_2-$
$R^2 = -CO-CH_3$

10 R^1 = H
$R^2 = -CO-CH_3$

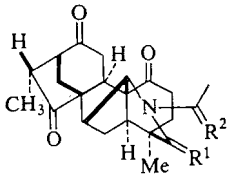
11 R^1 = Ms
$R^2 = -CO-CH_3$



12 R = $-CO-CH_3$
13 R = H



14



15 R^1 = O
$R^2 = H_2$

16 $R^1 = H_2$
R^2 = O

[2]It is remarkable that a dimethylacetal corresponding to **4**, which can be prepared from the precursor of compound **1** ($R^1 = -CH_2-O-CH_3$, $R^2 = -OCH_3$) in two steps is unreactive in the diene addition. This seems to be a striking example of steric hindrance.

Can. J. Chem. Downloaded from www.nrcresearchpress.com by 210.87.254.40 on 09/05/12
For personal use only.

vinylic H), 4.15, 4.77 (2d, J = 2 Hz, 1H each, exocyclic vinylic H), 5.45 (d, 2H, benzylic H).

Reduction of ketone **8** with $LiBH_4$ followed by acetylation with acetic anhydride and pyridine yielded 90% of the oily homogeneous diacetate **9** in which the stereochemistry of the two new chiral centers is left unassigned.

Hydrogenolysis of the benzyl group in compound **9** with Pd–charcoal in methanol gave the oily alcohol **10** and this material was mesylated with mesyl chloride and triethylamine in CH_2Cl_2 to the oily mesylate **11**.

The stage was now set for the rearrangement of the "denudatine" system **11** to the "napelline" system **12**. The rearrangement was accomplished in a yield of 95% by refluxing the mesylate **11** in glacial acetic acid for 2.5 h. The triacetate **12** was saponified with 5% methanolic KOH to the triol **13** and this material was oxidized with the CrO_3–dipyridine complex in CH_2Cl_2 to the homogeneous oily unsaturated triketolactam **14** in an overall yield of 90%; uv (EtOH) λ_{max}: 242 nm (log ε = 4.3); ir ($CHCl_3$): 1745 (cyclopentanone), 1710 (cyclohexanone), 1675 (cyclohexenone), 1650 (lactam) cm^{-1}; ^1H nmr ($CDCl_3$) τ: 3.80 (s, 1H, olefinic H).

Hydrogenation of the triketone **14** with Pd–$CaCO_3$ in ethanol gave quantitatively the saturated triketolactam **15** which was recrystallized from $CHCl_3$–ether and melted at 172–173°C. The totally synthetic racemate **15** was identical by all spectral and chromatographic criteria with the optically active compound of the same structure (mp 193°C) prepared many years ago in our laboratory (5). The methyl group in **15** and its derivatives is assigned the *endo* configuration. This configuration has been established in the optically active derivative by a mild acid catalyzed isomerization, allylic alcohol → ketone, and we agree with all the arguments recently summarized by Pelletier *et al.* in favour of the *endo* methyl stereochemistry of such isomerization products (cf. ref. 6). Infrared ($CHCl_3$): 1740 (cyclopentanone), 1710 (cyclohexanone), 1650 (lactam) cm^{-1}; ^1H nmr ($CDCl_3$) τ: 8.73 (m, 6H, C—CH_3, —CH_2—CH_3), 8.87 (d, J = 2 Hz, 3H, CH—CH_3). Reduction of the racemate **15** with $LiAlH_4$ as described for the optically active compound **15** (5) yielded racemic dihydronapelline.[3] Since dihydronapelline has been converted to napelline (1), the synthesis of **15** constitutes a formal synthesis of napelline.

We have described previously (1) the preparation of napelline from the triketo amide **16**. The same method should be applicable to the isomer **15** and since we have 300 mg of this racemic material in our hands, we hope to accomplish also a direct synthesis of racemic napelline in the near future.

Acknowledgements

We wish to thank the Natural Sciences and Engineering Research Council of Canada for an operating grant and the Canada Council for the award of an Izaak Walton Killam Scholarship to one of us (K.W.).

1. K. Wiesner, P.T. Ho, and C. S. J. Tsai. Can. J. Chem. **52**, 2353 (1974); K. Wiesner, P. T. Ho, C. S. J. Tsai, and Y. K. Lam. Can. J. Chem. **52**, 2355 (1974).
2. K. Wiesner, T. Y. R. Tsai, and K. P. Nambiar. Can. J. Chem. **56**, 1451 (1978); K. Wiesner. Pure Appl. Chem. **51**, 689 (1979); T. Y. R. Tsai, K. P. Nambiar, D. Krikorian, M. Botta, R. Marini-Bettolo, and K. Wiesner. Can. J. Chem. **57**, 2124 (1979).
3. K. S. Atwal, R. Marini-Bettolo, I. H. Sanchez, T. Y. R. Tsai, and K. Wiesner. Can. J. Chem. **56**, 1102 (1978).
4. S. P. Sethi. Ph.D. Thesis, University of New Brunswick, Fredericton, N.B. October, 1979.
5. K. Wiesner, Shô Itô, and Z. Valenta. Experientia, **14**, 167 (1958).
6. S. W. Pelletier, H. K. Desai, J. Finer-Moore, and N. V. Mody. J. Am. Chem. Soc. **101**, 6741 (1979).

[3]The reduction of **15** with hydride is known to yield a triol with all three alcoholic groups in the "natural napelline" configuration (formula **I**).

The structure of merosinigrin

MICHAEL BENN

Chemistry Department, The University of Calgary, Calgary, Alta., Canada T2N 1N4

Received March 3, 1980

This paper is dedicated to the memory of Dr. Léo Marion

MICHAEL BENN. Can. J. Chem. **58**, 1892 (1980).

On the basis of spectroscopic evidence, a new structure is proposed for merosinigrin, a transformation product of potassium allylglucosinolate (sinigrin).

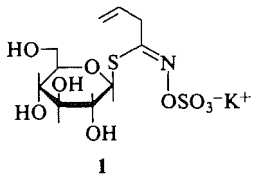
MICHAEL BENN. Can. J. Chem. **58**, 1892 (1980).

A partir des preuves spectroscopiques obtenues, on propose une nouvelle structure pour la mérosinigrine, un produit de transformation provenant de l'allylglucosinolate de potassium (sinigrine).

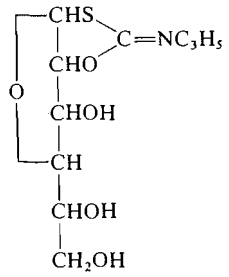
[Traduit par le journal]

Can. J. Chem. Downloaded from www.nrcresearchpress.com by 210.87.254.40 on 09/05/12
For personal use only.

In 1914, Schneider and Wrede (1) reported that the reaction of potassium allylglucosinolate (sinigrin, **1**) with methanolic potassium methoxide gave, besides 1-thioglucose, a small amount (at most 11%) of a crystalline compound which analysed as $C_{10}H_{15}O_5NS$ (**1** − $KHSO_4$). This substance, which they named merosinigrin, was highly dextrorotatory, formed a triacetate, did not reduce Fehling's reagent (even after prolonged boiling with dilute sulfuric acid), or yield lead sulfide when boiled with an alkaline solution of a lead salt. On the basis of this evidence, and accepting Gadamer's structure for sinigrin, Schneider and Wrede proposed that merosinigrin was the compound **2**.



1

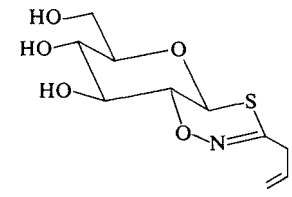


2

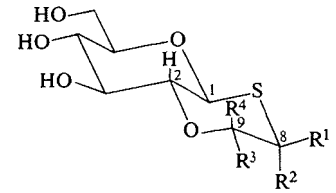
Following Ettlinger and Lundeen's deduction of **1** as the correct structure for sinigrin (2), Kjaer (3) suggested that merosinigrin was **3**.

Recently we had occasion to repeat Schneider and Wrede's experiment and isolated (in about 3% yield) material with physical constants in good agreement with those previously reported. With the availability of modern spectroscopic methods we undertook a reexamination of this merosinigrin with the results which we now present.

Our merosinigrin had mp 191–192°C (uncorr.) and $[\alpha]_D^{25}$ +158(±17)° (*c* 0.18, H_2O) (lit. (1) mp 191–192°C and $[\alpha]_D^{20}$ +149° (*c* 5.4, in H_2O)). The ir



3



4

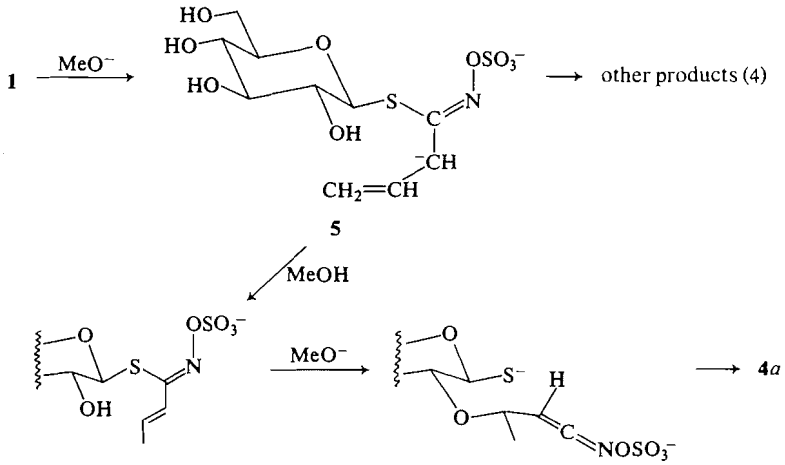
4a $R^1 = R^4 = H, R^2 = CN, R^3 = CH_3$
b $R^1 = R^3 = H, R^2 = CN, R^4 = CH_3$
c $R^1 = CN, R^2 = R^3 = H, R^4 = CH_3$
d $R^1 = CN, R^2 = R^4 = H, R^3 = CH_3$

spectrum contained absorptions at ν_{max} (KBr) 3480 and 3330 (br s, OH) and 2250 (wm) cm^{-1}, and there was no sign of absorptions due to C=C or C=N. A ^{13}C nmr spectrum (D_2O solution, CH_3OH internal reference (δ = 49.0 ppm)) had absorptions at δ: 19.0 (q), 35.2 (d), 60.6 (t), 70.0 (d), 73.3 (d), 74.0 (d), 75.1 (d), 81.4 (d), 83.0 (d), and 118.1 (s) ppm. The 200 MHz ^1H nmr spectrum (DMSO-d_6 solution, DMSO = δ 2.52 ppm) was also very revealing; δ: 1.29 (3H, d, J = 6.5 Hz), 3.1–3.55 (m, includes a DOH signal), 3.69 (1H, dd, J = 11 and 5.5 Hz), 3.91 (1H, dq, J = 6.5 and 2.5 Hz), 4.48 (1H, d, J = 2.5 Hz), 4.51 (1H, d, J = 8.3 Hz), 4.66 (1H, t, J = 5.5 Hz), 5.23 (1H, d, J = 5.5 Hz), and 5.35 (1H, d, J = 5.0 Hz). Mass spectra: 261 (M^+, in accord with $C_{10}H_{15}NO_5S$), with 145 amu as base-peak.

These data were clearly inconsistent with **3**, and

0008-4042/80/171892-02$01.00/0

©1980 National Research Council of Canada/Conseil national de recherches du Canada



SCHEME 1

instead suggested that merosinigrin was one of the isomers **4***a*–*c*.[1] (The fourth isomer, **4***d*, could be rejected on the basis of the small coupling constant, J = 2.5 Hz, between H-8 and H-9.) Distinction between these various possibilities followed from some nOe experiments. Irradiation of the methyl signal resulted in significant nOe enhancements (ca. 4% (difference experiment, coupled spectra)) of the signals for H-8 and H-9. Similar experiments, also at 200 MHz, in which H-9 was irradiated, were inconclusive, but at 400 MHz a ca.17% enhancement of the signal for H-2 was observed (this signal, a triplet at δ 3.23, J = 8.3 Hz, was identified by preliminary selective decoupling experiments), as well as ca.16% in H-8.

Accordingly we conclude that merosinigrin is **4***a*.

The formation of this compound from **1** can be rationalized by the reactions depicted in Scheme 1. The intermediate **5** has previously been postulated by Olesen-Larsen and co-workers to account for other products arising from the base-catalysed rearrangement of glucosinolates (5). The conformational preference of the cyano function is interesting and recalls the "anomeric effect", for although H-8 is easily exchanged for deuterium the nmr spectra showed no sign of epimerisation occurring at this centre during this process.

[1]A similar conclusion has been reached by Professor Peter Laur, Inorganic Chemistry Institute, R.W.T.H., Aachen, Bundesrepublik Deutschland (private communication).

Acknowledgements

We thank Dr. Tom Nakashima and Glen Bigam of the Chemistry Department, University of Alberta, for the nOe experiments. Thanks are also due to Professors Anders Kjaer, Martin Ettlinger, and Peder Olesen Larsen who at various moments stimulated my interest in the merosinigrin problem.

1. W. SCHNEIDER and F. WREDE. Ber. **47**, 2225 (1914).
2. M. G. ETTLINGER and A. J. LUNDEEN. J. Am. Chem. Soc. **78**, 4172 (1956).
3. A. KJAER. Fortschr. Chem. Org. Naturst. **18**, 122 (1960).
4. P. FRIIS, P. OLESEN-LARSEN, and C. E. OLSEN. J. Chem. Soc. Perkin. Trans. I, 661 (1977).

Can. J. Chem. Downloaded from www.nrcresearchpress.com by 210.87.254.40 on 09/05/12
For personal use only.

Biosynthesis of the antifungal sesquiterpene capsidiol. Confirmation of a hydride shift by ^2H magnetic resonance[1]

YUMIKO HOYANO,[2] A. STOESSL, AND J. B. STOTHERS

Agriculture Canada Research Institute and the Department of Chemistry, University of Western Ontario, London, Ont., Canada N6A 5B7

Received May 13, 1980

YUMIKO HOYANO, A. STOESSL, and J. B. STOTHERS. Can. J. Chem. **58**, 1894 (1980).

Direct evidence of a hydride shift in the biosynthesis of capsidiol has been obtained by incorporation studies utilizing deuteriated mevalonolactone (MVA-4,4-d_2) and ^{2}Hmr spectroscopy.

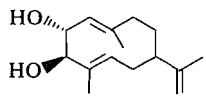
YUMIKO HOYANO, A. STOESSL et J. B. STOTHERS. Can. J. Chem. **58**, 1894 (1980).

Sur la base d'études d'incorporation utilisant la mévalonolactone deutérée (MVA-d_2-4,4) et à l'aide de la spectroscopie de RMN du ^{2}H, on a obtenu la preuve directe d'un glissement d'hydrure lors de la biosynthèse du capsidiol.

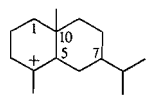
[Traduit par le journal]

Can. J. Chem. Downloaded from www.nrcresearchpress.com by 210.87.254.40 on 09/05/12
For personal use only.

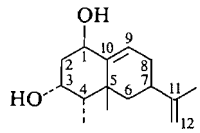
During the past decade, over twenty sesquiterpenes have been isolated from species of the *Solanaceae* under various stress conditions. Formation of most of these stress metabolites has been induced by fungal invasion of potato, aubergine, sweet pepper, jimson weed, and tobacco species (1, 2). Several, which exhibit antifungal activity, may have a role as post-infectional defensive agents (phytoalexins). The majority are bicyclic compounds, either of the eudesmane class or plausibly derived from eudesmanes by rearrangements of varying degrees of complexity. In recent years, the biosynthesis of several members of the series has been studied experimentally by several groups (3–6). For example, we recently utilized the double labelling technique with sodium acetate-1,2-$^{13}C_2$ to determine the carbon labelling patterns in ten sesquiterpenes induced by fungi in potatoes (4). It is apparent that, initially, cyclization of farnesyl pyrophosphate occurs to yield a germacrene; this is supported by the isolation of 2,3-dihydroxygermacrene (**1**) from jimson weed (7). Subsequent cyclization of these germacrene intermediates proceeds through eudesmane carbocations such as **2**. There appear to be a variety of ways in which the second cyclization may be triggered (1, 2), but, in general, the process would appear to require a hydride shift from C-5 to C-4. Direct support for this feature, however, has not been provided by the studies to date. We wish to present



1



2



3

results from deuterium incorporation experiments which establish the occurrence of such a hydride shift in the genesis of capsidiol (**3**), an antifungal stress metabolite isolable from tobacco, jimson weed, and sweet peppers (8).

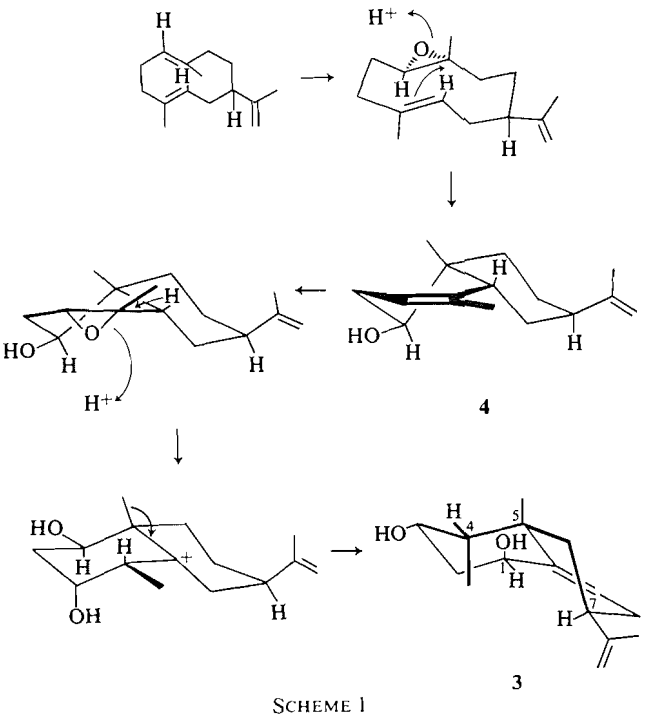
Incorporation studies by Brooks and co-workers (3) using sodium acetate-1,2-$^{13}C_2$ under stress conditions with sweet peppers revealed the carbon labelling pattern for **3** and confirmed that the angular methyl group arises by migration from the 10-position of an eudesmane-type intermediate. This appears to have been the first experimental demonstration of this long-postulated methyl shift in the eudesmane–eremophilane rearrangement (9). A number of possible pathways for the biosynthesis of **3** have been proposed (1) of which two could be subsequently discounted by structural revision of congeners which had been suggested to function as possible intermediates. However, a third alternative, which had been mechanistically the most attractive from the outset, is shown in Scheme 1 and includes sequential *syn* migration of hydrogen (C-5 → C-4) and methyl (C-10 → C-5), similar to the postulated biosynthesis of occidentalol (10). An interesting in vitro analogy for the generation of

[1]Part XXXIII of Nuclear magnetic resonance studies; for part XXXII see ref. 14. Part XXXV in the series Post infectional inhibitors from plants; for part XXXIV see ref. 15. Contribution No. 796 from the Agriculture Canada Research Institute.

[2]Present address: Department of Chemistry, University of Alberta, Edmonton, Alta.

0008-4042/80/171894-03$01.00/0

©1980 National Research Council of Canada/Conseil national de recherches du Canada



SCHEME 1

cis-decalins has been described (11) but we are unaware of in vivo demonstration of this sequence for the *cis* series. However, the corresponding hydride shift has been demonstrated for the *trans* series (12).

In the present instance, cyclization of a presumed simple germacrene induced by cleavage after epoxidation at one of the double bonds would give rise to the eudesmane analog **4**. A second epoxidation followed by acid-catalyzed cleavage sets the stage for a hydride shift (C-5 → C-4), the angular methyl shift (C-10 → C-5), and proton loss to form the 9,10-double bond in **3**. In the scheme, the skeletally bonded hydrogens shown are those originally at C-4 in the mevalonate precursors. To obtain evidence to support our proposed sequence, incorporation experiments utilizing mevalonolactone-4,4-d_2[3] were carried out following the method described previously (3). After isolation and recrystallization, **3** was acetylated to the corresponding diacetate because of its higher solubility. The ^{2}Hmr spectrum of capsidiol diacetate in Freon-11 contained three signals (see Fig. 1), one of which is significantly deshielded relative to the others. Clearly the deuterium atom from each of the three mevalonate units involved in the genesis of **3** is retained. Since the angular methyl group is bonded to a carbon originating from C-4 in mevalonate, a hydride (deuteride) shift has occurred. The low specific incorporation (0.3%) of mevalonate, as monitored by the presence of a small amount of radioactive mevalonolactone in the feeding experiments, clearly precludes other possible in-

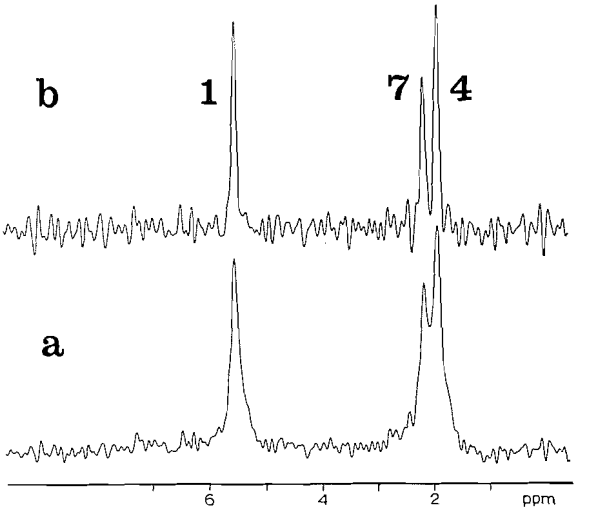


FIG. 1. 30.71 MHz ^{2}Hmr spectra of **3** in $CFCl_3$ (a) normal data processing, 4K transform, 1K spectral width (300 Hz illustrated), 11K transients, 30° flip angle, 0.40 s acquisition; (b) resolution enhanced spectrum, RE = 0.06.

[3]This compound was synthesized following the reported sequence for the 4-^{13}C labelled analog (13), using ethyl trideuterioacetate rather than ethyl [2-^{13}C]-acetate.

Can. J. Chem. Downloaded from www.nrcresearchpress.com by 210.87.254.40 on 09/05/12
For personal use only.

Can. J. Chem. Downloaded from www.nrcresearchpress.com by 210.87.254.40 on 09/05/12
For personal use only.

terpretations. The lowest field signal in the ^2H spectrum arises from deuterium on the C-1 carbinyl carbon. The chemical shift of this nucleus (5.52 ppm) is known from the proton spectrum and its separation, in ppm, from the 4-proton, coupled to the tertiary methyl protons, was determined by the required spin decoupling experiment. Irradiation at 1.95 ppm collapsed the methyl doublet (0.92 ppm) to a singlet, thus H-1 and H-4 are separated by 3.57 ppm. This is the separation between the highest and lowest field signals in the ^2H spectrum confirming the indicated assignments. The signal at intermediate field strength, 3.34 ppm upfield from the carbinyl resonance, is clearly attributable to the allylic deuterium at C-7. The relative intensity of this signal is noticeably smaller (~25%) than either of the others, presumably because of allylic exchange.

These results offer strong support for a sequence including *syn* migration of hydrogen and methyl. These data rule out an earlier suggestion that capsidiol, an 4-*epi*eremophilane, may arise from an eremophilane by a trivial epimerization (10).

Experimental

Feeding Experiments

Capsicum frutescens var. Red Sweet, harvested locally in the early ripening stage (red blush), was washed, halved, deseeded, and charged with 0.4 mL per half of a solution prepared by dissolving MVA-2-^{14}C (24.4 mg; 5.7 μCi from Amersham Corp., Oakville, Ont.) and MVA-4,4-$^2H_2$ (257.5 mg; >98% 4,4-$^2H_2$) in 96% EtOH (5 mL) and diluting to 560 mL with water. Approximately 1 h later, each half fruit was treated with 10 mL of a spore suspension of *Monilinia fructicola* prepared in the usual way (4). More MVA solution (1 mL per half fruit) was added 7 h after fungal inoculation and again after a further 16 h. The product was collected 48 h after fungal inoculation by decanting and rinsing the shells with water. The combined liquids (ca. 2 L) were extracted with 4 successive half volumes of Et_2O, which were washed with a little water. The residue obtained on evaporation of the extract was filtered in EtOAc, reevaporated (223 mg), and chromatographed over silica gel (Camag DF5, not activated, 225 g) in MeOH/$CHCl_3$ (1:9) in 25 mL fractions. Fractions 22–26 (105 mg) crystallized and were recrystallized from EtOAc and CH_2Cl_2 to constant specific radioactivity (4.96×10^5 cpm/mmol); specific activity of the MVA-2-^{14}C-4,4-$^2H_2$ under the same conditions, 5.20×10^6 cpm/mmol; hence, specific incorporation was 0.95% (~0.32% at each of 3 hypothetical sites). The purified capsidiol (61 mg, mp 150–152.5°C) was treated overnight at room temperature with pyridine (0.9 mL) and Ac_2O (0.6 mL). Evaporation furnished the pure diacetate-$^{14}C_x$-$^2H_2$ as an oil; ^{1}Hmr ($CFCl_3$) δ: 0.92 (d, *J* ~7 Hz, 3H, 4-Me), 1.37 (s, 3H, 5-Me), 1.72 (s, 3H, 11-Me), 1.98 (s, 3H), 2.01 (s, 3H), 4.67 (m, 2H, H-12), 5.52 (dd, $J = 2.3$ and 3.9 Hz, H-1), 5.59 (dt, *J*'s 12.6 and 4.8 Hz, H-3), 6.15 (dd, *J*'s 6.5 and 2.3 Hz, H-9), 1.95 (H-4, by spin decoupling), 2.14 (H-7, from the ^2H spectrum).

Nuclear Magnetic Resonance Spectra

The ^1H and ^2H spectra were recorded with a Varian XL-200 spectrometer at 200 and 30.7 MHz, respectively, using a solution of capsidiol diacetate-^2H_x in $CFCl_3$ (40 mg in 0.5 mL). The illustrated ^2H spectrum was obtained with proton noise decoupling.

Acknowledgements

We are grateful for the financial support of the Natural Sciences and Engineering Research Council of Canada. We wish to thank W. C. Jankowski of Varian Associates, Palo Alto, CA, for recording the nmr spectra, C. H. Unwin for supplying the *M. fructicola* spore suspension, and G. Rock for experimental assistance.

1. A. Stoessl, J. B. Stothers, and E. W. B. Ward. Phytochem. **15**, 885 (1976).
2. A. Stoessl, E. W. B. Ward, and J. B. Stothers. *In* Host plant resistance to pests. ACS Symposium Series, No. 62. *Edited by* P. A. Hedin. American Chemical Society, Washington, DC. 1977. pp. 61–77.
3. F. C. Baker, C. J. W. Brooks, and S. A. Hutchinson. J. Chem. Soc. Chem. Commun. 293 (1975); F. C. Baker and C. J. W. Brooks. Phytochem. **15**, 689 (1976).
4. A. Stoessl, J. B. Stothers, and E. W. B. Ward. Can. J. Chem. **56**, 645 (1978).
5. K. Sato, Y. Ishiguri, N. Doke, K. Tomiyama, F. Yogihashi, A. Murai, N. Katsui, and T. Masamune. Phytochem. **17**, 1901 (1978).
6. E. B. Kalan and S. F. Osman. Phytochem. **15**, 775 (1976).
7. A. Stoessl, J. B. Stothers, and E. W. B. Ward. J. Chem. Soc. Chem. Commun. 431 (1975).
8. M. Gordon, A. Stoessl, and J. B. Stothers. Can. J. Chem. **51**, 748 (1973); G. I. Birnbaum, A. Stoessl, S. H. Grover, and J. B. Stothers. Can. J. Chem. **52**, 993 (1974).
9. C. A. Miller and A. R. Pinder. J. Chem. Soc. Chem. Commun. 230 (1977).
10. R. M. Coates. Fortschn. Chem. Org. Naturst. **33**, 73 (1976).
11. M. Iguchi, M. Niwa, and S. Yamamura. J. Chem. Soc. Chem. Commun. 689 (1972).
12. C. J. W. Brooks and R. A. B. Keates. Phytochem. **11**, 3235 (1972).
13. D. E. Cane and R. H. Levin. J. Am. Chem. Soc. **98**, 1183 (1976).
14. A. K. Cheng and J. B. Stothers. Can. J. Chem. **56**, 1342 (1978).
15. A. Stoessl and J. B. Stothers. Z. Naturforsch. Teil C, **34**, 87 (1979).

Canadian Journal of Chemistry
Published by
THE NATIONAL RESEARCH COUNCIL OF CANADA

Journal canadien de chimie
Publié par
LE CONSEIL NATIONAL DE RECHERCHES DU CANADA

Volume 58 Number 18 September 15, 1980

Volume 58 numéro 18 15 septembre 1980

A note on the application of graph theory to the thermodynamic properties of isomeric alkanes

JOHN T. EDWARD[1]

Physicochimie des Solutions, LA CRNS 161, E.N.S.C.P., Université Pierre et Marie Curie, 11 Rue Pierre et Marie Curie, 75231 Paris, France

Received March 7, 1980

JOHN T. EDWARD. Can. J. Chem. **58**, 1897 (1980).

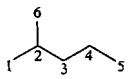
It has been claimed that trends in the thermodynamic properties of alkane isomers follow an ordering based on p_2 and p_3, the number of paths of length two or three, respectively (M. Randic and C. L. Wilkins. J. Phys. Chem. **83**, 1525 (1979)). A possible explanation of the approximate ordering of the partial molal volumes $\bar{V}^0$ of isomers in carbon tetrachloride at 25°C comes from the ordering, based on p_2 and p_3, of (*a*) the number N of methyl groups, and (*b*) the mole fraction Z_g of *gauche* arrangements in the different isomers. However, N and Z_g have opposite effects on $\bar{V}^0$, and specific cases of isomeric heptanes and nonanes are noted in which a reversal in trends in $\bar{V}^0$ may be expected.

JOHN T. EDWARD. Can. J. Chem. **58**, 1897 (1980).

On a prétendu que les tendances des propriétés thermodynamiques des alcanes isomères se classent en fonction de p_2 et p_3, le nombre de chemins de longueur deux ou trois respectivement (M. Randic et C. L. Wilkins, J. Phys. Chem. **83**, 1525 (1979)). Une explication possible du classement approximatif des volumes molaires partiels $\bar{V}^0$ des isomères en solution dans le tétrachlorure de carbone à 25°C vient du classement à partir de p_2 et p_3 (*a*) des nombres N de groupes méthyle et (*b*) de la fraction molaire Z_g des arrangements *gauches* des différents isomères. Cependant N et Z_g ont des effets opposés sur $\bar{V}^0$ et on a noté des cas spécifiques d'heptanes et de nonanes isomères pour lesquels on peut prévoir des tendances inverses de $\bar{V}^0$.

[Traduit par le journal]

A molecule may be regarded as a graph, with the atoms as points and the bonds as lines (1, 2). A path p_i in a molecular graph is a sequence of i adjacent bonds with no atom appearing more than once. The various paths found in the hexane isomer, 2-methyl pentane, are listed in Scheme 1 (cf. ref. 3). The numbers of paths of different length for this and for the other isomers of hexane are given in Table 1.



Path length i	Paths p_i	Numbers of path p_i
1	1–2, 2–3, 3–4, 4–5, 2–6	5
2	1–2–3, 2–3–4, 3–4–5, 1–2–6, 6–2–3	5
3	1–2–3–4, 6–2–3–4, 2–3–4–5	3
4	1–2–3–4–5, 6–2–3–4–5	2

SCHEME 1

A scrutiny of this and other tables of groups of isomers (3) shows that for any group p_1 must be identical, and the individual isomer is characterized (but not always completely (3)) by p_2, p_3, ... p_{n-1}, where n is the number of carbon atoms. Randic and Wilkins (3) found that trends in the thermodynamic properties of hydrocarbon isomers seemed to be determined chiefly (and perhaps entirely) by p_2 and p_3. To show trends, they displayed the properties of the isomers on grid graphs having p_2 and p_3 as coordinates; Figs. 1–3 are examples. In Figs. 1*a*, 2*a*, and 3*b* we display the partial molal volumes $\bar{V}^0$ in carbon tetrachloride at 25°C (4) of the isomers of hexane (Fig. 1*a*), of eight of the nine isomers of heptane (Fig. 2*a*), and of fifteen of the 35 isomers of nonane (Fig. 3*b*).

An examination of these figures shows that trends in $\bar{V}^0$ conform (with the exception of $\bar{V}^0$ of 3,3-dimethylpentane (Fig. 2*a*) and of 2,2- and 3,3-dimethylheptane (Fig. 3*b*), discussed below) to a (+, −) pattern: (+) indicating that in the direction of increasing p_2 (constant p_3), $\bar{V}^0$ increases; (−)

[1]On sabbatical leave from the Department of Chemistry, McGill University, Montreal, P.Q., Canada H3A 2K6.

0008-4042/80/181897-05$01.00/0
©1980 National Research Council of Canada/Conseil national de recherches du Canada

Can. J. Chem. Downloaded from www.nrcresearchpress.com by 210.87.254.105 on 09/05/12
For personal use only.

TABLE 1. Number of paths p_i of hexane isomers

Isomers	Symbol	Number of paths				
		p_1	p_2	p_3	p_4	p_5
n-Hexane	*n*	5	4	3	2	1
2-Methylpentane	2M	5	5	3	2	
3-Methylpentane	3M	5	5	4	1	
2,2-Dimethylbutane	$22M_2$	5	7	3		
2,3-Dimethylbutane	$23M_2$	5	6	4		

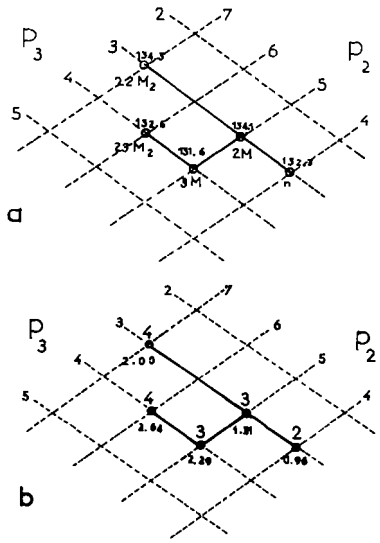


FIG. 1. Grid pattern for hexane isomers: (*a*) partial volumes $\bar{V}^0$ (in mL mol^{-1}; numbers above points); symbols of isomers (Table 1) below points; (*b*) numbers of methyl groups (above points); Z_g (below points).

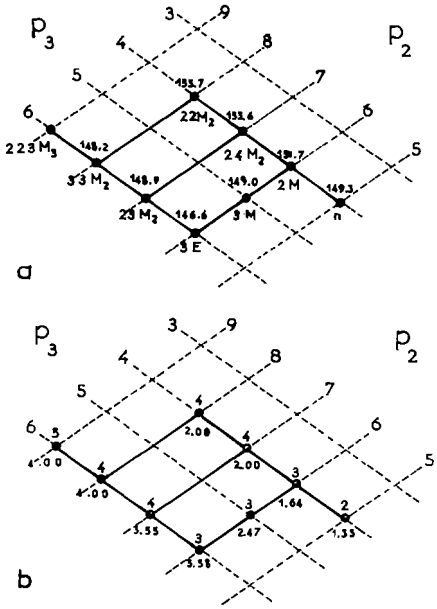


FIG. 2. Grid pattern for heptane isomers: (*a*) $\bar{V}^0$, above points; symbols below points (3E is 3-ethylpentane); (*b*) numbers of methyl groups, above points; Z_g, below points.

indicating that in the direction of increasing p_3 (constant p_2), $\bar{V}^0$ decreases. Randic and Wilkins consider that exceptions to trends may be due either to experimental error, or to the neglect of contributions from higher values of p_i; we show below that the exceptions noted above may be of more fundamental origin. However, the usefulness of the grid graphs in producing at least an approximate ordering of $\bar{V}^0$ is apparent. Randic and Wilkins found the graphs equally useful in showing trends in a large number of other properties: specific dispersions, molar volumes, heats of formation, molar refractions (trend (+,−)); surface tensions, heats of combustion, critical temperatures, volume molar factors, connectivity indices (5)(−,+); critical volumes, mean molecular radii as calculated by Altenburg (6), characteristic polynomials (7) (−,−); critical densities, critical pressures, molar magnetic susceptibilities, deviations of enthalpies of atomization from the values calculated by Somayaluju and Zwolinski (8), and Wiener's parameters ΔW and ΔP (+,+). Most of these molecular quantities are experimental, but some are theoretical (5–9). Discrepancies from the general trends were generally few and small; the occasional large discrepancy may indicate experimental error.

Randic and Wilkins point out that "there is as yet no theoretical basis for our ordering rule". A possible basis for the (+,−) trend in $\bar{V}^0$ emerges when we consider the equation recently (4) found to apply with reasonable accuracy to $\bar{V}^0$ of isomeric alkanes:

$$[1]\quad \bar{V}^0 = V_c + \sum_i n_i I_i - 2.5 Z_g$$

where V_c is a constant covolume of 11.61 mL mol^{-1}, I_i is the volume increment due to group i (—CH_3, 26.85; >CH_2, 17.36; >CH, 10.35; quaternary carbon 3.4 mL mol^{-1}); n_i is the number of groups i; and Z_g is the mole fraction of *gauche* conformations in a given isomer at 25°C. The cal-

Can. J. Chem. Downloaded from www.nrcresearchpress.com by 210.87.254.105 on 09/05/12
For personal use only.

Can. J. Chem. Downloaded from www.nrcresearchpress.com by 210.87.254.105 on 09/05/12
For personal use only.

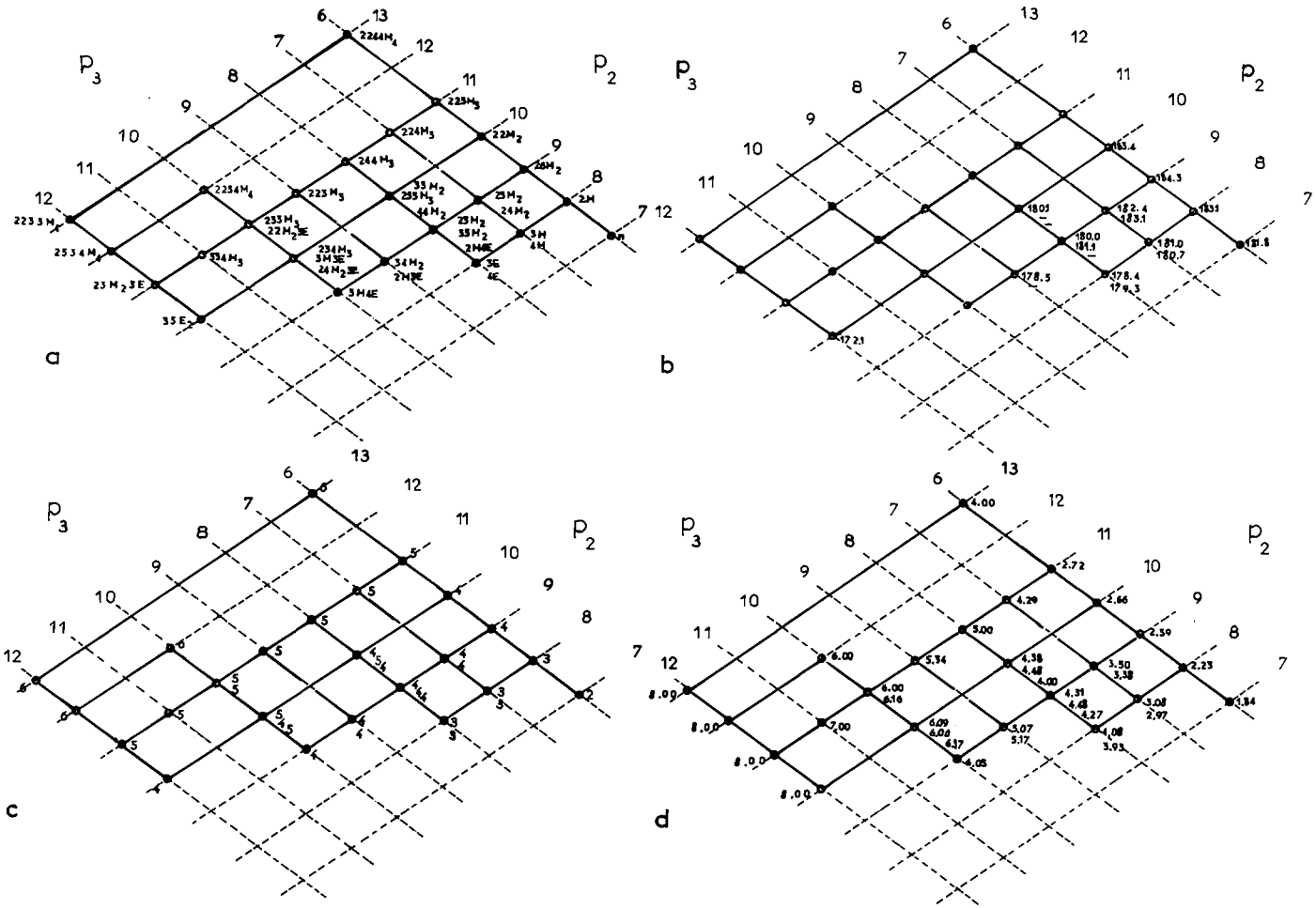


FIG. 3. Grid pattern for nonane isomers: (*a*) symbols for isomers; (*b*) $\bar{V}^0$; (*c*) numbers of methyl groups; (*d*) Z_v.

Can. J. Chem. Downloaded from www.nrcresearchpress.com by 210.87.254.105 on 09/05/12
For personal use only.

culation of Z_g follows a procedure described by Mann (10). The mole fraction γ of each different conformation, containing z_g *gauche* arrangements, is calculated by the methods of statistical mechanics; then $Z_g = \Sigma\gamma z_g$. In these calculations it is assumed that while two adjacent *gauche* arrangements g^+g^+ or g^-g^- are possible, g^+g^- or g^-g^+ arrangements contribute negligibly because they bring the terminal carbon atoms excessively close, and hence have excessively high energies.



The alkanes of an isomeric group all have the same number of carbon and hydrogen atoms, and so have $\bar{V}^0$ values approximately equal. The small differences from $\bar{V}^0$ of the *n*-alkane that come with branching, and an increase in p_2 and p_3, are associated (according to [1]) with changes in two molecular parameters:

(*1*) The number N of methyl groups increases. In fact, as shown in Figs. 1*b*, 2*b*, and 3*c*, N follows a (+,0) trend. This should cause $\bar{V}^0$ also to follow a (+,0) trend, since (in effect) the hydrogen atoms of methyl occupy more volume than the hydrogen atoms of methylene or methine.[2]

(*2*) Z_g increases with p_2 and p_3, following a (+,+) trend, except at high values of p_3, when it follows a (0,+) trend (Figs. 1*b*, 2*b*, and 3*d*). This should lead to a (−,−) or (0,−) trend in $\bar{V}^0$. The effects of the changes in N and Z_g oppose each other, so that the net result could be either a (+,−) or a (−,−) trend in $\bar{V}^0$, depending on whether N or Z_g was more important. In fact, with increasing branching the volume increase due to the greater number N of methyl groups seems to be more important than the volume decrease due to the increase in Z_g, so that an (approximately) (+,−) trend is observed.[3]

We may now consider the exceptions to this trend noted above. The trend would require $\bar{V}^0$ of 3,3- to be greater than $\bar{V}^0$ of 2,3-dimethylpentane (Fig. 2*a*). In fact, it is smaller, although the difference is less than the experimental error. This agrees with [1], which requires it to be smaller because, although it has the same N, it has a larger Z_g (Fig. 2*b*). Similarly, the (+,−) trend would require $\bar{V}^0$ of 2,2-dimethylheptane to be greater than $\bar{V}^0$ of 2,6-dimethylheptane (Fig. 3*a*). In fact, it is smaller (Fig. 3*b*) by an amount greater than experimental error. Again, N of the two isomers (Fig. 3*c*) is the same, but Z_g is greater for 2,2-dimethylheptane (Fig. 3*d*), so that the result agrees with [1]. Similar considerations apply to $\bar{V}^0$ of 3,3-dimethylheptane which, counter to a (+,−) trend, is smaller than V^0 of 3,5-dimethylheptane (Figs. 3*a* and 3*b*).

We can conclude that, to the extent that we can have confidence in [1], the (+,−) trend in $\bar{V}^0$ shown in Figs. 1*a*, 2*a*, and 3*b* should be approximate but not exact. Since Z_g affects not only $\bar{V}^0$ but also molar refractions and heats of combustion (10, 11), it seems likely that the same conclusions apply to these properties also.

A further test of these conclusions might come from determination of $\bar{V}^0$ of some of the twenty isomers of nonane not yet examined. Thus [1] predicts that the (+,−) trend in $\bar{V}^0$ in Fig. 3*b* should be violated in the following cases: 3,3- vs. 2,3-dimethylheptane and 2-methyl-4-ethylhexane; 3-methyl-3-ethyl- vs. 3-methyl-4-ethylhexane; and 2,2,3- vs. 2,3,4-trimethylhexane and 2,4-dimethyl-3-ethylpentane. This prediction is based on the Z_g values calculated for these and for twelve other isomers for the first time, and shown in Fig. 3*d*. An additional point of interest came out in these calculations. While, wherever possible, a chain molecule avoids a g^+g^- or g^-g^+ arrangement, for several of the nonane isomers of Fig. 3*a* this is not possible. One $g^{\pm}g^{\mp}$ arrangement is necessarily present in any staggered conformation of the following compounds: 2,2,4- and 2,4,4-trimethylhexane, 2,2-, 2,3-, and 2,4-dimethyl-3-ethylpentane, and 2,2,3,4-tetramethylpentane. Two such arrangements must be present in the staggered conformation of 2,2,4,4-tetramethylpentane (**1**).



1

The presence of such highly compressed arrangements might be expected to result in a pronounced drop in $\bar{V}^0$, and a pronounced rise in molar refractions and heats of combustion.

Acknowledgements

The hospitality and interest of Professor Schaal and financial support from the National Research Council of Canada, Le Centre National de la Recherche Scientifique de France Scientific Cooperation Program are warmly appreciated.

[2]Accepting a constant increment of 3.4 mL mol^{-1} for a carbon atom, the increment (in mL mol^{-1}) of a hydrogen atom varies according to its attachment as follows: CH_4, 9.2; CH_3, 7.8; CH_2, 7.0; CH, 7.0. (This corrects an error in ref. 4.) Possible reasons for this monotonic change are discussed in ref. 4.

[3]The exceptions to the (+,−) trend come from the fact that while Z_g increases continuously, N increases in stepwise fashion, and has the same value for each isomer of the aberrant pairs.

1. A. CAYLEY. Collected mathematical papers. Cambridge University Press. 1889–1897.
2. A. T. BALABAN (*Editor*). Chemical applications of graph theory. Academic Press, London. 1976.
3. M. RANDIC and C. L. WILKINS. J. Phys. Chem. **83**, 1525 (1979).
4. J. T. EDWARD, P. G. FARRELL, and F. SHAHIDI. J. Phys. Chem. **82**, 2310 (1978).
5. M. RANDIC. J. Am. Chem. Soc. **97**, 6609 (1975).
6. K. ALTENBURG. Kolloid. Z. **178**, 112 (1961).
7. H. HOSOYA. Bull. Chem. Soc. Jpn. **48**, 2332 (1977); **45**, 3415 (1972); Theor. Chim. Acta, **25**, 215 (1972).
8. G. R. SOMAYALUJU and B. J. ZWOLINSKI. J. Chem. Soc. Faraday Trans. II, **70**, 967 (1974).
9. H. WIENER. J. Am. Chem. Soc. **69**, 17 (1947); J. Phys. Chem. **52**, 425 (1948); **52**, 1082 (1948).
10. G. MANN. Tetrahedron, **23**, 3325 (1967).
11. N. L. ALLINGER. J. Am. Chem. Soc. **79**, 3943 (1957).

Can. J. Chem. Downloaded from www.nrcresearchpress.com by 210.87.254.105 on 09/05/12
For personal use only.

Thermodynamics of binary mixtures of 1,2-dichloroethane with aromatic hydrocarbons

RAM K. NIGAM, PREM P. SINGH, KRISHAN C. SINGH, MOHAN SINGH, AND RUCHI MISHRA

Department of Chemistry, Maharshi Dayanand University, Rohtak (Haryana), India

Received October 31, 1979

RAM K. NIGAM, PREM P. SINGH, KRISHAN C. SINGH, MOHAN SINGH, and RUCHI MISHRA. Can. J. Chem. **58**, 1902 (1980).

Molar excess volumes, V^E at 298.15 and 308.15 K, molar excess enthalpies H^E at 308.15 K, and total vapour pressure at 298.15 and 308.15 K have been measured for binary mixtures of 1,2-dichloroethane with aromatic hydrocarbons. The V^E and H^E data for an equimolar mixture at 308.15 K only have been utilized to predict V^E, H^E, and TS^E values (using Sanchez and Lacombe theory) for these mixtures as a function of temperature and composition. The agreement between the predicted and the corresponding experimental values is good so far as V^E and H^E data are concerned but the same is not true of the TS^E values.

RAM K. NIGAM, PREM P. SINGH, KRISHAN C. SINGH, MOHAN SINGH et RUCHI MISHRA. Can. J. Chem. **58**, 1902 (1980).

On a mesuré les volumes molaires en excès V^E à 298,15 et 308,15 K, les enthalpies molaires en excès H^E à 308,15 et la pression totale de vapeur à 298,15 et 308,15 K des mélanges binaires de dichloro-1,2 éthane avec des hydrocarbures aromatiques. On a utilisé uniquement les données de V^E, H^E d'un mélange équimolaire à 308,15 K pour prédire les valeurs de V^E, de H^E et de TS^E (en utilisant la théorie de Sanchez et Lacombe) de ces mélanges en fonction de la température et de la composition. L'accord est parfait entre les valeurs théoriques et expérimentales tant que les données de V^E et de H^E sont impliquées mais ce n'est pas le cas pour les valeurs de TS^E.

[Traduit par le journal]

Introduction

Sanchez and Lacombe have recently formulated a unified molecular theory (1–3) of liquid and gaseous mixtures. The theory (1–4) has been quite successful in describing/predicting not only the liquid–liquid and liquid–vapour equilibrium but also the lower critical solution temperature and the upper critical solution temperature for binary mixtures of non-electrolytes. Further, by allowing empty lattice sites on the lattice, this theory provides, unlike the lattice theory of Flory and Huggins (5), a means to calculate excess volumes for non-electrolytic fluids. In the present work we have employed this theory to predict molar excess volumes, V^E, molar excess enthalpies, H^E and TS^E values for binary mixtures of 1,2-dichloroethane with aromatic hydrocarbons at 308.15 and 298.15 K from *the corresponding* V^E *and* H^E *data for an equimolar mixture at 308.15 K only.*

Experimental

Analytical grade benzene, toluene, *o*-xylene, *m*-xylene, *p*-xylene, and 1,2-dichloroethane were purified by standard techniques (6, 7). The purity of the final samples was checked by density determination at 298.15 ± 0.01 K which agreed to within ± 0.00005 g cm^{-3} with their corresponding literature values (8–10).

Molar excess volumes were measured at 298.15 and 308.15 K as a function of composition using the direct dilatometric method (11). The temperature of the thermostatic bath was controlled to ±0.01 K and the uncertainty in the experimental V^E values is 0.5%.

Molar excess enthalpies as a function of composition were measured at 308.15 K in an adiabatic calorimeter described elsewhere (12). The time was recorded by an electronic timer (type 701, Systronics, Ahmedabad, India) which could read to ±0.0001 s. The temperature variation of the thermostatic bath was found to be within ±0.01 K and the uncertainty in H^E values is about 1.1%.

Total vapour pressures of these mixtures were determined by a static method described earlier (13). The apparatus was placed in a water thermostat which in turn was placed in another water bath. The temperature of the outer thermostat was controlled to ±0.01 K and the temperature drift in the inner thermostat was found to be less than ±0.003 K. The mercury heights in the manometer were read by a cathetometer which could read to ±0.001 cm. All vapour pressure measurements were reproducible to better than ±0.02 Torr.

Our measured vapour pressures at 298.15 K of benzene, *o*-xylene, and *p*-xylene compare within ±0.3% with their corresponding literature values (14, 15) at 298.15 K. However, our measured vapour pressures for toluene, *m*-xylene, and 1,2-dichloroethane compared within ±0.4% with those obtained from Antoine equation using the parameters given elsewhere (16).

Results

V^E data[1] at 298.15 and 308.15 K and H^E data[1] at 308.15 K were expressed by expressions of the type

[1] $$V^E(\text{cm}^3\ \text{mol}^{-1})/x_1(1 - x_1)$$

or $$H^E(\text{J mol}^{-1})/x_1(1 - x_1)$$

$$= \sum_{i=0}^{2} V_i \quad \text{or} \quad H_i(2x_1 - 1)^i$$

where V_i or H_i are adjustable parameters and x_1 is the mole fraction of 1,2-dichloroethane. These

[1]Complete set of data may be obtained, at a nominal charge, from the Depository of Unpublished Data, CISTI, National Research Council of Canada, Ottawa, Ont., Canada K1A 0S2.

0008-4042/80/181902-04$01.00/0

©1980 National Research Council of Canada/Conseil national de recherches du Canada

Can. J. Chem. Downloaded from www.nrcresearchpress.com by 210.87.254.40 on 09/05/12
For personal use only.

Can. J. Chem. Downloaded from www.nrcresearchpress.com by 210.87.254.40 on 09/05/12
For personal use only.

parameters were evaluated by fitting $V^E/x_1(1 - x_1)$ and $H^E/x_1(1 - x_1)$ to [1] by the method of least squares and are recorded together with the standard deviation of the molar excess volumes, $\sigma(V^E)$, and molar excess enthalpies, $\sigma(H^E)$, in Table 1.

The total vapour pressure data[1] for these mixtures at 298.15 and 308.15 K were used to evaluate molar excess Gibbs free energies of mixing, G^E, by Barker's method (17). The form of the function used for G^E, following Redlich and Kister (18), is

$$[2] \quad G^E/RT = x_1(1 - x_1) \sum_{i=0}^{2} G_i(2x_i - 1)^i$$

where G_i are adjustable parameters. These parameters are recorded in Table 1. The second virial coefficients for benzene were taken from literature (19) while those for toluene, *o*-xylene, *m*-xylene, and *p*-xylene and 1,2-dichloroethane were calculated from Berthelot's equation (20); the necessary critical constant data were taken from literature (21).

Discussion

V^E data for all these binary mixtures are positive and follow the sequence toluene < benzene < *o*-xylene ≈ *p*-xylene < *m*-xylene. On the other hand, while H^E values are positive over the entire 1,2-dichloroethane concentration range for 1,2-dichloroethane and benzene mixtures, they are negative for low and positive for high 1,2-dichloroethane concentration for the rest of these binary mixtures.

V^E, H^E, and TS^E data were examined for Sanchez and Lacombe's theory (1, 2), which is an improvement over the one proposed by Flory and Huggins (5). This visualizes that all fluids are lattice or Ising fluids and that some of the lattice sites are empty. Each molecule is then characterized by an energy parameter $\tilde{\varepsilon}^*$ (which is the energy required to create a lattice vacancy) and a parameter r (which is the measure of the repulsive or hard core part of the intermolecular potential). Further, each lattice site is assumed to have a coordination number Z and while mers at the chain ends have $Z - 1$ nearest non-bonded and one bonded neighbour, each interior r-mer is surrounded by $Z - 2$ nearest non-bonded neighbours. The number of configurations available to a r-mer occupying r sites and N_0 vacant sites were then obtained as suggested by Guggenheim (22–24).

In order to predict V^E, H^E, and TS^E values for the various mixtures at any temperature and composition, H^E and V^E values for an equimolar mixture at 308.15 K were used to evaluate $\tilde{\rho}_{mix}$ from [4] and $\tilde{\varepsilon}^*_{ij}$ from [3]

$$[3] \quad H^E = RTr_{mix}\{\tilde{\rho}\sum\sum\phi_i\phi_j\chi_{ij} + \sum(\tilde{\rho}_i\phi_i{}^0 - \tilde{\rho}\phi_i)/T_i\} + PV^E$$

TABLE 1. Parameters of eq. [1] along with standard deviation $\sigma(V^E)$ and $\sigma(H^E)$ for the various systems at 298.15 K and 308.15 K

System	T (°C)	V_0	V_1	V_2	h_0	h_1	h_2	G_0	G_1	G_2	V^E (cm³/mol)	H^E (J/mol)	χ_{12} (J/mol)
1,2-Dichloroethane + benzene	25	0.907	0.045	0.134	—	—	—	226.55	—	—	0.002	—	—
	35	0.871	−0.091	0.033	215.8	91.7	61.8	175.998	−34.84	—	0.003	1.8	−14.2
1,2-Dichloroethane + toluene	25	0.665	0.208	−0.057	—	—	——	531.19	50.81	62.71	0.002	—	—
	35	0.694	0.214	−0.043	−74.3	423.2	329.4	608.69	135.26	212.63	0.002	1.5	115.1
1,2-Dichloroethane + *o*-xylene	25	1.166	0.330	−0.085	—	—	—	889.11	121.21	45.86	0.003	—	—
	35	1.217	0.346	0.025	22.5	665.3	376.0	193.16	35.61	−45.86	0.003	3.0	202.3
1,2-Dichloroethane + *m*-xylene	25	1.413	0.427	−0.151	—	—	—	1251.99	311.32	615.21	0.003	—	—
	35	1.429	0.606	−0.154	155.4	809.4	306.8	716.55	114.51	335.09	0.002	3.4	181.6
1,2-Dichloroethane + *p*-xylene	25	1.013	0.442	−0.010	—	—	—	933.03	290.52	629.62	0.003	—	—
	35	1.079	0.384	0.064	−126.9	740.6	594.6	761.70	83.52	217.52	0.002	2.9	169.5

Compound	$\tilde{\varepsilon}^*$ (cal mol⁻¹)	$\tilde{v}^*$ (cm³ mol⁻¹)	r^0	T^* (K)	$\tilde{\rho}^*$ (g cm⁻³)
1,2-Dichloroethane	988	6.73	10.216	497	1.4356

Can. J. Chem. Downloaded from www.nrcresearchpress.com by 210.87.254.40 on 09/05/12
For personal use only.

TABLE 2. The comparison of V^E, H^E, and TS^E experimental and calculated values at 0.3, 0.5, 0.7 mole fractions of 1,2-dichloroethane

System	x_1	V^E (298.15 K) (cm^3/mol)		H^E (298.15 K) (J/mol)		TS^E (298.15 K) (J/mol)		V^E (308.15 K) (cm^3/mol)		H^E (308.15 K) (J/mol)		TS^E (308.15 K) (J/mol)	
		Calcd	Expt	Calcd	Expt	Calcd	Expt	Calcd	Expt	Calcd	Expt	Calcd	Expt
1,2-Dichloroethane + benzene	0.3	0.146	0.191	−116.1	41.7	−174.3	−5.8	0.169	0.192	−72.3	39.7	−158.2	−0.2
	0.5	0.211	0.227	68.0	65.1	−320.0	8.5	—	—	—	—	—	—
	0.7	0.152	0.199	47.3	79.0	−459.3	31.4	0.158	0.176	49.0	55.1	−490.6	11.1
1,2-Dichloroethane + toluene	0.3	0.152	0.120	−22.3	−48.5	1.7	−157.9	0.124	0.126	−42.3	−40.0	383.5	−163.6
	0.5	0.161	0.166	2.1	−26.9	− 6.0	−159.7	—	—	—	—	—	—
	0.7	0.128	0.155	38.8	21.9	−12.9	−96.0	0.164	0.162	50.0	31.0	170.9	−115.3
1,2-Dichloroethane + *o*-xylene	0.3	0.182	0.214	−6.5	−65.3	−66.9	−243.4	0.261	0.224	27.3	−38.5	−49.7	−74.6
	0.5	0.276	0.291	−33.9	−19.3	−60.0	−241.6	—	—	—	—	—	—
	0.7	0.251	0.270	64.1	48.5	−50.5	−149.9	0.248	0.286	95.7	73.3	−16.9	31.2
1,2-Dichloroethane + *m*-xylene	0.3	0.187	0.256	−48.6	−50.0	−13.2	−306.0	0.189	0.245	−37.2	−25.0	6.2	−177.2
	0.5	0.211	0.353	9.5	15.1	−23.1	−297.9	—	—	—	—	—	—
	0.7	0.265	0.328	87.0	95.0	−17.9	−214.7	0.265	0.345	128.1	110.9	−8.0	−60.4
1,2-Dichloroethane + *p*-xylene	0.3	0.147	0.175	−120.1	−99.0	41.5	−291.7	0.152	0.196	−70.3	−68.9	−30.5	−229.1
	0.5	0.215	0.253	−63.2	−64.5	32.1	−297.3	—	—	—	—	—	—
	0.7	0.198	0.249	33.8	17.4	−9.2	−224.1	0.236	0.261	41.6	55.5	−2.1	−118.7

[4] $$V^E = \left[\frac{1}{\tilde{\rho}_{mix}} - \sum \phi_i \tilde{v}_i\right] \overset{*}{v}_{mix} r_{mix}$$

where

[5] $$\phi_i^0 = (m_i/\overset{*}{\rho}_i \overset{*}{v}_i)/(\sum m_i/\overset{*}{\rho}_i \overset{*}{v}_i)$$

[6] $$\phi_i = (m_i/\overset{*}{\rho}_i)/(\sum m_i/\overset{*}{\rho}_i)$$

[7] $$m_i = x_i M_i/\sum x_i M_i$$

(M_i = molecular weight of component i in the mixture)

[8] $$\overset{*}{v}_{mix} = \sum \phi_i^0 \overset{*}{v}_i$$

[9] $$r_{mix} = \sum x_i (\overset{*}{v}_i r_i^0/\overset{*}{v}_{mix})$$

[10] $$X_{ij} = (\overset{*}{\varepsilon}_{ii} + \overset{*}{\varepsilon}_{jj} - 2\overset{*}{\varepsilon}_{ij})/RT$$

and

[11] $$\overset{*}{\varepsilon}_{mix} = \sum\sum \phi_i \phi_j \overset{*}{\varepsilon}_{ij}$$

All the parameters in eqs. [5]–[11] are known from the properties of pure compounds.

The $\overset{*}{\varepsilon}_{ij}$ and $\tilde{\rho}_{mix}$ values thus obtained were utilized to see as to how closely [12] was satisfied

[12] $$\tilde{\rho}_{mix}^2 + \frac{RT}{\overset{*}{\varepsilon}_{mix}}\left[\left(1 - \frac{1}{r_{mix}}\right)\tilde{\rho}_{mix} + \ln(1 - \tilde{\rho}_{mix})\right] + \frac{P_{mix}\overset{*}{v}_{mix}}{\overset{*}{\varepsilon}_{mix}} = 0$$

It was observed that [12] was satisfied to 0.01. In all subsequent evaluations of $\tilde{\rho}_{mix}$ for the mixture at any other temperature and composition, [12] was always solved to this accuracy by numerical techniques. The $\overset{*}{\varepsilon}_{ij}$ value thus obtained for the mixture from its V^E and H^E values for an equimolar mixture at 308.15 K was next used to calculate $\overset{*}{\varepsilon}_{mix}$ and $\tilde{\rho}_{mix}$ from [11] and [12] and hence V^E and H^E for the mixture at any other temperature and composition. These V^E and H^E values at 308.15 and 298.15 K are recorded in Table 2 and are also compared with their corresponding experimental values (the H^E data at 298.15 K were taken from the literature (25)). The corresponding TS^E values were then evaluated from

[13] $$TS^E = -RT[\sum x_i \ln x_i/\phi_i + r_{mix} \times (\tilde{v}_{mix} - 1)\ln(1 - \tilde{\rho}_{mix}) + \ln \tilde{\rho}_{mix} - \sum x_i\{r_i^0(\tilde{v}_i - 1)\ln(1 - \tilde{\rho}_i) + \ln \tilde{\rho}_i\}]$$

These TS^E values are recorded in Table 2 and are also compared with the corresponding experimental values. All the parameters in [3]–[13] have the same significance as suggested by Sanchez and Lacombe (1, 2). The parameters $\overset{*}{\varepsilon}$, $\overset{*}{v}$, r^0, $\overset{*}{T}$, and $\overset{*}{\rho}$ for benzene, toluene, *o*-xylene, *m*-xylene, and *p*-xylene were taken from the literature (1) while those for 1,2-dichloroethane were evaluated in the manner described by

Can. J. Chem. Downloaded from www.nrcresearchpress.com by 210.87.254.40 on 09/05/12
For personal use only.

Sanchez and Lacombe (1); the necessary vapour pressure data at various temperatures were taken from the literature (26) while the corresponding density data were obtained by extrapolating the available density data (10). These parameters are recorded in Table 1.

Examination of Table 2 reveals that this theory is reasonably successful in predicting V^E and H^E values for the various mixtures at 308.15 and 298.15 K. However the same is not true of the TS^E values.

The qualitative difference in the behaviour of 1,2-dichloroethane towards various hydrocarbons may be related to the difference in the pure component parameters ε^* and r. Thus relative to 1,2-dichloroethane, benzene among all the hydrocarbons has the smallest repulsive intermolecular potential. Consequently V^E for the binary mixtures 1,2-dichloroethane with aromatic hydrocarbons should vary in the order benzene < toluene < *o*-xylene ≈ *p*-xylene < *m*-xylene. This is really true of the binary mixtures of 1,2-dichloroethane with *o*-, *m*-, and *p*-xylenes. For the remaining two mixtures, the V^E data can be explained if it is assumed that these mixtures are characterized by the charge transfer interactions between the components of these mixtures also. The introduction of a CH_3 substituent in benzene as in toluene would then increase the π-electron density of the aromatic ring in toluene which would then be readily accommodated in the vacant *d* levels of Cl atoms of 1,2-dichloroethane, as compared to benzene. Since the observed V^E would be the net effect of the repulsive intermolecular potential and charge transfer interaction, V^E for toluene would be less than that for benzene in their binary mixtures with 1,2-dichloroethane.

Again the sign and magnitude of H^E depends primarily on the contribution of the terms in ref. 3. Since the contribution of first term in ref. 3 which depends on χ_{12} (value in Table 1) outweighs those due to $\sum_i(\tilde{p}_i\phi_i^0 - \tilde{p}\phi_i)/T_i$, H^E is negative. This is true for all except the binary mixtures of 1,2-dichloroethane with benzene. This may be attributed to the small negative χ_{12} value for this mixture which suggests that in this mixture the unlike interactions are energetically more favoured than the like ones. However, the close proximity of 2 Cl atoms of 1,2-dichloroethane in its interaction with the π-electrons of the benzene ring may give rise to a repulsive contribution and since the observed H^E is the cumulative sum of the contributions due to unlike and steric interactions, H^E for this mixture is positive.

Acknowledgement

R.M. acknowledges her grateful thanks to the M.D. University, Rohtak for the award of a University Fellowship.

1. R. H. LACOMBE and I. C. SANCHEZ. J. Phys. Chem. **80**, 2352 (1976).
2. R. H. LACOMBE and I. C. SANCHEZ. J. Phys. Chem. **80**, 2568 (1976).
3. I. C. SANCHEZ and R. H. LACOMBE. Macromolecules, **11**, 1145 (1978).
4. F. KIMURA and S. MURAKAMI. Fluid Phase Equilibra, **3**, 93 (1979).
5. P. J. FLORY. Principles of polymer chemistry. Cornell University Press, Ithaca, New York. 1953. Chapts. 12, 13.
6. R. K. NIGAM and B. S. MAHL. Indian J. Chem. **77**, 2081 (1973).
7. J. N. VIJ and B. S. MAHL. Thermochim. Acta, **12**, 155 (1975).
8. A. F. FORZIATI, A. R. GLASGOW, JR., C. B. WILLINGHAM, and F. D. ROSSINI. J. Res. Natl. Bur. Stand. **36**, 129 (1946).
9. H. PERKIN. J. Chem. Soc. London, **69**, 1025 (1896); J. TIMMERMANS. Physico chemical constants of pure organic compounds. Elsevier Publishing Company, Inc., New York. 1950.
10. G. W. SEARS and E. R. HOPKE. J. Am. Chem. Soc. **71**, 1632 (1949); **71**, 2575 (1949).
11. R. K. NIGAM and P. P. SINGH. Trans. Faraday Soc. **65**, 950 (1969).
12. R. K. NIGAM and B. S. MAHL. J. Chem. Soc. Faraday Trans. I, **68**, 1508 (1972).
13. R. K. NIGAM and B. S. MAHL. Indian J. Chem. **9**, 1250 (1971).
14. F. HOVORKA and D. DREISBACH. J. Am. Chem. Soc. **56**, 1664 (1934).
15. K. S. PITZER and D. W. SCOTT. J. Am. Chem. Soc. **65**, 803 (1943).
16. A. D. JOHN (*Editor*). Lange's handbook of chemistry. 11th ed. McGraw Hill Book Co. 1973. pp. 10–37, 10–45.
17. J. A. BARKER. Aust. J. Chem. **6**, 207 (1953).
18. O. REDLICH and A. I. KISTER. Ind. Eng. Chem. **40**, 345 (1948).
19. P. W. ALLEN, D. H. EVERETT, and M. F. PENNEY. Proc. R. Soc. A**212**, 149 (1952).
20. G. SCATCHARD and L. B. TICKNOR. J. Am. Chem. Soc. **74**, 3724 (1952).
21. R. C. REID and T. S. SHERWOOD. The properties of gases and liquids. McGraw Hill Book Co., New York. 1958. pp. 575, 583.
22. E. A. GUGGENHEIM. Proc. R. Soc. London, Ser. A, **183**, 203 (1944).
23. E. A. GUGGENHEIM. Mixtures. Oxford University Press, London. 1952. Chapts. X and XI.
24. E. A. GUGGENHEIM. Application of statistical mechanics. Oxford University Press, London. 1966. Chapts. 4, 7.
25. B. S. MAHL and J. R. KHURANA. J. Chem. Soc. Faraday Trans. **73**(1), 29 (1977).
26. H. R. PATEL, S. SUNDRAM, and D. S. VISHWANATH. J. Chem. Eng. Data, **24**(1), 41 (1979).

Determination of $D[C_6F_5CH_2—Br]$ by the toluene carrier method

R. JOHN KOMINAR AND MICHAEL J. KRECH
Chemistry Department, Wilfrid Laurier University, Waterloo, Ont., Canada N2L 3C5
AND
STANLEY JAMES W. PRICE[1]
Chemistry Department, University of Windsor, Windsor, Ont., Canada N9B 3P4

Received April 22, 1980

R. JOHN KOMINAR, MICHAEL J. KRECH, and STANLEY JAMES W. PRICE. Can. J. Chem. **58**, 1906 (1980).

The pyrolysis of $C_6F_5CH_2Br$ has been studied by the toluene carrier technique over the temperature range 727–800°C. Rate constants are based on analysis for residual parent compound by gas chromatography using an internal standard technique. In selected runs a material balance of 100 ± 2% was obtained for bromine based on $C_6F_5CH_2Br$ plus HBr. Within the limits of the experimental technique the process appears to be first order and homogeneous. In addition to HBr the other major products of the thermal decomposition are $C_6F_5CH_3$, $(C_6F_5CH_2)_2$, $C_6F_5CH_2CH_2C_6H_5$, and $(C_6H_5CH_2)_2$. The Arrhenius equation obtained is

$$\log k_1\,(s^{-1}) = 14.54 \pm 0.42 - (225000 \pm 6000)/19.1T$$

The log A value is very close to the value of 14.6 recommended by Benson and O'Neal for the decomposition of $C_6H_5CH_2Br$. The activation energy, 225 ± 6 kJ mol^{-1}, should be a reasonable estimate of $D[C_6F_5CH_2—Br]$.

R. JOHN KOMINAR, MICHAEL J. KRECH et STANLEY JAMES W. PRICE. Can. J. Chem. **58**, 1906 (1980).

Utilisant la technique du toluène comme vecteur, on a étudié la pyrolyse du $C_6F_5CH_2Br$ sur une échelle de température allant de 727 à 800°C. Les constantes de vitesse sont calculées à partir de l'analyse du composé initial résiduel par chromatographie en phase gazeuse en faisant appel à la technique d'une référence interne. Dans des expériences choisies, on a obtenu un bilan pondéral de 100 ± 2% pour le brome en se basant sur le $C_6F_5CH_2Br$ plus le HBr. A l'intérieur des limites de la technique expérimentale, la réaction semble être homogène et d'ordre un. En plus du HBr, les autres produits principaux de la décomposition thermique sont: $C_6F_5CH_3$, $(C_6F_5CH_2)_2$, $C_6F_5CH_2CH_2C_6H_5$ et $(C_6H_5CH_2)_2$. On obtient l'équation d'Arrhénius suivante:

$$\log k_1\,(s^{-1}) = 14{,}54 \pm 0{,}42 - (225000 \pm 6000)/19{,}1T$$

La valeur de log A est très près de celle de 14.6 recommandée par Benson et O'Neal pour la décomposition de $C_6H_5CH_2Br$. L'énergie d'activation de 225 ± 6 kJ mol^{-1} serait une évaluation raisonnable de $D[C_6F_5CH_2—Br]$.

[Traduit par le journal]

Introduction

No previous studies of the pyrolysis of bromomethylpentafluorobenzene have been reported. Szwarc, Ghosh, and Sehon have studied the decomposition of $C_6H_5CH_2Br$ in a toluene carrier system and report that the Arrhenius parameters for the rupture of the C—Br bond are $E = 211$ kJ mol^{-1} and log $A = 13.0$ (2). However, based on the rate constants from the work of Szwarc *et al.* and thermodynamic arguments, Benson and O'Neal suggest "preferred values" of $E = 237$ kJ mol^{-1} and log $A = 14.6$ (1). Studies of related compounds by X-ray photoelectron spectroscopy and evaluation by ACHARGE and CNDO/2 calculations would suggest a slightly lower electron density on the methyl carbon in $C_6F_5CH_2Br$ cf. $C_6H_5CH_2Br$ (3, 4). Thus, it might be expected that $D[C_6F_5CH_2—Br]$ would be slightly lower than $D[C_6H_5CH_2—Br]$. The A factors for the carbon–bromine bond dissociations in the two compounds should be very similar.

[1]To whom all correspondence should be addressed.

Experimental

Materials

(a) Bromomethylpentafluorobenzene

The $C_6F_5CH_2Br$ used was obtained from Imperial Smelting Corporation. Prior to use, $C_6F_5CH_2Br$ was vacuum distilled and the head and tail fractions were discarded. Analysis by gas chromatography (6 ft × 0.125 in. 15% Apiezon L on Chromosorb W, N_2 carrier, 30 cm^3/min, isothermal for 4 min at 100°C and temperature programmed from 100–160°C at 32°C/min) using a flame ionization detector, showed only minor impurities estimated at a maximum of 0.01% of the sample.

(b) Toluene

Toluene from sulfonic acid (Eastman Organic X325) was prepared for use by refluxing over sodium under vacuum and then degassing by bulb-to-bulb distillation.

(c) n-Undecane

n-Undecane used as the internal standard for gc analysis was obtained from BDH Chemicals Ltd. and used as received.

Apparatus and Procedure

The basic toluene carrier system has been previously described (5). The quantity of $C_6F_5CH_2Br$ required for a run was injected via a gas tight syringe through a rubber septum. This procedure was subsequently modified by adding stop-cocks to the line so that after injection of $C_6F_5CH_2Br$ it could be isolated, frozen down, and degassed to remove any traces of air dissolved in the $C_6F_5CH_2Br$ or admitted during injection. The stop-cocks

0008-4042/80/181906-03$01.00/0
©1980 National Research Council of Canada/Conseil national de recherches du Canada

Can. J. Chem. Downloaded from www.nrcresearchpress.com by 210.87.254.42 on 09/05/12
For personal use only.

TABLE 1. Selected results for the pyrolysis of bromomethylpentafluorobenzene*

T (K)	P (kPa)	t_c (s)	Decomposition (%)	Toluene / $C_6F_5CH_2Br$ (molar ratio)	k_1 (s^{-1})
784.5	4.32	3.19	70.3	101	0.382
784.4	4.38	3.23	69.7	153	0.369
780.8	4.46	3.52	64.1	242	0.291
773.7	4.54	3.73	56.9	118	0.225
763.3	4.48	3.44	41.2	30	0.154
759.0 P	4.35	1.54	16.7	223	0.118
758.1	4.34	2.80	27.7	257	0.116
756.8 P	4.22	1.65	16.3	186	0.108
756.5	4.48	3.57	30.6	88	0.102
754.1	4.34	2.79	22.5	257	0.0913
748.9 P	4.27	1.65	9.9	188	0.0633
746.0	4.48	3.59	20.3	88	0.0633
727.8	4.09	3.16	7.1	196	0.0235
727.4	4.09	3.11	7.7	184	0.0257

*P runs in packed reaction vessel, surface-to-volume ratio 17 times that in unpacked vessel.

could then be adjusted to allow the toluene to pick up the $C_6F_5CH_2Br$. All lines into and out of the reaction zone were wrapped with heating windings controlled by variacs, to prevent condensation. The section containing the $C_6F_5CH_2Br$ was separately wound with its own variac to control the concentration of $C_6F_5CH_2Br$ in the toluene stream. Total pressures were taken by a differential manometer, after $C_6F_5CH_2Br$ had been removed from the system, while only toluene was flowing. The reaction vessels were treated with hot fuming nitric acid prior to use. Residual acid was baked out under vacuum after a vessel was installed in the system.

Toluene, unreacted $C_6F_5CH_2Br$, HBr, and other condensibles were trapped at −80°C. In experiments where the amount of HBr produced was to be quantitatively determined, the liquid products were isolated, the cold bath removed, and 25 mL of standardized NaOH introduced into the flask. The entire contents were stirred for 10–15 min with a magnetic stirrer while under vacuum. The aqueous layer was separated and titrated with standard HCl. The organic layer was dried over $MgSO_4$, filtered, and transferred to a tared amber sample bottle with a Teflon lined top. The sample was weighed and a weighed amount of internal standard, *n*-undecane, added. In experiments where HBr analyses were not carried out, the collected liquid products were transferred directly to amber bottles, weighed, and a weighed amount of internal standard introduced. The samples were analyzed on a P.E. Model 3920 Gas Chromatograph for $C_6F_5CH_3$, $C_6F_5CH_2Br$, $(C_6H_5CH_2)_2$, $C_6F_5CH_2$—$CH_2C_6H_5$, and $(C_6F_5CH_2)_2$ (6 ft × 0.125 in. 15% Apiezon L on Chromosorb W, N_2 carrier 16 cm/min, isothermal at 125°C for 8 min then 32°/min to 180°C, 4 min hold at 180°C). The peak areas were determined using a Columbia Scientific Industries Model CSI 38 digital electronic integrator.

Results and Discussion

Selected experimental results are given in Table 1. They may be discussed in terms of the following mechanisms:

[1] $C_6F_5CH_2Br \rightarrow C_6F_5CH_2 + Br$

[2] $Br + C_6H_5CH_3 \rightarrow C_6H_5CH_2 + HBr$

[3] $C_6F_5CH_2 + C_6H_5CH_3 \rightarrow C_6F_5CH_3 + C_6H_5CH_2$

[4] $C_6F_5CH_2 + C_6H_5CH_2 \rightarrow C_6F_5CH_2CH_2C_6H_5$

[5] $2C_6H_5CH_2 \rightarrow (C_6H_5CH_2)_2$

[6] $2C_6F_5CH_2 \rightarrow (C_6F_5CH_2)_2$

In addition, trace quantities of hydrogen and methane were observed, indicating very slight decomposition of the toluene carrier (0.001–0.01%).

First order rate constants were based on analysis for undecomposed $C_6F_5CH_2Br$. In addition, in six runs the quantity of HBr produced was determined. The amount of decomposition in these runs ranged from 12% to 71%. In these runs a material balance based on HBr + $C_6F_5CH_2Br$ was obtained with an average deviation of ±2%. Values of k_1 at various concentrations are shown in Table 2. Within the limits of the experimental method these results would appear to be consistent with first order behaviour.

Representative analytical data for the products

TABLE 2. The effect of $C_6F_5CH_2Br$ concentration on k_1*

T (K)	$[C_6F_5CH_2Br]$ (mol cm^{-3} × 10^9)	k_1 (s^{-1})
746	0.82	0.063
	2.80	0.061
757	3.56	0.107
	8.05	0.102
765	2.59	0.148
	7.89	0.154
	23.6	0.154

*Toluene concentration in these runs approximately 7×10^{-7} mol cm^{-3}.

Can. J. Chem. Downloaded from www.nrcresearchpress.com by 210.87.254.42 on 09/05/12
For personal use only.

TABLE 3. Representative product distribution for products involving $C_6F_5CH_2$ and $C_6H_5CH_2$

	Concentration (mol × 10^5)			
T (K)	$C_6F_5CH_3$	$(C_6F_5CH_2)_2$	$(C_6H_5CH_2)_2$	$C_6F_5(CH_2)_2C_6H_5$
751	3.14	0.57	3.43	2.95
773	6.42	0.99	8.30	6.92
784	9.57	1.49	11.90	9.50
784	10.00	1.67	13.16	10.69
797	12.52	1.71	14.36	11.06
800	13.08	1.68	14.11	10.94

of reactions [3] through [6] are shown in Table 3. The amount of decomposition in the runs used in this table ranges from 20% to 90%. With the system used, quantitative recovery of the dimers formed in reactions [4]–[6] was often difficult. Based on analysis for residual $C_6F_5CH_2Br$, the recoveries of $C_6F_5CH_3$, $(C_6F_5CH_2)_2$, and $C_6F_5(CH_2)_2C_6H_5$ fell in the range of 82%–100% with an average recovery of 93%. Based on the yields of fluorinated products, the quantities of dibenzyl found are all within ± 10% of the expected values. The yields of the recombination products are in agreement with the expected and required constancy of the rate constant ratio k_5k_6/k_4^2.

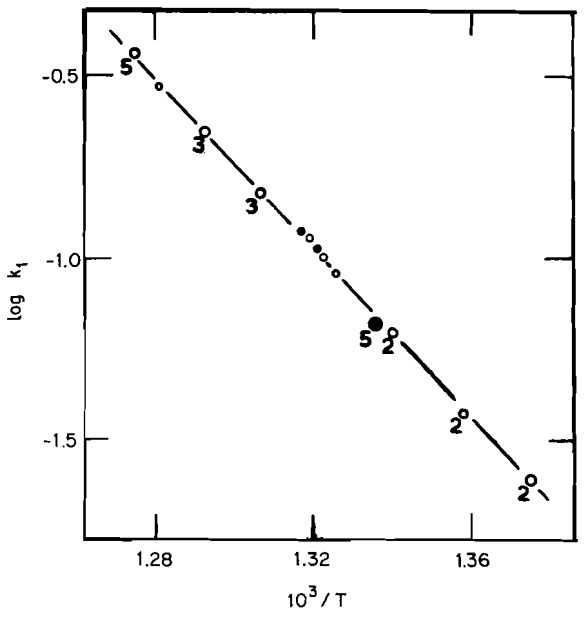


FIG. 1. Arrhenius plot for the decomposition of $C_6F_5CH_2Br$. Open circles: runs in unpacked reaction vessel. Full circles: runs in packed reaction vessel. Numbers are number of runs averaged to obtain the given point. Size of the point indicates the range of values.

The Arrhenius plot for values of k_1 is shown in Fig. 1. Approximately one-quarter of the experiments were carried out using a packed reaction vessel with a surface-to-volume ratio 17 times that of the unpacked vessel. No detectable surface effects were found. The data may be adequately represented by

$$\log k_1\,(s^{-1}) = 14.54 \pm 0.42 - (225000 \pm 6000)/19.1T$$

The error limits are based on two times the standard deviation. The activation energy, 225 ± 6 kJ mol^{-1}, should be a reasonable estimate of $D[C_6F_5CH_2—Br]$. The A factor is very close to the "preferred" value of 14.6 given by Benson and O'Neal for the pyrolysis of $C_6H_5CH_2Br$ (1) while the present activation energy is some 12 kJ mol^{-1} less than the estimated value for $C_6H_5CH_2Br$, giving a possible indication that fluorination of the aromatic ring slightly weakens the C—Br bond.

Acknowledgement

This work has been supported by a grant from the Natural Sciences and Engineering Research Council of Canada.

1. S. W. BENSON and H. E. O'NEAL. Natl. Stand. Ref. Data Ser. Natl. Bur. Stand. **21**, 511 (1970).
2. M. SZWARC, B. N. GHOSH, and A. H. SEHON. J. Chem. Phys. **18**, 1142 (1950).
3. B. C. TRUDELL and S. J. W. PRICE. Can. J. Chem. **55**, 1279 (1977).
4. B. C. TRUDELL and S. J. W. PRICE. Can. J. Chem. **56**, 538 (1978).
5. M. J. KRECH and S. J. W. PRICE. Can. J. Chem. **41**, 224 (1963).

Can. J. Chem. Downloaded from www.nrcresearchpress.com by 210.87.254.42 on 09/05/12
For personal use only.

The sonolysis of uracil

TAIN-JEN YU, RONALD G. SUTHERLAND, AND RONALD E. VERRALL[1]

Department of Chemistry and Chemical Engineering, University of Saskatchewan, Saskatoon, Sask., Canada S7N 0W0

Received August 28, 1979[2]

TAIN-JEN YU, RONALD G. SUTHERLAND, and RONALD E. VERRALL. Can. J. Chem. **58**, 1909 (1980).

The sonolysis of uracil (**1**) has been studied at 630 kHz in the presence of air, oxygen, nitrogen, and argon. The degradation products were identified by gc–ms analysis. Under aerated conditions the following products were found: uracil glycols (**7**), isobarbituric acid (**8**), *N*-formyl-*N'*-glyoxylurea (**6**), 5-hydroxyhydantoin (**9**), dialuric acid (**10**), alloxan monohydrate (**12**), parabanic acid (**13**), and oxaluric acid (**14**). In deaerated solutions **6**, **13**, and **14** were not observed but either 6-hydroxy-5,6-dihydrouracil (**17**) or its isomer (**18**) were detected in addition to **7**, **8**, **9**, **10**, and **12**. The observed products have been used to develop a possible mechanism for the sonolytic degradation and the results are similar to those obtained in radiolysis.

The sonolytic degradation of 5-bromouracil (**19**) is also reported; the products observed were 5-bromobarbituric acid (**20**), **12**, **13**, **14**, and **9** and these can be rationalized by a similar mechanistic scheme.

TAIN-JEN YU, RONALD G. SUTHERLAND et RONALD E. VERRALL. Can. J. Chem. **58**, 1909 (1980).

On a étudié la sonolyse de l'uracile (**1**) à 630 kHz en présence d'air, d'oxygène, d'azote et d'argon. On a identifié les produits de dégradation par spectrométrie de masse couplé à un chromatographe en phase gazeuse. En présence d'air, on obtient les composés suivants: le glycol d'uracyle (**7**), l'acide isobarbiturique (**8**), la *N*-formyl *N'*-gloxylurée (**6**), l'hydroxy-5 hydantoine (**9**), l'acide dialurique (**10**), le monohydrate l'alloxane (**12**), l'acide parabanique (**13**) et l'acide oxalurique (**14**). Dans des solutions en absence d'air, on n'observe pas les composés **6**, **13** et **14** mais on décèle les composés **7**, **8**, **9**, **10** et **12** avec en plus soit l'hydroxy-6 dihydro-5,6 uracile (**17**) soit son isomère (**18**). Sur la base des produits observés on a développé un mécanisme possible de la dégradation sonolytique et les résultats sont semblables à ceux obtenus par radiolyse.

On rapporte également la dégradation sonolytique de la bromo-5 uracile (**19**); les produits observés sont l'acide bromo-5 barbiturique (**20**), **12**, **13**, **14** et **9** et on peut les rationnaliser selon le même mécanisme.

[Traduit par le journal]

Introduction

Chemical reactions can be initiated by ultrasonic waves in liquids if the acoustic intensity is sufficient to induce cavitation (1,2). In this paper we report the sonolytic degradation of uracil (**1**) and it is part of a series (3, 4*a*) in which we examine the effect of ultrasound on biologically important molecules related to DNA and RNA. There are two other reports on the sonolysis of uracil in the literature (2, 5); however, the results of this study are much more detailed and demonstrate, for the first time, the use of the technique of gc–ms to separate and analyze the degradation products.

Since the radiolysis of uracil has been exhaustively investigated (6–14) and the primary reactions in the sonolysis of aqueous solutions (15–21) are known to be essentially similar to those produced in radiolytic reactions, the sonolysis and radiolysis results are compared and contrasted.

The sonolysis of 5-bromouracil (**19**) is also reported since the results obtained differ from those previously reported (5) where no degradation was observed.

Experimental

Ultrasonic Irradiation System and General Procedures

Irradiations were carried out with a Multisons MC 500-1 (Macrosonics Corporation, Cartaret, NJ) broad band generator coupled to a cobalt barium titanate transducer operated at 630 kHz with an average power output of 3.63×10^2 rads/s. Aliquots (50 mL) of aqueous solutions were insonated in a glass cell with a Mylar 500A plastic window (3, 22). A gas inlet was inserted into the glass cell and the solutions were saturated with the appropriate gas for at least 30 min prior to and during sonolysis when the experiment was carried out under air, O_2, N_2, or Ar atmosphere. Alternatively, a closed system was used without continuous bubbling of the gas during sonolysis in experiments when air was involved. The coupling liquid was an ethylene glycol – water mixture (60:40 by volume) whose temperature was maintained at 25°C. The aliquots were freeze-dried immediately after sonolysis and analyzed by gc–ms techniques.

A Cary 118 spectrophotometer was used to measure the change in absorbance at λ_{max} of the sample before and after sonolysis. Uracil absorbance was measured at 259.5 nm in a 1.0 cm quartz cell and that of 5-bromouracil at 276 nm. A Beckman Expandomatic SS-2 pH meter was used to measure the pH values before and after sonolysis.

General Analysis Procedures

After lyophilization the degradation products were converted to their trimethylsilyl (TMS) derivatives for gc–ms analysis (4*a*). Silylations were conducted by heating the reactants in an oil bath (150°C) for 10 min using the following proportions: one mg of the degradation products mixed with 100 μL of *N,O*-bis(trimethylsilyl)-trifluoroacetamide (BSTFA) and 100 μL of acetonitrile in a silylation vial (4*b*).

The gc–ms analyses were performed using a Finnigan Model 3300 gas chromatograph – mass spectrometer. Electron ionization (EI) spectra were obtained at an ionizing voltage of 70eV and the chemical ionization (CI) spectra were obtained using methane as the reagent gas. The chromatographic conditions were as follows: temperature program, 80–240°C at 4°C/min; injector temperature 250°C; detector temperature 280°C; air flow rate: 300 mL/min; hydrogen flow rate: 30 mL/min; and

[1]Author to whom correspondence should be addressed.

[2]Revision received June 4, 1980.

0008-4042/80/181909-07$01.00/0

© 1980 National Research Council of Canada/Conseil national de recherches du Canada

Can. J. Chem. Downloaded from www.nrcresearchpress.com by 210.87.254.105 on 09/05/12
For personal use only.

nitrogen flow rate: 30 mL/min. In the CI mode methane was used as the carrier gas for gc separation with a flow rate ca. 20 mL/min while the source pressure was optimized at 800 μm. Spectra were recorded at a rate of 2 s per scan. Accumulation of spectra and data manipulation were performed using a Finnigan Model 2300 INCOS data system.

The sonolytic degradation products were identified using both CI and EI mass spectra. Whenever possible final confirmation was made by comparison with authentic samples.

Materials

Uracil (Aldrich Chemical Co.) and 5-bromouracil (ICN·K&K Laboratories, Inc.) were recrystallized from triply distilled water before use. Urea (McArthur Chemical Co. Ltd.), alloxan, parabanic acid (Eastman Kodak Co.), isobarbituric acid, barbituric acid (Sigma Chemical Co.), and *p*-dimethylaminobenzaldehyde (J. T. Baker Chemical Co.) were used without further purification. BSTFA, acetonitrile, Pyrex columns (approximately 1.5 × 2 mm id), silylation vials, and column packing (8% SE-30 on AW-DMCS Chromosorb W, 80–100 mesh) were purchased from Chromatographic Specialties (Brockville, Ont.). Reagent grade tertiary butanol (Fisher Scientific Co.) was used without further purification.

The water used in this study was prepared by distillation of previously deionized water from alkaline permanganate followed by acidic perchromate solutions. All glassware used in these experiments was baked at 650°C before use.

Results and Discussion

The degradation products observed when 2 m*M* uracil solutions are insonated at 630 kHz for 80 min are dependent to some extent upon the gas used to saturate the aqueous solutions. In the presence of air or oxygen, eight degradation products have been identified: *N*-formyl-*N'*-glyoxylurea (**6**), uracil glycols (**7**), isobarbituric acid (**8**), 5-hydroxyhydantoin (**9**), dialuric acid (**10**), alloxan monohydrate (**12**), parabanic acid (**13**), and oxaluric acid (**14**). In the presence of nitrogen or argon six compounds were identified: uracil glycols (**7**), isobarbituric acid (**8**), 5-hydroxyhydantoin (**9**), dialuric acid (**10**), alloxan monohydrate (**12**), and either 6-hydroxy-5,6-dihydrouracil (**17**) or 5-hydroxy-5,6-dihydrouracil (**18**). Absorbance measurements showed that uracil was 74% degraded in the presence of air in a closed system without continuous air saturation and 60% with continuous gas saturation during insonation. The extent of degradation in oxygen was 52%, argon 49%, and nitrogen 10%, respectively. A pH decrease was observed during insonation under all conditions: from 6.5 to 3.4 in air; from 6.4 to 4.0 in oyxgen; and from 6.3 to 4.4 in argon or nitrogen. The degradation of 20 m*M* uracil solutions insonated in the presence of air for 80 min in a closed system was only 14% with an accompanying decrease in pH from 6.4 to 3.6. However, the products were found to be similar to those found at concentrations of 2 m*M*.

Figure 1 is an example of a reconstituted gc spectrum of the degradation products of uracil, in this case after 80 min insonation in a closed system

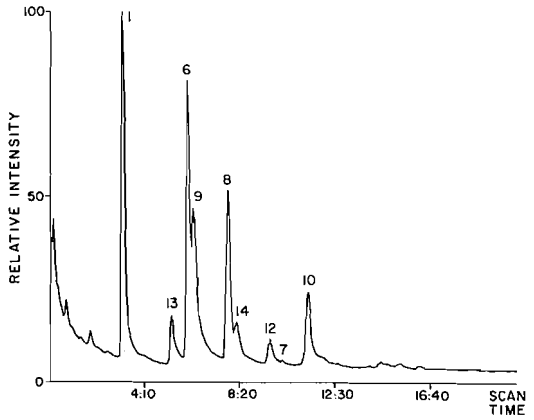


FIG. 1. A gc spectrum of 2 m*M* uracil insonated at 630 kHz for 80 min in the presence of air in a closed system. The gc conditions are given in the text. (Methane as the carrier gas.)

under air. It is very similar to that obtained when air is bubbled through continuously except that more parabanic acid and uracil glycols are present. Shorter insonation periods resulted in less degradation and a smaller pH drop, e.g. 30 min insonation in a closed system resulted in 27% degradation and a pH decrease from 6.4 to 3.8; however, the product profile is similar. Longer insonation periods resulted in almost complete conversion with 97% degradation in 120 min. The addition of tertiary butanol resulted in scavenging of the primary radicals and only 2% degradation in 80 min under argon; the pH change was unaffected by the lack of degradation. The relative product yields under a variety of conditions are given in Table 1.

The gc spectrum of the degradation products of 2 m*M* 5-bromouracil (**19**) insonated at 630 kHz for 80 min in the presence of air in a closed system is shown in Fig. 2; here the conversion is 59% and the pH dropped from 5.7 to 2.8. Six compounds were identified: 5-bromobarbituric acid (**20**), dialuric acid

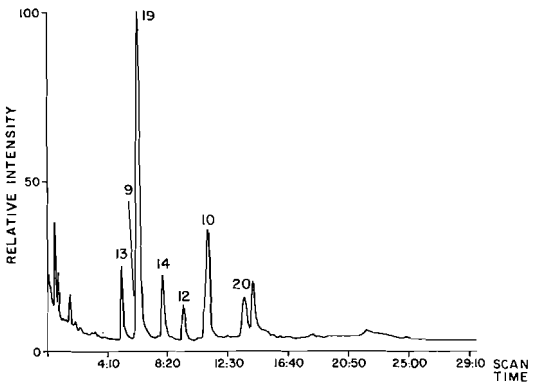


FIG. 2. A gc spectrum of 2 m*M* 5-bromouracil insonated at 630 kHz for 80 min in the presence of air in a closed system. The gc conditions are given in the text. (Methane as the carrier gas.)

Can. J. Chem. Downloaded from www.nrcresearchpress.com by 210.87.254.105 on 09/05/12
For personal use only.

Can. J. Chem. Downloaded from www.nrcresearchpress.com by 210.87.254.105 on 09/05/12
For personal use only.

TABLE 1. Products expressed as a percentage of the total sonolytic degradation products for uracil and 5-bromouracil solutions[a]

Degradation products	2 m*M* Uracil, air (30 min, closed system)	2 m*M* Uracil, air (80 min, closed system)	2 m*M* Uracil, air (80 min, open system)	2 m*M* Uracil, air (120 min, closed system)	20 m*M* Uracil, air (80 min, closed system)	2 m*M* Uracil, O_2 (80 min)	2 m*M* Uracil, Ar (80 min)	2 m*M* Uracil, N_2 (80 min)	2 m*M* 5-Bromouracil, air (80 min, closed system)
Parabanic acid	1	6	18	19	2	4			18
N-formyl-*N'*-glyoxylurea	21	34	26	29	36	34			
5-Hydroxyhydantoin	13	19	19	16	13	24	33	25	[d]
Isobarbituric acid	27	21	16	5	23	5	24[c]	29[c]	
Oxaluric acid	4	5	6	9	3	1			15
6-Hydroxy-5,6-dihydrouracil or 5-hydroxy-5,6-dihydrouracil							[c]	[c]	
Alloxan monohydrate	5	3	1	6[b]	3	12	15	15	8
Uracil glycols	3	0.5	1		7	4	15	12	
Dialuric acid	7	9	6	4	8	12	7	12	27
5-Bromobarbituric acid									10
Unidentified compounds	19	2.5	7	12	5	4	6	7	22

[a]Calculations are based on taking the peak heights of the gc spectra. Estimates obtained from gc peak height for unreacted uracil and from absorbance loss of uracil due to sonolytic degradation differ by 10–15% from previous method.
[b]These two gc peaks cannot be resolved. Mass spectra indicate major component is alloxan monohydrate.
[c]The gc peaks of these isomers and isobarbituric acid are unresolvable. Mass spectra show the latter is the major component.
[d]The gc peak of 5-hydroxyhydantoin is masked by that of 5-bromouracil.

Can. J. Chem. Downloaded from www.nrcresearchpress.com by 210.87.254.105 on 09/05/12
For personal use only.

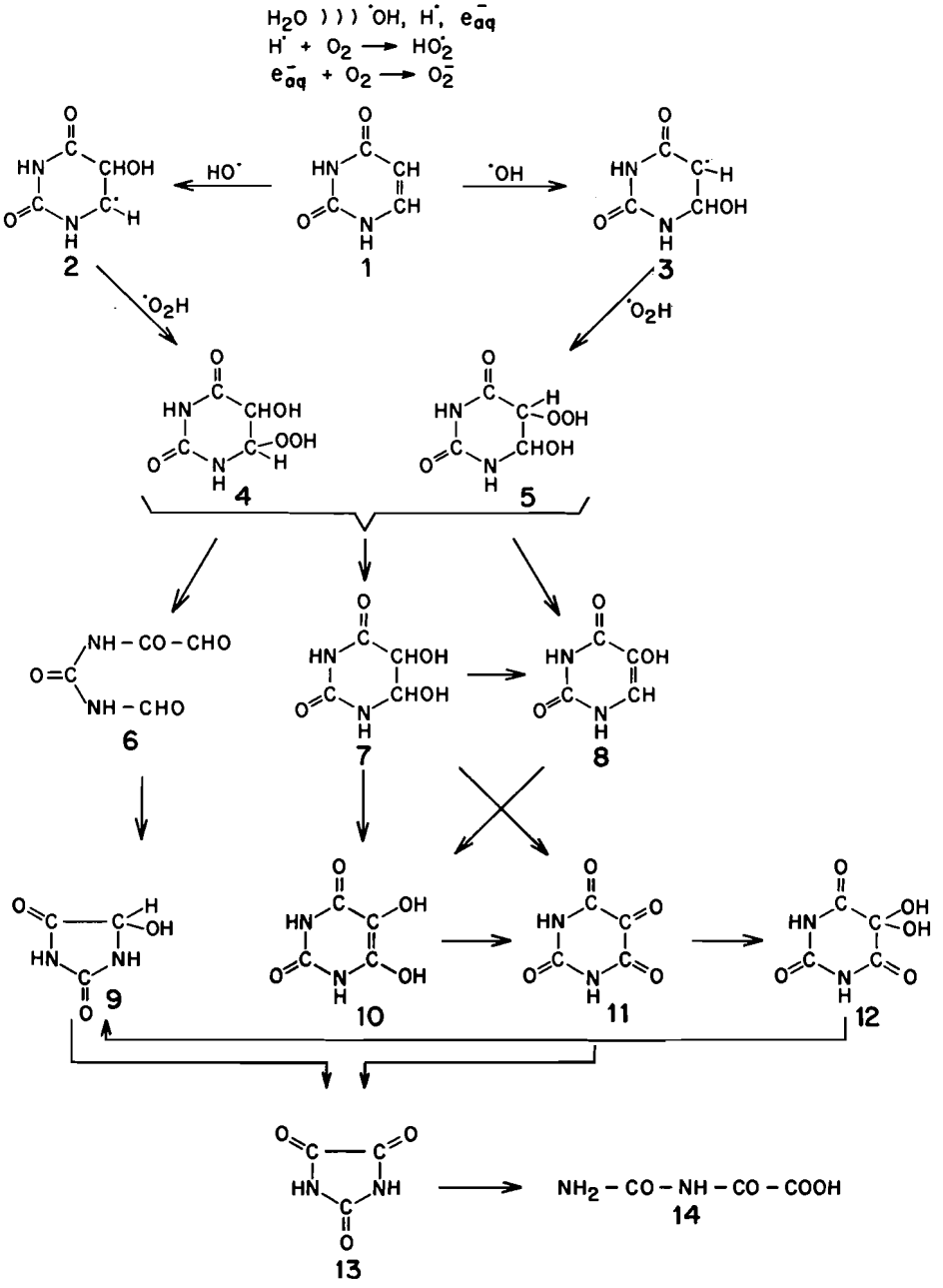


FIG. 3. Proposed sonolytic mechanism of degradation of aqueous uracil solutions in aerated state.

(**10**), alloxan monohydrate (**12**), parabanic acid (**13**), oxaluric acid (**14**), and 5-hydroxyhydantoin (**9**). The peak for **9** overlaps that of **19** but its presence was confirmed by its mass spectrum. Attempts to identify urea using *p*-dimethylaminobenzaldehyde (23) were negative.

The sonolytic degradation products of uracil under aerated conditions are quite similar to those reported (12, 14) for radiolytic degradation in air and this suggests that the mechanism of degradation may be similar. A sonolytic mechanism for uracil in the presence of air or oxygen is summarized in Fig. 3 and described as follows:

During cavitation the primary species produced are $OH^{\cdot}$, $H^{\cdot}$, and e^-_{aq} and in the presence of air (oxygen) the following two reactions occur.

[1] $e^-_{aq} + O_2 \rightarrow O_2^-$

[2] $^{\cdot}H + O_2 \rightarrow HO_2^{\cdot}$

The initial step in sonolysis under these condi-

Can. J. Chem. Downloaded from www.nrcresearchpress.com by 210.87.254.105 on 09/05/12
For personal use only.

tions is the addition of an hydroxyl radical across the 5,6 double bond of uracil (**1**) to form the adducts **2** and **3**, which is followed by $HO_2^{\cdot}$ reacting with the radical adducts to form the hydroperoxides **4** and **5**. These give rise to the uracil glycols (**7**) by the loss of oxygen.[3] Isobarbituric acid (**8**) could be formed by two distinct pathways, from the hydroperoxides by the loss of hydrogen peroxide or from uracil *cis*-glycol by the loss of water. *N*-formyl-*N'*-glyoxylurea (**6**) is a major degradation product in contrast with the radiolytic results (11, 14). It probably results from ring opening of the hydroperoxides since it is not observed in the absence of oxygen, i.e., sonolysis in the presence of N_2 or Ar.

Dialuric acid (**10**) could be produced both by the dehydrogenation of uracil glycols or by the oxidation of isobarbituric acid (24). Alloxan (**11**), detected in radiolysis (12, 14) studies was not found in sonolysis, but its monohydrate (**12**) was. Compound **11** could be an oxidation product of dialuric acid (24), the yield of which is lowered by oxygen, but it could also be formed through dehydrogenation of uracil glycols.

5-Hydroxyhydantoin (**9**) may be derived from the peroxides through *N*-formyl-*N'*-glyoxylurea (10) and also from alloxan monohydrate through a rearrangement process since it was still observed in the absence of oxygen where peroxides are not formed.

Parabanic acid (**13**) may arise from oxidation of 5-hydroxyhydantoin (10) or from rearrangement of alloxan (24). Further hydrolysis of parabanic acid would lead to open chain products like oxaluric acid (**14**).

One of the major differences between the degradation products in radiolysis and sonolysis is the lower yield of uracil glycols in the latter. This may be explained by a faster transformation into isobarbituric acid under acidic conditions (8). Urea and formylurea were both detected in radiolysis (12, 14) but not in sonolysis. It has been reported (3) that the amount of urea formed decreases with increasing insonation time but neither urea nor formylurea were detected when uracil was insonated for 30 min. The acidic condition arising from sonolysis may accelerate their decomposition, but authentic samples were stable under the same pH conditions in the absence of an ultrasonic field and could be detected. This leads one to conclude that the non-detection of urea and formylurea may be due to condensation reactions from *N*-formyl-*N'*-glyoxylurea and may also explain the rather high yields of the latter.

[3]The sterochemistry of these glycols can be either *cis* or *trans* but these cannot be distinguished by the gc–ms technique.

In the absence of oxygen fewer degradation products are detected in sonolysis than in radiolysis (8, 14). A suggested mechanism is shown in Fig. 4 and the rationale is as follows. Since oxygen is absent then hydrogen atoms and hydrated electrons are present in addition to hydroxyl radicals (cf. eqs. [1] and [2]). Hydroxyl radical attack on the 5,6 double bond of uracil occurs as before producing the adducts **2** and **3**. However, since no HO_2 radicals are present to scavenge adducts, these undergo the disproportionation observed in radiolysis (14, 25, 26) to form uracil (**1**) or uracil (**1**) and its glycols (**7**). This would also account for the lower conversion of uracil. Isobarbituric acid (**8**), dialuric acid (**10**), and alloxan (**11**) or alloxan monohydrate (**12**) can arise from uracil glycols as before and 5-hydroxyhydantoin (**9**) from alloxan monohydrate. *N*-formyl-*N'*-glyoxylurea, parabanic acid, and oxaluric acid are not formed because of the lack of oxygen.

Either 6-hydroxy-5,6-dihydrouracil (**17**) or its isomer (**18**) may occur through addition of a water molecule to the hydrogen uracil adducts **15** and **16** in the presence of H_2O_2 (14). Both of these isomers can be derived by attack of either an hydrated electron or hydrogen atom on uracil (14). Both products **17** and **18** are formed in radiolytic studies (14). While the fragmentation pattern of these compounds may be different, it is difficult to establish in this case since **17** or **18**, or a mixture of both, overlaps with **8** which is a major component. However, it has been stated (27) that the 5-hydrogen uracil adduct is more stable than the 6-hydrogen uracil adduct in radiolysis. No evidence has been obtained for the formation of dimers although they have been observed in radiolysis. Some of higher molecular weight species were observed in the mass spectra but we have not yet identified them.

Six products have been identified in the sonolysis of 5-bromouracil (**19**) in the presence of air. They are dialuric acid (**10**), 5-bromo-barbituric acid (**20**), alloxan monohydrate (**12**), parabanic acid (**13**), oxaluric acid (**14**), and 5-hydroxyhydantoin (**9**). On the basis of these degradation products the mechanism proposed for the sonolysis of uracil in air has to be modified to account for the isolation of **10** and **20**. These can be derived from the bromine-containing analogue of **7**, 5-bromo-5,6-dihydroxy-dihydrouracil. Dialuric acid (**10**) would be formed by the elimination of hydrogen bromide and **20** by the loss of water from the glycol. The other products can be accounted for as in the scheme for uracil (Fig. 3). The lower sonolytic conversion is likely due to the electron withdrawing effects of bromine (5). The pH drops have previously been observed

Can. J. Chem. Downloaded from www.nrcresearchpress.com by 210.87.254.105 on 09/05/12
For personal use only.

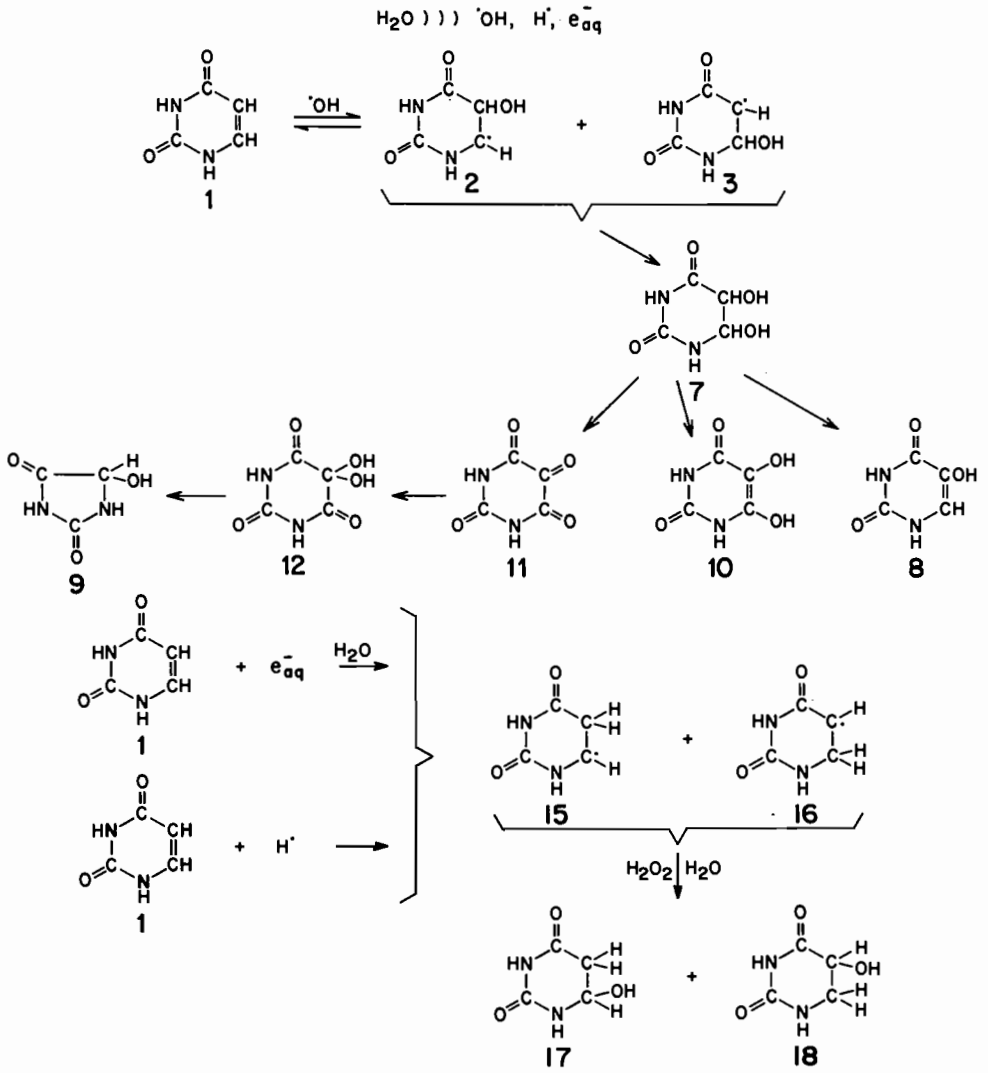


FIG. 4. Proposed sonolytic mechanism of degradation of aqueous uracil solutions in deaerated state.

in the sonolysis of water alone (28) but some of the identified products could accentuate the increase in acidity.

Finally, other work in this laboratory (4) has shown that a train of gas bubbles in a sonic field can have a detrimental effect on cavitation. For short insonation periods (<15 min), it has been found that conversion is reduced under these conditions compared with simply presaturating the solution for long periods and insonating in the absence of a continuous gas stream. However, for long insonation periods, the latter procedure does not assure a steady state concentration of dissolved gas because of degassing. This may explain the different conversions reported between closed and open systems. Furthermore, since it was very difficult to control the bubble flow of gases, the values of conversion as calculated from absorbance data may not be quite comparable under different gases. However, it is interesting to note that there is a difference in sonolytic effects of dissolved gases observed in this study (air > O_2 > Ar > N_2) and others (2,5) (Ar > O_2 > air > N_2).

Acknowledgements

The authors wish to acknowledge the use of the gc–ms facility of the National Research Council of Canada Prairie Regional Laboratory and to thank Mr. L. Hogge for his technical assistance. One of us (T.J.Y.) acknowledges the award of a University of Saskatchewan Postdoctoral Fellowship. Financial support from the Natural Sciences and Engineering

Research Council of Canada to R.G.S. and R.E.V. is gratefully acknowledged.

1. H. G. FLYNN. Physics of acoustic cavitation in liquids. *In* Physics acoustics. Vol. 1. Part B. *Edited by* W. P. Mason. Academic Press, New York. 1964.
2. I. E. EL'PINER. Ultrasound, its physical, chemical and biological effects. *Edited by* Consultants Bureau, New York, NY. 1964.
3. E. L. MEAD, R. G. SUTHERLAND, and R. E. VERRALL. Can. J. Chem. **53**, 2394 (1975).
4. (*a*) W. CRAIG. Ph.D. Dissertation, Department of Chemistry, University of Saskatchewan, 1979; (*b*) G. W. GEHRKE and C. D. RUYLE. J. Chromatogr. **38**, 473 (1968); G. W. GEHRKE and D. B. LAKINGS. J. Chromatogr. **61**, 45 (1971).
5. J. R. MCKEE, C. L. CHRISTMAN, W. D. O'BRIEN, JR., and S. Y. WANG. Biochemistry, **16**, 4651 (1977).
6. M. N. KHATTAK and J. H. GREEN. Aust. J. Chem. **18**, 1847 (1965).
7. M. N. KHATTAK and J. H. GREEN. Int. J. Radiat. Biol. **11**, 577 (1966).
8. K. C. SMITH and J. E. HAYS. Radiat. Res. **33**, 129 (1968).
9. A. NICOLAN, M. MCMILLAN, and R. O. C. NORMAN. Biochim. Biophys. Acta, **174**, 413 (1969).
10. M. C. PEUZIN, J. CADET, M. POLVERELLI, and R. TEOULE. Biochim. Biophys. Acta, **209**, 573 (1970).
11. R. PLETICHA-LANSKY. Tsitol. Genet. **6**, 400 (1972).
12. R. DUCOLOMB, J. CADET, and R. TEOULE. Bull. Soc. Chim. Fr. 1167 (1973).
13. P. C. SHRAGGE, A. J. VARGHESE, J. W. HUNT, and C. L. GREENSTOCK. Radiat. Res. **60**, 250 (1974).
14. G. A. INFANTE, P. JIRATHANA, E. J. FENDLER, and J. H. FENDLER. J. Chem. Soc. Faraday Trans. I, **70**, 1162 (1974).
15. A. WEISSLER. J. Am. Chem. Soc. **81**, 1977 (1959).
16. R. RIVAYRAND and M. HAISSINSKY. J. Chim. Phys. **59**, 623 (1962).
17. M. ANBAR and I. PECHT. J. Phys. Chem. **68**, 352 (1964).
18. M. HAISSINSKY and R. KLEIN. J. Chim. Phys. Phys. Chim. Biol. **65**, 326 (1968).
19. M. A. MARGULIS and A. N. MAL'TSEV. Russ. J. Phys. Chem. **42**, 1412 (1968).
20. M. ANBAR and I. PECHT. J. Phys. Chem. **68**, 1460 (1968).
21. C. SEHGAL, R. P. STEER, R. G. SUTHERLAND, and R. E. VERRALL. J. Phys. Chem. **81**, 2618 (1977).
22. L. A. SPURLOCK and S. B. REIFSNEIDER. J. Am. Chem. Soc. **92**, 6112 (1970).
23. G. W. WATT and J. D. CHRISP. Anal. Chem. **26**, 452 (1954).
24. R. PLETICHA-LANSKY and J. J. WEISS. Anal. Biochem. **16**, 510 (1966).
25. E. S. HILL. J. Biol. Chem. **85**, 713 (1929–1930).
26. G. SCHOLES. Progr. Biophys. Mol. Biol. **13**, 59 (1963).
27. P. NETA. Radiat. Res. **49**, 1 (1972).
28. E. L. MEAD, R. G. SUTHERLAND, and R. E. VERRALL. Can. J. Chem. **54**, 1114 (1976).

Can. J. Chem. Downloaded from www.nrcresearchpress.com by 210.87.254.105 on 09/05/12
For personal use only.

An experimental evaluation of nonselective proton spin–lattice relaxation rates: analyses of data for the eight isomeric 2,3,4-tri-*O*-acetyl-1,6-anhydro-β-D-hexopyranoses[1]

KLAUS BOCK,[2,3] LAURANCE D. HALL, AND CHRISTIAN PEDERSEN[3]

Department of Chemistry, The University of British Columbia, Vancouver, B.C., Canada V6T 1W5

Received January 4, 1980

KLAUS BOCK, LAURANCE D. HALL, and CHRISTIAN PEDERSEN. Can. J. Chem. **58**, 1916 (1980).

The nonselective spin–lattice relaxation rates (R_1-values) have been determined for all of the ring protons of the eight isomers of 2,3,4-tri-*O*-acetyl-1,6-anhydro-β-D-hexopyranose as 0.1 molar solutions in benzene-d_6. The effects on the proton R_1-values of changes in solvent, concentration, temperature, and proton impurities are documented and ^{13}C R_1-values are given to show that the first two sets of variations are due to changes in motional correlation times of the molecules. The proton relaxation data can be fitted by regressional analyses to a single set of interproton relaxation contributions, the numerical values of which accord with a $^1C_4$ conformation for the pyranose ring somewhat distorted by the 1,6-anhydro bridge.

KLAUS BOCK, LAURANCE D. HALL et CHRISTIAN PEDERSEN. Can. J. Chem. **58**, 1916 (1980).

On a déterminé les vitesses de relaxation spin–réseau non sélectives (valeur R_1) de tous les protons du cycle des 8 isomères du tri-*O*-acétyl-2,3,4 anhydro-1,6 β-D-hexopyrannose dans des solutions 0.1 molaire dans le benzène-d_6. On a étudié les effets des variations du solvant, de la concentration, de la température et des impuretés du proton sur les valeurs R_1 des protons et on donne les valeurs R_1 du ^{13}C pour montrer que les deux premiers ensembles de variation sont dus aux changements des temps de corrélation du mouvement des molécules. Les données de relaxation du proton peuvent s'adapter par analyse régressive à un ensemble simple de contributions de relaxation interproton, dont les valeurs numériques sont en accord avec une conformation $^1C_4$ du cycle pyrannose quelque peu déformée par le pont anhydro-1,6.

[Traduit par le journal]

Introduction

Previous studies (2) have demonstrated that the spin–lattice relaxation rates of the protons of complex organic molecules can be measured under conditions where the intramolecular dipole–dipole mechanism provides the dominant source of relaxation. Under these circumstances, the nonselective relaxation rate of any proton or any set of equivalent protons, $R_1^A(NS)$ can be represented by the summation

$$R_1^A(NS) = \frac{3}{2}\left(\sum_i \rho^A_{(i\rightarrow A)}\right)$$

where the terms $\rho_{i\rightarrow A}{}^A$ represent the specific relaxation contributions between A and the other protons. One of the principal purposes of this study is to show that these interproton relaxation contributions can be obtained by a regressional analysis of the nonselective relaxation rates of a series of configurationally related compounds. The eight possible isomers of the 2,3,4-tri-*O*-acetyl-1,6-anhydro-β-D-hexopyranoses were eminently suitable substrates for several reasons, but principally because they each give 100 MHz spectra, in benzene-d_6 solutions, which are sufficiently dispersed to allow the R_1-value of almost every proton to be separately determined.

It is appropriate to preface a discussion of these data with a brief summary of the various assumptions which are implicit in this approach and which have to be either confirmed or eliminated by suitable quality-control experiments. The first requirement is that it should be possible to properly define a spin–lattice relaxation rate for a scalar-coupled proton. We shall initially assume that the initial slope approximation (3) of the total magnetization intensity of the components of a multiplet resonance satisfies that requirement. The second requirement is that it is possible to intercompare data obtained from different molecules measured at different times in different solutions. This requirement has been tested by a series of independent quality-control experiments and has been fully justified. As will be seen, this aspect of our work provides the second major theme for this study; surprisingly, we can find no equivalent evidence in the literature. Several additional assumptions are also pertinent to any attempts to use these interproton ρ-values as the basis of structural assignments and although they are not of principal concern here, they will be briefly discussed towards the end of this paper.

It is also appropriate to summarize in eq. [1] a simplified formulation for the intramolecular dipole–dipole mechanism which applies equally well

[1]Part 11 of a series, Application of pulsed nuclear magnetic resonance spectroscopy. For Part 10 see ref. 1.

[2]Visiting Associate Professor at the University of British Columbia, 1974–1975.

[3]Department of Organic Chemistry, The Technical University of Denmark, DK-2800 Lyngby, Denmark.

0008-4042/80/181916-07$01.00/0

©1980 National Research Council of Canada/Conseil national de recherches du Canada

Can. J. Chem. Downloaded from www.nrcresearchpress.com by 210.87.254.105 on 09/05/12
For personal use only.

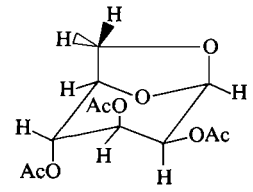
Can. J. Chem. Downloaded from www.nrcresearchpress.com by 210.87.254.105 on 09/05/12
For personal use only.

to the ^1H and ^{13}C relaxation rates to be discussed here.

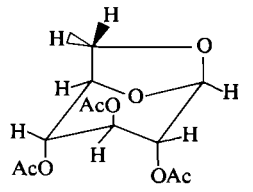
$$[1]\quad \frac{1}{T_1^A} = R_1^A = C \cdot \tau_c \cdot \left(\sum_i r_{A,i}^{-6}\right)$$

Discussion and Results

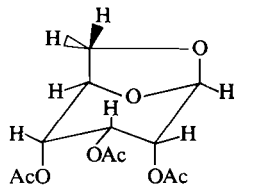
The first series of experiments intended to document the variations in proton R_1-values which accompany changes in solvent, solute concentration, and temperature used 2,3,4-tri-*O*-acetyl-1,6-anhydro-β-D-mannopyranose (**1**) as solute.



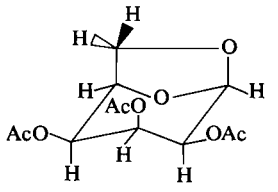
1



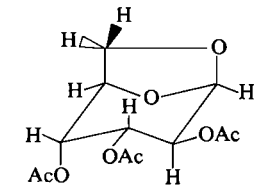
2



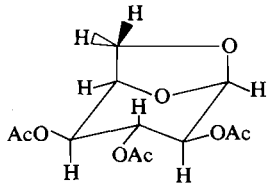
3



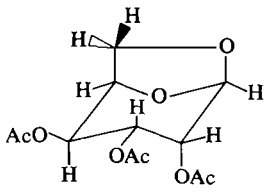
4



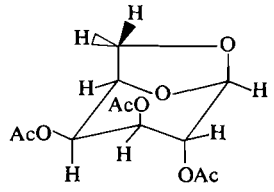
5



6



7



8

The data in Table 1 illustrate the variations of R_1-values[4] as the solvent is varied from benzene-d_6, to acetone-d_6, to chloroform-d, to dimethylsulphoxide-d_6, with the concentration of **1** held constant at 0.1 *M*; only one of several possible series of comparisons is emphasised in the table. These data demonstrate the rather substantial effect of solvent changes on ^1H R_1-values; for the H-1 resonance, the value changes from 69 ms^{-1} in acetone-d_6 to 143 ms^{-1} in dimethylsulphoxide-d_6. The clear inference here is *that comparisons between different molecules can only be made for data obtained in the same solvent*,[5] and, although we provide no experimental documentation here, it is obvious that the solutions used should all be free of paramagnetic impurities, including dissolved oxygen.

Using the same solute (**1**) a series of solutions in benzene-d_6 were prepared, with concentrations 0.05, 0.1, 0.2, 0.5, and 1.0 *M*. An almost linear increase in relaxation rate with increase in concentration was observed and these data are summarized in Table 2. It follows from this experiment *that comparisons between molecules in different solutions should be conducted at a standardized concentration*, but that if the concentration has to be varied for any reason, it may be possible to make an interpolative correction.

Using a 0.1 *M* sample of **1** in benzene-d_6 the effects of variation of the temperature were also studied.

The results are presented in Table 3 and it is clearly seen *that comparisons of data between different molecules should be conducted at the same temperature*.

If the relaxation of the protons of **1** occurs exclusively via the dipole–dipole mechanism, then two sources are possible for the above variations: either the correlation time of the molecules is dependent on the solvent, concentration, and temperature, or *inter*molecular relaxation is making a substantial contribution; or possibly both effects are operating simultaneously. We shall now provide evidence which suggests that the former effect is the dominant one.

It is well known (4) that ^{13}C spin–lattice relaxation rates provide a qualitative measure of the motional correlation time of a molecule. Without going into great detail here, the relaxation rates listed in Table 4 imply two points. First, that 2,3,4-tri-*O*-acetyl-β-D-mannopyranose (**1**) tumbles isotropically in solution; thus the ring carbon atoms bearing a single proton have essentially identical R_1-values, whereas C-6, which bears two protons, relaxes approximately twice as fast. More important for the

[4]Throughout this work, (ms^{-1}) is used in abbreviation for (s^{-1}) × 10^{-3}. Thus an R_1-value of 200 ms^{-1} is equivalent to a value of 0.2 s^{-1}; the equivalent relaxation time is 5 s.

[5]A referee suggested that there will probably be better agreement between the T_1's in *some* of the solvents studied if a correction is made for their different viscosities. We concur with this statement, but draw attention to the need to specify only "some" solvents. With this reservation in mind we do not recommend the practice of using macroscopic viscosities to correct for changes in a *molecular* event.

Can. J. Chem. Downloaded from www.nrcresearchpress.com by 210.87.254.105 on 09/05/12
For personal use only.

TABLE 1. Variation with solvent of the proton spin–lattice relaxation rates (ms^{-1}) of 2,3,4-tri-*O*-acetyl-1,6-anhydro-β-D-mannopyranose (**1**)

Solvent[a]	H-1[b]	H-2[b]	H-3[b]	H-4[b]	H-5[b]	H-6[c]	H-6'[c]	Average change
C_6D_6[d]	112	224	191	220	213	658	645	—
Ratio $(CD_3)_2CO/C_6D_6$	0.615	0.645	0.694	0.676	0.676	0.769	0.769	0.69
Ratio $CDCl_3/C_6D_6$	1.275	1.35	1.33	1.43	1.39	1.33	1.41	1.35
Ratio $(CD_3)_2SO/C_6D_6$	2.63	3.13	3.03	2.94	3.13	3.33	3.45	3.09

[a] All solutions were 0.1 *M*.
[b] Values ±5%.
[c] Values ±10%.
[d] The data for the C_6D_6 solution at 35°C are given in ms^{-1}, and for the other solutions are given as a ratio of the equivalent value found in C_6D_6.

TABLE 2. Effect on the proton spin–lattice relaxation rates (ms^{-1}) of changing the concentrations of 2,3,4-tri-*O*-acetyl-1,6-anhydro-β-D-mannopyranose (**1**) in C_6D_6 solutions at 35°C

Concentration (molarity)	H-1[a]	H-2[a]	H-3[a]	H-4[a]	H-5[a]	H-6[b]	H-6'[b]	Average change
0.1	112	224	191	220	213	658	645	—
Ratio 0.05/0.1	0.89	0.94	0.95	0.92	0.91	0.87	0.86	0.91
Ratio 0.2/0.1	1.19	1.19	1.27	1.22	1.19	1.25	1.24	1.22
Ratio 0.5/0.1	1.59	1.53	1.54	1.58	1.54	1.58	1.58	1.56
Ratio 1.0/0.1	2.51[c]	2.03	1.81[c]	2.01	2.17	2.27	2.28	2.15

[a] Values ±5%.
[b] Values ±10%.
[c] These two resonances were partly overlapping in the 1 *M* solution, and it is thus difficult to determine the relaxation rate accurately.

TABLE 3. Variation with temperature of the proton spin–lattice relaxation rates (ms^{-1}) of 2,3,4-tri-*O*-acetyl-1,6-anhydro-β-D-mannopyranose (**1**), 0.1 *M* in benzene-d_6, measured at 270 MHz

Temperature (K)	H-1	H-2	H-3	H-4	H-5	H-6	H-6'	Average change
285	163	334	279	310	302	917	901	—
Ratio 285/295	1.22	1.29	1.24	1.21	1.20	1.15	1.18	1.21
Ratio 285/305	1.37	1.48	1.35	1.38	1.32	1.32	1.37	1.37
Ratio 285/315	1.63	1.72	1.60	1.61	1.57	1.62	1.60	1.62

TABLE 4. ^{13}C R_1-values (ms^{-1}) for 2,3,4-tri-*O*-acetyl-1,6-anhydro-β-D-mannopyranose (**1**) in different solvents and at different concentrations for C_6D_6 measured at 67.89 MHz at 35°C using the inversion recovery method

Concentration	C-1	C-2	C-3	C-4	C-5	C-6	$\frac{\Sigma C\text{-}1\text{–}C\text{-}5}{5}$	Ratio	Ratio from ^1H-data
0.1 *M* in C_6D_6	376	414	398	409	423	682	404	—	—
0.1 *M* in $CDCl_3$	637	504	582	524	660	996	581	1.44	1.36
0.1 *M* in DMSO-d_6	1104	1290	1206	1186	1272	2164	1211	3.00	2.97
0.1 *M* in $(CD_3)_2CO$	254	244	254	268	354	602	275	0.68	0.66
0.5 *M* in C_6D_6	578	592	577	580	713	1102	608	1.51	1.56
10 *M* in C_6D_6	795	765	773	764	346	1411	809	2.00	2.11

present discussion is the fact that the ^{13}C R_1-values show quantitatively the same trend as the proton values, increasing as the solvent is changed from acetone, to benzene, to chloroform, to dimethylsulphoxide. If the changes in ^1H R_1-values had been solely due to solvation effects then only minor changes would have been anticipated in the relaxation rates of the ^{13}C nuclei, each of which is effectively shielded by its proton substituent.

Although the above evidence clearly indicates the importance of changes in molecular correlation times on the observed R_1-values, it seemed worthwhile attempting to measure any *inter*molecular relaxation for **1** in benzene-d_6 solution. It is well known that benzene preferentially solvates organic molecules which bear a carbonyl substituent and thus makes it more likely that intermolecular relaxation from the solvent may occur.

TABLE 5. Proton spin–lattice relaxation rates (ms^{-1}) for 2,4,5-tri-*O*-acetyl-1,6-anhydro-β-D-mannopyranose (**1**) showing the effects of added C_6H_6 on a solution in C_6D_6

Solvent[a]	H-1	H-2	H-3	H-4	H-5	H-6	H-6′
C_6D_6 (99.5%)	112	224	191	220	213	658	645
C_6D_6 + 5% C_6H_6	112	220	194	212	215	680	680
C_6D_6 + 50% C_6H_6[b]	136	243	214	227	234	680	680

[a]All solutions were 0.1 M.
[b]Values ±15% (see footnote [5] in text).

Accordingly the proton R_1-values were determined for **1** in three separate benzene-d_6 solutions, each 0.1 *M* in **1** and containing respectively 0.5% C_6H_6, 5% C_6H_6, and 50% C_6H_6. The latter concentration corresponds to ca. 10 *M* C_6H_6, hence these three solutions contained molar ratios of **1**/C_6H_6 of approximately 1, 10, and 100. Although the design of this experiment is not flawless (for example, it is assumed that **1** has the same correlation time in a C_6H_6 and a C_6D_6 solution), the data given in Table 5 are, nevertheless, of interest. Even a 100-fold excess of C_6H_6 only increases the relaxation rate of the ring protons of **1** by ca. 11%.[6] We infer from these results that the relaxation of **1** is largely dominated by the intramolecular mechanism even in the presence of ca. 10 *M* C_6H_6, and in 99.5% C_6D_6 this statement must be even closer to reality. Of course, this experiment tells us nothing about *inter*-molecular interactions between individual molecules of **1**; we shall return to this point at the end of this section.

Thus providing that both solvent and solute concentration, along with temperature and paramagnetic impurities, are held constant it should be possible to compare the proton relaxation data of a series of molecules whose size and overall conformational symmetry are similar. The data for the isomeric derivatives **1**–**8** summarized in Table 6 clearly support this conclusion.

These data can be used in several different ways. In the present discussion we wish to illustrate a simple, almost naive, level of intercomparisons which we hope will illustrate the very direct relationships which exist between molecular configuration and nonselective proton relaxation rates, and we have deliberately chosen to avoid more comprehensive forms of regressional analysis for the present.

According to the simplified formulation for the dipole–dipole relaxation mechanism, the relaxation efficiency between two protons of an isotropically tumbling molecule falls off as the sixth power of the interproton separation (eq. [1]). It follows then, that nearest-neighbour, proton–proton interactions will be the dominant source of relaxation contributions. In the present system, the relaxation of H-1 should be dominated by the contribution from H-2; and to a first approximation 2/3 $R_1{}^1$ will be equal to $\rho_1{}^1(2 \rightarrow 1)$. The $R_1{}^1$-values for the compounds cited in Table 6 fall between 104 and 120 ms^{-1} with a mean value of 111 ms^{-1} which implies that the nearest neighbour approximation is an adequate one. By the same token the relaxation of H-2 should now be dominated by contributions from both H-1 and H-3, thus

$$2/3\, R_1{}^2 = \rho_1{}^2(1 \rightarrow 2) + \rho_1{}^2(3 \rightarrow 2)$$

Since $\rho_1{}^1(2 \rightarrow 1) = \rho_1{}^2(1 \rightarrow 2)$ and we already have a value for the former, it is a trivial matter to calculate the value of $\rho_1{}^2(3 \rightarrow 2)$. For H-2 the situation can be somewhat more complex because it is feasible, in e.g. compounds **4** and **6**, for H-2 to receive an additional relaxation contribution from H-4; but this contribution would depend on the configurations at C-2 and at C-4 and would be detectable when the arithmetic was performed for several compounds.

It is possible with a computer program[7] to make a least-squares fit to a set of equations of this type using the relaxation contributions listed in Table 7. Without labouring individual intercomparisons further, it is interesting to see the results in Table 6 (calculated values) of this trivial form of regressional analysis. The agreement between the observed relaxation rates and the "calculated" values is very close indeed.

Only compound **3**, 2,3,4-tri-*O*-acetyl-1,6-anhydro-β-D-allopyranose, differs substantially more from the observed values than the experimental error (±5%) (Table 6). This could be explained by an extra degree of freedom in the motion of this molecule, e.g. a conformational equilibrium between different twist forms for the 6-membered

[6]This experiment can only be considered accurate within ±15%, because of dynamic range problems due to the large signal from C_6H_6.

[7]A basic program was written by Mr. H. Thøgersen for BNC-12 computers. This program will estimate the best fit (using a least-squares fit) to n unknowns in $n + x$ ($x \geq 1$) equations.

Can. J. Chem. Downloaded from www.nrcresearchpress.com by 210.87.254.105 on 09/05/12
For personal use only.

Can. J. Chem. Downloaded from www.nrcresearchpress.com by 210.87.254.105 on 09/05/12
For personal use only.

TABLE 6. Proton spin–lattice relaxation rates (ms^{-1}) for the isomeric 2,3,4-tri-*O*-acetyl-1,6-β-D-hexopyranoses in C_6D_6 solutions (0.1 *M*), and calculated relaxation rates (see Table 7)

2,3,4-Tri-*O*-acetyl-1,6-anhydro-D		H-1[a]	H-2[a]	H-3[a]	H-4[a]	H-5[a]	H-6[a]	H-6'[b]
Mannopyranose	obs.	112	224	191	220	213	658	645
(1)	calcd.	114	228	206	240	198		
Glucopyranose	obs.	109	171	151	241	221	821	742
(2)	calcd.	92	184	184	240	198		
Allopyranose	obs.	120	261	332	268	202	783	
(3)	calcd.	92	206	309	262	198		
Talopyranose	obs.	101	256	227	254	197	516	615
(4)	calcd.	114	255	228	255	220		
Altropyranose	obs.	113	172	207	274	209	869	857
(5)	calcd.	114	148	229	262	198		
Idopyranose	obs.	104	159	149	153	210	785	658
(6)	calcd.	114	156	150	156	220		
Gulopyranose	obs.	115	209	—	—	209	701	692
(7)	calcd.	92	206			220		
Galactopyranose	obs.	—	159	—	219	210	542	650
(8)	calcd.		184		228	220		

[a]±5%.
[b]±10%.

TABLE 7. Specific, interproton relaxation contributions ρ-values (ms^{-1}) for the isomeric 2,3,4-tri-*O*-acetyl-1,6-anhydro-β-D-hexopyranoses in C_6D_6 solutions (0.1 *M*) obtained using a regressional analysis (4) from the data in Table 6

Interaction	$\rho_{e,e}$	$\rho_{e,a}$	$\rho_{a,a}$	$\rho_{3,6}$	$\rho_{4,6}$	$\rho_{5,6}$	$\rho_{2,4}$[a]	$\rho_{2,4}$[b]
Rate	61	76	23	54	37	71	18	5

[a]Data from talosan derivative (**4**).
[b]Data from idosan derivative (**6**).

TABLE 8. Proton spin–lattice relaxation rates (ms^{-1}) of 2,3,4-tri-*O*-acetyl-1,6-anhydro-β-D-glucopyranose (**2**) and its perdeuterioacetyl derivative (**2***a*) in C_6D_6 solution (0.1 *M*)

Compound	H-1	H-2	H-3	H-4	H-5
2	109	171	151	241	221
2*a*	93	142	130	214	188
Difference	16	29	21	27	33

ring. This could cause the proton–proton distances to be changed, but a conformational equilibrium could also offer an alternative source of relaxation (5). This explanation is supported by an X-ray examination of 1,6-anhydro- β-D-allopyranose (6), which shows that this compound even in the crystal adopts three different conformations with the 6-membered ring flattened.

The interproton relaxation contributions obtained from the above regressional analyses are summarized in Table 7. These values include contributions from the acetate methyl protons. These latter contributions are readily detectable in a comparison of the R_1-values of **2** with those of its 2,3,4-tri-*O*-(*trideuteroacetyl*) derivative (Table 8). In concluding this paper we wish to mention three additional experiments which both support and extend the above discussions.

It is now possible to measure a *selective* R_1-value for any well resolved resonance **1**: simply, a selective 180°-pulse is applied to the resonance of interest and then the rate of recovery of the magnetization of that resonance is monitored in the usual fashion with a nonselective 90° (7). Theory states (8) that the ratio of this value, compared with the value obtained via a conventional, nonselective inversion–recovery experiment will be 1.5:1 if all of the relaxation of that proton comes from the dipole–dipole mechanism,[8] if none of its relaxation is dipolar then the ratio will be unity. The ratios found for the H-1 and H-4 resonances of **1** in 0.1 *M* deuterobenzene-d_6 solution were 1.46 and 1.50. It seems reasonable to infer from this experiment that the relaxation of all the protons of **1**, and by inference of all of the protons of the other seven isomers, are mediated by the dipole–dipole mechanism; and on the basis of the data given in Table 5 it

[8]The relationship between this experiment and the nuclear Overhauser effect is not accidental.

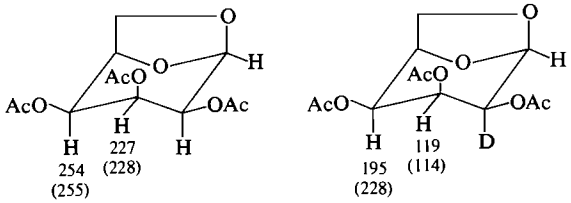
TABLE 9. Comparison of the proton spin–lattice relaxation rates (ms^{-1}) of 2,3,4-tri-*O*-acetyl-1,6-anhydro-β-D-mannopyranose (**1**) in C_6D_6 solution (0.1 *M*) measured at 100, 90, 270, and 300 MHz[a]

Observing frequency	H-1	H-2	H-3	H-4	H-5	H-6	H-6′
100 MHz 35°C	112	224	191	220	213	658	645
90 MHz 25°C	134 (1.20)	259 (1.15)	229 (1.20)	259 (1.18)	251 (1.18)	802 (1.22)	775 (1.20)
270 MHz 25°C	134 (1.20)	258 (1.15)	225 (1.18)	256 (1.16)	252 (1.18)	799 (1.21)	762 (1.18)
300 MHz 27°C	138 (1.23)	266 (1.19)	239 (1.25)	273 (1.24)	272 (1.28)	855 (1.30)	826 (1.28)

[a] Values in parentheses are the ratios to the values measured at 100 MHz.

also seems reasonable to infer that *intra*molecular dipole–dipole relaxation is dominant.

In a separate experiment, the magnitudes of several of the interproton relaxation contributions were confirmed by examination of a specifically deuterated analog, 2,3,4-tri-*O*-acetyl-2-deutero-1,6-anhydro-D-talopyranose (**4**), which was kindly provided by Professor H. Paulsen (Hamburg). The relaxation data for that compound are appended to the structural formula below.



Comparison between these data and those of the normal compound with a proton at C-2 gave a direct estimate of the interactions from H-2 to H-3 and H-4; the figures obtained by regressional analysis are listed in parentheses. The use of specific deuteration in relaxation studies of carbohydrates has been discussed in detail elsewhere (9).

Finally, the relaxation rates for **1** at 300 MHz, using a Varian SC300 spectrometer, at 270 MHz, using a Bruker HX-270 spectrometer, and at 90 MHz, using a Bruker WH-90 spectrometer are summarized in Table 9, together with their ratios to the corresponding values measured at 100 MHz. It can be seen that the ratios are essentially constant, proving that it is possible to determine and compare relaxation rates reliably even if they are obtained on different spectrometers.

Conclusions

The data reported here indicate that it is feasible to intercompare the proton spin–lattice relaxation rates of a series of organic molecules in separate solutions. It is necessary to work in a common solvent, at constant concentration and temperature, and care must be taken to exclude paramagnetic impurities, including dissolved oxygen. This finding has a number of important implications. It means that it is possible to intercompare proton R_1-values in much the same way as chemical shifts and coupling constants, ascribing observed changes to specific chemical or stereochemical differences between the compounds. It also implies that regressional analysis methods can be used to evaluate relaxation data obtained from a series of compounds; this complements methods based on either specific deuteration (8) or multiple, selective-pulse relaxation determinations (2).

Experimental

The preparation of samples, the measurements of spin–lattice relaxation rates, and the subsequent data processing all followed procedures described previously (9).

Samples of the derivatives were available from other studies.

Acknowledgements

This work was supported by operating grants to one of us (L.D.H.) from the National Research Council of Canada (A 1905) and from the Alfred P. Sloan Foundation. K.B. wishes to thank N.A.T.O., the Otto Moensted Foundation, and the University of British Columbia for their financial support of his sabbatical leave during 1974–1975. This paper was written under the aegis of a N.A.T.O. Research grant (1275). We thank Dr. Howard Hill of Varian Associates for performing the T_1-experiments at 300 MHz. The 270 MHz Bruker spectrometer was provided by the Danish Natural Science Research Council.

1. K. BOCK, R. BURTON, and L. D. HALL. Can. J. Chem. **55**, 1045 (1977).

Can. J. Chem. Downloaded from www.nrcresearchpress.com by 210.87.254.105 on 09/05/12
For personal use only.

2. (*a*) L. D. HALL. Chem. Can. **28**, 19 (1976); (*b*) L. D. HALL. Chem. Soc. Rev. **4**, 401 (1975).
3. L. D. HALL and H. D. W. HILL. J. Am. Chem. Soc. **98**, 1269 (1976).
4. J. M. BERRY, L. D. HALL, and K. F. WONG. Carbohydr. Res. **56**, C 16 (1977).
5. K. BOCK, L. D. HALL, and C. PEDERSEN. Can. J. Chem. **58**, 1923 (1980).
6. K. BOCK, R. NORRESTAM, and C. PEDERSEN. Acta Crystallogr. To be published.
7. K. BOCK, R. BURTON, and L. D. HALL. Can. J. Chem. **55**, 1045 (1977); L. D. HALL, K. F. WONG, and H. D. W. HILL. J. Chem. Soc. Chem. Commun. 951 (1979).
8. R. FREEMAN, H. D. W. HILL, B. L. TOMLINSON, and L. D. HALL. J. Chem. Phys. **61**, 4466 (1976).
9. K. F. WONG. Ph.D. Thesis, University of British Columbia, 1979; L. D. HALL, K. F. WONG, W. E. HULL, and J. D. STEVENS. J. Chem. Soc. Chem. Commun. 953 (1979).
10. C. M. PRESTON and L. D. HALL. Carbohydr. Res. **37**, 267 (1974).

Can. J. Chem. Downloaded from www.nrcresearchpress.com by 210.87.254.105 on 09/05/12
For personal use only.

A survey of the proton spin–lattice relaxation rates of selected furanose derivatives[1]

KLAUS BOCK,[2] LAURANCE D. HALL, AND CHRISTIAN PEDERSEN[2]

Department of Chemistry, The University of British Columbia, Vancouver, B.C., Canada V6T 1W5

Received January 4, 1980

KLAUS BOCK, LAURANCE D. HALL, and CHRISTIAN PEDERSEN. Can. J. Chem. **58**, 1923 (1980).

The non-selective proton spin–lattice relaxation rates of 3,5-di-*O*-acetyl-2,6-dibromo-2,6-dideoxy-D-mannono (**1**), or -glucono (**2**), 1,4-lactone, methyl-α,(β)-D-ribofuranoside (**3**), methyl-α,(β)-D-arabinofuranoside (**4**), methyl-α(β)-D-xylofuranoside (**5**), 3,5-di-*O*-acetyl-1-*O*-benzoyl-2,6-dibromo-2,6-dideoxy-α and β-D-mannofuranose (**6**) and (**7**), 3,5-di-*O*-acetyl-6-bromo-2,6-dideoxy-D-*arabino*-1,4-lactone (**8**), and 2,3,5,6-tetra-*O*-acetyl-1,4-anhydro-D-mannitol (**9**) have been measured at 270 MHz. Substantial differences are found for the R_1-values of epimeric pairs of substances which can be used for structural evidence. The anomalous R_1-values in deuteriochloroform for the H-2, H-3, and H-4 resonances of **1** are discussed.

KLAUS BOCK, LAURANCE D. HALL et CHRISTIAN PEDERSEN. Can. J. Chem. **58**, 1923 (1980).

On a mesuré à 270 MHz les vitesses de relaxation spin–réseau non sélectives du proton des composés suivants: di-*O*-acétyl-3,5 dibromo-2,6 didéoxy-2,6 D-mannono (**1**) ou glucono (**2**) lactone-1,4; α(β)-D-ribofurannoside de méthyle (**3**); α(β)-D-arabinofurannoside de méthyle (**4**); α(β)-D-xylofurannoside de méthyle (**5**); di-*O*-acétyl-3,5 *O*-benzoyl-1 dibromo-2,6 didéoxy-2,6 α et (β)-D-mannofurannose (**6**) et (**7**); di-*O*-acétyl-3,5 bromo-6 didéoxy-2,6 D-arabino lactone-1,4 (**8**) et tétra-*O*-acétyl-2,3,5,6 anhydro-1,4 D-mannitol (**9**). On a trouvé des différences importantes pour les valeurs R_1 des paires de substances épimères qui peuvent être utilisées comme preuves de structure. On discute des valeurs R_1 anormales des résonances des protons en positions 2, 3 et 4 dans le deutériochloroforme.

[Traduit par le journal]

Introduction

Although many unambiguous methods are available for assigning the configurations and conformations of pyranose sugars in solution, application of those same techniques to furanose derivatives is often less satisfactory, and in many instances the results are ambiguous. For example, measurements (2) of proton (^{1}H) vicinal coupling constants and chemical shifts have met with variable success as have equivalent studies (3) based on natural abundance carbon-13 (^{13}C) nuclear magnetic resonance (nmr) spectra.

Encouraged by the substantial differentials which have been observed in the proton spin–lattice relaxation rates (R_1-values) of many families of pyranose sugars (4–6) we have undertaken a survey of the R_1-values of epimeric pairs of furanose sugars which were available from other studies. Two reports (7, 8) describing the same type of measurements on furanose derivatives have recently been published.

It will be recalled (9) that the spin–lattice relaxation[3] of most protons of diamagnetic organic molecules appears to be dominated (10) by the intramolecular dipole–dipole mechanism (11), the form of which is given in eq. [1], where R_1^A(NS) is the composite, nonselective relaxation rate of a nucleus A, separated by a distance (r_{AB}) from another nucleus B located in the same molecule. As a result, interproton relaxation contributions fall very rapidly with increase in internuclear distance

$$[1] \quad R_1^A(\mathrm{NS}) = 3/2\hbar^2\gamma_A^2\gamma_B^2\, T_c(A-B) r_{AB}^{-6}$$

and hence composite proton relaxation rates are dominated by nearer neighbour interactions. From this it follows that any structural change, such as inversion of configuration at an individual carbon atom, which causes changes in interproton distances should cause detectable changes in the R_1-values of protons which are spatially close to that centre; and as a corollary it follows that the R_1-values of protons remote from that centre should remain unchanged.

As will be seen below, several series of furanose derivatives accord with the above expectation and it seems reasonable to infer that proton R_1-values can provide valuable new structural information for such derivatives.

Results and Discussion

The primary structures of derivatives **1** and **2** have been previously assigned by unambiguous chemical interconversions (12) and also by ^{1}H and ^{13}C nmr spectroscopy, the vicinal ^{1}H—^{1}H coupling constants of both epimers (Table 1) showing the values anticipated for molecules which favour the $^3T_4$ conformation (**A**). That the R_1-values of H-5,

[1]This paper forms part 12 of a series, Applications of pulsed nuclear magnetic resonance spectroscopy. For part 11 see ref. 1.

[2]Department of Organic Chemistry, The Technical University of Denmark, DK-2800 Lyngby, Denmark.

[3]For a completely detailed discussion of spin–lattice relaxation of the protons of scalar-coupled spin systems the reader is referred to ref. 9*c*. A brief summary is given in ref. 1.

0008-4042/80/181923-06$01.00/0

©1980 National Research Council of Canada/Conseil national de recherches du Canada

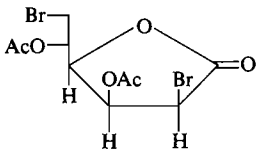
Can. J. Chem. Downloaded from www.nrcresearchpress.com by 210.87.254.6 on 09/05/12
For personal use only.

Can. J. Chem. Downloaded from www.nrcresearchpress.com by 210.87.254.6 on 09/05/12
For personal use only.

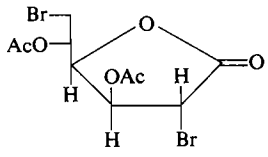
TABLE 1. Chemical shifts (δ-values), $^1H—^1H$ coupling constants (Hz), and proton spin–lattice relaxation rates (R_1-values, $s^{-1} \times 10^3$) for derivatives **1** and **2** measured at 270 MHz in deuteriobenzene solution (0.1 *M*) at 293 K

Compound	Parameter	Proton H-2	H-3	H-4	H-5	H-6	H-6′
1	δ-value	4.90	5.87	4.86	5.28	3.73	3.68
	J-value	$J_{23} = 5.0$	$J_{34} = 3.5$	$J_{45} = 9.5$	$J_{56} = 3.0$	$J_{56'} = 3.7$	$J_{66'} = 12.0$
	R_1-value	278	345	333	303	833	909
2	δ-value	4.16	5.52	5.09	5.31	3.79	3.67
	J-value	$J_{23} = 0$	$J_{34} = 3.4$	$J_{45} = 9.6$	$J_{56} = 3.0$	$J_{56'} = 4.2$	$J_{66'} = 12.0$
	R_1-value	137	250	270	263	833	833

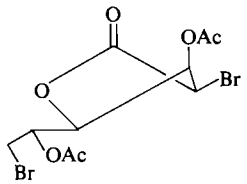
H-6, and H-6′ are closely similar for both compounds immediately suggests that they both tumble in solution with approximately the same motional correlation time (which was subsequently confirmed by the ^{13}C R_1-values, *vide infra*). On that basis the enhancement (ca. 100%) of the R_1-value of H-2 of **1**, compared with its counterpart in **2**, can be ascribed to its *cis*-relationship with H-3. The somewhat smaller rate enhancements observed for the H-3 and H-4 resonances of **1** further confirm this configurational assignment.



1



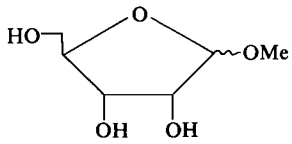
2



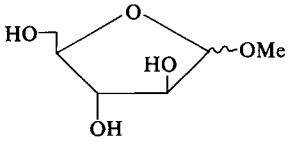
A

When a mixture of both anomeric forms is available, studies on the mixture can give useful structural information (4). For example, the R_1-values of the H-1 protons of anomeric mixtures of the known (13) methyl ribofuranosides (**3**), methyl arabinofuranosides (**4**), and methyl xylofuranosides (**5**) show the anticipated differentials with the *cisoid* relationship between H-1 and H-2, again resulting in an enhanced R_1-value. This dependence parallels that reported by Preston (14) for the 1,2:5,6-di-*O*-isopropylidene derivatives of α-D-gluco- and allo-furanose, and also results described in a more recent report (8).

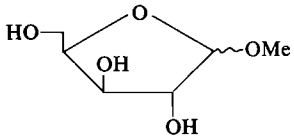
It is interesting to note that even though R_1-values are concentration dependent (1) the ratio between the R_1-values of methyl α- and β-D-ribofuranoside is independent of the relative



3



4



5

amount of the two compounds present and of the total concentration. It furthermore appears that the ratios between the R_1-values of the anomeric pairs for arabino- and xylofuranose derivatives are almost the same as the one found for ribofuranose.

Derivatives **6** and **7** exemplify a pair of epimers for which the vicinal $^1H—^1H$ coupling constants are essentially identical (Table 3). The previous (15) assignment of the anomeric configuration was based on intercomparison of the $[\alpha]_D$-values and ^{13}C nmr chemical shifts, which implied that **6** was the α-anomer, with the interconversion of both **6** and **7** to the same glycosyl bromide being cited as evidence that the configurations at all other centers were identical.

The enhanced R_1-values observed for H-1 and H-2 of **7** implied that these protons have a *cis*-relationship, in accord with the previously assigned structure.

The data for derivatives **8** and **9** demonstrate that methylene protons which, as a result of their closeness, tend to relax each other very efficiently, can pick up sufficient relaxation from other protons in the same molecule to evidence a configurational change at a vicinal carbon atom. Thus the H-2 resonances of **8**, for which an unequivocal assignment can be based on their vicinal coupling constants with H-3 (Table 3), show a 21% rate enhancement for the proton which is *cis* to H-3.

The H-1 resonances of **9** cannot be distinguished

TABLE 2. Spin–lattice relaxation rates (R_1-values, $s^{-1} \times 10^3$) for anomeric protons in derivatives **3**, **4**, and **5** measured at 270 MHz in D_2O at 300 K

Compound	Methyl D-ribofuranoside (3)		Methyl D-xylofuranoside (5)		Methyl D-arabinofuranoside (4)		Methyl[a] D-ribofuranoside (3)	
Anomer	α	β	α	β	α	β	α	β
Concentration (M)	0.3	0.3	0.3	0.3	0.4	0.2	0.3	0.5
R_1-value	318	248	308	225	252	358	385	301
Ratio $R_1 cis/R_1 trans$	1.28		1.37		1.42		1.28	

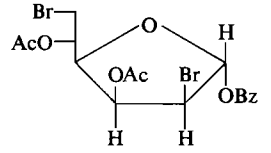
[a]Values obtained on same sample at 90 MHz at 295 K gave $R_1(\alpha) = 515$ and $R_1(\beta) = 398\ s^{-1} \times 10^3$, i.e. a ratio of 1.29.

TABLE 3. Proton chemical shifts (δ-values), ^1H—^1H coupling constants (J-values, Hz), and proton spin–lattice relaxation rates (R_1-values, $s^{-1} \times 10^3$) for derivatives **6**, **7**, **8**, and **9**, measured at 270 MHz in deuteriochloroform (0.1 M) at 293 K

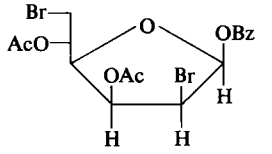
Compound	Parameter	Proton						
		H-1	H-2	H-3	H-4	H-5	H-6	H-6′
6	δ-value	6.59	4.60	5.69	4.64	5.27	3.75	3.63
	J-value	$J_{12} = 4.5$	$J_{23} = 5.0$	$J_{34} = 4.0$	$J_{45} = 9.0$	$J_{56} = 3.0$	$J_{56'} = 4.5$	$J_{66'} = 11.8$
	R_1-value	296	694	794	725	524	1540	1640
7	δ-value	6.63	4.45	5.84	4.57	5.22	3.70	3.63
	J-value	$J_{12} = 4.8$	$J_{23} = 5.0$	$J_{34} = 4.6$	$J_{45} = 9.5$	$J_{56} = 3.0$	$J_{56'} = 3.8$	$J_{66'} = 11.8$
	R_1-value	504	969	774	714	538	1490	1530
8	δ-value	H_2' 2.93	2.59	5.63	4.75	5.28	3.79	3.68
	J-value	$J_{2'3} = 6.0$ $J_{22'} = 14.0$	$J_{23} = 0$	$J_{34} = 3.5$	$J_{45} = 9.5$	$J_{56} = 3.0$	$J_{56'} = 4.0$	$J_{66'} = 12.0$
	R_1-value	1042	862	455	417	333	980	1031
9	δ-value	(1) 3.98 (1′)3.72	5.37	5.55	4.65	5.28	4.44	3.98
	J-value	$J_{11'} = 9.0$ $J_{1'2} = 6.8$	$J_{12} = 6.8$ $J_{23} = 5.0$	$J_{34} = 4.1$	$J_{45} = 9.0$	$J_{56} = 2.3$	$J_{56'} = 5.1$	$J_{66'} = 12.5$
	R_1-value	(1′) 962 (1)1163	578	585	641	503	1389	1449

on the basis of their vicinal couplings, but it seems eminently reasonable to assign the high field resonance to H-1α merely on the basis of its enhanced R_1-value.

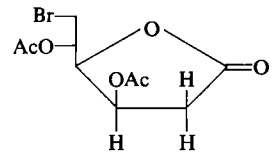
In all of the above experiments we have directed attention to the nonselective proton R_1-values and have ignored the various quality control experiments which can be used (9) to independently probe the validity of some of the assumptions which are implied in these simple intepretations. In the final section of this paper we shall discuss briefly two of these controls as applied to derivatives **1** and **2**.



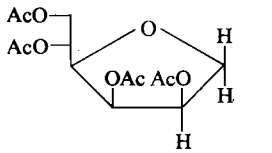
6



7



8



9

Fundamental to any intercomparison of the proton R_1-values of an epimeric pair of substances is the assumption that both epimers tumble in solution at the same rate (actually a more rigorous condition is implied, namely that both the molecules also tumble isotropically and hence that the motional correlation times for all interproton vectors are identical; we shall ignore that extra subtlety here) (16). Previously in this discussion we used the near identity of the R_1-values of the H-5, H-6, and H-6′ protons for **1** and **2** to justify that assumption, but independent evidence from the carbon-13 R_1-values will now be cited. As we have shown elsewhere (9*c*, 17), ^{13}C R_1-values are directly proportional to the motional correlation times of the ^{13}C–^1H vectors. It follows then that the near identity of the individual ^{13}C R_1-values for **1** and **2** indicates that these substances tumble with approximately the same rates in both deuteriobenzene and deuteriochloroform (Table 4). Al-

Can. J. Chem. Downloaded from www.nrcresearchpress.com by 210.87.254.6 on 09/05/12
For personal use only.

TABLE 4. Carbon-13 chemical shifts (ppm, from internal TMS), $^{13}C-^{1}H$ nuclear Overhauser enhancement factors (η-values, % of maximum possible value), and spin–lattice relaxation rates (R_1-values, s^{-1}) for **1** and **2** measured at 303 K at 22.63 MHz in deuteriochloroform and deuteriobenzene (1.0 *M*). The nOe experiments were performed at 67.89 MHz at 305 K on 0.5 *M* samples

Compound	Parameter	Solvent	C-2	C-3	C-4	C-5	C-6
1	δ-value	$CDCl_3$	42.9	68.7	77.6	66.8	32.3
	η-value	$CDCl_3$	97	107	94	107	94
	R_1-value	$CDCl_3$	1.64	1.64	1.56	1.61	2.94
	δ-value	C_6D_6	43.2	68.6	77.6	66.8	32.7
	η-value	C_6D_6	97	107	94	111	107
	R_1-value	C_6D_6	1.64	1.59	1.59	1.59	2.94
2	δ-value	$CDCl_3$	38.0	73.5	77.9	66.7	32.3
	η-value	$CDCl_3$	91	97	97	100	97
	R_1-value	$CDCl_3$	1.82	1.47	1.52	1.56	2.63
	δ-value	C_6D_6	38.1	73.3	77.9	66.7	32.5
	η-value	C_6D_6	107	107	104	111	104
	R_1-value	C_6D_6	1.92	1.69	1.67	1.67	2.86

though in this instance the R_1-values are essentially independent of the solvent, this is not invariably so. Indeed, as we have found (1) during a study of the tri-*O*-acetyl-1,6-anhydro-β-D-hexopyranoses, R_1-values in either acetone or dimethylsulphoxide solutions are very different from those in either benzene or chloroform. It follows from this that *intercomparisons between pairs of epimers must be made using a common solvent.*

A second assumption which we have not thus far questioned concerns the extent to which the protons are relaxing via the dipole–dipole mechanism. Clearly any major deviation from this assumption could irreversibly confuse interpretations of proton R_1-values. Fortunately a quantitative quality control has been developed. Briefly, the normal (18) two-pulse relaxation experiment is modified (19, 20) so that the 180°-pulse now selectively perturbs only the resonance of choice (A, say) rather than all the protons; the recovery of the magnetization of A is then monitored using the usual nonselective 90°-pulse and the resultant data processed to give the *single-selective* spin–lattice relaxation rate of A, $R_1^{A}(S)$. Theory then states (10) that if proton A is relaxing exclusively via the dipole–dipole mechanism with the other protons, the ratio of the normal nonselective R_1-value of A, $R_1^{A}(NS)$ to the single selective value, $R_1^{A}(S)$ will be 1.5. If none of the relaxation of A is mediated by the dipole–dipole mechanism then the ratio will be unity; thus the dynamic range of this ratio varies between 1 and 1.5. Our previous experience (10, 14, 19)[4] with methine and methylene protons is that 1.5 ratios are invariably obtained and it seems reasonable to assume that unless peculiar circumstances pertain, most protons in medium sized molecules can relax exclusively with other protons in the same molecule. We shall now present an apparent exception to this seemingly general rule.

As can be seen from Table 5, a change in solvent to deuteriochloroform for compounds **1** and **2** results in a drastic change of the R_1-values for H-2, H-3, and H-4 for **1** compared to the values obtained in deuteriobenzene (Table 1). In contrast to that, the R_1-values for H-5, H-6, and H-6′ for **1** and all the R_1-values for **2** are only changed as would expected *due* to a change of the solvent (1).

Selective T_1-experiments on H-2 and H-4 of **1** in deuteriochloroform gave ratios to nonselective values of 1.04. The same experiment performed on H-5 of **1** in deuteriochloroform or H-4 of **1** in deuteriobenzene gave a ratio of 1.30, whereas measurements on H-2 and H-4 of **2** in deuteriochloroform gave values of ca. 1.40. This clearly indicates that the H-2, H-3, and H-4 resonances of **1** in deuteriochloroform are availing themselves of some alternative source of relaxation or the initial slope approximation used in the evaluation of the nonselective R_1-values is seriously in error. The other protons for **1** and **2** seem, from the selective T_1-experiments, to obtain, within experimental error, most of their relaxation from protons within the same molecule. A possible source of relaxation for protons H-2 and H-4 in **1** could arise from a pseudorotation (21) of the five membered ring with a frequency component close to the resonance frequency of the nuclei, which is supported by the frequency dependence of the R_1-values (Table 5).

Conclusion

We have clearly demonstrated that epimeric pairs of furanose derivatives can be distinguished via comparison of their nonselective proton spin–lattice relaxation rates, the salient feature being the substantial enhancement of R_1-value in-

[4]L. D. Hall, K. F. Wong, and H. D. W. Hill. J. Chem. Soc. Chem. Commun. 951 (1979).

Can. J. Chem. Downloaded from www.nrcresearchpress.com by 210.87.254.6 on 09/05/12
For personal use only.

TABLE 5. Proton spin–lattice relaxation rates (R_1-values, $s^{-1} \times 10^3$) for derivatives **1** and **2** measured in deuteriochloroform solutions (0.1 *M*) at 293 K at 90 and 270 MHz. Single-selective R_1-values are indicated in parentheses, along with the calculated ratios for R_1(NS):R_1(SS)

Compound	Frequency	H-2	H-3	H-4	H-5	H-6	H-6′
1	90 MHz	769	588	667	385	1260	1240
	270 MHz	1250 (1200; 1.04)	833	1111 (1066; 1.04)	417 (325; 1.28)	1250	1250
2	90 MHz	238	370	417	417	1180	1240
	270 MHz	244 (176; 1.39)	345	370 (864; 1.40)	385	1160	1250

duced by a *cis* interaction between protons on adjacent carbons. Thus the proton relaxation method shows great promise as a powerful tool in structural studies of furanoses and further studies of other classes of these important derivatives are clearly warranted. The abnormal relaxation behaviour of some of the resonances of derivative **1** has been rationalized and although we believe that this is rather rare, it would seem prudent that any quantitative or critical structural study should incorporate, in addition to the conventional nonselective R_1-measurements, measurements of single-selective R_1-values.

Experimental

The nmr spectra were measured on Bruker HX-270 or WH-90 instruments operating in the Fourier transform mode. The ^{1}H nmr spectra at 270 MHz were obtained at 293 K using a 90° pulse of 12 μs for deuteriochloroform and deuteriobenzene samples and 17 μs for water samples (22), 16K of computer memory, and a spectral width of 3000 Hz. The ^{1}H nmr spectra at 90 MHz were obtained at 293 K using a 90° pulse of 6.5 μs, 8K of computer memory and a spectral width of 1000 Hz. The ^{13}C nmr spectra at 67.89 MHz were obtained at 305 K using a 90° pulse of 12 μs, 16K of computer memory, and a spectral width of 10 000 Hz. The ^{13}C nmr spectra at 22.63 MHz were obtained at 305 K using a 90° pulse of 16.5 μs, 8K of computer memory and a spectral width of 5000 Hz.

The T_1-experiments were performed using the inversion–recovery method (18) using the initial slope approximation ($T \leq T_1$) (10). The R_1-values were determined both from a regressional semilogarithmic fit with $T \leq T_1$ and also from an experimental fit to all the relaxation data.[5] The agreement between these two values was in general within 5%, which was also considered the experimental error.[6]

[5]Program written for BNC-12 computer in BASIC by H. Thøgersen, Lyngby, based on ref. 23.

[6]A referee queried if the 5% error estimate is reasonable; we believe that it is, at least within certain contexts (see ref. 1). Thus, the R_1-values reported here are "repeatable" within 5% when measured on the same sample, using the same spectrometer, and even with intercomparison between *different* samples on the *same* spectrometer appear to be equally reproducible. Furthermore, even if their absolute magnitudes are in substantial error, the *relative* magnitudes for the protons of any one compound are not. It is worth noting that the accuracy of R_1-values obtained with a superconducing solenoid exceeds that from an electromagnet system. Likely this reflects both the enhanced sensitivity of the superconducting spectrometer together with the increased overall stability of the B_0-field.

The solutions were made up in the appropriate solvents and degassed by bubbling nitrogen through the solution for 5 min. The selective proton relaxation rates were obtained using the decoupler as source for the selective field (20).

The ^{13}C nOe factors were determined using the gated technique (25).

Compounds 3,5-di-*O*-acetyl-2,6-dibromo-2,6-dideoxy-D-mannono (**1**) or -glucono (**2**), 1,4-lactone, 3,5-di-*O*-acetyl-1-*O*-benzoyl-2,6-dibromo-2,6-dideoxy-α and β-D-mannofuranose (**6**) and (**7**), 3,5-di-*O*-acetyl-6-bromo-2,6-dideoxy-D-*arabino*-1,4-lactone (**8**), and 2,3,5,6-tetra-*O*-acetyl-1,4-anhydro-D-mannitol (**9**) were all available from other studies (12, 15). Compounds α,β**3**, α,β**4**, and α,β**5** were synthesized as mixtures according to published methods (13). Their identities were checked by comparison of ^{13}C chemical shifts with values published (3).

Acknowledgements

This study was supported by a joint research grant from N.A.T.O. (Grant No. 1275) to whom we are indebted. The nmr spectrometers were available through grants from the Danish Natural Science Research Council.

1. K. BOCK, L. D. HALL, and C. PEDERSEN. Can. J. Chem. **58**, 1916 (1980).
2. G. KOTOWYCZ and R. U. LEMIEUX. Chem. Rev. **73**, 669 (1973), and references cited therein.
3. R. G. S. RITCHIE, N. CYR, B. KORSCH, H. J. KOCH, and A. S. PERLIN. Can. J. Chem. **53**, 1424 (1975).
4. (*a*) L. D. HALL and C. M. PRESTON. Chem. Commun. 1319 (1972); (*b*) L. D. HALL and C. M. PRESTON. Carbohydr. Res. **49**, 3 (1976).
5. C. M. PRESTON and L. D. HALL. Carbohydr. Res. **37**, 267 (1974).
6. C. W. M. GRANT, L. D. HALL, and C. M. PRESTON. J. Am. Chem. Soc. **95**, 7742 (1973).
7. (*a*) A. P. ZENS, T. A. BRYSON, R. B. DUNLAP, R. R. FISCHER, and P. D. ELLIS. J. Am. Chem. Soc. **98**. 7559 (1976); (*b*) K. BOCK and L. D. HALL. J. Carbohydr. Nucleosides Nucleotides, **4**, 83 (1977).
8. S. TRAN-DINH, J.-M. NEUMANN, J.-M. THIÉRY, T. HUYNH-DINH, J. IGOLEN, and W. GUSCHLBAUER. J. Am. Chem. Soc. **99**, 3267 (1977).
9. (*a*) L. D. HALL. Chem. Soc. Rev. **4**, 401 (1975); (*b*) L. D. HALL. Chem. Can. **28**, 19 (1976); (*c*) K. F. WONG. Ph.D. Thesis, University of British Columbia, Vancouver, Canada. 1979.
10. L. D. HALL and H. D. W. HILL. J. Am. Chem. Soc. **98**, 1269 (1976).
11. A. ABRAGAM. The principles of nuclear magnetism. Oxford University Press, London. 1961. Chapts. 2 and 8.
12. K. BOCK, I. LUNDT, and C. PEDERSEN. Carbohydr. Res. In press.

Can. J. Chem. Downloaded from www.nrcresearchpress.com by 210.87.254.6 on 09/05/12
For personal use only.

13. C. T. BISHOP and F. P. COOPER. Can. J. Chem. **41**, 2743 (1963).
14. C. M. PRESTON. Ph.D. Thesis, University of British Columbia, Vancouver, Canada. 1975.
15. K. BOCK and C. PEDERSEN. To be published.
16. J. M. BERRY, L. D. HALL, and K. F. WONG. Carbohydr. Res. **56**, C 16 (1977).
17. K. BOCK and L. D. HALL. Carbohydr. Res. **40**, C 3 (1975).
18. R. L. VOLD, J. S. WAUGH, M. P. KLEIN, and D. E. PHELPS. J. Chem. Phys. **48**, 3831 (1968).
19. R. FREEMAN, H. D. W. HILL, B. L. TOMLINSON, and L. D. HALL. J. Chem. Phys. **61**, 4466 (1974).
20. K. BOCK, R. BURTON, and L. D. HALL. Can. J. Chem. **55**, 1045 (1977).
21. O. RÖDER, H. D. LÜDEMANN, and E. VON GOLDAMMER. Eur. J. Biochem. **53**, 517 (1975).
22. K. BOCK. To be published.
23. M. SAAS and D. ZIESSOW. J. Magn. Reson. **25**, 263 (1977).
24. D. CANET. J. Magn. Reson. **23**, 361 (1976).

Can. J. Chem. Downloaded from www.nrcresearchpress.com by 210.87.254.6 on 09/05/12
For personal use only.

Nucleophilic addition to 4-acetyl-1-methylpyridinium iodide studied by ^{1}H nmr

LIANG K. TAN AND MICHAEL COCIVERA[1]

Guelph–Waterloo Centre for Graduate Work in Chemistry, University of Guelph, Guelph, Ont., Canada N1G 2W1

Received April 8, 1980

Can. J. Chem. Downloaded from www.nrcresearchpress.com by 210.87.254.5 on 09/05/12
For personal use only.

LIANG K. TAN and MICHAEL COCIVERA. Can. J. Chem. **58**, 1929 (1980).

The ^{1}H nuclear magnetic resonance spectra obtained during the addition of amines to 4-acetyl-1-methylpyridinium iodide in aqueous solution provide data for the kinetic parameters associated with: (*1*) the rapid equilibrium of the addition step to form the carbinolamine intermediate; (*2*) the rate determining dehydration step to form the *syn* and *anti* imines; and (*3*) the *anti* to *syn* isomerization. Depending on the amine used, (*1*) can result in methyl proton exchange that is either fast or slow relative to the chemical shift between the acetyl-CH_3 resonance of 4-acetyl-1-methylpyridinium iodide and the corresponding one due to carbinolamine. The line width data and the equilibrium constant K_n, which is determined by flow uv, provide values for the rate constants (k_n and k_{-n}) of the forward and reverse steps of the equilibrium. The logarithm of k_n does not correlate with log K_n or pK_a of the amines. In addition, the enthalpy change ΔH for the equilibrium step is found not to depend significantly on the nature of the amine. It remains relatively constant at about -11 kcal M^{-1}. The dehydration step is subject to general acid and base catalysis with the effect decreasing in the order hydrazine, hydroxylamine, semicarbazide, and methoxyamine. For hydrazine and hydroxylamine, the *syn*/*anti* ratios are pH dependent. For hydrazine and semicarbazide the *anti* to *syn* imine conversion depends on pH. The occurrence of *anti* to *syn* isomerism indicates that the dehydration of carbinolamine gives the *anti* imine as the product of kinetic control.

LIANG K. TAN et MICHAEL COCIVERA. Can. J. Chem. **58**, 1929 (1980).

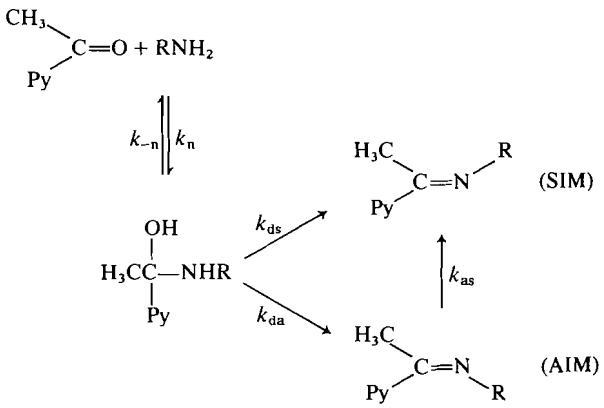
Les spectres rmn du ^{1}H obtenus lors de la réaction d'addition des amines sur l'iodure d'acétyl-4 méthyl-1 pyridinium en solution aqueuse fournissent des données sur les paramètres cinétiques associés à: (*1*) l'équilibre rapide de l'étape d'addition qui conduit à la carbinolamine intermédiaire, (*2*) la déshydratation qui est l'étape déterminante lors de la formation des imines *syn* et *anti* et (*3*) l'isomérisation *anti* à *syn*. Selon l'amine utilisée, (*1*) peut provoquer l'échange de proton du méthyle qui peut être rapide ou lent par rapport au déplacement chimique entre la résonance du CH_3 du groupe acétyle de l'iodure d'acétyl-4 méthyl-1 pyridinium et la résonance correspondante due à la carbinolamine. Les données sur la largeur du pic et la constante d'équilibre K_n qui est déterminée par uv à écoulement fournissent les valeurs des constantes de vitesse (k_n et k_{-n}) des étapes directe et inverse de l'équilibre. Le logarithme de k_n ne correspond pas au log K_n ou au pK_a des amines. De plus, on a trouvé que la variation d'enthalpie, ΔH, de l'équilibre ne dépend pas d'une façon importante de la nature de l'amine. Elle demeure relativement constante aux environs de -11 kcal M^{-1}. L'étape de déshydratation est sujette à une catalyse générale par les acides et par les bases dont l'effet décroît dans l'ordre: hydrazine, hydroxylamine, semicarbazide et méthoxyamine. Dans le cas de l'hydrazine et de l'hydroxylamine, les rapports *syn*/*anti* dépendent du pH. Dans le cas de l'hydrazine et de la semicarbazine, l'isomérisation *anti*–*syn* dépend du pH. Cette isomérisation *anti*–*syn* indique que la déshydratation de la carbinolamine donne comme produit cinétique l'imine *anti*.

[Traduit par le journal]

Introduction

The use of ^{1}H nuclear magnetic resonance (nmr) spectroscopy has provided detailed information concerning various steps associated with the nucleophilic addition to carbonyl compounds (1). As part of a continuing study, we have undertaken the investigation of the addition of α-effect nucleophiles to 4-acetyl-1-methylpyridinium iodide (AMPI), which has a structure not unlike that of 4-formyl-1-methylpyridinium iodide, a compound used to study transamination (2). Of particular interest is information about the rate of nucleophilic addition as well as the rates of formation of the imine isomers. Hydroxylamine (HA), hydrazine (HYD), methoxyamine (MA), and semicarbazide (SM) were used as the nucleophiles because they represent a range of pK_a values.

Because of the detailed information available in the nmr spectrum, it is possible to measure directly the rate constants for the reaction steps indicated in Scheme 1 in which Py denotes methylpyridinium iodide.



SCHEME 1

Experimental

Chemicals

AMPI was prepared from 4-acetylpyridine (vacuum distilled before use) and methyl iodide in benzene. It was recrystallized from acetonitrile giving red-brown crystals with mp 177–179°C,

[1]Author to whom correspondence may be addressed.

0008-4042/80/181929-10$01.00/0

©1980 National Research Council of Canada/Conseil national de recherches du Canada

Can. J. Chem. Downloaded from www.nrcresearchpress.com by 210.87.254.5 on 09/05/12
For personal use only.

which agreed with the previously reported value (3). Methoxyamine hydrochloride was recrystallized from absolute alcohol; imidazole was recrystallized twice from benzene; and diazabicyclooctane (Dabco) was purified by sublimation under reduced pressure. The oxazolidine of 4-acetylpyridine was prepared from 4-acetylpyridine (vacuum distilled) and 2-amino-2-methyl propan-1-ol according to the procedure reported in the literature (4). It was purified by distillation under reduced pressure (bp 85°C/1.0 Torr), solidifying immediately into white crystals. The oxazolidine of AMPI was prepared from the oxazolidine of 4-acetylpyridine and methyl iodide in anhydrous ether and recrystallized from acetonitrile giving light brown crystals with mp 167–169°C. The oxazolidine of acetone was prepared using the same procedure (4) and was purified by distillation under reduced pressure (bp 56°C/5.9 Torr). Other chemicals were obtained from suppliers and used without purification.

Kinetics

The kinetic measurements involved either line shape analysis of ^{1}H nmr spectra or determination of the time dependence of spectra obtained using a Varian HA 100-15 operating at 100 MHz (1). In either case, the reaction mixture was made by mixing equal volumes of aqueous AMPI and nucleophile solutions at an ionic strength of 1.30 *M* (KCl) and 30 ± 0.1°C. To determine time dependent spectra when the reaction was slow, temperature equilibration was done outside the nmr probe in a bath at 30.0 ± 0.1°C. The intensity of each signal was obtained from the ratio of its measured intensity to the intensity of the internal reference signal. In this manner, changes in magnetic field homogeneity during the period of the reaction did not affect the intensities of the signals being studied. For the same purpose, the line width measurements were also obtained relative to the line width for the internal reference signal in all runs.

The equilibrium constant K_n for the addition step forming the carbinolamine was determined at several temperatures by flow uv using a Cary 118 spectrometer as described previously (1).

Results and Discussion

Spectra

Figure 1 illustrates representative 100 MHz proton resonance spectra observed at 30°C for static spinning samples under the following conditions: A, 0.100 *M* AMPI solution buffered at pH 7.0; B, reaction mixture containing 0.100 *M* AMPI and 0.150 *M* HA solution (pH 7.0) immediately after mixing: C, reaction mixture of 0.100 *M* AMPI and 0.200 *M* MA solution (pH 7.0) immediately after mixing; D, same conditions as B but 9.0 minutes after mixing; E, reaction mixture B at the end of the reaction.

The two signals in Fig. 1A are assigned to be the

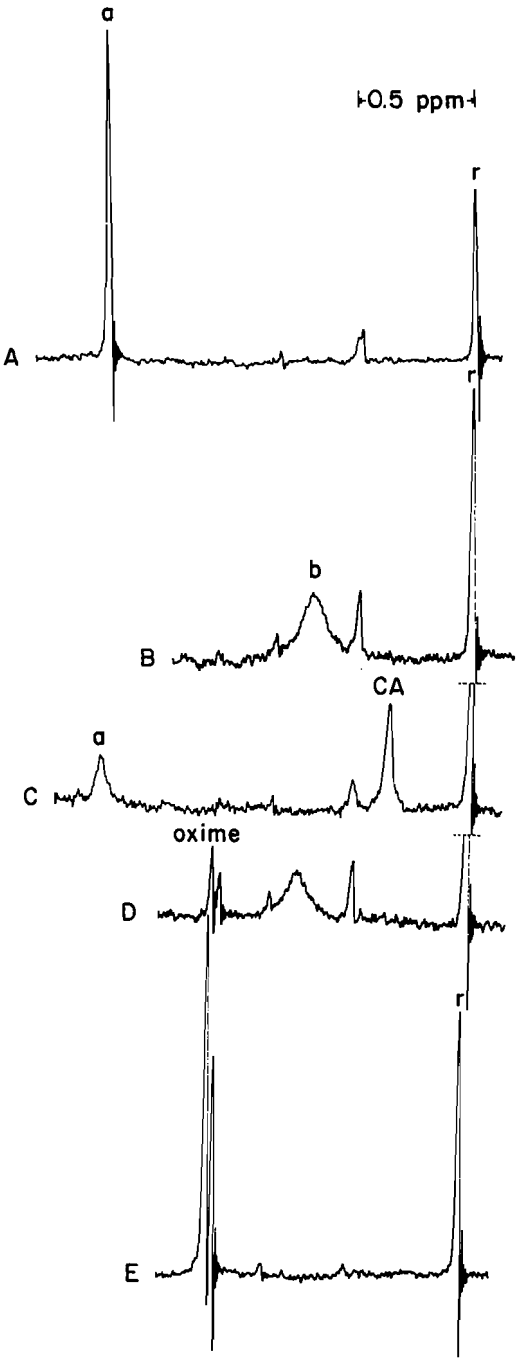


FIG. 1. Proton nmr spectra of aqueous solutions obtained at 100 MHz and 30°C. Only the portion of the spectral range upfield from water signal is illustrated. The most upfield signal (labeled r) in each spectrum is the methyl proton resonance of *tert*-butyl alcohol, which acts as intensity and line width internal reference. (A) Solution buffered at pH 7.0 with 0.350 *M* phosphate, containing 0.100 *M* AMPI. Signal labeled a is due to the acetyl CH_3-proton resonance of AMPI. The two small signals have not been identified, although the signal at higher field may be due in part to the hydrate of AMPI and to methyliodide. These signals are observed in the other spectra, although the intensity of the higher field signal has decreased at the end of the reaction (cf. (E)). (B) Reaction mixture of 0.100 *M* AMPI and 0.150 *M* HA, buffered with 0.350 *M* phosphate at pH 7.0, immediately after mixing. (C) Reaction mixture of 0.100 *M* AMPI and 0.200 *M* MA, buffered with 0.200 *M* phosphate at pH 7.0, immediately after mixing. (D) Reaction mixture as in (B), 9.0 min after mixing. (E) Reaction mixture as in (B), at the end of the reaction. For the assignment and chemical shifts of the resonances, see the text.

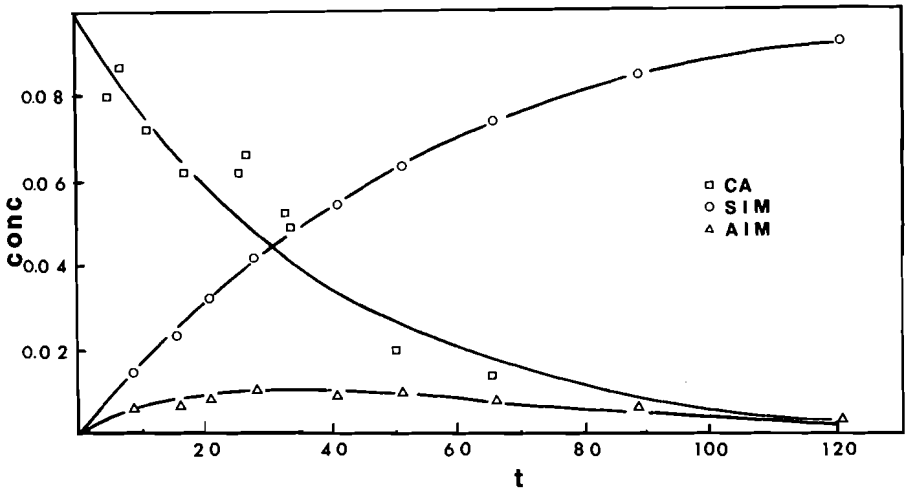


FIG. 2. Molar concentration of CA, SIM, and AIM as a function of time in minutes for an aqueous solution of 0.100 *M* AMPI and 0.405 *M* HYD buffered with 0.400 *M* Dabco (after mixing) at pH 8.2 and 30°C. The solid lines represent the simulated time dependences based on rate constants obtained by an iterative method (see text).

carbonyl CH_3-proton resonance of the AMPI (labeled a), and the CH_3-proton resonance of *tert*-butyl alcohol, which serves as the internal reference signal (labeled r). The broad signal (labeled b) in Fig. 1B, which is observed immediately after mixing with HA, is assigned to be the coalescence signal as a result of exchange between carbinolamine (CA) intermediate and AMPI (1*c*, 5) for the following reasons. The chemical shift of the broad signal is between the chemical shift of the acetyl-CH_3 resonance of AMPI and the expected CA-CH_3 resonance. This broad signal appears before the oxime signals grow (Figs. 1B, D, and E) and is a transient whose rate of decay is the same as the rate of growth for the *syn* and *anti* oximes (Fig. 2). That the broadening is a result of a fast exchange process is proved by the following observations. The line width and chemical shift of this signal are dependent upon the HA initial concentration when the initial concentration of AMPI is held constant, i.e., increasing the initial concentration of HA increases the line width of this signal and causes it to move upfield. A similar line width effect (1*c*, 5) is observed when HYD is used as the nucleophile.

On the other hand, when either MA or SM is the nucleophile, slow exchange (1*b*, *e*, 5) is observed, i.e., the acetyl-CH_3 resonance due to AMPI and the corresponding signal due to CA are not coalesced and can be observed separately (Fig. 1C for MA). In this case, the line widths but not the chemical shifts of these resonances are dependent on the concentration of nucleophile. Consequently the chemical shift between CH_3-proton resonances due to AMPI and CA can be measured directly. On the other hand, for HA and HYD, this chemical shift is obtained from the nucleophile concentration dependence of the chemical shift of the coalescence signal and the value for the equilibrium constant K_n (1, 5), which is discussed below. As expected, these chemical shift values are almost identical for all four nucleophiles (Table 1). In addition, they agree closely with the one for the structurally similar oxazolidine of AMPI (δ, 1.68).

TABLE 1. Chemical shifts[a] in H_2O at 30°C

Nucleophile	Carbinolamine[b]	Dehydration product	
		syn	*anti*
Hydroxylamine	1.57±0.02	2.32	2.29[c]
Methoxyamine	1.58±0.001	2.31	2.30
Hydrazine	1.61±0.002	2.20	2.26
Semicarbazide	1.69±0.001	2.32	2.35[d]

[a]Relative to TMS in ppm.
[b]The pH of the solutions is adjusted to 7.5 using phosphate for HA, MA, and SM. Solutions of pH 9.7 using Dabco are used for HYD.
[c]At pH 9.2 *syn* oxime has a chemical shift δ of 2.28 and the corresponding *anti* isomer is 2.30. This may be due to the deprotonation of H on =N—OH group at such high pH. Assignment of signals is based on ref. 7. See text.
[d]Resonances are well resolved with almost no overlap.

Equilibrium Constants

For evaluation of the kinetic parameters of both the rapid preequilibrium and the dehydration steps, K_n was measured using flow uv (1*e*) as described below, and the pK_a of CA for each nucleophile was estimated by starting with the pK_a value for a corresponding base and adjusting for substituent effects using σ* values (6) for —OH, —NH_2, —OCH_3, and —$NHCONH_2$ groups. Since a σ* value for the pyridyl-*N*-methyl iodide group does not appear to

Can. J. Chem. Downloaded from www.nrcresearchpress.com by 210.87.254.5 on 09/05/12
For personal use only.

Can. J. Chem. Downloaded from www.nrcresearchpress.com by 210.87.254.5 on 09/05/12
For personal use only.

be available, its effect was estimated by comparison of the pK_a values for the oxazolidine of AMPI (pK_a, 3.47) and the oxazolidine of acetone (pK_a, 7.06).[2] Using this approach, the estimated pK_a values for CA derived from HA, HYD, MA, and SM are 2.3, 4.7, 0.8, and 2.7, respectively.

The constant K_n for the equilibrium between AMPI and CA was determined for each nucleophile by measuring the decrease in absorbance at wavelength 278 nm when AMPI and nucleophile solutions are mixed. In order to simplify the mathematical analysis, the pH was sufficiently high so that protonation of the nucleophile was negligible. Solutions buffered with phosphate at pH 8.0 were used for HA, MA, and SM, and solutions buffered with Dabco at pH 10.0 were used for HYD. Under these conditions, less than two percent of the nucleophile is protonated, and the concentration of protonated carbinolamine (CAH^+) is negligible. The absorbance of CA is taken into account by assuming its molar absorptivity is the same as that for the structurally similar oxazolidine of AMPI. Based upon these considerations, K_n is determined at different temperatures using the expression

$$[1] \quad K_n = \frac{(A_3 - A_1 - A_2)\varepsilon_A}{b^0[A_1(\varepsilon_{CA} - \varepsilon_N) - (A_3 - A_2)\varepsilon_A]}$$

in which A_1, A_2, and A_3 represent the absorbance of AMPI solution, nucleophile solution, and the mixed solution, respectively. In all cases, the absorbance is measured when the liquid is flowing, b^0 is the initial concentration of nucleophile, and ε is the molar absorptivity at 278 nm.[3] Subscripts A, N, and CA denote AMPI, nucleophile, and carbinolamine, respectively. As mentioned above, ε_{CA} is assigned the molar absorptivity of the oxazolidine of AMPI (299.4 M^{-1} cm^{-1}). Values reported in Table 2 are averages of three nucleophile concentrations. For SM and MA, which exhibit slow exchange, K_n may also be calculated directly from the areas for the CH_3-proton resonances of AMPI and CA at 30°C, and the respective values of 6.8 ± 0.7 and 16 ± 2 M^{-1} agree well with the values in Table 2. Each of these nmr values is an average of about twenty experiments over the pH range 6.0 to 9.2. The enthalpy (ΔH°) of this equilibrium step, which is calculated from the relation

$$\ln K_n = -\Delta H^\circ/RT + C$$

by linear least squares, does not appear to depend significantly on the nature of the nucleophile (Table 2).

Preequilibrium Rates

Using these data, the rate constants k_n and k_{-n} (Scheme 1) were evaluated from line width data for slow and fast exchange as described previously (1). For slow exchange (1*b*, *e*, 5), the reciprocal of the exchange lifetime for AMPI and CA has the relations $1/\tau_A = \Delta_A$ and $1/\tau_{CA} = \Delta_{CA}$, in which $\Delta = \pi(\Delta\nu_e - \Delta\nu_o)$, $\Delta\nu$ is the width at half height of the appropriate signal, and the subscripts e and o denote exchange and no exchange, respectively. For CA, $\Delta\nu_o$ is obtained from a freshly prepared solution of oxazolidine of AMPI. The exchange lifetime τ is related to the rate contants by the equations: $1/\tau_{CA} = k_{-n}$ and $1/\tau_A = k_n[N]$ in which [N] is the equilibrium concentration of the nucleophile free base. The results for MA are listed in Supplementary Table 3. Each number is an average of at least three measurements.[4] Although the precision of the values appears very satisfactory, the rate constants are probably accurate to within 15% at the concentrations employed, since $\Delta\nu_o$ is about 1.7 Hz and $\Delta\nu_e$ varies from 3 to 6 Hz as the concentration of MA increases. The fact that the ratio of k_n/k_{-n} is about 16.0 M^{-1}, which differs by only 9% from the equilibrium constant K_n determined by flow uv (14.6 M^{-1}), provides substantiation of the reliability of the data in Supplementary Table 3. For SM, $(\Delta\nu_e - \Delta\nu_o)$ is small, varying from 0.2 to 0.9 Hz, depending on the concentration of SM employed, so that the data must be considered semiquantitative with k_n and k_{-n} equal to 5 and 0.9 M^{-1} s^{-1} respectively. The ratio of these two numbers gives a value of about 5.5 M^{-1} which is within 16% of K_n measured by flow uv (6.52 M^{-1}).

For HA and HYD, which cause fast exchange, the exchange lifetime (1, 5) is calculated using the equation $\Delta = P_A P_{CA} \delta^2 \tau$, in which $\Delta = \pi\{\Delta\nu_e - P_A(\Delta\nu_o)_A - P_{CA}(\Delta\nu_o)_{CA}\}$, $1/\tau - k_n[N] = k_{-n}$, and [N] is the equilibrium concentration of nucleophile free base. For these two nucleophiles, Δ makes a major contribution to the line width of the coalescence signal. Rate constants listed in Supplementary Table 3 are averages of at least three runs.

In general, data for the four nucleophiles show that k_n and k_{-n} are independent of pH and buffer

[2]These values take into account the decomposition of oxazolidines in acid media.

[3]HA and MA have negligible absorbance at the wavelength of the experiment, while HYD and SM have molar absorptivities of 2.17 and 0.221 M^{-1}cm^{-1} respectively.

[4]All of the data for HYD along with those for MA and HA are on file in Supplementary Table 3, which contains 426 values obtained for various buffers and pH values. This information can be obtained, at a nominal charge, from the Depository of Unpublished Data, CISTI, National Research Council of Canada, Ottawa, Ont., Canada K1A 0S2.

Can. J. Chem. Downloaded from www.nrcresearchpress.com by 210.87.254.5 on 09/05/12
For personal use only.

TABLE 2. Equilibrium constant (K_n) at ionic strength 1.30 M (KCl)

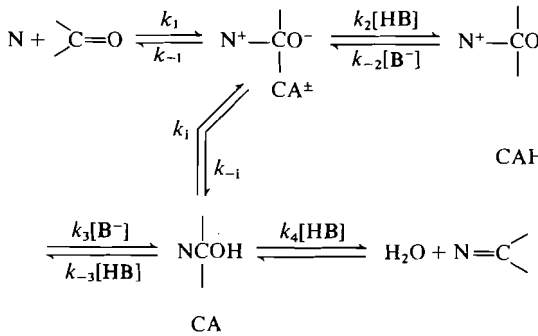
	Nucleophile			
Temperature (°C)	Hydroxylamine	Hydrazine	Methoxyamine	Semicarbazide
70	5.14±0.15	1.65±0.12	1.68±0.13	0.90±0.08
60	8.97±0.53	3.82±0.27	2.82±0.16	1.51±0.15
50	14.9 ±0.3	6.47±0.16	4.76±0.10	2.25±0.14
40	26.4 ±1.4	10.3 ±0.2	8.12±0.07	3.75±0.16
30	50.8 ±2.0	17.4 ±1.1	14.6 ±0.5	6.52±0.27
20	101.0 ±9.0	29.4 ±1.5	26.9 ±1.0	11.1 ±0.3
$\Delta H°$(kcal M^{-1})	−11.8	−11.0	−11.0	−10.0

TABLE 3. Values for pK_a, K_n, and the addition rate constant k_n for each nucleophile

		AMPI			Pyruvate anion[c]	
Nucleophile	pK_a	pH Range	K_n M^{-1}	k_n[a,b] M^{-1} s^{-1}	K_n M^{-1}	k_n M^{-1} s^{-1}
Semicarbazide	3.86	6.0–9.2	6.5	5±0.8	12.0	49
Methoxyamine	4.80	6.0–9.2	14.6	56±4	36.5	102[d]
Hydroxylamine	6.17	6.4–9.2	50.8	24000±2600	54.3	63000
Hydrazine	8.20	7.0–9.2	17.4	4600±400	24.0	14500

[a]The k_n data listed for AMPI are average values obtained from all the results given in Supplementary Table 3.
[b]The buffers and their concentration ranges were: sodium phosphate, 0.100–0.350 M; imidazole, 0.200–0.800 M; and Dabco, 0.200–0.800 M. The ionic strength was held constant at 1.3 M (KCl).
[c]Data for pyruvate anion are taken from ref. 1*e*.
[d]Calculated based on slow exchange since both the ketone and carbinolamine signals can be observed. Previously (1*e*) interpreted as fast exchange.

concentration, as well as independent of the concentration of the nucleophile. These results agree with the mechanism formulated previously (1*b*, *e*) for the nucleophilic addition to other carbonyl compounds (Scheme 2). Since the only steps in this sequence that are independent of acid and base catalysis are the addition step to form $CA^{\pm}$ and direct interconversion of $CA^{\pm}$ to CA, our experimental results are consistent either with this path or with a rate-determining formation of $CA^{\pm}$. A similar conclusion was reached for addition to pyruvate anion (1*e*). As with the pyruvate anion, we find that a good free energy relationship between k_n and either K_n or K_a is not obtained, although K_n appears to give a better fit than K_a for the four nucleophiles (Table 3).[5] While AMPI and the pyruvate anion show the same trend in values for k_n vs. nucleophile, the relative magnitudes differ substantially (Table 3). Understanding these differences will require a systematic study of a number of electrophiles. In contrast with AMPI, 4-formylpyridine reacts with secondary amines such as piperazine and sarcosine via both uncatalyzed and catalyzed routes. For the uncatalyzed addition by sarcosine at 25°C, the rate constant is 1.0×10^4 M^{-1} s^{-1} (2*c*).



SCHEME 2

Product Time Dependence

The time dependence of the *syn* (SIM) and *anti* (AIM) imines provides values for the rate constants (k_{ds} and k_{da}) for the dehydration step and also the rate constant (k_{as}) for the isomer conversion step on Scheme 1. Assignment of the acetyl-related CH_3 signals (Table 1) for the SIM and AIM products obtained with the four nucleophiles is based on the work of Karabatsos and co-workers (7). Figure 2 illustrates a representative time dependence for the concentration of SIM and AIM using HYD. The decay of AIM and growth of SIM indicate that dehydration of CA gives AIM as the product of kinetic control. The AIM to SIM interconversion is slower for the other three nucleophiles. In addition,

[5]Data in Table 3 are average values obtained from all the results given in Supplementary Table 3.

Can. J. Chem. Downloaded from www.nrcresearchpress.com by 210.87.254.5 on 09/05/12
For personal use only.

for HYD and SM this interconversion is pH dependent as discussed below. Isomeric interconversion has been noted before but not studied in the detail reported here (1*a*, *f*).

Analysis of the time dependence has involved two independent sets of data: (*1*) those for CA, which provide values for the total dehydration rate constant $k_d = k_{ds} + k_{da}$; and (*2*) those for AIM and SIM, which provide values for k_{ds}, k_{da}, and k_{as} as well as the dehydration rate constant k_d. First, consider the dehydration step. Because of the magnitude of K_n for each nucleophile, the equilibrium concentrations of AMPI and CA are appreciable during the dehydration reaction, which, therefore, cannot be treated as either pure first order or pure second order reaction. Consequently the value for $(k_{ds} + k_{da})$ has been calculated using the expression (1*f*): $\ln [AMPI]_t = (k_{ds} + k_{da})\beta t + C$ in which $[AMPI]_t$ is the total concentration of AMPI and β is $K_n[N]/(K_n[N] + 1)$.[6] In this expression [N], which is the concentration of nucleophile free base, is time dependent, i.e., for each value of t, [N] was calculated using the appropriate equilibrium constants taking into account the amount of AMPI and nucleophile that had been converted to product. A least-squares fit of $\ln [AMPI]_t$ vs. βt provided the value for $(k_{ds} + k_{da})$. The limitations of this approach have been discussed previously (1*f*). This approach was used for the decay data of the coalescence signal of (AMPI + CA) and the growth data for SIM plus AIM. For the latter the growth of the sum of the intensities of the two signals (AIM + SIM) was used since isomerization also occurs. The results from the growth and decay data are in close agreement. For example, at pH 7.5 and 0.200 *M* phosphate, values of 10.4×10^{-2} min^{-1} and 8.7×10^{-2} min^{-1} were obtained for the decay and growth, respectively, using 0.150 *M* HA as the nucleophile. In practice, because the signals of SIM and AIM were not exchange broadened, they were used predominantly to obtain values for the dehydration rate constants, some of which are listed for HYD in Table 4.[7]

To calculate values of k_{as}, the rate constant for conversion of AIM to SIM when HYD or SM is the nucleophile, an iterative program (Fortran IV, ref. 1*g*) was used to analyze the time dependence data of SIM and AIM in terms of the equations

$$\begin{aligned} d[CA]/dt &= -(k_{ds} + k_{da})[CA] \\ d[SIM]/dt &= k_{ds}[CA] + k_{as}[AIM] \\ d[AIM]/dt &= k_{da}[CA] - k_{as}[AIM] \end{aligned} \quad [2]$$

These equations do not include a term for SIM to AIM conversion because AIM converts completely to SIM for these two nucleophiles. The values for $(k_{ds} + k_{da})$ and k_{as} listed in Table 4[7,8] were obtained in this manner using k_{ds}/k_{da} ratios obtained from initial SIM/AIM intensity ratios that had been obtained by extrapolation. A measure of the internal consistency of the various treatments is given by the following values for $(k_{ds} + k_{da})$ obtained for the reaction between 0.100 *M* AMPI and 0.405 *M* HYD buffered with 0.400 *M* Dabco at pH 8.2: 3.4×10^{-2} min^{-1} (decay of CA, least squares), 3.8×10^{-2} min^{-1} (growth of SIM + AIM, least squares), and 3.5×10^{-2} min^{-1} (iterative treatment of AIM and SIM time dependences).

For all nucleophiles (Table 4 and Supplement), $(k_{ds} + k_{da})$ appears to be independent of nucleophile concentration but is dependent on pH and phosphate buffer concentration. In addition $(k_{ds} + k_{da})$ for HA is dependent on Dabco concentration. Consequently, the dehydration step is subject to a general acid and base catalysis. The slope and intercept (k_4^0) of the plot of $(k_{ds} + k_{da})$ vs. buffer concentration, which was calculated by least-squares fit, are listed in Table 5. Assuming a linear relationship between the slope and the fraction of buffer existing in its acid form, the general acid k_4^{GA} and general base k_4^{GB} catalytic rate constants are calculated (Table 5). With the four nucleophiles, k_4^{GA} is found always to be higher than k_4^{GB} for phosphate buffer, and the order of decreasing magnitude of k_4^{GA} or k_4^{GB} is HYD > HA > SM > MA, whereas the order for pK_a is HYD > HA > MA > SM. In the case of HA, Dabco appears to be a general base catalyst.

The values for k_4^0 are listed in Table 5 for all the buffers. For the cases in which Dabco and imidazole had a negligible catalytic effect, extrapolation provided only a minor correction. For a given nucleophile, the good agreement between k_4^0 values obtained at the same pH for different buffers indicates the reliability of the nmr technique in this type of study. The pH dependence of k_4^0 was analyzed according to the relation, $k_4^0 = k_h + k_4^+[H^+] + k_4^-[OH^-]$, where k_h is the rate constant for the dehydration of CA in the absence of H_3O^+ or OH^- catalysis. For HYD, a linear correlation between

[6] In view of the low estimated pK_a values for CA derived from each of the nucleophiles, no correction for protonation of CA (1*f*) is necessary for the pH range employed.

[7] Additional listings for HYD along with data for HA, SM, and MA are found in Supplementary Table 4. This table is also available from the Depository of Unpublished Data, see footnote 4.

[8] Isomerization may occur either via CA or the diamine formed by reversible addition of HYD or SM to the imine (or both). The present data are insufficient to allow a choice. Consequently a more complicated analysis has not been attempted.

TABLE 4. Kinetic data for the dehydration of carbinolamine and the conversion of *anti* to *syn* isomer

pH	[Buffer][a] (total), *M*	[Hydrazine][b] (total), *M*	k_{ds}/k_{da}[c]	$(k_{ds} + k_{da}) \times 10^2$ min^{-1}	$k_{as} \times 10^2$ min^{-1}
			Phosphate		
7.5	0.100	0.306	0.9±0.1	7.70±0.75	3.1±0.1
		0.408	0.8±0.0	8.41±0.91	4.9±0.5
		0.510	0.9±0.1	7.76±0.50	5.4±0.2
	0.200	0.306	1.0±0.1	9.55±0.30	2.8±0.3
		0.408	0.9±0.1	11.3 ±0.58	4.0±0.1
		0.510	0.9±0.0	11.7 ±0.95	4.4±0.3
	0.350	0.306	1.1±0.0	15.2 ±0.79	2.5±0.2
8.0	0.100	0.310	1.1±0.1	3.95±0.05	2.8±0.2
		0.413	1.1±0.1	5.32±0.32	3.7±0.1
		0.516	1.3±0.1	5.18±0.19	4.7±0.2
	0.200	0.310	1.1±0.1	5.38±0.26	2.3±0.2
		0.413	1.2±0.1	6.42±0.21	3.2±0.1
		0.516	1.0±0.1	6.16±0.8	4.5±0.2
	0.300	0.310	1.0±0.1	8.00±0.33	2.1±0.1
			Imidazole		
7.0	0.200	0.514	0.5±0.0	18.0 ±1.8	10.6±0.6
		0.610	0.5±0.0	14.5 ±0.3	13.7±0.9
	0.400	0.411	0.5±0.1	15.7 ±0.7	11.8±0.6
		0.514	0.5±0.0	18.5 ±2.2	15.4±2.3
		0.610	0.5±0.1	16.8 ±2.3	13.1±0.2
	0.600	0.514	0.6±0.1	19.5 ±1.4	16.1±3.5
		0.610	0.5±0.0	16.6 ±3.9	15.4±2.4
	0.800	0.411	0.5±0.0	19.4 ±3.1	16.2±3.7
		0.514	0.5±0.1	18.4 ±0.9	23.4±4.9
7.5	0.200	0.408	1.0±0.0	5.9 ±0.4	5.7±0.1
		0.511	1.1±0.1	5.7 ±0.5	7.6±0.6
	0.400	0.302	1.0±0.1	6.8 ±0.2	5.5±0.4
		0.408	1.1±0.1	7.2 ±0.4	6.1±0.4
	0.600	0.302	1.0±0.0	7.6 ±0.9	5.8±1.2
		0.408	1.2±0.1	8.7 ±1.0	5.2±0.4
		0.511	1.0±0.1	7.5 ±0.6	8.3±0.4
	0.800	0.302	1.0±0.2	8.8 ±0.7	6.8±1.2
		0.408	1.1±0.1	9.2 ±0.2	6.7±1.3

[a]Total concentration after mixing, includes all degrees of protonation.
[b]Total initial concentration after mixing, includes all degrees of protonation. The free base nucleophile was used in calculation. The initial concentration of AMPI after mixing was 0.100 *M* in all runs.
[c]Determined by extrapolation of the ratio [SIM]/[AIM] to zero time. Each value listed is the average of three determinations.

$[H^+]$ and k_4^0 obtains over the whole pH range, 7.0 to 9.2, and k_4^+ and k_h are listed in Table 5. For HA, k_4^0 correlates with either $[H^+]$ or $[OH^-]$ depending upon the pH range (Table 5). In both cases, the intercept k_h is identical as would be expected for the proposed model. Over the pH range employed, MA and SM exhibit an identical $[H^+]$ dependence as indicated by the k_4^+ value in the table. The intercept k_h for these two sets of data indicates that k_h is probably reliable to within about a factor of two. The dependence of these parameters (k_4^+ and k_h) on pK_a has been examined. While k_4^+ increases monotonically with pK_a, the linear free energy correlation is marginal (Fig. 3). A better correlation is obtained for k_h, which may, however, be fortuitous in view of the semiquantitative nature of these data (Fig. 3).

The k_{ds}/k_{da} ratio is independent of the nature and concentration of the buffer (Table 4 and Supplement). However it depends on the pH employed when HYD and HA are the nucleophiles. In the case of HYD a plot of k_{ds}/k_{da} vs. pH (Fig. 4) could be interpreted as having a sigmoid form with an inflection point at about pH 8.2. The corresponding plot for HA does not bend over for the highest pH (9.2) employed (Fig. 4). For SM and MA, k_{ds}/k_{da} is independent of pH in the range 6.0 to 7.5.

It is interesting to speculate about the cause of

Can. J. Chem. Downloaded from www.nrcresearchpress.com by 210.87.254.5 on 09/05/12
For personal use only.

Can. J. Chem. Downloaded from www.nrcresearchpress.com by 210.87.254.5 on 09/05/12
For personal use only.

TABLE 5. Kinetic parameters for buffer catalysis of the dehydration step and isomerization step

Nucleophile	Buffer	pK_a	pH	Concentration range (total) M	Fraction[a] of acid	Slope[b] $\times 10^3$ $min^{-1}\ M^{-1}$	k_4^{GB} $\times 10^2$ $min^{-1}\ M^{-1}$	k_4^{GA} $\times 10^2$ $min^{-1}\ M^{-1}$	$k_{as}^0 \times 10^2$ min^{-1}	$k_4^0 \times 10^{3b}$ min^{-1}	k_4^+ $min^{-1}\ M^{-1}$	$k_h \times 10^4$ min^{-1}
Hydroxylamine ($pK_a = 6.17$)	Phosphate	6.37	7.5	0.100–0.350	0.0690	53.1	4.7[c]	22.5[c]		2.3		
			7.0	0.100–0.350	0.190	92.7				5.5		
			6.4	0.100–0.500	0.483	123				17.6		
			6.0	0.100–0.650	0.701	176				31.5	3.0	27
	Imidazole	7.24	7.5	0.200–0.800	[d]					1.8		
			7.0	0.200–0.800	[d]					4.8		
			6.4	0.200–0.800	[d]					18.4		
	Dabco	9.40	9.2	0.200–0.800	0.612	19	3.9[c]	0.6[c]		7.4		
			8.7	0.200–0.800	0.834	11.6				4.8	0.0029[e]	29
			8.2	0.200–0.800	0.941	8.2				3.0		
Hydrazine ($pK_a = 8.20$)	Phosphate	6.37	8.0	0.100–0.300	0.0229	159	9.4[c]	293[c]	$3._3$	30.9		
			7.5	0.100–0.350	0.0690	290			$5._3$	50.4		
	Imidazole	7.24	8.2	0.200–0.800	[d]				$3._6$	26.1		
			7.5	0.200–0.800	[d]				$5._3$	47.5	130	140
			7.0	0.200–0.800	[d]				15	150		
	Dabco	9.40	9.2	0.200–0.800	[d]				$6._6$	12.4		
			8.7	0.200–0.800	[d]				$3._7$	17.8		
			8.2	0.200–0.800	[d]				$3._6$	26.2		
Semicarbazide ($pK_a = 3.86$)	Phosphate	6.37	7.5	0.100–0.350	0.0690	7.7	0.55[c]	5.0[c]	$0._1$	0.4		
			7.0	0.100–0.350	0.190	14.9			$0._4$	1.7	1.2	0.97
			6.5	0.100–0.350	0.426	25.0			$0._9$	3.3		
			6.0	0.100–0.650	0.701	36.4			$2._6$	12.3		
Methoxyamine ($pK_a = 4.80$)	Phosphate	6.37	7.5	0.100–0.350	0.0690	4.8	0.22[c]	0.6[c]		0.4		
			7.0	0.100–0.350	0.190	9.7				1.5	1.2	0.43
			6.5	0.100–0.500	0.426	15.4				3.7		
			6.0	0.100–0.650	0.701	28.0				12.2		

[a]Fraction of buffer in the acid form.
[b]Obtained by least squares fit of $(k_{ds} + k_{da})$ vs. the total concentration of buffer.
[c]Obtained from a plot of slope vs. fraction of acid.
[d]Not dependent on the concentration of buffer.
[e]Value for k_4^-.

Can. J. Chem. Downloaded from www.nrcresearchpress.com by 210.87.254.5 on 09/05/12
For personal use only.

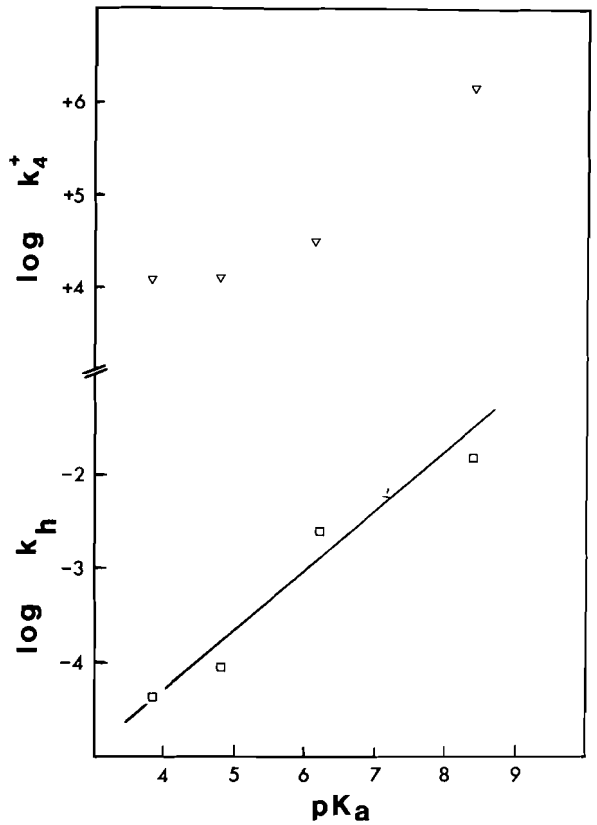


FIG. 3. The logarithm of hydronium ion catalysis (k_4^+) and the logarithm of water catalysis (k_h) for the dehydration step, plotted as a function of the pK_a of the nucleophiles. The solid line represents a least-squares fit of the data (see text).

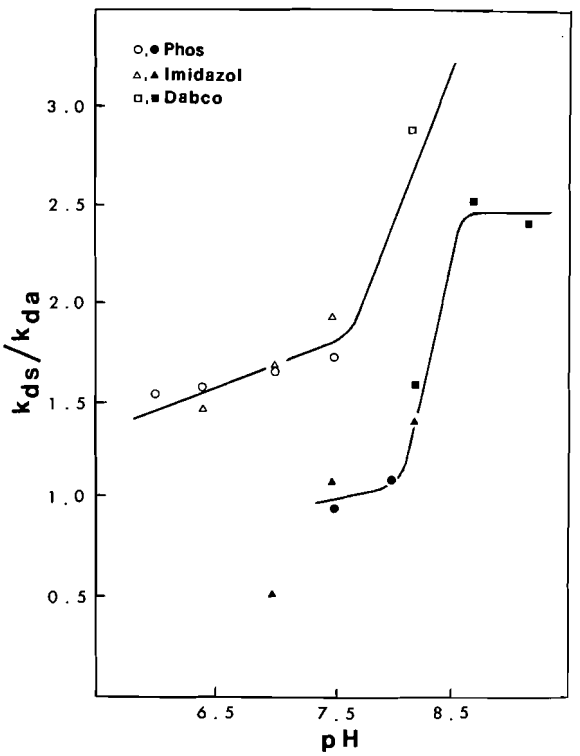
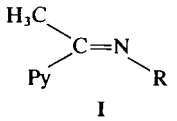


FIG. 4. The pH dependence of the ratio of k_{ds}/k_{da}. Each point represents the average value of k_{ds}/k_{da} at a given pH using several buffer concentrations. Data represented by open symbols are for nucleophile HA, and data represented by solid symbols are for nucleophile HYD. At pH 9.2, the value of k_{ds}/k_{da} is 4.3 The solid lines represent qualitative visual fits of the data.

these different responses to pH, assuming that they represent titration curves. Since there appears to be no buffer effect on the k_{ds}/k_{da} ratio, the pH effect for HYD and HA may reflect the degree of protonation of CA rather than acid or base catalysis. This protonation must occur at a position that can influence the dehydration of CA to form more *anti* isomer (structure **I**) than the unprotonated form (R



I

equals NH_2 or OH). Since there is no reason to suspect that protonation of the nitrogen atom bonded to carbon can affect the stereochemistry of the dehydration of CA, we have considered the possibility that the stereochemistry is affected by protonation at the R group and that the protonated forms are $-NH_3^+$ and —OH for CA derived from HYD and HA respectively. According to this description the orienting effect would be due to an interaction between these protonated R-groups and the π electrons of pyridine. Likewise, the absence of a pH effect for MA and SM could be explained by the fact that $-OCH_3$ and $-NHCONH_2$ are not protonated significantly in the pH range employed. The pK_a for $Py(CH_3)C(OH)NHNH_3^+$ is estimated to be 6.4 by adjusting the pK_a of hydrazine for substituent effects based on a ρ value of about -3 (8) and σ^*_{XNH} values for CH_3 and CH_2OH that have been estimated from σ^* values (6) assuming the relation $\sigma_X = 2.8\sigma_{XCH_2}$ holds when the CH_2 group is replaced by the isoelectronic NH group. The σ^* value for the Py group is estimated from the pK_a values for the oxazolidines of acetone and AMPI. Although this estimated pK_a value should be considered approximate (predicted and measured values can differ by 0.5 units (6)), the two-unit difference between this value and that obtained from Fig. 4 is probably too large.[9] Consequently, the evidence for this model is conflicting, i.e., on the one hand a pH response for HYD and HA differs from that for SM and MA in a manner expected for the model, but on the other hand there is insufficient

[9]Altering the sigmoid curve to include the point at low pH in Fig. 4 does not change the inflection point appreciably.

agreement between the predicted pK_a value for the CA of HYD and the inflection point in Fig. 4. In this regard, the pK_a for CA of HA was not estimated since the data in Fig. 2 are insufficient to give a clear indication of the inflection point. It should be noted that the *syn* and *anti* oxime CH_3-proton resonances are pH dependent (below pH 8.7 $\delta_{syn} > \delta_{anti}$, at pH 8.7 $\delta_{syn} = \delta_{anti}$, and above pH 8.7 $\delta_{syn} < \delta_{anti}$).

As indicated above, the SIM/AIM ratio is also time dependent with AIM converting completely to SIM. This conversion was not studied for HA and MA because of the long time period involved. For HYD and SM, the values for k_{as} calculated using the iterative method are listed in Table 4 and Supplement. The values for SM in the pH range 6.0 to 7.5 exhibit no dependence on SM concentration but show an increase (except for pH 7.0) as the phosphate buffer concentration is increased (unfortunately, the trends are not sufficiently large relative to the precision to allow quantitative analysis of the data). In addition k_{as} decreases monotonically by about a factor of 20 as the pH is increased from 6.0 to 7.5 (Table 4 and Supplement). For HYD, k_{as} does not appear to depend on the concentration of either Dabco or imidazole. There appears to be a slight dependence on HYD concentration, but the data are erratic and the trend barely exceeds experimental error (Table 4 and Supplement). As with SM, k_{as} depends on pH, but the effect is not as large and k_{as} appears to level off when the pH exceeds 8.2. To check the effect of pH on k_{as}, values of k^0_{as} (Table 5) were obtained by extrapolation to zero buffer concentration. While this extrapolation makes a small correction to k_{as}, the values in Table 5 should be considered semiquantitative in view of the precision indicated in Table 4. Nevertheless, the data are sufficiently quantitative to indicate a linear dependence on $[H^+]$ for SM. On the other hand k_{as} for HYD appears to go through a minimum although the accuracy decreases as the pH increases because the AIM signal becomes small.

Although not conclusive, the pH dependence of k^0_{as} indicates that isomerization may proceed in part via a mechanism in which the imine is protonated at the doubly-bonded nitrogen atom. A similar study of HA and MA was not attempted because the isomerization is slower for these nucleophiles. At any rate AIM converts completely to SIM for each of the nucleophiles. Consequently SIM appears to be the thermodynamically stable isomer, and the dehydration of CA gives the *anti* imine as the product of kinetic control.

Acknowledgment

This work was supported in part by a grant from the Natural Sciences and Engineering Research Council of Canada.

1. (*a*) M. COCIVERA, A. EFFIO, H. E. CHEN, and S. VAISH. J. Am. Chem. Soc. **98**, 7362 (1976); (*b*) M. COCIVERA and K. W. WOO. J. Am. Chem. Soc. **98**, 7366 (1976); (*c*) M. COCIVERA and A. EFFIO. J. Am. Chem. Soc. **98**, 7371 (1976); (*d*) M. COCIVERA, V. MALATESTA, K. W. WOO, and A. EFFIO. J. Org. Chem. **43**, 1140 (1978); (*e*) V. MALATESTA and M. COCIVERA. J. Org. Chem. **43**, 1737 (1978); (*f*) M. COCIVERA, K. W. WOO, and P. LIVANT. Can. J. Chem. **56**, 473 (1978); (*g*) P. LIVANT and M. COCIVERA. J. Org. Chem. **43**, 3011 (1978).
2. (*a*) B. H. JO, V. NAIR, and L. DAVIS. J. Am. Chem. Soc. **99**, 4467 (1977); (*b*) J. R. MALEY and T. C. BRUICE. J. Am. Chem. Soc. **90**, 2843 (1968); (*c*) R. N. F. THORNELEY and H. DIEBLER. J. Am. Chem. Soc. **96**, 1072 (1974); (*d*) J. R. MALEY and T. C. BRUICE. Arch. Biochem. Biophys. **136**, 187 (1970).
3. S. GINSBURG and I. B. WILSON. J. Am. Chem. Soc. **79**, 481 (1957).
4. J. KEANA, S. KEANA, and D. BEETHAM. J. Am. Chem. Soc. **89**, 3055 (1967).
5. J. POPLE, W. SCHNEIDER, and H. BERNSTEIN. High resolution nuclear magnetic resonance. McGraw-Hill, New York. 1959. p. 222.
6. J. CLARK and D. D. PERRIN. Q. Rev. **18**, 295 (1964).
7. (*a*) G. KARABATSOS and R. TALLER. Tetrahedron, **24**, 3347 (1968); (*b*) C. I. STASSINOPOULOU, C. ZIOUDROU, and G. J. KARABATSOS. Tetrahedron Lett. **35**, 3671 (1972).
8. F. E. CONDON. J. Am. Chem. Soc. **87**, 4491 (1965).

Can. J. Chem. Downloaded from www.nrcresearchpress.com by 210.87.254.5 on 09/05/12
For personal use only.

FOR ERRATA SEE
v 64 #12 1986 p 2477

Acylation of aromatic substrates with ketenes. II.[1] Hammett–Brown studies on substituted aromatic compounds

K. R. FOUNTAIN,[2] PAMELA HEINZE,[3] DAVE MADDEX,[4] GREG GERHARDT,[5] AND PAUL JOHN[6]

Northeast Missouri State University, Kirksville, MO 63501, U.S.A.

Received January 14, 1980

K. R. FOUNTAIN, PAMELA HEINZE, DAVE MADDEX, GREG GERHARDT, and PAUL JOHN. Can. J. Chem. **58**, 1939 (1980).

Competition reactions using dimethylketene (DMK) – aluminum chloride complexes on a variety of substituted benzene derivatives gave partial rate factors. The logs of these P_f^x values when plotted versus σ^+ values gave two line segments of $\rho = -6.59$ for less active substrates, and $\rho = -0.92$ for more active substrates. Similar results were found for diphenylketene ($\rho = -9.47$ and -1.07).

These results were rationalized by analogy to vinyl cation alkylations. A pair of π complexes (outer then inner) occur between initial approach of the reagent and final, product-determining π-complex formation. In one of these complexes the C=C bond of the ketene complex may be able to back-bond in a manner similar to that found in inorganic complexes of CO and metals.

K. R. FOUNTAIN, PAMELA HEINZE, DAVE MADDEX, GREG GERHARDT et PAUL JOHN. Can. J. Chem. **58**, 1939 (1980).

Des réactions de compétition entre le complexe de diméthylcétène (DMC) – chlorure d'aluminium et différents dérivés du benzène permettent d'obtenir des facteurs de vitesse partielle. Les courbes des logarithmes de valeurs de P_f^x en fonction des valeurs de σ^+ donnent deux segments de droite de pente $\rho = -6.59$ pour les composés moins réactifs et de pente $\rho = -0.92$ pour les composés plus réactifs. On obtient avec le diphénylcétène des résultats semblables ($\rho = -9.47$ et -1.07).

On rationalise ces résultats par analogie avec l'alkylation des cations vinyliques. Il se produit une paire de complexes π (externes aussi bien qu'internes) entre l'approche initiale du réactif et la formation finale d'un complexe π qui détermine la vitesse de la réaction. Dans l'un de ces complexes, la liaison C=C du complexe incluant le cétène peut établir une liaison inverse de façon analogue à celle trouvée dans les complexes inorganiques entre le CO et des métaux.

[Traduit par le journal]

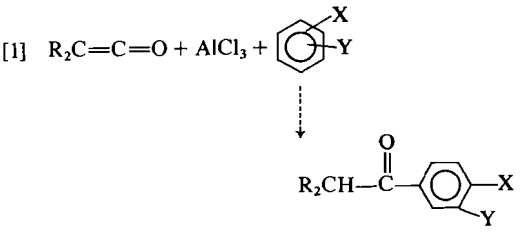
Our previous paper (1) reported the results of studies of substrate specificity using competition studies of benzene vs. toluene for Friedel–Craft acylations of dimethyl and diphenyl ketenes (DMK and DPK). Through a combination of kinetic isotope effect studies and the relative rates of acylations of benzene and toluene we were able to conclude that the ketene – aluminum chloride complex was more selective than an ordinary acyl chloride Friedel–Crafts reagent. The dimethylketene reagent was more reactive than the acetylium ion; the diphenylketene reagent was less reactive. Compared with the stereoelectronically similar vinyl cations the ketene – aluminum chloride complexes were also more selective.

These results indicated that the unique nature of the ketene – aluminum chloride reagent would be interesting to study. This paper deals with the Hammett–Brown linear free energy study of reactions of substituted aromatic substrates in competition for limited amounts of dimethyl and diphenylketene – aluminum chloride reagents.

[1]For paper I see ref. 1.
[2]Author to whom correspondence may be addressed.
[3]PRF Undergraduate Fellow, 1976–1977.
[4]Project SEED student, summer 1977.
[5]PRF Undergraduate Fellow, 1977–1978.
[6]NMSU Summer High School Trainee, 1979.

Results

The reaction which was studied was acylation of substituted benzenes with dimethylketene and diphenylketene (eq. [1]). R was Me or Ph and X and



Y were various substituents giving the substrates listed in Tables 1 and 2 along with the abbreviations for the substrates which are used in this paper.

The method used was a standard competition method in which a small amount of the ketene was allowed to react with a large excess of a mixture of two substrates (2).

Several points of explanation are needed for the competition studies with dimethylketenes as recorded in Table 1. First, the reaction mixtures using dimethylketene and the less activated substrates (entries 1–5 of Table 1) were difficult to analyze by gas chromatography, so extensive use was made of spiked samples for peak identification and artificial mixtures for quantitation of the areas

0008-4042/80/181939-08$01.00/0
©1980 National Research Council of Canada/Conseil national de recherches du Canada

Can. J. Chem. Downloaded from www.nrcresearchpress.com by 210.87.254.40 on 09/05/12
For personal use only.

Can. J. Chem. Downloaded from www.nrcresearchpress.com by 210.87.254.40 on 09/05/12
For personal use only.

TABLE 1. Relative rates of dimethylketene acylations

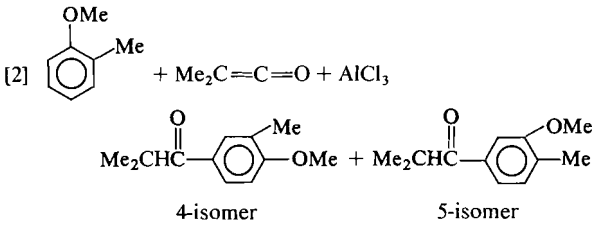
Substrate	Abbreviation	Area ratio[a]	RRF[b]	P_f^{x}[c]	log P_f^{x}	σ^+
1. Benzene	PhH	0.0193_5[d]	0.7547	1.000	0.000	0.000
2. Toluene	TolH	1.000	1.0000	380.2	2.5800	−0.306
3. *o*-Xylene	XylH	3.58	1.2191	455.4	2.6584	−0.375
4. Cumene	CumH	0.549	1.1090	153.5	2.1861	−0.276
5. *o*-Chlorotoluene	OClTolH	0.00245	0.877	0.718	−0.1439	+0.067
6. *o*-Bromoanisole[e]	OBrAnH	0.2187	0.2977	131.92	2.1203	−0.373
7. Anisole	AnH	5.152	1.0651	1249.3[a]	3.0960	−0.764
8. *o*-Methylanisole	OMeAnH					
(*a*) Reaction at 4-position		12.33	1.4440	2201[f]	3.3426	−0.833
(*b*) Reaction at 5-position		2.15	1.4440	385.0	2.5855	−0.259

[a]Relative to tolylketone.
[b]Defined as ((g of ketone x/unit area)/(g of tolyl ketone/unit area))$^{-1}$.
[c]P_f^{x} = area ratio × (area ratio toluene/area ratio benzene) × (1/RRF) × statistical factor × (mol. wt. benzene ketone/mol. wt. ketone).
[d]Ratio of (tolyl ketone area/phenyl ketone area) = (1.000/0.0193) = 51.69.
[e]Determined by liquid chromatography.
[f]Corrected for isomers.

TABLE 2. Relative rates of diphenylketene acylations

Substrate	Abbreviation	P_f^{x}	log P_f^{x}	σ^+
1. Benzene	PhH	1.000	0.000	0.000
2. Toluene	TolH	1042.1	3.01791	−0.306
3. *o*-Xylene	XylH	1365.2	3.1352	
4. *o*-Nitroanisole	ONAnH	54.48	1.7362	−0.102
5. *o*-Chlorotoluene	OClTolH	0.088	−1.0555	0.067
6. *o*-Methylanisole	OMeAnH			
(*a*) Reaction at 5-position		464.2	2.6667	−0.259
(*b*) Reaction at 4-position		6228.2	3.7944	−0.833
7. Anisole	AnH	4223.6	3.5721	−0.764

of the peaks of interest. Second, all the singly substituted substrates (1, 2, and 4 of Table 1) and the doubly substituted ones, XylH, OClTolH, and OBrAnH (entries 3, 5, and 6, Table 1) gave only one product (1), namely, the ketone which resulted from substitution *para* to the most activating substituent. Third, *o*-methylanisole (entry 8) gave two products (eq. [2]) which were impossible to resolve



[2]

4-isomer 5-isomer

by gc. The nmr of the ketone mixture showed the presence of the 5-isomer in that the OCH_3 signals occurred at $\delta = 3.72$ (4-isomer) and 3.64 (5-isomer) in the ratio of 29:5. The aryl CH_3 signal was likewise broadened at $\delta = 2.14$. The percentage of the 5-isomer was thus 14.7% by nmr analysis. All of the calculations concerning the reaction of OMeAnH were corrected by this amount, and the P_f^{x} calculations for attack at the 5-position of OMeAnH are based on 14.7% of the 5-isomer present in the reaction mixture. In no other case did any other isomers in the dimethylketene acylations appear except for anisole (entry number 7) in which case the *o*/*p* ratio was 4.47×10^{-3} (1).

The results for competition reactions involving diphenylketene acylations are similarly reported in Table 2. Once again the OMeAnH gave two products in a manner entirely consistent with acylations of these substrates with dimethylketenes.

Hammett–Brown plots of P_f^{x} (partial rate factors) versus σ^+ values are displayed in Fig. 1 for competitions with methylketenes and in Fig. 2 for diphenylketenes. In Fig. 1 linear regression of σ^+ vs. log P_f^{x} for the moderately activated substrates 1 through 6 and for the reaction at the 5-position of OMeAnH (entry 8*a*) gave $\rho^+ = -6.59$ (correlation coefficient = 0.9488). The limiting value for the slope of the curve in the anisole and 4-(*o*-methylanisyl) end was determined graphically, as shown in the Fig. 1, to be −0.921. The Hammett–Brown plot is seen to go smoothly from a nearly straight line segment of slope nearly −6.59 to a segment of limiting slope −0.94 indicating a smooth change in mechanism (3, 4).

Figure 2 shows a similar treatment for acylation reactions using diphenylketenes. Linear regression for entries 1 through 5 and the 5-position of

Can. J. Chem. Downloaded from www.nrcresearchpress.com by 210.87.254.40 on 09/05/12
For personal use only.

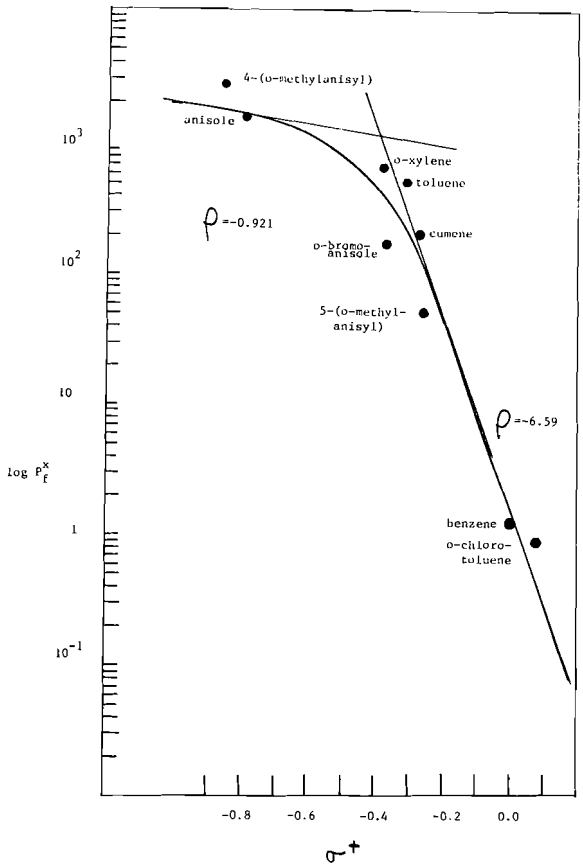


FIG. 1. Hammett–Brown plot for acylations with ketenes (DMK).

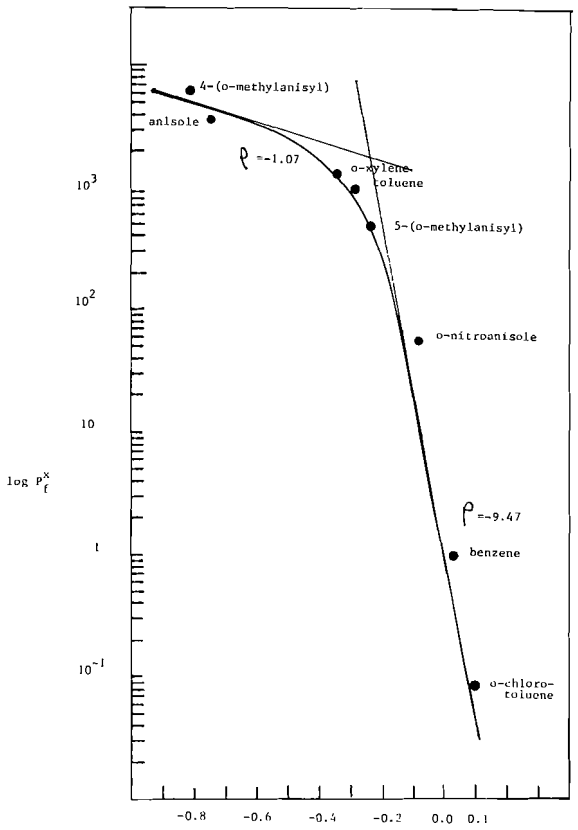


FIG. 2. Hammett–Brown plot of P_f^x for ketene acylations (DPK).

OMeAnH (Table 2, 6*a*) gave a ρ^+ value of -9.47 (correlation coefficient = -0.9667). The limiting value for ρ^+ in the upper region of the curve (large $-\sigma^+$ values) was determined graphically, as shown in Fig. 2, to be -1.07. The Hammett–Brown plot for diphenylketene acylations shows the same general pattern as the plot for dimethylketene (a line correlating moderately activated substrates, and one line correlating highly activated substrates).

It is apparent that, as the ρ^+ value shifts from near -6 to -10 to near -1.0, selectivity is decreased but not drastically so, i.e., *o*/*p* ratio of anisole is 4.47×10^{-3} and no *meta* isomer is found (1). (As little as 0.1% could have been detected.) Thus, although reactivity increases drastically (less negative ρ^+ value), selectivity (5) remains high. The line segments in the Hammett–Brown plots for reactive anisole derivatives resemble the Hammett–Brown plot for vinyl cation alkylation (6) ($\rho^+ = -2.567$), and the reactions are of similar selectivity. The plots for moderately active benzene derivatives resemble ordinary acetylation ($\rho^+ = -9.1$) but with exceptional selectivity (i.e., no *meta* isomers) (5).

Discussion

Stang and Anderson (6) have also reported unusually high positional selectivity combined with very low substrate selectivity. They explained this dilemma of how an intermolecularly nonselective species with a low ρ value (-2.567 for vinyl cations) acquires such great intramolecular selectivity by postulating the existence of two transition states prior to the formation of the usual σ complex (6).

> The first transition state determines the intermolecular selectivity (ρ) and the second transition state determines the intramolecular selectivity (isomer distribution). The low value of ρ indicates that the alkylating agent shows little differentiation between various monosubstituted aromatic rings, based on the electron-donating or withdrawing ability of the substituent. As an electrophilic species approaches an aromatic ring, electrons will flow out of the π cloud of the ring and toward the electrophilic species. The π cloud can be said to be disrupted to the extent that electrons are lost in the transition state. Since the substituent will act to stabilize the growing positive charge on the ring by electron donation, one would expect that the substituents most able to donate electrons (CH_3O, CH_3) would react much faster (sic) than substituents that are less able to donate electrons (H, Cl) to the disrupted π system. However, since all substituents

react at (sic) similar rates (low ρ value), the π system must not be significantly disrupted in the transition state. Hence the first transition state must, therefore, resemble an "inner" π complex rather than a σ complex which involves a greater disruption of the π system.

Such descriptions of inner π complexes as models for transition states of electrophilic aromatic substitutions also appear in the literature of aromatic nitration (7). They are not, however, without controversy (8, 9). Typically the formation of these π complexes is as depicted in eq. [3] (8, 10). The

[3] 

"Outer" complex π-Complex benzonium ion σ Complex

"outer" complex forms first, is transformed to an "inner" complex (the benzonium ion), and finally the product-determining σ complex is formed. These ideas can be summarized as in Fig. 3, the potential energy diagram for electrophilic substitution. In cases where formation of the benzonium ion π complex is rate limiting one would observe this transition state to be higher than for benzonium ion formation (dotted line in Fig. 3).

Applying these ideas to the reaction of aromatic substrates with ketene–$AlCl_3$ complexes we see that as long as one is acylating moderately active substrates the reaction is very much like acetylation (ρ = −9.1) (5).

With greatly activated substrates such as the anisole derivatives the reaction behaves like that for vinyl cations. π-Complexes similar to those postulated for vinyl cations must apply in the reactions of ketenes with very activated substrates.

There remains to be explained the difference in behavior between the acylations of modestly active substrates with ketenes and the alkylation of similar substrates with vinyl cations. In the latter case no change in slope was observed in the Hammett plot (ρ = −2.507) for toluene, benzene, fluorobenzene, and chlorobenzene. In the case of the ketene–$AlCl_3$ complexes resonance stabilization involving the oxygen atom undoubtedly stabilizes the complex and makes it less reactive than a vinyl cation (1). Using the k(Tol)/k(Ph—H) ratios as a measure of the kinetic stability of the ketene–$AlCl_3$ complexes and including the k(Tol)/k(Ph—H) (= 6.76) ratio for the electronically similar vinyl cations (6) one can order the series of species (of course, neglecting solvent differences) in the order of kinetic stability:

$$\underset{k(\text{Tol})/k(\text{Ph—H})\ 6.76}{Ph—\overset{+}{C}=CMe_2} < \underset{47.3}{Cl_3\bar{A}l—O—\overset{+}{C}=CMe_2}$$

$$< \underset{117\ (8,\ 10)}{Cl_3\bar{A}lO—\overset{Cl}{\overset{|}{C}}—\overset{+}{C}Me} < \underset{125\ (8,\ 10)}{O=\overset{+}{C}—Me} < \underset{173}{Cl_3\bar{A}l—O—\overset{+}{C}=CPh_2}$$

There are two surprises in these data. One is that the kinetic stability of the dimethylketene – aluminum chloride complex does not resemble more closely the kinetic stability of the vinyl cation, because the DMK–$AlCl_3$ complex resembles the vinyl cation electronically. The second is that the diphenylketene – aluminum chloride complex differs greatly in reactivity from the dimethylketene – aluminum chloride complex.

The difference between the DMK–$AlCl_3$ complex and a vinyl cation seems to involve the greater stability in the DMK-complex due to delocalization of charge as in **1**.

$$Me_2C=\overset{+}{C}—O—\bar{A}lCl_3 \longleftrightarrow Me_2C=C=\overset{+}{O}—\bar{A}lCl_3$$

1

Of course, one must also keep in mind that the DMK–$AlCl_3$ complex is a neutral compound and the vinyl cation is positively charged. The origin of the greater kinetic stability of the DPK–$AlCl_3$ complex compared to the DMK–$AlCl_3$ complex is more obscure.

In what follows below we extend the idea of rate limiting π-complex formation in terms of the unique stereoelectronic features of ketenes (and vinyl cations). If a unified mechanism connects the electronically similar vinyl cations and DMK or DPK–$AlCl_3$ complexes, the rationalization must contain the following features. It must explain why a vinyl cation behaves as though it forms a substrate-selecting π complex before a product-selecting σ complex in both greatly activated systems and in modestly activated systems. It must

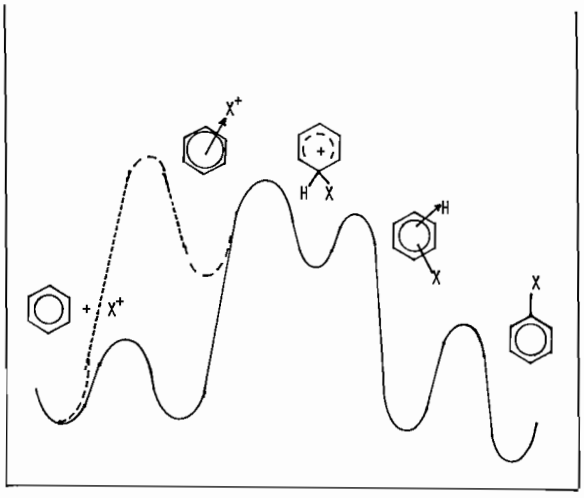


FIG. 3. Potential energy diagram for electrophilic substitution.

Can. J. Chem. Downloaded from www.nrcresearchpress.com by 210.87.254.40 on 09/05/12
For personal use only.

Can. J. Chem. Downloaded from www.nrcresearchpress.com by 210.87.254.40 on 09/05/12
For personal use only.

also explain why the less reactive DMK–$AlCl_3$ complex behaves similarly to an ordinary acylation in attacking modestly activated rings, yet behaves like a vinyl cation for highly activated rings. Lastly, it must explain why the DPK–$AlCl_3$ complex is greatly substrate selective with modestly activated rings, but with very activated rings behaves like DMK–$AlCl_3$ or a vinyl cation.

There are basically two types of orbital interactions possible, from first principles, in π-complex formation. These are shown in Figs. 4 and 5. We will label the interaction in Fig. 4 as a parallel approach and that of Fig. 5 as a perpendicular approach. The approach of Fig. 4 is described by Olah *et al.* (10) as a "benzonium ion" π complex. The second type of orbital interaction in Fig. 5 is taken to be similar to that postulated by Woodward and Hoffman (11) for $\pi^2s + \pi^2a$ processes, especially those that involve ketenes. Because of the unique stereoelectronic properties of any ketene – aluminum chloride complex the approach of the reagent to the substrate can involve both of these types of orbital interactions as in Fig. 6. Both types of overlaps may make significant contributions to the stability of the transition states before the ultimate product controlling σ complex. Note that in this scheme it is necessary to consider the HOMO–LUMO interaction between the substrate and the electrophilic reagent *and* the LUMO–HOMO interaction between the two. This is in clear contrast to the theoretical consideration of only the interaction between LUMO of the electrophile and HOMO of the substrate (12).

When a very reactive vinyl cation approaches a moderately active ring, π-complex formation takes place readily, involving both modes of bonding. As the "benzonium" π complex is formed, charge is placed more on the ring than in the "outer complex" formation. This additional charge on the ring causes back-bonding, of the type in Fig. 5, from the π orbital of the vinyl cation to the LUMO of the ring. This occurs in even moderately activated rings because of the great reactivity of the vinyl cation. When a more stable DMK–$AlCl_3$ complex approaches a moderately activated ring, sufficient charge is not transferred to the ring to allow significant amounts of back bonds, as in Fig. 5, to occur, due to the greater kinetic stability of the complex. Thus a normal course of events is followed in which a rate-determining σ complex occurs. With the more activated anisole derivatives more stabilization of the charge in the π complex (benzonium ion) occurs which in turn allows more back-bonding from the π orbitals of the C=C bond in the DMK–$AlCl_3$ complex to occur with the ring. Thus when activated species of rings are approached by the DMK or DPK–$AlCl_3$ complex, the reaction resembles alkylation by a vinyl cation. The decrease in ρ value for the DPK–$AlCl_3$ complex is probably due to the conjugation of the C=C π bond with the phenyl rings, thus making it less available for back-bonding and correspondingly the DPK–$AlCl_3$ complex would be more sensitive to substituents on the benzene ring.

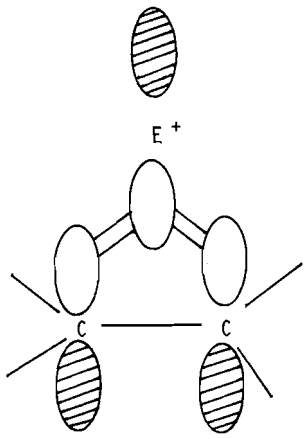


FIG. 4. Parallel approach.

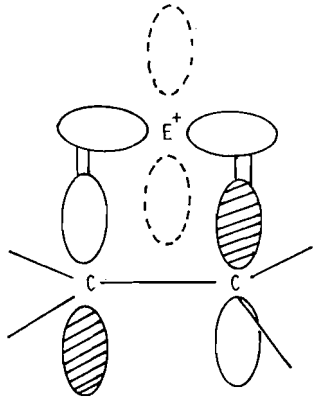


FIG. 5. Perpendicular approach.

This rationalization explains why the change in rate limiting step occurs with anisole and its derivatives for DMK– or DPK–$AlCl_3$ complexes, but not for vinyl cations. The interactions of the phenyl rings on DPK–$AlCl_3$ with the remainder of the molecule are not clear at the present time, so we cannot rationalize why the DPK–$AlCl_3$ complex is so kinetically stable; yet it behaves like a vinyl cation with active rings.

Experimental

General

Infrared spectra are neat or Nujol mulls except where noted, and are run on a Beckman IR4. The nmr spectra are run in the solvents noted with TMS or DSS as internal standard.

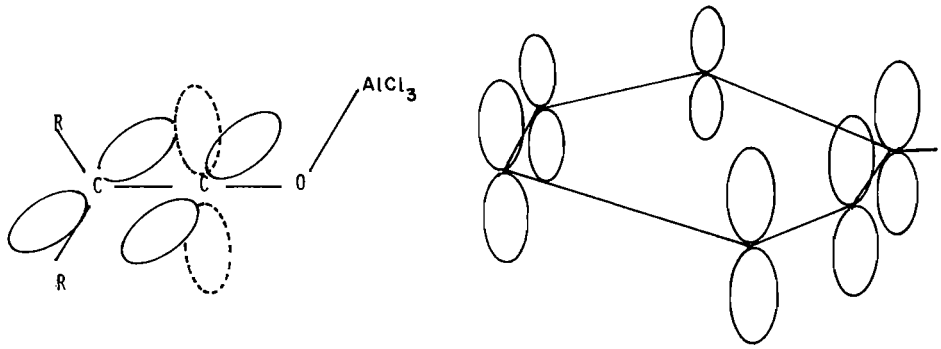


FIG. 6. Substituted ketene–$AlCl_3$ complex approaching a substituted benzene ring illustrating both parallel and perpendicular approaches in ketone acylations.

Statistical Analysis

The slopes of the two lines in Figs. 1 and 2 were calculated by means of a Texas Instruments TL-55 hand calculator using the regression routine provided.

Microanalytical work was done by Galbraith Labs, Knoxville, TN, or by Industrial Testing Laboratory, Inc., St. Louis, MO. All chemicals were reagent grade Eastman or Aldrich products.

Preparation of Ketenes

Dimethylketene was prepared by the pyrolysis of dimethylmalonic anhydride as per Staudinger *et al.* (12). The material thus obtained was distilled twice before use and opened only to a dry nitrogen atmosphere.

Diphenylketene was made by debromination of α,α-bromodiphenylacetyl bromide (13) with triphenyl phosphine in ligroin. The dibromotriphenyl phosphorane was filtered through a sintered glass funnel and hydroquinone (0.1 g) was added. The ligroin was removed by distillation under reduced pressure and the residue distilled to give yields of 60–85% of diphenylketene.

Preparation of Authentic Aryl Isopropyl Ketones

The preparations of authentic materials have been reported in ref. 1.

Competition Experiments with Dimethylketene

General Procedure

Dimethylketene generated and purified as reported above was added to a 20-fold excess of a 50 mol% mixture of each substrate. Aluminum chloride was added portionwise with mechanical stirring, and the reactions were stirred one hour after the addition was completed. Work-up was as recorded above.

Gas chromatographic analysis was done on a Perkin-Elmer 3920 instrument (TC Bridge) with a 6 ft 10% Carbowax 20 M on 80/100 Chromosorb W column at a temperature of 190°C, He flow rate of 30 mL/min.

Relative response factors were determined by mixing known concentrations, in hexane, of ketones (in g/100 mL) and determining the ratios of areas. This procedure gives a relative response factor (RRF) of (area/g of ketone I)/(area/g of ketone II). These are summarized in Table 3. All competitions were done by comparing the rates of reaction with toluene for experimental convenience. The rate constant ratios were determined by the formula

$$\frac{k_a}{k_b} = \frac{[AX]}{[BX]} \Big/ \frac{[A_0]}{[B_0]}$$

TABLE 3. Relative response factors for ketones from acylation with dimethylketene

Ketone from	Retention time (min)	RRF[a]	(Standard deviation)
1. Benzene	3.15	0.7547	(0.0492)
2. Toluene	4.20	1.0000	—
3. *o*-Xylene	6.55	1.2191	(0.0087)
4. *o*-Chlorotoluene	7.80	0.8771	(0.0214)
5. *o*-Methylanisole	15.25	1.2990	(0.0071)
6. Anisole	12.90	1.0651	(0.0115)
7. Cumene	8.15	1.1090	(0.0019)
8. *o*-Bromoanisole[b]	4.43	0.2977	(0.0009)

[a]RRF = (area of ketone/g ketone)/(area of tolyl ketone/g tolyl ketone).
[b]This compound was determined by liquid chromatography on a Waters 6000 dual pump instrument equipped with a 660 Solvent Programmer and a 440 UV-Detector. The column was a Whatman Partisil 10M9 ODS2 column 250 mm × 9.40 mm (id). Flow rate was 2.0 mL/min of 15% H_2O–methanol.

In all cases the substrate ratios to ketene were large enough to insure small errors in the rate ratios (2). In the cases involving the very active anisoles, relative rates of anisole vs. *o*-methyl anisole were used as a check on the accuracy of the relative rates vs. toluene. The former figures were used in the Hammett study. Integration was done by a Spectra Physics electronic integrator.

Authentic samples of ketones were mixed to give artificial mixtures as a check on the accuracy of the integration technique. It was found that at very high ratios the integrator consistently overestimated the amount of the smaller component. Corrections were applied where appropriate or the run was redone using a larger amount of less active substrate.

The benzene–toluene ratios were determined in this way using ratios of 1:1 benzene–toluene, 3:1, and 5:1. These results are summarized in Table 4.

The results for the 5:1 experiment were used to determine the toluene/benzene ratio as follows.

(Note: (RRF benzene/toluene)/(RRF toluene/ketone x)
= RRF benzene/ketone x)

k(Substrate)/k(Benzene)
= area ratio × 1/RRF × statistical factor
× mol. wt. isobutyrophenone/mol. wt. substituted isobutyrophenone

$= 51.86 \times 1/0.7547 \times 6 \times 148/162$

$= 376.7$

Can. J. Chem. Downloaded from www.nrcresearchpress.com by 210.87.254.40 on 09/05/12
For personal use only.

TABLE 4. Relative areas of ketones in benzene–toluene competition

Ratio of benzene–toluene	Moles of substrate:moles ketene	Ketone areas (area tolyl/area phenyl)
1:1	$(0.65 + 0.65)/1.313 \times 10^{-2} = 99$	52.34
3:1	$(1.95 + 0.65)/1.41 \times 10^{-2} = 184$	50.95
5:1	$(3.25 + 0.65)/1.52 \times 10^{-2} = 257$	51.86

TABLE 5. Rates of acylations relative to benzene

Substrate	Area ratio	Statistical factor	Mol. wt. ratio	P_f^x[a]	σ^+
1. Benzene	0.0193	1.000	1.000	1.00	0.000
2. Toluene	1.000	6	148/162	380.2	−0.306
3. *o*-Xylene	3.58	3	148/176	455.4	−0.375
4. Cumene	0.549	6	148/190	153.5	−0.276
5. *o*-Chlorotoluene	0.0033	6	148/196.45	0.718	+0.0070
6. Anisole	88.44	6	148/178	1259.7	−0.764
7. *o*-Methylanisole	649.52	6	148/192	2959.7	−0.833
8. *o*-Bromoanisole[b]	4.573	6	148/255.9	131.9	−0.373

[a] P_f^x = area ratio × 1/RRF × area tolyl ketone/area phenyl ketone × statistical factor × mol. wt. ratio (2).
[b] Determined by lc on the instrument described in footnote (*b*) of Table 3.

In a similar manner all the ketones were determined with the results in Table 5. In each case the reactions were done as competition of a given substrate with toluene. They are corrected relative to benzene by the toluene/benzene reactivity ratio. It was convenient to use toluene as the fundamental comparison reagent because benzene gave very low yields with dimethylketene, probably due to reaction of dimethylketene with itself to give dimer and then further reaction with $AlCl_3$.

Competitions with Diphenylketenes

A typical experiment involved adding a known amount of freshly prepared distilled diphenylketene to a large excess of a 50:50 mixture of hydrocarbons (mole:mole) present in a large molar excess. Thus 0.05 mol of diphenylketene was added to 2.0 mol of *o*-methylanisole and 20 mol of toluene in a flask fitted for mechanical stirring. Through a solids hopper, with the flask maintained at 25°C, 5.22 g (2.5 equivalents) of aluminum chloride was added rapidly, but not so as to cause a great temperature change. The reaction was quenched in 200 mL of dilute (6 *N*) HCl – ice water. The separated organic layer was washed with three 100 mL portions of NaOH, dried over $MgSO_4$, and the solvent removed on a rotary evaporator.

Analysis of the residues from this and all of the other reaction mixtures was done via liquid chromatography. The apparatus was a Waters hplc apparatus including a UL 6 injection loop, a pair of 6000 pumps, a 440 uv detector, and a 660 solvent programmer. The column was a Whatman Partisil 10M9 ODS2 reverse phase 250 mm × 9.40 mm. Flow rate was 2.5 mL/min of 25% H_2O – methanol.

The relative response factors at 254 mm for the ketones were determined from authentic mixtures of samples of known concentration. The RRF factors relative to toluene or benzene are recorded in Table 6 as well as the area ratios, which were determined from the integrator of a Soltec Model 250A recorder.

The partial rate factors in Table 2 are obtained from the area ratios as follows:

P_f^x = area ratio ÷ RRF × statistical factor × area toluene/area benzene.

When the area ratio was determined by competition with benzene, the last multiplier was omitted.

The benzene–toluene area ratio was obtained from an experiment in which the (moles of benzene/moles of toluene) starting material was 10 (1).

TABLE 6. Area ratios and RRF factors for diphenylketene competitions

Experiment	Substrate	Area ratio[a]	RRF[c]
1	*o*-Nitroanisole	4.3426[b]	0.3691
2	*o*-Chlorotoluene	4.529[b]	0.4185[b]
3	Benzene	4.44×10^{-2}	0.7720
4	Toluene	1	—
5	*o*-Xylene	3.03	1.1570
6	Anisole	2.128	0.5251
7	*o*-Methylanisole	6.366	0.8670
8	5-Isomer of *o*-methylanisole	0.298	0.3437

[a] Relative to toluene except as noted by footnote *b*.
[b] Relative to benzene.
[c] RRF = (area ketone 1/g ketone 1/mol. wt. ketone 1)/(area ketone 2/g ketone 2/mol. wt. ketone 2).
= (area ketone 1/area ketone 2)/(g ketone 2/g ketone 1)/(mol. wt. ketone 1/mol. wt. ketone 2)
= (area 1/mole 1/area 2/mole 2)

Acknowledgment

Acknowledgment is made to the donors of the Petroleum Research Fund, administered by The American Chemical Society, for support of this work.

1. K. R. FOUNTAIN, P. HEINZE, M. SHERWOOD, D. MADDEX, and G. GERHARDT. Can. J. Chem. **58**, 1198 (1980).
2. N. S. ISAACS. Experiments in physical organic chemistry. Macmillan Co., London. 1969. p. 3.
3. J. E. LEFFLER and E. GRUNWALD. Rates and equilibria of organic reactions. John Wiley and Sons, Inc., New York. 1963. p. 200.

Can. J. Chem. Downloaded from www.nrcresearchpress.com by 210.87.254.40 on 09/05/12
For personal use only.

4. L. M. STOCK and H. C. BROWN. Advances in physical organic chemistry. *Edited by* V. Gold. Academic Press, New York. 1963. p. 43.
5. L. M. STOCK. Aromatic substitution reactions. *Edited by* K. L. Rinehart. Prentice-Hall, Inc., Englewood Cliffs, NJ. 1968. p. 67.
6. P. J. STANG and A. G. ANDERSON. J. Am. Chem. Soc. **100**, 1520 (1978).
7. S. J. KUHN and G. A. OLAH. J. Am. Chem. Soc. **83**, 4564 (1961).
8. G. A. OLAH. Acc. Chem. Res. **4**, 240 (1971).
9. J. H. RIDD. Acc. Chem. Res. **4**, 248 (1971).
10. G. A. OLAH, S. KOBAYASHI, and M. TASHIRO. J. Am. Chem. Soc. **94**, 7448 (1972).
11. R. B. WOODWARD and R. HOFFMAN. The conservation of orbital symmetry. Verlag Chemie Academic Press, Inc., Weisheim. 1971. p. 164ff.
12. H. STAUDINGER, H. SCHLUBACH, and H. SCHNEIDER. Helv. Chim. Acta, **6**, 287 (1963).
13. S. D. DARLING and R. L. KIDWELL. J. Org. Chem. **33**, 3974 (1968).

Can. J. Chem. Downloaded from www.nrcresearchpress.com by 210.87.254.40 on 09/05/12
For personal use only.

Chemical shift correlated two-dimensional nmr spectroscopy and its application to solving the proton nmr spectra of oligoribonucleotides

ALEX D. BAIN,[1,2] RUSSELL A. BELL,[2] JEREMY R. EVERETT,[3] AND DONALD W. HUGHES[4]

Department of Chemistry, McMaster University, 1280 Main Street West, Hamilton, Ont., Canada L8S 4M1

Received February 13, 1980

ALEX D. BAIN, RUSSELL A. BELL, JEREMY R. EVERETT, and DONALD W. HUGHES. Can. J. Chem. **58**, 1947 (1980).

An alternative two-dimensional nmr pulse sequence, (90°–t_1/2–90°–t_1/2–FID), correlates the chemical shifts of coupled nuclei. The application of this technique to the solution of the complicated proton nmr spectra of oligoribonucleotides is discussed.

ALEX D. BAIN, RUSSELL A. BELL, JEREMY R. EVERETT et DONALD W. HUGHES. Can. J. Chem. **58**, 1947 (1980).

Une rmn alternative à impulsion (90°–t_1/2–90°–t_1/2–FID) coordonne les déplacements chimiques des noyaux couplés. On discute de l'application de cette technique à la résolution des spectres rmn compliqués d'oligoribonucléotide.

[Traduit par le journal]

Introduction

The principles of two-dimensional (2D) Fourier Transform (FT) nmr spectroscopy are very similar to those of normal one-dimensional (1D) FT nmr spectroscopy. In the normal 1D experiment, magnetization, due to all the spins, is created in the x,y plane by a pulse of radiofrequency energy. During the free induction decay (FID) the magnetization is sampled at regularly incremented times t_2. The resulting data are Fourier transformed to give the normal spectrum in which intensity is plotted as a function of a frequency axis f_2.

A 2D FT nmr (1, 2) experiment is similar if we consider the detector to be one of the lines in the 1D nmr spectrum. Magnetizations corresponding to all the lines in 1D spectrum are created by an initial pulse. The magnetizations rotate in the x,y plane for a certain time, after which each magnetization has a characteristic phase determined by its Larmor frequency. A second pulse, called the mixing pulse, will now transfer phase information from one magnetization to other magnetizations in a selective fashion. Thus, at the end of time t_1, the phase of a given magnetization depends on both its own Larmor frequency and the Larmor frequencies of any other magnetizations that were mixed with it. This given magnetization may now be sampled and Fourier transformed in exactly the same manner as the 1D experiment, and in addition, the experiment is repeated over regularly incremented times t_1. This yields a spectrum in f_2 for each t_1 value used. The phase dependence, as a function of t_1, of a magnetization corresponding to a line in f_2 allows that magnetization to act as a selective detector of only the magnetizations to which it is connected. Usually, this connection is via scalar coupling (2) although chemical exchange (3) and dipolar coupling (4, 5) are also possible connection mechanisms. A second Fourier transformation of each data point in f_2 as a function of t_1 leads to a single 2D nmr spectrum in which signal intensity is plotted as a function of two orthogonal frequency axes, f_2, the "normal" axis of the 1D experiment, and f_1, the second frequency axis. Each line in f_2, serving as a detector, displays what it has detected along the second frequency dimension f_1.

Just what appears in the second dimension depends upon the spin system, and the nature of the pulse sequence used on it. In the case of a 90°–t_1/2–180°–t_1/2–FID sequence (2) applied to a weakly coupled spin system, a line in a multiplet in f_2 is mixed only with the symmetrically disposed line on the other side of the multiplet, giving a single line in f_1 for each line in f_2. When strong coupling is present (6) or the 180° pulse is changed to any other angle $x°$ ($x \neq n \times 180°, n = 0, 1, 2, 3 \ldots$) the situation is more complex. More lines appear in f_1 because, in general, a line in the spectrum in f_2 associated with a particular nucleus can be mixed with any other line belonging to that same nucleus or another nucleus coupled to it, provided that this other nucleus is also affected by the pulse. This means that with respect to the evolution time t_1, modulation may be detected at frequencies involving both coupling constants and chemical shift differences. Thus, by the use of this 2D chemical shift correlated nmr spectroscopy, the relative chemical shift of a nucleus may be found from the spectra of any nucleus coupled to it, as in the INDOR experiment

[1]Present address: Bruker Spectrospin (Canada) Ltd., 2410 Dunwin Dr., Unit 4, Mississauga, Ont., Canada L5L 1J9.

[2]Authors to whom correspondence should be addressed.

[3]Present address: Dept. of Chemistry, Otto Maass Chemistry Bldg., McGill University, 801 Sherbrooke Street, W., Montreal, P.Q., Canada H3A 2K6.

[4]Present address: The Research Institute, The Hospital for Sick Children, 555 University Avenue, Toronto, Ont., Canada M5G 1X8.

0008-4042/80/181947-10$01.00/0

©1980 National Research Council of Canada/Conseil national de recherches du Canada

Can. J. Chem. Downloaded from www.nrcresearchpress.com by 210.87.254.6 on 09/05/12
For personal use only.

TABLE 1. The predicted and observed f_1 frequencies of the low field AH-1′ transition in f_2 for 5′-AMP

Peak no.[a]	Origin of line	$\nu_{obs.}$ (Hz)[b]	$\nu_{pred.}$ (Hz)[b]
7	$-(\omega_{1'}+J/2)]/2$	−0.2	0.0
6	$-(\omega_{1'}-J/2)]/2$	2.6	2.5
5	$[(\omega_{1'}+J/2)\ -(\omega_{2'}+J)]/2$	59.5	59.3
4	$-\omega_{2'}]/2$	62.1	61.8
3	$-(\omega_2-J)]/2$	64.2	64.3
9	$+(\omega_{1'}+J/2)]/2$	−21.8	−22.2
10	$+(\omega_{1'}-J/2)]/2$	−24.6	−24.7
11	$[(\omega_{1'}+J/2)\ +(\omega_{2'}+J)]/2$	−81.2	−81.5
1	$+\omega_{2'}]/2$	82.5[c]	82.7[c]
2	$+(\omega_{2'}-J)]/2$	80.2[c]	80.2[c]
8	$[(\omega_{1'}+J/2)]/2$	−11.1[d]	−11.1[d]

[a]See Fig. 4(A).
[b]$\nu_{obs.}$ = observed peak frequency in f_1 in Hz. $\nu_{pred.}$ = predicted peak frequency in f_1 in Hz (using data in Table 4).
[c]Folded lines (f_1 spectral width = ±83.3 Hz).
[d]Phantom.

TABLE 2. The predicted and observed f_1 frequencies of the low field AH-2′ transition in f_2 for 5′-AMP

Peak no.[a]	Origin of line	$\nu_{obs.}$ (Hz)	$\nu_{pred.}$ (Hz)
11	$-(\omega_{2'}+J)]/2$	−0.1	0.0
10	$-\omega_{2'}]/2$	2.7	2.5
9	$-(\omega_{2'}-J)]/2$	5.4	5.0
8	$-(\omega_{3'}+J)]/2$	9.5	9.3
7	$[(\omega_{2'}+J)\ -\omega_{3'}]/2$	11.8[b]	11.5
6	$-(\omega_{3'}-J)]/2$	13.7[b]	14.0
13	$-(\omega_{1'}+J/2)]/2$	−59.3	−59.3
12	$-(\omega_{1'}-J/2)]/2$	−56.9	−56.8
2	$+(\omega_{2'}+J)]/2$	26.2[c]	25.9[c]
3	$+\omega_{2'}]/2$	23.5[c]	23.4[c]
4	$+(\omega_{2'}-J)]/2$	20.6[c]	20.9[c]
5	$+(\omega_{3'}+J)]/2$	16.9[c]	16.5[c]
6	$[(\omega_{2'}+J)\ +\omega_{3'}]/2$	13.7[b,c]	14.4[c]
7	$+(\omega_{3'}-J)]/2$	11.8[b,c]	11.9[c]
15	$+(\omega_{1'}+J/2)]/2$	−81.7	−81.5
1	$+(\omega_{1'}-J/2)]/2$	83.3[c]	82.7[c]
14	$[(\omega_{2'}+J)]/2$	−70.2[d]	−70.4[d]

[a]See Fig. 4(C).
[b]Coincidence of peaks.
[c]Folded lines.
[d]Phantom.

(7). A proton spectrum may be correlated with itself (1) or with the ^{13}C or ^{31}P (8–12) spectra of the same molecule.

In this paper we use 2D chemical shift correlated nmr spectroscopy and a $90°-t_1/2-90°-t_1/2-FID$ pulse sequence to help unravel the complicated proton nmr spectra of 5′-adenosine monophosphate (5′-AMP) and cytidyl-3′,5′-adenosine (CpA). We further show how details of the effects in the 2D spectra may be calculated for an ABX-type spin system.

Experimental

The nucleotides were lyophilised from D_2O and then dissolved in 100% D_2O which contained 0.01 *M* sodium phosphate buffer (pD 7.0) and 1.0 *M* sodium chloride. The solution concentrations of 5′-AMP and CpA were 0.41 and 0.25 *M* respectively and the sample temperatures were 71 ± 2°C.

Spin-echo FID's were accumulated at 90 MHz on a Bruker WH90 spectrometer equipped with a BNC-12 data system and a NIC-293 I/O controller. The pulse sequence used was $90°-t_1/2-90°-t_1/2-FID$ (t_2). A total acquisition time t_2 of 4 s over 2K data points gave an f_2 sweep width of ∼±250 Hz. Four pulse sequences were used to accumulate the 5′-AMP FID's, eight were used in the case of CpA. The evolution time t_1 was incremented by 0.003 s 180 times from an initial value of 0.001 s. The sweep width in f_1 was thus ±83.3 Hz. Delay times of 4 s and 6 s between pulse sequences were used in the accumulation of the data on CpA and 5′-AMP respectively. The FID data were transferred to and processed on a Nicolet 1180 computer system. Nicolet kindly provided the data transfer program.

Results

5′-Adenosine Monophosphate

Table 1 gives the predicted and observed f_1 frequencies in the 2D spectrum of the low field (f_2) H-1′ transition of 5′-AMP. Tables 2 and 3 give the

Can. J. Chem. Downloaded from www.nrcresearchpress.com by 210.87.254.6 on 09/05/12
For personal use only.

TABLE 3. The predicted and observed f_1 frequencies of the lowest field AH-3′ transition in f_2 for 5′-AMP

Peak no.[a]	Origin of line	$\nu_{obs.}$ (Hz)	$\nu_{pred.}$ (Hz)
5	$-(\omega_{3'}+J)]/2$	0.1	0.0
4	$-\omega_{3'}]/2$	2.6[b]	2.2
3	$[(\omega_{3'}+J)\ -(\omega_{3'}-J)]/2$	4.8[b]	4.6
	$-(\omega_{2'}+J)]/2$	[c]	−9.3
	$-\omega_{2'}]/2$	[c]	−6.9
	$-(\omega_{2'}-J)]/2$	[c]	−4.4
2	$+(\omega_{3'}+J)]/2$	7.9[d]	7.2[d]
3	$+\omega_{3'}]/2$	4.8[b,d]	5.1[d]
4	$[(\omega_{3'}+J)\ +(\omega_{3'}-J)]/2$	2.6[b,d]	2.6[d]
1	$+(\omega_{2'}+J)]/2$	15.7[d]	16.5[d]
	$+\omega_{2'}]/2$	[c]	14.1[d]
	$+(\omega_{2'}-J)]/2$	[c]	11.6[d]
6	$[(\omega_{3'}+J)]/2$	−79.6[e]	−79.7[e]

[a]See Fig. 4(D).
[b]Coincidence of peaks.
[c]Not observed.
[d]Folded lines.
[e]Phantom.

corresponding data for the lowest field H-2′ and H-3′ transitions respectively. Table 4 lists the f_2 frequencies (relative to the carrier) of all the transitions in the H-1′, H-2′, and H-3′ multiplets.

Cytidyl-3′,5′-adenosine

Table 5 lists the f_1 frequencies and their analysis for the low field AH-1′ transition in CpA. Tables 6 and 7 list corresponding data for the high field CH-5 transition and low field CH-1′ transition respectively.

Discussion

The frequencies of lines that appear in a 2D FT nmr spectrum can be worked out in terms of the mixing of magnetizations corresponding to connected f_2 transitions (13). However, since it is difficult to represent the magnetizations in a coupled spin system in three-dimensional space (14), the determination of the details of intensities and phase relationships in the spectra requires more sophisticated calculation. This can be done using standard techniques, in which the effect of pulses on spin wavefunctions is calculated (1). A more efficient and elegant technique is to calculate the effect of pulses on the magnetizations directly, using single transition operators (14, 15) or the superspin formalism (16, 17). We feel the latter method provides the simplest method of calculation and gives the clearest picture of what is going on, particularly with regard to the formation of spin echoes (18, 19). The details of the superspin analysis of the ABX system (16) and of a general 2D FT nmr experiment (17) have been published elsewhere. However, we outline the theory below.

TABLE 4. A table of frequencies in f_2 in Hz for all the transitions of the H-1′, H-2′, and H-3′ spin multiplets in 5′-AMP

Proton	f_2 Transition frequency (Hz)[a]
H-1′	−22.2
	−27.2
H-2′	−140.8
	−145.8
	−150.7
H-3′	−159.5
	−163.8
	−168.8

[a]Relative to the carrier frequency at 0 Hz.

At equilibrium the only nonzero part of the density matrix is associated with a superspin of 1, representing the total magnetization of all the spins (20, 21). This means that the first pulse creates only single quantum coherence; in other words, it excites only the transitions we normally observe in a spectrum. This is a general result for any nonselective pulse on any type of spin system. In terms of our formalism, this coherence, corresponding to a transition frequency ω_i, is made up of two counterrotating components. These are associated with superspin z components of +1 and −1 and evolve in time as $\exp(i\omega_i t)$ and $\exp(-i\omega_i t)$. Note that these are positive and negative absolute frequencies representing the two senses of precession around the static magnetic field B_0. However, associated with the radio-frequency field are two counterrotating frames of reference, so that each sense of rotation is detected in its own rotating frame and appears as a frequency relative to the carrier.

The magnetizations created by the first pulse evolve at their characteristic frequencies until a second pulse is applied. The second pulse mixes the magnetizations so that lines in the spectrum

Can. J. Chem. Downloaded from www.nrcresearchpress.com by 210.87.254.6 on 09/05/12
For personal use only.

TABLE 5. The observed peaks in the f_1 spectrum of the low field AH-1′ transition $(\omega_{A1'} + J/2)$ in f_2 for CpA and their analysis

Peak no.[a]	Origin of line	$\nu_{obs.}$ (Hz)[b]	$\nu_{imp.}$ (Hz)[c]
5	$[(\omega_{A1'} + J/2)$ $-(\omega_{A1'} + J/2)]/2$	−0.1	−13.2
4	$-(\omega_{A1'} - J/2)]/2$	2.4	−18.2
3	$-(\omega_{A2'} + J)]/2$	60.8	−135.0
2	$-\omega_{A2'}]/2$	64.0	−141.4
1	$-(\omega_{A2'} - J)]/2$	65.8	−145.0
7	$[(\omega_{A1'} + J/2)$ $+(\omega_{A1'} + J/2)]/2$	−12.5	−12.5
8	$+(\omega_{A1'} - J/2)]/2$	−14.9	−16.4
9	$+(\omega_{A2'} + J)]/2$	−73.1	−132.8
	$+\omega_{A2'}]/2$	[d]	—
10	$+(\omega_{A2'} - J)]/2$	−78.1	−142.8
6	$[(\omega_{A1'} + J/2)]/2$	−6.0[e]	−12.0

[a]See Fig. 6(A).
[b]$\nu_{obs.}$ = observed peak frequency in f_1 in Hz.
[c]$\nu_{imp.}$ = implied f_2 frequency of the corresponding connected transition (in Hz relative to the carrier at 0 Hz).
[d]Not observed.
[e]Phantom peak.

TABLE 6. The observed peaks in the f_1 spectrum of the high field CH-5 transition in f_2 for CpA and their analysis

Peak no.[a]	Origin of line	$\nu_{obs.}$ (Hz)[b]	$\nu_{imp.}$ (Hz)[b]
5	$[(\omega_{C5} - J/2)$ $-(\omega_{C5} - J/2)]/2$	0.1	26.0
6	$-(\omega_{C5} + J/2)]/2$	−4.1	−17.6
12	$-(\omega_{C6} + J/2)]/2$	−83.3	140.8
11	$-(\omega_{C6} - J/2)]/2$	−78.9	132.0
4	$-(\omega_{C1'} + J/2)]/2$	7.6	−41.0
3	$-(\omega_{C1'} - J/2)]/2$	9.8	−45.4
9	$[(\omega_{C5} - J/2)$ $+(\omega_{C5} - J/2)]/2$	−25.0	−25.0
8	$+(\omega_{C5} + J/2)]/2$	−20.8	−15.8
1	$+(\omega_{C6} + J/2)]/2$	57.8	141.4
2	$+(\omega_{C6} - J/2)]/2$	54.3	134.4
10	$+(\omega_{C1'} + J/2)]/2$	−32.8	−39.8
	$+(\omega_{C1'} - J/2)]/2$	[c]	—
7	$[(\omega_{C5} - J/2)]/2$	−12.3[d]	−24.6

[a]See Fig. 6(B).
[b]See Table 5.
[c]Not observed.
[d]Phantom.

show modulation with respect to the evolution time t_1. If we collect the spectrum immediately after the second pulse, we get a two-dimensional correlated spectrum (1). Delaying the acquisition by a time equal to the interval between the pulses (i.e. a spin echo sequence) splits the spectrum into two parts, which we have called an additive and subtractive spectrum (13).

The additive spectrum arises from coherence which is mixed by the pulse with coherence precessing in the same sense. The frequencies (with respect to the carrier) add, and the lines in the f_1 spectrum appear $(\omega_i + \omega_j)/2$ where ω_i is the f_2 frequency of the line itself and ω_j is any other f_2 frequency that can be mixed in. The subtractive spectrum results from the mixing of coherence of opposite senses of precession and the lines in f_1 appear at $(\omega_i - \omega_j)/2$. The intensities of these lines are a sensitive function of the flip angle of the second pulse. For a $90°-t_1/2-180°-t_1/2$–FID pulse sequence, the additive spectrum disappears and in weakly coupled systems, the subtractive spectrum is particularly simple, since all but one of the expected lines have zero intensity. This results in a J-resolved 2D nmr spectrum (2). In the general case for a $90°-t_1/2-x°-t_1/2$–FID pulse sequence, some of the lines in the subtractive spectrum (e.g. $(\omega_i - \omega_i)/2$) have positions that are independent of the static field B_0. This means that they are unaffected by B_0 inhomogeneity and are responsible for spin echo formation (18, 19). Other lines in the subtractive spectrum and in general all the lines in the additive spectrum will suffer a broadening in f_1 due to B_0 inhomogeneity. The extent of this broadening is determined by how strongly the f_1 frequency at the start of acquisition depends on B_0. In general

Can. J. Chem. Downloaded from www.nrcresearchpress.com by 210.87.254.6 on 09/05/12
For personal use only.

TABLE 7. The observed peaks in the f_1 spectrum of the low field CH-1′ transition $(\omega_{C1'} + J/2)$ in f_2 for CpA and their analysis

Peak no.[a]	Origin of line	$\nu_{obs.}$ (Hz)[b]	$\nu_{imp.}$ (Hz)[b]
7	$-(\omega_{C1'} + J/2)]/2$	0.0	−40.9
6	$-(\omega_{C1'} - J/2)]/2$	2.3	−45.2
3	$-(\omega_{C2'} + J)]/2$	66.0	−172.9
2	$[(\omega_{C1'} + J/2) - \omega_{C2'}]/2$	68.0	−176.9
1	$-(\omega_{C2'} - J)]/2$	70.8	−182.5
9	$-(\omega_{C5} + J/2)]/2$	−11.8	−17.3
8	$-(\omega_{C5} - J/2)]/2$	−7.8	−25.3
11	$+(\omega_{C1'} + J/2)]/2$	−40.0	−40.0
12	$+(\omega_{C1'} - J/2)]/2$	−42.4	−43.9
4	$+(\omega_{C2'} + J)]/2$	60.9[c]	−170.7
	$[(\omega_{C1'} + J/2) + \omega_{C2'}]/2$	[c]	—
5	$+(\omega_{C2'} - J)]/2$	56.5[c]	−179.5
	$+(\omega_{C5} + J/2)]/2$	[c]	—
	$+(\omega_{C5} - J/2)]/2$	[c]	—
10	$[(\omega_{C1'} + J/2)]/2$	−19.9[d]	−39.8

[a]See Fig. 6(C).
[b]See Table 5.
[c]Not observed.
[d]Phantom peak.
[e]Folded lines.

the f_1 spectrum will consist of an additive and a subtractive spectrum plus one more line, a "phantom", due to coherence created by the second pulse (22). This is illustrated in Fig. 1, which shows the f_1 spectrum of a single uncoupled line (the AH-2 proton in CpA) obtained from a $90°$–t_1/2–$90°$–t_1/2–FID experiment. The subtractive line appears at 0.2 Hz ($(\omega_i - \omega_i)/2 = 0$ Hz, ω_i = 178.5 Hz in f_2 relative to the carrier) and the additive line appears at 12.8 Hz ($(\omega_i + \omega_i)/2 = 178.5$ Hz which folds to $178.5 - 2 \times 83.3 = 11.8$ Hz). The line at −76.9 Hz is the phantom ($\omega_i/2 = 89.3$ Hz which folds to $89.3 - 166.7 = -77.4$ Hz). Digitization in both f_2 and f_1 accounts for the frequency discrepancies. The subtractive line is the narrowest, since the B_0 effects have cancelled out; the phantom has only dephased for $t_1/2$, so it is not as broad as the additive line which has been dephasing for a full t_1.

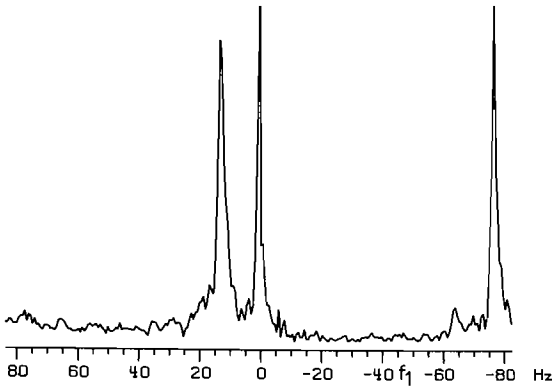


FIG. 1. The real f_1 spectrum of the AH-2 proton in CpA.

Since only single quantum coherence was present before the second pulse, no new frequencies will appear in f_1; only combinations of those observed in f_2. More pulses are needed to create multiple quantum coherence (23). The additive spectrum can be suppressed by a more complex series of pulses (24), leaving only the subtractive spectrum.

We have written a computer program which simulates the experiment based on the pulse sequence α_1–t_1/2–α_2–t_1/2–FID, where α_1 and α_2 are the flip angles of the two pulses, applied to an ABX spin system. The program was written in BASIC on

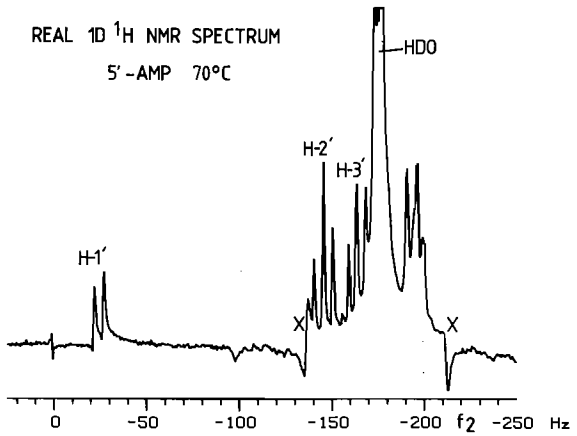


FIG. 2. The 1D ^{1}H nmr spectrum of 5′-AMP in the region of the ribose protons. X indicates a sideband of the strong, residual HDO resonance. Phase errors exist since the spectrum is the transform of an FID from the 2D experiment with the minimum evolution time t_1. The f_2 frequencies are relative to the carrier frequency at 0 Hz.

Can. J. Chem. Downloaded from www.nrcresearchpress.com by 210.87.254.6 on 09/05/12
For personal use only.

Can. J. Chem. Downloaded from www.nrcresearchpress.com by 210.87.254.6 on 09/05/12
For personal use only.

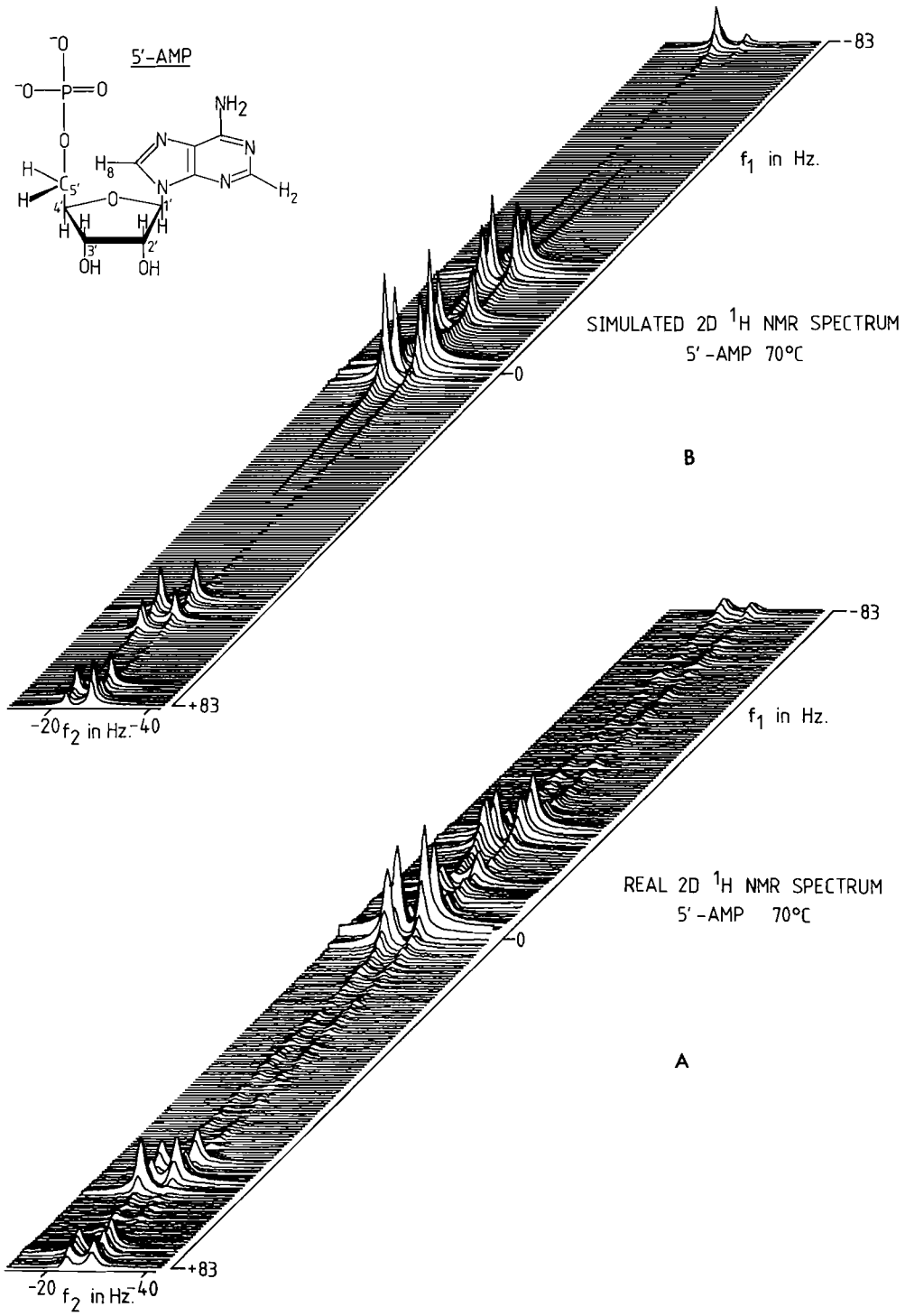


FIG. 3. (A) The real 2D ^{1}H nmr spectrum of 5'-AMP in the region of the H-1' proton; (B) the simulated 2D ^{1}H nmr spectrum of 5'-AMP in the region of the H-1' proton. The chemical shifts and coupling constants used in the simulation were derived from Table 4. 100° pulses were used.

Can. J. Chem. Downloaded from www.nrcresearchpress.com by 210.87.254.6 on 09/05/12
For personal use only.

a NICOLET 1180 computer; a listing of the program is available from A.D.B.

Analysis of the ^1H Chemical Shift Correlating 2D nmr Spectrum of 5′-AMP

Figure 2 shows the normal 1D ^1H nmr spectrum of 5′-AMP. This spectrum has been recorded many times (25, 26) and its analysis is well documented, but we shall use it here to illustrate our method. The H-1′, H-2′, and H-3′ multiplets are all clearly visible in the 1D spectrum and the exact f_2 frequencies of the transitions in these multiplets are given in Table 4. We shall start our analysis with the H-1′ proton and see how the f_1 spectrum of each transition in f_2 can be predicted from a knowledge of the f_2 transition frequencies of all the appropriate coupled lines.

Figure 3(A) shows the real 2D nmr spectrum in the region of the H-1′ proton. Figure 3(B) shows the simulation of this region produced by our calculation program. With the exception of a few minor intensity differences, the agreement between the real and simulated spectra is good.

Figures 4(A) and 4(B) show the real and simulated f_1 spectra of the low field transition in f_2 of the H-1′ proton. Table 1 gives the predicted and observed f_1 frequencies in this spectrum, a total of eleven lines. The table also lists the origin of all these lines. The low field H-1′ magnetization mixed with itself in both an additive and subtractive sense to give the lines at -21.8 and -0.2 Hz respectively. It also mixed with its upfield partner to give the lines at -24.6 and 2.6 Hz. Since the H-1′ proton is coupled to the H-2′ proton, the low field H-1′ transition also mixed with each of the three H-2′ magnetizations to give lines at -81.2, 82.5, and 80.2 Hz from additive mixing and lines at 59.5, 62.1, and 64.2 Hz from subtractive mixing. All these lines were predicted correctly to within the limits of digitization (0.9 Hz), by the simple addition and subtraction of the appropriate connected f_2 frequencies. This analysis accounts for ten lines; the eleventh is a phantom line and occurs at one half the f_2 frequency of the H-1′ transition, i.e. -11.1 Hz.

The spectrum of H-2′ is a doublet of doublets due to coupling to both H-1′ and H-3′. However, since the two coupling constants are similar in magnitude, the two central lines overlap to give the appearance of a triplet. One of the two overlapped lines is connected progressively to H-1′, and the other is connected regressively, in the generalized sense of these terms (1). In the f_1 spectrum of H-1′ the two lines due to the mixing of the H-1′ magnetization with these two central lines of H-2′ are 180°

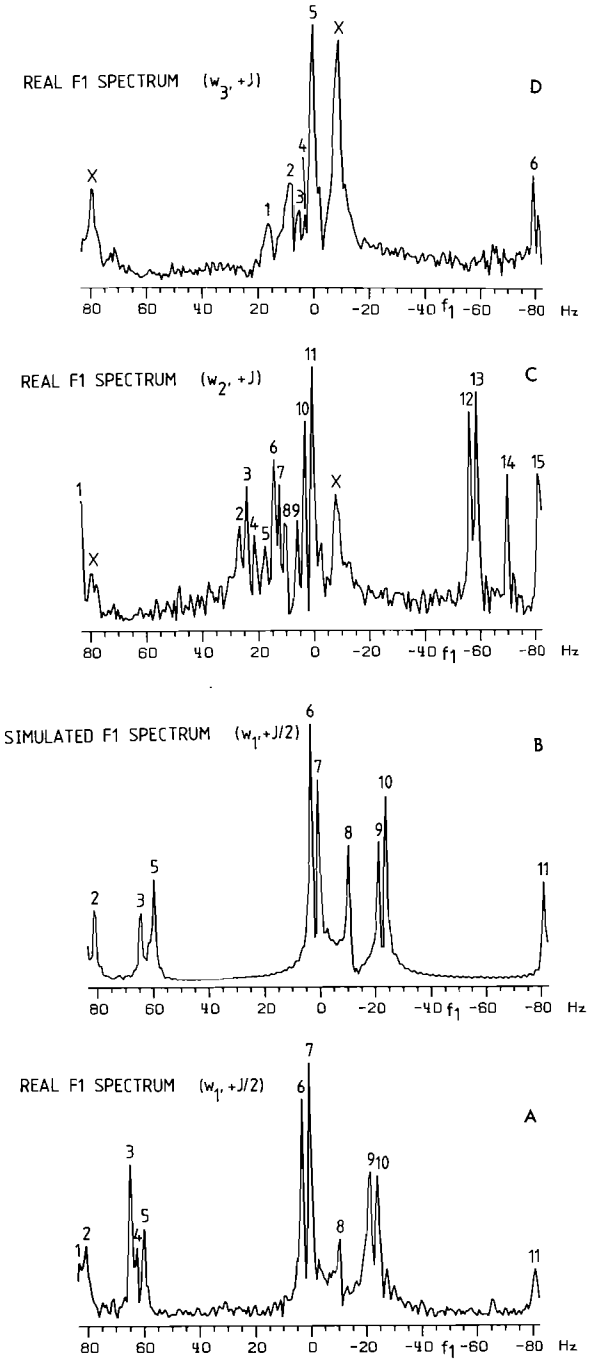


FIG. 4. (A) The real f_1 spectrum of the low field (f_2) H-1′ transition in 5′-AMP; (B) the simulated f_1 spectrum of the low field (f_2) H-1′ transition in 5′-AMP; (C) the real f_1 spectrum of the lowest field (f_2) H-2′ transition in 5′-AMP. X indicates lines due to the overlap from the f_1 spectrum of the HDO peak; (D) the real f_1 spectrum of the lowest field (f_2) H-3′ transition in 5′-AMP. X indicates lines due to the overlap from the f_1 spectrum of the HDO peak.

Can. J. Chem. Downloaded from www.nrcresearchpress.com by 210.87.254.6 on 09/05/12
For personal use only.

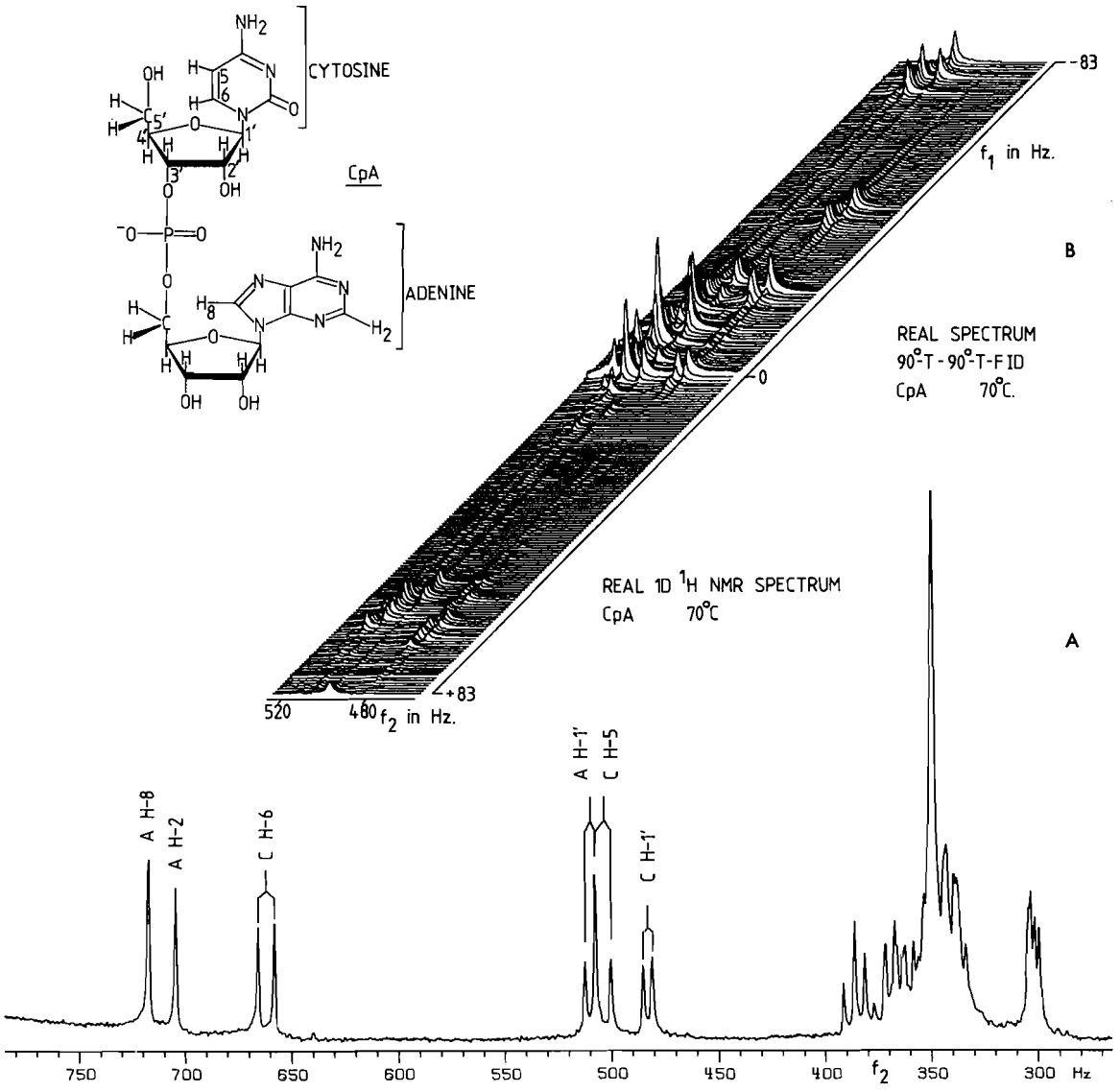


FIG. 5. (A) The 1D ^{1}H nmr spectrum of CpA. The f_2 frequencies are calibrated using internal *tert*-butanol; (B) the real 2D ^{1}H nmr spectrum of CpA in the region of the H-5 and H-1′ protons.

out of phase with one another. Since they overlap in f_1, they partially cancel each other out, leaving a very weak central line in the triplet in f_1, as can be seen in Fig. 4. This is a common feature when coherence is transferred between nuclei (2).

Figure 4 also shows the real f_1 spectra of the lowest field AH-2′ and AH-3′ transitions. Tables 2 and 3 give the predicted and observed frequencies of the lines in the f_1 spectra which were again calculated on the basis of the simple addition and subtraction of the appropriate f_2 frequencies given in Table 4. As before, agreement between predicted and observed f_1 frequencies was good. No lines in the f_1 spectrum of the H-3′ transition which indicated mixing with the H-4′ proton could be identified. However, the H-4′ proton is the C part of an ABCDX spin system, and as such it probably has an extremely complicated signal, many of the lines of which would be very weak (26).

Thus we can account for all of the lines in the 2D nmr spectrum of this relatively simple compound. We shall now turn our attention to the analysis of the more complicated spectrum of CpA.

Analysis of the Chemical Shift Correlated 2D nmr Spectrum of CpA

Figure 5 shows the normal 1D nmr spectrum of CpA. The 1D ^{1}H nmr spectrum has been recorded

Can. J. Chem. Downloaded from www.nrcresearchpress.com by 210.87.254.6 on 09/05/12
For personal use only.

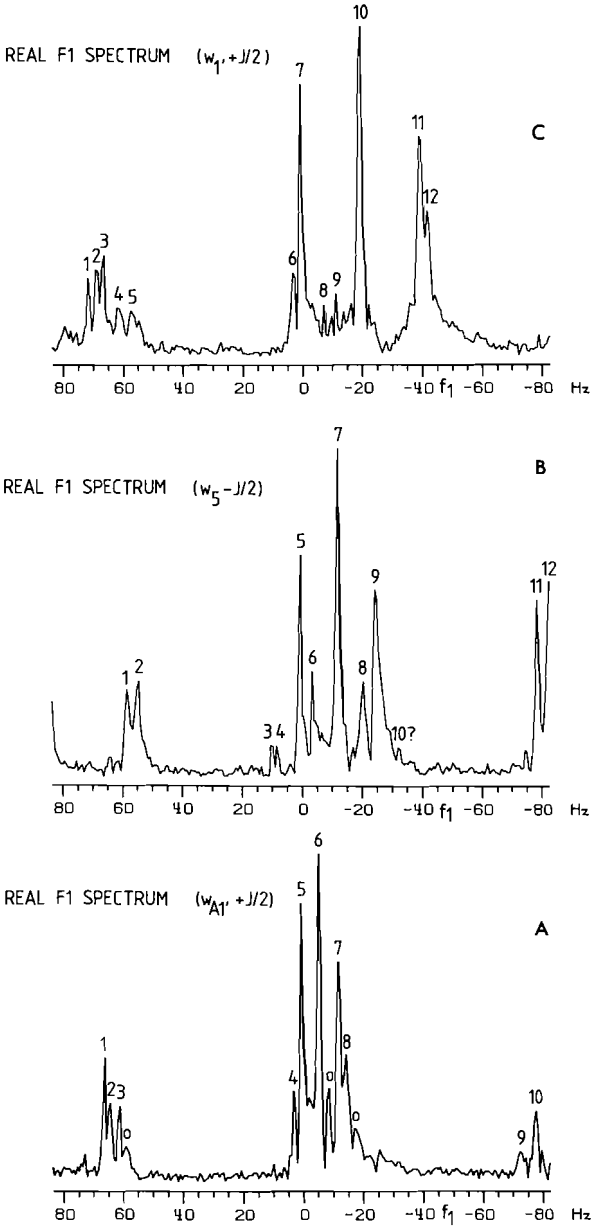


FIG. 6. (A) The real f_1 spectrum of the low field (f_2) AH-1′ transition in CpA. Overlapped lines from other f_1 spectra are indicated by O; (B) the real f_1 spectrum of the high field (f_2) CH-5 transition in CpA; (C) the real f_1 spectrum of the low field (f_2) CH-1′ transition in CpA.

at superconducting field strengths by Sarma and co-workers (27) who used simulation/iteration methods to analyse the spectrum. The results obtained here from the 2D analysis agree in general; however, differences in temperature, concentration, and solvent prevent direct comparison.

Figure 5 shows the real 2D nmr spectrum in the region of the AH-1′, CH-5, and CH-1′ resonances. Figure 6(A) shows the real f_1 spectrum of the low field AH-1′ transition. An analysis of this spectrum in terms of the mixing of the appropriate AH-1′ and AH-2′ magnetizations is given in Table 5. This analysis allowed the location of the AH-2′ resonance as a pseudo triplet at ~ -140 Hz from the carrier in f_2. This signal can be distinctly seen in the normal 1D spectrum. A similar analysis applied to the f_1 spectra of the f_2 transitions of the newly-located AH-2′ proton allowed the assignment of the AH-3′ proton as the pseudo triplet at ~ -159 Hz from the carrier in f_2.

Figure 6(B) shows the real f_1 spectrum of the high field CH-5 transition and Fig. 6(C) shows the real f_1 spectrum of the low field CH-1′ transition. Table 6 gives an analysis of the f_1 spectrum of the CH-5 transitions in f_2. An interesting feature of this spectrum is that it reveals the presence of a connection between the CH-1′ and the CH-5 protons via a five bond coupling. The two weak lines at 7.6 and 9.8 Hz are due to subtractive mixing with CH-1′. If these lines were perfectly resolved, they would form a doublet of doublets with a large splitting (observed) due to $^3J_{(H2'—H1')}$ and a smaller splitting (unresolved in the experiment) due to $^5J_{(H5—H1')}$. The lines split by this latter coupling overlap and partially cancel in the f_1 spectrum because they are of opposite phase; if the coupling constant was 0 Hz, they would cancel exactly. The digitization in this experiment was not good enough to measure this coupling, but the peaks in the f_1 spectrum were a clear indication of the presence of the $^5J_{H,H}$ coupling. Similar small $^5J_{H,H}$ couplings in similar systems have been observed in the past (25).

Table 7 gives an analysis of the f_1 spectrum of the low field CH-1′ transition in f_2. Aside from confirming the presence of the $^5J_{H,H}$ coupling this spectrum revealed the exact chemical shift of the CH-2′ "triplet" which was completely hidden in the 1D spectrum under a residual solvent signal and a mass of other resonances.

Conclusion

A new pulse sequence (13, 24) for 2D nmr spectroscopy has been described which allows chemical shift correlations between coupled nuclei to be made. The technique has been shown to be invaluable in the determination of the precise location of buried resonances and also in the discovery of small, long-range couplings not normally detected by 1D nmr spectroscopy. As such this new technique promises to be very useful to practising chemists especially, since the spectra may be accumulated and processed in a matter of a few hours on standard spectrometers.

This technique is a development of a previous one (1) in which there was no delay after the mixing

pulse. The advantage of inserting the second delay is that it allows the partial cancellation of B_0 inhomogeneity in f_1. With a more sophisticated pulse sequence (24) which suppresses the additive spectra a further advantage is accrued in that the f_1 width can be reduced to the largest chemical shift difference between two coupled nuclei rather than being equal to the f_2 width. This saves time and data storage.

Acknowledgements

We thank the Natural Sciences and Engineering Research Council of Canada, and McMaster University for their support.

1. W. P. AUE, E. BARTHOLDI, and R. R. ERNST. J. Chem. Phys. **64**, 2229 (1976).
2. R. FREEMAN and G. A. MORRIS. Bull. Magn. Reson. **1**, 5 (1979).
3. B. H. MEIER and R. R. ERNST. J. Am. Chem. Soc. **101**, 6441 (1979).
4. L. MÜLLER, A. KUMAR, T. BAUMANN, and R. R. ERNST. Phys. Rev. Lett. **32**, 1402 (1974).
5. R. K. HESTER, J. L. ACKERMAN, V. R. GROSS, and J. S. WAUGH. Phys. Rev. Lett. **34**, 993 (1975).
6. G. BODENHAUSEN, R. FREEMAN, G. A. MORRIS, and D. L. TURNER. J. Magn. Reson. **31**, 75 (1978).
7. V. J. KOWALEWSKI. Prog. Nucl. Magn. Reson. Spectrosc. **5**, 1 (1969).
8. A. A. MAUDSLEY, L. MÜLLER, and R. R. ERNST. J. Magn. Reson. **28**, 463 (1977).
9. G. BODENHAUSEN and R. FREEMAN. J. Magn. Reson. **28**, 471 (1977).
10. R. FREEMAN and G. A. MORRIS. J. Chem. Soc. Chem. Commun. 684 (1978).
11. G. BODENHAUSEN and R. FREEMAN. J. Am. Chem. Soc. **100**, 320 (1978).
12. P. H. BOLTON and G. BODENHAUSEN. J. Am. Chem. Soc. **101**, 1080 (1979).
13. A. D. BAIN, R. A. BELL, J. R. EVERETT, and D. W. HUGHES. J. Chem. Soc. Chem. Commun. 256 (1980).
14. S. VEGA and A. PINES. J. Chem. Phys. **66**, 5624 (1977).
15. A. WOKAUN and R. R. ERNST. J. Chem. Phys. **67**, 1752 (1977).
16. A. D. BAIN. J. Magn. Reson. **37**, 209 (1980).
17. A. D. BAIN. J. Magn. Reson. In press.
18. A. D. BAIN. Chem. Phys. Lett. **57**, 281 (1978).
19. A. A. MAUDSLEY, A. WOKAUN, and R. R. ERNST. Chem. Phys. Lett. **55**, 9 (1978).
20. A. D. BAIN and J. S. MARTIN. J. Magn. Reson. **29**, 125 (1978).
21. A. D. BAIN and J. S. MARTIN. J. Magn. Reson. **29**, 137 (1978).
22. G. BODENHAUSEN, R. FREEMAN, R. NIEDERMEYER, and D. L. TURNER. J. Magn. Reson. **26**, 133 (1977).
23. A. WOKAUN and R. R. ERNST. Chem. Phys. Lett. **52**, 407 (1977).
24. K. NAGAYAMA, K. WÜTHRICH, and R. R. ERNST. Biochem. Biophys. Res. Commun. **90**, 305 (1979).
25. D. B. DAVIES. Prog. Nucl. Magn. Reson. Spectrosc. **12**, 135 (1978).
26. J. R. EVERETT, D. W. HUGHES, A. D. BAIN, and R. A. BELL. J. Am. Chem. Soc. **101**, 6776 (1979).
27. F. S. EZRA, C. KEE, N. S. KONDO, S. S. DANYLUK, and R. H. SARMA. Biochemistry, **16**, 1977 (1977).

Can. J. Chem. Downloaded from www.nrcresearchpress.com by 210.87.254.6 on 09/05/12
For personal use only.

The metabolism of 2-hydroxymethyl-3-methylquinoxaline-di-*N*-oxide in the chicken, rat, and dog

S. K. FIGDOR AND D. C. HOBBS

Drug Metabolism Department, Pfizer Inc., Groton, CT 06340, U.S.A.

Received September 27, 1979[1]

This paper is dedicated to Prof. Karel Wiesner on the occasion of his 60th birthday

S. K. FIGDOR and D. C. HOBBS. Can. J. Chem. **58**, 1957 (1980).

2-Hydroxymethyl-3-methylquinoxaline-di-*N*-oxide (GS-7443) is rapidly metabolized in the chicken, rat, and dog to 3-carboxy-2-methylquinoxaline-1-oxide and a conjugate of 3-carboxy-2-methylquinoxaline-di-*N*-oxide. No appreciable amounts of other metabolites nor unchanged GS-7443 could be detected in the excreta from these animals. There were minor quantitative differences in the relative amounts of the two metabolites; moreover, the conjugating group employed by the chicken is different from that of the dog but the material being conjugated is the same. Although measurable tissue levels of drug-related material were noted in several organs of the chicken 6 days after drug administration, all chicken tissues examined were cleared of radioactivity within 21 days.

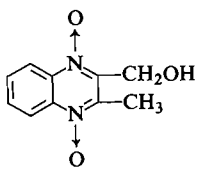
S. K. FIGDOR et D. C. HOBBS. Can. J. Chem. **58**, 1957 (1980).

Le di-*N*-oxyde de l'hydroxyméthyl-2 méthyl-3 quinoxaline (GS-7443) est métabolisé rapidement chez le poulet, le rat et le chien en oxyde-1 de la carboxy-3 méthyl-2 quinoxaline et en son espèce conjugée, le di-*N*-oxyde de la carboxy-3 méthyl-2 quinoxaline. On n'a pas pu déceler des quantités appréciables d'autres métabolites ou de GS-7443 de départ dans les excrétions de ces animaux. Quantitativement il y a très peu de différences entre les deux métabolites; de plus, le groupe conjugué employé par le poulet est différent de celui employé par le chien mais c'est le même produit qui devient conjugué. Bien qu'on ait pu déceler des quantités mesurables des drogues mentionnées dans les tissus de plusieurs organes du poulet six jours après que les drogues eurent été administrées, toute la radioactivité des tissus examinés disparait après 21 jours.

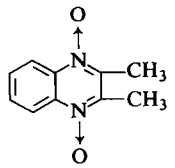
[Traduit par le journal]

Introduction

Quinoxaline-1,4-di-*N*-oxides were synthesized in the early 1940's and evaluated as human chemotherapeutic agents. A variety of undesirable side effects rendered these compounds unsuitable for clinical therapy. However, as a result of the effective antibacterial activity shown by this group of chemicals, a renewed interest in quinoxalines emerged for uses as antiinfective agents in food producing animals. 2-Hydroxymethyl-3-methylquinoxaline-di-*N*-oxide (GS-7443, **1**) was first described by Francis *et al.* in 1956 (1) as one of the metabolites of 2,3-dimethylquinoxaline-di-*N*-oxide (**2**) in sheep. The occurrence of further and additional metabolic transformations was not excluded since only a small percent of administered **2** was recovered unchanged.



1 GS-7443



2

GS-7443 has been shown in our laboratory to be an extremely effective gram negative chemotherapeutant for poultry with antibacterial activity extending to Terramycin resistant *E. coli*. In connection with its proposed use in food producing animals, the distribution and metabolism of GS-7443 in the chicken and appropriate experimental animal species, such as the rat and dog, was of interest.

Results

Excretion of Radioactivity

In the chicken, rat, and dog a dose of 30 mg/kg was rapidly excreted and most of the dose was recovered during the 24 h period following administration of the drug (Table 1). In the rat and dog approximately two-thirds of the administered radioactivity was recovered in urine and the remainder in the feces.

Paper chromatography indicated that the excreta of all animals contained two major metabolites of differing polarities. No GS-7443 (**1**) was observed. Thin layer chromatography also indicated the presence of trace amounts of several other radioactive materials not seen on papergrams; these were not investigated further but may have included degradation products of the polar metabolite (see below). Semi-quantitative information regarding the relative amounts of the two major metabolites was derived from the papergram scans as indicated in Table 2.

In the chicken and dog the polar metabolite predominated whereas in the rat the converse was observed.

[1]Revision received May 22, 1980.

0008-4042/80/181957-05$01.00/0

©1980 National Research Council of Canada/Conseil national de recherches du Canada

Can. J. Chem. Downloaded from www.nrcresearchpress.com by 210.87.254.42 on 09/05/12
For personal use only.

TABLE 1. Recovery of radioactivity following oral administration of ^{14}C-GS-7443 (percent of administered dose)

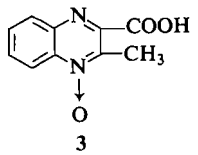
Chicken		Rat			Dog		
Time (h)	Combined excreta	Time (h)	Urine	Feces	Time (h)	Urine	Feces
0–24	88	0–21	61	14	0–24	59	11
24–48	11	21–44	2	<0.1	24–48	5	14
48–72	1	44–120	1	<0.1	48–96	0.4	3.6

TABLE 2. Relative amounts of metabolites of GS-7443

	Metabolite No. 1 (non-polar)	Metabolite No. 2 (polar)
Chicken	35	65
Rat	55	44
Dog	30	70

Isolation of Metabolite No. 1, the Non-polar Metabolite

Rat and dog urine and aqueous extracts of chicken excreta (suitably diluted with excreta from animals receiving non-labeled drug to provide sufficient material for isolation) were first passed through a cation exchange column (water elution) with purification and little loss of radioactivity. The lyophilized and reconstituted eluates when chromatographed on Sephadex G-10 columns gave a complete separation of the two metabolites, the polar material (metabolite No. 2) emerging first. In the case of the rat and dog, fractions containing metabolite No. 1 were lyophilized and the residue crystallized from water. This material, recrystallized from chloroform–hexane (mp 148°C), was anionic (electrophoresis) and had a uv spectrum in methanol indicative of a mono-*N*-oxide; λ_{max}: 325 (ε 8200), 243 (ε 28 200) nm (2). The nmr spectrum showed aromatic and *C*-methyl protons only. Thus the non-polar metabolite No. 1 is very likely 3-carboxy-2-methylquinoxaline-1-oxide, **3**. This was



3

confirmed by mass spectral analysis, which also excluded the isomeric 4-oxide, and by elemental analysis (*Anal.* calcd. for $C_{10}H_8N_2O_3$: C 58.82, H 3.95%; found: C 57.61, H 3.92%). Confirmation for assignment of the position of the *N*-oxide was also provided by subsequent synthesis of **3**. This compound (position of *N*-oxide unspecified) has also been isolated from urine of mice and dogs following the administration of **2** (3). The identity of metabolite No. 1 from the chicken was established by isotope dilution. To the appropriate Sephadex eluate containing the labeled nonpolar chicken metabolite was added crystalline metabolite No. 1 isolated from dogs receiving nonlabeled GS-7443. Several crystallizations from water and chloroform–hexane to constant specific activity established that the two were identical. Paper chromatography of this recrystallized material in three different systems showed that radioactivity aligned with **3**.

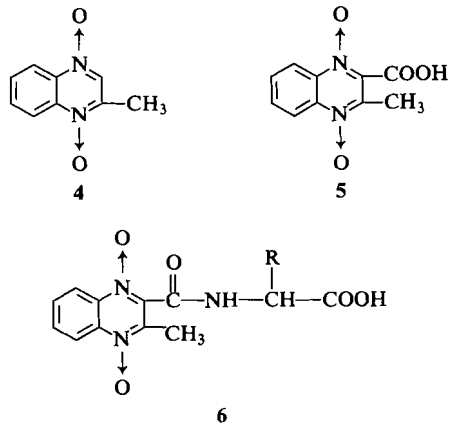
Isolation of Metabolite No. 2, the Polar Metabolite

Metabolite No. 2 as obtained from the Sephadex G-10 column was free of any other labeled material. It was also anionic (electrophoresis) but the uv spectrum was indicative of a di-*N*-oxide (maxima at 237, 261, 351, and 367 in water; at 235, 270, and 377 in methanol). Its early emergence from the Sephadex column and polarity suggested a conjugate. Treatment with glucuronidase and sulfatase, however, caused no change in the material.

One lot of the conjugated metabolite No. 2 from the dog, free of other labeled material, was converted on standing to an anionic nonpolar material with a uv spectrum similar to that of the conjugate and distinguishable from **3** by paper chromatography (R_f 0.6 on system D-20) and electrophoresis. This conversion could not be repeated with other lots of metabolite No. 2 and remains unexplicable, although it may have been due to residues of a peptidase introduced from tissue samples. On silica gel chromatography the purified material was converted to a neutral substance with a uv spectrum again similar to that of metabolite No. 2 conjugate. The neutral material, after purification on a small Sephadex G-10 column, was characterized as 2-methylquinoxaline-di-*N*-oxide (**4**) by comparison of its infrared and mass spectra with those of an authentic specimen. The anionic unconjugated material is very likely 2-methyl-3-carboxyquinoxaline-di-*N*-oxide (**5**) which was decarboxylated to **4** during silica gel chromatography. On silica gel chromatography **4** was also obtained in poor

Can. J. Chem. Downloaded from www.nrcresearchpress.com by 210.87.254.42 on 09/05/12
For personal use only.

Can. J. Chem. Downloaded from www.nrcresearchpress.com by 210.87.254.42 on 09/05/12
For personal use only.



4 5 6

yield directly from the conjugate. The isolation of **4** from chicken excreta by this method was also possible (see below). The decarboxylation of **5** has precedence since, in attempts to synthesize **5** by oxidation of the corresponding aldehyde with *m*-chloroperbenzoic acid, **4** could be isolated in good yield. The acid **5** is probably linked to an amino acid residue since metabolite No. 2 conjugate **6** is also anionic.

Metabolite No. 2 from the chicken, although having a similar uv spectrum, could be distinguished from the dog metabolite No. 2 by Sephadex chromatography of a mixture of non-labeled dog metabolite and labeled chicken metabolite (fractions analyzed by uv and radioactivity). The chicken metabolite, however, also yielded **4** on silica gel chromatography. The difference between metabolites No. 2 of the two species appears to reside in the nature of the conjugating group.

Further comparison of dog and chicken metabolites No. 2, and the identification of 2-methylquinoxaline-1,4-di-*N*-oxide as one product obtained from the polar metabolites of dog and chicken, were carried out as follows. Crude dog metabolite No. 2 free of metabolite No. 1 was slurried overnight with silica gel in chloroform–methanol – acetic acid (80:15:5). The supernatant liquid from this slurry was then examined by paper chromatography and compared with the major radioactive fraction resulting from silica gel chromatography of the crude chicken metabolite No. 2 fraction. The paper chromatograms were very similar and revealed one minor and two major components. One of the major components aligned with the reference standard, 2-methylquinoxaline-di-*N*-oxide (**4**), in two paper and two thin-layer systems. It is estimated that this compound comprises from 40 to 50% of the mixture. The two other components, neither of which has been identified and neither of which is unaltered metabolite No. 2, may result from decomposition of the polar metabolite by alternative reactions. 2-Methylquinoxaline-di-*N*-oxide (**4**) was also isolated from the chicken silica gel chromatography reaction mixture by isotope dilution.

TABLE 3. Distribution of radioactivity, calculated as μg GS-7443 per g tissue, in the chicken after a single oral dose of GS-7443-^{14}C

	Days after 30 mg/kg GS-7443		
Tissue	6[a]	14	21
Kidney	0.32	0	0
Liver	3.5[b]	0.35	0
Skin	0.14	0	0
Heart	0.15	0	0
Lung	< 0.5	0	0
Stomach	0[c]	0	0
Light muscle	0	0	0
Dark muscle	0	0	0

[a]Average of three chickens.
[b]Average of five chickens.
[c]0 = < 0.1 μg GS-7443 equivalent per gram of tissue.

Distribution of Radioactivity

Since GS-7443 was proposed for use as an antibacterial agent it was important to determine whether drug related residues were present in chicken tissues after GS-7443 administration. The distribution of radioactivity in various tissues of the chicken is shown in Table 3. Animals were "stressed" for four days on chicken feed containing 250 g/ton non-labeled GS-7443, then dosed orally with 30 mg/kg labeled GS-7443, and maintained on regular chicken feed prior to sacrifice. Paper chromatograms of extracts of chicken liver revealed the same distribution of radioactivity as extracts of chicken excreta, with approximately the same relative proportions of the two metabolites. Thus liver, which retains radioactivity longer than the other tissues, is cleared by 21 days, and the residue contained in liver appears to be the same as the excreted metabolites.

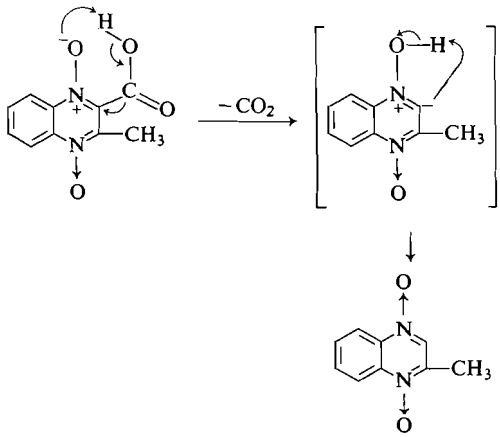
Discussion

The oxidative metabolic conversion of 2,3-dimethylquinoxaline-di-*N*-oxide (**2**) to GS-7443 (**1**) earlier detected in the sheep (1) appears to be merely part of a general oxidative sequence ending with the carboxylic acid. Although no unchanged GS-7443 could be detected in the excreta of the three species of the present study, the presence of GS-7443 in sheep's urine might simply be a function of metabolism in sheep. An alternative explanation may involve the considerably larger doses administered at an earlier step in the oxidative sequence (2,3-dimethylquinoxaline, **2**) and the in-

Can. J. Chem. Downloaded from www.nrcresearchpress.com by 210.87.254.42 on 09/05/12
For personal use only.

ability of sheep to further metabolize all of the resulting oxidized transformation product (2-hydroxymethyl-3-methylquinoxaline, **1**).

In the rat, dog, and chicken the mono-*N*-oxide carboxylic acid **3** is excreted exclusively in the uncoupled form whereas the corresponding di-*N*-oxide **5** is eliminated entirely as the conjugate. Although the latter acid was not obtained from the conjugate in pure form for characterization, its identity would appear to rest on a fairly firm foundation for several reasons. (*1*). Its formation from GS-7443 is metabolically reasonable, particularly since the corresponding mono-*N*-oxide is readily formed. (*2*). The limited analytical data on the acid are consistent with its formation. (*3*). The facile decarboxylation to 2-methylquinoxaline-di-*N*-oxide has precedent in synthetic studies and is mechanistically explicable:



The adjacent *N*-oxide must participate, since in its absence (in **3**) there is no decarboxylation under identical conditions.

The proposal regarding the nature of the conjugating group is speculative but an amino acid function is reasonable in light of the electrophoretic studies which indicate that the polar conjugate is acidic. The dissimilarity of the conjugating functions in the chicken and dog is clearly evident from the chromatographic studies on Sephadex columns. The amino acids for the dog and chicken may be glycine and ornithine, respectively, since a similar relationship is well known for other aromatic acids (4).

Experimental

Materials

Synthesis of GS-7443 Uniformly Labeled with Carbon-14 in the Benzene Ring

2,3-Dimethylquinoxaline-^{14}C

To 25 mL of benzene was added 0.532 g uniformly labeled ^{14}C-*o*-phenylenediamine (specific activity 1.18 mCi per mmol, Nuclear Research Chemicals, Inc., Orlando, Florida), 4.5 g nonradioactive *o*-phenylenediamine purified by recrystallization and sublimation, and 4.4 g freshly distilled diacetyl. The reaction mixture was stirred at reflux with a Dean–Stark water take-off tube for 5.5 h. After this period an aliquot was removed and assayed by paper chromatography. At this time no *o*-phenylenediamine remained in the reaction mixture and the entire solution was concentrated to dryness *in vacuo*. Yield was 7.38 g, 5.12 mCi.

*2,3-Dimethylquinoxaline-1-*N*-oxide-*^{14}C

2,3-Dimethylquinoxaline-^{14}C (7.38 g) was dissolved in 12 mL of glacial acetic acid with gentle warming. To this solution was added with stirring 9.3 g of 40% peracetic acid. The amount of added peracetic acid represents a 4% excess over one equivalent. The solution was allowed to stir at 35°C overnight. The following morning the reaction solution was diluted with 50 mL of water, extracted with 2 × 50 mL of chloroform, the chloroform in turn washed with one additional 50 mL portion of water. The combined chloroform filtrates were dried over sodium sulfate, filtered, and concentrated *in vacuo* to a small volume. The chloroform concentrate was added to a column of 400 g of Fischer's absorption alumina (80–200 mesh) in chloroform, and 125 mL chloroform fractions were collected. Paper chromatographic assay followed by radio scanning of all fractions indicated that fractions 1–3 consisted primarily of unreacted starting material, fractions 4–12 were the pure mono-*N*-oxide, and subsequent fractions from 13–16 contained mixtures of the mono-*N*-oxide and the di-*N*-oxide. Fractions 4–12, pure mono-*N*-oxide, were combined and concentrated to dryness; yield 5.109 g.

2-Acetoxymethyl-3-methylquinoxaline-^{14}C

2,3-Dimethylquinoxaline-1-*N*-oxide-^{14}C (5.109 g) was dissolved in 11 mL of acetic anhydride and the reaction mixture stirred at reflux for 1 h. At the end of this period the solution was concentrated to an oily residue under vacuum, redissolved in approximately 10 mL of ethanol, and again concentrated to dryness *in vacuo*. The crude reaction mixture was added to a 300 g column of acid-washed Florisil in chloroform and 500 mL of chloroform fractions were eluted. Each fraction was again assayed by paper chromatography, radio scanned, and appropriate fractions combined. In this manner, 6.4 g of 2-acetoxymethyl-3-methylquinoxaline-^{14}C was obtained.

*2-Acetoxymethyl-3-methylquinoxaline-di-*N*-oxide-*^{14}C

To a solution of 6.4 g of 2-acetoxymethyl-3-methylquinoxaline-^{14}C in 100 mL of chloroform was added slowly with stirring 16 g of 85% *m*-chloroperbenzoic acid. The reaction mixture was stirred at room temperature for 20 min and then slowly brought to reflux and subsequently refluxed a total of 16 h. The reaction mixture was cooled to room temperature, the solid material removed by filtration, and the filter cake repulped with several small portions of chloroform. The chloroform filtrate and washings were combined and washed with two 100 mL portions of saturated sodium bicarbonate, two 100 mL portions of water, and the aqueous phases, in turn, passed through four 100 mL portions of chloroform. The chloroform extracts were combined, dried over sodium sulfate, and concentrated to dryness *in vacuo*. Yield was 7.35 g.

*2-Hydroxymethyl-3-methylquinoxaline-di-*N*-oxide-*^{14}C*, GS-7443 (1)*

The total crude reaction product obtained from the previous reaction (7.35 g) was dissolved in 25 mL of concentrated HCl and stirred at room temperature overnight. The reaction mixture was poured into a separatory funnel, 50 mL of chloroform was added, and 100 mL of saturated sodium bicarbonate solution was slowly added with shaking. The reaction mixture was extracted with four 100 mL chloroform portions which were, in

Can. J. Chem. Downloaded from www.nrcresearchpress.com by 210.87.254.42 on 09/05/12
For personal use only.

turn, passed through four 50 mL aqueous washings. The combined chloroform extracts were dried over sodium sulfate, filtered, and concentrated to dryness *in vacuo*; yield, 5.22 g. The crude reaction product was purified by crystallization from a mixture of chloroform and acetonitrile with the addition of Darco and subsequently recrystallized once from chloroform and twice from acetone. The final product, 0.760 g, melting point 186–187°C, had a specific activity of 0.55 μCi/mg. No contaminating materials were visible in radio scans of the chromatographed product.

Methods

Radiometric Methods

All radioactive samples were measured in a Nuclear Chicago Model 725 liquid scintillation spectrometer. Quenching corrections were made by the internal standard procedure employing ^{14}C-toluene. Nonaqueous samples were assayed in a scintillator consisting of 0.3% 2,5-diphenyloxazole (PPO) and 0.01% *p*-bis[2-(5-phenyloxazolyl)]benzene (POPOP) in toluene. Aqueous samples (urine, water) were counted in a similar scintillator in which the solvent was 30% ethanol in toluene (30/70 scintillator). A maximum of 0.2 mL of aqueous solution was assayed in 15 mL of scintillator solution.

Feces were assayed by homogenizing in a Waring Blender with an equal weight of water and lyophilizing the resulting slurry. Samples of the dried powdered feces weighing approximately 50 mg were burned in an atmosphere of oxygen in a Schöniger combustion flask with an ethanolamine – ethyl cellosolve (1:2) mixture to trap $^{14}CO_2$. Aliquots of this solution were counted in 30/70 scintillator solution.

Chicken feces were assayed by dissolving from 2 to 25 mg of the lyophilized powder in a small volume of Hyamine (Packard Instrument Co., Downers Grove, IL), followed by the addition of 15 mL 30/70 scintillator solution.

Tissues were assayed by homogenizing 1 g of fresh wet tissue with 3 mL Hyamine in a Potter–Elvehjem tissue grinder. One mL of the resulting clear solution, equivalent to 0.25 g fresh tissue, was dissolved in 15 mL 30/70 scintillator solution and counted.

In vivo Experiments

Chickens, rats, and dogs received labeled drug as aqueous solutions by stomach tube at a level of 30–70 mg/kg and were thereafter kept in plastic or stainless steel metabolism cages. Nonlabeled drug at the same dose levels was also administered to accumulate sufficient amounts of metabolites to facilitate isolation; the rats received the nonlabeled GS-7443 in the drinking water (0.5 mg/mL). Because of the known (2) photoinstability of quinoxaline-*N*-oxides, all animals were maintained in darkened rooms (chickens and dogs) or in light-tight enclosures (rats). Experimental procedures were carried out in darkened rooms wherever possible.

Aqueous extracts of dog and rat feces were used to merely establish (paper chromatography) the similarity between fecal and urinary metabolites; lyophilized chicken feces preextracted with hexane to remove inactive oily material also provided the basis for the isolation of metabolites.

Chromatography

Paper chromatographic systems used were system D-20 (chloroform–ethanol – formic acid, 2:1:2, lower phase), system BCF (benzene–chloroform, 1:1, saturated with formamide), system 80 (methyl isobutyl ketone – formic acid – water, 2:1:1, upper layer), and benzene–acetone – formic acid – water (10:5:2:6). The BCF gave a good separation of GS-7443 from its metabolites, and the other systems resolved the two metabolites. Thin-layer chromatography was performed with chloroform–methanol – acetic acid (80:15:5), chloroform – ethyl acetate – formic acid (50:40:10), and 5% acetic acid in ethyl acetate. Electrophoresis was on Whatman #ET-1 paper in a pH 7.0, 0.05 *M* sodium acetate buffer at 300 V and 50 mA. Radioactivity was localized on the paper strips with a Vanguard Model 880 Autoscanner; thin layer plates were evaluated with the Vanguard tlc attachment or by autoradiography using Kodak type F X-ray film.

Column chromatography was performed on Sephadex G-10 in water, silica gel H in chloroform–methanol – acetic acid (80:15:5), and on a cation exchange resin (Dowex 50, H form). Aliquots of individual fractions were assayed for radioactivity by liquid scintillation counting.

Physical Measurements

The nmr spectra were obtained on a Varian A-20 instrument with tetramethylsilane calibration. The mass spectra were run on an Atlas model CH_4 instrument.

1. J. FRANCIS, J. K. LANDQUIST, A. A. LEVI, J. A. SOLK, and J. M. THORP. Biochem. J. **63**, 455 (1956).
2. J. K. LANDQUIST. J. Chem. Soc. 455 (1953).
3. J. R. VALENTA, J. R. E. HOOVER, and J. F. PAGANO. Antimicrob. Agents Chemother. 453 (1966).
4. R. T. WILLIAMS. Detoxication mechanisms. Chapman and Hall, Ltd., London. 1959.

EOR ERRATA SEE
v.60;#6.19.82...P.812

ERRATA

Metal complexes as antioxidants. 8. A kinetic and product study of the reaction of tertiary alkylperoxy radicals with cobalt(II) acetylacetonate[1]

J. A. HOWARD AND S. B. TONG[2]

Division of Chemistry, National Research Council of Canada, Ottawa, Ont., Canada K1A 0R9

Received February 25, 1980

J. A. HOWARD and S. B. TONG. Can. J. Chem. **58**, 1962 (1980).

tert-Butylperoxy radicals react rapidly with $Co(acac)_2$ in non-polar solvents and rate constants measured by kinetic electron spin resonance spectroscopy obey the Arrhenius equation $\log (nk/M^{-1}\,s^{-1}) = (8.9 \pm 0.7) - (4.7 \pm 1.5)/\theta$, where $\theta = 2.303RT$ kcal mol^{-1} and n is ~ 0.1. Cumylperoxy radicals react with $Co(acac)_2$ to give mainly α-cumyl alcohol and acetophenone. There is no evidence for the formation of "long-lived" alkylperoxy radicals co-ordinated to cobalt (III) or a stable alkylperoxo cobalt(III) complex in these systems.

J. A. HOWARD et S. B. TONG. Can. J. Chem. **58**, 1962 (1980).

Les radicaux *tert*-butylperoxy réagissent rapidement avec $Co(acac)_2$ dans des solvants non polaires et la constante de vitesse mesurée par la résonance paramagnétique électronique cinétique obéit à l'équation d'Arrhénius: $\log (nk/M^{-1}\,s^{-1}) = (8{,}9 \pm 0{,}7) - (4{,}7 \pm 1{,}5)/\theta$ où $\theta = 2{,}303RT$ kcal mol^{-1} et n est $\sim 0{,}1$. Les radicaux cumylperoxy réagissent avec $Co(acac)_2$ pour donner principalement l'alcool α cumylique et l'acétophénone. Dans ces systèmes, on n'a pas pu mettre en évidence la formation de radicaux alkylperoxy de "longue vie" coordonnés au cobalt(III) ou d'un complexe stable alkylperoxocobalt(III).

[Traduit par le journal]

Introduction

Although there is an extensive literature concerned with liquid phase hydrocarbon autoxidation and hydroperoxide decomposition initiated by soluble cobalt complexes (1–7) there have been comparatively few studies of the reaction of these complexes with alkylperoxy radicals. It is, however, known that cobalt(II) complexes can undergo a chain termination reaction with alkylperoxy radicals, reaction [1] (8–10), while it has been reported that co-ordinatively unsaturated cobalt(III) complexes form a stable paramagnetic complex with $RO_2^{\bullet}$, reaction [2] (11–14).

[1] $RO_2^{\bullet} + Co(II) \rightarrow Co(III) + \text{products}$

[2] $ROOH + Co(II) \rightarrow Co(III)\cdots RO_2^{\bullet}$

The studies that have been made on the reaction of alkylperoxy radicals with cobalt(II) complexes have yielded rate constants in the range $2 \times 10^4 - 8 \times 10^5\ M^{-1}\,s^{-1}$ at temperatures of 60–74°C (8–10). These rate constants are, however, rather unreliable because they have been obtained *indirectly* relative to other rate constants for reactions of alkylperoxy radicals.

In this paper we present the results of a *direct* study of the reaction of the *tert*-butylperoxy radical with $Co(acac)_2$ using the kinetic electron spin resonance spectroscopic method that has been successful for direct studies of the reactions of $t\text{-}BuO_2^{\bullet}$ with hindered and non-hindered phenols and aromatic amines (15, 16), trivalent phosphorus compounds (17), alkyl hydroperoxides (18), and organo-tin and -lead compounds (19). In addition we report a product study of the reaction of cumylperoxy with this complex.

Experimental

Materials

$Co(acac)_2$ (Alfa, Ventron) was recrystallized from methanol and heated under vacuum at 50°C for 2 days. Standard solutions of this material were prepared immediately before use. Azocumene was prepared by the method of Nelsen and Bartlett (20) and di-α-cumyl hyponitrite by the method of Kiefer and Traylor (21). Di-*tert*-butyl ketone was obtained from Chemical Samples Co. Solvents were purified by standard procedures.

Radical Generation

tert-Butylperoxy radicals were generated by photolysis of di-*tert*-butyl ketone in oxygen- or air-saturated toluene. The concentration of this radical after the light was masked was followed by time resolved electron spin resonance spectroscopy (17). The induction period (15) and titration (16) methods were used to estimate the number of *tert*-butylperoxy radicals destroyed by each molecule of $Co(acac)_2$, i.e., the stoichiometric factor, n.

Cumylperoxy radicals were produced by thermolysis of azocumene in oxygen-saturated solvent at 323 K. In the presence of $Co(acac)_2$ rates of oxygen absorption were slightly faster than rates of production of cumyl radicals and slightly more than the theoretical concentration of oxygen was absorbed. For instance, azocumene (0.0245 M) in chlorobenzene containing $Co(acac)_2$ (0.049 M) absorbed oxygen at an initial rate of $2 \times 10^{-6}\ M\,s^{-1}$ whereas the calculated initial rate of production of cumyl radicals was $1.6 \times 10^{-6}\ M\,s^{-1}$ and 0.057 M of oxygen were absorbed.

Product Analysis

Products from reaction of cumylperoxy, cumyloxy, and cumyl hydroperoxide with $Co(acac)_2$ were analyzed, after distillation from inorganic products, either by gas chromatography or high performance liquid chromatography. The gas chromatograph was a Varian 2800 equipped with a 12% OV-101

[1]NRCC No. 18477.

[2]NRCC Research Associate 1977–1979.

0008-4042/80/181962-04$01.00/0

©1980 National Research Council of Canada/Conseil national de recherches du Canada

Can. J. Chem. Downloaded from www.nrcresearchpress.com by 210.87.254.6 on 09/05/12
For personal use only.

Can. J. Chem. Downloaded from www.nrcresearchpress.com by 210.87.254.6 on 09/05/12
For personal use only.

on Chromosorb W (80/100 mesh) column (12 ft × 1/8 in.) and a flame ionization detector. The liquid chromatograph was a Spectra Physics 3500 equipped with a Brown-Lee RP-8 column and uv detector (254 nm); the eluting solvent was H_2O–CH_3CN (65:35, v/v).

Cobalt(III) yields were determined by uv-spectroscopy at 594 nm using a Hewlett-Packard 8450 A UV/VIS Spectrophotometer.

Results and Discussion

Kinetics

Photochemically generated *tert*-butylperoxy radicals decayed rapidly in the presence of excess $Co(acac)_2$ in the temperature range 183–213 K. Plots of ln [*t*-BuO_2·] against time were linear, indicating exponential radical decay, i.e.,

$$-d[t\text{-}BuO_2\cdot]/dt = k_\psi[t\text{-}BuO_2\cdot]$$

where k_ψ is the pseudo-first-order rate constant.

Values of k_ψ appeared to be linearly dependent on the concentration of $Co(acac)_2$ (Table 1) implying that this reaction obeys the rate law

$$-d[t\text{-}BuO_2\cdot]/dt = nk[t\text{-}BuO_2\cdot][Co(acac)_2]$$

where n is the stoichiometric factor and k is the bimolecular rate constant for reaction of the *tert*-butylperoxy radical with $Co(acac)_2$.

$$[1a] \quad t\text{-}BuO_2\cdot + Co(acac)_2 \xrightarrow{nk} \text{Products}$$

Unfortunately nk could only be measured over a narrow range of $Co(acac)_2$ concentrations because above $\sim 10^{-3}$ M the concentration of *t*-BuO_2· was too small to give meaningful decay kinetics while below $\sim 10^{-4}$ M the complex was consumed very rapidly by continuous photolysis.[3]

Values of nk fell in the range 2×10^3 to 1.1×10^4 M^{-1} s^{-1} from 183 to 213 K (Table 1) and a plot of log (nk/M^{-1} s^{-1}) against the reciprocal of the absolute temperature gave

$$\log (nk/M^{-1}\ s^{-1}) = (8.9 \pm 0.7) - (4.7 \pm 1.5)/\theta$$

where $\theta = 2.303\ RT$ kcal mol^{-1}.

This pre-exponential factor is similar to the *A*-factor of 2.9×10^9 M^{-1} s^{-1} reported by Shcheredin and Denisov (8) for reaction of the poly(peroxystyryl)peroxy radical with $Co(acac)_2$ obtained indirectly from a study of the influence of $Co(acac)_2$ on the autoxidation of styrene. The Russian workers, however, reported an activation energy of 7.8 kcal mol^{-1}, ~3 kcal mol^{-1} larger than our value.

Rate constants for reaction of 2-cyano-2-propylperoxy and poly(peroxystyryl)peroxy radicals with $Co(acac)_2$ have been reported to be 2.3×10^4 M^{-1} s^{-1} and 3.5×10^4 M^{-1} s^{-1}, respectively at 74°C (8). Our Arrhenius equation predicts a value significantly larger and our rate constants are in better agreement with rate constants that have been obtained by the chemiluminescence technique (9, 10).

[3] $Co(acac)_2$ at these concentrations in nonpolar solvents is monomeric (22).

TABLE 1. Kinetic data for reaction of *t*-BuO_2· with $Co(acac)_2$[a]

Temperature (K)	10^4[$Co(acac)_2$] (M)	k_ψ (s^{-1})	10^{-3} nk (M^{-1} s^{-1})
213	2.3	2.46	10.7
203	3.03	1.85	6.1
203	4.54	2.65	5.85
203	4.62	2.7	5.8
193	7.57	2.07	2.74
193	9.1	2.2	2.44
183	4.54	0.8	1.75
183	4.62	0.65	1.4
183	7.57	1.25	1.65
183	7.57	1.45	1.9

[a] In toluene.

Stoichiometric Factor

The simplest mechanism for destruction of alkylperoxy radicals by $Co(acac)_2$ involves the electron transfer reaction

$$RO_2\cdot + Co(II) \rightarrow RO_2^-Co(III)$$

and a stoichiometric factor of 1.

We could not estimate this parameter by the induction period method because the concentration of *tert*-butylperoxy increased in a pulsating manner during continuous photolysis and did not reach the uninhibited rate of radical production. On the other hand this technique works very well for 2,6-di-*tert*-butyl-4-methylphenol and gave a stoichiometric factor of 2 for this compound. The difference in the [*t*-BuO_2·]–time profiles for these two inhibitors is illustrated in Fig. 1.

Typical data obtained by the titration method are given in Table 2 and suggest that the stoichiometric factor is ~0.1 which is similar to the value of 0.26 reported by Shcheredin and Denisov (8).

Reaction Products

The organic product yields from reaction of cumylperoxy, cumyloxy, and cumyl hydroperoxide with $Co(acac)_2$ at 323 K are summarized in Table 3. Acetophenone (K) and α-cumyl alcohol (A) were the major organic reaction products and the total yield of these products, [A] + [K], was ~70% from cumylperoxy, ~90% from cumyloxy, and ~100% from cumyl hydroperoxide. Clearly the reaction products $PhCMe_2OOCo(acac)_2$ and $PhCMe_2OCo(acac)_2$ are not stable under our ex-

TABLE 2. Titration of t-$BuO_2\cdot$ with $Co(acac)_2$ at 183 K

$10^5[t\text{-}BuO_2\cdot]_0$ (M)	$10^5[Co(acac)_2]_0$ (M)	$10^5[t\text{-}BuO_2\cdot]_f$ (M)	$10^5\Delta[t\text{-}BuO_2\cdot]^a$ (M)	n
0.446	2.31	0.285	0.16	0.07
0.367	2.04	0.064	0.30	0.15
0.39	2.16	0.087	0.30	0.14
0.47	2.0	0.26	0.2	0.1
0.41	2.1	0.21	0.2	0.1
0.39	2.2	0.21	0.2	0.1
0.43	0.21	0.41	0.02	0.1

[a]Concentration of t-$BuO_2\cdot$ destroyed by the concentration of $Co(acac)_2$ given in column 2.

TABLE 3. Organic products from reaction of cumylperoxy, cumyloxy, and cumene hydroperoxide with $Co(acac)_2$ at 323 K

Radical/hydroperoxide (M)[a]	$[Co(acac)_2]_0$ (M)	Product	
		Acetophenone (M)	α-Cumyl alcohol (M)
$PhCMe_2O_2\cdot$ (0.044)[b]	0.049	0.013	0.017
$PhCMe_2O_2\cdot$ (0.022)[b]	0.049	0.003	0.012
$PhCMe_2O_2\cdot$ (0.043)[c]	0.049	0.009	0.02
$PhCMe_2O\cdot$ (0.040)[b]	0.0465	0.002	0.0033
$PhCMe_2OOH$ (0.009)[b]	0.0042	0.003	0.006
$PhCMe_2OOH$ (0.1)[b]	0.0001	0.028	0.07

[a]Calculated from $2e[In_2]$ where $e = 0.9$ and is the efficiency of radical production from the initiator In_2.
[b]In chlorobenzene.
[c]In *tert*-butylbenzene.

FOR ERRATA SEE 1982...P.812

ERRATA

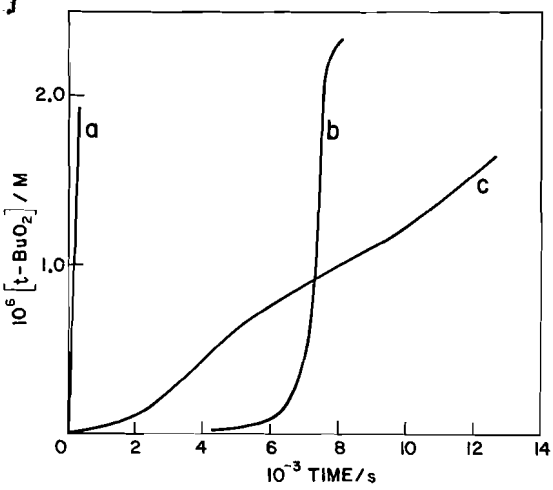


FIG. 1. The accumulation of t-$BuO_2\cdot$ with respect to time during photolysis of oxygen-saturated toluene containing di-*t*-butyl ketone at 303 K: (*a*) no additive; (*b*) 2,6-di-*tert*-butyl-4-methylphenol (2.4×10^{-5} M); (*c*) $Co(acac)_2$ (2.4×10^{-5} M).

perimental conditions. Interestingly pumping the chlorobenzene from decomposition of cumyl hyponitrite in the presence of $Co(acac)_2$ into a trap at the temperature of liquid nitrogen gave an initial yield of [A] + [K] ~ 70%. Addition of fresh chlorobenzene followed by distillation gave more A (~20%) but no K.

Cumylperoxy radicals reacted with an equivalent concentration of $Co(acac)_2$ in PhCl to give [A]/[K] = 1.3 whereas in the absence of the complex [A]/[K] was 0.6. This ratio increased to 4 when $[Co(acac)_2]_0$ was twice the initial concentration of azocumene. A higher value of [A]/[K] (2.2) was also observed when *tert*-butylbenzene was used as solvent instead of chlorobenzene.

Cumyloxy radicals in the presence of an equivalent concentration of $Co(acac)_2$ gave principally α-cumyl alcohol ([A]/[K] = 16.5) a result which is consistent with the recent finding by Niki, Kudo, and Kamiya (23) that a fraction of the *tert*-butoxy radicals from di-*tert*-butyl peroxyoxalate are reduced mainly to *tert*-butyl alcohol by $Co(acac)_2$. These workers concluded that the balance of t-$BuO\cdot$ were tied up as t-$BuOCo(acac)_2$.

Decomposition of cumyl hydroperoxide by catalytic and stoichiometric concentrations of $Co(acac)_2$ gives [A]/[K] = 2–2.5, ratios similar to ratios obtained from cumylperoxy rather than cumyloxy radicals.

We have not made a thorough investigation of the fate of $Co(acac)_2$ in its reactions with $PhCMe_2O_2\cdot$ and $PhCMe_2O\cdot$. Quantitative concentrations of $Co(acac)_3$ would, however, appear to be formed in these systems, i.e.,

$$3Co(acac)_2 \rightarrow 2Co(acac)_3$$

Complexed Peroxy Radicals

Tkáč and co-workers (12–14) have reported that reaction of an alkyl hydroperoxide with $Co(acac)_2$

Can. J. Chem. Downloaded from www.nrcresearchpress.com by 210.87.254.6 on 09/05/12
For personal use only.

Can. J. Chem. Downloaded from www.nrcresearchpress.com by 210.87.254.6 on 09/05/12
For personal use only.

gives a paramagnetic complex-bonded peroxy radical, $Co^{III}(acac)_2 \cdots RO_2^{\bullet}$, in which the radical is rendered persistent at ambient temperatures by co-ordination with cobalt(III).

Such a species should have been formed by reaction of t-$BuO_2^{\bullet}$ with $Co(acac)_2$ because co-ordinatively unsaturated Co(III) is formed which would be expected to complex with another t-$BuO_2^{\bullet}$ in the system. We could, however, find no experimental evidence for the formation of such a "complexed" radical.

In addition we have not been able to prepare $Co^{III}(acac)_2 \cdots RO_2^{\bullet}$ using *tert*-butyl hydroperoxide and $Co(acac)_2$ as described by Tkáč (13). A possible explanation for the apparent inconsistency in this work is that Tkáč isolated t-$BuOOCo(acac)_2$ which in solution could give t-BuOOH and $HOCo(acac)_2$ by reaction with adventitious water. Reaction of t-BuOOH with cobalt would then appear to give "persistent" t-$BuO_2^{\bullet}$ by the continuous generation method described by Ingold (24).

Conclusions

tert-Butylperoxy radicals react rapidly with $Co(acac)_2$ and the bimolecular rate constants obey the Arrhenius equation

$$\log (nk/M^{-1}\,s^{-1}) = (8.9 + 0.7) - (4.7 + 1.5)/\theta$$

This equation almost certainly applies to other alkylperoxy radicals since the rate of such a fast reaction should not depend on the nature of R in $RO_2^{\bullet}$.

The reaction of $RO_2^{\bullet}$ with $Co(acac)_2$ probably involves coordination of the radical with the complex followed by electron transfer to give $ROOCo(acac)_2$. Alkylperoxo cobalt(III) complexes have in fact been isolated after reaction of 4-alkyl-2,6-di-*tert*-butylphenols with molecular oxygen in the presence of bis(3-salicylideneaminopropyl) amino cobalt(II) in aprotic solvents (25, 26).

Hydrolysis of $ROOCo(acac)_2$ by adventitious water would give ROOH and $HOCo(acac)_2$ and the hydroperoxide would be rapidly reduced by $Co(acac)_2$. Such a mechanism is consistent with the similarity between the products obtained from reactions of $PhCMe_2O_2^{\bullet}$ and $PhCMe_2OOH$ with $Co(acac)_2$ and the low stoichiometric factors.

[3] $RO_2^{\bullet} + Co(acac)_2 \rightleftarrows RO_2^{\bullet} \cdots Co(acac)_2 \rightarrow RO_2Co(acac)_2$

[4] $ROOCo(acac)_2 + H_2O \rightarrow ROOH + HOCo(acac)_2$

[5] $ROOH + Co(acac)_2 \rightarrow RO^{\bullet} + HOCo(acac)_2$

[6] $RO^{\bullet} + Co(acac)_2 \rightarrow ROCo(acac)_2$

Alternatively, in the absence of water, $ROOCo(acac)_2$ could react with $Co(acac)_2$ (8) by an electron transfer process, a mechanism which is also consistent with the reaction products and stoichiometry.

[7] $ROOCo(acac)_2 + Co(acac)_2 \rightarrow [R\bar{O}OCo(acac)_2 + C\dot{o}(acac)_2] \rightarrow RO^{\bullet} + (acac)_2CoOCo(acac)_2$

We cannot, of course, rule out the possibility that the alkylperoxo cobaltic acetylacetonate undergoes O—O bond homolysis,

[8] $ROOCo(acac)_2 \rightarrow RO^{\bullet} + {}^{\bullet}OCo(acac)_2$

The marked difference between [A]/[K] for reaction of $PhCMe_2O_2^{\bullet}$ and $PhCMe_2O^{\bullet}$ with $Co(acac)_2$ would, however, appear to rule out the intermediacy of free alkoxy radicals.

Further work is in progress in our laboratory to determine the influence of the ligands attached to Co(II) on this chain terminating reaction.

1. W. A. Waters. Discuss. Faraday Soc. **46**, 158 (1968).
2. C. Walling. J. Am. Chem. Soc. **91**, 7590 (1969).
3. W. A. Waters. J. Am. Oil Chem. Soc. **48**, 427 (1971).
4. R. A. Sheldon and J. K. Kochi. Oxid. Combust. Rev. **5**, 135 (1973).
5. R. A. Sheldon and J. K. Kochi. Adv. Catal. **25**, 272 (1976).
6. J. F. Black. J. Am. Chem. Soc. **100**, 527 (1978).
7. A. T. Betts and N. Uri. Adv. Chem. **76**, 160 (1968).
8. V. P. Shcheredin and E. T. Denisov. Izv. Akad. Nauk Ser. Khim. 1428 (1967).
9. E. M. Tochina, L. M. Postnikov, and V. Yu. Shlyapintokh. Izv. Akad. Nauk Ser. Khim. 71 (1968).
10. A. L. Aleksandrov, G. I. Solov'ev, and E. T. Denisov. Izv. Akad. Nauk Ser. Khim. 1527 (1972).
11. R. W. Brandon and C. S. Elliot. Tetrahedron Lett. 4375 (1967).
12. A. Tkáč, K. Vesely, and L. Omelka. J. Phys. Chem. **75**, 2575 (1971); **75**, 2580 (1971).
13. A. Tkáč, K. Vesely, L. Omelka, and R. Prikryl. Collect. Czech. Chem. Commun. **40**, 117 (1975).
14. A. Tkáč. Degradation and stabilization of polyolefins. Polymer Symposia, **57**, 121 (1976).
15. J. A. Howard and E. Furimsky. Can. J. Chem. **51**, 3738 (1973).
16. J. H. B. Chenier, E. Furimsky, and J. A. Howard. Can. J. Chem. **52**, 3682 (1974).
17. E. Furimsky and J. A. Howard. J. Am. Chem. Soc. **95**, 369 (1973).
18. J. H. B. Chenier and J. A. Howard. Can. J. Chem. **53**, 623 (1975).
19. E. Furimsky and J. A. Howard. J. Organomet. Chem. **46**, C45 (1972).
20. S. F. Nelsen and P. D. Bartlett. J. Am. Chem. Soc. **88**, 137 (1966).
21. H. Kiefer and T. G. Traylor. Tetrahedron Lett. 6163 (1966).
22. F. A. Cotton and R. H. Soderberg. Inorg. Chem. **3**, 1 (1964).
23. E. Niki, M. Kudo, and Y. Kamiya. Oxid. Commun. **1**, 33 (1979).
24. K. U. Ingold. J. Phys. Chem. **76**, 1385 (1972).
25. A. Nishinaga, H. Tomita, and T. Matsuura. Tetrahedron Lett. 2893 (1979).
26. A. Nishinaga, H. Tomita, and T. Matsuura. Tetrahedron Lett. 1261 (1980).

A convection-free electrolysis cell in which a steady state is attainable

M. ALISON ARMITAGE, GERALD A. BRYDON,[1] PAUL J. J. CONNELLY,[2] CHUMMER J. E. FARINA, HEATHER L. GORDON, KEITH B. OLDHAM, AND TADASHI YANAGI[3]

Department of Chemistry, Trent University, Peterborough, Ont., Canada K9J 7B8

Received March 24, 1980

M. ALISON ARMITAGE, GERALD A. BRYDON, PAUL J. J. CONNELLY, CHUMMER J. E. FARINA, HEATHER L. GORDON, KEITH B. OLDHAM, and TADASHI YANAGI. Can. J. Chem. **58**, 1966 (1980).

Studies of a cell consisting of a sheet of a porous medium soaked with an aqueous electrolyte solution containing the mercurous ion and sandwiched between mercury pools show that steady-state electrolysis may be attained in the absence of convection. Several different porous matrices have been studied and, in some cases, a very simple model of the pore structure predicts behaviour close to that observed experimentally.

M. ALISON ARMITAGE, GERALD A. BRYDON, PAUL J. J. CONNELLY, CHUMMER J. E. FARINA, HEATHER L. GORDON, KEITH B. OLDHAM et TADASHI YANAGI. Can. J. Chem. **58**, 1966 (1980).

L'étude d'une cellule, consistant en une lame de substance poreuse imprégnée d'une solution aqueuse d'un électrolyte contenant un ion mercureux et plaçée entre deux bains de mercure, indique que l'électrolyse dans l'état stationnaire peut être réalisée en l'absence de convection. On a étudié plusieurs matrices poreuses différentes et dans certains cas un modèle très simple de la structure des pores prédit un comportement qui se rapproche de celui observé expérimentalement.

[Traduit par le journal]

Can. J. Chem. Downloaded from www.nrcresearchpress.com by 210.87.254.42 on 09/05/12
For personal use only.

At working electrodes to which transport occurs by planar semiinfinite diffusion, steady-state electrolysis is not theoretically possible in the absence of convection. Under such conditions at spherical electrodes, steady-state electrolysis is achieved (1) but only at times long in comparison with r^2/D where r is the radius of the spherical electrode and D is the diffusion coefficient of the electroactive species. With a finite electrolysis cell, in which parallel planar electrodes are separated by a distance L, the attainment of a convection-free steady state is again theoretically possible (provided that the anode reaction is the converse of that at the cathode), but its realization requires the passage of times large in comparison with L^2/D. Special fabrication techniques are needed to achieve values of r or L less than about 10^{-4} m, and since D in aqueous solutions is typically 10^{-9} m^2 s^{-1}, one must wait for at least 1 min to achieve such steady states. In most circumstances, however, 1 min is ample time for natural convection to develop as a result of density gradients generated by the electrolysis itself. Accordingly, almost all non-equilibrium electrochemical experiments can be classified into one of two categories: either non-steady-state (i.e. transient) techniques in which convection is absent, or steady-state techniques in which convection (natural or artificial) is present. It is disappointing that steady-state convection-free conditions are difficult to achieve, because steady-state results are easier to interpret than transient results and convection is notoriously difficult to treat quantitatively.

The forces that give rise to natural convection must operate over rather large distances to be effective. Consequently, convection in an electrolysis cell can be inhibited by compartmentalizing the electrolyte solution into small intercommunicating chambers, as occurs when the electrolyte solution is absorbed into a porous matrix. This is the principle that is exploited in the cell that is the subject of this article. It consists of a sheet of porous material soaked in electrolyte solution and then sandwiched between mercury electrodes. In its performance this cell displays no effect that can be attributed to convection. In addition to preventing convection, the porous sheet serves the function of accurately positioning the two electrodes parallel to each other with an interelectrode spacing L equal to the sheet's thickness. No third electrode is present in the cell, both mercury pools being "working" electrodes.

When the cell solution contains a concentration C of mercurous ion and any potential E in the range from zero to about 1.5 V is applied across the cell, the negative electrode functions as a cathode at which the reaction

[1] $Hg_2^{2+} + 2e \rightarrow 2Hg$

occurs, while at the other electrode the complementary anodic reaction

[2] $2Hg \rightarrow Hg_2^{2+} + 2e$

takes place. Alternatively, if the cell solution initially contains a concentration $2C/n$ of the ion M^{n+}

[1]Present address: Department of Chemistry, Dawson College, Westmount, P.Q., Canada H3Z 1W7.

[2]Present address: School of Medicine, University of Toronto, Toronto, Ont., Canada.

[3]Present address: Department of Nuclear Engineering, University of Osaka, Osaka, Japan.

0008-4042/80/181966-07$01.00/0

©1980 National Research Council of Canada/Conseil national de recherches du Canada

Can. J. Chem. Downloaded from www.nrcresearchpress.com by 210.87.254.42 on 09/05/12
For personal use only.

(such as Pb^{2+} or Tl^{+}), then no current flows through the polarized cell unless E is large enough to effect the electroreduction

[3] $M^{n+} + ne \rightarrow M(Hg)$

at the negative electrode. The anode reaction is again described by eq. [2], so that M^{n+} is continuously replaced by Hg_2^{2+}. In these circumstances, by the time that the steady state is reached, the cell functions exactly as if it had originally contained a concentration C of mercurous ions. Other electroreducible species, such as oxygen, are likewise replaced by equivalent concentrations of mercurous ion prior to the attainment of a steady state, the overall cell reaction being

[4] $O_2 + 4H^+ + 4Hg \rightarrow 2H_2O + 2Hg_2^{2+}$

in the case of dissolved oxygen.

Supporting electrolyte has been present in all our experiments. A low pH is generally necessary to inhibit the formation of insoluble mercuric species, especially at the anode. In a few of our experiments the electrolyte solution was neutral but contained a large concentration of iodide ion; the steady-state anodic and cathodic reactions were then

[5] $Hg + 4I^- \rightleftarrows HgI_4^{2-} + 2e$

because HgI_4^{2-} is the thermodynamically stable species under these conditions. These latter experiments (and others in which I^- plus I_3^- served as the redox pair) will not be reported here.

The complexity and heterogeneity of the pore geometry impedes an exact treatment of electrochemical transport in our cell. Instead, one must resort to models. A simple, but surprisingly successful, model envisages the pore structure as a bundle of non-intersecting tubules, all of length λL, which penetrate the porous matrix from one surface to the other. This so-called "uniform tortuosity model" predicts that the steady-state current is given by

[6] $$I_\infty = \frac{2nAFCD\theta}{\lambda^2 L} \tanh \frac{nFE}{2RT}$$

when supporting electrolyte is in excess (2). In this equation n equals 2, A is the area of each of the electrodes, θ is the porosity of the matrix (the fraction of its volume that is void, an independently measurable quantity), λ is its tortuosity and other symbols have either been defined earlier or are accorded their usual significances. Alternative models (2, 3) lead to different predictions but all models that treat the matrix as uniform (in the sense that there is no systematic variation in its structure on proceeding from one internal subregion of the matrix to another) lead to the conclusion that the quantity

[7] $$\frac{LI_\infty}{2nAFCD} \coth \frac{nFE}{2RT}$$

is a constant less than unity. In an experiment in which no porous matrix whatever was present (not an experimentally realizable situation, of course), expression [7] would be unity; the fractional value of this quantity thus represents the extent to which an actual matrix impedes the steady-state diffusion of mercurous ion from anode to cathode. Different models interpret this dimensionless quantity differently, but all predict its constancy. The experimental work of Topol and Oldham (4) demonstrated the constancy of expression [7], for a given matrix, and our own data have confirmed this.

In most of our studies (and all those reported in detail here) the solution soaking the porous matrix contained mercurous ion plus excess supporting electrolyte and the experiment was commenced by applying the potential step 0.0 V $\rightarrow E$ across the previously short-circuited cell. Because reactions [1] and [2] are fast and the cell resistance is very small, the initial current is immeasurably large. However, I falls rapidly and after several seconds approaches its steady-state value I_∞, as exemplified in Fig. 2. The transient phase of the experiment may be treated theoretically if one adopts the uniform tortuosity model. The prediction is that

[8a] $$\frac{\lambda I}{nAFC\theta} \coth \frac{nFE}{2RT} = \left(\frac{D}{\pi t}\right)^{1/2} \sum_{j=-\infty}^{\infty} \exp \frac{-j^2\lambda^2 L^2}{4Dt}$$

[8b] $$= \frac{2D}{\lambda L} \sum_{j=-\infty}^{\infty} \exp \frac{-4j^2\pi^2 Dt}{\lambda^2 L^2}$$

these two expressions being mathematically equivalent (2). At short times only the $j = 0$ term in [8a] is significant and reduction to

[9] $$(I\sqrt{t})_{t\rightarrow 0} = \frac{nAFC\theta}{\lambda} \sqrt{\frac{D}{\pi}} \tanh \frac{nFE}{2RT}$$

Can. J. Chem. Downloaded from www.nrcresearchpress.com by 210.87.254.42 on 09/05/12
For personal use only.

ensues. $I\sqrt{t}$ is predicted to be almost constant over the time range $0 < t < 2t_2$ where t_2 is the time it takes for the current I to fall to twice its ultimate I_∞ value. Over a somewhat larger time range, in fact for $0 < t < 8t_2$ approximately, the $j = 0, \pm 1$ terms in [8*a*] are important but those with $|j| > 1$ can be ignored. Under these circumstances one can show that a plot of the logarithm of $2(I\sqrt{t})_0/[I\sqrt{t} - (I\sqrt{t})_0]$ versus $1/t$ should yield a straight line passing through the origin and that the gradient of this line

$$[10] \quad \frac{d}{d(1/t)} \ln \frac{2(I\sqrt{t})_0}{I\sqrt{t} - (I\sqrt{t})_0}$$

is a constant equal to $\lambda^2 L^2/4D$. At longer times [8*b*] is a more useful expression and there exists a wide time range over which only the $j = 0, \pm 1$ terms in this equation are important. During this period (approximately $2t_2 < t < \infty$) the logarithm of $2I_\infty/[I - I_\infty]$ should give a linear plot versus t, extrapolating through the origin and having a gradient

$$[11] \quad \frac{d}{dt} \ln \frac{2I_\infty}{I - I_\infty}$$

equal to $4\pi^2 D/\lambda^2 L^2$. Of course, as $t \to \infty$, eq. [8*b*] shows that I approaches the constant I_∞ given by eq. [6].

The interpretation of the transient phase of an experiment is very model-dependent, though few models more complex than the uniform tortuosity model are capable of explicit solution. However, one conclusion, namely that the quantity

$$[12] \quad \frac{(I\sqrt{t})_{t\to 0}}{nAFC} \sqrt{\frac{\pi}{D}} \coth \frac{nFE}{2RT}$$

is a constant less than unity, is common to all models that treat the matrix as uniform. This dimensionless constant is predicted to equal the fraction of the cathode area that is exposed to the electrolyte solution (3).

In our laboratory several studies have been, or are being, conducted using the convection-free cell. The purpose of the present article is to describe the perfecting of the experimental technique, and to report on the testing of the uniform tortuosity model by the analysis of steady-state and transient results.

Experimental

A typical solution used to soak the porous matrix in these studies had the composition 5.00 m*M* $Hg_2(NO_3)_2$ + 50 m*M* HNO_3 + 2.0 *M* KNO_3 and was prepared by direct weighing of the ingredients and their dissolution in deionized water. The Hg_2^{2+} ion concentration was confirmed by titration with a standard ferric ion solution (5). Stock solutions were deaerated by the passage of argon and were stored under argon and over mercury.

All the experiments reported in this article employed one or other of the following porous media: (*i*) A felted glass fibre matrix known as "GF-81" and marketed (by W. & R. Balston Limited, London, England) for filtration and chromatographic support purposes. This material was purchased as large sheets and was trimmed to circles of about 60 mm diameter before use. (*ii*) Another porous medium sold primarily for filtration purposes is the "MF-Millipore" (Millipore Corporation, Bedford, MA) manufactured from mixed esters of cellulose. In the particular form used in this research, however, the membranes (manufacturer's code THWP102F0) are marketed for surgical use in nerve and tissue repair. This MF material was obtained as sterile 10 cm × 10 cm squares of nominal 25 μm thickness and 0.45 μm pore size. The squares were quartered for use in electrochemical and other measurements. (*iii*) "Whatman No. 5" filter paper (also manufactured by W & R Balston). Circles of 70 mm diameter (0.19 mg ash per circle) were invariably used. These three porous media, which we shall refer to as "glass", "esters", and "cellulose" matrices, were selected for study because they are manufactured with closely-controlled physical properties and because they span a range of porosities and thicknesses, as shown in Table 1. Before use, all matrices were thoroughly rinsed in deionized water and allowed to air-dry (as purchased, the filter paper was significantly contaminated by chloride ion).

Thicknesses were measured by placing the matrix, soaked with the solution to be used electrochemically, between optically flat glass plates mounted on a specially-constructed micrometer. This device is designed to exert on the matrix a pressure (usually 10.8 kPa) equal to that it would experience in the electrochemical cell. Double layers of a matrix were employed to investigate the dependence upon thickness.

Knowing the external dimensions of a matrix, the porosity was determined by comparing its dry weight with the apparent mass when the matrix is suspended in the electrolyte solution (of known density). These data also permit a determination of ρ, the density of the fibres from which the matrix is constructed. Values of ρ, which are also listed in Table 1, were calculated as a means of checking the validity of the porosity measurements.

The soaking of a matrix in electrolyte solution – whether for a thickness measurement, a porosity measurement, or an electrochemical experiment – was carried out very carefully so as to exclude the possibility of air pockets being trapped in the pores. The dry matrix was positioned above a pool of electrolyte solution in a vessel from which the air was then evacuated. After 10 min the matrix was dislodged and caused to fall into the pool. Atmospheric pressure was restored after the matrix had lain beneath the surface of the solution for several minutes. Prior to transfer to the electrochemical cell, each face of the matrix was wiped with a glass rod to dislodge excess liquid.

Figure 1 is a cross-sectional diagram of the electrochemical cell, which consists of three polymethylmethacrylate parts. The soaked matrix is firmly clamped between raised annular rings on the inward-facing faces of the left and right sections of the cell. An outer sleeve serves to locate the two cell sections opposite each other. The matrix is thus exposed to three chambers; a left

TABLE 1. Physical properties of the three matrices. Values represent averages of many independent measurements, together with standard deviations

Matrix	L/μm	θ	ρ/g cm^{-3}
Glass	358 ± 16	0.927 ± 0.005	2.13 ± 0.11
Esters	22.3 ± 0.5	0.648 ± 0.010	1.56 ± 0.04
Cellulose	272 ± 14	0.748 ± 0.008	1.50 ± 0.03

Can. J. Chem. Downloaded from www.nrcresearchpress.com by 210.87.254.42 on 09/05/12
For personal use only.

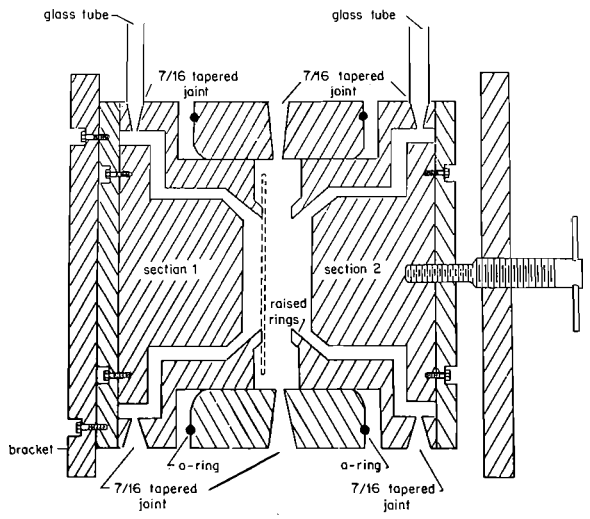


FIG. 1. A cross-sectional diagram of the cell. In operation sections 1 and 2 are firmly forced together, clamping the porous matrix (shown by dashed lines) between the raised rings. The matrix is thus exposed to three chambers.

chamber and a right chamber, each of which meets the matrix in an area

[13] $A = 1134\ \text{mm}^2$

which is accurately defined by the 38.0 mm inner diameter of the raised rings; and a peripheral chamber which surrounds all the surfaces of the matrix beyond the 46.0 mm outer diameter of the raised rings.

Two ports communicate with each chamber, one with its lowest point, the other with its highest point, so that fluids can be introduced. Glass sighting tubes fit into the three upper ports. After introducing a soaked matrix into the cell, argon is passed through the three chambers to remove the air that entered during assembly. Then the two lower ports serving the left and right chambers are commoned and carefully-purified mercury is admitted. The mercury level is allowed to rise slowly and evenly until both chambers are entirely filled and the menisci have reached predetermined levels in the sighting tubes.

In early experiments the peripheral chamber was filled with the same solution in which the matrix had been soaked. However, after results showed that this had no effect, the peripheral chamber was more often left empty. In some experiments that we discuss later, anomalous results could be attributed to the cellulose matrix being "too wet". The problem was corrected by passing dry argon through the peripheral chamber for a sufficient time; water evaporated into the argon and the excess solution was thereby wicked away from the electrochemical cell.

To perform an electrochemical experiment the interconnection between the two mercury pools is broken and a constant potential E is applied between the pools. More often than not E was in the range 100–150 mV, for which values the hyperbolic term in expresssions [7] and [12] is effectively unity. However, experiments employing potentials less than this gave results that, after correction by multiplication by the hyperbolic cotangent term, were indistinguishable from those which engendered complete concentration polarization. The electrical potential step was applied using a Model 170 Electrochemical System (Princeton Applied Research Corporation, Princeton, New Jersey), and the XY recorder which is an integral part of the instrument was used to monitor the current–time response.

The cell was not thermostatted. Experiments were conducted at an ambient temperature close to 294 K.

Results and Discussion

Figure 2 is a typical current–time trace. As predicted, the current does approach a constant steady-state value I_∞ at long times. Figure 3 is a typical plot of $I\sqrt{t}$ versus t. The $I\sqrt{t}$ product is predicted to be a constant at small times but this is not exactly what is observed. Instead we found $I\sqrt{t}$ to be almost constant over a range of short times, but with a small rise as $t \rightarrow 0$. This is precisely what would occur if the pores, on average, experience a slight flaring as they reach the cathode surface, as one might well expect to be the case. As illustrated in Fig. 3, we choose to associate $(I\sqrt{t})_0$ with the minimum value of $I\sqrt{t}$, acquired over a range of times close to t_2.

The results of numerous experiments employing a variety of L, C, and E values are assembled into Table 2 which reports, for each of the three matrices, average values of the dimensionless expressions [7] and [12] along with the corresponding standard deviations. Expression [13] for A together with the value

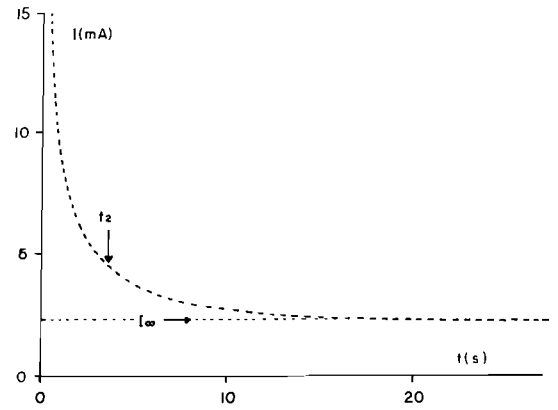


FIG. 2. A typical current versus time graph. t_2 is the time after which the current has fallen to a value twice that of the ultimate steady-state current I_∞.

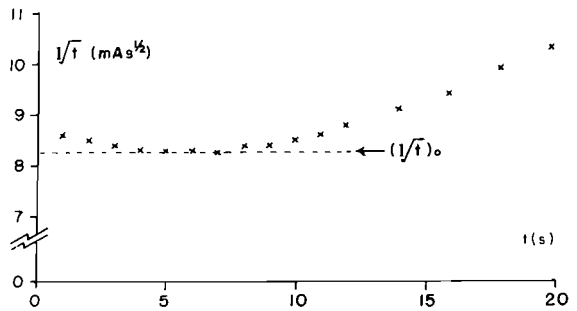


FIG. 3. A constant value of $I\sqrt{t}$ is predicted at short times. As this typical graph shows, experimental values pass through a shallow minimum.

TABLE 2. Values of dimensionless expressions that all models predict should be constant and less than unity

Matrix	Expression [7]	Expression [12]
Glass	0.797 ± 0.032	0.944 ± 0.033
Esters	0.480 ± 0.065	0.691 ± 0.080
Cellulose without drying	0.277 ± 0.020	0.421 ± 0.017
Cellulose after drying	0.341 ± 0.026	0.452 ± 0.045

[14] $D = 946\ \mu m^2\ s^{-1}$

(6) were used in compiling the tabulated data.

The constancy of expressions [7] and [12] is predicted by all models whereas, it will be recalled, the linearity of the graphs exemplified by Figs. 4 and 5 is predicted only by the uniform tortuosity model. These figures, which are typical, show that the plots are indeed linear over the time ranges predicted by the model. The gradients of many such graphs were measured and Table 3 is a compilation of such data. Notice that the glass and cellulose matrices generate graphs of comparable slopes, but that the slopes of the graphs produced by the esters matrix differ by two orders of magnitude, largely because this matrix is much thinner than the other two.

In some experiments with the cellulose matrix, when the applied potential was in the range 50–100 mV, erratic currents were obtained. The potential range in which these anomalies were found corresponds to that in which polarographic maxima are common and we believe the two phenomena have related causes. Large electroosmotic forces must operate in our cell, and it appears that their sign is such as to push the solution towards the cathode. Normally these forces do not result in any movement of the electrolyte solution because mercury from the anode cannot enter the pores to replace the migrating solution. However, with the cellulose matrix, it appears that the standard soaking and wiping procedure leaves sufficient solution adhering to the surface of the matrix that small pockets, sustained by electroosmosis, can develop between the mercury cathode and the matrix itself. Motion within these pockets is, we believe, responsible for the anomalous currents. As mentioned, we found that the anomalies disappear after dry argon is passed for a sufficient length of time through the peripheral chamber. If the drying is continued for too long, a precipitous fall in current ensues; a "sufficient" length of time is one that just fails to cause this condition.

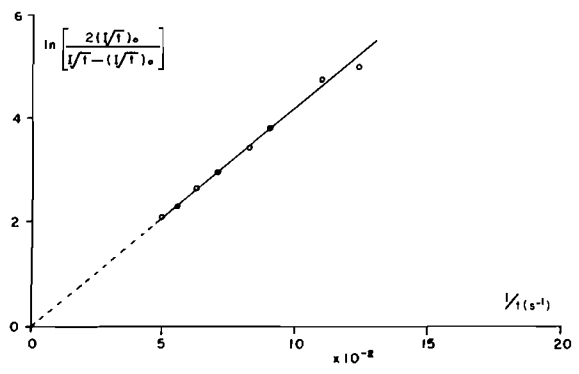


FIG. 4. The uniform tortuosity model predicts that the graph of which a typical example is shown should be linear at short times and should extrapolate through the origin.

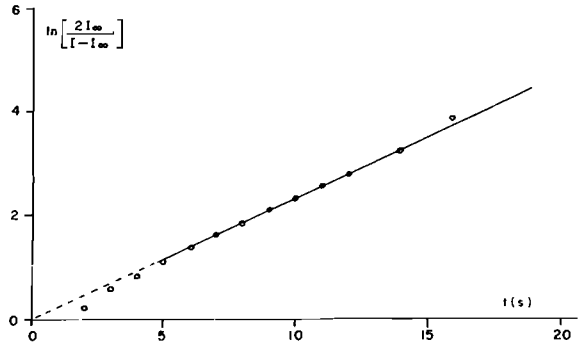


FIG. 5. According to the uniform tortuosity model the plot exemplified in this figure should be linear, except at short times, and should extrapolate through the origin.

For the three matrices that we report in this article, one sample is very like the next, but nevertheless there is more scatter in our results than one would find in a typical series of electrochemical experiments that did not employ porous media. Taking this into account, the data in Table 2 can be considered to display adequate constancy, implying that the model-independent aspects of the theory of cell operation are satisfactory. Note that the value of expression [12] is in each case about 30% larger than the value of expression [7]. In the absence of a model, no particular structural significance can be attached to the numerical values of the constants in Table 2, except that one might expect some correlation with the porosities of the matrices. This expectation is not borne out, however, because the sequence of porosities

[15] glass > cellulose > esters

does not match the sequence of magnitudes of expression [7] and [12], namely

[16] glass > esters > cellulose

One might conclude that the cellulose matrix impedes the progress of Hg_2^{2+} ions, and restricts their

Can. J. Chem. Downloaded from www.nrcresearchpress.com by 210.87.254.42 on 09/05/12
For personal use only.

TABLE 3. Values of the gradients given by expressions [10] and [11], and of the product of these gradients, for each matrix. The uniform tortuosity model predicts that the product should be π^2 (= 9.87)

Matrix	Expression [10]/s	Expression [11]/s^{-1}	Product
Glass	38.5 ± 1.5	0.245 ± 0.009	9.44 ± 0.38
Esters	0.321 ± 0.012	32.7 ± 2.6	10.51 ± 0.81
Cellulose without drying	42.1 ± 2.2	0.230 ± 0.012	9.77 ± 0.84
Cellulose after drying	32.2 ± 1.3	0.274 ± 0.013	8.83 ± 0.67

TABLE 4. Values of the tortuosity λ calculated by various methods according to the uniform tortuosity model. [7], [12], [10] and [11] refer to the quantities denoted by those expressions

Matrix	$\sqrt{\frac{\theta}{[7]}}$	$\frac{\theta}{[12]}$	$\frac{\sqrt{4D[10]}}{L}$	$\frac{2\pi}{L}\sqrt{\frac{D}{[11]}}$
Glass	1.08 ± 0.03	0.98 ± 0.03	1.07 ± 0.06	1.09 ± 0.06
Esters	1.16 ± 0.11	0.94 ± 0.11	1.56 ± 0.05	1.52 ± 0.09
Cellulose without drying	1.64 ± 0.08	1.78 ± 0.07	1.47 ± 0.09	1.48 ± 0.09
Cellulose after drying	1.48 ± 0.08	1.65 ± 0.17	1.28 ± 0.07	1.36 ± 0.08

access to the cathode, more than would be expected on the basis of the porosity of this matrix.

Let us now turn to the question of how well the predictions of the uniform tortuosity model are borne out by experiment. Recall that the model predicts that expressions [10] and [11] will equal $\lambda^2L^2/4D$ and $4\pi^2D/\lambda^2L^2$ respectively. The product of these expressions should therefore be π^2. Table 3 incorporates a column which lists average values of the products of expressions [10] and [11], together with standard deviations. With one exception the products are, indeed, within about one standard deviation of π^2. Even the exception lies only 1.55 standard deviations from π^2 and such a departure would be expected once in eight cases if the model were true.

Another way of testing the uniform tortuosity model is by comparing the values of λ calculated by different methods. The tortuosity λ is, in fact, calculable by four independent methods according to the model: (*i*) The uniform tortuosity model predicts that expression [7] is a constant equal to θ/λ^2. Since θ is measurable independently, λ can be calculated. (*ii*) Similarly, expression [12] equals θ/λ according to the model, whereby λ is calculable. (*iii*) Since the model predicts that expression [10] equals $\lambda^2L^2/4D$ and L and D are known, λ can be calculated. (*iv*) Likewise expression [11] equals $4\pi^2D/\lambda^2L^2$ according to the model, whereby λ is calculable. Tortuosity values calculated in this variety of ways are assembled into Table 4. The tabulation shows that the λ values calculated by method (*ii*) are discordant, and that in two cases this method produces nonsensical values of less than unity. It comes as no surprise that method (*ii*) fails to agree with the others; this method utilizes the $(I\sqrt{t})_{t\to 0}$ datum which (see Fig. 3) is ill-defined in practice. If one excludes values given by method (*ii*), excellent agreement is found between the remaining three values for the glass and cellulose matrices, with less satisfactory concordance in the case of the esters matrix.

The linearity of the graphs exemplified in Figs. 4 and 5, together with the fact that the linear sections extrapolate naturally through the origin, is further indirect evidence in support of the uniform tortuosity model. To assess the extent to which these graphs accurately diagnose the uniformity of pore tortuosities, we simulated a matrix in which the pores were non-intersecting tubules but in which all tortuosities between 1.00 and 2.00 occur with equal frequency. Synthetic current–time data were then generated and subjected to the logarithmic analyses of methods (*iii*) and (*iv*). Figures 6 and 7 show the results. The full lines in these figures span the time ranges in which the uniform tortuosity model predicts linearity. Notice that the lines are decidedly curved. Moreover, notice that if each curve were to be approximated by a "best" straight line, this would not extrapolate through the origin. Evidently heterogeneity in pore tortuosities can be detected quite easily in attempting to employ methods (*iii*) and (*iv*).

The dashed lines in Figs. 6 and 7 are forced through the origin. Analysis of the gradients of these lines according to methods (*iii*) and (*iv*) leads

Can. J. Chem. Downloaded from www.nrcresearchpress.com by 210.87.254.42 on 09/05/12
For personal use only.

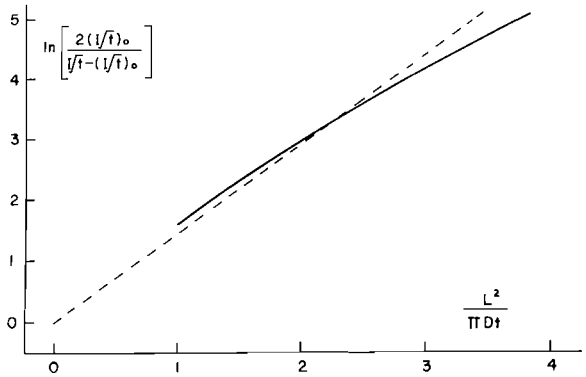


FIG. 6. The full curve is based on simulated data for a matrix in which tortuosities between 1.00 and 2.00 are equally probable. The dashed line has been forced through the origin.

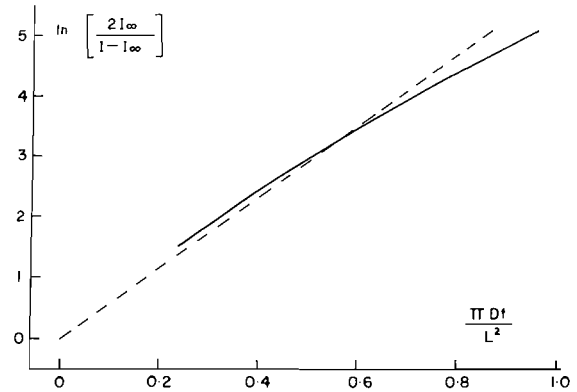


FIG. 7. The full and dashed lines have the same significance as those in Fig. 6.

to λ values of 1.38 and 1.48 respectively. From these gradients one can show that the product that the model predicts to be π^2 when tortuosities are uniform is only 8.21 when tortuosities range from 1.00 to 2.00. Evidently the π^2 test is quite discriminating.

Conclusions

The most significant result of the study reported here is the successful design and construction of an electrochemical cell in which steady-state electrolysis is established in the absence of convection. Experimental techniques have been perfected to a point at which reproducibility is better than 10% (see Table 2) between replicate experiments. The dependence of the steady-state current on thickness, concentration, and applied potential is as predicted by the model-independent theory.

The π^2 test of the uniform tortuosity model is surprisingly successful for all three matrices and has been shown to be discriminating. The intercomparison presented as Table 4 is less satisfactory but, for the glass and cellulose matrices, the agreement of three independent measurements of tortuosity is remarkably close. Moreover, the numerical tortuosity values that the model generates — 1.08 for the glass matrix and about 1.45 for the cellulose — are very reasonable values for matrices of 93% and 75% porosity respectively.

The success of the model does not, of course, imply that the pores of these media are actually non-intersecting tubules of common length. Rather it indicates that, under the imposed electrochemical conditions, the matrices facilitate the passage of a current of similar magnitude to that predicted by the simple model.

Acknowledgements

We are grateful for the financial support of the Defence Research Board of the Department of National Defence, the National Research Council of Canada, and the Natural Sciences and Engineering Research Council of Canada. The summertime participation of undergraduate students in this project was made possible by a generous grant from Canadian Industries Limited.

1. H. A. LAITINEN and I. M. KOLTHOFF. J. Am. Chem. Soc. **61**, 3344 (1939).
2. K. B. OLDHAM and L. E. TOPOL. J. Phys. Chem. **71**, 3007 (1967).
3. K. B. OLDHAM. Final Report on Extramural Grant DRB5480-32 to Defence Research Establishment Ottawa, National Defence Headquarters, Ottawa K1A 0Z4, August 1975.
4. L. E. TOPOL and K. B. OLDHAM. J. Phys. Chem. **73**, 1455 (1969).
5. A. I. VOGEL. Inorganic quantitative analysis. 3rd ed. Longmans, London. 1961. pp. 398–399.
6. B. R. CHAPMAN and K. B. OLDHAM. Unpublished results.

Can. J. Chem. Downloaded from www.nrcresearchpress.com by 210.87.254.42 on 09/05/12
For personal use only.

γ-Radiosensitized isomerization of gaseous butenes and methylbutenes

GUY J. COLLIN

Département des Sciences pures, Université du Québec à Chicoutimi, Chicoutimi (Qué.), Canada G7H 2B1

AND

JAN A. HERMAN

Centre de Recherches sur les Atomes et Molécules et Département de Chimie, Université Laval, Québec (Qué.), Canada G1K 7P4

Received October 22, 1979[1]

GUY J. COLLIN and JAN A. HERMAN. Can. J. Chem. **58**, 1973 (1980).

We have studied the isomerization of butenes and methylbutenes by noble gas-sensitized radiolysis. The isomerization of isobutene to but-2-ene is more efficient in the presence of xenon than in the presence of krypton or argon. The isomerization of but-1-ene into isobutene has a low radiolytic yield and occurs only in the presence of small quantities of dimethylamine. These observations are in agreement with the isomerization of the excited parent ion.

In the methylbutene systems, whatever the sensitizing agent, isomerization occurs with a high radiolytic yield. Thus, a chain mechanism is needed to explain the results. The addition of dimethylamine has a reverse effect relative to that observed in but-1-ene. It is concluded that the mechanism invoked for the butene systems is not adequate for explaining the isomerization observed in the methylbutene systems.

GUY J. COLLIN et JAN A. HERMAN. Can. J. Chem. **58**, 1973 (1980).

Nous avons étudié, par radiolyse sensibilisée aux gaz nobles, l'isomérisation des butènes et des méthylbutènes. L'isomérisation de l'isobutène en butène-2 est surtout efficace lors de la radiolyse sensibilisée au xénon. L'isomérisation du butène-1 en isobutène est de peu d'importance et n'est révélée que par l'addition de diméthylamine. Ces observations sont en accord avec un mécanisme mettant en jeu l'isomérisation de l'ion parent excité.

L'isomérisation des méthylbutènes a lieu quelle que soit la nature de l'agent sensibilisateur et se fait avec des rendements radiolytiques impliquant un mécanisme en chaîne. L'addition de diméthylamine a un effet opposé à celui observé dans le butène-1. On en conclut que le mécanisme valide pour les butènes n'est pas approprié pour expliquer l'isomérisation observée dans les méthylbutènes.

Introduction

The isomerization of radical-cations formed by the ionization of C_4H_8 alkenes is well known. For example, P. Ausloos *et al.* have shown that direct photoionization of one of the butenes induces the formation of others in various amounts depending on the wavelength of the uv lamp, pressure, additives, ... (1). $[C_4H_8]^+$ ions formed through various radiolytical techniques have also been prepared, and each of them isomerizes (2). The same trend was observed in the photoionization of several methylbutenes. For example, the photoionization of 3-methyl but-1-ene gives rise to an extensive formation of 2-methyl but-2-ene (3), and the same was also observed in the gaseous radiolysis (4). However, in this last case, another mechanism was thought to be responsible for the observations: it was proposed that the isomerization takes place through protonated methylbutene (4). In this paper we have extended our previous studies to the γ-sensitized radiolysis of butenes and methylbutenes in order to shed more light on the isomerization processes.

Experimental

The experimental methods have already been described (3, 4). Butenes and methylbutenes are from the American Petroleum Institute and have better than 99.9% purity. Rare gas, ammonia, nitric oxide, and oxygen, are Research grade products from Matheson of Canada (≥99.9% purity). They were used without further purification following vacuum degassing (10^{-5} Torr – 1.3×10^{-3} N m^{-2}). Dimethylamine was also used as received from Matheson of Canada.

The samples were prepared in a Pyrex vacuum line (mercury free) equipped with Teflon stopcocks and Wallace and Tiernan metallic membrane manometers.

All irradiation techniques have also been described (4). Dosimetry was carried out by measuring the saturation current and the W (rare gas) values were used to calculate dose rates. The dose rates measured in each of the rare gases were 5.20×10^{13}, 1.04×10^{14}, and 1.68×10^{14} eV cm^{-3} min^{-1} in 100 Torr (13300 N m^{-2}) of argon, krypton, and xenon, respectively. Analysis of the irradiated samples (irradiation time: 120 min) was carried out by gas chromatography. It is sufficient to say that but-1-ene, the couple 1,3-butadiene + isobutene, *cis*-, and *trans*-but-2-ene were separated on a squalane column. Finally, an alumina column (temperature programmed between 50 and 120°C – 1°C/min) was used to analyse 1,3-butadiene.

Each irradiation was carried out at least twice. The reproducibility was better than ± 10% unless otherwise indicated.

Results and Discussion

The yields of the products are indicated in the tables as $G(x)$ values: the number of x molecules

[1]Revision received June 24, 1980.

0008-4042/80/181973-06$01.00/0

©1980 National Research Council of Canada/Conseil national de recherches du Canada

Can. J. Chem. Downloaded from www.nrcresearchpress.com by 210.87.254.105 on 09/05/12
For personal use only.

Can. J. Chem. Downloaded from www.nrcresearchpress.com by 210.87.254.105 on 09/05/12
For personal use only.

formed per 100 eV energy absorbed by the sensitizing rare gas. We have only given the yields of pertinent products and the reader is encouraged to refer to a recent paper by one of us, especially for details concerning the mechanistic interpretation (5). Allene is generally thought to be formed in the fragmentation of a neutral excited or superexcited molecule (6), and its radiolytic yield is rather insensitive to the addition of oxygen, ammonia, or dimethylamine. The complex behaviour of the yields of isobutane–isobutene system (7), *n*-butane – linear butene system (8), or isopentane–methylbutene system (9) is apparent from the effect of different additives.

(a) The Case of Isobutene

The xenon-sensitized radiolysis of isobutene induces isomerization of the parent molecule: the G(but-2-ene) value being 0.23 and 0.48 in the absence and presence, respectively, of dimethylamine. These observations are in line with the following reactions:[2]

[1] $Xe^+ + \text{iso-}C_4H_8 \rightarrow [\text{iso-}C_4H_8^*]^+ + Xe$ $\quad \Delta H = -282 \text{ kJ mol}^{-1}$

[2] $[\text{iso-}C_4H_8^*]^+ \rightarrow [2\text{-}C_4H_8^*]^+$ $\quad \Delta H = 0.0 \text{ kJ mol}^{-1}$

[3] $2\text{-}C_4H_8^+ + \text{iso-}C_4H_8 \rightleftarrows \text{iso-}C_4H_8^+ + \textit{cis}\text{-}2\text{-}C_4H_8$ $\quad \Delta H = +9.9 \text{ kJ mol}^{-1}$

[4] $2\text{-}C_4H_8^+ + (CH_3)_2NH \rightarrow (CH_3)_2NH^+ + \textit{cis}\text{-}2\text{-}C_4H_8$ $\quad \Delta H = -80 \text{ kJ mol}^{-1}$

Assuming that dimethylamine intercepts the majority of the $2\text{-}C_4H_8^+$ ions (8), the G(process [4]) is at least equal to 0.48. Thus, this last value is a lower value for the radiolytic yield of process [2]. The radiolytic yield of the Xe^+ ions is equal to 100 eV divided by the average energy, W, required to produce an ion pair in xenon: W(xenon) = 21.9 eV (11) and $G(Xe^+) = 4.57$. Thus it turns out that around 11% of the initially formed Xe^+ ions give rise to the formation of but-2-ene and the $G([C_4H_8^*]^+)$ value is at least 0.48. In fact, the noble gas ion may transfer its charge to any of the additives (the ionization potential of the added noble gas is higher than that of any additive) so that the yield of isobutene radical cations is less than that of the yield of the noble gas ions. There, more than 11% of the Xe^+ ions which react with isobutene leads to its isomerization.

In the photoionization experiments, the isomerization quantum yield was observed to be very sensitive to the energy content of the parent ion. At 10.0 eV (960 kJ mol^{-1}), less than 2% of the parent ions isomerise to the but-2-ene structure. This percentage increases to 13 at 11.6–11.8 eV at a pressure of 1 Torr. Moreover, the increase of the pressure has a strong reverse effect: in the presence of 266 Torr of neon, the isomerization of the parent ion drops from 13 to less than 2% (1). In the present study, the isomerization seems more important since the 11% value (see above) was measured at 300 Torr and is relatively much less sensitive to pressure. This would indicate that the parent isobutene ion has more internal energy than in the 11.6–11.8 eV photolytic experiments. The exothermicity of process [1] must be shared among the products. The rare gas atom may only support kinetic energy (the available energy is far from sufficient to produce a metastable noble gas atom). Thus, it may be assumed that most if not all of the exothermicity of process [1] is located in the butene radical cation (12).

In this interpretation is correct, i.e. the energy content of the butene cation is higher than 11.6–11.8 eV, it would eliminate the involvement of the dimer noble gas ion. The appearance potential of Xe_2^+ ion is close to 11.3 eV. Energy transfer from this dimer ion would release less energy and the butene cations would contain less internal energy that when they are formed in the direct photo-

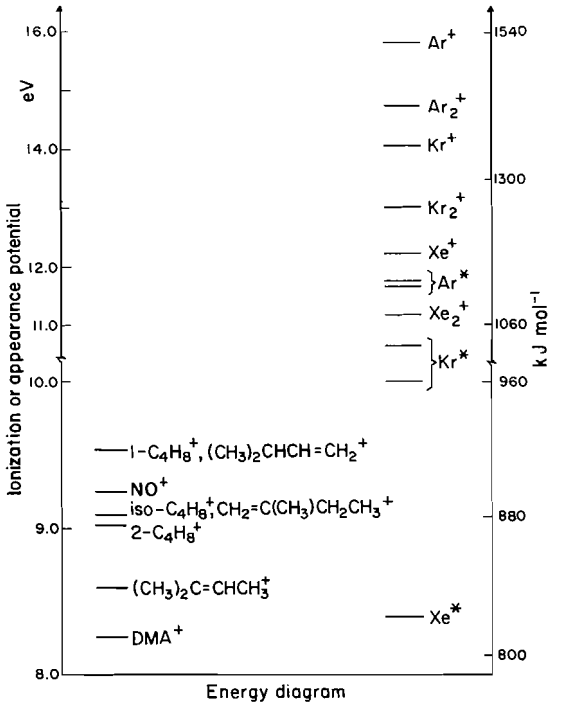


FIG. 1. Schematic energy diagram of the ionization potential or appearance potential of various butenes, methylbutenes, and additives.

[2]All the values of enthalpy changes refer to ground state species. The ΔH_f^0 (values) are from ref. 10.

TABLE 1. Noble gas sensitized-radiolysis of isobutene[c]

	Xenon							Krypton		Argon		
Noble gas	50[a]	70	70	70	100	100	300	100	100	100	100	100
Isobutene	0.5	0.7	0.7	0.7	1.0	1.0	1.0	1.0	1.0	1.0	1.0	1.0
Oxygen	—	0.2	0.2	0.2	0.2	0.4	0.2	0.5	0.2	—	0.5	0.2
Dimethylamine	0.5	—	0.5	1.4	0.5	—	0.5	—	0.5	—	—	0.5
Ammonia	—	—	—	—	—	0.2	—	0.3	—	—	—	—
G(propene)	0.24	0.23	0.17	0.15	0.16	0.30	0.14	0.42	0.44	0.60	0.58	0.46
G(*trans*-but-2-ene)	0.26	0.12	0.25	0.27	0.31	0.17	0.25	0.03	0.08	n.m.	0.05	0.06
G(*cis*-but-2-ene)	n.m.[b]	0.10	0.20	0.22	0.25	0.16	0.18	0.05	0.05	n.m.	0.04	0.05

[a]In Torr (1 Torr = 133 N m^{-2}).
[b]n.m. ≡ not measured.
[c]G(but-1-ene) = 0.00 in all experiments. Other yields may be found in ref. 5.

TABLE 2. Xenon-sensitized radiolysis of linear butenes

	But-1-ene			*cis*-But-2-ene	
Xenon[a]	145	147	230	147	149
Butene	1.54	1.51	2.97	1.54	1.52
Oxygen	0.76	0.49	0.96	0.61	0.55
DMA	—	0.49	0.87	—	0.73
G(allene)	0.30	0.30	0.29	0.12	0.10
G(propene)	0.60	0.57	0.44	0.50	0.34
G(*n*-butane)	0.43	0.12	0.22	0.01	0.02
G(isobutene)[b]	0.00	0.10	0.21	0.17	0.15
G(*trans*-but-2-ene)	0.32	0.58	0.91	3.8	1.2
G(*cis*-but-2-ene)	0.44	0.50	0.76	—	—
G(but-1-ene)	—	—	—	0.00	0.00

[a]All compositions are expressed in Torr (1 Torr = 133 N m^{-2}).
[b]The reproducibility is not better than ±20% for the isobutene yields.

ionization at 11.6–11.8 eV (Fig. 1). In photoionization experiments part of the photon energy is taken by the electron. This part is, however, small and may be ignored here.

The butene cations formed in process [1] have an internal energy of about 12.1 eV — the ionization potential of xenon (12) — above the ground state of neutral butene molecules. Thus, it is likely that some of these excited cations decompose, since the appearance potentials of several ionic fragments is lower than 12.1 eV (5). For example, Fig. 2 shows the variation of G(propene) value with pressure, in the xenon-, krypton-, and argon-sensitized radiolysis of isobutene. This product is, at least partly, the result of the chemistry of $C_3H_5^+$ ions formed in the decomposition of internally excited [iso-C_4H_8*]$^+$ ions (7, 13). This assumption is in agreement with the increase of the G(propene) values with increase of ionization potential of the noble gas (Fig. 1). It is also worthwhile to note the very low G(but-2-ene) values measured in the krypton- and argon-sensitized radiolytic experiments. In these cases, the energy released in the charge transfer from the noble gas ion to isobutene is too large, and the internally excited isobutene cation decomposes preferentially.

[5] $Kr^+ + \text{iso-}C_4H_8 \rightarrow Kr + [\text{iso-}C_4H_8^*]^+$ $\Delta H = -462$ kJ mol^{-1}

[6] $Ar^+ + \text{iso-}C_4H_8 \rightarrow A + [\text{iso-}C_4H_8^*]^+$ $\Delta H = -629$ kJ mol^{-1}

But-1-ene was not observed as a product (Table 1). The isomerization process

[7] $\text{iso-}C_4H_8^+ \rightarrow \text{1-}C_4H_8^+$ $\Delta H = 54$ kJ mol^{-1}

is strongly endothermic, and, as such, is not a favoured chemical path.

(b) The Case of Linear Butene

Table 2 shows the $G(C_4H_8)$ values measured in the but-1-ene and *cis*-but-2-ene systems. But-1-ene has a higher ionization potential (IP = 9.58 eV) than any of the other butenes. If other butene radical cations are formed in the but-1-ene system, a charge acceptor should be added in order to reveal the presence of such positive ions through charge transfer process. Thus, the formation of isobutene, and the increase of the G(but-2-ene) values upon addition of dimethylamine (IP = 8.24 eV) may be ascribed to the charge transfer process similar to process [4]. The situation is reversed in the *cis*-but-2-ene system, since this compound has a low ionization potential (see Fig. 1).

Can. J. Chem. Downloaded from www.nrcresearchpress.com by 210.87.254.105 on 09/05/12
For personal use only.

Can. J. Chem. Downloaded from www.nrcresearchpress.com by 210.87.254.105 on 09/05/12
For personal use only.

TABLE 3. γ-Sensitized radiolysis of 3-methyl but-1-ene[a]

Noble gas	Xenon[b]						Krypton		Argon	
Oxygen	0.45	0.50	0.80	0.40	—	—	—	—	—	0.45
Nitric oxide	—	—	—	—	0.29	1.77	0.41	0.43	0.8	—
Dimethylamine	—	0.90	2.3	—	—	—	—	—	—	—
Ammonia	—	—	—	0.50	—	—	—	—	—	—
G(2-methyl but-1-ene)	0.32	0.21	0.21	0.45	0.35	0.24	0.11	0.12	0.15	0.28
G(2-methyl but-2-ene)	2.7	1.12	1.12	2.2	2.6	2.4	0.76	0.95	1.0	1.6
G(isopentane)	0.15	0.02	0.02	0.02	0.08	0.06	0.06	0.06	0.06	0.11

[a]Typical composition: noble gas: 3-methyl but-1-ene (145:1.45 ± 0.10 Torr — 19000:190 ± 15 N m^{-2}).
[b]In the 147 nm (xenon resonance line) of the 3-methyl but-1-ene: O_2 mixture (10:1.0 Torr — 1330:133 N m^{-2}), the Φ(2-methyl but-2-ene) and Φ(2-methyl but-1-ene) values are 0.00 and 0.10, respectively. The same values measured in the xenon (150 Torr — 20000 N m^{-2})-sensitized photolysis of the same mixture are 0.00 and 0.08, respectively.

TABLE 4. γ-Sensitized radiolysis of 2-methyl but-2-ene[a]

Noble gas	Xenon		Krypton		Argon	
Oxygen	0.70	—	0.21	—	0.20	—
Nitric oxide	—	0.25	—	0.43	—	0.37
G(3-methyl but-1-ene)	0.011	0.007	0.015	0.00	0.02	0.01
G(2-methyl but-1-ene)	0.55	0.52	0.60	0.55	0.58	0.62
G(isopentane)	0.24	0.13	0.18	0.28	0.36	0.25

[a]Typical mixtures: noble gas:2-methyl but-2-ene (100:1.0 Torr — 13000:133 N m^{-2}).

TABLE 5. γ-Sensitized radiolysis of 2-methyl but-1-ene[a]

Noble gas	Xenon			Krypton		Argon		
Oxygen	0.82	—	—	0.50	—	0.38	—	—
Nitric oxide	—	0.73	0.80	—	0.73	—	0.44	0.73
Dimethylamine	—	—	0.80	—	—	—	—	0.80
G(3-methyl but-1-ene)	0.03	0.015	0.015	0.14	0.02	0.13	n.m.	0.03
G(2-methyl but-2-ene)	4.1	3.3	1.05	4.5	3.1	7.0	4.6	0.7
G(isopentane)	1.0	0.58	0.07	0.83	0.03	1.1	1.5	0.0

[a]Typical mixtures: noble gas:2-methyl but-1-ene (145 ± 10:1.45 ± 0.10 Torr — 19000 ± 1300:190 ± 130 N m^{-2}). The G(2-methyl but-2-ene) values are ±20%.

In the but-1-ene system, the amount of dimethylamine is probably sufficient to intercept all 2-$C_4H_8^+$ ions (8) (no attempt was made to get a "plateau" value). However, the G(2-C_4H_8) value may be as high as 1.80. Taking into account the possible fragmentation of the internally excited but-1-ene ions (see, for example, the formation of propylene (5)), it can be seen that the majority of the non-decomposing but-1-ene ions isomerize to but-2-ene (1). Conversely, the yield of isobutene is very low. Taking into account the large uncertainties in its measurement, it can be said that the isomerization of but-1-ene ion to isobutene is not an efficient process (14).

In the *cis*-but-2-ene system, the formation of the *trans*-isomer may be ascribed to various mechanisms and, as such, will not be discussed here. However, it seems that the formation of the isobutene structure is slightly easier here than in the previous system (14). This result is also in agreement with the photoionization experiments (1).

(c) The Case of the Methylbutenes

A glance at Tables 3, 4, and 5 exemplifies the high radiolytic yields of isomers formed in each system. Thus, the yields of isomers are much larger than those measured in the above-mentioned butene systems. In some cases, the total G(isomer) values were larger than the expected G(noble gas ion) values: $G(Xe^+) = 4.57$, $G(Kr^+) = 4.15$, and $G(Ar^+) = 3.80$ (11). In one case, not indicated in Table 5, a G(2-methyl but-2-ene) value of 10.0 was obtained! Thus a chain mechanism seems more appropriate to explain these high figures.

Moreover, whatever the sensitizing noble gas is, the isomerization is important. The excess energy available from the charge transfer process from Kr^+ and Ar^+ ions does not seem to decrease the importance of the isomerization process by favouring the decomposition of the internally excited $[C_5H_{10}{}^*]^+$ ions. This observation is contrary to the trend observed in the isobutene system.

The effect of the addition of nitric oxide or dimethylamine is not the one expected on the grounds

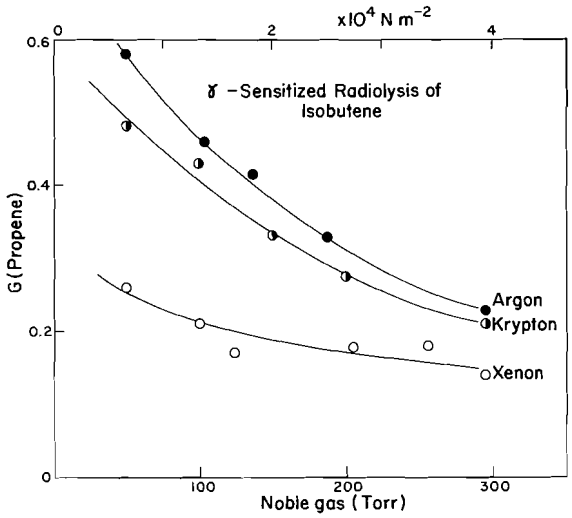


FIG. 2. The G(propene) values measured in the noble gas sensitized radiolysis of isobutene vs. the total pressure.

of the charge transfer process from any $C_5H_{10}^+$ ion. Thus, in the 3-methyl but-1-ene system, the ionization potentials of 2-methyl but-1-ene and 2-methyl but-2-ene are lower than the parent molecule (see Fig. 1). In the presence of only xenon, 3-methyl but-1-ene, and oxygen, there is no positive charge transfer from the expected 2-methyl but-1-ene and 2-methyl but-2-ene positive ions to any of the additives. The addition of nitric oxide or, much better, of dimethylamine should favour the positive charge transfer process, and an increase in the yield of isomer is expected. In fact the lower yields were measured in the presence of this additive. This observation would eliminate the parent ion as the intermediate involved in the isomerization reaction.

Finally, the addition of ammonia in the 3-methyl but-1-ene system (Table 3) has an interesting effect: it decreases the 2-methyl but-2-ene yield and it increases that of the 2-methyl but-1-ene. This effect was also observed in the radiolysis of 3-methyl but-1-ene sensitized by methane although it was much more important: the 2-methyl but-1-ene yield was larger than that of 2-methyl but-2-ene (9).

Although no definitive proof can be invoked to support this mechanism, together with the need for a chain mechanism, it is tempting to link the above-mentioned observation to the isomerization of a $C_5H_{11}^+$ ion, as was proposed in previous papers (4, 9).

[8] $RH^+ + (CH_3)_2CHCH{=}CH_2 \rightarrow R + [(CH_3)_2CHCHCH_3]^+$

[9] $[(CH_3)_2CHCHCH_3]^+ + (CH_3)_2CHCH{=}CH_2 \rightarrow (CH_3)_2C{=}CHCH_3 + [(CH_3)_2CHCHCH_3]^+$

$\Delta H = -13.6$ kJ mol^{-1}

[10] $[(CH_3)_2CHCHCH_3]^+ \rightarrow [(CH_3)_2CCH_2CH_3]^+$

$E_A = +9$ kJ mol^{-1} (4)

$\Delta H = -46$ kJ mol^{-1}

[11] $[(CH_3)_2CCH_2CH_3]^+ + (CH_3)_2CHCH{=}CH_2 \rightarrow CH_2{=}C(CH_3)CH_2CH_3 + [(CH_3)_2CHCHCH_3]^+$

$\Delta H = +39$ kJ mol^{-1}

[12] $[(CH_3)_2CCH_2CH_3]^+ + (CH_3)_2CHCH{=}CH_2 \rightarrow (CH_3)_2C{=}CHCH_2 + [(CH_3)_2CHCHCH_3]^+$

$\Delta H = +3.2$ kJ mol^{-1}

Of course, the formation of the various C_5H_{10} isomers in the presence of dimethylamine may partly be the result of the isomerization of the parent radical cations. The isomerization processes of radical cations become smaller with increasing molecular size (15, 16). Finally, it should be added that *cis*- and *trans*-pent-2-ene have been observed in the radiolysis of methylbutenes at 77 K. The formation of these products has been related to the isomerization of the parent ion through a cyclopropane structure: various dimethylcyclopropanes were also observed (17).[3]

Acknowledgments

We should like to thank the ministère de l'Éducation du Québec, programme FCAC for financial help throughout this work. The assistance of Mme Deslauriers in analytical work is also very much appreciated.

1. L. W. SIECK, S. G. LIAS, L. HELLNER, and P. AUSLOOS. J. Res. Natl. Bur. Stand. **76**A, 115 (1972).
2. P. S. GILL, Y. INEL, and G. G. MEISELS. J. Chem. Phys. **54**, 2811 (1971); S. G. LIAS and P. AUSLOOS. J. Res. Natl. Bur. Stand. **75**A, 591 (1971).
3. H. GAGNON, G. J. COLLIN, and C. BERTRAND. J. Phys. Chem. **78**, 98 (1974); G. J. COLLIN and C. BERTRAND. J. Photochem. **3**, 123 (1974).
4. G. J. COLLIN. Can. J. Chem. **54**, 3050 (1976); G. J. COLLIN and J. A. HERMAN. J. Chem. Soc. Faraday Trans. I, **74**, 1939 (1978).
5. J. A. HERMAN. Can. J. Chem. **57**, 2633 (1979).
6. J. A. HERMAN, K. HERMAN, and P. AUSLOOS. J. Chem. Phys. **52**, 28 (1970); G. J. COLLIN. Can. J. Chem. **51**, 2853 (1973).
7. J. A. HERMAN and G. J. COLLIN. Can. J. Chem. **47**, 3837 (1969).

[3]NOTES ADDED IN PROOF:

Recently Lias *et al.* have studied the isomerization processes of *trans*-but-2-ene to isobutene in an ion cyclotron resonance spectrometer. The isomerization process is explained in terms of a proton transfer process through a long-lived ($M{\cdot}sec$-$C_4H_9^+$) complex capable of isomerization towards the ($M{\cdot}t$-$C_4H_9^+$) structure (18).

As suggested by one of the referees, we have performed a few xenon-photosensitized experiments ($\lambda = 147$ nm) (see footnote *b* in Table 3). Clearly the energy transfer from metastable xenon atom does not result in 2-methyl but-2-ene formation.

Can. J. Chem. Downloaded from www.nrcresearchpress.com by 210.87.254.105 on 09/05/12
For personal use only.

8. S. G. LIAS and P. AUSLOOS. J. Am. Chem. Soc. **92**, 1840 (1970); J. NIEDZIELSKI, W. MAKULSKI, H. ZUCHMANTOWICZ, and J. GAWLOWSKI. Nukleonika, **24**, 1169 (1979).
9. G. J. COLLIN. Can. J. Chem. **54**, 555 (1976).
10. H. M. ROSENSTOCK, K. DRAXL, B. W. STEINER, and J. T. HERRON. J. Phys. Ref. Data, **6**, Suppl. No 1 (1977) and references therein.
11. D. W. HUYTON and T. W. WOODWARD. Radiation Res. Rev. **2**, 205 (1970), and references cited therein.
12. S. G. LIAS and P. AUSLOOS. *In* Ion–molecule reactions, their role in radiation chemistry. Am. Chem. Soc. Washington, 1975.
13. F. B. ABRAMSON and J. H. FUTRELL. J. Phys. Chem. **72**, 1994 (1968).
14. R. P. MORGAN, P. J. DERRICK, and A. G. LOUDON. J. Chem. Soc. Perkin Trans. II, 478 (1979).
15. T. NISHISHITA, F. M. BOCKHOFF, and F. W. MCLAFFERTY. Org. Mass Spectrom. **12**, 16 (1977); J. NISHISHITA and F. W. MCLAFFERTY. Org. Mass Spectrom. **12**, 75 (1977).
16. K. LEVSEN and J. HEINBRECHT. Org. Mass Spectrom. **12**, 131 (1977).
17. C. D. WAGNER. J. Phys. Chem. **71**, 3445 (1967).
18. S. G. LIAS, D. M. SHOLD, and P. AUSLOOS. J. Am. Chem. Soc. **102**, 2540 (1980).

Can. J. Chem. Downloaded from www.nrcresearchpress.com by 210.87.254.105 on 09/05/12
For personal use only.

The reaction between 2,2-di(4-nitrophenyl)1,1,1-trifluoroethane and *tert*-butoxide ion in *tert*-butyl alcohol solvent

ARNOLD JARCZEWSKI[1] AND KENNETH T. LEFFEK

Department of Chemistry, Dalhousie University, Halifax, N.S., Canada B3H 4J3

Received March 13, 1980

ARNOLD JARCZEWSKI and KENNETH T. LEFFEK. Can. J. Chem. **58**, 1979 (1980).

The reaction between 2,2-di(4-nitrophenyl)1,1,1-trifluoroethane and excess sodium *tert*-butoxide in *tert*-butyl alcohol takes place rapidly to yield first the olefin, by elimination of HF. This is followed by a slower addition of *tert*-butoxide to the olefin, which upon reaction with the solvent gives the *tert*-butyl ether as the final product. The blue anions involved in each of these reactions are observed.

Rate constants, the primary deuterium kinetic isotope effects, and the activation parameters have been measured for the appearance of the initial blue colour and also for the formation of the olefin. It is concluded that the reaction proceeds by a reversible E1cB mechanism.

ARNOLD JARCZEWSKI et KENNETH T. LEFFEK. Can. J. Chem. **58**, 1979 (1980).

La réaction entre le di(nitro-4 phényl)-2,2 trifluoro-1,1,1 éthane et un excès de *tert*-butylate de sodium dans l'alcool *tert*-butylique se produit rapidement et conduit en premier lieu à l'oléfine par élimination de HF. Cette étape est suivie d'une addition lente de *tert*-butylate sur l'oléfine qui, par réaction avec le solvant, conduit à l'éther *tert*-butylique comme produit final. On a observé les anions bleus impliqués dans chacune de ces réactions.

On a mesuré les constantes de vitesse, les effets isotopiques cinétiques primaires du deutérium et les paramètres d'activation de l'apparition de la couleur bleue initiale et également de la formation de l'oléfine. On en conclut que la réaction se fait suivant un mécanisme reversible E1cB.

[Traduit par le journal]

Introduction

In an earlier publication (1) the β-elimination reaction of 2,2′-di(*p*-nitrophenyl)-1,1,1-trifluoroethane initiated by sodium methoxide in methanol was investigated. It was concluded from the magnitude of the second-order rate constant and the lack of a primary detuerium isotope effect that the reaction proceeded via an $(E1cB)_R$ mechanism, eqs. [1] and [2], with k_{-1} [BH] very much greater than k_2.

[1] $B^- + (pNO_2C_6H_4)_2CH{-}CF_3$

k_{-1} ⇅ k_1

$(pNO_2C_6H_4)_2C^-{-}CF_3 + BH$

[2] $(pNO_2C_6H_4)_2C^-{-}CF_2 \xrightarrow{k_2} (pNO_2C_6H_4)_2C{=}CF_2 + X^-$

When the above substrate is mixed with sodium *tert*-butoxide in *tert*-butyl alcohol, a blue colour appears immediately. Since the *tert*-butoxide is a stronger base than methoxide, k_1 should be larger for *tert*-butoxide. *tert*-Butyl alcohol is a less polar solvent than methanol which should give a smaller k_2 for *tert*-butyl alcohol. Therefore, it would be expected that the carbanion would be more stable and exist in larger concentration in *tert*-butoxide/*tert*-butyl alcohol than in methoxide in methanol. If the blue colour observed is due to the anion of the substrate, it should be possible to observe all three rate processess k_1, k_{-1} [BH], and k_2 for this reaction.

Results and Discussion

The substrate in *tert*-butyl alcohol solvent has a uv absorption peak at 267 nm. The spectrum of a mixture of the substrate ($5 \times 10^{-5}M$) and sodium *tert*-butoxide ($5 \times 10^{-3}M$) in *tert*-butyl alcohol, taken a few minutes after mixing, shows no peak at 267 nm, but a new peak at 325 nm and a broad peak at 510–530 nm. The 325 nm peak is assigned to the product olefin (1).

This spectrum is not stable and changes markedly over a period of several hours. The change is dependent upon the conditions under which the reaction mixture was prepared, so all solutions for the experiments were made up and stored in an atmosphere of dry nitrogen. Under these conditions the product peak disappears after 3–4 hours and is replaced by a peak at 267 nm, while the absorption in the visible region shifts to about 600 nm.

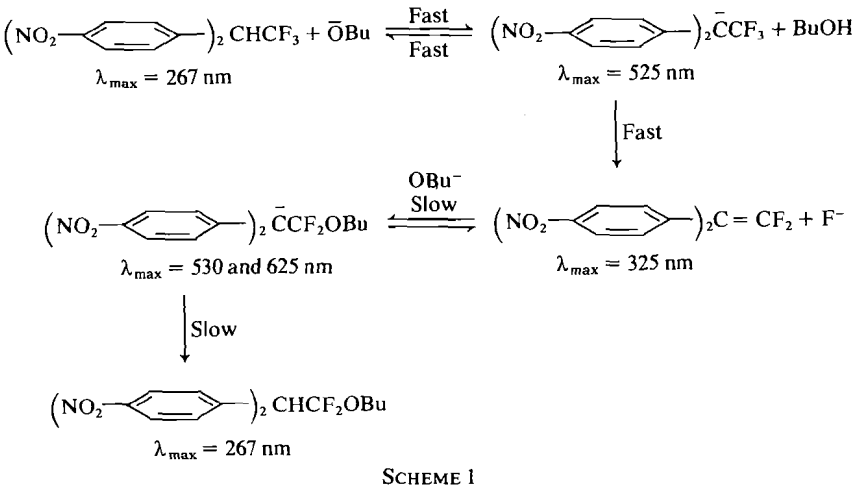
It is concluded that the product 2,2-di(4-nitrophenyl)-1,1-difluoroethylene is undergoing a further reaction, the products of which have absorption spectra quite similar to the substrate and

[1]Visiting Scientist 1978.

0008-4042/80/181979-04$01.00/0

© 1980 National Research Council of Canada/Conseil national de recherches du Canada

Can. J. Chem. Downloaded from www.nrcresearchpress.com by 210.87.254.42 on 09/05/12
For personal use only.



SCHEME I

its anion. The most likely reaction is the addition of *tert*-butoxide ion to the olefin to yield an anion which by reaction with solvent can yield the ether as the final product. Such a reaction of methoxide ion with fluoro-olefins has been observed by Miller *et al.* (2).

Reaction of 2,2-Di(4-nitrophenyl)1,1-difluoroethylene with tert-*Butoxide Ion*

The olefin was prepared by reaction of the trifluoride with sodium methoxide in methanol as previously described (1). This material dissolved in *tert*-butyl alcohol showed a single broad absorption peak at 336 nm. Upon addition of sodium *tert*-butoxide, no blue colour appeared immediately, but after a few minutes the colour appeared together with a peak in the 260–270 nm region, while the olefin peak fell. The reaction was complete after about four hours, after which the colour faded while the 260–270 nm peak continued to increase.

The complete reaction sequence of the trifluoride with sodium *tert*-butoxide is set out in Scheme 1.

Kinetic Investigation of Formation of Initial Carbanion

The appearance of the initial blue colour was followed at 525 nm using a stopped-flow spectrophotometer. Pseudo first-order rate constants were measured in the presence of a large excess of base using the usual technique for organic proton transfer reactions (3). The half-life of the first-order reactions varied between three and ten seconds depending on the conditions of base concentration and temperature. The correlation coefficients for the Guggenheim plot were usually 0.998 or better. The observed first-order rate constants were plotted against the base concentration and the second-order rate constants were calculated from the slope of the graph. The measurements were carried out for both the normal and deuterated trifluoride at five different temperatures and these results are shown in Table 1. The intercepts of the plots of observed first-order constants against base concentration for the hydrogen compound have values of 0.045 to 0.06 s^{-1}, which give an average equilibrium constant for anion formation of 533 ± 15 L mol^{-1}.

Whether the base takes part in the reaction as an ion-pair or as free *tert*-butoxide is difficult to determine. There is no doubt (4–7) that a large part of the *tert*-butoxide is present, in solutions of the concentrations used in this work, as ion-pairs and larger aggregates. However, it has been shown that the dissociated *tert*-butoxide ion has a much greater chemical reactivity than the ion-pairs (5). Also, when this same assumption was made for methoxide and ethoxide, we were able to derive dissociation constants for the ion-pairs of these bases from kinetic measurements which were in agreement with those calculated from conductance data (8). The latter method has yielded a value of 0.0016 for potassium *tert*-butoxide (7) and if this value is assumed for sodium *tert*-butoxide, the observed first-order rate constants, k_H, in Table 1 may be analysed according to eq. [3]

$$[3] \quad k_H = k_{2H(ip)}\, c(1-\alpha) + k_{2H(i)}\, c\alpha$$

where $k_{2H(ip)}$ and $k_{2H(i)}$ are the second-order rate constants for the reaction with ion-pairs and free ions of base, respectively; c is the total base concentration, and α is the degree of ionization. A plot of $k_H/c\alpha v((1-\alpha)/\alpha)$ is linear with a slope of $k_{2H(ip)}$ and an intercept $k_{2H(i)}$. The difficulty with an analysis such as this is that the possible error in the derived rate constants is very large compared to the magnitude of the rate constants themselves. However, it does show that $k_{2H(ip)}$ is about 10 times smaller than $k_{2H(i)}$. Thus, about 90% of the reaction proceeds via the dissociated *tert*-butoxide ion.

Can. J. Chem. Downloaded from www.nrcresearchpress.com by 210.87.254.42 on 09/05/12
For personal use only.

TABLE 1. Rate constants and isotopic rate ratios for the appearance of the absorption peak at λ_{max} 525 nm in the reactions of $CF_3CH(4\text{-}NO_2C_6H_4)_2(k_H)$ and $CF_3CD(4\text{-}NO_2C_6H_4)_2(k_D)$ with sodium *tert*-butoxide in *tert*-butyl alcohol

Temperature (°C)	$10^3[\bar{O}Bu]$ (M)	$10k_H$ (s^{-1})	$10k_D$ (s^{-1})	k_{2H} (L mol^{-1} s^{-1})	k_{2D} (L mol^{-1} s^{-1})	k_{2H}/k_{2D}
26.0	2.0	0.94	0.53			
	3.0	1.12	0.74			
	4.0	1.38	0.88	23.5	16.6	1.42
	5.0	1.63	1.07			
	6.0	1.86	1.20			
30.0	2.0	1.02	0.55			
	3.0	1.21	0.74			
	4.0	1.54	0.94	25.2	19.0	1.33
	5.0	1.75	1.15			
	6.0	2.01	1.30			
35.0	2.0	1.10	0.56			
	3.0	1.40	0.76			
	4.0	1.61	1.00	28.4	21.3	1.33
	5.0	1.95	1.18			
	6.0	2.24	1.42			
40.0	2.0	1.19	0.58			
	3.0	1.50	0.79			
	4.0	1.77	1.09	30.7	23.7	1.30
	5.0	2.13	1.28			
	6.0	2.41	1.52			
45.0	2.0	1.31	0.59			
	3.0	1.66	0.82			
	4.0	1.94	1.14	36.0	28.2	1.28
	5.0	2.28	1.44			
	6.0	2.80	1.69			

The second-order rate constants yield $\Delta H^{\ddagger}_H = 3.5 \pm 0.3$ kcal mol^{-1}, $\Delta S^{\ddagger}_H = -40.6 \pm 1.0$ cal mol^{-1} deg^{-1}, $\Delta H^{\ddagger}_D = 4.4 \pm 0.3$ kcal mol^{-1}, $\Delta S^{\ddagger}_D = -38.3 \pm 0.9$ cal mol^{-1} deg^{-1}. These enthalpies of activation are quite low, but do compare reasonably with the value of 6.4 kcal mol^{-1} observed (3) for the proton transfer from di-(4-nitrophenyl)methane to *tert*-butoxide in *tert*-butyl alcohol containing 10% toluene, particularly since the addition of toluene to the solvent increases the enthalpy of activation (9). The entropies of activation are very similar for these two reactions, except that for the trifluoride ($\Delta S^{\ddagger}_D - \Delta S^{\ddagger}_H$) is positive, the usual result for primary deuterium isotope effects, whereas the methane gave a value of ($\Delta S^{\ddagger}_D - \Delta S^{\ddagger}_H$) which was −2.4 cal mol^{-1} deg^{-1}. Thus, for the methane the istope effect on the entropy of activation reinforces that on the enthalpy of activation, giving $k_H/k_D = 7.2$ at 30°C, whereas in the present case the two effects cancel each other to a large extent, giving $k_H/k_D = 1.3$ at 30°C. Such a small isotopic rate ratio is very unusual for a proton transfer reaction from a carbon acid. However, McLennan and Wong (10) have reported k_H/k_D values of 5.4 at 30°C for methoxide ion in methanol and 3.4 at 45°C for ethoxide ion in ethanol for the dehydrochlorination reaction of $DDT(pClC_6H_4)_2CHCCl_3$. For this reaction evidence was presented that the rate determining step was the formation of the carbanion (11). For the dehydrochlorination of 2,2-di(4-nitrophenyl)1,1,1-trichloroethane, the same workers reported k_H/k_D values of 4.95 and 3.82 at 30°C for methoxide in methanol and *tert*-butoxide in *tert*-butyl alcohol (11). Thus, fairly small isotopic rate ratios may be expected for the *tert*-butoxide reaction.

Rate of Olefin Formation

The rate of appearance of the olefin product was measured using the same technique as above, following the reaction at 325 nm. Both the normal and deuterated trifluorides were used and these gave identical first-order rate constants. The plots of k_{obs} versus base concentration passed through the origin and yielded the second order rate constants shown in Table 2. The second order rate constants yield $\Delta H^{\ddagger} = 2.4 \pm 0.3$ kcal mol^{-1}, $\Delta S^{\ddagger} = -45.0 \pm 1.0$ cal mol^{-1} deg^{-1}.

The second-order rate constant at 30°C (17.5 L $mol^{-1}s^{-1}$) is about 29 times faster than the corresponding constant for the methoxide reaction (1) which is comparable to the butoxide/methoxide ratio of 36 found by McLennan and Wong for 2,2′-di(4-nitrophenyl)1,1,1-trichloroethane at 30°C (12).

Can. J. Chem. Downloaded from www.nrcresearchpress.com by 210.87.254.42 on 09/05/12
For personal use only.

TABLE 2. Rate constants for the appearance of olefin product (λ_{max} 325 nm) in the reaction of $CF_3CH(4\text{-}NO_2C_6H_4)_2$ with sodium *tert*-butoxide in *tert*-butyl alcohol

Temperature (°C)	$10^3[\bar{O}Bu]$ (M)	$10^2 k$ (s^{-1})	k ($L\ mol^{-1}\ s^{-1}$)
26.0	2.85	5.00	
	4.75	7.67	
	7.13	12.1	16.9
	9.03	14.5	
	10.9	18.6	
30.0	2.85	5.43	
	4.75	8.19	
	7.13	13.1	17.5
	9.03	16.4	
	10.9	19.5	
35.0	2.85	5.73	
	4.75	8.91	
	7.13	13.4	19.2
	9.03	17.0	
	10.9	20.8	
40.0	2.85	6.08	
	4.75	9.49	
	7.13	14.4	20.5
	9.03	18.0	
	10.9	23.0	
45.0	2.95	6.35	
	4.75	9.90	
	7.13	15.4	22.3
	9.03	19.8	
	10.9	24.8	

Comparing the second-order rate constant for the *tert*-butoxide elimination, the trifluoro compound is 12 to 13 times slower than the trichloro compound (12). This seems to be a reasonable ratio for the relative reactivity of the two compounds, although it is unfortunate that we have no comparison of the activation parameters.

In the kinetic treatment of this reaction, is has been implicitly assumed that there is a preequilibrium between the initial state and the carbanion ion-pair, which means that the rate constant, k, for olefin appearance (Table 2) is made up of k_1k_2/k_{-1} [BH] as defined by eqs. [1] and [2].

The values of k_1 and k_{-1} [BH] are obtained from the proton transfer step. For the normal substrate, k_1 is k_{2H} from Table 1, 25.2 L $mol^{-1}s^{-1}$ at 30°C, and k_{-1} [BH] is the intercept of the plot of k_H against base concentration, that is, 0.05 s^{-1} at 30°C. The rate constant for olefin appearance, from Table 2, is 17.5 L $mol^{-1}s^{-1}$ at 30°C. These values yield k_2 = 0.035 s^{-1}. Thus, k_2 is not significantly lower than k_{-1} [BH] so that to treat the reaction as a preequilibrium may yield observed rate constants containing some systematic error. However, the data fit the preequilibirum mechanism excellently, so that it would not be possible to find a better fit using the kinetic equation for consecutive reactions. Hammett (13) has noted the difficulty of recognizing a multistep reaction as such from the deviation from first-order behaviour because the deviation is very small when the rate constants for each step are slightly different.

It is concluded that this reaction proceeds by a reversible E1cB mechanism, since there is no kinetic isotope effect on the rate of olefin production. However, the mechanism must be fairly close to the transition point between the $(E1cB)_R$ and the irreversible E1cB mechanisms, since k_2 is not a great deal smaller than k_{-1} [BH].

Experimental

Materials

Tertiary butyl alcohol (Baker Analyzed Reagent) was dried overnight with Molecular Sieve Type 3A and then with calcium hydride. The alcohol was then fractionally distilled from dibutyl phthalate. The fraction boiling at 82.4°C was collected and stored in a vessel protected from moisture and CO_2 under dry O_2-free nitrogen.

Sodium *tert*-butoxide solutions were prepared by dissolving clean sodium metal in *tert*-butyl alcohol in flasks protected from moisture and CO_2. The concentration of the stock solution was determined by titration with standard HCl solution using methyl red as indicator.

The preparation of 2,2'-(4-nitrophenyl)1,1,1-trifluoroethane and its deuterated analogue were described in an earlier publication (1).

Kinetic Measurements

The kinetic runs were carried out with a Durrum stopped-flow spectrophotometer using the standard technique previously described (14).

Acknowledgement

The authors are grateful for financial support by the Natural Sciences and Engineering Research Council of Canada.

1. J. KURZAWA and K. T. LEFFEK. Can. J. Chem. **55**, 1696 (1977).
2. W. T. MILLER, JR., E. W. FAGER, and P. H. GRISWOLD. J. Am. Chem. Soc. **70**, 431 (1948).
3. J.-H. KIM and K. T. LEFFEK. Can. J. Chem. **52**, 592 (1974).
4. D. J. CRAM, B. RICKBORN, C. A. KINGSBURY, and P. HABERFIELD. J. Am. Chem. Soc. **83**, 3678 (1961).
5. D. J. CRAM, C. A. KINGSBURY, and B. RICKBORN. J. Am. Chem. Soc. **83**, 3688 (1961).
6. W. H. SAUNDERS, JR., D. G. BUSHMAN, and A. F. COCKERILL. J. Am. Chem. Soc. **90**, 1775 (1968).
7. J. R. JONES. Prog. React. Kinet. **7**, 1 (1973).
8. K. T. LEFFEK and A. SUSZKA. Can. J. Chem. **53**, 1537 (1975).
9. A. JARCZEWSKI, P. PRUSZYNSKI, and K. T. LEFFEK. Can. J. Chem. **53**, 1176 (1975).
10. D. J. MCLENNAN and R. J. WONG. Tetrahedron Lett. 2887 (1972).
11. D. J. MCLENNAN and R. J. WONG. J. Chem. Soc. Perkin Trans. II, 526 (1974).
12. D. J. MCLENNAN and R. J. WONG. J. Chem. Soc. Perkin Trans. II, 1373 (1974).
13. L. P. HAMMETT. *In* Physical organic chemistry. 2nd ed. McGraw-Hill Book Co., New York. 1970. p. 88.
14. A. JARCZEWSKI and K. T. LEFFEK. Can. J. Chem. **50**, 24 (1972).

Can. J. Chem. Downloaded from www.nrcresearchpress.com by 210.87.254.42 on 09/05/12
For personal use only.

An investigation of anthraquinone-catalysed alkaline pulping via component modeling and electron spin resonance experiments

M. B. HOCKING,[1] H. I. BOLKER, AND B. I. FLEMING

Department of Chemistry, Pulp & Paper Building, McGill University, 3420 University Street, Montreal, P.Q., Canada H3A 2A7

Received March 21, 1980

M. B. HOCKING, H. I. BOLKER, and B. I. FLEMING. Can. J. Chem. **58**, 1983 (1980).

The radical anion of anthraquinone ($AQ^{\cdot -}$) has been generated by the reduction of anthraquinone (AQ) with sugars in aqueous alkaline solution. This appears to be the first time that the radical has been observed (esr spectrometry) in an entirely aqueous medium. Alkaline methanol solutions of AQ, when irradiated with light, yielded colourless solutions also exhibiting strong esr signals characteristic of $AQ^{\cdot -}$.

The ability of various carbohydrate and lignin preparations to reduce AQ, or to oxidize the reduced forms of AQ, was also investigated, both by direct observation and by electrode potential measurements. In very concentrated alkali, AQ was reduced by glucose to a green solid thought to be a quinhydrone.

M. B. HOCKING, H. I. BOLKER et B. I. FLEMING. Can. J. Chem. **58**, 1983 (1980).

On a produit l'anion radical de l'anthraquinone ($AQ^{\cdot -}$) en réduisant l'anthraquinone (AQ) par les sucres dans une solution aqueuse basique. Il semble que c'est la première fois qu'on observe le radical (spectroscopie de rpe) dans un milieu complètement aqueux. Quand on irradie les solutions basiques de méthanol de AQ, on obtient des solutions incolores qui montrent également de forts signaux caractéristiques du $AQ^{\cdot -}$ en rpe.

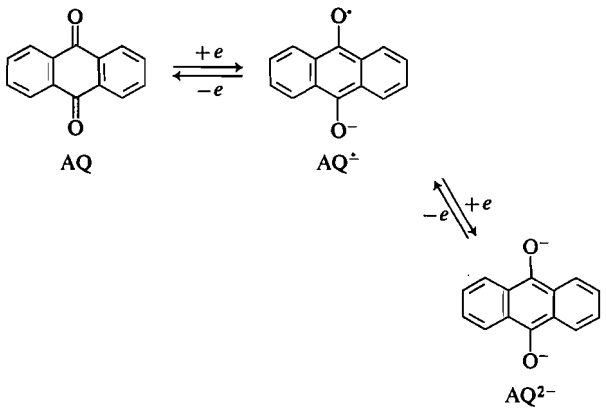
En utilisant l'observation directe et les mesures de potentiel d'électrode on a également étudié la capacité qu'ont diverses préparations de sucre ou de lignine, de réduire AQ ou d'oxyder les formes réduites de AQ. En solution basique très concentrée, le glucose réduit le AQ en un solide vert que l'on pense être une quinhydrone.

[Traduit par le journal]

Introduction

Interest in the chemistry of anthraquinone (AQ) has recently been revived, because a discovery of considerable industrial importance has revealed that in small quantities it accelerates the alkaline delignification of wood (1) and increases the yield of residual carbohydrate fibres. Proposed mechanisms (2–4) consider AQ to function as a redox catalyst by transferring electrons to lignin from a predominantly carbohydrate source. However, the nature of the species formed when AQ is reduced in alkaline solutions is far from clear (3). Although the red color of alkaline reduced AQ solutions has been ascribed to the dianion, AQ^{2-} (5, 6), one might also expect the semiquinone anion radical ($AQ^{\cdot -}$) to absorb light in the visible region (7–10). The anion radicals of amino- (10) and sulphonated- (8) anthraquinones have been reported to absorb between 450 and 520 nm, and there are reports that $AQ^{\cdot -}$ itself is red (9, 11). There are also reports that it is yellow (in aqueous methanol (12)) and pale brown (in pyridine (13)).

One investigation indicated that AQ may have as many as 5 stable reduced forms (including 2 radicals) in alkaline media (12), and there is always the possibility that $AQ^{\cdot -}$, if formed, may disproportionate rapidly to a mixture of AQ and AQ^{2-} (14).



The picture is further complicated by the variety of solvents used in previous experimental work.

When formed by electrolysis, photolysis, radiolysis, or chemical oxidation–reduction, $AQ^{\cdot -}$ is very stable in organic solutions (14–23), and in aqueous organic solutions (9, 12, 17, 24–29). Consequently, the esr spectrum of the radical is very well known, and all the 25 theoretical lines (24) have been observed in aqueous methanol (10% H_2O) solution (12). We have not, however, found any reports of esr spectra of the radical anion in 100% aqueous solution, although one paper indicated that $AQ^{\cdot -}$ formed at a pH above 12 in aqueous solution when an AQ-treated graphite electrode was maintained at a suitably low potential (30). In this work, our aim has been to identify the various

[1]Visiting Professor. Present address: Department of Chemistry, University of Victoria, Victoria, B.C., Canada V8W 2Y2.

0008-4042/80/181983-10$01.00/0

©1980 National Research Council of Canada/Conseil national de recherches du Canada

Can. J. Chem. Downloaded from www.nrcresearchpress.com by 210.87.254.105 on 09/05/12
For personal use only.

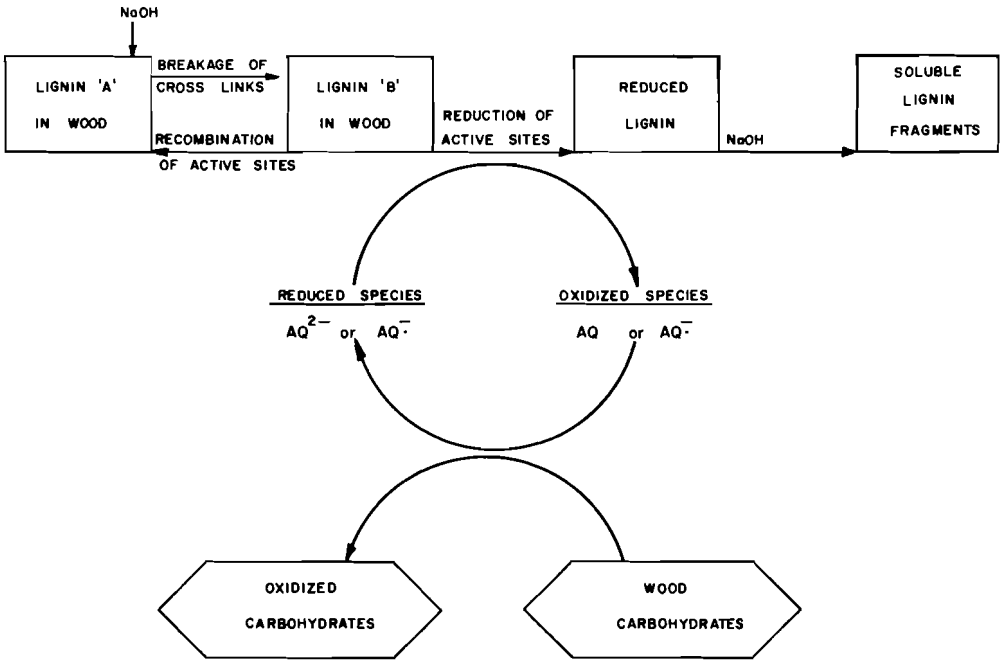


FIG. 1. Proposed mechanism for delignification rate enhancement in alkaline pulping with anthraquinone (3).

reduced states of anthraquinone in 100% aqueous solution, and to evaluate the stability of $AQ^{\cdot-}$ in aqueous alkaline media, with the objective of contributing to the detailed understanding of the catalytic role of AQ in alkaline pulping (Fig. 1).

In polarographic investigations, AQ showed only one wave in aqueous alkaline solution (3), indicating that the radical anion was not formed at a mercury electrode under reducing conditions.

We now report the preparation of the radical anion $AQ^{\cdot-}$ from anthraquinone by chemical reduction in aqueous alkaline solution. Although all the aqueous radical-containing solutions were red, alkaline methanolic solutions of AQ, after exposure to light, remained virtually colorless, yet still showed strong esr signals due to the radical anion.

As a step towards further elucidating the chemistry of the pulping process, modeling experiments were done in order to determine which wood components are capable of reducing AQ to the dianion, i.e. of acting as the source of electrons for AQ. Another part of the work describes tests conducted to determine those wood components present which were capable of accepting electrons from reduced AQ, i.e. AQ dianion.

Experimental

Anthraquinone (AQ) supplied by the Aldrich Chemical Co. was precipitated in fine particle size by adding a saturated solution in 50 mL dimethylformamide at 120°C, while hot, to 10 L of vigorously stirred cold water. The precipitated AQ was filtered off, washed with deionized water, and dried at 60°C.

Aqueous solutions of sodium and potassium hydroxides of all concentrations were freshly prepared for each series of experiments from distilled water and the appropriate base, and were sparged with high purity nitrogen (< 10 ppm O_2) for 1 h prior to use.

Solvents were commercially dried varieties which had been stored over fresh Molecular Sieve 4A for at least 24 h prior to use, and were used without any further precautions to exclude moisture. Sodium ethoxide and methoxide were freshly prepared for each experiment by the addition of the appropriate mass of clean sodium to the appropriate dry alcohol in a reflux assembly fitted with a drying tube.

Electron Paramagnetic Resonance Experiments

Electron paramagnetic resonance experiments were conducted on a Varian V4501-B spectrometer fitted with a rectangular TE_{104} dual sample cavity. Further instrumental details are given elsewhere (31).

The various reduced AQ solutions to be examined were loaded into standard epr capillaries (1.0 × 90 mm nominal) from serum capped preparation flasks via a gas tight polypropylene syringe fitted with a needle long enough to reach the bottom of the capillary. The transfer was conducted in a dry box flushed with high-purity nitrogen gas bubbled through three flasks of Fieser's deoxygenating solution (32), and thence through a tube (5 × 100 cm) packed with indicating Drierite. The liquid levels in the filled esr capillaries were dropped 2 to 3 mm by touching the surfaces with filter paper, and the tubes were sealed with Five-minute Epoxy cement (Lepage's Ltd.). At least 20 min setting time was allowed before tubes were withdrawn from the nitrogen atmosphere.

An internal standard of benzoquinone radical anion placed in the second cavity of the spectrometer was used to calibrate the line width of the AQ radical anion spectra. The radical solution

Can. J. Chem. Downloaded from www.nrcresearchpress.com by 210.87.254.105 on 09/05/12
For personal use only.

Can. J. Chem. Downloaded from www.nrcresearchpress.com by 210.87.254.105 on 09/05/12
For personal use only.

was prepared by a variation of the flow system developed by Venkatamaran (33). Hydroquinone (50.0 mg) was dissolved in 15 mL of 95% ethanol and 20 drops (0.46 mL) of 0.1 *M* aqueous sodium hydroxide added while this solution was exposed to air. Portions of the yellow solution obtained were sealed into several esr capillaries within 10 min according to the procedure outlined above, and gave the expected strong five-line esr signal of about 2.4 G line-width. The signal decreased to about 1/20 of its original intensity (1/2 h after preparation) 4 h after it was first observed. All sealed esr tubes now looked colorless to the eye. An open tube showed a thin brown line at the open end. For AQ samples having low radical concentrations, the hydroquinone charge was decreased to 5.0 mg.

To determine the absolute number of spins of AQ radical anion samples, fresh diphenylpicrylhydrazyl (DPPH, mp 135–139°C, 19.7 mg) was finely ground and thoroughly dispersed into 13.8 g of previously powdered sodium chloride (Fisher) containing less than 7×10^{-4} mg iron/g. When well packed, this powder had a bulk DPPH concentration of 5×10^{-3} *M*. Samples of exact known weight were sealed in esr capillaries with epoxy and the integrated area (by weighing) of the single line spectrum was used as a standard for determining numbers of spins. Determination of the absolute number of spins of the various AQ samples was simplified by irradiating the sample with sufficient power to saturate the sample and cause collapse of the normal 13 or 19 line spectra (31) to a single line of similar line width to that of DPPH. The absolute number of spins in a sample containing AQ radical anions was estimated by simultaneously scanning both samples and DPPH in the dual cavity probe, with a modulation amplitude high enough to cause saturation. The gain settings required to obtain the same peak area for sample and reference were then compared (34). For greater accuracy, the whole procedure was repeated with the reference DPPH and the sample positions reversed in the cavities of the spectrometer and the average of the two gain ratios was used to determine the absolute number of spins. It was then possible to relate the absolute number of spins of other AQ samples by comparing their signal strengths to that of the calibrated AQ sample, both now run under ordinary conditions.

Redox Potential Measurements

These were made in a closed cell containing a smooth platinum electrode with a saturated calomel reference electrode (Fisher No. 13-639-115 and 13-639-51 respectively). The voltage was measured with a high impedance (10^{12} ohm) voltmeter (Aardvark Instrument Co., Model PEC-VM) whose output was fed to a pen recorder.

Glucose (1.0 g), sodium dithionite (1.0 g), and cellobiose (1.0 and 2.0 g) were added to 25 mL of freshly nitrogen-purged sodium hydroxide (1.0 *M*), and the change in potential was recorded as a function of time. A parallel set of experiments was conducted in 1.0 *M* aqueous potassium hydroxide. Attempts to obtain redox potential curves for cellobiose in KOH solution failed to yield reproducible results.

Reduction of Anthraquinone by Glucose

One example (No. 22-1) is described. A suspension of 25 mg of AQ (0.120 mmol) in 25 mL 1.0 *M* aqueous sodium hydroxide (previously sparged with nitrogen, 1 h) placed in a serum-capped Erlenmeyer flask was magnetically stirred for 5 min while flushing with nitrogen via two syringe needles through the serum cap. Stirring was stopped, 21.6 mg (0.120 mmol) of glucose was added, the serum cap was replaced and wired on, and nitrogen flushing was continued for 2 min before stirring was resumed. The exit flushing needle was removed before the nitrogen entry needle to give a positive pressure of 7 kPa. In 3 h the originally white suspension had become slightly pink, and in 47 h had become a clear deep red solution. Details of other experiments with glucose as reductant are given in Table 1. Reductions in nonaqueous or aqueous-organic media (Table 2) were conducted in a manner strictly parallel to the aqueous reductions.

Reduction of Aqueous Anthraquinone by Sodium Dithionite

These experiments were conducted in a similar manner to the aqueous sugar reductions except that preparation No. 15-1 was carried out in a stoppered, magnetically stirred, completely full one liter Erlenmeyer flask in the open air, and the resulting solution was then transferred to esr capillaries in a nitrogen box. Details are given in Table 3.

Reduction of Aqueous Anthraquinone by Cellobiose

The sugar (123 mg; 0.360 mmol) was added to a previously nitrogen-purged flask containing a suspension of AQ (25 mg; 0.120 mmol) in 25 mL 1.0 *M* sodium hydroxide. A serum cap was wired on and the system was flushed with nitrogen through two needles for a further 5 min before leaving a slight positive nitrogen pressure. This suspension was then magnetically stirred for 1 h, with no change in appearance, whereupon it was placed in a water bath at 50°C. In 1 h the suspension had become red, and most of the AQ had dissolved. A trace of undissolved AQ remained after 1.5 h, but the suspension had become a clear deep red solution after 15 h stirring.

Reduction of Aqueous Anthraquinone by Cellulose and Lignin Preparations

Three suspensions of AQ (10 mg) in 10 mL of 1.0 *M* sodium hydroxide in screw-capped Reacti-Flasks[2] fitted with Teflon-lined silicone rubber septa and Teflon-covered stirring bars were prepared in a nitrogen-flushed glove-bag. Samples of Whatman No. 1 filter paper, cotton linters, and hydrocellulose (35) were finely chopped, a weighed sample (202 ± 2 mg) of each was added to a flask, and the flasks were tightly closed. Stirring 24 h at room temperature (21°C) induced no change in appearance. All the flasks were placed in a stirred oil bath which was gradually heated to 70°C over 8 h while stirring of the contents of each flask was continued. The paper experiment showed no change, while after 2 h at 65–70°C the linters and hydrocellulose mixtures had become colored. The observations, set out in Table 4, indicate that hydrocellulose in aqueous alkali reduced AQ more effectively than linters, while filter paper failed to reduce AQ.

Cuoxam lignin (200 mg) prepared as described in ref. 36 also failed to reduce AQ (10 mg) in aqueous alkali below 150°C (Table 4). A second sample was heated at 160°C without any red color being produced. Dioxane lignin (37) gave a dark solution at room temperature, and thus could not be tested. Periodate lignin (38) gave a brownish-red supernatant after 30 min at 25°C indicating reduction of AQ. A control experiment without AQ had a quite different brown color. Because of the seemingly different behaviour of cuoxam and periodate lignins towards AQ, we examined the redox potentials of 1 *M* sodium hydroxide containing these materials. As anticipated, periodate lignin gave a low potential (−0.62 V after 10 min at 25°C) while cuoxam lignin yielded a less powerfully reducing solution (−0.42 V vs. SCE).

A further experiment with 207.2 mg of finely chopped Whatman No. 1 filter paper placed in a Reacti-Flask[2] with 10 mL of 20 *M* aqueous sodium hydroxide and 10.0 mg of AQ, with the same precautions as above, was heated with stirring to 150°C during 1 h in a stirred oil bath without any visible change. After 1.7 h at 157°C the flask contents became a pale reddish brown color, and after a further 0.5 h a green upper layer appeared. The

[2]Supplied by Pierce Company, Rockford, Illinois. Flasks larger than the 10 mL size do not withstand the pressure developed in this experiment.

TABLE 1. Stoichiometry and rate of reduction of anthraquinone (AQ) by glucose (Gluc) in aqueous suspensions at room temperature

Experiment No.	Gluc:AQ, mmoles	Base, and concentration	Volume of solution mL	Time (h) to Initial dianion[a]	Time (h) to Total solution of AQ[b]	Remarks
22–1	0.12 0.12	NaOH, 1 *M*	25	3	48	Strong $AQ^{\cdot -}$ radical signal equivalent to 1% of the AQ present
22–2	0.36 0.12	NaOH, 1 *M*	25	0.3	10	Weak $AQ^{\cdot -}$ radical signal
24–1	0.24 0.12	NaOH, 1 *M*	25	16	—	About 1/5 of AQ dissolved in 48 h[c]
24–2	0.06 0.12	NaOH, 1 *M*	25	8	—	About 1/2 of AQ dissolved in 48 h[c]
57–1	0.17 0.10	NaOH, 20 *M*	20	0.17	5.25	Final dark green *suspension*[d]
57–2	0.17 0.10	NaOH, 5 *M*	20	0.75	5.25	Deep red solution
57–3	0.17 0.10	NaOH, 1 *M*	20	3.5	8	Deep red solution
57–4	0.17 0.10	NaOH, 0.25 *M*	20	4.5	9.5	Deep red solution
55–3	0.12 0.05	H_2O only	10	—	—	No change in 22 h stirring
55–3	0.12 0.05	H_2O, + 1 mL 5 *M* $NaOC_2H_5/C_2H_5OH$	11	10	—	Initially, yellow suspension[e]
67–2	0.36 0.12	KOH, 1 *M*	25	0.6	4	Deep red, no radicals detected

[a]The time at which the first pink coloration was detectable from the initially white suspensions.
[b]The time at which a clear (non-turbid) deep red solution was obtained.
[c]After 48 h stirring at room temperature the mixture was gradually heated to 93°C over 48 h. The color of the reaction with 0.024 mmol glucose gradually faded to white, the other showed no change.
[d]Color change sequence observed was: 5 min, yellow; 10 min, pale brown; 15 min, greenish brown; 30 min, brownish green; 45 min, green suspension; gradually during next 4.5 h becoming a very dark green suspension. Pressure filtration under nitrogen yielded a clear colorless filtrate without a detectable esr signal and a green precipitate. On exposure to air the green solid did not change in appearance during three days, but had become white in one month.
[e]Initial yellow suspension gradually became a stable yellow orange suspension after 7 h.

flask was swirled occasionally while heating for another 0.5 h without any further change, so the temperature of the bath was raised during the next 0.5 h to 169°C. At this point the flask contents became a pale purple color, again with the green upper layer present. After 1.7 h at this temperature with no further visible change the flask exploded.

Oxidation of Reduced AQ by Model Wood Components

Anthraquinone (8.2 mg, 0.04 mmol) and 1.0 *M* aqueous sodium hydroxide (10 mL) were added to each of six Reacti-Flasks under nitrogen in a glove bag and, 16 h later, glucose (14 mg, 0.08 mmol) was added, yielding, after standing overnight, a red solution of reduced AQ. Dioxane lignin, periodate lignin, cuoxam lignin, cotton linters, Whatman filter paper, and hydrocellulose in 200 ± 2 mg amounts were added to the flasks in turn. The dioxane lignin dissolved immediately to give a solution too dark for further observation. In the other mixtures, the red color was unchanged after 72 h at 25°C. Upon gradually heating to 160°C, there was little change in the flasks containing carbohydrates. The periodate lignin mixture became too dark for further observation above 100°C, but the paler cuoxam lignin mixture was seen to lose some of its color above 120°C.

This interaction of reduced AQ and lignin was observed by polarography in the following way. The AQ (6 mg), hydrocellulose (40 mg), and 1 *M* NaOH (7.5 mL) were placed in Pyrex glass tubes (1/2 in. × 6 in.) sealed at one end and fitted at the other with a Teflon valve (Omnifit 022 BAA). One of the tubes also contained cuoxam lignin (60 mg). The tubes were purged with nitrogen before the chemicals were added, otherwise no precautions were taken to exclude traces of air. The sealed tubes were heated in a glycol bath for 30 min at 140°C, and then, by inverting the tubes and opening their valves, the contents could be transferred under pressure to a nitrogen-purged polarograph cell; DC polarograms were recorded immediately on a Princeton Applied Research 174A polarograph with a model 303 dropping mercury electrode.

Results and Discussion

The Identity of the Reduced AQ Species

Solutions of reduced AQ, prepared in a variety of ways, were examined by esr spectroscopy in an attempt to discover the conditions giving radical anions. AQ reduced with an excess of sodium dithionite (Table 3) in 1 *M* NaOH (No. 15-1) gave a deep red solution which had no esr signal in the total absence of oxygen. When air was admitted to the sample tube, a fully resolved 19-line spectrum appeared (Fig. 2), and gradually increased in intensity. Alkaline dithionite thus seems to reduce AQ completely to the dianion; partial oxidation generates the radical anion.

AQ reduced with 3 mol of glucose per mol of AQ in 1 *M* NaOH (Table 1; No. 22-2) gave a deep red solution which exhibited a weak 19-line esr signal. As can be seen from the redox potential curves in

Can. J. Chem. Downloaded from www.nrcresearchpress.com by 210.87.254.105 on 09/05/12
For personal use only.

TABLE 2. Reduction of anthraquinone (AQ) by glucose (Gluc) in non-aqueous suspensions at room temperature

Experiment No.	Gluc:AQ mmoles	Base, and amount, mmol	Solvent, and vol. of solution	Time to color change	Remarks
51–3	0.0 0.10	NaOH, 10	50% Aqueous ethanol, 20 mL	No change	Remained as white suspension
55–3a	0.12 0.05	Nil	Water, 10 mL	No change	White solid suspension
55–2a	0.12 0.05	Nil	Ethanol, 100% 10 mL	No change	White solid suspension
55–2b	0.12 0.50	$NaOC_2H_5$, 15, in 3 mL	As above, base added after 23 h	1 h[a]	An initial cream-colored suspension[a]
51–2	0.12 0.10	NaOH, 10	50% Aqueous ethanol, 20 mL	5 min, yellow 80 min, green	90% of AQ dissolved; stable green color
55–1a	0.12 0.05	Nil	Dimethylformamide (DMF), 10 mL	No change	30 min to stable colorless solution
55–1b	0.12 0.05	$NaOC_2H_5$, 5, in 1 mL C_2H_5OH	DMF, 10 mL, base added after 23 h	Instant dark green when base added	Stable suspension
63–3	0.84 0.28	$NaOCH_3$, 50	Methanol, 50 mL	1 h, green 15 h, red	Near solution, radicals present
67–1	0.0 0.280	$NaOCH_3$, 50	Methanol, 50 mL	[b]	Nearly all AQ dissolved in 5 h, no radicals unless irradiated

[a]Color change sequence observed was: 1 h, pale cream; 80 min, yellow; 110 min, green; 2 h, dark green suspension and nearly all in solution; 3 h, brownish red and all dissolved; 7 h, deep red and stable color.
[b]No color change in subdued light, became yellow in daylight or under fluorescent lights.

TABLE 3. Sodium dithionite reductions of anthraquinone (AQ) in aqueous suspensions

Experiment No.	$Na_2S_2O_4$:AQ, (mmol)	Base, and amount (mmol)	Solvent (volume of solution)	Time to color change	Remarks
15–1	11.0 5.0[a]	NaOH (1000)	H_2O (1 L)	10 min, pink 4 h, deep red	Turbid suspension No radicals observed
62–1	0.42 0.14	KOH (30)	H_2O (30 mL)	10 s, pink 0.3 h, deep red	Turbid suspension Clear solution
63–2	0.42 0.14	NaOH (30)	H_2O (30 mL)	10 s, pink 0.3 h, deep red	Turbid suspension Clear solution
21–12	0.87 0.48	NaOH (400)	H_2O (20 mL)	10 min, yellow 4 h, brown	Turbid suspension After 48 h became a dark green suspension, see text

[a]Anthraquinone used was not previously reprecipitated, i.e. it had a large particle size.

Figs. 3 and 4, alkaline glucose solutions have less reducing power than dithionite solutions. Decreasing the amount of glucose to 1 mol per mol of AQ in 1 *M* NaOH (Table 1; No. 22-1) gave a deep red solution with a strong 19-line esr signal. The absolute concentration of $AQ^{\cdot -}$ was close to 1% of the total AQ present and did not diminish over a period of 3 months when the solution was in a sealed capillary, kept in subdued light at room temperature. When the amount of glucose was decreased to 0.5 or 0.25 mol per mol of AQ, the amount of AQ dissolved decreased correspondingly and pink suspensions were obtained. The reduction mechanism and equilibria appear to favour the formation of the stoichiometric equivalent of AQ^{2-} rather than $AQ^{\cdot -}$.

AQ reduced with 3 mol equivalents of glucose in 1 *M potassium* hydroxide (Table 1; No. 67-2) gave a deep red solution but *no esr signal* in absence of oxygen (less than $1 \times 10^{-7} M$ radical species present). A possible explanation for the failure of KOH solutions to produce radicals lies in the slightly

Can. J. Chem. Downloaded from www.nrcresearchpress.com by 210.87.254.105 on 09/05/12
For personal use only.

Can. J. Chem. Downloaded from www.nrcresearchpress.com by 210.87.254.105 on 09/05/12
For personal use only.

TABLE 4. Reduction of anthraquinone in 1 *M* aqueous sodium hydroxide[a] by model wood components

Temperature, °C	Time, h	Filter paper, Whatman No. 1	Cotton linters	Hydrocellulose	Cuoxam lignin	Periodate lignin
21	24	White suspension, chopped pieces, non-dispersed	Off-white suspension	White suspension	Light brown solution, brown and white solids underneath	Brownish red solution,[b] brown solid
21–70	8	No change	Pink suspension	Deep orange color	No change	No change
70–100	1	No change	Red suspension, part of AQ dissolved	Intense red color	No change	No change
100	3	No change	No change	Red, all AQ dissolved	No change	Solution too dark for further observation
100–130	1	No change	Intense red color, nearly all AQ in solution	No change	Brown solution, no evidence of AQ reduction	
130	3.5	No change	Intense red color, all AQ appears to be in solution, linters well dispersed	No change	No change	
130–150	0.5	Pale yellow mixture	No change	Intense red-brown	No change	
150	0.5	As above, fiber well dispersed	No change	Dark red-brown	No change	
150–210	2	Color faded to white	Red color retained, approx. 0.2 mL volume loss	Red color retained	Brown solution, no red color	

[a]See Experimental for full details.
[b]A control sample without AQ gave a brown solution.

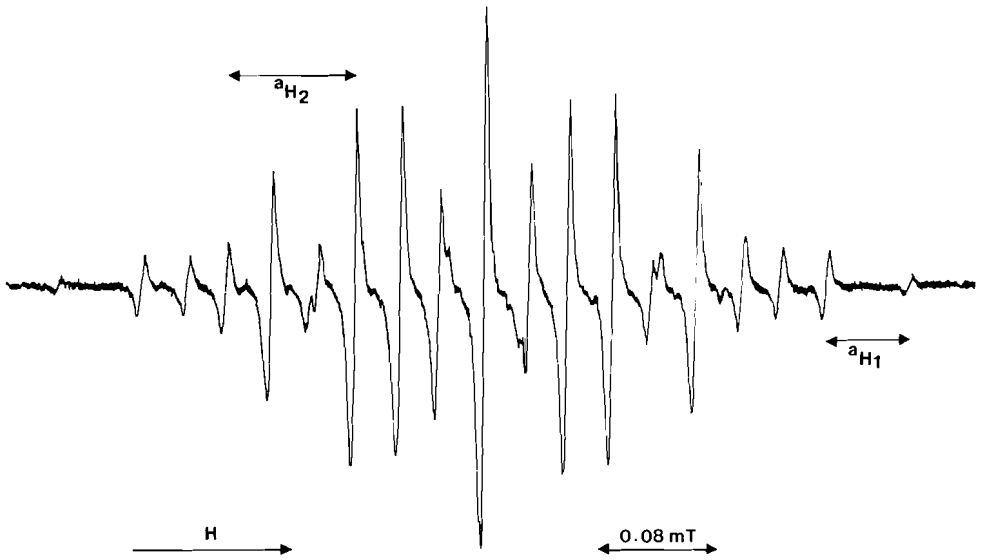


FIG. 2. Electron spin resonance spectrum of anthraquinone radical anion in aqueous 1.0 *M* sodium hydroxide at room temperature, produced by initial reduction with excess sodium dithionite followed by partial oxidation with air (No. 15-1).

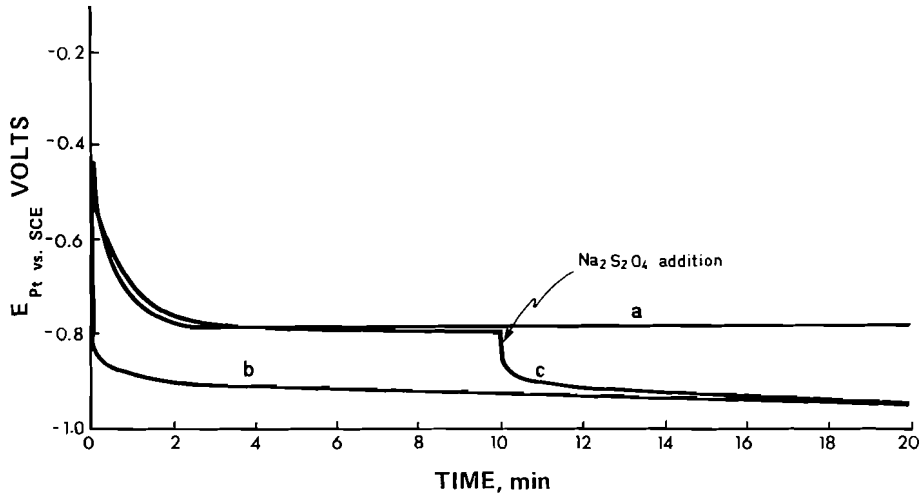


FIG. 3. Redox potential vs. time for (a) 1 g glucose (0.22 *M*), (b) dithionite (1 g), and (c) glucose followed by dithionite, when mixed with 1 *M* sodium hydroxide (25 mL) solution at 23°C.

lower redox potentials observed in KOH solutions of carbohydrates (Fig. 4, lowest curve).

In 1 *M* methanolic $NaOCH_3$, AQ was reduced by 3 equivalents of glucose to a deep red solution which gave a very intense 13-line esr spectrum (No. 63-3, Fig. 5) for $AQ^{\cdot -}$. A 13-line spectrum is commonly observed for $AQ^{\cdot -}$ in methanol solution (29), because the coupling constants of the anion radicals are solvent-dependent (18, 24). The overlapping of lines which produces a 13-line spectrum is also the main reason for the increased signal intensity.

When glucose was omitted from a methanolic AQ solution containing $NaOCH_3$, the solution remained colorless and gave no esr signal (Table 2, No. 67-1). But, when exposed to light, the solution became pale yellow and slowly faded to colorless again. Both of the latter solutions showed very strong 13-line esr spectra of $AQ^{\cdot -}$. The formation of radicals by photoreduction has been noted previously (16, 23), but *colorless* solutions giving the esr spectra of $AQ^{\cdot -}$ have not been reported. In absence of oxygen, the radical anions are stable over long periods (3 months) and do not yield any colored products.

Formation of a Green Material

When an excess of sodium ethoxide was added to

Can. J. Chem. Downloaded from www.nrcresearchpress.com by 210.87.254.105 on 09/05/12
For personal use only.

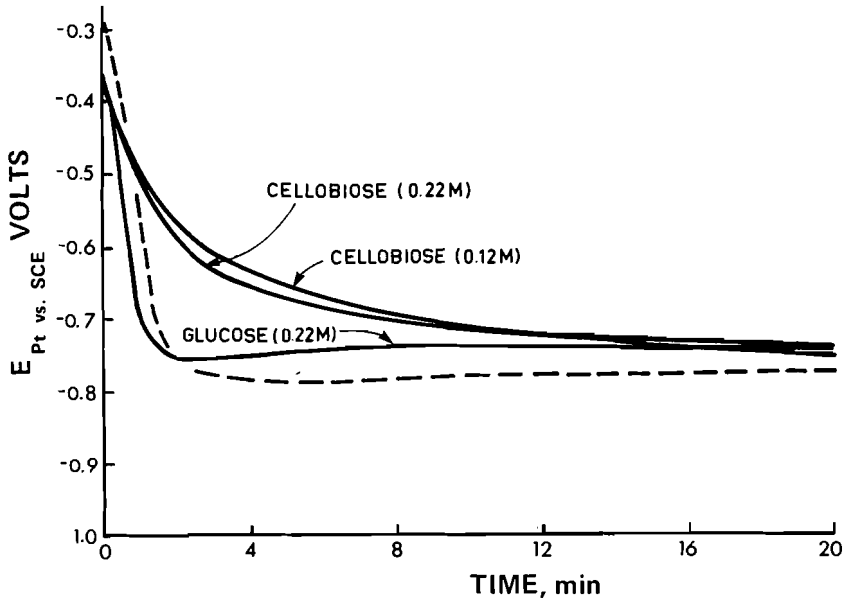


FIG. 4. Redox potential curves for glucose and cellobiose in 1 *M* sodium hydroxide at 23°C. The dotted line was produced by glucose (0.22 *M*) in 1 *M* potassium hydroxide at 23°C.

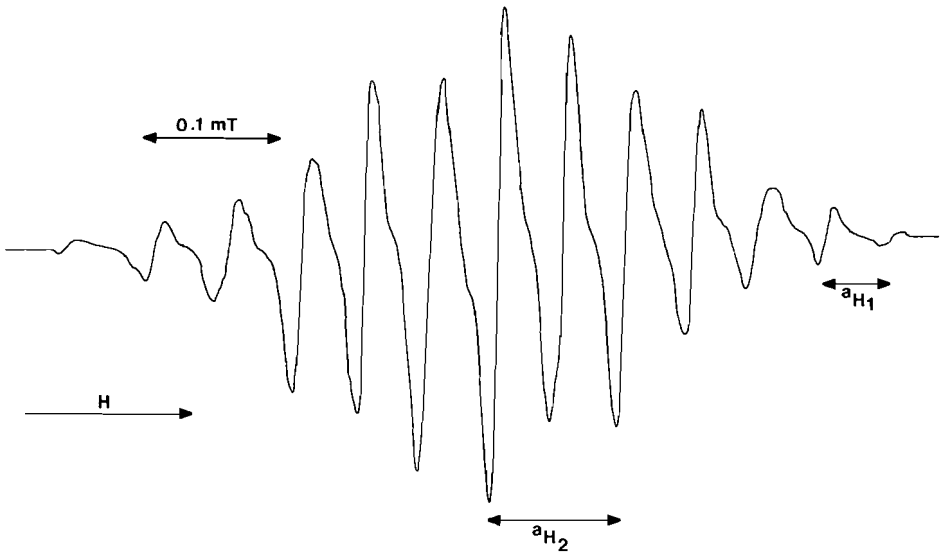


FIG. 5. Electron spin resonance spectrum of anthraquinone radical anion in methanolic 1.0 *M* sodium methoxide after exposure to light (No. 67-1).

a colorless ethanolic suspension of AQ containing glucose, it yielded a dark green suspension in 2 h, and gradually formed a stable red solution over a 7-h period (Table 2, No. 55-2b). Control mixtures of AQ and glucose in ethanol (Table 2, No. 55-2a) or water (Table 2, No. 55-3a), but with no base, and solutions with base but no glucose (No. 51-3) gave no visible reaction. Dark green solutions were obtained from AQ, glucose, and base in dimethylformamide (No. 55-1b); in the absence of base, there was no color (Table 2, No. 55-1a).

When AQ was added to a 1 *M* solution of sodium methoxide in methanol in the presence of 3 equivalents of glucose, a dark green suspension formed in 1 h, then gradually became a red solution (Table 2, No. 63-3). The green material was obtained as a stable end-product when AQ was reduced in 20 *M* aqueous sodium hydroxide with 1.7 equivalents of glucose (Table 1, No. 57-1) or sodium dithionite. When the green suspension from glucose reduction was pressure-filtered under N_2 and the filtrate examined by esr, no signal was observed. The dark

Can. J. Chem. Downloaded from www.nrcresearchpress.com by 210.87.254.105 on 09/05/12
For personal use only.

TABLE 5. DC polarographic measurement of the oxidation of reduced AQ by cuoxam lignin

	Color of suspension	Height of AQ[a] wave (I_d), μA	AQ concentration, ppm[b]		Redox potential (V) of liquor (Hg vs. SCE)
			Reduced	Oxidized	
AQ + hydrocellulose + 1 *M* NaOH	Deep red	9.0	152	2	−0.84
AQ + hydrocellulose + cuoxam lignin + 1 *M* NaOH	Orange	2.1	29	7	−0.78

[a]Measurements made at 95 ± 5°C in liquor blown out of a glass digester tube previously heated at 140°C.
[b]Calibrated with AQ standards in alkaline sodium dithionite solution at 25°C (39).

green precipitate from either source appears to be reasonably stable in air (footnote *d*, Table 1; Table 3).

Deffner and Brunner (12) have reported the formation of green solutions by partial oxidation of anthrahydroquinone solutions in methanol. They considered the color to be caused by quinhydrone formation. This concept is supported by our observation that, when the whole green suspension in 20 *M* NaOH was injected into 80 mL 1 *M* NaOH (oxygen-free conditions), a red solution and a white precipitate formed instantly, evidently by disproportionation. Filtration under nitrogen allowed separation of the white solid, which was anthraquinone (by mp, mixture mp, and ir) and comprised about one half of the initial anthraquinone. Exposure of the red filtrate to air, with stirring, rapidly generated a white suspension in a colorless solution, which on filtration yielded further anthraquinone.

Components of Wood Capable of Reducing AQ

Glucose reduced AQ rapidly at room temperature in 1 *M* aqueous sodium hydroxide, but not as rapidly as sodium dithionite. This is predicted by the redox potential curves (Fig. 3) wherein dithionite is shown to be the more powerful reductant. The asymptotic minimum potential recorded for glucose in the absence of AQ was −0.78 V (Pt vs. SCE), and is reached about 2 min after mixing in NaOH solution.

The stoichiometry of the reduction was approximately 1:1 on a molar basis, glucose to AQ (see Table 2), and was demonstrated to occur at sodium hydroxide concentrations of 0.25 *M* to 5.0 *M*, and probably also at 20 *M* but with a different final product.

Cellobiose was found to reduce AQ slowly at room temperature in 1 *M* aqueous sodium hydroxide, but rapidly at 50°C. The asymptotic minimum redox potential recorded for cellobiose in 1 *M* sodium hydroxide was about the same as that of glucose (−0.75 V, Pt vs. SCE) but is more slowly attained (Fig. 4).

Cotton linters in 1 *M* aqueous sodium hydroxide began to reduce AQ at 70°C (Table 5), with rapid reduction occurring at 130°C. Hydrocellulose produced from these linters by acid hydrolysis (35) was more active, with full reduction occurring at 100°C. Whatman No. 1 filter paper, on the other hand, did not reduce AQ even at 150°C in 1 *M* sodium hydroxide. When the experiment was repeated at 170°C in 20 *M* sodium hydroxide, a pale purple solution and green upper phase were evidence of some slight AQ reduction, but the process was apparently accompanied by decarboxylation of some of the hydrolytic products and caused gas release which, possibly accompanied by some attack of the glass, ruptured the flask.

Cuoxam lignin did not reduce AQ in aqueous alkali in contrast to periodate lignin which, in contact with aqueous NaOH, was found to give much lower redox potentials than cuoxam lignin.

Components of Wood Capable of Oxidizing Reduced AQ

Reduced AQ solutions were treated under oxygen-free conditions with wood components in excess to test their ability to oxidize the red solution, i.e. to participate in the upper half of the proposed AQ redox pulping cycle (Fig. 1). None of the materials listed in Table 4 produced any noticeable oxidation during 3 days at room temperature, or when heated slowly to 130°C. Periodate lignin, as expected, did not oxidize the red solution up to 100°C, at which point the solution became dark. Polarograph measurements showed that cuoxam lignin was able to oxidize solutions of reduced AQ at 140°C (Table 5). Hydrocellulose was the preferred reagent for the reduction of AQ in this experiment because, unlike glucose, it did not form dark-colored products during the reaction.

Conclusions

It now seems quite clear that the red form of

Can. J. Chem. Downloaded from www.nrcresearchpress.com by 210.87.254.105 on 09/05/12
For personal use only.

reduced AQ is the dianion. The radical anion is colorless, or, at most, pale yellow. Under conditions of high base strength, a green substance, possibly a quinhydrone, may be observed.

The maximum concentration of radical anion observed in the aqueous room temperature experiments amounted only to 1% of the AQ charge, although the possibility exists of higher equilibrium radical concentrations at pulping temperature (170°C).

In aqueous alkaline solution AQ can be reduced by polysaccharide end groups, but the ease of reduction, as judged by the temperature required, seems to be a function of chain length, the order of reduction efficiency being: glucose > cellobiose > hydrocellulose > cotton linters > filter paper. This conclusion is supported, at least for glucose/cellobiose, by both the much slower development of the asymptotic minimum redox potential and the slightly less negative asymptotic minimum reached for the same molar concentrations (Fig. 4).

Two insoluble lignin preparations behaved differently towards AQ in alkaline solution. Periodate lignin was able to reduce AQ under alkaline conditions at room temperature, but cuoxam lignin did not. On the contrary, when heated to 140°C, alkaline solutions of reduced AQ were oxidized by cuoxam lignin. The difference in behavior doubtless stems from the modification of lignin during isolation. Periodate lignin is considerably demethylated and oxidized during isolation (40) and it is thus not a particularly good model for virgin lignin. Cuoxam lignin, on the other hand, has chemical and physical properties which resemble more closely those of lignin in wood (41).

Acknowledgements

The authors are indebted to S. M. Mattar for the esr spectra. They are also grateful to Dr. A. S. Perlin for helpful discussion, and (MBH) to Dr. Perlin and the Department of Chemistry, McGill University for providing support facilities during his tenure of the Harold Hibbert Memorial Fellowship. Part of this work was also supported by an IRAP grant from the National Research Council of Canada.

1. H. H. HOLTON. Pulp Paper Can. **78** (10), 19 (1977); U.S. Pat. 4,012,280 (March, 1977).
2. L. LOWENDAHL and O. SAMUELSON. Tappi, **61** (2), 19 (1978).
3. B. I. FLEMING, G. J. KUBES, J. M. MACLEOD, and H. I. BOLKER. Tappi, **61** (6), 43 (1978).
4. K. IIYAMA, A. G. KULKARNI, Y. NOMURA, and J. NAKANO. J. Jpn. Wood Res. Soc. **24**, 766 (1978).
5. R. L. EDSBERG, D. EICHLIN, and J. J. GARIS. Anal. Chem. **25**, 798 (1953).
6. P. H. GIVEN, M. E. PEOVER, and J. SCHOEN. J. Chem. Soc. 2674 (1958).
7. K. DEUCHERT and S. HUNIG. Angew. Chem. Int. Ed. Engl. **17**, 875 (1978).
8. I. V. KHUDYAKOV and V. A. KUZ'MIN. Russ. Chem. Rev. **44**, 801 (1975).
9. P. R. RAO and E. HAYON. J. Phys. Chem. **77**, 2274 (1973).
10. B. E. HULME, E. J. LAND, and G. O. PHILLIPS. Trans. Faraday Soc. **68**, 1992 (1972).
11. S. COFFEY. Chem. Ind. 1068 (1953).
12. U. DEFFNER and E. BRUNNER. Z. Phys. Chem. **51**, 290 (1966).
13. A. K. GUPTA. J. Chem. Soc. 3479 (1952).
14. D. E. G. AUSTEN, P. H. GIVEN, D. J. E. INGRAM, and M. E. PEOVER. Nature, **182**, 1784 (1958).
15. S. K. WONG, W. SYTNYK, and J. K. S. WAN. Can. J. Chem. **50**, 3052 (1972).
16. R. W. BRANDON and E. A. C. LUCKEN. J. Chem. Soc. 4273 (1961).
17. M. R. DAS and G. K. FRAENKEL. J. Chem. Phys. **42**, 1350 (1965).
18. E. W. STONE and A. H. MAKI. J. Chem. Phys. **36**, 1944 (1962).
19. V. H. RINKEL and W. WINDSCH. Z. Phys. Chem. **227**, 281 (1964).
20. B. J. TABNER and J. R. ZDYSIEWICZ. J. Chem. Soc. 1659 (1971).
21. G. R. STEVENSON, A. E. ALGERIA, and A. M. BLOCK. J. Am. Chem. Soc. **97**, 4859 (1975).
22. R. POINTEAU, J. FAVEDE, and P. DELHAES. J. Chim. Phys. **61**, 1129 (1964).
23. J. H. SHARP, T. KUWANA, A. OSBORNE, and J. N. PITTS. Chem. Ind. 508 (1962).
24. G. VINCOW and G. K. FRAENKEL. J. Chem. Phys. **34**, 1333 (1961).
25. B. VENKATAMARAN, B. G. SEGAL, and G. K. FRAENKEL. J. Chem. Phys. **30**, 1006 (1959).
26. H. L. STRAUSS and G. K. FRAENKEL. J. Chem. Phys. **35**, 1738 (1961).
27. M. R. DAS and B. VENKATARAMAN. J. Chem. Phys. **35**, 2262 (1961).
28. B. ELSCHNER, R. NEUBERT, H. BERG, and D. TRESSELT. Z. Chem. **1**, 361 (1961).
29. M. ADAMS, M. S. BLOIS, and R. H. SANDS. J. Chem. Phys. **28**, 774 (1958).
30. O. S. KSENZHEK, S. A. PETROVA, S. V. OLEINIK, and V. Z. MOSKOVSKII. Elektrokhimiya, **13**, 182 (1977); Chem. Abstr. **86**, 129946t (1977).
31. M. B. HOCKING and S. M. MATTAR. To be published.
32. L. F. FIESER and M. FIESER. Reagents for organic synthesis. Vol. I. Wiley, New York. 1967. p. 393.
33. B. VENKATAMARAN, B. G. SEGAL, and G. K. FRAENKEL. J. Chem. Phys. **30**, 1006 (1959).
34. K. HALBACH. Phys. Rev. **119**, 1230 (1960).
35. D. W. CLAYTON and L. M. MARRACCINI. Sven. Papperstidn. **69**, 311 (1966).
36. J. J. RENARD, D. M. MACKIE, and H. I. BOLKER. Pap. Puu, **57**, 786 (1975).
37. J. M. PEPPER, P. E. T. BAYLIS, and E. ADLER. Can. J. Chem. **37**, 1241 (1959).
38. P. F. RITCHIE and C. B. PURVES. Pulp Pap. Mag. Can. **48** (12), 74 (1947).
39. B. I. FLEMING, G. J. KUBES, J. M. MACLEOD, and H. I. BOLKER. Tappi, **62** (7), 55 (1979).
40. H. I. BOLKER. Natural and synthetic polymers. Dekker, New York. 1974. p. 596.
41. B. I. FLEMING and H. I. BOLKER. To be published.

Can. J. Chem. Downloaded from www.nrcresearchpress.com by 210.87.254.105 on 09/05/12
For personal use only.

Quantitative prediction of stereochemistry in the reduction of cyclohexanones by sodium borohydride

R. MURUGAN

University Service and Instrument Centre, Madurai Kamaraj University, Madurai-625 021, India

Received April 11, 1980

R. MURUGAN. Can. J. Chem. **58**, 1993 (1980).

An extremely simple method is presented for quantitatively predicting the stereochemical product ratio in the reduction of alkylcyclohexanones by sodium borohydride. Accurate predictions are made except in the cases of highly hindered ketones.

R. MURUGAN. Can. J. Chem. **58**, 1993 (1980).

On présente une méthode quantitative extrêmement simple qui permet de prévoir le rapport des produits stéréochimiques de la réduction des alkylcyclohexanones par le borohydrure de sodium. Les prévisions sont justes sauf dans le cas de cétones fortement encombrées.

[Traduit par le journal]

Can. J. Chem. Downloaded from www.nrcresearchpress.com by 210.87.254.105 on 09/05/12
For personal use only.

Introduction

Reduction of cyclohexanones by sodium borohydride and other similar reducing agents has attracted much attention. Many ideas and theories have been advanced to account for the interesting stereochemical control exhibited in these reactions (1–10). In contrast, however, much less attention has been paid to the matter of quantitatively predicting these stereochemical product ratios, with only two approaches, those of Wigfield (11) and of Wipke and Gund (12), having been presented in the literature.

Discussion

The method presented here is an extremely simple, yet useful, empirical method that applies to the reduction of cyclohexanones by sodium borohydride. The assumptions made for the quantitative prediction are as follows.

(*1*) Changes in stereoselectivity from one ketone to another are simply the consequence of differential steric impedance between ketone and reducing agent.

(*2*) The difference in stereoselectivity between a substituted cyclohexanone and cyclohexanone is assumed to be due to the substituent present in the cyclohexanone ring. For example, the stereoselectivity of cyclohexanone and 3-methyl cyclohexanone are respectively (product ratio, axial/equatorial) A/E (cyclohexanone) = 86:14 and A/E (3-methyl cyclohexanone) = 87:13. That is, a 3e methyl group has no effect on the stereoselectivity in the reduction of cyclohexanone by sodium borohydride.

(*3*) The stereoselectivity of free cyclohexanone is taken as the base value for the calculation.

(*4*) The increments are given for calculating the percentage of equatorial alcohol formed. Positive increment values are given for substituents which hinder equatorial attack of the reagent, negative increment values are given for substituents which hinder axial attack of the reagent, and zero values for substituents which do not hinder either axial or equatorial attack of the reagent. From previous work and from models it is clear that 2e(6e) and 3a(5a) substituents hinder axial attack and so are given negative increment values; 2a(6a) and 4a substituents hinder equatorial attack and so are given positive increment values; 3e(5e) and 4e substituents do not hinder equatorial or axial attack and so are given zero values.

(*5*) The effect due to two or more substituents on the stereoselectivity is assumed to be additive.

From a detailed study of the stereoselectivity of the different cyclohexanones (16) the increment values for methyl substituents at various positions in the cyclohexanone ring are given in Table 1. For substituents other than the methyl group the increment values are also given in Table 1.

For example, the calculation of percentage of equatorial alcohol formed for 2,4,4-trimethyl cy-

TABLE 1. Increment values for substituents at various positions in the cyclohexanone ring for calculating percentage of equatorial alcohol

	Nature of substituent			
Position	Methyl	—CH_2— of cyclic or acyclic side chain	*i*-Propyl	*tert*-Butyl
2e	−12	−16	−20	−24
2a	+14			
3e	0	−1	−2	−3
3a	−40			
4e	0	0	0	−2
4a	+6			

0008-4042/80/181993-03$01.00/0

© 1980 National Research Council of Canada/Conseil national de recherches du Canada

Can. J. Chem. Downloaded from www.nrcresearchpress.com by 210.87.254.105 on 09/05/12
For personal use only.

TABLE 2. Calculated and observed stereochemical product ratio from ketone reduction with sodium borohydride

No.	Ketone	% Equatorial alcohol Calculated	Observed
	Cyclohexanone (base value)	86	86
1.	4-Methyl cyclohexanone	86	86
2.	3-Methyl cyclohexanone	86	87
3.	2-Methyl cyclohexanone	74	70
4.	*trans*-3,4-Dimethyl cyclohexanone	86	88
5.	*cis*-3,5-Dimethyl cyclohexanone	86	86
6.	2,2-Dimethyl-4-*tert*-butyl cyclohexanone	90	92
7.	2,4,4-Trimethyl cyclohexanone	80	82
8.	3,3,5-Trimethyl cyclohexanone	46	48
9.	*cis*-2,6-Dimethyl cyclohexanone	62	62
10.	3,3-Dimethyl cyclohexanone	46	48
11.	4-*tert*-Butyl cyclohexanone	88	88
12.	3-*tert*-Butyl cyclohexanone	83	83
13.	2-*tert*-Butyl cyclohexanone	62	50
14.	Menthone (*trans*-5-methyl-2-*i*-propyl cyclohexanone)	66	69
15.	3,3-Dimethyl-5-*n*-butyl cyclohexanone	45	45
16.	2-Ethyl cyclohexanone	70	65
17.	2-*n*-Butyl cyclohexanone	70	65
18.	Androstan-3-one	92	91
19.	Cholestan-2-one	44	46
20.	Cholestan-3-one	92	94
21.	Cholestan-7-one	74	73
22.	*trans*-10-Methyl-2-decalone	91	85
23.	*trans*-9-Methyl-2-decalone	45	41
24.	2,5,5-Trimethyl cyclohexanone	34	29
25.	*trans*-3,4-Dimethyl cyclohexanone	86	88
26.	3,3,5,5-Tetramethyl cyclohexanone	6	5
27.	*cis*-2-Methyl-4-*tert*-butyl cyclohexanone	76	79
28.	*trans*-1-Decalone	69	68

clohexanone (Fig. 1) is: base value = 86%; Me at 2e = −12; Me at 4a = +6; Me at 4e = 0. Calculated total = 80%; observed total = 82%.

Calculated percentage of equatorial alcohols using this method and the experimentally observed (11,12,15,16,17) values are shown in Table 2. Examination of Table 2 makes it clear that there is good agreement between the calculated and the experimental values. The method is able to predict satisfactorily for a good number of cyclohexanones including steroidal ketones. The prediction for the ketone, 3,3,5,5-tetramethyl cyclohexanone, is in excellent agreement with the observed value. For 2-substituted cyclohexanones, the difference in value is tolerable for the methyl group but is higher for the *tert*-butyl group, which may be due to the participation of the less stable conformation (13,14) in the reduction process.



FIG. 1

The major limitation of this method is the oversimplification which would lead to predictions of less than 0% or greater than 100% of the equatorial alcohol if too many critical substituents are present. 11-Keto steroids and axial *cis*-2,6-dimethyl cyclohexanones respectively would be examples of this problem. In most cases, however, the prediction is simpler to obtain and as accurate as the method of Wigfield, and far simpler and more accurate than the approach of Wipke and Gund.

Acknowledgements

My thanks are due to Professor D. C. Wigfield, Carleton University, Ottawa, Canada, for his valuable comments during the preparation of this paper. My thanks are also due to Mr. S. Perumal, School of Chemistry, Madurai Kamaraj University, for the discussion that I had with him regarding this paper.

1. J. C. RICHER. J. Org. Chem. **30**, 324 (1965).
2. J. A. MARSHALL and R. D. CAROLL. J. Org. Chem. **30**, 2748 (1965).
3. H. B. BURGI, J. D. DUNITZ, J. M. LEHN, and G. WIPFF. Tetrahedron, **30**, 1563 (1974).

4. W. G. DAUBEN, G. J. FONKEN, and D. S. NOYCE. J. Am. Chem. Soc. **78**, 2579 (1956).
5. J. W. CONFORTH, R. H. CONFORTH, and K. K. MATHEW. J. Chem. Soc. 112 (1959).
6. H. HAUBENSTOCK and E. L. ELIEL. J. Am. Chem. Soc. **84**, 2363 (1962).
7. M. CHREST, H. FELKIN, and N. PRUDENT. Tetrahedron Lett. 2199 (1968).
8. M. CHREST and H. FELKIN. Tetrahedron Lett. 2205 (1968).
9. E. L. ELIEL and Y. SENDA. Tetrahedron, **26**, 2411 (1970).
10. D. H. WERTZ and N. L. ALLINGER. Tetrahedron, **30**, 1579 (1974).
11. D. C. WIGFIELD. Can. J. Chem. **55**, 646 (1977).
12. W. T. WIPKE and P. GUND. J. Am. Chem. Soc. **98**, 8107 (1976).
13. D. C. WIGFIELD and D. J. PHELPS. J. Am. Chem. Soc. **96**, 543 (1974).
14. D. C. WIGFIELD, S. FEINER, and D. J. PHELPS. J. Org. Chem. **40**, 2533 (1975).
15. B. RICKBORN and M. T. WUESTHOFF. J. Am. Chem. Soc. **92**, 6894 (1970).
16. D. C. WIGFIELD and D. J. PHELPS. J. Org. Chem. **41**, 2396 (1976).
17. M. P. DOYLE, C. C. MCOSKER, N. BALL, and C. T. WEST. J. Org. Chem. **42**, 1922 (1977).

Can. J. Chem. Downloaded from www.nrcresearchpress.com by 210.87.254.105 on 09/05/12
For personal use only.

The synthesis and chlorinolysis of 5-phenyl-2,4,5-trithiapentane-2,2-dioxide

TERENCE PATRICK AHERN, RICHARD FRANCIS LANGLER,[1] AND ROBERT LEONARD MCNEIL
Chemistry Department, Dalhousie University, Halifax, N.S., Canada B3H 4J3

Received March 26, 1980

TERENCE PATRICK AHERN, RICHARD FRANCIS LANGLER, and ROBERT LEONARD MCNEIL. Can. J. Chem. **58**, 1996 (1980).

Application of mercaptide anions to the dechlorination of an α-polychlorosulfonyl substrate has provided the key step in a successful synthesis of the title compound. 5-Phenyl-2,4,5-trithiapentane-2,2-dioxide undergoes chlorinolysis in an aqueous medium to yield products consistent with the view that α-sulfonyl oxodichlorosulfonium chlorides and α-sulfonyl dichlorosulfonium chlorides may undergo unusually facile Pummerer rearrangements.

TERENCE PATRICK AHERN, RICHARD FRANCIS LANGLER et ROBERT LEONARD MCNEIL. Can. J. Chem. **58**, 1996 (1980).

L'application des anions thiolates à la déchloration d'un substrat α-polychlorosulfonyle s'avère l'étape clé d'une synthèse satisfaisante du composé mentionné dans le titre. Le phényl-5 trithia-2,4,5 pentane dioxyde-2,2 subit une chlorolyse en milieu aqueux et conduit à des composés qui sont en accord avec le fait que les chlorures d'α-sulfonyloxodichlorosulfonium et les chlorures d'α-sulfonyldichlorosulfonium peuvent subir aisément des transpositions de Pummerer.

[Traduit par le journal]

Introduction

For some time now, we have been studying the pathways followed by sulfur compounds upon chlorinolysis in aqueous and nonaqueous media (1–6). In an earlier report (7), we have described the aqueous chlorinolysis of **1** which furnishes **2** as shown in eq. [1].

[1] $\underset{\mathbf{1}}{CH_3SO_2CH_2SCH_2Ph} \xrightarrow[HOAc]{Cl_2/H_2O} \underset{\mathbf{2}}{CH_3SO_2CCl_2SO_2Cl} + PhCH_2Cl + PhCH_2OAc$

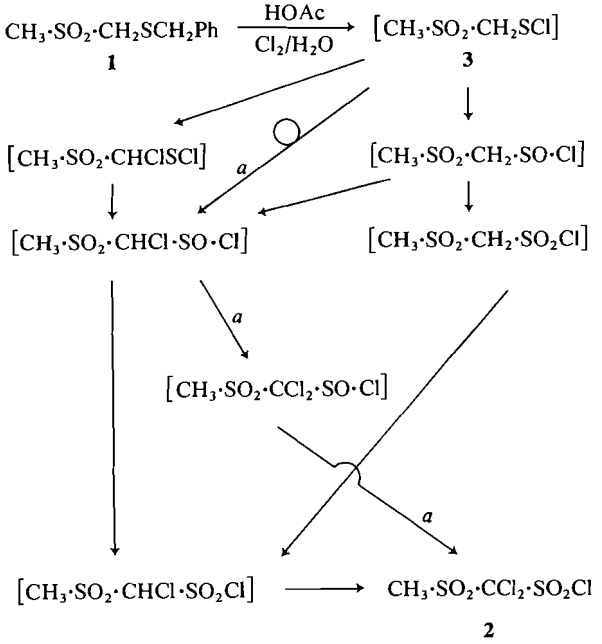
Our conclusions about the pathway for the conversion **1** → **2** are presented as pathway *a* in Scheme 1.

We have undertaken the synthesis of $CH_3SO_2CH_2SSPh$ (**4**) with the expectation that aqueous chlorinolysis of **4** would accomplish the conversion **4** → **3** → **2** if pathway *a* is correct.

Results and Discussion

The synthesis of **4** is depicted in Scheme 2. An attempt to dechlorinate **6** with the reagent system of choice, based on a previous report (6), was complicated by an unwanted substitution reaction as shown in eq. [2].

[2] $\underset{\mathbf{6}}{CH_3SO_2CCl_2S{-}OCH_3} \xrightarrow[CH_3OH/CH_3ONa]{PhCH_2SH} \underset{\mathbf{7}}{CH_3SO_2\overset{\overset{SCH_2Ph}{|}}{CH}{-}S{-}OCH_3}$



SCHEME 1

The mass spectrum of **4** showed an interesting new rearrangement.[2] A fragmentation scheme consistent with the observed data is presented in Scheme 3.

Chlorinolysis of **4** in aqueous acetic acid gave **2** and benzenesulfonyl chloride in good yields as shown in eq. [3].

[3] $\underset{\mathbf{4}}{CH_3SO_2CH_2SSPh} \xrightarrow[HOAc]{Cl_2/H_2O} \underset{\mathbf{2}}{CH_3SO_2CCl_2SO_2Cl} + PhSO_2Cl$

[1]Author to whom correspondence should be directed at the Chemistry Department, Mount Allison University, Sackville, N.B., Canada E0A 3C0.

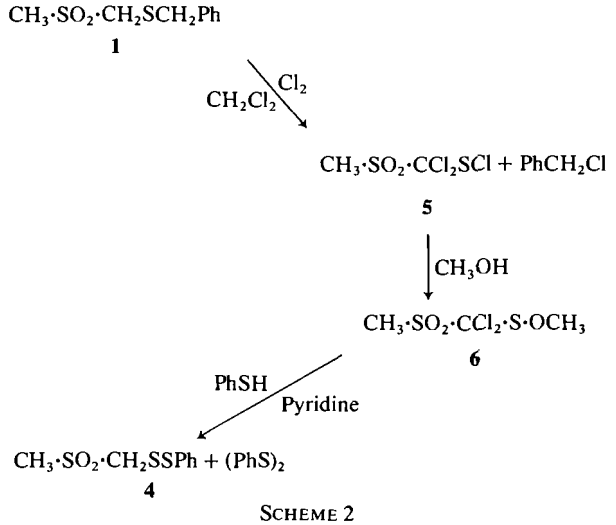
[2]There has been recent interest in the mass spectra of disulfides (8).

0008-4042/80/181996-03$01.00/0

© 1980 National Research Council of Canada/Conseil national de recherches du Canada

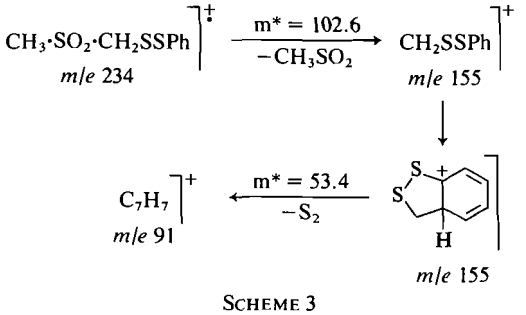
Can. J. Chem. Downloaded from www.nrcresearchpress.com by 210.87.254.6 on 09/05/12
For personal use only.

Can. J. Chem. Downloaded from www.nrcresearchpress.com by 210.87.254.6 on 09/05/12
For personal use only.



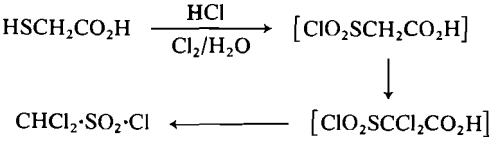
SCHEME 2

This result makes it unnecessary to invoke chlorosulfide or sulfoxide intermediates in the chlorinolysis of **1**, although it does not rigorously exclude them.



SCHEME 3

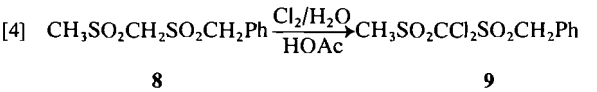
We have recently become aware of a study of the chlorinolysis of thioglycolic acid (9, 10). The proposed pathway, which avoids Pummerer rearrangements altogether, is shown in Scheme 4.



SCHEME 4

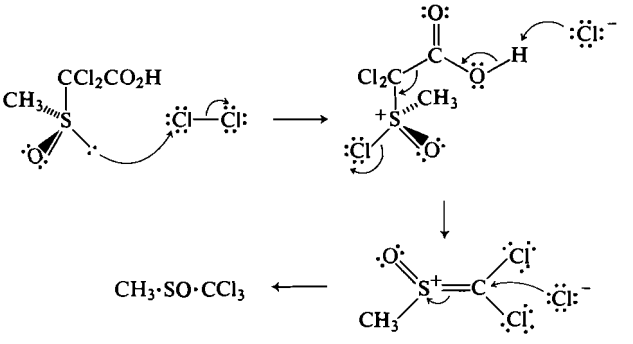
Since we have demonstrated (1) that a related substrate incorporates chlorine on carbon by Pummerer rearrangements and that decarboxylation occurs from an oxochlorosulfonium chloride salt (*vide* Scheme 5) we presumed that the rationale shown in Scheme 4 was in error. In any case, in our system, a disulfonyl methylene would not be expected to chlorinate by an acid catalyzed mechanism and would be unlikely to react (via the anion) with chlorine at a meaningful rate in aqueous acetic acid containing HCl.

To confirm our assumptions we have subjected the model disulfone **8** to aqueous chlorinolysis.



The surprising result shown in eq. [4] invalidates our assumptions and requires consideration of both $CH_3SO_2CH_2SO_2Cl$ and $CH_3SO_2CHClSO_2Cl$ as intermediates in the chlorinolysis of **1**. A preliminary kinetic study[3] of the reaction in eq. [4] indicates that it is base catalyzed but remains rapid enough under the reaction conditions to occur at a significant rate.

While the results from the chlorinolysis of **4** lend further support to Scheme 1 (pathway *a*), the results from the chlorinolysis of **8** introduce three pathways (Scheme 1) which proceed through the



SCHEME 5

sulfone sulfenyl chloride **3** and are consequently equally as reasonable as those portrayed in Scheme 1 (pathway *a*).

It is now clear that conclusive evidence concerning the facility of Pummerer rearrangements in α-sulfonyl sulfenyl and α-sulfonyl sulfinyl chlorides will only come from chlorinolyses of the appropriate substrates in an *anhydrous medium*.

In conclusion, the present results combined with our previous report (7), while not conclusive, offer tantalizing support for the possibility that α-sulfonyl sulfinyl chlorides may undergo very facile Pummerer rearrangements when treated with chorine. Since it is unlikely that such behaviour would be uniquely induced by a neighbouring sulfonyl group, there is now a reasonable probability that the chlorination of thioglycolic acid (9, 10) proceeds through an α-carboxy sulfinyl chloride which would undergo unusually facile Pummerer rearrangement.

Pending further investigation, it must remain unclear which is the preferred pathway for the

[3]R. F. Langler, K. P. Murray, and J. A. Pincock. Unpublished results.

Can. J. Chem. Downloaded from www.nrcresearchpress.com by 210.87.254.6 on 09/05/12
For personal use only.

chlorinolyses of **1** and thioglycolic acid, viz. (*i*) conversion to the unchlorinated sulfonyl chloride with chlorine incorporation on carbon as the final process or (*ii*) conversion to the chlorinated sulfinyl chloride with oxidation of the sulfinyl chloride to the sulfonyl chloride as the terminal step.

Experimental

General

The ir spectra were recorded on a Perkin-Elmer 237B grating spectrophotometer. The nmr spectra were obtained on a Varian T60 instrument using TMS as the internal standard. The mass spectra were recorded on a Dupont CEC model 21-104 mass spectrometer. Samples were directly introduced using an all glass probe and the spectra run at 30 eV with a source temperature of 150°C. Melting points were determined on a Fisher–Johns melting point apparatus and are uncorrected.

Preparation of 5

Chlorine (ca. 200 mL/min) was bubbled into a solution of the sulfone-sulfide **1** (5.25 g) (7) in methylene chloride (25 mL) until the temperature of the reaction mixture fell 1–2°C below ambient temperature (ca. 1 h). The solution was concentrated and the residue rectified at reduced pressure affording the sulfone-sulfenyl chloride **5** (5.22 g) which was identical with previously described material (7).

Preparation of 6

The sulfenyl chloride **5** (3.910 g) was dissolved in methanol (100 mL) and the solution refluxed for 0.5 h. The methanol was evaporated and the residue chromatographed on silica gel (300 g) employing 1% v/v methanol in chloroform (100 mL aliquots) elution. Fractions 7–10 were combined and concentrated affording the sulfenate ester **6** (1.722 g). Upon recrystallization **6** had mp 43–44°C; ir ($CHCl_3$): 1340 and 1150 cm^{-1}; nmr ($CDCl_3$) δ: 4.06 (3H, s) and 3.30 (3H, s); ms *m/e*: 149 (18.5%), 147 (69.0%), 145 (100%), 81 (20.6%), and 79 (61.8%). *Anal.* calcd. for $C_3H_6Cl_2O_3S_2$: C 16.00, H 2.68; found: C 15.91, H 2.73.

Reaction of 6 with $PhCH_2SH$

Crude sulfenate ester **6** was prepared as described above from the sulfenyl chloride **5** (1.279 g). Unchromatographed **6** was added to a solution of sodium methoxide (from 0.265 g sodium) and phenylmethanethiol (2.8 mL) in methanol (50 mL). The reaction mixture was stirred overnight. Methylene chloride (200 mL) was added and the resultant solution washed with water (100 mL). The organic phase was dried, concentrated, and the residue chromatographed on silica gel (300 g) employing 1% v/v methanol in chloroform (100 mL aliquots) for elution. Fractions 15–17 were combined affording clean sulfone-sulfide-sulfenate ester **7** (0.227 g, mp 72–74°C); ir ($CHCl_3$): 1310 and 1130 cm^{-1}; nmr ($CDCl_3$) δ: 7.23 (5H, s), 4.00 (3H, s), 3.97 (1H, s), 3.76 (2H, s), and 3.00 (3H, s); ms *m/e*: 278 (15.1%) and 91 (100%). *Anal.* calcd. for $C_{10}H_{14}O_3S_3$: C 43.14, H 5.06; found: C 42.98, H 5.28.

Preparation of 4

Benzenethiol (5.898 g) and chromatographed sulfenate ester **6** (3.0136 g) were added to dry pyridine (100 mL) and the reaction mixture stirred at ambient temperature for 0.5 h. Methylene chloride (200 mL) was added and the resultant solution washed with 5% HCl (100 mL aliquots) until the aqueous pH remained acidic. The organic layer was dried and concentrated and the residue chromatographed on silica gel (600 g) employing chloroform (100 mL fractions) for elution. Fractions 53–64 were combined and retained affording clean **4** (1.410 g). Upon recrystallization the sulfone disulfide had mp 64–66°C; ir: 1320 and 1130 cm^{-1}; nmr[4] ($CDCl_3$) δ: 7.23 (5H, m), 4.06 (2H, s), and 2.93 (3H, s); ms *m/e*: 234 (M^+, 8.5%), 155 (63.8%), 109 (76.5%), and 91 (100%). *Anal.* calcd. for $C_8H_{10}O_2S_3$: C 41.00, H 4.30; found: C 41.36, H 4.35.

Chlorinolysis of 4

The sulfone disulfide **4** (4.025 g) was added to a solution of glacial acetic acid (25 mL) and water (5 mL); Cl_2 (ca. 200 mL/min) was bubbled into the reaction mixture for 1 h 15 min. The solvent was distilled off at reduced pressure. The residue was rectified at 0.6 Torr affording benzenesulfonyl chloride (1.702 g) which was identical with authentic material by ir, nmr, ms, and bp. The distillation residue was the dichlorosulfone sulfonyl chloride **2** (2.858 g) which was identical to previously obtained samples (7) by ir, bp, and nmr. A sample (1.464 g) of **2** was hydrolyzed by our reported procedure (7) furnishing dichloromethyl methyl sulfone (0.583 g after recrystallization).

Chlorinolysis of 8

The disulfone **8** (0.500 g) was added to a solution of glacial acetic acid (25 mL) and water (5 mL); Cl_2 (ca. 200 mL/min) was bubbled into the reaction mixture for 45 min. Water (50 mL) was added and the resultant mixture washed with methylene chloride (100 mL). The organic layer was washed with 2.5% NaOH (two 50-mL aliquots). The organic layer was dried and concentrated affording the dichlorodisulfone (**9**) (0.639 g). Upon recrystallization the product was shown to be identical with previously obtained material (11) by nmr, ir, mp, and ms.

Acknowledgements

We gratefully acknowledge the technical assistance of Mr. F. Haley and Mr. J. Sutton. We are indebted to Dr. J. H. Kim who ran the mass spectra. We thank Dalhousie University for financial support in the form of a grant from the Research Development Fund.

1. R. F. Langler, Z. A. Marini, and E. S. Spalding. Can. J. Chem. **57**, 3193 (1979).
2. D. G. Kay, R. F. Langler, and J. E. Trenholm. Can. J. Chem. **57**, 2185 (1979).
3. H. O. Fong, W. R. Hardstaff, D. G. Kay, R. F. Langler, R. H. Morse, and D. N. Sandoval. Can. J. Chem. **57**, 1206 (1979).
4. T. P. Ahern, D. G. Kay, and R. F. Langler. Can. J. Chem. **56**, 2422 (1978).
5. R. F. Langler, Z. A. Marini, and J. A. Pincock. Can. J. Chem. **56**, 903 (1978).
6. R. F. Langler and J. A. Pincock. Can. J. Chem. **55**, 2316 (1977).
7. W. R. Hardstaff, R. F. Langler, J. Leahy, and M. J. Newman. Can. J. Chem. **53**, 2664 (1975).
8. M. E. Alonso, H. Aragona, A. W. Chitty, R. Compagnone, and G. Martin. J. Org. Chem. **43**, 4491 (1978).
9. T. Kempe and T. Norin. Acta Chem. Scand. **27**, 1451 (1973).
10. T. Kempe and T. Norin. Acta Chem. Scand. Ser. B, **28**, 609 (1974).
11. W. R. Hardstaff and R. F. Langler. Org. Mass Spectrom. **10**, 215 (1975).

[4]Admixture of authentic $CH_3SO_2CH_2SPh$ established a significant difference in the chemical shifts of the methylene protons from those of **4**. $CH_3SO_2CH_2SPh$ has been described previously (2).

Canadian Journal of Chemistry
Published by
THE NATIONAL RESEARCH COUNCIL OF CANADA

Journal canadien de chimie
Publié par
LE CONSEIL NATIONAL DE RECHERCHES DU CANADA

Volume 58 Number 19 October 1, 1980 Volume 58 numéro 19 1 octobre 1980

The iron(III)-catalyzed oxidation of EDTA in aqueous solution

RAMUNAS J. MOTEKAITIS, ARTHUR E. MARTELL, AND DAVID HAYES
Coordination Chemistry Consultants, Route 5, Box 1255, College Station, Bryan, TX 77840, U.S.A.
AND
WAYNE W. FRENIER
Dowell Division, Dow Chemical U.S.A., Tulsa, OK 74102, U.S.A.
Received February 19, 1980

RAMUNAS J. MOTEKAITIS, ARTHUR E. MARTELL, DAVID HAYES, and WAYNE W. FRENIER. Can. J. Chem. **58**, 1999 (1980).

At temperatures above 100°C iron(III) oxidizes coordinated EDTA to ethylenediaminetriacetic acid in aqueous solution in the absence of molecular oxygen. The reaction proceeds with an activation energy of 28.6 kcal/mol, and its rate is directly proportional to the concentration of Fe(III) and inversely proportional to pH. At 125°C, the halflife of Fe(III) in the presence of excess EDTA is about 3 h at pH 9.3, but increases to >70 h at pH 5.4. The reaction is stoichiometric and no other reaction products or by-products were detected by nmr, gc, and gc – mass spectroscopy. In the presence of oxygen iron catalyzes quantitative oxidation of ethylenediamine-*N,N,N',N'*-tetraacetic acid (EDTA) to ethylenediaminetriacetic acid. The copper(II)–EDTA chelate undergoes a similar reaction but higher temperatures (≲170°C) are required. Iron(III) also oxidizes nitrilotriacetic acid (NTA) to iminodiacetic acid (IDA) and glycine. The hydrolyzed species Fe(OH)EDTA is shown to be the reactive intermediate, and the well-known $(Fe–EDTA)_2O^{4-}$ μ-oxo dimer is shown not to exist at elevated temperatures (above 100°C). Probable mechanisms are proposed for these reactions and comparisons are made with earlier work.

RAMUNAS J. MOTEKAITIS, ARTHUR E. MARTELL, DAVID HAYES et WAYNE W. FRENIER. Can. J. Chem. **58**, 1999 (1980).

A des températures supérieures à 100°C, en solution aqueuse et en l'absence d'oxygène moléculaire, le fer(III) oxyde le EDTA coordonné en acide éthylènediaminetriacétique. L'énergie d'activation de la réaction est de 28.6 kcal/mol et sa vitesse est directement proportionnelle à la concentration de Fe(III) et inversement proportionnelle au pH. A 125°C, la période de demi-vie du Fe(III) en présence d'un excès de EDTA est d'environ de 3 h à un pH de 9.3 mais elle augmente au delà de 70 h à un pH de 5.4. La réaction est stoechiométrique et la rmn, la chromatographie en phase gazeuse et la spectroscopie de masse couplée à la chromatographie en phase gazeuse n'ont pas permis de déceler d'autres réactions ou d'autres produits secondaires. En présence d'oxygène, le fer catalyse l'oxydation quantitative de l'acide éthylènediamine-*N,N,N',N'*-tétracétique (EDTA) en acide éthylènediaminetriacétique. Le chélate cuivre(II)–EDTA subit une réaction analogue mais à des températures plus élevées (≲170°C). Le fer(III) oxyde également l'acide nitriloacétique (NTA) en acide iminodiacétique (IDA) et en glycine. On montre que les espèces hydrolysées du type Fe(OH)EDTA sont les réactifs intermédiaires et que le dimère bien connu $(Fe–EDTA)_2O^{4-}$ et μ oxo n'existe pas à des températures élevées (au-dessus de 100°C). On propose les mécanismes probables de ces réactions et on établit des comparaisons avec un travail antérieur.

[Traduit par le journal]

Introduction

The coordination chemistry of ethylenediamine-*N,N,N',N'*-tetraacetic acid (EDTA) in aqueous solution at normal temperatures (0–100°C) and pressures is well understood in terms of its coordination reactions with metal ions, and the reactions involved are described by appropriate equilibrium constants (1). The ability of EDTA to form stable, soluble metal chelates in solution has resulted in a wide variety of chemical, analytical, and industrial applications for EDTA including water softening, scale removal, and preservative action through the suppression of catalytic effects of metal ion impurities (2). For applications involving high temperatures, there are many reactions that limit the lifetime of EDTA in solution that are not encountered in moderate temperature ranges. In addition to changes in the magnitudes of the thermodynamic parameters, the values of which vary greatly with temperature, there are also extensive changes in

0008-4042/80/191999-07$01.00/0
©1980 National Research Council of Canada/Conseil national de recherches du Canada

Can. J. Chem. Downloaded from www.nrcresearchpress.com by 210.87.254.105 on 09/05/12
For personal use only.

Can. J. Chem. Downloaded from www.nrcresearchpress.com by 210.87.254.105 on 09/05/12
For personal use only.

the hydrolytic stability of the free ligand (3). Indeed, it has been shown that at 175°C and pH 9.4 the EDTA molecule splits via hydrolysis into equimolar amounts of iminodiacetic acid (IDA) and 2-hydroxyethyliminodiacetic acid (HEIDA), at a rate having a half-life of about 4 h (4).

Another important high-temperature degradative pathway becomes available at high temperature when EDTA is bound to a metal ion which has a stable lower valence state (e.g., Fe(III), Cu(II), Co(III), etc.). In these systems the EDTA becomes oxidized by an internal electron transfer process involving the coordinated metal ion. This paper describes a study of the rates and probable mechanism of the oxidation of EDTA by coordinated Fe(III), and of catalytic processes based on this reaction involving molecular oxygen.

Experimental

Reagents

EDTA, iron(III) salts, and other compounds were reagent grade quality materials and were used as received without further purification.

Kinetics

The kinetic experiments were carried out with a Parr glass-lined 2 L stirred autoclave. Appropriate quantities of an inorganic iron(III) salt and EDTA were mixed, diluted with water, and the pH was adjusted to the desired value (usually 9.3) with ammonia or sodium hydroxide. The reaction mixture was heated quickly to the desired temperature under an inert atmosphere and aliquots were removed at predetermined time intervals for spectrophotometric measurement of Fe(III)EDTA concentration. The analysis was made at room temperature by observing the intensity of the 475 nm band which is a quantitative measure of the concentration of $[(Fe(III)EDTA)_2O]$ (5, 6). The equilibrium constant for the dimerization of Fe(III)EDTAOH^{2-} was redetermined for the conditions employed in this investigation ($10^{1.88}$ at 25°C) while the pK_a used for the equilibrium

$$Fe(III)EDTA \rightleftharpoons Fe(III)EDTAOH^{2-} + H^+ \text{ is } 7.58.$$

The analytical samples taken from the autoclave were also analyzed for residual EDTA by nmr spectrometry in D_2O/NaOD solvent systems after removal of the Fe(III) ion.

Product Analysis

The determination of reaction products was made initially through nmr chemical shift assignments, which were subsequently confirmed by glc and mass spectrometry measurements on methyl ester derivatives of the reaction products. These analytical results were compared with parallel measurements of standard compounds considered to be probable candidates for the reaction products and intermediates.

Instrumentation

Visible spectra were recorded with a Cary model 14 spectrophotometer equipped with a thermostatted cell compartment. The temperature of the 1.000 cm matched cells was controlled at 25.0°C with a Haake refrigerated constant temperature bath. The nmr spectra were measured at 36°C with a Varian T-60 spectrometer equipped with a variable temperature probe. Precision nmr tubes were employed, and samples were prepared in NaOD/D_2O solutions with internal trimethylsilylpropanesulfonic acid (TMS*) as reference. The reaction vessel was a 2-L, glass-lined all titanium stirred pressure vessel equipped with a sampling stopcock, stainless steel valve, titanium tube gas inlet and outlet, thermometer well, and a pressure gauge. Gas chromatograms were obtained with a Hewlett-Packard Model 5830A gas chromatograph equipped with both TC and FI detectors. The gc mass spectrograms were measured on esterified samples with a Hewlett-Packard Model HP-5982-59-33 at the Texas A&M Center for trace characterization. Column conditions were 150–250°C at 16°/min, 3% OV-1, 1/8 in. × 10 ft, 20 mL/min flow rate.

Synthesis of Ethylenediaminetriacetic Acid (ED3A) from EDDA

Ethylenediamine-*N,N'*-diacetic acid (EDDA) lactam (0.050 mol) was treated with 8.34 g (0.06 mol) $BrCH_2COOH$ and NaOH while maintaining the pH of the solution between 7–9 at 35°C. After 24 h, the solution was passed through a DOWEX 50WX-8 column in acid form, and the amino acid fraction was concentrated to 25 mL. Crystals of ED3A lactam formed when the solution was allowed to stand for 12 h.

Molecular weight calculated for $C_8H_{12}N_2O_5 \cdot H_2O$ 252; found by titration 254: nmr 3.93 (1), 3.47 (3), 3.30 (1), 3.13 (1), 2.87 (3) in the ratio 1:1:1:1:1.

Conversion of EDTA to ED3A

Refluxing Procedure

A solution containing 19 g (0.065 mol) of ethylenediaminetetraacetic acid disodium salt dihydrate and 24 g (0.056 mol) $Fe(SO_4)_2 \cdot NH_4 \cdot 12H_2O$ was prepared in about 75 mL H_2O by careful addition of a solution containing 7.0 g NaOH in about 10 mL H_2O adjusted to 100 mL and was refluxed under a blanket of oxygen for 168 h. The red Fe_2O_3 precipitate was filtered off and a part of the filtrate was reserved for analysis. Standard Fisher esterification with MeOH was employed to volatilize the amino carboxylic acids for the determination of conversion to reaction product by gas chromatography. The ratio of ED3A/EDTA found was 2.5:1 representing better than 50% conversion with substantial IDA and HEIDA as primary contaminants. Purification was effected by passing 10 mL of the reaction mixture through a DOWEX 50 W X-8 column in the H^+ form using 25 mL wet resin/10 mL of solution, and eluting with water. EDTA passed through unhindered in the first 250 mL of eluate, while the second 250 mL contained almost pure ED3A lactam. The only contaminant appeared to be a trace of IDA.

In the above procedure, ammonia was also used to make the initial solution basic with almost identical results but slightly lower yield.

Autoclave Procedure

A solution containing 58.4 g (0.20 mol) EDTA, 96.0 g (0.20 mol) $FeNH_4(SO_4)_2$, and made basic with 75 mL concentrated NH_3 was heated at 142–145°C for 6 h in a 2-L autoclave initially pressurized to 100 lb/in.^{2}. The resulting Fe_2O_3 was filtered off and all volatiles were removed with a rotary evaporator. Some water was replaced, the solution was acidified, and an equivalent of $FeCl_3$ solution was added. Dilution with isopropyl alcohol (2:1 v/v C_3H_7OH:H_2O) gave 20 g ferric ED3A (34%) as a tan powder. The iron was removed by raising the pH to 10, followed by centrifugation and ion exchange chromatography as described above.

Results and Discussion

Stoichiometry

It was found that when a solution containing 1.00 mol Fe(III) and 1.50 mol EDTA adjusted to pH 9.3 is heated to 175°C, a reaction occurs within minutes to produce a yellow green solution of

Can. J. Chem. Downloaded from www.nrcresearchpress.com by 210.87.254.105 on 09/05/12
For personal use only.

1.00 mol Fe(II)EDTA containing 0.50 mol of an oxidized reaction product. Also, it has been shown in separate experiments that the Fe(II)EDTA complex is stable under these reaction conditions toward any further decomposition for at least 24 h. When a solution containing a 1:1 ratio of Fe(III) to EDTA is heated at pH 9.3 and at 175°C, the same reaction takes place, except that one third of the iron(III) precipitates as ferric oxide, Fe_2O_3. Several experiments were run with ratios of [EDTA]/[Fe(III)] greater than 1.5, with no change in the results; i.e., excess EDTA was inert under the reaction conditions employed, as would be expected from previous work on this ligand (3, 4). Figure 1 illustrates the nmr evidence for these reactions. The nmr spectra (after removal of iron) show that the initial sample taken at just above 100°C is essentially pure EDTA. At $t = 0$, the evidence presented indicates that the reaction is already more than half complete, while the spectra at $t = 0.33$ h and at 3.0 h show that no further changes occur on this time scale. Also, integration over the ethylene proton peaks indicates the ultimate formation of a product in the ratio of 1 mol decomposed product to 2 mol of unchanged EDTA.

The above observations are consistent with the proposed stoichiometry shown in eqs. [1] and [2] for the reactions involving 1.5:1 and 1:1 ligand-to-metal molar ratios, respectively.

[1] $2\text{Fe(III)EDTA} + \text{EDTA} \xrightarrow[\text{pH 9.3}]{175^\circ\text{C}} 2\text{Fe(II)EDTA} + \text{EDTA}_{\text{decomp}}$

[2] $3\text{Fe(III)EDTA} \rightarrow 2\text{Fe(II)EDTA} + (1/2)\text{Fe}_2\text{O}_3 + \text{EDTA}_{\text{decomp}}$

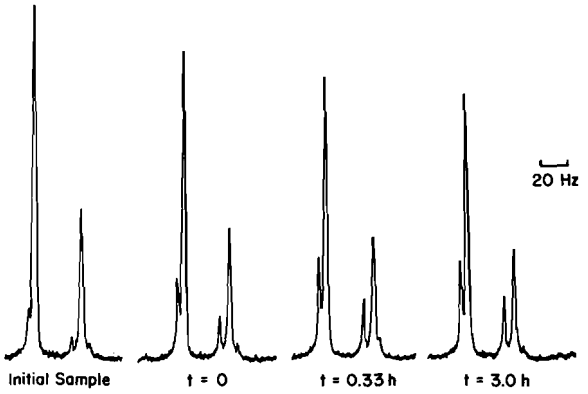


FIG. 1. Proton nmr spectra (after removal of metal ion) of samples of a 1:1 molar ratio of EDTA to Fe(III) after heating to various times at 175°C. The pH was adjusted at room temperature to 9.3 with ammonia. The initial sample is the spectrum taken when the temperature was near 100°C. At $t = 0$ the autoclave contents are at 175°C. After $t = 0.33$ h, the system ceases to react. The heating rate was such that it took 15 min for the temperature to rise from 145 to 175°C.

It is therefore concluded that two electrons are transferred to two Fe(III) ions from one ligand molecule.

Mechanistic Considerations

In order to work out the mechanism of this redox reaction, reaction rates were measured under several sets of conditions. It was found that the rate of reaction is proportional to the concentration of total Fe(III) present. A typical example of the kinetic method employed is illustrated in Fig. 2, in which the ordinate represents the natural logarithm of the total Fe(III) concentration. The Fe(III) concentration was measured spectrophotometrically from the intensity of the 475 nm band ($\varepsilon = 180\ M^{-1}\ cm^{-1}$) which actually is a measure of the room temperature concentration of the μ-oxo dimer, $Fe_2L_2O^{4-}$ in equilibrium with Fe(III)L(OH). The total Fe(III) concentration was computed using the previously measured (*vide supra*) equilibrium constants and standard mass balance equations. Similar kinetic plots were obtained for several pH values at temperatures ranging from 102–143°C. The first order rate constants for the disappearance of Fe(III) thus obtained are presented in Table 1.

It was concluded on the basis of the temperature dependence of the dimerization equilibrium of the hydrolyzed chelate that the reactive species in the

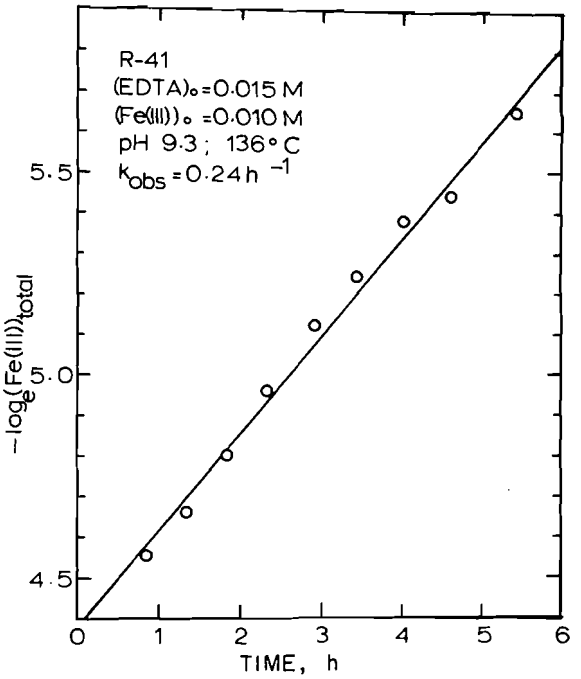


FIG. 2. A plot of the natural logarithm of total remaining Fe(III) concentration vs. time for the system: $[\text{EDTA}]_{\text{initial}} = 1.5 \times 10^{-3}\ M$, $[\text{Fe(III)}]_{\text{initial}} = 1.0 \times 10^{-2}\ M$, pH = 9.3, $t = 136$°C. Slope = $k_{\text{obs}} = 0.24\ \text{h}^{-1}$.

Can. J. Chem. Downloaded from www.nrcresearchpress.com by 210.87.254.105 on 09/05/12
For personal use only.

redox reaction is $Fe(OH)EDTA^{2-}$. Figure 3 contains a plot of log K_D vs. $1/T$ where T is the temperature in degrees Kelvin and K_D is defined by eq. [3].

$$[3] \quad 2\,FeL(OH)^{2-} \rightleftharpoons (FeL)_2O^{4-}$$
$$K_D = [(FeL)_2O^{4-}]/[FeL(OH)^{2-}]^2$$

Each equilibrium point was measured spectrophotometrically in 10° intervals from 25 to 95°C. The ΔH of dimerization was determined from the slope and was found to be -11.6 kcal/mol. The actual concentrations of $Fe(OH)EDTA^{2-}$ and EDTA—Fe—O—Fe—$EDTA^{4-}$ are plotted in Fig. 4 for a 0.0100 M solution of FeEDTA. These plots clearly show that as the temperature is raised at pH 9.30, the predominant species becomes Fe(OH)EDTA.

Additional evidence for implicating mononuclear Fe(OH)EDTA as the reactive intermediate comes from a pH dependence study on the rate of reaction. Table 1 shows that as the pH is lowered, the rate of the oxidation reaction decreases. At 136°C, pH 9.3, the rate constant is 0.24 h^{-1}, at 7.4 it is 0.13 h^{-1}, while at pH 5.4 the reaction practically ceases. Since the pK_a for the hydrolysis of the Fe(III)EDTA chelate is 7.58 (5, 6) (reaction [4]), the observed trend in reaction rates with pH at con-

$$[4] \quad FeL^{-1} \rightleftharpoons FeLOH^{2-} + H^+$$

stant temperature is explained in terms of the concentration of the reactive monohydroxo form of the metal chelate, $FeLOH^{2-}$. The energy of activation for the oxidation at pH 9.30 was found to be 28.6 kcal/mol.

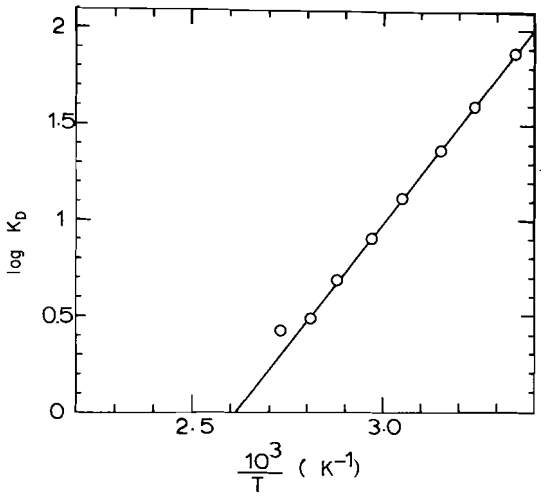


FIG. 3. Plot of log K_D vs. reciprocal of the absolute temperature; $K_D = [Fe_2EDTA_2O^{4-}]/[Fe(OH)EDTA^{2-}]^2$. From the slope, $\Delta H = -11.6$ kcal/mol.

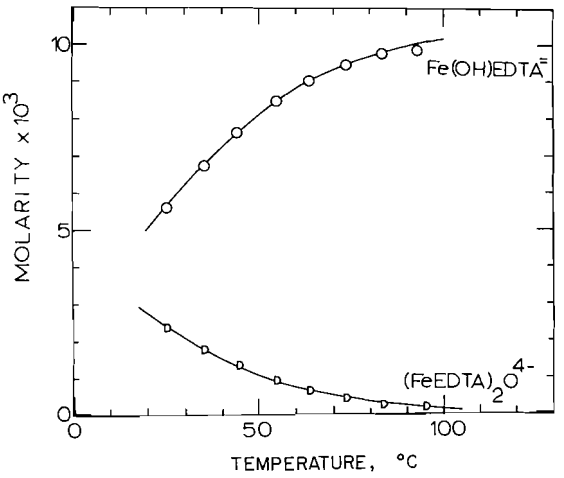


FIG. 4. For initial concentrations of $[Fe(III)]_0 = 0.010\,M$ and $[EDTA]_0 = 0.015\,M$, pH = 9.3, the calculated concentrations of monomer, $Fe(OH)EDTA^{2-}$, and dimer, $Fe_2EDTA_2O^{4-}$, are plotted as a function of temperature. By extrapolation to $t >$ 100°C, the predominant species is $Fe(OH)L^{2-}$, with less than 1% of the iron(III) in the form of the μ-oxo dimer.

TABLE 1. First order rate constants for the oxidation of EDTA by Fe(III)[a]

t (°C)	pH	k (h^{-1})
143	9.30	0.38
136	9.30	0.24
135	9.30	0.22
102	9.30	0.0092
137	7.4	0.13
135	5.4	<0.01

[a] The molar composition of all runs was 0.010 M Fe^{3+}, 0.015 M EDTA; pH was adjusted with NH_3 to 9.30; NaOH was used to adjust lower pH runs.

Identification of Products

Although nmr was very useful in following the reaction rates through the disappearance of EDTA an unambiguous determination of reaction products formed could not be made on the basis of proton nmr measurements alone. Table 2 lists the chemical shifts of several reference compounds which were required for identification of the products formed in this study. Although the chemical shifts are indeed similar, there are differences in the relative integrated intensities of the peaks. Although the spectra were all run in basic $NaOD/D_2O$ solution, in practice the chemical shifts relative to TMS* do vary somewhat as a function of pH, concentration, and the presence of even traces of paramagnetic ions, thus making absolute assignments tenuous. For example, the spectra in Fig. 1 beyond $t = 0$ are consistent with but not necessarily limited to the interpretation that the only reaction product is ethylenediaminetriacetic acid, ED3A.

TABLE 2. Proton magnetic resonance spectra (60 MHz) of reference compounds measured in 0.15 *M* D_2O solutions containing 5% NaOD; chemical shifts are reported in Hz relative to trimethylpropanesulfonate (TMS*)

Compound	Chemical shifts (relative intensities)	
	Acetate	Ethylene
Ethylenediaminetetraacetic acid	190 (4)	160 (2)
Ethylenediamine-*N,N,N'*-triacetic acid[a]	194 (1), 191 (2)	160 (2)
Ethylenediamine-*N,N'*-diacetic acid	190 (1)	160 (1)
Glycine	186	

[a] To obtain nmr spectrum of ED3A the pure lactam was heated on a steam bath with 7 *M* NaOH for 1 h. Solvent was stripped off, D_2O added, and the spectrum was run.

TABLE 3. Gas chromatographic – mass spectral parameters of methylated reference compounds used for identification of reaction products of Fe(III)-catalyzed oxidation of EDTA

Retention time (min)	Standard	Mass, form	Last four peaks				Strongest peak
1.7	IDA	161, diester	130.0	146.1	161.1	162.0	102.0
3.5	HEIDA	173, monoester lactone	171.0	173.1	174.1	175.1	114.0
4.1	S-EDDA	172, monoester lactam	173.1	174.0	186.1	187.0	85.1
5.2	U-EDDA	172, monoester lactam	157.1	163.0	172.1	173.0	113.1
6.7	ED3A	244, diester lactam	213.1	215.1	244.1	245.1	185.1
8.1	EDTA	348, tetraester	317.1	348.2	349.2	350.2	174.1

Because of these uncertainties, a more direct measurement involving gc and gc – mass spectrometry determinations was selected. A number of standards were run individually and the retention times in the order of increasing elution time are shown in Table 3. Although mass spectra generally have many peaks, it is sufficient for most analytical purposes to consider the four peaks having the highest molecular weights, plus the major, or the highest intensity peak.

The gas chromatogram of a typical sample taken from the initial reaction mixture having a 3:1 molar ratio of EDTA to Fe(III), heated at 130°C, consisted of two major peaks, which were found at 6.7 min, with the first peak smaller than the second. The mass spectrograms were identical with those previously obtained for ED3A and EDTA respectively. This result clearly supports the conclusion that in the absence of oxygen, at pH 9.30 the reaction involves the conversion of EDTA to ED3A until all Fe(III) present has been reduced.

In another experiment a sample at pH 9.3 containing a 10:1 molar ratio of EDTA to Fe(III) under a blanket of 92 psig oxygen was heated for 3 h at 135°C. When this reaction mixture was analyzed by gc – mass spectrometry, the gas chromatogram again possessed only two peaks, at 6.7 min and at 8.1 min. In this case, the ED3A peak was about twice as large as the remaining EDTA. Thus it appears that in this system EDTA becomes catalytically oxidized to ED3A according to the following scheme:

[5] $2Fe(III)EDTA + EDTA \rightarrow 2Fe(II)EDTA + ED3A$

[6] $Fe(II)EDTA \xrightarrow{O_2} Fe(III)EDTA$

This catalytic cycle would continue until either the oxygen or the reducing agent (EDTA) becomes exhausted.

The explanation now offered for the nearly stoichiometric conversion of EDTA to ED3A involves the possible combination of three favorable reaction rates: at 135°C the oxidation of Fe(II)EDTA to Fe(III)EDTA by molecular oxygen is almost instantaneous. This means that Fe(III)EDTA is regenerated as rapidly as EDTA is oxidized by Fe(III)EDTA. Secondly, at 135°C, the hydrolysis reaction of EDTA to form IDA and HEIDA is negligible (4). This means that the thermal degradation products would not form from the excess EDTA employed in the reaction. Finally, at 135°C, the reaction of interest proceeds at a convenient rate, with a half-life of about 3 h.

The stoichiometric nature of the oxidation of EDTA requires further discussion in view of the low yields reported above in the adaptation of the reaction for the synthesis of ED3A from EDTA. The magnitudes of the yields reported were

Can. J. Chem. Downloaded from www.nrcresearchpress.com by 210.87.254.105 on 09/05/12
For personal use only.

primarily a reflection of the percent conversion of EDTA, rather than the result of the formation of by-products which were apparently produced in very small amounts. The reported yields would have been greatly increased by separation and recycling of the unreacted EDTA remaining in the reaction mixtures.

Other Systems

In order to confirm the generality of the metal aminocarboxylate redox reaction several other systems were studied. It was found that a 1:1 Cu:EDTA solution, buffered with ammonia to pH 9.30 and heated at 175°C, also undergoes a first order redox reaction in which EDTA is converted to ED3A as the major product. In 24 h under these conditions about 40% ED3A was formed with the remainder of the EDTA found unreacted. Other minor components identified were IDA and HEIDA. Copper(II) was converted to Cu(0). In the absence of oxygen the copper(II)EDTA reaction is interpreted as proceeding in the manner shown in reaction [7].

[7] $\mathrm{CuEDTA} \rightarrow \mathrm{Cu(0)} + \mathrm{ED3A}$

The rate constant for this reaction was determined to be $0.024\ \mathrm{h}^{-1}$. Thus the copper(II) reaction is much slower at comparable temperatures than is the corresponding Fe(III)EDTA redox reaction.

In order to determine the susceptibility of a similar chelating agent to oxidative attack by Fe(III), NTA was investigated under similar conditions with a large excess of ligand-to-metal ion, and in the presence of oxygen. After 24 h at 135°C, the major product identified by gas chromatography was IDA along with lesser amounts of glycine and unreacted NTA. Similarly, when a 2:1 molar ratio of NTA to Fe(III) was heated at 175°C, the following reaction appeared to take place nearly quantitatively:

[8] $2\mathrm{Fe(III)(NTA)_2} \rightarrow 2\mathrm{Fe(II)NTA} + \mathrm{IDA} + \mathrm{NTA}$

Related Studies

A number of studies have been made which indicate that EDTA is oxidized by metal ions at or near room temperature. Lambert and Jones (7) found that at 50°C in aqueous solution hexacyanoferrate(III) oxidizes EDTA according to the following ultimate stoichiometry:

[9] $\mathrm{EDTA^{4-}} + 4\mathrm{Fe(CN)_6^{3-}} + 4\mathrm{OH^-} \rightarrow$ Oxidized organic products $+ 4\mathrm{Fe(CN)_6^{4-}}$

The organic products suggested are IDA and glycolic acid, but were not rigorously shown to be present. The nature of the reaction products was inferred by analogy with the oxidation of EDTA by its own *N,N'*-dioxide.

Hanna and co-workers (8–10) studied the oxidation of EDTA by Ce(IV) in sulfuric acid (8) and perchloric acid (9, 10) media. They found that 4 mol of Ce(IV) per mol of EDTA are required for the initial reaction, but that ultimately 14 mol of Ce(IV) are reduced. The mechanism suggested is represented by reaction [10].

[10] $2\mathrm{Ce(IV)} + \rangle\mathrm{N{-}CH_2CO_2H} \rightarrow \rangle\mathrm{N^+{=}CH_2} + \mathrm{CO_2} + 2\mathrm{Ce(III)} + \mathrm{CO_2} + \mathrm{H^+}$

Thus each acetate function of EDTA is indicated as undergoing a two electron oxidative decarboxylation. The products suggested are the result of a series of such steps in which acetate functions are removed, producing a mixture of the tri-, di-, and monoacetates of ethylenediamine as well as ethylenediamine itself.

Rao (11), on the other hand, observed only a single stoichiometric redox reaction involving a 9:1 molar ratio of Ce(IV) to EDTA. Conflicting results involving earlier work by others were also pointed out by Rao (11).

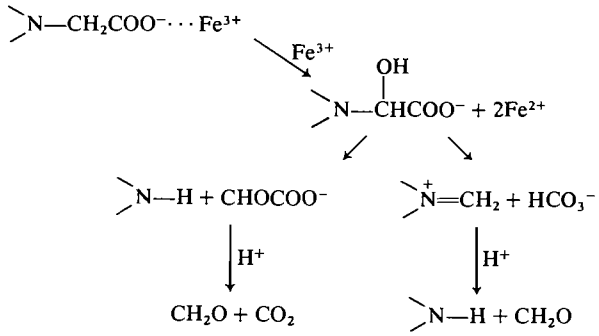
In an environmentally important study, Lockhart and Blakeley (12) investigated photolytic degradation of the Fe(III)EDTA chelate in the presence of oxygen over a period of several days. The products identified include ED3A, iminodiacetic acid (IDA), ethylenediaminediacetic acid (EDDA) (both isomers), ethylenediaminemonoacetic acid (EDMA), and glycine. The reaction was run at pH values of 4.5, 6.9, and 8.5. The following stoichiometry was suggested as the first step in this complex reaction:

[11] $2\mathrm{FeEDTA^-} + 2\mathrm{H_2O} + \mathrm{O_2} \xrightarrow{h\nu} 2\mathrm{CO_2} + 2\mathrm{CH_2O} + 2\mathrm{OH^-} + 2\mathrm{FeED3A}$

In contrast to the rather non-specific nature of the photochemical and redox reactions described above, the thermal Fe(III)EDTA oxidation as described in this work is a highly specific reaction. In the absence of oxygen at pH 9.3 and at temperatures above 100°C Fe(III) continues to oxidize EDTA as long as any is left in the reaction mixture. Two mol of Fe(III) are needed for each mol of triacetate formed. The ferrous ion produced is present in the reaction mixture as the Fe(II)–EDTA chelate, and in separate experiments it has been found to be stable indefinitely at the temperatures employed in this study.

On the basis of the evidence obtained in this research, and the redox reactions of similar systems described above, the mechanism now suggested for Fe(III)-catalyzed oxidation of EDTA is the following:

Can. J. Chem. Downloaded from www.nrcresearchpress.com by 210.87.254.105 on 09/05/12
For personal use only.



The alternate routes indicated for the fission of the acetate group from EDTA cannot be distinguished from each other on the basis of evidence now available. Further investigation of these systems to obtain details of the rate-determining electron-transfer step, and to determine the conditions favoring formaldehyde or glyoxylic acid as the final reaction product seems warranted.

1. R. M. SMITH and A. E. MARTELL. Critical stability constants. Vol. 1. Plenum Publishing Corp., New York. 1974.
2. S. CHABEREK, JR. and A. E. MARTELL. Organic sequestering agents. John Wiley and Sons, Inc., New York. 1959.
3. A. E. MARTELL, R. J. MOTEKAITIS, A. R. FRIED, J. S. WILSON, and D. T. MACMILLAN. Can. J. Chem. **53**, 3471 (1975) and references therein.
4. R. J. MOTEKAITIS, D. HAYES, A. E. MARTELL, and W. W. FRENIER. Can. J. Chem. **57**, 1018 (1979).
5. R. L. GUSTAFSON and A. E. MARTELL. J. Phys. Chem. **67**, 576 (1963) and references therein.
6. G. MCLENDON, R. J. MOTEKAITIS, and A. E. MARTELL. Inorg. Chem. **15**, 2306 (1976).
7. D. G. LAMBERT and M. M. JONES. J. Am. Chem. Soc. **88**, 4615 (1966).
8. S. HANNA, E. M. NICHOLSON, and R. HESSLEY. Z. Anal. Chem. **258**, Part 2, 126 (1972).
9. S. HANNA, S. ATTIGA, W. CARROLL, and W. WEBB. Z. Anal. Chem. **260**, 371 (1972).
10. S. HANNA, W. CARROLL, S. ATTIGA, and W. WEBB. Z. Naturforsch, **30b**, 409 (1975).
11. G. N. RAO. Indian J. Chem. **8**, 328 (1970).
12. H. LOCKHART and R. BLAKELEY. Environ. Sci. Tech. **9**, 1035 (1975).

Can. J. Chem. Downloaded from www.nrcresearchpress.com by 210.87.254.105 on 09/05/12
For personal use only.

The role of the molecular environment for the primary photoprocesses of phenol in solution

J. ZECHNER, G. KÖHLER, G. GRABNER, AND N. GETOFF[1]

Institut für Theoretische Chemie und Strahlenchemie der Universität Wien und Ludwig Boltzmann Institut für Strahlenchemie, Währingerstraße 38, A-1090 Vienna, Austria

Received April 9, 1980

J. ZECHNER, G. KÖHLER, G. GRABNER, and N. GETOFF. Can. J. Chem. **58**, 2006 (1980).

Quantum yields of fluorescence as well as of solvated electron and H atom formation have been measured for phenol in several pure solvents and mixtures of varying polarity. The influence of excitation energy has been studied by excitation of phenol in the first and second excited singlet states. The solvent dependences of fluorescence and photoejection parameters are strongly correlated. The results are interpreted in terms of specific solute–solvent interactions, in particular H-bonded structures.

J. ZECHNER, G. KÖHLER, G. GRABNER et N. GETOFF. Can. J. Chem. **58**, 2006 (1980).

On a mesuré les rendements quantiques de fluorescence ainsi que les rendements d'électrons solvatés et de formation d'atomes d'hydrogène pour le phénol dans plusieurs solvants purs et dans des mélanges de différentes polarités. On a étudié l'influence de l'énergie d'excitation en excitant le phénol dans ses premier et deuxième états singulets excités. L'influence du solvant sur la fluorescence et les paramètres de photoéjection sont fortement reliés. On interprète les résultats en fonction d'interactions spécifiques solvant–soluté en particulier en terme de structures comportant des liaisons hydrogène.

[Traduit par le journal]

Introduction

Solvent effects on photophysical properties of molecules are well known from studies of spectral energy shifts between gas phase and solution. Many of the effects observed could be explained by a general theory of electrostatic interactions (1). However, the influence of solute–solvent interactions on excited state decay processes and primary photochemical reactions is less well understood.

As various studies carried out during the last years have demonstrated, simple aromatic molecules such as phenols, anilines, indoles, and aromatic amino acids share the interesting photophysical property of having a fluorescence quantum yield (Q_F) which is not independent of the energy of excitation (2–5). It has been early recognized that this effect is strongly influenced by the solvent environment: the dependence of Q_F on excitation energy is pronounced in hydrocarbon solvents, small in polar organic solvents, but notable again in water (2, 6). A correlation between the effect on Q_F and the hydrogen bonding capability of the solvent was suggested in the case of phenol (7). Furthermore, a connection with excitation energy-dependent H atom abstraction in hydrocarbon solvents and formation of hydrated electrons in aqueous solutions was established (7–11).

A few studies carried out on indolic compounds have sought to clarify the role of the solvent by studying the dependence of the excitation energy effect on general liquid state parameters, such as the static dielectric constant (12) or Kosower's micropolarity parameter Z (6, 13). These investigations showed that there is no simple relationship between solvent and fluorescence behaviour in the case of the systems studied; the decrease of Q_F at higher excitation energies is related to the static dielectric constant in a non-linear way (12). The behaviour of Q_F in different classes of solvents (hydrocarbons, polar organic solvents, water) is reflected in a different dependence on Z within each of these classes (13).

The aim of the present study was to obtain more information about solvent effects on primary photoprocesses from S_1 and S_2 states of phenol. To this effect, the influence of excitation energy on the fluorescence quantum yield as well as on electron photoejection and H atom formation by OH bond rupture has been investigated in pure polar and apolar solvents and in solvent mixtures. Particular attention has been paid to the possible role of specific solute–solvent interactions on these processes.

Experimental Section

All chemicals used were reagent grade (E. Merck, Darmstadt). Phenol was further purified by sublimation under low pressure, diethyl ether by column distillation, methanol and propanol-2 by distillation under addition of 2,4-dinitrophenyl hydrazine and sulfuric acid, cyclohexane by column chromatography with alumina Woelm B, activity I. Four times distilled water was used for the preparation of aqueous solutions. The purity of all solvents was checked by fluorescence measurements. 2-Chloro-ethanol was kept overnight over K_2CO_3 and then distilled under reduced pressure. Oxygen-free solutions were obtained by saturation with argon. For steady-state irradiations, phenol concentration was 0.01 M. Temperature was kept constant at 30°C.

[1]To whom all correspondence should be addressed.

0008-4042/80/192006-05$01.00/0

©1980 National Research Council of Canada/Conseil national de recherches du Canada

Can. J. Chem. Downloaded from www.nrcresearchpress.com by 210.87.254.105 on 09/05/12
For personal use only.

Can. J. Chem. Downloaded from www.nrcresearchpress.com by 210.87.254.105 on 09/05/12
For personal use only.

Ultraviolet absorption spectra were obtained on a Perkin-Elmer spectrophotometer (Coleman 575). Details of fluorescence measurements (2, 7) as well as of steady-state irradiations at 254 and 229 nm (11), actinometry at these wavelengths (11, 14, 15), and the design of irradiation vessels (16) have been described in detail. Absolute fluorescence quantum yields are based on $Q_F = 0.95$ for 9,10-diphenylanthracene in cyclohexane (17). Changes in refractive indices were taken into account for measurements of absolute yields in other solvents (refs. 2, 18*a*, data about refractive indices were taken from ref. 18*b*).

H atoms originating from excitation of phenol react with the organic solvents used in this work by H atom abstraction. The resulting H_2 was collected in a vacuum line in connection with a gas chromatograph and determined quantitatively (11). Corrections were made for the concurrent reaction of H atoms with phenol using the following rate constants

$$k(\mathrm{H} + \text{phenol}) = 1.8 \times 10^9\ M^{-1}\ s^{-1}\ (19)$$

$$k(\mathrm{H} + \text{methanol}) = 2.5 \times 10^6\ M^{-1}\ s^{-1}\ (20)$$

$$k(\mathrm{H} + \text{propanol-2}) = 6.7 \times 10^7\ M^{-1}\ s^{-1}\ (20)$$

$$k(\mathrm{H} + \text{cyclohexane}) = 4 \times 10^7\ M^{-1}\ s^{-1}\ (21)$$

2-Chloroethanol was used as a specific scavenger for solvated electrons in a concentration of 0.06 *M*; the Cl^- resulting from this reaction was determined by potentiometric titration with $AgNO_3$. The Cl^- yield can be taken as a quantitative measure of the amount of electron photoejection (22).

Results

The characteristic feature of the excitation energy dependence of the fluorescence of phenolic (2, 7) and indolic (3, 5, 6) compounds is a drop of Q_F in the region of overlap between the S_1 and S_2 absorption bands. Q_F is constant within each absorption band. The effect is formally described by the parameter β defined by

$$[1]\quad \beta = Q_F(\lambda_{exc})/Q_F(S_1)$$

β can be equated to the internal conversion efficiency from S_2 to S_1. Figure 1 shows the characteristic behaviour of β for phenol dissolved in cyclohexane – diethyl ether mixtures of varying composition. The lowest value of β is obtained in pure cyclohexane, whereas it is near to 1 in pure diethyl ether.

The two wavelengths at which the steady-state irradiations have been carried out, 254 and 229 nm, fall into the S_1 and S_2 states of phenol. For the processes of photoejection of electrons and H atoms, we define the parameter α in an analogous way to the definition of β:

$$\alpha_{e,H} = Q_{e,H}^{229} - \beta^{229} \times Q_{e,H}^{254}$$

Inasmuch as there is good evidence that α is also constant for excitation within S_1 or S_2 (8, 11), α and β can be related to each other (23). Table 1 shows the quantum yields of fluorescence, electron and H atom formation, as well as the values of β, α_e, and α_H for phenol in various solvents.

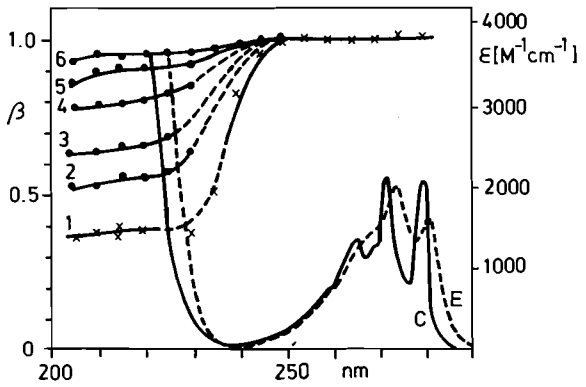


FIG. 1. Dependence of β on excitation wavelength for phenol in cyclohexane – diethyl ether mixtures. (*1*) Pure cyclohexane; (*2*) 0.027 *M*, (*3*) 0.058 *M*, (*4*) 0.15 *M*, (*5*) 0.55 *M* diethyl ether in cyclohexane; (*6*) pure diethyl ether. Curves *C* and *E*: absorption spectra of phenol in cyclohexane and diethyl ether.

β is the lowest in cyclohexane, not much below unity in alcohols, and intermediate in water. Q_e is considerably higher in water than in alcohols, and below the detection limit in cyclohexane. Very few H atoms are ejected in water and alcohols, whereas this is the main photolytical process in cyclohexane. All photolytical processes are more efficient at higher excitation energy ($\alpha > 0$). All these results can be attributed to phenol monomers; indeed, dimer formation in hydrocarbon solution, where it must be expected to be the strongest, is less than 5% for a phenol concentration of 0.01 *M*, as used in the steady-state irradiations (7).

The behaviour of the quantum yields and of the parameters α and β is shown in Figs. 2 and 3 for phenol dissolved in mixtures of H_2O and methanol, and in Fig. 4 for mixtures of cyclohexane and methanol.

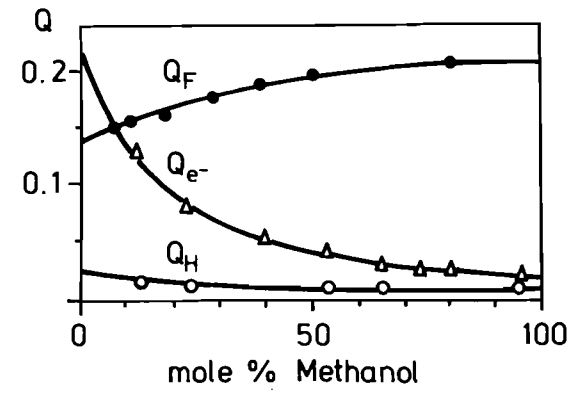


FIG. 2. Quantum yields of fluorescence (Q_F), solvated electrons (Q_e), and H atoms (Q_H) as a function of methanol content in water for solutions of phenol (excitation in S_1 at 30°C).

In figure 2 the scale is to be divided by a factor of 10 for Qe and for Q_H. ERRATA

FOR ERRATA SEE V59#12 19.81 P 1744

FOR ERRATA SEE v59 #2 19...81...P...1744

In figure 3 the scale is to be divided by a factor of 10 for α_e and by a factor of 3 for $\alpha_{(e+H)}$.

TABLE 1. Quantum yields of fluorescence (Q_F), solvated electrons (Q_e), and H atoms (Q_H), and values of β, α_e, and α_H for phenol in various solvents at 30°C (see text for definition of α and β)

ERRATA

Solvent	$Q_F(S_1)$	β^{229}	Q_e^{254}	Q_e^{229}	α_e	Q_H^{254}	Q_H^{229}	α_H
Water	0.14	0.71	0.021	0.033	0.018	0.002	0.064	0.06
Cyclohexane	0.08	0.37	$< 10^{-3}$	$< 10^{-3}$	—	0.11	0.55	0.51
Methanol	0.21	0.93	1.8×10^{-3}	$(1.80 \pm 0.1) \times 10^{-3}$	—	0.001	0.003	0.002
Propanol-2	0.22	0.93	4.5×10^{-4}	1×10^{-3}	$< 10^{-3}$			
tert-Butanol	0.22	0.93	5.7×10^{-4}	1×10^{-3}	$< 10^{-3}$			

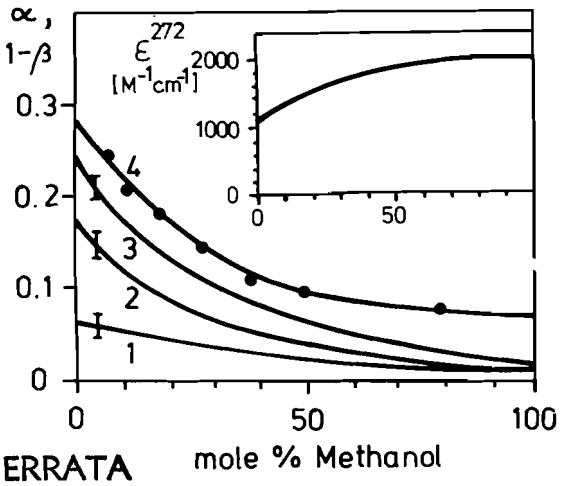


FIG. 3. α_H (*1*), α_e (*2*), $\alpha_{(e+H)}$ (*3*), and $1 - \beta$ (*4*) as a function of methanol content in water for solutions of phenol (see text for definition of α and β). Insert: extinction coefficient of phenol as a function of methanol content in water at 272 nm.

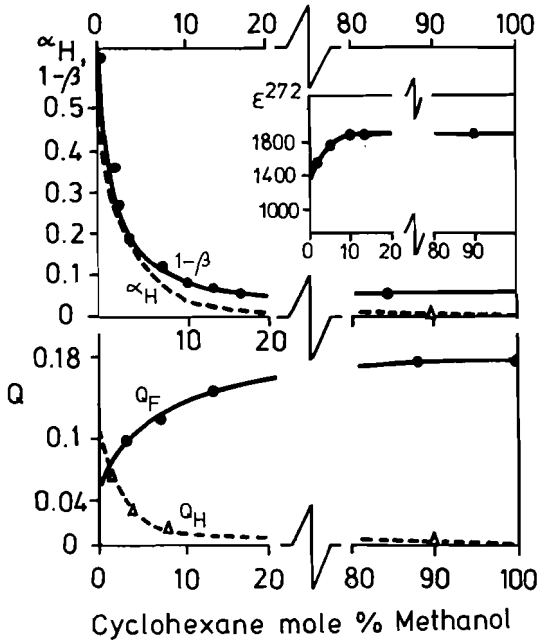


FIG. 4. Quantum yields of fluorescence (Q_F) and H atoms (Q_H) and values of α_H and $1 - \beta$ as a function of methanol content in cyclohexane for solutions of phenol (see text for definition of α and β). Insert: extinction coefficient (ε^{272}, M^{-1} cm^{-1}) of phenol as a function of methanol content in cyclohexane at 272 nm.

The effect of solvent composition on the extinction coefficient at a fixed wavelength within S_1 is also exhibited. The results show a remarkable parallelism in the sense that all parameter variations occur in the same ranges of solvent composition. In addition, the changes in the yields of fluorescence and photolytical processes show opposite trends.

Discussion

The results of the present work confirm our previous conclusion (7, 8, 11, 23) that excitation of phenol both in its S_1 and S_2 state can lead to formation of solvated electrons and/or H atoms. The quantum yields for excitation in S_2 are higher, which results in efficient competition to the very fast process of internal conversion to S_1. This state of affairs holds in all solvents as well as in all mixtures investigated in this work. It must be noted that the relation between the α's and β is not quantitative: as shown explicitly in Figs. 3 and 4, α is always smaller than $1 - \beta$. This is most probably due to geminate recombination processes which do not populate the fluorescent state.

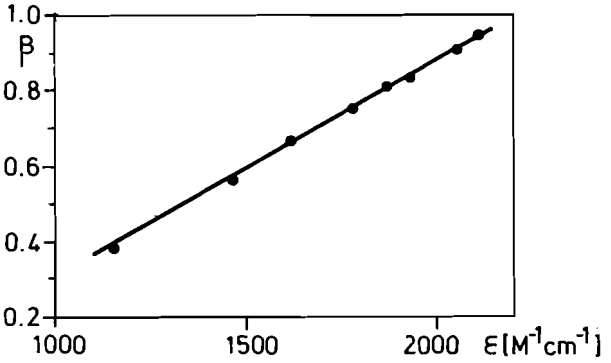


FIG. 5. Correlation plot of β (excitation at 215 nm) vs. the extinction coefficient (ε^{267}, M^{-1} cm^{-1}) at 267 nm for phenol in cyclohexane – diethyl ether mixtures.

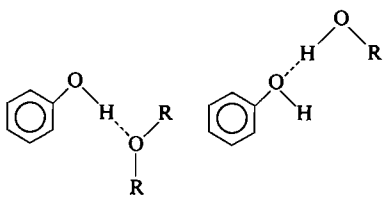
Can. J. Chem. Downloaded from www.nrcresearchpress.com by 210.87.254.105 on 09/05/12
For personal use only.

Can. J. Chem. Downloaded from www.nrcresearchpress.com by 210.87.254.105 on 09/05/12
For personal use only.

In order to answer the question of the possible mechanisms of solvent action, we may note that solvent effects on photoprocesses, in a way analogous to spectral energy shift phenomena (1), fall into two broad categories: (*a*) solvent effects caused by physical perturbation of the relevant molecular states of the chromophore; (*b*) specific chemical solvent effects like hydrogen bond formation, proton or charge transfer, solvent-dependent aggregation and others.

Electrostatic effects on excited energy levels are theoretically well understood (24) and corroborated by emission and absorption spectroscopy with the notable exception of hydrogen bond-forming solvents (25). Accordingly, these models do not apply to shift phenomena in aqueous solutions of phenolic compounds (1, 25). This observation is in broad agreement with the inadequacy of general liquid state parameters, such as the static dielectric constant or Kosower's parameter Z, to account for the observed solvent effect on photophysical and photochemical processes of these compounds, especially in aqueous solutions and in aqueous/organic mixtures. Indeed, a correlation of the data of the present work with these parameters leads to results which are very similar to those reported in the literature for indolic compounds (6, 12, 13), and which yield little information about the mechanisms responsible for the observed effects.

It seems therefore more promising to look to specific solute–solvent interactions to explain the behaviour of phenol. Hydrocarbons, alcohols, and water may be considered as three classes of solvents which specifically alter the solute's photophysical and photochemical behaviour. Indeed, while several hydrogen-bonded structures of different stoichiometry can be envisaged for phenol in hydroxylic solvents (26), there is a characteristic difference between the probability of occurrence of the two simplest structures in alcohols and in water (26, 27):



Type I Type II

R = H or alkyl group

Type I structures, where phenol acts as the proton donor, are predominant in ethers and alcohols. They result in a red shift of absorption and emission spectra as compared to hydrocarbon solutions. The solvation structure of these systems can be expected to exhibit a single well-defined pattern, as the occurrence of several isosbestic points in the absorption spectra of phenol in cyclohexane–dioxane mixtures demonstrates (25, 28). In contrast, phenol acts as proton acceptor in *Type II structures*; this type of hydrogen bond may be responsible for the blue shift of the absorption spectra of phenol and anisole in water.

This classification of solvents according to different hydrogen-bonded structures can easily be correlated with an analogous classification according to our experimental results: (*a*) In hydrocarbon solutions (no H-bonded structures in dilute solutions), the rupture of the OH bond is the main photochemical event. The quantum yield of this process is higher at higher excitation energy, which is reflected in a corresponding decrease of Q_F (see Table 1). (*b*) In alcohols, H atom formation is almost completely suppressed. e^-_{sol} are formed with a comparably very low yield. Concurrently, β is near unity (Table 1). It appears that Type I structures have a strong stabilizing effect in the sense that OH bond rupture is efficiently reduced (29). As Figs. 2, 3, and 4 show, addition of moderate concentrations of methanol to either cyclohexane or water are sufficient to achieve this effect. (*c*) In aqueous solutions, Q_H is very small, but the formation of e^-_{sol} is of importance; both processes, along with fluorescence, are dependent on excitation energy (Table 1). The different behaviour of aqueous and alcoholic solutions is at least partly attributable to variations in electron solvation ability; however, the predominance of Type II structures in water may also play a role, as witnessed by the observation that anisole, which can only participate in Type II structures, shows almost constant Q_F with respect to excitation energy both in hydrocarbons and in alcohols, but not in water (7).

This classification according to H-bonded structures does not distinguish between possible differences between the ground state and the excited states of the solute with respect to solute–solvent interactions. Such differences should eventually show up in a comparison of the influence of solvent composition on absorption parameters (transition energies, extinction coefficients) on the one hand, and emission parameters and photochemical yields on the other. In Fig. 5, we show a correlation plot between the values of β and of the extinction coefficient at 267 nm (S_1 band) for phenol in cyclohexane – diethyl ether mixtures. This plot yields a correlation coefficient of 0.997

and thus suggests a similar dependence of both β and ε on the solvent structure.

In conclusion there is no evidence for the contribution of others than the ground state solvent configuration for photoprocesses occurring from S_2 states in the particular case of phenol.

Acknowledgements

The authors are grateful to the Fonds zur Föderung der Wissenschaftlichen Forschung (Project No. 2248) for financial support.

1. M. F. NICOL. Appl. Spectrosc. Rev. **8B**, 183 (1974).
2. G. KÖHLER and N. GETOFF. Chem. Phys. Lett. **26**, 525 (1974).
3. I. TATISCHEFF and R. KLEIN. Excited states of biological molecules. *Edited by* J. B. Birks. John Wiley and Sons. 1976. p. 375.
4. G. KÖHLER, C. ROSICKY, and N. GETOFF. Excited states in organic chemistry and biochemistry. *Edited by* B. Pullman and N. Goldblum. Reidel. 1977. p. 303.
5. H. B. STEEN. J. Chem. Phys. **61**, 3997 (1974).
6. I. TATISCHEFF and R. KLEIN. Photochem. Photobiol. **22**, 221 (1975).
7. G. KÖHLER and N. GETOFF. J. Chem. Soc. Faraday I, **72**, 2101 (1976).
8. J. ZECHNER, G. KÖHLER, G. GRABNER, and N. GETOFF. Chem. Phys. Lett. **26**, 525 (1974).
9. J. ZECHNER, G. KÖHLER, N. GETOFF, I. TATISCHEFF, and R. KLEIN. J. Photochem. **9**, 304 (1978).
10. G. KÖHLER, J. ZECHNER, G. GRABNER, and N. GETOFF. 7th Int. Congr. Photobiol. Roma, 1976. Poster p11.
11. G. GRABNER, G. KÖHLER, J. ZECHNER, and N. GETOFF. Photochem. Photobiol. **26**, 449 (1977).
12. L. KEVAN and H. B. STEEN. Chem. Phys. Lett. **34**, 184 (1975).
13. I. TATISCHEFF, R. KLEIN, T. ZEMB, and M. DUQUESNE. Chem. Phys. Lett. **54**, 394 (1978).
14. M. NEUMANN-SPALLART and N. GETOFF. Radiat. Phys. Chem. **13**, 109 (1979).
15. W. D. WILSON and J. F. FOSTER. Biochem. Biophys. Res. Commun. **38**, 552 (1970).
16. N. GETOFF and G. O. SCHENCK. Photochem. Photobiol. **8**, 167 (1968).
17. W. W. MANTULIN and J. R. HUBER. Photochem. Photobiol. **17**, 139 (1973).
18. (*a*) J. N. DEMAS and G. A. CROSBY. J. Phys. Chem. **75**, 991 (1971); (*b*) International Critical Tables. Natl. Res. Counc. U.S.A., *Edited by* E. W. Washbum. McGraw Hill. 1926.
19. E. J. LAND and M. EBERT. Trans. Faraday Soc. **63**, 1181 (1967).
20. R. W. FESSENDEN and N. C. VERMA. Faraday Discuss. **63**, 104 (1977).
21. M. C. SAUER, JR. and I. MANI. J. Phys. Chem. **72**, 3856 (1968).
22. G. GRABNER, J. ZECHNER, G. KÖHLER, and N. GETOFF. To be published.
23. G. GRABNER, G. KÖHLER, J. ZECHNER, and N. GETOFF. J. Phys. Chem. In press.
24. (*a*) Y. OOSHITA. J. Phys. Soc. Jpn. **9**, 594 (1954); (*b*) E. LIPPERT. Z. Naturforsch. **10**a, 541 (1955); E. G. MCRAE. J. Phys. Chem. **61**, 562 (1957).
25. D. A. CHIGNELL and W. B. GRATZER. J. Phys. Chem. **72**, 2934 (1968).
26. G. NEMETHY and A. RAY. J. Phys. Chem. **77**, 64 (1973).
27. M. ITO. J. Mol. Spectrosc. **4**, 125 (1960).
28. H. BABA and S. SUZUKI. J. Chem. Phys. **35**, 1118 (1961).
29. K. HARA and H. BABA. J. Chem. Soc. Faraday II, **72**, 1100 (1975).

Can. J. Chem. Downloaded from www.nrcresearchpress.com by 210.87.254.105 on 09/05/12
For personal use only.

Cyclopentadienyl platinum(IV) complexes: ^1H, ^{13}C nuclear magnetic resonance and optically active shift reagent study

GORDON HAMER[1] AND ALAN SHAVER[2]

Department of Chemistry, McGill University, 801 Sherbrooke St. W., Montreal, P.Q., Canada H3A 2K6

Received February 4, 1980

GORDON HAMER and ALAN SHAVER. Can. J. Chem. **58**, 2011 (1980).

The ^1H and ^{13}C nmr parameters for the recently reported complexes $(\eta^5\text{-}C_5H_5)PtR_1R_2R_3$ where R_1, R_2, and R_3 are combinations of CH_3, C_2H_5, and $C(O)CH_3$ groups are reported and compared to those for known octahedral di- and trimethylplatinium (IV) complexes. The C_5H_5 group has a relatively weak nmr *trans*-influence. A chiral shift reagent study on complex **5** ($R_1 = C(O)CH_3$, $R_2 = CH_3$, and $R_3 = C_2H_5$) resolved the peaks due to the enantiomers, consistent with its structure and establishing its stereochemical stability. The four groups attached to the platinum atom in **5** differed greatly in their sensitivity to the shift reagent. The methyl groups in complex **4** ($R_1 = C(O)CH_3$, and $R_2 = R_3 = CH_3$) become diastereotopic in the presence of chiral shift reagent. The J(Pt—H) values for **5** were not affected by the shift reagent.

GORDON HAMER et ALAN SHAVER. Can. J. Chem. **58**, 2011 (1980).

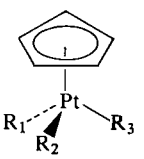
On rapporte les paramètres de la rmn du ^1H et du ^{13}C pour les complexes $(\eta^5\text{-}C_5H_5)PtR_1R_2R_3$ où R_1R_2 et R_3 sont des combinaisons des groupes CH_3, C_2H_5 et $C(O)CH_3$, décrits récemment et on les compare à ceux de complexes octaédriques connus de di- et triméthylplatine(IV). Le groupement C_5H_5 a une influence *trans* relativement faible en rmn. L'utilisation d'un réactif de contact chiral sur le complexe **5** ($R_1 = C(O)CH_3$, $R_2 = CH_3$ et $R_3 = C_2H_5$) a permis de résoudre les bandes provenant des énantiomères et qui sont en accord avec leur structure tout en révélant leur stabilité stéréochimique. Les quatres groupes attachés à l'atome de platine dans le composé **5** diffèrent notamment par leur sensibilité au réactif de contact. Les groupes méthyles du complexe **4** ($R_1 = C(O)CH_3$ et $R_2 = R_3 = CH_3$) deviennent diastéréotopiques en présence du réactif de contact. Les valeurs de J(Pt—H) du composé **5** ne sont pas affectées par le réactif de contact.

[Traduit par le journal]

Introduction

There is a great deal of activity in the emerging field of chiral organometallics (1, 2) and catalysts. Most systems studied to date contain relatively easily dissociated ligands such as carbonyls, phosphines, or olefins. Previously, we reported (3) the synthesis of complexes of platinum(IV) containing the cyclopentadienyl ligand and three alkyl groups: $(\eta^5\text{-}C_5H_5)PtR_1R_2R_3$.

Complex **1** had been reported earlier (4) but complexes with other than three methyl substituents were unknown. The pseudotetrahedral or piano stool arrangement of the ligands (5) confers optical isomerism upon complex **5**. In addition, complexes **1–6** are interesting metal alkyls that bear no easily dissociated ligands. Their reactivity to electrophilic metal–carbon bond cleavage reagents is quite different from other organometallics (3). This new class of compounds has been fully characterized by ^1H and ^{13}C nmr spectroscopy. Also the dependence of the ^1H nmr spectrum of **4** and **5** upon the addition of optically active europium shift reagent was studied.



1 $R_1 = R_2 = R_3 = CH_3$
2 $R_1 = R_2 = CH_3$, $R_3 = C_2H_5$
3 $R_1 = CH_3$, $R_2 = R_3 = C_2H_5$
4 $R_1 = C(O)CH_3$, $R_2 = R_3 = CH_3$
5 $R_1 = C(O)CH_3$, $R_2 = CH_3$, $R_3 = C_2H_5$
6 $R_1 = C(O)CH_3$, $R_2 = R_3 = C_2H_5$

Experimental

The complexes were prepared as previously described (3). The ^{13}C and ^1H nmr spectra were measured in $CDCl_3$ solution at 36 ± 2°C on a Bruker WH-90 spectrometer operating in the pulsed Fourier transform mode at 22.6 MHz and 90.0 MHz, respectively. The ^{13}C spectra were determined with noise-modulated proton decoupling. Chemical shifts are reported relative to TMS as internal reference. Proton spectral analyses of compounds **2**, **5**, and **6** were carried out with the Bruker NMRSIMIT program on an Aspect 2000 computer. The shift reagent, tris[3-trifluoromethylhydroxymethylene-*d*-camphorato]europium(III) (trade name Eu-Opt) was purchased from Alfa Inorganics and used without further purification. A weighed portion of the reagent was placed in a disposable pipette which was long enough to be inserted to the bottom of the nmr tube. A small filter-plug of Kimwipe® was wedged in the neck of the pipette and one or two pieces of molecular sieve placed above the plug. By sucking the sample past the plug the reagent was dissolved. The solution was forced back into the nmr tube, the plug serving to filter any undissolved particles or impurities. Additional portions of reagent were added in the same way.

Results and Discussion

The ^1H and ^{13}C nmr parameters are given in

[1]Present address: Xerox Research Centre of Canada, 2480 Dunwin Dr., Mississauga, Ont., Canada L5L 1J9.

[2]To whom all correspondence should be addressed.

0008-4042/80/192011-05$01.00/0

©1980 National Research Council of Canada/Conseil national de recherches du Canada

Can. J. Chem. Downloaded from www.nrcresearchpress.com by 210.87.254.42 on 09/05/12
For personal use only.

TABLE 1. ^{1}H nmr parameters for some Pt(IV) alkyl complexes

Compound	R_1	R_2	R_3	Chemical shifts[a] [J(Pt–H)][b] Cp	CH_3	CH_2CH_3[c]	CH_2CH_3[c]	C(O)CH_3
1	Me	Me	Me	5.650(5.9)	0.916(82.4)			
2	Me	Me	Et	5.635(5.9)	0.867(83.1)	1.695(−77.1)[d]	1.328(+59.7)[d]	
3	Me	Et	Et	5.633(5.9)	0.859(84.0)	[e]	[e]	
4	Ac	Me	Me	5.842(5.7)	1.160(84.7)			2.476(7.0)
5	Ac	Me	Et	5.845(5.7)	1.128(85.9)	1.953(e)[f] 2.179(e)	1.320(+66.8)	2.503(6.2)
6	Ac	Et	Et	5.857(5.5)		1.959(e)[f] 2.074(e)	1.300(+68.9)	2.558(5.1)
7	Ac	Me	Me[g]		1.13(65.0)			3.07(15.5)
8	Me	Me	Me[h]		0.91(72.8)[i] 1.23(63.6)[j]			

[a] ±0.002 ppm.
[b] Absolute values (except *c*), in Hz ± 0.15.
[c] Calculated values.
[d] ^3J(H—H) = +7.5 Hz.
[e] Not calculated.
[f] ^3J(H—H) = +7.5 Hz, ^2J(H_A—H_B) = −9.6 Hz.
[g] Reference 7.
[h] Reference 8.
[i] *trans* to 1.
[j] *trans* to Me_3As.

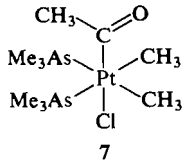
TABLE 2. ^{13}C nmr parameters for some Pt(IV) alkyl complexes

Compound	R_1	R_2	R_3	Chemical shifts[a] [J(Pt—C)][b] Cp	CH_3	CH_2CH_3	CH_2CH_3	C(O)CH_3	C(O)CH_3
1	Me	Me	Me	95.85(8.8)	−20.72(714.8)				
2	Me	Me	Et	96.41(8.8)	−20.02(750.0)	2.89(693.4)	23.09(43.0)		
3	Me	Et	Et	97.02(10.7)	−18.90(786.1)	2.98(728.5)	22.70(43.9)		
4	Ac	Me	Me	97.32(12.7)	−17.57(741.2)			194.26(996.1)	48.81(195.3)
5	Ac	Me	Et	98.01(14.6)	−16.66(780.3)	8.20(718.7)	23.35(42.0)	195.25(1034.2)	49.59(192.4)
6	Ac	Et	Et	98.87(15.6)		8.93(756.3)	23.30(42.0)	196.34(1077.1)	50.24(187.0)
7	Ac	Me	Me[c]		3.5(583)			193.2(851)	36.4(22)
8	Me	Me	Me[c]		−0.7(623)[d] 2.0(556)[e]				

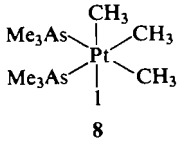
[a] ±0.04 ppm.
[b] Absolute values in Hz ± 0.9.
[c] Reference 9.
[d] *trans* to 1.
[e] *trans* to $(CH_3)_3As$.

Tables 1 and 2. The values appear within the normal range for such compounds (6). It is interesting to compare **1–6** to complexes **7** (7) and **8** (8, 9). The coupling of the methyl and acyl groups to platinum-195 is greater in **1–6** than in **7** or **8** (with the exception of ^3J(Pt—C(O)CH_3)). Since the C_5H_5 ring is a uninegative, six electron "tridentate" ligand it is formally equivalent to the two $(CH_3)_3As$ groups and a halide ligand. Trends in platinum–ligand coupling constants in complexes such as **7** and **8** are usually discussed in terms of *trans*- and *cis*-influences (9, 10) which are related to the hybridization of the central platinum atom and steric effects respectively. In the case of **1–6** the situation is complicated by the fact that the C_5H_5 ring is both "*cis*" and "*trans*" to the remaining groups. Since the *trans*-influence is considered dominant, it is reasonable to conclude that the hybridization of the central platinum atom in **1–6** concentrates more *s*-character in the platinum–alkyl bonds than exists in **7** and **8**. This is consistent with the postulate that there is low *s*-character in the M or C orbitals used in the M—C bond (11) to the *pentahapto*cyclopentadienyl ligand.

The similarity of the chemical shifts for the acyl carbon atoms in **4**, **5**, **6**, and **7** to those in unsaturated aldehydes and ketones is noted (12). The infrared stretching frequencies for the carbonyl groups in **4**, **5**, and **6** are in the range



7



8

Can. J. Chem. Downloaded from www.nrcresearchpress.com by 210.87.254.42 on 09/05/12
For personal use only.

TABLE 3. Ranges of the ^1H and ^{13}C nmr parameters for the cyclopentadienyl ring in complexes of platinum in oxidation states II and IV

Type of complex	Range of δ (range of coupling constant)[a]	
	C_5H_5[J(Pt—H)][b]	C_5H_5[J(Pt—C)][b]
η^1-CpPt(II)	6.46–5.89(28.0–43.5)[10]	115.2–116.5(87.8–96.8)[2]
η^5-CpPt(II)	6.26–5.07(10.5–19.0)[19]	93.2–94.1(3.8–8.4)[2]
η^5-CpPt(IV)	5.633–5.857(5.50–5.86)[6]	95.85–98.87(8.8–15.6)[6]

[a]Data collected from refs. 21, 22, and this work.
[b]The superscript beside each coupling constant is the number of complexes included in the range.

1699–1662 cm^{-1} (3) expected for unsaturated ketones (13). However, the ^{13}C chemical shift for the acyl carbon atom in $(\eta^5\text{-}C_5H_5)Fe(CO)_2[C(O)CH_3]$ is 254.4 ppm (14) and the stretching frequency is 1655 cm^{-1} (15), significantly different from **4**, **5**, and **6**. Many metal-acyls have reduced stretching frequencies due to metal → acyl d_π–p_π backbonding (16). The spectroscopic data for **4**, **5**, **6**, and **7** is consistent with there being little backbonding, as expected for a metal in a high oxidation state.

It is often difficult to distinguish between *monohapto* and *pentahapto* bonding modes for the C_5H_5 ligand. For molecules that do not contain complicated ligands infrared spectroscopy can sometimes be useful (17). In the nmr spectrum, however, both bonding modes result in only a single band. Chemical shift arguments have been used for the assignment (18) but this is not reliable in our opinion. The shifts of C_5H_5 rings in either bonding mode are dependent on solvent, temperature, and the presence of other ligands (19, 20). However, the coupling between platinum-195 and the ring provides a facile diagnostic test for both the bonding mode of the ring and the oxidation state of the metal atom. In Table 3 ranges of nmr parameters are given for three different combinations of bonding mode and oxidation state. The platinum(II) data are taken from earlier work (21, 22) while those for platinum(IV) are from this work. The coupling constants form mutually exclusive sets thus the bonding mode of the ring and the oxidation state of the metal can be determined simply and unambiguously from the ^1H nmr spectrum.

The ^1H nmr spectra of the ethyl groups in **2**, **3**, **5**, and **6** were very complex. Second order effects due to the similarity of the shifts of the methylene and the methyl groups plus the presence of platinum coupling generated a multitude of peaks. The $PtCH_2CH_3$ spectrum of $CpPtMe_2Et$, **2**, was analyzed iteratively as an A_2B_3X spin system. The analysis requires that ^2J(Pt—H) and ^3J(Pt—H) have opposite signs (23*a*); ^2J(Pt—H) in methyl derivatives of platinum(II) and (IV) has previously been shown to be negative (23*b*). In $CpPtMeEt_2$, **3**, CpPtMeAcEt, **5**, and $CpPtAcEt_2$, **6**, the ethyl CH_2 protons are non-equivalent. The CH_2CH_3 spectra of **5** and **6** were analyzed iteratively as ABC_3 systems; due to its greater complexity, no attempt was made to analyze **3**. Values of ^3J(Pt—H) were obtained for **5** and **6** by simulation of the CH_3 group high field satellite spectra. Precise values of ^2J(Pt—H) could not be obtained due to poor resolution of the low field satellite lines and band overlap with the acyl resonance.

Trends in the shifts and coupling constants were observed for **1**–**6**. There are two sub-groups of complexes: (*a*) $CpPtMeR_2R_3$ and (*b*) $CpPtAcR_2R_3$ where R_2, R_3 = Me, Et. Within each group the proton chemical shifts and couplings are very little affected by increasing Et substitution. The polar acyl group deshields the C_5H_5, CH_3, and CH_2 protons. The ^{13}C shifts are more sensitive to acyl substitution which produces downfield shifts for all carbons (again with the exception of the methyl carbon of Et). The magnitude of J(Pt—C) increases with increasing substitution for all J's except for $^2J(PtC(O)CH_3)$ which decreases. It is difficult to establish more quantitative trends since the Et substituent is a rather weak perturbation of the Pt—C bonding.

Addition of Eu-Opt to a sample of **5** causes a shift of the ^1H nmr resonances to low field (24) due to complexation of the acyl-oxygen atom with the europium reagent. Figure 1 plots the change in chemical shift (Δδ) of the four ligands as a function of the shift reagent to substrate molar ratio (R). The $C(O)CH_3$ and CH_3 groups are the most sensitive, while the CH_2CH_3 and C_5H_5 groups are affected little. This is of some interest since previous studies on organometallic complexes have indicated that the C_5H_5 group was very sensitive (25–27). However, most of these complexes did not have simple alkyl groups near the complexing ligand.

Figure 2 plots the diastereotopic splitting (ΔΔδ) vs. R. The splitting is greatest for the CH_3 group, least for the C_5H_5 group, while the CH_2CH_3 and $C(O)CH_3$ ligands are intermediate. Thus while the

Can. J. Chem. Downloaded from www.nrcresearchpress.com by 210.87.254.42 on 09/05/12
For personal use only.

Can. J. Chem. Downloaded from www.nrcresearchpress.com by 210.87.254.42 on 09/05/12
For personal use only.

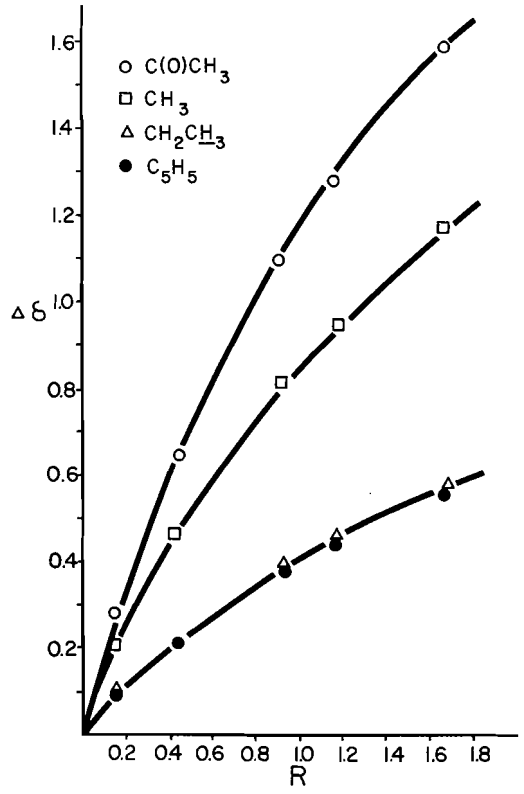


FIG. 1. Change in chemical shift (Δδ) vs. molar ratio of shift reagent/**5** (*R*).

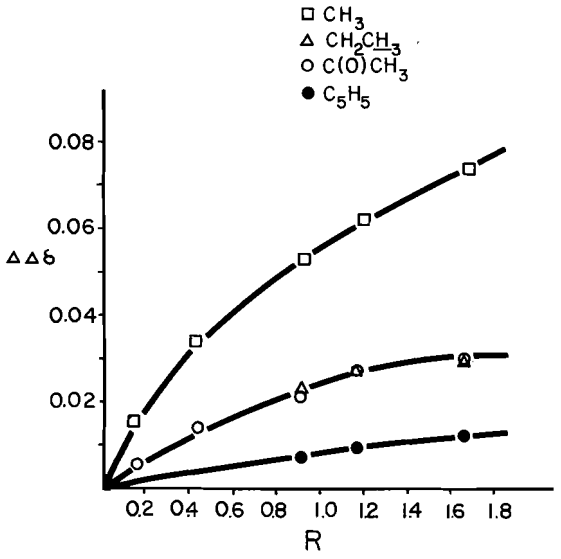


FIG. 2. The splitting of the peaks (ΔΔδ) vs. molar ratio of shift reagent/**5** (*R*).

$C(O)CH_3$ group was shifted the most its splitting was fairly weak, being comparable to CH_2CH_3 and C_5H_5 ligands. Figure 3 relates Δδ to ΔΔδ. It seems particularly significant that there is no positive correlation between a group's shift sensitivity (Δδ) and its tendency to split (ΔΔδ).

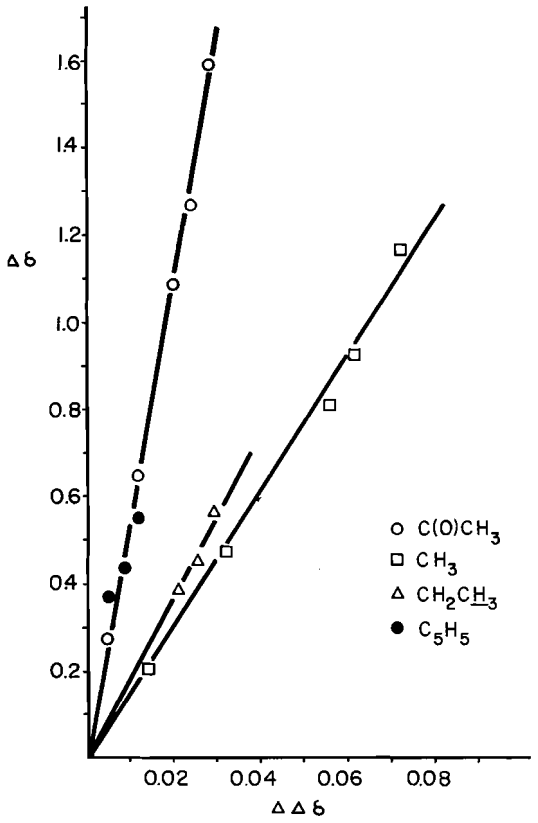


FIG. 3. Change in chemical shift (Δδ) vs. the splitting of the peaks (ΔΔδ).

The splitting of the peaks is due to the diastereotopic interaction of the two enantiomers of **5** with the chiral shift reagent (28, 29). Two reasons are generally invoked to explain this splitting: one is geometry, the other, differing equilibrium constants for the complexes formed. The geometry of the two complexes between the enantiomers of **5** and Eu-Opt are different since Eu-Opt is "resolved". A chiral pocket in Eu-Opt can be envisioned, into which one isomer fits one way, the other isomer, another. Therefore, the platinum–methyl group for example would be in two different magnetic environments and hence have different chemical shifts, giving rise to splitting. Geometry is also the reason that molecules such as DMSO and other organic (30) and inorganic molecules (31) show splitting in their spectra. Uncomplexed, these molecules have a mirror plane of symmetry; however, complexation removes this. Such an effect was observed for complex **4** which has two methyl groups related by a mirror plane that passes through the $C(O)CH_3$ group. In the

Can. J. Chem. Downloaded from www.nrcresearchpress.com by 210.87.254.42 on 09/05/12
For personal use only.

presence of Eu-Opt two peaks due to the methyl groups are observed while the acyl-methyl and the cyclopentadienyl group each give only one peak. Such splitting cannot be due to a difference in equilibrium constants since only one type of complex is formed. These observations prove that geometry alone could account for the nmr resolution of chiral complexes such as **5**.

Differences in equilibrium constants have also been postulated as a reason for the splitting and resolution of the spectra of chiral molecules (28, 29). The diastereomeric complexes formed between **5** and Eu-Opt might well have different equilibrium constants and this would cause different shifts and hence splitting of peaks. We feel that the difference between the equilibrium constants is likely to be small due to the similarity of the two sides of the molecules as viewed down the Pt—$C(O)CH_3$ bond (i.e. CH_2CH_3 vs. CH_3).

The subtle nature of the phenomenon is particularly evident in the differences in the sensitivities of the different groups in **5**. Each functional group behaves differently with the most shifted group (i.e. $C(O)CH_3$) not being the most split. This sort of behaviour is also evident in the data reported by other investigators (29, 31). No facile explanation for these observations is at hand.

Previous to this study no organometallic compound having extensive metal-to-hydrogen spin–spin coupling has been subjected to a lanthanide shift reagent study. We were interested to see if the $J(^{195}Pt—H)$ values for the four groups on **5** would vary upon addition of Eu-Opt. They do not. This is consistent with studies on organic compounds where variations in coupling constants are observed only in rather specialized cases involving changes in conformation upon complexation (32).

In conclusion, the chiral shift reagent study on **5** is consistent with its expected chiral nature and indicates that it is configurationally stable on the nmr time scale. It should in principle be possible to resolve complex **5**.

Acknowledgements

This work was supported by the National Research Council of Canada and the Quebec Department of Education.

1. M. D. Fryzuk and B. Bosnich. J. Am. Chem. Soc. **99**, 6262 (1977).
2. H. Brunner. Top. Current Chem. **56**, 67 (1975).
3. A. Shaver. Can. J. Chem. **56**, 2281 (1978).
4. S. D. Robinson and B. L. Shaw. Z. Naturforsch. B**18**, 507 (1963); J. Chem. Soc. 1529 (1965).
5. G. W. Adamson, J. C. J. Bart, and J. J. Daly. J. Chem. Soc. A, 2616 (1971).
6. B. E. Mann. Adv. Organomet. Chem. **12**, 135 (1974).
7. T. G. Appleton, H. C. Clark, and L. E. Manzer. J. Organomet. Chem. **65**, 275 (1974).
8. H. C. Clark and L. E. Manzer. Inorg. Chem. **12**, 362 (1973).
9. H. C. Clark, L. E. Manzer, and J. E. H. Ward. Can. J. Chem. **52**, 1973 (1974).
10. T. G. Appleton, H. C. Clark, and L. E. Manzer. Coord. Chem. Rev. **10**, 335 (1973).
11. G. M. Bodner, B. N. Storhoff, D. Doddrell, and L. J. Todd. J. Chem. Soc. D, 1530 (1970).
12. J. B. Stothers. Carbon-13 nmr spectroscopy. Academic Press, New York. 1972. p. 283.
13. I. Fleming and D. H. Williams. Spectroscopic methods in organic chemistry. McGraw-Hill, Toronto. 1966.
14. L. F. Farnell, E. W. Randall, and E. Rosenberg. Chem. Commun. 1078 (1971).
15. R. B. King. J. Am. Chem. Soc. **85**, 1918 (1963).
16. J. D. Bibler and A. Wojcicki. Inorg. Chem. **5**, 889 (1966).
17. F. A. Cotton and T. J. Marks. J. Am. Chem. Soc. **91**, 7281 (1969).
18. (*a*) Yu. K. Grishin, N. M. Sergoyev, and Yu. A. Ustynyuk. Org. Magn. Reson. **4**, 337 (1972); (*b*) P. Fischer, J. Stadelhofer, and J. Weidlein. J. Organomet. Chem. **116**, 65 (1976).
19. A. Shaver. Unpublished results.
20. J. L. Calderon and F. A. Cotton. J. Organomet. Chem. **30**, 377 (1971).
21. R. J. Cross and R. Wardle. J. Chem. Soc. A, 2000 (1971).
22. H. C. Clark and A. Shaver. Can. J. Chem. **54**, 2068 (1976).
23. (*a*) S. F. A. Kettle. J. Chem. Soc. 6664 (1965); (*b*) R. G. Kidd and R. J. Goodfellow. *In* NMR and the periodic table. *Edited by* R. K. Harris and B. E. Mann. Academic Press, London. 1978. p. 256 and references therein.
24. K. A. Kime and R. E. Sievers. Aldrichim. Acta, **10**, 54 (1977).
25. T. J. Marks, J. S. Kristoff, A. Alich, and D. F. Shriver. J. Organomet. Chem. **33**, C35 (1971).
26. D. L. Reger. Inorg.Chem. **14**, 660 (1975).
27. T. C. Flood and D. L. Miles. J. Am. Chem. Soc. **95**, 6460 (1973); T. C. Flood, F. J. DiSanti, and D. L. Miles. J. Chem. Soc. Chem. Commun. 336 (1975).
28. M. D. McCreary, D. W. Lewis, D. L. Wernick, and G. M. Whitesides. J. Am. Chem. Soc. **96**, 1038 (1974).
29. H. L. Georing, J. N. Eikenberry, G. S. Koermer, and C. J. Lattimer. J. Am. Chem. Soc. **96**, 1493 (1975).
30. R. R. Fraser, M. A. Petit, and M. Miskow. J. Am. Chem. Soc. **94**, 3253 (1972).
31. L. F. Lindoy and W. E. Moody. J. Am. Chem. Soc. **99**, 5863 (1977).
32. A. F. Cockerill, G. L. O. Davies, R. C. Harden, and D. M. Rackham. Chem. Rev. **73**, 553 (1973).

An experimental evaluation of simplified procedures for determining the proton spin–lattice relaxation rates of natural products[1]

LAWRENCE D. COLEBROOK[2] AND LAURANCE D. HALL[3]

Department of Chemistry, University of British Columbia, Vancouver, B.C., Canada V6T 1W5

Received December 27, 1979

LAWRENCE D. COLEBROOK and LAURANCE D. HALL. Can. J. Chem. **58**, 2016 (1980).

A general discussion is given of the determination of the proton spin–lattice relaxation rates of natural products, with particular emphasis on use of the null-point method which, for the systems studied here, gives identical results with those obtained via the conventional (and relatively time consuming) computational method.

LAWRENCE D. COLEBROOK et LAURANCE D. HALL. Can. J. Chem. **58**, 2016 (1980).

On présente une discussion générale sur la détermination des vitesses de relaxation spin–réseau du proton des produits naturels en mettant l'accent sur l'utilisation de la méthode du point zéro, qui, dans le cas des systèmes étudiés, donne des résultats identiques à ceux obtenus au moyen de méthodes conventionnelles de calculs qui sont relativement longues.

[Traduit par le journal]

Introduction

Although the development of pulse Fourier transform (F.t.) nuclear magnetic resonance (nmr) spectrometers has made the measurement (1) of proton spin–lattice relaxation rates (R_1 values) routine, relatively few such studies have thus far been reported for complex natural products, studies of carbohydrate (2) and nucleoside (3) derivatives providing the principal exceptions, with a lesser emphasis on other compounds (4). There are many good reasons for this neglect, not the least of which is the substantial amount of time which is required to process the experimental data using conventional methods. The main thrust of this report is to delineate some simple experimental procedures whereby proton R_1 values can be obtained rapidly and without prejudicing either the numerical accuracy, or the chemical significance, of the resultant data.

Results and Discussion

The Relaxation Mechanism

The diagnostic potential of proton R_1 values depends on the fact (5) that it is possible experimentally to ensure that the spin–lattice relaxation of the protons of a diamagnetic molecule is dominated by the intramolecular dipole–dipole (D.D.) mechanism, the complete formulation of which, for non-selective excitation, is given in eq. [1].

$$[1]\quad R_1(\mathrm{ns}) = \frac{\gamma_D^2\gamma_R^2h^2}{r^6(\mathrm{D,R})}I(I+1)\left\{\frac{\tau_c}{1+\omega_0^2\tau_c^2} + \frac{4\tau_c}{1+\omega_0^2\tau_c^2}\right\}$$

Providing that the molecule is tumbling in the extreme narrowing limit ($\omega_0^2\tau_c^2 \ll 1$), the simplified formulation, eq. [2] can be used. This makes clear

$$[2]\quad R^R(\mathrm{ns}) = K\sum\frac{\gamma_R^2\gamma_D^2}{r^6(\mathrm{D,R})}\tau_c(\mathrm{D,R})$$

the dependence of the observed relaxation rate on three experimentally manipulatable parameters; γ_D, the magnetogyric ratio of the donor nuclide, D, which contributes to the relaxation of the receptor nucleus, R; r(D,R), the internuclear distance separating each pair of donor and receptor nuclides, and τ_c(D,R), the motional correlation time of the vector between D and R.

The dependence on γ_D^2 generally results in the domination of the relaxation by the other protons in the system, these being the only nuclides with a high value of γ. Hall and Hill have previously described (6) a rigorous quality control experiment whereby the extent to which the relaxation of a proton arises via dipole–dipole interactions with the other protons of a diamagnetic system may be quantitatively ascertained; experience in this laboratory over the past seven years suggests that few protons of medium size (200–700 dalton) diamagnetic molecules will show appreciable relaxation contributions from any other mechanism. The dependence on the inverse sixth power of the inter-proton separations is illustrated graphically in Fig. 1 which indicates some of the interesting

[1]A complete account of this work was presented at the Fourth International Meeting on Nuclear Magnetic Resonance Spectroscopy, July 2–7, 1978, York, England.

[2]Permanent address: Department of Chemistry, Concordia University, 1455 de Maisonneuve Blvd., W., Montreal, P.Q., Canada H3G 1M8.

[3]To whom all correspondence should be addressed.

0008-4042/80/192016-08$01.00/0

©1980 National Research Council of Canada/Conseil national de recherches du Canada

Can. J. Chem. Downloaded from www.nrcresearchpress.com by 210.87.254.6 on 09/05/12
For personal use only.

Can. J. Chem. Downloaded from www.nrcresearchpress.com by 210.87.254.6 on 09/05/12
For personal use only.

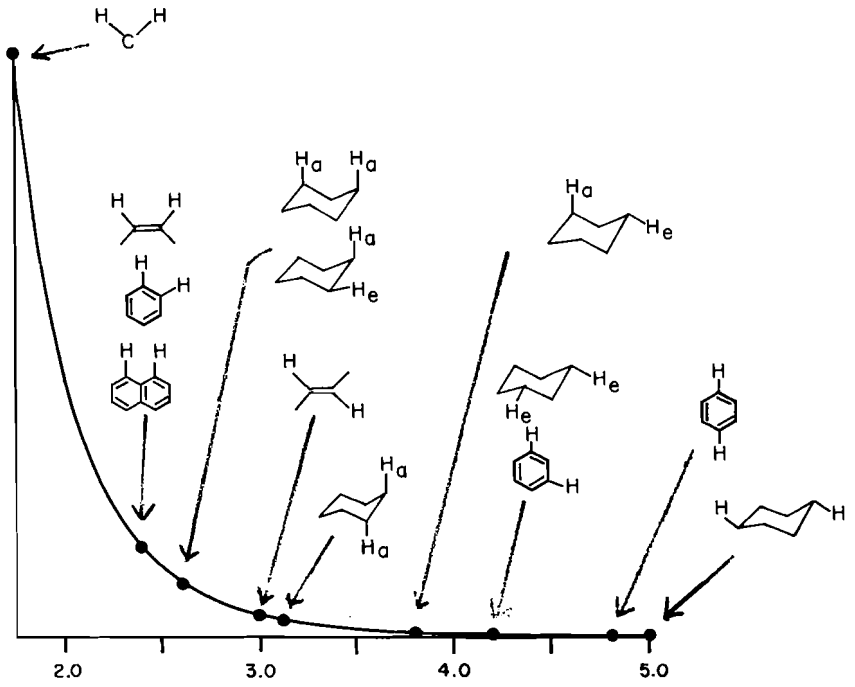


FIG. 1. Plot of the relative relaxation efficiency between two protons versus the inverse sixth power of their internuclear separation (derived from measurements of Dreiding Stereomodels).

stereochemical dependencies which can be anticipated for natural products. We shall return later to the dependence on τ_c(D,R).

Sample Preparation

The experimental precautions required (2*a*, *b*) to ensure that the intramolecular dipole–dipole mechanism R_1^A(DD), is at least dominant (and probably exclusive), are nicely illustrated with reference to eq. [3], which summarizes the probable relaxation contributions for any proton, A. Intermolecular contributions, R_1^A(inter), between the protons of different solute molecules are minimized

$$[3] \quad R_1^A(\text{ns}) = R_1^A(\text{DD}) + R_1^A(\text{inter}) + R_1^A(\text{solvent}) + R_1^A(\text{para})$$

by working at high dilution, typically 0.1 *M* or less. Contributions from the solvent, R_1^A(solvent), will be zero if the solvent contains no strongly magnetic nuclei (for example, CS_2 or CCl_4) or can be reduced substantially if a perdeuterated solvent is used.[4] Insofar that most F.t. nmr spectrometers require a deuterium resonance for the field-frequency lock system, the latter choice of solvent is the more common, and for proton R_1 values of 0.2 s^{-1} or more this is perfectly acceptable.[5]

The principal sources[6] of paramagnetic impurities, R_1^A(para), are solid particles of decayed automobile (readily removed by filtration) and dissolved oxygen; the latter can be removed either by repeated "freeze–pump–thaw" cycles, or by sparging with a stream of nitrogen gas, followed by sealing under vacuum. However, these procedures are inconvenient and time consuming, especially if many samples are to be studied and, as it happens, are unnecessary for qualitative studies of the protons of natural products having R_1 values of 0.2 s^{-1} or more. This follows from knowledge that the relaxation contribution from dissolved oxygen is approximately 0.2 s^{-1}.

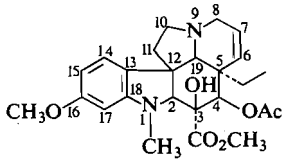
The data for vindoline (**1**) in deuterochloroform solution (Fig. 2 and Table 1) are typical, and show that dissolved oxygen has essentially no effect on the relative disposition of the proton R_1 values.

[4]From eq. [1] it can be seen that the relaxation efficiency of a donor nucleus is proportional to $\{I(I+1)\gamma^2\}$, from which it follows by simple numerical substitution that relaxation from a deuterated species will be ca. 6.3% that of the equivalent protio species.

[5]We strongly caution against using this procedure for small organic molecules having R_1 values of 0.1 s^{-1} or less.

[6]Deuterium oxide can also contain significant quantities of dissolved paramagnetic metal ions which can substantially affect protons which have very long R_1 values, especially if the solute molecule has a high affinity for metal ions.

Can. J. Chem. Downloaded from www.nrcresearchpress.com by 210.87.254.6 on 09/05/12
For personal use only.



1

Acquisition of Relaxation Data and Calculation of R_1 *Values*

In a conventional, non-selective[7] "two-pulse" (1) or "three-pulse" (7) sequence, the spins of interest are first "heated" by application of a 180° pulse then, after the lapse of some defined delay period (t), during which some of the excess energy leaks to the lattice, the residual magnetization is monitored using a non-selective 90°-pulse. Generally, a series of 30, or so, partially relaxed spectra[8] are obtained in this fashion, and the resultant spectra plotted in the form of a stack plot (Fig. 3). Although this is a reasonably efficient process, the subsequent calculation of the R_1 values (see Experimental section) is, unfortunately, rather time-consuming. As a result, we strongly recommend for all *qualitative* (and some quantitative) studies a simpler and more rapid procedure in which the R_1 value of each resonance is taken directly from its null point using the relationship $R_1 = 0.69/t$, where t is the delay time (in s) of the two-pulse, partially relaxed spectrum for which the magnetization of that proton has reached its null point. Given an adequate number of partially relaxed spectra and the excellent sensitivity of pulse F.t. proton spectrometers, the null point can generally be determined within 0.1 s. The R_1 values obtained for **1** in ca. 15 min from the data given in Fig. 3 are compared in Fig. 4 with the values obtained by a least-squares fit procedure which took ca. 12 hours' work; clearly the two sets of data are in excellent agreement.

The advantages of the null point approach are that it is rapid (visual inspection of the partially relaxed spectra) and that an estimate can often be obtained for overlapping resonances; this latter feature is particularly important for natural products where conventional data processing is frequently precluded. Furthermore, because the nmr spectra are plotted directly it is applicable to F.t. instruments which lack any data storage device.

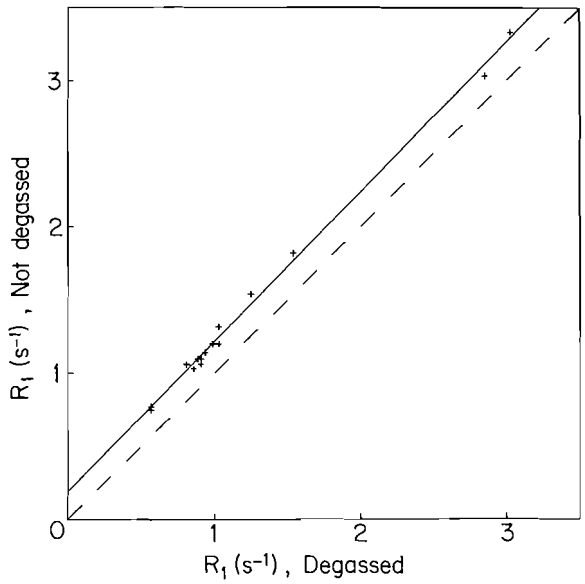


FIG. 2. Plot of the proton R_1 values for vindoline (0.1 M in $CDCl_3$ solution) determined by the null point method. Ordinate values, measured without degassing; abscissa values measured after six freeze–pump–thaw cycles followed by sealing under vacuum.

On the debit side, errors in setting the duration of the 180° pulse are more serious than in the conventional two-pulse method and for some resonances the null point method may violate the initial slope approximation (8); the experimental precautions required to minimize this danger are summarized in the Experimental section. However, based on experience with about 40 natural products and a large number of carbohydrate derivatives (9) we believe that, with care and a good spectrometer, the total accrued error of the method is unlikely to compromise the chemical significance of any R_1 values, and in most instances the numerical accuracy can compare favourably with that of the conventional, and more laborious, computational procedures.

Use of R_1 *Values for the Assignment of Proton Resonances*

Relaxation data can be used in a wide variety of ways. At the simplest level, the partially relaxed spectra themselves can be illuminating since they often enable otherwise overlapping resonances to be separately resolved. For example, the components of the overlapping signals near 2.6 δ in the spectrum of **1** have distinctly different relaxation rates (0.8–1.8 s^{-1}), enabling the chemical shift of a relatively sharp, slowly relaxing signal at 2.66 δ to be identified as that of H-19.

Because of the inverse distance dependence,

[7]An experiment in which the 180° pulse is applied simultaneously to all of the proton spins. In contrast, a single selective R_1 value is obtained (6) from an experiment in which only one proton resonance is subjected to the 180° pulse.

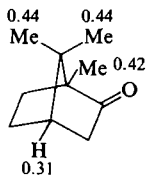
[8]The intensity of the resulting resonances then depends on the relative magnitudes of the chosen delay time (t) and the R_1 value of each individual resonance; for $t \gg T_1$ the nuclei will have recovered their thermal equilibrium with the lattice when the sampling pulse is applied and they will give the normal, positive-going resonance; for $t \ll T_1$ the resonance signal will be negative-going because the magnetization is still inverted.

TABLE 1. Spin–lattice relaxation rates (R_1 values, s^{-1}) for vindoline **1** (0.1 *M*)

Proton[c]	Solvent				
	δ $(CD_3)_2CO$	$CDCl_3$ (degassed)	$CDCl_3$ (not degassed)	C_6D_6 (not degassed)	$(CD_3)_2CO$ (not degassed)
N-1 CH_3	2.63	1.25	1.54	1.30	0.79
C-2	3.62	0.99	1.20	1.06	0.63
C-3 OH	8.50	0.81	1.06	0.77	0.39
OCH_3	3.75	1.03	1.32	1.11	0.77
C-4 H	5.37	0.91	1.10	1.06	0.59
CH_3	1.95	1.03	1.20	1.03	0.74
C-5 CH_2	1.13, 1.63	3.03	3.33	3.13	1.96
CH_3	0.44	1.54	1.82	1.72	1.10
C-6	5.16	0.91	1.06	1.01	0.62
C-7	5.83	0.86	1.03	0.99	0.63
C-8	~3.4	2.86	3.03	2.86	1.72
C-10	~2.6	3.3[a]	3.3[a]	[b]	[b]
C-11	~2.3			[b]	1.72
C-14	7.07	0.94	1.14	1.06	0.64
C-15	6.31	0.57	0.77	0.71	0.47
C-16 OCH_3	3.71	0.89	1.10	0.96	0.69
C-17	6.18	0.57	0.75	0.77	0.48
C-19	2.66	[b]	[b]	[b]	0.95

[a] Approximate estimation.
[b] Resonance masked.
[c] The assignments given here are based on the work of Gorman *et al.* (16).

protons which are spatially isolated will relax more slowly than those which are in close proximity; this often allows for the identification of methine and hydroxyl protons. For example, the resonance of the relatively isolated bridgehead proton of camphor, **2**, is easily identified as a triplet at 2.04 δ



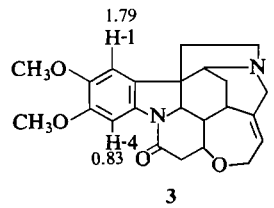
2

because it relaxes more slowly ($R_1 = 0.31\ s^{-1}$) than any other of the skeletal protons (0.4–0.5 s^{-1}), all of which have a *geminal* neighbour (cf. Fig. 1).

It is important to note that "spatial proximity" often involves interactions with protons on pendant substituents or on adjacent rings, and this can often facilitate the otherwise ambiguous spectral assignments. For example, one of the two aromatic protons of brucine, **3**, relaxes 2.15 times faster than the other. Consideration of the relaxation pathways of these two protons with those on other rings indicates that H-1 should relax faster than H-4, thereby providing an unambiguous assignment for those two resonances.

Effects of Molecular Motion on Proton R_1 *Values*

In addition to the pronounced distance dependence alluded to earlier, full interpretation of proton R_1 values often involves consideration of the effects of the motional correlation times (τ_c values) of the individual inter-proton vectors (10). These values reflect the tumbling rate of the molecule as a whole (which need not necessarily be isotropic (10*a*)) plus any additional degrees of motional freedom such as the internal motion of a side-chain with respect to a ring, an excellent example of which is the motion of the methyl and other side-chain protons of a steroid. An *increase* in the rate of motion is equivalent to a decrease in τ_c and hence a *decrease* in relaxation efficiency. From the practical standpoint, however, it is more important to recognize that molecular tumbling rates depend on three experimental variables, temperature, solvent, and solute concentration. As an illustrative example, Fig. 5 shows the effect of changing solvent on the R_1 values of **1**. This is why it is usual practice to keep all three of the above parameters constant if meaningful intercomparisons are to be made between the R_1 values of different substances (11). Even then difficulties arise for molecules of differing molecular mass or shape, and we suggest that a plausible procedure for such systems is to nor-



3

Can. J. Chem. Downloaded from www.nrcresearchpress.com by 210.87.254.6 on 09/05/12
For personal use only.

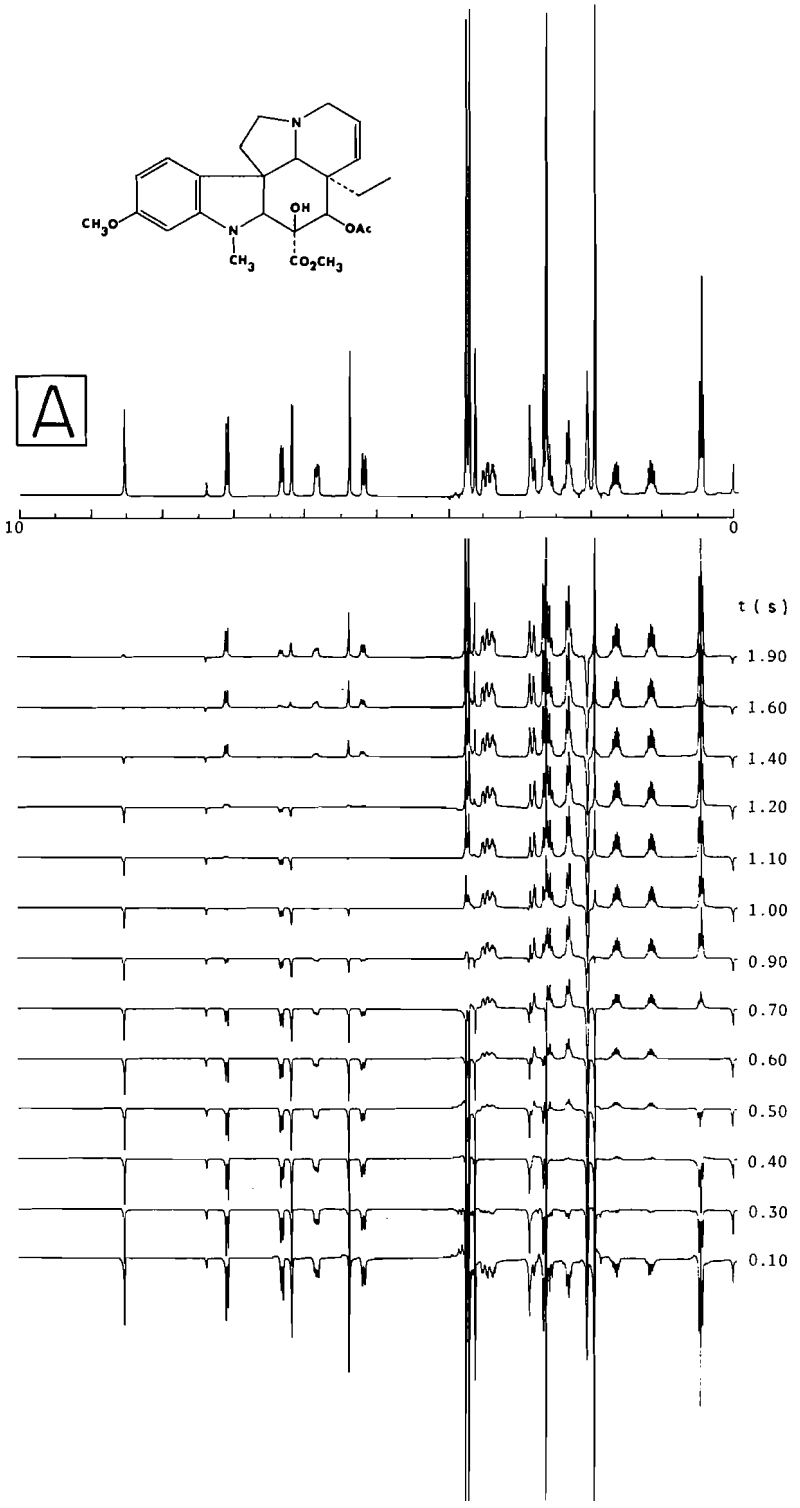


FIG. 3. Proton nmr spectra (270 MHz) of vindoline (0.1 *M* in acetone-d_6, without degassing). *A* shows the normal spectrum measured with four transients, measurement sweep width 3 kHz, 16 K data points. The remaining spectra were obtained under the same operating conditions using a 180°–*t*–90° two pulse sequence; the delay times (*t*, s) are indicated to the right of the spectra.

Can. J. Chem. Downloaded from www.nrcresearchpress.com by 210.87.254.6 on 09/05/12
For personal use only.

Can. J. Chem. Downloaded from www.nrcresearchpress.com by 210.87.254.6 on 09/05/12
For personal use only.

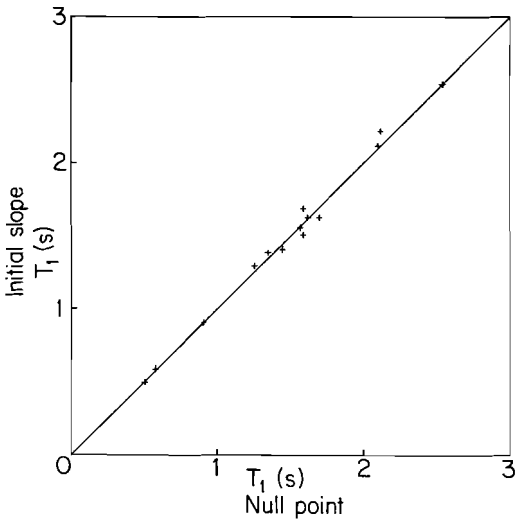


FIG. 4. Plot of the R_1 values for vindoline (0.1 *M* in acetone-d_6, without degassing). The data on the ordinate were obtained by the null point method and those on the abscissa from the initial slope method using a least-squares fit.

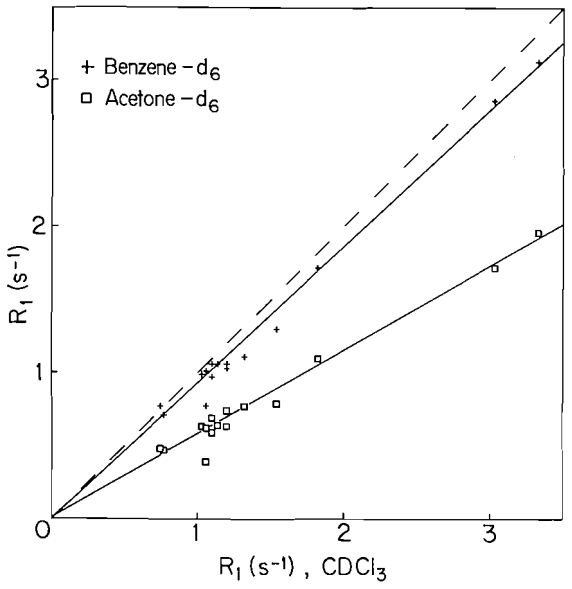
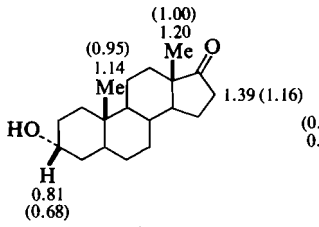
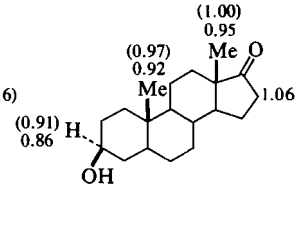


FIG. 5. Proton R_1 values for vindoline obtained by the null point method with the ordinate showing the data measured in $CDCl_3$ solution (0.1 *M*). The abscissa shows the data for 0.1 *M* solutions in benzene-d_6 (+) and in acetone-d_6 (□), measured at the same temperature.

malize the observed R_1 values to that of a particular proton which has a closely similar environment in the separate molecules under study. For example, the R_1 values for the protons of androsterone, **4**, and its C-3 epimer epiandrosterone, **5**, are distinctly different at each site, even though the two molecules were studied under identical conditions. Evidently these two epimers have sufficiently different molecular interactions with the solvent that their overall tumbling motion is significantly different. However, when the R_1 values are normalized (values in parentheses) to those of the 18-methyl group, chosen for this purpose because that group is remote from the site of epimerization, the R_1 values of H-16 and H-19 show excellent agreement between the epimers. In contrast, the axial proton at C-3 in **5** relaxes 34% faster than its equatorial counterpart in **4**. This rate enhancement for an axial

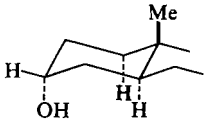


4



5

proton was first observed for pyranose carbohydrates (2*b*) and simply reflects the shorter internuclear separation between H-3 axial and the axial protons at positions 1 and 5 as compared with those of H-3 equatorial. Clearly this dependence has substantial diagnostic potential yet, it would not be detectable without the normalization procedure.



Conclusions

We believe that the spin–lattice relaxation rates of the protons of natural products have substantial diagnostic potential for practicing chemists since they contain information concerning the overall steric environment and molecular motion of each proton. We suggest that access to this information can be rapidly obtained via measurements of null point R_1 values, using a normalization procedure if intercomparisons are to be made between the R_1 values of substances which have different molecular sizes or which have to be studied in different solvents. Given the substantially higher sensitivity of the proton nmr experiment compared with that of ^{13}C nmr there seems to be a strong case for using the former rather that the latter method to study molecular motion of natural products; indeed when limited quantities of material are available measurement of ^{13}C R_1 values may be impossible.

It seems appropriate to end with a comment concerning the null point method, which has previously been regarded by many workers as being so fraught with pitfalls as to be worthless. We feel that

Can. J. Chem. Downloaded from www.nrcresearchpress.com by 210.87.254.6 on 09/05/12
For personal use only.

it is important to recall that those opinions were largely based on attempts to measure ^{13}C R_1 values with spectrometers which were only capable of producing rather long 180° pulses (typically 120 μs); thus the criteria (12) for a good 180° pulse over the entire spectral width (typically 5 kHz) were far more demanding than those required by the proton experiments described here and could not, in fact, be achieved. Even so, the purity of the 180° pulse is still critical, and all reports describing null point R_1 values should be accompanied either by an intercomparison between data obtained by the conventional and the null point methods or by an experimental evaluation of the performance of the spectrometer vis-à-vis the effectiveness of the 180° pulse.

It seems clear from the experiments which we have performed with our spectrometer that any additional errors associated with the null point method are rather small compared wtih those implicitly associated with the conventional two pulse determination of spin–lattice relaxation rates. Nevertheless, it would clearly be preferable if any remaining reservations held by others could be professionally resolved; in this regard the recent report by Levitt and Freeman (13) describing the use of composite pulses to minimize errors in R_1 determinations resulting from infidelities in the 180° pulse is welcome indeed. An appraisal of that procedure in the context of proton relaxation studies of complex natural products is deferred until a later date.

Experimental

Samples

All solvents were stored over molecular sieves prior to use. All solutes gave proton nmr spectra in entire accord with the assigned structures and showed no resonances from impurities.

All solutions were filtered through glass or cotton-wool directly into precleaned nmr tubes. Degassing was performed either by six consecutive freeze–pump–thaw cycles followed by sealing under vacuum, or by sparging with a slow stream of oxygen-free nitrogen followed by sealing with a rubber septum cap.

The Spectrometer

All measurements were made with a home-built 270 MHz spectrometer which was assembled at the Universtiy of British Columbia from what was originally a Nicolet TT-23 spectrometer operating at 100 MHz, and a Nicolet 1080 computer. The operating frequency was increased to 270 MHz by externally heterodyning against 170 MHz from a frequency synthesizer, and the 270 MHz signal was amplified using a home-built 50 W class C power amplifier. The single coil probe for 5 mm sample tubes and 6.5 Tesla superconducting solenoid were from Oxford Instruments. Although no field-frequency lock was used, the observed frequencies changed by less than ±0.2 Hz per hour.

Many of the data reported were obtained with the instrument based on a Nicolet 1180 computer (40 k), a Nicolet 293A pulse programmer, and a Diablo high density disk drive (model 30).

Criteria for 180° Pulse

Before each measurement, the 180° pulse duration was optimized by finding the length which produced a null in the amplitude of the free induction decay signal. Typically the duration was ca. 25 μs; this corresponds to a total pulse width of ca. 40 kHz which is far in excess of the ca. 3 kHz spectral widths of interest; and according to the calculations of Meakin and Jesson (12) under these conditions both intensity and phase errors would be negligible.[9]

Data Acquisition and Processing

Spectra were measured using the two-pulse, 180°–t–90° inversion-recovery sequence (1) with averaging of four free induction decay signals. The delay between each sequence was at least five times the estimated value of the longest T_1. Typically, data for about 30 values of t were separately averaged, filtered, Fourier transformed, phase corrected, and stored automatically on disk for later processing, the appropriate range of t values having been selected either by preliminary experiments or by experience. The longest value of t was chosen so that all peaks had relaxed through their null points.

R_1 values were determined by the "null" method, using extrapolation between data sets straddling the null point itself. The same partially relaxed spectra were used for conventional calculations of R_1 values. The intensity(ies) of the component(s) of each resonance were obtained from the computer peak printout; for multiplet resonances these were summed. The total magnetization intensity for each resonance was then processed in the usual fashion (14, 15) to give an R_1 value. In partial cognizance of the requirements of the initial slope approximation (8), the R_1 values were then recalculated using the data obtained during the first calculated T_1 period of the individual proton. R_1 values could typically be measured with a reproducibility of ±1–4% using the null point method, and with a standard (random) error of 1–4% by the conventional (regression) method. Additional systematic errors inherent in the two-pulse method may also be present.

Acknowledgments

It is a pleasure for one of us (L.D.C.) to thank the University of British Columbia for the facilities provided for his sabbatical leave during 1977–1978 when this study was performed. Funds for the components of the 270 MHz spectrometer were provided by the Chemistry Department, University of British Columbia and by the President's Emergency Research Equipment Fund of the University of British Columbia. Both authors wish to thank the National Research Council of Canada for operating grants.

1. R. L. VOLD, J. S. WAUGH, M. P. KLEIN, and D. E. PHELPS. J. Chem. Phys. **48**, 3831 (1968).
2. (*a*) C. W. M. GRANT, L. D. HALL, and C. M. PRESTON. J. Am. Chem. Soc. **95**, 7742 (1973); (*b*) L. D. HALL and C. M. PRESTON. Chem. Commun. 1319 (1972); Carbohydr. Res. **37**, 267 (1974); (*c*) L. D. HALL and C. M. PRESTON. Car-

[9]This procedure provides no information concerning the homogeneity of the radiofrequency field induced by the pulse; we shall not discuss the subtleties of this point here because this is an implicit limitation built into the instrument by the design of the probe, over which the operator has no control.

bohydr. Res. **49**, 3 (1976); (*d*) L. D. HALL and K. F. WONG. Anomeric effect. *Edited by* W. A. Szarek and D. Horton. Am. Chem. Soc. Symp. Ser. **87**, 30 (1979); (*e*) L. D. HALL, K. F. WONG, W. E. HULL, and J. D. STEVENS. Chem. Commun. 953 (1979).

3. K. AKASAKA, T. IMOTO, S. SHIBATA, and H. HATANO. J. Magn. Reson. **18**, 328 (1975); A. P. ZENS, T. J. WILLIAMS, J. C. WISOWATY, R. R. FISCHER, R. B. DUNLAP, T. A. BRYSON, and P. D. ELLIS. J. Am. Chem. Soc. **97**, 2850 (1975); K. BOCK and L. D. HALL. J. Carbohydr. Nucleosides, Nucleotides, **4**, 83 (1977).
4. (*a*) R. L. VOLD, R. R. VOLD, and D. CANET. J. Chem. Phys. **66**, 1202 (1977); (*b*) L. D. HALL, K. F. WONG, and H. D. W. HILL. Chem. Commun. 951 (1979).
5. I. SOLOMON. Phys. Rev. **99**, 559 (1955); A. ABRAGAM. The principles of nuclear magnetism. Oxford Univ. Press. 1961.
6. H. D. W. HILL and L. D. HALL. J. Am. Chem. Soc. **98**, 1269 (1976).
7. R. FREEMAN and H. D. W. HILL. J. Chem. Phys. **54**, 3367 (1971).
8. R. FREEMAN, S. WITTEKOEK, and R. R. ERNST. J. Chem. Phys. **52**, 1529 (1970).
9. L. D. HALL and S. SUKUMAR. To be published.
10. (*a*) D. E. WOESSNER. J. Chem. Phys. **37**, 647 (1962); (*b*) J. K. M. SANDERS, J. C. WATERTON, and I. S. DENNISS. J. Chem. Soc. Perkin I, 1150 (1978); (*c*) N. NICCOLAI, M. P. DE LEON DE MILES, S. P. HEHIR, and W. A. GIBBONS. J. Am. Chem. Soc. **100**, 6528 (1978).
11. L. D. HALL. Chem. Soc. Rev. **4**, 401 (1975); Chem. Can. **28**, 19 (1976).
12. P. MEAKINS and J. P. JESSON. J. Magn. Reson. **11**, 182 (1973); **13**, 354 (1974).
13. M . H. LEVITT and R. FREEMAN. J. Magn. Reson. **33**, 473 (1979).
14. C. M. PRESTON. Ph.D. Thesis, University of British Columbia, Vancouver, B.C. 1975.
15. K. F. WONG. Ph.D. Thesis, University of British Columbia, Vancouver, B.C. 1979.
16. M. GORMAN, N. NEUSS, and K. BIEMANN. J. Am. Chem. Soc. **84**, 1058 (1962).

Can. J. Chem. Downloaded from www.nrcresearchpress.com by 210.87.254.6 on 09/05/12
For personal use only.

C-Nucleosides and related compounds. XV. The synthesis of D,L-2′-*epi*-showdomycin and D,L-showdomycin

GEORGE JUST, T. J. LIAK, MU-ILL LIM, PIERRE POTVIN, AND YOULA S. TSANTRIZOS
Department of Chemistry, McGill University, Montreal, P.Q., Canada H3C 3G1

Received March 26, 1980

GEORGE JUST, T. J. LIAK, MU-ILL LIM, PIERRE POTVIN, and YOULA S. TSANTRIZOS. Can. J. Chem. **58**, 2024 (1980).

The conversion of the Diels–Alder adduct of methyl β-nitroacrylate with furan to the title compounds and to D,L-2,5-anhydroglucose derivatives is described.

GEORGE JUST, T. J. LIAK, MU-ILL LIM, PIERRE POTVIN et YOULA S. TSANTRIZOS. Can. J. Chem. **58**, 2024 (1980).

On décrit la transformation du produit de la réaction Diels–Alder du méthyle β-nitroacrylate avec le furane en dérivés du D,L-2,5-anhydroglucose, en D,L-2′-*épi*-showdomycine, et en showdomycine.

Can. J. Chem. Downloaded from www.nrcresearchpress.com by 210.87.254.40 on 09/05/12
For personal use only.

As part of a programme to synthesize *C*-nucleosides, we were interested in developing a method to prepare an arabinose derivative **8**, bearing at the anomeric center a functionalized carbon atom, which could serve as a precursor for the synthesis of compounds such as *ara*-showdomycin (**9***b*).

Reaction of furan with methyl β-nitroacrylate gave the known adducts **1***a* and **1***b* (1). Prolonged treatment with *m*-chloroperbenzoic acid gave epoxides **2***a* and **2***b*, which upon treatment with diazabicyclo[5.4.0]undec-5-ene (DBU) gave olefinic epoxide **3**. As expected (2*a*), nmr analysis of this compound revealed that the stereochemistry of the epoxide function was *exo*, since the coupling constant between the bridgehead protons and the *endo*-protons α to the epoxide was 0 Hz (dihedral angle ~ 90° (2*b*)).

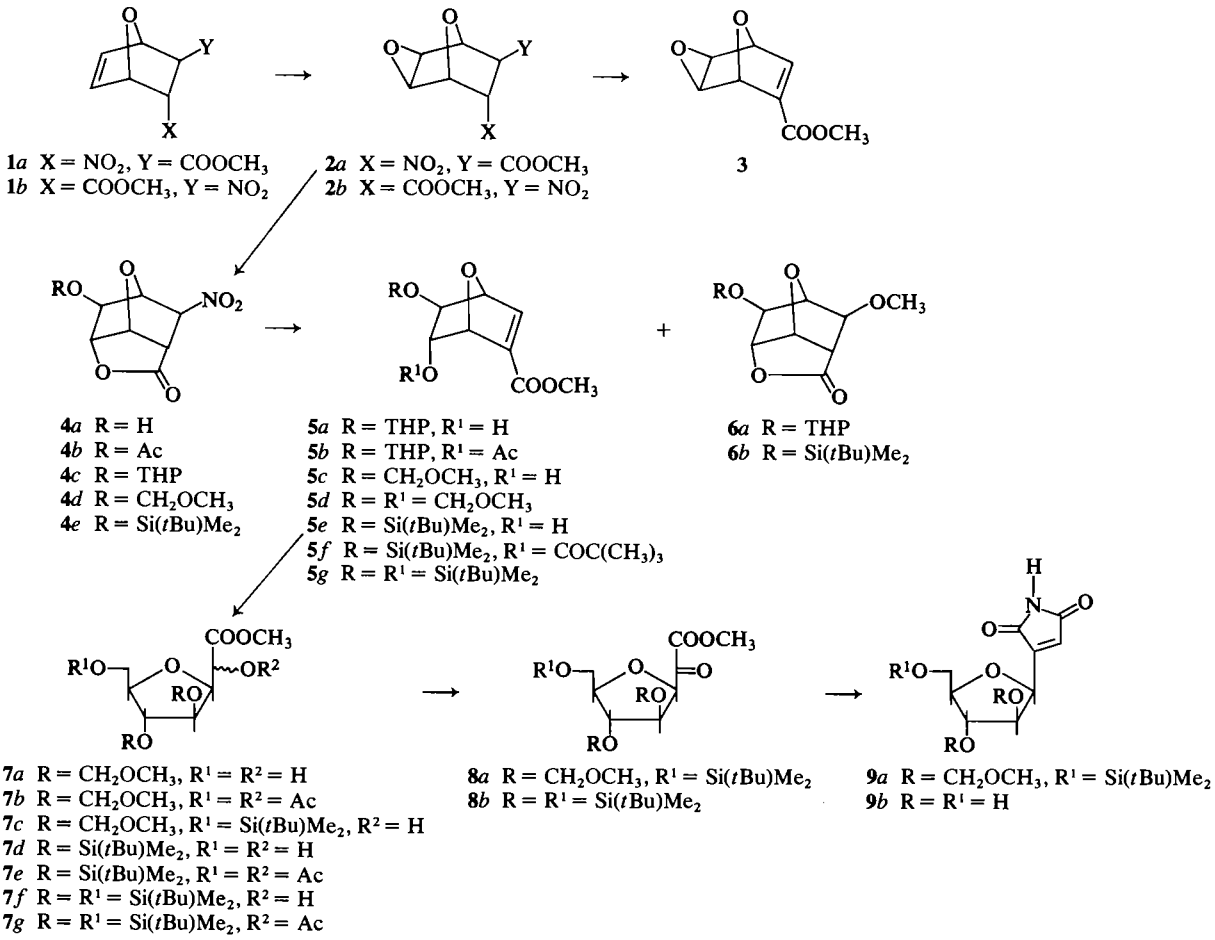
Treatment of *endo*-carbomethoxy epoxide **2***b* with acetic acid and hydrochloric acid at 95°C for 2 h gave lactone **4***a* in 60% yield. There is ample precedent that lactonizations of this type proceed in the manner depicted, and it has been recently reconfirmed in an unambiguous manner for a closely related system (12).

Attempts to acylate hydroxy lactone **4***a* with acetic anhydride or pivaloyl chloride in pyridine failed, leading to decomposition products. However, acetylation using acidic conditions gave acetate **4***b* in good yield. Tetrahydropyranyl ether **4***c* could also be easily prepared.

Attempts to transform lactone **4***c* into the α,β-unsaturated ester **5***a* using one or more equivalents of sodium methoxide in methanol, the conditions which had cleanly converted the corresponding bromolactone in the bicyclo[2.2.1]heptane series to an analogous compound (3), failed because of the formation of the sodium salt of **4***c*. However, treatment of **4***c* with DBU in methanol gave ester **5***a*, accompanied by varying amounts of **6***a*. From the relative ratios of **5***a* to **6***a* as a function of reaction time, it was obvious that **5***a* was transformed to **6***a*. Compound **5***a* was characterized as its acetate **5***b*. At this point, it became apparent that the tetrahydropyranyl protecting group obscured the nmr spectrum of **5***a* and **5***b* enough to make some of the assignments doubtful. The reaction sequence was therefore repeated with the dimethyl-*tert*-butylsilyl ether lactone **4***e*, providing **5***e* and **6***b*; **5***e* was characterized as its pivalate **5***f*. Since Just and Ouellet (3) subsequently established in the analogous carbocyclic series that the pivalate group interacted with the hydroxy group generated in the subsequent ozonolysis–reduction sequence **5** → **7**, it was decided to block the hydroxy group in **5***e* as its dimethyl-*tert*-butylsilyl ether **5***g* (4). Silylation of **5***e* proceeded in an unpredictable manner, providing the disilylation product **5***g*, except for one instance, in low yield.

Ozonolysis of the olefin **5***g*, followed by treatment with dimethyl sulfide and the reduction of the resulting keto aldehyde, obtained in part as its hydrate, with 4 equivalents of lithium tri-*tert*-butoxyaluminum hydride, gave diol ester **7***d*. Selective silylation of **7***d* gave the trisilyl ether **7***f*. That the silylation had proceeded with the desired selectivity was proven by acetylation, where only one proton was shifted downfield from 2.96 to 3.63 ppm. Oxidation (5) of **7***f* provided the relatively unstable ketoester **8***b*. Because of the low silylation yield encountered at one stage in this sequence, the methoxymethyl protecting group (6) was used in the analogous sequence **4***d* → **5***d* → **7***c* → **8***a*. In this sequence, considerable difficulty was experienced when the method worked out for the transformation **4***c* → **5***a* was applied to transformation **4***d* → **5***c*, and it had to be modified. The highest reproducible yields (40–50%) of **5***c* were obtained

0008-4042/80/192024-10$01.00/0
©1980 National Research Council of Canada/Conseil national de recherches du Canada



when **4***d* was boiled for 7 hours with triethylamine in dry methanol. It was transformed to its methoxymethyl ether **5***d* in high yield. The structure and stereochemistry of **5***d* follow from its mode of formation and nmr spectrum, which indicated that H4 was split by H3 (2 Hz), whereas the coupling constant H4—H5 was close to 0 Hz, indicating an *exo*-configuration of the 5-substituent. On the other hand *J*(H1—H6) was 4 Hz as expected, indicating that the 6-substituent was *endo*. This was confirmed by the fact that *J*(H5—H6) was close to 0 Hz.

Ozonolysis of **5***d*, followed by reduction with dimethylsulphide and lithium aluminum tri-*tert*-butoxyhydride, gave diol **7***a*, characterized as its diacetate **7***b*. Selective silylation with *tert*-butyldimethylsilyl chloride gave monosilyl ether **7***c*. Silyl ether **7***c* seemed to consist of one diastereomer only. The stereochemistry at C2 was of no consequence, since the next step involved oxidation (5) to ketoester **8***a*.

Whereas the ozonolysis, reduction, and oxidation sequence should not have affected the stereochemistry at $C2^1$, $C3^1$ and $C4^1$, there was some doubt about the stereochemistry at $C1^1$ especially in ketoester **8***a*. The following spectral and chemical data support the assignment of stereochemistry made: whereas the nmr spectrum of **7***c* in deuterochloroform or benzene was uninformative, addition of Eu(fod)$_3$ to the deuterobenzene solution of **7***c* allowed an assignment of most signals. The lowest-field signal (1H, C2) appeared as a doublet (J = 8 Hz). The $C1^1$-proton appeared at somewhat higher field as a doublet of doublets ($J_{2,1'}$ = 8 Hz, $J_{1',2'}$ = 4 Hz). This latter coupling constant is indicative of a *cis* relation (8, 20) for $H1^1$—$H2^1$. The $H3^1$ proton consisted of a 4-line system (J_a, $J_b \simeq$ 2 Hz, 2.5 Hz). The $C4^1$-proton consisted of complex signal which did not permit first order interpretation. The appearance of the protons corresponding to $C1^1$, $C2^1$, $C3^1$, $C4^1$, and $C5^1$ was similar in ketoester **8***a* and in showdomycin analogs **9***a* and **9***b*, except

Can. J. Chem. Downloaded from www.nrcresearchpress.com by 210.87.254.40 on 09/05/12
For personal use only.

Can. J. Chem. Downloaded from www.nrcresearchpress.com by 210.87.254.40 on 09/05/12
For personal use only.

for the absence of C2—C1^1 coupling in **8***a* and for the appearance of a 2 Hz long-range coupling between the olefinic proton of the heterocycle and C1^1—H. The stereochemical assignment was confirmed by the following conversion. Compound **5***d* was ozonized at −78°C and the ozonide reduced with borohydride to the corresponding triol (**7***a*, $COOCH_3$=CH_2OH). Without purification, the triol was oxidized with periodate to give 2,5-anhydroglucose **10**, which existed predominantly in the hemiacetal form shown, as indicated by spectral and microanalytical data. The formation of a hemiacetal proves that triol **7***a* ($COOCH_3$=CH_2OH) and therefore triol derivative **7***c* had most likely the same *cis* configuration at C1^1 and C4^1.

Compound **10** was transformed to the thiazolidine acetate **11***b* and the α,β-unsaturated ester **12***b*, using the methods described for the analogous anhydroallose (1). Both types of compounds have been shown to be versatile precursors to *C*-nucleosides (10).

Compound **8***a* was obtained from nitroacrylate adduct **1***b* in an overall yield of 6.5% in 8 steps.

Following procedures used for the synthesis of showdomycin (21) and showdomycin analogues (13, 14), the ketoester **8***a* was reacted with 1 equivalent of carbamoylmethylenetriphenylphosphorane (7) in chloroform at room temperature for 2 h. The reaction gave a single major product together with considerable amounts of polar by-products. Purification of the crude product by flash chromatography (19) using petroleum ether – ethylacetate (3:1) gave the maleimide **9***a* in an overall yield of 40% from the hydroxy ester **7***c*. The nmr spectrum of this substance clearly showed the disappearance of the methyl ester group, the presence of a single NH proton at δ 8.08 and a vinyl proton at δ 6.39. The ir spectrum showed characteristic absorptions at 1790 and 1740 cm^{-1} for the carbonyl function and at 1665 cm^{-1} for the olefinic bond. In the mass spectrum, the molecular ion peak was found at *m/e* 431 and other major peaks at *m/e* 400 ($M^+ - OCH_3$) and 374 ($M^+ - C(CH_3)_3$). Furthermore, the uv spectrum revealed the typical maleimide chromophore having absorption maximum at 222 nm ($\log \varepsilon = 4.2$).

Completion of the synthesis of 2′-*epi*-showdomycin then only required removal of the protecting groups. Treatment of **9***a* with 80% aqueous trifluoroacetic acid led to the simultaneous removal of both *tert*-butyldimethylsilyl and methoxymethyl groups. Subsequent purification on silica gel plates gave crystalline D,L-2′-*epi*-showdomycin **9***b*, mp 170–171°C, in 60% yield. The uv spectrum of the product showed an absorption at 222 nm and the molar extinction coefficient ($\log \varepsilon$ 4.36) was also in accord with that of the known showdomycin (8), thus confirming the structure of the aglycon moiety of **9***b*. The ir data and elemental analysis were consistent with the structure of **9***b*. Furthermore, this compound was fully identified by its mass spectrum.

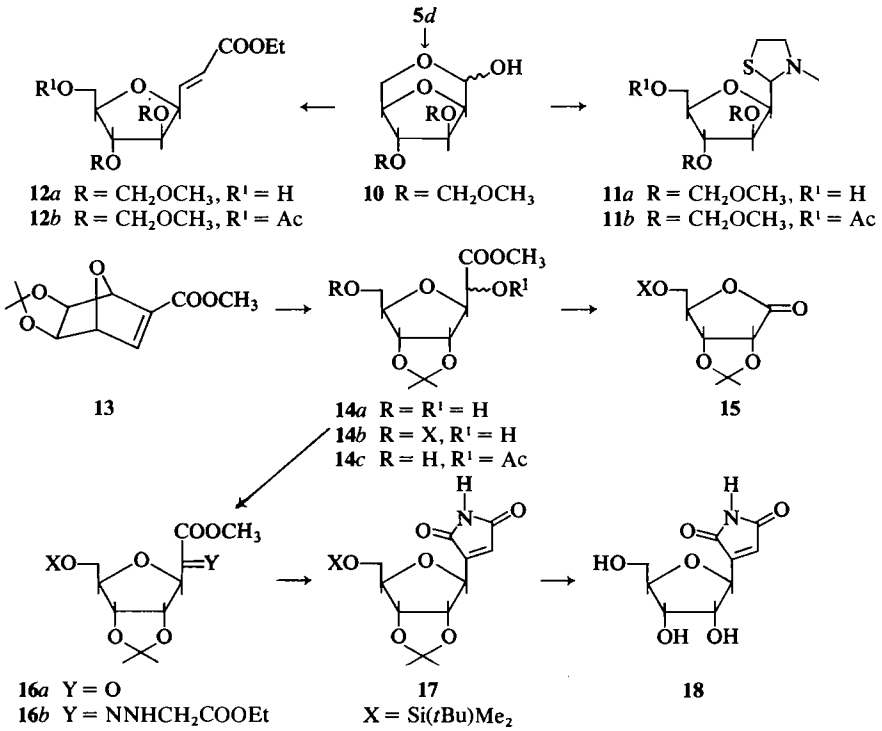
The mass spectrum of 2′-*epi*-showdomycin **9***b* was quite typical of other *C*-nucleosides (9) and showed a minor molecular ion peak at *m/e* 229 and an abundant peak at *m/e* 211 corresponding to loss of water from the molecular ion. The base peak was found at *m/e* 126 (B + 30) where B was the heterocyclic aglycon. The B + 30 peak is strongly suggestive of a formyl type residue attached to the base. Comparison of the major peaks of showdomycin with those of 2′-*epi*-showdomycin **9***b* revealed considerable similarity in the fragmentation pattern.

The nmr spectrum of **9***b* showed clearly H4 as a doublet coupled to H1^1 ($J_{1',4}$ = 2 Hz), and H1^1 as a doublet of doublets ($J_{1',4}$ = 2 Hz, $J_{1',2'}$ = 4 Hz). A coupling constant of 4 Hz indicates *cis*-related protons. Comparison of spectra (8, 20) of *C*-nucleosides and sugars having a β-configuration at the anomeric centre to related compounds having the α-configuration shows that the chief difference is that the coupling constant corresponding to $J_{1',2'}$ in the α-anomers, having otherwise identical stereochemistry, is close to 0 Hz. We are therefore quite convinced that the stereochemistry of **9***b* is as indicated.

The overall yield for the formation of 2′-*epi*-showdomycin, based on the *exo*-nitro adduct **1***b*, was 1.6%.

The synthesis of D-showdomycin **18**, first accomplished by Kalvoda *et al.* (11) and improved by Trümmlitz and Moffatt (21), was carried out in a similar manner for the racemate, and is described below.

The readily available bicyclic ester **13** (1) was ozonolysed at −78°C, and the resulting ozonide reduced with dimethyl sulphide. The resulting ketoester aldehyde, which, when freshly prepared, seems to contain 60% of the expected aldehyde (by nmr), was normally obtained as its hydrate. Its reduction with 2.5 equivalents of lithium aluminum tri-*tert*-butoxy hydride gave diol **14***a*, presumably as a mixture of diastereoisomers, in 60–78% yield, based on **13**. It was characterized as its diacetate **14** (R = R^1 = Ac). When treated with one equivalent of *tert*-butyldimethylsilyl chloride, **14***b* was obtained. Its structure followed from the fact that acetylation gave **14***c*, in which the proton α to the acetate



function had shifted downfield by 1 ppm with respect to the same proton in **14***b*. Further confirmation was derived from the fact that the di-*tert*-butyldimethylsilyl ether of **14***a* could be selectively hydrolysed to an isomeric monosilylether **14** (R = H, R^1 = Si (*t*Bu)Me_2), acetylation of which gave **14** (R = Ac, R^1 = Si (*t*Bu)Me_2) in which two protons shifted downfield by 0.8 ppm. Oxidation of alcohol **14***b* with a variety of reagents such as ruthenium tetroxide (5), *N*-bromosuccinimide (15), or Collins reagent (16) resulted in either decomposition, formation of lactone **15**, or formation of the desired ketoester **16** in an irreproducible manner. However, with acetic anhydride – dimethylsulfoxide (17), the unstable ketoester **16** could be obtained in 80% yield. The analogous oxidation of related compounds such as the carbocyclic analog of **14***b* (13, 14) had never given rise to this type of erratic behaviour.

Treatment of the crude ketoester **16** with carbamoylmethylenetriphenylphosphorane (7) gave D,L-showdomycin derivative **17**, in 35% yield. The nmr spectrum of **17** was fully consistent with the structure assigned. In particular, the isopropylidene group gave two well-spaced singlets (18) indicating that only the desired "β-anomer" was obtained. Hydrolysis gave D,L-showdomycin, mp 143–144°C. Its mass spectrum was identical to that of naturally occurring showdomycin (9*a*).

Attempts to prepare pyrazomycin by cyclization of **16***a*, which had been successful for analogous compounds in the carbocyclic (13) and other series, was unsuccessful, and no pure D,L-pyrazomycin could be obtained from **16***a*, although the uv spectrum of a purified sample indicated that it had been formed in very low yield.

Experimental

Melting points were determined on a Gallenkamp block and are uncorrected. Preparative thin layer chromatography was performed using Merck HF-254 and Brinkmann HF-254 silica gel on 20 cm × 20 cm plates. Merck silica gel 60 and Woelm neutral alumina were used for column chromatography. Woelm silica gel 32–63 μ was used for flash chromatography. Mass spectra were obtained on AE1-MS-902 or LKB-900 mass spectrometers at 70 eV using a direct-insertion probe. Nuclear magnetic resonance spectra were recorded on Varian Associates T-60, T60A, HA-100, or Bruker FT90 spectrometers. Infrared spectra were obtained on a Unicam SP1000 and Perkin–Elmer 257 and 297 ir spectrophotometers. Ultraviolet spectra were determined with a Unicam SP-800 or a Cary 17 spectrophotometer. Microanalyses were carried out by Dr. C. Daessle, Montreal.

3-Exo-*carbomethoxy*-*2*-endo-*nitro*-*5,6*-exo-*epoxido*-*7*-*oxabicyclo*[*2.2.1*]*heptane* (2a)

To a solution of **1***a* (2.02 g, 10 mmol) in methylene chloride (40 mL) was added by portions a solution of 85% *m*-chloroperbenzoic acid (2.49 g, 14 mmol) in methylene chloride (40 mL). The mixture was stirred for 2 days at room temperature. Excess peracid was then destroyed by addition of 10% sodium sulfite solution. The organic phase was washed with 5% aqueous sodium bicarbonate and water and dried ($MgSO_4$). Solvent removal left an oil which was crystallized from ethyl ether. Recrystallization from chloroform–hexane gave 1.31 g

Can. J. Chem. Downloaded from www.nrcresearchpress.com by 210.87.254.40 on 09/05/12
For personal use only.

Can. J. Chem. Downloaded from www.nrcresearchpress.com by 210.87.254.40 on 09/05/12
For personal use only.

(60%) of **2***a*, mp 100–101°C; ir (KBr) ν_{max}: 1745 (C=O), 1550 (C—NO_2) cm^{-1}; nmr (DMSO-d_6) δ: 3.52 (m, 2H), 3.69–3.76 (s + m, 4H), 4.83 (s, 1H), 4.94 (d, 1H, J = 5 Hz), 5.53 (t, 1H, J = 4 Hz); mass spectrum (70 eV) *m/e*: 215 (M^+), 184 ($M^+ - OCH_3$), 169 ($M^+ - NO_2$), 109 ($M^+ - COOCH_3 - HNO_2$). *Anal.* calcd. for $C_8H_9NO_6$: C 44.65, H 4.17, N 6.51; found: C 44.54, H 4.44, N 6.77.

2-Endo-*carbomethoxy-3*-exo-*nitro-5,6*-exo-*epoxido-7-oxabicyclo[2.2.1]heptane* (**2**b)

To a solution of **1***b* (3.03 g, 15 mmol) in methylene chloride (50 mL) was added dropwise a solution of 85% *m*-chloroperbenzoic acid (3.66 g, 17 mmol) in methylene chloride (50 mL). Stirring was continued for 2 days at room temperature. The reaction mixture was washed with 10% sodium sulfite (3 × 30 mL) and 5% sodium bicarbonate solution, water, and finally with brine. Drying over sodium sulfate and evaporation gave 2.44 g (74.4%) of **2***b* as an oil which was crystallized from methanol and recrystallized from chloroform, mp 109–110°C; ir (KBr) ν_{max}: 1745 (C=O), 1550 (C—NO_2) cm^{-1}; nmr (DMSO-d_6) δ: 3.66 (m, 2H), 3.73 (s, 3H), 3.93 (t, 1H, J = 4 Hz), 4.88 (d, 1H, J = 5 Hz), 5.10 (s, 1H), 5.25 (d, 1H, J = 4 Hz); mass spectrum (70 eV) *m/e*: 215 (M^+), 169 ($M^+ - NO_2$), 109 ($M^+ - COOCH_3 - HNO_2$). *Anal.* calcd. for $C_8H_9NO_6$: C 44.65, H 4.17, N 6.51; found: C 44.66, H 4.34, N 6.68.

5-*Carbomethoxy-2,3*-exo-*epoxido-7-oxabicyclo[2.2.1]-hept-5-ene* (**3**)

A solution of **2***a* (319 mg, 1.48 mmol) and DBU (281 mg, 1.77 mmol) in methylene chloride (10 mL) was refluxed for 40 min. The mixture was diluted with methylene chloride, washed with 0.1 *N* hydrochloric acid three times, with water, then evaporated to dryness, leaving a syrup which was purified by eluting it through a column of silicic acid using chloroform. Crystallization of the major product from carbon tetrachloride – hexane gave 152 mg (61%) of **3**, mp 76–77°C; ir (KBr) ν_{max}: 1700 (C=O), 1595 (C=C) cm^{-1}; nmr ($CDCl_3$) δ: 3.48 (d, 1H, J = 3.5 Hz), 3.62 (d, 1H, J = 3.5 Hz), 3.75 (s, 3H), 4.88 (d, 1H, J = 2 Hz), 5.00 (s, 1H), 7.26 (d, 1H, J = 2 Hz); mass spectrum (70 eV) *m/e*: 168 (M^+), 153 ($M^+ - CH_3$), 139, 136 ($M^+ - CH_3OH$). *Anal.* calcd. for $C_8H_8O_4$: C 57.14, H 4.80; found: C 57.37, H 4.85. Using the conditions described above, **2***b* was transformed to **3**, identical in all respects with **3** obtained from **2***a*.

5-Exo-*6*-endo-*dihydroxy-3*-exo-*nitro-7-oxabicyclo-[2.2.1]heptane-2*-endo-*carboxylic Acid γ-Lactone* (**4**a)

A solution of **2***b* (3.12 g, 15 mmol) in acetic acid (60 mL), hydrochloric acid (30 mL), and water (30 mL) was heated at 95–100°C for 2 h. After cooling to room temperature, the solvents were evaporated *in vacuo* to dryness and the residue was coevaporated with ethanol. The black residue was dissolved in hot acetone and treated with charcoal. The filtrate was concentrated to afford a yellow oil. Crystallization from acetone–chloroform gave 2.34 g (60%) of **4***a*, mp 170–171°C; ir (KBr) ν_{max}: 3500 (OH), 1800 (lactone), 1575 (C—NO_2) cm^{-1}; nmr ($(CD_3)_2CO$) δ: 3.36 (bs, 1H), 3.63 (d, 1H, J = 5 Hz), 4.10 (s, 1H), 4.60 (d, 1H, J = 5 Hz), 5.25 (s, 1H), 5.33 (s, 1H), 5.60 (t, 1H, J = 5 Hz); mass spectrum (70 eV) *m/e*: 201 (M^+), 155 ($M^+ - NO_2$). *Anal.* calcd. for $C_7H_7NO_6$: C 41.79, H 3.48, N 6.96; found: C 41.66, H 3.75, N 7.17.

5-Exo-*acetoxy-6*-endo-*hydroxy-3*-exo-*nitro-7-oxabicyclo-[2.2.1]heptane-2*-endo-*carboxylic Acid γ-Lactone* (**4**b)

A mixture of **4***a* (165 mg) and acetic anhydride (2 mL) containing one equivalent of *p*-toluenesulfonic acid monohydrate was stirred at room temperature for 30 min. The resulting solid was collected by filtration and washed with cold water to give 139 mg (70%) of analytically pure **4***b*, mp 198–200°C; ir (KBr) ν_{max}: 1800 (lactone), 1745 (C=O), 1560 (C—NO_2) cm^{-1}; nmr (DMSO-d_6) δ: 2.08 (s, 3H), 3.62 (d, 1H, J = 5 Hz), 4.82 (d, 1H, J = 5 Hz), 4.98 (s, 1H), 5.36 (s, 1H), 5.62 (t, 1H, J = 5 Hz), 5.83 (s, 1H); mass spectrum (70 eV) *m/e*: 243 (M^+), 196 ($M^+ - NO_2$), 155, 109. *Anal.* calcd. for $C_9H_9NO_7$: C 44.44, H 3.70, N 5.76; found: C 44.24, H 3.73, N 5.41.

6-Endo-*hydroxy-3*-exo-*nitro-5*-exo-*tetrahydropyranyl-oxy-7-oxabicyclo[2.2.1]heptane-2*-endo-*carboxylic Acid γ-Lactone* (**4**c)

To a solution of **4***a* (1.0 g, 5 mmol) and *p*-toluenesulfonic acid (10 mg) in acetone was added dihydropyran (2 mL). The mixture was stirred at room temperature for 4 h and then evaporated, leaving a solid residue. Recrystallization from acetone–hexane gave 1.21 g (85%) of **4***c*, mp 123–124°C; ir (KBr) ν_{max}: 1800 (lactone), 1560 (C—NO_2), 1040 cm^{-1}; nmr ($(CD_3)_2CO$) δ: 1.57 (m, 6H), 3.33–3.57 (m, 3H), 3.90 (s, 1H), 4.36–4.70 (m, 2H), 5.03 (bs, 2H), 5.23 (t, 1H, J = 4 Hz). *Anal.* calcd. for $C_{12}H_{15}NO_7$: C 50.53, H 5.26, N 4.91; found: C 50.43, H 5.47, N 5.12.

6-Endo-*hydroxy-3*-exo-*nitro-5*-exo-*methoxy-methyloxy-7-oxabicyclo[2.2.1]heptane-2*-endo-*carboxylic Acid γ-Lactone* (**4**d)

To a stirred solution of **4***a* (1.33 g, 6.6 mmol) and methylal (5 mL) in tetrahydrofuran (30 mL) was added phosphorus pentoxide (about 5 g). After standing for 1.5 h at room temperature the mixture was filtered and the residue was washed with tetrahydrofuran. The filtrate was evaporated to dryness. The residue was dissolved in ethyl acetate and washed with 5% sodium bicarbonate solution, water, and brine. Evaporation of the dried organic phase gave 1.53 g (93%) of **4***d* as an analytically pure solid, mp 154–155°C; ir (KBr) ν_{max}: 1800 (lactone), 1560 (C—NO_2) cm^{-1}; nmr ($(CD_3)_2CO$) δ: 3.06 (s, 3H), 3.36 (d, 1H, J = 5 Hz), 3.86 (s, 1H), 4.40 (d, 1H, J = 5 Hz), 4.43 (s, 2H), 5.23 (s, 2H), 5.50 (t, 1H, J = 5 Hz); mass spectrum (70 eV) *m/e*: 245 (M^+), 199 ($M^+ - NO_2$). *Anal.* calcd. for $C_9H_{11}NO_7$: C 44.08, H 4.52, N 5.71; found: C 44.22, H 4.75, N 5.54.

6-Endo-*hydroxy-3*-exo-*nitro-5*-exo-*tert-butyldimethylsilyloxy-7-oxabicyclo[2.2.1]-heptane-2*-endo-*carboxylic Acid γ-Lactone* (**4**e)

To a solution of **4***a* (2.01 g, 10 mmol) in tetrahydrofuran (20 mL) and dimethylformamide (20 mL) was added dimethyl-*tert*-butylsilyl chloride (2.26 g, 15 mmol) and imidazole (1.70 g, 25 mmol). The reaction mixture was stirred at room temperature for one day. After evaporation of the solvents the residue was dissolved in ethyl acetate, washed with water, dried, and evaporated. The residue was chromatographed on a column of silicic acid (40 g) using methylene chloride. Crystallization from hexane gave 2.84 g (90%) of **4***e*, mp 112–113°C; ir (Nujol) ν_{max}: 1800 (lactone), 1560 (C—NO_2) cm^{-1}; nmr ($CDCl_3$) δ: 0.16 (s, 6H), 0.95 (s, 9H), 3.76 (d, 1H, J = 5 Hz), 4.00 (s, 1H), 4.58 (d, 1H, J = 5 Hz), 4.84 (s, 1H), 5.14 (s, 1H), 5.51 (t, 1H, J = 5 Hz); mass spectrum (70 eV) *m/e*: 315 (M^+), 258 ($M^+ - C(CH_3)_3$). *Anal.* calcd. for $C_{13}H_{21}NO_6Si$: C 49.52, H 6.67, N 4.44; found: C 49.77, H 6.87, N 4.56.

5-*Carbomethoxy-3*-endo-*hydroxy-2*-exo-*tetrahydro-pyranyloxy-7-oxabicyclo[2.2.1]hept-5-ene* (**5**a) *and* 6-Endo-*hydroxy-3*-exo-*methoxy-5*-exo-*tetrahydro-pyranyloxy-7-oxabicyclo[2.2.1]heptane-2*-endo-*carboxylic Acid γ-Lactone* (**6**a)

A solution of **4***c* (336 mg, 1.18 mmol) and DBU (205 mg, 0.13 mmol) in methanol – methylene chloride (1:1) was refluxed for 45 min. The solvents were then evaporated and the residue was dissolved in chloroform, washed with 0.1 *N* hydrochloric acid (3×) and water, dried (Na_2SO_4), and evaporated. The residue was applied on silica gel plates using chloroform. Elution

Can. J. Chem. Downloaded from www.nrcresearchpress.com by 210.87.254.40 on 09/05/12
For personal use only.

of the major, more polar, band gave 220 mg (70%) of **5***a* as an oil; ir ($CHCl_3$) ν_{max}: 3480 (OH), 1720 (C=O), 1625 (C=C) cm^{-1}; nmr ($CDCl_3$) δ: 1.68 (m, 6H), 2.70 (bs, 1H), 3.65 (m, 2H), 3.76 (s, 4H), 4.25 (d, 1H, J = 4 Hz), 4.76 (m, 1H), 5.00–5.08 (m, 2H), 7.17 (d, 1H, J = 2 Hz). *Anal.* calcd. for $C_{13}H_{18}O_6$: C 57.77, H 6.71; found: C 57.65, H 6.58. Elution of the minor, less polar, band gave 45 mg (14%) of **6***a*, mp 134–136°C; ir (KBr): 1800 (lactone) cm^{-1}; nmr ($CDCl_3$) δ: 1.66 (m, 6H), 2.73 (d, 1H, J = 4 Hz), 3.40 (s, 3H), 3.50–4.00 (m, 4H), 4.56 (d, 1H, J = 4 Hz), 4.67–4.90 (m, 2H), 5.36 (t, 1H, J = 5 Hz); mass spectrum (70 eV) *m/e*: 270 (M^+), 238 ($M^+ - CH_3OH$). *Anal.* calcd. for $C_{13}H_{18}O_6$: C 57.71, H 6.71; found: C 57.82, H 6.71.

*3-*Endo-*acetoxy-5-carbomethoxy-2-*exo-*tetrahydropyranyloxy-7-oxabicyclo[2.2.1]hept-5-ene (5b)*

A solution of **5***a* (91 mg) and acetic anhydride (1 mL) in pyridine (2 mL) was stirred overnight at room temperature. The mixture was then evaporated to dryness *in vacuo*. The residue was dissolved in chloroform and washed with water. The dried organic phase was evaporated and purified by chromatography on a silica gel plate using ethyl ether, giving 70 mg (67%) of **5***b* as an oil which solidified on standing, mp 81–82°C; ir ($CHCl_3$) ν_{max}: 1740 (C=O), 1625 (C=C) cm^{-1}; nmr ($CDCl_3$) δ: 1.69 (m, 6H), 1.96 (s, 3H), 3.47 (m, 1H), 3.76 (s + m, 5H), 4.76 (bs, 1H), 5.05 (m, 2H), 5.16 (d, 1H, J = 4 Hz), 7.17 (d, 1H, J = 2 Hz); mass spectrum (70 eV) *m/e*: 312 (M^+), 281 ($M^+ - OCH_3$), 228 ($M^+ - O(CH_2)_4CH$). *Anal.* calcd. for $C_{15}H_{20}O_7$: C 57.68, H 6.46; found: C 57.47, H 6.49.

*5-Carbomethoxy-3-*endo-*hydroxy-2-*exo-*methoxymethyloxy-7-oxabicyclo[2.2.1]hept-5-ene (5c)*

A solution of **4***d* (1.2 g, 4.89 mmol) and triethylamine (510 mg, 3 mmol) in dry methanol (60 mL) was refluxed for 8 h. Then the solution was filtered to remove small amounts of precipitate and the filtrate was evaporated to dryness. The residue was dissolved in chloroform, washed twice with water, dried over sodium sulfate, and evaporated. The oil obtained was chromatographed on a column of alumina using 3:1 chloroform – ether and slowly increasing the polarity to pure ethyl ether. Compound **5***c* was obtained as a colourless oil in 40% yield (500 mg); ir ($CHCl_3$) ν_{max}: 3500 (alcohol), 1730 (ester), 1625 (olefin) cm^{-1}; nmr ($CDCl_3$) δ: 2.89 (bs, 1H, OH), 3.20 (s, 3H, CH_2OCH_3), 3.51 (d, 1H, $CHOCH_2OCH_3$, J = 1 Hz), 3.73 (s, 3H, $COOCH_3$), 4.22 (dd, 1H, $CHOH$, J = 1, 4 Hz), 4.71 (s, 2H, CH_2OCH_3), 4.92–5.04 (m, 2H, bridgeheads), 7.06 (d, 1H, J = 2 Hz, C=CH) ppm. *Anal.* calcd. for $C_{10}H_{14}O_6$: C 52.17, H 6.13; found: C 52.08, H 6.28.

*5-Carbomethoxy-2-*exo-*3-*endo-*dimethoxymethyloxy-7-oxabicyclo[2.2.1]hept-5-ene (5d)*

To a stirred solution of **5***c* (1.3 g, 5.6 mmol) in dry chloroform (50 mL) were added methylal (10 mL) and approximately 3 g of phosphorus pentoxide. After 2 h at room temperature, the mixture was poured into 5% sodium bicarbonate solution. The organic layer was washed with water, dried over sodium sulfate, and evaporated to dryness. The residue was purified on a column of silicic acid using chloroform–hexane – ethyl ether (10:6:1), giving 1.3 g (84%) of **5***d* as a homogeneous syrup; ir ($CHCl_3$) ν_{max}: 1730 (ester), 1625 (olefin) cm^{-1}; nmr ($CDCl_3$) δ: 3.36 (2s, 3H + 3H, CH_2OCH_3), 3.66 (d, 1H, CH_3OCH_2OCH, J = 0.8 Hz), 3.76 (s, 3H, $COOCH_3$), 4.20 (dd, 1H, CH_3OCH_2OCH, J = 0.8, 4 Hz), 4.66 (q, 2H, OCH_2, J = 3, 6 Hz), 4.76 (s, 2H, OCH_2), 4.99 (d, 1H, CH=CH—CH, J = 2 Hz), 5.12 (d, 1H, CH=C—CH, J = 4 Hz), 7.15 (d, 1H, C=CH, J = 2 Hz); ms (70 eV) *m/e*: 259 ($M^+ - CH_3$), 243 ($M^+ - OCH_3$), 213 ($M^+ - CH_3OCH_2O$), 148. *Anal.* calcd. for $C_{12}H_{18}O_7$: C 52.55, H 6.62; found: C 52.38, H 6.53.

*5-Carbomethoxy-3-*endo-*hydroxy-2-*exo-*tert-butyldimethylsilyloxy-7-oxabicyclo[2.2.1]hept-5-ene (5e) and 6-*Endo-*hydroxy-3-*exo-*methoxy-5-*exo-*tert-butyldimethylsilyloxy-7-oxabicyclo[2.2.1]heptane-2-*endo-*carboxylic Acid γ-Lactone (6b)*

To a stirred refluxing solution of DBU (635 mg) in methylene chloride – methanol (15:15 mL) was added dropwise a solution of **4***e* (1.22 g, 3.8 mmol) in methylene chloride (15 mL). The mixture was kept refluxing for an additional 15 min. After evaporation of the cooled solution the residue was dissolved in chloroform, washed with dilute hydrochloric acid and water, dried over sodium sulfate, and evaporated. The residue was chromatographed on a column of silicic acid using chloroform, giving 976 mg (84%) of the more polar **5***e* as a colorless syrup; ir ($CHCl_3$) ν_{max}: 3500 (OH), 1725 (C=O), 1620 (C=C) cm^{-1}; nmr ($CDCl_3$) δ: 0.13 (s, 6H), 0.97 (s, 9H), 3.37 (bs, 1H), 3.66 (s, 1H), 3.76 (s, 3H), 4.13 (d, 1H, J = 5 Hz), 4.75 (d, 1H, J = 2 Hz), 5.01 (d, 1H, J = 5 Hz), 7.08 (d, 1H, J = 2 Hz). The less polar compound **6***b* (62 mg) was also obtained; ir ($CHCl_3$): 1800 (lactone) cm^{-1}; nmr ($CDCl_3$) δ: 0.15 (s, 6H), 0.85 (s, 9H), 2.67 (d, 1H, J = 5 Hz), 3.33 (s, 3H), 3.62 (s, 1H), 3.68 (s, 1H), 4.30–4.50 (m, 2H), 5.63 (m, 1H).

*5-Carbomethoxy-3-*endo-*pivaloyloxy-2-*exo-*tert-butyldimethylsilyloxy-7-oxabicyclo[2.2.1]hept-5-ene (5f)*

A mixture of **5***e* (320 mg, 1 mmol) and pivaloyl chloride (1 mL) in dry pyridine (5 mL) was stirred overnight at room temperature and then evaporated to dryness *in vacuo*. The mixture was coevaporated with toluene as a chaser, dissolved in chloroform, and washed with 5% hydrochloric acid and water. The dried organic phase was chromatographed on a column of silicic acid (act. III) using ethyl ether – hexane (1:1), giving 300 mg (89%) of **5***f* as a syrup that solidified on standing, mp 48–49°C; ir (neat) ν_{max}: 1760, 1750 (C=O), 1630 (C=C) cm^{-1}; nmr ($CDCl_3$) δ: 0.10 (s, 6H), 0.87 (s, 9H), 1.13 (s, 9H), 3.72 (s, 3H), 3.80 (bs, 1H), 4.80 (bs, 1H), 4.88 (d, 1H, J = 5 Hz), 5.25 (d, 1H, J = 5 Hz), 7.28 (d, 1H, J = 2 Hz); mass spectrum (70 eV) *m/e*: 369 ($M^+ - CH_3$), 353 ($M^+ - OCH_3$), 327 ($M^+ - C(CH_3)_3$), 258, 201. *Anal.* calcd. for $C_{19}H_{32}O_6Si$: C 59.35, H 8.39; found: C 59.66, H 8.28.

*5-Carbomethoxy-2-*exo-*3-*endo-*di-O-*tert-*butyldimethylsilyloxy-7-oxabicyclo[2.2.1]hept-5-ene (5g)*

The mixture of **5***e* (1.14 g, 3.8 mmol), dimethyl-*tert*-butylsilyl chloride (1.44 g, 9.5 mmol) and imidazole (610 mg, 8.9 mmol) in dimethylformamide (20 mL) was stirred at room temperature for 6 h and then evaporated to dryness. The residue was dissolved in ethyl acetate, washed with water and with brine, dried over sodium sulfate, and evaporated. The resulting syrup was chromatographed on a column of silicic acid using ethyl ether – hexane (1:1), giving 600 mg (51%) of **5***g* as an oil which solidified on standing, mp 90–91°C; ir (KBr) ν_{max}: 1738 (C=O), 1630 (C=C) cm^{-1}; nmr ($CDCl_3$) δ: 0.10 (s, 12H), 0.83 (s, 9H), 0.90 (s, 9H), 3.54 (bs, 1H), 3.64 (s, 3H), 4.02 (d, 1H, J = 4 Hz), 4.62 (d, 1H, J = 1 Hz), 4.85 (d, 1H, J = 4 Hz), 7.02 (d, 1H, J = 2 Hz). *Anal.* calcd. for $C_{20}H_{38}O_5Si_2$: C 57.97, H 9.18; found: C 57.88, H 9.27.

Methyl 2-(2¹,3¹-Di-O-methoxymethyl-β-D,L-arabinofuranosyl) Glycolate (7a)

Through a solution of **5***d* (327 mg, 1.19 mmol) in dry methylene chloride at −78°C was bubbled ozone until a faintly blue color was observed. Excess ozone was flushed with dry nitrogen while the system was kept at −78°C and dimethyl sulfide (0.5 mL) was added. The mixture was allowed to rise to room temperature over a period of 5 h. The solution was then evaporated to dryness. To a precooled solution of the residue in freshly distilled tetrahydrofuran (50 mL) at 0°C was added lithium tri-*tert*-butoxyaluminum hydride (0.91 g, 3.57 mmol).

Can. J. Chem. Downloaded from www.nrcresearchpress.com by 210.87.254.40 on 09/05/12
For personal use only.

The resulting clear solution was then allowed to warm to room temperature and stirred overnight under dry nitrogen. A solution of ammonium sulfate (2 g) in water (2 mL) and Celite (1 g) were added to the reaction at 0°C. The mixture was stirred for 30 min and finally filtered over a layer of Celite. Following evaporation of the solvent the residue was dissolved in ethyl acetate, washed with water, dried ($MgSO_4$), and evaporated. The crude clear oil was crystallized from chloroform–hexane giving 222 mg (60%) of **7***a* as white crystals, mp 70–71°C; ir ($CHCl_3$) ν_{max}: 3500 (alcohol), 1745 (ester) cm^{-1}; nmr ($CDCl_3$) δ: 3.33 (s, 3H), 3.36 (s, 3H), 3.67–3.96 (m, 6H), 4.06–4.56 (m, 5H), 4.56–4.83 (m, 5H) ppm. *Anal.* calcd. for $C_{12}H_{22}O_9$: C 46.45, H 7.15; found: C 46.28, H 7.28.

Methyl 2-O-acetyl-2-(5¹-O-acetyl-2¹,3¹-di-O-methoxymethyl-β-D,L-arabinofuranosyl) Glycolate (7b)

The compound 7*a* (73 mg) was acetylated using acetic anhydride (1 mL) and pyridine (1 mL) with stirring overnight. After evaporation to dryness the residue was chromatographed on a column of silicic acid using ethyl ether – hexane (1:1) giving 84 mg (92%) of 7*b* as an oil; ir (neat) ν_{max}: 1745, 1755 (C=O) cm^{-1}; nmr ($CDCl_3$) δ: 2.00 (s, 3H), 2.03 (s, 3H), 3.21 (s, 3H), 3.24 (s, 3H), 3.26 (s, 3H), 3.90–4.13 (m, 5H), 4.13–4.30 (m, 1H), 4.32 (d, 2H, J = 1 Hz), 4.40 (s, 2H), 4.86 (s, 0.5H), 5.0 (s, 0.5H); mass spectrum (70 eV) *m/e*: 363 ($M^+ - OCH_3$), 317, 289 ($M^+ - COCH_3 - CH_3OCH_2OH$). *Anal.* calcd. for $C_{16}H_{26}O_{11}$: C 48.73, H 6.60; found: C 48.63, H 6.88.

*Methyl 2-(2¹,3¹-Di-O-methoxymethyl-5¹-O-*tert*-butyldimethylsilyl-β-D,L-arabinofuranosyl) Glycolate (7c)*

A mixture of **7***a* (169 mg, 0.54 mmol), dimethyl-*tert*-butylsilyl chloride (82 mg, 0.54 mmol), and imidazole (92 mg, 1.35 mmol) in dimethylformamide (5 mL) was stirred at room temperature for 18 h. Then the reaction mixture was added to 60 mL of ethyl ether and washed three times with water, dried, and evaporated, leaving a syrup. The latter was chromatographed on a column of silicic acid eluting with ethyl ether – hexane (2:1) giving 197 mg (85%) of **7***c* as an oil which crystallizes below room temperature; ir ($CHCl_3$) ν_{max}: 3500 (alcohol), 1745 (ester) cm^{-1}; nmr ($CDCl_3$) δ: 0.10 (s, 6H), 0.96 (s, 9H), 3.32 (s, 3H), 3.36 (s, 3H), 3.48 (m, 1H), 3.60–4.00 (m, 6H), 4.08–4.43 (m, 4H), 4.62 (bs, 4H) ppm. *Anal.* calcd. for $C_{18}H_{36}O_9Si$: C 50.94, H 8.94; found: C 50.68, H 8.37.

*Methyl 2-(2¹,3¹-Di-O-*tert*-butyldimethylsilyl-β-D,L-arabinofuranosyl) Glycolate (7d)*

After reductive ozonolysis of **5***g* (386 mg, 0.93 mmol) in methylene chloride, the solution was washed with brine twice, dried, and evaporated. To a solution of the residue in dry tetrahydrofuran (40 mL) was added lithium tri-*tert*-butoxyaluminum hydride (945 mg, 3.72 mmol) at 0°C. The resulting clear mixture was allowed to warm to room temperature and stirred overnight under nitrogen. A solution of ammonium sulfate (2 g) in water (2 mL) and Celite (1 g) were added to the reaction mixture at 0°C. The mixture was stirred for 30 min and finally filtered over a layer of Celite. The residue was washed with tetrahydrofuran. Following evaporation of the solvent the residue was dissolved in ethyl acetate, washed with water, dried, and evaporated. The residue was purified on silica gel plates using ethyl ether – hexane (2:1), giving 250 mg (59%) of 7*d* as an oil; ir ($CHCl_3$) ν_{max}: 3500 (OH), 1745 (C=O) cm^{-1}; nmr ($CDCl_3$) δ: 0.10 (m, 12H), 0.86 (s, 9H), 0.90 (s, 9H), 1.96 (bs, 1H), 2.70 (bs, 1H), 3.53–4.36 (m, 10H). *Anal.* calcd. for $C_{20}H_{42}O_7Si_2$: C 53.33, H 9.33; found: C 53.00, H 9.17.

*Methyl 2-O-acetyl-2-(5¹-O-acetyl-2¹,3¹-di-O-*tert*-butyldimethylsilyl-β-D,L-arabinofuranosyl) Glycolate (7e)*

The compound 7*d* (126 mg) was acetylated with acetic anhydride (1 mL) and pyridine (1.5 mL). After the usual work-up, the crude product was purified by column chromatography (aluminum oxide act. III) using ethyl ether – hexane (1:2) to give 136 mg (91%) of **7***e* as an oil which solidified on standing, mp 74–77°C; ir (KBr) ν_{max}: 1755 (C=O), 1240, 1080 cm^{-1}; nmr ($CDCl_3$) δ: 0.13 (m, 12H), 0.96 (s, 18H), 2.03 (s, 3H), 2.10 (s, 3H), 3.76 (s, 3H), 3.90–4.33 (m, 6H), 4.70, 4.96 (bs, 0.5H each); mass spectrum (60 eV) *m/e*: 519 ($M^+ - CH_3$), 503 ($M^+ - OCH_3$), 477 ($M^+ - C(CH_3)_3$). *Anal.* calcd. for $C_{24}H_{46}O_9Si_2$: C 53.93, H 8.61; found: C 54.12, H 8.84.

*Methyl 2-(2¹,3¹,5¹-Tri-O-*tert*-butyldimethylsilyl-β-D,L-arabinofuranosyl) Glycolate (7f)*

To a solution of 7*d* (106 mg, 0.24 mmol) in dimethylformamide (5 mL) was added dimethyl-*tert*-butylsilyl chloride (36 mg, 0.24 mmol) and imidazole (40 mg, 0.6 mmol). The mixture was stirred at room temperature for 21 h. The solvent was evaporated *in vacuo* and the residue was coevaporated several times with ethyl acetate. The residue was dissolved in chloroform, washed with water, dried, and evaporated. The resulting syrup was chromatographed on a column of alumina using ethyl ether – hexane (1:2) to give 125 mg (94%) of 7*f* as an oil; ir ($CHCl_3$) ν_{max}: 3500 (OH), 1730 (C=O) cm^{-1}; nmr ($CDCl_3$) δ: 0.10 (m, 18H), 0.92 (m, 27H), 2.96 (bs, 1H), 3.30–3.90 (m, 5H), 3.90–4.45 (m, 5H). *Anal.* calcd. for $C_{26}H_{56}O_7Si_3$: C 55.32, H 9.93; found: C 55.59, H 9.84.

*Methyl 2-O-acetyl-2-(2¹,3¹,5¹-tri-O-*tert*-butyldimethylsilyl-β-D,L-arabinofuranosyl) Glycolate (7g)*

The compound **7***f* (125 mg, 0.22 mmol) was acetylated with acetic anhydride (1.5 mL) and pyridine (1.5 mL). After the usual work-up the crude product was chromatographed on a column of alumina using ethyl ether – hexane (1:1) to give 134 mg (100%) of **7***g* as an oil which solidified on standing, mp 68–72°C; ir (KBr) ν_{max}: 1760 (C=O), 1080, 840 cm^{-1}; nmr ($CDCl_3$) δ: 0.10 (m, 18H), 0.87 (bs, 27H), 2.06 (s, 3H), 3.63 (m, 1H), 3.71 (s, 3H), 3.85–4.33 (m, 5H), 4.70, 4.85 (two bs, 1H). *Anal.* calcd. for $C_{28}H_{58}O_8Si_3$: C 55.45, H 9.55; found: C 55.16, H 9.32.

*Methyl 2-(2¹,3¹-Di-O-methoxymethyl-5¹-O-*tert*-butyldimethylsilyl-β-D,L-arabinofuranosyl) Glyoxylate (8a)*

To a solution of **7***c* (424 mg, 1 mmol) in carbon tetrachloride (40 mL) were added ruthenium dioxide dihydrate (20 mg) and a solution of sodium periodate (856 mg, 4 mmol) in water (40 mL). The pH of the reaction mixture was controlled between 6 and 7 by the addition of a 5% sodium bicarbonate solution. After 6 h, stirring at room temperature or until a yellow color persisted, the reaction was terminated by adding a few drops of isopropyl alcohol. After collection of the black precipitated solid (RuO_2) on Celite, the organic phase was washed with water and brine, dried over magnesium sulfate, and evaporated, leaving 359 mg of crude **8***a* as a low mp white solid (less than 25°C). Attempted purification by chromatography on silicic acid led to partial decomposition and accordingly the material was used directly in the next step; ir (neat) ν_{max}: 1750, 1775 (ketone, ketoester) cm^{-1}; nmr ($CDCl_3$) δ: 0.08 (s, 6H), 0.86 (s, 9H), 3.13 (s, 3H), 3.25 (s, 3H), 3.36–3.58 (m, 2H), 3.72 (s, 3H), 3.76 (m, 1H), 4.13 (bs, 1H), 4.30 (m, 1H), 4.40–4.70 (m, 4H), 5.06 (d, 1H, J = 5 Hz) ppm.

*Methyl 2-(2¹,3¹,5¹-Tri-O-*tert*-butyldimethylsilyl-β-D,L-arabinofuranosyl) Glyoxylate (8b)*

To the mixture of **7***e* (416 mg, 0.74 mmol) in carbon tetrachloride (40 mL) and ruthenium dioxide dihydrate (20 mg) was added a solution of sodium periodate (633 mg) in water (40 mL). The pH of the mixture was controlled between 6 and 7 by the addition of a 5% sodium bicarbonate solution. After vigorously stirring at room temperature until a yellow color persisted, a few drops of isopropyl alcohol were added to terminate the reaction. Ruthenium dioxide was removed on Celite and the organic

Can. J. Chem. Downloaded from www.nrcresearchpress.com by 210.87.254.40 on 09/05/12
For personal use only.

phase was washed with water and brine, dried ($MgSO_4$), and evaporated, giving 353 mg of crude **8***b*; ir ($CHCl_3$) ν_{max}: 1750, 1730 (C=O) cm^{-1}; nmr ($CDCl_3$) δ: 0.13 (m, 18H), 0.86 (m, 27H), 3.76–4.00 (m, 5H), 4.13 (m, 1H), 4.33 (m, 1H), 4.53 (bs, 1H), 4.66 (d, 1H, J = 4 Hz).

*2-(2¹,3¹-Di-O-methoxymethyl-5¹-O-*tert*-butyldimethylsilyl-β-D,L-arabinofuranosyl)maleimide (9*a*)*

A solution of carbamoylmethylenetriphenylphosphorane (400 mg, 1.2 mmol) and the crude ketoester **8***a* (450 mg, 1.07 mmol) in freshly distilled chloroform (20 mL) was stirred at room temperature for 2 h. The solvent was then evaporated and the residue was purified by chromatography on a silica gel column using petroleum ether – ethyl acetate (3:1), giving 216 mg (47%) of solid **9***a*, mp 49–50°C; ir ($CHCl_3$) ν_{max}: 3460, 3250 (alcohol, amine), 1740, 1790 (maleimide), 1655 (olefin) cm^{-1}; nmr ($CDCl_3$, D_2O), 100 MHz δ: 0.10 (s, 6H, $Si(CH_3)_2$), 0.82 (s, 9H, $C(CH_3)_3$), 3.20 (s, 3H, OCH_3), 3.26 (s, 3H, OCH_3), 3.53–3.70 (m, 2H, $SiOCH_2CH$), 3.70–4.10 (m, 1H, $SiOCH_2CH$), 4.30 (d, 1H, OCH_2OCH, J = 2 Hz), 4.50 (d, 1H, OCH_2OCH, J = 4 Hz), 4.65 (q, 2H, CH_3OCH_2), 4.80 (q, 2H, CH_3OCH_2), 5.0 (q, 1H, "anomeric" proton, J_1 = 4 Hz, J_2 = 3 Hz), 6.39 (d, 1H, C=CH, J = 2 Hz); ms (70 eV) *m/e*: 431 (M^+), 400 ($M^+ - OCH_3$), 374 ($M^+ - C(CH_3)_3$), 328. *Anal.* calcd. for $C_{19}H_{33}NO_8Si$: C 52.90, H 7.66, N 1.62; found: C 52.68, H 7.76, N 1.49.

*2¹-*Epi*-showdomycin (9*b*)*

A solution of **9***a* (212 mg, 0.5 mmol) in a mixture of trifluoroacetic acid – water–tetrahydrofuran (4:1:1) (12 mL) was stirred at room temperature for 4 h. After evaporation to dryness *in vacuo* the residue was crystallized from acetone–hexane to give 68 mg (60%) of **9***b* with mp 170–171°C; ir (KBr) ν_{max}: 3470, 3110 (alcohol, amine), 1775, 1720 (maleimide), 1625 (olefin) cm^{-1}; uv (λ_{max}^{EtOH}): 222 nm (log ε 4.36); nmr (D_2O), 100 MHz δ: 3.8–3.9 (m, 2H, $HOCH_2$—CH), 4.1–4.25 (m, 1H, $HOCH_2CHO$), 4.28 (q, 1H, J_1 = 2 Hz, J_2 = 3 Hz), 4.55 (q, 1H, J_1 = 2 Hz, J_2 = 4 Hz), 5.1 (q, 1H, "anomeric" H, J_1 = 2 Hz, J_2 = 4 Hz), 6.85 (d, 1H, C=CH, J = 2 Hz); ms (70 eV) *m/e*: 229 (M^+), 211 ($M^+ - H_2O$), 180, 140 ($M^+ - HOCHCH_2B$), 127 (B + 31), 126 (B + 30), 110, 87, 85, 69, 57, 55, 45, 44, 43, 32, 31, 28 (B is maleimide). *Anal.* calcd. for $C_9H_{11}NO_6$: C 47.16, H 4.80, N 6.15; found: C 47.05, H 4.75, N 6.08.

3,4-Di-O-methoxymethyl-2,5-anhydro-D,L-glucose (10)

To a solution of **5***d* (230 mg, 0.84 mmol) in methylene chloride was bubbled ozone until a faintly blue color was observed. Excess ozone was flushed with dry nitrogen and evaporation of solvent left a white foam. The ozonide in isopropanol was treated with sodium borohydride (500 mg) at 0°C and then refluxed for 4 h. The solution was then cooled in an ice-bath and stirred with 50% aqueous acetic acid (10 mL) for 30 min and evaporated *in vacuo*. The residue was coevaporated with ethanol and dissolved in water and stirred with sodium periodate (300 mg) for 1 h at room temperature. The resulting precipitate was removed by filtration on cotton and the filtrate extracted with chloroform three times. The organic phase was dried and evaporated, giving 77 mg (37%) of **10** as a colorless syrup; ir ($CHCl_3$) ν_{max}: 3500, 3420 (OH), 2840, 2800 cm^{-1}; nmr ($CDCl_3$) δ: 3.36 (bs, 6H), 3.56 (bs, 1H), 3.90 (m, 1H), 3.93–4.27 (m, 3H), 4.36 (m, 2H), 4.72 (m, 4H), 4.98 (bs, 1H). *Anal.* calcd. for $C_{10}H_{18}O_7$: C 47.99, H 7.25; found: C 47.65, H 7.51.

N-methyl 2-(2¹,3¹-Di-O-methoxymethyl-β-D,L-arabinofuranosyl) Thiazolidine and its 5¹-Acetate (11b)

To a solution of **10** (77 mg, 0.31 mmol) in dry benzene (15 mL) was added *N*-methylthioethanolamine (31 mg, 0.34 mmol). The reaction mixture was stirred overnight at room temperature. After evaporation of the solvent the crude product (**11***a*) was directly acetylated with acetic anhydride in pyridine. The compound (**11***b*) was purified by a column of alumina using chloroform to give 86 mg (77%) of **11***b* as a colorless oil; ir ($CHCl_3$) ν_{max}: 2870, 2830 (N—CH_3), 1755 (C=O) cm^{-1}; nmr ($CDCl_3$) δ: 2.03 (s, 3H), 2.30, 2.40 (s + s, 3H), 2.60–3.26 (m, 4H), 3.30 (s, 3H), 3.40 (s, 3H), 3.90–4.23 (m, 6H), 4.37–4.53 (m, 1H), 4.57–4.76 (m, 4H); mass spectrum (70 eV) *m/e*: 365 (M^+), 333 ($M^+ - CH_3OH$), 318 ($M^+ - CH_2SH$), 102. *Anal.* calcd. for $C_{15}H_{27}NO_7S$: C 49.32, H 7.40, N 3.84, S 8.77; found: C 49.53, H 7.60, N 4.08, S 8.53.

Ethyl trans*-3-(2¹,3¹-Di-O-methoxymethyl-β-D,L-arabinofuranosyl) Acrylate (12a)*

To a solution of crude **10** (144 mg, 0.58 mmol) in methylene chloride (10 mL) was added carbethoxymethylenetriphenylphosphorane (242 mg, 0.69 mmol). After 4 h at room temperature, the solvent was evaporated and the residue was partitioned between chloroform and water. The organic phase was dried over sodium sulfate and evaporated. The residue was chromatographed on a column of alumina using chloroform, eluting 143 mg (79%) of **12***a* as a chromatographically homogeneous syrup; ir ($CHCl_3$) ν_{max}: 3500 (OH), 1730 (C=O), 1680 (C=C) cm^{-1}; nmr ($CDCl_3$) δ: 1.23 (t, 3H, J = 7 Hz), 2.23 (t, 1H, J = 6 Hz), 3.26 (s, 3H), 3.30 (s, 3H), 3.53–4.30 (m, 8H), 4.52 (d, 2H, J = 2 Hz), 4.60 (s, 2H), 5.98 (d, 1H, J = 14 Hz), 6.85 (dd, 1H, J = 14 Hz, J = 4 Hz); mass spectrum (70 eV) *m/e*: 320 (M^+), 289 ($M^+ - OCH_3$), 243, 230 ($M^+ - 2CH_3OCH_2$). *Anal.* calcd. for $C_{14}H_{24}O_8$: C 52.49, H 7.55; found: C 52.48, H 7.62.

Ethyl trans*-3-(5¹-O-acetyl-2¹,3¹-di-O-methoxymethyl-β-D,L-arabinofuranosyl) Acrylate (12b)*

The compound **12***a* (40 mg, 0.13 mmol) was acetylated using acetic anhydride (1 mL) and pyridine (2 mL). Evaporation to dryness and separation on a column of alumina, eluting with chloroform gave 40 mg (89%) of **12***b* as a colorless oil; ir ($CHCl_3$) ν_{max}: 1750, 1730 (C=O), 1680 (C=C) cm^{-1}; nmr ($CDCl_3$) δ: 3.27 (t, 3H, J = 6 Hz), 2.06 (s, 3H), 3.28 (s, 3H), 3.33 (s, 3H), 3.90–4.30 (m, 8H), 4.57 (d, 2H, J = 2 Hz), 4.62 (s, 2H), 6.02 (d, 1H, J = 14 Hz), 6.88 (dd, 1H, J = 14 Hz, J = 4 Hz); mass spectrum (70 eV) *m/e*: 362 (M^+), 331 ($M^+ - OCH_3$), 317 ($M^+ - 2CH_3O$), 272 ($M^+ - 2CH_3OCH_2$). *Anal.* calcd. for $C_{16}H_{26}O_9$: C 53.03, H 7.23; found: C 53.10, H 7.32.

Diol 14a from Olefin 13

The olefin **13** (452 mg, 2 mmol) in dry methylene chloride (50 mL) was treated with ozone at −78°C until the blue colour persisted. The excess ozone was removed by bubbling in dry nitrogen gas, and then 1 mL of dimethyl sulfide was added at −78°C. The solution was then allowed to warm up to room temperature with stirring, at which time it was evaporated.

To the resulting oily residue in dry tetrahydrofuran (THF), (50 mL) at 0°C under a nitrogen atmosphere was added lithium aluminum tri-(*tert*-butoxy) hydride (7.0 mmol, 1.78 g). After stirring at 0°C for 3 h, ammonium sulfate (2 g) in 10 mL of water was added, and the stirring continued for another 30 min. The mixture was then filtered, and the residue washed with 25 mL of THF, the combined filtrates were evaporated to dryness and the resulting residue was dissolved in ethyl acetate (50 mL), washed with brine (20 mL × 3), dried (Na_2SO_4), and evaporated to afford 315 mg (65%) of diol **14***a*; ir ($CHCl_3$) ν_{max}: 3650–3350 (OH), 1755 (C=O), 1395 cm^{-1}; nmr ($CDCl_3$) δ: 1.33 (s, 3H), 1.52 (s, 3H), 3.66 (d, 2H, J = 4.0 Hz, CH_2OH), 3.76 (s, 3H, $COOCH_3$), 3.78–4.85 (m, 7H, two deuterium exchangeable protons) ppm; ms (80°C) *m/e*: 262 (M^+), 247 ($M^+ - CH_3$), 230 ($M^+ - CH_2OH$), 203 ($M^+ - COOCH_3$), 201, 187, 185, 173 ($M^+ - CHOHCOOCH_3$), 169, 139, 85, 83. *Anal.* calcd. for $C_{11}H_{18}O_7$: C 50.38, H 6.91; found: C 50.59, H 6.76.

Can. J. Chem. Downloaded from www.nrcresearchpress.com by 210.87.254.40 on 09/05/12
For personal use only.

*Diacetate 14 (R = R¹ = Ac) from Diol 14*a

The diol **14***a* (131 mg, 0.5 mmol) was stirred overnight at room temperature in 5 mL pyridine – acetic anhydride (3:2). After the removal of the solvent, chloroform (25 mL) was added to the residue and the solution washed with dilute hydrochloric acid (10 mL × 2), water (10 mL × 2), dried (Na_2SO_4), and evaporated. The diacetate **14** (R = R¹ = Ac) was obtained in quantitative yield; ir ($CHCl_3$) ν_{max}: 1765 and 1755 (C=O), 1390 cm^{-1}; nmr ($CDCl_3$) δ: 1.35 (s, 3H), 1.52 (s, 3H), 2.08 (s, 3H, CO*CH*$_3$), 2.19 (s, 3H, COC*H*$_3$), 3.75 (s, 3H, COOC*H*$_3$), 4.12 (bs, 2H, C*H*$_2$OCOCH$_3$), 4.22–4.95 (m, 4H), 5.12 (d, *J* = 4 Hz, C*H*OCOCH$_3$) ppm; ms (150°C) *m/e*: 346 (M^+), 331 ($M^+ - CH_3$), 287 ($M^+ - COOCH_3$), 271, 245, 243, 229, 215, 211, 201, 179, 169. *Anal.* calcd. for $C_{15}H_{22}O_9$: C 52.03, H 6.35; found: C 52.33, H 6.75.

*Monosilylated Diol 14*b *from Diol 14*a

To the diol **14***a* (524 mg, 2 mmol) and imidazole (340 mg, 5 mmol) in *N,N*-dimethylformamide (5 mL) was added *tert*-butyldimethylchlorosilane (302 mg, 2 mmol). After stirring at room temperature for 18 h, the solvent was removed under high vacuum. To the residue was then added ethyl acetate (50 mL) and the solution was washed with water (20 mL × 3), dried (Na_2SO_4), and evaporated. The crude product was chromatographed on silica gel. Elution with ether–hexane (1:1) afforded 677 mg (90%) of the silyl ether **14***b*; ir ($CHCl_3$) ν_{max}: 3550 and 3400 (OH), 1770 (C=O), 1395 cm^{-1}; nmr ($CDCl_3$) δ: 0.13 (s, 6H, Si(C*H*$_3$)$_2$), 0.92 (s, 9H, Si—*t*Bu), 1.32 (s, 3H), 1.50 (s, 3H), 3.73 (bs, 5H, COOC*H*$_3$ and C*H*$_2$OSi), 3.86–4.82 (m, 6H) ppm; ms (180°C) *m/e*: 361 ($M^+ - CH_3$), 317 ($M^+ - COOCH_3$), 287 ($M^+ - CHOHCOOCH_3$), 261 ($M^+ - (CH_3)_2Si$—*t*Bu), 201. *Anal.* calcd. for $C_{17}H_{32}O_7Si$: C 54.25, H 8.51; found: C 54.55, H 8.72.

*Monoacetate 14*c *from Monosilylated Diol 14*b

The acetate **14***c* was prepared from the alcohol **14***b* by the usual acetylation procedure; ir ($CHCl_3$) ν_{max}: 1770 (C=O), 1395 cm^{-1}; nmr ($CDCl_3$) δ: 0.08 (s, 6H, (C*H*$_3$)$_2$), 0.8 (s, 9H, Si—*t*Bu), 1.32 (s, 3H), 1.50 (s, 3H), 2.11 (s, 3H, COC*H*$_3$), 3.60 (d, 2H, *J* = 5 Hz, C*H*$_2$OSi), 3.68 (s, 3H, COOC*H*$_3$), 3.83–4.78 (m, 4H), 5.08 (d, 1H, *J* = 5 Hz, C*H*OCOCH$_3$) ppm; ms (170°C) *m/e*: 403 ($M^+ - CH_3$), 387 ($M^+ - OCH_3$), 361 ($M^+ - t$Bu), 303 ($M^+ - (CH_3)_2Si$—*t*Bu), 261, 243, 201.

Silylated Diol 14 (R = R¹ = (CH$_3$*)*$_2$*Si*—t*Bu) from Diol 14*a

The disilyl ether **14** (R = R¹ = $(CH_3)_2Si$—*t*Bu) was prepared with two equivalents of *tert*-butyldimethylchlorosilane from **14***a* by the usual silylation procedure; nmr ($CDCl_3$) δ: 0.07 (s, 12H, 2 Si(C*H*$_3$)$_2$), 0.89, 0.92 (each s, 18H, 2 Si—*tBu*), 1.29 (s, 3H), 1.49 (s, 3H), 3.56 (m, 2H), 3.63 (s, 3H, COOC*H*$_3$), 3.80–4.72 (m, 5H) ppm.

Monosilylated Diol 14 (R = H, R¹ = (CH$_3$*)*$_2$*Si*—t*Bu) from Silylated Diol 14 (R = R¹ = (CH*$_3$*)*$_2$*Si*—t*Bu)*

Disilyl ether **14** (R = R¹ = $(CH_3)_2Si$ +) (490 mg, 1 mmol) was stirred in a solution of acetic acid – water–THF (3:1:1) (5 mL) at room temperature for 20 h. After evaporation of the solution, chloroform (40 mL) was added to the residue, which was washed with saturated sodium bicarbonate solution (15 mL × 2), water (15 mL), then dried (Na_2SO_4) and evaporated. The alcohol **14** (R = H, R¹ = $(CH_3)_2Si$ +) was obtained in 90% yield; ir ($CHCl_3$) ν_{max}: 3550 (OH), 1770 (C=O), 1400, 1395 cm^{-1}; nmr ($CDCl_3$) δ: 0.08, 0.11 (each s, 6H, Si(C*H*$_3$)$_2$), 0.95 (s, 9H, Si—*t*Bu), 1.33 (s, 3H), 1.54 (s, 3H), 2.77 (bs, 1H, O*H*), 3.66 (m, 2H, C*H*$_2$OH), 3.76 (s, 3H, COOC*H*$_3$), 3.96–4.82 (m, 5H) ppm.

Monoacetate 14 (R = Ac, R¹ = (CH$_3$*)*$_2$*Si*—t*Bu) from Monosilylated Diol 14 (R = H, R¹ = (CH*$_3$*)*$_2$*Si*—t*Bu)*.

Monoacetate **14** (R = Ac, R¹ = $(CH_3)_2Si$—*t*Bu) was prepared from alcohol **14** (R = H, R¹ = $(CH_3)_2Si$—*t*Bu) by the usual acetylation procedure; ir ($CHCl_3$) ν_{max}: 1760 (C=O), 1400, 1390 cm^{-1}; nmr ($CDCl_3$) δ: 0.08, 0.11 (each s, 6H, Si(C*H*$_3$)$_2$), 0.92 (s, 9H, Si—*t*Bu), 1.32 (s, 3H), 1.53 (s, 3H), 2.03 (s, 3H, COC*H*$_3$), 3.70 (s, 3H, COOC*H*$_3$), 4.12 (s, 2H, C*H*$_2$OCOCH$_3$), 4.16–4.85 (m, 5H) ppm.

*Lactone 15 from Monosilylated Diol 14*b

To alcohol **14***b* (94 mg, 0.25 mmol) in methylene chloride (5 mL) was added 15 equivalents of chromium trioxide – pyridine complex in methylene chloride (10 mL). After stirring for 30 min at room temperature, the solution was decanted from the black residue, and the residue was triturated with anhydrous ether (20 mL). The combined organic layers were washed with 5% HCl (15 mL), saturated sodium bicarbonate solution (15 mL), and brine (15 mL), followed by drying (Na_2SO_4) and evaporation. Recrystallization from petroleum ether (bp 30–60°C) afforded 59 mg (78%) lactone **15**; ir ($CHCl_3$) ν_{max}: 1800 (lactone C=O), 1395 cm^{-1}; nmr ($CDCl_3$) δ: 0.07 (s, 6H, Si(C*H*$_3$)$_2$), 0.86 (s, 9H, Si—*t*Bu), 1.36 (s, 3H), 1.44 (s, 3H), 3.73 (m, 2H, C*H*$_2$OSi), 4.29–4.79 (m, 4H) ppm; ms (270°C) *m/e*: 287 ($M^+ - 15$), 258, 217. *Anal.* calcd. for $C_{14}H_{26}O_5Si$: C 55.63, H 8.61; found: C 55.98, H 8.94.

*Keto-ester 16 from Monosilylated Diol 14*b

Alcohol **14***b* (320 mg, 1 mmol) was stirred in dimethyl sulfoxide – acetic anhydride (3:2) (3 mL) overnight at room temperature. The solution was further stirred for 15 min after the addition of chloroform (25 mL) and saturated Na_2CO_3 solution (15 mL). The organic layer was washed with water (10 mL × 2), dried (Na_2SO_4), and evaporated. The unstable keto-ester **16** was obtained in 80% yield; ir ($CHCl_3$) ν_{max}: 1755 and 1745 (C=O), 1400, 1390 cm^{-1}; nmr ($CDCl_3$) δ: 0.07 (s, 6H, Si(C*H*$_3$)$_2$), 0.86 (s, 9H, Si—*t*Bu), 1.37 (s, 3H), 1.52 (s, 3H), 3.67 (m, 2H, C*H*$_2$OSi), 3.80 (s, 3H, COOC*H*$_3$), 4.06–4.96 (m, 4H) ppm.

D,L-Showdomycin Derivative 17 from Keto-ester 16

To keto-ester **16** (374 mg, 1 mmol) in dry chloroform (10 mL) was added carbamoylmethylenetriphenylphosphorane (319 mg, 1 mmol). After stirring at room temperature for 3 h, the crude product was purified by silica plates to afford 134 mg (35%) of D,L-showdomycin derivative **17**; ir ($CHCl_3$) ν_{max}: 3480 (maleimide NH), 2985, 2895, 1795, 1745, 1395 cm^{-1}; uv (EtOH) λ_{max}: 222 nm (ε 13 400), shoulder ~ 275 nm (ε 1430); nmr ($CDCl_3$) δ: 0.07 (s, 6H, Si(*CH*$_3$)$_2$), 0.87 (s, 9H, Si—*tBu*), 1.35 (s, 3H), 1.57 (s, 3H), 3.66 (m, 2H, *CH*$_2$OSi), 4.13 (bm, 1H), 4.55–4.82 (m, 3H), 6.41 (t, 1H, *J* = 2 Hz), 7.99 (bm, 1H, N*H*) ppm; ms (150°C) *m/e*: 368 ($M^+ - CH_3$), 326 ($M^+ - t$Bu), 268 ($M^+ - (CH_3)_2Si$—*t*Bu).

D,L-Showdomycin 18 from D,L-Showdomycin Derivative 17

To showdomycin derivative **17** (383 mg, 1 mmol) was added 3 mL of trifluoroacetic acid – water 4:1. After stirring at room temperature for 10 min, the solution was evaporated to dryness. Recrystallization from benzene–acetone afforded 176 mg (77%) D,L-showdomycin **18**, mp 143–144°C; nmr (acetone-d_6) δ: 3.15–4.75 (m, 10H), 6.60 (t, 1H, *J* = 2 Hz); ms (180°C) *m/e*: 229 (M^+), 211 ($M^+ - H_2O$), 180, 156, 152, 140, 139, 127 (B + 31), 126 (B + 30), 123, 110, 85, 73.

*Hydrazone 16*a *from Keto-ester 16*

To keto-ester **16** (374 mg, 1 mmol) and pyridine (87 mg, 1.1 mmol) in methanol (10 mL) was added ethyl hydrazinoacetate hydrochloride (170 mg, 1.1 mmol). After stirring at room temperature overnight, the solution was evaporated to dryness. Chloroform (40 mL) was added to the residue, which was washed (2 × 15 mL H_2O), dried (Na_2SO_4), and evaporated. The crude product was purified by silica plates to afford 389 mg (82%) hydrazone **16***a* as *syn*- and *anti*-isomers. (*Syn*-isomer) ir ($CHCl_3$) ν_{max}: 3300 (NH), 2985, 2890, 1760 (C=O), 1700 (C=N), 1400, 1390 cm^{-1}; uv (EtOH) λ_{max}: 294 nm (ε 13 800);

nmr ($CDCl_3$) δ: 0.05 (s, 6H, $Si(CH_3)_2$), 0.89 (s, 9H, Si—*t*Bu), 1.26 (t, 3H, $J = 7$ Hz, CH_2CH_3), 1.34 (s, 3H), 1.52 (s, 3H), 3.57 (d, 2H, $J = 5$ Hz, CH_2OSi), 3.73 (s, 3H, $COOCH_3$), 3.86–5.05 (m, 8H), 10.21 (bm, 1H, N*H*); ms (140°C) *m/e*: 474 (M^+), 459 ($M^+ - CH_3$), 417 ($M^+ - t$Bu).

Acknowledgement

We wish to thank the Natural Sciences and Engineering Research Council of Canada for generous financial support.

1. G. JUST, A. MARTEL, K. GROZINGER, and M. RAMJEESINGH. Can. J. Chem. **53**, 131 (1975).
2. (*a*) H. B. HENBEST and B. NICHOLLS. J. Chem. Soc. 221 (1959); (*b*) M. I. LIM. Ph.D. Thesis, McGill University, Montreal, P.Q., 1976.
3. G. JUST and R. OUELLET. Can. J. Chem. **54**, 2925 (1976).
4. E. J. COREY and A. VENKATESWARLU. J. Am. Chem. Soc. **94**, 6190 (1972).
5. V. M. PARIKH and J. K. N. JONES. Can. J. Chem. **43**, 3452 (1965).
6. K. FUJI, S. NAKANO, and E. FUJITA. Synthesis, 276 (1975).
7. S. TRIPPETT and D. M. WALKER. J. Chem. Soc. 3874 (1959).
8. Y. NAKAGAWA, H. KANO, Y. TSUKUDA, and H. KOYAMA. Tetrahedron Lett. 4105 (1967).
9. (*a*) L. B. TOWNSEND and R. K. ROBINS. J. Heterocycl. Chem. **6**, 459 (1969); (*b*) P. F. CRAIN, J. A. MCCLOSKEY, A. F. LEWIS, K. H. SCHRAM, and L. B. TOWNSEND. J. Heterocycl. Chem. **10**, 843 (1973).
10. (*a*) H. P. ALBRECHT, D. B. REPKE, and J. G. MOFFATT. J. Org. Chem. **39**, 2176 (1974); (*b*) G. JUST and M. RAMJEESINGH. Tetrahedron Lett. 985 (1975).
11. L. KALVODA, J. FARKAS, and F. SORM. Tetrahedron Lett. 2297 (1970).
12. D. E. RYONO and G. M. LONDON. J. Am. Chem. Soc. **98**, 1889 (1976).
13. G. JUST and S. KIM. Tetrahedron Lett. 1063 (1976).
14. G. JUST and G. P. DONNINI. Can. J. Chem. **55**, 2998 (1977).
15. L. F. FIESER and S. RAJAGOPALAN. J. Am. Chem. Soc. **71**, 3935 (1949).
16. R. RATCLIFFE and R. RODEHORST. J. Org. Chem. **35**, 4000 (1970).
17. J. S. BRIMACOMBE. Angew. Chem. Int. Ed. Engl. **8**, 401 (1969).
18. J.-L. IMBACH, J.-L. BARASCUT, B. L. KAM, and C. TAPIERO. Tetrahedron Lett. 129 (1974).
19. W. C. STILL, M. KAHN, and A. MITRA. J. Org. Chem. **43**, 2923 (1978).
20. N.M.R. Spectra Catalogue. *Compiled by* N. S. Bhacca, D. P. Hollis, L. F. Johnson, and E. A. Pier. Varian Associates, U.S.A. 1963.
21. G. TRÜMMLITZ and J. G. MOFFATT. J. Org. Chem. **38**, 1841 (1973).

Can. J. Chem. Downloaded from www.nrcresearchpress.com by 210.87.254.40 on 09/05/12
For personal use only.

Cycloaddition reactions of *meso*-ionic oxazolone with cinnamaldehyde anils

BIR SAIN, GOPALAKRISHNA THYAGARAJAN, AND JAGIR S. SANDHU
Regional Research Laboratory, Jorhat-785006, India

Received January 16, 1980

BIR SAIN, GOPALAKRISHNA THYAGARAJAN, and JAGIR S. SANDHU. Can. J. Chem. **58**, 2034 (1980).

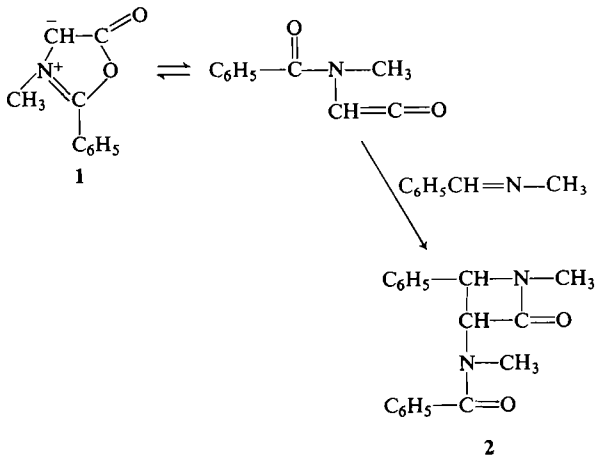
During the reaction of the azlactone **5** with different cinnamaldehyde anils, we obtained α-pyridones with no evidence for the formation of β-lactams. The products have been characterized through elemental and spectral analyses.

BIR SAIN, GOPALAKRISHNA THYAGARAJAN et JAGIR S. SANDHU. Can. J. Chem. **58**, 2034 (1980).

La réaction de l'azalactone **5** avec différents anils de l'aldéhyde cinnamique a conduit à des α pyridones sans formation apparente de β lactames. On a caractérisé les composés par des analyses élémentaires et spectrales.

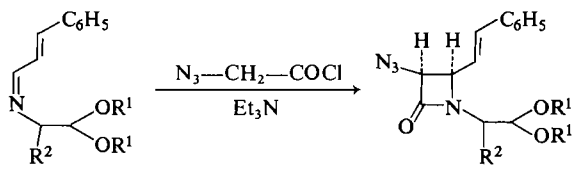
[Traduit par le journal]

Huisgen first discovered that azlactones (Δ^2-oxazolin-5-ones) can undergo cycloaddition reactions with a variety of multiple bonds (1), with the elimination of carbon dioxide. However, benzylidene-methylamine reacted with oxazolone **1** to give a β-lactam structure **2**, the formation of which was explained via ketene intermediate (2).



1 **2**

Addition reactions of ketene on to C=N bonds have been of much interest in view of conflicting reports. In particular the products obtained from cinnamaldehyde anils had been in considerable controversy. Staudinger (3) claimed the formation of β-lactams from dimethyl ketene and diphenyl ketene, whereas Pfleger and Jager (4) claimed the formation of α-pyridones, when phenyl ketene and ketene were used. Recently Doyle *et al.* (5) have prepared β-lactam precursors **4** from **3** for the synthesis of their nuclear analogs of β-lactam antibiotics.[1]

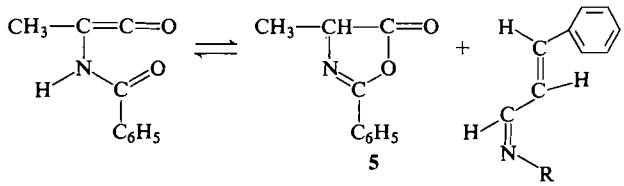


3 **4**

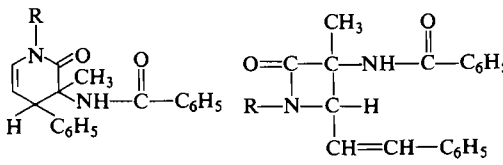
a $R^1 = CH_3$, $R^2 = H$
b $R^1 = C_2H_5$, $R^2 = COOC_2H_5$

Just *et al.* (6) have also demonstrated the formation of *cis* β-lactams when the *N*-alkyl part is replaced by aromatic amines; however, in some cases β-lactams formed were found not to have *cis* geometry.

We have used azlactone **5** (which on analogy to Huisgen's findings can equilibrate to ketene) and are able to obtain α-pyridones, with no evidence for the formation of β-lactams.



5 **6**(*a–h*)



7(*a–h*) **8**(*a–h*)

a R = C_6H_5
b R = $C_6H_4OCH_3(p)$
c R = $C_6H_4Br(p)$
d R = $C_6H_4Cl(p)$
e R = $C_6H_3Cl_2(2,4)$
f R = $C_6H_4CH_3(p)$
g R = CH_3
h R = C_6H_{11}

[1]Azido-acetyl chloride and cinnamaldehyde anils reacted in the presence of triethylamine to give β-lactam analogs. T. W. Doyle, personal communication.

0008-4042/80/192034-04$01.00/0
©1980 National Research Council of Canada/Conseil national de recherches du Canada

Can. J. Chem. Downloaded from www.nrcresearchpress.com by 210.87.254.5 on 09/05/12
For personal use only.

Can. J. Chem. Downloaded from www.nrcresearchpress.com by 210.87.254.5 on 09/05/12
For personal use only.

Equimolecular quantities of oxazolone **5** and anil **6***a* dissolved in dry benzene and allowed to stand at room temperature gave on evaporation a white crystalline solid, mp 240°C, in 85% yield. The ir(KBr) spectral analysis clearly ruled out the formation of any β-lactam of the type **8***a*, which is likely to absorb well above 1740 cm^{-1} (5). A strong band at 1699 cm^{-1}, weaker ones at 1667 cm^{-1} and 3350 cm^{-1}, corresponded to amide and NH respectively. The nmr spectrum ($CDCl_3$) δ: 8.12(s, 1H), 7.24–7.67(m, 15H), 6.43(dd, 1H), 5.23(dd, 1H), 5.00(m, 1H), 1.15(s, 3H) is consistent with structure **7***a*. The position of olefinic protons did not show significant shift even when the *N*-aryl group was replaced by an *N*-alkyl group (see **7** (*g* and *h*), Table 2). Presumably this behaviour is because of the 2-keto group present, which influences the electronic distribution significantly. The mass spectrum showed a molecular ion at *m/e* 382 (0.02%) and major fragments at 261(80%), 260(100%), 232(10%), 208(40%), 206(30%), 105(50%), and 77(30%). Plausible schemes showing these fragmentations are given below.

The reaction was generalized by employing different cinnamaldehyde anils using aromatic as well as aliphatic amines. In all the cases investigated we obtained α-pyridone analogs of **7***a* only and there was no evidence for the formation of β-lactam analogs of **8***a*. The characteristics of these pyridones thus obtained are given in Tables 1 and 2.

Duran *et al.* (7, 8) described the formation of α-chloro-2-pyridones from cinnamylidene anils and dichloro ketene and proposed two mechanistic pathways. One involved a dipolar intermediate and the other an acyl intermediate. In our case the reaction appears to proceed through dipolar intermediate **9** since the reaction rate was found to be dependent on the nucleophilicity of nitrogen.

Further investigation using differently substituted azlactones and imines is in progress.

Experimental

Melting points were taken in open capillary on a Büchi apparatus and are uncorrected. The nmr spectra were recorded on a Varian-A-60T instrument with chemical shift values recorded in δ parts per million relative to internal standard (tetramethylsilane). Mass spectra were determined on a AEI MS 30 instrument. The infrared spectra were recorded on a Perkin Elmer 237B ir spectrometer.

Can. J. Chem. Downloaded from www.nrcresearchpress.com by 210.87.254.5 on 09/05/12
For personal use only.

TABLE 1. Characteristics of pyridones

Compound No.	R	Melting point (cinnamaldehyde anil)°C	Yield (pyridone) %	Melting point (pyridone) °C	Formula	Analysis (%) Calculated C	H	N	Halogen	Found C	H	N	Halogen
7a (9)	C_6H_5	107	85	240	$C_{25}H_{22}N_2O_2$	78.53	5.76	7.33	—	78.68	5.72	7.31	—
7b	$C_6H_4OCH_3(p)$	120	90	225	$C_{26}H_{24}N_2O_3$	75.73	5.82	6.79	—	75.80	5.80	6.78	—
7c	$C_6H_4Br(p)$	117	90	248	$C_{25}H_{21}BrN_2O_2$	65.08	4.55	6.07	17.34	65.04	4.54	6.04	17.28
7d	$C_6H_4Cl(p)$	105	85	260	$C_{25}H_{21}ClN_2O_2$	72.03	5.04	6.72	8.51	72.05	5.03	6.70	8.50
7e	$C_6H_3Cl_2(2,4)$	115	25	190	$C_{25}H_{20}Cl_2N_2O_2$	66.53	4.43	6.21	15.73	66.55	4.42	6.20	15.72
7f	$C_6H_4CH_3(p)$	85	90	237	$C_{26}H_{24}N_2O_2$	78.78	6.06	7.07	—	78.89	6.05	7.06	—
7g	CH_3	40	70	194	$C_{20}H_{20}N_2O_2$	75.00	6.25	8.75	—	75.05	6.25	8.74	—
7h	C_6H_{11}	bp 180–185/12 Torr	70	180	$C_{25}H_{28}N_2O_2$	77.32	7.21	7.21	—	77.33	7.20	7.20	—

TABLE 2. Spectral data of pyridones

Compound No.	Infrared (cm^{-1})	Nuclear magnetic resonance (δ)	Mass spectra *m/e* (%)
7a	3350, 3025, 1699, 1667, 1645	8.12(s, 1H), 7.24–7.67(m, 15H), 6.43(dd, 1H), 5.23(dd, 1H), 5.00(m, 1H), 1.15(s, 3H)	382(0.02), 261(80), 260(100), 232(10), 208(40), 206(30), 105(50), 77(30)
7b	3350, 3025, 1700, 1667, 1645	8.18(s, 1H), 7.20–7.75(m, 14H), 6.43(dd, 1H), 5.25(dd, 1H), 5.07(m, 1H), 3.67(s, 3H), 1.16(s, 3H)	412(0.05), 291(80), 290(100), 262(4), 238(10), 236(10), 105(15), 77(12)
7c	3350, 3020, 1695, 1665, 1648	8.18(s, 1H), 7.30–7.72(m, 14H), 6.40(dd, 1H), 5.24(dd, 1H), 5.03(m, 1H), 1.17(s, 3H)	462(0.02), 460(0.02), 339(65), 338(100), 310(10), 286(25), 284(20), 105(60), 77(40)
7d	3350, 3025, 1695, 1665, 1648	8.17(s, 1H), 7.32–7.70(m, 14H), 6.45(dd, 1H), 5.27(dd, 1H), 5.00(m, 1H), 1.17(s, 3H)	416(0.01), 295(70), 294(100), 266(6), 242(22), 240(20), 105(70), 77(55)
7e	3345, 3020, 1690, 1661, 1647	8.17(s, 1H), 7.27–7.70(m, 13H), 6.45(dd, 1H), 5.27(dd, 1H), 5.00(m, 1H), 1.17(s, 3H)	450(0.01), 329(20), 328(15), 294(90), 276(40), 274(30), 105(100), 77(50)
7f	3355, 3025, 1695, 1665, 1645	8.12(s, 1H), 7.17–7.70(m, 14H), 6.40(dd, 1H), 5.22(dd, 1H), 5.02(m, 1H), 2.20(s, 3H), 1.14(s, 3H)	396(0.04), 275(80), 274(100), 246(6), 222(20), 220(22), 105(30), 77(20)
7g	3365, 3025, 1675, 1662, 1648	8.02(s, 1H), 7.28–7.75(m, 10H), 6.33(dd, 1H), 5.20(dd, 1H), 5.03(m, 1H), 2.48(s, 3H), 1.07(s, 3H)	320(0.05), 199(80), 198(100), 146(45), 105(50), 77(10)
7h	3355, 3010, 1695, 1665, 1645	8.00(s, 1H), 7.23–7.70(m, 10H), 6.37(dd, 1H), 5.18(dd, 1H), 4.97(m, 1H), 1.50(m, 11H), 1.07(s, 3H)	388(0.01), 267(50), 266(100), 214(70), 105(75), 77(25)

The anils **6** described in this study were prepared by known methods and mp/bp values agreed with those recorded in the literature.

Typical Procedure for the Formation of Oxazolone 5

A suspension of DL-α-benzoyl alanine (1.93 g, 0.01 mol) in acetic anhydride (30 mL) was warmed to 50°C. A clear solution was obtained in about 15 min. Acetic acid and excess acetic anhydride were rapidly removed *in vacuo* at 50°C (bath temperature); the residue thus obtained was dissolved in 10 mL of dry benzene. This solution of oxazolone **5** (0.01 mol) was directly used for reaction purposes.

General Procedure for the Reaction between Schiff Bases and Oxazolone

To a solution of cinnamylidene–aniline **6***a* (2.07 g, 0.01 mol) in 10 mL of dry benzene, a solution of oxazolone **5** (0.01 mol) in dry benzene (10 mL) was added at room temperature. The mixture was allowed to stand for 16 h, and the separated solid filtered to give 2.8 g of pyridone. An additional 0.447 g of the compound was obtained by evaporating the filtrate *in vacuo* and working up the residue. The product obtained was crystallized from benzene. Total yield 85%, mp 240°C.

Pyridones **7** (*b–f*) were similarly prepared. Pyridone **7***g* and **7***h* could be obtained only when the reaction was allowed to proceed at 4°C for 12 h. In all the cases benzene was used as the solvent for crystallization.

Acknowledgements

The authors wish to thank the Analytical Chemistry Division for spectral analyses.

1. H. GOTTHARDT, R. HUISGEN, and H. O. BAYER. J. Am. Chem. Soc. **92**, 4340 (1970), and references cited therein.
2. R. HUISGEN. Aromaticity, Chem. Soc. special publication No. 21, 51 (1967).
3. H. STAUDINGER. Ann. Chem. **356**, 51 (1907).
4. R. PFLEGER and A. JAGER. Chem. Ber. **90**, 2460 (1957).
5. T. W. DOYLE, B. BELLEAU, B. LUH, C. F. FERRARI, and M. P. CUNNINGHAM. Can. J. Chem. **55**, 468 (1977), and references cited therein.
6. G. JUST, A. UGOLINI, and R. ZAMBONI. Synth. Commun. **9**(2), 117 (1979).
7. F. DURAN and L. GHOSEZ. Tetrahedron Lett. 245 (1970).
8. Ger. Patent Nos. 2,046,822 (1970); 2,046,823 (1970); 2,046,824 (1970).
9. S. MOHAN, B. KUMAR, and J. S. SANDHU. Chem. Ind. 671 (1971).

Can. J. Chem. Downloaded from www.nrcresearchpress.com by 210.87.254.5 on 09/05/12
For personal use only.

Spectral and photochromic properties of two long-chain spiropyranindoline monolayers at the air–solid interface[1]

MARCEL MORIN, ROGER M. LEBLANC, AND ILONA GRUDA

Groupe de Recherche en Biophysique, Département de Chimie–Biologie, Université du Québec à Trois-Rivières, Trois-Rivières (Qué.), Canada G9A 5H7

Received January 21, 1980

MARCEL MORIN, ROGER M. LEBLANC, and ILONA GRUDA. Can. J. Chem. **58**, 2038 (1980).

Some long-chain spiropyranindolines have been studied at the air–water and the air–solid interfaces. We have measured the surface pressure – area isotherms of these compounds and two of them are characterized by a solid film. We have also investigated the spectroscopic properties (uv–visible) of these spiropyranindolines in monolayer and in solution. The deposition of monolayers on quartz slides allowed the study of the photochromic properties of these compounds at the air–solid interface. The 3′,3′-dimethyl-1′-hexadecyl-6-nitrospiro(2H-1-benzopyran-2,2′-indoline), irradiated at 253.7 nm, showed the appearance of a new absorption band at 570 nm which varied in intensity when the number of monolayers and the time of irradiation were changed.

MARCEL MORIN, ROGER M. LEBLANC et ILONA GRUDA. Can. J. Chem. **58**, 2038 (1980).

L'étude de quelques spiropyranindolines possédant un substituant à longue chaîne a été effectuée aux interfaces air–eau et air–solide. Nous avons mesuré les isothermes de pression de surface de ces substances à l'interface air–eau. Deux d'entre elles sont caractérisées par un film solide. Les propriétés spectroscopiques (uv–visible) de ces spiropyranindolines ont été étudiées en solution et en monocouche. La déposition de monocouches sur lamelles de quartz a permis l'étude des propriétés photochromiques de ces substances à l'interface air–solide. Le 3′,3′-diméthyl-1′-hexadécyl-6-nitrospiro (2H-1-benzopyran-2,2′-indoline), irradié à 253.7 nm, a démontré l'apparition d'une nouvelle bande d'absorption à 570 nm dont l'intensité varie avec le nombre de monocouches et le temps d'irradiation.

Introduction

The photochromic process involves a reversible modification in the structure of molecules during irradiation. There has been an increasing interest in the understanding of the mechanisms of these processes, their kinetics and their fatigue phenomena in solution as well as in solid films or membranes (1).

Spiropyranindolines are well-known for their photochromic properties. The spectral, electrical, and photochromic properties of these compounds have been widely studied (1–5). In solid films, there are many studies on the photochromic properties of the spiropyrans alone (6–8) or complexed with polymers (9–12). These photochromic properties were investigated by uv–visible spectroscopy (1–5, 7–13) or by uv–laser irradiation (14, 15).

Recently, Kato *et al.* (13) have prepared photoresponsive membranes by incorporating a photochromic spiropyran with phosphatidylcholine in a cellulose acetate membrane. The membrane-bound spiropyran exhibited normal photochromism: a colorless form under visible light irradiation and a colored form under uv light irradiation. Only one study has investigated the photochromic properties of a spiropyranindoline in monomolecular state. In their paper, Polymeropoulos and Mobius (16) reported the surface pressure and surface potential properties of mixed monolayers of a long-chain spiropyran with tripalmitine as well as the photochromic properties of these mixed monolayers. They observed, from their experiments, a photochromic reaction not only in a monomolecular film at the air–water interface but also in a monolayer system at the air–solid interface.

Recently, we synthesized nine long-chain spiropyranindolines (17) and studied the monolayer properties of these compounds at air–water interface. Two of them showed a solid isotherm at relatively high surface pressure[2] (above 15 mN m^{-1}) while the others exhibited some inflections in the isotherms between 5 and 15 mN m^{-1}, probably due to some modifications in the conformation of the compounds during the compression.

We present in this paper the surface-pressure properties of some long-chain spiropyranindolines at the air–water interface. Their spectral properties in monolayers as well as in solution along with their photochromic properties at the air–solid interface are described.

Experimental

Material

The 3′,3′-dimethyl-1′-hexadecyl-6-nitrospiro-(2H-1-benzopyran-2,2′-indoline) and 1,3-dimethyl-3-hexadecyl-8′-nitro-

[1]Part III of Photochromic Studies in Monolayers.

[2]In our previous paper (17), these two spiropyranindolines were mentioned as compounds **7***c* and **8***b*. We must read **8***c* instead of **8***b*, i.e. 1,3-dimethyl-3-hexadecyl-8′-nitrospiro-(indoline-2,3′-(3H)-naphtho(2,1-*b*)-pyran).

0008-4042/80/192038-06$01.00/0

©1980 National Research Council of Canada/Conseil national de recherches du Canada

Can. J. Chem. Downloaded from www.nrcresearchpress.com by 210.87.254.40 on 09/05/12
For personal use only.

Can. J. Chem. Downloaded from www.nrcresearchpress.com by 210.87.254.40 on 09/05/12
For personal use only.

spiro)indoline-2,3′-(3H)-naphtho(2,1-*b*)-pyran) were synthesized and purified according to the method described previously (17). Absolute ethanol (95%) and certified grade *n*-hexane (99 mol% pure) (Fisher Sci. Co., Montreal) were used, without purification, as solvents in spectroscopic experiments.

For all the monolayer experiments, "Analar" grade diethyl ether (BDH Chemicals, Montreal) was used as spreading solvent. Phosphate buffer was prepared from certified ACS grade sodium phosphate monobasic and dibasic (Fisher Sci. Co., Montreal). Arachidic acid (99+% pure) was purchased from Applied Sciences Laboratories, State College, PA. Distilled water was prepared by, first, filtering and demineralizing tap water on a Super-Q™ Millipore system (Millipore Co., Mississauga, Ontario) and, subsequently, by distilling twice on a glass system, using potassium permanganate and sodium hydroxide in the first distillation. Finally, the distilled water was filtered in Millipore (0.22 μ) to eliminate all particles and microorganisms.

Quartz cells (path length of 1, 2, and 10 mm) for spectroscopic studies in solution were obtained from Hellma Canada Ltd., Toronto. Quartz slides (5.00 cm × 2.50 cm × 0.10 cm) for spectroscopic studies in monolayers were purchased from Esco Products, NJ, U.S.A. The low pressure mercury light source (253.7 nm, 2.5 mW) was purchased from Sargent-Welch Co., Montreal.

Absorption spectra were recorded on Perkin-Elmer Coleman 124 or Unicam SP-1800 spectrophotometers.

Methods

For the determination of the surface pressure – area isotherms and the deposition of the monolayer on slide, we utilized a simple Langmuir-type film balance described elsewhere (18, 19). The calibration of the balance was achieved with arachidic acid and the sensitivity of the balance was 0.229 ± 0.005 mN m^{-1} deg^{-1}. To adjust the pH of the subphase to 7.5–8.0, we used sodium phosphate (10^{-3} mol dm^{-3}). The water temperature was maintained at 18.0 ± 0.5°C and the room temperature at 19.0 ± 1.0°C.

The monolayers were formed at the air–water interface by delivering the spreading solution (100 μL) at 5 mm above the water surface with a Hamilton microsyringe and by compressing the molecules manually at a constant speed of 2.8 $Å^2$ $molecule^{-1}$ min^{-1}. Approximately 10 min were allowed to let the solvent evaporate and the molecules equilibrate before starting compression. The isotherms were repeated at least five times each so as to obtain a good reproducibility of the results (±1–2 $Å^2$ $molecule^{-1}$ and ±0.2 mN m^{-1}).

To clean the quartz slides, we immersed them in hot sulfochromic acid or in a mixture of concentrated sulfuric acid and hydrogen peroxide 50% (1:1 v/v) for about 10 min. After that, the slides were rinsed many times, with bi-distilled water. Then the slides were dried in a stream of nitrogen.

For the deposition of the monolayer on the quartz slide, the following method was used: first, the slide was dipped into the trough to a depth of 3.2 cm with the help of an electric motor which lowered and raised the vertically clamped slide at a constant speed of 0.25 rpm. Then, the water surface was cleaned (18) and we spread 100 μL of the spiropyran solution on the water surface. We compressed the molecules to a surface pressure of 15 mN m^{-1}. At that pressure, the slide was raised and the monolayer transferred from the water surface to the slide, each side of the slide having one monolayer. We should note that, during the deposition of the monolayer, we must always apply a constant pressure of 15 mN m^{-1}, otherwise we will have some irregularities in the aggregation of the molecules in monolayer. The deposition ratio normally obtained has a value of 1.0 ± 0.1; it is defined as A_1/A_s where A_1 is the decrease of area occupied by the monolayer at the air–water interface and A_s is the area coated by the monolayer at the air–solid interface.

After the deposition of the monolayer on the slide, the absorption spectrum was recorded as described elsewhere (18). We needed five slides, each having one monolayer on each side, to get a good spectrum with a sufficient absorbance.

Finally, the irradiation of the monolayers was carried out by putting the five slides in front of a low pressure mercury light source (λ_{exct} = 253.7 nm; $I_o = 3.17 \times 10^{15}$ photons s^{-1}). The support with the slides was placed at about 3 cm from the source. After irradiation, the absorption spectrum was recorded the same way as before irradiation.

Results and Discussion

Π-A *Curves*

The surface pressure – area (Π–*A*) isotherm is normally used as the characteristic description of an insoluble monolayer at the air–water interface. It corresponds to the relationship between the surface pressure observed and the area occupied on the water surface by the molecules of the film. The surface pressure – area isotherms of the spiroindolinobenzopyran (**1***a*) and the spiroindolinonaphthopyran (**2***a*) are shown in Fig. 1. Each curve was recorded at least five times and the maximum variation between the different runs was not more than ±2 $Å^2$ $molecule^{-1}$. The shape of the curve is typical of the condensed monolayers, i.e. solid films (20).

The limiting area per molecule is situated at 20.9

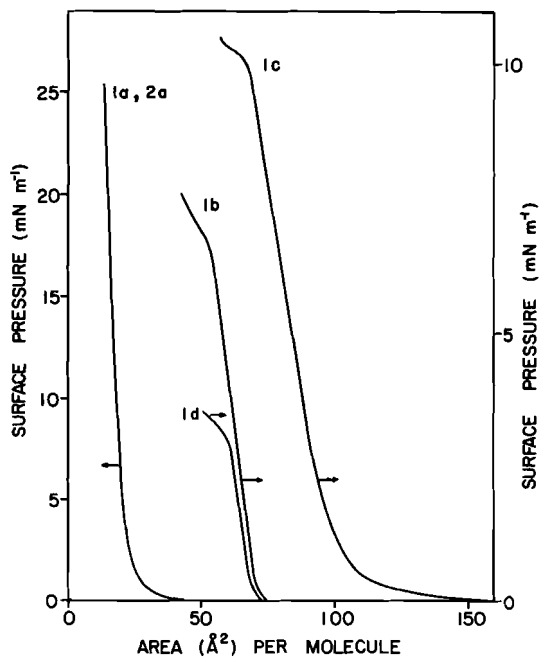
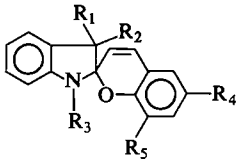
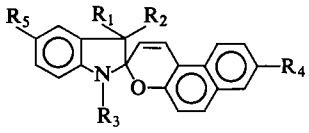


FIG. 1. Pressure-area isotherms of compounds **1***a*, **1***b*, **1***c*, **1***d*, and **2***a* on phosphate buffer (pH 7.6) at the air–water interface. *T*: 18.5 ± 0.5°C.

TABLE 1. Structure of the spiropyranindolines

Compound	R_1	R_2	R_3	R_4	R_5
					
1*a*	CH_3	CH_3	$C_{16}H_{33}$	NO_2	H
1*b*	CH_3	CH_3	$C_{16}H_{33}$	H	OCH_3
1*c*	CH_3	$C_{16}H_{33}$	CH_3	H	OCH_3
1*d*	CH_3	$C_{16}H_{33}$	CH_3	NO_2	H
					
2*a*	CH_3	$C_{16}H_{33}$	CH_3	NO_2	H
2*b*	CH_3	CH_3	$C_{16}H_{33}$	H	H
2*c*	CH_3	CH_3	$C_{16}H_{33}$	NO_2	H
2*d*	CH_3	CH_3	$C_{16}H_{33}$	H	NO_2

$Å^2$ for compound 1*a* and 19.9 $Å^2$ for compound 2*a*. These spiropyrans have a molecular area almost identical with the molecular cross-sectional areas of fatty acids like stearic and arachidic acids. The compression of the spiropyranindoline films was stopped before the collapse of the monolayers which is well beyond a surface pressure of 30 mN m^{-1}.

On the basis of these results, we can affirm that the long aliphatic chain of the spiropyranindolines (1*a*, 2*a*) is oriented perpendicularly at the air–water interface (Π greater than 15 mN m^{-1}), the rest of the molecule being more or less immersed in water. The three other spiroindolinobenzopyrans (1*b*, *c*, *d*; Table 1) form liquid films as shown in Fig. 1. However, the three other spiroindolinonaphthopyrans (2*b*, *c*, *d*; Table 1) form isotherms with a surface pressure between 0 and 2 mN m^{-1} and a molecular area between 60 and 20 $Å^2$.

Our results show that in the spiropyranindoline series there is a very narrow range of structures allowing the formation of a solid monolayer at air–water interface. It is quite evident that a strongly hydrophilic substituent is indispensable to immerse the whole aromatic part of the molecule into the subphase, which makes possible a strong interaction between the aliphatic chains. Two hydrophilic centers of a spiropyranindoline, the amino nitrogen and the oxygen of the pyran ring, have too weak polar characteristics to immerse the polycyclic part of the molecule. Adding a methoxy group does not increase enough hydrophilic interactions. The much more polar nitro group seems to be sufficiently hydrophilic hence only nitrospiropyranindolines give solid monolayers.

Another important factor is the position of the aliphatic chain. As one can see in Table 1 and Fig. 1, in the benzopyran series, the chain at 1′ gives a solid monolayer whereas in the naphthopyran series the long chain must be at 3′. This phenomenon is more difficult to justify. The examination of molecular models shows that spiropyrans may exist in two conformations determined by the C—O—C angle in the pyran ring. Probably only in one of the two conformations (Fig. 2, conformation **I**), the aliphatic chains may come close enough to allow a strong chain–chain interaction. The equilibrium ratio of the conformers depends on structural factors and is difficult to evaluate. We suppose that the formation of a solid monolayer with strong chain–chain interactions is possible only for conformation **I** and that the inflections in the isotherms may be due to the change of the conformation equilibrium during compression.

Absorption Spectroscopy

The monolayer spectra of compounds 1*a* and 2*a* were recorded at room temperature and are shown in Figs. 3 and 4. Table 2 presents the absorption maxima for the compounds 1*a* and 2*a* in solution in ethanol, *n*-hexane, and in the monomolecular state, respectively.

In ethanol solution, the spectrum shows absorption in both regions, ultraviolet and visible. In the monomolecular state, only ultraviolet region presents maxima for both compounds; in the visible, compound 1*a* does not show any absorption while compound 2*a* shows two shoulders.

If we compare, for each compound, the spectrum in monolayer with those in solution (Figs. 3, 4, and Table 2), we could note that some bands, present in solution, completely disappear in monolayer.

Can. J. Chem. Downloaded from www.nrcresearchpress.com by 210.87.254.40 on 09/05/12
For personal use only.

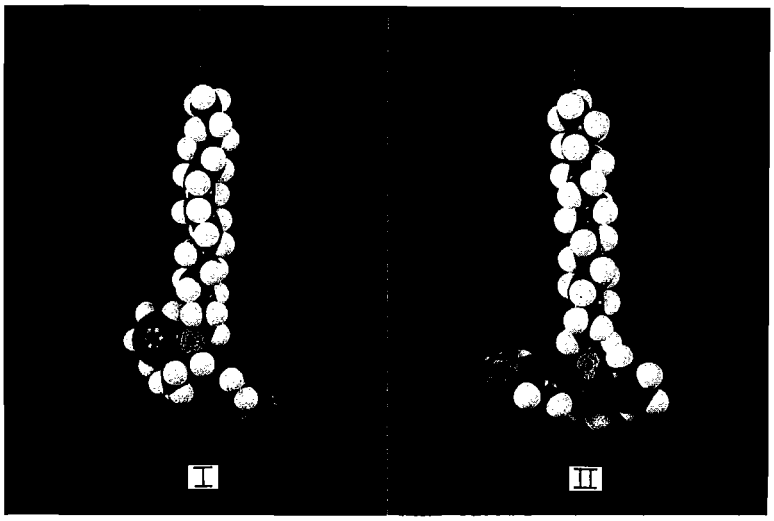


FIG. 2. Models of compound 1*a* at the air–water interface: conformation I (model A) and conformation II (model B).

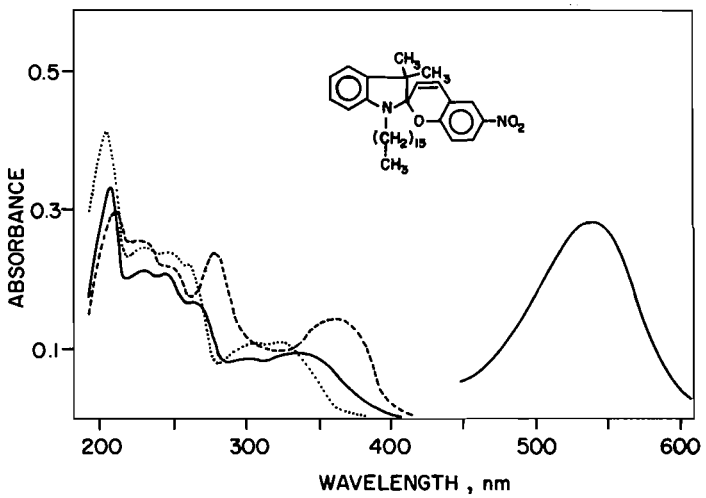


FIG. 3. Absorption spectra of compound 1*a* respectively in ethanol (—), *n*-hexane (· · ·) and monolayer at the air–solid interface (---).

Also, for both compounds, the spectra in the monolayer show a red shift compared to the solution spectra.

The spectral behavior of both compounds in monolayers may be due to the fact that the molecules are present in aggregates and are in distinct geometry compared to the solution, where the polarity of the solvent plays an important role in the shifts.

Photochromism

The photochromism of the two spiropyrans was studied as a function of time of irradiation when the compounds are irradiated with uv light at 253.7 nm.

When colorless films of compound 1*a* are irradiated with uv light at a suitable wavelength, one can observe the appearance and increase in intensity of the absorption band in the visible region and the decrease of the bands in the uv region. Figure 5 represents typical spectra obtained at different times of irradiation for compound 1*a*. The irradiation effect could be explained by the fact that a new isomer is formed with a new band in the visible region. Thus the change in the spiropyran molecule from colorless to colored form results in the change of its absorption spectrum in both uv and visible region (8).

Our experiments have shown that the maximum coloration is obtained after about 15 min of irradiation, depending on the number of monolayers; if we

Can. J. Chem. Downloaded from www.nrcresearchpress.com by 210.87.254.40 on 09/05/12
For personal use only.

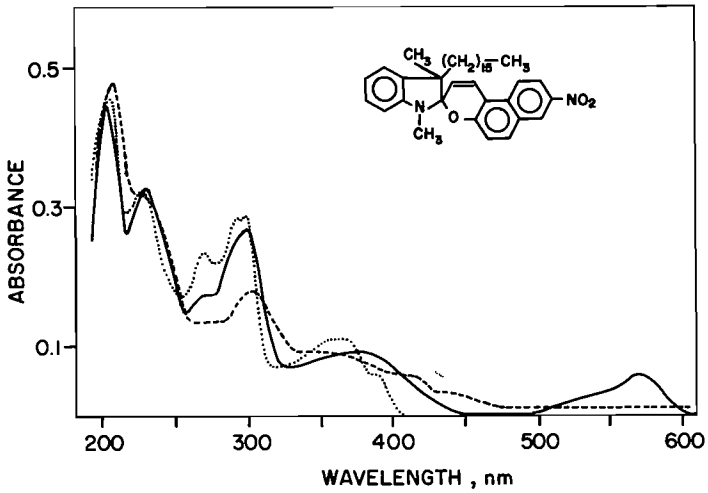
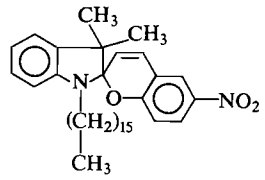
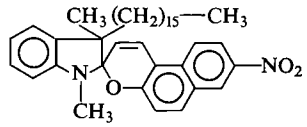


FIG. 4. Absorption spectra of compound **2***a* respectively in ethanol (—), *n*-hexane (· · ·), and monolayer at the air–solid interface (---).

TABLE 2. Spectral characteristics of compounds **1***a* and **2***a*

Compounds (concentration: 10^{-3}–10^{-5} *M*)	$\lambda_{max} \pm 0.5$ nm		
	Ethanol solution	*n*-Hexane solution	Monomolecular state
	205.4	203.3	209.5
	226.5	226.5	227.0
	243.5	244.0	248.0
	265.0	250.5*	276.5
	303.5	263.5*	364.0
	335.5	302.5	
	541.5†	323.0	
	201.0	202.7	205.0
	229.5	224.3	230.0*
	248.0*	268.5	303.0
	270.0	291.7	350.0*
	298.0	297.0	412.0*
	346.5*	335.5*	452.0*
	370.0	354.0	
	385.0*	365.5	
	538.0*	390.0*	
	573.0		

*Shoulder.
†In our previous paper (17), it should read 541.5 nm instead of 590.0 nm for the spectral characteristics of compounds **7***e*.

continue the irradiation after that time, the absorption bands in the uv region still slowly decrease and those in the visible region also begin to decrease in intensity. After 15 min irradiation, an equilibrium is reached and further irradiation causes degradation of both isomers.

We have also observed the process of decoloration of these monolayers. We noted, after 5 h in darkness, a decoloration of about 75% and a complete decoloration after at least 10 h. Furthermore, it seems from Tyczkowski and Kryosewski (8) that the best photochromic properties are shown by the spiropyrans which, in position R_4, have a nitro group as a substituent. This generally agrees with the observation of photochromic properties of spiropyrans in solution and shows the important role played by the nitro group and its position in the molecule of spiropyran in the process of photocoloration (8).

The absorption spectrum of compound **2***a* was

Can. J. Chem. Downloaded from www.nrcresearchpress.com by 210.87.254.40 on 09/05/12
For personal use only.

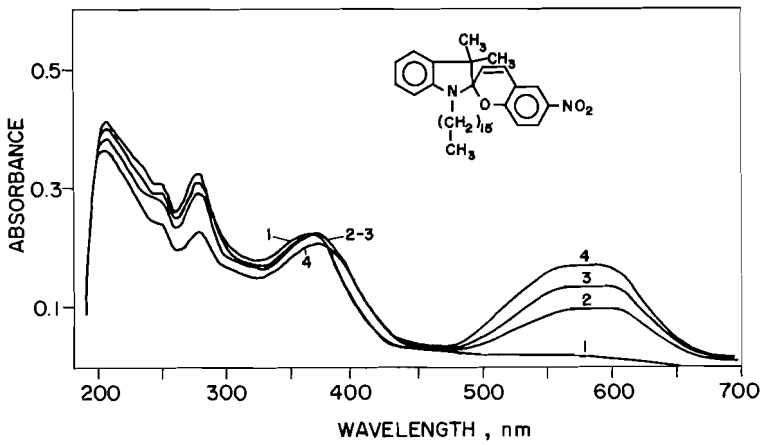


FIG. 5. Absorption spectra of compound 1*a* in monolayer before irradiation (curve *1*), after 2 min (curve *2*), 5 min (curve *3*), and 15 min (curve *4*) of irradiation.

taken after 2.5 and 15 min of irradiation under the same experimental conditions as for compound **1***a*. However, for this compound no change was observed in the spectrum after irradiation. Nevertheless, that does not mean that the compound **2***a* does not respond to irradiation. It might be possible that the reaction occurs in a very fast time, too fast to be observed by conventional spectroscopy.

Acknowledgements

The authors are grateful to Mr. Gaétan Munger for his contribution to this work. Financial assistance was provided by the Ministère de l'Education du Québec and the Natural Sciences and Engineering Research Council of Canada.

1. R. C. BERTELSON. *In* Photochromism. Vol. III. Techniques of chemistry. *Edited by* G. H. Brown. Wiley-Interscience, New York. 1971.
2. T. BERCOVICI, R. HEILIGMAN-RIM, and E. FISCHER. Mol. Photochem. **1**, 23 (1969).
3. A. A. PARSHUTKIN and V. A. KRONGAUZ. Mol. Photochem. **6**, 437 (1974).
4. P. APPRIOU, R. GUGLIELMETTI, and F. GARNIER. J. Photochem. **8**, 145 (1978).
5. V. A. KUZMIN, Y. N. MALKIN, and E. R. ZAKHS. Photogr. Sci. Eng. **23**, 20 (1979).
6. T. NAKAYAMA, I. SHIMIZU, H. KOKADO, and E. INOUE. Bull. Chem. Soc. Jpn. **44**, 3203 (1971).
7. M. KRYSZEWSKI, S. SAPIEHA, J. TYCZKOWSKI, and M. ZIELINSKI. Pr. Nauk. Inst. Chem. Org. Fiz. Politech. Wroclaw. 7, 390 (1974).
8. J. TYCZKOWSKI and M. KRYSZEWSKI. Rocz. Chem. Ann. Soc. Chim. Polon. **51**, 89 (1977).
9. M. V. R. SAHYUN. Photogr. Sci. Eng. **16**, 63 (1972).
10. E. MOHN. Appl. Opt. **12**, 1570 (1973).
11. D. G. WILSON and H. G. DRICKAMER. J. Chem. Phys. **63**, 3649 (1975).
12. D. GAUDE, M. LE BACCON, R. GUGLIELMETTI, and R. GAUTRON. Bull. Soc. Chim. Fr. **9–10**, 11-489 (1979).
13. S. KATO, M. AIZAWA, and S. SUZUKI. J. Membr. Sci. (*a*) **1**, 289 (1976); (*b*) **2**, 39 (1977).
14. S. MASLOWSKI, H. P. VOLLMER, and A. G. ZOOP. Z. Angew. Phys. **26**, 212 (1969).
15. V. A. MURIN, V. F. MANDZHIKOV, S. G. KUZMIN, and V. A. BARACHEVSKII. Opt. Spectrosc. **37**, 216 (1974).
16. E. E. POLYMEROPOULOS and D. MOBIUS. Ber. Bunsenges. Phys. Chem. **83**, 1215 (1979).
17. I. GRUDA and R. M. LEBLANC. Can. J. Chem. **54**, 576 (1976).
18. S. HOTCHANDANI, R. M. LEBLANC, and F. BOUCHER. Vision Res. **15**, 605 (1975).
19. H. P. POMMIER, J. BARIL, I. GRUDA, and R. M. LEBLANC. Can. J. Chem. **57**, 1377 (1979).
20. G. L. GAINES, JR. Insoluble monolayers at liquid–gas interface. Wiley-Interscience, New York, NY. 1966. Chapt. 4.

Can. J. Chem. Downloaded from www.nrcresearchpress.com by 210.87.254.40 on 09/05/12
For personal use only.

Base-catalysed ring opening of *N*-(aminothioxomethyl)-5,6-dihydro-2-methyl-1,4-oxathiin-3-carboxamides

MARSHALL KULKA

Uniroyal Limited, Research Laboratories, Guelph, Ont., Canada N1H 6N3

Received April 7, 1980

MARSHALL KULKA. Can. J. Chem. **58**, 2044 (1980).

The condensation of 5,6-dihydro-2-methyl-1,4-oxathiin-3-carbonyl isothiocyanate (**1**) with ethyl 3-phenylamino-2-butenoate (**2**) has yielded a mixture of ethyl 1,4-dihydro-2-(5,6-dihydro-2-methyl-1, 4-oxathiin-3-yl)-6-methyl-1-phenyl-4-thioxo-5-pyrimidine carboxylate (**3**) and *N*-[(phenylamino)thioxomethyl]-5,6-dihydro-2-methyl-1,4-oxathiin-3-carboxamide (**4**, R′ = phenyl). It has been discovered that compounds **4**, in general, rearrange to 1-substituted-2,3-dihydro-5-[(2-hydroxyethyl)thio]-6-methyl-2-thioxo-4(1*H*)-pyrimidinones (**5**) at room temperature when stirred with dilute aqueous sodium hydroxide. The products of the reaction of 5,6-dihydro-2-methyl-1,4-oxathiin-3-carbonyl isothiocyanate (**1**) and phenylhydrazine, when treated with dilute aqueous sodium hydroxide, did not yield the rearrangement product **5** (R′ = NHC_6H_5). Instead, a mixture of the two triazole-3-thiones **9** and **10** was formed. *N*,2-Bis(5,6-dihydro-2-methyl-1,4-oxathiin-3-carbonyl)hydrazinecarbothioamide (**12**) with dilute aqueous sodium hydroxide yielded one rearrangement product (out of a possible four), namely, 5-6-dihydro-2-methyl-*N*-[1,2,3,4-tetrahydro-5-[(2-hydroxyethyl)thio]-6-methyl-4-oxo-2-thioxo-1-pyrimidinyl]-1,4-oxathiin-3-carboxamide (**13**).

MARSHALL KULKA. Can. J. Chem. **58**, 2044 (1980).

La condensation du dihydro-5,6 méthyl-2 oxathiinne-1,4 carbonylisothiocyanate-3 (**1**) sur le phénylamino-3 butène-2 oate d'éthyle (**2**) donne un mélange de dihydro-1,4 (dihydro-5,6 méthyl-2 oxathiinne-1,4 yl-3)-2 méthyl-6 phényl-1 thioxo-4 pyrimidine-5 carboxylate d'éthyle (**3**) et de *N*-[(phénylamino) thioxométhyl]dihydro-5,6 méthyl-2 oxathiinne-1,4 carboxamide-3 (**4**, R′ = phényle). On a découvert que d'une façon générale, les composés du type **4** se transposent en dihydro-2,3 [(hydroxy-2 éthyl) thio]-5 méthyl-6 thioxo-2 pyrimidinones-4 (1*H*) (**5**) substituées en position 1 quand on les agite à la température ambiante avec une solution aqueuse diluée d'hydroxyde de sodium. On n'obtient pas de composé de transposition **5** (R′ = NHC_6H_5) lorsqu'on traite les produits de la réaction du dihydro-5,6 méthyl-2 oxathiinne-1,4 carbonylisothiocyanate-3 (**1**) avec la phénylhydrazine par une solution aqueuse diluée d'hydroxyde de sodium. On obtient de préférence un mélange de deux triazolethiones-3 (**9** et **10**). Le composé *N*,-bis(dihydro-5,6 méthyl-2 oxathiinne-1,4 carbonyl-3)-2 hydrazinecarbothioamide (**12**, traité par une solution aqueuse diluée d'hydroxyde de sodium, donne un seul des quatre produits de transposition possibles soit le dihydro-5,6 méthyl-2 *N*-[tétrahydro-1,2,3,4 [(hydroxy-2 éthyl)thio]-5 méthyl-6 oxo-4 thioxo-2 pyrimidyl-1] oxathiium-1,4 carboxamide (**13**).

[Traduit par le journal]

The systemic fungicides, 5,6-dihydro-2-methyl-1,4-oxathiin-3-carboxanilide (Vitavax ®[1]) and its sulfone (Plantvax®[1]) were discovered (1) in 1966 and are now used worldwide for combatting fungal pathogens of plants and are saving food crops from destruction. This has stimulated great interest in the chemistry and biological activity of the 1,4-oxathiins. A recent paper published from this laboratory (2) records ring opening reactions of some dihydro-1,4-oxathiins. The purpose of this paper is to describe further work on the ring opening reactions of 3-carbonyl substituted-5,6-dihydro-1,4-oxathiins through base-catalysed nucleophilic attack on carbon-2.

The condensation of 5,6-dihydro-2-methyl-1,4-oxathiin-3-carbonyl isothiocyanate (**1**) with ethyl 3-phenylamino-2-butenoate (**2**) (3) yielded a mixture of two compounds. These were separated by hand-picking into yellow crystals and into white crystals. The yellow crystals were identified by elemental analysis and nmr spectrum as ethyl 1,4-dihydro-2-(5,6-dihydro-2-methyl-1,4-oxathiin-3-yl)-6-methyl-1-phenyl-4-thioxo-5-pyrimidine-carboxylate (**3**) and the white crystals as *N*-[(phenylamino)thioxomethyl]-5,6-dihydro-2-methyl-1,4-oxathiin-3-carboxamide (**4**, R′ = phenyl). These assignments are in agreement with that of Goerdeler and Gnad (4) who found similar products from the condensation of benzoyl isothiocyanate with **2**.

A better method for the separation of the mixture of **3** and **4** was sought and it became apparent that the use of aqueous sodium hydroxide should provide an easy method of separation. Dilute aqueous sodium hydroxide dissolved the white crystals, **4** (R′ = phenyl) and the yellow crystals (**3**) could be filtered off in pure form. However, acidification of the basic solution did not yield **4** (R′ = phenyl). Instead, another compound was obtained which was identified by elemental analysis and nmr spectrum as 2,3-dihydro-5-[(2-hydroxyethyl)thio]-6-methyl-1-phenyl-2-thioxo-4(1*H*)-pyrimidinone (**5**, R′ = phenyl).

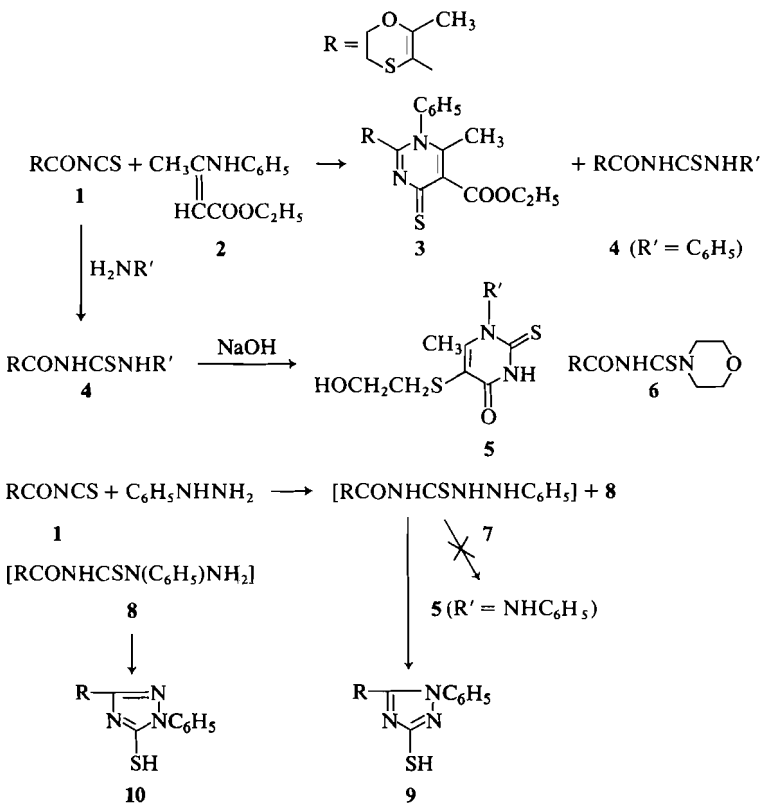
This rearrangement by ring opening of the dihydro-1,4-oxathiin, **4**, through intramolecular nucleophilic attack at carbon-2 under the mild con-

[1]®UNIROYAL's registered trademark.

0008-4042/80/192044-05$01.00/0

© 1980 National Research Council of Canada/Conseil national de recherches du Canada

Can. J. Chem. Downloaded from www.nrcresearchpress.com by 210.87.254.105 on 09/05/12
For personal use only.



ditions of dilute aqueous sodium hydroxide at room temperature to form **5** appears to be a general reaction. Thirteen *N*-(aminothioxomethyl)-5,6-dihydro-2-methyl-1,4-oxathiin-3-carboxamides (**4** where R′ = H, 1-methylethyl, *n*-butyl, *n*-hexyl, *n*-octyl, 2-phenylethyl, dimethylamino, phenyl, 4-chlorophenyl, 4-methoxyphenyl, 2-methylphenyl, 2-furanylmethyl, and 2-pyridinyl) were synthesized through the condensation of 5,6-dihydro-2-methyl-1,4-oxathiin-3-carbonyl isothiocyanate (**1**) with the corresponding primary amines. These oxathiin-3-carboxamides (**4**) rearranged readily to the corresponding 1-substituted-2,3-dihydro-5-[(2-hydroxyethyl)thio]-6-methyl-2-thioxo-4(1*H*)-pyrimidinones (**5**) when dissolved in dilute aqueous sodium hydroxide at room temperature. This rearrangement is similar to that previously found (2) in which *N*-[(phenylamino)carbonyl]-5,6-dihydro-2-methyl-1,4-oxathiin-3-carboxamide (the oxygen analog of **4**, R′ = phenyl), was converted to 5-[(2-hydroxyethyl)thio]-6-methyl-1-phenyluracil (the oxygen analog of **5**, R′ = phenyl). However, the oxygen analog of **4** (R′ = phenyl), required heating under reflux in toluene with sodium hydride instead of dilute aqueous sodium hydroxide at room temperature for the rearrangement.

The aqueous base-catalysed rearrangement is limited to those *N*-(aminothioxomethyl)-5,6-dihydro-2-methyl-1,4-oxathiin-3-carboxamides (**4**) in which the amino nitrogen bears at least one hydrogen atom. Thus *N*-[(4-morpholinyl)thioxomethyl]-5,6-dihydro-2-methyl-1,4-oxathiin-3-carboxamide (**6**), which was prepared through the condensation of 5,6-dihydro-2-methyl-1,4-oxathiin-3-carbonyl isothiocyanate (**1**) with morpholine, remained unchanged when treated with dilute aqueous sodium hydroxide.

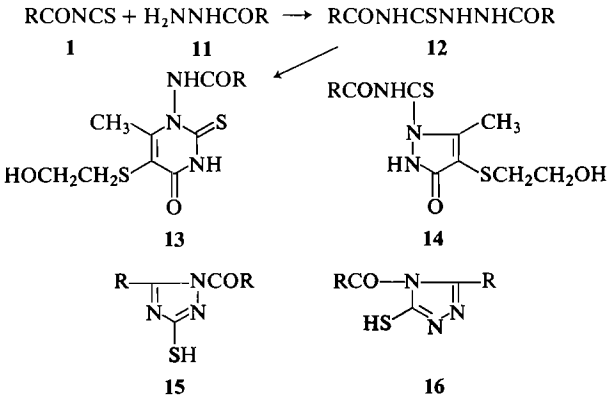
Another case where the 1,4-oxathiin ring resists opening in the presence of aqueous base was encountered. The mixture of **7** and **8** formed by the condensation of **1** with phenylhydrazine, when treated with aqueous sodium hydroxide did not yield any of the rearrangement product **5** (R′ = NHC_6H_5). Instead, another mixture was formed which was separated by fractional precipitation from sodium hydroxide into two compounds. The nmr spectra showed that these compounds contained the 1,4-oxathiin ring and they were identified as (5,6-dihydro-2-methyl-1,4-oxathiin-3-yl)-1,2,4-triazole-3-thiones **9** and **10**. Sufficient evidence is not available at the present time to distinguish between **9** and **10**. The formation of the

Can. J. Chem. Downloaded from www.nrcresearchpress.com by 210.87.254.105 on 09/05/12
For personal use only.

Can. J. Chem. Downloaded from www.nrcresearchpress.com by 210.87.254.105 on 09/05/12
For personal use only.

triazole-3-thiones **9** and **10** from 5,6-dihydro-2-methyl-1,4-oxathiin-3-carbonyl isothiocyanate (**1**) and phenylhydrazine is in agreement with the work of Pohloudek-Fabini and Schroepl (5) who found the formation of the benzene analogs from benzoyl isothiocyanate and phenyl hydrazine.

N,2-Bis(5,6-dihydro-2-methyl-1,4-oxathiin-3-carbonyl)hydrazinecarbothioamide (**12**), which was readily prepared through the condensation of 5,6-dihydro-2-methyl-1,4-oxathiin-3-carbonyl isothiocyanate (**1**) with 5,6-dihydro-2-methyl-1,4-oxathiin-3-carboxylic acid hydrazide (**11**), appears to be a versatile compound. It could theoretically rearrange in base to form four different compounds, two (**13** and **14**) resulting from nucleophilic attacks at the carbon-2 position of each of the oxathiin rings and two (**15** and **16**) resulting from the ring



R = 5,6-dihydro-2-methyl-1,4-oxathiin-3-yl

closures at each of the carbonyl groups. Actually when **12** was treated with aqueous sodium hydroxide at room temperature, one compound was obtained in good yield. The nmr spectrum of this compound showed the presence of a (2-hydroxyethyl)thio group. This indicates that the product is neither **15** nor **16** and that a nucleophilic attack on carbon-2 must have occurred to form either the structure **13** or **14**. At the present time evidence is insufficient to distinguish between the structures **13** and **14**. The structure **13** is tentatively assigned to this compound on the basis that in general pyrazolinones are more difficult to form than 2-thioxo-4(1*H*)-pyrimidinones. The 2-thioxo-4(1*H*)-pyrimidinone, structure **13** is indicated also by the comparison of its nmr spectra with that of model compounds such as 2,3-dihydro-5-[(2-hydroxyethyl)thio]-6-methyl-1-phenyl-2-thioxo-4(1*H*)-pyrimidinone (**5**, R′ = phenyl).

Experimental

The nmr spectra were recorded using an R-20 Hitachi Perkin-Elmer spectrometer and are expressed in ppm (δ values) relative to tetramethylsilane as internal standard. Infrared spectra were obtained on Perkin-Elmer 237B or 521 grating ir spectrometers. Melting points were determined on a Gallenkamp melting point apparatus and are uncorrected.

Ethyl 1,4-Dihydro-2-(5,6-dihydro-2-methyl-1,4-oxathiin-3-yl)-6-methyl-1-phenyl-4-thioxo-5-pyrimidinecarboxylate (3) and N-*[(Phenylamino)thioxomethyl]-5,6-dihydro-2-methyl-1,4-oxathiin-3-carboxamide (4 R′ = Phenyl)*

To a mixture of 5,6-dihydro-2-methyl-1,4-oxathiin-3-carboxylic acid (20 g, 0.125 mol) and chloroform (50 mL) was added thionyl chloride (25 mL) and the reaction mixture was heated at 50–55°C for 1 h. The solvent and excess thionyl chloride were removed *in vacuo*, the last traces by alternate addition and removal of toluene. The residual acid chloride was dissolved in dry acetone (30 mL) and the solution added portionwise to a solution of ammonium thiocyanate (9.6 g) in acetone (60 mL). The reaction mixture was let stand 4 h and then treated with ethyl 3-(phenylamino)-2-butenoate (3) (25.6 g, 0.125 mol). The resulting reaction mixture was allowed to stand overnight and then poured into cold water. The precipitated oil which soon solidified was filtered, pulverized, washed with cold methanol, and then crystallized from 95% ethanol. This yielded a mixture of yellow and white crystals which were separated by picking with a pair of tweezers. The yellow crystals, *ethyl 1,4-dihydro-2-(5,6-dihydro-2-methyl-1,4-oxathiin-3-yl)-6-methyl-1-phenyl-4-thioxo-5-pyrimidinecarboxylate* (**3**) melted at 225–227°C (dec.). Infrared (KBr): 3040, 750, 700 (aromatic), 1730 (ester), 1060 (C=S) cm^{-1}. Nuclear magnetic resonance ($CHCl_3$): 7.65–7.18 (5H, m, aromatic), 4.35 (2H, q, J = 7 Hz, CH_2), 4.05 (2H, m, CH_2O), 2.50 (2H, m, CH_2S), 1.88 (3H, s, CH_3), 1.80 (3H, s, CH_3), 1.38 (3H, t, J = 7 Hz, CH_3). *Anal.* calcd. for $C_{19}H_{20}N_2O_3S_2$: C 58.76, H 5.19, N 7.21; found: C 59.04, H 5.37, N 7.38.

The white crystals melted at 112–113°C and were identical with N-*[(phenylamino)thioxomethyl]-5,6-dihydro-2-methyl-1,4-oxathiin-3-carboxamide* (**4**, *R′ = phenyl*) prepared by the condensation of 5,6-dihydro-2-methyl-1,4-oxathiin-3-carbonyl isothiocyanate (**1**) and aniline (general method described below). Infrared (KBr): 3360 (NH), 1670 (CONH), 1590, 730, 690 (aromatic) cm^{-1}. The nmr spectrum was consistent with that of the structure **4** (R′ = phenyl), (see below).

2,3-Dihydro-5-[(2-hydroxyethyl)thio]-6-methyl-1-phenyl-2-thioxo-4(1H)-pyrimidinone (5, R′ = Phenyl)

In another experiment, the mixture of **3** and **4** (R′ = phenyl) prepared from 20 g of 5,6-dihydro-2-methyl-1,4-oxathiin-3-carboxylic acid (see above) was stirred with 3% aqueous sodium hydroxide (50 mL) for 1 h, filtered, washed with water, and the yellow product crystallized from ethanol yielding 10.3 g of yellow crystals, mp 224–226°C (dec.), identical with ethyl 1,4-dihydro-2-(5,6-dihydro-2-methyl-1,4-oxathiin-3-yl)-6-methyl-1-phenyl-4-thioxo-5-pyrimidinecarboxylate (**3**) (see above). The aqueous alkaline filtrate was acidified, the white precipitate filtered, washed with water, dried, and crystallized from ethanol–dioxane. The white crystals (9.1 g) melted at 193–195°C and did not depress the melting point of 2,3-dihydro-5-[(2-hydroxyethyl)thio]-6-methyl-1-phenyl-2-thioxo-4(1*H*)-pyrimidinone (**5**, R′ = phenyl) prepared from **4** (R′ = phenyl) through base-catalysed rearrangement (see below).

Preparation of N-*(Aminothioxomethyl)-5,6-dihydro-2-methyl-1,4-oxathiin-3-carboxamides (4)*

A reaction mixture of 5,6-dihydro-2-methyl-1,4-oxathiin-3-carboxylic acid (0.25 mol), chloroform (50 mL), and thionyl chloride (40 mL) was heated at 50–55°C until dissolved (1 h). Then the solvent and excess thionyl chloride were removed *in vacuo* at 50–60°C, the last traces by alternate addition and removal of toluene. The residual acid chloride which solidified was dissolved in dry acetone (40 mL) and the solution added to a

Can. J. Chem. Downloaded from www.nrcresearchpress.com by 210.87.254.105 on 09/05/12
For personal use only.

cold solution of ammonium thiocyanate (20 g, 0.26 mol) in acetone (100 mL). The resulting reaction mixture was allowed to stand 4 h and then treated portionwise with the amine (0.25 mol) in acetone (25 mL), keeping the temperature at 30–35°C by cooling on a water bath. After allowing the reaction mixture to stand overnight it was poured into cold water. The precipitate was filtered, washed with water, and crystallized from methanol or toluene. N-*[(Phenylamino)thioxomethyl]-5,6-dihydro-2-methyl-1,4-oxathiin-3-carboxamide* (**4**, *R′ = phenyl*), mp 112–113°C, yield, 70%; nmr ($CDCl_3$): 12.50 (1H, s, NH), 9.20 (1H, s, NH), 7.8–7.1 (5H, m, aromatic), 4.40 (2H, m, CH_2O), 2.90 (2H, m, CH_2S), 2.30 (3H, s. CH_3). *Anal.* calcd. for $C_{13}H_{14}N_2O_2S_2$: C 53.06, H 4.80, N 9.52; found: C 53.21, H 4.87, N 9.43. N-*[(2-Pyridylamino)thioxomethyl]-5,6-dihydro-2-methyl-1,4-oxathiin-3-carboxamide* (**4**, *R′ = 2-pyridyl*), mp 143–145°C, yield, 60%; nmr ($CDCl_3$): 12.95 (1H, s, NH), 9.14 (1H, s, NH), 8.75 (1H, d, J = 8 Hz, aromatic), 8.40 (1H, m, aromatic), 7.70 (1H, m, aromatic), 7.10 (1H, m, aromatic), 4.40 (2H, m, CH_2O), 2.92 (2H, m, CH_2S), 2.30 (3H, s, CH_3). *Anal.* calcd. for $C_{12}H_{13}N_3O_2S_2$: C 48.81, H 4.44, N 14.23; found: C 49.02, H 4.48, N 14.23.

Other compounds in this series, for which yields, analyses, and nmr spectra are available from the Depository of Unpublished Data,[2] are **4**, where R′ is in turn H, mp 170–172°C; —$CH(CH_3)_2$, mp 84–86°C; *n*-C_4H_9, mp 70–72°C; *n*-C_6H_{13}, mp 51–52°C; *n*-C_8H_{17}, mp 39–40°C; —$CH_2CH_2C_6H_5$, liquid; —$N(CH_3)_2$, mp 149–150°C; 4-ClC_6H_4—, mp 136–138°C; 4-$CH_3OC_6H_4$—, mp 128–130°C; 2-$CH_3C_6H_4$—, mp 112–114°C; 2-furanylmethyl, mp 101–103°C.

N-*[(4-Morpholinyl)thioxomethyl]-5,6-dihydro-2-methyl-1,4-oxathiin-3- carboxamide* (**6**)

This was prepared from 5,6-dihydro-2-methyl-1,4-oxathiin-3-carbonyl isothiocyanate (**1**) and morpholine by the method described above for **4**, mp 134–135°C, yield, 67%. Nuclear magnetic resonance ($CDCl_3$): 8.30 (1H, s, NH), 4.35 (2H, m, CH_2O), 3.78 (8H, s, $4CH_2$), 2.82 (2H, m, CH_2S), 2.23 (3H, s, CH_3). *Anal.* calcd. for $C_{11}H_{16}N_2O_3S_2$: C 45.83, H 5.60, N 9.72; found: C 46.09, H 5.53, N 9.71.

This compound remained unchanged when stirred in 2% aqueous sodium hydroxide for 24 h.

1-Substituted-2,3-dihydro-5-[(2-hydroxyethyl)thio]-6-methyl-2-thioxo-4(1H)-pyrimidinones (**5**) *from* **4** *by Base-catalysed Rearrangement*

The *N*-(aminothioxomethyl)-5-6-dihydro-2-methyl-1,4-oxathiin-3-carboxamide (**4**) (0.1 mol) was added to 2% aqueous sodium hydroxide (2 L) and the reaction mixture stirred at room temperature for 20 h. The solution was filtered, the filtrate neutralized, and the precipitate filtered, washed with water, dried, and crystallized from alcohol. This gave the rearrangement products in high yields. In the case of **5**, R′ = 1-methylethyl, the rearrangement was not complete so it was heated at 50°C for an additional hour. *1-Phenyl-2,3-dihydro-5-(2-hydroxyethylthio)-6-methyl-2-thioxo-4(1H)-pyrimidinone* (**5**, *R′ = phenyl*), mp 194–195°C, yield, 80%; nmr (DMSO-d_6): 12.80 (1H, m, NH), 7.5–7.1 (5H, m, aromatic), 4.70 (1H, m, OH), 3.50 (2H, m, CH_2O), 2.82 (2H, m, CH_2S), 2.12 (3H, s, CH_3). *Anal.* calcd. for $C_{13}H_{14}N_2O_2S_2$: C 53.06, H 4.80, N 9.52; found: C 53.14, H 4.77, N 9.82. *1-(2-Pyridyl)-2,3-dihydro-5-(2-hydroxyethylthio)-6-methyl-2-thioxo-4(1H)-pyrimidinone* (**5**, *R′ = 2-pyridyl*), mp 226–227°C (dec.), yield, 87%; nmr (DMSO-d_6): 12.90 (1H, m, NH), 8.58 (1H, m, aromatic), 8.0 (1H, m, aromatic), 7.50 (2H, m, aromatic), 4.70 (1H, m, OH), 3.50 (2H, m, CH_2O), 2.83 (2H, m, CH_2S), 2.10 (3H, s, CH_3). *Anal.* calcd. for $C_{12}H_{13}N_3O_2S_2$: C 48.81, H 4.44, N 14.23; found: C 49.14, H 4.48, N 13.97.

Other compounds in this series, for which yields, analyses and nmr spectra are available from the Depository of Unpublished Data,[2] are **5**, where R′ is in turn H, mp 180–182°C (dec.), —$CH(CH_3)_2$, mp 155–157°C; *n*-C_4H_9, mp 115–117°C; *n*-C_6H_{13}, 111–112°C; *n*-C_8H_{17}, mp 102–104°C; —$CH_2CH_2C_6H_5$, mp 156–158°C —$N(CH_3)_2$, mp 143–145°C; 4-ClC_6H_4, mp 228–230°C; 4-$CH_3OC_6H_4$, mp 193–194°C; 2-$CH_3C_6H_4$, mp 202–204°C; 2-furanylmethyl, 134–135°C.

*1,2-Dihydro-5-(5,6-dihydro-2-methyl-1,4-oxathiin-3-yl)-1-phenyl-3*H*-1,2,4-triazole-3-thione* (**9**) *and 2,4-Dihydro-5-(5,6-dihydro-2-methyl-1,4-oxathiin-3-yl)-2-phenyl-3*H*-1,2,4-triazole-3-thione* (**10**)

5,6-Dihydro-2-methyl-1,4-oxathiin-3-carbonyl isothiocyanate (**1**) (0.25 mol) in toluene (200 mL) was treated with a solution of phenylhydrazine (27 g) in toluene (50 mL), while the temperature was maintained at 30–35°C, and then left to stand overnight. The reaction mixture was filtered, washed with toluene, and the combined filtrate and washings were evaporated to "dryness" at reduced pressure. The liquid residue which would not solidify was stirred with 3% aqueous sodium hydroxide (1.5 L) for 20 h, filtered, and then neutralized. The semi-solid precipitate was filtered, washed, dried, and separated into two compounds by fractional precipitation from dilute aqueous sodium hydroxide followed by crystallization from ethanol. The compound which was more soluble in aqueous sodium hydroxide melted at 173–175°C and is tentatively assigned the structure **9**, yield, 6.0 g. Infrared (KBr): 1560 (—C=N—), 760, 690 (aromatic) cm^{-1}; nmr (DMSO-d_6): 7.61 (5H, s, aromatic), 4.35 (2H, m, CH_2O), 3.10 (2H, m, CH_2S), 1.58 (3H, s, CH_3), SH is too broad for reading. *Anal.* calcd. for $C_{13}H_{13}N_3OS_2$: C 53.61, H 4.52, N 14.43; found: C 53.99, H 4.84, N 14.42.

The compound which was less soluble in aqueous sodium hydroxide is tentatively assigned the structure **10**. It melted at 212–214°C, yield, 5.5 g; nmr (DMSO-d_6): 13.75 (1H, m, D_2O exchangeable, SH), 8.10 (2H, m, aromatic), 7.55 (3H, m, aromatic), 4.40 (2H, m, CH_2O), 3.15 (2H, m, CH_2S), 2.07 (3H, s, CH_3). *Anal.* calcd. for $C_{13}H_{13}N_3OS_2$: C 53.61, H 4.52, N 14.43; found: C 53.84, H 4.75, N 14.62.

N,*2-Bis(5,6-dihydro-2-methyl-1,4-oxathiin-3-carbonyl)hydrazinecarbothioamide* (**12**)

5,6-Dihydro-2-methyl-1,4-oxathiin-3-carbonyl isothiocyanate (**1**) (0.125 mol) in warm toluene (120 mL) was treated with a suspension of 5,6-dihydro-2-methyl-1,4-oxathiin-3-carboxylic acid hydrazide (22 g) (2) (**11**) in toluene (120 mL) and 5 drops of triethylamine. After stirring the reaction mixture at room temperature overnight it was cooled, filtered, washed, dried, and crystallized from toluene–methanol, mp 166–168°C, yield 34.2 g (73%); nmr ($CDCl_3$): 13.35 (1H, m, NH), 9.93 (1H, m, NH), 9.12 (1H, s, NH), 4.48 (4H, m, $2CH_2O$), 3.00 (4H, m, $2CH_2S$), 2.33 (6H, s, $2CH_3$). *Anal.* calcd. for $C_{13}H_{17}N_3O_4S_3$: C 41.60, H 4.57, N 11.20; found: C 41.54, H 4.68, N 11.32.

Rearrangement of N,*2-bis(5,6-dihydro-2-methyl-1,4-oxathiin-3-carbonyl)hydrazinecarbothioamide* (**12**) *to 5,6-Dihydro-2-methyl-*N*-[1,2,3,4-tetrahydro-5-[(2-hydroxyethyl)thio]-6-methyl-4-oxo-2-thioxo-1-pyrimidinyl]-1,4-oxathiin-3-carboxamide* (**13**)

N,2-Bis(5,6-dihydro-2-methyl-1,4-oxathiin-3-carbonyl)hydrazinecarbothioamide (**12**) (15 g) was added to 2% aqueous sodium hydroxide (1.2 L) and the reaction mixture stirred overnight. It was then filtered and the cold filtrate acidified. The white precipitate was filtered, washed, dried, and recrystallized from ethanol, mp 203–205°C, yield 12.5 g (83%). Infrared (KBr): 3340 (OH and NH), 1690 (CO), 1660, 1580 (amide) cm^{-1}; nmr (DMSO-d_6): 13.0 (1H, m, NH), 10.70 (1H, m, NH), 4.75 (1H, m,

[2]This information may be obtained, at a nominal charge, from the Depository of Unpublished Data, CISTI, National Research Council of Canada, Ottawa, Ont., Canada K1A 0S2.

OH), 4.35 (2H, m, CH_2O), 3.50 (2H, s, CH_2O), 3.05 (2H, m, CH_2S), 2.80 (2H, m, CH_2S), 2.43 (3H, s, CH_3), 2.15 (3H, s, CH_3). *Anal.* calcd. for $C_{13}H_{17}N_3O_4S_3$: C 41.60, H 4.57, N 11.20; found: C 41.74, H 4.58, N 11.10.

Acknowledgements

Grateful acknowledgement is made to W. R. Boos, Murray Ross, Mary Ann Fitzsimmons, and Helen Van Veggel for providing the analysis and the nmr and ir spectra.

1. (*a*) B. VON SCHMELING and M. KULKA. Science, **152**, 659 (1966); (*b*) B. VON SCHMELING, M. KULKA, D. S. THIARA, and W. A. HARRISON. U.S. patents 3,249,499 (1966); 3,393,202 (1968); 3,399,214 (1968); and 3,402,241 (1968); Canadian patents 787,893 (1968); 791,151 (1968); 824,243 (1970); and 825,665 (1969).
2. M. A. CORBEIL, M. CURCUMELI-RODOSTAMO, R. J. FANNING, B. A. GRAHAM, M. KULKA, and J. B. PIERCE. Can. J. Chem. **51**, 2650 (1973).
3. S. COFFEY, J. K. THOMSON, and F. J. WILSON. J. Chem. Soc. 856 (1936).
4. J. GOERDELER and J. GNAD. Ber. **98**, 1531 (1965).
5. R. POHLOUDEK-FABINI and E. SCHROEPL. Pharm. Zentralhalle, **107**, 736 (1968); Chem. Abstr. **70**, 77870m (1969).

Can. J. Chem. Downloaded from www.nrcresearchpress.com by 210.87.254.105 on 09/05/12
For personal use only.

Ozonolysis of olefins containing monochloro substituted double bonds[1]

HELMUT KEUL AND KARL GRIESBAUM[2]

Engler–Bunte Institut, Bereich Petrochemie, Universität Karlsruhe (T.H.), D-7500 Karlsruhe, W. Germany

Received March 27, 1980

HELMUT KEUL and KARL GRIESBAUM. Can. J. Chem. **58**, 2049 (1980).

Ozone cleavage of 12 substituted vinyl chlorides (**1**) in methanol occurred such that the chlorinated moiety of the double bond afforded the carbonyl fragment (i.e. acyl chloride) and the nonchlorinated moiety afforded the carbonyl oxide fragment. All of these fragments underwent secondary reactions: formyl chloride gave carbon monoxide and hydrogen chloride; all other acyl chlorides yielded the corresponding methyl esters. The carbonyl oxides were converted into the corresponding methoxy hydroperoxides. Under the influence of hydrochloric acid unsubstituted and monosubstituted methoxy hydroperoxides were dehydrated to form the corresponding methyl esters, whereas the disubstituted methoxy hydroperoxide of acetone produced the cyclic trimeric peroxide of acetone.

HELMUT KEUL et KARL GRIESBAUM. Can. J. Chem. **58**, 2049 (1980).

Le clivage par l'ozone dans le méthanol de 12 chlorures vinyliques substitués (**1**) se produit d'une façon telle que la partie chlorée de la double liaison conduit au fragment porteur du groupement carbonyle (i.e. chlorure d'acyle) et la partie non chlorée fournit le fragment porteur de l'oxyde de carbonyle. Tous ces fragments subissent des réactions secondaires: le chlorure de formyle donne le monoxyde de carbone et le chlorure d'hydrogène; tous les autres chlorures d'acyles conduisent aux esters méthyliques correspondants. Les oxydes de carbonyle sont transformés en méthoxy hydroperoxydes monosubstitués correspondants. Sous l'action de l'acide chlorhydrique, les méthoxyhydroperoxydes non substitués et monosubstitués donnent, par déshydratation, les esters méthyliques, alors que le méthoxyhydroperoxyde disubstitué de l'acétone produit le peroxyde cyclique trimère de l'acétone.

[Traduit par le journal]

Introduction

The reaction of ozone with organic compounds containing chloro substituted double bonds attracts increasing attention from the standpoint of ecological chemistry. In recent years, a number of papers have appeared which were concerned with the rate of attack, with the reaction course, and with the reaction products of the ozonolysis of olefins containing 1,2-dichloro substituted double bonds (1–5). By contrast, to our knowledge, there is no systematic investigation of the course and the products of the ozone cleavage of olefins containing monochloro substituted double bonds. On the other hand, however, compounds containing such structural moieties are important chemical products. Their behavior towards ozone may, therefore, have far-reaching consequences, both from the standpoint of stability and from the standpoint of ecology if such compounds are exposed to or emitted to the environment.

In the present paper we report the ozonolysis of 12 model compounds (**1***a*–**1***l*) containing monochloro substituted double bonds. They have been selected such that the double bonds exhibit different types of substitution. From preliminary results it became evident that their ozonolysis in nonparticipating solvents affords very complicated product mixtures, including oligomeric peroxidic materials. Therefore, the ozonolyses were carried out in the participating solvent methanol.

A priori, one might anticipate two sets of primary products upon ozone cleavage of **1**, viz. either fragment pair **2** and **3** formed by route *A* or fragment pair **4** and **5** formed by route *B* in Scheme 1. Of these, the chlorinated fragments **3** and **4** would not be stable under the reaction conditions, but would be converted into the corresponding methyl esters of structure **7** (6),[3] so that they could not be expected to furnish information about the actual mode of cleavage. Fragments **2** and **5**, on the other hand, were expected to be recognizable in the form of the methoxy hydroperoxide **6** and as such, respectively. The ratio of their occurrence could thus provide evidence for the relative importance of routes *A* and *B*.

Results

Substrates **1***a*–*g* and **1***i*–*l* were ozonized in methanol solution at −78°C and they reacted spontaneously with ozone under these conditions. Due to its lower solubility, substrate **1***h* was ozonized in methanol at ambient temperatures. Its reaction with ozone was slow, and some ozone passed the reaction vessel unconsumed.

[1]Presented in part at the annual conference of the Chemical Institute of Canada, Montreal, May 29–June 2, 1977. Preliminary publication in Angew. Chem. **87**, 748 (1975); Angew. Chem. Int. Ed. Engl. **14**, 716 (1975).

[2]Author to whom correspondence should be addressed.

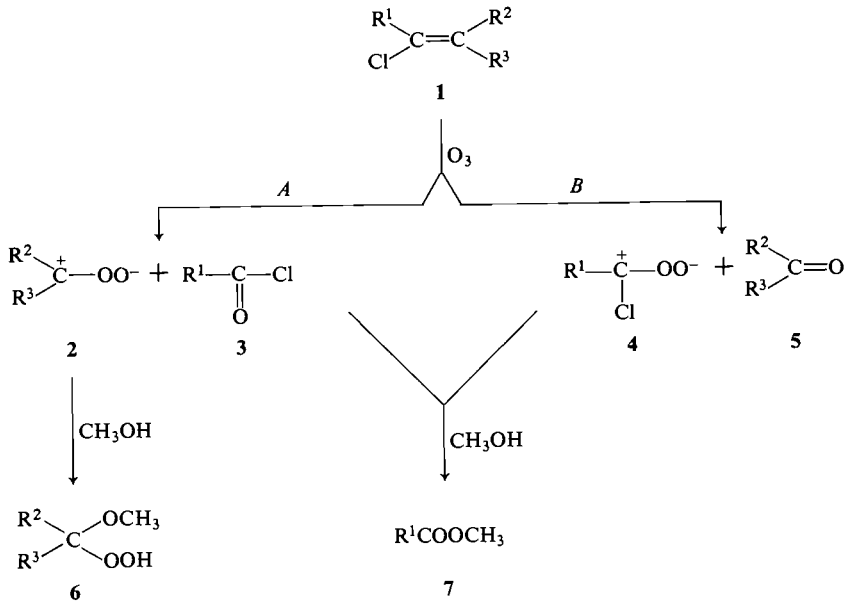
[3]In previous work we have shown that the ozonolysis of olefins containing 1,2-dichloro substituted double bonds in methanol affords ester fragments from each moiety of the double bond. This means that carbonyl oxides of type **4** are converted into esters in the presence of alcohols.

0008-4042/80/192049-06$01.00/0

©1980 National Research Council of Canada/Conseil national de recherches du Canada

Can. J. Chem. Downloaded from www.nrcresearchpress.com by 210.87.254.42 on 09/05/12
For personal use only.

Can. J. Chem. Downloaded from www.nrcresearchpress.com by 210.87.254.42 on 09/05/12
For personal use only.

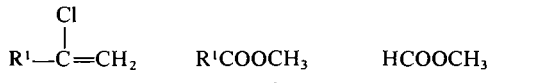


	a	*b*	*c*	*d*	*e*	*f*	*g*	*h*	*i*	*j*	*k*	*l*
R^1	*t*-Bu	CH_3CHCl	$ClCH_2$	C_6H_5	H	H	CH_3	C_6H_5	$(CH_2)_3$	$(CH_2)_4$	CH_3	$CH(CH_2)_3$
R^2	H	H	H	H	Et	C_6H_5	H	H			CH_3	CH_3
R^3	H	H	H	H	H	H	CH_3	C_6H_5	H	H	CH_3	CH_3

SCHEME 1. Possible fragmentation patterns of olefins containing monochloro substituted double bonds.

Immediately after the ozonolysis reaction, all reaction mixtures gave positive peroxide tests. When the cold solutions were allowed to warm up, exothermic reactions occurred as the mixtures had reached approximately room temperature. The intensity of these reactions was different, depending on the structure of the substrates ozonized. The ozonized solutions of the substrates **1***e*, **1***g*, **1***i*, and **1***j* reacted so vigorously that the mixtures came to reflux. After completion of these reactions the peroxide contents of the solutions had disappeared. The ozonized solutions of the substrates **1***a–d* and of substrates **1***f* and **1***h* reacted less vigorously. Their peroxide contents had also decreased but not disappeared after the exothermic reactions had ceased. After prolonged standing at ambient temperatures or heating of the samples to 30–60°C, however, no peroxidic material was left. The ozonized solutions of the trisubstituted substrates **1***k* and **1***l* exhibited only a weak exothermic reaction, and the reaction mixtures remained strongly peroxidic even after prolonged standing at ambient temperatures.

For structural identification of the ozonolysis products, the peroxide free reaction mixtures obtained from the substrates **1***a–j* were analyzed by glc with the help of authentic samples. The quantitative determination of the reaction products was carried out by nmr spectroscopy, using 1,1,1-trichloroethane as a standard. The products from the ozonolysis of **1***d*, **1***f*, **1***h*, **1***i*, and **1***j* were also isolated. The results obtained are given in Table 1. The 2-chloroalkenes of structures **1***a–d* afforded the corresponding methyl esters **8***a–d* in yields of 80–95% and methyl formate (**9**) in yields of 65–80%. The low yields of methyl formate (**9**) may be due to losses owing to its high volatility.



1*a–d* **8***a–d* **9**

The 1-chloroalkenes of structures **1***e* and **1***f* gave the corresponding methyl esters **10***e* and **10***f* in 85% and 75% yield, respectively, but no detectable amounts of methyl formate. In the off-gases from the ozonolysis reactor, carbon monoxide and carbon dioxide were qualitatively detected by glc analysis.

TABLE 1. Ozonolysis of olefins containing monochloro substituted double bonds in methanol

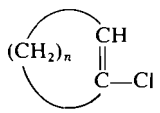
Substrate			Reaction conditions				^{1}H nmr analysis			Reaction products	
Type	mg	mmol	MeOH mL	Temp. °C	Post-treatment °C	h	Standard mg	mmol	δ $COOCH_3$ ppm	Structure	Yield (%)*
1*a*	826	7	8	−78	Room temperature	15	924	7	3.66 3.73	$(CH_3)_3CCOOCH_3$ $HCOOCH_3$	95 80
1*b*	620	5	6.2	−78	Room temperature	15	660	5	3.76 3.73	$CH_3CHClCOOCH_3$ $HCOOCH_3$	91 80
1*c*	1100	10	11	−78	Room temperature	15	1320	10	3.76 3.73	$ClCH_2COOCH_3$ $HCOOCH_3$	80 66
1*d*	690	5	7	−78	30	3	660	5	3.91 3.73	$C_6H_5COOCH_3$ $HCOOCH_3$	95 (85)† 65
1*e*	450	5	4.5	−78	None		660	5	3.66	$CH_3CH_2COOCH_3$	85
1*f*	6900		69	−78	60	3	—	—	—	$C_6H_5COOCH_3$	85†
1*g*	450	5	4.5	−78	None		1320	5	3.63	2 CH_3COOCH_3	95
1*h*	6420		64	R.T.	60	3	—	—	—	$C_6H_5COOCH_3$	64†
1*i*	1020	10	10	−78	None		1320	10	3.65	$CH_3OOC(CH_2)_3COOCH_3$	96 (81)†
1*j*	580	5	5.8	−78	None		660	5	3.65	$CH_3OOC(CH_2)_4COOCH_3$	94 (83)†
1*k*	520	5	5	−78	Room temperature	15	660	5	3.63	$[(CH_3)_2COO]_3$ CH_3COOCH_3	34† 95
1*l*	1440	10	14	−78	Room temperature	15	—	—	—	Not identified	

*Determined by nmr analysis unless mentioned otherwise.
†Yield of isolated product.

$R^2CH{=}CHCl$ R^2COOCH_3

1*e*, **1***f* **10***e*, **10***f*

The acyclic chloroalkenes **1***g* and **1***h* yielded nearly two equivalents of the corresponding methyl ester fragments **11***g* and **11***h*, respectively. The cyclic chloroalkenes **1***i* and **1***j* produced in high yields the corresponding dimethyl esters **12***i* and **12***j*, respectively.

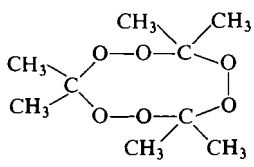
$R(Cl)C{=}CHR$ $RCOOCH_3$ 

1*g*, **1***h* **11***g*, **11***h* **1***i*, **1***j*

$CH_3OOC{-}(CH_2)_n{-}COOCH_3$

12*i*, **12***j*

From the persistently peroxidic reaction mixtures obtained by ozonolysis of **1***k*, the trimeric peroxide of acetone (**13**) precipitated upon prolonged standing. It was isolated in 34% yield. In the mother liquors, methyl acetate (**14**) was detected in approximately 95% by nmr analysis.

$(CH_3)_2C{=}C(Cl)CH_3$  CH_3COOCH_3

1*k* **13** **14**

From the also persistently peroxidic reaction mixture obtained by ozonolysis of **1***l* no products could be identified at this stage of the analysis. The course of the reaction could, however, be elucidated by the trapping experiments discussed in the following section.

Reaction Course

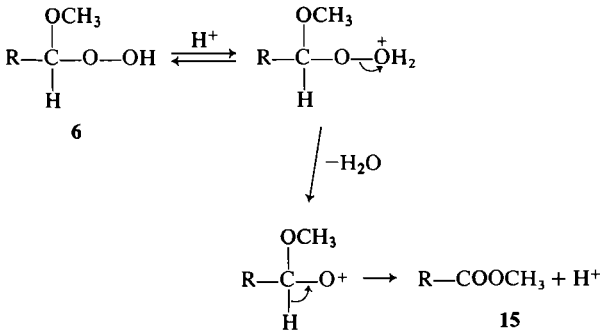
The foregoing results can be readily rationalized by the following sequence of reactions. In the first step the chlorinated double bonds in the substrates **1***a*–*l* are predominantly cleaved so as to form acyl chlorides (**3**) and nonchlorinated carbonyl oxides (**2**), i.e. cleavage occurs by route *A* in Scheme 1. This is in line with the previous experience that in the ozonolysis of unsymmetrically substituted olefins the carbonyl oxide fragment is preferentially formed at the carbon atom which is tied to the least electron deficient substituents (7). Thus, for 1-chloro-2-butene and for 3-chloropropene the ozone cleavage was reported to afford the corresponding nonchlorinated carbonyl oxides in proportions of 89% and 83%, respectively (8).

In secondary steps, substituted acyl chlorides are solvolyzed by methanol to form the corresponding methyl esters (**7**) and hydrogen chloride, formyl chloride is decomposed to carbon monoxide and hydrogen chloride, and the carbonyl oxides (**2**) are trapped by methanol to form the corresponding methoxy hydroperoxides (**6**). In the presence of hydrogen chloride, the latter apparently are not

Can. J. Chem. Downloaded from www.nrcresearchpress.com by 210.87.254.42 on 09/05/12
For personal use only.

stable and undergo further reactions. The rates, the courses, and the results of these further reactions are different, depending on the structure, i.e. the substituents R^2 and R^3, of **6**.

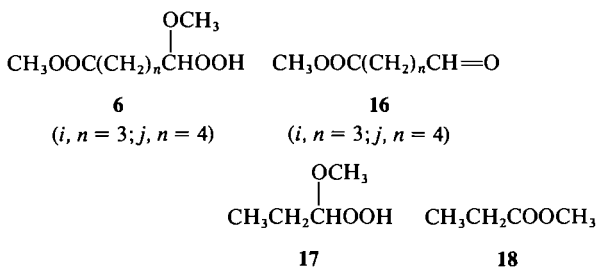
Methoxy hydroperoxides bearing two (**6***a–d*) or at least one hydrogen atom at the central carbon position (**6***e–j*) are converted into the corresponding methyl esters **15**. This conversion occurs probably by acid catalyzed intramolecular dehydration:



The conversion of the unsubstituted (**6***a–d*) and of the phenyl substituted methoxy hydroperoxides (**6***f*, **6***h*) into the corresponding esters (**15**) was rather slow. Hence they could be detected in the reaction mixtures by nmr spectroscopy (δ 4.87 ppm, s, CH_2-group in **6***a–d*; δ 5.70 ppm, s, CH-group in **6***f* or **6***h*). Their gradual conversion into methyl formate and methyl benzoate, respectively, could be also followed by nmr spectroscopy.

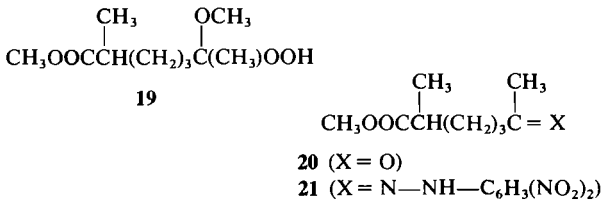
Conversion of the monoalkyl substituted methoxy hydroperoxides (i.e. **6***e*, **6***g*, **6***i*, and **6***j*) into the corresponding esters (**15**) was very fast, as indicated by vigorous exothermic reactions. Nevertheless, the intermediacy of these hydroperoxides as precursors form the esters **15** could be ascertained in some cases and thus rendered likely for the other cases by the following experiments. When the freshly ozonized solutions of 1-chlorocyclopentene (**6***i*) and of 1-chlorocyclohexene (**6***j*) were treated with one equivalent of sodium methoxide in methanol at −78°C, the corresponding methoxy hydroperoxides **6***i* and **6***j* could be preserved. Subsequent reduction of the latter with dimethyl sulfide afforded the corresponding ester-aldehydes **16**. Treatment of **6***j* or of independently prepared **17** with a solution of hydrogen chloride in methanol, on the other hand, produced in good yields dimethyladipate (**12***j*) and methyl propionate (**18**), respectively.

Methoxy hydroperoxides bearing no hydrogen atom at the central carbon position are not converted into esters under the prevailing conditions, i.e. by hydrogen chloride at ambient temperatures. The methoxy hydroperoxide **6***k* is partly converted



into the trimeric peroxide **13**. This was confirmed by treatment of independently prepared, authentic **6***k* with a solution of hydrochloric acid in methanol. It afforded **13** along with other nonidentified products but no detectable amounts of methyl acetate.

The methoxy hydroperoxide **19**, which is formed by ozonolysis of **1***l*, also undergoes secondary reactions under the influence of hydrogen chloride, but none of the products were identified. The formation and existence of **19** itself, however, was definitely established. Treatment of the freshly ozonized mixture with sodium methoxide at −78°C preserved **19**, which was subsequently isolated at room temperature. Its reduction with triphenyl phosphine afforded the expected ketoester **20**, which was characterized as its derivative **21**.



Materials and Methods

Materials

The substrates **1***a* (9), **1***b* (10), **1***c* (11), **1***d* (12), **1***e* (13), **1***f* (14), **1***g* (15), **1***h* (16), **1***i* (17), **1***j* (18), **1***k* (19), and **1***l* (20) were prepared by known procedures. Methanol was of analytical grade and was dried by refluxing over magnesium shavings. Stock solutions of hydrochloric acid in methanol were prepared by introducing gaseous anhydrous hydrogen chloride into methanol at 0°C and titration of these solutions with aqueous sodium hydroxide using phenolphthalein as indicator. Stock solutions of sodium methoxide were prepared by adding the appropriate amount of sodium to anhydrous methanol.

Analytical Methods

Gas–liquid chromatographic analyses were carried out on a Varian model 1440 unit with flame ionization detector; stainless steel columns: 0.3 × 500 cm, 5% Nitrilesiliconoil XE 60 on Chromosorb G. Conditions: 60°C to 160°C at 4°C per min, injection block 200°C, N_2 stream 30 mL/min. Nuclear magnetic resonance spectra were recorded on a Varian model A 60 spectrometer.

General Procedure for the Ozonolysis and for the Analysis of the Reaction Products

Mixtures of the substrates **1** and of methanol in the ratios given in Table 1 were ozonized at the temperatures indicated in Table 1. Ozone treatment was terminated when the solutions

Can. J. Chem. Downloaded from www.nrcresearchpress.com by 210.87.254.42 on 09/05/12
For personal use only.

TABLE 2. Isolation of ester products

Substrate		Methanol	Reaction temperature	Ester products			
					Yield		
Type	g	mL	°C	Structure	g	(%)	Boiling point
1*d*	6.90	69	−78	$C_6H_5COOCH_3$	5.78	(85)	96–98°C/24 Torr
1*f*	6.90	69	−78	$C_6H_5COOCH_3$	5.20	(76)	96–98°C/24 Torr
1*h*	6.42	64	Room temperature	$C_6H_5COOCH_3$	5.22	(64)	98°C/24 Torr
1*i*	5.10	51	−78	$(CH_2)_3(COOCH_3)_2$	6.50	(81)	93°C/10 Torr
1*j*	5.00	50	−78	$(CH_2)_4(COOCH_3)_2$	6.20	(83)	110°C/13 Torr

assumed a blue color. Excess ozone was removed by a stream of nitrogen and a sample of the cold crude reaction mixture was tested for its peroxide content by its reaction with sodium iodide. The ozonolysis products of all substrates (**1***a–l*) gave positive peroxide tests. Then the crude reaction mixtures were allowed to warm up. When they had reached temperatures between 0°C and room temperature, exothermic reactions set in.

For the products derived from ozonolysis of **1***e*, **1***g*, **1***i*, and **1***j* these reactions were so vigorous that intermittent cooling was necessary. When the reaction had ceased, the solutions were free of peroxide. The final products were identified by glc analysis by coinjection with authentic samples. Quantitative determination of the products occurred by nmr spectroscopy; 1,1,1-trichloroethane was added to the mixture in amounts equivalent to the substrate used (Table 1) and the esters were determined on the basis of their CH_3O-signals.

The products derived from ozonolysis of **1***a–d*, **1***f*, and **1***h* reacted less vigorously and no cooling was necessary. The mixtures remained peroxidic after the exothermic reaction had terminated. Equivalent amounts of 1,1,1-trichloroethane was added (Table 1) and the mixtures were analyzed by nmr. In the ozonolysis products of **1***a–d* the singlet CH_2-signal of the corresponding methoxy hydroperoxide (**6***a*) appeared at 4.87 ppm. In the ozonolysis products of **1***f* and of **1***h* the singlet CH-signal of the corresponding methoxy hydroperoxide (**6***f*) appeared at δ 5.70 ppm. Upon standing for approximately 15 h at room temperature or after warming to 30°C for approximately 3 h, the peroxide contents of all samples and the signals at 4.87 ppm and 5.70 ppm, respectively, had disappeared. The glc and nmr analyses showed only the peaks and signals, respectively, of the corresponding ester fragments. Their yields were again determined on the basis of the CH_3O-signals of the methyl ester groups with the help of 1,1,1-trichloroethane as a standard (Table 1).

The products derived from the ozonolysis of **1***k* and of **1***l* gave only weak exothermic reactions and they remained strongly peroxidic. From the ozonolysis product of **1***k*, solid **13** had precipitated after the mixture was left at room temperature for 15 h. The solid was filtered off, washed with methanol, and dried; yield 148 mg (34%); mp 96–97°C (lit. (21) mp 96–97°C). To the mother liquor 1,1,1-trichloroethane was added in amounts equivalent to the substrate **1***k* used (Table 1), and the mixture was analyzed by nmr spectroscopy. The amount of methyl acetate was quantitatively determined on the basis of its CH_3O-signal (Table 1); other signals in the spectrum were not assigned. The reaction products obtained from the ozonolysis of **1***l* could not be identified on the basis of the nmr spectrum of the crude reaction mixture.

General Procedure for the Ozonolysis and Subsequent Isolation of Ester Products

Mixtures of the substrates **1***d*, **1***f*, **1***h*, **1***i*, or **1***j* and methanol were ozonized in the ratio and at the temperatures listed in Table 2. The end of the ozonolysis was indicated by the appearance of a blue color if the ozonolysis was carried out at −78°C; it was detected by the disappearance of the substrate by glc analysis if the ozonolysis was carried out at room temperature. The reaction mixtures were flushed with nitrogen and then allowed to warm up, whereby exothermic reactions occurred. When they had ceased, the mixtures were heated to 60°C for 3 h and then the methanol was distilled off. The residue was dissolved in ether, sequentially washed with a 10% aqueous solution of sodium hydroxide and with water, and dried over sodium sulfate. After removal of ether, the residue was submitted to a vacuum distillation. The results are summarized in Table 2. The glc and nmr analyses of the distilled products showed in each case no detectable amounts of impurities.

*Identification of Methoxy Hydroperoxides **6**i, **6**j, and **19** as Reaction Intermediates*

*Identification of **6**i*

A mixture of 1.02 g (10 mmol) **1***i* and 10 mL methanol was ozonized at −78°C until the solution turned blue. Excess ozone was removed by a stream of nitrogen and 2.3 mL of a precooled 10% solution of sodium methoxide in methanol was immediately added to the cold reaction mixture. The mixture was allowed to warm up to room temperature and the precipitated sodium chloride was removed. To the peroxidic mother liquor 1.24 g (20 mmol) of dimethyl sulfide was added and the mixture was left standing for 1 h. Then the volatile components were removed under vacuum on a rotary evaporator. The residual aldehyde-ester **16***i* was converted into its 2,4-dinitrophenylhydrazone derivative; mp (recrystallized from cyclohexane) 105–106°C (lit. (22) mp 105–106°C); yield 1.7 g (55%); ^1H nmr ($CDCl_3$, TMS) δ: 1.83–2.25 (broad signal, 2H), 2.33–2.73 (broad signal, 4H), 3.70 (s, 3H), 7.60 (t, J = 4.5 Hz, 1H), 7.91 (d, J = 9.5 Hz, 1H), 8.4 (dd, J = 9.5 Hz, J = 2.4 Hz, 1H), 9.11 (d, J = 2.4 Hz, 1H), 11.05 (broad signal, 1H).

*Identification of **6**j*

A mixture of 580 mg (5 mmol) **1***j* in 5.8 mL methanol was ozonized, subsequently treated with sodium methoxide (1.15 mL of a 10% solution in methanol) and with 0.62 g (10 mmol) dimethylsulfide, and then worked up as described above. The residual aldehyde-ester **16***j* was converted into its 2,4-dinitrophenylhydrazone derivative: mp (recrystallized from cyclohexane) 104–105°C (lit. (23) mp 104–105°C); yield 0.8 g (50%). ^1H nmr ($CDCl_3$, TMS) δ: 1.57–1.90 (broad signal, 4H), 2.27–2.67 (broad signal, 4H), 3.69 (s, 3H), 7.54 (t, J = 5.2 Hz, 1H), 7.91 (d, J = 9.5 Hz, 1H), 8.40 (dd, J = 9.5 Hz, J = 2.56 Hz, 1H), 9.11 (d, J = 2.56 Hz, 1H), 11.05 (broad signal, 1H).

*Identification of **19***

A mixture of 720 mg (5 mmol) **1***l* and 7.2 mL methanol was ozonized, subsequently treated with sodium methoxide (1.15 mL of a 10% solution in methanol), and warmed up to room temperature. After removal of the sodium chloride, methanol was removed under vacuum on a rotary evaporator. The residue was dissolved in ether, washed with water, dried over

Can. J. Chem. Downloaded from www.nrcresearchpress.com by 210.87.254.42 on 09/05/12
For personal use only.

Can. J. Chem. Downloaded from www.nrcresearchpress.com by 210.87.254.42 on 09/05/12
For personal use only.

sodium sulfate, and the ether distilled off. The residue was 1 g (91%) of essentially pure methoxy hydroperoxide **19**; ^{1}H nmr (CCl_4, TMS) δ: 1.15 (d, J = 7.0 Hz, 3H), 1.32 (s, 3H), 1.40–1.78 (broad signal, 6H), 2.45 (m, 1H), 3.32 (s, 3H), 3.68 (s, 3H).

A solution of 1 g (4.5 mmol) of **19** and 1.44 g (5.5 mmol) of triphenyl phosphine in 10 mL of hexane was refluxed for 1 h. Then the mixture was separated by preparative thin layer chromatography (silica gel, dichloromethane) to give **20**; ^{1}H nmr (CCl_4, TMS) δ: 1.08 (d, J = 7.0 Hz, 3H), 1.33–1.63 (broad signal, 4H), 2.00 (s, 3H), 2.20–2.50 (broad signal, 3H), 3.60 (s, 3H).

The keto-ester **20** was converted into its 2,4-dinitrophenylhydrazone (**21**). Melting point (recrystallized from cyclohexane) 89–90°C; ^{1}H nmr ($CDCl_3$, TMS) δ: 1.19 (d, J = 6.96 Hz, 3H), 1.47–1.83 (broad signal, 4H), 2.07 (s, 3H), 2.27–2.70 (broad signal, 3H), 3.69 (s, 3H), 7.94 (d, J = 9.5 Hz, 1H), 8.40 (dd, J = 9.5 Hz, J = 2.56 Hz, 1H), 11.04 (broad signal, 1H). *Anal.* calcd. for $C_{15}H_{20}N_4O_6$: C 51.13, H 5.72, N 15.90; found: C 51.13, H 5.71, N 15.94.

Treatment of Methoxy Hydroperoxides **6***j*, *17, and* **6***k with Hydrochloric Acid*

Treatment of **6***j*

A mixture of 580 mg (5 mmol) **1***j* in 5.8 mL methanol was ozonized at −78°C and treated with sodium methoxide (1.15 mL of a 10% solution in methanol) as described above. After warming to room temperature and removal of methanol on a rotary evaporator, the crude methoxy hydroperoxide **6***j* is obtained as residue; ^{1}H nmr ($CDCl_3$, TMS) δ: 3.50 (s, 3H), 3.68 (s, 3H), 4.72 (t, J = 5.0 Hz, 1H). To this crude **6***j* 5 mL of a 1 N solution of hydrogen chloride in methanol was added at room temperature. A vigorous exothermic reaction ensued. After it had ceased, the mixture was analyzed by glc and by nmr spectroscopy. Dimethyl adipate was the only product detected.

Treatment of **17**

To a mixture of 1.06 g (10 mmol) **17** (24) in 1 mL of methanol was added 10 mL of a 1 *N* solution of hydrogen chloride in methanol. To avoid losses during the exothermic reaction, the mixture was cooled with ice water and then left standing for 3 h at room temperature. After addition of 1.32 g (10 mmol) of 1,1,1-trichloroethane, nmr analysis showed the presence of 90% of methyl propionate (**18**).

Treatment of **6***k*

To a mixture of 1.06 g (10 mmol) **6***k* (25) in 1 mL of methanol was added 10 mL of a 1 *N* solution of hydrogen chloride in methanol. After standing overnight, crystalline **13** had precipitated and was collected by filtration; yield 260 mg (30%); mp 96–97°C; mixture mp with an authentic sample (21) showed no depression; ^{1}H nmr ($CDCl_3$, TMS) δ: 1.45 (s). Nuclear magnetic resonance analysis of the mother liquor showed as the major component additional **13**, along with signals of unidentified components; however, no methyl acetate was detected.

1. D. G. Williamson and R. J. Cvetanović. J. Am. Chem. Soc. **90**, 4248 (1968).
2. K. Griesbaum and P. Hofmann. J. Am. Chem. Soc. **98**, 2877 (1976).
3. C. W. Blume, I. C. Hisatsune, and J. Heicklen. Int. J. Chem. Kinet. **8**, 235 (1976).
4. S. Schulte-Hostede, S. Gäb, and F. Korte. Chem. Ber. **111**, 2646 (1978).
5. S. Gäb, S. Nitz, H. Parlar, and F. Korte. Chem. Ber. **111**, 1440 (1978).
6. G. Nagendrappa and K. Griesbaum. J. Agric. Food Chem. **26**, 581 (1978).
7. P. S. Bailey. Ozonation in organic chemistry. Vol. I (appeared as Vol. 39 in the series Organic chemistry). Academic Press, New York, NY. 1978. pp. 119–129.
8. S. Fliszár and M. Granger. J. Am. Chem. Soc. **92**, 3361 (1970).
9. P. D. Bartlett and L. J. Rosen. J. Am. Chem. Soc. **64**, 544 (1942).
10. D. V. Tischtschenko. Zh. Obshch. Khim. **8**, 1242 (1938).
11. A. L. Henne and F. W. Haeckel. J. Am. Chem. Soc. **63**, 2692 (1941).
12. Ch. Dufraisse and J. E. Viel. Bull. Soc. Chim. Fr. **37**, 874 (1928).
13. A. L. Henne and J. B. Hinkamp. J. Am. Chem. Soc. **67**, 1197 (1945).
14. C. Forrer. Ber. **17**, 983 (1884).
15. A. L. Henne and J. B. Hinkamp. J. Am. Chem. Soc. **67**, 1194 (1945).
16. J. J. Sudborough. J. Chem. Soc. **71**, 220 (1897).
17. E. A. Braude and W. F. Forbes. J. Chem. Soc. 1755 (1951).
18. E. A. Braude and J. A. Coles. J. Chem. Soc. 2014 (1950).
19. A. A. Béhal. Ann. Chim. **15**, 284 (1888).
20. H. Kwart and D. M. Hoffman. J. Org. Chem. **31**, 419 (1966).
21. A. Baeyer and V. Villiger. Ber. **33**, 859 (1900).
22. S. D. Mikhao, V. M. Berezovskii, and N. A. Preobrazhenskii. Zh. Obshch. Khim. **32**, 2829 (1962); Chem. Abstr. **58**, 8897e (1963).
23. H. A. Staab and H. Bräunling. Justus Liebigs Ann. Chem. **654**, 119 (1962).
24. J. Renard and S. Fliszár. Can. J. Chem. **47**, 3333 (1969).
25. R. Criegee. *In* Methoden der organischen Chemie. Vol. III/8. 4th ed. Houben Weyl. Georg Thieme Verlag, Stuttgart. 1952. p. 32.

Nickel(II)-binding to the NH_2-terminal peptide segment of human serum albumin: ^{13}C- and ^1H-nuclear magnetic resonance investigation

JEAN-PIERRE LAUSSAC[1] AND BIBUDHENDRA SARKAR[2]

The Research Institute, The Hospital for Sick Children, Toronto, Ont., Canada M5G 1X8 and the Department of Biochemistry, University of Toronto, Toronto, Ont., Canada M5S 1A8

Received February 29, 1980

JEAN-PIERRE LAUSSAC and BIBUDHENDRA SARKAR. Can. J. Chem. **58**, 2055 (1980).

Recent studies have shown that Ni(II) in human blood serum is bound to albumin and the binding site is located at the NH_2-terminus of the protein. In this article, the nature of the Ni(II)-binding site of the NH_2-terminal tripeptide segment of human albumin: L-aspartyl-L-alanyl-L-histidine-*N*-methyl amide (AAHNMA) is reported as deduced by ^{13}C- and ^1H-nmr spectroscopy. The ^{13}C spectrum shows that the Ni(II) complex is in slow exchange on the nmr time scale, and resonances for Ni(II)–peptide complex and metal-free peptide are observed clearly in the pH range 6.4 to 9.1. The Asp COO^- carbon is most affected by Ni(II) binding. The imidazole ring system also shows large variation. Furthermore, the results implicate the involvement of the NH_2 group. The introduction of Ni(II) ion into the solution containing peptide causes profound changes in the ^1H-nmr spectra in the pH range 6.4 to 9.1. Most significantly, there is a complete disappearance of Ala and His N—H protons which confirm the coordination of these two peptide nitrogens. The measurement of the ^{13}C spin–lattice relaxation times (T_1) for AAHNMA and its 1/1 complex provide confirmatory evidence for the existence of a definite complex. The overall results suggest that Ni(II) forms complex with the NH_2-terminal peptide of human albumin involving the α-NH_2, N(3) imidazole, two deprotonated peptide nitrogens, and Asp COO^- group in a pentacoordinated structure.

JEAN-PIERRE LAUSSAC et BIBUDHENDRA SARKAR. Can. J. Chem. **58**, 2055 (1980).

Des études récentes ont montré que, dans le sérum humain, le Ni(II) se lie à l'albumine; cette protéine présente un site de fixation fort qui a été identifié comme étant le site NH_2-terminal. Nous avons étudié la complexation par spectroscopie de rmn des noyaux ^{13}C et ^1H, du Ni(II) avec le fragment tripeptidique NH_2-terminal de la serumalbumine: L-Asp-L-Ala-L-His-*N*-methyl amide (AAHNMA). Dans l'intervalle de pH 6,4 à 9,1, nous observons en ^{13}C que le système est en échange lent. Le carbone AspCOO^- est le plus affecté à la complexation; de la même façon, les carbones du cycle imidazole montrent un important déplacement chimique. Ces résultats sont confirmés par les spectres en résonance du proton qui, dans le même intervalle de pH, montrent de larges variations. Dans le DMSO-d_6, il est intéressant de constater la disparition des protons amides Ala et His N—H qui confirme la coordination de ces deux azotes. Les mesures du temps de relaxation spin–réseau (T_1) en résonance du ^{13}C sur le peptide libre et complexé sont également discutées et confirment les résultats obtenus en ^{13}C et ^1H (δ). L'ensemble de ces données montrent que le nickel se trouve dans un environnement pentacoordonné, les sites de complexation étant le α-NH_2, le N(3) imidazole, les deux azotes peptidiques et le groupement carboxyl AspCOO^-.

Introduction

Metal toxicity caused by environmental pollution or occupational exposure in industry is of great concern around the world. Studies have revealed an association between Ni(II) exposure and nasal carcinoma (1, 2). An investigation of workers at a nickel refinery in Norway found that the degree of epithelial keratinization was more pronounced in the Ni(II) exposed group than in the controls (3). It has been observed that there is a high level of Ni(II) in the blood of healthy individuals in a mining town in North America (4). Very little is known, however, about how this metal is handled by the body or transported.

In our continuing investigation of the biological transport of metals and their toxic effects in humans (5–8), we have recently found that Ni(II) in human blood serum is bound to albumin and to L-histidine (9). From previous reports it appears that the Ni(II)-binding site of human albumin is located at the NH_2-terminus of the protein (10) but the structure of the binding site remains unknown. The synthesis of the NH_2-terminal tripeptide segment of human albumin: L-aspartyl-L-alanyl-L-histidine-*N*-methyl amide in this laboratory (11) has made it possible to investigate the Ni(II)-binding to human albumin in detail.

Nuclear magnetic resonance (nmr) spectroscopy is a well-established method for studying the structure of metal–ligand complexes. The measurable quantities such as chemical shifts, spin–spin coupling constants, and nuclear relaxation times can provide direct information on molecular dynamics and structure. In this article we report the structure of the Ni(II)-binding site of the peptide fragment representing the NH_2-terminus sequence of human albumin as deduced by ^{13}C- and ^1H-nmr spectroscopy.

Experimental Section

The tripeptide, L-aspartyl-L-alanyl-L-histidine-*N*-methyl amide (AAHNMA) was synthesized according to the procedure described earlier (11). D_2O from Merck, Sharp and Dohme, Canada, was used as a solvent. Stock solutions of $NiCl_2$ (Fisher

[1]Present address: Laboratoire de Chimie de Coordination, CNRS, 205 Route de Narbonne, 31400 Toulouse, France.

[2]To whom all correspondence should be addressed.

0008-4042/80/192055-06$01.00/0

©1980 National Research Council of Canada/Conseil national de recherches du Canada

Can. J. Chem. Downloaded from www.nrcresearchpress.com by 210.87.254.40 on 09/05/12
For personal use only.

TABLE 1. ^{13}C-nmr data for AAHNMA and Ni(II)–AAHNMA in D_2O at different pH values

	^{13}C-nmr at pH =							
	6.4		7.0		8.0		9.1	
Carbon	Free	1/1	Free	1/1	Free	1/1	Free	1/1
Asp COO^-	178.48	189.44	178.90	189.38	180.22	189.39	181.06	189.38
Ala CO	177.03	182.02	177.03	181.82	177.32	181.74	177.52	181.63
His CO	174.77	177.33	175.25	177.27	175.64	177.28	175.74	177.30
Asp CO	172.49	Broad	173.75	180.49	175.64	180.53	179.44	180.77
C(2)	136.80	138.84	137.73	138.78	138.33	138.78	138.46	138.93
C(4)	132.49	135.62	134.10	135.61	135.01	135.61	135.26	135.60
C(5)	119.66	117.10	119.60	117.03	129.70	117.05	119.75	117.30
His Cα	55.68	58.63	56.08	58.57	56.33	58.56	56.34	58.55
Asp Cα	53.10	Broad	53.34	59.31	54.05	59.51	54.47	59.16
Ala Cα	52.39	54.68	52.33	54.65	52.44	54.66	52.46	54.74
Asp Cβ	39.76	Broad	40.64	Broad	42.99	42.60	44.48	42.75
His Cβ	29.46	31.76	30.35	31.69	30.77	31.68	30.84	31.73
NH CH_3	28.37	28.43	28.27	28.33	28.31	28.33	28.33	28.33
Ala CH_3	18.74	20.95	18.69	20.85	18.68	20.83	18.67	20.80

TABLE 2. ^{1}H-nmr data for AAHNMA and Ni(II)-AAHNMA in D_2O at different pH values

	^{1}H-nmr at pH =							
	6.4		7.0		8.0		9.1	
Hydrogen	Free	1/1	Free	1/1	Free	1/1	Free	1/1
C(2)H	8.39	7.55	8.01	7.55	7.81	7.54	7.77	7.55
C(5)H	7.28	6.95	7.10	6.95	7.05	6.95	7.03	6.95
His CHα	4.63	4.05	4.57	4.04	4.55	4.04	4.55	4.05
Ala CHα	4.38	3.71	4.34	3.71	4.31	3.71	4.27	3.71
Asp CHα	4.26	3.63	4.17	3.63	3.91	3.63	3.72	3.62
His CH_2	3.22	3.00	3.14	3.00	3.11	3.00	3.11	3.00
Asp CH_2	2.83	2.53	2.77	2.53	2.63	2.53	2.54	2.53
NH CH_3	2.76	2.61	2.74	2.61	2.72	2.61	2.74	2.61
Ala CH_3	1.37	1.30	1.34	1.30	1.31	1.28	1.30	1.29

complex is in slow exchange on the nmr time scale, and resonances for Ni(II)–peptide complex and metal-free peptide are observed clearly in the pH range 6.4 to 9.1.[3] Since the system is in slow exchange, it is possible to unequivocally assign the carbon resonances for the Ni(II) complex. The method used for the assignment of the proton bearing carbon resonances was specific irradiation of the directly bonded ^{1}H resonances; in the same way carboxyl and carbonyl carbons are assigned by off-resonance techniques. The individual chemical shifts ($\Delta = \delta_{1/1\ \text{complex}} - \delta_{\text{free peptide}}$) for all carbons are shown in Fig. 2. All the carbons are shifted downfield except the C(5) imidazole which is shifted upfield. The Asp Cβ shows a downfield shift at low pH but at pH 9.1 it is shifted upfield. The Asp COO^- carbon is affected most of all by Ni(II) binding ($\Delta = 8.32$ ppm at pH = 9.1), which is consistent with carboxylate–Ni(II) coordination. The imidazole ring system also shows large variation, for example, $\Delta = -2.45$ ppm for the C(5) carbon. The Ala Cβ carbon is also affected (not the His-$NHCH_3$), but here the shift must be due largely to conformational effects. Indeed, the CPK space-filling model building indicates that the Ala Cβ is near the carboxylate group. The amino titration ($pK = 7.73$) affects the Asp CO more strongly than Asp COO^- and the β carbon more strongly than the nearest α carbon. But upon complexation, the Ni(II)-binding to the NH_2-terminal and COO^-

[3]Species analysis of the Ni(II)–AAHNMA system in 0.15 *M* NaCl, 25°C shows the presence of four complex species MA ($\log \beta_{101} = 5.50$), MA_2 ($\log \beta_{102} = 11.56$), $MH_{-1}A_2$ ($\log \beta_{1-12} = 4.75$), and $MH_{-2}A$ ($\log \beta_{1-21} = -5.94$) in the pH range 5.0–10.0. At pH 9, $MH_{-2}A$ is the only complex species present in the system. The spectrum of this species is that of typical diamagnetic Ni(II) complex. Results of the magnetic moment measurements are consistent with a diamagnetic system (34).

Can. J. Chem. Downloaded from www.nrcresearchpress.com by 210.87.254.40 on 09/05/12
For personal use only.

Can. J. Chem. Downloaded from www.nrcresearchpress.com by 210.87.254.40 on 09/05/12
For personal use only.

Scientific Company) were prepared and calibrated titrimetrically. Nickel(II) was added with a Hamilton microliter syringe from a stock solution to obtain appropriate [AAHNMA]/[Ni(II)] ratios. The pH was varied by adding NaOD or DCl to the solution. All quoted pH values have meter readings which are uncorrected for D_2O solutions. It was assumed that pD and pH values of this solution were not significantly different for the interpretation of the results (12).

Carbon-13 spectra were recorded at 25.2 MHz on a Varian XL-100-15-NMR spectrometer operating in the pulse-Fourier transform mode. Probe temperature, under proton decoupled conditions, was 32 ± 3°C. All chemical shifts were reported in ppm downfield from internal DSS. The deuterium resonance of the solvent D_2O was used for the lock signal and the concentration of the solution was 0.1 *M*.

Spin–lattice relaxation time (T_1 in s) measurements were performed by the inversion recovery method (13) by the use of the $(180°-\tau-90°-T)_n$ pulse sequence method where τ is a variable delay time, T is at least five times longer than the longest T_1 to be measured. The value of the spin–lattice relaxation time is given by using semi-logarithmic plot:

$$A = A_\infty[1 - 2\exp(-\tau/T_1)]$$

where A is the observed intensity and A_∞ is the equilibrium intensity. The nmr spectra were generally obtained for 10 different τ values and T_1 was calculated from the slopes of a plot of $\ln|A_\infty - A|$ vs. τ. Samples with a volume of 1.5 mL (0.3 *M*) were prepared in 12-mm nmr tubes and were degassed five times using the freeze–pump–thaw technique. The accuracy of T_1 values was ±10%.

Nuclear Overhauser enhancement (nOe) was measured by comparing the integrated intensities of the ^{13}C resonances in proton noise-decoupled spectra and coupled spectra. The proton-bearing α, β, and imidazole carbons yielded enhancement of 2.8 ± 0.1.

The proton magnetic resonance studies were performed on a Varian HR.220 FT NMR spectrometer. Chemical shifts were reported in ppm downfield from internal DSS. Samples run in D_2O or in DMSO-d_6 were replaced in 5-mm tubes and the spectrometer locked directly on the solvent resonance.

Results and Discussion

^{13}C- and ^1H-Nuclear Magnetic Resonance Studies of Free Peptide

Carbon-13 and proton nmr results of free peptide are shown at various pH values in Tables 1 and 2. Assignments were made with homonuclear decoupling experiments, spectra of free amino acids, and analysis of pH dependent resonances. The assignments are also consistent with some of the results reported recently on the ^{13}C-nmr spectra of the peptide (14).

pH Studies

There are some important aspects of the results with ^{13}C chemical shift titration:

1. All the carbon resonances are affected except the methyl carbons, Ala Cα, and C(5) where no significant change in chemical shift is observed from pH 6.4 to 9.1.

2. The shifts are downfield with increasing pH. The phenomenon of downfield shifts with deprotonation for ^{13}C resonances has been previously noted (15, 16).

3. The amino titration affects the Asp CO more strongly than Asp COO^- and the β carbon more strongly than the nearby α carbon (pK_a = 7.73). The titration of imidazole group (pK_a = 6.55) affects the quaternary C(4) resonance far more than those of the C(2) and C(5). This has been explained by predominance of N(1)H tautomer form (17, 18). The invariability of the C(5) chemical shift suggests that the N(1)H form remains predominant, but the charge redistribution in the imidazole ring has probably been modified by an intramolecular interaction (*vide infra*) (19).

Proton nmr spectra also show changes in the chemical shifts as a result of deprotonating the imidazole ring of His and Asp—NH_2 terminal, all resonances being shifted upfield with increasing pH (20). This opposite phenomenon, compared to those of ^{13}C resonances which show only downfield shifts with deprotonation, has been explained by several authors (17, 21). In accordance with the data on histidine residues, the lower field resonance which exhibits the greater pH shift is identified with the C(2)H proton, and the upper field resonance with the C(5)H hydrogen. C(2)H is the most affected (0.62 ppm) of all protons. It is known that the proton resonances of the imidazole residue are sensitive to pH changes. The amino titration affects more strongly the Asp α (0.54 ppm) than the Asp β (0.29 ppm).

Interestingly, the changes in pH do not cause any large changes in the vicinal coupling constants, indicating that protonation or deprotonation occurs without major alterations in rotamer populations around the bonds.

Spectra in DMSO-d_6

The use of DMSO-d_6 as a solvent for ^1H-nmr studies allows direct observation of the exchangeable protons. These protons have all been assigned by homonuclear spin decoupling of the CH and CH_3 resonances. Double resonance experiments demonstrate that the two doublets at δ 8.93 ppm ($^3J_{NH-\alpha CH}$ = 5.9 Hz) and δ 8.35 ppm ($^3J_{NH-\alpha CH}$ = 8.2 Hz) originate from the NH groups of the alanine and histidine residues. Decoupling also identifies the quadruplet at δ 7.85 ppm ($^3J_{NH-\alpha CH_3}$ = 4.5 Hz) with the NH of CH_3—NH. The resonance from the imidazole N(1)H can be accounted at δ 11.95 ppm.

^{13}C- and ^1H-Nuclear Magnetic Resonance Studies of Nickel(II)–Peptide Complex

^{13}C-Nuclear Magnetic Resonance Studies

The ^{13}C spectrum (Fig. 1) shows that the Ni(II)

Can. J. Chem. Downloaded from www.nrcresearchpress.com by 210.87.254.40 on 09/05/12
For personal use only.

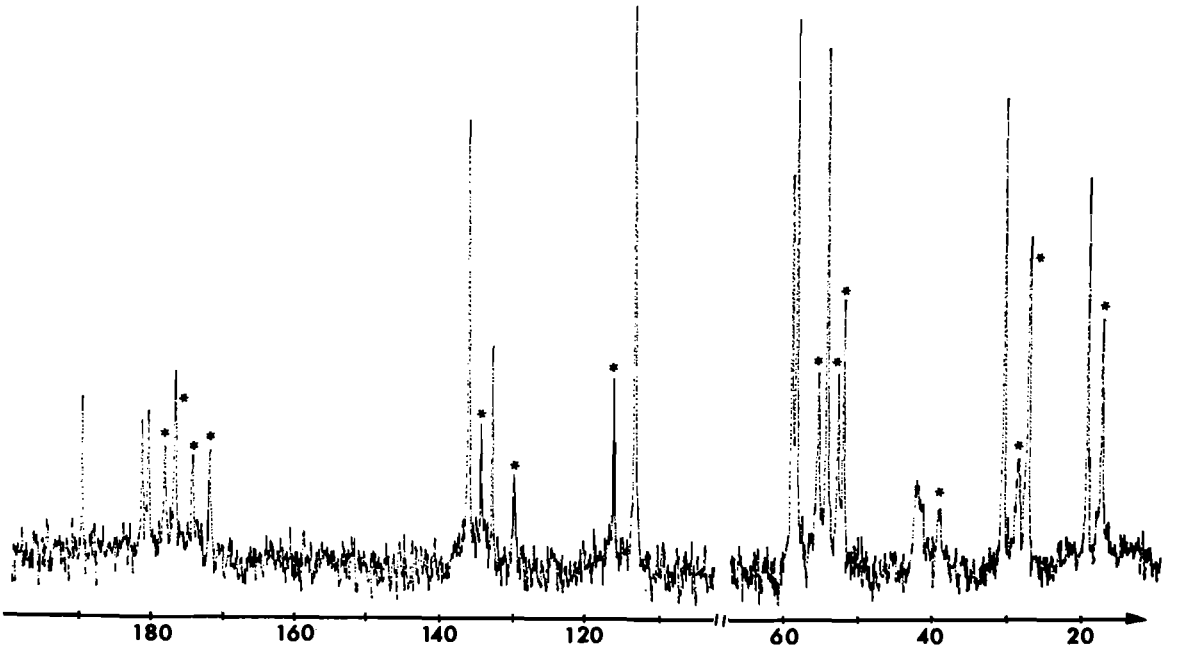


FIG. 1. ^{13}C-nmr spectrum of AAHNMA:Ni(II) (3/2) in D_2O at pH 7.0. Peak with * is free peptide; peak without *is Ni(II)–peptide complex.

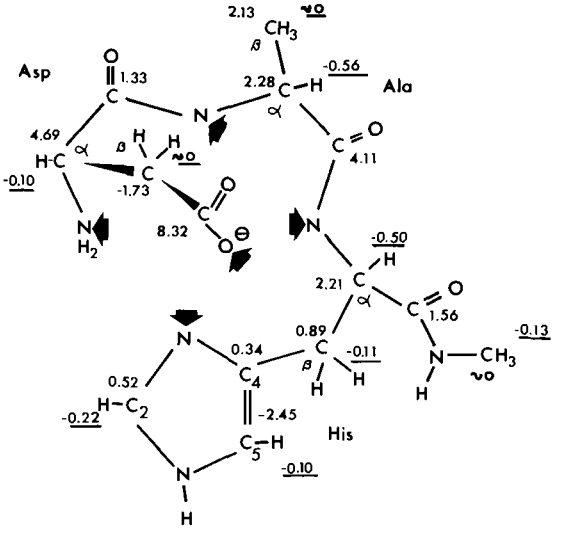


FIG. 2. Chemical shift ($\Delta = \delta_{1/1\ \text{complex}} - \delta_{\text{free peptide}}$) for the 1/1 AAHNMA–Ni(II) complex in D_2O at pH 9.1. Underlined numbers represent ^{1}H values and numbers without underline shows ^{13}C values in ppm. Arrows are directed toward the proposed site of Ni(II)-binding to the peptide.

group affects the α carbon (4.69 ppm) more strongly while in the case of β carbon, we observe a shielding effect (−1.73 ppm) at pH 9.1.

^{1}H-Nuclear Magnetic Resonance Studies

The introduction of Ni(II) ion into the solution containing peptide causes profound changes in the ^{1}H-nmr spectra in the pH range 6.4 to 9.1 in 1/1 Ni(II):AAHNMA solution. There are overall upfield chemical shifts for all protons. The same phenomenon has been observed for different Ni(II) complexes with peptides (22, 23). Many upfield chemical shifts are observed for imidazole residues C(2)H (0.22 ppm), C(5)H (0.10 ppm), and also the CHα protons (Asp α (0.10 ppm), Ala α (0.56 ppm), His α (0.50 ppm)) all at pH 9.1. For all groups which are affected by titration, the upfield chemical shifts are more pronounced in case of complexation (Asp $CH_2\beta$, Asp CHα, C(2)H, and C(5)H) than deprotonation at pH 9.1. It appears that the pronounced upfield shifts induced by diamagnetic nickel ion result from the diamagnetic metal ion and not from the ligand involved. Most significantly, in DMSO-d_6 solution containing Ni(II)—AAHNMA, there is a complete disappearance of Ala and His N—H protons, which confirms the coordination of these two peptide nitrogens. It is known that the metal ion promotes the ionization of peptide protons with subsequent binding to the negatively charged nitrogen atom (24, 25).

Studies of Spin–Lattice Relaxation Times

The ^{13}C spin–lattice relaxation times (T_1) for AAHNMA and its (1/1) Ni(II) complex have been determined at pH 7.0 and 10.0. NT_1 values, where N is the number of directly bonded hydrogen atoms, are given in Table 3. In general, ^{13}C spin–lattice relaxation times of protonated carbons of large molecules are relatively easy to relate to

TABLE 3. Spin–lattice relaxation values (NT_1's) (s) measured for AAHNMA and its 1:1 Ni(II)–complex

	Spin–lattice relaxation value								
	Ala–CH_3	His NH–CH_3	His Cβ	Asp Cβ	Ala Cα	Asp Cα	His Cα	C(5)	C(2)
				pH = 7					
Free peptide	1.35	2.60	0.40	0.52	0.36	0.35	0.30	0.36	0.38
Ni(II)-complex	1.00	1.15	0.18	*	0.15	*	0.17	0.19	0.19
Ratio	1.35	2.3	2.2		2.4		1.8	1.9	2.0
				pH = 10.0					
Free peptide	1.35	2.50	0.46	0.62	0.40	0.40	0.35	0.40	0.38
Ni(II)-complex	1.00	1.20	0.32	0.36	0.25	0.29	0.25	0.23	0.21
Ratio	1.35	2.1	1.4	1.7	1.6	1.4	1.4	1.7	1.8

*Peak is broadened.

dynamic properties of the molecules in solution. This is because the ^{13}C relaxation of such carbons is dominated by a single relaxation mechanism, namely the ^{13}C–^1H dipolar interaction with the directly bonded hydrogen (26, 27). Indeed, in our case, the nuclear Overhauser enhancement (nOe) factor was found to be 2.8, within experimental error (pH = 10.0), and at our magnetic field (25.2 MHz), the ^{13}C–^1H dipolar relaxation satisfies the extreme narrowing conditions. Therefore, we have the relation: $NT_1 = f(1/\tau_{eff})$ where τ_{eff} is the isotropic rotational correlation time. In the present conditions, more rapid rotational motion (shorter rotational correlation time) is reflected in a longer value of NT_1. A large decrease is observed for T_1 values in Ni(II) binding. These data suggest that complexation results in a rigidification and a restriction of segmental motion (28). The present T_1 measurement shows that the 1/1 Ni(II)–AAHNMA complex moiety is more rigid than the free peptide.

There is little effect of pH change on the relative mobilities of the individual residues in AAHNMA and its complex as manifested in the NT_1 values (Table 3). Nevertheless, the values for the majority of the nuclei at neutral pH are lower than those at basic pH, except those of methyl groups which have the same mobility in both pH's. However, it should be pointed out that the observed change approaches the experimental error. In the case of the free peptide the observation is consistent with the resonance intensities and linewidths near the pK values of the imidazole (6.55) and Asp (7.73) titrating groups. It is known that certain resonances which are sensitive to titration undergo a broadening effect in the pH range near the pK of the titrating group (29). The difference for the 1/1 complex at pH 7.0 and 10.0 is more significant. The ^{13}C nmr spectra show a different behavior with pH changes. In acidic solution (pH 2.5) the signals of the Asp COO^-, Asp Cα, and Asp Cβ are broadened and they disappear with increasing pH (3.5), but again appear and sharpen when the pH rises above 5.0. In this condition and in the absence of all the available nitrogen ligands, the ionized carboxyl group of aspartic residue is involved in paramagnetic complex formation. But within the pH range 6 to 10, a diamagnetic species is observed (magnetic moment measurements show a diamagnetic complex at pH 9.0). The visible spectra support the conclusions drawn from the nmr results. These data are consistent with previously observed species distribution as a function of pH for the system AAHNMA/Cu(II) (30). However, at pH 7.0 we have a small amount of paramagnetic species; for this reason the NT_1 values obtained at neutral pH for the Ni(II)–complex (1/1) are lower than those for basic pH, which give a different correlation time (*vide infra*). Within the experimental errors for the same pH, all the three different α carbons had identical ^{13}C T_1 values; this would be strong evidence for isotropic rotation of compounds in D_2O. We find that this relaxation time corresponds to an isotropic rotational correlation time $\tau_{eff} = 1.6 \times 10^{-10}$ s (pH = 7.0) and 1.3×10^{-10} s (pH = 10) for complex. This value for AAHNMA may be compared with correlation times estimated for the peptide TRF (thyrotropin releasing factor) (1.2×10^{-10} s at pH 9.9) which have similar molecular weights (31).

The β carbons of Asp and His residues in the free peptide and complexes show greater motion than the corresponding Cα. For example at pH = 10.0, the ratio of their T_1 Asp is 1.5. The substantially lower T_1 ratio (1.2) of 1/1 complex at the same pH suggests that in this case the side chain of Asp experiences restricted mobility about the Cα—Cβ bond, which is consistent with the involvement of COO^- group. The T_1's of the protonated carbons of the histidine ring in free peptide are similar to that of the β-carbon suggesting a restricted rotation of the ring about the Cα—Cβ bond. The side chain of Asp is slightly more mobile than the His residue. For example, the Cβ/Cα His ratio is ~1.3 at pH 7.0 and 10.0 in the free peptide. The lower ratio and the

Can. J. Chem. Downloaded from www.nrcresearchpress.com by 210.87.254.40 on 09/05/12
For personal use only.

invariability of the C(5) chemical shift by titration suggests a slightly higher proportion of the N(1)H tautomer that could be stabilized by an intramolecular interaction.

The largest values of NT_1 in Table 3 are observed for the methyl groups. Here, the rotational motion about their axis is expected to make a dominant contribution. Comparison of the NT_1 for methyl groups with those for the corresponding Cα (Ala) shows a ratio of 3.8 (pH 7.0) and 3.4 (pH 10.0) in free peptide and 6.5 (pH 7.0) and 4.0 (pH 10.0) upon Ni(II) binding. The ratio of the NT_1 value for the methyl group to the NT_1 value for the central residue Cα increased with increasing distance from the central Cα. The maximum ratio for a freely rotating methyl group attached directly to a rigid backbone undergoing isotropic reorientation is 9 (26).

Structure of the Nickel(II)–Peptide Complex

Assuming that the (1/1) Ni(II)–AAHNMA complex tumbles isotropically, the overall results provide confirmatory evidence for the existence of a definite complex. The above results suggest that Ni(II) forms complex with this peptide involving the α-NH_2, N(3) imidazole, two deprotonated peptide nitrogens, and the Asp COO^- group in a pentacoordinated structure as shown by the arrows in Fig. 2. Nickel(II) complexes are commonly found to be square planar or octahedral. However, Sacconi and co-workers (32) first reported a pentacoordinated Ni(II) complex and since then several such complexes have been found.

There is considerable similarity in the binding properties of Ni(II)–AAHNMA and those of Ni(II) – human albumin (10). The involvement of the histidine residue in the third position in the polypeptide chain is reinforced by the recent results[4] of Ni(II)-binding to dog albumin where the histidine is replaced by a tyrosine residue (33). Taking all these into account, it appears that the Ni(II)-binding site of human albumin is similar to that found in the Ni(II)–AAHNMA complex. Detailed studies are underway with human albumin.

Acknowledgements

The research was supported by the Medical Research Council of Canada. J.-P. L. acknowledges the financial support from CNRS (France) – NRC (Canada) Scientific Exchange Programme.

[4]Nickel(II)-binding to dog albumin determined by equilibrium dialysis in 0.1 *M* *N*-ethylmorpholine–HCl buffer at pH 7.5, 6°C, and ionic strength 0.16 show the lack of a specific Ni(II)-binding site apparent in human albumin. The visible spectra as a function of pH of Ni(II) – human albumin and Ni(II) – dog albumin are also different (35).

1. E. A. PEDERSEN, A. C. HØGETVEIT, and A. ANDERSEN. Int. J. Cancer, **12**, 32 (1973).
2. F. W. SUNDERMAN, JR. Prev. Med. **5**, 279 (1976).
3. W. TORJUSSEN and L. A. SOLBERG. Acta Otolaryngol. **82**, 266 (1976).
4. M. D. MCNEELY, M. W. NECKAY, and F. W. SUNDERMAN, JR. Clin. Chim. **18**, 992 (1972).
5. E. HORAK, F. W. SUNDERMAN, JR., and B. SARKAR. Res. Commun. Chem. Pathol. Pharmacol. **14**, 153 (1976).
6. B. SARKAR. *In* Metal ligand interactions in organic chemistry and biochemistry. Part 1. *Edited by* B. Pullman and N. Goldblum. D. Reidel Publishing Co., Dordrecht-Holland. 1977. p. 193.
7. S. H. LAURIE, D. H. PRIME, and B. SARKAR. Can. J. Chem. **57**, 1411 (1979).
8. B. SARKAR. 62nd Canadian Chemical Conference, Vancouver, Canada. 1979. p. 39.
9. M. LUCASSEN and B. SARKAR. J. Toxicol. Environ. Hlth. **5**, 897 (1979).
10. J. O'C. WESTERIK and B. SARKAR. Proc. Can. Fed. **18**, 286 (1975).
11. K. S. N. IYER, S. LAU, S. H. LAURIE, and B. SARKAR. Biochem. J. **169**, 61 (1978).
12. G. C. K. ROBERTS, D. H. MEADOWS, and O. JARDETZKY. Biochemistry, **8**, 2053 (1969).
13. R. FREEMAN and H. D. W. HILL. J. Chem. Phys. **56**, 3367 (1971).
14. H. LAKUSTA, C. M. DEBER, and B. SARKAR. Can. J. Chem. **58**, 757 (1980).
15. P. C. LAUTERBUR. Appl. Spectrosc. **24**, 450 (1970).
16. G. JUNG, E. BREITMAIER, and N. VOELTER. Eur. J. Biochem. **24**, 438 (1972).
17. A. R. QUIRT, J. R. LYERLA, JR., I. R. PEAT, J. S. COHEN, W. F. REYNOLDS, and M. H. FREEDMAN. J. Am. Chem. Soc. **96**, 570 (1974).
18. W. F. REYNOLDS, I. R. PEAT, M. H. FREEDMAN, and J. R. LYERLA, JR. J. Am. Chem. Soc. **95**, 328 (1973).
19. P. PTAK. Inf. Chim. **147**, 237 (1975).
20. O. H. SACHS, A. N. SCHECHTER, and J. S. COHEN. J. Biol. Chem. **246**, 6577 (1971).
21. W. J. HORSLEY and H. J. STERNLICHT. J. Am. Chem. Soc. **90**, 3738 (1968).
22. M. K. KIM and A. E. MARTELL. J. Am. Chem. Soc. **91**, 872 (1969).
23. H. KOZLOWSKI. Inorg. Chim. Acta, **31**, 135 (1978).
24. R. MATHUR and R. B. MARTIN. J. Phys. Chem. **69**, 668 (1965).
25. R. NAKON and R. J. ANGELICI. J. Am. Chem. Soc. **96**, 4178 (1974).
26. D. DODDRELL, V. GLUSHKO, and A. ALLERHAND. J. Chem. Phys. **56**, 3683 (1972).
27. K. F. KUHLMANN, D. M. GRANT, and R. K. HARRIS. J. Chem. Phys. **52**, 3439 (1970).
28. K. WUTHRICH. *In* NMR in biological research: peptides and proteins. North-Holland Publishing Company, Amsterdam. 1976.
29. S. KITAGAWA, K. YOSHIKAWA, and I. MORISHIMA. J. Phys. Chem. **82**, 89 (1978).
30. J.-P. LAUSSAC and B. SARKAR. J. Biol. Chem. In press.
31. R. DESLAURIERS, W. H. MCGREGOR, D. SARANTAKIS, and I. C. P. SMITH. Biochemistry, **13**, 3443 (1974).
32. L. SACCONI, P. L. ORIOLI, and M. DI VAIRA. J. Am. Chem. Soc. **87**, 2059 (1965).
33. J. W. DIXON and B. SARKAR. J. Biol. Chem. **249**, 5872 (1974).
34. J. GLENNON and B. SARKAR. To be published.
35. B. SARKAR. Unpublished results.

Can. J. Chem. Downloaded from www.nrcresearchpress.com by 210.87.254.40 on 09/05/12
For personal use only.

Hydrolytic behavior of two β-lactams and their corresponding imidate salts. New evidence for stereoelectronic control

PIERRE DESLONGCHAMPS AND MAURICE CARON[1,2]

Laboratoire de Synthèse Organique, Département de Chimie, Faculté des Sciences, Université de Sherbrooke, Sherbrooke (Qué.), Canada J1K 2R1

Received April 23, 1980

PIERRE DESLONGCHAMPS and MAURICE CARON. Can. J. Chem. **58**, 2061 (1980).

The basic hydrolysis and the concurrent carbonyl–oxygen exchange of ^{18}O-labelled *N*-phenyl-4-phenyl-2-azetidinone (**5***) and *N*-2,6-dimethylphenyl-2-azetidinone (**6***) have been studied. β-Lactam **5*** was easily hydrolysed and showed no carbonyl–oxygen exchange with 0.1 *N* sodium hydroxide (dioxane–water, 9:1). Under the same conditions, β-lactam **6*** gave no exchange and was found resistant to basic hydrolysis. Hydrolysis and exchange was observed when **6*** was refluxed with 0.1 *N* and 1 *N* sodium hydroxide in water.

The hydrolysis of the corresponding imidate salts **7** and **8** was also investigated. Under basic conditions, salt **7** gave an 8:2 mixture of ester amine **9** and β-lactam **5**, while under acidic conditions the hydrochloride salt of ester amine **9** was the only product. Under basic conditions, the imidate salt **8** produced only the β-lactam **6**, and under acidic conditions, a 3:7 mixture of the hydrochloride salt of **10** and β-lactam **6**. Under stronger acidic conditions (≥3 *N* HCl), **8** gave only the starting β-lactam **6**.

The results of these hydrolysis reactions are easily explained on the basis of the stereoelectronic theory for the cleavage of tetrahedral intermediates, and by taking into account that the nitrogen of tetrahedral intermediates must be either protonated under acidic conditions, or hydrogen bonded with the solvent under basic conditions in order to observe the cleavage of the C—N bond.

PIERRE DESLONGCHAMPS et MAURICE CARON. Can. J. Chem. **58**, 2061 (1980).

L'hydrolyse basique et l'échange O-18 au carbonyle de la *N*-phényl phényl-4 azétidinone-2 (**5***) et de la *N*-diméthyl-2,6 phényl azétidinone-2 (**6***) ont été étudiées. La β-lactame **5*** s'hydrolyse facilement et ne subit pas d'échange O-18 au carbonyle avec l'hydroxyde de sodium 0.1 *N* (dioxanne–eau, 9:1). Dans les mêmes conditions, la β-lactame **6*** ne subit pas d'échange et résiste à l'hydrolyse basique; ce n'est qu'à reflux avec l'hydroxyde de sodium 0.1 *N* et 1 *N* dans l'eau que la lactame **6*** s'hydrolyse et subit l'échange.

L'hydrolyse des sels imidates correspondants **7** et **8** fut aussi étudiée. En milieu basique, le sel **7** donne un mélange 8:2 d'ester-amine **9** et de β-lactame **5** et en milieu acide, il donne l'hydrochlorure de l'ester-amine **9** comme produit unique. En milieu basique l'imidate **8** donne seulement la β-lactame **6** et en milieu acide il donne un mélange (3:7) de l'hydrochlorure de **10** et de β-lactame **6**. En milieu plus acide (≥HCl 3 *N*) l'imidate **8** donne uniquement la β-lactame **6** de départ.

Les résultats de ces réactions d'hydrolyse sont expliqués facilement par la théorie stéreoélectronique sur le bris des intermédiaires tétraédriques en tenant compte que le bris du lien C—N d'un intermédiaire tétraédrique ne peut se faire que si l'azote (de l'intermédiaire tétraédrique) est soit protoné en milieu acide, soit lié par un pont hydrogène avec le solvant en milieu basique.

We have recently shown that carbonyl–oxygen exchange concurrent with the basic hydrolysis of ^{18}O-labelled amides is a powerful technique to demonstrate the importance of stereoelectronic effects in the cleavage of tetrahedral intermediates (1, 2). In the course of this work, we have also shown conclusively that the nitrogen of tetrahedral intermediates in the T^- ionic form must be hydrogen bonded with the solvent in order to observe the cleavage of the C—N bond. For instance, *N*-2,6-dimethylphenyl *N*-methylformamide **1** (Scheme 1) was found to be resistant to basic hydrolysis, and this result was explained by the fact that in the corresponding tetrahedral intermediate **2**, the presence of the two methyl groups on the phenyl ring prevents the formation of a hydrogen bond between the tertiary nitrogen and water.

We have also described that the basic hydrolysis of imidate salts **3** (3) and **4** (4) gave only the corresponding amide alcohol products. Again, these results were explained by the fact that the nitrogen in their corresponding tetrahedral intermediates cannot form a hydrogen bond with the solvent.

In order to emphasize these results, we have undertaken the study of the carbonyl–oxygen exchange in the basic hydrolysis of ^{18}O-labelled β-lactams **5*** and **6***. We have also studied the acid and basic hydrolysis of the corresponding imidate salts **7** and **8** which can either give the β-lactams **5** and **6** or the ester amines **9** and **10** respectively. We wish now to report this work.

Synthesis of β-Lactams and Imidate Salts

N-phenyl-4-phenyl-2-azetidinone (**5**) was prepared by utilizing the Reformatsky reaction (5) with ethyl bromoacetate and the imine **11** (Scheme 2) derived from benzaldehyde and aniline. Compound **5** was also produced by the zinc reduction of

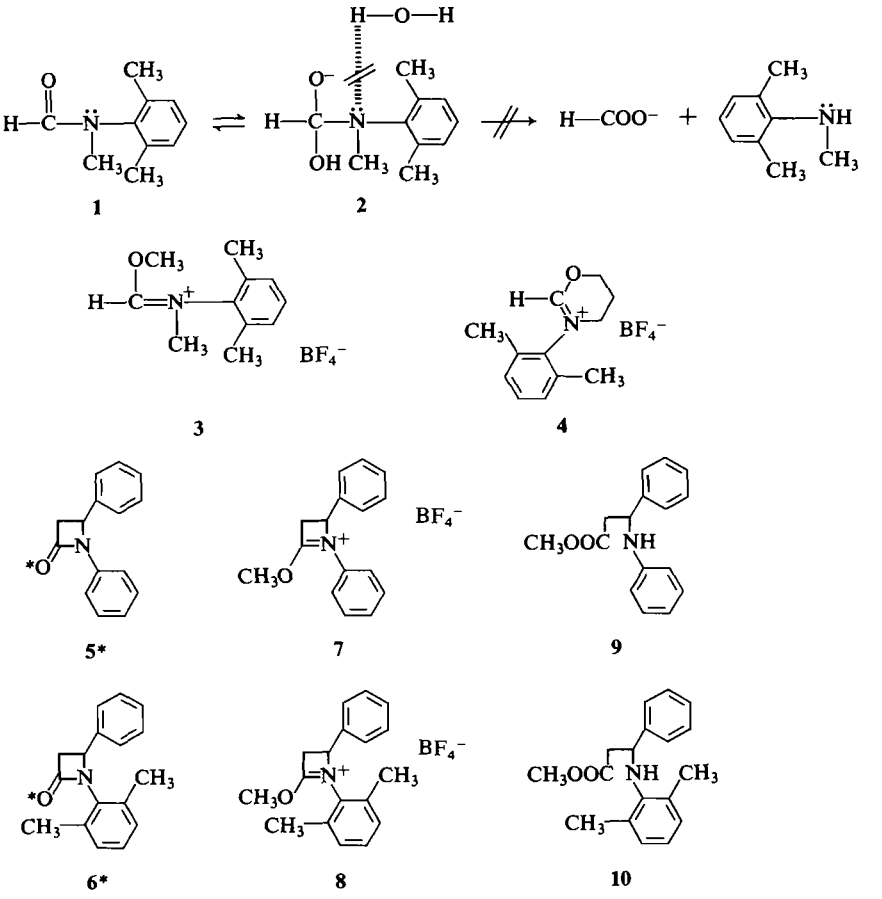
[1]Holder of a scholarship from the Ministère de l'Education of Québec.

[2]Taken in part from the M.Sc. thesis, Université de Sherbrooke, 1979.

0008-4042/80/192061-08$01.00/0

©1980 National Research Council of Canada/Conseil national de recherches du Canada

Can. J. Chem. Downloaded from www.nrcresearchpress.com by 210.87.254.5 on 09/05/12
For personal use only.



SCHEME 1 (O* = ^{18}O)

dichlorolactam **12** which was obtained by the condensation of imine **11** with dichloroketene (6). Condensation of dichloroketene with imine **13**, derived from benzaldehyde and 2,6-dimethyl aniline, gave the dichlorolactam **14**. Reduction of **14** with zinc yielded the desired *N*-2,6-dimethylphenyl-2-azetidinone (**6**).[3]

The imidate salts **7** and **8** were prepared by the reaction of trimethyloxonium tetrafluoroborate on the corresponding β-lactams **5** and **6** (8). The ^{18}O-labelled products were obtained in the following manner. Hydrolysis of imidate salt **7** with ^{18}O-labelled water gave ^{18}O-labelled ester amine **9*** which was converted into ^{18}O-labelled **5*** by the action of ethyl magnesium bromide (9). Reaction of imidate salt **8** with ^{18}O-labelled water gave directly the ^{18}O-labelled β-lactam **6***. Alkylation of β-lactam **6*** with trimethyloxonium tetrafluoroborate gave ^{18}O-labelled imidate salt **8***.

[3]A different β-lactam derived from 2,6-dimethylaniline has been synthesized recently (7).

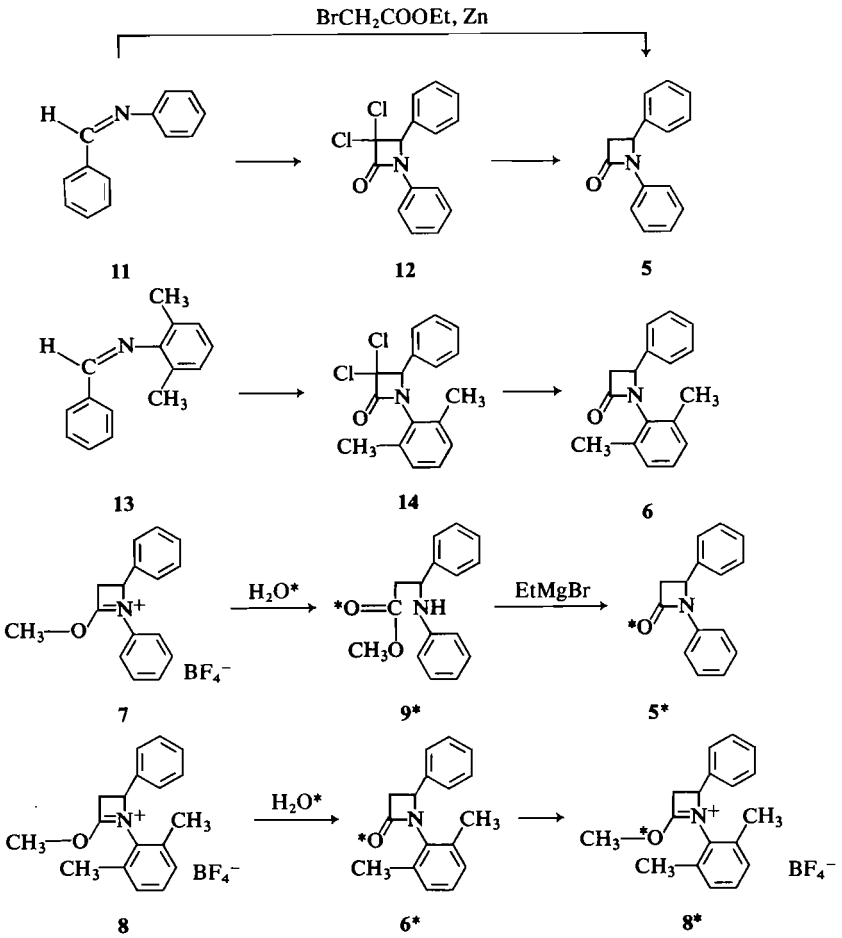
Results and Discussion

β-Lactams **5*** and **6*** were hydrolysed at reflux temperature with 0.1 *N* and 1 *N* sodium hydroxide. The results are described in Table 1.

Concurrent carbonyl–oxygen exchange was not observed during the basic hydrolysis of β-lactam **5***. We have previously predicted and shown (1, 2) that tertiary amides do not undergo carbonyl–oxygen exchange concurrent to hydrolysis, thus compound **5*** behaves like a typical tertiary amide.[4] β-Lactam **5*** must therefore react with hydroxide ion to give, with stereoelectronic control (10), the tetrahedral intermediate **15**. The intermediate **15** has proper electron pair orientation to eject either the unlabelled OH group or the amino group, yielding either the labelled β-lactam **5*** or the hy-

[4]Formamides are essentially the only exceptions, in these compounds, the energy barrier for conformational change in the corresponding tetrahedral intermediate is lower than usual due to the presence of the hydrogen atom which is smaller than an alkyl group (2).

Can. J. Chem. Downloaded from www.nrcresearchpress.com by 210.87.254.5 on 09/05/12
For personal use only.



SCHEME 2

drolysis product **16**. Since the nitrogen of the tetrahedral intermediate **15** can easily form a hydrogen bond with the solvent, the ring opening barrier is low. Consequently, conformational change (and appropriate proton transfer) to give the intermediate **17** which would then yield the unlabelled β-lactam **5** or the hydrolysis product **16**, cannot compete with the breakdown of **15** with stereoelectronic control.[5]

The β-lactam **6*** is hydrolysed at a considerably slower rate than the β-lactam **5*** and contrary to **5***, **6*** does undergo concurrent carbonyl–oxygen exchange. These results can also be readily explained: **6*** can form first the tetrahedral intermediate **18**. However, the barrier to ring opening of the intermediate **18** is raised on account of steric hindrance to hydrogen bonding. Conformational change (**18** → **20**) can therefore compete with hydrolysis, with the result that carbonyl–oxygen exchange (**20** → **6**) is observed.

The hydrolyses of imidate salts **7** and **8** were carried out under a range of pH conditions at room temperature and the results are summarized in Table 2.

We have previously shown that the hydrolysis of *syn* and *anti* imidate salts can be understood by taking into consideration the principle of stereoelectronic control and the ionic form of the tetrahedral intermediate which depends upon the pH of the medium.[6]

[5]The absence of carbonyl–oxygen exchange in **5*** can also be explained if the cleavage **15** → **16** occurs at a faster rate than the cleavage **15** → **5**. The cleavage **15** → **16** would be unusually fast due to the release of strain caused by the opening of the four-membered ring.

[6]The tetrahedral intermediate exists in the T^- ionic form **31** (Scheme 5) under strongly basic conditions (pH > 11), in the T^0 form **30** or the kinetically equivalent $T^{\pm}$ ionic form **29** at a pH corresponding to the pK_a of the tetrahedral intermediate (pH ≃ 10), and the T^+ ionic form **28** under acidic conditions. Also, the tertiary nitrogen in the T^- ionic form **31** must be able to form a hydrogen bond with water (**32**).

Can. J. Chem. Downloaded from www.nrcresearchpress.com by 210.87.254.5 on 09/05/12
For personal use only.

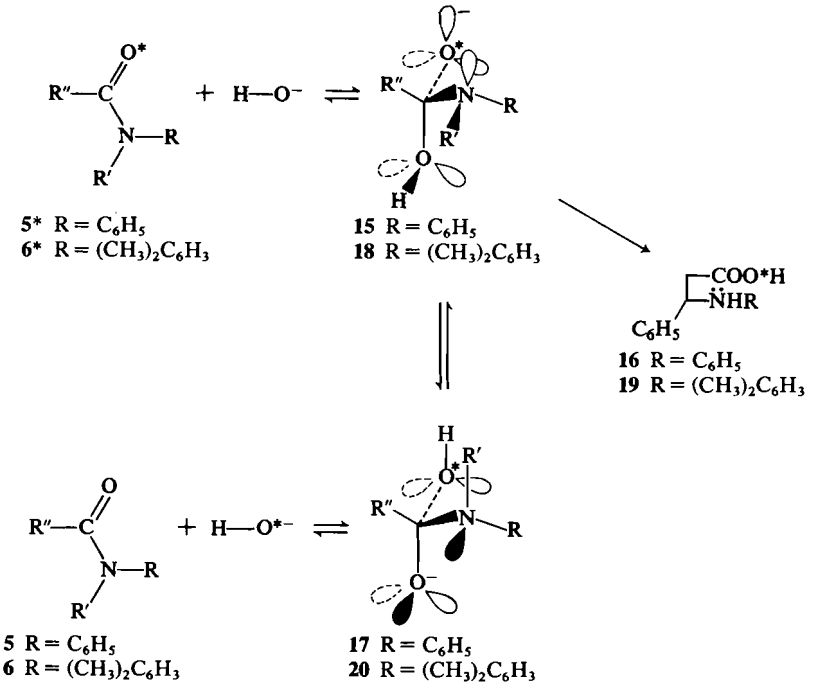
Can. J. Chem. Downloaded from www.nrcresearchpress.com by 210.87.254.5 on 09/05/12
For personal use only.

TABLE 1. Hydrolysis and carbonyl–oxygen exchange with β-lactams **5*** and **6*** at reflux temperature

NaOH	Medium	β-Lactam	Time (h)	Hydrolysis (%)	Exchange (%)
0.1 *N*	Water–dioxane (1:9)	**5**	0.08	10	0
0.1 *N*	Water–dioxane (1:9)	**5**	0.5	64	0
0.1 *N*	Water–dioxane (1:9)	**5**	0.75	71	0
0.1 *N*	Water —	**5**	0.42	74	0
0.1 *N*	Water–dioxane (1:9)	**6**	63	0	0
0.1 *N*	Water–dioxane (1:9)	**6**	215	0	0
0.1 *N*	Water–dioxane (1:9)	**6**	784	0	0
0.1 *N*	Water —	**6**	63	1[a]	3
1.0 *N*	Water —	**6**	168	8	19
1.0 *N*	Water —	**6**	336	24	40

[a]Detected by ^{1}H nmr.

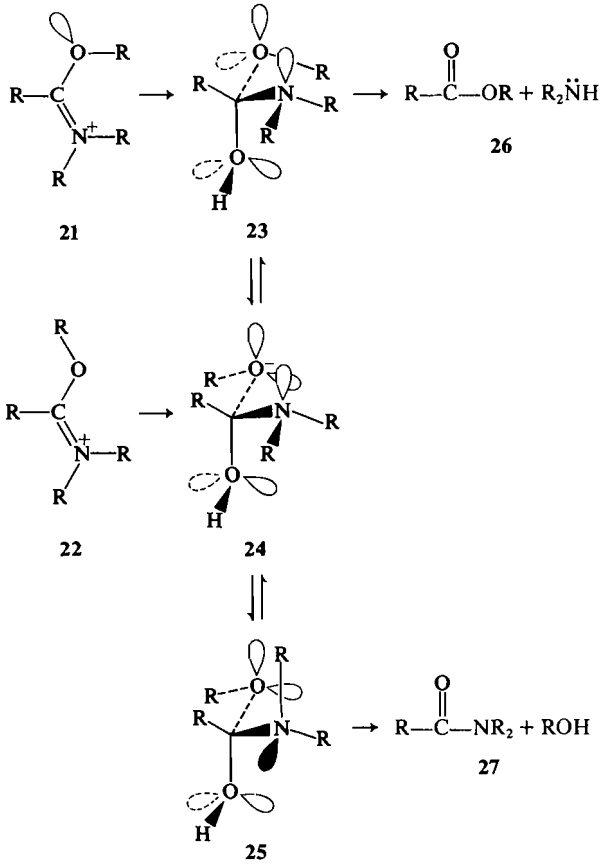
It is necessary to summarize this rationalization. The *anti* form **21** (Scheme 4) of an imidate salt gives the intermediate **23** in which the cleavage of the C—N bond to yield **26** can take place with stereoelectronic control regardless of whether **23** exists in the T^+, $T^\pm$, or T^- ionic form. The *syn* form **22** of an imidate salt gives first the intermediate **24** which cannot break down with stereoelectronic control; it therefore undergoes a conformational change to either **23** or **25**. The T^- ionic form of **25** can break down with stereoelectronic control. Assuming that both conformational changes, **24** → **23** and **24** → **25**, can take place, *syn* imidate salts will give a mixture of ester amine and amide alcohol products **26** and **27** under strongly basic conditions. The $T^\pm$ and T^+ ionic forms of intermediate **25** cannot undergo a cleavage of the C—O bond with stereoelectronic control because the nitrogen electron pair is no more available. Consequently, *syn* imidate salts will give the ester amine product **26** only, under such conditions. Thus, in résumé, *anti* imidate salts always give the ester amine product **26** over the complete range of pH values, whereas *syn* imidate salts yield the ester amine product **26** under acidic conditions, and a mixture of ester amine and amide alcohol products **26** and **27** under basic conditions. These conclusions have been previously verified experimentally (3, 4, 11).



SCHEME 3

TABLE 2. Hydrolysis of imidate salts at various pH values at room temperature

Medium	Imidate salt 7		Imidate salt 8	
	β-Lactam 5 (%)	Ester-amine 9 (%)	β-Lactam 6 (%)	Ester-amine 10 (%)
1.0 *N* NaOH	20	80	100	0
pH 12.7	12	88	100	0
pH 9	0	100	100	0
pH 7	0	100	100	0
pH 4	0	100	68	32
0.1 *N* HCl	0	100	56	44
0.5 *N* HCl	0	100	65	35
1.5 *N* HCl	0	100	87	13
3.0 *N* HCl	0	100	100	0
6.0 *N* HCl	0	100	100	0



SCHEME 4

Under basic conditions (pH > 11), imidate salt **7** yields a mixture of ester amine **9** and β-lactam **5**, and from pH 9 to 6 *N* hydrochloric acid, the only product formed is the ester amine **9**. Consequently imidate salt **7**, which very likely exists as a mixture of *syn* and *anti* isomers (11), reacts normally.

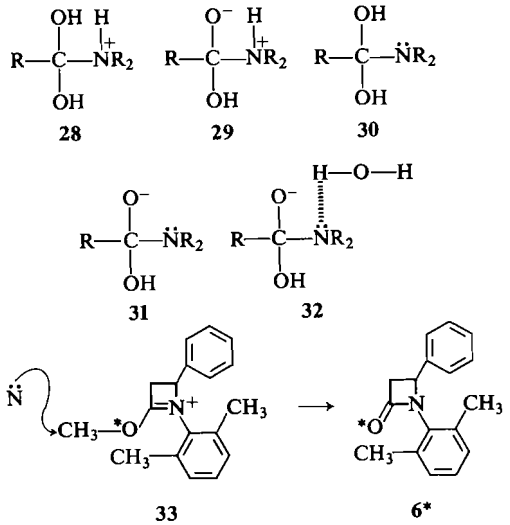
If one of the parameters that we have discussed in the hydrolysis of *syn* and *anti* imidate salts is changed, for instance if there is a situation where there is considerable steric hindrance at the tetrahedral intermediate level which will prevent protonation of the tertiary nitrogen, different results should be obtained. We believe that this is indeed the case with imidate salt **8** in which the two methyl groups on the *N*-phenyl substituent render the nitrogen electron pair in the corresponding tetrahedral intermediate unavailable to approach by a molecule of water or a proton donor source.

Imidate salt **8** when hydrolysed under strongly basic conditions gave the β-lactam **6** only. This result shows that if **23** is formed, it cannot break down, **23** is therefore converted into **25** (or an equivalent) which yields the β-lactam **6** (or **27**). At pH 7–9, the β-lactam **6** is again the only hydrolysis product. Under these conditions, the tetrahedral intermediate must first exist in the T^0 form, but T^0 is no longer easily converted into the $T^{\pm}$ ionic form necessary for the breakdown because of the unusual steric hindrance to proton transfer. The absence of ester amine **10** (or **26**) is therefore readily understood in this case. As soon as the nitrogen can be protonated (≃pH 4), ester amine **10** starts to be formed (32%). It is, however, remarkable that the formation of T^+ is not complete at pH 4, indicating that even under acidic conditions it is not easy to protonate the tertiary nitrogen.

The unexpected gradual decrease of ester amine **10** under stronger acidic conditions suggests a change in the reaction mechanism. This was verified by carrying out the hydrolysis of ^{18}O-labelled imidate salt **8***: at pH 4, the β-lactam **6** produced from **8*** did not contain ^{18}O, at higher pH (0.1 *N* HCl) there was a 25% transmission of the ^{18}O label, and with 3 *N* hydrochloric acid there was a complete transmission of the ^{18}O-label from the imidate salt **8** to the β-lactam **6**.

Formation of β-lactam **6** from salt **8** can either occur via the formation of a tetrahedral intermediate or by an S_N2 type displacement reaction on

Can. J. Chem. Downloaded from www.nrcresearchpress.com by 210.87.254.5 on 09/05/12
For personal use only.



SCHEME 5

the methoxy group (**33** → **6***). If the imidate salt **8** contains an ^{18}O atom, this label should be lost if the first mechanism is operative, but it should be totally transmitted into the β-lactam (**6***) in the second mechanism (12).

The results obtained with ^{18}O-labelled imidate salt **8*** clearly indicate that the displacement reaction can compete with the other at pH lower than 4 and it becomes the only reaction under strong acid conditions. An attractive explanation for this change of mechanism is simply that under increasingly acidic conditions, water becomes a weaker nucleophile, and the tetrahedral intermediate formation can no longer compete with the displacement reaction which can take place for instance with chlorine ion. The formation of methyl chloride was indeed observed by nmr spectroscopy under strong acidic conditions.

Experimental

The ir spectra were taken on a Perkin-Elmer 257 spectrophotometer. The ultraviolet (uv) spectra were registered on a Varian Techtron 635 spectrophotometer. Proton nmr spectra were recorded on a Varian A-60 or a Bruker WP-60 instrument. The following abbreviations have been used: s: singlet; d: doublet; dd: doublet of doublet; t: triplet; m: multiplet. Chemical shifts are reported in δ values relative to tetramethylsilane as internal standard.

Mass spectral assay were obtained using a Hitachi-Perkin-Elmer RMU-6-A instrument at 70 eV. Percentages of ^{18}O were calculated using the formula:

$$\%\ ^{18}O = \frac{100\,(P+2)}{P+(P+2)}$$

where P is the height of the parent peak and $(P+2)$ is that of the parent peak plus two m/e units. The percentage exchange is thus

$$\%\ \text{exchange} = \frac{(\%\ ^{18}O \text{ before hydrolysis}) - (\%\ ^{18}O \text{ after hydrolysis})}{(\%\ ^{18}O \text{ before hydrolysis})} \times 100$$

Microanalyses were carried out by Dr C. Daessle, Organic Microanalyses, Montreal. Anhydrous sodium sulfate was used as the drying agent in working reactions. Imines **11** and **13** are known compounds and were prepared by standard procedures (13). Cycloaddition leading to dichlorolactam **12** and the Reformatsky reaction giving the β-lactam **5** were also previously reported in the literature (5, 6).

Imine 11

Melting point 52–53°C (lit. (13) 51–54°C); ir ($CHCl_3$): 1630 cm^{-1}; nmr ($CDCl_3$) δ: 8.20 (1H, s, C_6H_5—C*H*=NC_6H_5), 7.95–7.18 (5H, m, C_6H_5CH=NC_6H_5), 7.13 (5H, m, C_6H_5—CH=NC_6H_5).

Imine 13

Boiling point 110°C/0.4 Torr; ir ($CHCl_3$): 1642 cm^{-1}; nmr ($CDCl_3$) δ: 8.00 (1H, s, C_6H_5C*H*=N—), 7.70 (2H, m, C_6H_5—CH=N—), 7.28 (3H, m, C_6H_5CH=N—), 6.85 (3H, m, C_6H_5CH=N—$C_6H_3(CH_3)_2$), 2.07 (6H, s, —$NC_6H_3(CH_3)_2$).

Dichlorolactam 12

Melting point 162–163°C; ir ($CHCl_3$): 1785 cm^{-1}; nmr ($CDCl_3$) δ: 7.17 (10H, m, two phenyls), 5.37 (1H, s, C_6H_5—C*H*—N—C_6H_5); ms m/e: 292 (M^+), 294 ($M+2$), 296 ($M+4$), 256 (M^+ – HCl).

Dichlorolactam 14

Imine **13** (12.4 g, 59.5 mmol) and triethylamine (12.5 mL, 89.2 mmol) were dissolved in dry benzene (200 mL). At room temperature was added, dropwise, a solution of dichloroacetyl chloride (8.6 mL, 89.2 mmol) in benzene (40 mL). The mixture was stirred at room temperature for 1 h. Then the solution was washed with 5% hydrochloric acid, water, dried, and evaporated. The residue was filtered on silica gel with chloroform – ethyl acetate (9:1). The isolated oil crystallized when treated with methanol giving dichlorolactam **14** (14.9 g, 78%); mp 98–99°C; ir ($CHCl_3$): 1795 cm^{-1}; nmr ($CDCl_3$) δ: 7.17 (5H, s, C_6H_5), 6.92 (3H, s, N—$C_6H_3(CH_3)_2$), 5.70 (1H, s, —C*H*C_6H_5), 2.35 (6H, s, $C_6H_3(CH_3)_2$); ms m/e: 320 (M^+), 322 ($M+2$), 324 ($M+4$), 284 (M^+ – HCl). *Anal.* calcd. for $C_{17}H_{15}NOCl_2$: C 63.76, H 4.72, Cl 22.15; found: C 63.83, H 4.55, Cl 22.25.

β-*Lactam 5*

The dichlorolactam **12** (52.3 mg, 0.18 mmol) was dissolved in glacial acetic acid (2 mL) containing traces of water. Zinc dust (64 mg, 0.97 mmol) was added and the mixture was refluxed for 3 h. A second portion of zinc dust (100 mg, 1.53 mmol) and glacial acetic acid (3 mL) containing traces of water were added and the reflux was maintained for 2 h. The zinc was filtered and the solvent was evaporated to dryness using benzene. Purification of the residue by thick layer chromatography on silica gel gave pure β-lactam **5** (32 mg, 80%); mp 153–154°C (lit. (5) 153–154°C); uv (dioxane) λ_{max}: 251 nm (ε 9 143), 285 nm (ε 565); ir ($CHCl_3$): 1760 cm^{-1}; nmr ($CDCl_3$) δ: 7.23 (10H, m, two phenyls), 5.02 (1H, dd, J_1 = 5.6 Hz, J_2 = 2.7 Hz, —C*H*—N), 3.59 and 2.93 (2H, dd, J_1 = 5.6 Hz, J_2 = 2.7 Hz, J_3 = 15.2 Hz, CH_2—CH—N); ms m/e: 223 (M^+), 180 ($M^+ - CH_3C{\equiv}O^+$).

The β-lactam **5** was also synthesized using Gilman's procedure (5) and showed identical physical and spectroscopic properties.

β-*Lactam 6*

The dichlorolactam **14** (27 mg, 0.08 mmol) was dissolved in glacial acetic acid (4 mL) containing traces of water. Zinc dust (556 mg, 8.5 mmol) was added and the mixture was refluxed 4 h. The zinc was filtered and the solvent was evaporated to dryness using benzene. Purification of the residue by thick layer chromatography on silica gel gave pure β-lactam **6** (11 mg, 51%); mp 90–91°C; uv (dioxane) λ_{max}: 245 nm (ε 2 709), 287 nm (ε 287); ir ($CHCl_3$): 1750 cm^{-1}; nmr ($CDCl_3$) δ: 7.25 (5H, s, C_6H_5), 6.95

Can. J. Chem. Downloaded from www.nrcresearchpress.com by 210.87.254.5 on 09/05/12
For personal use only.

Can. J. Chem. Downloaded from www.nrcresearchpress.com by 210.87.254.5 on 09/05/12
For personal use only.

(3H, s, $C_6H_3(CH_3)_2$), 5.12 (1H, dd, J_1 = 5.1 Hz, J_2 = 2.9 Hz, —C*H*—N), 3.49 and 3.22 (2H, dd, J_3 = 15.1 Hz, J_1 = 5.1 Hz, J_2 = 2.9 Hz, CH_2—CH—N), 2.21 (6H, s, $2CH_3$); ms *m/e*: 251 (M^+), 208 ($M^+ - CH_3C{\equiv}O^+$). *Anal.* calcd. for $C_{17}H_{17}NO$: C 81.24, H 6.82; found: C 80.92, H 7.07.

Imidate Salt 7

The β-lactam **5** (261 mg, 1.17 mmol) was added to trimethyloxonium tetrafluoroborate (173 mg, 1.17 mmol) suspended in dichloromethane (10 mL). The mixture was stirred overnight at room temperature. Evaporation of the solvent and recrystallization from dichloromethane–ether mixture gave pure **7** (311 mg, 82%); mp 129°C (dec); ir (CH_2Cl_2): 1670 cm^{-1}; nmr (CD_2Cl_2) δ: 7.43 (5H, s, $C_6H_5\overset{+}{N}$—), 7.34 (5H, s, C_6H_5—CH), 5.75 (1H, dd, J_1 = 1.8 Hz, J_2 = 4.4 Hz, C_6H_5CH—$CH_2\overset{+}{N}$), 4.54 (3H, s, OCH_3), 4.34 and 3.53 (2H, dd, J_3 = 17.2 Hz, J_1 = 1.8 Hz, J_2 = 4.4 Hz, CH_2—CH—C_6H_5).

Imidate Salt 8

The β-lactam **6** (111 mg, 0.44 mmol) was added to trimethyloxonium tetrafluoroborate (65 mg, 0.44 mmol) suspended in dichloromethane (10 mL). The mixture was stirred overnight at room temperature. Evaporation of the solvent and recrystallization from dichloromethane–ether mixture gave pure **8** (114 mg, 73%); mp 148–149°C (dec); ir (CH_2Cl_2): 1675 cm^{-1}; nmr (CD_2Cl_2) δ: 7.40 (5H, m, C_6H_5—CH), 7.14 (3H, m, C_6H_3—$(CH_3)_2$—$\overset{+}{N}$), 5.88 (1H, dd, J_1 = 2.3 Hz, J_2 = 3.9 Hz, C_6H_5CH—CH_2—$\overset{+}{N}$), 4.60 (3H, s, OCH_3), 4.59 and 4.19 (2H, dd, J_3 = 17.3 Hz, J_2 = 3.9 Hz, J_1 = 2.3 Hz, CH_2—CH—C_6H_5), 2.54 (3H, s, CH_3), 1.97 (3H, s, CH_3).

Ester Amine 9

The β-lactam **5** (52 mg, 0.23 mmol) was refluxed with sodium methoxide (19.3 mg) in methanol (15 mL) for 2 h. The solvent was evaporated and the residue diluted with water (10 mL). The solution was extracted with chloroform. The chloroform extracts were dried and evaporated. Pure ester amine **9** was obtained (56 mg, 96%); mp 105.5–106°C (lit. (14) 106–107°C); uv (methanol) λ_{max}: 213 nm (ε 6 684), 248 nm (ε 8 379), 295 nm (ε 1 275); ir ($CHCl_3$): 3420, 1745 cm^{-1}; nmr ($CDCl_3$) δ: 7.34 (5H, m, C_6H_5—CH), 7.29–6.51 (5H, m, C_6H_5—N), 4.86 (1H, t, *J* = 6.6 Hz, *CH*—C_6H_5), 4.56 (1H, m, N—*H*), 3.66 (3H, s, OCH_3), 2.83 (2H, d, *J* = 6.6 Hz, CH_2COOCH_3); ms *m/e*: 255 (M^+), 182 ($M^+ - CH_2COOCH_3$). The ester amine **9** isolated from the hydrolysis of imidate salt **7** was identical to the material prepared by the action of sodium methoxide on the β-lactam **5**.

Ester Amine 10

The ester amine **10** was isolated from the hydrolysis of imidate salt **8** with hydrochloric acid 0.1 *N*; uv (methanol) λ_{max}: 218 nm (ε 10 354), 244 nm (ε 7 651); ir ($CHCl_3$): 1740 cm^{-1}; nmr ($CDCl_3$) δ: 7.27 (5H, s, C_6H_5—CH), 6.90 (3H, m, C_6H_3—$(CH_3)_2$), 4.70 (1H, t, *J* = 7.0 Hz, *CH*—C_6H_5), 3.58 (3H, s, OCH_3), 2.90 (2H, d, *J* = 7 Hz, CH_2COOCH_3), 2.18 (6H, s, $2CH_3$); ms *m/e*: 283 (M^+), 210 ($M^+ - CH_2COOCH_3$).

β-*Lactam 5**

To the imidate **7** (96 mg, 0.30 mmol) was added $H_2{}^{18}O$ (70 μL ca. 95% enriched) followed by $H_2{}^{16}O$ (50 μL). The mixture was left overnight at room temperature. Water was added (5 mL) and the solution was extracted with dichloromethane and dried. The crude product (74 mg, 0.29 mmol) was dissolved in dry ether (30 mL) and under nitrogen was treated with ethyl magnesium bromide (434 μL of 0.67 *N* solution). The solution was stirred for 30 min and 10% ammonium chloride solution (30 mL) was added. The aqueous phase was extracted with ether and dried. β-Lactam **5*** was purified by thick layer chromatography on silica gel (57 mg, 88%). The β-lactam **5*** contained 61% of ^{18}O; ir ($CHCl_3$): 1760 (C=O), 1730 (C=^{18}O) cm^{-1}; ms *m/e*: 225 (*M* + 2) (61%), 223 (M^+). The nmr was identical to the unlabelled β-lactam **5**.

β-*Lactam 6**

To the imidate **8** (218 mg, 0.62 mmol) was added $H_2{}^{18}O$ (200 μL ca. 95% enriched) followed by $H_2{}^{16}O$ (400 μL). The mixture was left overnight at room temperature. Water was added (5 mL) and the solution was extracted with dichloromethane and dried. The crude product was purified by thick layer chromatography on silica gel (118 mg, 76%). The β-lactam **6*** contained 43% of ^{18}O; ir ($CHCl_3$): 1750 (C=O), 1720 (C=^{18}O) cm^{-1}; ms *m/e*: 253 (*M* + 2) (43%), 251 (M^+). The nmr was identical to the unlabelled β-lactam **6**.

Basic Hydrolysis and Concurrent Carbonyl–Oxygen Exchange Experiments (Typical Procedure)

β-*Lactam 5**

The labelled β-lactam **5*** (57 mg, 0.25 mmol) (^{18}O = 61%) was dissolved in dioxane (30 mL) and sodium hydroxide (1.0 *N*, 4.56 mL) was added. The solution was refluxed and at convenient times 5 mL aliquots were withdrawn and poured over hydrochloric acid (1.2 *N*, 1 mL). This solution was extracted several times with dichloromethane and dried. The percentage of hydrolysis was established by nmr spectroscopy. The methine resonance (C_6H_5—C*H*N) appears at higher field in the amino acid (4.88 δ) than in the β-lactam (5.02 δ) in chloroform. Unreacted β-lactam **5*** was purified by thick layer chromatography and submitted to mass spectroscopy. For each aliquot withdrawn material recovered was greater than 84% and β-lactam **5*** isolated revealed a constant incorporation of ^{18}O (61%).

Hydrochloride salt of amino acid **16**: mp 134–136°C (lit. (14) 135–136°C); ir ($CHCl_3$): 3600–2800, 1720 cm^{-1}; nmr ($CDCl_3$) δ: 7.34 (5H, s, C_6H_5—CH), 7.08–6.48 (8H, m, C_6H_5N and $\overset{+}{N}H_2$, COOH), 4.88 (1H, t, *J* = 6.8 Hz, CHC_6H_5), 2.87 (2H, d, *J* = 6.8 Hz, CH_2COOH).

β-*Lactam 6**

The labelled β-lactam **6*** (13 mg, 0.05 mmol) (^{18}O = 43%) was dissolved in dioxane (15 mL) and sodium hydroxide (1.0 *N*, 1.70 mL) was added. The solution was refluxed under argon and after a desired time the reaction was completely stopped. The solution was extracted with dichloromethane and dried. The aqueous phase was acidified with 1.2 *N* hydrochloric acid, extracted with dichloromethane, and dried. The percentage of hydrolysis was established according to the material isolated (greater than 90%). Under this condition β-lactam **6*** did not exchange and revealed constant incorporation of ^{18}O (43%). The identical procedure was used when hydrolysis and exchange took place with sodium hydroxide (0.1 *N* and 1.0 *N*, no dioxane).

Hydrochloride salt of amino acid **19**: mp 150–165°C (sublimes slowly); ir ($CHCl_3$): 3600–2400, 1720 cm^{-1}; nmr ($CDCl_3$) δ: 7.34 (3H, s, $\overset{+}{N}H_2$ and COO*H*), 7.18 (5H, m, C_6H_5—CH), 6.85 (3H, m, $C_6H_3(CH_3)_2$), 4.60 (1H, t, *J* = 7.1 Hz, *CH*—CH_2COOH), 2.90 (2H, d, *J* = 7.1 Hz, CH—CH_2—COOH), 2.08 (6H, s, $2CH_3$).

Imidate Salt Hydrolysis

Typical Procedure

To the imidate salt **7** or **8** (=0.05 mmol) was added water (8 mL) at the desired pH. Both imidate and hydrolysis products were insoluble and the heterogeneous solution was left overnight unstirred.[7] Dichloromethane (15 mL) was added and the solution was neutralized with solid sodium carbonate when solutions were acidic. The aqueous phase was extracted with

[7]Complete hydrolysis was verified by nmr spectrum from crystals taken out from water and dissolved in deuterated dichloromethane. With imidate **7** hydrolysis was complete after 4 h.

dichloromethane and dried. The nmr spectrum was recorded and the ratio of the hydrolysis products determined. The material recovered from extractions was greater than 90%. The methine resonances of the ester amine **9** and the β-lactam **5** appear at 4.86 and 5.02 δ respectively in chloroform. The methine resonance of the ester amine **10** and the β-lactam **6** appear at 4.70 and 5.12 δ respectively. In the case of hydrolysis under acidic conditions, the solution was neutralized before extraction. The ester amine **9** was also obtained by the reaction of sodium methoxide on the β-lactam **5**.

Labelled imidate **8*** (27% O^{18}) was submitted to the same procedure. Mass spectroscopy revealed 27% of ^{18}O in β-lactam **6*** isolated from the hydrolysis with 3.0 *N* hydrochloric acid. Hydrolysis with 0.1 *N* hydrochloric acid gave 6.8% of ^{18}O incorporated in β-lactam **6*** and the unlabelled β-lactam **6** was isolated when imidate **8*** was hydrolysed at pH 4.

Formation of Methyl Chloride

Imidate salt **8** (22 mg, 0.06 mmol) was dissolved in deuterated dichloromethane (0.6 mL) and a solution of deuterated hydrochloric acid (3 *N*, 0.25 mL). The mixture was left for 1.5 h and then vigorously shaken. The nmr spectrum of the dichloromethane phase was recorded and revealed a singlet at 2.88 δ which corresponds to that of methyl chloride. Addition of a few drops of a saturated solution of methyl chloride in deuterated dichloromethane enhanced the singlet at 2.88 δ. Addition of methanol into the nmr tube gave a new singlet at 3.27 δ.

Acknowledgements

Support for this work by the National Research Council of Canada, and by the Ministère de l'Education, Québec, is gratefully acknowledged.

1. P. DESLONGCHAMPS, U. O. CHERIYAN, A. GUIDA, and R. J. TAILLEFER. Nouv. J. Chim. **1**, 235 (1977).
2. P. DESLONGCHAMPS, P. GERVAL, U. O. CHERIYAN, A. GUIDA, and R. J. TAILLEFER. Nouv. J. Chim. **2**, 631 (1978).
3. P. DESLONGCHAMPS, U. O. CHERIYAN, J. P. PRADERE, P. SOUCY, and R. J. TAILLEFER. Nouv. J. Chim. **3**, 343 (1979).
4. P. DESLONGCHAMPS, U. O. CHERIYAN, and R. J. TAILLEFER. Can. J. Chem. **57**, 3262 (1979).
5. H. GILMAN and M. SPEETER. J. Am. Chem. Soc. **65**, 2255 (1943).
6. F. DURAN and L. GHOSEZ. Tetrahedron Lett. 245 (1970); A. K. BOSE and M. S. MANHAS. Tetrahedron Lett. 2823 (1972).
7. W. KUNZ and H. KRISTINSON. Helv. Chim. Acta, **62**, 872 (1979).
8. H. MEERWEIN, W. FLORIAN, N. SCHÖN, and G. STOPP. Ann. **641**, 1 (1961).
9. H. B. KAGAN and J. L. LUCHE. Bull. Soc. Chim. Fr. **6**, 3500 (1969).
10. P. DESLONGCHAMPS. Tetrahedron, **31**, 2463 (1975); Heterocycles, **7**, 1271 (1977).
11. P. DESLONGCHAMPS, C. LEBREUX, and R. J. TAILLEFER. Can. J. Chem. **51**, 1665 (1973); P. DESLONGCHAMPS, S. DUBE, C. LEBREUX, D. R. PATTERSON, and R. J. TAILLEFER. Can. J. Chem. **53**, 2791 (1975); P. DESLONGCHAMPS and R. J. TAILLEFER. Can. J. Chem. **53**, 3029 (1975).
12. R. A. MCCLELLAND. J. Am. Chem. Soc. **97**, 3177 (1975).
13. L. A. BIGELOW and H. EATOUGH. *In* Org. Synth. Coll. Vol. I. John Wiley & Sons, Inc., New York, NY. 1932. p. 80.
14. A. W. BURGSTAHLER. J. Am. Chem. Soc. **73**, 3021 (1951).

Can. J. Chem. Downloaded from www.nrcresearchpress.com by 210.87.254.5 on 09/05/12
For personal use only.

2-Epi- and 15-dihydro-2-epilubimin: new stress compounds from the potato[1,2]

A. STOESSL AND J. B. STOTHERS

Agriculture Canada Research Institute and the Department of Chemistry, University of Western Ontario, London, Ont., Canada N6A 5B7

Received May 30, 1980

A. STOESSL and J. B. STOTHERS. Can. J. Chem. **58**, 2069 (1980).

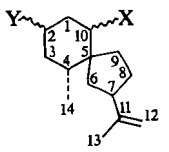
The complement of sesquiterpenoidal stress compounds produced in the interaction of potato with the pathogenic fungus, *Alternaria solani*, includes representatives of a new stereochemical series, 2-epilubimin (**1**) and its reduction product, 15-dihydro-2-epilubimin (**3**). Their structures were deduced from ^{13}C and ^{1}H magnetic resonance data.

A. STOESSL et J. B. STOTHERS. Can. J. Chem. **58**, 2069 (1980).

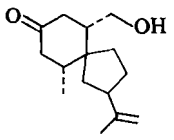
Le complément des composés sesquiterpéniques de stress qui proviennent de l'interaction entre la pomme de terre et le champignon pathogène *Alternaria solani* comprend des composés caractéristiques d'une nouvelle série stéréochimique, l'épilubimine-2 (**1**) et son produit de réduction la dihydro-15 épilubimine-2 (**3**). On a déduit leurs structures à partir de données de la rmn du ^{13}C et du ^{1}H.

[Traduit par le journal]

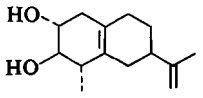
Fungal infection or treatment with certain chemicals induces the formation of complex mixtures of bicyclic sesquiterpenoids in potato tubers (1–4). Some of these stress metabolites, of which eighteen have been characterized, are considered to be phytoalexins, i.e., post-infectional defensive agents, on the basis of their fungitoxic properties. A close overall biosynthetic relationship between these compounds is abundantly clear, since all can be, at least formally, derived from eudesmane precursors (1). However, with respect to details, some of the relationships remain obscure. For instance, the predominant vetispirane subgroup of these compounds has hitherto been found to occur in two stereochemical forms, a normal series as represented by lubimin (**2**) and 15-dihydrolubimin (**4**) and a 10-epi series with 10-epilubimin (**5**) and 15-dihydro-10-epilubimin (**6**) as examples. Compound **4** accumulates in large amounts in potatoes invaded by *Glomerella cingulata* and certain other fungi as well as in pure cultures of these fungi supplemented with **2** (5); there is, therefore, no doubt that it is mainly a product of fungal reduction of **2**. In contrast, in potatoes inoculated with *Monilinia fructicola*, very small amounts of **6** have been found, accompanied by even smaller traces of **4** (6). It is not yet clear to what extent these two compounds, under these conditions, are products of potato or fungal metabolism, nor whether the dihydroepi compound is a precursor for, or a product of, **5**. It is clear, however, from these and other data that the



1 X = α-CHO; Y = β-OH
2 X = α-CHO; Y = α-OH
3 X = α-CH_2OH; Y = β-OH
4 X = α-CH_2OH; Y = α-OH
5 X = β-CHO; Y = α-OH
6 X = β-CH_2OH; Y = α-OH



7



8

invading fungus can exert a considerable effect on the spectrum of compounds produced, at least in part, as a result of its own metabolic activity but possibly also by specific effects on biosynthetic pathways of the potato tissue. We have recently extended our investigations of these phenomena to the interaction of potatoes with *Alternaria solani*. This fungus was chosen both because of our interest in its metabolism (7) and because it is an important pathogen of solanaceous crops (8). These experiments led to the discovery of yet another stereochemical series among the vetispirane family. Two new compounds have been isolated in small amounts from potatoes inoculated with mycelial suspensions of *A. solani* and their structures elucidated by spectroscopic methods. We wish to present these results to characterize the 2-epi series of these stress metabolites.

[1]Part XXXVI of "Postinfectional inhibitors from plants". For Part XXXV see ref. 12, Contribution No. 800 from the Research Institute.

[2]Part 89 of ^{13}Cmr studies. For Part 88 see ref. 13; for Part 87, ref. 7.

0008-4042/80/192069-04$01.00/0

©1980 National Research Council of Canada/Conseil national de recherches du Canada

Can. J. Chem. Downloaded from www.nrcresearchpress.com by 210.87.254.40 on 09/05/12
For personal use only.

TABLE 1. ^{13}C shielding values[a] for the stress metabolites 1–4[b]

Compound	C-1	C-2	C-3	C-4	C-5	C-6	C-7	C-8	C-9	C-10	C-11	C-12	C-13	C-14	C-15
1	42.5	65.0	37.9	35.2	47.6	32.2	47.2	31.1	25.1	54.2	147.5	108.7	21.3	16.2	206.3
2	41.8	69.3	40.3	41.0	46.9	33.3	47.4	32.6	25.9	58.4	147.3	108.8	21.2	16.4	205.0
3	41.0	66.1	38.3	35.6	47.3	34.1	47.3	32.5	24.1	43.6	148.3	108.1	21.6	16.6	64.4
4	40.6	69.9	40.8	41.2	46.7	36.7	47.4	32.7	25.4	48.5	148.1	108.2	21.5	16.7	64.1

[a]In ppm from internal TMS for $CDCl_3$ solutions (5–10%, w/v).
[b]Data for 2 and 4 taken from ref. 6.

The first compound, 2-epilubimin (**1**), was isolated as an oil having the constitution $C_{15}H_{24}O_2$ by precise mass measurement. The ^1H and ^{13}Cmr spectra indicated the presence of an aldehyde, a hydroxyl group, and a terminal double bond. In addition, the ^1Hmr spectrum revealed a secondary methyl group and the fact that the double bond is part of an isopropenyl group. All spectra closely resembled those exhibited (9) by lubimin (**2**) but with some significant and informative differences, attributed to stereochemical modification. Specifically, the width of the carbinyl proton absorption for **1** was smaller (14 vs. 32 Hz) and this pattern was centred at lower field (4.14 vs. 3.69 ppm). These differences suggest an axial orientation for the hydroxyl group in **1** as opposed to its equatorial disposition in **2**. The formyl proton appearing as a doublet at 9.92 ppm, $J \sim 3$ Hz, was shown by decoupling experiments to be vicinal to a proton at 2.71 ppm; the latter multiplet, a doublet of triplets, was collapsed to a four-line X pattern by irradiation of the formyl proton. This behavior is identical to that found for **2** and the widths of the X patterns are the same for each (16 Hz), indicating that the methine proton on carbon bearing the formyl group is axial in each. Furthermore, irradiation at 1.8 ppm collapsed the carbinyl proton pattern to a triplet and that at 2.71 ppm to a doublet indicating that the hydroxyl and formyl groups are bonded to carbons separated by a common methylene group. The methine proton at 2.71 ppm is 0.45 ppm less shielded than the corresponding proton in **2**; a similar difference was found for the methine proton on carbon bearing the secondary methyl group, while the latter is similarly shielded in each, 0.90 and 0.94 ppm. The shift of 0.45 ppm for each of these protons is consistent with an axial orientation for the hydroxyl function. The signals characterizing the isopropenyl group for **1** and **2** gave rise to very similar patterns in both ^1H and ^{13}C spectra. The major differences in the ^{13}C spectra of **1** and **2** (see Table 1) were the shieldings observed for three of the methine carbons. The carbinyl carbon of **1** at 65.0 ppm is 4.3 ppm upfield from that for **2** while the methine signal at 54.2 ppm is 4.2 ppm upfield from the C-10 absorption in **2**. The latter signal was unequivocally identified in the spectrum of **2** for material obtained from incorporation experiments utilizing sodium acetate-$^{13}C_2$ (6). The highest field methine absorption for **1** at 35.2 ppm is 5.8 ppm upfield from that for C-4 in **2**. It may be noted that the fourth methine signal for **1** is essentially the same as the C-7 signal in **2** (47.2 vs. 47.4 ppm). The upfield shifts for the three methine carbons in **1** constitute strong supporting evidence for an axial 2-hydroxyl substituent. Thus, the nmr evidence led to the 2-epi assignment for **1**, the first example of this stereochemical series.

The structural characterization of the second compound as the 15-dihydro derivative **3** was straightforward since **3** was formed from **1** on treatment with sodium borohydride as evidenced by its chromatographic behavior. The close resemblance of the ^{13}C spectra of **3** and **4** mirrored that described above for **1** and **2** in that three of the methine carbons were distinctly shielded (by 3.7–5.7 ppm) for **3** vs. **4** while the remaining carbons exhibited similar shieldings in both compounds (see Table 1). These three upfield shifts signal the axial disposition of the hydroxyl group. The ^1Hmr spectrum for **3** was also closely similar to that for **4** with the important difference in the band width and position of the carbinyl methine absorption analogous to that described above for **1** and **2**. For **3**, this pattern is deshielded by 0.5 ppm and is much narrower. The patterns for the methylene protons of the hydroxymethyl group in **3** and **4** were essentially identical, appearing as the AB portion of an ABX spectrum with $\delta_{AB} = 0.67$ ppm. This shift difference may be contrasted with the 0.15 ppm difference previously recorded for the isomeric 10-epi-dihydro derivative **6** (6).

As noted above, the reduction of **2** to **4** by the fungus accounted for most, if not all, of the **4** which accumulated in the potato – *Glomerella cingulata* interaction (9). *Alternaria solani* has also been demonstrated to effect this reduction (10). Preliminary evidence (see Experimental) indicates that a similar reduction of **1** by *A. solani* is responsible for the formation of **3** in the interaction of the fungus

Can. J. Chem. Downloaded from www.nrcresearchpress.com by 210.87.254.40 on 09/05/12
For personal use only.

Can. J. Chem. Downloaded from www.nrcresearchpress.com by 210.87.254.40 on 09/05/12
For personal use only.

with potato. It is of some interest to note that we were able to detect 2-epilubimin (**1**) in only one, although **3** was isolated from each of three separate experiments. The functional and biogenetic significance of the 2-epi compounds in the complex array of stress metabolites produced by infected potatoes is unclear. With compounds **1** and **3** in hand, we were able to check the product of a potato – *Monilinia fructicola* interaction for their presence; **3** was detected but only in vanishingly small amount. The apparently differential effect of different fungi on the spectrum of stress metabolites produced will receive further attention.

Experimental

Nuclear Magnetic Resonance and Mass Spectra

The spectra were recorded with Varian XL-100-12 and XL-100-15 spectrometers using $CDCl_3$ solutions (5–10%, w/v) of the stress metabolites. Proton spectra were obtained on the first instrument using c.w. operation while Fourier transform methods were used on the second to obtain the ^{13}C spectra. For the latter, square-wave modulated proton decoupling gave completely decoupled spectra and single frequency proton irradiation gave off-resonance decoupled spectra. Shielding data (±0.05 ppm) are given relative to internal TMS. Mass spectra were obtained from a Varian MAT 311A system.

Feeding Experiments and Fungal Cultures

Potatoes, var. Kennebec, purchased locally, were stored at ca. 4°C and were 4–7 months old when used. These were inoculated as described previously (6) except that suspensions of homogenized mycelium of *A. solani* in water containing streptomycin (200 ppm) were used instead of spore suspensions.

Monilinia fructicola (Wint.) Honey was from a culture routinely maintained at the Research Institute; it was used as a spore suspension containing ca. 2×10^5 spores/mL.

Alternaria solani (Ell. & Mart.) Jones & Grout was a pigment-producing strain kindly provided by Prof. U. Matern, University of Freiburg, West Germany, and routinely maintained on V-8 juice agar. Inoculum from an agar slope was grown in 6 Erlenmeyer flasks (200 mL capacity) containing medium T (11) (25 mL/flask) for 10–12 days when the mycelia were collected, rinsed with sterile water, homogenized, and resuspended in medium T contained in Roux bottles (100 mL in each of 40–60 bottles).

Column chromatography was done on silica gel, Camag DF5, not activated, using ca. 1 g/mg substance, and MeOH/Et_2O 5:95 as solvent (25 mL fractions) unless otherwise specified. Precoated silica gel plates (0.2 mm; Macherey-Nagel Polygram Sil N-HR/UV) were used for tlc, with MeOH/Et_2O 5:95, MeOH/$CHCl_3$ 5:95, and *i*PrOH/EtOAc 5:95 as standard irrigants. Vanillin (0.5%) in phosphoric acid (50%) was used as chromogenic reagent at 110°C.

Isolation of Metabolites

Incubation of ca. 30 kg of potatoes with a mycelial suspension of *Alternaria solani*, grown in 3 Roux bottles for 12 days, furnished a diffusate from which 310 mg of ether-soluble material was extracted after 2 days as previously described (6). On column chromatography, the extract yielded the known compounds lubimin (**2**), 10-epilubimin (**5**), and isolubimin (**7**) as a mixture (fractions 50–59; 25 mg; identification by ^{13}Cmr); practically pure **2** (fractions 60–69; 53 mg); rishitin (**8**) admixed with unidentified compounds (fractions 91–95; 18.6 mg); and crystalline **4** (fractions 107–116; 32.7 mg). Fractions 41–48 (9.4 mg) consisted of essentially pure **1**. Fractions 96–106 (26 mg) were rechromatographed (40 g silica gel; 10 mL fractions) to yield crude **3** (6.9 mg). This was combined with similar material (26 mg) from two similar experiments and purified by rechromatography in *i*-PrOH/EtOAc (5:95).

2-Epilubimin (1)

This compound was isolated as an oil. *Exact mass* calcd. for $C_{15}H_{24}O_2$: 236.1776; found (high resolution ms): 236.1775; ir (liq. film): 1710 cm^{-1}; ^1Hmr ($CDCl_3$) δ: 0.90 (d, J = 7 Hz, 3H), 1.71 (bs, 3H), 2.71 (m, 1H), 4.14 (tt, 1H), 4.69 (m, 2H), 9.92 (d, $J \sim 3$ Hz, 1H).

Treatment of a small amount (< 1 mg) with $NaBH_4$ (a few grains) in MeOH at ice-temperature gave, after several hours and upon ether extraction of the acidified solution, the reduced product **3** as judged by R_f (0.26 in *i*PrOH/EtOAc 5:95, 0.17 in MeOH/$CHCl_3$ 5:95) and the characteristic red color with the vanillin reagent.

About 4.5 mg of **1** in 96% EtOH (0.9 mL) was injected under sterile conditions into the medium below a 7-day old culture of *A. solani* in a Roux bottle. After 48 h, the mycelium was filtered off and the filtrate extracted with Et_2O. The complex extract (22 mg) contained no detectable starting material but a small amount of substance indistinguishable from **3** by tlc in 3 systems.

15-Dihydro-2-epilubimin (3)

This compound occurred as a viscous oil which did not crystallize even upon sublimation (60°C). The ms showed only a very small molecular ion at *m/e* 238 (< 1%); hence the elementary composition was confirmed on the $M^+ - H_2O$ ion. *Exact mass* calcd. for $C_{15}H_{26}O_2 - H_2O$: 220.1827; found: 220.1825; ^1Hmr ($CDCl_3$) δ: 0.88 (d, J = 7 Hz, 3H), 1.79 (bs, 3H), 3.31 (dd) and 3.98 (dd) forming the AB portion of an ABX pattern, J_{AB} = 11 Hz, 4.11 (m, 1H), 4.71 (m, 2H).

The ether extract (21.2 mg) obtained from potatoes (25 kg) incubated with a spore suspension of *M. fructicola* in the usual way was chromatographed by our standard procedure. Fractions 41–46 (1–2 mg) contained a small amount (~0.4 mg) of **3** as judged by careful chromatographic comparisons. Fractions 47–62 on rechromatography yield crude hydroxylubimin (8 mg) and **6** (5.2 mg) identified by their ^1Hmr spectra (7). The yields of **2** and **8** in this experiment were 19 and 13 mg, respectively.

Acknowledgements

We are grateful to C. H. Unwin for supplying fungal cultures, to H. Schroeder and D. Hairsine for measuring proton and mass spectra, and to G. L. Rock for skilled experimental assistance. We wish to thank the Natural Sciences and Engineering Research Council of Canada for financial support.

1. A. Stoessl, E. W. B. Ward, and J. B. Stothers. *In* Host plant resistance to pests. ACS Symposium Series, No. 62. *Edited by* P. A. Hedin. American Chemical Society, Washington, DC. 1977. pp. 61–77.
2. D. Gross. Biochem. Physiol. Pflanz. **174**, 327 (1979); J. Kuć and N. Lisker. *In* Biochemistry of wounded plant tissues. *Edited by* G. Kahl. De Gruyter, Berlin. 1978. pp. 203–242.
3. A. Murai, N. Katsui, F. Yagihashi, T. Masamune, Y. Ishiguri, and K. Tomiyama. J. Chem. Soc. Chem. Commun. 670 (1977); T. Masamune, A. Murai, and N. Katsui. Kagaku To Seibutsu, **16**, 648 (1978).

4. D. T. COXON, K. R. PRICE, J. B. STOTHERS, and A. STOESSL. J. Chem. Soc. Chem. Commun. 348 (1979).
5. E. W. B. WARD and A. STOESSL. Phytopathology, **67**, 468 (1977).
6. A. STOESSL, J. B. STOTHERS, and E. W. B. WARD. Can. J. Chem. **56**, 645 (1978).
7. A. STOESSL, C. H. UNWIN, and J. B. STOTHERS. Tetrahedron Lett. 2481 (1979).
8. D. F. HEALD. Manual of plant diseases. 2nd ed. McGraw-Hill, New York and London. 1933.
9. A. STOESSL, J. B. STOTHERS, and E. W. B. WARD. Can. J. Chem. **53**, 3351 (1975).
10. A. STOESSL. In preparation.
11. P. BRIAN, P. J. CURTIS, and H. G. HEMMING. Proc. Roy. Soc. Ser. B, **135**, 106 (1947).
12. Y. HOYANO, A. STOESSL, and J. B. STOTHERS. Can. J. Chem. **58**, 1894 (1980).
13. D. T. COXON, K. R. PRICE, J. B. STOTHERS, and A. STOESSL. J. Chem. Soc. Chem. Commun. 348 (1979).

Can. J. Chem. Downloaded from www.nrcresearchpress.com by 210.87.254.40 on 09/05/12
For personal use only.

Reactions of singlet oxygen. Part V. Dye sensitized photooxidation of *m*-hydroxydiphenylamine[1]

NATHU RAM AND K. S. SIDHU

Department of Chemistry, Punjabi University, Patiala-147002, India

Received May 29, 1979[2]

NATHU RAM and K. S. SIDHU. Can. J. Chem. **58**, 2073 (1980).

Methylene blue sensitized photooxidation of *m*-hydroxydiphenylamine gives *N*-(3-hydroxyphenyl)-*p*-benzoquinoneimine as the primary product in acetonitrile–water medium. The experimental results are in good agreement with the theoretical plots calculated on the basis of the reaction undergoing through the participation of $O_2(^1\Sigma_g^+$ or $^1\Delta_g)$ as well as the excited dye interacting with the substrate. β-Value and rate constant of reactivity of *m*-hydroxydiphenylamine with singlet oxygen have been calculated. The effects of β-carotene, 1,4-diazabicyclo[2,2,2]octane, triethylamine, allyl thiourea, 2,5-diphenylfuran, and dielectric of different solvents show the participation of singlet oxygen at low substrate concentration and interaction of the excited dye with the substrate at its high concentrations. The data on oxygen concentration effect fit into the derived rate expressions. No complexation between methylene blue and *m*-hydroxydiphenylamine is observed.

NATHU RAM et K. S. SIDHU. Can. J. Chem. **58**, 2073 (1980).

L'oxydation photochimique de la *m*-hydroxydiphénylamine sensibilisée par le bleu de méthylène donne la *N*-(hydroxy-3 phényl) *p*-benzoquinoimine comme produit principal dans un milieu acétonitrile–eau. Les résultats expérimentaux sont en parfait accord avec les courbes théoriques calculées en se basant sur les réactions se produisant avec la participation de O_2 ($^1\Sigma_g^+$ ou $^1\Delta_g$) tant que le colorant excité interagit avec le substrat. On a calculé la valeur β et la constante de vitesse de réactivité de la *m*-hydroxydiphénylamine avec l'oxygène singulet. Les effets du β carotène, du diaza-1,4 bicyclo[2,2,2] octane, de la triéthylamine, de l'allylthiourée, du diphényl-2,5 furanne et les effets diélectriques des différents solvants mettent en évidence la participation de l'oxygène singulet à faible concentration et l'interaction du colorant excité avec le substrat à forte concentration. Les données des effets de la concentration de l'oxygène s'adaptent aux expressions dérivés de vitesse. On n'a pas observé de complexation entre le bleu de méthylène et la *m*-hydroxydiphénylamine.

[Traduit par le journal]

Introduction

Photosensitized oxidations of amines and other compounds have been studied (1–10) and it is well known that dyes act as sensitizers in a large number of these reactions (1, 5–10). In some of these systems *in situ* formation of singlet $O_2(^1\Sigma_g^+$ or $^1\Delta_g)$ is reported (1, 5, 6, 9, 10), whereas in others interaction of the excited dye with the substrate has been postulated (7, 8). Photooxidation of anthracene and 2,3-dimethylbut-2-ene sensitized by rose bengal and methylene blue leads to the formation of 9,10-endoperoxide (11) and 3-hydroperoxy-2,3-dimethylbut-1-ene (12), respectively. Kautsky proposed that these types of reactions involve the participation of singlet oxygen (13) and this has been confirmed by other workers (14, 15).

Dye sensitized photooxidation of mono-, di-, and tri-*n*-butylamines has been suggested to take place without the participation of singlet oxygen (16). The dye sensitization reaction in the flash photolysis of amines has been observed not to involve singlet oxygen ($^1O_2$) as a reactive intermediate (7) but the dye radical anions have been observed as a result of an electron transfer from amine to the excited triplet dye. The final products have been suggested to be formed by the proton transfer from amine radical ion and the following reactions of the resulting amine radical with oxygen. The uncertainty about the generation of $^1O_2$ in dye-sensitized oxidation of amines is due to the intrinsic possibility of hydrogen abstraction and exciplex formation by the dyes.

It has been a point of controversy whether the dye sensitization reactions take place through the participation of $^1O_2$ or through hydrogen abstraction or electron transfer processes. In certain cases the comparison of the photosystems with the one in which singlet oxygen is generated by chemical methods (14) or electrodeless discharge (15) is expected to help in sorting out the reaction paths. Limonene gives rise to the same product distribution and kinetic features in both sensitized photooxidation and chemically produced singlet oxygen oxidations (17). But Bartholomew and Davidson have pointed out that there is a competition between the two primary processes viz. energy transfer from the excited sensitizer to oxygen and substrate (8). The efficiency of each path depends upon the concentration of the reactants as well as the rate constants of the two processes. Davidson *et al.* have recently postulated that both the mechanisms are operative in rose bengal sensitized

[1]For Part IV, see ref. 1.

[2]Revision received May 29, 1980.

0008-4042/80/192073-07$01.00/0

© 1980 National Research Council of Canada/Conseil national de recherches du Canada

Can. J. Chem. Downloaded from www.nrcresearchpress.com by 210.87.254.105 on 09/05/12
For personal use only.

Can. J. Chem. Downloaded from www.nrcresearchpress.com by 210.87.254.105 on 09/05/12
For personal use only.

photooxidation of triethylamine (18, 19). This work was undertaken to ascertain the role of singlet oxygen as the reactive intermediate and to lay down the detailed mechanism for the photosensitized oxidation reaction of *m*-hydroxydiphenylamine (HDPA). It was hoped that the study would clarify the interactions of triplet methylene blue with the constituents of the system, particularly at varying concentrations of HDPA.

Experimental

High purity BDH (AR) grade solvents were distilled before use. *m*-Hydroxydiphenylamine (K & K Lab., U.S.A.) was crystallized from benzene – petroleum ether to sharp melting point 81°C. Stock solutions were prepared in blackened standardized volumetric flasks. The other reagents were of high purity and were crystallized to sharp melting points before use.

A Pyrex cell (20 mm diameter × 130 mm) with a narrow capillary for passing gases along the side of the cell was used for photolysis purposes. The capillary was so adjusted as not to be in the light path. The cell was fitted with a condenser at the top and cold water was circulated through it in order to avoid excessive evaporation of the solvent. A white mercury lamp (Philips, India; 125 W) fed from a stabilized power supply was used as a light source. The light was filtered through an optically flat glass plate with cut off at 4700 Å. The emission of the lamp was monitored through the current flowing in the circuit and was found to be constant. Presaturated oxygen gas was passed through the solution at suitable rates. The reaction was found to be very slow in pure acetonitrile, and in order to get reasonable conversions, 4% water was added to the medium except when otherwise stated.

For kinetic runs the reaction was monitored on a precalibrated Hilger and Watt's spectrophotometer at 4900 Å where the product has maximum extinction coefficient in the visible region. Aliquots of 3 mL were withdrawn from the photolysis cell at different intervals of time and were transferred back to the cell after absorbance measurements. Absorbances were measured in Pyrex cell of 10 mm path length.

Results and Discussion

N - (3 - Hydroxyphenyl) - *p* - benzoquinoneimine (HPBQ) was the only primary product as reported earlier (1). Since amines have a lone pair of electrons on nitrogen, there exists the possibility of complexation of amines with the dye (may be charge transfer type (20, 21)) and this can influence the reaction (22, 23). The effect of concentration of methylene blue (MB) was, therefore, examined and the results are given in Table 1. The relative reaction rate increases with the increase in MB concentration and in the region of essentially complete absorption of incident radiation any further increase in MB concentration ceases to affect the rate. This rules out the possibility of any role of complexation because if the complex would have been formed the rate would have increased more at higher concentrations of the dye since the concentration of the complex is expected to be more at higher concentrations of the dye. Furthermore, no product was observed in the absence of light which negates any ground state complexation of amine with the dye.

TABLE 1. Effect of concentration of methylene blue*

[MB] × 10^5, *M*	Relative reaction rate†
0.850	1.00
2.125	1.67
4.250	2.33
6.375	2.50
10.625	2.67
14.875	2.87

*HDPA = 8.0×10^{-4} *M*; O_2 flow rate = 25 mL min^{-1}; solvent = acetonitrile:water::24:1.
†Relative reaction rates have been calculated from the linear plots of [HPBQ] vs. time of irradiation.

Charge transfer complexation was further examined by obtaining the visible spectra of 1.0×10^{-5} *M* MB in acetonitrile–water in the presence of varying amounts of HDPA (1.0×10^{-4} *M* to 8.0×10^{-2} *M*). No spectral shift was observed which supports the absence of any such complexation.

The dielectric of the medium plays an important role in the reactions where amines are involved or where the transition state has some charge separation (24). The effect of dielectric of the medium was examined by varying the proportion of water in the acetonitrile–water solvent and the results are given in Fig. 1. A linear plot of log *R* vs. $1/\varepsilon_0$ (*R* = relative reaction rate; ε_0 = dielectric constant of the medium) shows a good correlation between the solvent polarity and relative rate. A specific solvent effect because of intermolecular interaction can

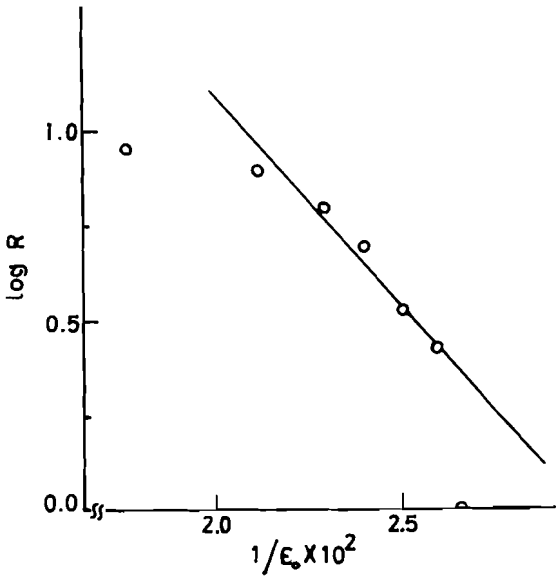


FIG. 1. Plot of log *R* vs. $1/\varepsilon_0$; HDPA = 2.0×10^{-3} *M*; MB = 9.0×10^{-5} *M*.

Can. J. Chem. Downloaded from www.nrcresearchpress.com by 210.87.254.105 on 09/05/12
For personal use only.

influence either the rate of deactivation or rate of reactivity of singlet oxygen and this may be the basis for anomalous behaviour observed at very low and high concentrations of water (water varied from 0 to 40%) (25). The lifetime of singlet oxygen decreases with the increase in water concentration (τ for singlet oxygen is 2 μs and 30 μs in water and acetonitrile respectively) which shows that it is the dielectric which affects the rate and not the lifetime of singlet oxygen.

An electron transfer from the substrate to the dye has been established in some systems (7). The effect of HDPA concentration was studied to examine this possibility in the present system and Fig. 2 gives the results. The relative rate of oxygenation first increases and then decreases after reaching a maximum value. This indicates that the reaction may involve more than one path. One may consider the following scheme to explain the observed results.

[1] $D + h\nu \longrightarrow {}^1D$

[2] ${}^1D \xrightarrow{k_1} D + h\nu'$

[3] ${}^1D \xrightarrow{k_2} D$

[4] ${}^1D \xrightarrow{k_3} {}^3D$

[5] ${}^3D \xrightarrow{k_4} D$

[6] ${}^3D + {}^3O_2 \xrightarrow{k_5} D + O_2({}^1\Delta_g)$

[7] $O_2({}^1\Delta_g) \xrightarrow{k_6} {}^3O_2$

[8] $O_2({}^1\Delta_g) + A \xrightarrow{k_7} [O_2({}^1\Delta_g)\cdots A] \longrightarrow \text{Products}(AO_2)$

[9] ${}^3D + A \xrightarrow{k_8} [{}^3D\cdots A] \xrightarrow{O_2} AO_2$

[10] ${}^1D + A \xrightarrow{k_9} D + A$

D = Dye; ${}^1D$, ${}^3D$ are the first excited singlet and triplet states of the dye respectively; A = HDPA.

SCHEME 1

If the reaction solely occurs with the participation of singlet oxygen, steady state treatment of steps [1] to [8] gives

$$[11]\quad \phi_{AO_2} = \phi_{{}^1O_2}\frac{\alpha_1[A]}{[A] + \beta}$$

where $\beta = k_6/k_7$, ϕ_{AO_2} = quantum yield of product formation; α_1 = fraction of the complex $[O_2({}^1\Delta_g)\cdots A]$ giving products and $\phi_{{}^1O_2}$ = quantum yield of singlet oxygen formation

$$[12]\quad \phi_{{}^1O_2} = \frac{k_3}{k_1 + k_2 + k_3} \times \frac{k_5[{}^3O_2]}{k_4 + k_5[{}^3O_2]}$$

A theoretical plot based on eq. [11] can be made if

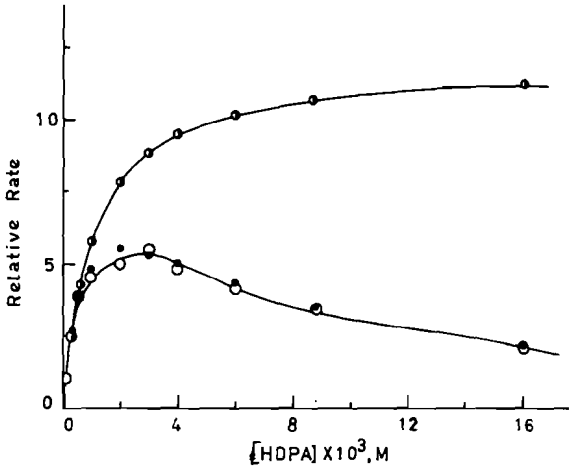


FIG. 2. Effect of concentration of HDPA; ○, experimental; ●, calculated for reaction occurring via $^1O_2$ and triplet dye; ◑, calculated for reaction occurring via $^1O_2$; MB = 9.0×10^{-5} *M*; solvent = acetonitrile:water::24:1.

β is known. Equation [11], when rewritten in the form

$$[13]\quad [AO_2]^{-1} = (\phi_{{}^1O_2}\alpha_1 I_a)^{-1}(1 + k_6/k_7[A])$$

where I_a is the number of mole quanta absorbed per litre during irradiation, can be used for the evaluation of β. A plot of $[AO_2]^{-1}$ vs. $[A]^{-1}$ gives a straight line with β equal to the ratio of the slope and intercept on the $[AO_2]^{-1}$ axis. The results are given in Fig. 3 which gives a β value of 11.04×10^{-4} *M*. With the calculated value of β and known value of rate

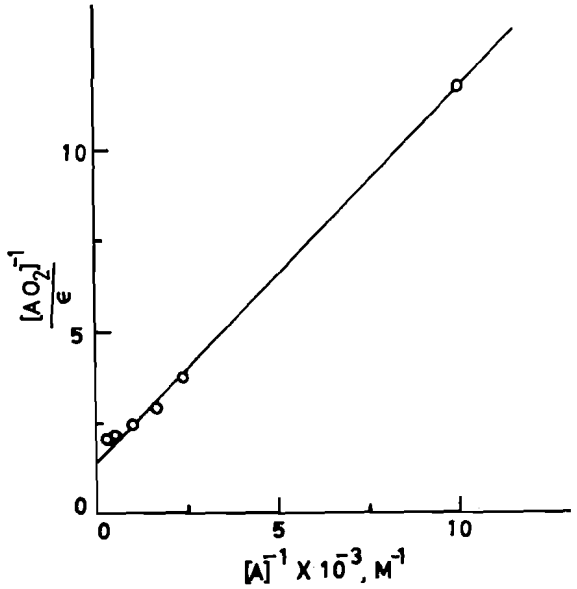


FIG. 3. Plot of $[AO_2]^{-1}$ vs. $[A]^{-1}$ (i.e. 1/product vs. 1/substrate); MB = 9.0×10^{-5} *M*; solvent = acetonitrile: water::24:1.

Can. J. Chem. Downloaded from www.nrcresearchpress.com by 210.87.254.105 on 09/05/12
For personal use only.

constant of deactivation of singlet oxygen ($k_6 = 3.33 \times 10^4\ s^{-1}$) in acetonitrile (26), the rate constant of reactivity of HDPA with singlet oxygen (k_7) comes out to be 3.02×10^7 L mol^{-1} s^{-1}.

A theoretical curve based on eq. [11] with the calculated β value agrees well with the experimental points at low HDPA concentrations (Fig. 2) but there is a complete divergence at its higher concentrations. The decrease in the rate cannot be due to triplet energy transfer to the substrate because this process is strongly endothermic and is bound to be inefficient (27). The observed decrease in the rate beyond 3.0×10^{-3} *M* HDPA concentration points to an alternate pathway since the product remains the same.

The interaction of the triplet dye with the substrate is an obvious pathway. However, deactivation of the singlet dye must also be considered as reported in the literature (18, 19). The steady-state treatment of Scheme 1 now gives

$$[14]\quad \phi_{AO_2} = \frac{k_3[A]}{(k_1 + k_2 + k_3 + k_9[A])(k_4 + k_5[^3O_2] + k_8[A])}\left(\frac{k_5 k_7 \alpha_1 [^3O_2]}{k_6 + k_7[A]} + k_8\alpha_2\right)$$

where α_2 = fraction of the complex $[^3D\cdots A]$ giving products.

The singlet–singlet energy transfer at high amine concentration is not possible because of the endothermicity of the process (MB and HDPA have first excited singlet state energies 44.3 kcal and 80 kcal, respectively). Furthermore, the interaction of amine with singlet dye is not expected because the rate constant for the decay of singlet dye is very high ($\sim 2.5 \times 10^9\ s^{-1}$). For an appreciable interaction the amine concentration should be very high as compared to the one used here.

Using literature values for some of the rate constants (19), calculated value of β, $k_9(k_1 + k_2 + k_3)^{-1} = k_9\tau \simeq 40$ (19), $\alpha_1 = 0.15$ and $\alpha_2 = 0.007$, a plot based on eq. [14] can be obtained between the theoretical values of relative reaction rate and HDPA concentration which agrees well with the experimentally observed points. The values of α_1 and α_2 have been adjusted and a good fit of the data shows that the reaction follows both the reaction paths.

Oxygen is expected to strongly influence the reaction both at low and high amine concentrations since it is one of the reactants. Its effect has been examined both at low and high HDPA concentrations and Fig. 4 gives the results. Equation [11], when rewritten in the form

$$[15]\quad [AO_2]^{-1} = \left\{\frac{k_3\alpha_1[A]I_a}{(k_1 + k_2 + k_3)([A] + \beta)}\right\}^{-1} \times \left(1 + \frac{k_4}{k_5}[^3O_2]^{-1}\right)$$

predicts a linear relationship between $[AO_2]^{-1}$ and $[^3O_2]^{-1}$ at constant amine concentration which is in agreement with the observed results (Fig. 4, curve I). This shows the participation of singlet oxygen at low amine concentration.

The curve showing the oxygen concentration effect at high HDPA concentration is linear and passes through the origin (Fig. 4, curve II). This is not explained by eq. [14] which predicts a non-zero rate at zero oxygen concentration. However, if the following processes are considered together with steps [1] to [5], the predicted rate may agree with the observed rate.

$$[16]\quad {}^3D + A \xrightarrow{k_{10}} [^3D\cdots A]$$

$$[17]\quad [^3D\cdots A] \xrightarrow{k_{11}} D + A$$

$$[18]\quad [^3D\cdots A] + {}^3O_2 \xrightarrow{k_{12}} AO_2$$

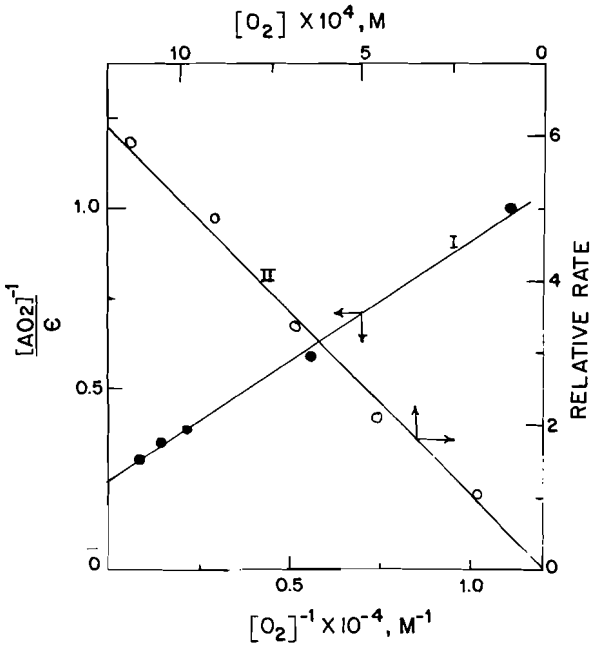


FIG. 4. Effect of oxygen concentration; curve I, HDPA = 8.0×10^{-4} *M*; curve II, HDPA = 8.8×10^{-3} *M*; MB = 9.0×10^{-5} *M*; solvent = acetonitrile:water::24:1.

This gives the quantum yield of product formation as

$$[19]\quad \phi_{AO_2} = \frac{k_3 k_{10} k_{12}[A][^3O_2]}{(k_1 + k_2 + k_3)(k_{11} + k_{12}[^3O_2])(k_4 + k_{10}[A])}$$

which is obviously for high HDPA concentration where the role of the singlet oxygen is negligible. Equation [19] predicts a direct linear relationship between rate and oxygen concentration at constant amine concentration (as observed) if $k_{12}[^3O_2]$ is neglected in comparison to k_{11}; this is reasonable because step [17] involves back electron transfer from dye to amine and is known to be an efficient process (8). It is, therefore, apparent that at high concentrations of HDPA triplet dye is interacting with the substrate and singlet oxygen is not being formed.

In order to further examine the role of singlet oxygen the effect of singlet oxygen quenchers, 1,4-diazabicyclo[2,2,2]octane (DABCO) (28) and β-carotene (29) were examined separately at low and high concentrations of HDPA and the results are given in Fig. 5. For low concentrations the data fit into the Stern-Volmer equation

$$[20]\quad \phi_0/\phi = 1 + \frac{k_q[Q]}{k_6 + k_7[A]}$$

where k_q is the quenching rate constant of singlet oxygen by the quencher Q; ϕ_0 and ϕ are the quantum yields in the absence and presence of the quencher respectively. From the slopes of the lines 1 and 2 the quenching efficiency of β-carotene has been found to be 0.39×10^3 times more than DABCO which can be compared with a reported value of 0.79×10^3 for hexamethyleneammonium hexamethylenedithiocarbamate in ethanol (30). This is in good agreement with the present results, particularly in view of the expected difference in reactivity of the substrate. However, the quenching by DABCO at high HDPA concentrations (Fig.5, curve 3) is nearly 11 times less efficient, showing that at high amine concentrations singlet oxygen does not significantly contribute to the reaction. Further increase in HDPA concentrations is certain to further decrease the contribution of singlet oxygen. The lowering in the reaction rate at high substrate concentrations can, therefore, be attributed to electron transfer exciplex formation mechanism since the product remains the same.

To further substantiate the role of singlet oxygen the effect of triethylamine (TEA), which is a good acceptor of singlet oxygen and as good a quencher as DABCO (31, 32) was studied and the results are given in Table 2. The relative reaction rate decreases with the increase in TEA concentration. Quenching of triplet methylene blue by TEA can be competitive with quenching of singlet oxygen by TEA in its effect on relative overall reaction quantum yields. This is directly related to the solvent used, the lifetime of singlet oxygen in that solvent,

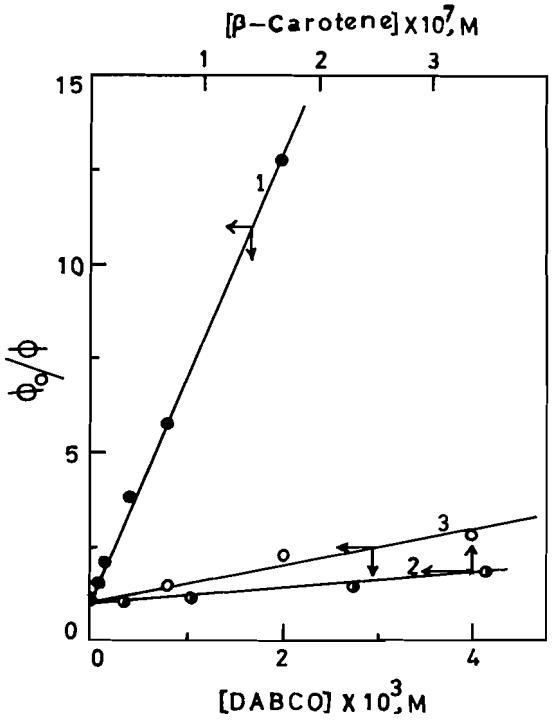


FIG. 5. Effect of DABCO and β-carotene on the rate of reaction; ϕ and ϕ_0 are the reaction rates with and without quenchers respectively. Curve 1 is for DABCO and curve 2 for β-carotene; HDPA = 8.0×10^{-4} *M*; curve 3 is for DABCO; HDPA = 8.8×10^{-3} *M*. MB = 9.0×10^{-5} *M*; solvent = acetonitrile:water::24:1.

TABLE 2. Effect of adding triethylamine (TEA)*

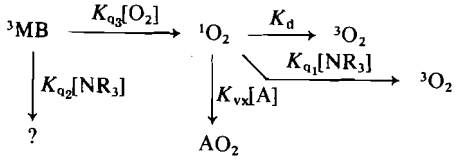
[TEA] × 10^5, *M*	Relative reaction rate†
0.00	1.000
0.15	0.826
2.88	0.652
5.76	0.522
28.80	0.304

*HDPA = 8.0×10^{-4} *M*; MB = 9.0×10^{-5} *M*; solvent = acetonitrile:water::24:1; O_2 flow rate = 25 mL min^{-1}.
†Relative reaction rates have been calculated from the linear plots of [HPBQ] vs. time of irradiation.

Can. J. Chem. Downloaded from www.nrcresearchpress.com by 210.87.254.105 on 09/05/12
For personal use only.

Can. J. Chem. Downloaded from www.nrcresearchpress.com by 210.87.254.105 on 09/05/12
For personal use only.

etc. Unfortunately, not all of the needed rate constants are available for methylene blue, TEA, and singlet oxygen in acetonitrile. However, the lifetime of singlet oxygen is known and if one assumes that the other quenching rate constants by TEA are the same in acetonitrile as they are in methanol, then the following arguments can be made.



$$K_d = \frac{1}{\tau_{1_{O_2}}} \cong \frac{1}{57 \times 10^{-6}} \cong 1.7 \times 10^4$$

$$K_{q_1}[NR_3] \cong 2.8 \times 10^8 [5.8 \times 10^{-5}] \cong 1.6 \times 10^4$$

Thus, then two values are nearly equal, and the calculated efficiency of the photo-oxidation reaction is expected to be 50%, which was found experimentally (Table 2).
Also

$$K_{q_3}[O_2] \cong 3 \times 10^9 [2 \times 10^{-3}] \cong 6.0 \times 10^6$$

$$K_{q_2}[NR_3] \cong 4.7 \times 10^7 [5.8 \times 10^{-5}] \cong 2.7 \times 10^3$$

Thus, the quenching of triplet state at the concentrations of amine used is much slower than the quenching of the triplet state of the dye by oxygen. This shows that the effect of TEA is on singlet oxygen and not on the triplet state of the dye and the observed decrease can be safely attributed to the quenching of singlet oxygen.

Singlet oxygen is known to react with 2,5-diphenylfuran (DPF) very efficiently (25) and the effect of its addition was studied at low HDPA concentrations. The extent of the reaction decreases in the initial stages of the reaction and after a time, which increases with the increase in DPF concentration, becomes equal to the rate in the absence of the quencher. This effect is due to the rapid consumption of DPF because k(DPF)/k(HDPA) = 6.3.

In order to further examine the electron transfer from the substrate to the triplet dye the effect of addition of allyl thiourea (ATU), a reducing agent, was examined and the results are given in Table 3. The efficiency of the reaction decreases with increase in ATU concentration which negates the possibility of the semiquinone form of the dye as an intermediate since in that case the reaction would have increased (30). It is thus apparent that the reaction takes place through singlet oxygen at low HDPA concentrations.

TABLE 3. Effect of adding allyl thiourea (ATU)*

[ATU] × 10⁴, M	Relative reaction rate†
0	1.000
4	0.888
10	0.815
20	0.777
80	0.704‡

*HDPA = 8.0 × 10⁻⁴ M; MB = 9.0 × 10⁻⁵ M; solvent = acetonitrile:water::24:1; O_2 flow rate = 25 mL min⁻¹.
†Relative reaction rates have been calculated from the linear plots of [HPBQ] vs. time of irradiation.
‡Calculated from the initial part of the curve as it became non-linear after 20 min.

The effects of viscosity and dielectric of the medium have been reported elsewhere (1). However, in order to examine the properties other than dielectric and viscosity of the solvent which might influence the reaction, the effect of various solvents was examined at low and high HDPA concentrations and the results are given in Table 4. The relative reaction rate is maximum in ethylene glycol and minimum in acetonitrile. If we look at the viscosities of these solvents the rates increase with the increase in viscosity but not regularly. The increase in the relative reaction rate cannot be attributed to the viscosity alone because there is a simultaneous change in the dielectric of the medium. A lot of other effects like quenching of some triplet states by oxygen in a non-energy transfer process, hydrogen bonding ability, and stabilization of transition state involved can also occur and their extent is different in different solvents. Unfortunately, very little is known about the quenching of different excited states in various solvents which makes it difficult to work out the absolute values of reaction rates. The higher rate in ethylene glycol, however, can be taken to support the participation of singlet oxygen as reported previously (25). It appears that the electron transfer mechanism is also influenced

TABLE 4. Effect of various solvents*

Solvent	Viscosity† (η) (cP)	Dielectric† (ε_0)	Relative reaction rate‡ A	B
Acetonitrile	0.345	37.50	1.00	1.00
Methanol	0.593	32.53	—	2.83
Ethanol	1.194	24.30	1.36	3.33
2-Propanol	2.370	18.30	3.33	3.67
Ethyleneglycol	15.600	37.70	4.85	4.50

*MB = 9.0 × 10⁻⁵ M; O_2 flow rate = 25 mL min⁻¹.
†Values from ref. 33.
‡Relative reactions rates have been calculated from the linear plots of [HPBQ] vs. time of irradiation. The HDPA used for A and B is 8.0 × 10⁻⁴ M and 1.6 × 10⁻² M respectively.

by the hydrogen bonding ability of the hydroxylic solvents. The effect is, however, complex and defies a simple correlation. Thus we conclude that the methylene blue sensitized photooxidation of HDPA proceeds through the participation of singlet oxygen as well as electron transfer exciplex formation and the efficiency of each path is dependent upon substrate concentration.

Acknowledgement

We are thankful to the Council of Scientific and Industrial Research, New Delhi, for financial assistance.

1. N. RAM, W. R. BANSAL, B. V. PANDAV, and K. S. SIDHU. Indian J. Chem. **15B**, 820 (1977).
2. H. GAFFRON. Chem. Ber. **60**, 2229 (1927).
3. R. F. BARTHOLOMEW and R. S. DAVIDSON. J. Chem. Soc. C, 2342 (1971).
4. R. F. BARTHOLOMEW and R. S. DAVIDSON. J. Chem. Soc. C, 2804 (1971).
5. M. H. FISCH, J. C. GRAMAIN, and J. A. OLESEN. J. Chem. Soc. Chem. Commun. 663 (1971).
6. M. H. FISCH, J. C. GRAMAIN, and J. A. OLESEN. J. Chem. Soc. Chem. Commun. 13 (1970).
7. R. F. BARTHOLOMEW and R. S. DAVIDSON. J. Chem. Soc. Chem. Commun. 1174 (1970).
8. R. F. BARTHOLOMEW and R. S. DAVIDSON. J. Chem. Soc. C, 2347 (1971).
9. W. R. BANSAL, S. PURI, and K. S. SIDHU. Bull. Chem. Soc. Jpn. **47**, 2329 (1974).
10. W. R. BANSAL, N. RAM, and K. S. SIDHU. Indian J. Chem. **13**, 987 (1975).
11. C. S. FOOTE, S. WEXLER, W. ANDO, and R. HIGGINS. J. Am. Chem. Soc. **90**, 975 (1968).
12. G. O. SCHENCK and K. H. SCHULTE-ELTE. Annalen, **618**, 185 (1958).
13. H. KAUTSKY. Biochem. Z. **291**, 271 (1937).
14. C. S. FOOTE and S. WEXLER. J. Am. Chem. Soc. **86**, 3879 (1964); **86**, 3880 (1964).
15. E. J. COREY and W. C. TAYLOR. J. Am. Chem. Soc. **86**, 3881 (1964).
16. F. C. SCHAEFER and W. D. ZIMMERMANN. J. Org. Chem. **35**, 2165 (1970).
17. C. S. FOOTE, S. WEXLER, and W. ANDO. Tetrahedron Lett. **46**, 4111 (1965).
18. R. S. DAVIDSON and K. R. TRETHEWAY. J. Chem. Soc. Chem. Commun. 674 (1975).
19. R. S. DAVIDSON and K. R. TRETHEWAY. J. Chem. Soc. Perkin Trans. II, 169 (1977); 173 (1977); 178 (1977).
20. R. S. MULLIKEN. J. Am. Chem. Soc. **74**, 811 (1952).
21. M. MATAGA. Bull. Chem. Soc. Jpn. **31**, 487 (1958).
22. K. M. C. DAVIS and M. F. FARMER. J. Chem. Soc. B, 859 (1968).
23. W. C. MEYER. J. Phys. Chem. **74**, 2118 (1970).
24. C. S. FOOTE and R. W. DENNY. J. Am. Chem. Soc. **93**, 5168 (1971).
25. R. H. YOUNG, K. WEHRLY, and R. L. MARTIN. J. Am. Chem. Soc. **93**, 5774 (1971).
26. P. B. MERKEL and D. R. KEARNS. J. Am. Chem. Soc. **94**, 7244 (1972).
27. J. G. CALVERT and J. N. PITTS, JR. Photochemistry. John Wiley and Sons, Inc., New York, 355 (1967).
28. C. OUANNES and T. WILSON. J. Am. Chem. Soc. **90**, 6527 (1968).
29. C. S. FOOTE and R. W. DENNY. J. Am. Chem. Soc. **90**, 6233 (1968).
30. T. YAMASE, H. KOKADO, and E. INOUE. Bull. Chem. Soc. Jpn. **45**, 726 (1972).
31. W. F. SMITH. J. Am. Chem. Soc. **94**, 186 (1972).
32. G. O. SCHENCK. Ind. Eng. Chem. **55**, 40 (1963).
33. Handbook of chemistry and physics. The Chemical Rubber Publishing Co., U.S.A. 1962.

Can. J. Chem. Downloaded from www.nrcresearchpress.com by 210.87.254.105 on 09/05/12
For personal use only.

Vibrational spectroscopic studies of molecular associations by local anesthetics

M. GUÉRIN,[1] J.-M. DUMAS,[1] AND C. SANDORFY

Département de Chimie, Université de Montréal, C.P. 6210, Succ. A, Montréal (Qué.), Canada H3C 3V1

Received April 22, 1980

M. GUÉRIN, J.-M. DUMAS, and C. SANDORFY. Can. J. Chem. **58**, 2080 (1980).

Infrared spectroscopic studies have been performed on H-bonding for a number of local anesthetics: benzocaine, procaine, tetracaine, lidocaine, dibucaine, and three barbiturates: phenobarbital, pentobarbital, and thiopental. All these compounds have a marked tendency for self-association. When they are put into contact with systems containing H-bonds of the N—H---O=C$\diagdown$, N—H---N, or O—H---O types, however, the degree of self-association decreases and new H-bonds are formed at the expense of the former. The possible consequences of this for the chemical mechanism of anesthesia are briefly discussed.

M. GUÉRIN, J.-M. DUMAS et C. SANDORFY. Can. J. Chem. **58**, 2080 (1980).

Les liaisons hydrogène formées par les anesthésiques locaux: benzocaïne, procaïne, tetracaïne, lidocaïne et dibucaïne ont été examinées par les méthodes de la spectroscopie infrarouge. Trois barbituriques: phenobarbital, pentobarbital et thiopental ont été également étudiés. Tous ces composés montrent une nette tendance à l'auto-association. Cependant quand ils sont mis en contact avec des systèmes qui contiennent les liaisons hydrogène du type N—H---O=C, N—H---N ou O—H---O, la proportion des molécules auto-associées diminue et de nouvelles liaisons hydrogène hétéro-associées sont formées. Les conséquences que cela peut avoir pour le mécanisme de l'anesthésie sont brièvement discutées.

Introduction

Molecular associations of *general* (inhalation) anesthetics have been the topic of previous publications from this laboratory (1–5). Particular emphasis has been laid on the dissociative effect exerted by halofluorocarbon anesthetics on hydrogen bonds. This effect was studied by measuring infrared spectra of model systems containing H-bonds of the

N—H---O=C$\diagdown$, N—H---N, and O—H---O

types and anesthetics like chloroform, halothane, methoxyflurane, ··· . Such H-bonds are needed to keep in the right conformation the macromolecules (lipids and proteins) forming the membrane of the nerve cell. Perturbing them might alter the permeability of the membrane thereby interfering with the normal functioning of the nervous system. It has been proposed, on the basis of the results obtained, that while lipid solubility and hydrophobic interactions are necessary to bring the anesthetic into the membrane, both hydrophobic and polar interactions (among these the perturbation and formation of H-bonds) have to be invoked in order to explain the anesthetic action at the molecular level. Polar interactions might not be important for weak anesthetic action but they appear to be essential when potent anesthetics are required. It is not intended to elaborate here on the theories of anesthesia, however. Instead, we are going to report on the extension of our studies to local anesthetics.

Local anesthetics generally contain two or more strongly associative groups. Since this is so, it seemed to us of interest to examine the associations of a number of local anesthetics with similar model systems. The question as to whether there are analogies between the behavior of general and local anesthetics seemed to us a particularly intriguing one.

Two categories of anesthetics have been examined. (*a*) Benzylalcohol, benzocaine, procaine, tetracaine, lidocaine, and dibucaine; while some of these can exert anesthetic action both as neutral molecules and positive ions, only the neutral molecules have been studied. (*b*) Phenobarbital, pentobarbital, and thiopental.

Contrary to general anesthetics, local anesthetics have a strong tendency to self-association. It has become clear after some preliminary measurements that the best way to investigate their associations is to study the competition between self-association and hetero-association (formation of H-bonded species in which the proton donor and the proton acceptor are different molecules) in the presence of selected perturbers. This can be done through infrared spectroscopic methods. The perturbers were *N*,*N*-dimethylacetamide (NNDA), *N*-methylacetamide (NMA), and benzylalcohol. NNDA is a proton acceptor while NMA and benzylalcohol can act both as proton donors and proton acceptors. These "perturbers" were chosen to represent associative sites in the membrane. Benzylalcohol was used both as a "perturber" and an "anesthetic". In most cases the concentration of

[1]Permanent address: Laboratoire de Physico-Chimie des Diélectriques, Université de Poitiers, Poitiers, France.

0008-4042/80/192080-09$01.00/0

©1980 National Research Council of Canada/Conseil national de recherches du Canada

Can. J. Chem. Downloaded from www.nrcresearchpress.com by 210.87.254.42 on 09/05/12
For personal use only.

Can. J. Chem. Downloaded from www.nrcresearchpress.com by 210.87.254.42 on 09/05/12
For personal use only.

the perturber was kept low so that its self-association could be disregarded. The concentrations of the anesthetics were in the range of concentrations used in clinical practice or lower (see, for example, Adriani *et al.* (6)).

Experimental

The infrared spectra were measured on a Perkin-Elmer model 621 spectrometer at room temperature, using standard techniques. Those of the compounds in category (*a*) were measured in CCl_4 solutions, those in category (*b*) in CH_2Cl_2 since they did not show sufficient solubility in CCl_4.

Benzylalcohol was a Baker Analyzed Reagent, *N,N*-dimethylacetamide and *N*-methylacetamide were high purity Eastman products. They were further purified by vacuum distillation under dry nitrogen atmosphere and were kept on molecular sieves. Benzocaine was a high purity Eastman product and was used without further purification. The other compounds of category (*a*) were Astra or Winthrop products. The free bases were obtained from their hydrochlorides by adding KOH and were extracted with ether. Spectrograde CCl_4 was kept on molecular sieves in a dry box.

The barbiturates were May and Baker U.S.P. Products. Phenobarbital was used without further purification. Pentobarbital and thiopental were prepared from the aqueous solutions of their sodium salts (May and Baker) by adding 10% HCl, extracting with ether and rinsing with water. They were dried at 105°C and kept in a desiccator.

Fisher spectral analyzed CH_2Cl_2 was dried on P_2O_5, distilled, and kept on molecular sieves in a dry box.

The solutions were prepared immediately before measuring the spectra.

The infrared spectra of the self-associated molecules are presented in apparent molar extinction coefficients (ε, in L mol^{-1} cm^{-1}) against wavenumbers in cm^{-1}. The ε values are apparent since to compute them the overall concentrations were used, the proportion of the free and the various associated species being undetermined. The other spectra are plotted in absorbance against wavenumbers in cm^{-1}.

The chemical formulas of the compounds treated in this paper are given in Fig. 1 for convenience.

Results and Discussion

(I) Self-association of "Caine" Type Anesthetics

It is necessary to have at our disposal the absorption curves of the anesthetics at various concentrations so that we can assess the extent of perturbation exerted by the added perturber.

Figure 2 shows the spectrum of benzylalcohol. The free band is at 3619 cm^{-1} for a concentration of about 3×10^{-3} *M* in CCl_4. The band exhibits a shoulder at its high frequency side. This is due to rotational isomerism about the C—O bond as has been shown for a number of alcohols by Krueger, Jan, and Wieser (7). The relative intensities of the band and the shoulder appear to be independent of concentration. In the given range of concentrations the only associated species that can be seen in the spectrum is the dimer whose band, near 3500 cm^{-1}, increases in intensity with increasing concentration.

Benzocaine and procaine have nearly identical spectra and only that of benzocaine is shown (Fig. 3). The two NH stretching bands of the primary amino group are at 3500 and 3410 cm^{-1}. The shoulder at 3383 cm^{-1} disappears upon dilution and must belong to an associated species. In the spectrum of tetracaine (Fig. 4), a secondary amine, the free band is double. As in the previous case this is believed to be due to rotational isomerism. At higher concentrations the associated band is well pronounced at 3387 cm^{-1}.

As to the nature of self-association in tetracaine this is likely to involve mostly N—H---N (tertiary) association but N—H---C=O (ester) and N—H---N—H are probably also involved. While no quantitative studies are reported here it is noteworthy that the relative intensity change in the carbonyl band is less than what is observed for the NH band.

Dibucaine is a secondary amide; its spectrum is very similar to that of tetracaine. Lidocaine is also a secondary amide but with the nitrogen (not the carbonyl) linked to the benzene ring. Its spectrum is apparently simple (Fig. 5). The peak is near 3320 cm^{-1} and at low concentrations it appears to be nearly symmetrical. At higher concentrations, however, the lower frequency side increases in intensity and the band becomes asymmetrical. Thus the peak at 3320 cm^{-1} is likely to correspond to the free species while the associated band is centered near 3225 cm^{-1}.

The carbonyl bands of these anesthetics decrease in intensity upon self-association. At the low concentrations used, however, the associated carbonyl band could not be observed, being hidden under the low frequency wing of the free band.

The curves in Figs. 2 to 5 are to be compared to those presented in the next section in order to assess the changes brought about by hetero-association. As is seen the concentrations of the anesthetics were chosen so that little self-association occurs.

(II) Hetero-associations of "Caine" Type Anesthetics

In Figs. 6, 8, and 10 two curves are shown. The dashed curves are the sum of the curves of the (unmixed) anesthetic and the perturber. They were obtained by putting into the sample beam two cells in a row. The solid lines represent the spectra of the mixture of the anesthetic and the perturber at the same concentrations. Thus whatever difference is observed between the two curves is a consequence of association between the anesthetic and the perturber.

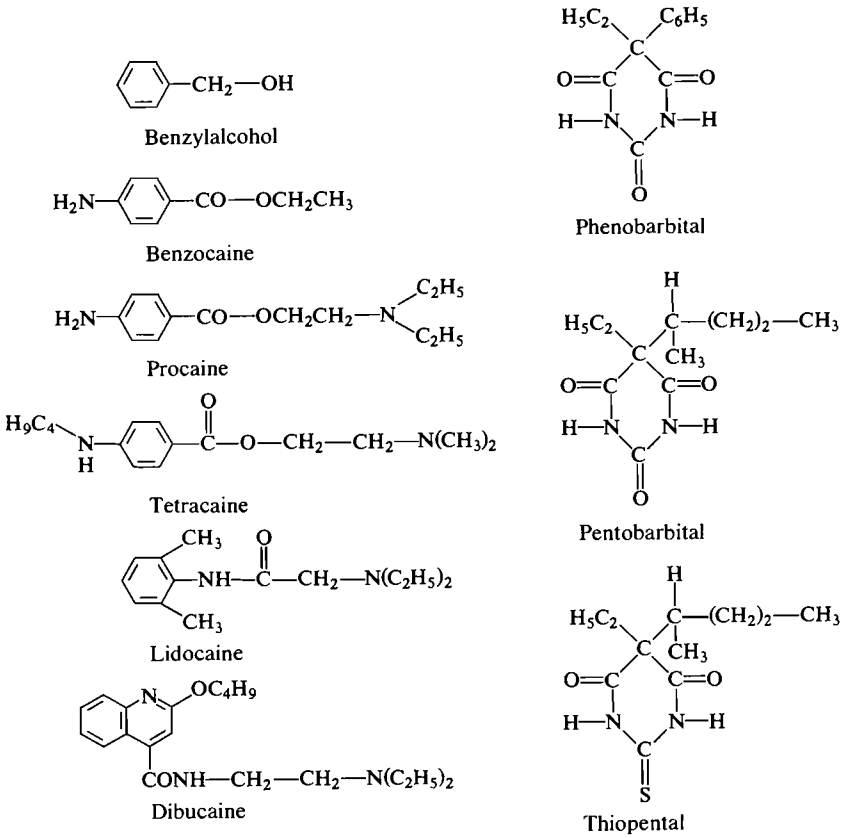


FIG. 1. Formulas of the compounds examined.

In Figs. 7 and 9 the absorption curves of the anesthetic, the perturber, and their mixture are given separately.

(a) Association with N,N-*Dimethylacetamide*

The effect of adding benzylalcohol to NNDA is shown in Figs. 6 and 7. The free band of the alcohol decreases in intensity and an intense new band appears near 3440 cm^{-1} representing the hydrogen bond formed between the "anesthetic" (benzylalcohol) and the perturber (NNDA). Since at the same time the carbonyl band of NNDA becomes asymmetrical with a shoulder appearing at its low wavenumber side we can assign the new band to O—H---O=C bonds. Some O—H---N type H-bonds might also be present.

Benzocaine and procaine again give practically identical spectra. Figures 8 and 9 show the spectra of the procaine + NNDA system. Upon mixing, new bands appear which can only belong to the N—H bonds of procaine hydrogen bonded to NNDA. The new band of lower frequency (3350 cm^{-1}) is largely free-standing while the one of higher frequency (about 3450 cm^{-1}) becomes a shoulder. The main observation from the point of view of this study is that these bands cannot belong to self-associated procaine. As has been shown above (Fig. 3) the associated band for the latter species is at 3383 cm^{-1} and it is easily distinguished from the new bands due to procaine-NNDA association.

The tetracaine + NNDA system gives similar results although the observed spectral change is less spectacular (Fig. 10). Upon mixing the intensity of the NH stretching band of tetracaine diminishes and a new band appears with maximum at about 3350 cm^{-1}, which can only correspond to tetracaine–NNDA association. The NH band for self-association is at distinctly higher frequencies, about 3387 cm^{-1}. Thus here again we observe the trend favoring mixed association.

Similar observations are made on the dibucaine + NNDA system despite the fact the proton donor NH group is engaged in an amide linkage in this molecule. The new band appears near 3300 cm^{-1} (Fig. 11). Self-associated dibucaine has its band at

Can. J. Chem. Downloaded from www.nrcresearchpress.com by 210.87.254.42 on 09/05/12
For personal use only.

Can. J. Chem. Downloaded from www.nrcresearchpress.com by 210.87.254.42 on 09/05/12
For personal use only.

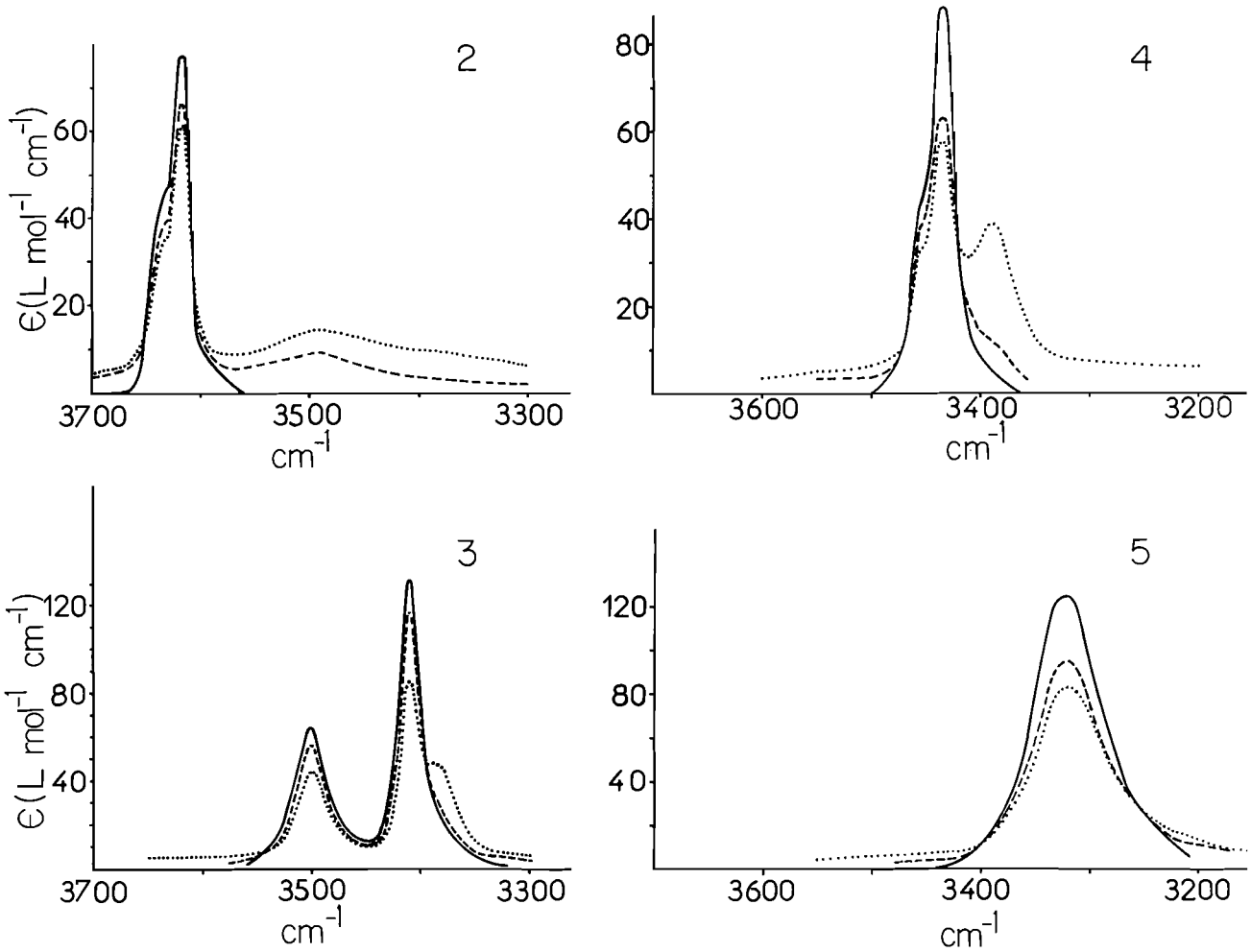


FIG. 2. The XH stretching region of the infrared spectrum of benzylalcohol in carbon tetrachloride. —, $c = 2.938 \times 10^{-3}$ mol L^{-1}; ---, $c = 5.745 \times 10^{-2}$ mol L^{-1}; ···, $c = 1.049 \times 10^{-1}$ mol L^{-1}.

FIG. 3. The XH stretching region of the ir spectrum of benzocaine in carbon tetrachloride. —, $c = 9.752 \times 10^{-3}$ mol L^{-1}; ---, $c = 3.203 \times 10^{-2}$ mol L^{-1}; ···, $c = 1.600 \times 10^{-1}$ mol L^{-1}.

FIG. 4. The XH stretching region of the ir spectrum of tetracaine in carbon tetrachloride. —, $c = 6.363 \times 10^{-4}$ mol L^{-1}; ---, $c = 2.774 \times 10^{-2}$ mol L^{-1}; ···, $c = 2.068 \times 10^{-1}$ mol L^{-1}.

FIG. 5. The XH stretching region of the ir spectrum of lidocaine in carbon tetrachloride. —, $c = 8.336 \times 10^{-4}$ mol L^{-1}; ---, $c = 2.759 \times 10^{-2}$ mol L^{-1}; ···, $c = 1.965 \times 10^{-1}$ mol L^{-1}.

Can. J. Chem. Downloaded from www.nrcresearchpress.com by 210.87.254.42 on 09/05/12
For personal use only.

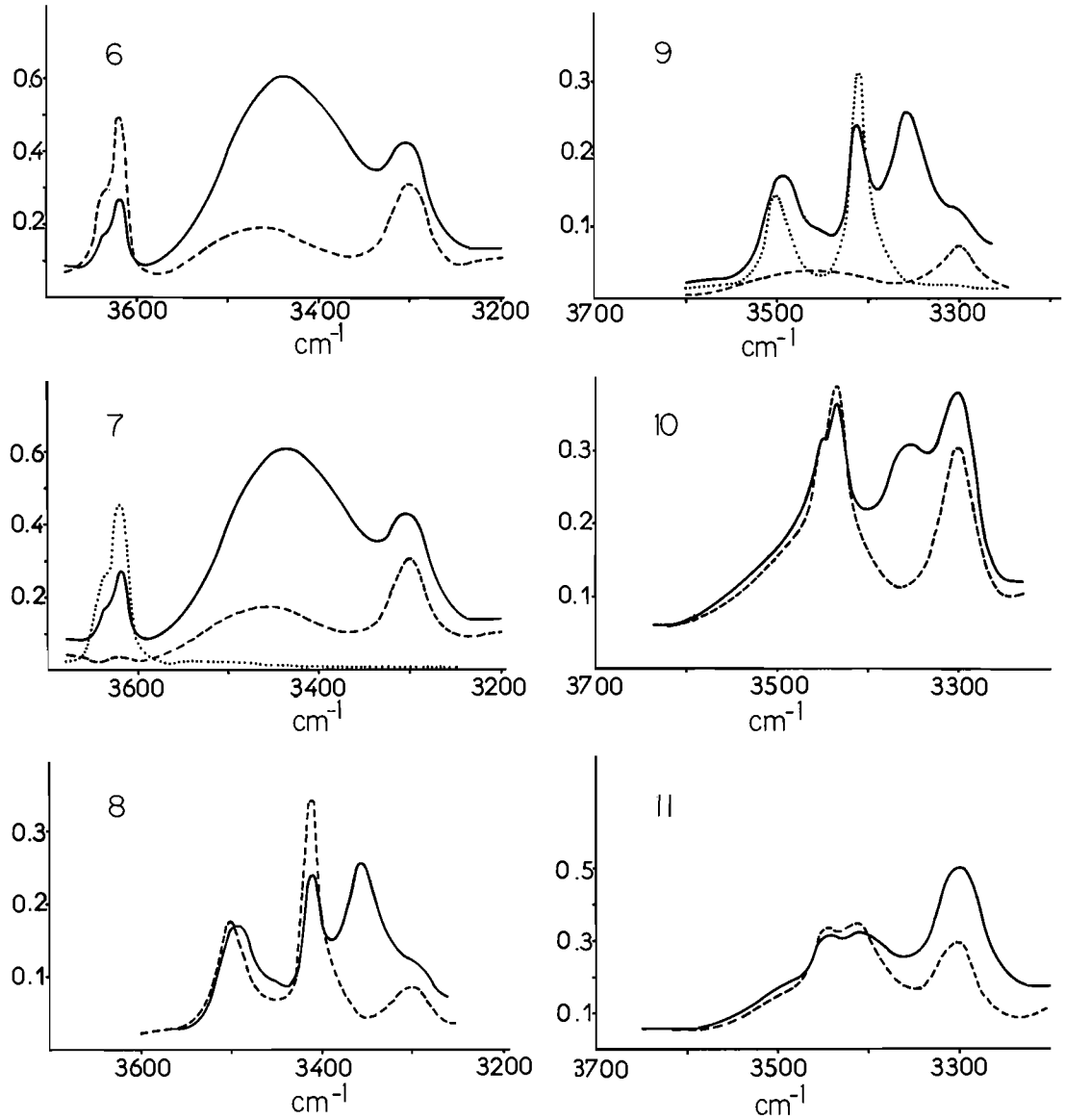


FIG. 6. ---, summation spectrum of unmixed benzylalcohol (1.370×10^{-2} mol L^{-1}) and *N*,*N*-dimethylacetamide (1.434×10^{-1} mol L^{-1}); —, mixture of the two at the same concentrations.

FIG. 7. ···, the ir spectra of benzylalcohol (1.370×10^{-2} mol L^{-1}); ---, *N*,*N*-dimethylacetamide (1.434×10^{-1} mol L^{-1}); —, mixture of the two at the same concentrations.

FIG. 8. ---, summation spectrum of unmixed procaine (2.631×10^{-2} mol L^{-1}) and *N*,*N*-dimethylacetamide (1.368×10^{-1} mol L^{-1}); —, mixture of the two at the same concentrations.

FIG. 9. ··· the ir spectra of procaine (2.631×10^{-2} mol L^{-1}); --- *N*,*N*-dimethylacetamide (1.368×10^{-1} mol L^{-1}); —, mixture of the two at the same concentrations.

FIG. 10. ---, summation spectrum of unmixed tetracaine (7.330×10^{-3} mol L^{-1}) and *N*,*N*-dimethylacetamide (1.375×10^{-1} mol L^{-1}); —, mixture of the two at the same concentrations.

FIG. 11. ---, summation spectrum of unmixed dibucaine (9.655×10^{-3} mol L^{-1}) and *N*,*N*-dimethylacetamide (1.210×10^{-1} mol L^{-1}); —, mixture of the two at the same concentrations.

3335 cm^{-1}. As in the previous case self-association seems to involve both N—H---O=C and N—H---N type H-bonds.

Unfortunately, in the case of the lidocaine + NNDA system, the bands of the self-associated and the mixed complex coincide and the new band cannot be discerned. The observed intensity in the spectral region concerned is, however, higher; indicating that such mixed complexes are formed.

The observations made on the NNDA +

Can. J. Chem. Downloaded from www.nrcresearchpress.com by 210.87.254.42 on 09/05/12
For personal use only.

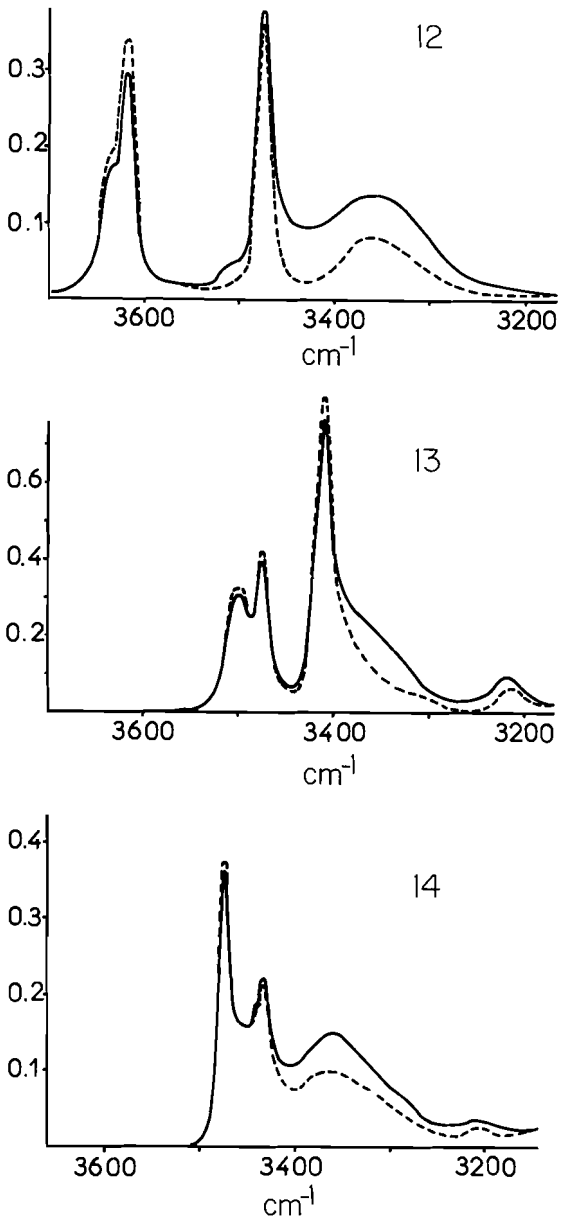


FIG. 12. --- summation spectrum of unmixed benzylalcohol (3.156×10^{-2} mol L^{-1}) and *N*-methylacetamide (2.045×10^{-2} mol L^{-1}); —, mixture of the two at the same concentrations.

FIG. 13. ---, summation spectrum of unmixed procaine (4.000×10^{-2} mol L^{-1}) and *N*-methylacetamide (1.904×10^{-2} mol L^{-1}); —, mixture of the two at the same concentrations.

FIG. 14. ---, summation spectrum of unmixed tetracaine (1.916×10^{-2} mol L^{-1}) and *N*-methylacetamide (2.059×10^{-2} mol L^{-1}); —, mixture of the two at the same concentrations.

anesthetic systems are not surprising and are in line with general knowledge on H-bonding. NNDA (which in this context represents an associative site in proteins) dissociates some of the H-bonds in self-associated local anesthetics replacing them by H-bonds with itself, representing an associative site in the membrane. While in our experiments NNDA was in great excess, this is in line with clinical conditions where the anesthetic is always applied at low concentrations.

(b) Associations between N*-Methylacetamide (NMA) and "-caine" Anesthetics*

Figure 12 shows the ir spectrum of a mixture of NMA and benzylalcohol (the alcohol playing the role of anesthetic). There is a broad region of absorption superimposed on the bands of the components extending from about 3550 to 3200 cm^{-1} which is readily assigned to O—H---O=C H-bonding. (The band and the shoulder at 3620 cm^{-1} are free OH while the band at 3475 cm^{-1} is the free NH band of NMA.) There is a fair amount of evidence in the literature that the carbonyl group is the more eligible proton acceptor in NMA. The contribution of O—H---N type H-bonds is probably minor. Another possibility is H-bonding between the NH group of NMA as the proton donor and the alcohol as the proton acceptor. This has been ascertained by measuring the spectrum of a mixture of NMA and the methylether of benzylalcohol, $C_6H_5CH_2OCH_3$. A slight broadening and intensification of the bonded NH absorption region was observed. Anyway, as expected, the new absorption region can only correspond to hetero-association.

Procaine with NMA (and similarly benzocaine) give the results shown in Fig. 13. The bands at 3500 and 3410 cm^{-1} (superimposed on the broad associated band) are the NH stretching bands of the primary amino group of procaine while the band at 3475 cm^{-1} belongs to the secondary amino group of NMA. The new band of the mixture appears clearly in the 3350 cm^{-1} region. Thus just as for benzylalcohol hetero-association is demonstrated at concentrations where little self-association takes place.

In tetracaine conditions are similar except that this molecule has a greater tendency to self-association than the previous ones (Fig. 14). The band at 3475 cm^{-1} belongs to the free NH stretching vibration of NMA while the band at 3430 cm^{-1} belongs to the NH group of tetracaine. The sum-curve exhibits a broad band with maximum at 3365 cm^{-1} but the increased absorption of the complex in this region indicates the trend for hetero-association. It is good to point out in this respect that both NMA and tetracaine contain a secondary NH and a C=O group so that both can enter self-association with the same type of N—H---O=C H-bond as the one responsible for hetero-association.

Dibucaine and lidocaine behave similarly.

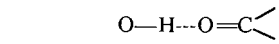
Can. J. Chem. Downloaded from www.nrcresearchpress.com by 210.87.254.42 on 09/05/12
For personal use only.

(c) Benzylalcohol as Representative of a Membrane Site (Protein Side Chain, for example)

With procaine (and benzocaine) (Fig. 15), at concentrations where no self-association occurs in either procaine or the alcohol, new absorption regions appear in the difference spectrum near 3550, 3450, and 3300 cm^{-1}. The first two are readily assigned to OH groups associated with the proton acceptors present in procaine, namely, the ester, the amino-group, or the phenyl ring. In all likelihood the most affected of these is the ester group. Its carbonyl band (at 1710 cm^{-1}) decreases in intensity and a shoulder appears at its low frequency wing. The broad feature around 3300 cm^{-1} probably contains more highly associated species in which further alcohol molecules rally the procaine–alcohol dimer. H-bonds in which the amino group is the proton donor and the phenyl ring of the OH group of benzylalcohol the acceptor are also possible. The shoulder at 3383 cm^{-1} seems to be eligible for this assignment. This has been confirmed by using the methylether of benzylalcohol instead of the alcohol itself.

The observations that can be made for tetracaine, dibucaine, and lidocaine are similar. For dibucaine (Fig. 16) in the spectrum of the mixture a well pronounced new shoulder appears near 3480 cm^{-1} and a broad band is centered around 3350 cm^{-1}.

As in the examples above, the main observation is that hetero-association occurs at concentrations where little or no self-association is observed. The pattern of these associations is believed to be complicated involving more than one associative site in the "caines" and in benzyl alcohol. The



interaction is likely to be the most important one. As to the N—H---phenyl H-bonds these were shown to exist in the case of complexes between *N*-methylacetamide and various phenyl derivatives (9) and they might make some contribution.

III. Barbiturates

In the spectrum of a 4×10^{-3} mol L^{-1} solution of phenobarbital in CH_2Cl_2 only the free NH stretching band is seen at 3365 cm^{-1}. In the carbonyl region the three well known bands are found at 1762, 1740, and 1714 cm^{-1}. The assignment of these bands has been the subject of much discussion (10–13) (for a review see ref. 10). The band of the highest frequency (1760 cm^{-1}) is thought to belong to the carbonyl in the 2 position (between the two NH groups) mainly on the ground that the replacement of its oxygen by sulfur displaces this band

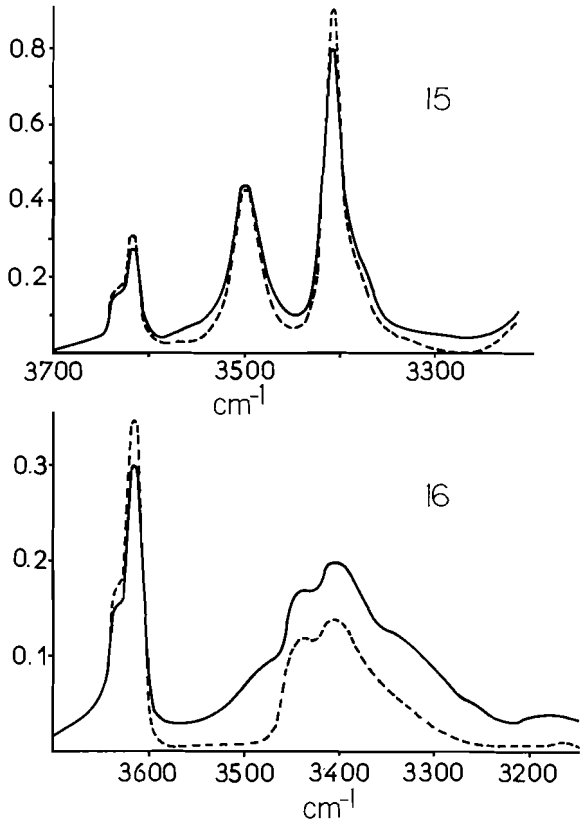


FIG. 15. ---, summation spectrum of unmixed benzylalcohol (3.002×10^{-2} mol L^{-1}) and procaine (4.663×10^{-2} mol L^{-1}); —, mixture of the two at the same concentrations.

FIG. 16. ---, summation spectrum of unmixed benzylalcohol (3.399×10^{-2} mol L^{-1}) and dibucaine (1.939×10^{-2} mol L^{-1}); —, mixture of the two at the same concentrations.

whereas the 1738 and 1712 cm^{-1} bands are unshifted.

In a 1:20 mixture of 4×10^{-3} mol L^{-1} phenobarbital and NNDA the intensity of the free NH band diminishes but the weak associated band is overlapped by solvent absorption. The amide I (carbonyl) band is at 1635 cm^{-1}. The most conspicuous change with respect to the spectrum of phenobarbital itself is a sizeable decrease in the intensity of the 1762 cm^{-1} band which becomes a shoulder. The other two carbonyl bands undergo very slight bathochromic shifts only.

There is no indication for enolization in the spectrum.

Entirely similar observations are made when pyridine is used instead of NNDA. The loss of intensity of the 1762 cm^{-1} band is even more pronounced.

At somewhat higher concentrations (3×10^{-2} mol L^{-1}) self-associated phenobarbital exhibits a weak and broad NH band at about 3225 cm^{-1}. At 3

Can. J. Chem. Downloaded from www.nrcresearchpress.com by 210.87.254.42 on 09/05/12
For personal use only.

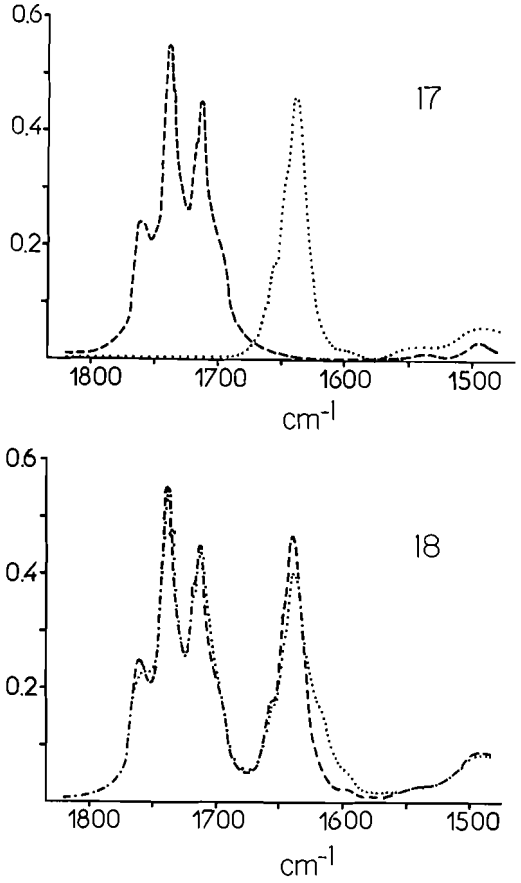


FIG. 17. The double bond stretching region of the ir spectra of phenobarbital (3.0×10^{-2} mol L^{-1}) --- and *N*,*N*-dimethylacetamide (4.8×10^{-2} mol L^{-1}) ···.

FIG. 18. The double bond stretching region of the ir spectra of phenobarbital (3.0×10^{-2} mol L^{-1}) and *N*,*N*-dimethylacetamide. ---, summation curve, ···, mixture of the two at the same concentrations.

$\times 10^{-2}$ mol L^{-1} a pronounced shoulder appears near 1610 cm^{-1}. This band, which can only belong to associated NNDA, does not appear in pure NNDA at the same concentration so it cannot belong to self-association. The 1762 cm^{-1} band decreases in intensity as before (Figs. 17 and 18).

The only explanation of these facts appears to be that a H-bond is formed in which an N-H group of phenobarbital is the proton donor and the carbonyl of NNDA is the proton acceptor. This implies that the intensity of the 1762 cm^{-1} band decreases due to the indirect effect of H-bond formation by its NH neighbors and that the associated NH stretching band is too weak to be seen. The latter assumption is not unusual. These bands are often very weak.

The observation that phenobarbital can form H-bonds with an amide (supposed to represent the peptide H-bond) even at concentrations where self-association with its own carbonyls is already significant might be important for its anesthetic action.

If instead of NNDA we use NMA (2:1 to the concentration of phenobarbital in CH_2Cl_2) we find the free NH band of the amide at 3462 cm^{-1} and the free NH band of phenobarbital at 3368 cm^{-1}. In $CHCl_3$ solution ($3 \times 10^{-2} M$ for phenobarbital), where there is less overlap by the solvent bands, the associated NH band of phenobarbital appears at about 3225 cm^{-1}. The associated NH band of the amide is not seen. The 1762 cm^{-1} carbonyl band of phenobarbital, however, diminishes in intensity just like in NNDA and the associated amide carbonyl band is clearly distinguished at 1615 cm^{-1}. Thus it must be assumed that in this case too the association consists of the formation of H-bonds in which the NH of phenobarbital is the proton donor and the amide carbonyl is the proton acceptor. Conditions might change with concentration and environment but it appears that at low anesthetic concentrations similar to those used in clinical practice, this is the pattern of association and that it is favored with respect to self-association of the anesthetic.

Pentobarbital and thiopental behave similarly. For pentobarbital the carbonyl bands are at 1759, 1736, and 1708 cm^{-1}. For thiopental they are at 1740 and 1706 cm^{-1}; a band at 1508 cm^{-1} has been assigned to the N—C=S group by different authors (10, 14). No separate discussion seems to be necessary.

Conclusions

Our spectroscopic study indicates that while local anesthetics have a tendency to self-association, they prefer hetero-association when put into contact with H-bond systems like those which occur in cell membranes. In other words, just as for general (inhalation) anesthetics, mutual perturbations between local anesthetics and H-bonds present in the membrane can be expected to alter the conformation of the macromolecules forming the membrane. This, in turn, could affect the permeability of the membrane and perturb the nervous system. Whereas general and local anesthetics exert different physiological effects, the chemical mechanism of their action — through perturbing molecular associations — might be similar.

Acknowledgements

The work reported in this paper is the result of a cooperative effort involving the Laboratory of Professor M. Gomel from the Université de Poitiers, France and our laboratory at the Univer-

sité de Montréal. Our thanks are due to the France–Québec scientific exchange programme for making possible the stay of M. G. in Montréal. Furthermore, this work is a part of a programme of research under the Killam Memorial Scholarship granted to one of us (C.S.) by the Canada Council. Financial help from the Natural Sciences and Engineering Research Council of Canada and the Ministère de l'Education du Québec is also gratefully acknowledged.

Our thanks are due to Dean Julien Braun, Dr. R. Denis, and Dr. H. H. Mantsch for giving us the benefit of their experience on various aspects of this work.

1. T. Di Paolo and C. Sandorfy. J. Med. Chem. **17**, 809 (1974).
2. R. Massuda and C. Sandorfy. Can. J. Chem. **55**, 3211 (1977).
3. A. Nagyrévi and C. Sandorfy. Can. J. Chem. **55**, 1593 (1977).
4. G. Trudeau, K. C. Cole, R. Massuda, and C. Sandorfy. Can. J. Chem. **56**, 1681 (1978).
5. C. Sandorfy. Anesthesiology, **48**, 357 (1978).
6. J. Adriani, R. Zepernik, J. Arens, and E. Authement. Clin. Pharmacol. Therap. **5**, 49 (1964).
7. P. J. Krueger, J. Jan, and H. Wieser. J. Mol. Struct. **5**, 375 (1970).
8. P. J. Krueger and B. F. Hawkins. Can. J. Chem. **51**, 3250 (1973).
9. I. Suzuki, M. Tsuboi, and T. Shimanouchi. J. Chem. Phys. **32**, 1263 (1960).
10. R. J. Mesley. Spectrochim. Acta, **26A**, 1427 (1970).
11. W. C. Price, J. E. S. Bradley, R. D. B. Fraser, and J. P. Quilliam. J. Pharm. Pharmacol. **6**, 522 (1954).
12. S. Pinchas. Spectrochim. Acta, **22**, 1889 (1966).
13. S. Goeneshea. Z. Anal. Chem. **218**, 416 (1966).
14. C. N. R. Rao and R. Venkataraghavan. Spectrochim. Acta, **18**, 541 (1962).

Can. J. Chem. Downloaded from www.nrcresearchpress.com by 210.87.254.42 on 09/05/12
For personal use only.

Thermolysis and photolysis of 3,3:4,4-dibutano-1,2-dioxetane[1]

KARL R. KOPECKY AND JUAN A. LOPEZ SASTRE[2]

Department of Chemistry, University of Alberta, Edmonton, Alta., Canada T6G 2G2

Received April 14, 1980

KARL R. KOPECKY and JUAN A. LOPEZ SASTRE. Can. J. Chem. **58**, 2089 (1980).

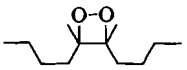
Thermolysis of 5×10^{-3} *M* 3,3:4,4-dibutano-1,2-dioxetane **2**, $E_a = 25.3 \pm 0.3$ kcal/mol, $\Delta S^{\ddagger} = 0 \pm 2$ eu, in degassed decane solution at 42°C produced a 300:1 ratio of cyclopentanone **3**:4-pentenal, **4**. From the quantum yield of photolysis of **3** to **4**, determined to be 0.27 using 313 nm light, it is calculated that 2.5% excited **3** is formed on thermolysis of **2**. Photolysis of (>380 nm) 5×10^{-4} *M* **2** produces a 54:1 ratio of **3**:**4** corresponding to a 13.5% yield of excited **3**. Excited state yields determined by measuring luminescence of benzene solutions of **2** containing DPA and DBA were 1×10^{-4}% singlet and 8.7% triplet. The reason for the 300% discrepancy between the two methods for determining excited state yields is not known.

KARL R. KOPECKY et JUAN A. LOPEZ SASTRE. Can. J. Chem. **58**, 2089 (1980).

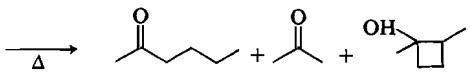
Pour la thermolyse à 42°C d'une solution 5×10^{-3} *M* de dibutano-3,3:4,4 dioxétane-1,2 (**2**) dans du décane dégazée, $E_a = 25.3 \pm 0.3$ kcal/mol, $\Delta S\ddagger = 0 \pm 2$ eu on obtient comme produits de la cyclopentanone (**3**) et du pentène-4 al (**4**) dans un rapport de 200:1. En se basant sur un rendement quantique de 0.27 pour la photolyse de **3** en **4**, valeur obtenue en utilisant de la lumière à 313 nm, on a calculé que la thermolyse de **2** conduit à 2.5% de **3** à l'état excité. La photolyse d'une solution 5×10^{-4} *M* de **2** (~380 nm) conduit à **3** et **4** dans un rapport de 54:1 correspondant à un rendement de 13.5% de **3** à l'état excité. Les rendements de l'état excité déterminés par la mesure de la luminescence des solutions de **2** dans du benzène contenant du DPA et du DBA sont de 1×10^{-4}% pour le singulet et 8.7% pour le triplet. On ne peut pas expliquer la différence de 300% qui existe entre les deux méthodes de détermination des rendements de l'état excité.

[Traduit par le journal]

Yields of carbonyl compounds formed in the excited state on thermolysis have usually been determined by measuring either the amount of photo product formed (1) or light emitted from fluorescers (2) after energy transfer to appropriate acceptors (for a review see ref. 3). Only a few dioxetanes have been prepared which could yield directly photolabile products (4). The yield of excited state formed could then be determined directly by measuring the amount of rearranged or decomposition product formed if the quantum yield for the photoreaction of the carbonyl compound has been determined independently. The only dioxetane for which the yields of excited state products formed has been determined by both methods is 3,4-di-(1-butyl)-3,4-dimethyldioxetane, **1**. However, the yields of excited 2-hexanone formed as determined from the distribution of thermolysis products [1],

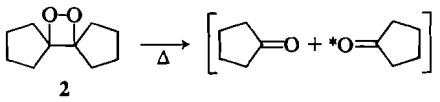
[1] 

1

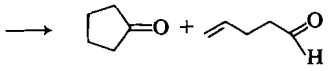


3.5% triplet and 5%, singlet (4*b*, *c*), are quite different from those determined by chemiluminescence measurements, 25% triplet and 0.08% singlet (4*f*).

The present paper reports a study of the decomposition of 3,4:3,4-dibutano-1,2-dioxetane, **2** (11,12-dioxadispiro[4.0.4.2] dodecane) which yields directly a product, cyclopentanone, **3**, which if produced in the excited state would yield 4-pentenal, **4**, [2].

[2] 

2

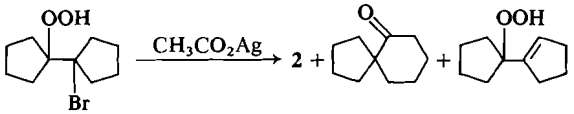


3 **4**

The thermolysis and photolysis of **2** were carried out and the yield of excited **3** formed on thermolysis of **1** was determined both from the ratio of **3**:**4** produced and from measurement of light emitted in the presence of 9,10-dibromoanthracene (DBA) and 9,10-diphenylanthracene (DPA) (2).

Results

Only ~4% of **2** was produced on treatment of 1-bromo-1′-hydroxycyclopentylcyclopentane, **5**, with silver acetate, [3].

[3] 

5 **6** **7**

[1]This research was supported by the National Research Council of Canada.

[2]Present address: Departamento de Quimica Organica, Universidad de Granada, Granada, Spain.

0008-4042/80/192089-04$01.00/0

©1980 National Research Council of Canada/Conseil national de recherches du Canada

Can. J. Chem. Downloaded from www.nrcresearchpress.com by 210.87.254.5 on 09/05/12
For personal use only.

TABLE 1. Product ratios from thermolysis and photolysis of **2** in decane

Temperature (°C)	Concentration (*M*)	**3**/**4**[a]	Total yield (%)	% excited state
42	5.5×10^{-3} [b]	415 ± 25	109	1.7
42	5.5×10^{-4} [c]	300 ± 40	108	2.5
0	5×10^{-4} [d]	54 ± 5	97	13.5

[a] Average of two runs.
[b] Thermolysis, aerated.
[c] Thermolysis, degassed.
[d] Photolysis through a 380 nm cutoff filter.

The main products were spiro[4.5]decan-6-one, **6**, and 1-hydroperoxy-1- (1-cyclopentyl)cyclopentane, **7**, which were isolated in 44 and 15% yields, respectively. Most of the ketone **6** in the crude reaction mixture was converted to the semicarbazone and pure **2** could then be isolated in ~1% yield by repeated column chromatography at −30°C. The hydroperoxide **7** appeared to be the exclusive product formed on treatment of **5** with base (5) and also in the photosensitized oxygenation of cyclopentylidenecyclopentane.

Rates of thermolysis of **2** in benzene were obtained by monitoring the luminescence of solutions of **2** containing DBA (2, 3, 6). At 40.9 and 60.4°C the rates were 5.44 ± 0.05 and 58.4 ± 0.08 × 10^{-5} s^{-1}, respectively; $E_a = 25.3 \pm 0.3$ kcal/mol, $\Delta S^{\ddagger} = 0 \pm 2$ eu (40°C). The stability of **2** is quite similar to that of tetramethyldioxetane (6).

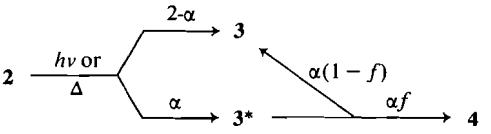
The yields of excited singlet and triplet **3** formed from thermolysis of **2** in benzene, as determined by measuring the luminescence intensities of solutions of **2** as a function of DPA and DBA concentration (2, 3, 7), were 1 × 10^{-4} and 8.7%, respectively, based on the luminol light standard (7).

The product distributions resulting from thermolysis of 5.5 × 10^{-3} *M* and photolysis of 5 × 10^{-4} *M* **2** in decane are given in Table 1. The only product detected besides **3** and **4** was a very small amount of an unidentified material that was eluted from the gc just after air. Quantum chain decomposition (8) of **2** should be negligible because of the low concentrations used and the short lifetime of triplet **3** (9). The ratio **3**/**4** is greater in aerated solutions because oxygen quenches some excited **3**, resulting in a decreased yield of **4** (10).

Decomposition of **2** according to Scheme 1 leads to an expression [4] for the yield α of excited **3**

$$[4] \quad \alpha = 2/(3/4 + 1)f$$

formed in terms of the product ratio **3**/**4** and *f*, the quantum yield for formation of **4** from **3**. This quantum yield depends on the conditions of the reaction, being 0.37 in neat **3** (10) and is somewhat lower in dilute benzene solution as indicated by two



SCHEME 1

determinations which, however, differ by a factor of two: 0.24 (9) and 0.11 (11). The quantum yield was redetermined by irradiating decane solutions of **3** with 313 nm light in a merry-go-round apparatus using as actinometer 2-hexanone, decane solutions of which were irradiated in parallel with those of **3**. A value of 0.19 (12) was used for the quantum yield of acetone formation from 2-hexanone, which is independent of temperature (13). The quantum yield for formation of **4** from **3** was found to be 0.27 at both 22 and 40°C. This is in close agreement with the higher of the previous solution values and there is little, if any, effect of temperature on this quantum yield.

The yields (Table 1) of excited **3** formed from thermolysis and photolysis of **2** were calculated using this value for the quantum yield.

Discussion

The two methods used here for determining the yield of excited **3** formed on thermolysis of **2** give results that differ by a factor of about three, with the yield as determined by product distribution being the lower. A similar discrepancy occurs with the dioxetane **1** which yields 2-hexanone on thermolysis. Attention had been focused on the anomalously high yield of excited singlet 2-hexanone formed from **1** as calculated from the product distribution (4*b*, *c*). It has been pointed out that only a small difference in product ratios would result in a much smaller calculated yield of excited singlet (4*f*). Nevertheless, the fact remains that the absolute yield of products is such that the total yield of excited states calculated this way (assuming that the yield of excited singlet is very small) is only about a fifth of that derived from measurement of luminescence intensities from solutions containing fluorescers: ~5 vs. ~25%.

Can. J. Chem. Downloaded from www.nrcresearchpress.com by 210.87.254.5 on 09/05/12
For personal use only.

Can. J. Chem. Downloaded from www.nrcresearchpress.com by 210.87.254.5 on 09/05/12
For personal use only.

The yields of excited state products formed on photolysis of **1**, ~5%, and **2**, ~14%, also appear to be lower than might be expected on the basis of results reported for photolysis of tetramethyldioxetane. Irradiation of the latter dioxetane with 360 nm light produces about 53 (14) to 65% (15) total yield of excited acetone, as determined by trapping experiments with appropriate alkenes.

The reasons for the discrepancies between the two methods for measuring the yields of excited state from **1** and **2** are not known. Although the yields of **4** from **2** and of acetone and dimethylcyclobutanols from **1** are low and subject to error, they should be in error by as much as 300 to 500%. Nor should measurement of the absolute light intensities from solutions of DBA be in error by this amount. Since the excited state yields obtained via luminescence in the presence of DBA agree well with those obtained by various chemical trapping experiments (3, 16), we conclude that the DBA results obtained here are more likely to be the correct ones. It is possible that anomalously high efficiencies could be obtained by the DBA method however, if there were a bimolecular reaction between DBA and **2**. The effect of DBA concentration on the rate of thermolysis of **2** was not determined, but no effect with DBA has been observed in several other systems (2, 3, 6), so it is not likely that there will be an effect with **2**.[3]

Further studies using a 1,2-dioxetane which can be prepared in higher yield than either **1** or **2** and which produces a ketone whose photolysis proceeds with a high quantum yield are in order.

Experimental

Melting points and boiling points are uncorrected. Nuclear magnetic resonance spectra were recorded with a Varian analytical spectrometer Model A-60. Gas chromatography was carried out on an Aerograph A-90-P3 gas chromatograph using a 10 ft × 1/4 in. stainless steel column packed with 15% dinonylphthalate on 60/80 chromosorb W operating at 145°C. Decane was purified by shaking several times with concentrated H_2SO_4 and then with water. After drying ($MgSO_4$) it was distilled at reduced pressure.

Preparation of **5** and manipulations with concentrated, crude solutions of **2** were carried out behind shields with the aid of tongs while hands were protected with heavy canvas gloves.

Cyclopentylidenecyclopentane

This material was prepared by pyrolysis of the corresponding orthoformate ester (17). A mixture of 50 g 1,1′-dihydroxycyclopentylcyclopentane (18) and 47 mL triethyl orthoformate was heated at 135°C until no more ethanol distilled, 4 h. The temperature was raised to 175°C and kept there until no more ethanol distilled, 3 h. The residue was distilled through a spinning band column to give 27.7 g (69%) of product, bp 87°C/23 Torr, n_D^{22} 1.4896 (lit. (19) bp 76°C/13 Torr, n_D^{20} 1.4934).

1-Bromo-1′-hydroperoxycyclopentylcyclopentane, 5

A dry ether solution of the crude title compound, prepared from 10 g of cyclopentylidenecyclopentane by the usual method (5), was treated with 10 g of 1,4-diaza[2.2.2]bicyclooctane and the resulting solution kept at −78°C for several hours. The white precipitate which formed was filtered on a precooled funnel, washed with ether at −78°C, and then shaken with a mixture of ether and water. The ether layer was shaken several times with water, dried, and concentrated at 0°C under reduced pressure. The semisolid residue was crystallized from 30 mL isopentane at −78°C. Three crops of crystals were obtained, 8.6 g (47%), mp 35–36°C; τ(CCl_4) 1.73 (s, 1H, 8.02 (broad, 18H)) (required ratio 1:16); 99.5% active oxygen.

This material is extremely unstable. Impure material exploded at 10°C soon after solvent was removed. Pure material invariably explodes within a minute at 50°C. It may be stored for several weeks as the 1,4-diaza[2.2.2]bicyclooctane complex at −10°C.

Product Distribution from Reaction of 1-Bromo-1′-hydroperoxycyclopentylcyclopentane with Silver Acetate

A solution of 2.5 g of **5** in 10 mL benzene was added to a suspension of 2 g silver acetate in benzene at 5°C. The mixture was stirred at 5°C for 30 min, filtered, and the filtrate concentrated at 20°C under vacuum. The residue was chromatographed on a 1.5 × 30 cm column of silica gel at −40°C. The column was eluted with Skelly B containing gradually increasing amounts of ether. The eluent was analyzed by tlc (the tlc plate was visualized by heating after spraying with sulfuric acid) and by testing for luminescence by adding a few drops of eluent to a hot solution of DBA. Four fractions were isolated: fraction *1*, 0.63 g, was luminescent and shown by tlc and gc to be < 90% **6** and < 10% **2** (as cyclopentanone by gc); fraction *2*, 0.14 g, was pure **6** identical (ir and nmr) with an authentic sample (20); fraction *3*, 0.27 g, was pure **7**; and fraction *4*, 0.06 g was an unidentified, fragrant oil.

In a separate experiment the crude product from treatment of 1.1 g **5** with silver acetate at 5°C in isopentane, after removal of solvent at 0°C, was taken up in 10 mL ether and the resulting solution added slowly to a stirred suspension of 1 g lithium aluminum hydride in 40 mL ether at −40°C. The reaction mixture was allowed to come to 20°C and, after workup, the crude product was chromatographed on 20 g silica gel. All the 1,1′-dihydroxycyclopentylcyclopentane, the product of reduction of **1** was eluted pure in one fraction, 0.03 g (4%), mp and mixed mp with authentic material 109–110°C. The yield of diol should represent the yield of **2** (6).

3,3:4,4-Dibutano-1,2-dioxetane 2

A solution of 10.4 g **5** in 50 mL Skelly B was added dropwise to a stirred suspension of 25 g silver acetate in 500 mL Skelly B at 20°C. The mixture then was stirred 5 min and filtered. The filtrate was evaporated under reduced pressure and the residual yellow oil poured into a saturated aqueous solution containing 5 g semicarbazide hydrochloride and 7.5 g sodium acetate. Methanol was added until the mixture became homogeneous. This was cooled to −10°C for 1 h and filtered. The precipitate was washed with pentane and the filtrate shaken with several portions of pentane. The combined pentane solutions were shaken with sodium bicarbonate, dried, and concentrated under vacuum. The residual yellow oil was chromatographed at −30°C on a 2 × 30 cm column of silica gel using 2% ether in 2-methylbutane as eluant. Fractions, 10 mL each, containing dioxetane (luminescence on addition to hot benzene solutions of DBA)

[3]A referee has noted that the quantum yield for photolysis of **2** appears to be concentration dependant, increasing with increasing concentration, but that if the reverse were true and an excimer were formed in thermolysis of **2**, then the DBA and chemical measures of efficiency might be reconciled.

Can. J. Chem. Downloaded from www.nrcresearchpress.com by 210.87.254.5 on 09/05/12
For personal use only.

were combined, concentrated, and the residual yellow oil rechromatographed in this way. After a total of four chromatographs 0.049 g (1%) of yellow needles were isolated, mp 55–56°C (from 2-methylpentane), 93% active oxygen.

1-Hydroperoxy-1-(1-cyclopentenyl)cyclopentane, 7

(*A*) A stirred solution of 1.36 g cyclopentylidenecyclopentane and 30 mg methylene blue in 30 mL 1:1 methanol–benzene was irradiated at 10°C under oxygen with two 200 W incandescent lamps until 300 mL oxygen had been taken up. The reaction mixture was poured into ice water, and the resulting mixture was extracted with ether (3 × 50 mL). The combined ether layers were shaken with water, brine, dried, and concentrated under vacuum at 0°C. The residual oil was chromatographed on a 1.5 × 20 cm column of silica gel using 5% ether in pentane as eluant to give 1.30 g (80%) of **7** as a clear oil; τ (CCl_4) 2.07 (s, 1H, OOH); 4.43 (1H, vinyl H), 7.67 (broad, 4H), 8.25 (broad, 10H). No evidence for the presence of dioxetane could be detected by tlc in the crude product.

(*B*) A solution of 1.25 g **5** in 10 mL methanol was added to a solution of 1 g NaOH in 10 mL cold methanol. After 10 min the reaction mixture was worked up as above to give 0.055 g (65%) **7**. No dioxetane could be detected by tlc in the crude product.

Kinetic Studies

Rates of thermolysis were determined by the luminescence decay method using the apparatus described previously (6) at 60.4 and 40.9°C with 5×10^{-4} *M* and 1.4×10^{-3} *M* solution of **2**, respectively, in aerated benzene also containing 10^{-2} *M* DBA. Rates were followed for at least three half-lives of decomposition. Rate constants obtained were 5.92 and 5.76×10^{-4} s^{-1} and 5.39 and 5.49×10^{-5} s^{-1} at 60.2 and 40.9°C, respectively.

Excited State Yields from 2 from Luminescence Intensities

The apparatus and methods used have been described (7). Plots of the reciprocal of the light intensity vs. the reciprocal of fluorescer concentration for 2.8×10^{-3} *M* solutions of **2** in benzene were made. Experiments with DBA were conducted at 40.9°C and those with DPA at 60.4°C because emission was so weak at 40.9°C. The apparatus was calibrated with a solution of tetramethyldioxetane containing DBA (7). The yield of triplet acetone formed from tetramethyldioxetane was taken to be 31% (7) and the efficiency of energy transfer from triplet **3** to give singlet DBA was taken as 0.2 (3). The absolute light intensities of infinite fluorescer concentrations were then determined from the intercepts of the plots and the excited state yields were calculated as described (7).

Photolysis and Thermolysis of 2

Solutions of 5.5×10^{-3} *M* **2** in purified decane were heated at 42°C in sealed ampoules for 10 half lives of decomposition. Degassed solutions were prepared using 3 freeze–thaw cycles under 1×10^{-3} Torr. Degassed solutions of 5×10^{-4} *M* **2** in purified decane were irradiated at 0°C with a 200 W medium pressure Hanovia lamp through a CS-562 filter (380 nm cutoff). The resulting solutions were then analyzed by gc. The ratios of **3**:**4** were determined with the aid of calibration charts which were constructed with solutions containing known amounts of **3** and authentic (21) **4** that bracketed the experimental values.

Quantum Yield of Photolysis of 3

Degassed decane solutions 1.0 *M* in **3** in Pyrex tubes were irradiated on a merry-go-ground apparatus with a 200 W medium pressure Hanovia lamp and a potassium chromate filter to isolate the 313 nm line. As actinometers degassed decane solutions 1.0 *M* in 2-hexanone were irradiated in parallel. Irradiations were carried out to less than 3% decomposition. The amounts of **4** and acetone were determined by gc using solutions of known concentrations of these materials to make calibration charts. The quantum yield of acetone formation from 2-hexanone was taken to be 0.19 (12).

1. E. H. White, J. Wiecko, and D. E. Roswell. J. Am. Chem. Soc. **91**, 5194 (1969).
2. T. Wilson and A. P. Schaap. J. Am. Chem. Soc. **93**, 4126 (1971).
3. T. Wilson. *In* MTP Int. Rev. Sci. Chem. Kinet. Ser. Two. *Edited by* D. R. Herschbach. Butterworths, London. 1976. p. 265.
4. (*a*) W. H. Richardson, F. C. Montgomery, and M. B. Yelvington. J. Am. Chem. Soc. **94**, 9277 (1972); (*b*) T. R. Darling and C. S. Foote. J. Am. Chem. Soc. **96**, 1625 (1974); (*c*) C. S. Foote and T. R. Darling. Pure Appl. Chem. **41**, 495 (1975); (*d*) H. E. Zimmerman and G. E. Keck. J. Am. Chem. Soc. **97**, 3527 (1975); (*e*) H. E. Zimmerman, G. E. Keck, and J. L. Pfledderer. J. Am. Chem. Soc. **98**, 5574 (1976); (*f*) E. J. H. Bechara, A. L. Baumstark, and T. Wilson. J. Am. Chem. Soc. **98**, 4648 (1976).
5. K. R. Kopecky, J. H. van de Sande, and C. Mumford. Can. J. Chem. **46**, 25 (1968).
6. K. R. Kopecky, J. E. Filby, C. Mumford, P. A. Lockwood, and J.-Y. Ding. Can. J. Chem. **53**, 1103 (1975).
7. K. R. Kopecky and J. E. Filby. Can. J. Chem. **57**, 283 (1979).
8. P. Lechtken, A. Yekta, and N. J. Turro. J. Am. Chem. Soc. **95**, 3027 (1973).
9. P. J. Wagner and R. W. Spoerke. J. Am. Chem. Soc. **91**, 4437 (1969).
10. P. Dunion and C. N. Trumbone. J. Am. Chem. Soc. **87**, 4211 (1965).
11. J. C. Dalton, K. Dawes, N. J. Turro, S. D. Weiss, J. A. Barltrop, and J. D. Coyle. J. Am. Chem. Soc. **93**, 7213 (1971).
12. S. Murov. Handbook of photochemistry. Marcell Dekker, New York. 1973. p. 127.
13. M. V. Encina, A. Nogales, and E. A. Lissi. J. Photochem. **4**, 75 (1975).
14. N. J. Turro, P. Lechtken, A. Lyons, R. R. Hautala, E. Carnahan, and T. J. Katz. J. Am. Chem. Soc. **95**, 2035 (1973).
15. P. Lechtken and H.-C. Steinmetzer. Chem. Ber. **108**, 3159 (1975).
16. (*a*) J.-Y. Koo and G. B. Schuster. J. Am. Chem. Soc. **77**, 5403 (1977); (*b*) W. Adam, C.-C. Cheng, O. Cueto, K. Sakanishi, and K. Zinner. J. Am. Chem. Soc. **101**, 1324 (1979).
17. G. Cranck and F. W. Eastwood. Aust. J. Chem. **17**, 1392 (1964).
18. A. A. Scheibmann. Tetrahedron Lett. 4271 (1970).
19. R. Criegee, E. Vogel, and H. Hoger. Chem. Ber. **85**, 144 (1952).
20. H. Hart and L. Lerner. J. Org. Chem. **32**, 2669 (1967).
21. L. K. Montgomery and J. W. Matt. J. Am. Chem. Soc. **89**, 6556 (1967).

Solvolysis of specifically C-6 deuterated 7-halonorbornyl brosylates; stereoselectivity of proton loss for "E1-like" 1,3-elimination in locked bicyclo[2.2.1]heptyl systems

NICK HENRY WERSTIUK, FRANK PETER CAPPELLI, AND GEORGE TIMMINS

Department of Chemistry, McMaster University, Hamilton, Ont., Canada L8S 4M1

Received May 1, 1980

NICK HENRY WERSTIUK, FRANK PETER CAPPELLI, and GEORGE TIMMINS. Can. J. Chem. **58**, 2093 (1980).

We have solvolyzed the *syn*-7-chloro-*endo*-6-*d*, *anti*-7-chloro-*endo*-6-*d*, *syn*-7-chloro-*exo*,*exo*-5,6-d_2, *anti*-7-chloro-*exo*,*exo*-5,6-d_2, *syn*-7-bromo-*endo*-6-*d*, and *anti*-7-bromo-*endo*-6-*d* norbornyl brosylates **1***c*, **2***c*, **1***d*, **2***d*, **1***e*, and **2***e* in 80:20 ethanol–water buffered with NaOAc, isolated the 3-halonortricyclenes, the products of 1,3-elimination, and assayed for deuterium mass spectrometrically. Analysis of the deuterium-loss data established that there is a 10:1 to 15:1 preference for loss of an *endo*-6-proton for formation of the 7-halonortricyclenes from the 7-halonorbornyl cations. The isotope effects for "E1-like" 1,3-elimination are 1.78, 1.71, 1.53, and 1.52 for **1***c*, **2***c*, **1***e*, and **2***e*, respectively. That there is an increase in the degree of 1,3-elimination in the solvolysis of *anti*-7-chloro-*exo*-2-norbornyl brosylate-*exo*-3-*d* (**3**) relative to the non-deuterated brosylate indicates that the destabilizing effect of the β-deuterium at C-3 leads to an increase in the degree of 1,3-elimination from C-6.

NICK HENRY WERSTIUK, FRANK PETER CAPPELLI et GEORGE TIMMINS. Can. J. Chem. **58**, 2093 (1980).

Nous avons solvolysé les brosylates des chloro-7-*syn d*-6-*endo* (**1***c*), chloro-7-*anti d*-6-*endo* (**2***c*), chloro-7-*syn* d_2-5,6-*exo*-*exo* (**1***d*), chloro-7-*anti* d_2-5,6-*exo*-*exo* (**2***d*), bromo-7-*syn d*-6-*endo* (**1***e*) et bromo-7-*anti d*-6-*endo* (**2***e*) norbornyles dans une solution à 80:20 éthanol–eau tamponnée avec du AcONa, nous avons isolé les halogéno-3 nortricyclènes, produits d'une élimination 1,3 et nous avons dosé le deutérium par spectrométrie de masse. Une analyse des données relatives à la perte de deutérium établit qu'il y a une préférence allant de 10:1 à 15:1 pour la perte proton 6-*endo* lors de la formation des halogèno-7 nortricylènes à partir des cations halogèno-7 norbornyles. Les effets isotopiques pour l'élimination "pseudo E-1" sont respectivement de 1.78, 1.71, 1.53 et 1.52 pour **1***c*, **2***c*, **1***e* et **2***e*. Le fait qu'il y a une augmentation du degré d'élimination 1,3 au cours de la solvolyse du brosylate du chloro-7-*anti d*-3-*exo* norbornyle-2-*exo* (**3**) par rapport au brosylate non deutéré indique que l'effet déstabilisant du deutérium en β conduit à une augmentation du degré d'élimination à partir du carbone en position 6.

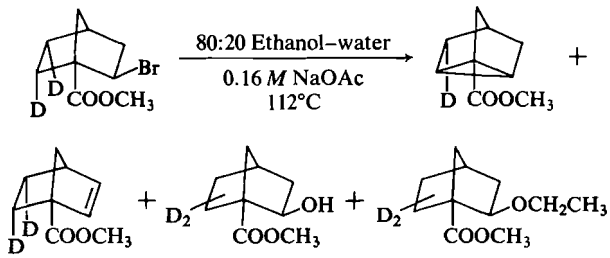
[Traduit par le journal]

Introduction

The mechanistic details of 1,2-elimination have been probed extensively and the results are documented in many substantial reviews. However, 1,3- and 1,4-elimination reactions have not been studied as extensively although there has been a gradual increase in activity in the field over the past decade. 1,3-Elimination occurs in acyclic and cyclic systems and developments in the area have been documented in several recent publications (1, 2).

Our interest in detailing the mechanism of $H^+(D^+)$ catalyzed ring-opening of nortricyclenes (4–6) led us to study the stereochemistry of the reverse process, "E1-like" 1,3-elimination. In a previous study we established that there is at least a 15:1 preference for loss of an *endo* proton (deuteron) for formation of methyl 1-nortricyclene carboxylate from deuterated methyl *exo*-2-bromo-1-norbornanecarboxylate via 1,3-elimination (Scheme 1).

In this publication we report the results of our study. As in the case of solvolysis of the locked system methyl *exo*-2-bromo-1-norbornanecarboxylate (Scheme 1), we find that there is at least a 15:1 preference for loss of an *endo* proton for 1,3-(6,2)-elimination in the case of *syn*-7- and *anti*-7-chlorobrosylates **1***c* and **2***c*. In the case of the *syn*-7- and *anti*-7-bromobrosylates **1***e* and **2***e*, the *endo* preference appears to be reduced somewhat.



SCHEME 1

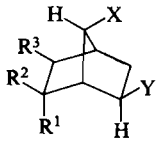
Results

Preparation of Substrates

While the non-deuterated *syn*- and *anti*-chlorohydrins, the precursors of the brosylates **1***a* and **2***a*, were prepared by the method of Roberts (3), the *syn*- and *anti*-bromohydrins were obtained via the acid-catalyzed ring-opening of 3-bromonortricyclene (4). The deuterated chloro and bromobrosylates **1***c*, **1***e*, **2***c*, and **2***e* were prepared from the corresponding deuterated chlorohydrins and bromohydrins that were obtained via acid-catalyzed ring-opening of 3-chloro- and 3-bromonortricyclene in deuterated medium (4). That

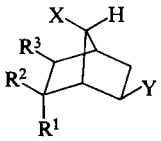
0008-4042/80/192093-07$01.00/0

©1980 National Research Council of Canada/Conseil national de recherches du Canada



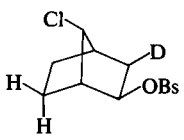
1

a $R^1 = R^2 = R^3 = H$, X = Cl, Y = OBs
b $R^1 = R^2 = R^3 = H$, X = Br, Y = OBs
c $R^1 = D$, $R^2 = R^3 = H$, X = Cl, Y = OBs
d $R^1 = H$, $R^2 = R^3 = D$, X = Cl, Y = OBs
e $R^1 = D$, $R^2 = R^3 = H$, X = Br, Y = OBs



2

a $R^1 = R^2 = R^3 = H$, X = Cl, Y = OBs
b $R^1 = R^2 = R^3 = H$, X = Br, Y = OBs
c $R^1 = D$, $R^2 = R^3 = H$, X = Cl, Y = OBs
d $R^1 = H$, $R^2 = R^3 = D$, X = Cl, Y = OBs
e $R^1 = D$, $R^2 = R^3 = H$, X = Br, Y = OBs

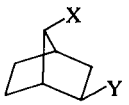


3



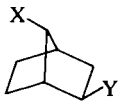
4

a X = Cl
b X = Br



5

a X = Cl, Y = OH
b X = Cl, Y = OEt
c X = Br, Y = OH
d X = Br, Y = OEt



6

a X = Cl, Y = OH
b X = Cl, Y = OEt
c X = Br, Y = OH
d X = Br, Y = OEt

the deuterium in **1***c*, **1***e*, **2***c*, and **2***e* was 80–90% stereochemically pure *endo* at C-6 was established by ^{1}H nmr and ir spectroscopy (4).

To prepare *syn*-7-chloro-*exo*-2-norbornyl brosylate-*exo*,*exo*-5,6-d_2 (**1***d*), we converted norbornene-*endo*,*endo*-5,6-d_2 into the *syn*-7-chlorohydrin via Roberts' method and brosylated the deuterated chlorohydrin. We began the synthesis of *anti*-7-chloro-*exo*-2-norbornyl brosylate-*exo*,*exo*-5,6-d_2 (**2***d*) with a $LiAlD_4$ reduction of acetoxynorbornadiene that yielded *anti*-7-norbornenol-*exo*,*exo*-5,6-d_2. The dideuterated norbornenol was converted into *anti*-7-chloronorbornene-*exo*,*exo*-5-6-d_2 (5), the chloronorbornene was hydroborated, and the deuterated chlorohydrin was brosylated. That the deuterium was at least 90% stereochemically pure *exo* was established by ^{1}H nmr spectroscopy (5). *Anti*-7-chloro-*exo*-2-norborneol-*exo*-3-*d*, the precursor of brosylate **3***a*, was prepared by deuteroboration of *anti*-7-norbornenyl chloride. To establish that the deuterium was located specifically *exo* at C-3, we recorded the ^{1}H nmr spectra of the deuterated and nondeuterated chlorohydrins in the presence of Eu(fod)$_3$ (5).

Identification of Products

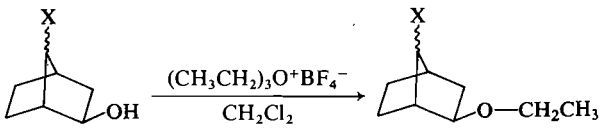
A large scale solvolysis of the *syn*-chlorobrosylate **1***a* yielded a mixture of products that were separated by preparative glpc. While the major products of solvolysis of **1***a* were identified as **4***a*, **5***a*, **5***b*, **6***a*, and **6***b* by comparison of their ^{1}H nmr spectra to those of authentic samples, the major products from the *anti*-chlorobrosylate **2***a* were identified simply by analytical glpc retention times. The major products, **4***b*-*d*, **5***c*-*d*, **5***d*-*d*, **6***c*-*d*, and **6***d*-*d*, of solvolysis of the deuterated *syn*- and *anti*-bromobrosylates **1***e* and **2***e* were isolated by preparative glpc from a large scale solvolysis and identified by ^{1}H nmr spectroscopy. Authentic samples of the 7-halo-*exo*-2-norbornyl ethyl ethers **5***b*, **5***d*-*d*, and **6***d*-*d* were prepared from the corresponding halohydrins and $(CH_3CH_2)_3\overset{+}{O}BF_4^-$ (Scheme 2).

Determination of Relative Yields of Products

To determine the relative yields of the products (Table 1), we extracted solvolysis solutions obtained from γ-KIE studies (5) as described in the Experimental.

Determination of Deuterium Losses

To determine the deuterium losses we carried out large scale solvolyses of the deuterated brosylates **1***c*, **1***d*, **1***e*, **2***c*, **2***d*, and **2***e*, isolated the 3-halonortricyclenes by preparative glpc, and assayed for deuterium mass spectrometrically. The isotopic compositions of the starting brosylates and the 3-halonortricyclenes and the deuterium losses are listed in Table 2.



SCHEME 2

Discussion

It is clear from Table 2 that there is an *endo* stereoselectivity for loss of a proton (deuteron) from C-6 of the 7-halobrosylates. This result is

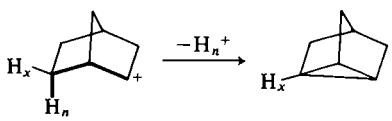


TABLE 1. Relative percent yields of solvolysis products[a]

Brosylate	Δ	*Syn*-OEt	*Anti*-OEt	*Syn*-OH	*Anti*-OH	Other
Syn-7-chloro-*exo*-2- (**1***a*)[b]	30	24	11	23	8	4
Syn-7-chloro-*exo*-2-*endo*-6-*d* (**1***c*)	20	31	10	30	8	1
Anti-7-chloro-*exo*-2- (**2***a*)[b]	21	5	36	4	29	5
Anti-7-chloro-*exo*-2-*endo*-6-*d* (**2***c*)	13	4	40	3	33	7
Syn-7-bromo-*exo*-2- (**1***b*)	25	37	12	22	1	3
Syn-7-bromo-*exo*-2-*endo*-6-*d* (**1***e*)	18	39	10	28	2	4
Anti-7-bromo-*exo*-2-(**2***b*)	10	9	48	5	20	8
Anti-7-bromo-*exo*-2-*endo*-6-*d* (**2***e*)	7	8	56	5	16	7
Syn-7-chloro-*exo*-2- (**1***a*)[b]	35	21	11	19	11	3
Syn-7-chloro-*exo*-2-*exo*,*exo*-5,6-d_2 (**1***d*)	20	27	11	25	17	0
Anti-7-chloro-*exo*-2- (**2***a*)[b]	20	7	39	5	23	6
Anti-7-chloro-*exo*-2-*exo*,*exo*-5,6-d_2 (**2***d*)	22	6	38	4	23	7
Anti-7-chloro-*exo*-2- (**2***a*)[b]	19	7	40	5	22	7
Anti-7-chloro-*exo*-2-*exo*-3-*d* (**3***a*)	28	7	36	5	18	6

[a]The relative percent yields were determined by electronic integration of peak areas and are averages of at least four determinations. The average error was ±10%.
[b]Since the product ratios were determined for different runs, the results give an indication of the reproducibility of the experiments.

TABLE 2. Deuterium content of 7-halobrosylates and 3-halonortricyclenes

					3-Halonortricyclene				
	Composition[a]			Excess *d*	Composition			Excess *d*	Fractional % deuterium
Brosylate	d_0	d_1	d_2	per molecule	d_0	d_1	d_2	per molecule	loss
Syn-7-chloro- (**1***c*)	3.3	95.0	1.7	0.98	78.1	21.7	0.2	0.22	77.6
Anti-7-chloro- (**2***c*)	3.6	95.2	1.2	0.97	77.2	22.7	0.1	0.23	76.3
Syn-7-chloro- (**1***d*)	4.7	6.0	89.3	1.85	6.9	9.1	84.0	1.77	3.2
Anti-7-chloro- (**2***d*)	7.3	3.4	89.3	1.82	7.2	9.2	88.6	1.81	0.5
Syn-7-bromo- (**1***e*)	4.3	94.0	1.7	0.97	61.5	38.4	0.1	0.39	59.8
Anti-7-bromo- (**2***e*)	5.6	92.5	1.9	0.97	67.9	30.6	1.4	0.39	64.8

[a]Determined by analysis of the corresponding 7-halonorbornanones.

consistent with our previous finding that loss of an *endo* proton from C-6 of a locked norbornyl system is preferred over loss of an *exo* proton by 15:1 (*vide supra*) and indicates that the semi-U path (6) is preferred. From the data listed in Table 1 it is possible to evaluate the elimination isotope effects (EIE's) using eq. [1] that was described previously

$$[1]\quad \left(\frac{k_H}{k_D}\right)^{1,3\text{-Elimination}} \simeq \left(\frac{\%\ \text{Elimination (H)}}{\%\ \text{Substitution (H)}}\right) \Big/ \left(\frac{\%\ \text{Elimination (D)}}{\%\ \text{Substitution (D)}}\right)$$

(7). The EIE's are 1.78, 1.71, 1.58, and 1.52 for **1***c*, **2***c*, **1***e*, and **2***e*, respectively. Based on an *endo*-6-*d* stereochemical purity of 90% for 7-chlorobrosylates **1***c* and **2***c*, an 80% stereochemical purity for 7-bromobrosylates **1***e* and **2***e*, and a series of *endo*:*endo* preferences, we have calculated the expected relative yields of the 3-halonortricyclenes and the isotopic compositions using eq. [2] and [3] that were developed previously (7).

$$[2]\quad \left(\frac{\%\ d_n\ \text{Species}}{100}\right)\left(\begin{array}{c}\text{Fractional}\\ \text{amount}\\ \textit{endo-d}\ \text{or}\\ \textit{exo-d}\end{array}\right)\left(\begin{array}{c}\text{Assumed}\\ \text{preference}\end{array}\right)\left(\frac{1}{\text{EIE}}\right)\left(\begin{array}{c}\text{Relative}\\ \text{yield of}\\ \Delta_H\end{array}\right) = \left(\begin{array}{c}\text{Relative yield}\\ \text{of } d_x \text{ species}\end{array}\right)$$

$$(x = n - 1)$$

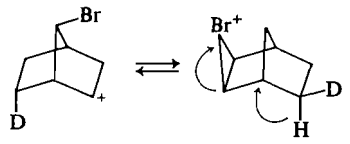
TABLE 3. Relative percent yields and isotopic composition of 3-halonortricyclenes; comparison of calculated and experimental values

Substrate	Stereochemical purity (%)	Assumed *endo*:*exo* preference[a]	Composition d_0	d_1	d_2	Relative % yield Δ
Syn-7-Cl- (**1***c*)	90	5:1	62.2	33.8	—[b]	23.7
		10:1	73.8	26.2	—	21.0
		15:1	77.1	22.9	—	20.1
		20:1	78.7	21.3	—	19.7
			(78.1)	(21.7)	(0.2)[c]	(20)
Anti-7-Cl- (**2***c*)	90	5:1	67.1	32.9	—	17.0
		10:1	74.8	25.2	—	15.1
		15:1	77.9	22.1	—	14.5
		20:1	79.6	20.4	—	14.2
			(77.2)	(22.7)	(0.1)[c]	(13)
Syn-7-Br- (**1***e*)	80	5:1	62.1	37.9	—	21.9
		10:1	67.1	37.9	—	19.7
		15:1	68.7	31.3	—	19.2
			(61.5)	(38.5)	(0.1)[c]	(18)
Anti-7-Br- (**2***e*)	80	5:1	63.3	36.7	—	9.0
		10:1	68.7	31.3	—	8.3
		15:1	70.9	29.1	—	7.9
		20:1	80.9	19.1	—	6.8
			(67.9)	(30.6)	(1.4)[c]	(7)

[a]The EIE's for **1***c*, **2***c*, **1***e*, and **2***e* are 1.78, 1.71, 1.58, and 1.52, respectively.
[b]The small amounts of d_2 species (Table 2) were omitted in the analysis using eq. [2].
[c]Experimentally observed values.

[3] Relative yield $\Delta_D = \Sigma$ relative yields of d_x species

The results are listed in Table 3. It is clear from the data that there is a 10:1 to 15:1 preference for loss of an *endo* proton (deuteron) for "E1-like" 1,3-elimination from **1***c*, **2***c*, and **2***e*. The reason for the reduced stereoselectivity for proton loss from **1***e* is not obvious although it is possible that the *syn*-7-bromo-2-norbornyl cation **7** rearranges to the *exo* bromonium ion **8**

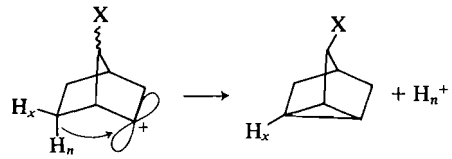


7 **8**

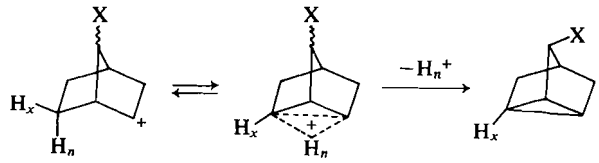
which leads to 3-bromonortricyclene via loss of an *endo* proton.

Since E1-like 1,3-elimination of a proton (deuteron) from the 7-halonorbornyl cations should be the reverse of the $H^+(D^+)$ catalyzed ring-opening of the corresponding 3-halonortricyclenes, the stereochemistry of the 1,3-elimination should be related to the stereochemistry of the ring-opening. As we have documented in preceding papers (4, 8) this is, in fact, the case because 3-chloronortricyclene and 3-bromonortricyclene are preferentially ring-opened by *edge-wise* attack on the most basic bond of the three-membered ring by D^+ to form, in our view, classical 7-halonorbornyl cations (Scheme 3).

It is of interest to speculate on the nature of the transition state of 1,3-elimination. Does proton (deuteron) loss occur from the classical species **9** or from an edge-protonated (deuteronated) nortricyclene **10** which is one of the intermediates of

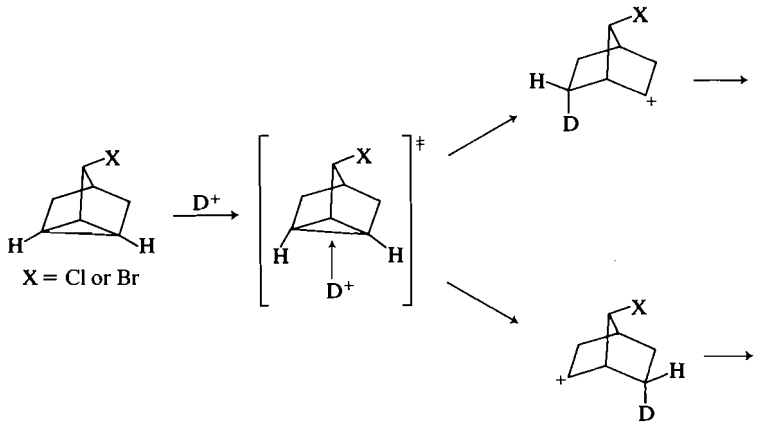


9 (X = Cl or Br)



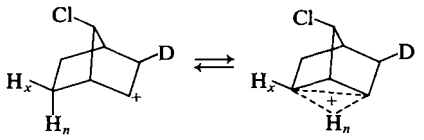
9 (X = Cl or Br) **10**

solvolysis? That cleavage of an *exo* C—H bond (semi-W type path) is preferred for steric and perhaps stereoelectronic reasons as well (9) in the case of homoenolization of bicyclo[2.2.1]heptanones such as fenchone suggests that proton (deuteron) loss from locked 7-halonorbornyl cations occurs from an edge-protonated nortricyclene.



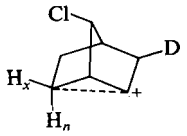
SCHEME 3

Interestingly, we find that there is a substantial increase (Table 1) relative to the non-deuterated brosylate **2***a*, in the degree of 1,3-elimination when *anti*-7-*exo*-3-*d* brosylate **3** is solvolyzed. If elimination does indeed occur from an edge-protonated (deuteronated) nortricyclene **10**, which along with the classical species **9** is one of the intermediates in the solvolysis reaction, then introduction of the β-deuterium at C-3 would cause an increase in the equilibrium population of this edge-protonated species and thereby result in an increase in 1,3-elimination. Another possibility is that the decrease in stability of **11** relative to the non-deuterated



11

species is compensated by homohyperconjugation to the *exo* and *endo* C—H bonds at C-6, with the result that the C—H bonds at C-6 are activated and undergo cleavage more readily.



Experimental

General

Nuclear magnetic resonance spectra were recorded on Varian T-60, A-60, and HA-100 spectrometers with tetramethylsilane (TMS) as the internal standard. Samples were dissolved in either carbon tetrachloride or carbon disulfide and chemical shifts are expressed in parts per million downfield from internal tetramethylsilane. Infrared spectra were recorded on Perkin Elmer 337 and Beckman IR-5 infrared spectrometers and the samples were dissolved in carbon tetrachloride or carbon disulfide. Spectra were calibrated with a polystyrene thin film and peak positions are expressed in cm^{-1}. Mass spectra were recorded on a Hitachi-Perkin Elmer RMU-6A spectrometer at 80 eV and deuterium assays were performed at 10–15 eV. Analytical gas liquid partition chromatograms (glpc) were obtained on a Varian Aerograph Model 204B dual column analytical gas chromatograph equipped with dual flame ionization detectors using helium as the carrier gas. The helium flow rate was usually 20–30 mL/min. Product ratios were determined by an Aerograph Model 485 electronic digital integrator. Preparative gas liquid partition chromatography was carried out on a Varian Aerograph Model A-90-P gas chromatograph equipped with a thermal conductivity detector at a helium flow rate of 50–60 mL/min. Melting points were recorded on a Kofler hot-stage apparatus and are uncorrected. Boiling points are also uncorrected. Pentane was stirred vigorously over fuming sulfuric acid, washed with sodium bicarbonate solution, dried, and distilled. Dry ether refers to ether that was distilled from lithium aluminum hydride. Pyridine was refluxed over barium oxide for 48 h and distilled. All solutions were dried with either anhydrous sodium sulfate or magnesium sulfate.

Preparation of Brosylates

The brosylates were prepared from the appropriate halohydrins via the method described in a preceding publication (5).

Deuterium Assay of Brosylates

Since both the deuterated halohydrins and their corresponding halobrosylates gave weak parent ions when analyzed by mass spectrometry, the determination of deuterium content of these compounds by this method was not reliable. Therefore, we determined the deuterium content mass spectrometrically by analyzing the corresponding deuterated haloketones which were obtained by oxidation of the deuterated halohydrins.

Identification of Products

Syn-7-chloro-*exo*-2-norbornyl brosylate (5.5 g) and buffered 80:20 ethanol–water (75 mL) were magnetically stirred in a round-bottomed flask and heated in an oil bath at 56 ± 2°C for 36 h. All the brosylate dissolved after several hours. After the reaction mixture cooled to room temperature, it was extracted with pentane (3 × 200 mL). Water (700 mL) was added to the aqueous layer and further extractions with ether (3 × 250 mL) were carried out. The pentane and ether extracts were combined and washed with water (2 × 100 mL), saturated bicarbonate solution (2 × 100 mL), water (2 × 150 mL), and dried. After the solvent was removed under reduced pressure, a yellow residue remained which was found by analytical glpc on a 1/8 in. × 10 ft 10% Carbowax column at 170°C to contain five major products.

Each product was collected by preparative glpc on a 1/4 in. × 10 ft 15% FFAP column at 175°C. In order of increasing retention time, the products were identified as, 3-chloronortricyclene (**4***a*), *anti*-7-chloro-*exo*-2-norbornyl ethyl ether (**6***b*), *syn*-7-chloro-*exo*-2-norbornyl ethyl ether (**5***b*), *syn*-7-chloro-*exo*-2-norbornanol (**5***a*), and *anti*-7-chloro-*exo*-2-norbornanol (**6***a*). Careful analysis of the ^{1}H nmr spectrum of **4***a* revealed that chloronorbornenes, the products of 1,2-elimination, were not present. When the fourth product, *syn*-7-chloro-*exo*-2-norbornanol, was subjected to analytical glpc on a 1/8 in. × 10 ft 10% Carbowax column at 175°C, the glpc peak had an appreciable shoulder. A small portion of the sample was oxidized as previously described to the corresponding chloroketones (5). By comparison of retention times, it was shown with analytical glpc on a 1/8 in. × 10 ft 10% Carbowax column at 145°C that the contaminant was *exo*-3-chloro-2-norbornanone. The ratio of *syn*-7-chloro-2-norbornanone to *exo*-3-chloro-2-norbornanone was determined to be 9:1 and establishes that the solvolysis of *syn*-7-chloro-*exo*-2-norbornyl brosylate yields small amounts of *exo*-3-chloro-*exo*-2-norbornanol. *Anti*-7-chloro-*exo*-2-norbornyl brosylate (4.00 g) was solvolyzed in buffered 80:20 ethanol–water (100 mL) and worked up as described above. The products which had identical retention times to the products from **1***a* were isolated by preparative glpc and subjected to mass spectrometric analysis. The mass spectra of the products were identical in all respects to the mass spectra of **4***a*, **5***a*, **5***b*, **6***a*, and **6***b* isolated from solvolysis of **1***a*. Compound **4***a*: ir (CS_2); 3075, 2940, 1308, 1292, 1244, 958, 858, 825, 719; ^{1}H nmr (CS_2, 60 MHz) δ: 3.98 (sharp m, 1H, H-3), 2.18 (broad m, 2H, H-4 and *syn*-7-H), 1.8–1.3 (6H, nortricyclyl envelope); ms *m/e*: 128, 130(M^+), 93, 91, 79, 77, 66, 65, 58. Compound **6***b*: ir (CS_2); 2960, 1244, 1100, 1063; ^{1}H nmr (CS_2, 60 MHz) δ: 4.13 (sharp m, 1H, H-3), 2.48 (broad m, 2H, —O—CH_2CH_3), 2.33 (broad m, 2H, H-1 and H-4), 2.3–1.6 (norbornyl envelope), 1.22 (t, 3H, J = 7 Hz, O—CH—CH_3); ms *m/e*: 176, 174(M^+), 139, 138, 93, 91, 79, 77, 72, 67. Compound **5***b*: ir (CS_2); 2960, 1365, 1348, 1305, 1244, 1115, 1068; ^{1}H nmr (CS_2, 60 MHz) δ: 3.78 (sharp m, 1H, H-7), 3.40 (broad m, 2H, —O—CH_2—CH_3), 2.40 (m, 1H, H-1 or H-4), 2.25 (m, 1H, H-1 or H-4), 2.2–1.4 (norbornyl envelope), 1.15 (t, 3H, J = 7 Hz, —O—CH_2—CH_3); ms *m/e*: 176, 174(M^+ very weak), 138, 93, 91, 72, 67, 65. Compound **5***a*: ir (CS_2); 3580, 2960, 1245, 1088, 1050, 1018; ^{1}H nmr (CS_2, 60 MHz) δ: 4.02 (sharp m, 1H, H-7), 3.75 (broad pentuplet, 1H, H-2), 2.42 (broad m, 2H, H-1 and H-4), 2.2–1.0 (norbornyl envelope and —O—H); ms *m/e*: 131, 129(M^+ − OH), 110, 93, 91, 67, 66. Compound **6***a*: ir (CS_2); 3620, 3400, 2960, 1245, 1084, 1002; ^{1}H nmr (CS_2, 60 MHz) δ: 4.22 (sharp m, 1H, H-7), 3.83 (dd, 1H, J = 7, 1.5 Hz, H-2), 2.08 (s, 1H, —O—H), 2.4–1.0 (norbornyl envelope); ms *m/e*: 130, 128($M^+ - H_2O$), 110, 93, 91, 87, 79, 66, 67.

Determination of Deuterium Losses from Chlorobrosylates

In a typical reaction, buffered 80:20 ethanol–water (35–45 mL) was heated at 63 ± 2°C in an oil bath in a round-bottomed flask equipped with a reflux condenser and a calcium chloride drying tube. The deuterated chlorobrosylate (0.17 g of **1***c* and 0.50 g of **2***c*, 0.17 g of **1***d*, and 0.18 g of **2***d*) was added to the solution and the mixture was heated for about 50 h. Water (500 mL) was added and the mixture was extracted with ether. After the solvent was distilled off and the residue was concentrated to 0.05 mL, the total reaction mixture was subjected to preparative glpc on a 1/4 in. × 10 ft. 15% Carbowax column at 110°C in one injection and the fraction corresponding to 3-chloronortricyclene was collected in a U-shaped tube cooled in liquid nitrogen. Analysis of a mixture of 3-chloronortricyclene, *exo*-5-chloronorbornene, and *endo*-5-chloronorbornene by preparative glpc under the conditions described above revealed that the compounds were separated from each other. Compound **4***d-d* from **2***c*: ms *m/e*: M^+ 128, 129, 130, 131; 77.2% d_0, 22.8% d_1, 0.1% d_2, (0.23 excess d per molecule). Compound **4***a-d* from ms *m/e*: M^+ 128, 129, 130, 131; 78.1% d_0, 21.7% d_1, 0.2% d_2 (0.22 excess d per molecule). Compound **4***a-d* from **1***d*: ms *m/e*: M^+ 128, 129, 130, 131; 6.9% d_0, 9.1% d_1, 84.0% d_2 (1.77 excess d per molecule). Compound **4***a-d* from **2***d*: ms *m/e*: M^+ 128, 129, 130, 131; 7.2% d_0, 9.2% d_1, 88.6% d_2 (1.81 excess d per molecule).

Determination of Products and Deuterium Losses for Solvolysis of Bromobrosylates

Deuterated *syn*-bromobrosylate **1***e* (1.2 g) was dissolved in buffered (0.04 *M* NaOAc) 80:20 ethanol–water (25.6 mL) and the solution was heated at 65 ± 1°C for 24 h. Water was added (100 mL) and the mixture was extracted with purified pentane (4 × 50 mL). The combined extracts were washed with water (3 × 40 mL), dried, and the solvent was removed by distillation through a 15 in. glass helices-packed column. Analytical glpc analysis on a 1/8 in. × 12 ft 10% FAPP column at 150°C showed that **4***b*, **5***c*, **5***d*, **6***c*, and **6***d* comprised >85% of the reaction mixture. Three of the major products **4***b-d*, **5***d-d*, and **5***c-d* were isolated by preparative glpc on a 1/4 in. × 8 ft 15% Carbowax column at 150°C. Compound **4***b-d*: ^{1}H nmr (CS_2, 100 MHz) δ: 4.28 (sharp m, 1H, H-3), 2.03 (sharp m, 1H, H-4), 1.97 (d with fine structure, 1H, H-5), 1.5–1.0 (nortricyclyl envelope, < 5H); ms *m/e*: M^+ 172, 174; 61.5% d_0, 38.4% d_1, 0.1% d_2; (0.39 excess d per molecule). Compound **5***d-d*: ^{1}H nmr (CS_2, 100 MHz) δ: 3.69 (m, 1H, H-7), 3.33 (broad m, 3H, H-2 and —O—CH_3—), 2.38 (broad d, 1H, H-1), 2.25 (broad t, 1H, H-4), 2.15–1.25 (norbornyl envelope), 1.09 (t, J = 6.5 Hz, —CH_3). Compound **5***c-d*: ^{1}H nmr (CS_2, 100 MHz) δ: 3.26 (sharp m, 1H, H-7), 2.05 (broad p, 1H, H-2), 2.25 (broad m, 2H, H-1 and H-4), 2.03 (d, 1H, J = 11 Hz, —OH), 1.9–0.9 (norbornyl envelope).

Deuterated *anti*-bromobrosylate **2***c* (2.76 g) was dissolved in buffered 80:20 ethanol–water (55.2 mL) and the solution was heated at 65 ± 1°C for 24 h. Water was added (200 mL) and the mixture was extracted with purified pentane (4 × 100 mL) and after the usual workup the three major products were isolated by preparative glpc. The nmr of the nortricyclene was identical to that of **4***b-d* isolated from the solvolysis of **1***e*; ms *m/e*: M^+ 172, 174; 67.9% d_0, 30.6% d_1, 1.4% d_2 species (0.34 excess d per molecule). Compound **6***d-d*: ^{1}H nmr (CS_2, 100 MHz) δ: 4.06 (sharp m, 1H, H-7), 3.30 (broad m, 3H, H-2 and —O—CH_2—CH_3), 2.28 (broad m, 1H, H-1), 2.20 (broad t, 1H, H-4), 2.1–1.2 (norbornyl envelope), 1.10 (t, 3H, J = 6.5 Hz, —O—CH_2—CH_3). Compound **6***c-d*: ^{1}H nmr (CS_2, 100 MHz) δ: 4.13 (sharp m, 1H, H-7), 2.70 (dd, 1H, J = 8, 2.5 Hz, H-2), 3.35 (s, 1H, —OH), 2.25 (broad t, 1H, H-4), 2.13 (broad m, 1H, H-1), 2.1–1.9 (norbornyl envelope).

Syn-*7-chloro*-exo-*2-norbornyl Ethyl Ether*

Compound **5***a* (0.10 g) was dissolved in methylene chloride (3 mL) in a round-bottomed flask fitted with a nitrogen inlet and a calcium chloride drying tube. The system was flushed with nitrogen for 15 min. To this solution was added 0.12 g of triethyloxonium fluoroborate and the mixture was magnetically stirred for 24 h at 25°C. Water (10 mL) was added and the solution was extracted with methylene chloride (3 × 15 mL). The combined extracts were washed with water (2 × 10 mL) and dried. After the solution was concentrated under reduced pressure, analytical glpc analysis on a 1/8 in. × 10 ft. 15% FFAP column at 190°C showed one major product. The major product was isolated by preparative glpc on a 1/4 in. × 10 ft 15% FFAP column at 175°C as a clear liquid and identified as *syn*-7-chloro-*exo*-2-norbornyl ethyl ether. Infrared (CS_2): 1365, 1348, 1320, 1305, 1265, 1245, 1190, 1115(s), 1070: ^{1}H nmr (CS_2, 100 MHz) δ: 3.72 (s with fine structure, 1H, H-7), 3.32 (m, 3H, H-2 and —O—CH_2—), 2.33 and 2.30 (broad s, each 1H, H-1 and H-4), 2.12–1.02 (m, 6H, norbornyl envelope), 1.09 (t, 3H, J = 8 Hz, —CH_3).

Syn-*7-bromo*-exo-*2-norbornyl Ethyl Ether*

Deuterated *syn*-bromohydrin **5***c-d* (0.065 g, >95% pure) was dissolved in dry CH_2Cl_2 (2 mL) in a 5 mL two-necked flask and N_2 was slowly bubbled through the solution for 15 min. Freshly distilled thiethyloxonium tetrafluoroborate (0.15 g) was added and the flask was flushed with dry N_2 and stoppered. After 24 h water (10 mL) was added, the mixture was extracted with ether (3 × 10 mL), and the combined layers were washed with water (2 × 10 mL) and dried. Distillation of the solvent gave an oil that was composed of five major products of which the *syn*-bromoether was the major component as established by preparative glpc on a 1/4 in. × 8 ft 15% Carbowax column at 155°C. The ^1H nmr (CS_2, 100 MHz) was identical in all respects to the spectrum of the ether isolated from solvolysis of **1***e*.

Anti-*7-bromo*-exo-*2-norbornyl Ethyl Ether*

Deuterated *anti*-bromohydrin (0.059 g, 95% pure) was dissolved in dry CH_2Cl_2 (2 mL) and treated in the normal manner with triethyloxonium tetrafluoroborate. After workup the *anti*-bromoether that was the major component of the five major products of the reaction was isolated by preparative glpc on a 1/4 in. × 8 ft 15% Carbowax column at 150°C. The nmr was identical to that of the deuterated *anti*-7-bromo ether isolated from solvolysis of **2***e*.

Determination of Relative Yields of Products

The solutions from the kinetic runs (5) of the *non*-deuterated brosylates **1***a*, **1***b*, **2***a*, and **2***b* and the deuterated brosylates **1***d*, **1***e*, **2***d*, **2***e*, and **3** were combined and water (10–20 mL) was added. The mixtures were extracted with ether (2 × 80 mL, 1 × 30 mL), the combined extracts were washed with water (20 mL), saturated aqueous $NaHCO_3$ (2 × 20–35 mL), water (3 × 15–30 mL), and dried. The solvent was carefully distilled off through a 30 cm glass-helices column and the residues were analyzed by analytical glpc on a 1/8 in. × 10 ft 10% Carbowax column at 155°C. Peak areas were determined with a Varian Aerograph Model 485 electronic integration.

Acknowledgement

We thank the Natural Sciences and Engineering Research Council of Canada for financial support.

1. F. G. Bordwell and B. B. Jarvis. J. Am. Chem. Soc. **95**, 3585 (1973).
2. A. Nickon, J. R. Simmons, and B. Ho. J. Org. Chem. **42**, 800 (1977), and references cited therein.
3. J. D. Roberts, F. O. Johnson, and R. A. Carboni. J. Am. Chem. Soc. **76**, 5692 (1954).
4. N. H. Werstiuk, G. Timmins, and F. P. Cappelli. Can. J Chem. **58**, 1709 (1980).
5. N. H. Werstiuk, G. Timmins, and F. P. Cappelli. Can. J. Chem. **58**, 1738 (1980).
6. A. Nickon and N. H. Werstiuk. J. Am. Chem. Soc. **89**, 3914 (1967).
7. N. H. Werstiuk. Can. J. Chem. **53**, 26 (1975).
8. N. H. Werstiuk and F. P. Cappelli. Can. J. Chem. **58**, 1725 (1980).
9. A. L. Johnson, J. B. Stothers, and C. T. Tan. Can. J. Chem. **53**, 212 (1975).

Photolyse du butyne-1 dans la région de 147 à 174 nm

HÉLÈNE DESLAURIERS, JOVETTE DESCHÊNES ET GUY J. COLLIN[1]

Département des Sciences Pures, Université du Québec à Chicoutimi, Chicoutimi (Qué.), Canada G7H 2B1

Reçu le 14 avril 1980

HÉLÈNE DESLAURIERS, JOVETTE DESCHÊNES et GUY J. COLLIN. Can. J. Chem. **58**, 2100 (1980).

La photolyse du butyne-1 a été observée à 147, 163 et 174 nm. Les principaux produits C_1 à C_5 ont été mesurés dans le monomère pur ou en présence d'additifs et à différentes pressions (0,5 à 100 Torr – 65 à 13 300 N m^{-2}). Le radical méthyle est l'espèce intermédiaire dont le rendement est le plus important. L'acétylène, l'éthylène et le vinylacétylène sont produits en présence d'intercepteur radicalaire et proviennent probablement de la fragmentation de la molécule photoexcitée. On a noté en outre une forte polymérisation même en présence d'intercepteur radicalaire, et la presque impossibilité d'intercepter les radicaux C_3H_3 par l'iodure d'hydrogène. Des réactions secondaires diverses interviennent très certainement et compliquent l'interprétation. Par exemple l'augmentation du rendement en éthylène sur addition d'oxygène est difficilement explicable sur la notion simple habituellement admise de l'interception des radicaux libres par cet additif.

HÉLÈNE DESLAURIERS, JOVETTE DESCHÊNES, and GUY J. COLLIN. Can. J. Chem. **58**, 2100 (1980).

We have studied the 147, 163, and 174 nm photolysis of 1-butyne. Several products from C_1 to C_5 were observed under various conditions such as in the presence of additives, or at different pressures between 0.5 and 100 Torr (65 to 13 300 N m^{-2}). The methyl radical is the most important radical intermediate. Acetylene, ethylene, and vinylacetylene are produced in the presence of radical scavengers and are probably the result of the fragmentation of the photoexcited molecule. Propargyl radicals are thought to be produced but appear not to be scavenged by hydrogen iodide. Polymerization was observed even in the presence of radical scavengers. Secondary processes are numerous and make the interpretation of our results difficult; for example, the ethylene quantum yield increased upon addition of 10% oxygen, the simple radical scavenging effect of this additive does not explain such an effect.

Introduction

La photolyse des oléfines entre 147 et 174 nm a montré un effet de pression fort intéressant (1, 2). Dans certains cas des informations sur la chimie des radicaux allyles ont été obtenues (3, 4). Il est intéressant d'étudier la famille des alcynes pour voir si des informations similaires peuvent être obtenues sur les radicaux propargyles et ses dérivés. Le choix du butyne-1 pour aborder cette étude est lié à différents facteurs secondaires. Il est intéressant à priori d'étudier aussi la fragmentation de la molécule excitée. En particulier, il est nécessaire de savoir si les liaisons C—C en position β de la triple liaison sont aussi importantes dans la photolyse des alcynes que dans celle des oléfines (1, 2). Le butyne-1 permet de comparer l'importance de la scission de la liaison C—C située en position β par rapport à celle située en α de la triple liaison.

Le butyne-1 a déjà fait l'objet d'une étude à 123,6, 147 et au-dessus de 220 nm (5). Mis à part la réaction de fragmentation du radical butènyle-1 aucun effet de pression n'a été mentionné, il est vrai dans un domaine de pression restreint. Nous avons repris l'étude à 147 nm en ajoutant l'effet de l'iodure d'hydrogène et en élargissant l'échelle de pression.

Méthode expérimentale

Matériaux

Le butyne-1 est un produit API de pureté moléculaire affichée 99,94 ± 0,03%. L'analyse chromatographique de ce produit montre la présence d'une impureté dont le temps de rétention correspond à celui du méthyl-3-butyne-1-ène-3: 1470 ppm ainsi que de méthyl-3-butène-1: 38 ppm. L'oxygène (99,99%), l'oxyde nitrique (99,0%) et le propane (99,99%) sont des produits de qualité recherche de la compagnie Matheson du Canada. L'iodure d'hydrogène et le sulfure d'hydrogène sont les produits perdeutériés de la compagnie Merck, Sharp et Dohme du Canada (99,9%).

Préparation et irradiation des échantillons

Les échantillons sont utilisés après avoir été dégasés sous vide (10^{-5} mm mercure) dans une rampe en Pyrex équipée de valves en Téflon, de manomètres à membrane métallique Wallace et Tierman et d'une pompe à diffusion à huile située en amont d'une pompe mécanique. Les techniques d'irradiation ont été décrites et l'actinométrie est faite en comparant les chromatogrammes obtenus avec ceux obtenus lors de la photolyse du *cis*-butène-2 (6) ou du propène (2).

Les lampes utilisées sont elles aussi connues. La lampe au xénon (147 nm – 8,4 eV) est monochromatique (7), celle au brome (≈163 nm – 7,6 eV) (9) et celle à l'azote (≈174 nm – 7,1 eV) (8) le sont beaucoup moins. Le coefficient d'absorption du butyne-1 est de 800 ± 50 et de 250 ± 30 atm^{-1} cm^{-1}, respectivement à 147 et à 163 nm (9) et celui de l'iodure d'hydrogène est de 50 ± 20 atm^{-1} cm^{-1} à 147 nm (10*a*). Sans avoir trouvé ou mesuré le coefficient d'absorption du DI à 163 et à 174 nm, l'addition de cet intercepteur (25%) au butyne-1 ne provoque pas de diminution notable d'absorption de la lumière par l'alcyne. Celui de H_2S est de 285 atm^{-1} cm^{-1} à 147 nm et il est probablement plus faible à 163 et 174 nm (10*b*).

Analyse

Les produits sont analysés par chromatographie en phase gazeuse par ionisation de flamme en utilisant une colonne de squalane (25% – 8 m) à la température de la chambre (11). Une colonne de *n*-octane/Porasil C permet en outre d'extraire le rendement en propane ainsi que celui en butène-1.

[1]Auteur auquel toute correspondance devrait être envoyée.

0008-4042/80/192100-08$01.00/0

©1980 National Research Council of Canada/Conseil national de recherches du Canada

Can. J. Chem. Downloaded from www.nrcresearchpress.com by 210.87.254.6 on 09/05/12
For personal use only.

Can. J. Chem. Downloaded from www.nrcresearchpress.com by 210.87.254.6 on 09/05/12
For personal use only.

Résultats

Avant de présenter les résultats qui accompagnent le texte, il y a lieu de parler ici de la difficile reproductibilité rencontrée dans l'expérimentation. Contrairement aux précédentes études faites avec les oléfines, la fenêtre, qui sépare la lampe d'irradiation de la chambre réactionnelle, devient de plus en plus opaque au fur et à mesure que les temps de photolyse s'additionnent. La fig. 1 montre le nombre de photons émis par seconde après des temps variables de photolyse du mélange butyne-1:oxygène (100:10). La mesure est faite en photolysant le *cis*-butène-2 (6, 7). Le remplacement de l'oxygène par l'oxyde nitrique ne modifie pas substantiellement la décroissance de la transmission de la fenêtre. Evidemment, le nettoyage de la fenêtre avec un solvant habituel (acétone, tétrachlorure de carbone, ...) permet de retrouver la transmission initiale. Cette perte de transmission est encore plus sévère lors de la photolyse du monomère pur. Il s'ensuit que chaque irradiation de butyne-1 est encadrée par deux irradiations de *cis*-butène-2 pour les fins de l'actinométrie. Mais même dans ce cas, la précision de la mesure n'est au mieux connue qu'à ±10%. Les rendements quantiques ont été calculés en faisant la moyenne arithmétique de l'intensité de la lampe déterminée avant et après chaque photolyse. Aux résultats qui accompagnent le texte et qui apparaissent dans les tableaux et les figures, il faut ajouter les suivants.

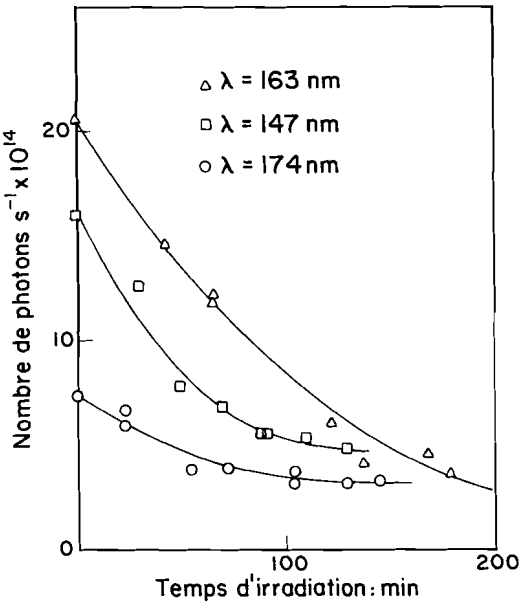


FIG. 1. Intensité du flux photonique entrant dans la chambre réactionnelle, mesurée à travers la photolyse du *cis*-butène-2. Les temps d'irradiations sont ceux des photolyses de butyne-1 qui sont effectuées entre les photolyses de butène-2; note: l'échelle pour la lampe à xénon (147 nm) doit être divisée par 10.

A 163 nm

1. La photolyse du mélange butyne-1:DI:SF_6 (50:1,25:x Torr) avec x variant entre 0 et 150 Torr, ne montre aucune variation substantielle des rendements quantiques des produits, sauf celui attribuable à l'effet de pression (voir plus loin).

2. Le pentadiène-2,3 est observé dans la photolyse du butyne-1 pur: $\Phi = 0{,}028$ à 10 Torr.

3. L'addition de l'oxyde nitrique a un effet similaire à celui de l'oxygène (tableau 1) sauf en ce qui a trait au rendement quantique en éthylène. Ce dernier diminue d'environ 50%: $\Phi(C_2H_4) = 0{,}04_5$, $0{,}05_5$ et 0,06 à 1,0, 5,0 et 10,0 Torr respectivement.

A 147 nm

Les résultats sont comparables à ceux déjà publiés par Hill et Doepker (5). On note par exemple des valeurs $\Phi_{O_2}(C_2H_4)$ environ deux fois plus importantes que celles de $\Phi_{NO}(C_2H_4)$. Nos rendements quantiques sont en général un peu plus élevés sauf ceux relatifs au vinylacétylène. Par contre nous observons un effet de pression sur la majorité des produits. Par exemple ces auteurs indiquent une valeur $\Phi_{NO}(C_4H_4)$ de 0,33 constante entre 0,5 et 20 Torr. Notre étude entre 0,5 et 90 Torr montre une variation faible certes, mais nette entre 0,5 et 90 Torr: $\Phi_{O_2}(C_4H_4)$ varie de 0,25 et 0,13.

Discussion

Photolyse à 163 nm

Le tableau 1 résume les principaux résultats obtenus dans la photolyse du butyne-1 dans différentes conditions. Les produits majeurs qui apparaissent lors de l'irradiation du produit pur sont l'éthane, l'allène et le vinylacétylène. En présence d'oxygène, le rendement en éthane disparaît, laisse inchangés ceux en allène et en vinylacétylène et augmente, double, celui en éthylène. En présence d'iodure d'hydrogène, le méthane est de loin le produit majeur avec un rendement quantique qui dépasse la valeur 1/2. Toujours en présence d'iodure d'hydrogène, les rendements en allène et en vinylacétylène ne sont pas perturbés, tandis que celui en butène-1 s'accroît de façon substantielle.

L'effet de l'addition de l'iodure d'hydrogène dans ces systèmes est relativement bien connu (11–13): il sert d'intercepteur radicalaire.

[1] $R + DI \rightarrow RD + I$

Ainsi la croissance du rendement en méthane en

Can. J. Chem. Downloaded from www.nrcresearchpress.com by 210.87.254.6 on 09/05/12
For personal use only.

TABLEAU 1. Photolyse du butyne-1 à 163 nm. Rendements quantiques

Butyne-1	1,0[a]	10,0	1,0	10,0	1,0	10,0	1,0	5,0
Oxygène[b]	—	—	0,1	1,0	—	—	—	—
DI	—	—	—	—	0,25	2,5	—	—
D_2S	—	—	—	—	—	—	0,2	1,0
Méthane	$0,03_5$	$0,03_8$	$0,02_0$	$0,02_5$	0,65	0,61	0,60	0,70
Acétylène	$0,05_2$	$0,04_5$	0,10	0,08	$0,06_4$	$0,04_8$	0,08	0,09
Ethylène	$0,06_1$	$0,06_1$	$0,10_7$	0,11	0,07	0,06	0,10	0,10
Éthane	0,18	0,11	0,00	0,00	0,05	0,04	0,16	0,14
Propyne	$0,03_1$	$0,01_5$	0,00	0,00	0,05	0,05	0,02	0,01
Allène	0,18	0,06	0,17	0,09	0,18	0,08	0,27	0,16
Propane	0,03	0,01	0,00	0,00	0,00	0,00	n.m.[c]	n.m.
Vinylacétylène	$0,12_5$	0,13	0,11	0,12	0,15	0,14	0,09	0,10
Butène-1	0,07	0,05	0,00	0,00	0,10	0,18	n.m.	n.m.
Butadiène-1,2	0,06	0,05	0,005	0,04	$0,00_5$	n.m.	n.m.	n.m.
Butatriène (?)[d]	0,03	0,03	0,00	0,00	0,00	0,00	n.m.	n.m.
Méthyl-2-butène-1	0,03	0,02	0,00	0,00	n.m.	n.m.	n.m.	n.m.

[a]En Torr (1 Torr = 133 N m^{-2}).
[b]Effet de l'oxyde nitrique similaire sauf pour la valeur $\Phi_{NO}(C_2H_4)$; voir résultats.
[c]n.m.: non mesuré.
[d]Identification très incertaine; voir réf. 13.

présence de cet additif est liée à la présence de radicaux méthyles. En supposant en outre qu'en présence d'oxygène ou d'oxyde nitrique tous les radicaux méthyles libres sont interceptés par l'un ou l'autre de ces deux additifs, la relation suivante peut être utilisée pour la mesure de rendements quantiques du radical méthyle:

$$[A] \quad \Phi(CH_3) = \Phi_{DI}(CH_4) - \Phi_{O_2 \text{ ou } NO}(CH_4)$$

ou

$$[B] \quad \Phi(CH_3) = \Phi_{D_2S}(CH_4) - \Phi_{O_2 \text{ ou } NO}(CH_4)$$

L'effet est sans doute similaire à celui de l'hydrogène sulfuré (11–13). Les deux relations [A] et [B] permettent de déterminer un rendement en radicaux méthyles de l'ordre de 0,62 ± 0,06. Ce rendement en radicaux méthyles est suffisant pour expliquer la formation de l'éthane dans la photolyse du produit pur, et est conforme à la disparition de ce produit lors des photolyses réalisées en présence d'oxygène ou d'oxyde nitrique. Cette proposition, de même que les relations [A] et [B], excluent la possibilité de réactions entre les radicaux méthyles et le monomère.

Un second produit important obtenu en présence de DI est le butène-1. Sur la base de la réaction [1], la formation de ce produit est liée à la présence de radicaux C_4H_7. La voie la plus directe pour la formation de ces radicaux C_4H_7 est celle de l'addition d'atome d'hydrogène sur le monomère (5, 14).

$$[2] \quad H + CH_3CH_2C{\equiv}CH \rightarrow CH_3CH_2\dot{C}{=}CH_2^* \qquad \Delta H = -200 \text{ kJ mol}^{-1} \quad \text{(réf. 15)}^2$$

$$[3] \quad CH_3CH_2\dot{C}{=}CH_2^* + M \xrightarrow{k_s} CH_3CH_2\dot{C}{=}CH_2 + M$$

$$[4] \quad CH_3CH_2\dot{C}{=}CH_2^* \xrightarrow{k_d} CH_3 + CH_2{=}C{=}CH_2(A) \qquad \Delta H = +150 \text{ kJ mol}^{-1}$$

Un deuxième intermédiaire radicalaire est donc l'atome d'hydrogène. Le radical vinylique C_4H_7 formé dans la réaction [2] est vibrationnellement excité: il doit être stabilisé par collision, sans quoi il a toutes chances de se fragmenter en un radical méthyle et en allène. Le mécanisme réactionnel proposé ([3] et [4]) est régi par la relation bien connu de Stern–Volmer (16):

$$[C] \quad [\Phi(A)]^{-1} = [\Phi_0(A)]^{-1} + [\Phi_0(A)]^{-1}(k_s/k_d)[M]$$

où Φ et Φ_0 sont les rendements quantiques à pression quelconque et à pression nulle; A est l'allène; k_s et k_d, respectivement, les constantes d'ordre deux et d'ordre un des réactions [3] et [4]; et [M] tient lieu de pression. Cette relation linéaire de $[\Phi(A)]^{-1}$ en fonction de la pression est présentée à la fig. 2. La courbure observée n'est pas importante compte tenu de l'incertitude expérimentale, mais n'est pas non plus impossible (16). D'autre part, le rendement en atome d'hydrogène dépend lui aussi de la pression (voir plus loin): il diminue probablement légèrement lorsque la pression croît. Ce qui doit ajouter à la non-linéarité de la relation [C]. Par conséquent, il ne peut se calculer avec une relation aussi simple que les relations [A] ou [B]: il faut tenir compte de l'effet de pression et

$$[D] \quad \Phi[H] \simeq \Phi_{DI}(C_2H_5CH{=}CH_2) + \Phi_{DI}(CH_2{=}C{=}CH_2) - \Phi_{O_2 \text{ ou } NO}(C_2H_5CH{=}CH_2) - \Phi_{\text{moléculaire}}(CH_2{=}C{=}CH_2)$$

Comme le rendement en butène-1 en présence d'oxygène est nul, l'expression [D] se simplifie. Il

[2]Les valeurs thermodynamiques usuelles sont tirées de Rosenstock et coll. (15) (voir le tableau 5).

TABLEAU 2. Photolyse du mélange butyne-1:DI (5:x Torr) à 163 nm

x	$\Phi(C_4H_4)$	$CH_3C{\equiv}CH$	$CH_2{=}C{=}CH_2$	$C_2H_5CH{=}CH_2$	[D']
0,0	0,13	—[a]	0,13	—[a]	—
0,26	$0,12_6$	$0,05_4$	0,13	$0,23_4$	0,36
0,49	$0,12_2$	$0,08_1$	$0,12_5$	0,20	0,32
0,71	$0,11_3$	$0,03_9$	$0,09_2$	0,21	0,30
0,99	$0,10_8$	$0,08_5$	0,11	0,15	0,26
1,21	$0,10_5$	$0,05_2$	0,09	0,18	0,27

[a] $\Phi_{O_2}(CH_3C{\equiv}CH) = 0,00$ et $\Phi_{O_2}(C_2H_5CH{=}CH_2) = 0,00$.

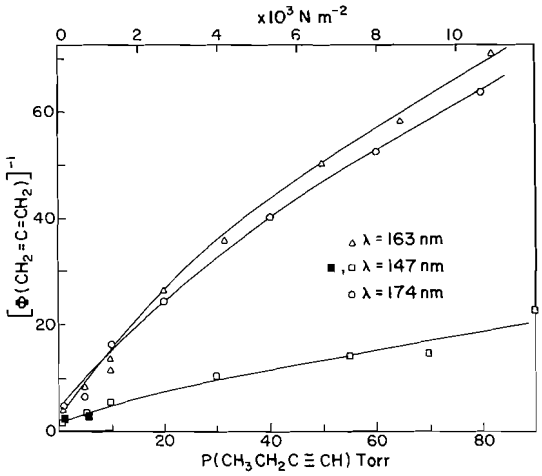


FIG. 2. Inverse du rendement quantique de l'allène en fonction de la pression de butyne-1 dans le mélange butyne-1: oxygène (100:10) ■: voir réf. 5.

reste cependant à évaluer le rendement $\Phi_{\text{moléculaire}}(CH_2{=}C{=}CH_2)$. La réaction [4] est un processus qui se fait avec une fréquence de l'ordre de grandeur de celle de collision à une pression de 1 Torr (133 N m^{-2}) ([4] est en compétition avec [3]). Donc l'oxygène et l'oxyde nitrique ajouté en faible proportion sont incapables d'intercepter les radicaux chauds $C_4H_7{}^*$. Par conséquent la réaction [4] génère l'allène même en présence de ces additifs (5). Il existe cependant au moins une autre possibilité de formation de l'allène par décomposition de la molécule photoexcitée

[5] $CH_3CH_2C{=}CH + h\nu \rightarrow CH_3CH_2C{\equiv}CH^{**}$

[6] $CH_3CH_2C{\equiv}CH^{**} \rightarrow (C_4H_6{}^{**}) \rightarrow CH_2{=}C{=}CH_2 + CH_2$

$\Delta H = +418$ kJ mol^{-1}

Cette possibilité est à éliminer. En effet, on admet généralement dans ces systèmes que la fragmentation directe des molécules photoexcitées se fait avec une fréquence beaucoup plus grande que la fréquence de collision sous pression normale ou de la réaction d'isomérisation. Dans ces conditions, la fig. 2 montre que la réaction [6] a un rendement quantique maximum inférieur à 0.02. La même conclusion a été proposée à 147 nm (5). En ignorant cette possibilité, la relation [D] se réduit à

[D'] $\Phi(H) = \Phi_{DI}(C_2H_5CH{=}CH_2) + \Phi_{DI}(CH_2{=}C{=}CH_2)$

et le rendement quantique en atome d'hydrogène est voisin de 0,29 ± 0,03. Cette valeur est probablement une valeur par défaut. En effet, l'interception des atomes d'hydrogène par le butyne-1 est en compétition avec celle par l'iodure d'hydrogène. Malgré un pourcentage élevé de DI (25%) (tableau 1) le rendement en allène ne semble pas être altéré tout au moins à l'incertitude expérimentale près. Le tableau 2, montre une étude plus systématique de l'effet de DI. La valeur de [D'] montre une variation à la baisse lorsque la concentration de DI croît. Compte tenu de l'incertitude expérimentale, on peut estimer que la variation de la concentration de DI de 5 à 25% fait diminuer la valeur de [D'] de 25%. De telle sorte que la valeur de [D'] est plutôt voisine de 0,4 ± 0,05 avec un rapport $k(H + DI)/k(H + C_2H_5C{\equiv}CH)$ voisin de 2,3 ± 0,3. La formation de méthyl-2-butène-1 en l'absence d'additifs est explicable par la combinaison des radicaux méthyles et butényles issus des réactions [2] et [3].

Un troisième radical est aussi révélé par l'addition de DI ou de D_2S: le radical éthyle. Les deux relations [A] et [B] appliquées au rendement en éthane sont contradictoires: $\Phi_{DI}(C_2H_5) = 0,45$ et $\Phi_{D_2S}(C_2H_5) = 0,15$ et l'explication de ces différents effets n'est pas aisée. Notons cependant la formation du propane attribuable à la combinaison des radicaux méthyles et éthyles, formation qui disparaît en présence d'oxygène ou d'oxyde nitrique.

Un autre produit révélé par l'usage de DI est le radical C_3H_3 via la formation du propyne. La réaction [1] appliquée à cette formation entraîne la relation suivante.

[E] $\Phi(C_3H_3) = \Phi_{DI}(CH_3C{\equiv}CH) - \Phi_{O_2 \text{ ou } NO}(CH_3C{\equiv}CH)$

et $\Phi(C_3H_3) \simeq 0,05 \pm 0,01$

Le rendement en propyne obtenu en présence de D_2S est beaucoup plus faible que celui mesuré en présence de DI. La structure du radical C_3H_3

Can. J. Chem. Downloaded from www.nrcresearchpress.com by 210.87.254.6 on 09/05/12
For personal use only.

Can. J. Chem. Downloaded from www.nrcresearchpress.com by 210.87.254.6 on 09/05/12
For personal use only.

suggérée partir de la structure de monomère est le radical propargyle $CH_2C{\equiv}CH$:

[7] $CH_3CH_2C{\equiv}CH^{**} \rightarrow \dot{C}H_3^* + \dot{C}H_2C{\equiv}CH^*$
$\Delta H = +320$ kJ mol^{-1} (réf. 17)[3]

[8] $\dot{C}H_2C{\equiv}CH^* + M \rightarrow \dot{C}H_2C{\equiv}CH + M$

[9] $\dot{C}H_2C{\equiv}CH^* \rightarrow C_3H_2 + H$
$\Delta H = +347$ kJ mol^{-1} (?)

[10] $\dot{C}H_2C{\equiv}CH^* \rightleftarrows CH_2{=}C{=}\dot{C}H^*$

[11] $CH_2{=}C{=}\dot{C}H^* + M \rightarrow CH_2{=}C{=}\dot{C}H + M$

[12] $\dot{C}H_2C{\equiv}CH \rightleftarrows CH_2{=}C{=}\dot{C}H$

où R* est un fragment primaire qui emporte une part inconnue de l'excédent de l'énergie du photon. L'interception du radical propargyle $\dot{C}H_2C{\equiv}CH$ par D_2S est une réaction endothermique, la chaleur de la liaison $H{-}CH_2C{\equiv}CH$ étant plus faible que celle de la liaison H—SH: $D(H{-}CH_2C{\equiv}CH)$ = 89,3 kcal mol^{-1} (18) et $D(H{-}SH)$ = 90,5 kcal mol^{-1} (19). Sur cette base et de façon similaire à l'interception des radicaux allyles, l'hydrogène sulfuré ne doit pas intercepter les radicaux propargyles (11). Le radical propargyle est cependant en résonance électronique avec la structure allènique. Des études théoriques (20) tout autant expérimentales (21) ont montré que le radical propargylique est probablement plus stable que le radical allènique. Expérimentalement, Kebarle et coll. ont montré que le rapport des concentrations à l'équilibre favorise le radical propargylique dans un rapport 3 à 1. Compte tenu de la valeur du rendement $\Phi_{DI}(CH_3C{\equiv}CH)$, la valeur du rendement en allène provenant de l'interception du radical allènique par DI ne devrait pas dépasser 0,02, une valeur de l'ordre de grandeur de l'incertitude expérimentale sur la mesure du rendement de l'allène. En ajoutant cette dernière valeur à celle de $\Phi_{DI}(C_3H_3)$ trouvée plus haut à partir de la formation du propyne, on observe un rendement maximum en radicaux C_3H_3 de 0,07.

L'iodure d'hydrogène n'est sans doute pas un excellent intercepteur radicalaire lorsqu'il s'agit de radicaux très insaturés comme C_2H ou C_3H_3 (13) surtout en présence d'un monomère dont on connaît peu de chose sur sa réactivité vis-à-vis les radicaux. Il faut d'ailleurs ajouter ici que le radical C_2H ne réagit pas avec l'oxyde nitrique (22) mais qu'il réagit passablement vite avec les alcanes et les oléfines: l'un des produits majeurs de telles interactions est l'acétylène (22, 23).

Il faut aussi traiter de la formation de l'éthylène et de l'acétylène. La formation de radicaux éthyles se relie simplement à la fragmentation de la molécule photoexcitée.

[13] $CH_3CH_2C{\equiv}CH^{**} \rightarrow C_2H_5^* + C_2H^*$
$\Delta H = +419$ kJ mol^{-1}

[14] $C_2H_5^* \rightarrow C_2H_4 + H$ $\Delta H = 79$ kJ mol^{-1}

[15] $C_2H_5^* + M \rightarrow C_2H_5 + M$

La relation de Stern–Volmer s'applique également au rendement en éthylène (fig. 3) et les commentaires faits précédemment pour la courbure de la droite de Stern–Volmer s'appliquent aussi ici. Il faut cependant mentionner l'effet différent de l'oxygène et de l'oxyde nitrique: $\Phi_{O_2}(C_2H_4) > \Phi_{NO}(C_2H_4)$. A basse pression, la valeur $\Phi_{O_2}(C_2H_4)$ est le double de la valeur $\Phi_{NO}(C_2H_4)$ (tableau 1). Cette différence a aussi été observée par Hill et Doepker (5). Les notions simples, ou peut-être trop simplistes, de l'interception des radicaux libres par les intercepteurs utilisés ne donnent pas un éclairage suffisant pour fins d'explication.

Une autre possibilité de formation de l'éthylène est la libération d'une molécule d'éthylène et d'acétylène à partir de la molécule photoexcitée. Cela nécessite évidemment l'isomérisation de la molécule photoexcitée

[16] $CH_3CH_2C{\equiv}CH^{**} \rightarrow (C_4H_6)^{**} \rightarrow C_2H_4^* + C_2H_2^*$
$\Delta H = +27{,}2$ kcal mol^{-1}

Les remarques faites à propos de la réaction [6] s'appliquent encore. D'autre part si l'excédent de l'énergie du photon est localisée dans l'éthylène, cette molécule a suffisamment d'énergie pour se fragmenter à nouveau en acétylène. Il faut rappeler ici que l'énergie minimum des photons est de 680 kJ einstein^{-1} à 174 nm. Dans ces conditions, la réaction [16] ne pourrait rendre compte que de la formation de l'éthylène et de l'acétylène (fig. 4) à haute

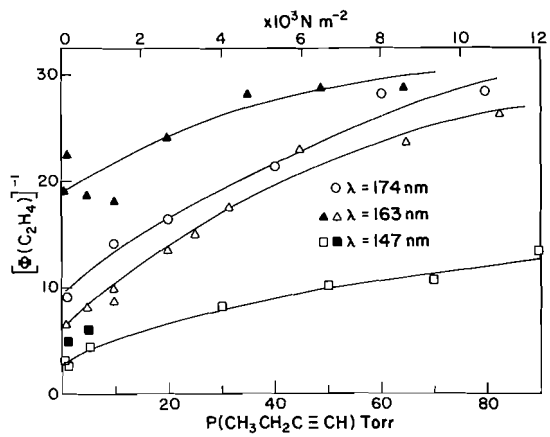


FIG. 3. Inverse du rendement quantique de l'éthylène en fonction de la pression de butyne-1. Le mélange contient 10% d'oxygène (△, ○, □) ou 5% d'oxyde nitrique ■ (réf. 5).

[3] $\Delta H_f^0(\dot{C}H_2C{\equiv}CH) \simeq 82$ kcal mol^{-1}. Voir la réf. 17.

Can. J. Chem. Downloaded from www.nrcresearchpress.com by 210.87.254.6 on 09/05/12
For personal use only.

pression. Dans ce cas $\phi([16]) \leq 0{,}04$. Inversement, il faut ajouter que des états excités à longue durée de vie ont été postulés pour l'acétylène (24). Cette possibilité n'a cependant pas été retenue pour les alcynes supérieurs (25). Notons en outre que les états excités du type Rydberg ont été observés dans cette région (9, 26).

Finalement, un dernier produit dont le rendement est plutôt insensible aux additifs est le vinylacétylène. Son rendement varie avec la pression (fig. 5). Deux possibilités sont disponibles:

[17] $CH_3CH_2C{\equiv}CH^{**} \rightarrow H_2 + CH_2{=}CHC{\equiv}CH$
$\Delta H = +120$ kJ mol^{-1}

[18] $CH_3CH_2C{\equiv}CH^{**} \rightarrow H + CH_3\dot{C}HC{\equiv}CH^{*}$
$\Delta H = +361$ kJ mol^{-1} (réf. 17*c*)[3]

[19] $CH_3\dot{C}HC{\equiv}CH^{*} \rightarrow H + CH_2{=}CHC{\equiv}CH$
$\Delta H \simeq +195$ kJ mol^{-1}

[20] $CH_3CHC{\equiv}CH^{*} + M \rightarrow CH_3CHC{\equiv}CH + M$

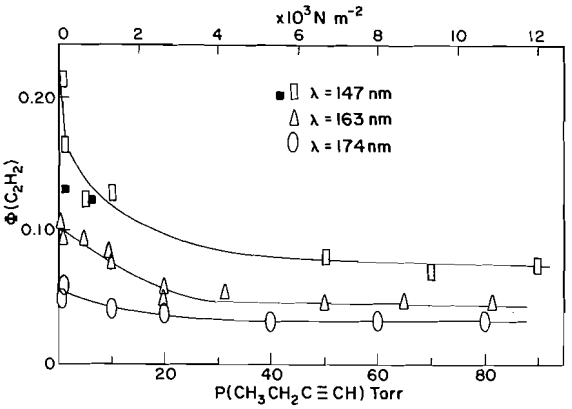


FIG. 4. Rendement quantique de l'acétylène en fonction de la pression de butyne-1 dans le mélange butyne-1:oxygène (100:10); ■ (réf. 5).

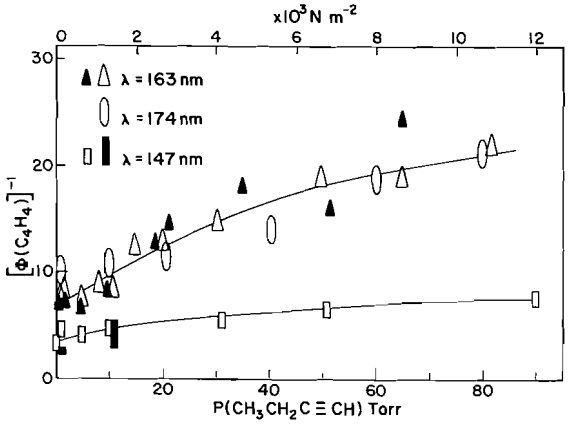


FIG. 5. Inverse du rendement quantique en vinylacétylène en fonction de la pression de butyne-1. Le mélange contient 10% d'oxygène (■, □, ○, △) ou 5% d'oxyde nitrique (▲). ■ (réf. 5).

La réaction [17] a contre elle les mêmes remarques faites à propos de la réaction [16]: l'effet de pression doit porter sur un état excité à longue vie. Les réactions [18] à [20] sont plus conformes à ce qui a été observé avec les oléfines (1, 2). La réaction [18] est la réaction majeure observée dans la photolyse sensibilisée par le mercure (21). Contrairement au radical propargylique où la forme allènique est moins stable, le radical $CH_3CHC{\equiv}CH$ semble exister plus facilement sous la forme allènique $CH_3CH{=}C{=}CH$ (21). Le produit résultant de sa combinaison avec le radical méthyl est observé dans le système pur sous forme de pentadiène-2,3.

Il est intéressant maintenant de faire les bilans. Puisque deux sources de radicaux méthyles ont été identifiées, le rendement du processus primaire [7] est au plus égal au rendement en radicaux méthyles diminué du rendement en allène: réaction [4]. Le tableau 1 permet ainsi de calculer $\phi([7]) \simeq 0{,}50 \pm 0{,}05$. Par contre, la mesure du rendement $\Phi(C_3H_3) \simeq 0{,}07$ calculée plus haut est insuffisante. Le produit C_3H_2 s'il est formé n'a pas été analysé. Le processus primaire [13] est au plus égal à la somme des rendements en radicaux éthyles et en éthylène. L'effet de DI, évalue à $0{,}11 \pm 0{,}02$ la valeur maximum de $\phi([13])$. Si la réaction [16] participe aussi à la formation de l'éthylène, alors $\phi([13]) \simeq 0{,}07$. A nouveau on ne retrouve pas le complément c'est-à-dire le radical C_2H. Finalement la mesure du rendement en vinylacétylène à pression nulle donne une valeur minimum à la somme $\phi([17]) + \phi([18]) \geq 0{,}15$. La mesure du rendement en radicaux $CH_3CHC{\equiv}CH$ ou $CH_3CH{=}C{=}CH$ est difficile de telle sorte qu'il devient impossible de faire le bilan complet du comportement de la molécule photoexcitée. Un fait cependant demeure, c'est l'abondante "polymérisation" du butyne-1 (fig. 1). La réactivité du radical C_2H (et probablement du radical C_3H_3) envers le monomère explique cette polymérisation. Ajoutons enfin, qu'un état photoexcité du monomère à temps de vie long n'est pas improbable bien que rien ici ne permet de le justifier.

A 147 nm

Les produits sont identiques à ceux mesurés à 163 nm. Cependant les rendements quantiques sont plus élevés (tableau 3). L'effet de pression est aussi beaucoup plus faible qu'à 163 nm (figs 2, 5). Ces deux arguments favorisent à la fois la plus grande décomposition et/ou la plus grande importance des fragmentations secondaires, et/ou la plus grande fréquence de fragmentation de l'isomère du monomère à long temps de vie.

L'application du modèle développé à 163 nm

Can. J. Chem. Downloaded from www.nrcresearchpress.com by 210.87.254.6 on 09/05/12
For personal use only.

TABLEAU 3. Photolyse du butyne-1 à 147 nm. Rendements quantiques

Butyne-1	1,0[a]	10,0	1,0	5,0	1,0	10,0	1,0	10,0
Oxygène	—	—	0,1	1,0	—	—	—	—
Oxyde nitrique	—	—	—	—	0,1	1,0	—	—
DI	—	—	—	—	—	—	0,26	2,5
Méthane	0,07	0,10	0,04	0,03	0,03	0,05	1,2	1,1
Acétylène	0,12	0,10	$0,16_5$	0,10	0,14	0,10	0,09	0,13
Ethylène	0,14	0,07	0,38	0,20	0,13	0,10	0,12	0,12
Ethane	0,36	0,12	0,02	0,00	n.m.[b]	0,00	0,11	0,11
Propyne	0,01	0,00	0,00	0,00	0,00	0,00	0,09	0,15
Allène	0,51	0,15	0,63	0,25	0,52	0,18	0,27	0,20
Propane	0,07	0,05	0,00	0,00	0,00	0,00	0,00	0,00
Vinylacétylène	0,31	0,26	0,27	0,25	0,36	0,27	0,27	0,24
Butadiène-1,2	0,06	0,08	n.m.	n.m.	$0,01_5$	0,02	0,00	0,00
Butatriène (?)[c]	0,06	0,07	n.m.	n.m.	0,00	0,00	0,00	0,00
Butène-1	0,14	0,23	n.m.	n.m.	0,00	0,00	0,40	0,40
Méthyl-2-butène-1	0,06	0,07	n.m.	n.m.	0,00	0,00	0,00	0,00

[a]En Torr (1 Torr = 133 N m^{-2}).
[b]n.m.: non mesuré.
[c]Identification très incertaine; voir réf. 13.

conduit à des rendements à 147 nm qui sont les suivants: $\phi([7]) \simeq 0,9$, $\phi([13]) \simeq 0,13$, $\phi([16]) = 0,10$ et $\phi([17]) \geq 0,33$, soit un total de 1,46! C'est évidemment une valeur trop élevée à moins d'admettre l'amorce d'un mécanisme en chaîne. L'impossibilité à nouveau d'intercepter les radicaux C_3H_3 et C_2H par DI, et l'accumulation de polymère sur la fenêtre, l'augmentation du rendement en éthylène sur addition d'oxygène conduit à proposer un mécanisme radicalaire de polymérisation. Certaines de ces chaînes en croissance peuvent donner lieu à la libération d'une part des produits mesurés et expliquer ainsi la valeur de 1,46 calculée plus haut. Il faut aussi mentionner que les atomes d'iode libérés dans la réaction (1) peuvent ne pas être inertes.

Vers 174 nm

Les rendements mesurés sont très semblables à ceux mesurés à 163 nm (tableau 4 et figs 2–5). Une exception toutefois, le rendement en acétylène semble un peu plus faible surtout en présence d'oxygène.

TABLEAU 4. Photolyse du butyne-1 vers 174 nm. Rendements quantiques

Butyne-1	0,5[a]	1,0	1,0	10,0
Oxygène	—	—	0,05	0,5
Méthane	0,03	$0,03_5$	0,030	0,011
Acétylène	0,05	0,07	0,06	0,04
Ethylène	0,05	0,07	0,11	0,07
Ethane	0,19	0,21	0,02	0,00
Propane	0,03	0,03	0,00	0,00
Propyne	0,00	0,005	0,00	0,00
Allène	0,21	0,22	0,21	0,06
Vinylacétylène	0,12	0,15	0,14	0,10
Butadiène-1,2	0,06	0,07	n.m.	n.m.[b]
Butène-1	n.m.	$0,07_5$	0,01	0,00
Butatriène (?)[c]	0,02	0,02	0,00	0,00
Pentyne-1	0,02	0,03	n.m.	n.m.
Pentadiène-2,3 ou -1,2	0,03	0,03	n.m.	n.m.

[a]En Torr (1 Torr ≡ 133 N m^{-2}).
[b]n.m.: non mesuré.
[c]Identification très incertaine; voir réf. 13.

Conclusion

Le spectre d'absorption du butyne-1 est connu (9). En-dessous de 159 nm et jusque vers 121,8 nm (le potentiel d'ionisation du butyne-1), Nakayama et Watanabe ont proposé trois séries de bandes Rydberg. Par contre au-dessus de 165 nm et jusque vers 200 nm, un large continuum avec un maximum à 177 nm a été enregistré. Sur celui-ci on croît pouvoir distinguer de faibles bandes de type Rydberg (27). Ainsi, l'absorption à 147 nm a lieu dans une zone d'absorption Rydberg sans qu'on sache très bien ce qui se passe au-dessus de 160 nm. Le présent travail n'aide pas non plus. Finalement, il est difficile de quantifier l'importance de la scission de la liaison C—C située en position β par rapport à celle située en α. Disons qu'elle semble être la plus importante. Par rapport aux oléfines cependant, elle l'est moins. Par contre la scission C—H semble être ici plus importante (1, 2, 7, 8).

Remerciements

Nous voudrions remercier vivement le Conseil de recherches en sciences naturelles et en génie du Canada qui nous a permis de faire cette étude, et l'Université du Québec à Chicoutimi qui a défrayé le salaire de l'un d'entre nous (J.D.).

1. G. J. COLLIN, H. DESLAURIERS et S. AUCLAIR. Can. J. Chem. **57**, 863 (1979).
2. G. J. COLLIN, H. DESLAURIERS et J. DESCHÊNES. Can. J. Chem. **57**, 870 (1979).
3. G. J. COLLIN et H. DESLAURIERS. Nouv. J. Chim. **3**, 701 (1979).

Can. J. Chem. Downloaded from www.nrcresearchpress.com by 210.87.254.6 on 09/05/12
For personal use only.

4. G. J. COLLIN et H. DESLAURIERS. Int. J. Chem. Kinet. **XII**, 17 (1980).
5. K. L. HILL et R. D. DOEPKER. J. Phys. Chem. **76**, 1112 (1972).
6. G. J. COLLIN et P. M. PERRIN. Can. J. Chem. **50**, 2823 (1972); A. WIĘCKOWSKI et G. J. COLLIN. J. Phys. Chem. **81**, 2592 (1977).
7. R. GORDEN, JR., R. E. REBBERT et P. AUSLOOS. NBS Technical Note 496 (1969).
8. A. WIĘCKOWKSI et G. J. COLLIN. Can. J. Chem. **56**, 1435 (1978).
9. T. NAKAYAMA et K. WATANABE. J. Chem. Phys. **40**, 558 (1964).
10. (*a*) P. AUSLOOS, R. E. REBBERT et S. G. LIAS. J. Photochem. **2**, 267 (1974); (*b*) K. WATANABE et A. S. JURSA. J. Chem. Phys. **41**, 1650 (1964).
11. R. A. HIVELY. Anal. Chem. **35**, 1921 (1963).
12. G. J. COLLIN et K. BUKKA. J. Photochem. **6**, 381 (1976/77).
13. Z. DIAZ et R. D. DOEPKER. J. Phys. Chem. **81**, 1442 (1977).
14. J. A. KERR. Compr. Chem. Kinet. **18**, 39 (1976).
15. H. M. ROSENSTOCK, K. DRAXL, B. W. STEINER et J. T. HERRON. J. Phys. Chem. Ref. Data, **6**, Suppl. no. 1 (1977).
16. W. FORST. *Dans* Theory of unimolecular reactions. Academic Press Inc., New York, NY. 1973.
17. (*a*) J. L. FRANKLIN et O. K. S. SHAMA. Adv. Mass. Spectrom. **6**, 947 (1974); (*b*) K. D. KING. Int. J. Chem. Kinet. **X**, 545 (1978); (*c*) W. TSANG. Int. J. Chem. Kinet. **X**, 687 (1978).
18. K. D. KING et T. T. NGUYEN. J. Phys. Chem. **83**, 1940 (1979).
19. R. J. WANG et S. W. BENSON. Int. J. Chem. Kinet. **XI**, 579 (1979).
20. A. HINCHLIFFE. J. Mol. Struct. **36**, 162 (1977).
21. P. KEBARLE. J. Chem. Phys. **39**, 2218 (1963).
22. A. M. TARR, O. P. STRAUSZ et H. E. GUNNING. Trans. Faraday Soc. **61**, 1946 (1965).
23. A. M. TARR, O. P. STRAUSZ et H. E. GUNNING. Trans. Faraday Soc. **62**, 1221 (1966).
24. L. J. STIEF, V. J. DECARLO et R. J. MATOLONI. J. Chem. Phys. **42**, 3131 (1965).
25. L. J. STIEF, V. J. DECARLO et W. A. PAYNE. J. Chem. Phys. **54**, 1913 (1971).
26. S. HAMAI et F. HIRAYAMA. J. Chem. Phys. **71**, 2934 (1979).
27. W. M. FLICKER, O. A. MOSHER et A. KUPPERMAN. J. Chem. Phys. **69**, 3311 (1978).
28. W. J. HERE, J. A. POPLE, W. A. LATHAN, L. RADON, E. WASSERMAN et Z. R. WASSERMAN. J. Am. Chem. Soc. **98**, 4378 (1976).
29. H. OKABE et V. H. DIBELER. J. Chem. Phys. **59**, 2430 (1973).

Annexe

Les valeurs thermodynamiques utilisées dans ce travail sont indiquées dans le tableau 5.

TABLEAU 5. Enthalpies de formation à 25°C

Espèce chimique	ΔH_f^0 (kJ mol^{-1})	Réf.
$CH_3CH_2\dot{C}{=}CH_2$	≈184	*a*
$CH_3CH_2C{\equiv}CH$	165,0	15
$CH_3\dot{C}HC{\equiv}CH$	308	*b*
$CH_2{=}CHC{\equiv}CH$	315	15
$CH_2{\equiv}C{\equiv}CH_2$	192	15
$\dot{C}H_2C{\equiv}CH$	343	17*b*,*c*
$\dot{C}_3H_2$ (?)	472	28
$\dot{C}_2H_5$	107	15
C_2H_4	52	15
$\dot{C}_2H_2$	227	15
$\dot{C}{\equiv}CH$	530 ± 10	17*a*, 29
CH_3	142	15
CH_2	390	15
H	220	15

[a] $\Delta H_f^0(CH_3\dot{C}HCH{=}CH_2)$ = 127,6 kJ mol^{-1} (15)[2] et $\Delta H_f^0(CH_3CH_2\text{-}\dot{C}{=}CH_2) \approx \Delta H_f^0(CH_3\dot{C}HCH{=}CH_2)$ + énergie de résonance de radical allylique.
[b] $\Delta H_f^0(CH_3C{\equiv}C\dot{C}H_2)$ = 308 kJ mol^{-1} (17*c*)[3].

Photolyse du butyne-2 dans la région de l'uv sous vide

JOVETTE DESCHÊNES, HÉLÈNE DESLAURIERS ET GUY J. COLLIN[1]

Département des Sciences Pures, Université du Québec à Chicoutimi, Chicoutimi (Qué.), Canada G7H 2B1

Reçu le 14 avril 1980

JOVETTE DESCHÊNES, HÉLÈNE DESLAURIERS et GUY J. COLLIN. Can. J. Chem. **58**, 2108 (1980).

La photolyse dans l'uv sous vide du butyne-2 a été étudiée à 147, 163 et 174 nm. L'usage de l'iodure d'hydrogène montre l'importance du radical méthyle dans la fragmentation de la molécule photoexcitée. On en conclut que la fragmentation principale de la molécule photoexcitée implique la rupture de la liaison C—CH_3: $\Phi_{147} \simeq 0.9$ et $\Phi_{163} \simeq 0.8$. On n'a cependant pas pu mesurer convenablement le rendement de la contrepartie, soit le radical C_3H_3. La diminution rapide de la transmission de la fenêtre suggère qu'une polymérisation radicalaire se fait même en présence d'oxygène ou d'oxyde nitrique. Finalement, on a pu suivre la variation du rendement du propyne et en vinylacétylène en fonction de la pression. Le premier produit est le résultat de la fragmentation du radical butènyle vibrationnellement excité tandis que le deuxième est probablement le résultat de la fragmentation du radical C_4H_5.

JOVETTE DESCHÊNES, HÉLÈNE DESLAURIERS, and GUY J. COLLIN. Can. J. Chem. **58**, 2108 (1980).

The vacuum uv photolysis of gaseous 2-butyne has been studied at 147, 163, and 174 nm. The use of hydrogen iodide as radical scavenger shows the importance of methyl radical formation in the fragmentation of the photoexcited molecule. It is concluded that the principal fragmentation of the photoexcited molecule involves the cleavage of a C—CH_3 bond: $\Phi_{147} \simeq 0.9$ and $\Phi_{163} \simeq 0.8$. Unfortunately, it was not possible to scavenge the corresponding C_3H_3 radicals. From the fast decrease of the transparency of the window it is concluded that an important radical polymerization takes place, even in the presence of oxygen or nitric oxide. Finally, from the pressure effect, it is shown that propyne results from the fragmentation of the vibrationally excited butenyl radical and vinylacetylene arises from the fragmentation of an excited C_4H_5 radical.

Introduction

A la suite de nos études sur le comportement photochimique sur les oléfines (1), nous avons pensé faire des études similaires sur les alcynes. La raison principale de cet intérêt réside dans le fait que la spectroscopie des deux familles de composés est assez différente. Alors que les oléfines (sauf l'éthylène) présentent peu de structure dans le spectre d'absorption et que celui-ci correspond surtout à une absorption de type $N \rightarrow V, (\pi, \pi^*)$, les alcynes ont un spectre d'absorption très structuré qui correspond à une absorption de type Rydberg vers 140–180 nm (2, 3).

Nous avons donc entrepris une étude similaire à celle faite sur les oléfines. Ce rapport présente les résultats obtenus avec le butyne-2. Avec le butène-2, la fragmentation de la molécule photoexcitée a lieu par moitié par scission de la liaison C—C située en α de la double liaison et par moitié par scission de la liaison C—H située en β par rapport à la double liaison (4). Le but premier est ici évidemment de voir si cette caractéristique est maintenue.

Méthode expérimentale

Les lampes de photolyse ont été décrites dans la publication précédente de ce journal, de même que la nature et la qualité de certains produits et les techniques d'analyse (5, 6). Le butyne-2 est un produit API de pureté 99,95 ± 0,04%. L'analyse révèle des quantités mineures de vinylacétylène (1,1 ppm) et de butyne-1 (5,0 ppm). Tous ces produits sont utilisés tel que reçus après avoir été dégasés dans un système à vide en Pyrex équipé de robinets en Téflon et de manomètres à membrane métallique Wallace et Tiernan. Dans la totalité des photolyses, le taux de conversion a été limité à moins de 0,5% (cas des monomères purs) et à moins de 0,1% dans le cas des irradiations en présence d'oxygène ou d'oxyde nitrique.

Le spectre d'absorption du butyne-2 est moins connu que celui du butyne-1. Une étude récente a montré que vers 174 nm, son coefficient d'absorption est supérieur à 1000 atm^{-1} cm^{-1} (3), de même qu'à 163 et à 147 nm (2).

Résultats

Les résultats expérimentaux sont exprimés dans les tableaux et les figures qui accompagnent le texte. Ils sont indiqués sous la forme de rendements quantiques. Ceux-ci ont été obtenus par comparaison avec ceux des produits obtenus dans la photolyse du *cis*-butène-2 (3) ou du propène (7) à la longueur d'onde d'intérêt.

A nouveau il faut mentionner la diminution de la transmission des fenêtres avec le temps d'irradiation du butyne-2 (fig. 1). Voir aussi la publication précédente de ce journal. La précision de la mesure des rendements quantiques qui en résulte a aussi été discutée précédemment.

Discussion

A 147 nm: les réactions radicalaires

Le tableau 1 montre la variété des produits obtenus lors de la photolyse du monomère pur, en présence d'iodure d'hydrogène ou d'oxyde nitrique. Les produits majeurs que sont l'éthane, les *cis*- et *trans*-butène-2 et le pentyne-2 disparaissent en présence d'oxygène ou d'oxyde nitrique. La

[1]Auteur auquel toute correspondance devrait être envoyée.

0008-4042/80/192108-07$01.00/0

©1980 National Research Council of Canada/Conseil national de recherches du Canada

Can. J. Chem. Downloaded from www.nrcresearchpress.com by 210.87.254.40 on 09/05/12
For personal use only.

Can. J. Chem. Downloaded from www.nrcresearchpress.com by 210.87.254.40 on 09/05/12
For personal use only.

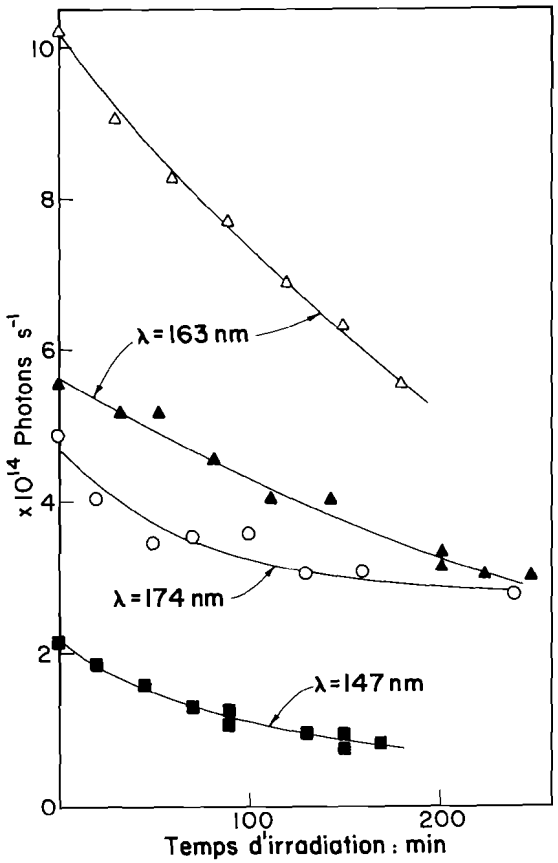


FIG. 1. Effet du temps de photolyse sur la transmission des fenêtres △, ○: mélange butyne-2:O_2 (100:10); ▲, ■: mélange butyne-2:NO (100:5). L'échelle doit être multipliée par 10 à 163 nm (△, ▲).

nature des mécanismes qui président à leur formation est donc très probablement radicalaire. Il en est de même pour certains C_4 et pour les C_5.

L'iodure d'hydrogène accroît fortement le rendement en méthane, et dans une moindre mesure ceux des butène-2 et du propyne. En admettant que l'iodure d'hydrogène intercepte les radicaux libres usuels (8–10):

[1] $R\cdot + HI \rightarrow RH + I$

la croissance du rendement en méthane, par exemple, est alors liée à la présence de radicaux méthyles. En supposant en outre qu'en présence d'oxygène ou d'oxyde nitrique, tous les radicaux libres sont interceptés, la relation suivante peut être utilisée pour la mesure des rendements quantiques des radicaux libres:

[A] $\Phi(R\cdot) = \Phi_{HI}(RH) - \Phi_{NO}(RH)$

Ainsi le produit majeur identifié est le radical méthyle: $\Phi(CH_3\cdot) \simeq 1{,}0$. De ce fait la formation de l'éthane dans le monomère pur est attribuable à la combinaison des radicaux méthyles.

La relation [A] permet aussi d'identifier les radicaux C_4H_7. La voie la plus simple pour la formation de cette espèce est l'addition d'un atome d'hydrogène sur le monomère. Un second intermédiaire est identifié: l'atome d'hydrogène. La mesure du rendement quantique est ici sujette à une sous-estimation. En effet, l'iodure d'hydrogène est en compétition avec le butyne-2 pour l'interception de ces atomes. Bien que le rapport des constantes de vitesse des réactions [2] et [3] ne soit pas disponible, la situation est probablement similaire à celle observée avec les alcènes (9), et la valeur $\Phi(C_4H_7) = \Phi_{HI}$(butène-2) donne probablement une valeur inférieure à la valeur réelle de $\Phi(H\cdot)$.

[2] $H + HI \rightarrow H_2 + I$

[3] $H + CH_3C{\equiv}CCH_3 \rightarrow CH_3CH{=}\dot{C}CH_3^*$

$\Delta H \simeq -175\ \text{kJ mol}^{-1}$

La combinaison des radicaux méthyles et butènyles explique la formation du méthyl-2-butène-2. Les radicaux butènyles formés dans le processus [3] sont vibrationnellement excités et doivent être auparavant stabilisés par collision.

[4] $CH_3CH{=}\dot{C}CH_3^* + M \xrightarrow{k_s} CH_3CH{=}\dot{C}CH_3$

[5] $CH_3CH{=}\dot{C}CH_3^* \xrightarrow{k_d} CH_3 + CH_3C{\equiv}CH(Py)$

$\Delta H = +138\ \text{kJ mol}^{-1}$

Un traitement cinétique simple conduit à la relation bien connue de Stern–Volmer (11):

[B] $[\Phi(Py)]^{-1} = [\Phi_0(Py)]^{-1} + [\Phi_0(Py)]^{-1}(k_s/k_d)[M]$

où l'indice zéro indique la mesure du rendement quantique obtenue par extrapolation à pression nulle; k_s et k_d sont les constantes d'ordre 2 et d'ordre 1 des réactions [4] et [5] respectivement; [M] est la pression dans le réacteur (fig. 2). Dans un article récent nous avons également proposé que le radical butènyle-2 excité peut aussi s'isomériser vers la forme allylique (7). La formation de butadiène-1,3, qui est formé par décomposition du radical α-méthallyle excité, peut donc aussi s'expliquer à partir du radical butènyle: $\Phi_{NO}(C_4H_6) \simeq 0{,}03$ à 147 nm (tableau 1).

Un autre radical mis en évidence par l'usage de l'iodure d'hydrogène est le radical C_3H_3. L'addition de cet additif fait croître à la fois le rendement en allène et en propyne (réaction [1]). La structure du monomère suggère le radical propynyle suivant: $CH_3C{\equiv}C^{\cdot}$. Par contre l'allène ne peut être formé

TABLEAU 1. Photolyse du butyne-2 à 147 nm

Butyne-2	1,0[a]	5,0	10,0	1,0	5,0	10,0	1,0	5,0	10,0
Oxyde nitrique	—	—	—	0,18	0,5	1,2	—	—	—
DI	—	—	—	—	—	—	0,28	1,07	1,90
Méthane	$0,06_4$[b]	0,07	0,06	0,03	0,04	$0,03_5$	1,10	0,97	0,91
Acétylène	0,13	0,11	$0,09_5$	$0,11_7$	$0,12_5$	$0,10_4$	0,15	0,12	0,10
Ethylène	$0,06_5$	0,08	0,07	0,05	0,06	0,07	0,11	0,11	0,10
Ethane	$0,18_6$	0,15	0,13	0,00	0,00	0,00	0,00	0,00	0,00
Propyne	$0,14_6$	0,09	0,06	0,11	0,08	0,07	0,29	0,26	0,18
Allène	$0,01_5$	$0,00_5$	0,00	0,00	0,00	0,00	0,06	0,06	$0,04_5$
Vinylacétylène	0,15	0,15	0,12	0,16	0,18	$0,16_5$	$0,16_9$	0,16	0,12
C_4H_6[c]	0,07	0,09	0,07	n.m.[d]	$0,03_5$	0,03	0,04	0,08	0,06
trans-Butène-2	$0,16_4$	0,23	0,22	0,00	0,00	0,00	0,24	0,33	0,32
cis-Butène-2	0,18	0,19	0,17	0,00	0,00	0,00	0,14	0,19	0,18
Butadiène-1,2	$0,07_4$	0,07	0,05	0,00	0,00	0,00	0,00	0,00	0,00
Pentyne-2	$0,14_2$	0,15	0,13	0,00	0,00	0,00	0,00	0,00	0,00
Méthyl-3-butadiène-1,2	$0,02_5$	$0,03_0$	$0,04_8$	0,00	0,00	0,00	0,00	0,00	0,00
Méthyl-2-butène-2	$0,04_8$	0,07	0,06	0,00	0,00	0,00	0,00	0,00	0,00

[a] En Torr (1 Torr = 133 N m^{-2}).
[b] Rendements quantiques.
[c] Butyne-1 + butadiène-1,3.
[d] n.m.: non mesuré.

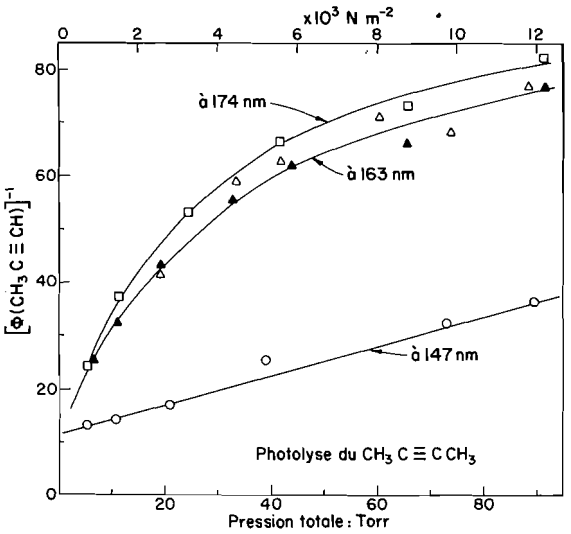


FIG. 2. Variation de l'inverse du rendement quantique du propyne en fonction de la pression à diverses longueurs d'onde. Mélange butyne-2:oxygène (100:10): □, △, ○; et butyne-2: oxyde nitrique (100:10): ▲.

qu'à partir du radical allènyle $CH_2{=}C{=}\dot{C}H$. Il y a donc lieu d'admettre un processus d'isomérisation soit de la molécule photoexcitée avant fragmentation, soit d'un fragment. Le radical allènyle est en résonance électronique avec le radical propargyle $^{\cdot}CH_2C{\equiv}CH$. Des études théoriques (12) tout autant qu'expérimentales (13) ont montré que l'équilibre favorise la structure propargyle dans un rapport de 3 à 1. On devrait donc trouver 3 fois plus de propyne que d'allène par interception des radicaux allènyles et propargyles par DI. Compte tenu de la formation de propyne par le processus [5], le rapport de 3 à 1 est à peu près conservé (tableau 1). De la même façon dans le produit pur on devrait retrouver trois fois plus de butyne-1 que de butadiène-1,2, produits issus de la réaction de combinaison des radicaux méthyles et allènyles et propargyles (13). On trouve en fait au moins autant de butadiène-1,2 que de butyne-1 dans le produit pur. Il doit donc y avoir une autre source radicalaire de butadiène-1,2. Cette interprétation suppose donc que tous les radicaux C_3H_3 n'ont pas la structure $CH_3C{\equiv}C^{\cdot}$ telle que suggérée par la structure du monomère.

Un autre radical est révélé par la présence de pentyne-2 et de méthyl-3-butadiène-1,2:

[6] $CH_3C{\equiv}C\dot{C}H_2 + \dot{C}H_3 \rightarrow CH_3C{\equiv}CCH_2CH_3$

[7] $CH_3C{\equiv}C\dot{C}H_2 \rightleftarrows CH_3\dot{C}{=}C{=}CH_2$

[8] $CH_3\dot{C}{=}C{=}CH_2 + \dot{C}H_3 \rightarrow (CH_3)_2C{=}C{=}CH_2$

En accord avec la prépondérance de la stabilité du radical propargylique sur celle du radical allènylique (13) le rendement en pentyne-2 est environ 5 fois supérieur à celui du méthyl-3-butadiène-1,2: $\Phi(C_5H_8) \simeq 0,18$ dans le produit pur.

Finalement il faut mentionner la légère augmentation du rendement en éthylène ($\simeq$0,07) et en acétylène ($\simeq$0,03) en présence d'iodure d'hydrogène ce qui, interprété sur la base de la réaction [1], est l'indice de formation des radicaux $C_2H_3\cdot$ et $C_2H\cdot$ et la relation [A] permet d'estimer les rendements $\Phi(C_2H_3\cdot) \simeq 0,05 \pm 0,02$ et $\Phi(C_2H\cdot) \simeq 0,01 \pm 0,01$. La structure du monomère oblige à admettre une isomérisation non négligeable soit de la molécule photoexcitée, soit de certains intermédiaires.

Can. J. Chem. Downloaded from www.nrcresearchpress.com by 210.87.254.40 on 09/05/12
For personal use only.

Can. J. Chem. Downloaded from www.nrcresearchpress.com by 210.87.254.40 on 09/05/12
For personal use only.

Il est dès lors tentant d'établir les bilans complets des rendements radicalaires via l'usage de l'iodure d'hydrogène. Il faut cependant faire les commentaires qui suivent. On a déjà mentionné l'interférence causée par l'addition de HI sur l'addition de l'atome d'hydrogène sur la triple liaison. Il faut aussi ajouter qu'on ne connaît finalement que peu de chose de la réactivité des radicaux sur les alcynes: la chimie des radicaux insaturés est d'autant plus méconnue que l'insaturation croît. Par exemple, le radical $C_2H\cdot$ s'il est présent, voir plus haut, à une chimie assez inhabituelle et ne semble pas intercepté par l'oxyde nitrique (14). Même en présence de quantités notables de NO, C_2H réagit avec le butène-2 et produit de l'acétylène et des pentadiènes (15). Que dire des radicaux C_3H_3 avec les alcynes?

La présence des radicaux C_4H_5, réactions [6]–[8], résulte soit de la rupture de la liaison C—H dans la molécule photoexcitée soit du transfert d'un atome d'hydrogène du monomère vers un radical

[9] $R + CH_3C{\equiv}CCH_3 \rightarrow RH + CH_3C{\equiv}C\dot{C}H_2$

Il est donc possible qu'une part de l'acétylène formé en présence d'oxygène résulte d'une telle réaction (voir plus loin).

A 147 nm: la fragmentation de la molécule photoexcitée

Le produit majeur identifié plus haut est le radical méthyle, et seulement un processus secondaire qui le produit semble bien identifié: réaction [5]. En soustrayant du rendement en méthane obtenu en présence d'iodure d'hydrogène celui du propyne obtenu en présence d'oxyde nitrique, on obtient un résidu en radicaux méthyles de l'ordre de 0,9 ± 0,05. Etant donné que d'autres processus secondaires non identifiés peuvent participer à ce rendement, cela donne une valeur maximum au processus primaire suivant: $\phi([11]) \leq 0{,}9 \pm 0{,}06$

[10] $CH_3C{\equiv}CCH_3 + h\nu \rightarrow CH_3C{\equiv}CCH_3{}^{**}$

[11] $CH_3C{\equiv}CCH_3{}^{**} \rightarrow CH_3 + CH_3C{\equiv}\dot{C}^{*}$

$\Delta H = +384\ \text{kJ mol}^{-1}$

Le rendement en radicaux C_3H_3 mesuré à travers l'effet de DI est beaucoup plus faible. D'après la discussion précédente

[C] $\Phi(C_3H_3) = \Phi_{HI}(\text{allène}) + \Phi_{HI}(\text{propyne}) - \Phi_{NO}(\text{propyne})$

Cette dernière relation donne un rendement $\Phi(C_3H_3)$ voisin de 0,20 ± 0,04. L'usage de DI n'est pas sans défaut. En particulier, son efficacité déficiente dans l'interception des radicaux C_3H_3 a déjà été mentionnée (10) et la chimie des radicaux C_3H_3 est vraiment mal connue. La valeur trouvée donne cependant une valeur minimum pour le processus [11] (voir plus bas).

L'autre radical qui a un rendement important est l'atome d'hydrogène. Le seul processus primaire évident est la rupture d'un lien C—H:

[12] $CH_3C{\equiv}CCH_3{}^{**} \rightarrow H + CH_3C{\equiv}C\dot{C}H_2{}^{*}$

$\Delta H = 374\ \text{kJ mol}^{-1}$

[13] $CH_3C{\equiv}C\dot{C}H_2{}^{*} \rightleftarrows CH_3\dot{C}{=}C{=}CH_2{}^{*}$

[14] $CH_3C{\equiv}\dot{C}CH_2{}^{*} \rightarrow CH_2{=}\dot{C}CH{=}CH_2{}^{*}$

[15] $CH_2{=}\dot{C}CH{=}CH_2{}^{*} \rightarrow H + CH{\equiv}CCH{=}CH_2$

Même en présence d'iodure d'hydrogène, il n'y a pas formation de butadiène-1,2. Par contre on observe une faible formation d'un mélange de butyne-1 et de butadiène-1,3. La formation de butadiène-1,3 est aussi possible à partir du radical butènyle (voir ci-haut). Le seul produit relié à la formation d'atome d'hydrogène est le vinylacétylène. Pour chaque molécule de ce produit, il y a libération d'un atome dans le processus primaire [12] et dans le processus secondaire [15]. Une autre possibilité serait évidemment l'élimination directe (en une étape) d'une molécule d'hydrogène:

[16] $CH_3C{\equiv}CCH_3{}^{**} \rightarrow (C_4H_6)^{**} \rightarrow H_2 + CH{\equiv}CCH{=}CH_2$

$\Delta H = 170\ \text{kJ mol}^{-1}$

L'effet de pression, sans être important, est notable (fig. 3). Un intermédiaire a donc un temps de vie suffisamment long pour être intercepté et stabilisé par collision. Cet intermédiaire peut être la molécule photoexcitée elle-même, une molécule très excitée, isomère du monomère, ou l'un des radicaux $C_4H_5{}^{*}$ (réactions [14] et [15]). Les

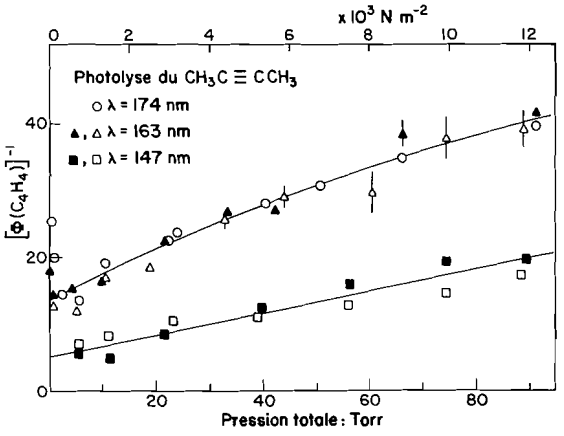


FIG. 3. Courbes de type Stern–Volmer. Variation de l'inverse du rendement quantique du vinylacétylène en fonction de la pression. Mélange butyne-2:oxygène (100:10): ○, △, □ et butyne-2:oxyde nitrique (100:10): ▲, ■.

Can. J. Chem. Downloaded from www.nrcresearchpress.com by 210.87.254.40 on 09/05/12
For personal use only.

courbes de type Stern–Volmer sont en accord avec une telle proposition.

Par contre, il est de coutume dans ce genre de travail d'admettre que les processus primaires, ceux qui impliquent la décomposition de la molécule photoexcitée, se font avec une fréquence beaucoup plus grande que la fréquence de collision. Ils ne sont donc pas sensibles à la pression. La seule exception notable est l'acétylène. Il faut se rappeler que l'absorption dans cette région met en jeu des états Rydberg, et le comportement de la molécule photoexcitée peut être particulier. Le haut rendement en hydrogène atomique favorise cependant les réactions [14] et [15]. En admettant que le mélange C_4H_6 obtenu en présence d'hydrogène consiste uniquement en butadiène-1,3, alors

$$[D] \quad \phi([12]) \geq \Phi_{NO}(C_4H_4) + \Phi_{HI}(C_4H_6) - \Phi_{NO}(C_4H_6)$$

Cette relation conduit à une valeur $\phi([12])$ de l'ordre $0{,}18 \pm 0{,}03$. Il y correspond un rendement en atome d'hydrogène de l'ordre égal à $\Phi(H) = \phi([12]) + \Phi(C_4H_4)$, soit $\Phi(H) \simeq 0{,}35$ et 0,30, à 1 et 10 Torr, respectivement. Ces valeurs sont minimum, car on ne sait rien de l'efficacité de l'interception des radicaux C_4H_5 par le HI.

Quant à la formation d'acétylène et d'éthylène (figs 4 et 5), on a déjà mentionné la réaction d'abstraction d'un atome d'hydrogène par le radical correspondant: processus [9]. On peut aussi proposer l'élimination d'une molécule d'acétylène

$$[17] \quad CH_3C{\equiv}CCH_3^{**} \rightarrow (C_4H_6^{**}) \rightarrow C_2H_2^* + C_2H_4^* \qquad \Delta H = +114 \text{ kJ mol}^{-1}$$

ou encore tout autre chemin mettant en cause les radicaux C_2H et C_2H_3. Il faudrait dans ces cas admettre une isomérisation importante de la molécule photoexcitée.

Cette proposition va à l'encontre des processus proposés dans le cas de la photolyse des oléfines. La présence d'états Rydberg dans cette région du spectre peut jouer un rôle particulier. La réaction [17] a contre elle le fait qu'il reste un excédent d'énergie de quelque 690 kJ mol^{-1} qu'il faut distribuer entre les fragments. L'éthylène aurait ainsi très probablement suffisamment d'énergie interne pour se fragmenter davantage.

A 163 nm

Les résultats sont similaires à ceux mesurés à 147 nm (tableau 2). La photolyse du monomère pur ou en présence d'oxyde nitrique conduit à des rendements qui sont en général 50% plus faibles ici comparativement à ceux discutés plus haut. Par

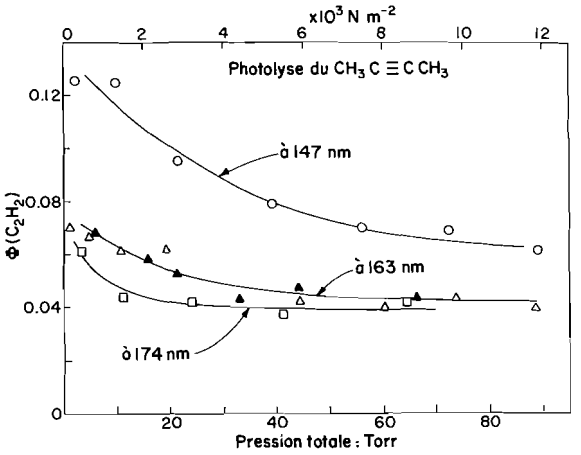


FIG. 4. Variation du rendement quantique de l'acétylène avec la pression à différentes longueurs d'onde. Mélange butyne-2:oxygène (100:10): ○, △, □ et butyne-2:oxyde nitrique (100:10): ▲.

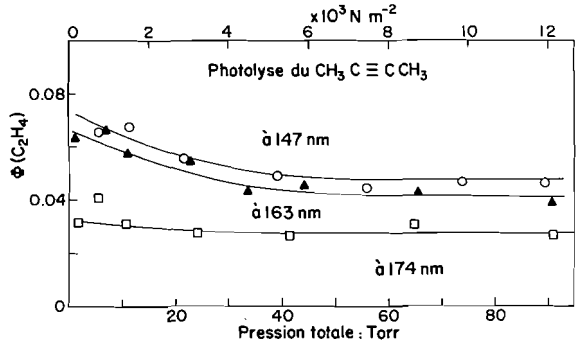


FIG. 5. Variation du rendement quantique de l'éthylène avec la pression à différentes longueurs d'onde. Mélange butyne-2:oxygène (100:10): ○, □; butyne-2:oxyde nitrique (100:10): ▲.

contre, les rendements en radicaux mesurés à travers l'effet de l'iodure d'hydrogène sont comparables. Sur la base de la relation [A], on obtient les valeurs suivantes: $\Phi(CH_3) = 0{,}87 \pm 0{,}03$; $\Phi(C_2H) \simeq 0{,}03$; $\Phi(C_2H_3) = 0{,}07$; $\Phi(C_3H_3) = 0{,}19$ (relation [C]). En outre, à 10 Torr, $\Phi(C_4H_7) = 0{,}53$. Par conséquent les rendements radicalaires ne sont pas ou peu affectés par la diminution de l'énergie photonique. Cette remarque est évidemment en faveur de la formation des radicaux par processus primaires, alors que les produits moléculaires le sont surtout par des processus secondaires. Les effets de pression (figs 2 à 5) sont aussi en accord avec une telle proposition. Sans reprendre au complet la discussion faite précédemment à 147 nm, la réaction [11] demeure la principale source de radicaux méthyles et du même coup c'est encore la

TABLEAU 2. Photolyse du butyne-2 à 163 nm

Butyne-2	1,0[a]	5,0	10,0	1,0	5,0	10,0	1,0	5,0	10,0	1,0	5,0	10,0
NO ou O_2	—	—	—	0,14	0,55	1,0	—	—	—	—	—	—
DI	—	—	—	—	—	—	0,27	1,0	0,9	—	—	—
D_2S	—	—	—	—	—	—	—	—	—	0,33	1,0	2,16
Méthane	$0,03^{b}$	0,03	0,03	$0,01_5$	$0,01_7$	$0,01_5$	0,91	0,92	0,81	0,78	0,70	0,72
Acétylène	0,06	$0,06_7$	0,06	0,06	0,06	0,06	0,10	0,09	0,07	0,16	0,09	0,15
Ethylène	0,04	0,06	0,06	0,02	0,04	0,04	0,10	0,11	$0,09_5$	0,09	0,09	0,09
Ethane	$0,10_5$	$0,09_4$	$0,08_5$	0,00	0,00	0,00	0,00	0,00	0,00	0,00	0,00	0,00
Propyne	$0,05_5$	$0,03_5$	0,03	$0,05_5$	0,0	0,03	$0,21_5$	0,16	$0,14_5$	0,19	0,12	0,11
Allène	0,00	0,00	0,00	0,00	0,00	0,00	$0,05_4$	0,05	0,04	0,00	0,00	0,00
Vinylacétylène	$0,07_3$	$0,07_2$	$0,06_2$	$0,07_4$	0,08	0,06	$0,09_4$	$0,09_5$	$0,08_0$	$0,08_7$	0,08	0,07
C_4H_6[c]	$0,04_5$	0,06	$0,06_1$	$0,00_4$	0,00	0,01	0,02	0,04	0,05	0,31	0,25	$0,23_5$
Butadiène-1,2	$0,03_3$	$0,03_3$	0,00	0,00	0,00	0,00	0,00	0,00	0,00	0,01	n.m.	0.02
trans-Butène-2	0,07	0,13	$0,13_5$	0,00	0,00	0,00	0,13	0,25	0,24	0,35	0,32	0,34
cis-Butène-2	n.m.[d]	n.m.	0,15	0,00	0,00	0,00	0,16	0,35	0,29	0,23	0,10	0,21
Pentyne-2	0,07	0,07	0,09	0,00	0,00	0,00	0,00	0,00	0,00	n.m.	n.m.	n.m.

[a]En Torr (1 Torr = 133 N m^{-2}).
[b]Rendements quantiques.
[c]Butyne-1 + butadiène-1,3.
[d]n.m.: non mesuré.

principale voie de fragmentation de la molécule photoexcitée: $\phi_{163}([11]) \leq 0,82 \pm 0,03$. Le rendement en vinylacétylène à pression nulle est voisin de 0,08: $\phi([15]) \simeq 0,08$ et $\phi([12]) \geq 0,08$. Une part des radicaux C_4H_5* formés par le processus [12] sont sans doute stabilisés par collision et il est difficile d'en évaluer la quantité. L'importance du rendement en pentyne-2 dans le système pur comparativement à ce qui est observé à pression nulle tend à montrer que le processus [12] est ici moins important qu'à 147 nm. On retrouve à nouveau une formation limitée d'éthylène et d'acétylène (figs 4 et 5) et de butadiène-1,3 + butyne-1.

L'effet de l'addition de l'hydrogène sulfuré est déroutant. Dans la photolyse du butyne-1, Doepker a observé que D_2S intercepte certains radicaux allènyles (10). Cette observation est en accord avec le fait que la liaison C—H dans l'allène est plus forte que la liaison HS—H. Une valeur de la liaison C—H dans l'allène a été calculée voisine de 108,1 kcal/mol (16), comparativement à 90,5 ± 1,1 kcal/mol dans le cas de la liaison HS—H (17). L'allène n'est pas un produit dans le présent mélange butyne-2:D_2S. Il n'y aurait donc pas ou peu de radicaux allènyles. L'isomérisation envisagée à 147 nm est donc de peu d'importance. Inversement, toujours dans le même travail, Doepker ne rapporte pas de formation de propyne dans le mélange $CH_3CH_2C{\equiv}CH$:D_2S. Le radical $^{\cdot}CH_2C{\equiv}CH$ ne serait pas intercepté par l'hydrogène sulfuré. Cette observation est en accord avec le fait que la liaison $CH{\equiv}CCH_2$—H est plus faible que la liaison HS—H: $D(CH{\equiv}CCH_2$—H) = 89,3 kcal/mol (18). Le propyne est aussi un produit de la photolyse du mélange butyne-2:D_2S. Par conséquent le radical intercepté par D_2S ne pourrait être que le radical $CH_3C{\equiv}C^{\cdot}$ en accord avec la structure du monomère d'une part, et en accord avec le fait que la chaleur de la liaison $CH_3C{\equiv}C$—H a été calculée voisine de 128 kcal/mol (16). Le rendement en radicaux propynyles est de l'ordre de 0,2, c'est-à-dire beaucoup moins que celui calculé à partir de la réaction [12]. Par conséquent les radicaux C_3H_3 disparaissent du milieu réactionnel, et HI est incapable de les titrer convenablement tout au moins sous la forme du produit propyne.

Remerciements

Nous tenons à exprimer notre gratitude au ministère de l'Education du Québec (programme FCAC) qui nous a soutenu monétairement pendant cette étude, de même que l'Université du Québec à Chicoutimi (FIR).

1. G. J. COLLIN. Rev. Chem. Interm. **2**, 377 (1979).
2. H. KAISER. Thèse de doctorat, Univ. Louis-Maximillien, Munich. 1970.
3. S. HAMAI et F. HIRAYAMA. J. Chem. Phys. **71**, 2934 (1979).
4. A. WIĘCKOWSKI et G. J. COLLIN. J. Phys. Chem. **81**, 2592 (1977).
5. R. GORDEN, JR., R. E. REBBERT et P. AUSLOOS. NBS, Technical Note 496 (1969).
6. A. WIĘCKOWSKI et G. J. COLLIN. Can. J. Chem. **56**, 1435 (1978); G. J. COLLIN, H. DESLAURIERS et S. AUCLAIR. Can. J. Chem. **57**, 863 (1979).
7. G. J. COLLIN, H. DESLAURIERS et J. DESCHÊNES. Can. J. Chem. **57**, 870 (1979).
8. P. AUSLOOS, R. E. REBBERT et S. G. LIAS. J. Photochem. **2**, 267 (1973/74).

Can. J. Chem. Downloaded from www.nrcresearchpress.com by 210.87.254.40 on 09/05/12
For personal use only.

9. G. J. COLLIN et K. BUKKA. J. Photochem. **6**, 381 (1976/77).
10. Z. DIAZ et R. D. DOEPKER. Phys. Chem. **81**, 1442 (1977).
11. W. FORST. *Dans* Theory of unimolecular reaction. Academic Press, New York, NY. 1973.
12. A. HINCHLIFFE. J. Mol. Struct. **36**, 162 (1977).
13. P. KEBARLE. J. Chem. Phys. **39**, 2218 (1963).
14. A. M. TARR, O. P. STRAUSZ et H. E. GUNNING. Trans. Faraday Soc. **61**, 1946 (1965).
15. A. M. TARR, O. P. STRAUSZ et H. E. GUNNING. Trans. Faraday Soc. **62**, 1221 (1966).
16. D. C. MCKEAN, J. L. DUNCAN et L. BATT. Spectrochim. Acta, **29**A, 1037 (1973).
17. P. J. WANG et S. W. BENSON. Int. J. Chem. Kinet. **XI**, 579 (1979).
18. K. D. KING et T. T. NGUYEN. J. Phys. Chem. **83**, 1940 (1979); W. TSANG. Int. J. Chem. Kinet. **X**, 687 (1978).

Annexe

Les valeurs thermodynamiques utilisées pour les valeurs ΔH (réaction) sont indiquées dans le tableau 5 du manuscrit précédent de ce journal.

Can. J. Chem. Downloaded from www.nrcresearchpress.com by 210.87.254.40 on 09/05/12
For personal use only.

Can. J. Chem. Downloaded from www.nrcresearchpress.com by 210.87.254.5 on 09/05/12
For personal use only.

On the evaluation of the nuclear electric quadrupole moment of vanadium-50

MAHMOUD ADAM HABAYEB AND O. E. HILEMAN, JR.

Department of Chemistry, McMaster University, Hamilton, Ont., Canada L8S 4M1

Received June 3, 1980

MAHMOUD ADAM HABAYEB and O. E. HILEMAN, JR. Can. J. Chem. **58**, 2115 (1980).

^{50}V- and ^{51}V-nmr relaxation spectra were recorded for neat $VOCl_3$ at 298 K. In addition, the line width at half-height ($W_{1/2}$) of each resonance was measured. The average $Q(^{50}V)/Q(^{51}V)$ ratio was calculated to be |3.55|. A quadrupole moment, $|Q|$, of ^{50}V was estimated using these data along with the reported Q values of ^{51}V. The magnetic moments, μ, of both isotopes were also evaluated from the ratio of their Larmor frequencies.

MAHMOUD ADAM HABAYEB et O. E. HILEMAN, JR. Can. J. Chem. **58**, 2115 (1980).

Opérant à 298 K, on a enregistré les spectres des relaxation en rmn du ^{50}V et du ^{51}V du $VOCl_3$ homogène. De plus, on a mesuré la largeur des raies à mi-hauteur ($W_{1/2}$) de chaque résonance. On a calculé un rapport moyen $Q(^{50}V/^{51}V)$ de |3,55|. On a évalué le moment quadrupolaire $|Q|$ du ^{50}V en utilisant ces données de concert avec des valeurs connues de Q du ^{51}V. On a également évalué les moments magnétiques, μ, des deux isotopes à partir du rapport de leur fréquences de Larmor.

[Traduit par le journal]

Introduction

Data from ^{50}V-nmr investigations of various vanadium (V) species present in neat liquids or solutions have not appeared frequently in the literature. Howarth and Richards (1) reported the line widths of the ^{50}V and ^{51}V resonances observed in $VOCl_3$ (neat). From these data and an estimated value of the nuclear electric quadrupole moment, Q, of ^{51}V they calculated a value of Q for ^{50}V. No authors — to the best of our knowledge — have reported the results of either T_1 or T_2 measurements on this nucleus.

The purpose of this communication is to report the results of an investigation of the nmr parameters of the ^{50}V nucleus in $VOCl_3$ (neat) using FT-nmr techniques. From these data and from ^{51}V-nmr parameters we estimated a new value of $|Q|$ for ^{50}V and confirmed the reported values of the magnetic moments, μ, for ^{50}V and ^{51}V (2).

Experimental Details

Preparation of Samples

Two samples of neat $VOCl_3$ were used in this work. The first was prepared in house as reported in the literature (3). The product was thrice distilled under N_2 at 10^{-3} Torr. The purified product was transferred to an 8 mm od nmr tube connected to the vacuum line. The tube was sealed off after collection of 4 mL of sample. The second sample was prepared by transferring, within a dry-box (N_2), stock material (Canadian Scientific Co.) to an 8 mm od nmr tube fitted with a Teflon connector/stopcock. The tube was connected to a vacuum line and the sample was degassed by the freeze/thaw method at 10^{-3} Torr (N_2). The tube was sealed off below the connector/stopcock while still connected to the line. Both samples were stored in the dark and at 0°C between nmr measurements. No differences in nmr observables were detected between the two samples.

^{50}V and ^{51}V NMR Measurements

^{50}V- and ^{51}V-nmr relaxation spectra were recorded at 8.97 and 23.66 MHz respectively in a magnetic field of 2.114 T using a pulse FT-nmr technique on a Bruker WH-90 nmr spectrometer interfaced with a Bruker BNC-12 data system. To obtain nmr spectra, the 8 mm sample tube was placed inside a 10 mm nmr tube. Field/frequency stabilization was achieved by locking on the ^{2}H resonance of C_6D_6 containing in the 10 mm tube. Also, the line widths at half-height ($W_{1/2}$) of the ^{50}V and ^{51}V resonances were measured at 24.94 and 65.79 MHz, respectively, in a magnetic field of 5.9 T using a pulse FT-nmr technique on a Bruker WM-250 nmr spectrometer.

Spin–lattice relaxation times (T_1's) measurements on ^{50}V and ^{51}V were performed in a magnetic field of 2.114 T using the usual 180–τ–90° (inversion recovery method) pulse sequence as described in the literature (4). Spin–spin lattice relaxation times (T_2) were obtained from natural line widths ($W_{1/2}$) given by $W_{1/2}$, Hz $= 1/\pi T_2$, where $W_{1/2}$ is the resonance line width at half-height. For T_1 measurements, typical spectral widths of 5 kHz and 8K of data memory were used. For normal ^{50}V and ^{51}V spectra, spectral widths of 12 kHz in 8K of data memory and 90° pulses (30 μs) were applied. All measurements were performed at 298 ± 1 K. The results are shown in Table 1.

Results and Discussion

For quadrupolar nuclei such as ^{50}V and ^{51}V the line width of each resonance is determined by the nuclear quadrupole moment of each isotope and the molecular correlation time as given in eq. [1] (5):

$$[1]\quad \pi W_{1/2} = \frac{1}{T_1} = \frac{1}{T_2} = \frac{3(2\pi)^2}{40}\,\frac{(2I+3)}{I^2(2I-1)} \times (e^2Qq/h)^2(1+\eta^2/3)\tau_c$$

The various symbols used above have their usual meaning. The individual values of q, η, and τ_c are identical for the isotopic pair. Thus, eq. [1] may be

0008-4042/80/192115-03$01.00/0

©1980 National Research Council of Canada/Conseil national de recherches du Canada

Can. J. Chem. Downloaded from www.nrcresearchpress.com by 210.87.254.5 on 09/05/12
For personal use only.

TABLE 1. Various nmr parameters for the ^{50}V and ^{51}V isotopes

Nucleus	$W_{1/2}$, Hz*	T_2, ms†	$W_{1/2}$, Hz	T_1, ms	T_2, ms	μ
^{50}V	55	5.8	69 ∓ 2	5 ∓ 1	4.6	3.3413
^{51}V	90	3.5	20 ∓ 1	18 ∓ 2	$1.6 \times 10^{+1}$	5.1419

*$W_{1/2}$ values were reported in ref. 1.
†T_2 values were estimated from $W_{1/2}$ values given in ref. 1.

TABLE 2. The quadrupole moment values of ^{50}V and ^{51}V

Method	Q of ^{51}V (barn)*	$\|Q\|$ of ^{50}V (barn) from T_1 values† and $W_{1/2}$ values†	
Optical hyperfine structure	0.28 ∓ 0.15	1.01 ∓ 0.055	0.98 ∓ 0.52
Nmr	0.007	0.025	0.024
Nmr	0.26	0.94	0.92
Atomic beam magnetic resonance	−0.049	0.18	0.17
Optical hyperfine structure	−0.04	0.14	0.14
Shell model	−0.047	0.17	0.16
Configuration mixing	−0.03	0.11	0.10
Collective model	+0.04	0.14	0.14
	−0.12	0.43	0.42

*Values of Q of ^{51}V were reported in ref. 6.
†T_1 and $W_{1/2}$ values are given in Table 1.

used to evaluate $|Q|$ of ^{50}V if Q of ^{51}V is known and $W_{1/2}$ and T_1 values of both ^{50}V and ^{51}V resonances are determined.

One of the main difficulties in calculating $|Q|$ values for ^{50}V by this method is the wide range of ^{51}V Q values reported in the literature (6). Representative values are included in Table 2. Several of these, namely, 0.28, 0.26, −0.12, and 0.007 b, have been called into question and then were ruled out as reasonable values by Saraswati (6). In addition, the short relaxation times obtained in the present work (18 ± 2 ms) along with that reported by Gillen and Noggle (23 ms) (7) for the ^{51}V nucleus in $VOCl_3$ (neat) indicate that the value of Q for ^{51}V must be larger than 0.007 b.

Using T_1 and $W_{1/2}$ values of the isotopic pair in this work, the various ^{51}V Q values reported by Saraswati (6) and eq. [1], the $Q(^{50}V)/Q(^{51}V)$ ratios were calculated to be |3.5| from $W_{1/2}$ data and |3.6| based on T_1 measurements. With these ratios, the various $|Q|$ values of ^{50}V shown in Table 2 were calculated.

Using the known viscosity of neat $VOCl_3$ (η = 0.68 cP at 30°C) (7, 8), an estimate of an average weighted molecular radius, a = 2.80 Å and the Debye equation $\tau_c = 4\pi a^3\eta/KT$ gives $\tau_c = 15 \times 10^{-12}$ s.[1] With this τ_c value, ^{51}V-T_1 value, asymmetry parameter value reported by Allerhand (10), and eq. [1] we calculated e^2Qq/h = 2.98 MHz. This value is significantly less than that reported by Allerhand (10) for solid $VOCl_3$ (5.4 MHz).

Howarth and Richards (1) reported $W_{1/2}$ values of 55 and 90 Hz for the ^{50}V and ^{51}V resonances, respectively.[2] In contrast, our values for the isotopic pair are 69 ± 2 and 20 ± 1 Hz. This discrepancy may be due to sample characteristics. A second suggestion is that the relaxation rates are frequency dependent. Values of $\omega_0\tau_c$ for both isotopes, however, are in the extreme narrowing condition ($\omega_0\tau_c \ll 1$). This proposal was confirmed by the observation that our T_1 and T_2 values for each nucleus of the isotopic pair are equal within experimental error. In addition, the observed line widths were found to be insensitive to changes in the applied magnetic field strength. In contrast, the data of ref. 1 lead to calculated values of T_2 that are not equal to the experimentally determined T_1 values for each nucleus.

Finally, to evaluate the magnetic moments of both isotopes it was necessary to measure the ratios of their Larmor frequencies. These ratios are: $\nu(^{51}V)/\nu(^1H)$ = 0.263022 (10), $\nu(^{50}V)/\nu(^1H)$ = 0.099700 (10), and $\nu(^{51}V)/\nu(^{50}V)$ = 2.638129 (10). Using the magnetic moment of the proton in H_2O (μ_p = 2.7927740 (11)) reported by Cohen and Taylor

[1]The V—O and V—Cl bond distances are 1.56 Å and 2.12 Å, respectively. The oxygen and chlorine ionic radii are 0.66 Å and 0.90 Å, respectively (9). To calculate a, the oxygen and chlorine ionic radii were added to the V—O and V—Cl distances and then the weighted average was estimated.

[2]These line widths were obtained by multiplying the values reported in ref. 1 by $\sqrt{3}$ since these values are absorption derivative line widths and must be corrected for comparison in Table 1.

(11) and a similar procedure to that reported by Kautt *et al.* (12) for the calculation of μ of ^{95}Mo and ^{97}Mo isotopes, one can calculate the μ values of ^{50}V and ^{51}V nuclei. The results are shown in Table 1. These magnetic moment values are in good agreement with those reported in the literature (2). Minor differences may be due to the fact that no diamagnetic corrections were made in the present work.

Acknowledgements

The financial support of the Natural Sciences and Engineering Research Council of Canada, Strategic Grants Program is gratefully acknowledged. We also thank Drs. G. Schrobilgen and D. Eaton for helpful discussions, Mr. B. Sayer for recording the ^{50}V- and ^{50}V-nmr spectra, and C. Rodgers of Bruker Canada Ltd., Mississauga, Ont., for recording the spectra on Bruker WM-250 spectrometer.

1. O. HOWARTH and R. E. RICHARDS. Proc. Phys. Soc. London, **84**, 326 (1964).
2. G. H. FULLER. J. Phys. Chem. Ref. Data, **2**, 663 (1973).
3. G. BAUER (*Editor*). Handbook of preparative inorganic chemistry. Vol. 12, 2nd ed. Academic Press, New York, NY. 1965. pp. 1264–1265.
4. D. SHAW. *In* NMR and the Periodic Table. *Edited by* R. K. Harris and B. E. Mann. Academic Press, New York, NY. 1978. p. 41.
5. A. ABRAHAM. The principles of nuclear magnetism. Oxford University Press, London. 1961. p. 314.
6. V. SARASWATI. J. Phys. Soc. Jpn. **23**, 763 (1967).
7. K. T. GILLEN and J. H. NOGGLE. J. Chem. Phys. **53**, 801 (1970).
8. N. N. RUBAN and S. M. ISAEVA. Tr. Inst. Met. Obgash. Akad. Nauk Kaz. USSR, **18**, 32 (1966).
9. R. C. WEAST (*Editor*). CRC handbook of chemistry and physics. 60th ed. CRC Press, Boca Raton, Florida. 1979–80. pp. F214–F218.
10. A. ALLERHAND. J. Chem. Phys. **52**, 2162 (1970).
11. E. R. COHEN and B. N. TAYLOR. J. Phys. Chem. Ref. Data, **2**, 663 (1973).
12. W. D. KAUTT, H. KRÜGER, O. LUTZ, H. MAIER, and A. NOLLE. Z. Naturforsch. **31a**, 351 (1976).

Oxidation of substituted aromatic compounds by peroxydisulphate. Homolytic benzylation and oxidative coupling reaction

ANGELO CLERICI AND OMBRETTA PORTA

Istituto di Chimica del Politecnico, Via Golgi 39, 20133 Milano, Italia

Received May 26, 1980

ANGELO CLERICI and OMBRETTA PORTA. Can. J. Chem. **58**, 2117 (1980).

Under the same experimental conditions 4-methoxytoluene brings about homolytic benzylation of isoquinoline while 3,4-dimethoxytoluene gives a coupling reaction. Proton loss by the radical cation X—$\overset{+\cdot}{\text{Ph}}$—$CH_3$ in the former case and its electrophilic attack to the starting aromatic in the latter account for these experimental findings.

ANGELO CLERICI et OMBRETTA PORTA. Can. J. Chem. **58**, 2117 (1980).

Dans les mêmes conditions expérimentales, le méthoxy-4 toluène amène à une benzylation homolytique de l'isoquinoléine alors que le diméthoxy-3,4 toluène donne lieu à une réaction de couplage. On peut expliquer ces observations par la perte d'un proton du radical cation X—$\overset{+\cdot}{\text{Ph}}$—$CH_3$ dans le premier cas et par l'attaque électophilique du radical cation sur le cycle aromatique de départ dans le deuxième cas.

[Traduit par le journal]

Several reports on oxidation reactions of ring-substituted benzenes by peroxydisulphate are now available in the recent literature (1–7); the one-electron oxidation of the aromatic ring to a radical cation is commonly postulated in reactions involving the radical anion $SO_4^{-\cdot}$. Our previous studies (8) showed this possibility for $SO_4^{-\cdot}$, easily obtainable from thermal decomposition of peroxydisulphate, to transfer an electron from aromatics having a relatively low oxidation potential, such as compound **1** where X = H and Y = CH_2CH_2-COOH. It is also known that the Ag^{2+} species, formed in the Ag^+-catalyzed decomposition of peroxydisulphate, is considered able to oxidize the aromatic ring to the radical cation **2** in the initial step (9, 10) (Scheme 1).

An undoubted case of formation of **2** (X = $CH(CH_3)_2$ and Y = H) is given by *p*-cimene oxidation with Co(III)acetate in which an almost quantitative yield of benzyl radical was described (11).

0008-4042/80/192117-03$01.00/0

©1980 National Research Council of Canada/Conseil national de recherches du Canada

Can. J. Chem. Downloaded from www.nrcresearchpress.com by 210.87.254.5 on 09/05/12
For personal use only.

(11) and a similar procedure to that reported by Kautt *et al.* (12) for the calculation of μ of ^{95}Mo and ^{97}Mo isotopes, one can calculate the μ values of ^{50}V and ^{51}V nuclei. The results are shown in Table 1. These magnetic moment values are in good agreement with those reported in the literature (2). Minor differences may be due to the fact that no diamagnetic corrections were made in the present work.

Acknowledgements

The financial support of the Natural Sciences and Engineering Research Council of Canada, Strategic Grants Program is gratefully acknowledged. We also thank Drs. G. Schrobilgen and D. Eaton for helpful discussions, Mr. B. Sayer for recording the ^{50}V- and ^{50}V-nmr spectra, and C. Rodgers of Bruker Canada Ltd., Mississauga, Ont., for recording the spectra on Bruker WM-250 spectrometer.

1. O. HOWARTH and R. E. RICHARDS. Proc. Phys. Soc. London, **84**, 326 (1964).
2. G. H. FULLER. J. Phys. Chem. Ref. Data, **2**, 663 (1973).
3. G. BAUER (*Editor*). Handbook of preparative inorganic chemistry. Vol. 12, 2nd ed. Academic Press, New York, NY. 1965. pp. 1264–1265.
4. D. SHAW. *In* NMR and the Periodic Table. *Edited by* R. K. Harris and B. E. Mann. Academic Press, New York, NY. 1978. p. 41.
5. A. ABRAHAM. The principles of nuclear magnetism. Oxford University Press, London. 1961. p. 314.
6. V. SARASWATI. J. Phys. Soc. Jpn. **23**, 763 (1967).
7. K. T. GILLEN and J. H. NOGGLE. J. Chem. Phys. **53**, 801 (1970).
8. N. N. RUBAN and S. M. ISAEVA. Tr. Inst. Met. Obgash. Akad. Nauk Kaz. USSR, **18**, 32 (1966).
9. R. C. WEAST (*Editor*). CRC handbook of chemistry and physics. 60th ed. CRC Press, Boca Raton, Florida. 1979–80. pp. F214–F218.
10. A. ALLERHAND. J. Chem. Phys. **52**, 2162 (1970).
11. E. R. COHEN and B. N. TAYLOR. J. Phys. Chem. Ref. Data, **2**, 663 (1973).
12. W. D. KAUTT, H. KRÜGER, O. LUTZ, H. MAIER, and A. NOLLE. Z. Naturforsch. **31a**, 351 (1976).

Oxidation of substituted aromatic compounds by peroxydisulphate. Homolytic benzylation and oxidative coupling reaction

ANGELO CLERICI AND OMBRETTA PORTA

Istituto di Chimica del Politecnico, Via Golgi 39, 20133 Milano, Italia

Received May 26, 1980

ANGELO CLERICI and OMBRETTA PORTA. Can. J. Chem. **58**, 2117 (1980).

Under the same experimental conditions 4-methoxytoluene brings about homolytic benzylation of isoquinoline while 3,4-dimethoxytoluene gives a coupling reaction. Proton loss by the radical cation X—$\overset{+\cdot}{\text{Ph}}$—$CH_3$ in the former case and its electrophilic attack to the starting aromatic in the latter account for these experimental findings.

ANGELO CLERICI et OMBRETTA PORTA. Can. J. Chem. **58**, 2117 (1980).

Dans les mêmes conditions expérimentales, le méthoxy-4 toluène amène à une benzylation homolytique de l'isoquinoléine alors que le diméthoxy-3,4 toluène donne lieu à une réaction de couplage. On peut expliquer ces observations par la perte d'un proton du radical cation X—$\overset{+\cdot}{\text{Ph}}$—$CH_3$ dans le premier cas et par l'attaque électophilique du radical cation sur le cycle aromatique de départ dans le deuxième cas.

[Traduit par le journal]

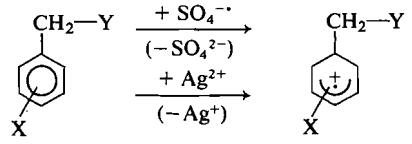
Several reports on oxidation reactions of ring-substituted benzenes by peroxydisulphate are now available in the recent literature (1–7); the one-electron oxidation of the aromatic ring to a radical cation is commonly postulated in reactions involving the radical anion $SO_4^{-\cdot}$. Our previous studies (8) showed this possibility for $SO_4^{-\cdot}$, easily obtainable from thermal decomposition of peroxydisulphate, to transfer an electron from aromatics having a relatively low oxidation potential, such as compound **1** where X = H and Y = CH_2CH_2-COOH. It is also known that the Ag^{2+} species, formed in the Ag^+-catalyzed decomposition of peroxydisulphate, is considered able to oxidize the aromatic ring to the radical cation **2** in the initial step (9, 10) (Scheme 1).

An undoubted case of formation of **2** (X = $CH(CH_3)_2$ and Y = H) is given by *p*-cimene oxidation with Co(III)acetate in which an almost quantitative yield of benzyl radical was described (11).

0008-4042/80/192117-03$01.00/0

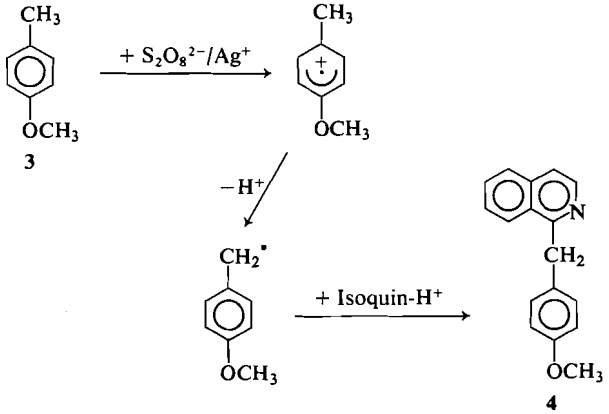
©1980 National Research Council of Canada/Conseil national de recherches du Canada

Can. J. Chem. Downloaded from www.nrcresearchpress.com by 210.87.254.42 on 09/05/12
For personal use only.



SCHEME 1

In view of this general interest in reactions leading to side-chain functionalization of alkylaromatic compounds, we happened to investigate the oxidation of 4-methoxytoluene (**3**) with the peroxidisulphate–silver(I) salt system in the presence of protonated isoquinoline. Homolytic benzylation (12) occurs at position 1 of the heteroaromatic base and 1-(4-methoxybenzyl)-isoquinoline (**4**) was the only reaction product along with traces of 4-methoxybenzaldehyde (Scheme 2).



SCHEME 2

A typical run is as follows: isoquinoline (0.03 mol), concentrated H_2SO_4 (0.015 mol), compound **3** (0.1 mol), $AgNO_3$ (0.006 mol) in 30 mL of CH_3CN/H_2O (1:1) solution, were kept at 50°C for 3 h while slowly adding $(NH_4)_2S_2O_8$ (0.03 mol) in 10 mL of H_2O to the mixture. Product **4** (1.15 g) was obtained as a thick oil after work-up (12). Its purity (≥99%) was checked by glc analysis. Yield based on starting isoquinoline: 15% in moles; ^1H nmr ($CDCl_3$) δ: 3.7 (3H, CH_3O—, s); 4.6 (2H, —CH_2Ph, s); 6.7 ($2H_{ar}$, in α to —CH_2—, d); 7.2 ($2H_{ar}$, in α to —OCH_3, d); 7.4 ($4H_{ar}$, C_6H_4, m); 8.15 ($1H_{ar}$, in β to N, m); 8.5 ($1H_{ar}$, in α to N, d); ms *m/e*: 249 ($M^{+\cdot}$), 234, 217, 128, 121, 91.

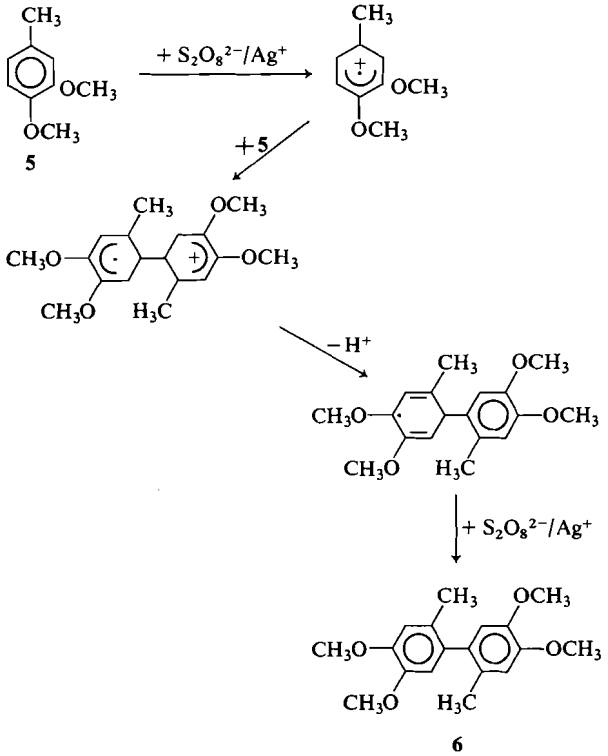
On replacing isoquinoline with quinoline, under the same experimental conditions and with the same molar ratio, homolytic benzylation occurs at positions 2 and 4 giving a mixture of isomers in the ratio 1:4, revealed by glc analysis. The isomer mixture (2.40 g) was obtained as an oil after work-up. Yield based on starting quinoline: 33% in moles; ms *m/e*: 249 ($M^{+\cdot}$), 234, 217, 128, 121, 91.

The success of these first results prompted us to extend the oxidation with $S_2O_8^{2-}/Ag^+$ to 3,4-dimethoxytoluene (**5**) with the aim of exploiting the synthetic potentiality of the reaction for a one-step synthesis of a precursor of papaverine, 1-(3,4-dimethoxybenzyl)-isoquinoline.

Surprisingly, we did not obtain any product resulting from the attack of the 3,4-dimethoxybenzyl radical to the protonated isoquinoline. The only reaction product was 2,2′-dimethyl-4,5,4′,5′-tetramethoxybiphenyl (**6**) along with traces of 3,4-dimethoxybenzaldehyde. The mechanism of this coupling reaction seems, in our viewpoint, compatible with the sequence in Scheme 3, reaction of $S_2O_8^{2-}/Ag^+$ with the aromatic substrate with generation of the radical cation, followed by reaction of this electrophile with the activated starting aromatic followed by oxidative rearomatization.

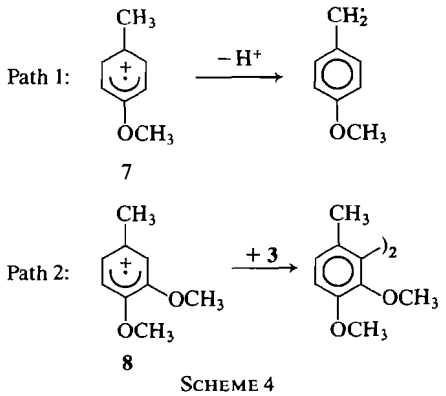
A similar result is given in the oxidation of 4-bromoveratrole with thallium(III)trifluoroacetate for which an analogous mechanism was considered (13).

A typical run (in the absence of the protonated aromatic base) is as follows: **5** (0.026 mol), $AgNO_3$ (0.0065 mol) in 20 mL of CH_3CN/H_2O (1:1) solution were kept for 4 h at 50°C while slowly adding $(NH_4)_2S_2O_8$ (0.013 mol) in 10 mL of H_2O to the initial mixture. Product **6** (1.80 g) was obtained as



SCHEME 3

Can. J. Chem. Downloaded from www.nrcresearchpress.com by 210.87.254.42 on 09/05/12
For personal use only.



SCHEME 4

pale yellow needles after work-up and hexane–ether recrystallization (mp 121–122°C). Its purity (≥99%), isomer free, was checked by glc analysis. Conversion: 70%. Yield based on converted aromatic: 65%; yield based on the dipersulphate: 92%; ^1H nmr ($CDCl_3$) δ: 2.0 (6H, $2CH_3$—, s); 3.8 (6H, $2CH_3O$—, s); 3.9 (6H, $2CH_3O$—, s); 6.65 ($2H_{ar}$, s); 6.8 ($2H_{ar}$, s); ms *m/e*: 302 ($M^{+\cdot}$), 287, 259, 244, 152, 151. *Anal.* calcd. for $C_{18}H_{22}O_4$: C 71.40, H 7.40, O 21.20; found: C 71.48, H 7.35, O 21.17.

Concluding, these findings indicate that when only one electron-donating group, such as —OCH_3, is present in the aromatic ring the proton loss by the radical cation **7** to give the benzyl radical is the favoured process (path 1), while the introduction of a second —OCH_3 group, increasing the stabilization of the radical cation **8**, makes the proton loss slower than the electrophilic attack to the starting aromatic (path 2) (Scheme 4).

1. R. O. C. NORMAN, P. M. STOREY, and P. R. WEST. J. Chem. Soc. B, 1087 (1970).
2. H. HEY, G. H. JONES, and M. J. PERKINS. J. Chem. Soc. Perkin Trans. I, 118 (1972).
3. A. LEDWITH, P. J. RUSSEL, and L. M. SUTCLIFFE. J. Chem. Soc. Perkin Trans II, 630 (1973).
4. C. WALLING and D. CAMAIONI. J. Am. Chem. Soc. **97**, 1603 (1975).
5. M. E. SNOOK and G. A. HAMILTON. J. Am. Chem. Soc. **96**, 860 (1974).
6. P. NETA, V. MADHOVAN, H. ZIMEL, and R. W. FESSENDEN. J. Am. Chem. Soc. **99**, 163 (1977).
7. P. MAGGIONI and F. MINISCI. Chim. Ind. Milan, **61**, 101 (1979).
8. A. CLERICI, F. MINISCI, and O. PORTA. Tetrahedron Lett. 4183 (1974).
9. K. NYBERG and L. G. WISTRAND. J. Org. Chem. **43**, 2613 (1978).
10. C. WALLING and D. CAMAIONI. J. Am. Chem. Soc. **100**, 4814 (1978).
11. A. ONOPCHENKO, J. G. D. SCHULZ, and R. SEEKIRCHER. J. Org. Chem. **37**, 1414 (1972).
12. A. CLERICI, F. MINISCI, and O. PORTA. Tetrahedron, **29**, 2775 (1973).
13. A. MCKILLOP, A. G. TURREL, and E. TAYLOR. J. Org. Chem. **42**, 764 (1977).

Can. J. Chem. Downloaded from www.nrcresearchpress.com by 210.87.254.42 on 09/05/12
For personal use only.

Canadian Journal of Chemistry
Published by
THE NATIONAL RESEARCH COUNCIL OF CANADA

Journal canadien de chimie
Publié par
LE CONSEIL NATIONAL DE RECHERCHES DU CANADA

Volume 58 Number 20 October 15, 1980 Volume 58 numéro 20 15 octobre 1980

Linear peptide alkaloids from the sponge *Cliona celata* (Grant). Celenamides C and D

RICHARD J. STONARD AND RAYMOND J. ANDERSEN
Departments of Oceanography and Chemistry, The University of British Columbia, Vancouver, B.C., Canada V6T 1W5
Received May 8, 1980

RICHARD J. STONARD and RAYMOND J. ANDERSEN. Can. J. Chem. **58**, 2121 (1980).

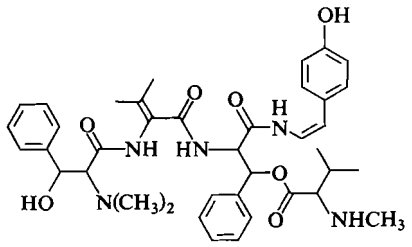
Celenamides C (**7**) and D (**8**), two novel alkaloids closely related to peptide alkaloids found in higher plants, have been isolated as their penta (**12**) and nonacetyl (**13**) derivatives, respectively, from acetylated extracts of the sponge *Cliona celata* (Grant). The structure elucidation of **7** and **8** is described.

RICHARD J. STONARD et RAYMOND J. ANDERSEN. Can. J. Chem. **58**, 2121 (1980).

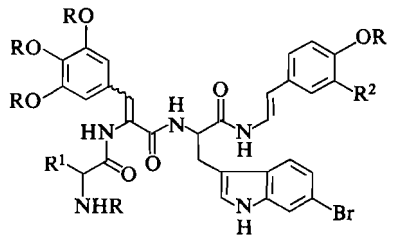
On a isolé deux nouveaux alcaloïdes les célénamides C (**7**) et D (**8**) qui s'apparentent beaucoup aux alcaloïdes peptidiques que l'on trouve dans les plantes supérieures. On les obtient sous forme de dérivés penta (**12**) et non acétylés (**13**) à partir des extraits acétylés de l'éponge *Cliona celata* (Grant). On décrit la détermination de la structure des composés **7** et **8**.

[Traduit par le journal]

We have recently reported the structural elucidation of two novel linear peptide alkaloids (**1**) which bear close resemblance to cyclopeptide alkaloids isolated from several terrestrial plant families (2) and to the linear peptide alkaloid lasoidine A (**1**) obtained from an African Rhamnaceae (3). Celenamides A (**2**) and B (**3**) were isolated as their hexacetyl derivatives **4** and **5**, respectively, from British Columbia and Californian samples of the ubiquitous burrowing sponge *Cliona celata* (Grant). Clionamide (**6**) (4) was the major metabolite present in both collections. In this paper we wish to describe the structure determination of celenamides C (**7**) and D (**8**), two minor metabolites of *C. celata* collected from Howe Sound, British Columbia (−20 m). Celenamide D (**8**) represents the first nonindolic linear peptide alkaloid isolated from *Cliona* and it is a rare example of a dehydropeptide possessing multiple aromatic dehydroamino acid residues.[1]



1



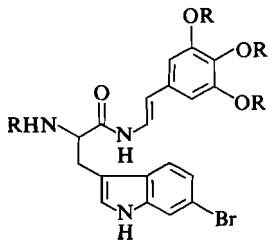
2	R = H	R^1 =	R^2 = OH
3	R = H	R^1 =	R^2 = OH
4	R = Ac	R^1 =	R^2 = OAc
5	R = Ac	R^1 =	R^2 = OAc
7	R = H	R^1 =	R^2 = H
12	R = Ac	R^1 =	R^2 = H

Acetylated celenamides were obtained from crude acetylated methanol extracts of *C. celata* by silica column chromatography employing a stepwise methylene chloride – ethyl acetate gradient. Analysis of the column eluate by high pressure liquid chromatography (hplc) and ^{1}H nmr indicated that the fraction eluting with 25% EtOAc in CH_2Cl_2 was composed of a mixture of several acetyl-

[1]For examples of aromatic dehydroamino acid containing peptides, see ref. 5.

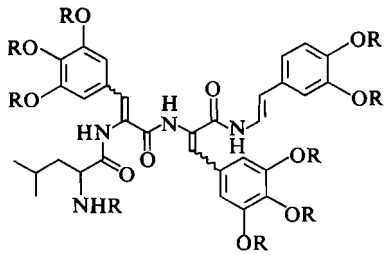
0008-4042/80/202121-06$01.00/0
©1980 National Research Council of Canada/Conseil national de recherches du Canada

Can. J. Chem. Downloaded from www.nrcresearchpress.com by 210.87.254.40 on 09/05/12
For personal use only.



6 R = H
9 R = Ac

celenamides (Fig. 1a). Subsequent fractions were comprised of mixtures of hexacetylcelenamide A (**4**), B (**5**), and tetracetylclionamide (**9**) (6) (e.g. Fig. 1b). Repetitive silica preparative thin layer chromatography (ptlc) of the acetylcelenamide containing fractions afforded **4** (0.03% wet weight), **5** (0.02%), and the more minor components, pentacetylcelenamide C (**12**, ~0.003%), and nonacetylcelenamide D (**13**, ~0.002%) as noncrystalline solids. The homogeneity of compounds **4**, **5**, **12**, and **13** was established by hplc, ^{1}H nmr, and electron-impact mass spectroscopy (eims).



8 R = H
13 R = Ac

^{1}H nmr analysis demonstrated that the ptlc bands corresponding to the hplc peaks observed at $R_T \sim 6$–8 min as shown in Fig. 1a were composed of a complex mixture of acetylcelenamide related compounds.

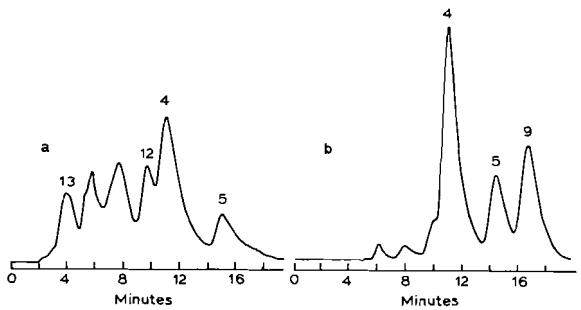


FIG. 1. High pressure liquid chromatography of acetylcelenamides eluted from silica gel G with (a) CH_2Cl_2–EtOAc (4:1); (b) CH_2Cl_2–EtOAc (2:1). Analysis conditions: LiChrosorb Si60 (10μ, 4 × 250 mm); solvent, CH_2Cl_2—CH_3CN (4:1); flow rate, 1.2 mL/min; room temperature; A 290 nm.

The 270 MHz ^{1}H nmr spectrum of pentacetylcelenamide C (**12**) showed remarkable similarity to the spectrum displayed by hexacetylcelenamide A (**4**, Table 1). Comparison of the two spectra indicated the presence of resonances corresponding to a 1,4-disubstituted phenyl ring in the spectrum of **12**, in contrast to the presence of signals resulting from a 1,3,4-trisubstituted phenyl ring in the spectrum of **4**.[2] The eims of **12** (Table 2) contained major fragment ions corresponding to 4-acetoxystyrylamine (ion **d**, n = 1) and 4-hydroxystyrylamine. Hence, **12** must encompass the gross structure of **4** but with a C-terminal (*E*)-4-acetoxystyrylamino residue instead of the (*E*)-3,4-diacetoxystyrylamino grouping present in **4**. It was also evident from eims that the amino acid sequence of **12** corresponded to that of **4** (Table 2).

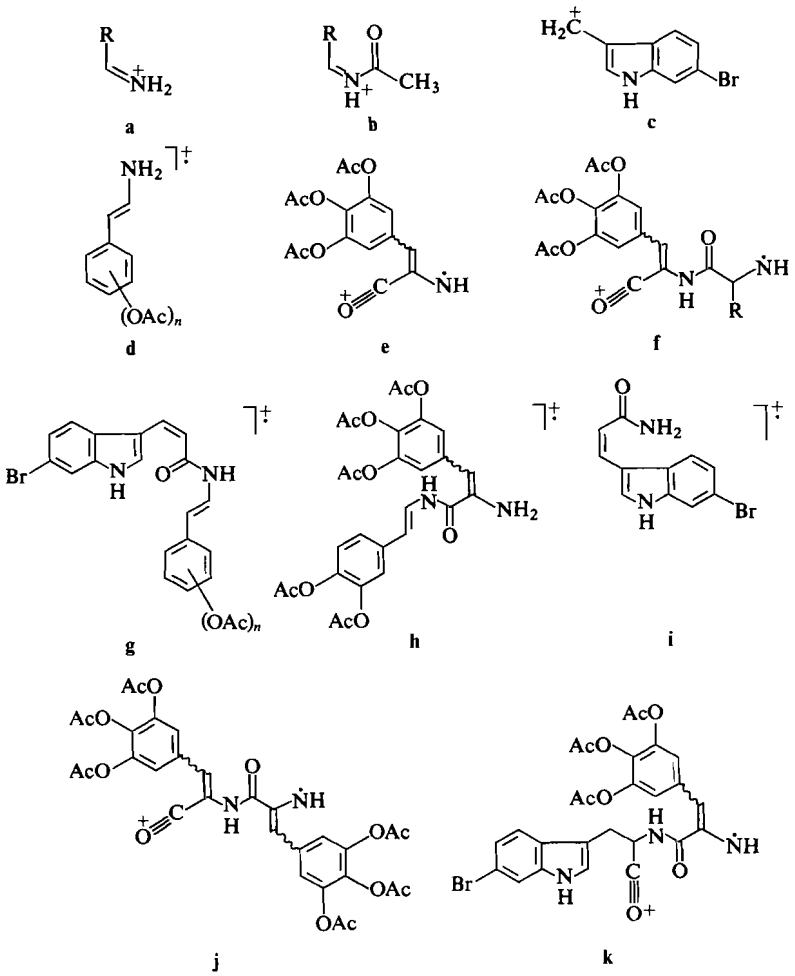
Confirmation of the proposed structure for **12** was provided by chemical degradation. Hydrolysis with hydrochloric acid in acetonitrile at room temperature afforded a primary amide (**14**) which was identical (see Tables 1 and 2) to the primary amide obtained when **4** was treated in a similar fashion.

It was immediately apparent from ^{1}H nmr studies (Table 1) that, unlike hexacetylcelenamide A (**4**), B (**5**), and pentacetylcelenamide C (**12**), nonacetylcelenamide D (**13**) did not possess a 6-bromotryptophan residue and that leucine (αCH δ 4.48 m, NH 7.91 d, J = 5 Hz) represented the sole α-amino acid in the molecule. Ions **a** (*m/e* 86) and **b** (*m/e* 128) observed in the eims (Table 2) defined acetylleucine as the N-terminal residue. Characteristic resonances at δ 6.60 (d, J = 15 Hz), 7.59 (dd, J = 10, 15 Hz), and 9.65 (d, J = 10 Hz) in the ^{1}H nmr spectrum of **13** suggested the presence of a C-terminal styrylamine residue. Intense fragment ions at *m/e* 235 (ion **d**), 193, and 151 in the eims (Table 2) further suggested that the C-terminus was an (*E*)-3,4-diacetoxystyrylamine[2] group as in **4** and **5**. This was confirmed by hydrolysis with hydrochloric acid in acetonitrile at room temperature to give the primary amide **15**. The ^{1}H nmr (δ 6.53 and 7.30 (each 1H, s); Table 1), ir (3640, 3540 cm^{-1}), and mass spectra (Table 2) of **15** indicated that the C-terminal styrylamine present in **13** was absent in **15** and that the C-terminal residue of **15** was protected as a primary amide as a result of the *trans*-substituted enamide hydrolysis.

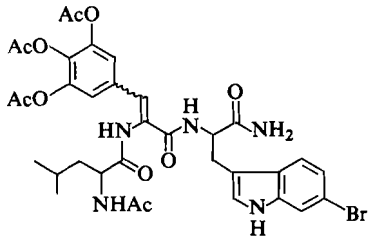
The remaining structural features of nonacetyl-

[2]Ozonolysis (*1*. O_3, −78°C, CH_3OH *2*. $(CH_3)_2S$) of a mixture of acetylcelenamides similar in composition to that shown in Fig. 1a afforded 3,4,5-triacetoxy-, 3,4-diacetoxy-, and 4-acetoxybenzaldehyde as the only isolable products. The substitution pattern of each of the benzaldehydic products was determined by comparison with synthetic samples.

Can. J. Chem. Downloaded from www.nrcresearchpress.com by 210.87.254.40 on 09/05/12
For personal use only.

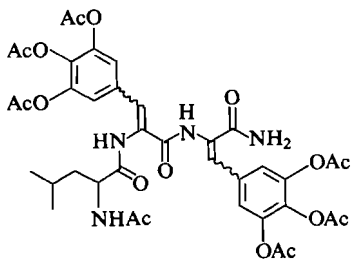


celenamide D (**13**) were elucidated by ^{1}H nmr (Table 1). Two uncoupled olefinic signals at δ 7.06 and δ 7.59, two highly deshielded NH singlets at δ 9.18 and δ 9.89, and two 2H aromatic singlets at δ 7.43 and 7.47 clearly indicated the presence of two 3,4,5-triacetoxy-α,β-didehydrophenylalanine[2] residues. The observation of fragment ions **j** (*m/e* 638), **h** (*m/e* 554), **f** (*m/e* 432), and **e** (*m/e* 319) in the eims of **13** (Table 2) furnished conclusive evidence for this proposal. Hence, the structure of nonacetylcelenamide D (**13**) must be as shown.



14

The nature of the naturally occurring sponge metabolites was demonstrated by a small scale isolation procedure employing acetic anhydride-d_6 as acetylating agent. The ^{1}H nmr of the ptlc purified



15

deuteroacetylcelenamide mixture did not display any resonances corresponding to phenolacetate or acetamide. Hence, **12** and **13** must exist in the sponge as their nonacetylated precursors celenamide C (**7**) and celenamide D (**8**).

Can. J. Chem. Downloaded from www.nrcresearchpress.com by 210.87.254.40 on 09/05/12
For personal use only.

Can. J. Chem. Downloaded from www.nrcresearchpress.com by 210.87.254.40 on 09/05/12
For personal use only.

TABLE 1. 270 MHz ^{1}H nmr spectra[a] chemical shift[b]

Proton position[c]	9	4	12	13	14[d]	15	Multiplicity (Hz)
Indole H_1	10.22	10.19	10.21	—	10.16	—	bs
H_2	7.20	7.31	7.32	—	7.26	—	d, 2.2
H_4	7.59	7.62	7.64	—	7.64	—	d, 8.8
H_5	7.16	7.16	7.15	—	7.15	—	dd, 1.4, 8.8
H_7	7.57	7.57	7.55	—	7.58	—	d, 1.4
Trp NH	7.41 d, 8	7.91 d, 10	7.88 d, 9	—	7.81 d, 8	—	—
CH_2	3.14 dd, 6, 15	3.26 dd, 11, 15	3.28 dd, 11, 15	—	3.25 dd, 11, 15	—	—
	3.28 dd, 7, 15	3.54 dd, 4, 15	3.55 dd, 4, 15	—	3.51 dd, 4, 15	—	—
CH	4.77 ddd, 6, 7, 8	4.75 ddd, 4, 10, 11	4.77 ddd, 4, 9, 11	—	4.66 ddd, 4, 8, 11	—	—
Leu NH	—	7.93	7.94	7.91	7.91	7.76	d, 5
CH_2	—	1.73	1.75	1.78	1.67	1.71	m
CH	—	4.32	4.32	4.48	4.28	4.38	m
i-PrCH	—	1.86	1.89	1.86	1.87	1.85	m
$(CH_3)_2$	—	0.97, 1.02	0.98, 1.03	0.95, 0.98	0.95, 0.99	0.94, 0.99	d, 7
—NH*Ac*	1.91	1.98	1.99	1.90	1.98	1.88	s
—O*Ac*	2.26 6H	2.25 3H	2.24 3H	2.26 9H	2.28 9H	2.24 6H	s
	2.27 3H	2.27 3H	2.28 6H	2.27 3H	—	2.27 3H	s
	—	2.28 9H	2.29 3H	2.29 3H	—	2.29 6H	s
	—	—	—	2.31 9H	—	2.30 3H	s
—NHC*H*=CH	7.46	7.50	7.51	7.59	—	—	dd, 10, 15
—NHCH=C*H*	6.14	6.54	6.56	6.60	—	—	d, 15
—N*H*CH=CH	9.54	9.51	9.46	9.65	—	—	d, 10
Phenyl H	7.13 2H	7.17 2H	7.23 2H	7.43 2H	7.21 2H	7.38 2H	s
	—	7.15 d, 9, 1H	7.04 d, 9, 2H	7.15 d, 9, 1H	—	—	—
	—	7.24 d, 2, 1H	7.38 d, 9, 2H	7.26 d, 2, 1H	—	—	—
	—	7.23 dd, 2, 9, 1H	—	7.28 dd, 2, 9, 1H	—	—	—
	—	—	—	7.47 2H	—	7.44 2H	s
—CO(NHR)C=C*H*	—	6.80	6.84	7.06, 7.59	6.88	7.09, 7.41	s
—CO(N*H*R)C=CH	—	9.44	9.46	9.18, 9.89	9.33	9.10, 9.54	each 1H, s
—$CONH_2$	—	—	—	—	6.51, 7.21	6.53, 7.30	each 1H, s

[a]All ^{1}H nmr spectra were recorded in $(CD_3)_2CO$.
[b]In ppm from internal tetramethylsilane.
[c]Assignments were made by extensive decoupling and D_2O exchange experiments.
[d]Derived from **4** or **12**.

Can. J. Chem. Downloaded from www.nrcresearchpress.com by 210.87.254.40 on 09/05/12
For personal use only.

TABLE 2. Electron-impact mass spectra[a]

Fragment ion[b]	4	5	12	13	14[c]	15	
a[g]	86(34)	—	86(30)	86(73)	86(87)	86(15)	R = C_4H_9
	—	72(78)	—	—	—	—	R = C_3H_7
b[g]	128(15)	—	128(17)	128(43)	128(83)	128(9)	R = C_4H_9
	—	114(38)	—	—	—	—	R = C_3H_7
c[d,g]	210/208(20)	210/208(74)	210/208(6)	—	210/208(91)	—	
d[e,g]	235(13)	235(40)	—	235(60)	—	—	$n = 2$
	—	—	177(10)	—	—	—	$n = 1$
e[e,g]	319(2)	319(5)	319(1)	319(11)	319(16)	319(1)	
f[e,g]	432(5)	—	432(3)	432(39)	432(6)	432(4)	R = C_4H_9
	—	418(2)	—	—	—	—	R = C_3H_7
g[d,e]	484/482(2)	484/482(4)	—	—	—	—	$n = 2$
	—	—	n.o.[f]	—	—	—	$n = 1$
h[e]	—	—	—	554[h](5)	—	—	
i[d,g]	—	—	—	—	266/264(34)	—	
j[e]	—	—	—	638(1)	—	638(0.1)	
k[d,e]	585/583(1)	585/583(1)	n.o.[f]	—	585/583(1)	—	

[a]Only fragments relevant to the structure assignment are presented (see Experimental).
[b]Fragment ion designations refer to structures in the text. Intensities are given in parentheses.
[c]Derived from **4** and **12**. Intensities shown are for the hydrolysis product of **12**.
[d]1:1 Ion intensity.
[e]Consecutive losses of C_2H_2O (*m/e* 42) are observed from these ions (see Experimental).
[f]Ions above *m/e* 432 are of low intensity.
[g]Exact mass measurement obtained.
[h]Distinguished from ion **j** fragmentation by high-resolution ms of daughter ions.

Experimental

Low-resolution and high-resolution mass spectra were recorded on A.E.I. MS-902 and MS-50 spectrometers, respectively. Infrared spectra were recorded on a Perkin-Elmer Model 710B spectrometer. Optical rotations were measured on a Perkin-Elmer Model 241C polarimeter using a 10 cm microcell. The ^{1}H nmr spectra were recorded on a Nicolet-Oxford-270 spectrometer with tetramethylsilane ($\delta = 0$) as an internal reference. High pressure liquid chromatography (hplc) was performed on a Perkin-Elmer Series 2 instrument equipped with a Perkin-Elmer LC55 uv detector system and a Hewlett-Packard 18850A microprocessor.

Isolation of Pentacetylcelenamide C (12) and Nonacetylcelenamide D (13)

The sponge *Cliona celata* (450 g wet weight) was collected by hand using SCUBA in Howe Sound, British Columbia (−20 m). The crude sponge metabolites were extracted, acetylated, and the acetylated residue fractionated on a column of silica gel G as previously described (1). Pure pentacetylcelenamide C (**12**; 12 mg, ~0.003% wet weight) and nonacetylcelenamide D (**13**; 10 mg, ~0.002% wet weight) were obtained as noncrystalline solids following repeated silica ptlc (20 × 20 cm, 1.0 mm) using chloroform–methanol (14:1) as the developing solvent. High pressure liquid chromatographic analysis of column and ptlc purified components was performed as described in Fig. 1.

Pentacetylcelenamide C (**12**): $[\alpha]_D^{25}$ +14°(*c* 0.30, acetone); ir ($CHCl_3$): 3300 (broad), 1780, 1660 (broad); ^{1}H nmr (see Table 1); ms (see Table 2) *m/e* (ion **f**): 432 (3), 390 (3), 348 (3), 306 (1); (ion **e**): 319 (1), 277 (3), 235 (5), 193 (5); (ion **d**): 177 (10), 135 (20); base peak 43.

Nonacetylcelenamide D (**13**): $[\alpha]_D^{25}$ −25° (*c* 0.54, acetone); ir ($CHCl_3$): 3300 (broad), 1780, 1680 (broad); ^{1}H nmr (see Table 1); ms (see Table 2) *m/e* (ion **j**): 638 (1), 596 (2), 554 (5), 512 (11), 470 (11);[3] (ion **h**): (554, 512, 470),[3] 428 (9), 386 (6), 344 (2); (ion **f**): 432 (39), 390 (53), 348 (53), 306 (26); (ion **e**): 319 (11), 277 (26), 235 (60),[3] 193 (19); (ion **d**): 235,[3] 193 (61), 151 (67); base peak 43.

[3]These ions were not distinguished by high-resolution ms.

Hydrolysis of Pentacetylcelenamide C (12) with Hydrochloric Acid

Pentacetylcelenamide C (**12**, 3 mg) was dissolved in acetonitrile (15 mL) and concentrated HCl (0.1 mL in 2 mL CH_3CN) was added. After 24 h at room temperature the solvent was evaporated and the residue purified by ptlc ($CHCl_3$–CH_3OH, 5:1) to give the primary amide **14** (1 mg). Compound **14** was identical (tlc, ^{1}H nmr (Table 1), ms (Table 2)) to the hydrolysis product isolated following similar treatment of hexacetylcelenamide A (**2**).

Hydrolysis of Nonacetylcelenamide D (13) with Hydrochloric Acid

Nonacetylcelenamide D (**13**, 8 mg) was treated with HCl and the reaction mixture purified as described for **12**, to give the primary amide **15** (3 mg): ir (CH_3CN): 3640, 3540, 3350, 1780, 1680 (broad); ^{1}H nmr (see Table 1); ms (see Table 2) *m/e* (ion **j**): 638 (0.1), 596 (0.2), 554 (0.5), 512 (1), 470 (1), 428 (1), 386 (1); (ion **f**): 432 (2), 390 (3), 348 (3), 306 (2); (ion **e**): 319 (1), 277 (3), 235 (5), 193 (4); base peak 43.

Isolation with Acetic Anhydride-d_6

A small scale isolation procedure (40 g wet weight of sponge) employing acetic anhydride-d_6 (10 mL, 99 + atom %, Aldrich) as the acetylating agent yielded a mixture of deuteroacetylated celenamides following silica ptlc ($CHCl_3$–CH_3OH, 14:1). The hplc of this mixture was analogous to that shown in Fig. 1a. The ^{1}H nmr (270 MHz, acetone-d_6) indicated the absence of signals arising from naturally occurring acetamides (—NHCOCH_3) and phenolacetates (Ph—OCOCH_3).

Acknowledgments

The financial assistance of the Natural Sciences and Engineering Research Council of Canada is

gratefully acknowledged. One of us (R.J.S.) thanks the Natural Sciences and Engineering Research Council of Canada for a post-graduate scholarship. The authors would like to thank Mike LeBlanc for assistance in collecting the sponge.

1. R. J. STONARD and R. J. ANDERSEN. J. Org. Chem. In press.
2. (*a*) M. PAÏS and F.-X. JARREAU. *In* Chemistry and biochemistry of amino acids, peptides and proteins. Vol. 1. *Edited by* B. Weinstein. Marcel Dekker, New York. 1971. Chapt. 5; (*b*) R. TSCHESCHE and E. U. KAUBMANN. *In* The alkaloids. Vol. 15. *Edited by* R. H. F. Manske. Academic Press, Inc., New York. 1975. Chapt. 4.
3. J. MARCHAND, M. PAÏS, X. MONSEUR, and F.-X. JARREAU. Tetrahedron, **25**, 937 (1969).
4. R. J. ANDERSEN and R. J. STONARD. Can. J. Chem. **57**, 2325 (1979).
5. (*a*) J. C. SHEEHAN, D. MANIA, S. NAKAMURA, J. A. STOCK, and K. MAEDA. J. Am. Chem. Soc. **90**, 462 (1968); (*b*) W. L. MEYER, G. E. TEMPLETON, C. I. GRABLE, C. W. SIGEL, R. JONES, S. H. WOODHEAD, and C. SAUER. Tetrahedron Lett. 2357 (1971).
6. R. J. ANDERSEN. Tetrahedron Lett. 2541 (1978).

Can. J. Chem. Downloaded from www.nrcresearchpress.com by 210.87.254.40 on 09/05/12
For personal use only.

Studies on nucleation phenomena occurring in aqueous solutions supersaturated with calcium sulfate. III. The cation:anion ratio

DOUGLAS M. KELLER, RONALD E. MASSEY, AND O. E. HILEMAN, JR.
Department of Chemistry, McMaster University, Hamilton, Ont., Canada L8S 4M1

Received March 7, 1980

DOUGLAS M. KELLER, RONALD E. MASSEY, and O. E. HILEMAN, JR. Can. J. Chem. **58**, 2127 (1980).

Nucleation rates from solutions of calcium sulfate dihydrate were measured at constant supersaturation but at varying cation:anion ratios. Induction times were also measured. The values of each were found to be dependent on the Ca:SO_4 ratio. The results of empirical modeling studies are reported. These suggest that ion pair formation has an impact on the nucleation event beyond that of ion removal.

DOUGLAS M. KELLER, RONALD E. MASSEY et O. E. HILEMAN, JR. Can. J. Chem. **58**, 2127 (1980).

On a mesuré les vitesses de nucléation ainsi que les temps d'induction à partir de solutions de sulfate de calcium dihydraté sursaturé à niveau constant mais où l'on fait varier les rapports cation/anion. On a trouvé que les valeurs de ces deux mesures dépendent du rapport Ca:SO_4. On rapporte les résultats d'études faites à l'aide de modèles empiriques. Les résultats suggèrent que la formation des paires d'ions a un impact sur la nucléation en plus de l'élimination de l'ion.

[Traduit par le journal]

Introduction

Crystal nucleation from supersaturated solution is frequently studied by mixing together solutions that separately contain each of the moieties that comprise the precipitate. One of two experimental approaches has been used in most of these experiments: mixing together a series of reagent solution pairs each of increasing stoichiometric concentration levels; or, mixing together a series of reagent solution pairs prepared so that the concentration level across the final set of solutions of one of the moieties of interest is constant while that of the other is increasing across the members of the set. With each approach the supersaturation is calculated from the original solution compositions. Either the supersaturation level at the onset of particle formation or the rate of new particle formation (rate of nucleation) at each supersaturation level is determined experimentally. Then various parameters important in nucleation theory are evaluated using eq. [1].

$$[1] \qquad J = A \exp\left[-\beta\sigma^3 v^2 (kT)^{-3} (\ln S)^{-2}\right]$$

where J is the rate of new crystal formation (nucleation) in $cm^{-3}\ s^{-1}$; β is a shape factor for the newly forming phase; σ is the surface energy in ergs cm^{-2}; v is the volume of the monomer in the newly forming phase in cm^3; A is a pre-exponential factor; and k and T have their usual definitions. For strong electrolytes nucleating from aqueous solutions the supersaturation, S, is defined by eq. [2].

$$[2] \qquad S = [(\mathrm{IP})(K_{sp})^{-1}]^{r/n}$$

where $M_mX_x(s) \rightarrow mM^{q+} + xX^{r-}$; (IP) = ion product = $\{M\}^m\{X\}^x$; $n = m + x$; $mq + x(-r) = 0$; and K_{sp} has its usual definition.

By convention, the value of S at the point where J equals 1.0 $cm^{-3}\ s^{-1}$ is called the critical supersaturation, S^*. For ease of comparison with other studies, values of S^* along with estimates of n^*, r^*, and ΔG^* are usually reported. These are calculated using eqs. [3], [4], and [5].

$$[3] \qquad n^* = 2\beta\sigma^3 v^2 (kT \ln S^*)^{-3}$$

$$[4] \qquad r^* = 2\sigma v (kT \ln S^*)^{-1}$$

$$[5] \qquad \Delta G^* = \beta\sigma^3 v^2 (kT \ln S^*)^{-2}$$

where n^*, r^*, and ΔG^* are the critical number of monomers in an embryo, the critical radius of an embryo, and the critical free energy of an embryo, respectively.

The question of the effect of a changing cation:anion ratio across a suite of experimental runs —a feature of the second experimental approach noted above—on the values of the various nucleation and critical parameters has, to our knowledge, never been discussed in the literature. Mealor and Townshend (1) reported that during their studies on $BaSO_4$ nucleation a change in crystal size and morphology was observed as the initial $[Ba^{2+}]$:$[SO_4^{2-}]$ ratio changed through a series of experimental runs. These authors also noted a dependence of the slope of plots of the log (particle concentration) vs. log (reactant concentration) on the cation:anion ratio with the largest slope occurring when the ratio has a value of one.

The authors report in this paper the results of a set of experiments designed to examine the ques-

0008-4042/80/202127-05$01.00/0

©1980 National Research Council of Canada/Conseil national de recherches du Canada

Can. J. Chem. Downloaded from www.nrcresearchpress.com by 210.87.254.42 on 09/05/12
For personal use only.

TABLE 1. Initial experimental conditions for and the results obtained from the nucleation experiments*

Parameter	Value										
	E16	E17	E18	E19	E20	E21	E22	E23	E24	E25	E26
$[NO_3^-]$	0.202	0.248	0.272	0.286	0.332	0.350	0.428	0.464	0.496	0.606	0.700
$[I^-]_i$	0.350	0.350	0.350	0.350	0.350	0.350	0.350	0.350	0.350	0.350	0.350
$[S_2O_8^{2-}]_i$	0.152	0.124	0.113	0.107	0.0923	0.0875	0.0715	0.0661	0.0614	0.0505	0.0438
$[NH_4^+]$	0.350	0.350	0.350	0.350	0.350	0.350	0.350	0.350	0.350	0.350	0.350
$[K^+]$	0.303	0.248	0.226	0.214	0.185	0.175	0.143	0.132	0.123	0.101	0.0876
$[Ca^{2+}]_i$	0.101	0.124	0.136	0.143	0.166	0.175	0.214	0.232	0.248	0.303	0.350
$[Ca^{2+}]_i/[SO_4^{2-}]_i$	0.333	0.500	0.602	0.668	0.899	1.00	1.50	1.75	2.02	3.00	4.00
$J' \times 10^{-4}$ (cm^{-3} s^{-1})	39.2	35.8	398	646	359	222	71.1	35.1	9.07	—	9.59
$\tau \times 10$ (s)	660	540	300	300	300	420	720	840	1320	4200	4800

*$[\ ]_i$ = initial analytical concentrations of species in solution directly involved in the reactions of interest; $[SO_4^{2-}]_i = 2[S_2O_8^{2-}]_i$; $S_i = 34.46$; $T = 307.5 \pm 1.0$ K; J' = the experimentally determined rate of new particle formation per unit time and volume (2); τ = the time interval between the attainment of a time independent supersaturation and a time independent rate of nucleation.

tion of the impact on the experimental observables and on the various nucleation parameters of a changing cation:anion ratio at constant analytical ion product using calcium sulfate dihydrate as a model system.

Experimental Details and Results

The nucleation from solution experiments were carried out using the droplet technique coupled with *in situ* generation of the solute of interest (DTiGS). Events within the droplet population were recorded photomicrographically using dark field illumination. The information contained on the resulting 35 mm slides was used to obtain the number of particles formed in the population as a function of droplet volume and time. From these data values of J' were calculated.

The supersaturation required to overcome the barrier to $CaSO_4 \cdot 2H_2O$ nucleation from solution was generated using the iodide–peroxydisulfate reaction. The initial ion product ($[Ca^{2+}]_i[SO_4^{2-}]_i$) was set at a value of 0.03063 in each experiment but the initial ($[Ca^{2+}]_i$:$[SO_4^{2-}]_i$) ratio varied from 0.330 to 4.00 across the set of experiments. The generation reaction was initiated by mixing a solution containing Ca^{2+}, $S_2O_8^{2-}$, K^+, and NO_3^- with a solution containing NH_4^+ and I^-. The initial solution composition for each experiment in the series is shown in Table 1. Droplets were prepared from these reaction mixtures. The results of the nucleation events within the populations were recorded photomicrographically and then the data analysis was carried out following standard procedures reported elsewhere (2). The results are recorded in Table 1.

Discussion

The various J' values recorded in Table 1 for the nucleation of $CaSO_4 \cdot 2H_2O$ from solution were determined at the same analytical supersaturation level but at differing cation:anion ratios. A statistical analysis of these data led to the data of Table 2: the confidence levels at which the individual ln J' values are significantly different from that of ln J' for experiment E21 (cation:anion ratio = 1.00). We conclude from these data that the ln J' values observed for all cation:anion ratios differ significantly from that value observed for a cation:anion ratio equal to 1.00.

TABLE 2. Levels of confidence at which values of ln J_{EN}' are significantly different from ln J_{E21}' at one degree of freedom

Comparison	Level of confidence (%)
E16–E21	95
E17–E21	95
E18–E21	85
E19–E21	90
E20–E21	80
E22–E21	95
E23–E21	95
E24–E21	99
E25–E21	—
E26–E21	99

In addition to a changing cation:anion ratio, the composition of each solution in the series was rather different from that of the others. Thus the question of the impact of this compositional variation on the extent of ion pair formation, on ion activities, and on the ion product was considered. Data for the analytical solubility of the precipitate in the various reaction solutions were taken from ref. 3. The K_{sp} and the ion pair formation constant values used were those reported by Liu and Nancollas (4). The results of an iterative calculation that combines together equilibrium considerations and the extended Debye–Hückel theory are included in Table 3 as $[\alpha]$ (Ca^{2+} as ion pairs (mol L^{-1})), the activities of $\{Ca^{2+}\}$ and $\{SO_4^{2-}\}$, and the ionic activity product in the reaction solution just before the nucleation event.

An analysis of the $[\alpha]$ values suggests that those calculated for experiments E18 through E23 are not statistically different from each other and have a mean value of $0.514 \times 10^{-1} \pm 0.014 \times 10^{-1}$ (absolute, 95% C.I.). The ionic activity product values

Can. J. Chem. Downloaded from www.nrcresearchpress.com by 210.87.254.42 on 09/05/12
For personal use only.

TABLE 3. Results of the iterative calculation that corrects for ion pair formation and ionic strength effects*

Item	Value										
	E16	E17	E18	E19	E20	E21	E22	E23	E24	E25	E26
$[\alpha] \times 10$	0.473	0.502	0.511	0.513	0.520	0.520	0.513	0.508	0.498	0.473	0.449
$[NO_3^-]_f \times 10$	2.02	2.48	2.72	2.86	3.32	3.50	4.28	4.64	4.96	6.06	7.00
$[I^-]_f \times 10$	0.470	1.02	1.24	1.36	1.65	1.75	2.07	2.18	2.27	2.49	2.62
$[SO_4^{2-}]_j \times 10$	2.56	1.98	1.75	1.63	1.33	1.23	0.917	0.815	0.730	0.538	0.428
$[NH_4^+]_f \times 10$	3.50	3.50	3.50	3.50	3.50	3.50	3.50	3.50	3.50	3.50	3.50
$[K^+]_f \times 10$	3.03	2.48	2.26	2.14	1.85	1.75	1.43	1.32	1.23	1.01	0.876
$[Ca^{2+}]_j \times 10$	0.538	0.738	0.849	0.917	1.14	1.23	1.63	1.81	1.98	2.56	3.05
$[Ca^{2+}]_j/[SO_4^{2-}]_j$	0.210	0.373	0.486	0.564	0.860	1.00	1.77	2.23	2.71	4.76	7.14
$[Ca^{2+}]_j[SO_4^{2-}]_j \times 10^4$	138	146	149	149	151	151	149	148	145	138	131
μ	1.07	1.02	1.01	1.00	1.01	1.02	1.07	1.11	1.14	1.27	1.40
$f_{SO_4} \times 10$	1.49	1.52	1.53	1.53	1.53	1.52	1.49	1.48	1.46	1.40	1.36
$f_{Ca} \times 10$	1.36	1.34	1.33	1.33	1.33	1.34	1.36	1.38	1.39	1.45	1.50
$\{Ca^{2+}\} \times 10^2$	0.732	0.986	1.13	1.22	1.52	1.64	2.22	2.50	2.76	3.71	4.58
$\{SO_4\} \times 10^2$	3.82	3.01	2.68	2.49	2.03	1.87	1.37	1.20	1.07	0.754	0.580
$\{Ca^{2+}\}/\{SO_4^{2-}\}$	0.191	0.327	0.422	0.489	0.750	0.877	1.62	2.08	2.59	4.92	7.89
$\{Ca^{2+}\}\{SO_4^{2-}\} \times 10^4$	2.80	2.97	3.02	3.04	3.08	3.08	3.04	3.00	2.94	2.80	2.65

*[ ]$_f$ and [ ]$_j$ = analytical concentrations of species in solution after the generation and ion pair formation reactions have reached equilibrium; [α] = mol L^{-1} Ca^{2+} reacted to form ion pairs; ion pair formation constant = 169; $f_{Ca}f_{SO_4}$ = 0.020352 ± 0.000039 = ionic activity coefficient product for Ca^{2+} and SO_4^{2-}; $K_{sp} = 2.58 \times 10^{-5}$; μ = ionic strength of the solution just before the nucleation event takes place. See Appendix for the method of calculation used to generate the data of this table.

were also subjected to statistical analysis. It was found that, within experimental and calculational uncertainties, those values noted for experiments E17 through E24 are members of the same set with a mean value of 3.02 ± 0.08 (absolute, 95% C.I.) × 10^{-4}.

Plots of ln J' as a function of the ln (cation:anion ratio) either at constant initial ion product or at constant activity product are shown in Fig. 1. The logarithmic scales are used for convenience only. Also, adjacent points, except those at the apparent maximum, have been joined together by straight lines to aid in the visualization of data trends. The apparent maximum in ln J' cannot be located with precision, but it seems to occur at a cation:anion ratio of less than 1.0. The data shown in Fig. 1 suggest that the assumption of the independence of observed nucleation rates from changing cation:anion ratios at a constant ion product level must be questioned.

The induction times, the time interval between the attainment of a time independent supersaturation value and a steady state nucleation rate, observed in this set of experiments are noted in Table 1 and are also shown in Fig. 1. It is quite clear that the measured values depend on changes in the cation:anion ratio. Also, the values seem to go through an apparent minimum at a ratio of 0.75 ± 0.1.

It is tempting to note at this point that the ratio of the diffusion coefficients for Ca^{2+}:SO_4^{2-} is about 0.8, a number close to that of the cation:anion ratio at the apparent peak and apparent minimum in the

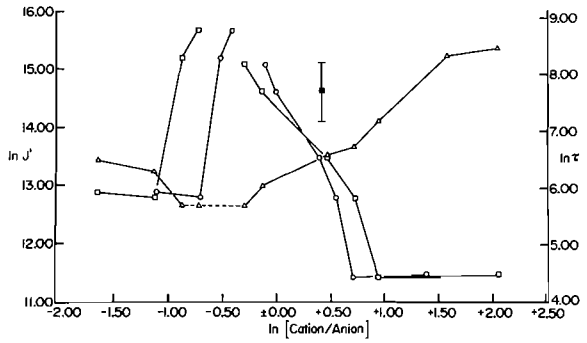


FIG. 1. A plot showing ln J' vs. ln $[[Ca]_i/[SO_4]_i]$ (○), ln J' vs. ln $[\{Ca\}/\{SO_4\}]$ (□), and ln τ vs. ln $[\{Ca\}/\{SO_4\}]$ (△). ■, 95% C.I.

ln J' and ln τ curves, respectively. This may be a coincidence or it may suggest that a diffusion mechanism is controlling the nucleation rate. With data limited to one system only, it is rather difficult to evaluate either hypothesis.

Empirical modeling studies were initiated to gain some insight into the nature of the dependence of the observed J' values on the cation:anion ratio. Two approaches were used. Firstly various alternative models for the estimation of the supersaturation were evaluated. The details of each are shown in Table 4. The resulting values of S were then substituted into eq. [1] and J' values were determined. The fit of these values to those determined experimentally is indicated by the parameter r^2 in Table 4. Secondly, various alternative models for the estimation of the rate of nucleation at constant supersaturation but at various cation:anion

Can. J. Chem. Downloaded from www.nrcresearchpress.com by 210.87.254.42 on 09/05/12
For personal use only.

Can. J. Chem. Downloaded from www.nrcresearchpress.com by 210.87.254.42 on 09/05/12
For personal use only.

TABLE 4. Empirical models for the estimation of S values

Variable	Variable value													
A'	[α]	[α]	[α]	[α]	[α]	[α]	[α]	[α]	[α]	[α]	[α]	[α]	[α]	[α]
B'	{Ca}	[Ca]	{SO_4}	[SO_4]	[Ca][SO_4]	[Ca]	{Ca}	{Ca}{SO_4}	[SO_4]	[Ca][SO_4]$^{-1}$	[Ca][SO_4]	{Ca}{SO_4}$^{-1}$
C'	{SO_4}	[SO_4]	1	1	1	1	1	1	1	1	1	1
D'	1	1	0	0	0	0	0	0	0	0	0	0
r^2	0.7690	0.7145	0.5809	0.5764	0.5684	0.5682	0.5592	0.5420	0.5410	0.5196	0.5149	0.5052

*IP = $aA' + bB' + cC' + dD'$; r^2 = a "goodness of fit" parameter. Best fit values: $a = 96.03$; $b = 34.68$; $c = 35.24$; $d = -3.235$; $r^2 = 0.7690$.

TABLE 5. Empirical models for the estimation of $\ln J_{(S)}$'*

Variable	Variable value													
A''	α	α	α	α	α	α	[Ca]	α	α	α	α	α	α	{Ca}
B''	{Ca}	[Ca]	{SO_4}	[SO_4]	[Ca]	{Ca}	[SO_4]	{Ca}{SO_4}	[Ca][SO_4]$^{-1}$	[Ca][SO_4]	{Ca}{SO_4}$^{-1}$	{SO_4}
C''	{SO_4}	[SO_4]	1.0	1.0	1.0	1.0	1.0	1.0	1.0	1.0	1.0	1.0
D''	1.0	1.0	0.0	0.0	0.0	0.0	0.0	0.0	0.0	0.0	0.0	0.0
r^2	0.7740	0.7239	0.5895	0.5848	0.5765	0.5675	0.5492	0.5442	0.5269	0.5196	0.5121	0.5048

*$\ln J' = aA'' + bB'' + cC'' + dD'' + \ln A - \beta\sigma^3 v^2 (kT)^{-3} (\ln S)^{-2}$; best fit values: $a = 2424$, $b = 873$, $c = 889$, $d = -142$, $r^2 = 0.7740$; $a = 2625$, $b = c = 959$, $d = -156$, $r^2 = 0.7660$.

ratios were evaluated. The details of each are shown in Table 5. Models with calculated r^2 values less than 0.5000 were not included in either Tables 4 or 5.

Generally, r^2 values calculated for models that do not include [α] are rather low (below 0.5). This observation suggests that the presence of ion pairs in the solution has an impact on the nucleation event beyond that of the removal of ionic participants. This suggestion is strengthened by the observation that the adjustable parameter for [α] in the best models is ~3 × that for the individual ions. Representatives of these best models, one from each approach, are shown as eqs. [6] and [7].

$$[6] \quad \ln J' = -\beta\sigma^3 v^2 (kT)^{-3} \{\tfrac{1}{2}[\ln (96.03[\alpha] + 34.68\{Ca\} + 35.24\{SO_4\} - 3.235 - \ln K_{sp}]\}^{-2} + \ln A$$

$$[7] \quad \ln J'_{(S)} = 2424[\alpha] + 873\{Ca^{2+}\} + 889\{SO_4^{2-}\} - \beta\sigma^3 v^2 (kT)^{-3} (\ln S)^{-2} + \ln A - 142$$

Either of the equations may be used in the calculation of nucleation parameters from data obtained during studies on solutions supersaturated with $CaSO_4 \cdot 2H_2O$ at constant supersaturation but with changing cation:anion ratios.

Acknowledgements

The authors acknowledge the financial assistance provided by the National Advisory Committee on Water Resources Research of the Department of Energy, Mines and Resources and by the National Sciences and Engineering Research Council of Canada.

1. D. MEALOR and A. TOWNSHEND. Talanta, **13**, 1069 (1966).
2. R. E. MASSEY and O. E. HILEMAN, JR. Can. J. Chem. **55**, 1285 (1976).
3. R. E. MASSEY. Ph.D. Thesis. McMaster University. Hamilton, Ont. 1974.
4. S.-T. LIU and G. H. NANCOLLAS. J. Cryst. Growth **6**, 281 (1970).

Appendix

The following method was used to calculate the data shown in Table 3.

$$[A1] \quad Ca_{(aq)}^{2+} + SO_{4(aq)}^{2-} \overset{K_1}{\rightleftarrows} CaSO_{4(aq)} \overset{K_2}{\rightleftarrows} CaSO_4 \cdot 2H_2O_{(s)}$$

$$K_{sp}^{-1}$$

$$[A2] \quad K_1 = \{CaSO_4\}/\{Ca^{2+}\}\{SO_4^{2-}\} = 1.69 \times 10^2$$

[A3] $\alpha = Ca^{2+}(\text{mol L}^{-1})$ that form ion pairs

[A4] $$2\alpha = [Ca^{2+}]_i + [SO_4^{2-}]_i + (K_1 f_{Ca} f_{SO_4})^{-1} - \{[Ca^{2+}]_i + [SO_4^{2-}]_i + (K_1 f_{Ca} f_{SO_4})^{-1}]^2 - 4[Ca^{2+}]_i[SO_4^{2-}]_i\}^{1/2}$$

[A5] $$\mu = {}^{1/2}\{\Sigma C_k Z_k^2 + 4[([Ca^{2+}]_i - \alpha) + ([SO_4^{2-}]_i - \alpha)]\}$$

[A6] $$f_{Ca} f_{SO_4} = \exp\left[\frac{-4\bar{A}\mu^{1/2}}{1 + \bar{B}\bar{a}_{Ca}\mu^{1/2}} + \frac{-4\bar{A}\mu^{1/2}}{1 + \bar{B}\bar{a}_{SO_4}\mu^{1/2}}\right]$$

where $\bar{A} = 1.1725$; $\bar{B} = 0.3286$; $\bar{a}_{Ca} = 4.03$; $\bar{a}_{SO_4} = 4.56$; C_k and Z_k are the concentrations and charges of ions in solution other than Ca^{2+} and SO_4^{2-}.

Can. J. Chem. Downloaded from www.nrcresearchpress.com by 210.87.254.42 on 09/05/12
For personal use only.

The adsorption and the reaction of NH_3 and NO_x on supported V_2O_5 catalysts: effect of supporting materials

MAKI TAKAGI-KAWAI, MITSUYUKI SOMA, TAKAHARU ONISHI, AND KENZI TAMARU

Department of Chemistry, Faculty of Science, The University of Tokyo, Hongo, Bunkyo-ku, Tokyo 113, Japan

Received April 8, 1980

MAKI TAKAGI-KAWAI, MITSUYUKI SOMA, TAKAHARU ONISHI, and KENZI TAMARU. Can. J. Chem. **58**, 2132 (1980).

The effects of supporting materials (Al_2O_3, SiO_2, TiO_2) on the catalytic activity and selectivity of V_2O_5 in the reduction of NO_x with ammonia are reported. The adsorbed state and the reactivity of the surface species were examined by an ir spectroscopy together with volumetric measurements, and the electronic state and the surface composition were studied by XPS.

The reactivity of an adsorbed ammonia (NH_4^+) for NO_2 over the supported catalysts was in the following increasing order, $TiO_2 > Al_2O_3 > SiO_2$. NH_4^+(ad) and NO_2(ad) were both reactive species in the reaction over V_2O_5, V_2O_5/Al_2O_3, and V_2O_5/TiO_2. Among these catalysts, the oxidized surface of V_2O_5/TiO_2 adsorbs NO as NO_2(ad), i.e. the reactive species, whereas other catalysts did not adsorb NO unless oxygen coexisted in the gas phase. In the case of V_2O_5/SiO_2, the reaction between NH_4^+(ad) and NO_2(ad) was very slow, while the surface oxygen was easily removed by the reduction with NH_3 and resupplied by the introduction of NO on the surface. This leads to the N_2O formation through so-called redox mechanism. The NH_4^+(ad) on V_2O_5/SiO_2 showed an ir absorption band at 1435 cm^{-1} which was much higher than those on other catalysts, and XPS measurement suggested that V_2O_5 on SiO_2 is electrically isolated.

MAKI TAKAGI-KAWAI, MITSUYUKI SOMA, TAKAHARU ONISHI et KENZI TAMARU. Can. J. Chem. **58**, 2132 (1980).

On présente les effets des supports (Al_2O_3, SiO_2, TiO_2) sur l'activité catalytique et la sélectivité du V_2O_5 lors de la réduction de NO_x par l'ammoniac. On a étudié l'état adsorbé et la réactivité des espèces à la surface par spectroscopie ir de concert avec des mesures volumétriques alors que l'on a étudié l'état électronique et la composition de la surface par XPS.

La réactivité de l'ammoniac adsorbé (NH_4^+) vis-à-vis le NO_2 sur les catalyseurs varie dans l'ordre croissant suivant: $TiO_2 > Al_2O_3 > SiO_2$. Le NH_4^+(ad) et le NO_2(ad) sont les deux espèces réactives dans la réaction sur le V_2O_5, V_2O_5/Al_2O_3 et V_2O_5/TiO_2. Parmi ces catalyseurs, la surface oxydée du V_2O_5/TiO_2 adsorbe le NO sous forme de NO_2(ad), i.e. l'espèce réactive, alors que les autres catalyseurs n'adsorbent pas le NO sauf si l'oxygène coexiste dans la phase gazeuse. Dans le cas du V_2O_5/SiO_2, la réaction entre le NH_4^+(ad) et le NO_2(ad) est très lente alors que l'oxygène de la surface est facilement enlevé par une réduction par le NH_3 et redéposé par l'introduction de NO sur la surface. Ceci conduit à la formation de NO_2 selon un mécanisme de pseudo redox. Le NH_4^+(ad) sur le V_2O_5/SiO_2 montre une bande d'adsorption dans l'infrarouge à 1435 cm^{-1} qui est plus haute que celle des autres catalyseurs et une mesure par XPS suggère que le V_2O_5/SiO_2 est isolé électriquement.

[Traduit par le journal]

Introduction

It has been shown previously that the reduction of NO by NH_3 proceeds over V_2O_5 in the presence of oxygen via the reaction between adsorbed NH_4^+(ad) and NO_2(ad) to form N_2 and H_2O (1), as follows.

$$NO + (1/2)O_2 \longrightarrow NO_2(ad)$$

$$NH_3 + \text{≡}OH \longrightarrow \text{≡}O^-—NH_4^+(ad)$$

$$NO_2(ad) + \text{≡}O^-—NH_4^+(ad) \longrightarrow N_2 + 2H_2O + \text{≡}O$$

SCHEME 1

In practice, various supports such as TiO_2, Al_2O_3, or SiO_2, are usually used for this reaction. It is generally accepted that the catalytic activity of V_2O_5 depends markedly on the material used for its support (2, 3). Moreover, when SiO_2 is used as the support, N_2O is formed as one of the reaction products, which is different from other cases (2). In order to elucidate the effect of the support on the catalytic activity and the selectivity for this reaction, we have studied adsorption and reactivity of surface species by means of ir and XPS methods. This paper describes the results on the adsorbed state of surface species and their reactivity studied by ir and volumetric methods. Furthermore, XPS data are also presented on the electronic state of the supported catalysts and the surface species, and the composition of the catalyst surfaces. The mechanism of the reaction is briefly discussed on the basis of these data.

Experimental

The ir measurements were carried out as described previously (4), using a Nihon Bunko IRA-2 or a JEOL JIR10 spectrometer (FT-IR). The catalyst powders (30–50 mg) were formed into disks which were 20 mm in diameter. These catalysts were heated in the ir cell under vacuum at 400°C for 2 h and then oxidized with 100 Torr of oxygen at the same temperature for 1 h before use. One to two g of catalysts were used for volumetric measurements. XPS measurements were taken using a McPherson ESCA 36. The catalysts were treated in a vacuum line and then mounted into the vacuum chamber of the spectrometer without getting into contact with air (O_2), using a dry-box purged by dry N_2 gas. The supported catalysts were prepared as described previously (1), by impregnating the supports with V_2O_5 saturated solution of oxalic acid. Commercial V_2O_5 (Nakarai Chemicals, special grade) was used. γ-Al_2O_3, SiO_2, and TiO_2

0008-4042/80/202132-06$01.00/0

©1980 National Research Council of Canada/Conseil national de recherches du Canada

Can. J. Chem. Downloaded from www.nrcresearchpress.com by 210.87.254.105 on 09/05/12
For personal use only.

Can. J. Chem. Downloaded from www.nrcresearchpress.com by 210.87.254.105 on 09/05/12
For personal use only.

(Anatase form) were obtained from Degussa Co. Ltd. The oxidized surface was obtained by treating the catalysts with 100 Torr of O_2 at 300°C for 1 h then evacuated at room temperature. The reduced surface was obtained by reducing the oxidized surface with 30 Torr of NH_3 at 200°C for 1 h followed by the evacuation for 1 h at the same temperature. For ir measurements, 23 wt% V_2O_5 supported catalysts were used unless mentioned. The reaction products, N_2 and N_2O, were detected by gas-chromatography, using molecular sieve 13X and Porapac Q columns of 4 m long at room temperature. Chemically pure NO (Takachiho Chemical Co., Ltd) was used without further purification. NO_2 was prepared by oxidizing NO with oxygen, then purified by distillation under vacuum until colourless crystals at liquid nitrogen temperature were obtained. NH_3 was purified by distillation.

Results

I. Adsorption of NO, NO_2, and NH_3 on Supported V_2O_5 Catalysts: IR and Volumetric Measurements

Adsorption of NO and NO_2

When 50 Torr of NO was introduced onto oxidized or reduced surface of V_2O_5, V_2O_5/Al_2O_3, or V_2O_5/SiO_2 at room temperature, it gave no change in ir spectra and no decrease in the pressure of NO. By introducing mixed NO and O_2, NO_2(ad) was adsorbed on each catalyst giving ir spectra shown in Fig. 1. The adsorption of NO_2 gas gave the same spectra as that obtained for the mixed NO and O_2 gases. This means that unless oxygen was also present in the gas phase, NO was not adsorbed on the oxidized surface of V_2O_5/Al_2O_3, V_2O_5/SiO_2, nor V_2O_5 alone.

The V_2O_5 catalyst on TiO_2 support, on the other hand, exhibited a very different behaviour as will be described below. On the oxidized surface of V_2O_5/TiO_2, the adsorption of NO was detected to give a single absorption band at 1620 cm^{-1}, which was the same as that obtained when NO_2 gas itself or the mixture of NO and O_2 was introduced on the oxidized or reduced catalyst. It was assigned to the antisymmetric stretching of NO_2(ad) (1). After V_2O_5/TiO_2 was reduced by 30 Torr of ammonia, followed by a 1.5 h evacuation at 400°C, the adsorption of NO was not detected by ir nor was the decrease in the NO pressure by volumetric measurement observed. Moreover, when NO_2(ad) formed upon introduction of NO on the oxidized surface of V_2O_5/TiO_2 was desorbed by evacuating at 160°C, NO was not adsorbed any more on the surface at room temperature. These facts suggest that NO was oxidized by the surface oxygen of V_2O_5/TiO_2 to form NO_2(ad), and the amount of adsorbed NO as NO_2(ad) on the oxidized surface of V_2O_5/TiO_2 was equal to the amount of surface active oxygen.

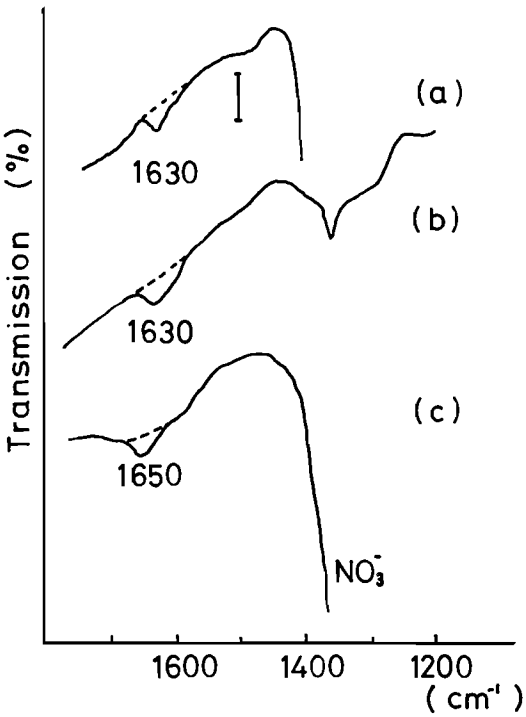


FIG. 1. Infrared spectra of adsorbed NO_2(ad) by the introduction of NO + O_2 onto the oxidized surface of (*a*) V_2O_5, (*b*) V_2O_5/Al_2O_3, and (*c*) V_2O_5/SiO_2. The bar shows the transmission of 10%. NO_3^- is formed on the NaCl window of the ir cell; 50 Torr of NO and 10 Torr of O_2 were introduced at room temperature. The spectra were taken after the gas phase was evacuated.

On the oxidized surface of TiO_2 itself, NO was also adsorbed as NO_2(ad) to give a single absorption band at 1620 cm^{-1} (Fig. 2*a*). The adsorption of NO_2 gas over oxidized or reduced TiO_2 gave a spectrum with two absorption bands at 1630 and 1200 cm^{-1} (Fig. 2*b*). These bands exhibited no changes in intensity when TiO_2 was heated to 160°C, whereas the adsorbed NO over the oxidized surface of TiO_2 in the form of NO_2(ad) could be desorbed at this temperature. Although the surface active oxygen forms NO_2(ad) from NO on the TiO_2 surface, the reactivity of NO_2(ad) on V_2O_5/TiO_2 was much higher than that on TiO_2 alone, as will be seen in the following section.

Adsorption of NH_3

The adsorption of NH_3 on the supported catalysts was examined as follows: 30 Torr of NH_3 was introduced onto the oxidized surface of each catalyst at room temperature and the ir spectra were taken after the gas was evacuated at the same temperature (Figs. 3, 4). Table 1 shows the positions and assignments of the ir absorption bands

Can. J. Chem. Downloaded from www.nrcresearchpress.com by 210.87.254.105 on 09/05/12
For personal use only.

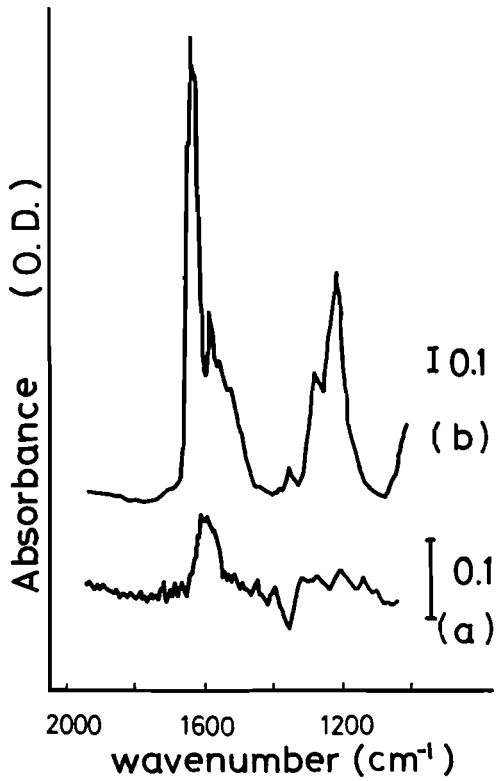


FIG. 2. Adsorption of (*a*) NO and (*b*) NO_2 on oxidized surface of TiO_2.

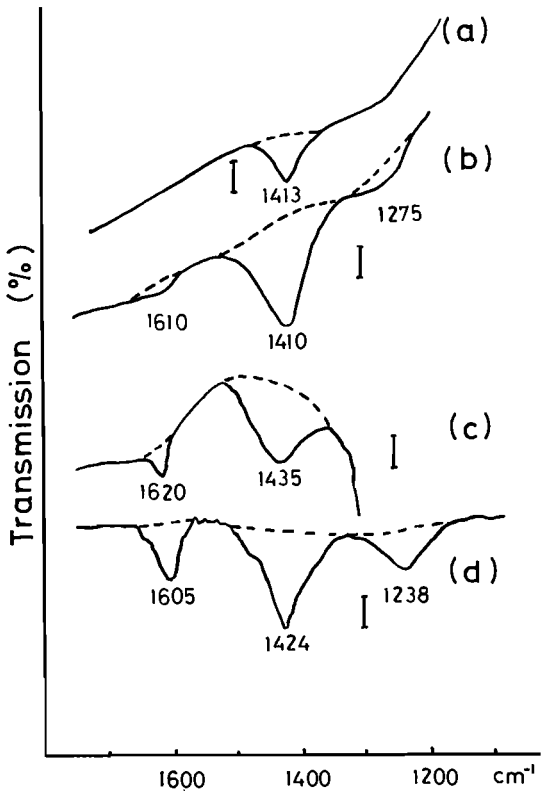


FIG. 3. Infrared spectra of adsorbed ammonia at room temperature on (*a*) V_2O_5, (*b*) V_2O_5/Al_2O_3, (*c*) V_2O_5/SiO_2, and (*d*) V_2O_5/TiO_2; 30 Torr of NH_3 was introduced over the catalysts followed by the evacuation at room temperature. Bars show the transmission of 10%.

due to the adsorbed ammonia, and N1*s* binding energies obtained by XPS. The adsorption of ammonia on V_2O_5 and V_2O_5/Al_2O_3 have been discussed previously (1). The TiO_2 supported catalyst showed absorption bands at 1424, 1605, and 1238 cm^{-1}, which were assigned to symmetric deformation of NH_4^+(ad), degenerate and symmetric deformation of NH_3(ad), respectively, as in the case of V_2O_5/Al_2O_3. The SiO_2 supported catalyst showed two bands at 1620 and 1435 cm^{-1} due to NH_3(ad) and NH_4^+(ad). Binding energies of N1*s* of the adsorbed species were 400 and 401 eV for NH_3(ad) and NH_4^+(ad), respectively, which gave a good correspondance with the ir results.

Reactivity of the Adsorbed Species

The reaction between adsorbed ammonia and gaseous NO_2 was carried out over each of the supported catalysts. Figure 5 shows the amount of N_2 production with time for a unit amount of preadsorbed ammonia. V_2O_5/TiO_2 exhibited the highest activity, V_2O_5/Al_2O_3 exhibited an activity of the same order of magnitude as that of the unsupported V_2O_5, whereas V_2O_5/SiO_2 showed an activity 1/10 that of V_2O_5/Al_2O_3.

It was found that the adsorbed ammonia on V_2O_5, V_2O_5/Al_2O_3, and on V_2O_5/SiO_2 reacted with NO_2 to form N_2, but did not react with NO. No decrease in the ir band of adsorbed ammonia and no N_2 production were observed by the introduction of NO. On the other hand, when NO was introduced over the surface of V_2O_5/TiO_2 preadsorbed with ammonia at room temperature, N_2 was formed at the initial stages (Fig. 5*d*). This suggests that the reaction takes place until the active oxygen on the surface of V_2O_5/TiO_2 is exhausted. The large enhancement of reactivity of system (*a*) over system (*d*) may be due to difference in the total amount of available NO_2(ad) on the surface of the catalysts.

The reaction between two adsorbates, NH_4^+(ad) and NO_2(ad), was examined separately by ir measurement. In order to observe these two adsorbates together, the pressure of NH_3 and NO_2 were carefully controlled. The band intensity of adsorbed ammonia (NH_4^+) on V_2O_5, V_2O_5/Al_2O_3, and V_2O_5/TiO_2 decreased gradually by the introduction of NO_2 or NO + O_2. That of NO_2(ad), on the other hand, decreased by the introduction of ammonia.

Can. J. Chem. Downloaded from www.nrcresearchpress.com by 210.87.254.105 on 09/05/12
For personal use only.

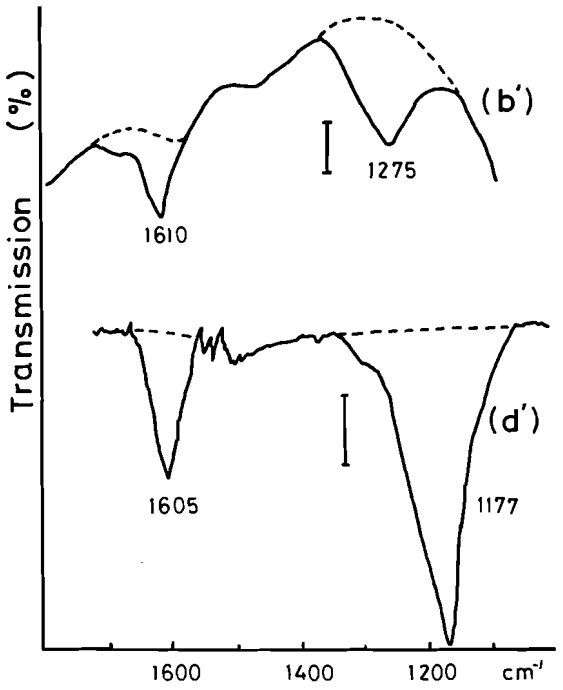


FIG. 4. Infrared spectra of adsorbed ammonia on oxidized surface of supports. (*b'*) on Al_2O_3 and (*d'*) on TiO_2. Ammonia was not adsorbed on SiO_2 surface at room temperature. Bars show the transmission of 10%.

TABLE 1. Adsorption of ammonia on V_2O_5 catalysts, ir and XPS measurements, and the assignment of the adsorbed species are listed*

	Ir (cm^{-1})	Assignment	XPS(Nls) (eV)
V_2O_5	1413	$\delta_s NH_4^+$	400.9
V_2O_5/Al_2O_3	1410	$\delta_s NH_4^+$	401.0
	1610	$\delta_d NH_3$	400.2
	1275	$\delta_s NH_3$	
Al_2O_3	1610	$\delta_d NH_3$	400.0
	1275	$\delta_s NH_3$	
V_2O_5/SiO_2	1435	$\delta_s NH_4^+$	401.0
	1620	$\delta_d NH_3$	
SiO_2	None		None
V_2O_5/TiO_2	1424	$\delta_s NH_4^+$	401.0
	1605	$\delta_d NH_3$	399.4
	1238	$\delta_s NH_3$	
TiO_2	1605	$\delta_d NH_3$	399.6
	1177	$\delta_s NH_3$	
NH_4VO_3	1410	$\delta_s NH_4^+$	400.9

*δ_d: degenerate deformation; δ_s: symmetric deformation.

For both cases, N_2 was formed in the gas phase. The band intensity of two adsorbates on V_2O_5/SiO_2, however, did not decrease by the introduction of each gas. The reaction between the two adsorbates for the V_2O_5/Al_2O_3 and V_2O_5/SiO_2

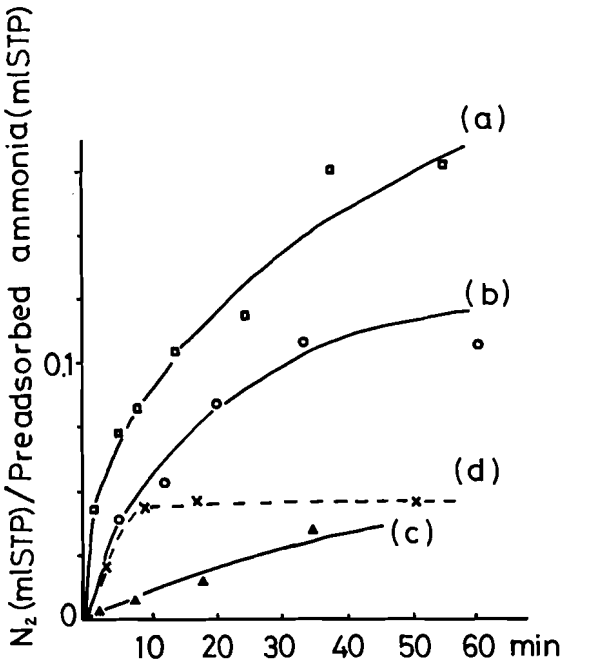


FIG. 5. Reaction between NO_2 and adsorbed ammonia at room temperature (25°C) on 23 wt% V_2O_5 supported catalysts. The amount of N_2 production divided by the amount of preadsorbed ammonia is plotted. (*a*) V_2O_5/TiO_2, (*b*) V_2O_5/Al_2O_3, (*c*) V_2O_5/SiO_2. The broken line (*d*) shows the reaction between adsorbed ammonia and NO gas over V_2O_5/TiO_2. The experimental conditions are as follows: amount of catalyst in g, adsorbed ammonia in mL STP/g, and NO_2 in Torr, V_2O_5/Al_2O_3, 1.68, 20.7, 22; V_2O_5/SiO_2, 1.30, 27.0, 19; V_2O_5/TiO_2, 1.00, 18.0, 22.

are shown in Fig. 6. The decrease of the absorption bands on V_2O_5/Al_2O_3 were observed with time and they were found to vanish in 20 min at room temperature, whereas those on V_2O_5/SiO_2 remained almost unchanged. Both adsorbates NH_4^+(ad) and NO_2(ad) on V_2O_5/SiO_2, which reacted readily on other V_2O_5 catalysts to form N_2, were comparatively inert.

The reactivity of NO_2(ad) on TiO_2 was examined by both ir and volumetric methods. The absorption band of NO_2(ad) on TiO_2 showed no change by the introduction of NH_3 at room temperature, except that extra absorption bands by adsorbed ammonia appeared in the spectrum. In the case of V_2O_5/TiO_2, adsorbed NO_2(ad) readily reacted with NH_3 at room temperature to form N_2.

II. N_2O Formation from NO and NH_3 over V_2O_5/SiO_2 Catalyst

When NO was introduced at 300°C onto V_2O_5/SiO_2, which was reduced by 100 Torr of ammonia at 200°C for 1 h, N_2O was detected in the gas phase, whereas N_2O production was not detected

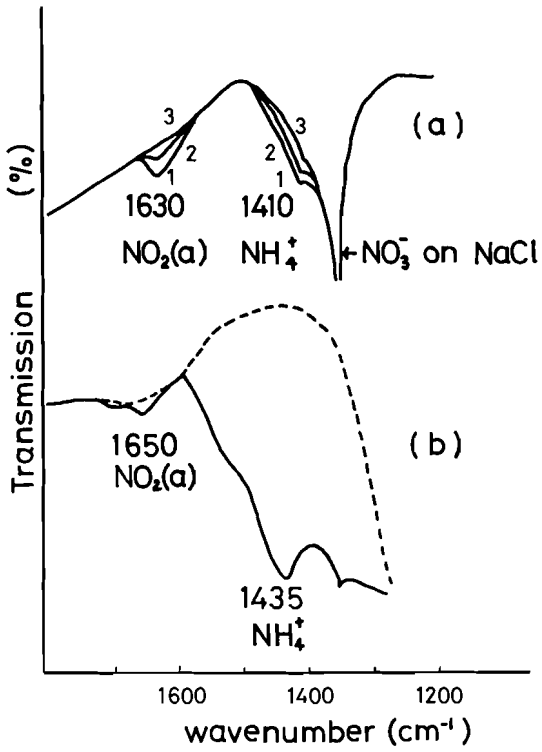


FIG. 6. Infrared spectra of the adsorbates on (*a*) V_2O_5/Al_2O_3, (*b*) V_2O_5/SiO_2. *1*, *2*, *3* in (*a*) show the decrease in the intensity of the absorption bands. The broken line shown in (*b*) is the background spectrum before the adsorption.

over V_2O_5 alone or V_2O_5/Al_2O_3. The changes in the amount of surface oxygen due to the surface treatment and the reaction were examined. It was found that the ratio of XPS emission peak area of O1*s* to that of V2*p* on V_2O_5/SiO_2 decreased by about 10% of its initial value when it was reduced by 30 Torr of NH_3 at 200°C for 1 h followed by evacuation at the same temperature. It increased to restore the original value when the reduced catalyst was exposed to 100 Torr of NO at 300°C for 1 h. In the case of V_2O_5 alone or V_2O_5/Al_2O_3, the ratio of XPS peak area of O1*s*/V2*p* stayed constant within experimental error after the surface was treated by NH_3. For SiO_2 alone, the ratio of O1*s* to Si2*p* exhibited no change due to the surface treatment.

III. XPS Measurement of V_2O_5 Catalysts

The effect of the support on the electronic state of V_2O_5 was examined by XPS. Table 2 shows the binding energies of $V2p_{3/2}$ of V_2O_5 supported over Al_2O_3, SiO_2, and TiO_2. For V_2O_5/SiO_2 the binding energy of V obtained from the $V2p_{3/2}$ shifted to a value 0.8–0.9 eV higher than that for V_2O_5 itself, whereas that for V_2O_5/Al_2O_3 gave a shift of only about 0.3 eV. These shifts in binding energy are

TABLE 2. Binding energies obtained by XPS (Au $4f_{7/2}$ = 83.7eV)*

	$V(2p_{3/2})$	O(1*s*)	Al(2*s*)	Si(2*p*)
V_2O_5	516.8	529.9		
23% V_2O_5/Al_2O_3	517.2	530.8	118.6	
23% V_2O_5/SiO_2	517.7	532.6		103.2
23% V_2O_5/TiO_2	516.9	529.9		
Al_2O_3		531.3	119.2	
SiO_2		532.6		103.2
TiO_2		529.9		

*Each catalyst was oxidized in 100 Torr of oxygen at 300°C for 1 h, and then evacuated for 30 min after cooling down to room temperature.

observed in the region where the content of V_2O_5 is less than 30 wt% for V_2O_5/SiO_2. In the case of V_2O_5/TiO_2, $V2p_{3/2}$ was observed at 516.9 eV, which was the same as that of V_2O_5 alone.

When Au was evaporated over 10% V_2O_5/SiO_2, the peak of $V2p_{3/2}$ was observed at 516.9 eV (the same value as V_2O_5 itself), whereas it was shifted to 517.8 eV without Au evaporation. The location of other emission peaks such as O1*s* or Si2*p* apparently stayed unchanged.

Discussion

(a) Surface Adsorbates of V_2O_5 Catalysts

It was demonstrated accordingly by ir and volumetric methods that NO was not adsorbed on the oxidized or reduced surface of V_2O_5, V_2O_5/Al_2O_3, or V_2O_5/SiO_2 unless oxygen was also present in the gas phase. Furthermore, we could see that NO with O_2 or NO_2 was adsorbed on these catalysts in the form of NO_2(ad). However, on the oxidized surface of V_2O_5/TiO_2, NO could be adsorbed as NO_2(ad) without gaseous oxygen. Although the same feature was observed for the TiO_2 support only, NO_2(ad) adsorbed on TiO_2 was entirely different in reactivity from that on V_2O_5/TiO_2. NO_2(ad) on V_2O_5/TiO_2 reacted to form N_2 when NH_3 was introduced to the surface at room temperature, leaving adsorbed NH_3 on the surface. On the other hand, NO_2 adsorbed on TiO_2 did not react with NH_3. The amount of NO adsorbed as NO_2(ad) on the oxidized surface of 23 wt% V_2O_5/TiO_2 was 0.2 mL STP/g, whereas that of ammonia was 19.0 mL STP/g. This means that the amount of surface active oxygen on V_2O_5/TiO_2 which adsorbs NO as NO_2(ad) is about 1/100 of adsorbed ammonia. If we assume that the V_2O_5 is uniformly supported on the surface of the support (as in the case of SiO_2 or Al_2O_3 supported catalysts), the amount of ammonia adsorbed is about 1/2 of the surface V atoms on the catalyst.

Several ir absorption peaks in the region, 1100–1600 cm^{-1} may be assigned to surface ammonia NH_3(ad) and NH_4^+(ad). These NH_4^+(ad)

Can. J. Chem. Downloaded from www.nrcresearchpress.com by 210.87.254.105 on 09/05/12
For personal use only.

Can. J. Chem. Downloaded from www.nrcresearchpress.com by 210.87.254.105 on 09/05/12
For personal use only.

and NH_3(ad) species could be well correlated with the XPS peaks which reflected the charge distribution in the molecules, and the ir peaks due to NH_3(ad) on the supports could be easily separated from the NH_4^+(ad) on V_2O_5.

NO_2(ad) and NH_4^+(ad) were both revealed to be the reactive species on V_2O_5, V_2O_5/Al_2O_3, and V_2O_5/TiO_2. Among them, NH_4^+(ad) on V_2O_5/TiO_2 reacted with NO to form N_2 until the surface active oxygen which forms NO_2(ad) from NO are exhausted. These facts suggest that the mechanism of the reduction of NO_x by NH_3 on V_2O_5/TiO_2 catalysts could also be described as that proposed for V_2O_5 only or V_2O_5/Al_2O_3 (1) (Scheme 1). It could be expected that under low NO pressure condition (in the practical system, NO is a few hundred ppm), where the rate of NO_2 formation in the gas phase should be slow, V_2O_5/TiO_2 can show high activity for the reduction of NO_x by NH_3 compared with that over the other supported catalysts, such as V_2O_5/Al_2O_3 or V_2O_5/SiO_2, because of the existence of the active oxygen on V_2O_5/TiO_2 to form reactive NO_2(ad) on the surface.

(b) Redox Mechanism over V_2O_5/SiO_2 to Form N_2O

It is well known that N_2O is formed by the reaction of NO with NH_3 over V_2O_5/SiO_2 (2). The observed changes in the amount of surface oxygen on V_2O_5/SiO_2 (section II) indicated that when V_2O_5 is supported on SiO_2, the oxygen on V_2O_5 is easily reduced by NH_3, while the reoxidation of the reduced surface by NO takes place, which offers a new route to the formation of N_2O. It was also demonstrated that the surface reaction between NH_4^+(ad) and NO_2(ad) is slow (or does not occur) on the V_2O_5/SiO_2 (Fig. 6) and this catalyst exhibited low activity in the reaction of NH_4^+(ad) with gaseous NO_2 (Fig. 5). Accordingly, on V_2O_5/SiO_2, there is a route to form N_2O via the so-called redox mechanism. It should be mentioned that the surface oxygen could be easily removed by NH_3 at 200°C, which means that even though the surface was oxidized at the initial stage, it could be easily reduced when NH_3 was present in the system.

(c) Electronic State of V_2O_5 Catalysts

The shift in the binding energy of V ($V2p_{3/2}$) when V_2O_5 is supported on SiO_2 can be attributed to two effects; the chemical effect or the relaxation effect. If the change in the observed binding energy of $V2p_{3/2}$ is due to the chemical effect, that is, the electronic state of vanadium is changed when supported on SiO_2, then the shift should be observed also after the evaporation of Au on the surface of V_2O_5/SiO_2, which was not the case in this study. The fact that V2*p* on SiO_2 is shifted toward higher binding energy without Au evaporation seems to suggest that V_2O_5 is electrically isolated when supported on SiO_2. The shifts in photoelectron peaks due to the local electric isolation and the local difference in chemical activity on a surface of a catalyst have been reported (5).

1. M. TAKAGI, T. KAWAI, M. SOMA, T. ONISHI, and K. TAMARU. J. Phys. Chem. **80**, 430 (1976); M. TAKAGI, T. KAWAI, M. SOMA, T. ONISHI, and K. TAMARU. J. Catal. **50**, 441 (1977).
2. A. UENO, N. TODO, M. KURITA, H. HAGIWARA, A. NISHIJIMA, T. SATO, and Y. KIYOZUMI. Chem. Lett. 557 (1979).
3. S. KASAOKA, T. YAMANAKA, and E. SASAOKA. Nenryo Kyokai-Shi, **56**, 834 (1977).
4. Y. NOTO, K. FUKUDA, T. ONISHI, and K. TAMARU. Trans. Faraday Soc. **63**, 2300 (1967).
5. J. S. BRINEN. J. Electron Spectrosc. **5**, 377 (1974); Acc. Chem. Res. **9**, 86 (1976).

Superoxide mediated autoxidation of hydrocarbons

EDWARD LEE-RUFF AND NEIL TIMMS

Department of Chemistry, York University, 4700 Keele Street, Downsview, Ont., Canada M3J 1P3

Received September 12, 1979[1]

EDWARD LEE-RUFF and NEIL TIMMS. Can. J. Chem. **58**, 2138 (1980).

Potassium superoxide was found to initiate autoxidations of fluorene, diphenylmethane, and distyrylmethane. In each case the oxidation results in the formation of ketones as primary products. Kinetics of the fluorene and diphenylmethane oxidations showed typical sigmoidal autoxidation rate profiles. External hydroperoxides did not affect the rates of these reactions, however, these were efficiently transformed to ketones in the presence of O_2^-. A mechanism for these autoxidations is proposed.

EDWARD LEE-RUFF et NEIL TIMMS. Can. J. Chem. **58**, 2138 (1980).

On a trouvé que le superoxyde de potassium initie l'autoxydation du fluorène, du diphénylméthane et du distirylméthane. Dans chaque cas, l'oxydation conduit à la formation de cétones comme produits primaires. Les cinétiques de l'oxydation du fluorène et du diphénylméthane montrent un profil de vitesse typique d'une autoxydation sigmoidale. Les hydroperoxydes extérieurs n'affectent pas les vitesses de ces réactions; cependant elles sont transformées efficacement en cétones en présence d'ions O_2^-. On propose un mécanisme pour ces réactions d'autoxydations.

[Traduit par le journal]

As part of a program on the study of the organic chemistry of superoxide (1), we became interested in the possible involvement of O_2^- in autoxidation reactions. The effect of metal and metal ions in the enhancement of autoxidation rates is well documented (2, 3) and has been rationalized in terms of the involvement of these in interfering with the chain initiating and propagating steps in the basic autoxidation scheme. It is conceivable that in the presence of metals and reducing metal ions superoxide may be produced and involved in the autoxidation scheme shown below.

Initiation: $M^{+n} + O_2 \rightarrow M^{+n+1} + O_2^-$

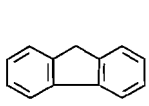
$R^- + O_2 \rightarrow R^\cdot + O_2^-$

$O_2^-(M^{+n+1}) + RH \rightarrow HO_2^- + R^\cdot$

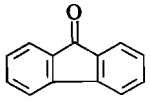
Chain propagation: $R^\cdot + O_2 \rightarrow RO_2^\cdot$

$RO_2^\cdot + RH \rightarrow R^\cdot + ROOH \rightarrow$ oxidation products

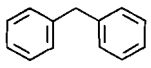
Superoxide, once formed from one electron reduction of triplet oxygen by either reducing species such as metals, metal ions, or even organic anions in base-catalyzed autoxidations, may abstract a hydrogen atom from the hydrocarbon to initiate the chain process. This step might be expected to be more efficient with O_2^- than with triplet oxygen and lead to rate enhancements. Triplet oxygen singlet substrate interactions in the ground state are spin forbidden and require appreciable activation energies. In the transformation of the primary hydroperoxides (ROOH) to more stable oxidation products, O_2^- may act as one electron reducing agent or a base (4) to produce other free radicals leading to chain branching and an acceleration of rates. On the other hand, superoxide may also participate in the chain terminating steps as a radical scavenger or as a reducing species of alkyl radicals leading to shorter chains and a deceleration of the overall rate. In order to evaluate the effect of superoxide in autoxidation reactions we studied the oxidation of hydrocarbons possessing benzylic and allylic hydrogens such as fluorene (**1**), diphenylmethane (**2**), and distyrylmethane (**3**) with oxygen in the presence of catalytic amounts of potassium superoxide. In all cases ketones **4**, **5**, and **6** were



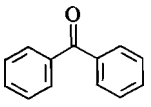
1



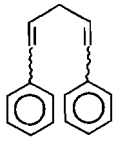
4



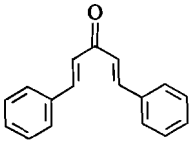
2



5



3



6

formed as major products accompanied by trace amounts of hydrocarbon dimers. That these were not direct superoxide oxidations was seen by the stoichiometry of these transformations. Catalytic amounts of O_2^- down to 1/100 equivalent were sufficient to cause these transformations to proceed

[1]Revision received July 3, 1980.

0008-4042/80/202138-04$01.00/0

©1980 National Research Council of Canada/Conseil national de recherches du Canada

Can. J. Chem. Downloaded from www.nrcresearchpress.com by 210.87.254.40 on 09/05/12
For personal use only.

Can. J. Chem. Downloaded from www.nrcresearchpress.com by 210.87.254.40 on 09/05/12
For personal use only.

to completion although the rates were significantly lowered with decreasing O_2^- concentrations. There were complications with the distyrylmethane oxidation in that a mixture of products consisting of ketone **6**, benzaldehyde, and cinnamic acid was obtained whose composition depended on the amount of superoxide initially present in the system. It was subsequently shown that benzaldehyde and cinnamic acid are secondary products derived from the direct oxidation by O_2^- of ketone **6** under the same conditions. Similar observations have been made by Poupko and Rosenthal (5). The rate profile (Figs. 1 and 2) shows the typical curve for an autoxidation reaction characterized by an induction period followed by an acceleration in rate and then a deceleration towards completion. The maximum rates are seen to depend on hydrocarbon concentrations with the rate increasing with RH concentration. It can also be seen from the rate profiles that the induction period is also affected by RH concentration in an inverse way. That these transformations are not base-catalyzed by O_2^- or spurious hydroxide was shown by similar experiments using potassium hydroxide in identical concentrations. Although autoxidations did occur under the latter conditions, the rates of the reactions were anywhere from 20 to 100-fold slower. The effect of varying superoxide concentration on the rate of oxygen uptake is seen to follow a similar pattern with rates and induction periods being affected by O_2^- concentration.

Table 1 summarizes the kinetic data of the fluorene oxidations. Oxygen consumption is close to but never exceeds 1 suggesting that if hydroperoxides are formed their subsequent transformation to ketones does not involve a second equivalent of oxygen but possibly a base-catalyzed

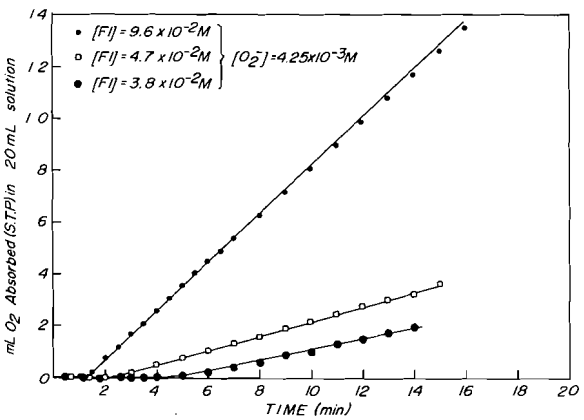


FIG. 1. Rate profile for fluorene autoxidation mediated by O_2^- (25°C), varying fluorene concentration.

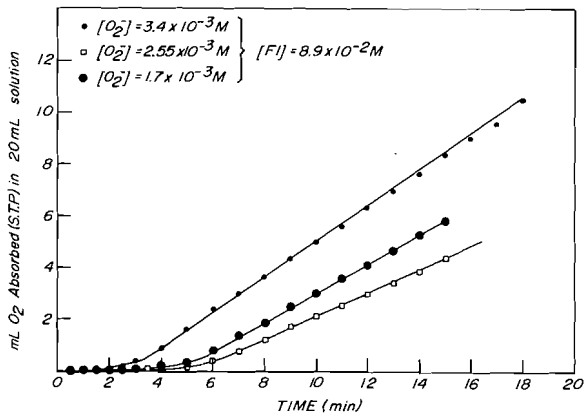


FIG. 2. Rate profile for fluorene autoxidation mediated by O_2^- (25°C), varying O_2^- concentration.

degradation. Independent studies on the fluorenyl hydroperoxide reaction with potassium superoxide as well as with potassium hydroxide showed a complete conversion to fluorenone *in the absence of oxygen*. With superoxide, oxygen evolution was associated with these transformations. The autoxidation rates represent lower limits since a two phase system is used and limited by the rate of oxygen diffusion into the liquid solution. The experimental orders in hydrocarbon and superoxide concentrations and bimolecular rate constants are tabulated in Table 2. In both the fluorene and diphenylmethane oxidations the order in hydrocarbon concentration is greater than 1 and that for superoxide is less than 1. It is also seen that the rate for fluorene autoxidation is about 30 times faster than for diphenylmethane. This is consistent with the relative order for hydrogen abstraction of fluorene and diphenylmethane as reported by Russell (6). At 90°C the rate of hydrogen abstraction of fluorene by alkyl peroxy radicals is more than 3 times as fast as in diphenylmethane. Assuming positive activation energies it would be expected that these rate differences would be larger at lower temperatures. However, direct quantitative comparisons cannot be made between our results and those of Russell since the latter were obtained for constant rate of chain initiation which is not the case in the present work. Our kinetic data for fluorene oxidation are also consistent with those reported by Ohkatsu and co-workers (7), who studied these oxidations using electrogenerated O_2^- with tetraethylammonium phosphate as the supporting electrolyte in pyridine solutions. However, they report that diphenylmethane oxidation is 3.5 times faster than fluorene oxidation. It may be that

Can. J. Chem. Downloaded from www.nrcresearchpress.com by 210.87.254.40 on 09/05/12
For personal use only.

TABLE 1. Kinetics of fluorene oxidation in DMSO (25±1°C)

Run	Rate of O_2 consumed			
	Fluorene ($10^2 \times M$)	Superoxide ($10^3 \times M$)	$10^7 \times (M/s)$	Equiv. O_2/equiv. fluorene[a]
1	3.8	4.25	1.38	0.93
2	4.7	4.25	2.08	0.83
3	9.6	4.25	6.67	0.78
4	8.9	1.7	3.17	0.86
5	8.9	2.55	4.17	0.91
6	8.9	3.4	5.17	0.83

[a]Based on volume of oxygen consumed after 24 to 26 h corrected to STP.

TABLE 2. Kinetic data for O_2^- autoxidations

	Order in RH	Order in O_2^-	k (L/mol − s)
Fluorene	1.6	0.66	1.02×10^{-3}
Diphenylmethane	1.4	0.54	2.88×10^{-5}

solvent effects and the nature of the gegenion may contribute to rate differences and even reversals in rate orders.

Following the basic autoxidation scheme the rate of oxidation can be expressed by the equation:

$$R = \frac{k_2[O_2]R_i^{1/2}(k_3[RH] + k_6^{1/2}R_i^{1/2})}{k_3k_4^{1/2}[RH] + k_2k_6^{1/2}[O_2] + (k_4k_6R_i)^{1/2}}$$

By making the approximation that the rate initiation R_i is rate determining the above expression can be reduced to:

$$R = \frac{k_2k_3[O_2][RH]R_i^{1/2}}{k_3k_4^{1/2}[RH] + k_2k_6^{1/2}[O_2]}$$

Basic Autoxidation Scheme

Production of R· or $RO_2^·$ radicals: initiation rate = R_i

$$R^· + O_2 \xrightarrow{k_2} RO_2^·$$

$$RO_2^· + RH \xrightarrow{k_3} RO_2H + R^·$$

$$\left.\begin{array}{ll} 2R^· & \xrightarrow{k_4} \\ R^· + RO_2^· & \xrightarrow{k_5} \\ 2RO_2^· & \xrightarrow{k_6} \end{array}\right\} \text{inert products}$$

For sufficiently high oxygen pressures the rate expression can be further simplified to one involving first order in hydrocarbon concentration and independent of oxygen concentration, i.e.

$$R = k[RH]R_i^{1/2}$$

If one proposes that in the presence of superoxide, the dominant initiation process is hydrogen abstraction from hydrocarbon RH by O_2^- the rate expression becomes:

$$R = k[RH]^{3/2}[O_2^-]^{1/2}$$

The experimental orders (Table 2) fall within the range of the predicted rate equation suggesting O_2^- is primarily involved in the rate determining initiation step of these oxidations. Studies on the rates of autoxidation in the presence of fluorenyl hydroperoxide (10^{-4} M) showed a minimal decrease in the rate attributable to the reaction of O_2^- with hydroperoxide as described above. This would suggest that hydroperoxides are not responsible for autocatalysis under these conditions. The initiation rate constant k_i can be estimated from values of k_6 and k_3 of 6×10^5 and 10 L/mol-s respectively for γ-methylcrotylbenzene (12), a related system. A value of 5.3×10^{-3} L/mol-s is calculated for fluorene hydrogen abstraction by O_2^-. This is about three orders of magnitude slower than the corresponding hydrogen abstractions by peroxy radicals in line with the expected decreased reactivity of radical anions towards hydrogen abstaction. It is noteworthy that such a slow initiation step is more compatible with a hydrogen abstraction by O_2^- rather than a proton abstraction. Work is in progress to investigate the nature of these radicals by spin-trapping experiments.

Experimental

Diphenylmethane was redistilled from a commercial sample. Distyrylmethane (mixture of isomers) was prepared by Wittig reaction of 1,3-dibromopropane with benzaldehyde (8). Fluorene was recrystallized from a commercial sample. Fluorenyl hydroperoxide was prepared according to the method of Hock *et al.* (9). *Trans* dibenzalacetone was synthesized according to a literature method (10).

Qualitative Experiments

Solutions (50 mL) of hydrocarbon (10^{-2} to 10^{-3} M) in dimethyl sulfoxide containing 10^{-4} M potassium superoxide were placed in a gas bubbler. Oxygen gas was passed through the solution for 1–2 h. The solutions were diluted with 200 mL of water and extracted with 3 × 50 mL of ether. The ether extracts were dried with anhydrous magnesium sulfate and evaporated.

Can. J. Chem. Downloaded from www.nrcresearchpress.com by 210.87.254.40 on 09/05/12
For personal use only.

The residue was chromatographed on a silica gel column (hexane–benzene 1:1). The nonpolar fractions (<5%) were identified as dimeric material from their mass spectra ($2M^+ - 2$). The ketone fractions (>90%) were compared with authentic material.

The fluorenyl hydroperoxide oxidation was carried out as follows: 50 mg of hydroperoxide (9) in 5 mL of benzene was added to 2 mL of a suspension of 100 mg of finely crushed KO_2 in benzene in a closed system saturated with N_2. Evolution of a gas was observed during addition. After the addition was complete the mixture was poured into 10 mL of water – crushed ice mixture. The solution was extracted with ether and the ether layer worked up in the usual manner to give 40 mg of fluorenone. The same procedure was repeated using KOH instead of KO_2.

Oxidation of Distyrylmethane (3) and Dibenzalacetone (6) with Potassium Superoxide

A solution containing 0.5 g of distyrylmethane (**3**) (mixture of isomers) in 50 mL dimethyl sulfoxide was placed in a gas bubbler. Oxygen was passed through the solution for 2 h. The solution was added to 200 mL of water and extracted with 3 × 50 mL of ether. The combined ether extract was dried with anhydrous magnesium sulfate and evaporated. The residue was chromatographed on a silica gel column. Hexane–benzene 1:1 eluted 45 mg of benzaldehyde (dinitrophenylhydrazone mp 235–236°C (lit. (11) mp 237°C)), and 340 mg of *trans* dibenzalacetone, mp 109–110°C, identical by ir spectroscopy to *trans* dibenzalacetone prepared according to ref. 10. The aqueous solution was neutralized with concentrated HCl and extracted with 2 × 50 mL of ether. The ether extract was washed neutral with water, dried with $MgSO_4$, and evaporated to give 64 mg of *trans* cinnamic acid, mp 131°C. This was identical by ir with an authentic sample. Mixture melting point showed no depression.

The control oxidation of dibenzalacetone with potassium superoxide was carried out as follows. To a solution of 0.5 g of dibenzalacetone in 50 mL dimethyl sulfoxide was added 0.5 g of KO_2. The solution turned to an orange-brown colour after a few minutes. After stirring for 2 h the mixture was added to 200 mL water and worked up in the same way as above yielding 0.15 g of benzaldehyde and 0.24 g of cinnamic acid.

Kinetic Runs

In a closed system consisting of a gas burette and a reaction assembly with an addition flask was introduced 10 mL of a dimethyl sulfoxide solution containing potassium superoxide. A 10 mL solution containing the hydrocarbon was introduced into the addition funnel. The reaction assembly was equilibrated with oxygen for one hour. The hydrocarbon solution was rapidly added to the reaction flask and the oxygen uptake was followed by gas burette reading and corrected to STP.

Acknowledgement

We would like to thank the Imperial Oil Company of Canada for financial support of this project.

1. E. Lee-Ruff. Chem. Soc. Rev. **2**, 195 (1977).
2. F. W. Heaton and N. Uri. J. Lipid Res. **2**, 152 (1961).
3. A. T. Betts and N. Uri. Makromol. Chem. **95**, 22 (1966).
4. J. W. Peters and C. S. Foote. J. Am. Chem. Soc. **98**, 873 (1976).
5. I. Poupko and I. Rosenthal. J. Phys. Chem. **77**, 1722 (1973).
6. G. A. Russell. J. Am. Chem. Soc. **78**, 1047 (1956).
7. M. Tezuka, Y. Ohkatsu, and T. Osa. Bull. Chem. Soc. Jpn. **48**, 1471 (1975).
8. G. Wittig, H. Eggers, and P. Duffner. Justus Liebigs Ann. Chem. **619**, 10 (1958).
9. H. Hock, S. Long, and G. Knauel. Ber. **83**, 227 (1950).
10. A. H. Blatt. Org. Synth. Coll. Vol. II. J. Wiley, New York. 1950. p. 167.
11. R. L. Shriner, R. C. Fuson, and D. Y. Curtin. Systematic identification of organic compounds. J. Wiley, New York. 1964.
12. J. L. Boland. Trans. Faraday Soc. **46**, 358 (1950).

Kinetic deuterium isotope effects and kinetic solvent isotope effects for the solvolyses in water and in water + acetonitrile mixtures related to a series of substituted benzyl nitrates

MOHAMMED AHSAN AND ROSS ELMORE ROBERTSON
Department of Chemistry, University of Calgary, Calgary, Alta., Canada T2N 1N4
MICHAEL JESSE BLANDAMER
Department of Chemistry, University of Leicester, Leicester, England
AND
JOHN MARSHALL WILLIAM SCOTT
Department of Chemistry, Memorial University, St. John's, Nfld., Canada A1B 3X7
Received March 25, 1980

MOHAMMED AHSAN, ROSS ELMORE ROBERTSON, MICHAEL JESSE BLANDAMER, and JOHN MARSHALL WILLIAM SCOTT. Can. J. Chem. **58**, 2142 (1980).

In aqueous solution, the α-deuterium isotope effects in the solvolyses of benzyl nitrates derivatives depend on the nature of the substituent in the benzene ring. In addition, the isotope effect for some derivatives depends on mole fraction of added acetonitrile while for others the isotope effect is insensitive to solvent composition. However, the kinetic solvent isotope effects for *para*-methyl and *meta*-trifluoromethyl derivatives remain unchanged when acetonitrile is added. These observations are accounted for in terms of a model which describes the solvolytic reaction as a two-stage process and contrasts the relative importance of bond-making and bond-breaking.

MOHAMMED AHSAN, ROSS ELMORE ROBERTSON, MICHAEL JESSE BLANDAMER et JOHN MARSHALL WILLIAM SCOTT. Can. J. Chem. **58**, 2142 (1980).

En solution aqueuse, les effets isotopiques des deutérium α observés lors des solvolyses de nitrates de benzyles dépendent de la nature du substituant fixé sur le cycle. De plus les effets isotopiques de quelques dérivés dépendent de la fraction molaire d'acétonitrile ajouté alors que d'autres effets isotopiques sont indépendants de la composition du solvant. Cependant les effets isotopiques cinétiques du solvant pour les dérivés *para*-méthylé et *méta*-trifluorométhylé demeurent les mêmes quand on ajoute de l'acétonitrile. On interprète ces observations en fonction d'un modèle qui décrit la réaction de solvolyse, une réaction en deux étapes où s'opposent les importances relatives de la rupture et de la formation d'une liaison.

[Traduit par le journal]

Introduction

In principle, a detailed understanding of the mechanism of solvolytic reactions involving organic substrates of the general form RX should be forthcoming from a study of the α-deuterium isotope effects as measured by the ratio k_H/k_D. A similar comment applies to the information provided by the kinetic solvent isotope effect as measured by the ratio k_{H_2O}/k_{D_2O}. However, as more information became available the interpretation of these isotope effects became less clear-cut. Thus Shiner (1) attempted to use k_H/k_D as an indicator of the extent of nucleophilic involvement in the rate determining step for displacement of chloride ion. However, Bentley and Schleyer (2) argue that the reference value of k_H/k_D is not known for systems where nucleophilic driving forces are absent. Turning to the solvent isotope effect, there was reason to anticipate that in terms of the Ingold description (3), the ratios would follow the sequence $1° > 2° > 3°$. However, these ratios for displacement of halide, nitrates, and sulphonates from a saturated carbon atom are often close to unity (4), the slight deviation from unity being partially attributed to initial state differences (5).

The work reported in this paper was prompted by the observations of Koshy and Robertson (6, 7). For a series of benzyl nitrates in water, the α-k_H/k_D ratios vary between 0.99 and 1.18 per deuterium atom. Moreover it was noted (7) that the latter ratios correlated with the heat capacities of activation, $\Delta C_p^{\ddagger}$, calculated from the dependence of rate constant for solvolysis in water on temperature. However, a reappraisal (8) of the latter dependence has indicated that the calculated $\Delta C_p^{\ddagger}$-quantity is an artefact of the mechanism which is more correctly described in terms of a two-stage process. This raises the question of whether a similar model could account for the isotope effects. The data reported in this paper for the solvolysis of a series of substituted benzyl nitrates prompt the development of such a model. Here the reaction proceeds through an intermediate which is characterized by appreciable charge separation in the C—X bond. The transition state characterizing the next stage is appreciably ionic whereas the nucleophile H_2O (D_2O) is reactant-like, whether the reacting carbon centre is primary, secondary, or tertiary. This new model shifts the emphasis away from the traditional assumption which stresses the compensation be-

0008-4042/80/202142-04$01.00/0
©1980 National Research Council of Canada/Conseil national de recherches du Canada

Can. J. Chem. Downloaded from www.nrcresearchpress.com by 210.87.254.5 on 09/05/12
For personal use only.

TABLE 1. α-Deuterium isotope effects for hydrolysis of benzyl nitrates

Nitrate	Solvent acetonitrile/H_2O (mole fraction)	Temperature (°C)	$k_H \times 10^4\ s^{-1}$	$k_D \times 10^4\ s^{-1}$	k_H/k_D*
p-Methylbenzyl	0.00 $Y = 3.493$	25.901	5.49 ±0.019	3.96 ±0.028	1.18
	0.05 $Y = 2.323$	25.901	2.468 ±0.005	1.816 ±0.003	1.166
	0.10 $Y = 1.923$	53.288	20.70 ±0.09	16.04 ±0.03	1.136
	0.20 $Y = 1.038$	53.288	2.872 ±0.013	2.524 ±0.003	1.066
Benzyl	0.00	53.408	2.373 ±0.009	1.892 ±0.018	1.119
	0.05	53.408	0.9747±0.0026	0.791 ±0.0027	1.109
	0.1	53.408	0.4035±0.0015	0.343 ±0.0015	1.084
	0.2	53.408	0.0782±0.0003	0.0721±0.0003	1.041
p-Br-benzyl	0.00	65.258	3.76 ±0.009	3.279 ±0.015	1.071
	0.05	65.258	1.458 ±0.003	1.304 ±0.005	1.057
	0.10	65.258	0.5856±0.0022	0.5359±0.0021	1.045
	0.20	65.258	0.1193±0.0006	0.1316±0.0004	0.9521
o-Methylbenzyl	0.00	53.444	40.49 ±0.13	30.93 ±0.13	1.144
	0.05	53.444	13.95 ±0.05	10.85 ±0.05	1.134
	0.10	53.444	5.140 ±0.014	4.075 ±0.005	1.123
	0.20	53.444	0.7534±0.0023	0.6749±0.0012	1.057
m-CF_3-benzyl	0.00	86.179	2.535 ±0.009	2.605 ±0.004	0.973
	0.05	86.179	0.9736±0.0015	1.008 ±0.003	0.965
	0.1	86.179	0.4221±0.0007	0.4349±0.0006	0.971

*Per *d*.

TABLE 2. α-Deuterium isotope effect for solvolysis of benzyl chlorides

Chloride	Acetonitrile (mole fraction)	Temperature °C	$k_H \times 10^4\ s^{-1}$	$k_D \times 10^4\ s^{-1}$	k_H/k_D
p-Me-benzyl	0.00	25.860	4.91 ±0.018	3.75 ±0.014	1.144
	0.05	25.860	1.95 ±0.022	1.54 ±0.01	1.125
	0.10	25.860	0.495±0.012	0.395±0.011	1.119
Benzyl	0.00	51.373	2.520±0.009	2.301±0.003	1.047
	0.05	51.373	1.011±0.0003	0.954±0.003	1.029
	0.10	58.498	0.151±0.0015	0.708±0.003	1.029
	0.20	70.553	1.125±0.003	1.086±0.005	1.018
p-Br-benzyl	0.00	60.215	3.170±0.005	3.067±0.002	1.016
	0.05	60.215	1.318±0.002	1.294±0.002	
	0.10	60.215	0.715±0.003	0.709±0.002	1.004
	0.20	80.120	4.18 ±0.01	4.14 ±0.007	1.005

tween bond-making and bond-breaking in displacement reactions.

Results

The α-deuterium isotope effects for the solvolysis of various benzyl nitrates in water are reported in Table 1. The ratios range from 1.16 for *o*-methylbenzyl nitrate to 0.986 for the *m*-trifluoromethyl derivative showing that α-deuteration can increase or decrease the rate constant.

A more interesting trend is observed when the solvent is changed by adding acetonitrile. In some cases the ratio k_H/k_D changes; in the case of *o*-methylbenzyl nitrate, the ratio shifts from 1.158 to 1.070 when the mole fraction of acetonitrile increases from 0 to 0.20. However, the ratio for some substrates is insensitive to the mole fraction of added acetonitrile, e.g. *m*-trifluorobenzyl nitrates. A similar solvent dependence of k_H/k_D is observed for the solvolyses of three benzyl chlorides (Table 2).

The effect of added acetonitrile on the kinetic

Can. J. Chem. Downloaded from www.nrcresearchpress.com by 210.87.254.5 on 09/05/12
For personal use only.

TABLE 3. Kinetic solvent isotope effect for hydrolysis of benzyl nitrates

Nitrate	Temperature (°C)	Acetonitrile (mole fraction)	$k_{H_2O} \times 10^{-4}$ s^{-1} calculated (7)	$k_{D_2O} \times 10^{4}$ s^{-1}	k_{H_2O}/k_{D_2O}
p-CH_3-benzyl	25.901	0.00	5.487	5.03±0.03	1.09_1
		0.02	2.885	2.64±0.014	1.09_2
m-CF_3-benzyl	86.181	0.00	2.535	2.37±0.01	1.07(4)*
		0.10	0.398±0.002	0.422	1.06(4)*

*Adjusted to 25°C.

solvent isotope effect is shown in Table 3 for two benzyl nitrates. Here we note that this isotope effect is insensitive to the solvent composition.

In summary the data show (*1*) how the α-deuterium isotope effects depend on the substituent in the benzene ring; (*2*) how the ratio of k_H/k_D may or may not depend on the solvent composition; and (*3*) how the solvent isotope effect is unchanged when acetonitrile is added. In the following section we attempt to formulate a model which accounts for these observations.

Discussion

It could be argued that the ratio k_H/k_D reflects the balance of bond-breaking and bond-making in a chemical solvolytic reaction which proceeds by a process characterized by one activation barrier/transition state. In these terms the data require that there is a larger degree of bond-breaking or charge-separation in the *p*-methyl derivative than in the *m*-CF_3 derivative, yet the latter is the less reactive by a factor of 5.7×10^3 at 25°C. With decrease in ionizing power of solvent, the same model suggests that less bond-breaking is required at the transition state for the *p*-Me derivative. In contrast the ratio k_H/k_D for the less reactive *m*-CH_3 derivative is insensitive to solvent composition. The difference between these trends for *m*-CF_3 and CH_3 derivatives must be contrasted with the insensitivity of the kinetic solvent isotope effect on addition of acetonitrile. Clearly the kinetic solvent isotope effect for reaction in the pure solvents does not stem from the inherent differences between the structural properties of the H_2O and D_2O. If this were so, we would anticipate that the solvent isotope effect would diminish when acetonitrile is added. The difficulties in the interpretation outlined above stem from the hypothesis (9) which argues that nucleophilic driving forces lower the activation energy for the displacement process by reducing the large heterolytic gas phase enthalpies to thermally available energies in solution. Thus even direct reactions of nucleophiles with triarylcarbonium ions require an activation energy although *no* bonds are broken and *no* incoming group/leaving group repulsions are present (10, 11).

The above arguments lead us to propose a different model for these reactions which is consistent with the observed α-deuterium and solvent isotope effects. The solvolytic reaction in water is treated in terms of a two-stage process along the lines visualized by Albery and Robinson (12), by Sneen (13), and by our recent calculations (8) concerning the dependence of rate constants on temperature. In these terms, the experimental rate constant is a function of parameters (8, 12) describing the formation of an intermediate and its subsequent chemical reaction with the solvent. The formation of the intermediate involves charge separation within the C—X bond; the intermediate is stabilized by solvation interactions. At this stage the charge separation is incomplete. Interaction of the intermediate with water leading to initiation of bond-making necessitates some critical level of positive charge being localized on the reacting carbon in the *subsequent* transition state. Further, the degree of bond separation at the transition state depends on the substrate. The small kinetic solvent isotope effect arises from the fact that the water nucleophile is reactant-like at the transition state. However, for different substrates, the C—X distance at the transition state is characteristic of the substrate. Subsequent reorganization leading to products occurs beyond the transition state and is not kinetically significant. The variation of the α-*d* ratios is a consequence of varying degrees of separation of the incipient anion at the transition state. Hence across a range of related substrates, this distance will change, resulting in a different k_H/k_D ratio and, more importantly, in different sensitivities to added cosolvent.

Clearly, the level of charge localized on the reacting carbon at the transition state is an important parameter in relation to the initiation of nucleophilic attack. The ability of the carbonium ion to disperse positive charge will be reflected in greater separation of the heterolysing fragments before the required level of charge at the reacting carbon

Can. J. Chem. Downloaded from www.nrcresearchpress.com by 210.87.254.5 on 09/05/12
For personal use only.

is attained. This hypothesis is consistent with Ritchie's observations (10). Triarylcarbonium ions which are efficient at delocalizing charge react the slowest. Indeed the barrier in these reactions may largely reflect the energy required to "relocalize" the charge in these highly delocalized systems. For any comparable level of bond extension the smaller charge on the reacting extracyclic carbon atom results in a greater separation of charges in, for example, *p*-methylbenzyl nitrate relative to the *m*-trifluoromethyl substrate.

Experimental

The substituted benzyl chlorides and nitrates were prepared as described by Koshy and Robertson (6, 14). As a further refinement after reduction of the corresponding acids, the alcohols were purified by a zone–freeze–melt operation. Where comparison was possible (for hydrolysis in water), agreement with the rate constants calculated from the Valentiner constants reported by Koshy was excellent.

Acetonitrile was reagent grade and solutions were made up to the indicated composition with distilled water.

The rates were determined by conductance as described by Robertson and Sugamori (15). Temperatures were determined using a platinum resistance thermometer. The isotope effects were determined in pairs of cells run simultaneously, and so the effect of temperature variation was minimized. The rate constants were calculated by a Moore-type equation (16) which uses a nonlinear least-squares procedure coupled with an iterative calculation, the latter refining an estimated rate constant for the reaction.

Acknowledgement

The assistance of an operating grant from the National Research Council of Canada is gratefully acknowledged.

1. J. V. SHINER, JR. *In* Isotope effects in chemical reactions. *Edited by* C. J. Collins and N. S. Bowman. A. C. S. Monograph #16. van Nostrand, Rheinhold Co., New York. 1970. Chapt. 2.
2. T. W. BENTLEY and P. VON R. SCHLEYER. Adv. Phys. Org. Chem. **14**, 1 (1976).
3. C. K. INGOLD. *In* Structure and mechanism in organic chemistry. Cornell University Press, Ithaca, NY. 1953. Chapt. 7.
4. P. M. LAUGHTON and R. E. ROBERTSON. *In* Solute–solvent interactions. *Edited by* J. F. Coetzee and C. D. Ritchie. Marcel Dekker, New York. 1969. Chapt. 7.
5. R. E. ROBERTSON. Phys. Org. Chem. **4**, 213 (1967).
6. K. M. KOSHY and R. E. ROBERTSON. J. Am. Chem. Soc. **96**, 914 (1974).
7. K. M. KOSHY and R. E. ROBERTSON. Can. J. Chem. **52**, 2660 (1974).
8. M. J. BLANDAMER, R. E. ROBERTSON, J. M. W. SCOTT, and A. VRIELINK. J. Am. Chem. Soc. **102**, 2585 (1980).
9. R. E. ROBERTSON, R. L. HEPPOLETTE, and J. M. W. SCOTT. Can. J. Chem. **37**, 803 (1959).
10. C. D. RITCHIE. Acc. Chem. Res. **5**, 348 (1972).
11. S. H. MORRIS, J. M. W. SCOTT, and F. STEELE. Can. J. Chem. **55**, 686 (1977).
12. W. J. ALBERY and B. H. ROBINSON. Trans. Faraday Soc. **65**, 980 (1969).
13. R. A. SNEEN. Acc. Chem. Res. **6**, 46 (1973).
14. K. M. KOSHY. Ph.D. Thesis, University of Calgary, Calgary, Alta. 1973.
15. R. E. ROBERTSON and S. E. SUGAMORI. J. Am. Chem. Soc. **91**, 7254 (1969).
16. P. MOORE. J. Chem. Soc. Faraday Trans. I, 180 (1972).

Can. J. Chem. Downloaded from www.nrcresearchpress.com by 210.87.254.5 on 09/05/12
For personal use only.

Rates of OH radical reactions. VII. Reactions of OH and OD radicals with n-C_4H_{10}, n-C_4D_{10}, H_2 and D_2, and of OH with *neo*-C_5H_{12} at 297 K[1]

GEORGE PARASKEVOPOULOS AND WING S. NIP[2]

Division of Chemistry, National Research Council of Canada, Ottawa, Ont., Canada K1A 0R9

Received June 5, 1980

GEORGE PARASKEVOPOULOS and WING S. NIP. Can. J. Chem. **58**, 2146 (1980).

Absolute rate constants of hydrogen and deuterium atom abstraction by OH and OD radicals from n-C_4H_{10}, n-C_4D_{10}, H_2 and D_2, and by OH radicals from *neo*-C_5H_{12} have been measured at room temperature in the gas phase using the flash photolysis-resonance absorption technique. The rate constants in units of $cm^3\ mol^{-1}\ s^{-1}$ were found to be:

$k_{OH+n\text{-}C_4H_{10}} = 1.61 \pm 0.13 \times 10^{12}$ $\quad$ $k_{OH+neo\text{-}C_5H_{12}} = 5.48 \pm 0.59 \times 10^{11}$

$k_{OH+n\text{-}C_4D_{10}} = 4.20 \pm 0.41 \times 10^{11}$ $\quad$ $k_{OH+D_2} = 1.27 \pm 0.11 \times 10^{9}$

$k_{OD+n\text{-}C_4H_{10}} = 1.66 \pm 0.13 \times 10^{12}$ $\quad$ $k_{OD+H_2} = 3.70 \pm 0.25 \times 10^{9}$

$k_{OD+nC_4D_{10}} = 4.84 \pm 0.38 \times 10^{11}$ $\quad$ $k_{OD+D_2} = 1.33 \pm 0.13 \times 10^{9}$

The quoted errors are the 95% confidence limits. A kinetic isotope effect was observed when hydrogen was replaced by deuterium in the paraffin and H_2, whereas there was no significant effect when OH was replaced by OD.

GEORGE PARASKEVOPOULOS et WING S. NIP. Can. J. Chem. **58**, 2146 (1980).

Les constantes de vitesse absolues pour l'abstraction d'atomes d'hydrogène et de deutérium de n-C_4H_{10}, n-C_4D_{10}, H_2 et D_2 par les radicaux OH et OD, et d'atomes d'hydrogène de *néo*-C_5H_{12} par OH, ont été mesurées en phase gazeuse, à température ambiente. Les radicaux OH et OD sont produits par photolyse-éclair et détectés par spectrométrie d'absorption de résonance. Les constantes de vitesse en unités de $cm^3\ mol^{-1}\ s^{-1}$ sont:

$k_{OH+n\text{-}C_4H_{10}} = 1.61 \pm 0.13 \times 10^{12}$ $\quad$ $k_{OH+neo\text{-}C_5H_{12}} = 5.48 \pm 0.59 \times 10^{11}$

$k_{OH+n\text{-}C_4D_{10}} = 4.20 \pm 0.41 \times 10^{11}$ $\quad$ $k_{OH+D_2} = 1.27 \pm 0.11 \times 10^{9}$

$k_{OD+n\text{-}C_4H_{10}} = 1.66 \pm 0.13 \times 10^{12}$ $\quad$ $k_{OD+H_2} = 3.70 \pm 0.25 \times 10^{9}$

$k_{OD+n\text{-}C_4D_{10}} = 4.84 \pm 0.38 \times 10^{11}$ $\quad$ $k_{OD+D_2} = 1.33 \pm 0.13 \times 10^{9}$

Les écarts correspondent au niveau de confiance de 95%. On observe un effet isotopique sur les constantes de vitesse lorsque le deutérium substitue l'hydrogène dans n-C_4H_{10} et H_2 mais le remplacement de OH par OD ne produit aucune variation significative de ces constantes.

Introduction

Hydroxyl radical reactions play an important role in combustion and atmospheric chemistry and therefore there is a need for accurate values of their kinetic parameters for use in numerical modeling of these processes. Hydrogen abstraction rate data for the reactions of OH and OD with paraffins and deuterated paraffins are also of fundamental interest to chemical kinetics in that they may provide insights into the reactivity of OH radicals and may enable eventual prediction of the rate constants of such reactions.

In the present paper, which is part of a program of kinetic studies of OH radical reactions, we report absolute rate constants at 297 K for the reactions of OH and OD with n-C_4H_{10}, n-C_4D_{10}, H_2 and D_2, and of OH with *neo*-C_5H_{12}, measured in the gas phase using the flash photolysis – resonance absorption technique. Rate constants from previous studies have been reported only for the reactions of OH with n-C_4H_{10} (1), *neo*-C_5H_{12} (1), and D_2 (2–4); there have been no measurements for the other reactions studied in this work.

Experimental

The apparatus and experimental technique have been described in detail before (5, 6) and will be mentioned here briefly. The apparatus consists of a fast flash photolysis system coupled to a spectrophotometric detection system. The OH and OD concentrations were monitored by following the time-resolved attenuation of the OH or OD resonance radiation (Q_1^3 rotational line at 308.15 nm for OH and Q_1^5 rotational line at 307.60 nm for OD, of the (0,0) band of the $A^2\Sigma^+ \rightarrow X^2\Pi$ transition) produced by a microwave discharge in a flowing low pressure Ar/H_2O or Ar/D_2O mixture. The radiation was detected with a photomultiplier (EMI 9783B) mounted on the exit slit of a 1 m Czerny-Turner monochromator (Jarrell-Ash). The signal was amplified, filtered, recorded in digital form and accumulated in a signal averager from which it was transferred to an on line PDP 11/10 minicomputer for further processing (5, 6). Signal averaging improved the signal-to-noise ratio and rates in the range (0.5–6) $\times 10^4\ s^{-1}$ were measured using 16 to 48 flashes.

The OD (0,0) band has been analyzed by Clyne *et al.* (7). The

[1]NRCC No. 18524.

[2]NRCC Research Associate 1976–1979. Present address: Lumonics Research Ltd., Kanata, Ont., Canada K2K 1Y3.

0008-4042/80/202146-04$01.00/0

©1980 National Research Council of Canada/Conseil national de recherches du Canada

Can. J. Chem. Downloaded from www.nrcresearchpress.com by 210.87.254.40 on 09/05/12
For personal use only.

Can. J. Chem. Downloaded from www.nrcresearchpress.com by 210.87.254.40 on 09/05/12
For personal use only.

emission spectrum of the OD (0,0) band from our resonance lamp is shown in Fig. 1. Experiments, in which different low partial pressures of D_2O in He were flashed at constant flash energy (150 J), showed the expected logarithmic dependence of the maximum OD absorption (which in the absence of another reactant corresponds to the initial OD absorption (5, 6)) on the pressure of D_2O for absorptions of up to 30%, indicating that Beer's law is obeyed in this range. Our rate measurements were made at initial absorptions in the range 4 to 15%.

Two sources of OH/OD radicals were used in this work. The flash photolysis of small pressures (0.3–0.6) Torr of H_2O or D_2O at the vacuum uv ($\lambda > 165$ nm) was used with H_2, D_2, and *neo*-C_5H_{12} which are transparent at this wavelength. For these conditions the initial OH/OD concentration estimated approximately from the initial absorption of the OH/OD resonance radiation (5, 6) was (4–8) $\times 10^{-11}$ mol cm^{-3}. With the butanes, however, which absorb very weakly at 165 nm (8) and may be photodissociated, we used the flash photolysis of N_2O/H_2 or N_2O/D_2 mixtures with light of wavelength $\lambda > 200$ nm as a source of OH/OD. (A filter 8 mm deep of O_2 at 600 Torr eliminated radiation below 200 nm.) This technique, in which $O(^1D)$ atoms from the photolysis of N_2O react rapidly with H_2 or D_2 to give OH or OD radicals, has been used before in this laboratory and is described in more detail in ref. 9. The OH/OD concentration was estimated (9) to be $\sim(1–2) \times 10^{-11}$ mol cm^{-3}, i.e. about 4 to 8 times lower than that from the photolysis of H_2O/D_2O. From the relative rates of the reactions of $O(^1D)$ with H_2 (10), D_2 (11), N_2O (12), and *n*-C_4H_{10} (13), and the concentrations used (see Table 1 below), we estimated that virtually all the $O(^1D)$ atoms will react with H_2 or D_2 and not with N_2O or the butanes.

The materials used were of the highest available purity (generally 99.95–99.999%) and with the exception of H_2, D_2, and He were thoroughly degassed before use. Mass spectrometric analysis of *n*-C_4D_{10} and D_2 confirmed the stated minimum D atom content of >98% and >99.5% respectively. The N_2O, Matheson 98%, was used after degassing and bulb-to-bulb distillation *in vacuo* in which only the middle fraction was retained.

Results and Discussion

Various aspects of the experimental conditions, procedure, and treatment of the data are given in refs. 5 and 6. The concentration of the other reactant [RH] was always much greater than the initial OH concentration so that the reaction was pseudo first order. The pseudo first order rate constant, k_I, was obtained from the linear plots of ln [OH] against time as described before (5, 6).

For the experiments in which OH was formed by photolysis of H_2O or D_2O, the values of k_I obtained over a range of [RH] concentrations are related to the second order rate constant, k_{II}, by the equation $k_I = \alpha + k_{II}[RH]$ (5, 6). Representative plots of k_I against [RH] for the reactions of OD with H_2 and D_2 are shown in Fig. 2. The second order rate constants, k_{II}, were obtained from the slopes of these plots by weighted least square fits, as described before (5, 6). The measured values of k_{II} for the reactions of OH with D_2 and *neo*-C_5H_{12} and of OD with H_2 and D_2 together with the experimental conditions are given in Table 1.

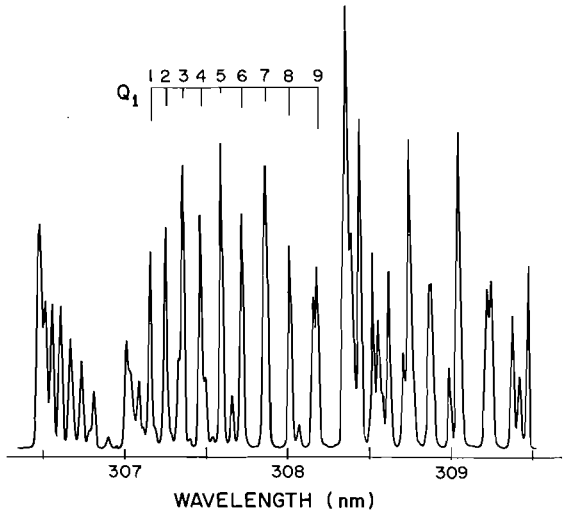


FIG. 1. Emission spectrum of OD (0,0) band of the $A^2\Sigma^+ \rightarrow X^2\Pi$ transition.

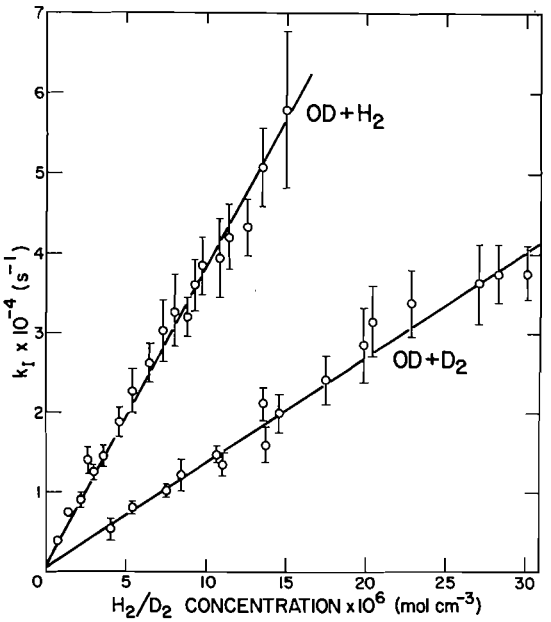


FIG. 2. Plot of the pseudo first order rate constant, k_I, against the concentration of H_2 and D_2 for the reactions of OD with H_2 and D_2.

For the experiments in which OH was produced by photolysis of N_2O/H_2, N_2O/D_2 mixtures, the values of k_I measured at constant $[H_2]$ concentration and over a range of [RH] concentrations are related to the second order rate constants k_{II} of H_2 and RH by the equation (9)

$$k_I = k_{II}^{(H_2)}[H_2] + k_{II}^{(RH)}[RH]$$

Can. J. Chem. Downloaded from www.nrcresearchpress.com by 210.87.254.40 on 09/05/12
For personal use only.

TABLE 1. Measured values of the second order rate constants, k_{II}, at 297 ± 2 K[a]

Reaction	k_{II}[b] (cm^3 mol^{-1} s^{-1})	Number of experiments
OH + *neo*-C_5H_{12}	$5.48 \pm 0.59 \times 10^{11}$	26
OH + D_2	$1.27 \pm 0.11 \times 10^9$	17
OD + H_2	$3.70 \pm 0.25 \times 10^9$	20
OD + D_2	$1.33 \pm 0.13 \times 10^9$	16
OH + *n*-C_4H_{10}	$1.61 \pm 0.13 \times 10^{12}$	14
OH + *n*-C_4D_{10}	$4.20 \pm 0.41 \times 10^{11}$	14
OD + *n*-C_4H_{10}	$1.66 \pm 0.13 \times 10^{12}$	11
OD + *n*-C_4D_{10}	$4.84 \pm 0.38 \times 10^{11}$	11

[a]The experimental conditions were as follows: flash photolysis of H_2O or D_2O; $H_2O/D_2O \approx$ (0.3–0.6) Torr, [OH] ≈ (4–8) × 10^{-11} mol cm^{-3}, (4–8) flashes of 150 J per mixture. Flash photolysis of N_2O/H_2 or N_2O/D_2; the ratios N_2O/H_2 and N_2O/D_2 were constant and equal to 0.1 (i.e., in mol cm^{-3} $[N_2O] = 2.7 \times 10^{-7}$, $[H_2] = 2.7 \times 10^{-6}$, and $[N_2O] = 5.4 \times 10^{-7}$, $D_2 = 5.4 \times 10^{-6}$) [OH] ≈ (1–2) × 10^{-11} mol cm^{-3}, 1 flash of 150 J per mixture.
[b]The indicated uncertainties are the 95% confidence limits calculated from the standard deviation and Students *t* distribution (14).

Plots of k_I against [RH] for the reactions of the butanes are shown in Fig. 3. The values of $k_{II}^{(RH)}$ (slope) and $k_{II}^{(H_2)}[H_2]$ (intercept) were obtained by weighted least square fits of the equation above to the data (9). The k_{II} values for the butanes and the experimental conditions are given in Table 1. The average values of the intercepts for the reactions of OH and OD are:

$$\text{Intercept}_{(OH)} = k_{II}^{(H_2)}[H_2] = 1.02 \pm 0.10 \times 10^4 \text{ s}^{-1}$$

$$\text{Intercept}_{(OD)} = k_{II}^{(D_2)}[D_2] = 0.756 \pm 0.080 \times 10^4 \text{ s}^{-1}$$

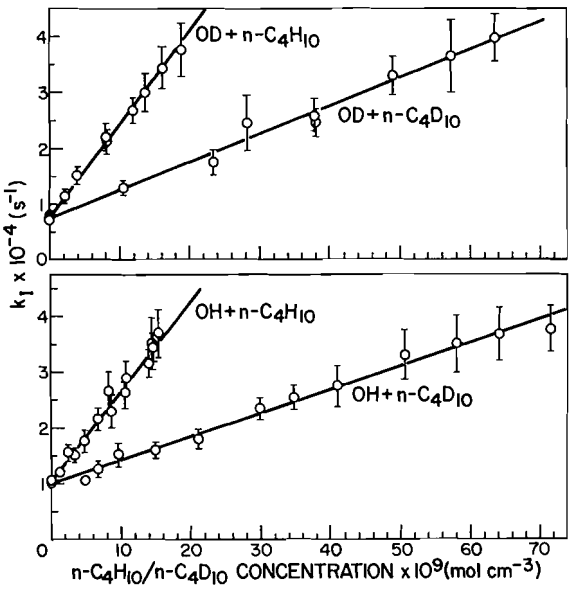


FIG. 3. Plots of the pseudo first order rate constant, k_I, against the concentration of the butanes for the reactions of OH and OD with *n*-C_4H_{10} and *n*-C_4D_{10}.

from which we calculate the second order rate constants for OH + H_2 and OH + D_2 to be in cm^3 mol^{-1} s^{-1}, $k_{II}^{(H_2)} = 3.78 \pm 0.37 \times 10^9$ and $k_{II}^{(D_2)} = 1.40 \pm 0.15 \times 10^9$ which agree well with our previous and present direct determinations of $3.5 \pm 0.16 \times 10^9$ (5) and $1.33 \pm 0.06 \times 10^9$ for OH + H_2 and OH + D_2 respectively; the uncertainties are 1 standard deviation.

In the experiments with H_2, D_2, and neopentane a variation of the OH/OD concentration by a factor of 5–10 effected by varying both the pressure of H_2O (0.2–2) Torr and the flash energy (30–350) J did not change the measured rates within the experimental error, indicating that there is no significant interference from secondary reactions of OH/OD radicals with the products of the primary reaction (5, 6). The same is true, of course, for the reactions of the butanes for which we used OH concentrations 4–8 times lower than with neopentane.

The total pressure was 50 Torr for the experiments with the butanes and 150 Torr (made up with He) with neopentane. It was demonstrated, by varying the total pressure, that the measured rate constants were independent of pressure.

Comparison of Rate Constant Values

As mentioned in the Introduction, rate constants have been reported only for the reactions of OH with *n*-C_4H_{10}, *neo*-C_5H_{12}, and D_2. All rate constants quoted below are in units of cm^3 mol^{-1} s^{-1}. For *n*-C_4H_{10} our value ($1.61 \pm 0.13 \times 10^{12}$) agrees very well with those measured by Greiner (15) ($1.55 \pm 0.10 \times 10^{12}$), Stuhl (16) ($1.42 \pm 0.21 \times 10^{12}$), and Perry *et al.* (17) ($1.64 \pm 0.16 \times 10^{12}$). It also agrees within the large error limits with the relative values determined by Gorse and Volman (18) and Campbell *et al.* (19); these, however, depend on the rate constant of the reference reaction OH + CO which has been found to be pressure dependent (20). On the other hand the value of Gordon and Mulac (21) ($2.54 \pm 0.10 \times 10^{12}$) and of Morris and Niki (22) (2.45×10^{12}) are significantly higher (~50%) than all the other determinations. In view of the good agreement among the majority of the data from very different experimental techniques and conditions, a value of $k_{n\text{-}C_4H_{10}} = 1.6 \pm 0.2 \times 10^{12}$ cm^3 mol^{-1} s^{-1} is recommended for use in photochemical air pollution models.

Our value for *neo*-C_5H_{12} ($5.48 \pm 0.59 \times 10^{11}$) lies between the absolute value of Greiner (15) ($4.97 \pm 0.28 \times 10^{11}$) and the relative value (reference reaction OH + *n*-butane) reported by Darnall *et al.* (23) ($6.26 \pm 1.02 \times 10^{11}$); it agrees well with both within the experimental uncertainty.

TABLE 2. Kinetic isotope effect; relative values k_H/k_D and k_{OH}/k_{OD} for the reactions of OH and OD with H_2, D_2, n-C_4H_{10}, and n-C_4D_{10}

Reaction	k_H/k_D
OH + H_2 (D_2)	2.75[a]
OD + H_2 (D_2)	2.78
OH + n-C_4H_{10} (n-C_4D_{10})	3.83
OD + n-C_4H_{10} (n-C_4D_{10})	3.43

Reaction	k_{OH}/k_{OD}
H_2 + OH (OD)	0.94[a]
D_2 + OH (OD)	0.95
n-C_4H_{10} + OH (OD)	0.97
n-C_4D_{10} + OH (OD)	0.87

[a]The value of $k_{OH+H_2} = 3.49 \pm 0.16 \times 10^9$ was taken from our earlier determination by the same technique (5).

Finally, there is excellent agreement among all the reported rate constants for OH + D_2, i.e., this work ($1.27 \pm 0.11 \times 10^9$), Greiner (2) ($1.27 \pm 0.16 \times 10^9$), Stuhl and Niki (3) ($1.24 \pm 0.18 \times 10^9$), and Smith and Zellner (4) ($1.32 \pm 0.24 \times 10^9$).

Kinetic Isotope Effect

Table 2 lists the ratios k_H/k_D and k_{OH}/k_{OD} at room temperature for the reactions studied. A kinetic isotope effect was observed when hydrogen was replaced by deuterium in the paraffin and H_2 whereas there was no significant effect when OH was replaced by OD. Similar isotope effects have been reported for hydrogen atom abstraction by OH and OD radicals from CH_4 and C_2H_6 (2) and by CH_3 and CD_3 radicals from H_2 and D_2 (24).

Acknowledgment

The authors wish to thank Dr. R. Overend who participated in the early measurements with neopentane.

1. R. ATKINSON, K. R. DARNALL, A. C. LLOYD, A. M. WINER, and J. N. PITTS, JR. Adv. Photochem. **11**, 375 (1979).
2. N. R. GREINER. J. Chem. Phys. **48**, 1413 (1968).
3. F. STUHL and H. NIKI. J. Chem. Phys. **57**, 3671 (1972).
4. I. W. M. SMITH and R. ZELLNER. J. Chem. Soc. Faraday Trans. II, **70**, 1045 (1974).
5. R. P. OVEREND, G. PARASKEVOPOULOS, and R. J. CVETANOVIĆ. Can. J. Chem. **53**, 3374 (1975).
6. R. OVEREND and G. PARASKEVOPOULOS. J. Phys. Chem. **82**, 1329 (1978).
7. M. A. A. CLYNE, J. A. COXON, and A. R. WOON FAT. J. Mol. Spectrosc. **46**, 146 (1973).
8. H. OKABE and D. A. BECKER. J. Chem. Phys. **39**, 2549 (1963).
9. W. S. NIP and G. PARASKEVOPOULOS. J. Chem. Phys. **71**, 2170 (1979).
10. G. PARASKEVOPOULOS and R. J. CVETANOVIĆ. J. Am. Chem. Soc. **91**, 7572 (1969).
11. R. F. HEIDNER III and D. HUSAIN. Int. J. Chem. Kinet. **5**, 819 (1973).
12. G. PARASKEVOPOULOS, V. B. SYMONDS, and R. J. CVETANOVIĆ. Can. J. Chem. **50**, 1838 (1972).
13. P. MICHAUD, G. PARASKEVOPOULOS, and R. J. CVETANOVIĆ. J. Phys. Chem. **78**, 1457 (1974).
14. R. J. CVETANOVIĆ, D. L. SINGLETON, and G. PARASKEVOPOULOS. J. Phys. Chem. **83**, 50 (1979).
15. N. R. GREINER. J. Chem. Phys. **53**, 1070 (1970).
16. F. STUHL. Z. Naturforsch. **28A**, 1383 (1973).
17. R. A. PERRY, R. ATKINSON, and J. N. PITTS, JR. J. Chem. Phys. **64**, 5314 (1976).
18. R. A. GORSE and D. H. VOLMAN. J. Photochem. **3**, 115 (1974).
19. I. M. CAMPBELL, B. J. HANDY, and R. M. KIRBY. J. Chem. Soc. Faraday Trans. I, **71**, 867 (1975).
20. R. OVEREND and G. PARASKEVOPOULOS. Chem. Phys. Lett. **49**, 109 (1977).
21. S. GORDON and W. A. MULAC. Int. J. Chem. Kinet. Symposium No. **1**, 289 (1975).
22. E. D. MORRIS, JR., and H. NIKI. J. Phys. Chem. **75**, 3640 (1971).
23. K. R. DARNALL, R. ATKINSON, and J. N. PITTS, JR. J. Phys. Chem. **82**, 1581 (1978).
24. T. G. MAJURY and E. W. R. STEACIE. Can. J. Chem. **30**, 800 (1952).

Can. J. Chem. Downloaded from www.nrcresearchpress.com by 210.87.254.40 on 09/05/12
For personal use only.

Potentiometric measurement of H^+ concentrations for aluminum orthophosphate titration curves

DONALD S. GAMBLE

Chemistry and Biology Research Institute, Agriculture Canada, Ottawa, Ont., Canada K1A 0C6

Received February 4, 1980

DONALD S. GAMBLE. Can. J. Chem. **58**, 2150 (1980).

A potentiometric titration method of measuring accurate H^+ concentrations is demonstrated for aluminum orthophosphate solutions. A calibration procedure has been used which permitted the glass electrode to be used as a concentration probe instead of as a quasi-activity probe. The random error "background noise" has been reduced by the use of Fortran computing for chemical calculations, data handling and sorting, and averaging by least squares polynomial fits. The distribution of experimental errors along the sample titration curve is indicated by estimates for its various regions.

DONALD S. GAMBLE. Can. J. Chem. **58**, 2150 (1980).

On démontre une méthode de titrage potentiométrique qui permet de mesurer avec précision les concentrations en ions H^+ des solutions d'orthophosphate d'aluminium. On a utilisé un procédé d'étalonnage qui permet d'employer une électrode de verre comme sonde de concentration et non comme sonde de quasi activité. On a réduit l'erreur fortuite due au bruit de fond en utilisant la méthode Fortran pour les calculs chimiques et la manipulation des données pour trouver les moyennes par la méthode des moindres carrés. La distribution des erreurs expérimentales le long de la courbe de titration de l'échantillon est indiquée par des évaluations faites pour ses différentes sections.

[Traduit par le journal]

Introduction

The reactions of orthophosphate with Al^{III} have been extensively investigated because of their importance to soil fertility and environmental quality (1–5). The existing literature is largely concerned with the preparation and properties of solid products, however, with very limited success having been reported for the investigations of solution species. A number of authors found evidence of solution complexes, but were unable to determine their chemical compositions or stability constants (6–12). In 1931 Bjerrum and Dahm were able to estimate the orders of magnitude for stability constants, only by postulating some solution complexes (6).

A fuller understanding of these reactions will require that solution or colloidal sol species, and solid products, be investigated together. The hydrogen ion is a key chemical reactant governing the composition of the solutions or colloidal sols, and the glass pH electrode is one of the few suitable probes available. Veith, for example, has used the inflection points in the pH titration curves of aluminum orthophosphate samples for determining the stoichiometric composition of precipitates (12). A rare and important precedent for the present Al^{III} orthophosphate investigations is the work of Childs (13). He applied glass electrode measurements of H^+ concentrations to the study of metal ion orthophosphate species in solution. Al^{III} was not included in his work, however.

It is now evident that in addition to titration equivalence points, investigations of solution species in systems such as the present one require accurate measurements of H^+ concentrations. A number of authors have pointed out or demonstrated this same requirement for various chemical problems (14–27). A concentration probe is evidently required. When used for conventional pH measurements, however, the glass electrode is instead a quasi-activity probe. This has been emphasized by the discussions of Irving *et al.* (17), McBryde (19, 28), Hedwig and Powell (23), and Bates (18). There are four fundamental reasons for this.

The first three of these are the systematic errors described in the literature. These include the activity coefficient and liquid junction potential effects, and as emphasized by Bates (18), the unknown relationship of standard buffer systems such as that of the U.S. National Bureau of Standards to Lewis and Randall standard states. Relatively high concentrations are usually used for the constant ionic strength method of minimizing or fixing the magnitudes of these systematic errors (18, 19, 23, 28, 29). Investigations of soil solutions and fresh surface waters require that a low ionic strength procedure also be developed.

The practical importance of the fourth type of error has been less widely recognized. Gamble has observed two categories of random errors in the H^+ concentration measurement of acid–base titration curves (22, 24, 25). These were the random scatter within a run, and the randomly occurring biases found in any collection of replicate runs. These errors can be appreciable, and Childs (20), for

0008-4042/80/202150-08$01.00/0

©1980 National Research Council of Canada/Conseil national de recherches du Canada

Can. J. Chem. Downloaded from www.nrcresearchpress.com by 210.87.254.5 on 09/05/12
For personal use only.

Can. J. Chem. Downloaded from www.nrcresearchpress.com by 210.87.254.5 on 09/05/12
For personal use only.

example, has reported an error in a calibration constant for his H^+ concentration measurements of ± 0.04 log unit. This translates to an error of $\pm 9.7\%$.

Any investigation of the solution or colloidal sol chemical species will require a sequence of chemical calculations. Since such calculations tend to magnify and accumulate the original errors of measurement, the four types of errors may seriously restrict the interpretation of calculated results. The objective of this work is therefore to develop and demonstrate a potentiometric titration method of measuring H^+ concentrations in aqueous Al^{III} orthophosphate systems. It is intended that such titration curves be used for future investigations of the solution or colloidal sol species in low ionic strength systems. The chemical calculations required for this purpose make it necessary that the above four types of errors be minimized.

Experimental Work

Equipment

1, Orion model 801 digital pH meter, with a Metrohm micro combination pH electrode, model EA 147; *2*, 5.000 mL microburett in a constant temperature room at 23.0 ± 1°C; *3*, 150 mL thermostatted titration beaker, fitted with a magnetic stirrer and N_2 flow fittings; *4*, constant temperature bath, at 25.000 ± 0.005°C; *5*, Perkin Elmer 124 UV–visible spectrophotometer and 1 cm quartz cells.

The combination electrode, pH meter, and connecting cables were shielded, grounded, and free from field effects (30).

Chemicals

Water was redistilled under N_2. The 0.1 *N* NaOH was Fisher Certified Sodium Hydroxide Solution, Lot 784814. The concentration specified by Fisher is 0.1000 within the outer limits of ±0.2%. A check against U.S. National Bureau of Standards Acid Potassium Phthalate Standard Sample 185d verified the concentration to within 0.1%. All other chemicals were of reagent grade.

Standard Stock Solutions

A calibration solution containing H_3PO_4 and NaCl, and an experimental stock solution containing $AlCl_3$ and H_3PO_4 were prepared gravimetrically from NaCl crystals and from analysed stock solutions. H_3PO_4 analysis was by titration end point, while Al^{III} analysis was done by the 8-hydroxyquinoline photometric method. J. T. Baker "Dilute-it" Aluminum Standard was used for the analysis. Aliquots (100 g) of these Standard Stock Solutions were used for calibration and sample titrations.

Instrument Calibration Titrations

An instrument calibration titration was run before each experimental sample titration. Each of the calibration titrations had 70 to 80 data points, with voltage readings being taken 1 min after the additions of standard base. The experimental conditions for calibration are given in Table 1. The volume increments of standard base listed there were arranged according to the shape of the calibration curve. The purpose of this was to optimize the density and distribution of data points along the curve. This is especially important at the first orthophosphate equivalence point, where the curve drops steeply between 0.185 and 0.070 V. Without careful planning there would be serious gaps in the calibration curve. A related procedure has been found in the literature. The limited use of acetic acid titrations for H^+ concentration calibrations was reported by Rajan and Martell in 1964 (26).

Experimental Sample Titration

Sample solutions initially contained 0.722×10^{-3} *m* total orthophosphate, 0.751×10^{-3} *m* total Al^{III}, and 2.253×10^{-3} *m* Cl^-. Aliquots (10.000 g) were titrated with the 0.1 *N* standard NaOH at 25.00°C. Voltage readings were taken 1 min after additions of standard base. A typical sample run had 56 V vs. mL data points. In contrast to the calibration titrations, the sample titrations had volume increments of titrant constant at 0.05 mL.

Data Processing and Calculations

The raw data consist of potentiometric titrations of orthophosphoric acid calibration solutions, and of experimental sample solutions. A typical experiment is shown in Fig. 1, with the calibration conditions being given in Table 1. Random error "background noise" was reduced by averaging a substantial amount of data from four replicate experiments. The production of an averaged sample titration curve in H^+ molalities from four or more experiments in this way requires a considerable amount of data processing and chemical calculations. These have been programmed in Fortran IV, and are done in five stages: *1*, the calculation of H^+ molalities for the orthophosphoric acid instrument calibration titrations; *2*, the sorting of the calibration data into a series of curves having decade ranges of H^+ molalities; *3*, the matching of experimental sample data to the Decade Range calibration curves; *4*, the production of H^+ molality vs. mL data points for sample titration curves; *5*, final averaging by the method of least squares, to produce an averaged sample titration curve.

Two Fortran programs were used for the present work, the first of which executed the first four stages. The first stage of the computing requires that the first two orthophosphoric acid dissociation equilibria be known as functions of total orthophate concentration, at the experimental temperature. Experimental data from the literature (31–36) have been recalculated to give the equilibrium concentration quotients on the molal scale, K_1 and K_2, as polynomials in C_p, total orthophosphate concentration. Although a separate investigation of K_1 and K_2 is in progress, the essential features of the calculations can be outlined here. The calculations were based on the original electrochemical measurements of Bates (31), Nims (32), and Lugg (33), with hydrogen and Ag–AgCl electrodes in cells without liquid junctions. The unsurpassed quality of these data makes them uniquely valuable for instrument calibration. Bates correctly pointed out at the time of publication that the lack of suitable

TABLE 1. H^+ molality vs. potential instrument calibration curves [a]

Approximate ranges			ΔV
Standard NaOH (mL)	E (V)	m_H	Increments of standard base (mL)
0.000 to 0.850	0.234 to 0.185	0.966×10^{-3} to 1.04×10^{-4}	0.050
0.850 to 1.05	0.185 to 0.070	1.04×10^{-3} to 1.99×10^{-6}	0.010
1.050 to 1.800	0.070 to −0.031	1.99×10^{-6} to 1.17×10^{-8}	0.020

[a] Experimental conditions for the potentiometric titration: temperature, 25.00°C; standard stock solution, 1.0×10^{-3} *m* H_3PO_4, 1.0×10^{-3} *m* NaCl; 100.0000 g aliquot; standard base, 0.1 *N* NaOH.

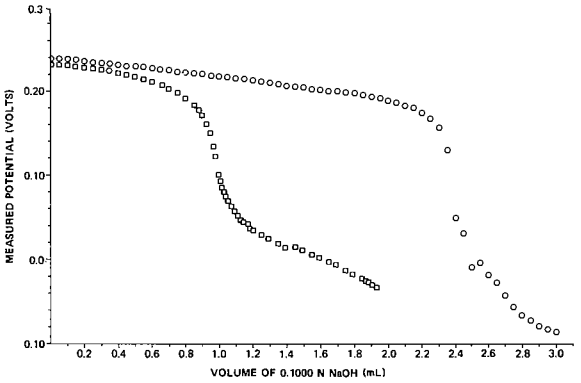


FIG. 1. The calibration and sample titration curves of a typical experiment. See Table 1 and the text for the experimental conditions. ⊡, calibration run. ⊙, experimental sample run.

activity coefficient data precluded the calculation of concentration quotients. Subsequent developments have since made such calculations feasible. First, McBryde (28) has suggested that Debye–Hückel calculations are a reasonable approximation for ionic strengths up to 0.1 *M*. Secondly, Elmore *et al.* (35) have concluded from their comparison of experimental methods that for constant ionic strengths up to almost 1 *m*, $\gamma_{\pm} = (\gamma_H\gamma_{Cl})^{1/2}$ has the same values in orthophosphate–chloride mixed solutions as in HCl solutions. It is proposed that these rather high concentration limits given by McBryde and by Elmore *et al.* are excellent justification for the use of the published HCl $\gamma_{\pm}$ values of Harned and Owen (36) in orthophosphate–chloride solutions of approximately 10^{-3} *m*. It has also been assumed that the experimental $\gamma_{\pm}$ values are preferable to the theoretical calculations. The resulting polynomials are used as input for the first Fortran program. The K_1 and K_2 polynomials have been prepared for use within the orthophosphate range $0 < C_p < 2 \times 10^{-3}$ *m*. The present work is confined to orthophosphate concentrations less than 1×10^{-3} *m*. The changes in the first and second H^+ dissociation equilibria are nonetheless significant. Over the range $0 < C_p < 1 \times 10^{-3}$ *m*, K_1 increases 6.9% with increasing C_p, while the increase for K_2 is 17.8%.

The calibration data are sorted into Decade Ranges of H^+ molality, for the purpose of optimizing the quality of the least squares fits. If too wide a range of values is fitted, then the manipulation of the normal equations results in the calculation of small differences between relatively larger numbers. This can give unreliable values for the H^+ molality vs. volts polynomial coefficients (37).

Stages 3 and 4 of the computing calculate H^+ molalities for experimental sample titrations, from experimental volts and the fitted Decade Range calibration curves. Each calibration curve is generally fitted to a set of polynomials up to the sixth degree.

The calibration polynomials having the best fits were chosen from the printout of the first Fortran IV program. Table 2 lists the computing results for the selection of Decade Range instrument calibration curves, and their use for the calculation of H^+ molalities in the sample titrations. The last column in Table 2 gives the numbers of sample titration data points used with each Decade Range calibration curve for the calculation of the sample H^+ molalities. These numbers resulted from the computerized matching of sample data to the calibration curves.

Stage 4 of the computing averages the calibration data, but leaves the experimental sample data unaveraged. This is done in the last stage, using the second Fortran IV program. The Stage 5 computing is summarized in Table 3. For this final averaging in Stage 5, the experimental sample titration curve was fitted in four sections. These sections were chosen as seen in Tables 3 and 4 according to the shape of the titration curve and the ranges of m_H values. The reason for doing this was again to achieve the best least squares fits to polynomials. These sections were made to overlap, and the fitted polynomials used were those that give the lowest standard deviations consistent with agreement of values at the overlaps. The results are listed in Tables 3 and 4. The overlap values have been averaged in Table 4.

The two Fortran programs, labelled TE17 and TE04, are available from the Depository of Unpub-

Can. J. Chem. Downloaded from www.nrcresearchpress.com by 210.87.254.5 on 09/05/12
For personal use only.

TABLE 2. Instrument calibration for H^+ molality determinations: decade range calibration curves at 25.00°C; results from four runs, averaged by Fortran IV Program TE17

Curve no.	H^+ molality range	Volts range	Polynomial degree	Number of calibration data points	Calibration titration error: ±σ molality	±% at mid range: σ	±% at mid range: Standard error	Number of sample data points
1	9.8×10^{-4} to 7.3×10^{-5}	0.237 to 0.181	3	72	4.68×10^{-5}	8.89	1.05	138
2	7.7×10^{-5} to 2.0×10^{-5}	0.186 to 0.160	4	36	7.03×10^{-6}	14.5	2.45	15
3	7.1×10^{-6} to 7.3×10^{-7}	0.161 to 0.073	6	36	6.31×10^{-7}	16.1	2.72	7
4	8.9×10^{-7} to 6.9×10^{-8}	0.097 to 0.003	4	89	4.76×10^{-8}	9.93	1.05	9
5	7.7×10^{-8} to 1.3×10^{-8}	0.017 to −0.028	3	86	1.24×10^{-8}	27.6	2.99	10
6	7.9×10^{-9} to 1.7×10^{-9}	−0.015 to −0.035	1	11	2.23×10^{-9}	46.5	14.7	8

TABLE 3. Experimental sample titration curve at 25.00°C; four runs averaged by least squares fits to polynomials, with Fortran Program TE04

Section of sample titration curve	H^+ molality range	0.1 *N* NaOH mL range	Polynomial degree	Number of sample data points	Sample titration error: ±σ molality	±% at mid range: σ	±% at mid range: Standard error
1	8.0×10^{-4} to 1.6×10^{-4}	0.300 to 1.800	4	121	1.79×10^{-5}	3.73	0.340
2	1.6×10^{-4} to 5.1×10^{-6}	1.800 to 2.300	5	39	8.06×10^{-6}	9.76	1.58
3	5.1×10^{-6} to 1.1×10^{-7}	2.300 to 2.500	4	18	2.54×10^{-7}	4.88	1.18
4	1.1×10^{-7} to 6.0×10^{-8}	2.500 to 2.750	1	22	1.74×10^{-7}	204.7	44.7

lished Data.[1] Descriptions of the programs are included. The orthophosphoric acid data required as input for TE17 are attached to it.

Results and Discussion

The Quality of the Titration Curve

The experimental objective has been achieved with the aluminum orthophosphate titration curve shown in Fig. 3. Table 4 lists it in digital form, for use in future calculations. The ionic strengths are relevant to soil solutions and fresh surface waters. The high ionic strength procedures found in the literature are not applicable to these cases, but instead are most properly used for such systems as blood and sea water.

Activity coefficient and liquid junction potential effects, which contribute systematic errors, have been minimized. Exact calculations of activity coefficient errors are not practical, because of the lack of the required data for these mixed solutions. Considering the compositions given in Table 1 and the text for calibration and sample solutions, however, it is inferred from the data of Harned and Owen (36) and Robinson and Stokes (38) that the activity coefficient errors should have an upper limit of about 1%. In comparison, Feldman has reported that H^+ concentrations estimated from conventional pH measurements may have errors of 10% to 25% (29). By using some measurements by Harned (39), Feldman has also given estimates of liquid junction potentials. From the application of his estimates to the present experimental work, it is concluded that the liquid junction potential errors

[1]Complete set of data is available, at a nominal charge, from the Depository of Unpublished Data, CISTI, National Research Council of Canada, Ottawa, Ont., Canada K1A 0S2.

Can. J. Chem. Downloaded from www.nrcresearchpress.com by 210.87.254.5 on 09/05/12
For personal use only.

in the titration curve are about 0.1% to 0.2%. Somewhat more important than these systematic errors are the random errors from the glass electrode measurements. Two typical sample titration runs in Fig. 2 illustrate the titration curve biases. In addition to the random scatter within a run, a set of replicate runs shows these biases also to be random. This random error "background noise" has been averaged out by the method of least squares. The details given in Tables 2 and 3 and Fig. 2 are quite consistent with earlier work done with a humic polyelectrolyte (22, 24, 25). The final result is the averaged titration curve given in Table 4. Its shape is shown in Fig. 3. The total errors in Table 4 have been estimated from the calibration and sample data of Tables 2 and 3.

It is evident from the error estimates in Table 4 that the part of the titration curve which may be used for detailed chemical calculations includes the region from 1×10^{-5} *m* down to 1×10^{-7} *m* H^+. This region of the curve is very important to natural systems such as soil solutions. The calibrations for this region reported in the earlier work were unsatisfactory (22, 24, 25). The orthophosphoric acid calibration has made a substantial improvement, with data gaps being avoided. The range of H^+ concentrations between 1×10^{-7} *m* and 1×10^{-8} *m* is also of great practical interest. Unfortunately, the errors of measurement become large here. The uses of the fourth section of the curve in Table 4 will be limited to preliminary and semiquantitative estimates of chemical properties. The reason for this indicated by the data of Tables 2 and 3 is poor electrode response in the potential region of 0.0 to −0.06 V. Although this disturbing result remains generally unrecognized, evidence of it has persisted in the literature for more than forty years (13, 16, 19, 23, 24, 28, 40, 41). For example, earlier titrations with fulvic acid had an average error of ±30%, in the region 1×10^{-5} to 1×10^{-9} *m* H^+ (24). Hedwig and Powell (23), Childs (20), and Tanford (40) have all reported unsatisfactory glass electrode measurements in this concentration range. As long

TABLE 4. Averaged $AlPO_4$ titration curve at 25.00°C: data for calculations[a,b]

Section of curve	No.	0.1 *N* NaOH (mL)	m_H	Standard error in m_H; % at mid range
1	1	0.3000	8.0147×10^{-4}	1.46
	2	0.3500	7.7365×10^{-4}	
	3	0.4000	7.4531×10^{-4}	
	4	0.4500	7.1662×10^{-4}	
	5	0.5000	6.8772×10^{-4}	
	6	0.5500	6.5876×10^{-4}	
	7	0.6000	6.2989×10^{-4}	
	8	0.6500	6.0122×10^{-4}	
	9	0.7000	5.7288×10^{-4}	
	10	0.7500	5.4496×10^{-4}	
	11	0.8000	5.1759×10^{-4}	
	12	0.8500	4.9084×10^{-4}	
	13	0.9000	4.6479×10^{-4}	
	14	0.9500	4.3953×10^{-4}	
	15	1.0000	4.1511×10^{-4}	
	16	1.0500	3.9158×10^{-4}	
	17	1.1000	3.6900×10^{-4}	
	18	1.1500	3.4740×10^{-4}	
	19	1.2000	3.2681×10^{-4}	
	20	1.2500	3.0725×10^{-4}	
	21	1.3000	2.8872×10^{-4}	
	22	1.3500	2.7122×10^{-4}	
	23	1.4000	2.5476×10^{-4}	
	24	1.4500	2.3930×10^{-4}	
	25	1.5000	2.2482×10^{-4}	
	26	1.5500	2.1129×10^{-4}	
	27	1.6000	1.9866×10^{-4}	
	28	1.6500	1.8688×10^{-4}	
	29	1.7000	1.7588×10^{-4}	
	30	1.7500	1.6559×10^{-4}	
	31	1.8000	1.5594×10^{-4}	
Overlap average		1.8000	1.5568×10^{-4}	
2	32	1.8000	1.5541×10^{-4}	3.87
	33	1.8500	1.4143×10^{-4}	
	34	1.9000	1.3018×10^{-4}	
	35	1.9500	1.1850×10^{-4}	
	36	2.0000	1.0494×10^{-4}	
	37	2.0500	8.9325×10^{-5}	
	38	2.1000	7.2270×10^{-5}	
	39	2.1500	5.4756×10^{-5}	
	40	2.2000	3.7672×10^{-5}	
	41	2.2500	2.1367×10^{-5}	
	42	2.3000	5.1945×10^{-6}	
Overlap average		2.3000	5.1137×10^{-6}	
3	43	2.3000	5.0328×10^{-6}	3.90
	44	2.3500	1.6522×10^{-6}	
	45	2.4000	4.3350×10^{-7}	
	46	2.4500	1.6357×10^{-7}	
	47	2.5000	8.0698×10^{-8}	
Overlap average		2.5000	1.09×10^{-7}	
4	48	2.5000	1.37×10^{-7}	47.3
	49	2.5500	1.22×10^{-7}	
	50	2.6000	1.06×10^{-7}	
	51	2.6500	9.11×10^{-8}	
	52	2.7000	7.58×10^{-8}	
	53	2.7500	6.04×10^{-8}	

[a]Numbers of significant figures are to be inferred from the standard errors. Data handling errors should be minimized by completing all computing and calculations before the final rounding off.

[b]See Table 2 and the deposited material for experimental and data processing details.

Can. J. Chem. Downloaded from www.nrcresearchpress.com by 210.87.254.5 on 09/05/12
For personal use only.

Can. J. Chem. Downloaded from www.nrcresearchpress.com by 210.87.254.5 on 09/05/12
For personal use only.

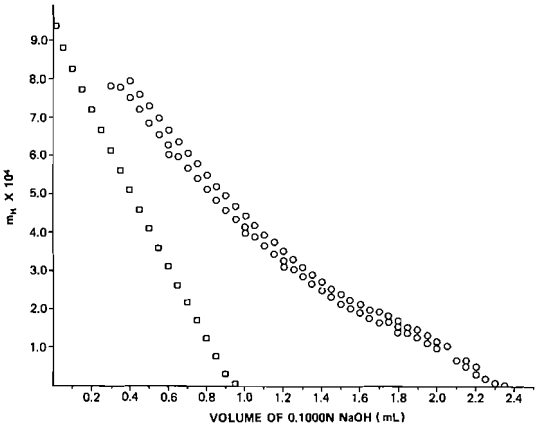


FIG. 2. Typical titration curves at 25.00°C, before final averaging. ⊙, sample runs. ⊡, instrument calibration run. See Table 1 for experimental conditions. The values $K_1 = 7.91 \times 10^{-3}$ and $K_2 = 7.47 \times 10^{-8}$ were generated and used by Fortran Program TE17. See the material in the Depository of Unpublished Data.

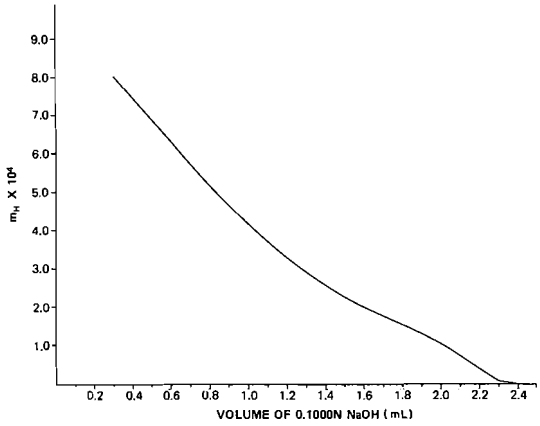


FIG. 3. $AlPO_4$ titration at 25.00°C. Final averaged curve. The values $K_1 = 7.91 \times 10^{-3}$ and $K_2 = 7.47 \times 10^{-3}$ were generated and used by Fortran Program TE17. See the material in the Depository of Unpublished Data.

ago as 1935, Ellis and Kiehl found the problem to be greatest in pure water of low conductivity (41). They postulated the generation and slow dissipation of electric charges.

Properties and Significance of the Titration Curve

The titration curve is intended for use in future work, for detailed chemical calculations and interpretation. This will require that the precipitation which gradually develops during the titration be characterized.

It is anticipated that some unknown number of chemical species will exist, including Al^{III}, orthophosphates, and aluminum orthophosphates. Their physical states might include true solution, colloidal sol, and the precipitate in physical suspension. Some sort of true or metastable equilibrium distribution of H^+ among these chemical species and physical states is also expected. It should be recognized that this phenomenon partly controls the solution phase concentrations of H^+, but does not interfere with its measurement by the electrode system. It is in fact seen as potentially the basis of a method for characterizing the system. Pending such future work, some important features of the titration curve may be examined immediately.

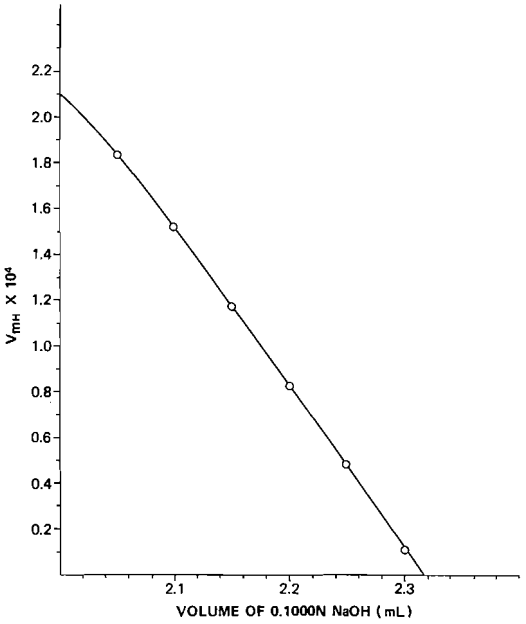


FIG. 4. Gran's plot for the averaged titration curve of Fig. 3. First equivalence point at 2.320 mL of 0.1 *N* standard NaOH.

The first feature to note is the sharp break in the curve, seen in Fig. 3 just beyond 2.3 mL. A very definitive Gran's plot was obtained for this break, indicating an equivalence point of 2.320 mL of 0.1 *N* standard base. This corresponds to 3.214 mol of H^+ per mole of total orthophosphate and 3.090 mol of H^+ per mole of total Al^{III} (= ±0.2%). Gran originally proposed his function in the form $V \times 10^{k - pH}$ (42). With the titration curve in terms of H^+ molalities, this reduces to the simpler form Vm_H. This is seen in Fig. 4.

The next feature of the curve is a low "bump" between 1.6 and 1.8 mL, in Fig. 3. Although this shape is quite subtle, two important observations concerning it may be made in Fig. 2. The first is that this curve shape is reproduced in each of the replicate runs. In addition, it does not reflect any structural feature of the calibration curves. It is therefore postulated that this effect is real. It may be

related to the onset of precipitation, since turbidity first appears in this part of the titration.

A third characteristic is noted between 2.3 and 2.5 mL. The low slope indicates relatively greater buffering, which may also be related to precipitation.

The Advantages and Limitations of the Experimental Method

Earlier versions of this potentiometric method have been used for fulvic acid, which is a purely organic polyelectrolyte. A more developed version has now been demonstrated for a totally inorganic system. This potentiometric titration procedure is therefore proposed as a quite general experimental method. It is possible that in future investigations of the acidic properties of samples, experimentalists might want to consider determining their own K_a concentration quotients for the calibrating weak acid. Two existing procedures for converting the glass electrode to a concentration probe are based on the use of known concentrations of strong acids, and could be employed in the evaluation of such reference K_a values. In one of these (22, 24, 25), computer calculations of sample K_a's are based directly on instrument calibrations with known HCl concentrations. In the other method (19, 28), standard buffers are checked against known concentrations of strong acids in a two-step calibration procedure. The alternative method presented here permits the required K_a's for the calibrating weak acid to be generated from computerized data. These data have been recalculated for this purpose from the hydrogen electrode measurements of Bates, Nims, and Lugg. Overall, this approach offers three distinct advantages, including the previously mentioned solutions to the high constant ionic strength and calibration curve gap problems. Thirdly, glass electrode measurements are unlikely to match the quality of the hydrogen electrode measurements, and thus the use of computer generated reference K_a values as described is recommended. Two important limitations in the present "state of the art" identified in this study should be emphasized. The first is the poor response region in glass electrode measurements. A reduction of this problem should be sought. The other limitation exists in the reduction of the random error "background noise". It might well be argued that four, or even six replicate experiments are insufficient for averaging out the random biases of titration curves. The practical restriction encountered in this problem is the cost of experimental time and labour. The solution to the problem must lie with the development of an improved system of instrumentation and data processing.

Acknowledgement

Mr. D. A. Gordon contributed to this work with experimental skill and great patience.

1. J. M. SADLER and J. W. B. STEWART. Residual fertilizer phosphorus in western Canadian soils: a review. Saskatchewan Institute of Pedology Publ. No. R136 (1974).
2. C. V. COLE, G. S. INNIS, and J. W. B. STEWART. Ecology, **58**, 1 (1977).
3. C. CHANG and S. J. RACZ. Can. J. Soil Sci. **57**, 271 (1977).
4. G. H. NEILSEN and A. F. MACKENZIE. Can. J. Soil. Sci. **57**, 465 (1977).
5. M. D. WEBBER. Soil Sci. **125**, 107 (1978).
6. N. BJERRUM and C. R. DAHM. Z. Phys. Chem. Bodenstein-Festband, 627 (1931).
7. H. L. BOHN and M. PEECH. Soil Sci. Soc. Am. Proc. **33**, 873 (1969).
8. P. H. HSU. Interactions between aluminum and phosphate in aqueous solution. Adv. Chem. Ser. Number 73. Trace inorganics in water. Am. Chem. Soc. 1968.
9. R. F. JAMESON and J. E. SALMON. J. Chem. Soc. 4013 (1954).
10. J. E. SALMON and J. G. L. WALL. J. Chem. Soc. 1128 (1958).
11. S. MATTSON. Soil Sci. **30**, 459 (1930).
12. J. A. VEITH. Z. Pflanzenernaehr. Bodenkd. **140**, 91 (1977).
13. C. W. CHILDS. Inorg. Chem. **9**, 2465 (1970).
14. J. A. VEITH. Z. Pflanzenernaehr. Bodenkd. **141**, 29 (1978).
15. J. A. VEITH and G. SPOSITO. Soil Sci. Am. J. **41**, 870 (1977).
16. H. J. K. POWELL and N. F. CURTIS. J. Chem. Soc. B, 1205 (1966).
17. H. M. IRVING, M. G. MILES, and L. D. PETTIT. Anal. Chim. Acta, **38**, 475 (1967).
18. R. G. BATES. Determination of pH. Theory and practice. 2nd ed. John Wiley and Sons. 1973.
19. W. A. E. MCBRYDE. Analyst, **96**, 739 (1971).
20. C. W. CHILDS. J. Phys. Chem. **73**, 2956 (1969).
21. C. W. CHILDS and D. D. PERRIN. J. Chem. Soc. A, 1039 (1969).
22. D. S. GAMBLE. Can. J. Chem. **48**, 2662 (1970).
23. G. R. HEDWIG and H. K. POWELL. Anal. Chem. **43**, 1206 (1971).
24. D. S. GAMBLE. Can J. Chem. **50**, 2680 (1972).
25. R. D. BURCH, C. H. LANGFORD, and D. S. GAMBLE. Can. J. Chem. **56**, 1196 (1978).
26. K. S. RAJAN and A. E. MARTELL. Inorg. Nucl. Chem. **26**, 789 (1964).
27. R. GUEVREMONT and D. L. RABENSTEIN. Can. J. Chem. **55**, 4211 (1977).
28. W. A. E. MCBRYDE. Analyst, **94**, 337 (1969).
29. I. FELDMAN. Anal. Chem. **28**, 1859 (1956).
30. W. H. BECK, A. E. BOTTOM, and A. K. COVINGTON. Anal. Chem. **40**, 501 (1968).
31. R. G. BATES. J. Res. Natl. Bur. Stand. **47**, 127 (1951).
32. L. F. NIMS. J. Am. Chem. Soc. **56**, 1110 (1934).
33. J. W. H. LUGG. J. Am. Chem. Soc. **53**, 1 (1931).
34. R. G. BATES and S. F. ACREE. J. Res. Natl. Bur. Stand. **30**, 129 (1943).
35. K. L. ELMORE, J. D. HATFIELD, R. L. DUNN, and A. D. JONES. J. Phys. Chem. **69**, 3520 (1965).
36. H. S. HARNED and B. B. OWEN. The physical chemistry of electrolyte solutions. 3rd ed. Am. Chem. Soc. Monograph Series. Reinhold Publishing Corporation, New York. 1958.
37. D. D. MCCRACKEN and W. S. DORN. Numerical methods and Fortran programming; with applications in engineering and science. John Wiley, New York. 1964.

Can. J. Chem. Downloaded from www.nrcresearchpress.com by 210.87.254.5 on 09/05/12
For personal use only.

38. R. A. ROBINSON and R. H. STOKES. Electrolyte solutions. 2nd ed. Butterworths, London. 1959.
39. H. S. HARNED. J. Phys. Chem. **30**, 433 (1926).
40. C. TANFORD. J. Am. Chem. Soc. **72**, 441 (1950).
41. S. B. ELLIS and S. J. KIEHL. J. Am. Chem. Soc. **57**, 2139 (1935).
42. G. GRAN. Analyst, **77**, 661 (1952).

Appendix

Iterative Calculation Procedure for m_H

In the Fortran Program TE17, H^+ molality is estimated from the material balance relations for total phosphate and for total titratable acid in the appropriate region of the titration curve, and with K_1, K_2, and K_3 evaluated as described above. The molalities of H_3PO_4, $H_2PO_4^-$, HPO_4^{2-}, and PO_4^{3-} and final values of H^+ molality are iteratively calculated together from the material balance relation for total orthophosphate and the equations for K_1, K_2, K_3, and K_w. The concentrations of H_3PO_4 and PO_4^{3-} are of course frequently expected to become unimportant.

Can. J. Chem. Downloaded from www.nrcresearchpress.com by 210.87.254.5 on 09/05/12
For personal use only.

Pyrones. VI.[1] The total synthesis of phacidin

GERALD ARTHUR POULTON[2] AND TERRY DONALD CYR
Department of Chemistry, University of Victoria, Victoria, B.C., Canada V8W 2Y2

Received April 14, 1980

GERALD ARTHUR POULTON and TERRY DONALD CYR. Can. J. Chem. **58**, 2158 (1980).

Phacidin (4-methoxy-6-nonanoyl-2*H*-pyran-2-one-3-carboxaldehyde) is synthesized from triacetic acid lactone in four steps.

GERALD ARTHUR POULTON et TERRY DONALD CYR. Can. J. Chem. **58**, 2158 (1980).

On a synthétisé la phacidine (méthoxy-4 nonanoyl-6 2*H*-pyrannone-2 carboxaldéhyde-3) en 4 étapes à partir de la lactone de l'acide triacétique.

[Traduit par le journal]

Phacidin, **1**, a metabolic product of the canker fungus *Potebniamyces balsamicola* var. *boycei* Funk, has been shown to be a methoxypyrone derivative (1) possessing potentially useful antifungal activity (2). The synthesis of phacidin was required in order to verify the assignment of structure and to provide an alternate source of the compound. Herein we report an unambiguous synthesis of phacidin from 4-hydroxy-6-methyl-2*H*-pyran-2-one (triacetic acid lactone, **2**) in an overall yield of 13%.

Experimental

Nuclear magnetic resonance data were obtained on a Perkin Elmer R12B (60 MHz) or R32 (90 MHz) instrument (proton) or Nicolet TT-14 (15.1 MHz) instrument (carbon) in $CDCl_3$ solution and are referenced to internal TMS. Mass spectra (70 eV) were obtained using the Hitachi-Perkin Elmer RMU-7E, ultraviolet spectra in 95% EtOH on the Beckman SP800, and infrared spectra on the Perkin Elmer 283 instruments. All mp are uncorrected.

*4-Hydroxy-6-nonyl-2*H*-pyran-2-one (**3**)*

To triacetic acid lactone (3), (**2**, 6 g, 47.6 mmol) dissolved in dry THF (100 mL) and HMPT (20 mL) at −78°C under a nitrogen atmosphere was added *n*-butyllithium (62 mL of 1.7 *M* solution in hexane, 105 mmol). The mixture was allowed to warm to 0°C, stirred for 2 h, and then 1-bromooctane (9.66 g, 50 mmol) was added. The solution was stirred for 14 h at −5°C, then treated with ice-water (100 mL) and the hexane layer separated. The aqueous layer was extracted with pentane (3 × 50 mL), then acidified with dilute HCl (5%) to pH 6. The resulting solution was extracted with ether (3 × 10 mL), the ether extracts washed with water followed by saturated NaCl solution, and then dried (Na_2SO_4). Chromatography of the crude material obtained from these extracts on Florisil using ethyl acetate/pentane (1:1) gave 4-hydroxy-6-nonyl-2*H*-pyran-2-one, 3.9 g (34%), mp 78–79°C (hexane); ν_{max} (KBr); 1704, 1665, 1634 cm^{-1}; λ_{max} (95% EtOH): 282 (log ε = 3.85), 238 (3.86), and 203 nm (4.32); ^1H nmr ($CDCl_3$) δ: 11.1 (bs, 1H, OH), 6.02 (bd, J = 4.5 Hz, 1H, H-5), 5.60 (d, J = 4 Hz, 1H, H-3), 2.48 (t, J = 7 Hz, 2H, $ArCH_2$), 1.8–1.0 (m, 14H, $(CH_2)_7$), and 0.88 (t, J = 7.5 Hz, 3H, nonyl-CH_3); ^{13}C nmr ($CDCl_3$) δ: 172.9 (s, C-4), 168.6 (d, J = 2.0 Hz, C-2), 167.3 (m, C-6), 101.4 (dd, J = 174.7, 2.5 Hz, C-5), 89.8 (d, J = 170.5 Hz, C-3), 33.7 (C-7), 31.9 (C-13), 29.3 and 29.0 (C-9–C-12), 26.7 (C-8), 22.7 (C-14), and 14.1 (C-15); ms *m/e* (relative intensity): 239 (6.5), 238 (21, M^+), 178 (30), 163 (25), 140 (18), 139 (98), 137 (20), 136 (39), 127 (15), 126 (31), 112 (16), 111 (87), 110 (15), 98 (46), 97 (31), 95 (21), 85 (31), 84 (69), 83 (21), 82 (38), 81 (20), 71 (25), 69 (53), 57 (31), 55 (39), 45 (30), 44 (10), 43 (100), and 41 (36). *Anal.* calcd. for $C_{14}H_{22}O_3$: C 70.55, H 9.30; found: C 70.43, H 9.25%.

*4-Methoxy-6-nonyl-2*H*-pyran-2-one (**4**)*

To 4-hydroxy-6-nonyl-2*H*-pyran-2-one (100 mg, 0.42 mmol) and anhydrous K_2CO_3 (380 mg, 2.75 mmol) in 2-butanone (20 mL) was added dimethyl sulfate (64 mg, 0.50 mmol). The mixture was heated to reflux under a dry nitrogen atmosphere for 3 h, additional dimethyl sulfate (64 mg, 0.50 mmol) added, and the heating continued for an additional 20 h. After cooling, the reaction mixture was filtered and evaporated *in vacuo*. Chromatography on silica gel with ethyl acetate/pentane (1:3) yielded 4-methoxy-6-nonyl-2*H*-pyran-2-one (**4**), 91 mg (86%), mp 58–59°C (pentane); ν_{max} (KBr): 1736, 1648, 1565 cm^{-1}; λ_{max} (95% EtOH): 279 nm (log ε = 3.99); ^1H nmr δ: 5.86 (d, J = 2.5 Hz, 1H, H-5), 5.48 (d, J = 2.5 Hz, 1H, H-3), 3.87 (s, 3H, OCH_3), 2.49 (t, J = 8 Hz, 2H, CH_2Ar), 2.0–1.1 (m, 14H, $(CH_2)_7$), and 0.90 (bt, 3H, nonyl-CH_3); ^{13}C nmr δ: 171.3 (m, J = 1.9, 2.9 Hz, C-4), 165.8 (dt, J = 5.7, 2.1 Hz, C-6), 165.0 (s, C-2), 99.6 (dt, J = 171.0, 3.8 Hz, C-5), 87.5 (dd, J = 168.8, 2.9 Hz, C-3), 55.9 (OCH_3), 33.7 (C-7), 31.9 (C-13), 29.3 and 29.0 (C-9–C-12), 26.7 (C-8), 22.7 (C-14), and 14.1 (C-15); ms *m/e* (relative intensity): 253 (5), 252 (26, M^+), 223 (3), 152 (62), 140 (74), 125 (100), 112 (16), 111 (11), 98 (32), and 69 (29). *Anal.* calcd. for $C_{15}H_{24}O_3$: C 71.39, H 9.59; found: C 71.47, H 9.52%.

*4-Methoxy-6-nonyl-2*H*-pyran-2-one-3-carboxaldehyde (**5**)*

To 4-methoxy-6-nonyl-2*H*-pyran-2-one (500 mg, 2.0 mmol) in 1,1-dichloromethyl methyl ether (5 mL) at −5°C under a dry nitrogen atmosphere was added dropwise titanium tetrachloride (2.2 mL, 20 mmol); the evolved HCl was removed by the continuous nitrogen flow, while stirring was continued for 14 h, and the temperature allowed to reach 15°C. Ice and diethyl ether were added, cautiously. The ether layer was washed with water (2 × 25 mL), saturated aqueous sodium chloride (25 mL), dried (Na_2SO_4), evaporated, and the product recrystallized from cyclohexane: 4-methoxy-6-nonyl-2*H*-pyran-2-one-3-carboxaldehyde, (**5**), 487 mg (87%), mp 66–70°C; ν_{max} (KBr): 1750, 1727, 1654, 1629 cm^{-1}; λ_{max} (95% EtOH): 322 (log ε = 3.08), 247 (2.76), and 227 nm (3.17); ^1H nmr ($CDCl_3$) δ: 10.11 (s, 1H, CHO), 6.12 (s, 1H, H-5), 4.02 (s, 3H, OCH_3), 2.56 (t, J = 6 Hz, 2H, CH_2Ar), 1.95–1.1 (m, 14H, $(CH_2)_7$), and 0.88 (bt, 3H, nonyl-CH_3); ^{13}C nmr ($CDCl_3$) δ: 186.5 (d, J = 182.4 Hz, CHO),

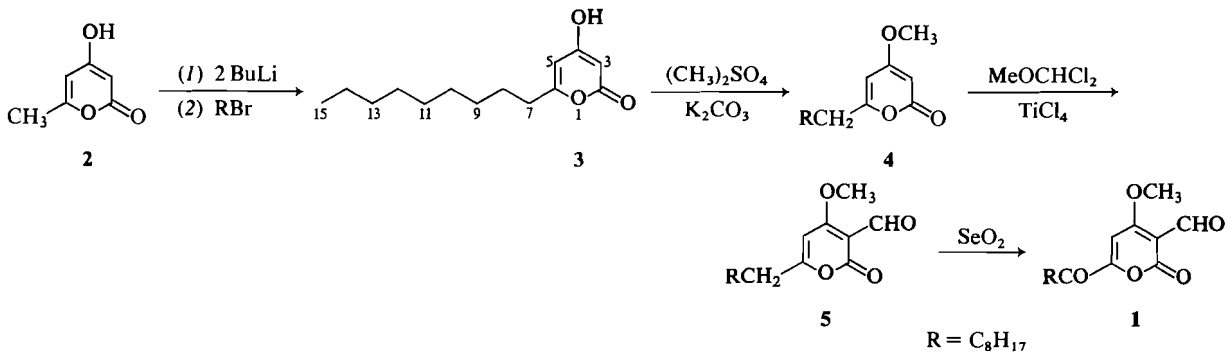
[1]Part V in this series: D. L. McGillivray and G. A. Poulton, Org. Mass Spectrom. **15**, 31 (1980).

[2]Author to whom correspondence should be addressed.

0008-4042/80/202158-03$01.00/0

©1980 National Research Council of Canada/Conseil national de recherches du Canada

Can. J. Chem. Downloaded from www.nrcresearchpress.com by 210.87.254.5 on 09/05/12
For personal use only.



174.6 (dd, J = 2.9, 2.9 Hz, C-4), 174.4 (dt, J = 4.7, 2.6 Hz, C-6), 162.2 (d, J = 3.3 Hz, C-2), 102.1 (dd, J = 23.9, 4.2 Hz, C-3), 94.3 (dt, J = 170.4, 3.5 Hz, C-5), 57.7 (OCH_3), 35.3 (C-7), 31.9 (C-13), 29.4, 29.2 and 29.0 (C-9–C-12), 26.8 (C-8), 22.6 (C-14), and 14.0 (C-15); ms *m/e* (relative intensity): 281 (26), 280 (47, M^+), 253 (18), 252 (100), 251 (78), 224 (18), 223 (100), 181 (28), 177 (35), 167 (44), 163 (20), 154 (20), 153 (92), 140 (48), 125 (23), 123 (54), 110 (27), 95 (20), 69 (29), 57 (19), 56 (27), and 55 (31). *Anal.* calcd. for $C_{16}H_{24}O_4$: C 68.55, H 8.69; found: C 68.62, H 8.71%.

*4-Methoxy-6-nonanoyl-2*H*-pyran-2-one-3-carboxaldehyde (1)*

4-Methoxy-6-nonyl-2*H*-pyran-2-one-3-carboxaldehyde (30 mg, 0.12 mmol) and freshly sublimed selenium dioxide (110 mg, 1.0 mmol) in *m*-xylene (2 mL) were heated to reflux with vigorous stirring under dry nitrogen for 30 min. The mixture was then cooled, evaporated *in vacuo*, added to ether (40 mL), filtered, and the organic layer washed with water (2 × 25 mL), saturated aqueous sodium chloride (25 mL), and dried (Na_2SO_4). The reaction mixture contained unreacted starting material (18 mg) and the desired product (**1**) which was isolated by preparative tlc: 4-methoxy-6-nonanoyl-2*H*-pyran-2-one-3-carboxaldehyde, 6.5 mg (53%, based on reacted starting material), mp 111–114°C (cyclohexane) (lit. (1) mp 112–113°C); ν_{max} (KBr): 1729, 1701, 1688 and 1617 cm^{-1}; λ_{max} (95% EtOH): 342 ($\log \varepsilon$ = 3.97), 272 (3.28), and 223 nm (4.13); ^1H nmr ($CDCl_3$) δ: 10.22 (s, 1H, CHO), 7.08 (s, 1H, H-5), 4.13 (s, 3H, OCH_3), 2.94 (t, J = 7 Hz, 2H, CH_2CO), 1.9–1.1 (m, 12H, $(CH_2)_6$), and 0.88 (t, J = 6 Hz, 3H, nonanoyl-CH_3); ms *m/e* (relative intensity): 294 (3.5, M^+), 266 (3), 265 (0.5), 238 (1), 154 (12), 153 (100), 141 (6), 125 (12), 123 (4), 71 (11), 69 (15), 57 (17), 55 (16), 43 (16), and 41 (15).

Results and Discussion

Addition of two moles of *n*-butyllithium to triacetic acid lactone **2** (4) results in the rapid formation of the dilithio dianion (5, 6) as a white precipitate which dissolved almost immediately upon addition of 1-bromooctane, leading to smooth monoalkylation at the 7 position. Alkylation of the ring at C-5 which has been observed (5) as a competing process (e.g. when $NaNH_2/NH_3$ was used) does not appear to be occurring under the conditions used here. This product, 4-hydroxy-6-nonyl-2*H*-pyran-2-one (**3**), was then *O*-alkylated using conditions which have been shown (7) to produce only 4-methoxy-2*H*-pyran-2-ones. Diazomethane or other nonbasic methylation systems, which can result in the formation of mixtures containing the isomeric 2-methoxy-4*H*-pyran-4-ones, were not used in order to avoid ambiguities in the synthesis. The product of *O*-methylation of **3** with dimethyl sulfate was assigned the structure 4-methoxy-6-nonyl-2*H*-pyran-2-one (**4**) by analogy with the literature findings (7) and on the basis of a detailed spectral analysis. The carbonyl stretching frequencies found for isomeric pairs of 4-methoxy-2-pyrones and 2-methoxy-4-pyrones have been reported (5) to be diagnostic, although experience has shown that care must be taken in making an assignment of structure when both isomers are not available for direct comparison (8). The CO absorption in 2-pyrones is generally in the 1740–1720 cm^{-1} range, and between 1680 and 1650 cm^{-1} in 4-pyrones; our methylated product had an absorption band at 1736 cm^{-1}, agreeing best with the 2-pyrone assignment. Similar arguments can be presented using the uv data (4-methoxy-6-methyl-2*H*-pyran-2-one, 280 nm; 2-methoxy-6-methyl-4*H*-pyran-4-one, 240 nm (8); compound **4**, 279 nm).

The assignment of a 2-pyrone structure to **4** was further confirmed by the subsequent transformation; 2-pyrones are known (9) to undergo electrophilic substitution with ease at C-3, while 4-pyrones are inert (see for example ref. 10) to most similar processes. One-step electrophilic formylation with dichloromethyl methyl ether (11) gave an excellent yield of the aldehyde **5**; introduction of the aldehyde group at C-3 rather than C-5 follows the normal behaviour of 2-pyrones (9) and can be supported by the following nmr data. Using the known compounds 4-methoxy-6-methyl-2*H*-pyran-2-one (nmr signals at 5.44, H-3, and 5.84 ppm, H-5 (12)) and 3-acetyl-4-methoxy-6-methyl-2*H*-pyran-2-one (nmr signal at 6.11 ppm, H-5 (13)) as models, the assignment of ring proton resonances in 4-methoxy-6-nonyl-2*H*-pyran-2-one (**4**) is made as 5.48 (H-3) and 5.86 (H-5), and in the

Can. J. Chem. Downloaded from www.nrcresearchpress.com by 210.87.254.5 on 09/05/12
For personal use only.

aldehyde **5** as 6.12 (H-5). The parallel is clear, indicating the C-3 has been substituted.

Assignments of structures **4** and **5** are also supported by interpretation of the ^{13}C nmr data.

Oxidation of pyrone methyl groups is known to be practicable (14) as a result of the pseudoaromatic nature of the ring. Thus, treatment of the nonylpyrone **5** with freshly sublimed selenium dioxide in refluxing *m*-xylene gave a modest yield of the nonanoyl compound **1**. The spectral properties of this synthetic material were identical with those of the natural product, thus confirming the structure of phacidin to be 4-methoxy-6-nonanoyl-2*H*-pyran-2-one-3-carboxaldehyde.

Acknowledgement

The authors gratefully acknowledge the provision of research funds and the award of the Lewis J. Clark Fellowship (to T.D.C.) by the University of Victoria.

1. G. A. POULTON, T. D. CYR, and E. E. MCMULLAN. Can. J. Chem. **57**, 1451 (1979).
2. A. S. SEKHON and A. FUNK. J. Antimicrobial Chemother. **3**, 95 (1977).
3. N. C. BROWN and G. S. PALL. S. A. Patent No. 67 00 6159; Chem. Abstr. **70**, 87585m (1969).
4. M. A. BUTT and J. A. ELVIDGE. J. Chem. Soc. 4483 (1963).
5. M. P. WACHTER and T. M. HARRIS. Tetrahedron, **26**, 1685 (1970).
6. E. M. KAISER, J. D. PETTY, and P. L. A. KNUTSON. Synthesis, 509 (1977).
7. J. D. BU'LOCK and H. G. SMITH. J. Chem. Soc. 502 (1960).
8. D. HERBST, W. B. MORS, O. R. GOTTLIEB, and C. DJERASSI. J. Am. Chem. Soc. **81**, 2427 (1959).
9. N. P. SHUSHERINA, N. D. DMITRIEVA, E. A. LUK'YANETS, and R. YA. LEVINA. Russ. Chem. Rev. **36**, 175 (1967).
10. M. GHOSAL and D. N. CHAUDHURY. J. Org. Chem. **28**, 583 (1963).
11. A. RIECHE, H. GROSS, and E. HÖFT. Organic Syntheses Coll. Vol. V. John Wiley & Sons, Inc., New York, NY. 1973. p. 49.
12. P. BEAK and H. ABELSON. J. Org. Chem. **27**, 3715 (1962).
13. T. D. CYR and G. A. POULTON. Can. J. Chem. **56**, 1796 (1978).
14. E. SUZUKI, R. HAMAJIMA, and S. INOUE. Synthesis, 192 (1975).

Can. J. Chem. Downloaded from www.nrcresearchpress.com by 210.87.254.5 on 09/05/12
For personal use only.

Studies of silyl and germyl Group VI species. Part IV. Dimethyl- and tetramethyl-disilyl chalcogenides and related species

JOHN E. DRAKE, BORIS M. GLAVINČEVSKI,[1] AND RAYMOND T. HEMMINGS[2]

Department of Chemistry, University of Windsor, Windsor, Ont., Canada N9B 3P4

Received November 21, 1979

JOHN E. DRAKE, BORIS M. GLAVINČEVSKI, and RAYMOND T. HEMMINGS. Can. J. Chem. **58**, 2161 (1980).

The symmetrically substituted disilyl chalcogenides $(Me_nH_{3-n}Si)_2E$ where E = O, S, Se, Te; $n = 0 \rightarrow 3$, have been prepared and characterized spectroscopically and by cleavage reactions. The synthetic routes include reactions of halogenosilanes with water, mercury(II) sulfide, lithium telluride, and complex thio- and seleno-aluminates. The spectroscopic properties of the $(MeH_2Si)_2E$ and $(Me_2HSi)_2E$ species, which have not been reported previously, are discussed in some detail.

JOHN E. DRAKE, BORIS M. GLAVINČEVSKI et RAYMOND T. HEMMINGS. Can. J. Chem. **58**, 2161 (1980).

On a préparé des chalcogénides disilylés $(Me_nH_{3-n}Si)_2E$ ou E = O, S, Se, Te; $n = 0 \rightarrow 3$ symétriquement substitués et on les a caractérisé par spectroscopie et par des réactions de clivage. Les différentes synthèses font intervenir les réactions des halogénosilanes avec l'eau, le sulfure mercurique, le tellurure de lithium et les complexes de thio et de sélénoaluminates. On discute en détail des propriétés spectroscopiques des composés $(MeH_2Si)_2E$ et $(Me_2HSi)_2E$ nouveaux.

[Traduit par le journal]

Introduction

The parent disilyl chalcogenides $(H_3Si)_2E$ (1–4) and $(Me_3Si)_2E$ (5–8) where E = O, S, Se, Te, have been known for some time. As a continuation of our investigations on silyl and germyl Group VI species (9, 10) we report herein the preparation of the disilyl chalcogenides $(Me_nH_{3-n}Si)_2E$, where E = O, S, Se, Te; $n = 0 \rightarrow 3$. Comparisons are made of reactions of halogenosilanes with water, mercury(II) sulfide, lithium telluride, and complex thio- or seleno-aluminates. The chalcogenides are characterized by their ^1H nmr, infrared, Raman, and mass spectral parameters and analysed by their cleavage reactions with anhydrous hydrogen halides, chalcogenides, and methoxytributylstannane.

Experimental

All manipulations were carried out on a conventional vacuum line equipped with greaseless stopcocks. Halogeno-silanes (11) and -germanes were either commercially obtained or prepared by literature methods. Lithium telluride, Li_2Te, was prepared from the elements in liquid NH_3(9). Complex thio- and seleno-aluminates were prepared from $LiAlH_4$ (12) and hydrogen sulfide and hydrogen selenide were obtained via the hydrolysis of the respective aluminum chalcogenides (13). Other materials were of commercial origin.

Infrared spectra were recorded on a Beckman IR12 spectrometer with expansion facilities, using a 90 mm gas cell fitted with KBr windows. The low volatile species were recorded as smears between CsI plates in an air-tight device. The Raman spectra were recorded on a Spectra Physics 700 spectrometer using the argon ion laser exciting line at 488.0 nm with the liquids held in sealed capillaries (ca. 2 mm id). Slitwidths used were 8 cm^{-1} (routine scans), 4 cm^{-1}; and 2 cm^{-1}. Strong bands were estimated to ± 1 cm^{-1} and weaker bands to ± 4 cm^{-1}. The same capillaries were used for the ^1H nmr spectra, recorded on a JEOL C60-HL instrument. Mass spectra were recorded at 70 eV on a Varian GMAT CH5 spectrometer fitted with a greaseless vacuum inlet system.

Reactions of Halogenosilanes with Water

In a typical experiment, MeH_2SiI (0.70 g, 4.07 mmol) was condensed under vacuum conditions, into a reaction vessel (ca. 40 mL) containing degassed distilled water (ca. 8 mL). The contents were allowed to react at room temperature with occasional shaking of the vessel. After ca. 20 min, the volatile material was allowed to distill through a series of U-traps held at −45, −78, and −196°C. The fraction at −78°C was passed again through traps held at −45, −78, and −196°C to give $(MeH_2Si)_2O$ (0.21 g, 1.97 mmol; 96%, identified spectroscopically) at −78°C. By a similar procedure Me_2HSiI (0.54 g, 2.9 mmol) was reacted with H_2O (ca. 6 mL) to give $(Me_2HSi)_2O$ (0.185 g, 1.38 mmol). The analogous reactions of Me_3SiBr (0.41 g, 2.68 mmol) and H_3SiBr (0.29 g, 2.61 mmol) with H_2O (ca. 6 mL) gave $(Me_3Si)_2O$ (0.21 g, 1.29 mmol, 96%) and $(H_3Si)_2O$ (0.095 g, 1.22 mmol, 93%, collected at −126°C) and the purity was confirmed by their vibrational (14), ^1H nmr (8, 15), and mass spectral $((C_5H_{15}Si_2O)^+$ *m/e* 147–149, 78.6%; $(H_nSi_2O)^+$ *m/e* 72–80, 73.6%) parameters.

Reactions of Iodosilanes with Mercuric Sulfide

Details of these reactions have appeared elsewhere (16). The overall yield of the disilthianes, based on the corresponding iodosilane consumed, was 94%. The purity was confirmed by their spectroscopic parameters (14, 16). The parent species $(H_3Si)_2S$ and $(Me_3Si)_2S$ gave ms peaks at *m/e* 88–96 $(H_nSi_2S)^+$ and *m/e* 178–181 $(C_6H_{18}Si_2S)^+$.

Reactions of Halogenosilanes with Complex Thio- and Seleno-aluminates

Typically, H_3SiI (0.38 g, 2.40 mmol) was condensed into the reaction vessel containing the seleno-aluminate and allowed to react at −45°C for ca. 2 h, with occasional shaking of the reaction vessel. Fractionation of the volatile material through U-traps held at −78 and −196°C gave $(H_3Si)_2Se$ (0.14 g, 0.99 mmol,

[1]Present address: Division of Chemistry, National Research Council of Canada, Ottawa, Ont., Canada K1A 0R9.

[2]Present address: Department of Chemistry, Scarborough College, University of Toronto, West Hill, Ont., Canada M1C 1A4.

0008-4042/80/202161-06$01.00/0

©1980 National Research Council of Canada/Conseil national de recherches du Canada

Can. J. Chem. Downloaded from www.nrcresearchpress.com by 210.87.254.42 on 09/05/12
For personal use only.

Can. J. Chem. Downloaded from www.nrcresearchpress.com by 210.87.254.42 on 09/05/12
For personal use only.

83%; ms peak *m/e* 130–146 $(H_nSi_2Se)^+$) at −78°C and Me_2O and traces of H_3SiSH (17) at −196°C. Similar sets of experiments using MeH_2SiI (0.52 g, 3.02 mmol), Me_2HSiI (0.68 g, 3.66 mmol), and Me_3SiBr (0.44 g, 2.89 mmol) with excess of seleno-aluminate in the absence of solvent at room temperature for ca. 3 h afforded the corresponding disilselenanes: $(MeH_2Si)_2Se$ (0.24 g, 1.42 mmol, 94%); $(Me_2HSi)_2Se$ (0.315 g, 1.60 mmol, 87%); and $(Me_3Si)_2Se$ (0.20 g, 0.89 mmol, 62%; ms peak *m/e* 220–230 $(C_6H_{18}Si_2Se)^+$). The analogous reactions with thioaluminate gave similar yields of the disilthianes.

Reactions of Halogenosilanes with Lithium Telluride

The reactions were carried out in essentially the same manner as in the synthesis of telluro-germanes (9). Typically, H_3SiI (1.05 g, 6.65 mmol), MeH_2SiI (1.37 g, 7.97 mmol), Me_2HSiCl (1.08 g, 11.42 mmol), and Me_3SiCl (1.12 g, 10.31 mmol) with excess of Li_2Te in ether gave $(H_3Si)_2Te$ (0.565 g, 2.98 mmol, 90%; ms peak *m/e* 178–194 $(H_nSi_2Te)^+$); $(MeH_2Si)_2Te$ (0.77 g, 3.54 mmol, 89%), $(Me_2HSi)_2Te$ (1.30 g, 5.29 mmol, 92%), and $(Me_3Si)_2Te$ (1.35 g, 4.93 mmol, 95%, ms peak *m/e* 268–278 $(C_6H_{18}Si_2Te)^+$).

Reactions of Disilyl Chalcogenides with H_2E where E = O, S, or Se

Typically $(Me_3Si)_2Te$ (0.27 mmol) and H_2S (1.9 mmol) were condensed into a semi-micro nmr tube which was then sealed and allowed to warm to room temperature. After ca. 10 min the ^1H nmr spectrum showed the resonances to be expected for $(Me_3Si)_2Te$ δ(Me) 0.58 ppm and H_2S δ(SH) 0.78 ppm relative to $(Me_3Si)_2O$. After ca. 2 h, tellurium was deposited on the walls of the tube and additional resonances had appeared assignable to Me_3SiSH (18). Further examination showed resonances at 0.65 and −7.9 ppm in the ratio 9:1 assignable to the new tellurol Me_3SiTeH, and H_2Te could also be detected (δ = 5.41) (17). Similarly $(Me_3Si)_2Te$ (0.22 mmol) reacted with H_2Se with formation of Me_3SiSeH (δMe 0.44, δSeH 2.26 ppm) and H_2Te. Alternatively, the silane thiols and selenols, $Me_nH_{3-n}SiEH$ (E = S, Se; $n = 0, 3$) were formed as reported elsewhere (17) from the corresponding sulfides and selenides with H_2S and H_2Se, respectively. Similar reactions with H_2O gave the corresponding disiloxanes.

Cleavage Reactions of Disilthianes and Disilselenanes with Hydrogen Halides

Typically $(Me_2HSi)_2Se$ (1.40 mmol) and HBr (3.12 mmol) were condensed into a 25 mL reaction vessel held at −196°C. The reactants were warmed to room temperature and allowed to react for ca. 30 min. Fractionation of the volatile products gave Me_2HSiBr (2.76 mmol, 99%) in a trap held at −78°C and a mixture of H_2Se and unreacted HBr in one held at −196°C. Similarly, the other species gave quantitative amounts of the corresponding halide.

Reaction of $(Me_2HSi)_2Te$ with Air

When the telluride $(Me_2HSi)_2Te$ (0.36 g, 1.46 mmol) was exposed to air, tellurium was deposited immediately. Fractionation gave H_2Te, which readily decomposed on warming to H_2 and Te, traces of $(Me_2HSi)_2$ and some $(Me_2HSi)_2O$. The ^1H nmr spectrum of the mixture showed resonances at δ(SiH) 4.71, 3.75 and δ(Me) 0.15 ppm relative to TMS. The Raman features characteristic for $(Me_2HSi)_2O$ were ν(SiH) 2128 sh,p; ν_s(SiO) 547 cm^{-1} m,p; and for $(Me_2HSi)_2$ (36) at ν(SiH) 2106 vs,p; ν(Si—Si) 408 cm^{-1} vs,p.

Reaction of $(Me_2HSi)_2O$ with n-Bu_3SnOMe

Typically $(Me_2HSi)_2O$ (0.27 g, 2.0 mmol) was distilled into a reaction vessel (ca. 25 mL) containing 6.1 mmol of degassed *n*-Bu_3SnOMe. The reactants were isolated and allowed to react at room temperature for ca. 22 h with occasional shaking. Fractionation of the volatile material gave $[Me_2(MeO)Si]_2O$ (0.36 g, 1.85 mmol, ^1H nmr (C_6H_{12}) δ(MeO) 3.41 ppm; ms peak *m/e* 179–181 (100%) $(Me_5Si_2O_3)^+$; XPS binding energies (eV) Si 2*p*, 107.1; C 1*s*, 292.15 and 289.25; O 1*s* 537.65) condensing in a trap held at −23°C, whilst an involatile material remained in the reaction vessel.

Results and Discussion

In keeping with the well known heavy-metal salt exchange series (16, 19) iodosilanes are readily converted to disilthianes when passed as gases over mercury(II) sulfide, i.e.

$$[1]\quad 2Me_nH_{3-n}SiI + HgS \xrightarrow[-HgI_2]{25°C} (Me_nH_{3-n}Si)_2S\ (n = 0 \rightarrow 3)$$

Although Li_2S and Li_2Se may be used to prepare the thio- and seleno-silanes (9) the corresponding lithium aluminate salts, $LiAl(EH)_4$ or $LiAlE_2$, may be substituted. These salts are easily prepared and with iodo- or bromo-silanes react readily to give $(Me_nH_{3-n}Si)_2E$ (E = S, Se). The methylated silane is added to the solid aluminate in absence of solvent. The yields are high for the reactions carried out at room temperature, and there is no disproportionation. This method has been well established in the synthesis of methyl-thio and -seleno silanes and germanes (20) but the thermal instability of H_2Te makes it inconvenient for the preparation of the symmetrically disubstituted silyl tellurides. However, these are efficiently prepared from Li_2Te and the corresponding halogenosilane, e.g.

$$[2]\quad 2Me_2HSiCl + Li_2Te \rightarrow (Me_2HSi)_2Te + 2LiCl$$

The yields are high even when the reaction is carried out at room temperature in ether and there is no disproportionation of the product $(Me_2HSi)_2Te$.

The disilyl chalcogenides are all clear, colorless liquids, but $(Me_3Si)_2Se$ and the telluro species soon become pale yellow to brownish at room temperature. The hydridic species $(H_3Si)_2Se$ and $(H_3Si)_2Te$ do not disproportionate at room temperature unless they are stored for several weeks. All of these compounds are sufficiently volatile that they can be easily handled under vacuum line conditions, provided contact with silicone-grease is kept to a minimum. The thio-, seleno-, and telluro-silanes react rapidly with oxygen or H_2O to give the corresponding siloxane and H_2E, i.e.

$$[3]\quad (Me_nH_{3-n}Si)_2E + H_2O \rightarrow (Me_nH_{3-n}Si)_2O + H_2E \qquad (E = S, Se, Te)$$

A similar reaction leading to $Me_nH_{3-n}SiEH$ occurs with excess of the corresponding hydrogen chalcogenide, H_2E (17). Unlike the germyl analogues (9), the disilyl chalcogenides may also be intercon-

Can. J. Chem. Downloaded from www.nrcresearchpress.com by 210.87.254.42 on 09/05/12
For personal use only.

verted by exchange with a "lighter" hydrogen chalcogenide. For example, a tellurosilane can be converted to a selenosilane $(Me_nH_{3-n}Si)_2Se$ or $Me_nH_{3-n}SiSeH$ via cleavage with H_2Se while a thiosilane may be produced by using H_2S. These reactions also present a convenient route to the formation and identification of silanetellurols, e.g.

[4] $(Me_3Si)_2Te + H_2Se \rightarrow Me_3SiSeH + Me_3SiTeH$

When an excess of H_2Se or H_2S is used, the reactions occur with quantitative formation of Me_3SiSeH or Me_3SiSH and H_2Te. Previous methods have typically given poor yields. Elimination of tellurium may result from the thermal instability of Me_3SiTeH or H_2Te. Similarly, elimination of tellurium, resulting in the formation of disilane and disiloxane, is also observed when $(Me_2HSi)_2Te$ is exposed to air, or when tellurosilanes are sealed in cyclohexane solution. Disiloxane, in contrast with other Group VI analogues, reacts smoothly with *n*-Bu_3SnOMe to give $[Me_2(MeO)Si]_2O$. This methoxydisiloxane is identified by its parent peak in the mass spectrum and its ^1H nmr spectrum. Two C 1*s* signals are observed in XPS in the expected intensity ratio of 1:2 at 292.15 eV (typical of MeO) and 289.25 eV (typical of MeSi).

Characterization of the Disilyl Chalcogenides

(i) ^1H Nuclear Magnetic Resonance Spectra

The ^1H nmr spectra (Table 1) not only provided the initial characterization for the calcogen compounds, but also confirmed their purity (>99%) based on the absence of any other proton-containing species. All of the chalcogenides give first order spectra consistent with the free rotation about the skeletal bonds.

As methyl groups substitute for protons along a series $(H_3Si)_2E \rightarrow (MeH_2Si)_2E \rightarrow (Me_2HSi)_2E$ there is a successive down-field shift in the SiH resonance. However, the change is relatively small for E = O (4.61 → 4.69 ppm) and large for E = Te (3.71 → 4.82 ppm) with the sulfides and selenides falling in between, suggesting that the contributing factors must be quite complex. For the series $(H_3Si)_2E$ and $(MeH_2Si)_2E$, the SiH chemical shift moves to higher field in the order O → S → Se → Te as would be expected on the basis of a decreasing inductive effect. This order is maintained in related compounds such as Me_2HSiX (X = F, Cl, Br, I) (21) and in the germanes $(Me_nH_{3-n}Ge)_2E$ (E = O, S, Se, Te) (9). However, in the $(Me_2HSi)_2E$ series the order of high field shift changes to Te → Se → O → S, indicating that the factors contributing to the "methyl shifts" outweigh the inductive effect. The chemical shift of the methyl resonances in all cases decreases (shifts to higher field) with increasing methyl substitution, but increases as the chalcogen changes from O → S → Se → Te. This is the case for the methyl proton shifts in the corresponding halogenosilanes (20) and related halogeno- and chalco-germanes (9, 22, 23). This general feature appears to be more related to the size of the substituents and hence has been attributed to anisotropy and related effects (24). Satellites arising from proton coupling with the magnetic isotope of selenium (^{77}Se) and tellurium (^{125}Te) are observed, indicating that there is no rapid exchange of silyl groups under these conditions. The hydridic chalcogenols H_3SiEH (E = S, Se) give long range, first-order coupling as do the related germyl species H_3GeEH (9, 17). However, coupling involving the hydrogen of the EH entity in Me_3SiEH with the methyl protons is not observed. The sequential shifts in both SiH_3 and CH_3 proton resonances follow the trends observed for the symmetric species and the shifts of the EH proton resonances are close to the values for Et_3SiEH chalcogenols (25).

TABLE 1. The ^1H nmr parameters of $(Me_nH_{3-n}Si)_2E$ species[f]

Compound	δ(Me)	δ(SiH)	$\lvert J_{HH}^{vic}\rvert$	$\lvert J_{^{29}SiH}\rvert$	$\lvert J_{^{13}CH}\rvert$
$(H_3Si)_2O$[a]	—	4.61	—	221.5	—
$(MeH_2Si)_2O$[b]	0.28	4.66	3.33	213.0	121.5
$(Me_2HSi)_2O$[b]	0.14	4.69	2.85	204.9	120.0
$(Me_3Si)_2O$[b,c]	0.06	—	—	—	118.0
$(H_3Si)_2S$[a]	—	4.35	—	223.7	—
$(MeH_2Si)_2S$[b]	0.49	4.47	3.83	214.7	123.0
$(Me_2HSi)_2S$[b]	0.38	4.63	3.39	205.1	121.2
$(Me_3Si)_2S$[b,c]	0.31	—	—	—	119.3
$(H_3Si)_2Se$[a]	—	4.12	—	224.0	—
$(MeH_2Si)_2Se$	0.59	4.43	3.98	215.8	124.5
$(Me_2HSi)_2Se$	0.51	4.73	3.54	205.5	121.4
$(Me_3Si)_2Se$[c]	0.42	—	—	—	120.6
$(H_3Si)_2Te$[d]	—	3.71	—	224.4	—
$(MeH_2Si)_2Te$	0.73	4.25	4.14	216.2	125.3
$(Me_2HSi)_2Te$	0.63	4.82	3.74	206.0	122.7
$(Me_3Si)_2Te$[c,e]	0.58	—	—	—	121.5

[a]Reference 15.
[b]Reference 21.
[c]Reference 8.
[d]Reference 4.
[e]Compare with δ(Me) 0.67 ppm of $(Me_3Si)_2Te$ (C_6H_{12} solution) in ref. 19 and 0.60 ppm (CCl_4 solution) in ref. 8.
[f]All the spectra were recorded using a JEOL C-60HL high resolution spectrometer operating at 60 MHz at room temperature. Chemical shifts (δ ± 0.02 ppm) are in ppm to low field of internal tetramethylsilane in CCl_4 solution (5% v/v). Chemical shifts of the tellurides were measured relative to cyclohexane. Deviations for coupling constants of neat liquids are *J*(HH) ± 0.05 Hz, *J*(SiH) ± 1 Hz, *J*(CH) ± 0.2 Hz.

(ii) Vibrational Spectra

The observed ir and Raman spectra for the two series $(MeH_2Si)_2E$ and $(Me_2HSi)_2E$ are given in Tables 2 and 3, respectively. The assignments are based on comparisons of the spectra along the series E = O → S → Se → Te taking into account previous assignments for MeH_2SiX and Me_2HSiX

TABLE 2. The ir and Raman spectra (cm^{-1}) of the dimethyldisilyl chalcogenides[a]

Tentative assignment		$(MeH_2Si)_2O$		$(MeH_2Si)_2S$		$(MeH_2Si)_2Se$		$(MeH_2Si)_2Te$	
		Ir (gas)	Raman (liq)	Ir (gas)	Raman (liq)	Ir (gas)	Raman (liq)	Ir (liq)	Raman (liq)
$\nu(CH_3)$	(a)	2970 mw	2967 m, dp	2979 m	2973 m, dp	2975 m	2967 m, dp	2966 m	2965 m, dp
	(s)	2908 vw	2908 vs, p	2912 mw	2909 vs, p	2906 w	2903 vs, p	2903 mw	2901 s, p
$\nu(SiH_2)$		2157 vs	2159 vs, p	2159 vs	2159 vs, p	2158 vs	2155 vs, p	2151 vs	2147 s, p
$\delta(CH_3)$	(a)	1418 vw	1422 w, dp	1417 wbr	1418 brw, dp	1418 w	1418 w, dp	1413 m	1411 w, dp
	(s)	1265 s	1259 m, p	1261 m	1255 m, p	1262 m	1251 m, p	1246 s	1249 m, p
$\delta(SiH_2)$	(sc)	970 s	974 m, dp	949 s	944 m, dp	942 sh	936 m, dp	935 s	931 m, dp
$\rho(CH_3)$	(s)	919 vs	916 wbr	909 s	907 w, p	900 sh	896 m, p	877 vs	877 s, p
	(a)	877 m	866 mw, dp	873 vs	868 mw, dp	870 vs	868 brsh, dp	834 vs	835 wsh, dp
$\nu(SiC)$		766 m	756 s, p	745 ms	743 s, p	737 s	733 s, p	720 vs	721 s, p
$\delta(SiH_2)$	(wag)		720 vs, p	699 w	698 s		693 s, p		685 s, p
	(tw)		695 sh, dp		672 sh, dp		657 sh, dp		638 br, dp
$\rho(SiH_2)$		518 w	519 mw, p	510 ms	505 ms, p	495 w	493 m, p	475 mw	473 w, p
$\nu(SiE)$	(a)	1085 vs			489 sh	388 m		332 s	
	(s)	ca. 575 vw	581 vs, p		461 vs, p		380 vs, p		328 vs, p
$\delta(CSiE)$	(a)				221 sh, dp				
	(s)		261 sh		198 s, p		186 s, p		173 s, p
$\delta(ESiE)$			227 m, p		119 w, p		ca. 96 p		ca. 85 vw, p

[a]Spectra recorded at room temperature. m = medium, s = strong, w = weak, v = very, sh = shoulder, br = broad, ms = moderately strong, p = polarized, dp = depolarized.

TABLE 3. The ir and Raman spectra (cm^{-1}) of the tetramethyldisilyl chalcogenides[c]

Tentative assignment		$(Me_2HSi)_2O$		$(Me_2HSi)_2S$		$(Me_2HSi)_2Se$		$(Me_2HSi)_2Te$	
		Ir (gas)	Raman (liq)	Ir (gas)	Raman (liq)	Ir (liq)	Raman (liq)	Ir (liq)	Raman (liq)
$\nu(CH_3)$	(a)	2965 m	2966 m, dp	2965 s	2967 m, dp	2965 ms	2962 m, dp	2959 ms	2961 m, dp
	(s)	2907 w	2904 vs, p	2905 m	2903 vs, p	2901 m	2902 vs, p	2899 m	2899 vs, p
$\nu(SiH)$		2125 s	2129 vs, p	2130 vs	2137 s, p	2136 vs	2138 s, p	2130 vs	2135 s, p
$\delta(CH_3)$	(a)	1425 w	1425 w, dp	1425 m	1425 w, dp	1426 w	1423 w, dp	1421 m	1416 w, dp
		1393	1399 w, dp	1398 sh[a]	1396 w, dp	1394 sh	1392 w, dp	1393 sh	1391 w, dp
	(s)	1265 s	1258 m, p	1255 vs	1254 m, p	1254 vs	1254 m, p	1250 vs	1253 mw, p
$\rho(CH_3)$	(a)	915 s	907 mw, dp	896 vs	894 mw, dp	893 vs	885 m	874 vs	877 m
	(s)	886 vs	880 w	869 vs	860 w	854 vs	862 wsh	851 vs	847 vwsh
	(a, s)	836 m	836 mw, p	833 vs	841 wsh	831 vs	837 wsh	829 wsh	835 vwsh
$\nu(SiC)$	(a)	774 m	764 m, dp	768 s	767 m, dp	765 ms	765 mw, dp	758 ms	762 w, dp
	(s)	670 w	670 vs, p	663 ms	667 vs, p	657 ms	664 s, p	662 sh	661 ms, p
$\delta(SiH)$	(s)	ca. 730 vw	748 m, p	716 ms	715 m, p	703 ms	702 m, p	684 s	688 m, p
	(a)	630 w	626 m, dp	635 m	633 m, dp	632 m	634 mw, dp	628 m	629 sh, dp
$\nu(SiE)$	(a)	1074 vs		489 vs		379 vs		326 s	
	(s)	ca. 565 vw	547 vs, p	472 sh[a] 460 vwsh	{472 vs, p 459 sh, p	372 vwsh[b]	{387 vs, p 373 sh, p		{335 vs, p 323 sh, p
$\delta(CSiC)$			285 sh	254 w[a]	255 m, p		250 m, p		240 m, p
$\delta(CSiE)$	(s)		259 sh		215 sh		199 sh		
	(a)		211 sh		188 s, p		184 s, p		177 s, p
$\delta(SiESi)$			193 s, p		103 mw, p		89 wsh		ca. 78 w

[a]Liquid.
[b]Gas.
[c]See footnote to Table 2.

Can. J. Chem. Downloaded from www.nrcresearchpress.com by 210.87.254.42 on 09/05/12
For personal use only.

Can. J. Chem. Downloaded from www.nrcresearchpress.com by 210.87.254.42 on 09/05/12
For personal use only.

(X = F, Cl, Br, I) (26). The skeletal vibrational frequences are very close to the values reported for the parent species $(H_3Si)_2E$ (4, 27, 28) and $(Me_3Si)_2E$ (14). As the chalcogen changes in the series $(MeH_2Si)_2E$, the Si—E—Si stretching vibrations give a sequence of bands which fall at: 1085 vs and 581 vs,p (O); 461 vs,p (S); 388 m and 380 vs,p (Se); 332 s and 328 cm^{-1} vs,p (Te). Clearly, the ir counterpart for ν(SiS) remains unobserved but appears at 489 cm^{-1} in the dimethylated analogue. The small separation between the asymmetric and symmetric modes in the heavier chalcogenides relative to the large split in the oxides is as expected for an Si—E—Si angle close to 90° in all compounds except the oxide. The frequency shifts of ν(SiE) for the other series $(Me_2HSi)_2E$ appear to follow the same trend, but the result of extra methyl groups on these frequencies can be seen in the Raman spectra. As expected, ν(SiO) occurs as a single peak at lower frequency 547 cm^{-1} while the heavier Si—E—Si stretches show a new band as a shoulder on the low frequency side. The shoulder can be resolved into a distinct band as illustrated in Fig. 1. The occurrence of this splitting appearing at 472 vs,p and 459 sh,p (S); 387 vs,p, and 373 sh,p (Se); 335 vs,p and 323 cm^{-1} sh,p (Te) is thought to arise from possible conformational effects. Apparently, this doublet feature appears to be characteristic only for the $(Me_2HSi)_2S,Se,Te$ since ν(Ge—E—Ge) appears as a single band in the related germyl species (9). In the low frequency region of the Raman spectra the SiESi and CSiE deformations are clearly observed. The resulting trend of decreasing deformation frequencies for SiESi along the series confirmed that the heavy atom skeletons are bent at the central atom like the related species. The splitting between the two CSiE deformations decreases as the chalcogen becomes heavier and in the case of $(MeH_2Si)_2Se,Te$ and $(Me_2HSi)_2Te$ become coincident. The methyl stretching and deformation modes are unambiguously assigned in the expected 2979–2899 cm^{-1} and 1426–1246 cm^{-1} regions as are the SiH stretches at 2159–2125 cm^{-1}. The assignment of the remaining vibrations for the $Me_nH_{3-n}Si$-moieties are comparable to the related halogenosilanes (26).

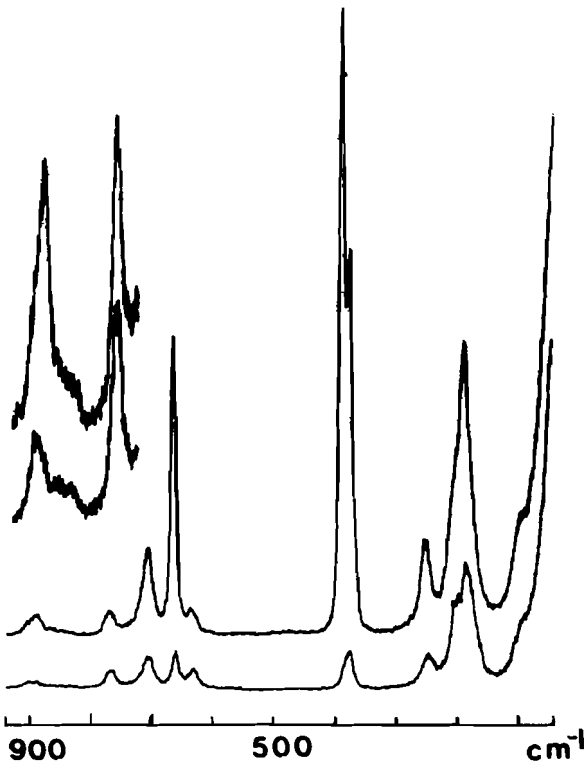


FIG. 1. Partial Raman spectrum of $(Me_2HSi)_2Se$.

(iii) Mass Spectra

In a preceding paper (29) we reported a detailed study of the mass spectra of $(Me_3Si)_2E$ series, so we describe here only the characteristic features associated with $(MeH_2Si)_2E$ and $(Me_2HSi)_2E$ where E = O, S, Se, Te. The observed cluster ions are collected in Tables 4 and 5, along with their relative abundances. Examination of the data shows that the molecular ion (M^+ or $(M - nH)^+$) is present in every case and the sequence of decreasing relative abundance on going through the series O → S → Se → Te apparently parallels the thermal stability of the species or the Si—E—Si bond strength on electron impact. Aside from the telluro species, the molecular ion is predominant for $(MeH_2Si)_2E$ while silicon–methyl bond cleavage appears in greater abundance for $(Me_2HSi)_2E$ species. The fact that the Si—O bond is stronger than the Si—S, Si—Se, or Si—Te bond is shown by the lesser fragmentation of the Si—O—Si linkage. The contribution of the $(Me_3Si)^+$ ion arises as in the dimethylated ger-

TABLE 4. Ion clusters in the mass spectra of the dimethyldisilyl chalcogenides[a]

Ion fragment	Relative abundance (%)			
	E = O	E = S	E = Se	E = Te
$(Me_2H_nSi_2E)^+$	41.6	36.9	32.8	17.3
$(MeH_nSi_2E)^+$	17.4	17.5	12.0	5.5
$(H_nSi_2E)^+$	20.2	6.1	3.4	4.2
$(H_nSi_2)^+$	[b]	7.5	7.2	7.7
$(MeH_nSiE)^+$	9.3	13.9	29.5	41.9
$(MeH_nSi)^+$	4.7	10.0	9.6	14.5
$(H_nSiE)^+$	5.3	4.9	3.6	6.4
$(H_nSi)^+$	1.5	3.2	1.9	2.5

[a]The value of n is summed from 0 → 2 for Si and 0 → 4 for Si_2.
[b]Contribution summarized with $(MeH_nSiE)^+$.

TABLE 5. Ion clusters in the mass spectra of the tetramethyldisilyl chalcogenides[a]

Ion fragment	Relative abundance (%)			
	E = O	E = S	E = Se	E = Te
$(Me_4H_nSi_2E)^+$	35.5	13.3	13.9	8.2
$(Me_4H_nSi_2)^+$	—	—	—	5.8
$(Me_3H_nSi_2E)^+$	40.9	28.8	15.6	1.2
$(Me_3H_nSi_2)^+$	—	—	—	1.7
$(Me_2H_nSi_2E)^+$	3.0	7.5	0.5	—
$(Me_2H_nSi_2)^+$	—	—	—	1.4
$(MeH_nSi_2E)^+$	1.8	1.1	—	—
$(MeH_nSi_2)^+$	—	—	—	11.4
$(Me_3H_nSi)^+$	6.0	14.3	17.6	—
(Me_2H_nSiE)		7.6	15.0	27.1
$(H_nSi_2E)^+$				
$(H_nSi_2)^+$	—	—	—	1.1
$(Me_2H_nSi)^+$	6.1	7.9	16.1	15.2
$(MeH_nSiE)^+$		8.2	8.0	17.9
$(MeH_nSi)^+$	3.7	5.3	7.5	5.3
$(H_nSiE)^+$		3.0	2.6	1.8
$(H_nSi)^+$	3.0	3.0	3.2	1.9

[a]The value of n is summed from $0 \rightarrow 1$ for Si and $0 \rightarrow 2$ for Si_2.

myl species (9) from a migration of a methyl group from one silicon atom to the other. However, an interesting feature is the elimination of tellurium leading to $(Me_2HSi)_2^+$ species, suggesting that Te elimination noted for reactions could be intramolecular.

Acknowledgement

We thank the Natural Sciences and Engineering Council of Canada for financial support.

1. A. STOCK, C. SOMIESKI, and R. WINTGEN. Chem. Ber. **50**, 1754 (1917).
2. B. J. AYLETT, H. J. EMELÉUS, and A. G. MADDOCK. Research, **6**, 305 (1953).
3. H. J. EMELÉUS, A. J. MACDIARMID, and A. G. MADDOCK. J. Inorg. Nucl. Chem. **1**, 194 (1955).
4. H. BÜRGER and U. GOETZE. Inorg. Nucl. Chem. Lett. **3**, 549 (1967).
5. R. O. SAUER. J. Am. Chem. Soc. **66**, 1707 (1944).
6. C. EABORN. J. Chem. Soc. 3077 (1950); Nature, 165 (1950); 685 (1950).
7. M. SCHMIDT and H. RUF. Z. Anorg. Allgem. Chem. **32**, 270 (1963).
8. K. A. HOOTON and A. L. ALLRED. Inorg. Chem. **4**, 671 (1965).
9. J. E. DRAKE, B. M. GLAVINČEVSKI, H. E. HENDERSON, and R. T. HEMMINGS. Can. J. Chem. **56**, 465 (1978).
10. J. E. DRAKE, B. M. GLAVINČEVSKI, and R. T. HEMMINGS. J. Inorg. Nucl. Chem. **41**, 457 (1979).
11. J. E. DRAKE, B. M. GLAVINČEVSKI, R. T. HEMMINGS, and H. E. HENDERSON. Inorg. Synth. **19**, 268 (1979).
12. J. E. DRAKE, B. M. GLAVINČEVSKI, R. T. HEMMINGS, and H. E. HENDERSON. Inorg. Synth. In press.
13. G. R. WAITKINS and R. SHUTT. Inorg. Synth. **2**, 183 (1946); A. TIAN and S. AUBANEL. Compt. Rend. Trav. Faculte Sci. Marseille, **1**, 97 (1942).
14. H. BÜRGER and U. GOETZE. Spectrochim. Acta, **24A**, 2003 (1968).
15. E. A. V. EBSWORTH and J. J. TURNER. J. Phys. Chem. **67**, 805 (1963).
16. J. E. DRAKE, B. M. GLAVINČEVSKI, R. T. HEMMINGS, and H. E. HENDERSON. Inorg. Synth. **19**, 274 (1979).
17. C. GLIDEWELL, D. W. H. RANKIN, and G. M. SHELDRICK. Trans. Faraday Soc. 1409 (1969).
18. T. SAKAKIBARA, T. HIRABAYASHI, and Y. I. SHII. J. Organomet. Chem. **46**, 231 (1972).
19. A. G. MACDIARMID. Q. Rev. **10**, 208 (1956).
20. G. K. BARKER, J. E. DRAKE, and R. T. HEMMINGS. J. Chem. Soc. Dalton, 450 (1974); J. W. ANDERSON and J. E. DRAKE. Inorg. Nucl. Chem. Lett. 1007 (1971).
21. E. A. V. EBSWORTH and S. G. FRANKISS. Trans. Faraday Soc. 1574 (1967); 1518 (1963).
22. G. K. BARKER, J. E. DRAKE, and R. T. HEMMINGS. Can. J. Chem. **52**, 2622 (1974).
23. J. E. DRAKE and R. T. HEMMINGS. Can. J. Chem. **51**, 302 (1973).
24. H. SCHMIDBAUR and I. RUIDISH. Inorg. Chem. **3**, 599 (1964).
25. A. N. EGOROCHKIN, N. S. VYAZANKIN, M. N. BOCHKAREV, V. T. BYCHKOV, and A. I. BUROV. Zh. Obshch. Khim. **38**, 396 (1968); M. N. BOCKAREV, L. P. SANINA, and N. S. VYAZANKIN. **39**, 135 (1969).
26. A. J. F. CLARK. Ph.D. Thesis, University of Windsor, Windsor, Ont. 1979.
27. E. A. V. EBSWORTH, R. TAYLOR, and L. A. WOODWARD. Trans. Faraday Soc. **55**, 211 (1959).
28. J. E. DURIG, M. J. GLANAGAN, and V. F. KALASINSKI. J. Chem. Phys. **66**, 2775 (1977); Spectrochim. Acta, **34A**, 63 (1978).
29. J. E. DRAKE, B. M. GLAVINČEVSKI, and C. WONG. J. Inorg. Nucl. Chem. **42**, 175 (1980).

Can. J. Chem. Downloaded from www.nrcresearchpress.com by 210.87.254.42 on 09/05/12
For personal use only.

Hydrolysis and carbonyl-oxygen exchange in tertiary amides. Estimation of the free energy changes for breakdown and conformational changes of tetrahedral intermediates

PIERRE DESLONGCHAMPS, ROGER BARLET,[1] AND ROLAND J. TAILLEFER

Département de Chimie, Faculté des Sciences, Université de Sherbrooke, Sherbrooke (Qué.), Canada J1K 2R1

Received May 1, 1980

PIERRE DESLONGCHAMPS, ROGER BARLET, and ROLAND J. TAILLEFER. Can. J. Chem. **58**, 2167 (1980).

Second order rate constants were measured at several temperatures for the basic hydrolysis and for concurrent carbonyl-oxygen exchange with solvent for *N*-benzyl-*N*-methylformamide-^{18}O, *N*-benzyl-*N*-methyltrideutéroacetamide-^{18}O, and *N*-benzyl-*N*-methyl-α,α-dideuteropropionamide-^{18}O. Carbonyl-oxygen exchange with solvent is rationalized by invoking a conformational change in the tetrahedral intermediate. Energy barriers for these conformational changes are estimated to be of the order of 5.6, 8.0, 8.2 kcal/mol respectively for the above amides.

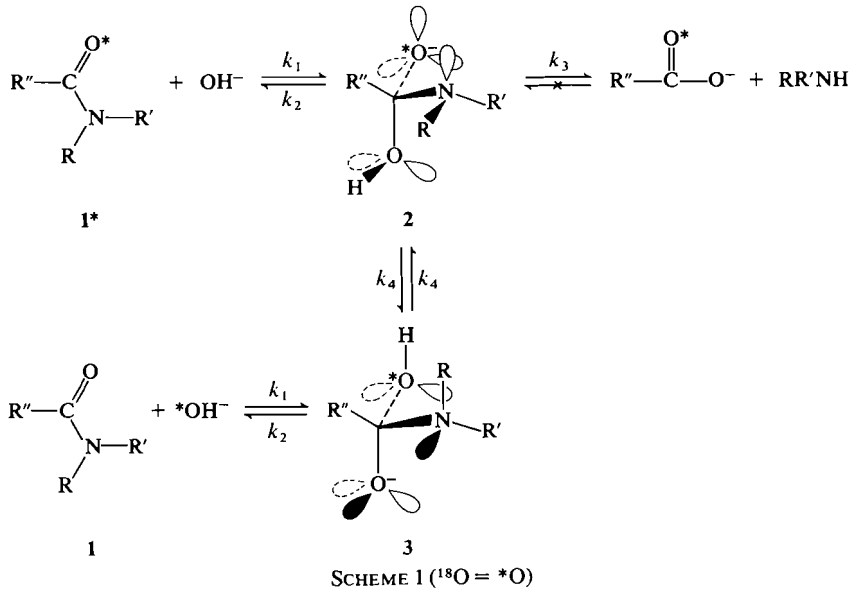
PIERRE DESLONGCHAMPS, ROGER BARLET et ROLAND J. TAILLEFER. Can. J. Chem. **58**, 2167 (1980).

On a mesuré les constantes de vitesse de 2e ordre à plusieurs températures pour l'hydrolyse basique et l'échange concurrente d'oxygène avec le solvant pour le *N*-benzyl-*N*-méthylformamide-^{18}O, le *N*-benzyl-*N*-méthyl-trideutérioacétamide-^{18}O et le *N*-benzyl-*N*-méthly-α,α-dideutériopropionamide-^{18}O. L'échange de l'oxygène du carbonyle avec le solvant est expliqué en invoquant un changement conformationnel au niveau de l'intermédiaire tétraédrique. Les barrières pour ces changements conformationnels sont de l'ordre de 5.8, 8.0 et 8.2 kcal/mol respectivement pour ces trois amides.

Application of the theory of stereoelectronic control to the cleavage of tetrahedral intermediates (1) which are formed during the basic hydrolysis of carbonyl-^{18}O amides has led to the following predictions: primary and secondary amides, but not tertiary amides or secondary and tertiary lactams, could give rise to isotope exchange with solvent, concurrent with hydrolysis (2).

The basic postulate is that a stereoelectronically controlled nucleophilic attack by hydroxide ion on the ^{18}O-labeled amide **1*** (Scheme 1) gives specifically the tetrahedral conformer **2**, which exists in the monoanionic form (T^-) above pH 11. The second postulate is that the energy barrier for the stereoelectronically controlled breakdown of **2** is lower than that for its conformational change.

In the case of primary or secondary amide, the R group in intermediate **2** is a hydrogen atom. It is assumed that proton transfer on the two oxygens can take place prior to the breakdown of intermediate **2** (3). The same assumption is also made for proton exchange on the nitrogen (**2** ⇄ **3**) which



SCHEME 1 (^{18}O = *O)

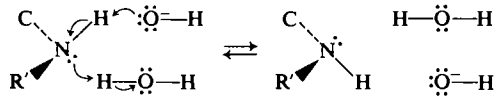
[1]Laboratoire de Chimie Organique, Université Scientifique et Médicale de Grenoble, St-Martin-d'Hères, B.P. 53, 38041 Grenoble, France.

0008-4042/80/202167-06$01.00/0

©1980 National Research Council of Canada/Conseil national de recherches du Canada

Can. J. Chem. Downloaded from www.nrcresearchpress.com by 210.87.254.5 on 09/05/12
For personal use only.

must occur via the following process which, we think, has also a low energy barrier.



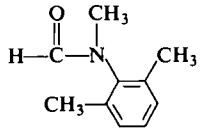
The N—H as well as the O—H bond can therefore be considered equivalent to a nonbonded electron pair. Under these conditions, intermediate **2** has proper electron pair orientation to give the starting amide **1*** and the hydrolysis products or the unlabeled amide **1** via **3**. As k_2 is larger than k_3 (OH being a better leaving group than NH_2), primary and secondary amides should exhibit significant exchange, a prediction which is supported by experiments (4). Consequently, in the case of primary and secondary amides, there is no need to postulate a conformational change prior to breakdown in order to observe carbonyl-oxygen exchange.[2]

In tertiary amides, intermediate **2** can fragment in only two ways, yielding the starting labeled amide **1*** or the hydrolysis products. In order to observe carbonyl-oxygen exchange, intermediate **2** must be converted first into another conformer such as **3** which can give unlabeled amide **1** or the hydrolysis products. Oxygen exchange in tertiary amides depends therefore on the relative ease by which **2** can yield **3** or the hydrolysis products by direct fragmentation. The change of **2** into **3** can be obtained by either a 120° rotation around the C—N bond, or by an inversion of the nitrogen atom followed by a 60° rotation, with appropriate proton transfer on oxygens. For conformational change to occur at rates competitive with fragmentation, it is necessary that the energy of activation for the conformational change be less than or comparable to that for fragmentation.

We have initially obtained experimental evidence that tertiary amides and secondary and tertiary lactams do not undergo carbonyl-oxygen exchange, confirming the above postulate (2). Since then, we have observed that *N*,*N*-disubstituted formamides (5) gave significant oxygen exchange at room temperature and at 90°C during their basic hydrolysis at pH 13. These results, in contradiction with the initial predictions, can, however, be easily interpreted. The energy barrier to rotation of **2** to **3** is lowered when R″ = H compared to R″ = alkyl (5).

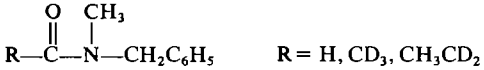
It was also shown (5) that in tertiary acetamides and propionamides, isotopic exchange with the solvent, which was negligible, or absent, at room temperature became significant at 90°C. Further, the exchange rate increased with temperature more rapidly than did the hydrolysis rate.

This phenomenon was explained by taking into account that the nitrogen atom of the tetrahedral intermediate must be hydrogen-bonded to the solvent in order to observe hydrolysis. This association, which favors the heterolytic cleavage but disfavors the rotation step necessary for exchange, becomes less important at higher temperature, and the exchange rate is therefore favored over that of hydrolysis by an increase of temperature. This solvent effect was clearly shown with *N*-2,6-dimethylphenyl-*N*-methylformamide (**4**), in which steric effects inhibit such hydrogen bonding. Indeed, this formamide does not hydrolyse (0.15 *N* KOH, 90°C, 70 h) but undergoes considerable carbonyl-oxygen exchange (91%) (5).



4

We now report the rates of hydrolysis and carbonyl ^{18}O exchange with solvent ($D_2{}^{16}O$) of amides **5** in order to estimate the magnitude of the energies involved in these processes. α-Deuterated amides were required because under our experimental conditions (KOD, D_2O) hydrogen–deuterium exchange occurred.



5

Experimental

Vapor-phase chromatographic (vpc) analyses and separations were carried out on a Varian Aerograph instrument model 920 with a thermal conductivity detector. The columns used were 10% Versamid 900 (5 ft × 1/4 in.) and 5% SE-30 (5 ft × 1/4 in.), both on Chromosorb W, 100–200 mesh. Infrared spectra were taken on a Perkin-Elmer spectrometer model 257. Proton nmr spectra were recorded on a Varian A-60 instrument, or a Bruker WP-60 instrument. Chemical shifts are reported in δ values relative to tetramethylsilane as the internal standard. Constant temperature baths were obtained using a Thermistemp YSI model 71 temperature controller. Temperatures were constant within ±0.25°C.

Mass spectra were obtained using a Hitachi-Perkin-Elmer RMU-6A instrument at 70 eV. Percentages of ^{18}O were obtained by measuring the peak height of the parent peak (P) and that of the parent peak plus two mass units (P + 2). These heights were corrected for background if necessary. The unlabeled amides (^{16}O) presented a small P + 2 peak due to natural abundance ^{18}O,

[2]The rapid oxygen exchange in primary and secondary amides can also be explained by the rapid interconversion of **2** and **3** via a conformational change. The energy barrier for the interconversion of **2** and **3** in intermediates derived from primary and secondary amides must be lower than that from tertiary amide because the substitutents on the nitrogen are smaller.

Can. J. Chem. Downloaded from www.nrcresearchpress.com by 210.87.254.5 on 09/05/12
For personal use only.

Can. J. Chem. Downloaded from www.nrcresearchpress.com by 210.87.254.5 on 09/05/12
For personal use only.

^2H, ^{13}C, the percentage of which was subtracted from the (P + 2) peak in the sample. After these corrections, the percentage ^{18}O was given by

$$\%^{18}O = \frac{100\,(P+2)}{P+(P+2)}$$

Each assay was an average of 25 scans.

Syntheses

Unlabeled amides were prepared by standard procedures. Their physical properties corresponded to literature values and their spectra were in accord with their structures. α-Deuteroamides were obtained by base catalysed hydrogen–deuterium exchange in CH_3O^-/CH_3OD at 80°C ($CD_3CON(CH_3)$–$(CH_2C_6H_5)$) or 50°C ($CH_3CD_2CON(CH_3)$–$(CH_2C_6H_5)$). Three to four exchange cycles were necessary to completely deuterate the amides. *N*-Methyl-*N*-benzylformamide-^{18}O (**5***, R = H) was prepared as previously reported (5). Other labeled amides were prepared as described in Scheme 2.

N-*Methyl*-N-*benzyltrideuteroacetamide*-^{18}O

Method A

Trimethyloxonium tetrafluoroborate (225 mg, 1.51 mmol) was added to freshly distilled methylene chloride (5 mL). Trideuteroacetamide (133 mg, 0.93 mmol) dissolved in methylene chloride (10 mL) was added and the mixture was stirred at room temperature overnight. Filtration and solvent evaporation gave the acetamidate (220 mg, 90%) present in both the *E* and *Z* configurations.

Sodium metal (28 mg, 1.2 mmol) was added to methanol-*O*-*d* (200 μL). When all the sodium had reacted, $D_2{}^{18}O$ (22 μL, 50% ^{18}O, Merck, Sharp and Dohme) was then added, followed by the mixture of acetamidate salts (0.83 mmol) dissolved in methanol-*O*-*d* (100 μL). The solution was stirred for two hours. Methylene chloride was then added, and the mixture was filtered. The filtrate was evaporated to dryness. Nuclear magnetic resonance analysis of the residue showed 75% amide and 25% amine. The mixture was then dissolved in water and the solution was saturated with ammonium chloride. The solution was then extracted several times with methylene chloride. After drying, solvent evaporation gave 0.62 mmol of amide (overall yield 66%) containing 18.8% ^{18}O.

Method B

Trideuteroacetyl chloride (407 mg, 5 mmol, >99% d_3, Merck, Sharp and Dohme) was placed in a septum sealed test tube in which two needles were placed in order to circulate dry nitrogen. $H_2{}^{18}O$ (0.91 μL, 46 mmol) was added and the solution was stirred overnight. The solution was then cooled to 0°C and phosphorus trichloride (168 μL) was slowly added followed by methylene chloride (2 mL, freshly distilled from P_2O_5). The solution was left warming to room temperature for one hour to eliminate the HCl produced. The solution was then cooled again and methylbenzylamine (2 mL, 17 mmol) was slowly added. The solution was left standing for 3–4 hours. Aqueous hydrochloric acid (50% 1 *N*, 50% saturated aqueous NaCl solution) was then added and the solution was extracted with methylene chloride. The organic solution was then washed with bicarbonate, dried, and evaporated. Purification by vpc (Versamid, 180°C) gave 313 mg (total yield 38%) of labeled amide containing 54% ^{18}O.

N-*Methyl*-N-*benzyl*-α,α-*dideuteropropionamide*-^{18}O

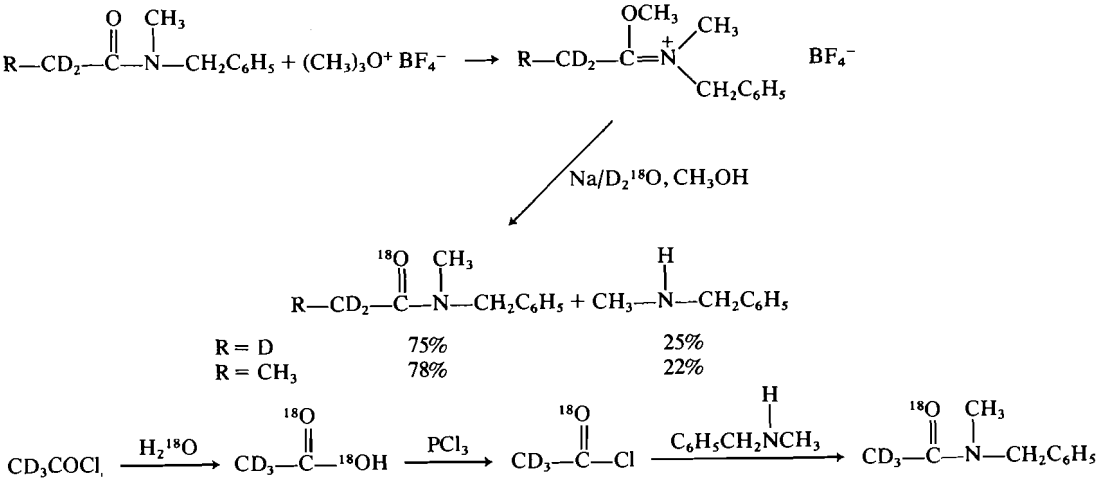
This compound, which was prepared by utilizing method A, was isolated in 78% total yield and contained 20% ^{18}O.

Kinetics

The hydrolyses were done in deuterated buffer solutions of total ionic strength of 0.5 *M*, adjusted with KCl. Potassium hydroxide solutions (KOD) were prepared by adding potassium metal to D_2O. Concentrations were 0.25 to 0.36 *N*.

The labeled amides were dissolved in the buffer solutions at the appropriate temperature such that their final concentrations were 0.028 *M* to 0.035 *M*. At appropriate times, samples were removed, quenched with solid ammonium chloride, and assayed directly by nmr spectroscopy integration for the percentage of amide (*N*-methyl peak) and the percentage of amine (*N*-methyl peak). The sample was then extracted several times with methylene chloride. After drying and evaporation of solvent, the unreacted amide was isolated by preparative vpc, and assayed for ^{18}O by mass spectroscopy.

For the case of *N*-methyl-*N*-benzylformamide where the working temperatures were lower (27–45°C), two parallel reactions were made. One was in an nmr tube and nmr analysis was made without quenching by transferring the tube to the nmr probe kept at the same temperature as that of the run. In this case the time of the point was taken as the median time before and after the FT accumulations. The second parallel reaction was done in a reaction vessel. Samples were removed, quenched as above, and extracted rapidly for mass spectral assay.



SCHEME 2

Can. J. Chem. Downloaded from www.nrcresearchpress.com by 210.87.254.5 on 09/05/12
For personal use only.

TABLE 1. Rate constants for hydrolysis and for ^{18}O exchange in amides[a]



R	[OD⁻](*M*)	*T*(°C)	k_h^1(s⁻¹)	k_h(L mol⁻¹ s⁻¹)	k_{ex}^1(s⁻¹)	k_{ex}(L mol⁻¹ s⁻¹)
H	0.360	10	1.19×10^{-5}	3.32×10^{-5}	3.31×10^{-6}	9.19×10^{-6}
		27	4.31×10^{-5}	1.20×10^{-4}	1.43×10^{-5}	3.97×10^{-5}
		37	8.20×10^{-5}	2.28×10^{-4}	3.46×10^{-5}	9.61×10^{-5}
		45	1.59×10^{-4}	4.41×10^{-4}	7.56×10^{-5}	2.10×10^{-4}
CD_3	0.305	40	2.72×10^{-6}	8.93×10^{-6}	2.63×10^{-7}	8.62×10^{-7}
		55	5.86×10^{-6}	1.92×10^{-5}	1.10×10^{-6}	3.61×10^{-6}
		70	1.99×10^{-5}	6.53×10^{-5}	—	—
		85	4.49×10^{-5}	1.47×10^{-4}	1.36×10^{-5}	4.46×10^{-5}
CH_3CD_2	0.305	60	4.61×10^{-6}	1.51×10^{-5}	8.39×10^{-7}	2.75×10^{-6}
		70	8.89×10^{-6}	2.91×10^{-5}	2.34×10^{-6}	7.67×10^{-6}
		80	1.58×10^{-5}	5.17×10^{-5}	5.83×10^{-6}	1.91×10^{-5}
		90	2.61×10^{-5}	8.55×10^{-5}	1.14×10^{-5}	3.74×10^{-5}

[a]Errors in pseudo-first order constants are estimated to be less than ±5%.

Results

Table 1 lists the data obtained for hydrolysis and exchange of amides **5** (R = H, CD_3, CH_3CD_2). Pseudo-first order rate constants were found by following the disappearance of starting amide (k_h^1) or following the disappearance of the ^{18}O-label (k_{ex}^1) in the starting amide. Second order rate constants were obtained by dividing the pseudo-first order constants by the base concentration. This assumes the rate law described by eq. [1]. However, second order terms in hydroxide ion concentration (eq. [2]) have sometimes been observed (6) in amide hydrolysis. That such was not the case under our conditions is shown in Table 2. The second order rate constants are the same within experimental error for each base concentration.

$$[1] \quad \text{Rate} = k\,[\text{amide}]\,[OH^-]$$

$$[2] \quad \text{Rate} = k'\,[\text{amide}]\,[OH^-] + k''\,[\text{amide}]\,[OH^-]^2$$

The activation parameters, found by plotting ln (k/T) vs. $1/T$ where k is the second order rate constant for hydrolysis (k_h) or exchange (k_{ex}), are summarized in Table 3.

TABLE 2. Second order rate constants for amides **5** hydrolyses

R	[OD⁻](*M*)	*T*(°C)	k_h^1(s⁻¹)[a]	k_h(L mol⁻¹ s⁻¹)[b]
H	0.2915	27	3.08×10^{-5}	1.05×10^{-4}
	0.185		1.95×10^{-5}	1.06×10^{-4}
CH_3CD_2	0.305	60	4.61×10^{-6}	1.51×10^{-5}
	0.254		4.00×10^{-6}	1.57×10^{-5}
CH_3CD_2	0.305	90	2.59×10^{-5}	8.50×10^{-5}
	0.254		2.08×10^{-5}	8.17×10^{-5}
	0.173		1.42×10^{-5}	8.22×10^{-5}

[a]Pseudo-first order rate constants.
[b]Second order rate constants $k_h^1 = k_h/[OD^-]$.

Discussion

The activation parameters for hydrolysis $\Delta H_h^{\ddagger}$, $\Delta S_h^{\ddagger}$, and $\Delta G_h^{\ddagger}$, described in Table 3 are in accord with values obtained previously on similar amides (7, 8). The large negative entropy of activation agrees with the fact that the nitrogen in the tetrahedral intermediate must form a hydrogen bond with the solvent in order to observe hydrolysis. As expected, the formamide is more reactive towards hydrolysis than the other two amides.

Comparison of the activation parameters for carbonyl-oxygen exchange and for hydrolysis show that in the case of formamide, the rate of exchange is only slightly lower than that of hydrolysis, whereas in the case of acetamide and propionamide, the exchange occurs at a significantly lower rate. These results are in accord with our previous studies (2, 4).

In order to obtain a free energy diagram for hydrolysis and carbonyl-oxygen exchange, it is necessary to analyze in more detail the mechanism of these two processes. Consider the following simple mechanism for amide hydrolysis, where A is the amide, T, the tetrahedral intermediate, and P, the products

$$A + OD^- \underset{k_2}{\overset{k_1}{\rightleftharpoons}} T \xrightarrow{k_3} P$$

Application of the steady-state approximation for this mechanism gives

$$k_h = k_1 k_3/(k_2 + k_3)$$

Under the present conditions, because there is isotope exchange with solvent, k_3 must be the rate determining step and since an OH group is a better leaving group than an R_2N group, we must have k_2

TABLE 3. Activation parameters for hydrolysis and ^{18}O exchange of amides **5**

R	$k_h^{25°}$[a] (L mol^{-1} s^{-1})	$\Delta H_h^{\ddagger}$ (kcal mol^{-1})	$\Delta S_h^{\ddagger}$ (eu)	$\Delta G_{h-25°}^{\ddagger}$ (kcal mol^{-1})	$k_{ex}^{25°}$[a] (L mol^{-1} s^{-1})	$\Delta H_{ex}^{\ddagger}$ (kcal mol^{-1})	$\Delta S_{ex}^{\ddagger}$ (eu)	$\Delta G_{ex-25°}^{\ddagger}$ (kcal mol^{-1})
H	1.15×10^{-4}	12.4±0.3	−34.9±0.5	22.8	3.56×10^{-5}	15.3±0.6	−27.5±1.9	23.5
CD_3	2.75×10^{-6}	13.3±0.2	−39.3±0.5	25.0	1.54×10^{-7}	19.0±0.3	−25.9±0.9	26.7
CH_3CD_2	1.27×10^{-6}	13.4±0.5	−40.5±1.3	25.5	6.85×10^{-8}	20.7±1.0	−21.8±2.8	27.2

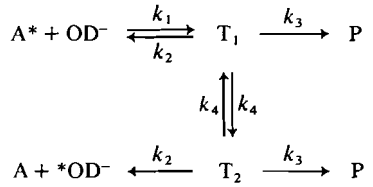
[a]Extrapolated.

$\gg k_3$ and hence

[3] $k_h = K k_3$

where $K = k_1/k_2$, the equilibrium constant for tetrahedral intermediate formation.

For the exchange mechanism, we must consider two conformations of the tetrahedral intermediate:



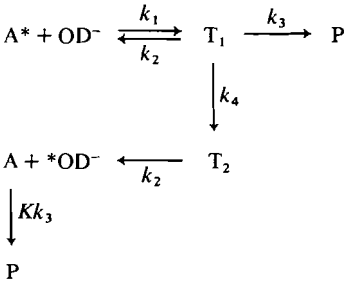
where A* is the labeled amide, A the unlabeled amide, and T_1 and T_2 are conformers **2** and **3** of Scheme 1. In this mechanism, formation of T_2 from A and $^*OD^-$ is considered negligible because the labeled deuteroxide is diluted in the D_2O pool. Further, if we consider the methyl and the benzyl substituents on nitrogen as very similar groups,[3] then T_1 and T_2 are close to mirror images so that their interconversions go at similar rates (k_4). Steady-state treatment on this mechanism gives

$$k_{ex} = k_1 k_2 k_4/(k_2 + k_3)(k_2 + k_3 + 2k_4)$$

As before, $k_2 \gg k_3$. Also, if we assume that the decomposition of T_1 into starting material is a much easier process than conformational changes, then $k_2 \gg k_4$. If $k_2 \gg k_3 + 2k_4$, then

[4] $k_{ex} = k_1 k_2 k_4/k_2^2$
$= K k_4$

If these approximations hold, the exchange mechanism is effectively reduced to



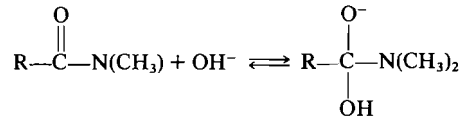
[3]The Taft's ρ* value for a benzyl group is +0.22 compared to 0.0 for methyl. Also, Taft's steric parameter is −0.33 for the benzyl group compared to 0.0 for the methly group (9).

i.e. once the first tetrahedral intermediate T_1 is formed it will go back to starting A* and OD^- most of the time. However, every so often T_1 will evolve to products via k_3 or to T_2 via k_4. Once T_2 is formed on the other hand, it decomposes rapidly to unlabeled amide and $^*OD^-$.

To estimate the constants k_3 and k_4 in eq. [3] and [4], the knowledge of the equilibrium constant K for tetrahedral intermediate formation is required. Recently, Guthrie (7) has estimated these equilibrium constants for *N*,*N*-dimethylformamide and *N*,*N*-dimethylacetamide. They are shown in Table 4, together with the value calculated for the propionamide using the ρ* value defined by the points R = H, and R = CH_3. Assuming the benzyl group is not very different from a methyl group,[3] and neglecting the solvent isotope effect and the secondary isotope effects in the acetamide and propionamide, these equilibrium constants can then be used to estimate k_3 and k_4. These are shown in Table 5 and illustrated in Fig. 1.

Table 5 shows that the free energy of activation for the tetrahedral intermediate decomposition step (k_3, $\Delta G_3^{\ddagger}$) does not vary considerably with the amide structure, while that for the conformational change at the nitrogen (k_4, $\Delta G_4^{\ddagger}$) varies appreciably from the formamide to the acetamide (or propionamide) case. It is expected that the conformational change step would be influenced appreciably by the steric interaction of the R group. These differences in $\Delta G_4^{\ddagger}$ militate against interpreting the k_4 step as a proton transfer step. The free energy for

TABLE 4. Equilibrium constant for tetrahedral intermediate formation[a]



R	$K(M^{-1})$	$\Delta G°$ (kcal mol)
H	1.1×10^{-13}	17.7
CH_3	1.7×10^{-14}	18.8
C_2H_5	1.2×10^{-14}[b]	19.0

[a]In aqueous solution at 25°C; standard state for water is the pure liquid at unit activity; standard state for solutes is 1 *M* aqueous solution with an infinitely dilute reference state (7).
[b]Calculated from the ρ* value defined by the R = H, CH_3 points.

Can. J. Chem. Downloaded from www.nrcresearchpress.com by 210.87.254.5 on 09/05/12
For personal use only.

TABLE 5. Estimated rate constants found in this work[a]

R	$K(M^{-1})^b$	$\Delta G^{\circ b}$ (kcal/mol)	k_3 (s^{-1})	$\Delta G_3^{\ddagger}$ (kcal/mol)	k_4 (s^{-1})	$\Delta G_4^{\ddagger}$ (kcal/mol)
H	1.1×10^{-13}	17.7	1.0×10^{9}	5.2	3.2×10^{8}	5.8
CD_3	1.7×10^{-14}	18.8	1.6×10^{8}	6.2	9.0×10^{6}	8.0
CH_3CD_2	1.2×10^{-14}	19.0	1.1×10^{8}	6.5	5.7×10^{6}	8.2

[a]25°C.
[b]From Table 4, cf. text.

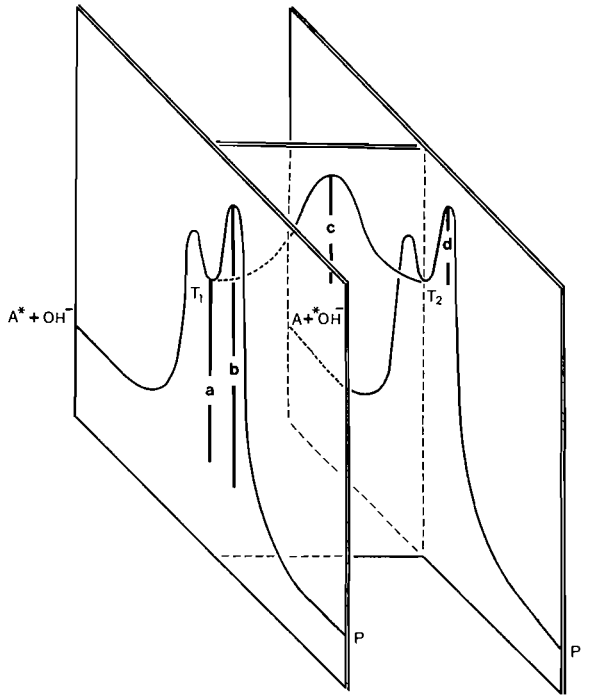
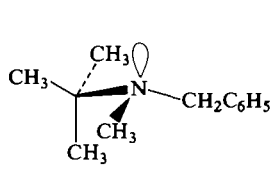


FIG. 1. Free energy diagram (kcal/mol) for hydrolysis and carbonyl oxygen exchange. (a) ΔG° for formamide is 17.7, for acetamide 18.8, and for propionamide is 19.0; (b) $\Delta G_h^{\ddagger}$ for formamide is 22.8, for acetamide 25.0, and for propionamide is 25.5; (c) $\Delta G_4^{\ddagger}$ for formamide is 5.8, for acetamide 8.0, and for propionamide is 8.2; (d) $\Delta G_3^{\ddagger}$ for formamide is 5.2, for acetamide 6.2, and for propionamide is 6.5.

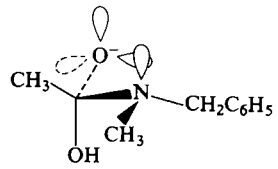
such a step would not vary much from R = H to R = CH_3CD_2.

In summary, the above interpretation of the results obtained indicates that carbonyl-oxygen exchange with solvent, concurrent to the hydrolysis of tertiary amides, arises through a rate determining step which involves a conformational change at the nitrogen in the tetrahedral intermediate. The free energy changes for these conformational changes have been estimated to be of the order of 5.8, 8.0, and 8.2 kcal/mol^{-1} for formamides, acetamides, and propionamides respectively.

It is interesting to compare *tert*-butylbenzylmethylamine (**6**) and the tetrahedral intermediate **7** derived from *N*-benzyl-*N*-methylacetamide which have a similar degree of substitution.



6



7

The rotation barrier for the $(CH_3)_3C$—N bond and the nitrogen inversion barrier in *tert*-butylbenzylmethylamine have been found identical and estimated at 6.2 kcal/mol (10). The slightly higher value of 8.0 kcal/mol for the intermediate **7** may be due to an electronic reason, related to the anomeric effect (11).

This work constitutes further evidence in favor of the principle of stereoelectronic control which governs the cleavage of tetrahedral intermediates in hydrolysis reactions.

Acknowledgements

This research was supported by the Natural Sciences and Engineering Research Council of Canada and by the Ministère de l'Education de Québec.

1. P. DESLONGCHAMPS. Pure Appl. Chem. **43**, 351 (1975); Tetrahedron, **31**, 2463 (1975); Heterocycles, **7**, 1271 (1977).
2. P. DESLONGCHAMPS, U. O. CHERIYAN, A. GUIDA, and R. J. TAILLEFER. Nouv. J. Chim. **1**, 235 (1977).
3. M. EIGEN. Angew. Chem. Int. Ed. Engl. **3**, 1 (1964).
4. M. L. BENDER. Chem. Rev. **60**, 53 (1960); S. L. JOHNSON. *In* Advances in physical organic chemistry. Vol. 5. *Edited by* V. Gold. Academic Press, London. 1967. pp. 237–331.
5. P. DESLONGCHAMPS, P. GERVAL, U. O. CHERIYAN, A. GUIDA, and R. J. TAILLEFER. Nouv. J. Chim. **2**, 631 (1978).
6. S. S. BIECHLER and R. W. TAFT, JR. J. Am. Chem. Soc. **79**, 4927 (1957).
7. J. P. GUTHRIE. J. Am. Chem. Soc. **96**, 3608 (1974).
8. P. D. BOLTON and G. L. JACKSON. Aust. J. Chem. **24**, 969 (1971).
9. R. D. GILLION. *In* Introduction to physical organic chemistry. *Edited by* Addison-Wesley, Don Mills, Ont. 1970. p. 158.
10. C. H. BUSHWELLER, J. W. O'NEIL, and H. S. BILOFSKY, J. Am. Chem. Soc. **93**, 542 (1971).
11. R. U. LEMIEUX and S. KOTO. Tetrahedron, **30**, 1933 (1974), and references therein.

Can. J. Chem. Downloaded from www.nrcresearchpress.com by 210.87.254.5 on 09/05/12
For personal use only.

Synthesis of ring A of ambruticin and proof of its absolute stereochemistry

GEORGE JUST AND PIERRE POTVIN[1]

Department of Chemistry, McGill University, Montreal, P.Q., Canada H3A 2K6

Received May 26, 1980

GEORGE JUST and PIERRE POTVIN. Can. J. Chem. **58**, 2173 (1980).

Appropriately derivatized ambruticin was converted by reductive ozonolysis to tetrahydropyran **9***c* and cyclopropane **12***a*, which were synthesized from L-arabinose and (*R*)-Feist's acid in an unambiguous manner.

GEORGE JUST et PIERRE POTVIN. Can. J. Chem. **58**, 2173 (1980).

L'ambruticine, sous forme derivée, fut convertie en tétrahydropyranne **9***c* et cyclopropane **12***a*, qui furent eux-mêmes synthétisés de manière non-ambigüe à partir du L-arabinose et de l'acide de Feist résolu.

Can. J. Chem. Downloaded from www.nrcresearchpress.com by 210.87.254.105 on 09/05/12
For personal use only.

Ambruticin, a novel antifungal agent, has been assigned structure **11**, based on X-ray diffraction studies (1). We were interested in developing an efficient synthesis of this compound, starting from chiral precursors corresponding to the three ring-systems, and therefore had to know the absolute stereochemistry of **11**, since most inexpensive chiral precursors are not available in both enantiomeric forms.

Because of the ready availability of both D- and L-arabinose, it was decided to synthesize ring A from L-arabinose (**1**), and to compare it to the appropriately modified ozonolysis fragment derived from ambruticin.

Reaction of the known aldehyde **3***a* (2) with methyl 3-nitropropionate (3) and potassium *tert*-butoxide in tetrahydrofuran gave adduct **4***a* as a mixture of isomers, which was acetylated *in situ* using acetic anhydride and 4-dimethylaminopyridine to give acetates **4***b*. Elimination of acetic acid with triethylamine and reduction with sodium borohydride (12) gave **4***c* as a mixture of diastereomers.

Treatment of **4***c* with diazabicycloundecene (DBU) in chloroform gave the α,β-unsaturated ester **6***a* in 45% yield, based on aldehyde **3***a*. Partial hydrolysis of **6***a* with acetic acid (4) gave diol **6***b*. All attempts to effect ring closure failed, and seemed to result in elimination of the vinylogously β-alkoxy group at C5 of **6***a*, followed by further reaction which we did not care to investigate. The failure to close the ring was attributed to strain generated in forming the *trans*-fused trioxahydrindanes of type **9** (RR=CMe_2).

The sequence was therefore repeated using 2,3-*O*-dibenzyl-4,5-*O*-isopropylidene-L-arabinose, **3***b*, prepared from the dithioacetal **2** by partial ketalization with acetone – pyridinium *para*-toluenesulfonate (5), followed by benzylation (6) and hydrolysis of the thioacetal using iodine in water (7) to give unstable **3***b* (**2** → **2***b* → **2***c* → **3***b*). Reaction of **3***b* with methyl 3-nitropropionate, followed by the steps outlined above for diacetonide **3***a* (**3***b* → **5***a* → **5***b* → **5***c* → **7***a* → **7***b*) using modified experimental conditions gave dibenzyloxy diol **7***b* in 25–30% yield, based on **3***b*. This time, ring-closure could be effected smoothly by boiling **7***b* in toluene in the presence of a catalytic amount of sodium methoxide, and slowly distilling off the methanol formed in the reaction. This reaction gave bicyclic lactone **8**, mp 154–156°C, $[\alpha]_D^{21}$ −6.4°, in 51% yield, and ensured the *cis*-stereochemistry of the two chains attached to the tetrahydropyran ring. Reaction of lactone **8** with sodium methoxide in methanol gave **9***a*. Considerable difficulties were encountered in removing the benzyl groups of **9***a* by catalytic hydrogenation. However, treatment of **9**a with trimethylsilyl iodide gave **9***b* which was isolated in modest yield and characterized as its tribenzoate **9***c* (mp 134–136°C, $[\alpha]_D^{21}$ +11.1°).

(*R*,*R*)-Feist's acid **13**, mp 198–199°C, $[\alpha]_{546}^{21}$ +172°, (lit. (8) mp 203–205°C, $[\alpha]_{546}^{25}$ +176°), resolved through its quinine salt (8),[2] was hydrogenated over palladium on charcoal to give (*S*,*S*)-**10**, mp 162.5–163.5°C, $[\alpha]_D^{21}$ +92.4° (lit. (9) mp 130–131°C, 147° for *rac*-**10**). Diborane reduction gave (*S*,*S*)-**12**, which was characterized as its dibenzoate (*S*,*S*)-**12***a*, $[\alpha]_D^{21}$ −12.9°.

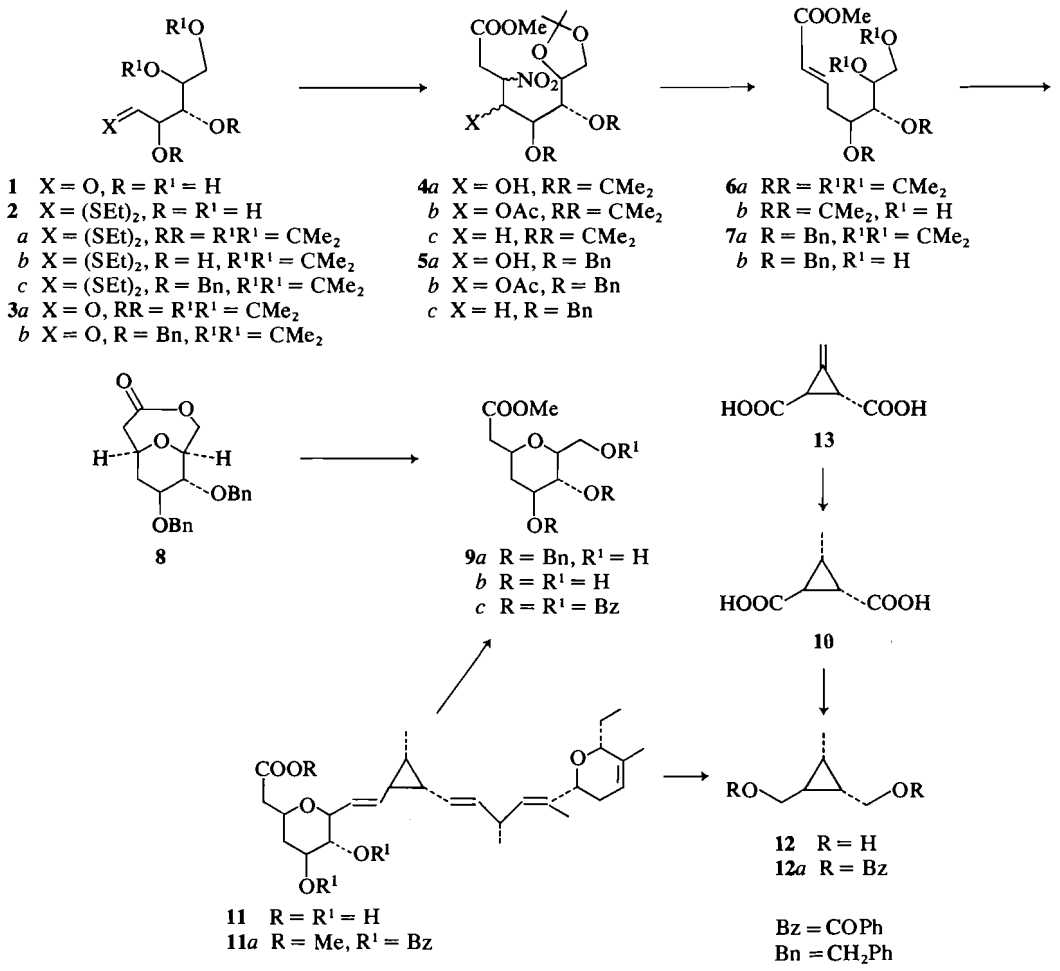
In order to correlate ambruticin **11** with **9***c* and **12***a*, it was transformed to its methyl ester dibenzoate **11***a* by reaction with diazomethane, followed by benzoyl chloride – pyridine. Ozonolysis in methylene chloride at −78°C, followed by treatment with dimethylsulfide and zinc borohydride, gave a mixture of alcohols, from which could be isolated diol **12** and triol **9***b*. These were separately transformed to their respective perbenzoates **12***a*

[1]Holder of a N.S.E.R.C. Scholarship, 1979–1981, and a D.G.E.S. Scholarship, 1978–1980.

[2]We found the presence of some water essential for crystallizing the quinine salt from ethanol.

0008-4042/80/202173-05$01.00/0

©1980 National Research Council of Canada/Conseil national de recherches du Canada



([α]$_D^{21}$ −9.0°) and **9***c* (mp and mixture mp 132–134°C, [α]$_D^{21}$ +8.6°). The spectra (200 MHz ^{1}Hmr, ir, mass) of **9***c* obtained from ambruticin were identical to those of **9***c* obtained from L-arabinose.

Compound **12***a* was chromatographically homogeneous (tlc, hplc, flash chromatography (10)), but minor differences in the 200 MHz ^{1}Hmr and ir spectra of **12***a* obtained from ambruticin from those of **12***a* obtained from (*R*,*R*)-Feist's acid suggest the presence of an unidentified contaminant, which explains the slightly lower optical rotation of natural-source **12***a*. In view of the report (1) that ozonolysis of the ambruticin system had failed to give identifiable products, we were satisfied that the similarities in optical rotation of the synthetic and natural-source perbenzoates **9***c* and **12***a* prove that the absolute stereochemistry of ambruticin is as depicted in formula **11**.

Experimental

Thin-layer chromatography was performed on Merck Silica Gel 60 aluminum-backed plates. Flash chromatography was done using Woelm Silica (32–63 μ) using predistilled solvents. Petroleum ether used was the fraction boiling in the 30–60°C range. The nmr spectra (all in $CDCl_3$) were recorded on Varian T-60A or XL-200 instruments; infrared spectra were measured on a Perkin-Elmer 297 spectrometer. Optical rotations were measured in a 1 dm cell on a Perkin-Elmer 141 polarimeter. Melting points were measured on a Gallenkamp block and are uncorrected. Elemental analyses were performed by Midwest Microlab Ltd., Indianapolis. High pressure liquid chromatography was performed on an Altex 300 instrument, equipped with an ultraviolet detector, using an analytical column of silica gel (10 μ spherical).

Diisopropylidene α,β-Unsaturated Ester **6**a

Methyl 3-nitropropionate (3) (0.26 g, 2 mmol) in 3 mL of dry THF was added dropwise to a stirred suspension of potassium *tert*-butoxide (0.22 g, 2 mmol) in 6 mL of dry THF, at 0°C under a dry N_2 atmosphere. After stirring the yellow solution for 15 min, a solution of 2,3;4,5-di-*O*-isopropylidene-L-arabinose **3***a* (2) (0.46 g, 2 mmol) in 3 mL of dry THF was added dropwise. After stirring a further 30 min at room temperature, tlc (3:2 ether – petroleum ether) indicated complete adduct formation. After neutralization (using 0.53 mL of a 20% THF solution of acetic acid), acetic anhydride (0.20 mL, 2.2 mmol) and a catalytic amount of 4-dimethylaminopyridine were added to the intermediate nitro-alcohols **4***a*. After stirring for 2 h at room temperature, the reaction mixture consisted of acetates **4***b* and some

Can. J. Chem. Downloaded from www.nrcresearchpress.com by 210.87.254.105 on 09/05/12
For personal use only.

Can. J. Chem. Downloaded from www.nrcresearchpress.com by 210.87.254.105 on 09/05/12
For personal use only.

elimination product. Triethylamine (0.26 mL, 2 mmol) was added, and the mixture was filtered and evaporated to dryness. The residue was dissolved in acetonitrile (4 mL) and treated with excess sodium borohydride while stirring at room temperature for 1 h. The reaction mixture was diluted with ether (20 mL), filtered, and evaporated, and the residue, mainly **4***c*, was dissolved in $CHCl_3$ (20 mL) and brought to reflux. To this solution was added DBU (0.30 mL, 2 mmol), dropwise. After 30 min, at which time the elimination was complete (tlc), the solution was washed twice with KH_2PO_4 buffer (pH 4.4) and once with brine, while reextracting the aqueous layers with $CHCl_3$ (3 times). The combined organic layers were dried ($MgSO_4$) and evaporated to dryness to give 750 mg of crude product, which was purified by flash chromatography using 10% ethyl acetate – petroleum ether to give 0.24 g of pure **6** (45%), as a slightly yellow oil which gave hexane-soluble crystals on standing, mp 38.5–41.5°C; $[\alpha]_D^{21}$ −19.3° (*c* 2.56, $CHCl_3$); ir (neat): 1725 ($COOCH_3$), 1660 (CH=CH) cm^{-1}; 60 MHz nmr δ: 1.38 and 1.41 (2 bs, 12H, isopropylidene), 2.11–2.84 (m, 2H, CH=CH—C*H*$_2$—CH), 3.31–4.21 (m, 5H), 3.70 (s, 3H, OCH_3), 5.86 (2t, 1H, *J* = 1.5, 15 Hz, CH_3OOCCH=CH), 6.96 (2t, 1H, *J* = 7, 15.5 Hz, CH_3OOCCH=C*H*); mass spectrum (70 eV) *m/e* (rel. %): 315 (1.2) ($M^+ + CH_3$), 300 (0.9) (M^+), 299 (2.9) ($M^+ - H$), 287 (2.5), 286 (12.7), 285 (77.7) ($M^+ - CH_3$), 143 (100), 101 (96.5). *Anal.* calcd. for $C_{15}H_{24}O_6$: C 59.98%, H 8.05%; found: C 60.08%, H 7.92%.

Monoisopropylidene α,β-*Unsaturated Ester* 6b

A solution of di-isopropylidene ester **6***a* (0.24 g, 0.8 mmol) in 2.4 mL of 80% aqueous acetic acid was stirred for 3 h at 55°C. The reaction mixture was evaporated to near dryness, then diluted with ethyl acetate and washed twice with saturated $NaHCO_3$ solution (2×) and water (1×). The washings were reextracted with ethyl acetate (2×). The combined organic layers were dried ($MgSO_4$) and evaporated to give crude diol **6***b* containing some tetraol. This was purified by flash chromatography, using ethyl acetate as eluent to give 0.15 g of pure **6***b* (72%) as a slightly yellowish oil; $[\alpha]_D^{21}$ −27.9° (*c* 2.73, $CHCl_3$); ir (neat): 3420 (b, OH), 1710 (b, $COOCH_3$), 1655 (CH=CH) cm^{-1}; 60 MHz nmr δ: 1.40 (bs, 6H, isopropylidene), 2.40–2.73 (m, 2H, CH=CH—C*H*$_2$—), 2.93 (bs, 2H, O*H*), 3.47–4.27 (m, 5H), 3.70 (s, 3H, OC*H*$_3$), 5.94 (2t, 1H, *J* = 1.5, 15 Hz, CH_3OOC-C*H*=CH), 7.05 (2t, 1H, *J* = 7, 15 Hz, CH_3OOCCH=C*H*); mass spectrum (70 eV) *m/e* (rel. %): 256 (0.5), 247 (0.6), 246 (2.1), 245 (16.7), 242 (0.2) ($M^+ - H_2O$), 241 (0.1), 59 (100). *Anal.* calcd. for $C_{12}H_{20}O_6$: C 55.37%, H 7.75%; found: C 55.21%, H 7.90%.

*4,5-*O*-Isopropylidene-*L*-arabinose Diethyldithioacetal* 2b

A suspension of 22 g of L-arabinose diethyldithioacetal **2** (11) (0.090 mol) in 900 mL of acetone (freshly distilled over $KMnO_4$) and 22 mL of 2,2-dimethoxypropane (0.18 mol) was treated with 1.12 g of pyridinium *p*-toluenesulfonate (5) (4.5 mmol), and allowed to stir for 90 min. The reaction mixture was evaporated, dissolved in $CHCl_3$, and washed twice with water. The $CHCl_3$ solution was then dried ($MgSO_4$) and evaporated. The crude crystalline product was recrystallized from hot toluene to give 38.3 g of pure monoacetonide **2***b* (74%), mp 75–76°C, $[\alpha]_D^{22}$ +76.5° (*c* 0.83, $CHCl_3$) (lit. (4) mp 70–72°C, $[\alpha]_D^{20}$ −68.9° (*c* 2.19, $CHCl_3$) for the D-arabinose derivative). We report here, for the first time, spectral data for **2***b*: 60 MHz nmr ($CDCl_3$ + D_2O) δ: 1.27 (t, 6H, *J* = 7.5 Hz, SCH_2CH_3), 1.33 and 1.40 (2s, 6H, isopropylidene), 2.66 and 2.68 (2q, 4H, *J* = 7.5 Hz, SCH_2CH_3), 3.60–4.14 (m, 6H); mass spectrum (70 eV) *m/e* (rel. %): 296 (3.7) (M^+, *S*-cluster), 283 (0.5), 282 (0.6), 281 (3.8) ($M^+ - CH_3$), 263 (0.5), 256 (0.3), 236 (0.5), 235 (3.5) (M^+ − SEt), 135 (100).

*2,3-Di-*O*-benzyl-4,5-*O*-isopropylidene-*L*-arabinose Diethyldithioacetal* 2c

A 50% oil suspension of sodium hydride (5.81 g, 121 mmol) was washed by successively stirring and decanting with *n*-hexane (3×) and dry THF (1×), under an inert atmosphere (N_2). After cooling to 0°C, dry THF (100 mL) was added, 14.83 g of monoacetonide **2***b* was stirred in (50 mmol), and a crystal of imidazole added to accelerate anion formation. The evolution of H_2 was complete when the reaction mixture became homogeneous, at which time 14.4 mL of benzyl bromide (121 mmol) was added, followed by 0.92 g of tetra-*n*-butyl ammonium iodide (2.5 mmol). The reaction mixture was allowed to warm up to room temperature and stir for 3 h or when tlc (15% ethyl acetate in petroleum ether) showed the complete disappearance of **2***b*. Florisil (3.5 g, 100–200 mesh, Fisher) was added and the whole was transferred to a 500 mL round-bottomed flask, where it was evaporated to near-dryness under reduced pressure. The crude mixture was then repeatedly triturated with portions of petroleum ether to extract the product. After evaporation of the petroleum ether solution, one obtained 26.18 g of crude yellow dibenzyl compound **2***c* (quantitative yield) contaminated with some residual benzyl bromide. Although this crude product tended to darken at room temperature, the darkening is considerably slowed at −20°C, and it can be used directly for the next transformation. An analytically pure sample could be obtained through flash chromatography, using 7% ethyl acetate – petroleum ether as eluent, to give a stable, colorless oil; $[\alpha]_D^{21}$ −29.6° (*c* 3.15, $CHCl_3$); ir (neat): no assignable absorptions, 1500, 1455, 1380, 1370, 1070, 700 cm^{-1}; 60 MHz nmr δ: 1.23 and 1.24 (2t, 6H, *J* = 7.5 Hz, SCH_2CH_3), 1.34 and 1.42 (2s, 6H, isopropylidene), 2.66 and 2.69 (2q, 4H, *J* = 7 Hz, SCH_2CH_3), 3.64–4.44 (m, 6H), 4.78 and 4.83 (s and ABq, 4H, *J* = 11 Hz, C*H*$_2$φ), 7.31 (bs, 10H, φ); mass spectrum (70 eV) *m/e* (rel.%): 476 (0.6) (M^+, S-cluster), 461 (0.6) ($M^+ - CH_3$), 410 (0.7) (M^+ − SEt), 358 (0.5), 357 (1.7), 91 (100). *Anal.* calcd. for $C_{26}H_{36}O_4S_2$: C 65.50%, H 7.61%, S 13.45%; found: C 65.76%, H 7.50%, S 11.90%.

*2,3-*O*-Dibenzyl-4,5-*O*-isopropylidene-*L*-arabinose* 3b

The dithioacetal **2***c* (10.4 g, 22 mmol) in 150 mL of acetone and 25 mL of water was treated with 4 g of sodium bicarbonate (48 mmol) and, with slow portionwise addition at 0°C with good stirring, 6.1 g of iodine (24 mmol). After the addition, the mixture was allowed to warm up to room temperature and to stir overnight. Further portions of 6.1 g of iodine and 4 g of sodium bicarbonate were added in the morning at 0°C, and stirring was continued at room temperature for a further 8–10 h, at which time the excess iodine was destroyed by adding saturated sodium thiosulfate solution. After partial evaporation of the acetone, the product was extracted into ethyl acetate (3 × 50 mL) and the combined extracts washed with water (3 × 15 mL). After drying ($MgSO_4$) and evaporation of solvent, the crude product was purified by flash chromatography, using 15% ethyl acetate in petroleum ether. In one run 1.39 g of starting dithioacetal (13%) and 3.85 g of the unstable aldehyde **3***b* (yield 55%, based on converted starting material) were obtained. Other runs furnished **3***b* in 42–92% yield. Aldehyde **3***b* must be used immediately.

Compound **3***b* $[\alpha]_D^{22}$ +6.0° (*c* 1.46, $CHCl_3$); ir (neat): 1730 (CHO), 1612, 1495, 1455 cm^{-1}; 60 MHz nmr δ: 1.23 and 1.31 (2s, 6H, isopropylidene), 3.50–4.02 (m, 5H), 4.25 and 4.38 (s and ABq, 4H, *J* = 10.5 Hz, C*H*$_2$φ), 6.80 and 6.85 (2s, 10H, φ), 9.09 (d, 1H, *J* = 1 Hz, CHO).

*Dibenzylisopropylidenyl-*α,β-*unsaturated Ester* 7a

To a solution of methyl 3-nitropropionate (0.56 g, 4.2 mmol) and diisopropyl amine (0.46 mL, 3.3 mmol) in dry DMF (6 mL) was added 1.11 g of aldehyde **3***b* (3 mmol) in 1 mL of dry DMF. After stirring for 6 h at room temperature, 60 mL of water was added, and the product mixture was extracted into ether (3 × 30 mL). The ether layers were washed with water (5 × 15 mL), and the combined ether layers were dried ($MgSO_4$) and evapo-

Can. J. Chem. Downloaded from www.nrcresearchpress.com by 210.87.254.105 on 09/05/12
For personal use only.

rated to give an oily mixture of nitro-alcohols **5***a* and excess methyl 3-nitropropionate. This was dissolved in 6 mL of anhydrous ether, and 0.56 mL of acetic anhydride (6 mmol) and a catalytic amount of 4-dimethylaminopyridine were added. The solution was allowed to stir for 2 h at room temperature, after which time 0.84 mL of triethylamine (6 mmol) was added, and the mixture was stirred a further 2 h. The solution was washed with KH_2PO_4 buffer (pH 4.4) and water, and the aqueous solutions reextracted once with ether. The combined ether layers were dried ($MgSO_4$) and evaporated to give crude nitro-olefin, as an oil. This was treated as before, for **6**, to give 1.10 g of crude **7***a*, which was purified by flash chromatography using 15% ethyl acetate in petroleum ether, to yield 0.34 g of pure **7***a* (25%) as an oil, $[\alpha]_D^{22}$ +4.3° (*c* 1.62, $CHCl_3$); ir (neat): 1725 ($COOCH_3$), 1660 (CH=CH) cm^{-1}; 60 MHz nmr δ: 1.28 and 1.37 (2s, 6H, isopropylidene), 2.22–3.07 (m, 2H, CH=CH—C*H*$_2$), 3.35–4.26 (m, 5H), 3.58 (s, 3H, OC*H*$_3$), 4.38 and 4.53 (s and ABq, 4H, *J* = 10.5 Hz, C*H*$_2$φ), 5.58 (2t, 1H, *J* = 1.5, 15 Hz, CH_3OOC-C*H*=CH), 6.63 (2t, 1H, *J* = 7, 15 Hz, CH_3OOCCH=C*H*), 7.03 and 7.06 (2s, 10H, φ); mass spectrum (70 eV) *m/e* (rel. %): 291 (0.6), 274 (0.2), 259 (0.9), 243 (0.6), 241 (0.1), 91 (100). *Anal.* calcd. for $C_{26}H_{32}O_6$: C 70.89%, H 7.32%; found: C 70.85%, H 7.41%.

Dibenzyldihydroxy-α,β-unsaturated Ester **7**b

Isopropylidene compound **7***a* (0.36 g, 0.8 mmol) was stirred for 3 h at 55°C in 4 mL of 80% aqueous acetic acid. The reaction mixture was worked up as before, for **6***a*, to give 0.29 g of diol **7***b* (88%) as a colorless oil which can be used as is for the next transformation. An analytical sample was obtained by flash chromatography, using 60% ethyl acetate in petroleum ether as eluent; $[\alpha]_D^{21}$ −0.92° (*c* 2.18, $CHCl_3$); ir (neat): 3460 (OH), 1715 ($COOCH_3$), 1650 (CH=CH) cm^{-1}; 60 MHz nmr δ: 2.30 (b, 2H, O*H*), 2.37–3.13 (m, 2H, —CH=CH—C*H*$_2$), 3.30–4.20 (m, 5H), 3.67 (s, 3H, OC*H*$_3$), 4.48 and 4.52 (2s, 4H, C*H*$_2$φ), 5.76 (2t, 1H, *J* = 1, 15 Hz, CH_3OOC—C*H*=CH), 6.81 (2t, 1H, *J* = 7, 15 Hz, CH_3OOCCH=C*H*), 7.20 (s, 10H, φ).

Dibenzyl Lactone **8**

The acyclic diol **7***b* (0.57 g, 1.4 mmol) in 14 mL of toluene was treated with 0.28 mL of a 0.5 *N* methanolic solution of sodium methoxide (0.14 mmol) at room temperature. A yellowish color was immediately discharged, and tlc indicated complete conversion to an intermediate C3-epimeric mixture of cyclic alcohols **9***a*. The solution was heated for 6 h at 20–80°C in an open flask while allowing a slow distillation of solvent, and replacing it with more toluene from time to time. While still warm, the solution was neutralized with methanol- and toluene-washed Dowex 50W-X8 resin (H^+), and allowed to cool. The resin was filtered off, washed with toluene, and the combined filtrate and washings were evaporated to give a quantitative yield of crude crystalline product. This was purified by flash chromatography, using 30% ethyl acetate in petroleum ether, followed by recrystallization from hot toluene to give 0.27 g of pure lactone **8** (51%), mp 154–156°C; $[\alpha]_D^{21}$ −6.4° (*c* 2.25, $CHCl_3$); ir ($CHCl_3$): 1715 (lactone), 1490, 1445, 1112, 1070 cm^{-1}; 60 MHz nmr δ: 1.23–2.51 (2m, 4H, ROOC—C*H*$_2$— and C*H*$_2$—CH(OBn)—), 2.91–4.31 (m, 6H), 4.53 and 4.81 (s and ABq, 4H, *J* = 11 Hz, C*H*$_2$φ), 7.13 (bs, 10H, φ); mass spectrum (70 eV, C.I.) *m/e* (rel. %): 355 (19.3), 313 (14.8), 286 (19.3), 285 (26.1), 284 (42.0), 283 (20.5), 267 (83), 256 (100); *Anal.* calcd. for $C_{22}H_{24}O_5$: C 71.72%, H 6.57%; found: C 71.50%, H 6.45%.

Dibenzyloxyhydroxymethyl Tetrahydropyran **9**a

Lactone **8** (0.11 g, 0.3 mmol) in 12 mL of methanol was treated with 0.6 mL of a 0.5 *N* methanolic sodium methoxide solution (0.3 mmol) at room temperature, and conversion to **9***a* seems to be immediate by tlc. After neutralization with methanol-washed Dowex-50W-X8 resin (H^+) and filtration, the solvent was evaporated to give a quantitative yield of oily **9***a* (0.115 g), which was used as is for the next step; $[\alpha]_D^{21}$ −6.9° (*c* 1.81, $CHCl_3$); ir (neat): 3440 (b, OH), 1730 ($COOCH_3$) cm^{-1}; 60 MHz nmr δ: 1.40–2.63 (m, 5H, CH_3OOC—C*H*$_2$—, —C*H*$_2$—CH(OBn)—, and O*H*), 3.13–4.23 (m, 6H), 3.69 (s, 3H, OCH_3), 4.68 and 4.82 (s and ABq, 4H, *J* = 11 Hz, C*H*$_2$φ), 7.37 (bs, 10H, φ); mass spectrum (70 eV) *m/e* (rel. %): 310 (1.3) ($M^+ - CH_2\phi + H$), 309 (8.2) (M^+—$CH_2\phi$), 203 (3.9), 187 (0.5), 186 (1.0), 185 (12.3), 91 (100).

Synthetic Tribenzoate **9**c

A solution of 90 mg of cyclic alcohol **9***a* (0.225 mmol) in 9 mL of dry methylene chloride was treated with 0.13 mL of trimethylsilyl iodide (0.91 mmol), at room temperature, under an atmosphere of N_2. Thin-layer chromatography indicated almost complete and immediate conversion to a very polar compound or complex. After stirring for 2 h, the reaction was quenched with methanol, the solvent evaporated, and the residue taken up in 1 mL of dry pyridine, to which was added 0.12 mL of benzoyl chloride (1.01 mmol), and a trace of 4-dimethylaminopyridine. After stirring overnight and stirring with H_2O for 1 h, the solution was diluted with chloroform (20 mL), washed with 0.5 *N* HCl (2 × 10 mL), saturated $NaHCO_3$ (2 × 10 mL), and water (1 × 10 mL). The aqueous layers were reextracted once each with chloroform (10 mL) and the combined organic layers were dried ($MgSO_4$), evaporated, and coevaporated with toluene (to rid the product of the last traces of pyridine) to give crude tribenzoate **9***c* along with some benzoyl chloride and an unidentified less polar compound present in significant amounts. Flash chromatography, using 25% ethyl acetate in petroleum ether gave 19 mg of pure crystalline tribenzoate **9***c* along with less pure fractions. Recrystallization from ether – petroleum ether gave material with mp 134–136°C; $[\alpha]_D^{21}$ +11.1° (*c* 0.95, $CHCl_3$); ir (film from solution): 1725 (b, $COOCH_3$, φCOO), 1600, 1582 cm^{-1}; 200 MHz nmr δ: 1.79 (q, 1H, *J* = 11 Hz), 2.12 (m and ABq of d, 3H, *J* = 6, 7, 15 Hz), 3.64 (s, 3H, OCH_3), 4.02 (m, 1H), 4.19 (m, 1H), 4.48 (ABq of d, *J* = 3, 5.5, 12 Hz), 5.44 (t of d, 1H, *J* = 4.5, 10 Hz), 5.54 (t, 1H, *J* = 10 Hz), 7.33–7.60 and 7.93–8.06 (m, 15H, φCOO—); mass spectrum (70 eV), *m/e* (rel.%): 289 (0.5), 288 (3.3), 275 (0.3), 263 (0.3), 105 (100), 77 (20.9). *Anal.* calcd. for $C_{30}H_{28}O_9$: C 67.66%, H 5.30%; found: C 67.37%, H 5.31%.

Diacid **10**

Partially resolved (*R*,*R*)-Feist's acid (88 mg, $[\alpha]_{546}^{22}$ +172° (*c* 0.6 EtOH), (lit. (8) $[\alpha]_{546}^{25}$ +176° (*c* 0.7, EtOH)) was hydrogenated in a Parr apparatus at 40 psi, using dry H_2 gas in 10 mL ethyl acetate over 10 mg of 5% Pd on charcoal. After 1 h, the catalyst was filtered off and washed several times with ethyl acetate, and the combined filtrate and washings were evaporated to give 90 mg of crude diacid **10**, mp 162.5–163.5°C, $[\alpha]_{546}^{21}$ +110°, $[\alpha]_D^{21}$ +92° (*c* 0.8, EtOH). When recrystallized from ether – petroleum ether, the diacid gave mp 163–164°C. No evidence for the formation of 2-ethylsuccinic acid could be found, as had been reported (9). We report here, for the first time, spectral data for **10**: 60 MHz nmr δ: 1.31 (d, 3H, *J* = 5.5 Hz, CH_3), 1.61–2.51 (m, 3H), 11.70 (bs, 2H, COOH); mass spectrum (70 eV) *m/e* (rel. %): 127 (1.9), 126 (5.1) ($M^+ - H_2O$), 100 (12.9) ($M^+ - CO_2$), 99 (100) ($M^+ - COOH$). *Anal.* calcd. for $C_6H_8O_4$: C 50.00%, H 5.60%; found: C 49.75%, H 5.75%.

Synthetic Dibenzoate **12**a

A solution of 21 mg of diacid **10** (0.15 mmol) in 1.5 mL of dry THF was treated with 0.38 mL of a 1 *M* THF solution of BH_3 (0.38 mmol) by dropwise addition at room temperature, under a dry N_2 atmosphere. A precipitate was immediately formed, accompanied by the evolution of gas. After stirring for 1 h,

Can. J. Chem. Downloaded from www.nrcresearchpress.com by 210.87.254.105 on 09/05/12
For personal use only.

methanol was added, and the whole evaporated to dryness. Methanol was again added and evaporated three times to complete the distillation of trimethyl borate. The residue after the final evaporation was dissolved in 2 mL of pyridine, and treated with 0.05 mL of benzoylchloride (0.45 mmol), and a trace of 4-dimethylaminopyridine. After work-up as with **9***c*, the crude dibenzoate was purified by flash chromatography, using 5% ethyl acetate in petroleum ether to give 31 mg of pure dibenzoate **12***a* (66%) as an oil, $[\alpha]_D^{22} -12.9°$ (*c* 1.53, $CHCl_3$); ir (neat): 1710–1730 (4 pks, ϕCOO), 1602, 1585 cm^{-1}; 200 MHz F.T. nmr δ: 1.03–1.44 (m, 3H ring H), 1.17 (s, 3H, CH_3), 4.06 and 4.26–4.49 (d of d + m, 4H, CH_2OBz), 7.34–7.58 and 8.02 (m + d, 10H, ϕCOO); mass spectrum (70 eV) *m/e* (rel. %): 324 (0.2) (M^+), 219 (0.1) ($M^+ - \phi CO$), 205 (0.4), 204 (4.2), 203 (30.5), 105 (100). *Anal.* calcd. for $C_{18}H_{20}O_4$: C 74.05%, H 6.22%; found: C 73.79%, H 6.34%.

*Methyl 5,6-Dibenzoyloxypolyangioate (Ambruticin Methyl Ester Dibenzoate) 11*a

Methyl 5,6-dihydroxypolyangioate **11** (R = Me) (1), obtained from the sodium salt of ambruticin by acidification (Dowex 50W-X8 resin in ethanol) and methylation (CH_2N_2 in ether), was benzoylated in the usual manner for 2 days, and, after normal work-up, was purified by flash chromatography, using 20% ethyl acetate in petroleum ether to give dibenzoate **11***a* as a yellowish oil, ir (neat): 1725 (b, COOR), 1665 (w), 1600, 1580 cm^{-1}; 200 MHz nmr δ: 0.59–1.00 (m, 10H), 1.15–1.91 (m, 6H), 1.58 and 1.60 (2s, 6H, CH_3), 1.99–2.09 (m, 1H), 2.38–2.77 (m + ABq of d, 3H, J = 6,7,16 Hz), 3.00 (q, 1H), 3.70 (s, 3H, OCH_3), 3.82 (d of d, 1H, J = 3, 10 Hz), 3.94 (d of d, 1H, J = 6.5, 10 Hz), 4.03–4.19 (m, 2H), 4.95 (d of d, 1H, J = 9, 16 Hz), 5.17–5.58 (m, 7H), 7.39–7.65 and 7.83–8.13 (m, 10H, ϕ); mass spectrum (70 eV C.I.) *m/e* (rel. %): 697 (19.1) ($M^+ + 1$), 681 (3.8) ($M^+ - 15$), 680 (9.9), 573 (1.5), 559 (1.2), 531 (4.8), 479 (6.3), 467 (2.2), 456 (2.2), 454 (15.6), 435 (23.9), 357 (11.6), 331 (27.1), 263 (10.6), 209 (43.5), 193 (29.4), 123 (100), 105 (13.5).

*Ozonolytic Cleavage of 11*a*: Natural-source Tribenzoate 9*a *and Dibenzoate 12*a

Dibenzoate **11***a* (50 mg, 0.07 mmol) in 75 mL of dry methylene chloride was ozonolysed at −78°C until the blue color persisted. After flushing the excess ozone with a stream of nitrogen, 1 mL of dimethylsulfide was added at −78°C and the mixture was allowed to warm up to room temperature with stirring. To this was added 4.3 mL of a 0.14 *M* solution of zinc borohydride in ether (large excess), and the mixture was stirred a further 90 min while a precipitate formed. Enough saturated ammonium chloride solution was then added slowly to dissolve the precipitate and destroy excess borohydride. After separating the organic layer, the aqueous layer was extracted with ethyl acetate (6 × 40 mL), evaporated to near-dryness and reextracted with ethyl acetate (2 × 20 mL). The combined organic layers were dried ($MgSO_4$) and evaporated to give a crude mixture of alcohols. Flash chromatography of the mixture, eluting with 1:1 ethyl acetate – acetone (distilled over $KMnO_4$), furnished 3.7 mg of diol **12**, which when benzoylated as with synthetic **12**, gave 3.1 mg of dibenzoate **12***a* (13% from **11***a*), $[\alpha]_D^{21} -9.0°$ (*c* 0.15, $CHCl_3$), after hplc, using a mixture of ethyl acetate (2%), and methanol (0.3%) in petroleum ether. The remaining fractions after flash chromatography were combined, evaporated, and the residue was resubmitted to flash chromatography, eluting this time with 1:1 ethyl acetate – petroleum ether to give 22 mg of alcohol **9***c* (R^1 = H), which was immediately benzoylated as with synthetic **9***b* to afford 8.1 mg of pure crystalline tribenzoate **9***c* (21%, based on **11***a*), $[\alpha]_D^{21} +8.6°$ (*c* 0.4, $CHCl_3$), mp and mixture mp with synthetic **9***c* 132–134°C after recrystallization from ether – petroleum ether.

Dibenzoate **12***a* so prepared ran as one spot together with synthetic **12***a* on tlc, and was also homogeneous on flash chromatography and hplc analytical columns. Its spectra (200 MHz ^{1}Hmr, ir, and mass) were nearly superimposable with those of synthetic **12***a*, indicating the presence of a contaminant. Tribenzoate **9***c* so prepared had spectra (200 MHz nmr, ir, E.I. mass) superimposable with those of synthetic **9***c*. Mass spectrum (70 eV C.I.): *m/e* (rel. %): 533 (8.1) ($M^+ + 1$), 425 (3.8), 413 (3.1), 412 (11.6), 411 (50.8) ($M^+ - \phi COO$), 123 (100) ($\phi COOH_2^+$), 105 (33.8).

Acknowledgements

We thank Dr. N. Elmore for generously providing a sample of the sodium salt of ambruticin, A. Ugolini for the 200 MHz nmr spectra, and Dr. O. Mamer and associates for the mass spectra. Financial support by the Natural Sciences and Engineering Research Council of Canada is also gratefully acknowledged.

1. D. T. Connor, R. Clive Greenough, and M. von Strandtmann. J. Org. Chem. **42**, 3664 (1977).
2. H. Zinner, E. Wittenberg, and G. Rembarz. Chem. Ber. **92**, 1614 (1959).
3. P. Bakuzis, M. L. F. Bakuzis, and T. F. Weingartner. Tetrahedron Lett. 2371 (1978).
4. H. Zinner, G. Rembarz, and H.-P. Klöcking. Chem. Ber. **90**, 2688 (1957).
5. (*a*) M. Miyashita, A. Yoshikoshi, and P. A. Grieco. J. Org. Chem. **42**, 3772 (1977); (*b*) R. Sterzycki. Synthesis, 724 (1979).
6. S. Czernecki, C. Georgoulis, and C. Provenlenghiou. Tetrahedron Lett. 3535 (1976).
7. C. A. Russell and L. A. Ochrymowycz. J. Org. Chem. **34**, 3618 (1969).
8. W. von E. Doering and H. D. Roth. Tetrahedron, **26**, 2825 (1970).
9. (*a*) F. Feist. Ann. **436**, 125 (1924); (*b*) M. G. Ettlinger. J. Chem. Soc. 922 (1957); (*c*) G. A. R. Kon and H. R. Nanji. J. Chem. Soc. 2557 (1932).
10. W. Clarke Still, M. Kahn, and A. Mitra. J. Org. Chem. **43**, 2923 (1978).
11. H. Zinner, H. Brandner, and G. Rembarz. Chem. Ber. **89**, 800 (1956).
12. A. Hassner and C. Heathcock. J. Org. Chem. **29**, 1350 (1964).

Kinetic studies of the reactions of 2,4,6-trinitrotoluene and 2,4,6-trinitrotoluene-d_3 with ion-paired KOBu^t and free *tert*-butoxide ion in *tert*-butanol

ALBERT R. NORRIS

Department of Chemistry, Queen's University, Kingston, Ont., Canada K7L 3N6

Received May 22, 1980

ALBERT R. NORRIS. Can. J. Chem. **58**, 2178 (1980).

The reactions of 2,4,6-trinitrotoluene (TNT) and TNT-d_3 (deuterated methyl group) with tetra-*n*-butylammonium *tert*-butoxide and with potassium *tert*-butoxide (KOBu^t), in the absence and presence of the crown ethers 18-crown-6, and dicyclohexyl-18-crown-6, have been studied kinetically in *tert*-butanol at 30.0°C. Evidence is presented to support the suggestion that, at ratios of crown ether to base > 1, the reactive base species is free *tert*-butoxide ion and that this rapidly reacts with TNT or TNT-d_3 to form, in each case, a mixture of σ-complex and purple anion. Specific rate constants for the reactions of free *tert*-butoxide ion and ion-paired KOBu^t with TNT and TNT-d_3 to form both σ-complex and purple anion are compared.

ALBERT R. NORRIS. Can. J. Chem. **58**, 2178 (1980).

On a étudié la cinétique des réactions du trinitro-2,4,6 toluène (TNT) et du TNT-d_3 (groupe méthyle deutéré) avec le *tert*-butylate de tétra-*n*-butylammonium et avec le *tert*-butylate de potassium (*t*BuOK) en l'absence et en présence des éthers 18-couronne-6 et dicyclohexyl-18 couronne-6 dans le *tert*-butanol à 30°C. On apporte des données pour appuyer la suggestion qu-à des rapports d'éther couronne/base > 1 l'espèce basique réactive est l'ion *tert*-butylate libre et cet ion réagit rapidement avec le TNT ou le TNT-d_3 pour former dans chaque cas un mélange d'un complexe σ et d'un anion pourpre. On compare la constante de vitesse spécifique des réactions de l'ion *tert*-butylate libre et de la paire d'ion *t*BuOK avec le TNT et le TNT-d_3 pour former le complexe σ et l'anion pourpre.

[Traduit par le journal]

Introduction

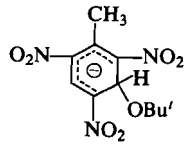
The reactions of nitroaromatic compounds with alkoxide ions in alcohols or dipolar aprotic solvents can lead to a variety of reaction products including σ- and π-complexes, radical anions, and anions derived via loss of a proton from the nitroaromatic (1).

We have previously reported on the σ-complex formation reactions of 1,3,5-trinitrobenzene (TNB) and 1,3,5-trideutero-2,4,6-trinitrobenzene (TNB-d_3) (2) and the σ-complex formation and proton abstraction reactions of 2,4,6-trinitrotoluene (TNT) and 2,4,6-trinitrotoluene fully deuterated at the methyl position (TNT-d_3) with alkoxide ions (RO^-) in the corresponding alcohols (ROH) (3–5).

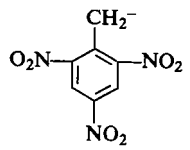
The results of kinetic and spectrophotometric studies of the reactions of *tert*-butoxide ion ($^-$OBu^t) with TNT and TNT-d_3 in *tert*-butanol were interpreted in terms of a simultaneous formation of σ-complex and "purple anion", **1** and **2**, and **3** and **4**, respectively, in each system (5).

These products were considered to result from the interactions of substrate with ion-paired KOBu^t, although the reaction of substrate with free *tert*-butoxide ion could not be ruled out with absolute certainty. In both systems, the purple colored anion, TNT^- (**2**) or TNT-d_2^- (**4**), predominated over σ-complex at equilibrium. The equilibrium constant (K) for the formation of **2** at 30.0°C was determined to lie between 5×10^4 and 10^6 M^{-1}.

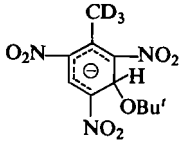
In an attempt to gain more detailed information concerning the role of ion-pairing in determining both the reactivity of the *tert*-butoxide ion and the relative stabilities of both σ-complex and purple anion in these systems, we have studied the reactions of TNT and TNT-d_3 with tetra-*n*-butylammonium *tert*-butoxide ((*n*-BU)$_4$NOBu^t) and with potassium *tert*-butoxide in the absence



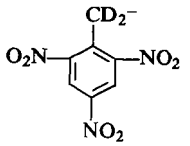
1



2



3



4

and presence of the added polyethers 1,4,7,10,13,-16-hexaoxacyclooctadecane (18-crown-6) and 2,3,11,12-dicyclohexano-1,4,7,10,13,16-hexaoxyacyclooctadecane (DCH-18-crown-6) (6–8).

Results and Discussion

Kinetic Studies Employing TNT as Substrate (30.0°C)

Over the range of stoichiometric base concen-

0008-4042/80/202178-05$01.00/0

©1980 National Research Council of Canada/Conseil national de recherches du Canada

Can. J. Chem. Downloaded from www.nrcresearchpress.com by 210.87.254.105 on 09/05/12
For personal use only.

Can. J. Chem. Downloaded from www.nrcresearchpress.com by 210.87.254.105 on 09/05/12
For personal use only.

trations ([KOBu^t]$_0$) $1.15 \times 10^{-3} M$ to $1.80 \times 10^{-2} M$, in the absence of added crown ether, at each base concentration employed and at each wavelength at which absorbances (A) were measured (420, 520, and 650 nm), plots of log ($A_\infty - A_t$) versus time were linear to at least 80% completion of reaction. For a given concentration of base, the slopes of the log ($A_\infty - A_t$) versus time plots ($\equiv k_{obs}/2.303$) were, within experimental error, independent of the initial concentration of TNT (1.0×10^{-5} to $5.0 \times 10^{-5} M$) and of the wavelength at which values of A were measured. The plot of k_{obs} versus [KOBu^t]$_0$ was linear, passed through the origin, and possessed a slope of $7{,}600 \pm 400\ M^{-1}\ s^{-1}$. A slope of $7{,}000 \pm 400\ M^{-1}\ s^{-1}$ for the k_{obs} versus [KOBu^t]$_0$ plot was reported earlier (5).

The measured A_∞ values at 420, 520, and 650 nm point to the exclusive formation of only purple anion **2** in the reaction process described above. This result is completely in accord with the observations made in previous studies (5).

At any given [KOBu^t]$_0$ over the range $1.15 \times 10^{-3} M$ to $1.15 \times 10^{-2} M$, the addition of crown ether resulted in a marked enhancement in the rate of change in absorbance at 420, 520, or 650 nm. For each of the three wavelengths at which absorbances (A) were measured, plots of log ($A_\infty - A_t$) versus time were linear to at least 80% completion of reaction. The magnitudes of k_{obs} were experimentally reproducible to ±5% and were, within experimental error, independent of the wavelength at which values of A were measured and independent of [TNT]$_0$ ($1.0 \times 10^{-5} M$ to $5.0 \times 10^{-5} M$). At any fixed initial concentration of base in the range [KOBu^t]$_0$ $1.50 \times 10^{-4} M$ to $10.0 \times 10^{-4} M$, k_{obs} values increased linearly with increasing ratio of [crown ether]$_0$/[KOBu^t]$_0$ and reached a maximum value, k_{obs} (max), at a ratio of [crown ether]$_0$/[KOBu^t]$_0 \geq 1$. Within experimental error, k_{obs} (max) at a given [KOBu^t]$_0$ was the same for both polyethers employed in these studies.

Values of k_{obs} (max) at 30.0°C plotted versus the [KOBu^t]$_0$ are shown in Fig. 1. The slope of the resulting straight line, which passes through the origin, is $6.5 \pm 0.5 \times 10^5\ M^{-1}\ s^{-1}$ and is, within experimental error, the same for both 18-crown-6 and DCH-18-crown-6.

At the same stoichiometric concentration of *tert*-butoxide ion, the reaction of TNT with (n-butyl)$_4$NOBu^t was found to be very much more rapid than the reaction of TNT with KOBu^t. In the reactions of TNT with (n-butyl)$_4$NOBu^t, absorbances recorded at 420 and 520 nm yielded log ($A_\infty - A_t$) versus time plots linear to approximately

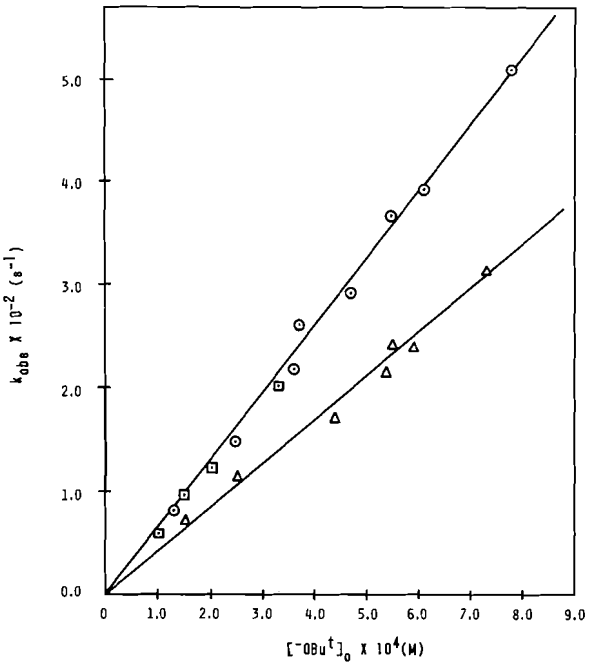


FIG. 1. k_{obs} versus [$^-$OBu^t]$_0$ for the following reactions at 30.0°C in *tert*-butanol: ⊙ 2,4,6-trinitrotoluene–KOBu^t–18-crown-6 at ratios of 18-crown-6 to KOBu$^t \geq$ 2:1; ⊡ 2,4,6-trinitrotoluene–(C_4H_9)$_4$NOBu^t; △ 2,4,6-trinitrotoluene-d_3–KOBu^t–18-crown-6 at ratios of 18-crown-6 to KOBu$^t \geq$ 2:1.

80% completion of the reaction. At a given [(n-butyl)$_4$NOBu^t]$_0$ in the range 1.0×10^{-4} to $5.0 \times 10^{-4} M$, k_{obs} values were independent of the [TNT]$_0$ (1.0×10^{-5} to $5.0 \times 10^{-5} M$) and the wavelengths at which values of A were recorded. The k_{obs} values could, however, only be obtained with a reproducibility of from ±10 to ±15% in this system as compared to a reproducibility of ±5% in the TNT–KOBu^t and TNT–KOBu^t–crown ether reaction systems. The plot of k_{obs} versus [(n-butyl)$_4$NOBu^t]$_0$ was linear, passed through the origin and possessed a slope of $6 \pm 1 \times 10^5\ M^{-1}\ s^{-1}$ (see Fig. 1).

In these fast reactions of TNT with (n-butyl)$_4$NOBu^t and KOBu^t–crown ether, at ratios of [crown ether]$_0$/[KOBu^t]$_0$ of from 2:1 to 16:1, the recorded A_∞ values at 420, 520, and 650 nm were consistent with the formation of a reaction mixture consisting of 60 ± 5% σ-complex **1** and 40 ± 5% purple anion **2**. This ratio was essentially constant over the entire range of [KOBu^t]$_0$ and ratios of [crown ether]$_0$/[KOBu^t]$_0$ (when ≥ 1) utilized in these studies.

Following the rapid formation of this mixture of products was a comparatively slow reaction leading to the formation of **1** as the exclusive nitro-

Can. J. Chem. Downloaded from www.nrcresearchpress.com by 210.87.254.105 on 09/05/12
For personal use only.

aromatic species in solution. Values of k_{obs} for this slow reaction were, within experimental error, independent of the wavelength at which values of A were measured, independent of $[TNT]_0$, independent of $[KOBu^t]_0$, and at any given $[KOBu^t]_0$, independent of $[crown\ ether]_0/[KOBu^t]_0$ ratio at ratios ≥ 1. The mean value of k_{obs} for the slow reaction was $0.10 \pm 0.02\ s^{-1}$ at 30.0°C.

Kinetic Studies Employing TNT-d_3 as Substrate (30.0°C)

In the absence of crown ether, over the range of $[KOBu^t]_0$ 1.15×10^{-3} to $1.15 \times 10^{-2}\ M$, absorbances recorded at 430 nm yielded log $(A_\infty - A_t)$ versus time plots linear to approximately 60 to 70% completion of reaction. The slopes of these lines were, at a constant $[KOBu^t]_0$, independent of $[TNT\text{-}d_3]_0$. A plot of k_{obs} versus $[KOBu^t]_0$ was linear, passed through the origin, and yielded a slope of $1{,}800 \pm 100\ M^{-1}\ s^{-1}$.

At any fixed concentration of $KOBu^t$ over the range $[KOBu^t]_0$ 1.15×10^{-3} to $1.15 \times 10^{-2}\ M$, addition of crown ether resulted in a marked increase in the rate of increase in absorbance at 430 nm. Plots of log $(A_\infty - A_t)$ versus time were linear to at least 80% completion of the reaction. The slopes of these plots were experimentally reproducible to ±5% and were, within experimental error, independent of $[TNT\text{-}d_3]_0$ (1.0×10^{-5} to $6.0 \times 10^{-5}\ M$). At any fixed, initial concentration of base in the range $[KOBu^t]_0$ 1.50×10^{-4} to $1.50 \times 10^{-3}\ M$, k_{obs} increased linearly with increasing ratio of $[crown\ ether]_0/[KOBu^t]_0$ and reached a maximum value, k_{obs} (max), at ratios of $[crown\ ether]_0/[KOBu^t]_0 \geq 1$. Within experimental error, k_{obs} (max) for the reaction of TNT-d_3 with $[KOBu^t]_0$ was the same for both polyethers used in the studies. For a fixed $[KOBu^t]_0$ over a wide range of initial base concentrations and with $[crown\ ether]_0/[KOBu^t]_0$ ratios of from 1:1 to 16:1, the average ratio of k_{obs} (max) for TNT/k_{obs} (max) for TNT-d_3 at 30.0°C, was found to be 1.58 ± 0.02 (mean of 21 runs).

Values of k_{max} (TNT-d_3) at 30.0°C plotted as a function of $[KOBu^t]_0$ are shown in Fig. 1. The slope of the resulting straight line, which passes through the origin, is $4.2 \pm 0.4 \times 10^5\ M^{-1}\ s^{-1}$.

In the reactions of TNT-d_3 with $KOBu^t$–crown ether at ratios of $[crown\ ether]_0/[KOBu^t]_0$ of from 2:1 to 16:1 the A_∞ values at 430, 520, and 600 nm are consistent with the formation of σ-complex **3** and the purple anion **4**, in the ratio of 90 ± 5:10 ± 5.

A further slow reaction following the rapid formation of the above reaction mixture followed the same pattern as observed in the slow reaction in the TNT–$KOBu^t$–crown ether system. The k_{obs} in this case was $0.030 \pm 0.005\ s^{-1}$ at 30.0°C, independent of $[TNT\text{-}d_3]_0$, $[KOBu^t]_0$, and at a fixed $[KOBu^t]_0$, independent of $[crown\ ether]_0/[KOBu^t]_0$ ratio.

At any given stoichiometric concentration of *tert*-butoxide ion over the range $1.0 \times 10^{-4}\ M$ to $1.5 \times 10^{-3}\ M$, the rates of reaction of both TNT and TNT-d_3 are much greater when either $KOBu^t$, in the presence of crown ether, or $(n\text{-butyl})_4NOBu^t$ is used as a source of the *tert*-butoxide ion than when $KOBu^t$ is used as a source of the *tert*-butoxide ion. For any given $[^-OBu^t]_0$, the maximum k_{obs} in the $KOBu^t$–crown ether systems is achieved at $[crown\ ether]_0/[KOBu^t]_0 \geq 1$. Also, for any given $[^-OBu^t]_0$, both crown ether–$KOBu^t$ combinations at ratios of $[crown\ ether]_0/[KOBu^t]_0 > 1$ and $(n\text{-butyl})_4NOBu^t$ lead, within experimental error, to the same k_{obs} (Fig. 1). It seems reasonable therefore to associate the reactions of TNT and TNT-d_3 with $(n\text{-butyl})_4NOBu^t$ and with $KOBu^t$–crown ether combinations, at ratios $[crown\ ether]_0/[KOBu^t]_0 > 1$, as reactions of substrate with free *tert*-butoxide ion (7, 8).

If, as suggested previously, the reactive form of base when $KOBu^t$ is present in *tert*-butanol at 30.0°C is the ion-paired $KOBu^t$ species then, at any given stoichiometric concentration of *tert*-butoxide ion, the ratio of k_{obs} for the reaction of TNT with free *tert*-butoxide ion to k_{obs} for the reaction of TNT with ion-paired $KOBu^t$ species is of the order of 86. For the case of TNT-d_3 as substrate, the corresponding ratio of k_{obs} values at any given stoichiometric concentration of *tert*-butoxide ion is approximately 228. The ratio is not the same for the two substrates because k_{obs} is a pseudo-first order rate constant relating to the disappearance of substrate (TNT or TNT-d_3) along two competing pathways and the proportion of reaction along each pathway is not the same for the two substrates.

More meaningful comparisons of rate constants may be achieved as follows. If we consider that TNT and TNT-d_3 undergo essentially irreversible reaction with free *tert*-butoxide ion via parallel first order reaction paths then

[1] $k_{obs}\,(max) = (k_1 + k_2)[^-OBu^t]_0$

for the TNT system and

[2] $k_{obs}\,(max) = (k_3 + k_4)[^-OBu^t]_0$

for the TNT-d_3 system. In each case, k_n is the specific rate constant associated with the formation of species n according to the rate law

[3] $-d[substrate]/dt = k_n[substrate][^-OBu^t]_0$

Also, for the proposed reaction scheme

[4] $k_1/k_2 = [\mathbf{1}]/[\mathbf{2}]$

and

[5] $k_3/k_4 = [3]/[4]$

at any time t during the initial fast reaction (9).

Hence, from the slopes of the plots of k_{obs} (max) versus $[^-OBu^t]_0$ in Fig. 1 we have that

[6] $k_1 + k_2 = 6.5 \times 10^5\ M^{-1}\ s^{-1}$

and

[7] $k_3 + k_4 = 4.2 \times 10^5\ M^{-1}\ s^{-1}$

Since in the reaction of TNT-d_3 with free $^-OBu^t$ the initial fast reaction is associated with the formation of **3** and **4** in a 90 to 10 ratio, the values of k_3 and k_4 are calculated to be $\geq 3.8 \times 10^5\ M^{-1}\ s^{-1}$ (maximum value $4.2 \times 10^5\ M^{-1}\ s^{-1}$) and $4.2 \times 10^4\ M^{-1}\ s^{-1}$, respectively at 30.0°C.

Assuming that there is no kinetic isotope effect associated with the formation of the σ-complexes **1** and **3**, we obtain a value of k_1 of $\geq 3.8 \times 10^5\ M^{-1}\ s^{-1}$ at 30.0°C. Since

$$k_1 + k_2 = 6.5 \times 10^5\ M^{-1}\ s^{-1}$$

we find a maximum value of k_2 of $2.7 \times 10^5\ M^{-1}\ s^{-1}$ (minimum value $2.3 \times 10^5\ M^{-1}\ s^{-1}$). A summary of the values of the specific rate constants k_1, k_2, k_3, and k_4 is presented in Table 1.

The values of the specific rate constants k_2 and k_4 suggest that a kinetic isotope effect of 6.4 is associated with the formation of **2** and **4** via reaction of substrate with free *tert*-butoxide ion. This may be compared to a kinetic isotope effect of 8 ± 1 reported earlier (5) for the formation of **2** and **4** via the reaction of substrate and ion-paired KOBu^t. Kinetic isotope effects of 8.4 ± 1.4 and 7.0 ± 0.5 have been reported for the formation of **2** and **4** by reaction of substrate with free isopropoxide ion in isopropanol and free ethoxide ion in ethanol, respectively (3, 4).

The k_1 and k_2 values, obtained as outlined above, predict a 58.5 to 41.5 ratio of **1** to **2** at the completion of the initial fast reaction. This is in very good agreement with the 60 ± 5 to 40 ± 5 ratio observed experimentally.

The values of the specific rate constants listed in Table 1 clearly indicate that, in the reactions of TNT and TNT-d_3 to form both σ-complex (**1** or **3**) and purple anion (**2** or **4**), free *tert*-butoxide ion is a far more reactive species than is ion-paired KOBu^t. Higher reactivities of free ions as compared to ion pairs have been observed previously in both nucleophilic displacement (7, 8, 10) and electron transfer processes (11, 12). One way in which the results may be rationalized is in terms of a concept involving ion-pairing equilibria in the transition state complex (13). To the extent that charge is dispersed in the transition state relative to the reactants, ion pairing is expected to be less important in the transition state and the reaction is therefore faster for the freer species. Our higher ratio of k(free $^-OBu^t$)/k(KOBu^t) for formation of the extensively charge delocalized σ-complex (~270) as compared to the less extensively charge delocalized purple anion (~ 46) seems to be in accord with this proposal.

TABLE 1. Specific rate constants for the reactions of TNT and TNT-d_3 with free and ion-paired *tert*-butoxide ion in *tert*-butanol at 30.0°C

Species formed	k^a for ion paired KOBu^t ($M^{-1}\ s^{-1}$)	k^b for free $^-OBu^t$ ion^b ($M^{-1}\ s^{-1}$)	$\frac{k_n\text{ (free }^-OBu^t)}{k_n\text{ (KOBu}^t)}$
1	1.4×10^3	3.8×10^5	2.7×10^2
2	7.0×10^3	2.7×10^5	0.39×10^2
3	1.4×10^3	3.8×10^5	2.7×10^2
4	8.0×10^2	4.2×10^4	0.53×10^2

[a]Obtained as described in ref. 5.
[b]Obtained as described in the text.

Based on studies of the reactions of sodium isopropoxide with TNT and TNT-d_3 in isopropanol, it was concluded that free isopropoxide ion was more reactive than sodium isopropoxide in the proton transfer reaction but possessed comparable reactivity to the ion-pair in the σ-complex formation reaction (4). Different orders of reactivity in the sodium isopropoxide and potassium *tert*-butoxide systems might well arise because of differences in steric properties and solvation requirements in the two base systems. Further speculation on this point must await a direct study, following procedures described in this paper, of the reactivity of free isopropoxide ion with TNT and TNT-d_3.

Experimental

Materials

The preparation and purification of TNT and TNT-d_3 were as previously described (3, 4). Reagent grade *tert*-butanol was refluxed over Linde 4 Å Molecular Sieve for several hours, then distilled under nitrogen. Only the middle fraction of the distillate was retained. Solutions of potassium *tert*-butoxide were prepared and standardized as previously described (5). The crown ethers, 18-crown-6 and dicyclohexyl-18-crown-6, obtained from PCR Research Chemicals Inc., were dried to constant weight *in vacuo* before use and weighed and handled under an atmosphere of dry nitrogen. Eastman tetra-*n*-butylammonium hydroxide titrant in methanol (1 *M*) was used as received. Solutions containing tetra-*n*-butylammonium *tert*-butoxide were prepared following the procedure outlined by Guthrie *et al.* (14) and standardized in the same manner as the solutions of potassium *tert*-butoxide. Different batches of tetra-*n*-butylammonium *tert*-butoxide yielded reproducible kinetic results only when the evaporation and pumping down procedure used to remove methanol was repeated at least 4 times. Stock solutions (~ 10^{-1} *M*) were a pale yellow color but the solutions used in the kinetic runs (~ 10^{-4}–10^{-3} *M*) were colorless.

Can. J. Chem. Downloaded from www.nrcresearchpress.com by 210.87.254.105 on 09/05/12
For personal use only.

Procedure

The equipment and procedures used in carrying out kinetic measurements and in obtaining spectral data for the σ-complex and the purple anion have been described previously (3–5).

Acknowledgements

Financial support by the Natural Sciences and Engineering Research Council of Canada is acknowledged. The author is indebted to Dave Creber, Nancy Lever, and John Patterson for their assistance in carrying out the experimental work and to Dr. K. E. Russell for discussions concerning the interpretation of the experimental results.

1. E. BUNCEL, A. R. NORRIS, and K. E. RUSSELL. Q. Rev. London, **22**, 123 (1968); M. R. CRAMPTON. Adv. Phys. Org. Chem. **7**, 211 (1969); M. J. STRAUSS. Chem. Rev. **70**, 667 (1970).
2. L. H. GAN and A. R. NORRIS. Can. J. Chem. **49**, 2490 (1971).
3. E. BUNCEL, A. R. NORRIS, K. E. RUSSELL, and R. TUCKER. J. Am. Chem. Soc. **94**, 1646 (1972).
4. E. BUNCEL, A. R. NORRIS, K. E. RUSSELL, P. SHERIDAN, and H. WILSON. Can. J. Chem. **52**, 1750 (1974).
5. E. BUNCEL, A. R. NORRIS, K. E. RUSSELL, and H. WILSON. Can. J. Chem. **52**, 2306 (1974).
6. C. J. PEDERSEN and H. K. FRENDSDORFF. Angew. Chem. Int. Ed. Engl. **11**, 16 (1972).
7. R. A. BARTSCH. Acc. Chem. Res. **8**, 239 (1975), and references cited therein.
8. D. J. RABER, J. M. HARRIS, and P. v. R. SCHLEYER. *In* Ions and ion pairs in organic reactions. Vol. 2. *Edited by* M. Szwarc. Wiley, New York. 1974.
9. A. A. FROST and R. G. PEARSON. Kinetics and mechanism. Wiley, New York. 1961.
10. A. JARCZEWSKI, G. SCHROEDER, and K. T. LEFFEK. J. Chem. Soc. Perkin Trans. II, 866 (1979).
11. S. BANK and D. A. JUCKETT. J. Am. Chem. Soc. **97**, 567 (1975).
12. B. BOCKRATH and L. M. DORFMAN. J. Phys. Chem. **77**, 2618 (1973).
13. J. G. PACIFI, J. GARST, and E. G. JANZEN. J. Am. Chem. Soc. **87**, 3014 (1965); J. F. GARST. *In* Solute–solvent interactions. *Edited by* J. F. Coetzee and C. D. Ritchie. Marcel Dekker, New York, NY. 1969. p. 570.
14. R. D. GUTHRIE, G. R. WEISMAN, and L. G. BURDON. J. Am. Chem. Soc. **96**, 6955 (1974).

Can. J. Chem. Downloaded from www.nrcresearchpress.com by 210.87.254.105 on 09/05/12
For personal use only.

Aminomethylation of *N*-propargylphosphoramides. Synthesis of unsymmetrical acetylenic diamines

BERNARD CORBEL,[1] JEAN-PAUL PAUGAM, AND GEORGES STURTZ

Laboratoire de Chimie Hétéro-organique, ERA CNRS No. 612, Faculté des Sciences, Université de Bretagne Occidentale, F-29283 Brest, France

Received April 14, 1980

BERNARD CORBEL, JEAN-PAUL PAUGAM, and GEORGES STURTZ. Can. J. Chem. **58**, 2183 (1980).

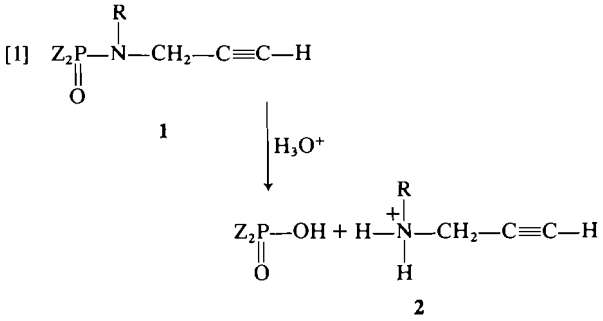
The preparation of *N*-alkyl-*N*-(4-dialkylamino-2-butynyl)phosphoramides **3** using the Mannich reaction is described. The acidic hydrolysis of those phosphoramides leads to unsymmetrical acetylenic diamines **4**.

BERNARD CORBEL, JEAN-PAUL PAUGAM et GEORGES STURTZ. Can. J. Chem. **58**, 2183 (1980).

On décrit la préparation des phosphoramides de *N*-alkyle et de *N*-(dialkylamino-4 butyne-2)yle **3** à l'aide de la réaction de Mannich. L'hydrolyse acide de ces phosphoramides conduit aux diamines acétyléniques dissymétriques **4**.

Introduction

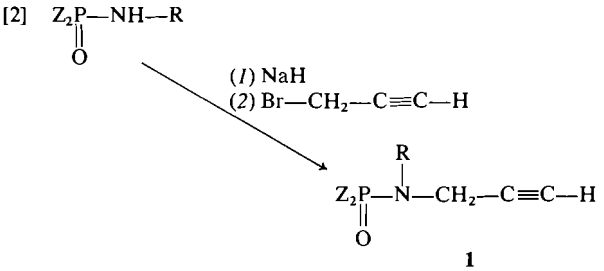
The propargylic ammonium salts **2** have been shown to act as specific irreversible inhibiting substrates for certain flavin-linked oxidases (1). We have recently shown that such compounds are readily prepared by the acid-catalysed hydrolysis of phosphoramides of the type **1** (eq. [1])



[1] $Z_2P(=O)-N(R)-CH_2-C\equiv C-H \xrightarrow{H_3O^+} Z_2P(=O)-OH + H-\overset{+}{N}(R)-CH_2-C\equiv C-H$

1 → **2**

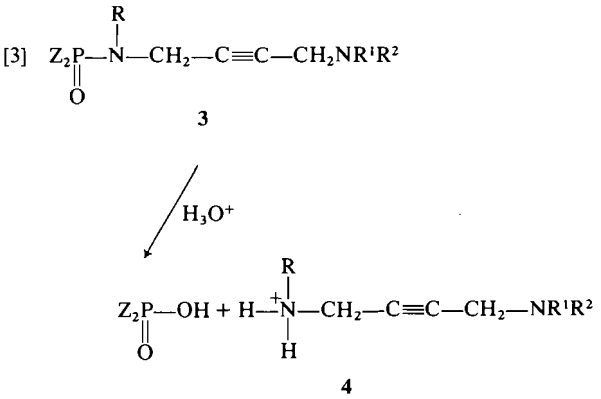
The phosphoramides in turn are obtained by the simple route shown in eq. [2] (2).



[2] $Z_2P(=O)-NH-R \xrightarrow[(2)\ Br-CH_2-C\equiv C-H]{(1)\ NaH} Z_2P(=O)-N(R)-CH_2-C\equiv C-H$

1

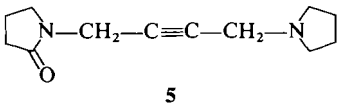
We now wish to report that aminomethylation of **1** leads to the unsymmetrical acetylenic derivatives **3** which are readily hydrolysed to unsymmetrical acetylenic diamines **4** (eq. [3])



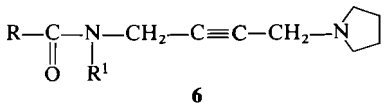
[3] $Z_2P(=O)-N(R)-CH_2-C\equiv C-CH_2NR^1R^2 \xrightarrow{H_3O^+} Z_2P(=O)-OH + H-\overset{+}{N}(R)-CH_2-C\equiv C-CH_2-NR^1R^2$

3 → **4**

The amides **3** themselves are also of considerable pharmacological interest due to their structural relationship to the potent muscarinic agent oxotremorine **5** (3)[2] and the recently described carboxamides **6** (4).



5



6

Results and Discussion

The *N*-propargylphosphoramides **1**, prepared according to eq. [2], were aminomethylated by first heating **1** with paraformaldehyde in dioxane containing Cu_2Cl_2 and then adding a secondary amine (eq. [4]).

[1]Author to whom correspondence should be addressed.

[2]See also ref. 1*b*, p. 1538.

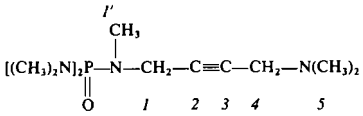
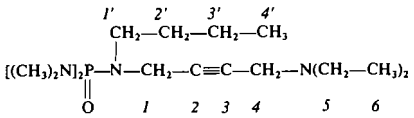
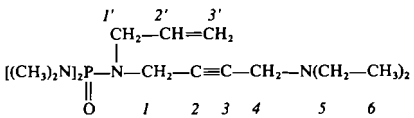
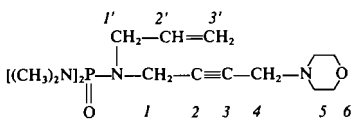
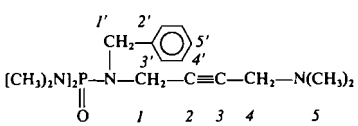
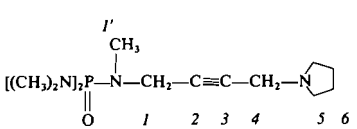
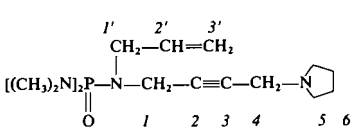
0008-4042/80/202183-06$01.00/0

©1980 National Research Council of Canada/Conseil national de recherches du Canada

Can. J. Chem. Downloaded from www.nrcresearchpress.com by 210.87.254.105 on 09/05/12
For personal use only.

Can. J. Chem. Downloaded from www.nrcresearchpress.com by 210.87.254.105 on 09/05/12
For personal use only.

TABLE 1. Physical characteristics of the phosphoramides **3** (eq. [4])

Entries	Phosphoramides 3	Molecular formula	Boiling point °C (Torr)	n_D^t	% Yield	^{1}H nmr δ ppm from TMS (δ = 0), *J* in Hz	^{13}C nmr δ ppm from TMS (δ = 0), J_{C-P} in Hz
3a		$C_{11}H_{25}N_4OP$ (260.2)	$133_{(0.05)}$	1.4840^{20}	90	2.29 (s, 6H); 2.73 (d, 3H, J_{P-H} = 8.6); 3.26 (t, 2H, J_{H-H} = 1.7); 3.84 (2t, 2H, J_{P-H} = 9.2).	C-1′ 33 (d, J_{CNP} = 3.6); C-1 38.1 (d, J_{CNP} = 6.1); C-2 80.7 (d, J_{CCNP} = 3.6); C-3 77.8; C-4 47.2; C-5 43.3.
3b		$C_{16}H_{35}N_4OP$ (330.2)	$140_{(0.01)}$	1.4800^{18}	61	1.07 (t, 9H); 1.44 (m, 4H); 2.59 (q, 4H, J_{H-H} = 7.1); 3.08 (m, 2H); 3.43 (t, 2H, J_{H-H} = 1.6); 3.85 (2t, 2H, J_{P-H} = 9.7).	C-1′ 44.6 (d, J_{CNP} = 3); C-2′, 3′, 4′ 29.5, 19.6, 13.4; C-1 34.8 (d, J_{CNP} = 5.5); C-2 80.6 (d, J_{CCNP} = 3); C-3 77.5; C-4 40; C-5 46.6; C-6 12.
3c		$C_{15}H_{31}N_4OP$ (314.2)	$152_{(0.05)}$	1.4885^{16}	70	1.07 (t, 6H); 2.59 (q, 4H, J_{H-H} = 7.1); 3.42 (t, 2H, J_{H-H} = 1.7); 3.5–4 (m, 4H); 5–6.1 (m, 3H).	C-1′ 48 (d, J_{CNP} = 3.6); C-2′ 134.3 (d, J_{CCNP} = 3); C-3′ 117.9; C-1 34.9 (d, J_{CNP} = 5.5); C-2 81 (d, J_{CCNP} = 3); C-3 78; C-4 40.5; C-5 47.2; C-6 12.5.
3d		$C_{15}H_{29}N_4O_2P$ (328.2)	$186_{(0.05)}$	1.5062^{17}	60	2.55 (m, 4H); 3.32 (t, 2H, J_{H-H} = 1.7); 3.55–4.02 (m, 8H); 5.02–5.91 (m, 3H).	C-1′ 47.9 (d, J_{CNP} = 3.6); C-2′ 134.1 (d, J_{CCNP} = 3); C-3′ 117.6; C-1 34.7 (d, J_{CNP} = 6.1); C-2 81.5 (d, J_{CCNP} = 3.1); C-3 77.9; C-4 47.1; C-5 51.9; C-6 66.5.
3e		$C_{17}H_{29}N_4OP$ (336.2)	$179_{(0.05)}$	1.5258^{18}	64	2.31 (s, 6H); 3.29 (t, 2H, J_{H-H} = 1.7); 3.71 (2t, 2H, J_{P-H} = 9.7); 4.32 (d, 2H, J_{P-H} = 8.6); 7.33 (m, 5H).	C-1′ 48.8 (d, J_{CNP} = 4.2); C-2′ 137.6 (d, J_{CCNP} = 3.6); C-3′, 4′ 128.5, 128.3; C-5′ 127.2; C-1 35.1 (d, J_{CNP} = 5.5); C-2 81 (d, J_{CCNP} = 3); C-3 79.2; C-4 48; C-5 44.1.
3f		$C_{13}H_{27}N_4OP$ (286.2)	$140_{(0.01)}$	1.4965^{20}	88	1.85 (m, 4H); 2.5–2.9 (m, 19H); 3.44 (t, 2H, J_{H-H} = 1.6); 3.82 (2t, 2H, J_{P-H} = 9.2).	C-1′ 33.8 (d, J_{CNP} = 3.6); C-1 39 (d, J_{CNP} = 6.1); C-2 80.6 (d, (J_{CCNP} = 4.2); C-3 79.4; C-4 43.4; C-5 52.5; C-6 23.8.
3g		$C_{15}H_{29}N_4OP$ (312.2)	$156_{(0.01)}$	1.4976^{22}	80	1.8 (m, 4H); 3.4 (t, 2H, J_{H-H} = 1.8); 3.5–4 (m, 4H); 5–6 (m, 3H).	C-1′ 47.1 (d, J_{CNP} = 3.6); C-2′ 133.4 (d, J_{CCNP} = 3); C-3′ 116.8; C-1 34 (d, J_{CNP} = 5.5); C-2 79.8 (d, J_{CCNP} = 2.5); C-3 77.6; C-4 42.1; C-5 51.4; C-6 22.8.

Can. J. Chem. Downloaded from www.nrcresearchpress.com by 210.87.254.105 on 09/05/12
For personal use only.

TABLE 1 (*Concluded*)

Entries	Phosphoramides 3	Molecular formula	Boiling point °C (Torr)	n_D^t	% Yield	^{1}H nmr δ ppm from TMS (δ = 0), J in Hz	^{13}C nmr δ ppm from TMS (δ = 0), J_{C-P} in Hz
3*h*		$C_{16}H_{30}N_3O_3P$ (343.2)	Crude		95	2.4 (m, 9H); 2.8 (d, 3H, J_{P-H} = 9.5); 3.1–3.6 (m, 6H); 3.9 (2t, 2H, J_{H-H} = 9.5).	C-1′ 33 (d, J_{CNP} = 3.4); C-1 38.6 (d, J_{CNP} = 6.8); C-2, C-3, C-7, C-8 79.8; C-4 48; C-5 39.8; C-6, C-9 43.2, 44.7; C-10 44.1.
3*i*		$C_{13}H_{25}N_2O_3P$ (288.1)	$134_{(0.01)}$	1.4720[18]	80	1.86 (m, 4H); 2.7 (m, 4H); 2.8 (d, 3H, J_{P-H} = 9.2); 3.5 (t, 2H, J_{H-H} = 1.8); 3.91 (2t, 2H, J_{P-H} = 9.2).	C-1′ 33.3 (d, J_{CNP} = 3.9); C-1 38.9 (d, J_{CNP} = 6.8); C-2 79.9 (d, J_{CCNP} = 2); C-3 79.8, C-4 43.2; C-5 52.5; C-6 23.9.
3*j*		$C_{11}H_{23}N_2O_3P$ (262.1)	$110_{(0.01)}$	1.4560[19]	90	2.23 (s, 6H); 2.67 (d, 3H, J_{P-H} = 9.3); 3.17 (t, 2H, J_{H-H} = 1.7); 3.7 (2t, 2H, J_{P-H} = 9.2).	C-1′ 33.3 (d, J_{CNP} = 3.6); C-1 38.9 (d, J_{CNP} = 6.1); C-2 80.7 (d, J_{CCNP} = 4.2); C-3 79; C-4 48; C-5 44.1.

Aminomethylation of propargylic derivatives carrying a variety of other functional groups such as hydroxyl, carbonyl, or nitrile, had previously been described (5). The experimental procedure used by us was adapted from Mornet and Gouin (6).

The aminomethylation of **1** was followed by gas chromatography and found to be complete within 5 min irrespective of the nature of the secondary amine employed. The aminomethylated products **3** were obtained as colorless oils after purification by vacuum distillation. They are indefinitely stable when stored in a refrigerator but deteriorate and turn brown upon standing at room temperature. The yields of the isolated products **3** produced according to eq. [4], together with some physical properties and spectroscopic data (^{1}H and ^{13}C nmr), are given in Table 1.

The deviation of the yields from the quantitative conversions of **1** → **3** indicated by the vpc analysis is due to some mechanical loss but primarily to decomposition if the distillation temperatures were excessively high (entries *d*, *e*). Neither changes in the nature of Z ($(CH_3)_2N$— to EtO—) nor use of different secondary amines had significant effect on the rate of aminomethylation of **1** and the product yield.

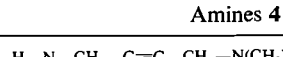
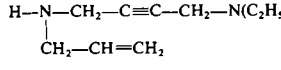
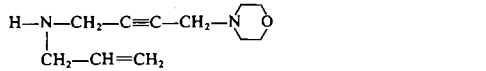
The phosphoramides **3** were cleaved to the diamines **4** upon refluxing in 3 *N* hydrochloric acid for 12 h. During the reflux period the solutions turned light yellow and dark brown respectively when purified samples of **3** or crude products were used. Workup of the reaction mixture followed by vacuum distillation gave the diamines **4** in good to excellent yields (Table 2). The spectroscopic and analytical data were in full agreement with the proposed structures. The compounds decompose unless stored at cold temperatures.

The use of the diamine **4***a* in the Mannich reaction followed by hydrolysis afforded the triamine **4***h* in 60% overall yield. The sequence suggests the possibility of preparing polyamines of the type **7**.

7

Can. J. Chem. Downloaded from www.nrcresearchpress.com by 210.87.254.105 on 09/05/12
For personal use only.

TABLE 2. Physical characteristics of the acetylenic diamines 4 (eq. [3])

Entries	Amines 4	Molecular formula	Boiling point °C (Torr)	% Yields[a]	^{1}H nmr
4*a*		$C_7H_{14}N_2$ (126.1)	$78_{(15)}$	75 (a), 79 (b)	2.22 (s, 1H); 2.31 (s, 6H); 2.48 (s, 3H); 3.23 (t, 2H, J_{HH} = 1.9); 3.41 (t, 2H).
4*b*		$C_{12}H_{24}N_2$ (196.2)	$90_{(0.05)}$	85	1.06 (t, 9H, J = 7.1); 1.12 (s, 1H); 1.41 (m, 4H); 2.24–2.84 (m, 6H); 3.4 (s, 4H).
4*c*		$C_{11}H_{20}N_2$ (180.2)	$120_{(10)}$	81	1.07 (t, 6H, J = 7.1); 1.32 (s, 1H); 2.55 (q, 4H); 3.44–3.56 (m, 6H); 4.95–6.25 (m, 3H).
4*d*		$C_{11}H_{18}N_2O$ (194.1)	$110_{(0.05)}$	82	1.32 (s, 1H); 2.57 (m, 4H); 3.19–3.55 (m, 6H); 3.72 (m, 4H); 4.95–6.25 (m, 3H)
4*e*		$C_{13}H_{18}N_2$ (202.1)	$114_{(0.01)}$	90	1.53 (s, 1H); 2.31 (s, 6H); 3.25 (t, 2H, J = 1.7); 3.43 (t, 2H); 3.86 (s, 2H); 7.25 (m, 5H).
4*f*		$C_9H_{16}N_2$ (152.1)	$59_{(0.01)}$	94 (c), 92 (d)	1.4 (s, 1H); 1.8 (m, 4H); 2.48 (s, 3H); 2.63 (m, 4H); 3.42 (s, 4H).
4*g*		$C_{11}H_{18}N_2$ (178.1)	$84_{(0.01)}$	92	1.4 (s, 1H); 1.84 (m, 4H); 2.68 (m, 4H); 3.2–3.8 (m, 6H); 5–6.4 (m, 3H).
4*h*		$C_{12}H_{21}N_3$ (207.2)	$129_{(0.05)}$	60 (e)	1.3 (s, 1H); 2.29 (s, 6H); 2.36 (s, 3H); 2.45 (s, 3H); 3.14–3.49 (m, 8H).

[a]Yields were calculated for distilled compounds (a) from 3*a*; (b) from 3*j*; (c) from 3*f*; (d) from 3*i*; (e) from 1*a*.

TABLE 3. Physical characteristics of the *N*-alkylphosphoramides (eq. [2])

$Z_2P(=O)-N(R)-H$	Molecular formula or literature values	Boiling point °C (Torr)	n_D^t	% yields[a]
$[(CH_3)_2N]_2P(=O)-N(CH_3)-H$	Lit. (7) $bp_{3\,Torr}$ 137–143°C, 47% yield	$114_{(0.05)}$	1.4622^{23}	83
$(C_2H_5O)_2P(=O)-N(CH_3)-H$	Lit. (8) $bp_{15\,Torr}$ 130°C, 84% yield	$85_{(0.01)}$	1.4245^{18}	94
$[(CH_3)_2N]_2P(=O)-N(C_4H_9)-H$	$C_8H_{22}N_3OP$ (207.1)	$131_{(0.05)}$	1.4591^{18}	81
$[(CH_3)_2N]_2P(=O)-N(CH_2-CH=CH_2)-H$	$C_7H_{18}N_3OP$ (191.1)	$128_{(0.05)}$	1.4721^{18}	77
$[(CH_3)_2N]_2P(=O)-N(CH_2-C_6H_5)-H$	$C_{11}H_{20}N_3OP$ (241.1)	Melting point 93°C	—	82

[a]Yields are quoted for distilled or recrystallized (CH_2Cl_2 – petroleum ether) compounds.

The pharmacological properties of the new acetylenic compounds **3** and **4** as possible specific inhibiting substrates similar to **2**, **5**, and **6** are being investigated.

Experimental

General Comments

Infrared spectra were recorded as thin films on a Perkin Elmer 257 spectrometer. The main stretching frequencies were, for compounds **3***a–g* ν(P=O) = 1215 cm^{-1}, ν((P)—N—C) = 985 cm^{-1}, ν(P—N—(C)) = 745 cm^{-1}; for compounds **3***g–j* ν(P=O) = 1250 cm^{-1}; for amines **4**, ν(N—H) = 3260 cm^{-1}.

The ^1H nmr spectra were taken on a JEOL C60HL spectrometer at 60 MHz, in $CDCl_3$ with TMS as internal standard (δ = 0); ^{31}P nmr were taken on the same spectrometer at 24.3 MHz using a ^{31}P probe, the chemical shifts being taken from 85% H_3PO_4 used as external reference. For compounds **3***a–g* ^{31}P nmr δ: 22.2 ± 0.3 ppm (neat), **3***h–j* ^{31}P nmr δ: 9.3 ± 0.3 ppm (10% $CDCl_3$). The ^{13}C nmr spectra were determined on a JEOL FX60 FT nmr spectrometer interfaced to a Texas Instruments JEOL JEC 980 B computer (24K), with TMS as internal standard. Pulse widths were in the range 4–8 μs, pulse repetition 2.5 s, frequency bandwidth 2500 Hz, impulsion number 800–8000; the resolution was between 0.6 to 0.9 Hz.

The decoupling techniques, including proton noise decoupling, coherent off-resonance decoupling, gated noise decoupling (for undecoupled spectra), or low noise decoupling (51 dB) were used for the assignment of signals. The ^1H and ^{13}C chemical shifts of the diethoxy and bis-dimethylamido phosphoryl are omitted in Table 2; (CH_3—N—P) ^1H nmr δ: 2.69 ± 0.01 ppm, doublet, J_{P-H} = 9.6 ± 0.1 Hz; ^{13}C nmr δ: 36.5 ± 0.3 ppm, doublet, J_{CNP} = 3.7 Hz; (CH_3—CH_2—O—P) ^1H nmr δ: 1.35 ± 0.04 ppm, triplet; δ: 4 ± 0.01 ppm, pentuplet, $J_{H-H} = J_{P-H}$ = 7 Hz; ^{13}C nmr δ: 16.1 ± 0.1 ppm, doublet, J_{CCOP} = 7 Hz; δ: 62.2 ± 0.1 ppm, doublet, J_{COP} = 4.9 Hz. The signs of coupling constants have not been established and absolute values only are tabulated.

Mass spectroscopic data were obtained on a Varian MAT-311 spectrograph from Université de Rennes. Found M^+ are in agreement with the calculated values. The microanalyses showed the following maximum deviations from the calculated values: C, ±0.25; H, ±0.2.

Gas chromatographic analyses were carried out on a Girdel 3000 model with flame ionization detector, fitted with steel tube (150 cm × 0.125 cm) packed with 10% (w/w) SE-30 on 80–100 mesh Chromosorb W-AW DMCS, N_2 being the carrier gas (25–30 mL/min). Boiling points and melting points (Köfler) are not corrected.

N-*Alkyl*-N-*(2-propynyl)phosphoramides 1*

These compounds have been obtained from *N*-alkylphosphoramides and propargylbromide (1) (eq. [2]).

N-*Alkylphosphoramides*

The compounds have been prepared either through the slightly modified procedure of Arceneaux *et al.* (7) or Sauders *et al.* (8) (procedure (*a*)), or using the two-phase transfer process which has also been reported by Zwierzack (9) (procedure (*b*)).

Procedure (a)

To a cold solution (−10 to +10°C) of 3 mol of primary amine[3] in dried ether (400 mL) was added dropwise an ethereal solution of chlorophosphate (1 mol in 150 mL ether). After awhile, a white solid appeared. After the addition was complete, the reaction mixture was then allowed to warm to room temperature and stirred for about 2–3 h. The hydrochloride salt was filtered off, the filtrate washed with water, and then dried over $MgSO_4$. Evaporation of the solvent, followed by vacuum distillation, gave the title compounds.

Procedure (b)

To a cold mixture (0–5°C) of 0.22 mol of amine, 20% sodium hydroxide (80 mL), and benzyltriethylammonium chloride (2 g) in methylene chloride (80 mL) was added dropwise, under stirring, a solution of bis-dimethylamidochlorophosphate (0.2 mol) in methylene chloride (50 mL). After the addition was complete, the reaction mixture was kept at 0°C for 1 h and then allowed to warm to room temperature. The phosphoramide was extracted once with methylene chloride (80 mL) and twice with chloroform (2 × 80 mL). The organic phase was dried over $MgSO_4$. After evaporation of the solvents, the vacuum distillation or crystallization gave the title compounds. Infrared spectra: ν(NH) = 3195 ± 5 cm^{-1}; ν(P=O) = 1195 ± 5 cm^{-1}.

The products obtained by these procedures are collected in Table 3.

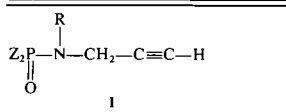
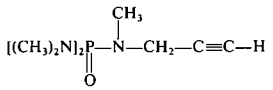
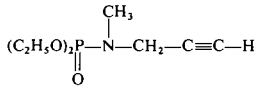
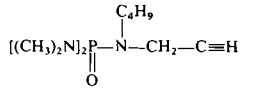
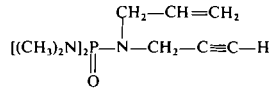
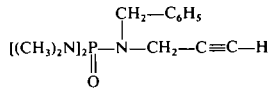
N-*Alkyl*-N-*(2-propynyl)phosphoramides 1*

To a stirred suspension of 1 mol NaH (previously washed twice with dried ether and once with THF) in 250 mL anhydrous THF was added dropwise 1 mol of *N*-alkylphosphoramide at

[3]Triethylamine was used as an acid acceptor when the amine was expensive. The yields were in the same range as when 2 equivalents of amine were employed.

Can. J. Chem. Downloaded from www.nrcresearchpress.com by 210.87.254.105 on 09/05/12
For personal use only.

TABLE 4. Physical characteristics of the *N*-alkyl-*N*-propargylphosphoramides **1** (eq. [2])

 1	Molecular formula	Boiling point, °C (Torr)	n_D^t	% yields[a]
	$C_8H_{18}N_3OP$ (203.1)	$109_{(0.05)}$; Melting point 62°C.	—	92
	$C_8H_{16}NO_3P$ (205.1)	$68_{(0.01)}$	1.4420^{18}	89
	$C_{11}H_{24}N_3OP$ (245.2)	$124_{(0.05)}$	1.4740^{21}	79
	$C_{10}H_{20}N_3OP$ (229.1)	Melting point 68°C	—	84
	$C_{14}H_{22}N_3OP$ (279.2)	Melting point 120°C	—	77

[a]Yields are quoted for distilled or recrystallized (CH_2Cl_2 – petroleum ether) compounds.

such a rate as to maintain a gentle reflux. The reaction was completed by heating (~1 h reflux) until the H_2 evolution had ceased. The reaction mixture was cooled between −10°C and −20°C and propargyl bromide (1.1 mol in 100 mL THF) was added slowly during which time sodium bromide precipitated.

After the addition was complete, the reaction mixture was stirred and allowed to warm to room temperature over 1 h. It was cautiously (it might contain excess NaH) hydrolysed and extracted once with ether (200 mL) and three times with chloroform (3 × 200 mL). The organic phase was dried over $MgSO_4$. After evaporation of the solvents, the crude products were purified by recrystallization (CH_2Cl_2 – petroleum ether) or distillation under vacuum (Table 4). Infrared spectra: ν(C—H_{free}) = 3200 cm^{-1}, ν(C—H_{ass}) = 3170 cm^{-1}, ν(C≡C) = 2100 cm^{-1}, ν(P=O) = 1195 cm^{-1}; (—CH_2—C≡C—H) ^{1}H nmr δ: 3.75 (2d, 2H, J_{P-H} = 9.7 Hz, J_{H-H} = 2.4 Hz); δ ~ 2.3 (t, 1H) sensitive to concentration; ^{13}C nmr $\delta_{(C-1)}$: 38.7 (d, J_{CNP} = 6 Hz), $\delta_{(C-2)}$: 80 ± 0.4 (d, J_{CCNP} = 3 Hz) $\delta_{(C-3)}$: 72.2 ± 0.1.

All attempt to prepare compounds **1** using the phase transfer process failed.

An excess of NaH can lead to a propargylic rearrangement. To avoid this undesired reaction the excess NaH can be removed by decanting after the amide formation is complete if the sodium salt of the amide is soluble (R = C_4H_9—, $PhCH_2$—, CH_2=CH—CH_2—). Alternatively, the reaction mixture is kept below 0°C during and after the propargyl bromide addition. In the latter case hydrolysis is done at 0°C.

N-*Alkyl*-N-*(4-dialkylamino-2-butynyl)phosphoramides 3*

A mixture of 0.1 mol of propargylic phosphoramide **1**, 0.2 mol of paraformaldehyde, and 0.2 g of Cu_2Cl_2 in dioxane (150 mL) became yellowish when heated to 60–70°C. A solution of the secondary amine (0.11 mol in 20 mL of dioxane or in water for dimethylamine) was quickly added (2 min). The reaction was complete within 5 min as shown by vpc. The dioxane was evaporated and the mixture was washed with water (100 mL) and extracted with chloroform (3 × 80 mL). The organic phase was dried over $MgSO_4$ and the solvent evaporated. Distillation of the crude products under vacuum gave the title compounds (see Table 1).

N-*Alkyl*-N-*(4-dialkylamino-2-butynyl)amines 4*

N-Alkyl-*N*-(4-dialkylamino-2-butynyl) phosphoramide (0.05 mL) was hydrolysed by refluxing with 300 mL of 3 *N* hydrochloric acid for about 10 to 12 h. After cooling, the reaction mixture was made alkaline to pH 12 by addition of commercial sodium hydroxide (40% w/w). Extraction with chloroform (3 × 80 mL), drying over $MgSO_4$, and evaporation of the solvent gave the desired amines which were purified by distillation (see Table 2).

Acknowledgements

The financial assistance of CNRS (France) is gratefully acknowledged. We wish to thank Mr J. Y. Le Gall for measuring ^{13}C nmr spectra.

1. (*a*) Monoamine oxidase and its inhibition. CIBA Foundation Symposium 39. Elsevier, Amsterdam. 1976; (*b*) A. BURGER. Medicinal chemistry. 3rd ed. Wiley Interscience, New York, NY. 1970. p. 1489.
2. B. CORBEL, J. P. PAUGAM, M. DREUX, and P. SAVIGNAC. Tetrahedron Lett. 835 (1976).
3. B. KARLEN. Acta Pharm. Suec. **7**, 169 (1970).
4. U. SVENSSON, U. HACKSELL, and R. DAHLBOM. Acta Pharm. Suec. **15**, 67 (1978).
5. E. R. H. JONES, I. MARSZAK, and H. BADER. J. Chem. Soc. 1578 (1947); I. MARSZAK and A. MARSZAK-FLEURY. Bull. Soc. Chim. Fr. 1305 (1950); J. A. GAUTIER, M. MIOCQUE, and L. MASCRIER-DEMAGNY. C. R. Acad. Sci. Ser. C, **264**, 778 (1967); M. F. SHOSTAKOVSKII, A. S. ATAVIN, and N. V. EGOROV. Zh. Org. Khim. **3**, 429 (1967); Chem. Abstr. **67**, 11122 (1967).
6. R. MORNET and L. GOUIN. Bull. Soc. Chim. Fr. 206 (1974).
7. R. L. ARCENEAUX, J. G. FRICK, E. K. LEONARD, and J. D. REID. J. Org. Chem. **24**, 1419 (1959).
8. B. C. SAUNDERS, G. J. STACEY, F. WILD, and I. G. E. WILDING. J. Chem. Soc. 699 (1948).
9. A. ZWIERZAK. Synthesis, 507 (1975).

Can. J. Chem. Downloaded from www.nrcresearchpress.com by 210.87.254.105 on 09/05/12
For personal use only.

Mass spectrometry of diamantane and some adamantane derivatives

ROBERT J. WALTMAN AND A. CAMPBELL LING[1]

Department of Chemistry, San Jose State University, San Jose, CA 95192, U.S.A.

Received December 21, 1979[2]

ROBERT J. WALTMAN and A. CAMPBELL LING. Can. J. Chem. **58**, 2189 (1980).

The mass spectrometric fragmentation of adamantane, adamantane-d_{16}, diamantane, 1- and 2-adamantanol, and 3,5,7-trimethyl-1-adamantanol has been re-examined, and new data for diamantane and 3,5,7-trimethyl-1-adamantanol are presented in more detail. Metastable peak data have been used to support potential fragmentation pathways. Simple statistical considerations applied to peak intensity data seem to indicate that ionization occurs at the primary bridgehead in both adamantane and diamantane, and that loss of a primary hydrogen is favored over loss of a secondary hydrogen atom.

ROBERT J. WALTMAN et A. CAMPBELL LING. Can. J. Chem. **58**, 2189 (1980).

On a examiné de nouveau la fragmentation en spectrométrie de masse de l'adamantane, de l'adamantane-d_{16}, du diamantane, des adamantanols 1 et 2 et du triméthyl-3,5,7 adamantanol-1 et on présente avec plus de détails les données relatives au diamantane et au triméthyl-3,5,7 adamantol-1. On a utilisé le pic métastable pour appuyer les voies potentielles de fragmentation. De simples considérations statistiques faites sur les données d'intensité du pic semblent indiquer que l'ionisation se produit au niveau de la tête de pont primaire de l'adamantane et du diamantane et que la perte d'un hydrogène primaire est favorisée par rapport à la perte d'un atome d'hydrogène secondaire.

[Traduit par le journal]

Introduction

The polycyclic compound adamantane (tricyclo[3.3.1.$1^{3,7}$]decane) has proven to be of great interest to physical chemists and radiation chemists. In particular, adamantane provides a relatively inert isolation matrix for a variety of purposes, including those involving electron spin resonance (esr) studies of organic radical species formed via molecular fragmentation induced by radiolytic or photolytic processes. Compared to inert gas matrices or SF_6, or glassy organic matrices such as 2-methylpentane and 2-methyltetrahydrofuran, adamantane matrices doped with suitable solutes provide narrow-line (often less than 1 G) well resolved isotropic esr spectra for radicals derived from the solute up to a molecular size equivalent to approximately C_{10}. Further, these solute esr spectra are obtained via a solid isolation matrix with a usable temperature range from approximately 150°C down to accessible cryogenic temperatures, and exhibiting radical half-lives that are often in excess of several days, even at temperatures up to 100°C (1).

Diamantane (pentacycl[7.3.1.$1^{4,12}$.$0^{2,7}$.$0^{6,11}$]tetradecane mp 244–245°C, also known as "congressane") can also be used for the same purpose, although it offers no advantages over adamantane as an isolation matrix (2).

The mechanism of radical formation in adamantane (or diamantane) itself, undoped with any solute, has produced a major controversy concerning the nature of the initial step produced by ionizing radiation; apparently conflicting data exist concerning the identity of the initial radical obtained from a variety of investigative techniques, including: ENDOR studies (3), X-band and Q-band esr (4), spin trapping and scavenger studies (5), product analyses, and semi-empirical calculations (6). These data are summarized in ref. 2. The major point of contention is whether the 1-hydrogen (bridgehead) or a 2-hydrogen atom (secondary position) is lost to form the adamantyl radical on radiolysis of the pure solid, or whether a stabilized radical formed by C—C bond cleavage could occur (7). In order to provide further data that might aid in clarifying this controversy, we have examined some adamantane derivatives subjected to radiolysis via the electron beam source of a conventional mass spectrometer.

Experimental Section

All compounds used (adamantane, adamantane-d_{16}, diamantane, 1- and 2-adamantanol, and 3,5,7-trimethyl-1-adamantanol) were obtained from commercial sources. Mass spectra were taken via a Hitachi Perkin-Elmer RMU-9 mass spectrometer at an ionization energy of 80 eV, or from a Varian EM-600 mass spectrometer at 70 eV.

Results and Discussion

Diamantane

The mass spectrum of diamantane, like adamantane (8), is highly unusual in that the molecular ion peak (*m/e* 188) is also the base peak (Fig. 1*b*). The great stability of the molecular ion for diamantane is attributed to the nearly strain free interlocking system of rings and the structure's

[1]To whom all correspondence should be addressed.

[2]Revision received June 27, 1980.

0008-4042/80/202189-07$01.00/0

©1980 National Research Council of Canada/Conseil national de recherches du Canada

Can. J. Chem. Downloaded from www.nrcresearchpress.com by 210.87.254.6 on 09/05/12
For personal use only.

Can. J. Chem. Downloaded from www.nrcresearchpress.com by 210.87.254.6 on 09/05/12
For personal use only.

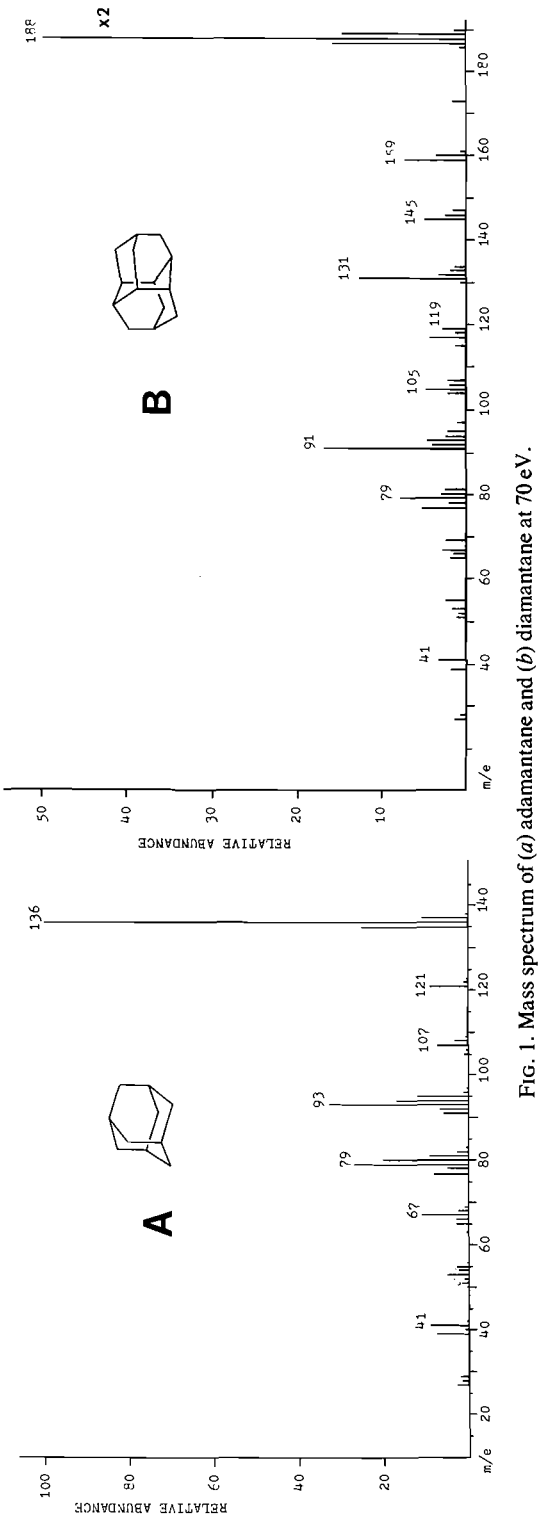


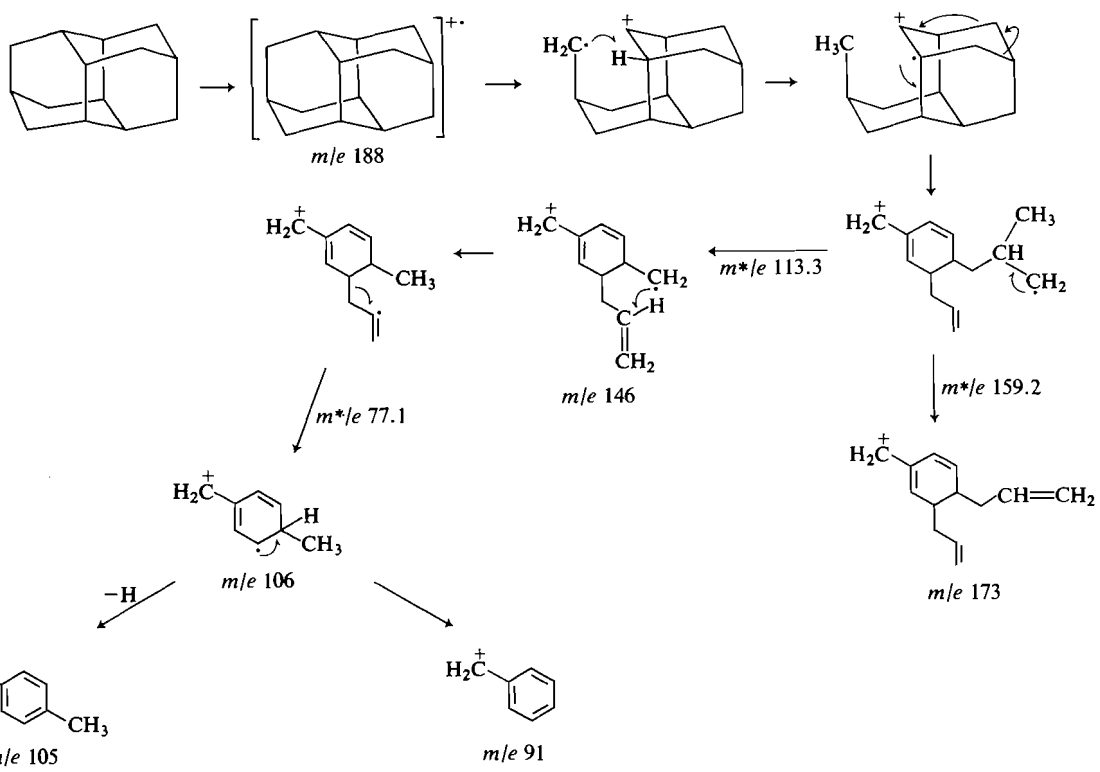
FIG. 1. Mass spectrum of (*a*) adamantane and (*b*) diamantane at 70 eV.

ability to easily accommodate the loss of an electron. The molecular ion base peak is seen to be ca. five times greater in intensity than the next most abundant fragment ion at *m/e* 91, an unusual feature. Cupas *et al.* (9) suggested this ion at *m/e* 91 results from a symmetrical splitting of the diamantane molecular ion into two equal fragments, followed by rearrangement and loss of three hydrogen atoms from one of the fragments to yield the tropylium ion $C_7H_7^+$ (10). However, Cupas *et al.* did not report metastable peaks or any other evidence to support such a fragmentation pathway, nor have we been able to observe any metastable peaks to support this particular hypothesis. Further, Fig. 1*b* shows a relative intensity of only ca. 3% for the half-mass peak at *m/e* 94. In contrast to diamantane, many polycyclic compounds which undergo symmetrical splitting into two equal fragments, e.g. pentacyclodecanes (11), usually show a large half-mass peak intensity (they are often the base peak) reflecting the relatively low energy pathway available for such a fragmentation. We therefore suggest an alternate pathway for the formation of the *m/e* 91 ion observed, and which we tentatively assign to the benzyl $C_7H_7^+$ fragment at this time. This is a multistep process involving fragmentation to produce phenylalkyl ions and various C_1–C_4 fragments, as shown in Scheme 1. Metastable peak data, on which we base our scheme, are shown in Table 1.

Further evidence to support Scheme 1 is provided by pyrolysis studies of adamantane (12) and 1-nitroadamantane (13) in which decomposition of both compounds resulted primarily in the formation of a mixture of benzene and mono- and dialkylbenzenes. Also, mass spectrometric studies of some substituted adamantanes by Dolejsek *et al.* (8) has shown that various phenylalkyl ions could be formed on fragmentation of some adamantane derivatives. We suggest that the same type of fragment ions are produced from the adamantane homolog, diamantane, as shown in Scheme 1. The great abundance of the *m/e* 91 peak in the mass spectrum of diamantane (Fig. 1) suggests intrinsic stability, such as is conferred by a delocalized system, and thus we suggest that a reasonable assignment for this fragment could well be the benzyl ion (**1**).

3,5,7-Trimethyl-1-adamantanol

For many singly substituted adamantane derivatives, the mass spectral fragmentation patterns observed are substantially similar regardless of whether the substituent is at the 1- or 2-position.



I

SCHEME 1

However, for other substituents, there are significant differences in fragmentation pathways, and it is pertinent to our discussion of the new data for this substituted adamantane to compare and contrast these aspects using 1- and 2-adamantanol as illustrative examples (8, 14). Although both charge site initiation and radical site initiation stemming from a saturated oxygen atom can cause reaction, it appears that 1-adamantanol favors a radical site initiation process while 2-adamantanol favors charge site initiation. These contrasting behavioral patterns are well illustrated in Fig. 2, where mass spectra for 1- and 2-adamantanol are shown. In 2-adamantanol, the major fragmentation pathway results in loss of the hydroxyl group as H_2O after an initial hydrogen atom transfer (which offsets the radical site's tendency to initiate a reaction) to yield the *m/e* 134 base peak. The mass spectrometry of 2-adamantanol has been discussed briefly by Greidanus (14).

For 1-adamantanol, in which elimination of the hydroxyl group is not the key fragmentation mech-

TABLE 1. Metastable ion peaks m^*/e in diamantane for transformations of the type $A^+ \rightarrow B^+ + C$

A (*m/e*)	B (*m/e*)	C	*m*/e* Observed	*m*/e* Calculated
$C_{14}H_{20}^+$ (188)	$C_{13}H_{17}^+$ (173)	CH_3	159.2	159.2
$C_{14}H_{20}^+$ (188)	$C_{12}H_{15}^+$ (159)	C_2H_5	134.6	134.5
$C_{14}H_{20}^+$ (188)	$C_{11}H_{14}^+$ (146)	C_3H_6	113.3	113.4
$C_{14}H_{20}^+$ (188)	$C_{10}H_{11}^+$ (131)	C_4H_9	91.3	91.3
$C_{11}H_{14}^+$ (146)	$C_8H_{10}^+$ (106)	C_3H_4	77.1	77.0
$C_{10}H_{11}^+$ (131)	$C_7H_7^+$ (91)	C_3H_4	63.2	63.2
$C_7H_7^+$ (91)	$C_5H_5^+$ (65)	C_2H_2	46.4	46.4
$C_6H_7^+$ (79)	$C_6H_5^+$ (77)	H_2	75.1	75.1

Can. J. Chem. Downloaded from www.nrcresearchpress.com by 210.87.254.6 on 09/05/12
For personal use only.

Can. J. Chem. Downloaded from www.nrcresearchpress.com by 210.87.254.6 on 09/05/12
For personal use only.

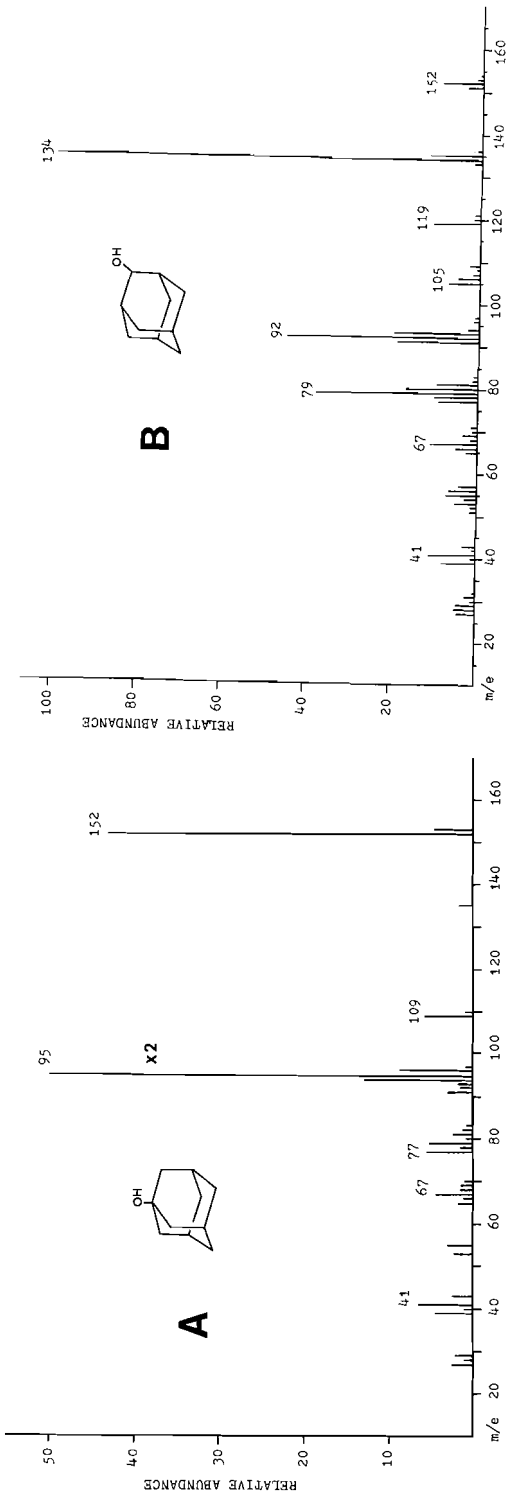
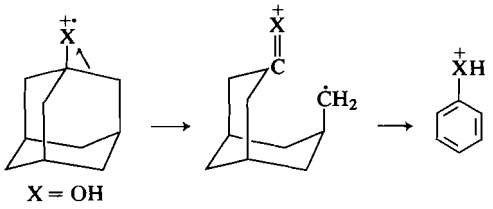


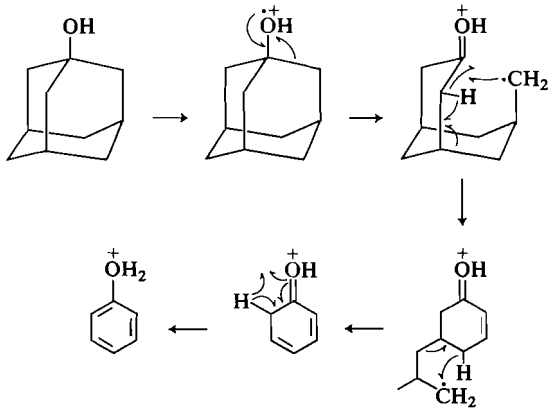
FIG. 2. Mass spectra of (*a*) 1-adamantanol and (*b*) 2-adamantanol at 70 eV.



SCHEME 2

anism, Dolejsek *et al.* (8) proposed the formation of a protonated phenol structure for the *m/e* 95 base peak involving the transfer of two hydrogen atoms and splitting-off of a $C_4H_9^{\cdot}$ neutral radical. This is shown in Scheme 2.

Utilizing this general approach proposed by Dolejsek and co-workers, we can postulate a more specific fragmentation pathway for 1-adamantanol, shown in Scheme 3, which accounts satisfactorily for the mass spectrum displayed in Fig. 2*a*.



SCHEME 3

More importantly, these data are pertinent to the fragmentation pattern we have observed for TMA, shown in Fig. 3.[3] In this previously unstudied compound, three of the four bridgehead positions are substituted with methyl groups. The most apparent changes in the mass spectrum of TMA occurred in the relative intensities of the molecular ion peaks (43% for 1-adamantanol and 26% for TMA), and in the appearance of a $(M - CH_3)^+$ peak (molecular ion minus a methyl group) in TMA, although the corresponding $(M - H)^+$ fragment (molecular ion minus a hydrogen atom) was absent in the spectrum of 1-adamantanol. This is not unusual, however, since the possibility for fragmentation usually increases with the size of the alkyl substituent.

The base peak of TMA occurs at *m/e* 123. In conjunction with this, we observed the presence of

[3]For simplicity, 3,5,7-trimethyl-1-adamantanol is referred to as TMA.

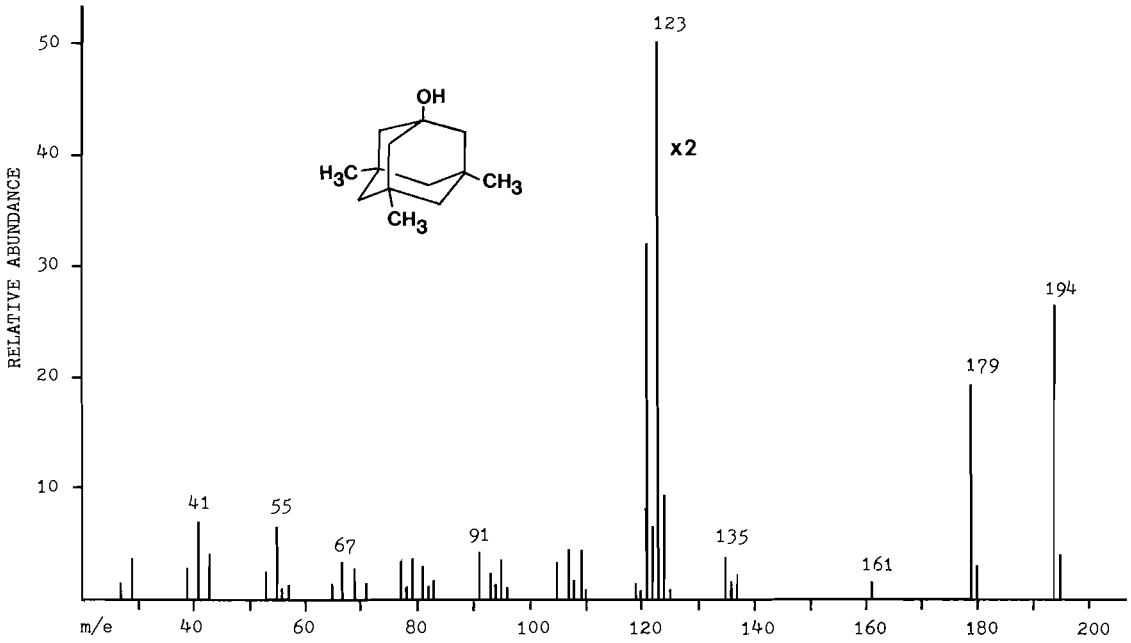


FIG. 3. Mass spectrum of 3,5,7-trimethyl-1-adamantanol at 70 eV.

TABLE 2. Metastable ion peaks m^*/e in 3,5,7-trimethyl-1-adamantanol for transformations of the type $A^+ \rightarrow B^+ + C$

A (*m/e*)	B (*m/e*)	C	*m*/e* Observed	*m*/e* Calculated
$C_{13}H_{22}O^+$ (194)	$C_{12}H_{19}O^+$ (179)	CH_3	165.2	165.2
$C_{13}H_{22}O^+$ (194)	$C_8H_{11}O^+$ (123)	C_5H_{11}	78.0	78.0
$C_8H_{11}O^+$ (123)	$C_8H_9^+$ (105)	H_2O	89.4	89.6
$C_{12}H_{19}O^+$ (179)	$C_{12}H_{17}^+$ (161)	H_2O	145.0	144.8
$C_{12}H_{19}O^+$ (179)	$C_8H_9O^+$ (121)	C_4H_{10}	82.0	81.8

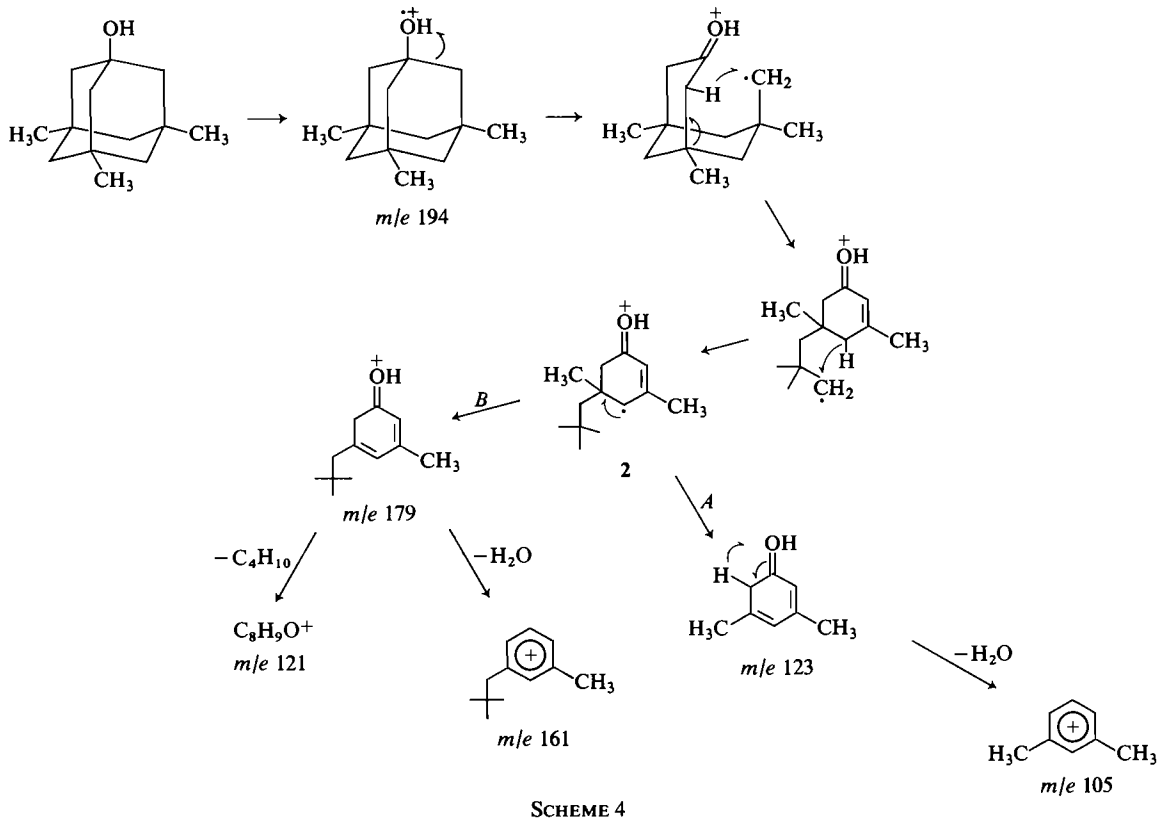
a metastable peak at m^*/e 78.0 (calcd. 78.0) and postulate that transformation 2 of Table 2 could well be the key fragmentation pathway for TMA. This pathway is similar to that given in Scheme 3 for 1-adamantanol, with formation of a corresponding protonated phenol structure as originally proposed by Dolejsek *et al.* (8). To account for the major peaks in the mass spectrum from this totally bridgehead-substituted adamantane, particularly the *m/e* 121, 123, and 179 peaks, we made a careful search for metastable peaks in the range *m/e* 75 through 194, inclusively. These data are recorded in Table 2. A possible fragmentation pathway based on these data is shown in Scheme 4. From the intermediate **2**, since the preferred fragmentation pathway results from loss of the larger alkyl group, the relative abundance of the *m/e* 123 peak (path A) is much greater than the *m/e* 179 peak (path B). It is interesting to note that when TMA undergoes the same postulated fragmentation pathway as 1-adamantanol in Scheme 3, the three major peaks at *m/e* 121, 123, and 179, as well as the *m/e* 105 and 161 peaks, can be accounted for from the common ancestor **2** in Scheme 4.

Summary

Metastable peak data were collected for diamantane and 3,5,7-trimethyl-1-adamantanol, and possible fragmentation pathways were presented based on these and other data (8, 12, 13). All data appear to indicate that fragmentation of these polycyclic compounds via electron beam bombardment or via pyrolysis results primarily in the formation of alkyl-substituted benzenes.

Athough the effects on molecules of different radiation sources can differ, the results are often found to be the same; for example, the work of Filby *et al.* (15) has shown that identical results are

Can. J. Chem. Downloaded from www.nrcresearchpress.com by 210.87.254.6 on 09/05/12
For personal use only.



SCHEME 4

obtained from both electron beam and γ-radiolysis of adamantane in the pure phase solid state. Electron beam bombardment via mass spectrometry (ca. 70 eV) of adamantane and diamantane yielded $(M - H)^+$ peaks of relative intensity 25% to 16%, respectively, while loss of the hydrogen atom from both adamantane and diamantane is thought to be the primary reaction seen via esr following γ-radiolysis of the pure solids. It appears then that gas phase isolated molecular ionization events differ substantially to the events occurring in condensed phase solid state processes (a prima facie result of the hindered energy transfer capabilities inherent to gas phase species). Further, since the origin of the hydrogen atom that is lost on ionization is yet unknown, these data from mass spectral analysis have not allowed us to identify the initial radical and/or ionic species formed on radiolysis. Deuterium labeling studies at either the bridgehead or secondary position may be helpful but will not necessarily be definitive due to isotope effects and possibly random H-atom rearrangements which are so prominent in the mass spectrometry of many saturated alicyclic and polycyclic hydrocarbons.

Substitution of the four bridgehead positions with deuterium atoms might provide more helpful data concerning initial H-atom loss in these three dimensional cage-like molecules, but synthesis does not appear to be practical at this time. Also, despite the availability of the perdeuterated adamantane-d_{16}, the mass spectrum is essentially the same as that of adamantane when the mass of the heavier isotope of hydrogen is considered, and thus no new data are obtained. However, although simple statistical considerations can be misleading, it is interesting to consider further the relative ratios of $(M - H)^+$ peaks for the two compounds. The ratios observed, 25% and 16% for adamantane and diamantane, respectively, suggest a greater participation by the bridgehead hydrogens in H-atom loss processes as compared with the secondary positions. In support of this hypothesis, we note that although diamantane has eight bridgehead hydrogen atoms, compared to only four in adamantane (see Fig. 1), they form two distinct populations, and only two of these eight bridgehead H-atoms (called "primary bridgehead H-atoms") are comparable to the four in adamantane. The ratio of the number of primary bridgehead H-atoms in adamantane to those in diamantane is thus 2 to 1, respectively, and this is approximately reflected in the experimental ratio of relative intensities of the

Can. J. Chem. Downloaded from www.nrcresearchpress.com by 210.87.254.6 on 09/05/12
For personal use only.

$(M - H)^+$ peaks for adamantane and diamantane (25 to 16, respectively). Further, the number of secondary H-atoms in adamantane and diamantane are the same, so we might have predicted equal peak intensities if these were the major participants. Coupled with data reported by others, in particular the work of Filby and Gunther (15), this suggests to us that on irradiation, the bridgehead H-atoms of adamantane and diamantane may play a greater role in H-atom loss processes than the H-atoms at the secondary sites.

1. (*a*) S. DiGregorio, M. B. Yim, and D. E. Wood. J. Am. Chem. Soc. **95**, 8457 (1973); (*b*) D. M. Camaioni, H. F. Walker, J. E. Jordan, and D. W. Pratt. J. Am. Chem. Soc. **95**, 7978 (1973); (*c*) M. E. Manzuk, D. L. Winters, G. J. Hyfantis, and A. C. Ling. Int. J. Radiat. Biol. **26**, 51 (1974); (*d*) R. E. Linder, D. L. Winters, and A. C. Ling. Can. J. Chem. **54**, 1405 (1976); **54**, 1971 (1976); (*e*) D. R. Gee, L. Fabes, and J. K. S. Wan. Chem. Phys. Lett. **7**, 311 (1970).
2. G. J. Hyfantis and A. C. Ling. Can. J. Chem. **52**, 1206 (1974).
3. R. V. Lloyd and M. T. Rodgers. Chem. Phys. Lett. **17**, 428 (1972).
4. A. C. Ling and L. Kevan. J. Phys. Chem. **80**, 592 (1974).
5. G. J. Hyfantis and A. C. Ling. Chem. Phys. Lett. **24**, 335 (1974).
6. K. Hattenbach and E. Vom Baur. Atomkernenergie, **11**, 262 (1962).
7. L. Bonnazola and R. Marx. Chem. Phys. Lett. **8**, 413 (1971).
8. Z. Dolejsek, S. Hala, V. Hanus, and S. Landa. Collect. Czech. Chem. Commun. **31**, 435 (1966).
9. C. Cupas, P. von R. Schleyer, and D. J. Trecker. J. Am. Chem. Soc. **87**, 917 (1965).
10. P. N. Rylander, S. Meyerson, and H. M. Grubb. J. Am. Chem. Soc. **79**, 842 (1957).
11. W. L. Dilling and M. L. Dilling. Tetrahedron, **23**, 1225 (1967).
12. B. A. Kazanskii, E. A. Shokova, and T. V. Kosteleva. Izv. Akad. Nauk SSSR, Ser. Khim. **11**, 2640 (1968).
13. A. I. Feinstein, E. K. Fields, P. J. Ihrig, and S. Meyerson. J. Org. Chem. **36**, 996 (1971).
14. J. W. Greidanus. Can. J. Chem. **49**, 3210 (1971).
15. W. G. Filby and K. Gunther. Z. Naturforsch. **27**, 1289 (1972).

Can. J. Chem. Downloaded from www.nrcresearchpress.com by 210.87.254.6 on 09/05/12
For personal use only.

Photocycloaddition of 2-methyl-1,4-naphthoquinone to enol esters. A photochemical approach to benzofuran derivatives

HSING-JANG LIU AND WING HONG CHAN

Department of Chemistry, University of Alberta, Edmonton, Alta., Canada T6G 2G2

Received May 26, 1980

HSING-JANG LIU and WING HONG CHAN. Can. J. Chem. **58**, 2196 (1980).

Naphthoquinone **1** undergoes facile photocycloaddition with vinyl acetate and isopropenyl acetate to give cyclobutane derivatives in excellent yields. The photocycloaddition reactions were found to be completely regioselective; in the case of vinyl acetate, a mixture of epimeric acetates **2** and **3** was obtained and in the case of isopropenyl acetate, a single adduct **7** was formed. Treatment of the photoadducts with dilute sulfuric acid resulted in skeletal rearrangement giving naphthofurans **4** and **8**.

HSING-JANG LIU et WING HONG CHAN. Can. J. Chem. **58**, 2196 (1980).

La cycloaddition photochimique de la naphtaquinone **1** sur les acétates de vinyle et d'isoprényle se fait facilement et conduit avec d'excellents rendements aux dérivés du cyclobutane. On a trouvé que les réactions de photocycloaddition sont complètement régiosélectives. Dans le cas de l'acétate de vinyle, on obtient un mélange des acétates épimères **2** et **3** et seul l'adduit **7** se forme dans le cas de l'acétate d'isoprényle. Lorsqu'on traite les adduits photochimiques par de l'acide sulfurique dilué, il en résulte une transposition du squelette qui conduit aux naphtofurannes **4** et **8**.

[Traduit par le journal]

Can. J. Chem. Downloaded from www.nrcresearchpress.com by 210.87.254.40 on 09/05/12
For personal use only.

It has been well established that conjugated enones undergo photocycloaddition reactions with olefinic and acetylenic compounds resulting in cyclobutane ring formation, a process which has found extensive use in organic synthesis.[1] In contrast, 2-ene-1,4-diones usually react photochemically with compounds containing carbon–carbon multiple bond by a different route giving rise to oxetanes or products derived from oxetanes and only limited number of examples are known to produce cyclobutane rings.[2] We wish to report the photocycloaddition of 2-methyl-1,4-naphthoquinone (**1**) to vinyl acetates, which proceeds regiospecifically to give cyclobutane derivatives in excellent yield. As well, we wish to illustrate the application of this method to the construction of benzofuran systems which are of considerable interest in natural product chemistry.[3]

Naphthoquinone **1** and vinyl acetate reacted cleanly and rapidly when a benzene solution was irradiated with a 450 W Hanovia high-pressure quartz mercury-vapor lamp through a Pyrex filter. The reaction was complete within 1 h and a mixture of two epimeric adducts **2** and **3** (4:1 by nmr integration) was isolated in virtually quantitative yield. The two epimers, which were inseparable by thin-layer or column chromatography, could be partially separated by crystallization using dichloromethane–cyclohexane which gave the pure crystalline minor isomer **3**, mp 115–116°C. The regiochemistry of the products was suggested by the nmr spectra[4] showing in each case a doublet of doublets (δ 5.07 for the major product and δ 5.20 for the minor) for the methine proton adjacent to the acetoxy group. The *cis* stereochemistry of the ring junction was indicated for each compound since these compounds[5] were recovered intact after prolonged treatment with *p*-toluenesulfonic acid in benzene (16). Furthermore, in the nmr spectrum of the minor product the acetoxy group appeared at δ 2.04 as a singlet while the major product gave a singlet at δ 1.94. The appearance of the acetoxy group at rather high field in the latter case suggested that it is in close proximity to the aromatic ring and is shielded by it. Structure **2** was assigned accordingly.

The photocycloaddition reaction was found to be completely regioselective; no isomers other than **2** and **3** were detected. Although the reasons for the profound selectivity remain unclear, the observed regiochemistry is expected in view of the previous observation (16, 17) that the photocycloaddition of 2-alkyl-2-cyclohexenones to olefins proceeds with difficulty whereas 3-alkyl-2-cyclohexenones undergo facile photocycloaddition reactions with vinyl acetate to give head-to-tail adducts as the major products.

[1]For reviews see ref. 1.

[2]See ref. 2 for an extensive review of the work in this area prior to 1973. Additional examples are to be found in refs. 3–14.

[3]For examples of existing methods for the preparation of benzofuran systems and natural products containing them see ref. 15.

[4]Since the major product **2** could not be obtained in pure form, its analysis was based on the nmr spectrum of the 4:1 mixture of **2** and **3** which showed a minor set of signals identical with those of pure **3**.

[5]The 4:1 mixture was used.

0008-4042/80/202196-03$01.00/0

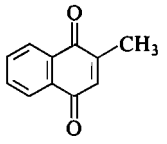
©1980 National Research Council of Canada/Conseil national de recherches du Canada

Can. J. Chem. Downloaded from www.nrcresearchpress.com by 210.87.254.40 on 09/05/12
For personal use only.

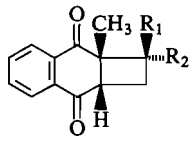
Treatment of the mixture of **2** and **3** with aqueous 5% sulfuric acid in refluxing tetrahydrofuran for 16 h gave, in 92% yield, naphthofuran **4**, mp 120–121°C, resulting apparently from an array of reactions including hydrolysis, retro-aldol, aromatization, hemiacetal formation, and dehydration. When the pure minor isomer **3** was subjected to the same acid treatment, a comparable yield of naphthofuran **4** was obtained. In addition to spectroscopic evidence, the structure of **4** was further confirmed by acetylation with acetic anhydride in pyridine to give the corresponding acetate **5**, mp 70–71°C.

By suitable choice of the two counterparts involved in the photocycloaddition, the above two-step sequence could, in principle, be extended to the preparation of naphthofurans possessing general formula **6**. A further example is illustrated below.

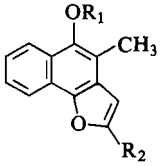
Irradiation of quinone **1** and isopropenyl acetate in benzene for 1 h gave, in quantitative yield, a single adduct **7** the nmr spectrum of which showed a doublet of doublets at δ 2.63 for the methine proton and a singlet for the acetoxy group at an abnormally high field of δ 1.63 in agreement only with the assigned structure. When exposed to dilute sulfuric acid in refluxing tetrahydrofuran for 30 h, the adduct **7** underwent skeletal rearrangement giving naphthofuran **8** in 75% yield.



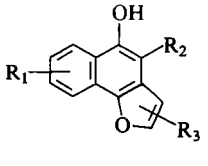
1



2 $R_1 = H; R_2 = CH_3COO$
3 $R_1 = CH_3COO; R_2 = H$
7 $R_1 = CH_3; R_2 = CH_3COO$



4 $R_1 = R_2 = H$
5 $R_1 = CH_3COO; R_2 = H$
8 $R_1 = H; R_2 = CH_3$



6

Experimental

General

Melting points were determined on a Kofler hot stage apparatus and are uncorrected. Elemental analyses were performed by the microanalytical laboratory of this department. Infrared spectra were recorded on a Perkin-Elmer model 457 spectrometer and were obtained on solutions in chloroform. Nuclear magnetic resonance spectra were recorded on a 90 MHz Perkin-Elmer 32 spectrometer and, except where otherwise stated, were obtained on solutions in chloroform-*d* with tetramethyl silane as an internal reference. Mass spectra were recorded using A.E.I. model MS 50 mass spectrometer.

Photocycloaddition of 2-Methyl-1,4-naphthoquinone (1)

(A) With Vinyl Acetate

A solution of 2-methyl-1,4-naphthoquinone (**1**) (8.5 g, 0.049 mol) and vinyl acetate (86 g, 1 mol) in benzene (90 mL) was irradiated at room temperature for 1 h using a 450 W Hanovia high-pressure quartz mercury-vapor lamp through a Pyrex filter. Concentration of the reaction mixture gave an oil which was chromatographed on silica gel. Elution with benzene gave a mixture of epimeric acetates **2** and **3** (12.5 g, 98% yield). The ir and mass spectra of the mixture were similar to those of the minor isomer (see below). The nmr spectrum of the mixture displayed two partly superimposed sets of signals in an integral ratio of 4:1. The major set contained the following signals: δ 1.54 (s, 3H, CH_3), 1.94 (s, 3H, CH_3COO), 5.07 (dd, 1H, $J = J' =$ 8 Hz, OCH), 7.64–7.89 (complex, 2H, aromatic), and 7.91–8.22 (complex, 2H, aromatic) and the signals of the minor set were found to coincide with those of the pure minor isomer (see below). The minor isomer **3** was obtained in pure form by crystallization and showed the following physical data: mp 115–116°C (dichloromethane–cyclohexane); ir 1740 (ester), 1685, 1675 (ketones), and 1590 cm^{-1} (benzene); nmr δ 1.47 (s, 3H, CH_3), 2.04 (s, 3H, CH_3COO), 2.42–3.18 (complex, 3H, CH_2 and CH), 5.20 (dd, 1H, $J = J' = 8$ Hz, COOCH), 7.69–7.88 (complex, 2H, aromatic), and 7.97–8.21 (complex, 2H, aromatic); mass spectrum M^+ 258.0922 (calcd. for $C_{15}H_{14}O_4$: 258.0892). *Anal.* calcd. for $C_{15}H_{14}O_4$: C 69.76, H 5.46; found: C 69.50, H 5.41.

(B) With Isopropenyl Acetate

Under similar conditions, a solution of naphthoquinone **1** (5 g, 0.029 mol) and isopropenyl acetate (58 g, 0.58 mol) in benzene (60 mL) was irradiated for 1 h. Concentration followed by column chromatography on silica gel eluting with benzene gave acetate **7** (7.87 g; 100% yield): ir 1735 (acetate), 1680 (ketones), and 1590 cm^{-1} (benzene); nmr δ 1.47 (s, 3H, CH_3), 1.58 (s, 3H, CH_3), 1.63 (s, 3H, CH_3COO), 2.63 (dd, 1H, $J = 8$, $J' = 4$ Hz, CH), 2.82–3.13 (complex, 2H, CH_2), 7.64–7.80 (complex, 2H, aromatic), and 7.89–8.13 (complex, 2H, aromatic); mass spectrum *m/e* (M − 42) 230.0940 (calcd. for $C_{14}H_{14}O_3$: 230.0943). *Anal.* calcd. for $C_{16}H_{16}O_4$: C 70.58, H 5.92; found: C 70.28, H 5.91.

Conversion of Acetates 2 and 3 to Naphthofuran 4

The mixture of epimeric acetates **2** and **3** (4:1 ratio, 410 mg, 1.59 mmol) was dissolved in tetrahydrofuran (10 mL) and 5% aqueous sulfuric acid (10 mL) was added. The resulting solution was refluxed under a nitrogen atmosphere for 16 h, cooled to room temperature, and extracted with methylene chloride. Drying ($MgSO_4$), filtration, and concentration gave an oil which was chromatographed on silica gel. Elution with a solution of 5% ether in benzene gave naphthofuran **4** (290 mg, 92% yield): mp 120–121°C (benzene–cyclohexane); ir 3600 (OH), 1595 and 1580 cm^{-1} (aromatic); nmr (C_6D_6) δ 2.01 (s, 3H, CH_3), 4.27 (s, 1H, OH), 6.48, 7.32 (both d, 1H each, $J = 2$ Hz, OCH=CH), 7.13–7.47 (complex, 2H, aromatic), and 8.09–8.47 (complex, 2H, aromatic); mass spectrum M^+ 198.0680 (calcd. for $C_{13}H_{10}O_2$: 198.0681). *Anal.* calcd. for $C_{13}H_{10}O_2$: C 78.77, H 5.09; found: C 78.94, H 5.05.

When 258 mg of the pure crystalline acetate **3** was treated with sulfuric acid under the same conditions, 180 mg (91% yield) of naphthofuran **4** was obtained.

Acetylation of Naphthofuran 4

A solution of **4** (85 mg, 0.43 mmol) and acetic anhydride (0.5 mL) in pyridine (1 mL) was stirred at room temperature. After 24 h, the reaction mixture was poured into ice-cold water and extracted with methylene chloride. The extracts were washed with 1 *N* hydrochloric acid, saturated aqueous sodium carbonate solution, and water. The usual work-up of the organic solution followed by chromatography of the crude product on silica gel with benzene elution gave acetate **5** (98 mg, 95% yield): mp 70–71°C (benzene); ir 1755 (ester), 1595 and 1575 cm^{-1} (aromatic); nmr δ 2.41, 2.46 (both s, 3H each, 2 × CH_3), 6.88, 7.72 (both d, 1H each, J = 2 Hz, OCH=CH), and 7.21–8.38 (complex, 4H, aromatic); mass spectrum M^+ 240.0785 (calcd. for $C_{15}H_{12}O_3$: 240.0786).

Conversion of Acetate 7 to Naphthofuran 8

To a solution of acetate **7** (520 mg, 1.91 mmol) in tetrahydrofuran (12 mL) was added 5% aqueous sulfuric acid (12 mL). After refluxing for 30 h, the reaction mixture was cooled to room temperature and extracted with methylene chloride. The usual work-up of the extracts followed by column chromatography of the crude product on silica gel with ether–benzene (1:20) elution gave naphthofuran **8** (304 mg, 75% yield): mp 117–118°C (chloroform – petroleum ether); ir 3620 (OH) and 1590 cm^{-1} (aromatic); nmr δ 2.33 (s, 3H, CH_3), 2.47 (d, J = 1 Hz, CH_3), 4.78 (br s, 1H, OH), 6.38 (q, 1H, J = 1 Hz, OC=CH), 7.31–7.59 (complex, 2H, aromatic), and 8.07–8.22 (complex, 2H, aromatic); mass spectrum M^+ 212.0829 (calcd. for $C_{14}H_{12}O_2$: 212.0833).

Acknowledgements

We are grateful to the Natural Sciences and Engineering Research Council of Canada and the University of Alberta for financial support.

1. (*a*) P. E. Eaton. Acc. Chem. Res. **1**, 50 (1968); (*b*) P. G. Bauslaugh. Synthesis, 287 (1970); (*c*) P. de Mayo. Acc. Chem. Res. **4**, 41 (1971).
2. J. M. Bruce. The chemistry of the quinonoid compounds. Part 1. *Edited by* S. Patai. Interscience, New York. 1973. Chapt. 9.
3. P. Yates and G. V. Nair. Synth. Commun. **3**, 337 (1973).
4. N. Ishibe and Y. Yamaguchi. J. Chem. Soc. Perkin I, 2618 (1973).
5. Z. Yoshida, M. Kimura, and S. Yoneda. Tetrahedron Lett. 2519 (1974); Chem. Lett. 519 (1975).
6. T. Otsuki. Bull. Chem. Soc. Jpn. **47**, 3084 (1974); **49**, 2596 (1976).
7. N. J. Bunce and M. Hadley. Can. J. Chem. **53**, 3240 (1975).
8. N. Ishibe, K. Hashimoto, and Y. Yamaguchi. J. Chem. Soc. Perkin I, 318 (1975).
9. K. Maruyama, Y. Naruta, and T. Otsuki. Bull. Chem. Soc. Jpn. **48**, 1553 (1975).
10. M. Oda, H. Oikawa, N. Fukazawa, and Y. Kitahara. Tetrahedron Lett. 4409 (1977).
11. M. Oda, H. Oikawa, Y. Kanao, and A. Yamamuro. Tetrahedron Lett. 4905 (1978).
12. E. A. Fehnel and F. C. Brokaw. J. Org. Chem. **45**, 578 (1980).
13. R. M. Wilson and A. K. Musser. J. Am. Chem. Soc. **102**, 1720 (1980).
14. K. Maruyama and N. Narita. Bull. Chem. Soc. Jpn. **53**, 757 (1980).
15. P. Cagniant and D. Cagniant. Advances in heterocyclic chemistry. Vol. 18. *Edited by* A. R. Katritzky and A. J. Boulton. Academic Press, New York. 1975. pp. 337–482.
16. E. J. Corey, J. D. Bass, R. LeMahieu, and R. B. Mitra. J. Am. Chem. Soc. **86**, 5570 (1964).
17. H. J. Liu and T. Ogino. Tetrahedron Lett. 4937 (1973).

Can. J. Chem. Downloaded from www.nrcresearchpress.com by 210.87.254.40 on 09/05/12
For personal use only.

Canadian Journal of Chemistry
Published by
THE NATIONAL RESEARCH COUNCIL OF CANADA

Journal canadien de chimie
Publié par
LE CONSEIL NATIONAL DE RECHERCHES DU CANADA

Volume 58 Number 21 November 1, 1980

Volume 58 numéro 21 1 novembre 1980

Vinyl ether hydrolysis. XIV. 2-Methoxy-2,3-dihydropyran: concurrent reaction of vinyl ether and acetal functional groups[1]

R. A. BURT, Y. CHIANG, AND A. J. KRESGE[2]

Department of Chemistry, University of Toronto, Scarborough College, West Hill, Ont., Canada M1C 1A4

Received May 1, 1980

R. A. BURT, Y. CHIANG, and A. J. KRESGE. Can. J. Chem. **58**, 2199 (1980).

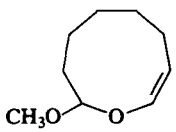
The hydrolysis of 2-methoxy-2,3-dihydropyran shows a normal isotope effect ($k_H/k_D > 1$) under catalysis by the hydrogen ion and gives an accurately linear dependence of reaction rate upon undissociated acid concentration in cyanoacetic acid and formic acid buffer solutions. This substrate, therefore, unlike its higher homolog, 9-methoxyoxacyclonon-2-ene, provides no evidence in support of an anything but a normal mechanism for vinyl ether hydrolysis. Analysis of the hydrogen isotope effect suggests that a minor amount (8%) of this hydrolysis occurs via reaction of the acetal functional group.

R. A. BURT, Y. CHIANG et A. J. KRESGE. Can. J. Chem. **58**, 2199 (1980).

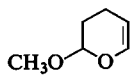
L'hydrolyse du méthoxy-2 dihydro-2,3 pyranne catalysée par l'ion hydrogène, montre un effet isotopique normal ($k_H/k_D > 1$) et sa vitesse de réaction dépend d'une façon précise et linéaire de la concentration en acide non dissocié dans des solutions tampons d'acides cyanoacétique et formique. Dans le cas de ce substrat, contrairement à son homologue supérieur, le méthoxy-9 oxacyclononène-2, toutes les données indiquent que la réaction se produit par un mécanisme d'hydrolyse normal pour les éthers vinyliques. L'analyse de l'effet isotopique de l'hydrogène suggère qu'une partie infime (8%) de cette hydrolyse se produit par l'intermédiaire de la réaction du groupe fonctionnel acétal.

[Traduit par le journal]

In order to gain information which might be of use in understanding the unusual hydrolytic behavior of 9-methoxyoxacyclonon-2-ene,[3] **1** (1), we have investigated the acid-catalyzed hydrolysis of the related substance, 2-methoxy-2,3-dihydropyran, **2**. The hydrolysis of a homolog of **2**, 2-ethoxy-2,3-dihydropyran, had been examined before (2), but that study was limited to HCl solutions. In dilute aqueous HCl, **1** behaves normally in a manner characteristic of the hydrolysis of its vinyl ether functional group. In carboxylic acid buffer solutions, however, its behavior deviates from that of all other vinyl ethers examined so far, and we were particularly interested, therefore, in studying a similarly substituted vinyl ether in these media.



1



2

Experimental

Materials

2-Methoxy-2,3-dihydropyran was purchased from the Aldrich Chemical Company. Its proton nmr spectrum was consistent with its structure and showed no sign of impurities, but kinetic data for the hydrolysis of the commercial material nevertheless sometimes produced curved first-order plots. Samples freshly purified by gas chromatography, on the other hand, were well behaved, and kinetic measurements were therefore carried out on material purified in this way.

Acids were best available commercial grades and were used without further treatment. Solutions were made using either deionized H_2O purified further by distillation from alkaline permanganate or D_2O as received (Merck); buffer solutions were prepared by adding requisite amounts of aqueous sodium hydroxide to acid solutions.

Kinetics

Rates of reaction were measured spectroscopically by following the decrease in the intense absorption of the vinyl ether chromophore of the substrate in the region 210–220 nm. A Cary

[1]Part XIII: Y. Chiang, W. K. Chwang, A. J. Kresge, and S. Szilagyi. Can. J. Chem. **58**, 124 (1980).

[2]Author to whom correspondence should be addressed.

[3]The name of **1** in the Hantzsh–Widman system of nomenclature for heterocyclic compounds is 2-methoxy-2,3,4,5,6,7-hexahydrooxonin.

0008-4042/80/212199-04$01.00/0

©1980 National Research Council of Canada/Conseil national de recherches du Canada

Can. J. Chem. Downloaded from www.nrcresearchpress.com by 210.87.254.42 on 09/05/12
For personal use only.

Can. J. Chem. Downloaded from www.nrcresearchpress.com by 210.87.254.42 on 09/05/12
For personal use only.

118C spectrometer was used with thermostatted cell compartment operating at 25.0 ± 0.02°C. Acid or buffer solutions were first allowed to come to thermal equilibrium with the cell compartment. A few microliters of substrate, dissolved in either water or methanol, were then added. The mixture was shaken, and a continuous recording of absorbance as a function of time was begun. Substrate concentrations were chosen to give convenient initial absorbance values; when methanol stock solutions were used, the final methanol concentration in the reaction mixture was never greater than 0.2%.

For the faster runs, absorbance recording was continued for 10–12 half-lives and first-order rate constants were obtained as slopes of plots of $\ln (A - A_\infty)$ vs. time. When freshly purified substrate was used, these data adhered to the first-order rate law accurately. Infinite-time readings were not made for the slower runs, and these data were analyzed by the Guggenheim (3) or Swinbourne methods (4).

Results

First-order rate constants for the hydrolysis of 2-methoxy-2,3-dihydropyran were determined in dilute hydrochloric acid solutions using H_2O and D_2O as the solvents. The data are summarized in Table 1. In each case, rates of reaction were found to be accurately proportional to hydrochloric acid concentrations, and second-order hydrogen ion catalytic coefficients were therefore obtained by linear least-squares analysis of the relationship between first-order rate constants and acid concentration. Intercepts proved to be zero within the experimental uncertainty indicating no uncatalyzed reaction. The results provide the isotope effect $k_{H^+}/k_{D^+} = 1.56 \pm 0.06$.

Rate measurements were also made in formic acid and cyanoacetic acid buffer solutions; these data are summarized in Table 2. In each case, rate constants were determined in series of buffer solutions of constant stoichiometric buffer ratio but varying buffer concentration. Because the buffer acids were moderately strong and the buffer concentrations were low, the hydrogen ion concentrations of these series of solutions were not quite constant. Small adjustments were therefore made to the observed rate constants to correct for this "buffer failure"; these corrections were made as before (5) using activity coefficients recommended by Bates (6) and the hydrogen ion catalytic coefficient determined in HCl solutions. First-order rate constants adjusted in this way were linear functions of undissociated acid concentration, indicating adherence to the expected rate law, eq. [1]. The data were therefore fitted to this expression by least-squares analysis and values of k_{H^+} were calculated using hydrogen ion concentrations estimated for the buffer failure corrections. This treatment gave values, $k_{H^+} = (1.66 \pm 0.02) \times 10^{-2}\ M^{-1}\ s^{-1}$ and $(1.64 \pm 0.04) \times 10^{-2}\ M^{-1}\ s^{-1}$ for the cyanoacetic and formic acid solutions respectively, in excellent agreement with the result obtained in HCl solutions, $k_{H^+} = (1.67 \pm 0.02) \times 10^{-2}\ M^{-1}\ s^{-1}$.

$$[1] \quad k_1 = k_{H^+}[H^+] + k_{HA}[HA]$$

TABLE 1. Rates of hydrolysis of 2-methoxy-2,3-dihydropyran in aqueous hydrochloric acid solutions at 25°C[a]

Acid concentration (M)	$10^3\ k\ (s^{-1})$
H_2O	
0.020	0.337, 0.325, 0.329
0.040	0.646, 0.646, 0.650, 0.659, 0.658
0.060	0.925, 0.950, 1.01, 1.00, 1.01
0.080	1.33, 1.31, 1.32, 1.33, 1.37, 1.34
0.100	1.66, 1.65
$k_1 = (-1.35 \pm 1.31) \times 10^{-5} + (1.67 \pm 0.02) \times 10^{-2}$[HCl]	
D_2O	
0.058	0.648, 0.647
0.087	0.999
0.116	1.27, 1.24, 1.31, 1.28
$k_1 = (3.58 \pm 3.92) \times 10^{-5} + (1.07 \pm 0.04) \times 10^{-2}$[DCl]	

[a]Ionic strength = concentration of acid; error limits are standard deviations of mean values.

TABLE 2. Rates of hydrolysis of 2-methoxy-2,3-dihydropyran in aqueous (H_2O) carboxylic acid buffer solutions[a]

10^2[HA] (M)	$10^5\ k\ (s^{-1})$
HA = CH_2CNCO_2H; [HA]/[NaA] = 0.61	
0.49	2.73
0.98	3.45
1.47	3.82
1.96	4.12
2.45	4.38
$k_{adj} = (4.06 \pm 0.04) \times 10^{-5} + (1.29 \pm 0.27) \times 10^{-4}$[HA]	
$k_{H^+} = (1.66 \pm 0.02) \times 10^{-2}\ M^{-1}\ s^{-1}$	
HA = HCO_2H; [HA]/[NaA] = 1.96	
0.78	0.693
1.56	0.753
2.35	0.839
3.13	0.833
3.91	0.863
$k_{adj} = (7.62 \pm 0.20) \times 10^{-6} + (2.77 \pm 0.79) \times 10^{-5}$[HA]	
$k_{H^+} = (1.64 \pm 0.04) \times 10^{-2}\ M^{-1}\ s^{-1}$	

[a]Ionic strength maintained at 0.040 M by adding NaCl; error limits are standard deviations of mean values.

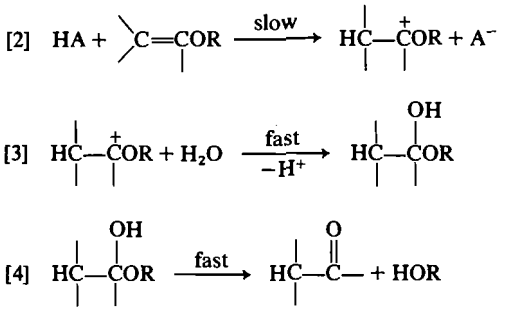
Discussion

Reaction Mechanism

With the sole exception of 9-methoxyoxacyclonon-2-ene, **1**, all vinyl ethers examined so far hydrolyze through rate-determining proton transfer from the catalyzing acid to the β-carbon atom of the vinyl ether functional group, eq. [2]. Hydration

Can. J. Chem. Downloaded from www.nrcresearchpress.com by 210.87.254.42 on 09/05/12
For personal use only.

of the thus formed cation (eq. [3]) and decomposition of the ensuing hemiacetal intermediate (eq. [4]) then proceed in subsequent rapid reaction steps.



This mechanism is characterized by solvent isotope effects of appreciable magnitude in the normal direction, $k_{H^+}/k_{D^+} = 2$–4 (7), and significant general acid catalysis with a linear dependence of reaction rate upon general acid concentration, eq. [1] (5). The hydrolysis of 9-methoxyoxacyclonon-2-ene, **1**, follows this pattern in dilute mineral acid solutions, giving $k_{H^+}/k_{D^+} = 4.2 \pm 0.2$ (1). In carboxylic acid buffers, however, this reaction shows a curved dependence of rate upon general acid concentration and a saturation of buffer catalysis at moderate undissociated acid concentrations.[4] The nonlinear nature of the relationship between specific first-order rates of disappearance of substrate and undissociated acid concentration is reinforced by the fact that hydrogen ion catalytic coefficients calculated by forcing a linear dependence, i.e. by fitting the data to eq. [1], are far in excess of values determined directly in mineral acid solutions.

These buffer solution data can be fitted to a hydrolysis reaction scheme in which the initial proton transfer step, eq. [2] is reversible and some subsequent step is rate-determining. The data adhere to such a mechanism well, and they give reasonable values of the parameters which may be obtained from the analysis (1). It was originally suggested that the subsequent slow step might be hydration of the cation formed by proton transfer, eq. [3]. However, recent measurements of the rate of reaction of alkoxy-substituted carbonium ions with water (8) suggest that this reaction, in the case of the cation formed from 9-methoxyoxacyclonon-2-ene, is likely to be a diffusion-controlled process. It therefore cannot be slower than reversion of the proton transfer step, but decomposition of the hemiacetal intermediate, eq. [4], appears still to be a viable possibility for the slow step.

The homolog of 9-methoxyoxacyclonon-2-ene examined in the present study, 2-methoxy-2,3-dihydropyran (**2**) shows no such unusual behavior. In dilute mineral acid solutions its hydrolysis gives a normal solvent isotope effect, $k_{H^+}/k_{D^+} = 1.6$. (This value may be somewhat low for a substrate of this reactivity, but that can be understood in terms of an expected competing hydrolysis of the acetal functional group in this molecule; *vide infra*.) The reaction follows the normal pattern in buffer solutions as well, giving an accurately linear dependence of rate upon undissociated acid concentration. The data obtained in solutions of the weaker of the two buffer acids investigated here, for which unusual behavior is the more likely, are displayed in Fig. 1. It may be seen that there is no indication of curvature and that the intercept (= $k_{H^+}[H^+]$, cf. eq. [1]), obtained by least-squares analysis agrees very well with the value expected on the basis of the known hydrogen ion concentration and the hydrogen ion catalytic coefficient determined directly in mineral acid solutions. The data obtained in buffer solutions of the other carboxylic acid used in this study show similar conformity with normal behavior.

Thus, though structurally similar to 9-methoxyoxacyclonon-2-ene, 2-methoxy-2,3-dihydropyran does not behave in a manner which suggests that the initial protonation step in its vinyl ether hydrolysis reaction is a reversible process. It is unlike its higher homolog in this respect. It is interesting that this dissimilarity extends to a difference in reactivity: the value of k_{H^+} for 2-methoxy-2,3-dihydropyran is 0.0167 M^{-1} s^{-1} while that for 9-methoxyoxacyclonon-2-ene is 8.1 M^{-1} s^{-1}, some 500 times greater.

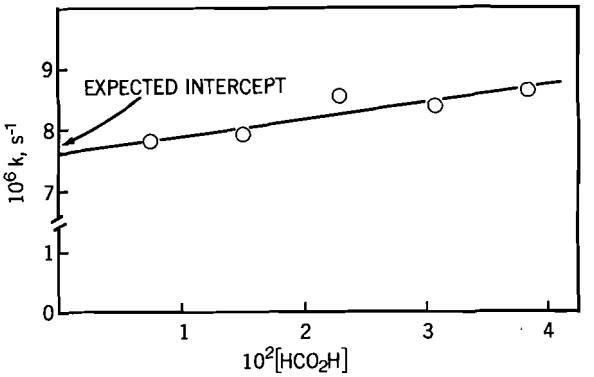


FIG. 1. Relationship between the rate of hydrolysis of 2-methoxy-2,3-dihydropyran in formic acid buffer solutions and buffer acid concentrations.

[4]In acetic acid buffers, saturation appears at [HOAc] = 0.01 M (1); a curved dependence of rate upon undissociated acid concentration has also been observed in methoxyacetic acid buffers (personal communication from Professor V. P. Vitullo).

Can. J. Chem. Downloaded from www.nrcresearchpress.com by 210.87.254.42 on 09/05/12
For personal use only.

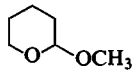
Concurrent Acetal Hydrolysis

The 2-methoxy-2,3-dihydropyran molecule contains an acetal function in addition to its vinyl ether group. Since the reactivity of acetals in acid-catalyzed hydrolysis is generally similar to that of vinyl ethers, reaction by way of this second functional group might be expected to occur. The two hydrolysis reactions will give the same products, glutaraldehyde and methanol, and they cannot be distinguished on that basis. They will, however, show different solvent isotope effects, and this difference has in fact been used to estimate the amount of reaction occurring by each route in the case of the closely related substance, 2-ethoxy-2,3-dihydropyran (2).

The method makes use of dihydropyran, **3**, and 2-methoxytetrahydropyran, **4**, as monofunctional



3



4

models for the vinyl ether and acetal functions of the difunctional substrate. If solvent isotope effects on the hydrogen ion-catalyzed hydrolysis of these model compounds are assumed to be the same as the isotope effects on the hydrolysis of the corresponding functional groups in the difunctional substrate, then eqs. [5] and [6] may be written. Here

$$[5] \quad k_{H^+} = k_{VE} + k_A$$

$$[6] \quad k_{D^+} = ak_{VE} + bk_A$$

k_{H^+} and k_{D^+} are rate constants for the overall hydrolysis of the difunctional substrate in H_2O and in D_2O respectively, k_{VE} and k_A are the rate constants for the vinyl ether and acetal hydrolysis components of the overall rate in H_2O, and a and b are isotope effects (k_{D^+}/k_{H^+}) on the vinyl ether and acetal reactions respectively, as determined by measurements on the model compounds. With $a = (2.21)^{-1}$ and $b = (0.340)^{-1}$ (2), this analysis gives 67% reaction by the vinyl ether pathway and 33% by the acetal pathway for 2-ethoxy-2,3-dihydropyran (2), and 92% reaction by the vinyl ether pathway and 8% by the acetal pathway for the substrate studied here, 2-methoxy-2,3-dihydropyran.

It is significant that the relative amounts of reaction by the two pathways for these two substrates do not differ very much, for the substitution of an ethoxy group for a methoxy group is but a minor structural change. What difference there is is produced principally by a change in the rate constant for reaction of the acetal group (Table 3), in keeping with the fact that the structural change occurs in this function and that it should therefore have more effect here than on the reactivity of the more remote vinyl ether group. It is significant as well that changing methoxy to ethoxy raises the rate of acetal hydrolysis, for this is the direction of the change in the hydrolysis rates of the monofunctional model substrates, 2-methoxytetrahydropyran and 2-ethoxytetrahydropyran (9). The effect in the models, however, amounts to only a factor of 1.2, which is considerably less than the 6-fold difference found here. This suggests that the assumption of transferability of isotope effects may not be entirely justified.

TABLE 3. Estimated rate constants for concurrent vinyl ether and acetal hydrolysis in 2-alkoxy-2,3-dihydropyrans

Substrate	$10^2 k_{H^+}$ (M^{-1} s^{-1}) Vinyl ether pathway	Acetal pathway
2-Methoxy-2,3-dihydropyran	1.55	0.13
2-Ethoxy-2,3-dihydropyran	1.73	0.82

Acknowledgements

We are grateful to the Natural Sciences and Engineering Research Council of Canada and the Connaught Fund of the University of Toronto for their financial support of this research.

1. J. D. COOPER, V. P. VITULLO, and D. L. WHALEN. J. Am. Chem. Soc. **93**, 6294 (1971).
2. A. KANKAANPERA. Acta Chem. Scand. **23**, 1465 (1969).
3. E. A. GUGGENHEIM. Philos. Mag. **2**, 538 (1926).
4. E. S. SWINBOURNE. J. Chem. Soc. 2371 (1960).
5. A. J. KRESGE, H. L. CHEN, Y. CHIANG, E. MURRILL, M. A. PAYNE, and D. S. SAGATYS. J. Am. Chem. Soc. **93**, 413 (1971).
6. R. G. BATES. Determination of pH. John Wiley and Sons, New York. 1973. p. 49.
7. A. J. KRESGE, D. S. SAGATYS, and H. L. CHEN. J. Am. Chem. Soc. **99**, 7228 (1977).
8. P. R. YOUNG and W. P. JENCKS. J. Am. Chem. Soc. **99**, 8238 (1977); R. A. MCCLELLAND and M. AHMAD. J. Am. Chem. Soc. **100**, 7031 (1978).
9. A. KANKAANPERA and A. MIKKI. Suom. Kemistil. B, **41**, 42 (1968).

Vinyl ether hydrolysis. XV. Methyl β,β-di-*tert*-butylvinyl ether: buttressing steric effects[1]

Y. CHIANG, A. J. KRESGE,[2] T. T. TIDWELL, AND P. A. WALSH

Department of Chemistry, University of Toronto, Scarborough College, West Hill, Ont., Canada M1C 1A4

Received April 28, 1980

Y. CHIANG, A. J. KRESGE, T. T. TIDWELL, and P. A. WALSH. Can. J. Chem. **58**, 2203 (1980).

The highly congested molecule, methyl β,β-di-*tert*-butylvinyl ether, undergoes reaction in dilute aqueous mineral acid solutions by a normal vinyl ether hydrolysis mechanism and gives an unrearranged aldehyde product. The *tert*-butyl groups retard the rate of hydrolysis, but the effect of *cis* and *trans* substituents is not cumulative; this is attributed to a repulsive nonbonded interaction, relieved in the course of reaction, between the ether oxygen atom and the *cis*-*tert*-butyl group buttressed by the *trans*-*tert*-butyl group.

Y. CHIANG, A. J. KRESGE, T. T. TIDWELL et P. A. WALSH. Can. J. Chem. **58**, 2203 (1980).

L'éther méthyl β,β di-*tert*-butylvinyle, une molécule fortement encombrée, réagit dans des solutions aqueuses diluées d'acide minéral selon un mécanisme normal d'hydrolyse d'éther vinylique et conduit à l'aldéhyde non transposé. Le groupe *tert*-butyle retarde la vitesse d'hydrolyse, mais l'effet des substituants en position *cis* et *trans* n'est pas cumulatif. Ceci est attribué à l'interaction répulsive non liée notée au cours de la réaction entre l'atome d'oxygène de l'éther et le groupe *tert*-butyle en position *cis* comprimé par le groupe *tert*-butyle en position *trans*.

[Traduit par le journal]

Substitution of small alkyl groups such as methyl at the β-carbon atom of vinyl ethers is known to depress the rate of acid-catalyzed hydrolysis of these substances (1). The effect is thought to operate through lowering of the energy of the initial state of this reaction, via the well-known ability of alkyl groups to stabilize carbon–carbon double bonds (2). Two groups are more effective than one and, though there are differences which can be attributed to different steric requirements of *cis* and *trans* isomers, the effects are cumulative, i.e. two groups exert an influence roughly equal to the product of the effects of the two groups taken separately.

The bulky *tert*-butyl group conforms to this pattern of reactivity in part; introduction of a single *tert*-butyl group in either the *cis* or the *trans* position at the β-carbon atom of ethyl vinyl ether lowers the rate of hydrolysis of this substance (3). We have found, however, that disubstitution is surprisingly ineffective in producing a further lowering of reactivity, and that methyl β,β-di-*tert*-butylvinyl ether is in fact an order of magnitude more reactive than it would be were the effects of the individual *tert*-butyl groups cumulative.

This behavior is remarkable in view of the fact that interference between the geminal *tert*-butyl groups of the substrate should increase as the trigonal carbon atom to which they are attached becomes tetrahedral during the course of the hydrolysis reaction, eq. [1] (4). The combined bulk

$$[1]\quad (t\text{-Bu})_2C{=}CHOMe \xrightarrow[H_2O]{H^+} (t\text{-Bu})_2CHCHO + MeOH$$

of two *tert*-butyl groups at the reaction site might also impede approach of the electrophilic reagent (H^+); tri-*tert*-butylethylene is known to add bromine only slowly because of steric hindrance (5). These effects would serve to produce a rate retardation *greater* than the product of the retardations shown by the *cis* and *trans* monosubstituted substrates separately, rather than the *less* than cumulative retardation actually observed.

Experimental

Materials

Methyl β,β-di-*tert*-butylvinyl ether was prepared from the corresponding acetal which was made by heating β,β-di-*tert*-butylacetaldehyde (6) with trimethyl orthoformate and a catalytic amount of *p*-toluenesulfonic acid. The acetal was not purified; upon introduction onto a gas chromatography column (Carbowax 20M, 210°C) it eliminated methanol and formed the vinyl ether. The latter was characterized by proton nmr; δ: 5.77 (s, 1H), 3.55 (s, 3H), 1.25 (2, 9H), 1.17 (s, 9H); and by elemental analysis. *Anal.* calcd. for $C_{11}H_{22}O$: C 77.58%, H 13.02%; found: C 77.46%, H 13.30%. Samples for kinetic measurements were purified by gas chromatography.

Acids were best available commercial grades and were used without further treatment. Solutions were made using either deionized H_2O purified further by distillation from alkaline permanganate or D_2O (Merck) as received.

Product Analysis

A reaction mixture was prepared by combining 10 μL of methyl β,β-di-*tert*-butylvinyl ether and 0.5 mL of 1 *M* aqueous HCl. This two-phase system was agitated in an ultrasonic cleaning bath for 15 min to disperse the organic component, and it was then allowed to stand at room temperature for 3 h. After this time the mixture was extracted with 0.2 mL of CCl_4 and a proton nmr spectrum of the extract was taken. This showed a mixture of the starting vinyl ether and the expected hydrolysis product, di-*tert*-butylacetaldehyde (δ: 9.70 (d, 1H), 1.72 (d, 1H),

[1]Part XIV: R. A. Burt, Y. Chiang, and A. J. Kresge. Can. J. Chem. **58**, 2199 (1980).

[2]Author to whom correspondence should be addressed.

0008-4042/80/212203-04$01.00/0

©1980 National Research Council of Canada/Conseil national de recherches du Canada

Can. J. Chem. Downloaded from www.nrcresearchpress.com by 210.87.254.5 on 09/05/12
For personal use only.

1.23 (s, 18H)) in a 2:1 ratio; no other substances could be detected, even when the spectrum was measured at the highest possible sensitivity.

Kinetics

Rates of reaction were determined spectroscopically by monitoring the decrease in the intense absorption of methyl β,β-di-*tert*-butylvinyl ether at 205–215 nm. Measurements were made using a Cary 118C spectrometer with cell compartment thermostatted at 25.0 ± 0.02°C. Acid solutions were allowed to come to temperature equilibrium with the cell compartment and reactions were then initiated by adding a few μL of substrate, dissolved in ethanol, to the equilibrated solutions and shaking the resultant mixtures. Since methyl β,β-di-*tert*-butylvinyl ether is only very sparingly soluble in water, care had to be taken to insure that shaking did produce homogeneous solutions. Ethanol concentrations in the final reaction mixtures were never greater than 0.2%.

For the faster runs, continuous records of absorbance as a function of time were made out to 10–12 half-lives and first-order rate constants were evaluated as slopes of plots of ln $(A - A_\infty)$ vs. time. With the slower runs, absorbance readings were recorded at preset time intervals out to 2–3 half-lives and rate constants were determined by the Guggenheim (7) or Swinbourne (8) methods.

Results

First-order rate constants for the hydrolysis of methyl β,β-di-*tert*-butylvinyl ether were determined in solutions of $HClO_4$ and HCl in H_2O and in solutions of DCl in D_2O. The data are summarized in Table 1.

In each kind of solution first-order specific rates proved to be accurately proportional to acid concentration, and second-order rate constants were therefore calculated by dividing the first-order rate constants by acid molarity. The results obtained from $HClO_4$ and HCl solutions are in good agreement with one another, $k_{H^+} = 0.352 \pm 0.013$ and $0.337 \pm 0.012\ M^{-1}\ s^{-1}$; combination of these two values by taking a simple average gives $k_{H^+} = 0.344 \pm 0.009\ M^{-1}\ s^{-1}$ as the best estimate of this catalytic coefficient. That, together with the result from DCl solutions, gives the isotope effect $k_{H^+}/k_{D^+} = 2.82 \pm 0.18$.

TABLE 1. Rates of hydrolysis of methyl di-*tert*-butylvinyl ether in aqueous solution at 25°C[a]

10^2 Acid concentration (M)	$10^2\ k_{obs}$ (s^{-1})
$HClO_4$	
11.8	4.30, 4.34, 4.34
9.4	3.38, 3.43, 3.42
7.1	2.52, 2.53, 2.50
5.9	2.07, 2.12, 2.06
4.7	1.60, 1.60, 1.64
2.4	0.774, 0.787, 0.783
$k_{H^+} = (3.52 \pm 0.13) \times 10^{-1}\ M^{-1}\ s^{-1}$	
HCl	
10.0	3.50, 3.48, 3.50
8.0	2.80, 2.71, 2.77
6.0	2.08, 2.03, 2.02
4.0	1.32, 1.32, 1.35
2.0	0.631, 0.647, 0.633
$k_{H^+} = (3.37 \pm 0.12) \times 10^{-1}\ M^{-1}\ s^{-1}$	
DCl	
11.6	1.51, 1.48
9.2	1.15, 1.14, 1.19, 1.13
7.0	0.809, 0.803, 0.826
4.6	0.593, 0.554
2.3	0.257, 0.249
$k_{D^+} = (1.22 \pm 0.07) \times 10^{-1}\ M^{-1}\ s^{-1}$	

[a]Ionic strength = acid concentration.

Discussion

Reaction Mechanism

The mechanism by which virtually all vinyl ethers hydrolyze consists of rate-determining proton transfer from a catalyzing acid to the substrate, eq. [2],

$$[2]\quad R_2C{=}CHOR \xrightarrow[\text{slow}]{HA} R_2CHCHOR^+$$

followed by rapid hydration of the ensuing cation, eq. [3], and decomposition of the hemiacetal intermediate, eq. [4].

$$[3]\quad R_2CHCHOR^+ \xrightarrow[\text{fast}]{H_2O,\ -H^+} R_2CHCH(OH)OR$$

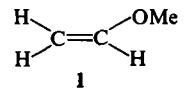
$$[4]\quad R_2CHCH(OH)OR \xrightarrow[\text{fast}]{} R_2CHCHO + HOR$$

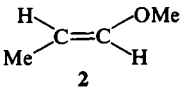
A reaction scheme such as this is characterized by kinetic isotope effects of appreciable magnitude in the normal direction ($k_H/k_D > 1$). The fact that the isotope effect observed here is as great as it is, $k_{H^+}/k_{D^+} = 2.8 \pm 0.2$ indicates that this mechanism operates in the case of the present reaction as well. This conclusion is reinforced by the excellent agreement between this isotope effect and the value predicted for a vinyl ether of the present substrate's reactivity, $k_{H^+}/k_{D^+} = 2.7$, from a correlation of isotope effects on the hydrolysis of a large group of vinyl ethers known to react by the mechanism of eqs. [2]–[4] (9).

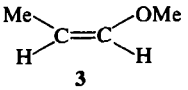
Reactivity

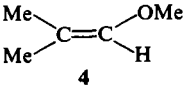
Methyl *trans*-propenyl ether, **2**, is only 0.095 times as reactive to hydrogen ion-catalyzed hydrolysis as methyl vinyl ether, **1** (9). The *cis* isomer, **3**, also shows reduced reactivity, but the factor by which it differs from the unsubsituted parent, **1**, is somewhat weaker, 0.34 (9); this difference is probably due to steric acceleration produced by relief of crowding between the vicinal methyl and methoxyl groups situated on the same side of the double bond

Can. J. Chem. Downloaded from www.nrcresearchpress.com by 210.87.254.5 on 09/05/12
For personal use only.


1
1.00


2
0.095

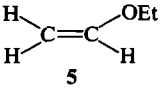

3
0.34

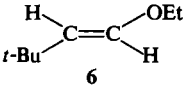

4
0.033

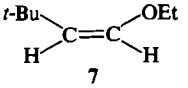
in the *cis* isomer. Methyl isobutenyl ether, **4**, is still less reactive than either of the propenyl derivatives, and it is interesting that the factor by which its rate constant is lower than that of the parent ether (**1**), 0.033 (9), is very nearly equal to the product of the reductions in reactivity shown individually by the two propenyl ethers: $0.095 \times 0.34 = 0.032$.

These comparisons are for hydrolysis reactions conducted in wholly aqueous solution. A similar pattern is shown by the hydrolysis of ethyl analogs in 80% aqueous dioxane (3): CH_2=CHOEt, 1.00; *trans*-MeCH=CHOEt, 0.12; *cis*-MeCH=CHOEt, 0.39; Me_2C=CHOEt, 0.029. Here again the reactivity of the isobutenyl derivative is consistent with the product of the reductions shown by the propenyl ethers, though in this case the quantitative agreement is less exact: $0.12 \times 0.39 = 0.047$.

Data are also available for the hydrolysis in 80% aqueous dioxane of the two mono-*tert*-butyl substituted vinyl ethers, **6** and **7**. Once again β-alkyl


5


6


7

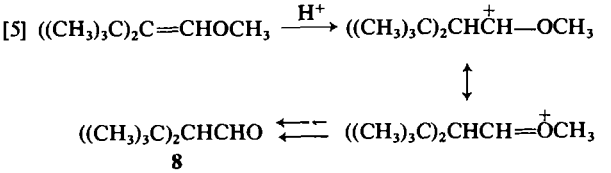
substitution produces a reduction in reaction rate, and as before the *trans* isomer gives the stronger effect, 0.066 (*trans*) vs. 0.47 (*cis*). The product of these two factors would put the relative reactivity of methyl β,β-di-*tert*-butylvinyl ether at ca. 0.03, if the retardations due to the *cis* and *trans tert*-butyl groups were cumulative. The actual rate reduction seen by comparing the rate constant determined here with $k_{H^+} = 0.76\ M^{-1}\ s^{-1}$ for methyl vinyl ether (9) is only 0.45. This makes β,β-di-*tert*-butyl substitution 14 times less effective at retarding vinyl ether hydrolysis than is β,β-dimethyl substitution: k_{H^+} (*t*-Bu_2C=CHOMe)/k_{H^+} (Me_2C=CHOMe) = 14.

It seems likely that this difference in behaviour between the *tert*-butyl and methyl systems originates in buttressing steric effects present in the di-*tert*-butyl substrate. A simple geometrical calculation shows that the distance separating the oxygen atom of a *cis*-β-*tert*-butylvinyl ether from the central carbon atom of the *tert*-butyl group would be only 2.8 Å if all bond lengths and bond angles had their normal values. This is much shorter than the sum of the van der Waals radius of oxygen, 1.40 Å (10), and even the minimum radius of a *tert*-butyl group, 2.44 Å (11). The molecule will therefore distort to relieve the nonbonded repulsion implied by this short distance, and it will probably do this by opening up the C=C—C and C=C—O bond angles; in *cis*-2-butene similar strain is relieved through opening of the C=C—C angle to 127°, and calculations suggest that in *cis*-1,2-di-*tert*-butylethylene there is a further opening to 135° (12). A similar accommodation to relieve nonbonded repulsion between oxygen and the *cis*-*tert*-butyl group in β,β-di-*tert*-butylvinyl ethers can occur only at the expense of increasing repulsion between the two *tert*-butyl groups themselves, which is already quite severe; the strain energy of 1,1-di-*tert*-butylethylene has been estimated to be 12 kcal mol^{-1} (13). The second *tert*-butyl group of the β,β-di-*tert*-butylvinyl ether will therefore buttress the first, augmenting nonbonded repulsion between the oxygen atom and the *tert*-butyl group *cis* to it. Some of this increased strain will be relieved when the requirement for coplanarity of substituents on the carbon–carbon double bond is removed as the hydrolysis reaction takes place, and an increased rate of reaction will result.

It is typical that only a small portion of the strain resulting from the *cis* arrangement of two bulky groups is translated into an enhanced reactivity. Even for 1,2-di-*tert*-butylethylene the *cis*/*trans* rate ratio for protonation is only 3.8 (14).

Reaction Products

Highly congested systems such as that investigated here are prone to rearrangement; this is especially likely if their reactions produce cations which can be transformed to more stable species (4, 5, 15). The ion produced by straightforward protonation of the β-carbon of the present substrate is an alkoxy substituted cation stabilized by resonance (eq. [5]); its rearrangement is therefore apt to be an


[5] $((CH_3)_3C)_2C$=$CHOCH_3$ $\xrightarrow{H^+}$ $((CH_3)_3C)_2\overset{+}{C}HCH$—$OCH_3$ ↕ $((CH_3)_3C)_2CHCHO$ ⇄ $((CH_3)_3C)_2CHCH$=$\overset{+}{O}CH_3$

8

unfavorable process. This is supported by the fact that the only product of this reaction which we were able to detect was the expected, unrearranged aldehyde, β,β-di-*tert*-butylacetaldehyde, **8**.

Can. J. Chem. Downloaded from www.nrcresearchpress.com by 210.87.254.5 on 09/05/12
For personal use only.

Acknowledgements

We are grateful to the Natural Sciences and Engineering Research Council of Canada and the Petroleum Research Fund of the American Chemical Society for their financial support of this research. Part of this work was done at Stanford University where T.T.T. was on sabbatical leave in 1978–1979.

1. Y. CHIANG, W. K. CHWANG, A. J. KRESGE, and S. SZILAGYI. Can. J. Chem. **58**, 124 (1980).
2. J. HINE. Structural effects on equilibria in organic chemistry. John Wiley, New York. 1975. pp. 265–276.
3. T. OKUYAMA, T. FUENO, H. NAKATSUJI, and J. FURUKAWA. J. Am. Chem. Soc. **89**, 5826 (1967).
4. H. C. BROWN and R. S. FLETCHER. J. Am. Chem. Soc. **71**, 1845 (1949); H. C. BROWN. Rec. Chem. Prog. **14**, 83 (1953).
5. G. J. ABRUSCATO and T. T. TIDWELL. J. Org. Chem. **37**, 4151 (1972).
6. M. S. NEWMAN, A. ARKELL, and T. FUKUNAGA. J. Am. Chem. Soc. **82**, 2498 (1960).
7. E. A. GUGGENHEIM. Philos. Mag. **2**, 538 (1926).
8. E. A. SWINBOURNE. J. Chem. Soc. 2371 (1960).
9. A. J. KRESGE, D. S. SAGATYS, and H. L. CHEN. J. Am. Chem. Soc. **99**, 7228 (1977).
10. L. PAULING. The chemical bond. Cornell University Press, Ithaca, NY. 1967. p. 152.
11. M. CHARTON. Prog. Phys. Org. Chem. **8**, 247 (1971).
12. A. GREENBERG and J. F. LIEBMAN. Strained organic molecules. Academic Press, New York. 1978. p. 108.
13. O. ERMER and S. LIFSON. Tetrahedron, **30**, 2425 (1973).
14. W. K. CHWANG and T. T. TIDWELL. J. Org. Chem. **43**, 1904 (1978).
15. P. D. BARTLETT and M. S. SWAIN. J. Am. Chem. Soc. **77**, 2801 (1955); P. D. BARTLETT and M. STILES. J. Am. Chem. Soc. **77**, 2806 (1955).

Can. J. Chem. Downloaded from www.nrcresearchpress.com by 210.87.254.5 on 09/05/12
For personal use only.

The mechanism of the reaction of the Nash and the Sawicki aldehyde reagent

BRUCE JON COMPTON AND WILLIAM C. PURDY

Department of Chemistry, McGill University, 801 Sherbrooke St. W., Montreal, P.Q., Canada H3A 2K6

Received March 7, 1980

BRUCE JON COMPTON and WILLIAM C. PURDY. Can. J. Chem. **58**, 2207 (1980).

Synthetic and chromatographic studies are presented on the Nash and Sawicki colorimetric methods for quantitating formaldehyde. It is shown that the actual color-forming agent in the Nash method is an isolable iminodione formed *in situ* by reaction of the two components. Explanation is given for differences between these two methods.

BRUCE JON COMPTON et WILLIAM C. PURDY. Can. J. Chem. **58**, 2207 (1980).

On présente des études chromatographiques de synthèse en rapport avec les méthodes colorimétriques de Nash et de Sawicki relatives à la détermination quantitative de la formaldéhyde. On montre que l'agent qui est de fait responsable de la formation de la couleur, dans la méthode de Nash, est une iminodione que l'on peut isoler et qui se forme *in situ* par la réaction de deux réactifs. On donne une explication des différences qui apparaissent entre ces deux méthodes.

[Traduit par le journal]

Introduction

Both the colorimetric methods of Nash (1) and of Sawicki and Carnes (2, 3) involve a condensation reaction between formaldehyde and a reagent consisting of a β-diketone and ammonium acetate. In the Nash method, based on the Hantzsch pyridine synthesis (4, 5), formaldehyde reacts with a reagent consisting of 2,4-pentanedione and concentrated (~ 2 *M*) ammonium acetate (reaction 10). The chromophore, 3,5-diacetyl-2,6-dihydrolutidine (**4**), exhibits fluorescence (6). The method of Sawicki and Carnes (2) uses dimedone (5,5-dimethyl-1,3-cyclohexanedione) as the β-diketone. The reaction of formaldehyde, dimedone, and ammonium acetate (reaction 11) was first described by Vorländer and co-workers (7–9). The product, **9**, exhibits approximately 100 times greater fluorescence than the product (**4**) from 2,4-pentanedione (2).

Reactions 1–4 (Fig. 1) are possible pathways by which the Nash method can proceed. Similarly, reactions 5–9 (Fig. 2) are possible pathways for the Sawicki reagent. Reactions 1, 3, and 5–9 have been described in various places in the literature (see Experimental). Reaction 2 has not previously been reported. None of these reactions have been discussed with reference to either of the two reagents studied here.

While it was our intention to study these two methods from the standpoint of achieving greater sensitivity for formaldehyde in a continuous-flow analyzer, we discovered a general lack of understanding of the basic chemistry underlying these two methods.

Our experimental approach was to demonstrate that reactions 1–9 can occur under the conditions used for the two methods. Compounds **1–9** were then synthesized and used as standards to investigate the mechanism of the Nash and Sawicki methods. This study bridges the gap between organic and analytical work and has resulted in a superior aldehyde reagent (10).

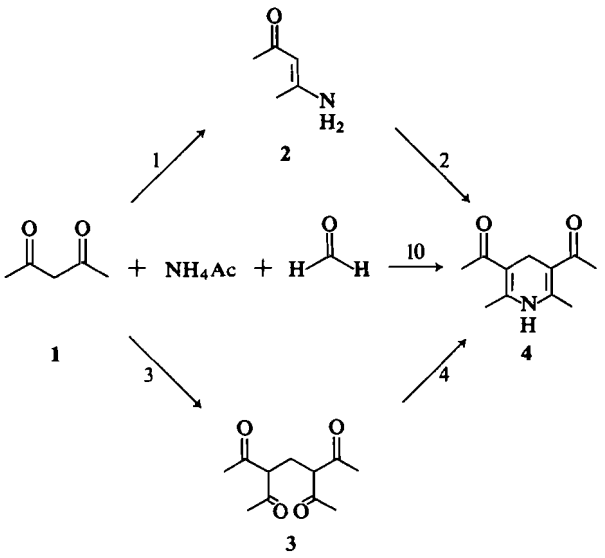


FIG. 1. The reactions and intermediates found with the Nash method.

Experimental

Two methods, a synthetic and an analytical assay procedure, were used to determine the mechanistic aspects of the reactions of interest (reactions 10 and 11). First the reaction pathways illustrated in Figs. 1 and 2 were carried out using preparative synthetic procedures. Once standards were obtained for each of the compounds shown in these two figures, assays utilizing high-performance liquid chromatography (hplc) were developed and used to monitor the actual reactions of Nash and Sawicki. Efforts were made to run all synthetic reactions under conditions similar to those found in the analytical assay systems for formaldehyde (1, 2) as well as by an alternative method from the literature. Yields were unoptimized.

0008-4042/80/212207-05$01.00/0

©1980 National Research Council of Canada/Conseil national de recherches du Canada

Can. J. Chem. Downloaded from www.nrcresearchpress.com by 210.87.254.42 on 09/05/12
For personal use only.

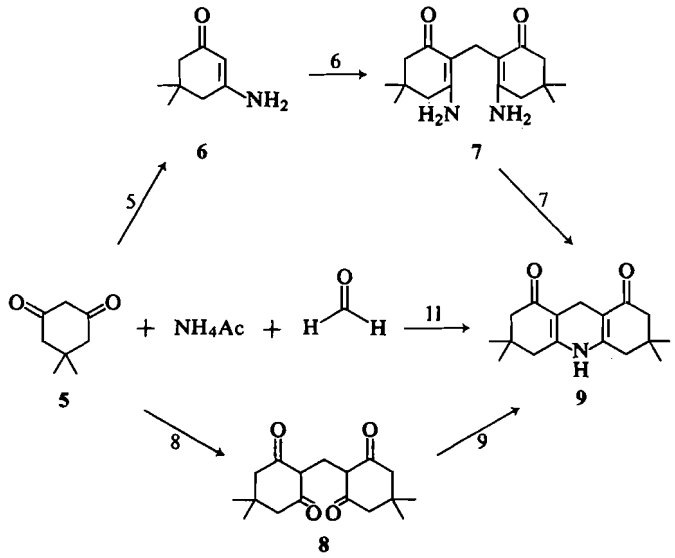


FIG. 2. The reactions and intermediates found with the Sawicki method.

Synthetic Procedures

Compound 2, 4-Amino-3-penten-2-one (Fluoral-P)

Twenty mL of 2,4-pentanedione in 50 mL of 4 *M* ammonium acetate, pH 5.5, was heated to 80°C for 3 h, extracted into chloroform, and vacuum distilled (bulb-to-bulb, 5 Torr, 64°C) to give a clear viscous liquid which solidified upon cooling (yield 32%, 5.66 g; mp 45°C; recrystallized from ethyl acetate – petroleum ether). Structural assignment was based on chemical (conversion of **2** to **4** with formaldehyde) and spectral data (ir, chloroform: 3500 (s), 3120–3440 (b), 3200 (s), 1624 (s), 1597 (s); ^{1}H nmr, 200 MHz, D-chloroform, δ: 2.75 (3), 2.87 (3), 5.87 (2), 8.10 (1), all singlets; ms (C_5H_9NO): 99.0674, and microanalysis C 61.03 (60.61), H 9.30 (9.09), N 14.38 (14.31), theoretical in parentheses. This compound was also synthesized by an alternative route (10) modified from the literature (11).

Compound 3, 3,3'-Methylene-bis-(2,4-pentanedione)

To one mL of 2,4-pentanedione in 20 mL of 99% methanol – 1% acetic acid was added 4 mL of 37% aqueous formaldehyde. After 10 min of stirring and evaporation, a white crystalline mass was isolated; this was recrystallized from ethyl acetate, yield 89%, 0.923 g; mp 140–142°C; ir 3200–3600 (b), 1695 (s); nmr δ: 1.3(3), 2.2(3), 2.6(1), 3.6(2), all singlets; ms: 212, 150, 112, 109, 43 (base). The melting point data indicate that the di-intramolecular hydrogen-bonded species was isolated since the free and mono-intramolecular hydrogen-bonded species have already been assigned different melting points (12).

Compound 4, 3,5-Diacetyl-1,4-dihydro-2,6-lutidine

The method of Erikson and Biggs (13) was used. Also, **2** was employed by reaction with formaldehyde in pH 2.25 phosphate buffer or **3** with molar ammonium acetate, pH 6.0, after 30 min of stirring. Compound **4** was recrystallized from methanol, mp 204–205°C (lit. (1) mp 200°C; (13) mp 201–205°C), with yields greater than 90%.

Compound 6, 5,5-Dimethyl-3-aminocyclohex-2-en-1-one

The method of Greenhill (14) was used (yield 81%) as well as a method similar to that described for **2** (yield 27%, mp 166.5–167°C (lit. (14) mp 164–165°C)).

Compound 7, 2,2'-Methylene-bis-(5,5-dimethyl-3-aminocyclohex-2-en-1-one)

The method of Greenhill (14) was used. In addition, this compound was isolated whenever attempts were made to convert **6** to **9** by the rapid addition of formaldehyde (mp 241–242°C (lit. (14) mp 242°C)).

Compound 8, Bis-(4,4-dimethyl-2,6-dioxocyclohexyl) Methane

The method of Horning and Horning (15) was used (yield 95%). Also this product was isolated when following the synthetic method of Sawicki and Carnes (2) for **9** if formaldehyde is added at a rate faster than dropwise (mp 191–191.5°C (lit. (16) mp 189–190°C; (15) mp 191–191.5°C)).

Compound 9, 3,3,6,6-Tetramethyl-1,2,3,4,5,6,7,8,9,10-decahydro-1,8-acridinedione

The method of Sawicki and Carnes (2) was used and the product was recrystallized from acetone (yield 10%; mp 298–301°C (lit. (17) mp 296–297°C)). Also **9** was synthesized by heating **8** in 2 *M* ammonium acetate (pH 5.5) for 3 h at 80°C or directly from **6** or **7** by modifying the alternate method for **7** to include overnight heating at 80°C.

Equipment and Chemicals

The hplc studies were conducted using a system previously described (18) except that the normal phase mode was employed with a μ-Porasil column (Waters Associates, Milford, CT). Spectral studies were made with a Cary Model 17 Spectrophotometer (Varian Associates, Palo Alto, CA) and an Aminco SPF-125 Spectrofluorometer (American Instrument Co., Silver Spring, MD).

All organic reagents were purchased from Aldrich Chemical Co. (Milwaukee, WI) and all inorganic reagents such as ammonium acetate from Anachemia Chemicals Ltd. (Montreal, P. Q.). All solvents were from American Chemicals Ltd. (Montreal, P.Q.) and were either reagent or "spectrograde" quality. Formaldehyde (37% reagent grade) was purchased from American Chemicals.

Assay Conditions

The chromatographic conditions and retention data (k') are summarized in Table 1. Reactions 10 and 11 as well as those involving the conversion of **6** to **9** (reactions 6 and 7) were investigated under the following conditions. To a preincubated (either 5 or 30 min) mixture of 0.1 *M* 2,4-pentanedione (1 mL in methanol) and molar ammonium acetate (2 mL at pH 5.5) at 22°C was added 1 mL of 1.26×10^{-2} *M* formaldehyde. Samples were

Can. J. Chem. Downloaded from www.nrcresearchpress.com by 210.87.254.42 on 09/05/12
For personal use only.

TABLE 1. Chromatographic conditions and data used in studying the reactions between formaldehyde, ammonium acetate, and dimedone or 2,4-pentanedione

	Reaction systems	
	Dimedone	2,4-Pentanedione
Mobile phase	Ethyl acetate:petroleum ether: methanol (60:40:0.5)	Ethyl acetate:petroleum ether: acetic acid (59:40:1)
Column	μ-Porasil	μ-Porasil
Flow rate	2 mL/min	2 mL/min
λ's monitored	254 and 397	254 and 285
Injection volume	25 μL	25 μL
Standard concentration (ranges)	2×10^{-9}–2×10^{-8} mol/injection	10^{-9}–10^{-6} mol/injection

Compound	*k'* Data*	
2		2.3
3		1.4
4		3.2
5	3.0	
6	6.0	
7	2.0	
8	0.0	
9	1.5	

*k' has the usual meaning of (retention volume − void volume)/void volume.

introduced directly from the reaction mixture into the chromatographic system at the times indicated in Fig. 3.

The analysis of the dimedone system was similar to that of the pentanedione except that the concentrations were changed slightly, 1 mL of $1.0 \times 10^{-1} M$ formaldehyde, 1 mL of $2.0 M$ ammonium acetate, pH 5.5, and 1 mL of $0.1 M$ dimedone in methanol. Preincubation was carried out for 5 min and a white precipitate, compound **8**, formed but dissolved during the course of the analysis.

For the study of the conversion of **6** to **9**, 25 μL of $1.0 \times 10^{-3} M$ **6** in methanol was added to 1 mL of $1.24 \times 10^{-1} M$ formaldehyde and 1 mL of a $0.5 M$ phosphate buffer, pH 2.25. The mixture was incubated at 22°C and assayed after one hour.

Results and Discussion

The original objective of this study was to compare the dimedone and 2,4-pentanedione reactions for the determination of formaldehyde. Although the relative fluorescence intensity of **9** was found to be 70 times greater than **4** (cf. 100 times (2)), this was of little use when considered in the context of a mechanized reaction system for detecting formaldehyde. The production of **9** was very slow in comparison to **4** and the reaction involving 2,4-pentanedione produced at room temperature a steady-state fluorescence in approximately 1 hour while the dimedone reaction required at least 3 hours to reach steady-state fluorescence. This is not surprising when one compares the conditions recommended by Nash (1) and Sawicki and Carnes (2) for their respective methods.

Another problem involved the preparation and usage of the Nash and Sawicki reagents. Many different accounts have been given for the storage and use of the Nash reagent. For instance the reagent was reported to be usable after preparation but had to be discarded after two days (19). In another instance the Nash reagent was to be used within one hour of preparation and discarded after that time (20).

In his original communication Nash (1) describes the shift of the "first ultraviolet absorption band" which stabilizes in 24 h at a position approximately 18 nm higher in wavelength. This corresponds to the formation of compound **2** in solution (λ_{max} 271.7 nm, $\log \varepsilon = 3.43$). Nash also showed that the reaction rate for the condensation reaction (assumed first order), when measured with one-day-old reagent, gave two distinct rate constants during the course of the reaction. The initial rate was fast but then it slowed as the reaction progressed to about 50% completion. The inflection between the two rates was approximately the same with regard to the degree of completion of the reaction at two different temperatures (5° and 37°C). Up to the present this was the only attempt at a detailed study of the Nash reagent.

The reagent of Sawicki and Carnes (2) has been prepared by several methods. When cyclohexanedione was used as the β-diketone, they recommended allowing the reagent to stand overnight before usage. However, when the reagent was prepared with dimedone, it was used immediately and discarded after 6 h. Cyclohexanedione and dimedone were investigated throughout this present study but only the results

Can. J. Chem. Downloaded from www.nrcresearchpress.com by 210.87.254.42 on 09/05/12
For personal use only.

Can. J. Chem. Downloaded from www.nrcresearchpress.com by 210.87.254.42 on 09/05/12
For personal use only.

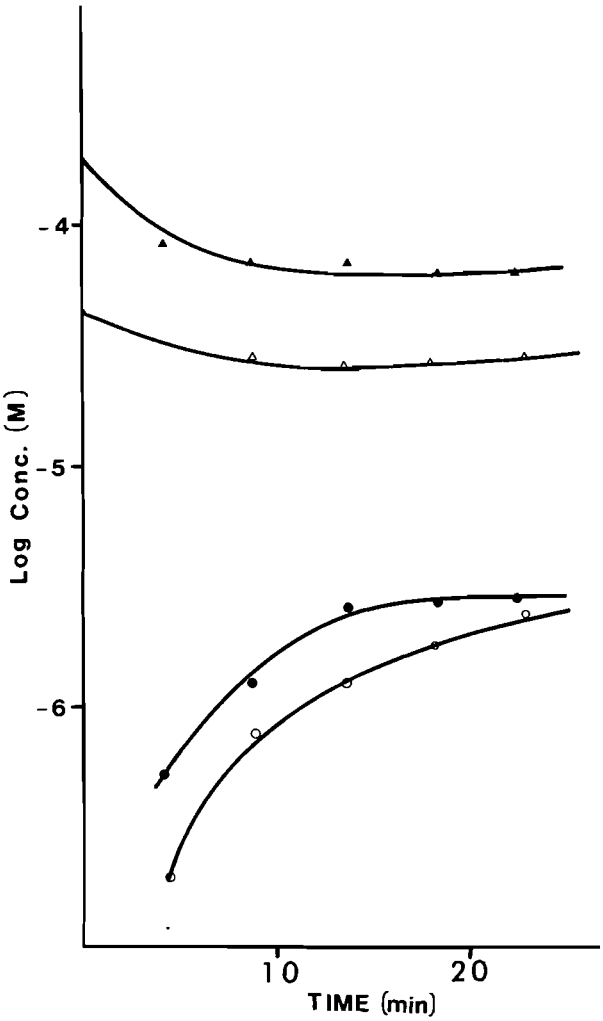


FIG. 3. Effect of preincubation and formaldehyde addition on the concentration of Fluoral-P (**2**) and the formation of **4** (○ = **4**, 5-min incubation; ● = **4**, 30-min incubation; △ = **2**, 5-min incubation; ▲ = **2**, 30-min incubation).

for dimedone are reported. The intermediates found with cyclohexanedione are very similar to those isolated for dimedone. Cyclohexanedione is quite heat sensitive (supplied with 3% NaCl stabilizer added) while dimedone is not. It reacts with ammonia (gas or as ammonium acetate solution) about twice as fast as dimedone. When preparing the respective iminodiones, dimedone containing reaction mixtures can be heated to 80°C while cyclohexanedione reactions were run at 22°C. The explanation for these differences centers around the steric effects of the 5-methyl groups which affect the coplanarity of the iminodione system (21). However, we could find no reason to treat these two reagents differently except that the dimedone-based reagent was less reactive.

This study aids our understanding of the two reagents. The hplc assay system indicated that in the Nash method the formation of **2** occurred *in situ*. Thus, as can be seen from Fig. 3, compound **2** is already present at $t = 0$ due to the 5-min preincubation of 2,4-pentanedione with ammonium acetate. Upon addition of formaldehyde there is a decrease in the concentration of **2** and the appearance and increase of **4** to a steady state.

Figure 3 also shows a duplicate experiment in which the 2,4-pentanedione is preincubated with ammonium acetate for 30 min. Greater concentrations of **2** and a faster rate of formation of **4** are noted. The reaction conditions which were used in this assay system correspond to those normally described in the literature for the Nash method.

The reaction sequence found to occur in the method of Sawicki and Carnes (2) has been partially described with regard to the identity of the intermediates (18, 22) and the general reaction sequence (14, 23, 24), but not in the context of the original reaction by Vorländer (7–9) nor from an analytical point of view (i.e., with Sawicki's assay system in mind). The results of the study of reaction 10 indicate that compound **8** is formed immediately followed by the final product, **9**. No other reaction intermediates were detected in the system. When compound **6** was assayed under conditions which had been determined would give the optimum rate of hydroacridine production, the bis-iminodione (**7**) was first detected and then the final product, **9**.

Thus it appears that reactions 1 and 2 are the ones which normally occur in the reagent mixture of Nash and the iminodione exists *in situ*. In the Nash method addition of formaldehyde yields the hydrolutidine (**4**) product directly from compound **2**, Fluoral-P.

The active agent in the Nash reagent, 4-amino-3-penten-2-one, has been studied in some detail and is a very useful aldehyde reagent (10). At pH 2.2 this compound reacts almost instantaneously with formaldehyde to form **4**. Reaction with other aldehydes is slower but selective for this class of compounds. Further studies are being carried out to characterize this reagent.

The reaction sequence which occurs with the Sawicki reagent depends greatly on how the reagent is prepared and used. In the case of dimedone, if the advice of Sawicki and Carnes (2) is followed, the events which occur follow the pathways of reactions 8 and 9. However, for the cyclohexanedione reagent, reactions 6 and 7 would be

followed because overnight storage of a reagent consisting of cyclohexanedione and ammonium acetate would produce the iminodione. This same sequence of events would occur for dimedone if the reagent were stored overnight. Compound **6** also has potential as an aldehyde reagent. However, no reproducible standard curve could be generated for the reaction of **6** with formaldehyde. An explanation for this follows.

The main difference between the Nash and Sawicki reagents is the relative reaction rates for conversion of **2** to **4** vs. **6** to **9**. In the reaction sequence of the Nash method there is no detectable intermediate between compounds **2** and **4**. The Sawicki reaction sequence, on the other hand, will go through an intermediate (**7**) which is isolable and stable. In the Sawicki method the final ring-closure step (reaction 7) to the chromophore product is acid catalyzed (12). While both **2** and **6** are susceptible to hydrolysis to their respective diones, the condensation reaction of **2** to yield **4** (2) is fast enough to be competitive with the hydrolysis reaction. As an aldehyde reagent, **2** is stored in acetonitrile. Since its reaction with formaldehyde is most rapid at pH 2.25 (10), it is used in conjunction with a buffer of low pH. No similar reagent system could be developed for compound **6**. Thus, the hydrolysis of **6** to **5** becomes the dominant reaction.

Some data exist on the acid hydrolysis of the iminodione (25) and they support our observations. A significant decrease in the hydrolysis rate occurs if the reagents are used in the pH range of the Nash and Sawicki methods (pH 5.0–7.0). However, these higher pH values do not favor rapid reactions between the reagents and formaldehyde.

While **2** has been useful to us as an aldehyde reagent, it would be desirable to develop further this family of compounds (the iminodiones). This would provide a wide choice of sensitivities and reactivities for aldehydes. Other iminodiones will represent a greater challenge with respect to optimizing reaction conditions. However, mechanized continuous-flow methods which give more reproducible reaction conditions should be of great utility in meeting this challenge.

Acknowledgements

The authors acknowledge the assistance of J. Honek, M. Mancini, and G. Lajoie, Jr. and the financial support of the Medical Research Council of Canada.

1. T. NASH. Biochem. J. **55**, 416 (1953).
2. E. SAWICKI and R. A. CARNES. Mikrochim. Acta, 148 (1968).
3. E. SAWICKI and R. A. CARNES. Mikrochim. Acta, 602 (1968).
4. A. HANTZSCH. Ber. **17**, 1515 (1884).
5. A. HANTZSCH. Ber. **18**, 1774 (1885); **18**, 2579 (1885).
6. S. BELMAN. Anal. Chim. Acta, **29**, 120 (1963).
7. D. VORLÄNDER and O. STRAUSS. Justus Liebigs Ann. Chem. 375 (1899).
8. D. VORLÄNDER and F. KALKOW. Justus Liebigs Ann. Chem. 356 (1899).
9. D. VORLÄNDER and J. ERIG. Justus Liebigs Ann. Chem. 294 (1897); 314 (1897).
10. B. J. COMPTON and W. C. PURDY. Anal. Chim. Acta. In press.
11. M. J. LACEY. Aust. J. Chem. **23**, 841 (1970).
12. B. D. WILSON. J. Org. Chem. **28**, 314 (1963).
13. J. M. ERIKSON and H. G. BIGGS. J. Chem. Educ. **50**, 631 (1973).
14. J. V. GREENHILL. J. Chem. Soc. C, 2699 (1971).
15. E. C. HORNING and M. G. HORNING. J. Org. Chem. **11**, 95 (1946).
16. D. PITEA and G. FAVINI. J. Chem. Soc. Perkin Trans. II, 291 (1971).
17. G. Y. VANAG and E. I. STANKEVICH. Zh. Obshch. Khim. **30**, 3287 (1960).
18. B. J. COMPTON, W. C. PURDY, and D. J. PHELPS. Anal. Chim. Acta, **105**, 409 (1977).
19. M. E. ROYER and H. KO. Anal. Biochem. **29**, 405 (1969).
20. F. G. SOLONI. Clin. Chem. **17**, 529 (1971).
21. D. PITEA and G. FAVINI. J. Chem. Soc. Perkin Trans. II, 142 (1972).
22. D. VORLÄNDER. Z. Anal. Chem. **77**, 241 (1929).
23. M. WINTER and W. DEMOLE. Helv. Chim. Acta, **44**, 271 (1961).
24. A. SONN and H. SCHREIBER. J. Prakt. Chem. **155**, 65 (1940).
25. K. DIXON and J. V. GREENHILL. J. Chem. Soc. Perkin Trans. II, 164 (1973).

Can. J. Chem. Downloaded from www.nrcresearchpress.com by 210.87.254.42 on 09/05/12
For personal use only.

Effet d'engrenage. VIII. Extension à des dérivés fonctionnels de l'alanine[1]

BRUNO BLAIVE, CHRISTIAN ROUSSEL ET JACQUES METZGER

Institut de Pétroléochimie et de Synthèse Organique Industrielle, Faculté d'Aix-Marseille III, Rue H. Poincaré, 13013 Marseille, France

ET

JAN SANDSTRÖM

Division of Organic Chemistry 1, Chemical Center, University of Lund, P.O. Box 740, S-220 07 Lund 7, Sweden

Reçu le 22 février 1980

BRUNO BLAIVE, CHRISTIAN ROUSSEL, JACQUES METZGER et JAN SANDSTRÖM. Can. J. Chem. **58**, 2212 (1980).

L'effet d'engrenage a été découvert et étudié la première fois sur des molécules où les groupements en interaction sont des substituants alkyles. Pour se rapprocher de modèles biochimiques, cet effet est étudié ici lorsqu'un des groupements en interaction est asymétrique et fonctionnel. Dix-huit composés nouveaux, dérivés de l'alanine, ont été préparés dans ce but, et étudiés par rmn et rmn dynamique. L'effet d'engrenage est bien observé, et il apparait comme un moyen de moduler l'interaction de deux fonctions actives.

BRUNO BLAIVE, CHRISTIAN ROUSSEL, JACQUES METZGER, and JAN SANDSTRÖM. Can. J. Chem. **58**, 2212 (1980).

The gear effect has been discovered and studied for the first time on molecules where the interacting groups were alkyl substituents. In order to be closer to biochemical models, this effect has now been studied where one interacting group is asymmetric and functional. For this purpose eighteen new compounds derived from alanine have been prepared and studied by nmr and dynamic nmr. The gear effect is operating, and it appears to be a suitable means to modulate the interaction of two active functions.

Introduction

Rappelons que la notion nouvelle d'effet d'engrenage (1–5) traduit la possibilité de transmettre, à longue distance, une information conformationnelle, par l'intermédiaire de groupements alkyles convenablement placés. Ces groupements alkyles se comportent comme les roues dentées d'un engrenage, même si les rotations ne sont pas toujours concertées (3).

Les molécules sur lesquelles cet effet a été mis en évidence la première fois sont les hétérocycles Δ_4-thiazolinethione-2 portant en position 3, 4 et 5 du cycle des groupements alkyles sans carbone asymétrique.

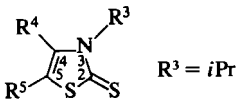


FIG. 1

Il était important, pour se rapprocher de modèles biochimiques (6, 7), d'étudier l'effet d'engrenage lorsque les groupements en interaction sont asymétriques et fonctionnels. Dans une molécule où les groupements en interaction portent des fonctions actives, l'effet d'engrenage peut être un moyen d'écarter ou de rapprocher l'une de l'autre deux fonctions (8, 9).[2]

Pour faire une telle étude, le cycle des Δ_4-thiazolinethione-2 a été conservé, et comme fonction active, un groupement carboxy a été introduit dans le substituant R^3, à proximité du groupement thiocarbonyle très réactif. La famille des acides **2–9** a donc été choisie pour cette étude. Afin d'éliminer les éventuelles liaisons hydrogène, les esters méthyliques correspondant **2′–9′** ont été préparés également.

Les effets observés dans ces deux familles de composés (R^3 = $CH(Me)CO_2H$ ou R^3 = $CH(Me)CO_2Me$) seront fréquemment comparés à ceux observés antérieurement (1) pour des groupements non fonctionnels (R^3 = *i*Pr).

Nous allons d'abord décrire les conformères observés, puis étudier leurs pourcentages, enfin donner la valeur des barrières de rotation autour de la liaison C—N.

Les conformères

L'étude par rmn du proton, à différentes températures, des composés **2–9** et **2′–9′** en solu-

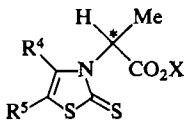
[1]Ce travail résume partiellement la Thèse de Spécialité de B. Blaive, Université d'Aix-Marseille III, 1976.

[2]Ces auteurs ont utilisé le composé R^5 = H, R^4 = H, R^3 = $CH(Me)CO_2H$ pour complexer l'argent entre le groupement carboxy et le soufre; on peut penser qu'une modulation de la distance entre ces deux groupements peut conduire à une modulation de la constante de complexation.

0008-4042/80/212212-09$01.00/0

©1980 National Research Council of Canada/Conseil national de recherches du Canada

Can. J. Chem. Downloaded from www.nrcresearchpress.com by 210.87.254.5 on 09/05/12
For personal use only.



		R^5	H	H	H	H	Me	Me	Me	Me
		R^4	Me	Et	*i*Pr	*t*Bu	H	Me	Et	*i*Pr
No. du composé	acide	X = H	**2**	**3**	**4**	**5**	**6**	**7**	**8**	**9**
	ester	X = Me	**2′**	**3′**	**4′**	**5′**	**6′**	**7′**	**8′**	**9′**

FIG. 2

TABLEAU 1. Déplacements chimiques (ppm) et constantes de couplage (Hz) des protons des acides **2–9** (R^3 = CH(Me)CO_2H) et du composé **2″** (R^5 = H, R^4 = Me, R^3 = *i*Pr), en solution dans CD_3COCD_3 (b désigne un pic mal résolu)

No. du composé	*T* (°C)	R^5	R^4	R^3	
				H	Me
2	30	6,55 s	2,32 s	vers 6,08 d	1,66 d
	−50	6,73 s	2,42 s 2,35 s	5,20 q 6,52 q	1,78 d (6,6) 1,62 d (7,3)
3	Amb.	6,20 s	1,05 t 2,55 q		1,68 d
	−40	6,68 s	1,28 t 2,68 q	5,18 q 6,57 q	1,78 d (6,8) 1,58 d (7,4)
4	30	6,63 s	vers 2,90 b 1,30 d	vers 5,3 b	1,74 d
	−30	6,72 s 6,88 s	3,07 1,28 d (7,5) vers 2,73 1,33 d (7,5)	5,22 q 6,64 q	1,81 d (6,8) 1,62 d (7,4)
5	30	6,65 s	1,47 s	5,39 q	1,88 d
	−30	6,70 s	1,45 s	5,45 q	1,82 d (6,5)
6	Amb.	2,16 d	7,30 s	6,13 b	1,63 d
7	30	2,16 s et 2,24 s		vers 6,15	1,69 d
	−50	2,21 s		5,19 q 6,58 q	1,75 d (6,8) 1,58 d (7,2)
8	34	2,20 s	1,19 t 2,69 q		1,76 d
	−46	2,22	1,17 t 2,70 q	5,12 q 6,62 q	1,78 d (6,7) 1,58 d (7,2)
9	−20	2,30 s	2,77 Hept. 1,29 d	5,16 q 6,68 q	1,78 d (6,4) 1,56 d (7,4)
2″	−28	6,62	2,32 s 2,54 s	4,7 5,89	1,49 d 1,81 d

tion dans CD_3COCD_3, montre l'existence de plusieurs conformères.

Composés 2–5

Dans les spectres de rmn à température ambiante (tableau 1), la présence de signaux mal résolus ne s'explique que si les molécules sont en équilibre entre plusieurs conformations, ayant des durées de vie de 1 à 10^{-3} seconde. Il ne peut s'agir d'énantiomères se convertissant par une inversion à l'azote, puisque les trois liaisons de l'azote sont dans un même plan, comme les rayons X le montrent (10). Les conformères se différencient donc par la rotation des substituants R^3, R^4, R^5.

Par ailleurs, la variation du déplacement chimique à température ambiante du groupement méthyle de R^3, lorsque R^4 varie:

R^4	Me	Et	*i*Pr	*t*Bu
δ_{ppm}	1,66	1,68	1,74	1,88

est trop importante pour s'expliquer seulement par la variation de l'anisotropie due à R^4. Elle montre que les molécules se répartissent entre plusieurs conformères avec des populations qui dépendent fortement du substituant R^4.

A basse température, le méthyle du groupement

Can. J. Chem. Downloaded from www.nrcresearchpress.com by 210.87.254.5 on 09/05/12
For personal use only.

Can. J. Chem. Downloaded from www.nrcresearchpress.com by 210.87.254.5 on 09/05/12
For personal use only.

R^3 des composés **2–4** apparait sous la forme de deux doublets, au lieu d'un seul à température ambiante. De même, le signal de l'hydrogène méthinique de R^3, se dédouble en deux quadruplets bien résolus: la rotation du groupement R^3 autour de la liaison C—N devient lente à basse température, et deux positions privilégiées de R^3 apparaissent.

On peut identifier les conformères d'une part en attribuant à un même conformère des signaux d'un même spectre dont les intensités sont dans un rapport simple, d'autre part en remarquant la similitude des déplacements chimiques à −50°C des doublets suivants

R^4	Me	Et	*i*Pr	*t*Bu
δ_{ppm}	1,78	1,80	1,80	1,82

et de même la similitude des déplacements chimiques des doublets

R^4	Me	Et	*i*Pr
δ_{ppm}	1,62	1,59	1,62

de plus, **5** ne présente qu'un seul conformère, dont les signaux sont ainsi facilement repérables.

Nous appellerons I le conformère correspondant aux valeurs de δ proches de 1,80 ppm, II celui qui correspond aux valeurs proches de 1,60 ppm.

Pour déterminer la position du groupement R^3 dans les conformères I et II, on peut admettre qu'un hydrogène du groupement R^3 est déblindé lorsqu'il est à proximité du soufre exocyclique (1); alors dans les conformères I le groupement méthyle est proche du soufre, tandis que l'hydrogène méthinique en est éloigné; dans les conformères II, c'est l'inverse.

A un observateur placé dans le plan du cycle et sur le prolongement de la liaison C—N (vision de Newman, réf. 31), le groupement R^3 apparaitrait donc dans deux positions proches de celles-ci:

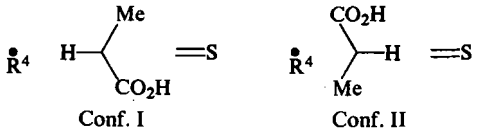


FIG. 3

Deux conformères semblables ont été mis en évidence (1) dans les composés analogues avec R^3 = *i*Pr. Pour un conformère donné (I ou II), on constate un bon accord entre les déplacements chimiques des acides (R^3 = $CH(Me)CO_2H$) et ceux des composés analogues avec R^3 = *i*Pr. Cependant le remplacement d'un méthyle de R^3 = *i*Pr par le groupement CO_2H entraîne une inversion du déplacement chimique du méthyle en position 4; elle montre que l'effet anisotrope du CO_2H prend le pas sur l'effet stérique (11).

Composés 6–9

De façon très similaire, on voit en rmn l'existence des conformères I et II (tableau 1).

Dans le cas du composé **9**, à −32°C les conformères I et II sont bien visibles, et le signal du méthyle de R^3 dans le conformère I est un doublet parfaitement résolu. Lorsqu'on abaisse la température, ses pics s'élargissent puis se dédoublent, et à −73°C on observe très nettement deux doublets au lieu d'un. Au contraire le doublet représentant le méthyle de R^3 dans le conformère II reste bien résolu entre −32 et −73°C. Il y a donc à −73°C trois conformères I_A, I_B et II, ce qui avait déja été observé pour des composés voisins (3, 4, 12).

Composés 2′–9′

Comme les acides **2–9**, les esters **2′–9′** admettent deux conformères I et II que l'on peut mettre en évidence et identifier par rmn (tableau 2).

La substitution de CO_2Me à CO_2H dans R^3 laisse presque inchangés les déplacements chimiques des protons, dans un conformère comme dans l'autre (comparaison des tableaux 1 et 2). On retrouve même, dans le composé **2′**, le fait étonnant que le méthyle en position 4 soit moins blindé dans le conformère I que dans le II. Le déplacement chimique du méthyle de l'ester est assez constant dans un conformère donné; contrairement à l'hydrogène méthinique ou au méthyle de R^3, l'ester est moins déblindé dans le conformère où il est le plus proche du soufre.

On remarque que dans le substituant R^3 la constante de couplage est toujours plus élevée pour le conformère II que pour le I.

Pourcentages des conformères

A basse température, les pourcentages p_I et $p_{II} = 1 - p_I$ des conformères I et II ont été obtenus en mesurant la surface des pics de rmn. De la température où l'échange commence jusqu'à la température T_c de coalescence, p_I a été obtenu par optimisation lors de l'étude complète de forme de courbe (13). Aux températures supérieures à T_c, il est difficile d'avoir une valeur juste de p_I.

Valeurs des pourcentages

Les figures 5(a) et 5(b) montrent l'évolution de p_I quand la taille du substituant R^4 varie. Dans les séries **2–5** et **2′–5′** (R^5 = H), la croissance de p_I quand la "grosseur" de R^4 augmente parait normale (14). Par contre, dans les séries **6–9** et **6′–9′**

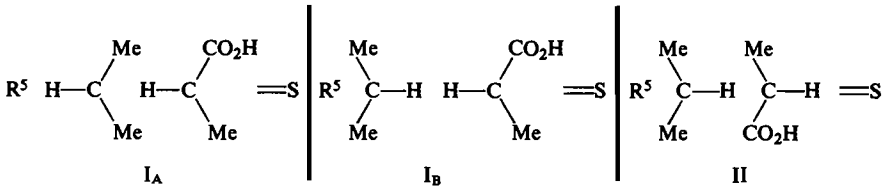


FIG. 4

TABLEAU 2. Déplacements chimiques (ppm) et constantes de couplage (Hz) des protons des esters **2'**–**9'** (R^3 = $CH(Me)CO_2Me$) en solution dans CD_3COCD_3 (b désigne un pic mal résolu)

No. du composé	T (°C)	R^5	R^4	R^3 H	R^3 Me	R^3 Ester Me
2'	33	6,60 s	2,31 s	vers 5,95 b	1,68 d	3,73 s
	−50	6,78 s	2,44 2,28	5,27 q 6,58 q	1,77 d (6,7) 1,61 d (7,6)	3,66 3,81
3'	33	6,56 s	2,62 q 1,27 t	vers 5,74 b	1,70 d	3,70 s
	−50	6,72	2,70 1,28 t	5,25 q 6,45	1,76 d (5,9) 1,58 d (6,6)	3,64 3,78
4'	33	6,63 s	2,89 mult. 1,29 deux d	vers 5,55 b	1,75 d	3,70 s
	−50	6,79 6,95	3,06 mult. 1,28 d 1,36 d	5,33 q vers 6,67	1,78 d (7,4) 1,61 d (6,7)	3,68 3,81
5'	33	6,63 s	1,45 s	5,39 q	1,86 d (6,6)	3,67
	−50	6,73 s		5,49 q		3,64 s
6'	33	2,23	7,24	5,85 q	1.64 d	3,73 s
	−50	2,27	7,46	5,83 q	1,68 d (7,4)	3,74 s
7'	33	2,18 s	2,18 s	5,98 b	1,66 d	3,73 s
	−50	vers 2,2	vers 2,2 2,33 s	5,21 q 6,58 q	1,74 d (7) 1,57 d (7,5)	3,64 3,80
8'	33	2,19 s	2,66 deux q 1,15 t	5,45 b	1,73 d (7)	3,69 s
	−50	2,23 s	2,71 q 1,14 t 2,77 q	5,17 q 6,65 q	1,75 d (7,5) 1,56 d	3,64 3,77
9'	33	2,25 s	1,33 deux d		1,62 d	3,74 s
	−50	2,26 2,31	vers 2,6 1,27 d 1,36 d	5,26 q 6,70 q	1,75 d 1,54 d	3,64 3.79

(R^5 = Me), les points bas correspondant aux composés **9** et **9'** sont surprenants.

Ces courbes donnant p_I en fonction de R^4 sont très semblables à celles qui avaient été obtenues[1] pour les séries analogues avec R^3 = *i*Pr. Les valeurs très faibles de p_I correspondant aux composés R^5 = Me, R^4 = *i*Pr montrent que l'on ne peut expliquer les interactions stériques en assimilant le substituant R^4 à un volume simple, comme une sphère ou un cône (15). De plus, la différence d'allure des courbes R^5 = H et R^5 = Me montre que la nature du substituant en position 5 a un effet important sur la conformation de R^3. On peut donc parler de transmission conformationnelle par le groupement R^4. Comparons globalement les pourcentages des conformères dans les séries R^3 = *i*Pr, R^3 = $CH(Me)CO_2H$ et R^3 = $CH(Me)CO_2Me$; le remplacement d'un méthyle du groupement R^3 = *i*Pr par un groupement CO_2H ou CO_2Me favorise le conformère I (sauf dans le cas de **9**). On peut envisager *a priori* trois causes possibles de la stabilisation de la conformation I dans les acides et les esters: (*1*) soit une interaction intramoléculaire stabilisante entre le groupement acide ou ester et le thiocarbonyle dans la conformation I; une éventuelle liaison hydrogène dans la conformation II entre l'hydrogène méthinique de R^3 et le soufre exocyclique n'est pas une explication possible, car elle stabiliserait davantage la conformation II des acides et des esters que celle des composés alkyles; (*2*) soit un phénomène d'autoassociation se produisant préférentiellement dans la conformation I (une telle explication n'est envisageable que dans le cas des acides); (*3*) soit un accroissement, dans les acides et les esters, de la différence d'énergie de solvatation entre les deux conformations.

Can. J. Chem. Downloaded from www.nrcresearchpress.com by 210.87.254.5 on 09/05/12
For personal use only.

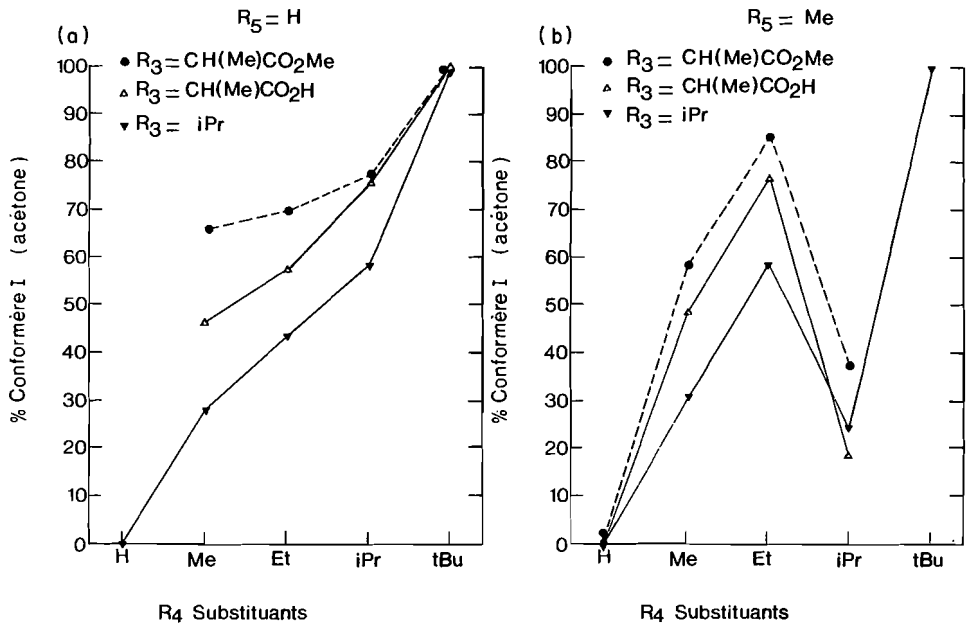


FIG. 5. Pourcentage de conformère I des acides **2–9** (R^3 = $CH(Me)CO_2H$) et des esters **2'–9'** (R^3 = $CH(Me)CO_2Me$); le pourcentage de conformère I des composés à substituant alkyle $R^3 = i$Pr est redonné pour comparaison. (a). Composés correspondant à R^5 = H. (b). Composés correspondant à R^5 = Me. Dans le cas de **9**, à −74°C les doublets correspondant aux conformères I_A et I_B ne sont pas assez séparés pour qu'on puisse mesurer avec précision les pourcentages p_{I_A} et p_{I_B}; cependant, p_{I_A} et p_{I_B} paraissent voisins l'un de l'autre. (no., p_I (%), T (°C); **2**, 46, −56; **3**, 57, −51; **4**, 75, −61; **5**, 100, −30; **6**, 0, amb.; **7**, 48, −53; **8**, 76, −46; **9**, 18, −32.)

Etude des liaisons hydrogène par infrarouge

L'absorption infrarouge des acides **2** et **5** a été mesurée; elle a été rendue difficile par la faible solubilité des composés dans tous les solvants utilisables en ir. Le spectre d'absorption de **5** dissous dans CCl_4 à la concentration de $2{,}6 \times 10^{-3}$ mol/L a l'allure suivante.

Ce spectre varie avec la dilution: à la concentration de $1{,}7 \times 10^{-4}$ mol/L, les intensités relatives des bandes sont différentes, le massif vers 3000 cm^{-1} est moins large, 3200 à 2800 cm^{-1}; I_B/I_A a décru faiblement, et l'intensité relative I_D/I_C a diminué énormément.

La forte variation, avec la concentration, du pourcentage de molécules où existe une liaison hydrogène montre que les liaisons hydrogène sont intermoléculaires. Une partie importante des molécules est sous forme de dimères (liaisons acide–acide). Par contre l'existence d'une liaison hydrogène intramoléculaire est très improbable. Une liaison hydrogène intramoléculaire engageant le soufre exocyclique aurait formé un cycle à 7 chaînons, analogue à ceux qui stabilisent probablement l'isomère *trans* de peptides (16–18); toutefois, de tels cycles sont moins fréquents dans la littérature que ceux à 6 ou 5 chaînons.

TABLEAU 3. Spectre d'absorption de **5** en ir

Bande 3532 cm^{-1} (intensité I_A)	ν_{OH} sans liaison hydrogène
Massif 3300 à 2800 cm^{-1} (I_B)	ν_{OH} avec liaison hydrogène
Bande 1767 cm^{-1} (I_C)	$\nu_{C=O}$ sans liaison hydrogène
Bande 1721 cm^{-1} (I_D)	$\nu_{C=O}$ avec liaison hydrogène

L'intensité de la bande à 1721 cm^{-1} étant légèrement supérieure à celle de la bande à 1767 cm^{-1}

On peut faire des conclusions identiques pour le composé **2**. Les constantes d'association en dimères cycliques sont du même ordre pour les composés **2** et **5**, environ 100 $L \cdot mol^{-1}$ dans $CHCl_3$.

Il résulte de cette étude que ce ne sont pas des liaisons hydrogène qui sont responsables de l'accroissement du pourcentage de la conformation I lorsqu'on substitue $R^3 = CH(Me)CO_2H$ à $R^3 = i$Pr. En effet, d'une part il n'y a pas de liaison hydrogène intramoléculaire, d'autre part les autoassociations par liaisons hydrogène ne peuvent stabiliser préférentiellement la conformation I, car on observerait alors une constante d'autoassociation plus forte pour le composé **5**, qui est totalement sous la forme I, que pour le composé **2**, ce qui n'est pas le cas.

Variation des pourcentages des conformères avec la température

La figure 6 représente, pour six composés, la variation du pourcentage de I avec la température. On remarque que cette variation est importante

Can. J. Chem. Downloaded from www.nrcresearchpress.com by 210.87.254.5 on 09/05/12
For personal use only.

TABLEAU 4. Température de coalescence T_c en degré Celsius, et durée de vie $\tau(T)$ à une température T, du conformère I (τ^{-1} est la constante de vitesse de l'échange I → II) des acides **2–4** et **7–9** en solution dans CD_3COCD_3

No. du composé	**2**	**3**	**4**	**7**	**8**	**9**
T_c	−20	0	15	−15	12	I ⇌ II + 20 $I_A \rightleftharpoons I_B$ − 55
τ (s)	0,005	0,023	0,077	0,0065	0,055	0,08
T (°C)	(−1,0)	(−2,6)	(0,3)	(−2,3)	(0,0)	(−0,7)

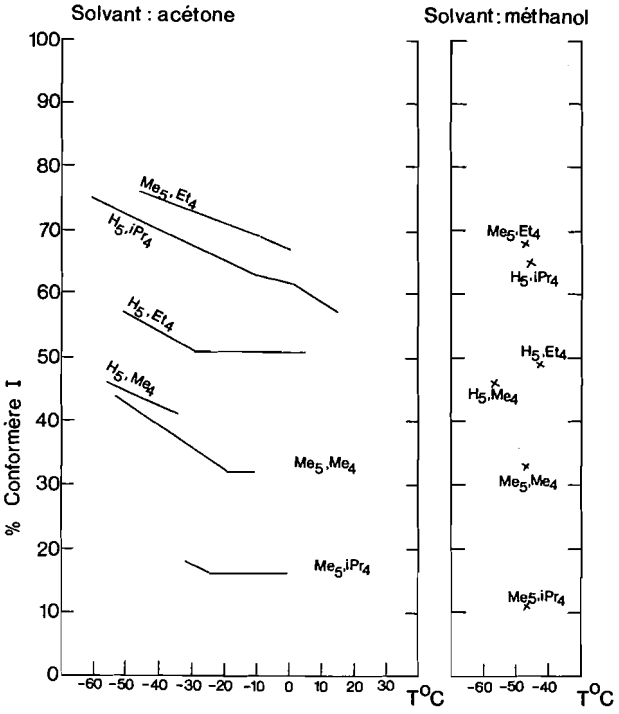


FIG. 6. Variation avec la température du pourcentage de conformère I des acides (R^3 = CH(Me)CO_2H) **2–4** et **7–9**. La méthode d'obtention de p_I aux températures où l'échange I ⇌ II est rapide étant peu précise, la partie droite de chaque courbe est approximative.

(elle peut atteindre 20%), et que le conformère I est toujours défavorisé quand la température croît.

Au contraire, dans la série analogue avec R^3 = *i*Pr, le pourcentage de I reste constant quand T varie (3). Pour expliquer cette variation avec la température, il faut imaginer qu'un phénomène sensible à la température est susceptible de stabiliser un conformère plus que l'autre. On pourrait trouver une explication plausible de la variation du pourcentage de I avec la température si les associations en dimères se faisaient préférentiellement dans certaines conformations; mais nous avons vu qu'aux erreurs expérimentales près, les associations en dimères ne semblent pas préférentielles. Toutefois l'étude par ir a été faite dans CCl_4 et à température ambiante, tandis que l'étude par rmn a été faite dans CD_3COCD_3 et à basse température.

Barrières de rotation autour de la liaison C—N (sp^3 − sp^2)

Les paramètres d'activation $\Delta G^{\ddagger}$, $\Delta H^{\ddagger}$, $\Delta S^{\ddagger}$ relatifs au passage du conformère I au conformère II ont été mesurés par la méthode de la rmn dynamique (13, 19, 20) pour les acides **2–4** et **7–9** (tableau 5). Pour cela, la constante de vitesse d'échange a été mesurée pour chaque composé à une quinzaine de températures différentes, l'analyse complète de forme de courbe portant sur le signal du méthyle de R^3. On constate (tableau 4) que la température de coalescence T_c croît avec la taille du substituant R^4, c'est-à-dire avec l'empêchement à la rotation autour de la liaison C—N; T_c croît également avec la taille de R^5. La différence des déplacements chimiques étant peu variable suivant les composés, la variation de T_c indique la variation de la barrière.

Les valeurs de $\Delta G^{\ddagger}$ et $\Delta H^{\ddagger}$ sont comprises entre 13 et 15 kcal mol^{-1}, donc nettement inférieures aux 23 kcal nécessaires pour que les conformères soient séparables à température ambiante.

On remarque que $\Delta G^{\ddagger}$ augmente régulièrement avec la "grosseur" du substituant R^4. L'évolution de $\Delta H^{\ddagger}$ est moins régulière. Les valeurs de $\Delta S^{\ddagger}$ sont assez dispersées; en particulier la valeur correspondant au composé **4** est élevée, mais cette valeur est peu précise, à cause de la démesure de p_I par rapport à p_{II}, qui rend malaisée l'étude par rmn dynamique. Cependant la valeur moyenne (∼ − 7 cal) des $\Delta S^{\ddagger}$ trouvés est voisine des valeurs correspondant à la rotation de substituants dans divers composés (21, 22). Le tableau 5 redonne également les valeurs de $\Delta G^{\ddagger}$ trouvées antérieurement pour la série analogue R^3 = *i*Pr, étudiée (1) dans $CDCl_3$.

La figure 7 représente, en fonction du substituant R^4, la différence

$$\Delta G^{\ddagger}_{(I \rightarrow II)} - \tfrac{1}{2}\Delta G_{(I \rightarrow II)} \text{ à } 298 \text{ K}$$

où la différence d'enthalpie libre ΔG a été calculée à partir des pourcentages des conformères; cette

Can. J. Chem. Downloaded from www.nrcresearchpress.com by 210.87.254.5 on 09/05/12
For personal use only.

Can. J. Chem. Downloaded from www.nrcresearchpress.com by 210.87.254.5 on 09/05/12
For personal use only.

TABLEAU 5. (*a*) Paramètres d'activation de la transformation conformère I → conformère II, pour les acides **2–4** et **7–9** (R^3 = $CH(Me)CO_2H$) dans CD_3COCD_3; (*b*) valeur de $\Delta G^{\neq}$ à 298 K pour les composés analogues avec $R^3 = i$Pr, dans $CDCl_3$ (sauf contre-indication)[a]

	Valeur					
Paramètre	R^4 = Me R^5 = H	R^4 = Et R^5 = H	$R^4 = i$Pr R^5 = H	R^4 = Me R^5 = Me	R^4 = Et R^5 = Me	$R^4 = i$Pr R^5 = Me ($I_A + I_B \rightarrow$ II)
(*a*) $R^3 = CH(Me)CO_2H$						
$\Delta S^{\neq}$ calcd.	−7,9 ± 1,8	−7,2 ± 0,6	2,8 ± 3,5	−1,6 ± 1,2	−12,0 ± 1,9	−7,1 ± 2,0
$\Delta H^{\neq}$ kcal	10,89 ± 0,44	11,80 ± 0,14	15,4 ± 1,0	12,63 ± 0,31	11,20 ± 0,54	12,55 ± 0,53
$\Delta G^{\neq}_{298}$ kcal	13,24 ± 0,09	13,94 ± 0,02	14,60 ± 0,07	13,11 ± 0,05	14,78 ± 0,05	14,68 ± 0,07
(p_I)	(46)	(57)	(75)	(48)	(76)	(18)
(*b*) $R^3 = i$Pr						
$\Delta G^{\neq}_{298}$ kcal	14,1	14,4	15,4	14,0 (14,2 dans CD_3COCD_3)	15,0	15,6 dans $CHCl_2F$
(p_I)	(28)	(43)	(58)	(30)	(58)	(24)

[a]Sous chaque valeur de $\Delta G^{\neq}$ est redonnée la valeur de p_I correspondante (entre parenthèses, en %).

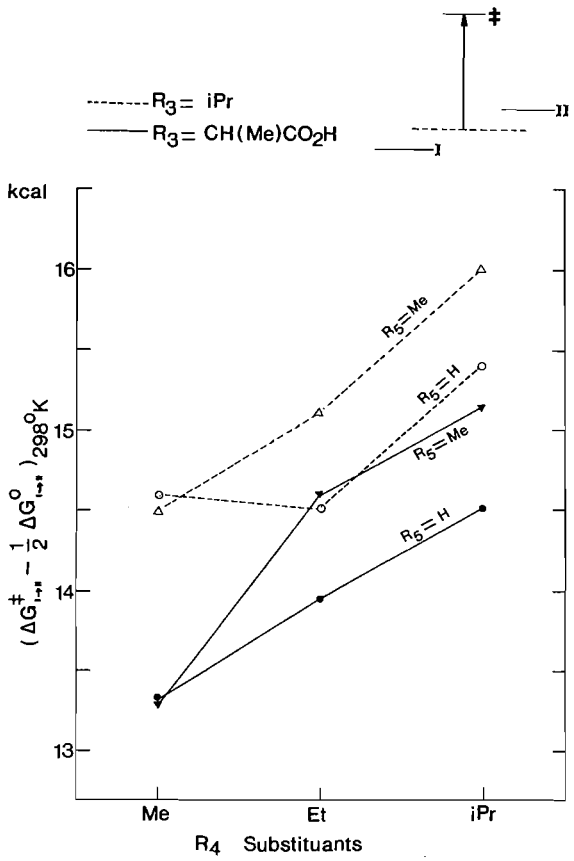


FIG. 7. Variation, en fonction du substituant R^4, de la barrière de rotation $\frac{1}{2}(\Delta G^{\neq}_{I\rightarrow II} + \Delta G^{\neq}_{II\rightarrow I}) = \Delta G^{\neq}_{I\rightarrow II} - \frac{1}{2}\Delta G^{0}_{I\rightarrow II}$ des acides **2–4** et **7–9** (R^3 = $CH(Me)CO_2H$) et des composés alkyles correspondant ($R^3 = i$Pr).

différence représente la moyenne entre $\Delta G^{\neq}_{(I\rightarrow II)}$ et $\Delta G^{\neq}_{(II\rightarrow I)}$. On remarque une diminution générale de $\Delta G^{\neq} - \frac{1}{2}\Delta G$ quand on passe de $R^3 = i$Pr à R^3 = $CH(Me)CO_2H$, et nous n'en voyons pas l'explication; ce résultat rappelle un phénomène analogue observé à propos de l'équilibre conformationnel de cyclohexanes substitués (23).[3] Par ailleurs, on remarque pour les composés ayant un substituant R^4 petit (R^4 = Me) que $\Delta G^{\neq}$ n'est pas changé lorsqu'on passe de R^5 = H à R^5 = Me.

Les valeurs de $\Delta G^{\neq}$ sont assez précises pour mériter une interprétation quantitative, hors de notre portée pour le moment.

Conclusion

Il résulte de cette étude qu'il est possible de moduler la proximité de deux fonctions actives, telles qu'une fonction thiocarbonyle et une fonction acide carboxylique par exemple, à l'aide de l'effet d'engrenage.

L'influence de la nature du groupement "transmetteur" R^4 est analogue à celle trouvée pour des composés ayant des substituants alkyles uniquement. Mais la sensibilité des pourcentages des conformères à la température est propre aux groupements fonctionnels.

Les valeurs des pourcentages des conformères et des barrières de rotation, mesurées avec précision, se joignent à un lot de valeurs semblables mesurées antérieurement dans une famille de composés très homogène. Nous voyons comme intérêt de ces données de fournir à terme des tests aux modèles théoriques ou semi-empiriques représentant les interactions d'atomes non liés, pour lesquelles les

[3]Les enthalpies libres relatives à l'équilibre conformationnel des cyclohexanes substitués par des groupements CH_3, CO_2H, CO_2CH_3 sont respectivement ΔG = 1,70; 1,35; 1,27 de sorte que dans ce cas tout se passe en apparence comme si les tailles des substituants étaient dans l'ordre $CH_3 > CO_2H > CO_2CH_3$. On peut penser à rapprocher cet ordre également de la valeur relative des pourcentages des conformères des composés $R^3 = i$Pr, $R^3 = CH_2(Me)CO_2H$, $R^3 = CH_2(Me)CO_2Me$.

Can. J. Chem. Downloaded from www.nrcresearchpress.com by 210.87.254.5 on 09/05/12
For personal use only.

données concernant des interactions de groupements polaires sont en nombre limité.

La mise en place d'un substituant R^3 chiral est une première étape de l'introduction de deux asymétries (dans R^3 et R^4), qui conduira à des diastéréoisomères.

Partie expérimentale

Préparation des composés 2–9 et 2′–9′

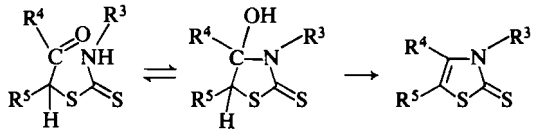
Les acides **2–9** ont été préparés en faisant réagir (5) une cétone α-bromée R^4-CO—CH(Br)-R^5 ou α-chlorée, avec un dithiocarbamate R^3-NH—CS_2^-.

Bromation des cétones

La chloracétone est commerciale; le propanal est brômé en bromo-2 propanal par le bromure de dioxanne (24). Les autres cétones sont brômées par le brôme, en présence d'acide bromhydrique, dans le méthanol, à température ambiante (25, 26).

Préparation du dithiocarbamate

Le sulfure de carbone et l'alanine réagissent en milieu basique pour donner le dithiocarbamate (27) HO_2C—CH(Me)—NH—CS_2^-, Na^+ (ou K^+); dans le méthanol (8) la réaction ne dure qu'une heure et a un excellent rendement.



(A) (B) (C)

La réaction entre la cétone bromée et le dithiocarbamate qui conduit au composé (A) puis à la Δ_4-thiazolinethione-2 (C), est un cas particulier de la réaction de Hantzsch (8, 28).

On passe finalement à la forme fermée déshydratée (C) en acidifiant à pH 2 avec HCl, puis en chauffant le mélange en contrôlant par uv l'avancement de la réaction (A) ⇄ (B) → (C); (A) absorbe en uv dans l'eau aux alentours de 250 nm, (B) de 275 nm et (C) de 319 nm.

Nous n'avons pu obtenir l'acide correspondant à R^5 = Me et R^4 = *t*Bu. L'intermédiaire non cyclisé (A) a été obtenu sans difficultés. Nous pensons avoir mis en évidence par uv le composé (C) correspondant, mais nous n'avons pu l'isoler; il est probable qu'il s'hydrate pour redonner (A).

Les esters ont été préparés par action du diazométhane sur les acides (29, 30). Le rendement est de 100%. Ces valeurs ont été obtenus: no., rendement, pf (isomère L, racémique DL), spectre de masse (70 eV); **2**, 85, (159, 170), 203(100) 158(30) 131(74) 86(28) 72(29) 45(35); **3**, 85, (128, 104), 217(100) 172(31) 145(67) 144(35) 45(47) 41(35); **4**, 55, (—, 116), 231(100) 186(24) 159(36) 158(63) 144(36) 45(45) 41(41); **5**, 80, (224, 223), 245(100) 200(34) 158(51) 45(34) 41(54); **6**, 70, (126, —), 203(100) 158(50) 131(68) 72(23) 59(22); **7**, 68, (154, 148), 217(100) 172(24) 145(52) 85(16) 59(18); **8**, 30, (171, 171), 231(100) 186(34) 159(60) 158(34) 59(51) 41(25); **9**, 49, (137, —), 245(100) 200(29) 173(29) 172(58) 158(31) 59(74) 41(35); **2′**, (76, —); **3′**, huile; **4′**, (—, 110); **5′**, (194, —); **6′**, huile; **7′**, huile; **8′** (110, —); **9′**, (80, —).

Les spectres de masse et rmn sont en accord avec les structures attendues.

Mesures de résonance magnétique nucléaire

Les spectres de rmn du proton ont été enregistrés à 100 MHz sur un spectromètre JEOL JNM-MH-100 muni d'un contrôleur de température VT 3-C. Les composés ont été étudiés en solution dans l'acétone à la concentration de 0,4 mol L^{-1} environ.

Les constantes de vitesse d'échange ont été choisies de façon que le signal théorique (13) du méthyle de R^3 coïncide au mieux avec le signal expérimental. Le signal théorique est tracé pour diverses valeurs des paramètres, à l'aide d'un ordinateur Hewlett-Packard 9820 A équipé d'une table traçante 9862 A, et comparé visuellement au signal expérimental. Le temps de relaxation T_2 est déduit de la largeur à mi-hauteur du signal du ou des protons du substituant R^5 (19, 20).

Les paramètres d'activation sont calculés à partir des droites ($-\log\tau(T)$, $1/T$), et les erreurs sont évaluées statistiquement, en utilisant un seuil de confiance de 90%.

Remerciements

Nous remercions M. R. Gallo de l'I.P.S.O.I., qui a étudié par rmn dynamique les composés **2** et **8**, ainsi que M. B. Mille du Laboratoire du Professeur J. Chouteau à Marseille, Mlle. E. Gentric et M. J. Lauransan de la Faculté de Brest, qui ont étudié par ir les composés **2** et **5** et mesuré leurs constantes d'autoassociation.

1. C. ROUSSEL, M. CHANON et J. METZGER. Tetrahedron Lett. 1861 (1971).
2. C. ROUSSEL. Thèse Sciences, Université de Provence, Marseille. 1973.
3. C. ROUSSEL, A. LIDEN, M. CHANON, J. METZGER et J. SANDSTRÖM. J. Am. Chem. Soc. **98**, 2847 (1976).
4. A. LIDEN, C. ROUSSEL, T. LILJEFORS, M. CHANON, R. E. CARTER, J. METZGER et J. SANDSTRÖM. J. Am. Chem. Soc. **98**, 2853 (1976).
5. C. ROUSSEL, R. BARONE et M. CHANON. Thiazole and its derivatives. *Dans* The chemistry of heterocyclic compounds. *Edité par* J. Metzger. J. Wiley, New York. 1979.
6. M. P. SCHWEIZER, J. T. WITKOWSKI et R. K. ROBINS. J. Am. Chem. Soc. **93**, 277 (1971).
7. N. YATHINDRA et M. SUNDARALINGHAM. Biochem. Biophys. Res. Commun. **56**, 119 (1974).
8. G. M. HAIST, W. J. HUMPHLETT et J. R. KING. Brevet enregistré en France no. 69.33284 par Eastman Kodak.
9. R. W. LAMON et W. J. HUMPHLETT. J. Heterocycl. Chem. **4**, 605 (1967).
10. G. PEPE et M. PIERROT. Acta Crystallogr. Sect. B, **32**, 1317 (1976); **32**, 1321 (1976).
11. C. ROUSSEL, J. M. BERNASSAU, R. GALLO et J. METZGER. Org. Magn. Reson. **8**, 453 (1976).
12. A. LIDEN, C. ROUSSEL, M. CHANON, J. METZGER et J. SANDSTRÖM. Tetrahedron Lett. **41**, 3629 (1974).
13. I. O. SUTHERLAND. Annual reports on nmr spectroscopy. Vol. 4. *Edité par* E. F. Mooney. Academic Press, New York. 1971.
14. E. L. ELIEL, N. L. ALLINGER, S. J. ANGYAL et G. A. MORRISON. Conformational analysis. Wiley Interscience, New York. 1965.
15. J. D. MORRISON et H. S. MOSHER. Asymmetric organic reactions. Prentice Hall Inc., New Jersey. 1971.
16. C. A. EVANS et D. L. RADENSTEIN. J. Am. Chem. Soc. **96**, 7312 (1974).
17. V. MADISON et J. SCHELLMAN. Biopolymers, **9**, 511 (1970).
18. S. MIZUSHIMA. Adv. Protein Chem. **9**, 299 (1954).
19. L. M. JACKMAN et F. A. COTTON. Dynamic nuclear resonance spectroscopy. Academic Press, New York. 1975.
20. J. SANDSTRÖM. Etude des processus dépendant du temps.

Détermination des durées de vie. S.E.T.A.R.–C.N.R.S., Stage R.M.N., L.C.O.P. Nantes, mai 1974.
21. A. J. M. REUVERS, A. SINNEMA, T. J. NIEUWSTAD, F. VAN RANTWIJK et M. VAN BEKKUM. Tetrahedron, **27**, 3713 (1971).
22. J. PEELING, T. SCHAEFER et C. M. WONG. Can. J. Chem. **48**, 2840 (1970).
23. J. A. HIRSCH. Top. Stereochem. **1**, 199 (1967).
24. M. POITE. Thèse Sciences, Marseille. 1962. p. 71.
25. C. ROUSSEL. Thèse de Spécialité, Marseille. 1970.
26. C. ROUSSEL, A. BABADJAMIAN, M. CHANON et J. METZGER. Bull. Soc. Chim. Fr. 1087 (1971).
27. B. HOLMBERG. Chem. Abstr. **32**, 6246 (1938).
28. M. CHANON et J. METZGER. Bull. Soc. Chim. Fr. 2842 (1968).
29. T. J. DE BOER et H. J. BACKER. Organic Syntheses, Coll. Vol. IV. 1963. p. 250.
30. J. D. ROBERTS. J. Am. Chem. Soc. **73**, 760 (1951).
31. W. G. DAUBEN et K. S. PITZER. Conformational analysis. *Dans* Steric effects in organic chemistry. *Edité par* M. S. Newman. J. Wiley, New York. 1956. p. 5.

Can. J. Chem. Downloaded from www.nrcresearchpress.com by 210.87.254.5 on 09/05/12
For personal use only.

Pyrochlores. XI. High-pressure studies of the antimonates $A_2Sb_2O_7$ (A = Ca, Sr, Cd) and preparation of the weberite $Sr_2Bi_2O_7$[1]

OSVALD KNOP
Department of Chemistry, Dalhousie University, Halifax, N.S., Canada B3H 4J3
AND
GERARD DEMAZEAU AND PAUL HAGENMULLER
Laboratoire de Chimie du Solide du CNRS, Université de Bordeaux I, 33405 Talence, France
Received April 11, 1980

OSVALD KNOP, GERARD DEMAZEAU, and PAUL HAGENMULLER. Can. J. Chem. **58**, 2221 (1980).

Reactive hot-pressing experiments at 60–70 kbar and 700–900°C indicate that the relative stability of the pyrochlore and weberite phases of the $A_2Sb_2O_7$ (A = Ca, Sr, Cd) antimonates depends primarily on the effective size of A^{2+} and the covalency of the A—O bond working in conjunction. The analogous bismuthate(V) $Sr_2Bi_2O_7$, obtained by hot pressing of $SrBiO_{3-x}$ with an excess of $KClO_3$, has been shown to have the weberite-type structure.

OSVALD KNOP, GERARD DEMAZEAU et PAUL HAGENMULLER. Can. J. Chem. **58**, 2221 (1980).

L'étude sous hautes pressions (60–70 kbar) des oxydes $A_2Sb_2O_7$ (A = Ca, Sr, Cd), dans un domaine de température compris entre 700 et 900°C, a montré que la stabilité relative des phases pyrochlore et wébérite dépendait de la taille de l'ion A^{2+} ainsi que de la covalence de la liaison A—O. L'oxyde de bismuth(V), $Sr_2Bi_2O_7$, obtenu par action sous haute pression de $KClO_3$ sur $SrBiO_{3-x}$, présente la structure wébérite.

Introduction

The antimonates $Ca_2Sb_2O_7$ and $Cd_2Sb_2O_7$ crystallize with structures of both the pyrochlore (*P*) and the weberite (*W*) type, but $Sr_2Sb_2O_7$ is only known as a weberite (2). The following is an account of an investigation undertaken to examine the possibility of the $W \rightarrow P$ conversion under pressure suggested in ref. 2, and to explore the possibility of existence of the corresponding $A_2Bi_2O_7$ phases containing Bi(V).

Experimental

The $A_2Sb_2O_7$ antimonates (Table 1) were prepared by firing dry-mixed reactants of high purity in air (cf. ref. 2).[2] The products were ground and refired as necessary. The maximum firing temperature was chosen so as to keep possible weight loss by volatilization to a minimum, consistent with the formation of a well-defined product of the intended crystal structure. The antimonic acid used was prepared by hydrolyzing purified $SbCl_5$ in ice and H_2O_2. The composition of the air-dried acid was $Sb_2O_5 \cdot 3.67\ H_2O$ (as determined by the method outlined in ref. 4).

A sample of the $Cd_2Sb_2O_7(W)$ described in ref. 5 was kindly supplied by Dr. B. Raveau.

The high-pressure experiments were carried out in a belt-type apparatus, with the samples contained in sealed Au or Pt capsules. $KClO_3$ in excess was used an an oxidant in the reactive hot-pressing runs. The perovskite $SrBiO_{3-x}$ used in the synthesis of $Sr_2Bi_2O_7$ has been prepared by heating SrO + Bi_2O_3 in oxygen under pressure.

X-ray powder diffraction patterns were obtained either in 114.6 mm diameter cameras with Straumanis-type film mounting, or with a Guinier camera, or with a Philips powder diffractometer. Owing to a certain diffuseness of the high-angle lines in the powder photographs, the unit-cell dimensions listed in Table 2 were evaluated by least-squares from low- and medium-angle peaks of the diffractograms, using high-purity Mo or KCl powders as internal standards. The small discrepancies in the unit-cell dimensions between the present work and ref. 2 are attributable in part to the difference in the evaluation procedure and in part to genuine slight differences between samples of the same nominal composition but prepared on different occasions.

Results

Phase-transformation Experiments

The available evidence indicates that the mean linear unit-cell dimension $\bar{a} = (V/Z)^{1/3}$ of a particular *W* phase at room temperature is larger than that of the corresponding *P* phase (cf. Fig. 3 of ref. 2 and Table 2). This points to the possibility of a $W \rightarrow P$ transformation under pressure. The actual values of the difference $\Delta\bar{a} = \bar{a}(W) - \bar{a}(P)$ are difficult to establish with any accuracy, as is evident from an examination of the $\bar{a}$ values of Table 2: the observed $\Delta\bar{a}(Cd_2Sb_2O_7)$ is so small as to be indeterminate, $\Delta\bar{a}(Ca_2Sb_2O_7)$ is of the order of 0.2% of $\bar{a}$, and $\Delta\bar{a}$ estimated for $Sr_2Sb_2O_7$ (the *P* phase has never been reported) is about 1% of $\bar{a}$. The Sr weberite would therefore be expected to transform more readily than the Ca and Cd weberites. However, heating $Ca_2Sb_2O_7(W)$ and $Sr_2Sb_2O_7(W)$ at 800–900°C at 78 kbar for 20 min resulted merely in an improved crystallinity of the two weberites, as evidenced by the sharpening of the lines in the X-ray powder patterns of the pressed compounds.

[1]For Part X, see ref. 1.

[2]The products described in Tables 1 and 2 are the same as those used by Ferguson (3) in his Mössbauer ^{121}Sb study of these antimonates.

0008-4042/80/212221-04$01.00/0
©1980 National Research Council of Canada/Conseil national de recherches du Canada

Can. J. Chem. Downloaded from www.nrcresearchpress.com by 210.87.254.6 on 09/05/12
For personal use only.

Can. J. Chem. Downloaded from www.nrcresearchpress.com by 210.87.254.6 on 09/05/12
For personal use only.

TABLE 1. Details of preparation of the $A_2Sb_2O_7$ antimonates

A	Type	Colour*	Reactants†	Heat treatment‡
Ca	*P*	Yellowish	$Ca(NO_3)_2 \cdot 4H_2O$ + a.a.	Fusion at 200°C; 400/1, 620/20, 700/35, 700/86
Ca	*W*	White	$CaCO_3$ + a.a.	400/24, 800/24, 1000/140, 1000/24, 1000/24, 1200/20
Sr	*W*	White	$SrCO_3$ + a.a. §	400/24, 800/48, 900/36
Cd	*P*	Greenish	$CdCO_3$ + a.a. §	150/20, 400/48, 700/24

*Powdered final product.
†a.a. = antimonic acid (see text).
‡400/24 stands for 400°C for 24 h etc.
§MCO_3 + a.a. treated *in situ* with dilute acetic acid and the resulting acetate dehydrated and decomposed by slowly raising the temperature to the first value indicated.

TABLE 2. Lattice parameters (Å) of $A_2Sb_2O_7$ antimonates

A	Type	*a*	*b*	*c*	$\bar{a}$	Reference
Ca	*P*	*10.32			5.16	16
		10.321(8)			5.161	2
		10.33			5.17	This work
Ca	*W*	*7.29	7.46	10.20	5.18	8
		*7.29	7.44	10.18	5.17	17
		7.290	7.460	10.222	5.180	This work
		†7.298	7.466	10.201	5.180	This work
Sr	*W*	*7.46	7.68	10.38	5.30	8
		7.451	7.683	10.363	5.293	11
		7.452	7.687	10.381	5.297	This work
		†7.463	7.685	10.377	5.299	This work
Cd	*P*	10.270(2)			5.135	7
		10.259(1)			5.130	2
		10.27			5.135	6
		10.273(3)			5.137	This work
Cd	*W*	*7.22	7.34	10.16	5.13	8
		7.222	7.341	10.189	5.131	5, 11

*Converted from kX.
†78 kbar/800–900°C/20 min.

Reactive hot-pressing was therefore tried. A mixture of CdO + Sb_2O_3 + $KClO_3$(excess) was heated at 800°C and 60 kbar for 30 min. The sample was then quenched by cutting furnace power while maintaining the pressure. After quenching the pressure was gradually reduced to atmospheric over several hours. The product was a mixture of a poorly crystallized *P* phase and KCl. Using CaO instead of CdO under the same conditions yielded what appeared to be a mixture of the *P* and *W* phases and KCl. The similarity of the main features of the diffraction patterns of the two phases and the rather poor crystallinity did not permit an unambigous conclusion, but the *P* phase seemed to dominate. With SrO, only $Sr_2Sb_2O_7$(*W*) formed. The results of these and additional experiments at 800°C and 60 kbar can be summarized as follows:

Intended composition	Phase obtained
$Cd_2Sb_2O_7$	*P*
$CaCdSb_2O_7$	*P*
$Ca_2Sb_2O_7$	*P*+*W*
$CaSrSb_2O_7$	*W*
$Sr_2Sb_2O_7$	*W*

Later in the investigation a sample of $Cd_2Sb_2O_7$(*W*) (5) became available. Powder patterns (diffractometer and Guinier) of a product obtained by heating this material at ~700°C and 65 kbar for 20 min showed that the weberite had transformed completely into a well-defined *P* phase. On the other hand, a DTA run up to 1200°C (Pt capsule, Al_2O_3 reference) in stagnant air gave no indication of a transformation.

Can. J. Chem. Downloaded from www.nrcresearchpress.com by 210.87.254.6 on 09/05/12
For personal use only.

Strontium Bismuthate(V)

The brownish-orange product obtained by heating an intimate mixture of $SrBiO_{3-x}$ and $KClO_3$ for 15 min at 730°C and 60 kbar was a mixture of KCl and a relatively well-crystallized phase whose X-ray diffraction pattern could be indexed on an orthorhombic unit cell with $a = 7.70$ Å, $b = 7.91$ Å, and $c = 10.58$ Å. There is little doubt that this phase was the weberite $Sr_2Bi_2O_7$. Its $\bar{a}$ value, 5.44 Å, is about 2.6% larger than that of $Sr_2Sb_2O_7(W)$. The product was not analyzed chemically, partly because the quantity involved was quite small and partly because of the high accuracy that would have been required to establish with any confidence departures from oxygen stoichiometry of the weberite: the loss of as much as one oxygen per $Sr_2Bi_2O_7$ (corresponding to $Sr_2Bi^{III}Bi^{V}O_6$) would amount to a weight loss of only 2.3%. In the circumstances such an accuracy could not be hoped for.

Similar experiments designed to prepare the corresponding Ca bismuthate gave products with complex, poorly defined powder patterns, difficult to identify with confidence and most likely mixtures.

Discussion

The results obtained in the high-pressure experiments can be explained if we assume that at 60–65 kbar and 700–800°C the volume relationships are as represented schematically in Fig. 1. On this reasonable assumption it is clear that $Cd_2Sb_2O_7(P)$ and $Sr_2Sb_2O_7(W)$ will not transform under pressure but $Cd_2Sb_2O_7(W)$ will. For $Ca_2Sb_2O_7$ the difference between $\bar{a}(P)$ and $\bar{a}(W)$ must be very small. Which phase is obtained will depend on how the experimental conditions affect the delicate balance of the different factors (including kinetic) that determine the relative stability of the P and W phases, as shown by the formation of a $P + W$ mixture in the reactive hot pressing on one hand and the failure of the well-defined W phase to transform on the other.

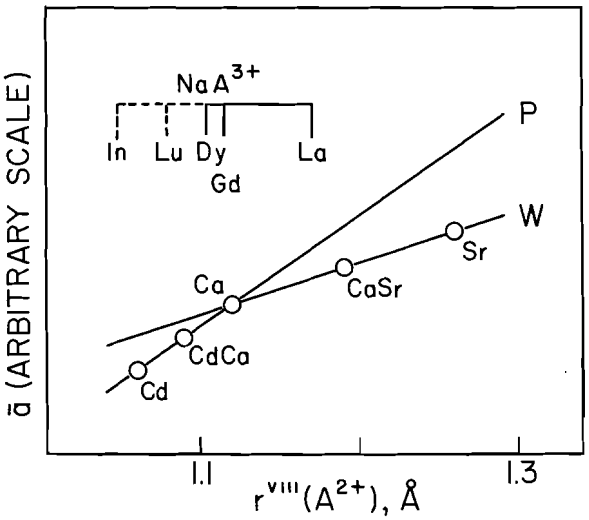


FIG. 1. Schematic representation of the pyrochlore–weberite volume relationships, at 60–65 kbar and 700–800°C, of the $A_2Sb_2O_7$ and $AA'Sb_2O_7$ antimonates.

The unexplained failure of some experiments designed to prepare $Cd_2Sb_2O_7(W)$ at atmospheric pressure (2, 6, 7) and the success of others, under seemingly identical conditions (5, 8), is undoubtedly also related to the small, pressure-dependent $\Delta\bar{a}$ of this antimonate. In the absence of compressibility data it cannot be decided whether the P–W phase relationship of Fig. 3 of ref. 2 holds at 1 atm and the P and W lines become inverted as the pressure increases, or whether the limited accuracy of the $\bar{a}$ values and the smallness of $\Delta\bar{a}$ are sufficient to introduce ambiguity into the relative positions of the P and W lines in the 1 atm plot.

The occurrence of the $NaLnSb_2O_7$ (Ln = La, Pr, Nd, Sm, Eu, Gd, Dy) antimonates as weberites (6, 9) is consistent with the volume relationships of Fig. 1. It is interesting to note that while Desgardin *et al.* (9) prepared $NaDySb_2O_7$ as a weberite, Burchard and Rüdorff (6) reported that they were unable to obtain a W phase of this composition; their experiments designed to yield $NaLnSb_2O_7$ (Ln = Dy, Er, Lu, Y) and $NaInSb_2O_7$ weberites resulted in mixtures of the unreacted sesquioxide and a P phase of unknown composition. It thus appears that Dy may be at the limit of the $NaLnSb_2O_7(W)$ field and occupies a position analogous to that of Ca in the $A_2^{2+}Sb_2O_7(W)$ series.

A further observation of interest concerns the effective ionic radius of Cd^{2+} in the W antimonates. A linear regression of $\bar{a}(W)$ on $r^{viii}(A^{2+})$ (or on the mean r^{viii} for the mixed weberites) shows clearly (Fig. 2) that Shannon's (10) $r^{viii}(Cd^{2+})$ value of 1.10 Å is too high relative to his values for Ca^{2+} (1.12 Å) and Sr^{2+} (1.26 Å). The regression equation, $\bar{a}(W) = 4.228 + 0.84r^{viii}(A^{2+})$ (14 $\bar{a}$ values, $r^2 = 0.994$, $\sigma = 0.003$ Å), requires 1.063 Å for Cd^{2+}. It also shows that the $\bar{a}$ value of 5.201 Å calculated from the unit-cell dimensions of $CdSrSb_2O_7$ (11) is lower than would be expected for $r^{viii}(Cd^{2+}) = 1.063$ Å. This is consistent with the Cd,Sr ordering reported to exist in this weberite (11).

Examination of the combined observations on $A_2Sb_2O_7$ antimonates appears to indicate that the two primary structure-determining factors are the effective size of A^{2+} and the covalency of the A—O

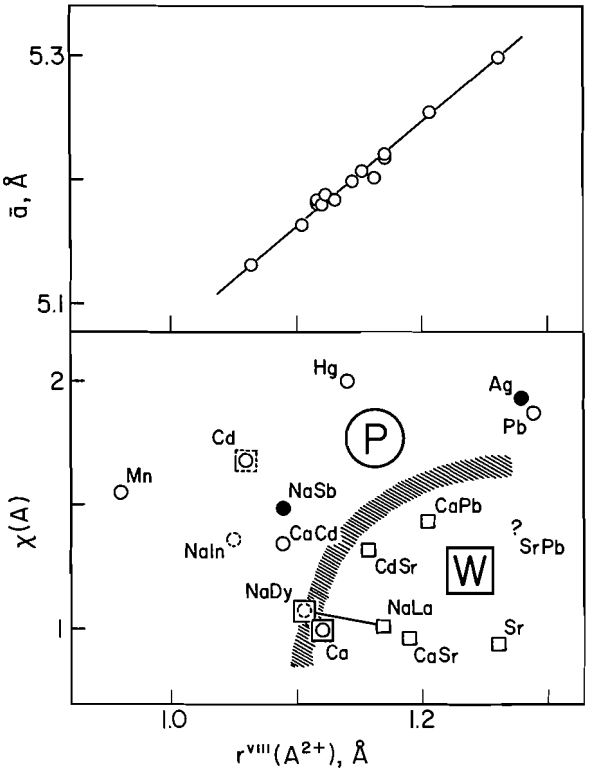


FIG. 2. (*Top*) Linear regression of $\bar{a}$ on $r^{VIII}(A^{2+})$ for $A_2Sb_2O_7(W)$. Shannon's (10) effective ionic radii are used throughout except for Cd^{2+} (see text). (*Bottom*) Pyrochlore–weberite stability relationship in dependence on the effective ionic radius $r^{VIII}(A^{2+})$ and electronegativity $\chi(A)$. Open circles, $A_2Sb_2O_7$ and $AA'Sb_2O_7$ pyrochlores. Full circles, defect antimonate pyrochlores. Squares, $A_2Sb_2O_7$ and $AA'Sb_2O_7$ weberites.

bond, and that these two factors work in conjunction. The relative *P–W* stability (within the ionic-size tolerance limits of these phases) is shown, in dependence on $r^{VIII}(A^{2+})$ and Allred's (12) electronegativity $\chi(A)$, in Fig. 2.[3] It is seen that large cations of low electronegativity favour the weberite structure. This crude separation of the *P* and *W* fields leaves out additional factors, e.g. the details of the *p–T* behaviour of the individual compounds and kinetic factors which may override the thermodynamic stability relationships and lead to formation of metastable phases. It contains no provision to account for the existence of the trigonal distortion observed in $Pb_2Sb_2O_7(P)$ (which is probably due to the lone pair on Pb^{2+}), for the effect of nonstoichiometry on the symmetry of the crystal structure, or for ordering in solid solutions $A_{2-x}A'_xSb_2O_7$, such as described in ref. 11. However, the *general* features of Fig. 2 appear to be valid.

The $Sr_2Bi_2O_7$ weberite appears to be one of the few genuine stoichiometric oxygen compounds of Bi(V). It is noted that neither of the two recently investigated mixed-valence compounds related to $Sr_2Bi_2O_7$, the golden $Ba_2Bi^{III}Bi^VO_6$ (13), and the brownish-black $(K_{1.14}Bi^{III}_{0.37})(Bi^{III}_{0.27}Bi^V_{1.73})[O_{4.9}(OH)_{1.1}](OH)_{0.8}$ (14), is a weberite. The former is an ordered perovskite with temperature-induced transitions, whilst the latter is a highly disordered pyrochlore, $\bar{a} = 5.483$ Å. If $r^{VI}(Sb^{5+})$ is taken to be 0.59 Å, the corresponding value of $r^{VI}(Bi^{5+})$, as estimated from the known Bi—O distances in the intensely yellow Na_3BiO_4 (isostructural with Na_3SbO_4) (15) and taking $r^{VI}(O^{2-}) = 1.40$ Å, is 0.64 Å. The straight line obtained by plotting $\bar{a}(Sr_2Sb_2O_7)$ and $\bar{a}(Sr_2Bi_2O_7)$ against these radii is parallel to that for Na_3SbO_4 and Na_3BiO_4. This may be taken as further evidence in support of our contention that our preparation was in fact $Sr_2Bi_2O_7$.

[3]Of the antimonates included in Fig. 2 the following have been described previously: Mn, Pb (2); Ag (4); NaSb (4, 6); Hg (18); CdSr (11); CaPb (6); NaLn (Ln = La to Dy) (6, 9). An attempt to prepare $SrPbSb_2O_7(W)$ failed (6).

Acknowledgments

We wish to thank Dr. B. Raveau for supplying a generous sample of $Cd_2Sb_2O_7(W)$. Financial support received by one of us (O.K.) under the CNRS/NRCC agreement on cooperative research during his stay at the Laboratoire de Chimie du Solide du CNRS is gratefully acknowledged.

1. W. W. BARKER, P. S. WHITE, and O. KNOP. Can. J. Chem. **54**, 2316 (1976).
2. F. BRISSE, D. J. STEWART, V. SEIDL, and O. KNOP. Can. J. Chem. **50**, 3648 (1972).
3. B. J. FERGUSON. M.Sc. thesis. Dalhousie University, Halifax, N.S. 1974.
4. D. J. STEWART, O. KNOP, C. AYASSE, and F. W. D. WOODHAMS. Can. J. Chem. **50**, 690 (1972).
5. G. DESGARDIN, G. JEANNE, and B. RAVEAU. C.R. **279C**, 565 (1974).
6. G. BURCHARD and W. RÜDORFF. Z. Anorg. Allg. Chem. **454**, 107 (1979).
7. J.-Y. MOISAN, J. PANNETIER, and J. LUCAS. C.R. **271C**, 403 (1970).
8. A. BYSTRÖM. Ark. Kemi Miner. Geol. **18A**, No. 21 (1944).
9. G. DESGARDIN, C. ROBERT, and B. RAVEAU. J. Inorg. Nucl. Chem. **39**, 907 (1977).
10. R. D. SHANNON. Acta Crystallogr. A, **32**, 751 (1976).
11. G. DESGARDIN, C. ROBERT, and B. RAVEAU. Can. J. Chem. **54**, 1665 (1976).
12. A. L. ALLRED. J. Inorg. Nucl. Chem. **17**, 215 (1961).
13. G. THORNTON and A. J. JACOBSON. Acta Crystallogr. B, **34**, 351 (1978); D. E. COX and A. W. SLEIGHT. Acta Crystallogr. B, **35**, 1 (1979).
14. J. TREHOUX, F. ABRAHAM, and D. THOMAS. J. Solid State Chem. **21**, 203 (1977).
15. B. SCHWEDES and R. HOPPE. Z. Anorg. Allg. Chem. **393**, 136 (1972).
16. M. BACCAREDDA. Gazz. Chim. Ital. **66**, 539 (1936).
17. K. H. BUTLER, M. J. BERGIN, and V. M. B. HANNAFORD. J. Electrochem. Soc. **97**, 117 (1950).
18. A. W. SLEIGHT. Inorg. Chem. **7**, 1704 (1968).

Can. J. Chem. Downloaded from www.nrcresearchpress.com by 210.87.254.6 on 09/05/12
For personal use only.

SO_2 diffusion through acetonitrile-saturated perfluorosulfonic acid membranes

FRANK M. KIMMERLE AND RAYMOND BREAULT

Department of Chemistry, Université de Sherbrooke, Sherbrooke, P.Q., Canada J1K 2R1

Received April 1, 1980

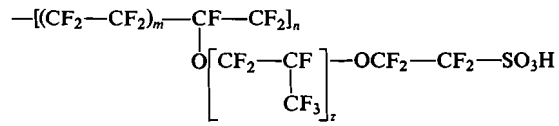
FRANK M. KIMMERLE and RAYMOND BREAULT. Can. J. Chem. **58**, 2225 (1980).

The diffusion coefficient of SO_2 and acetonitrile in Nafion perfluorinated ion exchange membranes have been determined from chromatographic measurements of SO_2 concentration and the isotopic ratios in acetonitrile solutions. The diffusion coefficients vary with residual water content and attain values about one fifth those reported for water-saturated membranes falling in the range $1-2 \times 10^{-7}$ cm^2 s^{-1}. Values obtained for Teflon reinforced material indicates diffusion takes place over an effective surface more than twice the optically open area.

FRANK M. KIMMERLE et RAYMOND BREAULT. Can. J. Chem. **58**, 2225 (1980).

Les coefficients de diffusion D_{SO_2} et D_{CH_3CN} dans les membranes d'échangeur d'ion perfluorinés ont été déterminés à partir des mesures chromatographiques et isotopiques en milieu acétonitrile. Les coefficients dépendent de la concentration résiduelle en eau et atteingent finalement des valeurs un cinquième à celles observées dans les membranes saturés en eau, soit de $1 à 2 \times 10^{-7}$ cm^{-2} s^{-1}. Des valeurs mesurées pour un matériel renforci par un tissu de Teflon indiquent que la diffusion a lieu sur une surface plus que deux fois importante que la surface apparente à l'examen microscopique.

Cation exchange membranes in general and perfluorosulfonic acid membranes in particular have attracted a lot of attention in the electrochemical industry. Dupont's Nafion® materials are described (1) as copolymers of tetrafluoroethylene and monomers such as perfluoro-3,6-dioxa-4 methyl-7-octensulfonic acid, typified by the chemical formula



where m = 5 to 13.5, n = ca. 1000, and z = 1, 2, 3 ...

The sulfonic acid groups may be assumed (2) to line the walls of a conductive network of a series of pores and cavities that permeate the otherwise hydrophobic fluoropolymer. The transport properties are largely governed by the equivalent weight (ew) of the polymer, the amount of water retained by the hydrophilic R—SO_3H groups, and the extent of cation exchange that has taken place. Ion exchange membranes are available in various forms including Nafion membrane 110: a homogeneous film 10 mils thick ew = 1100, Nafion membrane 125: a homogeneous film 5 mils thick ew = 1200, and Nafion membrane 427: a 7 mils thick film of ew = 1200 perfluorosulfonic acid resin laminated with a Basket Weave Teflon® supporting cloth.[1]

The membranes have been widely used as separators in water electrolysis (4) and chlor-alkaline cells (3, 5), and have been investigated as membranes in the production of alkali metal carbonates (6) and suggested for use in metal recovery as well as in battery, fuel cell, and dialysis applications (7). No specific mention of these solid polymer membranes in connection with aprotic electrolytes appears in the literature. We now have reason to believe that small polar molecules including acetonitrile, methylformate and methylacetate are readily retained within the cavities of the membrane. Data will be presented here showing that acetonitrile and SO_2 possess mobilities of the same order of magnitude as the water molecule in aqueous electrolytes. Work currently in progress indicates that cation transport remains high and anion transport remains negligibly small in membranes equilibrated with respect to aprotic electrolytes.

Will (8) recently investigated the diffusion of bromine in bromide solution through Nafion perfluorinated membranes, showing that D_{Br_2} depends on the chemical nature of the diffusing species as well as the counter cation. In order to minimize the number of experimental parameters, this exploratory work avoids the use of a supporting electrolyte and other solutes. Moreover, extrapolation of our results to real systems, including the commercially available Li/SO_2 batteries would be premature since only SO_2/CH_3CN ratios below 0.01 were investigated.

Experimental

Chromatographic Measurements

The effect of membrane equivalent weight, its pretreatment, and temperature were studied by following the SO_2 concentration in the two compartment cell shown in the schematic drawing of Fig. 1. The two halves, having a volume of 3.1 and 150 mL respectively, were separated by the semipermeable membrane held between two stainless steel flanges exposing an area A 2.5 cm in diameter.

The larger of the two compartments was filled with an

[1]Registered trademark of E. I. du Pont de Nemours and Company.

0008-4042/80/212225-05$01.00/0

©1980 National Research Council of Canada/Conseil national de recherches du Canada

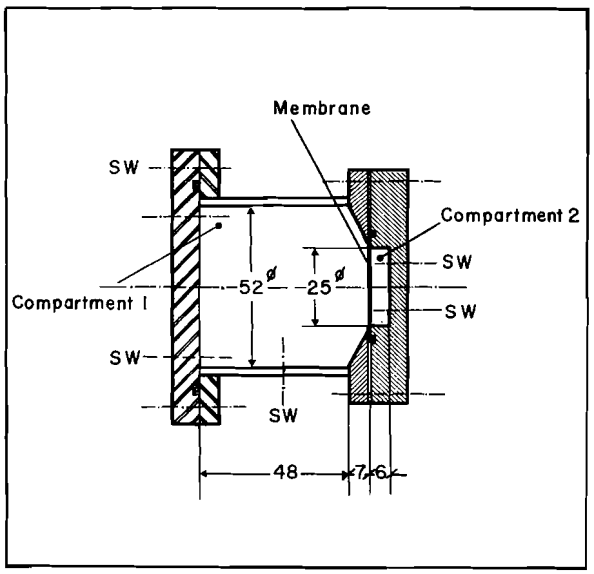


FIG. 1. Sectional view of diffusion cell. Dimensions in mm, material SS-316, Teflon seal, SW: Swagelok® male connectors 1/8 in.

~0.2 *M* SO_2/acetonitrile solution, the smaller with pure acetonitrile. Samples (5.0 μL) were withdrawn through septums held in 1/8 in. Swagelock® ports and analysed by measuring the ratio of the chromatographic peak areas SO_2/CH_3CN in both compartments. The separation of SO_2 and acetonitrile using a Carbowax 200 column at 100°C in a Gow-Mac chromatograph proved very reliable and allowed sufficient time to change the attenuation factor. As verified by iodometric titrations the peak ratio remained proportional to the SO_2 concentrations up to 0.5 *M*. Relative concentrations could be measured to within 0.5% and the concentration of the SO_2 in the larger compartment remained constant to within 1% throughout any one run.

Mass Spectrometric Measurements

The smaller of the two compartments was filled with deuterated acetonitrile and the larger with CH_3CN. Samples (5 μL) from both compartments were analysed by mass spectrometry over a period of several hours and the diffusion rate of acetonitrile was calculated from the variation of the peak ratio at $m/e = 44$ and $m/e = 41$. The spectra for ten repetitive scans were averaged to yield relative results for the m/e ratio 41/44 accurate to within 2% for the smaller compartment. The m/e ratio 44/41 for the larger compartment proved less reliable since the mass ratio remained below 2% even when diffusion equilibrium had been reached.

Acetonitrile Solutions and Membrane Pretreatment

Acetonitrile was purified following the method outlined by O'Donnel *et al.* (9). Water was removed by distillation from molecular sieves or calcium hydride and typical Karl Fisher analysis indicated less than 400 ppm H_2O. A SO_2 stock solution was prepared by bubbling SO_2 gas through dried and purified acetonitrile at room temperature. Test solutions (0.2 *M*) were prepared by volumetric dilution and their SO_2 content determined exactly by iodiometric titration (10) using dead stop end point detection. The Nafion membranes were boiled in dried acetonitrile for periods up to 100 h and immediately mounted in the cell.

Mathematical Treatment

The mathematical analysis of the results assumes steady state diffusion inside the membrane and a uniform concentration throughout the two compartments. For the diffusion of SO_2 from the large compartment [1] through a membrane of thickness l to the smaller compartment [2] it follows (11) that

$$[1]\quad \log_e \left\{\frac{{}^1_0[SO_2] - {}^2_0[SO_2]}{{}^1[SO_2] - {}^2[SO_2]}\right\} = \frac{AD_{SO_2}}{l}\left\{\frac{1}{V_1} + \frac{1}{V_2}\right\}\Delta t$$

Furthermore, since ${}^1[SO_2] = {}^1_0[SO_2]$, to within 1% throughout the run, and the initial concentration in the smaller compartment, ${}^2_0[SO_2] = 0$, the diffusion coefficient could be obtained from a logarithmic plot:

$$[2]\quad \log_e \left\{\frac{{}^1[SO_2] - {}^2[SO_2]}{{}^1[SO_2]}\right\} = \frac{AD_{SO_2}}{l}\left\{\frac{1}{V_1} + \frac{1}{V_2}\right\}t$$

For the diffusion of acetonitrile, equal diffusion coefficients were assumed for the two isotopes. Equal amounts of CH_3CN should diffuse from the larger to the smaller compartment as amounts of CD_3CN would diffuse in the opposite direction. Using expressions analogous to eq. [1] and the simplifying assumption that ${}^1[Cd_3CN] \simeq {}^1_0[CD_3CN] \simeq 0$ to within 1%, and ${}^1[CH_3CN] = {}^1_0[CH_3CN] \simeq 1.0$, the isotopic ratio in the smaller compartment was expected to vary as:

$$[3]\quad \log_e \left\{\frac{{}^2[CH_3CN]}{{}^2[CD_3CN]} + 1\right\} = \frac{AD_{CH_3CN}}{l}\left\{\frac{1}{V_1} + \frac{1}{V_2}\right\}t$$

Results and Discussion

The perfluorosulfonic acid products were not attacked by boiling acetonitrile and their appearance remained unchanged. After drying the membranes in air a net weight loss of the order of 1% was observed with respect to the original material at 35% humidity. Subsequent ir spectra of the membrane with respect to Nafion products evacuated at 0.1 Torr were almost identical to those of an acetonitrile film and the original OH band of water-boiled Nafion membranes could no longer be detected. DTA analysis revealed a weight loss peak some 20°C below that found for the original material and, as verified by Karl Fisher analysis, less than 0.05% H_2O could subsequently be extracted. When only one surface of the membranes was exposed to acetonitrile or its vapours, temporary puckering and distortion of the flat surface occurred which could be removed by plunging the entire film into the solvent. With some practice smooth films could be mounted in the diffusion cell and the two compartments filled with solvent and solution without undue exposure to the ambient air.

The increase in SO_2 concentration in the 3 mL compartment with time is shown in Fig. 2 for various Nafion membranes in acetonitrile containing 0.2 *M* SO_2. As expected from Will's work on Br_2 diffusion (8), SO_2 diffuses more rapidly in the lower equivalent weight product and across the thinner membranes. The diffusion across the membrane #427, consisting

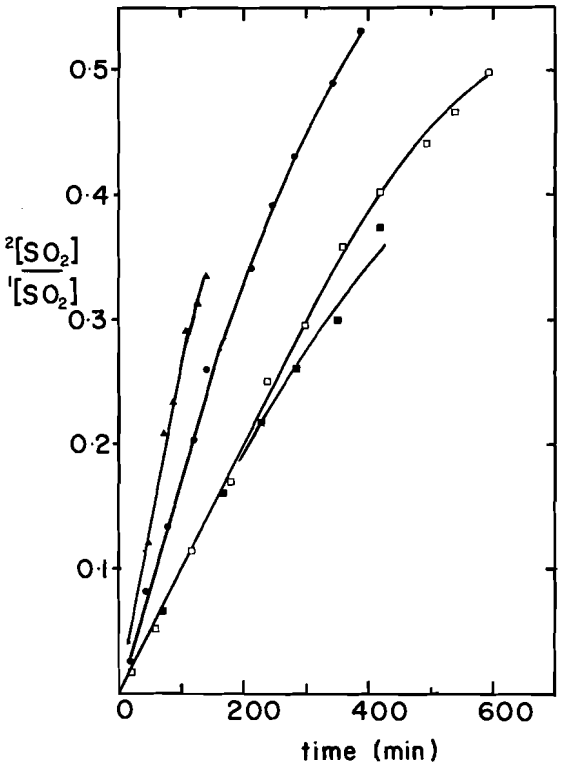


FIG. 2. SO_2 concentration ratio as a function of time. Membrane acetonitrile boiled for 20 h; ▲, membrane #110; ●, membrane #125; ■, membrane #120; □, membrane #427.

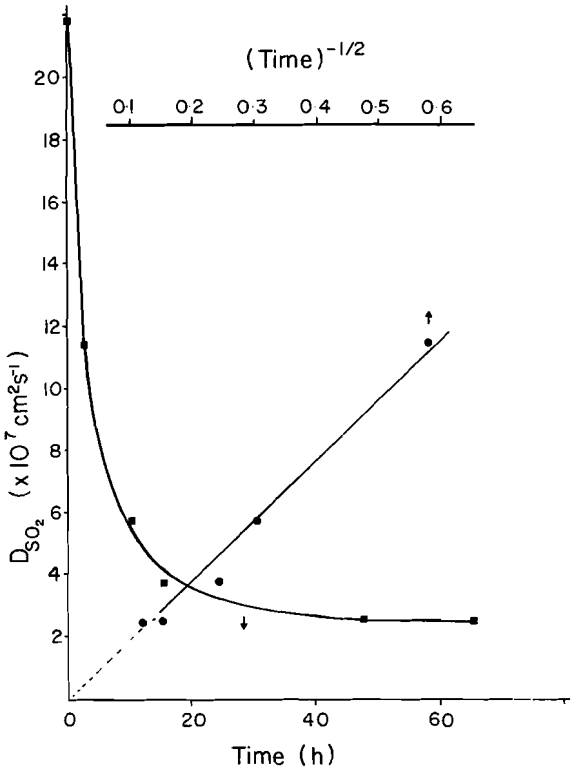


FIG. 3. Variation of diffusion coefficient D_{SO_2} with the extent of acetonitrile leaching for Nafion 110. Lower scale: τ, hours of contact with boiling CH_3CN; upper scale: $\tau^{-1/2}$.

of 0.007 in. sheet of 1200 equivalent weight perfluoronated membrane laminated to a woven Teflon fabric, is marginally greater than across a 0.010 in. thickness of the same composition.

Diffusion coefficients for membranes acetonitrile-boiled for 1 h were up to twice as great as those observed for membranes boiled overnight. Similarly, acetonitrile containing 0.5% H_2O yielded D_{SO_2} values about twice those observed in dried CH_3CN solution. Clearly the acetonitrile can replace the water molecule within the membrane given sufficient time and subsequent diffusion within the pores is slowed down appreciably. Figure 3 illustrates this effect for the Nafion 110 membrane. The diffusion coefficient diminishes as $\tau^{-1/2}$ where τ represents the numbers of hours the membrane was contacted with boiling acetonitrile. Water seems to be leached slowly from the membrane and if perfectly anhydrous conditions could be maintained, D_{SO_2} might drop to zero. In actual practice no further decrease in D was observed after 75 h even for the thicker or higher molecular weight membranes and these residual values are discussed further below.

The increase in the isotopic ratio CH_3CN/CD_3CN follows the same general behaviour as the SO_2 concentration in the smaller compartment. Diffusion coefficients were calculated from data such as presented in Table 1 using a least squares fit to eqs. [2] and [3], respectively. Most runs were abandoned after 7 h but linear plots were obtained for periods up to 30 h, SO_2 ratios up to 90%, and CH_3CN/CD_3CN ratios up to 3. The diffusion coefficients listed in Table 2 represent average values of duplicate or triplicate runs calculated using the membrane thickness measured for acetonitrile-boiled products listed in column 3. Unlike SO_2 diffusion coefficient, D_{CH_3CN} varied little with the membrane leaching time. After the initial 1 h boiling time essentially constant values were obtained indicating that the transport mechanism is fundamentally different from that of the strong Lewis acid SO_2.

Plots of log D versus $1/K$ over the temperature interval 20 to 60°C indicate an activation energy for diffusion of SO_2 of 23 kJ/mol for the 1100 equivalent weight product, only somewhat higher than that observed for concentrated aqueous NaOH solution (2). Since the diffusion processes do not seem drastically different from diffusion in aqueous solution it may be instructive to compare the D_{SO_2} values with those predicted by Gierke's cluster model (2).

TABLE 1. SO_2 and isotopic composition: time variation membrane #120, $T = 25 \pm 1$°C, membrane leached with boiling acetonitrile for 20 h*

t (min)	m/e ratio 41/44	log [ratio + 1]	t (min)	$\frac{^2[SO_2]}{^1[SO_2]}$	log [1 − ratio]
13	0.045	0.044	65	0.062	−0.064
71	0.148	0.138	123	0.1136	0.121
132	0.270	0.239	208	0.209	0.235
191	0.355	0.304	250	0.241	0.276
253	0.486	0.396	317	0.285	0.336
313	0.636	0.492	350	0.300	0.357
413	1.141	0.761	418	0.374	0.469

*D_{CH_3CN}, 4.26 × 10^{-7} cm² s^{-1}, D_{SO_2}, 3.39 × 10^{-7} cm² s^{-1}.

TABLE 2. Diffusion coefficients in Nafion perfluorosulfonic acid membranes, $T = 25 \pm 1$°C

Identification	Equivalent weight	Thickness	Pore diameter* (Å)	D_{SO_2}* (10^{-7} cm² s^{-1}) Expt.	Calcd.	D_{H_2O}	D_{CH_3CN}
110	1100	0.250±0.008 mm	16	2.22	7.2	12.8	9.0
120	1200	0.275±0.009 mm	12	1.12	4.2	6.9	4.05±0.2
125	1200	0.134±0.003 mm	12	1.26			
427	1200	0.007 in. (nominal)	12	1.71			

*Prediction from data of ref. 2 (Gierke).

Thus, the diffusion coefficient D_{SO_2} in the membrane can be estimated from the free diffusion in acetonitrile, $D_{SO_2}^0$, the pore diameter, D_p, the Bragg spacing of the clusters, d, and an effective diameter of the SO_2 molecule σ_{SO_2}:

$$[4] \quad \frac{D_{SO_2}}{D_{SO_2}^0} = \frac{\pi}{4d^2}(D_p - \sigma_{SO_2})^2$$

From the polarographic reduction of SO_2 in acetonitrile we obtain $D_{SO_2}^0 = 2.15 \times 10^{-5}$ cm² s^{-1}, from van der Waals radii we estimate $\sigma_{SO_2} = 4.6$ Å and the other parameters are taken from Gierke's work. The experimental results are almost four times lower than the results predicted by this model. Although acetonitrile can obviously diffuse across the Nafion membranes, it does not simply replace water molecules as the transport media within the cavities of the membranes. Given the same ratios of the diffusion coefficients in the 1100 and 1200 ew films (1.85 in both acetonitrile and water-saturated products) and the similar value of the diffusional activation energy (20–25 kJ/mol) it seems likely that the transport takes place through fewer cavities but in essentially the same manner in both water- and acetonitrile-saturated membranes. The diffusion process might therefore involve only cavities containing a certain minimum number of water molecules.

For the laminated product Nafion 427 Grot (7) claimed that the open area of the T-12 weave is about 25% according to optical measurements, a value confirmed by our microscopic examination. Since the separator material is identical to that used in the homogeneous Nafion 120 and Nafion 125 products, an effective diffusion coefficient D_{SO_2} of about 3×10^{-8} cm² s^{-1} might be expected if only 25% of the material were available for diffusion. This is clearly not the case.

The experimental value 1.71 ± 0.04 × 10^{-7} cm² s^{-1} is even greater than that found in the uniform 1200 ew materials 120 and 125. We have no satisfactory explanation for this observation. Possibly the laminated material is attacked by the prolonged leaching or the Teflon cloth contributes to the transport of SO_2. D values calculated after a pretreatment of 20 h differed little from those obtained after 100 h leaching with boiling acetonitrile in contrast to all other materials examined.

Isotopic measurements indicated $D_{CH_3CN} = 0.38 \times 10^{-6}$ cm² s^{-1} for the Nafion 120 membrane and $D_{CH_3CN} = 0.24 \times 10^{-6}$ cm² s^{-1} for the diffusion across the perfluorosulfonic acid layer of the Nafion 427 membrane. If we can attribute the difference to a partial blocking of the surface by the Teflon cloth, we would estimate an open area of 0.24/0.38 = 67%. Since only one surface is reinforced and the diffusional process does not take place entirely in one straight direction, part of the membrane blocked by the Teflon cloth undoubtedly contributes to the diffusion. For acetonitrile solutions, which wet

Teflon, the effective blockage (33%) may be less than in aqueous solutions and represents less than half of the effect simple optical measurements predict (78%).

Acknowledgements

The authors wish to thank C. P. Vijayan for help in designing the diffusion cell and are pleased to acknowledge the support of this work through an operating grant of the Natural Sciences and Engineering Research Council of Canada.

1. A. EISENBERG and M. KING. Ion-containing polymers. Vol. 2. Polymer physics. Academic Press, New York. 1977. p. 162 ff.
2. T. D. GIERKE. Ionic clustering in Nafion perfluorosulfonic acid membranes and its relationship to hydroxyl rejection and chlor-alkali efficiency. Presented at the 152nd National Meeting, The Electrochemical Society, Atlanta, GA, October 10–14, 1977.
3. B. E. KURTZ and R. H. FITCH. Chlorine/caustic soda production in a permselective membrane cell. Presented at the 153rd National Meeting, The Electrochemical Society, Seattle, WA, May 21–26, 1978.
4. J. E. HARRAR and R. J. SHERRY. Anal. Chem. **47**, 601 (1975).
5. H. L. YEAGER and A. STECK. Anal. Chem. **51**, 862 (1979).
6. R. L. RESPIRIS and T. J. GILLIGAN. Membrane cell process for the electrosynthesis of alkali metal carbonates. Presented at the 153rd National Meeting, The Electrochemical Society, Seattle, WA, May 21–26, 1978.
7. W. GROT. Chem. Eng. Tech. **50**, 299 (1978).
8. F. G. WILL. J. Electrochem. Soc. **126**, 36 (1979).
9. J. F. O'DONNEL, J. T. AYRES, and C. K. MANN. Anal. Chem. **37**, 1161 (1965).
10. A. I. VOGEL. Text-book of quantitative inorganic analysis. 3rd ed. Longman, London. 1962. p. 370.
11. W. JOST. Diffusion. Academic Press, New York. 1960. p. 436 ff.

Processus primaire de la photolyse et de la photo-oxydation de l'*o*-phényl-phénol

LOUISE-MARIE COULANGEON, GILLES PERBET, PIERRE BOULE ET JACQUES LEMAIRE

Laboratoire de Photochimie, U.E.R. Sciences Exactes et Naturelles et Ecole Nationale Supérieure de Chimie, Université de Clermont II, Ensemble Universitaire des Cézeaux, B.P. 45, 63170 Aubière

Reçu le 5 mars 1980

LOUISE-MARIE COULANGEON, GILLES PERBET, PIERRE BOULE et JACQUES LEMAIRE. Can. J. Chem. **58**, 2230 (1980).

En solution aqueuse, l'*o*-phényl-phénol présente une double fluorescence qui traduit un équilibre de déprotonation dans l'état excité singulet. Cette propriété permet d'interpréter l'influence de l'oxygène sur la production photochimique primaire des radicaux phénoxy. On montre que, seul l'état excité singulet de la forme phénolate donne lieu à la photo-éjection d'électrons. L'oxygène inhibe la recombinaison des électrons éjectés avec les radicaux phénoxy. D'autres capteurs d'électrons comme les Cd^{2+} ou NO_3^- sont également susceptibles d'accroître le rendement quantique de disparition de l'*o*-phényl-phénol en solution dégazée. L'effet de l'oxygène au niveau du processus primaire permet d'interpréter les résultats acquis en photo-oxydation de dérivés phénoliques donnant naissance à des radicaux phénoxy inoxydables.

LOUISE-MARIE COULANGEON, GILLES PERBET, PIERRE BOULE, and JACQUES LEMAIRE. Can. J. Chem. **58**, 2230 (1980).

The dual fluorescence observed in aqueous solution of *o*-phenyl-phenol is attributed to a deprotonation equilibrium in the excited singlet state. The effect of oxygen on the primary photochemical process of formation of phenoxy radicals can be explained in a parallel study of the variations of fluorescence and photo-oxidation quantum yields of this phenolic compound at different pH. It is shown that photoionisation occurs only from the excited singlet state of the phenolate form. Oxygen inhibits recombination of the solvated electron and phenoxy radical. Increase of quantum yield for the disappearance of irradiated *o*-phenyl-phenol in degased solution also is observed in the presence of electron scavengers like Cd^{2+} or NO_3^- ions. Even when the phenoxy radicals are not able to react with oxygen, quantum yield for the disappearance of the phenolic compounds is higher in an aerated than in a degassed solution; the oxygen effect on the primary photochemical step may explain this difference.

Introduction

Le comportement photochimique de composés phénoliques en solution aqueuse diluée, aérée ou désoxygénée a été souvent étudié par des techniques de photolyse par éclairs ou de photolyse laser. Ces techniques permettent de déterminer la concentration des espèces radicalaires formées et leur cinétique de disparition (1–4). Les processus primaires de photodéélectronation sont également appréhendés par des techniques pulsées, comme celles récemment rapportées par Mialocq et ses collaborateurs (5).

La photolyse et la photo-oxydation des dérivés phénoliques en solution aqueuse impliquent en fait une formation primaire de radicaux phénoxy et d'électrons et une succession de processus secondaires mettant en jeu ces espèces réactives. Les résultats acquis en photolyse par éclairs ne permettent pas à eux seuls de comprendre le comportement de ces composés sous irradiation continue et à des intensités incidentes très inférieures à celles utilisées en techniques rapides. Depuis 1972, notre laboratoire s'est engagé dans une étude détaillée de l'évolution des phénols les plus simples, en solution diluée, sous excitation monochromatique et continue à 253,7 nm (6–8). Les objectifs de ces études étaient: de mesurer les rendements quantiques de disparition de dérivés phénoliques et d'étudier leurs variations avec les paramètres macroscopiques habituels (température, O_2 dissous, pH, concentration initiale, longueur d'onde d'excitation, ...); d'établir un bilan matière (au moins à faible taux de conversion); de proposer un mécanisme de photo-oxydation.

Nous avons, en particulier, remarqué que les radicaux phénoxy issus des différents phénols peuvent participer à trois processus prépondérants, soit une oxydation soit une dimérisation, soit une disproportionnation (ou dismutation). Dans des conditions expérimentales analogues (O_2 dissous, température, pH), l'importance relative de ces trois processus dépend essentiellement du phénol examiné. Le tableau 1 regroupe les principaux résultats acquis sur la photo-oxydation (irradiation en solution aérée) et sur la photolyse (irradiation en solution dégazée) de sept dérivés phénoliques simples.

On remarque que même dans les cas où les radicaux phénoxy sont inoxydables, le rendement quantique de photo-oxydation reste très supérieur au rendement de photolyse; nous avons donc été amenés à reconnaître la nécessité d'une étape primaire de production des radicaux phénoxy "assistée" par l'oxygène (l'exemple le plus significatif étant constitué par l'hydroquinone ou les radicaux phénoxy sont inoxydables). Or, les mesures de fluorescence montrent que l'oxygène dissous n'est pas susceptible de réagir avec le niveau excité singulet de courte durée de vie ($\tau = 7 \times 10^{-9}$ s pour le phénol). Et, la seule interaction rapportée entre

0008-4042/80/212230-06$01.00/0
©1980 National Research Council of Canada/Conseil national de recherches du Canada

Can. J. Chem. Downloaded from www.nrcresearchpress.com by 210.87.254.105 on 09/05/12
For personal use only.

Can. J. Chem. Downloaded from www.nrcresearchpress.com by 210.87.254.105 on 09/05/12
For personal use only.

TABLEAU 1. Caractéristiques cinétiques et analytiques de la photolyse et de la photo-oxydation des phénols

Composé phénolique étudié	Solution	Rendement quantique de disparition	Processus prépondérant de disparition des radicaux phénoxy	Photoproduits principaux pour un degré d'avancement de l'ordre de 0,2
Phénol (6)	Dégazée	0,004	Duplication	Dihydroxybiphényles
	Aérée	0,12	Oxydation suivie d'une dismutation ou d'une duplication	Trihydroxybiphényles (50%); tétrahydroxybiphényles (12%) hydroquinone et pyrocatéchol (15%); benzoquinone (15%)
Hydroquinone (Dihydroxy-1,4 benzène) (8)	Dégazée	0,004	Dismutation	Trihydroxybenzène (70%); hydroquinone (30%)
	Aérée	0,020		
Pyrocatéchol (Dihydroxy-1,2 benzène) (8)	Dégazée	0,001	Duplication	Biphényles tétrahydroxylés
	Aérée	0,007		
Résorcinol (Dihydroxy-1,3 benzène) (8)	Dégazée	0,001	Duplication	Biphényles tétrahydroxylés
	Aérée	0,035	Oxydation suivie d'une dismutation	Hydroxy-*p*-benzoquinone (28%); trihydroxy-1,2,4 benzène (40%)
Hydroxy-hydroquinone (Trihydroxy-1,2,4 benzène) (9)	Dégazée	0,004	Dismutation	Hydroxy-*p*-benzoquinone (100% à l'instant initial)
	Aérée	0,020		
Pyrogallol (Trihydroxy-1,2,3 benzène) (9)	Dégazée	0,008	Dismutation	Purpurogalline
	Aérée	0,030	Dismutation ou oxydation suivie d'une dismutation	Purpurogalline (30%); dihydroxy-quinones (25%); tétrahydroxy-benzène (25%)
Phloroglucinol (Trihydroxy-1,3,5 benzène) (9)	Dégazée	0,0001	Oxydation suivie d'une dismutation	Tétrahydroxy-benzène; quinones
	Aérée	0,010		

Can. J. Chem. Downloaded from www.nrcresearchpress.com by 210.87.254.105 on 09/05/12
For personal use only.

l'état excité triplet du phénol et l'oxygène consisterait en une complexation du niveau triplet de la forme neutre; ce complexe est alors capable, sous forte intensité lumineuse, de donner naissance par processus biphotonique à un radical phénoxy (2); sous faible intensité lumineuse, on ne connaît pas la réactivité de ce complexe.

L'étude de l'intervention de l'oxygène sur les processus photochimiques primaires, difficile pour la plupart des phénols simples, s'est avérée possible dans le cas de l'*o*-phényl-phénol. Comme nous allons le voir, cette molécule présente une double fluorescence qui traduit l'existence d'un équilibre de déprotonation dans l'état excité singulet. Cette propriété intéressante peut alors permettre d'élucider le mécanisme d'intervention de l'oxygène.

Techniques expérimentales

Les solutions aqueuses d'*o*-phényl-phénol ont été préparées à partir d'un produit Aldrich (99%). Les mélanges tampons ont été réalisés selon (10) à l'aide des substances suivantes: acide sulfurique Prolabo R. P. Normapur de pH = 0, à pH = 1; acide citrique Merck "pro analysi" de pH = 1,17 à pH = 6,69; phosphates monopotassique et disodique R.A.L. de pH = 5,29 à pH = 8,04; acide borique Merck "pro analysi" de pH = 7,61 à pH = 12,38; hydroxyde de sodium Prolabo R.P. Normapur pour pH > 12.

Les forces ioniques des solutions d'*o*-phényl-phénol tamponnées varient de 0,006 à 0,033 *M*.

Le nitrate de potassium utilisé est un produit Prolabo R.P. pour analyses, le sulfate de cadmium $3CdSO_4,8H_2O$, un produit Merck pour analyses.

Les spectres d'absorption ont été mesurés sur un spectrophotomètre Cary 118C à double faisceau; les mesures d'émission de fluorescence ont été réalisées sur un spectrofluorimètre Perkin-Elmer MPF-3L, équipé d'une lampe au Xénon Osram XBO de 150 W. Les solutions d'*o*-phényl-phénol dans l'eau ont été irradiées à 296 nm ou à 313 nm à l'aide d'un monochromateur Bausch et Lomb "haute intensité", équipé d'une lampe à vapeur de mercure "haute pression" Osram HBO 200 W. Le flux du faisceau d'irradiation est mesuré avec un phototube R.C.A. 935 et un galvanomètre A.O.I.P G.223. Ce dispositif est préalablement étalonné par une actinométrie basée sur la photoréduction du ferrioxalate de potassium (11). Les rendements quantiques de disparition initiale ont été mesurés par spectrofluorimétrie aussi bien en milieu aéré qu'en milieu dégazé. La désoxygénation des solutions a été réalisée par des cycles de congélation et de pompage sous vide dans l'azote liquide.

Résultats expérimentaux

Dans toute cette étude, nous nous sommes intéressés uniquement au comportement photochimique de l'*o*-phényl-phénol excité dans son premier état singulet.

Propriétés absorbantes et émissives de l'o-phényl-phénol

Nous avons examiné l'influence du pH sur les spectres d'absorption et de fluorescence de l'*o*-phényl-phénol dans l'eau. Le tableau 2 mentionne les propriétés absorbantes et émissives de la molécule, en solution aqueuse diluée. Les fluorescences observées ne dépendent pas de l'oxygène dissous, quel que soit le pH de la solution et elles sont invariantes après désoxygénation complète de la solution.

L'évolution comparée des spectres d'absorption et d'émission avec le pH et l'existence d'une double émission ($1 < pH < 10$) traduisent un équilibre acide–base dans l'état excité singulet, comme cela a déjà été mis en évidence pour différents composés phénoliques (12, 13) et tout particulièrement pour le naphtol-2 (13–15). La relation déduite du cycle de Förster (16):

$$pK = pK^* + 2{,}1 \times 10^{-3}\Delta\nu \quad (cm^{-1})$$

conduit à $pK^* = 0$ ou à $pK^* = 3$ selon que $\Delta\nu$ représente respectivement la différence de fréquences des maximums d'émission ou d'absorption. La courbe *a* de la fig. 1 représente les variations du rapport entre l'intensité d'émission à $\lambda_{max} = 413$ nm à différents pH à l'intensité d'émission à pH = 14. Cette courbe indique que le pK^* (S_1) est effectivement compris entre 1 et 1,5.

Etude cinétique de la photolyse et de la photo-oxydation de l'o-phényl-phénol

En milieu dégazé, le rendement quantique de disparition (ϕ_0) est indépendant de la concentration initiale et du pH de la solution; il est égal à 0,002 en milieu de pH variable entre 5 et 14 ($\lambda_{exc} = 296$ ou 313 nm).

Dans l'eau et en solution aérée, le rendement quantique de disparition ($\phi_0{}^{O_2}$) de l'*o*-phényl-phénol à 296 nm est indépendant de la concentration initiale (tableau 3). On note que comme dans le cas du phénol, des diphénols et triphénols le rendement quantique de disparition est beaucoup plus faible en photolyse qu'en photo-oxydation. Le rendement quantique initial de photo-oxydation ($\phi_0{}^{O_2}$) varie avec le pH de la solution; sur la fig. 1, la courbe *b* représente les variations du rapport des valeurs des rendements quantiques de photo-oxydation mesurées à différents pH à celle mesurée

TABLEAU 2. Propriétés absorbantes et émissives de l'*o*-phényl-phénol en solution aqueuse

pH	Absorption transition $S_0 \rightarrow S_1$	Emission transition $S_1 \rightarrow S_0$
0–1	$\lambda_{max} = 282$ nm ($\varepsilon_{max} = 4000\ M^{-1}\ cm^{-1}$)	$\lambda_{max} = 345$ nm
1–10	$\lambda_{max} = 282$ nm	$\lambda_{max} = 345$ et 413 nm
10–14	$\lambda_{max} = 310$ nm ($\varepsilon_{max} = 5750\ M^{-1}\ cm^{-1}$)	$\lambda_{max} = 413$ nm
$pK(S_0) \simeq 10$		$1 < pK^*(S_1) < 1{,}5$

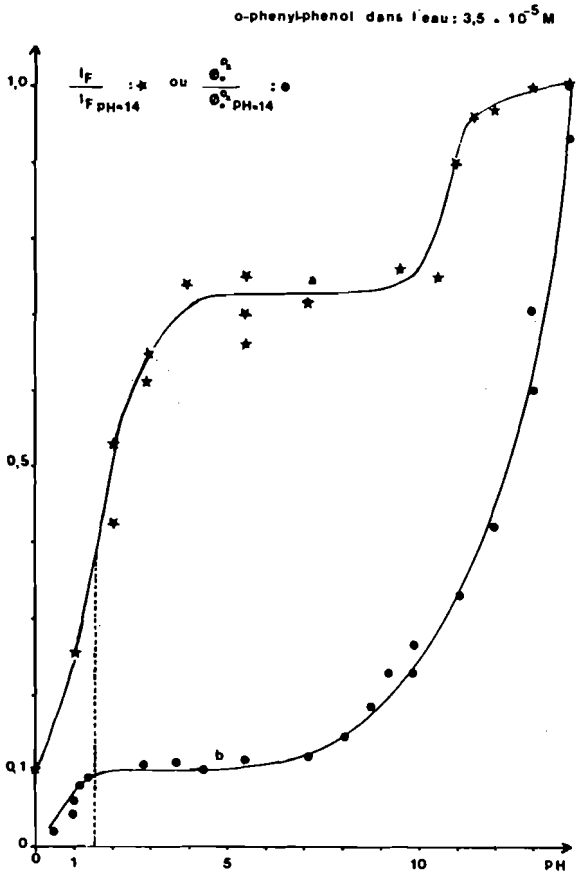


FIG. 1. (*a*) Variations du rapport I_F à $\neq$ pH/I_F à pH = 14 de l'intensité de fluorescence à 413 nm mesurée à différents pH à l'intensité de cette même fluorescence à pH = 14 pour une solution aqueuse d'*o*-phényl-phénol ($3,5 \times 10^{-5}$ *M*). (*b*) Variations du rapport $\phi_0^{O_2}$ à $\neq$ pH/$\phi_0^{O_2}$ à pH = 14 des valeurs des rendements quantiques $\phi_0^{O_2}$ de photo-oxydation mesurés à différents pH à celle mesurée à pH = 14, pour une solution d'*o*-phényl-phénol ($3,5 \times 10^{-5}$ *M*).

à pH = 14 ($\phi_{0\ ^2} = 0,15$). La confrontation des courbes *a* et *b* nous permettra par la suite de proposer un mécanisme primaire pour la formation des radicaux phénoxy issus de l'*o*-phényl-phénol.

La photo-oxydation de l'*o*-phényl-phénol à 296 nm conduit à la formation d'un produit absorbant à 250 nm et non émissif, et un produit émetteur en milieu neutre à 355 nm et absorbant à 320 nm. Le produit absorbant à 250 nm est identifié à la phényl-*p*-benzoquinone. Le produit émetteur à 355 nm n'a pas pu être isolé dans ces solutions où la solubilité de l'*o*-phényl-phénol est limitée à 3×10^{-4} *M*.

Dans le cas analogue de la photo-oxydation du phénol, les produits émetteurs à 340 nm en milieu neutre ou acide et à 390 nm en milieu basique ont été identifiés à différents trihydroxydiphényles représentant 50% du phénol transformé. Nous admettrons donc que le produit émetteur à 355 nm est un trihydroxytétraphényle.

TABLEAU 3. Rendements quantiques initiaux de photo-oxydation de l'*o*-phényl-phénol ($\lambda_{exc} = 296$ nm, pH = 5,5, oxygène dissous 3×10^{-4} *M*)

o-Phényl-phénol (*M*)	($\phi_0^{O_2}$)
$1,45 \times 10^{-4}$	$0,01_9 \pm 0,002$
$3,50 \times 10^{-4}$	$0,01_9 \pm 0,002$ $0,02_0 \pm 0,002$ $0,01_4 \pm 0,002$ $0,02_1 \pm 0,002$
$1,45 \times 10^{-5}$	$0,02_0 \pm 0,002$
$3,50 \times 10^{-6}$	$0,01_5 \pm 0,002$

*Influence des capteurs d'électrons sur la photolyse et la photo-oxydation de l'*o*-phényl-phénol*

La production de radicaux phénoxy à partir de la forme phénolate excitée dans son plus bas niveau singulet s'accompagne de photo-éjection d'électrons. Ce processus a été particulièrement étudié dans le cas du phénol (17, 18) et du β-naphtol (19). Comme nous allons le voir, nous proposons une recombinaison partielle des radicaux phénoxy avec les électrons solvatés pour interpréter les cinétiques différentes de disparition des phénols en photolyse et en photo-oxydation. La vitesse de conversion de l'*o*-phényl-phénol en radicaux phénoxy, ne se recombinant pas avec les électrons éjectés, dépend de la présence d'un capteur d'électrons. Nous rapportons l'influence de Cd^{2+} et NO_3^- sur le rendement quantique de disparition de l'*o*-phényl-phénol en solution aqueuse dégazée (ϕ_0).

Jusqu'à présent, et particulièrement dans le cas du phénol et du β-naphtol, c'est le protoxyde d'azote N_2O qui a été choisi comme capteur d'électrons. L'emploi des ions Cd^{2+} en milieu acide et de NO_3^- en milieu basique est préférable car le contrôle de la concentration des capteurs et des effets parasites est plus facile.

L'ion Cd^{2+} est susceptible de réagir avec les électrons hydratés avec des constantes de vitesse proches de 5×10^{10} M^{-1} s^{-1}; ces constantes de vitesse varient peu avec la concentration du capteur quand celle-ci est comprise entre 0,1 et 0,5 *M* (5, 20, 21). La constante de vitesse de capture des électrons hydratés par NO_3^- est voisine de 2×10^{10} M^{-1} s^{-1} quand la concentration d'ions NO_3^- est comprise entre 0,01 et 0,75 *M* (5, 22, 23).

Le tableau 4 rassemble les rendements quantiques initiaux de disparition en milieu dégazé (ϕ_0) en présence de sulfate de cadmium ou de nitrate de potassium, de même que les conditions expérimentales.

Can. J. Chem. Downloaded from www.nrcresearchpress.com by 210.87.254.105 on 09/05/12
For personal use only.

TABLEAU 4. Rendement quantique initial de disparition de l'*o*-phényl-phénol irradié à 296 nm en solution dégazée (concentration initiale $2{,}40 \times 10^{-5}$ *M*)

Concentration (*M*) du sulfate ou du nitrate			ϕ_0
$3CdSO_4,8H_2O$	$\lambda_{exc} = 296$ nm	pH = 5–6	
	10^{-5}		$0{,}008 \pm 0{,}002$
	5×10^{-5}		$0{,}01_8 \pm 0{,}004$
	10^{-4}		$0{,}02_0 \pm 0{,}004$
	$1{,}60 \times 10^{-3}$		$0{,}02_3 \pm 0{,}004$
	$1{,}60 \times 10^{-3}$		$0{,}02_4 \pm 0{,}004$
	$9{,}10 \times 10^{-3}$		$0{,}02_3 \pm 0{,}004$
KNO_3	$\lambda_{exc} = 313$ nm	pH = 14	
	2×10^{-3}		$0{,}06_0 \pm 0{,}006$
	5×10^{-3}		$0{,}08_0 \pm 0{,}008$
	7×10^{-3}		$0{,}10_7 \pm 0{,}01$
	10^{-2}		$0{,}16_9 \pm 0{,}02$
	5×10^{-2}		$0{,}17_0 \pm 0{,}02$

Aux concentrations utilisées, le sulfate de cadmium a l'avantage de ne pas absorber à 296 nm. Mais il ne peut être évidemment utilisé en milieu basique. Dans les solutions de pH égal à 14, nous avons dû employer du nitrate de potassium. L'ion nitrate absorbe avec un maximum à 300 nm; il est photostable sous excitation à 313 nm en solution dégazée.

Les rendements quantiques apparaissant dans le tableau 4 sont calculés en tenant compte de l'absorption parasite de NO_3^-. Les ions nitrate à fortes concentrations sont susceptibles de désactiver la fluorescence de l'*o*-phényl-phénolate (fig. 2); mais aux concentrations inférieures à 10^{-2} *M*, cette désactivation reste de faible importance.

Le tableau 4 montre que l'addition de capteur provoque l'augmentation du rendement de photolyse jusqu'à une valeur limite indépendante de la concentration de capteur. Cette valeur limite est généralement supérieure au rendement quantique de disparition du phénol irradié en présence d'oxygène.

Discussion

Aux erreurs expérimentales près, les courbes *a* et *b* de la fig. 1 présentent des points d'inflexion dans le même domaine de pH. On peut donc en conclure que la formation des radicaux phénoxy met en jeu l'état excité singulet de la forme phénolate. C'est d'ailleurs le même mécanisme qui a été proposé par Grabner *et al.* (18) pour le phénol et par Ottolenghi (19) pour le β-naphtol. Ainsi les courbes *a* et *b* permettent d'atteindre le p*K* de l'état excité singulet ($1 < pK^* < 1{,}5$) et celui de l'état fondamental ($pK \simeq 10$).

Si on voulait interpréter la formation des radicaux phénoxy par la déélectronation du niveau triplet de la forme phénolate ou phénol, il faut admettre, compte tenu de l'invariance des rendements quantiques de photo-oxydation ($\phi_0{}^{O_2}$) entre pH = 2 jusqu'à pH = 7, que la durée de vie de l'état triplet de la forme phénolate soit inférieure à 10^{-8} s, soit supérieure à 10^{-2} s. Si la déélectronation était issue du niveau triplet de la forme phénolate, il faudrait admettre que le processus de déélectronation contrôle la durée de vie, et que ce processus est toujours plus rapide que la protonation entre pH = 2 et pH = 7, soit: k_e (constante de déélectronation) $> \overleftarrow{k}[H^+]$, où $\overleftarrow{k}$ est la constante d'un processus contrôlé par la diffusion, et où:

$$[H^+] = \tau = 1/k_e < 10^{-8} \text{ s}$$

Si la déélectronation était issue du niveau triplet de la forme phénol, il faudrait admettre que la population de ce niveau soit indépendante du pH, et donc que la durée de vie du niveau triplet de la forme phénolate soit plus grande que la vitesse initiale de protonation, soit:

$$\tau > \overleftarrow{k}[H^+] \quad \text{où } [H^+] = 10^{-8}$$

$$\tau > 10^{-2} \text{ s}$$

La durée de vie d'un niveau triplet de la forme phénolate ne peut vérifier l'une ou l'autre de ces deux inégalités.

On constate que l'excitation directe de la forme phénolate est beaucoup plus efficace pour la production des radicaux phénoxy que l'excitation de la forme phénol dans le domaine de pH où se produit la déprotonation du niveau excité singulet. On peut interpréter ce résultat en admettant que la déélectronation se produit sur les niveaux vibrationnels excités (photo-ionisation) alors que l'équilibre de déprotonation se produit sur les niveaux vibrationnels les plus bas. La même hypothèse a été avancée pour le β-naphtol par Goldschmidt et Stein (24).

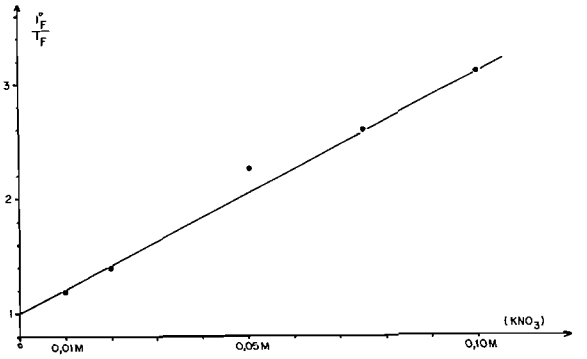


FIG. 2. Etude de l'extinction de fluorescence de l'*o*-phényl-phénolate par le nitrate de potassium. Variations du rapport I_F^0/I_F en fonction de la concentration de nitrate de potassium (KNO_3). (I_F^0 est l'intensité à 413 nm de fluorescence de l'*o*-phényl-phénolate et I_F l'intensité de fluorescence en présence de nitrate de potassium.)

Can. J. Chem. Downloaded from www.nrcresearchpress.com by 210.87.254.105 on 09/05/12
For personal use only.

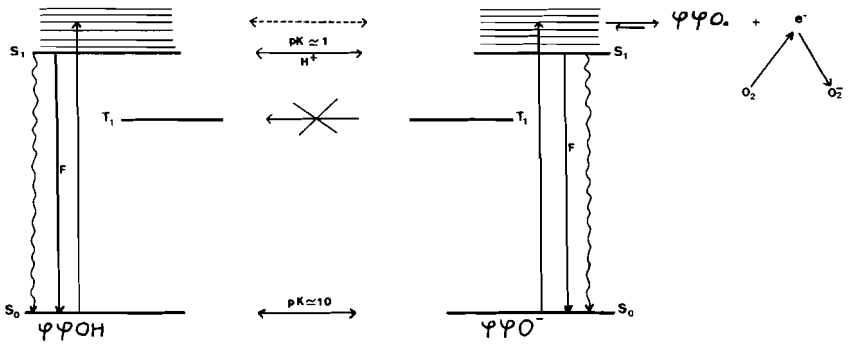


FIG. 3. Diagramme énergétique illustrant le mécanisme de production des radicaux phénoxy.

La fig. 3 résume le mécanisme de formation des radicaux phénoxy assisté par l'oxygène. Les radicaux apparaissent à la suite de déprotonation et de déélectronation successive dans les états excités. L'oxygène qui ne peut intervenir sur les états excités singulets pourrait alors augmenter le rendement quantique de disparition de l'*o*-phényl-phénol en solution aérée, en inhibant la recombinaison de l'électron solvaté et des radicaux phénoxy. Cette hypothèse est confirmée par l'influence des capteurs d'électrons utilisés.

L'introduction d'ions Cd^{2+} et NO_3^- entraîne effectivement l'augmentation de la vitesse de disparition de l'*o*-phényl-phénol en inhibant la recombinaison radical–électron. A une concentration de Cd^{2+} supérieure à 10^{-4} *M*, et à une concentration de NO_3^- supérieure à 10^{-2} *M*, le rendement quantique de photolyse devient indépendant de la concentration de capteur. Dans ces conditions, tous les électrons éjectés sont piégés par les capteurs Cd^{2+}, NO_3^- et le rendement de formation des radicaux phénoxy, égal d'ailleurs au rendement de photo-éjection, peut alors être atteint. Aux concentrations d'oxygène dissous dans l'eau, $[O_2] = 3 \times 10^{-4}$ *M* (25), la capture des électrons est pratiquement totale. La disparition du phénol irradié en solution aérée peut être simplement justifiée par le processus photochimique primaire. Il n'est donc pas nécessaire de supposer que le phénol disparaisse par une réaction thermique secondaire mettant en jeu soit O_2^-, soit des radicaux phénoxy.

En conclusion, l'excitation de la forme neutre de l'*o*-phényl-phénol dans son premier état excité singulet donne lieu successivement à une déprotonation, puis à une déélectronation. La présence d'oxygène augmente la vitesse de production de radicaux phénoxy disponibles; l'oxygène, comme les ions Cd^{2+} ou NO_3^- inhibe la recombinaison des électrons éjectés avec les radicaux phénoxy. Nous examinons actuellement la généralisation de ce mécanisme aux autres dérivés phénoliques.

1. (*a*) L. I. GROSSWEINER, G. W. SWENSON et E. F. ZWICKER. Science, 141 (1963); 805 (1963); 1042 (1963); 1180 (1963); (*b*) G. DOBSON et L. I. GROSSWEINER. Trans. Faraday Soc. **61**, 708 (1965); (*c*) L. I. GROSSWEINER. Photophysiology, **5**, 1 (1970).
2. J. FEITELSON, E. HAYON et A. TREININ. J. Am. Chem. Soc. **95**, 1025 (1973).
3. H. I. JOSCHEK et S. I. MILLER. J. Am. Chem. Soc. **88**, 3269 (1966); **88**, 3273 (1966).
4. M. COCIVERA, M. TOMKIEWICZ et A. GROEN. J. Am. Chem. Soc. **94**, 6598 (1972).
5. J. C. MIALOCQ, J. SUTTON et P. GOUJON. J. Chem. Phys. Sous presse.
6. J. AUDUREAU, C. FILIOL, P. BOULE et J. LEMAIRE. J. Chim. Phys. **73**, 613 (1976).
7. G. PERBET, L.-M. COULANGEON, P. BOULE et J. LEMAIRE. J. Chim. Phys. **75**, 1096 (1978).
8. G. PERBET, C. FILIOL, P. BOULE et J. LEMAIRE. J. Chim. Phys. **76**, 89 (1979).
9. G. PERBET. Thèse de 3o cycle. Photolyse et photo-oxydation de dérivés phénoliques en solution aqueuse diluée. Université de Clermont II. 1979.
10. W. PALMER. Experimental physical chemistry. Cambridge University Press. 1954. p. 231.
11. J. G. CALVERT et J. N. PITTS. Photochemistry. Wiley. 1966. p. 783.
12. E. L. WEHRY et L. B. ROGERS. Spectrochim. Acta, **21**, 1976 (1965).
13. A. WELLER. Progress in reaction kinetics. Vol. 1. *Edité par* G. Porter. Pergamon Press. 1961. p. 189.
14. N. M. TRIEFF et B. R. SUNDHEIM. J. Phys. Chem. **69**, 2044 (1965).
15. TH. FÖRSTER. Z. Elektrochem. **54**, 531 (1950).
16. TH. FÖRSTER. Z. Elektrochem. **54**, 42 (1950).
17. J. JORTNER, M. OTTOLENGHI et G. STEIN. J. Am. Chem. Soc. **85**, 2712 (1963).
18. G. GRABNER, G. KÖHLER, J. ZECHNER et N. GETOFF. Photochem. Photobiol. **26**, 449 (1977).
19. M. OTTOLENGHI. J. Am. Chem. Soc. **85**, 3557 (1963).
20. J. H. BAXENDALE, E. M. FIELDEN et J. P. KEENE. Proc. R. Soc. London, A**286**, 320 (1965).
21. R. K. WOLFF, J. E. ALDRICH, T. L. PENNER et J. W. HUNT. J. Phys. Chem. **79**, 210 (1975).
22. J. E. ALDRICH, M. J. BRONSKILL, R. K. WOLFF et J. W. HUNT. J. Chem. Phys. **55**, 538 (1971).
23. C. D. JONAH, J. R. MILLER, E. J. HART et M. S. MATHESON. J. Phys. Chem. **79**, 2705 (1975).
24. C. R. GOLDSCHMIDT et G. STEIN. Chem. Phys. Lett. **6**, 299 (1970).
25. S. L. MUROV. Handbook of photochemistry. M. Dekker Inc., New York, NY. 1973. p. 89.

Can. J. Chem. Downloaded from www.nrcresearchpress.com by 210.87.254.105 on 09/05/12
For personal use only.

The kinetics of internal energy randomisation in thermal unimolecular reactions

HUW OWEN PRITCHARD

Centre for Research in Experimental Space Science, York University, Downsview, Ont., Canada M3J 1P3

Received March 20, 1980

HUW OWEN PRITCHARD. Can. J. Chem. **58**, 2236 (1980).

The aim of this paper is to present a minimal theory of thermal unimolecular reactions, including explicitly the kinetics of intramolecular randomisation processes. A quasi-diatomic model is formulated and, within the framework of the model, both first- and second-order randomisation processes among reactant and product states are examined.

It is concluded that a vital mechanism for the intramolecular energy randomisation in thermal unimolecular reactions is a collisional one. On this assumption, a straightforward derivation of the Polanyi–Wigner specific rate function, as we have reinterpreted it, becomes possible.

At the same time, anomalies in the fall-off curves for the thermal isomerisations of methyl isocyanide and ethyl isocyanide can be accounted for very simply: in the former case, values for both the first- and second-order randomisation rate constants can be derived, but in the latter case it is only possible to establish a lower limit for the second-order randomisation rate constant.

HUW OWEN PRITCHARD. Can. J. Chem. **58**, 2236 (1980).

Cet article a pour but de présenter une théorie minimale des réactions unimoléculaires thermiques incluant explicitement la cinétique du mode de distribution au hasard intramoléculaire. On formule un modèle quasi-diatomique et on examine à l'intérieur du squelette de ce modèle le mode de distribution au hasard d'ordre 1 et d'ordre 2 entre les réactifs et les produits.

On conclut que le méchanisme essentiel de l'énergie intramoléculaire de la distribution au hasard dans des réactions thermiques unimoléculaires est un mécanisme de collision. Sur cette base, il devient possible de dériver directement la fonction de vitesse spécifique de Polanyi–Wigner telle que nous l'avons réinterprété.

En même temps, on peut simplement tenir compte des anomalies dans l'abaissement des courbes des isomérisations thermiques des isocyanures de méthyle et d'éthyle: dans le premier cas, les valeurs des constantes de vitesse d'ordre un et d'ordre deux de la distribution au hasard peuvent être dérivées mais dans le second cas on peut seulement établir une limite inférieure pour la constante de vitesse d'ordre deux de la distribution au hasard.

[Traduit par le journal]

I. Introduction

We have recently reformulated the original concept of Polanyi and Wigner (1) in discrete rather than in classical terms, and have found that it is possible to make very simple calculations of the specific rate constants for thermal unimolecular reactions (2). This reformulation presupposes a knowledge of the vibrational and rotational properties of the reactant molecule and the energy barrier for the reaction, and just simply by classifying states as reactive or unreactive, calculations of specific rate constants superior to any hitherto obtained are possible. It appears, therefore, that despite all the emerging complexities in the descriptions of highly vibrationally excited molecules resulting from contemporary laser studies, it is nevertheless possible to present a very simple description of thermal unimolecular reactions. In the following pages, I will present a very simple model for a thermal unimolecular reaction, including *explicit* consideration of the intramolecular randomisation processes; moreover, I hope that the extreme simplicity of the model will lend itself to a ready identification of the implicit assumptions, so that they can be thoroughly examined as and when necessary in the future.

II. List of Symbols

Table 1 is a list of symbols used in this presentation: where numerical values of the represented quantities are used in this paper, units are given if necessary.

III. A Quasi-diatomic Model for Thermal Unimolecular Reactions

Imagine a polyatomic molecule isolated in space, in an infinitely large box whose walls have a temperature of absolute zero: i.e. the molecule is in a perfectly field-free space. The molecule is vibrationally and/or rotationally excited to some energy which is *below* the lowest threshold for any reaction; the molecule's translational energy is, of course, immaterial. In this energy range, the molecule has available to it a series of non-adiabatic states; each of these states has a *nodeless* vibrational wave function (3, 4), regardless of the degree of vibrational excitation. For CO_2, there will be about 3×10^5 states per wavenumber just below the reaction threshold, and comparable figures for methyl isocyanide or cyclobutane are about 1×10^8 or 2×10^{15} states per wavenumber respectively (these state densities are estimated for adiabatic states, but

0008-4042/80/212236-10$01.00/0

©1980 National Research Council of Canada/Conseil national de recherches du Canada

Can. J. Chem. Downloaded from www.nrcresearchpress.com by 210.87.254.40 on 09/05/12
For personal use only.

Can. J. Chem. Downloaded from www.nrcresearchpress.com by 210.87.254.40 on 09/05/12
For personal use only.

the density of non-adiabatic states will be very similar). At this point, we assume these non-adiabatic states are strictly orthogonal (whatever that may mean) to each other, they are infinitely narrow, they are all distinct, and therefore they cannot change into each other without external influence. We then have to consider the influences which can broaden these states, cause them to overlap, and thus change into each other. Given our premise of quasi-diatomic non-adiabatic and non-interacting states, there are only two kinds of external influence we can consider; radiation broadening, i.e. first-order processes, and collisional broadening, i.e. second-order process.

Since the inception of the theory of unimolecular reactions more than 50 years ago, it has been axiomatic that internal energy randomisation was a property of the reacting molecule *itself* — hence the term intramolecular — although there have been a few tentative suggestions in recent years (5–8) that such randomisation could be a collisional process. It is not the purpose of this paper to try to make theoretical predictions of the respective time scales for such processes; rather, it is to recognise that both first- and second-order randomisation processes *may* play a part, and to examine the consequences in respect of the observed overall kinetics. Thus, for the time being, I will make only very brief allusion to the intrinsic nature of these two classes of randomisation processes:

First-order Processes

Even in the rigorous absence of an imposed electromagnetic field, there is a broadening of the levels due to spontaneous emission. In principle therefore, the conversion of one state into an adjacent state can be described by spontaneous emission followed by reabsorption of the same quantum (9); likewise, in the normal presence of ambient black body radiation, stimulated radiative interconversions of a similar type will not be negligible. Whether or not there are, in addition, any "spontaneous" mechanisms within the framework of this model will remain to be seen as the ideas of Czub and Wolniewicz (3) are extended to polyatomic molecules. Nevertheless, it seems fairly well established that in the energy range of interest (i.e. just above reaction threshold),[1] we should expect to find first-order randomisation processes taking place with rate constants $\mu_1 \approx 10^{12}\ s^{-1}$ (8).

Second-order Processes

If we examine the Lennard–Jones interactions between a pair of typical organic molecules (10), we find that they exceed the spacing between the molecular energy levels, even at very considerable distances. For example, typical values of the interaction potential $V(\bar{r})$ at the mean intermolecular separation $\bar{r}$ are

p (Torr)	$\bar{r}$ (Å)	$V(\bar{r})$ (cm^{-1})
1000	30	2.5×10^{-1}
1	300	2.5×10^{-7}
10^{-3}	3000	2.5×10^{-13}

In theory, at least, it is possible to calculate the changes in the energy levels of a molecule due to the interaction $V(\bar{r})$, but at the present time, we have no basis for correlating the magnitudes of these shifts with the magnitude of $V(\bar{r})$, since such calculations are totally intractable. A cautious view would be that if $V(\bar{r}) > [\rho(E)]^{-1}$, then collisional scrambling is a possibility. Figure 1 shows a plot indicating the pressures at which $V(\bar{r})$ equals $[\rho(E)]^{-1}$ for various molecules — in other words, the threshold for the scrambling of energy levels within the molecule by pressure broadening; the points shown on this graph correspond to the mean spacings between states at the thermal threshold, and are therefore a guide for consideration in thermal reactions — other values of the spacings would have to be used at other energies, i.e. for chemical activation experiments, or for molecular states below threshold. I regard it as axiomatic that $\rho(E)$ in this context is the total density of rotational and vibrational states, since the randomising collisions, by definition, have large impact parameters and there seems to be no reason

[1]Of course, for the consideration of thermal reactions, it does not matter *at all* whether randomisation takes place *below* the thermal threshold. Above threshold, it is normal to ascribe a width to each state having a finite lifetime with respect to predissociation. These widths are very large indeed in the present model — for example, the bending mode of methyl isocyanide ($\nu = 263\ cm^{-1}$) has an equivalent width above threshold of $\Gamma = 263/\pi \approx 85\ cm^{-1}$. Such broad states would overlap with many, many millions of passive molecular states, and this could be regarded as a built-in mechanism for randomisation. I suspect that this is not so, and that these widths may only have meaning within the context of a collision experiment: in other words, if we fire the two molecular fragments towards each other and observe a phase shift; alternatively, if the rupture has taken place and we try to make observations on the trajectories of the two fragments in an attempt to deduce the initial energy. Whether or not these overlaps actually constitute a mechanism for randomisation within the framework of the quasi-diatomic model is not obvious; it would seem however, that unlike collisional randomisation, all first-order randomisation processes will be restricted by optical selection rules and/or conservation of angular momentum to either zero or small change in rotational quantum number.

Can. J. Chem. Downloaded from www.nrcresearchpress.com by 210.87.254.40 on 09/05/12
For personal use only.

TABLE 1. List of symbols and their definition

Symbol	Definition
a_{ij}	Relaxation matrix (as defined in eq. [1] or [2]). Units: s^{-1}
c	Velocity of light
d, d_k	Rate constant for decay to products from a single state k. Units: s^{-1} (only two values allowed, either $d_k = 0$ or $d_k = d = 2cv\ s^{-1}$)
δ	Mean lifetime of an "active" state ($=d^{-1}$). Units: s
δ_{ij}	Kronecker delta
E	Energy (usually in the continuous representation). Units: cm^{-1}
E_∞	Activation energy at infinite pressure. Units: cm^{-1}
ε_k	Energy of kth microscopic level. Units: cm^{-1}
g_k	Degeneracy of kth microscopic level
k	Boltzmann's constant
$k(E)$	Specific rate constant for decay to products at energy E (continuous representation). Units: s^{-1}
k_i	Effective rate constant for decay to products from ith energy grain. Units: s^{-1}
k_{uni}	Overall unimolecular rate constant. Units: s^{-1}
m_k	Fraction of the reactant molecules *within one grain* in the kth energy level. Units: normalised such that $\sum m_k = 1$
$\tilde{m}_k$	Equlibrium value of m_k
[M]	Concentration of inert gas molecules
μ	Conventional collisional relaxation rate constant. Units: when this symbol appears in an equation, the units are always s^{-1}; however, in the text, it always represents the second-order rate constant for relaxation, in $Torr^{-1}\ s^{-1}$
μ_1	First-order rate constant for randomisation *within a specified grain*. Units: s^{-1}
μ_2	Second-order rate constant for randomisation *within a specified grain* via long-range interaction. Units: see μ
μ_r	Randomisation rate constant, $r = 1$ or 2 as appropriate
n_i	Fraction of the reactant molecules in the ith energy grain. Units: normalised such that $\sum n_i = 1$
$\tilde{n}_i$	Equilibrium value of n_i
ν	Frequency of critical vibration. Units: cm^{-1}
P	Pressure. Units: Torr
p_{ij}	Probability, per collision, of a transition *from* state i *to* state j in the reactant molecule
$Q(T)$	Partition function (rotation–vibration)
$\bar{r}$	Mean intermolecular separation at pressure P
$\rho(E)$	Density of states (continuous representation)
Σ'	Summation over only those states having non-zero decay rate constants
t	Time
T	Temperature
$V(r)$	Long-range intermolecular interaction potential
Z	Gas-kinetic collision number
Z'	Collision number for bimolecular randomisation processes

why significant redistribution of angular momentum should not take place, even though the total energy interchange is minute. In the light of Fig. 1, the conclusion reached below that the second-order randomisation rate constant, μ_2, appears to increase with increasing state density is not surprising. I might add also that theories of pressure broadening

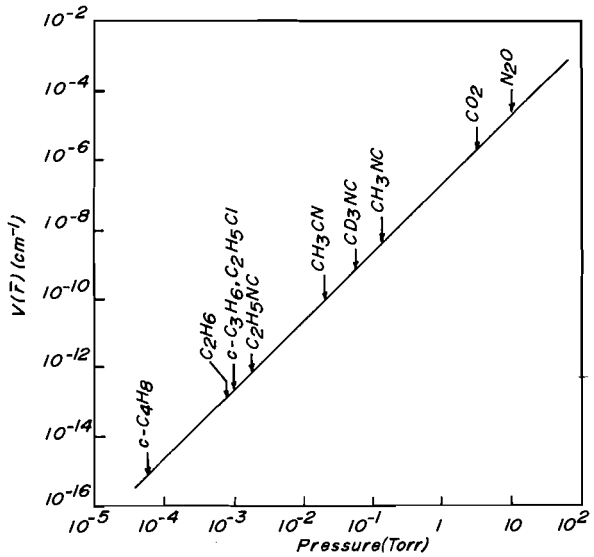


FIG. 1. Thresholds for internal energy randomisation. The arrows mark the pressures above which the estimated intermolecular potential exceeds the mean spacing between the molecular energy levels.

are reasonably well advanced, and that it may well be possible to make better empirical estimates of these thresholds than those depicted here.

IV. Summary of Existing Formulation

The following is a brief summary of our recent master-equation formulation of thermal unimolecular reactions (11), presented simply to introduce the required notation. The reactant molecule X was considered to possess a denumerable set of rotation–vibration states whose populations at thermal equilibrium are denoted by $\tilde{n}_i$, with normalisation such that $\sum \tilde{n}_i = 1$. Transitions among the various states are induced by collisions with inert molecules M: the collision number between X and M is Z and p_{ij} represents the probability per collision of a transfer *from* state i *to* state j. This relaxation process may be characterised by solving for the eigenvalues and eigenvectors of the relaxation matrix

$$[1]\quad a_{ij} = Z[\mathrm{M}]\left\{(1-\delta_{ij})p_{ji} - \delta_{ik}\sum_k (1-\delta_{ik})p_{ik}\right\}$$

The reaction is regarded as a perturbation of this relaxation process: above the thermal threshold, spontaneous decay to products may occur from various states with rate constants k_i, and the overall rate constant k_{uni} is given by the shift in the absolute magnitude of the zero eigenvalue of [1]. In the special case where the p_{ij} are taken to be the strong- or scaled strong-collision probabilities (12, 13) viz.

$$[2]\quad a_{ij} = \mu\{(1-\delta_{ij})\tilde{n}_i - \delta_{ij}(1-\tilde{n}_i)\}$$

Can. J. Chem. Downloaded from www.nrcresearchpress.com by 210.87.254.40 on 09/05/12
For personal use only.

it is possible to write the expression for k_{uni} in a very simple form (14), i.e.

$$[3] \quad k_{uni} = \frac{\mu\sum\tilde{n}_i k_i(\mu + k_i)^{-1}}{1 - \sum\tilde{n}_i k_i(\mu + k_i)^{-1}}$$

where μ is the rate constant for the internal relaxation (equivalent to $\lambda Z[M]$ in conventional treatments, λ being the "collision efficiency"). Equation [3] (since it is identical with the more cumbersome expressions we gave earlier) reproduces the fall-off curves for many thermal unimolecular reactions with high precision (11).

V. Derivation of the Quantised Form for the Specific Rate Function

We showed recently that reformulation in quantum terms of the original idea of Polanyi and Wigner (1) leads to remarkably good predictions for the specific rate functions $k(E)$ for simple unimolecular reactions (2). The formulae we proposed were evolved by intuitive reasoning, and no attempt was made at a theoretical justification: however, within the framework of the quasi-diatomic model, it is a simple matter to derive the basic formula used. The essence of the reformulation was that if more energy than the critical energy is to be found in a certain assumed critical vibration, the molecule will react within that vibrational period, but if the molecule possesses the same amount of energy distributed in any other fashion, it is unreactive: the specific rate constant is then simply the time constant for the vibrational disruption multiplied by the ratio of the "active" to the "passive" states.

Within the framework of the quasi-diatomic model, we can make a simple distinction between these active and passive states: an active state is one for which the vibrational motion will carry the system irrevocably into nuclear configurations which can be classed as products; a passive state on the other hand is one in which the motion is confined by the generalised internuclear potential at all extremes to nuclear configurations which can only be classed as reactant. We need not specify at this stage the mechanisms by which the intramolecular relaxation takes place, so that passive states are converted into active states, and vice-versa; we will assume, however, on the basis of the arguments given above, that there is a collisional component which will dominate at sufficiently high pressure.

We write the master equation for the *overall* reaction as

$$[4] \quad \frac{dn_i}{dt} = [M]Z\sum_j [p_{ji}n_j - p_{ij}n_i] - k_i n_i$$

where n_i now denotes the population in group of adjacent energy levels which form a "grain" within the calculation. This grain (above threshold) comprises two kinds of states, those whose motions are bounded at all extremities, and have infinite lifetime, and those which will transform the molecule into products within the period of the vibration: all these latter states have the same lifetime of $(2c\nu)^{-1}$ s, where ν is the frequency of the vibration in wavenumber units.

We now examine the relaxation in competition with the decay processes *within* the grain. We may write another master equation for the grain itself as

$$[5] \quad \frac{dm_k}{dt} = [M]Z'\sum_l [p_{lk}m_l - p_{kl}m_k] - d_k m_k$$

where Z' is the collision number appropriate to the long-range encounters which cause randomisation (estimated for example from arguments such as depicted in Fig. 1), and d_k is the rate constant for decay of the specific state, which is either zero for a passive state, or $d = 2c\nu\ s^{-1}$ for an active state. We may also accept intuitively that the transition probabilities p_{lk} etc. are strong collision probabilities, as would be defined by an expression analogous to eq. [2], but with a relaxation rate constant μ_2. The rate constant for decay from the grain therefore becomes the same (provided that $\sum\tilde{m}_k$ is renormalised to unity) as the strong collision expression for the unimolecular rate constant, eq. [3], viz.,

$$[6] \quad k_i = \frac{\mu_2\sum\tilde{m}_k d_k(\mu_2 + d_k)^{-1}}{1 - \sum\tilde{m}_k d_k(\mu_2 + d_k)^{-1}}$$

which simplifies[2] enormously when all the d_k are either zero or d to a simple Lindemann form (15)

$$[7] \quad k_i = \frac{\mu_2 d\sum'\tilde{m}_k}{\mu_2 + d - d\sum'\tilde{m}_k}$$

where $\sum'$ denotes the summation over only those states k for which $d_k \neq 0$. Assuming we are at the high-pressure limit *with respect to the randomisation process*, then k_i for the grain becomes simply $d\sum'\tilde{m}_k$, i.e. d times the fraction of states within the grain which decay with time constant d. Hence, for each grain i, we are justified in identifying its decay rate constant k_i with the quantity $d\sum'\tilde{m}_k$ at the energy of the ith grain.

Now, since the energy difference across the grain

[2]One may have to be careful about the use of this formula, which is only valid when γ (the eigenvalue) $\ll \mu$ (the relaxation rate), which is *usually* the case. The exact solution for γ is (16)

$$\gamma[(\gamma - \mu) - d(1 - \sum'\tilde{m})] = (\gamma - \mu)d\sum'\tilde{m}$$

which easily reduces to [7] when $\gamma \ll \mu$; otherwise, the correct solution is

$$\gamma = \tfrac{1}{2}[(\mu + d) - \{(\mu + d)^2 - 4\mu d\sum'\tilde{m}\}^{1/2}]$$

Can. J. Chem. Downloaded from www.nrcresearchpress.com by 210.87.254.40 on 09/05/12
For personal use only.

is infinitesimal, all states in the grain have the same Boltzmann factor $\exp(-\varepsilon_k/kT)$, whence $\tilde{m}_k = g_k/\sum g_k$, i.e. $d\sum' \tilde{m}_k = d\sum' g_k/\sum g_k$. Thus, k_i becomes $d\sum' g_k/\sum g_k$, or in continuous terms $d\rho_{n-1}'(E - E_\infty)/\rho(E)$ which is the simplest form used in ref. 2, i.e. eqs. [6*a*] and [7*a*] of that paper.

VI. Randomisation Kinetics

Equations [4]–[7] provide a direct method for incorporating the kinetics of randomisation into the calculation of the specific rate constant k_i: if the randomisation rate constant μ_2 is very large, then k_i is simply $d\sum' g_k/\sum g_k$ as we have suggested before (2), but if μ_2 becomes rate-limiting, then a lower effective value of k_i from eq. [7] ensues. Moreover, although we have written eq. [7] on the assumption of second-order randomisation processes only, with μ_2 proportional to pressure, we can also use [7] to introduce first-order randomisation processes simply by keeping the relaxation rate constant μ_1 = constant, independent of pressure.

At the moment, the formulation of k_i we have given above and in ref. 2 is very primitive, and the precise rules for its proper implementation have yet to be worked out. Consequently, for the practical calculations reported below, it is preferable to use the most accurate specific rate functions attainable, i.e. the Slater–Forst specific rate function (2, 11), slightly reinterpreted in the light of this new formulation. Thus, I will identify the term $d\sum' \tilde{m}_k$ in [7] with the Slater–Forst specific rate function $k(E)$, whence the rate constant for decay from a grain becomes

$$[8] \quad k_i = \mu_r k(E)/(\mu_r + 2c\nu - k(E))$$

where μ_r is the randomisation rate, either first- or second-order as appropriate (cf. Section II above for explanation concerning the units of μ_r); I will also assume for the time being that μ_r remains the same from grain to grain, although I will conclude below that μ_2 is probably a function of state density — a problem for examination at a later date.

Figure 2 shows the results of assuming only first-order randomisation processes to be operative, using the methyl isocyanide isomerisation reaction as an example. The top curve is the standard fall-off curve, which corresponds to an essentially infinite rate of randomisation, and the other four curves, in descending order, correspond to fixed values for the randomisation rate constants of 10^{13}, 10^{12}, 10^{11}, and 10^{10} s^{-1} respectively. All the curves merge at infinitely low pressure: this is because, from [8], $k_i = \mu_1 \times \alpha_i$, whence substitution into [3] gives the usual expression for the low-pressure limiting overall rate, but a different high-pressure rate for each value of μ_r.

Figure 3 shows the results of a similar calculation,

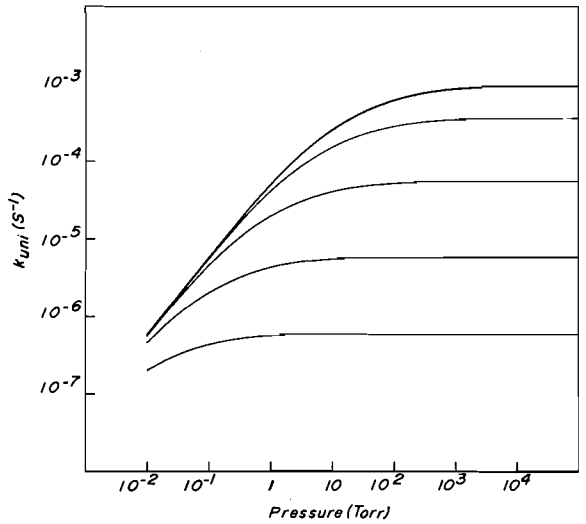


FIG. 2. Fall-off curves for the thermal isomerisation of methyl isocyanide at 230.4°C considering only first-order randomisation processes. In descending order, the curves correspond to values of $\mu_1 = \infty$, 10^{13}, 10^{12}, 10^{11}, and 10^{10} s^{-1} respectively.

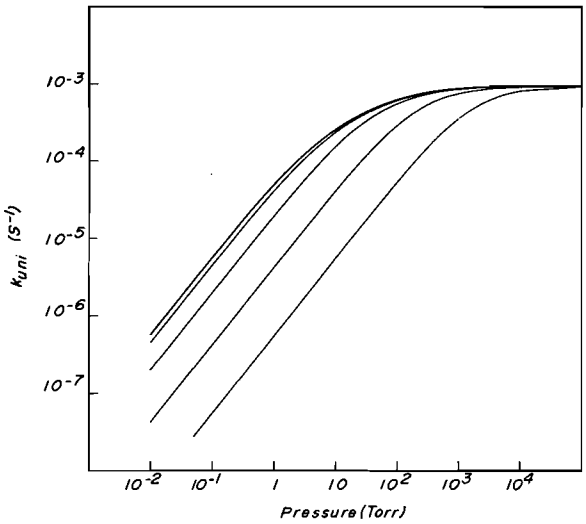


FIG. 3. Fall-off curves for the thermal isomerisation of methyl isocyanide at 230.4°C considering only second-order randomisation processes. In descending order, the curves correspond to values of $\mu_2 = \infty$, 10^{13}, 10^{12}, 10^{11}, and 10^{10} $Torr^{-1}$ s^{-1} respectively.

but this time assuming that only second-order randomisation processes are operative, with rate constants (again independent of total energy), in descending order, of 10^{13}, 10^{12}, 10^{11}, and 10^{10} $Torr^{-1}$ s^{-1} respectively; again, the topmost curve is the standard fall-off curve corresponding to an essentially infinite randomisation rate constant. Again, inspection of [8] shows how this behaviour arises: μ_r is now identified as μ_2 which is proportional to pressure,

Can. J. Chem. Downloaded from www.nrcresearchpress.com by 210.87.254.40 on 09/05/12
For personal use only.

whence at high pressure, $k_i = k(E)$ and the normal high-pressure limiting rate ensues from [3]. The low-pressure limiting rate for k_i from [8] is however βP, and substitution of this into [3] gives a different low-pressure limit for the overall rate for each value of β, i.e. for each value of μ_2.

Notice that neither first-order nor second-order randomisation gives rise to false high-pressure limits (i.e. plateaux in the overall rate constant at intermediate pressures), such as have been postulated on several occasions (8, 17–19) on the basis of less rigorous arguments.

VII. An Assumption

Unimolecular reaction theories in the past have always accepted that the rate constant at the high-pressure limit was given by the sum $\sum \tilde{n}_i k_i$, or its continuous equivalent $[Q(T)]^{-1}\int \rho(E)k(E)\,dE$: it is also implicit that k_i or $k(E)$ are "natural" rate constants, i.e. not rate-limited by "hidden" processes such as randomisation. The results of the preceding section show that if only first-order randomisation is allowed, we can never realise this high-pressure limit unless the first-order randomisation rate constant is infinite, which is untenable: thus, second-order randomisation is a necessity in order to achieve the conventional high-pressure limiting rate constant.

In addition, in deference to the universally held belief that first-order randomisation processes are a reality (8), I will accept that there is also a first-order component, guaranteeing that we also approach the conventional magnitude of $\mu\sum'\tilde{n}/(1 - \sum'\tilde{n})$ for the limiting value of the low-pressure rate constant: second-order randomisation alone would not allow this.

Thus, in fact, we have a twin postulate, that *both* first- and second-order randomisation processes must be invoked in any rigorous treatment of thermal unimolecular reactions.

VIII. Randomisation among Product States

The arguments I have presented so far consider only randomisation amongst the reactant states but, of course, randomisation amongst product states will also occur and, in fact, in isomerisation reactions such randomisation is vital in the quasi-diatomic model for the reaction to occur.

If we consider the isomerisation of methyl isocyanide again, we may represent a quasi-diatomic potential for this process in some such generalised form as shown in Fig. 4. The shaded portion on the left side represents all those passive states whose motions are confined entirely within the reactant configuration space, and on the right side, we have all those passive states lying within the product configuration space. Since this reaction is strongly

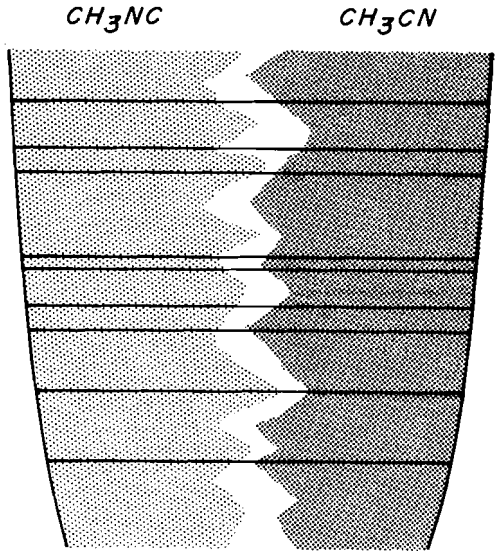


FIG. 4. Schematic pseudo-potential for the isomerisation of methyl isocyanide to methyl cyanide. The lightly shaded portion on the left represents passive states which lie entirely within the *reactant* configuration space: there are roughly 1.9×10^8 such states per wavenumber just above threshold. The more heavily shaded portion on the right represents passive states which lie entirely within the *product* configuration space: there are roughly 1.1×10^{10} such states per wavenumber in this energy range. The solid lines represent the active states, or connecting states, i.e. those states for which the molecule makes excursions through both reactant and product configurations within one vibrational period: these are fewer than 100 such states per wavenumber just above threshold, but the density of such states increases rapidly with increasing energy.

exothermic, there are many more product states than reactant states at any particular value of the total energy: nevertheless, all states are *bound* in the sense that none of them is connected with a translational continuum. The solid lines on this diagram represent those states which are common to reactant and product: according to our previous arguments (2), these are states with more than about 50 quanta in the C—N—C bending mode of the reactant, or because of microscopic reversibility, they also correspond exactly to a series of C—C—N bending states of the product. Consequently, a methyl isocyanide molecule is not transformed into a methyl cyanide molecule simply by the accumulation of more than 50 quanta in this certain vibration, since although it will have all the spatial attributes of a cyanide molecule half a vibrational period later, it will have reverted to an isocyanide molecule after another half-period. Thus, unless "fixed" as cyanide by randomisation processes, "reaction" does not take place.

Let us suppose for the moment that randomisation rate constants are equal in both the reactant and

Can. J. Chem. Downloaded from www.nrcresearchpress.com by 210.87.254.40 on 09/05/12
For personal use only.

product configuration, and that only second-order randomisation is important. Figure 5 depicts the decay from an assembly of states, initially normalised to unity, and with the origin of the horizontal axis coincident with the transition from the left-hand to the right-hand side of Fig. 4. For the first half-vibration, i.e. $\delta = (2cv)^{-1}$ s, systems are "killed" to product states with the randomisation rate constant μ_r: then for the next period of δ seconds, the vibrational excursion is through *reactant* configurations and during this time the molecule will be randomised to reactant states, and so on. Thus, the total chance of ending up as product is the ratio of the sum of the unshaded strips to the total area, viz.

$$[9] \quad \text{Fraction} = \frac{\sum_{n=0}^{\infty} \int_{2n\delta}^{(2n+1)\delta} \exp(-\mu_r t)\, dt}{\int_0^{\infty} \exp(-\mu_r t)\, dt}$$

If $\mu_r \gg 2cv$, this ratio is 1, and if $\mu_r \ll 2cv$, it is 0.5. Figure 6 shows the form of the overall reaction rate for values of the randomisation rate constant of, in descending order, 10^{13}, 10^{12}, 10^{11}, and 10^{10} $\text{Torr}^{-1}\,\text{s}^{-1}$, respectively. In this case, both limiting rates are the usual ones: the high-pressure rate because $k_i = d\sum' g_k$ as usual, and the low-pressure rate because, although $k_i = 0.5d\sum' g_k$, the overall rate, by eq. [3], is independent of k_i in the limit.

If, on the other hand, we had chosen to perform the calculation for first-order randomisation only, a series of curves like those shown in Fig. 2 would have been obtained, except that the lowest one of the

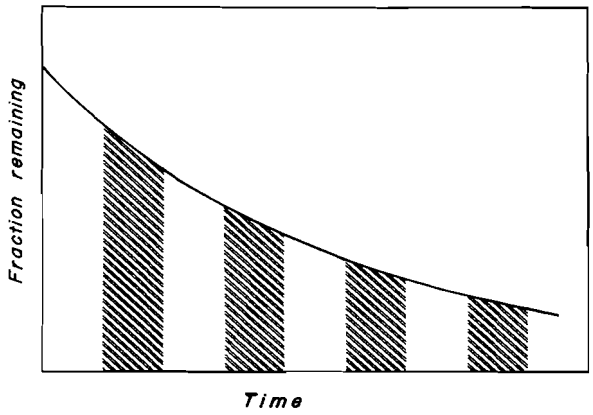


FIG. 5. Representation of the rate of stabilisation of interesting molecules by randomisation when the randomisation rate constant is the same in both reactant and product manifolds. The unshaded portions represent the vibrational half-periods when the nuclear excursions are through product configurations, and the shaded portions represent the vibrational half-periods when the nuclear configurations have the characteristics of the reactant molecule.

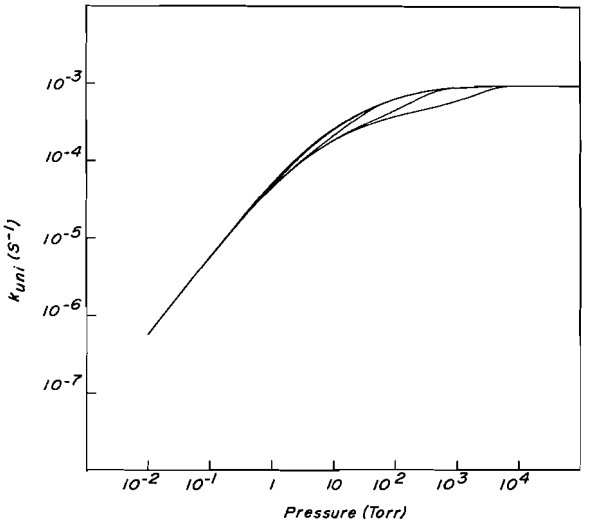


FIG. 6. Fall-off curves for the thermal isomerisation of methyl isocyanide at 230.4°C considering only second-order randomisation in both reactant and product manifolds. In descending order, the curves correspond to $\mu_2 = \infty$, 10^{13}, 10^{12}, 10^{11}, and 10^{10} $\text{Torr}^{-1}\,\text{s}^{-1}$ respectively.

set (i.e. for $\mu = 10^{10}\,\text{s}^{-1}$) would have a high pressure limiting rate just a little more than half the normal high-pressure rate.

As we will show below, the randomisation rate constant — at least the second-order one — appears to be a function of the density of state in the vicinity of the level being considered. Consequently, it is only for thermoneutral or endothermic isomerisation reactions that such manifestations of *product* non-randomisation might be observed — assuming, since we have yet to establish it below, that the effect of non-randomisation can be observed at all in thermal reactions.

When we turn to fragmentation reactions, the situation is rather different. In these cases, the right-hand wall of the pseudo-potential in Fig. 4 is absent, and hence, once the system emerges into the right-hand side representing product configurations, fragmentation is irrevocable. The particles are now moving with momenta such that, in the absence of external influences, they will inevitably recede to infinity: our picture of a randomising event is that it is something rather weak — in other words, it may change the energy of the system very slightly, but it can never *reverse* the total relative momentum (or momenta if we include rotation) of the two massive fragments; this could only be done by a *collision* in the normal sense, and this constitutes the back-reaction. Thus, product randomisation, although it will take place, will have no effect upon the *rate* of unimolecular fragmentation reactions.

Can. J. Chem. Downloaded from www.nrcresearchpress.com by 210.87.254.40 on 09/05/12
For personal use only.

IX. A Summary of the Experimental Data for Methyl Isocyanide

The landmark experimental results of Schneider and Rabinovitch (20, 21) on the thermal isomerisation of methyl isocyanide have been compared with theory on a number of occasions (11, 20–24) and the conclusion has always been that the theory does not exactly match the experimental results to the same degree that it does for (say) the isomerisation of cyclopropane (11). The discrepancies are similar (20) at each of the three temperatures studied by Schneider and Rabinovitch, and since the data for the temperature of 230.4°C are the most extensive, I will confine my attention to this set of data. The situation was confused recently by the emergence of another set of data from this laboratory (25): these experiments were not undertaken for the purposes of testing unimolecular reaction theory, and were confined to a very limited pressure range (2–100 Torr); their comparison with unimolecular reaction theory was only suggested later (11) in order to try to throw some more light on the nature of these generally agreed discrepancies. It turns out that over their limited pressure range, not only do the data of Collister and myself (25) agree very well with those of Schneider and Rabinovitch, but they also fit superbly to standard unimolecular fall-off curves corresponding to a somewhat lower high-pressure limit than that of Schneider and Rabinovitch (cf. Fig. 14 of ref. 11). Since then, we have undertaken a new series of experiments to determine which high-pressure limiting rate constant is correct, and we confirm that the value of Schneider and Rabinovitch is the correct one.[3]

X. Treatment of Alkyl Isocyanide Isomerisations including Randomisation Processes

Methyl Isocyanide

Previous theoretical treatments of this reaction have always chosen the pressure shift in such a way as to achieve the best compromise fit between theory and experiment over the whole pressure range (11, 20–24). Knowing now that first-order randomisation will ensure that the low-pressure limit coincides with the standard low-pressure limit, and that second-order randomisation will do likewise at the high-pressure limit (cf. Figs. 2 and 3), I have re-plotted the data slightly differently in Fig. 7. The dashed line is the standard unimolecular calculation (11, 15) using a collisional relaxation rate constant $\mu = 1.20 \times 10^6$ Torr^{-1} s^{-1} and the solid line shows the effect of including both first- and second-order randomisation, with rate constants $\mu_1 = 4.0 \times 10^{12}$ s^{-1} and $\mu_2 = 1.25 \times 10^{12}$ Torr^{-1} s^{-1} respectively. The agreement with the data of Schneider and Rabinovitch is virtually exact.

Perdeuteriomethyl Isocyanide

One example does not prove a theory: it is necessary to examine other similar reactions to see whether they behave equally well without making any further unjustifiable assumptions. To this end, Fig. 8 shows the fall-off data of Schneider and Rabinovitch (20, 27) for CD_3NC compared with three theoretical models: the dashed curve is again the standard unimolecular calculation (11, 15) and the dotted curve is the calculation using *the same* collisional relaxation and randomisation rate parameters as were used for CH_3NC in Fig. 7; quite unambiguously, this curve does not fit the data. The solid curve shows the plot obtained using the constants $\mu = 1.30 \times 10^6$ Torr^{-1} s^{-1}, $\mu_1 = 5.0 \times 10^{12}$ s^{-1}, and $\mu_2 = 3.0 \times 10^{12}$ Torr^{-1} s^{-1} respectively. The only *significant* difference in the parameters required to achieve this exact fit is that the second-order

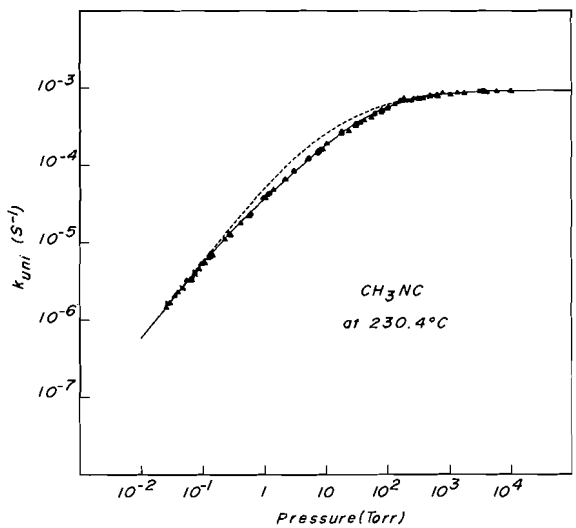


FIG. 7. Fall-off curves for the thermal isomerisation of methyl isocyanide at 230.4°C. The points represent the results of Schneider and Rabinovitch (20, 21) with the experiments in packed vessels marked by tags. The dashed line is the standard fall-off calculation without considering randomisation. The solid line includes both first-order and second-order randomisation effects, with $\mu = 1.20 \times 10^6$ Torr^{-1} s^{-1}, $\mu_1 = 4.0 \times 10^{12}$ s^{-1}, $\mu_2 = 1.25 \times 10^{12}$ Torr^{-1} s^{-1}.

[3]We (26) carried out experiments using about 50 Torr of CH_3NC pressurised with helium in a 10 mL steel vessel at 200°C; at this temperature, the Collister and Pritchard limit is 5.1×10^{-5} s^{-1} whereas the Schneider and Rabinovitch limit is 7.3×10^{-5} s^{-1}. We observed rate constants as high as 6.4×10^{-5} s^{-1} and extrapolated our results between 7 and 8×10^{-5} s^{-1} at infinite pressure: this proves conclusively (cf. also footnote 23 of ref. 8) that, despite superficial appearances, the infinite-pressure limit extrapolated from our own experiments (25) is not the correct one.

Can. J. Chem. Downloaded from www.nrcresearchpress.com by 210.87.254.40 on 09/05/12
For personal use only.

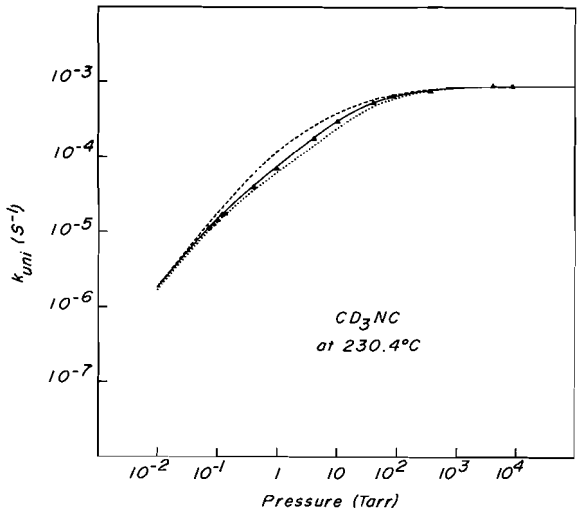


FIG. 8. Fall-off curves for the thermal isomerisation of perdeuteriomethyl isocyanide at 230.4°C. The points represent the results of Schneider (20). The dashed line is the standard fall-off calculation without considering randomisation. The dotted line includes both first-order and second-order randomisation, but with constants appropriate to methyl isocyanide as in Fig. 7. The solid line uses $\mu = 1.30 \times 10^6$ Torr^{-1} s^{-1}, $\mu_1 = 5.0 \times 10^{12}$ s^{-1}, $\mu_2 = 3.0 \times 10^{12}$ Torr^{-1} s^{-1}.

randomisation rate constant is about $2\frac{1}{2}$ times as large, which I think is quite reasonable in view of the fact that CD_3NC has 6 or 7 times the density of states of CH_3NC. The only questionable point is that μ for CD_3NC appears to be very slightly greater than that for CH_3NC, contrary to the general trend found at lower temperatures in ultrasonic relaxation experiments (28).

Schneider and Rabinovitch (27) also conducted another extensive set of experiments in which they measured the relative rate ratios for isomerisation of CH_3NC and CD_3NC, and although the general trends are well represented by standard unimolecular calculations (11, 27), there are some inexplicable discrepancies. Figure 9 shows these experimental ratios compared with the results of standard theory (dashed line) and with those calculated using the relaxation and randomisation rate parameters chosen separately in Figs. 7 and 8. Whilst this method of presentation is not entirely independent of the preceding arguments because of the remarkable internal consistency of Schneider's earlier (19) and later (27) results, it does suggest quite strongly that the unexplained "bump" in the ratios just below 1 Torr arises from the differences in randomisation rates between the two isotopic variants of the reactant molecule. Notice that in this plot, the rate constant ratio itself is plotted, rather than its logarithm as in previous presentations (11, 27).

Ethyl Isocyanide

Rabinovitch and co-workers (29, 30) have published equally remarkable sets of experimental data for the thermal isomerisations of both C_2H_5NC and C_2D_5NC. Again, as we have noted previously (11), there appears to be a slight anomaly in the observed fall-off behaviour for C_2H_5NC between 10^{-2} and 1 Torr, rather like that found for CH_3NC between 1 and 100 Torr, and which can probably be accounted for in the same fashion. Unfortunately, because of the onset of the wall activation mechanism at the lowest pressures, it is not possible to make a definitive choice for the primary energy relaxation rate constant μ. In consequence, it is not possible to derive accurate values for the two randomisation rate constants μ_1 and μ_2 in ethyl isocyanide. However, it is clear that the value of μ_2 used for methyl isocyanide is hopelessly wrong for ethyl isocyanide, and the value for the ethyl compound has to be 1×10^{14} Torr^{-1} s^{-1} *at the very least*; it is not possible to make such a categorical statement about

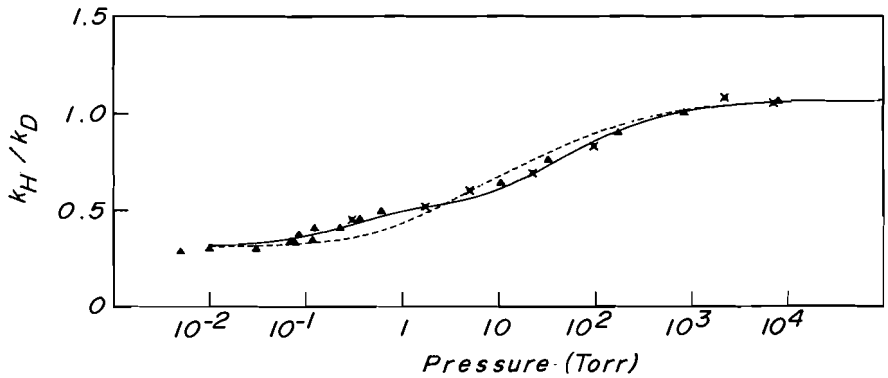


FIG. 9. Kinetic isotope effect k_H/k_D for CH_3NC and CD_3NC isomerisation as a function of pressure at 230.4°C. The points represent the two sets of ratio measurements made by Schneider and Rabinovitch (27). The dashed line uses standard fall-off calculations for each molecule, whereas the solid line allows for reactant-state randomisation with the respective rate constants as used in Figs. 7 and 8.

μ_1, but it seems that a value rather similar to those used for the two methyl isocyanides would not be inappropriate. An experimental determination of the gas-phase second-order limit for ethyl isocyanide would be extremely valuable indeed, as it would provide definitive information on the general behaviour of these first- and second-order randomisation rate constants as a function of molecular complexity.

XI. Summary

I have presented a model for the explicit inclusion of the kinetics of internal energy randomisation within the usual unimolecular fall-off calculations, and shown how the method can be applied to the thermal isomerisations of methyl and ethyl isocyanide.

I have concluded that it is sensible to admit the existence of both first-order and second-order randomisation mechanisms, with rate constants μ_1 and μ_2 respectively. The principal consideration here is the general success of earlier unimolecular reaction theories in reproducing fall-off characteristics: these earlier calculations are equivalent to the present treatment with either $\mu_1 \rightarrow \infty$ or $\mu_2 \rightarrow \infty$ or both; however, once both μ_1 and μ_2 take on rate-limiting values, it is necessary to postulate the *significant* involvement of both randomisation mechanisms in order to maintain the traditional forms for the high- and low-pressure limits.

Numerical application of this formulation to the two symmetrical isotopic forms of methyl isocyanide and (as best I can) to ethyl isocyanide suggests very strongly that the second-order randomisation rate increases markedly with increasing density of states, an observation which can easily be rationalised with arguments suggested by Fig. 1. On the other hand, until a true low-pressure limiting rate can be determined for ethyl isocyanide, there is no strong evidence to suggest that the first-order randomisation rate constant differs very much from $5 \times 10^{12}\ s^{-1}$.

The quasi-diatomic model used in these calculations provides a simple vehicle for treating randomisation processes, and leads directly to a very simple formulation of the specific rate constant for unimolecular decay. It is not necessary to understand the exact details of the processes causing randomisation in order to model practical reaction processes. However, the second-order process is clearly a collisional one, and the elucidation of the precise nature of the first-order randomisation process (or processes) may well be facilitated considerably through this approach, once the full implications of the nodeless quality of *all* vibrational wave functions (3, 4) are worked out.

Acknowledgements

I would like to thank M. D. Clarkson, B. F. Gray, G. Hunter, S. R. Singh, and A. W. Yau for help and advice.

1. M. Polanyi and E. Wigner. Z. Phys. Chem. **139**, 439 (1928).
2. H. O. Pritchard, G. M. Diker, and A. W. Yau. Can. J. Chem. **58**, 1516 (1980).
3. J. Czub and L. Wolniewicz. Mol. Phys. **36**, 1301 (1978).
4. G. Hunter. Int. J. Quantum Chem. **17**, 133 (1980).
5. D. W. Placzek, B. S. Rabinovitch, and F. H. Dorer. J. Chem. Phys. **44**, 279 (1966).
6. S. Nordholm and S. A. Rice. J. Chem. Phys. **62**, 157 (1975).
7. K. V. Reddy and M. J. Berry. Chem. Phys. Lett. **52**, 111 (1977).
8. I. Oref and B. S. Rabinovitch. Acc. Chem. Res. **12**, 166 (1979).
9. W. Heitler. Quantum theory of radiation. Clarendon Press, Oxford. 1954.
10. J. O. Hirschfelder, C. F. Curtiss, and R. B. Byrd. Molecular theory of gases and liquids. John Wiley, New York. 1954.
11. A. W. Yau and H. O. Pritchard. Can. J. Chem. **56**, 1389 (1978).
12. S. Nordholm. Chem. Phys. **29**, 55 (1978).
13. H. O. Pritchard and A. Lakshmi. Can. J. Chem. **57**, 2793 (1979).
14. S. R. Singh and H. O. Pritchard. Chem. Phys. Lett. **73**, 191 (1980).
15. H. O. Pritchard and S. R. Singh. In preparation.
16. S. R. Singh. Unpublished results.
17. O. K. Rice. Z. Phys. Chem. B, **7**, 226 (1930).
18. D. L. Bunker and W. L. Hase. J. Chem. Phys. **59**, 4621 (1973).
19. E. Thiele, M. F. Goodman, and J. Stone. Chem. Phys. Lett. **69**, 18 (1980).
20. F. W. Schneider. Ph.D. Thesis, University of Washington, 1962.
21. F. W. Schneider and B. S. Rabinovitch. J. Am. Chem. Soc. **84**, 4215 (1962).
22. W. Forst. *In* Reaction transition states. *Edited by* J. E. Dubois. Gordon and Breach, London. 1972. p. 75.
23. W. Forst. J. Phys. Chem. **76**, 342 (1972).
24. M. Christianson, D. Price, and R. Whitehead. J. Phys. Chem. **78**, 2326 (1974).
25. J. L. Collister and H. O. Pritchard. Can. J. Chem. **54**, 2380 (1976).
26. M. T. J. Glionna and H. O. Pritchard. Unpublished results.
27. F. W. Schneider and B. S. Rabinovitch. J. Am. Chem. Soc. **85**, 2365 (1963).
28. J. D. Lambert. Vibrational and rotational relaxation in gases. Clarendon Press, Oxford. 1977.
29. K. M. Maloney and B. S. Rabinovitch. J. Phys. Chem. **73**, 1652 (1969).
30. K. M. Maloney, S. P. Pavlou, and B. S. Rabinovitch. J. Phys. Chem. **73**, 2756 (1969).

Can. J. Chem. Downloaded from www.nrcresearchpress.com by 210.87.254.40 on 09/05/12
For personal use only.

Spin–lattice relaxation in MBBA and MBBA – carbon tetrachloride mixtures

MARGARET A. HELDMAN AND D. F. R. GILSON[1]

Department of Chemistry, McGill University, Montreal, P.Q., Canada H3A 2K6

Received May 28, 1980

MARGARET A. HELDMAN and D. F. R. GILSON. Can. J. Chem. **58**, 2246 (1980).

The spin–lattice relaxation time has been measured at 33 MHz as a function of temperature for the liquid crystal MBBA and mixtures with carbon tetrachloride. The behaviour of T_1 close to the nematic–isotropic transition can be explained if the correct order fluctuation dependence is included. Diffusion constants calculated from fits to the self-diffusion contribution to relaxation are in agreement with existing results.

MARGARET A. HELDMAN et D. F. R. GILSON. Can. J. Chem. **58**, 2246 (1980).

On a mesuré le temps de relaxation–spin réseau à 33 MHz en fonction de la température du cristal liquide MBBA et de ses mélanges avec le tétrachlorure de carbone. On peut expliquer le comportement du T_1 près de la transition nématique–isotrope si l'on inclut l'ordre correct de l'influence de la fluctuation. Les constantes de diffusion ainsi calculées cadrent avec la contribution d'auto-diffusion à la relaxation et sont en accord avec les résultats existants.

[Traduit par le journal]

Introduction

The mechanism of proton spin–lattice relaxation in nematic liquid crystals has been a subject of controversy. The two principal theories are the order director fluctuation mechanism of Pincus (1), which requires a dependence on the inverse square root of the Larmor frequency, and the self-diffusion theory due to Blinc (2) which involves a simple square root dependence. At first sight, an easy distinction between the two mechanisms should be obtainable by measuring the dispersion of T_1 as a function of the frequency of measurement but the experimental results have been inconclusive in that they do not provide an unambiguous interpretation even when extended over a very wide range of frequencies. Each approach has been modified in efforts to solve the conflict. The Pincus theory was changed to incorporate a squared dependence on the order parameter (3) and by the inclusion of a cut-off frequency above which the order fluctuation mechanism does not operate (4). The self-diffusion model was extended by using a step-width parameter and a frequency independent term in the relaxation rate (5). In both cases these changes appeared to give agreement with the experimental results, but by incorporating both order fluctuations and diffusive motion together with a cross correlation term, Ukleja, Pirs, and Doane (6) proposed an improved overall theory capable of explaining the available experimental results for both PAA (*p*-azoxyanisole) and MBBA (*p*-methoxybenzylidene-*n*-*p*-butylaniline). However, this theory was later criticized on the grounds that it could not adequately explain the deuterium spin–lattice relaxation times in MBBA (7). Subsequently, measurements of T_1 for MBBA were extended into the kilohertz range by Graf, Noack, and Stohrer (8) who explained their results by dropping the cross-correlation term in favour of a molecular rotational correlation time for motion about the short molecular axis. The theory which now emerges for spin–lattice relaxation in MBBA is that order fluctuations provide the dominant mechanism at low Larmor frequencies while self-diffusion is responsible at high frequencies and at lower temperatures. Near the nematic to isotropic transition the rotational process becomes of comparable importance. Each relaxation process is weighted by the number of contributing spins.

In nearly all studies of MBBA the emphasis has been on the frequency dispersion and not on the temperature dependence of T_1. Graf *et al.* (8), for instance, covered the frequency range from 2 kHz to 270 MHz but only at four temperatures, 18, 27, 35, and 45°C. In earlier work (9, 10), we have obtained the order parameter (S) dependence upon temperature for pure MBBA and for MBBA doped with various solutes and shown that the order parameter is a universal function of reduced temperature in all cases. It seemed worthwhile to explore the temperature dependence of T_1 in MBBA (pure and doped) in greater detail, specifically in terms of the reduced temperature. Carbon tetrachloride was chosen as a non-proton containing solute molecule.

Experimental

MBBA was prepared by the condensation reaction between freshly distilled *p*-anisaldehyde and *n*-butylaniline and vacuum distilled three times. The nematic to isotropic transition temperature was 44°C. Since reduced temperature scales are used in the present study no attempts were made to obtain extremely pure material. Solutions with carbon tetrachloride were prepared

[1]To whom all correspondence should be addressed.

0008-4042/80/212246-04$01.00/0

©1980 National Research Council of Canada/Conseil national de recherches du Canada

Can. J. Chem. Downloaded from www.nrcresearchpress.com by 210.87.254.105 on 09/05/12
For personal use only.

with 9.1 and 18.4 mol% solute and carefully degassed by freeze–pump–thaw cycling.

Spin–lattice relaxation times were measured on a Spin-Lock CPS-2 pulse spectrometer at 33 MHz using a $\pi-\tau-\pi/2$ sequence with delay times up to $1.3T_1$ used in the analysis. Free induction decays were captured with a Biomation model 805 transient recorder and subsequently plotted on a strip chart recorder. The sample temperature was controlled by a heated or cooled flow of nitrogen gas and measured with a copper–constantan thermocouple placed next to the sample.

Results and Discussion

The T_1 versus temperature plots are shown in Fig. 1. The relaxation time increases with increasing temperature but shows some levelling-off as the nematic–isotropic transition is approached. This effect has been observed previously (11) in a variety of liquid crystals but has been given little attention. The presence of CCl_4 as a solute decreases T_1 and also reduces the nematic temperature range and the ability to supercool the solution below the nematic–solid transition. Thus the results for the 18 mol% solution show greater scatter and are less satisfactory.

In previous applications of the order fluctuation theory various simplifications and approximations have been applied. The order fluctuation rate is given by

$$[1]\quad (T_{1OF})^{-1} = A\omega^{-1/2} + B = \frac{9}{4\sqrt{2\pi}}\frac{\gamma^4 h^2}{r^6}\frac{S^2 kT\eta^{1/2}\omega^{-1/2}}{K^{3/2}}$$

where S is the order parameter; η, the average viscosity; K, the average elastic constant; r, the internuclear separation (2.44 Å); and γ, the magnetogyric ratio, and other symbols have their usual significance. The elastic constant and viscosity are anisotropic properties and, because these are not necessarily known in sufficient detail, are replaced by average quantities. The expressions S^2/K and $T\eta^{1/2}/K^{1/2}$ are commonly assumed to vary little with temperature and therefore this contribution to the relaxation rate is taken to be temperature independent. The term B can be neglected. Graf *et al.* (8) included the viscosity as an Arrhenius-type dependence, $\eta(T) = \eta_0 \exp(-E_\eta/RT)$, in the Pincus–Doane factor, A, and a similar function for the self-diffusion term, $D(T) = D_0 \exp(-E_D/RT)$ with $D = d^2/(6\tau_{SD})$ from the Torrey formalism for self-diffusion spin–lattice relaxation (12, 13), where d is the distance of closest approach of neighbouring molecules and is equated with the mean squared flight distance. For the rotational contribution a weighting factor, ε, reflecting the anisotropy of the ellipsoids of rotation about the long and short molecular axes, and a correlation time, τ_S, again in a thermally activated mode, were included. Graf *et al.* made a computer fit to the T_1 frequency dispersion at each temperature optimizing the six parameters A, D, d, ε, τ_{SD}, and H_z (the local dipolar field) and thus to E_η, E_D, and E_S and the appropriate pre-exponential factors, the local field term can, however, be neglected for high frequency studies. This procedure led to acceptable values for the activation energy terms and good agreement with the frequency dispersion curves.

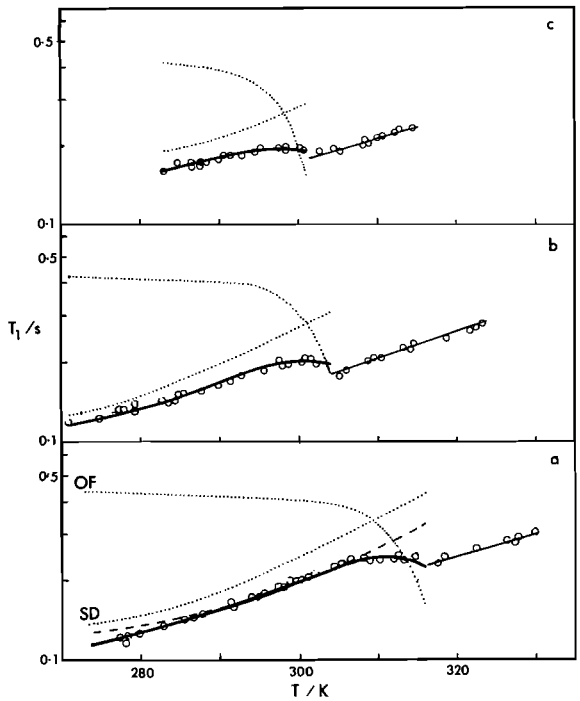


FIG. 1. Experimental spin–lattice relaxation times vs. temperature plots for (*a*) MBBA, (*b*) mole fraction CCl_4 0.091, (*c*) mole fraction CCl_4 0.183. The solid lines are the calculated dependences, the dotted line in (*a*) is calculated using the Graf–Noack–Stohrer approach.

However, when this method was applied to the temperature dependence of T_1 of MBBA at 33 MHz the dotted line of Fig. 1(*a*) was obtained. The behaviour of the spin–lattice relaxation time in the temperature region close to the nematic–isotropic transition is not explained by this theory. Experimental observations of properties such as the elastic constants, viscosity, and order parameter show that they vary quite rapidly in the vicinity of the transition. The viscosity of MBBA, in fact, shows an increase with increasing temperature. We have taken advantage of the fact that these properties

Can. J. Chem. Downloaded from www.nrcresearchpress.com by 210.87.254.105 on 09/05/12
For personal use only.

TABLE 1. Self-diffusion parameters

Mole fraction CCl_4	τ_0^{SD} (s)	D_0 ($m^2\ s^{-1}$)	E_{SD} (kJ mol^{-1})	d (Å)
0	$2.08\times10^{-15}\pm1.9\times10^{-17}$	6.68×10^{-6}	-32.2 ± 0.25	2.89 ± 0.11
0.09	$6.15\times10^{-16}\pm3.3\times10^{-18}$	2.36×10^{-5}	-35.4 ± 0.11	2.97 ± 0.06
0.18	$1.98\times10^{-17}\pm4.0\times10^{-19}$	9.73×10^{-4}	-45.2 ± 0.40	3.40 ± 0.23
0[a]	1.30×10^{-16}	3.45×10^{-5}	-36.4	

[a]Reference 8.

follow a reduced temperature behaviour and can be described by functions of T^*, where $T^* = T/T_N$. In Fig. 2 the Pincus–Doane factor, A, for MBBA is plotted as a function of T^*. The single constant approximations were used with values for K_{ii} and η taken from the literature (14–17), plus the S values of Lee (10). Obviously, approximations about the temperature constancy of A do not hold above $T^* \sim 0.98$ which may be responsible for the failure of the Graf–Noack–Stohrer theory to explain the observed temperature dependence.

The order fluctuation contribution to the total relaxation, $(T_{1\,OF})^{-1}$, can thus be calculated using only observed experimental data and subtracted, using the weighting factor 8/12 suggested by Graf *et al.*, from the experimental spin–lattice relaxation rate to give the contribution due to self-diffusion. The relaxation arising from rotational motion was calculated and found to be too small both at 33 MHz and close to the transition to be important. This procedure is applicable to the carbon tetrachloride solutions as well as to MBBA itself since the reduced temperature behaviour is followed.

In applying the Torrey formalism (12, 13) to the calculation of the self-diffusion relaxation the following parameters are involved; the diffusion constant, D, via $D = \langle r^2\rangle/6\tau_{SD}$, where $\langle r^2\rangle$ is the mean squared flight distance and τ_{SD} the mean time between flights, d the distance of closest approach of spins of neighbouring molecules, and the spin-density or number of protons per unit volume. In principle all these terms are temperature and concentration dependent. The ratio of flight distance to distance of closest approach can be used as an optimization parameter (7), or assumed to be unity. Graf *et al.* (8) neglected the temperature variation of the spin density and allowed d to be a temperature dependent variable. In the present treatment we have chosen to limit the number of temperature dependent variables and thus have optimized the T_{1SD} variation to τ_{SD} and d at each concentration. The value of d obtained in this way thus be subject to these assumptions.

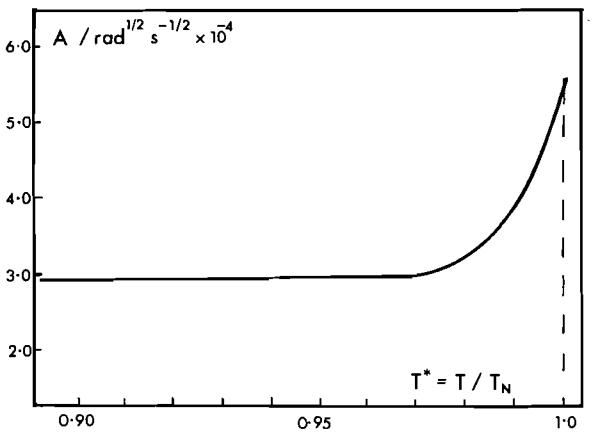


FIG. 2. Dependence of the Pincus–Doane factor A on reduced temperature.

For MBBA the optimization was extended to include the frequency dependence data at fixed temperatures (values taken from the various literature sources) together with the present results. For the carbon tetrachloride solutions the spin densities were calculated using the data given by Gierke and Flygare (18). The results are given in Table 1. The following trends are apparent, the activation energies and the distance of closest approach increase with increasing CCl_4 concentration. The latter term, however, is to be considered in the context of the approximations and assumptions mentioned above. If the expressions for τ_{SD} are converted to diffusion constants using these distances then values of D of 1.04×10^{-7}, 5.47×10^{-8}, and 2.58×10^{-8} $cm^2\ s^{-1}$ for MBBA and the 9 and 18 mol% solutions respectively at $T^* = 0.915$. At the nematic to isotropic transition these values are 3.23×10^{-7}, 2.01×10^{-7}, and 1.38×10^{-7} $cm^2\ s^{-1}$. These diffusion constants for MBBA are in good agreement with those reported by other authors (19, 20) (in the range 1×10^{-7} to 4×10^{-7} $cm^2\ s^{-1}$) although most studies have been limited to a single temperature and very few measurements exist of the activation energies for self-diffusion. There is certainly a need, as Wade has said, for much more work on the role of diffusion as a re-

Can. J. Chem. Downloaded from www.nrcresearchpress.com by 210.87.254.105 on 09/05/12
For personal use only.

laxation mechanism in liquid crystals (21). The decrease in diffusion constant for increasing concentration of CCl_4 parallels the observations of Gierke and Flygare (18) who showed that the viscosities of MBBA – carbon tetrachloride mixtures increased with concentration. Presumably this is due to charge transfer complex formation (22) affecting the effective size and shape of the diffusing species.

Conclusions

The experimental temperature dependence of the spin–lattice relaxation time in MBBA at 33 MHz can be explained by a model which includes only order director fluctuations and self-diffusion mechanisms. The order fluctuation term is not temperature independent but can be expressed as a function of reduced temperature. A fit of the remaining contribution to a self-diffusion mechanism gives reasonable parameters even though the number of variables was limited.

1. P. PINCUS. Solid State Commun. **7**, 415 (1969).
2. M. VILFAN, R. BLINC, and J. W. DOANE. Solid State Commun. **11**, 1073 (1972).
3. J. W. DOANE and D. L. JOHNSON. Chem. Phys. Lett. **6**, 291 (1970).
4. J. W. DOANE, C. E. TARR, and M. A. NICKERSON. Phys. Rev. Lett. **32**, 622 (1974).
5. R. BLINC, M. VILFAN, and V. RUTAR. Solid State Commun. **17**, 171 (1975).
6. P. UKLEJA, J. PIRS, and J. DOANE. Phys. Rev. A**14**, 414 (1976).
7. V. RUTAR, M. VILFAN, R. BLINC, and E. BOCK. Mol. Phys. **35**, 721 (1978).
8. V. GRAF, F. NOACK, and M. STOHRER. Z. Naturforsch. **32a**, 61 (1977).
9. B. KRONBERG, D. F. R. GILSON, and D. D. PATTERSON. J. Chem. Soc. Faraday Trans. 2, **72**, 1673 (1976).
10. Y. P. LEE and D. F. R. GILSON. J. Chem. Phys. **70**, 2042 (1979).
11. C. L. WATKINS and C. S. JOHNSON. J. Phys. Chem. **75**, 2452 (1971).
12. H. C. TORREY. Phys. Rev. **92**, 962 (1953).
13. J. F. HARMON and B. H. MULLER. Phys. Rev. **182**, 400 (1969).
14. I. HALLER. J. Chem. Phys. **57**, 1400 (1972).
15. S. A. SHAYA and H. YU. J. Chem. Phys. **63**, 221 (1975).
16. Y. S. LEE, S. L. GOLUB, and G. H. BROWN. J. Phys. Chem. **76**, 2409 (1972).
17. P. MARTINODY and S. CANDAU. Mol. Cryst. Liquid Cryst. **14**, 243 (1971).
18. T. D. GIERKE and W. H. FLYGARE. J. Chem. Phys. **61**, 2231 (1974).
19. F. RONDELEZ. Solid State Commun. **14**, 815 (1974).
20. H. HAKEMI and M. LABES. J. Chem. Phys. **63**, 3708 (1975).
21. C. G. WADE. Ann. Rev. Phys. Chem. **28**, 47 (1977).
22. R. F. WEIMER and J. M. PRAUSNITZ. J. Chem. Phys. **42**, 3643 (1965).

Can. J. Chem. Downloaded from www.nrcresearchpress.com by 210.87.254.105 on 09/05/12
For personal use only.

On the ion exchange sorption of some complex cations and their nature of interaction with chromium ferrocyanide gel

ISHWARI P. SARASWAT, SURESH K. SRIVASTAVA, SURENDRA K. VERMA, AND ASHOK K. SHARMA

Department of Chemistry, University of Roorkee, Roorkee-247 672, India

Received October 24, 1979[1]

ISHWARI P. SARASWAT, SURESH K. SRIVASTAVA, SURENDRA K. VERMA, and ASHOK K. SHARMA. Can. J. Chem. **58**, 2250 (1980).

The sorption of ammine complex cations of Co(III), viz. $[Co(NH_3)_6]^{3+}$ and $[Co(en)_3]^{3+}$, on the H^+ form of chromium ferrocyanide gel has been studied under static conditions. It is observed that the majority of these complex cations (90%) are sorbed by ion-exchange process. The extent of desorption of these complex ions with some uni- and bivalent cations is in the order $K^+ > NH_4^+ > Ba^{2+} > Sr^{2+} > Ca^{2+} > Mg^{2+}$.

Infrared, Mössbauer, and magnetic susceptibility studies on the air-dried and powdered gel in H^+ form and loaded with $[Co(NH_3)_6]^{3+}$, $[Co(en)_3]^{3+}$, Fe^{3+}, and La^{3+} ions show that prussiate compounds are not formed during the gel formation and the sorbed cations are held by the electrostatic attraction forces in the matrix, which is strained by the sorption of the big cations.

ISHWARI P. SARASWAT, SURESH K. SRIVASTAVA, SURENDRA K. VERMA et ASHOK K. SHARMA. Can. J. Chem. **58**, 2250 (1980).

On a étudié, dans des conditions statiques, l'adsorption des cations complexes aminés du Co(III) du type $[Co(NH_3)_6^{3+}$ et $[Co(en)_3]^{3+}$ sous la forme protonée du gel de ferrocyanure de chrome. On a observé que la plus grande partie des cations complexes (90%) sont adsorbés par un procédé d'échange d'ions. Le taux de désorption de ces ions complexes avec quelques cations mono et bivalents a varié selon l'ordre suivant: $K^+ > NH_4^+ > Ba^{2+} > Sr^{2+} > Ca^{2+} > Mg^{2+}$.

Des études infrarouges et de susceptibilité de Mossbauer et magnétique sur le gel sous forme H^+ séché à l'air, pulvérisé et chargé en ions $[Co(NH_3)_6]^{3+}$, $[Co(en)_3]^{3+}$, Fe^{3+} et La^{3+} montrent que les composés du type pruissiate ne se forment pas pendant la formation du gel et que les cations adsorbés sont retenus par des forces électrostatiques sur la matrice qui est tendue par l'adsorption de gros cations.

[Traduit par le journal]

Introduction

Recently, we have reported the kinetics and thermodynamics of exchange of some complex cations (1), viz. $[Co(NH_3)_6]^{3+}$ and $[Co(en)_3]^{3+}$, on chromium ferrocyanide gel (CFC). However, some aspects such as the nature of binding between the exchanger and the sorbed species, etc., could not be well understood on the basis of kinetic and thermodynamic data alone. Therefore, it looks essential to carry out further investigations on the sorption behaviour of CFC towards these complex cations. As the exchanger has been found to be amorphous on X-ray analysis (2) and is opaque to most spectroscopic investigations, the experimental informations at the molecular level are limited. However, infrared (ir), Mössbauer effect (Me), and magnetic susceptibility (ms) studies could provide useful informations. In the present article, the sorption and desorption of these complex cations under static conditions have been reported and the results have been supplemented by ir, Me, and ms data to explain the mechanism of uptake and the nature of interaction between the gel and the sorbed cations.

Experimental

Chromium ferrocyanide gel, $K_6Cr_2[Fe(CN)_6]_3 \cdot 16H_2O$, was synthesized under optimum experimental conditions (exchange capacity 3.65 mequiv./g) and analyzed as reported earlier (2). The chromium–iron ratio of the product was 0.66. The thermogravimetric analysis of CFC showed a sharp inflexion point at 174°C, thus indicating the complete loss of water. The water content in the gel had been calculated by heating the exchanger to a constant weight at 180°C.

The complexes of cobalt, viz. hexammine cobalt(III) chloride and trisethylenediamine cobalt(III) chloride, were prepared using standard methods (3). Infrared spectra of the compounds were examined (4(*a*), (*c*)) and their purity was ascertained by the gravimetric estimations (5) of cobalt(III).

The gel was converted into H^+ form by the treatment with 1 *M* HCl. It was then saturated with different cations of interest by immersing in their salt-solutions (0.01 *M*) for long enough time (48 h). The samples were then repeatedly washed with deionized water to remove the adherent ions and dried at room temperature.

pH-measurements were made with a pH-meter, model pH 821, E.C.I., India, and the solutions of complexes were determined spectrophotometrically with a Unicam-500.

Sorption and Desorption Studies

The sorption of complex cations on the H^+ form of CFC, (100–170) B.S.S. mesh size of mean radius $(6.80 \pm 0.40) \times 10^{-3}$ cm, was studied as a function of initial solution concentration (pH 2 ± 0.02) using 0.1 g and 0.05 g of exchanger for $[Co(en)_3]^{3+}$ and $[Co(NH_3)_6]^{3+}$, respectively. The final volume of solution was 10 mL in each case. The solutions were shaken intermittently and, after equilibrium was attained (48 h), were filtered and spectrophotometrically estimated for the complex cations. The distribution coefficients of the complex cations were also determined as a function of the initial pH of the solution. The influence of HNO_3 and NH_4NO_3 concentrations on the distribution coefficients was also investigated at 0.005 *M*

[1]Revision received May 30, 1980.

0008-4042/80/212250-05$01.00/0

©1980 National Research Council of Canada/Conseil national de recherches du Canada

Can. J. Chem. Downloaded from www.nrcresearchpress.com by 210.87.254.42 on 09/05/12
For personal use only.

Can. J. Chem. Downloaded from www.nrcresearchpress.com by 210.87.254.42 on 09/05/12
For personal use only.

initial solution concentration of the complex cations. The calculations of K_d values (mL/g) were made as:

K_d = (Milliequivalents of complex cations sorbed at equilibrium per Milliequivalents of complex cations in solution at equilibrium) (V/m)

where V is the volume of solution and m is the mass of the exchanger sample.

For desorption studies, the weighed samples of CFC in H^+ form were first equilibrated with the solutions of $[Co(NH_3)_6]^{3+}$ and $[Co(en)_3]^{3+}$ of known concentrations (0.01 M) and volumes sufficiently high to saturate the samples and sorption per gram of the exchanger was calculated for each complex species. Equal amounts of these saturated samples (0.1 g) were then placed in contact with solutions of different concentrations of the desorbing salts and after the equilibrium was attained (48 h), the complex cations released were estimated. The desorbing salts used were NH_4Cl, KCl, $MgCl_2$, $CaCl_2$, $SrCl_2$, and $BaCl_2$ and at equilibrium the percentage of desorption was calculated as:

$$\% \text{ Desorption} = 100 \times \frac{\text{Milliequivalents of complex cations released at equilibrium for 1 g of CFC}}{\text{per milliequivalents of complex cations required to saturate 1 g of CFC in } H^+ \text{ form}}$$

All measurements were carried out under static conditions at 25 ± 0.2°C.

Recording of Infrared Spectra

The infrared spectra of dried and powdered samples of CFC in H^+ form and those loaded with Fe^{3+}, La^{3+}, and complex cations, $[Co(NH_3)_6]^{3+}$ and $[Co(en)_3]^{3+}$, were recorded at room temperature (25°C) in KBr pallets on Beckmann IR-20 spectrophotometer.

Mössbauer Resonance Spectra

Mössbauer measurements were made on air-dried samples at room temperature. The studies with samples dried in vacuum and with wet samples were not carried out because of the likelihood of structural changes (6). Spectra were recorded on a Mössbauer spectrometer employing a 256 channel analyzer and Elscint type constant acceleration velocity drive. ^{57}Co in Pd matrix of intensity 2 m Ci was used as the source. Sodium nitroprusside (SNP), which gives a well resolved quadrupole split doublet of 1.7048 ± 0.0025 mm s^{-1} (7), was used for calibrating the instrument and the reported value of chemical shift is with respect to this standard. In order to minimize the error, the spectra were recorded for sufficiently long time, and at least 2×10^4 counts per channel were recorded.

Magnetic Measurements

Magnetic susceptibility measurements were carried out on a Gouy balance at room temperature. The powdered samples were well packed into a cylindrical glass tube and suspended by a fine fibre in a homogeneous magnetic field of intensity 8.5×10^3 G, generated by an electro-current stabilizer (UNICO). A semi-micro Mettler balance was employed for suspending and weighing the samples.

The ir, Me, and ms studies were performed with CFC in H^+ form and loaded with the complex cations, $[Co(NH_3)_6]^{3+}$ and $[Co(en)_3]^{3+}$. In order to compare the results similar investigations were made with CFC loaded with Fe^{3+} and La^{3+} ions.

Results and Discussion

Sorption and Desorption of Complex Cations

Figure 1 presents the influence of HNO_3 and NH_4NO_3 concentrations on the distribution coefficients (K_d) of the complex cations at initial solution concentration 0.005 M. It is clear from the figure that the K_d values for the two complex cations show little change at lower acid as well as ammonium ion concentrations. Further, in separate experiments carried out at the same initial concentration of the complex cations (0.005 M), the distribution coefficients for $[Co(NH_3)_6]^{3+}$ and $[Co(en)_3]^{3+}$, 570 ± 15 and 117 ± 8, respectively, do not show appreciable change with the variation of initial pH of the solutions (adjusted by HNO_3 or NH_4OH) in the range 2–7, suggesting that the influence of H^+ and NH_4^+ ions on K_d values at such low concentrations is negligible. The observed levelling of the plots (Fig. 1) in lower concentration range of H^+ and NH_4^+ (particularly in case of $[Co(en)_3]^{3+}$) may be due to the saturation of CFC by complex cations. Above the concentration of 0.5 M, the influence of H^+ or NH_4^+ ions becomes dominant, resulting in the abrupt fall in K_d values (Fig. 1). The break in the curves (Fig. 1) at concentration 0.5 M is probably due to a change in the sorption behaviour of CFC caused either by the high concentrations of H^+ and NH_4^+ or by the oxidizing medium. The inhomogeneity of the exchanger may also be responsible for this effect. Since the exchanger is fairly stable (2) in the solutions of salts and mineral acids at the concentrations under study and no oxidative effect of HNO_3 is observed (8), the abrupt change in the straight

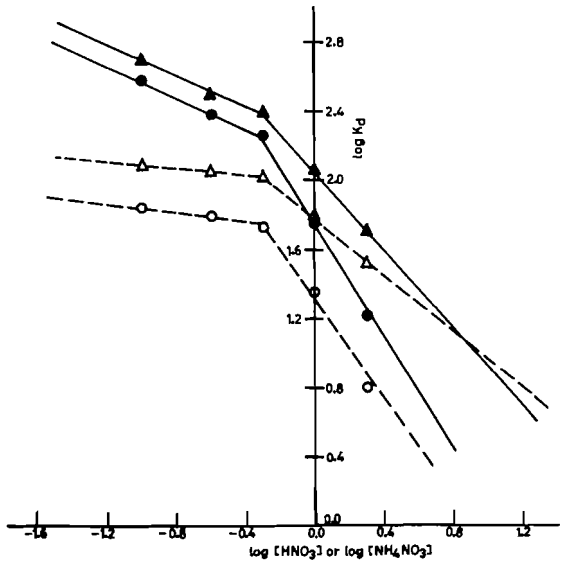


FIG. 1. Variation of K_d of complex cations with HNO_3(○,●) and NH_4NO_3 (△,▲) concentration at 25°C. Broken curves for $[Co(en)_3]^{3+}$ and solid curves for $[Co(NH_3)_6]^{3+}$.

Can. J. Chem. Downloaded from www.nrcresearchpress.com by 210.87.254.42 on 09/05/12
For personal use only.

line plots (Fig. 1) may be attributed to the increasing sorption competence of H^+ and NH_4^+ ions and also to the inhomogeneity of the exchanger material. This behaviour is analogous to that observed for the sorption of Cs^+ on CFC (8). Similar results have also been observed by Krtil in the case of vanadium ferrocyanide (9) and tungsten ferrocyanide (10), and by Ganzerli-Valentini *et al.* in the case of zinc ferrocyanide (11).

As none of the straight line plots in Fig. 1 has a slope equal to the valence of the complex cations (+3), the sorption of $[Co(NH_3)_6]^{3+}$ and $[Co(en)_3]^{3+}$ may not be solely ascribed to an ion-exchange mechanism. However, in separate experiments performed at 0.01 *M* initial solution concentration of complex cations and without adding any NH_4^+ or H^+ cations from outside, it is observed by measuring the pH of the solutions initially and after the equilibrium has been attained that, within the limits of experimental error, the major part of the uptake (90%) for both complex cations is followed by an equivalent release of H^+ ions and hence by the ion-exchange mechanism. The rest of the uptake (10%) may be due to some non-exchangeable processes like physical adsorption and co-ion inclusion.

The dependence of the extent of sorption on the initial solution concentration of complex cations has been depicted in Fig. 2, in terms of sorption isotherms. The values of saturation capacity for $[Co(NH_3)_6]^{3+}$ and $[Co(en)_3]^{3+}$ are 3.55 mequiv./g and 0.86 mequiv./g, respectively. The saturation capacity for $[Co(NH_3)_6]^{3+}$, within 4%, is equal to the values of saturation capacity for Cs^+ (3.70 mequiv./g) and Tl^+ (3.50 mequiv./g) determined radiometrically using ^{134}Cs and ^{204}Tl (12) and to the apparent exchange capacity of CFC (3.65 mequiv./g) determined by K–H exchange (2). This suggests that almost all the pores inside the exchanger are sufficiently large to accommodate $[Co(NH_3)_6]^{3+}$ ions and thus making all the exchanging sites accessible to it. The low saturation capacity of $[Co(en)_3]^{3+}$ is due to its larger size which does not permit its passage through the pores of narrower mesh-regions. Moreover, the $[Co(en)_3]^{3+}$ ions which have undergone exchange at the easily available exchanging sites during the initial stages of equilibration may also block the pores in CFC, thus preventing the further entry of $[Co(en)_3]^{3+}$ ions and limiting the extent of exchange to such a low value.

The desorption of complex cations by some univalent and bivalent cations has been shown in Figs. 3 and 4, respectively. It is clear from the figures that the desorption is higher for the cations of smaller hydrated sizes (13). This is in accordance to the

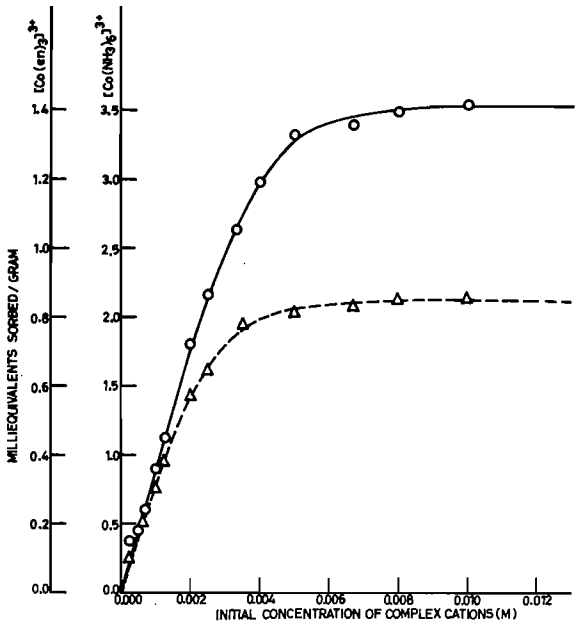


FIG. 2. Sorption isotherms of complex cations at 25°C; (○) for $[Co(NH_3)_6]^{3+}$ and (△) for $[Co(en)_3]^{3+}$.

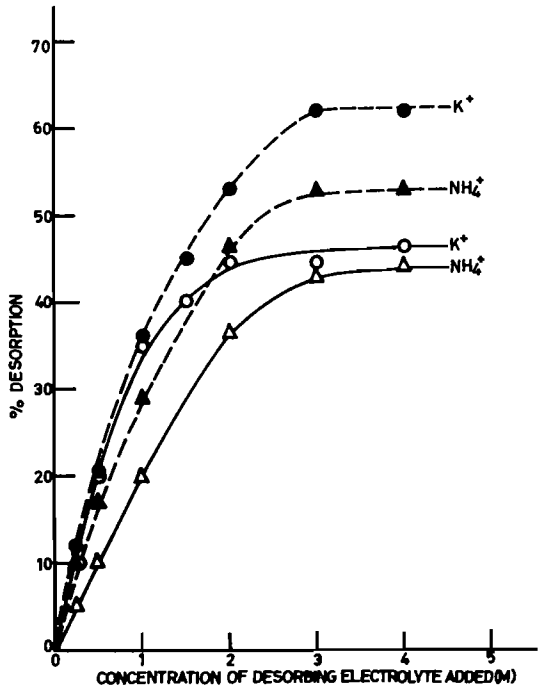


FIG. 3. Desorption of complex cations by K^+ and NH_4^+ at 25°C. Broken curves for $[Co(en)_3]^{3+}$ and solid curves for $[Co(NH_3)_6]^{3+}$.

common selectivity sequence of ion-exchangers:

$$K^+ > NH_4^+ > Ba^{2+} > Sr^{2+} > Ca^{2+} > Mg^{2+}$$

The total desorption of complex cations is not possible and much of them (35% to 55% in case of K^+

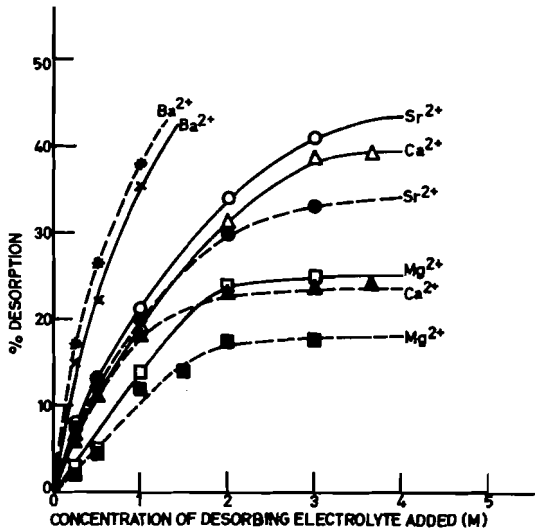


FIG. 4. Desorption of complex cations by bivalent metal ions at 25°C. Broken curves for $[Co(en)_3]^{3+}$ and solid curves for $[Co(NH_3)_6]^{3+}$.

and NH_4^+) remains in the exchanger material. Such hysteresis as well as a slow desorption are quite common with inorganic ion-exchangers (14). Further, it is quite interesting to note that among these two, the extent of desorption of $[Co(en)_3]^{3+}$ is higher for K^+, NH_4^+, and Ba^{2+} ions; however, it is less for Sr^{2+}, Ca^{2+}, and Mg^{2+} as compared to that of $[Co(NH_3)_6]^{3+}$. It can be argued here that the sorbed $[Co(en)_3]^{3+}$ cations, which block the pores in CFC, alter the pore dimensions in such a manner that the ions of hydrated sizes (13) bigger than Ba^{2+}, viz. Sr^{2+}, Ca^{2+}, and Mg^{2+}, have to encounter with the greater steric hindrance and to a certain degree their passage through the pores of inadequate mesh-regions may also be prevented, resulting in the relatively smaller extent of desorption of $[Co(en)_3]^{3+}$ as compared to that of $[Co(NH_3)_6]^{3+}$ ions.

Nature of Interaction between CFC and the Sorbed Cations

Infrared Studies

The infrared spectrum of chromium ferrocyanide in H^+ form shows absorption bands at 3400–3000, 2080, 1610, 580, 530, and 400 cm^{-1}. The broad band in the region 3400–3000 cm^{-1} is characteristic of interstitial water molecules and OH groups (15), while the band at 1610 cm^{-1} is due to HOH bending mode (15). The sharp band at 2080 cm^{-1} and another at 580 cm^{-1} are characteristic of cyanide (*4b*), and Fe—C stretching frequencies (*4b*). A strong band at 530 cm^{-1} may be assigned to bonding between chromium and oxygen which is in accordance with a similar band reported in the case of chromium(III) hydroxide gel (17). The Cr—N stretching mode, reported by Nakamoto *et al.* (18) at 444 cm^{-1}, shifts to lower frequency region, 400 cm^{-1} in the present case, thereby suggesting a weak bond formation.

In the infrared spectra of CFC loaded with $[Co(NH_3)_6]^{3+}$ and $[Co(en)_3]^{3+}$ cations, i.e. of CFC/$Co(NH_3)_6^{3+}$ and CFC/$Co(en)_3^{3+}$ systems, respectively, the intensity of the band at 400 cm^{-1} is significantly reduced. It may be argued that as a result of sorption of these large size complex cations, the strength of the Cr—N bond is weakened. Besides this, some new features emerged in the spectra recorded for these products. In case of CFC/$Co(NH_3)_6^{3+}$, the new peaks appeared at 1320 and 800 cm^{-1} are the high intensity peaks observed in the ir spectrum of pure $[Co(NH_3)_6]Cl_3$ complex (*4a*). Similarly, in the case of CFC/$Co(en)_3^{3+}$, the appearance of additional peaks at 1460, 1150, and 1050 cm^{-1} are due to the sorbed $[Co(en)_3]^{3+}$ ions (*4c*).

The spectra recorded for CFC loaded with Fe^{3+} and La^{3+} are identical to that observed for H^+ form. This indicates that the sorbed cations do not react chemically with CFC but are held by the electrostatic attraction forces in the matrix of the exchanger.

Mössbauer Studies

Mössbauer spectrum of the H^+ form of CFC shows only a single unsplit resonance line indicating octahedral symmetry and zero electric field gradient. This shows that the prussiate compounds (*19a*) are not formed during gel formation. In prussiate ion, e.g. in sodium nitrosyl prussiate, $Na_2[Fe^{II}(en)_5NO]$, etc., one of the cyano group is replaced by another ligand which gives rise to the quadrupole split doublet. Further, an isomeric shift of 0.16 ± 0.02 mm s^{-1} with respect to sodium nitroprusside observed in the Mössbauer spectrum of CFC indicates the existence of ferrocyanide group in the exchanger. However, the observed line-width is 0.46 mm s^{-1}, which is more than 0.23 mm s^{-1} reported for ferrous complexes (19). This is ascribed to some sort of distortion (*19b*) of the octahedral cyanide cage around Fe(II) in CFC.

Sorption of the complex cations, viz. $[Co(NH_3)_6]^{3+}$ and $[Co(en)_3]^{3+}$, does not affect the observed isomeric shift and the general character of the spectrum. Further, the sorption of Fe^{3+} (1.35 mequiv./g) and La^{3+} (2.90 mequiv./g) does not give rise to any new absorption peak in the Mössbauer spectrum. This also indicates that the interaction between sorbed cations and CFC is very weak.

The observed line-widths for Fe^{3+}, $[Co(NH_3)_6]^{3+}$, and $[Co(en)_3]^{3+}$ sorbed CFC are

Can. J. Chem. Downloaded from www.nrcresearchpress.com by 210.87.254.42 on 09/05/12
For personal use only.

0.50, 0.51, and 0.57 mm s^{-1}, respectively. From this, it is concluded that the sorption of relatively larger cations causes strain in the gel structure, thereby providing some inhomogeneity at iron(II) site in the ferrocyanide ion. This argument is further supported by the thermodynamic data for the exchange of the complex cations where the observed increase in the entropies of activations (ΔS^*) have been associated with the deformations in the exchanger matrix (1).

Magnetic Susceptibility Studies

The magnetic moment (μ_{eff}) of CFC in H^+ form is 8.00 ± 0.25 BM, which may be attributed to the presence of the two ionic chromium (20) in the molecule of the exchanger, $K_6Cr_2[Fe(CN)_6]_3 \cdot 16H_2O$. Although the experimentally observed value is higher than the reported value, 3.87 BM for one Cr^{3+} ion (20), within the limits of experimental error the two are in close agreement.

The magnetic moment of CFC loaded with complex cations, viz. $[Co(NH_3)_6]^{3+}$ and $[Co(en)_3]^{3+}$, is the same as observed in H^+ form. Since these complex ions have zero moment (16), the same value of μ_{eff} indicates that complex cations do not undergo exchange with Cr^{3+} ions. The sorption of Fe^{3+} and La^{3+} also does not cause any change in the magnetic moment of CFC. However, in case of Fe^{3+}, which possesses five unpaired electrons, an increase in μ_{eff} value is expected. It appears that Fe^{3+} ions are sorbed on CFC as hydrocomplex, i.e. $[Fe(H_2O)_6]^{3+}$, and thus do not cause any appreciable change in μ_{eff} of the exchanger.

Acknowledgements

Thanks are due to Professor W. U. Malik, Head of the Department for his interest and valuable discussion in carrying out these investigations. One of the authors (A.K.S.) would like to express appreciation for the financial support provided by C.S.I.R., India.

1. I. P. Saraswat, S. K. Srivastava, and A. K. Sharma. Can. J. Chem. **57**, 1214 (1979).
2. W. U. Malik, S.K. Srivastava, V. M. Bhandari, and S. Kumar. J. Inorg. Nucl. Chem. **38**, 342 (1976).
3. G. G. Schlessinger. Inorganic laboratory preparations. Chemical Publishing Co., Inc., New York, NY. 1962. pp. 176, 177, 186, 187.
4. K. Nakmoto. Infrared spectra of inorganic and coordination compounds. John Wiley, New York. 1963. (*a*) pp. 143–145; (*b*) 166–171; (*c*) 186, 187.
5. A. I. Vogel. A text book of quantitative inorganic analysis including elementary instrumental analysis. 3rd ed. Longmans. 1961. p. 530.
6. I. P. Suzdalev, A. S. Plachinda, E. Markarov, and V. A. Dolgopolov. Zh. Fiz. Khim. **41**, 2831 (1967).
7. N. N. Greenwood and T. C. Gibb. Mössbauer spectroscopy. Chapman and Hall Ltd., London. 1971. pp. 182, 183.
8. W. U. Malik, S. K. Srivastava, R. P. Singh, and S. Kumar. J. Radioanal. Chem. **36**, 469 (1977).
9. J. Krtil. J. Chromatogr. **20**, 384 (1965).
10. J. Krtil. J. Inorg. Nucl. Chem. **27**, 233 (1965).
11. M. T. Ganzerli-Valentini, S. Meloni, and V. Maxia. J. Inorg. Nucl. Chem. **34**, 1427 (1972).
12. A. K. Sharma. Ph.D. Thesis, Roorkee University, India. 1979.
13. R. Kunin. Ion exchange resins. 2nd ed. John Wiley and Sons, Inc., New York. 1958. p. 27.
14. F. Helfferich. Ion exchange. McGraw-Hill Book Company, Inc. 1962. pp. 188–193.
15. P. J. Lucchesi and W. A. Glasson. J. Am. Chem. Soc. **78**, 1347 (1956).
16. A. W. Adamson. J. Phys. Chem. **56**, 858 (1952).
17. P. Ratnasamy and A. J. Leonard. J. Phys. Chem. **76**, 1838 (1976).
18. K. Nakamoto, J. Fujita, and H. Murata. J. Am. Chem. Soc. **80**, 4817 (1958).
19. E. Fluck. *In* Advances in inorganic chemistry and radiochemistry. Vol. 6. Academic Press, New York. 1964. (*a*) pp. 464–466; (*b*) 461–462.
20. P. W. Selwood. Magnetochemistry. 2nd ed. Interscience Publishers Inc., New York. 1964. p. 159.

Can. J. Chem. Downloaded from www.nrcresearchpress.com by 210.87.254.42 on 09/05/12
For personal use only.

^{51}V FT-nmr investigations of metavanadate ions in aqueous solutions

MAHMOUD ADAM HABAYEB AND O. E. HILEMAN, JR.
Department of Chemistry, McMaster University, Hamilton, Ont., Canada L8S 4M1

Received February 20, 1980

MAHMOUD ADAM HABAYEB AND O. E. HILEMAN, JR. Can. J. Chem. **58**, 2255 (1980).

^{51}V-nmr chemical shifts, line widths, and area ratios obtained for various vanadium(V) species in aqueous solutions as a function of counter ion, pH, and analytical vanadium concentration changes are reported. From these data the eight vanadium(V) species shown to be present in significant amounts are identified. In the pH range 8.5 to 7.0, ^{51}V-nmr resonances were observed at 574 ppm and 582 ppm. The 574 ppm resonance is assigned to both $V_3O_9^{3-}$ and $V_4O_{12}^{4-}$ while the 582 ppm resonance has been assigned to the $V_6O_{17}^{4-}$ species. The suggestion that tetra alkyl ammonium cations stabilize $V_4O_{12}^{4-}$ species in solution is confirmed.

MAHMOUD ADAM HABAYEB et O. E. HILEMAN, JR. Can. J. Chem. **58**, 2255 (1980).

On rapporte les déplacements chimiques en rmn du ^{51}V, les largeurs des pics et les rapports de surfaces obtenus pour différentes espèces de vanadium(V) en solutions aqueuses en fonction de l'ion opposé, du pH et des changements de concentration du vanadium. A partir de ces données, on a identifié les 8 espèces de vanadium(V) présentes en quantités appréciables. On a observé, dans l'intervalle de pH allant de 8,5 à 7,0, les résonances du ^{51}V à 574 et 582 ppm. La résonance à 574 ppm est attribuée aux ions $V_3O_9^{3-}$ et $V_4O_{12}^{4-}$ tandis que la résonance à 582 ppm est attribuée à l'espèce $V_6O_{17}^{4-}$. On confirme le fait que les cations tétraalkylammonium stabilisent l'ion $V_4O_{12}^{4-}$.

[Traduit par le journal]

Introduction

Vanadium(V) speciation in aqueous solutions has been studied in detail (1–19). A variety of techniques — ranging from salt cryoscopy (1, 3) and diffusion coefficient measurements (4, 5) to potentiometric (6, 7), light scattering (9–10), ^{51}V-nmr (11–14), Raman spectroscopy (15–17), and spectrochemical measurements (20–24), have been utilized. The results of these investigations have been summarized in Fig. 1 of ref. 21 and suggest that vanadium(V) speciation is both pH and solute concentration sensitive.

There is a point of controversy, however, in the isopolyanion series $(VO_3)_n^{n-}$. Several potentiometric (6, 7) and spectrophotometric measurements (20–24) that were conducted at low solute concentration have led to the conclusion that the metavanadate ion is present in solution as the trimer "$V_3O_9^{3-}$" in the pH range of 9.0 to 7.0, while cryoscopic (1) and diffusion coefficient calculations (4) support the existence of the tetramer, "$V_4O_{12}^{4-}$". Recent Raman data (15–17) suggested the presence of a cyclic polymer, but failed to show whether this polymer is a trimer or a tetramer. Also, recent depolarized light scattering results (10) can be best explained if based on the presence of a tetramer. Finally, ^{51}V-nmr spectra (11–14) reported in the literature show two partially resolved resonances corresponding to two or more closely related species in the pH range 9.0 to 7.0. These resonances have been assigned to acyclic and cyclic $(VO_3)_n^{n-}$ type species, but to the best of our knowledge, no specific assignment of each of the two resonances has been attempted. Recently, the authors were encouraged by the report of the successful synthesis of hydrogen tetravanadate "$HV_4O_{12}^{3-}$" and hydrogen decavanadate "$H_nV_{10}O_{28}^{(6-n)-}$" anions as discrete polyanions (25). This suggests the possibility of a definitive assignment of these observed resonances.

The purpose of this work is the study of the speciation of metavanadate ions in solution as a function of pH, counter ion, and V(V) concentration using ^{51}V FT-nmr. In addition, particular attention is given to the assignment of the two resonances previously attributed to the isopolyanion series $(VO_3)_n^{n-}$.

Experimental Details

Preparation of Samples

(*a*) Aqueous sodium metavanadate solutions: isopolyvanadate stock solutions (0.25 *M*, 0.5 *M*, and 1.1 *M*) were prepared by dissolving the appropriate amounts of $NaVO_3$ as supplied (Fisher Scientific Co.) in boiling distilled water under nitrogen. The stock solutions were allowed to cool to room temperature and then were diluted to volume. Each was divided into several samples. The pH of each sample was adjusted using concentrated HCl or 4.5 *N* NaOH. The pH measurements were obtained at 298 ∓ 2 K using a Corning pH meter-130 equipped with a Fisher 13-639-51 glass electrode and Beckman 41263 reference electrode. The standard deviation in the pH values was ∓0.05. The samples were stored under N_2 at room temperature for 3–4 days before ^{51}V-nmr spectra were recorded. Check ^{51}V-nmr spectra were obtained two months later.

(*b*) $NaVO_3$–$[(CH_3)(CH_2)_3]_4NBr$ solutions: tetra-*n*-butyl ammonium bromide (16.0 g) (abbreviated as TBA-Br) (Eastman Organic Chemicals) were dissolved in 500 mL of a solution (0.0989 *M*) that contained 2.04 g of $NaVO_3$ (0.0334 *M*). This stock solution was stirred under N_2 overnight before being

0008-4042/80/212255-07$01.00/0
©1980 National Research Council of Canada/Conseil national de recherches du Canada

Can. J. Chem. Downloaded from www.nrcresearchpress.com by 210.87.254.6 on 09/05/12
For personal use only.

Can. J. Chem. Downloaded from www.nrcresearchpress.com by 210.87.254.6 on 09/05/12
For personal use only.

divided into 50-mL samples. The pH of each was adjusted by addition of concentrated HCl or 2.0 *N* NaOH.

(*c*) Preparation of $[N(C_4H_9)_4]_{6-n}H_nV_{10}O_{28}$: this compound was prepared as reported in the literature (25, 26) by dissolving either 1.1 g of V_2O_5 (J. T. Baker Chemical Co.) in 250 mL of 0.1 *N* $[(CH_3)_4NOH{\cdot}5H_2O]$ (Eastman Organic Chemicals) solution or by dissolving 1.20 g of $NaVO_3$ (Canadian Scientific Products Ltd.) in 150 mL of solution containing 6.14 g of tetra-*n* butyl ammonium chloride (Eastman Organic Chemicals) and 4.0 g of NaOH (Fisher Scientific Co.). Any residue was filtered out. The solution was stirred under N_2 for 3 days. The pH was maintained at 6.5. Acetone was added in 25 mL aliquots (a total of 200 mL) over a 2 h period. Within 24 h a yellow precipitate was observed. The supernatant liquid was decanted off. The precipitate was dissolved in distilled water and the pH was adjusted to the appropriate value using concentrated HCl or 2.0 *N* NaOH.

(*d*) Preparation of $[N(C_4H_9)_4]_3HV_4O_{12}$: $HV_4O_{12}^{3-}$ isopolyanion was prepared according to the procedure outlined in part (*c*) except that 0.56 g of $NaVO_3$ were dissolved in 100 mL of 10% tetra-*n*-butyl ammonium hydroxide (BDH) and the pH of the solution was maintained at 8.3 ± 0.2.

^{51}V-nmr Measurements

^{51}V-nmr spectra were recorded at 23.66 MHz in a magnetic field of 2.1 T using a pulse FT-nmr technique on a Bruker WH-90 spectrometer interfaced with Bruker BNC-12 data system. The ^2H-resonance of a C_6D_6 capillary (2 mm) contained in a normal 10 mm nmr sample tube provided field-frequency stabilization. Typical spectral widths of 12 kHz in 8K of data memory using a 90° pluse (30 μs) were used. Spectra were recorded using rotating, cylindrical 10 mm od samples that were referenced, externally, to neat liquid $VOCl_3$ at 298 ± 2 K. Chemical shift data were calculated in ppm with negative values in the low frequency direction relative to $VOCl_3$. The resolution of overlapping peaks and peak areas were calculated using the Nicolet-1180 Curve Analysis Program (CAP). The error associated with each chemical shift value is estimated at ±0.2 ppm in the high pH region and ±1 ppm in the low pH region. All reported line widths at half-height values ($W_{1/2}$) have an uncertainty of about ±5 Hz.

Results

A series of ^{51}V FT-nmr spectra of $NaVO_3$ solutions were recorded at various pH and V(V) concentration levels. Typical spectra for a solution containing 0.5 mol L^{-1} total V(V) as $NaVO_3$ at various pH levels are shown in Fig. 1. Figures 2 and 3 show the data obtained from aqueous metavanadate solutions containing TBA as counter ions at two pH levels, respectively.

Discussion

This section is comprised of two parts. The first is focussed on the variation in ^{51}V FT-nmr parameters — chemical shifts, resonance line widths and relative peak areas — at various V(V) molar concentrations in the pH ranges 14.0 to 10.0 and 5.0 to 1.0. The second deals with the nature and characterization of metavanadate ions in the intermediate pH range 10.0 to 5.0 using data obtained from ^{51}V FT-nmr and other related techniques. Assignment of the 574 ppm and 582 ppm resonances is also suggested in this section.

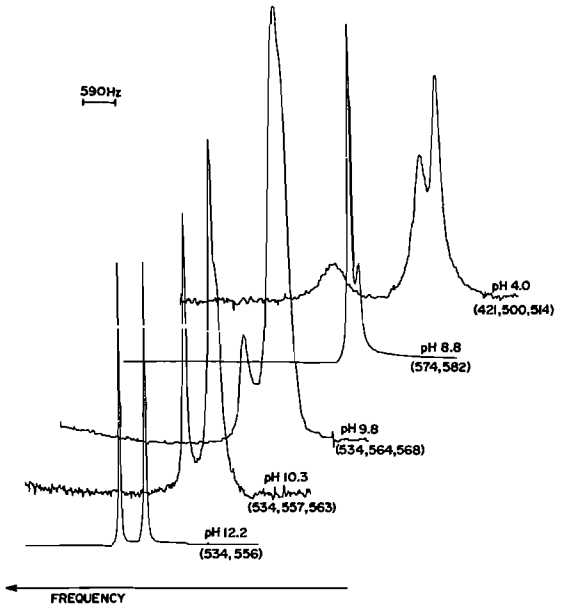


FIG. 1. Natural abundance ^{51}V-nmr spectra of 0.50 *M* metavanadate aqueous solutions at various pH levels (25°C and $I = 0.50$).

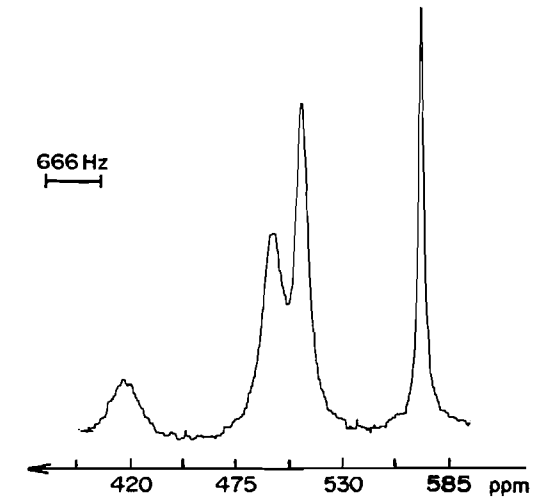


FIG. 2. ^{51}V-nmr spectrum of $V_{10}O_{28}^{6-}$ isopolyanion at pH 6.5. Resonances at 421, 496, and 512 ppm have been assigned to $V_{10}O_{29}^{6-}$ anion and the 574 ppm resonance is assigned to $V_4O_{12}^{4-}$ species. (TBA as counter ions.) $[NaVO_3] = 0.066$ *M*.

Variations of ^{51}V FT-nmr parameters with V(V) concentration change ($1.1 - 2.5 \times 10^{-1}$ *M*) and with pH change (14.0 to 10.0 and 5.0 to 1.0) observed in the present work are in general agreement with the continuous wave data reported by Howarth and Richards (11) and O'Donnell and Pope (14). Minor discrepancies are attributed to small pH variations, to the nature of the counter ions present in solution, and to the temperature at which the spectra were

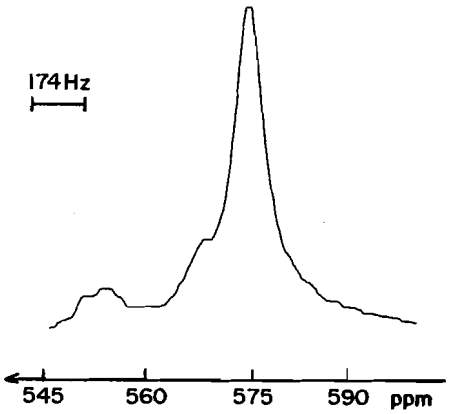


FIG. 3. ^{51}V-nmr spectrum of a metavanadate solution containing $V_4O_{12}^{4-}$ anion in the presence of TBA ions at pH = 8.3. $[NaVO_3] = 0.046\ M$.

recorded. Additionally, we are in general agreement with their arguments concerning changes in the line width and chemical shift values of the various resonances with changing pH and also with their assignments of the observed chemical shifts to the various vanadium(V) species present in solution.

We found our observed chemical shift values to be insensitive to ionic strength changes (0.25 to 0.45 (NaCl)) and to vanadium(V) concentration changes. No new resonances were observed when Na^+ was replaced with TBA as the counter ion in solution. The pH range of stability of the 574 ppm resonance, however, was extended to 10.0 from 9.7. At pH levels of 5.5 and below, only the resonances at 420, 495, and 510 ppm were observed and it was found that each chemical shift was pH sensitive. For example, the resonances shifted in the low frequency direction to 423, 507, and 527 ppm, respectively, as the pH decreased to 1.0. This sensitivity to pH changes is probably due to protonation reactions.

Our data suggest that the line widths are sensitive to pH and to vanadium(V) concentration changes. Generally, all resonances broadened significantly as the pH decreased and as the vanadium concentration increased.

The percentage total area of each ^{51}V FT-nmr resonance was dependent on the nature of the counter ion and strongly dependent on the pH at each vanadium concentration. At pH 14.0 only the 536 ppm resonance was observed. In the pH range 13.0 to 9.0, the percentage total area of the observed resonance at 534 ppm decreased from 93% to nearly zero, while the percentage total area of the resonance observed at 556 ppm increased to a maximum value of 25% at pH 10.0 and then decreased as the pH decreased to 9.0. Below pH 5.0, the intensity ratios of the three resonances observed have been reported to be 1:3:1 (11), 1:1:2 (12), and 1:2:2 (14, 27). Only the 1:2:2 ratio is in agreement with the crystalline structure of $V_{10}O_{28}^{6-}$ isopolyanion (28). The structure consists of ten VO_6 octahedra sharing edges, with two oxygen atoms in the interior of the molecule surrounded by six vanadium atoms in an octahedral geometry. This structure gives the ratio of the number of vanadium atoms occupying equivalent environments to be 2:4:4. The area ratios measured in the present work were close to 1:2:2 and were found to be independent of pH and total V(V) concentration. The ratios were sensitive to the time interval between the end of the pulse and accumulation of data points and approached 1:2:2 as the time delay decreased from 80 μs to 20 μs.

A summary of the variations of ^{51}V FT-nmr parameters with pH changes in the presence of Na^+ as a counter ion is given in Fig. 4 and in the presence of TBA is given in Fig. 5.

Variations of ^{51}V FT-nmr parameters with vanadium(V) concentration change (1.1 *M* to 0.033 *M*) and with pH change (intermediate range) observed in this work are shown in Table 1. For comparison, data from the literature (11, 12, 14) are also included in this table.

Howarth and Richards (11) observed only one resonance at 562 ppm which they assigned to $HV_2O_7^{3-}$, whereas Schneider and co-workers (12) observed resonances at 569 and 534 ppm which they assigned erroneously to the VO_3^- and $V_2O_7^{4-}$ species respectively.[1] Recently, O'Donnell and Pope (14) observed resonances at 535 ppm, 562 ppm, and 574 ppm and reported the coalescence of the latter two into a single resonance at 574 ppm as the pH decreased to 7.5. They attributed this behavior to a fast exchange between $HV_2O_7^{3-}$ and $(VO_3)_n^{n-}$ species. In our work, at pH 9.8, resonances at 534 ppm, 562 ppm, and 574 ppm were observed. As the solution was further acidified, a fourth appeared at 582 ppm — a resonance that has not been reported previously (11–14) in this pH range. The observation of partially resolved resonances at 562, 574, and 582 ppm indicates that the exchange rate between $HV_2O_7^{3-}$ and the species giving rise to the 574 and 582 ppm resonances is fairly fast.

In ref. 11, resonances were reported in the pH range 8.5 to 7.0 at 573 and 577 ppm that were as-

[1] ^{51}V-nmr chemical shifts from ref. 12 were obtained by subtracting the chemical shifts reported therein from 574 ppm. The authors of ref. 12 used the resonance of an aqueous NH_4VO_3 at pH 7.0 as a reference, while in effect, such solutions give rise to two resonances at 574 and 582 ppm relative to $VOCl_3$.

Can. J. Chem. Downloaded from www.nrcresearchpress.com by 210.87.254.6 on 09/05/12
For personal use only.

Can. J. Chem. Downloaded from www.nrcresearchpress.com by 210.87.254.6 on 09/05/12
For personal use only.

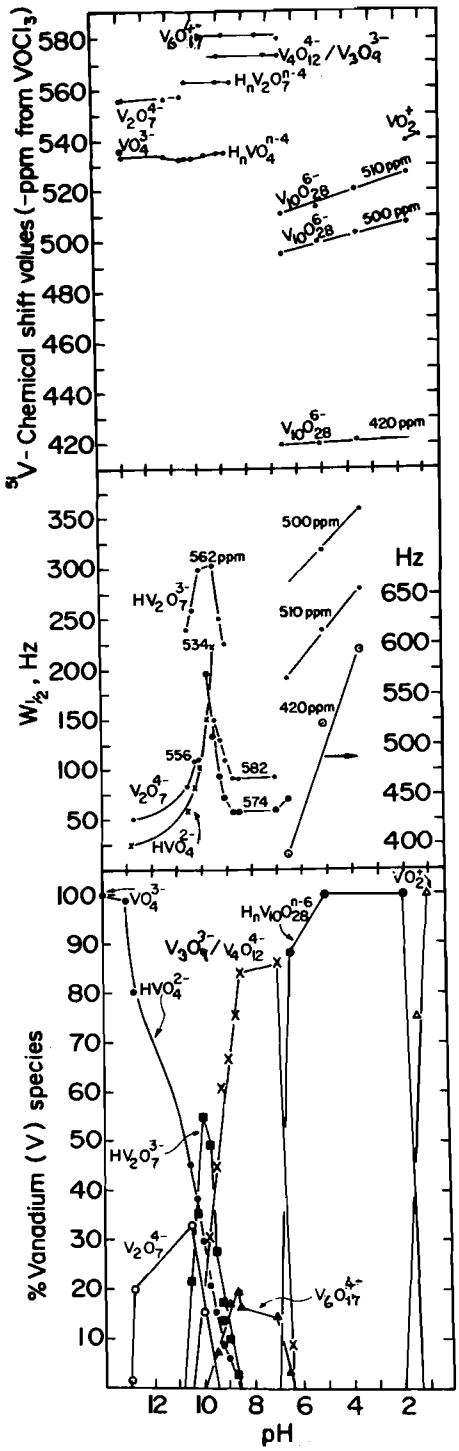


FIG. 4. ^{51}V-nmr chemical shifts, line widths, and % total areas of various vanadium(V) species as a function of pH at 0.25 *M* $NaVO_3$.

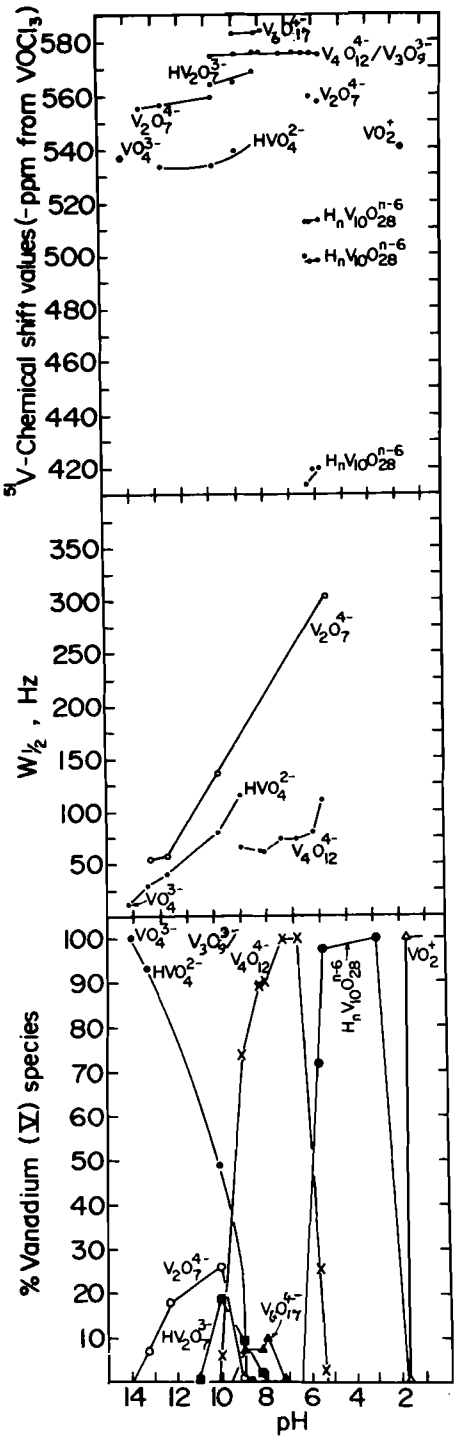


FIG. 5. ^{51}V-nmr chemical shifts, line widths, and % total areas of various vanadium(V) species in the presence of tetra-*n*-butyl ammonium ions at various pH levels and at 0.033 *M* $NaVO_3$.

TABLE 1. Comparison of ^{51}V FT-nmr chemical shift data of metavanadate ions at various pH levels

	Vanadium(V) species							
pH	$H_nVO_4^{(3-n)-}$	$H_nV_2O_7^{(4-n)-}$	VO_3^-	$(VO_3)_n^{n-}$†	$H_2V_4O_{13}^{4-}$	$V_3O_{10}^{5-}$	$V_6O_{17}^{4-}$	$V_{10}O_{28}^{6-}$	Reference
9.8–8.7		562							11
		534	569						12
	535	562		574					14
	534	562		574					This work
8.5–7.0			573	577					11
			574						12
				574					14
				574			582		This work
7.7–6.5*				574					This work
6.5–5.5								420,495,510	11
			574			410,500,516			12
				574	582				14
				574			582	419,495,510	This work
6.0–5.4*				574				419,495,512	This work

*Those metavanadate solutions contained TBA ions.
†n = 3 and/or 4.

signed to $(VO_3 \cdot H_2O^-)$ and $V_3O_9^{3-}$ or $V_4O_{12}^{4-}$, respectively. In refs. 12 and 14, however, only one resonance was reported at 574 ppm and this was assigned to VO_3^- in ref. 12 and to $(VO_3)_n^{n-}$ type species in ref. 14. In the present work resonances were observed at 574 and 582 ppm. The partial resolution of these implies a fairly fast rate of interconversion between the corresponding species giving rise to the resonances.

In the pH range 6.5 to 5.5, resonances were observed at 420, 495, 510, 574, and 582 ppm. Howarth and Richards (11) observed only the first three resonances and they assigned these to the $V_{10}O_{28}^{6-}$ anion. Schneider and co-workers (12) observed the first four resonances and incorrectly assigned them to $V_3O_{10}^{5-}$ and VO_3^- species. O'Donnell and Pope (14) observed resonances corresponding to $V_{10}O_{28}^{6-}$, $(VO_3)_n^{n-}$, and a resonance at 582 ppm which they assigned to an acyclic tetramer $H_2V_4O_{13}^{3-}$. For this assignment two ^{51}V-resonances should be observed. Our observation of five resonances indicates that $H_nV_{10}O_{28}^{(6-n)-}$ species are in equilibrium with the species giving rise to the 574 ppm and 582 ppm resonances. The large separation between the sub-set of three at higher frequency and the sub-set of two at lower frequency is indicative of a slow rate of exchange between the species giving rise to each sub-set. This slow rate of exchange could be rationalized if the vanadium coordination number of the species giving rise to the 574 ppm and 582 ppm resonances is four. In contrast, metavanadate solutions containing TBA as the counter ion exhibited resonances at 420, 495, 510, 556, and 574 ppm as shown in Fig. 2. This suggests that $H_nV_{10}O_{28}^{(6-n)-}$ anion disproportionates to $V_2O_7^{4-}$ and the species corresponding to 574 ppm.

As shown in Figs. 4 and 5, the line width of the 574 ppm resonance was always less than that of the 582 ppm resonance. This points out that the species giving rise to the 574 ppm resonance is either more symmetrical or has a smaller correlation time (τ_c) or both. Also, the insensitivity of the line widths and chemical shifts of both resonances to pH variations indicates no protonation occurred as the pH decreased from 8.5 to 7.0. As seen in Figs. 6 and 7, the percentage total area of the 574 ppm resonance was always larger than that of the 582 ppm resonance and the area ratios of the 574/582 resonances were found to be sensitive to changes in pH and V(V) concentration. As depicted in Fig. 7, this ratio decreased with increasing V(V) concentration.

Based on the observations noted in the intermediate pH range, we have assigned the 574 ppm resonance to both $V_3O_9^{3-}$ and $V_4O_{12}^{4-}$ species and the 582 ppm resonance to $V_6O_{17}^{4-}$ species.

It is generally recognized that metavanadate ions are present as $V_3O_9^{3-}$ in dilute solutions ($< 0.02\ M$) (1, 24, 29) and as $V_4O_{12}^{4-}$ in more concentrated solutions (2–5, 9, 10, 30, 31). Our observation that the area of the 574 ppm resonance was the largest in both dilute solutions ($[VO_3^-] = 1.9 \times 10^{-3}\ M$) and more concentrated solutions ($[VO_3^-] = 0.25\ M$) as tabulated in Table 2 suggests that this resonance corresponds to an equilibrium between $V_3O_9^{3-}$ and $V_4O_{12}^{4-}$ species. The observation of one resonance at 574 ppm suggests that the rate of interconversion between these species is fast and this

Can. J. Chem. Downloaded from www.nrcresearchpress.com by 210.87.254.6 on 09/05/12
For personal use only.

TABLE 2. ^{51}V FT-nmr chemical shift data of metavanadate solutions at various concentration levels

	V(V) species (mol/L)				
pH	VO_3^-	$V_2O_7^{4-}$	$H_nV_2O_7^{(4-n)-}$	$V_3O_9^{3-}$ and $V_4O_{12}^{4-}$	$V_6O_{17}^{4-}$
7.4	0.0019	554	568	573	
7.3	0.0034	555	568	574	
7.4	0.0058	553		573	581
7.7	0.0101	554	568	573	582
7.4	0.0226	553		573	581
7.1	0.249	—		573	581

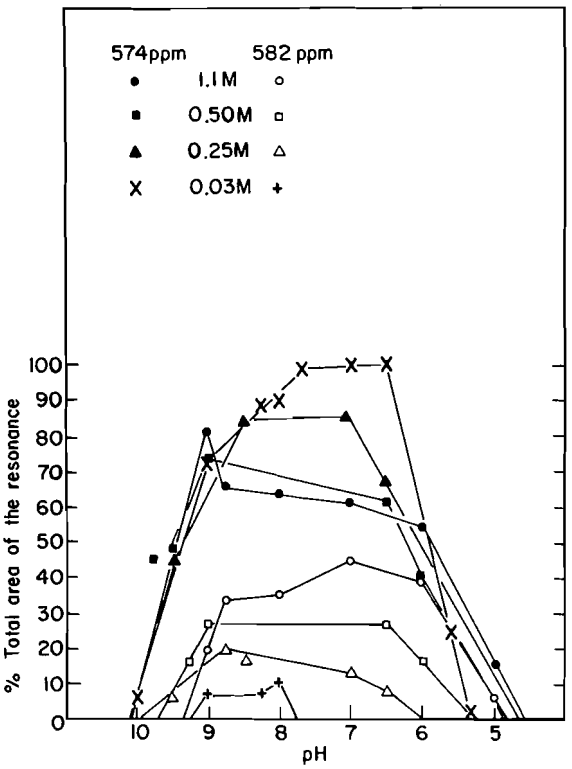


FIG. 6. Dependence of the % total areas of the 574 and 582 ppm resonances on pH and concentration changes.

value represents a weighted average of both resonances corresponding to $V_3O_9^{3-}$ and $V_4O_{12}^{4-}$ species.

A plot of ^{51}V-nmr chemical shifts vs. average change per vanadium atom (Z) based on the above assignments is shown in Fig. 8. This plot reveals — as pointed out elsewhere (11) — that the data fall into two distinct regions; one for vanadium species with a coordination number of four — VO_4^{3-}, $V_2O_7^{4-}$ and $H_nV_2O_7^{(4-n)-}$ — and a second for distorted octahedral species such as $V_{10}O_{28}^{6-}$ and $VO_2(H_2O)_4^+$. A discontinuity gap between these two regions is noted. The four coordinate series defines a straight line with the chemical shifts moving in the low frequency direction as Z de-

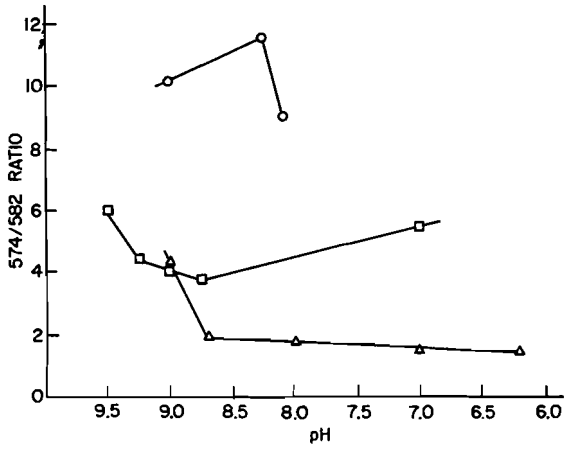


FIG. 7. A plot of the 574/582 ratio as a function of pH at various vanadium(V) concentration levels (○ = 0.033 M $NaVO_3$, TBA present; □ = 0.25 M $NaVO_3$, and △ = 1.1 M $NaVO_3$); T = 298 K.

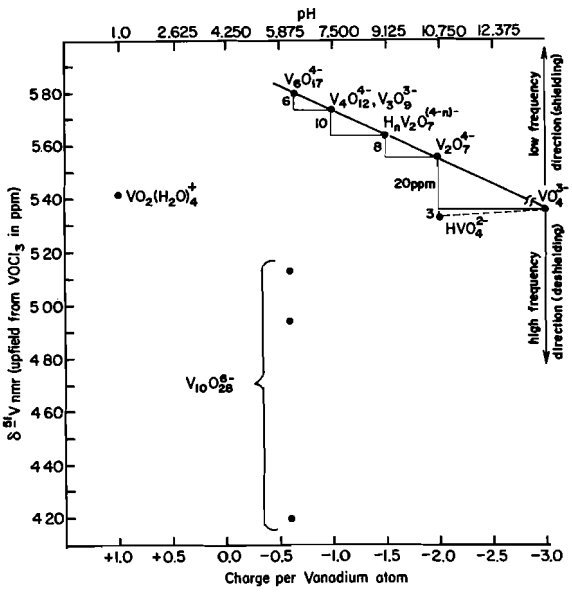
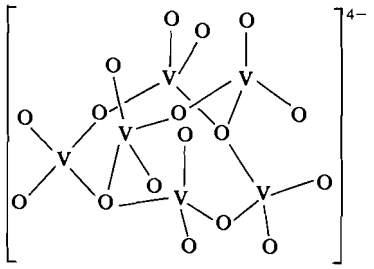


FIG. 8. A plot of ^{15}V-nmr chemical shift data vs. average charge per vanadium(V) atom. [$NaVO_3$] = 0.25 M.

Can. J. Chem. Downloaded from www.nrcresearchpress.com by 210.87.254.6 on 09/05/12
For personal use only.

creases. The 582 ppm resonance falls on this line if it is assigned to a four coordinated $V_6O_{17}^{4-}$ species. The data of Brito (32) support the presence of such a species in solution in the intermediate pH range.

A structure that is consistent with the requirements of one vanadium environment with four coordination sites and $Z = -0.67$ that gives rise to the 582 ppm resonance is shown below.



It consists of six VO_4 tetrahedra sharing two corner oxygen atoms to form three puckered eight-membered rings. The suggestion that the structure of $V_6O_{17}^{4-}$ anion in solution is composed of two cyclic trimers joined together through an oxygen atom may be ruled out by recognizing that such a structure gives rise to two vanadium atom environments.

Our proposed structure suggests that the formation of $V_6O_{17}^{4-}$ may occur by the reaction between $V_4O_{12}^{4-}$ and $V_2O_7^{4-}$ as shown by reaction [1].

[1] $$V_4O_{12}^{4-} + V_2O_7^{4-} + 4H^+ \rightleftarrows V_6O_{17}^{4-} + 2H_2O$$

Support for this hypothesis is based on our observation that the areas of the 554 ppm and 568 ppm resonances decreased while the areas of the 574 and 582 ppm resonances increased as the total vanadium concentration increased. It should be pointed out that in metavanadate solutions (0.033 *M*) containing TBA ions — in the pH range 7.7 to 6.5 — only a resonance at 574 ppm was observed. The resonance was fairly narrow ($W_{1/2}$ = 70 ± 5 Hz) which is indicative of a symmetrical environment about the vanadium atoms. The absence of the 582 ppm resonance suggests that TBA ions preferentially stabilize the $V_3O_9^{3-}$ and/or $V_4O_{12}^{4-}$ species through ion pair formation. Fuchs *et al.* (25, 26) determined the structure of a crystalline salt prepared from similar solutions. They reported the structure to be cyclic, consisting of four VO_4 tetrahedra sharing two oxygen corners to form a puckered eight-membered ring.

Acknowledgements

We thank the Natural Sciences and Engineering Research Council of Canada, Strategic Grants Program, for financial support; Drs. R. A. Bell, D. R. Eaton, and G. T. Schrobilgen for helpful discussions; and Mr. B. Sayer for technical assistance in recording the ^{51}V-nmr spectra. We also acknowledge a referee's question that led to the ^{51}V FT-nmr studies on dilute ($<10^{-2}$ *M*) metavanadate solution.

1. P. Z. Düllberg. Z. Phys. Chem. **45**, 129 (1903).
2. I. F. Jahr and H. Fuchs. Z. Naturforsch. **18**b, 1133 (1963).
3. A. W. Naumann and C. J. Hallada. Inorg. Chem. **3**, 70 (1964).
4. G. Jander and K. F. Jahr. Z. Anorg. Allg. Chem. **212**, 1 (1963).
5. J. Simon and K. F. Jahr. Z. Naturforsch. **19**b, 165 (1964).
6. N. Ingri and F. Brito. Acta Chem. Scand. **13**, 1971 (1959).
7. F. Brito, N. Ingri, and L. G. Sillen. Acta Chem. Scand. **18**, 1557 (1964).
8. R. S. Saxena and O. P. Sharma. J. Inorg. Nucl. Chem. **28**, 1881 (1966).
9. D. B. Copley, A. K. Banerjee, and S. Y. Tyree, Jr. Inorg. Chem. **4**, 1480 (1965).
10. A. Gaglani, N. Asting, and W. H. Nelson. Inorg. Chem. **13**, 1715 (1974).
11. O. W. Howarth and R. E. Richards. J. Chem. Soc. A, 864 (1965).
12. J. V. Hatton, Y. Saito, and G. W. Schneider. Can. J. Chem. **43**, 47 (1965).
13. A. Akasarailian, J. Lecuna, and R. Brito. Ann. Quim. **64**, 343 (1968).
14. S. E. O'Donnell and M. T. Pope. J. Chem. Soc. Dalton, 2290 (1976).
15. W. P. Griffith and T. D. Wickins. J. Chem. Soc. A, 1087 (1966).
16. W. P. Griffith and P. J. Lesniak. J. Chem. Soc. 1066 (1969).
17. W. P. Griffith. J. Chem. Soc. 905 (1967).
18. C. Liteanu, I. Lukas, and C. Strusievici. Omagin Reluca Ripan, 333 (1966).
19. P. Petrovic, O. Cutkova, and P. Schwendt. Chem. Zvesti. **27**, 752 (1973).
20. (*a*) D. L. Kepert. *In* Comprehensive inorganic chemistry. Vol. 4. *Edited by* J. C. Bailor, H. J. Emeleus, R. Nyholm, and A. F. Trotman-Dickinson. Pergamon Press, New York, NY. 1973. pp. 607–672. (*b*) R. H. Clark. *In* Comprehensive inorganic chemistry. Vol. 3. 1973. p. 521.
21. M. T. Pope and B. W. Dale. Q. Rev. Chem. Soc. **22**, 527 (1968).
22. D. L. Kepert. The early transition elements. Academic Press, London. 1972. pp. 181–187.
23. L. Newman, W. J. Lafleur, F. J. Brousaicles, and A. M. Ross. J. Am. Chem. Soc. **80**, 4491 (1958).
24. K. Schiller and E. Thilo. Z. Anorg. Allg. Chem. **310**, 261 (1961).
25. J. Fuchs, S. Mahjour, and J. Pickordt. Angew. Chem. Int. Ed. Eng. **15**, 374 (1976).
26. J. Fuchs, S. Mahjour, and R. Palm. Z. Naturforsch. **31**b, 544 (1976).
27. L. P. Kazansii and A. V. Spitsyn. Dokl. Akad. Nauk SSSR, **223**, 381 (1975).
28. H. T. Evans. Inorg. Chem. **5**, 967 (1966).
29. R. A. Robinson and D. A. Sinclair. J. Chem. Soc. 642 (1934).
30. J. F. Hazel, W. M. McNabb, and R. J. Santini, Jr. J. Phys. Chem. **57**, 681 (1953).
31. G. Schwarzenbach and G. Parissakis. Helv. Chim. Acta, **41**, 2042 (1958).
32. F. Brito. Acta Chem. Scand. **21**, 1968 (1967).

Can. J. Chem. Downloaded from www.nrcresearchpress.com by 210.87.254.6 on 09/05/12
For personal use only.

Ion molecule reactions in ethane. Thermochemistry and structures of the intermediate complexes: $C_4H_{11}^+$ and $C_4H_{10}^+$ formed in the reactions of $C_2H_5^+$ and $C_2H_4^+$ with C_2H_6

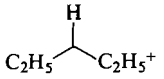
K. HIRAOKA[1] AND P. KEBARLE

Chemistry Department, University of Alberta, Edmonton, Alta., Canada T6G 2G2

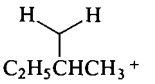
Received March 28, 1980

K. HIRAOKA and P. KEBARLE. Can. J. Chem. **58**, 2262 (1980).

The reactions of $C_2H_5^+$ and $C_2H_4^+$ with ethane were studied in a pulsed electron beam high ion source pressure mass spectrometer. Ethane at variable pressures in the 10–100 mTorr range in ~5 Torr hydrogen was used in experiments covering the temperature range −145 to 400°C. Reaction [7]: $C_2H_5^+ + C_2H_6 = sec\text{-}C_4H_9^+ + H_2$ was found to have a rate constant whose magnitude decreased with temperature: $k_7 = 10^{-5.12}\,T^{-2}$ (molecule^{-1} cm^3 s^{-1}). The reaction proceeds via a $C_4H_{11}^+(b)$ intermediate, which at low temperature can be stabilized and becomes the major product. The rate constant for thermal decomposition of $C_4H_{11}(b)$ by reaction [6t]: $C_4H_{11}^+(b) = sec\text{-}C_4H_9^+ + H_2$ could be measured. The activation energy was found to be $E_{6t} = 9.6$ kcal/mol. From consideration of the above data and the known ΔH_7, it was concluded that $C_4H_{11}^+(b)$ has the structure



Before dissociation to $sec\text{-}C_4H_9^+ + H_2$, this ion rearranges to

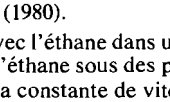


The barrier for this rearrangement is ~9.6 kcal/mol.

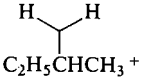
$C_2H_4^+$ reacts with C_2H_6 to give $C_4H_{10}^+(d)$ at low temperatures. At high temperatures $C_4H_{10}^+(d)$ becomes an intermediate in the dissociation to $sec\text{-}C_3H_7^+ + H_2$. The formation of $C_4H_{10}^+$ at low temperature has a rate constant whose magnitude decreases with temperature. The temperature dependence of the equilibrium constant K_{10} for the reaction [10]: $C_2H_4^+ + C_2H_6 = C_4H_{10}^+(d)$ could be determined. This led to $\Delta H_{10} = -15.3$ kcal/mol. The rate constant for the high temperature reaction [11]: $C_2H_4^+ + C_2H_6 = sec\text{-}C_3H_7^+ + H_2$ was $k_{11} = 8.4 \times 10^{-10} \exp(-3.9/RT$ kcal/mol) (molecule^{-1} cm^3 s^{-1}). A potential energy diagram for the reaction system is proposed. $C_4H_{10}^+(d)$ is probably a complex between $C_2H_4^+$ and C_2H_6 held largely by ion induced dipole process. Reaction [11] probably proceeds via $C_4H_{10}^+(d) \rightarrow n\text{-}C_4H_{10}^+ \rightarrow sec\text{-}C_3H_7^+ + H_2$. The barrier between $C_7H_{10}^+(d)$ and $n\text{-}C_4H_{10}^+$ is ~20 kcal/mol.

K. HIRAOKA et P. KEBARLE. Can. J. Chem. **58**, 2262 (1980).

On a étudié les réactions des ions $C_2H_5^+$ et $C_2H_4^+$ avec l'éthane dans un spectromètre de masse ayant une source d'ions à haute pression et un faisceau pulsé d'électrons. On a utilisé l'éthane sous des pressions allant de 10 à 100 mTorr et dans un intervalle de température allant de −145 à 400°C. On a trouvé que la constante de vitesse de la réaction [7]: $C_2H_5^+ + C_2H_6 = sec\text{-}C_4H_9^+ + H_2$ diminue avec la température $K_7 = 10^{-5,12}\,T^{-2}$ (molécule^{-1} cm^3 s^{-1}). La réaction se fait via un intermédiaire $C_4H_{11}^+(b)$ qui peut se stabiliser à basse température et devenir le produit majoritaire. On peut mesurer la constante de vitesse de la décomposition thermique du $C_4H_{11}^+(b)$ selon la réaction [6t]: $C_4H_{11}^+(b) = sec\text{-}C_4H_9^+ + H_2$. On a trouvé une énergie d'activation E_{6t} = 9,6 kcal/mol. En considérant les données précédentes et connaisant le ΔH_7, on en conclu que l'ion $C_4H_{11}^+(b)$ a la structure suivante



Cet ion se transpose en



avant sa dissociation en $sec\text{-}C_4H_9^+$ et H_2. La barrière d'énergie de cette transposition est d'environ 9,6 kcal/mol.

L'ion $C_2H_4^+$ réagit avec C_2H_6 pour donner $C_4H_{10}^+(d)$ à de basses températures. A des températures plus élevées, l'ion $C_4H_{10}^+$ devient un intermédiaire lors de la dissociation en $sec\text{-}C_3H_7^+ + H_2$. La constante de vitesse de la formation de $C_4H_{10}^+$ diminue avec la température. On peut déterminer l'effet de la température sur la constante d'équilibre K_{10} de la réaction [10]: $C_2H_4^+ + C_2H_6 = C_4H_{10}^+(d)$. Ceci conduit à une valeur de $\Delta H_{10} = -15,3$ kcal/mol. La constante de vitesse de la réaction [11] se produisant à haute température: $C_2H_4^+ + C_2H_6 = sec\text{-}C_3H_7^+ + H_2$ est de $k_{11} = 8,4 \times 10^{-10} \exp(-3,9/RT$ kcal/mol) (molécule^{-1} cm^3 s^{-1}). On propose un diagramme d'énergie potentielle de la réaction. L'ion $C_4H_{10}^+(d)$ est probablement un complexe entre $C_2H_4^+$ et C_2H_6 maintenu essentiellement par des forces dipolaires induites par l'ion. La réaction [11] se fait probablement par l'intermédiaire de: $C_4H_{10}^+(d) \rightarrow n\text{-}C_4H_{10}^+ \rightarrow sec\text{-}C_3H_7^+ + H_2$. La barrière entre $C_7H_{10}^+(d)$ et $n\text{-}C_4H_{10}^+$ est d'environ de 20 kcal/mol.

[Traduit par le journal]

---

[1]Present address: Faculty of Engineering, Yamanashi University, Takeda-4, Kofu, Japan 400.

0008-4042/80/212262-09$01.00/0

©1980 National Research Council of Canada/Conseil national de recherches du Canada

Can. J. Chem. Downloaded from www.nrcresearchpress.com by 210.87.254.105 on 09/05/12
For personal use only.

Can. J. Chem. Downloaded from www.nrcresearchpress.com by 210.87.254.105 on 09/05/12
For personal use only.

Introduction

Considerable information is available in the literature concerning the ion molecule reactions in ethane (see ref. 1 and references therein).

The present work concentrates on the temperature dependence of the reactions of two ions, $C_2H_5^+$ and $C_2H_4^+$, with ethane. $C_2H_6^+$, $C_2H_5^+$, and $C_2H_4^+$ are the three major ions produced by electron impact on ethane. The present work provided also information on the reactions of $C_2H_6^+$, but these did not have novel character and are therefore not discussed.

By covering a wide temperature range (−145 to 400°C) and working at a relatively high pressure of a third gas (~5 Torr H_2) information could be obtained not only on the temperature dependence of the reactions but also on some of the properties and energetics of the complexes and reaction intermediates $C_2H_5^+ \cdot C_2H_6$ and $C_2H_4^+ \cdot C_2H_6$. In this regard, the present work represents an extension of earlier results from this laboratory (2, 3) which dealt with the thermochemistry and the possible structures of $C_2H_7^+$, $C_3H_9^+$, and $C_4H_{11}^+$ formed by reactions of alkyl cations with hydrogen or suitable paraffins.

Experimental

The measurements were made with the pulsed electron beam high-pressure ion source mass spectrometer which has been described previously (4). A small amount of ethane (Phillips Research Grade) was introducted into hydrogen carrier gas (Linde U.H.P.) through a stainless steel capillary (0.3 mm × 1 m). Impurity (mainly water) was largely suppressed by passing the hydrogen through a liquid N_2 cooled molecular sieve 5 Å trap. The scatter of values of measured rate constants and equilibrium constants was within 20% when the ethane pressure was changed by a factor of more than 10.

Results and Discussion

(a) Production of Ions from Ethane

Results from four typical runs at four different temperatures are shown in Figs. 1–4. The primary ethane ions are most clearly displayed in Fig. 2 obtained at 12°C. The principal ion is $C_2H_5^+$ (~80% of total ionization). The next most abundant ion is $C_2H_4^+$ (~10%). These two major ions are probably produced by processes: [1]–[5].

[1] $e + H_2 = H_2^+ + 2e$ ~95%
$H^+ + H + 2e$ ~5%

[2] $e + C_2H_6 = C_2H_4^+$ (50%), $C_2H_3^+$ (15%), $C_2H_6^+$ (13%), C_2H_5 (10%)

[3] $H_2^+ + H_2 = H_3^+ + H$

[4] $H_2^+ + C_2H_6 = C_2H_4^+ + 2H_2$ 70%
$C_2H_6^+ + H_2$ 22%

[5] $H_3^+ + C_2H_6 = C_2H_5^+ + 2H_2$

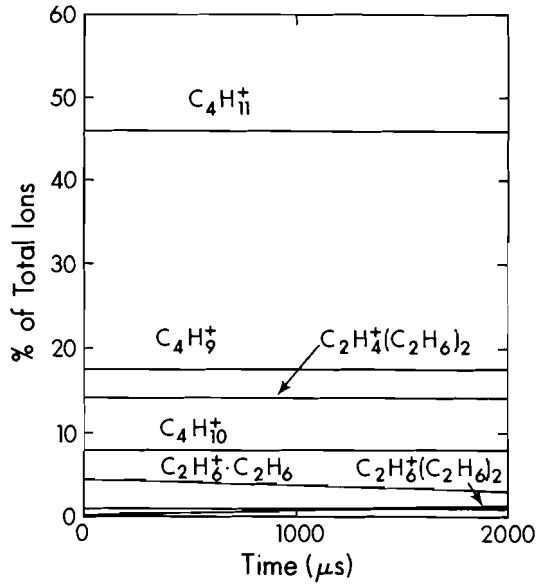


FIG. 1. Ions observed in 4 Torr H_2 containing 47 mTorr C_2H_6 at −145°C. The primary ethane ions produce "clusters" with ethane: $C_2H_6^+$ leads to $C_2H_6^+(C_2H_6)_n$, $C_2H_5^+$ leads to $C_4H_{11}^+$, some of which decomposes to $C_4H_9^+$, $C_2H_4^+$ leads to $C_4H_{10}^+$ and higher "cluster" $C_2H_4^+(C_2H_6)_2$. Reactions are very fast and therefore complete in a few microseconds.

The observed abundances of $C_2H_5^+$ and $C_2H_4^+$ in Fig. 2 can be approximately accounted as follows. Considering the preponderance of H_2 over C_2H_6, the principal ion is $C_2H_5^+$ produced by [1] → [3] → [5]. Some $C_2H_4^+$ is produced by the direct ionization of C_2H_6, process [2]. The electron impact ionization cross section of ethane is about 8 times larger than that of hydrogen and 50% of the ethane ionization leads to $C_2H_4^+$ (7). Some additional $C_2H_4^+$ is produced by [4]. This may be expected since $k_4/k_3 \approx 2.3$ (see Kim and Huntress (5) and Bowers and Elleman (6)) and 70% of the yield of [4] leads (5) to $C_2H_4^+$.

(b) Reactions $C_2H_5^+ \rightarrow C_4H_{11}^+ \rightarrow C_4H_9^+ + H_2$

The fate of the principal ion, $C_2H_5^+$, at different temperatures, can be deduced from Figs. 1–4. At the lowest temperature, −145°C Fig. 1, very fast reactions convert $C_2H_5^+$ to $C_4H_{11}^+$ and $C_4H_9^+$. The major product is $C_4H_{11}^+$. Near room temperature, 12°C Fig. 2, $C_2H_5^+$ is observed to decrease more slowly. The major product is $C_4H_9^+$, although some $C_4H_{11}^+$ is also formed. At longer reaction times ($t >$ 100 μs), the $C_4H_{11}^+$ is seen to decompose slowly to $C_4H_9^+$. The higher temperature run, 77°C Fig. 3, shows that the disappearance of $C_2H_5^+$ is much slower again, there is even less $C_4H_{11}^+$, and the $C_4H_{11}^+$ decomposes faster to $C_4H_9^+$. At the highest

Can. J. Chem. Downloaded from www.nrcresearchpress.com by 210.87.254.105 on 09/05/12
For personal use only.

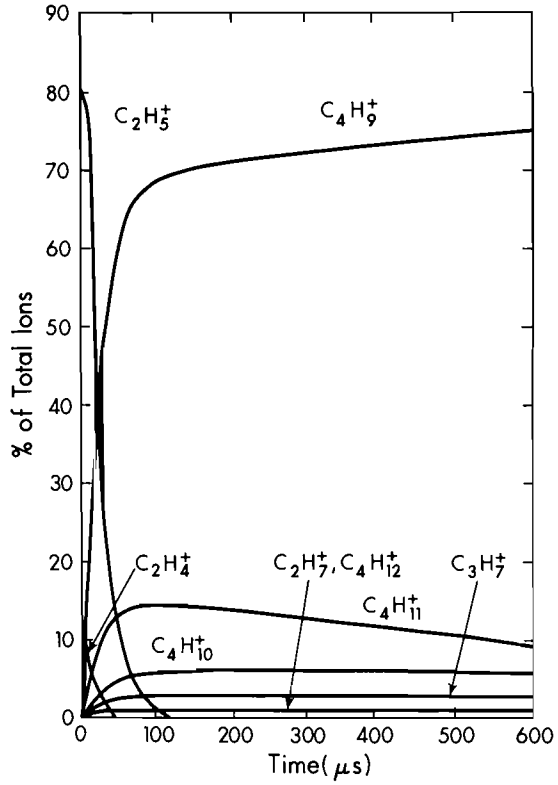


FIG. 2. Ions observed in 4 Torr H_2 containing 15 mTorr C_2H_6 at 12°C. At this temperature, the major ion $C_2H_5^+$ reacts more slowly than at −145°C. It yields mostly $C_4H_9^+$ and some $C_4H_{11}^+$. The $C_4H_{11}^+$ decomposes thermally to $C_4H_9^+$ at longer reaction times. $C_2H_4^+$ leads to $C_4H_{10}^+$ and $C_3H_7^+$.

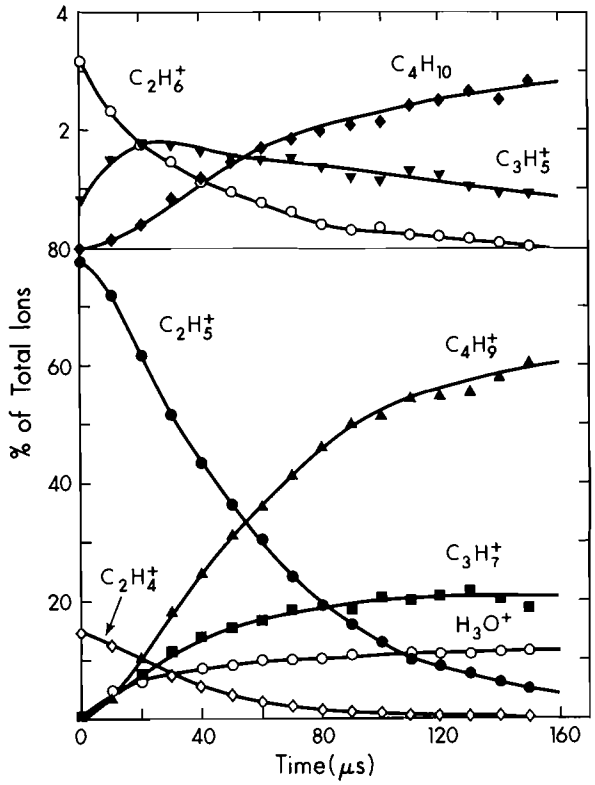


FIG. 3. Ions observed in 4 Torr H_2 containing 22 mTorr C_2H_6 at 77°C. $C_2H_5^+$ reacts more slowly at 77°C than at 12°C, major product is $C_4H_9^+$. Products of $C_2H_4^+$ are $C_4H_{10}^+$ and $C_3H_7^+$.

temperature, 352°C Fig. 4, disappearance of $C_2H_5^+$ is the slowest, $C_4H_9^+$ is the only observed product, since, presumably, the intermediate $C_4H_{11}^+$ is present at such low concentrations that it is not detected.

The observation that the rate of $C_2H_5^+$ disappearance decreases with temperature indicates that the formation of the observed $C_4H_{11}^+$ and $C_4H_9^+$ occurs via some intermediate reaction complex whose back decomposition to the initial reactants increases with temperature. A suitable reaction scheme is provided by reaction [6].

$$[6]\quad C_2H_5^+ + C_2H_6 \underset{r}{\overset{f}{\rightleftarrows}} (C_4H_{11}^+)^*$$

$$(C_4H_{11}^+)^* \xrightarrow{d} C_4H_9^+ + H_2$$

$$(C_4H_{11}^+)^* + M \xrightarrow{s} C_4H_{11}^+(b) + M$$

$$C_4H_{11}^+(b) \xrightarrow{t} C_4H_{11}^+(a) \rightarrow C_4H_9^+ + H_2$$

The $(C_4H_{11}^+)^*$ formed by [6f] is excited since its formation from $C_2H_5^+$ and C_2H_6 is exothermic. Some of the $(C_4H_{11}^+)^*$ undergoes reverse dissociation by [6r], this reverse dissociation increases with temperature. The reverse dissociation may be accompanied by hydride transfer. The hydride transfer may be made visible by using deuterium labelled compounds like C_2H_6 and C_2D_6 (see Ausloos *et al.* (8)). The $(C_4H_{11}^+)^*$ may decompose directly to $C_4H_9^+ + H_2$. This occurs to some extent even at the lowest temperature (see Fig. 1). Some of the $(C_4H_{11}^+)^*$ is stabilized by third body collisions, [6s]. At low temperatures, the stabilized $C_4H_{11}^+(b)$ does not decompose (Fig. 1). At higher temperatures, the $C_4H_{11}^+(b)$ undergoes thermal decomposition [6t], see Figs. 2, 3. The significance of the notation $C_4H_{11}^+(b)$ and $C_4H_{11}^+(a)$ will be explained later.

Plots of log $[C_2H_5^+]$ versus time were made for a series of runs in which the H_2 pressure was approximately constant but for which the temperature and ethane concentration was varied. It was found that the rate of disappearance of $C_2H_5^+$ was first order in the C_2H_6 concentration. In the higher temperature range 70–350°C, the observed $C_4H_{11}^+$ concentration was extremely low. For these condi-

Can. J. Chem. Downloaded from www.nrcresearchpress.com by 210.87.254.105 on 09/05/12
For personal use only.

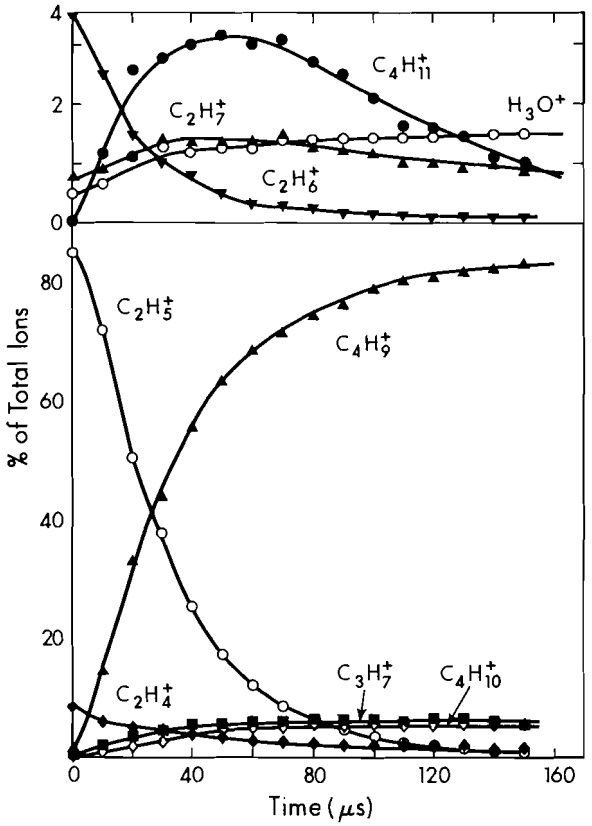


FIG. 4. Ions observed in 4 Torr H_2 containing 52 mTorr of C_2H_6 at 352°C. $C_2H_5^+$ reacts slowly to yield $C_4H_9^+$, concentration of $C_4H_{11}^+$ intermediate too low to detect. $C_2H_4^+$ leads to $C_3H_7^+$ and some small concentration of stable $C_4H_{10}^+$.

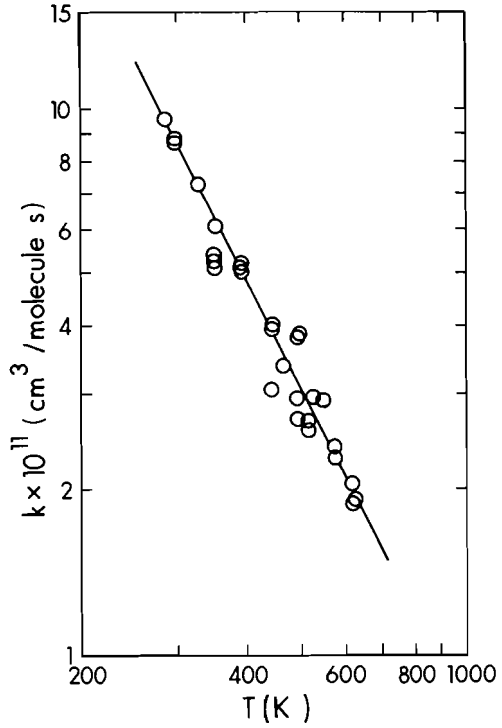


FIG. 5. Plot of rate constant k_7 for reaction [7]: $C_2H_5^+ + C_2H_6 = C_4H_9^+ + H_2$. From rate of disappearance of $C_2H_5^+$ in temperature region where concentration of $C_4H_{11}^+$ intermediate is very low. Reaction shows negative temperature dependence which can be expressed as $k_7 = 10^{-5.12}\,T^{-2}$ (cm^3 molecule^{-1} s^{-1}).

tions the disappearance of $C_2H_5^+$ can be represented by reaction [7].

[7] $C_2H_5^+ + C_2H_6 = C_4H_9^+ + H_2$

Rate constants k_7, obtained from log $[C_2H_5^+]$ versus time plots in this temperature range, are shown in Fig. 5 which is a plot of log k_7 versus log T. A straight line is obtained which defines eq. [8].

[8] $k_7 = 10^{-5.12}\,T^{-2}$ (cm^3 molecule^{-1} s^{-1})

Bennett *et al.* (1) have determined previously k_7 at two different temperatures, $k_7 = 2.5 \times 10^{-10}$ at 189 K and $k_7 = 5 \times 10^{-11}$ at 410 K. Equation [8] predicts, in good agreement, $k_7 = 2.2 \times 10^{-10}$ and $k_7 = 4.5 \times 10^{-11}$ (all values in molecule^{-1} cm^3 s^{-1}) for the same two temperatures.

The negative temperature dependence of [7] is typical for a reaction which proceeds via an excited intermediate, i.e. $(C_4H_{11}^+)^*$, whose reverse reaction to $C_2H_5^+ + C_2H_6$ [6r] increases faster with temperature than the forward decomposition; [6d] and [6s] followed by [6t].

The rate of the thermal decomposition of $C_4H_{11}^+(b)$, i.e. reaction [6t] could be determined in the temperature range 12°C to 70°C. At these temperatures $C_4H_{11}^+$ is formed and decomposes (see Figs. 2 and 3). A series of runs in this temperature range provided the data for the determination of the rate constants k_{6t}. An Arrhenius plot of k_{6t} is shown in Fig. 6. Actually two plots are given in Fig. 6 because of a certain ambiguity in the evaluation of k_{6t}. In one treatment of the data, k_{6t} was obtained by plotting log $[C_4H_{11}^+]$ versus t at long reaction times. This treatment is fully justified for conditions like those in Fig. 2 where the production of $C_4H_{11}^+$, from $C_2H_5^+$, is finished in a short time. However, at higher temperatures (see Fig. 3) the production of $C_4H_{11}^+$ is slower, while the decomposition is faster. This means that practically over all the observed time, $C_4H_{11}^+$ is produced, by [6f, s], and decomposes by [6t], so that one must treat $C_4H_{11}^+$ as an intermediate in the consecutive sequence $C_2H_5^+ \rightarrow C_4H_{11}^+ \rightarrow C_4H_9^+$. The steeper Arrhenius line in Fig. 6 was obtained by treating the high temperature concentrations as a consecutive reaction. The true temperature dependence of k_{6t} probably lies somewhere between the two plots.

Can. J. Chem. Downloaded from www.nrcresearchpress.com by 210.87.254.105 on 09/05/12
For personal use only.

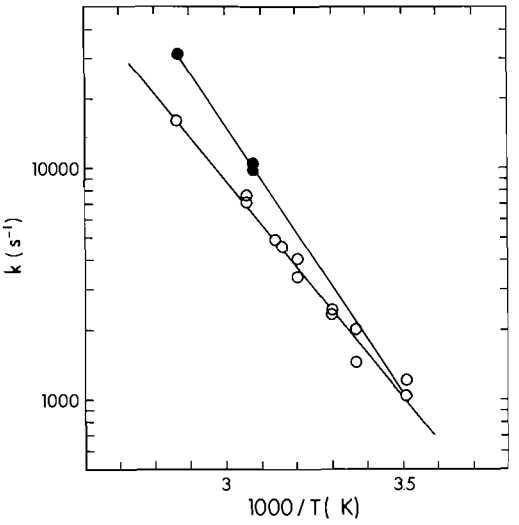


FIG. 6. Arrhenius plot of rate constant k_{6t} for thermal decomposition: $C_4H_{11}^+ \rightarrow C_4H_9^+ + H_2$. Depending on treatment of data (see text), two activation energies can be obtained, the lesser slope leads to 8.6 kcal/mol, the steeper slope to 10.6 kcal/mol.

Therefore the activation energy E_{6t} should be between the two slopes of the plots, i.e. $8.6 < E_{6t} < 10.6$ kcal/mol (see Fig. 6).

A potential energy diagram for the reaction system [6] is shown in Fig. 7. The diagram takes into account that the overall reaction to $C_4H_9^+$ has no activation energy and has a negative temperature dependence. The potential energy barrier 9.6 kcal/mol is based on the average activation energy E_{6t} from Fig. 6. The exothermicity of reaction [7] shown in the potential energy diagram as 20.8 kcal/mol was calculated using the following literature data: $\Delta H_f(C_2H_5^+) = 219$ kcal/mol (9), $\Delta H_f(sec\text{-}C_4H_9^+) = 178$ kcal/mol. This last value is based on the results of Lossing and Maccoll (10), but the enthalpy was reduced by 5 kcal/mol.[2] We have assumed that the $C_4H_9^+$ formed in reactions [6], [7] is $sec\text{-}C_4H_9^+$, following Ausloos *et al.* (8) who on the basis of neutral product analysis and deuterium labelling deduced this structure for the ion formed from $C_2H_5^+$ and C_2H_6. The well depth of 13 ± 3 kcal/mol for the $C_4H_{11}^+(b)$ compound is a somewhat arbitrary number. In earlier work (3), it was found that $\Delta H = -6.6$ kcal/mol for the reaction $C_2H_5^+ + CH_4 = C_3H_9^+$ (see Fig. 7, *II*). One can expect that the reaction $C_2H_5^+ + C_2H_6 = C_4H_{11}^+$ should be considerably more exothermic since the Lewis basicity of ethane should be much larger than that of methane. This is suggested by the Brönsted acidities, i.e. proton affinities which are: $PA(CH_4) = 127$ kcal/mol, $PA(C_2H_6) = 140$ kcal/mol (11). Furthermore, since reaction [7] was found to have no activation energy, the well depth in Fig. 7, *I* must be deeper than the 9.6 kcal/mol potential energy barrier. On the basis of these considerations we chose 13 ± 3 kcal/mol for the well depth.

The potential energy diagram of a related system studied earlier (3) is shown in Fig. 7, *II*. This is reaction [9].

[9] $C_2H_5^+ + CH_4 \rightleftarrows C_3H_9^+ \rightarrow C_3H_7^+ + H_2$

The rate for the reaction $C_2H_5^+ + CH_4 = C_3H_7^+ + H_2$ was found to increase with temperature. This increase corresponded to an activation energy of 2.5 kcal/mol. The equilibrium $C_2H_5^+ + CH_4 = C_3H_9^+(b)$ proved measurable. The temperature dependence of the equilibrium constant gave $\Delta H = -6.6$ kcal/mol. This is the well depth shown in Fig. 7, *II*. The potential energy barrier of 9.1 kcal/mol was obtained by adding the activation energy of 2.5 kcal/mol to the well depth 6.6 kcal/mol. For the present system, experimental conditions could not be found for which the equilibrium $C_2H_5^+ + C_2H_6 = C_4H_{11}^+$ could be observed. This is in line with the potential energy diagram in Fig. 7, *I* which shows a smaller internal potential barrier for the dissociation to $C_4H_9^+ + H_2$ that the well depth which corresponds to the barrier for back dissociation $C_4H_{11}^+ \rightarrow C_2H_5^+ + C_2H_6$. It is interesting to note that the internal barriers for the two systems in Fig. 7 are quite similar, i.e. both around 9 kcal/mol. In earlier work (2), it was found that $C_2H_5^+$, $sec\text{-}C_3H_7^+$, and $t\text{-}C_4H_9^+$ form only very weakly bonded complexes with H_2. These complexes were assigned the structures **A** (see Fig. 7). The structures in which the bonding comes about from the alkyl cation interacting with the electrons of a C—H bond (see Fig. 7) were called structures **B**. In analogy with that earlier work (2), we assign the $C_4H_{11}^+(b)$ ion of reaction [6] a **B** type structure. The weakly bonded $C_4H_{11}^+(a)$, precursor in the dissociation to $sec\text{-}C_4H_9^+ + H_2$ in the potential energy diagram Fig. 7, *I*, is assumed to have structure **A**. With these assignments, the barriers of ~9 kcal/mol in Fig. 7, *I* and *II* turn out to represent the barriers for rearrangement from structures **B** to structures **A**. We associate structures **B** as the precursors for dissociation to an alkyl cation and an alkane and as intermediates in hydride transfer reactions like $C_2H_5^+ + C_2H_6 = C_2H_6 + C_2H_5^+$. On the other hand, structures **A** are precursors to the dissociation to an alkyl cation and H_2.

[2]Houle and Beauchamp (9) found an I_p for $sec\text{-}C_3H_7$ radical that was 5 kcal/mol lower than that measured by Lossing and Maccoll (10). We have assumed that a similar difference exists also between the Lossing and Maccoll value for $sec\text{-}C_4H_9^+$ and the true value.

Can. J. Chem. Downloaded from www.nrcresearchpress.com by 210.87.254.105 on 09/05/12
For personal use only.

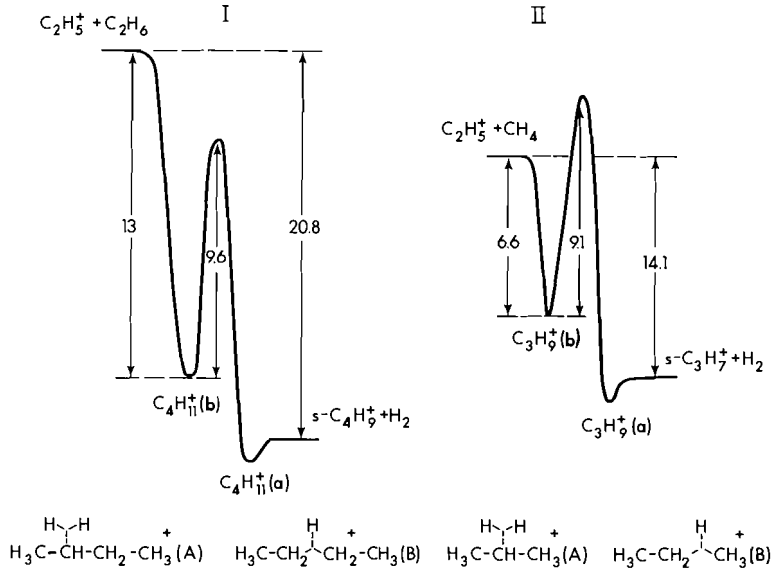


FIG. 7. Potential energy diagrams. Values given are in kcal/mol. *I*. Diagram for reaction system [6]. For origin of numbers see text. $C_4H_{11}^+(b)$ is suggested to have structure **B** and $C_4H_{11}^+(a)$ structure **A**. The barrier of 9.6 kcal/mol then corresponds to energy required for rearrangement **A** → **B**. *II*. Diagram for reaction $C_2H_5^+ + CH_4 \rightarrow C_3H_9^+(b) \rightarrow C_3H_9^+(a) \rightarrow sec\text{-}C_3H_7^+ + H_2$. From earlier work (3). Suggested structures for $C_3H_9^+(a)$ and (b) given above. The **A** structures are loose complexes of the alkyl cation and H_2. These species are of lower energies than the **B** species, however, they dissociate very easily to the alkyl cation and H_2, thus they are considered as the immediate precursors in the dissociation of a protonated alkane, to H_2 + alkyl$^+$. The **B** species behave as complexes of an alkyl cation and an alkane, i.e. ($C_2H_5{\cdot}CH_4^+$ and $C_2H_5^+{\cdot}C_2H_6$). They may be considered also as intermediates in hydride transfer reactions.

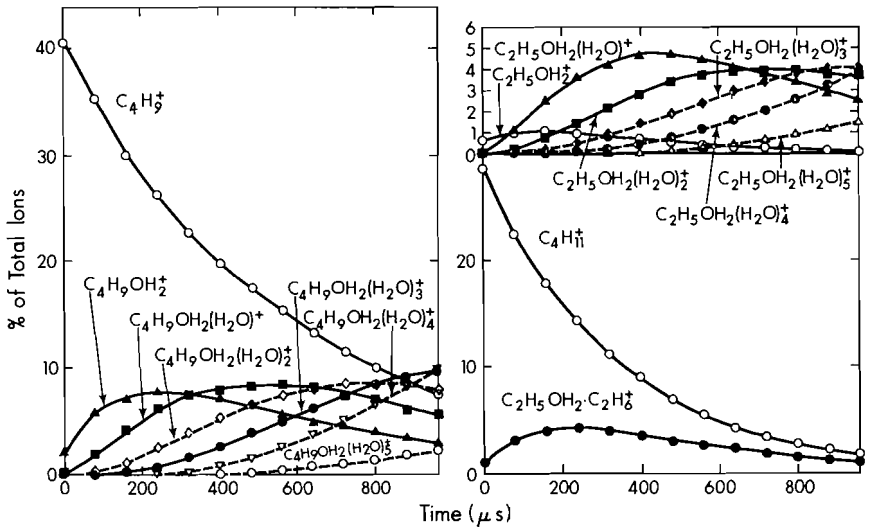


FIG. 8. Behavior of $C_4H_9^+$ and $C_4H_{11}^+$ on addition of traces of water, temperature −80°C, 4 Torr H_2, 55 mTorr C_2H_6.

Some experiments were made in which traces of water were added to the gas mixture. Typical results are shown in Fig. 8, *I* and *II*. Part *I* shows the disappearance of $C_4H_9^+$ and the resulting hydrates. Earlier work (12) from this laboratory showed that the monohydration of alkyl cations R^+ leads to the corresponding protonated alcohols ROH_2^+. Therefore the hydrates of *sec*-$C_4H_9^+$ are expected to correspond to hydrates of *sec*-butyl alcohol, $s\text{-}C_4H_9OH_2^+(H_2O)_n$. In all hydration experiments, it was found that the decrease of $C_4H_9^+$ was almost completely accounted for by the increase of $C_4H_9OH_2^+(H_2O)_n$. For example after 960 μs the decrease of $C_4H_9^+$ is 34% while the increase of corresponding hydrates is 35% (see Fig. 8).

The hydration reaction of $C_4H_{11}^+$ leads mostly to

Can. J. Chem. Downloaded from www.nrcresearchpress.com by 210.87.254.105 on 09/05/12
For personal use only.

the formation of $C_2H_5OH_2^+(H_2O)_n$. $C_4H_{11}\cdot H_2O^+$ is formed early but decreases with time. Only about two thirds of the decrease of $C_4H_{11}^+$ are accounted for by $C_4H_{11}H_2O^+$ and $C_2H_5OH_2(H_2O)_n^+$. The "missing" one third could be accounted for by the observed appearance of proton hydrates $H^+(H_2O)_n$. Similar results were observed in hydration experiments undertaken at different temperatures (−47, −65, −75°C).

It was suggested above that the $C_4H_{11}^+(b)$ has structure **B** (Fig. 7). This corresponds to an *n*-C_4H_{10} protonated on the central C—C bond. The proton affinities of the C—C protonated ethane and propane determined earlier (2) were: ~145 kcal/mol and ~152.8 kcal/mol.[3] From these values one can estimate a proton affinity for the central bond of *n*-butane of about 155 kcal/mol. This value is considerably lower than the $PA(H_2O)$ = 175 kcal/mol.[3] Proton transfer from $C_4H_{11}^+(b)$ to water is therefore an exothermic and likely reaction channel leading to the observed $H^+(H_2O)_n$. Ausloos and co-workers (8), in their study of the neutral products of the radiolysis of ethane, found *n*-butane as a product and suggested that it was formed by proton transfer from $C_4H_{11}^+$. The present results are consistent with the above finding. Thus we see that the $C_4H_{11}^+(b)$ is sufficiently butane-like to undergo proton loss and yield butane. On the other hand, the representation as a complex of $C_2H_5^+$ and C_2H_6 is also a valid partial description, since the reaction of water with $C_4H_{11}^+(b)$ leads largely to formation of $C_2H_5OH_2^+(H_2O)_n$, i.e. water, displaces ethane in the $C_4H_{11}^+(b)$ complex.

(c) Reactions $C_2H_4^+ + C_2H_6 = C_4H_{10}^+ \rightarrow C_3H_7^+ + CH_3$

At the lowest temperatures (−145°C, Fig. 1), $C_2H_4^+$ reacts with C_2H_6 to form aggregates $C_2H_4^+(C_2H_6)_n$. The ion with $n = 1$, $C_4H_{10}^+$ becomes the major product as temperature is increased to about 70°C (see Figs. 2 and 3). Around this temperature, the conversion of part of the $C_2H_4^+$ to $C_3H_7^+$ becomes noticeable. Unfortunately the exact amount of $C_3H_7^+$ originating from $C_2H_4^+$ cannot be established, since a small amount of $C_3H_7^+$ may be produced also from the reaction of $C_2H_5^+$ with C_2H_6. At 70°C the yields of $C_3H_7^+$ and $C_4H_{10}^+$ from $C_2H_4^+$ are of similar magnitude. At higher temperatures, the yield of $C_3H_7^+$ increases rapidly relative to that of $C_4H_{10}^+$. From 170°C to 352°C, the disappearance of $C_2H_4^+$ could be almost completely accounted for by the formation of $C_3H_7^+$, although a small amount of $C_4H_{10}^+$, ca. 15% of the initial $C_2H_4^+$, was formed even at the highest temperature (see Fig. 4).

The intensity ratio $C_2H_4^+/C_4H_{10}^+$ was observed to become constant at longer reaction times in the temperature range 45–80°C. It was assumed that this was due to establishment of the equilibrium [10].

[10] $C_2H_4^+ + C_2H_6 + M = C_4H_{10}^+(d) + M$

A number of runs were made in that range and the equilibrium constant K_{10} determined. A van't Hoff plot of the data is shown in Fig. 9. The plot leads to $\Delta H_{10} = -15.3 \pm 3$ kcal/mol and $\Delta S_{10}^0 = -21 \pm 4$ cal/deg.

The rate of $C_2H_4^+$ disappearance at higher temperatures, where the dominant reaction product was $C_3H_7^+$, was used to evaluate the rate constant for reaction [11].

[11] $C_2H_4^+ + C_2H_6 = C_3H_7^+ + CH_3$

k_{11} was found to increase with temperature. An Arrhenius plot of k_{11} is shown in Fig. 10. The straight line leads to a pre-exponential factor $A_{11} = 8.4 \times 10^{-10}$ molecule^{-1} cm^3 s^{-1} and an activation energy $E_{11} = 3.9$ kcal/mol.

The formation of $C_4H_{10}^+$ from $C_2H_4^+ + C_2H_6$,

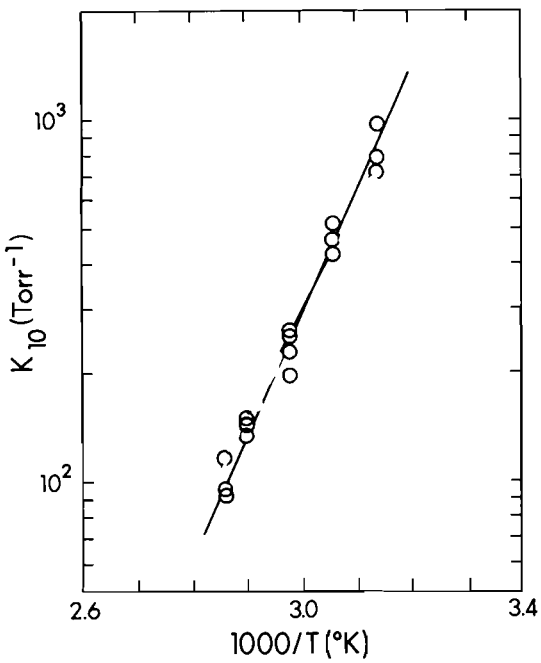


FIG. 9. van't Hoff plot of equilibrium constant K_{10} for reaction [10]: $C_2H_4^+ + C_2H_6 = C_4H_{10}^+(d)$ leads to $\Delta H_{10} = -15.3$ kcal/mol $\Delta S^0_{10} = -21$ cal/deg mol. $C_4H_{10}^+(d)$ is believed to be a complex between $C_2H_4^+$ and C_2H_6 which is held largely by ion-induced dipole forces.

[3] From ref. 2 and ref. 10 but corrected upwards by 5 kcal/mol, see Houle and Beauchamp (9).

Can. J. Chem. Downloaded from www.nrcresearchpress.com by 210.87.254.105 on 09/05/12
For personal use only.

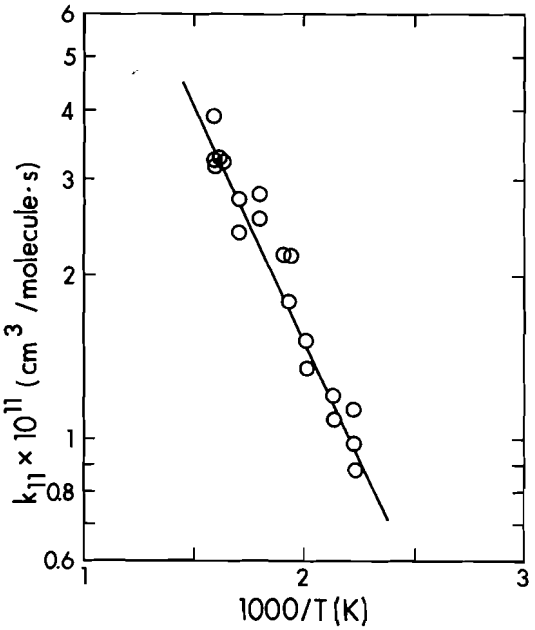


FIG. 10. Arrhenius plot of rate constant for reaction [11], $C_2H_4^+ + C_2H_6 = sec\text{-}C_3H_7^+ + CH_3$. Straight line obtained gives: $k_{11} = A \exp(-E_{11}/RT)$ with $A = 8.4 \times 10^{-10}$ molecule^{-1} cm^3 s^{-1} and $E_{11} = 3.9$ kcal/mol.

i.e., reaction [10], was first observed by Bennett *et al.* (1). These authors also reported on reaction [11], which had been observed earlier. Bennett *et al.* determined the rate constant for the overall disappearance of $C_2H_4^+$ at two temperatures 189 and 410 K. Expressed as second order rate constants their results were $K(189\ K) \approx 2 \times 10^{-10}$, $K(410\ K) \approx 0.1 \times 10^{-10}$ (molecule^{-1} cm^3 s^{-1}). According to our observations the temperature range 189 to 410 K covers two different regions. The low temperature region up to ~320 K where reaction [10] dominates. This reaction has a negative temperature dependence as found by Bennett *et al.* but is *third* order. An upper temperature region exists above 350 K where the second order reaction [11] dominates. This reaction rate *increases* with temperature. Thus no direct comparison with the rate constants quoted by Bennett *et al.* (1) can be made. In fact the results of Bennett *et al.* (Fig. 2, ref. 1) seem to indicate that in the experiments of Bennett *et al.* there was also a decrease of $C_2H_4^+$ rate of disappearance between 327 and 410 K. However the authors did not quote a rate constant for the run obtained at 327 K.

The potential energy diagram shown in Fig. 11 represents a rationalization of the experimental observations of the present work. The well of −15.3 kcal/mol for the formation of $C_4H_{10}(d)$ corresponds to ΔH_{10} obtained from the equilibrium measurements of reaction [10]. The barrier of 3.9 kcal/mol is the measured activation energy for the formation of $C_3H_7^+$ by reaction [11]. The rest of the data are based on information from the literature: $\Delta H_f(s\text{-}C_3H_7^+) = 187.3$ kcal/mol and $\Delta H_f(CH_3) = 34.9$ kcal/mol were taken from Houle and Beauchamp (9). $\Delta H_f(C_2H_4^+) = 253$ kcal/mol and $\Delta H_f(n\text{-butane}^+) = 213$ kcal/mol are from the NBS compilation (13). These data allow the calculation of the well of 19.8 kcal/mol for the formation of n-butane$^+$ from $C_2H_4^+$ and C_2H_6 and the exothermicity of 10.6 kcal/mol for the reaction $C_2H_4^+ + C_2H_6 = s\text{-}C_3H_7^+ + CH_3$. The potential energy barrier of 5.5 kcal/mol (see Fig. 11) was obtained from the difference of the appearance potential $AP(C_3H_7^+, n\text{-}C_4H_{10}) = 11.18$ eV (Chupka and Berkovitz, ref. 14) and the calculated energy for the dissociation $n\text{-}C_4H_{10} = s\text{-}C_3H_7^+ + CH_3 + e$, $\Delta H = 10.94$ eV obtained from the quoted data of Houle and Beauchamp (9). The barrier of 6.3 kcal/mol (see Fig. 11) was obtained from the difference of the appearance potential $AP(C_2H_4^+, n\text{-}C_4H_{10}) = 11.65$ (Chupka and Berkovitz, ref. 14) and $\Delta H = 11.38$ eV for the process $n\text{-}C_4H_{10}^+ = C_2H_4^+ + C_2H_6 + e$ calculated from $\Delta H_f(C_2H_4^+) = 253$ kcal/mol quoted above.

The species $C_4H_{10}^+(d)$ involved in equilibrium [10] is assumed not to be identical to $n\text{-}C_4H_{10}^+$ on the basis of the following considerations. Had $C_4H_{10}^+(d)$ been equal to $n\text{-}C_4H_{10}^+$, equilibrium [10] would not have been observed since $n\text{-}C_4H_{10}^+$ excited by some 15–20 kcal/mol dissociates predominantly to $C_3H_7^+ + CH_3$. This is evident from the breakdown graph for $n\text{-}C_4H_{10}^+$ obtained by Chupka and Berkovitz and others (14–16). Also, equilibrium [10] predicts a well for $C_4H_{10}^+(d)$ which is ~15 kcal/mol while the well of $n\text{-}C_4H_{10}^+$ is ~20

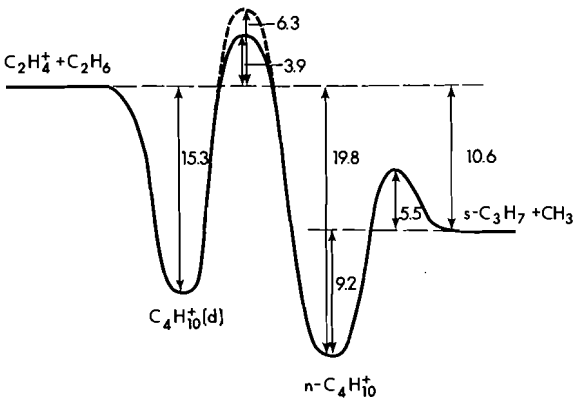


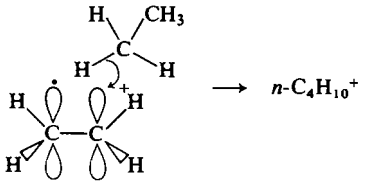
FIG. 11. Potential energy diagram showing intermediates in reactions of $C_2H_4^+ + C_2H_6$. Numbers give energies in kcal/mol. Data provide also a partial potential energy diagram for the decomposition of excited $n\text{-}C_4H_{10}^+$.

Can. J. Chem. Downloaded from www.nrcresearchpress.com by 210.87.254.105 on 09/05/12
For personal use only.

kcal/mol. The well of n-$C_4H_{10}^+$ may actually be even deeper than 20 kcal/mol. The onset of ionization of n-$C_4H_{10}^+$ from n-C_4H_{10} is very gradual (14), therefore the true adiabatic ionization potential might be a few kcal/mol lower than the value (13, 14) used for the evaluation of $\Delta H_f(n\text{-}C_4H_{10}^+)$. This expectation is also in line with the earlier mentioned observation that a small amount of relatively stable $C_4H_{10}^+$ was observed in our experiments at higher temperatures where most of the reaction of $C_2H_4^+$ with C_2H_6 leads to $C_3H_7^+ + CH_3$. This relatively stable $C_4H_{10}^+$ may be n-$C_4H_{10}^+$ formed by collisional stabilization of reaction product passing from left to right over the 3.9–6.3 kcal/mol activation barrier in Fig. 11. The formation of stabilized n-$C_4H_{10}^+$ may be expected to occur also at lower temperatures where $C_4H_{10}^+(d)$ is also formed. No distinction between the two species can be obtained by mass analysis; however, experiments in which traces of water were added, i.e. experiments like those shown in Fig. 8, showed that although most of the $C_4H_{10}^+$ was converted to $C_2H_9^+(H_2O)_n$, some small part stayed as $C_4H_{10}^+(H_2O)_n$. It is likely that the precursor of $C_2H_4^+(H_2O)_n$was $C_4H_{10}^+(d)$ while that of $C_4H_{10}^+(H_2O)_n$ was n-$C_4H_{10}^+$.

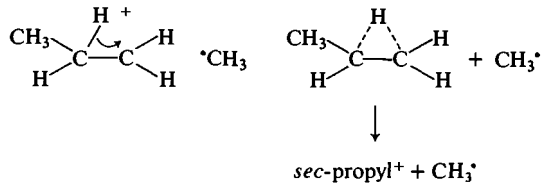
The structure and type of bonding in $C_4H_{10}^+(d)$ is unknown. One may consider a "physical" type of $C_2H_4^+ \cdot C_2H_6$ complex held together by ion induced dipole forces. This is in line with the easy conversion of $C_4H_{10}^+(d)$ to $C_2H_4^+(H_2O)$, but the binding energy $-\Delta H_{10} = 15.3$ kcal/mol appears rather large for such a complex.

The barrier 3.9–6.3 kcal/mol (Fig. 11) must be associated with the insertion of $C_2H_4^+$ into a C—H bond of C_2H_6 to produce n-$C_4H_{10}^+$. One may visualize such an insertion to occur by the electrophilic attack of an sp^2 hybridized $\dot{C}H_2$—CH_2^+ on the C—H bond of ethane as shown below:



Evidently the preparation of $\dot{C}H_2$—$\overset{+}{C}H_2$ as well as the formation of the intermediate will require energy so that the presence of an energy barrier of 3.9–6.3 kcal/mol for the reaction is not surprising.

The dissociation of n-$C_4H_{10}^+$ to sec-$C_3H_7^+ + CH_3$ occurs also in the electron impact fragmentation of n-C_4H_{10}. Wolkoff and Holmes (17), on the basis of the mass spectra of isotopically substituted n-butanes, have established that the methyl group comes mostly from terminal carbon of the n-butane$^+$. Therefore one may assume that the dissociation occurs via the intermediate shown below:



Prior to the appearance of the thermochemical data of Houle and Beauchamp (9), the dissocation of n-$C_4H_{10}^+$ to s-$C_3H_7^+ + CH_3$ was assumed to proceed without an activation energy barrier (see for example ref. 17). This assumption is not really plausible considering the requirement of a 1–2 hydrogen shift as indicated in process [13] above. The 5.5 kcal/mol barrier (Fig. 11) predicted by the modern thermochemical data (9) is a more believable result.

1. S. L. Bennett, S. G. Lias, and F. H. Field. J. Phys. Chem. **76**, 3919 (1972).
2. K. Hiraoka and P. Kebarle. J. Am. Chem. Soc. **98**, 6119 (1976).
3. K. Hiraoka and P. Kebarle. J. Chem. Phys. **62**, 2267 (1975); **63**, 394 (1976).
4. A. J. Cunningham, J. D. Payzant, and P. Kebarle. J. Am. Chem. Soc. **94**, 7627 (1972).
5. J. K. Kim and W. T. Huntress. J. Chem. Phys. **62**, 2820 (1975).
6. M. T. Bowers and D. D. Elleman. J. Chem. Phys. **51**, 4606 (1969).
7. Index of mass spectral data.
8. P. Ausloos, R. E. Rebbert, and L. W. Sieck. J. Chem. Phys. **54**, 2612 (1971).
9. F. A. Houle and J. L. Beauchamp. J. Am. Chem. Soc. **101**, 4067 (1979).
10. F. P. Lossing and A. Maccoll. Can. J. Chem. **54**, 990 (1976).
11. P. Kebarle. Ann. Rev. Phys. Chem. **28**, 445 (1977).
12. K. Hiraoka and P. Kebarle. J. Am. Chem. Soc. **99**, 360 (1977).
13. J. L. Franklin *et al.* Ionization potentials, appearance potentials and heats of formation of gaseous positive ions. HSRDS-NBS 26 (1969).
14. W. A. Chupka and J. Berkovitz. J. Chem. Phys. **47**, 2921 (1967).
15. W. A. Chupka and E. Lindholm. Ark. Fys. **25**, 349 (1963).
16. J. Sunner and I. Szabo. Int. J. Mass Spectrom. Ion Phys. **25**, 241 (1977).
17. P. Wolkoff and J. J. Holmes. J. Am. Chem. Soc. **100**, 7346 (1978).

Crown ether catalysis of decarboxylation and decarbalkoxylation of β-keto acids and malonates: a synthetic application

DUNCAN H. HUNTER,[1] VIJAY PATEL, AND RICHARD A. PERRY
Department of Chemistry, University of Western Ontario, London, Ont., Canada N6A 5B7

Received May 20, 1980

DUNCAN H. HUNTER, VIJAY PATEL, and RICHARD A. PERRY. Can. J. Chem. **58**, 2271 (1980).

The effect of 18-crown-6 ether on the decarboxylation rates of the sodium and potassium salts of 3-camphor carboxylic acid **1** and of 1-carbomethoxy-1-carboxycyclohexane **2** was studied. For **2** the K-18C6 salt reacted ca. 10^4 times faster than the parent acid. This remarkable difference in reactivity was used in developing a one-pot, two-step procedure for decarbalkoxylation of malonic esters. This procedure was then applied to a range of malonates, β-keto esters, and an α-cyano ester. The effect of 15C5, other cations, and good nucleophiles was also studied.

DUNCAN H. HUNTER, VIJAY PATEL et RICHARD A. PERRY. Can. J. Chem. **58**, 2271 (1980).

On a étudié l'effet de l'éther 18-couronne-6 sur la vitesse de décarboxylation des sels de sodium et de potassium de l'acide carboxylique-3 camphre **1** et du carbométhoxy-1 carboxy-1 cyclohexane **2**. Dans le cas du composé **2**, le sel K-18C6 réagit environ 10^4 fois plus vite que celui de l'acide apparenté. On a utilisé cette grande différence de réactivité pour développer une méthode en deux étapes et dans le même récipient permettant de décarboxyler des esters maloniques. On a appliqué cette méthode sur un certain nombre de malonates de β-céto esters et d'α-cyanoesters. On a également étudié l'effet du 15C5, d'autres cations et de bons nucléophiles.

[Traduit par le journal]

A prior study of the catalytic effect of crown ethers upon the rate of decarboxylation of carboxylate salts (1) revealed the importance of a number of governing factors among which was the stability of the resultant carbanion (R^-). It was found that if the corresponding hydrocarbon (RH) had a pK_a of ca. 30 or less, decarboxylation occurred under fairly mild conditions ($\leq 100°C$). Of the various acidifying groups which can provide a pK_a of less than 30, the carbonyl group occurs in a large number of compounds. This led us to look at the effect of crown ethers on the decarboxylation of both β-ketoacids and malonic acids with a view to synthetic applications.

Decarboxylation

Two carboxylic acids with β-carbonyl groups were chosen for the study of the effect of counterion on the rate of decarboxylation. Of these two the camphor-carboxylic acid **1** purchased was a mixture of *exo* and *endo*-isomers with the *endo*-CO_2H predominating. It was used as such without noticeably affecting our rate measurements. The 1-carbomethoxy-1-carboxycyclohexane **2** was prepared as described in the Experimental. The salts of both were prepared by titration and by lyophilization.

The rates of decarboxylation were measured for **1** and **2** and for their sodium and potassium salts in refluxing dioxane both in the absence and presence of 18-crown-6 ether (18C6). Benzene and tetrahydrofuran were used also to determine the sensitivity of rate to solvent. These rate data, expressed in terms of half-lives from a first order analysis are presented in Table 1. While these data show trends similar to those obtained earlier with triphenylacetates, the most dramatic comparison is of the acid forms of **2** and its potassium-crown ether complex salt form. The rate of decarboxylation changed by about 10^4 (250 000 min for **2**-H and 16 min for **2**-K,CE). This should be contrasted with the decarboxylation of **1** where the corresponding rate ratio is 20. Thus although the acid form of the malonate, **2**-H, decarboxylates much more slowly than the β-ketoacid, **1**-H, the K,CE salts react at almost the same rate. It is this dramatic rate enhancement that encouraged us to develop a crown ether assisted route for decarboxyalkylations applied, in particular, to the malonic ester synthesis as described in the following section.

The mechanism of decarboxylation of β-keto acids has received much attention and is thought to proceed through a cyclic state (for a recent critique see ref. 2). The reduced reactivity of **2** versus **1** is attributable in part to the reduced basicity of an ester carbonyl relative to a ketonic carbonyl (3) and to the relative stability of the two enolic intermediates.[2] It is tempting to attribute the similar rates of decarboxylation of the K^+,CE salts to similar stabilities of the resultant enolates; however, it is difficult to substantiate this suggestion. While the pK_a values of numerous ketones are available, esters have not proven amenable to measurement. What little data

[1]Author to whom correspondence may be addressed.

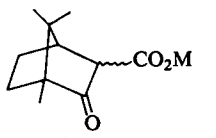
[2]The % enol for acetone is 10^{-5} (4) and is estimated to be $\sim 10^{-13}$ for ethyl acetate (J. P. Guthrie, unpublished results).

0008-4042/80/212271-07$01.00/0
©1980 National Research Council of Canada/Conseil national de recherches du Canada

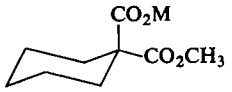
Can. J. Chem. Downloaded from www.nrcresearchpress.com by 210.87.254.6 on 09/05/12
For personal use only.

Can. J. Chem. Downloaded from www.nrcresearchpress.com by 210.87.254.6 on 09/05/12
For personal use only.

TABLE 1. Effect of counterion on the rate of decarboxylation of **1** and **2** at reflux



1



2

Solvent	Cation	Concentration, *M*	$t_{1/2}$, min[a]	Concentration, *M*	$t_{1/2}$, min[a]
Dioxane	H	0.060	160	0.015	250,000[b]
Dioxane	Na	0.054	2,200		
Dioxane	Na-18C6	0.038	340		
THF	Na-18C6	0.050	1,040		
Dioxane	K	0.023	1,040	0.044	2,100
Dioxane	K-18C6	0.040	8[c]	0.059	16
Benzene	K-18C6			0.076	120

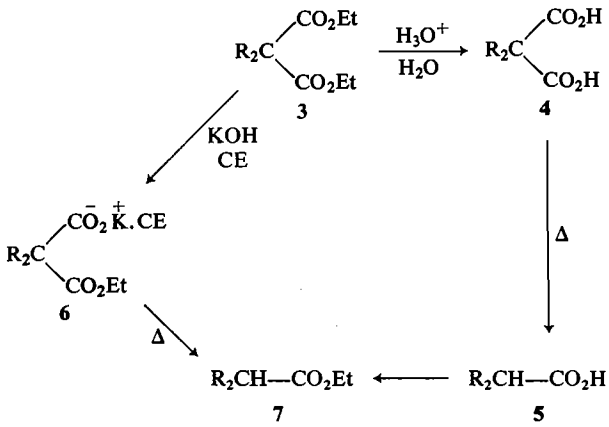
[a]Obtained from four points showing first order behaviour.
[b]Both a sealed tube and reflux experiment.
[c]Calculated from 75% reaction at 14 min and 87% reaction at 20 min.

there are suggest that acetone should be more acidic than ethyl acetate (5). But of the ketones, camphor is one of the less acidic ($pK_a^{DMSO} = 30.40$; cf. phenylcyclohexyl ketone = 26.7).[3] Thus it may be that camphor and methyl cyclohexylcarboxylate do have similar acidities.

Interpretation of the effect of added 18C6 is complicated by the fact that the reactions run in the absence of crown ether were heterogeneous. But certainly one role of the crown ether is to dissolve the salts and in the case of **1** this has led to a rate enhancement of 7 for the sodium salt and of 130 for the potassium salt. The potassium salt of **2** showed a similar rate enhancement. The replacement of dioxane by benzene in this case led to an eight-fold decrease in rate but of course the reaction temperature has been reduced by about 20° (100 to 80°C). In the case of the sodium salt of **1** the change from dioxane to THF led to only a 3-fold drop in rate in spite of a temperature drop of 35°. This seems consistent with the earlier observations (1) of the effect of solvent on decarboxylation rates.

Decarbalkoxylation

The greatly enhanced rate of decarboxylation of the potassium-crown ether salt of **2** relative to the acid form of the malonic half ester made us turn our attention to malonic esters. As part of a traditional malonic ester synthesis, the diester **3** is first hydrolyzed to the diacid **4**, which is then heated to effect decarboxylation and the acid **5** is then often reesterified for further conversions (Scheme 1). As an alternative to this procedure we decided to explore the route via the salt of the half-ester **6** which in the presence of crown ether should decarboxylate under conditions much milder than those required for the diacid **4**. We were further encouraged in this regard by the realization that crown ethers also greatly accelerate the saponification of esters (6). If a selective saponification could be realized then both steps could be telescoped into a one-pot conversion of malonate **3** to acetate **7**.



SCHEME 1

Diethyl Butylmalonate

In this regard we studied the conversion of diethyl butylmalonate **8** under a variety of conditions to optimize yields and then looked at a number of other malonates. Initial attempts were directed at preparing and utilizing a 1:1 complex of KOH–18C6 in an aprotic solvent; protic solvents reduce the rate of decarboxylation. Attempts using solid KOH and equimolar 18C6 resulted in a largely insoluble reagent in a wide range of aprotic solvents (isooctane, benzene, dioxane, THF, pyridine, aceto-

[3]F. G. Bordwell, personal communication.

Can. J. Chem. Downloaded from www.nrcresearchpress.com by 210.87.254.6 on 09/05/12
For personal use only.

nitrile). Nonetheless these reaction mixtures were stirred for 0.5 h at 25°C and then refluxed for 20–24 h and gave quite similar product distribution; ~40% recovered **8**, ~40% ethyl caproate **9**, and ~20% of other products amongst which both butylmalonic acid and caproic acid were identified. The insoluble reagent seemed to favour complete saponification of the malonate rather than selective hydrolysis to the half-ester which is needed for a successful malonate to acetate conversion.

Attempts were made to enhance the solubility of the potassium hydroxide in benzene by preforming the crown ether complex initially in water followed by lyophilization and also directly in benzene by removing the water as an azeotrope. These attempts led to no improvement in the product distribution and again a largely insoluble reagent resulted.

A homogeneous reaction mixture was obtained in ethanol with KOH–18C6 and while this led to quite selective monohydrolysis there was incomplete decarboxylation after 24 h at reflux (10% recovered **8**, 40% **9**, 45% ethyl hydrogen butylmalonate $CH_3CH_2CH_2CH_2CH(CO_2H)CO_2Et$). In an attempt to maintain homogeneity but to enhance the rate of decarboxylation, a benzene–ethanol mixture (5 vol.% ethanol) was employed for the ambient temperature hydrolysis. For the decarboxylation step, the ethanol was removed by distillation from the refluxing reaction mixture with the concurrent addition of benzene to keep the volume approximately constant. This led to 97% conversion (vpc) after 24 h and yields (after distillation) of **9** of 72% at 5 h, 81% at 16 h, and 84% at 24 h.

At this stage the use of benzene was somewhat arbitrary but did present some practical advantages. Its boiling point was high enough to effect efficient decarboxylation and removal of the ethanol. The 18C6 could be removed and subsequently recovered by washing with KCl solution (7).

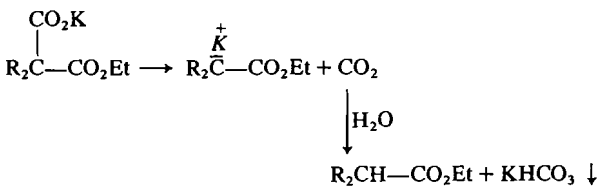
Comparison of Malonates

The near optimum yield of ethyl valerate from diethyl butylmalonate led us to apply this same two step one-pot procedure to other malonates (Table 2). These reactions, run on a 3 mmol scale, gave high yields (76–87%) of crude product sufficiently pure for further use. In some cases (runs 2, 4, 7, 9, 11) the reaction was run also on a 30 mmol scale and the product was distilled (>99% pure). As is evident in runs 2 and 4, the yields are affected by the volatility of the liquid products and a glc analysis of the crude reaction mixture showed better than 90% yields. Both monoalkyl and dialkylmalonates (runs 1–8) reacted under similar conditions to give comparable yields.

For most cases the hydrolysis step was complete in 1–3 h but the acidifying influence of a phenyl or nitro group led to competitive deprotonation of the malonic diester with consequent reduction in the rate of ester hydrolysis. The phenylmalonate (runs 10 and 11) proved to be borderline and an extended hydrolysis period sufficed to complete the reaction. However, in the case of the nitro-malonate the conversion to enolate was so complete that only starting material was recovered upon acidification. Thus, the presence of strong acidifying groups represents a limitation to this method of decarboxylation.

For most of the malonates in Table 2, a reflux period, after ethanol removal, of about 12–20 h was appropriate to complete decarboxylation. However there were two exceptions worth noting. The phenylmalonate (runs 10 and 11) proved very reactive once the ester hydrolysis was complete. In contrast, the decarboxylation of the cyclobutyl compound (run 6) was quite slow even in the higher boiling dioxane. Estimated half-lives for decarboxylation were ≥60 h in refluxing benzene and 12 h in refluxing dioxane compared with the cyclohexyl compound (run 7) with $t_{\frac{1}{2}}$ ~2 h (benzene). This reduced reactivity does not seem to reflect the stability of the derived anion (cyclobutylphenylketone pK_a^{DMSO} = 26.1; cyclohexylphenylketone pK_a^{DMSO} = 26.7[3]) and the source of this reduced reactivity remains a puzzle.

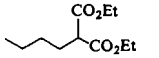
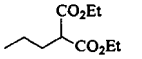
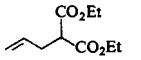
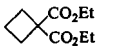
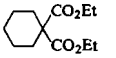
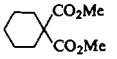
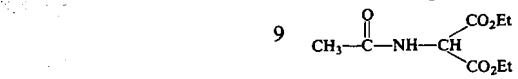
In one other case (run 9), dioxane was substituted for benzene but this was to enhance the solubility of the hydrolysis product to facilitate decarboxylation. It was also in this run that the usual precipitate of $KHCO_3$ was characterized and isolated in yields comparable to the product. Thus the CO_2 acts to trap the hydroxide generated during the final protonation producing an insoluble and unreactive precipitate.



This one-pot, two-step procedure for the decarbalkoxylation of malonate diesters to acetate esters gives good yields at moderate temperatures (80 or 100°C) under mildly basic conditions and acts to complement the other procedures for decarbalkoxylation. Thus the traditional three-step procedure (hydrolysis to the diacid, thermal decarboxylation, and re-esterification) gives comparable yields (73% ethyl caproate versus 75% of caproic acid (8); 59% ethyl valerate versus 60% (9); and 45% 2-heptanone versus 52–61% (10)). However, the present procedure employs basic rather than acidic conditions; the de-

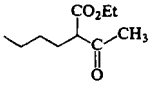
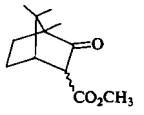
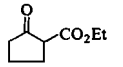
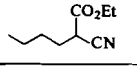
Can. J. Chem. Downloaded from www.nrcresearchpress.com by 210.87.254.6 on 09/05/12
For personal use only.

TABLE 2. Conditions and yields for one-pot decarbalkoxylation of malonates using equimolar KOH-18C6 in ethanol and benzene or dioxane

Run	Substrate: Nature	Substrate: Amount, g	Solvent[a]	Reaction time, h: ≤ 25°C[b]	Reaction time, h: Reflux	% SM	% Product: Crude[c]	% Product: Purified[b]
1		0.67	B	1.5	23	3	84	
2		6.7	B	10	13	3	93[d]	73
3		0.60	B	1	14	16	81	
4		6.0	B	9	13	5	95[e]	59
5		0.60	B	1	24	18	79	
6		0.61	D	0.5	40	5	76	
7		6.7	B	3	22	15		70
8		0.67	B	1	20		87[f]	
9		6.5	D	1	20	10	78	
			D	3	23			61
10		0.71	B	20	1	10	78	
11		7.1	B	22	3			65
12		0.60	B	2	24	92		

[a]B = benzene, D = dioxane. The large scale reactions were run using ca. 200 mL of solvent and the small scale in 50 mL.
[b]The reactants were mixed at ~10°C and allowed to warm to ambient temperature.
[c]Neat liquid analyzed for purity by nmr after solvent removal.
[d]Analyzed by glc.
[e]Distilled in runs 2, 4, 7, and 11 (>99% pure by glc) and recrystallized in run 9.
[f]Isolated as the ethyl ester.

TABLE 3. Conditions and yields for decarbalkoxylation of keto and cyanoesters using equimolar KOH-18C6 in ethanol and benzene or dioxane

Run	Substrate: Nature	Substrate: Amount, g	Solvent[a]	Reaction time, h: ≤ 25°C[b]	Reaction time, h: Reflux	% Product: Crude[c]	% Product: Purified[c]	% Other
13		0.56	B	16	2	86		
14		6.2	B	2	18		91	
15		0.47	B	2	20			50[d]
16		0.52	D	1	48	76	55	21[e]

[a]B = benzene, D = dioxane. Runs 13, 15, and 16 were in 50 mL of solvent and run 14 used 200 mL. In run 14 a 5 *M* KOH/H_2O solution was used rather than ethanol.
[b]The 18C6 was added after the hydrolysis period.
[c]The camphor was sublimed and the capronitrile was distilled.
[d]Ethyl hydrogen adipate.
[e]α-Cyanocaproic acid.

TABLE 4. Comparison of cations and crown ethers upon the reaction of diethyl butylmalonate with equimolar KOH/ethanol – benzene[a]

Run	Reagent[b]	Reflux period, h	% SM	% Product	% EHBM[c]
2	KOH, 18C6	24	3	84	
17	KOH, 15C5	50	12	51	14
18	NaOH, 18C6	44	14	33	17
19	NaOH, 15C5	43	7	50	15
20	$Ba(OH)_2$, 18C6	40	6	61	8
21	KOH, 0.2 18C6	42	10	72	
22	KOH, DB18C6	24	4	70	4
23	KOH, $N(n\text{Bu})_4\text{Br}$	22	8	73	
24	KOH, $N(n\text{Pr})_4\text{Br}$	21	6	57	
25	KOH, 0.5 $N(n\text{Bu})_4\text{Br}$	22	13	55	15

[a]The reagent solution was added to the substrate in benzene at ~10°C over 0.5 h and then warmed to 25°C for 1 h. The ethanol was removed by distillation during the first part of the reflux period.
[b]15C5 = 15-crown-5 ether; DB18C6 = dibenzo-18-crown-6 ether.
[c]Ethyl hydrogen butylmalonate.

carboxylation step is run at a lower temperature; and fewer steps are required.

Decarboxylation has also been effected with refluxing dimethylsulfoxide (11) containing water, sometimes with added salts, with yields comparable to the present study (76% $CH_3CONHCH_2CO_2Et$ in this study versus 70%; 78% ethyl phenylacetate in this study versus 90%; and 76% $(CH_2)_3CHCO_2Et$ in this study versus 80–90%). However, the present procedure employs a significantly lower temperature, 80–100°C versus 160°C; and uses slightly basic rather than neutral conditions.

There are some limitations to the present procedure: particularly acidic substrates can deprotonate rather than hydrolyze (e.g. diethyl nitromalonate); substrates containing base sensitive groups may not be satisfactory; and large amounts of 18C6 may be needed since equimolar quantities give optimum results. The importance of this latter factor is reduced since 18C6 is recoverable by the simple expedient of a KCl wash (7). There are a number of other procedures (12) for decarbalkoxylation but most have been developed for β-ketoesters.

α-*Cyano and* β-*Keto Esters*

Although the potassium-crown ether salt of camphor-3-carboxylic acid decarboxylated only 20 times faster than the acid (Table 1), the present procedure would allow a mildly basic alternative to the usual route. Consequently three β-ketoesters were investigated (Table 3; runs 13, 14, and 15) as well as an α-cyanoester (run 16).

The reactions of 3-carbethoxy-2-heptanone (run 13) and camphor-3-methylcarboxylate (run 14) proceeded in good yield, although in both these cases it was found the hydrolysis step proceeded more rapidly without 18C6, which was added after the initial step. The 2-carbethoxy cyclopentanone (run 15) gave the usual (13) ring opening reaction even in the presence of 18C6 and only traces of the desired product were observed. The ethyl α-cyanocaproate hydrolyzed readily (before adding the crown ether) but the decarboxylation was quite slow even in refluxing dioxane. Thus even after 48 h at reflux (run 16), there was isolated 21% of α-cyanocaproic acid. This reduced reactivity presumably reflects the reduced acidifying effect of a nitrile grouping (pK_a^{DMSO}: CH_3CN 31.3; CH_3COCH_3 26.5)[3] relative to a carbonyl.

Other Cations and Crown Ethers

A series of experiments was run using diethyl butylmalonate **8** under the standard conditions for decarbalkoxylation (1–2 h at ≤25°, 20–50 h at reflux) except that the reagent was altered by varying both the cation and the crown ether. Although no attempt was made beyond this to optimize either yields or conditions, some effects are apparent. The replacement of 18C6 (run 2) with 15C5 (run 17) led to reduced amounts of both hydrolysis and decarboxylation. The replacement of potassium by sodium led to reduced yields although in this case 15C5 (run 17) was better than 18C6 (run 18). These changes are consistent with the cation selectivity shown by crown ethers (14) and with the effect of cation on the rate of decarboxylation (Table 1).

Barium (run 20) was also chosen for its compatibility with 18C6 and gave moderate yields although long reflux periods were needed. Long reflux periods were needed when less than equimolar 18C6 was used (run 21). With less than equimolar 18C6, the reaction mixture remained gelatinous but nonetheless yields were quite good. However since the 18C6 can be recovered by KCl extraction, use of equimolar crown ether seems advisable. Dibenzo-18C6 (run 22) also gave reasonable yields but pre-

Can. J. Chem. Downloaded from www.nrcresearchpress.com by 210.87.254.6 on 09/05/12
For personal use only.

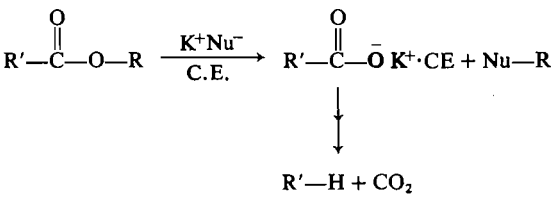
Can. J. Chem. Downloaded from www.nrcresearchpress.com by 210.87.254.6 on 09/05/12
For personal use only.

sented practical problems due to its reduced solubility. Of the cations and crown ethers surveyed, equimolar 18C6 and potassium hydroxide gave optimum yields in minimum time.

The effectiveness of quaternary ammonium cations was also explored albeit in a brief manner (runs 23, 24, and 25). While tetrapropylammonium bromide was effective, the longer chain tetrabutylammonium bromide, in equimolar amounts, behaved very similarly to K-18C6. A reduction in the amount of tetrabutylammonium bromide led to a reduction in yield both at the hydrolysis stage and at the decarboxylation stage. Although no attempt was made to optimize conditions it is fairly clear that tetrabutyl, or perhaps longer chain (15), quarternary ammonium salts can be very effective particularly on the large scale. This point deserves further study.

An S_N2 Route to Decarbalkoxylation

The feasibility of using 18C6 in combination with the salts of good nucleophiles to effect decarbalkoxylation was studied. The study with diethyl butylmalonate was limited to potassium iodide and



potassium cyanide with equimolar 18C6 in a number of solvents at reflux. The following combinations were attempted with no detectable reaction of the malonate: KI in benzene, 5% ethanol–benzene, dioxane, 5% ethanol–dioxane, acetonitrile, dimethylsulfoxide ($\leq$120°C); KCN in dioxane. The reluctance of diethyl butylmalonate to undergo even the first step made us look at the reactions of methyl oleate. Again there was no reaction with KI in tetrahydrofuran and in dioxane, and with KF in dioxane. There was reaction with potassium 2-propanethiolate in both tetrahydrofuran and dioxane but water may have been responsible for this result and the matter was not explored further.

It has been clearly demonstrated that both water and salts (KCN, NaCl, or LiCl) in refluxing dimethylsulfoxide (160°C) provide good yields in decarbalkoxylation without the use of crown ethers (11). If there is a catalytic effect of 18C6, it is not of sufficient magnitude to lower the reaction temperature to that of the solvents employed here ($\leq$100°C).

Experimental

The *d,l-3-camphorcarboxylic acid*, *diethyl* n-*butylmalonate*, *diethyl acetamidomalonate*, and *diethyl phenylmalonate* were purchased. *Diethyl propylmalonate*, *diethyl allylmalonate*, and *diethyl nitromalonate* were provided by F. H. Pattison and *2-carbethoxycyclopentanone* was provided by P. de Mayo. A sample of *3-carbethoxy 2-heptanone* was prepared in 70% yield by the procedure of Marvel and Hager (16). The *d,l-methyl-3-camphorcarboxylate* was prepared from commercial, d,l-3-camphorcarboxylic acid using the esterification procedure of Clinton and Laskowski (17). The ester was obtained as a mixture of 80% *endo*-CO_2CH_3 and 20% *exo*-CO_2CH_3 and was used as such. The *1-carbomethoxy cyclohexanecarboxylic acid* was prepared in 50% yield by the procedure of Reiffers, Wynberg, and Strating (18).

Diethyl-1,1-cyclobutanedicarboxylate was prepared by alkylation of diethylmalonate with 1,3-dibromopropane. The cyclobutyl compound was obtained in about 50% yield but contaminated with about 25% diethyl allylmalonate. The allylmalonate was removed by treatment with $KMnO_4$ and the net overall yield of purified cyclobutyl compound was 40%. The procedure follows.

A mixture of 1,3-dibromopropane (27.5 g, 0.136 mol) and diethyl malonate (21.5 g, 0.134 mol) in dry EtOH (125 mL) was added dropwise from one addition funnel into refluxing EtOH (100 mL) while simultaneously adding 150 mL of 1.7 *M* from another addition funnel, over a period of 2.5 h. After an additional half hour reflux, the solution was filtered, evaporated, and the residue extracted with CH_2Cl_2. The CH_2Cl_2 extracts were evaporated to give a liquid mixture (26.3 g) which was dissolved in glacial acetic acid (60 mL) and cooled to < 10°C. Solid $KMnO_4$ (15.0 g) was added in portions over 10 min and the exothermic reaction was maintained at < 50°C by external cooling for 3/4 hour. Dilute NaOH (100 mL) was added, and the mixture extracted with ether. The dried ether extracts were evaporated to yield a liquid which was distilled. After a forerun, the diethyl cyclobutanedicarboxylate was collected (10.83 g, bp 108–110°C (18 Torr)).

Diethyl 1,1-cyclohexanedicarboxylate was prepared by the reaction of diethyl malonate and 1,5-dibromopentane by the following procedure.

To 150 mL of 1.9 *M* sodium ethoxide in ethanol was added a solution of diethyl malonate (23.0 g, 0.144 mol) and 1,5-dibromopentane (34.5 g, 0.15 mol) in ethanol (150 mL) at reflux over 2.5 h. After an additional hour reflux the solution was cooled, pentane (100 mL) was added, and the solution filtered. The residue after evaporation of the filtrate was distilled and after a forerun of dibromopentane, the diethyl ester was collected (17.08 g, 52%, bp 83–92°C at 0.2–0.3 Torr; lit. (19) bp 100°C at 2 Torr).

Ethyl α-cyanocaproate was prepared by alkylation of ethyl cyanoacetate with butylbromide according to the following procedure. To 150 mL of 2.8 *M* sodium ethoxide in ethanol was added ethyl cyanoacetate (49.0 g, 0.43 mol) in EtOH (876 mL) followed by butyl bromide (60.5 g, 0.44 mol) in EtOH (75 mL). The solution was refluxed 8.5 h, cooled, filtered, and evaporated. The residue was extracted with pentane (200 mL), evaporated, and the resulting liquid distilled to give a forerun (25.1 g) followed by ethyl α-cyanohexanoate (30.53 g, 43%, bp. 140–144°C (134 Torr)).

The sodium and potassium salts of d,l-3-camphorcarboxylic acid and 1-carbomethoxy cyclohexanecarboxylic acid were prepared by lyophilization of an aqueous solution from titration of the corresponding acids (to the equivalence point). The 18C6 was prepared by the usual procedure (20).

Procedure for Decarboxylation

The decarboxylation reactions were run on doubly degassed solutions under an argon atmosphere. Typically 25 mL of solvent were used and sufficient substrate, 18C6, and glc

Can. J. Chem. Downloaded from www.nrcresearchpress.com by 210.87.254.6 on 09/05/12
For personal use only.

standard (mesitylene) to provide concentrations in the range of 0.02 *M* to 0.08 *M* were used. Aliquots of these solutions were removed to determine the progress of the reaction and for the heterogeneous reactions an attempt was made to remove representative samples. The aliquot was treated by extraction with water–pentane to remove the unreacted salt. After three water extractions and drying with sodium sulfate, the pentane layer was concentrated and analyzed by glc (5 ft × ¼ in. column of 5% SE-30 on 45–60 Chromosorb P).

Procedure for Decarbalkoxylations

The procedures described here for removal of a CO_2R group involve two distinct steps; first, low temperature hydrolysis of one of the ester groupings with an equimolar amount of potassium hydroxide in ethanol, and second, heating to reflux in benzene or dioxane to induce decarboxylation of the potassium carboxylate. The decarboxylation is facilitated by removal of the ethanol by distillation as the temperature is raised to reflux. In most reactions benzene was used as the solvent (Procedure A) while in some cases dioxane was used (Procedure B). In two cases KOH in water (Procedure C) replaced KOH in ethanol.

(*A*) *Benzene and Ethanol*

A mixture of benzene (20 mL) and potassium hydroxide in ethanol (2.8 mL (3.1 mmol) of 1.1 *M*) was added dropwise over about 25 min to a stirred solution of substrate (3.0 mmol) and 18C6 (3.0 mmol) in 30 mL of benzene at 5–10°C. After stirring several hours at room temperature to effect hydrolysis of the esters, the solution was heated to reflux. To facilitate the decarboxylation reaction about 10–15 mL of distillate was collected, resulting in removal of most of the ethanol. After the reflux period was over the reaction mixture was cooled and then acidified with 3 *M* hydrochloric acid. The benzene layer was washed three times with ca. 15 mL of saturated potassium chloride solution to remove the crown ether and then dried with sodium sulfate. The benzene was removed by distillation and the residual oil analyzed by glc and nmr.

For those reactions run on a 30 mmol scale, the residual oil was distilled and checked for purity by glc.

(*B*) *Dioxane and Ethanol*

Following procedure A, the dioxane–ethanol–hydroxide solution was added at < 15°C and the ethanol was removed by distillation until the temperature rose to 100°C. After the reflux period, the reaction mixture was cooled and 50 mL of pentane was added. (See below for acetamidoester isolation procedure.) Then 3 *N* hydrochloric acid and saturated potassium chloride solution were added and the above washing procedure followed. After evaporation of the solvent, if the crude material was contaminated with crown ether (20–50 mg), this was removed by filtration of a pentane solution through neutral alumina (1–2 g) and reevaporation. Since the acetamidoester was sparingly soluble in pentane and soluble in water, after the reaction was completed, the solution was filtered and evaporated. The residue was taken up in dichloromethane (50 mL), washed four times with saturated potassium chloride solution, dried, and evaporated to yield 54% ester and 10% diester. The combined washes were continuously extracted with ether, which was dried and evaporated to yield 24% ester product.

(*C*) *Benzene and Water*

To the compound (3.0 mmol) in benzene (50 mL) at 25°C was added 5 *N* aqueous potassium hydroxide solution (3.5 mmol, 0.7 mL). (If crown was also present then 6 mmol of potassium hydroxide were added.) After 3.5 h reflux, 18C6 (3.0 mmol) was added, the water distilled off as an azeotrope, and the solution refluxed for an additional 7.5 h. The isolation procedure of A was then followed.

Acknowledgments

The authors wish to acknowledge financial support from the Natural Sciences and Engineering Research Council of Canada.

1. D. H. Hunter, M. Hamity, V. Patel, and R. A. Perry. Can. J. Chem. **56**, 104 (1978).
2. M. W. Logue, R. M. Pollack, and V. P. Vitullo. J. Am. Chem. Soc. **97**, 6868 (1975).
3. (*a*) R. A. Cos, C. R. Smith, and K. Yates. Can. J. Chem. **57**, 2952 (1979); (*b*) R. A. McClelland and W. F. Reynolds. Can. J. Chem. **54**, 718 (1976); (*c*) D. G. Lee and M. H. Sadar. J. Am. Chem. Soc. **96**, 2862 (1974).
4. J. P. Guthrie and P. A. Cullimore. Can. J. Chem. **57**, 240 (1979).
5. R. G. Pearson and R. L. Dillon. J. Am. Chem. Soc. **75**, 2439 (1953).
6. C. J. Pedersen. J. Am. Chem. Soc. **89**, 7017 (1967).
7. D. H. Hunter and R. A. Perry. Synthesis, 37 (1977).
8. E. B. Vliet, C. S. Marvel, and C. M. Hsuek. Org. Synth. Coll. Vol. II. 1943. p. 416.
9. M. R. Loridjani and M. Vilkas. C.R. Acad. Sci. (Paris), **254**, 1090 (1962).
10. J. R. Johnson and F. D. Hager. Org. Synth. Coll. Vol. I. 1941. p. 351.
11. A. P. Krapcho, J. F. Weimaster, J. M. Eldridge, E. G. E. Jahngen, Jr., A. J. Lovey, and W. P. Stephens. J. Org. Chem. **43**, 138 (1978).
12. A. E. Greene, A. Cruz, and P. Crabbé. Tetrahedron Lett. 2707 (1976), and references therein.
13. R. Mayer. *In* Newer methods of preparative organic chemistry. Vol. 2. *Edited by* W. Foerst. Academic Press, New York. 1963. pp. 101–131.
14. (*a*) R. M. Izatt, R. E. Terry, R. L. Haymore, L. D. Hansen, N. K. Dalley, A. G. Avondet, and J. J. Christensen. J. Am. Chem. Soc. **98**, 7620 (1976); (*b*) R. M. Izatt, J. D. Lamb, R. E. Asay, G. E. Maas, J. S. Bradshaw, J. J. Christensen, and S. S. Moore. J. Am. Chem. Soc. **99**, 6134 (1977).
15. J. Dockx. Synthesis, 441 (1973).
16. C. S. Marvel and F. D. Hager. Org. Synth. Coll. Vol. I. 1941. p. 248.
17. R. O. Clinton and S. C. Laskowski. J. Am. Chem. Soc. **70**, 3135 (1948).
18. S. Reiffers, H. Wynberg, and J. Strating. Tetrahedron Lett. 3001 (1971).
19. V. P. Golmov. Zh. Obshch. Khim. **22**, 1944 (1922).
20. G. W. Gokel, D. J. Cram, C. L. Liotta, H. P. Harris, and F. L. Cook. J. Org. Chem. **39**, 2445 (1974).

Trihapto cycloheptatrienyl molybdenum and tungsten dicarbonyl compounds incorporating tridentate chelating dimethyl(1-pyrazolyl)(ethanolamine)gallate ligands

KENNETH S. CHONG AND ALAN STORR

Department of Chemistry, University of British Columbia, 2036 Main Mall, University Campus, Vancouver, B.C., Canada V6T 1W5

Received May 20, 1980

KENNETH S. CHONG and ALAN STORR. Can. J. Chem. **58**, 2278 (1980).

The synthesis and physical properties of a series of cycloheptatrienyl molybdenum and tungsten dicarbonyl compounds incorporating dimethyl(1-pyrazolyl)(ethanolamine)gallate ligands have been investigated. The monomeric, pseudo octahedral, complexes have the organogallate ligand occupying a set of facial positions with the cycloheptatrienyl ring situated opposite to the amino nitrogen atom. Proton nmr studies have shown the η^3-C_7H_7 ligand of the complexes to be fluxional in solution at room temperature. In the low temperature limiting ^1H nmr spectra of the complexes in solution, however, it is possible to distinguish all seven protons of the *static* η^3-C_7H_7 ring owing to the asymmetric nature of the octahedral molecules.

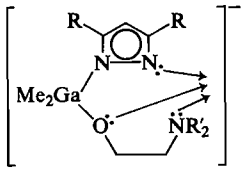
KENNETH S. CHONG et ALAN STORR. Can. J. Chem. **58**, 2278 (1980).

On a étudié la synthèse et les propriétés physiques des composés dicarboxylés du cycloheptatriénylmolybdène et du cycloheptatriényltungstène, incorporant les ligands gallate de diméthyl(pyrazolyl-1)(éthanolamine). Les complexes monomères pseudo-octaédriques ont le ligand organogallate dans un ensemble de positions faciales avec le cycle cycloheptatriényle situé à l'opposé de l'atome d'azote du groupe amine. Les études de la rmn du proton ont montré que le ligand η^3-C_7H_7 des complexes subit de fréquents changements en solution à la température de la pièce. Cependant à la basse température limite des spectres rmn du ^1H des complexes en solution, il est possible de distinguer chacun des sept protons du cycle η^3-C_7H_7 figé en raison de la nature asymétrique des molécules octaédriques.

[Traduit par le journal]

Introduction

Our continuing investigations into the coordinating properties of organogallate ligands of the type **1** has resulted in a series of dicarbonyl com-



1
R = H or Me
R′ = H or Me

plexes of molybdenum and tungsten containing both the ligand **1** and the cycloheptatrienyl ligand, η^3-C_7H_7. Previous investigations using these organogallate ligands **1** had resulted in a wealth of molybdenum and tungsten dicarbonyl derivatives of the general formula $LM(CO)_2X$ (where L = **1**; M = Mo or W; X = η^3-C_3H_5, η^3-C_4H_7 (1, 2), NO (1), and η^2-CH_2SMe (3)), and a series of nickel (4), iron (5), and manganese (5) nitrosyl derivatives. In addition a variety of complexes involving the first row transition elements (Mn → Zn) and the ligands **1** have been described (6–8). Cycloheptatrienyl complexes were of interest because of the ability of the C_7H_7 ligand to coordinate in a mono-, tri-, penta-, or hepta-hapto fashion to metal atoms, and also because of the unique fluxional properties displayed by this group in solutions of such complexes. In the present series of cycloheptatrienyl compounds the C_7H_7 group occupies one coordination site in the octahedral complexes in a trihapto fashion with the ligands **1** in a *fac* conformation. The nature of the ligands **1** imparts an asymmetry to the complexes and this is reflected in the detection of seven proton signals for the C_7H_7 group, in solution, in a low temperature ^1H nmr study.

Experimental

Air-sensitive materials were handled in a glove box under an atmosphere of oxygen-free dry nitrogen, in a nitrogen-blanketed apparatus, or on a high-vacuum line. Tetrahydrofuran (THF) was dried by refluxing over Na/benzophenone and was used immediately following distillation. Benzene was dried by refluxing over molten potassium followed by distillation. The ligands **1** were prepared as sodium salts in THF solution as described previously (1, 2, 7). $(C_7H_7)Mo(CO)_2I$ (9), $(C_7H_7)W(CO)_2I$ (10), and $(C_7H_7)^+BF_4^-$ (11) were prepared as described previously.

*Preparation of the Complexes $LM(CO)_2(C_7H_7)$ (L = **1**; M = Mo or W)*

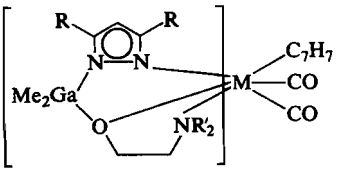
The preparations of the complexes $LM(CO)_2(C_7H_7)$ were all very similar and may be summarized by the following procedures. Analytical, ^1H nmr, and ir data for these complexes are given in Tables 1 and 2.

In a typical preparation, $(C_7H_7)Mo(CO)_2I$ (0.740 g, 2.0 mmol) was suspended in ~50 mL of benzene and 2.0 mmol of ligand **1** in THF added. The mixture was stirred for 1–2 days. Gradually the colour of the mixture changed from green to red–brown and a white precipitate formed. After filtration of the mixture, the solvent was removed from the filtrate under vacuo and the red–brown solid obtained recrystallized from benzene. The tungsten analogues were prepared similarly by

0008-4042/80/212278-08$01.00/0
©1980 National Research Council of Canada/Conseil national de recherches du Canada

Can. J. Chem. Downloaded from www.nrcresearchpress.com by 210.87.254.40 on 09/05/12
For personal use only.

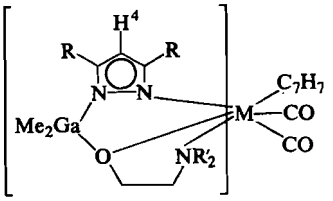
TABLE 1. Analytical and ir data for



			Calculated (%)			Found (%)			ν_{CO} (cm^{-1})†	
M	R	R′	C	H	N	C	H	N	CH_2Cl_2	C_6H_{12}
Mo*	H	H	44.8	5.0	8.2	44.7	5.1	8.2	1840, 1925	1858, 1935vs 1875, 1956m
Mo	Me	H	43.4	5.2	8.4	43.9	5.4	8.3	1835, 1922	1855, 1932
Mo	H	Me	43.4	5.2	8.4	42.6	5.0	8.3	1835, 1918	1853, 1929
Mo	Me	Me	45.7	5.8	8.0	45.3	5.8	7.9	1834, 1919	1849, 1928
W*	H	H	38.2	4.2	7.0	38.5	4.3	7.1	1827, 1915	i
W	Me	H	36.9	4.4	7.2	37.2	4.6	7.2	1822, 1914	i
W	H	Me	36.9	4.4	7.2	36.5	4.5	7.3	1825, 1913	1846, 1925
W	Me	Me	39.1	4.9	6.8	39.1	5.0	6.8	1821, 1912	1841, 1923

*Crystallized with 0.5 mol C_6H_6.
†vs = very strong, m = medium, i = insoluble.

TABLE 2. ^1H nmr data for



			τ (ppm)*				
M	R	R′	C_7H_7	H^4	R	R′	Ga—Me
Mo	H	H	4.74s	3.88t	2.36d, 2.85d		10.15s, 10.36s
			5.04s				9.66s, 10.20s
Mo	Me	H	4.83s	4.27s	7.53s, 8.03s		10.09s, 10.37s
Mo	H	Me	4.76s	3.91t	2.34d, 2.84d	7.51s, 8.59s	10.16s, 10.28s
Mo	Me	Me	4.83s	4.26s	7.46s, 8.02s	7.48s, 8.36s	10.08s, 10.26s
W	H	H	4.93s	3.98t	2.35d, 2.92d		10.17s, 10.42s
			5.21s	3.91t			9.67s, 10.26s
W	Me	H	5.01s	4.33s	7.56s, 8.08s		10.10s, 10.43s
W	H	Me	4.95s	4.00t	2.36d, 2.92d	7.35s, 8.61s	10.19s, 10.34s
W	Me	Me	5.00s	4.32s	7.50s, 8.07s	7.32s, 8.38s	10.10s, 10.30s

*Measured in C_6D_6 solution; s = singlet, d = doublet, t = triplet.

reaction of $(C_7H_7)W(CO)_2I$ with the organogallate ligands **1**. The yield of the desired product in these reactions was in the range of 50–70%. The complexes prepared were all air-stable in the solid state but in solution decomposed on prolonged exposure to air.

An alternative preparative route to these complexes involved reacting the $Na^+LM(CO)_3^-$ salts (1) with $(C_7H_7)^+BF_4^-$ in THF, followed by recrystallization of the crude product from benzene. However, the yields in these reactions were substantially lower, being in the range of 10–15%.

Preparation of the Complex
$[MeGa(N_2C_3H_3)_3]Mo(CO)_2(C_7H_7)$

This complex was prepared by reacting the ligand salt $Na^+MeGa(N_2C_3H_3)_3^-$ (12) (0.495 g, 1.60 mmol) with $(C_7H_7)Mo(CO)_2I$ (0.593 g, 1.60 mmol) in THF solution. The colour of the reaction mixture changed from green to a yellowish-brown colour, and a red–brown solid was obtained after removal of solvent under vacuum. This was extracted with and recrystallized from a benzene/heptane mixed solvent. The pure product was obtained as air stable orange–brown crystals. *Anal.* calcd. for $C_{19}H_{19}N_6O_2GaMo$: C 43.1, H 3.6, N 15.9; found: C 43.7, H 3.8, N 15.3. Ir spectra: $\nu_{CO}(cm^{-1})$ 1942, 1868 (cyclohexane); 1926, 1847 (Nujol). ^1H nmr (C_6D_6 solution, $\tau_{C_6H_6}$ = 2.84 ppm): $\tau_{(ppm)}$ = 1.66d(1), 1.93d(2) pyrazolyl-H_3; 3.25d(1), 2.79d(2) pyrazolyl-H_5; 3.95t(2), 4.32t(1) pyrazolyl-H_4; 4.73s(7) C_7H_7; 10.03s(3) GaMe (s = singlet, d = doublet, t = triplet. Relative intensities in parentheses. $J_{HCCH} \approx 2$ Hz for pyrazolyl-H_3, -H_5, -H_4 protons).

Can. J. Chem. Downloaded from www.nrcresearchpress.com by 210.87.254.40 on 09/05/12
For personal use only.

Can. J. Chem. Downloaded from www.nrcresearchpress.com by 210.87.254.40 on 09/05/12
For personal use only.

Preparation of the Complex

[MeGa($N_2C_5H_7$)$_2$(OH)]Mo(CO)$_2$(C_7H_7)

This complex was prepared by the reaction of the ligand salt $Na^+MeGa(N_2C_5H_7)_3^-$ (13) with $(C_7H_7)Mo(CO)_2I$ in THF solution. The origin of the hydroxy ligand in this type of reaction has been speculated upon previously (13). The crude product isolated from the reaction mixture was recrystallized from benzene to yield reddish brown crystals. *Anal.* calcd. for $C_{20}H_{25}N_4O_3GaMo$: C 44.9, H 4.7, N 10.5; found: C 45.1, H 4.4, N 10.1. Ir spectra: ν_{CO}(cm^{-1}) 1927, 1839 (CH_2Cl_2); 1911, 1809 (Nujol). ν_{OH}(cm^{-1}) 3575 (Nujol). ^1H nmr (C_6D_6 solution, $\tau_{C_6H_6}$ = 2.84 ppm): τ(ppm) = 4.44s(1), 4.56s(1) pyrazolyl-H_4; 4.89s(7) C_7H_7; 7.17s(3), 7.47s(3), 8.16s(3), 8.29s(3) pyrazolyl-Me_3 and -Me_5; 9.61s(1) OH; 10.07s(3) GaMe.

Spectra

Mass spectra were recorded on a Varian MAT CH4 mass spectrometer at 70 eV with a source temperature of 120–200°C. Infrared spectra were recorded on a Perkin-Elmer 457 spectrophotometer and ^1H nmr spectra on a Varian XL-100 spectrometer using FT techniques.

Results and Discussion

Analysis of mass spectral, ir, ^1H nmr, and preliminary X-ray structural data for the complexes listed in Tables 1 and 2 points to a monomeric pseudo octahedral structure for the compounds $LM(CO)_2(C_7H_7)$ (where L = **1**; M = Mo or W), with the cycloheptatrienyl ligand bonded in a trihapto fashion in one of the octahedral positions. The $LM(CO)_2(C_7H_7)$ compounds can be prepared by treating the carbonyl anions, $LM(CO)_3^-$, with tropenium salts, e.g. $(C_7H_7)^+BF_4^-$, but a more productive route to the same compounds was via the reaction of the $(C_7H_7)M(CO)_2I$ compounds with the ligand salts, Na^+L^-.

Infrared Spectra

With the exception of one complex the ν_{CO} region of the ir spectra of the $LM(CO)_2(C_7H_7)$ compounds (Table 1) in solution showed two sharp strong bands of approximately equal intensity, indicating a *cis* arrangement of the two CO ligands in the pseudo octahedral complexes (14). This does not distinguish between a *fac* or *mer* arrangement for the organogallate ligand, L, about the central molybdenum atom (7). However, a *fac* arrangement for this ligand is predicted on the following counts: (*i*) previous X-ray structural studies have demonstrated this arrangement in the similar complex $[Me_2Ga(N_2C_5H_7)(OCH_2CH_2NH_2)]Mo(CO)_2(\eta^3\text{-}C_4H_7)$ (2); (*ii*) the C_7H_7 compounds can be prepared from the anions, $LM(CO)_3^-$, which are known to have a *fac* arrangement for the ligand L (1); (*iii*) ^1H nmr studies are consistent with a *fac* arrangement for the organogallate ligand; and (*iv*) preliminary data from the crystal structure determination of $[Me_2Ga(N_2C_5H_7)(OCH_2CH_2NH_2)]Mo(CO)_2(C_7H_7)$ has shown the organogallate ligand to be *fac* and the cycloheptatrienyl ligand to be trihapto (15).

Two pairs of ν_{CO} bands were found in the ir spectrum of the complex $[Me_2Ga(N_2C_3H_3)(OCH_2CH_2NH_2)]Mo(CO)_2(C_7H_7)$ in cyclohexane solution in approximately a 6:1 intensity ratio. Taken together with the ^1H nmr data for this complex and for the analogous tungsten compound, these results indicate the presence of two positional isomers for these derivatives which both incorporate the least sterically demanding ligand **1** with R = R′ = H. The most likely positions of substitution for the C_7H_7 groups in these positional isomers, as indicated by molecular model studies, are opposite either the pyrazolyl or the amino nitrogen atoms. As observed previously for similar complexes (1, 12, 16, 17) the ν_{CO} bands for the tungsten compounds are approximately 10–15 cm^{-1} lower than those for the corresponding molybdenum compounds.

The two compounds, $[MeGa(N_2C_3H_3)_3]Mo(CO)_2(C_7H_7)$ and $[MeGa(N_2C_5H_7)_2(OH)]Mo(CO)_2(C_7H_7)$, both displayed two strong ν_{CO} bands in their ir spectra, consistent with a *cis* dicarbonyl grouping. In these two complexes a *cis* arrangement for the two CO groups is mandatory since the inflexibility of the tridentate chelating organogallate ligands dictates that they must adopt a facial configuration about the molybdenum atom in the pseudo octahedral complexes.

^1H Nuclear Magnetic Resonance Spectra

^1H nmr data for the complexes, $LM(CO)_2(C_7H_7)$, recorded in C_6D_6 solution, are listed in Table 2. In the majority of cases the presence of only one isomer is indicated in the solutions. Figure 1 shows the room temperature spectrum of the complex $[Me_2Ga(N_2C_3H_3)(OCH_2CH_2NMe_2)]Mo(CO)_2(C_7H_7)$. However, for the two complexes $[Me_2Ga(N_2C_3H_3)(OCH_2CH_2NH_2)]M(CO)_2(C_7H_7)$ (M = Mo or W), two sets of signals in an approximate 6:1 ratio were observed. In addition the ir spectrum of the compound where M = Mo, in cyclohexane solution (the compound where M = W was insoluble in cyclohexane), showed two pairs of ν_{CO} bands in approximately this same ratio of 6:1. These results may be explained by the presence of two positional isomers for these two complexes, as discussed above.

The observation that in solutions of all the complexes the ^1H nmr signal due to the C_7H_7 group was observed as one sharp singlet at room temperature, indicates that this group is involved in a rapid fluxional process. This premise was confirmed by a variable temperature ^1H nmr study of the complex $[Me_2Ga(N_2C_3H_3)(OCH_2CH_2NMe_2)]W$-

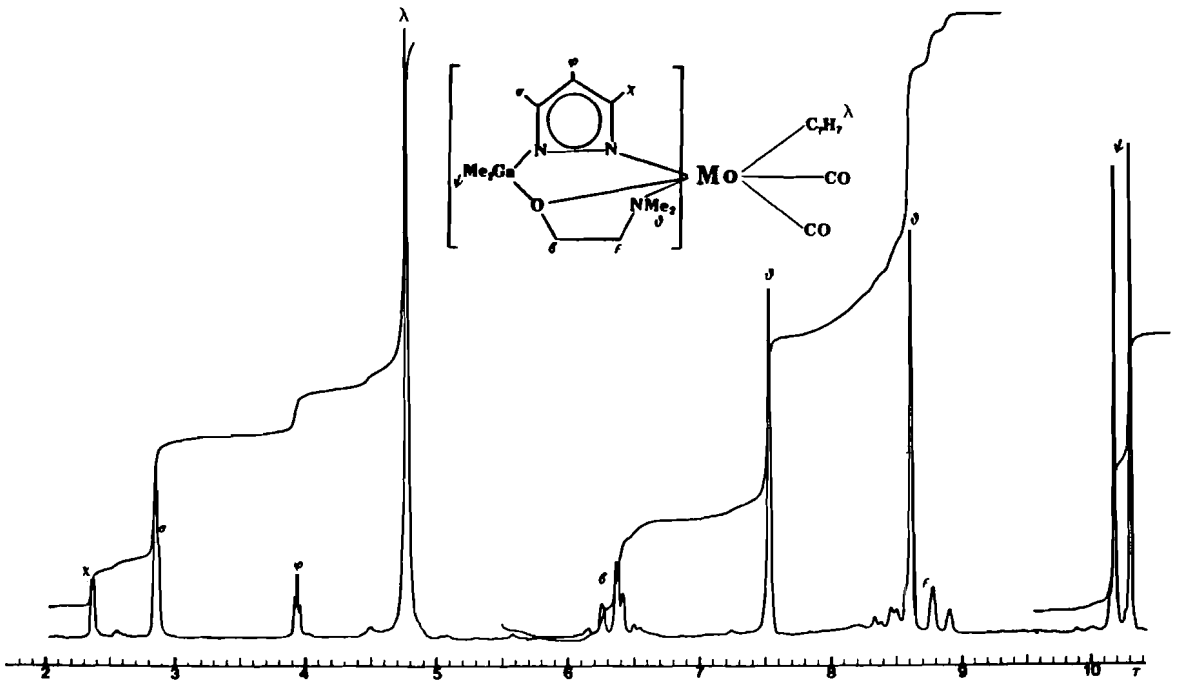


FIG. 1. Room temperature 100 MHz ^{1}H nmr spectrum of $[Me_2Ga(N_2C_3H_3)(OCH_2CH_2NMe_2)]Mo(CO)_2(C_7H_7)$ in C_6D_6 solution.

$(CO)_2(C_7H_7)$ in d_6-acetone solution (Fig. 2). As the sample solution was cooled the signal due to the C_7H_7 moiety successively broadened, disappeared, and finally reappeared as "five" distinct multiplets. The low temperature limiting spectrum was reached at -75°C and the C_7H_7 region of this spectrum is shown in Fig. 3 together with a computer simulated spectrum of the C_7H_7 protons. The assignments of the C_7H_7 protons are listed in Table 3 and are based on double resonance experiments. In Fig. 3 the three carbon atoms interacting with the tungsten atom in a trihapto "allylic" fashion are those bearing the protons *g*, *a*, and *b* with the central carbon atom bearing the proton *a*. Irradiation of the signal due to proton *a* caused the signal due to proton *g* to collapse to a doublet (the effect of this irradiation on the signal due to proton *b* could not be clearly seen because of coincident signals due to $-CH_2-$ protons). Conversely irradiation of the signals due to the protons *b* or *g* caused the signal due to proton *a* to collapse to a doublet as well as affecting the signals due to protons *c* and *f*. In addition it was noticed that irradiation of the proton *b* signal affected only the lowfield half of the *c*, *f* proton multiplet and irradiation of the proton *g* signal affected only the upfield half of the *c*, *f* proton multiplet. Irradiation of the lowfield half of the *c*, *f* proton multiplet reduced the upfield half of the *e*, *d* proton multiplet to a doublet and irradiation of the upfield half of the *c*, *f* proton multiplet reduced the lowfield half of the *e*, *d* proton multiplet to a doublet as well as reducing the *g* proton signal to a doublet. Finally irradiation of the lowfield half of the *e*, *d* proton multiplet reduced the upfield half of the *c*, *f* proton multiplet to a doublet while irradiation of the upfield half of the *e*, *d* proton multiplet reduced the lowfield half of the *c*, *f* proton multiplet to a doublet. These experiments fix the relative positions of the respective protons and since the highfield proton *a* is coupled to both the protons *b* and *g* (the other "1" proton multiplets) it must be the one associated with the central "allylic" carbon atom of the η^3-C_7H_7 group. The near identical computer simulated spectrum (based on the parameters given in Table 3) shown in Fig. 3 confirms unequivocally these assignments. The asymmetric nature of the complex, $[Me_2Ga(N_2C_3H_3)(OCH_2CH_2NMe_2)]W(CO)_2(C_7H_7)$, makes possible the observation of seven different proton signals due to the η^3-C_7H_7 group at low temperature in solution. This phenomenon eliminates any possibility of a monohapto cycloheptatrienyl group if it is assumed that such a ligand would freely rotate at -75°C. It is interesting to compare the low temperature limiting spectrum reported here with the spectra of other more symmetrical η^3-C_7H_7 complexes. Thus the low temperature solution ^{1}H nmr spectra of the

Can. J. Chem. Downloaded from www.nrcresearchpress.com by 210.87.254.40 on 09/05/12
For personal use only.

Can. J. Chem. Downloaded from www.nrcresearchpress.com by 210.87.254.40 on 09/05/12
For personal use only.



FIG. 2. Temperature dependent 100 MHz ^{1}H nmr spectrum of $[Me_2Ga(N_2C_3H_3)(OCH_2CH_2NMe_2)]W(CO)_2(C_7H_7)$ in d_6-acetone solution.

compounds $(\eta^3\text{-}C_7H_7)Co(CO)_3$ (18), $(\eta^5\text{-}C_5H_5)$-$Fe(CO)(\eta^3\text{-}C_7H_7)$ (19), and $(\eta^5\text{-}C_5H_5)Mo(CO)_2$-$(\eta^3\text{-}C_7H_7)$ (18, 20) each displayed four proton signals due to the $\eta^3\text{-}C_7H_7$ ring in the predicted intensity ratio of 1:2:2:2 with the central "allylic" proton again being to high field. Surprisingly, the low temperature solution ^{1}H nmr spectrum (21) of the pyrazolyl borate complex $[H_2B(N_2C_5H_7)_2]Mo$-$(CO)_2(C_7H_7)$ (22), which contains a B—H—Mo 2 electron-3 centre bond and a $\eta^3\text{-}C_7H_7$ ring (23), also shows only four signals due to the $\eta^3\text{-}C_7H_7$ ring protons. This is surprising since the cycloheptatrienyl group is asymmetrically positioned with respect to the pyrazolyl borate ligand, at least in the solid state, in the pseudo octahedral complex (23). In the present study the complex $[MeGa(N_2C_5H_7)_2(OH)]Mo$-

Can. J. Chem. Downloaded from www.nrcresearchpress.com by 210.87.254.40 on 09/05/12
For personal use only.

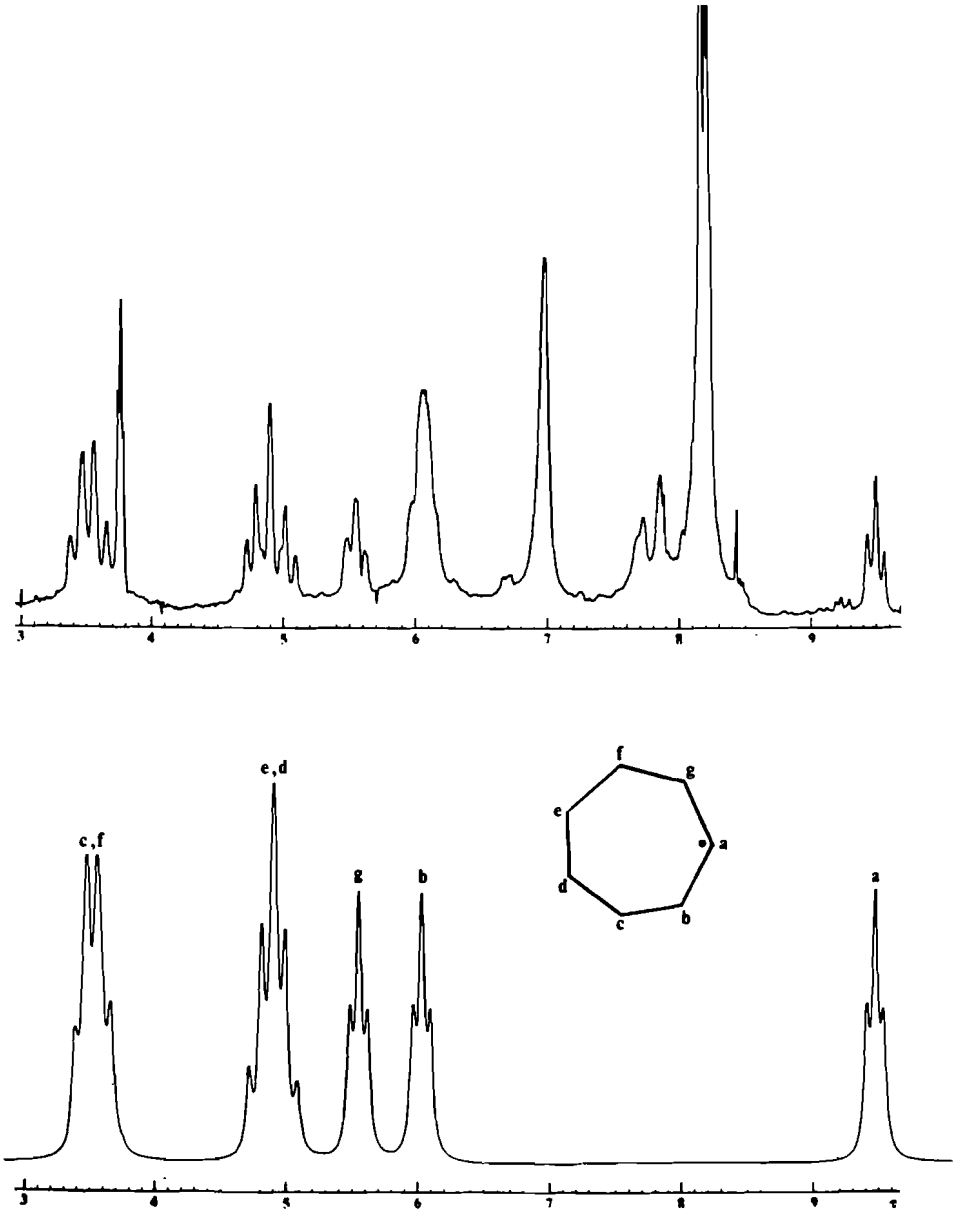


FIG. 3. Low temperature limiting ^1H nmr spectrum of C_7H_7 proton region of $[Me_2Ga(N_2C_3H_3)(OCH_2CH_2NMe)]W(CO)_2(C_7H_7)$ in d_6-acetone solution: experimental (top); computer simulated C_7H_7 proton spectrum (bottom).

$(CO)_2(C_7H_7)$ was synthesized to enable a comparison to be made of its low temperature ^1H nmr spectrum with those discussed above. The room temperature ^1H nmr of this complex in d_6-acetone solution was essentially identical with that of the C_6D_6 solution spectrum reported in the experimental section. Thus two equally intense pyrazolyl-H_4 proton signals, four equally intense pyrazolyl-Me signals, in addition to singlet resonances for the C_7H_7, OH, and GaMe protons, were observed. This spectrum indicates that the fluxional C_7H_7 group must be positioned opposite to one of the pyrazolyl nitrogens, rather than opposite to the OH group, in the pseudo octahedral complex. This arrangement would be expected on steric grounds (13), and should lead to an asymmetric environment for a "static" C_7H_7 group at low temperature in solution. Consequently, a similar low temperature ^1H nmr spectrum, for the C_7H_7 group, to that shown in Fig. 3 might be anticipated. Indeed, at $-82°C$, this

Can. J. Chem. Downloaded from www.nrcresearchpress.com by 210.87.254.40 on 09/05/12
For personal use only.

TABLE 3. Low temperature ^1H nmr data for the C_7H_7 ring in $[Me_2Ga(pz)(OCH_2CH_2NMe_2)]W(CO)_2(\eta^3\text{-}C_7H_7)$

Proton*	Chemical shift (τ)†	Coupling constants (Hz)	Pattern
a	9.39	$J_{ab} = 6.6, J_{ag} = 6.6$	Triplet
b	6.02‡	$J_{ba} = 6.6, J_{bc} = 7.0$	Not seen
c	3.46	$J_{cd} = 11.0, J_{cb} = 7.0$	Complex
d	4.96	$J_{de} = 9.5, J_{dc} = 11.0$	Complex
e	4.82	$J_{ef} = 12.0, J_{ed} = 9.5$	Complex
f	3.56	$J_{fg} = 7.0, J_{fe} = 12.0$	Complex
g	5.54	$J_{ga} = 6.6, J_{gf} = 7.0$	Distorted triplet

*See Fig. 3.
†Measured in d_6-acetone.
‡Calculated from position of C_7H_7 signal at room temperature.

type of pattern was observed with the central "allylic" proton again to highfield. A slight difference from the spectrum shown in Fig. 3 was that the two midfield triplets due to protons *g* and *b* were closer together causing an overlap of the two central lines to give an approximate 1:2:2:2:1 five line pattern. The low temperature ^1H nmr spectrum of the complex $[MeGa(N_2C_3H_3)_3]Mo(CO)_2(C_7H_7)$ at −82°C in d_6-acetone solution was not clearly resolved and unfortunately instrument limitations did not allow lower temperature spectra to be obtained. For this complex a low temperature limiting ^1H nmr spectrum of four signals for the C_7H_7 group might be expected since the tridentate chelating gallate ligand is now symmetrical and the complex is akin to those mentioned above (18–20). A tridentate chelating gallate ligand in this complex is consistent with its room temperature solution ^1H nmr spectrum (see Experimental) which shows the three pyrazolyl groups in two different environments in a 2:1 ratio. The unique pyrazolyl group would be positioned opposite to the C_7H_7 group in the pseudo octahedral complex. This arrangement is similar to that found for the pyrazolyl borate ligand in the related complex, $[PhB(N_2C_3H_3)_3]Mo(CO)_2(C_7H_7)$, for which the crystal structure has been determined (24). An earlier structural model suggested by Trofimenko for the compound of $[B(N_2C_3H_3)_4]Mo(CO)_2(C_7H_7)$ consisted of a bidentate chelating pyrazolyl borate ligand and a η^5-C_7H_7 ring (16). This model is also consistent with the ^1H nmr data, and was put forward on the basis of steric considerations and also on the grounds that the complex $[B(N_2C_3H_3)_4]Mo(CO)_2(C_5H_5)$ displays a bidentate pyrazolyl borate ligand and a η^5-C_5H_5 group, rather than a tridentate pyrazolyl borate ligand and a η^3-C_5H_5 group (25). It would appear, however, that in this type of complex the main driving force is the preference of the C_7H_7 ligand for η^3- rather than η^5-coordination, whereas for the C_5H_5 ligand this preference is reversed.

In order to provide a chemical proof of the trihapto nature of the C_7H_7 ring in the complexes $LM(CO)_2(C_7H_7)$ (where L = **1**; M = Mo or W), the preparation of "$Fe(CO)_3$" adducts was attempted. Thus if the $Fe(CO)_3$ moiety can be bound to the "butadiene" part of a coordinated η^3-C_7H_7 ring this has been taken as evidence for a trihapto as opposed to a penta- or hepta-hapto cycloheptatrienyl ring (26). Indeed, when an ethereal solution of $LMo(CO)_2(C_7H_7)$ (L = **1** where R = R′ = Me) and $Fe(CO)_5$ was subjected to uv radiation the complex $LMo(CO)_2(C_7H_7)\cdot Fe(CO)_3$ was formed. Unfortunately, however, the desired $Fe(CO)_3$ adduct could not be separated from the starting molybdenum complex using either column chromatography or fractional crystallization techniques. Nevertheless, the ir spectrum of the mixture of the $Fe(CO)_3$ adduct and the starting molybdenum complex in cyclohexane solution showed five ν_{CO} bands attributable to the $Fe(CO)_3$ adduct (in addition to the two ν_{CO} bands at 1928 and 1849 cm^{-1} due to the molybdenum starting material). These five bands occurred at 1924, 1837 (assigned to the $Mo(CO)_2$ moiety of the adduct) and 2045, 1979, and 1968 cm^{-1} (assigned to the $Fe(CO)_3$ grouping of the adduct). This pattern of five ν_{CO} bands is reminiscent of the patterns observed for a series of related compounds, $L'Mo(CO)_2(C_7H_7)\cdot Fe(CO)_3$ (where L′ = $[H_2B(N_2C_5H_7)_2]$ (21), $[HB(N_2C_3H_3)_3]$ (26), $[B(N_2C_3H_3)_4]$ (26), $[HB(N_2C_5H_7)_3]$ (26), and (η^5-C_5H_5) (27)), and strongly suggests a trihapto cyclohaptatrienyl ligand in the gallate complex.

Mass Spectra

All of the cycloheptatrienyl complexes described in this study were sufficiently volatile and stable to give readily observable parent ion signals in their mass spectra, which corresponded to the monomer species in the vapour phase. For the complexes $LM(CO)_2(C_7H_7)$ (where L = **1**; M = Mo or W) and the complex $[MeGa(N_2C_3H_3)_3]Mo(CO)_2(C_7H_7)$ the strongest signal in the spectra was due to the parent ion minus two CO groups, whereas for the compound $[MeGa(N_2C_5H_7)_2(OH)]Mo(CO)_2(C_7H_7)$ the strongest signal corresponded to the parent ion minus two CO groups and a dimethylpyrazole molecule. The appearance of signals due to other ions in all the spectra were accountable on predictable fragmentation patterns for the complexes. The intensity ratios of the individual peaks in all multi-line signals agreed closely with theoretical predictions based on the percentage isotope compositions of the contributing metal atoms.

Preliminary data (15) on the crystal structure determination of the complex, $[Me_2Ga(N_2C_5H_7)(OCH_2CH_2NH_2)]\ Mo(CO)_2(C_7H_7)$, has confirmed

the predicted "allylic" trihapto nature of the cycloheptatrienyl ligand, and the overall monomeric pseudo octahedral structure, for this complex. However, the position of substitution was found to be *trans* to the amino nitrogen rather than *trans* to the pyrazolyl nitrogen as found, or predicted, in related allyl or nitrosyl compounds (1, 2). On close inspection of molecular models this was not surprising since it became evident that the flattish *and* elongated shape of the η^3-C_7H_7 ring is best accommodated when it is aligned parallel to the pyrazolyl ring and to the two CO groups in the complex, i.e. opposite the amino nitrogen. In the position opposite the pyrazolyl nitrogen steric interactions involving the C_7H_7 group, particularly with the amino alcohol part of the gallate ligand, become more severe.

Acknowledgements

We thank the Natural Sciences and Engineering Research Council of Canada for financial support. We are grateful to Mr. P. Borda for C, H, N analyses, to Mr. J. Nip for mass spectra, and to Ms. M. Tracey for ^{1}H nmr spectra.

1. K. S. CHONG and A. STORR. Can. J. Chem. **57**, 167 (1979).
2. K. S. CHONG, S. J. RETTIG, A. STORR, and J. TROTTER. Can. J. Chem. **57**, 1335 (1979).
3. K. S. CHONG, S. J. RETTIG, A. STORR, and J. TROTTER. Can. J. Chem. **58**, 1080 (1980).
4. K. S. CHONG, S. J. RETTIG, A. STORR, and J. TROTTER. Can. J. Chem. **57**, 3107 (1979).
5. K. S. CHONG, S. J. RETTIG, A. STORR, and J. TROTTER. Can. J. Chem. **57**, 3113 (1979).
6. K. S. CHONG, S. J. RETTIG, A. STORR, and J. TROTTER. Can. J. Chem. **55**, 4166 (1977).
7. K. S. CHONG, S. J. RETTIG, A. STORR, and J. TROTTER. Can. J. Chem. **56**, 1212 (1978).
8. K. S. CHONG, S. J. RETTIG, A. STORR, and J. TROTTER. Can. J. Chem. **58**, 1091 (1980).
9. R. B. KING. Organometallic synthesis. Academic Press, New York. 1965.
10. R. B. KING and A. FRONZAGLIA. Inorg. Chem. **5**, 1837 (1966).
11. H. J. DAUBEN, L. R. HONNEN, and K. M. HARTMAN. J. Org. Chem. **25**, 1442 (1960).
12. K. R. BREAKELL, S. J. RETTIG, D. L. SINGBEIL, A. STORR, and J. TROTTER. Can. J. Chem. **56**, 2099 (1978).
13. K. R. BREAKELL, S. J. RETTIG, A. STORR, and J. TROTTER. Can. J. Chem. **57**, 139 (1979).
14. D. M. ADAMS. Metal–ligand and related vibrations. Edward Arnold Ltd., London. 1967. Chapt. 3.
15. K. S. CHONG, S. J. RETTIG, A. STORR, and J. TROTTER. Unpublished results.
16. S. TROFIMENKO. J. Am. Chem. Soc. **91**, 588 (1969).
17. S. TROFIMENKO. Inorg. Chem. **10**, 504 (1971).
18. M. A. BENNETT, R. BRAMLEY, and R. WATT. J. Am. Chem. Soc. **91**, 3089 (1969).
19. D. CIAPPENELLI and M. ROSENBLUM. J. Am. Chem. Soc. **91**, 6876 (1969).
20. J. W. FALLER. Inorg. Chem. **8**, 767 (1969).
21. J. L. CALDERON, F. A. COTTON, and A. SHAVER. J. Organomet. Chem. **42**, 419 (1972).
22. S. TROFIMENKO. Inorg. Chem. **9**, 2493 (1970).
23. F. A. COTTON, M. JEREMIC, and A. SHAVER. Inorg. Chim. Acta, **6**, 543 (1972).
24. F. A. COTTON, C. A. MURILLO, and B. R. STULTS. Inorg. Chim. Acta, **22**, 75 (1977).
25. J. L. CALDERON, F. A. COTTON, and A. SHAVER. J. Organomet. Chem. **37**, 127 (1972).
26. J. L. CALDERON, F. A. COTTON, and A. SHAVER. J. Organomet. Chem. **57**, 121 (1973).
27. F. A. COTTON and C. R. REICH. J. Am. Chem. Soc. **91**, 847 (1969).

Can. J. Chem. Downloaded from www.nrcresearchpress.com by 210.87.254.40 on 09/05/12
For personal use only.

Oxidation products of arachidonic acid. III. The synthesis of methyl 8*R*,9*R*,11*R*-, 8*S*,9*R*,11*R*-, and 8*S*,9*S*,11*R*-triacetoxyeicosa-5*Z*,12*E*,14*Z*-trienoate

GEORGE JUST AND CORINNE LUTHE[1]

Department of Chemistry, McGill University, Montreal, P.Q., Canada H3A 2K6

Received April 28, 1980

GEORGE JUST and CORINNE LUTHE. Can. J. Chem. **58**, 2286 (1980).

A stereospecific synthesis of the title compounds, starting from readily available glucose derivatives, is described, and methods for differentiating them and the already reported 8*R*,9*S*,11*R*-eicosatrienoate are discussed.

GEORGE JUST et CORINNE LUTHE. Can. J. Chem. **58**, 2286 (1980).

Une synthèse stéreospécifique des composés susnommés à partir du glucose est décrite, et des méthodes pour les différencier sont discutées.

Can. J. Chem. Downloaded from www.nrcresearchpress.com by 210.87.254.6 on 09/05/12
For personal use only.

In the second paper of this series (1), we described the synthesis of methyl 8*R*,9*S*,11*R*-trihydroxy-5*Z*, 12*E*,14*Z*-eicosatrienoate (**24***f*) from epoxide **13***a*, and gave the rationale for its preparation and that of the corresponding 8*S*,9*S*,11*R* (**25***d*), 8*R*,9*R*,11*R* (**22***f*), and 8*S*,9*R*,11*R* (**23***d*) isomers. In this communication, we would like to describe the synthesis of the latter three isomers, which follows the general scheme outlined for **24***f*.

The three chiral centers in **24** are directly related to those found in **13***a*. Similarly, those found in **22** correspond to the three chiral centers in epoxide **13** (3) (see **13** → **22**). Triol **23** has the stereochemistry of **22** except for an inversion at C(8), and a similar relation holds for **25** and **24**. The first task at hand was therefore to prepare **13** (3) in a simple and reproducible manner, and then to follow the synthetic scheme used for the preparation of **24**.

Although the stereochemistry at C(8) in **23** and **25** could have been built in at the epoxide stage using a C(5) epimer of either **13** or **13***a*, it was decided to introduce it at the latest possible stage in order to avoid unnecessary labor. Model studies on compounds of type **16** indicated that elimination reactions competed very strongly with displacement reactions at C(8). Use was therefore made of participation of a neighbouring acetate to invert the stereochemistry of the alcohol function at C(8). This is detailed in the second section of the paper.

The preparation of 1,2;5,6-di-*O*-isopropylidene-3-deoxy-α-D-xylohexofuranose (**8**) has been described (2) and consists in transforming diacetone glucose **1** to its tosylate **2**, pyrolyzing **2** at 210–220°C over soda-lime to give olefin **6**, and reducing **6** catalytically to **8**.

A clean partial hydrolysis (3) of the 5,6-*O*-isopropylidene group of **8** failed in our hands, so that a different 5,6-protecting group had to be used. Diacetone glucose tosylate **2** (2) was hydrolysed to the corresponding 5,6-diol **3**, which was then transformed to the corresponding 5,6-benzylidene derivate **4** and orthoester **5** by reaction with benzaldehyde/*p*-toluenesulfonic acid in benzene and trimethyl orthoformate respectively. Both compounds were obtained as a mixture of diastereomers, and were used as such. Treatment of the 5,6-benzylidene derivate **4** with soda-lime at 220°C/5 Torr did not yield any distillate, and raising the temperature only gave tars.

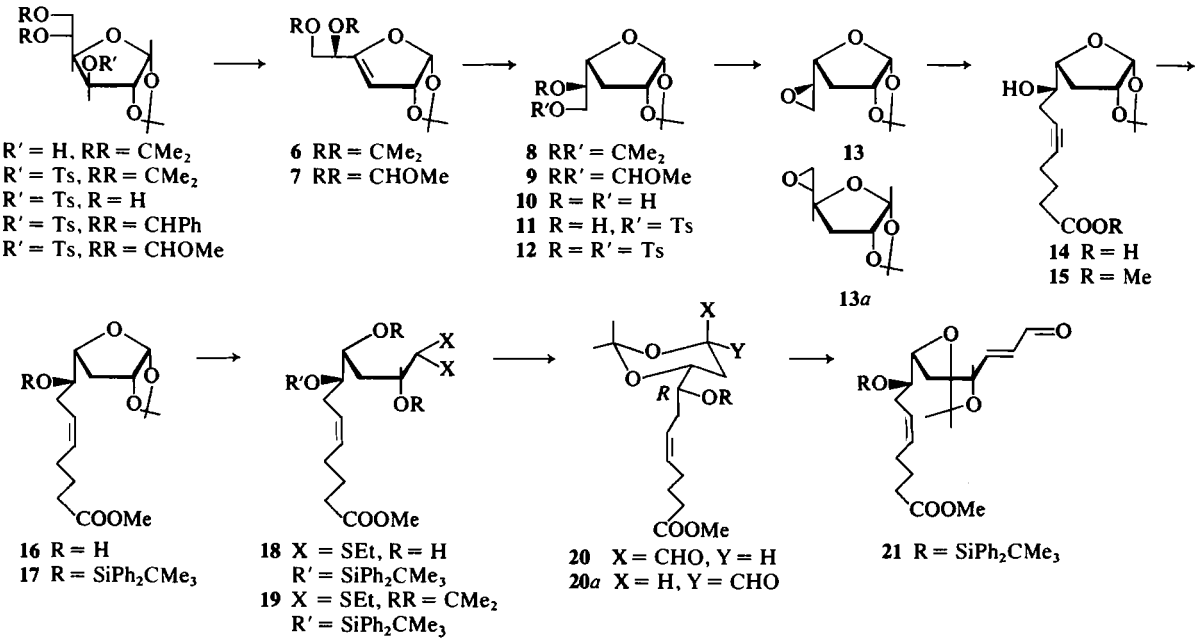
However, reaction of the orthoester **5** under the same conditions gave the extremely acid-sensitive **7**, which was immediately hydrogenated with Pd/C in acid-free ethyl acetate to give deoxy-diol **10** after brief acid treatment. Tosylation of crude **10** with one equivalent of *p*-toluenesulfonyl chloride/pyridine in chloroform gave monotosylate **11**, contaminated with 10–15% each of ditosylate **12** and diol **10**. Treatment of the crude tosylation mixture with 1 equivalent of aqueous methanolic potassium hydroxide, followed by distillation of the crude reaction mixture gave epoxide **13** in overall ~ 25% yield, based on glucose monotosylate **2**.

The sequence **13** → **22***a* followed the sequence **13***a* → **24***g* described (1), and the only differences noted were the acid sensitivity of aldehyde **20** with respect to its 9-isomer, and lower yields in the two consecutive Wittig reactions **20** → **21** → **22**. The proton α- to the aldehyde in **20** appeared as a triplet (dd, $J_{10,11} \cong 6.5$ Hz) and indicated an axial conformation of the aldehyde, in contrast to the corresponding aldehyde in the series leading to **24**, where the same proton appeared as a four line system (dd, $J_{10,11} \cong 5$ Hz, ~ 10 Hz) typical of an axial hydrogen. No isomerization had therefore taken

[1]Holder of a National Research Council of Canada Scholarship, 1977–1979, and a scholarship of the Ministry of Education of the Province of Quebec, 1977–1980.

0008-4042/80/212286-09$01.00/0

©1980 National Research Council of Canada/Conseil national de recherches du Canada



place during the transformation **19** → **20**. This was confirmed by the following experiment. Aldehyde **20** was dissolved in dry methanol saturated with potassium carbonate and was kept at room temperature for 6 hours. After this time, the isomerization of the axial aldehyde group of **20** to the diequatorial isomer **20***a* was complete. The coupling constant and chemical shift of the proton to the aldehyde was typical of an axial hydrogen (dd, $J_{10,11} \sim 5$ Hz, 10 Hz) and virtually identical to that of the corresponding aldehyde obtained in the 8*R*,9*S*,11*R* series (**24**), as were the chemical shifts of the aldehydic hydrogens in the two compounds. The isopropylidene methyls of **20***a* appeared at somewhat higher field than in the aldehyde of the 8*R*,9*S*,11*R* series (**24**), because of shielding due to the benzene rings of the *tert*-butyldiphenylsilyl group, as clearly demonstrated by inspection of models.

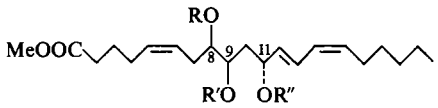
No isomerization occurred either during the Wittig reactions **20** → **21** → **22**, since (8*R*,9*R*,11*R*)-triacetate **22***g* was different by hplc from (8*S*,9*S*,11*R*)-triacetate **25***c* prepared below. Had isomerization taken place at C(11), the resulting triacetate would have had the 8*R*,9*R*,11*S*-configuration, and would therefore have had the same hplc behaviour as its (8*S*, 9*S*, 11*R*)-enantiomer **25***c*.

8*R*-*tert*-Butyldiphenylsilyloxy-9*R*,11*R*-di-*O*-isopropylidene ester **22***a* was obtained as a 9:1 mixture of 14*Z* and 14*E* isomers, as established by hplc, and was separated most efficiently at the triacetate stage **22***g*. Desilylation of **22***a* to alcohol **22***b* was effected by tetra-*n*-butylammonium fluoride in dry boiling THF. The acid removal of the isopropylidene group in **22***b* caused some difficulty, in contrast to its removal in **24***a*, in which the two substituents of the 1,3-dioxane ring are equatorial. This difficulty was caused by acid-catalysed trans-ketalization of **22***b* to the dioxolane **22***c*, which is considerably more stable to acid. This problem was resolved by acetylating **22***b*, and hydrolysing the resulting acetate **22***d* with aqueous methanolic hydrochloric acid. Work-up with basic resin gave a mixture of two acetates due to base-catalysed acetate migration. Base hydrolysis of the acetate mixture "(**22***e*)" gave triol **22***f*, which could not be separated into its geometric isomers. However, triacetate **22***g* (14*Z*/14*E* = 9:1) could be cleanly resolved.

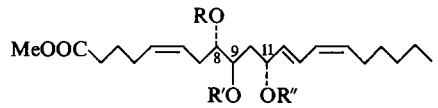
The conversions of appropriately derivatized triol ester **22** to its 8*S*-isomer **23**, and **24** to its 8*S*-isomer **25** were carried out in exactly the same manner, and no major differences were noted except for the considerably greater lability of mesylate **22***i* as compared to **24***b*. The sequence will therefore only be described for **24**. Alcohol **24***a* was mesylated, and the mesylate **24***b* subjected to acid hydrolysis. The reaction conditions for the hydrolysis were very critical, since the resulting alcohol **24***c* solvolyzed to furan **26***a*, identified by mass spectrometry and nmr only.

At room temperature, furan **26***a* started being detected by tlc after 40 min, in a reaction which was independent of acid concentration. The hydrolysis

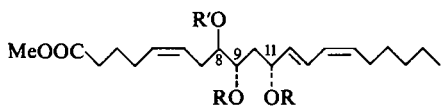
Can. J. Chem. Downloaded from www.nrcresearchpress.com by 210.87.254.6 on 09/05/12
For personal use only.



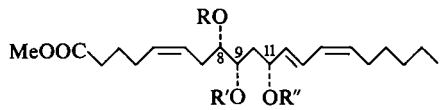
22 (8*R*, 9*R*, 11*R*)
a R = $SiPh_2CMe_3$, R′R″ = CMe_2
b R = H, R′R″ = CMe_2
c RR′ = CMe_2, R″ = H
d R = Ac, R′R″ = CMe_2
e R = Ac, R′ = R″ = H
f R = R′ = R″ = H
g R = R′ = R″ = Ac
h Me = R = R′ = R″ = H
i R = Ms, R′R″ = CMe_2
j R = Ms, R′ = R″ = H
k R = Ms, R′ = R″ = Ac



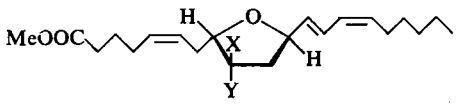
23 (8*S*,9*R*,11*R*)
a RR′ = $C(CH_3)OMe$, R″ = Ac
b R, R′ = H, Ac, R″ = Ac
c R = R′ = R″ = Ac
d R = R′ = R″ = H
e Me = R = R′ = R″ = H



24 (8*R*,9*S*,11*R*)
a RR = CMe_2, R′ = H
b RR = CMe_2, R′ = Ms
c R = H, R′ = Ms
d R = Ac, R′ = Ms
e R = R′ = Ac
f R = R′ = H
g RR = CMe_2, R′ = $SiPh_2CMe_3$



25 (8*S*,9*S*,11*R*)
a RR′ = $C(CH_3)OMe$, R″ = Ac
b R, R′ = H, Ac, R″ = Ac
c R = R′ = R″ = Ac
d R = R′ = R″ = H
e Me = R = R′ = R″ = H



26
a Y = OH, X = H (from gluco)
b Y = H, X = OH (from galacto)
c Y = OAc, X = H
d Y = H, X = OAc

reaction was therefore carried out with relatively strong acid (~0.1 *N*) and the product immediately worked up and acetylated with acetic anhydride/4-dimethylaminopyridine in ether. Flash-chromatography gave mesylate diacetate **24***d* in 60% yield, based on **24***a*. Solvolysis of the diacetoxymesylate **24***d* in methanol containing 1.1 equiv. of potassium acetate produced a less polar spot, presumably orthoester **25***a* which slowly hydrolyzed to a mixture of trihydroxydiacetates **25***b*. The orthoester was only identified by its acid-catalyzed conversion to **25***b*. The solvolysis mixture was then treated with some acetic acid to convert orthoester **25***a* to **25***b*, which was then reacetylated. The resulting triacetate **25***c* could be cleanly separated by hplc from triacetate **24***e*, obtained by acetylation of triol **24***f*. The structure of triacetate **25***c* was confirmed by the usual spectroscopic data. Treatment with methanolic sodium methoxide gave triol ester **25***e*.

When alcohol **22***b* was submitted to an analogous reaction sequence, triacetate **23***c* was obtained.

Triols **24***f* and **22***f*, which were obtained in relatively large quantities, proved to be rather unstable and decomposed even when kept under argon at −20°C. Their ^{1}Hmr spectra and optical rotations did not allow a clear differentiation, especially when only small samples were available. However, the corresponding triacetates **24***e* and **22***g* as well as **23***c* and **25***c* were quite stable and gave very characteristic ^{1}Hmr spectra, allowing a clear distinction (see Fig. 1). No single hplc system could be found in which all four isomers could be separated. Thus, on a reverse phase system (Microbondapak C_{18} ("Waters")), **24***e* and **25***c* had identical retention times, followed by **22***g* and **23***c*. $PGF_{2\alpha}$ methyl ester triacetate had a comparatively much shorter retention time on this system. When straight-phase conditions were employed (Lichrosorb Si-100 (Brownlee Labs.)), the

Can. J. Chem. Downloaded from www.nrcresearchpress.com by 210.87.254.6 on 09/05/12
For personal use only.

Can. J. Chem. Downloaded from www.nrcresearchpress.com by 210.87.254.6 on 09/05/12
For personal use only.

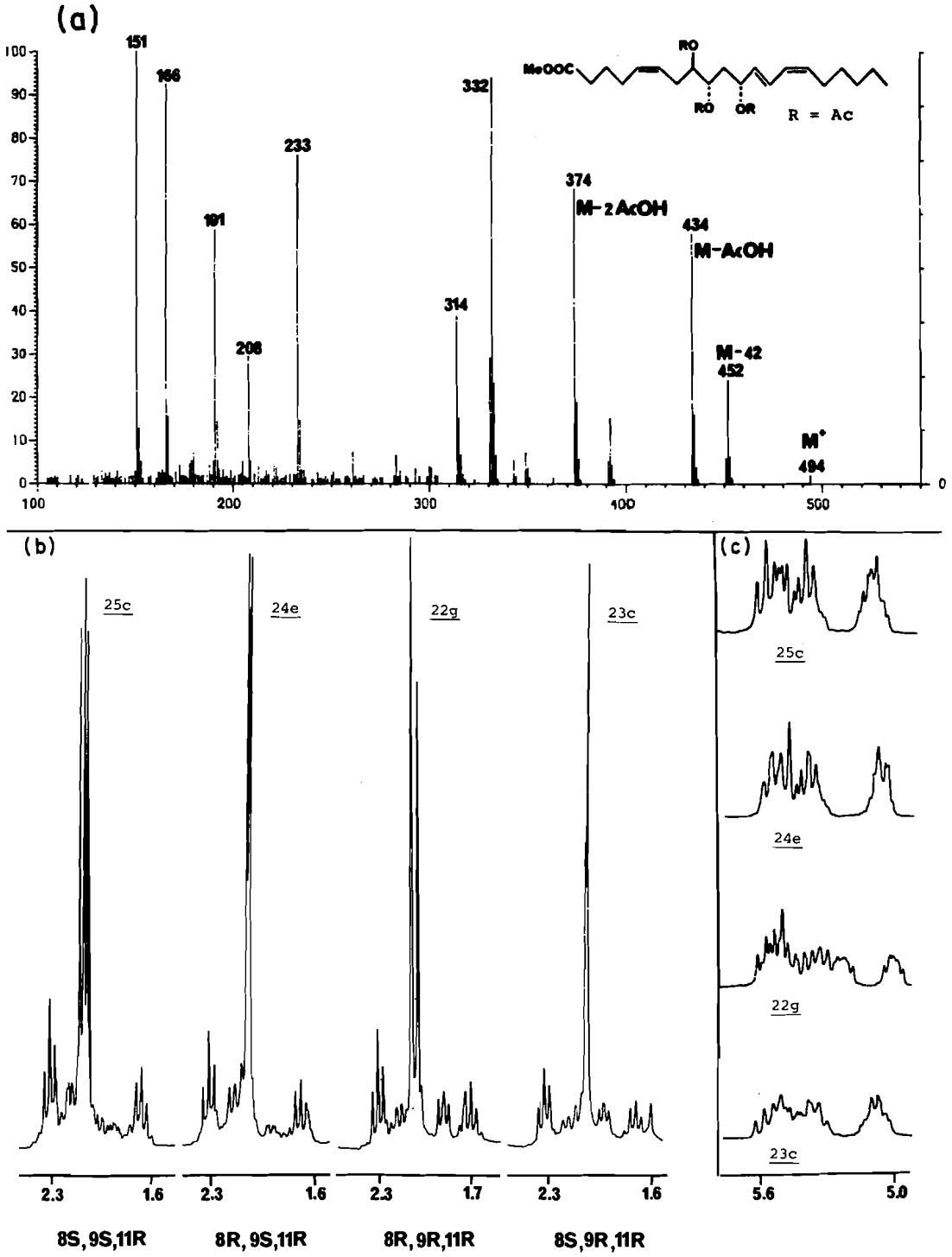


FIG. 1. (a) Mass spectrum of methyl 8*R*,9*S*,11*R*-triacetoxy-5*Z*,12*E*,14*Z*-eicosatrienoate (**24***e*) at 15 eV; (b) 200 MHz ^{1}Hmr spectra of 8*S*,9*S*,11*R*-, 8*R*,9*S*,11*R*-, 8*R*,9*R*,11*R*-, and 8*S*,9*R*,11*R*-triacetates **25***c*, **24***e*, **22***g*, and **23***c*, between 1.6–2.5 ppm; (c) 200 MHz ^{1}Hmr spectra of 8*S*,9*S*,11*R*-, 8*R*,9*S*,11*R*-, 8*R*,9*R*,11*R*-, and 8*S*,9*R*,11*R*-triacetates **25***c*, **24***e*, **22***g*, and **23***c*, between 5.0–5.7 ppm.

Can. J. Chem. Downloaded from www.nrcresearchpress.com by 210.87.254.6 on 09/05/12
For personal use only.

elution sequence was quite different, $PGF_{2\alpha}$ methyl ester triacetate having the same retention time as **24***e* and **23***c*, which were then followed by **22***g* and **25***c*.

The high-resolution mass spectra of the four acetates proved conclusively their structural identity. Their isomeric purity was ascertained by their 200 MHz ^{1}Hmr spectra, and the ^{13}Cmr of triacetates **22***g* and **25***c* and triol **24***f* (1).

Experimental

General

Mass spectra (ms) were obtained on a HP 5984 mass spectrometer or on a LKB-9000 mass spectrometer at 70 eV. Infrared (ir) spectra were obtained on a Perkin Elmer 297 spectrophotometer. Proton and carbon-13 magnetic resonance spectra were recorded on Varian T-60, T-60A, XL-200, and on Brucker FT 90 spectrometers. The hplc separations were performed on an Altex 300 instrument, using "Spherisorb $S_{10}W$" silica gel (Technical Marketing) and on a Waters 660, using Microbondapak C_{18} (reverse phase) and Lichrosorb Si-100 (straight phase) columns. Microanalyses were carried out by Mid-West Laboratories, Indianapolis, IN.

3-p-Toluenesulphonate of 1,2-O-Isopropylidene-α-D-glucofuranose (3)

A solution of tosylate **2** (2) (108 g, 0.26 mol) in MeOH (2 L) and 2.5 *M* aqueous H_2SO_4 (175 mL) was stirred at room temperature for 11 h. The solution was then neutralized with concentrated aqueous NaOH and the solvent was removed *in vacuo*; the residue was dissolved in CH_2Cl_2, dried over $MgSO_4$, and evaporated to give diol **3** as a hygroscopic solid in quantitative yield. Nuclear magnetic resonance ($CDCl_3$) δ: 1.26 (s, 3H, CH_3), 1.45 (s, 3H, CH_3), 2.42 (s, 3H, Ph—CH_3), 2.9–4.0 (m, 5H, C(5)H, C(6)H, 2OH (exchangeable with D_2O)), 4.14 (bdd, 1H, $J_{3,4} \sim 2.5$ Hz, $J_{4,5} \sim 2.5$ Hz, C(4)H), 4.56 (d, 1H, $J_{1,2} = 4$ Hz, C(2)H), 4.95 (d, 1H, $J_{3,4} = 2.5$ Hz, C(3)H), 5.79 (d, 1H, $J_{1,2} = 4$ Hz, C(1)H), 7.52 (4H, ABq, $\delta_{AB} = 0.48$, $J = 8$ Hz).

p-Toluenesulfonate of 1,2-O-Isopropylidene-5,6-O-methoxymethylidene-α-D-glucofuranose (5)

Diol tosylate **3** (79 g, 0.21 mol), *p*-toluenesulfonic acid (0.63 g), and trimethylorthoformate (100 mL) were refluxed for 0.5 h; saturated aqueous $NaHCO_3$ (100 mL) was then added, the excess trimethylorthoformate removed *in vacuo*, and the residue extracted with ether (3 × 600 mL). The ether extracts were washed with H_2O (3 × 100 mL), dried over $MgSO_4$, and evaporated *in vacuo* to give the oily orthoformate as a 2:1 mixture of diastereomers in quantitative yield. Nuclear magnetic resonance ($CDCl_3$) δ: 1.30 (s, 3H, CH_3), 1.47 (s, 3H, CH_3), 2.45 (s, 3H, Ph—CH_3), 3.17 (s, ~1H, OCH_3), 3.23 (s, ~2H, OCH_3), 3.90–4.43 (m, 4H, C(4)H, C(5)H, C(6)H), 4.80 (d, 1H, $J_{1,2} = 4$ Hz, C(2)H), 4.92 (d, 1H, $J_{3,4} = 2.5$ Hz, C(3)H), 5.52 (s, ~0.33 H, *H*—C—OCH_3), 5.65 (s, ~0.66 H, *H*—C—OCH_3), 7.62 (4H, ABq, $\delta_{AB} = 0.49$, $J = 8$ Hz).

1,2-O-Isopropylidene-5,6-O-methoxymethylidene-3-deoxy-D-erythro-3,4-hexofuranoside (7)

The pyrolysis reaction was carried out following an adaptation of the procedure described by Zinner *et al.* (2). Tosylate **5** (15 g, 36 mmol) was dissolved in benzene (50 mL) and powdered soda lime (60 g) was added; the solvent was then removed *in vacuo*, yielding an intimate mixture of substrate and base. (Note: Do not homogenize the granular mixture; this is important to prevent the soda lime from blowing over during the pyrolysis.) Vacuum (~5 Torr) was applied and the 250 mL flask was then immersed in a silicon oil bath at 225–235°C. After 10 min the product began to distill over and the vacuum was increased to ~0.5 Torr. The extremely acid labile vinyl ether **7** (2:1 mixture of diastereomers) was obtained as a colorless oil in 55–65% yield, and was at times contaminated with some starting material. Nuclear magnetic resonance ($CDCl_3$) δ: 1.41 (s, 6H, CMe_2), 3.30 (s, 3H, OCH_3), 3.73–4.30 (m, 2H, C(6)H), 4.40–4.90 (m, 1H, C(5)H), 5.15–5.36 (m, 2H, C(2)H, *H*—C—OMe), 5.76 (d, 1H, $J_{1,2} = 4$ Hz, C(1)H), 5.90–6.10 (m, 1H, C(3)H).

1,2-O-Isopropylidene-5,6-O-methoxymethylidene-3-deoxy-α-D-xylohexofuranose (9)

Olefin **7** (5 g, 20 mmol) in ethyl acetate (200 mL, freshly distilled from P_2O_5 after carbonate wash) was hydrogenated (40 lb H_2) using 5% Pd/C as catalyst (1.6 g). After 10 min the reaction mixture was filtered through Celite and the solvent removed *in vacuo* to give the desired deoxy-galacto-furanose **9** in ~90% yield. In spite of all precautions taken, **9** was always contaminated with its partial hydrolysis product **10**. Nuclear magnetic resonance ($CDCl_3$) δ: 1.22 (s, 3H, CH_3), 1.45 (s, 3H, CH_3), 1.53–2.16 (m, 2H, C(3)H), 3.15 (s, 1.5H, OCH_3), 3.19 (s, 1.5H, OCH_3), 3.19–4.76 (m, 5H, C(2)H, C(4)H, C(5)H, C(6)H), 5.50–5.66 (m, 2H, C(1)H, *H*—C—OMe).

1,2-O-Isopropylidene-3-deoxy-α-D-xylohexofuranose (10) (3)

Crude **9** (15.3 g, 62 mmol) was stirred at room temperature for 0.5 h in 200 mL concentrated HCl/H_2O/MeOH (0.01:1:100); solid $NaHCO_3$ (10 g) was then added to effect total hydrolysis of the formates formed. The MeOH was removed *in vacuo*, the residue dissolved in CH_2Cl_2, dried over $MgSO_4$, filtered, and the CH_2Cl_2 removed *in vacuo* to give diol **10** as a solid in quantitative yield. A sample, recrystallized from acetone:hexane, melted at 95.5–96°C (lit. (3) mp 97°C); nmr ($CDCl_3$) δ: 1.33 (s, 3H, CH_3), 1.57 (s, 3H, CH_3), 2.03–2.32 (m, 2H, C(3)H), 3.27 (bs, 2H, OH, exchangeable with D_2O), 3.33–4.43 (m, 4H, C(4)H, C(5)H, C(6)H), 4.68–4.93 (m, 1H, C(2)H), 5.83 (d, 1H, $J_{1,2} = 4$ Hz, C(1)H).

5,6-Anhydro-3-deoxy-1,2-isopropylidene-α-D-xylohexofuranose (13) (3)

To the crude diol **10** (12.7 g, 62 mmol) and *p*-toluenesulfonyl chloride (11.8 g, 62 mmol) under N_2 at 0°C, in CH_2Cl_2 (75 mL, distilled from P_2O_5) was added dropwise pyridine (11 mL) in 10 mL CH_2Cl_2. The reaction mixture was maintained at 0°C for 3 h and was stirred at room temperature for 20 h. The product was extracted with CH_2Cl_2 (2 × 700 mL); the extracts were washed with cold 1% HCl till the washings were acidic, and H_2O (4 × 100 mL). Evaporation gave mono-tosylate **11** in ~70% yield, contaminated with ~15% di-tosylate **12**. This crude residue was dissolved in MeOH/H_2O (300 mL/50 mL), cooled at 0°C, and 1 *N* KOH was added dropwise till the solution remained basic. The solution was neutralized with acidic resin (AM-120 H^+) and the solvents were removed *in vacuo*; the residue was redissolved in CH_2Cl_2, dried over $MgSO_4$, and the solvent removed *in vacuo*. Distillation (100°C/1 Torr) gave the epoxide **13** as an oil (crystallizes at 0°C, lit. (3) mp 27°C), in ~90% yield; nmr ($CDCl_3$) δ: 1.32 (s, 3H, CH_3), 1.54 (s, 3H, CH_3), 2.04–2.37 (m, 2H, C(3)H), 2.40–2.89 (m, 2H, C(6)H), 3.14–3.44 (m, 1H, C(5)H), 3.59–3.94 (m, 1H, C(4)H), 4.64–4.85 (m, 1H, C(2)H), 5.77 (d, 1H, $J_{1,2} = 4$ Hz, C(1)H).

Acid 14 and Methyl Ester 15

To 5-hexynoic acid (4) (2.2 g, 20 mmol) in 25 mL dry HMPA in an argon atmosphere at 5°C was added dropwise

Can. J. Chem. Downloaded from www.nrcresearchpress.com by 210.87.254.6 on 09/05/12
For personal use only.

n-BuLi in hexane (25 mL, 40 mmol). The colorless solution became bright orange. The epoxide **13** (1.9 g, 10 mmol) in 10 mL HMPA was added dropwise, the ice bath removed (precipitation of the dianion may otherwise occur), and the reaction mixture was stirred at room temperature for 20 h. Acetic acid (1.2 mL, 20 mmol) was then added and the solvents were removed by Kugelrohr distillation (110°C/0.1 Torr). The residue was stirred and shaken in cold 1 *N* aqueous HCl/ether, and was then extracted with ether (3 × 400 mL); the ether extracts were washed with saturated salt solution (4 × 100 mL), dried over $MgSO_4$, and evaporated to yield oily **14** which was methylated with ethereal diazomethane; excess methyl hexynoate was removed at 60°C/0.1 Torr, and the residual oil was purified by flash chromatography (5) (petroleum ether (30–50°C)/ethyl acetate 4.6:4.0) to yield 1.3 g (42% yield) of **15** as an oil. Infrared (neat): 1735 (C=O), 3490 (OH) cm^{-1}; nmr ($CDCl_3$) δ (glucose numbering): 1.33 (s, 3H, CH_3), 1.57 (s, 3H, CH_3), 1.60–2.63 (m, 10H, C(3)H, C(6)H, $CH_2CH_2CH_2$), 3.06 (d, 1H, $J_{5,OH}$ = 3.5 Hz, OH, exchangeable with D_2O), 3.65–4.43 (m, 2H, C(4)H, C(5)H), 3.68 (s, 3H, CO_2CH_3), 4.67–4.93 (m, 1H, C(2)H), 5.82 (d, 1H, $J_{1,2}$ = 4 Hz, C(1)H); ms (70 eV) *m/e*: 297 (M − CH_3), 173 (M − (CH_2—C≡C − $(CH_2)_3CO_2Me$)), 169 (CHOH—CH_2—C≡C$(CH_2)_3CO_2Me$)) 143 (*M* − 169); $[\alpha]_D^{20}$ −20.4° (*c* 4.90, $CHCl_3$). *Anal.* calcd. for $C_{16}H_{24}O_6$: C 61.54, H 7.69; found: C 61.79, H 7.40.

Z-Olefin 16 (6)

To nickel acetate (2.2 g, 8.8 mmol) in a three-neck flask equipped with a septum, was added 5 mL of 95% ethanol. The flask was connected to the hydrogenation apparatus and was flushed with hydrogen. The catalyst was produced by injecting 12.9 mL of a 0.5 *M* solution of sodium borohydride in 95% ethanol to the rapidly stirred solution of nickel acetate. The reaction vessel was reflushed with hydrogen and ethylene diamine (0.5 mL) was added. Hydrogenation was then initiated by introducing the acetylenic alcohol **15** (3.12 g, 10.0 mmol), in 10 mL ethanol, via the septum. Hydrogen uptake was quantitative within an hour and then virtually ceased. The reaction mixture was filtered through Celite, the ethanol was removed under reduced pressure, and the residue was extracted with ether (3 × 350 mL). The combined ether extracts were washed with H_2O (3 × 40 mL), dried over $MgSO_4$, and evaporated *in vacuo* to give the olefinic alcohol **16** in quantitative yield. Infrared (neat): 1735 (C=O), 3500 (OH) cm^{-1}; nmr ($CDCl_3$) δ (glucose numbering): 1.32 (s, 3H, CH_3), 1.54 (s, 3H, CH_3), 1.61–2.61 (m, 10H, C(3)H, C(6)H, $CH_2CH_2CH_2$), 2.89 (d, 1H, *J* ~ 3 Hz, OH, exchangeable with D_2O), 3.58–4.38 (m, 2H, C(4)H, C(5)H), 3.67 (s, 3H, CO_2CH_3), 4.68–4.93 (m, 1H, C(2)H), 5.41–5.68 (m, 2H, *Z*-CH=CH), 5.81 (d, 1H, $J_{1,2}$ = 4 Hz, C(1)H); Cmr ($CDCl_3$) δ: 173.67 (CO_2Me), 130.52 (C=C), 125.98 (C=C), 112.17, 105.92, 83.64, 80.56, 72.31, 51.11, 33.36, 33.14, 31.04, 26.78, 26.40, 25.75, 24.46, 23.81; *m/e* (trimethylsilylated sample): 313 (M − $SiMe_3$), 245 (M − CH_2HC=CH$(CH_2)_3COOMe$), 243 (Me_3SiOCH—CH_2CH=CH$(CH_2)_3CO_2Me$).

tert-*Butyldiphenylsilyl Ether 17*

To the alcohol **16** (2.53 g, 8.06 mmol) in dry dimethylformamide (15 mL) under N_2 was added *tert*-butylchlorodiphenylsilane (2.44 g, 8.86 mmol) and imidazole (1.21 g, 17.8 mmol); the reaction mixture was then stirred at 78°C for 17 h to effect complete silylation. Water (100 mL) was added and the product was extracted with ether (3 × 350 mL); the combined ether extracts were washed with H_2O (3 × 40 mL), dried over $MgSO_4$, and evaporated to afford the silylated alcohol, **17**, as a pale yellow oil, in quantitative yield. Nuclear magnetic resonance (glucose numbering) ($CDCl_3$) δ: 0.68–2.55 (m, 10H, C(3)H, C(6)H, $CH_2CH_2CH_2$), 1.05 (s, 9H, $SiCMe_3$), 1.28 (s, 3H, CH_3). 1.38 (s, 3H, CH_3), 3.54 (s, 3H, CO_2CH_3), 3.67–4.20 (m, 2H, C(4)H, C(5)H), 4.43–4.70 (q-like m, 1H, C(2)H), 5.08–5.38 (m, 2H, *Z*-HC=CH), 5.47 (d, 1H, $J_{1,2}$ = 4 Hz, C(1)H), 7.05–7.75 (m, 10H, $SiPh_2$); *m/e*: 537 (*M* − 15); $[\alpha]_D^{21}$ −41.44° (*c* 4.85, $CHCl_3$). *Anal.* calcd. for $C_{32}H_{44}O_6Si$: C 69.57, H 7.97; found: C 69.76, H 7.98.

*Methyl 8*R-tert-*Butyldiphenylsilyloxy-9*R,*11*R-*dihydroxy-9,11*-O-*isopropylidene-12,12-di(ethylthio)dodeca-5Z-enoate (19) from 17*

To the silylated alcohol **17** (1.5 g, 2.7 mmol) in ethanethiol (4 mL) at −10°C was added anhydrous zinc chloride (1.9 g, 14.0 mmol). After one hour at −10°C, the excess ethanethiol was removed at −10°C, *in vacuo*. The foamy residue was dissolved in ethyl acetate (50 mL) and aqueous $NaHCO_3$ (10 mL) was added; the precipitate which formed was filtered off and the filtrate was extracted with ethyl acetate (3 × 400 mL); the ethyl acetate extracts were washed with saturated salt solution (3 × 50 mL), dried over $MgSO_4$, and evaporated to give the thioacetal **18** in ~85% yield. Its nmr spectrum was consistent with the structure proposed.

To an aliquot of the crude product **18** (1.1 g, 1.8 mmol) in 50 mL acetone was added dimethoxypropane (5 mL) and *p*-toluenesulfonic acid (catalytic). After 15 min at room temperature the acetone was removed at reduced pressure and the residue extracted with ethyl acetate (3 × 400 mL); the ethyl acetate extracts were washed with aqueous $NaHCO_3$ (3 × 30 mL), saturated salt solution (3 × 30 mL), dried over $MgSO_4$, and evaporated to give the isopropylidene thioacetal **19** as a pale yellow oil in quantitative yield. Nuclear magnetic resonance ($CDCl_3$) δ: 1.05 (s, 9H, $SiCMe_3$), 1.17–2.93 (m, 16H, $5CH_2$, $2CH_3$), 1.22 (s, 6H, CMe_2), 2.65 (q, $J \simeq 7$ Hz, 4H, $2SCH_2CH_3$), 3.60 (s, 3H, CO_2CH_3), 3.60–4.17 (m, 4H, H—C—S, H—C—O), 5.13–5.57 (m, 2H, *Z*-HC=CH), 7.17–7.87 (m, 10H, $SiPh_2$); *m/e* (70 eV): 584 ($M^+ - CH_2C$-(OMe)OH), 135 ($CH(SEt)_2$, 100%); $[\alpha]_D^{22}$ 5.71° (*c* 2.75, $CHCl_3$). *Anal.* calcd. for $C_{36}H_{54}O_5S_2Si$: C 65.65, H 8.21, S 9.73; found: C 65.84, H 8.57, S 9.83.

*Methyl 8*R-tert-*Butyldiphenylsilyloxy-9*R,*11*R-*dihydroxy-9,11*-O-*isopropylidene-12-oxo-dodeca-5Z-enoate (20)*

To the dithioacetal **19** (0.49 g, 0.75 mmol) in acetone: water (26 mL: 2.6 mL) was added mercuric oxide (1.3 g, 6.1 mmol), and mercuric chloride (0.55 g, 2.0 mmol); the heterogeneous reaction mixture was stirred at room temperature for 6 h, and was then filtered into aqueous $NaHCO_3$ (100 mL); the filtrate was refiltered, the acetone removed *in vacuo*, and the residue extracted with CH_2Cl_2 (2 × 300 mL); the extracts were washed with aqueous KI (2 × 50 mL), saturated salt solution (3 × 50 mL), dried over $MgSO_4$, and evaporated to give (after flash chromatography, petroleum ether/ethyl acetate 7:2) the oily, somewhat unstable aldehyde **20**, in part as a hydrate, in 75% yield. Infrared (neat): 1737 (COOMe), 3450 (OH-hydrated aldehyde) cm^{-1}; nmr ($CDCl_3$) δ: 1.08 (s, 9H, $SiCMe_3$), ~1.1–2.5 (m, 10H, $5CH_2$), 1.23 (s, 3H, CH_3), 1.32 (s, 3H, CH_3), 3.48–3.95 (m, 2H, C(8)H, C(9)H), 3.61 (s, 3H, CO_2CH_3), 4.15 (dd, 1H, $J_{10e,11}$ = $J_{10a,11}$ ~ 6.5 Hz, C(11)H), 5.16–5.58 (m, 2H, *Z*-HC=CH), 7.18–7.88 (m, 10H, $SiPh_2$), 9.72 (s, 0.8H, CHO); $[\alpha]_D^{20}$ 4.4° (*c* 1.80, $CHCl_3$).

*Methyl 8*R-tert-*Butyldiphenylsilyloxy-9*R,*11*S-*dihydroxy-9,11*-O-*isopropylidene-12-oxo-dodeca-5Z-enoate (20*a*) from 20*

Aldehyde **20** (30 mg, 0.052 mmol) was dissolved in dry

Can. J. Chem. Downloaded from www.nrcresearchpress.com by 210.87.254.6 on 09/05/12
For personal use only.

methanol saturated with potassium carbonate and was kept at room temperature for 6 h to effect complete isomerization of the axial aldehyde to its equatorial epimer. The solution was then neutralized with weak acidic resin (IRC-50). Removal of the resin, followed by evaporation of the methanol gave the oily, somewhat unstable, aldehyde **20***a* in part as a hydrate, in ~90% yield; nmr ($CDCl_3$) δ: 0.73–2.37 (m, 10H, $5CH_2$), 1.04 (s, 9H, $SiCMe_3$), 1.25 (s, 3H, CH_3), 1.32 (s, 3H, CH_3), ~3.6–3.9 (m, 2H, C(8)H, C(9)H), 3.66 (s, 3H, CO_2Me), 4.13 (dd, 1H, $J_{10,11}$ ~ 3 Hz, 12 Hz, C(11)H), 5.3–5.6 (m, 2H, *Z*-HC=CH), 7.31–7.85 (m, 10H, $SiPh_2$), 9.58 (s, 0.4H, hydrated CHO); $[\alpha]_D^{22}$ −21° (*c* 0.95, $CHCl_3$).

*Methyl 8*R-tert-*Butyldiphenylsilyloxy-9*R,*11*R-*dihydroxy-9,11*-O-*isopropylidene-14-oxo-tetradeca-5Z,12*E-*dienoate (21)*

To aldehyde **20** (1.25 g, 2.26 mmol) in 15 mL dry dimethylformamide under N_2, was added formylmethylenetriphenylphosphorane (7) (0.76 g, 2.5 mmol). After 20 h stirring at room temperature, water (200 mL) was added to the reaction mixture which was then extracted with ether (3 × 300 mL); the ether extracts were then washed with H_2O (3 × 50 mL), dried over $MgSO_4$, and evaporated to give the α,β unsaturated aldehyde **21** in ~70% yield, after flash chromatography (petroleum ether/ethyl acetate 11:2). Infrared (neat): 1692 (CHO), 1738 (CO_2Me) cm^{-1}; nmr ($CDCl_3$) δ: 1.06 (s, 9H, $SiCMe_3$), ~1.2–2.4 (m, 10H, $5CH_2$), 1.26 (s, 3H, CH_3), 1.35 (s, 3H, CH_3), 3.65 (s, 3H, CO_2CH_3), 3.71–3.91 (m, 2H, C(8)H, C(9)H), 4.48–4.63 (m, 1H, C(11)H), 5.27–5.55 (m, 2H, *Z*-CH=CH), 6.51 (ABq, 2H, $J_{12,13}$ = 16 Hz, $J_{13,14}$ ~8 Hz, $J_{11,13}$ ~ 1.5 Hz, $J_{11,12}$ = 4 Hz, OCH(11)—C*H*(12)—CH(14)O), 7.33–7.87 (m, 10H, $SiPh_2$), 9.57 (d, 1H, $J_{13,14}$ = 8 Hz, CHO); $[\alpha]_D^{22}$ 12.1° (*c* 4.25, $CHCl_3$).

*Methyl 8*R-tert-*Butyldiphenylsilyloxy-9*R,*11*R-*dihydroxy-9,11*-O-*isopropylidene-eicosa-5Z,12*E,*14Z-trienoate (22*a*)*

To *n*-hexyltriphenylphosphonium bromide (1.36 g, 3.19 mmol) in dry THF (10 mL) under argon at room temperature was rapidly added *n*-BuLi (2.55 mmol). The reaction mixture turned red immediately; it was stirred for 10 min, cooled to −78°C, and then aldehyde **21** (0.88 g, 1.52 mmol, in 5 mL THF) was added slowly via syringe. The reaction was over immediately and was warmed up rapidly by immersion into a room temperature water bath. The reaction mixture was quenched with H_2O, the THF removed *in vacuo*, and the residue extracted with hexane (3 × 150 mL); the extracts were washed with H_2O (3 × 20 mL), dried over $MgSO_4$, and evaporated. Flash chromatography (petroleum ether/ethyl acetate 10:0.7) gave the desired 14-*Z* olefin **22***a*, contaminated with a small amount of its 14-*E* isomer, as an oil, in ~70% yield. A separation of the minor 14-*E* impurity could not be achieved at this stage of the synthesis. Nuclear magnetic resonance ($CDCl_3$) δ: 0.73–2.53 (m, 21H, $9CH_2$, $1CH_3$), 1.08 (s, 9H, $SiCMe_3$), 1.27 (s, 3H, CH_3), 1.35 (s, 3H, CH_3), 3.64 (s, 3H, CO_2CH_3), 3.67–3.70 (m, 2H, C(8)H, C(9)H), 4.13–4.57 (m, 1H, C(11)H), 5.10–6.75 (m, 6H, olefinic H's), 7.23–7.93 (m, 10H, $SiPh_2$); $[\alpha]_D^{21}$ 29.53° (*c* 3.20, $CHCl_3$).

*Methyl 8*R,*9*R,*11*R-*Trihydroxy-9,11*-O-*isopropylidene-eicosa-5Z,12*E,*14Z-trienoate (22*b*)*

A mixture of **22***a* (0.65 g, 1.0 mmol) and tetra-*n*-butyl ammonium fluoride (2.0 mmol) was stirred in dry tetrahydrofuran (10 mL) at 60°C under a nitrogen atmosphere for 2 h; the tetrahydrofuran was removed *in vacuo* and the residue was extracted with ether (3 × 150 mL), washed with H_2O (3 × 30 mL), dried over $MgSO_4$, and purified by flash chromatography (petroleum ether/ethyl acetate 4:1) to give an 80% yield of **22***b*, contaminated with traces of its 14-*E* isomer. Nuclear magnetic resonance ($CDCl_3$) δ: 0.67–2.57 (m, 21H, $9CH_2$, $1CH_3$), 1.42 (s, 6H, $C(Me)_2$), ~2.6 (bs, 1H, OH (exchangeable with D_2O)), 3.33–4.00 (m, 2H, C(8)H, C(9)H), 3.68 (s, 3H, CO_2CH_3), 4.17–4.62 (m, 1H, C(11)H), 5.23–6.78 (m, 6H, olefinic H's); $[\alpha]_D^{21}$ +52.64° (*c* 3.75, $CHCl_3$).

*Methyl 8*R-*Acetoxy-9*R,*11*R-*dihydroxy-9,11*-O-*isopropylidene-eicosa-5Z,12*E,*14Z-trienoate (22*d*) from 22*b

A solution of alcohol **22***b* (0.055 g, 0.14 mmol, 14*Z*/14*E* 9:1) in anhydrous ether (10 mL) containing dry acetic anhydride (1 mL) and 4-dimethylaminopyridine (catalytic) was stirred at room temperature for 0.5 h. The ether was then evaporated *in vacuo*, and excess reagents were removed by azeotroping with toluene. The residue was extracted with ether (3 × 150 mL), washed with cold 1 *N* aqueous HCl (2 × 20 mL), aqueous $NaHCO_3$ (2 × 20 mL), H_2O (2 × 20 mL), and dried over $MgSO_4$. Removal of the solvent yielded acetate **22***d* quantitatively; nmr ($CDCl_3$) δ: 0.59–2.56 (m, 21H, $9CH_2$, $1CH_3$), 1.37 (s, 6H, CMe_2), 2.09 (s, 3H, $COCH_3$), 3.67 (s, 3H, CO_2CH_3), 3.72–4.14 (m, 1H, C(9)H), 4.19–4.62 (m, 1H, C(11)H), 4.74–5.11 (m, 1H, C(8)H), 5.14–6.76 (m, 6H, olefinic H's).

*Methyl 8*R-*Acetoxy-9*R,*11*R-*dihydroxyeicosa-5Z,12*E,*14Z-trienoate (22*e*) from 22*d

Acetate **22***d* (14*Z*/*E* ≅ 9:1, 60 mg, 0.13 mmol) in 10 mL methanol and 2.5 mL 0.035 *N* aqueous HCl was stirred at room temperature for 2 h to effect complete hydrolysis. The solution was neutralized with basic resin (IR-45 OH) and the solvents removed *in vacuo*; the residue was redissolved in ether and dried over $MgSO_4$. Evaporation of the solvent gave diol **22***e*, as a 9:1 mixture of 14*Z* and *E* isomers, in quantitative yield; the minor 14*E* impurity was not separated at this stage of the synthesis. The nmr data showed the presence of two acetate peaks, in an approximate 2:3 ratio, indicative of acetate migration during the basic conditions of work-up. However, this was of no consequence since the acetate group would be removed in the next synthetic step; nmr ($CDCl_3$) δ: 0.64–2.61 (21H, $9CH_2$, $1CH_3$), 2.09 (s, ~1.8H, $COCH_3$), 2.13 (s, ~1.2H, $COCH_3$), 3.02 (bs, 2H, OH, exchangeable with D_2O), 3.69 (s, 3H, CO_2CH_3), ~3.7–~5.0 (m, 3H, three —O—C—*H*), 5.24–6.88 (m, 6H, olefinic H's).

*Methyl 8*R,*9*R,*11*R-*Trihydroxy-5Z,12*E,*14Z-eicosatrienoate (22*f*) from 22*e

Acetate diol **22***e* (55 mg, 0.13 mmol, 14*Z*/*E* ~ 9:1), in 10 mL dry MeOH containing a catalytic amount of sodium methoxide, was stirred for 0.5 h, and was then neutralized with weak acidic resin (IRC-50). Removal of the resin, followed by evaporation of the methanol, gave triol **22***f* in quantitative yield. Flash chromatography as well as hplc proved to be ineffective for separation of the 14*E* and *Z* isomers. Nuclear magnetic resonance ($CDCl_3$) δ: ~0.6–2.5 (m, 21H, $9CH_2$, $1CH_3$), ~2.5–3.2 (bs, 3H, OH, exchangeable with D_2O), 3.33–4.03 (m, 2H, C(8)H, C(9)H), 3.68 (s, 3H, CO_2CH_3), 4.33–4.77 (m, 1H, C(11)H), 5.23–6.85 (m, 6H, olefinic H's).

*Methyl 8*R,*9*R,*11*R-*Triacetoxy-5Z,12*E,*14Z-eicosatrienoate (22*g*) from 22*f

Triacetate **22***g* was synthesized in a manner analogous to that of triacetate **24***e* herein described. The 14*E* and *Z* isomers were separated by hplc (petroleum ether/ethyl acetate/MeOH 900:100:3). Nuclear magnetic resonance ($CDCl_3$) δ: 0.89 (t, 3H, $J_{19,20}$ ~ 6.5 Hz, CH_3), 1.20–2.44 (m, 18H, $9CH_2$), 2.04 (s, 3H, $COCH_3$), 2.08 (s, 6H, $2COCH_3$), 3.67 (s, 3H, CO_2CH_3), 4.93–5.06 (m, 2H, *H*C(8)OAc, *H*C(9)OAc), 5.15–5.64 (m, 5H, *H*C(11)OAc, 4 olefinic H's), 5.94 ("dd",

Can. J. Chem. Downloaded from www.nrcresearchpress.com by 210.87.254.6 on 09/05/12
For personal use only.

1H, $J_{13,14} = J_{14,15} \sim 11$ Hz, C(14)H), 6.55 ("dd", 1H, $J_{13,14} \sim 11$ Hz, $J_{12,13} \sim 15$ Hz, C(13)H); Cmr ($CDCl_3$) δ: 173.86 (*C*OOCH$_3$), 170.33 (O*C*OCH$_3$), 170.22 (O*C*OCH$_3$), 170.16 (OCOCH$_3$), 134.68 (C=C), 132.02 (C=C), 129.74 (C=C), 128.63 (C=C), 127.12 (C=C), 124.34 (C=C), 73.76, 70.46, 69.42, 51.46, 35.70, 33.35, 31.42, 29.19, 28.68, 27.79, 26.58, 24.60, 22.52, 21.16, 20.88, 20.80, 14.01; *m/e*: found 494.2881 (M^+), calcd.: 494.2877 (M^+); 435 (M^+ − OCOCH$_3$), 374 (M^+ − 2AcOH), 333 (M^+ − $(CH_2)_3CO_2Me$ − AcOH), 233 (M^+ − $CH_2CH{=}CH(CH_2)_3CI_2Me$ − 2AcOH); $[\alpha]_D^{22}$ 1.68° (*c* 3.10, $CHCl_3$).

*Methyl 8*R*-Mesyloxy-9*R*,11*R*-dihydroxy-9,11*-O*-isopropylidene-eicosa-5Z,12*E*,14Z-trienoate (22*i*) from 22*b*

To a mixture of alcohol **22***b* (20 mg, 0.05 mmol, 14*Z*/14*E* 9:1) and triethylamine (20 mg, 0.2 mmol) in dry methylene chloride (5 mL), under a nitrogen atmosphere, at 5°C, was added methanesulfonyl chloride (15 mg, 0.13 mmol). After 0.5 h the reaction mixture was extracted with ether (3 × 100 mL); the extracts were washed with cold aqueous 0.3% HCl (3 × 15 mL), H_2O (3 × 15 mL), dried over $MgSO_4$, and evaporated to give highly unstable mesylate **22***i* as an oil, in quantitative yield. It was reacted immediately to avoid decomposition; nmr ($CDCl_3$) δ: 0.7–2.6 (m, 21H, $9CH_2$, $1CH_3$), 1.38 (s, 6H, $2CH_3$), 3.03 (s, 3H, SO_2CH_3), 3.63 (s, 3H, CO_2CH_3), 3.75–4.75 (m, 3H, C(8)H, C(9)H, C(11)H), 5.20–6.73 (m, 6H, olefinic H's).

*Methyl 8*R*-Mesyloxy-9*R*,11*R*-diacetoxyeicosa-5Z,12*E*,14Z-trienoate (22*k*)*

Mesylate **22***i* (24 mg, 0.05 mmol, 14*Z*/*E* = 9:1) in 4 mL MeOH and 1 mL 1 *N* aqueous HCl was stirred at room temperature for 20 min to effect complete hydrolysis. Reaction time was kept at a minimum to avoid competitive furan (**26***b*) formation. The solution was neutralized with basic resin (IR-45 OH) and the solvents removed *in vacuo*; the diol mesylate **22***j* thus obtained was redissolved in ether, dried over $MgSO_4$, filtered, and acetic anhydride (0.5 mL, excess) and a catalytic amount of 4-dimethylaminopyridine were added. After 0.5 h the ether was evaporated *in vacuo* and excess reagents were removed by azeotroping with toluene. The residue was extracted with ether (3 × 100 mL); the extracts were then washed with cold 0.3% HCl (3 × 10 mL), H_2O (3 × 10 mL), and dried over $MgSO_4$. Removal of the solvent yielded the mesylate diacetate **22***k*, as an oil, in 90% yield; nmr ($CDCl_3$) δ: ~0.7–2.6 (m, 21H, $9CH_2$, $1CH_3$), 2.05 (s, 3H, $COCH_3$), 2.09 (s, 3H, $COCH_3$), 3.04 (s, 3H, SO_2CH_3), 3.66 (s, 3H, CO_2CH_3), ~4.5–6.7 (m, 9H, C(8)H, C(9)H, C(11)H, three HC=CH).

*Methyl 8*S*,9*R*,11*R*-Triacetoxy-5Z,12*E*,14Z-eicosatrienoate (23*c*)*

Mesylate diacetate **22***k* (20 mg, 0.038 mmol, 14*Z*/*E* = 9:1) and anhydrous potassium acetate (4 mg, 0.041 mmol) in 10 mL dry methanol were refluxed for 48 h under a nitrogen atmosphere. The reaction mixture was then cooled and a catalytic amount of aqueous acetic acid added; the methanol was removed *in vacuo*, and the remaining solvents azeotroped with toluene, to yield crude acetates **23***b*; these were then dissolved in 10 mL anhydrous ether, and 0.2 mL acetic anhydride and a catalytic amount of 4-dimethylaminopyridine were added; after 15 min the excess acetic anhydride and acetic acid were azeotroped off with toluene. The residue was extracted with ether (3 × 75 mL); the extracts were washed with cold aqueous 1% HCl (2 × 10 mL), H_2O (3 × 10 mL), and dried over $MgSO_4$; evaporation of the solvent, followed by purification of the crude triacetate by flash chromatography (petroleum ether/ethyl acetate 7.5:2) yielded **23***c* (14*Z*/*E* 9:1) in 75% yield. The minor 14*E* isomer was separated by hplc (petroleum ether/ethyl acetate/MeOH 850:100:3). Nuclear magnetic resonance ($CDCl_3$) δ: 0.90 (t, 3H, $J_{19,20} \sim 6$ Hz, CH_3), 1.22–2.48 (m, 18H, $9CH_2$), 2.05 (s, 6H, $2COCH_3$), 2.06 (s, 3H, $COCH_3$), 3.68 (s, 3H, CO_2CH_3), 5.01–5.20 (m, 2H, *H*C(8)OAc, *H*C(9)OAc), 5.29–5.66 (m, 5H, *H*C(11)OAc, 4 olefinic H's), 5.96 ("dd", 1H, $J_{13,14} = J_{14,15} \sim 11$ Hz, C(14)H), 6.57 ("dd", 1H, $J_{13,14} \sim 11$ Hz, $J_{12,13} \sim 15$ Hz, C(13)H).

*Methyl 8*R*-Mesyloxy-9*S*,11*R*-dihydroxy-9,11*-O*-isopropylidene-eicosa-5Z,12*E*,14Z-trienoate (24*b*)*

To a mixture of alcohol **24***a* (1) (0.10 g, 0.25 mmol) and methanesulfonyl chloride (0.043 g, 0.38 mmol) in dry methylene chloride (4 mL), under nitrogen, at 5°C, was added triethylamine (0.05 g, 0.50 mmol). After 0.5 h the reaction mixture was extracted with ether (3 × 150 mL); the extracts were washed with cold aqueous 1% HCl (3 × 20 mL) H_2O (3 × 20 mL), dried over $MgSO_4$, and evaporated to give mesylate **24**b as an oil in quantitative yield; nmr ($CDCl_3$) δ: ~0.6–2.7 (m, 21H, $9CH_2$, $1CH_3$), 1.42 (s, 3H, CH_3), 1.48 (s, 3H, CH_3), 3.07 (s, 3H, SO_2CH_3), 3.67 (s, 3H, CO_2CH_3), 3.87–4.93 (m, 3H, C(8)H, C(9)H, C(11)H), 5.20–6.82 (m, 6H, three HC=CH); $[\alpha]_D^{20}$ 5.87 (*c* 3.95, $CHCl_3$).

*Methyl 8*R*-Mesyloxy-9*S*,11*R*-diacetoxyeicosa-5Z,12*E*,14Z-trienoate (24*d*)*

Mesylate **24***b* (0.085 g, 0.175 mmol) in 8 mL methanol and 2 mL 0.5 *N* aqueous HCl was stirred at room temperature for 1 h to effect complete hydrolysis. Reaction time was kept at a minimum to reduce competitive furan (**26***a*) formation. The solution was neutralized with basic resin (IR-45 OH) and the solvents removed *in vacuo*; the diol mesylate **24***c*, thus obtained, was redissolved in ether, dried over $MgSO_4$, filtered, and acetic anhydride (2 mL, excess) and a catalytic amount of 4-dimethylaminopyridine (8) were added. After 0.5 h the ether was evaporated *in vacuo* and excess reagents were removed by azeotroping with toluene. The residue was extracted with ether (3 × 150 mL); the extracts were then washed with cold 1% HCl (3 × 20 mL), H_2O (3 × 20 mL), and dried over $MgSO_4$. Removal of the solvent yielded the mesylate diacetate **24***d* contaminated with furan byproduct **26***a*. Purification of the above mixture by flash chromatography (petroleum ether/ethyl acetate 7:3) gave mesylate **24***d* as an oil in 60% yield; nmr ($CDCl_3$) δ: ~0.66–2.86 (m, 21H, $9CH_2$, $1CH_3$), 2.06 (s, 3H, $COCH_3$), 2.10 (s, 3H, $COCH_3$), 3.04 (s, 3H, SO_2CH_3), 3.68 (s, 3H, CO_2CH_3), 4.69–6.78 (m, 9H, C(8)H, C(9)H, C(11)H, three HC=CH); $[\alpha]_D^{22}$ −4.0° (*c* 2.75, $CHCl_3$). Tetrahydrofuran **26***c*: nmr ($CDCl_3$) δ: 0.89 (t, 3H, $J_{19,20} \sim 6$ Hz, CH_3), ~0.94–2.54 (m, 18H, $9CH_2$), 2.12 (s, 3H, $COCH_3$), 3.68 (s, 3H, CO_2CH_3), 3.97–4.12 (m, 1H, C(8)H), 4.61–4.78 (m, 1H, C(11)H), ~5.3–5.7 (m, 5H, HC(9)OAc, 4 olefinic H's), 6.00 ("dd", 1H, $J_{13,14} = J_{14,15} \sim 11$ Hz, C(14)H), 6.55 ("dd", 1H, $J_{13,14} \sim 11$ Hz, $J_{12,13} \sim 15$ Hz, C(13)H); *m/e* (70 eV): 392 (M^+), 332 (M^+ − AcOH), 191 (M^+ − AcOH − $CH_2CH{=}CH(CH_2)_3CO_2Me$).

*Methyl 8*S*,9*S*,11*R*-Triacetoxyeicosa-5Z,12*E*,14Z-trienoate (25*c*)*

Mesylate diacetate **24***d* (50 mg, 0.094 mmol) and anhydrous potassium acetate (10.6 mg, 0.108 mmol) in 10 mL dry methanol was refluxed for ~48 h under a nitrogen atmosphere. The reaction mixture was then cooled and a catalytic amount of aqueous acetic acid added; the methanol was removed *in vacuo* and the remaining solvents azeotroped with toluene to yield crude acetates **25***b*; these were then dissolved in 10 mL anhydrous ether, and 0.5 mL acetic anhydride and a catalytic amount of 4-dimethylaminopyridine were added;

after 15 min the excess acetic anhydride and acetic acid were azeotroped off with toluene. The residue was extracted with ether (3 × 150 mL); the extracts were washed with cold 1% aqueous HCl (2 × 15 mL), H_2O (3 × 15 mL), and dried over $MgSO_4$; evaporation of the solvent, followed by purification of the crude triacetate by flash chromatography (petroleum ether/ethyl acetate 7.5:2), yielded **25***c* in 75% yield. Nuclear magnetic resonance ($CDCl_3$) δ: 0.89 (t, 3H, $J_{19,20} \sim$ 6.5 Hz, CH_3), 1.18–2.44 (m, 18H, $9CH_2$), 2.05 (s, 3H, $COCH_3$), 2.07 (s, 3H, $COCH_3$), 2.10 (s, 3H, $COCH_3$), 3.67 (s, 3H, CO_2CH_3), 4.98–5.16 (m, 2H, *H*C(8)OAc, *H*C(9)OAc), 5.26–5.64 (m, 5H, *H*C(11)OAc, 4 olefinic H's), 5.95 ("dd", 1H, $J_{13,14} = J_{14,15} \sim$ 11 Hz, C(14)H), 6.53 ("dd", 1H, $J_{13,14} \sim$ 11 Hz, $J_{12,13} \sim$ 15.5 Hz, C(13)H); Cmr ($CDCl_3$) δ: 173.88 (CO_2Me), 170.28 ($OCOCH_3$), 170.02 ($OCOCH_3$), 169.96 ($OCOCH_3$), 134.62 (C=C), 131.98 (C=C), 129.16 (C=C), 128.83 (C=C), 127.11 (C=C), 124.32 (C=C), 73.41, 71.58, 70.12, 51.46, 35.91, 33.34, 31.39, 29.16, 28.53, 27.76, 26.55, 24.59, 22.50, 21.24, 20.95, 20.88, 14.02; *m/e*: found: 494.2884 (M^+); calcd.: 494.2877 (M^+); 435 ($M^+ - OCOCH_3$), 374 (M^+ − 2AcOH), 333 ($M^+ - (CH_2)_3CO_2Me$ − AcOH), 233 ($M^+ - CH_2CH{=}CH(CH_2)_3CO_2Me$ − 2AcOH), $[\alpha]_D^{22}$ 1.60° (*c* 1.60, $CHCl_3$).

*Methyl 8*R,*9*S,*11*R-*Triacetoxy-5*Z,*12*E,*14*Z-*eicosatrienoate (24e) from 24*f

A solution of triol **24***f* (60 mg, 0.16 mmol) in 10 mL anhydrous ether containing dry acetic anhydride (1 mL) and 4-dimethylaminopyridine (catalytic) was stirred at room temperature for 0.5 h. The ether was then evaporated *in vacuo* and excess reagents were removed by azeotroping with toluene. The residue was extracted with ether (3 × 150 mL), washed with cold aqueous 1 *N* HCl (2 × 20 mL), aqueous $NaHCO_3$ (2 × 20 mL), H_2O (2 × 20 mL), and dried over $MgSO_4$. Removal of the solvent yielded triacetate **24***e* quantitatively; nmr ($CDCl_3$) δ: 0.90 (t, 3H, $J_{19,20} \sim$ 6.5 Hz, CH_3), 1.20–2.46 (m, 18H, $9CH_2$), 2.04 (s, 3H, $COCH_3$), 2.05 (s, 3H, $COCH_3$), 2.06 (s, 3H, $COCH_3$), 3.68 (s, 3H, CO_2CH_3), 4.98–5.14 (m, 2H, *H*C(8)OAc, *H*C(9)OAc), 5.28–5.64 (m, 5H, *H*C(11)OAc, 4 olefinic H's), 5.95 ("dd", 1H, $J_{13,14} = J_{14,15} \sim$ 11 Hz, C(14)H), 6.52 ("dd", 1H, $J_{13,14} \sim$ 11 Hz, $J_{12,13} \sim$ 15 Hz, C(13)H); *m/e*: found: 494.2884 (M^+), calcd.: 494.2877 (M^+); 435 ($M^+ - OCOCH_3$), 374 (M^+ − 2AcOH), 333 ($M^+ - (CH_2)_3CO_2Me$ − AcOH), 233 ($M^+ - CH_2CH{=}CH(CH_2)_3CO_2Me$ − 2AcOH); $[\alpha]_D^{22}$ − 1.20° (*c* 3.75, $CHCl_3$).

Acknowledgements

We wish to thank the Natural Sciences and Engineering Research Council of Canada for financial support, and A. Ugolini and O. Mamer for running 200 MHz ^{1}Hmr and mass spectra, respectively. We would like to thank, in particular, Dr. Ng Ying Kin for the hplc separations.

1. G. Just and C. Luthe. Can. J. Chem. **58**, 1799 (1980).
2. H. Zinner, G. Wulf, and R. Heinatz. Chem. Ber. **97**, 3536 (1964).
3. K. Antonakis, A. Dowgiallo, and L. Szabó. Bull. Soc. Chim. Fr. 1355 (1962).
4. G. Just, C. Luthe, H. Oh, and J. Montgomery. Synth. Commun. **9**, 613 (1979).
5. W. C. Still, M. Kahn, and A. Mitra. J. Org. Chem. **43**, 2923 (1978).
6. C. A. Brown and V. K. Ahuja. J. Chem. Soc. Chem. Commun. 553 (1973).
7. S. Trippet and D. M. Walker. J. Chem. Soc. 1266 (1961).
8. G. Höfle, W. Steglich, and H. Vorbrüggen. Angew. Chem. Int. Ed. Engl. **17**, 569 (1978).

Can. J. Chem. Downloaded from www.nrcresearchpress.com by 210.87.254.6 on 09/05/12
For personal use only.

3-Aminotropane-3-carboxylic acids. Preparation and properties

GREGORIO G. TRIGO, CARMEN AVENDAÑO, AND EMILIA SANTOS

Department of Organic and Pharmaceutical Chemistry, School of Pharmacy, Universidad Complutense, Madrid-3, Spain

AND

HALVOR N. CHRISTENSEN AND MARY E. HANDLOGTEN

Department of Biological Chemistry, University of Michigan, Ann Arbor, MI 48109, U.S.A.

Received May 13, 1980

GREGORIO G. TRIGO, CARMEN AVENDAÑO, EMILIA SANTOS, HALVOR N. CHRISTENSEN, and MARY E. HANDLOGTEN. Can. J. Chem. **58**, 2295 (1980).

The two isomers of 3-aminotropane-3-carboxylic acid have been prepared by hydrolysis of the two α- and β-tropane-3-spiro-5′-hydantoins whose configurations were determined by X-ray crystallography and ^{13}C nmr. The pK'_a values of these amino acids and the hydrolysis rates of their *N*-formyl derivatives have been determined to study the influence of the amino group in an axial or equatorial position. The biological transport – inhibitory action of the two tropane amino acids has also been compared.

GREGORIO G. TRIGO, CARMEN AVENDAÑO, EMILIA SANTOS, HALVOR N. CHRISTENSEN et MARY E. HANDLOGTEN. Can. J. Chem. **58**, 2295 (1980).

On a préparé les deux isomères de l'acide amino-3-tropane-carboxylique-3 par hydrolyse des deux α- et β-tropane-3-spiro-5′-hydantoïne dont les configurations ont été déterminées par rayons X et rmn ^{13}C. Les valeurs des pK'_a de ces aminoacides et les vitesses d'hydrolyse de leurs dérivés *N*-formylés ont été déterminées afin d'étudier l'influence du groupement amino en position axiale or équatoriale. On a comparé également l'action biologique d'inhibition du transport de ces deux aminoacides tropaniques.

Introduction

We have succeeded in preparing the epimeric tropane amino acids (**1**, **2**) and we hoped that with both epimers in hand we could contribute to the accumulated information relating to the configurational studies of aminocyclohexane- and aminocyclopentane carboxylic acids (1–4).

From the biological point of view, several diamino acids have been used to investigate transport properties of lysine analogs. Interest in them extends also to transport of neutral amino acids. 1-Methylpiperidine-4-amino-4-carboxylic acid, for instance, is effective in inhibiting uptake of the amino-*endo* isomer of the norbornane amino acid, BCH (2-aminobicyclo[2.2.1]heptane-2-carboxylic acid), that serves as a model substrate for system L, the system for neutral amino acids with bulky, apolar sidechains (5). The transport behavior of the two isomeric tropane amino acids (ATC) has been studied to see if the 2-carbon bridge might give some information about the space available around the receptor site for system L, where the amino acid is bound for transport.

Experimental

Infrared spectral data were obtained from a Perkin-Elmer 577 spectrophotometer. All compounds were compressed into KBr pellets. Nuclear magnetic resonance spectra were obtained from a Perkin-Elmer R-24 A (60 MHz) spectrometer. Elemental analyses were performed on a Carlo Erba 1104 analyzer. All melting points were uncorrected. Paper chromatography (*n*-BuOH/AcOH/H_2O 3 :1 :6) was used in the R_f determinations.

Synthesis

3α-Amino-1αH,5αH-tropane-3β-carboxylic Acid (1)

α-Tropane-3-spiro-5′-hydantoin (10 g), obtained by the Bucherer synthesis from tropinone (6), was heated with 60% sulphuric acid (85 mL), the solution was neutralized with barium carbonate, and filtered. The pure amino acid was isolated by passage over 54 mL of ion exchange resin (cationic Lewatit S100) using 0.25 *N* aqueous ammonia as eluent and removing the solvent in vacuum giving **1** (8 g, 89%); mp >300°C; R_f 0.19 (19°C); ir(KBr) ν_{max}: 3500–3250 (s), 2600–1900 (s), and 1600–1500 (s, b) cm^{-1}; ^{1}Hmr (D_2O) δ: 2.79 (s, 3H, N—CH_3). *Anal.* calcd. for $C_9H_{16}N_2O_2 \cdot 1H_2O$: C 53.44, H 8.97, N 13.85; found: C 53.30, H 9.09, N 13.95.

In order to remove the water, it was necessary to heat the compound at 100°C/0.05 Torr over P_2O_5 for 24 h. *Anal.* calcd. for $C_9H_{16}N_2O_2$: C 58.66, H 8.75, N 15.20; found: C 58.32, H 8.63, N 15.10.

N-*Formyl-3α-amino-1αH,5αH-tropane-3β-carboxylic Acid*

The formylamino acid can be prepared in 90% yield following essentially the procedure of du Vigneaud *et al.* for the formylation of DL-cystine (7). Acetic anhydride (13.5 mL) was added dropwise to a mixture of the amino acid (3 g) and 85% formic acid (42 mL) at a rate to maintain the temperature of the reaction mixture between 50–60°C. After the addition was complete, the mixture was stirred at room temperature for 1 h at the end of which time 13 mL of ice-water was added and the mixture concentrated at reduced pressure. The crude product was recrystallized from absolute ethanol; mp 294°C (dec.); ir(KBr) ν_{max}: 1685 (s) and 1500–1600 (b) cm^{-1}; ^{1}Hmr (D_2O) δ: 2.75 (s, 3H, N—CH_3), 7.95 (s, 1H, CHO). *Anal.* calcd. for $C_{10}H_{16}N_2O_3 \cdot 1H_2O$: C 52.15, H 7.87, N 12.16; found: C 52.40, H 8.06, N 11.82.

3β-Amino-1αH,5αH-tropane-3α-carboxylic Acid (2)

From the β-Hydantoin

Tropane-3-spiro-5′-hydantoin (7 g) obtained by the Read synthesis from tropinone (6), was heated with 60% sulphuric acid (35 mL) at 150°C for 24 h and the solution was treated as

0008-4042/80/212295-05$01.00/0

©1980 National Research Council of Canada/Conseil national de recherches du Canada

Can. J. Chem. Downloaded from www.nrcresearchpress.com by 210.87.254.5 on 09/05/12
For personal use only.

Can. J. Chem. Downloaded from www.nrcresearchpress.com by 210.87.254.5 on 09/05/12
For personal use only.

in **1** to give **2** (48 g, 80%); mp >300°C; R_f 0.25; ir(KBr) ν_{max}: 3130–2050 (s, b) and 1610–1515 (s, b) cm^{-1}; ^{1}Hmr (D_2O) δ: 2.8 (s, 3H, N—CH_3).

From the Aminonitrile

3-Aminotropane-3-carboxynitrile (16.1 g) obtained from tropinone by the Strecker synthesis (8) was treated at 0°C with fuming hydrochloric acid (120 mL) and set aside overnight. The solution was then diluted with water (68 mL) and boiled under reflux for 24 h. The pure β-amino acid was isolated by passage over an ion exchange resin (cationic Lewatit S100) (108 mL) using 1 *N* aqueous ammonia as eluent and removing the solvent in vacuum, giving **2** (4 g, 22%). *Anal.* calcd. for $C_9H_{16}N_2O_2 \cdot 1/2\,H_2O$: C 55.93, H 8.86, N 14.49; found: C 55.60, H 8.67, N 14.16.

On heating at 100°C/0.05 Torr over P_2O_5 for 24 h the water was removed. *Anal.* calcd. for $C_9H_{16}N_2O_2$: C 58.66, H 8.75, N 15.20; found: C 58.82, H 8.52, N 15.46.

N-*Formyl-3β-aminotropane-3-carboxylic Acid*

The formylamino acid was prepared following the procedure of Huffman (9). The acetic formic anhydride was prepared (but not isolated) by heating acetic anhydride (4.4 mL) and 98% formic acid (1.9 mL) for 2 h at 50–60°C in a flask equipped with a stirrer and drying tube. The solution was cooled to 27°C. A gradual addition of the amino acid **2** (1 g) was made over a 15-min period using a water bath to maintain a temperature below 39°C. The reaction mixture was stirred about 29 h at room temperature after which water (30 mL) was added. The solvent was removed *in vacuo* to furnish the crude product (1.1 g, 96%) which was crystallized from water–dimethoxyethane; mp 301–305°C (dec.); ir(KBr) ν_{max}: 1685 (s) and 1590 cm^{-1}; ^{1}Hmr (D_2O) δ: 2.85 (s, 3H, N—CH_3), 8.15 (d, 1H, CHO). *Anal.* calcd. for $C_{10}H_{16}N_2O_3$: C 56.58, H 7.59, N 13.20; found: C 56.37, H 7.71, N 12.90.

3α-Amino-3β-hydroxymethyl-1αH,5αH-tropane (3)

Lithium aluminum hydride (3.27 g) in tetrahydrofuran previously distilled from $LiAlH_4$ (182 mL) was heated under reflux for 10 min after which dry, finely powdered **1** (5.5 g) was added in small portions with efficient stirring. After the addition was completed, the solution was heated under reflux for a further 4 h. With external cooling the reaction mixture was worked up after the method of Mićović and Mihailović (10) and the inorganic solid was filtered off and extracted with tetrahydrofuran (2 × 30 mL). The tetrahydrofuran filtrate and the extracts were combined and the solvent removed at 20 Torr. The residue crystallized from benzene – light petroleum (bp 60–80°C) to give **3** (3 g, 60%); mp 61.5–63.5°C: ir(KBr) ν_{max}: 3415 and 3380 (b), 3160 (b), and 1595 (m) cm^{-1}; ^{1}Hmr ($CDCl_3$) δ: 3.1 (s, 2H, O—CH_2), 2.25 (s, 3H, N—CH_3). *Anal.* calcd. for $C_9H_{18}N_2O$: C 63.48, H 10.65, N 16.45; found: C 63.58, H 10.93, N 16.33.

Spiro[tropane-3,4′α-N-oxazolidine] (4)

3-Amino-3-hydroxymethyltropane (1.5 g) in dry benzene (16 mL) was heated under reflux for 9 h with 37% formalin solution (3 mL) and then a Dean–Stark water trap was adapted. The reflux was continued for 1 h after the formation of water ceased. The solvent was removed in vacuum and the residue was crystallized from ethyl acetate to give **4** as needles (1.3 g, 89.6%); mp 116–117°C; ir(KBr) ν_{max}: 3320 (s); ^{1}Hmr ($CDCl_3$) δ: 4.5 (s, 2H, N—CH_2—O), 3.25 (s, 2H, O—CH_2), 2.3 (s, 3H, N—CH_3). *Anal.* calcd. for $C_{10}H_{18}N_2O$: C 65.84, H 9.95, N 15.37; found: C 66.15, H 10.05, N 15.57.

Spiro[tropane-3,4′-N-oxazolidine-2′-one] (5)

3-Amino-3-hydroxymethyltropane (1.7 g) was heated with ethyl carbonate (1.18 g) and sodium methoxide (50 mg) and the ethanol formed eliminated by distillation. The solid residue was crystallized from ethanol–dimethoxyethane giving **5** (400 mg, 20.5%); mp 85–86°C; ir(KBr) ν_{max}: 3250 (b) and 1615 (s) cm^{-1}; ^{1}Hmr (D_2O) δ: 3.4 (s, 2H, O—CH_2), 2.95 (s, 3H, N—CH_3); *Anal.* calcd. for $C_{10}H_{16}N_2O_2 \cdot 3H_2O$: C 47.98, H 8.85, N 11.19; found: C 48.00, H 8.85, N 11.11.

pH Titration

The pK_a' values for the amino groups (—NH_2 and N—CH_3) and the carboxylic group of both α- and β-tropane amino acids were determined at 25°C by continuous titration of 0.1 *M* amino acid dissolved in 0.1 *M* NaCl solution with 1 *N* HCl and 1 *N* NaOH. Standard buffers, phosphate pH 7.00, and phthalate pH 4.01 (Curtin Matheson Scientific, Inc.), were used. The results were corrected for dilution. The pK_a' was calculated for each point using standard equations. Corrections for HCl serving to establish pH values of 3 and lower were made by the following standard method. We take the first equivalent of HCl added (measured here as $[Cl^-]$) to convert the amino acid R from $R^{+,-}$ to $R^{2+,-}$. Further HCl acts to form R^{2+} and free H^+ (or H_3O^+). Then by the law of electroneutrality, neglecting species at very low concentrations, we have

$$[Cl^-] = A_{H^+}/\gamma_{H^+} + [R^{2+,-}] + 2[R^{2+}]$$

where pH is taken to be $\log A_{H^+}$, and A_{H^+}/γ_{H^+} at the calculated ionic strength is taken to be $[H^+]$. Thus we apportioned the total amount of the amino acid present between the univalent cation $R^{2+,-}$ and the divalent cation R^{2+}, to obtain the ratio desired in $pH = pK_a' + \log([R^{2+,-}]/[R^{2+}])$.

Rate Constants for Hydrolysis of N-*Formyl Amino Acids*

Solutions (10 m*M*) of the *N*-formyl α- and β-amino acids were prepared in 1 *N* HCl at room temperature. Aliquots of 0.5 mL were added to individual test tubes and the tubes incubated at 50°C. The reaction was stopped after selected time intervals by adding 1 *N* NaOH and the tubes were placed on ice. The extent of hydrolysis was measured by the Rosen ninhydrin method (11) for the liberated free amino acid. The low chromogenicity of the β-amino isomer was compensated by increasing the time for colour development at 100°C from 15 min to one hour. All values were corrected for a zero-time blank. Total hydrolysis was obtained by autoclaving 2 or 3 h in a small volume of 6 *N* HCl in sealed tubes. The tubes were opened and the HCl removed by holding the samples overnight in an evacuated desiccator over NaOH pellets at room temperature.

Biological Transport Determinations

Ehrlich cells were propagated as usual in Swiss white mice, and separated and washed as usual in the Na^+-free media (12). The uptake during 30 s at 37°C was measured in about 5% suspensions in Na^+-free, choline-containing Krebs–Ringer bicarbonate medium in a 5% CO_2–O_2 atmosphere. Uptake was terminated by cold dilution and brief centrifugation. Adhering medium was blotted away from the cell pellet before weighing (13). The separated suspending medium and a sulfosalicylic acid extract of the cells were then counted for ^{14}C-BCH as usual (13, 14). Extracellular water was measured by the sucrose contained in the medium, which was retained in the cell pellet. The uptake of ^{14}C-BCH is recorded in mmol · Kg^{-1} cell water · $30\,s^{-1}$ in Fig. 1. The external concentration of BCH was nearly constant at $10^{-4}M$.

Results and Discussion

Configuration of α- *and* β-*Amino-isomers*

The acid hydrolysis of α- and β-tropane-3-spiro-

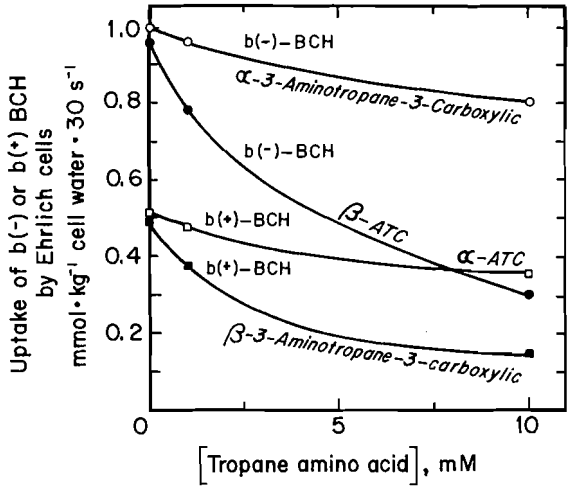


FIG. 1.

5′-hydantoins, whose configurations were determined by X-ray crystallography (15) and ^{13}C nmr data (16) gave the two α- and β-amino isomers of 3-aminotropane-3-carboxylic acids **1** and **2**. The amino acid obtained by hydrolysis of the 3-aminotropane-3-carboxynitrile was identical to the β-isomer **2** obtained from the β-hydantoin.

Lithium aluminum hydride reduction of **1** gave the corresponding aminoalcohol **3**, which was condensed with formaldehyde to give the spiro-4′-oxazolidine **4**. Condensation of **3** with ethyl carbonate gave the spiro-4′-oxazolidin-2-one **5** (Scheme 1).

*p*K′$_a$ *Determinations*

Compounds **1** and **2**, by potentiometric titration, gave the results shown in Table 1. Both tropane amino acids in water solution will be dipolar ions (α- or γ-zwitterions) (Fig. 2). By analogy with the results found in the above mentioned 1-methylpiperidine amino acid (5), the pK_3' value for the tropane amino acids is associated to a larger extent with the piperidine *N* than with the α-amino group. Furthermore, the ^1H nmr spectra in D_2O solution of both amino acids clearly show δ N—CH_3 values corresponding to a protonated piperidine nitrogen atom (pH of the solution 8.87 and 9.1 for the α-amino and β-amino isomers respectively).

Lowered values for pK_1' are characteristic for diamino acids in general (17), although the values of 1.2 and 1.5 are unexpectedly low. The lower value for compound **1** corresponds logically to the greater acidity of the equatorial carboxyl groups (18) together with the inductive effect of the closer approach of the carboxyl group to the piperidine *N*.

The small difference between the pK_3' values points to a less efficient solvation of the ammonium group in the γ-zwitterion for the α-amino isomer **1** than for the β-amino isomer **2**, probably due to the *cis*-relation with the carboxylate group in the first case.

Regarding the pK_2' values which are mainly attributed to the ionization of the —$\overset{+}{N}H_3$ group, the found differences show a weaker basicity for the β-amino isomer, with the NH_2 group in equatorial position. These results are in agreement with literature data for α-cyclohexaneamino acids (1, 3) but contradictory to the general consideration about the basic strength of axial and equatorial amino groups (19). Some authors (20) have explained the effect of a negative carboxylate group in weakening the acidity of the ammonium group only at great distances (up to $n = 3$ in $H_2N(CH_2)_nCOOH$ amino acids) as if the ionization of the ammonium group at short distances (α-amino acids) was accompanied by a net binding of water molecules, which, in our case and in the α-cyclohexaneamino acids may be more efficient when the α-amino group is in an equatorial position. In the tropane amino acid **2** obtained by the Strecker route, however, the nearness of the ammonium group and the tertiary nitrogen atom can also be implied.

Rate Constants for Hydrolysis of N-*Formyl Amino Acids*

Direct formylation with formic acid (7) was used to formylate **1** with 90% yield but did not give the formyl derivative of **2** in the same experimental conditions. This last derivative was obtained by reaction with acetic formic anhydride (9) with 96% yield.

We found that the 3β-formamidotropane-3α-carboxylic acid is hydrolyzed about 5 times as fast as the other isomer. The values of log $a/(a - X)$ versus

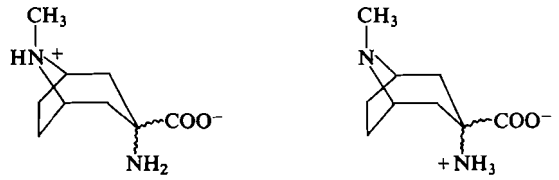


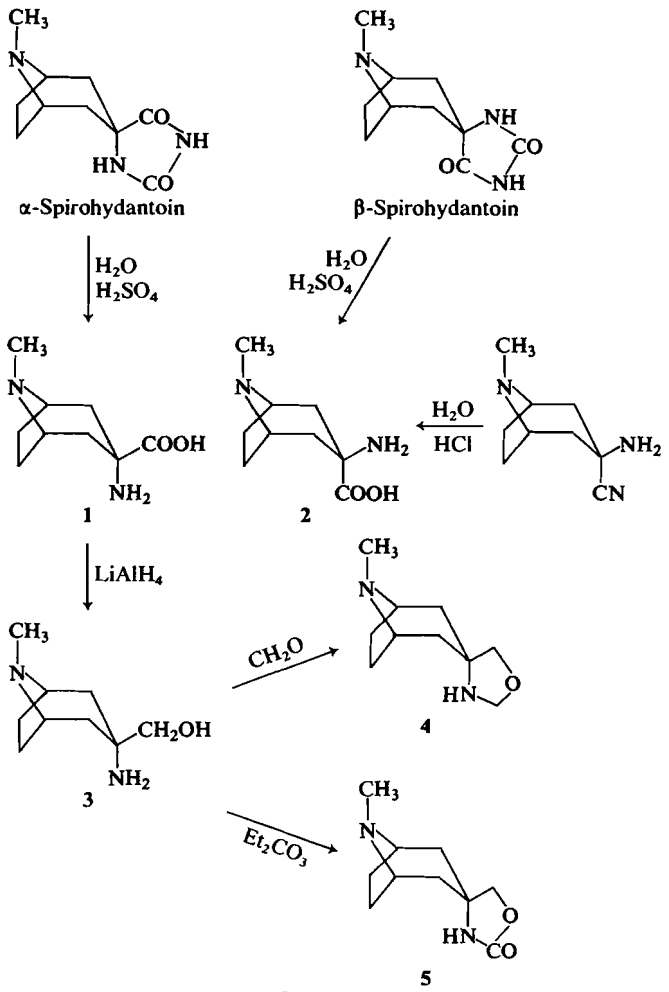
FIG. 2

TABLE 1. pK_a' values of the two isomers of 3-aminotropane-3-carboxylic acid[a]

Compounds	pK_1'	pK_2'	pK_3'
1	1.2	7.08	10.65
2	1.5	6.94	10.70

[a]Duplicate titrations were made consecutively for the two isomers, so the differences, probably even that in pK_3', are regarded as significant.

Can. J. Chem. Downloaded from www.nrcresearchpress.com by 210.87.254.5 on 09/05/12
For personal use only.



SCHEME 1

time appear to be about 0.82 and 0.16 min^{-1}, respectively, the quantity log $a/(a - X)$ being essentially linear with time. The lability of the *N*-formyl derivative of **2** to 1 *N* HCl was severe enough to allow a few percent of hydrolysis of the zero-time control sample held momentarily at room temperature and 3.5 h in ice-water while the experimental samples were held at 50°C.

The striking difference in the reactivity of the 3α- and 3β-*N*-formyltropane amino acids towards the acid hydrolysis is apparently due to the steric blockade of the axial 3-tropane derivatives by the C(6)—C(7) dimethylenic chain. Similar differences have been found in the hydrolysis and esterification of 3α- and 3β-tropane carboxynitriles (21). Furthermore the resistance to hydrolysis of 4-isopropyl- and 4-*tert*-butyl-1-amino-1-carboxynitrile hydrochlorides (α- and β-isomers) has been used as a clue to determine the configuration of the corresponding amino acids (22).

Biological Transport

The 3β-amino isomer **2** (β-ATC) is a good inhibitor of the uptake by the Ehrlich ascites tumor cell of the b(−)-BCH. The b(−) isomer of BCH has been shown to be the amino *endo* form (4). In *E. coli* it is the only one of the four BCH isomers taken up (23). The use of BCH as a system-specific model substrate is discussed elsewhere (24, 25). K_i for β-ATC is crudely estimated as 4 to 5 m*M* (Fig. 1).

The 3α-amino isomer (α-ATC) is only about one-seventh as effective (K_i roughly 25 to 42 m*M*). A rather smaller difference is seen for the two isomeric amino acids acting on the slow uptake of the less interesting (+) isomer of BCH.

By comparison with 1-methylpiperidine-4-amino-4-carboxylic acid (K_i = 1 m*M*) (5) we may suppose that the two-carbon bridge is unfavorable to affinity and that it is more unfavorable in **1** than in **2**. To evaluate the effect of the $CH_3—N<$ structure of the

Can. J. Chem. Downloaded from www.nrcresearchpress.com by 210.87.254.5 on 09/05/12
For personal use only.

tropane amino acids we have in mind to compare the results for the analogs in which this group is replaced by $\diagdown\!\diagup CH_2$.

1. L. MUNDAY. J. Chem. Soc. 4372 (1961).
2. R. J. W. CREMLYN. J. Chem. Soc. 3977 (1962); R. J. W. CREMLYN and M. CHISHOLM. J. Chem. Soc. **22**, 2269 (1967); Tetrahedron Lett. 1373 (1967); J. Chem. Soc. C, 1762 (1967); R. J. W. CREMLYN, R. M. ELLAM, and T. K. MITRA. Indian J. Chem. **8**, 218 (1970).
3. Y. MAKI and T. MASUGI. Chem. Pharm. Bull. Tokyo, **21**, 685 (1973).
4. H. S. TAGER and H. N. CHRISTENSEN. J. Am. Chem. Soc. **94**, 968 (1972).
5. H. N. CHRISTENSEN. J. Bioenerg. **4**, 433 (1974).
6. G. G. TRIGO and M. MARTINEZ. Pharmacia Mediterranea, **10**, 643 (1974).
7. V. DU VIGNEAUD, R. DORFMAN, and H. S. LORING. J. Biol. Chem. **98**, 577 (1932).
8. A. STRECKER. Ann. **155**, 177 (1870); F. TIEMANN. Ber. 381 (1880).
9. C. H. HUFFMAN. J. Am. Chem. Soc. **23**, 727 (1958).
10. V. M. MIĆOVIĆ and M. LJ. MIHAILOVIĆ. J. Org. Chem. **18**, 1190 (1953).
11. H. ROSEN. Arch. Biochem. Biophys. **67**, 10 (1957).
12. Y. INUI and H. N. CHRISTENSEN. J. Gen. Physiol. **50**, 203 (1966).
13. D. L. OXENDER and H. N. CHRISTENSEN. J. Biol. Chem. **238**, 3686 (1963).
14. P. R. PAL and H. N. CHRISTENSEN. J. Biol. Chem. **236**, 894 (1961).
15. P. SMITH-VERDIER, F. FLORENCIO, and S. GARCIA-BLANCO. Acta Crystallogr. Sect. B, **33**, 3381 (1977).
16. G. G. TRIGO, C. AVENDANO, E. SANTOS, J. T. EDWARD, and S. CH. WONG. Can. J. Chem. **57**, 1456 (1979).
17. R. M. C. DAWSON, D. C. ELLIOTT, W. H. ELLIOTT, and K. M. JONES (*Editors*). Data for Biochemical Research. University Press, Oxford. 1959. pp. 2–29; A. ALBERT. Biochem J. **50**, 690 (1952).
18. R. D. STOLOW. J. Am. Chem. Soc. **81**, 5806 (1959).
19. C. W. BIRD and R. C. COOKSON. J. Chem. Soc. 2343 (1960).
20. J. T. EDWARD, P. G. FARRELL, J. L. JOB, and B. POH. Can. J. Chem. **56**, 1122 (1978).
21. S. J. DAUM, C. M. MARTINI, R. K. KULLNIG, and R. L. CLARKE. J. Med. Chem. **18**, 496 (1975).
22. L. MUNDAY. Chem. Ind. 1057 (1960).
23. H. S. TAGER and H. N. CHRISTENSEN. J. Biol. Chem. **246**, 7572 (1971).
24. H. N. CHRISTENSEN, M. E. HANDLOGTEN, I. LAM, H. S. TAGER, and R. ZAND. J. Biol. Chem. **244**, 1510 (1969).
25. H. N. CHRISTENSEN. Adv. Enzymol. **49**, 41 (1978).

Can. J. Chem. Downloaded from www.nrcresearchpress.com by 210.87.254.5 on 09/05/12
For personal use only.

Canadian Journal of Chemistry
Published by
THE NATIONAL RESEARCH COUNCIL OF CANADA

Journal canadien de chimie
Publié par
LE CONSEIL NATIONAL DE RECHERCHES DU CANADA

Volume 58 Number 22 November 15, 1980

Volume 58 numéro 22 15 novembre 1980

Enthalpies of interaction of polar and nonpolar solutes with a perfluoro solvent

RICHARD FUCHS, L. ALAN PEACOCK, AND KAMALENDU DAS
Department of Chemistry, University of Houston, Central Campus, Houston, TX 77004, U.S.A.

Received February 27, 1980

RICHARD FUCHS, L. ALAN PEACOCK, and KAMALENDU DAS. Can. J. Chem. **58**, 2301 (1980).

Enthalpies of solution of 51 polar and nonpolar organic solutes have been determined in the solvent perfluoro-1,3-dimethylcyclohexane. The values have been combined with solute enthalpies of vaporization to give the enthalpies of transfer from vapor to solvent. These solvation enthalpies are for most solutes substantially less exothermic than those measured in other solvents. Polar interactions appear to be stronger than with hydrocarbon solvents; but this may result, in part, from incomplete dissociation of strongly associated solutes in the perfluoro solvent.

RICHARD FUCHS, L. ALAN PEACOCK et KAMALENDU DAS. Can. J. Chem. **58**, 2301 (1980).

On a déterminé les enthalpies de solution de 51 solutés organiques polaires et non polaires dans le perfluorodiméthyl-1,3 cyclohexane. On a combiné les valeurs obtenues avec les enthalpies de vaporisation des solutés pour obtenir les enthalpies de transfert de la vapeur au solvant. Dans la plupart des solutés, ces enthalpies de solvatation sont substantiellement moins exothermiques que celles mesurées dans d'autres solvants. Les interactions polaires semblent être plus fortes que celle intervenant dans les solvants hydrocarbonés, mais ceci peut provenir en partie d'une dissociation incomplète des solutés fortement associés dans le solvant perfluoré.

[Traduit par le journal]

The unusual solvent properties of completely fluorinated alkane derivatives (perfluoroalkanes) were first recognized more than three decades ago (1). These compounds show limited miscibility with nonpolar alkanes, and even less miscibility with polar liquids. On the other hand, the solubility of nitrogen (2) and of oxygen are greater than that in other solvents, and there has been wide interest in perfluorocarbons and perfluorocarbon derivatives as components of blood extenders.

The boiling points of perfluorocarbons are generally lower than those of the analogous hydrocarbons, as are the heats of vaporization (ΔH_v) in the few cases where comparison data are available (3). The fluorocarbon polarizability is slightly greater, and at equal separation the dispersion forces should be larger (4). The molar volume and mean radius are much larger, however, and at the greater distance the effective dispersion forces are smaller than in hydrocarbons.

We have recently measured the heats of solution (ΔH_s) of some polar molecules (5, 6) and nonpolar hydrocarbons (7) in the solvents cyclohexane, benzene, methanol, and dimethylformamide, and some additional hydrocarbon values (8) in acetic acid and in hexane. Values of ΔH_s have been combined with experimental (5) or literature (3) heats of vaporization (ΔH_v) to give enthalpies of transfer from vapor to solvent [$\Delta H(v \rightarrow S)$] (the solvation enthalpy). Comparison of $\Delta H(v \rightarrow S)$ for polar compounds and nonpolar model compounds has provided an estimate of the polar solute–solvent interactions (5–7). It is our eventual objective to evaluate the contributions of various types of intermolecular forces (dipole–dipole, dipole – induced dipole, dispersion, charge transfer, and hydrogen bonding) to overall solvent–solute interactions, using, in addition to model compounds, a series of diagnostic solvents.

One premise of this diagnosis has been used previously (7) to effect a rough separation of the dispersion and solvent cavity formation energy contributions to $\Delta H(v \rightarrow S)$, and will be used in the present study. When a straight chain alkane is dissolved in a nonpolar or slightly polar solvent, the observed $\Delta H(v \rightarrow S)$ results from exothermic dispersion interactions and an endothermic solvent cavity formation

0008-4042/80/222301-04$01.00/0
©1980 National Research Council of Canada/Conseil national de recherches du Canada

Can. J. Chem. Downloaded from www.nrcresearchpress.com by 210.87.254.42 on 09/05/12
For personal use only.

TABLE 1. Heats of solution and enthalpies of transfer from vapor to perfluoro-1,3-dimethylcyclohexane and cyclohexane at 25°C (kcal/mol)

Solute[a]	MV, mL[b]	ΔH_v[c]	ΔH_s PFDC[d]	$-\Delta H(v\rightarrow PFDC)$[e]	Polar[f]	$-\Delta H(v\rightarrow c\text{-}C_6)$[g]	Polar[h]
n-C_5	115.2	6.39±0.05	2.09	4.30		6.13	
n-C_6	130.5	7.54±0.01	2.46	5.08		7.27	
n-C_7	146.5	8.74±0.01	2.82	5.92		8.35	
n-C_8	162.6	9.92±0.01	3.14	6.78		9.48	
n-C_9	178.7	11.10±0.01	3.50	7.60		10.63	
n-C_{10}	194.9	12.28±0.01	3.83	8.45		11.73	
n-C_{12}	227.5	14.65±0.06	4.41	10.24		13.96	
2-MeC_4	116.4	6.03±0.05	2.35	3.68		5.88	
2,2-Me_2C_4	132.9	6.62±0.01	2.06	4.56		6.49	
2,2-Me_2C_5	148.7	7.75±0.01	2.38	5.37		7.52	
3,3-Me_2C_5	144.5	7.89±0.01	2.33	5.56		—	
2,2,4-Me_3C_5	165.1	8.40±0.01	2.46	5.94		8.20	
2-MeC_8	179.9	10.70±0.10[i]	3.26	7.44		10.35	
Et_4C	170.2	10.17±0.08[j]	2.92	7.25		9.98	
2,2,4,4-Me_4C_5	178.3	9.21±0.07[j]	2.60	6.61		9.14	
2,2,5,5-Me_4C_6	198.0	10.13±0.06[k]	3.02	7.11		9.94	
c-C_5H_{10}	94.1	6.85±0.01	2.16	4.69		6.82	
c-C_6H_{12}	108.1	7.90±0.01	2.69	5.21		7.88	
Me-*c*-C_6	127.6	8.45±0.01	2.74	5.71		8.46	
1,1-Me_2-*c*-C_6	143.7	9.05±0.05	2.75	6.30		9.00	
cis-1,2-Me_2-*c*-C_6	140.9	9.14±0.01	2.81	6.33		9.09	
c-C_7H_{14}	121.3	9.21±0.05	2.97	6.24		—	
c-C_8H_{16}	134.6	10.36±0.05	3.24	7.12		10.39	
1-C_5	109.4	6.09±0.03	2.23	3.86		5.81	
1-C_6	125.0	7.34±0.05	2.48	4.86		7.03	
1-C_7	140.9	8.52±0.04	2.74	5.78		8.17	
1-C_8	157.0	9.70±0.05	3.16	6.54		9.31	
1-C_9	173.1	10.88±0.05[i]	3.42	7.46		10.45	
1-C_{10}	189.3	12.06±0.05	3.80	8.26		11.57	
1-C_{12}	221.9	14.53±0.05	4.39	10.14		13.92	
trans-*t*-BuCH=CH-*t*-Bu	195.7	10.04±0.06[j]	3.33	6.71		9.86	
Cyclopentene	88.2	6.71±0.07	2.24	4.47		6.50	
Cyclohexene	101.3	8.00±0.08	2.55	5.45		7.90	
1-Me-cyclohexene	118.7	9.06±0.05	2.76	6.30		9.07	
Benzene	88.9	8.09±0.01	3.12	4.97		7.18	

energy. When an isomeric branched alkane with one or more quaternary carbon atoms is dissolved in the same solvent, the cavity energy is essentially unchanged, for branching has little effect on solute molar volume, and the shape or surface area of the cavity should have little influence, except with highly structured solvents such as water. However, dispersion interactions with the "buried" quaternary carbon atom are small or nil, and the $\Delta H(v\rightarrow S)$ difference between the straight chain and branched alkanes provides a measure of strength of dispersion interactions of which various solvents are capable.

The objective of the present study is to examine a perfluorocarbon solvent with respect to the capabilities for dispersion and polar interactions, and to compare these properties with those of a comparable hydrocarbon solvent. The perfluorocarbon chosen on the basis of availability, reasonably low vapour pressure, and relatively high purity is perfluoro-1,3-dimethylcyclohexane (PFDC).

Experimental

The solutes were commercial samples obtained from the Aldrich, Chemical Samples, and Fluka Companies (7, 8). All were stated to be of 99–99.9% purity, and are liquids at room temperature. Methyl *tert*-butyl ether (99.8%) was furnished by Professor N. L. Allinger. Cyclohexane (99+%) was obtained from Aldrich, and stored over 4A molecular sieve. Perfluoro-1,3-dimethylcyclohexane was furnished by PCR Research Chemicals Inc. After calorimetric use this solvent was recovered using three extractions with dichloromethane, followed by distillation through a short column. The material boiling at 100–102°C was collected for reuse.

The calorimetric procedure and apparatus have been described previously (7, 8). The calorimeters were immersed in water baths maintained at 25.00°C with regulation to ±0.002°C or better. Samples were introduced into the calorimeters from 10-, 20-, or 50-μL syringes. Heats of solution were corrected (0.02 kcal/mol less endothermic) to allow for the cooling due

Can. J. Chem. Downloaded from www.nrcresearchpress.com by 210.87.254.42 on 09/05/12
For personal use only.

TABLE 1 (*Concluded*)

Solute[a]	MV, mL[b]	ΔH_v[c]	ΔH_s PFDC[d]	$-\Delta H$(v→PFDC)[e]	Polar[f]	$-\Delta H$(v→*c*-C_6)[g]	Polar[h]
Toluene	106.3	9.08±0.01	3.21	5.87		8.31	
Acetone	73.5	7.48±0.02	3.53	3.95	−1.4[i]	4.79	−1.0[i]
2-Butanone	89.5	8.29±0.02	3.67	4.62	−1.2[i]	6.00	−1.0[i]
2-Heptanone	140.8	11.34±0.07[m]	3.99	7.35	−1.4	9.33	−1.0
4-Heptanone	139.7	11.10±0.09[n]	3.81	7.29	−1.4	9.35	−1.0
2-Nonanone	173.3	13.53±0.14[m]	4.80	8.73	−1.3	11.55	−1.0
5-Nonanone	173.1	13.12±0.09[m]	4.31	8.81	−1.4	11.42	−0.8
Cyclohexanone	103.6	10.77±0.05[n]	3.84	6.93	−1.7	9.00	−1.1
2,2,4,4-Me_4-3-pentanone	172.6	10.84±0.02	3.34	7.50	−0.9	9.85	−0.7
Me hexanoate	147.2	11.64±0.10	3.82	7.82		—	
Pyridine	80.6	9.61±0.01	3.99	5.64	−0.7[o]	7.65[t]	−0.5[o]
n-Butyl methyl ether	118.4	7.77±0.02	2.77	5.00	−0.7[p]	7.09[u]	−1.0[p]
tert-BuOMe	119.0	7.27±0.02	3.33	3.94	−0.3[q]	5.73[v]	0.2[q]
Aniline	91.1	13.33±0.01	1.55	11.78	−6.8[o]	9.11	−1.9[o]
*t*ert-Amyl alcohol	109.4	11.63±0.30	7.33	4.30	−0.6[q]	5.77[w]	0.1[q]
					−0.4[r]		−0.04[r]
1-Butanol	91.5	12.50±0.02	5.81	6.69	−3.2[i,s]	6.56[x]	−1.6[i,s]

[a]Abbreviations are those used in ref. 7: 2,2-Me_2C_4 is 2,2-dimethylbutane, 1-C_5 is 1-pentene.
[b]Molar volume.
[c]Heat of vaporization and uncertainty, kcal/mol, from ref. 3 unless otherwise indicated.
[d]Heat of solution in perfluoro-1,3-dimethylcyclohexane, ± 0.10 kcal/mol.
[e]ΔH(v→PFDC) = $\Delta H_s - \Delta H_v$.
[f]Polar interactions = ΔH(v→PFDC)(polar molecule) − ΔH(v→PFDC)(nonpolar model).
[g]Mainly from refs. 5–7.
[h]In cyclohexane.
[i]Estimated.
[j]Reference 11.
[k]Reference 8.
[l]Based on extrapolated value of ΔH(v→S) of hydrocarbon model.
[m]Reference 5.
[n]Mean of two experimental values. See ref. 5.
[o]Vs = benzene.
[p]Vs = *n*-pentane.
[q]Vs = 2-methylbutane.
[r]Vs = *tert*-butyl methyl ether.
[s]Vs = butane.
[t]ΔH_s = 1.96 kcal/mol.
[u]ΔH_s = 0.68 kcal/mol.
[v]ΔH_s = 1.54 kcal/mol.
[w]ΔH_s = 5.86 kcal/mol.
[x]ΔH_s = 5.94 kcal/mol.

to the sample temperature (22–23°C). This correction is based on the experimental heat of solution of 50 μL samples of perfluoro-1,3-dimethylcyclohexane at room temperature in perfluoro-1,3-dimethylcyclohexane (70 mL), and cyclohexane in cyclohexane.

A typical heat of solution involved a change of 0.2–0.4 cal, and a temperature change of 0.005 to 0.01°C. Sample concentrations were in the range of 1.5×10^{-3} to 10×10^{-3} *M*.

Results and Discussion

Experimental heats of solution in perfluoro-1,3-dimethylcyclohexane, and enthalpies of transfer from the vapor state to this solvent are presented in Table 1. The corresponding values of ΔH(v→S) for cyclohexane solvent (5–7) are also given for comparison, but heats of solution in cyclohexane appear (as a footnote) only if previously unreported.

Methylene Increment

The methylene increment in ΔH(v→S) represents the enthalpy difference between an endothermic solvent cavity formation term and exothermic contribution from the solvent–solute interactions. In the case of a nonpolar methylene group and nonpolar solvents the interactions are entirely dispersion forces. The mean increment (pentane–dodecane) in PFDC is -0.85 ± 0.04 kcal/mol, and for cyclohexane the value (7) (C_5–C_{16}) is -1.12 ± 0.02 kcal/mol. The methylene increment for six other solvents we have examined range from −0.91 kcal/mol in *N*,*N*-dimethylformamide to −1.17 kcal/mol in heptane. The values do not agree very well with those calculated (9) on the basis of the methanol–ethanol difference in the solvents cyclohexane (found −1.12, calcd. (9) −0.9), carbon tetrachloride (−1.12 vs. −0.8), and DMF (−0.91 vs. −0.6).

The methylene increment in PFDC is less exothermic than in any of the other solvents we have examined. The rather small increment in DMF can reasonably be attributed to a highly endothermic cavity formation term in this strongly associated solvent (7, 9). This is clearly not the case in a per-

Can. J. Chem. Downloaded from www.nrcresearchpress.com by 210.87.254.42 on 09/05/12
For personal use only.

Can. J. Chem. Downloaded from www.nrcresearchpress.com by 210.87.254.42 on 09/05/12
For personal use only.

fluorocarbon with particularly small values of ΔH_v (estimated to be 8.5–9.0 kcal/mol (4)) and cohesive energy density. The small methylene increment in PFDC must therefore result from particularly weak dispersion interactions with dissolved solute molecules.

Quarternary Carbon Atom Effect

Four of the hydrocarbons in Table 1 having quaternary carbon atoms (2,2-dimethylbutane, 2,2-dimethylpentane, 2,2,4,4-tetramethylpentane, and 2,2,5,5-tetramethylhexane) have molar volumes similar to those of the isomeric *n*-alkanes (mean difference 2.0 ± 1.2 mL; the molar volume contribution of CH_2 is 16 mL). Branching decreases heats of vaporization by a mean value of 0.98 ± 0.07 kcal/mol per quaternary carbon atom. The methylene increment in ΔH_v in *n*-alkanes and several other classes of straight chain compounds (10) is approximately 1.18 kcal/mol. Thus about 83% of the dispersion interactions of the "buried" carbon atom is lost by the difficulty of close approach by neighboring molecules. A similar situation occurs in solutions of the isomeric hydrocarbons. $\Delta H(v \rightarrow S)$ becomes less exothermic by 0.80 kcal/mol (methanol) to 0.98 kcal/mol (CCl_4) per quaternary carbon atom. In cyclohexane solutions the mean loss is 0.82 ± 0.06 kcal/mol, and in PFDC, 0.56 ± 0.08 kcal/mol per quaternary carbon atom. If we make the crude assumption that the equivalent of about 83% of the dispersion interactions of a methylene group is lost for each "buried" quaternary carbon atom present in a molecule, one concludes that the dispersion interactions of PCDC with a methylene group is less than 0.7 kcal/mol, compared with values of about 1.0–1.2 kcal/mol for other solvents.

Solvation of Polar Compounds

Almost all of the compounds in Table 1 having functional groups are more strongly solvated ($\Delta H(v \rightarrow S)$ more exothermic) in cyclohexane than in PFDC. The exceptions are 1-butanol and aniline, two strongly hydrogen bonded compounds. However, the polar contributions to solvent–solute interactions, taken as $\Delta H(v \rightarrow S)$ (polar compound) $- \Delta H(v \rightarrow S)$ (nonpolar model), is generally larger in PFDC. The nonpolar model is the hydrocarbon having the same number of carbon atoms as the ketone, ether, or alcohol. This provides comparisons of compounds with similar molar volumes, because of the very small contribution of an oxygen atom.

We have strong reservations about accepting the view that PFDC is capable of substantially stronger polar interactions than are hydrocarbon solvents. This is especially the case with hydrogen bonded solutes. 1-Butanol has such slight solubility in PFDC that studies of the concentration effect on ΔH_s were impossible. While typical calorimetric samples dissolve rapidly, and the system is thermally equilibrated in less than 2 min, the thermal effect with 1-butanol, and, hence, the solution process, required more than 30 min. We believe it quite likely that 1-butanol and aniline do not dissolve to give monomeric solute species, but retain appreciable hydrogen bonded association. The resulting values of ΔH_s are therefore less endothermic, and $\Delta H(v \rightarrow S)$ values are more exothermic, than would be the case if complete dissociation to monomer occurred. The association of *tert*-amyl alcohol (2-methyl-2-butanol) is probably considerably weaker, and a more realistic value of $\Delta H(v \rightarrow S)$ is obtained.

For the other polar solutes there appears to be a trend toward somewhat larger polar interactions with PFDC than with cyclohexane for the most polar solutes (ketones), but smaller differences for the less polar or sterically hindered compounds (ethers, 2,2,4,4-tetramethyl-3-pentanone). Whether this reflects greater association of the more polar compounds in PFDC solution, or a true ability of PFDC to undergo stronger polar interactions than can cyclohexane, cannot at present be stated with certainty. The uncertainties in ΔH_s(PFDC) are of the order of 0.10 kcal/mol. Four heats of solution are involved in a comparison of the polar interactions in PFDC vs. cyclohexane, with an overall uncertainty of ca. 0.20 kcal/mol. We therefore warn against overinterpretation of the data, when differences of only a few tenths of a kilocalorie per mole are observed.

Acknowledgement

This study was supported by the Robert A. Welch Foundation (Grant E-136).

1. R. L. Scott. J. Am. Chem. Soc. **70**, 4090 (1948).
2. J. C. Gjaldbaek and J. H. Hildebrand. J. Am. Chem. Soc. **71**, 3147 (1949).
3. J. B. Pedley and J. Rylance. Sussex–N.P.L. computer analysed thermochemical data: organic and organometallic compounds. University of Sussex, Brighton. 1977.
4. J. H. Hildebrand and R. L. Scott. The solubility of nonelectrolytes. 3rd ed. Dover Publications, New York, NY. 1964.
5. P. P. S. Saluja, L. A. Peacock, and R. Fuchs. J. Am. Chem. Soc. **101**, 1958 (1979).
6. R. Fuchs, T. M. Young, and R. F. Rodewald. J. Am. Chem. Soc. **96**, 4705 (1974).
7. P. P. S. Saluja, T. M. Young, R. F. Rodewald, F. H. Fuchs, D. Kohli, and R. Fuchs. J. Am. Chem. Soc. **99**, 2949 (1977).
8. R. Fuchs and L. A. Peacock. J. Phys. Chem. **83**, 1975 (1979).
9. J. N. Spencer, J. E. Gleim, C. H. Blevins, R. C. Garrett, and F. J. Mayer. J. Phys. Chem. **83**, 1249 (1979).
10. M. Mansson, P. Sellers, G. Stridh, and S. Sunner. J. Chem. Thermodyn. **9**, 91 (1977).
11. R. Fuchs and L. A. Peacock. Can. J. Chem. **57**, 2302 (1979).

Heat capacities of liquid ketones and aldehydes at 298 K[1]

RICHARD FUCHS

Department of Chemistry, University of Houston, Houston, TX 77004, U.S.A.

Received May 23, 1980

RICHARD FUCHS. Can. J. Chem. **58**, 2305 (1980).

The heat capacities of 25 liquid aliphatic, alicyclic, and aromatic ketones and aldehydes at 298.2 K and atmospheric pressure have been measured calorimetrically with a typical uncertainty of 0.5%. Additive parameters are proposed for estimating C_p(l) of ketones and aldehydes.

RICHARD FUCHS. Can. J. Chem. **58**, 2305 (1980).

Opérant à 298,2 K et sous la pression atmosphérique, on a mesuré, par calorimétrie avec une erreur type de 0,5%, les capacités calorifiques de 25 aldéhydes et cétones aliphatiques, alicycliques et aromatiques liquides. On propose des paramètres additifs pour évaluer le C_p(l) des cétones et des aldéhydes.

[Traduit par le journal]

Can. J. Chem. Downloaded from www.nrcresearchpress.com by 210.87.254.5 on 09/05/12
For personal use only.

Measurements of the heat capacities of many hydrocarbons and organic sulfur compounds in the liquid state have been reported, and useful schemes have been devised for the estimation of C_p(l) of additional compounds of these classes using additive group parameters (1, 2). Relatively few such data are available for many other common classes of compounds, and group parameters must be based on one or a few compounds, or may be totally unavailable. These classes include the esters, which have recently been examined (3), and the ketones and aldehydes, which are the subject of this study. A few values for some open chain aliphatic ketones have been reported previously (4, 5). This paper reports the heat capacities of 25 aliphatic, alicyclic, and aromatic ketones and aldehydes in the liquid state at 298.2 K and atmospheric pressure.

Experimental

Ketone and aldehyde samples were obtained from Fluka, Aldrich, and Chemical Samples Companies. All were stated by the suppliers to be of 99 mass% or greater purity by gas chromatographic analysis, and were used as received. Drying and redistillation of samples of propionaldehyde, cyclohexanone, acetophenone, and propiophenone through a short column did not significantly affect the measured heat capacities, although this procedure would remove adventitious water, condensation products, and oxidation products.

Calorimetry

Heat capacities of the liquids were measured in a 10 cm^3 or a 45 cm^3 vacuum jacketed glass isoperibol calorimeter fitted with a Teflon stopper through which pass thermistor, heating, and cooling probes. The thermistor ($2 \times 10^3\ \Omega$) is an arm of a Wheatstone bridge, the output of which is amplified by a Keithley Model 177 digital multimeter (which also serves as a null meter), and recorded on a potentiometric recorder. Full scale deflection results from a temperature change of 0.1 K. Measurements were made over 0.06 K increments within the range of 298.1–298.3 K, at ambient atmospheric pressure. The calorimeters were magnetically stirred continuously before, during, and following the heating period, using five revolutions s^{-1} synchronous motors. The stirring unit and calorimeter were immersed in a water bath at 298.15 ± 0.002 K. The heat capacity of each calorimeter (10 cm^3: 12.74 J K^{-1}; 45 cm^3: 33.47 J K^{-1}) was determined (for example, for the 10 cm^3 calorimeter) from the heating times required to produce equal recorder deflections for the systems calorimeter + 10 cm^3 water, and calorimeter + 10 cm^3 heptane. (C_p(l) = 75.25 J mol^{-1} K^{-1} for water (6); 225.0 J mol^{-1} K^{-1} for heptane, at 298.15 K (2).)

The heaters are metal film electronic resistors sealed in Teflon (temperature coefficient of resistance 50×10^{-6} K^{-1}), with resistances of 90.8 Ω and 561 Ω, for the smaller and larger calorimeter, respectively. Heater currents of 19.30×10^{-3} A were furnished by timed constant current sources, and monitored by a digital milliammeter in the heater circuit.

Each 10 cm^3 or 45 cm^3 sample was weighed in the sealed calorimeter. Values of C_p(l) were calculated from the mean of four to ten heating curves relative to water. Duplicate C_p(l) values determined from separate samples agreed to 1.1 J mol^{-1} K^{-1} or better (<0.5%). Appropriate heating periods (30–65 s) were used to produce recorder deflections of approximately 15 cm.

Sample heat capacities C_p(S) were calculated from the equation

$$C_p(\mathrm{S}) = [C_p(\mathrm{W}) + C_p(\mathrm{Cal})]\frac{\mathrm{defl(W)}}{\mathrm{defl(S)}} - C_p(\mathrm{Cal}) \times \frac{\text{molar mass(S)}}{\text{sample mass}}$$

where C_p(W) and C_p(Cal) are the heat capacities of the reference water sample and the calorimeter, respectively, and defl(W) and defl(S) are the recorder deflections produced by equal heat inputs into the water and ketone samples.

Results and Discussion

Of the heat capacities of liquid ketones and aldehydes in Table 1, 17 have not been previously reported. Eight others have been remeasured, giving values within 3.5 J mol^{-1} K (1.5%) of the literature values (1, 4, 5). (The mean difference is 1.6 J mol^{-1}

[1]This study was supported by the Robert A. Welch Foundation Grant E-136.

0008-4042/80/222305-02$01.00/0

©1980 National Research Council of Canada/Conseil national de recherches du Canada

TABLE 1. Heat capacities of liquid ketones and aldehydes at 298.2 K

Compound	C_p(l)/J mol^{-1} K^{-1} Experimental[a]	Calcd[b]	Calcd[c]
Acetone	124.9±0.1,[d] 125.4±0.3, 126.4[e]	125.5	126.4
2-Butanone	157.8±0.2, 158.6[f]	156.9	156.9
2-Pentanone	185.5±0.6, 184.1[f]	185.8	187.4
3-Pentanone	190.1±0.4, 189.6±1.0, 190.8[f]	188.3	187.0
2-Hexanone	214.8±1.1, 213.4[g]	214.6	217.6
3-Hexanone	216.9[g]	217.1	217.6
2-Heptanone	243.6±0.5,[d] 243.7±0.6	243.5	247.7
4-Heptanone	246.3±0.3	246.0	247.7
2-Octanone	276.9±0.9	274.1	278.2
5-Nonanone	307.1±0.9, 305.9±1.3, 303.6[g]	307.1	308.8
Cyclopentanone	154.5±0.3	155.6	154.0
Cyclohexanone	179.3±0.4, 180.2±0.5	181.6	177.4
Cycloheptanone	211.8±0.4	207.5	—
3-Methyl-2-butanone	180.6±0.6, 179.9[g]	180.7	180.3
3,3-Dimethyl-2-butanone	210.0±0.4, 206.9[g]	212.5	207.4
2-Methyl-3-hexanone	241.5±0.5	241.0	244.8
4-Methyl-2-pentanone	215.8±1.1	214.6	214.5
2,4-Dimethyl-3-pentanone	233.7[g]	236.0	234.3
Acetophenone	204.6±0.3,[d] 205.5±0.8[d]	202.9	212.5
Propiophenone	243.8±0.5,[d] 243.2±0.5,[d] 244.0±0.3[d]	234.3	243.1
4-Ethylacetophenone	260.7±0.3[d]	247.3	265.7
3-Methylbenzophenone	325.1±1.1	295.8	325.5
Propionaldehyde	137.2±0.7[d]	131.8	130.1[h]
Valeraldehyde	189.2±0.9[d]	189.5	190.8[h]
Trimethylacetaldehyde	186.2±0.5	184.1	180.7[h]
Benzaldehyde	177.9±0.5[d]	177.8	184.1[h]
Cinnamaldehyde	232.6±0.3	—	228.4[h]

[a]Each new value is listed together with the standard deviation of four to ten heating curves. When two or more new values are reported the measurements involve separately weighed samples.
[b]Values calculated using group parameters in Discussion section.
[c]From group parameters of Shaw (1).
[d]Measured in 45 cm^3 calorimeter.
[e]Reference 1.
[f]Reference 4.
[g]Reference 5.
[h]Value assigned to—CHO group is 62.9 J mol^{-1} K.

K^{-1} (0.79%).) Predictions of C_p(l) for the 10 straight chain ketones on the basis of Shaw's group values (1) show a mean difference from the experimental values of 2.0 J mol^{-1} K^{-1} (maximum, 3.8 J mol^{-1} K^{-1}). No distinction is made in this scheme between 2-ketones and symmetrical ketones.

The values proposed below provide C_p(l) values for the same ten compounds which differ from the experimental by an average of 0.8 J mol^{-1} K^{-1} (maximum, 2.9 J mol^{-1} K^{-1}). The new parameters (J mol^{-1} K^{-1}) are:

$$-\overset{\overset{O}{\|}}{C}- \text{ (51.9), (CO)}-CH_2- \text{ (31.4), (CO)}-\overset{|}{C}H- \text{ (18.4),}$$

$$\text{and } H-\overset{\overset{O}{\|}}{C}- \text{ (64.9)}$$

Shaw's values (1) for $-CH_3$ (36.8) and $-\overset{|}{C}H-$ (20.9) have been retained, as have our previous values (3) of $-C_6H_5$ (114.2), (CO)$-\overset{|}{C}-$ (10.0), and $-CH_2-$ (28.9 in straight chains of up to seven atoms; 30.5 for each additional CH_2 group). For ring CH_2 (25.9) the value of Chueh and Swanson (7) has been adopted; this avoids the use of ring corrections.

No value for the aldehyde group was estimated by Shaw (1). Using his parameters for other groups, an aldehyde value of 62.9 J mol^{-1} K^{-1} provides the best fit, although no single value is completely satisfactory. Neither set of parameters is consistently reliable in predicting the experimental values for aromatic ketones.

1. R. SHAW. J. Chem. Eng. Data, **14**, 461 (1969).
2. M. LURIA and S. W. BENSON. J. Chem. Eng. Data, **22**, 90 (1977).
3. R. FUCHS. J. Chem. Thermodyn. **11**, 959 (1979).
4. R. J. L. ANDON, J. F. COUNSELL, and J. F. MARTIN. J. Chem. Soc. A, 1894 (1968).
5. R. J. L. ANDON, J. F. COUNSELL, E. B. LEES, and J. F. MARTIN. J. Chem. Soc. A, 833 (1970).
6. D. W. OSBORNE, H. F. STIMSON, and D. C. GINNINGS. J. Res. Natl. Bur. Stand. **23**, 238 (1939).
7. C. F. CHUEH and A. C. SWANSON. Can. J. Chem. Eng. **51**, 596 (1973).

Can. J. Chem. Downloaded from www.nrcresearchpress.com by 210.87.254.5 on 09/05/12
For personal use only.

The gas phase acidities of fluorinated acetones. An ion cyclotron resonance investigation of the role of fluorine substituents in the stabilization of planar carbanions

R. FAIRD AND T. B. MCMAHON

Department of Chemistry, University of New Brunswick, P.O. Box 4400, Fredericton, N.B., Canada E3B 5A3

Received May 22, 1980

R. FAIRD and T. B. MCMAHON. Can. J. Chem. **58**, 2307 (1980).

The gas phase acidities of a series of fluorinated acetones and acetylfluoride have been determined. The results obtained are interpreted in terms of a model for fluorine substituents in planar carbanions in which fluorine exerts an overall stabilizing influence on enolate ions, but also has a component in the interaction which is destabilizing via a repulsive interaction between fluorine lone pair electrons and the carbanion centre. Comparisons with solution phase acidities are made and the validity of the model for fluorine substituents discussed.

R. FAIRD et T. B. MCMAHON. Can. J. Chem. **58**, 2307 (1980).

On a déterminé les acidités en phase gazeuse d'une série d'acétones fluorées et du fluorure d'acétyle. On a interprété les résultats obtenus en fonction d'un modèle pour les substituants fluorés dans les carbanions plans où le fluor exerce une influence stabilisatrice globale sur les ions énolates mais participe également à l'interaction déstabilatrice par l'intermédiaire d'une interaction répulsive entre la paire d'électrons libres du fluor et le centre du carbanion. On a établi des comparaisons avec les acidités en phase liquide et on discute de la validité du modèle pour les substituants contenant du fluor.

[Traduit par le journal]

Can. J. Chem. Downloaded from www.nrcresearchpress.com by 210.87.254.42 on 09/05/12
For personal use only.

Introduction

The effects of fluorine substituents on the stability and reactivity of ionic species have been of interest to physical organic chemists for several decades (1, 2). The relatively small size of the fluorine atom relative to hydrogen generally precludes any appreciable steric effects and thus any modification of chemical properties may be attributed to a combination of inductive, resonance, and hydrogen bonding interactions (2).

On positive charge centres, fluorine substituents have been shown on the basis of gas phase fluoride affinities to exert an ambiguous effect, being capable of both destabilizing cations by inductive electron withdrawal and stabilizing them by resonance delocalization of fluorine $2p$ electrons to the empy p lobe of an adjacent carbonium ion centre (3, 4). A similar ambiguity has been suggested for effects of fluorine substituents on carbanions, based on the relative solution acidities of some fluorinated carbon acids (5, 6). In the case of planar carbanions, it is suggested that fluorine substituents stabilize negative charge centres by inductive withdrawal but at the same time, destabilize them via electrostatic repulsion between the non-bonding fluorine $2p$ electrons and the adjacent carbanion electron pair (7, 8). This inference, however, is made on the basis of solution acidity data, and it is well known that solution phase acidities do not always reveal intrinsic relative anionic stabilities due to complications associated with solvation effects (9, 10).

The concept of fluorine as a carbanion destabilizing agent is supported, however, by a number of *ab initio* molecular orbital calculations. Brundle *et al.* (11) find that in planar systems, such as ethylene, substitution of fluorine for hydrogen gives rise to a strong C—F antibonding overlap resulting from mixing of the π group orbital with the fluorine σ atomic orbitals. This prediction is supported by the vibrational fine structure of the lowest energy band of the photoelectron spectrum of C_2F_4, corresponding to removal of an electron from a π molecular orbital exhibiting C—F antibonding character. Further evidence of a dual nature of fluorine substituents in carbanions is provided by the *ab initio* calculations of Burdon and co-workers (12) for four isomeric fluorocyclohexadienyl anions. These calculations show that the most stable fluorocyclohexadienyl anion is one in which fluorine is substituted in an *ipso* position where negative charge cannot be localized on the carbon bonded to fluorine in any of the conventional valence bond structures.

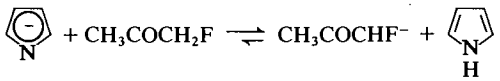
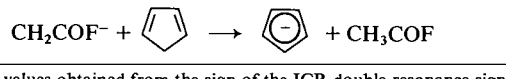
To date, the only comprehensive data obtained for gas phase carbanions containing fluorine substituents are those of Sullivan and Beauchamp for fluoroethyl carbanions (13). They find that the gas phase acidities of fluoroethanes are virtually independent of the number or position of fluorine substituents. This rather bizarre result indicates that fluorine substituents must participate in a very complex interaction with the charge center even in these sp^3 hybridized, nonplanar anions.

In order to clarify the effect of fluorine substituents on planar carbanions we have therefore undertaken the present study of the gas phase

0008-4042/80/222307-05$01.00/0

©1980 National Research Council of Canada/Conseil national de recherches du Canada

TABLE 1. Proton transfer reactions used to bracket the gas phase acidities of fluorinated acetones

Reaction	ΔG^0_{298} [a] (kcal/mol)	ΔS^0_{298} [b] (eu)	ΔH^0_{298} [c] (kcal/mol)	ΔH^0_{298} [d] (AH) (kcal/mol)
[1] 	$\lesssim 0$	−3.5	$\lesssim -1.0$	$\lesssim 358.5$
[2] $CH_3COCHF^- + CH_3NO_2 \rightarrow CH_2NO_2^- + CH_3COCH_2F$	<0	+2.3	<+0.7	>358.3
[3] $\phi CHCN^- + (CH_2F)_2CO \rightarrow CH_2FCOCHF^- + \phi CH_2CN$	<0	−1.1	<−0.3	<351.6
[4] $CH_2FCOCHF^- + CF_3COCH_3 \rightarrow CF_3COCH_2^- + (CH_2F)_2CO$	<0	+1.1	<+0.3	>350.6
[5] $HCO_2^- + (CHF_2)_2CO \rightarrow CHF_2COCF_2^- + HCO_2H$	<0	+0.4	<+0.1	<345.3
[6] $CHF_2COCF_2^- + CH_2FCO_2H \rightarrow CH_2FCO_2^- + (CHF_2)_2CO$	<0	−1.0	<−0.3	>337.3
[7] $CH_2FCO_2^- + CF_3COCHF_2 \rightarrow CF_3COCF_2^- + CH_2FCO_2H$	<0	+1.8	<+0.5	<338.1
[8] $CF_3COCF_2^- + HCl \rightleftharpoons Cl^- + CF_3COCF_2H$	$\lesssim 0$	−6.1	$\lesssim -1.8$	$\gtrsim 331.8$
[9] $CH_3COCHF^- + CH_3COF \rightarrow CH_2COF^- + CH_3COCH_2F$	<0	+2.1	<+0.6	<358.4
[10] 	<0	−0.4	<−0.1	>355.6

[a] ΔG values obtained from the sign of the ICR double resonance signal. A negative double resonance response indicates an exothermic reaction. In cases where ΔG is indicated as $\lesssim 0$ the double resonance response was found to be negative for reaction in the forward direction *and* positive for reaction in the reverse direction.

[b] S^0_{298} values for neutrals were either experimentally known data or calculated from group equivalent methods (21). S^0_{298} values for anions were estimated from known entropy data for isoelectronic neutrals or calculated from group equivalent and methods for isoelectronic neutrals making appropriate mass corrections for translational entropy.

[c] ΔH^0_{298} calculated from $\Delta G = \Delta H - T\Delta S$ at 298 K.

[d] ΔH^0_{298}(AH) is the enthalpy change for the reaction $AH \rightarrow A^- + H^+$, based on the acidity scale of Cumming and Kebarle (19). $\Delta H^0_{298}(AH) = D(A—H) - EA(A) + IP(H)$ where $D(A—H)$ is the homolytic bond dissociation energy, EA(A) is the radical electron affinity, and IP(H) the hydrogen atom ionization potential.

acidities of a series of fluorinated acetones. Upon deprotonation these species will yield enolate anions which have fluorine substituted in sp^2 hybridized carbon in a planar system. From observation of trends in gas phase acidities with increasing fluorine substitution, it should thus be possible to provide a clear assessment of the intrinsic role of fluorine substitution on stabilities of planar carbanions.

Experimental

All experiments were carried out on a Varian Instruments, V-5900 ICR spectrometer, extensively modified to permit routine operation in both conventional drift and trapped-ion modes as described by McMahon and Beauchamp (14). All other techniques and instrumentation associated with ion cyclotron resonance experiments have been described in detail previously (15).

All fluoroenolate ions were generated by proton transfer from the corresponding fluoroacetone to F^-, which was generated by dissociative electron attachment to NF_3 at 3.0 eV (16).

Fluoroacetone, 1,3-difluoroacetone, 1,1,1-trifluoroacetone, and 1,1,3,3-tetrafluoroacetone were obtained from I.C.N. Pharmaceuticals Inc. Pentafluoroacetone was purchased from Columbia Organic Chemicals, NF_3 was obtained from Air Products and Chemicals Ltd., and both acetylfluoride and 1,3-difluoroisopropyl alcohol were obtained from P.C.R. Inc. All other compounds used as reference acids were readily available reagent grade chemicals.

Results

Proton transfer reactions of the fluoroenolate ions were in general found to be very slow, a phenomenon commonly observed for charge delocalized ions (17). As a result, bimolecular proton transfer equilibria could not easily be attained under the typical operating conditions of the trapped-ion ICR experiment for most of the fluoroacetones studied. Therefore, all gas phase acidities were determined using the bracketing technique of observation of the exothermic direction of proton transfer to appropriate reference acids with the aid of ICR double resonance experiments (18). With the large number of appropriate reference acids available (9, 10, 19, 20) this method can, in general, yield gas phase acidity values accurate to within ± 1 kcal/mol.

As previously demonstrated (19, 20), deprotonation of species which yield charge delocalized anions may involve significant entropy changes, largely associated with restriction of internal rotations. Thus, in order to convert the approximate free energy changes obtained in the bracketing experiment to enthalpy changes some estimate of the entropy changes must be made. Cumming and Kebarle (19) have recently outlined a procedure for estimating entropy changes largely based on Benson's group additivity tables (21). We have used similar procedures to obtain estimates of entropy changes for proton transfer reactions of the fluoroacetones investigated here. In addition, in many cases, it was also possible to estimate absolute entropies of species using isoelectronic analogues also according to methods outlined by Benson (21).

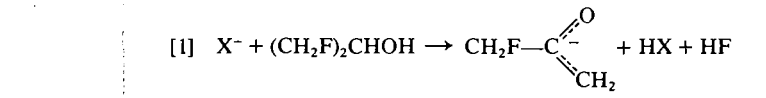
Shown in Table 1 are the proton transfer reactions used to ultimately bracket the gas phase acidity of each fluoroacetone, the free energy change inferred on the basis of the observed direction of proton transfer and double resonance experiments,

Can. J. Chem. Downloaded from www.nrcresearchpress.com by 210.87.254.42 on 09/05/12
For personal use only.

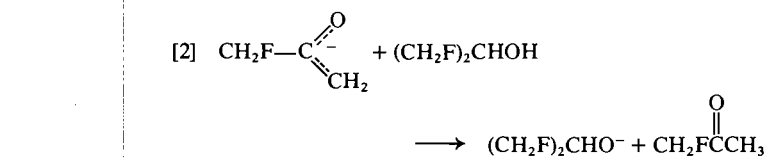
Can. J. Chem. Downloaded from www.nrcresearchpress.com by 210.87.254.42 on 09/05/12
For personal use only.

the estimated entropy change for each reaction and the resulting limits for the enthalpy change for each reaction at 25°C. The gas phase acidity of each fluorinated acetone, expressed as the difference in homolytic bond dissociation energy and the electron affinity of the corresponding free radical (D(R—H) – EA(R)), is shown in Table 2. Also shown are the electron affinities of each fluoroacetone enolate radical based on an assumed C—H bond dissociation energy of 98 kcal/mol. This latter quantity is based on observations that fluorine substitution has a minimal effect on the strength of adjacent C—H bonds in fluoromethanes (22) and the known C—H bond dissociation energy of acetone (23).

In a previous study of the gas phase negative ion chemistry of fluorinated alcohols (24), it was shown that a monofluoroacetone enolate ion could be produced by reaction of anions with 1,3-difluoroisopropylalcohol, reaction [1]



It was further shown that the enolate ion produced was more basic than that generated by simple proton abstraction from monofluoroacetone since the former ion was able to abstract a proton from 1,3-difluoroisopropylalcohol, reaction [2], while the latter was not.



This, and further proton transfer experiments involving the ion generated in reaction [1], establish that this species is a fluoroenolate in which fluorine is substituted remote from the carbanion centre and that the value of D(R—H) – EA(R) for the more weakly acidic site of fluoroacetone is 49 ± 2 kcal/mol (24).

In addition to the fluorinated acetones the gas phase acidity of acetylfluoride was also determined. The enolate derived from this compound will have fluorine substituted at an sp^2 hybridized carbon which does not have any appreciable negative charge localized on it in any resonance structures. Acidity data for this compound are also included in Tables 1 and 2.

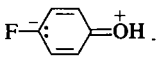
TABLE 2. Gas phase acidities of fluorinated acetones and acetylfluoride and electron affinities of the corresponding free radicals

Compound	D(AH) – EA(A)[a] (kcal/mol)	EA(A)[b] (kcal/mol)
CH_3COCH_3	54.9	43.1
CH_3*$COCH_2F$	49±2	49
CH_3COCH_2*F	43.5±0.5	54.5
$(CH_2F)_2CO$	36.0±0.5	62.0
CH_3COCF_3	35.2±0.1	62.8 (59.5±2.9[c])
$(CHF_2)_2CO$	26±3	72
CF_3COCHF_2	17.5±1	80.5
CH_3COF	42±1	56 (51.2±2.1[c])

[a]Calculated from the ΔH^0_{298}(AH) data of Table 1. Using a value of $\Delta H^0_{f298}(H^+)$ of 367.186 kcal/mol (29).
[b]Calculated from D(AH) – EA(A) values assuming a constant value of D(A—H) of 98 ± 2 kcal/mol, ref. 23.
[c]Determined from photodetachment thresholds for the enolate ions (30).

Discussion

The basis for the proposal that fluorine substituents may destabilize planar carbanions lies in observations of reduced kinetic and equilibrium acidities of a number of fluorinated carbon acids relative to their non-fluorinated analogues. For example, in solution both fluoronitromethane and difluoronitromethane have lower equilibrium acidity values than nitromethane itself (25). Similarly, 9-fluorofluorene is found to have a lower kinetic acidity than does fluorene (5). Unfortunately, all such arguments regarding the effect of fluorine substituents on carbanions are based on solution acidity measurements and it has been definitively shown recently that solution phase acidities do not always reflect true intrinsic relative anionic stabilities (9, 10). Gas phase acidity values, however, do provide an accurate measure of intrinsic anionic stabilities and should therefore be used to determine whether fluorine indeed does exert a destabilizing effect on planar carbanion centres. For example, one case used to support arguments of the destabilizing effect of fluorine substituents is the lower acidity in solution of *p*-fluorophenol relative to phenol (26, 27). In the gas phase, however, *p*-fluorophenol is appreciably more acidic than phenol although it is found to be less acidic than *m*-fluorophenol (10). The former result would thus indicate that in gas phase phenolate ions, fluorine substituents do not exert a *net* destabilizing effect. However, the greater acidity of *m*-fluorophenol relative to the *para* isomer suggests that the *p*-fluorophenolate ion may be destabilized somewhat due to the repulsive interaction between fluorine 2*p* electrons and negative charge localized onto the *para* ring position. Unfortunately, even this latter explanation is not completely unambiguous since an alternative argument involving preferential stabilization of the *neutral p*-fluorophenol resulting from charge separated resonance structures such as **I** is also possible.

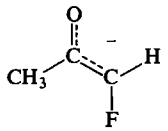


I

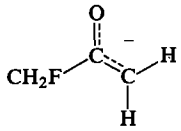
Can. J. Chem. Downloaded from www.nrcresearchpress.com by 210.87.254.42 on 09/05/12
For personal use only.

Almost no data are available for the solution acidities of fluorinated carbonyl compounds. One qualitative observation which has been made is the relative ease of formation of carbanions in mixtures of fluorinated acetate esters which are reacted in the presence of sodium hydride to effect a Claisen condensation (28). In all such cases, the fluorinated acetoacetic ester produced in greatest amount must have resulted from reaction of the carbanion containing the least number of fluorines. This result may be interpreted to indicate that the kinetic acidity of fluorinated acetate esters in solution decreases with increasing fluorine substitution.

The data presented in Tables 1 and 2 also show that a straightforward explanation of fluorine substituent effects in gas phase enolate ions is not possible. On the basis of arguments advanced from solution acidity data, it might have been anticipated that the fluorinated acetones with a fluorine α to the carbanion site would show a lower gas phase acidity than their analogues with no α fluorines. That this is not the case is most dramatically demonstrated by the 12 kcal/mol *increase* in the gas phase acidity of fluoroacetone relative to acetone. In this case, enolate **II**, the fluorine is substituted α to the carbanion site. However, even when the fluorine is remote from the carbanion centre as in the less stable form, **III**, of the fluoroacetone enolate, an increase of 6 ± 1 kcal/mol in acidity is still observed relative to acetone.



II



III

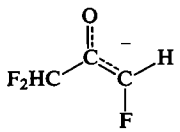
This order of acidity increase is paralleled in a comparison of data for 1,3-difluoroacetone and fluoroacetone. Addition of a remote fluorine to an enolate already bearing an α fluorine gives rise to a further increase of 7 ± 1 kcal/mol in acidity. Similarly, comparing difluoroacetone to the more weakly acidic site of fluoroacetone reveals a further 13 ± 2 kcal/mol increase in acidity by addition of an α fluorine to an enolate already having a remote fluorine substituent.

The gas phase acidity of 1,1,1-trifluoroacetone was found to be 19.7 kcal/mol greater than that of acetone. In this case of an enolate with three remote fluorines, the acidity difference from acetone is roughly equal to three times the acidity difference between the more weakly acidic site of fluoroacetone and acetone. This result would thus suggest a monotonic increase in acidity of acetones of approximately 6.5 kcal/mol for each remote fluorine substituent added. In addition, from the data for acetone, fluoroacetone, and difluoroacetone, it would appear that addition of a first α fluorine substituent to an enolate should give rise to an increase in acidity of the parent acetone of about 12 kcal/mol.

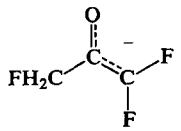
If the above postulates are correct, then it must be the case that addition of a second fluorine α to the carbanion centre cannot lead to an additive increase in acidity by an amount comparable to the first α fluorine. For example, for the gas phase acidity of pentafluoroacetone it would be calculated that addition of the second α fluorine leads to a further increase in acidity of only 6 ± 1 kcal/mol. Using this value for the increase in acidity resulting from a second α fluorine, it is possible to predict a difference in acidity between 1,1,3,3-tetrafluoroacetone and acetone of 31 kcal/mol. This agrees extremely well with the experimentally obtained value of 29 ± 3 kcal/mol.

Thus, for the fluorinated acetones studied here, all gas phase acidities may be interpreted on the basis of an increase in acidity of 6.5 kcal/mol relative to acetone for each remote fluorine substituent, 12 kcal/mol increase for the first α fluorine substituent, and a further 6 ± 1 kcal/mol increase for the second α fluorine substituent.

This order of substituent effects has important implications for the deduction of the detailed nature of fluorine in stabilization of enolate ions. It implies for example, that 1,1,1,3-tetrafluoroacetone, in which the resulting enolate would have three remote fluorines and one α fluorine, should be slightly more acidic than 1,1,3,3-tetrafluoroacetone where the resulting enolate has two remote and two α substituents. Similarly, it would be predicted that the more acidic site of 1,1,3-trifluoroacetone would be the less fluorinated methyl group to produce the enolate **IV** in preference to **V**.



IV



V

These postulates thus suggest that fluorine substituents can in fact have a destabilizing component in their interactions with planar carbanion centres which becomes manifest in highly fluorinated enolates of acetone.

The observed gas phase acidity of acetyl fluoride also supports this postulate. The acidity of acetyl fluoride is found to be roughly 1.5 kcal/mol greater

Can. J. Chem. Downloaded from www.nrcresearchpress.com by 210.87.254.42 on 09/05/12
For personal use only.

than that of fluoroacetone indicating that a fluorine substituted β to the charge centre is more effective in stabilization of the enolate ion than is an α fluorine substituent. The greater inductive effect resulting from closer proximity of the α fluorine to the carbanion centre in fluoroacetone enolate than in acetyl fluoride enolate is therefore counterbalanced by the repulsive electrostatic interaction which makes β fluorine substitution more energetically favourable.

Conclusion

The experimental data presented here lend some support to the hypothesis that fluorine substituents may play an ambiguous role in the stabilization of planar carbanions. Unlike the inference from solution acidity data, however, they do not support a *net* destabilization of planar carbanions with increasing fluorine substitution. Rather, the gas phase acidities show an *irregular* increase in carbanion stability with increasing fluorine substitution with multiple fluorine substitution frequently giving rise to carbanion formation which maximizes the number of remote substituents. The differences between the gas phase and solution results must therefore be largely a result of ion-pair and ion–solvent interactions in the solution acidity data which obscures the intrinsic electronic substituent effect.

Further studies of sp^2 and sp^3 hybridized fluorocarbanions are currently underway in our laboratory to investigate whether or not these phenomena are general for carbanions other than enolate ions.

Acknowledgement

The financial support of the Natural Sciences and Engineering Research Council of Canada is gratefully acknowledged.

1. M. HUDLICKY. Chemistry of organic fluorine compounds. MacMillan, New York. 1962.
2. W. A. SHEPPARD and C. M. SHARTS. Organic fluorine chemistry. Benjamin, New York. 1969.
3. N. C. BAIRD and R. K. DATTA. Can. J. Chem. **49**, 3708 (1971).
4. T. B. MCMAHON, R. J. BLINT, D. P. RIDGE, and J. L. BEAUCHAMP. J. Am. Chem. Soc. **94**, 8934 (1972).
5. A. STREITWEISER, JR. and F. MARES. J. Am. Chem. Soc. **90**, 2444 (1968).
6. H. G. ADOLPH and M. J. KAMLET. J. Am. Chem. Soc. **88**, 4761 (1966).
7. D. HOLTZ. Prog. Phys. Org. Chem. **8**, 1 (1971).
8. E. BUNCEL. Carbanions: mechanistic and isotopic aspects. Elsevier, Amsterdam. 1975.
9. T. B. MCMAHON and P. KEBARLE. J. Am. Chem. Soc. **98**, 3399 (1976).
10. T. B. MCMAHON and P. KEBARLE. J. Am. Chem. Soc. **99**, 2222 (1977).
11. C. R. BRUNDLE, M. B. ROBIN, N. A. KUEBLER, and H. BASCH. J. Am. Chem. Soc. **94**, 1451 (1972).
12. J. BURDON, I. W. PARSONS, and E. J. ARRAMIDES. J. Chem. Soc. Perkin II, 1201 (1979).
13. S. A. SULLIVAN and J. L. BEAUCHAMP. J. Am. Chem. Soc. **98**, 1160 (1976).
14. T. B. MCMAHON and J. L. BEAUCHAMP. Rev. Sci. Instrum. **43**, 509 (1972).
15. J. L. BEAUCHAMP. Ann. Rev. Phys. Chem. **22**, 517 (1971).
16. J. M. S. HENIS. *In* Ion molecule reactions. *Edited by* J. L. Franklin. Plenum, New York. 1972.
17. W. E. FARNETH and J. I. BRAUMAN. J. Am. Chem. Soc. **98**, 7891 (1976).
18. J. H. J. DAWSON and J. R. JENNINGS. Int. J. Mass Spectrom. Ion Phys. **25**, 47 (1977).
19. J. B. CUMMING and P. KEBARLE. Can. J. Chem. **56**, 1 (1978).
20. J. E. BARTMESS, J. A. SCOTT, and R. T. MCIVER, JR. J. Am. Chem. Soc. **101**, 6046 (1979).
21. S. W. BENSON. Thermochemical kinetics. Wiley, New York. 1968.
22. J. KERR and D. M. TIMLIN. Int. J. Chem. Kinet. **3**, 427 (1971).
23. F. ZABEL, S. W. BENSON, and D. M. GOLDEN. Int. J. Chem. Kinet. **10**, 295 (1978).
24. R. L. CLAIR and T. B. MCMAHON. Int. J. Mass Spectrom. Ion Phys. **33**, 21 (1980).
25. I. KNUNYANTS, L. GERMAN, and I. ROZHKOV. Isvest. Akad. Nauk SSSR, Ser. Khim. 1062 (1966).
26. G. BADDELEY, G. M. BENNET, S. GLASSTONE, and B. JONES. J. Chem. Soc. 1827 (1935).
27. J. BURDON, D. W. DAVIES, and G. DEL CONDE. J. Chem. Soc. Perkin II, 1205 (1979).
28. E. T. MCBEE, O. R. PIERCE, H. W. KILBOURNE, and E. R. WILSON. J. Am. Chem. Soc. **75**, 3152 (1953).
29. S. G. LIAS. *In* Kinetics of ion molecule reactions. *Edited by* P. Ausloos. Plenum, New York. 1979.
30. A. H. ZIMMERMAN, K. J. REED, and J. I. BRAUMAN. J. Am. Chem. Soc. **99**, 7203 (1977).

Etude des complexes chlorés de cadmium dans des mélanges HF/H_2O

HUGUES MÉNARD ET FRANCINE LEBLOND-ROUTHIER

Département de Chimie, Université de Sherbrooke, Sherbrooke (Qué.), Canada J1K 2R1

Reçu le 10 mars 1980

HUGUES MÉNARD et FRANCINE LEBLOND-ROUTHIER. Can. J. Chem. **58**, 2312 (1980).

La détermination des constantes de formation de $CdCl_2$, $CdCl^+$ et Cd^{2+} a été obtenue par polarographie dans des milieux HF/H_2O de 2,5 à 27,6 molaire.

HUGUES MÉNARD and FRANCINE LEBLOND-ROUTHIER. Can. J. Chem. **58**, 2312 (1980).

The formation constants of $CdCl_2$, $CdCl^+$, and Cd^{2+} have been determined by polarography from 2.5 to 27.6 molar in HF/H_2O.
[Journal translation]

Can. J. Chem. Downloaded from www.nrcresearchpress.com by 210.87.254.5 on 09/05/12
For personal use only.

Introduction

Depuis quelques années plusieurs articles (1, 2) ont démontré des méthodes simples de fabrication de capillaires polarographiques pouvant résister aux milieux extrêmement corrosifs pour le verre. C'est ainsi que maintenant il est possible de faire des analyses de métaux directement dans les milieux tel que HF, NaOH concentré par des techniques dérivées de la polarographie. Lors d'une étude sur la réduction de l'antimoine $Sb^{3+} \rightarrow Sb^0$ dans HF/H_2O, 40% en poids un déplacement anodique de la vague en présence de Cl^- a été mis en évidence. Ce déplacement a été attribué à un changement de la double couche à l'électrode de mercure. D'autre part, il est possible, par la même technique dans ces milieux, d'analyser la formation de complexes métalliques tels que:

$$Cd^{2+} + nCl^- \rightleftarrows CdCl_n^{(2-n)+}$$

Partie expérimentale

Appareil

Un polarographe modèle 174A (Princeton Applied Research) a été utilisé avec un système à trois électrodes. Une électrode de calomel saturée séparée de la solution à étudier par une jonction en Teflon poreuse a été utilisée comme réf. 3.

Produit

Les solutions ont été préparées à partir de HF 48% en volume (Allied Chemical). Les solutions de Cd^{2+} ont été faites à partir de CdO (Baker Anal. Reagent) et tout comme les solutions de chlorures sont issues de KCl (Baker).

Résultats et discussion

L'étude par polarographie a été faite pour la réduction du cadmium $Cd^{2+}/CdHg$ dans les milieux HF/H_2O et en milieu KF aqueux (0,1 à 2 *M*). L'addition de Cl^- dans ces milieux lors de l'analyse par polarographie nous donne un déplacement cathodique de la vague de réduction (Fig. 1). La réversibilité du système a été vérifier par l'analyse de la vague E vs. $\log [i/(i_d - i)]$ donne des droites dont les pentes sont de 29 mV. De plus, des études de voltamétrie cyclique ont démontré la réversibilité.

En utilisant la théorie de Deford–Hume (4) il est possible de déterminer les constantes de formation pour différents complexes à l'aide des données polarographiques, sachant que la réduction du Cd^{2+} est réversible. L'équation pour trouver $F_0(X)$, $F_0(X)$ étant une quantité expérimentalement mesurable (à force ionique constante) est:

$$[1] \quad F_0(X) = \sum_j \frac{K_j C_x{}^j f_x{}^j}{f_{nxj}} = \text{antilog } 0{,}435 \frac{nF}{RT} \times [(E_{1/2}{}^0)_s - (E_{1/2})_c] + \log \frac{I_s}{I_c}$$

où $(E_{1/2}{}^0)_s$ est le potentiel de demi-vague lorsqu'il n'y a pas d'espèces complexantes; $(E_{1/2})_c$, potentiel de demi-vague avec espèce complexante dans le milieu; I_s et I_c, les courants de diffusion sans et avec espèces complexantes. Le terme $\log (I_s/I_c)$ peut être négligé (5) car il contribue très peu à la fonction $F_0(X)$. L'expression $[(E_{1/2})_s - (E_{1/2})_c]$ est remplacée par $\Delta E_{1/2}$/ecs. Pour une réduction de deux électrons comme dans le cas du cadmium on aura:

$$[2] \quad F_0(X) = \text{antilog} - 33{,}28\,(\Delta E_{1/2})$$

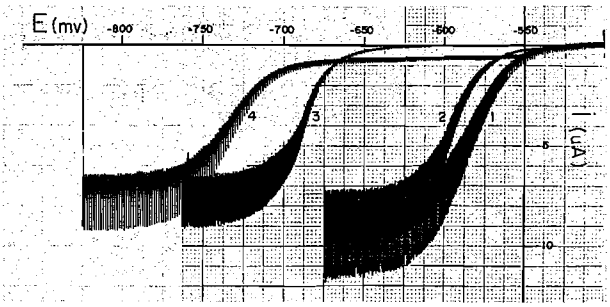


FIG. 1. Polarogrammes de Cd^{2+}/Cd^0 (Hg) dans HF 27,6 *M*, en présence de KCl; (*1*) 10^{-3} *M* CdO/HF 27,6 *M*; (*2*) *ibid* +0,0003 *M* KCl; (*3*) *ibid* +0,1 *M* KCl; (*4*) *ibid* +0,3 *M* KCl.

0008-4042/80/222312-02$01.00/0
©1980 National Research Council of Canada/Conseil national de recherches du Canada

Can. J. Chem. Downloaded from www.nrcresearchpress.com by 210.87.254.5 on 09/05/12
For personal use only.

En connaissant $F_0(X)$ on peut obtenir les fonctions $F_i(X)$ pour un complexe de degré supérieur. Ainsi:

[3] $F_i(X) = [F_0(X) - \beta_0]/c_x$

où β_0 est la constante de formation de l'ion seul et est égal à l'unité. c_x est la concentration analytique ajoutée de l'espèce complexante.

En traçant $F_i(X)$ versus c_x, l'extrapolation à $c_x = 0$ donnera β_1, la constante de formation du complexe de degré 1.

Le complexe du degré le plus élevé sera celui qui donne une droite parallèle à l'axe de la concentration. Nous devons remarquer que les constantes de formation des complexes de degré supérieur comportent une incertitude vu que l'extrapolation est plus ou moins précise pour donner β_i supérieur.

Le tableau 1 regroupe pour les différentes concentrations de HF les β_0, β_1, β_2 pour le système $CdCl_2$, $CdCl^+$, Cd^{2+} obtenu par graphique.

A l'aide des constantes il est possible de calculer le % de chacun des complexes présents pour différentes concentrations HF/H_2, les figs 2, 3 et 4.

Il apparaît clairement que le complexe $CdCl_2$ est plus facile à former en milieu pauvre en fluorure

TABLEAU 1. Système Cd—F—Cl

[HF] (*M*)	β_0	β_1	β_2
27,6	1,00	470 ± 20	1,7 × 10^5 ± 0,25 × 10^5
22,5	1,00	500 ± 50	3,5 × 10^4 ± 0,4 × 10^4
18	1,00	170 ± 50	4,550 ± 0,700
13	1,00	71 ± 1	540 ± 10
7	1,00	50 ± 7	190 ± 40
2,5	1,00	38 ± 4	65 ± 10

Force ionique non constante

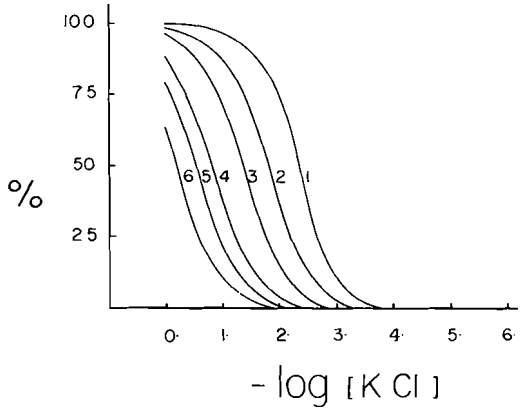


FIG. 2. Pourcentage de $CdCl_2$ présent dans les différents mélanges de HF–H_2O: (*1*) 27,6 *M*; (*2*) 22,5 *M*; (*3*) 18 *M*; (*4*) 13 *M*; (*5*) 7 *M*; (*6*) 2,5 *M*.

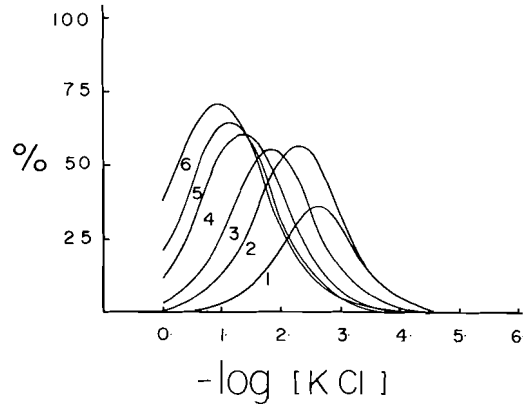


FIG. 3. Pourcentage de $CdCl^+$ présent dans les différents mélanges de HF–H_2O: (*1*) 27,6 *M*; (*2*) 22,5 *M*; (*3*) 18 *M*; (*4*) 13 *M*; (*5*) 7 *M*; (*6*) 2,5 *M*.

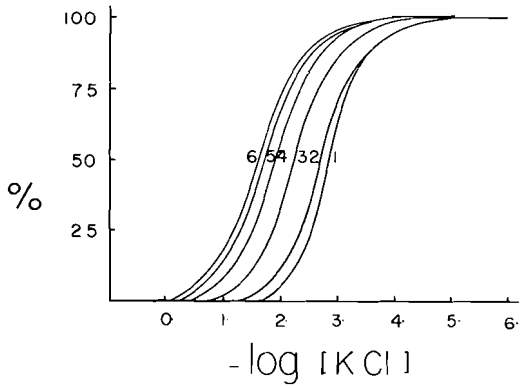


FIG. 4. Pourcentage de Cd^{2+} dans les différents mélanges de HF–H_2O: (*1*) 27,6 *M*; (*2*) 22,5 *M*; (*3*) 18 *M*; (*4*) 13 *M*; (*5*) 7 *M*; (*6*) 2.5 *M*.

libre c'est-à-dire [HF] élevé (6), qu'en milieu riche en F^-. D'autre par la concentration en $CdCl^+$ semble passer part un maximum tandis que la concentration en Cd^{2+} diminue en présence de chlorure si la concentration en [F^-] augmente.

Remerciements

Les auteurs sont reconnaissants des octrois de recherche du CRSNG et du M.E.Q. qui ont rendu ce travail possible.

1. H. MÉNARD et F. LEBLOND-ROUTHIER. Anal. Chem. **50**, 687 (1978).
2. J. DEVYNCK, B. TRÉMILLON, H. MÉNARD et G. COMARMOND. Can. J. Chem. **56**, 703 (1978).
3. F. LEBLOND-ROUTHIER. Thèse, Sherbrooke. 1977.
4. D. DEFORD et D. N. HUME. J. Am. Chem. Soc. **73**, 5321 (1951).
5. A. M. BOND et T. A. O'DONNELL. J. Electroanal. Chem. **26**, 137 (1970).
6. H. MÉNARD, J. P. MASSON, J. DEVYNCK et B. TRÉMILLON. J. Electroanal. Chem. **63**, 163 (1975).

Complexes of dithiobenzoic acids. III. ^1H and ^{13}C nuclear magnetic resonance studies of a series of *tetrakis*(dithiobenzoato)molybdenum(IV) complexes[1]

T. ROBERIE, N. S. BHACCA, D. LANKIN, AND J. SELBIN

Department of Chemistry, Louisiana State University, Baton Rouge, LA 70803, U.S.A.

Received May 16, 1980

T. ROBERIE, N. S. BHACCA, D. LANKIN, and J. SELBIN. Can. J. Chem. **58**, 2314 (1980).

A series of dithiocarboxalato (X-dtb) complexes of molybdenum(IV), $Mo(X\text{-}dtb)_4$, where the *para* substituent X = H, CH_3, CH_3O, F, C_6H_5, CHO, C_6H_5CO, or $(n\text{-}C_4H_9)_2N$, the parent acids and tetraalkylammonium salts were studied by ^1H and ^{13}C nmr in order to monitor the expected charge density shifts as a function of the group X. Analysis of the ^{13}C nmr data unexpectedly revealed an absence of delocalization of electron density either from molybdenum to ligand or from ligand to molybdenum.

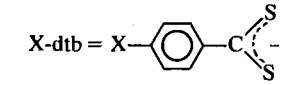
T. ROBERIE, N. S. BHACCA, D. LANKIN et J. SELBIN. Can. J. Chem. **58**, 2314 (1980).

Afin de pouvoir évaluer les déplacements de densité de charge résultant de la présence des groupes X, on a étudié, par la rmn du ^1H et du ^{13}C, une série de complexes dithiocarboxalato (X-dtb) du molybdenum(IV) $Mo(X\text{-}dtb)_4$ où le substituant X en position *para* = H, CH_3, CH_3O, F, C_6H_5, CHO, C_6H_5CO ou $(n\text{-}C_4H_9)_2N$ ainsi que les acides et les sels de tétraalkylammonium apparentés. L'analyse des données de la rmn du ^{13}C revèle une absence surprenante de délocalisation de la densité électronique soit du molybdène vers le ligand ou du ligand vers le molybdène.

[Traduit par le journal]

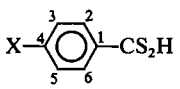
Introduction

In a previous paper (1) we reported the preparation and characterization of a number of (mostly new) dithiocarboxalato complexes of molybdenum(IV), $Mo(X\text{-}dtb)_4$, where the bidentate sulfur ligands are of the general type:

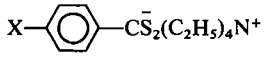


and X is H, CH_3, CH_3O, Cl, F, C_6H_5, CHO, C_6H_5CO, CH_3CO, or $(n\text{-}C_4H_9)_2N$. Visible–ultraviolet and infrared spectral data for the ligands, their tetraalkylammonium salts, and the molybdenum complexes were also reported and discussed. We now report the results of both ^1H and ^{13}C nmr studies of as many of those ligands, salts, and complexes as were stable enough and soluble enough to yield reproducible data. The primary purpose of the ^{13}C nmr study was to attempt to monitor the expected shifts of charge density either from ligand-to-metal or metal-to-ligand as a function of the electronic nature of the X group in the ligand molecule.

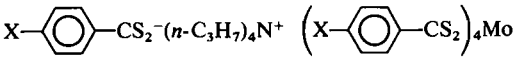
The compounds studied were the following acids (**1**), salts (**2** and **3**), and molybdenum(IV) complexes (**4**):



1



2



3

a (X = H)
b (X = CH_3)
c (X = CH_3O)
d (X = F)

4

e (X = C_6H_5)
f (X = CHO)
g (X = CH_3CO)
h (X = C_6H_5CO)

The more stable methylthioesters were used for nmr studies in place of the acids **1***a* and **1***d*.

Experimental

The preparations of the various ligands, salts, and complexes have already been described (1). The proton noise decoupled ^{13}C nmr spectra were obtained at ambient temperature on a JEOL FX-100 spectrometer. The solvent was $CDCl_3$ in all cases. Tetramethylsilane was added to the samples to serve as an internal standard. The ^1H nmr spectra were obtained at 60 MHz on a Varian A-60A spectrometer. The metal complexes were run at 60°C in saturated $CDCl_3$ solutions. A Varian Model 4343 temperature control was used to maintain the probe at this temperature. Ethylene glycol was used for the high temperature calibration.

Results and Discussion

The ^1H nmr data for the eight soluble Mo(IV) dithiocarboxalato complexes and for analogous complexes of both Ti(IV) and Sn(IV), ($Ti(\mathbf{1}a\text{-}H)_3Cl$, $Ti(\mathbf{1}c\text{-}H)_3Cl$, and $Sn(\mathbf{1}a\text{-}H)_2Cl_2$) were collected along with the data for the corresponding free acids and their tetraalkylammonium salts. The data reveal that the signals of the *ortho* protons of the Mo(IV) complexes are shifted slightly upfield (by 0.11–0.21 ppm) from their positions in the ligand acids, whereas the *meta* protons are essentially all unshifted. A possible explanation (*vide infra*) for this behavior is some sort of nonbonding

[1]Presented in part at the American Chemical Society Annual Meeting, Washington, DC, September 9–14, 1979.

0008-4042/80/222314-04$01.00/0

©1980 National Research Council of Canada/Conseil national de recherches du Canada

Can. J. Chem. Downloaded from www.nrcresearchpress.com by 210.87.254.42 on 09/05/12
For personal use only.

TABLE 1. ^{13}C chemical shifts (ppm) of the dithiobenzoic acids, tetraalkylammonium salts, and molybdenum(IV) complexes

Compound	Chemical shift						
	C_1	C_2	C_3	C_4	CCS	CH_3	CO
1*a*[a]	144.7	126.6	128.1	132.0	224.5[b]	20.5[c]	—
1*b*	140.9	126.9	128.9	144.3	224.3	21.6	—
1*c*	136.5	129.3	113.4	164.2	222.0	55.6	—
1*d*[a]	141.0	128.9	115.1	165.3	222.1[b]	20.6[c]	—
1*e*	141.9	126.8	127.4	145.9	223.8	—	—
1*f*	—	—	—	—	—	—	—
1*g*	146.0	126.9	128.2	139.7	223.9	26.8	197.0
1*h*	145.5	126.5	129.7	140.9	224.0	—	—
4*a*	140.8	123.1	128.2	132.8	216.0	—	—
4*b*	138.9	123.1	128.9	143.8	215.5	21.7	—
4*c*	135.1	125.1	113.4	165.0	214.4	55.6	—
4*d*	137.4	125.4	115.5	166.3	214.2	—	—
4*e*	139.7	123.6	127.0	145.3	214.6	—	—
4*f*	143.4	123.5	129.4	138.7	214.6	—	191.0
4*g*	142.8	123.3	128.2	139.7	214.9	26.8	196.9
4*h*	142.3	123.5	129.9	140.8	214.7	—	195.3
2*a*	153.4	126.7	126.7	128.7	253.6	—	—
2*b*	150.4	126.6	127.2	138.7	252.3	21.1	—
2*c*	145.5	128.8	111.6	161.1	251.0	55.6	—
2*d*	149.1	128.8	113.8	163.8	251.1	—	—
3*e*	151.7	127.4	125.1	140.7	252.1	—	—
3*f*	158.8	126.8	128.5	135.3	251.6	—	192.2
2*g*	157.4	126.3	127.1	136.2	252.2	26.8	198.0
3*h*	157.1	126.3	128.9	137.9	252.5	—	196.6

[a]The methyl ester of the ligand acid, used in place of the less stable acid.
[b]Corrected for the downfield shift due to the methyl group.
[c]Methyl carbon of the methylthioester.

d-orbital shielding effect associated with the partially occupied metal *d*-orbitals. Support, but not conclusive evidence, for this suggestion comes from the corresponding data for the Ti(IV) and Sn(IV) complexes which are d^0 and d^{10} systems, respectively, and where we have found no such shielding effect. However, we must recognize that in neither of these two cases are there *four* bidentate ligands crowded around the central metal as in the case of Mo(IV).

The ^{13}C nmr spectra of the six dithiobenzoic acids and the two thioesters were examined in the 0–320 ppm range, as were the spectra for the eight dithiobenzoate salts and the eight molybdenum(IV) complexes. The experimental data are collected in Table 1 for the acids, salts, and complexes.

The assignments of the four resonances observed in the aromatic (~110–160 ppm) region are relatively straightforward. For the methylester of the parent compound, dithiobenzoic acid, the assignment of the 132.0 resonance to C_4 is made on the basis that aromatic carbons *para* to an electron-withdrawing group generally fall in the 130–134 ppm range. The C_1 assignment follows from the absence of a nuclear Overhauser effect for this quaternary arene carbon, leading to its much reduced intensity relative to C_2 and C_3. These latter two assignments were made that the 128.5 resonance of benzene itself would be more affected by an *ortho* substituent, hence C_2 must be at 126.6, than by a *meta* substituent, hence C_3 resonates at 128.1. The dithio carbon assignment is unequivocal from previous studies of thioketones where this carbon appears above 200 ppm. The assignment of the methyl carbon in the parent as well as *para*-substituted derivatives is likewise straightforward from previously assigned CH_3 groups in monosubstituted benzenes with the same substituents. The assignments for the carbonyl carbon (where X = $COCH_3$ or COC_6H_5) are from previous assignments for acetophenone and benzophenone, respectively.

The assignment of the arene resonances in all of the *para-substituted* ligands were made in accord with shift increment calculations, made possible by the simple relationship (2)

$$\delta_c = 128.5 + \sum_i A_i(X)$$

Can. J. Chem. Downloaded from www.nrcresearchpress.com by 210.87.254.42 on 09/05/12
For personal use only.

Can. J. Chem. Downloaded from www.nrcresearchpress.com by 210.87.254.42 on 09/05/12
For personal use only.

where the arene carbon chemical shift, δ_c, is obtained by adding the sum of the chemical shift increments $A_i(X)$ for substituent X in the ith position. The shift parameters for the new groups obtained in this study are listed in Table 2. The excellent agreement we found between our calculated and observed resonances for the arene carbons (never larger than 3 ppm, but generally within a few tenths of a ppm) gives us confidence in our assignments. Further support for these assignments comes from the data for $^{19}F-^{13}C$ coupling constants recorded in Table 3 for the ester, salt, and complex of the *para* fluoro ligand.

Table 4 presents the displacements of the carbon chemical shifts of the dithiobenzoic acids after their complexation to molybdenum. As can be seen in Table 4 the largest effect, ~9 ppm upfield shift, due to the complexation is exhibited at the thiocarbonyl carbons. A somewhat lesser effect, ~3 ppm upfield shift, occurs at both the C_1 and C_2 (*ortho*) carbons whereas virtually no effect is felt by the C_3 (*meta*) and C_4 (*para*) carbons. The data in Table 4 strongly suggest the unexpected result that *there is essentially no delocalization of electron density from molybdenum orbitals into the π aromatic system or vice versa*. Such an effect would be expected to show up most clearly at the C_1 and C_4 carbons. The ~9 ppm upfield shift of the thiocarbonyl carbons as well as the smaller upfield shifts for C_1 and C_2 may be due to a nonbonding *d*-orbital shielding effect similar to that which has been proposed to account for proton shifts in transition metal hydrido complexes (3). On the other hand, the upfield shifts may have nothing at all to do with Mo, but rather may be a consequence of the clustering of four bidentate groups around the metal.

When we plotted the carbon-13 chemical shifts of the C_1, C_3, and C_4 carbons in the tetraalkylammonium salts and in the molybdenum complexes versus those same shifts in the free acids, we found excellent linear agreement. A sample of such plots is shown in Fig. 1. Particularly in the case of the C_3 and C_4 chemical shifts for the acids and their mo-

TABLE 2. Empirical parameters from this work for the calculation of chemical shifts in substituted benzenes

	A_i			
X	C_1	*ortho* (C_2)	*meta* (C_3)	*para* (C_4)
CS_2CH_3	+16.2	−1.9	−0.4	+3.5
CS_2^-	+24.9	−1.8	−1.8	+0.2
CS_2Mo	+12.3	−5.4	−0.3	+4.3

TABLE 3. $^{19}F-^{13}C$ coupling constants (Hz) for the *para* fluoro derivatives[a]

	Value		
Constant	Acid	Salt	Complex
$J(F-C_4)$	253.6	248.4	255.2
$J(F-C_3)$	21.5	21.5	22.3
$J(F-C_2)$	8.8	8.6	8.8
$J(F-C_1)$	3.2	2.6	3.2

[a]C_1, C_2, C_3, and C_4 refer to positions with respect to the dithiocarboxyl group.

TABLE 4. Displacements of the ^{13}C chemical shifts of the dithiobenzoic acids due to complexation[a]

	Displacement				
X	C_1	C_2	C_3	C_4	CSS
H	−3.9	−3.5	0.1	0.8	−8.5
p-CH_3	−2.0	−3.8	0.0	−0.5	−8.8
p-OCH_3	−1.4	−4.1	0.0	−0.2	−7.6
p-F	−3.6	−3.5	0.4	1.0	−7.8
p-Ph	−2.2	−3.2	−0.4	−0.6	−9.4
p-CHO[b]	—	—	—	—	—
p-$COCH_3$	−3.2	−3.6	0.0	0.0	−9.0
p-COPh	−3.2	−3.0	0.2	−0.1	−9.3

[a]Negative values denote upfield shifts due to complexation.
[b]Compound too insoluble for spectra to be obtained.

When we plotted the carbon-13 chemical shifts of the C_1, C_3, and C_4 carbons in the tetraalkylammonium salts and in the molybdenum complexes versus those same shifts in the free acids, we found excellent linear agreement. A sample of such plots is shown in Fig. 1. Particularly in the case of the C_3 and C_4 chemical shifts for the acids and their mo-

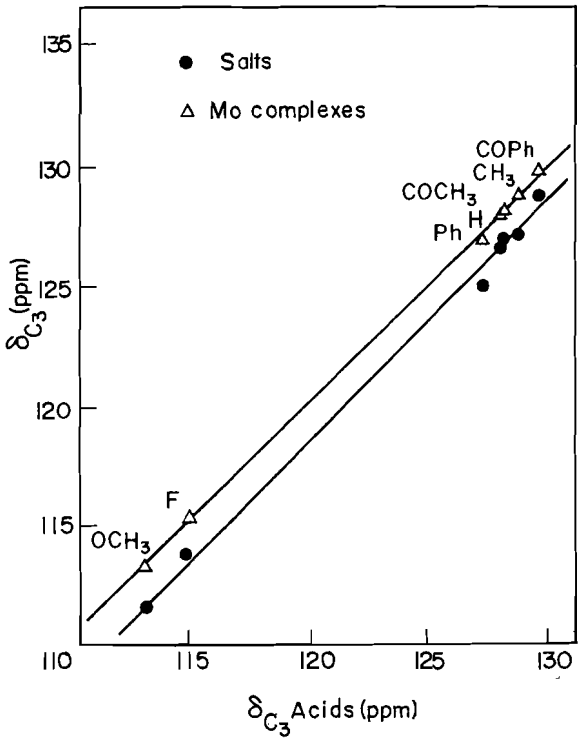


FIG. 1. ^{13}C chemical shifts of the C_3 carbon in the molybdenum complexes and the salts versus the ^{13}C chemical shifts of the C_3 carbon in the free acids (or methylesters).

lybdenum complexes we feel this agreement provides substantial evidence that there must be little or no delocalization of charge (either M → L or L → M) in these complexes. Thus any appreciable resonance interaction of the molybdenum with the π-aromatic system would be expected to involve both C_1 and C_4 carbons in these *para*-substituted ligands, which would alter the electron densities at these particular carbon atoms which should in turn be reflected in the ^{13}C chemical shifts; but it is not.

To further test our hypothesis we plotted the C_1 shifts in the salts, acids, and molybdenum complexes against both Hammett σ_p^+ constants and Taft σ_R^0 constants (4). The correlation coefficients for the salts, acids, and complexes which we found are for σ_p^+: 0.990, 0.941, and 0.966, respectively; and for σ_R^0: 0.962, 0.905, and 0.976, respectively. Although the correlations are not as good for the acids as they are for the salts and complexes, the plots do show that the electronic effects of the various substituents in the *para* position are at least similar in the free acids, the salts, and the complexes. Moreover the slopes of the corresponding three lines in our plots are very similar, suggesting that the transmission of the electronic effect of the substituent X is virtually unaltered in the acids, salts, and complexes. Thus these comparisons provide additional, if only slight evidence for a lack of delocalization of electron density from molybdenum to ligand or vice versa. We might note also that plots of the *electronegativities* of the substituents versus the C_4 chemical shifts in both the complexes (or acids) and the salts also showed good correlation, the correlation coefficients being 0.968 and 0.976, respectively. This correlation result is also expected (5) if there is no additional electron density effect imposed by the molybdenum–ligand interaction in the complexes.

1. T. ROBERIE, A. E. HOBERMAN, and J. SELBIN. J. Coord. Chem. **9**, 79 (1979).
2. F. W. WEHRLI and T. WIRTHLIN. Interpretation of carbon-13 nmr spectra. Heyden, PA. 1978.
3. A. K. BUCKINGHAM and P. J. STEPHENS. J. Chem. Soc. 2747 (1964).
4. O. EXNER. *In* Adv. in linear free energy relationships. *Edited by* N. B. Chapman and J. Shorter. Plenum Press, New York. 1972.
5. H. SPIESECKE and W. G. SCHNEIDER. J. Chem. Phys. **35**, 731 (1961).

Can. J. Chem. Downloaded from www.nrcresearchpress.com by 210.87.254.42 on 09/05/12
For personal use only.

The partitioning of tetrahedral intermediates of the hydrolysis of benzimidatonium ions in acid solutions

ROBERT A. MCCLELLAND AND JANET P. POTTER

Scarborough College, University of Toronto, West Hill, Ont., Canada M1C 1A4

Received March 20, 1980

ROBERT A. MCCLELLAND AND JANET P. POTTER. Can. J. Chem. **58**, 2318 (1980).

The products (a benzoate ester or an *N*,*N*-dimethylbenzamide) have been accurately determined for the hydrolysis of the *O*-ethyl-*N*,*N*-dimethylbenzimidatonium ion (**1**) and its 4-nitro derivative (**2**) in dilute and moderately concentrated H_2SO_4 solutions. In dilute acid the ratio of amide:ester is very small (0.0005–0.001). It is proposed that the ester product arises from the zwitterionic form of the tetrahedral intermediate of the hydrolysis. The small amount of amide is due to an S_N2 hydrolysis reaction and to the non-catalyzed breakdown of the neutral form of the tetrahedral intermediate, the relative contributions of the two being unknown. Although ester remains the major product throughout, at some intermediate acid concentration (20% H_2SO_4 for **1** and 35% H_2SO_4 for **2**) a sharp increase in the amide:ester ratio is observed, followed by a levelling-off. This change is shown to be associated with tetrahedral intermediate partitioning, and not the S_N2 reaction. It is argued that the strong acid product ratio represents the breakdown of the tetrahedral intermediate via cationic transition states. Two kinetically equivalent reactions are involved, the breakdown of the *N*-protonated tetrahedral intermediate producing a protonated ester and amine and the H^+-catalyzed breakdown of the neutral tetrahedral intermediate producing a protonated amide and alcohol. Analogous pathways are also observed for the decomposition in acid of the amide acetals $ArC(OMe)_2NMe_2$, and the two systems are compared. A similar effect of the aromatic substituent on the partitioning ratio is noted, but the tetrahedral intermediate exhibits a greater tendency for amine expulsion. A kinetic analysis produces the estimate of 10^{11} s^{-1} for the rate constant for the breakdown of the zwitterionic form of the tetrahedral intermediate. This very large rate explains why its decomposition remains important even in concentrated acids, where the amount of tetrahedral intermediate which actually exists as zwitterion must be extremely low.

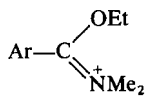
ROBERT A. MCCLELLAND et JANET P. POTTER. Can. J. Chem. **58**, 2318 (1980).

On a déterminé avec précision les quantités relatives des produits (un ester benzoique ou un *N*,*N*-diméthylbenzamide) de l'hydrolyse de l'ion *O*-éthyl *N*,*N*-diméthylbenzimidatonium (**1**) et de son dérivé nitré en position 4 (**2**) en solutions diluées et moyennement concentrées de H_2SO_4. En solution acide diluée le rapport amide/ester est très petit (0,0005–0,001). On croît que l'ester provient de la forme zwitterionique de l'intermédiaire tétraédrique de l'hydrolyse. La faible quantité d'amide est due à une réaction d'hydrolyse du type S_N2 et à la décomposition non catalysée de la forme neutre de l'intermédiaire tétraédrique dont les contributions relatives sont inconnues. Bien que l'ester demeure le produit principal de la réaction à des concentrations intermédiaires d'acide (20% et 35% de H_2SO_4 pour les composés **1** et **2** respectivement), on observe une nette augmentation du rapport amide/ester suivie d'un équilibre. On montre que ce changement est associé à la répartition de l'intermédiaire tétraédrique et non pas à une réaction S_N2. On suggère que le rapport de produits en milieu fortement acide représente la décomposition de l'intermédiaire tétraédrique via un état de transition du type cationique. Deux réactions cinétiquement équivalentes sont impliquées: la décomposition de l'intermédiaire tétraédrique *N*-protoné qui fournit un ester protoné et une amine et la décomposition catalysée par l'ion H^+ de l'intermédiaire tétraédrique neutre qui produit un amine et un alcool. On observe également un cheminement analogue lors de la décomposition des acétals des amides $ArC(OMe)_2NMe_2$ en milieu acide et on compare les deux systèmes. On note un effet semblable du substituant aromatique sur le rapport de répartition, mais l'intermédiaire tétraédrique montre une plus grande tendance à expulser l'amine. Une analyse cinétique permet d'évaluer à 10^{11} s^{-1} la constante de vitesse de décomposition de la forme zwitterionique de l'intermédiaire tétraédrique. Cette très grande vitesse explique pourquoi la décomposition demeure importante même en solutions concentrées d'acide où la quantité d'intermédiaire tétraédrique qui existe de fait sous forme de zwitterion doit être entièrement faible.

[Traduit par le journal]

We recently reported a kinetic and mechanistic study of the hydrolysis of amide acetals (1). These molecules model (2) in some respects the tetrahedral intermediates encountered in amide hydrolysis (3–7), ester aminolysis (8–13), and imidate hydrolysis (6, 9, 10, 12–20). As we pointed out (1), there is a difference in the behavior of the types of species in acid solutions. Whereas the tetrahedral intermediates generally breakdown with predominant, if not exclusive, loss of amine, the decomposition of the amide acetals occurs with loss of both amine and alcohol.

We report here an investigation undertaken to attempt to account for this difference, namely a study of the partitioning in relatively acidic solutions of the tetrahedral intermediates generated in the hydrolysis of the benzimidatonium ions **1** and **2**.



1, Ar = C_6H_5
2, Ar = 4-$NO_2C_6H_4$

Experimental

Materials

Sulfuric acid solutions were prepared and standardized as

0008-4042/80/222318-08$01.00/0

©1980 National Research Council of Canada/Conseil national de recherches du Canada

Can. J. Chem. Downloaded from www.nrcresearchpress.com by 210.87.254.6 on 09/05/12
For personal use only.

Can. J. Chem. Downloaded from www.nrcresearchpress.com by 210.87.254.6 on 09/05/12
For personal use only.

previously described (21). *O*-Ethyl-*N,N*-dimethylbenzimidatonium (**1**) borofluorate and *O*-ethyl-*N,N*-dimethyl-4-nitrobenzimidatonium (**2**) borofluorate were prepared by the *O*-ethylation of the appropriate *N,N*-dimethylbenzamide with triethyloxonium borofluorate (22), following a standard procedure (6). Amide and a 10–20% molar excess of alkylating agent were dissolved in anhydrous methylene chloride. The solution was allowed to stand overnight and anhydrous ether was added to precipitate the imidatonium salt. This was filtered in a water-free environment (glove box), and washed with a large quantity of anhydrous ether in order to remove unreacted amide. *O,N,N*,4-Tetramethylbenzimidatonium borofluorate was prepared by the reaction of the substituted benzamide and trimethyloxonium borofluorate (23), as previously described (6). We find that samples of this alkylating agent, either when obtained commercially (Cationics) or synthesized in our laboratories (23), do not consist entirely of methyl groups, but contain a small fraction (1–5%) of ethyl groups. This contamination is undoubtedly caused by incomplete replacement of ethyl by methyl in the synthesis from triethyloxonium borofluorate (23), and results in the presence of a small amount of *O*-ethyl imidatonium ion. This impurity, which only amounts to 1–5%, does not have any effect on the linearity of the first-order kinetic plots for the hydrolysis of the contaminated *O*-methyl imidatonium ion, but significantly interferes with our gc product analysis. For this reason we switched to *O*-ethyl for the latter.

Product Analysis

Gas Chromatographic Method

Imidatonium borofluorate (0.5 g) was dissolved in 100 mL of aqueous acid and immediately shaken three times with 100 mL of methylene chloride. The aqueous layer was placed in a water bath thermostatted at 25°C and after an appropriate period of time (see below) extracted with 300 mL of ether, followed by concentration of the ether layer. This sample was injected into a Varian Gas Chromatograph containing a 2 m × 6 mm column of 10% Carbowax 20 M on Chromosorb P with a column temperature of 130°C (unsubstituted system) or 180°C (4-nitro substituted compound).

This method provides the ratio of the ester product of the hydrolysis, ethyl benzoate or ethyl 4-nitrobenzoate, and the amide product of the hydrolysis, *N,N*-dimethylbenzamide or *N,N*-dimethyl-4-nitrobenzamide. This ratio was determined by comparing the relative areas under the gc peaks of the two products. The relative response of the two compounds on the gc instrument was determined using mixtures of authentic samples of the ester and amide, these mixtures being prepared in such a way that the relative amount of the two compounds present approximated that in the mixtures being obtained on hydrolysis. These synthetic mixtures also verified that the flame ionization detector of the gas chromatograph does have a linear response to the two products at the concentration levels involved. In general, with any sample four to six injections were made in a given experiment and the relative areas of each averaged.

This method requires that, under the conditions employed to hydrolyze the imidatonium ion, no ester can have hydrolyzed. (This is also true for the amide but the ester hydrolysis is much more rapid (5, 24).) Rate constants for the hydrolysis of the esters at 25°C were estimated by interpolation or extrapolation of literature values for methyl benzoate (24), with the reasonable assumption (25) being made that there are only minor differences with the two ethyl esters of this study. This rate constant was then used to determine the period of time for which the hydrolysis of the imidatonium ion could be allowed to run before significant hydrolysis of the ester occurred. As a general rule no study was carried out for a longer period of time than that which would result in 5% hydrolysis of the ester product. This problem becomes more severe as the sulfuric acid concentration is increased, due to the fact that the rates of hydrolysis of the benzimidatonium ions decrease with increasing acidity (6) whereas the rates of hydrolysis of the ethyl benzoates increase, at least up to 50–55% H_2SO_4 (24). This means that in the more concentrated acids the imidatonium hydrolysis cannot be allowed to proceed to completion before work-up and product analysis. In these cases we did verify that unreacted imidatonium ion does not affect this analysis. Eventually this problem does become too severe. The method cannot be employed in acids more concentrated than those reported in our results.

A second possible source of error in our analysis is contamination of the imidatonium ion by unreacted amide. We attempted to avoid this in several ways. An excess of alkylating agent was used in the preparation of the salt. This salt was washed with large quantities of ether, which will dissolve the amide but not the salt. Finally the aqueous acid solutions of imidatonium salts were immediately shaken with several portions of methylene chloride. Our reasoning behind this procedure is that the benzamides should distribute very strongly towards the organic phase, while the imidatonium salts remain in the aqueous phase. The hydrolysis of the latter fortunately is slow, with half-lives greater than 60 min even in water, so that little hydrolysis occurs during these initial washings. Even if hydrolysis does occur, it is still not a problem since the ester is also extracted into the organic phase. In other words, we start our analysis from the time immediately after the last washing.

Experimental justification that this procedure does provide the true product ratio comes from two observations. (*a*) In the hydrolysis of both imidatonium ions in dilute acids, a very small amount of amide is observed. Even in the unlikely event that all of this were to be due to unreacted amide, its quantity is very small. (*b*) In the more concentrated acids where the imidatonium ion hydrolysis could not be allowed to proceed to completion, experiments were carried out over varying periods of time corresponding to varying extents of hydrolysis. We find, however, as we should, the same ratio of the two products. If further hydrolysis of the ester were occurring, the amide:ester ratio would have shown an increase with time as more ester hydrolyzes. If, on the other hand, the initial sample were contaminated with amide, the amide:ester ratio would have shown a decrease with time, as more product with the actual amide:ester ratio is formed.

Nuclear Magnetic Resonance Method

This method was used to provide a further check on the gc results obtained with the 4-nitro compound in 40–50% H_2SO_4. The imidatonium ion salt (1 g) was dissolved in 100 mL of acid and left for 5–7 half-lives of hydrolysis. The resulting mixture was extracted with ether, the ether was then completely removed, and the nmr spectrum recorded. The relative yield of *N,N*-dimethyl-4-nitrobenzamide was determined by comparing the integration of the *N,N*-dimethyl doublet at δ 3.0 and δ 3.2 with the total integration of the aromatic protons. These are due to amide, ester, and carboxylic acid, the last compound being present since in this experiment the ester product has undergone further hydrolysis. We assume that once the contribution from the amide to the total aromatic integration is subtracted out, whatever remains is due to ester. This procedure is far less precise than the gc technique

Can. J. Chem. Downloaded from www.nrcresearchpress.com by 210.87.254.6 on 09/05/12
For personal use only.

because of the problems associated with exact nmr integration. It does, however, verify unambiguously that a significant quantity of amide is being formed from this ion in these acids.

^{18}O Tracer Study

O-Ethyl-*N,N*-dimethyl-4-nitrobenzimidatonium borofluorate (0.3 g) was dissolved in 48.6% H_2SO_4 (6 g) containing 7.3% ^{18}O. The labelled acid was prepared as previously described (26). After a period of time corresponding to 5 half-lives of hydrolysis of the imidatonium ion, the mixture was extracted with ether, the ether layer washed with aqueous Na_2CO_3 to remove 4-nitrobenzoic acid, dried ($MgSO_4$), and the ether removed. The resulting material, a mixture of ethyl 4-nitrobenzoate and *N,N*-dimethyl-4-nitrobenzamide, was analyzed on an AEI Model MS 902 mass spectrometer equipped with a Vacuumetrics ratiometer. Peaks due to both the ester and amide appeared in the mass spectrum. We measured, as described previously (26), the intensity ratio of the peaks at 179:177, these peaks being due to the amide. The amount of ^{18}O in the amide was then calculated, using the formula described previously (26), to be 8.1 ± 0.6%.

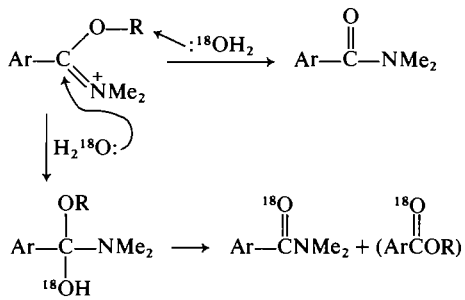
Kinetics

First-order rate constants for the hydrolysis of *O,N,N*,4-tetramethylbenzimidatonium borofluorate were measured at 25°C and ionic strength 0.1 by following spectroscopically the increase in absorbance at 240 nm which accompanies hydrolysis. Rate constants were calculated from the slopes of plots of ln $(A_\infty - A)$ versus time. Rate constants for the hydrolysis of **1** and **2** were measured in a similar way.

Results and Discussion

Importance of S_N2 Hydrolysis

Table 1 lists the relative amounts of amide product and ester product obtained in the hydrolysis of the imidatonium ions in various sulfuric acid solutions. The precautions and checks which ensure that the experimental method is providing the actual product ratio of the hydrolysis are described in the Experimental section. Another point which must be addressed before these ratios can be discussed in terms of tetrahedral intermediate partitioning is whether the amide does in fact come from the intermediate. An alternative route to this product is the S_N2 displacement outlined in reaction [1] (27, 28).

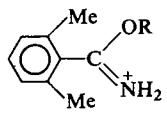


[1]

The S_N2 reaction has been observed in competition with tetrahedral intermediate formation (6, 27) with benzimidatonium ions, but only at higher sulfuric acid concentrations (60–65% H_2SO_4) and higher temperatures (85°C). Previous results would suggest that its importance is relatively small in more dilute acids at 25°C (6), except for benzimidatonium ions with *ortho* substituents (28).

We have carried out the appropriate labelling experiment for the hydrolysis of the 4-nitrobenzimidatonium ion in 48% H_2SO_4 at 25°C. These conditions do produce a substantial amount of amide (Table 1). Within experimental uncertainty this amide is found to contain an oxygen atom from the solvent, a result which unambiguously demonstrates (reaction [1]) that this product is derived from the tetrahedral intermediate, and not an S_N2 reaction.

For the hydrolysis of **2** in more dilute acids, and for the hydrolysis of **1** at all the acidities of Table 1, the yield of amide is small, and the labelling experiment could not satisfactorily be carried out. The following analysis does, however, provide some idea of the significance of the S_N2 reaction. The hindered benzimidatonium ions **3** hydrolyze via the S_N2 reaction to an extent greater than 99% in dilute acids (28). Extrapolation from higher temperatures provides a rate constant for the hydrolysis of **3***b* in 1.9% H_2SO_4 at 25°C of 4×10^{-8} s^{-1}. The *N,N,O*-trimethylbenzimidatonium ion hydrolyzes via the S_N2 reaction almost exclusively in 63% H_2SO_4 at 85.2°C (6, 27) with a rate constant of 2×10^{-6} s^{-1}. Under the same conditions, the rate constant for the hydrolysis of **3***a*, obtained by a short extrapolation,



3*a*, R = Me
b, R = Et

is 4×10^{-6} s^{-1} (28). If it is assumed that there is the same difference in rate between **3***b* and the *O*-ethyl-*N,N*-dimethylbenzimidatonium ion **1**, and more-

TABLE 1. Molar ratio of ester-to-amide in the products of hydrolysis at 25°C of the *O*-ethyl-*N,N*-dimethylbenzimidatonium ion (**1**) and the *O*-ethyl-*N,N*-dimethyl-4-nitrobenzimidatonium ion (**2**)

%H_2SO_4	Amide/ester[a] **1**	%H_2SO_4	Amide/ester[a] **2**
0.1	0.0006	0.1	0.0009 (0.00 nmr)
2.0	0.0004	8.0	0.0006
8.0	0.0006	13.0	0.0008
13.0	0.0007	25.5	0.0009
18.1	0.0019	29.5	0.0015
22.1	0.0040	35.7	0.018
25.5	0.0046	37.9	0.042
26.6	0.0045	39.6	0.068
29.5	0.0056	43.4	0.087 (0.07 nmr)
30.7	0.0056	45.4	0.108
33.5	0.0058	47.6	0.105
35.7	0.0065	48.2	0.109 (0.10 nmr)
		49.2	0.114

[a]We estimate the error to be about ±10%, increasing when the ratio is very small to ±50%.

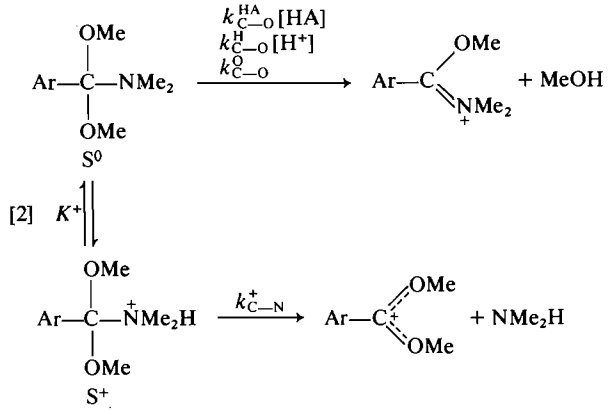
Can. J. Chem. Downloaded from www.nrcresearchpress.com by 210.87.254.6 on 09/05/12
For personal use only.

over that this difference is independent of temperature and acidity, the rate constant for S_N2 hydrolysis of **1** in 1.9% H_2SO_4 at 25°C is 2×10^{-8} s^{-1}. We have measured spectroscopically the rate constant for the hydrolysis of **1** in this acid at 25°C and obtain a value of 5×10^{-5} s^{-1}. Comparison of the two numbers suggests that a fraction 0.0004 of the hydrolysis is the S_N2 reaction. Although there is obviously uncertainty in the S_N2 rate because of the extrapolations and assumptions, this figure is remarkably similar to the fraction of amide actually produced (Table 1). For dilute acid solutions it seems reasonable to conclude therefore that a significant amount of amide is due to the S_N2 reaction, and is not derived from a tetrahedral intermediate. This is also probably true for **2**, although we can be less certain because the effect of substituents on the S_N2 reaction has not been fully evaluated.

Both ions show a relatively sharp increase in the yield of amide at some intermediate acidity (Table 1). The labelling experiment demonstrates for **2** that this change is associated with a change in partitioning of the tetrahedral intermediate. We feel that this is true for **1** also, although the actual increase in amide yield is not as great. Extrapolation, as described previously, shows that if the fraction of S_N2 hydrolysis is 0.0004 in dilute acid it should rise gradually, but only reach a value of 0.002 by 30–35% H_2SO_4, where the observed amide:ester ratio has risen to 0.006. This would imply that about two-thirds of the amide product in these acids comes from the tetrahedral intermediate. Considering the uncertainty in the extrapolations, a figure somewhere between 40 and 90% seems a more conservative estimate. It is difficult, however, to rationalize the sharp change in amide yield totally in terms of the S_N2 reaction.

Mechanisms

The general scheme which we proposed (1) for the primary decomposition pathways of an amide acetal is shown in reaction [2].



In neutral and basic solutions, decomposition occurs in a non-catalyzed reaction involving the neutral amide acetal S^0 and resulting in imidatonium ion and alcohol (C—O cleavage). In acid solutions decomposition involves two kinetically equivalent pathways, H^+-catalyzed C—O cleavage of S^0, and a non-catalyzed breakdown of the *N*-protonated amide acetal S^+. The latter reaction involves a C—N cleavage, and produces a dialkoxycarbonium ion and amine. The ratio of the two competing reactions is given by eq. [3].

$$[3] \quad \left(\frac{C—O}{C—N}\right)_{H^+} = \frac{k^{H}_{C-O}K^{+}}{k^{+}_{C-N}}$$

Table 2 lists the value of this ratio for the unsubstituted benzamide acetal and its 4-nitro derivative. It can be seen that both modes of cleavage are observed, particularly with the unsubstituted compound. There is a substantial substituent effect, the origin of which was discussed previously (1).

Table 3 lists values of the various constants of eq. [2]. These values refer to water and were estimated in the following way from actual kinetic results (1). For the 4-nitro derivative, the constants k^{O}_{C-O}, k^{H}_{C-O}, and pK^+ were determined previously in 30% dimethoxyethane (DME):water and 70% DME:water and these have simply been extrapolated to 0% DME. Values of the same three constants were obtained for

TABLE 2. Ratio of C—O cleavage to C—N cleavage for the breakdown in acid solutions of amide acetals and tetrahedral intermediates

	C—O/C—N	
Ar	$Ar—C(OMe)(OMe)—NMe_2$[a]	$Ar—C(OEt)(OH)—NMe_2$[b]
C_6H_5	0.9	~0.004
4-$NO_2C_6H_4$	16	0.1

[a]Ratio in 0.1 *M* HCl, from ref. 1.
[b]Ratio of amide:ester product in 30–35% H_2SO_4 for Ar = C_6H_5, and 45–50% H_2SO_4 for Ar = 4-$NO_2C_6H_4$. The number for Ar = C_6H_5 has been corrected for the S_N2 hydrolysis.

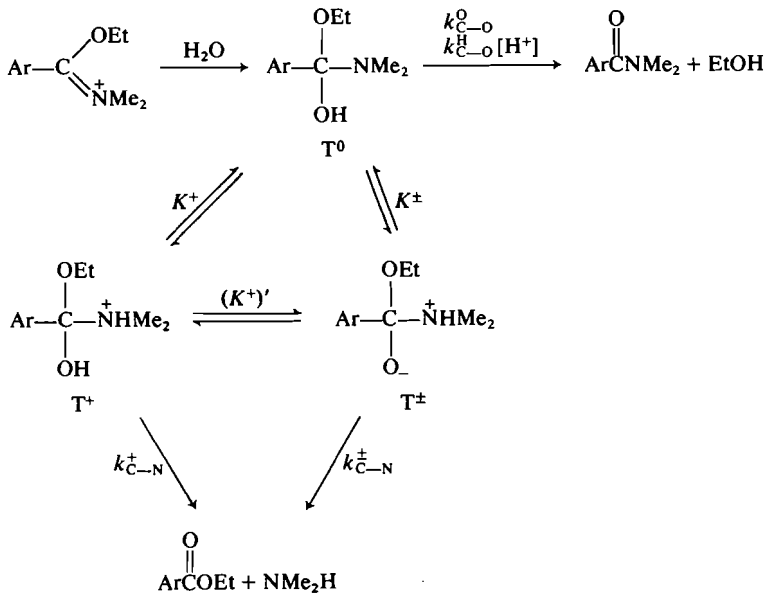
TABLE 3. Rate and equilibrium constants for the decomposition of $ArC(OMe)_2NMe_2$ in water at 25°C

	Value	
Constant	Ar = C_6H_5	Ar = 4-$NO_2C_6H_4$
pK^+	6	5
k^{O}_{C-O}, s^{-1}	10	1
k^{H}_{C-O}, M^{-1} s^{-1}	10^6	10^5
k^{+}_{C-N}, s^{-1}	1	10^{-2}

the unsubstituted compound, but only in 70% DME:water. The values in water have been estimated using the extrapolated values of the 4-nitro derivative and assuming that the substituent effect is the same as it is in 70% DME:water. Values of $k^{\pm}_{C-N}$ were not measured previously since C—N cleavage is not observed under the conditions used for the kinetic studies. However, from the values of k^{H}_{C-O} and pK^{+} estimated in water and the product ratios (Table 2) which were measured in water, $k^{\pm}_{C-N}$ can be calculated using eq. [3].

The tetrahedral intermediates of the hydrolysis of the imidatonium ions of the present study obviously break down in acid with a considerably smaller relative amount of C—O cleavage, a fact which has been recognized previously (6, 19). Equation [4] provides a general mechanism which will be used to account for the various observations.

[4]



This scheme is based on the generally accepted mechanism for imidate hydrolysis and ester aminolysis (12), omitting the anionic form of the tetrahedral intermediate which is not likely to be important in the acids involved here. This mechanism incorporates the basic features of the amide acetal system of reaction [2], with the addition of the zwitterion $T^{\pm}$, a structure obviously unattainable by an amide acetal.

The general analogy between the amide acetal and imidatonium ion systems is illustrated by the following. The acid C—O cleavage reaction of an amide acetal is a general acid-catalyzed reaction (and we have taken this to indicate that C—O bond breaking and proton transfer are concerted (29–34)). For the amide acetal $4\text{-}CH_3C_6H_4C(OMe)_2NMe_2$, a Bronsted α value of 0.61 was obtained (1). The microscopic reverse of this reaction is the general base catalyzed addition of methanol to the *O,N,N*,4-tetramethylimidatonium ion, and this must have a β value of 1 − α or 0.39 (29). We have measured rate constants for the hydrolysis of this ion. The reaction is general base catalyzed, as expected (19), and the Bronsted value is 0.39 (Table 4). (The exact agreement is probably somewhat fortuitous since slightly different α or β values are likely to be found for methanol and water (30).)

Partitioning of Tetrahedral Intermediate

Qualitatively, we interpret the behavior of the tetrahedral intermediates in the following way. In dilute acids the ester and amine products which predominate arise from breakdown of the zwitterion $T^{\pm}$. The very small amount of amide and alcohol products formed can be attributed to the S_N2 reaction and to the non-catalyzed breakdown of the neutral intermediate T^0 (or to a reaction which is

TABLE 4. Rate constants at 25°C and ionic strength 0.1 for the hydrolysis of the *O,N,N*,4-tetramethylbenzimidatonium ion

Catalyst	Rate constant
CH_3COO^-	$24 \times 10^{-5}\ M^{-1}\ s^{-1}$
$HCOO^-$	$9.8 \times 10^{-5}\ M^{-1}\ s^{-1}$
CH_2ClCOO^-	$4.4 \times 10^{-5}\ M^{-1}\ s^{-1}$
H_2O	$4.5 \times 10^{-5}\ s^{-1}$

Can. J. Chem. Downloaded from www.nrcresearchpress.com by 210.87.254.6 on 09/05/12
For personal use only.

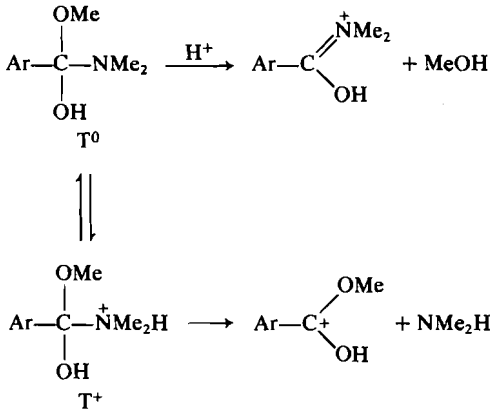
Can. J. Chem. Downloaded from www.nrcresearchpress.com by 210.87.254.6 on 09/05/12
For personal use only.

kinetically equivalent to this). The relative importance of these two pathways cannot be rigorously assessed, although as discussed previously the possibility does exist that the S_N2 reaction accounts for almost all of the amide product. Whatever the case, greater than 99.9% of the tetrahedral intermediates formed in dilute acid give rise to ester and amine products, via the zwitterionic form.

At some intermediate acid concentration there is a sharp increase in the relative yield of amide, followed by a levelling off. This change is associated with a change in the partitioning of the tetrahedral intermediate, and not the S_N2 reaction, and our proposal is that this represents a change-over from breakdown via neutral transition states to breakdown via cationic transition states. The ester and amine products arise from the cationic tetrahedral intermediate T^+, while amide and alcohol products come from the kinetically equivalent H^+-catalyzed breakdown of T^0.

The same two reactions are observed in acid solutions with amide acetals. Both systems show a similar dependency in their partitioning on the aromatic substituent (Table 2), the 4-nitro group significantly favoring expulsion of alcohol or C—O cleavage. This common behavior is in fact one of the pieces of evidence supporting our proposal that the strong acid reactions of the tetrahedral intermediates resemble those of the amide acetals.

There is also a difference in the two systems, in that for a given substituent considerably less alcohol expulsion is seen with the tetrahedral intermediate (Table 2). To explain this we note the presence of the OH group in the cations which are being formed from the tetrahedral intermediates (reaction [5]).



By serving as a hydrogen bond donor to a solvent water molecule, this group assists in the solvation of the positive charge (36). This results in a stabilization relative to an analogous cation where such hydrogen bonding is not possible. The amount of the stabilization which can be gained by such hydrogen bonding is dependent on the inherent stability of the cation in the first place, with less stable cations deriving a greater amount of stabilization (36). This means that there will be a greater relative increase in stabilization in changing from the dialkoxycarbonium ion to a protonated ester than in changing from the imidatonium ion to the protonated amide. Since the transition states leading to these cations will see the same effect, a *relative* favoring of C—N cleavage over C—O cleavage can be expected for the tetrahedral intermediate.

This effect of hydrogen bonding is seen very clearly in comparing the rates of water addition to the various cations. (For the protonated ions this involves the applying of a factor correcting for the amount of protonation to the rate of an acid-catalyzed hydrolysis (37).) The *O,N,N*-dimethylbenzimidatonium ion is only four times more reaction than protonated *N,N*-dimethylbenzamide (6). The phenyldimethoxycarbocation (38), on the other hand, hydrates 10^3–10^5 more readily than proton ated ethyl benzoate (24), the uncertainty in this number arising from the considerable extrapolation from concentrated acid solutions required to make the protonation correction.

A detailed quantitative treatment taking into account the interconversions and breakdowns of all three forms of the tetrahedral intermediate is difficult. One problem concerns the question as to whether the three forms of the intermediate can be regarded as being in equilibrium before breakdown, or whether it is necessary to account for proton transfer steps (11, 12, 29). We feel that the former is probably close to being the case in our system, particularly for the interconversion of T^0 and T^+. Equilibrium will exist if each of the three forms is converted to at least one of the other forms faster than it decomposes. This is undoubtedly true for T^0 since its rate of nitrogen protonation in these strong acids will be extremely rapid. It is probably also true for T^+. This will be deprotonated by solvent to form T^0 with a rate constant of the order of 10^4– 10^6 s^{-1}, an estimate based on the assumptions that the pK^+ value is 5–6, and that the reverse reaction, the protonation of T^0 by H^+, is diffusion limited with a rate constant of 10^{10}–10^{11} M^{-1} s^{-1}. The breakdown of T^+ to amide and protonated ester should be slower, even if as discussed previously it occurs at a rate several orders of magnitude greater than that of an amide acetal (see values of k_{C-N}^{+} in Table 3). The problem arises with $T^{\pm}$, which is known to undergo breakdown extemely rapidly, sufficiently rapidly that in some systems it is not in equilibrium with the other forms (11, 12, 29). Its protonation by H^+ to

Can. J. Chem. Downloaded from www.nrcresearchpress.com by 210.87.254.6 on 09/05/12
For personal use only.

form T^+ is however diffusion limited, and at the very high H^+ concentrations of this study, this reaction is also extremely rapid.

A second problem lies in the fact that our data refer to non-dilute acids, and this means that activity coefficients must be included. This is clearly difficult to do, particularly when it is considered that the activity coefficients of the proton, T^0, T^+, $T^\pm$, and the three transition states of reaction [4] are involved. To simplify matters we will assume that the $T^+ \rightleftarrows T^0$ equilibrium follows the H_0 acidity function, as does the rate of the H^+-catalyzed decomposition of T^0 ($k^H_{C-O}[H^+] = k^H_{C-O}h_0$). All other activity coefficients are ignored or assumed to cancel. We will also assume equilibrium exists between all three forms before breakdown. This treatment, of course, represents a considerable oversimplification, and we make no claim to rigor in the analysis. A semi-quantitative description is provided, however, of the important features.

These various assumptions produce eq. [6] for the partitioning of the tetrahedral intermediate in acid solutions.

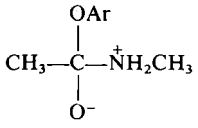
$$[6] \quad \frac{\text{Amide}}{\text{Ester}} = \left(\frac{C{-}O}{C{-}N}\right) = \frac{k^O_{C-O} + k^H_{C-O}h_0}{\frac{k^\pm_{C-N}}{K^\pm} + \frac{k^+_{C-N}}{K^+}h_0}$$

In dilute acid (low h_0) the C—O/C—N ratio is independent of acidity, with a value given by eq. [7].

$$[7] \quad \left(\frac{C{-}O}{C{-}N}\right)_{\text{low } h_0} = \frac{k^O_{C-O}K^\pm}{k^\pm_{C-N}}$$

This ratio is of course very small experimentally. A second acidity independent region is predicted for concentrated acids (high h_0) where, as has been discussed, the breakdown involves the amide acetal type of mechanisms. The (C—O/C—N) ratio is given by eq. [3], and has been discussed already.

Another parameter which can be obtained is the ratio $k^H_{C-O}K^\pm/k^\pm_{C-N}$, a quantity which is related to the acidity region where the change-over occurs from one behavior to the other. For the 4-nitro compound, the value of this ratio is $10^{-3}\ M^{-1}$. As discussed previously, the value of k^H_{C-O} should be similar to that for the analogous amide acetal, that is, $10^5\ M^{-1}\ s^{-1}$. A value of $K^\pm$ of 10^3 can also be estimated, using correlations suggested by Guthrie (2). (For Ar = Ph of reaction [4], these correlations produce $pK^+ = 4.8$ and $p(K^+)' = 8.1$.) Taken together the estimate for $k^\pm_{C-N}$ is $10^{11}\ s^{-1}$. This value is extremely large,[1] but it is not at all unreasonable when compared to rate constants measured or estimated for the decomposition of other zwitterions (12*b*, 20, 33, 39–43). For example, the rate of decomposition of **6** was calculated to be $3 \times 10^9\ s^{-1}$ (12*b*), a number of the same order of magnitude as the estimate for $T^\pm$. Moreover the rate for the latter should be somewhat larger, since its OEt should provide a greater push for amine expulsion than an OAr group.



6

This very large rate of zwitterion breakdown explains why this mode of decomposition can remain important into relatively concentrated acids where the amount of tetrahedral intermediate in zwitterionic form is extremely low. For example, in 20% H_2SO_4 approximately half of the ester product observed in the hydrolysis of the unsubstituted benzamidation ion is derived from the zwitterion with the remainder being derived from the *N*-protonated tetrahedral intermediate. However, in this acid the relative concentration at equilibrium of the zwitterion is only $1/10^{10}$ that of the *N*-protonated intermediate. Their equal contributions to product formation can be explained by the 10^{10} greater rate of decomposition of the zwitterion.

Acknowledgement

Continued financial support from the Natural Sciences and Engineering Research Council is gratefully acknowledged.

1. R. A. McClelland. J. Am. Chem. Soc. **100**, 1844 (1978).
2. J. P. Guthrie. J. Am. Chem. Soc. **96**, 3608 (1974).
3. M. L. Bender. Chem. Rev. **60**, 53 (1960).
4. C. A. Bunton, S. J. Farber, A. J. G. Milbank, C. J. O'Connor, and T. A. Turney. J. Chem. Soc. Perkin Trans. **2**, 1869 (1972).
5. C. R. Smith and K. Yates. J. Am. Chem. Soc. **93**, 6578 (1971).
6. C. R. Smith and K. Yates. J. Am. Chem. Soc. **94**, 8811 (1972).
7. R. A. McClelland. J. Am. Chem. Soc. **97**, 5281 (1975).
8. W. P. Jencks. Catalysis in chemistry and enzymology. McGraw-Hill, New York, NY. 1969. pp. 526–529.
9. W. P. Jencks and M. Gilchrist. J. Am. Chem. Soc. **90**, 2622 (1968).
10. G. M. Blackburn and W. P. Jencks. J. Am. Chem. Soc. **90**, 2638 (1968).
11. J. P. Fox and W. P. Jencks. J. Am. Chem. Soc. **96**, 1436 (1974).

[1]It is sufficiently large that the assumption that $T^\pm$ is in equilibrium with T^+ may be open to question. As suggested by a referee it is possible that the rate of breakdown of $T^\pm$ may be faster, and what is being observed is a change-over from rate-determining deprotonation to rate-determining cleavage. Although this possibly cannot be definitely ruled out, the analogy to the amide acetal chemistry in concentrated acids does suggest that there should be some breakdown by cationic transition states, as we have suggested in our general scheme.

12. A. C. SATTERTHWAIT and W. P. JENCKS. J. Am. Chem. Soc. (*a*) **96**, 7018 (1974); (*b*) **96**, 7031 (1974).
13. M. J. GRESSOR and W. P. JENCKS. J. Am. Chem. Soc. **99**, 6963 (1977); **99**, 6970 (1977).
14. G. L. SCHMIR and B. A. CUNNINGHAM. J. Am. Chem. Soc. **87**, 5692 (1965).
15. B. A. CUNNINGHAM and G. L. SCHMIR. J. Am. Chem. Soc. **88**, 551 (1966); **89**, 917 (1967).
16. R. K. CHATURVEDI and G. L. SCHMIR. J. Am. Chem. Soc. **90**, 4413 (1968).
17. T. C. PLETCHER, S. KOEHLER, and E. H. CORDES. J. Am. Chem. Soc. **90**, 7072 (1968).
18. T. OKUYAMA, T. C. PLETCHER, D. J. SAHN, and G. L. SCHMIR. J. Am. Chem. Soc. **95**, 1253 (1973).
19. V. F. SMITH and G. L. SCHMIR. J. Am. Chem. Soc. **97**, 3171 (1975).
20. Y. N. LEE and G. L. SCHMIR. J. Am. Chem. Soc. **100**, 6700 (1978); **101**, 3026 (1979).
21. K. YATES and R. A. MCCLELLAND. Can. J. Chem. **52**, 1098 (1974).
22. H. MEERWEIN. Org. Synth. **46**, 113 (1966).
23. H. MEERWEIN. Org. Synth. **46**, 120 (1966).
24. C. A. LANE, M. F. CHEUNG, and G. F. DORSEY. J. Am. Chem. Soc. **90**, 6492 (1968).
25. A. J. KIRBY. Comprehensive chemical kinetics. Vol. 10. *Edited by* C. H. Bamford and C. F. H. Tipper. Elsevier, New York, NY. 1972. pp. 57–207.
26. R. A. MCCLELLAND and M. AHMAD. J. Am. Chem. Soc. **99**, 5356 (1977).
27. R. A. MCCLELLAND. J. Am. Chem. Soc. **96**, 3690 (1974).
28. R. A. MCCLELLAND. J. Am. Chem. Soc. **97**, 3177 (1975).
29. W. P. JENCKS. Chem. Rev. **72**, 705 (1972).
30. N. GRAVITZ and W. P. JENCKS. J. Am. Chem. Soc. **96**, 507 (1974).
31. B. CAPON and K. NIMMO. J. Chem. Soc., Perkin Trans. 2, 1113 (1975).
32. J. M. SAYER and W. P. JENCKS. J. Am. Chem. Soc. **99**, 464 (1977).
33. W. P. JENCKS. Acc. Chem. Res. **9**, 425 (1976).
34. R. G. BERGSTROM, M. J. CASHEN, Y. CHIANG, and A. J. KRESGE. J. Org. Chem. **44**, 1639 (1979).
35. N. GRAVTIZ and W. P. JENCKS. J. Am. Chem. Soc. **96**, 489 (1974).
36. K. YATES and R. A. MCCLELLAND. Prog. Phys. Org. Chem. **11**, 323 (1974).
37. K. YATES. Acc. Chem. Res. **4**, 136 (1971).
38. R. A. MCCLELLAND and M. AHMAD. J. Am. Chem. Soc. **100**, 7031 (1978).
39. R. E. BARNETT and W. P. JENCKS. J. Am. Chem. Soc. **90**, 4199 (1968); **91**, 2358 (1969).
40. J. HINE and F. C. KOKESH. J. Am. Chem. Soc. **92**, 4383 (1970).
41. J. HINE, J. C. CRAIG, J. G. UNDERWOOD, and F. A. VIA. J. Am. Chem. Soc. **92**, 5194 (1970).
42. S. ROSENBERG, S. M. SILVER, J. M. SAYER, and W. P. JENCKS. J. Am. Chem. Soc. **96**, 7986 (1974).
43. R. KLUGER, J. CHIN, and W. W. CHOY. J. Am. Chem. Soc. **101**, 6976 (1979).

Can. J. Chem. Downloaded from www.nrcresearchpress.com by 210.87.254.6 on 09/05/12
For personal use only.

Aromatization and microbial hydroxylation of 3-^{18}O-testosterone

HERBERT L. HOLLAND AND GREGG J. TAYLOR
Department of Chemistry, Brock University, St. Catharines, Ont., Canada L2S 3A1

Received May 28, 1980

HERBERT L. HOLLAND and GREGG J. TAYLOR. Can. J. Chem. **58**, 2326 (1980).

3-^{18}O-Testosterone (**1**) is transformed to estradiol (**4**) by human placental microsomes, and to the 6β- and 11α-hydroxy derivatives **2** and **3** by *Rhizopus arrhizus*, without significant loss of label. Neither process is therefore one which involves reversible Schiff base formation at C-3 at any stage.

HERBERT L. HOLLAND et GREGG J. TAYLOR. Can. J. Chem. **58**, 2326 (1980).

La testostérone (**1**) marquée avec du ^{18}O en position 3 est transformée en estradiol (**4**) par les microsomes du placenta humain et en dérivés hydroxy-6β et 11α (**2** et **3**) sous l'action du *Rhizopus arrhizus*; ces réactions se produisant sans perte significative du marqueur. Aucune des étapes de chacune de ces méthodes ne fait donc intervenir la formation réversible d'une base de Schiff au niveau du carbone en position 3.

[Traduit par le journal]

Introduction

The intermediacy of Schiff bases during enzymatic transformations of substrates which contain a carbonyl group is well established for many systems; examples include the vitamin B_6 dependent reactions and tetrahydrofolate dependent transfer of a C_1 unit at the formaldehyde oxidation level (1).

Schiff base formation has been proposed to occur during enzymatic transformations of steroids. It has been suggested that the 3-ketosteroid Δ^4,Δ^5-isomerase from *Pseudomonas testosteroni* operates on a substrate bound to the enzyme as a Schiff base involving the C-3 carbonyl of the steroid and a primary amino group of the protein (2) (Fig. 1). This mechanism is supported by kinetic (2, 3) and spectroscopic (2) evidence in model studies. Conversely, Wilton (4) has shown that saturation of the Δ^4 double bond of 3-^{18}O-testosterone **1** by mammalian C-5α- or C-5β- reductases (to give **5** and **6**) involves retention of label, thus precluding the formation of a Schiff base intermediate in this case. A necessary corollary of reversible Schiff base formation is the exchange of the carbonyl oxygen of the substrate with water, leading to loss of label in the case of ^{18}O carbonyl labelled substrates; this point has not, however, been experimentally proven for the Δ^4,Δ^5-isomerase system.

In the present study we have used **1** as a substrate for both the human placental aromatase enzyme system (leading to estradiol, **4**), and the microbial C-6β and C-11α hydroxylation reaction of *Rhizopus arrhizus* (leading to **2** and **3** respectively). Both enzyme systems require Δ^4-3-keto functionality in the substrate, and both could potentially involve an intermediate Schiff base complex analogous to **7** (Fig. 1), in the former case with

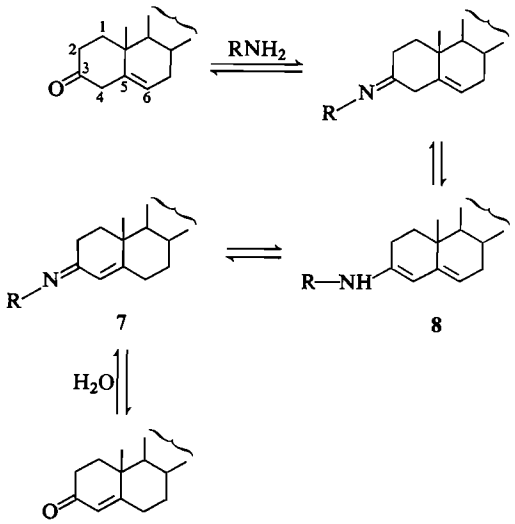


FIG. 1. Proposed mechanism of 3-ketosteroid Δ^4,Δ^5-isomerization (2).

binding of substrate to the enzyme during oxidative removal of C-19, followed by hydrolysis prior to oxidation of Ring A and liberation of the phenol **4**.

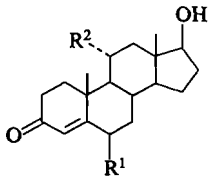
Results and Discussion

3-^{18}O-Testosterone (**1**), prepared in quantitative yield by acid catalysed exchange with ^{18}O-water in 2-propanol (4), was transformed to estradiol (**4**) in yields approaching 10% by a microsomal suspension obtained from human placentae. The results of these incubations are presented in Table 1. It is apparent from the retention of label in estradiol that any mechanism for the aromatase enzyme system which involves a Schiff base complex (analogous to structure **7** of Fig. 1) can be discounted.

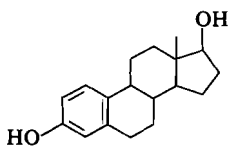
The slight loss of label in both recovered starting material and **4** is attributable to nonenzymic ex-

0008-4042/80/222326-03$01.00/0
©1980 National Research Council of Canada/Conseil national de recherches du Canada

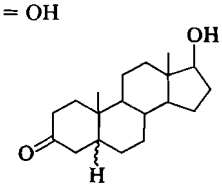
Can. J. Chem. Downloaded from www.nrcresearchpress.com by 210.87.254.42 on 09/05/12
For personal use only.



1 $R^1 = R^2 = H$, testosterone
2 $R^1 = OH, R^2 = H$
3 $R^1 = H, R^2 = OH$



4 Estradiol



5 C-5α H
6 C-5β H

change of label with water during the incubation. Control experiments confirm that work-up conditions do not lead to loss of label from **4** or recovered substrate, provided that the latter is isolated directly from the initial ethyl acetate extract before basification (see Experimental). In addition, incubation of **1** under normal conditions but with a deactivated microsome preparation resulted in comparable loss of label.

The demonstration that the conversion of **1** to **4** does not involve a Schiff base complex is of interest in view of the demonstrated capacity of human placental mitochondria to isomerize Δ^5-3-ketosteroids (5), a process which may involve such a mechanism (*vide supra*).

In a separate series of experiments we have studied the hydroxylation of **1** at C-6β and C-11α by the fungus *Rhizopus arrhizus* ATCC 11145 (Table 1). Previous work by the Oxford group (6) has established that the site of hydroxylation of an oxygenated steroid by a given fungus is often controlled by the position of oxygenation (usually carbonyl or alcohol) in the substrate, an effect which appears to be due to binding of the substrate to the active site of the enzyme through the polar oxygenated positions of the former. Alternatively, hydroxylation may be substrate specific, as in the C-6β hydroxylation by *Rhizopus arrhizus* which requires a Δ^4-3-ketosteroid and proceeds through a $\Delta^{3,5}$ intermediate (7). In either case, the substrate may bind to the enzyme as a Schiff base, which, in the case of hydroxylation at C-6β, could undergo subsequent ketimine–enamine tautomerism followed by oxidation and hydrolysis (**1** → **7** → **8** → **2**). The latter hypothesis is particularly attractive in view of the apparent similarities of the C-6β hydroxylation and Δ^4,Δ^5-isomerization processes, and the relative ease of the ketimine–enamine tautomerism compared with the analogous keto–enol interconversion (8–10). Our results (Table 1) clearly show, however, that hydroxylations at both the C-6β and C-11α positions of **1** proceed with retention of the oxygen label at C-3, so that once again Schiff base intermediates cannot occur. The slight loss of label with respect to substrate is again attributed to aqueous exchange during the lengthy incubation period (15 h). Under conditions which afforded acceptable yields of **2** and **3**, starting material could not be recovered.

We therefore conclude that interaction of the C-3 carbonyl oxygen of **1** with the enzyme during 11α hydroxylation does not involve reversible Schiff base formation, and that the C-6β hydroxylation, as previously reported (7), involves keto–enol rather than ketimine–enamine tautomerism.

TABLE 1. ^{18}O content of testosterone (**1**) and metabolites

Incubation	Steroid	% ^{18}O
R. arrhizus	**1** (Substrate)	74
	2	58
	3	59
Placental microsomes	**1** (Substrate)	63
	1 (Recovered)	58
	4	48,53, 54[a]

[a]Values from three independent incubations.

Experimental

Apparatus, Materials, and Methods

Melting points were determined on a Kofler heating stage and are uncorrected. Infrared spectra were recorded with a Perkin-Elmer 237B, ^{1}Hmr spectra with a Bruker WP-60 using $CDCl_3$ as solvent and TMS as internal standard, and mass spectra were obtained with an AEI MS 30. ^{18}O content was estimated by repeated scanning of the relevant ions and application of the appropriate corrections for natural isotopic abundances; values are accurate to ±1%. Thin-layer and preparative-layer chromatography were performed on Merck silica gel plates.

Rhizopus arrhizus ATCC 11145 was maintained on 4.5% malt agar slopes.

3-^{18}O-Testosterone (1)

This was prepared by a modification of the method of Wilton (4). Acid washed testosterone (200 mg) was added to a solution of 1 mL of HCl (4 m*M* in 2-propanol) and ^{18}O-water (95 at.% ^{18}O) (1 mL) in dry 2-propanol (20 mL) contained in an acid washed reaction vessel. The vessel was then flushed with nitrogen and maintained at 60–62°C for 24 h. The solvent and reagents were then removed and recovered on a vacuum line. The reaction was repeated using an additional 200 mg of starting material, employing the recovered reagents plus additional HCl. A quantitative yield of product was obtained in both runs. Mass spectral analysis indicated the following isotopic compositions: batch 1, 78% ^{18}O; batch 2, 63% ^{18}O. The material, although stored in a desiccator, showed a slight loss of isotopic enrichment over a period of 5–8 months (cf. values in Table 1).

Can. J. Chem. Downloaded from www.nrcresearchpress.com by 210.87.254.42 on 09/05/12
For personal use only.

Can. J. Chem. Downloaded from www.nrcresearchpress.com by 210.87.254.42 on 09/05/12
For personal use only.

Incubation of 3-^{18}O-Testosterone with Rhizopus arrhizus

The fungus was grown in a medium consisting of a solution of glucose (50 g), peptone (20 g), and corn steep liquor (5 mL) in tap water (1 L). A one-litre Erlenmeyer flask, containing 150 mL of the above medium, was sterilized by autoclaving at 15 psi for 20 min and allowed to cool. A sample of actively growing *Rhizopus arrhizus* was transferred from an agar slope to the above flask, which was then incubated on a rotary shaker (180 rpm) at 28°C for 72 h. The mycelium was then separated by filtration, washed by short maceration with distilled water, and resuspended in 0.1 *M* phosphate buffer (pH 7.0, 150 mL) in a one-litre Erlenmeyer flask. A solution of 3-^{18}O-testosterone (100 mg) in ethanol (2 mL) was then added to the flask, and incubation continued under the above conditions for a further 15 h. The mycelium and buffer were then separated by filtration and each extracted separately with dichloromethane. The mycelial extract yielded no detectable steroids (tlc). The buffer extract was evaporated to dryness to give a residue (110 mg) which after preparative layer chromatography (3% methanolic chloroform, two elutions) afforded 6β-hydroxy-3-^{18}O-testosterone (**2**) (27 mg from ethyl acetate/hexane) and 11α-hydroxy-3-^{18}O-testosterone (**3**) (44 mg from ethyl acetate/hexane), both identified by tlc and spectral (^{1}Hmr) comparisons with authentic unlabelled material. ^{18}O content is presented in Table 1.

Incubation of 3-^{18}O-Testosterone with Placental Microsomes

Human placentae (full term) were obtained immediately upon delivery at the St. Catharines General Hospital, and were transported on ice. The placentae were then washed in ice-water (or saturated KCl solution) and minced. The minced tissue was added to 200–300 mL of tris buffer of the following composition (g/L): sucrose (85.6), dithiothreitol (0.015), nicotinamide (0.005), tris HCl (0.24), tris base (0.06). The resulting suspension was homogenized in a Waring blender with frequent ice-cooling. The homogenate was then centrifuged at 10 000 g and 0°C for 30 min. The pellet was discarded and the resultant supernatant was centrifuged at 100 000 g and 0°C for 1 hour. The supernatant was then discarded and the resultant pellets were resuspended in the above buffer (50–100 mg/mL) using a Teflon homogenizer. The microsome suspensions prepared in this way retained their activity for several months when stored frozen at −20°C.

For the transformation of testosterone to estradiol, 5 units of glucose-6-phosphate dehydrogenase (Sigma type XV from Baker's Yeast, 10 units/mL in 5 m*M* sodium citrate) were added to a solution of glucose-6-phosphate (70 mg) and NADP (40 mg) in 0.1 *M* sodium phosphate buffer (pH 7.2, 15 mL). This mixture was incubated at 37°C for 30 min in order to generate NADPH. At this point, 5 mL of thawed placental microsome suspension was added, followed by the steroid substrate (2 mg in 400 μL 95% ethanol). Incubation at 37°C in a rotary incubator–shaker was carried out for 45–50 min. The incubation mixture was then extracted with ethyl acetate, and the extract dried over sodium sulphate and evaporated. Recovered starting material could be isolated directly from this fraction by plc. For the isolation of estradiol, the residue was dissolved in toluene and the resulting solution extracted with 0.1 *M* NaOH. The basic extract was then neutralized (0.1 *M* HCl) to pH 7 and extracted with ether. The ethereal extract was dried and evaporated. Estradiol was obtained from the residue by plc. The isotopic content is listed in Table 1.

Acknowledgements

We thank the Natural Sciences and Engineering Research Council of Canada for a Research Studentship (to G.J.T.) and for general financial support. Thanks are also due to Drs. J. N. Wood and J. Lo of the St. Catharines General Hospital for their invaluable cooperation in obtaining placentae for use in this study, and to Dr. P. Morand of the University of Ottawa for helpful discussion.

1. C. WALSH. Enzymatic reaction mechanisms. W. H. Freeman, San Francisco. 1979. pp. 777, 828.
2. W. F. BENISEK and A. JACOBSON. Bioorg. Chem. **4**, 41 (1975).
3. T. OKUYAMA, A. KITADA, and T. FUENO. Bull. Chem. Soc. Jpn. **50**, 2358 (1977).
4. D. C. WILTON. Biochem. J. **155**, 487 (1976).
5. D. P. EDWARDS, J. L. O'CONNOR, E. D. BRANSOME, and W. E. BRASELTON. J. Biol. Chem. **251**, 1632 (1976).
6. E. R. H. JONES, G. D. MEAKINS, J. O. MINERS, R. N. MIRRINGTON, and A. L. WILKINS. J. Chem. Soc. Perkin Trans. I, 1842 (1976), and references therein.
7. H. L. HOLLAND and P. R. P. DIAKOW. Can. J. Chem. **56**, 694 (1978); **57**, 436 (1979); **57**, 1585 (1979).
8. H. E. FERRAN, R. D. ROBERTS, J. N. JACOB, and T. A. SPENCER. J. Chem. Soc. Chem. Commun. 49 (1978).
9. R. D. ROBERTS and T. A. SPENCER. Tetrahedron Lett. 2557 (1978).
10. P. BOLLA and M. LEGRAND. Bull. Soc. Chim. Fr. 2143 (1973).

Electrophilic additions to strained alkenes. II. The reaction of benzeneselenenyl chloride with tricyclo[4.2.2.0^{2,5}]deca-3,7-diene derivatives[1,2]

DENNIS G. GARRATT[3]

Department of Chemistry, University of Ottawa, Ottawa, Ont., Canada K1N 9B4 and the Division of Chemistry, National Research Council of Canada, Ottawa, Ont., Canada K1A 0R6

AND

M. DOMINIC RYAN[4] AND ANN KABO

Department of Chemistry, University of Ottawa, Ottawa, Ont., Canada K1N 9B4

Received April 3, 1980

DENNIS G. GARRATT, M. DOMINIC RYAN, and ANN KABO. Can. J. Chem. **58**, 2329 (1980).

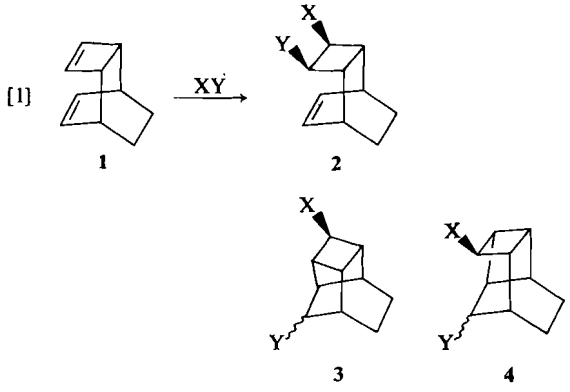
The reactions of benzeneselenenyl chloride with three derivatives of tricyclo[4.2.2.0^{2,5}]deca-3,7-diene have been investigated in four solvent systems: methylene chloride, acetic acid, acetic acid/$LiClO_4$, and methanol. Under conditions of kinetic control only products of *exo–anti* attack upon the cyclobutene moiety are isolable when the solvent system is methylene chloride or acetic acid. This observation also holds in acetic acid/$LiClO_4$ except in the case of dimethyl tricyclo[4.2.2.0^{2,5}]deca-3,7,9-triene-7,8-dicarboxylate where the major product is that of cross-bonding with solvent incorporation. In methanol products of solvent incorporation, transannular cross-bonding and lactonization (where possible) are observed. A general mechanistic scheme is proposed to account for these observations in accord with earlier results for the analogous arenesulphenylations.

DENNIS G. GARRATT, M. DOMINIC RYAN et ANN KABO. Can. J. Chem. **58**, 2329 (1980).

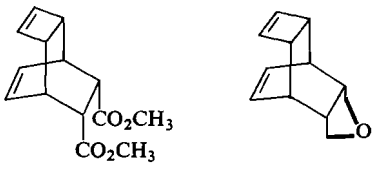
On a étudié la réaction du chlorure de benzènesélényle avec trois dérivés du tricyclo[4.2.2.0^{2,5}]décadiène-3,7 dans 4 systèmes de solvant: le chlorure de méthylène, l'acide acétique, l'acide acétique/$LiClO_4$ et le méthanol. Dans des conditions de contrôle cinétique, on n'a isolé que les produits résultant de l'attaque *exo–anti* sur le noyau cyclobutène dans le chlorure de méthylène ou l'acide acétique. Cette observation vaut également pour le système acide acétique/$LiClO_4$ à l'exception du tricyclo[4.2.2.0^{2,5}]-décatriène-3,7,9 dicarboxylate-7,8 de diméthyle où le produit principal est celui qui est réticulé avec incorporation de solvant. Dans le méthanol, on observe la formation de produits incorporant le solvant, de produits réticulés de façon transannulaire et de produits lactonisés (si il y a formation). On propose un mécanisme général qui tient compte à la fois de ces observations ainsi que des résultats obtenus antérieurement dans le cas d'arènesulphénylations analogues.

[Traduit par le journal]

The reactions of electrophiles with tricyclo-[4.2.2.0^{2,5}]deca-3,7-diene, **1**, and its derivatives usually occur via a predominantly *exo–syn* attack upon the cyclobutene moiety yielding products of 1,2-addition, **2**, or under certain conditions, trans-annular cyclization, **3** and/or **4** (2–10).



Mehta and Pandey (8) have recently reported the somewhat unprecedented nonstereospecific addition of benzenesulphenyl chloride to the cyclobutene moieties of dimethyl *endo,endo*-tricyclo[4.2.2.0^{2,5}]-deca-3,9-diene-7,8-dicarboxylate, **5**, and 4-oxatetra-cyclo[5.4.2.0^{2,6}.0^{8,11}]trideca-9,12-diene, **6**, yielding in each case a 3:1 mixture of *trans* and *cis* adducts. These results are at variance to those of Zefirov *et al.* (9) who simultaneously reported stereospecific *syn*



addition to **5** in nonpolar media such as carbon tetrachloride, and transannular cyclization to yield pentacyclic γ-lactones, **7** and/or **8**, in protic media such as acetic acid (eq. [2]). More recent studies by Kanematsu and co-workers (7) are at variance with both of the above, their analysis being consistent with stereospecific *anti* addition and the formation of a cross-bonded δ-lactone, **9**, instead of the γ-lactones previously described. No evidence was found for the

[1]Issued as NRCC No. 18549.

[2]For Part I see ref. 1.

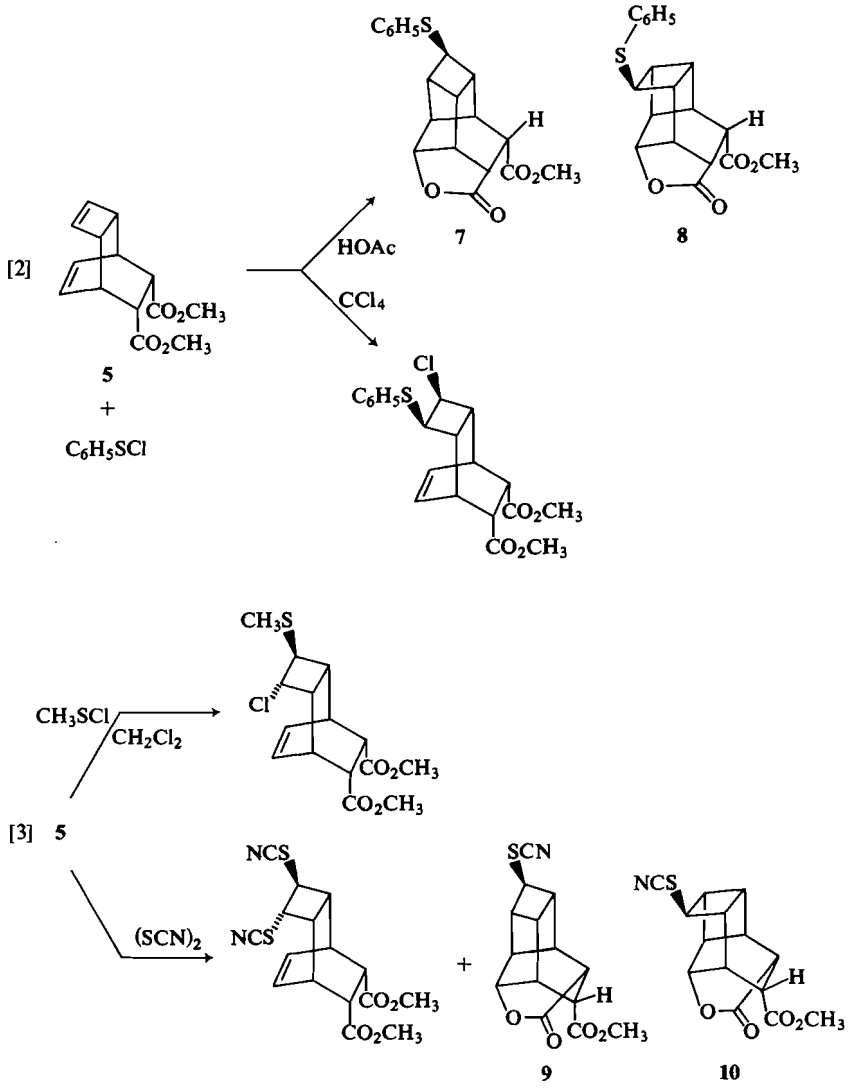
[3]Author to whom correspondence may be addressed at the National Research Council of Canada, 100 Sussex Dr., Ottawa, Ont., Canada K1A 0R6.

[4]Current address: Department of Chemistry, University of Toronto, Toronto, Ont., M5S 1A1.

0008-4042/80/222329-11$01.00/0

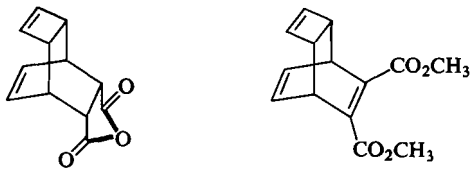
©National Research Council of Canada/Conseil national de recherches du Canada

Can. J. Chem. Downloaded from www.nrcresearchpress.com by 210.87.254.105 on 09/05/12
For personal use only.



analogous parallel bonded δ-lactone, **10**. Zefirov and co-workers have subsequently changed their interpretation to correspond with that of Kanematsu *et al.* and have supplied data from X-ray crystallographic investigations which substantiate the new findings (11–20) (eq. [3]).

During the course of our studies of the mechanism of areneselenenyl halide additions to olefinic substrates (21–33), we undertook an investigation of the reactions of benzeneselenenyl chloride with *endo*-tricyclo[4.2.2.$0^{2,5}$]deca-3,9-diene-7,8-dicarboxylate anhydride, **11**, dimethyl tricyclo[4.2.2.$0^{2,5}$]deca-3,7,9-triene-7,8-dicarboxylate, **12**, species **5**, and some related bicyclic alkenes (31). It was our aim to determine whether or not stereochemical constraints imposed by the configuration of the alkene would lead to nonstereospecific or perhaps *syn*-stereospecific addition, in contrast to the *normal stereospecific anti* mode of attack (22, 23, 26, 27, 31, 33–41).



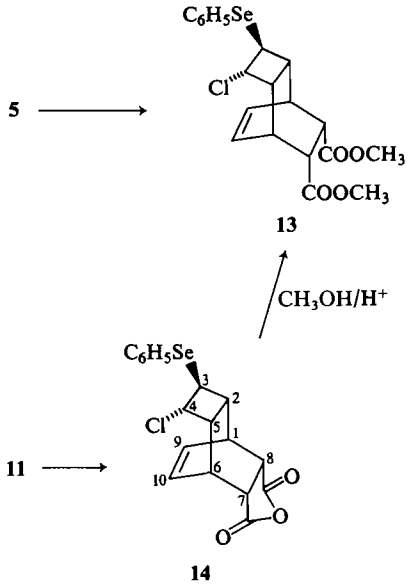
11 **12**

Results and Discussion

The reaction of benzeneselenenyl chloride with **5** at ambient temperature in methylene chloride, anhydrous acetic acid, or anhydrous acetic acid in the

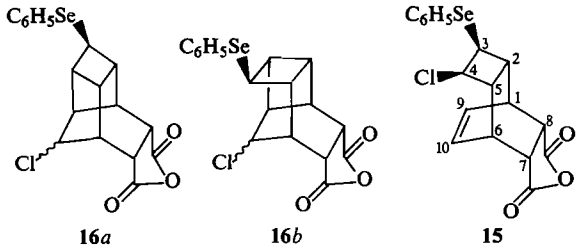
Can. J. Chem. Downloaded from www.nrcresearchpress.com by 210.87.254.105 on 09/05/12
For personal use only.

presence of 2.5 mole-equivalents of lithium perchlorate (relative to **5**) yields **13** in essentially quantitative yield. Under equivalent conditions benzeneselenenyl chloride gives upon addition to **11** the adduct **14**. Treatment of **14** with acidic (aqueous HCl) methanol gives **13**. Assignment of **13** and **14** as



the *trans* isomers of *exo* electrophilic attack upon the cyclobutene double bonds of **5** and **11**, respectively, follows from a comparison of the ms, ir, and ^1H and ^{13}C nmr spectral parameters with those of their sulphur analogues. The configuration of the sulphur analogue of **13** has been previously unambiguously determined by single crystal X-ray crystallographic studies by Zefirov and co-workers (13, 15).

In addition to the above, two further compounds, **15** and **16**, were observed as transient products during the course of the reaction of benzeneselenenyl chloride with **11**. Compound **15** is assigned as the product of *exo–syn* addition to the cyclobutene double bond. The ratio of **14** to **15** between 40 and 55% reaction was observed to be approximately 4:1 and to increasingly favour **14** as the reaction progresses. Compound **16** accounts for no more than 5% of the total product mixture during the course of the reaction, and unfortunately could not be isolated in a pure state. Attempts to separate **16** from **14** and **15** by chromatography on silica gel or Florisil led to the isomerization of **16** to **14** and/or **15**, irrespective of the nature of the eluting solvent. The absence of olefinic protons and the presence of an intact anhydride functionality allows us to tentatively assign **16** as either the cross-bonded, **16***a*, or parallel-bonded, **16***b*, pentacyclic anhydride.



With respect to the assignments of **13**, **14**, and **15** the following points are of note. First, the olefinic protons at C9 and C10 in **14** appear as two distinct doublets of doublets of doublets at δ 6.35 and 6.62 ppm, due presumably to unsymmetrical *endo* substitution, with a vicinal olefinic $^1H—^1H$ coupling of 7.0 Hz. In contrast, the olefinic protons at C9 and C10 of compound **15** appear as an apparent triplet centered at δ 6.56, indicative of essentially symmetric *endo* substitution at C3 and C4. This tentatively establishes **15** as the *cis* isomer of *exo–syn* addition (13, 42) as previously indicated.

Assignments were further corroborated by an analysis of chemical shifts and coupling constants of the protons at C3 and C4. The *exo* proton at C4 in the *trans* isomer **14** resonates at δ 4.17, exhibiting significant shielding due to the *cis* vicinal phenylseleno group as compared to the *endo* proton at C4 in the *cis* isomer **15** which resonates at δ 4.48. The *exo* and *endo* protons at C3 and C4, respectively, in species **14** exhibit a complex multiplet characteristic of the AB portion of an ABXX′ spin system.

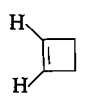
Confirmation that attack occurs at the cyclobutene double bond, and *not* at the double bond of the bicyclo[2.2.2]octene system, is based upon an analysis of their ^{13}C nmr spectra, and those of a series of model compounds (see Experimental and ref. 31). Chemical shift assignments have been based upon previously studied substituent effects and the magnitude of $^{13}C—^1H$ and $^{13}C—^{77}Se$ coupling interactions.

One-bond $^{13}C—^1H$ interactions are particularly useful, since it has been shown that the magnitude of the coupling increases markedly with increasing *s* character of the carbon hybridization (43, 44). Of paramount importance is the observation that the value of $^1J_{C,H}$ increases significantly in small rings, relative to moderately sized monocyclic or acyclic systems. Furthermore, the $^1J_{C,H}$ values for a series of low molecular weight polycyclic hydrocarbons have been found to correlate, at least qualitatively, with increasing ring strain. For example, the magnitude of $^1J_{C,H}$ for the olefinic carbon in cyclobutene, **17**, is greater than that in bicyclo[2.2.2]octene, **18**, by 5.5

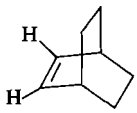
Can. J. Chem. Downloaded from www.nrcresearchpress.com by 210.87.254.105 on 09/05/12
For personal use only.

Can. J. Chem. Downloaded from www.nrcresearchpress.com by 210.87.254.105 on 09/05/12
For personal use only.

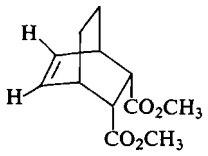
Hz (170 vs. 164.5). The value of the olefinic couplings is seen to increase slightly to 165.9 in dimethyl *endo,endo*-bicyclo[2.2.2]oct-5-ene-2,3-dicarboxylate, **19**, and even further to 167.4 Hz in *endo*-bicyclo-[2.2.2]oct-5-ene-2,3-dicarboxylic anhydride, **20**. We are thus able to assign the resonances at δ 129.1 ($^1J_{C,H}$ = 167.6 Hz) and δ 138.2 ($^1J_{C,H}$ = 171.9 Hz) to the cyclohexene and cyclobutene moieties of **11**, respectively. An examination of the olefinic one-bond $^{13}C—^1H$ couplings in **14** and **15** (167, 166 vs. 168, 167) supports our assignments in terms of attack on the cyclobutene double bond.



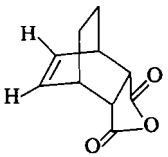
17



18

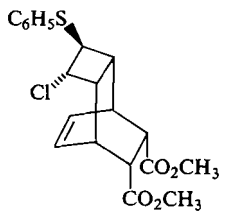


19

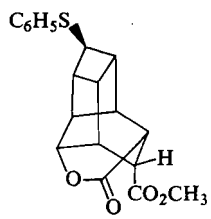


20

While the assignment of configuration to adducts **13–15** is quite straightforward, the rationalization for their formation proved to be somewhat more difficult. In particular, the observation of a single species **13** derived from **5** in protic media, such as acetic acid and acetic acid/$LiClO_4$ (Zefirov's dopping–addition conditions (12)) was unanticipated. Under equivalent conditions, for example, we found that benzenesulphenyl chloride reacts with **5**, in acetic acid, to give a 39:61 mixture of the *trans* adduct **21** and the δ-lactone, methyl (1*RS*,4*SR*,12*RS*)-4-phenylthio-9-oxapentacyclo[6.4.0.$0^{2,5}$.$0^{3,7}$.$0^{6,11}$]-dodeca-10-one-12-carboxylate, **22**. The identity of **22** was confirmed by the synthesis of an authentic sample by the procedure of Zefirov *et al.* (12).



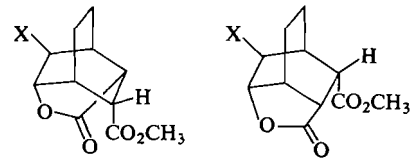
21



22

We note at this point that many investigators have claimed that selenenyl and sulphenyl halides must react by very similar, if not identical, mechanisms (45) because of the isosteric relationship found between organoselenium and organosulphur compounds. In this regard the absence of lactone products and/or products of solvent-incorporation, particularly in acetic acid/$LiClO_4$ (18, 46–50), was quite surprising. Our previous observation (31) that both benzeneselenenyl and benzenesulphenyl chlorides react with **19** in methylene chloride solution under ambient laboratory conditions of temperature, light, and atmosphere, to give mixtures of the γ- and δ-lactones, **23** and **24** (eq. [5]), served to substantiate our initial expectations.

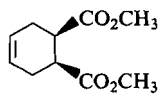
[5] **19** → X = ArSe, ArS



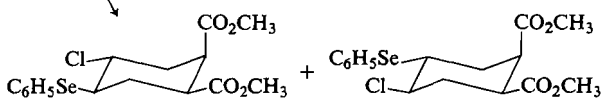
24 **23**

Intrigued by the very different propensities of **19** and **5** towards lactonization, we chose to investigate the related monocyclic diester **25**. Treatment of **25** with benzeneselenenyl chloride in methylene chloride did not, however, give the expected lactones. Instead, a mixture of 1:1 adducts **26** and **27**, formed in the ratio of 1:3, was isolated. Assignment of **26** and **27** was made on the assumption (33, 45) that the

[6]



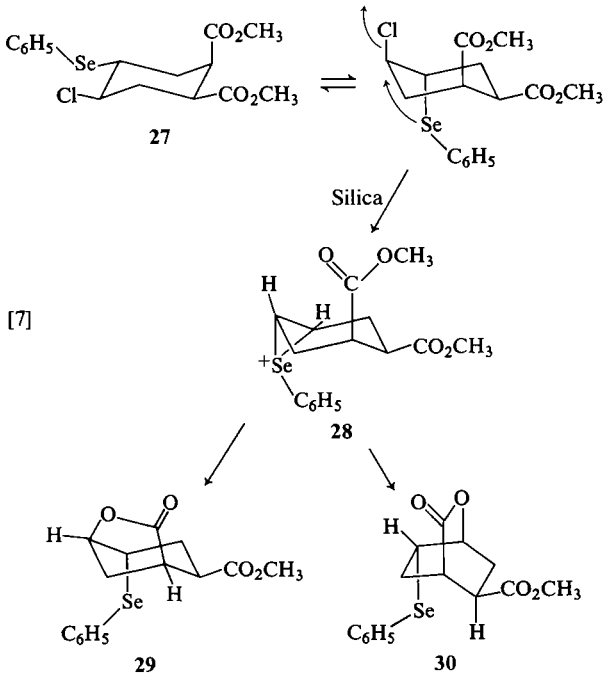
25



26 **27**

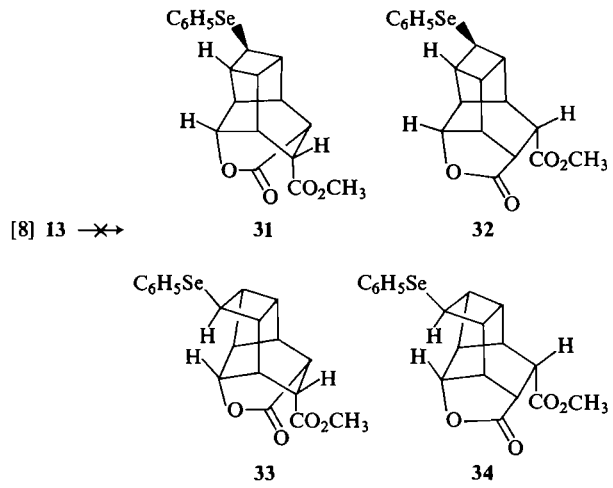
configurational-selectivity would be governed by steric approach control and that therefore attack occurs on the face of the double bond *anti* with respect to the diester moiety. Furthermore, only **27** has the correct configuration to allow lactonization with neighbouring group participation by selenium, through formation of the seleniranium ion **28**. Attempts to separate **26** and **27** by tlc on silica gel, using methylene chloride as eluant, were only partially successful. Compound **27** was converted under these conditions to a 2:1 mixture of the respective γ- and δ-lactones **29** and **30** in approximately 80% yield, based on **27**. Further chromatographic separations allowed for a mass conversion-isolation of greater than 95% based upon the total amount of **26** + **27** available. It is of interest to note that **26** is apparently isomerized to **27**, presumably via an elimination–readdition sequence on silica gel, thus

Can. J. Chem. Downloaded from www.nrcresearchpress.com by 210.87.254.105 on 09/05/12
For personal use only.



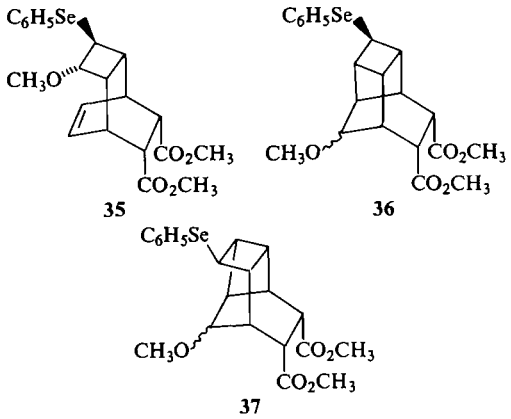
demonstrating the facile reversibility of these additions.

Attempts on our part to force the lactonization of **13** in a manner analogous to that above, either on preparative tlc plates or in a slurry of finely divided silica, were unsuccessful.



An alternative approach to the lactones **31**–**34**, however, now presented itself. Studies being carried out in our laboratory indicated that molecular rearrangements might occur during selenenyl chloride additions to alkenes when polar solvents such as methanol are used (33).

The reaction of **5** with benzeneselenenyl chloride in methanol gives, in contrast to our results in methylene chloride and acetic acid, three products in the relative proportions of 2:1:1. The major species was identified as **13**. The two remaining compounds are pentacyclic lactones. Surprisingly, no evidence is found for products of solvent-incorporation, such as **35**, **36**, or **37**. While one of the lactones could be readily assigned as **31**, methyl (1*RS*,4*SR*,12*RS*)-4-phenylseleno-9-oxapentacyclo[6.4.0.0^{2,5}.0^{3,7}.0^{6,11}]-dodeca-10-one-12-carboxylate, the product of δ-lactonization with cross-bonding, the configuration of the remaining lactone is still in doubt.



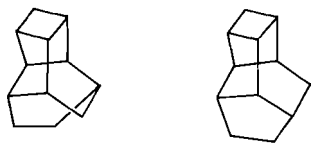
A tentative assignment of configuration to this lactone as **32** may, however, be made on the basis of force field calculations. In a recent publication Osawa *et al.* (51) proposed a steric interpretation of electrophilically induced transannular cyclization of juxtaposed double bonds. They observed that the course of an electrophilic addition to a molecule having two isolated double bonds in close proximity gives a transannular cross- or parallel-bridged product depending on the thermo-dynamic stability of the products. When the difference in calculated steric energies between neutral hydrocarbon skeletons of the cross and parallel adducts exceeds 10 kcal mol^{-1}, the more stable product is formed exclusively, whereas if the energy difference is less than 10 kcal mol^{-1} both types of transannular products may be formed.

If one makes the hypothesis, which seems reasonable, that the ring strain inherent in **31** and **32** bears the same relationship to the strain energy in **33** and **34** that the somewhat simpler hydrocarbon, tetracyclo[4.2.2.0^{2,5}.0^{3,7}]decane, **38**, has with respect to tetracyclo[4.4.0.0^{2,5}.0^{3,8}]decane, **39** (dihydrobasketane), then one would predict **31** and **32** to be favoured thermodynamically over **33** and **34**. This



Can. J. Chem. Downloaded from www.nrcresearchpress.com by 210.87.254.105 on 09/05/12
For personal use only.

follows from the calculated strain energies of **38** and **39** which are 54.35 and 67.03 kcal mol^{-1} as based on the Engler force field (52, 53) or 57.43 and 66.66 kcal mol^{-1} as based on the 1971–1972 Allinger force field (54–56). Extending this form of argument to the saturated hydrocarbon analogues of **31** and **32**, one notes that the calculated strain energies for pentacyclo[6.4.0.$0^{2,5}$.$0^{3,7}$.$0^{6,11}$]dodecane, **40**, and pentacyclo[5.4.1.$0^{2,9}$.$0^{3,6}$.$0^{4,8}$]dodecane, **41**, are 59.55 and

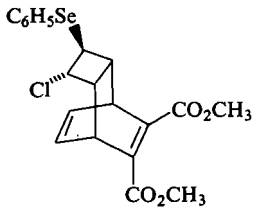


40 **41**

62.84 kcal mol^{-1} (51–53) respectively, or 61.21 and 68.53 kcal mol^{-1} (51, 54–56), respectively. From these data one predicts that **31** will be thermodynamically more stable than **32**. Indeed, we observe an isomerization of our second lactone, presumably **32**, upon standing, to **31** (room temperature, CD_2Cl_2).

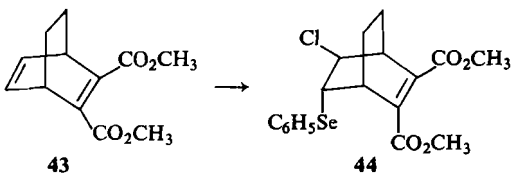
The reaction of benzeneselenenyl chloride with triene **12** gives, in either methylene chloride or acetic acid, a single product **42**, identified by comparison of its ^{13}C nmr parameters with those of the sulphur analogue, as the *trans* adduct of *exo–anti* attack, (eq. [9]). No evidence was found for attack upon either the C7—C8 or C9—C10 double bonds.

[9] **12** $\xrightarrow[\text{or HOAc}]{CH_2Cl_2}$ **42**



This result is of interest, since the related diene, dimethyl bicyclo[2.2.2]octa-2,5-diene-2,3-dicarboxylate, **43**, is observed to add benzeneselenenyl chloride to give **44**, (eq. [10]).

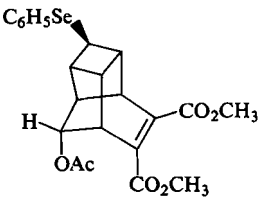
[10] **43** → **44**



Presumably, the absence of products derived from attack upon the C9—C10 double bond of **12** is the result of a deactivating effect by the dicarboxylate functionalities at C7—C8 and enhanced reactivity at C3—C4 by release of Baeyer ring strain upon addition to the cyclobutene moiety.

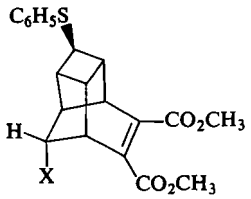
In contrast to our results with dienes **5** and **11**, the addition of benzeneselenenyl chloride to triene **12** in acetic acid/$LiClO_4$ gives, as the major product, the acetate of transannular addition, dimethyl *exo*-4-phenylseleno-*endo*-8-acetoxytetracyclo[4.2.2.$0^{2,5}$.$0^{3,7}$]deca-9-ene-9,10-dicarboxylate, **45**! The ratio of **42** to **45** is found to be 37:63 when 2.2 mole-equivalents (based on **12**) of lithium perchlorate are present.

It is constructive at this point to compare our data for areneselenenylation with those for arenesulphenylation carried out under identical conditions. As noted above, the reaction of benzeneselenenyl chloride with **12** gives only **42** in acetic acid. In contrast, we observe a 1:1 mixture of **42′** and **45′**, the sulphur analogues of **42** and **45**, respectively, when benzenesulphenyl chloride is allowed to react with

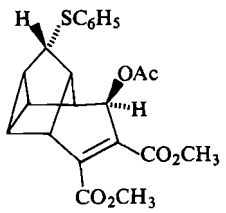


45

12 in acetic acid. Furthermore, while benzeneselenenyl chloride yields only **42** and **45** in acetic acid/$LiClO_4$, benzenesulphenyl chloride gives a complex mixture of at least five products! We have been able to identify and assign **42′**, **45′**, the cross-bonded chloride **46**, the cross-bonded perchlorate **47**, and the novel rearranged acetate **48**. The relative proportions of **42′**:**45′**:**46**:**47**:**48** were determined to be 8:59:11:9:13. The structures of these species are assigned in accord with the previously reported 2-nitrophenylthio derivatives (19).



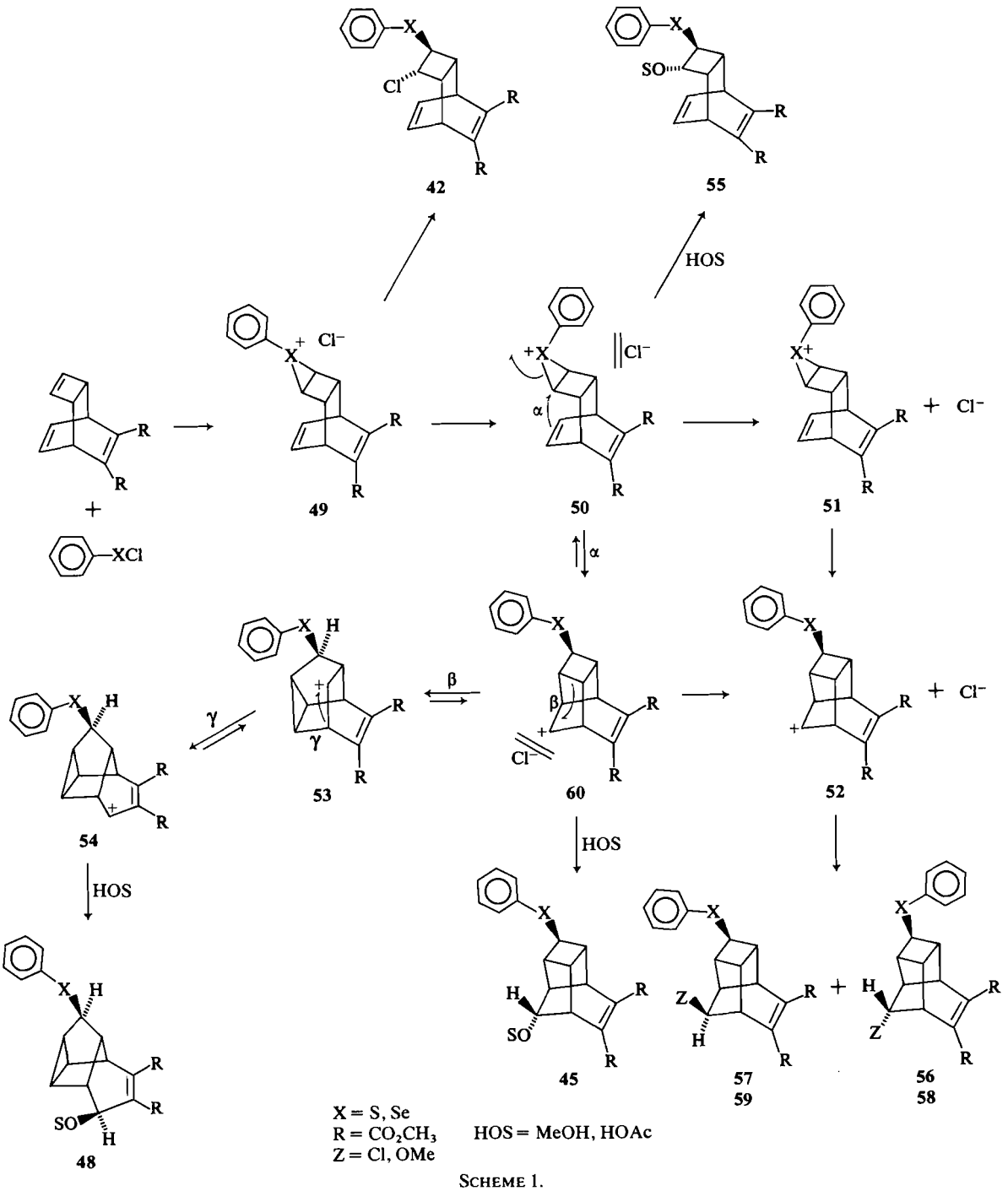
46 X = Cl
47 X = $OClO_4$



48

In comparing these reactions of benzeneselenenyl chloride and benzenesulphenyl chloride with substrates **5**, **11**, and **12**, it becomes apparent that areneselenenylation is much less affected by the change from a relatively nonpolar solvent, such as methylene chloride, to a moderately polar protic solvent, such as acetic acid or acetic acid/$LiClO_4$ than is arenesulphenylation. If one makes the

Can. J. Chem. Downloaded from www.nrcresearchpress.com by 210.87.254.105 on 09/05/12
For personal use only.



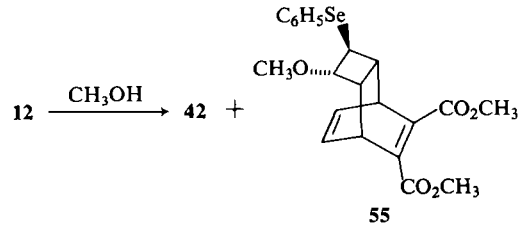
SCHEME 1.

assumption that the reaction hypersurfaces for areneselenenylation and arenesulphenylation are similar after the rate-determining step (45), the differences observed in product distributions might be accounted for in terms of the more efficient neighbouring group or bridging ability of selenium relative to sulphur. As the polarity of the reaction medium increases one begins to observe, in both reaction series, a competition between bridged ionic intermediates such as the seleniranium intimate ion-pair **49**, or its sulphur analogue **49′** (see Scheme 1), and the more loosely associated species, such as the

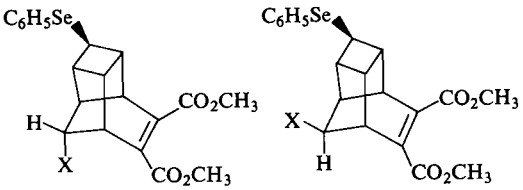
Can. J. Chem. Downloaded from www.nrcresearchpress.com by 210.87.254.105 on 09/05/12
For personal use only.

solvent-separated ion-pairs **50**, **50′**, the dissociated species **51**, **51′**, and free carbonium ions **52–54**.

In accord with this concept of a series of ion-pairs is the observation that benzeneselenenyl chloride reacts with **12** in methanol to give in addition to the *trans* chloride **42**, the analogous methoxy product **55**, the epimeric cross-bonded chlorides **56**, **57**, and the analogous epimeric methoxy adducts **58**, **59** (eq. [11]). When the reaction is carried out at 23–25°C



[11]



56 X = Cl
58 X = OMe

57 X = Cl
59 X = OMe

the relative proportions of **42**:**55**:**56**:**57**:**58**:**59** are found to be 55:14:6:1:14:10. Of particular note is the observation that both epimeric chlorides and methoxy adducts of cross-bonding are formed in methanol, whereas in acetic acid/$LiClO_4$ only one acetoxy species, **45**, is formed. This latter result suggests the possible role of a specifically solvated carbonium ion ion-pair such as **60** prior to formation of a free carbonium ion of type **52**.

Summary

Within the limits of our initial objectives, these results show a number of differences between the addition reactions of areneselenenyl and arenesulphenyl chlorides. Of particular importance is the observation of nonstereospecific addition to the cyclobutene double bond of **11** under conditions of kinetic control, followed by isomerization stereospecifically to the adduct of *exo–anti* addition! While this observation suggests the possible presence of two competitive reaction pathways, further mechanistic speculation should await more comprehensive studies including those which would specifically deal with the nature of the rate-determining step.

Experimental

General

All new compounds were separated and purified using preparative tlc performed on Analtech precoated plates, silica gel GF. Yields were determined by weighing the collected fractions and by nmr. The ^1H nmr spectra were obtained on a Varian Associates T60, EM 360, or HA 100 spectrometer. The ^{13}C nmr spectra were recorded on a Varian CFT20 or FT80-16K spectrometer operating in the Fourier Transform mode at 20.0 MHz. Infrared spectra were recorded on a Unicam 1100 or Perkin Elmer 257 spectrophotometer as CCl_4 solutions in NaCl cavity cells. Melting points were obtained on a Fisher-Johns block and are reported uncorrected. All new compounds gave acceptable elemental analyses: C, H, Cl, S, Se ± 0.35%. Elemental analyses were carried out by Scandinavian Microanalysis Laboratories, Herlev, or by Mr. H. Séguin, NRCC, Ottawa.

Benzeneselenenyl chloride was available commercially (Aldrich). Recrystallized prior to use from CCl_4, mp 63–64.5°C.

Benzenesulphenyl chloride was prepared from thiophenol (Aldrich) in 96% yield via the direct chlorination in CCl_4 at 0°C. Distilled under reduced pressure, bp 72°C/4 Torr. *Caution: this substance, although in use by various investigators for over thirty years, may spontaneously explode. A screw-capped bottle of triply distilled benzenesulphenyl chloride containing approximately 5–10 mL of the substance stored under argon, exploded in a refrigerator destroying not only the container but the desiccator in which it was stored!*

endo-*Tricyclo*[*4.2.2.0*^{2,5}]*deca-3,9-diene-7,8-dicarboxylate anhydride*, **11**, was prepared by the cycloaddition of maleic anhydride with 1,3,5,7-cyclooctatetraene (Aldrich) in chlorobenzene under reflux. Crystallized from benzene: mp 170–171°C; ir (KBr): 1850, 1760 cm^{-1}; ^1H nmr identical to that previously reported (31); ^{13}C nmr ($CDCl_3$): 36.9 (d, C1,6) $^1J_{C,H}$ = 140.8 Hz; 43.3 (d, C2,5) $^1J_{C,H}$ = 145.2 Hz; 138.2 (d, C3,4) $^1J_{C,H}$ = 171.9 Hz; 44.0 (d, C7,8) $^1J_{C,H}$ = 140.1 Hz; 129.1 (d, C9,10) $^1J_{C,H}$ = 167.6 Hz; 172.6 (s —C(=O)O—).

endo-*Bicyclo*[*2.2.2*]*oct-5-ene-2,3-dicarboxylate anhydride*, **20**, was prepared by the cycloaddition of maleic anhydride with 1,3-cyclohexadiene (Aldrich) in benzene under reflux. Recrystallized from benzene: mp 146–147°C; ir (NaCl, CCl_4): 1795, 1870 cm^{-1}; ^1H nmr ($CDCl_3$): 6.28 (m, 2H), 3.22 (bs, 2H), 2.98 (s, 2H), 1.55 (A_2B_2, 4H); ^{13}C nmr ($CDCl_3$): 31.6 (d, C1,4) $^1J_{C,H}$ = 143.8 Hz, $^2J_{CCH}$ = 6.2 Hz; 44.7 (d, C2,3) $^1J_{C,H}$ = 137.9; 133.0 (d, C5,6) $^1J_{C,H}$ = 167.4 Hz; 22.9 (t, C7,8) $^1J_{C,H}$ = 135.0 Hz; 172.9 (s —C(=O)O—).

Bicyclo[*2.2.2*]*oct-2-ene*, **18**, was purchased from Chemical Samples: ^{13}C nmr: 29.6 (d, C1,4) $^1J_{C,H}$ = 134.0 Hz; 134.3 (d, C2,3) $^1J_{C,H}$ = 164.5 Hz; 25.8 (t, C5,6,7,8) $^1J_{C,H}$ = 131.0 Hz, $^2J_{CCH}$ = 6.2 Hz.

Dimethyl endo,endo-*tricyclo*[*4.2.2.0*^{2,5}]*deca-3,9-diene-7,8-dicarboxylate*, **5**, was prepared from **11** by acid (HCl, 12 mol dm^{-3}) catalyzed esterification in anhydrous methanol. The diester was separated from unreacted anhydride on a silica gel column eluted with methylene chloride; ^1H nmr: 6.03 (m, 2H), 5.87 (bs, 2H), 3.60 (s, 6H), 2.5–3.3 (m, 6H); ^{13}C nmr: 37.6 (d, C1,6) $^1J_{CH}$ = 140.2 Hz, $^2J_{CCH}$ = 6.7 Hz, $^3J_{CCCH}$ = 6.8 Hz; 44.5 (d, C2,5) $^1J_{CH}$ = 145.5, $^2J_{CCH}$ = 5.2 Hz; 137.8 (d, C3,4) $^1J_{CH}$ = 169.8 Hz, $^2J_{CCH}$ = $^3J_{CCCH}$ = 6.4 Hz; 46.5 (d, C7,8) $^1J_{CH}$ = 133.5 Hz; 128.2 (d, C9,10) $^1J_{CH}$ = 167.3 Hz; 173.3 (s, CO_2CH_3) $^2J_{CCH}$ = 2.8 Hz; 51.6 (q, CH_3O_2) $^1J_{CH}$ = 146.8 Hz.

Dimethyl endo,endo-*bicyclo*[*2.2.2*]*oct-5-ene-2,3-dicarboxylate*, **19**, was prepared from **20** by acid (HCl, 12 mol dm^{-3}) catalyzed esterification in anhydrous methanol. Recrystallized from methanol: mp 64–67°C; ir: 1750 cm^{-1}; ^1H nmr: 6.35 (m, 2H), 3.42 (s, 6H), 3.00 (bs, 2H), 2.92 (bm, 2H), 1.52 (A_2B_2, 4H); ^{13}C nmr: 32.1 (d, C1,4) $^1J_{CH}$ = 140.2 Hz, $^2J_{CCH}$ = 6.2 Hz; 47.1 (d, C2,3) $^1J_{CH}$ = 133.5 Hz; 131.9 (d, C5,6) $^1J_{CH}$ = 165.9 Hz, $^2J_{CCH}$ = 3.4 Hz; 24.1 (t, C7,8) $^1J_{CH}$ = 132.0 Hz; 172.8 (s, CO_2CH_3); 51.0 (q, CH_3O_2) $^1J_{CH}$ = 146.8 Hz.

3,4-exo, exo-*Dibromo*-endo-*tricyclo*[*4.2.2.0*^{2,5}]*deca-9-ene-7,8-dicarboxylate anhydride* was prepared in accord with the pro-

Can. J. Chem. Downloaded from www.nrcresearchpress.com by 210.87.254.105 on 09/05/12
For personal use only.

cedure of Farnum and Snyder (2) and that of Sasaki *et al.* (6); ^{13}C nmr: 34.4 (d, C1,6); 47.2 (d, C2,5); 48.1 (d, C3,4); 43.7 (d, C7,8); 133.4 (d, C9,10); 171.8 (s, —C(=O)O—).

3-exo-*4*-endo-*Dibromo*-endo-*tricyclo*[*4.2.2.0*^{2,5}]*deca-9-ene-7,8-dicarboxylate anhydride* was prepared as above; ^{13}C nmr: 34.2 (d, C1); 43.7 (d, C2); 50.9 (d, C3); 49.2 (d, C4); 47.9 (d, C5); 34.6 (d, C6); 42.6 (d, C7); 43.6 (d, C8); 131.3 (d, C9); 135.5 (d, C10); 171.8, 171.7 (s, —C(=O)O—).

3-endo-*Chloro-4*-exo-*phenylthio*-endo-*tricyclo*[*4.2.2.0*^{2,5}]*deca-9-ene-7,8-dicarboxylate anhydride*, **14′**, was prepared by the reaction of benzenesulphenyl chloride with 1 molar-equivalent of diene **11** in methylene chloride or acetic acid solvent. Infrared (CCl_4): 1852, 1760 cm^{-1}; ^{1}H nmr: 6.64 (ddtt, 1H), 6.34 (ddtt, 1H), 4.44 (dd, 1H, J = 6.0, 6.5 Hz), 3.56 (ddd, 1H, J = 6.0, 6.4, 1.0 Hz), 2.4–3.4 (m, 6H); ^{13}C nmr: 33.4 (d, C1) $^1J_{CH}$ = 147.2 Hz; 43.2 (d, C2); 59.9 (d, C3) $^1J_{CH}$ = 161.0 Hz; 52.1 (d, C4) $^1J_{CH}$ = 148.0 Hz; 43.7 (d, C5); 34.2 (d, C6) $^1J_{CH}$ = 146.3 Hz; 42.3 (d, C7); 42.7 (d, C8); 131.1 (d, C9) $^1J_{CH}$ = 168.0 Hz; 135.5 (d, C10) $^1J_{CH}$ = 168.0 Hz; 171.8, 172.1 (s —C(=O)O—). Recrystallized from CH_2Cl_2: mp 188°C.

3-exo-*Phenylseleno-4*-endo-*chloro*-endo-*tricyclo* [*4.2.2.0*^{2,5}]-*deca-9-ene-7,8-dicarboxylate anhydride*, **14**, was prepared by the reaction of benzeneselenenyl chloride with 1 molar-equivalent of diene **11** in methylene chloride ($10\ t_{1/2}$ = 10 days), in glacial acetic acid ($10\ t_{1/2}$ = 3 h). Recrystallized from 1:1 *n*-pentane–methylene chloride: mp 154–158°C; ir ($CHCl_3$): 1795, 1870 cm^{-1}; ^{1}H nmr: 6.62 (tm, 1H), 6.35 (tm, 1H, J = 7.4 Hz), 4.17 (m, 1H, C*H*Cl), 4.05 (m, 1H), 2.8–3.5 (m, 6H); ^{13}C nmr: 34.7 (d, C1) $^1J_{CH}$ = 147.0 Hz; 47.6 (d, C2) $^1J_{CH}$ = 149.0 Hz; 49.8 (d, C3) $^1J_{CH}$ = 154.0 Hz; 60.0 (d, C4) $^1J_{CH}$ = 163.0 Hz; 43.6 (d, C5) $^1J_{CH}$ = 144.0 Hz; 33.7 (d, C6) $^1J_{CH}$ = 147.0 Hz; 42.8 (d, C7) $^1J_{CH}$ = 142.0 Hz; 41.4 (d, C8) $^1J_{CH}$ = 141.8 Hz; 134.7 (d, C9) $^1J_{CH}$ = 167.0 Hz; 132.2 (d, C10) $^1J_{CH}$ = 166.0 Hz; 171.4, 171.3 (s, —C(=O)O—); 132.8 (d, C_o); 129.3 (d, C_m); 127.4 (d, C_p); 130.6 (s, C_i) *C*Se; tlc, silica gel, R_f = 0.89 using 1:4 EtOAc–toluene as elutant.

3-exo-*Phenylseleno-4*-exo-*chloro*-endo-*tricyclo* [*4.2.2.0*^{2,5}]-*deca-9-ene-7,8-dicarboxylate anhydride*, **15**, observed in methylene chloride-d_2 in previous reaction between 20–50% completion; ^{1}H nmr: 6.56 (t, 2H), 4.48 (dd, 1H, C*H*Cl), 3.78 (dm, 1H, C*H*Se), 2.7–3.6 (m, 6H); ^{13}C nmr: 34.2 (d, C1); 45.3 (d, C2); 47.5 (d, C3); 61.1 (d, C4); 43.5 (d, C5); 33.2 (d, C6); 42.8 (d, C7); 41.4 (d, C8); 134.5 (d, C9,10); 171.6, 171.4 (s, —C(=O)O—).

Dimethyl 3-endo-*chloro-4*-exo-*phenylthio*-endo,endo-*tricyclo*[*4.2.2.0*^{2,5}]*deca-9-ene-7,8-dicarboxylate*, **21**, was prepared by the reaction of benzenesulphenyl chloride with 1 molar-equivalent of **5** in either methylene chloride (48% yield) or acetic acid (39% yield). Nuclear magnetic resonance data were ^{1}H nmr: 6.56 (tm, 1H), 6.37 (tm, 1H), 4.40 (dd, 1H, C*H*Cl), 3.5 (m, 1H, C*H*SPh), 3.58 (s, 6H, CO_2CH_3), 1.1–3.5 (m, 6H); ^{13}C nmr: 34.7 (d, C1); 46.5 (d, C2); 60.8 (d, C3); 51.8 (d, C4); 45.7 (d, C5); 35.0 (d, C6); 42.8 (d, C7); 43.9 (d, C8); 131.2 (d, C9); 133.9 (d, C10); 172.7, 172.3 (s, CO_2CH_3); 51.7, 51.6 (q, CH_3O_2).

Dimethyl 3-exo-*phenylseleno-4*-endo-*chloro*-endo,endo-*tricyclo*[*4.2.2.0*^{2,5}]*deca-9-ene-7,8-dicarboxylate*, **13**, was prepared by the addition of benzeneselenenyl chloride to 1 molar-equivalent of **5** in methylene chloride at 24°C (98%$^+$ yield by nmr, 93% isolated yield); ^{1}H nmr: 6.62 (tm, 1H), 6.41 (tm, 1H), 4.26 (dm, 1H, C*H*Cl), 3.7 (m, 1H, C*H*Se), 3.61 (s, 6H), 1.2–3.6 (m, 6H); ^{13}C nmr: 35.8 (d, C1); 46.2 (d, C2); 48.5 (d, C3); 60.7 (d, C4); 45.2 (d, C5); 34.1 (d, C6); 41.8 (d, C7,8); 133.1 (d, C9); 132.6 (d, C10); 172.2, 172.4 (s, CO_2CH_3); 51.4, 50.1 (q, CH_3O_2); 130.0 (d, C_o); 128.7 (d, C_m); 126.5 (d, C_p); tlc, silica gel, R_f = 0.59 using 1:4 EtOAc–toluene as elutant.

*Methyl (2*SR,*7*RS*)-2-phenylseleno-4-oxatricyclo*[*4.4.0.0*^{3,8}]-*deca-5-one-7-carboxylate*, **24**, was prepared as previously described (31). Recrystallized from $CHCl_3$: mp 114–116°C; ^{13}C nmr: 31.0 (d, C1); 42.1 (d, C2); 83.2 (d, C3); 176.7 (s, C=O, C5); 43.9 (d, C6); 40.3 (d, C7); 36.9 (d, C8); 22.7 (t, C9); 15.0 (t, C10); 171.9 (s, CO_2CH_3); 52.0 (q, CH_3O_2); tlc, silica gel, R_f = 0.36 using CH_2Cl_2 as elutant.

*Methyl (2*SR,*7*RS*)-2-phenylthio-4-oxatricyclo*[*4.4.0.0*^{3,8}]-*deca-5-one-7-carboxylate*, **24′**, was prepared as previously described (31). Recrystallized from $CHCl_3$, mp 109–112°C; ^{13}C nmr: 30.3 (d, C1); 45.9 (d, C2); 81.9 (d, C3); 176.5 (s, C=O, C5); 43.5 (d, C6); 40.3 (d, C7); 36.9 (d, C8); 21.0 (t, C9); 14.8 (t, C10); 172.0 (s, CO_2CH_3); 52.1 (q, CH_3O_2); tlc, silica gel, R_f = 0.41 using CH_2Cl_2 as elutant.

*Methyl (2*SR,*10*RS*) - 2 - phenylseleno - 4 - oxatricyclo -* [*4.3.1.0*^{3,7}]-*deca-5-one-10-carboxylate*, **23**, was prepared as previously described (31). Isolated in 25% yield under conditions of kinetic control. Recrystallized from $CHCl_3$, mp 118–125°C; ^{13}C nmr: 33.1 (d, C1); 47.8 (d, C2); 75.0 (d, C3); 175.7 (s, C=O, C5); 41.8 (d, C6); 36.3 (d, C7); 24.5 (t, C8); 20.5 (t, C9); 44.1 (d, C10); 172.9 (s, C=O); 51.6 (q, CH_3O_2); tlc, silica gel, R_f = 0.52 using CH_2Cl_2 as elutant.

*Methyl (2*SR,*10*RS*)-2-phenylthio-4-oxatricyclo*[*4.3.1.0*^{3,7}]-*deca-5-one-10-carboxylate*, **23′**, was prepared as previously described (31). Isolated in 22% yield under conditions of kinetic control; ^{13}C nmr: 32.4 (d, C1); 50.8 (d, C2); 74.4 (d, C3); 175.5 (s, C=O, C5); 41.8 (d, C6); 36.5 (d, C7); 24.2 (t, C8); 19.5 (t, C9); 43.4 (d, C10); 173.1 (s, CO_2CH_3); 51.4 (q, CH_3O_2); tlc, silica gel, R_f = 0.52 using CH_2Cl_2 as elutant.

Dimethyl cis-*cyclohex-4-ene-1,2-dicarboxylate*, **25**, was prepared by the acid (HCl, 12 mol dm^{-3}) catalyzed esterification in anhydrous methanol of the corresponding anhydride supplied by Mr. P. L. Beaulieu of these laboratories; ^{13}C nmr: 39.4 (d, C1,2) $^1J_{CH}$ = 131 Hz; 25.5 (tm, C3,5) $^1J_{CH}$ = 131 Hz; 124.8 (d, C4,5) $^1J_{CH}$ = 157.3 Hz; 173.4 (sm, CO_2CH_3); 51.4 (q, CH_3O_2) $^1J_{CH}$ = 146.9 Hz.

*Dimethyl(1*RS,*2*RS,*4*RS,*5*SR*)-1-phenylseleno-2-chlorocyclo-hexane-4,5-dicarboxylate*, **26**, prepared in 33% yield from **25** by the addition of benzeneselenenyl chloride in methylene chloride at room temperature; ^{13}C nmr: 46.6 (d, C1); 60.4 (d, C2); 30.2 (t, C3); 41.5 (d, C4); 39.6 (d, C5); 33.6 (t, C6); 172.6 (s, CO_2CH_3); 52.0 (q, CH_3O_2); 135.5 (d, C_o); 129.2 (d, C_m); 128.4 (d, C_p).

*Dimethyl (1*RS,*2*RS,*4*SR,*5*RS*)-1-phenylseleno-2-chlorocy-clohexane-4,5-dicarboxylate*, **27**, prepared in 67% yield as above; ^{13}C nmr: 46.0 (d, C1); 60.6 (d, C2); 33.2 (t, C3); 40.7 (d, C4); 41.2 (d, C5); 33.6 (t, C6); 172.7 (s, CO_2CH_3); 52.0 (q, CH_3O_2); 135.4 (d, C_o); 129.2 (d, C_m); 127.9 (d, C_p).

*Methyl (1*RS,*5*RS,*7*SR*)-5-phenylseleno-3-oxabicyclo-*[*2.2.2*] *oct-2-one-7-carboxylate*, **30**, from **27** above, on treatment with silica gel/CH_2Cl_2; ir (CCl_4): 1770, 1750 cm^{-1}; ^{13}C nmr: 41.9 (d, C1); 70.8 (d, C4); 47.7 (d, C5); 33.0 (t, C6); 42.0 (d, C7) 31.4 (t, C8); 172.5 (s, C=O, C2); 51.9 (q, CH_3O_2); 170.6 (s, CO_2CH_3); tlc, silica gel, R_f = 0.53 using CH_2Cl_2 as elutant.

*Methyl (1*SR,*2*SR,*4*SR*)-2-phenylseleno-7-oxabicyclo-*[*3.2.1*] *oct-5-one-4-carboxylate*, **29**, prepared as above; ir (CCl_4): 1770, 1748 cm^{-1}; ^{13}C nmr: 68.7 (d, C1); 51.7 (d, C2); 34.5 (t, C3); 43.9 (d, C4); 41.4 (d, C5); 172.9 (s, C=O, C6); 31.1 (t, C8); 51.9 (q, CH_3O_2); 170.6 (s, CO_2CH_3); tlc, silica gel, R_f = 0.33 using CH_2Cl_2 as elutant.

Dimethyl tricyclo[*4.2.2.0*^{2,5}]*deca-3,7,9-triene-7,8-dicarboxy-late*, **12**, was prepared by the cycloaddition of dimethyl acetylenedicarboxylate with 1,3,5,7-cyclooctatetraene (Aldrich) in chlorobenzene under reflux; ^{13}C nmr: 42.8 (dt, C1,6) $^1J_{CH}$ = 143.9 Hz, $^2J_{CCH}$ = 7.0 Hz; 43.9 (dm, C2,5) $^1J_{CH}$ = 146.7 Hz; 138.6 (d, C3,4) $^1J_{CH}$ = 172.7 Hz; 142.7 (s, C7,8); 129.3 (dm, C9,10) $^1J_{CH}$ = 170.4 Hz, $^2J_{CCH}$ = 3.0 Hz; 166.2 (sdq, CO_2CH_3)

Can. J. Chem. Downloaded from www.nrcresearchpress.com by 210.87.254.105 on 09/05/12
For personal use only.

$^3J_{CCCH}$ = 3.8 Hz, $^3J_{COCH}$ = 3.7 Hz; 51.6 (q, CH_3O_2) $^1J_{CH}$ = 147.4 Hz.

Dimethyl 3 - exo - phenylseleno - 4 - endo - chlorotricyclo - [4.2.2.0^{2,5}]deca-7,9-diene-7,8-dicarboxylate, **42**, was prepared in 97% yield by the reaction of benzeneselenenyl chloride with triene **12** in either methylene chloride or acetic acid; ^{13}C nmr: 42.4 (d, C1); 46.5 (d, C2); 49.2 (d, C3); 59.6 (d, C4); 43.7 (d, C5); 40.8 (d, C6); 141.7, 142.8 (s, C7,8); 134.7 (d, C9); 132.4 (d, C10); 165.2, 165.5 (s, CO_2CH_3); 52.0 (q, CH_3O_2); tlc, silica gel R_f = 0.54 when eluted with 1:9 EtOAc–toluene.

Dimethyl 3-exo-phenylthio-4-endo-chlorotricyclo[4.2.2.0^{2,5}]-deca-7,9-diene-7,8-dicarboxylate, **42′**, was prepared using benzenesulphenyl chloride as above in methylene chloride solution; ^{13}C nmr: 41.5 (d, C1); 44.4 (d, C2); 50.5 (d, C3); 57.2 (d, C4); 43.9 (d, C5); 41.3 (d, C6); 142.4, 142.6 (s, C7,8); 135.0 (d, C9); 133.9 (d, C10); 165.4, 165.5 (s, CO_2CH_3); 52.0, 52.3 (q, CH_3O_2); tlc, silica gel, R_f = 0.82 using 1:4 EtOAc–toluene.

Dimethyl (1RS,4SR,8SR)-4-phenylseleno-8-acetoxytetracyclo[4.2.2.0^{2,5}.0^{3,7}]deca-9-ene-9,10-dicarboxylate, **45**, gave ^{13}C nmr: 41.4 (d, C1); 39.6 (d, C2); 45.1 (d, C3); 52.0 (d, C4); 48.2 (d, C5); 38.3 (d, C6); 42.0 (d, C7); 78.1 (d, C8—OAc); 138.2, 139.9 (s, C9,10); 170.1 (s, $OCOCH_3$); 20.5 (q, $OCOCH_3$); 166.7, 167.7 (s, CO_2CH_3); 52.1 (q, CH_3O_2); tlc silica gel, R_f = 0.38 using 1:4 EtOAc–toluene.

Dimethyl (1RS,4SR,8SR)-4-phenylthio-8-acetoxytetra-cyclo-[4.2.2.0^{2,5}.0^{3,7}]deca-9-ene-9,10-dicarboxylate, **45′**, gave ^{13}C nmr: 41.3 (d, C1); 39.3 (d, C2); 46.5 (d, C3); 49.1 (d, C4); 47.3 (d, C5); 38.2 (d, C6); 44.3 (d, C7); 77.9 (d, C8 —OAc); 137.9, 139.7 (s, C9,10); 170.0 (s, $OCOCH_3$); 20.5 (q, $OCOCH_3$); 166.7, 167.7 (s, CO_2CH_3); 51.9 (q, CH_3O_2).

Dimethyl 5-phenylthio-10-acetoxytetracyclo[4.4.0.0^{2,4}.0^{3,7}]-deca-8-ene-8,9-dicarboxylate, **48**, gave ^{13}C nmr: 41.9 (d, C1); 21.7 (d, C2); 13.0 (d, C3); 24.0 (d, C4); 48.8 (d, C5); 46.9 (d, C6); 30.5 (d, C7); 138.1 (s, C8); 145.8 (s, C9); 87.3 (d, C10—OAc); 170.0 (s, $OCOCH_3$); 20.8 (q, $OCOCH_3$); 164.7, 167.4 (s, CO_2CH_3); 52.0 (q, CO_2CH_3).

Dimethyl 3 - exo - phenylseleno - 4 - endo - methoxytricyclo-[4.2.2.0^{2,5}]deca-7,9-diene-7,8-dicarboxylate, **55**, gave ^{13}C nmr: 43.8 (d, C1); 45.3 (d, C2); 50.9 (d, C3); 86.6 (d, C4—OCH_3); 44.2 (d, C5); 40.3 (d, C6); 138.4, 139.5 (s, C7,8); 52.0 (q, CH_3O_2); 135.4 (d, C9); 131.9 (d, C10); 53.8 (q, CH_3O); tlc, silica gel, R_f = 0.60 using 1:9 EtOAc–toluene as elutant.

Dimethyl (1RS,4SR,8SR)-4-phenylseleno-8-methoxytetra-cyclo[4.2.2.0^{2,5}.0^{3,7}]deca-9-ene-9,10-dicarboxylate, **58**, gave ^{13}C nmr: 41.0 (d, C1); 39.3 (d, C2); 45.1 (d, C3); 48.3 (d, C4); 44.2 (d, C5); 37.4 (d, C6); 43.2 (d, C7); 82.9 (d, C8); 53.8 (q, CH_3O); tlc, silica gel, R_f = 0.43 using 1:9 EtOAc–toluene as elutant.

Dimethyl (1RS,4SR,8RS)-4-phenylseleno-8-methoxytetra-cyclo[4.2.2.0^{2,5}.0^{3,7}]deca-9-ene-9,10-dicarboxylate, **59**, gave ^{13}C nmr: 41.1 (d, C1); 39.6 (d, C2); 42.8 (d, C3); 48.0 (d, C4); 45.3 (d, C5); 37.6 (d, C6); 42.0 (d, C7); 82.0 (d, C8); 52.8 (q, CH_3O); tlc, silica gel, R_f = 0.43 using 1:9 EtOAc–toluene as elutant.

Methyl (1RS,4SR,12RS)-4-phenylthio-9-oxapentacyclo-[6.4.0.0^{2,5}.0^{3,7}.0^{6,11}]dodeca-10-one-12-carboxylate, **22**, was prepared in accord with the procedure of Zefirov *et al.* (12) and gave ir (CCl_4): 1805, 1755 cm^{-1}; ^{13}C nmr: 35.3 (d, C1); 45.1 (d, C2); 48.9 (d, C3); 61.6 (d, C4); 45.3 (d, C5); 31.6 (d, C6); 50.7 (d, C7); 84.2 (d, C8); 176.0 (s, C=O, C10); 39.4 (d, C11); 44.8 (d, C12); 171.5 (s, CO_2CH_3); 52.4 (q, CH_3O_2).

Methyl (1RS,4SR,12RS)-4-phenylseleno-9-oxapentacyclo-[6.4.0.0^{2,5}.0^{3,7}.0^{6,11}]dodeca-10-one-12-carboxylate, **31**, was isolated from the reaction of benzeneselenenyl chloride with **5** using methanol as solvent. Infrared (CCl_4): 1811, 1760 cm^{-1}; ^{13}C nmr: 36.0 (d, C1); 45.8 (d, C2); 48.7 (d, C3); 60.9 (d, C4); 46.4 (d, C5); 34.5 (d, C6); 50.3 (d, C7); 84.4 (d, C8); 175.8 (s, C=O, C10); 37.3 (d, C11); 44.3 (d, C12); 171.6 (s, CO_2CH_3); 51.5 (q, CH_3O_2).

Methyl (1RS,4SR,12SR)-4-phenylseleno-9-oxapentacyclo-[6.4.0.0^{2,5}.0^{3,7}.0^{6,12}]dodeca-10-one-12-carboxylate, **32**, gave ^{13}C nmr: 38.5 (d, C1); 44.6 (d, C2); 48.7 (d, C3); 59.5 (d, C4); 46.0 (d, C5); 36.2 (d, C6); 50.2 (d, C7); 76.1 (d, C8); 175.1 (s, C=O, C10); 39.3 (d, C11); 43.5 (d, C12); 172.3 (s, CO_2CH_3); 51.3 (q, CH_3O_2).

Acknowledgement

Continued financial support from the Natural Sciences and Engineering Research Council of Canada for the portion of this work carried out at the University of Ottawa is gratefully acknowledged.

1. D. G. Garratt. Tetrahedron Lett. 1915 (1978).
2. D. G. Farnum and J. P. Snyder. Tetrahedron Lett. 3861 (1965).
3. T. Sasaki, K. Kanematsu, A. Kondo, and Y. Nishitani. J. Org. Chem. **39**, 3569 (1974).
4. T. Sasaki, K. Kanematsu, A. Kondo, and K. Okada. J. Org. Chem. **41**, 2231 (1976).
5. T. Sasaki, K. Kanematsu, and A. Kondo. J. Chem. Soc. Perkin Trans. I, 2516 (1976).
6. T. Sasaki, K. Kanematsu, and A. Kondo. J. Org. Chem. **39**, 2246 (1974).
7. A. Kondo, T. Yamane, T. Ashida, T. Sasaki, and K. Kanematsu. J. Org. Chem. **43**, 1180 (1978).
8. G. Mehta and P. N. Pandey. Tetrahedron Lett. 3567 (1975).
9. N. S. Zefirov, K. N. Sadovaya, V. N. Kirin, A. S. Koz'min, and I. V. Bodrikov. Zh. Org. Khim. **13**, 228 (1977).
10. G. Mehta, P. K. Dutta, and P. N. Pandey. Tetrahedron Lett. 445 (1975).
11. N. S. Zefirov, V. V. Ilyukhin, N. V. Belov, K. A. Potekhin, E. N. Kurkutova, Yu. T. Struchkov, V. N. Kirin, and A. S. Koz'min. Dokl. Akad. Nauk SSSR, **243**, 652 (1978); Chem. Abstr. **90**, 103547 (1979).
12. N. S. Zefirov, B. N. Kirin, K. A. Potekhin, A. S. Koz'min, N. K. Sadovaya, E. N. Kurkutova, and I. V. Bodrikov. Zh. Org. Khim. **14**, 1135 (1978).
13. N. S. Zefirov, V. N. Kirin, A. S. Koz'min, I. V. Bodrikov, K. A. Potekhin, and E. N. Kurkutova. Tetrahedron Lett. 2617 (1978).
14. N. S. Zefirov, N. V. Averina, A. M. Boganov, T. S. Kuznetsova, and S. S. Yarovi. Dokl. Akad. Nauk SSSR, **233**, 258 (1977).
15. K. A. Potekhin, E. N. Kurkutova, Yu. T. Struchkov, A. C. Koz'min, V. N. Kirin, N. S. Zefirov, V. V. Ilyukhin, and N. V. Belov. Dokl. Akad. Nauk SSSR, **242**, 832 (1978).
16. N. S. Zefirov, A. S. Koz'min, V. N. Kirin, V. V. Zhdankin, and I. V. Bodrikov. Zh. Org. Khim. **14**, 2615 (1978); Chem. Abstr. **90**, 137390 (1979).
17. N. S. Zefirov, A. C. Koz'min, V. N. Kirin, V. V. Zhdankin, and I. V. Bodrikov. Zh. Org. Khim. **14**, 2646 (1978).
18. W. A. Smit, N. S. Zefirov, I. V. Bodrikov, and M. Z. Krimer. Acc. Chem. Res. **12**, 282 (1979).
19. N. S. Zefirov, A. C. Koz'min, V. V. Zhdankin, V. N. Kirin, I. V. Bodrikov, B. B. Sedova, and V. G. Rau. Tetrahedron Lett. 3533 (1979).
20. N. S. Zefirov, V. N. Kirin, A. C. Koz'min, I. V. Bod-

RIKOV, K. A. POTEKHIN, and E. N. KURKUTOVA. Tetrahedron Lett. 1547 (1979).
21. D. G. GARRATT and G. H. SCHMID. Can. J. Chem. **52**, 1027 (1974).
22. D. G. GARRATT and G. H. SCHMID. Can. J. Chem. **52**, 3599 (1974).
23. G. H. SCHMID and D. G. GARRATT. Tetrahedron Lett. 3991 (1975).
24. D. G. GARRATT and G. H. SCHMID. Chem. Scr. **9**, 110 (1975).
25. D. G. GARRATT and G. H. SCHMID. J. Org. Chem. **42**, 1776 (1977).
26. D. G. GARRATT. Can. J. Chem. **56**, 2184 (1978).
27. G. H. SCHMID and D. G. GARRATT. Tetrahedron, **34**, 2869 (1978).
28. D. G. GARRATT, M. D. RYAN, and M. UJJAINWALLA. Can. J. Chem. **57**, 2145 (1979).
29. D. G. GARRATT. Can. J. Chem. **57**, 2180 (1979).
30. P. L. BEAULIEU, V. M. MORISSET, and D. G. GARRATT. Tetrahedron Lett. **21**, 129 (1980).
31. D. G. GARRATT, M. D. RYAN, and P. L. BEAULIEU. J. Org. Chem. **45**, 839 (1980).
32. D. G. GARRATT, P. L. BEAULIEU, and M. D. RYAN. Tetrahedron, **36**, 1507 (1980).
33. D. G. GARRATT and A. KABO. Can. J. Chem. **58**, 1030 (1980).
34. N. S. ZEFIROV, L. G. GURVICH, A. S. SHASHKOV, and W. A. SMIT. Zh. Org. Khim. **10**, 1786 (1974).
35. N. MIYOSHI, S. FURUI, S. MURAI, and N. SONODA. J. Chem. Soc. Chem. Commun. 293 (1975).
36. N. MIYOSHI, S. MURAI, and N. SONODA. Tetrahedron Lett. 851 (1977).
37. E. G. KATAEV, T. G. MANNAFOV, E. A. BERDNIKOV, and O. A. KOMAROVAKAYA. Zh. Org. Khim. **9**, 1983 (1973).
38. H. J. REICH. J. Org. Chem. **39**, 428 (1974).
39. K. B. SHARPLESS and R. F. LAUER. J. Org. Chem. **39**, 429 (1974).
40. D. L. J. CLIVE. J. Chem. Soc. Chem. Commun. 100 (1974).
41. D. LIOTTA and G. ZIMA. Tetrahedron Lett. 4977 (1978).
42. J. P. SNYDER and D. G. FARNUM. J. Org. Chem. **31**, 1699 (1966).
43. J. B. STOTHERS. *In* Carbon-13 nuclear magnetic resonance spectroscopy. Academic Press, New York. 1972.
44. F. W. WEHRLI and T. WIRTHLIN. *In* Interpretation of carbon-13 nmr spectra. Heyden & Sons, London. 1972. pp. 48–63.
45. G. H. SCHMID and D. G. GARRATT. *In* The chemistry of double bonded functional groups. *Edited by* S. Patai. Wiley & Sons, New York. 1977. Chapt. 9.
46. N. S. ZEFIROV, N. K. SADOVAJA, L. A. NOVGORODTSEVA, R. SH. ACHMEDOVA, S. V. BARANOV, and I. V. BODRIKOV. Tetrahedron, **35**, 2759 (1979).
47. N. S. ZEFIROV, N. K. SADOVAYA, A. M. MAGGERANOV, I. V. BODRIKOV, and V. R. KARTASKOV. Tetrahedron, **31**, 2948 (1975); Zh. Org. Khim. **10**, 2620 (1974).
48. N. S. ZEFIROV, N. K. SADOVAJA, L. A. NOVGORODTSEVA, and I. V. BODRIKOV. Zh. Org. Khim. **14**, 463 (1978).
49. N. S. ZEFIROV, N. K. SADOVAJA, A. M. MAGGARANOV, and I. V. BODRIKOV. Zh. Org. Khim. **13**, 245 (1977), and references cited therein.
50. N. S. ZEFIROV, N. K. SADOVAJA, R. SH. AKHMEDOVA, and I. V. BODRIKOV. Zh. Org. Khim. **14**, 612 (1978).
51. E. OSAWA, K. AIGAMI, and Y. INAMOTO. Tetrahedron, **34**, 509 (1978).
52. E. M. ENGLER, J. D. ANDOSE, and P. v. R. SCHLEYER. J. Am. Chem. Soc. **95**, 8005 (1973).
53. J. D. ANDOSE and K. MISLOW. J. Am. Chem. Soc. **96**, 2168 (1974).
54. N. L. ALLINGER, M. T. TRIBBLE, M. A. MILLER, and D. H. WERTZ. J. Am. Chem. Soc. **93**, 1637 (1971).
55. N. L. ALLINGER and J. T. SPRAGUE. J. Am. Chem. Soc. **94**, 5734 (1972).
56. N. L. ALLINGER, M. T. TRIBBLE, and M. A. MILLER. Tetrahedron, **28**, 1173 (1972).

Can. J. Chem. Downloaded from www.nrcresearchpress.com by 210.87.254.105 on 09/05/12
For personal use only.

Complete analysis of the ^{1}H nmr spectrum of tetrahydrothiophene

ANGEL LUIS ESTEBAN
Facultad de Ciencias, Alicante, Spain
AND
ERNESTO DÍEZ[1]
Departamentos de Electroquímica e Investigaciones Químicas, C.S.I.C., Universidad Autónoma, Cantoblanco, Madrid 34, Spain

Received April 30, 1980

ANGEL LUIS ESTEBAN and ERNESTO DÍEZ. Can. J. Chem. **58**, 2340 (1980).

The ^{1}H nmr spectrum of tetrahydrothiophene has been analyzed. The best set of coupling values (Hz) is: $^2J_A - {}^2J_B = 2.18$, $^3J_B^c = 5.53$, $^3J_B^t = 7.31$, $^3J_{AB}^c = 6.80$, $^3J_{AB}^t = 6.37$, $^4J_A^c = -0.32$, $^4J_A^t = 0.25$, $^4J_{AB}^c = 0.26$, $^4J_{AB}^t = -0.47$ (A and B refer to α- and β- protons and c and t denote respectively the same and opposite sides of the ring). The variances observed between the values of this set and those reported by Lozach *et al.*, particularly the interchange of the $^4J_A^c$ and $^4J_A^t$ couplings, are discussed and it is concluded that our set is the one that reproduces the most fine details of the spectrum profile. The proposed set has been selected as being the most physically meaningful, from amongst 24 equally valid sets of couplings, on the basis of a better agreement with the ^3J_B and $^4J_{AB}$ values calculated from a Karplus relationship and from the INDO-FPT method respectively. In these calculations it was assumed that the molecule was interconverting rapidly (on the nmr time scale) between two puckered conformations with C_2 symmetry. A detailed discussion of the dependence of the couplings on the height of the pseudorotational barrier and on the temperature indicate that the minimum values of the potential energy correspond to these conformations.

ANGEL LUIS ESTEBAN et ERNESTO DÍEZ. Can. J. Chem. **58**, 2340 (1980).

On a analysé les spectres rmn du ^{1}H du tétrahydrothiophène. Le meilleur ensemble de valeurs de couplage (Hz) est: $^2J_A - {}^2J_B = 2{,}18$, $^3J_B^c = 5{,}53$, $^3J_B^t = 7{,}31$, $^3J_{AB}^c = 6{,}80$, $^3J_{AB}^t = 6{,}37$, $^4J_A^c = -0{,}32$, $^4J_A^t = 0{,}25$, $^4J_{AB}^c = 0{,}26$, $^4J_{AB}^t = -0{,}47$ (A et B font référence aux protons α et β et c et t dénotent respectivement le même et le côté opposé du cycle). On discute des différences observées entre les valeurs de cet ensemble et celles rapportées par Lozach et ses collaborateurs, particulièrement l'échange mutuel des couplages $^4J_A^c$ et $^4J_A^t$ et on a conclu que notre ensemble est celui qui reproduit le mieux les détails les plus subtils du spectre. On a choisi l'ensemble proposé comme étant celui qui physiquement est le plus significatif parmi 24 ensembles de couplages également valables, en se basant sur un meilleur accord entre les valeurs de ^3J_B et $^4J_{AB}$ calculées respectivement à partir de la relation de Karplus et de la méthode INDO-FPT. Dans ces calculs, on a fait l'hypothèse que la molécule subit rapidement une interconversion (à l'échelle du temps de la rmn) entre deux conformations gauches avec une symétrie C_2. Une discussion détaillée de l'effet de la hauteur de la barrière pseudo-rotationnelle et de la température sur les couplages, indique que les valeurs minima de l'énergie potentielle correspondent à ces conformations.

[Traduit par le journal]

Introduction

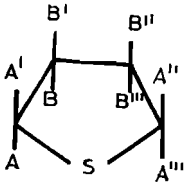
The ^{1}H nmr spectra of five-membered saturated rings of the type $(CH_2)_4X$, (X = O, S, Se, etc.), are being analysed by us (1, 2) with the aim of obtaining precise values of the proton–proton coupling constants to study the conformational behaviour in solution of these molecules. The spectra of tetrahydrofuran (THF, X = O) (1) and tetrahydroselenophene (THS, X = Se) (2) have been analysed by using a computer program written to carry out efficiently the spectral analysis for the $(AB)_4$ spin systems with C_{2v} symmetry (1). In this paper we report the complete analysis of the spectrum of tetrahydrothiophene (THT, X = S) which presents special difficulties arising from the small effect on the spectrum profile of the coupling differences ^2D, $^3D_{AB}$, and $^4D_{AB}$, as well as of the sign of ^4D_A, (the adopted notation is illustrated in the chart). A detailed study of the spectral dependence on these parameters has made possible a reliable determination of their values from spectra with optimum resolution. Some of our results differ from those obtained by Lozach *et al.* (3) who carried out a similar analysis in which these requirements were not so extensively satisfied. The values of the vicinal couplings for THT were first reported by Lambert *et al.* (4). The values for $^3J_B^c$ and $^3J_B^t$ were determined from the analysis of the ^{13}C satellites of THT-2,2′,5,5′-d_4 and those of $^3J_{AB}^c$ and $^3J_{AB}^t$ from the analysis of the proton spectrum of THT-2,2′,3,3′-d_4. These spectra were obtained with deuterium decoupling and the influence on the latter of $^3D_{AB}$ is so small that precise values for $^3J_{AB}^c$ and $^3J_{AB}^t$ cannot be determined from it.

The interpretation of the couplings of THF and THS in CS_2 solution could be satisfactorily made assuming the same conformational behaviour found in vapour phase studies, i.e., approximately free pseudorotation for THF (1) and fast inversion

[1]Author to whom correspondence may be addressed, at Facultad de Ciencias CII-103, Universidad Autónoma, Cantoblanco, Madrid 34, Spain.

0008-4042/80/222340-09$01.00/0
©1980 National Research Council of Canada/Conseil national de recherches du Canada

Can. J. Chem. Downloaded from www.nrcresearchpress.com by 210.87.254.42 on 09/05/12
For personal use only.



$$^2J_A = J_{AA'} \qquad ^2J_B = J_{BB'}$$

$$^2S = {}^2J_A + {}^2J_B \qquad ^2D = {}^2J_A - {}^2J_B$$

$$^3J^c_{AB} = J_{AB} \qquad ^4J^c_A = J_{AA'''}$$

$$^3J^t_{AB} = J_{AB'} \qquad ^4J^t_A = J_{AA''}$$

$$^3J^c_B = J_{BB'''} \qquad ^4J^c_{AB} = J_{AB'''}$$

$$^3J^t_B = J_{BB''} \qquad ^4J^t_{AB} = J_{AB''}$$

$$^nS_M = {}^nJ^c_M + {}^nJ^t_M \qquad n = 3, 4$$

$$^nD_M = {}^nJ^c_M - {}^nJ^t_M \qquad M = A, B, AB$$

between the two stable half-chair conformations with C_2 molecular symmetry for THS (2). For THT the far ir spectrum has been interpreted (5) in terms of a model of hindered pseudorotation with a potential barrier of 773 cm^{-1} separating two stable half-chair conformations. Likewise, the experimental electron diffraction data (6) were found to be in good agreement with the theoretical results obtained by assuming C_2 molecular symmetry. A detailed study of the dependence of couplings on the height of the barrier to pseudorotation and on the temperature confirm that, as for THF and THS, the conformational behaviour of THT in CS_2 solution is very similar to that in the vapour phase.

Spectral Analysis

The proton spectrum of THT was obtained on a Varian XL-100 spectrometer. The sample used, a solution of THT in CS_2 with TMS as an internal reference (molar fractions, $\chi_{THT} = 0.12$, $\chi_{TMS} = 0.08$ and $\chi_{CS_2} = 0.80$) was degassed by the freezing and thawing technique and sealed under vacuum. Sweep widths of 0.5 Hz cm^{-1} and sweep rates of 0.005 Hz s^{-1} were employed. Radiofrequency of low power (40 dB) was applied to avoid saturation. Under these experimental conditions the half-height line width was of 0.09 Hz. Peak frequencies were determined to $\pm$ 0.01 Hz by linear interpolation between readings from a frequency counter.

The analysis of the THT spectrum was carried out following the same steps as in the analysis of the similar THS spectrum (2) but particular difficulties arose because of the small effect on the THT spectrum of the coupling differences ^2D, $^3D_{AB}$, and $^4D_{AB}$, as well as of the sign of ^4D_A. In the first step, accurate values of the parameters $^3S_{AB}$, $^4S_{AB}$, ^3S_B, ^3D_B, ^4S_A, and ^4D_A were obtained from a fit of the line frequencies that depend only on these parameters. The spectrum calculated with these values and by taking $^2D = {}^3D_{AB} = {}^4D_{AB} = 0$ Hz and $^2S = -22$ Hz barely differs from the experimental spectrum, as can be seen in Fig. 1 where both spectra are shown for the high field signal zone. In the second step the values of ^2D, $^3D_{AB}$, and $^4D_{AB}$ were modified stepwise to correct these small differences in order to get a calculated spectrum as close as possible to the observed one, which allowed us to perform a reliable spectral assignment. Spectra were computed assuming that $^3D_B < 0$, $^4D_{AB} > 0$, and $^4D_A < 0$. The two first assumptions can be made to fit the experimental spectrum because, as has been discussed in ref. 1, there are several sets of couplings yielding an identical spectrum. The sign of ^4D_A was taken as negative, $^4D_A = -0.57$ Hz, by comparison with the value $^4D_A = -0.44$ Hz of THS, but the possibility of the positive sign for ^4D_A was also examined and is described below. In the third step, after accomplishing a satisfactory agreement between the experimental and the calculated spectra, an iterative refinement of the magnetic parameters was carried out from an assignment of 430 transitions out of 620 calculated transitions with an intensity greater than 0.05. The influence of ^2S on the spectrum is so small that one of the two couplings ^2J was kept constant in the iterative process, $^2J_B = -12.6$ Hz, since otherwise the problem would have remained undetermined. The first columns in Table 1 give the iterated magnetic parameter values, Set 1, together with their standard errors. The average deviation between observed and calculated line frequencies was 0.0153 Hz. An excellent agreement was obtained between the experimental spectrum and the simulated calculated spectrum as can be seen in Fig. 1, where both spectra appear for the high field signal zone, and in Fig. 2, where they appear for five signal zones selected from those where the effect of the ^2D, $^3D_{AB}$, and $^4D_{AB}$ parameters, and that of the ^4D_A sign, are more relevant.

Errors in the couplings and "vector errors" show similar features as in THF and THS (1, 2) except for the couplings ^2J. Since the ^2J_B coupling was kept constant in the iterative process the vector error ($\sim 0.7\ ^2S$) does not appear. This, in the case of THF and THS, has the largest error. The errors of the vector errors ($\sim 0.7\ ^3D_{AB}$), 0.022; ($\sim 0.7\ ^4D_{AB}$), 0.015; and ($\sim {}^2J_A$), 0.009 Hz, are the largest ones owing to the fact that the spectrum barely depends on the $^3D_{AB}$, $^4D_{AB}$, and ^2D parame-

Can. J. Chem. Downloaded from www.nrcresearchpress.com by 210.87.254.42 on 09/05/12
For personal use only.

Can. J. Chem. Downloaded from www.nrcresearchpress.com by 210.87.254.42 on 09/05/12
For personal use only.

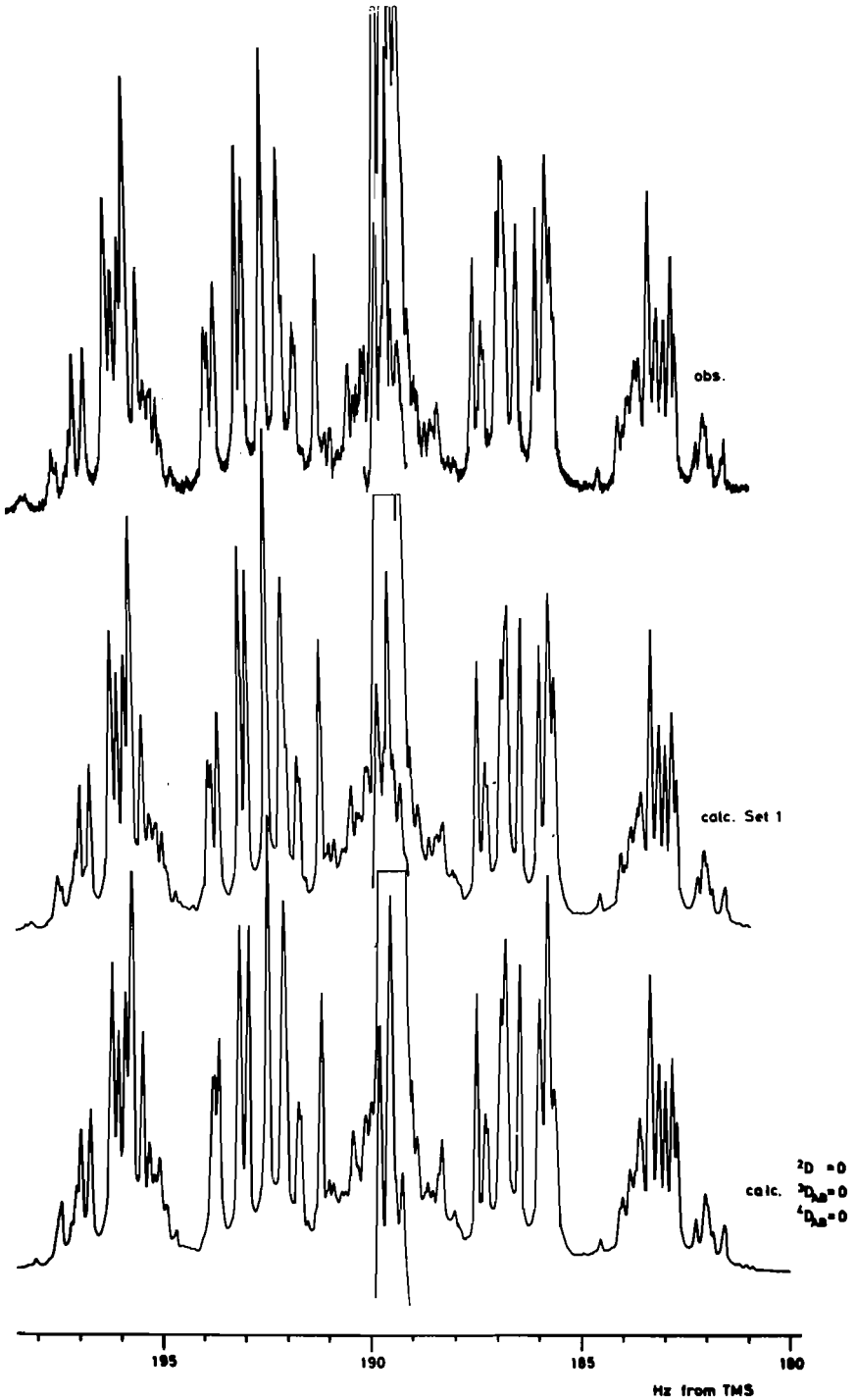


FIG. 1. Spectrum for protons B in THT. From top to bottom appears the observed spectrum, the spectrum calculated with the Set 1 values, and the spectrum calculated with the set values that result by taking $^2D = {}^3D_{AB} = {}^4D_{AB} = 0$ Hz (the values of the other parameters differ less than ± 0.02 Hz from the corresponding ones of Set 1).

TABLE 1. Chemical shifts (ν, Hz from TMS), coupling constants (J, Hz), and errors of parameter estimates for the ^{1}Hmr spectrum of tetrahydrothiophene

Parameter	Set 1[a]	Standard errors	Actual errors	Set 2[a]	Set 3[b]	Errors	Set 4[c]
ν_A	273.001	0.002	0.02	273.002	274.03	0.01	
ν_B	189.764	0.002	0.02	189.765	188.12	0.01	
$^2J_A - {}^2J_B$	2.184	0.009	0.05	2.163	1.9	0.2	
$^3J_B^c$	5.532	0.003	0.02	5.531	5.48	0.02	5.45
$^3J_B^t$	7.307	0.003	0.02	7.309	7.32	0.02	7.25
$^3J_{AB}^c$	6.802	0.016	0.1	6.765	6.55	0.2	6.66
$^3J_{AB}^t$	6.374	0.015	0.1	6.416	6.70	0.2	6.66
$^4J_A^c$	−0.318	0.002	0.02	0.251	0.25	0.02	
$^4J_A^t$	0.250	0.002	0.02	−0.317	−0.33	0.02	
$^4J_{AB}^c$	0.260	0.009	0.06	0.239	0.23	0.1	
$^4J_{AB}^t$	−0.469	0.009	0.06	−0.447	−0.43	0.1	

[a]This work. Iterated values with $^4D_{AB} < 0$, Set 1, and $^4D_{AB} > 0$, Set 2.
[b]Reference 2.
[c]Reference 1.

ters. Correspondingly, the couplings $^3J_{AB}$, $^4J_{AB}$, and ^2J_A present the largest errors amongst all couplings and the greatest correlation coefficients appear between the couplings $^3J_{AB}$, −0.99, and $^4J_{AB}$, −0.95. The actual errors of the parameters must be larger than those resulting from the fitting and can be estimated, from the effect of the parameters on the spectrum, to be ± 0.02 Hz for the couplings ^4J_A and ^3J_B and for the combinations $^3S_{AB}$ and $^4S_{AB}$, and ±0.05, ±0.1, and ±0.2 Hz for the differences ^2D, $^4D_{AB}$, and $^3D_{AB}$, respectively.

The interchange of the couplings $^4J_A^c$ and $^4J_A^t$, i.e. the change in the sign of ^4D_A, does not alter the spectrum if $^2D = {}^3D_{AB} = {}^4D_{AB} = 0$ Hz. Although the effect of these differences on the THS spectrum is small, the change in sign of ^4D_A sufficiently alters the spectrum so as to make possible its determination. When the values of the couplings $^4J_A^c$ and $^4J_A^t$ of Set 1 are interchanged most of the calculated lines are shifted less than 0.01 Hz. In the high field signal zone only one of each ten lines is shifted more than 0.01 Hz, without exceeding 0.02 Hz, whilst in the low field signal zone two of each ten lines are shifted more than 0.01 Hz, some of them reaching 0.033 Hz. From this calculated spectrum an assignment was made, including the same lines as in the previous one, and an iterative refinement of the magnetic parameter values was carried out. The interated parameter values, Set 2 in Table 1, practically do not differ from those of Set 1, except for the interchange of the couplings $^4J_A^c$ and $^4J_A^t$, and their standard errors are only slightly greater than those of Set 1. The average deviation between observed and calculated line freqencies, 0.0170 Hz, was only 0.0017 Hz greater than for Set 1. However, the agreement between the experimental spectrum and the simulated calculated spectrum is not as good as that obtained with Set 1 (see Fig. 2). This is mainly appreciated in zones where two very close lines are shifted in opposite directions by the change in the sign of ^4D_A. Such is the case for the two lines with experimental frequencies 265.25 and 265.32 Hz, whose calculated frequencies (intensities) are 265.25 (0.6) and 265.32 (1.0) Hz for Set 1 but 265.27 (0.6) and 265.29 (1.0) Hz for Set 2. On the other hand, the band with experimental frequency 265.99 Hz has three transitions assigned, those for Set 1 are spread over only 0.028 Hz, whilst for Set 2 they are spread over 0.076 Hz. Both situations, calculated lines too close or too separated, appear also in a few other signal zones making it evident that the sign of ^4D_A cannot be positive.

According to the small effect of the ^2D parameter on the THT spectrum the absolute values of the partial derivatives of the transition frequencies with respect to ^2D, $|\delta\nu_{k1}/\delta^2D|$, do not exceed 0.05 with the exception of about 30 weak lines, with intensities between 0.05 and 0.25, where these derivatives are close to 1.0. Most of these weak lines are obscured by others in their vicinity with a larger intensity but there are a few that can be picked out in the experimental spectrum. Such is the case for the four asterisked lines in Figs. $2c_1$ and $2d_1$ that can be used to test the reliability of the calculated values of ^2D, $^4D_{AB}$, and $^3D_{AB}$ as well as the sign of ^4D_A, since these lines are much more affected than their neighbours by changes in these parameters. As can be seen in Fig. $2c_3$, the reversing of the sign of ^4D_A causes the calculated ratio between the intensities of the bands at 198.16 and 198.28 Hz to be remarkably greater than the experimental ratio. When ^2D is changed by a given amount the asterisked lines are shifted approximately the same amount whilst the neighbouring lines remain practically un-

Can. J. Chem. Downloaded from www.nrcresearchpress.com by 210.87.254.42 on 09/05/12
For personal use only.

Can. J. Chem. Downloaded from www.nrcresearchpress.com by 210.87.254.42 on 09/05/12
For personal use only.

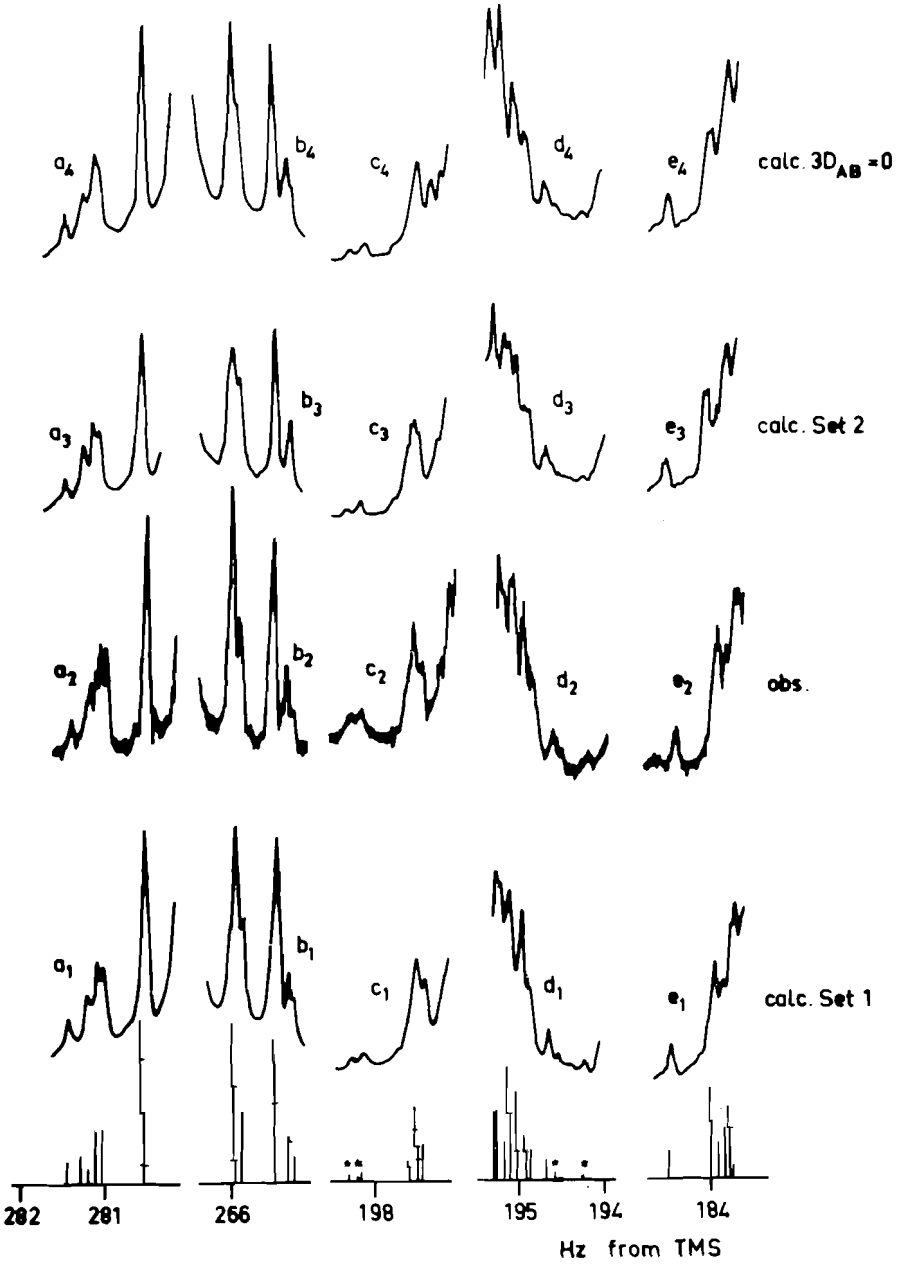


FIG. 2. THT spectrum for five signal zones selected from those where the effect of the ^2D, $^3D_{AB}$, and $^4D_{AB}$ differences, and that of the ^4D_A sign, are more relevant. From bottom to top appears the spectrum calculated with the Set 1 values, the observed spectrum, the spectrum calculated with the Set 2 values, and the spectrum calculated by taking $^3D_{AB} = 0$ Hz.

changed. When $^4D_{AB}$ is changed by a small amount, the asterisked lines are only shifted approximately a quarter of this amount but their intensities are also influenced, reducing to a half if $^4D_{AB}$ is decreased by 0.2 Hz and to zero if $^4D_{AB} = 0$ Hz. The effect of changing $^3D_{AB}$ is even less than for $^4D_{AB}$, and practically only affects the two outer lines. When $^3D_{AB}$ is changed by a small amount these two lines are shifted only approximately a tenth part of this amount. For $^3D_{AB} = 0$ they are shifted 0.05 Hz and these small shifts cause the two bands with experimental frequencies 198.16 and 198.28 Hz to appear too separated, 0.20 Hz, in the calculated spectrum, as can be seen in Fig. $2c_4$. Other disagreements between the experimental and the calculated spectra are due to shifts smaller than 0.03 Hz of

Can. J. Chem. Downloaded from www.nrcresearchpress.com by 210.87.254.42 on 09/05/12
For personal use only.

lines whose frequencies practically do not depend on ^2D. So the shoulder at 265.89 Hz, of the band at 265.99 Hz, does not clearly appear in Fig. $2b_4$ because the line assigned to the shoulder is shifted 0.01 Hz closer to the three lines assigned to the band. When the sign of $^3D_{AB}$ is reversed, the differences between the experimental and the calculated profiles are more evident, but if an iterative process is carried out using the resulting parameters as initial values, the sign of $^3D_{AB}$ is restored and the final values of the parameters are those of Set 1.

Discussion

The two sets of couplings resulting from our analysis of the ^{1}Hmr spectrum of THT with signs for the ^4D_A difference negative, Set 1, and positive, Set 2, are listed in Table 1 together with those reported by Lozach *et al.* (3), Set 3, and by Lambert *et al.* (4), Set 4. As discussed in the previous section, the choice of Set 1 as the correct solution, instead of Set 2, is unquestionable in spite of the small effect of the sign of ^4D_A on the THT spectrum. The actual errors of the $^3J_{AB}$, $^4J_{AB}$, and ^2D parameters are larger than those in the remaining couplings due to the small influence of $^3D_{AB}$, $^4D_{AB}$, and ^2D on the spectrum. Errors in the individual couplings, $^3J_{AB}$ and $^4J_{AB}$, arise mainly from the error involved in their differences, $^3D_{AB}$ and $^4D_{AB}$, as the error in their combinations $^3S_{AB}$ and $^4S_{AB}$ is only 0.02 Hz.

In Set 3, of Lozach *et al.*, the sign of ^4D_A is incorrect and therefore the couplings $^4J^c_A$ and $^4J^t_A$ are interchanged. With regard to the rest of the couplings the differences between the values of Sets 3 and 1 do not exceed ± 0.05 Hz except those of ^2D, $^3J^c_{AB}$, and $^3J^t_{AB}$, which are around ± 0.3 Hz. The differences between our $^3J_{AB}$ values and theirs arise mainly from the difference of -0.58 Hz in the $^3D_{AB}$ values, since the $^3S_{AB}$ values are closer (difference 0.07 Hz). The errors of the $^3J_{AB}$, $^4J_{AB}$, and ^2D parameters are larger in Set 3 than in Set 1 owing probably to the fact that the spectral resolution attained by Lozach *et al.*, for net THT, is not so good as that in this work, for a solution of THT in CS_2. The difference of resolution is evident by comparison of Fig. 1 with Fig. 2 of ref. 3. A very good spectral resolution is indispensable to obtain accurate values of these parameters owing to the small influence of the $^3D_{AB}$, $^4D_{AB}$, and ^2D differences over the THT spectrum.

Remarks similar to the aforementioned for the vicinal coupling values of Set 3 can be made for those of Set 4, of Lambert *et al.* The difference $^3D_{AB}$ of Set 4, equal to 0.00 Hz, is closer to the value of -0.15 Hz of Set 3 than to the value of 0.43 Hz of Set 1. Notwithstanding, we consider that our value is the most reliable. The $^3J_{AB}$ values of Set 4 were determined from the analysis of the proton spectrum of THT-2,2′,3,3′-d_4 obtained with deuterium decoupling. This spectrum corresponds to a spin system $[AB]_2$ and the influence on it of $^3D_{AB}$ is so small that this parameter can only be accurately determined from spectra with a resolution much better than that shown in the spectra reported in ref. 4.

As discussed in ref. 1, by carrying out certain concerted coupling interchanges from Set 1, 23 other parameter sets are obtained that yield an identical fit of the experimental spectrum. The final decision on selecting the physically meaningful set should be based upon a consideration of the relative magnitudes of $^3J^c_B$ and $^3J^t_B$, as well as $^4J^c_{AB}$ and $^4J^t_{AB}$ (or $^3J^c_{AB}$ and $^3J^t_{AB}$). These can be estimated from relations between coupling constants and conformational geometric parameters.

In the calculation of the ^3J_B, $^3J_{AB}$, and $^4J_{AB}$ couplings it was assumed that, as it seems to occur for the THF and THS molecules (1, 2), the conformational behaviour of the THT molecule in CS_2 solution is the same as in the vapour phase, i.e., a fast inversion between two puckered conformations with C_2 symmetry (5, 6). The vicinal ^3J couplings were calculated by using the Karplus equation with the coefficients given by Pachler and Wessels for ethane (7), where θ is the dihedral angle

$$[1] \quad {}^3J = 8.0 - 1.0\cos\theta + 6.0\cos 2\theta$$

H—C—C—H. The long-range ^4J couplings across a H—C—C—C—H′ path depend mainly on the dihedral angles ϕ, H—C—C—C, and ϕ', C—C—C—H′ and were calculated by using the INDO-FPT method (8) applied to propane with standard geometries. The dihedral angles were estimated from the electron diffraction values (6) of the intracyclic torsion angles S—C—C—C, $\psi_{AB} = \pm 40.4°$, and C—C—C—C, $\psi_B = \mp 52.5°$, assuming tetrahedral values for the bond angles; $\theta = \psi$ for $^3J^c$, $\theta = \psi - 120°$ for $^3J^t$, $(\phi, \phi') = (120° - \psi_B, 120° + \psi_{AB})$ for $^4J^c_{AB''}$, and $(\phi, \phi') = (120° - \psi_B, 240° + \psi_{AB})$ for $^4J^t_{A'B''}$ (angles ϕ and ϕ' are measured in the same sense from the C—C—C plane (9) and the unprimed H is in position B″).

The calculated coupling values, given in column 1 of Table 2, substantiate that $^3J^c_B < {}^3J^t_B$ and $^4J^c_{AB} > {}^4J^t_{AB}$ (and also, $^3J^c_{AB} > {}^3J^t_{AB}$), supporting the choice of Set 1, Table 1, as the most physically meaningful amongst the 24 parameter sets that yield an identical fit of the experimental spectrum. However, to confirm this selection, two points should be discussed in detail, the reliability of the J values given

Can. J. Chem. Downloaded from www.nrcresearchpress.com by 210.87.254.42 on 09/05/12
For personal use only.

by eq. [1] and by the INDO-FPT method, and the fact that the THT molecule in CS_2 solution has the same conformational behaviour as in the vapour phase.

The calculated vicinal coupling values are greater than the experimental ones (as in the case for THF (1) and THS (2)), owing to the use of an empirical Karplus equation for ethane without further corrections for the effects of bond angle changes and for the relative orientation of substituents. The latter effect is thought to be small, since it depends on the substituent electronegativity (10) and this one is very similar for the —S— and CH_3— groups. Corrections to the ^3J couplings, calculated from data in Table 3 of ref. 10 taking the effects of the —CH_2— and —S— groups equal to the effect of the —CH_3 group, are within −0.2 and −0.5 Hz. The effects of bond angle changes can be more important in this case, but their estimation (11) necessitates the knowledge of the values of the bond angles HCC and CCH′ which have not been measured with the required accuracy. Taking all this into consideration, the correlation between calculated and experimental ^3J couplings can be judged as satisfactory. The conclusion that $^3J^c_B < {}^3J^t_B$ can be safely established from the calculated ^3D_B value of −3.3 Hz, but the conclusion that $^3J^c_{AB} > {}^3J^t_{AB}$ has a limited significance because the values of the $^3J_{AB}$ couplings are very close. The second conclusion is not necessary for choosing Set 1. This choice can likewise be based on the firmer $^4J^c_{AB} > {}^4J^t_{AB}$ conclusion.

The $^4J_{AB}$ values calculated by the INDO-FPT method are in acceptable agreement with the experimental ones. According to Barfield *et al.* (9) the INDO-FPT method, as well as the sum of the EHMO and VB-SOT results, reproduces the experimental trends of the ^4J couplings: (*i*) couplings between equatorial protons ($\phi = \phi' = 180°$) are in the range +1 to +2 Hz, (*ii*) couplings between axial and equatorial protons ($\phi = 60°$, $\phi' = 180°$) are in the range 0.4 to 0.8 Hz and are probably negative in sign, and (*iii*) couplings between axial protons ($\phi = \phi' = 60°$) are in the range −0.3 to −0.9 Hz. The $^4J_{AB}$ values calculated from the sum of the EHMO and VB-SOT results (using the values in the last column of Table II of ref. 9), are $^4J^c_{AB} = 0.4$ Hz and $^4J^t_{AB} = 0.0$ Hz. Although these values are more positive than the experimental ones, they support, as do those calculated by the INDO-FPT method, the conclusion that $^4J^c_{AB} > {}^4J^t_{AB}$. This conclusion is in agreement with the aforementioned experimental trends of the ^4J couplings. In effect, the $^4J^c_{AB}$ coupling occurs, half the time, between near equatorial protons ("W" arrangement) and half between near axial protons. The average of both contributions must be positive. For the $^4J^t_{AB}$ coupling one contribution is probably negative, coupling between near axial–equatorial protons, and the other corresponds to a coupling path that differs from the "W" arrangement. Therefore, a smaller value for $^4J^t_{AB}$ than for $^4J^c_{AB}$ is reasonably expected.

The assumption that the THT molecule in solution has the same conformational behaviour as in the vapour phase, has been checked by comparison of the experimental J values with the calculated ones for different potential barriers to pseudorotation and, also, by analysing the dependence on temperature of the ^3J_B couplings. These studies require the simulation of the puckered conformations from the (q_0, ϕ) pseudorotational coordinates and the determination of the respective populations from the energy levels and wave-functions of the Hamiltonian for hindered pseudorotation (Case 3, formula 12 of ref. 12),

$$[2]\quad H(\phi) = BP_\phi^2 + (1/2)V_2(1 - \cos 2\phi) + (1/2)V_4(1 - \cos 4\phi) \ldots$$

The wave equation was solved by using the method described in ref. 13. Puckered conformations were generated by using the B_1 ring-puckering geometrical model that will be described elsewhere (14). The value taken for puckering amplitude, $q_0 = 0.474$ Å, was obtained by application of the Cremer and Pople method (15) to the electron diffraction molecular geometry of THT (6).

Calculated coupling constants of THT for different values of the two- and fourfold barriers to pseudorotation, V_2 and V_4, are given in Table 2. When V_2 increases, taking $V_4 = V_6 = 0$, (in fact, in the vapour phase the determined values of V_4 and V_6 are small (16) for $(CH_2)_4X$ molecules), the conformational behaviour changes from fast inversion between two puckered conformations with C_2 symmetry, $V_2 = -\infty$, to free pseudorotation, $V_2 = 0$, and to fast inversion between two puckered conformations with C_s symmetry, $V_2 = \infty$. The respective calculated values of ^3J, columns 1 to 3 of Table 2, increase for $^3J^c$ and decrease for $^4J^t$. Consequently, the value of $^3D_{AB}$ increases from 0.3 Hz for $V_2 = -\infty$, to 1.7 Hz for $V_2 = 0$, and to 3.8 Hz for $V_2 = \infty$. The experimental value $^3D_{AB} = 0.4$ Hz is close to the first one, corroborating that the preferred conformations are those with C_2 symmetry. The calculated value for free pseudorotation is larger than the experimental one and, in fact, for

TABLE 2. Calculated coupling constants[a] (J, Hz) of THT at 313 K for different values of the two- and fourfold barriers to pseudorotation[b] (V_2 and V_4, cm^{-1}). The Δ^3J values are the differences between the ^3J values at 365 K and at 215 K

Parameter	1	2	3	4	5	Exp[c]
V_2	$-\infty$	0	∞	−773	−220	−773
V_4	0	0	0	169	169	169
$^3J_B^c$	5.84	9.52	13.00	6.64	8.13	5.53
$\Delta^3J_B^c$	0	0	0	0.57	0.62	0.60
$^3J_B^t$	9.08	7.24	5.49	8.68	7.93	7.31
$\Delta^3J_B^t$	0	0	0	−0.29	−0.31	−0.10
$^3J_{AB}^c$	8.18	9.10	10.56	8.59	9.14	6.80
$\Delta^3J_{AB}^c$	0	0	0	0.24	0.24	—
$^3J_{AB}^t$	7.90	7.44	6.72	7.70	7.43	6.37
$\Delta^3J_{AB}^t$	0	0	0	−0.12	−0.12	—
$^4J_{AB}^c$	0.50	0.24	−0.09	0.44	0.32	0.26
$^4J_{AB}^t$	−0.49	−0.36	−0.21	−0.47	−0.41	0.47

[a]The ^3J and ^4J couplings were calculated respectively by the empirical Karplus eq. [1] and by the INDO-FPT method.
[b]Parameter B in [2] was considered equal to 2.35 cm^{-1} (5).
[c]V_2 and V_4 taken from ref. 5 and $\Delta^3J_B^c$ and $\Delta^3J_B^t$ from ref. 4.

molecules undergoing almost free pseudorotation, larger values of ^3D have been observed: ^3D = 1.9 Hz in cyclopentane (17) and $^3D_{AB}$ = 1.5 Hz, ^3D_B = 2.7 Hz in THF (1).

The temperature dependence of the ^3J_B couplings of THT in $CHCl_3$ solution has been observed by Lambert *et al.* (4). They found the following differences between the ^3J_B values at 365 K and at 215 K: $\Delta^3J_B^c$ = 0.60 Hz and $\Delta^3J_B^t$ = −0.10 Hz. The Δ^3J values, calculated by using the vapour phase barrier to pseudorotation of THT (5), are given in column 4 of Table 2 as well as the coupling values at 313 K. The calculated values $\Delta^3J_B^c$ = 0.57 Hz and $\Delta^3J_B^t$ = −0.29 Hz are in good agreement with the experimental ones, especially the former. In relation with the calculated coupling values, the agreement with the experimental ones is of similar quality as in the case of fast inversion between two puckered conformations with C_2 symmetry (column 1 of Table 2). The agreement is better for ^3D_B but worse for $^3D_{AB}$.

The calculated Δ^3J values depend on the height of the pseudorotational barrier. For $V_2 = -\infty$, C_2 molecular symmetry, and for $V_2 = V_4 = 0$, free pseudorotation, the couplings are independent of the temperature, $\Delta^3J = 0$. When V_2 changes from $-\infty$ to 0, the magnitude of each Δ^3J first increases and then, after reaching a maximum, decreases. The maxima which appear for $V_2 \simeq -550$ and $V_4 = 169$ cm^{-1}, are $\Delta^3J_B^c = 0.74$, $\Delta^3J_B^t = -0.37$, $\Delta^3J_{AB}^c = 0.29$, and $\Delta^3J_{AB}^t = -0.15$ Hz. After the maxima, for $V_2 = -220$ and $V_4 = 169$ cm^{-1}, the Δ^3J values, given in column 5 of Table 2, are very similar to those calculated for the experimental barrier to pseudorotation, given in column 4 of Table 2. However, the calculated ^3D_B and $^3D_{AB}$ values are in better agreement with the experimental ones in the latter than in the former case. Therefore, the barrier to pseudorotation of THT in solution seems to be close to that in the vapour phase. The error of the height of the pseudorotational barrier, −773 cm^{-1}, can be estimated at ±220 cm^{-1} (the calculated values of $^3J_B^c$ and $^3J_B^t$ are respectively 0.74 and −0.39 Hz, for $V_2 = -550$ cm^{-1}, and 0.41 and −0.20 Hz for $V_2 = -990$ cm^{-1}).

In conclusion, the above discussion supports the supposition that THT in CS_2 or $CHCl_3$ solution behaves conformationally as in the vapour phase and the choice of Set 1, Table 1, as the most physically meaningful. These conclusions are open to criticism because of the approximations used: calculation of the J values by an empirical Karplus equation and by the INDO-FPT method, assumption of a model of hindered pseudorotation, etc. However, the consistency of the results obtained by application of this approach to the $(CH_2)_4X$ molecules (1, 2) confirms its validity.

Acknowledgements

The authors are grateful to Dr. M. Rico, Instituto de Química Física "Rocasolano", Spain, for his valuable contributions during this research.

This study was supported by the Comisión Asesora de Investigación Científica y Técnica, Madrid.

1. E. DÍEZ, A. L. ESTEBAN, and M. RICO. J. Magn. Reson. **16**, 136 (1974).
2. A. L. ESTEBAN and E. DÍEZ. J. Magn. Reson. **36**, 113 (1979).
3. R. LOZACH, B. LEMARIE, and B. BRAILLON. J. Chim. Phys. **72**, 873 (1975).
4. J. B. LAMBERT, J. J. PAPAY, S. A. KHAN, K. A. KAPPAUF, and E. S. MAGIAR. J. Am. Chem. Soc. **96**, 6112 (1974).

Can. J. Chem. Downloaded from www.nrcresearchpress.com by 210.87.254.42 on 09/05/12
For personal use only.

5. D. W. WERTZ. J. Chem. Phys. **51**, 2133 (1969).
6. Z. NAHLOVSKA, B. NAHLOVSKY, and H. M. SEIP. Acta Chem. Scand. **23**, 3534 (1969).
7. K. G. R. PACHLER and P. L. WESSELS. J. Mol. Struct. **3**, 207 (1969).
8. J. A. POPLE and M. S. GORDON. J. Am. Chem. Soc. **89**, 4253 (1967).
9. M. BARFIELD, A. M. DEAN, C. J. FALLICK, R. J. SPEAR, S. STERNHELL, and P. W. WESTERMAN. J. Am. Chem. Soc. **97**, 1482 (1975).
10. K. G. R. PACHLER. Tetrahedron, **27**, 187 (1971).
11. M. KARPLUS. J. Am. Chem. Soc. **85**, 2870 (1973).
12. D. O. HARRIS, G. G. ENGERHOLM, CH. A. TOLMAN, A. C. LUNTZ, R. A. KELLER, H. KIM, and W. D. GWINN. J. Chem. Phys. **50**, 2438 (1969).
13. J. D. LEWIS, T. B. MALLOY, T. H. CHAO, and J. LAANE. J. Mol. Struct. **12**, 427 (1972).
14. E. DÍEZ, A. L. ESTEBAN, F. J. BERMEJO, and M. RICO. J. Phys. Chem. In press.
15. D. CREMER and J. A. POPLE. J. Am. Chem. Soc. **97**, 1354 (1975).
16. W. H. GREEN, A. B. HARVEY, and J. A. GREENHOUSE. J. Chem. Phys. **54**, 850 (1971).
17. R. L. LIPNICK. J. Mol. Struct. **21**, 411 (1974).

Can. J. Chem. Downloaded from www.nrcresearchpress.com by 210.87.254.42 on 09/05/12
For personal use only.

Oxidation products of arachidonic acid. IV. Model studies on the attachment of the C(13)—C(20) side-chain in the synthesis of tetrahydrofurans and pyrans 1, 2, and 3

GEORGE JUST AND DANILO CROSILLA

Department of Chemistry, McGill University, Montreal, P.Q., Canada H3A 2K6

Received April 28, 1980

GEORGE JUST and DANILO CROSILLA. Can. J. Chem. **58**, 2349 (1980).

The synthesis of methyl 15-hydroxy-8(*R*)-methoxy-11(*R*)-*p*-nitrobenzoyloxy-9(*S*),12(*R*)-oxy-eicosa-13-ynoate, an arachidonic acid metabolite derivative, is described. As well, methods for the attachment of the C(13)—C(20) prostaglandin side-chain to furanosides were studied and the results are described. The reduction of the C-15 keto group on a model compound was performed and was found to have the same behavior as in the prostaglandins.

A partial structure proof of Pace-Asciak's compound, 9,12-oxy-8,11,15- trihydroxy-13-enoic acid is given.

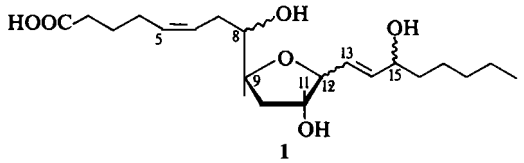
GEORGE JUST et DANILO CROSILLA. Can. J. Chem. **58**, 2349 (1980).

On décrit la synthèse de l'hydroxy-15 méthoxy-8(*R*) *p*-nitrobenzoyloxy-11(*R*) oxy-9(*S*), 12(*R*) eicosyne-13 oate de méthyle, un dérivé métabolique de l'acide arachidonique. On a également étudié les méthodes de fixation des carbones en position 13 à 20 de la chaîne latérale de la prostaglandine aux furannosides et on décrit les résultats. On a réalisé la réduction du groupe cétonique en position 15 sur un composé type et on a trouvé qu'il se comporte comme celui des prostaglandines.

On donne une preuve partielle de structure du composé de Pace-Asciak, l'acide oxy-9,12 trihydroxy-8,11,15 ène-13 oique.

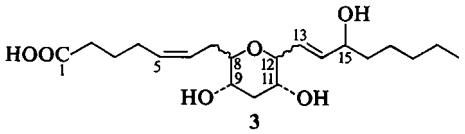
[Traduit par le journal]

In connection with the synthesis of oxidation products of arachidonic acid of type **1**, **2**, and **3**, isolated by Pace-Asciak and Wolfe (1) and Axelrod and co-workers (2), we had to work out procedures for attaching the C(13)—C(20) side-chain to furanose derivatives (for rationale of the choice of stereochemistry of the model compounds, see refs. 1, 3). In this paper, we wish to describe some model studies on this attachment and the synthesis of a derivative of type **1** having an acetylenic bond at Δ^{13}, which strongly supports the structure assigned to **1**.



1

2 5,6-dihydro-**1**



3

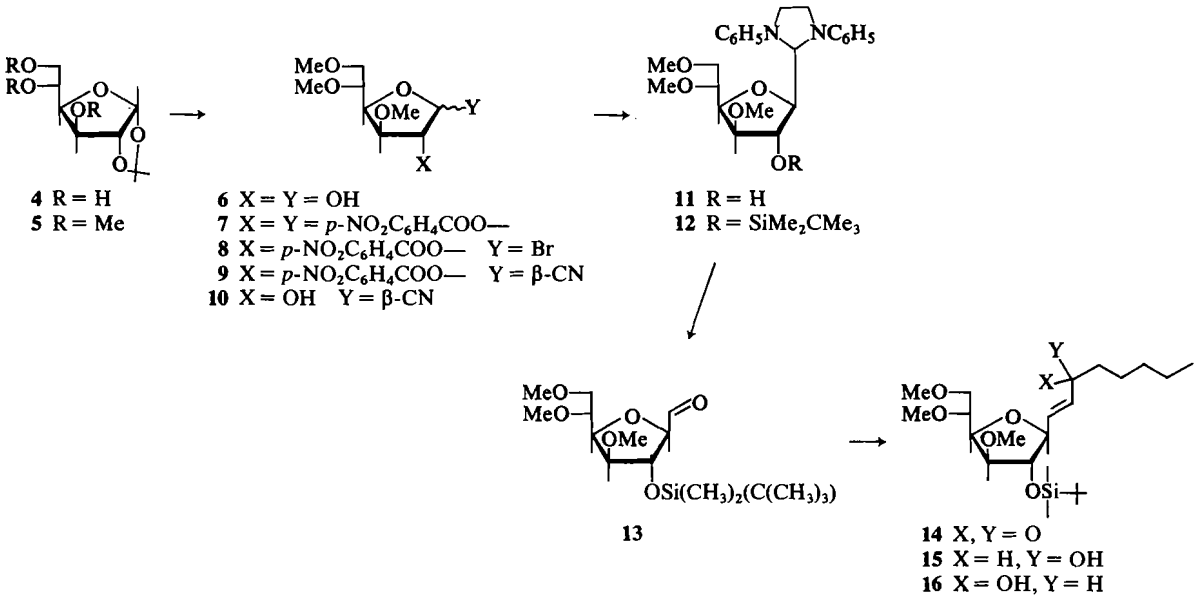
As a model, we used 1,2-*O*-isopropylidene-3,5,6-tri-*O*-methyl-α-D-glucofuranose (**5**), which is easily obtained by methylation (4) of the commercially available glucofuranose **4**. Hydrolysis of **5** with hydrochloric acid, followed by acetylation with *p*-nitrobenzoyl chloride in pyridine (5) gave **7** as a mixture of anomers. Treatment with hydrogen bromide in benzene at 0°C (6) transformed **7** to bromides **8**, which, when submitted to the action of mercuric cyanide in nitromethane (6), gave the β-cyanide **9** as one isomer only, as established by nmr which showed the C(1) hydrogen as a broad singlet ($J_{1,2} \cong 0$–1) indicating a $H_{1,2}$-dihedral angle of approximately 90°C. Alkaline hydrolysis gave the cyano alcohol **10**, which was reduced with Raney nickel in the presence of diphenylethylene diamine (7, 8) to the imidazoline **11**. It was protected as its *tert*-butyldimethylsilyl ether **12** (9). Hydrolysis of the nitrogen heterocycle with Dowex H^+ resin (7, 10) gave the aldehyde **13**, still having the same stereochemistry at the "anomeric center", since the coupling constant $H_{1,2}$ (glucose numbering) was still close to 0 Hz. Reaction of aldehyde **13** with dimethyl 2-oxoheptylphosphonate (11, 12) gave the α,β-unsaturated ketone **14**, which was reduced with sodium borohydride to a 1:1 mixture of diastereomeric alcohols (13) **15** and **16**. The less polar isomer was obtained pure by flash chromatography (14). Reduction of ketone **14** with L-Selectride (15) gave predominantly (85:15) the more polar isomer. No attempt was made to establish the configuration at C(15).

We next proceeded to apply this method to the molecule which had the proper functionalities for obtaining the desired arachidonic acid metabolite **2**. Acetylenic furanose **17** (3) was hydrogenated in ethyl acetate at 40 psi with platinum oxide to afford the saturated compound **18**. The isopropylidene group in compound **18** was hydrolyzed in an acetic acid – water mixture at 60°C to give the hemi-acetal **19** as a mixture of C-12 isomers. This diol was acylated with *p*-nitrobenzoyl chloride and pyridine

0008-4042/80/222349-09$01.00/0

©1980 National Research Council of Canada/Conseil national de recherches du Canada

Can. J. Chem. Downloaded from www.nrcresearchpress.com by 210.87.254.105 on 09/05/12
For personal use only.



4 R = H
5 R = Me

6 X = Y = OH
7 X = Y = *p*-$NO_2C_6H_4COO$—
8 X = *p*-$NO_2C_6H_4COO$— Y = Br
9 X = *p*-$NO_2C_6H_4COO$— Y = β-CN
10 X = OH Y = β-CN

11 R = H
12 R = $SiMe_2CMe_3$

13

14 X, Y = O
15 X = H, Y = OH
16 X = OH, Y = H

to afford the di-*p*-nitrobenzoate **20** as a mixture of C-12 isomers. Treatment of the di-*p*-nitrobenzoate with hydrogen bromide, followed by mercuric cyanide in the same manner as was done for compound **7**, afforded the cyano compound **22** as a mixture of (*R*) and (*S*) C-12 isomers. All the spectral data obtained for this compound were consistent with the proposed structure.

The next step in the synthesis would have been the hydrolysis of the *p*-nitrobenzoate function. However, all attempts to do so resulted in failures, and no clean hydrolysis product could be obtained. It is obvious that different protecting groups, which do not interfere in the reduction of the cyano function and would therefore obviate the hydrolysis step, will have to be used for successful completion of the sequence.

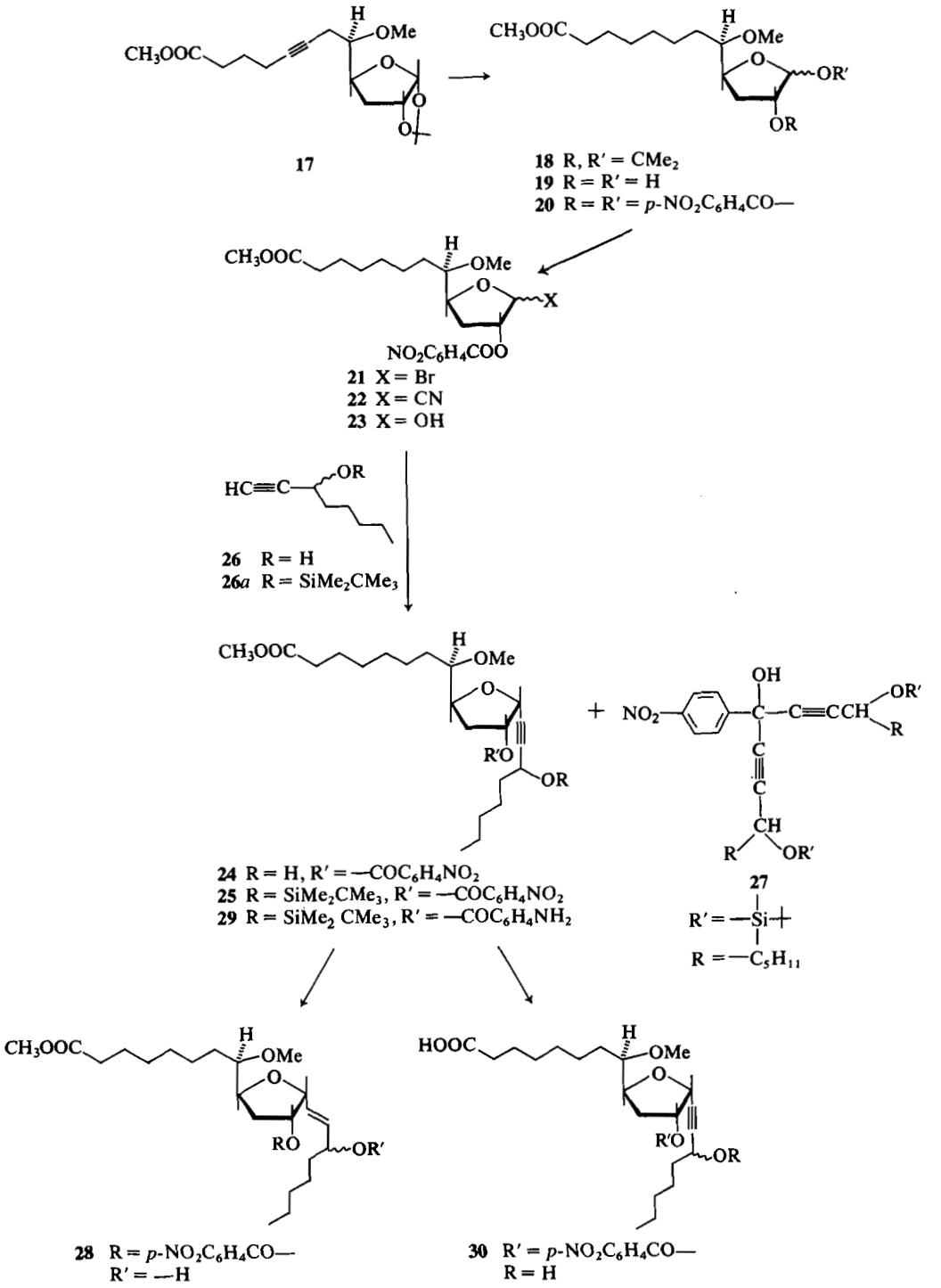
The second approach consisted in trying to add an appropriately substituted acetylenic anion to glycosyl bromide **21**, based on analogous work described by Buchanan *et al.* (16).

Oct-1-yn-3-ol (**26**) was converted to its *tert*-butyldimethylsilyl ether **26***a*, and its lithium salt reacted with glycosyl bromide **21** in dry tetrahydrofuran–hexamethylphosphoramide at −78°C. Four compounds were isolated from the reaction mixture by preparative tlc: (1) tertiary carbinol **27** (R_f 0.91) which arose by reaction of the acetylenic anion with a *p*-nitrobenzoate ester; (2) hemi-acetal **23** (R_f 0.18) which is the product of the reaction of **21** with water; (3) acetylenic silyl ether **25** (R_f 0.75); (4) acetylenic silyl ether **25** (R_f 0.60).

The compounds having R_f values of 0.75 and 0.60 were found to be the desired adducts epimeric at C-15. The stereochemistry at C-12 was assigned, based on the coupling constant between the C-12 and C-11 protons. The ^{1}Hmr spectrum of compound **25**, which has a R_f value of 0.75 and was the major component, displayed singlets at 0.20 ppm for the methyl groups on silicon, at 3.40 ppm for the methyl ether, at 3.60 ppm for the methyl ester, a multiplet between 4.80 and 5.10 ppm for the proton on C-11, a doublet at 6.00 ppm with a coupling constant of $J_{11,12}$ = 4 Hz, and a quartet at 8.00 ppm for the aromatic protons. Because of the large coupling constant between the C-11 and C-12 hydrogens an (*R*) stereochemistry was assigned to the C-12 carbon. The infrared spectrum had a carbonyl absorption at 1740 cm^{-1}, an aromatic absorption at 1610 cm^{-1}, and a nitro absorption at 1530 cm^{-1}. The spectral data for the compound having a R_f value of 0.60 were only slightly different from those of the above compound (having a R_f value of 0.75). The ^{1}Hmr spectrum of this isomer also had a coupling constant of 4 Hz for the hydrogens on C-11 and C-12. Because of the great similarity between their spectral data, the stereochemistry at C-15 could not be assigned to the two isomers.

Hydrolysis of either epimer **25** with 80% aqueous acetic acid at 80°C for 3 hours gave either epimer of **24**. All attempts to reduce either isomer of **24** to the corresponding olefin **28** by means of chromous sulfate (17, 18) or nickel boride (19, 20) failed, and resulted either in reduction of the nitro group of the benzoate function to give **29**, or the formation of mixtures from which no major fraction could be isolated. Attempts to hydrolyse the *p*-nitrobenzoate also failed, resulting either in the hydrolysis of the methyl ester function to the carboxylic acid **30**, or the formation of mixtures.

Can. J. Chem. Downloaded from www.nrcresearchpress.com by 210.87.254.105 on 09/05/12
For personal use only.

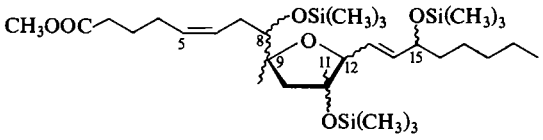


*Mass Spectral Comparisons of 15/16, 25, and 2*a

Comparison of **25** with the methylated and silylated natural product **2***a* reveals that the only basic difference is that there is a $\Delta^{13,14}$ acetylenic bond in **25** instead of an olefinic bond. Since compound **25** is a mixture and differs only in the chirality of the C-15 carbon, and since they have almost identical mass spectra, only one of them, that with R_f 0.75, will be discussed.

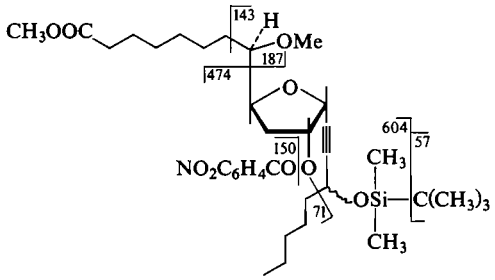
Examination of the mass spectrum of Pace-Asciak's compound **2***a* reveals that the C(1)—C(8) side-chain cleaves between C-7 and C-8 giving a

Can. J. Chem. Downloaded from www.nrcresearchpress.com by 210.87.254.105 on 09/05/12
For personal use only.



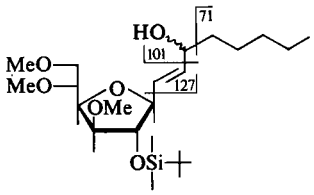
2*a*

fragment of mass 143 *m/e* having a small relative intensity. Examination of the mass spectrum of compound **25** (R_f 0.75), shown below, also displays the analogous fragment with a relative intensity of 4.8%. The base peak of compound **2***a* is the result of the fragmentation between C-8 and C-9, which corresponds exactly to the base peak of compound **25**. As well, both mass spectra display high intensities of a fragment of mass 71 *m/e* corresponding to the C_5H_{11} ion.



25

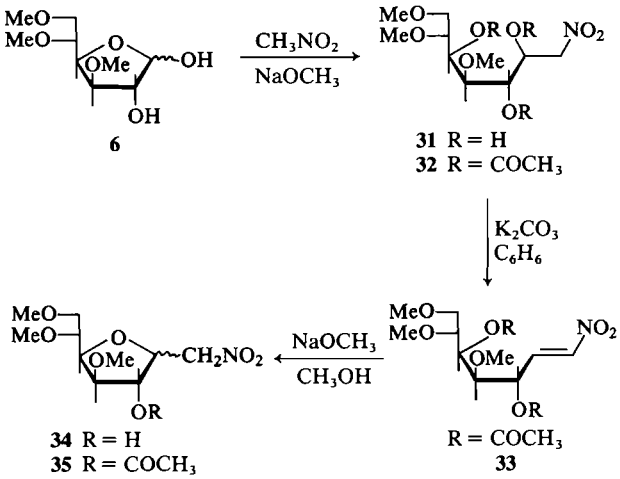
Comparison of the mass spectrum of a mixture of compounds **15** and **16** with the mass spectrum of compound **2***a* reveals that the fragment having a mass of 71 *m/e*, corresponding to C_5H_{11}, is very predominant in both. Cleavage between C-14 and C-15 in **2***a*, giving a fragment having a mass of 173 *m/e*, is also evident. Compounds **15** and **16** do not have a silyl ether at this position, but do cleave in the same manner giving a fragment with a mass of 101 *m/e*. A third fragment of Pace-Asciak's compound had a mass of 199 *m/e* corresponding to the cleavage between C-12 and C-13. The exact cleavage is observed in compounds **15** and **16** as shown below:



15, 16

From these brief comparisons, some evidence can be found in support of the structure **2***a* proposed by Pace-Asciak and Wolfe.

A third approach which was studied consisted of attaching a nitro alkane to a furanose, followed by dehydration and cyclization, as outlined (**6** → **31** → **32** → **33** → **34**). Reaction of furanose **6** with nitromethane gave nitrosugar **31** (21). Acetylation of **31** could only be carried out using acidic conditions, giving the unstable triacetate **32**, which spontaneously decomposed to give a 1:1 mixture of **32** and **33**



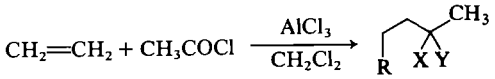
6

31 R = H
32 R = $COCH_3$

34 R = H
35 R = $COCH_3$

R = $COCH_3$
33

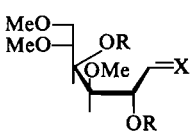
during work-up. When the mixture of **32** and **33** was treated with potassium carbonate (22) in benzene at 20°C for 6 h, an 82% yield of nitroolefin **33** was isolated. Cyclization with methanolic sodium methoxide gave what appeared to be furanose **34**. Acetylation provided acetate **35**. The structures of **34** and **35** were established by nmr only, but gave us confidence to proceed with a more elaborate nitroalkane **38**, which was prepared by an adaptation of the sequence described by Bakuzis *et al.* (23). The procedure consisted of treating acetyl chloride with ethylene and aluminum trichloride to give 1-chloro-3-butanone, and hence to the corresponding ketal **38**.



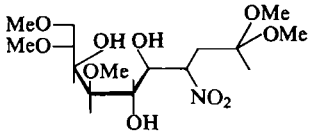
36 R = Cl X, Y = O
37 R = NO_2 X, Y = O
38 R = NO_2 X = Y = OMe

Reaction of **38** with **6** did not give any condensation product, and we therefore converted **6** to the corresponding free aldehyde **41** by first forming the thioacetal **39** (24, 25), converting the resulting diol to the acetonide **40** (26), and hydrolyzing the dithioacetal **40** to the aldehyde **41** (27, 28). Treatment of the aldehyde **41** with nitroalkane **38** and diisopropylamine in dimethylformamide (23), at room temperature for 3 h, afforded the adduct **42**, presumably as a mixture of diastereomers, in good yield.

Can. J. Chem. Downloaded from www.nrcresearchpress.com by 210.87.254.105 on 09/05/12
For personal use only.



39 R = H X = $(SEt)_2$
40 R, R = CMe_2, X = $(SEt)_2$
41 R, R = CMe_2, X = O



42

Having established that the addition of a more complex nitroalkane proceeded on the free aldehyde only, this sequence was applied to the synthesis of tetrahydrofuran **1**. This successful approach will be the subject of a separate communication (29).

Experimental

General

Melting points were determined on a Gallenkamp block and are uncorrected. Mass spectra (ms) were obtained on an AE1-MS-902 mass spectrometer or on an LKB-900 mass spectrometer using a direct insertion probe. Infrared (ir) spectra were obtained on Unicam SP1000 and 297 spectrophotometers. Ultraviolet spectra were obtained on a Cary 17 and rotations on a Perkin-Elmer 141 Polarimeter. Proton magnetic resonance (^{1}Hmr) spectra were recorded on Varian T-60, T-60A, and on Brucker FT 90 spectrometers using tetramethylsilane (TMS) as an internal standard. Chemical shifts are given in the δ scale in parts per million. Doublets (d), triplets (t), and quartets (q) were recorded at the center of the peaks, and multiplets (m) as their range of absorption; other abbreviations used: singlet (s) and broad (b). Chemical shifts were described as they appeared, even though they might represent a more complex splitting pattern.

Analytical thin-layer chromatography (tlc) was performed on silica gel-coated plates (Machery Nagel Polygram G or Merck Silica Gel 60) and on a preparative scale on silica gel (Merck HF 254) coated glass plates (20 cm × 20 cm × 1 mm). Merck silica gel 60, Woelm alumina (neutral), and Camag alumina (supplied by Ventron) were used for normal chromatography. Silica Woelm 32-63 was used for flash chromatography.

Solvents were reagent grade unless otherwise specified. All evaporations were done under reduced pressure (water aspirator) with a bath temperature of 25–40°C unless otherwise specified.

Elemental analyses were performed by Midwest Microlab Ltd., Indianapolis, IN.

1,2-O-Isopropylidene-3,5,6-tri-O-methyl-α-D-glucofuranose (5)

Sodium hydride (1.73 g of a 55% oil dispersion, 40 mmol), washed with *n*-pentane and after removal of the residual *n*-pentane, was added to dry dimethyl sulfoxide (18 mL). The resulting mixture was heated to 50°C for 45 min and then added to triol **4** (2.2 g, 10 mmol) in dry dimethyl sulfoxide (50 mL). A gel formed upon stirring for 30 min at 25°C, the viscous solution was cooled to 20°C, and methyl iodide (2.5 mL, 40 mmol) was added slowly. Water (500 mL) was then added, and the product was extracted with ether (3 × 100 mL). The extracts were washed with water (5 × 20 mL), dried ($MgSO_4$), and evaporated to give 2.5 g (95%) of **5**, as an oil; $[\alpha]_D^{22}$ −31.6° (*c* 6,90, chloroform). Infrared (film): ν_{max} 2970, 2920, 2880, 2800, 1370 cm^{-1}; ^{1}Hmr ($CDCl_3$) δ: 1.30 (s, 3H, CCH_3), 1.50 (s, 3H, CCH_3), 3.40 (s, 3H, OCH_3), 3.45 (s, 3H, OCH_3), 3.50 (s, 3H, OCH_3), 3.40–3.90 (m, 4H), 3.90–4.30 (m, 1H), 4.60 (d, $J_{2,1}$ = 4 Hz, 1H, C(2)H), 5.90 (d, $J_{1,2}$ = 4 Hz, 1H, C(1)H) ppm; ms (70 eV) *m/e*: 263 ($M^+ + 1$), 247 ($M^+ - 15$), 173 ($M^+ - CH(OCH_3)(CH_2OCH_3)$), 89, 45.

3,5,6-Tri-O-methyl-D-glucofuranose (6)

Ketal **5** (262 mg, 1 mmol) was heated at 70°C for 1.5 h in 10 mL of 0.5 *N* hydrochloric acid. After cooling and neutralization with sodium carbonate to pH 7.0, water was removed by azeotroping with toluene. The product was dissolved in hot ethyl acetate, filtered, and the solution was dried ($MgSO_4$). Removal of the ethyl acetate afforded 210 mg (95%) of the oily product **6**, as a mixture of anomers; $[\alpha]_D^{22}$ −34.5° (*c* 4.53, chloroform). Infrared (film) ν_{max}: 3400 (hydroxyl), 2960, 2910, 2800 cm^{-1}; ^{1}Hmr ($CDCl_3$) δ: 3.40 (s, 3H, OCH_3), 3.45 (s, 3H, OCH_3), 3.50 (s, 3H, OCH_3), 3.40–4.40 (m, 8H), 5.10 and 5.40 (s and d, 1H, C(1)H) ppm; ms (70 eV, probe temperature (PT) 37°C) *m/e*: 177 ($M^+ - CH_3OCH_2$), 89, 45; (PT 65°C) *m/e*: 204 ($M^+ - 18$), 89.

1,2-Di-O-p-nitrobenzoyl-3,5,6-tri-O-methyl-D-glucofuranose (7)

To the hemi-acetal **6** (444 mg, 2 mmol) in dry pyridine (5 mL) was added the *p*-nitrobenzoyl chloride (1.2 g, 6.5 mmol) in dry pyridine (25 mL) at 0°C under a nitrogen atmosphere. The mixture was stirred for 1 h at 0°C and set aside at −10°C for 2 days. The mixture was then allowed to warm to 20°C and added to a rapidly stirred ice-water mixture (250 mL) and the stirring was continued until all the ice had melted. The product, **7**, a mixture of α- and β-anomers (720 mg, 70%), was filtered, washed with ether, and recrystallized from acetone–water, mp 143–146°C; $[\alpha]_D^{22}$ −20.7° (*c* 4.51, chloroform). Infrared (KBr) ν_{max}; 2980, 2920, 2820, 1740 (carbonyl), 1620 (aromatic), 1540 (nitro) cm^{-1}; ^{1}Hmr ($CDCl_3$) δ: 3.55 (s, 3H, OCH_3), 3.60 (s, 3H, OCH_3), 3.70 (s, 3H, OCH_3), 3.40–4.10 (m, 3H), 4.10–4.30 (m, 1H), 4.40–4.70 (m, 1H), 5.70–5.90 (m, 1H, C(2)H), 6.70 and 6.90 (s and d, 1H, $J_{1,2}$ = 4 Hz, C(1)H), 8.10–8.50 (m, 8H, aromatic protons) ppm; ms (70 eV) *m/e*: 475 ($M^+ - CH_2OCH_3$), 150, 89. *Anal.* calcd. for $C_{23}H_{24}N_2O_{12}$: C 53.07, H 4.61, N 5.30; found: C 53.12, H 4.71, N 5.15.

2-O-p-Nitrobenzoyl-3,5,6-tri-O-methyl-β-D-glucofuranosyl Cyanide (9) and 2-O-p-Nitrobenzoyl-3,5,6-tri-O-methyl-D-glucofuranosyl Bromide (8)

A solution of the di-*p*-nitrobenzoate **7** (520 mg, 1 mmol) in dry benzene (4 mL) under a nitrogen atmosphere was saturated at 0°C with gaseous hydrogen bromide in the course of 30 min. The *p*-nitrobenzoic acid was filtered off and washed with more benzene. The benzene was then removed under vacuum (40°C) and the residue coevaporated with more benzene (4 mL). The syrupy material was dissolved in nitromethane (3 mL, dried by distillation over phosphorous pentoxide), and treated with mercuric cyanide (500 mg), predried at 140°C/15 Torr for 3 h. The whole reaction mixture was stirred at room temperature for 20 h under a nitrogen atmosphere. The insoluble portion was filtered off and washed with benzene. The filtrates were combined and evaporated under diminished pressure. The oil was then dissolved in ethyl acetate (5 mL) and washed with 5% potassium iodide solution (2 × 2 mL), water (2 × 2 mL), and dried ($MgSO_4$). Concentration under reduced pressure afforded the crude product **9** as an oil. Purification on an alumina column with a methylene chloride – chloroform (2:1) mixture afforded 204 mg (54%) of **9**, mp 111–113°C (methanol); $[\alpha]_D^{22}$ −46.0° (*c* 0.28, chloroform). Infrared (KBr) ν_{max}: 3000, 2940, 2910, 2830, 1730 (carbonyl), 1610 (aromatic), 1530 (nitro) cm^{-1}; ^{1}Hmr ($CDCl_3$) δ: 3.50 (s, 3H, OCH_3), 3.55 (s, 3H, OCH_3), 3.65 (s, 3H, OCH_3), 3.40–4.00 (m, 3H), 4.00–4.50 (m, 2H), 4.90 (s, 1H, C(1)H), 5.70 (s, 1H, C(2)H), 8.20–8.40 (m, 4H, aromatic protons) ppm; ms (70 eV) *m/e*: 336 (($M^+ + 1$) − 45), 335 ($M^+ - CH_2OCH_3$), 150, 89,

Can. J. Chem. Downloaded from www.nrcresearchpress.com by 210.87.254.105 on 09/05/12
For personal use only.

Can. J. Chem. Downloaded from www.nrcresearchpress.com by 210.87.254.105 on 09/05/12
For personal use only.

45. *Anal.* calcd. for $C_{17}H_{20}O_8N_2$: C 53.68, H 5.26, N 7.36; found: C 52.97, H 5.15, N 7.03.

*3,5,6-Tri-*O*-methyl-*β*-*D*-glucofuranosyl Cyanide (10)*

A solution of *p*-nitrobenzoate **9** (190 mg, 0.5 mmol) in tetrahydrofuran (3 mL) and 0.097 *N* aqueous sodium hydroxide (5.7 mL, 0.55 mmol) was stirred overnight at room temperature. The tetrahydrofuran was evaporated and the product extracted with ethyl acetate (2 × 20 mL). The organic layer was washed with water (1 × 10 mL), 10% sodium bicarbonate solution (1 × 10 mL), and with water (1 × 10 mL) again, then dried ($MgSO_4$). Purification on a silica gel column using chloroform–ether (5:1) as the eluent afforded 102 mg (62%) of pure **10** as an oil; $[\alpha]_D^{22}$ −60.1° (*c* 10.44, chloroform). Infrared (film) ν_{max}: 3400 (hydroxyl), 2990, 2940, 2840 cm^{-1}; ^{1}Hmr ($CDCl_3$) δ: 3.35 (s, 3H, OCH_3), 3.40 (s, 3H, OCH_3), 3.45 (s, 3H, OCH_3) 3.30–3.80 (m, 5H), 4.10–4.30 (m, 1H), 4.40–4.60 (m, 2H) ppm; ms (70 eV) *m/e*: 232, 89. *Anal.* calcd. for $C_{10}H_{17}NO_5$: C 51.95, H 7.36, N 6.06; found: C 51.92, H 7.39, N 5.81.

*1,3-Diphenyl-2-(3,5,6-tri-*O*-methyl-*β*-*D*-glucofuranosyl)imidazolidine (11)*

Cyanide **10** (231 mg, 1 mmol) was added to a vigorously stirred suspension of Raney nickel (1.8 g, 3.0 mL) in a solution of sodium hypophosphite (NaH_2PO_2) (943 mg) and *N*,*N*-diphenylethylenediamine (399 mg, 1.88 mmol) in pyridine, acetic acid, and water (2:1:1, 14 mL). The mixture was stirred at room temperature for 1.25 h and then filtered. The residue was extracted with chloroform (2 × 10 mL) and the combined extracts were diluted with chloroform and washed with water (3 × 20 mL), dried ($MgSO_4$), and concentrated to afford **11**. Purification on a silica gel column using ether–hexane (5:1) as the eluent afforded 300 mg (70%) of the pure product **11** as an oil; $[\alpha]_D^{22}$ −29.7° (*c* 4.00, chloroform). Infrared (film) ν_{max}: 3600, 3440 (hydroxyl), 2900, 2840, 1600 (aromatic), 1500 cm^{-1}; ^{1}Hmr (CCl_4) δ: 3.10 (s, 3H, OCH_3), 3.25 (s, 3H, OCH_3), 3.35 (s, 3H, OCH_3), 3.00–4.00 (m, 11H), 4.10–4.20 (m, 1H), 5.50 (d, 1H), 6.40–7.30 (m, 10H, aromatic protons) ppm; ms (70 eV) *m/e*: 101, 89, 45.

*1,3-Diphenyl-2-(2-*O*-(tert-butyldimethyl)silyl-3,5,6-tri-*O*-methyl-*β*-*D*-glucofuranosyl)imidazolidene (12) from Alcohol 11*

To alcohol **11** (250 mg, 0.58 mmol) in dry dimethylformamide (1 mL) was added *tert*-butyldimethylsilyl chloride (106 mg, 0.70 mmol) and imidazole (99 mg, 1.45 mmol). The resulting solution was stirred overnight at room temperature. Water (15 mL) was then added and the product extracted with ether (3 × 10 mL). The combined ethereal extracts were washed with water (3 × 10 mL), dried ($MgSO_4$), and concentrated. Crystallization from methanol afforded 250 mg (80%) of pure silyl ether **12**, mp 113–114°C; $[\alpha]_D^{22}$ −11.4° (*c* 5.33, chloroform). Infrared (KBr) ν_{max}: 2960, 2940, 2890, 2880, 1600 (aromatic), 1500, 1470, 1380 cm^{-1}; ^{1}Hmr (CCl_4) δ: 0.15 (s, 6H, $Si(CH_3)_2$), 0.90 (s, 9H, $C(CH_3)_3$), 3.30 (s, 4H), 3.60 (s, 9H), 3.20–3.80 (m, 5H), 3.90 (bd, 1H), 4.30 (s, 1H), 5.50 (d, 1H), 6.50–7.40 (m, 10H, aromatic protons) ppm: ms (15 eV) *m/e*: 542 (M), 223. *Anal.* calcd. for $C_{30}H_{46}N_2O_5Si$: C 66.42, H 8.49, N 5.16; found: C 66.22, H 8.49, N 5.18.

*2,5-Anhydro-3-*O*-(tert-butyldimethyl)silyl-4,6,7-tri-*O*-methyl-*D*-glycero-*D*-gulo-heptose (13)*

The protected aldehyde **12** (542 mg, 1 mmol) was stirred at 50°C in a 2:1 mixture of tetrahydrofuran and water (30 mL) containing Dowex 50W-X8 (H^+) resin (3.2 g) for 1 h. The resin was then filtered, and the tetrahydrofuran removed under vacuum. The product was extracted with ether (3 × 10 mL), dried ($MgSO_4$), and concentrated to afford 300 mg (86%) of pure aldehyde **13** as an oil; $[\alpha]_D^{22}$ +12.2° (*c* 8.80, chloroform). Infrared (film) υ_{max}: 2960, 2930, 2890, 2860, 2810, 1760 (carbonyl), 1460 cm^{-1}; ^{1}Hmr (CCl_4) δ: 0.10 (s, 6H, $Si(CH_3)_2$), 0.90 (s, 9H, $C(CH_3)_3$), 3.20 (s, 3H, OCH_3), 3.30 (s, 3H, OCH_3), 3.35 (s, 3H, OCH_3), 3.20–3.70 (m, 4H), 3.70–4.00 (m, 2H), 4.25 (s, 1H), 9.10 (s, 1H, CHO) ppm.

*E-1-(2-(*tert*-Butyldimethyl)silyl-3,5,6-tri-*O*-methyl-*β*-*D*-glucofuranosyl)-3-keto-1-octene (14)*

Sodium hydride (58% oil dispersion, 32 mg, 0.078 mmol) in dry 1,2-dimethoxyethane (4 mL) was cooled to 20°C and dimethyl 2-oxoheptylphosphonate (190 mg, 0.178 mL, 0.86 mmol) was added dropwise, with stirring, under a nitrogen atmosphere. After the addition, the solution was stirred at room temperature for 1 h. To this solution, the aldehyde **13** (300 mg, 0.86 mmol) in 1,2-dimethoxyethane (2 mL) was added dropwise, and the mixture was stirred at room temperature for 1.5 h. Dilution with water (10 mL) followed by ether extractions (3 × 10 mL) gave, after drying ($MgSO_4$) and purification on a silica gel column using an ether–hexane (1:1) mixture as the eluent, 300 mg (78%) of oily **14**; $[\alpha]_D^{22}$ −52.1° (*c* 5.07, chloroform). Infrared (film) ν_{max}: 2960, 2930, 2860, 2830, 1700, 1670 (carbonyl), 1630 (olefin) cm^{-1}; ^{1}Hmr (CCl_4) δ: 0.10 (s, 6H, $Si(CH_3)_2$), 0.90 (s, 9H, $C(CH_3)_3$), 1.00–1.90 (m, 9H), 2.40 (bt, 2H), 3.20 (s, 3H, OCH_3), 3.25 (s, 3H, OCH_3), 3.30 (s, 3H, OCH_3), 3.30–4.20 (m, 7H), 5.95 (B portion of an ABX system, 1H, $J_{1,2}$ = 14 Hz, $J_{1,3}$ = 1 Hz, OC(3)HC(2)H=C(1)*H*CO), 6.50 (A portion of an ABX system, 1H, $J_{2,1}$ = 14 Hz, $J_{2,3}$ = 6 Hz, C(3)HC(2)*H*=C(1)CHO) ppm; ms (15 eV) *m/e*: 444 (M^+), 387 ($M^+ - 57$), 355 ($M^+ - 89$), 89.

*E-1-(2-*tert*-Butyldimethyl)silyl-3,5,6- tri-*O*-methyl-*β*-*D*-glucofuranosyl)-3-hydroxyl-1-octene (15, 16)*

To the ketone **14** (150 mg, 0.34 mmol) in absolute ethanol (3 mL) at 0°C was added sodium borohydride (13 mg, 0.34 mmol), and the mixture stirred for 1 h at 0°C. Buffer (pH 4.4, 3 mL) was added and the solution allowed to warm up to room temperature. Evaporation *in vacuo*, and ether extraction (3 × 5 mL) gave 130 mg (85%) of **15/16** as a mixture of diastereomers. Infrared (film) ν_{max}: 3460 (hydroxyl), 2960, 2930, 2860, 2820, 1460 cm^{-1}; ^{1}Hmr (CCl_4) δ: 0.10 (s, 6H, $Si(CH_3)_2$), 0.90 (s, 12H, $C(CH_3)_3$, CH_2CH_3), 1.00–1.60 (m, 8H), 2.40 (bs, 1H), 3.20 (s, 3H, OCH_3), 3.30 (s, 3H, OCH_3), 3.30–3.70 (m, 6H), 3.75–4.00 (m, 2H), 5.40 (m, 2H, CH=CH) ppm; ms (70 eV) *m/e*: 428 ($M^+ - 18$), 389 ($M^+ - C(CH_3)_3$), 89, 57, 45. *Anal.* calcd. for $C_{23}H_{46}O_6Si$: C 61.88, H 10.31; found: C 62.03, H 10.32.

*E-1-(2-*tert*-Butyldimethyl)silyl-3,5,6-tri-*O*-methyl-*β*-*D*-glucofuranosyl)-3-hydroxyl-1-octene (15, 16)*

A tetrahydrofuran solution of L-Selectride (0.45 mL of a 1 *M* solution) was added over a 1 min period to a stirred solution of the ketone **14** (200 mg, 0.45 mmol) in tetrahydrofuran (1 mL) at −78°C, under a nitrogen atmosphere. After 1 hour the acetone–dry ice bath was replaced with an ice-water bath and 3 mL of a 7:5 mixture of 10% sodium hydroxide and 30% hydrogen peroxide was added, and the resulting solution was stirred overnight at room temperature. The aqueous layer was separated and extracted with hexane (3 × 10 mL). The combined organic layers were washed with water (2 × 2 mL), 10% sodium bisulfite solution (2 × 2 mL), and with saturated salt solution (1 × 2 mL). The organic solution was then dried ($MgSO_4$), filtered, and concentrated under reduced pressure to afford 100 mg (50%) of pure oily alcohols **15** and **16** as an approximately 85 (more polar): 15 (less polar) mixture of diastereomers, as established by thin layer chromatography. Infrared (film) ν_{max}: 3450 (hydroxyl), 2960, 2930, 2860, 1460 cm^{-1}; ^{1}Hmr (CCl_4) δ: 0.10 (s, 6H, $Si(CH_3)_2$), 0.90 (bs, 12H), 1.40 (m, 8H), 2.00 (bs, 1H), 3.30 (s, 3H, OCH_3), 3.35 (s, 3H, OCH_3), 3.40 (s, 3H, OCH_3), 3.40–4.20 (m, 8H), 5.55 (m, 2H, CH=CH) ppm.

*Methyl 11(*R*),12(*R*)-Isopropylidenedioxy-8(*R*)-methoxy-9(*S*),12(*R*)-oxy-dodecanoate (18)*

The alkyne **17** (940 mg, 2.88 mmol) was hydrogenated over-

Can. J. Chem. Downloaded from www.nrcresearchpress.com by 210.87.254.105 on 09/05/12
For personal use only.

night at 40 psi with platinum oxide (25 mg) catalyst in ethyl acetate (15 mL). The catalyst was then filtered and washed with more ethyl acetate (5 mL). Removal of the ethyl acetate from the combined organic layers under diminished pressure afforded crude product **18**, as an oil. Purification by flash chromatography (silica gel), using petroleum ether – ethyl acetate (3:1) as the eluent, afforded 577 mg (61%) of the pure product **18** as an oil; $[\alpha]_D^{22}$ −9.4° (*c* 6.05, chloroform). Infrared (film) ν_{max}: 2980, 2940, 2860, 1740 (carbonyl), 1460, 1430, 1380 cm^{-1}; ^{1}Hmr (CCl_4) δ: 1.25 (s, 3H, $C(CH_3)$), 1.40 (s, 3H, $C(CH_3)$), 1.20–2.00 (m, 12H), 2.00–2.40 (m, 2H), 3.10–3.30 (m, 1H), 3.35 (s, 3H, OCH_3), 3.60 (s, 3H, $COOCH_3$), 3.80–4.20 (m, 1H), 4.50–4.70 (m, 1H), 5.60 (d, 1H) ppm; ms (70 eV) *m/e*: 315 (M^+ − 15), 187, 155, 143, 85. *Anal.* calcd. for $C_{17}H_{30}O_6$: C 61.82, H 9.17; found: C 62.02, H 9.09.

*Methyl 11(*R*),12-Dihydroxy-8(*R*)-methoxy-9(*S*),12-oxy-dodecanoate (19)*

The isopropylidene compound **18** (330 mg, 1 mmol) was stirred in a mixture of acetic acid (2.9 mL) and water (5.5 mL) for 16 h at 60°C. Sodium chloride and saturated sodium chloride solution was then added and the product extracted with ethyl acetate (3 × 10 mL). The organic layers were washed with a mixture of saturated sodium bicarbonate and saturated sodium chloride solution until neutral. Drying ($MgSO_4$) and concentration afforded 190 mg (66%) of pure diol **19**, as an oil. Infrared (film) ν_{max}: 3400 (hydroxyl), 2940, 2860, 1740 (carbonyl) cm^{-1}; ^{1}Hmr ($CDCl_3$–D_2O) δ: 1.20–2.50 (m, 14H), 3.40 and 3.45 (s and s, 3H, OCH_3), 3.60 (s, 3H, $COOCH_3$), 3.10–3.50 (m, 1H), 4.00–4.50 (m, 2H), 5.10 and 5.30 (s and d, 1H) ppm; ms (70 eV) *m/e*: 241, 187, 125.

*Methyl 11(*R*),12-Di-*p*-nitrobenzoyloxy-8(*R*)-methoxy-9(*S*),12-oxy-dodecanoate (20)*

To dry pyridine (5 mL), under a nitrogen atmosphere, was added *p*-nitrobenzoyl chloride (302 mg, 1.63 mmol) and the mixture kept at 0°C. The diol **19** (150 mg, 0.52 mmol) in dry pyridine (1 mL) was added dropwise, and the resulting mixture was kept at 0°C for 1.5 h and then allowed to warm up to room temperature for 0.5 h. Water (60 mL) was then added and the product extracted with ether (3 × 10 mL). The combined ethereal extracts were washed with 1% hydrochloric acid (until acidic), water (1 × 10 mL), and dried ($MgSO_4$). Concentration under diminished pressure afforded 275 mg (90%) of di-*p*-nitrobenzoate **20** as an oil. Flash chromatography using petroleum ether – ethyl acetate (3:1) as the eluent afforded an analytically pure sample as a 1:1 mixture of epimers. Infrared (film) ν_{max}: 3110, 3080, 3050, 2840, 2860, 1730 (carbonyl), 1610 (aromatic), 1530 (nitro), 1435 cm^{-1}. ^{1}Hmr (CCl_4) δ: 1.10–1.70 (m, 10H), 1.90–2.60 (m, 4H), 3.20 (s, 3H, OCH_3), 3.40 and 3.60 (s and s, 3H, $COOCH_3$), 3.10–3.40 (m, 1H), 4.20–4.60 (m, 1H), 5.50 (bd, 1H), 6.35 and 6.60 (s and d, 1H), 7.90–8.20 (m, 8H, aromatic protons) ppm; ms (70 eV) *m/e*: 557 (M^+ − 31), 422 (M^+ − 166), 187, 166, 150. *Anal.* calcd. for $C_{28}H_{32}N_2O_{12}$: C 57.14, H 5.44, N 4.76; found: C 57.40, H 5.47, N 4.57.

*Methyl 12-Cyano-8(*R*)-methoxy-11(*R*)-p-nitrobenzoyloxy-9(*S*),12-oxy-dodecanoate (22) and Methyl 12-Bromo-8(*R*)-methoxy-11(*R*)-p-nitrobenzoyloxy-9(*S*),12-oxy-dodecanoate (21)*

The di-*p*-nitrobenzoate **20** (140 mg, 0.24 mmol) in benzene (1 mL) was reacted in the same manner as compound **7** to give the bromo compound **21**. Compound **21** was then reacted in the same manner as compound **8**, with powdered mercuric cyanide (133 mg) in nitromethane (1 mL) to afford crude compound **22**.

Purification by column chromatography (Al_2O_3), using petroleum ether – ethyl acetate (1:1) as the eluent, afforded 65 mg (61%) of the pure product **22** as an oil. Infrared (film) ν_{max}: 3110, 3080, 3060, 2940, 2860, 1730 (carbonyl), 1610 (aromatic), 1530 (nitro), 1435, 1410, 1350 cm^{-1}; ^{1}Hmr ($CDCl_3$) δ: 1.20–1.80 (m, 10H), 2.10–2.40 (m, 4H), 3.30–3.60 (m, 1H), 3.50 (s, 3H, OCH_3), 3.60 (s, 3H, $COOCH_3$), 4.00–4.60 (m, 1H), 4.70 (bs, 1H), 5.50–5.80 (m, 1H), 8.20 (bs, 4H) ppm.

*Methyl 15-Hydroxy-8(*R*)-methoxy-11(*R*)-p-nitrobenzoyloxy-9(*S*),12(*R*)-oxy-eicosa-13-ynoate (24)*

The silyl compound **25** (30 mg, 0.045 mmol (R_f 0.76)) was heated to 80°C for 3 h in 80% aqueous acetic acid (1 mL). Water (10 mL) was then added and the product extracted with ether (3 × 5 mL). The combined ethereal extracts were washed with saturated sodium bicarbonate solution (5 × 10 mL), water (1 × 5 mL), dried ($MgSO_4$), and concentrated under diminished pressure to afford the crude product. Purification by preparative plate chromatography, using petroleum ether – ethyl acetate (2:1) as the solvent, afforded 20 mg (81%) of pure oily alcohol **24** as a mixture of C-15 diastereomers. Infrared (film) ν_{max}: 3430 (hydroxyl), 2940, 2860, 1740 (carbonyl), 1720 (carbonyl), 1650, 1610 (aromatic), 1530 (nitro), 1350 cm^{-1}; ^{1}Hmr (90 MHz, $CDCl_3$) δ: 0.95 (bt, 3H), 1.25–2.50 (m, 22H), 3.30–3.55 (m, 2H), 3.50 (s, 3H, OCH_3), 3.75 (s, 3H, $COOCH_3$), 3.95–4.20 (m, 1H), 4.40–4.60 (m, 1H), 5.05–5.25 (m, 1H), 6.25 (d, 1H, $J_{12,11}$ = 4 Hz), 7.95–8.60 (q, 4H) ppm; ms (70 eV) *m/e*: 517, 425, 414, 190, 150.

*Methyl 15-(*tert*-Butyldimethyl)silyloxy-8(*R*)-methoxy-11(*R*)-p-nitrobenzoyloxy-9(*S*),12(*R*)-oxy-eicosa-13-ynoate (25)*

The lithium salt of the side-chain derivative **26***a* was prepared by treating **26***a* (375 mg, 1.5 mmol), in dry tetrahydrofuran (2 mL), with a 1.6 *M* solution of *n*-butyllithium in hexane (1 mL). This was stirred for 30 min, and added, dropwise, to a solution of the bromo compound **21** (251 mg, 0.5 mmol) in dry tetrahydrofuran (3 mL) and hexamethylphosphoramide (0.2 mL), at −78°C, under a nitrogen atmosphere. This mixture was stirred for 2 h at −78°C and quenched with buffer solution (pH 4.4). The tetrahydrofuran was removed under diminished pressure, water (5 mL) was added, and the product extracted with ether (3 × 10 mL). The combined ethereal extracts were washed with water (5 × 5 mL), dried ($MgSO_4$), and evaporated to afford the crude product **25**. Purification by preparative chromatography, using ethyl acetate – petroleum ether (1:3) as the solvent, afforded 80 mg (24%) of one diastereomer (R_f 0.76) and 60 mg (18%) of the other diastereomer (R_f 0.60).

Compound with R_f 0.76

Infrared (film) ν_{max}: 2960, 2930, 2860, 1740 (carbonyl), 1610 (aromatic), 1530 (nitro), 1460, 1435 cm^{-1}; ^{1}Hmr (CCl_4) δ: 0.20 (s, 6H, $Si(CH_3)_2$), 1.00 (s, 12H), 1.20–2.40 (m, 22H), 3.20–3.50 (m, 1H), 3.40 (s, 3H, OCH_3), 3.60 (s, 3H, $COOCH_3$), 3.80–4.10 (m, 1H), 4.20–4.60 (m, 1H), 4.80–5.10 (m, 1H), 6.00 (d, 1H, $J_{12,11}$ = 4 Hz, $OCHC{\equiv}C$), 7.70–8.30 (q, 4H, aromatic protons) ppm; ms (70 eV) *m/e*: 604 (M^+ − 57), 590 (M^+ − 71), 474 (M^+ − 187), 187, 150, 71, 57.

Compound with R_f 0.60

$[\alpha]_D^{22}$ 6.4° (*c* 1.05, chloroform); ^{1}Hmr (CCl_4) δ: 0.10 (s, 6H, $Si(CH_3)_2$), 1.00 (s, 12H), 1.10–2.50 (m, 22H), 3.20–3.50 (m, 1H), 3.40 (s, 3H, OCH_3), 3.60 (s, 3H, $COOCH_3$), 4.20–4.90 (m, 3H), 5.80 (d, 1H, $J_{12,11}$ = 4 Hz, $OCHC{\equiv}C$), 7.50–8.30 (q, 4H, aromatic protons) ppm; ms (70 eV) *m/e*: 646 (M^+ − 15), 604 (M^+ − 71), 474 (M^+ − 187), 187, 150, 71, 57, 45. *Anal.* calcd. for $C_{35}H_{55}NO_9Si$: C 63.54, H 8.32, N 2.12; found: C 63.80, H 8.40, N 1.92.

*3-(*tert*-Butyldimethyl)silyloxy-oct-1-yne (26*a*)*

To the alcohol **26** (1.26 g, 10 mmol) in dry dimethylformamide (3 mL) under nitrogen atmosphere was added *tert*-butyldimethylsilyl chloride (1.81 g, 12 mmol) and imidazole (1.70 g, 25 mmol). The resulting mixture was stirred overnight at room temperature. Water (30 mL) was then added and the product extracted with ether (3 × 50 mL). The combined ethereal ex-

Can. J. Chem. Downloaded from www.nrcresearchpress.com by 210.87.254.105 on 09/05/12
For personal use only.

tracts were washed with water (5 × 20 mL), dried ($MgSO_4$), and concentrated under diminished pressure to afford 2.20 g (92%) of the silylated compound **26***a*. Infrared (film) ν_{max}: 3320, 2960, 2940, 2860, 1470 cm^{-1}; ^{1}Hmr (CCl_4) δ: 0.20 and 0.22 (s and s, 6H, $Si(CH_3)_2$), 1.00 (bs, 12H), 1.20–1.80 (m, 8H), 2.30 (d, 1H, C≡CH), 4.20–4.50 (m, 1H) ppm.

*Methyl 11(*R*)-*p*-Aminobenzoyloxy-15-hydroxy-8(*R*)-methoxy-9(*S*),12(*R*)-oxy-eicosa-13-ynoate (29)*

The alkyne **25** (40 mg, 0.07 mmol) in *N*,*N*-dimethylformamide (0.4 mL) was added to a stirred mixture of 0.71 *N* $CrSO_4$ solution (0.4 mL) and water (0.1 mL) under a nitrogen atmosphere. The resulting solution turned from blue to green instantaneously and it was then stirred at room temperature for an additional 1.5 h. The solution was saturated with ammonium sulfate and extracted with ether (3 × 5 mL). The combined ethereal extracts were washed with water (3 × 5 mL), dried ($MgSO_4$), and concentrated under diminished pressure to afford the crude product **29**. Purification by preparative plate chromatography, using ethyl acetate – petroleum ether (2:1) as the solvent, afforded 30 mg (79%) of pure amine **29** as an oil. Infrared (film) ν_{max}: 3480 (amine), 3380 (hydroxyl), 2940, 2860, 1730 (carbonyl), 1630, 1610 (aromatic), 1430 cm^{-1}; ^{1}Hmr (90 MHz, $CDCl_3$) δ: 0.90 (bt, 3H), 1.20–1.90 (m, 18H), 2.00–2.50 (m, 4H), 3.45 (s, 3H, OCH_3), 3.39–3.60 (m, 3H), 3.70 (s, 3H, $COOCH_3$), 4.10–4.60 (m, 3H), 4.95–5.10 (m, 1H), 6.10 (d, 1H, $J_{12,11}$ = 4 Hz), 7.20 (q, 4H, aromatic protons) ppm; ms (70 eV) *m/e*: 517 (M^+), 486 (M^+ − 31), 330 (M^+ − 187), 187, 120 ($NH_2C_6H_4CO$), 92, 71, 45.

*1-Deoxy-1-nitro-4,6,7-tri-*O*-methyl-*D*-glycero(*D*-ido and *D*-gulo)-heptitols (31)*

The diol **6** (444 mg, 2 mmol) was dissolved in a mixture of methanol (2 mL) and nitromethane (1 mL) under a nitrogen atmosphere. To this was added a solution of sodium metal (70 mg) in dry methanol (1 mL). The resulting mixture was stirred overnight. The solvent was then removed under reduced pressure and the solid mass dissolved in water (5 mL). The aqueous solution was passed through a column of IR-120 (H^+ form) Amberlite resin (5 mL). The eluate was concentrated under reduced pressure and dried by azeotropic distillation with benzene (2 × 20 mL) to afford 510 mg (90%) of crude adduct**31**, homogeneous by thin layer chromatography, as an oil. Infrared (film) υ_{max}: 3350 (hydroxyl), 2980, 2920, 2810, 1560 (nitro) cm^{-1}; ^{1}Hmr ($CDCl_3$) δ: 3.10 (s, 3H, OCH_3), 3.20 (s, 6H, 2 OCH_3), 3.00–3.70 (m, 7H), 3.75–3.90 (m, 1H), 4.00–4.40 (m, 4H) ppm.

*3,5-Di-*O*-acetyl-1,2-dideoxy-1-nitro-4,6,7-tri-*O*-methyl-*D*-gluco-hept-1-enitol (33) and 1-Deoxy-1-nitro-2,3,5-tri-*O*-acetyl-4,5,7-tri-*O*-methyl-*D*-glycero(*D*-ido and *D*-gulo)-heptitols (32)*

A solution of the triol **31** (283 mg, 1 mmol) in acetic anhydride (6 mL) containing catalytic amounts of *p*-toluenesulfonic acid (50 mg) was stirred overnight at room temperature. The reaction mixture was then slowly poured on an aqueous solution of sodium bicarbonate and stirred for 30 min. The product was extracted with chloroform (3 × 10 mL). The extracts were washed with water (3 × 10 mL), dried ($MgSO_4$), and concentrated to afford the crude product (mixture of triacetate **32** and nitro-olefin **33**). This mixture was then dissolved in dry benzene (6 mL) and powdered anhydrous potassium carbonate (142 mg) was added. The suspension was stirred for 6 h at room temperature, and filtered through a Celite pad. The filtrate was concentrated to afford the crude product **33** as an oil. Purification through a silica gel column using ether as the eluent afforded 315 mg (90%) of pure nitro-olefin **33** as an oil, $[\alpha]_D^{22}$ −4.4° (*c* 3.20, chloroform). Infrared (film) ν_{max}: 2970, 2920, 2820, 1760 (carbonyl), 1660 (olefin), 1530 (nitro) cm^{-1}; uv λ_{max} (ethanol) 220 (ε 5560), 290 (ε 1500) (CH=CH—NO_2) nm; ^{1}Hmr (90 MHz, $CDCl_3$) δ: 2.00 (s, 3H, $OCOCH_3$), 2.20 (s, 3H, $OCOCH_3$), 3.40 (s, 3H, OCH_3), 3.50 (s, 3H, OCH_3), 3.65 (s, 3H, OCH_3), 3.30–3.80 (m, 3H), 3.90 (dd, 1H, $J_{4,5}$ = 3 Hz, $J_{4,3}$ = 6 Hz, C(4)H), 5.20 (dd, 1H, $J_{5,4}$ = 3 Hz, $J_{5,6}$ = 7 Hz, C(5)H), 5.80 (m, 1H, $J_{3,4}$ = 6 Hz, $J_{3,2}$ = 4 Hz, $J_{3,1}$ = 2 Hz, C(3)H), 7.02 (B portion of an ABX system, 1H, $J_{1,2}$ = 14 Hz, $J_{1,3}$ = 2 Hz, C(1)H), 7.42 (A portion of an ABX system, 1H, $J_{1,2}$ = 14 Hz, $J_{2,3}$ = 4 Hz, C(2)H) ppm; ms (70 eV) *m/e*: 305 (M^+), 290 (M^+ − $OCOCH_3$), 89, 45, 43.

*3,5,6-Tri-*O*-methyl-*D*-glucose 1,1-Diethylmercaptal (39) Using Zinc Chloride as the Catalyst*

The alcohol **6** (22 mg, 1 mmol) was added to ethanethiol (620 mg, 10 mmol, 0.74 mL). The mixture was cooled in an ice bath and anhydrous zinc chloride (250 mg) was added. The flask was stoppered and allowed to stand overnight in the freezer (−4°C). The ethanethiol was blown away with nitrogen and warming and the residue dissolved in ethyl acetate (5 mL). Sodium bicarbonate solution (5 mL) was added and the mixture filtered through a Celite pad. The precipitate was washed with more ethyl acetate (5 mL) and the combined filtrate and washings were separated from the aqueous layer. The aqueous layer was reextracted with ethyl acetate (3 × 5 mL). The combined extracts were dried ($MgSO_4$) and concentrated to afford 260 mg (79%) of pure product **39** as an oil. Infrared (film) ν_{max}: 3450 (hydroxyl), 2970, 2730, 2830, 1450, 1370 cm^{-1}; ^{1}Hmr ($CDCl_3$) δ: 1.30 (t, 6H, CH_2CH_3), 2.50–3.00 (m, 4H, CH_2CH_3), 3.40 (s, 3H, OCH_3), 3.50 (s, 3H, OCH_3), 3.70 (s, 3H, OCH_3), 3.20–4.20 (m, 9H) ppm; ms (15 eV) *m/e*: 328 (M^+), 296 (M^+ − 32), 193 (M^+ − $(CH_3CH_2S)_2CH$), 135, 119, 89, 45, 31.

4-Chlorobutan-2-one (36)

To dry methylene chloride (60 mL) was added aluminum trichloride (16.0 g, 0.12 mol), at 0°C, under a nitrogen atmosphere. Acetyl chloride (7.85 g, 7.13 mL, 0.1 mol) was added to this, dropwise, under a nitrogen atmosphere. Ethylene was then bubbled in at a rapid flow rate. Bubbling was continued for 30 min after the rapid uptake ceased. The ice bath was then removed and the mixture stirred for 1 hour at room temperature, poured on an ice-water mixture, and stirred for an additional hour. Extraction with methylene chloride (3 × 20 mL), drying of the extracts with $MgSO_4$, and removal of the solvent under reduced pressure afforded the crude product **36**. The product was purified by distillation to give 7.62 g (72%) of pure chloro compound **36**, bp 105–110°C. Infrared (film) ν_{max}: 2970, 1720 (carbonyl) cm^{-1}; ^{1}Hmr (CCl_4) δ: 2.10 (s, 3H, CH_3), 2.80 (t, 2H, CH_2CO), 3.60 (t, 2H, CH_2Cl) ppm.

4-Nitrobutan-2-one (37)

The chloro compound **36** (1.98 g, 0.0186 mol), potassium iodide (150 mg), and sodium nitrite (1.28 g, 0.0186 mol) were stirred overnight in dry dimethylsulfoxide (15 mL) at room temperature. Water (150 mL) was then added and the product extracted with ether (3 × 10 mL). The combined extracts were washed with water (3 × 10 mL), dried ($MgSO_4$), and evaporated under reduced pressure to afford the crude product **37**. The product was purified by distillation to give 1.1 g (50%) of the nitro ketone **37**, bp 90–93°C/2 Torr. Infrared (film) ν_{max}: 3000, 2960, 2920, 1720 (carbonyl), 1550 (nitro) cm^{-1}; ^{1}Hmr ($CDCl_3$) δ: 2.30 (s, 3H, CH_3), 3.20 (t, 2H, CH_2CO), 4.60 (t, 2H, CH_2NO_2) ppm.

2,2-Dimethoxy-4-nitrobutane (38)

The ketone **37** (480 mg, 4.1 mmol) was stirred overnight at room temperature with trimethylorthoformate (477 mg, 4.5 mmol, 0.492 mL) and methanol (0.2 mL) containing catalytic amounts of *p*-toluenesulfonic acid. Water (30 mL) and saturated sodium bicarbonate solution (1 mL) were then added and the resulting solution extracted with ether (3 × 30 mL). The extracts were dried ($MgSO_4$) and evaporated to afford the crude product **38**. Distillation (bp 60–65°C/1 Torr) of the crude product af-

Can. J. Chem. Downloaded from www.nrcresearchpress.com by 210.87.254.105 on 09/05/12
For personal use only.

forded 600 mg (90%) of pure nitro ketal **38**. Infrared (film) ν_{max}: 2990. 2940, 2830, 1550 (nitro), 1440, 1380, 1350 cm^{-1}; ^{1}Hmr (CCl_4) δ: 1.20 (s, 3H, CH_3), 2.30 (bt, 2H, $CH_2C(OCH_3)_2$), 3.10 (s, 6H, 2 OCH_3), 4.30 (t, 2H, CH_2NO_2) ppm.

2,4-O-Isopropylidene-3,5,6-tri-O-methyl-D-glucose 1,1-Diethylmercaptal (40)

To a solution of the dithioacetal **39** (328 mg, 1 mmol) in acetone (15 mL) was added anhydrous copper sulfate (750 mg) and 3 drops of concentrated sulfuric acid at room temperature. The resulting mixture was stirred overnight. The solution was then neutralized by bubbling in ammonia at room temperature until alkaline (pH 9). The blue precipitate was filtered (Celite) and concentrated to afford the crude product **40**. This was purified by flash chromatography (silica gel), using petroleum ether – ethyl acetate (4:1) as the eluent. Concentration of the appropriate fractions afforded 290 mg (78%) of pure isopropylidene compound **40** as an oil; $[\alpha]_D^{22}$ +4.2° (*c* 5.45, chloroform). Infrared (film) ν_{max}: 2970 (hydrocarbon), 2930, 2830, 1450, 1380, 1260 cm^{-1}; ^{1}Hmr (CCl_4) δ: 1.20 (t, 3H, CH_2CH_3), 1.30 (t, 3H, CH_2CH_3), 1.40 (s, 6H, $C(CH_3)_2$), 2.40–3.00 (m, 4H, CH_2CH_3), 3.30 (s, 3H, OCH_3), 3.40 (s, 3H, OCH_3), 3.50 (s, 3H, OCH_3), 3.20–4.10 (m, 7*H*) ppm; ms (15 eV) *m/e*: 368 (M^+), 233 ($M^+ - (CH_3CH_2S)_2CH$), 191, 135, 89.

2,4-O-Isopropylidene-3,5,6-tri-O-methyl-D-glucose (41)

The dithioacetal **40** (310 mg, 0.84 mmol) was stirred for 2.5 h with mercuric chloride (420 mg, 1.5 mmol) and mercuric oxide (420 mg, 1.94 mmol) in a mixture of water (0.2 mL) and acetone (3 mL), at room temperature. The mixture was then filtered through a Celite pad and the precipitate washed with acetone. The combined filtrate and washings were rid of acetone by evaporation and the resulting oil was treated with chloroform (10 mL). A white precipitate formed which was filtered off and washed with more chloroform (10 mL). The combined filtrates were washed with water (1 × 10 mL), 5% potassium iodide solution (2 × 5 mL), and again with water (1 × 10 mL). Drying ($MgSO_4$) of the chloroform layer and evaporation afforded 196 mg (89%) of pure aldehyde **41** as an oil; $[\alpha]_D^{22}$ +29.3° (*c* 0.72, chloroform). Infrared (film) ν_{max}: 3000, 2940, 2900, 2840, 1740 (carbonyl), 1460, 1380, 1370 cm^{-1}; ^{1}Hmr (CCl_4) δ: 1.38 (s, 3H, $C(CH_3)$), 1.42 (s, 3H, $C(CH_3)$), 3.30 (s, 6H, 2 OCH_3), 3.40 (s, 3H, OCH_3), 3.30–3.80 (m, 5H), 4.10 (bd, 1H), 9.60 (bs, 1H, CHO) ppm; ms (70 eV) *m/e*: 247 ($M^+ - 15$), 173 ($M^+ - CH(OCH_3)(CH_2OCH_3)$), 101, 89, 45, 31.

Nitro Alcohol (42)

The aldehyde **41** (170 mg, 0.65 mmol) was stirred at room temperature for 4 h with 2,2-dimethoxy-4-nitrobutane (**38**) (114 mg, 0.70 mmol) and diisopropylamine (73 mg, 0.72 mmol) in dry dimethylformamide (1 mL). Methanol (3 mL) was then added and the solution stirred for an additional 3 h. The methanol was then removed under vacuum and water (10 mL) was added. The product was extracted with ether (3 × 5 mL). The combined extracts were dried ($MgSO_4$) and concentrated to afford the crude product **42**. Purification through a silica gel flash column, using ethyl acetate – petroleum ether (2:1) as the eluent, afforded 232 mg (84%) of an oily mixture of diastereomeric nitroalcohols **42**; $[\alpha]_D^{22}$ +6.9° (*c* 0.29, chloroform). Infrared (film) ν_{max}: 3440 (hydroxyl), 2920, 2940, 2830, 1550 (nitro), 1380 cm^{-1}; ^{1}Hmr ($CDCl_3$) (R_f 0.36, ether) δ: 1.30 (s, 6H), 1.40 (s, 3H), 2.20–3.00 (m, 3H), 3.10 (s, 3H, OCH_3), 3.20 (s, 3H, OCH_3), 3.30 (s, 3H, OCH_3), 3.40 (s, 3H, OCH_3), 3.50 (s, 3H, OCH_3), 3.20–4.20 (m, 7H), 5.00 (m, 1H, $CHNO_2$) ppm; ^{1}Hmr ($CDCl_3$) (R_f 0.42, ether) δ: 1.40 (bd, 9H), 2.00–3.00 (m, 3H), 3.10 (s, 3H, OCH_3), 3.20 (s, 3H, OCH_3), 3.40 (s, 3H, OCH_3), 3.50 (s, 3H, OCH_3), 3.60 (s, 3H, OCH_3), 3.10–4.40 (m, 7H), 4.80–5.10 (m, 1H, $CHNO_2$) ppm; ms (70 eV) *m/e*: 379 ($M^+ - NO_2$), 89, 45.

Acknowledgements

We wish to thank the Natural Sciences and Engineering Research Council of Canada for financial support, Dr. O. Mamer for taking the mass spectra, and Dr. C. Pace-Asciak and Dr. L. S. Wolfe for helpful discussions.

1. (*a*) C. Pace-Asciak and L. S. Wolfe. Chem. Commun. 1235 (1970); (*b*) C. Pace-Asciak. Biochemistry, **10**, 3664 (1971).
2. (*a*) G. Bild, S. G. Bhat, C. S. Ramadoss, B. Axelrod, and C. Sweeley. Biochim. Biophys. Res. Commun. **81**, 486 (1978); (*b*) G. Bild, S. G. Bhat, C. S. Ramadoss, and B. Axelrod. J. Biol. Chem. **253**, 21 (1978).
3. G. Just and C. Luthe. Can. J. Chem. **58**, 1799 (1980).
4. H. E. Conrad. Methods in carbohydrate chemistry. Vol. VI. *Edited by* R. L. Whistler and J. N. Miller. Academic Press, New York. 1972. p. 361.
5. W. W. Zorbach and T. A. Payne, Jr. J. Am. Chem. Soc. **80**, 5564 (1958).
6. M. Bobek and J. Farkas. Collect. Czech. Chem. Commun. **34**, 247 (1969).
7. M. P. Albrecht, D. B. Repke, and J. C. Moffatt. J. Org. Chem. **38**, 1836 (1973).
8. C. M. Gupta, G. H. Jones, and J. G. Moffatt. J. Org. Chem. **41**, 3000 (1976).
9. E. J. Corey and A. Venkateswarlu. J. Am. Chem. Soc. **94**, 6190 (1972).
10. G. Trummlitz and J. G. Moffatt. J. Org. Chem. **38**, 1841 (1973).
11. E. J. Corey and G. T. Kwiatkowski. J. Am. Chem. Soc. **88**, 5654 (1966).
12. E. J. Corey, I. Vlattas, N. H. Andersen, and K. Harding. J. Am. Chem. Soc. **80**, 3247 (1968).
13. D. Brewster, M. Myers, J. Ormerod, M. E. Spinner, S. Turner, and A. C. B. Smith. Chem. Commun. 1235 (1972).
14. W. C. Still, M. Kahn, and A. Mitra. J. Org. Chem. **43**, 2923 (1978).
15. J. M. Fortunato and B. Ganem. J. Org. Chem. **41**, 2194 (1976).
16. J. G. Buchanan, A. R. Edgar, and M. J. Power. J. Chem. Soc. Chem. Commun. 346 (1972).
17. C. E. Castro. J. Am. Chem. Soc. **83**, 3262 (1961).
18. C. E. Castro and R. D. Stephens. J. Am. Chem. Soc. **86**, 4358 (1964).
19. C. A. Brown and V. K. Ahuja. J. Chem. Soc. Chem. Commun. 553 (1973).
20. H. C. Brown and C. A. Brown. J. Am. Chem. Soc. **85**, 1005 (1963).
21. D. T. Williams and M. B. Perry. Can. J. Chem. **47**, 2763 (1969).
22. M. M. A. Abdel-Rahman. Bull. Chem. Soc. Jpn. **50**, 1619 (1977).
23. P. Bakuzis, M. L. F. Bakuzis, and T. F. Weingartner. Tetrahedron Lett. **27**, 2371 (1978).
24. H. Zinner, H. Brandner, and G. Rembarz. Chem. Ber. **89**, 800 (1956).
25. P. G. Barry and B. M. Craig. Can. J. Chem. **33**, 716 (1955).
26. G. O. Aspinal and R. J. Ferrier. J. Chem. Soc. 1501 (1958).
27. H. Zinner, E. Wittenberg, and G. Rembarz. Chem. Ber. **92**, 1614 (1959).
28. B. T. Grobel and D. Seebach. Synthesis, 357 (1977).
29. G. Just, C. Luthe, and H. Oh. Tetrahedron Lett. 1001 (1980).

Physico-chemical studies on areno tropilidenes and tropones. II. The polarographic reduction and electrode kinetics of some furotropone derivatives

SAFAA H. ETAIW[1] AND MOHAMED EL-BORAI
Department of Chemistry, Faculty of Science, University of Tanta, Tanta, Egypt
AND
MOHAMED I. ISMAIL
Department of Chemistry, University of Ain, Shams, Egypt
Received October 2, 1979[2]

SAFAA H. ETAIW, MOHAMED EL-BORAI, and MOHAMED I. ISMAIL. Can. J. Chem. **58**, 2358 (1980).

The polarographic reduction of nine furotropone derivatives has been studied in Thiel buffers and in DMF. The reduction of compounds having two methyl or two phenyl groups proceeds via two electron waves along the whole pH range studied. The reduction of furotropone and derivatives having one substituent or three methyl groups proceeds via one reversible electron wave in acid media while in neutral and alkaline media two waves each corresponding to 1 F are observed. Above pH 12, the limiting current decreases and one wave appears, corresponding to 1 F. The values of n were determined coulometrically using the Ilkovic equation. All waves are diffusion controlled while the electrode process along these waves is irreversible. The rate constant, the free energy of activation, and the electron affinities of these compounds were computed.

SAFAA H. ETAIW, MOHAMED EL-BORAI et MOHAMED I. ISMAIL. Can. J. Chem. **58**, 2358 (1980).

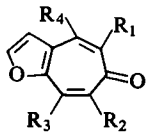
On a étudié la réduction polarographique de neuf dérivés de la furotropone dans des tampons de Thiel et dans la DMF. La réduction des composés possédant deux groupes méthyles ou phényles se fait par l'intermédiaire d'une vague à deux électrons dans tout l'intervalle du pH étudié. La réduction de la furotropone et de ses dérivés portant un substituant ou trois groupes méthyles se fait par l'intermédiaire d'une vague reversible à un électron en milieu acide tandis qu'en milieu neutre ou basique, on observe deux vagues correspondant chacune à 1 F. A un pH supérieur à 12, le courant limite diminue et il apparait une vague correspondant à 1 F. En faisant appel à l'équation d'Ilkovic et à la coulométrie on a déterminé les valeurs de n. La diffusion contrôle toutes les vagues alors que les réactions d'électrodes accompagnant ces vagues sont irréversibles. On a calculé la constante de vitesse, l'énergie d'activation et les affinités électroniques de ces composés.

[Traduit par le journal]

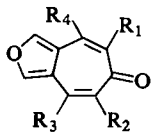
Introduction

Investigation of the polarographic reduction of the carbonyl or the quinonoid compounds has revealed that reduction at the dropping mercury electrode depends on the molecular structure, the composition of the solution (in particular hydrogen ion concentration), and electrode potential (1–9). In strong acid media, the reduction takes place by the uptake of one reversible electron forming a free radical while at high pH values two electrons are involved in the reduction process (1). The electroreduction of thiophenotropones was studied by Guilard and Fournari (10). They claimed that the polarograms consist of two reduction waves (pH 6.7), each corresponds to 1 F, producing the corresponding thiophenotropolones. In a previous article (11) we reported a detailed study on the electrochemical reduction of eleven thiophenotropones. The tropilidene ring proved to be inactive towards reduction and the reduction process was found to occur in three different ways depending on the pH value of the medium and the molecular structure.

In the course of our research, we have examined the electroreduction as well as the electrode kinetics of nine furotropone compounds **I** and **II** in Thiel buffer solutions of varying pH values. The electron affinities of these compounds were calculated regarding their polarographic behaviour in DMF.



I



II

Compound	Substituent			
	R_1	R_2	R_3	R_4
I*a*	H	H	H	H
b	OCH_3	H	H	H
c	H	OCH_3	H	H
d	CH_3	CH_3	H	H
e	ph	ph	H	H
f	CH_3	CH_3	H	CH_3
II*a*	H	H	H	H
b	H	OCH_3	H	H
c	ph	ph	H	H

[1]To whom all correspondence should be addressed.
[2]Revision received June 2, 1980.

0008-4042/80/222358-06$01.00/0
© 1980 National Research Council of Canada/Conseil national de recherches du Canada

Can. J. Chem. Downloaded from www.nrcresearchpress.com by 210.87.254.40 on 09/05/12
For personal use only.

Can. J. Chem. Downloaded from www.nrcresearchpress.com by 210.87.254.40 on 09/05/12
For personal use only.

Experimental

The furotropones were prepared according to the recommended procedure described by El-Borai *et al.* (12). The solids were purified by recrystallization from the appropriate solvents and their purity and identity were checked by mp determination, ^{1}Hmr, elemental analysis, and thin-layer chromatography. The polarograms were recorded by radiometer PO_4 type recording polarograph using a dropping electrode with $m = 2.45$ mg s^{-1} and $t = 3.6$ s at a height of 52 cm Hg and a kalousek polarographic cell with a thermostating jacket. The temperature was maintained with an ultrathermostat at 25 ± 0.1°C. A series of Thiel buffer solutions were used while after pH 12 a concentrated solution of NaOH was used to raise the pH of the medium. The compounds **I**, **II**, and **III** were dissolved in 20 vol% ethanol–water mixture. The polarograms in DMF were carried out using 0.1 *M* I^{-1} of *N*-tetrabutyl ammonium perchlorate as supporting electrolyte. Depolariser concentrations studied were 1×10^{-3} *M* at a μ of 0.1 (NaCl). A saturated calomel electrode (sce) was used as reference electrode. A radiometer pH meter type 63 fitted with a combined glass electrode type Gk 2301 C was employed for determination of pH. The instrument was accurate to ±0.01 pH unit. The electrolysis at controlled potential was made using a potentiostat Tacussel of type ASA 4/60. The electrolysis cell used was as that described by Peltier *et al.* (13).

Results and Discussion

The electroreduction of 1×10^{-3} *M* of furotropone derivatives recalls that of the carbonyl compounds (1, 11, 14–16). The polarograms of **I***a–c*, *f* and **II***a*, *b* show the same behaviour while those of **I***d*, *e* and **II***c* are identical (Fig. 1). The polarograms of **I***a*, *c*, *f* and **II***a*, *b* exhibit one reduction wave, A, in solutions of pH ≤ 4.3. Wave A corresponds to 1 F. However, the polarograms of **I***b* exhibit this behaviour in solutions of pH 2.3–7.5. Above pH 4.3 or 7.5, the polarograms consist of two reduction waves (A, B) of equal heights each corresponding to 1 F. The $E_{1/2}$ of wave A shifts to an apparent less negative potential while that of wave B suffers a slight shift in the same direction by increasing the pH value. At pH > 13 the height of wave B decreases until it vanishes at pH ≥ 13.4 and one wave, C, appears to correspond to 1 F. On the other hand, the polarograms of **I***d*, *e* and **II***c* consist of one reduction wave, D, over all the pH range from 2.3 to 12. The wave corresponds to 2 F and has a total height more or less equal to that of both waves A and B. As the pH increases, the height decreases until it attains the current corresponding to 1 F at pH ≃ 13.5.

The coulometric analysis under controlled potential and a μ of 0.1 proved that waves A, B, and C correspond to the uptake of one electron while wave D corresponds to the uptake of two electrons. Also, using the Ilkovic equation the number of electrons can be evaluated. The diffusion coefficient of the depolariser was determined from the molar volume applying "the Stocks–Einstein relation" [1].

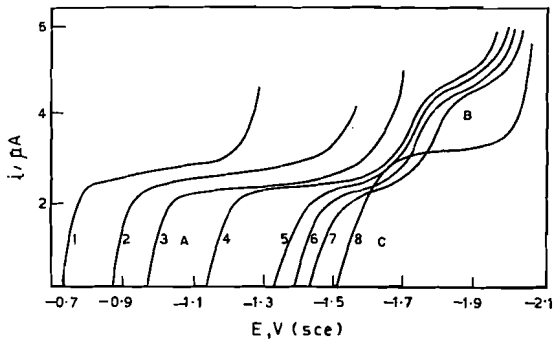


FIG. 1. The polarograms of 1 m*M* of **I***a* in Thiel buffer solutions at 25 ± 0.1°C, run and pH: (*1*) 2.30; (*2*) 3.50; (*3*) 4.30; (*4*) 5.50; (*5*) 7.50; (*6*) 8.70; (*7*) 10.20; (*8*) 13.40.

[1] $D_0 = 3.31 \times 10^{-5} (D/M)^{1/3}/\eta$ cm^2 s^{-1}

The values of the diffusion coefficient obtained by this method are reported in Table 1. The number of electrons evaluated using coulometry and Ilkovic equation are quite close to each other.

The waves A, B, C, and D proceed irreversibly as was indicated by the values of the slope of the straight lines obtained by applying the fundamental equation for polarographic data (17) and by the values of the transfer coefficient α (18). Also, all the waves are diffusion controlled as was indicated by the effect of mercury height on the limiting current, Table 1.

The $E_{1/2}$ of all waves shifts to less negative potential, however, the magnitude of shift for wave A is larger than that for wave B. The correlation of $E_{1/2}$ with pH is straight or in broken lines, depending on the nature of the wave and the molecular structure (Fig. 2). The number of protons involved in the reduction process for each wave was determined using relation [2] (Table 1).

[2] $\Delta E_{1/2}/\Delta\text{pH} = (0.059/\alpha n_a)(ZH^+)$

The correlation of i_1 with pH is straight or curved lines (Fig. 3), indicating that the limiting current decreases slightly as the pH increases. The validity of the Ilkovic equation was tested at pH 4.5 and 10.2. A satisfactory linear relation passing through the origin is obtained for waves A, B, and D. The values of i_1/C are constant, which suggests the possible application of the polarographic method for the determination of furotropone derivatives. Rate constants, k_e^0, and the free energy of activation, ΔG^*, are computed applying the different approaches proposed for analysis of irreversible

TABLE 1. Polarographic results[a] obtained for I and II

Compound	pH	$-E_{1/2}$ (V)	$D \times 10^6$ ($cm^2\ s^{-1}$)	Y^b	n_a	α	$\frac{\Delta E_{1/2}{}^b}{\Delta pH}$	ZH^+	K_e^0 ($cm\ s^{-1}$)	ΔG^* (kcal mol^{-1})
I*a*	2.30	0.76	5.289	11.70	1	0.69	0.09[c]	1.05	4.32×10^{-9}	84.32
	7.50	1.40[c]		10.32	1	0.61	0.026[c]	0.27	5.31×10^{-16}	121.93
		1.72[d]		9.70	1	0.57	0.005[d]	0.05	8.20×10^{-16}	129.95
	13.40	1.55		11.31	1	0.67	0.03[d]	—	2.40×10^{-17}	136.29
I*b*	2.30	0.85	8.351	10.93	1	0.64	0.087[c]	0.95	3.60×10^{-10}	93.93
	7.50	1.27[c]		10.50	1	0.62	0.020[c]	0.21	9.30×10^{-15}	121.33
		1.56[d]		9.30	1	0.55	0.027[d]	0.25	3.70×10^{-16}	128.66
	13.50	1.44		12.01	1	0.71	—	—	7.80×10^{-17}	135.77
I*c*	2.30	0.88	5.315	10.20	1	0.60	0.093[c]	0.95	7.30×10^{-10}	95.57
	7.50	1.44[c]		9.50	1	0.56	0.019[c]	0.18	3.80×10^{-15}	119.75
		1.75		8.51	1	0.50	0.056[d]	0.47	9.10×10^{-16}	127.65
	13.40	1.53		11.30	1	0.67	—	—	1.70×10^{-17}	133.52
I*d*	2.30	1.01	2.724	16.60	2	0.49	0.08	1.33	9.20×10^{-18}	122.29
	7.50	1.37		15.12	2	0.45	0.06	0.99	3.70×10^{-21}	166.92
	11.21	1.59		12.10	2	0.36		0.72	6.10×10^{-18}	167.55
	13.50	1.73		11.40	1	0.67		—	3.80×10^{-19}	157.11
I*e*	2.30	1.19	3.521	17.01	2	0.50		0.87	3.40×10^{-20}	163.82
	7.50	1.52		15.81	2	0.45		1.04	2.40×10^{-23}	178.99
	11.21	1.69		12.38	2	0.37	0.068	0.85	6.20×10^{-20}	148.83
	13.40	1.90		10.25	1	0.60		—	5.40×10^{-17}	143.66
I*f*	2.30	1.03	5.961	13.01	1	0.77	0.067[c]	0.87	2.38×10^{-14}	102.73
	7.50	1.38[c]		10.20	1	0.60	0.084[d]	0.58	1.80×10^{-18}	138.25
		1.70[d]		9.31	1	0.55	0.012[d]	0.11	3.50×10^{-17}	124.53
	13.40	1.75		12.02	1	0.71		—	2.90×10^{-19}	135.77
II*a*	2.30	0.70	4.207	10.92	1	0.64	0.084[c]	0.91	2.70×10^{-9}	73.85
	7.50	1.14[c]		10.63	1	0.63	0.031[c]	0.33	3.50×10^{-14}	119.21
		1.53[d]		9.38	1	0.55	0.01[d]	0.09	6.20×10^{-16}	120.14
	13.40	1.38		11.62	1	0.69		—	8.10×10^{-18}	145.85
II*b*	2.30	0.70	5.90	11.81	1	0.69	0.08[c]	0.94	7.10×10^{-11}	87.87
	7.50	1.10[c]		10.50	1	0.62	0.01[c]	0.10	5.30×10^{-13}	108.82
		1.50[d]		12.30	1	0.73	0.012[d]	0.15	6.30×10^{-16}	118.83
	13.40	1.36		17.50	1	0.68		—	7.30×10^{-18}	129.78
II*c*	2.30	1.12	3.578	17.32	2	0.51		0.59	5.30×10^{-18}	125.88
	7.50	1.28		15.41	2	0.46	0.034	0.52	1.90×10^{-19}	127.83
	11.21	1.40		12.31	2	0.37		0.42	4.10×10^{-20}	138.97
	13.50	1.47		10.82	1	0.64		—	9.40×10^{-22}	153.79

[a]The values of x in the relation $i_1 = kh^x$ are equal to 0.5–0.53 at different pH values.
[b]Y = the slope of the correlation of $\log i(i_1 - i)$ with E; the slopes are calculated by the method of least squares.
[c]Wave A.
[d]Wave B.

waves by Delahay (19) Strassner and Delahay (20), and Koutecky (21) and modified by Issa and Tharwat (22) (Table 1).

$$[3]\quad i_{irr}/(i_{rev} - i_{irr}) = 0.886\, K_e^0\, (t/d)^{1/2}$$

$$[4]\quad \log k_e^0 = \log \left(\frac{i_{irr}}{i_{rev} - i_{irr}}\right)_{E=0} + \log \frac{1}{0.886}\left(\frac{d}{t}\right)^{1/2}$$

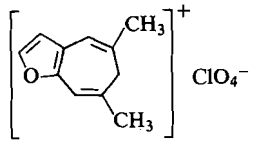
$$[5]\quad \Delta G^* = 5778.8\,(5.097 - \log k_e^0)$$

The low values of K_e^0 and the high values of ΔG^* support the irreversible nature of the waves.

Reduction Mechanism

In order to get precise information about the electroreduction of furotropone derivatives, one must consider the reduction of furotropilidene. Thus, we investigated the electroreduction of a perchlorate salt of type **III**.

The polarogram of 1×10^{-3} *M* of **III** in Thiel buffer solutions consists of one reduction wave



III

Can. J. Chem. Downloaded from www.nrcresearchpress.com by 210.87.254.40 on 09/05/12
For personal use only.

Can. J. Chem. Downloaded from www.nrcresearchpress.com by 210.87.254.40 on 09/05/12
For personal use only.

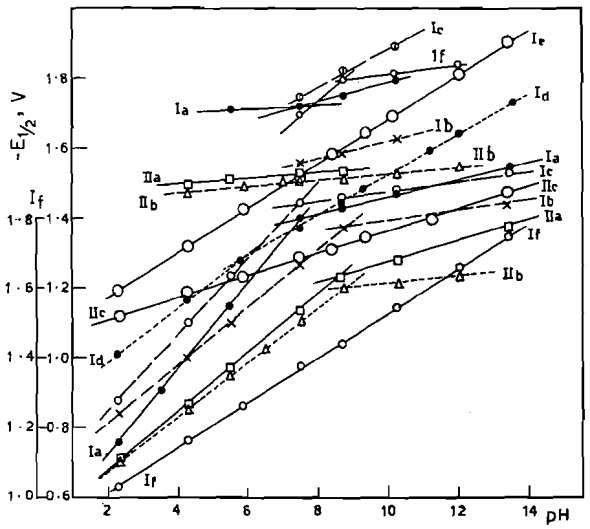


FIG. 2. The correlation of $E_{1/2}$ with pH.

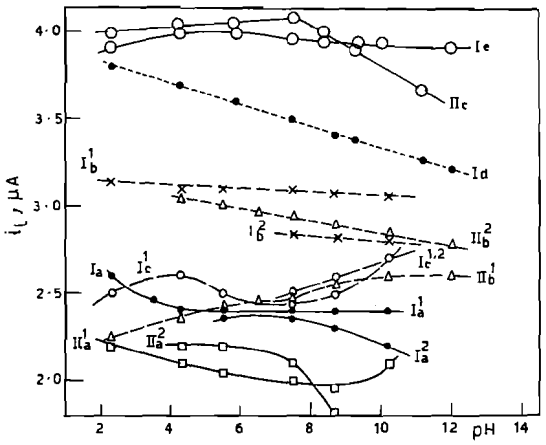


FIG. 3. The correlation of the limiting current with pH. (*1*) wave A; (*2*) wave B.

corresponding to 1 F at pH < 4.5. Within the pH range 4.5–7, a second wave appears, it almost has equal height as the first one (Fig. 4). Above pH 7 the polarograms suffer deformation since the compounds are hydrolysed. Khopin and Zhdanov (23) obtained similar results on studying the electroreduction of tropylium perchlorate salt. The first wave corresponds to the uptake of one electron forming a free radical which undergoes dimerisation. At pH > 4.5, the new wave can be attributed to the formation of furotropilidene since the reduction processes at these pH values involved the uptake of two electrons, as supported by coulometric analysis, and one proton.

$$\left.\begin{aligned}(C_{11}H_{11}O)^+ + e &\rightleftharpoons (C_{11}H_{11}O)^\cdot \\ 2(C_{11}H_{11}O)^\cdot &\rightarrow (C_{11}H_{11}O)_2\end{aligned}\right\} \quad \text{first wave, pH} < 4.5$$

$$\left.\begin{aligned}(C_{11}H_{11}O)^+ + 2e &\rightleftharpoons (C_{11}H_{11}O)^- \\ (C_{11}H_{11}O)^- + H^+ &\rightarrow C_{11}H_{12}O\end{aligned}\right\} \quad \text{pH} > 4.5$$

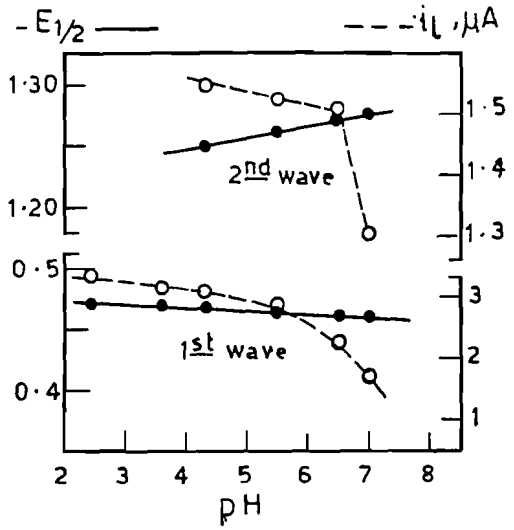
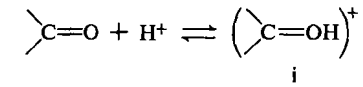


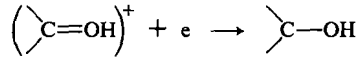
FIG. 4. The correlation of $E_{1/2}$ and i_l with pH for 0.5 m*M* **III**.

These results were further supported by electrolysis at controlled potential (13). The electrolysis was carried out in aqueous solution at pH 6 and at −1.37 V. After the extraction of the product of electrolysis, it was analysed by vapour phase chromatography. The electrochemical reduction was quantitative and three isomers of **III** were separated in proportions previously reported by El-Borai *et al.* (24). Thus the tropilidene ring is inactive towards reduction at the dropping mercury electrode under these experimental conditions.

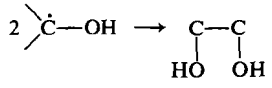
Wave A corresponds to the reduction of cation **i** and then forms the free radical **ii** which dimerises to form pinacol, **iii**.



i

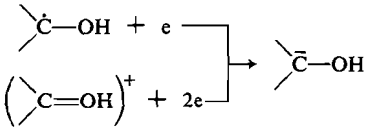


ii



iii

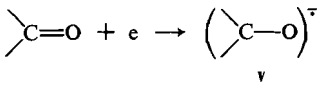
Wave B expresses the transformation of radical **ii** to alcohol **iv**.



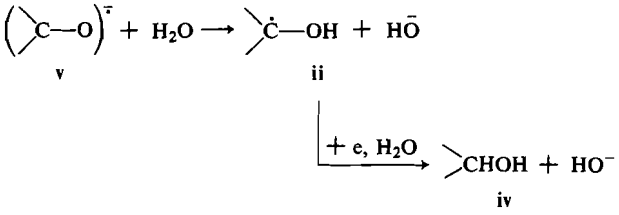
iv

Can. J. Chem. Downloaded from www.nrcresearchpress.com by 210.87.254.40 on 09/05/12
For personal use only.

Wave C corresponds to the direct reduction of the basic form to the anion radical **v** which is stable at pH ≥ 13.4.



On the other hand, wave D involves the formation of the anion radical **v** which reacts with one proton in acid media or with one mole of water in alkaline media to reproduce **ii**. Radical **ii** undergoes further reduction to form alcohol **iv**.



Effect of Molecular Structure on $E_{1/2}$

Consulting the half wave potentials of furotropone derivatives at one and the same pH value, one can conclude that the increase of electron density on the tropilidene ring, consequently the polarisation of the carbonyl group, renders the half wave potentials to be shifted to more negative values. The derivatives of **I** have more negative half wave potentials than the corresponding derivatives of **II**. Also, the increase of donor character of the substituent shifts the reduction wave A to more negative potential so that it intermingles with wave B to form wave D as observed in the polarograms of **Id**, *e* and **IIc**. In these compounds the carbonyl group tends to be completely polarised in the ground state facilitating the formation of the anion free radical **v** on reduction.

The Correlation of Half Wave Reduction Potentials with Absolute Electron Affinities

The potential determining step in the polarographic reduction of a compound has been assumed to be the reversible addition of an electron to the molecule so that the half wave reduction potential is a measure of the electron affinity of the compound according to eq. [6].

$$[6] \quad -E_{1/2} = \text{E.A.} - \Delta G_{sol} - \text{constant}$$

The constant term depends upon the reference electrode and is 5.07 eV for the saturated calomel electrode. The difference in solvation energies for the negative ion and the neutral, ΔG_{sol}, is often assumed to be constant for CT acceptors; in spite of the fact that the correlation of half wave reduction potentials with absolute E.A. values for aromatic hydrocarbons indicates that this quantity is not constant, at least in the case of dioxane and dimethoxyethanol as solvents (25). Briegleb (26) and Farragher and Page (27) calculated average values of −3.66 and −2.37 eV for ΔG_{sol}, respectively.

Chen and Wentworth (28) used the absolute E.A. values of 22 acceptors and calculated an average value of -2.58 ± 0.26 eV for ΔG_{sol}. Thus eq. [7] can be used to calculate the E.A. values from half wave reduction potentials vs. the saturated calomel electrode (29–34).

$$[7] \quad \text{E.A.} = -E_{1/2} + 2.49 \pm 0.26 \text{ eV}$$

The half wave potentials of furotropones recorded in DMF and the corresponding electron affinities are listed in Table 2. The correlation of E.A. values with $E_{1/2}$ values of furotropones gives an excellent linear relationship, (Fig. 5).

TABLE 2. Electron affinities and $E_{1/2}$'s of **I** and **II** measured in DMF

Compound	$-E_{1/2}$ (V)	E.A. (eV)
I*a*	1.51	0.98
b	1.57	0.92
c	1.53	0.96
d	1.75	0.74
e	1.70	0.79
f	1.76	0.73
II*a*	1.48	1.01
b	1.35	1.14
c	1.60	0.89

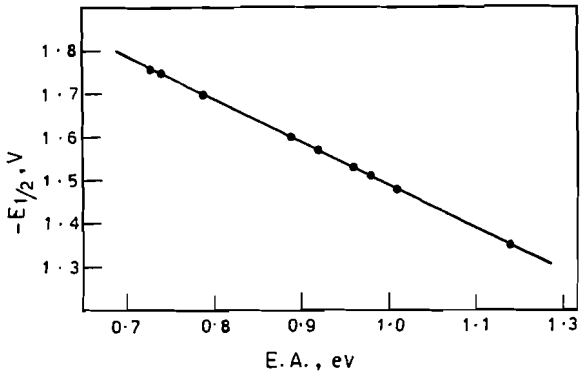


FIG. 5. The correlation of $E_{1/2}$'s with electron affinities of **I** and **II**.

1. L. HOLLECK and H. MERSON. Z. Elektrochem. **57**, 944 (1953).
2. R. JONES and T. MEL. Aust. J. Chem. **15**, 492 (1962).
3. H. SHIGEO and S. NORIKO. Bull. Chem. Soc. Jpn. **43**, 2083 (1970).
4. E. MUELLER and W. DILGER. Chem. Ber. **106**, 1643 (1973).
5. B. SHASHI and N. R. BANNERJEE. Indian J. Chem. **15**(A), 777 (1977).
6. I. M. ISSA, S. H. ETAIW, R. M. ISSA, and A. K. ABD-ELKADER. Ann. Chim. **67**, 211 (1977).

7. J. C. VIRE and Q. J. PATRIACHE. Analusis, **6**, 155 (1978).
8. S. H. ETAIW. Ann. Chim. **68**, 57 (1978).
9. A. M. KUTNEVICH, A. P. RUDENKO, L. L. RODINA, and F. PRAGST. Zh. Org. Khim. **14**, 1343 (1978).
10. R. GUILARD and P. FOURNARI. C. R. Acad. Sci. Paris, t.**273**, 160 (1971).
11. S. H. ETAIW, M. ISMAIL, and M. EL-BORAI. Can. J. Chem. **58**, 263 (1980).
12. M. EL-BORAI, R. GUILARD, and P. FOURNARI. Bull. Soc. Chim. Fr. **7**, 1383 (1974).
13. D. PELTIER, M. LE GUYADER, and J. TACUSSEL. Bull. Soc. Chim. 2609 (1963).
14. D. CHANTAL and L. MICHELLE. Bull. Soc. Chim. Fr. **5–6**, 817 (1976).
15. A. RUSINA, J. VOLKE, J. CERNAK, T. KOVAC, and V. KALTAR. J. Electroanal. Chem. Interfacial Electrochem. **50**, 351 (1974).
16. M. B. FLEURY. Actual Chim. Anal. Org. Pharm. Bromatol, **22**, 69 (1973).
17. L. MEITES. Polarographic techniques. 2nd ed. Interscience Publishers, New York – London – Sydney. 1965.
18. D. R. CROW. Polarography of metal complexes. Academic Press, London and New York. 1969. p. 39.
19. P. DELAHAY. J. Am. Chem. Soc. **73**, 4944 (1951).
20. J. E. STRASSNER and P. DELAHAY. J. Am. Chem. Soc. **74**, 6232 (1952).
21. J. KOUTECKY. Chem. Listy, **47**, 323 (1953).
22. I. M. ISSA and M. THARWAT. Electrochim. Acta, **17**, 1065 (1972).
23. A. M. KHOPIN and S. I. ZHDANOV. Electrokhimiya, **4**, 228 (1968).
24. M. EL-BORAI, G. GUILARD, P. FOURNARI, Y. DUSAUSOY, and J. PROTAS. Bull. Soc. Chim. Fr. **7**, 75 (1977).
25. R. S. BECKER and E. C. M. CHEN. J. Chem. Phys. **45**, 2403 (1966).
26. G. BRIEGLEB. Angew. Chem. Int. Ed. Engl. **3**, 617 (1964).
27. A. L. FARRAGHER and F. M. PAGE. Trans. Faraday Soc. **63**, 2369 (1967).
28. E. C. M. CHEN and W. E. WENTWORTH. J. Chem. Phys. **63**, 3183 (1975).
29. F. M. PAGE and G. C. GOODE. Negative ions and the magnetron. Wiley Interscience, New York. 1969.
30. M. E. PEOVER. Trans. Faraday Soc. **58**, 1656 (1962); **58**, 2370 (1962); **60**, 417 (1964); **60**, 479 (1964).
31. M. E. PEOVER. Nature, London, **191**, 702 (1961); **193**, 475 (1962).
32. M. E. PEOVER. J. Chem. Soc. 2540 (1962).
33. K. M. C. DAVIS, P. R. HAMMOND, and M. E. PEOVER. Trans. Faraday Soc. **61**, 1516 (1965).
34. A. H. MAKI and D. H. GESKE. J. Am. Chem. Soc. **83**, 1852 (1961).

Can. J. Chem. Downloaded from www.nrcresearchpress.com by 210.87.254.40 on 09/05/12
For personal use only.

Theoretical and experimental conformational preferences of the aldehyde and fluoroaldehyde groups in 2-methylbenzaldehyde, 2-trifluoromethylbenzaldehyde, and 4-chloro-2-methylbenzoyl fluoride. Proximate couplings

TED SCHAEFER, SALMAN R. SALMAN,[1] AND TIMOTHY A. WILDMAN
Department of Chemistry, University of Manitoba, Winnipeg, Man., Canada R3T 2N2

Received May 29, 1980

TED SCHAEFER, SALMAN R. SALMAN, and TIMOTHY A. WILDMAN. Can. J. Chem. **58**, 2364 (1980).

On the basis of long-range spin–spin coupling constants, the O-*syn* conformation of 2-methylbenzaldehyde in CCl_4 solution at 305 K is favored over the O-*anti* form by a free energy of 0.5$_3$ kJ/mol. This number is compatible with other experiments, as well as with STO-3G MO calculations in which the geometry of the substituents is optimized. The latter yield 0.52 kJ/mol in the internal energy difference. In benzene solution, 2-trifluoromethylbenzaldehyde exists in the O-*anti* form to the extent of at least 95% at 305 K. In CCl_4 solution at this temperature, the population of the O-*syn* conformer of 4-chloro-2-methylbenzoyl fluoride is likely 75% or more of the total, in semiquantitative agreement with STO-3G optimization procedures. Substantial proximate couplings exist between ^1H and ^{19}F nuclei in the sidechains of the latter two compounds and are compared with INDO MO FPT computations. These yield negative values for $^5J_o^{CHO,CF_3}$ in 2-trifluoromethylbenzaldehyde, whereas the experimental value is 2.23 Hz.

TED SCHAEFER, SALMAN R. SALMAN et TIMOTHY A. WILDMAN. Can. J. Chem. **58**, 2364 (1980).

En se basant sur les constantes de couplage spin–spin à longue distance on peut conclure que la conformation O-*syn* du méthyl-2 benzaldéhyde en solution dans le CCl_4 à 305 K est favorisée par rapport à la forme O-*anti* par une différence d'énergie libre de 0,53 kJ/mol. Cette valeur est compatible avec d'autres expériences ainsi qu'avec des calculs OM STO-3G dans lesquels on maximise la géométrie des substituants. Ces derniers donnent une différence d'énergie interne de 0,52 kJ/mol. En solution dans le benzène, au moins 95% du trifluorométhyl-2 benzaldéhyde existe sous la forme O-*anti* à 305 K. En solution dans le CCl_4 à cette température, probablement 75% ou plus du fluorure de chloro-4 méthyl-2 benzyle existe dans la conformation O-*syn*; cette conclusion est en accord semi-quantitatif avec les méthodes de maximisation du STO-3G. Des couplages approximatifs substantiels existent entre les noyaux de ^1H et de ^{19}F des chaînes latérales des deux derniers composés et on les compare aux valeurs obtenues par calculs OM INDO FPT. Ces derniers conduisent à des valeurs négatives de $^5J_o^{CHO,CF_3}$ pour le trifluorométhyl-2 benzaldéhyde alors que la valeur expérimentale est de 2,23 Hz.

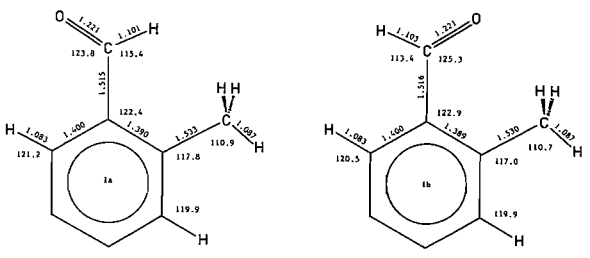
[Traduit par le journal]

Introduction

The conformational behaviour of the aldehyde and the fluoroaldehyde groups has been investigated for benzaldehyde and benzoyl fluoride and a number of their derivatives by a variety of techniques (1–18). In solution at least (1, 14), the twofold barrier to rotation about the exocyclic carbon–carbon bond is 31.4 kJ/mol for benzaldehyde and 29.3 kJ/mol for benzoyl fluoride, so that at ambient temperatures the molecules are effectively planar. Substitution at both *ortho* positions by chlorine atoms or methyl groups causes a twist about the exocyclic bond (12, 19), as shown by the appearance of spin–spin couplings over six bonds, $^6J_p^{H,CHO}$ and $^6J_p^{H,CFO}$, involving the *para* ring protons in such derivatives. The stereospecificity of long-range couplings from ring protons to the sidechain protons or ^{19}F nuclei allows deductions about the degree of twisting.

Asymmetric substitution patterns in the ring yield rapidly interconverting O-*syn* and O-*anti* isomers, whose populations can also be deduced from long-range couplings (8–11). At sufficiently low temperatures, ^{13}C or ^1H nmr spectra of both isomers are detectable and their peak areas give the population ratios (2, 3). The latter are not always in agreement with those found at room temperature, a fact perhaps attributable to varying solvent effects (20) in the experiments; particularly if the conformational isomers have rather different dipole moments (11).

If these moments are rather similar, then the two methods should agree. For example, the O-*anti* form, **1***a*, of 2-methylbenzaldehyde, cannot have a dipole moment very different from that of the O-*syn* form, **1***b* (structure **1**). Because ^1H and ^{13}C nmr data at low temperatures are available (2, 3), it is of



Structure **1**

[1]Present address: Department of Chemistry, University of Baghdad, Iraq.

0008-4042/80/222364-05$01.00/0

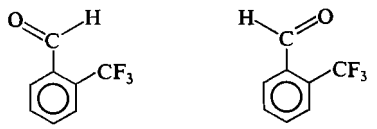
©1980 National Research Council of Canada/Conseil national de recherches du Canada

Can. J. Chem. Downloaded from www.nrcresearchpress.com by 210.87.254.6 on 09/05/12
For personal use only.

Can. J. Chem. Downloaded from www.nrcresearchpress.com by 210.87.254.6 on 09/05/12
For personal use only.

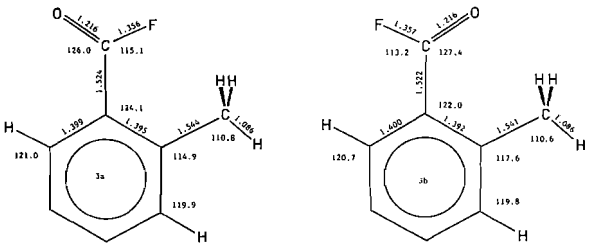
interest to see whether the use of stereospecific coupling constants at ambient temperatures will yield compatible population ratios or whether there exists a fundamental flaw in the assumptions (11) about such couplings.

In another vein, considerable effort has been expended in the elucidation of so-called "through-space" coupling constants (21–24). These exist when the coupled nuclei, although separated by four or more formal bonds, approach each other rather closely; or when the bonds containing these nuclei are juxtaposed in certain orientations. Considered rigorously, all couplings are transmitted through space, so that these couplings should probably be called proximate. Such couplings may well occur in the O-*anti* forms, **2***a*, of 2-trifluoromethylbenzaldehyde and **3***a*, of 4-chloro-2-methylbenzoyl fluoride (structure **3**).



2*a* O-*anti* **2***b* O-*syn*

Structure **2**



Structure **3**

Accordingly, the ^{1}H nmr spectra of **1** to **3** (the chlorine substituent in **3** unfortunately was necessary to allow a precise spectral analysis) were analyzed. The spectral parameters yield the *a*:*b* ratio and also emphasize the elusiveness of a satisfactory model for the proximate couplings in at least one of these compounds.

Experimental

Compounds **1** and **2** came from Aldrich and Chemical Procurement Laboratories, respectively. **3** was prepared from the acid by reaction with diethylaminosulfur trifluoride (DAST) in the accepted way (25). Nuclear magnetic resonance samples were prepared as degassed solutions in 5 mm od glass tubes and contained a small amount of tetramethylsilane (TMS). Compounds **1** and **3** were examined as 9.5 and 10.0 mol% solutions in CCl_4, respectively, whereas **2** had to be used as 6.0 mol% solution in C_6D_6 for reasons of chemical shift dispersion.

The ^{1}H nmr spectra were calibrated in the frequency sweep mode on an HA100 spectrometer at a probe temperature of 305 K. Markers were placed at ca. 5 Hz intervals, frequencies of sweep and lock (provided externally for stability) oscillators were read, and interpolation between these marker frequencies gave peak positions whose root-mean-square deviations were typically ≤ 0.02 Hz. Weak irradiation with a second radiofrequency field (26) yielded the relative signs of coupling constants.

Molecular orbital calculations were performed on an IBM System 360/168, or an Amdahl 470/V7, at the STO-3G (27) and INDO or CNDO (28) levels of molecular orbital theory.

Results and Discussion

Spectral Analyses

Performed with the computer program LAME (29, 30), the analyses gave the spectral parameters for **1** to **3**. Full results are given for 2-methylbenzaldehyde in Table 1, while the couplings to the sidechains in **2** and **3** are found in Table 2. Figure 1 displays the observed and calculated methyl ^{1}H nmr spectra for **1**.

Conformational Equilibrium in 2-Methylbenzaldehyde, 1

As discussed in detail previously (11), there is no evidence that $^5J_m^{H,CHO}$ is other than zero for H-3 in **1***a* or H-5 in **1***b*. Furthermore, the sum of the $^5J_m^{H,CHO}$ values in **1** is 0.76_8 Hz and is 0.76_0 Hz in benzaldehyde (31), suggesting a negligible intrinsic substituent perturbation of $^5J_m^{H,CHO}$ in **1**. Accordingly, the ratio of O-*syn* to O-*anti* forms is 55/45 in CCl_4 at 305 K.

At 113 K in $CHFCl_2$ solution (2), peak areas of ^{13}C and/or ^{1}H nmr spectra of the separate conformers yield the above ratio as 36 to 64. From the

TABLE 1. ^{1}H nmr spectral parameters at 100.001 MHz for a 9.5 mol% solution of 2-methylbenzaldehyde in CCl_4 at 305 K

Parameter[a]	Value	Parameter	Value
ν_{CHO}	1015.818(3)[b]	$^4J_o^{H,CH_3}$	−0.756(2)
ν_{CH_3}	262.234(2)	$^5J_4^{H,CH_3}$	0.349(2)
ν_3	717.336(2)	$^5J_6^{H,CH_3}$	0.367(2)
ν_4	737.328(3)	$^6J_p^{H,CH_3}$	−0.574(2)
ν_5	728.259(2)	$^4J_o^{H,CHO}$	−0.249(2)
ν_6	768.776(2)	$^5J_3^{H,CHO}$	0.424(3)
$^3J_{34}$	7.637(3)	$^5J_5^{H,CHO}$	0.344(3)
$^3J_{45}$	7.422(3)	$^6J_p^{H,CHO}$	≤ 0.03[d]
$^3J_{56}$	7.665(3)	Root-mean-square	0.013
$^3J_{35}$	1.233(3)	deviation	
$^3J_{46}$	1.502(3)	Peaks observed	145
$^3J_{36}$	0.514(2)	Peaks calculated	653
$^5J_o^{CHO,CH_3}$	≤ 0.4[d]	Peaks assigned	306[c]

[a]Chemical shifts in Hz to low field of internal TMS.
[b]Numbers in parentheses are standard deviations in the last significant figure.
[c]Many overlapping peaks were assigned only when no ambiguity existed.
[d]From decoupling experiments.

TABLE 2. Long-range $^1H,^1H$ and $^1H,^{19}F$ coupling constants in 2-trifluoromethylbenzaldehyde, **2**, and in 4-chloro-2-methylbenzoyl fluoride, **3**

	Value			Value	
Parameter[a,b]	2[c]	3[d]	Parameter	2	3
$^5J_o^{X,R}$	2.23	1.84	$^4J_o^{H,X}$	−0.15	−0.43
$^4J_o^{H,R}$	−0.64	−0.73	$^5J_3^{H,X}$	0.00	1.67
$^5J_4^{H,R}$	0.93	—	$^5J_5^{H,X}$	0.82	0.56
$^5J_6^{H,R}$	0.75	0.35	$^6J_p^{H,X}$	−0.06	—
$^6J_p^{H,R}$	−0.68	−0.60			

[a]In the formula 1-COX-2-CR_3-benzene.
[b]To an estimated accuracy of 0.02 Hz, the standard deviations lying between 0.004 and 0.01 Hz.
[c]6 mol% in benzene-d_6.
[d]10 mol% in CCl_4.

enthalpy and entropy data obtained in that work (2), it is clear that the O-*syn* population can become greater than 50% at 305 K (formally 72 ± 20%). In another investigation (3) at 128 K in a $CCl_2F_2/CHFCl_2$ solution, the ratio was 50/50 as obtained from ^{13}C nmr peak areas of the two conformers. The dipole moments of two conformers may differ by only 5% (see a later section) and therefore medium perturbations of the conformational equilibrium are probably small.

Shift reagents added to a solution of **1** in CCl_4 caused chemical shift dispersion interpretable as arising from a roughly 50/50 mixture of **1***a* and **1***b* (4).

We take these comparisons to mean that $^5J_m^{H,CHO}$ is a reliable indicator of the conformer preferences in **1**.

The negligible magnitude of $^6J_p^{H,CHO}$ in **1** suggests that the aldehyde group is essentially coplanar with the aromatic framework. Indeed, the barrier to interconversion of the conformers is ca. 28 kJ/mol (2, 3), similar to benzaldehyde and much larger than kT at 305 K. Therefore effectively planar conformations are a reasonable conclusion.

Molecular Orbital Calculations on 1

A standard geometry (32) at the STO-3G level gave the O-*syn* form as 11 kJ/mol less stable than the O-*anti* conformer. Therefore a geometry optimization was performed, beginning with benzaldehyde itself. No reliable structural data are available for this molecule, the geometry of the aldehyde group in acetaldehyde having been assumed for the microwave studies (16, 33). The structural results are set out in structure **1**. The O-*syn* form is favored by 0.52 kJ/mol, presumably the major part of the internal energy difference. The experimental value is 0.53 ± 0.05 kJ/mol in the free energy for a 9.5 mol% solution in CCl_4 at 305 K. The contribution of internal motions to the internal energy and to the entropy could be calculated from statistical

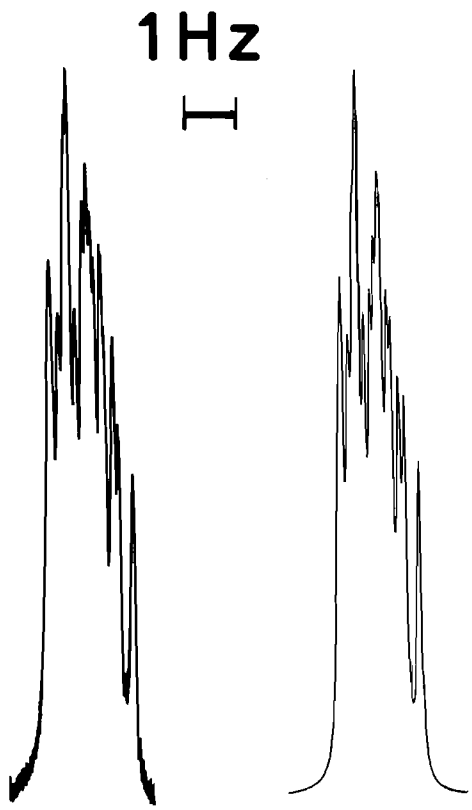


FIG. 1. The experimental and theoretical methyl proton ^1H nmr spectra at 100 MHz for a 9.5 mol% solution of 2-methylbenzaldehyde in CCl_4 at 305 K. The spectrum was recorded while decoupling the aldehyde proton. The theoretical spectrum used the parameters in Table 1. There is some disagreement in the middle region of the two spectra, attributable to slight differences in line width or shape and/or to variations of up to 0.02 Hz in some of the long-range couplings. Iteration on ring proton transitions only did not produce variations larger than 0.002 Hz in the crucial couplings, $^5J_m^{H,CHO}$. The assumed linewidth at half height was 0.10 Hz. The coupling between the aldehyde and methyl protons amounts to ca. 0.04 Hz in magnitude.

mechanics. However, one must know the molecular partition function. This requires a good knowledge of the potential energy surface for all internal motions, but this knowledge is unavailable. The STO-3G results may be considered encouraging.

STO-3G calculations underestimate dipole moments, being 1.92 D for benzaldehyde (3.21 K is the gas phase value (33)), and 2.00 and 1.71 D for the O-*anti* and O-*syn* forms, respectively. INDO MO dipole moments are usually more realistic. They are 2.75 D for benzaldehyde (11) and 2.58 and 2.71 D for the O-*anti* and O-*syn* forms, respectively, for the geometries in structure **1**. The small difference between the INDO MO dipole moments suggest relatively small solvent perturbations of the conformational equilibrium.

For the geometries in structure **1**, INDO MO

Can. J. Chem. Downloaded from www.nrcresearchpress.com by 210.87.254.6 on 09/05/12
For personal use only.

Can. J. Chem. Downloaded from www.nrcresearchpress.com by 210.87.254.6 on 09/05/12
For personal use only.

FPT calculations gave $^5J^{CHO,CH_3}$ as 0.00 Hz for the O-*anti* form and 0.32 Hz for the O-*syn* form. Therefore the calculations predict 0.17 Hz for the observed equilibrium, an overestimate of about 0.1 Hz. It appears that proximate coupling between the aldehyde and methyl protons is indeed very small.

Conformational Behavior of 2-Trifluoromethylbenzaldehyde, 2

Coupling between the aldehydic proton and H-3 in **2** was not observed, so that at least 95% of **2** exists in the O-*anti* form, **2***a* (in 2-fluorobenzaldehyde the sum of the $^5J_m^{H,CHO}$ values is 0.86 ± 0.04 Hz (11), whereas $^5J_5^{H,CHO}$ is 0.82 ± 0.02 Hz in **2**). In other words, a close proximity of the C=O and C—F dipoles in the orientation implied by **2***b* is unlikely. Alternatively, the C—H dipole of the aldehyde group may be attracted to the C—F dipoles in the CF_3 group.

The 0.06 Hz magnitude of $^6J_p^{H,CHO}$ is compatible with a slight average twist, perhaps as large as 10 to 12° (19), of the aldehyde group about the C—C bond in **2***a*; suggesting that interaction of the CHO and CF_3 moieties is net repulsive even when the C—H bond is *syn* to CF_3.

$^5J_o^{CHO,CF_3}$ is 2.23 Hz and is no doubt a proximate coupling (no coupling was observed for the *para* isomer). Extensive INDO MO FPT calculations with standard (32) and other reasonable geometries always yield this coupling as negative, as do CNDO MO FPT approaches. As there exists no doubt of the experimental sign (both multiple resonance experiments and the peak distribution in the aldehyde ^{1}H nmr spectrum gave positive signs), the theoretical results are disconcerting in view of the good agreement between theory and experiment for other proximate ^{1}H,^{19}F couplings involving the CF_3 group, e.g., that in 2-trifluoromethylphenol (34).

Conformational Equilibrium for 4-Chloro-2-methylbenzoyl Fluoride, 3

$^5J_m^{H,F}$ in benzoyl fluoride derivatives is somewhat dependent on intrinsic (nonstereospecific) substituent perturbations (13, 31, 35). For example, $^5J_m^{H,F}$ in benzoyl fluoride is 1.33 Hz (31), whereas it is 1.29 (1.30) Hz (35) in the presence of a *para* chlorine (methyl) substituent. Because of synthetic difficulties (13) no compound has been prepared in which a conformer analogous to either **3***a* or **3***b* is the only one in solution. Therefore it is not known whether the coupling to H-3 in **3***a* or to H-5 in **3***b* vanishes. However, because the internal rotational barrier in benzoyl fluoride is again large compared to *kT* (6, 7, 14), a discussion in terms of O-*syn* and O-*anti* conformers is sensible at ambient temperatures.

Whether the two conformers are those in which the lowest energy corresponds to coplanarity of the CFO and ring moieties cannot be said. However, in 2,6-dimethylbenzoyl fluoride substantial twisting (perhaps by 20°) about the exocyclic C—C bond was indicated by the observed $^6J_p^{H,F}$ and by the proximate $^5J_o^{F,CH_3}$ values (12).

A consistent description of the conformational equilibrium of **3** can be reached as follows. The sum of the two $^5J_m^{H,F}$ numbers in **3** is 2.23 Hz. If $^5J_3^{H,F}$ and $^5J_5^{H,F}$ are zero in the O-*anti* and O-*syn* forms, respectively, it follows that the O-*anti* conformer is 25% abundant in CCl_4 solution at 305 K. For this population distribution, the INDO MO FPT calculations (12) of $^5J_o^{F,CH_3}$ give good agreement (1.87 Hz) with the observed value of 1.84 Hz for a twist angle of 1° in both forms. If the latter rises to 20°, the calculated $^5J_o^{F,CH_3}$ drops to 0.33 Hz for the indicated conformer populations (the calculations assumed that one C—H bond of the methyl group eclipses the C_2—C_3 bond of the ring).

The error in the estimate of the conformer distribution is uncertain; yet, because the two $^5J_m^{H,F}$ couplings differ by a factor of three, it is very likely that the O-*syn* form is by far the most abundant.

Molecular Orbital Calculations on 2-Methylbenzoyl Fluoride

Partial optimization of the geometry at the STO-3G level of MO theory gave the results in structure **3**. The O-*syn* form is calculated as 6.64 kJ/mol lower in energy (enthalpy, apart from a $P\Delta V$ term and the contribution of internal motions) than the O-*anti* form, corresponding to 93% O-*syn*. The free energy difference between **3***a* and **3***b* is 2.8 kJ/mol in CCl_4 solution at 305 K, corresponding to ≥75% O-*syn*. If the entropy difference between the conformers is small and if the chlorine substituent *para* to the COF group exerts a minor influence on conformational stability, the STO-3G numbers overestimate the preference for the O-*syn* form by about 4 kJ/mol.

Solvent stabilization of the conformers should be similar for both forms because INDO MO computations on the STO-3G geometries in structure **3** yielded very similar dipole moments, 3.38 and 3.46 D for the O-*syn* and O-*anti* forms, respectively. The slightly larger dipole moment calculated for the O-*anti* form *is* consistent with a small shift towards the latter in solution.

It is of interest that, for the STO-3G geometries, INDO MO FPT calculations suggest that $^5J^{F,CH_3}$ is −0.45 Hz, in obvious disagreement with experiment and with the calculations mentioned in the

Can. J. Chem. Downloaded from www.nrcresearchpress.com by 210.87.254.6 on 09/05/12
For personal use only.

previous section. The latter agreed with the observed value of 1.84 Hz. This fact can be traced to the geometry of the CFO group in the two computations. In the previous calculation, the geometry of the COF group was taken as that in acetyl fluoride (also assumed in the microwave work (6)). In the O-*anti* form a large coupling (26 Hz) is predicted between ^{19}F and the proton in the methyl C—H bond eclipsing the ring (rear-lobe interaction (22)). It is this coupling which dominates the calculated average. In the STO-3G geometry, this rear-lobe coupling sinks to 2.1 Hz because the distance between the fluorine atom and the carbon atom of the methyl group has increased by 0.45 Å.

It is tempting to suggest that the observed 1.84 Hz for $^5J^{F,CH_3}$ proves the existence of an appreciable amount of the O-*anti* conformer of **3** because the INDO MO FPT calculations find substantial positive values only for the rear-lobe orientation of the C—F and C—H bonds and because (22) this prediction is independent of the intervening electronic structure. However, it is clear that, although the $^5J^{F,H}$ numbers for the ring protons also indicate the presence of appreciable amounts of the O-*anti* form, the quantitative agreement with $^5J^{F,CH_3}$ mentioned in the previous section must be viewed as a coincidence. The sensitivity of $^5J^{F,CH_3}$ to internuclear distances probably means that this coupling must be restricted to a qualitative indicator of conformational populations.

Conclusions

Satisfactory agreement exists between various experimental determinations and optimized STO-3G calculations of the conformational equilibrium for 2-methylbenzaldehyde. 2-Trifluoromethylbenzaldehyde exists predominantly (>95%) in the O-*syn* conformation in benzene solution. For 4-chloro-2-methylbenzoyl fluoride in CCl_4 solution experiment and theory are in semi-quantitative agreement; the O-*syn* form being present to the extent of 75% or more. The proximate coupling, $^5J_o^{CHO,CF_3}$, in 2-trifluoromethylbenzaldehyde is 2.2 Hz; in disagreement with the negative values calculated by INDO MO FPT for reasonable geometries.

Acknowledgments

We are grateful to Dr. L. Kruczynski for the synthesis of the benzoyl fluoride derivative, to the Natural Sciences and Engineering Research Council of Canada for financial support and to the University of Manitoba for some computer time.

1. F. A. L. Anet and M. Ahmad. J. Am. Chem. Soc. **86**, 119 (1964).
2. L. Lunazzi, A. Ticca, D. Macciantelli, and G. Spunta. J. Chem. Soc. Perkin II, 1121 (1976).
3. T. Drakenberg, R. Jost, and J. M. Sommer. J. Chem. Soc. Perkin II, 1682 (1975).
4. M. Grimand and G. Pfister-Guillouzo. Org. Magn. Reson. **7**, 386 (1975).
5. R. Benassi, L. Schenetti, and F. Taddei. J. Chem. Soc. Perkin II, 545 (1979).
6. T. C. Wong and E. E. Burnell. J. Magn. Reson. **22**, 227 (1976).
7. R. K. Kakar. J. Chem. Phys. **56**, 1189 (1972).
8. S. Forsén, B. Akermark, and T. Alm. Acta Chim. Scand. **18**, 2313 (1964).
9. G. J. Karabatsos and F. M. Vane. J. Am. Chem. Soc. **85**, 3886 (1963).
10. D. G. Kowalewski and S. Castellano. Mol. Phys. **16**, 567 (1969).
11. R. Wasylishen and T. Schaefer. Can. J. Chem. **49**, 3216 (1971).
12. T. Schaefer, K. Chum, K. Marat, and R. E. Wasylishen. Can. J. Chem. **54**, 800 (1976).
13. T. Schaefer, K. Marat, K. Chum, and A. F. Janzen. Can. J. Chem. **55**, 3936 (1977).
14. F. A. L. Anet and M. Ghiaci. J. Chem. Soc. Chem. Commun. 588 (1979).
15. R. E. Klinck, D. H. Marr, and J. B. Stothers. J. Chem. Soc. Chem. Commun. 409 (1967).
16. R. K. Kakar, E. A. Rinehart, C. R. Quade, and T. Kojima. J. Chem. Phys. **52**, 3803 (1970).
17. T. Drakenberg, J. Sommer, and R. Jost. J. Chem. Soc. Perkin II, 363 (1980).
18. F. A. Miller, W. G. Fateley, and R. E. Witowski. Spectrochim. Acta, **23A**, 891 (1967).
19. C. L. Bell, S. S. Danyluk, and T. Schaefer. Can. J. Chem. **47**, 3529 (1979).
20. R. J. Abraham and E. Bretschneider. *In* Internal rotation in molecules. *Edited by* W. J. Orville-Thomas. Wiley, New York. 1974.
21. J. Hilton and L. H. Sutcliffe. Prog. Nucl. Magn. Reson. **10**, 27 (1975).
22. R. E. Wasylishen and M. Barfield. J. Am. Chem. Soc. **97**, 4545 (1975).
23. W. J. E. Parr and T. Schaefer. Can. J. Chem. **54**, 3564 (1976).
24. T. Schaefer, W. Niemczura, C. M. Wong, and K. Marat. Can. J. Chem. **57**, 807 (1979).
25. L. N. Markovskij, V. E. Pashinnik, and A. V. Kirsanov. Synthesis, 787 (1973).
26. R. Freeman and W. A. Anderson. J. Chem. Phys. **37**, 2053 (1962).
27. W. J. Hehre, W. A. Lathan, R. Ditchfield, M. D. Newton, and J. A. Pople. Quantum Chemistry Program Exchange, **11**, 236 (1979).
28. P. A. Dobosh. Quantum Chemistry Program Exchange, **11**, 141 (1979).
29. S. M. Castellano and A. A. Bothner-By. J. Chem. Phys. **41**, 3863 (1964).
30. C. W. Haigh and J. M. Williams. J. Mol. Spectrosc. **32**, 398 (1969).
31. R. J. Kostelnik, M. P. Williamson, D. E. Wisnosky, and S. M. Castellano. Can. J. Chem. **47**, 3313 (1969).
32. J. A. Pople and M. Gordon. J. Am. Chem. Soc. **89**, 4254 (1967).
33. Y. Kawashima and K. Kozima. Bull. Chem. Soc. Jpn. **47**, 2879 (1974).
34. T. Schaefer and J. B. Rowbotham. Chem. Phys. Lett. **29**, 633 (1974).
35. H. Bildsøe and K. Schaumburg. J. Magn. Reson. **14**, 223 (1974).

Rearrangement studies with ^{14}C. XLIV. Ion-pairs and dissociated ions in the solvolysis of triphenyl[2-^{14}C]vinyl and trianisyl[2-^{14}C]vinyl bromides in 70% acetic acid – 30% water[1]

CHOI CHUCK LEE AND ERIC C. F. KO

Department of Chemistry and Chemical Engineering, University of Saskatchewan, Saskatoon, Sask., Canada S7N 0W0

AND

ZVI RAPPOPORT

Department of Organic Chemistry, The Hebrew University of Jerusalem, Jerusalem, Israel

Received May 13, 1980

CHOI CHUCK LEE, ERIC C. F. KO, and ZVI RAPPOPORT. Can. J. Chem. **58**, 2369 (1980).

In the solvolysis of triphenyl[2-^{14}C]vinyl bromide (**1**-Br-2-^{14}C) in 70% HOAc – 30% H_2O, the presence of up to 30 equiv. of added NaOAc or 25 equiv. of added Et_4NBr did not significantly change the extent of scrambling of the label from C-2 to C-1 in the reaction product. The mean scrambling value observed for **1**-Br-2-^{14}C under a variety of conditions was 14.7 ± 0.7%. On the other hand, in the similar solvolysis of trianisyl[2-^{14}C]vinyl bromide (**2**-Br-2-^{14}C), the extent of scrambling in the product was found to decrease with increasing amounts of added NaOAc. The observed scramblings varied from a mean of 27.7% to 5.7%, respectively, for reactions without and with 10 *M* added NaOAc. With **1**-Br-2-^{14}C, the possibility is considered that ionization proceeds only to an ion-pair in which the scrambling via 1,2-phenyl shift is not affected by the presence of added OAc^-. In the case of **2**-Br-2-^{14}C, further dissociation to the free trianisylvinyl cation took place and in the dissociated ion, competition between the scrambling process and capture reactions with all the nucleophiles present resulted in a decrease in the extent of scrambling with the presence of the more nucleophilic OAc^-. Using the extents of scrambling as well as product data, various ratios including k_{SOH}/k_r, k_{OAc}/k_r, k_{OAc}/k_{H_2O}, and k_{OAc}/k_{HOAc}, are evaluated.

CHOI CHUCK LEE, ERIC C. F. KO et ZVI RAPPOPORT. Can. J. Chem. **58**, 2369 (1980).

Lors de la solvolyse du bromure (Br-**1**-^{14}C-2) de triphénylvinyle (^{14}C-2) dans une solution aqueuse de AcOH à 70%, l'addition de 30 équiv. de AcONa ou de 25 équiv. de Et_4NBr n'affecte pas d'une façon significative le degré de distribution au hasard du marqueur entre C-2 et C-1 dans le produit de la réaction. La valeur moyenne observée pour le mélange est de 14,7 ± 0,7% dans le cas du Br-**1** ^{14}C-2 sous différentes conditions. D'autre part, on a trouvé que la solvolyse du bromure (Br-**2**-^{14}C-2) de trianisylvinyle (^{14}C-2) dans les mêmes conditions provoquent une distribution au hasard dont le degré diminue avec une augmentation de AcONa ajoutée. Les taux de distribution au hasard observés varient d'une moyenne de 27,7% à 5,7% respectivement dans les réactions se faisant avec ou sans addition de AcONa 10 *M*. Dans le cas du Br-**1**-^{14}C-2, on considère la possibilité d'une ionisation se faisant au moyen d'une paire d'ions dans lesquels la distribution au hasard, qui provient d'un glissement 1,2 du phényle, n'est pas affectée par la présence du AcO^-. Dans le cas du Br-**2**-^{14}C-2, une dissociation plus poussée du cation trianisylvinyle se produit et dans l'ion dissocié la compétition entre les réactions de distribution au hasard et celle de capture avec tous les nucléophiles présents provoque une diminution du degré de distribution au hasard avec la présence du AcO^- plus nucléophile. En utilisant les degrés de distribution au hasard observées ainsi que les données relatives aux produits obtenus on a évalué plusieurs rapports comprenant: k_{SOH}/k_r, k_{AcO}/k_r, k_{AcO}/k_{H_2O} et k_{AcO}/k_{AcOH}.

[Traduit par le journal]

β-Aryl rearrangements arising from 1,2-aryl shifts across the double bond of triarylvinyl cations have been extensively studied (1, 2). Degenerate rearrangements from 1,2-phenyl or 1,2-anisyl shifts in triphenylvinyl or trianisylvinyl cationic systems have been investigated under a variety of conditions (3–9). It is generally agreed that the dissociated "free" trianisylvinyl cation can be formed from trianisylvinyl substrates (6, 7, 9, 10). However, the extent of scrambling observed during solvolyses of triphenyl[2-^{14}C]vinyl triflate (**1**-OTf-2-^{14}C) in HOAc, HCOOH, or CF_3COOH was found to be unaffected by the presence of 1.1 equiv. of the conjugate base of the respective solvents (3). Moreover, in the solvolysis of triphenyl[2-^{14}C]vinyl bromide (**1**-Br-2-^{14}C) in 70% HOAc – 30% H_2O, the presence of about 3 equiv. of NaOAc or NaBr did not change the extent of degenerate rearrangement (8). It was, therefore, suggested that the rearrangement in the triphenylvinyl cationic system proceeds at the ion-pair stage rather than at the free cation stage (3, 8). This suggestion is consistent with the expected substituent effects on the stability of cationic intermediates in solvolytic reactions. The triphenylvinyl cation would be less stable than the trianisylvinyl cation, and its reaction should proceed to an earlier intermediate stage than the dissociated "free' cation in Winstein's solvolysis scheme (11, 12). Indeed, in the decomposition of triphenyl[2-^{14}C]vinylphenyltriazene (**1**-NNNHPh-2-^{14}C) which presumably proceeds via the free cation, no rearrangement was observed when the decomposition was carried out in HOAc,

[1]Vinylic cations from solvolysis, part 32, from the Hebrew University of Jerusalem.

0008-4042/80/222369-08$01.00/0

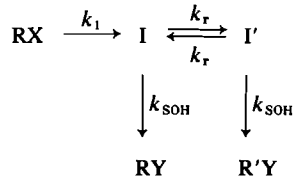
©1980 National Research Council of Canada/Conseil national de recherches du Canada

Can. J. Chem. Downloaded from www.nrcresearchpress.com by 210.87.254.5 on 09/05/12
For personal use only.

Can. J. Chem. Downloaded from www.nrcresearchpress.com by 210.87.254.5 on 09/05/12
For personal use only.

CF_3COOH, or acetone–H_2O–$HClO_4$ (7). On the other hand, the decomposition of trianisyl[2-^{14}C]-vinylphenyltriazene (**2**-NNNHPh-2-^{14}C) in HOAc and in HOAc + 1.7 equiv. NaOAc resulted in about 38% and 17% scramblings, respectively, of the label from C-2 to C-1. The decrease in scrambling in the presence of NaOAc was attributed to a competition between the rearrangement process and reaction of the dissociated trianisylvinyl cation with the more nucleophilic acetate ion (7).

Vinylic solvolyses are often carried out in the presence of an added base, such as the conjugate base of the solvent, in order to avoid the possible addition–elimination (Ad_E–E) reaction with the liberated acid (13). Since capture of the cation by either the solvent or its conjugate base would lead to the same product, it would be of interest to ascertain whether the solvent or the conjugate base is the capturing nucleophile. Previous analyses on changes in the selectivity constants for triarylvinyl cations (14, 15) and on the effects of different acetate concentrations on *cis* ⇄ *trans* isomerization accompanying solvolyses of *cis*- and *trans*-1,2-dianisyl-2-phenylvinyl bromides (16) have led to the suggestion that the acetate ion is the capturing nucleophile in HOAc, at least for relatively stable α-arylvinyl cations. Another approach to an evaluation of the capture ratio for a triarylvinyl cation by OAc^- and by HOAc (k_{OAc}/k_{HOAc}) can be based on data from degenerate rearrangements. For a mechanism as depicted in Scheme 1, where I and I′ are the unrearranged and rearranged cation or ion-pair intermediates, eq. [1] holds for reactions at completion.



SCHEME 1

[1] $[RY]/[R'Y] = 1 + (k_{SOH}/k_r)$

For the decomposition of **2**-NNNHPh-2-^{14}C in HOAc or HOAc–NaOAc (7), I and I′ would be the unrearranged and rearranged trianisyl[2-^{14}C]vinyl and trianisyl[1-^{14}C]vinyl cations, giving rise to trianisyl[2-^{14}C]vinyl and trianisyl[1-^{14}C]vinyl acetates (**2**-OAc-2-^{14}C and **2**-OAc-1-^{14}C) as products. Furthermore, a statistical factor of 2 should be applied in the k_r process (17), giving rise to eq. [2].

[2] [**2**-OAc-2-^{14}C]/[**2**-OAc-1-^{14}C] = $1 + (k_{SOH}/2k_r)$

Using the mean scrambling values of 38.1 and 16.8%, respectively, for the decomposition of **2**-NNNHPh-2-^{14}C in HOAc and in HOAc with 1.7 equiv. (0.24 *M*) NaOAc (7), and since neat HOAc corresponds to a concentration of 17.5 *M*, eqs. [3] and [4] are derived from eq. [2].

[3] $17.5k_{HOAc}/2k_{r(An)} = 0.62$

[4] $(17.5k_{HOAc} + 0.24k_{OAc})/2k_{r(An)} = 3.95$

From eqs. [3] and [4], the dimensionless k_{OAc}/k_{HOAc} is calculated to be 3.9×10^2.

The above k_{OAc}/k_{HOAc} ratio of about 390 is, of course, calculated for the selective capture, by OAc^- and HOAc, of the "hot" trianisylvinyl cation derived from the decomposition of **2**-NNNHPh-2-^{14}C which presumably took place via the diazonium ion. Under solvolytic conditions, this ratio may very well be quite different. In any event, when the concentration of HOAc compared to that of OAc^- is large, there is the possibility that the previously observed (3, 8) insensitivity of the extent of scrambling to the presence of added OAc^- ion in the less selective triphenylvinyl cationic system may be due to a predominant product formation from capture of a free ion by the excess HOAc. Such an alternative explanation would invalidate the suggestion that the rearrangement occurs in the ion-pair stage for the triphenylvinyl cationic system. In an attempt to clarify the situation, we have carried out further solvolytic studies with triphenyl[2-^{14}C]vinyl bromide (**1**-Br-2-^{14}C) in 70% HOAc – 30% H_2O (by volume) in the presence of large amounts of added NaOAc or Et_4NBr. The solvent system of 70% HOAc – 30% H_2O was chosen (8) because reaction of **1**-Br-2-^{14}C in pure HOAc, with or without added NaOAc, was impractically slow. For comparison, experiments were also carried out to study the effects of added NaOAc and/or Et_4NBr on the extent of scrambling observed during solvolyses of trianisyl[2-^{14}C]vinyl bromide (**2**-Br-2-^{14}C) in 70% HOAc – 30% H_2O.

Results and Discussion

The labeled **1**-Br-2-^{14}C and **2**-Br-2-^{14}C were prepared as previously described (3, 5, 9). The solvolyses in 70% HOAc, carried out in sealed tubes, have also been described earlier (8). With **1**-Br-2-^{14}C as substrate, the reactions were effected in the presence of up to 30 equiv. of added NaOAc at 150 ± 2°C for 2 days. One experiment was also done in the presence of 25 equiv. of Et_4NBr, but the reaction time was increased to 4 days. The reaction products, 1,2,2-triphenyl[1,2-^{14}C]ethanone (**3**-1,2-^{14}C) or **3**-1,2-^{14}C and triphenyl[1,2-^{14}C]vinyl acetate (**1**-OAc-1,2-^{14}C), were degraded via $LiAlH_4$

TABLE 1. Data from the solvolysis of triphenyl[2-^{14}C]vinyl bromide (**1**-Br-2-^{14}C) in 70% HOAc – 30% H_2O at 150 ± 2°C for 2 days

Expt.	[**1**-Br-2-^{14}C] (m*M*)	[NaOAc] (m*M*)	$\frac{[NaOAc]}{[\textbf{1}\text{-Br-2-}^{14}C]}$	[Et_4NBr] (m*M*)	$\frac{[Et_4NBr]}{[\textbf{1}\text{-Br-2-}^{14}C]}$	% reaction[a]	% scrambling in product
1	25	—	—	—	—	61[b]	15.3[b,c]
2	25	78	3	—	—	65[b]	14.9[b]
3	25	—	—	75[d]	3	56[b]	15.0[b]
4	15	75	5	—	—	64	15.3
5	15	150	10	—	—	62	14.0
6	15	225	15	—	—	63	15.1
7	15	300	20	—	—	64	14.1
8	15	375	25	—	—	64	14.3
9	25	750[e]	30	—	—	41[e]	14.6[f]
10	15	—	—	375	25	54[g]	14.1
						Mean	14.7±0.7

[a]From titration of the liberated bromide.
[b]Data from ref. 8. The recovered unconsumed reactant was found to show essentially no scrambling (0.5% or less) (8).
[c]The only product was 1,2,2-triphenylethanone. A control experiment showed that an initial addition of 25 m*M* triphenylvinyl acetate to the reaction mixture was completely hydrolyzed to the ketone.
[d]NaBr was used instead of Et_4NBr (8).
[e]Salting out of the substrate resulted in its incomplete dissolution. The lower extent of reaction was apparently due to this incomplete dissolution.
[f]The product was 86% ketone and 14% acetate as estimated by nmr. A control experiment showed that an initial addition of 25 m*M* triphenylvinyl acetate to the reaction mixture resulted in its extensive but not complete hydrolysis to the ketone.
[g]After 4 days.

reduction to 1,2,2-triphenyl[1,2-^{14}C]ethanol (**4**-1,2-^{14}C) followed by $KMnO_4$ oxidation to diphenyl [^{14}C]ketone (**5**-^{14}C) to give the extent of scrambling of the label from C-2 to C-1. These procedures have also been reported previously (3, 8). The results, together with some related data from an earlier study (8), are summarized in Table 1.

With **2**-Br-2-^{14}C as substrate, the solvolyses were carried out at 120 ± 1°C for different lengths of time in the presence of various amounts of added NaOAc and/or Et_4NBr. The product mixture, **2**-OAc-1,2-^{14}C and 1,2,2-trianisyl[1,2-^{14}C]ethanone (**6**-1,2-^{14}C), was also reduced with $LiAlH_4$ to 1,2,2-trianisyl[1,2-^{14}C]ethanol (**7**-1,2-^{14}C) and then oxidized to dianisyl[^{14}C]ketone (**8**-^{14}C) to give the extent of scrambling, again using previously described procedures (9). In some of the experiments with **2**-Br-2-^{14}C, the possibility of scrambling in the recovered, unconsumed reactant was also investigated using a previously reported method (9). After the $LiAlH_4$ treatment of a mixture of product and unconsumed reactant, the latter was converted to trianisyl[1,2-^{14}C]ethene (**9**-1,2-^{14}C) which was separated from the **7**-1,2-^{14}C by passage through an alumina column. Ozonolysis of **9**-1,2-^{14}C gave **8**-^{14}C and the extent of scrambling in the unconsumed reactant. The results are summarized in Table 2.

From Table 1, it is seen that for the solvolysis of **1**-Br-2-^{14}C in 70% HOAc at 150 ± 2°C for 2 days, both the extent of reaction and the extent of scrambling in the product were virtually independent of large changes in the concentration of the added NaOAc or in the NaOAc:substrate ratio. In the presence of 750 m*M* NaOAc (Expt. 9, Table 1), an appreciable salting out of the **1**-Br-2-^{14}C took place resulting in the incomplete dissolution of the substrate. The lower extent of reaction observed in this experiment apparently reflected the reaction of only a fraction of the substrate that was in solution.

A rate increase at higher NaOAc concentrations could have been anticipated as a result of a normal salt effect (18). Alternatively, if products were formed from the free, dissociation triphenylvinyl cation, a greater extent of product formation with a consequent decrease in external ion return and an increase in rate would be expected at higher salt concentrations. The insensitivity of the extent of reaction to changes in [NaOAc] would suggest that neither of these effects were very large in the solvolysis of **1**-Br-2-^{14}C in 70% HOAc.

Previously, it was shown that the extent of scrambling in the product from solvolysis of **1**-Br-2-^{14}C in 70% HOAc was independent of reaction time (8), and this was as expected since no significant scrambling was observed in the recovered, unconsumed reactant (8). However, it is of interest to note that the presence of added Br^- ion did decrease the rate of reaction (Expt. 3 and 10, Table 1). Such a common ion rate depression has often been attributed to a return to covalent reactant from the dissociated ions. If such an external ion return were involved in the present studies with **1**-Br-2-^{14}C, one would expect the observation of scrambling in the recovered reactant, but this was not the case.

Thus the results from the solvolysis of **1**-Br-2-^{14}C in 70% HOAc still present a dilemma in their in-

Can. J. Chem. Downloaded from www.nrcresearchpress.com by 210.87.254.5 on 09/05/12
For personal use only.

Can. J. Chem. Downloaded from www.nrcresearchpress.com by 210.87.254.5 on 09/05/12
For personal use only.

TABLE 2. Data from the solvolysis of trianisyl[2-^{14}C]vinyl bromide (2-Br-2-^{14}C) in 70% HOAc – 30% H_2O at 120 ± 1°C

Expt.	[2-Br-2-^{14}C] (mM)	[NaOAc] (mM)	$\frac{[NaOAc]}{[2\text{-Br-2-}^{14}C]}$	[Et_4NBr] (mM)	$\frac{[Et_4NBr]}{[2\text{-Br-2-}^{14}C]}$	Reaction time (min)	% reaction[a]	% scrambling in product	$k_{SOH'}/k_{r(An)}$[i]	k_{OAc}/k_{SOH}[i] (M^{-1})	$k_{OAc}/k_{r(An)}$[j] (M^{-1})
1	5.9	—	—	—	—	5	53	27.5[c]			
2	5.9	—	—	—	—	60	100	27.9			
3	5.9	—	—	59	10	12	52	27.5[c]			
4	6.0	—	—	176	30	12	46	27.6[c]			
5	5.8	—	—	176	30	150	100	28.0 (27.7)[e]	3.2		
6	5.9	—	—	500	85	12	50[b]	19.4[d]			
7	5.9	—	—	1000	169	12	38[b]	17.6[d]			
8	6.0	—	—	2000	333	12	23[b]	11.8[d]			
9	6.0	6	1	—	—	60	100	27.7	3.2		
10	6.0	30	5	—	—	60	100	25.9	3.7	5.2	16.6
11	5.9	60	10	—	—	5	56	25.3[c]			
12	5.9	60	10	59	10	12	48	25.2[c]			
13	5.8	178	30	—	—	5	56	24.9[c]			
14	5.9	178	30	—	—	60	100	24.1			
15	6.0	178	30	177	30	12	52	24.8[c]			
16	5.8	178	30	177	30	150	100	24.8 (24.7)[f]	4.1	1.6	5.1
17	5.9	300	50	—	—	60	100	24.8	4.1	0.9	3.0
18	47.0	473	10	—	—	60	99	24.0	4.3	0.7	2.3
19	5.9	590	100	—	—	60	100	23.8			
20	5.9	590	100	590	100	150	100	23.8 (23.8)[g]	4.4	0.6	2.0
21	5.9	900	150	—	—	60	100	22.9	4.7	0.5	1.7
22	6.0	1144	190	—	—	60	100	22.1	5.0	0.5	1.6
23	6.0	1410	235	—	—	60	100	21.0			
24	47.0	1410	30	—	—	60	99	21.6 (21.3)[h]	5.4	0.5	1.6
25	6.0	2500	420	—	—	60	100	18.2	7.0	0.5	1.5
26	6.1	3500	580	—	—	60	100	15.7	8.7	0.5	1.6
27	6.0	4700	780	—	—	60	100	13.4	10.9	0.5	1.6
28	5.8	6070	1050	—	—	60	100	10.7	14.7	0.6	1.9
29	5.9	8020	1350	—	—	60	100	8.9	18.5	0.6	1.9
30	5.8	10000	1720	—	—	60	100	5.7	31.1	0.9	2.8

[a]From titration of the liberated bromide ion.
[b]Estimated by isotope dilution.
[c]The recovered unconsumed reactant showed essentially no scrambling (1% or less).
[d]The recovered unconsumed reactant showed scramblings of 2, 5, and 9%, respectively, for Expt. 6, 7 and 8.
[e]Mean value for Expt. 1–5.
[f]Mean value for Expt. 13–16.
[g]Mean value for Expt. 19–20.
[h]Mean value for Expt. 23, 24.
[i]$k_{SOH'} = k_{HOAc}[HOAc] + k_{H_2O}[H_2O] + k_{OAc}[OAc^-]$; $k_{SOH} = k_{HOAc}[HOAc] + k_{H_2O}[H_2O]$, for Expt. 1–5 with no added OAc^-, $k_{SOH'}/k_{r(An)} = k_{SOH}/k_{r(An)} = 3.2\ M^{-1}$.
[j]From $(k_{OAc}/k_{SOH}) \times 3.2\ M^{-1}$.

Can. J. Chem. Downloaded from www.nrcresearchpress.com by 210.87.254.5 on 09/05/12
For personal use only.

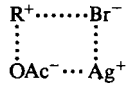
terpretation. On the one hand, the insensitivity of the extent of scrambling to the presence of added OAc^- or Br^- would suggest that the species undergoing scrambling is not affected by the added nucleophiles, and such a species could be an ion-pair. On the other hand, the common ion rate depression indicates the probable formation of and returns from dissociated free ions, and this is inconsistent with the absence of scrambling in the recovered reactant. Resolution of this dilemma will require further experimentation, including more detailed kinetic studies and possibly an investigation to ascertain if anion exchange occurs between the substrate and some added [^{82}Br]bromide. It is, however, of interest to report at this time the results given in Table 1, which show that added NaOAc, even in an amount sufficiently large to salt out some of the substrate (Expt. 9, Table 1), still failed to cause any detectable change in the extent of scrambling.

It has been pointed out that in the present studies with 1-Br-2-^{14}C, the product was mainly 1,2,2-triphenyl[1,2-^{14}C]ethanone (3-1,2-^{14}C). As indicated in footnotes *c* and *f* of Table 1, under the reaction conditions employed, most, if not all, of any acetate product, 1-OAc-1,2-^{14}C, that might have been formed would be hydrolyzed to the ketone. However, for the reaction in 70% HOAc in the presence of 0.75 *M* added NaOAc (Expt. 9, Table 1), some acetate product did survive, the ratio of ketone: acetate being 86:14. Recent reactivity–selectivity studies in mixed solvents assumed that the ratio of the capture products was given by the ratio of the bimolecular rates of reaction with the solvent components (19). With this assumption and using 12.2 *M* and 16.7 *M*, respectively, as [HOAc] and [H_2O] for 70% HOAc – 30% H_2O, eq. [5] may be written for Expt. 9, Table 1.

$$[5] \quad (12.2k_{HOAc} + 0.75k_{OAc})/16.7k_{H_2O} = 14/86$$

The product ratio of 14/86 is the minimum since some of the acetate formed must have been hydrolyzed to the ketone. If it were assumed further that capture by acetate is dominant over capture by HOAc, i.e. $0.75k_{OAc} \gg 12.2k_{HOAc}$, then from eq. [5] a minimum value for k_{OAc}/k_{H_2O} of 3.6 is obtained. Thus if the assumption of $0.75k_{OAc} \gg 12.2k_{HOAc}$ holds, the finding that some acetate has survived in Expt. 9, Table 1, would suggest that product forming capture by OAc^- is faster than by H_2O.

An interesting question is whether the possible involvement of ion-pairs in 70% HOAc can be extrapolated to pure HOAc. The occurrence of 1,2-phenyl shifts in the ion-pair stage was suggested by the similar extent of scrambling (6–7%) observed in the solvolysis of 1-OTf-2-^{14}C in HOAc and in HOAc containing 0.55 *M* NaOAc (3). The coincidence that 6–7% scrambling was also obtained in the solvolysis of 1-Br-2-^{14}C or 1-Br-2-^{13}C in HOAc–AgOAc (4) would be inconsistent with an ion-pair mechanism since the difference in the counter ions would be expected to affect the extent of scrambling in the ion-pairs. However, these difficulties could be rationalized from consideration of the scrambling data obtained in the solvolyses of 1-Br-2-^{14}C in aqueous HOAc (8). While solvolysis of 1-Br-2-^{14}C in pure HOAc is too slow for practical study, reactions of 1-Br-2-^{14}C in HOAc–H_2O containing different amounts of the two solvent components have been carried out. The extent of scrambling was found to increase with increasing amounts of HOAc, the scramblings varying from a mean of 9.6% in 50% HOAc to a mean of 18.4% in 90% HOAc (8). An extrapolated value of about 20% scrambling would be obtained for pure HOAc, and this value is quite different from the 6–7% scrambling found for the acetolysis of 1-OTf-2-^{14}C, indicating that the leaving group indeed exerts an effect on the extent of scrambling. It is probable that the reactions of 1-Br-2-^{14}C with HOAc–H_2O and with HOAc–AgOAc may follow different mechanisms. It may be suggested that in the presence of AgOAc, a quadrupolar type of intermediate, formulated as **10**, may be obtained. Such an intermediate could give rise to a product with a lesser extent of scrambling than that observed for solvolysis in HOAc–H_2O. A similar type of interaction may be proposed to account for the observation of a net retention of the *cis*- or *trans*-configuration in the reaction of *cis*- or *trans*-1-phenylpropen-1-yl bromide with CF_3COOAg in isopentane (20).



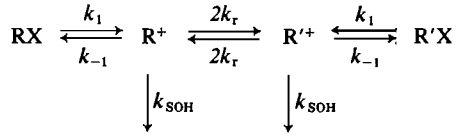
10

In considering the scrambling results given in Table 2 for the solvolysis of 2-Br-2-^{14}C in 70% HOAc, an obvious difference in behavior from that of 1-Br-2-^{14}C is that the extent of scrambling in the product is decreased by the presence of added NaOAc. It should be noted, however, that relatively small changes in [NaOAc] did not give a measurable decrease in scrambling, as may be seen from Table 2 in that the mean scrambling value for Expt. 1–5 is the same as that observed for Expt. 9, and similarly, there is no significant difference in the mean scrambling for Expt. 13–16 and the scrambling for Expt. 17. Since the precision in measuring ^{14}C scramblings in this and previous studies could show variations as large as ±1%, it is

Can. J. Chem. Downloaded from www.nrcresearchpress.com by 210.87.254.5 on 09/05/12
For personal use only.

not surprising that small changes would not be detectable. In considering all the scrambling data in Table 2 as a whole, it is clear that there is a decrease in the extent of scrambling with increasing amounts of added NaOAc.

It is also apparent from Table 2 that for a given concentration of added NaOAc, and with the Et_4NBr concentration of up to 177 m*M*, the scrambling found in the product did not change with the extent of reaction (e.g. Expt. 1–5, Table 2, no NaOAc, scrambling of 27.7 ± 0.3%; Expt. 13–16, Table 2, 178 m*M* NaOAc, scrambling of 24.7 ± 0.6%). This independence of scrambling in the product with reaction time is consistent with the finding that in some of these experiments which did not go to completion, the recovered, unconsumed reactant showed very little scrambling (1% or less). Yet under these conditions, the presence of added Et_4NBr did cause a decrease in reaction rate as indicated by the % reaction determined for the individual runs. Thus similar to the behavior of **1**-Br-2-^{14}C, when the solvolysis of **2**-Br-2-^{14}C was carried out in the presence of up to 177 m*M* Et_4NBr, there was a rate depression but the recovered reactant was not significantly scrambled. When the concentration of Et_4NBr was much higher (0.5–2.0 *M*, Expt. 6–8, Table 2), significant extents of scrambling were observed in the recovered reactant, indicating return from scrambled ionic species to covalent reactant. In these three experiments (Expt. 6–8, Table 2), the scrambling in the product also increased with an increase in the extent of reaction, and this is as expected for a reaction which involves returns to give scrambled reactant (8, 9).



SCHEME 2

The behavior of **2**-Br-2-^{14}C during its solvolysis in 70% HOAc as discussed above may be explained by a mechanism as depicted in Scheme 2, where X^- is Br^- and R^+ and R'^+ are the unrearranged and rearranged trianisyl[2-^{14}C]vinyl and trianisyl[1-^{14}C]vinyl cations, respectively. In this scheme, the product-forming ionic species is the dissociated cation, and processes leading to the formation of scrambled reactant, R'X, are also included. At complete reaction, eq. [6] can be used to calculate

$$[6] \quad [ROS]/[R'OS] = 1 + (k_{SOH}/2k_{r(An)})$$

$k_{SOH}/k_{r(An)}$, even if there were returns to R'X after partial reaction (6). Since eq. [6] does not involve the concentration of the substrate, the extent of scrambling should be independent of substrate concentration, and this is found (cf. e.g. Expt. 23 and 24, Table 2).

For the solvolysis of **2**-Br-2-^{14}C in the presence of 177 m*M* Et_4NBr or less, the extent of returns from the $k_{-1}[Br^-]$ process is relatively small. Hence the scrambling found in the recovered reactant is low (1% or less) and it does not significantly affect the extent of scrambling in the product with changing extents of reaction. At high concentrations of added Br^- as in Expt. 6–8, Table 2, the extent of returns from the $k_{-1}[Br^-]$ process is sufficiently large to give significant amounts of scrambling in the recovered reactant, and the scrambling in the product also varies with changes in the extent of reaction as was observed. Moreover, since the dissociated ion can undergo competitively 1,2-anisyl shift and capture reactions with the various nucleophiles that are prssent, the addition of the more nucleophilic OAc^- ion to the reaction mixture would favor the formation of more unrearranged product at the expense of the 1,2-shift process, resulting in the observed decrease in scrambling with increasing amounts of added OAc^-.

In the product forming processes, k_{SOH} is the pseudo first order rate constant for the bimolecular capture of the cation by all the nucleophiles present. A separation of the effects of added OAc^- in the 70% HOAc – 30% H_2O solvent system may be facilitated by the definitions given in eqs. [7] and [8].

$$[7] \quad k_{SOH} = k_{HOAc}[HOAc] + k_{H_2O}[H_2O] = 12.2k_{HOAc} + 16.7k_{H_2O}$$

$$[8] \quad k_{SOH'} = k_{OAc}(OAc^-] + k_{HOAc}[HOAc] + k_{H_2O}[H_2O] = k_{OAc}[OAc^-] + k_{SOH}$$

Using the scrambling data in Table 2 for experiments that were carried to completion or the mean scrambling values for the various series of experiments in which the scrambling was independent of reaction time, applying eq. [6], $k_{SOH'}/k_{r(An)}$ can be calculated from eq. [9].

$$[9] \quad (100 - \%\text{scrambling})/\%\text{scrambling} = 1 + (k_{SOH'}/2k_{r(An)})$$

These calculated $k_{SOH'}/k_{r(An)}$ results are given in Table 2. For Expt. 1–5 in which no acetate was added, the $k_{SOH'}/k_{r(An)}$, of course, is the same as $k_{SOH}/k_{r(An)}$. It is seen that $k_{SOH'}/k_{r(An)}$ increases with increasing amounts of added OAc^-, and this change

Can. J. Chem. Downloaded from www.nrcresearchpress.com by 210.87.254.5 on 09/05/12
For personal use only.

is in the direction expected since the addition of OAc^- favors product formation, the $k_{SOH'}$ process, at the expense of scrambling, the $k_{r(An)}$ process.

For Expt. 1–5, Table 2, with no added acetate and with a mean scrambling value of 27.7%, and for Expt. 10, Table 2, with 30 m*M* of added acetate and a scrambling value of 25.9%, eqs. [10] and [11], respectively, can be written.

[10] $k_{SOH}/k_{r(An)} = 3.2$

[11] $k_{SOH'}/k_{r(An)} = (0.03k_{OAc} + k_{SOH})/k_{r(An)} = 3.7$

From eqs. [10] and [11], eqs. [12] and [13] can be obtained.

[12] (From [11]/[10]) $k_{OAc}/k_{SOH} = 5.2\,M^{-1}$

[13] (From [12] × [10]) $k_{OAc}/k_{r(An)} = 5.2 \times 3.2 = 16.6\,M^{-1}$

The ratios of k_{OAc}/k_{SOH} and $k_{OAc}/k_{r(An)}$ have a unit of M^{-1} because k_{SOH} is a pseudo first order rate constant and no composite concentration for the $HOAc–H_2O$ solvent system was used in the calculations. These ratios, calculated for different amounts of added OAc^-, are included in Table 2.

It is seen from Table 2 that these selectivity ratios, k_{OAc}/k_{SOH} and $k_{OAc}/k_{r(An)}$, are not constant, showing variations with changing amounts of added OAc^-. Clearly, the activities of the acetate ion rather than its concentrations are involved in the rates of reaction, and correction of such effects would be more drastic at higher concentrations. Thus there should be a decrease in these ratios with increasing concentrations of added acetate. Reduction of the activities of the solvent components by their involvement in the solvation shells of the added salts should also change the k_{OAc}/k_{SOH} and $k_{OAc}/k_{r(An)}$ ratios, but in an opposite direction, causing an increase in these ratios with increasing concentrations of added acetate. These two opposing effects could qualitatively explain the trend of behavior for k_{OAc}/k_{SOH} and $k_{OAc}/k_{r(An)}$ with changing concentrations of added acetate. With increasing $[OAc^-]$, there is initially a sharp decrease in these selectivity ratios, but on further increases in acetate concentration, these ratios decline more gradually, reaching an essentially constant level and then eventually rises slightly at very high acetate concentrations, conforming to expectation from two opposing effects.

Ionic strength and salt effects might also affect the selectivity ratios, k_{OAc}/k_{SOH} and $k_{OAc}/k_{r(An)}$. The rate of reaction between oppositely charged ions, i.e. the capture of the trianisylvinyl cation by the acetate anion or the k_{OAc} process, should decrease with increasing ionic strength, whereas the rearrangement by 1,2-shift and the capture of the cation by the neutral solvent components, the k_r and k_{SOH} processes, should be less affected. The net result would be a decrease in k_{OAc}/k_{SOH} and $k_{OAc}/k_{r(An)}$ with increasing concentrations of added salts. However, on considering, for example, Expt. 13–16, Table 2, it is seen that in these experiments with 178 m*M* of added NaOAc, the absence or presence of 177 m*M* of added Et_4NBr gave essentially the same extent of scrambling and the same calculated k_{OAc}/k_{SOH} and $k_{OAc}/k_{r(An)}$ ratios. The ionic strength of the reaction mixture is obviously different in the absence or in the presence of added Et_4NBr, but its lack of influence on the extent of scrambling would suggest that the effect of ionic strength cannot be a major factor in causing the variations in the k_{OAc}/k_{SOH} and $k_{OAc}/k_{r(An)}$ ratios.

In the experiments with **2**-Br-2-^{14}C as recorded in Table 2, no systematic analysis was done on the acetate to ketone (**2**-OAc-1,2-^{14}C:**6**-1,2-^{14}C) ratios in the reaction products; although in a few cases when the product was examined by nmr, both **2**-OAc-1,2-^{14}C and **6**-1,2-^{14}C were detected. In contrast to the extensive hydrolysis of the acetate to ketone during the solvolysis of **1**-Br-2-^{14}C, the shorter reaction times employed in the studies with **2**-Br-2-^{14}C presumably may have been more favorable for the survival of some of the acetate product. A few control experiments on product distribution have been carried out with non-radioactive **2**-Br. The solvolysis of 5.9 m*M* **2**-Br in 70% HOAc at 120°C for 4 min (conditions similar but not identical to Expt. 1, Table 2) resulted in the formation of 27% acetate (**2**-OAc) and 73% ketone (**6**). When this experiment was repeated but with 5.9 m*M* of **2**-OAc added initially to the reaction mixture, analysis of the product mixture showed that 57% of the added acetate has survived and was not hydrolyzed to the ketone. Thus correcting for the 57% survival of acetate under these conditions, the 27% acetate that was formed should have been 27/0.57 = 47%. Similarly, the solvolysis of 5.9 m*M* **2**-Br in 70% HOAc at 120°C for 4 min and with the presence of 183 m*M* NaOAc (conditions similar but not identical to Expt. 13, Table 2) gave a 50:50 ratio for **2**-OAc and **6**. Again a reaction under the same conditions but with 5.9 m*M* of **2**-OAc also present showed 71% survival of the added acetate. Correcting for the 71% survival, the 50% acetate that was formed should have been 50/0.71 = 70% under these conditions.

From the above product analyses, using the corrected **2**-OAc contents of 47% and 70%, respectively, for reactions without and with the presence of 183 m*M* added NaOAc, and relationships as em-

Can. J. Chem. Downloaded from www.nrcresearchpress.com by 210.87.254.5 on 09/05/12
For personal use only.

ployed in eq. [5], eqs. [14] and [15] are obtained.

[14] $12.2k_{HOAc}/16.7k_{H_2O} = 47/53$

[15] $(0.183k_{OAc} + 12.2k_{HOAc})/16.7k_{H_2O} = 70/30$

From [14] and [15], the selectivity ratios, k_{HOAc}/k_{H_2O}, k_{OAc}/k_{H_2O}, and k_{OAc}/k_{HOAc}, for the trianisylvinyl cation, can be calculated as 1.2, 1.3×10^2, and 1.1×10^2, respectively. It is of interest to note that the k_{HOAc}/k_{H_2O} value of 1.2 indicates a similar magnitude for the nucleophilicities of the two solvent components in 70% HOAc, in contrast to the much larger difference in nucleophilicities for the two pure solvents, HOAc and H_2O (21, 22). Probably, in a mixed solvent system, extensive intermolecular H-bonding may tend to equalize the nucleophilicities of the two solvent components. The k_{OAc}/k_{HOAc} value of 1.3×10^2 calculated from the present work is different from the value of 3.9×10^2 derived from data obtained in the decomposition of **2**-NNNHPh-2-^{14}C (7), although the two values are in the same order of magnitude. It is reasonable to expect such differences since the trianisylvinyl cation in the two studies are generated by different methods in different solvent systems.

Experimental

Solvolyses of Triphenyl[2-^{14}C]vinyl Bromide (1-Br-2-^{14}C)

Except for modifications in the relative amounts of substrate and added salt, the procedure used in the present work on the solvolysis of **1**-Br-2-^{14}C in 70% HOAc was essentially the same as reported previously (8). A typical experiment is described below (Expt. 4, Table 1).

A solution of 100 mg (0.30 mmol) of **1**-Br-2-^{14}C and 123 mg (1.5 mmol) of NaOAc in 20 mL of 70% HOAc in a sealed tube was heated in an oil bath at 150 ± 2°C for 2 days. After cooling in an ice bath, the tube was opened and about 200 mg of ordinary 1,2,2-triphenylethanone was added as carrier. The material was then extracted with $CHCl_3$ (3 × 25 mL) and the extract washed with dilute $NaHCO_3$ solution and with H_2O. The liberated Br^- in the combined aqueous phase was titrated potentiometrically with $AgNO_3$ to give the extent of reaction. The organic extract, after drying over $MgSO_4$, was worked up as described previously (8), including separation of the product from the unconsumed reactant by passage through an alumina column, conversion of the product to 1,2,2-triphenyl[1,2-^{14}C]ethanol by $LiAlH_4$ reduction, and $KMnO_4$ oxidation of the latter to diphenyl-[^{14}C]ketone to give the % scrambling, using procedures already reported (3, 8).

Solvolyses of Trianisyl[2-^{14}C]vinyl Bromide (2-Br-2-^{14}C)

The solvolyses of **2**-Br-2-^{14}C in 70% HOAc were carried out at 120 ± 1°C. The reaction conditions for the various experiments are given in Table 2. As an illustration, Expt. 15, Table 2, is described below.

A solution of 25.5 mg (0.060 mmol) of **2**-Br-2-^{14}C, 146 mg (1.78 mmol) of NaOAc and 372 mg (1.77 mmol) of Et_4NBr in 10 mL of 70% HOAc in a sealed tube was heated at 120 ± 1°C for 12 min. After cooling in an ice bath, the tube was opened and about 200 mg each of ordinary **2**-Br and **2**-OAc were added as carriers. The material was extracted with $CHCl_3$ (3 × 25 mL) and the extract washed with a dilute $NaHCO_3$ solution and then with H_2O. The Br^- in the combined aqueous phase was determined by potentiometric titration, the excess Br^- over the amount added as Et_4NBr gave the extent of reaction. The work-up procedure for the organic material was the same as described by Lee, Weber, and Obafemi (9), which included the following treatments. $LiAlH_4$ reduction effected the conversion of the product mixture (acetate **2**-OAc-1,2-^{14}C and ketone **6**-1,2-^{14}C) to 1,2,2-trianisyl[1,2-^{14}C]ethanol (**7**-1,2-^{14}C), and the unconsumed reactant to 1,2,2-trianisyl[1,2-^{14}C]ethene (**9**-1,2-^{14}C). After separation through an alumina column, the alcohol **7**-1,2-^{14}C was oxidized to dianisyl[^{14}C]ketone (**8**-^{14}C) to give the extent of scrambling in the product, while the olefin **9**-1,2-^{14}C was degraded by ozonolysis, also giving rise to **8**-^{14}C and the scrambling, if any, in the unconsumed reactant.

Acknowledgment

The financial support given by the Natural Sciences and Engineering Research Council of Canada is gratefully acknowledged.

1. P. J. Stang, Z. Rappoport, M. Hanack, and L. R. Subramanian. Vinyl cations. Academic Press, New York. 1979. Chapt. 6.
2. C. C. Lee. *In* Isotopes in organic chemistry. Vol. 5. Isotopes in cationic reactions. *Edited by* E. Buncel and C. C. Lee. Elsevier Scientific Publishing Co., Amsterdam. 1980. Chapt. 1.
3. C. C. Lee, A. J. Cessna, B. A. Davis, and M. Oka. Can. J. Chem. **52**, 2679 (1974).
4. F. H. A. Rummens, R. D. Green, A. J. Cessna, M. Oka, and C. C. Lee. Can. J. Chem. **53**, 314 (1975).
5. M. Oka and C. C. Lee. Can. J. Chem. **53**, 320 (1975).
6. Y. Houminer, E. Noy, and Z. Rappoport. J. Am. Chem. Soc. **98**, 5632 (1976).
7. C. C. Lee and E. C. F. Ko. Can. J. Chem. **54**, 3041 (1976).
8. C. C. Lee and E. C. F. Ko. Can. J. Chem. **56**, 2459 (1978).
9. C. C. Lee, U. Weber, and C. A. Obafemi. Can. J. Chem. **57**, 1384 (1979).
10. Z. Rappoport. Acc. Chem. Res. **9**, 265 (1976).
11. S. Winstein, B. Appel, R. Baker, and A. Diaz. Chem. Soc. Spec. Publ. **19**, 109 (1969).
12. S. Winstein, E. Clippinger, A. H. Fainberg, R. Heck, and R. C. Robinson. J. Am. Chem. Soc. **78**, 328 (1956).
13. Z. Rappoport and A. Gal. J. Chem. Soc. Perkin Trans. II, 301 (1973).
14. Z. Rappoport, P. Shulman, and M. Thuval (Shoolman). J. Am. Chem. Soc. **100**, 7041 (1978).
15. Z. Rappoport, Y. Apeloig, and J. Greenblatt. J. Am. Chem. Soc. **102**, 3837 (1980).
16. Z. Rappoport and Y. Apeloig. J. Am. Chem. Soc. **97**, 821 (1975).
17. C. C. Lee, E. C. F. Ko, and Z. Rappoport. Can. J. Chem. **58**, 884 (1980).
18. A. H. Fainberg and S. Winstein. J. Am. Chem. Soc. **78**, 2863 (1956).
19. A. Pross. Adv. Phys. Org. Chem. **14**, 169 (1977).
20. C. F. P. Kernaghan and H. M. R. Hoffmann. J. Am. Chem. Soc. **92**, 6988 (1970).
21. T. W. Bentley, F. L. Schadt, and P. v. R. Schleyer. J. Am. Chem. Soc. **94**, 992 (1972).
22. F. L. Schadt, T. W. Bentley, and P. v. R. Schleyer. J. Am. Chem. Soc. **98**, 7667 (1976).

Quand la résonance paramagnétique électronique de l'uranium(IV) est-elle observable?

EDGAR SOULIÉ et GÉRARD FOLCHER

Département de Physico-Chimie, Centre d'Etudes Nucléaires de Saclay, BP no 2, 91190 Gif-sur Yvette, France

ET

BASIL KANELLAKOPULOS

Institut für Heiße Chemie, Kernforschungszentrum, Karlsruhe, 7514 Eggenstein, Leoposdshafen, Allemagne Fédérale

Reçu le 17 avril 1980

EDGAR SOULIÉ, GÉRARD FOLCHER et BASIL KANELLAKOPULOS. Can. J. Chem. **58**, 2377 (1980).

Les ions non de Kramers peuvent avoir un niveau électronique fondamental non dégénéré. Si en outre le premier niveau électronique excité est à plus de 0,3 cm^{-1} du niveau fondamental, la résonance paramagnétique électronique ne peut pas être excitée en bande X. C'est le cas chaque fois que la susceptibilité magnétique de poudre présente un paramagnétisme indépendant de la température. Un exemple de cette situation est présenté, $U(cupferron)_4$, en contradiction avec les spectres rpe publiés.

EDGAR SOULIÉ, GÉRARD FOLCHER and BASIL KANELLAKOPULOS. Can. J. Chem. **58**, 2377 (1980).

For non-Kramers ions, the electronic ground state may be nondegenerate. Then, if the first electronic excited level lies more than 0.3 cm^{-1} above the ground state, no electron paramagnetic resonance can occur between them in the X band. This is the case whenever a temperature-independent paramagnetism is observed in the magnetic susceptibility of the powder. An example of this situation, conflicting with published epr spectra, is provided by $U(cupferron)_4$.

Conditions d'observation de la résonance paramagnétique électronique et susceptibilité magnétique

La transition résonnante entre deux niveaux d'énergie électronique ne peut avoir lieu que s'il existe deux tels niveaux, distants de $h\nu$ avec $\nu = 9{,}6 \pm 0{,}5$ GHz en bande X. Dans le cas des ions de Kramers à nombre impair d'électrons, les niveaux d'énergie dégénérés en champ nul sont généralement décomposés par le champ magnétique, et il existe une valeur du champ telle que l'écart en énergie atteigne juste le quantum hyperfréquence. Sous réserve de l'ordre de grandeur du temps de relaxation électronique, un signal de rpe est donc le plus souvent observable.

Dans le cas des ions non de Kramers, à nombre pair d'électrons, le niveau d'énergie fondamental en champ nul peut être un singulet et les niveaux excités s'en écartent tous de plusieurs cm^{-1} ou plusieurs dizaines ou centaines de cm^{-1}. Aucune transition résonnante ne peut alors être induite. Corrélativement, la suceptibilité magnétique à basse température est une constante (paramagnétisme de Van Vleck) (fig. 1).

En effet, l'effet Zeeman ne peut pas agir comme perturbation du premier ordre sur un niveau fondamental singulet, de sorte que dans la formule de Van Vleck (1) le coefficient $\varepsilon^{(1)}$ relatif au niveau fondamental est nul.

$$\chi^{para}_{molaire}(T) = \frac{N\beta}{k} \sum_{états\ i} \left[\frac{(\varepsilon_i^{(1)})^2}{T} - 2\varepsilon_i^{(2)} \right] \times \exp\left[-\frac{E_i^{(0)}}{T} \right] \Big/ \sum_{états\ i} \exp\left[-\frac{E_i^{(0)}}{T} \right]$$

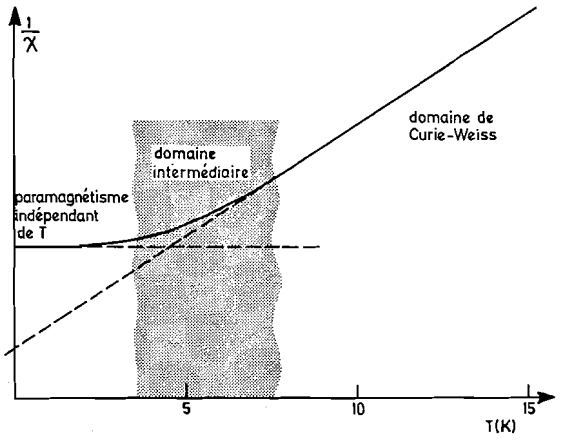


FIG. 1. Variation thermique de la susceptibilité paramagnétique χ d'un ion à nombre pair d'électrons dans le cas fréquent d'un niveau fondamental singulet et d'un premier niveau excité distant de quelques cm^{-1}. La susceptibilité est habituellement constante à très basse température, tandis qu'elle suit une loi de Curie–Weiss au-dessus d'une certaine température. Le domaine de température intermédiaire correspond au peuplement d'un premier état électronique excité, dont on peut, au moins grossièrement, estimer l'énergie: environ 2,5 cm^{-1} dans le cas représenté.

où

$$\varepsilon_i^{(1)} = \langle \psi_i | L_z + 2S_z | \psi_i \rangle$$

$$\varepsilon_i^{(2)} = \sum_{j(E_j^{(0)} \neq E_i^{(0)})} \frac{|\langle \psi_i | L_z + 2S_z | \psi_j \rangle|^2}{E_i^{(0)} - E_j^{(0)}}$$

pour la susceptibilité parallèle.

Une seconde possibilité est que le niveau fondamental soit un doublet non magnétique, c'est-à-dire non décomposé par le champ magnétique, quelle que soit sa direction.

0008-4042/80/222377-03$01.00/0

©1980 National Research Council of Canada/Conseil national de recherches du Canada

Can. J. Chem. Downloaded from www.nrcresearchpress.com by 210.87.254.40 on 09/05/12
For personal use only.

Can. J. Chem. Downloaded from www.nrcresearchpress.com by 210.87.254.40 on 09/05/12
For personal use only.

Cette situation se rencontre avec les états sous-tendant la représentation irréductible E du groupe O en symétrie cubique. Là encore, l'effet Zeeman du premier ordre est nul, il n'y a pas de signal observable par RPE, et la suceptibilité magnétique est une constante à température suffisamment basse. Il se peut enfin que le niveau fondamental soit un "quasi-doublet", dont les composantes sont très peu distantes. (D'après le théorème de Jahn–Teller, un niveau fondamental doublet au sens strict n'est pas possible.) Pour qu'une transition résonnante soit possible il faut que l'écart en champ nul ΔE soit inférieur à l'énergie du quantum hyperfréquence, donc $\nu < 0{,}3\,\text{cm}^{-1}$. L'effet Zeeman du second ordre, qui est alors du même ordre de grandeur que ΔE sépare davantage les composantes de ce doublet approché (fig. 2). Williams a montré (2) que contrairement au cas habituel, le champ magnétique hyperfréquence doit être parallèle au champ magnétique statique, car le facteur $g_\perp$ est nul, rigoureusement. Le cas d'un niveau fondamental quasi-doublet diffère des deux précédents par l'allure de la courbe de susceptibilité magnétique. Pour $kT > 5\,\Delta E$ soit $kT > \simeq 2{,}2$ K, la susceptibilité est pratiquement la même que celle d'un *vrai* doublet et suit la loi de Curie–Weiss.

Pour résumer cette discussion, une condition nécessaire (mais non suffisante) à l'observation d'un signal de résonance paramagnétique électronique d'un ion non de Kramers est que la susceptibilité magnétique ne reste pas quasi-constante au-dessous d'une température de l'ordre de 2 K.

Les faits expérimentaux

Aucune étude magnétochimique sur un composé de l'uranium(IV) n'a, à notre connaissance, montré l'existence d'un niveau fondamental "quasi-dégénéré" ($\Delta E < 0{,}3\,\text{cm}^{-1}$). La possibilité d'une résonance paramagnétique électronique[1] due à l'uranium(IV) est donc exceptionnelle. Une telle résonance a peut-être été observée sur un monocristal de CaF_2 dopé à l'uranium(IV) (3).

On a par contre montré (4) que le signal de résonance observé avec UF_4 (5) était en fait dû à des impuretés de fer et de nickel. Pour de nombreux composés d'uranium(IV), par exemple UCl_4 (6), $U(C_5H_5)_4$ (7), $U(acac)_4$ et $U(SO_4)_2{\cdot}4H_2O$ (8), le paramagnétisme devient constant à basse température (fig. 2). Une résonance associée à l'uranium(IV) est impossible dans ces composés.

Or, Miyake, Yoshimura et Imoto ont publié le spectre de résonance électronique du tétrakis-(cupferrato)-uranium(IV) (9), $U(C_6H_5{-}N_2O_2)_4$, en abrégé $U(cupf)_4$ et plus récemment celui du tétrakis-(néocupferrato)-uranium(IV) (10) obtenu à 77 K. Nous n'avons jamais pu obtenir de spectre du complexe dérivé du cupferron avec le spectromètre Varian V 4500-15, ni à 77 K, ni à 4,2 K.

Yoshimura *et al.* (11) ont mesuré la susceptibilité magnétique de $U(cupf)_4$ en fonction de la température depuis la température de l'hélium liquide jusqu'à la température ambiante. Leur fig. 2 (11) fait ressortir que l'inverse de la susceptibilité paramagnétique ne tend pas vers zéro mais vers une valeur finie correspondant à $\chi^{para}_{\text{molaire}} = 0{,}0175\,\text{cm}^3/\text{mol}$. Nos propres mesures confirment l'allure de la fig. 2. de Miyake *et al.*, bien que les valeurs que nous obtenons soient sensiblement plus faibles: $\chi^{para}_{\text{molaire}} \simeq 0{,}012\,\text{cm}^{-3}/\text{mol}$.

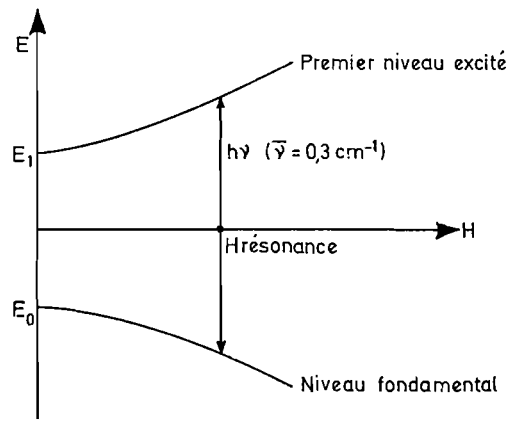


FIG. 2. Diagramme des niveaux d'énergie en fonction du champ magnétique appliqué dans le cas d'un "quasi-doublet" (au sens défini dans le texte). On notera que comme toute perturbation agissant au second ordre, l'effet Zeeman électronique augmente l'écart entre deux niveaux d'énergie par rapport à sa valeur en champ nul. La condition de résonance $h\nu = E_1(H) - E_0(H)$ implique donc $h\nu > E_1(H = 0) - E_0(H = 0)$, c'est-à-dire $E_1 - E_0 < 0{,}3\,\text{cm}^{-1}$ pour la rpe en bande X.

Conclusion

Nous en concluons donc que le signal de résonance que Miyake *et al.* (9) ont observé n'est pas dû à l'uranium(IV), mais à une impureté que nous n'avons pu identifier d'après leur spectre.

On ne doit pas être surpris par la présence d'un spectre d'impureté, en raison de la grande sensibilité de la résonance paramagnétique électronique. Ainsi avons-nous toujours obtenu deux signaux à température ambiante avec une solution aqueuse 1 M de tétrachlorure d'uranium. Nous avons attribué le signal sextuplet au manganèse divalent, et l'autre au fer trivalent. Les concentrations respectives de ces ions étaient $3 \times 10^{-6}\,M$ et $2 \times 10^{-5}\,M$. Par conséquent, l'élimination des signaux d'impureté exige d'amener les concentrations de certaines impuretés (métaux de transition) en-dessous de valeurs très faibles.

Enfin, nous suggérons que pour les composés d'uranium(IV) et plus généralement d'ions à nombre pair d'électrons, la susceptibilité paramagnétique de poudre soit toujours mesurée jusqu'à une température assez basse pour faire apparaître le palier de Van Vleck. Si ce palier n'apparaît pas à 4,2 K, comme cela se produit pour

[1] Il s'agit en fait plutôt d'une résonance paraélectrique comme l'a montré Williams (réf. 2, voir fig. 1).

$U[C_8H_4(C_6H_5)_4]_2$ (12), il faut diminuer la température jusqu'à 1 K ou mieux à 0,5 K, de telle façon qu'un niveau électronique fondamental "quasi-doublet", au sens indiqué plus haut, puisse le cas échéant être mis en évidence. C'est alors seulement qu'on pourrait entreprendre la recherche d'un signal rpe autentique.

Remerciements

E.S. remercie P. Rigny pour des discussions qui furent à l'origine de ce travail.

1. E. SOULIÉ et G. GOODMAN. Theor. Chim. Acta (Berl.), **41**, 17 (1976); Erratum, **51**, 259 (1979).
2. F. I. B. WILLIAMS. Proc. Phys. Soc. **91**, 111 (1967).
3. S. D. MCLANGHLAN. Phys. Rev. **150**, 118 (1966); G. C. WETSEL et P. L. DONOHO. Phys. Rev. **139**, A334 (1965); C. M. BOWDEN, H. C. MEYER, P. F. MCDONALD et J. D. STETTLER. J. Phys. Chem. Solids, **30**, 1535 (1969).
4. M. YA. SHCHERBAKOVA, S. P. GABUDA et YU. V. GAGARINSKI. Russ. J. Struct. Chem. **7**, 423 (1966).
5. S. N. CHOSH, W. GORDY et D. G. HILL. Phys. Rev. **96**, 36 (1954).
6. J. B. GRUBERT et H. G. HECHT. J. Chem. Phys. **60**, 1352 (1974); Erratum, **62**, 311 (1974).
7. H. D. AMBERGER, R. D. FISHER et B. KANELLAKOPULOS. Z. Naturforsch. **31**b, 12 (1976).
8. J. MULAK et A. CZOPNIK. Bull. Acad. Pol. Sci., Sér. Sci. Chim. **20**, 209 (1972); E. SOULIÉ. Proc. Int. Conf. Rare Earths and Actinides, Conference Series Number 37. The Institute of Physics, Bristol. 1978. pp. 166–172.
9. C. MIYAKE, T. YOSHIMURA et S. IMOTO. Chem. Phys. Lett. **4**, 275 (1969).
10. T. YOSHIMURA, C. MIYAKE et S. IMOTO. J. Inorg. Nucl. Chem. **37**, 739 (1975).
11. T. YOSHIMURA, C. MIYAKE et S. IMOTO. Bull. Chem. Jpn. **47**, 515 (1974).
12. N. EDELSTEIN, A. STREITWIESER, JR., D. G. MORRELL et R. WALKER. Inorg. Chem. **15**, 1397 (1976).

Can. J. Chem. Downloaded from www.nrcresearchpress.com by 210.87.254.40 on 09/05/12
For personal use only.

Sulfonation of strychnine and some related compounds by sulfur dioxide – manganese dioxide (the Leuchs reaction)

JOHN T. EDWARD, PATRICK G. FARRELL, SYED A. SAMAD, RICHARD WOJTOWSKI, AND SIN CHEONG WONG

Department of Chemistry, McGill University, 801 Sherbrooke St. West, Montreal, P.Q., Canada H3A 2K6

Received March 12, 1980

JOHN T. EDWARD, PATRICK G. FARRELL, SYED A. SAMAD, RICHARD WOJTOWSKI, and SIN CHEONG WONG. Can. J. Chem. **58**, 2380 (1980).

On the basis of pK measurements, ^{13}C nmr, and chemical arguments, the zwitterionic structures **3** and **4** have been assigned to the two minor products obtained by sulfonating strychnine or brucine in water with a mixture of sulfur dioxide and manganese dioxide. The same reagent sulfonates the quaternary salts of strychnine and brucine to give betaines, but fails to sulfonate many other strychnine derivatives as well as a number of other alkaloids examined.

JOHN T. EDWARD, PATRICK G. FARRELL, SYED A. SAMAD, RICHARD WOJTOWSKI et SIN CHEONG WONG. Can. J. Chem. **58**, 2380 (1980).

La sulfonation de la strychnine ou de la brucine en solution aqueuse par un mélange de bioxyde de soufre et de bioxyde de manganèse conduit entre autre à deux produits secondaires **3** et **4** auxquels on a attribué une structure de zwitterion en se basant sur des mesures de pK, sur la rmn du ^{13}C et sur des arguments chimiques. Le même réactif sulfone les sels quaternaires de la strychnine ou de la brucine en donnant des bétaines mais n'arrive pas à sulfoner les autres dérivés de la strychnine ainsi qu'un certain nombre d'autres alcaloïdes étudiés.

[Traduit par le journal]

In arriving at a structure for strychnine (**1**; R = H) and brucine (**1**; R = OMe), Robinson (1) and Woodward and Brehm (2) relied heavily on experimental data of Hermann Leuchs, who published 125 papers between 1908 (3) and (posthumously) 1949 (4). While the final structure has served to rationalize most of Leuchs' vast accumulation of data (see G. F. Smith (5) for an excellent review), one reaction has remained unexplained and, to our knowledge, unparalleled. This is a sulfonation reaction brought about by sulfur dioxide and manganese dioxide in warm water, which we propose to name the "Leuchs sulfonation reaction".

In 1908 Leuchs and Schneider (6) obtained a compound $C_{21}H_{22}O_5N_2S \cdot H_2O$ as colourless crystals from the clear solution obtained by bubbling sulfur dioxide through a warm aqueous solution of strychnine containing suspended manganese dioxide. This compound was designated strychninesulfonic acid-I (SSA-I) when it was found that work-up of the mother-liquors afforded isomeric acids SSA-II SSA-III (7). A similar series of isomeric brucinesulfonic acids (BSA-I, BSA-III, and BSA-IV) was obtained by applying the same reaction to brucine (8, 9).

Leuchs and his collaborators continued to study these sulfonic acids for more than 30 years (10–21), but most of their findings do not advance our understanding of the structures of the compounds. However, they did interrelate SSA-I and BSA-I by the observation that oxidation of 2-aminostrychninesulfonic acid-I (obtained by nitration of the aromatic ring followed by reduction) and of BSA-I with chromic acid removed the benzene ring and gave the same sulfonic-carboxylic acid (16). This showed that the sulfonic acid group is not attached to the aromatic ring in SSA-I and BSA-I. Likewise, it is not attached to the 11-position, because all of the various strychnine- and brucinesulfonic acids react at this position with benzaldehyde to form benzylidine derivatives (20).

These results indicate that the sulfonic acid group of SSA-I and BSA-I must be attached to some skeletal position to the right of the wavy line shown in **1**. Smith (5) suggested that the most likely positions for all the sulfonic acids would be on the carbon atoms adjacent to the basic nitrogen N(19), which would account for the isomerism. The formation of the sulfonic acids would then involve dehydrogenation followed by bisulfite addition.

On repeating Leuchs' procedures, we succeeded in obtaining strychninesulfonic acids -I, -II, and -III. Similarly, we obtained brucinesulfonic acids -I, -III, and -IV. Leuchs found this last compound difficult to isolate because of its tendency to form mixed crystals with BSA-III (9) but our modified procedure gave pure BSA-III and -IV.

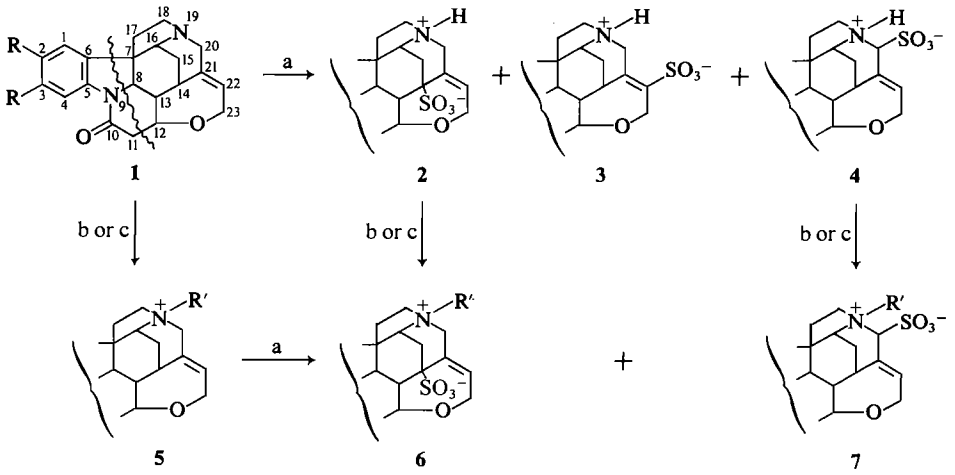
A comparison of the optical rotations of our products with those of Leuchs is given in Table 1. These suggest BSA-IV is the brucine analogue of SSA-II, and BSA-III that of SSA-III. The relations are confirmed by pK_{BH^+} measurements discussed below.

Because of the presence of the basic N(19) in

0008-4042/80/222380-06$01.00/0

©1980 National Research Council of Canada/Conseil national de recherches du Canada

Can. J. Chem. Downloaded from www.nrcresearchpress.com by 210.87.254.5 on 09/05/12
For personal use only.



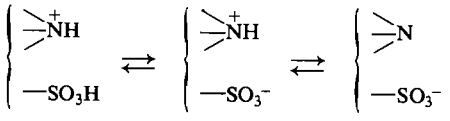
Reagents: a, SO_2/MnO_2; b, MeI or Me_2SO_4; c, $PhCH_2Br$

SCHEME 1

TABLE 1. Comparison of the optical rotations of strychninesulfonic acids (SSA) and brucinesulfonic acids (BSA) with those reported by Leuchs

	$[\alpha]_D^{25}$			$[\alpha]_D^{25}$	
SSA	Leuchs	This work	BSA	Leuchs	This work
I	−233°	−228°	I	−242°	−232°
II	−138°	−139°	IV	−122°	−121°
III	+163°	+176°	III	+157°	+151°

strychnine and brucine, the sulfonic acids must exist in neutral solution as zwitterions Z. This accords with their solubility characteristics. Thus SSA-I is almost insoluble in water, but dissolves readily in ammonium hydroxide, by loss of a proton from $\overset{+}{\diagdown\!\diagup}$N(19)—H to form the anion A, and in 20% hydrochloric acid, by addition of a proton to the sulfonic group to form the cation C, or to the amide group to form a tautomeric cation.



C Z A

X-ray diffraction studies of strychninesulfonic acid-I supplied by us to Professor L. Cartz and his colleagues (22) showed it to have the structure **2** (R = H), with the sulfonic acid group located at the allylic 14-position. This suggests the possible implication of the Δ^{21} double bond in the sulfonation reaction, a possibility supported by the failure of dihydrostrychnine (Δ^{21} saturated) to be sulfonated. On the other hand, the basic N(19) atom seems not to be involved in the reaction, because strychnine methosulfate (**5**; R = H, R′ = Me; counterion $MeOSO_3^-$) is sulfonated under Leuchs' conditions to give a sulfonic acid betaine. This betaine has the structure **6** (R = H, R′ = Me), since it is also obtained by treatment of SSA-I in alkaline solution (i.e., in the form A) with methyl iodide. Similarly, sulfonation of benzylstrychninium bromide (**5**; R = H, R′ = CH_2Ph; counterion Br^-) gave the betaine **6** (R = H, R′ = CH_2Ph). In addition, this reaction gave a second betaine, which could also be obtained by benzylation of SSA-III in alkaline solution; for reasons discussed below, we assign the structure **7** (R = H, R′ = CH_2Ph) to this betaine.

In similar fashion, brucine methosulfate (**5**; R = OMe, R′ = Me; counterion ion $MeOSO_3^-$) gave two betaines, one **6** (R = OMe, R′ = Me) and the other **7** (R = OMe, R′ = Me).

The pK_{BH^+} values for the reaction

$$Z \rightarrow A + H^+$$

of SSA-I, SSA-II, BSA-I, BSA-III, and BSA-IV were obtained by a solubility method (23, 24). Strychninesulfonic acid-III proved too soluble, and its pK_{BH^+} was determined by paper electrophoresis (23). The pK_{BH^+} values are listed in Table 2, along with the differences (ΔpK_{BH^+}) from the pK_{BH^+} in water of the unsubstituted bases, in this case strychnine or brucine (23).

This difference depends on the proximity of the sulfonic acid group to the ionizing $\overset{+}{\diagdown\!\diagup}$NH group. For the series of zwitterions **8** Rumpf (25) found ΔpK_{BH^+} to change with the number n of methylene

Can. J. Chem. Downloaded from www.nrcresearchpress.com by 210.87.254.5 on 09/05/12
For personal use only.

Can. J. Chem. Downloaded from www.nrcresearchpress.com by 210.87.254.5 on 09/05/12
For personal use only.

TABLE 2. The effect of the sulfonic acid group upon the pK_{BH+} values for strychnine and brucine

Compound	pK_{BH+}	ΔpK_{BH+} Experimental	ΔpK_{BH+} Calculated*	n
SSA-I	7.53	−0.9	−0.6	3
SSA-II	7.54	−0.9	−0.6	3
SSA-III	3.2	−5.2	−4.9	1
BSA-I	7.45	−1.0	−0.6	3
BSA-IV	7.43	−1.0	−0.6	3
BSA-III	3.12	−5.3	−4.9	1

*The ΔpK_{BH+} values of **8** for the n values shown.

carbon atoms between SO_3^- and NH_3^+:

n	1	2	3	4	5	10
ΔpK_{BH+}	−4.88	−1.43	−0.58	+0.02	+0.32	+0.72

The reason for the change in sign of ΔpK_{BH+} with n is discussed elsewhere (26); for the moment it suffices to note that the ΔpK_{BH+} for **8** ($n = 3$) is close to the ΔpK_{BH+} of SSA-I and BSA-I, which also have the ionizing NH^+ and SO_3^- groups separated by three carbon atoms. It consequently seems likely that

$$^-O_3S—(CH_2)_n—NH_3^+$$

8

ΔpK_{BH+} is determined mainly by the distance between SO_3^- and NH^+, i.e., by n, and only to a minor extent by the bulk of the molecule between the charged groups (counter to conventional Kirkwood–Westheimer theory (27)). On this basis, the ΔpK_{BH+} values of SSA-II, SSA-III, BSA-IV, and BSA-III suggest the n values indicated in the right-hand column of Table 2.

Further structural information was obtained from ^{13}C magnetic resonance spectroscopy. The ^{13}C signals of strychnine, SSA-I, SSA-II, and SSA-III in 70% aqueous perchloric acid are given in Table 3, together with their assignments and the multiplicity of each signal in the proton-coupled spectra.

Strychnine in dilute acid is protonated on N(19) (23); in 70% $HClO_4$ it is additionally protonated on the amide group, as shown by characteristic changes in the uv spectra. The assignments of Table 3 follow directly from those reported for the free base (28, 29), the hydrochloride (29), and the trifluoroacetate (28).

The ^{13}C spectrum of SSA-I, when compared with that of strychnine, is characterized by a large downfield shift (31 ppm) of the C(14) signal. This is due partly to the change from a tertiary to a quaternary carbon atom, and partly to the electronegativity of the sulfur atom of the sulfonic acid group. Other signals experiencing relatively large changes in position are C(12), C(15), C(18), C(21), and C(22),

TABLE 3. ^{13}C chemical shifts of strychnine and its sulfonic acids in 70% aqueous perchloric acid

Carbon number	Chemical shift (δ)* ppm Strychnine	SSA-I	SSA-II	SSA-III
1	134.5 (d)	134.6 (d)	134.5 (d)	134.5 (d)
2	141.4 (d)	141.6 (d)	141.5 (d)	141.2 (d)
3	141.7 (d)	141.9 (d)	141.9 (d)	141.9 (d)
4	130.2 (d)	130.2 (d)	130.2 (d)	130.1 (d)
5	147.8 (s)	148.0 (s)	147.5 (s)	146.9 (s)
6	143.1 (s)	142.8 (s)	142.4 (s)	144.2 (s)
7	62.4 (s)	62.5 (s)	62.5 (s)	61.2 (s)
8	74.5 (d)	74.4 (d)	73.8 (d)	74.9 (d)
10	182.5 (s)	182.4 (s)	182.4 (s)	182.5 (s)
11	52.2 (t)	52.4 (t)	51.8 (t)	52.4 (t)
12	86.2 (d)	82.0 (d)	85.8 (d)	86.4 (d)
13	56.8 (d)	56.6 (d)	55.8 (d)	59.3 (d)
14	40.2 (d)	71.2 (s)	42.3 (d)	36.0 (d)
15	35.3 (t)	39.6 (t)	35.3 (t)	36.3 (t)
16	71.2 (d)	71.2 (d)	71.3 (d)	73.4 (d)
17	48.2 (t)	48.9 (t)	47.8 (t)	47.2 (t)
18	64.4 (t)	66.2 (t)	64.4 (t)	67.0 (t)
20	63.1 (t)	62.5 (t)	58.7 (t)	73.8 (d)
21	142.2 (s)	134.6 (s)	147.6 (s)	144.6 (s)
22	147.0 (d)	155.8 (d)	157.7 (s)	141.9 (d)
23	75.3 (t)	75.7 (t)	76.6 (t)	77.0 (t)

*With respect to TMS; s = singlet, d = doublet, and t = triplet in the proton-coupled spectra.

which (with the exception of C(18) are all close to C(14).

The ^{13}C spectrum of SSA-II indicated that substitution has occurred on an sp^2-hybridized carbon atom. A proton-coupled doublet in the low-field portion of the spectrum of strychnine becomes a singlet in the spectrum of SSA-II. This, together with the information that the sulfonic group is probably 3 carbon atoms away from N(19) (Table 2), would place the sulfonic group on C(22) and give the structure **3**. As expected, the other signals experiencing relatively large changes from their positions in strychnine are those for C(13), C(14), C(20), C(21), and C(23), all close to C(22).

The ^{13}C spectrum of SSA-III indicates that substitution has occurred on an sp^3-hydridized methylene carbon atom (a proton-coupled triplet in the upfield portion of the spectrum of strychnine has changed into a doublet at lower field). This, together with the information that the sulfonic group is probably one carbon atom away from N(19) (Table 2), would place the sulfonic group on either C(18) or C(20). The shifts of the signals of nearby carbon atoms are more compatible with the C(20)-sulfonic acid of structure **4**.

These structures are supported by the rates of alkaline hydrolysis of the amide groups of the three sulfonic acids. SSA-II and SSA-III have about the same rate of hydrolysis in 2.5 N aqueous sodium

Can. J. Chem. Downloaded from www.nrcresearchpress.com by 210.87.254.5 on 09/05/12
For personal use only.

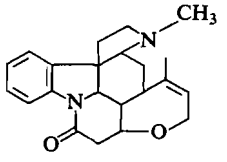
hydroxide whereas the rate for SSA-I is about 10 times slower,[1] and all hydrolyze more slowly than strychnine. These rates are in accord with the structures advanced above if the effect of the sulfonate group on the hydrolysis is taken to be a rate-retardation (through space). Some support for this assumption as to the influence of a negatively charged group upon the rate of base-catalyzed amide hydrolysis is obtained from the observation that the hippurate ion is hydrolyzed approximately 16 times more slowly than benzamide in 2.5 *N* aqueous sodium hydroxide at 70°C.[1]

The mechanism of Leuchs' reaction remains obscure. The reaction of manganese dioxide with sulfurous acid has been known since 1819 (30) to yield dithionate and some sulfate, through one- and two-electron oxidations:

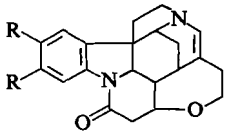
$$SO_3^- \xrightarrow{-e^-} \cdot SO_3^- \longrightarrow {}^-O_3S{-}SO_3^-$$

$$\cdot SO_3^- + H_2O \xrightarrow{-e^-} H_2SO_4$$

Reaction of $\cdot SO_3H$ with the allylic radicals produced by oxidation of strychnine with manganese dioxide could yield **2** and **4** (R = H). Analogous sulfonations of naphthols by sulfur dioxide – manganese dioxide are known (31). However, it is difficult to understand why the reaction proceeds only with strychnine, brucine, and their quaternary salts. The reaction fails with other alkaloids (codeine, quinine, cinchonine, rubijervine), and even with strychnine derivatives such as base-D (**9**) (32). It also fails with neostrychnine and neobrucine (**10**, R = H or OMe).



9



10

Experimental

Optical rotations were measured with a Perkin-Elmer 141 automatic polarimeter, infrared spectra with a Perkin-Elmer 257 spectrophotometer, and ^{13}C magnetic resonance spectra with a Bruker 22.63 MHz spectrometer locked to the resonance of D_2O contained in a capillary. Elemental analyses were performed by A. Bernhardt, West Germany.

*Sulfonation of Strychnine (**1**; R = H)*

Manganese dioxide was prepared by adding ethanol to a stirred solution of potassium permanganate (110 g) in water until a spot added to filter paper no longer showed a purple colour. The brown precipitate was filtered and washed thoroughly with water and, still wet, suspended in 1500 mL of distilled water. This brown suspension was added in ca. 100 mL portions to a solution of strychnine (40 g) in aqueous sulfur dioxide (2200 mL) at 50–55°C, while sulfur dioxide was bubbled through the solution. After the last of the manganese dioxide had dissolved, sulfur dioxide was bubbled through the solution at 50–55°C for another hour. From the hot solution strychninesulfonic acid-I (fraction A, 28 g) was removed by filtration.

The filtrate, after successive cooling, concentration, and finally chemical treatment, afforded the following fractions of crystalline material.

Fraction B (8.7 g), after 24 h in refrigerator; shown by tlc to be approximately 1:1 SSA-I and -II;

Fraction C (3.6 g), after concentration to 700 mL; shown by tlc to be approximately 1:2 SSA-I and -II;

Fraction D (1 g), after another 24 h in refrigerator; SSA-I.

Concentrated sulfuric acid (30 mL) was added to the filtrate from D and the solution was heated on the water bath for 10 h. Solid barium oxide was added to the hot solution with stirring to approximately pH 10. Inorganic material ($BaSO_4$, $Mn(OH)_2$) was removed by filtration from the alkaline solution, which was then cautiously neutralized with dilute sulfuric acid and filtered again. The neutral filtrate was concentrated to 50 mL and left in the refrigerator for 3 days, yielding fraction E (2.2 g), shown by tlc to contain SSA-I and -II and inorganic salt. The filtrate was concentrated and chromatographed on Florisil (180 g). Elution with water yielded some crystalline fractions of SSA-III (contaminated with inorganic material) and then noncrystalline fractions. These were evaporated to dryness, taken up in hot ethanol, and treated with potassium hydroxide in ethanol until the solution was strongly basic. An inorganic deposit was removed quickly by filtration of the hot solution. The filtrate after 4 days in the refrigerator deposited white needles (6 g) of the potassium salt of SSA-III, $[\alpha]_D^{20}$ +176° (water), giving only one spot on tlc with several different solvents.

Strychninesulfonic acid-I (22 g), $[\alpha]_D^{20}$ −228° (0.1 *N* NaOH) was obtained by recrystallization of fractions A and D from hot water.

Fractions B and C were combined and digested rapidly with 4 portions (25 mL) of boiling water to remove SSA-I. The final residue was recrystallized from a large amount of water, and yielded pure SSA-II (5 g), $[\alpha]_D^{20}$ −139° (0.1 *N* NaOH).

The potassium salt of SSA-III was dissolved in water, acidified with hydrochloric acid, and the solution evaporated to dryness. The residue was extracted quickly with hot anhydrous ethanol. The residue from evaporation of the ethanol, after wasteful crystallization from water, gave SSA-III, mp 289–291°C, $[\alpha]_D^{20}$ +176° (0.1 *N* NaOH).

*Sulfonation of Brucine (**1**; R = OMe)*

At 80–90°C

Following essentially the procedure described above for strychnine, manganese dioxide from 62 g of potassium permanganate was added to a solution of brucine hydrate (25 g) in water (400 mL) at 80–90°C through which sulfur dioxide was bubbled. The final solution (1400 mL) was treated with concentrated sulfuric acid (30 mL), heated on a water bath for 8 h, and allowed to stand at room temperature for 3 days. A crystalline deposit (fraction A (8.5 g)) was removed by filtration, and the filtrate after 3 days in the refrigerator deposited fraction B, which was removed, washed with cold water, and dried in air.

Fraction A was shown by tlc to be made up of BSA-III, BSA-IV, and some BSA-I. It was refluxed with stirring with nitromethane (500 mL) and the mixture left overnight at room temperature. The solid was removed by filtration, and the extraction in this manner repeated three times. The insoluble residue was recrystallized from water (500 mL), and gave pale tan plates of BSA-IV (2.1 g), $[\alpha]_D^{20}$ −121° (0.1 *N* NaOH).

[1]S. C. Wong, unpublished results.

Can. J. Chem. Downloaded from www.nrcresearchpress.com by 210.87.254.5 on 09/05/12
For personal use only.

The residue after evaporation of the combined nitromethane extracts was recrystallized from water (300 mL), with decolorization by sugar charcoal, giving feathery, colorless needles of BSA-III (3.9 g), $[\alpha]_D^{20}$ +151° (0.1 *N* NaOH).

Fraction B was shown by tlc to be BSA-I with a little BSA-III. It was stirred with boiling nitromethane, and the mixture left overnight at room temperature. The residue, recrystallized from water (150 mL) yielded colorless needles of BSA-I (9.5 g), $[\alpha]_D^{20}$ −232° (0.1 *N* NaOH).

At 97°C

The reaction was carried out as above but at about 97°C. After standing for 3 days at room temperature, the solution deposited fraction A (7.5 g), and the filtrate after 3 days in the refrigerator deposited fraction B (18 g).

Fraction A was shown by tlc to be BSA-III with a little BSA-I. After three recrystallizations from water, BSA-III (4.7 g) was obtained as colorless feathery needles, $[\alpha]_D^{20}$ +151° (0.1 *N* NaOH).

Fraction B was removed by filtration and washed with water. It was shown by tlc to be BSA-I with a little BSA-III. It was extracted three times with nitromethane, following the procedure for fraction B in the previous experiment, and then crystallized from water, to give BSA-I (9.5 g).

Anhydro-19-methylstrychninium-14-sulfonic Acid Hydroxide (6; R = H, R′ = Me)

From Strychnine Methosulfate (5; R = H, R′ = Me; Counterion $MeOSO_3^-$)

Strychnine methosulfate (33) (15 g) dissolved in water (750 mL) was treated with manganese dioxide (15 g) and sulfur dioxide according to the procedure described above. The solution on cooling deposited a white solid (9.6 g; 70% yield), which was recrystallized from water; white needles, mp 345–350°C (dec.), $[\alpha]_D^{20}$ −159° (in water), ν_{max}(KBr): 1170, 1060 (SO_3^-) cm^{-1}.

Anal. calcd. for $C_{22}H_{21}O_5N_2S \cdot 2H_2O$: C 56.9, H 6.1, N 6.0; found: C 56.7, H 6.1, N 6.0.

From Strychnine-14-sulfonic Acid (SSA-I) (2; R = H)

Methyl iodide (0.05 mL) was added to a solution of SSA-I (0.25 g) in 5% aqueous sodium hydroxide (20 mL). The product crystallized from the reaction mixture on standing at room temperature and proved identical (mp, ir) with the product above.

Sulfonation of Benzylstrychninium Bromide (5; R = H, R′ = CH_2Ph; Counterion Br^-)

Benzylstrychninium bromide, mp 308°C, was prepared by reaction of strychnine with benzyl bromide in 95% ethanol. The compound (20 g) was sulfonated under standard conditions to give a crystalline product (19.9 g) which showed three spots on thin-layer chromatography. Column chromatography of a portion (1.5 g) of the product on silica gel gave a first fraction of anhydro-19-benzylstrychninium-14-sulfonic acid hydroxide (**6**; R = H, R′ = CH_2Ph) (1.27 g; 85%), crystallizing from methanol in white flakes, mp 325–330°C, $[\alpha]_D^{20}$ −60° (MeOH), ν_{max}(KBr): 1170, 1060 (SO_3^-) cm^{-1}.

Anal. calcd. for $C_{28}H_{28}N_2O_5S \cdot 2H_2O$: C 62.2, H 6.0, N 5.2; found: C 62.2, H 5.9, N 5.4.

The same compound (mp, ir) crystallized from a solution of SSA-I (208 mg) and sodium bicarbonate (300 mg) in water treated with benzyl bromide (0.1 mL).

Later fractions from the chromatographic column gave anhydro-19-benzylstrychninium-20-sulfonic acid hydroxide (**7**; R = H, R′ = CH_2Ph) (35 mg; 2%), white flakes from methanol, mp 250°C (dec.), $[\alpha]_D^{20}$ +55° (MeOH), ν_{max}(KBr): 1190, 1050 (SO_3^-) cm^{-1}.

Anal. calcd. for $C_{28}H_{28}N_2O_5S \cdot 2H_2O$: C 62.2, H 6.0, N 5.2; found: C 62.5, H 5.9, N 5.2.

The same compound (mp, ir) was obtained by benzylation of SSA-III.

Sulfonation of Brucine Methosulfate (5; R = OMe, R′ = Me, Counterion $MeOSO_3^-$)

Brucine methosulfate (12 g) in water (800 mL) was sulfonated by the standard procedure. The resultant clear solution on standing for several days at room temperature deposited four crops of colorless needles of anhydro-19-methylbrucinium-14-sulfonic acid hydroxide (**6**; R = OMe, R′ = Me) (7.1 g; 64%), mp 350°C (dec.), $[\alpha]_D^{20}$ −113° (water), ν_{max}(KBr): 1140, 1055 (SO_3^-) cm^{-1}.

Anal. calcd. for $C_{24}H_{28}N_2O_7S \cdot H_2O$: C 56.9, H 6.0, N 5.5; found: C 57.0, H 5.9, N 5.6.

The same compound (mp, ir) was obtained by treatment of BSA-I (205 mg) in 1 mL of 10% aqueous sodium bicarbonate with methyl iodide (0.04 mL).

The mother liquors from the four crops of **6** (R = OMe, R′ = Me) were concentrated to 400 mL and left at room temperature for one week. Colorless flakes of anhydro-19-methylbrucinium-20-sulfonic acid hydroxide (**7**; R = OMe, R′ = Me) (1.3 g; 12%) crystallized out; mp 300–305°C (dec.), $[\alpha]_D^{25}$ −32° (water), ν_{max}(KBr): 1150, 1060 (SO_3^-) cm^{-1}.

Anal. calcd. for $C_{24}H_{28}N_2O_7S \cdot 2H_2O$: C 55.1, H 6.1, N 5.3; found: C 54.8, H 6.1, N 5.2.

The same compound (mp, ir) crystallized from a solution of BSA-III (100 mg) and sodium bicarbonate (50 mg) in water (0.5 mL) when treated with methyl iodide (0.02 mL).

Determination of Dissociation Constant by Paper Electrophoresis

The procedure of ref. 23 was followed, the relative mobility being given by the ratio of the distances moved in 45 min by strychninesulfonic acid-III (as a mixture of Z and A) to the distances moved by the standard picrate ion, which was essentially completely ionized (p*K* 0.38) at pH values higher than 2, and which could be located by its yellow color. Acrylamide was used as a neutral marker of electroendosmotic flow, and the zones of sulfonic acid and of marker were revealed by a permanganate–acetone spray (23) applied while the paper strips were still wet.

Acknowledgments

We are grateful to Dr. G. Welch, Dr. M. Kaufman, and Dr. G. A. Baramki for preliminary exploratory work, to Dr. D. M. Waldron-Edward for the loan of the paper electrophoresis apparatus, to Dr. A. S. Perlin, Dr. N. Cyr, and Dr. W. Dawson for ^{13}C nmr spectral measurements, and to the National Research Council of Canada for financial support.

1. R. Robinson. *In* Progress in organic chemistry. Vol. I. *Edited by* J. W. Cook. Butterworths, London. 1952. p. 12.
2. R. B. Woodward and W. J. Brehm. J. Am. Chem. Soc. **70**, 2107 (1948).
3. H. Leuchs. Ber. **41**, 1711 (1908).
4. H. Leuchs and M. Mengelberg. Chem. Ber. **82**, 250 (1949).
5. G. F. Smith. *In* The alkaloids. Vol. VIII. *Edited by* R. H. F. Manske. Academic Press, New York. 1965. p. 591.
6. H. Leuchs and W. Schneider. Ber. **41**, 4393 (1908).
7. H. Leuchs and W. Schneider. Ber. **42**, 2681 (1909).
8. H. Leuchs and W. Geiger. Ber. **42**, 3067 (1909).

9. H. LEUCHS. Ber. **67**, 1082 (1934).
10. H. LEUCHS and P. BOLL. Ber. **43**, 2362 (1910).
11. H. LEUCHS and W. GEIGER. Ber. **44**, 3049 (1911).
12. H. LEUCHS and J. WUTKE. Ber. **45**, 3686 (1912).
13. H. LEUCHS and K. FRICKER. Ber. **55**, 1244 (1922).
14. H. LEUCHS and H. ZANDER. Ber. **56**, 502 (1923).
15. H. LEUCHS and C. TAUBE. Ber. **57**, 1092 (1924).
16. H. LEUCHS, G. SCHLEMPP, and W. BAUR. Ber. **65**, 1121 (1932).
17. H. LEUCHS, G. SCHLEMPP, and A. DORNOW. Ber. **66**, 743 (1933).
18. H. LEUCHS and A. DORNOW. Ber. **66**, 1159 (1933).
19. H. LEUCHS and H. S. OVERBERG. Ber. **66**, 1711 (1933).
20. H. LEUCHS and F. RÄCK. Ber. **73**, 731 (1940).
21. H. LEUCHS and H. G. BOIT. Ber. **73**, 885 (1940).
22. D. S. SAKEGOWDA, L. CARTZ, and S. NATARAJAN. Acta Crystallogr. Sect. B, **29**, 2760 (1973).
23. J. T. EDWARD, P. G. FARRELL, S. A. SAMAD, and S. C. WONG. J. Org. Chem. **42**, 225 (1977).
24. A. ALBERT and E. P. SERJEANT. The determination of ionization constants. Chapman and Hall, London. 1971. p. 110.
25. P. RUMPF. Bull. Soc. Chim. Fr. **5**, 871 (1938); R. P. BELL. The proton in chemistry. Cornell University Press, Ithaca, NY. 1959. p. 101.
26. J. L. JOB. Ph.D. thesis, McGill University, Montreal, P.Q. 1973.
27. J. T. EDWARD, P. G. FARRELL, and J. L. JOB. J. Chem. Phys. **57**, 5251 (1972).
28. P. R. SRINIVASAN and R. L. LICHTER. Org. Magn. Reson. **8**, 198 (1976).
29. J. LEUNG and A. J. JONES. Org. Magn. Reson. **9**, 333 (1977).
30. Gmelins Handbuch der Anorganischen Chemie. 2nd ed. Schwefel. Syst. No. 9, Part B, Installment 2. Springer Verlag, Berlin. 1961. p. 958.
31. C. M. SUTER. The organic chemistry of sulfur. Tetracovalent sulfur compounds. Interscience Research Foundation, Santa Monica. 1969. p. 355.
32. O. ACHMATOWICZ and J. SZYCHOWSKI. Tetrahedron, Suppl. 8, Part I, 217 (1966).
33. W. H. PERKIN, R. ROBINSON, and J. C. SMITH. J. Chem. Soc. 1239 (1932).

Can. J. Chem. Downloaded from www.nrcresearchpress.com by 210.87.254.5 on 09/05/12
For personal use only.

Synthetic applications of α-hydroxydiazenes. III.[1] Uncatalyzed and phenol catalyzed hydroalkylation of alkenes and of azobenzene with alkylazodiphenylmethanols

DOMINIC W. K. YEUNG[2] AND JOHN WARKENTIN[3]

Department of Chemistry, McMaster University, Hamilton, Ont., Canada L8S 4M1

Received June 18, 1980

DOMINIC W. K. YEUNG and JOHN WARKENTIN. Can. J. Chem. **58**, 2386 (1980).

Alkylazodiphenylmethanols $(C_6H_5)_2C(OH)N{=}NR$, (R = $CH(CH_3)_2$, CH_2CH_3, CH_3), when decomposed in the presence of olefinic substrates or in the presence of azobenzene, hydroalkylate those substrates. Addition of R and H across the double bond of an unsymmetric alkene occurs with the regiochemistry expected for a radical mechanism, in which the group R adds first. Radical intermediates from decomposition of alkylazodiphenylmethanols have been demonstrated earlier with spin trapping experiments. The fact that addition of phenol can enhance the yield of hydroalkylation product suggests that the process is a radical chain reaction, with chain carrying steps consisting of the reactions:

(*i*) $R\cdot + CH_2{=}CHY \rightarrow RCH_2\dot{C}HY$

(*ii*) $RCH_2\dot{C}HY + (C_6H_5)_2C(OH)N_2R \rightarrow RCH_2CH_2Y + (C_6H_5)_2CO + N_2 + R\cdot$

One deuterioalkylation and some yield-optimizing experiments are also reported.

DOMINIC W. K. YEUNG et JOHN WARKENTIN. Can. J. Chem. **58**, 2386 (1980).

La décomposition des alkylazodiphénylméthanols $(C_6H_5)_2C(OH)N{=}NR$, (R = $CH(CH_3)_2$, CH_2CH_3, CH_3), en présence d'oléfines ou d'azobenzène conduit à l'hydroalkylation de ces substrats. L'addition de R et de H sur la double liaison d'un alcène asymétrique se produit selon la régiochimie attendue pour un mécanisme radicalaire dans lequel le groupe R s'additionne en premier. On a déjà démontré, par des expériences antérieures de piégeage de spin, l'existence de radicaux intermédiaires au cours de la décomposition des alkylazodiphénylméthanols. Le fait que l'addition du phénol puisse augmenter le rendement de l'hydroalkylation suggère que la réaction se déroule selon une réaction en chaîne propagée par les réactions suivantes:

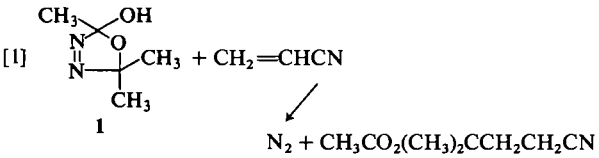
(*i*) $R\cdot + CH_2{=}CHY \rightarrow RCH_2\dot{C}HY$

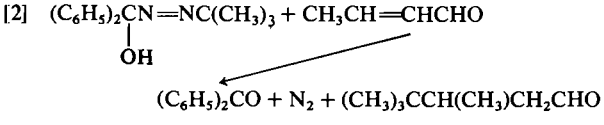
(*ii*) $RCH_2\dot{C}HY + (C_6H_5)_2C(OH)N_2R \rightarrow RCH_2CH_2Y + (C_6H_5)_2CO + N_2 + R\cdot$

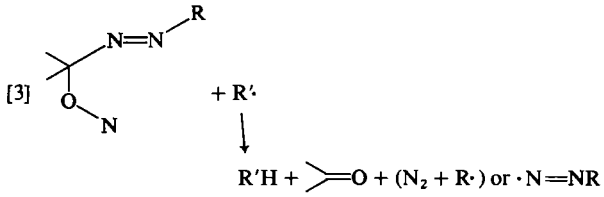
On rapporte également une deutérioalkylation et quelques expériences ayant pour but d'améliorer les rendements.

[Traduit par le journal]

A few years ago we reported some novel addition reactions to π-bonded systems, by reagents containing the alpha (α) hydroxydiazene (azocarbinol) functionality. For example, **1** reacted with acrylonitrile to yield 4-acetoxy-4-methylvaleronitrile, eq. [1] (1). Similarly, **2** reacted with crotonaldehyde to afford 3,4,4-trimethylpentanal, eq. [2] (2). Hydro-*tert*-butylations of π-bonded substrates with **2** occurred in higher overall yields if phenol was present at low concentration (2) and this observation, together with evidence for the intermediacy of *tert*-butyl radicals in thermolysis of **2** (3, 4) and 2-acetoxy-2-propyl radicals in thermolysis of **1** (5) led to the proposal of a radical chain mechanism for decomposition of those hydroxydiazene systems. The key step in that mechanism is radical abstraction of hydroxyl hydrogen from the hydroxydiazene in concert with C—N bond cleavage, thus avoiding formation of an alkoxy radical intermediate, eq. [3], and providing enough lower-

[1] 

[2] 

[3] 

ing of the free energy from formation of coproducts to allow even stabilized R· (e.g. phenoxy) to act as chain carriers.

It was of interest to try to establish the generality of the hydroalkylation reaction represented by eq.

[1]For parts I and II, see refs. 1 and 2.

[2]Present address: Alkaril Chemicals Ltd., Mississauga, Ont., Canada L5C 1V8.

[3]Author to whom correspondence should be addressed.

0008-4042/80/222386-08$01.00/0

©1980 National Research Council of Canada/Conseil national de recherches du Canada

Can. J. Chem. Downloaded from www.nrcresearchpress.com by 210.87.254.40 on 09/05/12
For personal use only.

Can. J. Chem. Downloaded from www.nrcresearchpress.com by 210.87.254.40 on 09/05/12
For personal use only.

[2] by testing systems which would have to generate secondary or primary free radicals. We also wanted to establish optimum conditions for hydroalkylation, and to attempt deuterioalkylation by the simple expedient of shaking the hydroxydiazene with D_2O prior to thermolysis. We report results of such work in this paper.

Methods and Results

2-Propylazodiphenylmethanol, **3**, was prepared from 2-propylmagnesium bromide and diphenyldiazomethane (6) as outlined in eqs. [4]–[6]. Ethylazodiphenylmethanol, **4**, was prepared by an analogous route. The appropriate benzophenone alkylhydrazones, eq. [4], can of course also be prepared from benzophenone and alkylhydrazine,[4] and the oxidation step, eq. [5], can also be carried out with bromine in acetic acid instead of lead tetraacetate, albeit in lower yield. Typical procedures are described below.

[4] $(C_6H_5)_2C{=}\overset{+}{N}{=}\overset{-}{N} + (CH_3)_2CHMgBr \xrightarrow[(2)\ H_3O^+]{(1)\ \text{Ether}} (C_6H_5)_2C{=}NNHCH(CH_3)_2$

[5] $(C_6H_5)_2C{=}NNHCH(CH_3)_2 + Pb(OAc)_4 \xrightarrow{CH_2Cl_2} (C_6H_5)_2\underset{\displaystyle OAc}{\underset{|}{C}}N{=}NCH(CH_3)_2$

[6] $(C_6H_5)_2\underset{\displaystyle OAc}{\underset{|}{C}}N{=}NCH(CH_3)_2 + 2CH_3Li \xrightarrow[(2)\ H_3O^+]{(1)\ -10°C} (C_6H_5)_2\underset{\displaystyle OH}{\underset{|}{C}}N{=}NCH(CH_3)_2$

3

Benzophenone-2-propylhydrazone

A solution of diphenyldiazomethane (2) (45.0 g, 0.23 mol) in 200 mL of anhydrous ether was added, during one hour, to a stirred solution of ice-cold, freshly-prepared 2-propylmagnesium bromide (0.34 mol). After addition was completed, the mixture was stirred for 30 min, during which time most of the red colour faded and a yellow precipitate was formed. The mixture was treated with cold, aqueous ammonium chloride, the ether layer was separated, and the aqueous layer was extracted twice with ether. The combined ethereal layers were dried over sodium sulfate before the ether was removed with a rotary evaporator. Benzophenone-2-propylhydrazone was obtained as a sticky, yellow oil in 90% yield; ir (CCl_4): 3275 (NH); ^1H nmr (CCl_4) δ: 1.08 (d, 6H), 3.12–3.65 (m, 1H), 4.89 (s, broad, 1H), 6.39–7.45 (m, 10H); *Mol. Wt.* (ms): 238.

Benzophenone Ethylhydrazone

This compound, prepared by the analogous procedure, was obtained as an oil in 80% yield; ir (CCl_4): 3260 (NH); ^1H nmr (CCl_4) δ: 1.12 (t, J = 7 Hz, 3H), 3.22 (q, J = 7 Hz, 2H), 4.92 (s, broad, 1H), 7.03–7.50 (m, 10H); *Mol. Wt.* (ms): 224.

Benzophenone Methylhydrazone

A mixture of benzophenone (0.30 mol), methyl hydrazine (0.33 mol), and glacial acetic acid (30 mL) in methanol (100 mL) was heated to reflux under nitrogen. After 2 h the flask was cooled with ice and the colourless crystals were filtered off. Recrystallization from hot methanol gave benzophenone methylhydrazone, mp 41–42°C (lit. (6), mp 42–43°C), in 65% yield.

2-Propylazodiphenylmethyl Acetate

A solution of benzophenone-2-propylhydrazone (11.9 g, 0.050 mol) in dichloromethane (50 mL) was added in the course of 20 min to a stirred, ice-cooled solution of lead tetraacetate (25 g, 0.055 mol) in dichloromethane (150 mL). An atmosphere of dry nitrogen was maintained over both solutions to prevent air oxidation of hydrazone to azohydroperoxide. After addition had been completed the mixture was stirred for 20 min more before ice water (150 mL) was added. The brown sludge which formed was removed by filtering the entire mixture through a bed of Celite. The organic layer was separated and washed, first with water and then with bicarbonate solution (5%), until it was free of acetic acid. After drying over Na_2SO_4 and evaporation of the solvent with a rotary evaporator, a pale yellow solid was obtained. Recrystallization from methanol gave 2-propylazodiphenylmethyl acetate, 70%, mp 69.5–70.5°C; ir: 1765 cm^{-1}; ^1H nmr (CCl_4) δ: 1.21 (d, J = 7 Hz, 6H), 2.03 (s, 3H), 3.87 (sept, J = 7 Hz, 1H), 7.08–7.48 (m, 10H). *Anal.* calcd. for $C_{18}H_{20}N_2O_2$: C 72.93, H 6.81, N 9.46; found: C 73.14, H 6.82, N 9.76.

Ethylazodiphenylmethyl Acetate

The above procedure gave, from benzophenone ethylhydrazone (0.050 mol), ethylazodiphenylmethyl acetate, 60%; mp 77–78°C; ir (CCl_4): 1765 cm^{-1}; ^1H nmr (CCl_4) δ: 1.29 (t, J = 7 Hz, 3H), 2.05 (s, 3H), 4.00 (q, J = 7 Hz, 2H), 7.08–7.52 (m, 10H). *Anal.* calcd. for $C_{17}H_{18}N_2O_2$: C 72.80, H 6.43, N 9.93; found: C 72.77, H 6.52, N 9.65.

Methylazodiphenylmethyl Acetate

The analogous procedure gave, from benzophenone methylhydrazone (0.050 mol), methylazodiphenylmethyl acetate in 45% yield; mp 124–125°C (lit. (9), mp 125–126°C); ir: 1750 cm^{-1}; ^1H nmr (CCl_4) δ: 2.06 (s, 3H), 2.86 (s, 3H), 7.13–7.53 (m, 10H).

2-Propylazodiphenylmethanol, 3

A solution of 2-propylazodiphenylmethyl acetate (14.8 g, 0.050 mol) in 200 mL of anhydrous ether, under nitrogen, was cooled to −10°C. Methyllithium (75 mL of 1.7 *M* reagent in ether, 0.13 mol) was added to the stirred solution by drops from a syringe, during 10 min. After 15 min more, ammonium chloride solution (saturated, ice-cold, 250 mL) was added slowly. After separation of the ether layer the aqueous phase was extracted three times with ether. The ethereal fractions were combined and dried with Na_2SO_4 before concentration (without heating) with a rotary evaporator. The pale yellow solid, after recrystallization from pentane, melted at 54–55°C (dec.); 70% yield; ^1H

[4] Such preparations, as well as handling of the hydrazones whatever their origin, must be done with care to prevent air oxidation to azohydroperoxides (7). The latter can be treated with triphenylphosphine to convert them to the desired azocarbinols (8). We have used this alternative approach to synthesize some azocarbinols and have developed a more convenient procedure (A. Nazran, to be published).

Can. J. Chem. Downloaded from www.nrcresearchpress.com by 210.87.254.40 on 09/05/12
For personal use only.

nmr (CCl_4) δ: 1.30 (d, J = 7 Hz, 6H), 4.03 (sept, J = 7 Hz, 1H), 5.63 (s, 1H), 7.07–7.53 (m, 10H). This product could not be analyzed and infrared spectra of freshly-prepared material showed a band at 1650 cm^{-1} (CO of benzophenone) which increased in intensity during successive scans as spontaneous decomposition progressed.

Ethylazodiphenylmethanol, 4

Deacylation of ethylazodiphenylmethyl acetate, as described above for the 2-propyl analogue, gave **4** as an unstable solid; mp 44–45°C (dec.); ^1H nmr (CCl_4) δ: 1.35 (t, J = 7 Hz, 3H), 4.05 (q, J = 7 Hz, 2H), 5.60 (s, 1H), 7.03–7.53 (m, 10H).

Methylazodiphenylmethanol, 5

Deacylation of methylazodiphenylmethyl acetate, as described above for the 2-propyl analogue, gave crude **5** as an oil; ^1H nmr (CCl_4) δ: 3.73 (s, 3H), 5.47 (s, 1H), 6.97–7.70 (m, 10H). Attempts to purify **5** were unsuccessful and subsequent experiments involving **5** were done with freshly-prepared but crude material.

Hydroalkylations of unsaturated compounds with 3, 4, and 5 were carried out in solvent benzene. In a typical procedure the unsaturated substrate (0.008 mol) was added to a solution of α-hydroxydiazene (0.002 mol) in benzene (4.0 mL) and the mixture was shaken until homogeneous. It was then warmed if necessary to initiate decomposition (typically to between 35° and 50°C was sufficient) and kept in that temperature range for 12–20 h. Evolution of gas was observed in all cases, either immediately after mixing or soon after warming to 35°C. Long after reaction appeared to be over, as judged by cessation of bubbling, the solution was subjected to bulb-to-bulb distillation, leaving behind telomeric material and benzophenone. The distillate was analyzed by glpc, with a column (10 ft × ¼ in.) packed with Carbowax 20 M (15%) on Chromosorb A (60–80 mesh) at 80–120°C with a helium flow rate between 45 and 60 mL/min, in a Varian Aerograph A90P3 instrument. Analytically pure products were isolated in this way for identification. Yields were estimated by addition of *tert*-butylbenzene to serve as internal standard, without correction for thermal conductivity differences.

Deuteriomethylation of Norbornene with 5-OD

A solution of methylazodiphenylmethanol (**5**, 1.0 g, 4.4 mmol) in benzene (10 mL) was stirred vigorously with D_2O (5 mL) for about 10 min before norbornene (1.6 g, 17.0 mmol) was added all at once. The resulting mixture was kept at 35°C, with vigorous stirring, for 36 h. The organic layer was separated and dried before bulb-to-bulb distillation, followed by addition of *tert*-butylbenzene and gas chromatography. A sample of 2-deuterio-*exo*-3-methylnorbornene was analyzed for deuterium content by ms: D_1 87%; D_0 13%.

Discussion

Results of reactions of hydroxydiazenes with olefinic substrates and with azobenzene are gathered in Tables 1–3. It is clear that **3**, **4**, and **5** act as agents for hydroalkylating olefinic and azo double bonds. It is also evident from the yield data that the efficiency of addition is very sensitive to substrate structure and that addition of an H-atom donor (phenol in the present case) can improve the yield of addition product. These observations can be accounted for in terms of the radical chain chemistry postulated for analogous hydro-*tert*-butylation with *tert*-butylazodiphenylmethanol (2).

The initiation step has not been identified but it is unlikely to be unimolecular homolysis according to eqs. [7] or [8], because the corresponding methyl ethers and acetates are very stable in benzene

[7] $(C_6H_5)_2\underset{\underset{OH}{|}}{C}-N=NR \longrightarrow (C_6H_5)_2\underset{\underset{OH}{|}}{C}\cdot + N_2 + R\cdot$

[8] $(C_6H_5)_2\underset{\underset{OH}{|}}{C}N=NR \longrightarrow (C_6H_5)_2\underset{\underset{OH}{|}}{C}\cdot + \cdot N=NR$

$(C_6H_5)_2\underset{\underset{OCH_3}{|}}{C}N=NR$ and $(C_6H_5)_2\underset{\underset{OCOCH_3}{|}}{C}N=NR$

under the reaction conditions. Possible mechanisms of initiation include molecule induced homolysis (17–20) and H-abstraction by dissolved ground state oxygen (2, 3). Once R· is generated in the presence of hydroxydiazene, phenol, and alkene, the expected chemistry is that of eqs. [9]–[15]. That is, R· can abstract from hydroxydiazene, or from phenol,[5] in unwanted reactions that lower the yield of RCH_2CH_2Y. Radical R· can also add to alkene, eq. [11], leading to a new radical which faces the same choices that R· has; H-abstraction from hydroxydiazene or from phenol and addition to alkene, eqs. [12]–[14].

[9] $R\cdot + (C_6H_5)_2\underset{\underset{OH}{|}}{C}N=NR \longrightarrow RH + (C_6H_5)_2CO + N_2 + R\cdot$

[10] $R\cdot + C_6H_5OH \longrightarrow RH + C_6H_5O\cdot$

[11] $R\cdot + CH_2=CHY \longrightarrow RCH_2\dot{C}HY$

[12] $RCH_2\dot{C}HY + (C_6H_5)_2\underset{\underset{OH}{|}}{C}N=NR \longrightarrow RCH_2CH_2Y + (C_6H_5)_2CO + N_2 + R\cdot$

[13] $RCH_2\dot{C}HY + C_6H_5OH \longrightarrow RCH_2CH_2Y + C_6H_5O\cdot$

[14] $RCH_2\dot{C}HY + \eta CH_2=CHY \longrightarrow$ telomers and polymers

[15] $C_6H_5O\cdot + (C_6H_5)_2\underset{\underset{OH}{|}}{C}N=NR \longrightarrow C_6H_5OH + (C_6H_5)_2CO + N_2 + R\cdot$

These reactions offer a rationale for the sensitivity of yields to structure and for the effects of phenol on the yields of hydroalkylation products. Rate constants for radical addition to $CH_2=CHY$ (eqs. [11], [14]) and for H-abstraction by $RCH_2\dot{C}HY$ (eqs. [12], [13]) depend on the substituent Y and it is not surprising that the outcome

[5] In the general case one should consider other H-donors, such as an olefinic substrate with a labile H-atom (e.g. allylic H), or the reaction products.

Can. J. Chem. Downloaded from www.nrcresearchpress.com by 210.87.254.40 on 09/05/12
For personal use only.

TABLE 1. Hydro-2-propylation with 2-propylazodiphenylmethanol (3)

Substrate	Product	Yield, %	^{1}H nmr (δ, $CDCl_3$)	Mol. wt. (ms)[b]
CH_2=CHCN	$(CH_3)_2CHCH_2CH_2CN$	53(75)[a]	0.91; d, J = 6.5 Hz, 6H 1.42–1.72; m, 3H 2.31; t, J = 7.0 Hz, 2H	97
CH_2=$CHCOCH_3$	$(CH_3)_2CHCH_2CH_2COCH_3$[c,d]	13(11)[a]	0.85; d, J = 6.0 Hz, 6H 1.37–1.58; m, 3H 2.08; s, 3H 2.38; t, J = 7.0 Hz, 2H	114
CH=$CHCOCH_3$ (*trans*)	$(CH_3)_2CHCH(CH_3)CH_2CHO$[e]	35(43)[a]	0.81; d, J = 6.5 Hz, 6H 1.01; d, J = 4.0 Hz, 3H 1.40–2.52; m, 4H 9.69; t, J = 3.0 Hz, 1H	114
CH_2=$CHCO_2CH_3$	$(CH_3)_2CHCH_2CH_2CO_2CH_3$	5(32)[a]	0.77; d, J = 6.0 Hz, 6H 1.34–1.47; m, 3H 2.18; d, J = 7.0 Hz, 2H 3.55; s, 3H	130
CH_2=$C(CH_3)O_2CCH_3$	$(CH_3)_2CHCH_2CH(CH_3)O_2CCH_3$	15(10)[a]	0.85; d, J = 6.5 Hz, 6H 1.15; d, J = 6.5 Hz, 3H 1.24–1.66; m, 3H 1.96; s, 3H 4.78–5.06; m,1H	144
	 [f]	22(0)[a]	0.74; d, J = 7.0 Hz, 6H 0.78–1.46; m,11H 2.10; s, broad, 2H	138
φN=Nφ	φNHN(φ)$CH(CH_3)_2$[g,h]	45	1.07; d, J = 7 Hz, 6H 4.09; sept, J = 7 Hz, 1H 4.98; s, 1H 6.47–7.04; m, 10H	226

[a]The number in parentheses is the yield of crude product from a run with phenol present; one mole per mole of 3.
[b]All the mass spectra also had the expected signal for the 2-propyl cation at *m/e* 43.
[c]The ^{1}H nmr and ir spectra of this product matched those reported (10).
[d]2,4-Dinitrophenylhydrazone, mp 90–91°C (lit. (11), mp 92–93°C).
[e]2,4-Dinitrophenylhydrazone, mp 92°C (lit. (12), mp 93–94°C).
[f]*Exo* geometry based on the stereochemistry of hydromethylation (see text).
[g]Melting point 86–87°C (lit. (13), mp 88.0–88.4°C).
[h]The yield of crude product was nearly quantitative, as judged by the ^{1}H nmr spectrum in the high field region. Isolation losses of this air-sensitive hydrazine were severe.

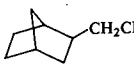
of the competition is olefin dependent in the presence or absence of phenol. There must be at least two counteracting effects of added phenol. First, it ought to lower the yield of RCH_2CH_2Y by capturing R· that would otherwise have added to alkene (eq. [10]). Second, it ought to raise the yield of RCH_2CH_2Y by capturing $RCH_2\dot{C}HY$ that would otherwise have added to alkene in telomerization or polymerization reactions (eq. [14]). Although one might predict that for some CH_2=CHY the yield should drop to zero at high phenol concentrations, because all R·'s get caught by phenol before they can add, one can not readily predict the effects of low phenol concentrations.

The experimentally observed effects are depicted graphically as Figs. 1–4, which show that yield optimization occurs at relatively high phenol concentration (ca 1.0–1.5 *M*). The other trend indicated by the figures is that the yields rise more rapidly with increasing [φOH] before the optimum is reached than they decline after the optimum concentration is exceeded. A qualitative diagram, Fig. 5, illustrates the probable origin of these trends.[6] In Fig. 5, the function A represents the fraction of $RCH_2\dot{C}HY$ that leads to RCH_2CH_2Y. That fraction should level off to a value of unity at high phenol concentrations but it should not go to zero when phenol is absent, because of other H-donors, notably azocarbinol, present. Function B represents, qualitatively, the fraction of R· that adds to alkene. That fraction will not be unity at [φOH] = 0, again because of H-donors like azocarbinol present in the medium, and it ought to go to zero at high [φOH]. The yield of RCH_2CH_2Y, expressed as a fraction, is the product of the fractions represented by curves A and B at a given [φOH]. Curve C, the yield curve,

[6]Quantitative analysis of the yield data could lead to values of ratios of rate constants and of rate constants themselves. Additional data will have to be gathered before that is attempted.

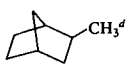
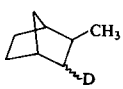
Can. J. Chem. Downloaded from www.nrcresearchpress.com by 210.87.254.40 on 09/05/12
For personal use only.

TABLE 2. Hydroethylation with ethylazodiphenylmethanol (4)

Substrate	Product	Yield, %[a]	^{1}H nmr (δ, $CDCl_3$)
CH_2=CHCN	$CH_3(CH_2)_3CN$	37(55)	0.83–1.13; m, 3H 1.37–1.90; m, 4H 2.20–2.43; m, 2H
CH_3CH=CHCHO	$CH_3CH_2CH(CH_3)CH_2CHO$[b]	34(42)	0.90; t, J = 7 Hz, 3H 0.96; d, J = 7 Hz, 3H 1.18–1.50; m, 2H 1.83–2.16; m, 1H 2.16–2.54; m, 2H 9.74; t, J = 2 Hz, 1H
CH_2=$CHCO_2CH_3$	$CH_3(CH_2)_3CO_2CH_3$[c,d]	5(13)	0.82–0.99; m, 3H 1.17–1.77; m, 4H 2.24–2.35; m, 2H 3.60; s, 3H
CH_2=$C(CH_3)O_2CCH_3$	$CH_3(CH_2)_2CH(CH_3)O_2CCH_3$[e]	9(7)	0.84–0.98; m, 3H 1.20; d, J = 7 Hz, 3H 1.30–1.63; m, 4H 2.00; s, 3H 4.82–5.01; m, 1H
		35(6)	0.74–1.51; m, 14H 1.95; m, 1H 2.16; m, 1H
φN=Nφ	φNHN(φ)CH_2CH_3[h]	23[i]	1.23; t, J = 7 Hz, 3H 3.56; q, J = 7 Hz, 2H 5.40; s, 1H 5.57–7.25; m, 10H

[a]The numbers in parentheses are yields of crude product, estimated by ^{1}H nmr spectroscopy, from a run with phenol present; one mole per mole of 4.
[b]The 2,4-dinitrophenylhydrazone melted at 93–94°C (lit. (14) mp 93.5–94.5°C). The ir and ^{1}H nmr spectra agree well with those reported in the literature (ref. 10, ^{1}H nmr #3696, ir #20785).
[c]The ^{1}H nmr and ir spectra (ref. 10, ^{1}H nmr #8096, ir #24944) in good agreement with those found in the present study.
[d]Molecular weight by mass spectrometry, 116, as required for $C_6H_{12}O_2$.
[e]Mass spectrometric molecular weight 130. Required for $C_7H_{14}O_2$, 130.
[f]Mass spectrometric molecular weight 124, as required.
[g]*Exo* geometry assigned on the basis of the stereochemistry of hydromethylation.
[h]Melting point 40–41°C (lit. (15), mp 38–40°C).
[i]The yield of crude product was quantitative, as judged by the ^{1}H nmr spectrum which showed only product signals in the high field region. Losses incurred during isolation are probably caused by air oxidation.

TABLE 3. Hydromethylation and deuteriomethylation with methylazodiphenylmethanol (5) and with methylazodiphenylmethanol-OD

Substrate	Product	Yield, %	^{1}H nmr (δ, $CDCl_3$)
CH_2=CHCN	$CH_3CH_2CH_2CN$[a]	32(52)[b]	1.09; t, J = 7 Hz, 3H 1.45–1.90; m, 2H 2.38; t, J = 7 Hz, 2H
CH=$C(CH_3)O_2CCH_3$	$CH_3CH_2CH(CH_3)O_2CCH_3$[c]	13	0.90; t, J = 7 Hz, 3H 1.22; d, J = 7 Hz, 3H 1.37–1.70; m, 2H 2.03; s, 3H 4.67–5.00; m, 1H
		59	0.80–1.53; m, 12H 1.83; m, 1H 2.16; m, 1H
		50	[e]
φN=Nφ	φNHN(φ)CH_3	27	3.10; s, 3H 5.23; s, 1H 6.53–7.25; m, 10H

[a]The ^{1}H nmr and ir spectra for this product agreed with published spectra (ref. 10 ^{1}H nmr #33, ir#261).
[b]The yield in parentheses is that for formation of crude product from a run in which phenol was present; one mole phenol per mole of 5.
[c]The ^{1}H nmr and ir spectra is in agreement with those published (ref. 10, ^{1}H nmr #6787, ir #5250).
[d]The ^{13}C nmr ($CDCl_3$) δ: 43.04(C-1), 36.41(C-2), 39.89(C-3),36.99(C-4), 30.07(C-5), 28.77(C-6), 34.82(C-7), 22.37(CH_3). The agreement of these values with those reported for *exo*-2-methylnorbornane (16) confirms the gross structure and the *exo* stereochemistry of our product.
[e]Deuterium content by ms, >87%. The ^{1}H nmr spectrum was qualitatively the same as that of the unlabelled compound. From the ^{2}H nmr spectrum the isomer ratio was 4:1, which was interpreted as 80% *exo*- and 20% *endo*- deuterio products (see text).

Can. J. Chem. Downloaded from www.nrcresearchpress.com by 210.87.254.40 on 09/05/12
For personal use only.

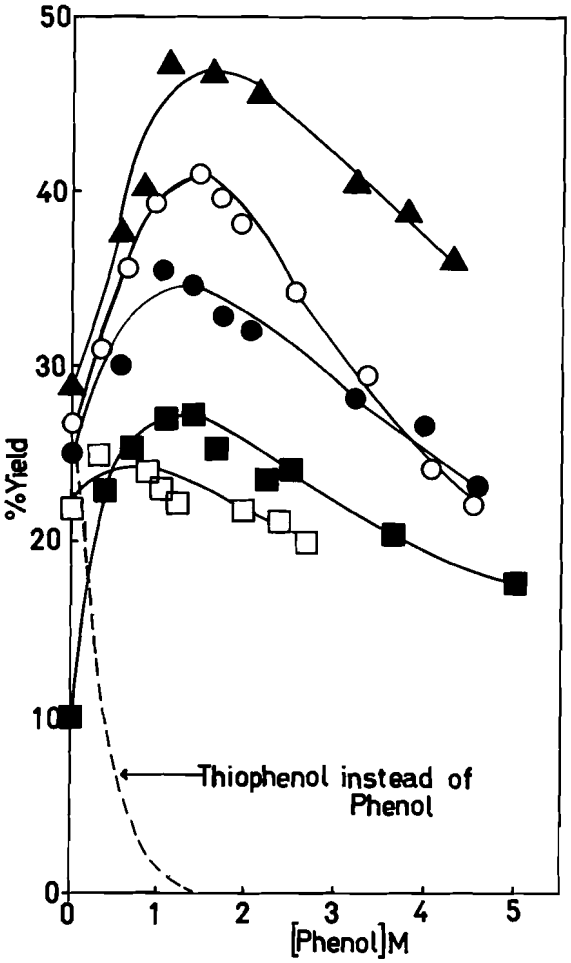


FIG. 1. Optimization of yield of adduct from 3 and crotonaldehyde. Crotonaldehyde concentrations (M, initial): △ 1.978, ○ 1.394, ● 3.484, ■ 0.348, □ 6.484, --- 1.394.

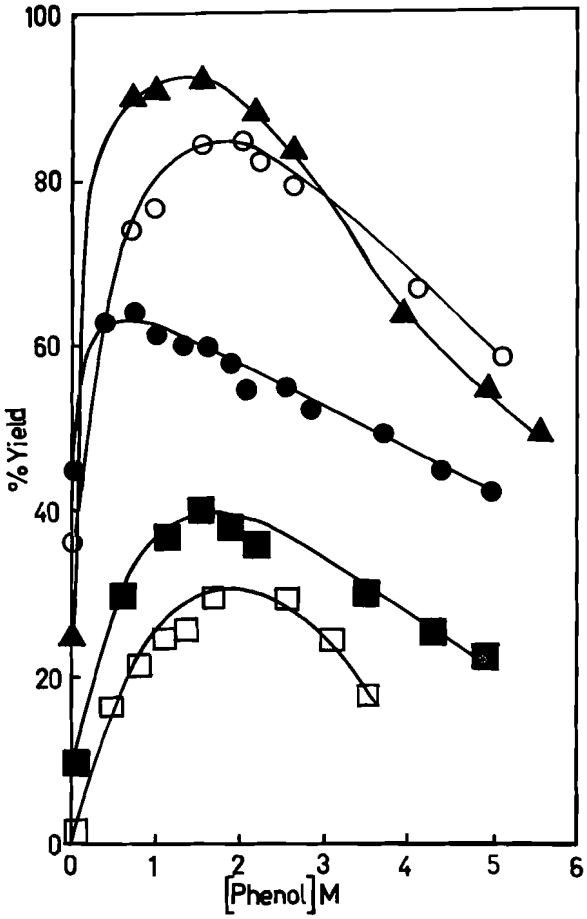


FIG. 2. Optimization of yield of adduct from 3 and acrylonitrile. Acrylonitrile concentrations (M, initial): ▲ 1.394, ○ 1.978, ● 0.348, ■ 3.484, □ 6.948.

was generated by multiplying points at corresponding [φOH] on curves A and B. From curves A and B, which were generated with the top curve of Fig. 1 as model, it follows that the rising part of the yield curve C represents a composite of two rapidly changing functions, operating in opposite senses, whereas the descending part represents a composite of one such function and a constant. Thus the general shape of the optimization curves in Figs. 1 and 2 appears to be accounted for satisfactorily.

The effect of added thiophenol (Fig. 1) can also be understood in terms of Fig. 5. Since thiophenol is much better than phenol as a H-donor to radicals,[7] the sloped portions of curves A and B should be much steeper than they are for the case of phenol. Thus the yield of RCH_2CH_2Y will be the product of unity and zero at relatively low [φSH] and a maximum, if any, at still lower [φSH] is not detectable.

Figure 2 shows the results of optimization experiments for hydro-2-propylation of acrylonitrile with 3. The yield curves are similar to those for addition to crotonaldehyde, with some notable differences. For instance, the maximum yield in the crotonaldehyde case is obtained with ca. 2 *M* crotonaldehyde and 1.5 *M* phenol. Lower or higher aldehyde concentrations lead to significant drops with roughly equal values at either 6.5 *M* or 0.35 *M* initial concentrations. In the acrylonitrile case the best yield is that for ca. 1.4 *M* substrate and 1.0 *M* phenol and the effects of going to higher substrate concentrations are more severe. There is also a discernible shift of the yield maxima, to higher phenol concentration, with increasing substrate concentration. Figure 3 illustrates the differences

[7]The chain transfer constant for 1-butanethiol is larger by a factor near 10^5 than that for phenol, toward polystyryl radicals (22). The analogous factor, toward polyvinylacetate radicals, is about 10^2 (22). Thiophenol is probably a chain transfer agent at least as good as butanethiol, in view of resonance stabilization, albeit little, in the phenylthiyl radical.

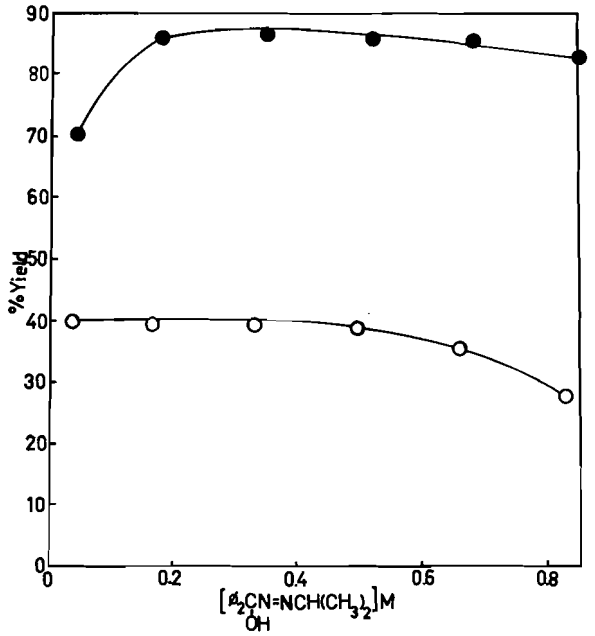


FIG. 3. Dependence of yield of adducts from **3** and olefinic substrates on initial concentration of **3**. Initial concentrations of phenol and substrate: ● [Phenol] = 0.712 M, [Acrylonitrile] = 1.445 M; ○ [Phenol] = 0.697 M, [Crotonaldehyde] = 1.396 M.

between the crotonaldehyde and acrylonitrile systems in the absence of phenol. That figure shows the points lying on the vertical axes of Figs. 1 and 2, plotted against substrate concentration at constant initial concentration of **3**. At low substrate concentration acrylonitrile gives the better yield while at high substrate concentration the reverse is true. The trends in Figs. 1, 2, and 3 are undoubtedly complex in origin, since it is likely that the two substrates are rather similar in their reactivities toward radicals.[8] Presumably the corresponding radical adducts have different k_p/k_{abstr} ratios for the two curves of Fig. 3 to cross.

Hydromethylation of norbornene occurs in the sense expected for radical (or polar) addition to that substrate. A large preference for initial *exo* attack is well known (22) and the tendency for overall *syn* addition by a radical mechanism has been accounted for in terms of steric effects (23). Our assignment of *exo* geometry for the methyl group in the hydromethylation and deuteromethylation products (Table 3) is based on the ^{13}C nmr spectra (16). Assignment of the location of deuterium, 80% *exo* and 20% *endo*, is based on the above mentioned

[8]For addition of CF_3 radicals the reactivity ratio, $k(CH_2{=}CHCN)/k(CH_2{=}CHCOCH_3)$ is about 0.13 (21). Although these are not ideal models for the additions in question, it is unlikely that acrylonitrile and crotonaldehyde are very different in their reactivities toward the 2-propyl radical.

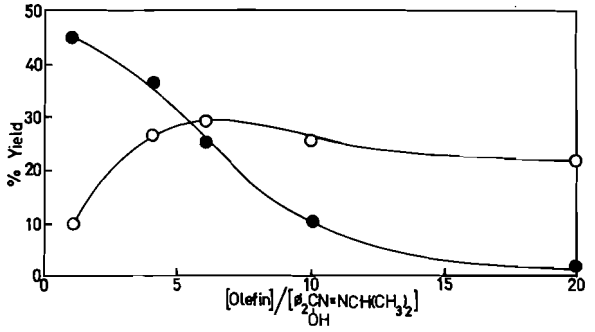


FIG. 4. Dependence of yield of adducts from **3** and olefinic substrates on the feed ratio. Substrates: ● acrylonitrile, ○ crotonaldehyde.

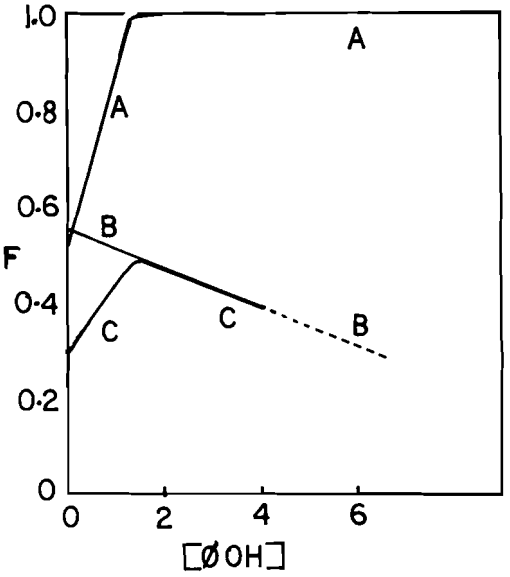


FIG. 5. Scenario for the variation with phenol concentration of: the fraction (F) of $RCH_2\dot{C}HY$ that becomes RCH_2CH_2Y, curve A; the fraction (F) of R· that becomes $RCH_2\dot{C}HY$, curve B; the fraction (F) of R· that becomes RCH_2CH_2Y, curve C. The latter is generated by taking the product of corresponding F-values on curves A and B; see text.

preferences for *syn* (*exo*, *exo*) addition of other addends. Although the generality of hydroxyl deuterium transfer to carbon has not been demonstrated with the one example cited, it is hard to imagine that it might fail entirely because of the expected isotope effect in the chain transfer step. Thus, hydroxydiazenes appear to be attractive reagents for deuteroalkylation of olefinic substrates.

In keeping with our earlier finding (3) azobenzene hydroalkylates much more efficiently than do olefinic substrates. Yields of raw product are nearly quantitative in some cases but losses incurred during separation of the sensitive 1-alkyl-1,2-diphenylhydrazines from excess azobenzene and

Can. J. Chem. Downloaded from www.nrcresearchpress.com by 210.87.254.40 on 09/05/12
For personal use only.

from benzophenone are substantial. The high efficiency of addition to azobenzene must mean that the rate constant for addition to form a resonance stabilized hydrazyl radical (24) is very much larger than that for abstraction of H from hydroxydiazene by R·. It is interesting that the hydrazyl radicals apparently abstract readily from the hydroxydiazene, suggesting again that the abstraction is concerted with other bond-breaking processes, for such a hydrazyl should be incapable of abstracting hydroxyl H from a simple alcohol.

In summary, the additions reported are potentially useful for the synthesis of ^{2}H- or ^{3}H-labelled and unlabelled small molecules. The radical chain mechanism used as a basis for discussion is a proposal which, although it appears to fit the observations, must still be regarded as tentative.[9]

Acknowledgement

We thank the Natural Sciences and Engineering Research Council of Canada (N.S.E.R.C.) for financial support.

1. P. KNITTEL and J. WARKENTIN. Can. J. Chem. **54**, 1341 (1976).
2. D. W. K. YEUNG and J. WARKENTIN. Can. J. Chem. **54**, 1345 (1976).
3. D. W. K. YEUNG and J. WARKENTIN. Can. J. Chem. **54**, 1349 (1976).
4. P. KNITTEL and J. WARKENTIN. Can. J. Chem. **54**, 1349 (1976).
5. P. KNITTEL and J. WARKENTIN. Can. J. Chem. **53**, 2275 (1975).
6. G. H. COLEMAN, H. GILMAN, C. E. ADAMS, and P. E. PRATT. J. Org. Chem. **3**, 99 (1938).
7. R. CRIEGEE and G. LOHAUS. Chem. Ber. **84**, 219 (1951).
8. M. SCHULZ, U. MISSOL, and H. BOHM. Z. Chem. **13**, 253 (1973); J. Prakt. Chem. **36**, 47 (1974).
9. D. C. IFFLAND, L. SALISBURY, and W. R. SCHAFER. J. Am. Chem. Soc. **83**, 747 (1961).
10. The Sadtler Standard Spectra. Sadtler research laboratories, Philadelphia, PA. ^{1}H nmr #5997, ir #17523.
11. M-C. CHIANG. J. Chin. Chem. Soc. Peking, **18**, 65 (1951).
12. E. I. KLIMOVA, E. G. TRESHCHOVA, and Y. A. ARBUZOV. Dokl. Akad. Nauk SSSR, **180**, 865 (1968).
13. J. W. B. REESOR and G. F. WRIGHT. J. Org. Chem. **22**, 375 (1957).
14. H. BRUNNER and E. H. FARMER. J. Chem. Soc. 1039 (1937).
15. K. BERG-NIELSEN and E. BERNATEK. Acta Chem. Scand. **26**, 4130 (1972).
16. J. B. STOTHERS, C. T. TAU, and K. C. TEO. Can. J. Chem. **51**, 2893 (1973).
17. C. WALLING, L. HEATON, and D. D. TANNER. J. Am. Chem. Soc. **87**, 1715 (1965).
18. K. R. KOPECKY and G. EVANI. Can. J. Chem. **47**, 4049 (1969).
19. W. A. PRYOR. Free radicals. McGraw-Hill, New York, NY. 1966. pp. 119–124, 180–188; W. A. PRYOR and T.-L. HUANG. Macromolecules, **3**, 500 (1970); W. A. PRYOR, J. H. COCO, W. H. DALY, and L. D. LASSWELL. Adv. Free-Radical Chem. **5**, 27 (1975); W. A. PRYOR, M. IINO, and G. R. NEWKOME. J. Am. Chem. Soc. **99**, 6003 (1977).
20. C. M. STARKS. Free radical telomerization. Academic Press, New York, NY. 1974. Tables 2.1 and 7.5, pp. 10 and 169, respectively.
21. H. C. LOW, J. M. TEDDER, and J. C. WALTON. Int. J. Chem. Kinet. **10**, 325 (1978).
22. T. G. TRAYLOR. Acc. Chem. Res. **2**, 152 (1969).
23. P. I. ABELL. *In* Free radicals. Vol. 2. *Edited by* J. K. Kochi. Wiley-Interscience, New York, NY. 1973. pp. 67, 73.
24. S. F. NELSEN. Free radicals. Vol. 2. *Edited by* J. K. Kochi. Wiley-Interscience, New York, NY. 1973. pp. 557–559.
25. S. HÜNIG and J. CRAMER. Angew. Chem. Int. Ed. Engl. **7**, 943 (1968); S. HÜNIG and G. BÜTTNER. Angew. Chem. Int. Ed. Engl. **8**, 451 (1969); G. BÜTTNER and S. HÜNIG. Chem. Ber. **104**, 1088 (1971); Chem. Ber. **104**, 1104 (1971); B. BÜTTNER, J. CRAMER, L. GELDERN, and S. HÜNIG. Chem. Ber. **104**, 1118 (1971).
26. E. SCHMITZ, R. OHME, and S. SCHRAMM. Angew. Chem. Int. Ed. Engl. **2**, 157 (1963); Justus Liebigs Ann. Chem. **702**, 131 (1967).
27. M. SCHULZ and U. MISSOL. Z. Chem. **14**, 265 (1974).

[9]An alternative mechanism, involving fragmentation of hydroxydiazene to ketone and alkyldiazene, $R_1R_2C(OH)N_2R_3 \rightleftarrows R_1R_2CO + HN_2R_3$, with the latter responsible for the hydroalkylation observed, must be considered. There is evidence for that process occurring, particularly under acidic or basic conditions but also under nominally neutral conditions (25–27). Preliminary experiments designed to test for the alkyldiazene pathway suggest that it is not general under our conditions although it could be a competitive mechanism.

Can. J. Chem. Downloaded from www.nrcresearchpress.com by 210.87.254.40 on 09/05/12
For personal use only.

Canadian Journal of Chemistry
Published by
THE NATIONAL RESEARCH COUNCIL OF CANADA

Journal canadien de chimie
Publié par
LE CONSEIL NATIONAL DE RECHERCHES DU CANADA

Volume 58 Number 23 December 1, 1980 Volume 58 numéro 23 1 décembre 1980

Can. J. Chem. Downloaded from www.nrcresearchpress.com by 210.87.254.40 on 09/05/12
For personal use only.

Muonium atoms observed in liquid hydrocarbons

YASUO ITO,[1] BILL W. NG, YAN-CHING JEAN,[2] AND DAVID C. WALKER
Chemistry Department and TRIUMF,[3] University of British Columbia, Vancouver, B.C., Canada V6T 1Y6

Received July 3, 1980

YASUO ITO, BILL W. NG, YAN-CHING JEAN, and DAVID C. WALKER. Can. J. Chem. **58**, 2395 (1980).

Muonium atoms have been observed in *n*-hexane, *c*-hexane, and tetramethylsilane at 295 or 273 K by the MSR technique. The yield of muonium in these non-polar liquids is found to be quite comparable to that observed previously in water, methanol, and ethanol. This suggests that neither the dielectric constant of the medium nor the free-electron mobility has a major influence on the formation process. This in turn supports the view that muonium formation does not mainly result from intraspur reactions in the terminal spur of the muon's track.

The chemical lifetime of muonium in these hydrocarbons is curtailed by spurious impurities so that high purity is required. In addition, however, there may be a chemical reaction between muonium and the hydrocarbon itself because the maximum lifetime found increases in the order of increasing bond energy. Reaction rate constants with added solutes have also been measured, and these observations open up the possibility of studying hydrophobic solutes and extending hydrogen-isotope studies to biologically-important media.

YASUO ITO, BILL W. NG, YAN-CHING JEAN et DAVID C. WALKER. Can. J. Chem. **58**, 2395 (1980).

On a observé des atomes de muonium dans le *n*-hexane, le *c*-hexane et dans le tétraméthylsilane à 295 ou 273 K par la technique de RSM. On a trouvé que le rendement en muonium dans ces liquides non polaires est tout à fait comparable à celui observé antérieurement dans l'eau, le méthanol et l'éthanol. Ceci suggère que ni la constante diélectrique du milieu ni la mobilité des électrons libres n'a d'influence sur la formation des muonium. Cette conclusion appuie le fait que la formation des muonium ne provient pas principalement de réactions à l'intérieur de la dernière cavité de la trajection du muon.

La présence d'impuretés parasites diminue la durée de vie du muonium dans ces hydrocarbures; il faut donc opérer avec des solvants d'une très grande pureté. De plus, il semble qu'une réaction chimique se produit entre le muonium et l'hydrocarbure puisqu'on a trouvé que la durée maximale de vie augmente avec l'énergie de liaison. On a mesuré également les constantes de vitesse en présence de solutés; ces observations ouvrent la possibilité d'étudier des solutés hydrophobes et d'étendre les études d'effets isotopiques de l'hydrogène aux milieux biologiquement importants.

[Traduit par le journal]

Introduction

The atom formed when a positive muon acquires an orbital electron is called muonium[4] and was first identified when energetic muons were stopped in gases (1). Although studied for more than a decade in gases and solids (2), only recently was the same species observed through its characteristic spin precession frequency of 1.4 MHz G^{-1} in a pure liquid, initially in water (3). It has subsequently been detected in methanol and ethanol at 295 K (4, 5) and in ether at ~162 K (6).

Muonium atoms (symbolized by Mu) are relatively short-lived due to the intrinsic lifetime of the muon which decays to a positron and two neutrinos with a mean lifetime of 2.2 μs. In the presence of reactive solutes the chemical existence of free Mu may be reduced further by reaction, and the chemical rate constant can be determined. In pure liquids there is also a spontaneous spin relaxation process of unknown origin characterized by the decay constant λ_0 (see later). This is significantly larger in neat alcohols than it is in water.

Muonium is of considerable interest from at least

[1]On leave from: Research Center for Nuclear Science and Engineering, University of Tokyo, Tokyo, Japan.

[2]Present address: Physics Department, University of Missouri, Kansas City, MO.

[3]TRIUMF stands for Tri University Meson Facility on the campus of the University of British Columbia.

[4]It should, more properly, have been called muium (despite the less mellifluous sound) in conformity with protium, deuterium, and tritium, because the suffix "onium" generally refers to species formed when a particle combines with its antiparticle, as in positronium and charmonium (though hydronium is an oddity).

0008-4042/80/232395-07$01.00/0
©1980 National Research Council of Canada/Conseil national de recherches du Canada

Can. J. Chem. Downloaded from www.nrcresearchpress.com by 210.87.254.40 on 09/05/12
For personal use only.

four points of view (2, 7). First, there is interest in the intrinsic properties and mode of formation of this unusual chemical species. Second, it can be used as a nuclear spin probe for radicals. Third, since Mu has essentially the same ionization energy and Bohr radius as a hydrogen atom, but 1/9th its mass, it is regarded as a super-light isotope of protium, deuterium, and tritium, and can be used as a sensitive probe of mass-dependent kinetic isotope effects. Fourth, since Mu is readily identified and monitored by single event nuclear physics counting techniques, it can be used as a handle on H-atom reactions which are not otherwise accessible to direct observation by conventional methods.

For these reasons its study has been intensely pursued during the past three years. For liquid phase studies most of this work has been in aqueous solution, but there is interest in trying to determine the reactivity of Mu in non-polar, hydrocarbon media. Of particular relevance to our own studies on micelles (8) is the reaction rate constant towards solutes held in the hydrocarbon centre of the micelle.

Experimental

Muonium is studied by the muon and muonium spin rotation methods (μSR and MSR) which have been described in detail elsewhere (2, 7, 9). Longitudinally spin-polarized muons from pion decays are made to impinge on a chemical sample where they come to rest and become incorporated in several different possible chemical states: either in diamagnetic states, or as free Mu atoms, or in free radicals (10). In the present experiments the 4.1 MeV "surface" μ^+ beam of the M20 channel at TRIUMF was used. The liquid samples were contained in Teflon cells having thin Mylar windows, as before (11). The sample cell was placed inside a pair of Helmholtz coils which provided a transverse magnetic field of 9.3 G for MSR and 80 G for μSR measurements.

In a typical experiment one obtains a time histogram of the MSR signal which is fitted by χ^2-minimization to eq. [1] (2, 7).

$$[1] \quad N = N_0 \exp(-t/\tau_\mu)[1 + A_\mu \cos(\omega_\mu t + \phi_\mu) + A_M \exp(-\lambda t) \cos(\omega_M t - \phi_M)] + B$$

where N_0 is a normalization factor, B the time-independent background, τ_μ the muon lifetime (2.2 μs), ω_μ and ω_M the muon and Mu spin-precession frequencies in the magnetic field, ϕ_μ and ϕ_M are the initial phases of these precessions, A_μ and A_M are the asymmetries of diamagnetic and muonium species, and λ is the muonium decay constant. The last three parameters are those of interest in the present study. All muons appear in diamagnetic states in CCl_4 (2, 7), therefore A_μ in CCl_4 is used as the 100% asymmetry reading (A_0). Thus the fraction of muons forming diamagnetic states (P_D) equals A_μ/A_0, and the fraction forming muonium (P_M) equals $2A_M/A_0$; the 2 arising from the fact that only half of the total muonium atoms have parallel electron and muon spins and are observable. In addition, λ is interpreted as a chemical rate constant (k_M) in the presence of a reactive solute at concentration [S] by application of eq. [2],

$$[2] \quad \lambda = \lambda_0 + k_M[S]$$

where λ_0 is the relaxation rate constant observed in the neat solvent (4, 7).

Oxygen had to be removed from the samples by continuous bubbling with helium gas throughout an experiment (12). In order to avoid excessive evaporation of either solvent or solute, the gas was passed through a prebubbler containing the same material, and to avoid back diffusion of O_2 a bubbler was also used on the gas line after the cell. The solvents studied were of reagent or spectroscopic grade to start with, but they were each further purified by collecting the middle fraction from a simple distillation column. In the case of *n*-hexane, cyclohexane, and tetramethylsilane (TMS), an attempt was made to reduce the concentration of unsaturated impurities by prior treatment of the starting materials with H_2SO_4, then washing with H_2O and drying over zeolite-4A before distillation. In the case of eicosane ($C_{20}H_{42}$), which is solid at 25°C, the material was deoxygenated by bubbling with He at ~50°C (where it is liquid) and then thermosealed in a polyethylene bag which then acted as the target cell. For dilute solutions of cyclohexane in methanol, methanol in water, and phenol in *n*-hexane the same solution was used in the prebubbler so that the solute concentration should not change during the course of the experiment because the gas should contain the equilibrium admixture of solution vapours before reaching the cell. All data reported were obtained from experiments conducted at ~295 K and 273 K.

Results

Typical time-histograms of the spin polarization are shown in Figs. 1, 2, and 3. The lines are the computer fits of the data to eq. [1] with the muon's exponential decay ($e^{-t/\tau}$) and the background (B) already removed. These MSR data were obtained in the low transverse magnetic field (9.3 G) and produce information on muonium signals precessing at the higher frequency. Thus the amplitude of the initial asymmetry is converted to P_M (as described in the Experimental section) and its decay is given as a decay constant λ. P_D values were obtained from the same solutions, but in separate μSR experiments conducted at higher field (80 G) in order to obtain good fits for the lower frequency precessions. In all cases two independent spectra were obtained, one from each of the positron telescopes. Figs. 1, 2, and 3 show the right-hand side spectra only but the data reported in Table 1 are the arithmetic means from the two detectors.

Figure 1*a* shows the histogram for water containing 20% methanol. The muonium asymmetry signal is seen to be relatively long-lived, falling to half magnitude in about 2 μs (in pure water the mean lifetime is normally 4 μs). By comparison the signal in neat methanol (Fig. 1*b*) is much shorter-lived, being ~0.4 μs and the fitting to eq. [1] is correspondingly less exact. Figure 2 shows the fitted histograms for purified TMS at 273 K and *n*-hexane at 295 K where the muonium lifetimes are ~1.5 and and ~1.0 μs respectively. For purified cyclohexane (not shown) at 295 K the lifetime of Mu is smaller but the asymmetry fit is good. However, in eicosane the fit is too poor to report, probably because of the presence of too much O_2 trapped in this solid hydrocarbon.

Can. J. Chem. Downloaded from www.nrcresearchpress.com by 210.87.254.40 on 09/05/12
For personal use only.

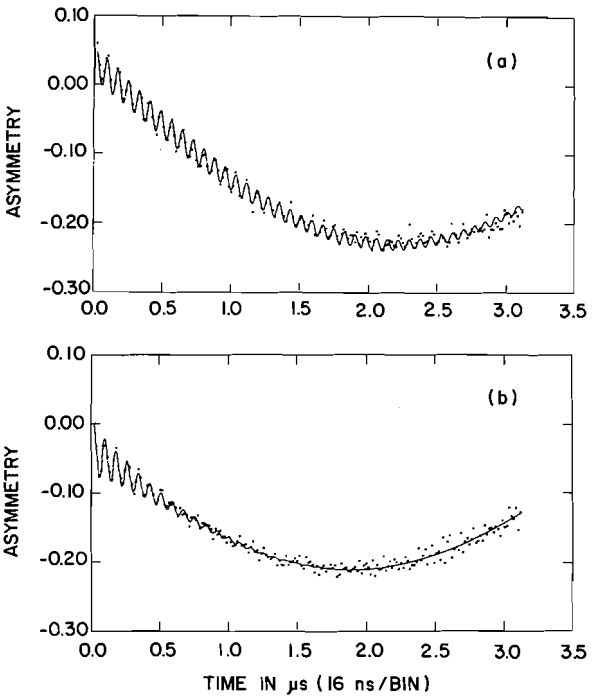


FIG. 1. MSR data and computer fits to eq. [1] for: (*a*) 20% by volume methanol in water; (*b*) purified methanol. The much faster decay of the muonium signal (higher frequency precession) in (*b*) compared to (*a*) is readily seen.

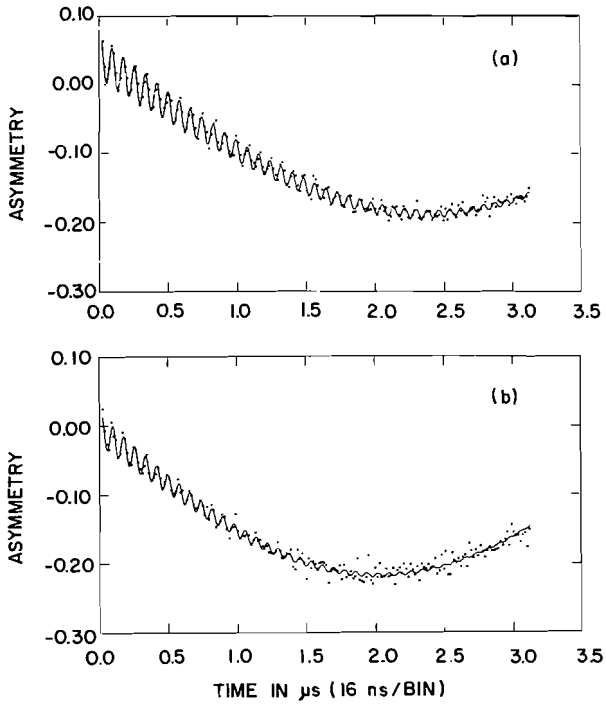


FIG. 2. MSR data and computer fits to eq. [1] for: (*a*) purified tetramethylsilane (TMS); and (*b*) purified *n*-hexane.

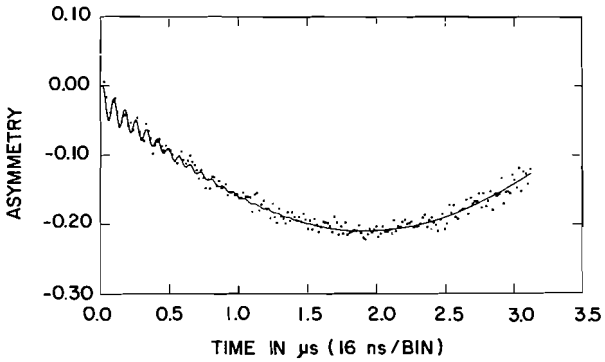


FIG. 3. MSR data and computer fit to eq. [1] for 1.9×10^{-4} *M* phenol in *n*-hexane.

The overall results are presented in Table 1, where the values obtained for P_D, P_M, P_L ($= 1 - P_D - P_M$), and λ are given for *n*-hexane, cyclohexane, TMS, methanol, and water. Data have previously been obtained for methanol (4, 5) and water (3, 11) and the means of the published values are given in Table 1 for comparison purposes. P_D values for all these liquids have been reported before as hot fractions (7).

During the course of these experiments several samples of each liquid were studied following different purification procedures and with different rates of bubbling by helium gas in the reaction cells. It became clear that both inherent impurities (probably carbonyl compounds and unsaturated hydrocarbons) as well as traces of O_2 in the liquids contributed to the muonium decay in all cases except water. O_2 is about 100-fold more soluble in the organic solvents than it is in water, and it probably diffuses into the cell because grease cannot be used at the pressure points between Teflon and Mylar in the cell construction when organic liquids are to be studied. Thus it was found that λ generally decreased somewhat when the gas bubbling rate was increased.

It should be emphasized, therefore, that the data reported here correspond to the longest-lived muonium signals that we obtained in the respective liquids. This does not affect P_M and P_D (indeed they are also the best "fits"), but it means that the values of λ given should merely be taken as *upper limits* at the moment.

Once the muonium decay constant λ has been determined for a particular sample of liquid it can be used as λ_0 in eq. [2] and the liquid employed as a solvent in the study of reaction rate constants of solutes. The example of phenol in *n*-hexane is shown in Fig. 3 and the result given in Table 2.

Discussion

These are the first reported observations of muonium in hydrocarbons, and the data show that

Can. J. Chem. Downloaded from www.nrcresearchpress.com by 210.87.254.40 on 09/05/12
For personal use only.

TABLE 1. Results obtained for P_D, P_M, P_L, and λ in *n*-hexane, *c*-hexane, tetramethylsilane (TMS), methanol, and water[a,b]

Liquid	P_D	P_M	P_L	$\lambda_0/10^6\ s^{-1}$
n-Hexane	0.65±0.02	0.13±0.02	0.22±0.04	1.0 ±0.5
c-Hexane	0.69±0.02	0.20±0.02	0.11±0.04	1.5 ±0.4
TMS	0.53±0.03	0.21±0.02	0.26±0.04	0.64±0.07
Methanol	0.62±0.01	0.23±0.02	0.15±0.02	2.3 ±0.4 (0.74)[c]
[d]	(0.61)	(0.19)	(0.20)	(0.75)
Water	0.62±0.01	0.20±0.01	0.18±0.01	0.25±0.08
[d]	(0.62)	(0.19)	(0.19)	(0.25)

[a] P_D, P_M, and P_L are the fractions of incident muons which are observed as diamagnetic species, free muonium atoms, or as neither of these ($P_L = 1 - P_D - P_M$), respectively. λ is the observed muonium spin relaxation rate constant.
[b] The values quoted are the mean of the values obtained independently from the left- and right-hand detectors. The error limits given cover the two values and each of their statistical errors only.
[c] Calculated for neat methanol from 20% methanol in water, from Table 2.
[d] Mean values of the data published previously in refs. 3, 4, 5, 11, and 16.

TABLE 2. Results obtained for λ in solutions (plus parameters calculated therefrom)

Composition	λ/s^{-1}	λ_0(solvent)/s^{-1}	$k_M/M^{-1}\ s^{-1}$	Calculated λ_0(solute)/s^{-1}
20% (vol) methanol in water	5.1×10^5	3.6×10^5[a]	3×10^4	0.74×10^6
1.9×10^{-4} *M* phenol in *n*-hexane	2.3×10^6	1.0×10^6	$7(\pm 2) \times 10^9$	—

[a] λ_0 in the sample of water used was considerably larger than is normal in pure water.

the yield of muonium atoms in these non-polar liquids is very similar to that found in water, methanol, and ethanol. In addition the chemical lifetime in highly purified saturated hydrocarbons is found to be comparable to that in water, and probably longer-lived than in aliphatic alcohols.

The main consequences of these findings are two-fold: first, they expand considerably the media and types of reactions in which the MSR technique can be used to study muonium chemistry; and second, they have strong implications concerning the proposed mechanisms by which muonium is formed.

(i) Muonium Reactivity

The origin of λ_0 in water has been discussed (11) but not resolved. There are reasons for believing it is not due to chemical reactions of Mu with either impurities or water itself based on its measured temperature dependence (13). Instead, it may be an artifact arising from the MSR equipment or technique rather than the chemical medium (9, 11). On the other hand, Mu reacts with neat methanol as reported by Percival *et al.* (4, 5) and as seen in Fig. 1. This reaction is probably a hydrogen abstraction reaction, as found with H atoms, but there is a very large inverse kinetic isotope effect (k_M/k_H equal to $\sim 10^{-2}$). Abstraction of hydrogen may also contribute to λ in the neat hydrocarbons studied here. Bearing in mind the fact that these values of λ are only upper limits (see previous section), the reported λ nevertheless increases systematically in the series TMS/*n*-hexane/*c*-hexane, as the $-CH_3$ groups are replaced by $>CH_2$ groups. This is to be expected if H-abstraction reactions contribute to λ since the C—H bond strength of methylene is slightly less than that of methyl.

In addition, the presence of O_2 is important in some solutions. For instance, in neat methanol $\lambda = 2.3 \times 10^6$ (Table 1), whereas from 20% methanol in water (Fig. 1*a*) one obtains $\lambda = 5.1 \times 10^5\ s^{-1}$ corresponding to λ_0 for neat methanol of $0.74 \times 10^6\ s^{-1}$ (Table 2). Since the methanol contains the same impurities in both cases, the difference in λ_0 probably arises from different residual O_2 concentrations. For the 20% solution the O_2 solubility will resemble that of water where the deoxygenation procedure used here has been shown to be adequate (12). That O_2 is involved in neat methanol is corroborated by the data of Percival *et al.* (4) which was obtained using freezing/pumping/thawing cycles to remove O_2 (see Table 1).

An example of the determination of the reaction rate constant of Mu with a solute in a hydrocarbon (for comparison with water) is provided by phenol in hexane as shown in Fig. 3 and Table 2. The value of k_M is found to be $(7 \pm 2) \times 10^9\ M^{-1}\ s^{-1}$ in hexane (Table 3), which is some three-fold faster than k_M for phenol in water (11). This in turn suggests that the enhanced reactivity seen for phenol embedded

TABLE 3. Comparison of P_M and $(1 - P_D)$ with properties of the liquid: (*i*) the fraction of electrons which escape intraspur neutralization in low LET radiolysis[a] (G_{fi}/G_t); (*ii*) the electron mobility (μ)[b]; and (*iii*) the static dielectric constant (ε)

Liquid	P_M	$(1 - P_D)$	G_{fi}/G_t	μ	ε
Water	0.20	0.38	0.62	0.002	78
Methanol	0.23	0.38	0.38	0.0006	33
TMS	0.21	0.47	0.16	100	1.8
c-Hexane	0.20	0.31	0.03	0.4	1.8
n-Hexane	0.13	0.35	0.03	0.08	1.8

[a] G_{fi} is the free ion yield (15) and G_t the total ionization yield taken to be 4.5 (±0.5) in all cases.
[b] μ is in $cm^2\ V^{-1}\ s^{-1}$, data from Allen (16).

in a micelle (8) may be due to the change from water to hydrocarbon as the environment for the reaction, rather than being connected with k_{diff} or with the collision frequency following an encounter.

Even though the origin of λ_0 in the different neat liquids remains unanswered, the empirical values can be used through eq. [2] to determine k_M in media, such as saturated hydrocarbons, in which the chemical lifetime of Mu is at least a few tenths of a microsecond. Thus one can use systems which resemble biologically-important media much more realistically than dilute aqueous solutions do.

(ii) Muonium Formation Mechanism

The values of P_D and P_M correspond to the primary disbursement of muons into diamagnetic states (including free or solvated μ^+, or molecules such as MuH, MuOH, $C_6H_{13}Mu$, etc.) or as free muonium atoms, respectively. To be observed with their spin polarizations precessing in phase, these states must have been formed within about 3×10^{-10} s of the time the energetic incident muon reached thermal energy, and they must still be present by the beginning of the detection period, $\sim 10^{-7}$ s. In all the cases reported here (though not in ice, for instance (4, 5)) there is a fraction of the incident muons, comparable in size to P_M, which does not appear as P_M or P_D. This is the "missing fraction" P_L (3). It may arise because of muon depolarization from either paramagnetic or diamagnetic states prior to $\sim 10^{-7}$ s or because of the initial incorporation of muons in free radicals, some of which have been studied at high fields (10).

The observation of a missing fraction in water when muonium was first identified in liquids (3), lead to the suggestion that some depolarization occurred by intraspur reactions, and thus to a "spur model" for muonium formation (4, 5) based on that for positronium formation (14). According to the spur model, muonium is formed by combination of a thermalized μ^+ with a free electron formed in the terminal spur of the muon's track. The immediate fate of μ^+ (and Mu), and therefore the measured yields of P_D and P_M, according to this model, should depend on both the chemical composition of the medium and those physical properties (such as dielectric constant and electron mobility) which determine the effective size and lifetime of spurs, and on the extent to which intraspur neutralization reactions occur.

However, the fact that P_M, as with P_D and P_L, is found to be nearly the same for both non-polar hydrocarbons and highly polar hydroxylic liquids, strongly suggests that the formation of muonium by intraspur neutralization reactions is not a dominant mechanism. Table 3 indicates how strikingly these data seem contrary to a spur model. It shows that P_M (and $(1 - P_D)$ to take account for possible changes in P_L) are essentially independent of: (*i*) the probability that the solvent positive ions and their concomitant electrons escape neutralization by each other in typical spurs produced in radiolysis by low linear-energy-transfer (LET) radiation; and (*ii*) the mobility of free electrons in the liquid. Thus one sees that P_M and $(1 - P_D)$ are essentially the same in water and in the hexanes, despite the fact that ~62%[5] of the cations in water avoid neutralization in the normal low LET distribution of spur sizes, whereas only ~3% do in the hexanes. Therefore, according to the spur model, P_M in hexane should have been much greater than both P_D in hexane and P_M in water. Both of these are clearly contrary to the results.

It could be argued that the terminal spur is likely to be a very small one, probably a single ion-pair spur. In which case μ^+ would be in competition with one solvent positive ion for the one free electron. The solvent ion has the advantage of always being formed very close to the electron but the muon has a higher mobility (at least prior to solvation), so it is not unreasonable to expect 20 to 40% of the muons to be neutralized — in a medium of a certain dielectric constant. For very short times water and hexane, for instance, have similar dielectric constants (high frequency values), but for times longer than the dielectric relaxation time ($\sim 10^{-11}$ s) they are dramatically different (see Table 3). The probability that an ion and an electron will neutralize when they are separated by distance r is given by eq. [3],

$$[3] \quad P(r) = 1 - \exp(-r_c/r) = 1 - \exp(-q^2/\varepsilon kTr)$$

where r_c is the Onsager critical escape radius (17), corresponding to the distance at which thermal

[5] For water, P_D equals very closely the electron (and ion) escape probability from low LET spurs (both happen to be ~62%). The values for other liquids, however, do not follow this correspondence at all.

Can. J. Chem. Downloaded from www.nrcresearchpress.com by 210.87.254.40 on 09/05/12
For personal use only.

Can. J. Chem. Downloaded from www.nrcresearchpress.com by 210.87.254.40 on 09/05/12
For personal use only.

motion overcomes the coulombic attraction, q is the unit change, ε the dielectric constant, and kT the thermal energy. For water ($\varepsilon = 78$), r_c is a mere 8 Å whereas for hexane $r_c \sim 300$ Å. Consequently, given a normal distribution of electron thermalization distances, a large fraction of ions escape neutralization in single ion-pair spurs in water, whereas only a very small fraction do in hexane. So the overall probability of Mu formation in hexane should be very much greater than in water, even if the formation occurs in small spurs.

It should also be noted that the spur model, as originally proposed to account for the inhibition of muonium depolarization by the presence of NO_3^- (4, 5), requires a large fraction of *sequential* intraspur encounters (μ^+ combining with e^- to form Mu followed by Mu encountering a further paramagnetic species). Sequential intraspur encounters are virtually impossible in a single ion-pair spur: they require either large spurs or overlapping spurs in a high LET track.

The probability of an ion being neutralized in a spur, and the time-scale over which it occurs, depend on the dielectric constant, the mean electron thermalization distance and the electron mobility. The latter property varies by more than five orders-of-magnitude for the liquids studied here (see Table 3). Mobility does not change simply according to the solvation energy but is exceptionally high for TMS which is a nearly-spherical molecule (18). This confers on the electrons in TMS a higher escape probability and shorter spur lifetime.

Recently there has been a suggestion (19) that the lifetime for muonium formation must be less than the solvation time of μ^+, otherwise μ^+ will be incorporated in a diamagnetic molecule. It was pointed out, however, that "radiation-chemical" intraspur neutralization reactions do not cease upon solvation of the ions and electrons (20, 21). In fact, the ease with which the neutralization energy is dissipated may well require some degree of solvation by at least one of the charged species involved. It is the dramatically different solvating powers of water and hexane which, again, put these two solvents on totally different planes as media for simple thermal neutralization reactions.

On the other hand, in the alternative model — the "hot model" — an epithermal muonium atom either forms a diamagnetic state (by abstracting a H atom, for instance) or is thermalized as Mu. The relative yields of P_D and P_M therefore depend primarily on the *chemical* composition and bonding rather than on physical properties: so they may well be similar for all saturated hydrogenated molecules, such as the hexanes, alcohols, and water.

This conclusion is further corroborated by the fact that an external electric field of 20 kV cm^{-1} had no effect on P_D in all the hydrocarbons studied so far (22).

Finally, one should examine why the spur model seems to have some support with respect to positronium formation (14, 23) yet is contradictory to the general points discussed herein, and to specific scavenger studies in water (20), with respect to muonium formation. There are three important differences between muons and positrons which will contribute to the end-of-tract events. First, as noted previously (21), the ionization energies of positronium and muonium are, respectively, less than and greater than the ionization energy of the molecules constituting the common liquids discussed here. Therefore, only in the case of the positron is there a gap in the kinetic energy below which it cannot undergo charge-exchange with the medium. Second, the linear-energy-transfer during the last few hundreds of eV of energy of the positron is thought to be some two orders-of-magnitude larger than that of the muon (24). The concept of a particle creating a sizable spur with its last 100 eV, or so, of energy is, therefore, much more reasonable for the positron than it is for the muon. Third, because of its much smaller mass, the thermalizing positron is more likely to be back-scattered, or to move under the influence of the Coulombic field, or to tunnel back into its track of radiation-produced free electrons.

Acknowledgments

We gladly acknowledge the collaboration and experimental assistance of members of the μSR group at TRIUMF, particularly J. H. Brewer, D. G. Fleming, D. M. Garner, and T. Suzuki; and help with some of the experiments by T. Q. Nguyen. This work was made possible by grants from the Natural Sciences and Engineering Research Council of Canada.

1. R. M. Mobley, J. M. Bailey, W. E. Cleland, V. W. Hughes, and J. E. Rothberg. J. Chem. Phys. **44**, 4354 (1966).
2. (*a*) J. H. Brewer, K. M. Crowe, F. N. Gygax, and A. Schenck. *In* Muon physics. *Edited by* V. W. Hughes and C. S. Wu. Academic Press, New York. 1975. p. 1; (*b*) J. H. Brewer and K. M. Crowe. Ann. Rev. Nucl. Part. Sci. **28**, 239 (1978).
3. P. W. Percival, H. Fischer, M. Camani, F. N. Gygax, W. Ruegg, A. Schenck, H. Schilling, and H. Graf. Chem. Phys. Lett. **39**, 333 (1976).
4. P. W. Percival, E. Roduner, and H. Fischer. *In* Positronium and muonium chemistry. *Edited by* H. J. Ache. Adv. Chem. Ser. 175. Am. Chem. Soc. 1979. p. 335.
5. P. W. Percival, E. Roduner, and H. Fischer. Chem. Phys. **32**, 353 (1978).
6. P. W. Percival. Private communication.

7. D. G. FLEMING, D. M. GARNER, L. C. VAZ, D. C. WALKER, J. H. BREWER, and K. M. CROWE. *In* Positronium and muonium chemistry. *Edited by* H. J. Ache. Adv. Chem. Ser. 175. Am. Chem. Soc. 1979. p. 279.
8. Y. C. JEAN, B. W. NG, Y. ITO, T. Q. NGUYEN, and D. C. WALKER. To be published.
9. D. M. GARNER. Ph.D. thesis, University of British Columbia, Vancouver, B.C. 1979.
10. E. RODUNER, P. W. PERCIVAL, D. G. FLEMING, J. HOCHMANN, and H. FISCHER. Chem. Phys. Lett. **57**, 37 (1978).
11. Y. C. JEAN, J. H. BREWER, D. G. FLEMING, D. M. GARNER, R. J. MIKULA, L. C. VAZ, and D. C. WALKER. Chem. Phys. Lett. **57**, 293 (1978).
12. Y. C. JEAN, D. G. FLEMING, B. W. NG, and D. C. WALKER. Chem. Phys. Lett. **66**, 187 (1979).
13. B. W. NG, Y. C. JEAN, Y. ITO, T. SUZUKI, and D. C. WALKER. J. Phys. Chem. To be published.
14. O. E. MÖGENSEN. J. Chem. Phys. **60**, 998 (1974).
15. A. O. ALLEN. NSRDS-NBS 57 (1976).
16. A. O. ALLEN. NSRDS-NBS 58 (1976).
17. L. ONSAGER. Phys. Rev. **54**, 554 (1938).
18. J-P. DODELET and G. R. FREEMAN. Can. J. Chem. **50**, 2667 (1972).
19. P. W. PERCIVAL. J. Chem. Phys. **72**, 2900 (1980).
20. D. C. WALKER, Y. C. JEAN, and D. G. FLEMING. J. Chem. Phys. **72**, 2902 (1980).
21. D. C. WALKER, Y. C. JEAN, and D. G. FLEMING. J. Chem. Phys. **70**, 4534 (1979).
22. Y. ITO, B. W. NG, Y. C. JEAN, and D. C. WALKER. To be published.
23. (*a*) G. DUPLATRE, A. G. MADDOCK, J. CH. ABBE, and A. HAESSLER. Chem. Phys. **28**, 433 (1978); (*b*) G. WIKANDER. Chem. Phys. **38**, 181 (1979); (*c*) W. BRANDT and J. WILKENFELD. Phys. Rev. B, **12**, 2579 (1975).
24. A. MOZUMDER. *In* Advances in radiation chemistry. Vol. I. *Edited by* M. Burton and J. L. Magee. Wiley, New York. 1969. p. 1.

Can. J. Chem. Downloaded from www.nrcresearchpress.com by 210.87.254.40 on 09/05/12
For personal use only.

Mechanistic study of the reaction of vitamin B_{12s} with 1,1-dichloro-2,2-bis(*p*-chlorophenyl)ethane

FARUK NOME AND DINO ZANETTE

Departamento de Química, Universidade Federal de Santa Catarina, 88.000 Florianópolis, S.C., Brasil

Received May 29, 1980

FARUK NOME and DINO ZANETTE. Can. J. Chem. **58**, 2402 (1980).

The reaction of vitamin B_{12s} with 1,1-dichloro-2,2-bis(*p*-chlorophenyl)ethane results in the formation of *trans*-4,4′-dichlorostilbene in a two-step process. In the first step, there is a nucleophilic attack by the cobalt(I) at C-1 resulting in the displacement of chloride ion and formation of an alkyl cobalamin with a chlorine atom on the α-carbon. The second step is a cobalt chloride α-elimination which proceeds through a carbenoid type intermediate that readily rearranges to the product.

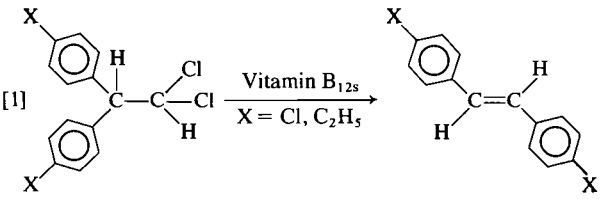
FARUK NOME et DINO ZANETTE. Can. J. Chem. **58**, 2402 (1980).

La vitamine B_{12s} réagit avec le dichloro-1,1 bis(*p*-chlorophényl)-2,2 éthane et conduit en deux étapes à la formation du dichloro-4,4′ stilbène *trans*. La première étape est une attaque nucléophile du cobalt(I) au niveau du carbone en position 1 qui provoque le déplacement de l'ion chlorure et conduit à la formation d'une cobalamine alkylée avec un atome de chlore sur la carbone en position α. La seconde étape consiste en une élimination α de cobalt et de chlore qui se fait via un intermédiaire du type carbénoïde qui se transpose facilement pour donner le produit final.

[Traduit par le journal]

Introduction

The reactions of vitamin B_{12} with a wide variety of inorganic and organic compounds, in aqueous and micellar environments, have been reported (1–6). It was recently demonstrated (7), that the reaction of vitamin B_{12s} with 1,1-dichloro-2,2-bis(*p*-chlorophenyl)ethane (DDD) results in the formation of *trans*-4,4′-dichlorostilbene (DCS). A similar reaction using 1,1-dichloro-2,2-bis(*p*-ethylphenyl)ethane resulted in the production of *trans*-4,4′-diethylstilbene (eq. [1]) (7). The above



[1]

described reactions appear to be mechanistically interesting since, for the product to be formed, two chlorine atoms must be eliminated and a phenyl migration should occur.

It is our purpose to report some studies on the interactions of vitamin B_{12s} with several possible intermediates, the results of which clarify the mechanism of this dechlorination reaction.

Experimental

All melting points are uncorrected. Infrared spectra were determined with a Perkin-Elmer 720 spectrophotometer. Nuclear magnetic resonance spectra were run in $CDCl_3$ on a Varian HA-100 spectrometer using tetramethylsilane as internal reference. Ultraviolet spectra were obtained in methanol by means of a Varian 634 spectrophotometer.

Vitamin B_{12a}, aquocobalamin, was purchased from Merck Chemical Co., 1,1-dichloro-2,2-bis(*p*-ethylphenyl)ethane from Chemical Service, and 1,1-dichloro-2,2-bis(*p*-chlorophenyl)-ethane (DDD) from Aldrich Chemical Co. The purity of the three reagents mentioned above was found to be satisfactory by thin-layer chromatographic analysis.

The intermediate 1-chloro-2,2-bis(*p*-chlorophenyl)ethane (DDMS) was prepared by a slight modification of a previously described procedure (8) and crystallized several times from ethanol, mp 51–51.5°C (lit. (8) mp 51–51.5°C). The observed nmr spectra (A_2B_2 aromatic protons, multiplet centered at 7.19 ppm, doublet at 3.95 ppm, and triplet at 4.25 ppm, integration 8:2:1) was identical with that reported elsewhere (9).

A sample of 2-chloro-1,2-diphenylethanol was prepared by the treatment of benzoin with thionyl chloride, in order to form desyl chloride, followed by sodium borohydride reduction (10). The compound presented fine structure in the 250–260 nm region, with a molar absorptivity of about 500, and when treated with zinc dust in acetic acid and crystallized afforded diamond-shaped irridescent plates of *trans*-stilbene as already described (10).

The compound 1-chloro-1,2-bis(*p*-chlorophenyl)ethane (DDMF) was prepared by treatment of a 10.0 g dry sample of 2,2-bis(*p*-chlorophenyl) acetic acid with lithium aluminum hydride in diethyl ether forming 2,2-bis(*p*-chlorophenyl)ethanol (yield 90%). Reaction of the alcohol (6.0 g) with thionyl chloride (1.7 mL) resulted in the formation of DDMF and DCS. The reaction mixture was purified by column chromatography using a 60 cm × 25 mm silica gel column and hexane (Ecibra) as the eluent. The uv spectra showed fine structure with maxima at 276.5, 268, and 261 nm; nmr showed an aromatic proton multiplet centered at 7.13 ppm, a doublet at 3.27 ppm, and a triplet at 4.90 ppm, integration 8:2:1. Besides, chemical treatment of a sample with alcoholic KOH resulted in quantitative transformation of DMF to DCS, as would be expected. All the other compounds were the best available reagent grade.

In a typical reaction, a solution of aquocobalamin (400 mg in 25 mL of water) was purged with purified nitrogen in a closed vessel through rubber septa for 2 h. A capillary tube punched just through the rubber septum provided the vent. Subsequent to deoxygenation, 200 mg of $NaBH_4$ was added, and the mixture

0008-4042/80/232402-04$01.00/0

©1980 National Research Council of Canada/Conseil national de recherches du Canada

allowed to react for 10 min. A solution of polyhalogenated hydrocarbon (30 times molar excess, dissolved in 250 mL of methanol, also purged for 2 h with purified nitrogen), was added and allowed to react. The reactions were monitored by thin-layer chromatography (using silica gel GF_{254}, type 60, Merck, and petroleum ether, fraction 30–60, Ecibra, as developing solvent). The colored solution was then extracted with several portions of chloroform to remove the organic fraction. The chloroform extract was rotary evaporated to dryness, and dried *in vacuo* in a Abderhaldem type apparatus over P_2O_5. The different products were separated by column chromatography using silica gel and then used for subsequent analysis. In all the reactions more than 90% of the organic compounds were recovered. In the reaction of vitamin B_{12s} with DDMS a vitamin B_{12} complex was formed. The alkyl cobalamin was purified by column chromatography using silica gel (Merck) and methanol as eluent. All the procedures for the isolation of the vitamin B_{12}–DDMS′ complex were done in the absence of light in order to prevent its photolysis.

Results and Discussion

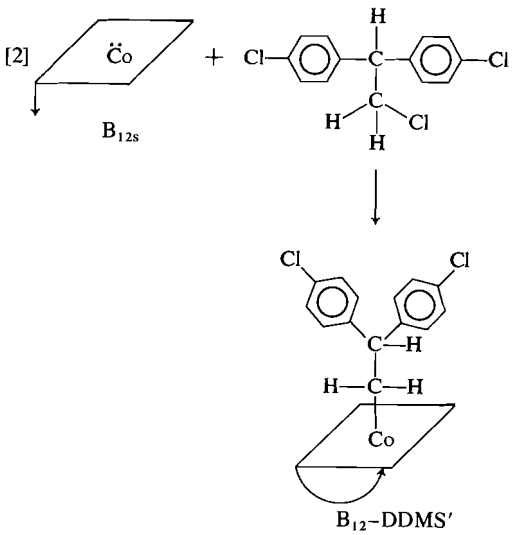
Vitamin B_{12s}, generated by the $NaBH_4$ reduction of aquocobalamin, appears to be the reactive species in the dechlorination of DDD. Indeed vitamin B_{12r}, generated by photolysis of methylcobalamin in a nitrogen atmosphere, does not react with DDD to produce DCS. Furthermore, if the Co(I) nucleophile is generated by an independent method, like treatment of the vitamin B_{12}–DDMS′ complex with base in a nitrogen atmosphere, DCS is also formed upon reaction with DDD. The first step of the reaction must be a nucleophilic attack of the cobalt(I) on DDD resulting in the formation of a vitamin B_{12}–DDD′ complex, a reaction which involves formation of a cobalt–carbon sigma (σ) bond and which is expected for a cobalt(I) supernucleophile such as vitamin B_{12s} (1, 2, 11).

Since DDD is present in large excess as compared with vitamin B_{12s} and the reaction goes to completion, it is obvious that the vitamin B_{12}–DDD′ complex must be unstable and regenerates the cobalt(I) nucleophile or vitamin B_{12r}, the latter of which is reduced by sodium borohydride to the vitamin B_{12s} form.

The main question to be answered in order to clarify the reaction pathway is whether the reaction proceeds via any isolable intermediate which subsequently reacts with vitamin B_{12s} to form DCS or, if the vitamin B_{12}–DDD′ complex directly decomposes to generate DCS.

There are three possible reactive intermediates to be formed upon decomposition of the vitamin B_{12}–DDD′ complex. Namely, 1,1-bis(*p*-chlorophenyl)-2-chloroethane (DDMS), 1,2-bis(*p*-chlorophenyl)chloroethane (DDMF), and 1,2-bis(*p*-chlorophenyl)-2-chloroethanol (DDMFOH). Thus in order to test the different reaction pathways, the compounds DDMS, DDMF, and an analog of DDMFOH were synthesized and their reactions with vitamin B_{12s} were investigated under conditions identical to those for which the reaction of DDD was studied.

DDMS reacts with vitamin B_{12s} in stoichiometric 1:1 proportion and all the excess of DDMS added can be recovered as unreacted material. Since DCS was not detected in the reaction mixture, and DDMS reacts in stoichiometric rather than catalytic proportions, it cannot be the reactive intermediate. Equation [2] describes the reaction occurring under our experimental conditions. Vitamin B_{12s} displaces chloride ion (detected by $AgNO_3$ titration) through a nucleophilic substitution process, forming a product which displays all the characteristics of a typical alkyl cobalamin. Treatment of the vitamin B_{12}–DDMS′ complex with hydroxide ion, using hexadecyldimethyl-2-hydroxyethyl ammonium bromide as catalyst, results in the formation of 1,1-bis(*p*-chlorophenyl)ethylene and vitamin B_{12a} as products, a result which is consistent with the proposed structure for the alkylcobalamin. Figure 1 shows a spectrum of the purified reaction product. As can be seen, the γ-band at 350 nm which is typical of vitamin B_{12a} is absent, and no sharp absorption band is observed in the 320–370 nm region. Indeed, the observed spectrum (Fig. 1, dotted line) is very similar to that reported for methyl cobalamin (2). Upon addition of 0.1 *M* hydrochloric acid, the alkylcobalamin turns yellow, reflecting the shift in the protonation equilibria of the benzimidazol in the fifth coordination position upon alkylation of the cobalt (Fig. 1, dashed line). Using the change in the absorption spectrum upon protonation, the pK_a for the base-on – base-



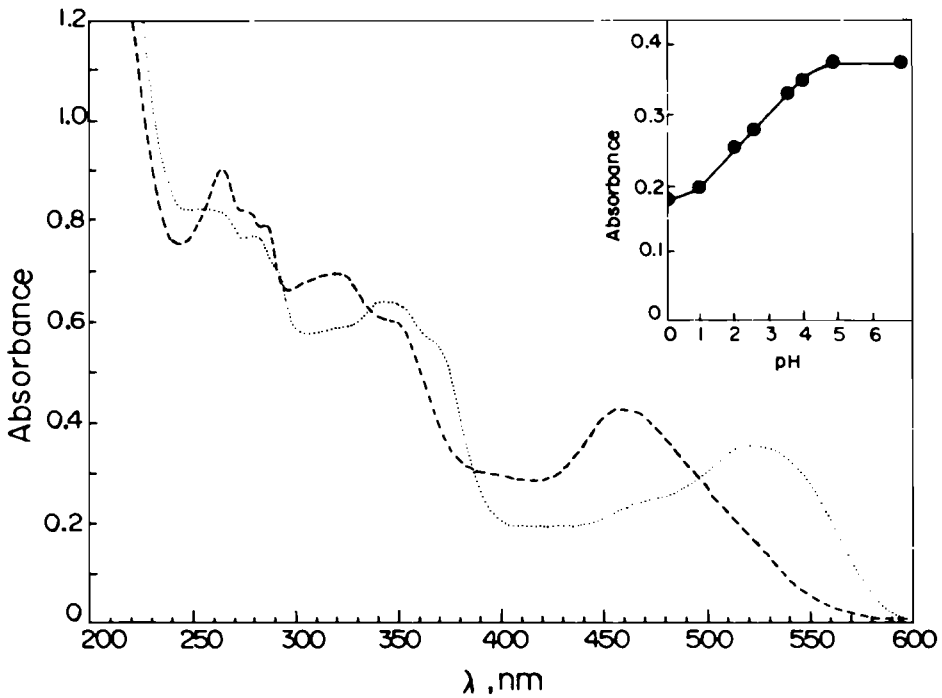
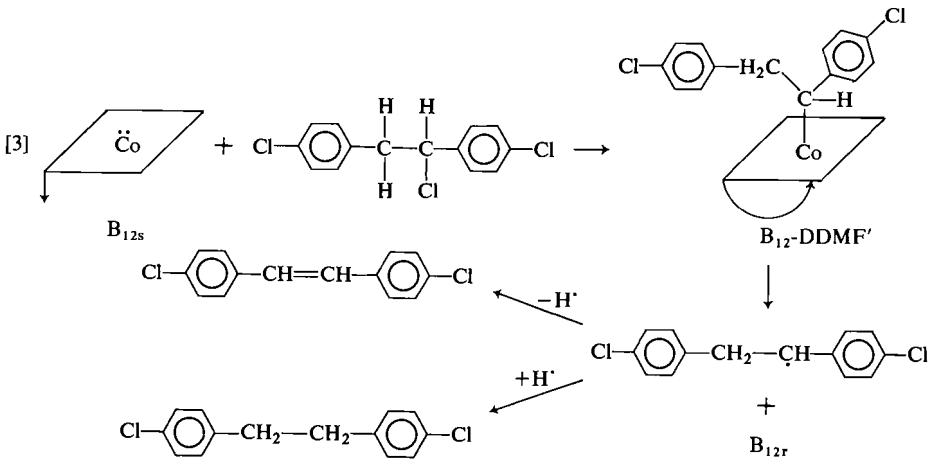


FIG. 1. Absorption spectrum of the vitamin B_{12}–DDMS′ complex at pH 7.0 (...) and pH 1.0 (---). The insert shows the absorbance at 462 nm as a function of pH.

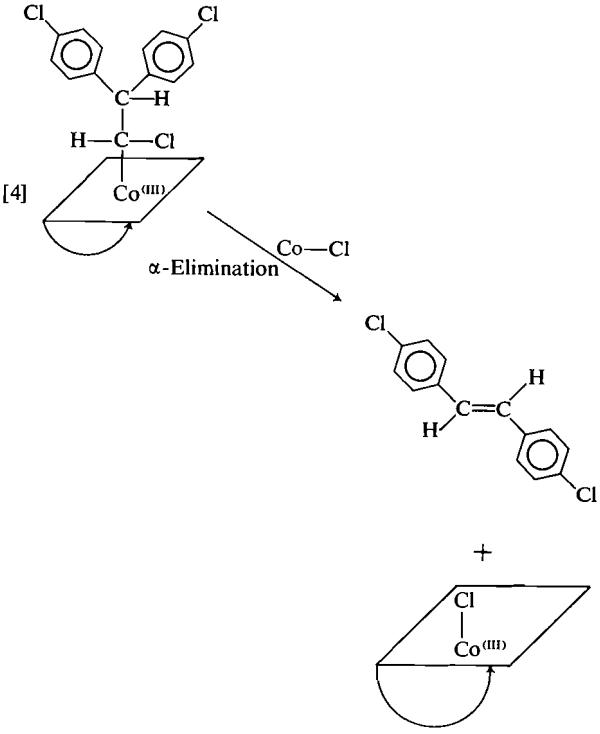
off equilibria was determined spectrophotometrically to be 2.5 (insert of Fig. 1). The obtained value is in close agreement with that normally reported for alkyl cobalamins (2).

Since DDMS was excluded as the reaction intermediate, the pathways involving phenyl migration and leading to the formation of DDMF and DDMFOH were analyzed. Under our experimental conditions 2-chloro-1,2-diphenylethanol, a chemical analog of DDMFOH without the chloro substituents in *para* position, did not react with vitamin B_{12s} to produce *trans*-stilbene and was therefore excluded as a possible reaction intermediate. Considering that the effect of the phenyl group should be somewhat between those of the *p*-ethylphenyl and *p*-chlorophenyl substituents, the choice of 2-chloro-1,2-diphenylethanol as an analog of DDMFOH seems reasonable since both DDD and 1,1-dichloro-2,2-bis(*p*-ethylphenyl)ethane react with vitamin B_{12s} to form the corresponding *trans*-stilbene. The interaction of DDMF with the cobalt(I) nucleophile was then investigated; eq. [3] describes our experimental results. Two organic products were detected in the analysis of the reaction mixture, namely DCS and 1,2-bis(*p*-chlorophenyl)ethane. Since the participation of vitamin B_{12s}, in the presence of $NaBH_4$, is catalytic, the vitamin B_{12}–DDMF′ complex formed upon nucleophilic attack of the cobalt(I) on DDMF must be unstable. The instability of the vitamin B_{12}–DDMF′ complex is not unexpected, since many examples are available showing the lack of stability of a cobalt–carbon bond involving a secondary carbon atom (2, 8). Thus, the reaction of isopropyl iodide with vitamin B_{12s} resulted in the production of vitamin B_{12r} via homolytic bond rupture of the initially formed alkyl cobalamin (11). Our results are entirely consistent with this type of mechanism, since homolytic cobalt–carbon bond cleavage of the vitamin B_{12}–DDMF complex would generate a free radical, which upon uptake or loss of a hydrogen atom will result in the formation of DCS and 1,2-bis(*p*-chlorophenyl)ethane respectively. Considering that in the reaction of vitamin B_{12s} with DDD only DCS was detected as reaction product, and that 1,2-bis(*p*-chlorophenyl)ethane could not be detected even in trace amounts, our evidence indicates that DDMF is not a reaction intermediate.

Thus, the reaction most likely proceeds directly from the vitamin B_{12}–DDD′ adduct to DCS without the participation of any isolable reaction intermediate; eq. [4] describes such a possibility. The vitamin B_{12}–DDD′ complex reacts via a cobalt chloride α-elimination to yield DCS and a vitamin B_{12} – chloride complex, in which the cobalt atom is formally in the Co(III) oxidation state. Hydrolysis of this complex will result in liberation of vitamin



B_{12a} and free chloride ion. The reaction described in eq. [4] is not unprecedented by any means, indeed it is analogous to the Simmons–Smith procedure (12), and to the reaction of organic *gem*-



dihalides with copper (13) among others (14), since the α-elimination will generate a carbene or carbenoid type intermediate which will readily rearrange to the products. Attempts to trap a free carbene using cyclohexene were unsuccessful, a result which was somewhat expected since DCS itself may act as a carbene trapping agent. Besides, alkylcarbenes generally undergo rearrangement so rapidly that additions to double bonds and insertion reactions, which are normally expected for carbene itself, are seldom found with alkyl carbenes. Our results seem to be more consistent with a carbenoid type intermediate rather than a totally free carbene. Accordingly, the rearrangement should occur concurrently with the α-elimination.

We are currently working on the development of a procedure for the synthesis of cyclopropane derivatives based on a modification of the above described reaction, using simple cobalt complexes.

Acknowledgement

The authors gratefully acknowledge financial assistance from the Conselho Nacional de Desenvolvimento Cientifico e Tecnológico-CNPq (Grants 2222.0070/78 and 1111.5805/79 to F.N.).

1. J. M. Pratt. Inorganic chemistry of vitamin B_{12}. Academic Press, New York. 1972.
2. R. H. Prince and D. A. Stotter. J. Inorg. Nucl. Chem. **35**, 321 (1973).
3. J. H. Fendler, F. Nome, and H. C. Van Woert. J. Am. Chem. Soc. **96**, 6745 (1975).
4. F. Nome and J. H. Fendler. J. Chem. Soc. Dalton Trans. 1212 (1976).
5. F. Nome and J. H. Fendler. J. Am. Chem. Soc. **99**, 1557 (1977).
6. G. C. Robinson, F. Nome, and J. H. Fendler. J. Am. Chem. Soc. **99**, 4969 (1977).
7. D. Zanette and F. Nome. J. Org. Chem. **44**, 2309 (1979).
8. S. J. Cristol, N. L. Hause, A. J. Quant, H. W. Miller, K. R. Eilar, and J. S. Meek. J. Am. Chem. Soc. **74**, 3333 (1952).
9. J. D. McKinney and N. K. Wilson. Mass spectrometry and nmr spectroscopy in pesticide chemistry. *Edited by* R. Haque and F. J. Biros. Plenum Press, New York, NY. 1974. p. 139.
10. L. F. Fieser and Mary Fieser. Reagents for organic synthesis. John Wiley and Sons Inc., New York, NY. 1967. p. 1161.
11. G. N. Schrauzer and E. Deutsch. J. Am. Chem. Soc. **91**, 3341 (1969).
12. H. E. Simmons, T. L. Cairns, S. A. Vladuchick, and C. M. Hoiness. Org. React. **20**, 1 (1973).
13. N. Kawabata, M. Naka, and S. Yamashita. J. Am. Chem. Soc. **98**, 2676 (1976).
14. G. Köbrich. Angew. Chem. Int. Ed. Engl. **11**, 473 (1972).

The crystal structure of 1-*O*-acetyl-17-*p*-bromobenzoylsideritol, a diterpenoid of the *ent*-atisane class

WILLIAM A. AYER AND JO-ANN H. FORSYTHE
Department of Chemistry, University of Alberta, Edmonton, Alta., Canada T6G 2G2
AND
LOUIS T. J. DELBAERE AND CAROLINE U. DELBAERE
Department of Biochemistry, University of Saskatchewan, Saskatoon, Sask., Canada S7N 0W0

Received July 3, 1980

This paper is dedicated to Prof. Raymond U. Lemieux on the occasion of his 60th birthday

WILLIAM A. AYER, JO-ANN H. FORSYTHE, LOUIS T. J. DELBAERE, and CAROLINE U. DELBAERE. Can. J. Chem. **58**, 2406 (1980).

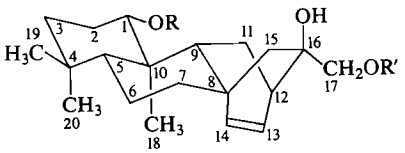
The crystal structure of 1-*O*-acetyl-17-*p*-bromobenzoylsideritol (*ent*-1α-acetoxy-16β-hydroxy-17-*p*-bromobenzoyloxyatis-13-ene) is presented. This crystal structure establishes unequivocally the structure of sideritol (**1**).

WILLIAM A. AYER, JO-ANN H. FORSYTHE, LOUIS T. J. DELBAERE et CAROLINE U. DELBAERE. Can. J. Chem. **58**, 2406 (1980).

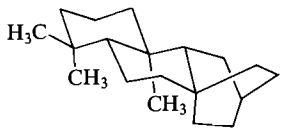
On présente la structure du cristal du *O*-acétyl-1 *p*-bromobenzoyl-17 sidéritol (*ent* acétoxy-1α hydroxy-16β *p*-bromobenzoyloxy-17 atisène-13). La structure du cristal établit de façon non équivoque la structure du sidéritol (**1**).

[Traduit par le journal]

Some time ago we proposed (1) structure **1** for sideritol, a diterpenoid isolated from *Sideritis angustifolia* Lag. (2). This was the first reported example of an oxygenated nitrogen-free diterpenoid of the *ent*-atisane type. The absolute configuration of **1** was established by correlation with *ent*-17-noratisane (**2**). The location of the secondary alcohol function at C-1 (as opposed to C-7) was based on the observation that the corresponding ketone showed a weakly positive Cotton effect in the circular dichroism (c.d.) spectrum. The stereochemistry at C-16 was assigned on the basis of the fact that the methylene group of the hydroxymethyl group (C-17) shows a significant downfield shift (in the ^1H nuclear magnetic resonance (^1H nmr) spectrum) when the C-13, C-14 double bond is hydrogenated (1). Although all the evidence presented is consistent with the assigned structure, we felt it desirable to confirm the assignment by means of a single crystal X-ray diffraction study. This seemed especially important with regard to the assignment of the position of the secondary hydroxyl group, since the c.d. assignment is based on steroidal analogies, and it is known that the presence of axial methyl groups at C-4 and C-10 in ring A ketones may lead to a distortion of ring A (3, 4), which might invalidate the argument.



1 R = R′ = H
3 R = Ac, R′ = H
4 R = Ac, R′ = —COPhBr



2

p-Bromobenzoylation of 1-*O*-acetylsideritol (**3**) in pyridine at room temperature provided the nicely crystalline 17-*O*-*p*-bromobenzoate **4**, mp 199–201°C, which crystallizes from ethyl acetate with the following crystal data:

$C_{29}H_{37}O_5Br$ mw = 545.1
$P2_1$, a = 15.307(3), b = 25.989(6), c = 6.929(2) Å, β = 101.5°, V = 2701.2 Å^3, Z = 4, ρ_c = 1.34 g/cm^3, $F(000)$ = 1144e.

Examination of the two strongest peaks on the Harker section (v = 1/2) and possible cross vectors provided the positions of the bromine atom of each of the two crystallographically independent molecules. Structure factors calculated for these bromine atoms produced an R index ($R = [\Sigma_{hkl}||F_o| - |F_d||]/[\Sigma_{hkl}|F_o|]$, where F_o and F_c are the observed and calculated structure factors, respectively) of 0.377. The remaining non-hydrogen atoms of the two molecules were located by means of subsequent difference maps calculated after including additional atoms in block-diagonal least-squares

0008-4042/80/232406-03$01.00/0
©1980 National Research Council of Canada/Conseil national de recherches du Canada

Can. J. Chem. Downloaded from www.nrcresearchpress.com by 210.87.254.40 on 09/05/12
For personal use only.

Can. J. Chem. Downloaded from www.nrcresearchpress.com by 210.87.254.40 on 09/05/12
For personal use only.

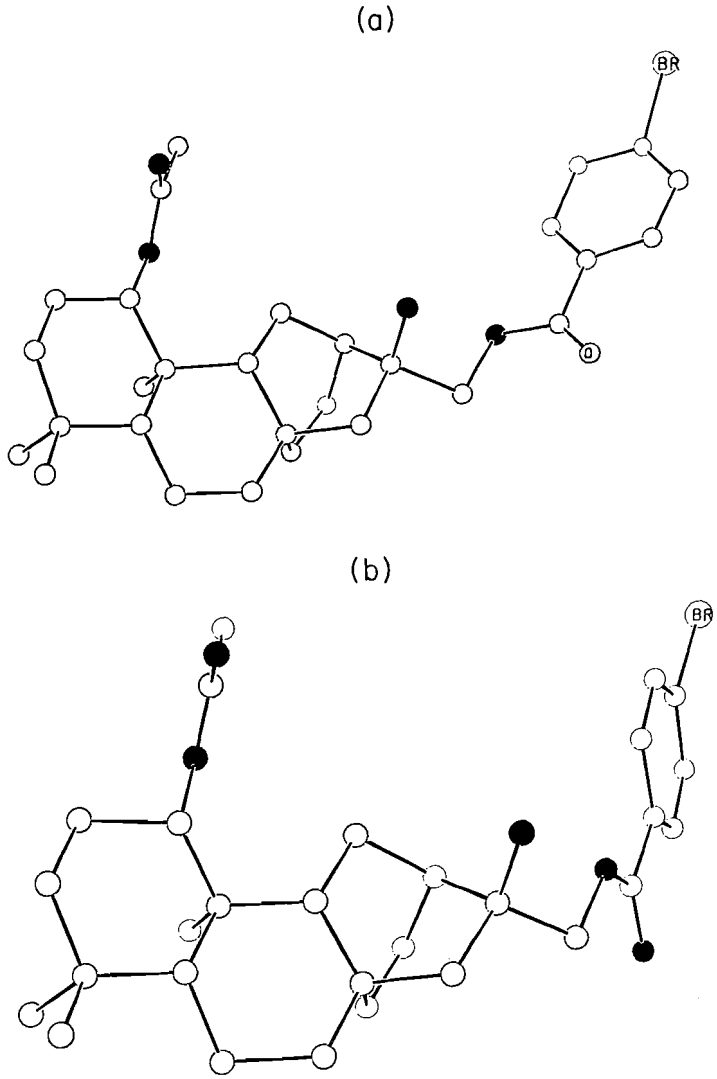


FIG. 1. Perspective view of the two crystallographically independent molecules (*a* and *b*) of 1-*O*-acetyl-17-*p*-bromobenzoylsideritol (**4**). The oxygen atoms of the molecules are illustrated as solid dark circles.

refinement. The quantity minimized was $\Sigma_{hkl}(|F_o| - k|F_c|)^2$, where k is the scale factor relating the observed and calculated structure amplitudes. The isotropic temperature factor refinement gave an index of 0.144. Further block-diagonal least-squares refinement, with anisotropic temperature factors for only the bromine and oxygen atoms lowered R to 0.108. Refining anisotropic temperature factors for all of the non-hydrogen atoms produced a final R index of 0.077.[1]

[1]Tables of atomic parameters, bond lengths and angles, and structure factors are available, at a nominal charge, from the Depository of Unpublished Data, CISTI, National Research Council of Canada, Ottawa, Ont., Canada K1A 0S2.

Perspective drawings of the two crystallographically independent molecules of **4** are shown in Fig. 1 (*a*) and (*b*). The conformation of the *p*-bromobenzoyl group around the C17—O17 bond varies in the two molecules due to crystal packing forces. There are two hydrogen bonds between the two crystallographically independent molecules, both from the tertiary hydroxyl group at C-16 of one molecule to the carbonyl oxygen atom of the acetyl group at C-1 of the other molecule; the distance between the oxygen atoms involved are 2.76 Å and 2.71 Å, respectively. The crystal structure shows that ring A is not distorted by the non-bonded interaction of the axial methyl groups at C-4 and

TABLE 1. Torsion angles (deg) around ring A of the two molecules of **4**

Atoms	Torsion angle (deg)		
	Molecule I	Molecule II	Average
C1—C2—C3—C4	−57	−57	−57
C2—C3—C4—C5	52	55	54
C3—C4—C5—C10	−48	−59	−54
C4—C5—C10—C1	45	58	51
C5—C10—C1—C2	−48	−63	−55
C10—C1—C2—C3	55	68	62

C-10. Table 1 gives the torsion angles around ring A for both independent molecules of **4**. The average torsion angles indicate that ring A has a regular chair conformation; the individual torsion angle differences between the two molecules are probably due to crystal packing forces. This, of course, does not mean that the ring A ketone is free from distortion. The crystal structure does, however, establish unequivocally the structure of sideritol.

Experimental

Mass spectra were recorded on an A.E.I. Model MS-9 mass spectrometer, ^{1}H nmr spectra were recorded on a Varian HR-10 spectrometer with tetramethylsilane as internal standard, and infrared spectra on a Perkin-Elmer Model 421 dual grating spectrometer.

The X-ray intensity data were collected from a crystal measuring 0.08 × 0.06 × 0.53 mm with a Picker FACS-1 diffractometer and a θ–2θ scan. The scan speed was 2° min^{-1} over a range of $(1.5 + 0.285 \tan\theta)°$ with Ni-filtered CuK_α radiation (λ = 1.5418 Å). A total of 1696 unique reflections with $2\theta < 80°$ were measured and 1257 had $I > 3\sigma(I)$. Lorentz and polarization corrections were applied but no absorption corrections were made. All crystallographic computations were carried out using the X-ray 70 system (5) on the Amdahl 470/V6 system at the University of Alberta.

*1-O-Acetyl-17-*p*-bromobenzoylsideritol (*ent*-1α-acetoxy-16β-hydroxy-17-*p*-bromobenzoyloxyatis-13-ene) (**4**)*

1-*O*-Acetylsideritol (**3**) (50 mg), pyridine (2 mL), and *p*-bromobenzoyl chloride (130 mg) were allowed to stir at room temperature for 24 h. The reaction mixture was then diluted with water and extracted with ether. The ether extracts were washed, dried, and concentrated. Chromatography over silica gel (eluent ethyl acetate) provided 1-*O*-acetyl-17-*p*-bromobenzoylsideritol (**4**) (41 mg), mp 199–201°C (from ethyl acetate). Ir (Nujol) cm^{-1}: 3500 medium (OH), 1720 (sh), 1708 strong (C=O), 1585 medium (aromatic); ^{1}H nmr ($CDCl_3$): δ 7.72 (4H, quartet, aromatic H's), 5.98 (2H, multiplet, H-13 and H-14). 4.55 (1H, apparent doublet of doublets, *J*'s 6 and 8 Hz, H-1β), 4.02 (2H, quartet, —CH_2—O—), 2.48 (1H, multiplet, H-12, 1.97 (3H, singlet, OCOCH_3), 0.86 (3H, s), 0.79 (3H, s), 0.73 (3H, s). Mass spectrum 70 eV, *m/e* (rel. int.): 546 (M^+ (^{81}Br) 2.2), 344 (1), 288 (12), 228 (60), 213 (13), 202 (12), 200 (12), 185 (28), 183 (28), 172 (40), 157 (16), 138 (14), 131 (16), 125 (16), 124 (100), 118 (12), 109 (48), 107 (12), 105 (22), 104 (36), 95 (16), 93 (14), 92 (22), 91 (48), 81 (42), 79 (12), 77 (10).

Acknowledgements

We thank the Natural Sciences and Engineering Research Council of Canada for financial support, Dr. Serafin Valverde for a supply of sideritol, and Professor M. James for the use of X-ray and computing facilities.

1. W. A. AYER, J. A. H. BALL, B. RODRÍGUEZ, and S. VALVERDE. Can. J. Chem. **52**, 2792 (1974).
2. C. VON CARSTEN-LICHTENFELDE, S. VALVERDE, and B. RODRÍGUEZ. Aust. J. Chem. **27**, 517 (1974).
3. N. L. ALLINGER, U. BURKERT, and W. H. DE CAMP. Tetrahedron, **33**, 1891 (1977).
4. U. BURKERT and N. L. ALLINGER. Tetrahedron, **34**, 807 (1978).
5. J. M. STEWART, F. A. KUNDELL, and J. C. BALDWIN. The X-ray 70 system. Computer Science Center, University of Maryland, College Park, MD. 1970.

Can. J. Chem. Downloaded from www.nrcresearchpress.com by 210.87.254.40 on 09/05/12
For personal use only.

Rydberg orbitals and the Woodward–Hoffmann procedure

C. SANDORFY

Département de chimie, Université de Montréal, Montréal (Qué.), Canada H3C 3V1

Received May 6, 1980

This paper is dedicated to Prof. R. U. Lemieux on the occasion of his 60th birthday

C. SANDORFY. Can. J. Chem. **58**, 2409 (1980).

It is argued that account should be taken of Rydberg states when the course of photochemical reactions is interpreted through correlation diagrams based on the principle of conservation of orbital symmetry. This is expected to be important for molecules whose lowest excited state has Rydberg character and a symmetry different from that of the lowest valence-shell type excited state.

C. SANDORFY. Can. J. Chem. **58**, 2409 (1980).

Il est nécessaire de tenir compte de l'existence d'états Rydberg quand on interprête le cours des réactions chimiques à la base de diagrammes de corrélation invoquant la conservation de la symétrie orbitale. Cela peut être important pour les molécules dont l'état excité de plus basse énergie a un caractère Rydberg et une symétrie différente de celle que possède la molécule dans son état excitée de valence de plus basse énergie.

Can. J. Chem. Downloaded from www.nrcresearchpress.com by 210.87.254.42 on 09/05/12
For personal use only.

One of the classical examples of the application of the principle of orbital symmetry conservation to the feasibility of thermal and photochemical reactions is the formation of cyclobutane from two ethylene molecules (1, 2). The first task is to choose the proper combinations of orbitals for two ethylenes approaching each other along the line containing the symmetry axis perpendicular to the molecular planes of both ethylenes, in the most symmetrical way. If π_1 and π_2 are the π orbitals of the two ethylenes which are filled and π^*_1 and π^*_2 those which are empty in the ground state, the proper combinations are $\pi_1 + \pi_2$ and $\pi_1 - \pi_2$ for the ground state and $\pi^*_1 + \pi^*_2$ and $\pi^*_1 - \pi^*_2$ for the excited states. The next step is to write down the relevant orbitals for the product, cyclobutane. For this, two pairs of π orbitals of the reactants have to transform into two σ orbitals of the product. Then we have a correlation diagram and if only we admit that the orbitals conserve their symmetry we can assess the height of the transition state that has to be reached in order to get from the reactants to the products. The characteristic symmetry elements in this case are the two planes perpendicular to the plane of the paper and S and A signify symmetrical and antisymmetrical with respect to these. Figure 1, adapted from Woodward and Hoffmann, illustrates the procedure. As is now well known the thermal reaction is "symmetry-forbidden", since in order to get from the reactants to the products while conserving symmetry the SA orbital of the ground state would become an antibonding orbital of high energy of the product. This would imply an unreasonably high activation energy. On the other hand, if one of the electrons is already in the AS excited state of the reactants it would correlate to a bonding orbital of the same symmetry of cyclobutane so that the photochemical reaction is symmetry allowed.

It is not intended to criticize this highly successful procedure. One might, however, make the following comment. Much depends on the selection of the relevant reactant and product orbitals. There is no argument about the ground state. As to the excited states of ethylene, however, it is known that the π^* orbital is in near coincidence with the 3*s* Rydberg orbital which does *not* have the same symmetry as the π^* orbital (3, 4). In the ultraviolet spectrum of ethylene itself the V $\leftarrow$ N (π,π^*) transition gives rise to a broad band whose maximum corresponding to the vertical transition is near 162 nm (61 700 cm^{-1}) from where it extends to about 210 nm (48 000 cm^{-1}) exhibiting complicated fine structure in the adiabatic part. The 3*s* $\leftarrow$ N Rydberg band ($^1B_{1u} \leftarrow {}^1A_g$; the (π,π^*) band is $^1B_{3u} \leftarrow {}^1A_g$ with the *X* axis taken along the C—C bond, and the *Z* axis perpendicular to the molecular plane) is superimposed to the wing of the intense (π,π^*) band and is centered at 174 nm (57 400 cm^{-1}). In many ethylene derivatives the Rydberg band is at lower frequencies and is clearly separated from the (π,π^*) band (3, 5–7). It is not intended to draw conclusions related to the course of the ethylene to cyclobutane reaction itself; it is only used as a model. It is conceivable, however, that in this or other similar cases the photochemical reaction chooses to proceed through the $(\pi,3s)$ excited state rather than through the (π,π^*) state. Then instead of the AS orbital (Fig. 1) we have a totally symmetrical (SS) Rydberg orbital.

Then, if conservation of orbital symmetry is stipulated this orbital cannot become the AS σ orbital of cyclobutane. However, the 3*s* Rydberg band of cyclobutane itself is at nearly the same energy as the one of ethylene and it is tempting to speculate that cyclobutane is first formed in *its* 3*s* state. In this way, orbital symmetry would be conserved.

0008-4042/80/232409-02$01.00/0

©1980 National Research Council of Canada/Conseil national de recherches du Canada

Can. J. Chem. Downloaded from www.nrcresearchpress.com by 210.87.254.42 on 09/05/12
For personal use only.

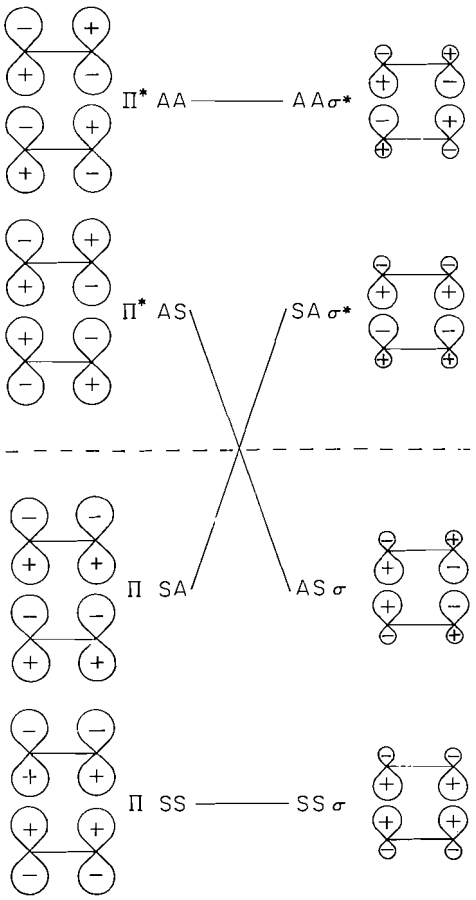


FIG. 1. Correlation diagram for the formation of cyclobutane from two molecules of ethylene. Adapted from R. B. Woodward and R. Hoffmann, The conservation of orbital symmetry. With permission from the authors and Verlag Chemie, GMBH.

Most known photochemical reactions lead to products in their electronic ground states. There are, however, cases in which the product is first obtained in an excited state and then it rids itself from the excitation energy by radiationless transition (8). If this was the case the yield would have a pronounced pressure dependence. It is to be remembered in this respect that Rydberg orbitals because of their large size are very sensitive to intermolecular interactions (9); therefore trimolecular collisions might be important for the kinetics of reactions occurring in such states. Many organic molecules have low-lying Rydberg states. Indeed, they are the lowest for many (10). Whether these considerations have any relevance to the particular case of the ethylene → cyclobutane reaction or not, the Rydberg route might turn out to be important for a number of photochemical reactions.

Similar considerations would apply to the method proposed by Salem *et al.* (11, 12) and by Dauben, Salem, and Turro (13) for the interpretation of the course of photochemical reactions. According to this method photochemical reactions proceed through primary products having the characteristics of diradicals. The procedure consists in enumerating the relevant reactant and primary product states and then constructing a correlation diagram so that symmetry and multiplicity are conserved. As the writer commented previously low-lying Rydberg states might play a role in this scheme too (10).

Caution should be exercised. States that are Rydberg at molecular distances may not remain so at the long internuclear distances involved with bond formation or dissociation. Every case would require a particular treatment. All that this brief note has been aiming at is to draw attention to a problem which might well turn out to be important for photochemistry.[1]

Acknowledgement

My thanks are due to Professor Roald Hoffmann for his valuable comments.

1. R. B. WOODWARD and R. HOFFMANN. J. Am. Chem. Soc. **87**, 395 (1965); **87**, 2046 (1965); **87**, 2511 (1965).
2. R. B. WOODWARD and R. HOFFMANN. The conservation of orbital symmetry. Verlag Chemie, Weinheim/Bergstrasse. 1970.
3. A. J. MERER and R. S. MULLIKEN. Chem. Rev. **69**, 639 (1969).
4. R. MCDIARMID. J. Chem. Phys. **55**, 4669 (1971).
5. M. B. ROBIN, R. R. HART, and N. A. KUEBLER. J. Chem. Phys. **44**, 580 (1962).
6. M. B. ROBIN. Higher excited states of polyatomic molecules. Vol. II. Academic Press, New York. 1975. p. 33.
7. G. BÉLANGER and C. SANDORFY. J. Chem. Phys. **55**, 2055 (1971).
8. TH. FÖRSTER. Ber. Bunsenges. Phys. Chem. **76**, 962 (1972).
9. M. B. ROBIN and N. A. KUEBLER. J. Mol. Spectrosc. **33**, 247 (1970).
10. C. SANDORFY. *In* Topics in current chemistry. Vol. 86. *Edited by* I. G. Csizmadia. Springer-Verlag. 1979. pp. 91–138.
11. L. SALEM. J. Am. Chem. Soc. **96**, 3486 (1974).
12. L. SALEM, C. LEFORESTIER, G. SEGAL, and R. WETMORE. J. Am. Chem. Soc. **97**, 479 (1975).
13. W. G. DAUBEN, L. SALEM, and N. J. TURRO. Acc. Chem. Res. **8**, 41 (1975).
14. N. D. EPIOTIS. Theory of organic reactions. Springer, New York. 1978.
15. N. D. EPIOTIS and S. SHAIK. J. Am. Chem. Soc. **100**, 1 (1978); **100**, 9 (1978).
16. J. MICHL. Photochem. Photobiol. **25**, 141 (1977).
17. R. P. STEINER and J. MICHL. J. Am. Chem. Soc. **100**, 6413 (1978).
18. J. MICHL. *In* Excited states in quantum chemistry. *Edited by* C. A. Nicolaides and D. R. Beck. Reidel, Dordrecht. 1979. pp. 417–435.

[1]Concerning theories of organic reactions the interested reader might like to consult the recent works of Epiotis (14), Epiotis and Shaik (15), and Michl (16–18).

The phenolic hydroxyl content of lignin in spruce wood

J.-M. YANG AND D. A. I. GORING

Pulp and Paper Research Institute of Canada and Department of Chemistry, McGill University, Montreal, P.Q., Canada H3A 2A7

Received October 1, 1979[1]

This paper is dedicated to Prof. Raymond U. Lemieux on the occasion of his 60th birthday

J.-M. YANG and D. A. I. GORING. Can. J. Chem. **58**, 2411 (1980).

Values of the phenolic hydroxyl content of the lignin in the secondary wall and cell corner middle lamella of the tracheids in black spruce wood were found by ultraviolet microscopy to be 0.12 and 0.06 PhOH/C_9 respectively. The overall value for the lignin in black spruce wood was 0.10 PhOH/C_9.

J.-M. YANG et D. A. I. GORING. Can. J. Chem. **58**, 2411 (1980).

Nous avons découvert, en utilisant la microscopie aux ultraviolets, que les valeurs absolues de la teneur en groupes hydroxyles phénoliques de la lignine dans la paroi secondaire et dans la lamelle moyenne aux coins de cellule des tranchéides d'épinette noire étaient de 0,12 et 0,06 PhOH/C_9 respectivement. La valeur globale de la lignine de l'épinette noire était de 0,10 PhOH/C_9.

Introduction

The proportion of phenylpropane units in lignin which contain free phenolic hydroxyl groups is a fundamental structural parameter of the lignin macromolecule (1, 2). Several techniques have been used for the determination of the PhOH[2] content of lignins from wood by the various laboratory and commerical methods of delignification (3). However, to date, no measurements have been reported of the PhOH content of lignin *in situ* in the wood. The purpose of the work described in the present paper was to make such measurements.

The spectroscopic $\Delta\varepsilon$ method of Aulin-Erdtman (4) has been used widely to determine the PhOH content of lignin. Applied microscopically in the ultraviolet it showed that the PhOH content of the lignin in the secondary walls of softwood tracheids is twice as great as that in the middle lamella (5). However, the $\Delta\varepsilon$ method is not absolute in the sense that it can be used by itself to determine the PhOH content. The method must be calibrated either by the use of model compounds (6, 7) or by measurements on a sample of lignin for which the PhOH content has been determined independently. A reliable chemical method for the determination of PhOH has been developed by Adler *et al.* (1) and Gierer *et al.* (8) in which the methoxyl group *vicinal* to the free phenolic hydroxyl group is converted into methanol by periodate oxidation and determined by gas chromatography.

In the present work the $\Delta\varepsilon$ method was calibrated by measurements on solutions of a milled wood lignin for which the PhOH content was measured by periodate oxidation. The calibration factor thus obtained was applied to $\Delta\varepsilon$ data determined microscopically on sections of spruce wood. In this manner values of the PhOH content of the lignin in the secondary wall and middle lamella of the tracheids in the wood were obtained.

Experimental

The milled wood lignin (MWL) was prepared from black spruce wood by the method of Björkman (9). Its elemental composition, methoxyl content, and carbohydrate content, are given in Table 1. Assuming the methoxyl content of "pure" MWL to be 15.7% (10), the sample used in the present work was taken to be 14.7/15.7 ≡ 94% pure. The impurity was probably acetic acid not completely removed in the preparation of the sample.

For measurement of $\Delta\varepsilon_{300}$, a 0.1% solution of MWL in *p*-dioxane was made up. Two millilitres of this solution was diluted to 25 mL with a 50/50 mixture of dioxane/water to give the neutral solution. The alkaline solution was made up by a similar dilution in a phosphate/NaOH buffer of pH 12. Ultraviolet spectra of the MWL solutions and solvent blanks were then recorded and $\Delta\varepsilon_{300}$ calculated from the difference in absorbances at 300 nm, ΔA_{300}, from

$$[1] \quad \Delta\varepsilon_{300} = \Delta A_{300}/Cl$$

in which C is the concentration of MWL corrected for the purity of the sample and l is the absorbance cell length (1 cm).

The experiment was then repeated using pure *p*-dioxane as the neutral solvent for dilution instead of the 50/50 mixture of dioxane/water.

The method of Gierer *et al.* (8) was used for the measurement of PhOH by gas chromatography. Chromasorb W was coated

TABLE 1. Elemental composition, methoxyl content, and carbohydrate content of MWL

Element or group	% (by weight)
Carbon	62.2
Hydrogen	6.2
Oxygen	28.7
Methoxyl	14.7
Carbohydrate	1.0

[1]Revision received June 16, 1980.

[2]In this paper, "PhOH" indicates a free phenolic hydroxyl group in the lignin polymer.

0008-4042/80/232411-04$01.00/0

©1980 National Research Council of Canada/Conseil national de recherches du Canada

Can. J. Chem. Downloaded from www.nrcresearchpress.com by 210.87.254.42 on 09/05/12
For personal use only.

Can. J. Chem. Downloaded from www.nrcresearchpress.com by 210.87.254.42 on 09/05/12
For personal use only.

with Triton X-100 dissolved in methanol. The stationary phase was then packed into a 2 m copper column in a Hewlett-Packard 402 High Efficiency Gas Chromatograph. About 40 mg of MWL was soaked in 1 mL of glacial acetic acid and then reacted with 7 mL of 0.133 mol/L periodate in 3:2 glacial acetic acid/distilled water at 4°C in a dark room. After the reaction, 3.5 μL of benzene was added as an internal standard. Three microlitres of the reaction products were injected into the column with a helium flow rate of 25 mL/min, a hydrogen flow rate of 25 mL/min, and an air flow rate of 200 mL/min.

As shown in Fig. 1, three peaks were obtained in the gas chromatogram after the periodate oxidation. They were for benzene, methanol, and methyl acetate. The methyl acetate was produced by reaction of some of the methanol with the glacial acetic acid.

The column was calibrated by substitution of pure methanol and pure methyl acetate for the MWL in the experiment described in the previous paragraph. As shown in Fig. 1, the methyl acetate gave a single peak while the methanol gave two peaks due to some conversion of the methanol into methyl acetate. Calibration curves were obtained by injecting known weight ratios of methanol/benzene and methyl acetate/benzene, measuring peak weight ratios by cutting out and weighing and plotting true weight ratios to peak weight ratios. The calibration curves were then used to determine the moles of MeOH and MeOAc produced by periodate oxidation of a known weight of MWL.

The moles of PhOH per C_9 residue in the MWL was then calculated from

$$[2]\quad \mathrm{PhOH/C_9} = \frac{184\,(\text{moles of MeOH} + \text{moles of MeOAc})}{\text{Weight of MWL}}$$

in which the monomer weight in MWL is taken to be 184 and the weight of the MWL is corrected for the purity of the sample.

Assuming that $\Delta\varepsilon_{300}$ is proportional to $\mathrm{PhOH/C_9}$ we may write

$$[3]\quad \mathrm{PhOH/C_9} = k\Delta\varepsilon_{300}$$

in which k is a constant. The value of k was then computed from $\Delta\varepsilon_{300}$ and $\mathrm{PhOH/C_9}$ obtained from eqs. [1] and [2] respectively. It is interesting to note that since corrections are made in both eqs. [1] and [2] for the purity of the MWL, the value of k obtained from eq. [3] is not affected by an error in the purity of the sample.

For measurements with the ultraviolet microscope, small chips 1 mm^2 × 7 mm were cut from the rings between 80 and 85 of a 183-year old black spruce tree (*Picea mariana* (Mill) BSP). The chips were embedded in Epon and ultrathin transverse sections of nominal thickness of 0.9 μm were cut with a diamond knife mounted on a Porter-Blum ultramicrotome. The sections were collected, soaked in a buffer solution of pH 12 for 30 min, and then some of them were transferred to a buffer solution of pH 6 for a further 30 min.

The sections were transferred to quartz slides and the transmittance at 300 nm was measured with a Leitz ultraviolet microscope. The microscopic methods used were essentially those of Scott *et al.* (11) and are given in greater detail elsewhere (12).

Absorbance was measured in the microscope for the S2 layer of the secondary wall and for the middle lamella at the cell corners. From the difference in absorbance from pH 12 to pH 6, $\Delta\varepsilon_{300}$ was computed by means of eq. [1]. For this purpose it was necessary to know the thickness of the section with accuracy. Accordingly the thickness of several sections was measured with a Zeiss interference microscope and the absorbance at 300 nm of the S2 layer on the same sections was measured on the uv microscope. From these data the relationship between section thickness and A_{300} was established, by means of which the values of ΔA_{300} could be normalized to correspond to a section thickness of 1.00 μm. The details of this procedure are given elsewhere (12).

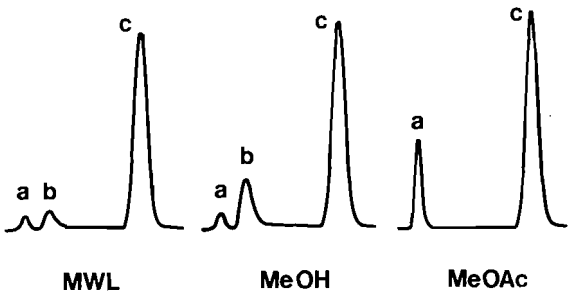


FIG. 1. Chromatograms obtained from MWL, methanol, and methyl acetate: peak *a*, methyl acetate; peak *b*, methanol; peak *c*, benzene.

Results

Considerable trial and error was necessary in preparing the solutions of MWL for the measurement of $\Delta\varepsilon_{300}$. It was found that a 0.1% solution of MWL in dioxane could be diluted 10-fold with the pH 12 buffer to give a clear, stable solution. However, this was not the case for the neutral system. A similar procedure with the pH 6 buffer or with distilled water gave a turbid solution and caused precipitation of the lignin. However, when the 0.1% solution of MWL in dioxane was diluted with a 50/50 mixture of dioxane and distilled water, the resulting solution was clear and stable and could be used for the measurement of $\Delta\varepsilon_{300}$.

As shown by the results in Table 2, $\Delta\varepsilon_{300}$ was virtually unchanged when dioxane instead of 50/50 dioxane/water was used for the dilution. This result indicates that the absorbance of the neutral solution is unaffected by the use of dioxane instead of water as solvent and thus supports the validity of the measurement of $\Delta\varepsilon_{300}$ by the method discussed above. The mean of the two results was used in the calculation of k by means of eq. [1].

Three determinations of the PhOH content of the MWL were made by the periodate oxidation method. The mean and mean deviation are given in Table 2.

The ultraviolet absorbances at pH 6 and pH 12 for the S2 layer and the cell corner middle lamella were measured 50 times each and a mean taken.

TABLE 2. $\Delta\varepsilon_{300}$ and $\mathrm{PhOH/C_9}$ for MWL

Parameter	Value
$\Delta\varepsilon_{300}$(dioxane/water)	2.45 $cm^{-1}g^{-1}L$
$\Delta\varepsilon_{300}$(dioxane)	2.35 $cm^{-1}g^{-1}L$
$\Delta\varepsilon_{300}$(mean)	2.40 $cm^{-1}g^{-1}L$
$\mathrm{PhOH/C_9}$	0.205 (±0.006)
k	0.085 cm g L^{-1}

TABLE 3. Calculation of the absolute values of $PhOH/C_9$ in the lignin of the secondary wall and middle lamella of spruce wood

Parameter	S2	ML
ΔA_{300}	0.028 (±0.005)	0.053 (±0.012)
Section thickness (μm)	1.00	1.00
Wt. conc. lignin (g g^{-1}) (14)	0.23	0.85
Vol. conc. lignin (g cm^{-3})	0.20	0.74
Δε (cm^{-1} g^{-1} L) (eq. [1])	1.4	0.7
$PhOH/C_9$ (eq. [3])	0.12	0.06

Values of ΔA_{300} normalized to a section thickness of 1 μm were then obtained. Three such sets of measurements were made and the mean value of ΔA_{300} and the mean deviation are given in Table 3.

The weight concentration of lignin for the secondary wall and cell corner middle lamella for spring wood in spruce was taken from the published data of Fergus *et al.* (13). By dividing by the factor of 1.15 to allow for the volume of the water swollen cell wall (14) the volume concentration of the lignin was obtained. Δε was then calculated from eq. [1] and from the values of Δε, the $PhOH/C_9$ for the secondary wall and middle lamella were calculated by means of eq. [3] to be 0.12 and 0.06, respectively.

As shown in Table 3 the experimental variation in ΔA_{300} is substantial and in the case for the cell corner middle lamella amount to ±23%. This large deviation is a clear manifestation of the difficulty of reproducing the measurement of ΔA_{300} from section to section. It is interesting to note, however, that the deviation in the ratio of $\Delta A_{300}(S2)/\Delta A_{300}(ML)$ was only about ±5% (12). This suggests that the variation in ΔA_{300} is due, in part, to the error in the determination of the thickness of the sections.

Discussion

The most significant characteristic of the results is the low values for the $PhOH/C_9$ ratio. If it is assumed that 72% of the lignin is in the secondary wall and 28% in the middle lamella and that the lignins in these two regions have the $PhOH/C_9$ ratios given in Table 3, the overall $PhOH/C_9$ of the lignin in black spruce can be calculated to 0.10. This result is considerably lower than the values of 0.19–0.20 reported by Chang *et al.* (15) for milled wood lignin and cellulolytic enzyme lignin from Norway spruce. The $PhOH/C_9$ values given in Table 3 are also lower than those reported in a previous paper from this laboratory (5). However, the previous results were not absolute but were based on the data published by Chang and coworkers (15).

It is interesting to note that Chang *et al.* (15) anticipated the low values of the PhOH content of the lignin in the wood. They noted that the phenolic hydroxyl content of the milled wood and cellulolytic enzyme lignins decreased with increase in molecular weight. They also found that reballmilling of cellulolytic enzyme lignin produced a decrease in the molecular weight and an increase in the $PhOH/C_9$ ratio. The authors then state "These results indicate that the molecular weight of lignin *in situ* is much higher than in the isolated lignins, and that its content of free phenolic hydroxyl groups ... may be even less than in the .. (cellulolytic enzyme lignin) preparations". Thus the high values of the $PhOH/C_9$ ratio in milled wood lignin may be artifacts caused by the isolation procedure and the lower values found in the present work for lignin in wood tissue may be more correct.

In spite of the agreement with the predictions of Chang *et al.* (15), we should consider the question as to whether the low values found for the $PhOH/C_9$ ratio in the present work are produced by some flaw in the experimental procedure followed. There seems to be three possible sources of error, as follows: (*1*) the determination of $PhOH/C_9$ by the method of periodate oxidation of MWL; (*2*) the determination of $\Delta\varepsilon_{300}$ for the dissolved MWL; (*3*) the microscopic determination of $\Delta\varepsilon_{300}$ on wood tissue with the uv microscope.

With respect to the accuracy of the method of periodate oxidation, it is interesting to note that the $PhOH/C_9$ ratio of 0.205 given in Table 2 is in good agreement with the value of 0.195 found by Chang *et al.* (15) using a similar method on milled wood lignin from Norway spruce. These authors also obtained a value of 0.202 using the Δε methods of Aulin-Erdtman (4) and Wexler (7). Thus it seems likely that the determination of the $PhOH/C_9$ ratio of the milled wood lignin used in the present work is correct.

The determination of $\Delta\varepsilon_{300}$ for the dissolved MWL may be questioned because of the use of different solvent systems for the neutral and alkaline solutions. However, the fact that the results were unchanged when pure dioxane was substituted from 50/50 dioxane/water for the neutral solution supports the reliability of the results obtained.

The most likely cause of error lies in the determination of $\Delta\varepsilon_{300}$ with the ultraviolet microscope. Usually absorbance measurements in the ultraviolet region are made on lignin in very dilute solutions (0.1 g L^{-1}) in a cell with path length of 1 cm. With the microscope the path length is the thickness of the section ($\sim 10^{-4}$ cm) and the concentration of lignin is from 200 to 800 g L^{-1}. In a

Can. J. Chem. Downloaded from www.nrcresearchpress.com by 210.87.254.42 on 09/05/12
For personal use only.

previous investigation (11), Beer's law was shown to be valid for aqueous solutions of lignosulphonate over a concentration range of 0.05 → 250 g L^{-1}. However, this may not be the case for $\Delta\varepsilon_{300}$. At the higher concentrations the ionization of the PhONa salt may be suppressed to give a smaller value of $\Delta\varepsilon_{300}$ than would have been obtained in a more dilute solution. It is interesting to note that, if this is the case, the error would be expected to be larger for the cell corner middle lamella because of the higher concentration of lignin in this tissue region. Thus the ratio of 2 previously found for the PhOH content in the cell wall lignin to that in the cell corner lignin may, in fact, be erroneously high (5).

A further source of error lies in the interference of the conjugated α-carbonyl groups. Goldschmid (16) has pointed out that the presence of such groups causes the 300 nm difference curve maximum to decrease. Sarkanen *et al.* (17, 18) have shown that the difficulty may be circumvented by borohydride reduction of the lignin prior to the determination. This step was not attempted in the present investigation. Instead it was assumed that the ratio of conjugated α-carbonyl groups to PhOH groups was the same in the MWL and the protolignin in the wood, in which case the effect would not produce an error in the determination of $PhOH/C_9$.

Further work will be necessary in order to test the findings of the present investigation. Perhaps the best approach, following in the footsteps of Bailey (19), would be to devise a suitable method for the preparation of gram quantities of pure middle lamella lignin directly from wood. Such a fractionation would permit unambiguous physical and chemical characterization of this important morphological region in wood. It is interesting to note that since this paper was first submitted for publication, Hardell *et al.* (20) have described a fractionation of spruce wood into different tissue regions. In qualitative agreement with our previous result (5), these authors found that the phenolic hydroxyl content of the lignin in the secondary wall was at least twice that of the lignin the middle lamella. However, no determination of the $PhOH/C_9$ ratio was reported.

1. E. ADLER, S. HERNESTAM, and I.WALLDÉN. Sven. Papperstidn. **61**, 641 (1958).
2. J. GIERER. Sven. Papperstidn. **73**, 571 (1970).
3. Y. Z. LAI and K. V. SARKANEN. *In* Lignins. *Edited by* K. V. Sarkanen and C. H. Ludwig. Wiley-Interscience, New York, NY. 1971. p. 201.
4. G. AULIN-ERDTMAN. Sven. Papperstidn. **57**, 745 (1954).
5. J.-M. YANG and D. A. I. GORING. Trans. Tech. Sect. CPPA, **4**, 2 (1978).
6. O. GOLDSCHMID. Anal. Chem. **26**, 1421 (1954).
7. A. S. WEXLER. Anal. Chem. **36**, 213 (1964).
8. J. GIERER, B. LENZ, I. NORÉN, and S. SÖDERBERG. Tappi, **47**, 233 (1964).
9. A. BJÖRKMAN. Sven. Papperstidn. **59**, 477 (1956).
10. A. BJÖRKMAN and B. PERSON. Sven. Papperstidn. **60**, 158 (1957).
11. J. A. N. SCOTT, A. R. PROCTER, B. J. FERGUS, and D. A. I. GORING. Wood Sci. Technol. **3**, 73 (1969).
12. J.-M. YANG. Ph.D. thesis. McGill University, Montreal, 1977.
13. B. J. FERGUS, A. R. PROCTER, J. A. N. SCOTT, and D. A. I. GORING. Wood Sci. Technol. **3**, 117 (1969).
14. P. A. AHLGREN, J. R. WOOD, and D. A. I. GORING. Wood Sci. Technol. **6**, 81 (1972).
15. H.-M. CHANG, E. B. COWLING, W. BROWN, E. ADLER, and G. MIKSCHE. Holzforschung, **29**, 153 (1975).
16. O. GOLDSCHMID. *In* Lignins. *Edited by* K. V. Sarkanen and C. H. Ludwig. Wiley-Interscience, New York, NY. 1971. p. 248.
17. K. V. SARKANEN, H.-M. CHANG, and G. G. ALLAN. Tappi, **50**, 583 (1967).
18. K. V. SARKANEN, H.-M. CHANG, and G. G. ALLAN. Tappi, **50**, 587 (1967).
19. A. J. BAILEY, Ind. Eng. Chem. Anal. Ed. **8**, 52 (1936).
20. H.-L. HARDELL, G. J. LEARY, M. STOLL, and U. WESTERMARK. Sven. Papperstidn. **83**, 44 (1980).

Can. J. Chem. Downloaded from www.nrcresearchpress.com by 210.87.254.42 on 09/05/12
For personal use only.

Conformation and crystalline structure of (2→1)-β-D-fructofuranan (inulin)

R. H. MARCHESSAULT,[1] T. BLEHA,[2] YVES DESLANDES,[1] and J.-F. REVOL[3]

Department of Chemistry, Université de Montréal, C.P. 6210, Succursale A, Montréal (Qué.), Canada H3C 3V1

Received May 20, 1980

This paper is dedicated to Prof. Raymond U. Lemieux on the occasion of his 60th birthday

R. H. MARCHESSAULT, T. BLEHA, YVES DESLANDES, and J.-F. REVOL. Can. J. Chem. **58**, 2415 (1980).

The crystalline conformation of inulin a (2→1)-β-D-fructofuranan has been determined based on conformational analysis coupled with X-ray and electron diffraction data. The energy contour maps as a function of three torsional angles ϕ, ψ, ω in the backbone were calculated taking into account van der Waals, torsional, and electrostatic interactions. Although several minima were observed, only two models are possible when one considers the information obtained from the diffraction data. The two models correspond to five-fold helices, one 5_4 (left-handed) and the other 5_1 (right-handed) with an advance per monomer of 2.16 Å, but with different conformational angles: $\omega = 60°$ and 180° respectively. Compared to the crystalline state torsion angles of polyethylene oxide analogs of inulin, large differences are noted. Steric interactions of the substituents and the exoanomeric effect are believed responsible for the observed conformational differences.

R. H. MARCHESSAULT, T. BLEHA, YVES DESLANDES et J.-F. REVOL. Can. J. Chem. **58**, 2415 (1980).

La conformation cristalline de l'inuline, un (2→1)-β-D-fructofuranan, a été déterminée en utilisant l'analyse conformationelle et les données expérimentales obtenues de la diffraction des rayons-X et de la diffraction électronique. Les cartes d'isoénergie en fonction des trois angles de torsion: ϕ, ψ, ω le long de la chaine furent calculées en considérant les interactions de van der Waals, les angles de torsion, et les interactions électrostatiques. Quoique plusieurs minima soient observés dans les cartes d'isoénergie, seulement deux modèles sont possibles si on considère l'information supplémentaire obtenue des clichés de diffraction (rayons-X et diffraction electronique sur cristaux uniques). Les deux modèles corespondent à des hélices de symétrie d'ordre 5, une 5_4 (hélice main gauche) et l'autre 5_1 (hélice main droite) ayant une avance par monomère de 2.16 Å; cependant elles ont differentes valeurs de l'angle de torsion: $\omega = 60°$ et 180° respectivement. A l'état solide, d'importantes différences sont observées entre les angles de torsion de l'inuline et celle de ses analogues de la famille des oxydes de polyéthylène. Les interactions stériques de substituants et l'effet éxo-anomérique sont probablement responsables pour ces différences.

Introduction

Although much progress has been made on the prediction of the conformational states of polysaccharides, almost all the work was concentrated on pyranose forms and little is known about the conformational structure of furanose polysaccharides. While a majority of carbohydrates in nature exist in the pyranose form, a number of biologically important molecules contain carbohydrate moieties with a 5-membered acetal ring. The furanose ring for example occupies a central position in the chemical structure of nucleic acids and in the important natural product of plants: sucrose.

For conformational studies of molecules such as polysaccharides a combined theoretical and experimental approach is the most powerful procedure (1–3). The role of theory in this procedure consists in assigning the preferred conformations on the basis of potential energy calculation for an isolated macromolecule. Although the evaluation of conformational energy is usually based on simple empirical potential functions the method as a whole has been remarkably successful for selecting the correct conformation when combined with some experimental evidence.

All previous stereochemical treatments have been devoted to pyranose polysaccharides and no attempts have been made for the furanose types, apart from the nucleic acid studies. One may expect that the conformational properties of pure furanans differ substantially from those for nucleic acids, mainly due to the absence of phosphate groups and the possibility of stacking interactions between bases in the latter. The enhanced flexibility of the furanose ring in comparison with the relatively rigid pyranose ring is the principal additional complicating factor in these calculations. As a first step in the explorations of furanans we decided to study inulin: a poly(2→1)-β-D-linked fructose (Fig. 1). Polyfructosans represent the most frequently occurring group of furanose polysaccharides (4). Besides inulin, the furanans include also levan which is poly(2→6)-β-D-linked fructose.

Inulin is a plant polysaccharide with a degree of polymerization of about 30 which varies with the

[1]Present address: Xerox Research Centre of Canada, 2480 Dunwin Drive, Mississauga, Ont., Canada L5L 1J9.

[2]Permanent address: Polymer Institute, Slovak Academy of Sciences, 80934 Bratislava, Czechoslovakia.

[3]Present address: Pulp and Paper Research Institute of Canada, 570 St. John's Boulevard, Pointe Claire, P.Q., Canada H9R 3J9.

0008-4042/80/232415-08$01.00/0

©1980 National Research Council of Canada/Conseil national de recherches du Canada

Can. J. Chem. Downloaded from www.nrcresearchpress.com by 210.87.254.42 on 09/05/12
For personal use only.

Can. J. Chem. Downloaded from www.nrcresearchpress.com by 210.87.254.42 on 09/05/12
For personal use only.

plant species and the life cycle. It serves as a reserve carbohydrate in the plant kingdom and is synthesized by successive addition of D-fructofuranose groups to sucrose (Gp-Ff), via the trisaccharide Gp-Ff-Ff (1-kestose), tetrasaccharide Gp-Ff-Ff-Ff (nystose), etc. Inulin solutions are universally used as a measure of the efficiency of glomerulal filtration in kidneys (5). Recently, oligomers of the inulin type have been identified as an important group of antigens forming immunobiological complexes with some myeloma immunoglubulins (6). Thus a knowledge of preferred conformations is basic to a development of the molecular biology aspects of inulin. Furthermore, as can be seen from the molecular formula in Fig. 1, inulin exhibits a unique structural feature within the family of polysaccharides, i.e. no bond of the furanose ring is part of the macromolecule backbone. Thus it is a biopolymer which has a close structural relation to the polyethyleneoxide class of synthetic polymers with general formula $-(O-CH_2-CR_1R_2)_n-$. However, it is not a polyether but a polyacetal.

In the present paper we wish to report the results of the conformational analysis for inulin type oligomers and polymers. From the calculated conformational energies the most probable helical conformations in the solid state are predicted and compared to some X-ray and electron diffraction data.

Conformational Analysis

A procedure as in the recent treatment of (1→6)-α-D-glucan conformations (7) was used. This involved an evaluation of the potential energy of the isolated inulin dimer molecule (inulobiose) as a function of three torsional angles ϕ, ψ, ω in the main backbone of the molecule. Figure 1 represents inulobiose in the extended all-*trans* conformation which corresponds to $\phi = \psi = \omega = 180°$. It is to be noted that in the fructofuranose moiety the anomeric carbon is C2. The definition of torsional angles $\phi = \theta(C1—C2—O—C1')$, $\psi = \theta(C2—O—C1'—C2')$, and $\omega = \theta(O—C1'—C2'—O')$ follows the proposed convention (8).

The geometrical parameters for the fructofuranose moiety were taken from the neutron-scattering investigation of crystalline sucrose (9). The glycosidic angle C1'O1'C2' was taken to be 114.0° and both O6 hydroxyl groups in inulobiose were fixed in a *trans* position with respect to C4—C5 bonds. Preliminary calculations revealed this position of the hydroxyl group as sterically favored in comparison with the *gauche* orientation as found in the sucrose structure. The ring conformation in this geometry is described as "envelope" (E_3) in which C3 is displaced out of the plane of the other four atoms: C2, O2, C5, C4 atoms (Fig. 2). This displacement in the opposite (*exo*) direction to C6 and O atoms represents the primary ring puckering and its value is 0.542 Å above the plane of atoms in question (10).

The potential energy of inulobiose was calculated taking into account van der Waals, torsional, and electrostatic interactions, also the energy of possible H-bonds between the two rings was considered. For van der Waals, torsional, and H-bond contributions the same potential functions as previously described (7) were used. All hydrogen atoms have been included in the calculations. An attempt has been made to include the electrostatic interactions between the point charges localized on each atom using the Coulomb law and dielectric constant $\varepsilon = 2$. The electrostatic term is usually of little importance in conformational analysis of polysaccharides (1) but may play an important role in polymers with a polyoxide main chain. Partial charges were evaluated using the following set of

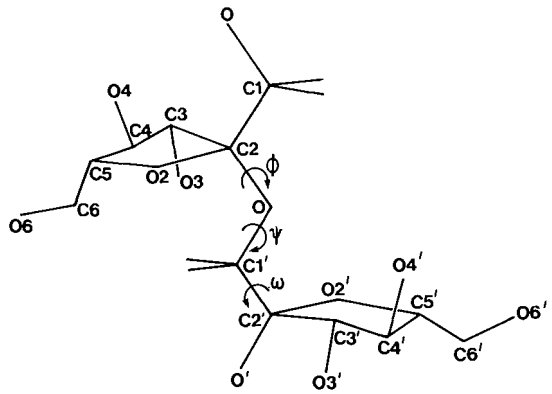


FIG. 1. Inulin-type difructosan molecule (inulobiose) in all-*trans* conformation $\phi = \psi = \omega = 180°$. Ring hydrogen atoms are not shown.

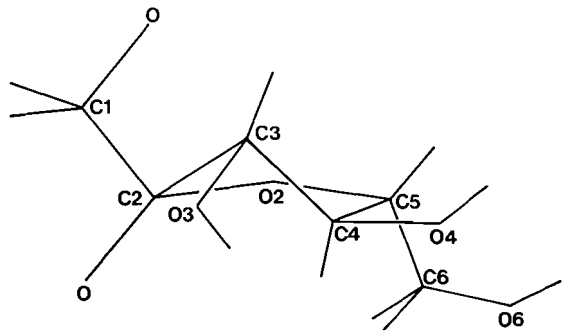


FIG. 2. Representation of ring puckering in fructofuranose moiety with C3 atom displaced out of plane formed by C2', O2', C5', and C4' atoms. Hydrogen atoms are omitted.

Can. J. Chem. Downloaded from www.nrcresearchpress.com by 210.87.254.42 on 09/05/12
For personal use only.

fixed bond dipoles: 0.82 D, 0.38 D, and 1.53 D for C—O, C—H, and O—H, respectively.

The ϕ,ψ isoenergy maps were constructed with a 10° grid. Each map was for a fixed value of ω which was changed at 20° intervals over the range $-180° < \omega < 180°$. Simultaneously, the helical parameters n (the number of residues per turn) and h (the projected height of the residue onto the helix axis) were calculated for each ϕ,ψ pair using the virtual bond method of generating the helical chains (11, 12).

Results

As for the dextran case (7), the allowed three dimensional conformational space is a "cylinder" with an irregular cross-section. The cylinder is extended parallel to the ω axis. Figures 3 and 4 show the ϕ,ψ sections computed for $\omega = 180°$ and $\omega = 60°$, respectively, without inclusion of the electrostatic term in the calculations. The allowed conformational space is restricted to the area around the position $\phi = 90°$, $\omega = 180°$. Variation of ω from $-180°$ to 180° results in only small changes in the cross-sectional shape of the allowed conformational ϕ,ψ space whose limit was arbitrarily set at an energy contour of 15 kcal/mol relative to the lowest calculated minimum on the map.

The minor influence of ω on the overall shape of "available" conformational space follows from the calculations regardless of electrostatic interactions. However, the situation is different when the local minima within a given cross-section are considered. For example, in the conformational map for $\omega = 180°$ (Fig. 3) the lowest minimum lies at $\phi = 70°$, $\psi = 120°$ and this mimimum is also the absolute minimum found for the whole (ϕ,ψ,ω) space in calculations performed without the electrostatic term. The second local minimum found for $\omega = 180°$ occurs at $\phi = 90°$, $\psi = 190°$ is about 1.62 kcal/mol higher than the absolute minimum. Finally, the third local minimum found in the "available" conformational space in Fig. 3 is situated at (140°,260°) 3.33 kcal/mol over the absolute minimum. Only this latter minimum is stabilized by one intramolecular hydrogen bond.

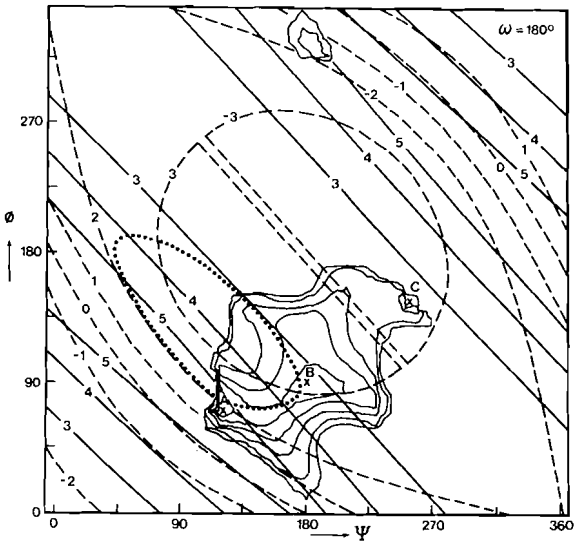


FIG. 3. ϕ,ψ conformational energy map for $\omega = 180°$. Relative isoenergy contours indicate energy values in kcal/mol relative to the lowest calculated minimum in the map. The full, dashed, and dotted curves represent the iso-n and iso-h contours and helices with $p = 10.8$ Å respectively.

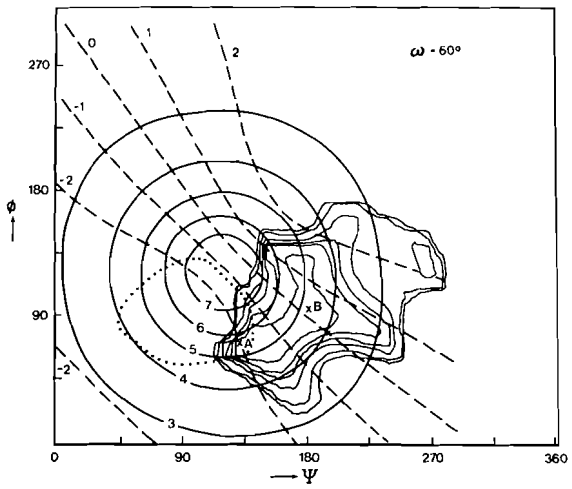


FIG. 4. ϕ,ψ conformation energy map for $\omega = 60°$. Relative isoenergy contours indicate energy values in kcal/mol relative to the lowest calculated minimum in the map. The full, dashed, and dotted curves represent the iso-n and iso-h contours and helices with $p = 10.8$ Å respectively.

The inclusion of the electrostatic term in the calculation changes the position of the minima and their relative stability. The local minimum (140°, 260°) is only 0.07 kcal/mol over the absolute minimum, now at (140°,140°), and the third mimimum (90°,190°) has the energy 4.06 kcal/mol. This and similar comparisons of conformational maps for other values of ω revealed that inclusion of the electrostatic term in our calculations manifests itself by enhanced stabilization of all conformations with intramolecular H-bond or bonds. This feature is due to the relatively high negative charges carried by hydrogen atoms of hydroxyl groups and their fixed position in the assumed rigid geometry of the inulobiose molecule. Since the contribution of H-bonds has already been included in the potential functions used it was judged that calculations with an electrostatic term overestimate the H-bond contribution. Therefore, most of our discussion

Can. J. Chem. Downloaded from www.nrcresearchpress.com by 210.87.254.42 on 09/05/12
For personal use only.

and subsequent conclusions are based on calculations without the electrostatic term.

The position and the sequence of minima for the ϕ,ψ map for $\omega = 60°$ (Fig. 4) duplicate the results for $\omega = 180°$. The lowest minimum is at (70°,135°), followed by conformations (90°,180°) with energy 0.55 kcal/mol and (130°,270°) with energy 3.62 kcal/mol. None of these minima are stabilized by an intramolecular H-bond. The maps in Figs. 3 and 4 are energetically preferred cross-sections of the general ϕ,ψ,ω hypersurface. This is supported by Fig. 5 showing the plot of minima energy for various ϕ,ψ maps, as a function of ω. Surprisingly, the third staggered position at $\omega = -60°$ results in a minimum with higher energy than an additional unexpected minimum at $\omega = -110°$.

Except for the range from $\omega = -80°$ to $\omega = 20°$ the lowest minimum (type A) in the ϕ,ω maps is always situated around $\phi = 70° \pm 10°$ and $\psi = 115° \pm 25°$. Only in the interval $-80° < \omega < 20°$ is this type of conformation slightly less favorable than conformations of type B: $\phi = +105° \pm 25°$, $\psi = -175° \pm 5°$; e.g. for $\omega = -60°$ the conformation (80°,130°) is 1.13 kcal/mol over the lowest minimum (130°, 180°). It should be noted that both above-mentioned minima are separated by a very low potential barrier. The third minimum (C) at about $\phi = 135° \pm 5°$ and $\psi = 265° \pm 5°$ is almost independent of ω, but is also the least important of the three.

The conformational maps for the ϕ,ψ,ω hypersurface clearly show that ϕ and ψ variations define the most important torsional potential interactions in the inulobiose molecule. The ϕ,ψ coupling restricts the polyoxyethylene-like main chain in (2→1)β-D-linked fructofuranans to a fairly narrow conformational space. On the other hand the ω torsional potential brings flexibility to the molecule since variation in ω brings about only a slight change in potential energy (within 5 kcal/mol for lowest minimum on each ϕ,ψ map (Fig. 5)). The most convenient aid for the selection of the main chain conformation of inulin in the solid state is the simultaneous use of the inulobiose ϕ,ψ isoenergy maps with n,h helical parameter maps. Using the virtual bond method (11, 12) we evaluated the helical parameters n and h for inulin in the whole ϕ,ψ,ω conformational space. The maps of n, the number of residues per turn of the helical chain and h, the projected height of the residue along the helix axis are given in Figs. 3 and 4 for two typical cases $\omega = 180°$ and $\omega = 60°$. Negative h values denote left-handed helices. For the map with $\omega = 180°$ the allowed space corresponds to helices with n from 2 to 6 all being right-handed except for the small area around the (140°,260°) minimum. The lowest minimum (type A) at (70°,120°) corresponds approximately to the integral right-handed helix with a five-fold screw axis and helix pitch ($p = n \times h$) equal to 8.94 Å. The minimum at (90°,190°) (type B) is close to a 3_1 symmetrical right-handed helix with 9.61 Å pitch. In the map with $\omega = 60°$ the allowed space corresponds both to right- and left-handed helices with n from 2 to 8. The lowest minimum on this map, at (70°,135°), implies again a 5_1 helix but left-handed with $p = 9.61$ Å. For the second minimum (90°,180°) $n = 4.58$ and $h = 0.04$ Å. Finally, the third minimum (120°,270°) predicts a right-handed helix with $n = 2.34$ and $h = 2.14$ Å.

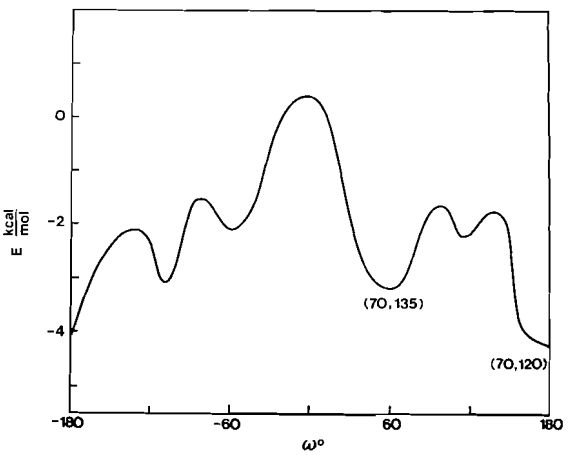


FIG. 5. The energy of lowest minimum on particular ϕ,ψ maps as a function of ω. Figures on the curve identify the ϕ,ψ positions of lowest minimum energy.

Recent work on the molecular and crystal structure of 1-kestose (13), which is a trisaccharide Gp-Ff-Ff containing the inulobiose moiety, fully supports the validity of the assumed geometry of the fructofuranose ring. For the second fructose unit in 1-kestose the *exo* E_3 envelope conformation is reported with the C3 atom displaced 0.63 Å from the plane of the other four atoms. The principal torsional angles determined for the inulobiose moiety in 1-kestose are as follows: $\phi = 80.5°$, $\psi = 190.3°$, and $\omega = 179.2°$ (13). As shown in Fig. 3 for $\omega = 180°$ this structure lies in the allowed conformational space and is situated very near to the local minimum B at (90°, 190°). In accordance with the computation, experimental data (13) confirmed also that there is no intramolecular hydrogen bond stabilizing the inulobiose structure in 1-kestose.

In the absence of other supporting experimental data it is difficult to predict unambiguously the crystalline chain conformation of inulin solely on the basis of energy calculations. Most probably this structure should have parameters similar to A or B type minima in the conformational map (Fig. 3), i.e. a helix with a three- to five-fold screw axis.

Can. J. Chem. Downloaded from www.nrcresearchpress.com by 210.87.254.42 on 09/05/12
For personal use only.

Diffraction Data

The electron and X-ray diffraction study on the inulin single crystals provided additional information for the interpretation of the stereochemical analysis. The sample used in this investigation was from Nutritional Biochemicals Corp., Cleveland, OH, and was used "as received". The agreement between the observed X-ray data (cf. below) and the information in the literature (14) was taken as confirmatory evidence that the sample was genuine. Liquid chromatography confirmed that the sample was polydisperse and easily degraded on heating in water (15).

Single crystals of inulin were prepared as follows: a 0.05% aqueous solution of inulin was dissolved in water at 45°C and cooled to about 1°C. After several days the solution appeared quite turbid and the crystals were collected by centrifugation. After successive washings in ethanol part of the suspension was used for the electron microscopy observations and the other part was spread on a Teflon plate. The film so obtained was extremely brittle and all attempts to prepare oriented films or fibers were ineffective. In another attempt to obtain oriented X-ray fiber diagrams it was assumed that during the film drying process the large faces of the crystals would align parallel to the plate surface. Therefore, the small pieces of dry film representing single crystal mats were vertically stacked together. With the X-ray beam parallel to the surface of the stack, an X-ray diagram was recorded on flat film using Cu Kα radiation. Probably due to the imperfect alignment of single crystals in the mats as well as of the single crystals themselves only a poorly oriented fiber diagram was obtained where the layer line assignments could only be made with difficulty. The density of dried inulin film was measured via flotation in a density gradient (CCl_4–$CHCl_3$) column and was found to be 1.54 ± 0.05 g cm^{-3}.

For electron microscopy observations, drops of the ethanol suspension of inulin single crystals were evaporated on carbon-coated grids. Observations were made with a Philips EM 300 transmission electron microscope operating at 60 kV for images and 100 kV for diffraction. The single crystals to be observed were either shadowed with tungsten or unshadowed. Gold was evaporated on some of the single crystal preparations for diffraction calibration.

An electron micrograph along with an electron diffraction pattern typical of inulin single crystals are shown in Fig. 6. The lamellar character of the crystals is undeniable but the perfection is far less than was observed in similar materials, e.g. wood xylan (16). In that case the hexagonal shape was almost perfect whereas here only occasional 120° angles are visible in the particulate product. At the edges of the thickened crystals single layer lamellae about 40–50 Å thick were always visible. The best diffraction data were recorded from moderately thickened uniform areas of the crystals and a sample diffractogram is shown in Fig. 6 along with a schematic interpretation.

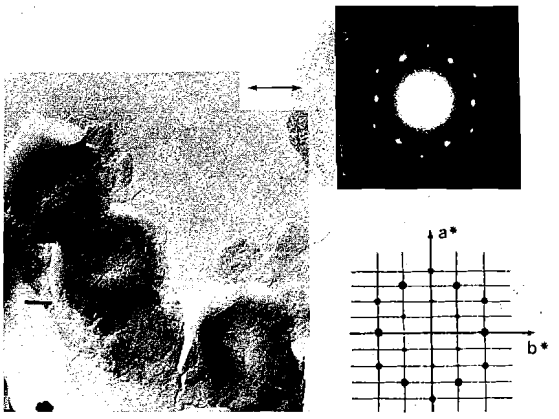


FIG. 6. Electron micrograph and electron diffraction pattern of single crystals of inulin along with a schematic relating the pseudohexagonal cell to the diffraction data. The 200 and 110 reflections in the schematic are masked by the central beam in the electron diffractogram (the arrow represents 0.5 μm).

Overall electron diffraction data indicate hexagonal symmetry in the base plane ($h\ k\ 0$). However, an orthorhombic (pseudo-hexagonal) unit cell provided the more correct base plane parameters a and b determined from electron diffraction data for this "dry" form with $a = 16.71$ Å and $b = 9.65$ Å. The "fiber repeat" was derived by a comparison of the electron diffractogram data and the X-ray diffraction data. Comparing all resolved ($h\ k\ 0$) reflections from the electron diffractogram with the X-ray data allowed indexation of the remaining X-ray reflections. The best fit between the calculated and observed d-spacings was found for $c = 10.8$ Å. Table 1 lists the d-spacings and their assignment.

One of the principal difficulties in this study was in appreciating the effect of hydration on the relative intensities of the diffraction data. An illustration of this difficulty can be had from Fig. 7 where diffractometer traces as a function of exposure to room humidity (r.h.) are shown. The first trace presumably corresponds closely to what would be observed in the electron microscope and shows a sharp reflection at $d = 8.35$ Å. This reflection is one of those observed in the electron diffractogram (0% r.h.) but it is absent in the 95% r.h. diffractometer scan. This problem had been alluded to previously by Katz and Derksen (14) but the data of Fig. 7 serves to illustrate one of the difficulties in com-

TABLE 1. Comparison of calculated and observed d spacing in "dry" form of crystalline inulin

Spacing	hkl	d_{calcd}	$d_{X\text{-}ray}$	$d_{el.\,diff.}$
1	001	10.8	10.70	
2	110 200	8.35	8.35	8.35
3	011	7.19	7.20	
4	211 002	5.42	5.34	
5	020 310	4.82	4.85	4.82
6	112 202	4.53	4.58	
7	220 400	4.17	4.17	4.17
8	212	4.10	4.04	
9	411 003 022	3.60	3.62	

paring electron diffraction data, necessarily recorded *in vacuo*, and X-ray data on polysaccharides.

From the comparison of the unit cell volume and the measured density it follows that there are 10 fructofuranose moieties per unit cell which is consistent with the presence of two chains in the unit cell with a five-fold screw axis (integral helix) along the c direction and a helix pitch $p = \pm 10.8$ Å. In this way the experimental data provided an additional restriction for the selection of the inulin chain conformation in the stereochemical analysis.

The ϕ,ψ variation of helix pitch for $p = \pm 10.8$ Å is plotted in Figs. 3 and 4. For $\omega = 60°$ (Fig. 4) it is possible to construct a model, left-handed (60°, 135°) which satisfies both conditions, i.e. $p = -10.8$ Å and a 5-fold. At $\omega = 180°$ (Fig. 3) a second model is found for the conformation about (75°,130°). Thus two low energy models can be proposed for the crystalline inulin chains. The model with $\omega = 180°$ (lowest energy) is shown in Fig. 8. The proposed conformation for $\omega = 180°$ is in an energy trough which includes the observed ϕ,ψ for the inulobiose end of 1-kestose; the latter almost coincides with the calculated energy minimum B in the map shown in Fig. 3.

Discussion

The area of allowed ϕ,ψ conformations which have been reported for all classes of polysaccharides with various types of linkages differs in their preference for a particular portion of ϕ,ψ space (17). So far no other polysaccharides exhibit

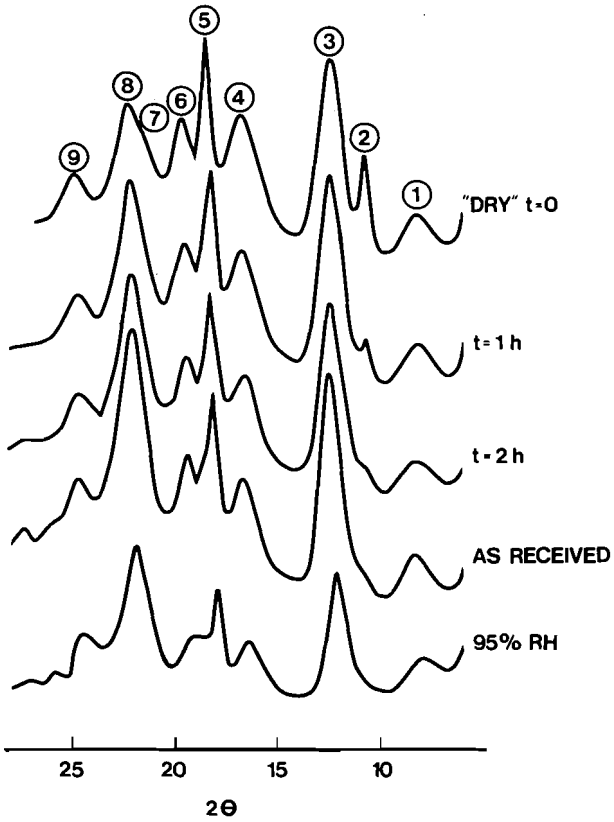


FIG. 7. X-ray diffractometer traces of a single sample of inulin powder recorded at various times after removal from a vacuum oven at 90°C. The last trace was recorded after the sample had been exposed to 95% relative humidity for 24 h.

minima in the same region of ϕ,ψ space as inulobiose, however for the structurally similar (1→6) linked α-D-glucans the allowed conformations are centered approximately around (0°,180°) (7).

Comparison with the polyoxyethylene class of synthetic macromolecules with general formula $[—CR_1R_2—O—CH_2—]_n$ is instructive for appreciating the strong (ϕ,ψ) coupling, as shown in Fig. 3. Only the conformational structure of the simplest synthetic polymers of this class has been determined (4, 5). In inulin the steric interactions of the "side group" correspond to $R_1 = R_2 = C_4O_4H_8$ and this ring substitution biases (ϕ,ψ) to rather unexpected values as may be seen by comparison with the crystalline state conformation of substituted polyoxyethylenes (18, 19) (Table 2). It should be noted that the regular (2→1)-β-D linkage in inulin results in an "isotactic" structure for inulin. The ω values for crystalline poly(alkyleneoxides) are either 180° or near to 60°, polyoxyethylene having two crystalline polymorphs. Both this comparison

Can. J. Chem. Downloaded from www.nrcresearchpress.com by 210.87.254.42 on 09/05/12
For personal use only.

Can. J. Chem. Downloaded from www.nrcresearchpress.com by 210.87.254.42 on 09/05/12
For personal use only.

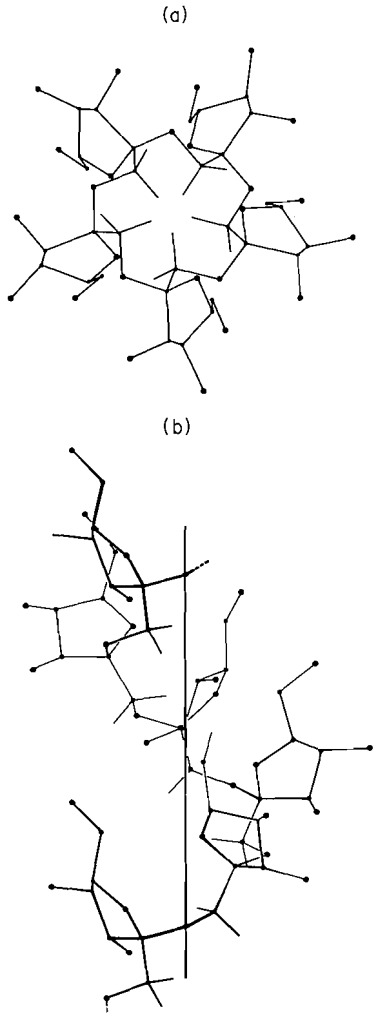


FIG. 8. The proposed conformation of the inulin (ω = 180°) chain in (*a*) *X–Y*, (*b*) *Y–Z* planes. The chain axis is along the *Z* axis and corresponds to a 5_1 helix. Hydroxyl and ring hydrogens are omitted.

as well as the potential energy diagram in Fig. 5 confirm that approximately 180° or 60° values for ω should be expected in the crystalline chain conformation of inulin.

Another comparison involving the ω values from Table 2 shows that all polymers prefer (approximately) the *trans* position, inulin being the most divergent from this rule. A similar comparison of ϕ values shows, however, that the ϕ values for poly(alkylene oxides) and inulin are quite different. This is probably related to the exoanomeric effect (20, 21) which provides additional non-bonded interaction due to oxygen–oxygen lone pair interactions of O2 and the glycosidic oxygen.

Some models of inulin were suggested previously (5, 6, 22). Phelps (22) claimed that the known

TABLE 2. Molecular conformation of isotactic poly-alkylene oxides $[—CHR—O—CH_2—]_n$ and inulin

R	ϕ	ψ	ω	Symmetry	Reference
H	183	184	68	(7/2) helix	25
	180	180	180	zig-zag	26
CH_3	165	195	180	(2/1) helix	27
$CH(CH_3)_2$	290	180	67	(2/1) helix	28
$C(CH_3)_3$	263	180	73	(9/4) helix	18
Inulin	75	130	180	(5/1) helix	This work

physicochemical data for the inulin molecule pointed to its conformation being a helix of four fructofuranose units per turn while Middleton (5) recommended a slightly lower value about 3.9 units per turn to avoid presumed steric repulsion of *n*th and (*n* + 4)th unit. Both these studies dealt with the conformation of inulin in solution and as is evident from our conformational maps several helix types are inside the favored area for ω = 180°. The conformation of inulin in solution can be expected to range, on the average, over all possible (ϕ,ψ,ω) combinations within the "allowed area" using the standard method of configurational statistics (23) to establish the probability of a given structure. Finally, the conformational energy maps in Figs. 3 and 4 should be relevant also in the structure-immunobiological activity relationship for fructofuranans (6, 24). Some myeloma immunoglobulins with anti-fructofuranan specificity have different complexing behaviour to (2→1)-β-D-linked and (2→6)-β-linked fructofuranan substrates (6). The conformational results presented in this paper can undoubtedly help in the elucidation of this difference.

Acknowledgements

Financial support from the National Research Council of Canada and the Ministère de l'Education du Québec made this work possible. The data for Fig. 7 were provided by Xerox Research Centre of Canada. The technical assistance of H. Morikawa of the Department of Agricultural Chemistry, University of Kyoto, is acknowledged.

1. D. A. BRANT. Q. Rev. Biophys. **9**, 527 (1976).
2. P. ZUGENMAIER and A. SARKO. Biopolymers, **15**, 2121 (1976).
3. P. R. SUNDARARAJAN, R. H. MARCHESSAULT, G. J. QUIGLEY, and A. SARKO. J. Am. Chem. Soc. **95**, 2001 (1973).
4. E. J. MCDONALD. Adv. Carbohydr. Chem. **2**, 253 (1946).
5. E. MIDDLETON. J. Membrane Biol. **34**, 93 (1977).
6. D. G. STREEFKERK and C. P. J. GLAUDEMANS. Biochemistry, **16**, 3760 (1977).
7. I. TVAROSKA, S. PÉREZ, and R. H. MARCHESSAULT. Carbohydr. Res. **61**, 97 (1978).

8. IUPAC-IUB Commission on Biochemcial Nomenclature. Arch. Biochem. Biophys. **145**, 405 (1971); J. Mol. Biol. **52**, 1 (1970).
9. G. M. BROWN and H. A. LEVI. Acta Crystallogr. B**29**, 790 (1973).
10. M. SUNDARALINGAM. J. Am. Chem. Soc. **87**, 599 (1965).
11. P. R. SUNDARARAJAN and R. H. MARCHESSAULT. Can. J. Chem. **53**, 3563 (1975).
12. P. R. SUNDARARAJAN. *In* Biomolecular structure, conformation, function and evolution. Pergamon Press, London. In press.
13. G. A. JEFFREY and Y. J. PARK. Acta Crystallogr. B**28**, 257 (1972).
14. J. R. KATZ and J. C. DERKSEN. Recl. Trav. Chim. Pays-Bas, **50**, 247 (1931).
15. M. D'AMBOISE, D. NOEL, and T. HANAI. Carbohydr. Res. **79**, 1 (1980).
16. R. H. MARCHESSAULT, F. F. MOREHEAD, N. M. WALTER, C. P. J. GLAUDEMANS, and T. E. TIMELL. J. Polym. Sci. **51**, 566 (1961).
17. D. A. REES. Polysaccharide shapes. Chapman and Hall, London. 1977.
18. M. SAKAKIHARA, Y. TAKAHASHI, M. TADOKORO, N. OGUNI, and H. TANI. Macromolecules, **6**, 205 (1973).
19. H. MATSUBAYASHI, Y. CHATANI, M. TADOKORO, P. DUMAS, N. SPASSKY, and P. SIGWALT. Macromolecules, **10**, 996 (1977).
20. R. U. LEMIEUX, S. KOTO, and D. VOISIN. *In* Anomeric effect. Am. Chem. Soc. Symp. Ser. 87. *Edited by* W. A. Szarek and D. Horton. 1979. p. 17.
21. S. PÉREZ and R. H. MARCHESSAULT. Carbohydr. Res. **65**, 114 (1978).
22. C. F. PHELPS. Biochem. J. **95**, 41 (1965).
23. P. J. FLORY. Statistical mechanics of chain molecules. Interscience, New York. 1969.
24. C. P. J. GLAUDEMANS. Adv. Carbohydr. Chem. Biochem. **31**, 313 (1975).
25. Y. TAKAHASHI, H. TADOKORO, and Y. CHATANI. J. Macromol. Sci. Phys. **2**, 361 (1968).
26. Y. TAKAHASHI and H. TADOKORO. Macromolecules, **6**, 672 (1973).
27. Y. TAKAHASHI, I. SUMITA, and H. TADOKORO. J. Polym. Sci. Polym. Phys. Ed. **11**, 2113 (1973).
28. Y. TAKAHASHI, H. TADOKORO, T. MIRANO, A. SATO, and T. TSURUTA. J. Polym. Sci. Polym. Phys. Ed. **13**, 285 (1975).

Can. J. Chem. Downloaded from www.nrcresearchpress.com by 210.87.254.42 on 09/05/12
For personal use only.

The kinetics and mechanism of acid catalysed hydrolysis of lactams

PETER WAN, TOMASZ A. MODRO, AND KEITH YATES[1]

Department of Chemistry, University of Toronto, Toronto, Ont., Canada M5S 1A1

Received April 14, 1980

This paper is dedicated to Prof. Raymond U. Lemieux on the occasion of his 60th birthday

PETER WAN, TOMASZ A. MODRO, and KEITH YATES. Can. J. Chem. **58**, 2423 (1980).

The acid-catalysed hydrolysis of lactams of ring size 4–7, and of *N*-ethylacetamide, has been studied at various temperatures in 0–70% aqueous sulfuric acids. The kinetics have been analysed by means of the *r*-hydration parameter treatment and the transition-state activity coefficient (TSAC) approach. Except for the β-lactam, all substrates show a strong positive rate dependence on water activity, indicating a tetrahedral intermediate type of mechanism ($A_{\delta}^{T}2$), similar to that found for simple (acyclic) amide hydrolyses; only the β-lactam shows a negative rate – water activity dependence, which is interpreted in terms of a unimolecular ($A_{N}^{R}1$) mechanism, involving rate-determining acylium ion formation. Similarly, all substrates except the β-lactam show a pronounced destabilization of the transition-state as acidity is increased, typical of oxonium ion species. The behaviour of the β-lactam resembles that of methyl mesitoate hydrolysis. Basicity constants for lactams of ring size 4–9 show a definite dependence on ring size, with the δ-lactam being unusually basic. Both rate and p*K* dependence on ring size are discussed in terms of ring strain and steric effects. The activation parameters, particularly $\Delta S^{\neq}$, are fully consistent with the conclusions drawn concerning transition-state hydration.

PETER WAN, TOMASZ A. MODRO et KEITH YATES. Can. J. Chem. **58**, 2423 (1980).

Opérant à diverses températures et dans des solutions où la concentration d'acide varie de 0 à 70%, on a étudié l'hydrolyse acido-catalysée des lactames cycliques de 4 à 7 chainons ainsi que de la *N*-éthylacétamide. On a analysé les cinétiques en traitant le paramètre d'hydratation *r* et en utilisant comme approche le coefficient d'activité de l'état de transition (CAET). A l'exception du β-lactame, tous les substrats ont une vitesse qui dépend fortement et d'une façon positive de l'activité de l'eau, ce qui suggère un mécanisme de type $A_{\delta}^{T}2$, faisant intervenir un intermédiaire tétraédrique semblable à celui trouvé au cours des hydrolyses d'amides simples (acycliques); seul le β-lactame a une vitesse qui depend d'une façon négative de l'activité de l'eau. Ceci est interprété en fonction d'un mécanisme unimoléculaire ($A_{N}^{R}1$) impliquant la formation de l'ion acylium dans l'étape déterminante. De la même manière, à l'exception du β-lactame, tous les substrats sont fortement déstabilisés dans l'état de transition lorsque l'acidité augmente; ceci est typique de l'ion oxonium. Le comportement du β-lactame ressemble à celui observé lors de l'hydrolyse du mésitoate de méthyle. Les constantes de basicité des lactames cycliques comportant de 4 à 9 chainons dépendent nettement de la taille du cycle, alors que le δ-lactame est anormalement basique. On discute de l'effet de la dimension du cycle sur la vitesse et le p*K* en fonction de la tension du cycle et des effets stériques. Les paramètres d'activation, et en particulier le $\Delta S^{\neq}$, sont en parfait accord avec les conclusions tirées au sujet de l'hydratation de l'état de transition.

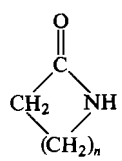
[Traduit par le journal]

Introduction

The acid-catalyzed hydrolysis of amides has been extensively investigated and the subject thoroughly reviewed (1). Although there has been general agreement for a long time on the predominant ($A_{O}^{T}2$) mechanism (2) of hydrolysis of simple amides, conclusive evidence has not been available until recently (3). The problem has been partly a result of inadequacies of the various treatments of kinetic acidity dependence which were available, and partly due to the difficulty of ruling out kinetically indistinguishable alternatives.

One of the fundamental problems associated with the mechanisms of amide (or lactam) hydrolysis is the site of protonation of the amido group. McClelland and Reynolds (4) appear to have resolved the question in favour of predominant oxygen protonation, in the equilibrium sense, but this does not eliminate the N-protonated form as a kinetically important species on the reaction pathway. There are four reasonable and distinct mechanistic schemes which must be considered in amide or lactam hydrolysis. Three of these (A-2 types) involve bimolecular rate-determining attack of water on the conjugate acid form (whether O- or N-protonated). The fourth (A-1 type) involves unimolecular rate-determining cleavage of the acyl–nitrogen bond of the N-protonated form. Smith and Yates (2) have categorized each of these mechanistic possibilities, using symbols analogous to the standard mechanistic symbols for acid- and base-catalyzed ester hydrolysis.

The acid-catalyzed hydrolysis of lactams has not been extensively studied, although various workers (5–7) have compared relative rates of hydrolysis for ring sizes from 4–7 atoms (n = 1–4).



n = 1, β-lactam; n = 2, γ-lactam;
n = 3, δ-lactam; n = 4, ε-lactam

[1]To whom all correspondence should be addressed.

0008-4042/80/232423-10$01.00/0

©1980 National Research Council of Canada/Conseil national de recherches du Canada

Can. J. Chem. Downloaded from www.nrcresearchpress.com by 210.87.254.42 on 09/05/12
For personal use only.

Can. J. Chem. Downloaded from www.nrcresearchpress.com by 210.87.254.42 on 09/05/12
For personal use only.

Mhala and Jagdale (8) have obtained the hydrolysis rate profile (as a function of acidity) for the ε-lactam at 97°C in sulfuric acid. Use of the Bunnett *w*-parameter treatment (9) led to a curved relationship and hence somewhat inconclusive results. Apart from these studies, hydrolysis rate – profiles have not been reported in the literature. For this reason we undertook a systematic study of lactams with n = 1–6, over the range 0–60% sulfuric acid, to examine their relative rates of hydrolysis and basicities as a function of ring size; also to determine, if possible, the general mechanism of lactam hydrolysis by using two more recently developed (10, 11) theoretical treatments of kinetic-acidity dependence.

Results and Discussion

Kinetics

The rates of hydrolysis of the β-, γ-, δ-, and ε-lactams, at different acid concentrations, were followed by ^{1}H nmr spectroscopy (see Experimental section). The rates of hydrolysis of *N*-ethylacetamide were also followed over the same range of acidity, to serve as a reference model for simple amide hydrolysis. All the reactions followed pseudo first order kinetics:

$$-\mathrm{d[lactam]}/\mathrm{d}t = k_2[\mathrm{lactam}][\mathrm{H^+}]$$
$$= k_\psi[\mathrm{lactam}]$$

The hydrolyses were generally measured at elevated temperatures due to the slowness of most of the reactions and the results extrapolated at 25°C using the Arrhenius relationship, for comparison purposes. These rate constants are listed in Table 1. The β-lactam, however, hydrolyses much more rapidly than the other substrates and was studied at 33°C. The rate profiles, as a function of acidity, are shown in Fig. 1. In all cases except for the β-lactam, the rate of hydrolysis passes through a maximum in the region 20–25% H_2SO_4. Such maxima are typical of many amide (2) and ester (12) hydrolyses, and are attributed to two opposing effects of increasing the acid concentration. On the one hand increased acidity raises the concentration of the reactive conjugate acid form of the substrate, but at the same time reduces the available water (i.e. the water activity) needed to complete the hydrolysis. This is true only of A-2 hydrolyses, since in A-1 reactions water does not intervene before or during the rate determining step. It can be seen from Fig. 1 (inset) that the β-lactam not only reacts much faster than all other substrates, but shows no sign of a rate maximum. The possibility of a very high maximum occurring outside the range of accessible rate measurements can almost certainly be ruled out for this lactam, since the rate increases monotonically (see Table 1) up to 82.5% H_2SO_4. It can be seen that over most of the acidity range studied, the rates are in the order

β- ≫ δ- > ε- > γ- > *N*-ethylacetamide

This is shown more quantitatively in Table 2 where the relative rate constants are compared at 20% H_2SO_4, which is near the rate maximum in most cases. The reasons for the very large rate enhancements (over *N*-ethylacetamide) in the six- and particularly the four-membered ring lactam will be discussed later.

Basicity Constants

Since none of the substrates studied possess strong chromophoric groups, basicity determinations were carried out essentially by the method of Lee and Sadar (13), using nmr spectroscopy. The ionization ratios (I = [SH$^+$]/[S]) obtained for aliphatic amides do not in general follow the H_A acidity function very well (14)

$$\log I = -mH_A + \mathrm{p}K_{\mathrm{SH^+}}$$

This function was based almost exclusively on aromatic amides (15), and the slopes m obtained with aliphatic amides are far from the required value of unity. It was therefore decided to use a recently developed and more generalized method (16) of determining the basicity constants. This employs the concept of "excess acidity" or the X-function, and is believed to give reliable estimates of p$K_{\mathrm{SH^+}}$ for any type of weak base. In this method pK values are obtained from

$$\log I - \log C_{\mathrm{H^+}} = m^*X + \mathrm{p}K_{\mathrm{SH^+}}$$

the intercepts of plots of ($\log I - \log C_{\mathrm{H^+}}$) versus X. The p$K_{\mathrm{SH^+}}$ values obtained for *N*-ethylacetamide and lactams with n = 1–6 are given in Table 3. It can be seen that the order of basicity is

δ- ≳ 9- > 8- > ε- > *N*-ethylacetamide > γ- > β-

which is quite different from the order of rates of hydrolysis for the five substrates studied kinetically.

It must be pointed out that the present p$K_{\mathrm{SH^+}}$ values differ significantly from previously reported values (17, 18), although as shown in Fig. 2 the trends in basicity with ring size are quite similar. We believe the values reported in the present work are more reliable, partly because no specific Hammett type acidity function was used in arriving at these values and partly because most of the previous data were obtained in anhydrous acetic acid and the pK's corrected to the aqueous scale (19). Also the two sets of values reported by Huisgen and

Can. J. Chem. Downloaded from www.nrcresearchpress.com by 210.87.254.42 on 09/05/12
For personal use only.

TABLE 1. Pseudo first order rate constants[a] in aqueous sulfuric acid at 25°C

% acid	$10^4 k_\psi$, β-propiolactam[b]	$10^8 k_\psi$, γ-butyrolactam	$10^7 k_\psi$, δ-valerolactam	$10^8 k_\psi$, ε-caprolactam	$10^8 k_\psi$, *N*-ethylacetamide[c]
5.1	1.39	10.2	11.0	30.2	3.31
10.5		18.6	21.4	67.6	7.76
15.5	8.62	25.7	28.2	91.2	11.8
20.3_5		30.9	29.5	97.7	13.5
22.5	34.4				
24.7		33.1	26.9	70.8	13.5
29.5		30.9	18.6	51.3	12.0
32.7	88.5				
34.9		24.6	12.0	31.6	10.0
36.0		22.9	8.91	28.2	9.33
37.0		20.9	8.13	25.7	9.12
39.0		18.2	6.76	20.9	8.13
40.2		17.4	6.17	19.1	8.13
41.8	272				
42.0		15.1	5.37	16.6	6.76
45.0		12.3	4.27	13.5	5.62
47.0		10.7	3.80	11.5	5.01
49.0		9.12	3.31	10.0	4.37
50.0		8.71	3.02	9.12	4.27
53.0		7.41	2.40	7.08	3.63
55.0		6.46	2.09	6.03	3.31
57.0		5.75	1.91	4.47	2.88
58.0		5.37	1.70	4.07	2.82
60.3	$>k_{41.8\%}$[d]	4.68	1.51	3.39	2.51
82.5	$>k_{60.3\%}$[d]				

[a]Values of k_ψ in s^{-1} obtained from Arrhenius relationship and rate data at higher temperatures. Actual rate constants obtained at different temperatures are listed in Tables of Supplementary Data.
[b]Measured at 33 ± 1°C.
[c]Measured at 25°C.
[d]In these acids, the reaction is too fast to measure k_ψ accurately. However the estimated rates show that these are higher than the values at lower acidity.

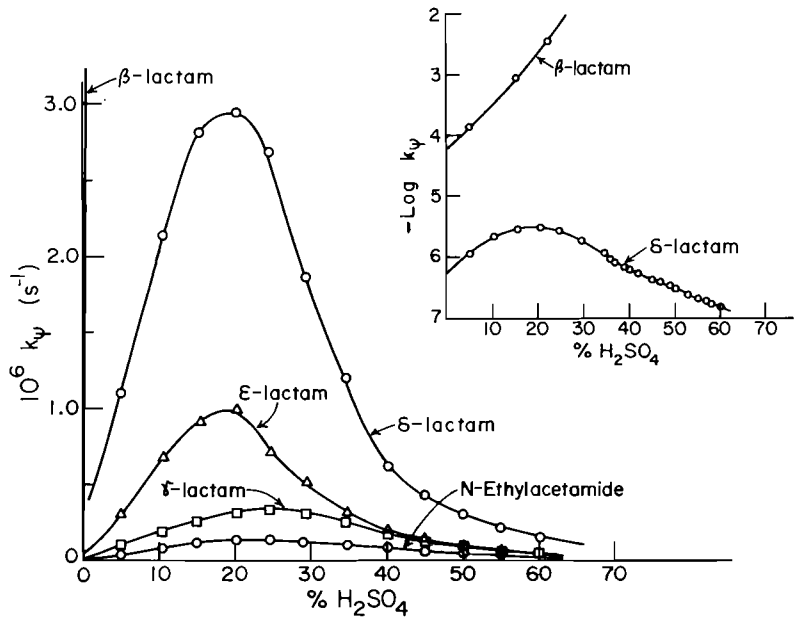
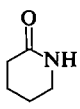
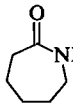
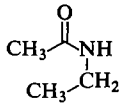


FIG. 1. Rate profiles of pseudo first order rate constants for lactam hydrolysis as a function of acid concentration (inset: logarithmic rate scale).

Can. J. Chem. Downloaded from www.nrcresearchpress.com by 210.87.254.42 on 09/05/12
For personal use only.

TABLE 2. Relative rates of hydrolysis at 25°C

Rate constant	Value				
					
k_0[a]	1.12×10^{-3}	3.98×10^{-6}	1.26×10^{-6}	1.0×10^{-6}	2.0×10^{-7}
k_0^{rel}	5600	19.9	6.3	5.0	1.0
k_ψ[b]	2.22×10^{-3}	2.95×10^{-6}	9.77×10^{-7}	3.09×10^{-7}	1.35×10^{-7}
k_ψ^{rel}	16 400	21.9	7.24	2.3	1.0

[a]In s^{-1}, obtained by extrapolation of log ($f_S f^*/k_0$) to zero acid concentration.
[b]In s^{-1}, measured at 20.35% H_2SO_4.

TABLE 3. Lactam pK_{SH^+} values

Lactam (or amide)	pK_{SH^+}	Rate maximum of acidity
N-Ethylacetamide	−0.49	~21% acid
β-Lactam (4)	−0.96	No observed maximum
γ-Lactam (5)	−0.65	~25%
δ-Lactam (6)	−0.18	~19.5
ε-Lactam (7)	−0.46	~20%
8-Lactam	−0.38	—[a]
9-Lactam	−0.18	—[a]

[a]Rates of hydrolysis not measured for these lactams.

co-workers (17), employing potentiometric and indicator methods, would suggest that lactams are much more basic than any other type of amide. Typical pK_{SH^+} values reported for aliphatic and aromatic secondary amides are in the range −0.7 to −4.0 (20). It is generally true that acyclic amides are weak bases with p*K* values less than zero,[2] whereas most of the values reported by Huisgen *et al.* (17) are positive. If the latter values were correct, it would suggest that lactams are anywhere from a factor of ten to a hundred times more basic than other types of amide. This does not seem reasonable in terms of structural factors, since it would be expected that the δ-lactam for example, which is relatively free of ring strain effects, would have a p*K* value close to those of typical open chain aliphatic amides. These structural effects will be discussed later. It is interesting that for the lactams which show a hydrolysis rate maximum, the acidity at which this occurs is in roughly the same order as the basicities of the substrates, which it should be if the previous explanation for the rate maxima is correct (see Table 3).

[2]This presented a problem in anchoring the H_A scale (15) since no simple amides could be found with p*K* values greater than zero, which would ionize significantly in the pH region. Even the pyridine-1-oxides subsequently used by Johnson, Katritzky, and Shakir (21) had negative p*K*'s in most cases.

Hydration Parameter Treatment

For the generalized reaction [1] it has been shown (22)

$$S + H^+ \underset{}{\overset{\text{fast}}{\rightleftharpoons}} SH^+ \quad [1]$$

$$SH^+ + rH_2O \xrightarrow{\text{slow}} \neq \longrightarrow \text{products}$$

(when certain assumptions are made) that the Bronsted rate equation may be written as

$$[2] \quad \log k_\psi + \log [(I + 1)/I] = r \log a_w + \text{constant}$$

where k_ψ is the observed pseudo first order rate constant, *I* is the ionization ratio $[SH^+]/[S]$, and a_w is the activity of water (32). Consequently a plot of the left side of eq. [2] versus log a_w should yield a straight line with slope *r*, which gives a measure of the change in hydration in going from the protonated species to the rate determining transition state. For typical A-2 ester hydrolyses *r* is about +2, and for A-1 pathways about −0.2 to −0.6 (12). Each of the lactams (except the β-lactam) and *N*-ethylacetamide, give two straight line regions,[3] as shown for the γ-lactam in Fig. 3. In the low acidity region an *r* value between +2 and +4 is obtained, as shown in Table 4, followed by a changeover around 40–45% H_2SO_4, to a lower but still positive slope of about +0.6 to +1.4. The implication here is that there are two A-2 mechanisms operating in lactam hydrolysis; one with a highly hydrated transition state, involving several water molecules, and as the acidity is increased (and the availability of water is decreased), a fairly sharp changeover occurs to a mechanism in which only one water molecule on average participates in

[3]The actual data used to construct these plots are given in the Tables of Supplementary Data. Complete set of data may be obtained, at a nominal charge, from the Depository of Unpublished Data, CISTI, National Research Council of Canada, Ottawa, Ont., Canada K1A 0S2.

Can. J. Chem. Downloaded from www.nrcresearchpress.com by 210.87.254.42 on 09/05/12
For personal use only.

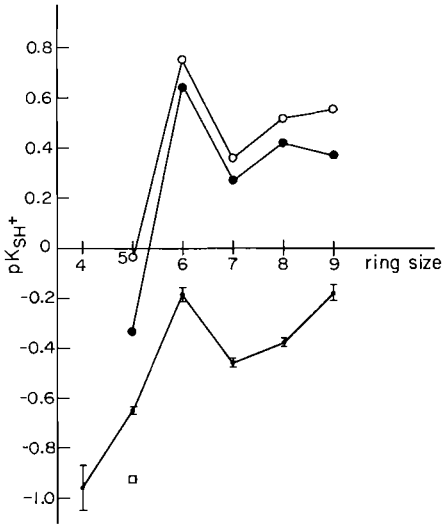


FIG. 2. Variation of lactam pK_{SH^+} values as a function of ring size (bars, nmr data from this work; open circles, potentiometric data from ref. 17; closed circles, indicator data from ref. 17; open square, spectrophotometric data from ref. 18).

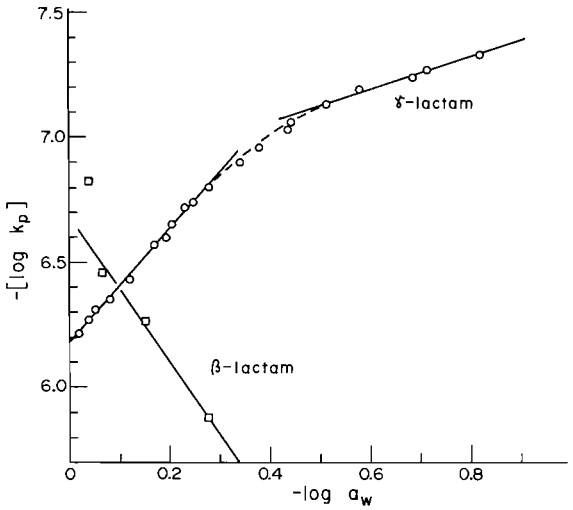
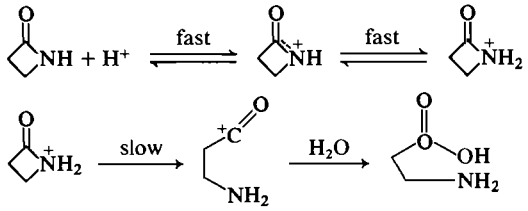


FIG. 3. Typical *r*-hydration parameter plots for lactam hydrolysis.

forming the tetrahedral-intermediate type of transition state.

The β-lactam is unusual, as shown in Fig. 3. The *r*-hydration parameter plot shows a distinctly *negative* dependence on water activity throughout, indicating a transition state which is less hydrated than its preceding conjugate acid. This is reasonable for an A-1 mechanism generating an acylium ion, since such an ion would almost certainly be much less hydrated than an oxonium ion-like lactam conjugate acid[4]



There is one other reasonable mechanistic possibility for the β-lactam, which would involve nucleophilic attack by water at C_β, with ring opening to give β-hydroxypropionic acid. An analogous mechanism has been shown to occur for β-lactone hydrolysis (23) using ^{18}O labelling. However, this mechanism can be ruled out in the present case, since the exclusive product of β-lactam hydrolysis is β-alanine, at all acidities.

Activation Parameters

For the δ-lactam, five different temperatures were used in the extrapolation of rate constants to 25°C. For both the γ- and ε-lactams six temperatures were employed.[5] In most cases, excellent linear Arrhenius plots were obtained, with correlation coefficients in the range 0.994–0.997. Values of $\Delta H^{\neq}$ and $\Delta S^{\neq}$ were obtained at different acidities, and typical values (at an acidity near the rate maximum) are given in Table 5. These values are fairly typical for A-2 reactions. Of more interest is the variation of $\Delta S^{\neq}$ with acid concentration. There are definite trends for each lactam, with $\Delta S^{\neq}$ changing from a larger negative value of around −27 to −30 eu in the more dilute acid region, to less negative values around −19 to −21 eu in more concentrated acids. This is shown in Fig. 4 for the γ-lactam, and implies that a change from a more- to a less-restricted transition state is occurring as the acidity is increased (or as a_w is decreased). This is fully consistent with the conclusion from the *r*-hydration parameter treatment, and indeed the changeover regions in the *r*-plots coincide reasonably well with the regions of levelling off of the $\Delta S^{\neq}$ values at higher acidities.

Unfortunately the β-lactam reacts too rapidly over most of the acidity range studied to allow accurate determination of its activation parameters. For the proposed A-1 mechanism for this lactam, both $\Delta H^{\neq}$ and $\Delta S^{\neq}$ would be expected to be significantly different from the values in Table 5, as

[4]Note that an A-1 mechanism leading to an acylium ion intermediate can only reasonably be written as proceeding via the minor N-protonated form.

[5]*N*-Ethylacetamide was studied at 25°C only, and the β-lactam at 33°C only.

TABLE 4. *r*-Hydration parameters for lactam hydrolysis

Substrate	Initial *r*-value	Final *r*-value	Acidity of changeover region
N-Ethylacetamide	2.1	0.6	~46% H_2SO_4
γ-Lactam	2.1	0.6	~47% H_2SO_4
δ-Lactam	4.4	1.0	~42% H_2SO_4
ε-Lactam	4.5	1.4	~41% H_2SO_4
β-Lactam	−2	—	—

TABLE 5. Activation parameters at 24.72% H_2SO_4

Lactam	$\Delta H^{\ddagger}$ (kcal mol^{-1})	$\Delta S^{\ddagger}$ (eu mol^{-1})	$\Delta S^{\ddagger}$ range[a]
γ-	19.6	−22.5	(−27 to −19)
δ-	17.9	−23.9	(−27 to −21)
ε-	18.4	−24.9	(−29 to −19)

[a]For the 5–60% H_2SO_4 region.

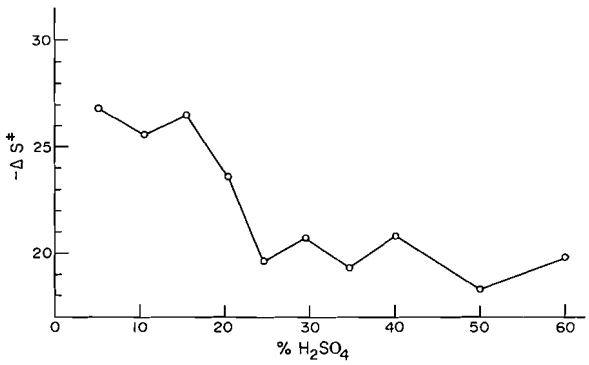


FIG. 4. Variation of $\Delta S^{\ddagger}$ as a function of acid concentration for hydrolysis of γ-butyrolactam.

well as the variation of $\Delta S^{\ddagger}$ with acidity.

TSAC Approach

For a reaction scheme such as that in reaction [1], application of transition state theory gives the following expression (11) for the observed rate constant

$$k_{\psi} = \frac{k_0}{K_{SH^+}} \frac{f_s}{f_{s\ddagger}} a_{H^+}$$

where k_0 is the rate constant for the slow step, K_{SH^+} is the substrate basicity constant, f_s and $f_{s\ddagger}$ are the substrate and transition state activity coefficients, respectively, and a_{H^+} is the hydronium ion activity. Rearranging and taking logarithms gives eq. [3],

$$[3] \quad \log (f_{s\ddagger}^*/k_0) = \log a_{H^+}^* - \log k_{\psi}^{corr} + \log f_s + pK_{SH^+}$$

where k_{ψ}^{corr} is the observed pseudo first order rate constant corrected for partial protonation of the substrate; i.e.

$$k_{\psi}^{corr} = k_{\psi}(1 + I)$$

where I is one ionisation ratio as defined in eq. [2]. Since activity coefficients for single ions are experimentally inaccessible, they are expressed as relative to a standard reference ion (24), usually the tetraethylammonium ion (TEA^+). This is indicated by starring such terms as $a_{H^+}^*$ and $f_{s\ddagger}^*$. The quantities on the right side of eq. [3] are all experimentally accessible, and since $\log f_{s\ddagger}^*$ must approach zero in dilute aqueous solution, $\log k_0$ can be obtained from the intercept of a plot of $\log (f_{s\ddagger}^*/k_0)$ versus acid concentration. Therefore it is possible to study the medium variation of $f_{s\ddagger}^*$, which should reflect the solvation requirements of the transition state.[6] This can then be interpreted in terms of possible transition state structures, by comparing the $\log f_{s\ddagger}^*$ behaviour with that of known stable cationic species, or with species involved in mechanisms which have been well-established.

Since $\log a_{H^+}$ values are already available (33), it was only necessary to measure $\log f_s$ values for the substrates of interest. This was done using a standard method (25) (see Experimental section) and the results are given in Table 6. The observed variations in $\log f_s$ (initial salting out, followed by a tendency to salt in at higher acidities) are typical of the behaviour of many weakly basic organic molecules (25). It was unfortunately impossible to measure $\log f_s$ for the β-lactam due to its high reactivity, so the values for *N*-ethylacetamide[7] were used to calculate $\log f_{s\ddagger}^*$ for this substrate. This should not cause any serious error since the total variations in all the $\log f_s$ values from 0–70% H_2SO_4 are of the order of one logarithmic unit or less. Plots of $\log f_{s\ddagger}^*$ versus acidity[3] are given for all the substrates in Fig. 5. It can be seen that the γ-, δ-, and ε-lactams, as well as *N*-ethylacetamide, show a

[6]The logarithms of activity coefficients determined in aqueous acidic media, with dilute aqueous solution as standard state, can be thought of as measures of the free energy change in transferring 1 mol of the species from pure water to the acid in question. When $\log f$ is positive the species is destabilized by acid, or "salts out". When $\log f$ is negative it is stabilized by acid, or "salts in".

[7]These were chosen as models for $\log f_s$ for the β-lactam since *N*-ethylacetamide hydrolyses most slowly of all the substrates studied. Hence its $\log f_s$ values should be the most reliable.

Can. J. Chem. Downloaded from www.nrcresearchpress.com by 210.87.254.42 on 09/05/12
For personal use only.

TABLE 6. Substrate activity coefficients in aqueous sulfuric acid at 25°C

	log f_s			
$\%H_2SO_4$	*N*-Ethylacetamide	δ-Lactam	γ-Lactam	ε-Lactam
5.1	0.18	0.2	0.15	0.31
10.5	0.30	0.3	0.25	0.50
15.5	0.42	0.4	0.35	0.60
20.3_5	0.53	0.45	0.48	0.68
24.7	0.50	0.6	0.60	0.75
29.5	0.40	0.5	0.70	0.78
34.9	0.25	0.5	0.80	0.80
40.2	0.10	0.4	0.80	0.77
50.0	−0.20	0.3	0.50	0.60
60.3	−0.43	0.2	0.0	0.35

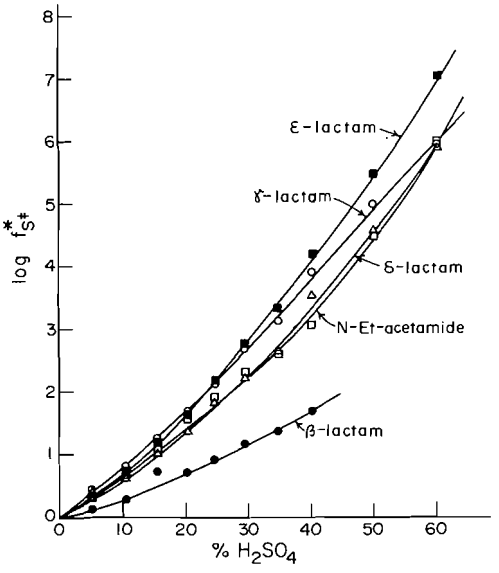


FIG. 5. Medium dependence of transition state activity coefficients for lactam hydrolysis.

strong destabilization with increasing acidity, with log $f_{s\ddagger}$* reaching values of 6–7 at around 60% H_2SO_4. This corresponds to a desolvation energy of about 8–9 kcal mol^{-1} over the range of acidity studied. This behaviour is typical of both stable oxonium ion species and of transition states in A_{Ac^2} ester hydrolysis (11). The curves in Fig. 5 are also very similar to the behaviour of log $f_{s\ddagger}$* found in various benzamide hydrolyses (3*a*). From these plots we can only conclude that all four of these substrates hydrolyse by way of an A-2 mechanism (more specifically A_O^T2), via a tetrahedral intermediate with strong oxonium ion character.[8]

[8]The curves in Fig. 5 do not suggest any change in mechanism at higher acidities, since the log $f_{s\ddagger}$ curves are smoothly monotonic, with no sharp breaks. In this sense the TSAC approach is less sensitive than the *r*-parameter treatment in determining the details of the mechanism.

The log $f_{s\ddagger}$* behaviour of the β-lactam is quite different. Although transition state destabilization does occur as the acidity is increased, this is much less pronounced than for the other substrates. The rate of change of log $f_{s\ddagger}$* with acidity is a factor of 2–3 less than that for the other lactams. Indeed the behaviour of the β-lactam is similar to that found for methyl mesitoate hydrolysis (11), which is known to involve an acylium ion mechanism. It seems clear from Fig. 5 that the β-lactam hydrolysis involves quite different mechanistic behaviour, and it is again concluded that this substrate reacts by an A-1 process (more specifically A_N^D1), via an acylium ion-like transition state.

As mentioned previously, the intercepts of the log ($f_{s\ddagger}$*/k_0) versus acidity plots give values of log k_0 which refer to the reactivity of the conjugate acid form of the substrate, in the limiting ideal dilute solution region. These values are thus corrected for differing degrees of protonation, and possibly different activity coefficient effects, and would be inaccessible experimentally in most cases due to the slowness of the reactions. The values of k_0 obtained are given in Table 2. It is interesting that the relative rates shown by these k_0 values are in the same order as those found from the observed pseudo first order rate constants, namely

β- ≫ δ- > ε- > γ- > *N*-ethylacetamide

The very high reactivity of the β-lactam conjugate acid relative to that of the other protonated species is thereby confirmed.

Effects of Ring Size

The relative rates of hydrolysis of all substrates except the β-lactam can be rationalized by considering two effects: substrate basicity and ring size effects. For reaction [1] the rate law can be written as

$$v = k_2K[H^+][S]$$

Can. J. Chem. Downloaded from www.nrcresearchpress.com by 210.87.254.42 on 09/05/12
For personal use only.

Can. J. Chem. Downloaded from www.nrcresearchpress.com by 210.87.254.42 on 09/05/12
For personal use only.

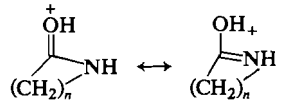
and

$$k_\psi = k_2 K[H^+]$$

where activity coefficient terms have been omitted for simplicity. Since $K (= 1/K_{SH^+})$ is the equilibrium constant for protonation of the substrate, the observed rate constant k_ψ should depend on lactam basicity. Comparing the data in Tables 2 and 3 it can be seen that the strongest base (δ-lactam; $pK_{SH^+} = -0.18$) also has the fastest rate of hydrolysis, followed by the ε-lactam ($pK_{SH^+} = -0.46$), with *N*-ethylacetamide ($pK_{SH^+} = -0.49$) and the γ-lactam ($pK_{SH^+} = -0.65$) reacting more slowly. Thus the three lactams reacting by the standard A_O^T2 mechanism have rates in the same order as their basicities. However, since relative substrate basicities are numerically smaller than relative rate factors, ring size effects must be important in determining relative reactivities. Brown and co-workers (26) have proposed the generalization that for cyclic compounds, reactivity depends on changes in internal strain (I-strain), as the transition state is approached. This I-strain is made up of various components, including bond angle distortion and bond opposition effects (26*c*). Since the rate-determining step in the A_O^T2 hydrolysis is addition of a water molecule to the carbonyl carbon to give a tetrahedral intermediate, the change from sp^2 to sp^3 hybridization should most favour the δ-lactam, which can accommodate the sp^3 carbon of the intermediate without any ring strain. (Also partial bond oppositions between the carbonyl–oxygen bond and the neighbouring C—H and N—H groups will be relieved.) For the γ-lactam, the relief of bond angle distortion would also be favourable, but formation of a tetrahedral intermediate would increase bond opposition forces. In the protonated form the five-membered ring is approximately planar with the sp^2 hybridized nitrogen and the N—H bond in the plane of the ring. On attack of water, the nitrogen hybridization reverts to sp^3 and the lone pair and N—H bond interactions with neighbouring bonds will disfavour the reaction.

A ground state effect is also operative in making the six-membered ring more reactive than the five-membered analogue. Fuji and co-workers (7) have shown that for a suitably substituted six-membered lactam, under conditions of thermodynamic control, the ring opens and prefers to close back to form a five-membered lactam. This shows that other things being equal, a five-membered lactam ring is more stable than the corresponding six-membered ring. Therefore the ground state energy of the γ-lactam is lower than what might have been expected, with the consequence that the activation energy for hydrolysis is increased (see Table 4). The ε-lactam presumably does not possess such ground state stabilization, and this, coupled with less serious bond opposition forces, and some ring strain at the transition state, causes this substrate to show reactivity intermediate between the δ- and γ-lactams. The β-lactam is different in the sense that although bond angle deformation would be significantly relieved in tetrahedral intermediate formation, bond opposition forces would be substantially increased. Also, since this ring is by far the most strained in either lactam or conjugate acid form, the strain can be relieved most readily by unimolecular ring opening.

The variations in basicity shown in Fig. 2 can most easily be explained simply in terms of ring strain effects in the neutral and protonated forms. Apart from the δ-lactam, basicity increases fairly monotonically with ring size and probably levels off somewhere around ring size 9 or 10 (this trend was also observed by Huisgen and co-workers (17)). If the two canonical forms of the O-protonated lactam are considered, the basicity will depend strongly on the ability of nitrogen to donate its pair of electrons to give a delocalized cation. Hence structure **II** will



I **II**

be more important in the conjugate acid than the analogous contributing structure in the neutral lactam. This will cause more serious ring strain the smaller the size of the lactam ring, and hence tend to reduce the basicity. As the rings become very large, such strain factors will become less important and the basicity would be expected to level off at a p*K* value similar to that of a typical secondary amide. Only the δ-lactam is unusual in that its base strength is much higher than expected. It is commonly observed (27) that for five-membered rings *exo* double bonds are preferred, while for six-membered rings *endo* double bonds are more stable, although these preferences are not easily rationalized. Therefore contributions from canonical form **II** in the protonated δ-lactam should be more important than in the γ-lactam case (and possibly the other lactams as well), leading to a higher basicity for the δ-lactam than its ring size would lead one to expect from the trends in Fig. 2. The β-lactam also may be unusual in the sense that although the major protonated species is still the O-protonated form, the stabilization produced by the nitrogen lone pair delocalization may be so

Can. J. Chem. Downloaded from www.nrcresearchpress.com by 210.87.254.42 on 09/05/12
For personal use only.

reduced that the N-protonated form (required for the A_N^D1 process) is relatively more important than it is for other lactam protonations.

Experimental

General

Infared spectra were taken from liquid films. Nuclear magnetic resonance spectra were run on Varian T60 and CFT-20 instruments, using $CDCl_3$ as solvent with TMS as internal standard, when required. Melting and boiling points are uncorrected.

Materials

CIL Reagent Grade sulfuric acid was appropriately diluted with distilled water and standardized at 25°C using an Anton Paar Model DMA 02C precision density meter and standard tables of densities (28). The γ-lactam (2-pyrrolidone) and δ-lactam (2-piperidone) were obtained from Aldrich. The ε-lactam (ε-caprolactam) was obtained from Eastman and recrystallized from ethanol to constant mp (66–67°C). The β-lactam (2-azetidinone) was prepared by the method of Birkofer and Schramm (29), with all reactions carried out under a nitrogen atmosphere. Mp 70–71°C (lit. (29) mp 72–74°C). Ir: 1760 cm^{-1} (strong); 3226 cm^{-1} (medium). Nmr: δ2.9 (m, 2H); δ3.2 (m, 2H); δ6.13 (broad, 1H). *N*-Ethylacetamide was prepared from acetic anhydride and ethylamine hydrochloride as follows. The anhydride (32 g) was added to a solution of the hydrochloride (20 g) in 500 mL water. A solution of sodium acetate (24 g) in 130 mL water was then added slowly, and the mixture cooled in an ice-bath. The solution was stirred for 2 h, followed by removal of the water under vacuum. The resulting slurry was filtered to give a viscous oil, which was fractionally distilled to give *N*-ethylacetamide (13 g) as a colorless liquid. Bp 104–106°C/20 mm (lit. (30) bp 104–105°C/18 mm). Further purification by column chromatography (alumina, methylene chloride) gave the essentially pure (>99%) amide, as determined by glpc. Ir: 1695 cm^{-1} (strong); 3225 cm^{-1} (medium). Nmr: δ1.1 (t, 3H); δ1.9 (s, 3H); δ3.2 (m, 2H); δ7.2 (broad, 1H).

Rate Measurements

The hydrolysis of *N*-ethylacetamide was followed at 25 ± 0.3°C, by taking samples periodically and recording their nmr spectra. The hydrolysis is slow enough ($t_{1/2}$ is several months at 25°C) that recording spectra at 33°C (the temperature of the spectrometer) should not materially affect the results. The growing area of the methyl signal due to acetic acid was followed, with the total area of the two methyl peaks (of the reactant and product) taken as 100%. Authentic samples of acetic acid were added at the end of the reaction and no additional peaks were observed. Plots of ln $[A_0]/[A_t]$ versus time were linear with correlation coefficients greater than 0.992 in almost all cases. For convenience, the hydrolyses of the lactams were studied at elevated temperatures (except for the β-lactam), again by following changes in the nmr spectra. Samples were quenched in ice before recording spectra. For the γ-lactam the methylene signal at the γ-position was used, since the change from a triplet in the lactam to a multiplet in the product was easy to detect. The spectrum of the hydrolysis product was indistinguishable from that of an authentic sample of 4-aminobutanoic acid in the appropriate sulfuric acid solution. In the case of the δ-lactam, the methylene signal at C_δ was followed. Again, comparison of the nmr spectrum of the product with that of an authentic sample of 6-aminovaleric acid showed no differences. A similar procedure was used to follow the hydrolysis of the ε-lactam. Mhala and Jagdale (8) also obtained a rate profile for this lactam at 97.0°C, which was one of the temperatures used in the present work. Although the shapes of the two profiles are similar, the rate maxima occur at different acidities. Since the acidity of the rate maximum for any amide or lactam hydrolysis should be near the position of half-protonation of the substrate (or pK_{SH^+} value), the position of the rate maximum found by Mhala and Jagdale (ca. 10% H_2SO_4) would suggest a substrate of much higher basicity than that found for any known amide or lactam. The position of the maximum found in the present work (ca. 20% H_2SO_4) is much nearer to both the pK_{SH^+} values measured, and to previously reported rate maxima for amide hydrolyses.

The hydrolysis of the β-lactam was followed at 33 ± 1°C, again using proton magnetic resonance spectroscopy. The hydrolysis product was in all cases β-alanine, as shown by comparison with authentic samples. At higher acidities the reaction is too fast to follow, but it was found that at 82% H_2SO_4, the hydrolysis is even faster than at 60% H_2SO_4, with $t_{1/2} < 10$ s. The actual rate constants determined at different temperatures are listed in the Tables of Supplementary Data.[3] These were converted to the values at 25°C given in Table 1 by extrapolation of plots at log k/T versus $1/T$.

*p*K *Determinations*

Lee and Sadar (13) have shown that ionization ratios, which are relatively free of errors due to medium effects, can be obtained from nmr spectra using the relationship

$$I = [SH^+]/[S] = (\Delta - \Delta_S)/\Delta_{SH^+} - \Delta$$

where Δ_S is the chemical shift difference between two sets of protons in the free base and Δ_{SH^+} is the chemical shift difference between the same two sets of protons in the conjugate acid form. Because the proton signals in the lactams do not occur as singlets, and because difficulty was encountered in following some proton chemical shifts, ^{13}C nmr was used for all substrates except the β-lactam, which reacts too rapidly for the use of ^{13}C spectra. Each signal could be followed readily and no multiplets were involved. For the β-lactam ^1H nmr was used, based on the central peaks of the two sets of triplets. Values of log I obtained this way were plotted according to the equation

$$\log I - \log C_{H^+} = m^*X + pK_{SH^+}$$

where X is the "excess acidity" (16) of the solution in question, and C_{H^+} is the stoichiometric hydrogen ion concentration. The pK_{SH^+} values in Table 3 were obtained from the intercepts. Medium effects on amide and lactam ionization ratios will be discussed in a forthcoming paper (31). They are not sufficiently serious in the present case to warrant extended discussion at this time, since the main use of the pK_{SH^+} values was for the TSAC treatment. Since K_{SH^+} is a constant in eq. [3], any uncertainty caused by medium effects would only affect the intercepts of the $\log f_{\neq}^*$ plots, and not $\log f_{s\neq}^*$ variation itself.

Substrate Activity Coefficients

The standard distribution method (25) was used, in which a stock solution of substrate in an inert organic solvent ($CHCl_3$) immiscible with water is shaken mechanically with the appropriate aqueous sulfuric acid until equilibrium is reached, and the concentration of substrate in both phases is then determined by ultraviolet spectrophotometry at 200–210 nm on a Cary 14 instrument. From these concentrations the two distribution coefficients D_0 (between water and the organic solvent), and D_x (between a given aqueous acid and the organic phase) can be obtained. The substrate activity coefficient f_s is then given by $f_s = D_0/D_x$. Since the substrates are very soluble in the aqueous phase, it was not possible to determine directly the small concentration left in the organic phase, after equilibration, because of interference by the chloroform absorption. As a result the concentration in the aqueous phase had to be determined very accurately, and the concentration left in the organic phase was

calculated from this and the known initial concentration. In the more strongly acidic solutions, it was also necessary to correct the aqueous phase concentration for partial protonation, using the K_{SH^+} values already determined.

Acknowledgements

Grateful acknowledgement is made to the Natural Sciences and Engineering Research Council of Canada for continued financial support and to the Ontario Government for a graduate scholarship (to P.W.).

1. B. C. CHALLIS and J. CHALLIS. The chemistry of amides. *Edited by* J. Zabicky. Interscience. 1970. p. 731; C. J. O'CONNOR. Q. Rev. **24**, 553 (1970); M. LILER. Reaction mechanisms in sulfuric acid. Academic Press, New York. 1971. p. 189.
2. C. R. SMITH and K. YATES. J. Am. Chem. Soc. **94**, 8811 (1972).
3. (*a*) T. A. MODRO, F. BEAUFAYS, and K. YATES. Can. J. Chem. **55**, 3050 (1977); (*b*) A. WILLIAMS. J. Am. Chem. Soc. **98**, 5645 (1976).
4. R. A. MCCLELLAND and W. F. REYNOLDS. J. Chem. Soc. Chem. Commun. 824 (1974).
5. A. K. BONETSKAYA, N. F. EROFEEVA, S. M. SKURATOV, and R. S. MUROMOVA. Izv. Vyssh. Uchebn. Zaved. Khim. Khim. Tekhnol. **4**, No. 1, 74 (1961); Chem. Abstr. **55**, 15071*h* (1961).
6. E. LAURENT, S. K. LEE, and N. PELLISSIER. J. Chem. Res. (S), 440 (1978).
7. T. FUJI, S. YOSHIFUJI, and A. TAMAI. Chem. Pharm. Bull. **19**, (2) 369 (1971).
8. M. MHALA and M. JAGDALE. Ind. J. Chem. **6**, 711 (1968).
9. J. F. BUNNETT. J. Am. Chem. Soc. **83**, 4968 (1961).
10. K. YATES and R. A. MCCLELLAND. J. Am. Chem. Soc. **89**, 2686 (1967).
11. K. YATES and T. A. MODRO. Acc. Chem. Res. **11**, 190 (1978).
12. K. YATES. Acc. Chem. Res. **4**, 136 (1971).
13. D. G. LEE and M. H. SADAR. J. Am. Chem. Soc. **96**, 2862 (1974).
14. V. C. ARMSTRONG and R. B. MOODIE. J. Chem. Soc. B, 275 (1968); K. YATES and J. B. STEVENS. Can. J. Chem. **43**, 529 (1965).
15. K. YATES, J. B. STEVENS, and A. R. KATRITZKY. Can. J. Chem. **42**, 1957 (1964).
16. R. A. COX and K. YATES. J. Am. Chem. Soc. **100**, 3861 (1978).
17. R. HUISGEN, H. BRADE, H. WALTZ, and I. GLOGGER. Chem. Ber. **90**, 1437 (1957).
18. P. O. VIRTANEN and T. SODERVALL. Suom. Kemistil. **40**, 337 (1967).
19. N. F. HALL and J. B. CONANT. J. Am. Chem. Soc. **49**, 3047 (1927); N. F. HALL and T. H. WERNER. J. Am. Chem. Soc. **50**, 2367 (1928); N. F. HALL. J. Am. Chem. Soc. **52**, 5115 (1930); H. LEMAIRE and H. J. LUCAS. J. Am. Chem. Soc. **73**, 5198 (1951).
20. M. LILER. J. Chem. Soc. B, 385 (1969); K. YATES and J. B. STEVENS. Can. J. Chem. **43**, 529 (1965).
21. C. D. JOHNSON, A. R. KATRITZKY, and N. SHAKIR. J. Chem. Soc. B, 1235 (1967).
22. K. YATES and R. A. MCCLELLAND. J. Am. Chem. Soc. **89**, 2686 (1967).
23. A. R. OLSON and J. L. HYDE. J. Am. Chem. Soc. **63**, 2459 (1941).
24. R. H. BOYD. J. Am. Chem. Soc. **85**, 1555 (1963).
25. K. YATES and R. A. MCCLELLAND. Prog. Phys. Org. Chem. **11**, 323 (1974).
26. (*a*) H. C. BROWN and K. ICHIKAWA. Tetrahedron, **1**, 221 (1957); (*b*) H. C. BROWN, F. S. FLETCHER, and R. B. JOHANNESEN. J. Am. Chem. Soc. **73**, 212 (1951); (*c*) H. C. BROWN and G. HAM. J. Am. Chem. Soc. **78**, 2735 (1956).
27. H. C. BROWN, J. H. BREWSTER, and H. SCHECHTER. J. Am. Chem. Soc. **76**, 467 (1954).
28. R. WEAST (*Editor*). Handbook of chemistry and physics. 56th ed. CRC Press, Cleveland. 1975. p. D263.
29. L. BIRKOFER and J. SCHRAMM. Liebigs Ann. Chem. 2195 (1975).
30. J. TITHERLEY. J. Chem. Soc. **79**, 401 (1901).
31. R. A. COX, T. A. MODRO, P. WAN, and K. YATES. Unpublished results.
32. C. R. SMITH and K. YATES. J. Am. Chem. Soc. **93**, 6578 (1971); W. F. GIAUQUE, E. W. HORNUNG, J. E. KUNZLER, and T. R. RUBIN. J. Am. Chem. Soc. **82**, 62 (1960).
33. T. A. MODRO, K. YATES, and J. JANATA. J. Am. Chem. Soc. **97**, 1492 (1975).

Can. J. Chem. Downloaded from www.nrcresearchpress.com by 210.87.254.42 on 09/05/12
For personal use only.

Deuterium and phosphorus-31 nuclear magnetic resonance of cholesteryl palmitate in dipalmitoylphosphatidylcholine model membranes

ROBERT J. CUSHLEY, HEINER GORRISSEN, AND STEPHEN R. WASSALL

Department of Chemistry, Simon Fraser University, Burnaby, B.C., Canada V5A 1S6

Received June 27, 1980

Dedicated to Prof. Raymond U. Lemieux on the occasion of his 60th birthday

ROBERT J. CUSHLEY, HEINER GORRISSEN, and STEPHEN R. WASSALL. Can. J. Chem. **58**, 2433 (1980).

Cholesteryl palmitate (CP) has been incorporated into vesicles of dipalmitoylphosphatidylcholine and dipalmitoylphosphatidylcholine/20 mol% cholesterol, in amounts up to 5 mol%. By means of ^{31}P lanthanide induced shifts the average diameter of these vesicles was calculated to be ~270 Å.

The ^{2}H spectral linewidths of selectively deuterated CP incorporated into liquid crystalline dipalmitoylphosphatidylcholine vesicles are ≤150 Hz, implying a low degree of order for the ester acyl chain. Addition of 20 mol% cholesterol to the vesicles increases the linewidths which, nevertheless, remain ≤185 Hz. The corresponding ^{2}H longitudinal relaxation times (≤450 ms) indicate that the fast segmental motions of the ester chain are slower than for the phospholipid chains.

ROBERT J. CUSHLEY, HEINER GORRISSEN et STEPHEN R. WASSALL. Can. J. Chem. **58**, 2433 (1980).

On a incorporé le palmitate de cholestéryle (PC) en quantité allant jusqu'à 5 mol% dans les vésicules de dipalmitoylphosphatidylcholine et de dipalmitoylphosphatidylcholine/20 mol% cholestérol. Au moyen des déplacements chimiques du ^{31}P induits par les lanthanides on a calculé que le diamètre moyen de ces vésicules est d'environ 270 Å. Les largeurs des raies des spectres rmn ^{2}H des PC deutérés sélectivement et incorporés dans les vésicules de dipalmitoylphosphatidylcholine cristallins à l'état liquide sont ≤150 Hz; ceci implique un faible degré d'ordre de la chaîne ester acyclique. L'addition de 20 mol% de cholestérol aux vésicules augmente la largeur des raies qui néanmoins restent à 185 Hz. Les temps de relaxation longitudinale correspondants du ^{2}H (≤450 ms) indiquent que les rapides mouvements des segments de la chaîne ester sont plus lents que ceux des chaînes phospholipides.

[Traduit par le journal]

Introduction

We have been studying the structure and properties of cholesteryl esters in various phospholipid membrane systems using a diversity of magnetic resonance techniques. In our initial study (1) we utilized ^{31}P nmr spectroscopy and found that cholesteryl palmitate (CP) increased the permeability of model membranes to ions, whereas cholesteryl linoleate did not. The behavior of the saturated ester CP in egg phosphatidylcholine bilayer systems was studied by epr of spin-labeled CP in multilayers (2, 3), as well as ^{13}C nmr difference spectroscopy (4) and ^{2}H nmr (using CP selectively deuterated in the acyl chain) (5, 6).

The epr studies indicated that only a small fraction of added ester (~0.85 mol%) intercalates between the phospholipid molecules while any excess ester forms solid patches (2). The epr studies of spin-labeled CP favor a "horseshoe" conformation for the intercalated, spin-labeled ester in the phospholipid multilayers with the ester linkage at the bilayer surface and with the chain and steroid moiety extending down into the bilayer interior. When selectively deuterated CP in an egg phosphatidylcholine multilamellar liposome system was studied using ^{2}H nmr spectroscopy, a smaller fraction of added ester (~0.2 mol%) was found to intercalate between egg phosphatidylcholine molecules (5). If the phospholipid is changed from phosphatidylcholine to sphingomyelin the amount of intercalated CP reaches 1.5 mol% (7).

When egg phosphatidylcholine bilayers are made by sonication of aqueous dispersions to form highly curved unilamellar vesicles, ester intercalation increases substantially, reaching as high as 5 mol% (6) while the ester chains appear more disordered compared to CP in multilamellar liposomes (5).

The present study is an attempt to determine the behavior of saturated cholesteryl ester in a highly curved bilayer composed of the completely saturated phospholipid, dipalmitoylphosphatidylchloline, both in the presence and absence of cholesterol (20 mol%). To do this, we used ^{2}H nmr spectroscopy of selectively deuterated cholesteryl palmitate in dipalmitoylphosphatidylcholine unilamellar vesicles.

Nuclear magnetic resonance experiments were also performed to determine whether the size of dipalmitoylphosphatidylcholine vesicles is affected by the incorporation of CP or CP/cholesterol. A ^{31}P nmr-lanthanide shift reagent technique was employed (8). Addition of the shift reagent to a sonicated dispersion separates the ^{31}P resonances from the inside and outside surfaces of the vesicles, and, from the relative intensity of the signals, an average vesicle radius may be estimated.

0008-4042/80/232433-09$01.00/0

©1980 National Research Council of Canada/Conseil national de recherches du Canada

Can. J. Chem. Downloaded from www.nrcresearchpress.com by 210.87.254.6 on 09/05/12
For personal use only.

Can. J. Chem. Downloaded from www.nrcresearchpress.com by 210.87.254.6 on 09/05/12
For personal use only.

Experimental

Materials

Cholesterol was obtained from Fisher Scientific Company and recrystallized from benzene before being used. Dipalmitoylphosphatidylcholine and cholesteryl palmitate were purchased from Sigma Chemical Company. Deteurium depleted water was obtained from Aldrich Chemical Company. Praseodymium nitrate was bought from Alfa Inorganics. Hexadecanoic-d_{31} acid, hexadecanoic-5,5,6,6,-d_4 acid, and hexadecanoic-11,11,12,12-d_4 acid were purchased from Merck, Sharp and Dohme, Canada, Ltd., whereas hexadecanoic-16,16,16-d_3 acid was obtained from Serdary Research Laboratories, London, Ont., Canada.

Syntheses of hexadecanoic-2,2-d_2 and 3,3-d_2 acids were described previously (6).

Deuterated cholesteryl esters were prepared from the corresponding deuterated fatty acids and cholesterol by the method of Grover and Cushley (9).

Preparation of Lipid Vesicles

Lipids were weighed directly into sample tubes and codissolved in a small amount (~2 mL) of chloroform–methanol (3:1). The solvent was then removed by evaporation under a stream of nitrogen and subsequent overnight pumping under high vacuum. Distilled or deuterium depleted water was added to the lipid mixture, the tube shaken vigorously on a vortex mixer and the resultant dispersion sonicated for ~15 min at ~50°C using a Biosonik III probe-type sonicator. The vesicles were then centrifuged for 15 min on a small laboratory centrifuge, in order to eliminate titanium fragments and undispersed lipid. The vesicles (~10% w/v) were used immediately for the nmr experiments. Samples in which a quantitative determination of the phospholipid and/or cholesteryl ester was required were subjected to an additional preparative ultracentrifugation for 3 h at 160 000 g on a Spinco Model L ultracentrifuge in order to remove any traces of residual undispersed lipid and multilamellar liposomes (10). The amount of phosphatidylcholine present in the suspension was quantified by phosphorus determination (11) while cholesteryl ester was determined as described by Rudel and Morris (12) or by ^{2}H nmr (6).

Nuclear Magnetic Resonance

Deuterium nmr experiments were performed at 15.4 MHz on a Varian XL 100-15 spectrometer interfaced to a NIC 1080 computer and operating in the pulse Fourier transform mode. Field stabilization was by means of an external ^{19}F field-frequency lock. Sufficient rf power was achieved by use of a 300 W ENI power amplifier. All experiments were performed at temperatures between 30–60°C as indicated throughout the text, the temperature being controlled by means of a gas-flow system.

Transverse relaxation times (T_2*) were measured from the ^{2}H nmr peak width at half-height, $\Delta\nu_{1/2}$. These spectra were obtained from the free induction decays (FID's) following a periodic sequence of 60–90° pulses. Longitudinal relaxation times (T_1) were measured by the inversion-recovery method (13),

$$[180°, \tau, 90°, \text{sample and add}, \tau_R]_N$$

where τ is the delay between the two pulses of the sequence, τ_R is the delay between subsequent pulse sequences ($\tau_R \geq 5T_1$ to ensure complete return to equilibrium), and N is the number of acquisitions. The errors in the relaxation measurements are reported in Tables 1 and 2. In all experiments a phase-alternating pulse sequence was used to minimize baseline errors.

The same spectrometer system and operating conditions were employed in the ^{31}P (40.5 MHz) nmr experiments. FID's were recorded in the presence of ^{1}H noise-decoupling (1 kHz bandwidth) and were collected both before and after addition of $Pr(NO_3)_3$ to the sonicated dispersions. Enough $Pr(NO_3)_3$ solution, approximately 50 μL of a 0.1 *M* solution to 2 mL samples of ~10% w/v vesicle dispersion, was added to produce a 150–200 Hz separation between signals from the inner and outer monolayers. Signal intensities were measured by integration of the spectra while ^{31}P chemical shifts were measured relative to an external H_3PO_4 (85%) reference. In order to eliminate Nuclear Overhauser Effects (NOE's) ^{1}H decoupling was gated on only during acquisition of the FID. Furthermore, sufficient time ($\geq 5T_1$) was left between successive rf pulses to allow complete recovery of the nuclear signals.

Results

Dipalmitoylphosphatidylcholine vesicles have been prepared which incorporate up to 5 mol% cholesteryl palmitate (CP). In order to prepare vesicles containing more than 1 mol% ester, excess CP must be added to the lipid mixture prior to sonication. The final amount of CP incorporated into the membrane may depend upon the length and power of sonication, and the temperature at which the sonication step is carried out.

The concentration of CP incorporated into the dipalmitoylphosphatidylcholine vesicles was measured in two ways. First, the amount of phospholipid in the suspension was quantified by the colorimetric determination of phosphorus (11), while the CP was determined using the phthalic dialdehyde method described by Rudel and Morris (12). Second, the ^{2}H nmr signal intensities for CP-d_{31} and natural abundance DOH in a carefully weighed amount of distilled water in the dipalmitoylphosphatidylcholine – cholesteryl palmitate-d_{31} vesicle system at 45°C were compared (6). The two methods agreed to within ±10%.

When 20 mol% cholesterol is added to the lipid preparation no reduction in the solubility of CP in the dipalmitoylphosphatidylcholine vesicle system is observed.

We have found that the ^{2}H nmr linewidths of deuterated CP in dipalmitoylphosphatidylcholine vesicles are independent of ester concentration. In addition, we observed that the ^{2}H nmr lineshape, hence $\Delta\nu_{1/2}$, was identical whether the vesicles were sized by preparative ultracentrifugation (see Experimental Section) or not, therefore, for the majority of the experiments the vesicles were not subjected to the ultracentrifugation step.

Deuterium nmr spectra for cholesteryl palmitate selectively deuterated at several positions along the acyl chain and incorporated into dipalmitoylphosphatidylcholine vesicles are shown in Fig. 1. The temperature of these runs was 45°C, which is just above the gel to liquid crystalline phase transition (T_m = 41°C) of the phospholipid. Included in Fig. 1 are the Lorentzian lineshapes giving the best

TABLE 1. Deuterium transverse relaxation times (T_2*) for selectively deuterated cholesteryl palmitate in dipalmitoylphosphatidylcholine vesicles

Position	45°C $\Delta\nu_{1/2}$ (Hz)	45°C T_2* ($\times 10^3$) (s)	55°C $\Delta\nu_{1/2}$ (Hz)	55°C T_2* ($\times 10^3$) (s)
	Without cholesterol			
2,2-d_2	150±20	2.1	110±15	2.9
3,3-d_2	80±10	4.0	58± 8	5.5
5,5,6,6-d_4	52± 6	6.1	33± 4	9.6
11,11,12,12-d_4	76± 8	4.2	42± 5	7.6
16,16,16-d_3	7± 1	45.5	5± 1	63.7
	With 20 mol% cholesterol			
2,2-d_2	180±25	1.8	140±20	2.3
3,3-d_2	160±25	2.0	110±15	2.9
5,5,6,6,-d_4	120±15	2.7	72± 8	4.4
11,11,12,12-d_4	185±30	1.7	180±25	1.8
16,16,16-d_3	21± 3	15.2	14± 2	22.7

TABLE 2. Deuterium longitudinal relaxation times (T_1) for selectively deuterated cholesteryl palmitate in dipalmitoylphosphatidylcholine vesicles

Position	T_1 ($\times 10^3$) (s) 45°C	T_1 ($\times 10^3$) (s) 55°C
2,2-d_2	6± 3	9± 4
3,3-d_2	9± 4	12± 5
5,5,6,6,-d_4	10± 4	14± 6
11,11,12,12-d_4	23± 8	35±10
16,16,16-d_3	330±30	450±50

fit to the experimental spectra. In most cases, a single Lorentzian function was found to give a good fit to the experimental spectrum. In spite of the good agreements between experimental and theoretical lineshapes, the possibility exists that our ^{2}H nmr spectra may actually be composed of a superposition of Lorentzian lines of different widths. From the signal-to-noise for our spectra we are unable to distinguish any superposition, hence, only a single Lorentzian function was fitted to the lineshape.

The ^{2}H nmr linewidths and the corresponding transverse relaxation times T_2* (where T_2* = $1/\pi\Delta\nu_{1/2}$) for a series of selectively deuterated esters at two temperatures above T_m, 45°C and 55°C, are given in Table 1. The linewidths are largest for the segment near the ester linkage, tend to decrease toward the terminal methyl group, and decrease when the temperature increases from 45°C to 55°C.

We have also obtained a ^{2}H nmr spectrum of CP-16,16,16-d_3 in dipalmitoylphosphatidylcholine vesicles at 30°C, i.e. below the gel to liquid crystalline phase transition of the phospholipid. The spectrum (not shown) was taken after performing an initial ^{2}H nmr run at 45°C and consisted of a signal approximately 200 Hz wide with an intensity of ~90% of that obtained at 45°C. Due to the large linewidth the 30°C run required 25 h in order to obtain sufficient signal-to-noise. After that time, the sample was warmed to 45°C and another spectrum taken at the higher temperature. The signal intensity in the final 45°C spectrum was ~80% of the intensity found in the original 45°C spectrum.

Deuterium nmr spectra of CP, selectively deuterated at various chain positions, in dipalmitoylphosphatidylcholine vesicles containing 20 mol% cholesterol, are presented in Fig. 2. The spectra were obtained at 45°C and have superimposed upon them the single Lorentzian function giving the best fit. Comparison with the spectrum for a similar position in the absence of cholesterol (Fig. 1) indicates that cholesterol produces a general increase in linewidth with an especially large increase at positions 11 and 12. The ^{2}H nmr linewidths and corresponding transverse relaxation times of selectively deuterated CP's in dipalmitoylphosphatidylcholine vesicles containing 20 mol% cholesterol are presented in Table 1. As seen above with vesicles composed of deuterated CP/dipalmitoylphosphatidylcholine alone, increasing the temperature from 45°C to 55°C results in a narrowing of the ^{2}H signal, and consequent increase in T_2*.

We have also measured the longitudinal relaxation times T_1 for selectively deuterated CP in dipalmitoylphosphatidylcholine vesicles and these are presented in Table 2. For all positions except the terminal methyl group the measured T_1's are very low (< 40 ms) while the T_1 for CP-16,16,16-d_3

Can. J. Chem. Downloaded from www.nrcresearchpress.com by 210.87.254.6 on 09/05/12
For personal use only.

Can. J. Chem. Downloaded from www.nrcresearchpress.com by 210.87.254.6 on 09/05/12
For personal use only.

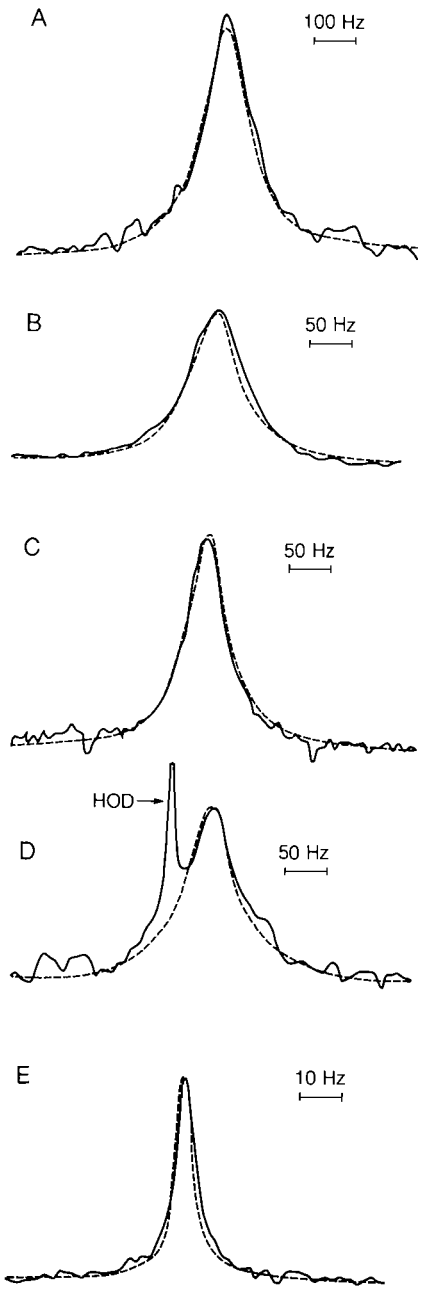


FIG. 1. Deuterium nmr spectra (—) and best-fit single Lorentzian lines (---) of selectively deuterated cholesteryl palmitate (~0.02 mol/mol phospholipid) in ~10% w/v dipalmitoylphosphatidylcholine vesicles at 45°C: *A*, 2,2-d_2; *B*, 3,3-d_2; *C*, 5,5,6,6-d_4; *D*, 11,11,12,12-d_4; *E*, 16,16,16-d_3. Spectral parameters: pulse width = 55 μs (90° flip angle); sweep width = 5000 Hz (*A*), 2500 Hz (*B*), 2000 Hz (*C*, *D*), 1000 Hz (*E*); pulse delay = 0.2 s (*A*, *B*), 0.25 s (*C*), 0.5 s (*D*), 2.4 s (*E*); No. of data points = 2K (*A*, *E*), 1K (*B*, *C*, *D*); No. of acquisitions = 3 800 – 114 000; please note that the plotted spectra represent expansions of the original ones, and the starting frequencies for each expansion are not the same.

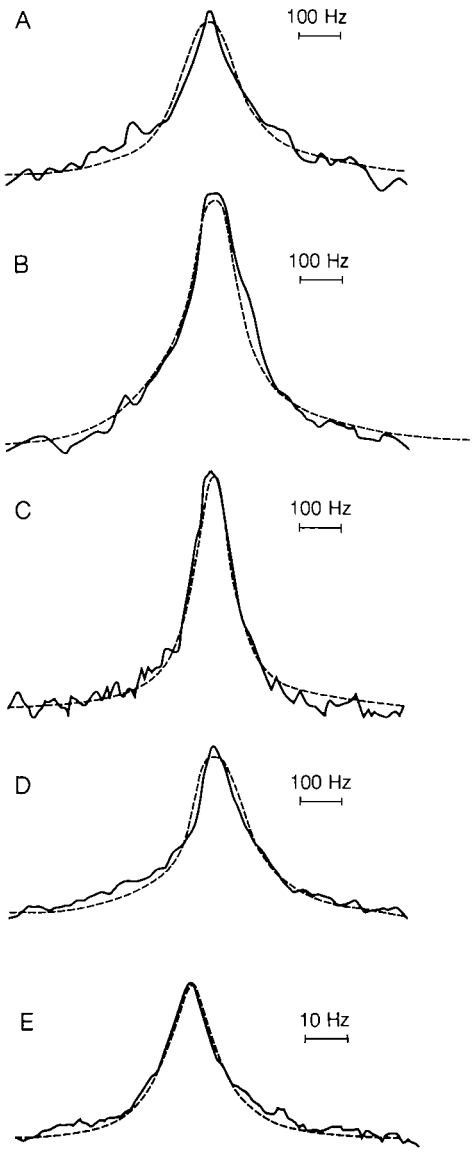


FIG. 2. Deuterium nmr spectra (—) and best-fit single Lorentzian lines (---) of selectively deuterated cholesteryl palmitate (~0.02 mol/mol total lipid) in ~10% w/v dipalmitoylphosphatidylcholine/20 mol% cholesterol vesicles at 45°C: *A*, 2,2-d_2; *B*, 3,3-d_2; *C*, 5,5,6,6-d_4; *D*, 11,11,12,12-d_4; *E*, 16,16,16-d_3. Spectral parameters: pulse width = 55 μs (90° flip angle); sweep width = 5000 Hz (*A*, *B*, *D*), 2000 Hz (*C*), 1000 Hz (*E*); pulse delay = 0.1 s (*A*, *B*, *D*), 0.25 s (*C*), 1 s (*E*); No. of data points = 1K (*A*, *B*, *D*), 2K (*C*, *E*); No. of acquisitions = 40 000 – 500 000.

at 45°C is 330 ms. Increasing the temperature from 45°C to 55°C causes T_1 to increase at all chain positions.

We have not determined T_1 values for deuterated CP in dipalmitoylphosphatidylcholine/20 mol% cholesterol vesicles since the larger linewidths in these cases would have required prohibitive

Can. J. Chem. Downloaded from www.nrcresearchpress.com by 210.87.254.6 on 09/05/12
For personal use only.

amounts of spectrometer time in order to achieve sufficient signal-to-noise.

The ^{31}P nmr spectra of sonicated dispersions of dipalmitoylphosphatidylcholine/CP and dipalmitoylphosphatidylcholine/20 mol% cholesterol/CP at 50°C following the addition of the lanthanide shift reagent $Pr(NO_3)_3$ are shown in Fig. 3. Addition of Pr^{3+} results in a downfield shift for phosphorus nuclei on the outer surfaces of the vesicles, whereas the upfield line is produced by phospholipids on the inner surfaces and is essentially unshifted. The ratio of the relative intensities of outside and inside ^{31}P nmr signals are $I_{out}/I_{in} = 1.9 \pm 0.2$ for dipalmitoylphosphatidylcholine/CP vesicles and $I_{out}/I_{in} = 1.7 \pm 0.2$ for dipalmitoylphosphatidylcholine/cholesterol/CP vesicles. Within the experimental uncertainty (±10%) these values agree with the value obtained for pure dipalmitoylphosphatidylcholine vesicles.

The outside–inside relative intensity may also be estimated by comparing the intensity of the upfield lines in Fig. 3 with that of the single ^{31}P signal observed for the same sample before the introduction of shift reagent. The ratios determined in this way are $I_{out}/I_{in} = 2.1 \pm 0.2$ and 1.9 ± 0.2 for dipalmitoylphosphatidylcholine/CP vesicles and dipalmitoylphosphatidylcholine/cholesterol/CP vesicles, respectively. However, these values may be slightly high, since some aggregation was seen to occur in the dispersions over the duration of the nmr experiment. This results in a progressive reduction in intensity of the narrow signals in the spectra recorded and makes the above comparison between spectra obtained before and after the lanthanide treatment subject to error. Therefore, the earlier stated ratios are preferred.

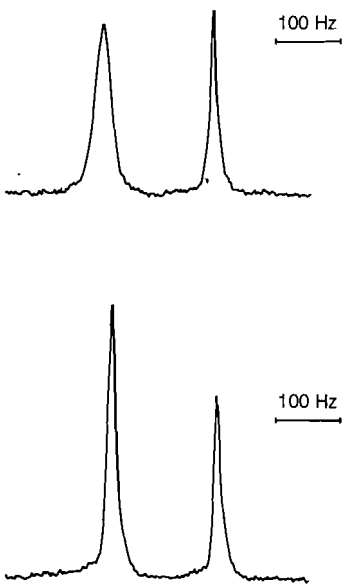


FIG. 3. Proton noise-decoupled ^{31}P nmr spectra at 50°C of sonicated dispersions after the addition of Pr^{3+}. The upper spectrum is for dipalmitoylphosphatidylcholine/CP vesicles whilst the lower one is for dipalmitoylphosphatidylcholine/cholesterol/CP vesicles. Spectral parameters: pulse width = 15 μs (90° flip angle); pulse delay $\tau_R = 15$ s; sweep width = 2000 Hz; No. of data points = 2K zero filled to 4K; line broadening = 2 Hz.

The linewidths of the upfield lines (at -1.5 ± 0.1 ppm) in the spectra of Fig. 3 are 13 Hz for the dipalmitoylphosphatidylcholine/CP vesicles and 12 Hz for the dipalmitoylphosphatidylchloline/cholesterol/CP vesicles while the widths of the signals (at -1.6 ± 0.1 ppm) of the corresponding samples prior to the addition of shift reagent are 15 and 16 Hz, respectively. On the other hand, the downfield signals are 31 Hz wide in the absence of cholesterol (at $+3.0 \pm 0.1$ ppm) and 17 Hz wide in the presence of cholesterol (at $+2.7 \pm 0.1$ ppm). The outside ^{31}P signals in the presence of cholesterol are unexpectedly, but reproducibly, less broadened.

Discussion

The results indicate that dipalmitoylphosphatidylcholine vesicles can incorporate up to 5 mol% CP, an amount identical to that incorporated into egg phosphatidylcholine vesicles (6). The solubility of the ester is not greatly reduced in the gel phase as evidenced by the ^2H nmr experiments conducted with a dipalmitoylphosphatidylcholine/CP-16,16,16-d_3 vesicle system both above and 10°C below the gel to liquid crystalline phase transition of the phospholipid. Indeed, the 10% loss in signal intensity observed at 30°C is attributed mostly, if not completely, to a small amount of vesicle aggregation (14). The additional ~10% loss in line intensity found when the sample was reheated above the phase transition lends support to this conclusion.

In an earlier study of the sphingomyelin/CP model membrane system (7), we also saw that ester solubility is independent of whether the phospholipid is in the gel or liquid crystalline phase. Our results contrast with the conclusion reached by Janiak *et al.* (15), who studied the related system, cholesteryl myristate/dimyristoylphosphatidylcholine/H_2O, using polarizing light microscopy, X-ray diffraction, and differential scanning calorimetry, and concluded that essentially all ester is forced out of the bilayer below the phospholipid phase transition temperature.

The 5 mol% maximum observed for the incorporation of CP in dipalmitoylphosphatidylcholine vesicles is several times higher than that found in

Can. J. Chem. Downloaded from www.nrcresearchpress.com by 210.87.254.6 on 09/05/12
For personal use only.

multilamellar liposomes prepared from the same phospholipid (28) and the same situation has also been encountered for the egg phosphatidylcholine/CP system (5, 6). The apparent increase in ester solubility upon going from liposomes to small vesicles may simply reflect sonication forcing an excess amount of cholesteryl ester into the bilayer, so that the final sample represents a supersaturated system. If this is the case, then the vesicles would try to achieve equilibrium by ejecting cholesteryl ester from the bilayer over a period of time. However, since the vesicles themselves have only a limited stability, such a process would be extremely difficult to prove.

On the other hand, ester solubility may actually be higher in a membrane of high curvature such as a unilamellar vesicle. A study by Pries and Klynstra (16) has established that areas of the intimal layer in animal aortas are enriched 4- to 5-fold in cholesteryl ester concentration, demonstrate enhanced permeability, and were said to be "predisposed to atherosclerosis" development. Such areas may contain cell membranes with small invaginations (endocytitic vacuoles) which, being more highly curved than the rest of the cell membrane, might dissolve more ester and lead to increased permeability of the intimal layer. We have previously established that cholesteryl palmitate enhances the permeability of model membranes (1).

Addition of 20 mol% cholesterol to the dipalmitoylphosphatidylcholine/CP-d_{31} vesicle system does not appear to decrease the amount of ester incorporated. This is in contrast to our previous observations on the egg phosphatidylcholine/CP-d_{31} system (6) in which 20 mol% cholesterol decreased the ester solubility at least by a factor of 2.

The size of the dipalmitoylphosphatidylcholine vesicles, as indicated by ^{31}P nmr, is not significantly changed either by the incorporation of CP or by the further incorporation of 20 mol% cholesterol. This behavior is identical to that reported previously for egg phosphatidylcholine vesicles (6). It is established in two ways. The first is based on the constant ratio, to within the experimental uncertainty, of the outside to inside phospholipid determined from ^{31}P nmr following addition of paramagnetic ions to the sonicated dispersions (Fig. 3). The average ratio found is I_{out}/I_{in} = 1.8 which is in agreement with the results obtained by de Kruijff *et al.* (17) for dipalmitoylphosphatidylcholine vesicles containing up to 50 mol% of cholesterol. Assuming an identical packing density of lipid in the two monolayers of a vesicle and taking a bilayer thickness of ~35 Å (18), an average vesicle diameter of ~270 Å is calculated from the ratio. This is well within the range of sizes that have been published for dipalmitoylphosphatidylcholine vesicles (19, 20).

The widths at half height $\Delta\nu_{1/2}$ of the ^{31}P nmr signals obtained with the sonicated dispersions of dipalmitoylphosphatidylcholine/CP and of dipalmitoylphosphatidylcholine/cholesterol/CP at 50°C are virtually identical to that for pure dipalmitoylphosphatidylcholine vesicles. This observation provides verification of unaltered vesicle size upon incorporation of CP or CP/cholesterol since the ^{31}P linewidth for a sonicated phospholipid dispersion is sensitive to the rate of vesicle tumbling and, hence, to vesicle size (17). The same conclusion may be reached from consideration of the unshifted (upfield) ^{31}P signals observed after addition of $Pr(NO_3)_3$ (Fig. 3).

Although it has no bearing on the present discussion, we have noted a smaller degree of broadening for the lanthanide shifted (downfield) resonance of the dipalmitoylphosphatidylcholine/cholesterol/CP vesicles which, we believe, has not been observed previously.

The ^{2}H nmr linewidths for selectively deuterated CP in dipalmitoylphosphatidylcholine vesicles decrease from 150 Hz at the 2 position to 7 Hz at the 16 position at 45°C (Table 1). Most of the variation occurs near the ends of the chain, with less change apparent in the central portion. The values are similar to those observed previously in egg phosphatidylcholine/*deutero*-CP vesicles (6). Such a profile in linewidth is in contrast to the characteristic plateau region observed by Stockton *et al.* (21) for selectively deuterated fatty acids incorporated into egg phosphatidylcholine vesicles. Furthermore, the linewidths reported for the corresponding chain positions of the fatty acid are, with the exception of the methyl group for which essentially the same widths are obtained, at least 4 times larger depending on temperature and chain position. This indicates that the behavior of the ester acyl chain in the bilayer is significantly different from that of a fatty acid. The similarity of the methyl linewidths is not surprising since the terminal methyl groups of hydrocarbon chains are known to have a high degree of motional freedom (22).

Reductions in linewidth at all positions along the acyl chain of selectively deuterated CP in dipalmitoylphosphatidylcholine vesicles accompany an increase in temperature from 45 to 55°C, whereas the additon of 20 mol% cholesterol increases the linewidths (Table 1). The trend in both cases is qualitatively in agreement with that observed for specifically deuterated stearic acids in-

Can. J. Chem. Downloaded from www.nrcresearchpress.com by 210.87.254.6 on 09/05/12
For personal use only.

tercalated in egg phosphatidylcholine vesicles (23). Stockton *et al.* (21), however, noted a decrease in vesicle tumbling rate due to an increase in vesicle size upon the addition of cholesterol which was partly responsible for the line broadening with the fatty acid. Our ^{31}P results, on the other hand, show that the size of the dipalmitoylphosphatidylcholine/CP vesicles is not altered by the presence of 20 mol% of cholesterol. Increased ^{2}H linewidths, including the especially large increase at chain positions 11 and 12, have also been reported for selectively deuterated CP in egg phosphatidylcholine vesicles (6).

A "plateau" in the spin–lattice relaxation rates $1/T_1$ is not apparent in the results obtained for selectively deuterated CP in dipalmitoylphosphatidylcholine vesicles (Table 2). Brown *et al.* (24) observed such a plateau for chain positions 2 to 10 in deuterated dipalmitoylphosphatidylcholine bilayers. Table 2 indicates a continuous decrease in $1/T_1$ towards the methyl end of the chain, the T_1's determined for the methylene segments of the ester being a factor of 2–3 shorter than for the corresponding chain positions of the phospholipid at comparable temperature. The largest difference (~3-fold) occurs near the ester linkage of CP (segments 2–6), whilst at positions 11 and 12 the difference is ~2-fold. Once again, the terminal methyl group is an exception, with the T_1 value for CP-16,16,16-d_3 being very close to that found for the CD_3 segment of dipalmitoylphosphatidylcholine-d_{62} (22). Raising the temperature is seen to increase the T_1's recorded for specifically deuterated CP in dipalmitoylphosphatidylcholine vesicles (Table 2), and is the same trend in T_1 reported for dipalmitoylphosphatidylcholine bilayers (24).

The positive temperature dependence of the T_1's observed for selectively deuterated CP in dipalmitoylphosphatidylcholine vesicles (Table 2) suggests that the molecular motions giving rise to the spin–lattice relaxation are in the short correlation time limit ($\omega_o^2\tau_c^2 \ll 1$). Hence, treating these fast motions as isotropic, an approximation which has been shown to be valid for the deuterated acyl chain segments of liquid crystalline dipalmitoylphosphatidylcholine bilayers (24), the relaxation rate $1/T_1$ may be related to a single, effective correlation time τ_c by (25)

$$[1] \quad \frac{1}{T_1} \approx \frac{3}{8}\left(\frac{e^2qQ}{\hbar}\right)^2 \tau_c$$

and e^2qQ/h is the static quadrupolar coupling constant and is 168 kHz for C—D bonds (26). Since the T_1 values measured for the methylene segments of deuterated CP are ~2–3 times shorter than the values for the corresponding chain positions in deuterated dipalmitoylphosphatidylcholine, we conclude, on the basis of eq. [1], that the effective correlation times must be ~2–3 times longer for the ester acyl chain. These longer τ_c's may be due to a slowing down of fast segmental motions of the ester chain as a result of steric interactions with the bulky cholesterol moiety. This effect would not be surprising if, for example, deuterated CP intercalated into the phospholipid bilayer in the form of a "horseshoe" as seems to be the case for spin-labelled CP (3). Space filling models show that hindrance to ester chain motions by the cholesterol moiety would then be expected to decrease markedly around chain positions 11 and 12 because the rigid cholesterol ring only extends to about these segments.

Assuming that the molecular motions contributing to the transverse relaxation observed for selectively deuterated CP in dipalmitoylphosphatidylcholine vesicles may be divided into two classes, one with a correlation time τ_c satisfying the condition $\omega_o^2\tau_c^2 \ll 1$ plus a second, much slower class, the linewidth may be written as the sum of two terms

$$[2] \quad \Delta\nu_{1/2} = \frac{1}{\pi T_2^*} = \frac{1}{\pi T_1} + \frac{1}{\pi(T_2)_{slow}}$$

This basic approach was adopted by Stockton *et al.* (21) to interpret the linewidths obtained with selectively deuterated stearic acids intercalated into egg phosphatidylcholine bilayers. They identified the slow motions producing line narrowing with vesicle tumbling together with lateral diffusion of lipid molecules in the bilayer. By replacing $1/\pi(T_2)_{slow}$ in eq. [2] by a term involving the segmental order parameter and an effective vesicle correlation time they were able to determine a profile of order along the fatty acid chain. A similar treatment was used in our earlier study of selectively deuterated CP in egg phosphatidylcholine vesicles (6) but, subsequently, we have discovered that the assumption that vesicle tumbling is the slow motion largely responsible for line narrowing may not be valid for cholesteryl esters in vesicles. This conclusion rests on the observation that the width of the ^{2}H resonance for CP-d_{31} in phospholipid vesicles appears to be independent of the suspending medium viscosity (29). Hence, in the case of selectively deuterated CP in dipalmitoylphosphatidylcholine vesicles, we choose not to specify the nature of the slow motions, and we prefer not to use the formalism of Stockton *et al.* (21). Neither do we wish to employ the alternate, more detailed, theory developed by Petersen and Chan (27), in which the effects of

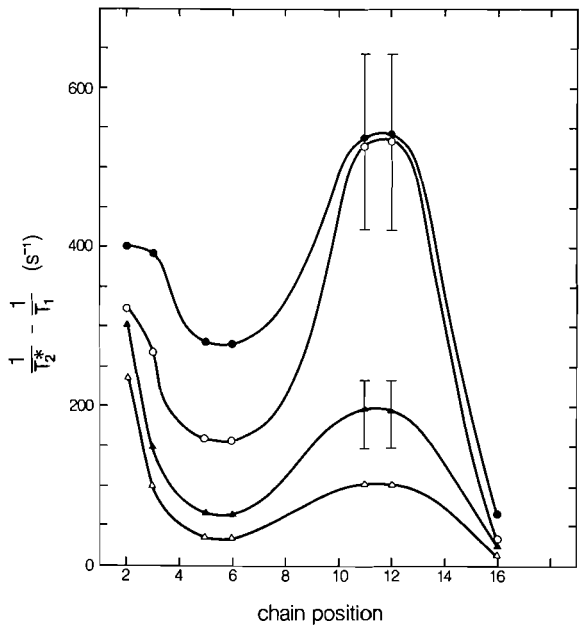


FIG. 4. Plot of $1/T_2^* - 1/T_1$ vs. chain position for selectively deuterated cholesteryl palmitate in dipalmitoylphosphatidylcholine or dipalmitoylphosphatidylcholine/20 mol% cholesterol vesicles: △, dipalmitoylphosphatidylcholine at 55°C; ▲, dipalmitoylphosphatidylcholine at 45°C; ○, dipalmitoylphosphatidylcholine/cholesterol at 55°C; ●, dipalmitoylphosphatidylcholine/cholesterol at 45°C. The indicated error bars are representative for positions 5,6 and 11,12 only; the actual error is higher at positions 2 and 3, and lower at position 16. Errors are lower at 55°C than at 45°C.

motional averaging due to slow reorientation of the lipid chain as a whole were included. Instead, we prefer to remain with the more general quantity $1/(T_2)_{slow}$ defined by eq. [2] and simply say that it reflects changes in disorder and/or rate of molecular motion along the ester chain.

The $1/(T_2)_{slow}$ values calculated for specifically deuterated CP in dipalmitoylphosphatidylcholine vesicles are plotted versus chain position in Fig. 4, as are the equivalent values estimated in the presence of 20 mol% cholesterol. The T_1's obtained for the samples without cholesterol were used in the latter estimations, and we feel this is not a serious approximation in the light of previous experience (6). A minimum around chain positions 5 and 6 followed by a maximum at positions 11 and 12 are characteristics of the plots, which clearly do not exhibit the plateau region seen for the C2–C10 part of the acyl chain in the order parameter profiles of deuterated phospholipids (21). This is another indication that the behavior of the ester chain differs considerably from that of the phospholipid chain. On the other hand, the fact that the $1/(T_2)_{slow}$ values are greater at the lower temperature and following the addition of cholesterol, corresponding to increased order and/or slower rates of motion for the ester chain, is qualitatively consistent with the changes observed for the phospholipid.

The origin of the maximum in $1/(T_2)_{slow}$ at chain positions 11 and 12 is unknown. In the absence of cholesterol, it appears to become less pronounced at the higher temperature when the dipalmitoylphosphatidylcholine bilayer is more disordered. The maximum is also seen to be greatly accentuated when order in the dipalmitoylphosphatidylcholine bilayer is made greater by addition of 20 mol% cholesterol. A similar change has been observed with egg phosphatidylcholine/deuterated CP vesicles (6). Explanation of the effect(s) responsible for the observations at the 11, 12 positions will require additional work.

1. B. J. FORREST and R. J. CUSHLEY. Atherosclerosis, **28**, 309 (1977).
2. A. K. GROVER and R. J. CUSHLEY. Atherosclerosis, **32**, 87 (1979).
3. A. K. GROVER, B. J. FORREST, R. K. BUCHINSKI, and R. J. CUSHLEY. Biochim. Biophys. Acta, **550**, 212 (1979).
4. R. J. CUSHLEY and B. J. FORREST. Can. J. Chem. **57**, 2364 (1979).
5. M. I. VALIC, H. GORRISSEN, R. J. CUSHLEY, and M. BLOOM. Biochemistry, **18**, 854 (1979).
6. H. GORRISSEN, A. P. TULLOCH, and R. J. CUSHLEY. Biochemistry, **19**, 3422 (1980).
7. A. L. MACKAY, S. R. WASSALL, M. I. VALIC, H. GORRISSEN, and R. J. CUSHLEY. Biochim. Biophys. Acta, **601**, 22 (1980).
8. V. F. BYSTROV, N. I. DUBROVINA, L. I. BARSUKOV, and L. D. BERGELSON. Chem. Phys. Lipids, **6**, 343 (1971).
9. A. K. GROVER and R. J. CUSHLEY. J. Labeled Compd. Radiopharm. **XVI**, 307 (1979).
10. Y. BARENHOLZ, D. GIBBES, B. J. LITMAN, J. GOLL, T. E. THOMPSON, and F. D. CARLSON. Biochemistry, **16**, 2806 (1977).
11. B. N. AMES. *In* Methods in enzymology. Vol. 8. *Edited by* E. F. Neufeld and V. Gimburg. Academic Press, New York. 1966. p. 115.
12. L. L. RUDEL and M. D. MORRIS. J. Lipid Res. **14**, 364 (1973).
13. R. L. VOLD, J. S. WAUGH, M. P. KLEIN, and D. E. PHELPS. J. Chem. Phys. **48**, 3831 (1968).
14. A. L. LARRABEE. Biochemistry, **18**, 3321 (1979).
15. M. J. JANIAK, D. M. SMALL, and G. G. SHIPLEY. J. Lipid Res. **20**, 183 (1979).
16. C. PRIES and F. B. KLYNSTRA. Lancet, 750 (1971).
17. B. DE KRUIJFF, P. R. CULLIS, and G. K. RADDA. Biochim. Biophys. Acta, **436**, 729 (1976).
18. M. H. F. WILKINS, A. E. BLAUROCK, and D. M. ENGELMAN. Nature New Biol. London, **230**, 72 (1971).
19. M. P. SHEETZ and S. I. CHAN. Biochemistry, **11**, 4573 (1972).
20. M. BLOOM, E. E. BURNELL, A. L. MACKAY, C. P. NICHOL, M. I. VALIC, and G. WEEKS. Biochemistry, **17**, 5750 (1978).
21. G. W. STOCKTON, C. F. POLNASZEK, A. P. TULLOCH, F. HASAN, and I. C. P. SMITH. Biochemistry, **15**, 954 (1976).

Can. J. Chem. Downloaded from www.nrcresearchpress.com by 210.87.254.6 on 09/05/12
For personal use only.

22. J. H. DAVIS. Biophys. J. **27**, 339 (1979).
23. G. W. STOCKTON, C. F. POLNASZEK, L. C. LEITCH, A. P. TULLOCH, and I. C. P. SMITH. Biochem. Biophys. Res. Commun. **60**, 844 (1974).
24. M. F. BROWN, J. SEELIG, and U. HABERLEN. J. Chem. Phys. **70**, 5045 (1979).
25. A. ABRAGAM. The principles of nuclear magnetism. Clarendon Press, Oxford. 1961. p. 313.
26. D. F. BURNETT and B. H. MULLER. J. Chem. Phys. **55**, 5929 (1971).
27. N. O. PETERSEN and S. I. CHAN. Biochemistry, **16**, 2657 (1977).
28. H. GORRISSEN, S. R. WASSALL, A. L. MACKAY, M. I. VALIC, and R. J. CUSHLEY. Unpublished results.
29. S. R. WASSALL, H. GORRISSEN, and R. J. CUSHLEY. To be published.

Can. J. Chem. Downloaded from www.nrcresearchpress.com by 210.87.254.6 on 09/05/12
For personal use only.

A nitrogen-15 nuclear magnetic resonance study of *N*-aryl phosphoramidates and phosphorimidates

G. W. BUCHANAN AND F. G. MORIN

Department of Chemistry, Carleton University, Ottawa, Ont., Canada K1S 5B6

AND

R. R. FRASER

Department of Chemistry, University of Ottawa, Ottawa, Ont., Canada K1N 9B4

Received March 14, 1980

This paper is dedicated to Prof. Raymond U. Lemieux on the occasion of his 60th birthday

G. W. BUCHANAN, F. G. MORIN, and R. R. FRASER. Can. J. Chem. **58**, 2442 (1980).

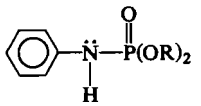
^{15}N nuclear magnetic resonance chemical shifts and one-bond ^{15}N—^{31}P couplings are reported for a series of five *N*-arylphosphoramidates and four *N*-arylphosphorimidates. Results are interpreted in terms of an extensively delocalized N lone pair in the phosphoramidates, with p_π–p_π donation into the aromatic ring being dominant over p_π–d_π donation from nitrogen to phosphorus.

G. W. BUCHANAN, F. G. MORIN et R. R. FRASER. Can. J. Chem. **58**, 2442 (1980).

On rapporte les ^{15}N rmn déplacements chimiques et les constantes de couplage entre ^{15}N et ^{31}P à travers une liaison pour cinq *N*-arylphosphoramidates et quatre *N*-arylphosphorimidates. Pour les phosphoramidates, on dit que la paire d'électrons sur l'azote est extrêmement délocalisée, et que la donation p_π–p_π vers le cycle de benzol est plus importante que la donation p_π–d_π de l'azote au phosphore.

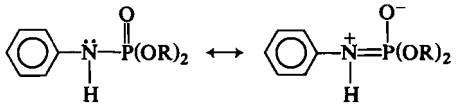
Introduction

Recently there has been considerable interest in the substituent effects of phosphorus-containing groups in electrophilic aromatic substitution reactions (1). In the case of a phosphorylated aniline (below), the phosphorus substituent can alter the behavior of the nitrogen lone pair and thereby

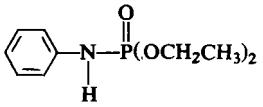


influence the site of electrophilic attack. Theoretically, there can be a competition between two opposing effects. The first is resonance p_π–p_π donation of the N lone pair to the adjacent aromatic ring, a well-recognized phenomenon in organic chemistry (2), which would lead to an increase in the electron densities (relative to benzene) at the *ortho* and *para* positions, and to *ortho–para* directing effects.

The competing phenomenon is p_π–d_π back donation from the N lone pair to a vacant 3*d* orbital of phosphorus, which would, if present, result in little discrimination between *o*, *m*, and *p* sites in electrophilic aromatic substitution reactions, i.e.:



Recently, ^{13}C nmr results (3), based on a dual substituent parameter approach (4), have been interpreted in terms of a dominance of N lone pair delocalization into the aromatic ring for the phosphorylated aniline shown below (R = CH_2CH_3).



By contrast, this substituted benzene was found to give *very low* discrimination between *o*, *m*, and *p* sites in electrophilic aromatic nitration (1), a result interpretable either in terms of strong involvement of the N lone pair in p_π–d_π back donation to phosphorus, or to reaction of the conjugate acid only.

In view of the uncertain nature of these results, we were motivated to examine some phosphorylated anilines by a technique which might provide direct information re: the nature of N—P bonding. ^{15}N nuclear magnetic resonance could present such an alternative, as it has been demonstrated (5) that both ^{15}N—^{31}P one bond couplings and ^{15}N shieldings are sensitive probes for structure and bonding in heterocyclic phosphoramidates.

Results and Discussion

The structures and numbering scheme for the compounds examined (**1–9**), are shown in Fig. 1, while Table 1 contains the ^{15}N—^{31}P couplings and ^{15}N chemical shifts. For both the phosphoramidate series and phosphorimidate series, the *p*-NO_2 derivatives were also synthesized (X = Y = H; Z = NO_2), but low solubilities precluded spectral determination.

0008-4042/80/232442-05$01.00/0

©1980 National Research Council of Canada/Conseil national de recherches du Canada

Can. J. Chem. Downloaded from www.nrcresearchpress.com by 210.87.254.42 on 09/05/12
For personal use only.

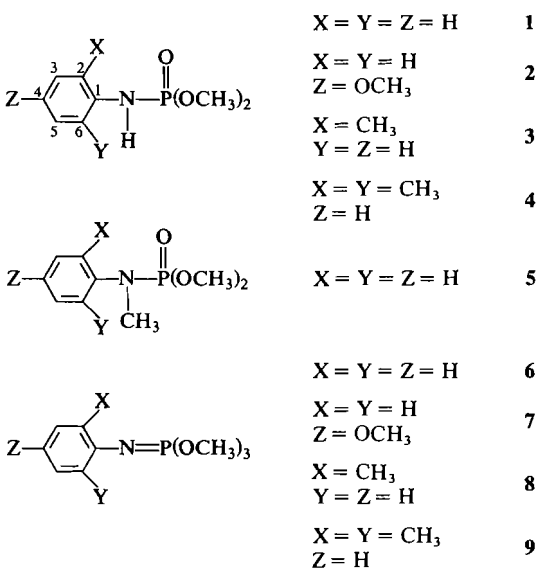


FIG. 1. Structures and numbering scheme.

TABLE 1. One bond $^{15}N—^{31}P$ couplings[a] and ^{15}N chemical shifts

Compound	$^1J_{NP}$ (Hz) ± 0.2	δ_N (ppm from NH_3) ± 0.1
1	42.6[b]	71.0
2	42.9[b]	63.8
3	44.3[b]	64.6
4	43.2[b]	56.0
5	42.8[c]	57.1
6	42.5[c]	71.3
7	42.6[c]	66.6
8	42.9[c]	66.9
9	44.1[c]	57.1

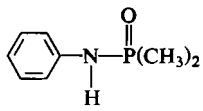
[a]Signs likely negative.
[b]For ca. 1.5 *M* solutions in $CDCl_3$.
[c]For ca. 1.5 *M* solutions in 3:1 ϕNH_2–$CHCl_3$.

One Bond Couplings

Although we have not determined them experimentally, the signs of the $^{15}N—^{31}P$ couplings in all these materials are almost assuredly negative (6). Several mechanisms may contribute to the coupling, but it has been demonstrated by a finite perturbation method (6), that the Fermi contact contribution can account for the observed coupling of −26.9 Hz in $[(CH_3)_2N]_3PO$.

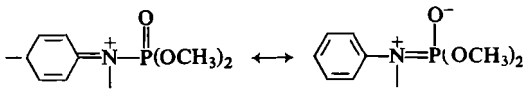
Via a series of double irradiation experiments (7), the sign of $^1J_{PN}$ in the phosphinamide below has been determined to be negative, the value being −0.5 Hz. If the Fermi contact mechanism dominates, then increasingly electronegative substituents bonded to N or P should make $^1J_{PN}$ more negative (6). Thus, the value of −42.6 Hz for **1** is, at least qualitatively, reasonable.

When purely trigonal planar geometry at N was



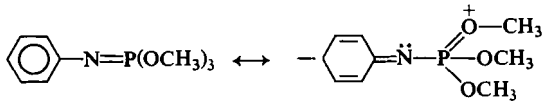
used in the Fermi contact calculations (6) for $[(CH_3)_2N]_3PO$, the calculated $^1J_{NP}$ was −39 Hz i.e. remarkably close to values for **1–9**. Furthermore, it has been found (5) for heterocyclic phosphoramidates, that $^1J_{PN}$ is -40.0 ± 2.5 Hz for compounds having sp^2 hybridized N atoms (8). In compounds with lower *s* character (i.e. sp^3 N), the value for $^1J_{NP}$ is ca. −10 Hz, again consistent with the Fermi contact formalism.

Accordingly, we interpret the ^1J results for **1–5** in terms of predominantly sp^2 hybridized N, but based on these data alone, we cannot distinguish between the relative contributions from the two resonance forms presented below.

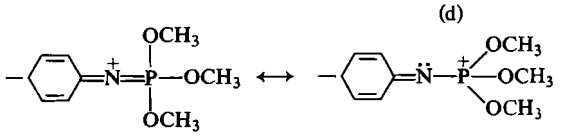


(a) (b)

For the phosphorimidates **6–9**, the $^1J_{PN}$ data again suggest sp^2 hybridized N, but one cannot, using ^1J data, evaluate the importance of contributions from resonance forms (c), (d), and (e) as shown below.



(d)



(c) (e)

Chemical Shifts of ^{15}N

Recently, it has been demonstrated (9) that ^{15}N nmr chemical shifts can be used to monitor steric inhibition to N lone pair delocalization into the aromatic ring of substituted anilines. Thus, assessment of the relative importance of resonance forms (a) and (b) above in the phosphoramidates should be possible using chemical shift trends.

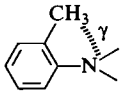
Both steric and electronic effects have been examined. The *para* —OCH_3 in **2** causes an upfield shift of 7.2 ppm vs. **1**, and the same trend is apparent in **7** vs. **6**. The magnitudes of these shifts are similar to those in substituted anilines (10).

Very substantial γ steric shifts are evident as well. Comparing data for **1** and **3**, replacement of one *ortho* H by a CH_3 produces an upfield shift of

Can. J. Chem. Downloaded from www.nrcresearchpress.com by 210.87.254.42 on 09/05/12
For personal use only.

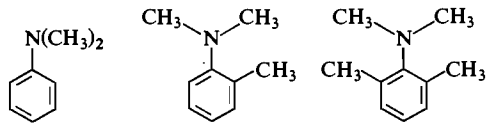
Can. J. Chem. Downloaded from www.nrcresearchpress.com by 210.87.254.42 on 09/05/12
For personal use only.

6.4 ppm at N. Such an effect can be attributed to the γ steric interaction depicted below



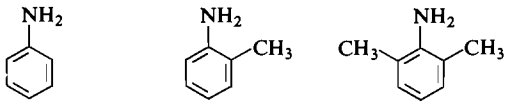
For secondary alkylamines (11), regression analysis of ^{15}N chemical shifts led to a value of −2.1 ppm for each γ interaction. In the present series of compounds, however, the γ shifts are considerably larger, since in **4**, containing two *ortho* CH_3 groups, the second CH_3 induces an additional shielding at N of 8.6 ppm.

The present findings can be compared to those for the *N*,*N*-dimethylanilines (9) shown below, where successive *ortho* methylations produce 10.7 and 16.8 ppm upfield shifts at N, respectively.



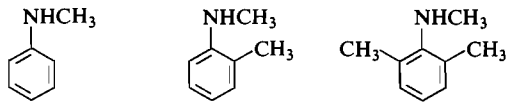
$\delta_N = 44.6$ $\delta_N = 33.9$ $\delta_N = 17.1$

In the *ortho*-alkylated materials, it was suggested that steric inhibition to N lone pair delocalization into the aromatic ring was the major cause of the upfield shielding effects at ^{15}N, and photoelectron spectral data are corroborative (12). For aniline itself, *ortho*-methylation produces much smaller γ effects at N (13).



$\delta_N = 56.5$ $\delta_N = 54.2$ $\delta_N = 51.0$

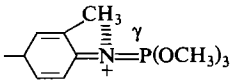
Unfortunately studies on the intermediate case, i.e. the N-methyl anilines, which would represent the closest analogy to the phosphoramidates **3** and **4** were not available. We have therefore measured the ^{15}N shifts for *N*-methylaniline, 2-methyl-*N*-methylaniline, and 2,6-dimethyl-*N*-methylaniline and the results are shown below.



$\delta_N = 54.0$ $\delta_N = 51.8$ $\delta_N = 41.5$

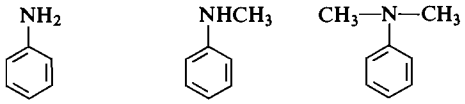
The first *ortho* group causes a minor shielding (2.2 ppm), whereas the second methyl induces a further shielding of 10.3 ppm. It appears then that the second *ortho* methyl generally has a larger influence on the ^{15}N shift than does the first in both the *N*-methyl aniline series and series **1**, **3**, **4**.

For the phosphorimidates **8** and **9**, one cannot invoke steric inhibition of resonance arguments to rationalize the upfield ^{15}N shifts on successive *ortho*-methylation. Clearly, contributions from resonance forms such as those depicted below are not subject to steric interference of N lone pair delocalization.



Thus, one can regard the upfield shifts in **8** and **9** vs. **6** as manifestations of normal γ effects, as depicted above. The ^{13}C shifts for carbons *para* to N in **6**, **8**, and **9** are nearly identical, in agreement with this argument (15), the values being 119.9, 120.0, and 120.2 ppm respectively.

In the case of the *N*-methyl phosphoramidate **5**, the ^{15}N resonance is shifted *upfield* by 13.9 ppm relative to **1**. By definition, this is termed an "α" effect, and can be contrasted with results for primary alkylamines (14), in which introduction of an "α" CH_3 group leads to an average *deshielding* at N of 8.7 ppm. There is, however, precedent for upfield α-methylation effects in aromatic amines, as is depicted below (13).



$\delta_N = 56.5$ $\delta_N = 52.8$ $\delta_N = 44.6$

A rationale for the aromatic amine results was recently put forward (9), involving reduced N lone pair delocalization into the aromatic ring as the N becomes more progressively alkylated. It was calculated (9), that the C(1)—N torsional angle remains unchanged as a result of N-methylation, and that the upfield α-methylation shift results from a change in the N lone pair energy relative to the benzene orbital energies.

The ^{13}C data (15) for phosphoramidates **4** and **5** vs. **1**, show substantially deshielded C-4 resonances (3–4 ppm) in the *ortho*-alkylated molecules vs. the non-hindered compound **7**, indicative of steric inhibition to N lone pair donation caused by *ortho* methylation.

Thus, we can conclude that N lone pair delocalization into the aromatic ring *is* an important process in phosphoramidates such as **1**, and accordingly the large amount of *meta* nitration product observed (1) is not likely to result from p_π–d_π back donation from N to P. Rather it is an indication that the reaction may proceed via the conjugate acid as originally suggested by Modro and Pioch (1).

Can. J. Chem. Downloaded from www.nrcresearchpress.com by 210.87.254.42 on 09/05/12
For personal use only.

Solvent Effects

Several practical problems arose during this work with respect to low ^{15}N signal intensity.[1] It is well known (16) that on irradiation of protons, the negative magnetogyric ratio for ^{15}N leads to a theoretical maximum of -3.93 for the nuclear Overhauser enhancement factor in the case of purely dipole–dipole H—^{15}N relaxation. Contributions from other mechanisms, however, can produce essentially zero ^{15}N signal intensity (16), and such mechanisms can be operative in compounds **5–9** in which there are no directly bonded H's on N to facilitate dipole–dipole relaxation. One method which we have used previously (5) to overcome this problem is the addition of $Cr(acac)_3$, but no beneficial effect of this reagent was observed for **5–9**.

Considerable success was obtained, however, by use of a 3:1 volume:volume mixture of aniline–$CHCl_3$ in place of $CDCl_3$ as solvent. In the case of **6** for example, a tenfold increase in the signal to noise ratio was observed in the ^1H decoupled spectrum. Furthermore no measurable solvent induced shifts or ^1J changes were noted between these two media. Several factors may be operative to increase the signal to noise ratio. Addition of aniline may increase the solution viscosity and thus lower the T_1. Additional protons in the medium will, on solute–solvent encounter, contribute to dipole–dipole relaxation of the ^{15}N nucleus, leading to a shortened T_1. Also, as the protons are decoupled, an *intermolecular* nuclear Overhauser effect resulting from the dipole–dipole relaxation can occur.

One could in principle test for the relative contributions of each effect noted above by measuring the viscosities, the ^{15}N T_1's and the nOe, but due to the lengthy time required for such experiments, they have not been carried out.

Experimental

Materials

Phosphoramidates **1**, **2**, and **3** were prepared by the following procedure. To a stirred solution of the corresponding aromatic amine (0.01 mol), triethylamine (0.01 mol), and CCl_4 (0.02 mol) in ether (20 mL) at 0°C, was added dropwise dimethyl phosphite (0.01 mol). The reaction mixture was stirred at room temperature overnight, solids removed by filtration, and the residue was evaporated to dryness. Recrystallization from the indicated solvent gave phosphoramidates in yields between 50–60%.

Compound **1**, recrystallized from hexane, mp 88–89°C (lit. (18) mp 88°C). Compound **2**, recrystallized from ethyl acetate and then hexane, mp 72.5–73.0°C (lit. (19) mp 109–110°C); ^1H nmr δ: 3.8 (d, J_{HP} = 12 Hz, CH_3O—P, 6H), 3.75 (s, CH_3—O—Ar, 3H), 7.0 (q, aromatic 4H), 7.3 (bs, —NH, 1H). Compound **3**, recrystallized from cyclohexane, mp 110–112°C (lit. (19) mp 110°C).

Phosphorimidates **6–9** were synthesized by reaction of the corresponding aromatic azide (20) with trimethyl phosphite. A typical procedure follows. In a 3-necked round bottom flask equipped with reflux condenser, stopper, and dropping funnel, was placed a stirring bar and trimethyl phosphite (0.022 mol) in ether (20 mL). The aromatic azide (0.02 mol) in ether (15 mL) was added dropwise with stirring. Stirring was continued overnight and then the solvent removed on a rotary evaporator. Only **6** could be distilled without rearrangement to *N*-methylphosphoramidates, however, **7**, **8**, and **9** showed expected ^1H and ^{13}C spectra after brief heating at < 50°C under vacuum to remove excess starting material.

Compound **6**, n_D^{20} = 1.5232 (lit. (18) n_D^{20} = 1.5232); compound **7**, n_D^{20} = 1.5281 (lit. (21) n_D^{20} = 1.5275); compound **8**, mp 40–41°C (lit. (19) bp 93–97°C/0.05 Torr); compound **9**, mp 36–36.5°C. *Anal.* calcd.: % C 54.32, H 7.45, N 5.76, P 12.73; found: % C 54.07, H 7.52, N 5.82, P 12.75.

The *N*-methyl compound **5** was prepared from **6** by heating in a pressure flask to 70°C in the presence of 1.0 equivalents of CH_3I (21). The product was purified by bulb to bulb distillation and gave a ^1H nmr spectrum consistent with its structure (21) i.e. δ: 3.2 (d, J_{HP} = 9.0 Hz, CH_3N, 3H), 3.8 (d, J_{HP} = 12.0 Hz, CH_3OP, 6H), 7.1–7.4 (m, 5H, aromatic).

Phosphoramidate **4** was prepared from phosphorimidate **9** as follows. Compound **9** (1.0 g) was adsorbed on a column of silica gel (30.0 g) in diethyl ether, and drawn onto the column. After standing for 24 h, the product was eluted with ether in 92% yield. Subsequent recrystallization from ethyl acetate–hexane gave **4**, mp 128–129°C; ^1H nmr δ: 2.4 (s, CH_3—, 6H), 3.8 (d, J_{HP} = 11.0 Hz, CH_3OP, 6H), 4.7 (bs, N—H, 1H), 7.0 (s, 3H, aromatic). *Anal.* calcd. for **4**: % C 52.40, H 7.04, N 6.11, P 13.51; found: % C 52.36, H 7.15, N 6.21, P 13.39.

N-Methyl-*o*-toluidine and *N*-methyl-2,6-dimethylaniline were prepared as described previously (22).

Spectra

The ^{15}N spectra were recorded with a Varian FT-80 nmr system at a frequency of 8.0603 MHz, using 10 mm sample tubes. Except as noted below all ^{15}N spectra were run using the deuterium of the solvent $CDCl_3$ for locking. In the cases of **5–9**, a coaxial D_2O capillary was used as a lock. The ^{15}N chemical shifts were measured relative to neat ^{15}N enriched aniline, and converted to the scale of δ_{NH_3} = 0 (17) using the conversion factor of 56.5 ppm for aniline → anhydrous ammonia (11).

Typical experimental conditions were: pulse width 30° to 50°; acquisition time 8 s; number of data points, 8000, sw = 500 Hz; and the number of transients ranged from 4000 to 20 000; ^{15}N enriched samples of **1** and **6** were used to optimize the instrument parameter settings.

[1]The practical problems in obtaining natural abundance ^{15}N spectra have been recently summarized (17).

Acknowledgments

G. W. Buchanan and R. R. Fraser thank the Natural Sciences and Engineering Research Council of Canada for financial support, and Mr. Raj Capoor for technical assistance.

1. T. A. Modro and J. Pioch. Can. J. Chem. **54**, 560 (1976).
2. C. K. Ingold. Structure and mechanism in organic chemistry. 2nd ed. G. Beel and Sons, London. 1969. Chapt. VI.
3. T. A. Modro. Phosphorus Sulfur, **5**, 331 (1979).

4. R. T. C. BROWNLEE and R. D. TOPSOM. Tetrahedron Lett. 5187 (1972).
5. G. A. GRAY, G. W. BUCHANAN, and F. G. MORIN. J. Org. Chem. **44**, 1768 (1979).
6. G. A. GRAY and T. A. ALBRIGHT. J. Am. Chem. Soc. **98**, 3857 (1976).
7. W. MCFARLANE and B. WRACKMEYER. Inorg. Nucl. Chem. Lett. **11**, 719 (1975).
8. G. W. BUCHANAN and F. G. MORIN. Can. J. Chem. **57**, 21 (1979).
9. M. P. SIBI and R. L. LICHTER. J. Org. Chem. **42**, 2999 (1977).
10. T. AXENROD, P. S. PREGOSIN, M. J. WIEDER, E. D. BECKER, R. B. BRADLEY, and G. W. A. MILNE. J. Am. Chem. Soc. **93**, 6536 (1971).
11. J. P. WARREN and J. D. ROBERTS. J. Phys. Chem. **78**, 2507 (1974).
12. T. KOBAYASHI and S. NAGAKURA. Bull. Chem. Soc. Jpn. **47**, 2563 (1974).
13. R. L. LICHTER and J. D. ROBERTS. Org. Magn. Reson. **6**, 636 (1974).
14. R. L. LICHTER and J. D. ROBERTS. J. Am. Chem. Soc. **94**, 2495 (1972).
15. G. W. BUCHANAN and F. G. MORIN. Org. Magn. Reson. In press.
16. R. L. LICHTER and J. D. ROBERTS. J. Am. Chem. Soc. **93**, 3200 (1973).
17. G. C. LEVY and R. L. LICHTER. Nitrogen-15 nuclear magnetic resonance spectroscopy. John Wiley & Sons, New York. 1979. Chapt. 2.
18. A. KABACHNIK and V. A. GILYAROV. Izv. Akad. Nauk USSR Otd. Khim. Nauk, 790 (1956). Chem. Abstr. **51**, 1823e (1957).
19. J. I. G. CADOGAN, J. D. SEARS, D. M. SMITH, and M. J. TODD. J. Chem. Soc. 2813 (1969).
20. P. A. S. SMITH and B. B. BROWN. J. Am. Chem. Soc. **73**, 2438 (1951).
21. V. A. GILYAROV, R. V. KUDRYAVTSEV, and M. I. KABACHNIK. Zh. Obshch. Khim. **36**, 708 (1966). Chem. Abstr. **65**, 8798c (1966).
22. R. R. FRASER. Can. J. Chem. **38**, 2226 (1960).

Can. J. Chem. Downloaded from www.nrcresearchpress.com by 210.87.254.42 on 09/05/12
For personal use only.

Diels–Alder cycloadditions of *N*-substituted-1,2-dihydropyridines with nitrosobenzene. Synthesis of 3-phenyl-2-oxa-3,6-diazabicyclo[2.2.2]oct-7-enes

EDWARD E. KNAUS[1] AND KAMLAKAR AVASTHI

Faculty of Pharmacy and Pharmaceutical Sciences, University of Alberta, Edmonton, Alta., Canada T6G 2N8

AND

C. S. GIAM

Department of Chemistry, Texas A & M University, College Station, TX 77843, U.S.A.

Received February 4, 1980

This paper is dedicated to Prof. Raymond U. Lemieux on the occasion of his 60th birthday

EDWARD E. KNAUS, KAMLAKAR AVASTHI, and C. S. GIAM. Can. J. Chem. **58**, 2447 (1980).

The regiospecific ($\pi 2 + \pi 4$) cycloaddition reaction of *N*-carbonyl-1,2-dihydropyridines **2** with nitrosobenzene afford a mixture of 3-phenyl-2-oxa-3,6-diazabicyclo[2.2.2]oct-7-ene rotamers **3** and **4**. Rotamers **3** and **4**, which differ in configuration at the carbonyl to nitrogen (amide) bond, exhibit dual resonances for C(1)H, C(5)H, and the N(6) acetyl (methoxycarbonyl) substituents. An ^{1}H nmr temperature study indicated that rotamers **3***a* and **4***a* coalesce at about 100°C.

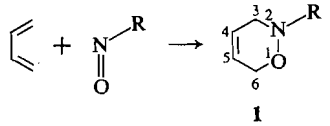
EDWARD E. KNAUS, KAMLAKAR AVASTHI et C. S. GIAM. Can. J. Chem. **58**, 2447 (1980).

La réaction de cycloaddition régiospécifique ($\pi 2 + \pi 4$) des *N*-carbonyldihydro-1,2 pyridines **2** avec le nitrosobenzène donne un mélange des rotamères **3** et **4** du phényl-3 oxa-2 diazo-3,6 bicyclo[2.2.2] octène-7. Les rotamères **3** et **4** dont la configuration diffère au niveau de la liaison carbonyle–azote (amide) montrent des doubles résonances pour C(1)H, C(5)H et pour les substituants sur le N(6) acétyle (méthoxycarbonyle). Une étude de rmn du ^{1}H en fonction de la température indique que les rotamères **3***a* et **4***a* se confondent aux environs de 100°C.

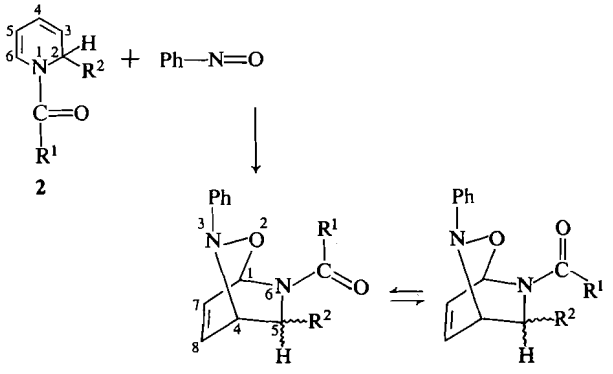
[Traduit par le journal]

The Diels–Alder reaction of dienamines with dienophiles is an attractive method for the synthesis of pharmacologically interesting bicyclic heterocycles (1). Several studies have shown that various *C*-nitroso compounds react readily with conjugated dienes to yield 3,6-dihydro-1,2-oxazines **1** (2, 3). It was therefore of interest to develop methods for the preparation of bicyclic heterocycles in which a 1,2-oxazine is fused to a tetrahydropyridine ring. The regiospecific ($\pi 2 + \pi 4$) cycloaddition reaction of *N*-substituted-1,2-dihydropyridines **2** with nitrosobenzene now provides a convenient route to exchanging 3-phenyl-2-oxa-3,6-diazabicyclo[2.2.2]oct-7-ene rotamers **3** and **4**.

Reaction of *N*-acetyl-2-phenyl-1,2-dihydropyridine **2***a* with nitrosobenzene proceeded smoothly in methylene chloride at 25°C under a nitrogen atmosphere with disappearance of the green color to afford a mixture of rotamers **3***a* and **4***a* (82.6%) which differ in configuration at the carbonyl to nitrogen (amide) bond. The ^{1}H nmr spectrum ($CDCl_3$, 25°C) exhibited dual absorptions at δ 6.06 and 6.87, 5.47 and 5.28, and 2.28 and 1.78 due to the C(1)H, C(5)H, and N(6)COMe groups of **3***a* and **4***a* respectively in a ratio of 18:82 as determined by integration. Double irradiation studies provide further evidence for the presence of the two rotational conformers **3***a* and **4***a*, which arise as a result of hindered internal rotation, since irradiation at 1.78 and 5.28 δ respectively results in saturation of the corresponding absorptions at 2.28 and 5.47 δ. An ^{1}H nmr temperature study effected on the 50:50



1



2 **3** **4**

a R^1 = Me, R^2 = Ph
b R^1 = Me, R^2 = *n*-Bu
c R^1 = CO_2Me, R^2 = H
d R^1 = CO_2Me, R^2 = *n*-Bu
e R^1 = CO_2Me, R^2 = Ph

[1]Author to whom inquiries should be addressed.

0008-4042/80/232447-05$01.00/0.

©1980 National Research Council of Canada/Conseil national de recherches du Canada

Can. J. Chem. Downloaded from www.nrcresearchpress.com by 210.87.254.5 on 09/05/12
For personal use only.

Can. J. Chem. Downloaded from www.nrcresearchpress.com by 210.87.254.5 on 09/05/12
For personal use only.

mixture of rotamers **3***a* and **4***a* in DMSO-d_6 indicated the coalescence temperature to be approximately 100°C where the N(6)COMe group appears as a sharp singlet at 2.15 δ. Upon cooling to 25°C the ratio of **3***a*:**4***a* returned to 50:50. The difference in the ratio of **3***a*:**4***a* in $CDCl_3$ (18:82) in comparison to DMSO-d_6 (50:50) is clearly a solvent effect. Dual absorptions for the —NCOMe group and protons on carbon adjacent to it have been observed in the ^{1}H nmr spectra of methyl 4-acetamido-4-deoxy-L-erythrofuranoside (4) and *N*-acetylimidazole (5). Protons adjacent to and in the nodal plane of the imide carbonyl group of *N*-acetylimidazole in a nonpolar solvent are shifted downfield as a result of the anisotropy of the acyl group (5) indicating that configurationally dependent changes in the chemical shifts of C(1)H and C(5)H are associated with their proximity to the acyl oxygen. On this basis it is expected that the C(1)H of **3***a* (6.06 δ) would appear at higher field than the C(1)H of **4***a* (6.87 δ) and the C(5)H of **3***a* (5.47 δ) would be deshielded relative to the C(5)H of **4***a* (5.28 δ). Similar shielding and deshielding effects were also observed for C(1)H and C(5)H for other compounds prepared as illustrated in Table 1.

Hart *et al.* (2) recently reported that nitrosobenzene adds regiospecifically to cyclohexadienones with the oxygen of the nitroso group being orientated toward the carbonyl group in the adduct. The regiospecificity of the cycloaddition reaction was rationalized using approximate frontal orbital theory. The most important interactions are between the HOMO of the dienone and the LUMO of nitrosobenzene. Coefficients are expected to be largest for these orbitals at C-3 of the *N*-substituted-1,2-dihydropyridine **2** and on the nitrogen of the nitroso group (2) leading to the formation of a C(3)N and C(6)O bond in the cycloaddition products.

The ^{1}H nmr spectra were also consistent with the assignment of the N—O orientation observed for the cycloadducts **3** and **4**. The coupling pattern observed for the mixtures of rotamers **3***a* and **4***a* in $CDCl_3$ fixed the low field bridgehead protons due to C(1)H adjacent to oxygen at 6.06 and 6.87 δ respectively and the high field bridgehead protons due to C(4)H adjacent to nitrogen at 4.6 δ. Kresze and Firl (6) have shown that the proton adjacent to oxygen, in adducts obtained from reaction of *p*-chloronitrosobenzene and a variety of 1,3-dienes, appears at lower field than that adjacent to nitrogen. The orientation of the N—O cycloaddition is therefore expected to be as illustrated for **3***a* and **4***a*.

The stereochemistry of the C-5 substituent (R^2) present in **3** and **4** has not been established. Examination of a Dreiding Model indicates that the dihedral angle for a C(4)H—C(5)H *exo–endo* interaction is very similar to that for an *exo–exo* interaction. The ^{1}H nmr spectrum of rotamers **3***c* and **4***c* support this observation since $J_{4,5}$ *exo* and $J_{4,5}$ *endo* are both 3.25 Hz. However, the large difference in the chemical shifts for the acetyl methyl groups of **3***a* and **4***a* (0.5 δ), relative to the difference in **3***b* and **4***b* (0.06 δ) indicates that the C(6) phenyl substituent does exhibit a significant shielding effect. The much larger chemical shift difference for the C(1)H (0.81 δ) compared with the C(5)H for the two rotamers **3***a* and **3***b* would suggest the R^2 substituent is in the *exo* position.

Reaction of *N*-acetyl-2-butyl-1,2-dihydropyridine **2***b* with nitrosobenzene afforded a mixture of 3-phenyl-5-butyl-6-acetyl-2-oxa-3,6-diazabicyclo[2.2.2]oct-7-ene rotamers **3***b* and **4***b* (51.8%). ^{1}H nuclear magnetic resonance spectrometry indicated that the ratio of **3***b*:**4***b* in deuterochloroform was 69:31. It is not clear why the ratio of **3***b*:**4***b* is so different from that of compounds *a*, *c*, *d*, and *e* (see Table 1). Similar reactions of nitrosobenzene with *N*-methoxycarbonyl-1,2-dihydropyridine **2***c*, *N*-methoxycarbonyl-2-butyl-1,2-dihydropyridine **2***d*, and *N*-methoxycarbonyl-2-phenyl-1,2-dihydropyridine **2***e* gave rise to mixtures of rotamers **3***c* and **4***c* (67.1%), **3***d* and **4***d* (51.8%), and **3***e* and **4***e* (75.9%) in ratios of 41:59, 29:71, and 11:89 respectively (see Table 1). It is not surprising that the products obtained in the latter reactions consist of a mixture of rotamers **3** and **4** since hindered internal rotation about the nitrogen to carbonyl bond has been observed in



N—COOMe systems such as 1,2-dimethoxycarbonyl-3,6-diphenyl-1,2,3,6-tetra-hydropyridazine **5** (7).

Adducts **3** and **4** having a N(6)COOMe substituent were less stable than those having a N(6)COMe or N(6)SO_2Me substituent. N(6)methoxycarbonyl adducts **3***e* and **4***e* having a C(5)Ph substituent were more stable than **3***c* and **4***c* having a C(5)*n*-Bu substituent which undergoes dissociation quite readily. The mass spectra for all adducts **3** and **4** did not exhibit molecular ions.

It was also of interest to examine a reaction which would give rise to a product in which hindered internal rotation about N(6) of the 2-oxa-3,6-diazabicyclo[2.2.2] oct-7-ene ring system was not possible. Reaction of *N*-methanesulfonyl-1,2-dihydropyridine **6** with nitrosobenzene afforded the N(6)SO_2Me product **7** which exhibited single absorptions for all nonequivalent protons.

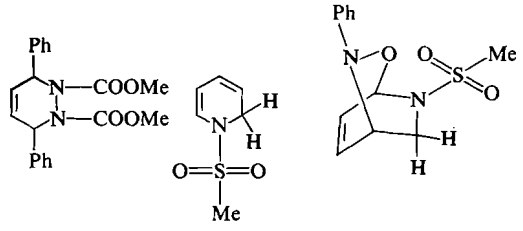
The reaction of 1,2-dihydropyridines with other

Can. J. Chem. Downloaded from www.nrcresearchpress.com by 210.87.254.5 on 09/05/12
For personal use only.

TABLE 1. ^{1}H nuclear magnetic resonance data for 3-phenyl-2-oxa-3,6-diazabicyclo[2.2.2]oct-7-enes **3** and **4**[a,b]

			Chemical shifts											
			Rotamers **3** and **4**[c]					Rotamer **3**			Rotamer **4**			
Compounds	R^1	R^2	R^2	C(4)H[d]	C(7)H[e]	C(8)H[f]	Ph	R^1	C(1)H[g]	C(5)H	R^1	C(1)H[g]	C(5)H	Ratio **3**:**4**[i,j]
3*a* and **4***a*	Me	Ph	7.15–7.44	4.6	6.82	5.86	6.96–7.12 7.14–7.44	2.28	6.06	5.47[h]	1.78	6.87	5.28[h]	18:82
3*b* and **4***b*	Me	*n*-Bu	0.8–1.0 1.1–1.5	4.54	6.7	6.16	6.94–7.12 7.2–7.32	2.18	5.8	4.34[k]	2.12	6.66	4.06[k]	69:31
3*c* and **4***c*	OMe	H	3.29(**3***c*)[l] 3.26(**4***c*)[l]	4.56	6.7	6.2	6.96–7.07 7.2–7.34	3.78	6.1	4.0[m]	3.75	6.2	4.0[m]	41:59
3*d* and **4***d*	OMe	*n*-Bu	0.84–0.96 1.2–1.46	4.5	6.66	6.1	6.96–7.1 7.2–7.3	3.80	6.1	4.15[k]	3.77	6.24	4.08[k]	29:71
3*e* and **4***e*	OMe	Ph	7.15–7.45	4.56	6.76	5.78	6.92–7.14	3.72	6.2	5.7	3.61	6.4	5.26	11:89

[a]Spectra were obtained in $CDCl_3$ at 25°C, chemical shifts are in δ units relative to tetramethylsilane, *J* are in Hertz, and all peaks had integrated areas appropriate to the structures. Double resonance experiments were used to confirm assignments and coupling constants *J*.
[b]The numbering system used is that shown for structures **3** and **4**.
[c]These chemical shifts were the same for both rotamers **3** and **4**.
[d]None of the compounds examined exhibited chemical shift nonequivalence for C(4)H. These peaks were d($J_{4,8}$ = 5.75 Hz) of d($J_{4,5}$ = 3.25 Hz) of d($J_{4,7}$ = 2 Hz).
[e]These peaks were d($J_{7,8}$ = 8 Hz) of d($J_{1,7}$ = 5.5 Hz) of d($J_{4,7}$ = 2 Hz).
[f]These peaks were d($J_{7,8}$ = 8 Hz) of d($J_{4,8}$ = 5.75 Hz) of d($J_{1,8}$ = 1.75 Hz).
[g]These peaks were d($J_{1,7}$ = 5.5 Hz) of d($J_{1,8}$ = 1.75 Hz).
[h]These peaks were d($J_{4,5}$ = 3.25 Hz).
[i]The ratio of rotamers as determined from integrals of C(1)H, C(5)H, and the R^2 substituent.
[j]The coupling constants *J*, for similar spin–spin interactions, were virtually identical for **3** and **4**.
[k]These peaks were t($J_{5,-CH_2}$ = 7 Hz) of d($J_{4,5}$ = 3.25 Hz).
[l]These peaks appeared as two closely overlapping d($J_{5,5}$ = 10 Hz) of d($J_{4,5}$ = 3.25 Hz).
[m]These peaks were d($J_{5,5}$ = 10 Hz) of d($J_{4,5}$ = 3.25 Hz).



5 6 7

electrophilic *C*-nitroso compounds (3) such as nitrosylcyanide, trifluoronitrosomethane, and nitrosocarbonyl compounds will be investigated to broaden the scope of this reaction.

Experimental

Melting points were determined with a Büchi capillary apparatus and are uncorrected. Infrared spectra (potassium bromide unless otherwise noted) were taken on a Perkin-Elmer 267 or Unicam SP 1000 spectrometer. Nuclear magnetic resonance spectra were determined for solutions in deuterochloroform or deuterodimethylsulfoxide with a Bruker WH-200 or WH-400 spectrometer. Double resonance studies were used to confirm assignments. *N*-Substituted-1,2-dihydropyridines **2***a–e* and **6** were prepared using published procedures (8–10).

*3,5-Diphenyl-6-acetyl-2-oxa-3,6-diazabicyclo[2.2.2]oct-7-ene Rotamers (***3**a *and* **4**a*)*

A solution of *N*-acetyl-2-phenyl-1,2-dihydropyridine **2***a* (3.15 g, 15.8 mmol) in 5 mL dry methylene chloride was added with stirring to a solution of nitrosobenzene (1.75 g, 16.3 mmol) in 30 mL dry methylene chloride, under a nitrogen atmosphere at 25°C. The reaction was allowed to proceed for 90 min during which the green color disappeared completely. Removal of the solvent *in vacuo* below 30°C gave a solid which was triturated with 75 mL *n*-hexane. The insoluble product was filtered, washed with 25 mL *n*-hexane, and recrystallized from acetone to yield a mixture of rotamers **3***a* and **4***a* (4.0 g, 82.6%) as white needles, mp 131–132°C (dec.); ir: 1665 (s, CO) cm^{-1}. *Anal.* calcd. for $C_{19}H_{18}N_2O_2$: C 74.48, H 5.93, N 9.15; found: C 74.38, H 5.88, N 9.08.

*3-Phenyl-5-*n*-butyl-6-acetyl-2-oxa-3,6-diazabicyclo[2.2.2.]-oct-7-ene Rotamers (***3**b *and* **4**b*)*

N-Acetyl-2-*n*-butyl-1,2-dihydropyridine (1.86 g, 10.38 mmol) was added with stirring to a solution of nitrosobenzene (1.1 g, 10.2 mmol) under a nitrogen atmosphere at 25°C and the reaction was allowed to proceed for 3 h. Removal of the solvent *in vacuo* at 25°C gave a solid residue which was purified using a neutral alumina oxide (75 g) column. Elution with 200 mL ether gave a viscous liquid which crystallized from 12 mL benzene–hexane (4:1 v/v) to afford 1.217 g of **3***b* and **4***b*. Concentration of the mother liquor gave a second crop of crystals (0.321 g) for a combined yield of 51.8%, mp 83–86°C (dec.); ir: 1655 (s, CO) cm^{-1}. *Anal.* calcd. for $C_{17}H_{22}N_2O_2$: C 71.28, H 7.75, N 9.79; found: C 71.22, H 7.86, N 9.79.

*3-Phenyl-6-methoxycarbonyl-2-oxa-3,6-diazabicyclo[2.2.2]-oct-7-ene Rotamers (***3**c *and* **4**c*)*

N-Methoxycarbonyl-1,2-dihydropyridine **2***c* (1.39 g, 10 mmol) was added with stirring to a solution of nitrosobenzene (1.07 g, 10 mmol) in 30 mL dry methylene chloride under a nitrogen atmosphere at 25°C. The reaction was allowed to proceed for 3 h during which the green color disappeared. Removal of the solvent *in vacuo* at 25°C gave a dark colored residue which on recrystallization from benzene–hexane (5:1 v/v) gave rotamers **3***c* and **4***c* as a pale yellow solid (1.65 g, 67.1%), mp 86°C (dec.); ir: 1720 (s, CO) cm^{-1}. *Anal.* calcd. for $C_{13}H_{14}N_2O_3$: C 63.39, H 5.73, N 11.38; found: C 62.88, H 5.49, N 11.50. A solid sample of **3***c* and **4***c* decomposed slowly on standing at 25°C over a period of a few days while ^1H nmr spectrometry indicated some dissociation in $CDCl_3$ after 1 h.

*3-Phenyl-5-*n*-butyl-6-methoxycarbonyl-2-oxa-3,6-diazabicyclo-[2.2.2]oct-7-ene Rotamers (***3**d *and* **4**d*)*

A solution of *N*-methoxycarbonyl-2-*n*-butyl-1,2-dihydropyridine **2***d* (0.918 g, 4.7 mmol) in 5 mL dry methylene chloride was added to a solution of nitrosobenzene (0.504 g, 4.7 mmol) in 30 mL dry methylene chloride with stirring under a nitrogen atmosphere at 25°C. The reaction was allowed to proceed for 16 h after which the solvent was removed *in vacuo* at 25°C. The dark residue was purified by elution from a neutral alumina oxide column (30 g) using first 50 mL hexane and then 200 mL benzene. Removal of the solvent from the benzene eluate afforded **3***d* and **4***d* as an oil (0.582 g, 41.6%); ir (film): 1720 (s, CO) cm^{-1}. Repeated attempts to obtain a satisfactory elemental analysis were not successful.

*3,5-Diphenyl-6-methoxycarbonyl-2-oxa-3,6-diazabicyclo-[2.2.2]oct-7-ene Rotamers (***3**e *and* **4**e*)*

A solution of *N*-methoxycarbonyl-2-phenyl-1,2-dihydropyridine **2***e* (2.86 g, 13.3 mmol) in 5 mL dry methylene chloride was added with stirring to a solution of nitrosobenzene (1.43 g, 13.3 mmol) in 30 mL dry methylene chloride under a nitrogen atmosphere at 25°C. The reaction was allowed to proceed for 3 h prior to removal of the solvent *in vacuo* below 30°C. The sticky semi-solid obtained was triturated with 100 mL hexane leaving a light green solid which was washed with 30 mL hexane to give **3***e* and **4***e* (3.26 g, 75.9%) as a crystalline light green solid, mp 129–131°C; ir: 1710 (s, CO) cm^{-1}. *Anal.* calcd. for $C_{19}H_{18}N_2O_3$: C 70.78, H 5.63, N 8.69; found: C 71.39, H 5.75, N 8.29.

*3-Phenyl-6-methanesulfonyl-2-oxa-3,6- diazabicyclo[2.2.2]-oct-7-ene (***7**)*

N-Methanesulfonyl-1,2-dihydropyridine **6** (1.9 g, 11.9 mmol) was added with stirring to a solution of nitrosobenzene (1.41 g, 13.1 mmol) in 30 mL dry methylene chloride under a nitrogen atmosphere at 25°C. The reaction was allowed to proceed for 3 h and the solvent was removed *in vacuo* below 30°C. The semi-solid residue obtained was triturated with hexane and then benzene. The insoluble residue was recrystallized from methylene chloride – hexane to afford **7** (1.63 g, 51.2%) as a white crystalline solid, mp 134–135°C (dec.); ir: 1155, 1340 (s, SO_2) cm^{-1}; ^1H nmr (DMSO-d_6) δ: 3.08 (s, 3H, SO_2Me), 3.2 (d, $J_{5,5}$ = 10.5 Hz of d, $J_{4,5}$ = 3.0 Hz, 1H, H-5*exo*), 3.82 (d, $J_{5,5}$ = 10.5 Hz of d, $J_{4,5}$ = 3.0 Hz, 1H, H-5*endo*), 4.96 (d, $J_{4,8}$ = 5.75 Hz of t, $J_{4,5}$ = 3.0 Hz of d, $J_{4,7}$ = 2.0 Hz, 1H, H-4), 5.86 (d, $J_{1,7}$ = 5.5 Hz of d, $J_{1,8}$ = 1.75 Hz, 1H, H-1), 6.24 (d, $J_{7,8}$ = 8.0 Hz of d, $J_{4,8}$ = 5.75 Hz of d, $J_{1,8}$ = 1.75 Hz, 1H, H-8), 6.76 (d, $J_{7,8}$ = 8.0 Hz of d, $J_{1,7}$ = 5.5 Hz of d, $J_{4,7}$ = 2.0 Hz, 1H, H-7), 6.92–7.08, 7.22–7.28 (m, 5H, Ph). *Anal.* calcd. for $C_{12}H_{14}N_2O_3S$: C 54.12, H 5.30, N 10.53, S 12.02; found: C 53.89, H 5.43, N 10.74, S 11.79.

Acknowledgements

We are grateful to the Natural Sciences and Engineering Research Council of Canada (Grant A0531) for financial support of this research and to the Department of Chemistry, University of Alberta for providing 200 and 400 mHz ^1H nmr spectra.

Can. J. Chem. Downloaded from www.nrcresearchpress.com by 210.87.254.5 on 09/05/12
For personal use only.

1. E. E. KNAUS, F. M. PASUTTO, and C. S. GIAM. J. Heterocycl. Chem. **13**, 481 (1976).
2. H. HART, S. K. RAMASWAMI, and R. WILLER. J. Org. Chem. **44**, 1 (1979).
3. G. W. KIRBY. Chem. Soc. Rev. **6**, 1 (1977).
4. W. A. SZAREK, S. WOLFE, and J. K. N. JONES. Tetrahedron Lett. 2743 (1964).
5. G. YAMAMOTO and M. RABAN. J. Org. Chem. **41**, 3788 (1976).
6. G. KRESZE and J. FIRL. Tetrahedron, **24**, 1043 (1968).
7. J. C. BRELIERE and J. M. LEHN. Chem. Commun. 426 (1975).
8. C. S. GIAM, E. E. KNAUS, and F. M. PASUTTO. J. Org. Chem. **39**, 3565 (1974).
9. F. W. FOWLER. J. Org. Chem. **37**, 1321 (1972).
10. E. E. KNAUS and K. REDDA. Can. J. Chem. **55**, 1788 (1977).

Can. J. Chem. Downloaded from www.nrcresearchpress.com by 210.87.254.5 on 09/05/12
For personal use only.

Conformational preferences about both exocyclic carbon–carbon bonds in some phenyl derivatives of ethane, propene, and 4-picoline

TED SCHAEFER, LEONARD J. KRUCZYNSKI, BERT KRAWCHUK, RUDY SEBASTIAN, JAMES L. CHARLTON, AND DAVID M. MCKINNON

Department of Chemistry, University of Manitoba, Winnipeg, Man., Canada R3T 2N2

Received January 18, 1980

This paper is dedicated to Prof. Raymond U. Lemieux on the occasion of his 60th birthday

TED SCHAEFER, LEONARD J. KRUCZYNSKI, BERT KRAWCHUK, RUDY SEBASTIAN, JAMES L. CHARLTON, and DAVID M. MCKINNON. Can. J. Chem. **58**, 2452 (1980).

The ^1H nmr spectra in solution of 1-*R*-(3,5-dibromophenyl) ethanes (R = CH_3, C_2H_5, *n*-C_3H_7 to *n*-C_6H_{13}, OH, F, Br), of 1-amino-2-(3,5-dichlorophenyl) ethane, of 3,5-dichloroallylbenzene, and of 4-(3,5-dibromobenzyl) pyridine are analyzed at 305 K. For the ethane derivatives, the populations of *anti* and *gauche* conformers are derived from the vicinal proton–proton coupling constants. The conformation about the C_1—C_α bond in both *gauche* and *anti* forms is discussed in terms of long-range couplings to the ring protons and some approximate barriers about this bond are suggested for both conformers. Greater rigidity exists in the *gauche* than in the *anti* conformations. In some cases the measurements are compared with extensive molecular orbital calculations, for example, for phenethylamine. The low-energy conformations and the barriers about the C_1—C_α bond are deduced for the allyl and pyridyl compounds.

TED SCHAEFER, LEONARD J. KRUCZYNSKI, BERT KRAWCHUK, RUDY SEBASTIAN, JAMES L. CHARLTON et DAVID M. MCKINNON. Can. J. Chem. **58**, 2452 (1980).

Opérant à 305 K, on a analysé les spectres rmn du ^1H de solutions des *R*-1 (dibromo-3,5 phényl) éthanes (R = CH_3, C_2H_5, *n*-C_3H_7 à *n*-C_6H_{13}, OH, F, Br), d'amino-1(dichloro-3,5 phényl)-2 éthane, du dichloro-3,5 allylbenzène et de la (dibromo-3,5 benzyl)-4 pyridine. Dans le cas des dérivés de l'éthane, on a évalué les populations des conformères *anti* et *semi-décalée* à partir des constantes de couplage des protons vicinaux. On discute de la conformation autour de la liaison C_1—C_α des deux formes *anti* et *semi-décalée* en fonction des couplages à longue distance avec les protons du cycle et on suggère pour les deux conformères des barrières approximatives pour la rotation autour de cette liaison. Il existe une plus grande rigidité dans la conformation *semi-décalée* par rapport à la forme *anti*. Dans certains cas, on compare les mesures aux longs calculs élaborés d'orbitales moléculaires effectués par exemple pour la phénylamine. On a évalué les conformations de faible énergie et les barrières à la rotation autour de la liaison C_1—C_α pour les composés allyliques et pyridiniques.

[Traduit par le journal]

Introduction

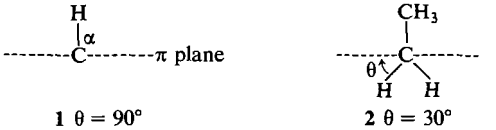
The use of stereospecific vicinal proton–proton coupling constants, $^3J^{H,H}$, in the derivation of *anti* and *gauche* populations of 1,2-disubstituted ethane derivatives is well known (1, 2). If the barrier to interconversion of the *anti* and *gauche* isomers is much larger than thermal energies, a condition reasonably well met by ethane derivatives near room temperature, then the assumption of effectively rigid[1] *gauche* and *anti* isomers in this procedure is reasonable.

On the other hand, in phenylethane derivatives the barrier to rotation about the C_1—C_α bond (sp^2—sp^3 bond) need not be large compared to thermal energies (3). Then the populations of the hindered rotor states, each of the latter corresponding to a different magnitude of a relevant coupling parameter, must be known when assessing conformational preferences. The *J* method (4) has been developed for this purpose and depends on the stereospecificity of the coupling over six bonds, ^6J_p, between an α proton and the ring proton or fluorine nucleus in the *para* position. As recently discussed in some detail (5), one may write

[1] $$^6J_p^{H,CH} = {}^6J_{90}\langle\sin^2\theta\rangle$$

where $^6J_{90}$ is the value of ^6J in **1** and $\langle\sin^2\theta\rangle$, the expected value of $\sin^2\theta$, can be calculated as a function of a presumed twofold barrier to internal rotation, V_2, in terms of a hindered rotor model (6). The experimental tests of this equation suggest strongly that $^6J_0$ ($\theta = 0°$) is negligibly small (5).

In an early experiment (3), the *J* method yielded **2** rather than **3** or **4** as the low-energy conformation about the C_1—C_α bond in 3,5-dibromophenylethane, in accord with a low resolution microwave study of phenylethane (7). In addi-



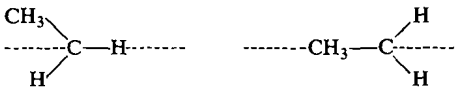
1 $\theta = 90°$ **2** $\theta = 30°$

[1]A rigorous procedure would consider the populations of torsional states within each conformer, each torsional state corresponding to a different ^3J.

0008-4042/80/232452-08$01.00/0

©1980 National Research Council of Canada/Conseil national de recherches du Canada

Can. J. Chem. Downloaded from www.nrcresearchpress.com by 210.87.254.6 on 09/05/12
For personal use only.



3 4 $\theta = 60°$

tion, the twofold barrier, V_2, was deduced as $1.2_2 \pm 0.08$ kcal/mol (1 cal = 4.184 J), in exact if fortuitous agreement with recent heat capacity data on the parent compound (8).

Unfortunately, the J method becomes relatively insensitive to V_2 above about 3 kcal/mol. Yet ^6J is still a good indicator of the preferred conformation at large V_2 values, the magnitudes of which are then large compared to thermal energies at ambient temperatures.

This paper combines the two procedures to provide an illustration of how a reasonable characterization of the conformations about both C_1—C_α and C_α—C_β bonds in some phenylethane derivatives can be achieved. In addition, conformations about the C_1—C_α bond in allylbenzene and 4-benzylpyridine derivatives are provided. The ^1H nmr measurements occur at 100 MHz, necessitating the use of substituents at the *meta* positions of the phenyl group. The necessity is purely tactical. At 500 MHz the substituents would be superfluous.

Experimental

The alkyl compounds were prepared from the commercial *p*-amino-4-*n*-alkylbenzenes in the obvious way and gave correct mass spectra. The synthesis of the alcohol and of the alkyl halides is as follows. To a solution of *p*-aminophenethyl alcohol (7.3 g, 0.053 mol) in 70 mL of tetrahydrofuran (THF) cooled to 0°C, add 6 mL Br_2 dropwise over 5 min. Add NaOH (2.4 g, 0.06 mol) in 10 mL of H_2O dropwise. During this addition an aqueous phase separates. The mixture is stirred violently for 5 min. If the aqueous phase is now acidic, add a drop of NaOH. Repeat until the aqueous phase remains basic. The phases are separated and the THF is pumped off, yielding maroon crystals of 3,5-dibromo-4-aminophenethyl alcohol. The yield is almost quantitative.

The amino group is removed in the standard way. Replacement of the hydroxyl group by bromine or fluorine proceeds as follows. To a solution of 5.0 g (0.018 mol) of 3,5-dibromophenethyl alcohol in 50 mL of diethyl ether, add 0.0357 mol (3.33 mL) of PBr_3 dropwise, then powdered $NaHCO_3$ (0.1 g at a time) till the mixture is basic to litmus. The ether layer is dried over $MgSO_4$. Evaporation leaves a brown oil; the yield is about 50% of 3,5-dibromophenethyl bromide.

To a solution of 1.71 g (0.0061 mol) of the alcohol in 50 mL of CH_2Cl_2 (dried over 5 Å sieve) cooled to −78°C (CO_2/acetone), add 0.982 g (0.0061 mol) of Et_2NSF_3 (Peninsular Chemicals) dropwise. The reaction is carried out under positive N_2 pressure. Stir for 1 h at room temperature. Add aqueous bicarbonate till basic to litmus. Dry CH_2Cl_2 layer over $MgSO_4$ and evaporate, leaving a brown liquid. The yield is ca. 60%. These compounds are not completely pure but give the correct mass and ^1H nmr spectra.

The 1-amino-2-(3,5-dichlorophenyl) ethane was prepared by reduction of the corresponding benzyl cyanide, whereas 3,5-dichloroallylbenzene came from a Grignard reaction in the standard way. The 4-(3,5-dibromobenzyl) pyridine was prepared from the 4-aminobenzyl precursor.

Solutions of various concentrations (see below) in CS_2 in 5 mm od nmr sample tubes were degassed by the freeze–pump–thaw technique and were flame-sealed. The sample tubes contained small amounts of tetramethylsilane (TMS). The ring ^1H nmr spectra were calibrated at a probe temperature of 305 K on an HA100 spectrometer in the frequency sweep mode. Markers were placed at ca. 5Hz intervals and their frequencies relative to the TMS frequency were determined from the lock and sweep frequencies. Repeating such a procedure four times yielded interpolated peak frequencies whose rms deviations were typically 0.02 Hz or less. The ^1H nmr spectra of the shorter sidechains were also calibrated.

Molecular orbital calculations (9, 10) were performed on an Amdahl 470/V7 system.

Results and Discussion

Spectral Analyses

These were done with the computer program LAME (11, 12) in the usual way. The analyses of the ring proton spectra as AB_2X_2 (X = α CH_2 protons) systems were straightforward. The analysis of the α and β methylene proton spectra as AA′BB′ spin systems proceeded as follows. In all cases the long-range coupling of the *alpha* methylene protons to the three ring protons complicated the procedure. Furthermore, as is well known (13), when the *anti* and *gauche* populations about the C_α—C_β bond are almost equal, only the sum of the two vicinal couplings, $^3J + {}^3J'$, within the AA′BB′ fragment can be extracted reliably. This condition applied to the 1-hydroxy, 1-fluoro, and 1-amino ethane derivatives.

For the 1-bromoethane derivative, although reliable ^2J values could be found, the ^3J and $^3J'$ numbers were strongly correlated (Table 1). In contrast, for the 1-methylethane compound, the ^3J and $^3J'$ numbers were reliable but the ^2J values had a correlation coefficient of unity and are therefore not known individually (high gain spectra did not alleviate these uncertainties).

In Table 1, the spectral parameters are tabulated for 1-bromo-2-(3,5-dibromophenyl) ethane and for 1-methyl-2-(3,5-dibromophenyl) ethane and illustrate the analytical quality. Coupling constants of interest to this paper are given for the other compounds in Table 2. The $^4J^{H,H}$ values indicate the spectral precision. The error in the coupling constants is taken as three times the standard deviation.

Figure 1 displays part of the methyl proton spectrum for 1-methyl-(3,5-dibromophenyl) ethane. It shows that $^4J^{CH_2,CH_3}$ in the propyl group must be negative.

Can. J. Chem. Downloaded from www.nrcresearchpress.com by 210.87.254.6 on 09/05/12
For personal use only.

Can. J. Chem. Downloaded from www.nrcresearchpress.com by 210.87.254.6 on 09/05/12
For personal use only.

TABLE 1. The ^1H nuclear magnetic resonance spectral parameters of 1-bromo-2-(3,5-dibromophenyl) ethane and 1-methyl-2-(3,5-dibromophenyl) ethane

Parameter[a]	1-Bromo[b]	1-Methyl[b]	Parameter[a]	1-Bromo[b]	1-Methyl[b]
ν_{CH_3}	—	92.818(5)[b]	$^3J_{H_1,H_2}$	6.726(9)[f]	6.391(9)
ν_1	342.911(2)	159.412(4)	$^3J'$	7.940(9)[f]	8.865(9)
ν_2	303.246(2)	250.	$^4J_m^{H,H}$	1.774(4)	1.777(2)
ν_0	722.362(3)	716.781(1)	$^4J_o^{H,CH_2}$	−0.542(4)	−0.594(2)
		716.759(4)[c]			−0.595(5)[c]
ν_p	747.324(3)	738.781(1)	$^6J_p^{H,CH_2}$	−0.384(5)	−0.428(2)
		738.298(1)[c]			−0.428(5)[c]
$^3J_{H,CH_3}$	—	7.349(4)[d]			—
$^4J_{CH_2,CH_3}$	—	−0.170(7)	Error (rms)	0.012	0.028[g]
$^2J_{H_1,H_1}$	−9.987(4)	−11.651(1.706)[e]	Largest correlation coefficient		—
$^2J_{H_2,H_2}$	−14.324(4)	−12.028(1.706)[e]		0.903[f]	1.000[e]

[a]In Hz at 100.01 MHz and 305 K; shifts relative to internal TMS.
[b]Concentration 11 mol% in CS_2.
[c]Concentration 6.8 mol% in CS_2.
[d]Numbers in parentheses are standard deviations in the last significant figure, except for footnote *e*.
[e]These couplings are individually uncertain, having a correlation coefficient of 1.000.
[f]These couplings have a correlation coefficient of 0.903.
[g]For the sidechain analysis, being 0.010 for the ring protons.

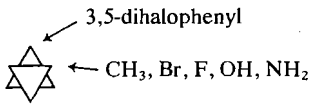
TABLE 2. Relevant coupling constants for some 1-*R*-2(3,5-dibromophenyl) ethanes, 3,5-dichloroallyl benzene,[a] and 4-(3,5-dibromobenzyl) pyridine

R	$^4J_o^{H,CH_2}$	$^6J_p^{H,CH_2}$	$^4J_m^{H,H}$	$^3J + {}^3J'$
CH_3[b]	−0.594(2)[g]	−0.428(2)	1.777(2)	15.26(2)
Br[b]	−0.542(4)	−0.384(5)	1.774(4)	14.67(2)
F[c]	−0.563(8)[h]	−0.416(5)	1.767(4)	12.27(8)
OH[d]	−0.525(5)	−0.380(4)	1.776(4)	12.91(1)
NH_2[e]	−0.523(9)	−0.368(7)	1.895(6)	13.23(8)
C_2H_5[f]	−0.634(10)	−0.423(8)	1.762(7)	—
n-C_3H_7[f]	−0.589(10)	−0.423(11)	1.766(8)	—
n-C_4H_9[f]	−0.590(10)	−0.426(10)	1.772(8)	—
n-C_5H_{11}[f]	−0.583(11)	−0.430(13)	1.771(9)	—
n-C_6H_{13}[f]	−0.583(14)	−0.444(13)	1.777(10)	—
Allyl[a] compound	−0.648(2)	−0.487(2)	1.903(2)	—
Pyridine[f] compound	−0.628(9)	−0.453(9)	1.757(7)	—

[a]Concentration 5 mol% in CCl_4 and 3,5-dichloroallylbenzene.
[b]Concentration 11 mol% in CS_2.
[c]Concentration 7 mol% in CS_2.
[d]Concentration 13 mol% in CS_2; $J + J'$ is 12.70 (8) Hz in a 1 mol% solution.
[e]Approximately 3 mol% in C_6D_{12} and is (3,5-dichlorophenyl).
[f]Approximately 10 mol% in CS_2.
[g]Numbers in parentheses give the standard deviation in the last significant figure.
[h]$^{5}J_o^{F,H} = +0.45_3$ Hz, $^2J^{H,F} = 47.0_1$ Hz, $^3J^{H,F} = 24.4_3$ Hz.

Conformation about the C_α—C_β Bond

The parameterization of Abraham and Gatti (1) was employed. Because $^3J + {}^3J'$ is most reliably known (Table 2), except for the methyl compound (Table 1), their eq. [5*c*] is appropriate. On the assumption that the entropy of one *gauche* form **5** is that of the *anti* form (*gauche* is favored by a statistical factor of 2), the enthalpy differences are 0.46 kcal/mol for CH_3 (*anti* more stable), 0.37 (Br), −0.04 (F), −0.02 (OH), and −0.15 (NH_2). The error is presumably about 0.1 kcal/mol (1).



5

1-Methyl-2-(3,5-dibromophenyl) Ethane

The present enthalpy difference agrees with the quoted 0.5 kcal/mol (14) for *n*-propylbenzene in CCl_4 solution and also with rough gas phase populations deduced from vibronic bands in a supersonic free jet (15). The equal populations of the *gauche* and *anti* conformers are also in accord with the observed $^4J^{CH_2,CH_3}$ of −0.17 Hz within the propyl group (Table 1) if theoretical ^4J values based on the valence bond – sum over triplets method (16) are used in a conformational averaging procedure. The theory yields −0.19 Hz. The alternative calculational methods (16) yield numbers up to 0.3 Hz at variance with the present experimental value. This coupling ranges between 0 ± 0.03 and -0.12 ± 0.03 Hz in a series of *n*-propyl derivatives (17).

Can. J. Chem. Downloaded from www.nrcresearchpress.com by 210.87.254.6 on 09/05/12
For personal use only.

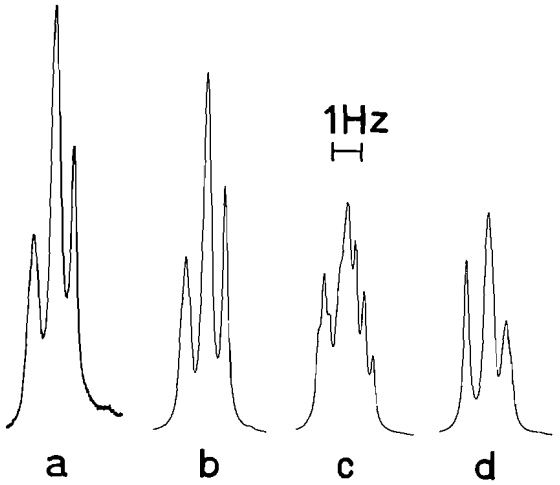


FIG. 1. One multiplet of the methyl ^{1}H nmr spectrum at 100 MHz and 305 K of an 11 mol% solution of 1-methyl-2-(3,5-dibromophenyl) ethane is displayed in *a*. In *b* to *d* the calculated multiplet is shown for $^4J^{CH_2,CH_3}$ equal to −0.17, 0.0, and +0.17 Hz, respectively. Clearly, this coupling is negative.

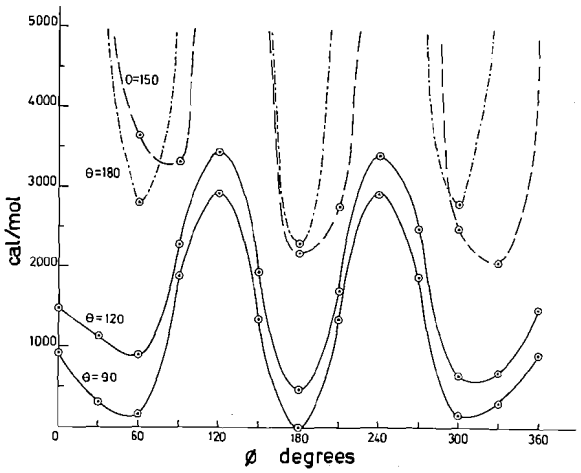


FIG. 2. A conformational energy diagram for 1-fluoro-2-phenylethane as calculated by the INDO MO approximation. The angles θ and φ are defined in **6** and **7** of the text. Only those conformations having an energy of ≤ 5 kcal/mol relative to θ = 90°, φ = 180° (perpendicular *anti* conformer) are shown.

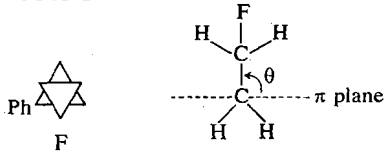
1-Bromo-(3,5-dibromophenyl) Ethane

The *anti–gauche* distribution is similar to that in the methyl compound. It may be noted that the respective $^2J^{H,H}$ values in the sidechain (Table 1) are apparently equal to those in toluene (18) and in methyl bromide (19). A similar comparison holds for phenylethane (20), toluene, and methane. Because the conformational averages of the H—H vector in the *alpha* methylene group with respect to the benzene π system must be quite different in the three phenyl compounds, doubt arises about the use of $^2J^{H,H}$ in conformational deductions for benzyl derivatives.

1-Fluoro-2-(3,5-dibromophenyl) Ethane

The negligible enthalpy difference between the *gauche* and *anti* rotamers *may* have to do with the small size of the fluorine atom, although arguments based on simple-minded steric effects are often wrong (21–23) when applied to ethane derivatives. For example, the *gauche* conformers of *n*-propyl derivatives are preferred by 0.47 ± 0.31, 0.5, and 0.28 ± 0.1 kcal/mol for the fluoride (24), chloride (25), and bromide (25), respectively.

In Fig. 2 the conformational energies are illustrated for 1-fluoro-2-phenylethane, as obtained from an INDO MO calculation with a standard geometry (26). The angles θ and φ are understood from **6** and **7**. According to these calculations, when θ = 90° the *gauche* form is 0.13 kcal/mol less stable than the *anti* form. On the other hand, STO 3G calculations gave the *gauche* form as 7.4 kcal/mol more stable for the same geometry (θ = 90° and unrelaxed bond angles). It is unlikely that the *meta* substituents and the solvent could cause the large discrepancy between the experimental and the STO 3G numbers. A full geometry optimization may reduce the discrepancy. An approximate analysis (27) of 1-fluoro-2-phenylethane ^{1}H nmr spectra for CS_2 solutions can be interpreted as yielding an *anti* fraction of 0.28, whereas the present study gives 0.32 for the 3,5-dibromophenyl derivative at 305 K.



6 φ = 60° **7** θ = 90°

It is interesting that $^5J_o^{H,F}$, the coupling involving the *ortho* protons, is +0.45 Hz. INDO MO FPT calculations give values ranging from −866 Hz for an unlikely crowded conformation (θ = 90°, φ = 0°) to +10.7 Hz. For a vanishing enthalpy difference, the computed value of $^5J^{H,F}$(θ = 90°, φ = 180°, 60°) is +0.32 Hz. According to Fig. 2, conformations for which θ = 120° are also appreciably populated. For example, if the θ = 120°, φ = 180° population is averaged in, the calculated $^5J^{H,F}$ increases by about 0.05 Hz. Of course, a proper averaging procedure would account for all hindered rotor states. These are not known (however, see below for a treatment of the θ torsion).

It is unlikely that the relatively low energies of the θ = 90° or 120°, φ = 0° conformers (C—F bond eclipsing the C_1—C_α bond) in Fig. 2 are realistic. The INDO results suggest such conformations are

Can. J. Chem. Downloaded from www.nrcresearchpress.com by 210.87.254.6 on 09/05/12
For personal use only.

about 2 kcal/mol more stable than those in which the C—F bond eclipses an alkyl C—H bond. A strong $\pi-\pi$ stabilization involving the *p* orbitals on the fluorine and the aromatic π system would cause such a preference, but is here considered as an artifact of the parameterization (as a matter of record, STO 3G gives $\theta = 90°$, $\phi = 0°$ as 14.5 kcal/mol less stable than $\theta = 90°$, $\phi = 180°$).

1-Hydroxy-2-(3,5-dibromophenyl) Ethane

The enthalpy differences favoring the *gauche* forms in 1 mol% (ca. 0.16 *M*) and 13 mol% solutions in CS_2 are 0.09 and 0.02 kcal/mol, respectively. The values of δ_{OH} are 1.62 and 3.88 ppm, respectively at 305 K. Extrapolation of δ_{OH} for a series of dilute solutions gave 1.01 ± 0.01 ppm for the shift at infinite dilution. Considerable self-association occurs at concentrations as high as 1 mol%, apparently favoring the *anti* form, presumably because the *gauche* form contains an intramolecular hydrogen bond involving the π electrons, so that intermolecular hydrogen bonding is more extensive in the extended conformation of the molecule.

For comparison, $J + J'$ is 13.0, 13.6_2, 13.9_2 Hz for 1.0, 5.0, 12.8 mol% solutions, respectively, of 2-phenylethanol in CS_2 at 305 K. Hence the *anti* form is favored by enthalpy differences of 0.02, 0.23, 0.33 kcal/mol for these solutions. If the accuracy is 0.1 kcal/mol, the 3,5-dibromophenyl substituent favors a *gauche* conformer somewhat more than does a phenyl substituent.[2]

Of course, the aim of the later sections is the characterization of the conformational preferences about the C_1—C_α bond in both *gauche* and *anti* forms by means of ${}^6J_p{}^{H,CH_2}$. This coupling is extractable at 100 MHz only for the 3,5-dibromophenyl compounds.

1-Amino-2-(3,5-dibromophenyl) Ethane

In C_6D_{12} (the compound is unstable in CS_2) the *gauche* form is energetically favored by 0.1_5 kcal/mol. Some PCILO computations (28) suggest minor influences of *meta* or *para* hydroxyl groups. A comprehensive theoretical investigation of phenethylamine, using a variety of semiempirical as well as *ab initio* STO 3G MO calculations, gives conflicting preferences of the *gauche* and *anti* forms (29). Empirical potential functions favor the *gauche* conformer (30). The STO 3G energies favor the *anti* form by 0.9 kcal/mol, whereas the semiempirical MO energies favor the *gauche* form by 1.1 kcal/mol. Insofar as the C_6D_{12} solvent is inert, our ${}^3J$ data agree with none of the MO methods (PCILO is somewhat related to MO approaches). The empirical force field calculations may be interpreted as favoring the *gauche* form of phenethylamine in the vacuum by ca. 0.2 kcal/mol in enthalpy (26). Apparently a water solvent will not change this conclusion by more than 0.1 kcal/mol for the neutral molecule.

Enrichment with ${}^{15}N$ could lead to nmr data relatable to the conformational preferences of the amino group.

Of course, the conformational preference about the carbon–carbon bond linking the phenyl moiety to the sidechain is also of interest. Here the long-range couplings between the ring protons and the *alpha* methylene protons become useful. Because most conformational theory is available for the amine, the next section begins with this molecule.

Conformational Preferences about the C_1—C_α Bond

As discussed in the introduction, conformation **2** is the low-energy form of phenylethane and ${}^6J_p{}^{H,CH_2}$ is directly related to the preferred conformation and the twofold barrier, V_2, of 1.2 kcal/mol (38). For the *anti* conformer of phenethylamine the calculations find the conformer analogous to **2** as stable, with a V_2 (Fig. 6 of ref. 29) ranging from 1.4 to 5 kcal/mol for different methods. If the molecule existed in the *anti* form only, the ${}^6J_p{}^{H,CH_2}$ of -0.37 Hz (Table 2) would give a $\langle \sin^2 \theta \rangle$ of 0.30 ± 0.02 and therefore a V_2 of more than 3 kcal/mol. Of course, the *anti* (extended) form would not be expected to have a much larger V_2 than phenylethane and the large apparent V_2 most probably arises from the presence of *gauche* conformers. For the *gauche* conformer, one intuits a conformation about the C_1—C_α bond in which one *alpha* C—H bond lies approximately in the aromatic plane (analogous to **3**). A rigid conformation of this kind would yield a ${}^6J_p$ of -0.47 Hz and relaxation of rigidity would *increase* the magnitude of ${}^6J_p$. The observed -0.37 Hz is therefore only in agreement with a conformation of type **2** for the *gauche* form also. Theory (29) agrees and explains this result as due to an electrostatic attraction between one N—H bond and the negatively charged carbon center *ortho* to the sidechain.

Now, it is evident from models that a conformation about the C_1—C_α bond of type **4** exhibits large steric hindrance to rotation about the C_1—C_α bond in the *gauche* form of the molecule. A reasonable picture emerges as follows. Attribute a V_2 of 1.2

[2]A 10 mol% solution of 2-(*p*-fluorophenyl) ethanol in CS_2 favors the *anti* form by 0.2_1 kcal/mol at 305 K.

Can. J. Chem. Downloaded from www.nrcresearchpress.com by 210.87.254.6 on 09/05/12
For personal use only.

kcal/mol to the *anti* form with a ^6J_p of −0.48 Hz, as in phenylethane. Then write 0.72 ^6J (*gauche*) + 0.28 (−0.48) = −0.37, where 0.28 is the *anti* population according to the ^3J numbers above. That yields ^6J in the *gauche* form as −0.33 Hz. If the *gauche* conformer were in a rigid form **2**, ^6J would be −0.31 ± 0.01 Hz because $^6J_{90}$ is −1.24 ± 0.04 Hz (3). For example, for 2,6-dichlorophenylethane, where V_2 must be > 5 kcal/mol, ^6J is −0.29 ± 0.02 Hz (3).

It follows that the barrier to rotation about the C_1—C_α bond is rather large, > 4 kcal/mol, in the *gauche* form of phenethylamine, as compared to the much smaller barrier in the *anti* form. The large difference in barriers is then a consequence of intramolecular hydrogen bonding in conformation **2** and probably of steric hindrance in conformation **4** of the *gauche* form.

The procedure above yields ^6J values of −0.33, −0.39, −0.30, and −0.38 Hz for the *gauche* forms corresponding to the substituents OH, F, Br, and CH_3 respectively. The largest V_2 therefore occurs for Br, as expected on steric grounds. The ^6J values are only compatible with a conformation **2** at C_1—C_α in both *anti* and *gauche*, so that the barrier to interconversion of the latter forms should be similar to the 3.5 kcal/mol in ethyl bromide (31, 32). The barrier to rotation about the C_1—C_α bond in the *gauche* form of the alcohol is the same as that in the amine. This is consistent with an enthalpy preference of 1.6 kcal/mol for the intramolecular hydrogen bond deduced from stretching band intensities (33). The 1 mol% solution of the alcohol gave ^6J as −0.36 ± 0.01 Hz (comparison with the 13 mol% solution indicated that ^6J is definitely of smaller magnitude in the 1 mol% solution) and yields ^6J in the *gauche* form as −0.31 Hz. To within experimental error this is the same as deduced for the higher concentration.

For the fluoride, the ^6J number implies a C_1—C_α barrier of 3 ± 1 kcal/mol in the *gauche* form. The INDO value in Fig. 2 is 2.7 kcal/mol (difference between $\theta = 90°, \phi = 60°$ and $\theta = 180°, \phi = 60°$) but of course, the present model assumes that V_2 in the *anti* form is 1.2 kcal/mol whereas INDO finds 2.3 kcal/mol for an *unrelaxed* geometry in the $\theta = 180°$ conformation (analogous to **4**), an overestimate of ca. 1 kcal/mol if the *anti* form has a C_1—C_α barrier of 1.2 kcal/mol.

The 1-alkyl substituents (R = CH_3 to *n*-C_6H_{13} in Table 2) cause ^6J values lying between −0.42 and −0.44 Hz, so that one has ^6J as −0.43 ± 0.02 Hz. Therefore the *gauche* barrier about C_1—C_α is 3.5 ± 1 kcal/mol, again in a region where the *J* method is insensitive.[3] Bromine (35) has a larger van der Waals volume than the methyl group (36) and the C—Br bond is also longer than the C—C bond. Therefore the higher barrier for the *gauche* 1-bromo compound is reasonable. The vibronic data (15) suggest two conformers of roughly equal abundance for the alkyl compounds. Models indicate that reasonable *gauche* conformations involve steric hindrance between the third CH_2 moiety and the *ortho* C—H bonds during rotation about the C_1—C_α bond for all the alkylethanes in Table 2.

If such steric interactions are important in these *gauche* alkyl conformations, replacement by other hydrocarbon groupings might well alter the barrier about the C_1—C_α bond. Therefore the two compounds below were examined.

3,5-Dichloroallylbenzene and 4-(3,5-Dibromobenzyl) Pyridine

^6J_p is −0.49 Hz in the allyl derivative, implying a barrier of 1.1 ± 0.2 kcal/mol about the C_1—C_α bond, the same as in phenylethane to within experimental error. (INDO MO FPT computations gave $^6J_{90}$ as −1.18 Hz, about 0.04 Hz larger than calculated for toluene, the latter agreeing with experiment. The stated error encompasses this range of $^6J_{90}$ values.) The INDO calculations, which give remarkably good conformational energy differences for hydrocarbons like phenylcyclopropane (37) and toluene (38), for example, suggest that for allylbenzene the stable conformation is of type **2** and that the olefinic bond is eclipsed by an *alpha* C—H bond (as in propene) in such a manner that the vinyl group points away from the benzene ring. The alternative eclipsed conformation, analogous to a *gauche* form for *n*-propylbenzene, in which the vinyl group points towards the aromatic moiety is 1.2 kcal/mol less stable. Accordingly, its population is small at ambient temperatures and the large barrier about C_1—C_α expected for such a conformer is not reflected in the observed barrier. In fact, for the favored conformer above, the distance of closest approach of the one olefinic C—H bond with an *ortho* C—H bond, as rotation occurs about the C_1—C_α bond, is somewhat less than the corresponding distance in phenylethane (Dreiding models).

In the pyridine derivative, ^6J is 0.45 ± 0.03 Hz,

[3]Spin–lattice relaxation times for ^{13}C nuclei of *p*-methoxybenzylidene-*p*-*n*-butylaniline in the isotropic phase (34) suggest that rotation about the C_1—C_α bond (*n*-butyl moiety) is hindered by 2.3 kcal/mol. This must be an *average* over the *anti* and *gauche* forms. If ^6J_p for the butyl compound in Table 2 is treated similarly one obtains an apparent barrier of 2.1 kcal/mol for rotation about the C_1—C_α bond.

corresponding to a $\langle \sin^2 \theta \rangle$ of $0.36_5 \pm 0.02$ and a V_2 of 1.6 ± 0.3 kcal/mol. To within experimental error, this is the same as the barriers derived for 4,4′-difluorodiphenylmethane and for 3,5-dibromodiphenylmethane (39). The discussion for these compounds concluded that the gable conformation, analogous to **2**, was preferred and that this conformation minimizes steric interactions between C—H bonds on neighbouring rings.

Concerning Various Assumptions

As in all other discussions of ^6J_p (5) it is assumed that the coupling is independent of the *meta* halogen substituents. This is certainly true for a variety of toluene derivatives, including *sym*-tetrafluorotoluene.[4] A recent ^{1}H nmr spectrum of ethylbenzene at 500 MHz (40) appears to have a ^6J identical to that in the 3,5-dibromo derivative. We also have reason to believe that ^6J_p in styrene and 3,5-dibromostyrene are identical.

Further, if the barriers about the C_1—C_α bond in the compounds discussed in this paper have their origin mainly in the steric hindrance between the sidechain and *ortho* C—H bonds, the *meta* substituents should play a minor role in determining their magnitudes. If the relative rigidity in the *gauche* form is indeed as marked as in the 1-bromo compound, it may be that the assumed statistical factor of 2 favoring the *gauche* form is an overestimate. In the absence of good partition functions the reduction in magnitude of this factor remains as an unsolved problem.

Of course, if the barrier about the C_1—C_α bond in the *anti* forms is greater than in phenylethane, a corresponding decrease in the barrier about the C_1—C_α bond in the *gauche* forms is implied by the present model. For example, if the barrier in the *anti* form of the phenethylamine derivative is as high as 2 kcal/mol, one deduces that the barrier in the *gauche* form is still > 4 kcal/mol.

If an alternative formulation (41) of the substituent dependence of the vicinal coupling constants in 1,2-disubstituted ethanes is employed, the *gauche* forms become ca. 0.1 kcal/mol more stable than above. However, the rigidity of the *gauche* forms, as obtained by calculations of ^6J in these forms, does not change appreciably.

Conclusions

A combination of the Karplus and J methods yields a plausible picture of the conformational populations about the C_α—C_β bond in 2-phenylethane derivatives, as well as the conformational preferences and rotational barriers about the C_1—C_α bond in the *gauche* and *anti* rotamers. The former are rather more rigid than the latter.

[4]R. Sebastian, unpublished work.

Acknowledgments

We are grateful to SSF Dottikon for a gift of 4-amino-*n*-propylbenzene, to the Natural Sciences and Engineering Research Council of Canada for financial support, and to T. Wildman for some STO 3G MO calculations. We thank a referee for useful comments.

1. R. J. Abraham and G. Gatti. J. Chem. Soc. B, 961 (1969).
2. R. J. Abraham and E. Bretschneider. *In* Internal rotations in molecules. *Edited by* W. J. Orville-Thomas. Wiley-Interscience, New York. 1974.
3. T. Schaefer, L. Kruczynski, and W. Niemczura. Chem. Phys. Lett. **38**, 498 (1976).
4. T. Schaefer, J. B. Rowbotham, W. J. E. Parr, K. Marat, and A. F. Janzen. Can. J. Chem. **54**, 1322 (1976).
5. T. Schaefer, W. Niemczura, and W. Danchura. Can. J. Chem. **56**, 2229 (1978); **57**, 355 (1979).
6. P. B. Ayscough, M. C. Brice, and R. E. D. McClung. Mol. Phys. **20**, 41 (1971).
7. M. S. Farag. Diss. Abstr. Int. B, **35**, 1594 (1974).
8. A. Miller and D. W. Scott. J. Chem. Phys. **68**, 1317 (1978).
9. P. A. Dobosh. Quantum chemistry program exchange, **11**, 141 (1979).
10. W. J. Hehre, W. A. Lathan, R. Ditchfield, M. D. Newton, and J. A. Pople. Quantum chemistry program exchange, **11**, 236 (1979).
11. C. W. Haigh and J. M. Williams. J. Mol. Spectrosc. **32**, 389 (1969).
12. S. Castellano and A. A. Bothner-By. J. Chem. Phys. **41**, 3863 (1964).
13. R. J. Abraham. The analysis of high resolution nmr spectra. Elsevier, Amsterdam. 1971.
14. E. I. Snyder. J. Am. Chem. Soc. **88**, 1165 (1965).
15. J. B. Hopkins, D. E. Powers, and R. E. Smalley. J. Chem. Phys. **71**, 3886 (1979).
16. M. Barfield, A. M. Dean, C. J. Fallick, R. J. Spear, S. Sternhell, and P. W. Westerman. J. Am. Chem. Soc. **97**, 1482 (1975).
17. G. Schrumpf. J. Magn. Reson. **6**, 243 (1972).
18. M. Barfield and D. M. Grant. J. Am. Chem. Soc. **85**, 1899 (1963).
19. H. J. Bernstein and N. Sheppard. J. Chem. Phys. **37**, 3012 (1962).
20. J. P. Bloxsidge, J. A. Elvidge, J. R. Jones, R. B. Mane, and M. Saljoughian. Org. Magn. Reson. **12**, 574 (1979).
21. C. A. Kingsbury. J. Chem. Educ. **56**, 431 (1979).
22. T. K. Brunck and F. Weinhold. J. Am. Chem. Soc. **101**, 1700 (1979); A. Gavezzotti and L. S. Bartell. J. Am. Chem. Soc. **101**, 5142 (1979).
23. E. Lombardi and G. Tarantini. Chem. Phys. Lett. **59**, 287 (1978).
24. E. Hirota. J. Chem. Phys. **37**, 283 (1962).
25. J. P. Lowe. Prog. Phys. Org. Chem. **6**, 1 (1968).
26. J. A. Pople and M. S. Gordon. J. Am. Chem. Soc. **89**, 4253 (1967).

Can. J. Chem. Downloaded from www.nrcresearchpress.com by 210.87.254.6 on 09/05/12
For personal use only.

27. H. BODOT, A. LERAY, and L. PUJOL. C.R. Acad. Sci. Ser. C, **265**, 842 (1967).
28. B. PULLMAN, J.-L. COUBEILS, PH. COURRIERE, and J.-P. GERVOIS. J. Med. Chem. **15**, 17 (1972).
29. M. MARTIN, R. CARBO, C. PETRONEGLO, and J. TOMASI. J. Am. Chem. Soc. **97**, 1338 (1975).
30. H. J. R. WEINTRAUB and A. J. HOPFINGER. J. Theor. Biol. **41**, 53 (1973).
31. D. R. LIDE. J. Chem. Phys. **30**, 37 (1959).
32. J. R. DURIG, W. E. BUCY, L. A. CARREIRA, and C. J. WURREY, J. Chem. Phys. **60**, 1754 (1974).
33. H. -H. KIRCHNER and W. RICHTER. Ber. Bunsenges. Phys. Chem. **81**, 1250 (1977).
34. H. M. HUTTON, E. BOCK, E. TOMCHUK, and R. Y. DONG. J. Chem. Phys. **68**, 940 (1978).
35. A. BONDI. J. Phys. Chem. **68**, 441 (1964).
36. M. CHARTON. J. Am. Chem. Soc. **91**, 615 (1969).
37. W. J. E. PARR and T. SCHAEFER. J. Am. Chem. Soc. **99**, 1033 (1977).
38. R. WASYLISHEN and T. SCHAEFER. Can. J. Chem. **50**, 1852 (1972).
39. T. SCHAEFER, W. NIEMCZURA, W. DANCHURA, and T. A. WILDMAN. Can. J. Chem. **57**, 1881 (1979).
40. Bruker advertisement. Am. Lab. **11**, No. 11. 24 (1979).
41. L. PHILLIPS and V. WRAY. J. Chem. Soc. Perkin Trans. II, 536 (1972).

Can. J. Chem. Downloaded from www.nrcresearchpress.com by 210.87.254.6 on 09/05/12
For personal use only.

The total synthesis of (±)hinesol and (±)epihinesol

JACQUES LAFONTAINE, MARCEL MONGRAIN, MIREILLE SERGENT-GUAY, LUC RUEST, AND PIERRE DESLONGCHAMPS

Laboratoire de Synthèse Organique, Département de Chimie, Faculté des Sciences, Université de Sherbrooke, Sherbrooke (Qué.), Canada J1K 2R1

Received December 28, 1979

This paper is dedicated to Prof. Raymond U. Lemieux on the occasion of his 60th birthday

JACQUES LAFONTAINE, MARCEL MONGRAIN, MIREILLE SERGENT-GUAY, LUC RUEST, and PIERRE DESLONGCHAMPS. Can. J. Chem. **58**, 2460 (1980).

The tricyclic ketal ketones **15***a* and **15***b* have been obtained in an isomeric ratio of 9:1 (**4** → **5** → **6** → **7** → **8** → **9** → **10** → **11** → **12** → **13** → **14** → **15***a* + **15***b*). Compound **15***a* was converted in seven (or eight) steps to (±)epihinesol (**3**) (**15***a* → **29** → **32** → **48** → **49** → **47** (or **32** → **39** → **38** → **44** → **47**) → **50** → **3**) and compound **38** was transformed into (±)hinesol (**2**) in five steps (**38** → **76** → **77** → **62** → **63** → **2**). The identity of epihinesol and agarospirol was confirmed by formation of a common epoxide.

JACQUES LAFONTAINE, MARCEL MONGRAIN, MIREILLE SERGENT-GUAY, LUC RUEST et PIERRE DESLONGCHAMPS. Can. J. Chem. **58**, 2460 (1980).

Les cétones cétales tricycliques **15***a* et **15***b* sont obtenues dans un rapport de 9 à 1 (**4** → **5** → **6** → **7** → **8** → **9** → **10** → **11** → **12** → **13** → **14** → **15***a* + **15***b*). Le composé **15***a* a donné le (±)épihinésol (**3**) en sept (ou huit) étapes (**15***a* → **29** → **32** → **48** → **49** → **47** (ou **32** → **39** → **38** → **44** → **47**) → **50** → **3**) et le composé **38** est transformé en (±)hinésol (**2**) en cinq étapes (**38** → **76** → **77** → **62** → **63** → **2**). L'identité de l'épihinésol et de l'agarospirol a été confirmée par formation d'un seul et même époxyde.

Introduction

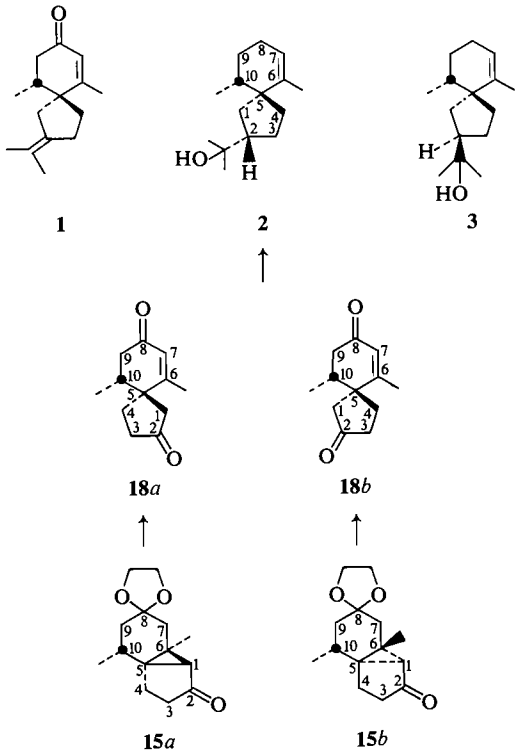
β-Vetivone (**1**) and hinesol (**2**) (Scheme 1) are naturally occurring members of the spiro[4.5]decane group of sesquiterpenes. Epihinesol (**3**) which is the isopropylol isomer of hinesol (**2**), has been proposed as the structure for the sesquiterpene agarospirol (1). The literature concerning the isolation, structure elucidation, and synthesis of these compounds has been reviewed (2, 3). More recent literature can be found in refs. 4–12.

We have reported in 1970 in a preliminary form (13) a synthesis of (±)epihinesol (**3**). We have since then successfully completed a synthesis of (±)-hinesol (**2**) by using the same key intermediate that we have utilized for the construction of (±)-epihinesol (**3**). We wish now to report in detail the synthesis of (±)hinesol (**2**) and (±)epihinesol (**3**).[1]

Synthetic Strategy

Skeleton

The conversion of the ketal diazoketone **14** (Scheme 2) into the spiro[4.5]decane enediketone **18** via the intermediates **15** and **16** constitutes the central idea of our synthetic scheme. The spiro compound **18** is indeed a very appealing key intermediate as ring A is complete for β-vetivone (**1**) and it should be easily converted to that of the hinesols. Furthermore, ring B of **18** has a ketone functionality to introduce either the isopropylidene group which is present in β-vetivone or the isopropylol group which is found in hinesol (**2**) and epihinesol (**3**).



SCHEME 1

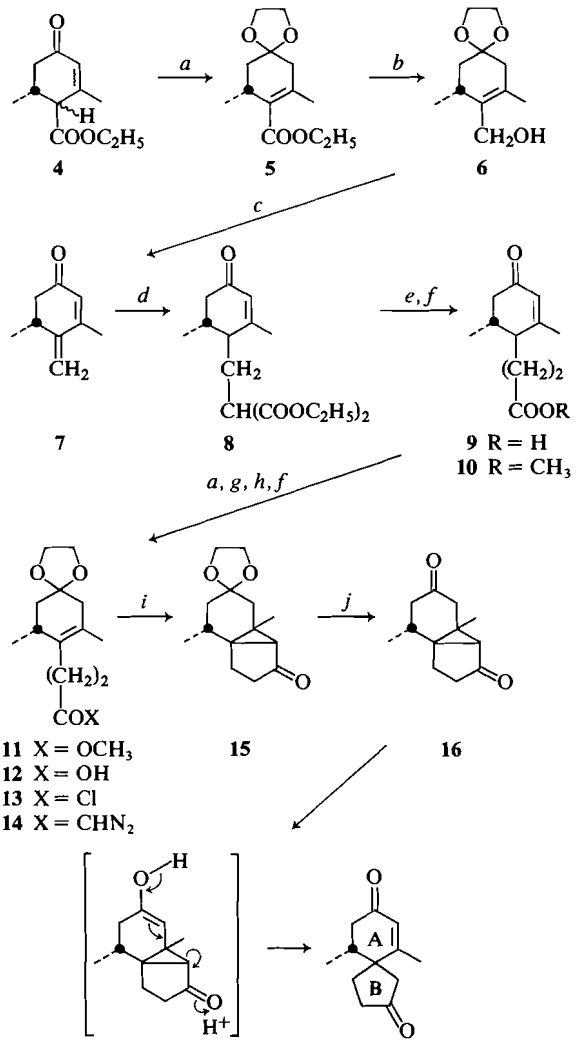
Our strategy was therefore based on the fol-

[1](±)Hinesol (**2**) and (±)epihinesol (**3**) have been converted into (±)β-vetivone (**1**) (14); our work can therefore be regarded as a synthetic route to (±)β-vetivone (**1**).

0008-4042/80/232460-17$01.00/0

© 1980 National Research Council of Canada/Conseil national de recherches du Canada

Can. J. Chem. Downloaded from www.nrcresearchpress.com by 210.87.254.40 on 09/05/12
For personal use only.



(*a*) $(CH_2OH)_2$, *p*-TsOH, benzene; (*b*) $LiAlH_4$, ether;
(*c*) HCl 2 *N*, THF; (*d*) $NaCH(COOC_2H_5)_2$, ethanol; (*e*) HCl 2 *N*, reflux;
(*f*) CH_2N_2, ether; (*g*) KOH, H_2O; (*h*) $(COCl)_2$, pyridine, benzene;
(*i*) Cu, benzene, reflux; (*j*) HCl 2 *N*, THF.

SCHEME 2

lowing facts: (*a*) the conversion of the ketal diazoketone **14** into the tricyclic ketal ketone **15** should be easily realized because this method is frequently used for internal cyclopropane ring formation (15–17), (*b*) the acid hydrolysis of **15** to give the cyclopropyl diketone **16** should proceed normally, and (*c*) compound **16** should undergo, under acidic conditions, a facile opening of the cyclopropane ring via the enol intermediate **17** to yield the desired spiro enedione **18**. The conversion of **16** into **18** could also be envisaged under basic conditions.

We were also convinced that the preparation of the ketal olefin diazoketone **14** could be realized starting from the substituted cyclohexenone methyl ester **10**. This was based on the well-known fact that ketalization of an α,β-cyclohexenone proceeds with concomitant migration of the double bond to give a β,γ-unsaturated ketal. Thus, **10** would first be transformed into the ketal methyl ester **11**. Basic hydrolysis of **11** would then give the ketal carboxylic acid **12** which could then be converted into the ketal diazoketone **14** via the acid chloride **13** by standard procedures. Finally, since the cyclohexenone methyl ester **10** is a relatively simple compound, its preparation should not create any major difficulty.

Control of Stereochemistry

The ketal diazoketone **14** which contains only one chiral center can give in principle two different adducts, the tricyclic ketal ketone **15***a* (Scheme 1) with the two methyl groups in a *cis* arrangement or the isomeric compound **15***b* having the two methyl groups in the *trans* configuration.

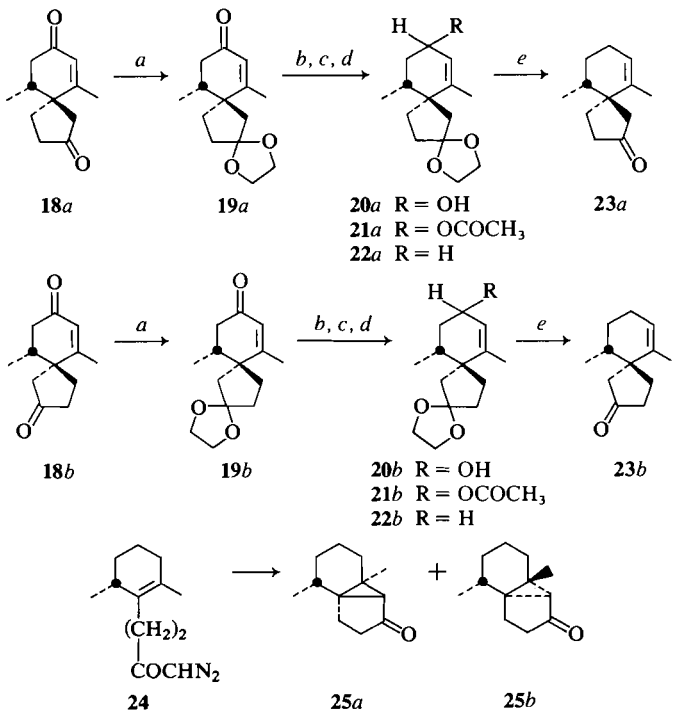
The *cis* (**15***a*) and the *trans* (**15***b*) isomers should give the spiro bicyclic enediketones **18***a* and **18***b* respectively. If **18***a* is obtained, completion of the synthesis requires the introduction of the isopropyl side chain in α-position to the carbonyl group (carbon-3) in the cyclopentane ring. On the other hand, if the other spiro bicyclic enediketone **18***b* is obtained, the isopropyl side chain will have to be attached directly to the ketone function (carbon-2) in **18***b*. Consequently, if one of the two isomers, **15***a* or **15***b* is formed preferentially, our synthetic route would permit a synthesis of β-vetivone with control of stereochemistry. We felt that there was a good possibility of obtaining some selectivity in the formation of the cyclopropane ring because the two faces of the double bond in the ketal diazoketone **14** have different environments.

We could not predict in advance how to control the extra chiral center which exists in the case of hinesol (**2**) and epihinesol (**3**). We were, however, confident of finding a solution by studying the reactivity of some of the key intermediates which would be obtained during the course of this investigation.

*Synthesis of the Ketal Diazoketone **14** and its Conversion into **15** and **18***

The enone ethyl ester **4** (Scheme 2) which is readily available by the condensation of two equivalents of ethyl acetoacetate and one of acetaldehyde (18) was selected as the starting material.

Can. J. Chem. Downloaded from www.nrcresearchpress.com by 210.87.254.40 on 09/05/12
For personal use only.



(*a*) $(CH_2OH)_2$, *p*-TsOH, benzene; (*b*) $LiAlH_4$, ether;
(*c*) $(CH_3CO)_2O$, pyridine; (*d*) Li, NH_3, ether;
(*e*) acetone, water, *p*-TsOH.

SCHEME 3

The enone ethyl ester **4** was first transformed into the ketal ethyl ester **5** which was then reduced to yield the crude ketal alcohol **6**. Treatment of **6** with aqueous acid gave the dienone **7** which was obtained pure by distillation.[2]

Michael addition of diethyl malonate to the dienone **7** gave the enone diethyl ester **8**.[3] The crude product **8** underwent hydrolysis and decarboxylation under reflux with aqueous acid to yield the enone monocarboxylic acid **9**. On esterification, **9** gave the enone methyl ester **10** which was purified by distillation.[4] The anticipated conversion of the enone methyl ester **10** into the ketal diazoketone **14** was realized without any difficulty.

On refluxing in benzene in the presence of copper, the ketal diazoketone **14** was smoothly converted into a mixture of the *cis* and the *trans* isomers **15***a* and **15***b* in a 9:1 ratio (Scheme 1). Both isomers could be obtained pure by chromatography. Treatment of the *cis* and the *trans* isomers **15***a* and **15***b* with hydrochloric acid (2 *N*) in tetrahydrofuran gave a good yield of the bicyclic enediketones **18***a* and **18***b* respectively.

We have firmly established the configuration of the *cis* and the *trans* tricyclic ketal ketones **15***a* and **15***b* by carrying out a chemical correlation between the bicyclic enediketones **18***a* and **18***b* and the two known bicyclic ketones **23***a* and **23***b* respectively (Scheme 3). Selective ketalization of **18***a* gave **19***a* which was reduced to the alcohol **20***a*. Acetylation of **20***a* gave the allylic acetate **21***a* which on chemical hydrogenolysis (21) produced the ketal olefin **22***a*. Acid hydrolysis of **22***a* gave the bicyclic ketone **23***a*. Compound **23***a* forms a mixture of two dinitrophenylhydrazone (DNP) derivatives (mp 107–108°C) which were separated by thin layer chromatography. These two DNP derivatives melt at 127–129°C and 150–151°C respectively. They are *syn* and *anti* geometrical isomers which are interconvertible at the temperature of their melting

[2]We first suspected that the dienone **7** would be unstable, readily aromatizing to yield 3,4,5-trimethylphenol. We found the contrary, compound **7** was remarkably stable under refluxing conditions with either potassium hydroxide (4 *N*) or potassium *tert*-butoxide in *tert*-butanol or hydrochloric acid (2 *N*). The conversion of dienone **7** into 3,4,5-trimethylphenol was finally achieved under refluxing conditions with perchloric acid in acetic acid!

[3]Cf. an analogous case in ref. 19.

[4]McCurry has prepared the same enone ester **10** utilizing a slightly different route (20). The ketal alcohol **6** was first converted into the corresponding ketal chloride **6** (OH=Cl) which was then displaced by the sodium salt of diethyl malonate.

Can. J. Chem. Downloaded from www.nrcresearchpress.com by 210.87.254.40 on 09/05/12
For personal use only.

Can. J. Chem. Downloaded from www.nrcresearchpress.com by 210.87.254.40 on 09/05/12
For personal use only.

points. They have been found to be identical with authentic samples.[5]

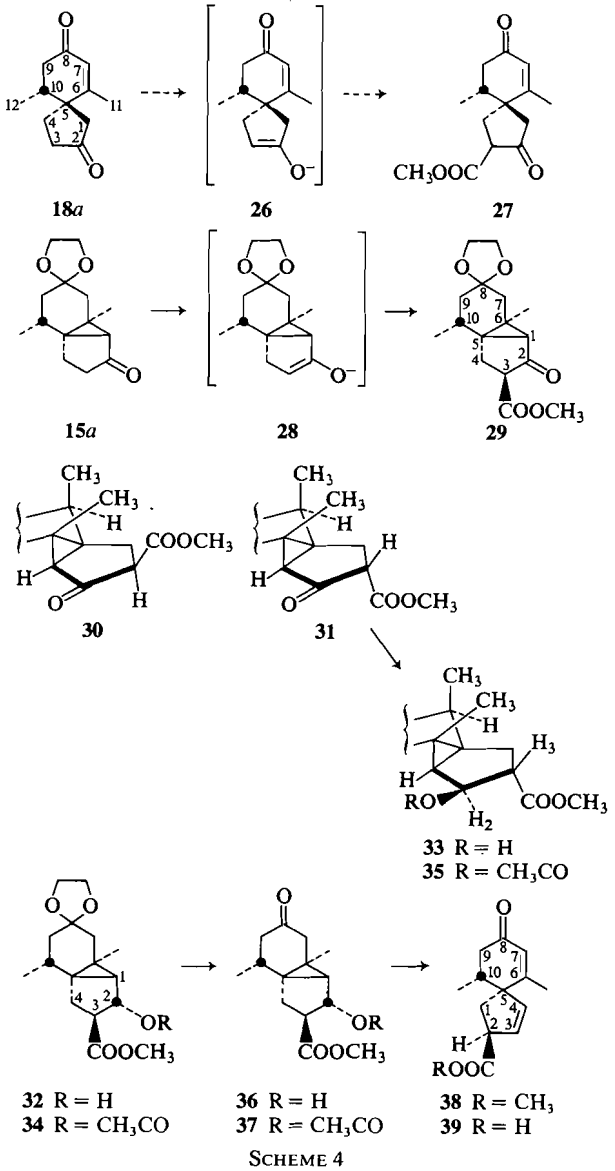
The isomeric bicyclic enediketone **18***b* was also converted by essentially the same procedure (**18***b* → **19***b* → **20***b* → **21***b* → **22***b* → **23***b*) to the isomeric bicyclic ketone **23***b* which was found to be identical with an authentic sample (22). The bicyclic ketone **23***b* gave also a mixture of two DNP derivatives (mp 78–88°C) which can be separated. They are *syn* and *anti* isomers (mp 113–114°C and 160–161°C) which are also interconvertible at their respective melting point temperatures.[6]

McCurry (20) has obtained the same mixture of *cis* and *trans* tricyclic ketal ketones **15***a* and **15***b* from the diazoketone **14**. He has also shown that the diazoketone **24** leads to a similar mixture of *cis* and *trans* tricyclic ketones **25***a* (89%) and **25***b* (11%). The isomeric ratios are essentially the same in both series (**14** and **24**), the presence of the ketal function in **14** has therefore no effect on the selectivity of the reaction. The selectivity can be explained if one considers the steric hindrance caused by the secondary methyl group; the carbenoid species resulting from the diazoketone in **14** (or in **24**) would simply prefer to attack on the face of the double bond which is *anti* to the secondary methyl group yielding the *cis* isomer **15***a* (or **25***a*) in preponderance.

Synthesis of (±)Epihinesol

The bicyclic enone **18***a* being the preponderant isomer, the next task consisted in finding a method for the introduction of an isopropylol or an isopropylidene group at carbon-3 (α to the carbonyl) in the five-membered ring (Scheme 4). A good approach appeared to be the introduction of a carbomethoxy group (**18***a* → **27**). Two main reasons guided this choice: (*a*) the subsequent manipulation of the ketone functions in **27** could presumably be easily achieved in the presence of the ester function, and (*b*) a carbomethoxy group is suitable for conversion by a Grignard reaction or its equivalent into an isopropylol group which in turn can be dehydrated to yield an isopropylidene group.

The introduction of a carbomethoxy group can be envisaged by the reaction of the enolate salt **26** with dimethyl carbonate. It could, however, be difficult to generate specifically the salt **26** as the hydrogens at positions 1, 9, and 11 of compound **18***a* might be equally susceptible to removal, yielding undesired enolate salts. Appropriate elimination of the carbonyl group at carbon-8 of **18***a* would still leave one competitive position (carbon-1) for enolate formation. These considerations led us to the conclusion that the precursor of the bicyclic enediketone **18***a*, the tricyclic ketal ketone **15***a*, would be a superior intermediate for the introduction of a carbomethoxy group. In compound **15***a*, only the desired enolate salt **28** can be formed. Furthermore, since compound **15***a* possesses a highly unsymmetrical rigid skeleton, there



SCHEME 4

[5]We are grateful to Professor James A. Marshall for an authentic sample of a mixture of the two DNP derivatives (mp 107–108°C) of the bicyclic ketone **23***a* (14). In this case also, separation gave two pure DNP derivatives (mp 127–129°C and 150–151°C).

[6]We are grateful to Professor Drury Caine (22) for an authentic sample of the bicyclic ketone **23***b*. This sample gave also two DNP derivatives (mp 113–114°C and 160–161°C).

Can. J. Chem. Downloaded from www.nrcresearchpress.com by 210.87.254.40 on 09/05/12
For personal use only.

was a very good possibility of obtaining only one of the two possible epimeric β-keto esters (**29**). It was important to us to achieve a control of stereochemistry at carbon-3 because this would permit a stereocontrolled synthesis of hinesol (**2**) or epihinesol (**3**).

Treatment of the *cis* tricyclic ketal ketone **15***a* with dimethyl carbonate in the presence of sodium hydride gave a crude product to which we have assigned the structure **29** with the carbomethoxy group *trans* to the tertiary methyl group. Examination of molecular models showed clearly that when the carbomethoxy group is *cis* to the tertiary methyl group, there is considerable steric hindrance between the two groups. Formulas **30** and **31** represent the two situations. The tricyclic ketal β-keto ester **29** was reduced with sodium borohydride to yield the tricyclic ketal alcohol ester **32** having the hydroxyl group *cis* to the tertiary methyl group. This assignment was simply based on the fact that the hydride reagent should reduce the carbonyl group from its least hindered face (cf. **31** → **33**). The tricyclic ketal alcohol ester **32** was further characterized by the preparation of the corresponding acetate derivative **34**. The assignment of the relative configuration of the carbomethoxy group was confirmed by a nuclear Overhauser effect study. Irradiation of the tertiary methyl group (1.24 δ) of compound **34** caused a 14% enhancement of the multiplet at 2.75 δ which corresponds to the hydrogen at carbon-3. This result shows that H3 is *cis* to the tertiary methyl group (cf. **35**).[7]

The next important operation was to verify if cyclopropane cleavage to yield a spiro[4.5]decane system would take place with the tricyclic ketal alcohol ester **32**. A brief treatment (10 min) of **32** with hydrochloric acid (1 *N*) gave the corresponding tricyclic ketone alcohol ester **36** which was further characterized as the acetate derivative **37**. If **36** was left for a longer period of time under these same acidic conditions, a new product was isolated which has the desired structure, the dienone ester **38**. When the reaction was carried out under reflux conditions for 4 hours, **32** as well as **36** gave the corresponding crystalline dienone carboxylic acid **39** directly in good yield. Treatment of the dienone ester **38** under similar conditions gave the dienone carboxylic acid **39**. Even if the desired product was the dienone ester **38**, we found it more convenient for purification purposes to use the experimental conditions leading to the dienone carboxylic acid **39** which could then be easily converted into the dienone ester **38** by esterification.

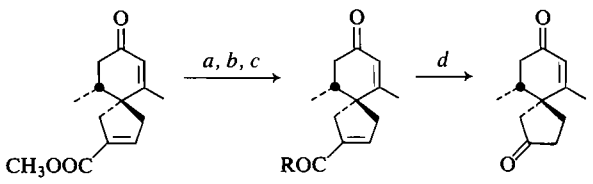
[7]We are grateful to Professors R. R. Fraser and J. K. Saunders who carried out this study for our laboratory.

The structure of the dienone ester **38** was rigorously established by carrying out a chemical correlation with the known bicyclic diketone **18***b* (Scheme 5). Treatment of the dienone ester **38** with sodium methoxide in methanol gave the conjugated ester **40** in good yield. The conjugated ester **40** was then hydrolysed to the corresponding carboxylic acid **41**. A Curtius degradation was realized by transforming **41** into its acid chloride **42** which was then converted into the azide **43**. Heating the azide **43** in water followed by the addition of dilute acid gave a product which was found identical with the bicyclic diketone **18***b* obtained previously.

The stereochemistry of the dienone ester **38** (Scheme 4) corresponds to that of epihinesol (**3**) and three further operations should yield the final product: (*a*) reduction of the cyclopentene double bond, (*b*) reductive elimination of the ketone carbonyl group, and (*c*) transformation of the carbomethoxy group into the isopropylol group.

The dienone ester **38** was first reduced with lithium tri-*tert*-butoxyaluminium hydride to give the allylic alcohol **44** (Scheme 6). We have postulated that the secondary hydroxyl group is *cis* to the secondary methyl group in **44** because this is the result of an attack by the bulky hydride on the pseudo-axial face of the conformation **45** of the dienone **38**. It is also possible that compound **38** exists in the other conformation **46** with the secondary methyl group in the pseudo-axial orientation where this methyl group has only one *gauche* interaction with the cyclopentene ring. If this is the case, reduction would simply occur on the least hindered face of the carbonyl group yielding the same allylic alcohol **44**. The allylic alcohol ester **44** was converted into the crystalline diol **47** by a Grignard reaction. The diol **47** was further characterized by the isolation of the monoacetate alcohol **50** upon acetylation.

The diol **47** was also obtained by reversing the sequence of operations. The isopropylol group was first introduced by a Grignard reaction on the tricyclic ketal alcohol ester **32** which gave the



40 **41** R = OH; **42** R = Cl; **43** R = N_3 **18***b*

(*a*) HCl 1 *N*, THF, reflux; (*b*) $(COCl)_2$, pyridine, CH_2Cl_2; (*c*) NaN_3, acetone; (*d*) THF, water, reflux and HCl 1 *N*, 0°C.

SCHEME 5

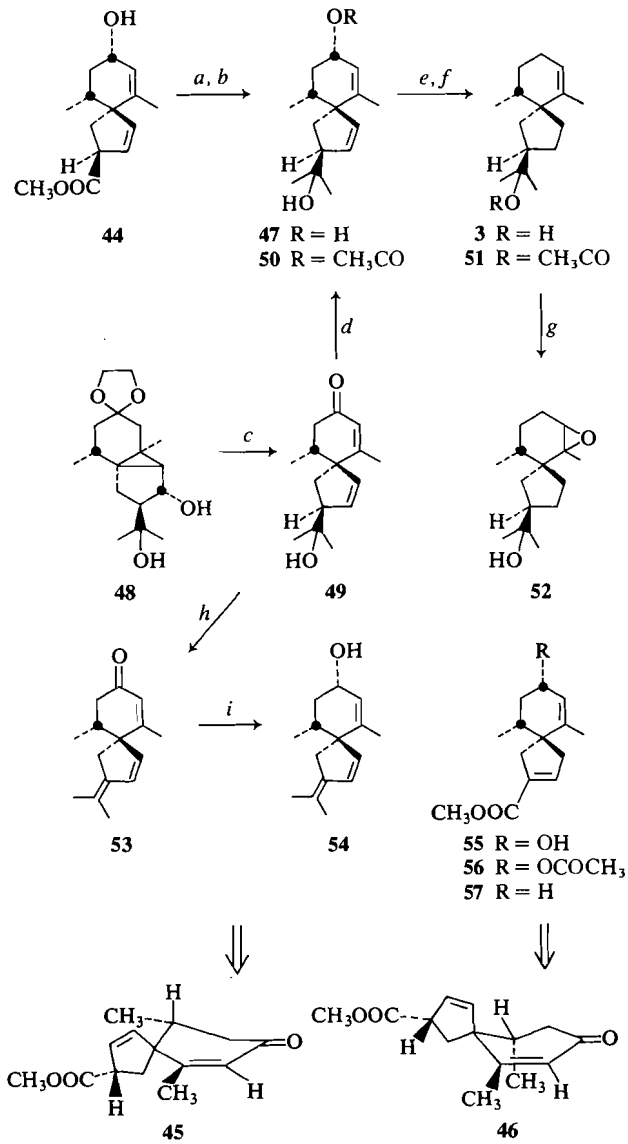
Can. J. Chem. Downloaded from www.nrcresearchpress.com by 210.87.254.40 on 09/05/12
For personal use only.

tricyclic ketal diol **48**. Treatment of **48** with aqueous acid yielded the expected dienone alcohol **49** which upon reduction with lithium aluminium hydride gave a product identical to diol **47**.

The hydrogenolysis of the allylic alcohol and the specific reduction of the cyclopentene double bond of the diol **47** were realized in a single operation. Treatment of the diol **47** with lithium in monoethylamine (23) gave epihinesol (**3**) in 55% yield. When the same reaction was carried out on the monoacetate alcohol **50**, epihinesol (**3**) was obtained in almost quantitative yield. The final proof that we had indeed produced epihinesol was carried out on the corresponding acetate **51** which was found to have the same retention time on vapor phase chromatography as that of an authentic sample of epihinesol acetate.[8,9]

The use of lithium in monoethylamine to specifically reduce the cyclopentene double bond (**47** or **50** → **3**) deserves some special comment. First, it is clear that we have not been able to selectively reduce this double bond by the usual method of hydrogenation using various catalysts. Unsuccessful experiments yielding complex mixtures were carried out with compounds **38**, **40**, **44**, **47**, **49**, **53**, and **54**. The dehydro β-vetivone **53** was obtained by dehydration of **49**. The allylic alcohol **54** was prepared by hydride reduction of **53**. Catalytic reduction of the allylic alcohol **55** prepared from **40** led to the hydrogenolysis product **57**. The same result was obtained from the corresponding allylic acetate **56**.

The disubstituted double bond of the cyclopentane ring should normally be hydrogenated at a faster rate than the trisubstituted double bond of the cyclohexane ring. The resistance to hydrogenation of the cyclopentene double bond can be explained by the steric hindrance caused by the two methyl groups of ring A; due to the spiro nature



(*a*) CH_3MgI, ether; (*b*) $(CH_3CO)_2O$, pyridine; (*c*) HCl 2 *N*, THF; (*d*) $LiAlH_4$, ether; (*e*) Li, $C_2H_5NH_2$, ether; (*f*) $(CH_3CO)_2O$, CH_3COONa;
(*g*) *m*-$ClC_6H_4CO_3H$, $CHCl_3$; (*h*) *p*-TsOH, benzene; (*i*) $LiAlH(O\text{-}t\text{-}Bu)_3$, ether, reflux

SCHEME 6

of these compounds, the cyclohexene ring is perpendicular to the plane of the cyclopentene ring (cf. **45**) and the two methyl groups of the cyclohexene ring protect both faces of the cyclopentene double bond. The catalyst cannot approach this double bond in the usual way to effectuate a reduction. We have finally used lithium in monoethylamine when we became aware that Benkeser *et al.* (23) had shown that this reagent also reduces disubstituted double bonds at a faster rate than trisubstituted double bonds.

[8]Hinesol and epihinesol have very similar infrared and proton nmr spectra and have an identical retention time on vpc. Their corresponding acetates have also very similar spectroscopic properties but have different retention times (vpc). We are very grateful to Professor J. A. Marshall who has carried out the vpc identification of our synthetic epihinesol acetate. We have since observed that hinesol and epihinesol differ in their ^{13}C nmr spectra (cf. Experimental).

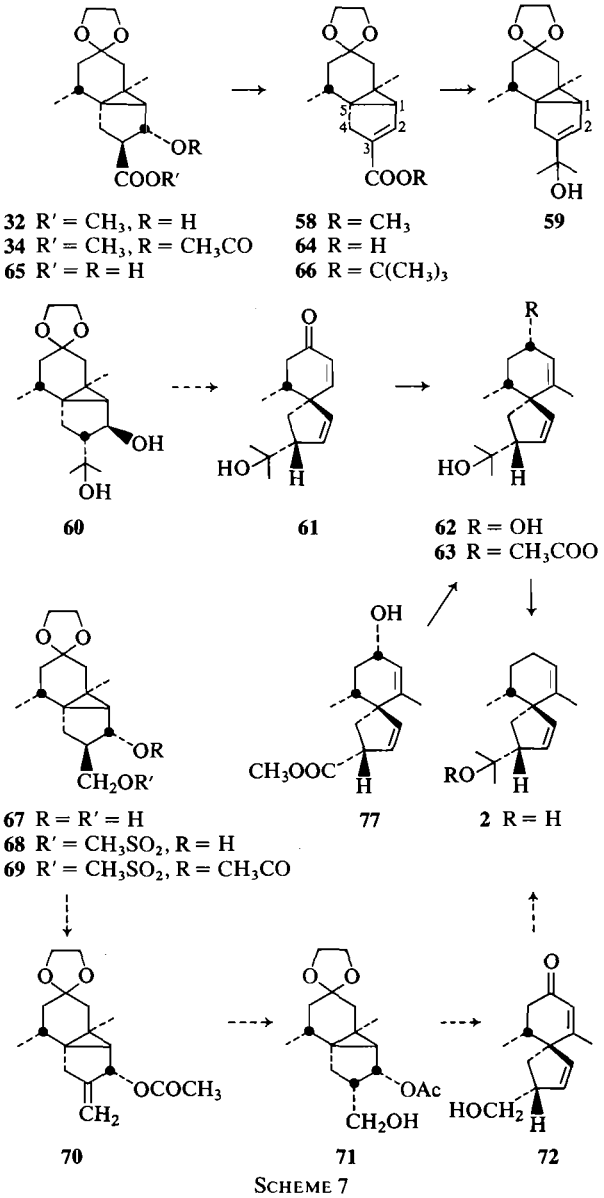
[9]Epihinesol (**3**) should in principle be identical with agarospirol (1), but the published nmr spectrum of agarospirol is not identical with the spectrum of epihinesol (**3**). We have not been able to obtain a sample of agarospirol. However, agarospirol gives a crystalline epoxide of which the proton nmr spectrum is essentially identical with the epoxide **52** obtained from epihinesol (**3**). We are grateful to Professor S. C. Bhattacharyya for this identification. It is therefore very likely that agarospirol is identical with epihinesol (**3**) if one makes the assumption that the published nmr spectrum comes from an impure sample of agarospirol.

Can. J. Chem. Downloaded from www.nrcresearchpress.com by 210.87.254.40 on 09/05/12
For personal use only.

Synthesis of (±)Hinesol (2)

It was possible to achieve the synthesis of (±)-epihinesol (**3**) with a complete control of stereochemistry from the tricyclic ketal ketone **15***a* because we were able to obtain the tricyclic ketal β-keto ester **29** in a specific manner. The next task was to achieve the synthesis of (±)hinesol (**2**), again having a control of stereochemistry for the isopropylol side chain.

The first approach that we considered was to reverse the chirality at carbon-3 in tricyclic compounds derived from the β-keto ester **29**. Our first attempt is outlined in Scheme 7. The plan was to dehydrate compound **32** to the conjugated methyl ester **58** followed by conversion of **58** into **59**. We then hoped that **59** could be transformed via hydroboration into the tricyclic ketal diol **60** which has the correct chirality at carbon-3 for the construction of hinesol (**2**). The formation of **60** was anticipated because it is the result of hydroboration on the least hindered face of the double bond in **59**. Treatment of **60** with aqueous acid would provide **61** which could then be transformed into hinesol (**2**) by a procedure (**61** → **62** → **63** → **2**) similar to that used in the synthesis of epihinesol (**3**).



SCHEME 7

Direct dehydration of the tricyclic ketal alcohol ester **32** was not successful. However, we found that treatment of the tricyclic ketal ester acetate **34** with potassium *tert*-butoxide in dry *tert*-butanol under reflux for 30 h gave a mixture of two carboxylic acids, the tricyclic ketal acid **65** and the conjugated acid **64**. The tricyclic ketal acid **65** could also be made by basic hydrolysis of **32** and esterification of the conjugated acid **64** with diazomethane gave the desired methyl ester **58**.

The fact that we obtained the two carboxylic acids **64** and **65** from **34** showed that the reaction medium was not completely dry. We have, however, succeeded in obtaining a completely dry mixture of potassium *tert*-butoxide in *tert*-butanol by adding a small quantity of maleic anhydride. Under this new condition, the medium becomes completely dry because maleic anhydride reacts with all the hydroxide in yielding maleic acid salt which does not interfere with the desired transformation. Thus, when compound **34** was refluxed for 72 h in *tert*-butanol containing two equivalents of potassium *tert*-butoxide and one equivalent of maleic anhydride, we obtained an essentially quantitative yield of the desired tricyclic ketal conjugated methyl ester **58**. When the same reaction was left for a longer period of time, the *tert*-butyl ester **66** was also formed, very likely via a *trans*-esterification mechanism with potassium *tert*-butoxide!

Reaction of the tricyclic ketal conjugated methyl ester **58** with methyl lithium gave the expected isopropylol derivative **59** in good yield. However, all attempts to carry out hydroboration of **59** with diborane or disyamyl borane failed to give the desired tricyclic ketal diol **60** and this approach was abandoned.

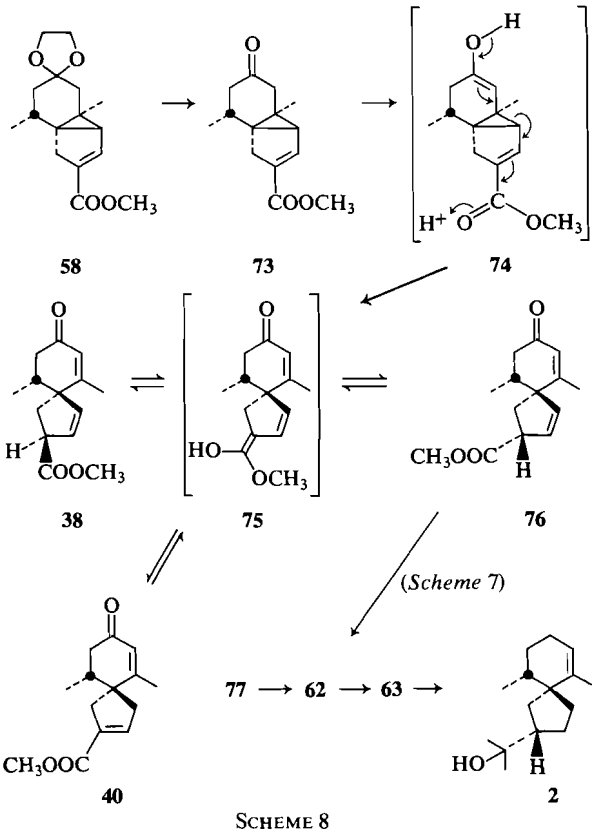
In our second attempt, we decided to transform the tricyclic ketal alcohol ester **32** into the acetate mesylate **69** in the hope that this product could undergo dehydromesylation to give the tricyclic ketal olefin **70**. Again hydroboration of **70** should give compound **71** which has its CH_2OH group properly oriented to eventually give hinesol (**2**) via

Can. J. Chem. Downloaded from www.nrcresearchpress.com by 210.87.254.40 on 09/05/12
For personal use only.

the intermediate **72**. This route had also to be abandoned because we have not been able to effect the dehydromesylation (**69** → **70**). The diol **67** was obtained by lithium aluminium hydride reduction of the tricyclic ketal alcohol ester **32**. The diol **67** was then mesylated to give **68** which after acetylation gave the acetate mesylate **69**.

At this stage, we completely changed our strategy in the following way. We first studied the mild acid hydrolysis of the tricyclic ketal conjugated ester **58**. Under acid conditions, **58** should first give the ketone **73** (Scheme 8) which should then enolise to give **74** which would undergo cyclopropane opening to yield a spiro[4.5]decane in which the ester should first be in its enol form **75**. The enol form **75** would then be protonated to give an ester. Since the formation of **75** would be generated under mild acid conditions, it will be protonated only once, and there should be no further equilibration of the resulting ester under these conditions. There are three different ways to protonate **75**. It can occur in two different ways at carbon-2, yielding the two isomeric esters **38** and **76**, or it can occur at carbon-4 giving the known conjugated ester **40**. We were hoping that protonation would occur at carbon-2 only, and that the protonation might occur stereospecifically to give the ester **76** only!

Treatment of **58** under mild acid gave a mixture of the two non-conjugated esters **76** (35%) and **38** (65%) but the conjugated ester **40** was not observed. This result showed that protonation is equally facile on either side of the enol of the ester function in **75**. It showed also that it is more difficult to protonate the position 4 in intermediate **75**. This led us to think that it might be possible to find some experimental conditions where the two non-conjugated esters **38** and **76** could be equilibrated while preventing the formation of the conjugated ester **40** which is the thermodynamically more stable isomer. We had already observed that when compound **38** was treated with sodium methoxide in methanol *under reflux*, it led to the exclusive formation of the conjugated ester **40**. We repeated this experiment *at room temperature* and under those new conditions the conjugated ester **40** was not observed but the unconjugated ester **38** underwent equilibration with its isomer **76**. We obtained a mixture of **76** and **38** in a 7:3 ratio. The major isomer **76** could be obtained pure by column chromatography. Having obtained **76**, we used the same strategy as in the case of epihinesol (**3**). Compound **76** was first reduced to give **77** (Scheme 7) which was then converted into **62** and then **63**. Reduction of **63** with lithium in monoethylamine gave a mixture of three products, from which (±)hinesol (**2**) was isolated.



SCHEME 8

Experimental

The ir spectra were taken on a Perkin-Elmer 257 spectrophotometer. The ultraviolet (uv) spectra were registered on a Varian Techtron 635 spectrophotometer. Proton nmr spectra were recorded on a Varian A-60 or a Bruker WP-60 instrument. The following abbreviations have been used: s, singlet; d, doublet; d of d, doublet of doublet; t, triplet; m, multiplet; and br, broad. Chemical shifts are reported in δ values relative to tetramethylsilane as internal standard. The ^{13}C nmr spectra were recorded on a Bruker H-90 instrument. Vapor phase chromatographic (vpc) analyses were carried out on a Varian, model 90-P.

The mass spectra were recorded on a Hitachi-Perkin-Elmer RMU-6 mass spectrometer. Microanalyses were carried out by Mr J. Tamas, Laboratoire de Microanalyses, Université de Sherbrooke; Schwarkkopf Microanalytical Laboratories, N.Y.; and by Dr C. Daessle, Organic Microanalyses, Montreal. Anhydrous magnesium sulfate was used as the drying agent in working reactions. Low boiling petroleum ether (bp 30–60°C) was used.

Ketal Ester **5**

Ketone ester **4** (50 g, 0.25 mol) (18) was dissolved in benzene (1 L) and mixed with ethylene glycol (30 mL) and *p*-toluenesulfonic acid (50 mg). The reaction mixture was refluxed for 40 h using a Dean–Stark water separator. The cooled reaction mixture was washed with saturated sodium carbonate and saturated sodium chloride. The dried solution was evaporated to give the crude ketal ester **5** (66 g) which was used without further purification. An analytical sample was prepared by microdis-

Can. J. Chem. Downloaded from www.nrcresearchpress.com by 210.87.254.40 on 09/05/12
For personal use only.

tillation *in vacuo*; ir ($CHCl_3$): 1725 cm^{-1}; nmr ($CDCl_3$) δ: 4.25 (2H, q, J = 7 Hz, OCH_2CH_3), 3.97 (4H, s, $2\,OCH_2$), 1.85 (3H, d, J = 1.8 Hz, CH_3—C3), 1.30 (3H, t, J = 7 Hz, OCH_2CH_3), and 1.07 (3H, d, J = 7 Hz, CH_3—C5); ms *m/e*: 240 (M^+). *Anal.* calcd. for $C_{13}H_{20}O_4$: C 65.00, H 8.33; found: C 64.63, H 8.29.

Ketal Alcohol 6

A solution of crude ketal ester **5** (66 g, 0.27 mol) in ether (200 mL) was slowly added to a suspension of lithium aluminium hydride (7 g) in ether (200 mL) and tetrahydrofuran. The mixture was heated at reflux for 10 h. After cooling to 0°C, water was carefully added to destroy the remaining lithium aluminium hydride followed by saturated sodium sulfate (200 mL) before extraction of the mixture with ether. The organic phase was dried and evaporated to give crude ketal alcohol **6** (48 g); ir ($CHCl_3$): 3350 and 1075 cm^{-1}; nmr ($CDCl_3$) δ: 4.28 (2H, s, CH_2OH), 3.93 (4H, s, $2\,OCH_2$), 1.73 (3H, s, CH_3—C3), and 1.15 (3H, d, J = 6 Hz, CH_3—C5); ms *m/e*: 198 (M^+).

Dienone 7

A solution of crude ketal alcohol **6** (48 g, 0.24 mol) in tetrahydrofuran (200 mL) and 2 *N* hydrochloric acid (200 mL) was stirred at room temperature for 10 h. The mixture was extracted with ether and the organic phase was dried and evaporated to give crude dienone **7** (25 g, 75%). The product was purified by distillation *in vacuo*; bp 65–68°C/0.8 Torr; uv (EtOH) λ_{max}: 273 nm (ε 16 300); ir ($CHCl_3$): 1665 cm^{-1}; nmr ($CDCl_3$) δ: 5.91 (1H, s, H—C2), 5.44 (2H, m, $=CH_2$), 2.86 (1H, m, H—C5), 2.38 (2H, m, H—C6), 2.09 (3H, d, J = 1.5 Hz, CH_3—C3), and 1.20 (3H, d, J = 7 Hz, CH_3—C5); ms *m/e*: 136 (M^+). *Anal.* calcd. for $C_9H_{12}O$: C 79.41, H 8.82; found: C 79.12, H 9.17.

3,4,5-Trimethylphenol

Dienone **7** (100 mg, 0.73 mmol) was added to glacial acetic acid (10 mL) containing perchloric acid (0.6 mL) and the mixture was heated at reflux for 24 h. After cooling, the mixture was basified by the addition of 10% sodium hydroxide and extracted with ether. The aqueous phase was reacidified and extracted with three volumes of ether. The latter organic extracts were dried and evaporated to give 3,4,5-trimethylphenol (60 mg, 60%); mp 109°C (from dichloromethane – petroleum ether); ir ($CHCl_3$): 3590, 3350, 1600, 1480, and 1135 cm^{-1}; nmr ($CDCl_3$) δ: 6.50 (2H, s, aryl—H), 4.60 (1H, br s, O—H), 2.22 (6H, s, $2\,CH_3$ on C3 and C5), and 2.08 (3H, s, CH_3—C4). The spectra of this compound were identical with those of a sample of authentic 3,4,5-trimethylphenol.

Enone Diester 8

Sodium metal (1.5 g) was added to a solution of dienone **7** (34 g, 0.25 mol) and diethyl malonate (48 g, 0.3 mol) in absolute ethanol under a nitrogen atmosphere. The reaction mixture was stirred at room temperature during 18 h and finally for 15 min at reflux. After cooling, water was added and the solution was neutralized with 0.5 *N* hydrochloric acid. Extraction with ether followed by drying and evaporation gave enone diester **8** (68 g, 92%). An analytical sample was prepared by microdistillation *in vacuo*; ir ($CHCl_3$): 1725 and 1665 cm^{-1}; nmr ($CDCl_3$) δ: 5.87 (1H, s, H—C2), 4.25 (4H, q, J = 7 Hz, $2\,OCH_2CH_3$), 3.55 (1H, m, $CH(CO_2C_2H_5)$), 2.00 (3H, d, J = 1.5 Hz, CH_3—C3), 1.28 (6H, t, J = 7 Hz, $2\,OCH_2CH_3$), and 1.05 (3H, d, J = 7 Hz, CH_3—C5); ms *m/e*: 296 (M^+). *Anal.* calcd. for $C_{16}H_{24}O_5$: C 64.86, H 8.10; found: C 64.11, H 8.22.

Enone Monocarboxylic Acid 9

Enone diester **8** (25 g, 0.1 mol) was added to hydrochloric acid (2 *N*, 500 mL) and the mixture was refluxed during 20 h. After cooling, the aqueous phase was extracted several times with ether. The combined organic extracts were dried and evaporated to give the crude enone monocarboxylic acid **9**; ir ($CHCl_3$): 3250 and 1725 cm^{-1}; nmr ($CDCl_3$) δ: 10.71 (1H, s, CO_2H), 6.05 (1H, br s, H—C2), 2.03 (3H, d, J = 1.5 Hz, CH_3—C3), and 1.08 (3H, d, J = 7 Hz, CH_3—C5).

Enone Methyl Ester 10

An excess of ethereal diazomethane was added to a solution of the crude enone monocarboxylic acid **9** in ether. The ether was evaporated to leave a yellow oil (22 g). An analytical sample of **10** was prepared by microdistillation *in vacuo*; ir ($CHCl_3$) 1730 and 1655 cm^{-1}; nmr ($CDCl_3$) δ: 6.05 (1H, br s, H—C2), 3.80 (3H, s, OCH_3), 2.03 (3H, d, J = 1.5 Hz, CH_3—C3), and 1.08 (3H, d, J = 7 Hz, CH_3—C5); ms *m/e*: 210 (M^+). *Anal.* calcd. for $C_{12}H_{18}O_3$: C 68.57, H 8.57; found: C 68.80, H 8.58.

Ketal Methyl Ester 11

Enone methyl ester **10** (39 g, 0.18 mol) was dissolved in benzene (1 L) and mixed with ethylene glycol (40 mL) and *p*-toluenesulfonic acid (200 mg). The reaction mixture was refluxed for 40 h using a Dean–Stark water separator. The cooled reaction mixture was washed with saturated sodium carbonate and saturated sodium chloride. The organic phase was dried, the solvent removed by distillation at reduced pressure, and the residue was purified by chromatography on Florisil. Ketal methyl ester **11** (34 g, 72%) was obtained by elution with benzene – petroleum ether (1:1); ir ($CHCl_3$): 1730 and 1070 cm^{-1}; nmr ($CDCl_3$) δ: 3.90 (4H, s, $2\,OCH_2$), 3.65 (3H, s, OCH_3), 1.65 (3H, d, J = 1.5 Hz, CH_3—C3), and 1.08 (3H, d, J = 7 Hz, CH_3—C5); ms *m/e*: 254 (M^+). *Anal.* calcd. for $C_{14}H_{22}O_4$: C 66.14, H 8.66; found: C 66.42, H 8.78.

Ketal Carboxylic Acid 12

Ketal methyl ester **11** (9.0 g, 0.035 mol) was added to a solution of potassium hydroxide (2.2 g) in water (50 mL). The mixture was refluxed during 3 h. After cooling, the reaction mixture was washed with ether, poured into a buffer solution (dipotassium phthalate – sodium hydroxide; pH = 5.5; 3.5 L), and extracted with ether. The organic phase was dried and evaporated to give ketal acid **12** as a difficult to crystallize solid (6 g); mp 72–73°C; ir ($CHCl_3$): 3100 and 1710 cm^{-1}; nmr ($CDCl_3$) δ: 10.71 (1H, s, O—H), 3.98 (4H, s, $2\,OCH_2$), 1.68 (3H, s, CH_3—C3), and 1.10 (3H, d, J = 7 Hz, CH_3—C5). *Anal.* calcd. for $C_{13}H_{20}O_4$: C 65.00, H 8.33; found: C 64.83, H 8.30.

Ketal Diazoketone 14 (via the Acid Chloride 13)

Ketal acid **12** (1.5 g, 6.2 mmol), dissolved in a solution of anhydrous benzene (40 mL) and anhydrous pyridine (0.7 mL), was added to a cooled (0°C) solution of freshly distilled oxalyl chloride (0.55 mL) in benzene (30 mL). The first 20 mL were added dropwise and the last 20 mL were added very rapidly. The mixture was stirred at room temperature for 2 h before filtration through cotton wool directly into a solution of diazomethane (1.5 g) in ether. The solution was immediately stripped of solvent at low temperature and the residue purified by chromatography on Florisil. Ketal diazoketone **14** was obtained as a yellowish oil (1.5 g) by elution with benzene; ir ($CHCl_3$): 2100 and 1645 cm^{-1}; nmr ($CDCl_3$) δ: 5.35 (1H, s, $COCHN_2$), 3.95 (4H, s, $2\,OCH_2$), 1.67 (3H, s, CH_3—C3), and 1.10 (3H, d, J = 7 Hz, CH_3—C5).

Tricyclic Ketal Ketones 15a and 15b

A solution of ketal diazoketone **14** (49.2 g) in anhydrous benzene (300 mL) was added during 1 h to a refluxing mixture of copper powder (18 g) and anhydrous benzene (500 mL) under a nitrogen atmosphere. After an additional 3.5 h at reflux, the mixture was cooled, filtered, and the benzene was evaporated. Potassium hydroxide solution (2 *N*, 700 mL) was added and the mixture was stirred at room temperature for 24 h. After cooling, the mixture was extracted with ether (4 × 250 mL). The organic extracts were dried and evaporated to leave a mixture of **15***a* and

Can. J. Chem. Downloaded from www.nrcresearchpress.com by 210.87.254.40 on 09/05/12
For personal use only.

15*b* (27 g). Vapor phase chromatographic analysis (SE-30 5% on Chromosorb W, 5 ft × ¼ in., 190°C, retention time: **15***a*, 5.2 min and **15***b*, 4.1 min) indicated a mixture of **15***a* and **15***b* in a 9:1 ratio.

A portion of the crude product (3.6 g) was purified by column chromatography with Florisil (benzene–ether, 9:1) to yield pure tricyclic ketal ketone **15***b* (150 mg) and pure tricyclic ketal ketone **15***a* (2.0 g).

Isomer **15**b: mp 62–63°C (ether – petroleum ether); ir ($CHCl_3$): 1700 cm^{-1}; nmr ($CDCl_3$) δ: 3.93 (4H, s, 2 OCH_2), 1.22 (3H, s, CH_3—C6), and 1.05 (3H, d, J = 6.5 Hz, CH_3—C10); ^{13}C nmr ($CDCl_3$): 215.0 (C2), 108.0 (C8), 64.4 (CH_2O), 64.2 (CH_2O), 44.8 (C5 or C6), 43.3 (C10), 42.8 (C3), 38.5 (C7), 38.1 (C9), 30.5 (C1), 29.2 (C5 or C6), 23.5 (C4), 19.3 (secondary CH_3), and 18.9 (tertiary CH_3); ms *m/e*: 236 (M^+).

Isomer **15**a: oil, an attempted microdistillation led to decomposition; ir ($CHCl_3$): 1700 cm^{-1}; nmr ($CDCl_3$) δ: 3.87 (4H, s, 2 OCH_2), 1.19 (3H, s, CH_3—C6), and 1.16 (3H, d, J = 6.5 Hz, CH_3—C10); ^{13}C nmr ($CDCl_3$): 214.9 (C2), 107.8 (C8), 63.8 (CH_2O), 63.7 (CH_2O), 44.7 (C10), 43.1 (C5 or C6), 42.6 (C3), 39.4 (C7), 37.8 (C9), 32.1 (C1), 29.8 (C5 or C6), 24.0 (C4), 18.9 (secondary CH_3), and 18.1 (tertiary CH_3); ms *m/e*: 236 (M^+).

Bicyclic Enediketone ***18***a

Tricyclic ketal ketone **15***a* (320 mg, 1.35 mmol) dissolved in tetrahydrofuran (20 mL) was mixed with aqueous hydrochloric acid (1 *N*, 5 mL) and heated (65°C, oil bath) for 1 h. The mixture was then poured into an excess of aqueous sodium bicarbonate (0.5 *N*) and extracted four times with dichloromethane. The extract was dried, filtered, and evaporated to dryness. Crystallization (ether–pentane) of the crude product (270 mg) and chromatography of the residual mother liquor afforded pure bicyclic enediketone **18***a* (242 mg, 90%); mp 102–102.5°C; ir ($CHCl_3$): 1750, 1670, and 1620 cm^{-1}; nmr ($CDCl_3$) δ: 5.84 (1H, br s, H—C7), 2.1–2.5 (9H, m), 1.94 (3H, d, J = 1.3 Hz, CH_3—C6), and 1.01 (3H, d, J = 6.7 Hz, CH_3—C10); ^{13}C nmr ($CDCl_3$): 216.7 (C2), 197.6 (C8), 163.5 (C6), 127.2 (C7), 48.1 (C10), 47.2 (C5), 42.0 (C9), 38.5 (C1), 36.8 (C3). 27.4 (C4), 21.1 (CH_3—C2), and 15.8 (CH_3—C10). *Anal.* calcd. for $C_{12}H_{16}O_2$: C 75.00, H 8.33; found: C 74.21, H 7.96.

Bicyclic Enediketone ***18***b

(a) From Tricyclic Ketal Ketone ***15***b

Tricyclic ketal ketone **15***b* (70 mg, 0.29 mmol) dissolved in tetrahydrofuran (5 mL) was mixed with hydrochloric acid (1 *N*, 1 mL) and heated (65°C, oil bath) for 1.5 h. The mixture was then poured into an excess of aqueous sodium bicarbonate (0.5 *N*) and extracted four times with dichloromethane. The extract was dried, filtered, and evaporated to dryness. Crystallization (ether–hexane) and chromatography of the residual mother liquor gave pure bicyclic enediketone **18***b* (50 mg, 86%) identical with the product obtained in procedure *b* (from conjugated acid **41**) described below.

(b) From Conjugated Carboxylic Acid ***41***

Conjugated carboxylic acid **41** (1.30 g, 5.9 mmol), dissolved in a solution of anhydrous dichloromethane (50 mL) and anhydrous pyridine (1.0 g), was added dropwise to a cooled (0°C) solution of oxalyl chloride (2.2 g) in dichloromethane (100 mL) under a nitrogen atmosphere. After completion of the addition (1.5 h) the mixture was stirred for an additional 3 h at room temperature. Filtration and evaporation gave the crude acid chloride **42** (1.35 g); ir ($CHCl_3$): 1735, 1655, 1620, and 1602 cm^{-1}; nmr ($CDCl_3$) δ: 7.27 (1H, s, H—C3), 5.85 (1H, s, H—C7), 1.97 (3H, d, J = 1.5 Hz, CH_3—C6), and 1.00 (3H, m, CH_3—C10).

Sodium azide (455 mg) in water (20 mL) was added dropwise to a cooled (0°C) solution of acid chloride **42** (1.35 g, 5.7 mmol) in acetone (20 mL) under a nitrogen atmosphere. The resulting solution was stirred for 3 h before the addition of saturated sodium chloride (100 mL) and extraction with dichloromethane. The organic phase was dried and evaporated to give the crude azide **43** (1.35 g); ir ($CHCl_3$): 2120, 1680, 1655, 1620, and 1605 cm^{-1}; nmr ($CDCl_3$) δ: 6.92 (1H, s, H—C3), 5.83 (1H, s, H—C7), 1.92 (3H, d, J = 1.0 Hz, CH_3—C6), and 0.97 (3H, m, CH_3—C10).

Azide **43** (1.35 g, 5.5 mmol) was added to a solution of tetrahydrofuran (100 mL) and water (100 mL). The mixture was refluxed during 2.5 h. After cooling to 0°C, aqueous hydrochloric acid (1 *N*, 50 mL) was added. The reaction mixture was stirred at 0°C for 2 h before the addition of saturated sodium chloride (100 mL) and extraction with dichloromethane. The organic phase was dried and evaporated. The residue was purified by thick layer chromatography on silica gel with ether–benzene (1:1). An analytical sample of **18***b* was obtained by crystallization from dichloromethane – petroleum ether (771 mg, 68% from conjugated carboxylic acid **41**); mp 68–69°C; uv (EtOH) λ_{max}: 241 nm (ε 14 600); ir ($CHCl_3$): 1730, 1655, and 1610 cm^{-1}; nmr ($CDCl_3$) δ: 5.92 (1H, s, H—C7), 1.98 (3H, d, J = 2.0 Hz, CH_3—C6), and 1.03 (3H, d, J = 6.5 Hz, CH_3—C10); ^{13}C nmr ($CDCl_3$): 216.7 (C2), 197.6 (C8), 163.4 (C6), 127 (C7), 48.0 (C5), 45.9 (C10), 42.1 (C9), 39.0 (C3), 36.7 (C1), 33.3 (C4), 21.6 (CH_3—C6), and 16.7 (CH_3—C10); ms *m/e*: 192 (M^+), 150, and 149. *Anal.* calcd. for $C_{12}H_{16}O_2$: C 74.97, H 8.39; found: C 74.85, H 8.52.

Bicyclic Ketal Enone ***19***a

Bicyclic enediketone **18***a* (790 mg, 4.11 mmol) was dissolved in anhydrous benzene (80 mL), and ethylene glycol (400 mg) and *p*-toluenesulfonic acid (38 mg) were added. The mixture was refluxed for 4 h using a Dean–Stark water separator. The cooled reaction mixture was diluted with ether (100 mL) and washed with aqueous sodium carbonate (10%, 100 mL) and water (100 mL). The organic phase was dried and evaporated to leave an oil which was purified by column chromatography on Florisil with ether–benzene (1:19) (935 mg, 96%). An analytical sample of **19***a* was prepared by microdistillation *in vacuo*; ir ($CHCl_3$): 1665, 1620, and 1120 cm^{-1}; nmr ($CDCl_3$) δ: 5.77 (1H, br s, H—C7), 3.92 (4H, s, 2 OCH_2), 1.98 (3H, d, J = 1.5 Hz, CH_3—C6), and 1.00 (3H, d, J = 6.5 Hz, CH_3—C10); ms *m/e*: 236 (M^+). *Anal.* calcd. for $C_{14}H_{20}O_3$: C 71.18, H 8.47; found: C 71.31, H 8.80.

Bicyclic Ketal Alcohol ***20***a *and its Acetate* ***21***a

Bicyclic ketal ketone **19***a* (450 mg, 1.9 mmol) dissolved in anhydrous ether (10 mL) was added to a suspension of lithium aluminium hydride (200 mg) in ether (15 mL). The mixture was then refluxed for 6 h and treated with saturated sodium sulfate solution. The aqueous phase was extracted with ether. Drying and evaporation of the organic phase gave ketal alcohol **20***a*; ir ($CHCl_3$): 3600 and 3450 cm^{-1}; nmr ($CDCl_3$) δ: 4.16 (1H, m, C*H*—OH).

The crude ketal alcohol **20***a* was dissolved in pyridine (10 mL) and acetic anhydride (10 mL) and left at room temperature. After 24 h the solvents were evaporated at reduced pressure using a water bath at 45°C. The residue was dissolved in chloroform (25 mL) and the solution was washed with saturated sodium bicarbonate. Drying and evaporation of organic phase gave the crude ketal acetate **21***a* which was purified by thick layer chromatography on silica gel with ether–benzene (1:2); ir ($CHCl_3$): 1715 cm^{-1}; nmr ($CDCl_3$) δ: 5.25 (2H, m, H—C7 and H—C8), 3.91 (4H, s, 2 OCH_2), 2.03 (3H, s, $COCH_3$), 1.80 (3H, s, CH_3—C6), and 1.03 (3H, d, J = 6 Hz, CH_3—C10); ms *m/e*: 280 (M^+).

Bicyclic Ketal Olefin ***22***a

Ketal acetate **21***a* (350 mg, 1.25 mmol) dissolved in ether (12 mL) was added to a solution of lithium (400 mg) in liquid

Can. J. Chem. Downloaded from www.nrcresearchpress.com by 210.87.254.40 on 09/05/12
For personal use only.

ammonia. After stirring for 3 h, solid ammonium chloride was added until the blue color disappeared. The solution was diluted with water and extracted several times with ether. The organic extracts were dried and evaporated. Chromatography of the residue on Florisil gave pure ketal olefin **22***a* (250 mg) as an oil after elution with ether – petroleum ether (9:1); nmr ($CDCl_3$) δ: 5.38 (1H, m, H—C7), 3.89 (4H, s, 2 OCH_2), 1.71 (3H, s, CH_3—C6), and 0.90 (3H, d, J = 1.5 Hz, CH_3—C10). *Anal.* calcd. for $C_{14}H_{22}O_2$: C 75.68, H 9.91; found: C 76.13, H 9.91.

*Bicyclic Enone 23*a

Purified bicyclic ketal olefin **22***a* (60 mg, 0.27 mmol) was dissolved in a solution of acetone (5 mL) and water (1 mL). *p*-Toluenesulfonic acid (15 mg) was added and the solution was stirred at room temperature. After 5 h the acetone was evaporated at reduced pressure and the residue was extracted with ether. The ether extracts were dried and evaporated. The residue was purified by thick layer chromatography on silica gel with ether–benzene (1:2) to give pure bicyclic enone **23***a* (44 mg) as an oil; nmr ($CDCl_3$) δ: 5.41 (1H, m, H—C7), 1.66 (3H, d, J = 1.5 Hz, CH_3—C6), 0.92 (3H, d, J = 6 Hz, CH_3—C10).

2,4-Dinitrophenylhydrazine (200 mg) was added to methanol (20 mL) containing concentrated sulfuric acid (6 drops). The above solution (10 mL) was added to bicyclic enone **23***a* (87 mg, 0.49 mmol) and the resulting solid was recrystallized five times from methanol (83 mg); mp 107–108°C; ms *m/e*: 358 (M^+). Thick layer chromatography on silica gel with benzene – petroleum ether (1:1) separated two products with R_f 0.64 and 0.49. Heating of either of these products returned the mixture. Analytical samples were prepared by recrystallization from methanol. Compound **I**, R_f 0.64; 43 mg (64%); mp 125–127°C; ms *m/e*: 358 (M^+). *Anal.* calcd. for $C_{18}H_{22}N_4O_4$: C 60.32, H 6.19; found: C 60.42, H 6.22. Compound **II**, R_f 0.49; 20 mg (11%); mp 150–151°C; ms *m/e*: 358 (M^+). *Anal.* calcd. for $C_{18}H_{22}N_4O_4$: C 60.32, H 6.19; found: C 59.45, H 6.20.

*Bicyclic Ketal Enone 19*b

Bicyclic enediketone **18***b* (403 mg, 2.1 mmol) was dissolved in anhydrous benzene (80 mL) and ethylene glycol (300 mg) and *p*-toluenesulfonic acid (23 mg) were added. The mixture was refluxed for 4 h using a Dean–Stark water separator. The cooled reaction mixture was diluted with ether (100 mL) and washed with aqueous sodium carbonate (10%, 100 mL) and water (100 mL). The organic phase was dried and evaporated to leave an oil which was purified by thick layer chromatography on silica gel with ether–benzene (1:1) (393 mg, 80%). An analytical sample of **19***b* was prepared by microdistillation *in vacuo*; uv (EtOH) λ_{max}: 242 nm (ε 13 900); ir ($CHCl_3$): 1650, 1602, and 1110 cm^{-1}; nmr ($CDCl_3$) δ: 5.85 (1H, s, H—C7), 3.97 (4H, s, 2 OCH_2), 2.03 (3H, d, J = 1.5 Hz, CH_3—C6), and 1.03 (3H, d, J = 6.5 Hz, CH_3—C10); ms *m/e*: 236 (M^+). *Anal.* calcd. for $C_{14}H_{20}O_3$: C 71.18, H 8.47; found: C 69.51, H 8.57.

*Bicyclic Ketal Alcohol 20*b *and its Acetate 21*b

Lithium tri-*tert*-butoxyaluminium hydride was added to a solution of bicyclic ketal ketone **19***b* (412 mg, 1.75 mmol) in ether (100 mL). The mixture was stirred at room temperature for 18 h before saturated sodium chloride (200 mL) was added and the mixture extracted with ether (2 × 200 mL). The organic extracts were dried and evaporated. The oily residue was purified by thick layer chromatography on silica gel using ether–benzene (1:4) to give bicyclic ketal alcohol **20***b* (343 mg, 83%) as an oil; ir ($CHCl_3$): 3600 and 3460 cm^{-1}; nmr ($CDCl_3$) δ: 5.39 (1H, br s, H—C7), 4.17 (1H, br s, H—C8), 3.92 (4H, s, 2 OCH_2), 2.53 (1H, s, O—*H*), 1.83 (3H, d, J = 1.0 Hz, CH_3—C6), and 1.02 (3H, d, J = 6.5 Hz, CH_3—C10); ms *m/e*: 238 (M^+).

Bicyclic ketal alcohol **20***b* (350 mg, 1.47 mmol) was dissolved in pyridine (15 mL) and acetic anhydride (10 mL) and stirred in the dark at room temperature. After 5 h the solution was cooled to 0°C and methanol (50 mL) was added. The solvents were evaporated and the residue was diluted with saturated sodium chloride (100 mL) and extracted with dichloromethane (3 × 100 mL). Drying and evaporation of the organic extracts gave the crude acetate **21***b* (395 mg); ir ($CHCl_3$): 1730 and 1250 cm^{-1}; nmr ($CDCl_3$) δ: 5.37 (2H, m, H—C7 and H—C8), 3.92 (4H, s, 2 OCH_2), 2.04 (3H, s, $COCH_3$), 1.84 (3H, br s, CH_3—C6), and 1.05 (3H, d, J = 6 Hz, CH_3—C10); ms *m/e*: 280 (M^+).

*Bicyclic Ketal Olefin 22*b

Ketal acetate **21***b* was reduced during 2 h with lithium in liquid ammonia as described above for ketal acetate **21***a*. The crude product was purified by thick layer chromatography on silica gel using ether–benzene (1:2) to give 125 mg (45%). An analytical sample of **22***b* was prepared by microdistillation *in vacuo*; nmr ($CDCl_3$) δ: 5.40 (1H, br s, H—C7), 3.92 (4H, s, 2 OCH_2), 1.75 (3H, br s, CH_3—C6), and 0.92 (3H, d, J = 7.0 Hz, CH_3—C10); ms *m/e*: 222 (M^+). *Anal.* calcd. for $C_{14}H_{22}O_2$: C 75.63, H 9.97; found: C 75.55, H 10.09.

*Bicyclic Enone 23*b

Bicyclic ketal olefin **22***b* (75 mg, 0.34 mmol) was dissolved in a solution of acetone (20 mL) and water (2 mL). *p*-Toluenesulfonic acid (20 mg) was added and the solution was stirred at room temperature. After 5 h, the acetone was evaporated at reduced pressure and the residue was diluted with saturated sodium carbonate solution (50 mL). Extraction with dichloromethane (3 × 50 mL) followed by drying and evaporation gave crude bicyclic ketal olefin **23***b* as an oil. Purification by thick layer chromatography on silica gel using benzene as eluent gave the pure product **23***b* (25 mg, 41%); ir ($CHCl_3$): 1740 cm^{-1}; nmr ($CDCl_3$) δ: 5.50 (1H, s, H—C7), 1.66 (3H, d, J = 1.0 Hz, CH_3—C6), and 0.90 (3H, d, J = 6.5 Hz, CH_3—C10); ms *m/e*: 178 (M^+).

A 2,4-dinitrophenylhydrazine solution (3 mL) was added to bicyclic enone **23***b* (25 mg, 0.14 mmol) and the resulting solid was recrystallized from methanol (43 mg); mp 78–88°C. Thick layer chromatography on silica gel with benzene – petroleum ether (1:1; three elutions) separated two products with R_f 0.64 and 0.55. Heating of either of these two products returned the mixture. Each derivative was recrystallized three times from methanol. Compound **I**, R_f 0.64; 21 mg (42%); mp 113–114°C; ms *m/e*: 358 (M^+). Compound **II**, R_f 0.55; 7 mg (14%); mp 160–161°C; ms *m/e*: 358 (M^+).

Tricyclic Ketal β*-Keto Ester 29*

Tricyclic ketal ketone **15***a* (9.5 g, 40.3 mmol) in anhydrous dimethyl carbonate (200 mL) was added to sodium hydride (5.3 g) and the mixture was refluxed under a nitrogen atmosphere during 10.5 h. After cooling to 0°C, a solution of acetic acid (200 mL) in ether (1.2 L) was carefully added. After dilution with water (1 L) the product was extracted with ether (2 × 500 mL). The organic phase was dried and evaporated to leave an amorphous solid (11.85 g); ir ($CHCl_3$): 1725 and 1700 cm^{-1}; nmr ($CDCl_3$) δ: 3.87 (4H, s, 2 OCH_2), 3.75 (3H, s, OCH_3), 1.22 (3H, s, CH_3—C6), and 1.21 (3H, d, J = 7.0 Hz, CH_3—C10); ms *m/e*: 294 (M^+).

Tricyclic Ketal Alcohol Ester 32

Sodium borohydride (1.6 g) was added to a solution of crude tricyclic ketal β-keto ester **29** (6.5 g, 22.1 mmol) in methanol (200 mL) at 0°C. After stirring for 3 h at the same temperature the solvent was evaporated and the residue was treated with saturated sodium chloride solution (300 mL). Extraction with ether (3 × 300 mL) followed by drying and evaporation of the ethereal extracts gave the crude tricyclic ketal alcohol ester **32** as an oil. This was purified by column chromatography on

Can. J. Chem. Downloaded from www.nrcresearchpress.com by 210.87.254.40 on 09/05/12
For personal use only.

Florisil using ether–benzene (15:85). An analytical sample of **32** was prepared by microdistillation *in vacuo*; 3.47 g (64% from **15**); ir ($CHCl_3$): 3580, 3460, 1720, and 1100 cm^{-1}; nmr ($CDCl_3$) δ: 4.88 (1H, m, H—C2), 3.86 (4H, s, 2 OCH_2), 3.72 (3H, s, OCH_3), 2.64 (1H, s, O—H), 1.35 (3H, s, CH_3—C6), and 1.06 (3H, d, J = 7 Hz, CH_3—C10); ms *m/e*: 296 (M^+). *Anal.* calcd. for $C_{16}H_{24}O_5$: C 64.84, H 8.17; found: C 64.54, H 8.12.

Tricyclic Ketal Ester Acetate 34

Tricyclic ketal alcohol ester **32** (325 mg, 1.1 mmol) was dissolved in pyridine (3 mL) and acetic anhydride (3 mL). The reaction mixture was stirred in the dark for 18 h. After cooling to 0°C, methanol (20 mL) was added and the solvents were evaporated at reduced pressure. The residue was diluted with water (100 mL) and extracted with dichloromethane (3 × 50 mL). The organic extracts were dried and evaporated to leave a solid. Crystallization from ether – petroleum ether gave pure tricyclic ketal ester acetate **34** (282 mg, 77%); mp 62–63°C; ir ($CHCl_3$): 1750–1720 cm^{-1}; nmr (100 MHz) ($CDCl_3$) δ: 5.68 (1H, t, J = 6.0 Hz, H—C2), 3.85 (4H, s, 2 OCH_2), 3.67 (3H, s, OCH_3), 2.75 (1H, m, H—C3), 2.41–2.03 (3H, m, H2—C1 and H—C10), 2.00 (3H, s, $COCH_3$), 1.86 (2H, s, H2—C7), 1.74 (1H, d, J = 6.0 Hz, H—C4), 1.46 (2H, m, H2—C9), 1.24 (3H, s, CH_3—C6), and 1.07 (3H, d, J = 7.0 Hz, CH_3—C10); ms *m/e*: 338 (M^+), 296, 295, and 278. *Anal.* calcd. for $C_{18}H_{26}O_6$: C 63.89, H 7.74; found: C 63.67, H 7.64.

Tricyclic Ketone Alcohol Ester 36

Hydrochloric acid (1 *N*, 50 mL) was added to a solution of tricyclic ketal alcohol ester **32** (212 mg, 0.74 mmol) in methanol (50 mL). After stirring for 10 min at room temperature the solution was neutralized by the addition of solid sodium carbonate and the methanol was evaporated. The product was extracted with dichloromethane and the organic extracts were dried and evaporated. Thick layer chromatography on silica gel with ether–benzene (1:1) gave tricyclic ketone alcohol ester **36** as an oil (151 mg, 80%). An analytical sample was prepared by microdistillation *in vacuo*; ir ($CHCl_3$): 3580, 3460, 1720, and 1700 cm^{-1}; nmr ($CDCl_3$) δ: 4.97 (1H, t, J = 6.0 Hz, H—C2), 3.75 (3H, s, OCH_3), 1.38 (3H, s, CH_3—C6), 1.09 (3H, d, J = 6.5 Hz, CH_3—C10); ms *m/e*: 252 (M^+), and 238. *Anal.* calcd. for $C_{14}H_{20}O_4$: C 66.65, H 7.99; found: C 66.39, H 8.06.

Tricyclic Ketone Acetate Ester 37

Tricyclic ketone alcohol ester **36** (133 mg, 0.53 mmol) was dissolved in a mixture of pyridine (1.5 mL) and acetic anhydride (1.5 mL) and left for 18 h at room temperature. After evaporation, water was added and the solution was extracted with dichloromethane. The organic extract was dried and evaporated to yield a crystalline product. Crystallization from ether – petroleum ether gave pure tricyclic ketone acetate ester **37** (115 mg, 74%); mp 119–120°C; ir ($CHCl_3$): 1720 (broad) cm^{-1}; nmr ($CDCl_3$) δ: 5.70 (1H, t, J = 6.0 Hz, H—C2), 3.70 (3H, s, OCH_3), 2.02 (3H, s, $COCH_3$), 1.72 (1H, d, J = 6 Hz, H—C4), 1.30 (3H, s, CH_3—C6), and 1.07 (3H, d, J = 6.5 Hz, CH_3—C10).

Dienone Ester 38

(a) From Tricyclic Ketone Alcohol Ester 36

A solution of tricyclic ketone alcohol ester **36** (150 mg, 0.51 mmol) in methanol (10 mL) was added to hydrochloric acid (1 *N*, 10 mL). After stirring for 30 min at room temperature the solvent was evaporated. The residue was diluted with sodium carbonate solution (10%, 100 mL) and extracted with dichloromethane (3 × 100 mL). The organic extracts were dried and evaporated to leave a solid which was recrystallized from petroleum ether to yield dienone ester **38** (91 mg, 77%); mp 78–79°C. The physical and chemical properties of this compound were identical with those of the product obtained in procedure *b*.

(b) From Dienone Carboxylic Acid 39

Ethereal diazomethane (18 mg/mL, 32 mL) was added to a solution of dienone acid **39** (1.73 g, 7.85 mmol) in dichloromethane (100 mL). After stirring for 10 min at room temperature the solvent was evaporated. The solid residue was crystallized from petroleum ether (1.65 g, 90%); mp 78–79°C; uv (EtOH) λ_{max}: 237 nm (ε 15 900); ir ($CHCl_3$): 1725, 1655, and 1610 cm^{-1}; nmr ($CDCl_3$) δ: 6.02 (1H, d of d, J = 6.0, 2.0 Hz, H—C4), 5.83 (1H, s, H—C7), 5.57 (1H, d of d, J = 6.0, 2.5 Hz, H—C3), 3.73 (1H, m, H—C2), 3.73 (3H, s, OCH_3), 1.83 (3H, d, J = 1.5 Hz, CH_3—C6), and 0.90 (3H, m, CH_3—C10); ms *m/e*: 234 (M^+) and 192. *Anal.* calcd. for $C_{14}H_{18}O_3$: C 71.77, H 7.75; found: C 71.76, H 8.03.

Dienone Carboxylic Acid 39

(a) From Tricyclic Ketal Alcohol Ester 32

Hydrochloric acid (1 *N*, 400 mL) was added to a solution of tricyclic ketal alcohol ester **32** (12.0 g, 40.5 mmol) in tetrahydrofuran (400 mL). After refluxing for 4 h the solvents were evaporated. The residue was diluted with water (500 mL), basified by the addition of solid potassium hydroxide, and then extracted with ether (2 × 200 mL). The aqueous phase was acidified with concentrated hydrochloric acid and extracted with dichloromethane (3 × 300 mL). The dichloromethane extracts were dried and evaporated. The solid residue was crystallized from ether (7.3 g, 82%); mp 163–165°C; uv (EtOH) λ_{max}: 240 nm (ε 15 800); ir ($CHCl_3$): 3600–2400, 1705, 1655, and 1610 cm^{-1}; nmr ($CDCl_3$) δ: 11.52 (1H, s, OH), 6.07 (1H, d of d, J = 6.0, 2.5 Hz, H—C4), 5.70 (1H, br s, H—C7), 5.59 (1H, d of d, J = 6.0, 2.5 Hz, H—C3), 3.92 (1H, m, H—C2), 1.85 (3H, d, J = 1.5 Hz, CH_3—C6), and 0.92 (3H, m, CH_3—C10); ms *m/e*: 220 (M^+). *Anal.* calcd. for $C_{13}H_{16}O_3$: C 70.89, H 7.32; found: C 70.64, H 7.11.

(b) From Tricyclic Ketone Alcohol Ester 36

Treatment of tricyclic ketone alcohol ester **36** under the conditions of procedure *a* gave the dienone carboxylic acid **39** in 84% yield; mp 163–164°C.

(c) From Dienone Ester 38

Treatment of dienone ester **38** under the conditions of procedure *a* gave the dienone carboxylic acid **39** in 94% yield; mp 163–165°C.

Conjugated Ester 40

Sodium methoxide (200 mg) was added to a solution of dienone ester **38** (1.45 g, 6.2 mmol). After refluxing for 6 h the solvent was evaporated. The residue was diluted with water (100 mL) and extracted with ether (3 × 100 mL). The organic extracts were dried and evaporated to leave an oil which was purified by thick layer chromatography on silica gel with ether–benzene (1:3) (1.18 g, 82%). An analytical sample of **40** was prepared by microdistillation *in vacuo*; uv (EtOH) λ_{max}: 235 nm (ε 17 500); ir ($CHCl_3$): 1705, 1655, 1610, and 1240 cm^{-1}; nmr ($CDCl_3$) δ: 6.84 (1H, br s, H—C3), 5.84 (1H, s, H—C7), 3.80 (3H, s, OCH_3), 1.95 (3H, d, J = 1.5 Hz, CH_3—C6), and 1.00 (3H, m, CH_3—C10); ms *m/e*: 234 (M^+) and 192. *Anal.* calcd. for $C_{14}H_{18}O_3$: C 71.77, H 7.75; found: C 71.77, H 7.88.

Conjugated Carboxylic Acid 41

Conjugated carboxylic acid **41** was obtained from conjugated ester in 88% yield following the procedure employed for the preparation of dienone carboxylic acid **39**. An analytical sample was prepared by recrystallization from dichloromethane – petroleum ether; mp 151°C; uv (EtOH) λ_{max}: 238 (ε 13 600); ir ($CHCl_3$): 3600–2400, 1675, 1655, 1635, and 1605 cm^{-1}; nmr ($CDCl_3$) δ: 10.55 (1H, s, O—H), 6.84 (1H, br s, H—C3), 5.79 (1H, d, J = 1.0 Hz, H—C7), 1.95 (3H, d, J = 1.0 Hz, CH_3—C6), 0.98 (3H, m, CH_3—C10); ms *m/e*: 220 (M^+) and 178. *Anal.* calcd. for $C_{13}H_{16}O_3$: C 70.89, H 7.32; found: C 70.22, H 7.22.

Can. J. Chem. Downloaded from www.nrcresearchpress.com by 210.87.254.40 on 09/05/12
For personal use only.

Allylic Alcohol Ester ***44***

Lithium tri-*tert*-butoxyaluminium hydride (1.7 g) was added to a solution of dienone ester **38** (500 mg, 2.14 mmol) in ether (100 mL). The mixture was stirred at room temperature for 4 h before hydrochloric acid (1 *N*, 200 mL) was added and the mixture extracted with ether (2 × 200 mL). The organic extracts were dried and evaporated. The oily residue was purified by thick layer chromatography on silica gel with ether–benzene (1:1) to give allylic alcohol ester **44** (310 mg, 62%) as an oil; ir ($CHCl_3$): 3600, 3450, and 1720 cm^{-1}; nmr ($CDCl_3$) δ: 5.84 (1H, d of d, J = 5.5, 2.0 Hz, H—C4), 5.42 (1H, br s, H—C7), 5.34 (1H, d of d, J = 5.5, 2.5 Hz, H—C3), 4.20 (1H, br s, H—C8), 3.70 (3H, s, OCH_3), 2.74 (1H, s, OH), 1.60 (3H, m, CH_3—C6), and 0.82 (3H, d, J = 6.0 Hz, CH_3—C10); ms *m/e*: 236 (M^+) and 218.

Bicyclic Diol ***47***

(a) From Allylic Alcohol Ester ***44***

Anhydrous ether (20 mL) and magnesium metal (250 mg) were placed in a dried flask under a positive pressure of nitrogen. A solution of methyl iodide (3.0 g) in anhydrous ether (25 mL) was added dropwise. A solution of allylic alcohol **44** (310 mg, 1.31 mmol) in anhydrous ether was then added at such a rate that maintained a gentle reflux. After the addition was completed, the mixture was refluxed for an additional 2 h before pouring it onto crushed ice (100 g) and extraction with ether (3 × 150 mL). The ethereal phase was dried and evaporated. The residue was crystallized from ether–pentane to give bicyclic diol **47** (222 mg, 72%) whose physical and spectral properties were identical with those of the product obtained by procedure *b* below.

(b) From Bicyclic Dienone Alcohol ***49***

Lithium aluminium hydride (300 mg) was added to a solution of bicyclic dienone alcohol **49** (578 mg, 2.47 mmol) in anhydrous ether (100 mL). The mixture was refluxed for 5 h. After cooling, water (200 mL) was added slowly and the resulting mixture extracted with ether (3 × 200 mL). The organic extracts were dried and evaporated. The solid residue was crystallized from ether–pentane to give bicyclic diol **47** (512 mg, 88%) and an analytical sample was prepared by recrystallization from the same solvent mixture; mp 118–120°C; ir ($CHCl_3$): 3600 and 3440 cm^{-1}; nmr ($CDCl_3$) δ: 5.90 (1H, d of d, J = 6.0, 2.0 Hz, H—C4), 5.42 (3H, s, CH_3—C7), 5.40 (1H, d of d, H—C3), 4.28 (1H, m, H—C8), 2.92 (1H, m, H—C2), 2.08 (2H, s, O—H), 1.63 (3H, s, CH_3—C6), 1.21 and 1.17 (total 6H, two s, isopropyl methyls), and 0.88 (3H, d, J = 6.0 Hz, CH_3—C10); ms *m/e*: 236 (M^+), 218, and 200. *Anal.* calcd. for $C_{15}H_{24}O_2$: C 76.23, H 10.24; found: C 76.35, H 10.35.

Tricyclic Ketal Diol ***48***

Anhydrous ether (50 mL) and magnesium metal (1.5 g) were placed in a dried flask under a positive pressure of nitrogen. A solution of methyl iodide (11 g) in anhydrous ether (50 mL) was added at a rate that maintained a gentle reflux. A solution of tricyclic ketal alcohol ester **32** (2.32 g, 7.9 mmol) in anhydrous ether (100 mL) was then added dropwise. After the addition was completed the mixture was refluxed for 3 h, allowed to cool, and poured onto a mixture of crushed ice and ammonium sulfate (200 g). Extraction with ether (3 × 200 mL) followed by drying and evaporation gave an oil which was purified by thick layer chromatography on silica gel with ether methanol (95:5) yielding tricyclic ketal diol **48**: (2.05 g, 88%); ir ($CHCl_3$): 3610 and 3460 cm^{-1}; nmr ($CDCl_3$) δ: 4.80 (1H, m, H—C2), 3.90 (4H, s, 2 OCH_2), 1.38 (3H, s, CH_3—C6), 1.24 and 1.20 (total 6H, two s, isopropyl methyls), and 1.09 (3H, d, J = 7.0 Hz, CH_3—C10); ms *m/e*: 296 (M^+) and 278.

Bicyclic Dienone Alcohol ***49***

Hydrochloric acid (2 *N*, 13 mL) was added to a solution of tricyclic ketal diol **48** (1.47 g, 5.14 mmol) in freshly distilled tetrahydrofuran (200 mL). After refluxing for 4 h under a positive pressure of nitrogen the solvent was evaporated. The residue was mixed with saturated sodium chloride (100 mL) and extracted with chloroform (3 × 100 mL). The chloroform extracts were dried and evaporated. The oily residue was purified by chromatography on Florisil and the crystalline compound **49** was obtained by elution with ether–benzene (1:3) (944 mg, 81%). An analytical sample was prepared by recrystallization from ether–pentane; mp 65–66°C; uv (EtOH) λ_{max}: 239 nm (ε 15 200); ir ($CHCl_3$): 3600, 3450, and 1665 cm^{-1}; nmr ($CDCl_3$) δ: 6.05 (1H, d of d, J = 6.0, 2.0 Hz, H—C4), 5.85 (1H, d, J = 1.0 Hz, H—C7), 5.62 (1H, d of d, J = 6.0, 3.0 Hz, H—C3), 3.02 (1H, m, H—C2), 2.08 (1H, s, O—H), 1.88 (3H, d, J = 1.0 Hz, CH_3—C6), 1.27 and 1.23 (total 6H, two s, isopropyl methyls), and 0.97 (3H, m, CH_3—C10); ms *m/e*: 234 (M^+) and 216. *Anal.* calcd. for $C_{15}H_{22}O_2$: C 76.88, H 9.46; found: C 77.13, H 9.63.

Bicyclic Monoacetate Alcohol ***50***

Bicyclic diol **47** (236 mg, 1.0 mmol) was dissolved in pyridine (5 mL) and acetic anhydride (5 mL) and left at room temperature in the dark. After 3 h the solvents were evaporated at reduced pressure and the residue was diluted with water (50 mL). Extraction with ether (3 × 50 mL) followed by drying and evaporation of the organic extracts gave the crude product. Purification by thick layer chromatography on silica gel using ether–benzene (1:10) gave pure bicyclic monoacetate alcohol **50** (252 mg, 91%). An analytical sample was prepared by recrystallization from ether–pentane; mp 84–85°C; ir ($CHCl_3$): 3600, 3450, 1715, and 1245 cm^{-1}; nmr ($CDCl_3$) δ: 5.87 (1H, d of d, J = 6.0, 2.0 Hz, H—C4), 5.33 (1H, d of d, J = 6.0, 2.5 Hz, H—C3), 5.23 (1H, br s, H—C7), 5.17 (1H, br s, H—C8), 2.83 (1H, m, H—C2), 1.98 (3H, s, $COCH_3$), 1.63 (3H, br s, CH_3—C6), 1.18 and 1.12 (6H, two s, isopropyl methyls), and 1.90 (3H, d, J = 6.5 Hz, CH_3—C10); ms *m/e*: 278 (M^+) and 218. *Anal.* calcd. for $C_{17}H_{26}O_3$: C 73.35, H 9.41; found: C 73.60, H 9.69.

(±)Epihinesol (3)

(a) From Bicyclic Diol ***47***

Finely divided lithium metal (70 mg) was added to ethylamine (25 mL). After 20 min a solution of bicyclic diol **47** (55 mg, 0.23 mmol) in ether was added. After stirring for 2.5 h, solid ammonium chloride was added until the blue color of the reaction mixture had just disappeared. The amine was evaporated and water (50 mL) was added to the residue. Extraction with ether (2 × 50 mL) followed by drying and evaporation of the organic phase gave the crude product. Purification by thick layer chromatography on silica gel using ether–benzene gave (±)-epihinesol (**3**) (29 mg, 56%) whose physical and chemical properties were identical with those of the product obtained by procedure *b* below.

(b) From Bicyclic Alcohol Acetate ***50***

(±)Epihinesol (**3**) was obtained from bicyclic monoacetate alcohol **50** in 92% yield by the procedure described above in *a*; ir ($CHCl_3$): 3600 and 3400 cm^{-1}; nmr ($CDCl_3$) δ: 5.05 (1H, m, H—C7), 1.66 (3H, d, J = 1.15 Hz, CH_3—C6), 1.15 (6H, s, isopropyl methyls), and 0.90 (3H, d, J = 6.5 Hz, CH_3—C10); ^{13}C nmr (CCl_4): 141.35 (C6), 122.25 (C7), 72.53 (C13), 54.79 (C2), 37.17 (C1 or C3), 33.79 (C5), 31.45 (C9), 30.09 (C1 or C3), 28.98 (C14 and C15), 28.59 (C4), 26.38 (C10), 24.18 (C11), 22.23 (C8), and 17.09 (C12); ms *m/e*: 222 (M^+) and 204.

Epihinesol Acetate ***51***

Sodium acetate (100 mg) was added to a solution of (±)-epihinesol (**3**) (84 mg, 0.38 mmol) in acetic anhydride (4 mL) and the mixture was heated to reflux. After 5 h the mixture was cooled to room temperature, saturated sodium carbonate (100 mL) was added, and the mixture was extracted with chloroform (3 × 100 mL). The organic extracts were dried and

Can. J. Chem. Downloaded from www.nrcresearchpress.com by 210.87.254.40 on 09/05/12
For personal use only.

evaporated to leave an oily residue which was purified by thick layer chromatography on silica gel using benzene. The purified product (77 mg, 77%) revealed the presence of only one component by vpc analysis; ir ($CHCl_3$): 1720 and 1270 cm^{-1}; nmr ($CDCl_3$) δ: 5.05 (1H, br s, H—C7), 1.90 (3H, s, $COCH_3$), 1.66 (3H, d, J = 1.5 Hz, CH_3—C6), 1.43 (6H, s, isopropyl methyls), and 0.90 (3H, d, J = 6.5 Hz, CH_3—C10); ms *m/e*: 264 (M^+) and 204.

Epihinesol Expoxide ***52***

A solution of *m*-chloroperbenzoic acid (195 mg) in chloroform (5 mL) was added to (±)epihinesol (**3**) (193 mg, 0.87 mmol) in chloroform (10 mL). After 36 h at 0°C the reaction mixture was diluted with chloroform (150 mL) and washed with saturated sodium carbonate (50 mL). The organic phase was dried and evaporated. The residue was purified by crystallization from petroleum ether (165 mg, 75%). An analytical sample of **52** was prepared by recrystallization from the same solvent; mp 94–95°C; ir ($CHCl_3$): 3600, 3460, and 800 cm^{-1}; nmr ($CDCl_3$) δ: 2.94 (1H, t, J = 2.5 Hz, H—C7), 1.31 (3H, s, CH_3—C6), 1.23 (6H, s, isopropyl methyls), and 0.82 (3H, d, J = 6.5 Hz, CH_3—C10); ms *m/e*: 238 (M^+). *Anal.* calcd. for $C_{15}H_{26}O_2$: C 75.58, H 11.00; found: C 75.36, H 10.82.

Dehydro β-Vetivone ***53***

p-Toluenesulfonic acid (1.4 g) was added to a solution of bicyclic dienone alcohol **49** (1.4 g, 6.0 mmol) in dry benzene (200 mL). The reaction mixture was refluxed for 4 h under a positive pressure of nitrogen. The cooled reaction mixture was diluted with saturated sodium carbonate (100 mL) and extracted with ether (2 × 100 mL). The organic extracts were decolorized with activated carbon and dried. Evaporation of the solvents left an oil which was purified by thick layer chromatography on silica gel using ether–benzene (1:9) to give crystalline dehydro β-vetivone **53** (1.03 g, 80%). An analytical sample was prepared by recrystallization from pentane; mp 79–80°C; uv (EtOH) λ_{max}: 244 nm (ε 16 800); ir ($CHCl_3$): 1665 and 1625 cm^{-1}; nmr ($CDCl_3$) δ: 6.65 (1H, d, J = 5.5 Hz, H—C4), 5.90 (1H, s, H—C7), 5.67 (1H, d, J = 5.5 Hz, H—C3), 1.88 (9H, m, CH_3—C6 and geminal methyls), and 0.87 (3H, m, CH_3—C10); ms *m/e*: 216 (M^+). *Anal.* calcd. for $C_{15}H_{20}O$: C 83.29, H 9.32; found: C 83.08, H 9.38.

Bicyclic Allylic Alcohol ***54***

Lithium tri-*tert*-butoxyaluminium hydride (5.0 g) was added to a solution of dehydro β-vetivone **53** (850 mg, 3.93 mmol) in anhydrous ether. The mixture was refluxed for 7 h. Saturated sodium chloride was added to the cooled reaction mixture followed by extraction with dichloromethane (3 × 200 mL). The organic extracts were dried and evaporated. The unstable residue was purified by thick layer chromatography on silica gel using ether–benzene (1:1) to give crystalline bicyclic allylic alcohol **54** (577 mg, 67%). An analytical sample was prepared by recrystallization from purified pentane (mp 100–101°C); ir ($CHCl_3$): 3600 and 3450 cm^{-1}; nmr ($CDCl_3$) δ: 6.55 (1H, d, J = 5.5 Hz, H—C4), 5.55 (1H, d, J = 5.5 Hz, H—C3), 5.48 (1H, br s, H—C7), 4.28 (1H, m, H—C8), 1.73 (6H, br s, geminal methyls), 1.58 (3H, br s, CH_3—C6), and 0.78 (3H, d, J = 6.0 Hz, CH_3—C10); ms *m/e*: 218 (M^+) and 200. *Anal.* calcd. for $C_{15}H_{22}O$: C 82.52, H 10.15; found: C 80.96, H 10.26.

Allylic Alcohol ***55***

Lithium tri-*tert*-butoxyaluminium hydride (1.5 g) was added to a solution of conjugated ester **40** (348 mg, 1.47 mmol) in ether (100 mL). The mixture was stirred at room temperature for 4 h before hydrochloric acid (1 *N*, 100 mL) was added and the mixture extracted with ether (2 × 200 mL). The organic extracts were dried and evaporated. The oily residue was purified by thick layer chromatography on silica gel using ether–benzene (1:1) to give allylic alcohol **55** (310 mg, 88%) as an oil; uv (EtOH) λ_{max}: 224 nm (ε 8 600); ir ($CHCl_3$): 3580, 3460, and 1700 cm^{-1}; nmr ($CDCl_3$) δ: 6.75 (1H, m, H—C3), 5.41 (1H, m, H—C7), 4.25 (1H, m, H—C8), 3.77 (3H, s, OCH_3), 1.67 (3H, m, CH_3—C6), 0.90 (3H, d, J = 6.0 Hz, CH_3—C10); ms *m/e*: 236 (M^+) and 218.

Allylic Acetate ***56***

Allylic alcohol **55** (150 mg, 0.63 mmol) was dissolved in pyridine (4.8 mL) and acetic anhydride (2.4 mL) and the reaction mixture was left in the dark for 24 h. Methanol (10 mL) was carefully added followed by evaporation *in vacuo*. The residue was diluted with saturated sodium chloride (100 mL) and the mixture extracted with dichloromethane (2 × 100 mL). The organic extracts were dried and evaporated to leave an oily residue which was purified by thick layer chromatography on silica gel using ether–benzene (1:5) to give pure allylic acetate **56** (133 mg, 76%); uv (EtOH) λ_{max}: 222 nm (ε 8 500); ir ($CHCl_3$): 1720 and 1705 cm^{-1}; nmr ($CDCl_3$) δ: 6.77 (1H, br s, H—C3), 5.35 (2H, m, H—C7 and H—C8), 3.78 (3H, s, OCH_3), 2.06 (3H, s, $COCH_3$), 1.68 (3H, m, CH_3—C6), and 0.71 (3H, d, J = 6.0 Hz, CH_3—C10); ms *m/e*: 278 (M^+) and 218.

Diene Ester ***57***

(a) From Allylic Alcohol ***55***

A solution of allylic alcohol **55** (124 mg, 0.52 mmol) in ethyl acetate was added to a rapidly stirred, prehydrogenated mixture of 10% palladium on carbon (35 mg) and ethyl acetate (10 mL) under a hydrogen atmosphere. The theoretical amount of hydrogen (11.8 mL) was consumed during 32 min and the mixture was filtered immediately with the aid of Celite. Evaporation of the filtrate and purification of the oily residue by thick layer chromatography on silica gel using ether–benzene (1:1) gave pure diene ester **57** (78 mg, 68%); uv (EtOH) λ_{max}: 225 nm (ε 6 950); ir ($CHCl_3$): 1700 and 1625 cm^{-1}; nmr ($CDCl_3$) δ: 6.73 (1H, br s, H—C3), 5.35 (1H, br s, H—C7), 3.75 (3H, s, OCH_3), 1.77 (3H, m, CH_3—C6), and 0.78 (3H, m, CH_3—C10); ms *m/e*: 220 (M^+).

(b) From Allylic Acetate ***56***

Allylic acetate **56** (65 mg, 0.23 mmol) was hydrogenated following procedure *a*. The purified product (33 mg, 64%) was obtained after thick layer chromatography on silica gel using ether–benzene (1:2). The physical and chemical properties of diene ester were identical to those of the product obtained from allylic alcohol **55**.

Tricyclic Ketal Conjugated Methyl Ester ***58***

(a) From Tricyclic Ketal Ester Acetate ***34***

Maleic anhydride (147 mg, 1.5 mmol) was added to a stirred solution of potassium *tert*-butoxide (purified by sublimation; 340 mg, 3 mmol) in anhydrous *tert*-butanol under a positive pressure of nitrogen. After a few minutes, tricyclic ketal ester acetate **34** (506 mg, 1.5 mmol) was added and the mixture was refluxed for 3 days. After cooling, the reaction mixture was added to brine (30 mL) and extracted with ether (3 × 20 mL). The organic extracts were washed with saturated sodium chloride (3 × 2 mL), dried, and the solvent evaporated to give pure crystalline **58** (416 mg, quantitative). An analytical sample was prepared by recrystallization from pentane (mp 67.5–68°C; uv (EtOH) λ_{max}: 265 nm (ε 8 350); ir ($CHCl_3$): 1707 and 1620 cm^{-1}; nmr ($CDCl_3$) δ: 6.76 (1H, br d of d, J = 4, 2 Hz, H—C2), 3.91 (4H, s, 2 OCH_2), 3.72 (3H, s, OCH_3), 1.11 (3H, d, J = 6.5 Hz, CH_3—C10), and 0.86 (3H, s, CH_3—C6); ms *m/e*: 278 (M^+). *Anal.* calcd. for $C_{16}H_{22}O_4$: C 69.04, H 7.97; found: C 69.16, H 8.34.

In another experiment using the following conditions, potassium *tert*-butoxide (228 mg, 1.94 mmol), freshly sublimed maleic anhydride (63 mg, 0.65 mmol), dry *tert*-butanol (23 mL), and tricyclic ketal ester acetate **34** (240 mg, 0.735 mmol), it was

found that compound **34** was converted into compound **58** (88%) after 1 h at room temperature.

(b) From Tricyclic Ketal Conjugated Carboxylic Acid 64

Ethereal diazomethane was added to a solution of tricyclic ketal conjugated carboxylic acid **64** (33 mg, 0.12 mmol) in ether (5 mL) until the yellow color persisted. After 20 min at room temperature the solvent was evaporated to leave tricyclic ketal conjugated methyl ester **58** in quantitative yield, identical with the material obtained from tricyclic ketal ester acetate **34** in *a* above.

Tricyclic Ketal Isopropylol 59

Methyl lithium (2 *M* in ether; 3 mL, 6 mmol) was added dropwise to a solution of tricyclic ketal conjugated methyl ester **58** (123 mg, 0.44 mmol) in anhydrous ether (15 mL) at 0°C under a positive pressure of nitrogen. The solution was stirred at 0°C for 20 min and then at room temperature. After 18 h the mixture was cooled to 0°C and water (25 mL) was added dropwise. Extraction with ether (3 × 15 mL) followed by drying and evaporation gave the desired tricyclic ketal isopropylol **59** (119 mg, 97%). An analytical sample was prepared by microdistillation *in vacuo*; ir ($CHCl_3$): 3605, 3470, and 1660 cm^{-1}; nmr ($CDCl_3$) δ: 5.56 (1H, m, H—C2), 3.89 (4H, s, 2 OCH_2), 1.33 (6H, s, isopropyl methyls), 1.11 (3H, d, J = 7 Hz, CH_3—C10), 0.83 (3H, s, CH_3—C6); ms *m/e*: 278 (M^+). *Anal.* calcd. for $C_{17}H_{26}O_3$: C 73.35, H 9.41; found: C 73.31, H 9.51.

Diene Diol 62

Methyl lithium (2 *M* in ether; 4.4 mL, 8.8 mmol) was added dropwise to a solution of diene alcohol ester **77** (134 mg, 0.57 mmol) in anhydrous ether (20 mL) at 0°C under a positive pressure of nitrogen. The solution was stirred 2 h at 0°C and then at room temperature. After 20 h the mixture was cooled to 0°C and saturated sodium chloride solution (20 mL) was added dropwise. The phases were separated and the aqueous phase was extracted with ether (3 × 10 mL). The combined organic extracts were dried and evaporated to give diene diol **62** as an oil. The product was purified by column chromatography on silica gel using ether. An analytical sample was prepared by microdistillation *in vacuo* (125 mg, 93%); ir ($CHCl_3$): 3610, 3450, 1665, and 1610 cm^{-1}; nmr ($CDCl_3$) δ: 5.96 (1H, d of d, J = 5.5, 1.75 Hz, H—C4), 5.5 (1H, m, H—C7), 5.50 (1H, d of d, J = 5.5, 3 Hz, H—C3), 4.3 (1H, m, H—C8), 1.66 (3H, m, CH_3—C6), 1.25 and 1.19 (total 6H, two s, isopropyl methyls), and 0.85 (3H, d, J = 6 Hz, CH_3—C10); ms *m/e*: 218 (M^+ − 18), 203 (M^+ − (18 + 15)), and 200 (M^+ − 36). *Anal.* calcd. for $C_{15}H_{24}O_2$: C 76.23, H 10.24; found: C 75.97, H 10.12.

Diene Alcohol Acetate 63

Diene diol **62** (125 mg, 0.53 mmol) was dissolved in pyridine (4 mL) and acetic anhydride (3.5 mL) and the reaction mixture was left in the dark under a positive pressure of nitrogen for 18 h. After cooling to 0°C, methanol was carefully added. The mixture was left to warm to room temperature before the addition of water (25 mL) and extraction with ether (4 × 15 mL). The organic extracts were washed with saturated sodium chloride (3 × 2 mL), dried, and evaporated to leave a yellow oil. Filtration through a column of silica gel with ether–benzene (1:1) gave crystalline diene alcohol acetate **63** (131 mg, 89%). An analytical sample was prepared by recrystallization from ether–pentane; mp 104–104.5°C; ir ($CHCl_3$): 3600, 3470, 1730, and 1667 cm^{-1}; nmr ($CDCl_3$) δ: 5.94 (1H, d of d, J = 5.75, 1.5 Hz, H—C4), 5.48 (1H, d of d, J = 6, 2.5 Hz, H—C3), 5.4 (2H, m, H—C7 and H—C8), 2.06 (3H, s, CH_3CO), 1.67 (3H, m, CH_3—C6), 1.27 and 1.20 (total 6H, two s, isopropyl methyls), 0.85 (3H, d, J = 6Hz, CH_3—C10); ms *m/e*: 278 (M^+).

Tricyclic Ketal Alcohol Carboxylic Acid 65

Aqueous sodium hydroxide (50%; 3 mL) was added to a stirred solution of tricyclic ketal alcohol ester **32** (312 mg, 1.05 mmol) in methanol (3 mL). After 4 h at room temperature, the methanol was evaporated and water (30 mL) was added. The mixture was extracted with ether, the aqueous phase acidified to pH = 6 with dilute hydrochloric acid and then extracted with dichloromethane (4 × 20 mL). The latter extracts were dried and evaporated to leave tricyclic ketal alcohol carboxylic acid **65** as a white solid (167 mg, 56%); mp 110–111°C; ir ($CHCl_3$): 3600, 3500–2500, and 1710 cm^{-1}; nmr ($CDCl_3$) δ: 6.77 (2H, br s, OH and CO_2H), 4.87 (1H, m, H—C2), 3.86 (4H, s, 2 OCH_2), 1.33 (3H, s, CH_3—C6), and 1.08 (3H, d, J = 6.5 Hz, CH_3—C10); ms *m/e*: 282 (M^+).

Tricyclic Ketal Conjugated Carboxylic Acid 64 and Tricyclic Ketal Alcohol Carboxylic Acid 65

Tricyclic ketal ester acetate **34** (103 mg, 0.3 mmol) was added to a solution of potassium *tert*-butoxide (104 mg, 0.9 mmol) in dry *tert*-butanol under a positive pressure of nitrogen. The mixture was refluxed for 30 h, cooled to 0°C, and brine (20 mL) was added. The mixture was extracted with ether (3 × 10 mL) which was washed with saturated sodium chloride, dried, and evaporated to give only *tert*-butanol. The aqueous phase was made slightly acidic (pH = 6–7) with dilute hydrochloric acid and extracted with ether (4 × 15 mL). These extracts were washed with saturated sodium chloride, dried, and evaporated to give tricyclic ketal conjugated carboxylic acid **64** (41 mg, 51%); ir ($CHCl_3$): 3500–2500, 1680, and 1620 cm^{-1}; nmr ($CDCl_3$) δ: 6.84 (1H, m, H—C2), 3.87 (4H, s, 2 OCH_2), 1.12 (3H, d, J = 7 Hz, CH_3—C10), and 0.87 (3H, s, CH_3—C6). The aqueous phase was further acidified to pH = 4 and extracted with ether (4 × 15 mL). These extracts were washed with saturated sodium chloride, dried, and evaporated to give tricyclic ketal alcohol carboxylic acid **65** (30 mg, 35%).

Tricyclic Ketal Conjugated tert-*Butyl Ester 66*

The procedure employed above for the preparation of the analogous methyl ester **58** was followed. In this case the following quantities were used; potassium *tert*-butoxide (792 mg, 7 mmol), *tert*-butanol (16 mL), maleic anhydride (232 mg, 2.36 mmol), and tricyclic ketal ester acetate **34** (800 mg, 2.36 mmol). A 5-day reaction time was used. The title compound was obtained in quantitative yield and could be crystallized with difficulty from pentane (mp 33–34°C). An analytical sample was prepared by microdistillation *in vacuo*; uv (EtOH) λ_{max}: 251 nm (ε 7 550); ir ($CHCl_3$): 1705 and 1627 cm^{-1}; nmr ($CDCl_3$) δ: 6.66 (1H, m, H—C2), 3.93 (4H, s, 2 OCH_2), 1.48 (9H, s, O—*tert*-butyl), 1.12 (3H, d, J = 7 Hz, CH_3—C10), and 0.87 (3H, s, CH_3—C6); ms *m/e*: 320 (M^+). *Anal.* calcd. for $C_{19}H_{28}O_4$: C 71.22, H 8.81; found: C 71.60, H 8.85.

Tricyclic Ketal Diol 67

Tricyclic ketal alcohol ester **32** (367 mg, 1.24 mmol) was added to a suspension of lithium aluminium hydride (170 mg) in anhydrous ether (100 mL). The mixture was heated at reflux for 5 h. After cooling, water (50 mL) was carefully added to destroy the remaining lithium aluminium hydride followed by saturated sodium chloride (100 mL) before extraction with ether (4 × 150 mL). The organic phase was dried and evaporated to leave an oily residue from which diol **67** (160 mg, 48%) was crystallized using ether. An analytical sample was prepared by crystallization from the same solvent (mp 114–115°C); ir ($CHCl_3$): 3580 and 3400 cm^{-1}; nmr ($CDCl_3$) δ: 5.47 (1H, m, H—C2), 3.88 (4H, s, 2 OCH_2), 3.60 (2H, m, CH_2—OH), 2.83 (2H, br s, 2 OH), 1.35 (3H, s, CH_3—C6), and 1.04 (3H, d, J = 7.0 Hz, CH_3—C10); ms *m/e*: 268 (M^+). *Anal.* calcd. for $C_{15}H_{24}O_4$: C 67.14, H 9.01; found: C 67.06, H 8.78.

Can. J. Chem. Downloaded from www.nrcresearchpress.com by 210.87.254.40 on 09/05/12
For personal use only.

Can. J. Chem. Downloaded from www.nrcresearchpress.com by 210.87.254.40 on 09/05/12
For personal use only.

Tricyclic Ketal Alcohol Mesylate 68

Tricyclic ketal diol **67** (77.2 mg, 0.29 mmol) was added to a solution of methane sulfonyl chloride (24.5 μL, 0.32 mmol) and pyridine (56 μL, 0.43 mmol) in dichloromethane maintained at 0°C. After an additional 3 days at 0°C, sodium bicarbonate solution (20%; 15 mL) was added, the mixture was extracted with dichloromethane (3 × 10 mL), and the organic extracts were washed with saturated sodium chloride until the aqueous wash was neutral. The organic phase was dried and evaporated to leave a mixture of starting material and the monomesylate **68**. The mixture was separated by thick layer chromatography on silica gel using ether to give tricyclic ketal diol **67** (33 mg) and tricyclic ketal alcohol mesylate **68** (51 mg, 51%). An analytical sample was not prepared due to the high lability of the product; ir ($CHCl_3$): 3600, 3460, 1365, and 1180 cm^{-1}; nmr ($CDCl_3$) δ: 4.45 (1H, m, H—C2), 4.20 (2H, d, J = 5.75 Hz, CH_2—OSO_2), 3.87 (4H, s, 2 OCH_2), 3.03 (3H, s, —OSO_2—CH_3), 1.34 (3H, s, CH_3—C6), and 1.06 (3H, d, J = 6.5 Hz, CH_3—C10).

Tricyclic Ketal Acetate Mesylate 69

The crude product (**67** and **68**, 166 mg) obtained from the mesylation of tricyclic ketal diol **67** (104 mg, 0.4 mmol) was dissolved in dry pyridine (3 mL) and acetic anhydride (2.5 mL) was added. After 18 h in the dark at room temperature, the solution was cooled to 0°C and methanol (2.5 mL) was carefully added. The solution was left to warm to room temperature before water (20 mL) was added and the mixture was extracted with ether (4 × 15 mL). The organic extracts were washed with brine (4 × 2 mL), dried, and evaporated to leave a mixture of diacetate and acetate mesylate **69**. The mixture was separated by thick layer chromatography on silica gel using ether to give the diacetate (57.5 mg) of **67** and tricyclic ketal acetate mesylate **69** (88 mg, 58% from diol **67**); ir ($CHCl_3$): 1730, 1365, and 1180 cm^{-1}; nmr ($CDCl_3$) δ: 5.39 (1H, m, H—C2), 4.23 (2H, d, J = 5 Hz, CH_2—OSO_2—), 3.88 (4H, s, 2 OCH_2), 3.04 (3H, s, —OSO_2—CH_3), 2.05 (3H, s, $COCH_3$), 1.29 (3H, s, CH_3—C6), and 1.10 (3H, d, J = 6.5 Hz, CH_3—C10).

Equilibration of Dienone Esters 76 and 38

Sodium methoxide (125 mg, 2.3 mmol) was added to dienone ester **38** (478 mg, 2 mmol) in anhydrous methanol (60 mL) and the mixture was left at room temperature for 4 h under an atmosphere of nitrogen. The methanol was evaporated, water (50 mL) was added and the mixture was extracted with ether (4 × 30 mL). The organic extract was washed with water, dried, filtered, and evaporated to yield a mixture (478 mg) of dienone ester **76** and **38** in a 7:3 ratio. Column chromatography with silica gel using benzene–ether (98:2) gave pure dienone ester **76** (175 mg) followed by a mixture of dienone ester **76** and **38**.

Dienone ester 76: mp 68.5–69°C; ir ($CHCl_3$): 1740, 1665, and 1625 cm^{-1}; nmr ($CDCl_3$) δ: 6.05 (1H, d of d, J = 5.5, 2.0 Hz, H—C4), 5.94 (1H, br s, H—C7), 5.60 (1H, d of d, J = 5.5, 2.5 Hz, H—C3), 3.78 (3H, s, OCH_3), 3.70 (1H, m, H—C2), 1.89 (3H, d, J = 1.5 Hz, CH_3—C6), and 0.92 (3H, d of d, J = 6.5 Hz, CH_3—C10); ms m/e: 234 (M^+), 219 ($M^+ - 15$), 202 ($M^+ - 32$), and 175 ($M^+ - 59$). *Anal.* calcd. for $C_{14}H_{18}O_3$: C 71.77, H 7.74; found: C 71.24, H 7.59.

Dienone Esters 38 and 76 from Tricyclic Ketal Conjugated Methyl Ester 58

Tricyclic ketal conjugated methyl ester **58** (35 mg, 0.126 mmol) dissolved in tetrahydrofuran (3 mL) was treated with hydrochloric acid (3 N, 2 mL) at room temperature. After stirring for 18 h, the mixture was poured into water and extracted four times with dichloromethane. The extract was dried and evaporated. The residue was dissolved in ether (4 mL) and treated with an excess of ethereal diazomethane (to esterify the small percentage of carboxylic acid formed). After evaporation, the product was purified by thin layer chromatography to yield a mixture (30 mg, ≈100%) of dienone esters **38** (65%) and **76** (35%). Crystallization of this mixture from ether–hexane gave pure dienone ester **38** (19 mg). Crystallization of the mother liquor (10 mg) with hexane gave pure dienone ester **76** (8 mg).

Diene Alcohol Ester 77

Sodium borohydride (55 mg, 1.45 mmol) was added to a solution of dienone ester **76** (134 mg, 0.57 mmol) in methanol (15 mL), maintained at 0°C by an ice bath. After an additional 4 h at 0°C, the solvent was evaporated and the residue was diluted with water (15 mL). The mixture was extracted with ether (4 × 10 mL). The ethereal extracts were washed with saturated sodium chloride (2 × 3 mL), dried, and evaporated to leave a colorless oil (140 mg). Filtration through a column of silica gel using ether gave the purified diene alcohol ester (135 mg, 100%). An analytical sample was prepared by microdistillation *in vacuo*; ir ($CHCl_3$): 3600, 3450, 1740, 1665, and 1625 cm^{-1}; nmr ($CDCl_3$) δ: 5.90 (1H, d of d, J = 5.5, 2 Hz, H—C4), 5.54 (1H, m, H—C7), 5.47 (1H, d of d, J = 5.5 Hz, H—C3), 4.27 (1H, m, H—C8), 3.75 (3H, s, OCH_3), 3.53 (1H, m, H—C2), 1.64 (3H, m, CH_3—C6), and 0.83 (3H, t, J = 6 Hz, CH_3—C10); ms m/e: 236 (M^+) and 218 ($M^+ - 18$). *Anal.* calcd. for $C_{14}H_{20}O_3$: C 71.16, H 8.53; found: C 70.93, H 8.52.

(±)Hinesol 2

Finely divided lithium metal (300 mg) was added to ethylamine (25 mL). When the metal was completely dissolved, a solution of bicyclic diene alcohol acetate **63** (130 mg, 0.47 mmol) in ether (5 mL) was added. After stirring for 6 h at room temperature, solid ammonium chloride was added until the blue color of the reaction mixture had just disappeared. The ethylamine was evaporated, water (50 mL) was added to the residue. Extraction with ether (4 × 20 mL) followed by drying and evaporation of the organic phase gave the crude product. This material was subjected to a column chromatography with silica gel. Elution with benzene gave a mixture (67 mg) of (±)-hinesol (**2**) and an unidentified product. Elution with ether gave another unidentified product (37 mg).

(±)Hinesol (**2**) was obtained pure (18 mg, 18%) by carrying out a second column chromatography with silica gel using a mixture of benzene and pentane (9:1). (±)Hinesol (**2**) (18 mg, 18%); ir (CCl_4): 3640, 3510, and 1660 cm^{-1}; nmr ($CDCl_3$) δ: 5.33 (1H, m, H—C7), 1.68 (3H, d, J = 1.5 Hz, CH_3—C6), 1.16 (6H, s, $(CH_3)_2C$), and 0.92 (3H, d, J = 6.5 Hz, CH_3—C10); ^{13}C nmr (CCl_4): 139.53 (C6), 121.34 (C7), 70.84 (C13), 51.15 (C2), 36.52 (C9), 35.61 (C1 or C3), 32.82 (C10), 31.78 (C5), 28.66 (C14 and C15), 28.46 (C1 or C3), 27.81 (C8), 27.36 (C4), 23.98 (C11), and 16.12 (C12).

Acknowledgements

We thank Professor J. K. Saunders for the interpretation of the ^{13}C nmr spectra.

Support for this work by the National Research Council of Canada, and by the Ministère de l'Education, Québec, is gratefully acknowledged.

1. K. R. Varma, M. L. Maheshwary, and S. C. Bhattacharyya. Tetrahedron, **21**, 115 (1965).
2. C. H. Heathcock. *In* The total synthesis of natural products. Vol. 2. *Edited by* J. ApSimon. John Wiley & Sons, Inc., New York. 1973. pp. 466–474.
3. J. A. Marshall, St. F. Brady, and N. H. Andersen. *In* Progress in the chemistry of organic natural products. Vol. 31. Springer-Verlag, Wien and New York. 1974. pp. 283–371.

4. E. PIERS and C. K. LAU. Synth. Commun. 7, 495 (1977).
5. W. G. DAUBEN and D. J. HART. J. Am. Chem. Soc. **99**, 7307 (1977).
6. K. YAMADA, S. GOTO, and H. NAGASE. J. Chem. Soc. Chem. Commun. 554 (1977).
7. E. WENKERT, B. L. BUCKWALTER, A. A. CRAVEIRO, E. L. SANCHEZ, and S. S. SATHE. J. Am. Chem. Soc. **100**, 1267 (1978).
8. D. A. CHASS, D. BUDDHASUKH, and P. D. MAGNUS. J. Org. Chem. **43**, 1750 (1978).
9. K. P. SUBRAHAMANIAN and W. REUSCH. Tetrahedron Lett. 3789 (1978).
10. D. T. COXON, K. R. PRICE, J. B. STOTHERS, and A. STOESSL. J. Chem. Soc. Chem. Commun. 348 (1979).
11. T. IBUKA, K. HAYASHI, H. MINAKATA, and Y. INUBUSHI. Tetrahedron Lett. 159 (1979).
12. T. IBUKA, K. HAYASHI, H. MINAKATA, Y. ITO, and Y. INUBUSHI. Can. J. Chem. **57**, 1579 (1979).
13. M. MONGRAIN, J. LAFONTAINE, A. BELANGER, and P. DESLONGCHAMPS. Can. J. Chem. **48**, 3273 (1970).
14. J. A. MARSHALL and P. C. JOHNSON. J. Chem. Soc. Chem. Commun. 391 (1968); J. Org. Chem. **35**, 192 (1970).
15. G. STORK and J. FICINI. J. Am. Chem. Soc. **83**, 4678 (1961).
16. M. M. FAWI and C. D. GUTSCHE. J. Org. Chem. **31**, 1390 (1966).
17. J. M. CONIA. Angew. Chem. Int. Ed. Engl. 7, 570 (1968).
18. E. C. HORNING, M. O. DENEKAS, and R. E. FIELD. *In* Org. Synth. Coll. Vol. 3. John Wiley and Sons, Inc., New York. 1955. p. 317.
19. R. L. MARKEZICH, W. E. WILLY, B. E. MCCARRY, and W. S. JOHNSON. J. Am. Chem. Soc. **95**, 4414 (1973).
20. P. M. MCCURRY, JR. Tetrahedron Lett. 1845 (1971).
21. A. S. HALLSWORTH, H. B. HENBEST, and T. I. WRIGLEY. J. Chem. Soc. 1969 (1957); J. A. MARSHALL and M. T. PIKE. J. Org. Chem. **33**, 435 (1968).
22. D. CAINE and J. B. DAWSON. J. Chem. Soc. Chem. Commun. 1232 (1970); D. CAINE, A. A. BOUCUGNANI, S. T. CHAO, J. B. DAWSON, and P. F. INGWALSON. J. Org. Chem. **41**, 1539 (1976).
23. R. A. BENKESER, J. J. HAZDRA, R. F. LAMBERT, and P. W. RYAN. J. Org. Chem. **24**, 854 (1959).

Can. J. Chem. Downloaded from www.nrcresearchpress.com by 210.87.254.40 on 09/05/12
For personal use only.

Photochemistry of *N*-nitroso-*N*-alkyl amino acids: a facile oxidative decarboxylation

YUAN L. CHOW, DOUGLAS P. HORNING, AND JOËL POLO
Department of Chemistry, Simon Fraser University, Burnaby, B.C., Canada V5A 1S6

Received March 3, 1980

This paper is dedicated to Prof. Raymond U. Lemieux on the occasion of his 60th birthday

YUAN L. CHOW, DOUGLAS P. HORNING, and JOËL POLO. Can. J. Chem. **58**, 2477 (1980).

Several *N*-alkyl or *N*-phenyl-*N*-nitroso α-amino acids were synthesized and were shown to photolytically rearrange to amidoximes with concurrent decarboxylation in solution or solid states without the presence of externally added acids. In contrast, *N*-nitrosonipecotinic acid, a *N*-nitroso β-amino acid, as well as *N*-nitrosopiperidine in the presence of acetic acid were not photolabile. The photolability of *N*-nitroso α-amino acids was ascribed to the presence of an intramolecular association between the nitrosamino and carboxyl groups through hydrogen bonding. The species having the hydrogen bonding through the nitroso oxygen in the *Z*-configuration was believed to be photolabile and decomposed to alkylideneimines as the primary product. The mechanism of the oxidative photorearrangement was discussed.

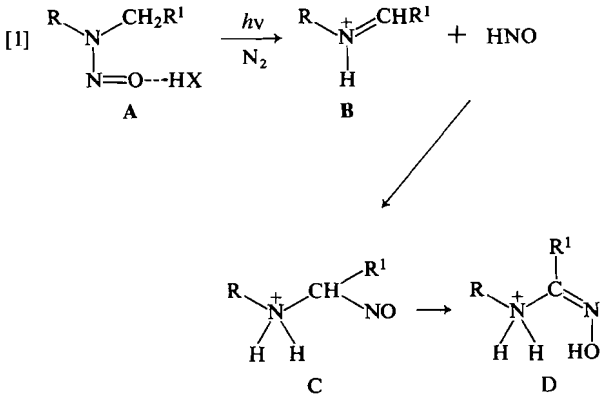
YUAN L. CHOW, DOUGLAS P. HORNING et JOËL POLO. Can. J. Chem. **58**, 2477 (1980).

On a synthétisé plusieurs acides α-aminés *N*-alkyles ou *N*-phényl-*N*-nitrosés et on a montré qu'ils se transposent photochimiquement en amidoximes tout en se décarboxylant et solution ou à l'état solide sans nécessiter d'addition d'acide. A l'opposé, l'acide *N*-nitrosonipécotinique, un acide β-aminé ayant un groupement *N*-nitroso, aussi bien que la nitrosopipéridine ne sont pas photolabiles en présence d'acide acétique. On attribue la photolabilité des *N*-nitroso α-amino acides à une association intramoléculaire entre les groupements nitrosoamino et carbonyle au moyen d'une liaison hydrogène. On croit que les espèces du groupement nitroso dans une configuration *Z* sont photolabiles et se décomposent principalement en alkylidèneimines. On discute du mécanisme de cette transposition photochimique.

[Traduit par le journal]

Introduction

It has been established by us (1, 2) as well as others (3, 4) that the presence of a strong acid is necessary for the efficient photorearrangement of dialkylnitrosamines[1] to give alkylideneimines and/or amidoximes therefrom (eq. [1]). However, we have also observed that an undegassed dilute methanol solution of *N*-nitroso-dimethylamine or -piperidine ($< 10^{-2}$ *M*) can be photodecomposed with reasonable quantum efficiency (0.2–0.4) when irradiated with a quartz filter (9). In apparent contradiction to this it has been reported (10) that dialkylnitrosamines photolytically decompose in *neutral* or *acidic* solutions without much difference in quantum efficiency. In preparative scale (ca. 0.1 *M* solution), it is demonstrated that irradiation of dialkylnitrosamines in neutral solution causes virtually no decomposition within the same or longer time interval required to cause clean photodecomposition in acidic solution. Our explanation of the apparent discrepancy is that in the undegassed solutions "acids" produced on irradiation catalyze the photodecomposition of nitrosamines. The small amounts and low concentrations of nitrosamines may make the quantum efficiency appear relatively high. Indeed, nitrosamines carrying activated α-hydrogen, such as *N*-nitrosodibenzylamine, can be partially photolyzed to afford dibenzylammonium nitrate on preparative scale but *only after prolonged irradiation* (4).

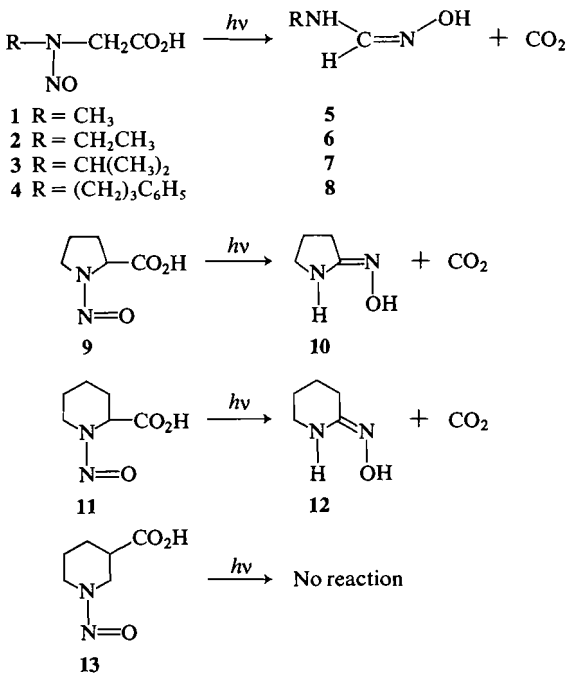
[1] 

Fifteen years ago, we published a brief communication (1) demonstrating the efficient photorearrangement of nitrosamines derived from α-amino acids in neutral solutions. Subsequently, various nitrosamines were shown to be environmental carcinogens widely distributed in food, tobacco smoke, cosmetics and drinks, etc. (11). Furthermore, it was shown these nitrosamines could be formed in the respective locales and even

[1]It must be emphasized that *N*-nitrosamides (5–7) and arylalkylnitrosamines (8) behave very differently in being photolabile in neutral solvents. Dibenzylnitrosamine (4) and *N*-nitrososarcosine methyl ester (9) undergo photolysis very slowly under nitrogen, but somewhat faster under oxygen, indicating that nitric acid is formed and catalyzes the photolysis.

0008-4042/80/232477-07$01.00/0
©1980 National Research Council of Canada/Conseil national de recherches du Canada

in the animal digestive system by *in situ* nitrosation (12). It is imperative that the chemical behavior of these nitrosamines be clarified as a basis for exploring their carcinogenic activity and controlling their formation. In this report we wish to reconfirm the need of acids for efficient photodecomposition of nitrosamines.



Results

As it was established that a strong acid was needed to induce efficient photodecomposition of simple nitrosamines (2, 3), it was thought a nitrosamine bearing a carboxylic acid group in the proximity (e.g., at the α-position) capable of donating the proton to the nitrosamino group might possess an intramolecular hydrogen bonded structure corresponding to that shown in eq. 1 and undergo photodecomposition efficiently. To demonstrate this proposal, *N*-nitrosated *N*-alkyl α-amino acids were chosen as the model compounds and some of these nitroso α-amino acids **1–4**, **9**, **11**, and **16** were synthesized from the corresponding D,L-α-amino acids. Except for nitroso amino acid **4**, other compounds were reported previously (1, 13–15). Nitroso amino acid **3** prepared by us melted 60° higher than reported (14) but was unambiguously characterized by spectroscopic data. The ^1H and ^{13}C nmr data for **1–4**, **9**, **11**, and **13** have been discussed separately with those for other nitroso compounds and their configurations and conformations in solid state as well as in solution (16) deduced. All these nitroso amino acids exhibited ir absorptions for the carbonyl at ca. 1720 cm^{-1} and for the nitrosamino group at ca. 1450 cm^{-1}. They showed typical uv absorptions for the nitrosamino group at ~350 nm (ε ~ 100) and 240 nm (ε ~ 10 000).

N-nitroso-*N*-phenylglycine (16) decomposed at the melting point to give CO_2 and *N*-nitroso-*N*-methylaniline. It was reported that the salts of some nitroso α-amino acids could be pyrolyzed to give the corresponding nitrosamines (16, 17). Pyrolytic decarboxylation of nitroso amino acids themselves to give the corresponding nitrosamines was, however, not a general reaction. Heating of *N*-nitrosopipecolinic acid (**11**) in toluene gave off CO_2 (73%) readily but also deposited much tar in which the presence of an unknown amide and a trace amount of *N*-nitrosopiperidine was noted.

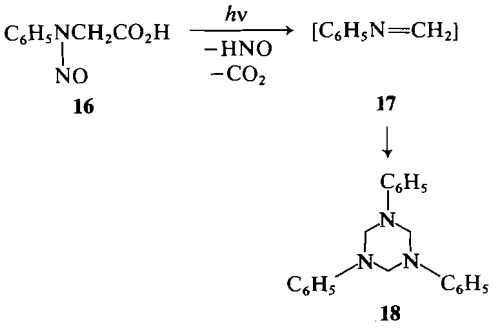
Alcoholic solutions of nitroso α-amino acids **1–4**, **9**, and **11** were smoothly photolyzed under nitrogen to give off CO_2, which may be trapped as barium carbonate, and to cause the disappearance of the $n \rightarrow \pi^*$ band at 350 nm. The uv spectra did not change at all when the solutions were kept in the dark at room temperature. The photolysates were evaporated to give crude products which showed ir and ^1H nmr spectra virtually identical to those of the amidoximes **5–8**, **10**, and **12**. The last two compounds were obtained previously in the photorearrangement of *N*-nitrosopyrrolidine and *N*-nitrosopiperidine (1, 2). Recrystallization of the crude products from benzene or cyclohexane afforded good to excellent yields of the amidoximes. In some cases, a small amount of the parent α-amino acids was present but readily separated by crystallization.

Whereas the *E–Z* isomerism could exist, only one isomer for each of the amidoximes **5–8**, **10**, and **12** was isolated and characterized. In analogy to **10** and **12**, the *Z*-configuration was assigned to formidoximes **5–8**. The assignments were supported by the fact that the chemical shifts of these formamidoxime protons at 7–6.6 ppm were very similar to those of *anti*-aldoxime protons at ca. 6.8 ppm (18). The strong and broad ir absorptions at 3200–2700 cm^{-1} also indicated the presence of intramolecular hydrogen bonding (19) which necessitated the *Z*-configuration. In addition, these compounds exhibited the characteristic C=N stretching mode at ca. 1680 cm^{-1} and the N—O stretching mode at ca. 900 cm^{-1}. Photolysis of nitroso α-amino acids **9** and **11** in ether or in acidic aqueous solution gave, in addition, hygroscopic amorphous solids which possessed very similar ir and ^1H nmr patterns to those of pyrrolidonoxime **2** and piperidonoxime **10**, respectively. The amorphous solid obtained from photolysis of **11** was converted to **10** either on attempted recrystallization by heat-

ing in solution or on treatment with a dilute aqueous hydrochloric acid. The amorphous solid obtained from photolysis of **9** exhibited nmr signals at 3.67(t), 2.83(t), and 2.23(m) and decomposed to a sticky resin on exposure to the air. These two compounds were tentatively assigned as the corresponding *E*-isomers of the amidoximes **10** and **12**, respectively. Although the presence of an acid for the photolysis of **9** and **11** is not essential, the yields of amidoximes **10** and **12** were higher and cleaner when hydrochloric acid or acetic acid was added in the photolysis. However, the rates of the photodecomposition were not affected even in the presence of 0.06 *N* hydrochloric acid or acetic acid. A thin solid film of **9** spread on a glass plate was also decomposed to **10** in a good yield.

Photolysis of a suspension of *N*-nitroso-*N*-(3-phenylpropyl) glycine (**4**) in water under nitrogen was interesting as it exhibited the emergence and subsequent dissipation of the absorptions at 328, 505, 540, and 720 nm, typical of a *C*-nitroso compound, upon irradiation. The formation of a *C*-nitroso intermediate was also indicated by the formation of a blue color which disappeared on prolonged irradiation. However, the product pattern was rather complex giving **8**, *N*-formyl-3-phenylpropylamine (**14**), 3-phenylpropylaminonitrosomethane (**15**), 3-phenylpropylamine, formaldehyde, the starting amino acid, and two more minor components that were not identified. The formamide **14** was identified by direct gc comparison with an authentic sample. Formaldehyde was isolated as the 2,4-dinitrophenylhydrazone from the distillate. The parent α-amino acid and 3-phenylpropylamine were isolated. One of the gc peaks was tentatively assigned to *C*-nitroso compound **15** on the basis of the mass spectra. This compound existed as an equilibrium mixture of the monomer and dimer in the gas chromatographic column showing a broadened gc peak with a shoulder. The ascending side of the peak showed a characteristic mass spectral pattern, very different from that of **8** but ascribable to the monomer of **15**. The tail-end of the peak showed a mass spectral pattern which could be rationalized as that of the dimer of **15** with reasonable fragmentation pathways. These fragmentation mechanisms are discussed in the thesis by one of us (J. Polo, see ref. 9).

Nitroso α-amino acid **16** was photolyzed readily either in ether or alcohol solution to afford excellent yields of hexahydro-*N*,*N*′,*N*″-triphenyl-*s*-triazine **18** which, unfortunately, was readily oxidized to a red oil and polymeric solid during work-up. With some difficulty, **18** was obtained in a pure state and showed a peculiar melting pattern as observed before (2). On storage, **18** deteriorated rapidly to a red tar. The formation of **18** suggested that formylideneaniline **17** must be formed as the intermediate since **18** could also be prepared from aniline and formaldehyde via the intermediacy of **17** (20).



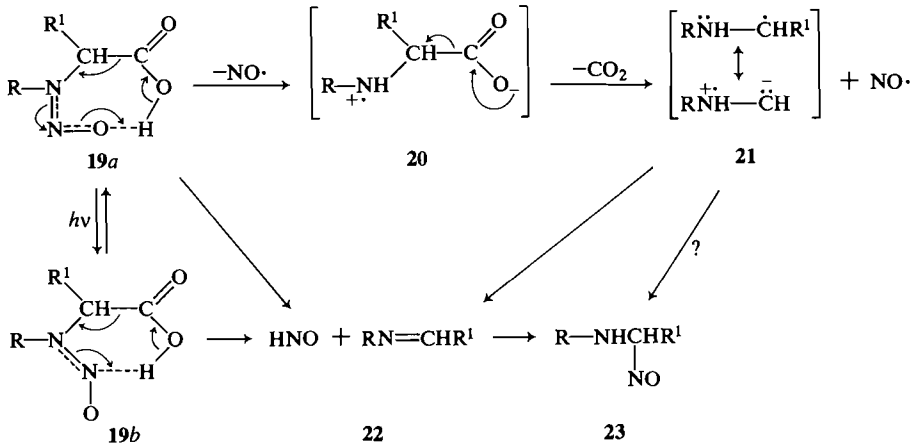
In contrast to the facile photolysis of *N*-nitroso α-amino acids as described above, *N*-nitrosonipecotinic acid (**13**), in ether, alcohol, or aqueous solution did not undergo photodecomposition noticeably even under prolonged irradiation. Nor did *N*-nitrosopiperidine undergo any significant photodecomposition in methanol when one or several equivalents of acetic acid were added.

Photolyses of *N*-nitroso α-amino acid in methanol were also carried out in the presence of cyclohexene or styrene in order to see if aminium radical addition reaction (21) could be observed. In these photolyses only amidoxime **5** and **10** were obtained, but no addition product to the olefins was isolated.

Discussion

In summary, the described results indicate, first of all, that a carboxylic acid located at an α-position of nitrosamines can act as a proton donor causing the nitrosamino group to become photosensitive. The demonstration assumes greater significance in terms of an entropic driving force when compared with the failure of *N*-nitroso β-amino acid **13** as well as *N*-nitrosopiperidine in the presence of acetic acid to undergo photodecomposition. Secondly, the photolysis of *N*-nitroso α-amino acids formally involves elimination of carbon dioxide and HNO to form alkylideneimines such as **17**, as the first step, which may react further to form amidoximes or hexahydro-*s*-triazines. Indeed, this photolysis is an efficient route to prepare amidoximes **5**–**8**, **10**, and **12** that are not readily obtained by other routes. The overall reaction pattern bears striking similarity to that of the acidic photolysis of dialkylnitrosamines (21). Mechanistically, the two types of photolyses may also share much similarity.

Owing to steric proximity to the nitrosamino group, the α-carboxyl group is more acidic (e.g., pK_a 3.2 for **1**). In our preliminary communication

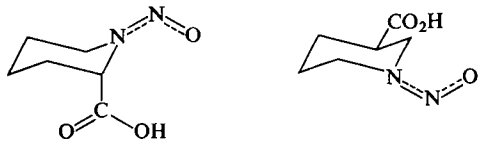


19a 20 21

19b 22 23

(1), it was proposed that these *N*-nitroso α-amino acids should be able to have an intramolecular association in the ground state through hydrogen bonding as depicted in **19***a* (*Z*-configuration) or **19***b* (*E*-configuration); these were assumed to be photolabile species. As nitrosamines are known to carry a high concentration of electron density at the oxygen atom and are alkylated with a carbonium ion at this position (22), **19***a* is favored as the photolabile species. In the *E*-configuration **19***b*, a hydrogen bonding with the lone pair electrons of the nitroso nitrogen is possible but, probably, less strong in view of the sp^2 orbital involved. Indeed, in the solid state, all these nitroso α-amino acids are known to have the *Z*-conformation **19***a* which is maintained in solution in the cases of **3** and **16** as demonstrated by ^1H and ^{13}C nmr spectroscopy (13, 16). However, **1**, **2**, **4**, **9**, and **11** isomerize slowly in solution to *Z*–*E* mixtures (13, 16). It has been shown that nitrosamines can undergo light induced *Z*–*E* isomerization in solution (23). As this isomerization is expected to occur concurrently during photoexcitation of nitroso α-amino acids, it is difficult to determine whether **19***a* or **19***b* is responsible for photoelimination. Since, qualitatively, **3** is much more efficiently photodecomposed than **1**, **2**, and **4**, it is apparently reasonable to assume that the *Z*-configuration **19***a* with the hydrogen bonding at the nitroso oxygen is responsible for the photolability in so far as these nitroso α-amino acids are concerned.

Such considerations based on ground state configuration become rather uncertain when the axial conformation of the carboxyl group (13) in **9** is taken into account to estimate the probability of the intramolecular hydrogen bonding (see **9***a*). According to Dreiding models, if a coplanar C_2C_6N—NO portion is assumed, the O---ON distance appears to be too far apart (>4 Å) to be in an effective hydrogen bonding distance. This suggests that the intramolecular association of the nitroso and carboxyl groups is far weaker than the acyclic cases discussed above. This situation is reflected in much slower photolysis of **9** than those of acyclic nitroso α-amino acids **1**–**4** when they are irradiated



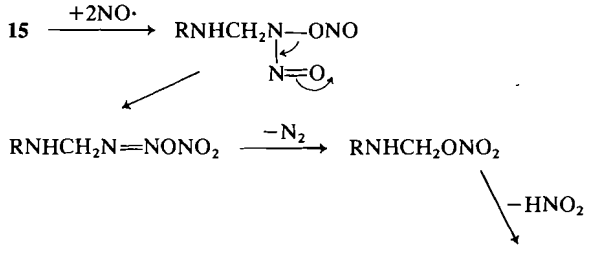
9*a* **13***a*

in a preparative scale in methanol solutions under comparable conditions. Most probably, conformational changes upon excitation bring the nearby groups in closer proximity to allow facile proton transfer which triggers the photodecomposition.

Regardless of *Z* or *E* configuration, such an intramolecular association with the strategically located acid group is undoubtedly necessary in rendering the nitrosamino group photolabile as indicated by certain evidence. Firstly, it is improbable, if not impossible, for **13** to assume a hydrogen bonded structure (see **13***a*); accordingly, **13** is not photolabile, as observed. Secondly, for efficient photolysis of *N*-nitrosopiperidine, the presence of a strong acid, such as hydrochloric, sulfuric, perchloric acid, etc., is required, but the presence of acetic acid shows no effects. Thirdly, the failure of externally added hydrochloric acid to influence the rates of photolysis of *N*-nitroso α-amino acids **1** and **9** indicated that the intramolecular proton donation dominates the catalytic process.

The intermediacy of alkylideneimine **22** and *C*-nitroso compound **3**, in analogy to acidic photolysis of nitrosamine, is clearly indicated by the formation of **18** (the trimer of **17**) from **16** and the formations of 3-phenylpropylamine, formalde-

hyde, and C-nitroso compound **16** from **4**. Under such mild conditions, formamide **14** is not likely derived from hydrolysis of **18** but more likely formed by photoinduced disproportionation of *C*-nitroso compound **15**, followed by the elimination as shown below. The formation of nitrates in photolysis of *C*-nitroso compounds has been well established (24). However, it is not well understood why **15** tautomerizes much more slowly in water than in methanol. It is probable that **15** is less soluble in water and preferentially stabilized by dimerization.



Mechanistically, the photoinduced elimination of carbon dioxide and HNO may be explained by the aminium radical route **20** → **21** → **22**, as aminium radicals are known to be the primary radical species in acidic photolysis of nitrosamines (25). Alternatively, a concerted elimination as shown in **19** may also look attractive. Such a process is indistinguishable from the above route since **20** could eliminate carbon dioxide rapidly to give resonance stabilized (26) α-amino radical **21**. Although attempts to trap the aminium radical **20** with cyclohexene or styrene have not been successful, this type of radical has been proposed as an intermediate in photosensitized decarboxylation of *N*-phenylglycines (27). It is also possible to write recombination of radical **21** with nitric oxide to give **23** directly. In view of good indications of the formation of **22**, such a process appears less likely.

Experimental

Unless specified otherwise the following general conditions were used. Infrared spectra (ir) were taken with a Perkin-Elmer Model 457 as liquid films or Nujol mulls. Ultraviolet spectra (uv) were recorded on a Unicam SP 800 or a Cary 17 spectrophotometer. Nuclear magnetic resonance spectra (nmr) were recorded on a Varian A56/60 or a Varian XL-100 spectrophotometer equipped with a Nicolet 1080 computer using TMS as internal standard. Melting points were measured on a Fisher-Johns hot stage and were not corrected. Elemental analyses were performed by Mr. M. K. Yang with a Perkin-Elmer 240 microanalyzer.

Preparation of N-*Nitroso* α-*Amino Acids.*

Commercially available proline, pipecolinic acid, sarcosine, and *N*-phenylglycine were recrystallized as the starting material. *N*-ethyl-, *N*-isopropyl-, and *N*-(3-phenylpropyl)glycine were prepared according to the reported procedure (14). These α-amino acids were nitrosated with sodium nitrite in aqueous solution containing hydrochloric acid to afford the nitroso compounds **1**–**4**, **9**, **11**, and **16**. The physical properties of most of these compounds were already reported in the literature (1, 13, 16).

N-Nitrososarcosine (**1**) was recrystallized from ethyl acetate: mp 69–70°C (13); ir: 1730 and 1440 cm^{-1}. The nmr spectrum recorded immediately after dissolution in $CDCl_3$ gave the two sets of singlets at 4.28–3.90 ppm and 4.98–3.13 ppm with the intensity ratio of 9:1. The ratios changed gradually to 1:1 after standing at room temperature in the dark.

N-Nitroso-*N*-ethylglycine (**2**) was obtained as yellow crystals: mp 83–85°C; ir: 3100–2600, 1730(s), 1460(s), 1305(s), 1210(s), 1110(s), and 700(s) cm^{-1}.

N-Nitroso-*N*-isopropylglycine (**3**) was recrystallized from water: mp 137–138°C (lit. (14) mp 76–78°C); ir: 3000–2600, 1730(s), 1240(s), 1070(m), 890(m), 690(m), and 650(s) cm^{-1}. *Anal.* calcd. for $C_5H_{10}N_2O_3$: C 41.09, H 6.90, N 19.17; found: C 41.22, H 6.85, N 19.22.

N-Nitroso-*N*-(3-phenylpropyl)glycine (**4**) was recrystallized from water: mp 106–108°C; ir: 3100–2840, 1730(s), 1450(m), 1310(s), 1285(s), 1210(s), 740(m), and 700(s) cm^{-1}. *Anal.* calcd. for $C_{11}H_{14}N_2O_3$: C 59.45, H 6.35, N 12.60; found: C 59.43, H 6.47, N 12.86.

N-Nitrosoproline (**9**): mp 104–106°C; ir: 3000–2500, 1720(s), 1370(s), 1200(m), 720(s), and 680(s) cm^{-1} (1).

N-Nitrosopipecolinic acid (**11**); mp 93–95°C; ir: 3200–2500, 1720(s), 1465(s), 1405(1), 1330(s), 1248(s), 1190(s), 1015(s), 930(s), and 740(s) cm^{-1} (1).

N-Nitroso-*N*-phenylglycine (**16**); mp 98–100°C (dec.) (15); ir: 3200–2600, 1720(s), 1590(m), 1495(m), 1295(s), 1262(m), 1150(s), and 962(s) cm^{-1}; ^1H nmr: 10.2, 7.20, and 4.75(s) ppm; ^{13}C nmr: 39.6, 120.1, 127.1, 129.6, 141, and 167.2 ppm. Nitroso compound **14** decomposed at the melting point to give an oil which was distilled to afford *N*-nitroso-*N*-methylaniline.

N-Nitrosonipecotinic acid (**13**) was recrystallized from ether: mp 110–112°C; ir: 3000–2500, 1700(s), 1462(s), 1348(s), 1290(s), 1170(s), 1000(m), 935(m), 865(m), and 660(s) cm^{-1}. The nmr spectrum of **13** showed complex signals in the 5.3–7.0 region obviously due to the *Z*–*E* isomers.

Photolysis of N-*Nitroso* α-*Amino Acids in Alcohol*

A solution of *N*-nitroso α-amino acid (~0.01 mol) in methanol or ethanol (120–150 mL) was purged with nitrogen and irradiated with a 200 W Hanovia medium pressure mercury lamp at the cooling water temperature. The uv absorption of the nitroso compound at ca. 350 nm decreased gradually as the irradiation progressed and disappeared completely in one to two hours. A small sample of the original solution kept in the dark at room temperature showed no decrease in the uv absorption. The photolysate was evaporated to afford a solid which showed virtually the same ir and nmr spectra as those of the corresponding amidoximes. A hot solution of this solid was filtered to give a small amount of α-amino acid. The filtrate was cooled to give crystalline amidoximes. Their physical properties are given below.

N-Methylformamidoxime (**5**, 572 mg, 72%) was obtained from benzene recrystallization as white plates: mp 134–135°C; ir: 3400(m), 3100–2900(b, m), 1680(m), 1320(m), 1290(m), 920(m), 900(m), and 750(m) cm^{-1}; ^1H nmr (D_2O): 7.00(s, 1H) and 2.88(s, 3H) ppm; ms *m/e* (%): 74.0486 (M^+, 69, calcd. for $C_2H_6N_2O$: 74.0480), 57(57), 42(54), 30(100), and 28(84). Sublimation at room temperature and at 1.5 Torr yielded an analytical sample. *Anal.* calcd. for $C_2H_6N_2O$: C 32.43, H 8.16, N 37.81; found: C 32.58, H 8.21, N 37.59.

N-Ethylformamidoxime (**6**) was recrystallized from benzene

as white crystals (449 mg, 69%): mp 81–83°C; ir: 3360(m), 3200(m, b), 2800(b, s), 1680(s), 1490(m), 1260(m), 1160(m), 940(s), 890(s), 750(m), and 730(m) cm^{-1}; ^1H nmr: 6.70(s,1H), 3.11(q, J = 7Hz, 2H), 2.10 (s, D_2O exch.), and 1.17 (6, J = 7 Hz, 3H) ppm; ms m/e (%): 88.0639 (M^+, 93, calcd. for $C_3H_8N_2O$: 88.0630), 73(67), 71(42), 55(58), 44(100), 43(62), 42(38) and 30(67). *Anal.* calcd. for $C_3H_8N_2O$: C 40.90, H 9.15, N 31.79; found: C 40.97, H 9.03, N 31.52.

N-Isopropylformamidoxime (**7**) was sublimed as white crystals (540 mg, 76%): mp 46–48°C; ir: 3380(m), 3250(b, m), 1675(s), 1380(d, m), 1340(m), 1270(m), 900(m), and 855(m) cm^{-1}; ^1H nmr (D_2O): 7.07 (s, 1H), 3.52 (sp, J = 7 Hz, 1H), and 2.20 (d, J = 7 Hz, 6H) ppm; ms m/e (%): 102.0799 (M^+, 36, calcd. for $C_4H_{10}N_2O$: 102.0793), 87(47.1), 71(15.5), 69(33), 60(32), 58(23), 44(100), 43(94), 42(69), 41(66), and 39(25). *Anal.* calcd. for $C_4H_{10}N_2O$: C 47.04, H 9.87, N 27.43; found: C 46.77, H 9.66, N 27.25.

N-(3-Phenylpropyl)formamidoxime (**8**) was recrystallized from cyclohexane as white plates (1.02 g, 82%): mp 100–101°C; ir: 3350(m), 3050(m), 2750(b, m), 1680(s), 1490(m), 1450(m), 1330(m), 1240(m), 900(s), 770(s), 740(s), and 690(s) cm^{-1}; ^1H nmr: 7.90 (bs, D_2O exch., 1H), 7.16 (m, 5H), 6.60 (bd, J = 6 Hz, changes to a sharp singlet after D_2O addition, 1H), 5.00 (bs, D_2O exch., 1H), 3.06 (bt, J = 8 Hz, changes to a sharp triplet after D_2O addition, 1H), 2.66 (t, J = 8 Hz, 2H), and 1.80 (qi, J = 8 Hz, 2H) ppm; ^{13}C nmr δ: 145.5(d), 142.0(s), 128.4(d), 125.9(d), 44.5(t), 33.7(t), and 32.8(t); ms m/e (%): 178.1125 (M^+, 18, calcd. for $C_{10}H_{14}N_2O$: 178.1125), 146(100), 117(60), 91(71), 73(60), and 57(58). *Anal.* calcd. for $C_{10}H_{14}N_2O$: C 67.39, H 7.92, N 15.72; found: C 67.48, H 7.96, N 15.80.

Photolysis of **4** *in Water*

A suspension of nitroso compound **4** (820 mg, 3.7 mmol) in water (230 mL) was photolyzed at room temperature under nitrogen for 4 h. On irradiation, the solution developed a violet-blue color and new absorptions at 328, 505, 540, and 725 nm which reached the maximum intensities after 30 min and faded away gradually to give a clear light brown solution at the end of the photolysis. The solution was concentrated under atmospheric pressure to about 40 mL. The distillate, on treatment with an ethanolic 2,4-dinitrophenylhydrazine solution, gave an orange precipitate of the 2,4-DNPH of formaldehyde, mp and mixture mp 164–166°C (from ethanol–water). The concentrated photolysate (pH = 6–7) was extracted with CH_2Cl_2 (3 × 20 mL) to give, after drying ($MgSO_4$) and evaporation, a brown semi-solid (346 mg). This crude mixture was triturated with hot cyclohexane to give a solution which on cooling afforded **8** (30 mg, 5%) as light brown plates; mp 91–94°C. The insoluble part was taken up in CH_2Cl_2 (20 mL) and washed several times with diluted HCl solution (0.5 *N*). The organic phase was further washed with water, dried ($MgSO_4$), and evaporated to yield a brown oil (280 mg); ir: 3200 (b, m), 1700(s), 1600(m), 1500(m), 1450(s), 1350(s), 1130(m), 750(m), and 700(s) cm^{-1}. This oil was analyzed by gc–ms (10% SE-30, 150°C to 250°C at 10°C/min) to give two major and two minor peaks: rt 2.5 min, **15**, 10%; rt 2.7 min, unknown, 5%; rt 3.6 min, unknown, 5%; rt 6.1 min, **14**, 23%. The peak at rt 2.5 min was shown to be composed of two components showing a shoulder on the decreasing side. The ascending side of the peak showed the mass peaks at m/e (%): 161(38), 148(57), 120(37), 118(17), 117(19), 105(50), 91(60), 74(100), and 42(30); the tail-end of the peak showed those at m/e (%): 251(13), 160(14), 147(29), 146(86), 117(40), 91(100), 71(13), and 56(81). The peak at rt 6.1 min was identified as *N*-formyl-3-phenylpropylamine **14** by the peak matching with an authentic sample and mass spectral pattern: 163 (M^+, 34), 118(62), 117(52), 105(18), 91(47), 77(15), and 59(100).

The aqueous photolysate was acidified to pH = 2–3 and extracted with ether (2 × 30 mL) to give, after drying ($MgSO_4$) and evaporation, unreacted *N*-3-(phenylpropyl)glycine (65 mg, 8%); mp 103–105°C. The water phase was then basified with 10% NaOH solution to pH = 10 and extracted with ether (3 × 20 mL) to give 3-phenylpropylamine (62 mg, 12%), as a yellow oil.

Formylation of 3-phenylpropylamine with chloral in $CHCl_3$ according to the procedure of Blicke and Lu (28) gave formamide **14** (70%) which was purified by distillation (bp 140°C/1 Torr); ir: 3280(m), 1655(s), 1520(m), 1490(m), 1450(m), 1380(m), 740(m), and 690(s) cm^{-1}; ms m/e (%): 163 (M^+, 7), 146(100), 117(31), 91(87), 65(18), and 59(25).

Photolysis of N-*Nitrosoproline* **9**

In Ether

On irradiation of an ether solution (200 mL) of **9** (535 mg, 3.7 mmol) at room temperature, under nitrogen, it gradually turned cloudy and an amorphous resin deposited on the wall of the photocell. After 75 min the absorptions at 381 and 368 nm disappeared completely. Concentration of the ether solution gave 2-pyrrolidonoxime **10** (185 mg, 50%) as white crystals; mp 150–152°C (from water); mixed with an authentic sample 156–158°C (2). The mother liquor was evaporated to give a resin which was taken up in hot benzene to give, on cooling, another crop of **10** (65 mg, 18%). The filtrate was evaporated to yield an amorphous solid which turned to a sticky resin on exposure to air. This solid was not soluble in acetone.

In Water and in the Presence of Hydrochloric Acid

Nitroso compound **9** (1.5 g, 0.01 mol) was photolyzed in water (200 mL) containing hydrochloric acid (7 mL, 2.8 *N*), at room temperature, under nitrogen. After 4 h of irradiation, the absorption band at 350 nm disappeared completely. The photolysate was filtered through a basic Dowex 3 (50 mL) column and the resulting filtrate (pH ≈ 5–6) was evaporated to dryness to give a yellowish oil. The residue was treated with hot isopropyl alcohol (25 mL) to leave a hygroscopic residue (350 mg); ^1H nmr δ: 3.67(t), 2.83(t), and 2.23(m). Cooling of the filtrate gave 2-pyrrolidonoxime hydrochloride (600 mg, 42%) as white crystals; mp 197–200°C (from isopropyl alcohol); ir: 2500–3200(b), 1690(s), 1555(w), 1310(m), 1060(s), and 990(s) cm^{-1}; ^1H nmr (D_2O) δ: 3.73 (t, J = 7 Hz, 2H), 2.9 (t, J = 7 Hz, 2H), and 2.27 (m, 2H). *Anal.* calcd. for $C_4H_8N_2O \cdot HCl$: C 35.17, H 6.64, N 20.51; found: C 35.58, H 6.85, N 20.07. Further evaporation of the mother liquor gave another crop of the hydrochloride of **10** (520 mg, 36%).

Photolysis of N-*Nitrosopipecolinic Acid* **11**

In Ether

An ether solution (200 mL) containing **11** (600 mg, 3.8 mmol) was photolyzed at room temperature, under nitrogen for 2 h until over 90% of the absorption at 350 nm had disappeared. The fluffy precipitate formed during the photolysis was filtered and turned to a resin upon exposure to air; ir: 3400–2500 (b, m), 1600–1650(s), and 1130(s) cm^{-1}. The ether solution was concentrated under vacuum and after cooling gave 2-piperidonoxime 12 (300 mg, 76%) as white crystals; mp 114–116°C (from benzene – petroleum ether); mixture mp with an authentic sample 114–116°C; ir and nmr spectra were identical to those of the authentic sample (2). The mother liquor was evaporated to dryness to give an amorphous solid with a strong pungent smell and whose ir spectrum was similar to that of **12**.

In Water and in the Presence of Hydrochloric Acid

A solution of **11** (1.82 g, 11.5 mmol) in water (200 mL) containing hydrochloric acid (2.85 *N*, 4.2 mL) was photolyzed for 9 h. The water phase was evaporated to dryness to give a yellowish residue which was taken up in ethanol. Addition of benzene gave hydrochloride of **12** (640 mg, 37%) as a white precipitate; mp 210–215°C; ir: 3150(m), 1665(s), and 1510(s) cm^{-1},

superimposable with that of an authentic sample of **12** hydrochloride (2). Further addition of petroleum ether gave an amorphous solid whose ir spectrum was similar to that of hydrochloride of **12**. Treatment of the amorphous solid with 1 *N* HCl and extraction with CH_2Cl_2 gave the hydrochloride of **12** (285 mg, 17%).

In another experiment, a solution of **11** (1.57 g, 10 mmol) in water (250 mL) and acetic acid (1.3 g, 20 mmol) was photolyzed for 4 h. Hydrochloric acid (2 *N*, 5 mL) was added to the photolysate and the resulting solution was boiled for 5 min. Usual work-up of the solution gave hydrochloride of **12** (560 mg, 37%) but no amorphous material. The mother liquor was dissolved in water, neutralized with Na_2CO_3, and extracted with ether to give **12** (530 mg, 46%).

In the Solid State

An ether solution of **9** (100 mg) was spread on a glass plate (20 × 20 cm) and the ether evaporated to give a thin film. This plate was irradiated through a Pyrex filter at room temperature for 4 h. The plate was washed with methanol and the solution evaporated. The residue was recrystallized from cyclohexane to give **10** (55 mg) and a small amount of pipecolinic acid.

Photolysis of N-*Nitroso*-N-*phenylglycine* **16**

A methanol solution (200 mL) of **16** (1.0 g) was photolyzed under nitrogen for 3 h until the absorption at 370 nm disappeared. The solvent was evaporated during which the solution became darker colored. The residue was taken up in ether and filtered. The ether solution was diluted with petroleum ether and cooled to give white crystals and some red oil. After filtration the crystals were washed with methanol to afford hexahydro-*N*,*N'*,*N''*-triphenyl-*s*-triazine **18** as white crystals which melted at 130–133°C but resolidified at 138°C and remelted again at 190–195°C (20); ir: 3100, 3060, 3040, 1595, 1575, 1500, 1228, 755, and 695 cm^{-1}; uv (EtOH): 280 nm (ε, 1770); ^1H nmr δ: 7.20 (m, 5H) and 4.94 (s, 2H). *Anal.* calcd. for $C_{21}H_{21}N_3$: C 80.10, H 6.67, N 13.33; found: C 80.49, H 6.54, N 13.38.

A solution of **18** rapidly gained color during heating or standing at room temperature. Concentration of the solution always gave red oil, the crystals, and some amorphous solid. On storage, crystalline **18** decomposed to a red oil in several days. Photolysis of **16** in ether, ethanol, or water gave similar results.

Comparative Photolysis of N-*Nitroso* α-*Amino Acids*

Solutions of **1** in methanol, and in methanol containing 0.06 *N* hydrochloric acid and acetic acid, were prepared. These solutions were photolyzed in a merry-go-round machine for 10 and 20 min without actinometry. The decrease of the 350 nm peaks was about the same for 3 solutions in each case. The same experiments were run with **11** to give similar results.

Methanol solutions (100 mL) containing nitroso α-amino acid **1**, **2**, **3**, and **11** (5×10^{-2} *M*) were irradiated in the same small scale apparatus with the same lamp. The reaction was followed by uv spectroscopy up to 65% completion for which **1**, **2**, and **3** required 1.1–1.3 h and **11** 2.5 h.

Acknowledgements

A substantial part of this work was carried out in the University of Alberta, Edmonton in 1964–1965. I (Y.L.C.) wish to express my thanks to my colleagues in that institute, for their hospitality. The authors also wish to thank the Natural Sciences and Engineering Research Council of Canada, Ottawa, for generous support of the project over the years.

1. Y. L. Chow. Tetrahedron Lett. 2333 (1964); 2473 (1965).
2. Y. L. Chow. Can. J. Chem. **45**, 53 (1967).
3. E. M. Burgess and J. M. Lavanish. Tetrahedron Lett. 1227 (1964).
4. T. Axenrod and G. N. A. Milne. Tetrahedron, **24**, 5775 (1968).
5. O. E. Edwards and R. S. Rosich. Can. J. Chem. **45**, 1287 (1967).
6. L. P. Kuhn, G. G. Kleinspehn, and A. C. Duckworth. J. Am. Chem. Soc. **89**, 3858 (1967).
7. Y. L. Chow and A. C. H. Lee. Chem. Ind. 827 (1967); Y. L. Chow, N. S. Tam, and A. C. H. Lee. Can. J. Chem. **47**, 2441 (1969).
8. M. Hoshino, H. Kokubun, and M. Koizumi. Bull. Chem. Soc. Jpn. **43**, 2796 (1970).
9. Y. L. Chow and D. P. Horning. Unpublished results; J. Polo. Ph.D. thesis, Simon Fraser University, Burnaby, B.C. 1979.
10. B. G. Gowenlock, J. Pfab, and G. C. Williams. J. Chem. Res. (s), 362 (1978).
11. E. A. Walker, M. Castegnaro, L. Griciute, and R. E. Lyle. Environmental aspects of *N*-nitroso compounds. I.A.R.C. Publication No. 19, International Agency for Research on Cancer. Lyon. 1978.
12. P. N. Magee, R. Montesano, and R. Preussman. Chemical carcinogens. *Edited by* E. C. Searle. American Chemical Society, Washington, DC. 1976. p. 491.
13. W. Lijinsky, L. Keefer, and J. Loo. Tetrahedron, **26**, 5137 (1970).
14. C. V. Greco, W. H. Nyberg, and C. C. Cheng. J. Chem. Pharm. Med. **5**, 861 (1962).
15. O. Fischer. Chem. Ber. **32**, 249 (1899).
16. Y. L. Chow and J. Polo. Org. Magn. Reson. **13**, 000 (1980). Submitted.
17. M. Nakajima and J. P. Anseline. Tetrahedron Lett. 4037 (1979).
18. E. Lustig. J. Phys. Chem. **65**, 491 (1961).
19. A. Palm and H. Herbin. Can. J. Chem. **32**, 858 (1954).
20. C. A. Bishoffe. Chem. Ber. **31**, 3250 (1898).
21. Y. L. Chow. Acc. Chem. Res. **7**, 354 (1973).
22. A. Schmidpeter. Tetrahedron Lett. 1421 (1963); S. Hünig, L. Geldern, and E. Lücke. Angew. Chem. **75**, 476 (1963).
23. C. J. Michejda, N. E. Davidson, and L. K. Keefer. J. Chem. Soc. Chem. Commun. 633 (1976).
24. Y. L. Chow, J. N. S. Tan, and K. S. Pillay. Can. J. Chem. **51**, 2477 (1973).
25. A. J. Cessna, S. E. Sugamori, R. W. Yip, M. P. Lau, R. S. Snyder, and Y. L. Chow. J. Am. Chem. Soc. **99**, 4044 (1977).
26. D. E. Wood and R. V. Lloyd. J. Chem. Phys. **52**, 3840 (1970).
27. R. S. Davidson, K. Harrison, and P. R. Steiner. J. Chem. Soc. C, 1682 (1971); 3480 (1971).
28. F. F. Blicke and C. J. Lu. J. Am. Chem. Soc. **74**, 3833 (1952).

Regioselectivity of metal hydride reductions of unsymmetrically substituted cyclic anhydrides. Systems where "steric hindrance along the preferred reaction path" rationalization is not applicable

MARGARET M. KAYSER AND PETER MORAND

Department of Chemistry, University of Ottawa, Ottawa, Ont., Canada K1N 9B4

Received February 11, 1980

This paper is dedicated to Prof. Raymond U. Lemieux on the occasion of his 60th birthday

MARGARET M. KAYSER and PETER MORAND. Can. J. Chem. **58**, 2484 (1980).

Metal hydride reductions of planar cyclic anhydrides such as methylmaleic or 3-substituted phthalic anhydrides occur preferentially at the sterically more hindered carbonyl function. This regioselectivity cannot be rationalized in terms of "the most favourable pathway for non-perpendicular attack by a nucleophile" since both carbonyl groups present are equally accessible to non-perpendicular approach. A study which takes into account the alkaline cation and inductive, mesomeric, and steric effects has been conducted for the reduction of several conjugated and aromatic anhydrides. A qualitative interpretation for the regioselectivities observed in these reductions (as well as in reductions already reported in the literature) is suggested. An early transition state for the catalyzed versus late transition state for the non-catalyzed process is proposed.

MARGARET M. KAYSER et PETER MORAND. Can. J. Chem. **58**, 2484 (1980).

Les réductions d'aldéhydes cycliques plans, tels l'anhydride maléique et l'anhydride phtalique substitué en position 3, au moyen d'hydrures métalliques se produisent préférentiellement au niveau de la fonction carbonyle la plus stériquement encombrée. On ne peut pas rationaliser cette régiosélectivité en fonction de la voie la plus favorable à une attaque non perpendiculaire du nucléophile puisque les deux groupes carbonyles présents sont également accessibles à une approche non perpendiculaire. On a réalisé une étude qui tient compte du cation alcalin et des effets inductifs, mésomériques et stériques lors de la réduction de plusieurs anhydrides conjugués et aromatiques. On suggère une interprétation qualitative de la régiosélectivité observée au cours de ces réductions (aussi bien qu'au cours des réductions déjà mentionnées dans la littérature). On propose un état de transition au début de la réaction catalysée par rapport à un état de transition apparaissant à la fin de la réaction non catalysée.

[Traduit par le journal]

Introduction

It has been demonstrated that unsymmetrically substituted cyclic anhydrides (1) and imides (2) are often reduced by metal hydrides preferentially or specifically at the sterically more hindered carbonyl group. Such regioselectivity has been rationalized in terms of the most favourable pathway for non-perpendicular attack (see Fig. 1) by a nucleophile on the carbonyl function (1,3,4). This rationalization, although very useful in explaining the selectivity of reduction in many unsymmetrical cyclic anhydrides and imides, is nonetheless only *one* of the factors contributing to the regioselectivity observed in these reactions (1,3).

Planar cyclic anhydrides (e.g. methylmaleic anhydride **1** or 3-nitrophthalic anhydride **9**) represent compounds in which the type of steric interactions discussed above is not operative, yet in most cases these anhydrides, also, are reduced preferentially at the more hindered carbonyl group (Table 1).

Metal Hydride Reductions of Substituted Maleic Anhydrides

Methylmaleic anhydride **1**, chloromaleic anhydride **2**, and phenylmaleic anhydride **3** are reduced with a high degree of selectivity at the carbonyl group adjacent to the substituent (Table 1). Methoxy substituted anhydrides **4** and **5** react preferentially at the carbonyl function adjoining the methoxy group. The regioselectivity of these reductions cannot be justified in terms of steric hindrance to non-perpendicular nucleophilic attack since the preferred reaction path leading to either carbonyl function is equally accessible.

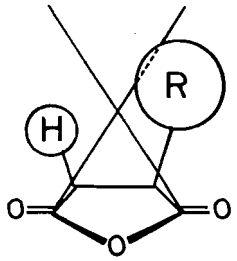


FIG. 1. At a distance of approximately 2 Å, approach to the carbonyl function next to the more highly substituted carbon atom is effectively "less hindered" than approach to the carbonyl group adjoining the unsubstituted carbon atom.

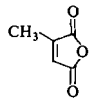
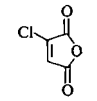
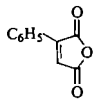
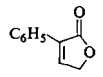
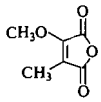
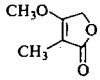
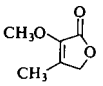
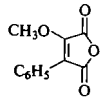
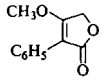
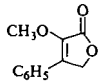
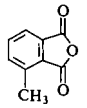
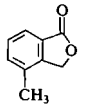
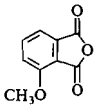
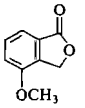
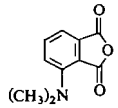
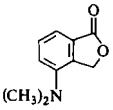
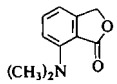
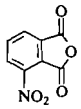
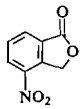
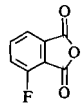
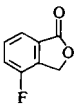
We would like to mention briefly explanations that have been offered to rationalize the above results. Knight and Pattenden (5) proposed two

0008-4042/80/232484-07$01.00/0

© 1980 National Research Council of Canada/Conseil national de recherches du Canada

Can. J. Chem. Downloaded from www.nrcresearchpress.com by 210.87.254.42 on 09/05/12
For personal use only.

TABLE 1. Metal hydride reductions of planar, cyclic anhydrides

Anhydride	No.	Lactonic products (*a*)	Lactonic products (*b*)	% Yield of lactonic product	Ratio (*a*) : (*b*)	Reference
	**1**			82–87[a] 80[b] 50	90 : 10[a] 85 : 15[b] 88 : 12	1 1 5
	**2**			30[a] 35[b]	90 : 10[a] 87 : 13[b]	
	**3**			50[a] 30[b]	75 : 25 67 : 33	
	**4**			70[e]	100 : —	5
	**5**			65[e]	100 : —	5
	**6**			77[d]	57 : 43[d]	11
	**7**			52[d]	87 : 13[d]	11
	**8**			45[d]	80 : 20[d]	11
	**9**			80[a] 75[b] 81[d]	67 : 33[a] 83 : 17[b] 100 : —[d]	1 11
	**10**			32[b] 49[c]	70 : 30[b] 84 : 16[c]	

[a]$LiAlH_4$ reduction.
[b]$NaBH_4$ reduction, general procedure (*b*).
[c]$NaBH_4$ reduction, general procedure (*c*).
[d]$NaBH_4$ reduction, no HCl or LiCl added (10).
[e]Total of lactone and hemiacylal.

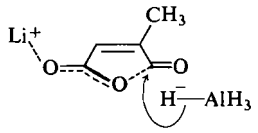
mechanisms, one suggesting initial complexation of the cation with the less-hindered carbonyl oxygen, followed by transfer of hydride to the more hindered carbonyl function **11** (6), and the other invoking an intermediate oxonium ion and an intramolecular four-centre mechanism **12** (5). These mechanisms do not take into account the catalytic activity of the counterion (1, 7, 8) and lack generality

Can. J. Chem. Downloaded from www.nrcresearchpress.com by 210.87.254.42 on 09/05/12
For personal use only.

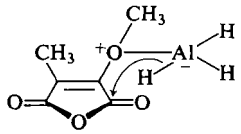
Can. J. Chem. Downloaded from www.nrcresearchpress.com by 210.87.254.42 on 09/05/12
For personal use only.

(since they can only be used to rationalize a specific case).

An alternate argument suggesting that the steric interactions between the substituent and the carbonyl group in **1** and **2** are relieved when the reaction proceeds from the reactants to the tetrahedral transition state assumes that the transition state in this case is "product-like" and consequently the observed regioselectivity reflects stability of the product. However, under normal reaction conditions fast, exothermic, kinetically-controlled reductions are believed to proceed through a "reactant-like" transition state (9). Thus we are faced with the controversial problem of fundamentally similar reactions having entirely different

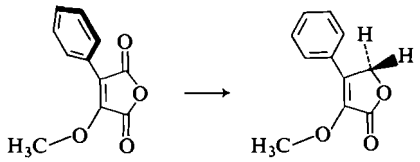


11



12

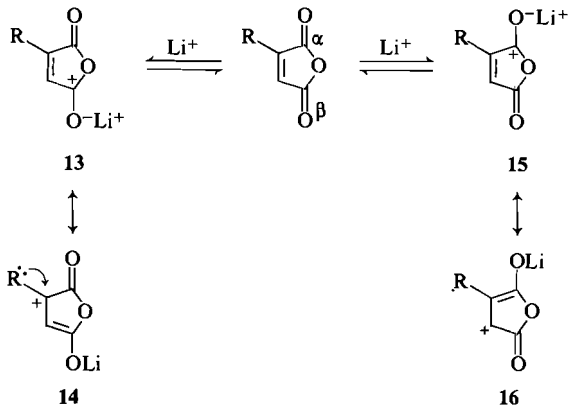
transition states (9). Moreover, preferential reduction of the carbonyl function neighbouring the methoxy rather than the phenyl substituent in **5** refutes "the more stable product" argument. The phenyl group which is twisted in the anhydride, could assume a position in conjugation with the double bond if the adjacent carbonyl group were reduced to give the lactone **5***b*. Yet despite this strongly stabilizing effect (favouring **5***b*) the only product obtained is lactone **5***a*.



5 **5***b*

We have suggested before (1) that there are two principal factors involved in controlling the regioselectivity in reductions by metal hydrides, namely, (*a*) preferential association of the cation with *one* of the carbonyl groups, and (*b*) rate of hydride transfer to the activated (by complexation with the cation) intermediate. For the conjugated and aromatic anhydrides reported in this paper, the major contribution is undoubtedly due to the factor (*b*).

The resistance of an enolized carbonyl group to reduction by metal hydrides has been recently demonstrated by Barton *et al.* (10). In the substituted maleic anhydrides both carbonyl groups can



13 **15**

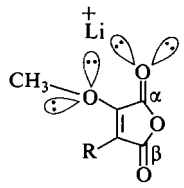
14 **16**

FIG. 2. The association of a cation with the carbonyl group is reversible. Thus, as the unstable intermediate **15** is reduced, the equilibrium shifts to the right. The overall effect is a highly regioselective reduction of the α-carbonyl group.

form enolates.[1] However, the unstable intermediate **15** will undergo preferential reduction even in the presence of **13**, since the latter possesses a higher degree of enolate character due to stabilization of the canonical form **14** by the substituent (see Fig. 2). Additional contributing factors such as the positive inductive effect of the methyl group in compound **1** and the formation of a cyclic chelated complex with the cation in methoxy substituted anhydrides **17** favour complexation with a cation, further promoting reduction at the α-carbonyl function.

Metal Hydride Reductions of ortho-*Substituted Phthalic Anhydrides*

Phthalic anhydrides constitute another class of compounds for which "steric hindrance along the preferred reaction path" argument cannot be used to rationalize observed regioselectivities. McAlees *et al.* (11) investigated sodium borohydride reductions of four *ortho*-substituted phthalic anhydrides



17

[1]The large proportion of 1,4 addition observed in $NaBH_4$ reductions of **2** and **3** confirms the importance of the contributing canonical forms such as **14** and **16** (see Experimental). The preference of $LiAlH_4$ for 1,2 addition to conjugated ketones (while $LiBH_4$ gives higher yields of 1,4 addition products) has been discussed by A. Loupy and J. Seyden-Penne, Tetrahedron Lett. 2571 (1978).

Can. J. Chem. Downloaded from www.nrcresearchpress.com by 210.87.254.42 on 09/05/12
For personal use only.

6, **7**, **8**, and **9** (Table 1). In all cases examined, hydride addition occurs preferentially at the carbonyl function *ortho* to the substituent. To account for the product distribution observed, the authors propose that nucleophilic attack at the carbonyl group *ortho* to the substituent results in relief of steric compression between this carbonyl group and the substituent. This argument implies an sp^3-hybridized ("product-like") transition state. It is generally assumed that steric effects are the major influence of a substituent in the *ortho* position, except when the substituent is of relatively small size (e.g. F) and induction and resonance become prominent (12, 13). Taking this into account, we decided to investigate the reduction of 3-fluorophthalic anhydride **10** in order to assess the extent of the *ortho* effect.

The reduction of **10**, under a variety of experimental conditions, yielded chiefly lactone **10***a* resulting from hydride addition to the carbonyl group *ortho* to the fluorine substituent. The isomeric lactone was always a minor product. These observations weaken considerably the interpretation based on the *ortho* effect and "product-like" transition state. Evidently, if the steric acceleration (due to the *ortho* effect) is not the principal factor governing regioselectivity of reduction in *ortho*-substituted phthalic anhydrides, the reaction must be controlled by inductive and mesomeric influences.

In view of the importance of catalysis by alkaline cation in metal hydride reductions (7, 8, 14, 15), an electron-donating substituent should promote complexation of a cation with the carbonyl group and consequently accelerate the reduction. Conversely, an electon-withdrawing group should decelerate the reaction. In the 3-substituted phthalic anhydrides we have two possible sites for reaction but since the intensity of inductive effect decreases sharply with distance, the activating or deactivating effect of the substituent in position 3 is felt most strongly by the adjacent (i.e. *ortho*) carbonyl function. Thus, we should expect increased selectivity for the *ortho* carbonyl group in phthalic anhydrides bearing an electron-donating substituent in position 3, while compounds with electron-attracting substituents should show a higher proportion of reduction at the *meta* carbonyl group. However, the problem becomes more complex when association with a cation is accompanied by electron delocalization (as is the case in aromatic and conjugated systems). In such instances when delocalization does occur, the relative rates of hydride transfer to the two possible intermediates may offset entirely

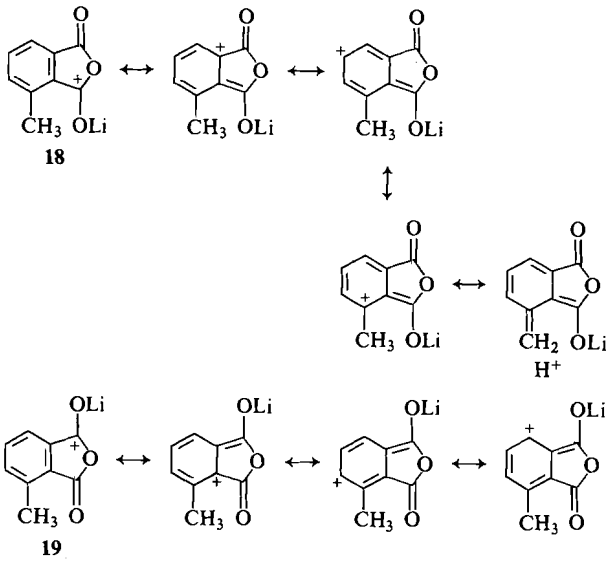
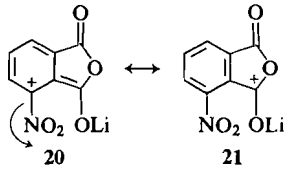


FIG. 3. The more stable intermediate **18** will be reduced at a slower rate than the less stable intermediate.

the regioselectivity anticipated on the basis of preferential association with the cation.

Let us consider an example. In the course of the reduction of 3-methylphthalic anhydride **6** the inductive electron-donating influence of the substituent promotes complexation with a cation at the *ortho* carbonyl group. But, at the same time, hydride transfer to the activated carbonyl function is retarded due to the greater stabilization of the intermediate **18** versus **19**. This augments the possibility of reduction at the *meta* carbonyl group (Fig. 3). When the substituent is electron-attracting, the deactivating inductive effect on the *ortho* carbonyl group is offset by the mesomeric effect. The enolized contributing structure **20** is quite unstable. The 3-nitrophthalic anhydride complex with a Li^+ cation may be expected to possess a higher proportion of non-enolized form **21**, which is particularly disposed toward reduction.



We may conclude that the ratios of the two lactones obtained represent a net effect of the opposing inductive and mesomeric influences. These ratios are different for various compounds (**6**, **7**, **8**, **9**, and **10**) since the magnitudes of the contributing effects are characteristic for each substituent.

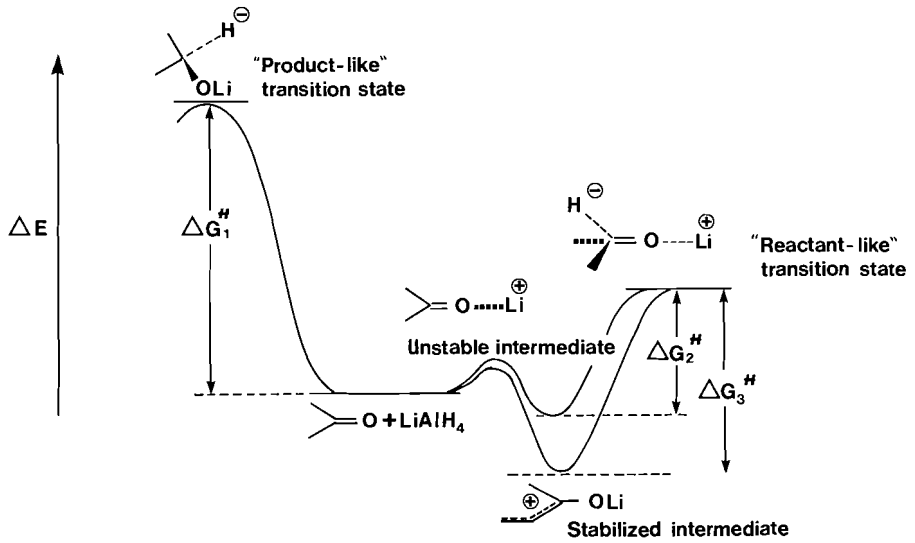


FIG. 4. Catalyzed and non-catalyzed reaction paths in metal hydride reductions.

The situation encountered in the reductions of phthalic anhydrides parallels that of the substituted maleic anhydrides. However, while in compound **1** inductive and mesomeric effects act in unison promoting reaction at the same (α) carbonyl function, in phthalic anhydrides the two influences oppose each other.

It is important at this stage to point out that although electrophilic assistance by an alkaline cation is necessary in reductions of saturated carbonyl compounds (7, 8), it is not "essential" when aromatic or conjugated systems are reduced (16). Apparently the electron-withdrawing aromatic ring (or a double bond) sufficiently lowers the energy level of the LUMO $\pi^*_{C=O}$, so that reaction can occur even in the absence of a cation, albeit at a slower rate. It is entirely possible that metal hydride reductions of aromatic compounds (especially those substituted with electron-withdrawing groups) may proceed through catalyzed or non-catalyzed processes. The slow, non-catalyzed reduction may be fundamentally different from the fast, exothermic reaction of the saturated ketone or aldehyde activated by complexation with an alkaline cation. In fact, it may very well proceed through the late, "product-like" transition state. In such a case the *ortho* effect of a substituent would become an important factor in determining the regioselectivity of the reaction.

The variations in the ratios of the two lactones obtained in reductions with $NaBH_4$ and $LiAlH_4$ support this interpretation. The most revealing is the series of reductions performed on 3-nitrophthalic anhydride **9**. The reduction of **9** with $NaBH_4$ in tetrahydrofuran (11), in the absence of an "effective" catalyst (Na^+ is a poor catalyst in comparison to Li^+), yields only lactone **9***a*. This suggests that the non-catalytic process and consequently the *ortho* effect is operative. When the same reaction was carried out in the presence of catalytic amounts of HCl, a mixture of two lactones (**9***a*:**9***b* = 83:17) was obtained. The percentage of **9***b* was still higher (33%) when the reduction was carried out in the presence of Li^+ cation.

Summary

In this paper we have suggested that the reduction by metal hydrides of aromatic and conjugated systems (especially those substituted with electron-withdrawing groups) may proceed through two competitive mechanisms: (*a*) one catalyzed by an alkaline cation and involving a "reactant-like" transition state; (*b*) the other non-catalytic process in which the transition state is "product-like".

The first mechanism is controlled by electronic effects while the *ortho* effect and the stability of the product are the dominant factors in the second. The catalyzed and non-catalyzed processes may be represented by the diagram depicted in Fig. 4.

Experimental

Melting points were determined on a Thomas–Hoover capillary melting point apparatus and are uncorrected. Infrared spectra were obtained on a Beckman IR-20 spectrophotometer and proton nmr spectra in $CDCl_3$, with TMS as internal standard, on a Varian HA-100 instrument. Tetrahydrofuran was distilled under nitrogen from lithium aluminum hydride into oven-dried flasks containing the lithium aluminum hydride.

Can. J. Chem. Downloaded from www.nrcresearchpress.com by 210.87.254.42 on 09/05/12
For personal use only.

Can. J. Chem. Downloaded from www.nrcresearchpress.com by 210.87.254.42 on 09/05/12
For personal use only.

The general procedures for the reductions were as follows. (*a*) Lithium aluminum hydride (0.005 mol) was placed in an oven-dried, three-neck flask into which 50 mL of tetrahydrofuran were subsequently distilled. The flask was fitted with an inlet post for syringes, gas outlet tube, thermometer, and magnetic stirrer. The flask, swept with a slow stream of nitrogen, was cooled in a dry ice – acetone bath. An anhydride (0.01 mol) dissolved in 25–30 mL of distilled tetrahydrofuran was injected into the flask. The temperature of the reaction mixture was maintained below −50°C throughout the addition process. The stirred solution was slowly warmed to 0°C over a period of 2 h. The flask was then cooled again to −20°C and 5 mL of 6 *N* HCl were added slowly. The reaction mixture was left overnight. The layers were separated and the aqueous layer extracted with ether. The combined organic layers were dried, the solvent evaporated, and the product analyzed by 100 MHz proton nmr. (*b*) Reductions with sodium borohydride were carried out as follows. A solution of an anhydride (0.01 mol) in dry tetrahydrofuran (50 mL) was added dropwise to a stirred, ice-cold suspension of $NaBH_4$ (0.01 mol) in tetrahydrofuran (50 mL). The reaction mixture was allowed to warm to room temperature and stirring was continued for an additional 2–3 h. During that period 3–4 drops of 6 *N* HCl were added to the reaction mixture. After quenching with 3 *N* HCl the layers were separated and the acidic aqueous layer was extracted with ether. The combined organic layers were dried over anhydrous $MgSO_4$ and the solvents removed. The crude product was analyzed by 100 MHz proton nmr. (*c*) An alternate procedure for the reduction with sodium borohydride involved addition of lithium chloride (0.01 mol) dissolved in tetrahydrofuran before the suspension of $NaBH_4$ (0.01 mol) in THF was added to the reaction vessel.

Reduction of Methyl Maleic Anhydride 1

Methyl maleic anhydride was reduced with $LiAlH_4$ as described in the general procedure. Upon work-up a yellow oil was recovered (82–87% yield). 100 MHz proton nmr of the crude product showed 4-hydroxy-3-methyl *cis* crotonic acid lactone **1***a* to be the major product. The mixture contained some unreacted anhydride (acid) and a small quantity of the isomeric lactone **1***b* (**1***a*:**1***b* = 90:10). The lactone **1***a* was purified by distillation at reduced pressure (17); ν_{max}: 1780 cm^{-1}; δ:2.16 (s, 3H, CH_3), 4.74 (s, 2H, CH_2O), 5.80 (m, 1H, H—C=C). The isomeric lactone **1***b* (18) showed δ:1.92 (m, CH_3), 7.22 (m, H—C=C—C=O).

The reduction of **1** with $NaBH_4$ according to the general procedure (*b*) gave lactone **1***a* as the principal product (**1***a*:**1***b* = 85:15).

Reduction of Chloromaleic Anhydride 2

Chloromaleic anhydride **2** was reduced with $LiAlH_4$ as described in the general procedure. The isolated product was a dark, brown oil sparingly soluble in chloroform. The crude material was repeatedly extracted with chloroform to give a mixture of products (30%). 100 MHz proton nmr analysis showed the ratio of two lactones to be **2***a*:**2***b* = 90:10. Separation on thick layer chromatography plates provided a sample of pure lactone **2***a* (19); ν_{max}: 1770 cm^{-1}; δ:4.85 (d, 2H, CH_2—O), 6.18 (t, 1H, H—C=C), and **2***b* (20): ν_{max}: 1770 cm^{-1}; δ:4.92 (d, 2H, CH_2—O), 7.54 (t, 1H, H—C=C—C=O).

The reduction of **2** with $NaBH_4$ according to the procedure (*b*) yielded lactonic product (35%) **2***a*:**2***b* = 87:13. The remaining crude material contained the unreacted diacid (ca. 10–15%) and reduction products (ca. 30%) resulting from 1,4 hydride addition to chloromaleic anhydride **2**.

Reduction of Phenylmaleic Anhydride 3

Phenylmaleic anhydride **3** was prepared according to the method of Miller *et al.* (21). It was reduced with $LiAlH_4$ according to the general procedure (*a*) to give a mixture of the lactones **3***a* and **3***b* in the proportions **3***a*:**3***b* = 75:25 (100 MHz nmr analysis). The total yield of the lactonic product was ca. 50%.

Separation by thick layer chromatography furnished both lactones displaying identical physical and spectroscopic properties to those published previously (22,23). Lactone **3***a*, ν_{max}: 1760 cm^{-1}; δ: 5.20 (d, 2H, CH_2—O), 6.34 (t, 1H, H—C=C), 7.35 (m, 5H); lactone **3***b*, ν_{max}: 1760 cm^{-1}; δ: 4.96 (2H), 7.46 (m, 4H), 7.80 (m, 2H).

The reduction of **3** with $NaBH_4$ (procedure (*b*)) gave a mixture of the two lactones **3***a* and **3***b* (ca. 30% **3***a*:**3***b* = 67:33), unreduced diacid (ca. 30%), and two saturated lactones (ca. 40%), 3-phenyl-γ-butyrolactone and 2-phenyl-γ-butyrolactone in the approximate ratio 2:1. These two last products are the result of 1,4 hydride addition, followed by 1,2 hydride addition.

Reduction of 3-Nitrophthalic Anhydride 9

Reduction of 3-nitrophthalic anhydride **9** by $LiAlH_4$ according to the general procedure yielded yellow crystalline product (80%). The 100 MHz proton nmr showed the presence of two lactones in the ratio **9***a*:**9***b* = 67:33.

4-Nitrophthalide **9***a*, mp 135–136°C (lit. (24) mp 136°C); ν_{max}: 1780 cm^{-1}; δ: 5.75 (s, 2H, CH_2—O), 7.82 (1H), 8.38 (2H). 7-Nitrophthalide **9***b*, mp 163°C; ν_{max} 1765 cm^{-1}; δ: 5.40 (s, 2H), 7.95 (m, 3H); *m/e*: 179 (M^+).

Reduction of **9** with $NaBH_4$ according to procedure (*b*) gave a mixture of two lactones (75%) **9***a*:**9***b* = 83:17.

Reduction of 3-Fluorophthalic Anhydride 10

Oxidation of 1-fluoronaphthalene with $KMnO_4$ gave 3-fluorophthalic acid in 47% yield, mp 185–187°C. Upon sublimation the 3-fluorophthalic acid was dehydrated to the corresponding anhydride **10**, mp 118–119°C; ν_{max}: 1805, 1875 cm^{-1}; δ: 7.70 (m).

Reduction of **10** with $NaBH_4$ according to the general procedure (*b*) yielded 32% of the lactonic product (**10***a*:**10***b* = 70:30) and 3-fluorophthalic acid. Separation on thick layer chromatography plates provided pure samples of the two lactones.

4-Fluorophthalide **10***a*, mp 160–162°C (lit. (25) mp 162–163°C); ν_{max}: 1790 cm^{-1}; δ: 5.32 (s, 2H, CH_2—O), 7.22 (m, 2H), 7.66 (m, 1H). 7-Fluorophthalide **10***b*, mp (62–64°C); ν_{max}: 1785 cm^{-1}; δ: 5.38 (s, 2H, CH_2—O), 7.60 (m, 3H).

Reduction of **10** with $NaBH_4$ according to general procedure (*c*) yielded a lactonic mixture (49%) **10***a*:**10***b* = 84:16.

Acknowledgement

We are grateful to the Natural Sciences and Engineering Research Council of Canada for financial support (Grant A 1918).

1. M. M. KAYSER and P. MORAND. Can. J. Chem. **56**, 1524 (1978).
2. J. B. WIJNBERG, W. N. SPECKAMP, and H. E. SCHOEMAKER. Tetrahedron Lett. 4073 (1974); J. B. WIJNBERG and W. N. SPECKAMP. Tetrahedron Lett. 4035 (1975).
3. M. KAYSER and P. MORAND. Tetrahedron Lett. 695 (1979).
4. R. SÜESS. Helvetica Chim. Acta, **60**, 1656 (1977); R. E. ROSENFIELD and J. D. DUNITZ. Helvetica Chim. Acta, **61**, 2176 (1978).
5. D. W. KNIGHT and G. PATTENDEN. J. Chem. Soc. Perkin Trans. I, 62 (1979).
6. J. J. BLOOMFIELD and S. L. LEE. J. Org. Chem. **32**, 3919 (1967).
7. J. L. PIERRE, H. HANDEL, and R. PERRAUD. Tetrahedron, **31**, 2795 (1975).

8. J. L. PIERRE and H. HANDEL. Tetrahedron Lett. 2317 (1974).
9. E. C. ASHBY and J. T. LAEMMLE. Chem. Rev. **75**, 521 (1975).
10. D. H. R. BARTON, R. H. HESSE, C. WILSHIRE, and M. PECHET. J. Chem. Soc. Perkin Trans. I, 1075 (1977).
11. A. J. MCALEES, R. MCCRINDLE, and D. W. SNEDDON. J. Chem. Soc. Perkin Trans. I, 2037 (1977).
12. J. F. BUNNETT and C. F. HAUSER. J. Am. Chem. Soc. **87**, 2214 (1965).
13. D. C. BERNDT and I. E. WARD. J. Org. Chem. **43**, 13 (1978); L. L. MCCOY and E. E. RIECKE. J. Am. Chem. Soc. **95**, 7407 (1973).
14. H. C. BROWN, E. J. MEAD, and B. C. RAO. J. Am. Chem. Soc. **77**, 6209 (1955).
15. P. T. LANSBURY and R. E. MACLEAY. J. Am. Chem. Soc. **87**, 831 (1965).
16. A. LOUPY, J. SEYDEN-PENNE, and B. TCHOUBAR. Tetrahedron Lett. 1677 (1976).
17. P. CAMBERE. Bull. Soc. Chim. Fr. 148 (1964); W. J. CONVADIE, C. F. GARBERS, and P. S. STEYN. J. Chem. Soc. 594 (1964).
18. C. J. CAVALLITO and T. H. HASKELL. J. Am. Chem. Soc. **68**, 2332 (1946).
19. R. C. LAROCK. J. Org. Chem. **40**, 3237 (1975).
20. S. DUCHER and A. MICHET. Bull. Soc. Chim. Fr. 4353 (1970).
21. L. MILLER, H. STANLEY, and D. MANN. J. Am. Chem. Soc. **71**, 374 (1949).
22. H. KOSUGI, S. SEKIGUCHI, R. SEKITA, and H. UDO. Bull. Chem. Soc. Jpn. **49**, 520 (1976).
23. G. W. PEROLD and H. K. HUNDT. J. Chem. Soc. C, 1924 (1966).
24. K. DIACONT and H. ANAU. Ber. **67**, 676 (1934).
25. R. V. BELINSKAYA and L. M. YAGUPOLSKII. Zh. Obshch. Khim. **38**, 1726 (1968).

Can. J. Chem. Downloaded from www.nrcresearchpress.com by 210.87.254.42 on 09/05/12
For personal use only.

The reduction of aryl trifluoromethyl ketones by sodium borohydride. The hydride transfer process

ROSS STEWART AND K. C. TEO

Department of Chemistry, University of British Columbia, Vancouver, B.C., Canada V6T 1W5

Received March 25, 1980

This paper is dedicated to Prof. Raymond U. Lemieux on the occasion of his 60th birthday

Can. J. Chem. Downloaded from www.nrcresearchpress.com by 210.87.254.6 on 09/05/12
For personal use only.

ROSS STEWART and K. C. TEO. Can. J. Chem. **58**, 2491 (1980).

The rates of reduction of 17 aryl trifluoromethyl ketones by sodium borohydride in 2-propanol have been measured. The rho (ρ) value is +3.12, excluding the 4-amino and 4-dimethylamino groups, which both lower the rate to a greater extent than their σ values predict. The close correspondence between substituent effects for hydride addition in the methyl and trifluoromethyl series (excluding the amino groups) suggests that normal substituent effects are to be expected for oxidation processes involving hydride removal in trifluoromethyl compounds. The present results are consistent with the oxidation of aryl trifluoromethyl carbinols by permanganate taking place by hydrogen atom abstraction. The effect of substituents on the rate of reduction of the trifluoromethyl ketones is almost identical to that on the equilibrium constant for formation of the ketone hydrates. The application of the reactivity–selectivity principle to the reduction reaction is also considered. Reduction of the 4-ethyl compound has $\Delta H^{\ddagger} = 2.7$ kcal mol^{-1} and $\Delta S^{\ddagger} = -38$ cal deg^{-1} mol^{-1}.

ROSS STEWART et K. C. TEO. Can. J. Chem. **58**, 2491 (1980).

On a mesuré les vitesses de réduction de 17 aryl trifluorométhylcétones par le borohydrure de sodium dans le propanol-2. La valeur rho (ρ) est de +3.12 en excluant les groupements amino-4 et diméthylamino-4 qui tous deux diminuent dans une proportion plus grande que celle prévue par leurs σ. L'étroite correspondance entre les effets de substituant lors de l'addition d'hydrure sur les cétones méthylées et trifluorométhylées (en excluant les groupement amino) suggère que les effets normaux de substituants sont à prévoir dans les réactions d'oxydation qui font intervenir une élimination d'hydrure dans les composés trifluorométhylés. Les résultats sont en accord avec l'hypothèse selon laquelle l'oxydation des aryltrifluorométhylcarbinols par le permanganate se fait par élimination d'hydrogène. L'effet des substituants sur la vitesse de réduction des trifluorométhylcétones est presqu'identique à celui sur la constante d'équilibre de la réaction de formation des énols. On considère également l'application du principe de réactivité–sélectivité à la réaction de réduction. Pour la réduction du composé portant un groupe éthyle en position 4 le $\Delta H^{\ddagger} = 2.7$ kcal mol^{-1} et le $\Delta S^{\ddagger} = 38$ cal deg^{-1} mol^{-1}.

[Traduit par le journal]

Introduction

Hydride transfer processes constitute an important class of oxidation–reduction reactions. Indeed, for organic compounds hydride transfer is one of the most frequently used 2-electron (2-equivalent) routes (1) between oxidants and reductants. A reaction that on first inspection appears to be a hydride transfer is the oxidation of alcohols to aldehydes or ketones by aqueous alkaline potassium permanganate (2). Since the isotope effect shows that the carbon–hydrogen bond is cleaved in the rate-controlling step and since the alkoxide ion is known to be an intermediate in the reaction, hydride transfer appears to be an attractive mechanism for the oxidation step, the driving force being provided by the negative charge on the alkoxide oxygen atom.

[1] $R_2CHOH + OH^- \rightleftharpoons R_2CHO^- + H_2O$

[2] $R_2CHO^- + MnO_4^- \longrightarrow R_2C{=}O + HMnO_4^{2-}(Mn^{V})$

[3] $(3\,Mn^{VI} \longrightarrow Mn^{VII} + 2\,Mn^{IV})$

However, there is one piece of evidence that has been known for some time that is inconsistent with such a mechanism for the rate-controlling step. When aryl trifluoromethyl carbinols, $ArCHOHCF_3$, are oxidized by aqueous permanganate there is no effect of ring substituents on the rate-controlling step; that is, the Hammett rho (ρ) value is roughly zero (2*b*). There is a substituent effect on the oxidation of these and other alcohols but in those cases in which the effect can be partitioned between step [1] and step [2] the substituent effect turns out to reside completely in step [1]. Furthermore, the sodium borohydride reduction of ketones is known to be a clear case of hydride addition to the carbonyl group (3) and since Bowden and Hardy (4) have shown that hydride *addition* to aryl methyl ketones[1] has a large positive rho, +3.06, it is to be expected that hydride *removal* would have a substantial negative rho.

Accordingly, the alternative mechanism, hydrogen-atom transfer, which is not expected to

[1]The ρ_{eq} for hydroxide addition to the carbonyl group of benzaldehydes is +2.76 (5).

0008-4042/80/232491-06$01.00/0

©1980 National Research Council of Canada/Conseil national de recherches du Canada

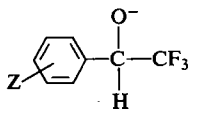
Can. J. Chem. Downloaded from www.nrcresearchpress.com by 210.87.254.6 on 09/05/12
For personal use only.

be as strongly affected by substituents, has been favoured (1). The driving force here would presumably be the relatively greater stability of the ketyl anion than the alkoxide ion.

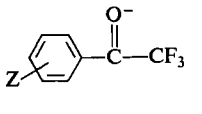
$$R_2CHO^- + MnO_4^- \longrightarrow R_2\dot{C}{-}O^- + HMnO_4^{-}\,(Mn)^{VI}$$

$$R_2\dot{C}{-}O^- + MnO_4^- \longrightarrow R_2C{=}O + MnO_4^{2-}\,(Mn)^{VI}$$

The above argument depends on the trifluoromethyl group, which has profound effects on reactivity in other systems (6), not having such an overwhelming electron-withdrawing effect that it obliterates the effects of the ring substituent Z on removal of a hydride unit from **1**. A test of the latter possibility can be made by comparing the effect of hydride addition to **2** with that for the analogous aryl methyl ketones. Accordingly, we have determined the effect of ring substituents on the reduction of aryl trifluoromethyl ketones by sodium borohydride.



1



2

Two ancillary benefits accrue from such a study. First, aryl trifluoromethyl ketone reduction has been widely used in biomimetic studies (7) and the present work should serve as a benchmark for substituent effects in such systems. Secondly, the reactivity difference between the methyl and trifluoromethyl systems is expected to be very large and should provide a further test of the reactivity–selectivity principle in aromatic systems (8).

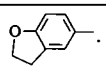
Results and Discussion

The reaction was initially investigated in several solvent systems. Aqueous solution has the advantage of being the medium in which the permanganate oxidation had been conducted; nonhydroxylic solvents such as dioxan have the advantage of not having hydrate or hemiacetal formation competing with the reduction. In the event, it was found that these systems gave very poor kinetic results and 2-propanol, the medium previously used in borohydride kinetic studies, was found to be preferable. Hemiacetal formation competes with the reduction but is much slower, being undetectable in the case of the 4-amino compound and proceeding at only 0.2% of the reduction rate for the unsubstituted compound.

The yield of alcohol is high, as expected (see Experimental). The rate data are given in Table 1.

TABLE 1. Second-order rates for reduction of aryl trifluoromethyl ketones by sodium borohydride in 2-propanol, 20°C

Substituent	k_2 (L mol^{-1} s^{-1})	Substituent	k_2 (L mol^{-1} s^{-1})
4-$(CH_3)_2N$	1.23	4-CH_3	198
4-NH_2	0.45	4-C_2H_5	276
4-HO	39.9	4-$(CH_3)_3C$	292
5′-Coumaranyl[a]	44.8	3-CH_3	386
4-CH_3O, 3-CH_3	47.8	H	625
4-C_2H_5	70.7	3-CH_3O	1070
4-CH_3O	71.7	4-F	1073
3,4-$(CH_3)_2$	191	4-Cl	2782
		4-Br	4212

[a]Aryl group is  .

Effect of Substituents

A Hammett plot, log k against σ, for 16 compounds is shown in Fig. 1. (The σ value for the coumaranyl group has not yet been determined; our results give a $\bar{\sigma}$ value of -0.38 for this group.) The rho value is 3.86 with a correlation coefficient of 0.9718.

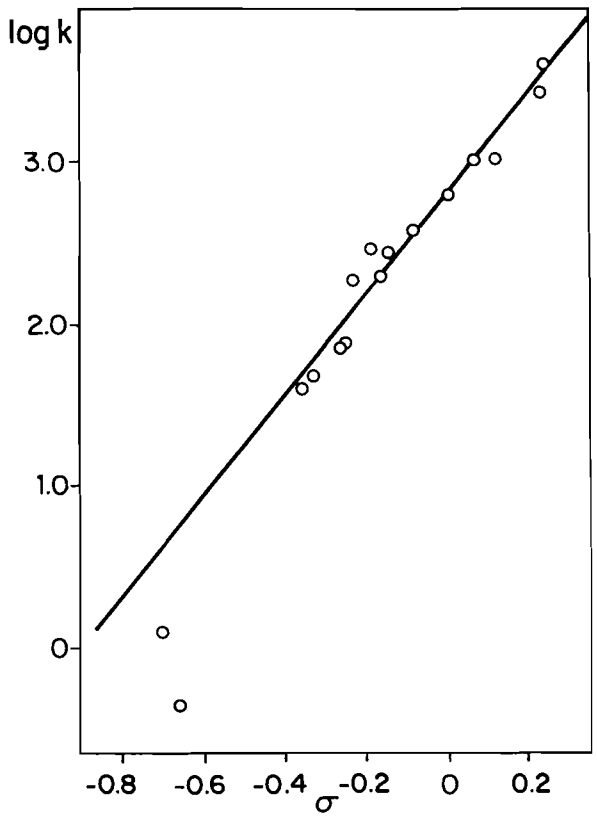


FIG. 1. Hammett plot for the reduction of substituted trifluoroacetophenones by sodium borohydride in 2-propanol at 20°C, $\rho = +3.12$, excluding 4-$(CH_3)_2N$ and 4-NH_2.

Can. J. Chem. Downloaded from www.nrcresearchpress.com by 210.87.254.6 on 09/05/12
For personal use only.

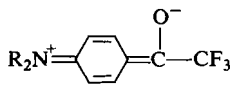
It is clear that the amino groups deviate markedly from the best line drawn for the other groups and the direction of deviation suggests that a σ^+ correlation would be more satisfactory. In fact, a plot of log k against σ^+ is not particularly good (correlation coefficient 0.9480), nor is a Yukawa–Tsuno plot (9), for which the highest correlation coefficient (0.9758) is obtained with the coefficient r set equal to 0.15.

For purposes of comparing the effect of ring substituents on the reduction of the methyl and trifluoromethyl series, either of the following treatments seems to be satisfactory. A direct comparison can be made of the six substituents that are common to the two series, excluding 4-methoxy which is grossly deviant in the Bowden and Hardy series. An excellent correlation is obtained when log k_{CF_3} (y axis) is plotted against log k_{CH_3} (x axis), the slope being 0.872 and the correlation coefficient 0.9969. This result suggests that borohydride reduction in the trifluoromethyl series is only slightly less sensitive to ring substituents than is the reaction with the methyl compounds.

An alternative approach is to use the rho value determined using all the groups in Fig. 1 except amino and dimethylamino. The rho of 3.12 (correlation coefficient 0.9798) is very slightly larger than the value of 3.06 found by Bowden and Hardy for the methyl ketones. Thus, in the case of hydride addition, replacing the hydrogen atoms of the methyl group with fluorine atoms causes virtually no change in the transmission of ring effects to the reaction site.

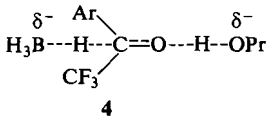
With regard to the hydride abstraction mechanism for the permanganate oxidation of trifluoromethyl carbinols, referred to in the Introduction, one can conclude that the trifluoromethyl group will not, in fact, obliterate the effect of ring substituents. Thus, the present results are consistent with the mode of carbon–hydrogen bond breaking in the alkoxide–permanganate reaction being homolytic. That is, as earlier argued (*1b*), hydrogen-atom transfer probably occurs, giving the ketyl anion as the initial product.

It does not seem possible to accommodate the effect on the borohydride reduction of all groups by any of the standard Hammett treatments and, accordingly, we simply assign a ρ value of 3.12 to the reaction, excluding the amino groups, which are more electron-donating (rate-retarding) than their σ values would suggest. It is clear, though, that the effect of these groups can be ascribed to conjugation in the neutral ketones, with the structure **3** being stabilized by the nearby trifluoromethyl group; just as in the ketone hydrate equilibrium, where a good σ^+ correlation has been obtained (10).



3

For the compounds common to the two series, borohydride reduction and hydration, there is a significant correlation. Figure 2 shows a plot of the logarithm of the reduction rate constant against the logarithm of the equilibrium constant for hydration. The slope of the line is only slightly greater than unity, 1.12. This result is consistent with Wigfield's view (3) that in the transition state for borohydride reduction in 2-propanol the hydride transfer is well advanced and is accompanied by proton transfer from the solvent to the carbonyl oxygen atom. Such a transition state, **4**, will closely resemble the carbonyl hydrate molecule if the new bonds are almost complete.[2]



4

The Reactivity–Selectivity Principle (RSP)

The borohydride reduction of a trifluoromethyl ketone is more than 10^5 times faster than that of the analogous methyl ketone yet the effect of substituents in the two series is little different, neglecting the amino compounds, which were not studied in the methyl series. This is in agreement with general experience that Hammett rho selectivity indices are not generally affected by reactivity changes. If they were, curved Hammett plots should be observed for series that cover a wide range of rates. Although Fig. 1 shows an apparent curvature (and in the direction expected if the RSP operated within the series) it seems unlikely that this effect is a simple manifestation of the RSP. Since the rates are very fast and the heats of activation very low any curvature would be expected to

[2]The fact that the borohydride reduction correlates better with σ than with σ^+ whereas the hydration equilibria are correlated better with σ^+ than with σ is paradoxical, considering that Fig. 2 indicates a similarity in substituent effects. A firmer distinction could be made between σ and σ^+ dependence in the reduction if groups more electron donating than *para*-halo were included. However, such compounds have reaction times of only a few seconds or less and it is impossible to measure faster rates by the technique we have used. Flow systems are difficult to use with 2-propanol because of competing hemiacetal formation and we were unable to obtain reproducible results with aprotic solvents.

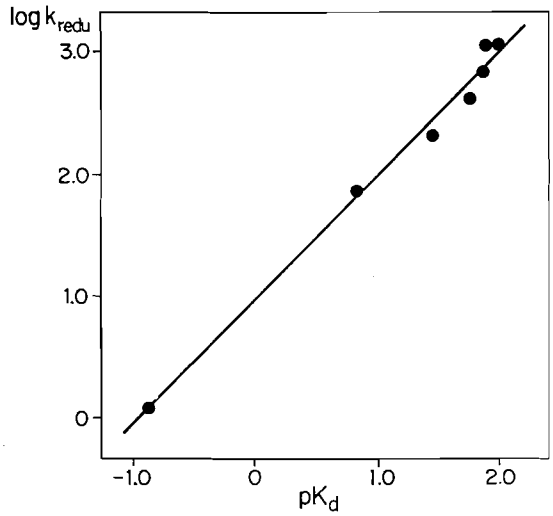


FIG. 2. Logarithm of the rate constant for borohydride reduction as a function of the logarithm of the equilibrium constant for hydration of the same ketone. The hydration constants (in the form pK_d, where d indicates dehydration) are from ref. 10. Slope = 1.12.

arise from the most reactive member of the series reacting less rapidly than predicted by a linear Hammett relation. This, in turn, would mean that the less reactive members would give a truer value of the reaction constant rho. In the present case, however, this would require a rho value considerably greater than 4.0 and it is difficult to imagine the trifluoromethyl series having a rho so much larger than that for the methyl series.

Activation Parameters

The activation enthalpy for the sodium borohydride reduction of 4-ethyl-α,α,α-trifluoroacetophenone is 2.7 kcal mol^{-1} (11.3 kJ mol^{-1}). The activation entropy is −38 cal deg^{-1} mol^{-1} (−159 J deg^{-1} mol^{-1}), falling in the range found for other borohydride reductions (4*a*, 11). The extremely small $\Delta H^{\ddagger}$ corresponds to a temperature coefficient of only 2% per degree at room temperature. Most ketone reductions by borohydride have $\Delta H^{\ddagger}$ values between 5 and 11 kcal mol^{-1}, and one might conclude that the reaction is enthalpy controlled. However, it is clear that the entropy of activation for the 4-amino compound, for example, must be very much more negative than that of the 4-ethyl compound since $\Delta\Delta G^{\ddagger}$ at 20°C for these two compounds is 3.7 kcal mol^{-1}, considerably greater than the $\Delta H^{\ddagger}$ for the 4-ethyl compound. That is, at least for the less reactive compounds, the reaction must be partly or entirely entropy controlled.

A Comment on the Use of the Hammett Relation for Comparing Reactivities in Two Series

The Hammett relation in its various forms correlates a vast body of physico-chemical data (9). However, because of the variability introduced by modified substituent constants σ^+, σ^-, σ^0 etc., the magnitude of a reported reaction constant rho may give a false impression of the sensitivity of the reaction to a change in ring substituents. Thus, for the borohydride reduction considered herein, the calculated rho value can be reported as +3.86 (using σ and all substituents) or the very much smaller value +1.83 (using σ^+ and all substituents), with comparable correlation coefficients in the two cases.

As a consequence we have found it more meaningful to compare directly two series of reactions, in one case the CF_3 and CH_3 ketones carrying the same ring substituents, and in the other case two different reactions, reduction and hydration, of the same CF_3 ketones. Such comparisons are not always possible nor, indeed, desirable, but they may be preferable to the powerful generality of the Hammett approach when it is unclear which set of substituent constants should be used.

Experimental

Materials

2-Propanol was distilled from sodium borohydride before use. Dioxan was distilled from sodium and benzophenone under nitrogen. The known ketones were prepared as previously described (10) and purified by chromatography. The ultraviolet and infrared spectroscopic data for all compounds are summarized in Table 2. Satisfactory nmr and high resolution mass spectra were obtained for all ketones used.

4-Amino-α,α,α-trifluoroacetophenone

Freshly prepared active manganese dioxide (12) (88 g) was stirred with a solution of 4-dimethylamino-α,α,α-trifluoroacetophenone (10) (2.0 g) in chloroform (450 cm^3) at room temperature for 91 h. The manganese dioxide was filtered off and washed with chloroform. Refiltration and evaporation of the combined solutions afforded 1.83 g of brown crystalline solid. The crude product was purified over an alumina column using ether/pentane and gave three fractions, the first consisting of 0.4 g of the monomethylamino compound (see below), the second containing 0.1 g of a mixture of this compound and the amino compound, and the third consisting of 0.4 g of the desired amino compound, mp 89.0–91.0°C.

Anal. calcd. for $C_8H_6NOF_3$: C 50.80, H 3.20, N 7.41; found: C 50.93, H 3.26, N 7.30.

4-Methylamino-α,α,α-trifluoroacetophenone

This compound was obtained as a fraction in the oxidative demethylation described above, mp 96.5–97.0°C.

Anal. calcd. for $C_9H_8NOF_3$: C 53.21, H 3.97, N 6.89; found: C 53.24, H 4.13, N 6.81.

5'-Coumaranyl-α,α,α-trifluoroacetophenone

A mixture of coumaran (5.6 g) and powdered anhydrous aluminum chloride was stirred in dry carbon disulfide (20 cm^3) for 15 min (13). Trifluoroacetic anhydride was added, and the mixture warmed until gas evolution ceased. The reaction mixture was decomposed with cold 5 *M* hydrochloric acid and extracted with ether, which was evaporated to give 6.2 g of a bright orange solid. The crude product was chromatographed over alumina and a pure sample obtained via glc.

Can. J. Chem. Downloaded from www.nrcresearchpress.com by 210.87.254.6 on 09/05/12
For personal use only.

Can. J. Chem. Downloaded from www.nrcresearchpress.com by 210.87.254.6 on 09/05/12
For personal use only.

TABLE 2. Spectroscopic data for substituted trifluoroacetophenones

Substituent	Ultraviolet[a] λ_{max}, nm	Ultraviolet[a] $\varepsilon_{max} \times 10^4$	Infrared[b,c] $\nu_{C=O}$, cm^{-1}
4-$(CH_3)_2N$	358	2.95	1680[d]
4-NH_2	355	2.55	1680[d]
5'-Coumaranyl	308	1.41	1700
4-HO	298	1.61	1693[d]
4-CH_3O, 3-CH_3	298	1.52	1707
4-CH_3O	294	1.97	1710
4-C_2H_5O	294	1.55	1708
3,4-$(CH_3)_2$	268	1.20	1715
4-C_2H_5	267	1.49	1718
4-CH_3	266	1.49	1718
4-$(CH_3)_3C$	267	1.65	1710[d]
H	255	1.32	1723
3-CH_3	260	1.21	1720
3-CH_3O	261	0.820	1722
4-F	266	0.943	1726
4-Cl	266	1.50	1725
4-Br	270	1.68	1722

[a]In 2-propanol.
[b]Liquid film, unless otherwise noted.
[c]The 3-Cl and 4-NO_2 compounds, which appear in the accompanying paper, both have their carbonyl band at 1730 cm^{-1}.
[d]In carbon tetrachloride.

Anal. calcd. for $C_{10}H_7O_2F_3$: C 55.57, H 3.26; found: C 55.83, H 3.31.

4-Ethoxy-α,α,α-trifluoroacetophenone

4-Bromophenetole (5.6 g) was converted to the Grignard reagent and treated with trifluoroacetic anhydride (3.0 g). Work-up gave 5.8 g of impure liquid which was purified by glc.

Anal. calcd. for $C_{10}H_9O_2F_3$: C 55.05, H 4.16; found: C 55.09, H 4.29.

4-tert-Butyl-α,α,α-trifluoroacetophenone

The Grignard procedure, as above, was used. The product was sublimed and gave a mp of 47.5–48.0°C.

Anal. calcd. for $C_{12}H_{13}OF_3$: C 62.60, H 5.69; found: C 62.59, H 5.50.

4-Ethyl-α,α,α-trifluoroacetophenone

The Grignard procedure gave a liquid which was purified by glc.

Anal. calcd. for $C_{10}H_9OF_3$: C 59.41, H 4.49; found: C 59.44, H 4.46.

3-Methyl-4-methoxy-α,α,α-trifluoroacetophenone

This compound was prepared from 2-methoxytoluene using the Friedel–Crafts reaction. A glc separated sample crystallized to give mp 28.0–29.5°C.

Anal. calcd. for $C_{10}H_9O_2F_3$: C 55.05, H 4.06; found: C 55.08, H 4.30.

3,4-Dimethyl-α,α,α-trifluoroacetophenone

The Grignard reagent from 3,4-dimethylbromobenzene was treated with trifluoroacetic anhydride and gave after work-up and glc purification a pure liquid sample.

Anal. calcd. for $C_{10}H_9OF_3$: C 59.41, H 4.49; found: C 59.70, H 4.55.

Kinetic Procedure

The rate was followed by measuring the disappearance of the ketone absorption peak in the ultraviolet. The substrate dissolved in dioxan (20–50 μL) was added to 3.0 cm^3 of a thermally equilibrated sample of 2-propanol in the spectrometer. The initial absorbance reading A_0 was taken and then 20–50 μL of a freshly prepared and standardized 2-propanol solution of sodium borohydride of concentration b was added. Three inversions of the cell were made and readings of absorption and time were begun. (For the very fast reactions the measured rate constant had some dependence on the way that the cell was handled after the borohydride was added.) The second-order rate constant was obtained by plotting $\log 4b(C_0 - C_t)/C_0(4b - C_t)$ against time, where C is concentration determined from absorbance using Beer's law. A linear regression analysis was performed on a programmable calculator and the second-order rate constant obtained from the slope.

Initial concentrations of ketone varied from $1.0 \times 10^{-5}M$ to $7.19 \times 10^{-5}M$, and the initial molar ratio of ketone to borohydride varied from 0.94 to 58. Good second-order plots were obtained.

The 4-hydroxy ketone behaves differently in that the reduction of the carbonyl group is accompanied by the appearance of a peak at 362 nm, which rises and eventually falls if sufficient borohydride is present. The absorption peak for the phenoxy anion of the ketone occurs at this wavelength and presumably the phenolic group in the hydroxy ketone is protonating the alkoxide reduction product. (There is no indication that the borohydride is being converted to molecular hydrogen by the phenol.) The overall rate of disappearance of ketone was corrected for partial conversion to phenoxide, based on the rate of appearance of the peak at 362 nm.

Substituent Constants

The σ values used are those of McDaniel and Brown (14) except for 4-$(CH_3)_2N$, for which a value of 0.70 has been used (15). The σ^+ values come from Okamoto and Brown (16) except for the following additions and emendations: (*a*) 4-$(CH_3)_2N$, −1.74; 5'-coumaranyl, −0.984; 4-CH_3O, −0.778; 4-C_2H_5O, −0.811 (17); (*b*) 4-NH_2, −1.31; 4-HO, −0.92; 4-C_2H_5, −0.30 (18); and (*c*) 3-CH_3, −0.098 (19).

Preparative Scale Reductions

The ketone (50–200 mg in 3 cm^3 of 2-propanol) was stirred with a 50% excess of sodium borohydride at room temperature. Acidification, filtration, and passage through an alumina column, followed by elution with ether and evaporation gave the following yields of alcohol (20, 21), with reaction times in parentheses: 4-$(CH_3)_2N$, 98% (16 h); unsubstituted, 85% (0.5 h); 3-NO_2, 95% (1 h).

The 4-dimethylamino alcohol has not been previously prepared. 4-Dimethylaminophenyl trifluoromethyl carbinol: mp 101–102°C.

Anal. calcd. for $C_{10}H_{12}NOF_3$: C 54.79, H 5.52, N 6.39; found: C 54.88, H 5.58, N 6.33.

1. (*a*) R. STEWART. Oxidation mechanisms. W. A. Benjamin, New York. 1964; (*b*) R. STEWART. *In* Isotopes in organic chemistry. Vol. 2. *Edited by* E. Buncel and C. C. Lee. Elsevier, Amsterdam. 1976.
2. (*a*) R. STEWART. J. Am. Chem. Soc. **79**, 3057 (1957); (*b*) R. STEWART and R. VAN DER LINDEN. Tetrahedron Lett. **2**, 28 (1960); (*c*) R. STEWART and R. VAN DER LINDEN. Discuss. Faraday Soc. **29**, 211 (1960).
3. (*a*) D. C. WIGFIELD. Tetrahedron, **35**, 449 (1979); (*b*) D. C. WIGFIELD and F. W. GOWLAND. Tetrahedron Lett. **24**, 2209 (1979); (*c*) M. J. S. DEWAR and M. L. MCKEE. J. Am. Chem. Soc. **100**, 7499 (1978).
4. K. BOWDEN and M. HARDY. Tetrahedron, **22**, 1169 (1966).
5. W. J. BOVER and P. ZUMAN. J. Chem. Soc. Perkin Trans. II, 786 (1973).
6. (*a*) D. M. LEMAL and L. H. DUNLOP. J. Am. Chem. Soc. **94**, 6562 (1972); (*b*) J. D. DILL, A. GREENBERG, and J. F.

LIEBMAN. J. Am. Chem. Soc. **101**, 6814 (1979); (*c*) D. G. LEE and R. STEWART. J. Org. Chem. **32**, 2868 (1967).
7. (*a*) J. J. STEFFENS and D. M. CHIPMAN. J. Am. Chem. Soc. **93**, 6694 (1971); (*b*) Y. OHNISHI and M. KITAMI. Tetrahedron Lett. **42**, 4033 (1978); (*c*) A. OHNO, H. YAMAMOTO, T. OKAMOTO, S. OKA, and Y. OHNISHI. Chem. Lett. (Jpn.), 65 (1978); (*d*) R. A. GASE. Doctorate Thesis, University of Amsterdam, 1979; (*e*) S. SHINKAI, H. HAMADA, Y. KUSANO, and O. MARABE. J. Chem. Soc. Perkin Trans. II, 699 (1979); (*f*) A. OHNO, M. IKEGUCHI, T. KIMURA, and S. OKA. J. Am. Chem. Soc. **101**, 7036 (1979); (*g*) P. VAN EIKEREN and D. L. GRIER. J. Am. Chem. Soc. **98**, 4655 (1976).
8. (*a*) C. D. JOHNSON. Chem. Rev. **75**, 755 (1975); (*b*) D. J. MCLENNAN. Tetrahedron, **34**, 2331 (1978).
9. C. D. JOHNSON. The Hammett equation. Cambridge University Press, London. 1973.
10. (*a*) R. STEWART and J. D. VAN DYKE. Can. J. Chem. **48**, 3961 (1970); (*b*) R. STEWART and J. D. VAN DYKE. Can. J. Chem. **50**, 1992 (1972).
11. D. C. WIGFIELD and D. J. PHELPS. J. Org. Chem. **41**, 2396 (1976).
12. D. G. LEE. *In* Oxidation. Vol. 1. *Edited by* R. L. Augustine. Marcel Dekker, New York. 1969.
13. G. CHATELUS. C.R. Acad. Sci. **224**, 201 (1946).
14. D. H. MCDANIEL and H. C. BROWN. J. Org. Chem. **23**, 420 (1958).
15. A. J. HOEFNAGEL and B. M. WEPSTER. J. Am. Chem. Soc. **95**, 5357 (1973).
16. Y OKAMOTO and H. C. BROWN. J. Org. Chem. **22**, 485 (1957).
17. H. C. BROWN, C. G. RAO, and M. RAVINDRATHAN. J. Am. Chem. Soc. **99**, 7663 (1977).
18. S. CLEMENTI and P. LINDA. J. Chem. Soc. Perkin Trans. II, 1887 (1973).
19. E. GLYDE and R. TAYLOR. J. Chem. Soc. Perkin Trans. II, 1463 (1975).
20. R. STEWART and R. VAN DER LINDEN. Can. J. Chem. **38**, 399 (1960).
21. R. STEWART, K. C. TEO, and L. K. NG. Can. J. Chem. **58**, 2497 (1980).

Can. J. Chem. Downloaded from www.nrcresearchpress.com by 210.87.254.6 on 09/05/12
For personal use only.

The reduction of aryl trifluoromethyl ketones by *N*-carbamoylmethyl-1,4-dihydronicotinamide

ROSS STEWART, K. C. TEO, AND L. K. NG

Department of Chemistry, University of British Columbia, Vancouver, B.C., Canada V6T 1Y6

Received March 25, 1980

This article is dedicated to Prof. Raymond U. Lemieux on the occasion of his 60th birthday

Can. J. Chem. Downloaded from www.nrcresearchpress.com by 210.87.254.42 on 09/05/12
For personal use only.

ROSS STEWART, K. C. TEO, and L. K. NG. Can. J. Chem. **58**, 2497 (1980).

The reaction of 15 aryl trifluoromethyl ketones with *N*-carbamoylmethyl-1,4-dihydronicotinamide has been studied in aqueous sulfolane buffer. The unsubstituted ketone and those containing electron-withdrawing groups in the ring have the following reaction characteristics: (*a*) a high yield of alcohol is obtained, (*b*) the observed reaction rate is independent of ring substituent; however, when corrections are made for degree of hydration of the ketones the rate is correlated with Hammett σ values with a rho of +1.98, (*c*) a secondary isotope effect of approximately 1.08 and primary isotope effects of 1.45–1.62 are observed at 43.4°C for the reaction of the dihydronicotinamide containing one or two atoms of deuterium at C-4, (*d*) $\Delta H^{\ddagger} = 15.2$ kcal mol^{-1}, and $\Delta S^{\ddagger} = -27.0$ cal deg^{-1} mol^{-1} for the unsubstituted compound, uncorrected for ketone hydration; $\Delta S^{\ddagger}$ for reaction of the unhydrated ketone and dihydronicotinamide is estimated to be −45 to −50 cal deg^{-1} mol^{-1}. The mechanism for the reduction is consistent with hydride transfer from reductant to oxidant, very possibly accompanied by blind-alley formation of an adduct between ketone hydrate and dihydronicotinamide. Ketones containing electron-donating groups in the ring react with the dihydronicotinamide in some undetermined way, giving little or no alcohol as product.

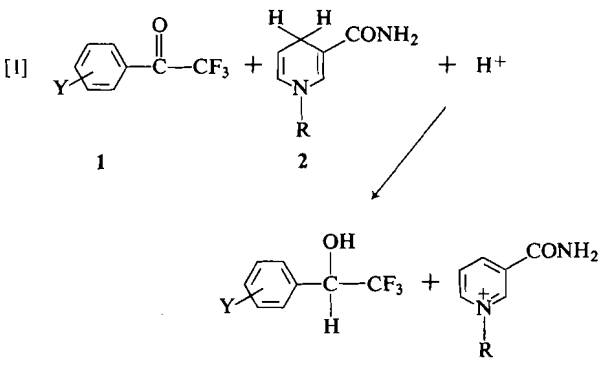
ROSS STEWART, K. C. TEO et L. K. NG. Can. J. Chem. **58**, 2497 (1980).

On a étudié la réaction de 15 aryl trifluorométhylcétones avec la *N*-carbamoylméthyldihydro-1,4 nicotinamide dans un tampon aqueux de sulfolane. La cétone non substitué et celle contenant des groupements électro-attracteurs sur le cycle ont les caractéristiques réactionnelles suivantes: (*a*) on obtient un fort rendement en alcool, (*b*) la vitesse de la réaction observée est indépendante du substituant fixé sur le cycle; cependant quand on fait des corrections pour tenir compte du degré d'hydratation des cétones, la vitesse se rapproche des valeurs σ de Hammett avec un rho de +1.98, (*c*) on observe un effet isotopique cinétique secondaire d'environ 1.08 et des effets isotopiques cinétiques primaires de 1.45–1.62 à 43.4°C pour la réaction de la dihydronicotinamide contenant un ou deux atomes de deutérium en C-4, (*d*) le $\Delta H^{\ddagger} = 15.2$ kcal mol^{-1} et le $\Delta S^{\ddagger} = -27$ cal deg^{-1} mol^{-1} pour les composés non substitués (ces valeurs ne sont pas corrigées pour tenir compte de l'hydratation de la cétone); pour la réaction de la cétone non hydratée et de la dihydronicotinamide on évalue que le $\Delta S^{\ddagger}$ se situe entre −45 et −50 cal deg^{-1} mol^{-1}. Le mécanisme de la réduction est en accord avec un transfert d'hydrure du réducteur à l'oxydant accompagné très probablement de la formation d'un adduit entre l'énol et la dihydronicotinamide. Les cétones ayant sur le cycle des groupements électro-donneurs réagissent avec la déhydronicotinamide d'une façon non encore connue en donnant peu ou pas d'alcool.

[Traduit par le journal]

Introduction

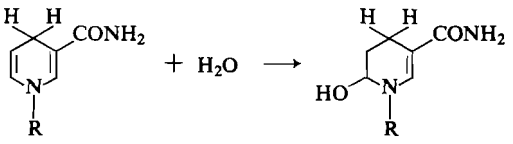
α,α,α-Trifluoroacetophenone (**1**, Y = H) has come to occupy an important place in the investigation of the mechanism of reduction of carbonyl compounds by nicotinamide coenzymes such as NADH and model compounds thereof (**2**) (1–7).



Steffens and Chipman studied the reaction of trifluoroacetophenone with *N*-alkyldihydronicotinamides and observed a disparity between the kinetic isotope effect and the partition isotope effect (as measured by the relative amounts of protium and deuterium in the alcohol reduction product) when the dihydronicotinamide was monodeuteriated at the 4-position (1). They concluded that an intermediate exists on the reaction pathway since the rate-determining and product-determining steps appear to be different. Recently van Eikeren *et al.* have carefully examined the course of the reaction of *N*-propyl and *N*-benzyl dihydronicotinamide with several carbonyl compounds, principally pyridine-2-carboxaldehyde but including trifluoroacetophenone (8, 9). They have shown that the hydration of dihydronicotinamides, which is a well known side reaction in dihydropyridine reductions, is catalyzed by the carbonyl compound under conditions where the usual acid-catalyzed reaction is quite slow.

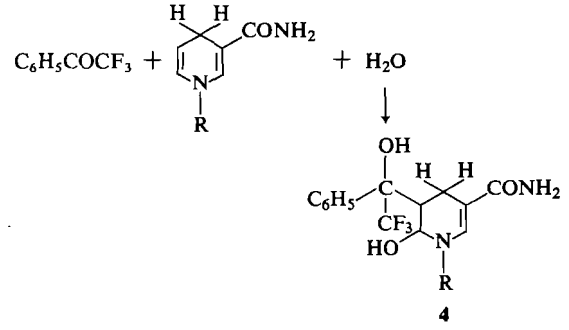
0008-4042/80/232497-07$01.00/0

©1980 National Research Council of Canada/Conseil national de recherches du Canada

[2] 

3

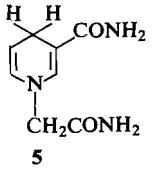
Furthermore, they showed that several carbonyl compounds, including trifluoroacetophenone, react in aqueous systems with the dihydronicotinamide to give adducts such as **4**.

[3] 

4

Although the normal acid-catalyzed reaction of dihydronicotinamides to give **3** is first order, the carbonyl-catalyzed hydration process and reaction [3] are both second order, and are kinetically equivalent to the oxidation process, eq. [1]. Thus following the disappearance of the dihydronicotinamide, the usual practice, can lead to a kinetic isotope effect that is too small, since only some of the dihydronicotinamide reacts by C—H(D) bond cleavage.

We have had a long-standing interest in the mechanism of organic oxidation processes and also in the hydration equilibria of trifluoroacetophenones. Accordingly, we have examined the reaction of a series of ring-substituted trifluoroacetophenones with *N*-carbamoylmethyl-1,4-dihydronicotinamide, **5**, in order to learn more about the oxidation process. We had earlier shown that **5** has reasonably good stability in aqueous solution, both in its reduced and in its oxidized forms (10).



5

Trifluoroacetophenone is highly hydrated in aqueous solution (11–13) and earlier workers realized that this caused the measured rate constant for reduction of this compound to be lower than the true bimolecular rate constant for reaction of carbonyl compound and reducing agent. We can calculate the equilibrium constant for hydration of aryl trifluoromethyl ketones in any mixture of water with sulfolane or dimethyl sulfoxide between 1 mole percent water and pure water (11). We have chosen to use 21.8% sulfolane – 78.2% water (v/v) buffered at an apparent pH of 8.3 for our studies. These conditions provide sufficient substrate solubility, coupled with decomposition rates that are tolerable. A higher pH would stabilize the dihydronicotinamide but would (*a*) increase the rate of decomposition of the pyridinium product (not a critical factor unless redox equilibrium were established) and (*b*) cause the aryl trifluoromethyl ketones containing strongly electron-withdrawing groups to form adducts with hydroxide ion (ionization of the ketone hydrates) (13). Higher sulfolane concentrations cause the equilibrium between ketone and ketone hydrate to become sluggish and thus complicate the kinetic treatment.

The effect of polar aprotic solvents such as dimethyl sulfoxide (DMSO) on ketone hydration and its effect on the oxidation process has not always been appreciated. Thus, when the reduction of trifluoroacetophenone by *N*-propyldihydronicotinamide was studied in mixtures of water and DMSO it was assumed that an increase in the water content of the system decreases the concentration of the free ketone (7). In fact, aqueous DMSO is unusual in that mixtures up to 85 mole percent DMSO actually produce a *higher* degree of hydration of trifluoroacetophenone than does pure water (12).

Results and Discussion

The rate measurements were made by following the disappearance in the ultraviolet of the 347.5 nm peak of **5** by one of the following means. The concentration of **1** was varied (Fig. 1) and the rate constant k_2' for the reaction of **1** with **5** determined from the slope. In each experiment an accompanying reaction was run in which the ketone was omitted and the first-order hydrolysis rate of **5**, k_{dec}, determined. We found that the latter quantity showed a greater variation than expected, the cause of which could not be traced. An enormous number of kinetic experiments would have to be performed to encompass all the envisaged substituent, isotopic, and temperature variations using the above procedure; thus, in some cases we simply subtracted the decomposition rate from the observed rate to obtain the pseudo first-order rate constant for the bimolecular process(es). Despite the variations in the decomposition rate referred to above, the error introduced when a considerable excess of ketone is used is quite small. The

Can. J. Chem. Downloaded from www.nrcresearchpress.com by 210.87.254.42 on 09/05/12
For personal use only.

Can. J. Chem. Downloaded from www.nrcresearchpress.com by 210.87.254.42 on 09/05/12
For personal use only.

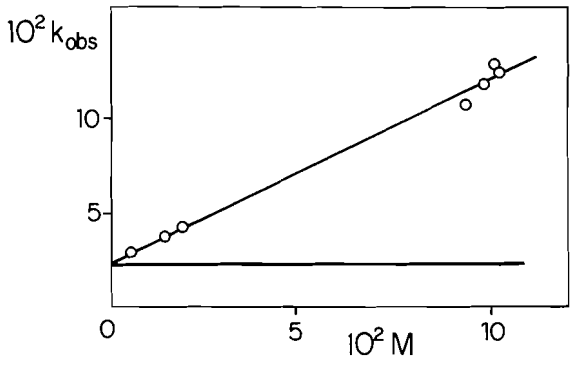


FIG. 1. Variation of k_{obs} with concentration of trifluoroacetophenone, T = 43.4°C. The horizontal line represents the decomposition rate of **5** (average of blanks accompanying reaction of **5** with ketone).

second-order rate constant k_2' was then obtained using eq. [4], where [ketone] is the total quantity of ketone added.

$$[4] \quad k_2' = (k_{obs} - k_{dec})/[\text{ketone}]$$

The values of k_2' obtained by one of the above procedures were then corrected for hydration of the ketone by using the equilibrium constant that is known, or that can be calculated, for each of the ketones (see Experimental) to give k_2, the true bimolecular rate constant for reaction of ketone and dihydronicotinamide. The results for 15 ketones are given in Table 1.

Substituent Effects

When the values of log k_2 and log k_2' are plotted against the Hammett substituent constant σ an interesting pattern emerges (Fig. 2). For the unsubstituted compound and those containing electron-withdrawing groups there is virtually no effect of substituent on the rate of reaction of the nicotinamide with the ketones, when no correction is made for the degree of hydration of the ketones. This tells us that the effect of substituents on the rate of reaction of these compounds is virtually identical to the effect of substituents on the equilibrium constant for hydration of the same compounds. For these compounds the rate constant corrected for the varying degrees of hydration of the ketones shows a large substituent effect. In the eight substituents ranging from Y = H to Y = 3-NO_2 the rho value is +1.98 (correlation coefficient 0.9908), showing that the reaction is subject to a strong electronic effect.

There is clearly a sharp break in the curve for the uncorrected rate constant k_2' as the σ values become negative, with the rate of reaction showing an increase with increasing electron donation by the substituent Y. When Y = 4-$(CH_3)_2N$ the degree of hydration is quite small and the values of k_2 and k_2' are almost identical. The two curves thus coalesce here, as expected.

The break in the curves in Fig. 2 is clearly caused by a second reaction of the dihydronicotinamide supplanting the reduction of ketone to alcohol, the following yields of alcohol being found using glc: 3-NO_2 (75%), 3-CF_3 (87%), unsubstituted (73%), 4-CH_3O (21%), 4-C_2H_5O (17%), 4-NH_2 (0.1%), 4-$(CH_3)_2N$ (0.1%).

We have been unable to positively identify the components of the mixture formed by the reaction of **5** with the amino compounds, but they appear to

TABLE 1. Rate data for reaction of aryl trifluoromethyl ketones with *N*-carbamoylmethyl-1,4-dihydronicotinamide[a]

Ring substituent	$[ZH_2O]/[Z]$[a,b]	$10^3 k_2'$ M^{-1} s^{-1}	$10^3 k_2$ M^{-1} s^{-1}
4-$(CH_3)_2N$	0.068	24.6	26.3
4-NH_2	0.34	10.9	14.6
5'-Coumaranyl[c]	1.13[d]	1.41	3.01
4-CH_3O	3.39	1.09	4.81
4-CH_3	14.1	0.362	5.47
4-C_2H_5	14.6[d]	0.267	4.15
4-$(CH_3)_3C$	17.4[d]	0.408	7.10
Unsubstituted	37.0	0.270	10.5
4-F	39.8	0.298	11.8
4-Cl	67.2[d]	0.293	20.0
4-Br	76.8[d]	0.330	25.7
3-F	155	0.336	52.3
3-Cl	178[d]	0.261	46.7
3-CF_3	224[d]	0.285	64.1
3-NO_2	691	0.345	239

[a]In 21.8% sulfolane – 78.2% water (v/v), pH 8.3, μ = 0.50, T = 43.4°C.
[b]ZH_2O = ketone hydrate, Z = ketone.
[c]Aryl structure is  .
[d]Calculated as described in experimental section using σ^+ values used in ref. 19.

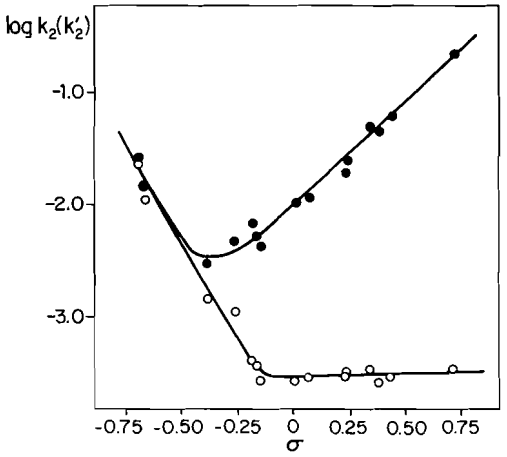


FIG. 2. Hammett plot for reaction of aryl trifluoromethyl ketones with **5**, T = 43.4°C. Open circles, log k_2'; closed circles log k_2. Sigma values those used in ref. 19.

Can. J. Chem. Downloaded from www.nrcresearchpress.com by 210.87.254.42 on 09/05/12
For personal use only.

TABLE 2. Primary isotope effects in the reaction of **5**-d and **5**-d_2 with aryl trifluoromethyl ketones $YC_6H_4COCF_3$[a]

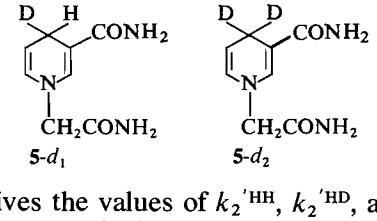
Y	$k_2'^{HH}$ $10^4\ M^{-1}\ s^{-1}$	$k_2'^{HD}$ $10^4\ M^{-1}\ s^{-1}$	$k_2'^{DD}$ $10^4\ M^{-1}\ s^{-1}$	T °C	Primary isotope effect, p[b]
3-CF_3	2.84	2.19	1.67	43.4	1.57
3-F	2.92	2.35	1.87	43.4	1.45
4-Cl	3.36	2.54	1.95	43.4	1.59
H	1.15	0.890	0.690	34.5	1.54
H	1.41	0.980	0.712	35.0	1.83
H	2.64	2.05	1.51	43.4	1.62
H	2.70	2.16	1.63	44.0	1.53
H	5.11	3.87	2.93	52.7	1.63
H	12.3	9.45	7.15	64.4	1.59

[a]In 21.8% sulfolane – 78.2% water (v/v), pH 8.3, $\mu = 0.50$.
[b]Calculated from eq. [5] using a value of s of 1.08.

include decomposition products of the dihydronicotinamide. The report of the formation of the adduct **4** appeared in the literature (8) after this work was completed and the analogous compound may also be a component of the mixture formed from the amino ketones. The possible catalytic effect of aromatic amino groups on the decomposition of **5** was checked by measuring its rate of decomposition in the presence of varying amounts of aniline and dimethylaniline. A catalytic effect was, indeed, observed but it is far too small to account for the rates of disappearance of **5** in the presence of the amino ketones. Thus, in order to double the rate of decomposition of **5** the presence of a roughly 80-fold excess of dimethylaniline was required, whereas this effect can be achieved with less than a 3-fold excess of 4-dimethylaminotrifluoroacetophenone.

Isotope Effects

The effects of deuterium substitution at the 4-position of **5** was examined for a number of ketones. The compound **5**-d_1 was prepared by the reduction of the pyridinium compound using sodium dithionite and D_2O; **5**-d_2 was prepared by a sequence of reductions and oxidations in the same manner.



5-d_1 **5**-d_2

Table 2 gives the values of $k_2'^{HH}$, $k_2'^{HD}$, and $k_2'^{DD}$ which are, respectively, the rate constants for the reaction of **5**, **5**-d_1, and **5**-d_2 with trifluoroacetophenone and four of its derivatives containing electron-withdrawing groups. Since such compounds give high yields of alcohol we assume that the isotope effects apply to the carbonyl reduction process. Both primary (p) and secondary (s) isotope effects will be associated with the hydrogen transfer process and, provided the kinetic data are sufficiently precise, both can be determined using the following relations.

$$[5]\quad k^{HH}/k^{DD} = p.s$$

$$[6]\quad k^{HD} = \frac{1}{2}\frac{k^{HH}}{p} + \frac{1}{2}\frac{k^{HH}}{s}$$

$$[7]\quad k^{DD}p^2 - 2k^{HD}p + k^{HH} = 0$$

Equations [5] and [6] (14) can be combined to give eq. [7], a quadratic which can be solved to give two roots, one of which corresponds to the primary isotope effect p. It can be easily shown that the other root is the secondary isotope effect s. We assign p to the larger and s to the smaller root. Equation [7] is sensitive to errors in the rate constants and imaginary roots can result if the rate data are not sufficiently precise.

Figure 3 shows rate plots for **5**, **5**-d_1, and **5**-d_2 reacting with 3-$CF_3C_6H_4COCF_3$. It is apparent from the slopes of the lines that isotopic substitution does not produce large rate changes. For this system the roots of eq. [7] are 1.19 and 1.43, the former presumably being s and the latter p. Because of the sensitivity of the roots of eq. [7] to experimental error in any one of the rate constants k^{HH}, k^{HD}, or k^{DD} we have concluded that it is preferable to calculate an average value of s for all systems that give real roots and then to apply this value to calculate p for the various systems studied. The rationale here is that s is not likely to be far from unity and is less likely to be affected by structural and mechanistic changes than is p. Indeed, previous workers who have used compounds analogous to **5** and **5**-d_1 have simply taken s to be unity and then calculated p from rate data on this basis (1, 8, 15). We have averaged the smaller of the real roots

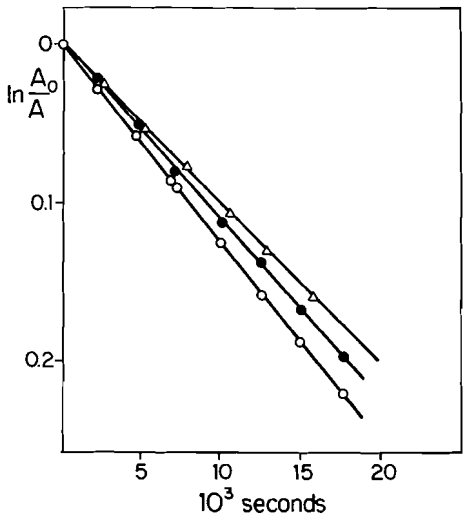


FIG. 3. Reaction of 3-$CF_3C_6H_4COCF_3$ with **5** (open circles), **5**-d_1 (closed circles), and **5**-d_2 (triangles). $T = 43.4°C$.

for all systems studied, giving a value for s of 1.08 (standard deviation ±0.11). The reaction site in the dihydronicotinamide changes from sp^3 to sp^2 during the reaction and such changes almost always produce small positive secondary deuterium isotope effects (16, 17) and our estimated value of 1.08 seems not unreasonable (see, however ref. 18). The primary isotope effects listed in Table 2 are based on this value of s and it is assumed that s does not change with changing temperature or substituent.

The values of p in Table 2 range from 1.45 to 1.83. Any variations of p with structure or with temperature are concealed by the limited precision of the rate data. One can conclude, however, that for the ketone reduction process the primary isotope effect is small and relatively insensitive to substituents in the ring of the ketone being reduced.

Activation Parameters

The data for the unsubstituted ketone in Table 2 give an apparent value of $\Delta H^{\ddagger}$ of 15.2 kcal mol^{-1} (63.5 kJ mol^{-1}) for reaction with **5**, the activation entropy being −27.0 cal deg^{-1} mol^{-1} (−113 J deg^{-1} mol^{-1}). These values are uncorrected for ketone hydration. Since the thermodynamic parameters of the dehydration step and the activation parameters of the reduction step(s) comprise the experimentally observed activation parameters, the entropy of activation of the reduction can be estimated as follows. The equilibrium hydration of the 4-methoxy compound has $\Delta H = -6.7$ kcal mol^{-1} and $\Delta S = -19.4$ cal deg^{-1} mol^{-1} (11), values which were observed to not change greatly when fairly large amounts of sulfolane were added. If ΔS for the hydration of the unsubstituted compound is also near −20 kcal mol^{-1} the entropy of activation for the rate-controlling step of the reduction must be a fairly large negative value, somewhere between −45 and −50 cal deg^{-1} mol^{-1}.

The primary isotope effects for reaction of the deuterated compound **5**-d_2 with trifluoroacetophenone corresponds to an energy difference of only 0.3 kcal mol^{-1} and the kinetic data are not sufficiently precise to allow the partition of this quantity between enthalpy and entropy with any precision. However, for both **5**-d_1 and **5**-d_2 a higher enthalpy of activation appears to be the source of most of the isotope effect.

Mechanism

It is clear from Fig. 2 that there are at least two different reactions taking place between aryl trifluoromethyl ketones and the dihydronicotinamide.

Consider first the reduction of ketone to alcohol, which predominates for ketones lacking an electron-donating substituent. This process is characterized by (*a*) a substantial positive rho, (*b*) a small primary isotope effect, and (*c*) a large negative entropy of activation. The simplest mechanism to be considered with respect to these criteria is hydride transfer to give pyridinium ion and alkoxide ion. Sodium borohydride reduction, which is a direct model for hydride transfer, has a rho of 3.12 in 2-propanol (19), somewhat larger than the value of 1.98 we observe. (The latter rho may be actually slightly larger since some of the competing reaction may be contributing to the reaction of the compounds containing less strongly electron-attracting groups.) Hydride transfer reactions often have modest isotope effects (20, 21) but they are not often as small as those observed herein. And finally, the entropy of activation seems rather large in magnitude for a simple bimolecular reaction between neutral molecules.

A number of possible intermediates have been suggested for reactions of dihydropyridines with oxidants, including charge-transfer complexes, complexes of radicals with radical-cations, and covalent adducts such as **4** (7, 8, 22, 23). A rapidly and reversibly formed intermediate lying on the reaction path, such as a charge-transfer or other complex, will have little effect on the overall rho or on the entropy of activation, provided it is not the major component at equilibrium. Though the size of the isotope effect would be a function of whatever species are involved in the carbon–hydrogen bond-breaking step, the present state of the art does not allow mechanism to be assigned on this basis with any degree of confidence (20, 24). Thus our

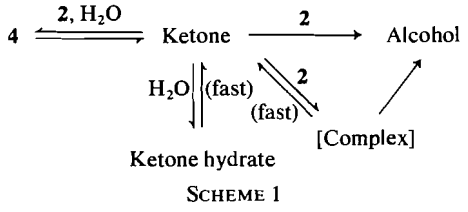
Can. J. Chem. Downloaded from www.nrcresearchpress.com by 210.87.254.42 on 09/05/12
For personal use only.

Can. J. Chem. Downloaded from www.nrcresearchpress.com by 210.87.254.42 on 09/05/12
For personal use only.

results are silent with respect to direct hydride transfer or net hydride transfer via an intermediate complex present in small concentration.

Adducts such as **4** are not on the reaction path; they could be slowly reconverted to reactants and eventually to redox products (8). If the measured rate of disappearance of dihydronicotinamide were due only to adduct formation the rho value would correspond to this process and there would be no isotope effect. A possible model for the adduct is the ketone hydrate and it may be significant that the effect of substituents on the equilibrium governing formation of the latter is identical to that which we observe in this work (25). The isotope effect can only be reconciled with this mechanism if the redox reaction has a substantial isotope effect and contributes significantly to the measured rate. Furthermore, the rho values for the redox reaction and adduct formation must not be drastically different in order that the isotope effect be relatively insensitive to substituent, as is observed. The large negative entropy of activation, 45–50 cal deg^{-1} mol^{-1}, is consistent with adduct formation, providing the transition state includes the three molecules required to form the adduct. Putting it another way, the measured value of -27 cal deg^{-1} mol^{-1} is consistent with adduct formation from a molecule of ketone hydrate and a molecule of dihydronicotinamide.

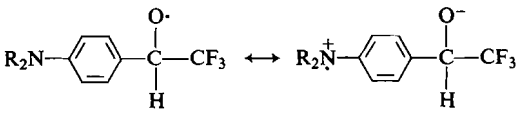
The results for the alcohol producing reaction appear to be best accommodated by the following mechanism (Scheme 1): a net hydride transfer, probably accompanied by some reversible formation of an adduct such as **4**, as suggested by van Eikeren *et al.* (8).



SCHEME 1

Were hydride transfer alone occurring one might have expected to find a somewhat higher rho, a somewhat higher primary isotope effect, and a somewhat less negative entropy of activation.

For ketones containing such groups as amino the reaction is mysterious, particularly so since we cannot identify the components in the mixture of products. It is difficult to see how a reaction between an aryl ketone and a dihydropyridine can have a negative rho, since the ketone itself is stabilized by groups such as amino. One possibility is hydrogen-atom transfer from the dihydropyridine to give the radical **6**, which would be stabilized by resonance in a way not open to ketones with electron-withdrawing groups in the ring. Such a radical might then decompose to give a mixture of products.



6

Summary

The reduction of aryl trifluoromethyl ketones to alcohols by *N*-carbamoylmethyl-1,4-dihydronicotinamide is facilitated by electron-withdrawing groups in the aryl ring but this effect is cancelled in aqueous systems by competing ketone hydrate formation. The mechanism appears to be hydride transfer, very possibly accompanied by blind-alley formation of an adduct between ketone hydrate and dihydronicotinamide. Electron-donating groups in the aryl ring favour a competing reaction that does not produce alcohol.

Experimental

Materials

The preparation of the ketones has been previously described (11–13, 19, 26) except for the following compounds.

3-Trifluoromethyltrifluoroacetophenone was prepared in 48% yield by the Grignard synthesis using *m*-trifluoromethylbromobenzene and trifluoroacetic acid (19); bp 59°C at 20 Torr. *Anal.* calcd. for $C_9H_4OF_6$: C 44.65, H 1.67; found: C44.75, H 1.69.

3-Chlorotrifluoroacetophenone was prepared by the Grignard method from *m*-iodochlorobenzene, bp 50°C at 9 Torr. *Anal.* calcd. for $C_8H_4OF_3Cl$: C 46.29, H 1.94; found: C 46.15, H 2.08.

N-Carbamoylmethyl-1,4-dihydronicotinamide **5** was prepared as previously described (10). The 4-deuterio compound **5**-d_1 was prepared in 83% yield (0.99 *d* at C-4 by nmr) by reduction of the pyridinium salt, using sodium dithionite and D_2O, using the general method of Caughey and Schellenberg (27). Four and one-half cycles of oxidation by chloranil followed by dithionite reduction in D_2O (27) gave the dideuterio compound **5**-d_2 containing 1.90 atoms of deuterium at C-4 by nmr. It was observed that the methylene protons of the carbamoylmethyl group at N-1 were almost completely deuterated in the product. It was assumed that this isotopic substitution had no effect on the redox reaction.

The pK_{BH^+} of **5** was determined spectrophotometrically using the 347.5 nm peak in the aqueous sulfolane system used for the kinetic experiments. An apparent pK_{BH^+} of 6.46 was obtained, based on glass electrode standardized against aqueous buffer. The pH of the aqueous sulfolane buffer system (21.8% sulfolane by volume) used in the kinetic experiments was 8.3 on the same basis. The buffer was 0.1 molar in each of triethanolamine and triethanolammonium chloride and 0.4 molar in sodium perchlorate.

Kinetic Procedure

The ketones and the dihydronicotinamide were dissolved in the aqueous sulfolane buffer to give stock solutions that were thermally equilibrated before the kinetic runs were begun. The peak for **5** at 347.5 nm has some ketone absorption in the case of

amino and alkoxy compounds. Since these were the compounds that gave higher rates than expected, additional experiments were undertaken using wavelengths as high as 380 nm. Although such measurements on the side of the absorption curve lacked some precision, they did not show any trend that would suggest the rates measured at 347.5 nm are spurious.

The second-order rate constant k_2' was corrected for ketone hydration as follows. The dehydration of trifluoromethyl ketones is governed by eq. [7], where Z is ketone and ZH_2O is ketone hydrate, W_0 is the hydration parameter, and pK_d the negative logarithm of the equilibrium constant for the reaction $ZH_2O \rightleftharpoons Z + H_2O$ in the standard state water (11, 12).

[7] $$W_0 = pK_d + \log [Z]/[ZH_2O]$$

[8] $$pK_d = 1.62\sigma^+ + 1.96$$

At 31.4°C eq. [8] holds for these ketones and K_d (standard state water) can be calculated for those compounds whose K_d values have not been previously determined (12). W_0 for 21.8% (v/v) aqueous sulfolane is 0.12 (11) and using this quantity and eqs. [7] and [8] gives eq. [9].

[9] $$\log [ZH_2O]/[Z] = 1.62\sigma^+ + 1.84$$

A temperature correction was made, based on the known heat of hydration of the 4-methoxy compound, $\Delta H = -6.7$ kcal mol^{-1} (11). Since the temperature correction is not large, $([ZH_2O]/[Z])^{43.4°} = ([ZH_2O]/[Z])^{31.4°}/1.55$, it is assumed that variations of ΔH with substituent do not give rise to significant errors.

In all cases examined the ketone – ketone hydrate relaxation rate was much faster than the reaction of the dihydronicotinamide.

The reaction products were isolated as follows. After standing for six days the reaction mixture on which the kinetics had been followed was extracted with an equal volume of ether–pentane (v/v = 1, four times). The combined organic extract was washed, dried, concentrated, and then subjected to analysis by gas–liquid chromatography and mass spectrometry. Authentic samples of alcohols were used for comparison of the chromatographic peaks in the reaction products.

Acknowledgement

The financial support of the Natural Sciences and Engineering Research Council of Canada is gratefully acknowledged.

1. J. J. Steffens and D. M. Chipman. J. Am. Chem. Soc. **93**, 6694 (1971).
2. Y. Ohnishi and M. Kitami. Tetrahedron Lett. **42**, 4033 (1978).
3. A. Ohno, H. Yamamoto, T. Okamoto, S. Oka, and Y. Ohnishi. Chem. Lett. (Jpn.), 65 (1978).
4. R. A. Gase. Doctorate Thesis, University of Amsterdam, Amsterdam, The Netherlands. 1979.
5. S. Shinkai, H. Hamada, Y. Kusano, and O. Marabe. J. Chem. Soc. Perkin Trans. II, 699 (1979).
6. A. Ohno, M. Ikeguchi, T. Kimura, and S. Oka. J. Am. Chem. Soc. **101**, 7036 (1979).
7. P. van Eikeren and D. L. Grier. J. Am. Chem. Soc. **98**, 4655 (1976).
8. P. van Eikeren, D. L. Grier, and J. E. Eliason. J. Am. Chem. Soc. **101**, 7406 (1979).
9. P. van Eikeren, P. Kenney, and R. Tokmakian. J. Am. Chem. Soc. **101**, 7402 (1979).
10. D. J. Norris and R. Stewart. Can. J. Chem. **55**, 1687 (1977).
11. R. Stewart and J. D. Van Dyke. Can. J. Chem. **50**, 1992 (1972).
12. R. Stewart and J. D. Van Dyke. Can. J. Chem. **48**, 3961 (1970).
13. R. Stewart and R. Van der Linden. Can. J. Chem. **38**, 399 (1960).
14. R. P. Bell and D. M. Goodall. Proc. R. Soc. London, Ser. A, **294**, 273 (1966).
15. D. J. Creighton, J. S. Hajdu, and D. S. Sigman. J. Am. Chem. Soc. **98**, 4619 (1976).
16. P. A. Rock (*Editor*). Isotopes and chemical principles. American Chemical Society, Washington, DC. 1975.
17. J. P. Klinman. *In* Isotope effects on enzyme catalyzed reactions. *Edited by* W. W. Cleland, M. H. O'Leary, and D. B. Northrop. Univ. Park Press, Baltimore. 1977.
18. P. van Eikeren and D. L. Grier. J. Am. Chem. Soc. **99**, 8057 (1977).
19. R. Stewart and K. C. Teo. Can. J. Chem. **58**, 2491 (1980).
20. R. Stewart. *In* Isotopes in organic chemistry. Vol. 2. *Edited by* E. Buncel and C. C. Lee. Elsevier, Amsterdam. 1976.
21. R. Stewart and T. W. Toone. J. Chem. Soc. Perkin Trans. II, 1243 (1978).
22. T. C. Bruice, L. Main, S. Smith, and P. Y. Bruice. J. Am. Chem. Soc. **93**, 7327 (1971).
23. G. Blankenhorn. Biochemistry, **14**, 3172 (1975).
24. H. Simon and A. Kraus. *In* Isotopes in organic chemistry. Vol. 2. *Edited by* E. Buncel and C. C. Lee. Elsevier, Amsterdam. 1976.
25. R. Stewart, L. K. Ng, and K. C. Teo. Tetrahedron Lett. **33**, 3061 (1979).
26. E. T. McBee, S. Resconich, L. R. Behohlav, and H. P. Braendlin. J. Org. Chem. **28**, 3579 (1963).
27. W. S. Caughey and K. A. Schellenberg. J. Org. Chem. **31**, 1978 (1966).

Can. J. Chem. Downloaded from www.nrcresearchpress.com by 210.87.254.42 on 09/05/12
For personal use only.

Horseradish peroxidase. XL. The oxidation of native enzyme to Compound II

ALEXANDER D. NADEZHDIN AND H. BRIAN DUNFORD
Department of Chemistry, University of Alberta, Edmonton, Alta., Canada T6G 2G2

Received February 1, 1980

This paper is dedicated to Prof. Raymond U. Lemieux on the occasion of his 60th birthday

ALEXANDER D. NADEZHDIN and H. BRIAN DUNFORD. Can. J. Chem. **58**, 2504 (1980).

The oxidation of native horseradish peroxidase to Compound II by photochemically generated inorganic free radicals $SO_4^{\cdot-}$, $Cl_2^{\cdot-}$, and $Br_2^{\cdot-}$ was observed. The rates of Compound II accumulation for different rates of free radical generation and different reagent concentrations have been measured. The interpretation of the experimental data allowed us to estimate the rates of the reactions $SO_4^{\cdot-}$ + HRP, $Br_2^{\cdot-}$ + HRP, and $Cl_2^{\cdot-}$ + HRP: (3–6) × 10^6 M^{-1} s^{-1}, (2.2–3.0) × 10^6 M^{-1} s^{-1}, and $\gtrsim 10^8$ M^{-1} s^{-1} respectively. Also obtained for all three oxidants were the ratios of the number of free radicals responsible for the heme oxidation to the total number of them attacking the enzyme.

ALEXANDER D. NADEZHDIN et H. BRIAN DUNFORD. Can. J. Chem. **58**, 2504 (1980).

On a observé l'oxydation de la peroxydase du raifort naturelle en un composé II par les radicaux inorganiques libres $SO_4^{\cdot-}$, $Cl_2^{\cdot-}$, $Br_2^{\cdot-}$ produits photochimiquement. On a mesuré la vitesse d'accumulation du composé II pour différentes vitesses de formation de radical libre et pour différentes concentrations de réactif. L'interprétation des données expérimentales nous permet d'évaluer la vitesse des réactions $SO_4^{\cdot-}$ + HRP, $Br_2^{\cdot-}$ + HRP et $Cl_2^{\cdot-}$ + HRP: (3–6) × 10^6 M^{-1} s^{-1}, (2.2–3.0) × 10^6 M^{-1} s^{-1} et $\gtrsim 10^8$ M^{-1} s^{-1} respectivement. On a également obtenu, pour les trois oxydants, les rapports entre le nombre de radicaux libres responsables de l'oxydation de l'hème et le nombre total de ceux qui attaquent l'enzyme.

[Traduit par le journal]

Introduction

Pulse and steady state radiolysis techniques have been used for more than a decade (1–5) for the study of enzyme reactions with free radical reductants such as e^-, ·H, or oxidants like ·OH, SCN^-, $Cl_2^{\cdot-}$, or $Br_2^{\cdot-}$. Rate constants, most of which are over 10^{10} $M^{-1}s^{-1}$, have been reported (1, 5, 7). In some cases the spectral changes caused by attack of free radicals were assigned to specific radical sites on the protein surface (6). Combined pulse radiolysis and enzyme inactivation studies of lysozyme, ribonuclease, trypsin, and α-chymotrypsin led to successful identification of the amino acid residues essential for enzymatic activity (2, 3). As was shown in ref. 4, many radicals by themselves are inefficient in the inactivation of trypsin.

In the case of the iron-containing hemoproteins, ferrocytochrome *c* and catalase, no appreciable oxidation of the heme iron by ·OH radicals was observed, while hydrated electrons reduce the heme group of ferricytochrome *c* very effectively but do not change the valence state of catalase iron (1, 5).

In this paper we report the results of a photochemical study of horseradish peroxidase (HRP) reactions with three inorganic free radicals $SO_4^{\cdot-}$, $Br_2^{\cdot-}$, and $Cl_2^{\cdot-}$. Sulfate radicals were produced in the water solution containing HRP and sodium persulfate under uv light irradiation according to the photochemical reaction (8):

$$[1]\quad S_2O_8^{2-} \xrightarrow{h\nu} 2SO_4^{\cdot-}$$

When sufficient amounts of sodium chloride and bromide were added to the system all primary $SO_4^{\cdot-}$ radicals were scavenged by Cl^- or Br^- and $Cl_2^{\cdot-}$ or $Br_2^{\cdot-}$ were produced (9–11):

$$SO_4^{\cdot-} + Cl^- \rightarrow SO_4^{2-} + Cl^{\cdot}$$

$$Cl^{\cdot} + Cl^- \rightarrow Cl_2^{\cdot-}$$

$$SO_4^{\cdot-} + Br^- \rightarrow SO_4^{2-} + Br^{\cdot}$$

$$Br^{\cdot} + Br^- \rightarrow Br_2^{\cdot-}$$

Materials and Methods

HRP (grade I) was purchased from Boehringer Mannheim GMBH as an ammonium sulfate precipitate. The stock solution was prepared by extensive dialysis against quintuply distilled water. The purity number (A_{403}/A_{280}) was in excess of 3.1. All other chemicals were reagent grade and used without further purification. The pH of all solutions was adjusted by adding dilute NaOH or H_2SO_4. All experiments were performed at room temperature. The light of a medium pressure mercury lamp was used for the photolysis. It was collimated with quartz lenses and a quartz filter was used for cutting off light of wavelengths shorter than 275 nm which destroys the enzyme. Monochromatic light with λ = 313 nm was obtained by using a resonance filter (Baird Atomic). Irradiations were carried out in a 1 cm spectrophotometric quartz cell which was transferred immediately at the end of photolysis to a Cary 219 spectrophotometer for recording the optical spectra. Concentrations of HRP used were fairly small so its absorbance did not exceed 0.1 in the spectral region 360–280 nm, important for the photochemical reaction [1]. HRP as well as its Compound II prepared by a conventional method, described in ref. 12, were stable

0008-4042/80/232504-04$01.00/0
©1980 National Research Council of Canada/Conseil national de recherches du Canada

Can. J. Chem. Downloaded from www.nrcresearchpress.com by 210.87.254.6 on 09/05/12
For personal use only.

Can. J. Chem. Downloaded from www.nrcresearchpress.com by 210.87.254.6 on 09/05/12
For personal use only.

under irradiation without persulfate for the periods of time typical for the photochemical experiments.

The following procedure was developed for determination of the $SO_4^{\cdot-}$ production rate. When the water solution containing $S_2O_8^{2-}$, ethyl alcohol, and tetranitromethane, $C(NO_2)_4$, was irradiated with uv light, the change in the optical spectrum was observed corresponding to accumulating nitroform anion, $C(NO_2)_3^-$, the product of tetranitromethane reduction. The rate of $C(NO_2)_3^-$ formation was directly proportional to $[S_2O_8^{2-}]$ and did not depend on tetranitromethane or alcohol concentrations over the concentration ranges: $[S_2O_8^{2-}] = 5 \times 10^{-4}$ to $10^{-2} M$, $[C(NO_2)_4] = 3 \times 10^{-5}$ to $6 \times 10^{-4} M$, $[C_2H_5OH] = 5 \times 10^{-2}$ to $4 \times 10^{-1} M$. No appreciable change of the spectra was observed in the dark or in the absence of either one of the three components under irradiation. Such behaviour was explained in terms of the following mechanism: $SO_4^{\cdot-}$ radicals formed in the primary photochemical step (reaction [1]) attack ethyl alcohol, producing free radicals which reduce tetranitromethane giving $C(NO_2)_3^{\cdot}$ as the final product. Hence the number of $SO_4^{\cdot-}$ radicals produced by light is equal to the number of $C(NO_2)_3^{\cdot}$ formed times n, where n depends on the total stoichiometry. The value of $n = 1 \pm 0.2$ was determined by using monochromatic light with $\lambda = 313$ nm for the photolysis of the system $S_2O_8^{2-}$–C_2H_5OH–$C(NO_2)_4$, and the following expression

$$n \cdot d[C(NO_2)_3^-]/dt = 2.3\, I_0 \cdot [S_2O_8^{2-}] \cdot \varepsilon_{313} \cdot \psi_{313} \cdot l$$

where I_0 is the light intensity at $\lambda = 313$ nm, measured by a standard procedure (13), ε the molar absorptivity of persulfate, ψ the quantum yield of reaction [1] equal to 0.75 (8), and l is the optical path length of the cell.

Results and Discussion

The effect of uv light on the solution containing HRP and $S_2O_8^{2-}$ is illustrated in Fig. 1 where the optical spectra before (curve 1) and after (curves 2 and 3) irradiation are shown. The well resolved isosbestic points at 338, 411, 450, and 524 nm and the directions of the changes clearly indicate the formation of the HRP Compound II, i.e. one-electron oxidation of the heme (14). The addition of a small excess of *p*-cresol to the irradiated solution led to almost complete (more than 95%) conversion back to the native enzyme (spectrum shown by the dotted line in Fig. 1). This provides another proof of Compound II formation in the course of HRP oxidation by $SO_4^{\cdot-}$ radicals. However, the photochemically formed Compound II was somewhat less stable than that obtained by conventional chemical methods (12) and this instability increased with increasing time of irradiation. Nevertheless, in the initial stages of photolysis the Compound II stability was good enough to enable quantitative measurements of the light induced spectral changes and to obtain the values of $R_{II} = d[\text{Compound II}]/dt$.

The irradiation of HRP–$S_2O_8^{2-}$ solutions containing NaCl or NaBr in amounts sufficient for scavenging of all primary $SO_4^{\cdot-}$ radicals produced qualitatively the same spectral change, i.e. the same product. Although the absolute rate of Compound II accumulation was dependent on the nature of the anions present, it did not depend on their amount provided [NaCl] or [NaBr] was over $10^{-2} M$. The measured values of R_{II} together with $SO_4^{\cdot-}$ radical generation rates for different concentration conditions with or without chloride or bromide salts are listed in Table 1.

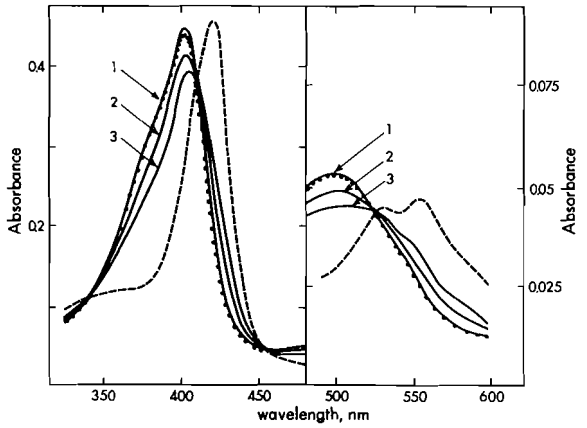


FIG. 1. Effect of uv light on the system HRP + $S_2O_8^{2-}$. The spectra shown are: 1, before irradiation; 2, after 250 s of irradiation; 3, after an additional 500 s under the light; .... after adding *p*-cresol to the irradiated solution; ---- spectrum of Compound II prepared by conventional method (12). [HRP] = $4.3 \times 10^{-6} M$, $[S_2O_8^{2-}] = 10^{-2} M$, pH = 6.3, 22°C.

The interpretation of the data must be empirical, since the radicals interact with the enzyme at several sites at least two of which are not equivalent. Nevertheless, a more detailed analysis is possible than in recent studies of the oxidation of Compound II to I (15, 16). Only a part of all $SO_4^{\cdot-}$ radicals captured by HRP react directly with the heme, the other part attacks different places on the enzyme surface, i.e. carbohydrate chains (17) or amino acid residues. If α is the ratio of the number of sulfate radicals responsible for the heme oxidation to the total number of $SO_4^{\cdot-}$ attacking HRP molecules (as shown in Fig. 2) then the rate of Compound II formation will be given by eq. [2]:

$$[2] \quad R_{II} = \alpha \cdot k\,[SO_4^{\cdot-}]\,[HRP]$$

where k is the total reaction rate constant of $SO_4^{\cdot-}$ scavenging by HRP. The recombination of $SO_4^{\cdot-}$

$$R^{\cdot} + HRP \begin{cases} \text{heme} \xrightarrow{\alpha k} \text{Compound II} \\ \text{protein} \xrightarrow{(1-\alpha)k} \text{Modified protein} \end{cases} + R^-$$

FIG. 2. Simplified scheme of HRP interaction with free radical oxidants. $R^{\cdot}$ corresponds to $SO_4^{\cdot-}$, $Br_2^{\cdot-}$, or $Cl_2^{\cdot-}$.

TABLE 1. The rates of Compound II accumulation under the different conditions; pH = 6.3 ± 0.1, 22°C

$10^6 \times$ [HRP], M	$10^3 \times [S_2O_8^{2-}]$, M	$10^9 \times R_{ph}$, $M\ s^{-1}$	$10^9 \times R_{II}$, $M\ s^{-1}$	R_{ph}/R_{II}	$10^{-2} \times (R_{II}/[HRP]^2)$, s^{-1}
		The system HRP + $S_2O_8^{2-}$			
3.0	2	3.6	1.1	3.3	1.2
3.0	4	7.2	2.0	3.7	2.2
3.0	8	14.4	3.3	4.4	3.7
1.6	4	7.2	1.53	4.7	6.3
1.6	8	14.4	3.0	4.8	12
4.0	8	14.4	3.9	3.7	2.4
4.0	2	3.6	1.4	2.6	0.9
2.0	8	14.4	3.7	3.9	9.3
0.6	8	14.4	1.8	8.0	50
1.0	8	14.4	2.4	6.0	24
0.5	4	7.2	1.1	6.5	44
1.0	10	18.2	2.6	7.0	26
1.0	6	11	2.2	5.0	21
2.0	4	7.2	2.2	3.3	5.5
1.4	12	21.4	3.9	5.5	19
2.0	6	11	2.4	4.6	5.9
4.2	10	18.2	5.4	3.3	3.1
0.9	7	12.9	1.9	6.7	26
2.7	7	2.9	3.1	4.1	4.3
		The system HRP + $S_2O_8^{2-}$ + NaCl (5×10^{-2} M)			
1.1	10	18.2	2.0	9.1	17
1.6	10	18.2	1.8	10.4	6.8
2.6	6	11	1.1	10	1.6
4.6	3	5.5	0.5	10	0.3
4.6	6	11	2.0	10	0.5
1.5	8	14	1.8	8.2	7.6
2.5	3	5.5	0.7	8.4	1.0
1.0	10	18.2	2.0	9.2	19
2.8	7	12.9	1.6	8.2	2.0
8.5	7	12.9	1.4	9.0	0.2
		The system HRP + $S_2O_8^{2-}$ + NaBr (5×10^{-2} M)			
1.5	14	25.8	1.7	15	7.3
3.0	10	18.2	1.9	9.6	2.1
4.0	4	7.2	1.1	6.5	0.7
1.6	15	27.6	1.7	16	6.8
2.5	10	18.2	1.3	10.5	2.1
4.0	7	12.9	1.3	9.9	0.8
2.0	12	21.4	2.0	11	4.9
2.0	5	9.2	8.7	10.5	2.2
1.1	10	18.2	1.1	16	9.0
3.9	10	18.2	2.2	8.2	1.4
2.2	10	18.2	1.5	12.3	3.0

radicals also occurs

[3] $SO_4^{\bar{}} + SO_4^{\bar{}} \xrightarrow{k_3} S_2O_8^{2-}$

According to the steady state approximation the rate of photochemical generation of $SO_4^{\bar{}}$ radicals (R_{ph}) must be equal to the overall rate of their consumption:

[4] $R_{ph} = k\,[SO_4^{\bar{}}]\,[HRP] + 2k_3\,[SO_4^{\bar{}}]^2$

Combining [4] with [2] one gets

$$R_{ph} = \frac{1}{\alpha} R_{II} + \frac{2k_3}{\alpha^2 k^2 [HRP]^2} \cdot R_{II}$$

or

[5] $$\frac{R_{ph}}{R_{II}} = \frac{1}{\alpha} + \frac{2k_3}{\alpha^2 k^2} \cdot \frac{R_{II}}{[HRP]^2}$$

According to [5] the plot of R_{ph}/R_{II} vs. $R_{II}/[HRP]^2$ will be a straight line. When $Cl_2^{\bar{}}$ or $Br_2^{\bar{}}$ is used instead of $SO_4^{\bar{}}$ the equation will still be valid provided the values of k, k_3, and α correspond to the new radicals.

In Fig. 3 the data from Table 1 are plotted according to eq. [5] for all three systems and straight line plots are obtained. The values of α and $2k_3/\alpha^2 k^2$ provided by the slopes and intercepts for

Can. J. Chem. Downloaded from www.nrcresearchpress.com by 210.87.254.6 on 09/05/12
For personal use only.

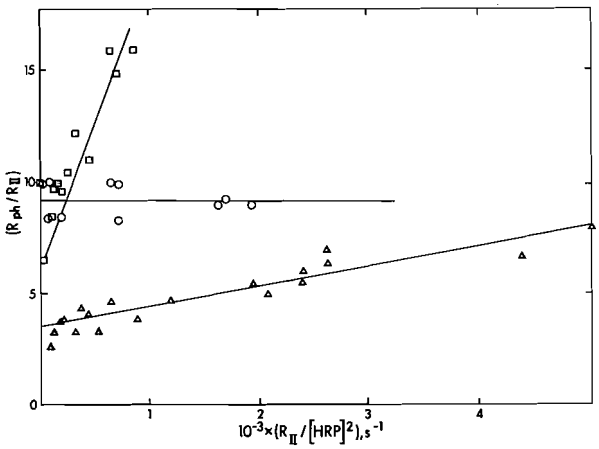


FIG. 3. Experimental data from Table 1 plotted according to eq. [5] in the coordinates R_{ph}/R_{II} and $R_{II}/[HRP]^2$. △△, $S_2O_8^{2-}$ + HRP; ⊙⊙, $S_2O_8^{2-}$ + HRP + NaCl; □□, $S_2O_8^{2-}$ + HRP + NaBr.

TABLE 2. The values of α, $2k_3/\alpha^2k^2$, and k

Radical	α	$2k_3/\alpha^2k^2$, M s	k, M^{-1} s^{-1}
$SO_4^{\bar{\cdot}}$	0.3	8.5×10^{-4}	$(3–6) \times 10^6$
$Br_2^{\bar{\cdot}}$	0.16	1.25×10^{-2}	$(2.2–3.0) \times 10^6$
$Cl_2^{\bar{\cdot}}$	0.11	$\lesssim 1 \times 10^{-4}$	$\gtrsim 10^8$

all three oxidants are listed in Table 2. The rate constants ($2k_3$) of the $SO_4^{\bar{\cdot}}$, $Br_2^{\bar{\cdot}}$, and $Cl_2^{\bar{\cdot}}$ recombination measured by different methods and gathered in ref. 18 are: $(0.75–3.6) \times 10^9$, $(1.6–2.6) \times 10^9$, and $(0.3–1.7) \times 10^{10}$ $M^{-1}s^{-1}$ respectively. Using these data and the values $2k_3/\alpha^2k^2$ from Table 2 we estimated the rate constants of HRP oxidation by $SO_4^{\bar{\cdot}}$, $Br_2^{\bar{\cdot}}$, and $Cl_2^{\bar{\cdot}}$ (k) and noted them in the last column of Table 2. Since no appreciable slope was observed in the $Cl_2^{\bar{\cdot}}$ plot in Fig. 3 only the lower limit of the $k(Cl_2^{\bar{\cdot}} + HRP)$ could be estimated.

Quite a surprising result of this study is that the rate constants for HRP oxidation by the powerful oxidants $SO_4^{\bar{\cdot}}$ and $Br_2^{\bar{\cdot}}$ are relatively low as compared with those for catalase or hemoglobin oxidation by ·OH radicals (over 10^{10} $M^{-1}s^{-1}$) (7) or for the reactions of $Br_2^{\bar{\cdot}}$ with tyrosine, tryptophan, and cysteine (over 10^7 $M^{-1}s^{-1}$) (2). The obvious conclusion is that the most easily oxidized amino acids mentioned above are not exposed on the surface of HRP.

Another feature is that there are about five different sites of the protein moiety in case of $Br_2^{\bar{\cdot}}$, eight of them in case of $Cl_2^{\bar{\cdot}}$, or two in case of $SO_4^{\bar{\cdot}}$ oxidized per one directly oxidized heme center. These oxidized locations on the protein surface can serve as good reductants for the newly formed Compound II which would account for its lower stability. On the other hand the oxidation of so many residues on the surface per one native enzyme – Compound II transformation has little effect on the enzyme integrity or its optical spectrum. This can be seen in Fig. 1 where the spectrum of the solution obtained after addition of *p*-cresol to the photochemically formed Compound II is shown. An appreciable part of HRP surface in solution is covered by carbohydrate chains (17), the destruction of which might not affect the integrity or catalytic activity of HRP and its compounds.

1. A. HENGLEIN, W. KARMANN, W. ROEBKE, and G. BECK. Makromol. Chem. **92**, 105 (1966).
2. G. E. ADAMS, J. E. ALDRICH, R. H. BISBY, R. B. CUNDALL, J. L. REDPATH, and R. L. WILLSON. Radiat. Res. **49**, 278 (1972).
3. G. E. ADAMS, R. H. BISBY, R. B. CUNDALL, J. L. REDPATH, and R. L. WILLSON. Radiat. Res. **49**, 290 (1972).
4. T. OVADIA. Isr. J. Chem. **10**, 1067 (1972).
5. K. NILSSON. Isr. J. Chem. **10**, 1011 (1972).
6. N. N. LICHTIN, J. OGDAN, and G. STEIN. Biochim. Biophys. Acta, **276**, 124 (1972).
7. M. ANBAR and P. NETA. Int. J. Appl. Radiat. Isot. **18**, 493 (1967).
8. M.-S. TSAO and W. K. WILMARTH. J. Phys. Chem. **63**, 346 (1959).
9. O. P. CHAWLA and R. W. FESSENDEN. J. Phys. Chem. **79**, 2693 (1975).
10. G. G. JAYSON, B. J. PARSONS, and A. J. SWALLOW. J. Chem. Soc. Faraday Trans. I, **69**, 1597 (1973).
11. M. S. MATHESON, W. A. MULAC, J. L. WEEKS, and J. RABANI. J. Phys. Chem. **70**, 2092 (1966).
12. W. D. HEWSON and H. B. DUNFORD. J. Biol. Chem. **251**, 6043 (1976).
13. C. G. HATCHARD and C. A. PARKER. Proc. R. Soc. London, Ser. A, **235**, 518 (1956).
14. H. B. DUNFORD and J. S. STILLMAN. Coord. Chem. Rev. **19**, 187 (1976).
15. W. D. HEWSON and L. P. HAGER. J. Biol. Chem. **254**, 3182 (1979).
16. A. NADEZHDIN and H. B. DUNFORD. Can. J. Biochem. **57**, 1080 (1979).
17. K. G. WELINDER. Eur. J. Biochem. **96**, 483 (1979).
18. A. B. ROSS and P. NETA. Rate constants for reactions of inorganic radicals in aqueous solution. NSRDS Natl. Bur. Stand. **65** (1979).

Can. J. Chem. Downloaded from www.nrcresearchpress.com by 210.87.254.6 on 09/05/12
For personal use only.

Nuclear analogs of β-lactam antibiotics. XIII. Structure activity relationships in the isocephalosporin series

TERRENCE W. DOYLE, JAMES L. DOUGLAS, BERNARD BELLEAU, TERRY T. CONWAY, C. F. FERRARI, DONALD E. HORNING, GARY LIM, BING-YU LUH, ALAIN MARTEL, MARCEL MENARD, AND L. R. MORRIS

Bristol Laboratories of Canada, 100 Industrial Boulevard, Candiac, P.Q., Canada J5R 1J1

AND

MARTIN MISIEK

Research Division, Bristol Laboratories, P.O. Box 657, Syracuse, NY 13201, U.S.A

Received March 31, 1980

This paper is dedicated to Prof. Raymond U. Lemieux on the occasion of his 60th birthday

TERRENCE W. DOYLE, JAMES L. DOUGLAS, BERNARD BELLEAU, TERRY T. CONWAY, C. F. FERRARI, DONALD E. HORNING, GARY LIM, BING-YU LUH, ALAIN MARTEL, MARCEL MENARD, L. R. MORRIS, and MARTIN MISIEK. Can. J. Chem. **58**, 2508 (1980).

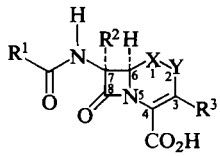
The general synthetic scheme to nuclear analogs of cephalosporins described in previous papers of this series is reviewed and the synthesis of a series of sidechain derivatives is given. Thus, systems of the following type were formed: carbacephems (A), 2-isocephems (B), *N*-2-isocephems (C), and *O*-2-isocephems (D). The *in vitro* microbiological activity of these compounds (with appropriate side-chains attached) is given, with comparison to analogous cephalosporins. Systems of type A, B, and C were only prepared with a 3-H or CH_3 substituent and had modest antibacterial activity. The *O*-2-isocephems (D) were prepared with a wide variety of sidechains at 3 and 7 and were found to have biological activity quite comparable to the cephalosporins. A more detailed biological examination (both *in vitro* and *in vivo*) of the *O*-2-isocephem analog (**19***i*) of cephalothin was made.

TERRENCE W. DOYLE, JAMES L. DOUGLAS, BERNARD BELLEAU, TERRY T. CONWAY, C. F. FERRARI, DONALD E. HORNING, GARY LIM, BING-YU LUH, ALAIN MARTEL, MARCEL MENARD, L. R. MORRIS et MARTIN MISIEK. Can. J. Chem. **58**, 2508 (1980).

On passe en revue le schéma de synthèse générale des analogues nucléaires des céphalosporines décrit antérieurement dans cette série et on rapporte la synthèse des dérivés de la chaîne latérale. On a ainsi préparé les systèmes suivants: carbacéphèmes (A), isocéphèmes-2 (B), *N*-isocéphèmes-2 (C) et *O*-isocéphèmes-2 (D). On donne l'activité microbiologique *in vitro* de ces composés (avec les chaînes latérales appropriées) par comparaison avec les céphalosporines analogues. On a préparé les composés de types A, B et C avec des substituants H-3 où CH_3 et ils ont une activité antibactérienne modérée. On a préparé les *O*-isocéphèmes-2 (D) ayant une grande variété de chaînes latérales en positions 3 et 7 et on leur a trouvé une activité tout à fait comparable à celle des céphalosporines. On a réalisé un examen biologique (*in vitro* et *in vivo*) plus détaillé de l'analogue *O*-isocéphème-2 (**19***i*) de la céphalothine.

[Traduit par le journal]

While literally thousands of semisynthetic penicillins and cephalosporins, obtained by manipulation of the C6 (or C7) amide side chains or the C3 side chain in the cephalosporins, are known, it is only relatively recently that β-lactam antibiotics extensively modified in the nucleus have been reported (for a recent review see ref. 1). Whether natural or synthetic in origin, these analogs have shattered many of the notions regarding the requirements for optimal activity which were current when we started our work. Our initial goals were rather modest ones, being to first examine whether or not it was necessary to retain the sulfur atom at position one in the cephalosporin ring **1** (Fig. 1) (X = S, Y = CH_2), and secondly if the heteroatom could be transposed to position 2 (X = CH_2, Y = O, S, N, etc.). In the previous papers of this series we have reported the syntheses of a variety of nuclear analogs of the cephalosporins in which the sulfur atom has been replaced by variously substituted carbon atoms and position two by various heteroatoms, as well as retaining a carbon atom



1

FIG. 1

(e.g. X has been CH_2, CHCl, $CH(CH_3)$, C=O, and Y has been O, S, SO, SO_2, NCO_2Et, NCH_3, CH_2, C=O, CHOR, CHBr, in Fig. 1) (2*a*–*l*). While this work was in progress, a number of other workers reported the syntheses of cephalosporin analogs having the type of substitutions in which we were interested. Lowe and co-workers (3) have reported the syntheses of the 2-isocepham and 2-isocephem systems (X = CH_2, Y = S), as have Bryan and co-workers (4). The latter workers have also reported the syntheses of a 1,2-benzofused cephalosporin (5) and several cephams incorporating two nitrogen atoms at positions 2 and 3 as well as a carbonyl at position 1 (6). A large series of

0008-4042/80/232508-16$01.00/0

©1980 National Research Council of Canada/Conseil national de recherches du Canada

Can. J. Chem. Downloaded from www.nrcresearchpress.com by 210.87.254.105 on 09/05/12
For personal use only.

Can. J. Chem. Downloaded from www.nrcresearchpress.com by 210.87.254.105 on 09/05/12
For personal use only.

1-oxadethiacephalosporins has been synthesized and these are reported to have quite good antibacterial activity (7). In addition to these cephalosporins, a number of papers have appeared which describe the total syntheses of a number of other β-lactam nuclear analogs, i.e., *N*-2-isopenams (8), 2-isopenams (9), clavulanic acid (10), oxapenems (11), penems (12), and thienamycin (13). In this paper we wish to more fully describe the biological activities of the compounds we have reported earlier (2) and to describe the synthesis and biological activities of a number of additional analogs.

Chemistry

Initially our goal was the development of a general stereoselective synthesis which would provide access to a variety of isocephalosporins. As the work proceeded, the following general considerations evolved.

1. The substituted β-lactam would be synthesized first in a stereospecific manner so as to provide an amide at the eventual C7 position which would be *cis* to the second ring.

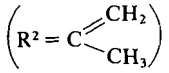
2. The substituent on the nitrogen atom of the initially-formed β-lactam would be used to form the second ring.[1]

3. The attached carbon atom at C4 in the initial azetidinone would be sp^2 hybridized so as to minimize problems inherent in the synthetic scheme chosen to form the β-lactam.

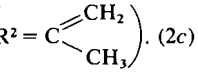
O-2-*Isocephems*

The synthetic scheme utilized for the majority of analogs we have synthesized may be illustrated by the synthesis of **8***a* ($R^1 = CH_3$) (Scheme I) (2*b*). Condensation of the amine **2** ($R^1 = CH_3$ throughout) with cinnamaldehyde gave **3** ($R^2 = CH{=}CH\phi$) which on treatment with azidoacetyl chloride in the presence of triethylamine gave the *cis* β-lactam **4***a* in good yield.[2] Ozonolysis of **4***a* gave **4***b* which was reduced by sodium borohydride to **4***c*. Compound **4***c* was converted to its mesylate **4***d* and hydrolysed to give a key intermediate **5***a*. When **5***a* was treated with base, cyclization occurred to the bicyclic β-lactam **6***a*. Reduction of **6***a* to the amine **7***a*, coupling to phenoxyacetic acid using EEDQ (14),[3] and hydrogenolysis of the benzyl ester gave the desired acid **8***a* ($R^1 = CH_3$, $R^2 = R^3 = H$). The syntheses of **8***b–d* were carried out similarly (2*b*) using the appropriately substituted amines **2**, or in the case of **8***b* starting from **9** (2*a*).

In the case of the *O*-2-isocephems carrying substituents at position 1, we employed either methacrylaldehyde or furfural as the aldehyde in the Schiff base forming step. Thus, treatment of **3**

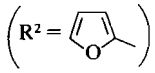


with azido acetyl chloride and TEA gave the β-lactam **4**



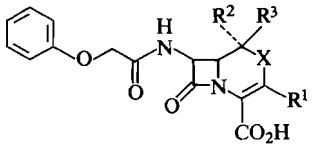
(2*c*)

Ozonolysis followed by sodium borohydride reduction gave two diastereoisomeric alcohols (**4**, $R^2 = \overset{*}{C}HOHCH_3$) which were separated by chromatography and carried through the same sequence of reactions to yield **8***e* and **8***f*. From the 4-furyl β-lactam **4**



was obtained **8***g* (2*d*) (Fig. 2).

One goal was the production of analogs having a 3-acetoxymethyl group in place of the 3-methyl group of **8***a*. Initially we had intended to produce these compounds via functionalization of **8***a* or **6***a*. A number of attempts to functionalize the 3-methyl group using NBS or other free radical oxidizing



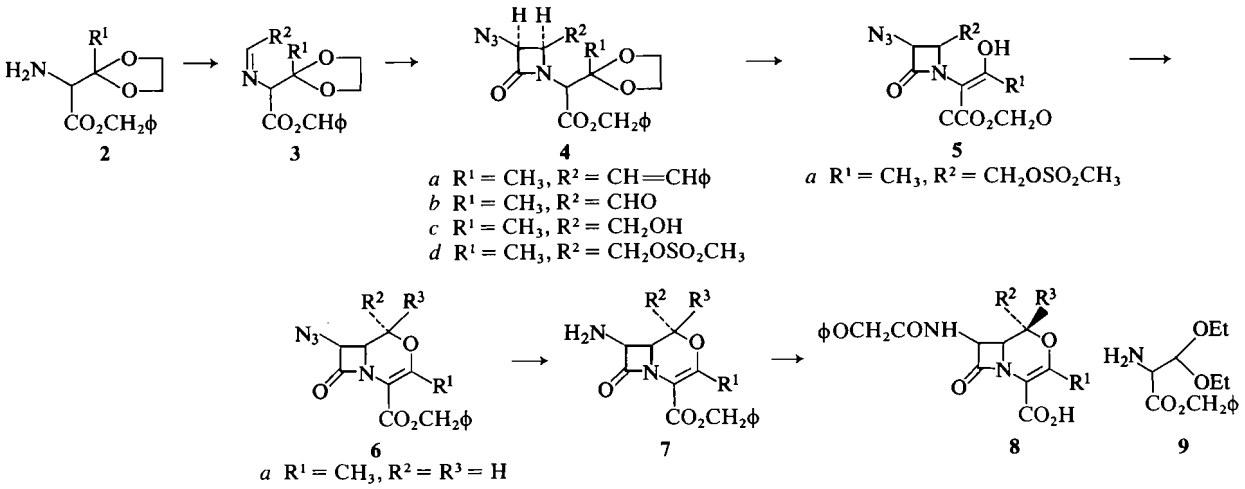
Compound	R^1	R^2	R^3	X
8*a*	CH_3	H	H	O
8*b*	H	H	H	O
8*c*	$CH_2\phi$	H	H	O
8*d*	$CH_2CH_2\phi$	H	H	O
8*e*	CH_3	CH_3	H	O
8*f*	CH_3	H	CH_3	O
8*g*	CH_3	—O—		O
8*h*	$CH_2CO_2CH_3$	H	H	O

FIG. 2

[1]Initially we attempted to use a variety of nitrogen blocking groups which we hoped to remove selectively, e.g. trityl, benzhydryl, and benzyl. The results were poor and the alternate approach of incorporating the *N*-blocking group in the final structure was decided on. The group at SKF has successfully utilized the first approach in their synthesis of the 2-isocephem system (4).

[2]The stereoselectivity of this and all other cycloadditions we have carried out in the course of our work has been very high, there being no detectable amounts of *trans* isomer formed.

[3]*N*-Ethoxycarbonyl-2-ethoxy-1,2-dihydroquinoline has been used extensively in the course of our studies for coupling sidechains to the nuclei.



SCHEME 1

agents failed (2*h*).[4] As part of this study, the treatment of the benzyl ester of **8***a* with a variety of strong bases, followed by treatment with electrophiles, was examined. For the most part, this resulted in the decomposition of starting material and no isolable products or in recovery of the starting material unchanged. Treatment of **10** with *n*-butyllithium followed by quenching with carbon dioxide resulted in the formation of a mixture of carboxylic acids, which was further treated with diazomethane to yield the methyl ester **11** in 3.5% overall yield from **10**. Hydrogenolysis of **11** gave the carboxylic acid **8***h* (Scheme 2).

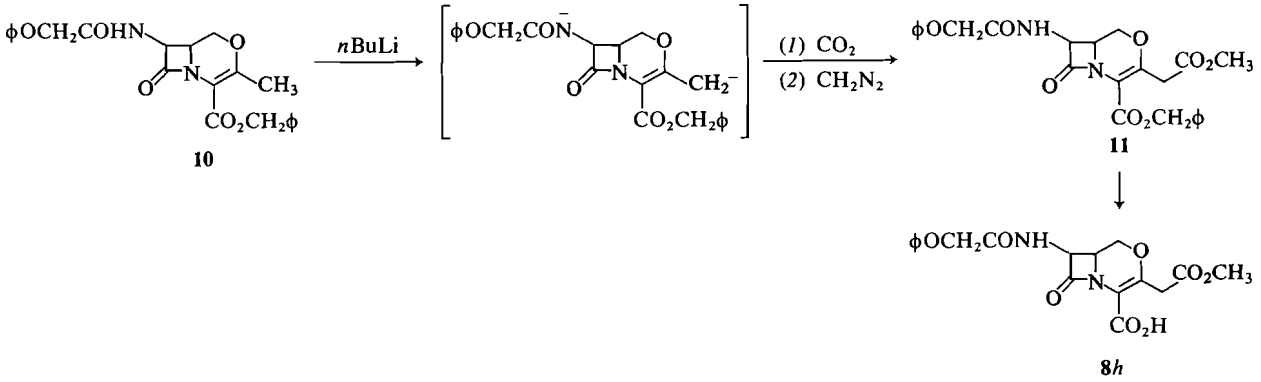
In view of the disappointing yield of **11**, further attempts to prepare the desired 3-acetoxymethyl compounds via direct functionalization of **6***a*, **8***a*, or **10** were abandoned. Routes based on amines such as **2** where $R^1 = CH_2OR$ also failed due to the fact that the presence of an α hetero atom rendered the subsequent hydrolysis of the ketals impossible without concomitant destruction of the β-lactam.[5] Fortunately, at about this time we discovered an alternate route to the desired compounds (2*h*). As part of our strategy to utilize the enol **5***a* to synthesize various other heteroatom substituted cephalosporins, the conversion of **5***a* to the dimesylate **12***a* or the mesylate triflate **12***b* had been carried out. This conversion was normally carried out by treating a mixture of the enol **5***a* plus either methane sulfonyl choride or triflic anhydride with one equivalent of triethylamine (TEA). On one occasion an excess of TEA was used and upon workup, instead of the desired **12**, compound **13** was obtained (Scheme 3). While **13** was unstable, it could be readily handled in solution. Halogenation of **13** with either bromine or iodine gave **14** as a mixture of geometrical isomers in excellent yields. When **14** was treated with potassium acetate in DMF, the desired 3-acetoxymethyl-*O*-2-isocephem **15***a* (R^1 = Bz) was produced in good yield. Attempted displacement of the 3-acetoxymethyl group by thiols failed. The hydrolysis of **15***a* to **15***c* did not proceed in good yield. Consequently, the solvolysis of **14***b* (R^1 = PNB) was carried out using potassium formate to yield **15***b* which could be hydrolysed to **15***c*. Treatment of **15***c* with sodium cyanate in trifluoroacetic acid gave the carbamate **15***d*. Mesylation of **15***c* gave **15***e* which was used to prepare **16***a–c* by displacement. While the displacements using the thiolates proceeded in good yield, that using 1-methyltetrazol-5-ol gave **16***c* in 22.5% yield. Compound **16***a* could also be prepared directly from **14***a* (R^1 = PNB). Thus, treatment of **14***a* with one equivalent of 1-methyltetrazole-5-thiol and TEA in CH_2Cl_2 gave **14***c* which was treated with potassium acetate in DMF to give **16***a*.

With compounds **6***a*, **15***a*, **15***d*, **16***a–c* readily available, the conversion of these to suitably substituted cephalosporin analogs was attempted next. We used two general methods to accomplish this goal. Reduction of the azide using hydrogen sulfide – triethylamine proceeded in good yield to give the amines **17***a*, *b* and **17***d–g*. In the case of **15***a* an alternate scheme was used. Hydrogenolysis of **15***a* over platinum accomplished both reduction of the azide and cleavage of the benzyl ester simultaneously to yield **17***c*. Compounds **17***a*, *b*, *d–g* were coupled to the appropriate carboxylic acids using EEDQ. Thus, from **17***a* we obtained **18***a–d*, from **17***b* compounds **18***e–g*, from **17***d* compound **18***h*, from **17***e* compounds **18***i–l*, from **17***f* compound **18***m*, and from **17***g* compound **18***n* (Scheme

[4]The SKF group has reported the successful bromination of the 2-isocephem system with NBS (4).

[5]M. Menard, unpublished results.

Can. J. Chem. Downloaded from www.nrcresearchpress.com by 210.87.254.105 on 09/05/12
For personal use only.

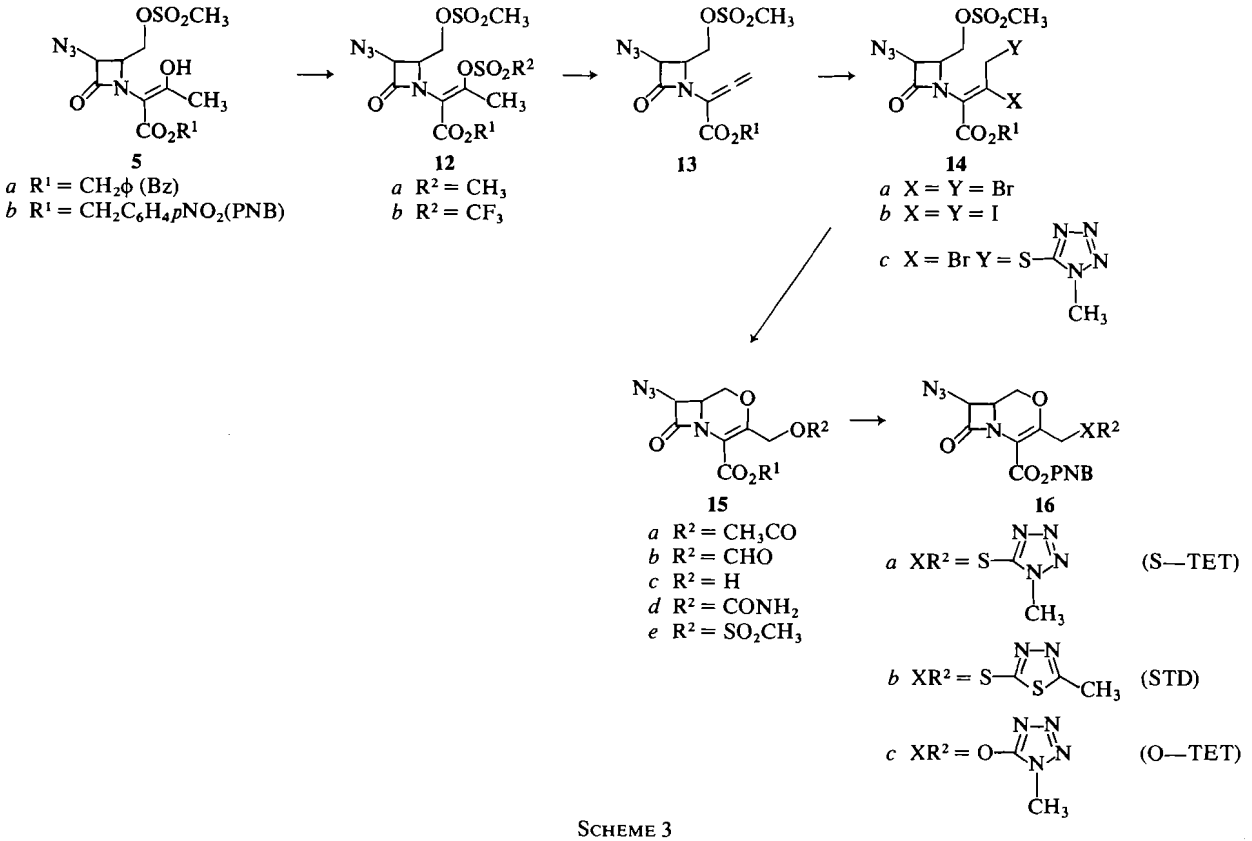


SCHEME 2

4), Hydrogenolysis of the benzyl or *p*-nitrobenzyl esters proceeded smoothly to give the corresponding carboxylic acids. In the cases of **18***b*, **18***c*, **18***e*, the secondary blocking groups on the sidechains were simultaneously deblocked. The azido function of **18***l* was reduced simultaneously with PNB removal to give **19***r*. A number of the final products were obtained via direct coupling of the acid chloride or mixed anhydrides to the amino acid. Thus, **17***c* was coupled with 4-chloromethylphenylacetyl chloride to give **20**. Reaction of **20** with thiourea gave **19***m*. Similarly, 2-(1-carbomethoxypropen-2-yl-aminomethyl)phenylacetic acid was coupled to **17***c* or **21** via the mixed anhydride procedure to yield **19***j* and **19***e*, respectively (Scheme 5). Compounds **19***k* and **19***l* were prepared via the method of Crast *et al.* (15).

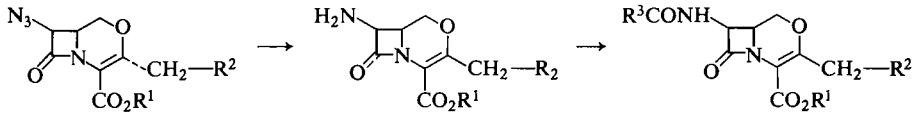
2-Isocephems, N-2-Isocephems, and Carbacephems

The facile ring closure of the enol mesylate **5***a* to give the *O*-2-isocephem system **6***a* encouraged us to further explore the chemistry of **5***a* with a view to preparing isocephalosporins having other hetero-

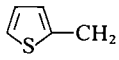
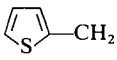
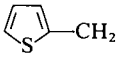
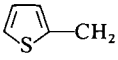
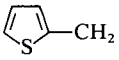
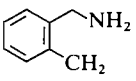


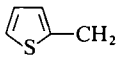
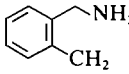
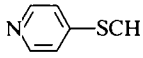
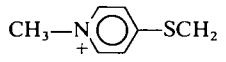
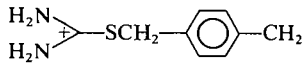
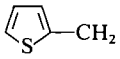
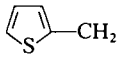
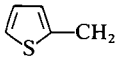
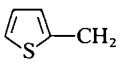
SCHEME 3

Can. J. Chem. Downloaded from www.nrcresearchpress.com by 210.87.254.105 on 09/05/12
For personal use only.



17 18 19 R¹ = H

Compound	R¹	R²	R³
17*a*	Bz	H	—
17*b*	Bz	OAc	—
17*c*	H	OAc	—
17*d*	PNB	$OCONH_2$	—
17*e*	PNB	S-TET	—
17*f*	PNB	S-TD	—
17*g*	PNB	O-TET	—
18*a*	Bz	H	ϕCH_2
18*b*	Bz	H	$\phi CH(NHCBz)$
18*c*	Bz	H	$\phi CH(CO_2Bz)$
18*d*	Bz	H	ϕOCH_2
18*e*	Bz	OAc	$\phi CH(NHCBz)$
18*f*	Bz	OAc	$NCCH_2$
18*g*	Bz	OAc	ϕOCH_2
18*h*	PNB	$OCONH_2$	
18*i*	PNB	S-TET	ϕOCH_2
18*j*	PNB	S-TET	$\phi CHOH$
18*k*	PNB	S-TET	
18*l*	PNB	S-TET	ϕCHN_3
18*m*	PNB	S-TD	
18*n*	PNB	O-TET	
18*o*	H	H	ϕOCH_2
19*a*	—	H	ϕCH_2
19*b*	—	H	$\phi CHNH_2$
19*c*	—	H	$\phi CHCO_2H$
19*d*	—	H	
19*e*	—	H	

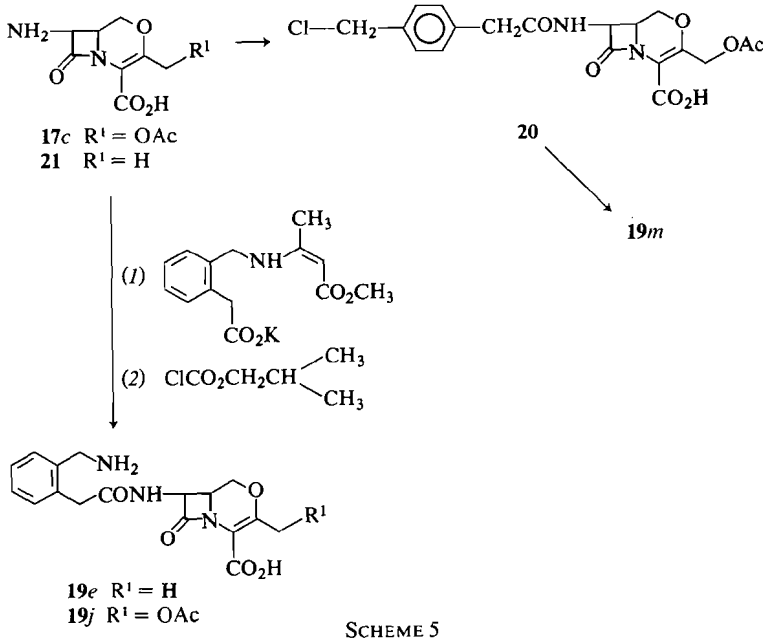
Compound	R¹	R²	R³
19*f*	—	OAc	ϕOCH_2
19*g*	—	OAc	$\phi CHNH_2$
19*h*	—	OAc	$CNCH_2$
19*i*	—	OAc	
19*j*	—	OAc	
19*k*	—	OAc	
19*l*	—	OAc	
19*m*	—	OAc	
19*n*	—	$OCONH_2$	
19*o*	—	S-TET	ϕOCH_2
19*p*	—	S-TET	
19*q*	—	S-TET	$\phi CHOH$
19*r*	—	S-TET	$\phi CHNH_2$
19*s*	—	STD	
19*t*	—	O-TET	

SCHEME 4

atoms at position 2. A number of attempts were made to prepare the ene thiol directly from the enol with no success. Consequently the enols were converted to their mesylates **22***a* or **22***b* as described earlier. Treatment of the dimesylate with hydrogen sulfide – triethylamine (Scheme 6) gave the desired 2-isocephem systems **23***a* and **23***b*. These were converted to their amides **24***a* and **24***b*. Compound **24***b* was converted by oxidation into the sulfoxide **24***c* and the sulfone **24***d*. Treatment of **24***c* with *tert*-butyl hypochlorite gave **24***e* (2*g*).

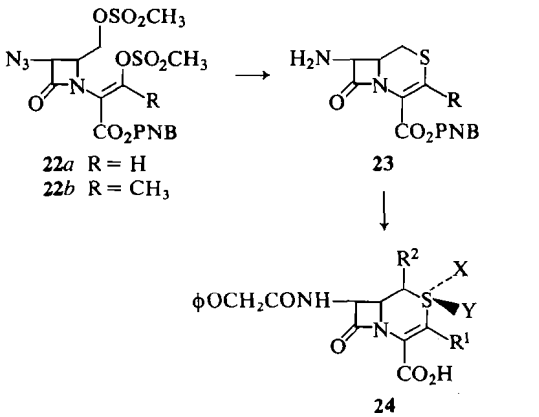
Similarly, treatment of **25***a* with monomethylamine (Scheme 7) or with ammonia followed by ethyl chloroformate gave the *N*-2-isocephems **26***a* and **26***b*. These were converted to **27***a* and **27***b*, respectively, in the usual fashion (2*f*).

Can. J. Chem. Downloaded from www.nrcresearchpress.com by 210.87.254.105 on 09/05/12
For personal use only.



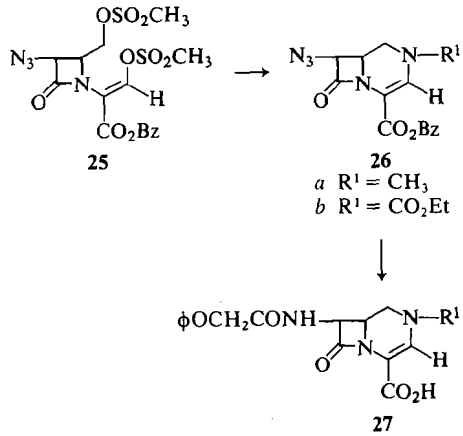
SCHEME 5

Encouraged by the successful syntheses of **24** and **27**, we next examined the reactions of **12***b* with various carbon nucleophiles (Scheme 8). Treatment of **12***b* with the sodium salts of dimethyl, dibenzyl, and di-*tert*-butyl malonate gave the cyclized products of **28***a*, *b*, and *c*, respectively. Compounds **28***a* and *b* were converted to compounds **30***a–e* (2*j*). When **28***c* (R = *tert*-butyl) was treated with acid and the resultant dicarboxylic acid **28** (R = H) decarboxylated there was obtained the Δ^2-cephalosporin analog **29**. This was converted



	R¹	R²	X	Y
a	H	H	—	—
b	CH_3	H	—	—
c	CH_3	H	O	—
d	CH_3	H	O	O
e	CH_3	Cl	O	—

SCHEME 6



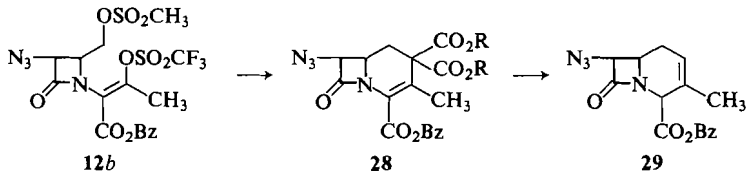
SCHEME 7

to **30***d* as described earlier (2*k*). Starting from **29** we have also synthesized compounds **30***e–j* (2*l*).

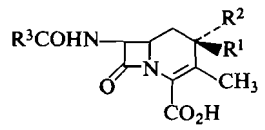
7-Methoxy Isocephalosporins

In view of the reported broadening of the antibacterial spectrum of cephalosporins by substitution with a 7-α-methoxy group (16), we decided to prepare 7-methoxy analogs of the 2-iso and the *O*-2-isocephems (2*i*). The method of Spitzer and Goodson (17) was chosen to introduce a thiomethyl group (Scheme 9). Thus, **31***a* (A = R^2 = H, R^3 = PNB, X = S) was treated with LDA followed by methoxycarbonylmethyl disulfide to give **31***b* (A = SCH_3, R^2 = H, R^3 = PNB, X = S). The Schiff base was hydrolysed to the amine which was acylated. Treatment of the sulfide with mercuric acetate in methanol (18) followed by hydrogenolysis of the

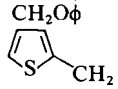
Can. J. Chem. Downloaded from www.nrcresearchpress.com by 210.87.254.105 on 09/05/12
For personal use only.



12*b* 28 29



30

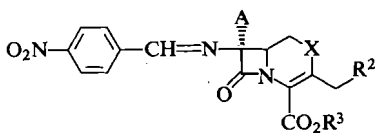
	R^1	R^2	R^3
a	CO_2CH_3	CO_2CH_3	$CH_2O\phi$
b	H, CO_2CH_3		$CH_2O\phi$
c	H, CO_2H		$CH_2O\phi$
d	H	H	$CH_2O\phi$
e	H	OH	$CH_2O\phi$
f	H	OAc	$CH_2O\phi$
g	—O—		$CH_2O\phi$
h	—O—CH_2CH_2—O—		$CH_2O\phi$
i	OH	H	$CH_2O\phi$
j	OAc	H	$CH_2O\phi$
k	OAc	H	

SCHEME 8

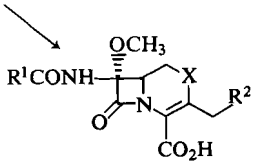
ester group gave **32***a* (R^1 = ϕOCH_2, R^2 = H, X = S). Compounds **32***b* and **32***c* were prepared similarly.

Biological Activity

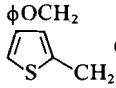
In vitro antibiotic activities for the cephalosporin analogs prepared were determined by a two-fold serial dilution assay in Difco nutrient broth by the method of Pursiano *et al.* (19). Results in terms of minimum inhibitory concentrations (MIC) in μg/mL are given in Tables 1–4. Bacterial strains utilized included gram positive organisms (*Streptococcus pyogenes*, *Staphylococcus aureus* Smith), a β-lactamase producing gram positive organism (*S. aureus* BX 1633), gram negative organisms (*Escherichia coli* Juhl, *Klebsiella pneumoniae* 9977, *Proteus mirabilis*), β-lactamase producing gram negative organisms (*E. coli* 9675, *K. pneumoniae* 15130, *P. morganii*, *Enterobacter cloacae*), and *Pseudomonas aeruginosa*. None of the compounds tested were active against *Pseudomonas* so it is not included in the tables. In the tables the effects of changing substituents at the 1, 2, 3, and 7 positions are demonstrated. As well, comparisons to cephalosporins are made.



31



32

	R^1	R^2	X
a	ϕOCH_2	H	S
b	ϕOCH_2	H	O
c		OAc	O

SCHEME 9

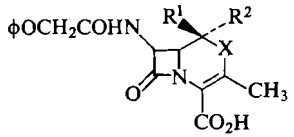
The limited amount of data in Table 1 demonstrates that substitution at position 1 seems to be deleterious to antibiotic activity. In particular, compare the lower activity of **8***f* or **8***g* with **8***a* and **24***e* with **24***c*.

Table 2 demonstrates the effect of varying the 2 substituent on antibiotic activity. For example, the nuclear analogs **8***a*, **24***a*, **24***b*, **27***b*, and **30***d* show that the 2-O analog is most active while the 2-S, CH_2, and 2-NCO_2Et analogs are of reduced activity but roughly equivalent to one another. However, oxidation of the 2-S gives sulfoxide **24***c* and sulfone **24***d* with close to the activity of **8***a*. Similarly, the 2-keto analog **30***g* has activity comparable to **8***a*. Except for the 2-β-acetoxy analog **30***j*, other sub-

Can. J. Chem. Downloaded from www.nrcresearchpress.com by 210.87.254.105 on 09/05/12
For personal use only.

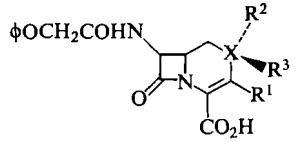
Can. J. Chem. Downloaded from www.nrcresearchpress.com by 210.87.254.105 on 09/05/12
For personal use only.

TABLE 1. Effect of substituents at C1 on antibacterial activity



Compound	X	R^1	R^2	*S. pyogenes*	*S. aureus* Smith	*S. aureus* BX1633	*E. coli* Juhl	*E. coli* 9675	*K. pneumoniae* 9977	*K. pneumoniae* 15130	*Proteus mirabilis*	*Proteus morganii*	*Enterobacter cloacae*
8*a*	O	H	H	0.5	0.5	32	63	>125	32	>125	16	>125	63
8*f*	O	CH_3	H	10	>125	>125	>125	>125	>125	>125	>125	>125	>125
8*g*	O	H	CH_3	10	>10	63	>125	>125	>125	>125	>125	>125	>125
8*h*	O	O		>125	>125	>125	>125	>125	>125	>125	>125	>125	>125
24*c*	SO	H	H	5	2.5	16	125	>125	63	>125	63	>125	125
24*e*	SO	Cl	H	8	16	63	>125	>125	>125	>125	>125	>125	>125

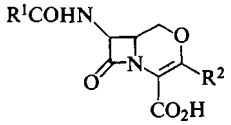
TABLE 2. Effects of substituents at position 2 on antibacterial activity



Compound	X	R^1	R^2	R^3	*S. pyogenes*	*S. aureus* Smith	*S. aureus* BX1633	*E. coli* Juhl	*E. coli* 9675	*K. pneumoniae* 9977	*K. pneumoniae* 15130	*Proteus mirabilis*	*Proteus morganii*	*Enterobacter cloacae*
8*a*	O	H	—	—	0.6	0.6	>125	63	>125	32	>125	63	>125	—
27*b*	NCO_2Et	H	—	—	2	8	125	>125	>125	>125	>125	>125	>125	>125
24*a*	S	H	—	—	2	2	16	>125	>125	125	>125	>125	>125	125
8*a*	O	CH_3	—	—	0.5	0.5	32	63	>125	32	>125	16	>125	63
24*b*	S	CH_3	—	—	16	32	63	>125	>125	>125	>125	>125	>125	>125
24*c*	S	CH_3	O	—	5	2.5	16	125	>125	63	>125	63	>125	125
24*d*	S	CH_3	O	O	2	4	63	>125	>125	125	>125	63	>125	>125
30*a*	C	CH_3	CO_2CH_3	CO_2CH_3	16	>125	>125	>125	>125	>125	>125	>125	>125	>125
30*b*	C	CH_3	H, CO_2CH_3		16	>32	63	>125	>125	>125	>125	>125	>125	>125
30*c*	C	CH_3	H, CO_2H		125	>125	125	>125	>125	>125	>125	>125	>125	>125
30*d*	C	CH_3	H	H	4	4	8	>125	>125	>125	>125	>125	>125	>125
30*e*	C	CH_3	OH	H	8	16	32	>125	>125	>125	>125	>125	>125	>125
30*f*	C	CH_3	OAc	H	125	125	>125	>125	>125	>125	>125	>125	>125	>125
30*g*	C	CH_3	O		0.13	0.5	125	>125	>125	63	>125	32	>125	>125
30*h*	C	CH_3	$O(CH_2)_2O$		16	16	>125	>125	>125	>125	>125	>125	>125	>125
30*i*	C	CH_3	H	OH	4	8	32	>125	>125	>125	>125	>125	>125	>125
30*j*	C	CH_3	H	OAc	0.5	2	4	>125	>125	>125	>125	>125	>125	>125

Can. J. Chem. Downloaded from www.nrcresearchpress.com by 210.87.254.105 on 09/05/12
For personal use only.

TABLE 3. Effect of substituents at C-3



Compound	R^1	R^2	*S. pyogenes*	*S. aureus* Smith	*S. aureus* BX1633	*E. coli* Juhl	*E. coli* 9675	*K. pneumoniae* 9977	*K. pneumoniae* 15130	*Proteus mirabilis*	*Proteus morganii*	*Enterobacter cloacae*
8*b*	ϕOCH_2	H	0.6	0.6	>125	63	>125	32	>125	63	>125	—
8*a*		CH_3	0.5	0.5	32	63	250	32	500	16	500	63
8*c*		$CH_2\phi$	0.25	0.25	>125	Inactive						
8*d*		$(CH_2)_2\phi$	0.03	0.06	>125	Inactive						
8*h*		$CH_2CO_2CH_3$	0.06	0.25	>125	125	>125	63	>125	32	>125	>125
19*f*		CH_2OAc	0.13	1	125	16	125	16	>125	4	>125	63
9*o*		CH_2STET	0.13	0.25	16	4	32	2	32	2	63	32
19*b*	$\phi CHNH_2$	CH_3	0.13	1	63	4	32	4	8	8	63	4
19*g*		CH_2OAc	0.06	1	8	1	4	1	8	0.5	32	2
19*r*		CH_2STET	0.25	4	125	4	16	1	16	2	16	8
19*d*		CH_3	0.25	0.5	16	16	63	4	32	4	>125	8
19*i*		CH_2OAc	0.03	0.5	2	8	63	1	63	1	>125	16
19*n*		CH_2OCONH_2	0.25	0.5	8	16	125	2	32	2	>125	16
19*p*		CH_2STET	0.016	0.13	2	1	16	0.25	8	0.13	32	1
19*s*		CH_2STD	0.008	0.06	2	4	23	0.5	32	0.5	32	4
19*t*		CH_2OTET	0.06	0.25	125	32	125	2	63	2	125	16

Can. J. Chem. Downloaded from www.nrcresearchpress.com by 210.87.254.105 on 09/05/12
For personal use only.

stituents at the 2-carbon (**30***a*–*c*, *e*, *f*, *h*) generally produced lessened activity. Thus it would appear that electron donation to the $\Delta^{3,4}$ double bond decreases antibiotic activity, and steric bulk at the 2 position also decreases activity.

Since the *O*-2-isocephem nucleus appeared to have the greatest potential for high antibiotic activity, an extensive series of 3 and 7 substituted analogs was prepared. Table 3 shows the effect of varying substituents at position 3. Increasing hydrophilic character at 3 (**8***a*, **8***c*, **8***d*) leads to an increase in activity against non-β-lactamase producing gram positive organisms but loss of activity against other organisms. For the 3-methylene substituted compounds, the order of activity is (with minor exceptions) as follows: S-tetrazole more active than S-thiadiazole, more active than acetoxy, more active than O-tetrazole, same as carbamate, more active than H. These are similar to the trends seen with cephalosporin 3-sidechains (20). The effect of varying 7-sidechains can be seen in Tables 3 and 4. In general, the phenylglycine group confers the highest activity followed by the thienylacetyl and the groups of compounds **19***m*, *j*, *k*, and *l*, with the phenoxyacetyl, cyanoacetyl, mandeloyl, and phenylmalonyl groups conferring the lowest activity. It should be noted that compounds with the phenylglycine sidechain (except for **19***b*) had poor chemical stability. These trends in activity seen with the various 7-sidechains parallel the trends seen with the cephalosporins with some exceptions. Notably the mandeloyl sidechain confers much poorer activity on the O-isocephem than one would expect from the corresponding cephalosporins.

A direct comparison between *O*-2-isocephems and cephalosporins with the same side-chains is given in Table 4. With certain combinations of sidechains, the *O*-2-isocephem is more active (**8***a*, **19***a*, *d*, *p*, *s*), with others the cephalosporin is more active (**19***h*, *j*, *k*, *l*, *m*, *q*), while the rest are more or less equivalent. With regard to individual strains of bacteria, the following generalizations can be made: the cephalosporins are more active than *O*-2-isocephems against staphylococci and β-lactamase producing strains of *E. coli*, *Klebsiella*, and *Proteus*. Thus it would seem that the *O*-2-isocephem and cephalosporin nucleii have about the same inherent activity but that the *O*-2-isocephem nucleus is more susceptible to β-lactamases. The 7-methoxy substituent appears to give some protection against β-lactamases but overall activity is reduced considerably (2*i*).

More extensive microbiological testing was carried out with several *O*-2-isocephems. Compound **19***i* (2*h*) (the cephalothin analog) can be taken as typical. Data comparing **19***i* (resolved) with cephalothin are presented in Fig. 3. Both are highly active against *S. aureus* with cephalothin being slightly better. Against the gram negative organisms, **19***i* is superior for the more sensitive strains, but this advantage is reduced for the more resistant strains (presumably which include many β-lactamase producers).

Table 5 shows the *in vivo* activity of compound **19***i* compared to cephalothin. Blood levels in mice are essentially equivalent. Both provide high protection for mice experimentally infected with *Streptococcus pyogenes* with **19***i* being somewhat superior.

In summary, various nuclear modifications of cephalosporins (carba, 2-iso, *N*-2-iso, *O*-2-iso) were found to have antibiotic activity. More extensive testing of *O*-2-isocephem analogs, both *in vitro* and *in vivo*, showed these compounds to have antibiotic activity similar to cephalosporins with only minor differences in detail.

Experimental

General

The ir spectra were recorded on a Unicam SP-200G spectrometer. The nmr spectra were determined on a Varian A60-A spectrometer using tetramethylsilane as an internal standard. Melting points were uncorrected and were determined on a Gallenkamp melting point apparatus. The analyses were performed by Micro-Tech Laboratories, Skokie, IL. Many of the final compounds were relatively unstable and were best submitted for microbiological testing without purification. Such products usually did not give satisfactory elemental analyses. However, spectral data indicated that they were ≥90% pure in most cases (unless otherwise indicated below). Extraction solutions were dried over sodium sulfate. All chromatographic purifications were carried out on activity III silica gel by the dry column technique.

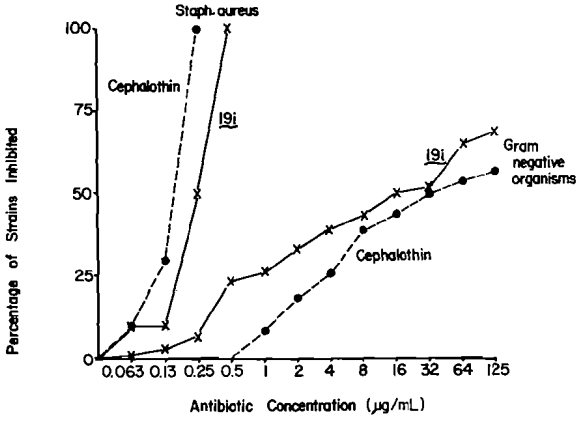
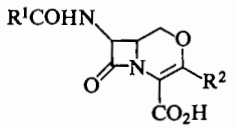


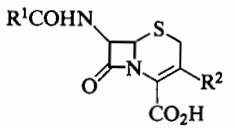
FIG. 3. Antibiotic susceptibility of 10 strains of *Staphylococcus aureus* and 54 strains of gram negative organisms to cephalothin and **19***i* in Mueller–Hinton medium. (Five strains each of *Enterobacter aerogenes* and *Ent. cloacae*, 10 strains each of *Escherichia coli*, *Klebsiella pneumoniae* and *Proteus mirabilis*, 5 strains each of *Proteus rettgeri* and *P. vulgaris*, 4 strains of *P. morganii*.)

Can. J. Chem. Downloaded from www.nrcresearchpress.com by 210.87.254.105 on 09/05/12
For personal use only.

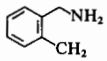
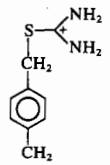
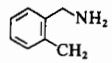
TABLE 4. Comparison of *O*-2-isocephems to cephalosporins



A

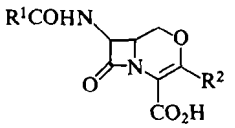


B

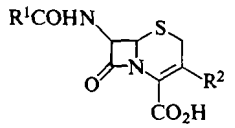
Compound	A B	R^1	R^2	*S. pyogenes*	*S. aureus* Smith	*S. aureus* BX1633	*E. coli* Juhl	*E. coli* 9675	*K. pneumoniae* 9977	*K. pneumoniae* 15130	*Proteus mirabilis*	*Proteus morganii*	*Enterobacter cloacae*
8*a*	A	ϕOCH_2	CH_3	0.5	0.5	32	63	>125	32	>125	16	>125	63
	B			2	1	2	>125	>125	>125	>125	>125	>125	>125
19*a*	A	ϕCH_2	CH_3	0.5	1	32	125	>125	16	125	16	>125	>125
	B			0.6	2.5	—	250	>250	32	>250	32	>250	>250
19*d*	A		CH_3	0.25	0.5	16	16	63	4	32	4	>125	8
	B			1	2	32	125	>125	16	125	16	>125	16
19*b*	A		CH_3	0.13	1	63	4	32	4	8	8	63	4
Cephalexin	B			0.3	1.3	4	8	16	4	16	4	>125	4
19*e*	A		CH_3	0.08	0.6	32	16	32	16	32	32	125	8
	B			0.3	1.3	8	32	63	32	63	32	>125	—
19*c*	A		CH_3	8	16	>125	125	125	63	>125	63	125	63
	B												
19*f* (2*h*)	A	ϕOCH_2	CH_2OAc	0.13	1	125	16	125	16	>125	4	>125	63
	B			0.016	0.062	—	>100	—	100	—	—	—	
19*i*	A		CH_2OAc	0.03	0.5	2	8	63	1	63	1	>125	16
Cephalothin	B			0.06	0.13	0.25	16	63	0.25	16	0.5	>125	2
19*g*	A		CH_2OAc	0.06	1	8	1	4	1	8	0.5	32	2
Cephaloglycine	B			0.13	0.5	2	2	4	1	2	1	63	1
19*h*	A	$NCCH_2$	CH_2OAc	0.25	2	8	32	125	16	125	32	>125	63
Cephacetrile	B			0.13	0.5	1	8	16	8	16	4	>125	8
19*m*	A		CH_2OAc	0.016	0.13	8	8	63	0.5	16	1	>125	8
	B			0.004	0.008	0.13	4	32	0.13	4	0.13	>125	1
19*j*	A		CH_2OAc	0.03	0.5	125	4	8	2	8	4	32	2
	B			0.03	0.13	0.25	1	4	1	2	1	63	0.5

Can. J. Chem. Downloaded from www.nrcresearchpress.com by 210.87.254.105 on 09/05/12
For personal use only.

TABLE 4 (*Concluded*)



A



B

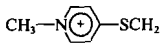
Compound	A B	R^1	R^2	*S. pyogenes*	*S. aureus* Smith	*S. aureus* BX1633	*E. coli* Juhl	*E. coli* 9675	*K. pneumoniae* 9977	*K. pneumoniae* 15130	*Proteus mirabilis*	*Proteus morganii*	*Enterobacter cloacae*
19*k*	A		CH_2OAc	0.13	1	63	32	125	2	>125	4	>125	32
Cephapirin	B			0.008	0.13	1.3	16	125	1	8	1	>125	8
19*f*	A		CH_2OAc	0.13	1	125	32	125	4	63	4	>125	32
	B			0.004	0.13	0.5	2	16	2	4	1	>125	8
19*q*	A		S-TET	0.25	2	16	8	63	4	63	2	32	32
Cefamandole	B			0.03	0.25	2	1	8	0.5	4	0.25	4	2
19*p*	A		S-TET	0.016	0.13	2	1	16	0.25	8	0.13	32	1
	B			0.06	0.13	0.5	4	16	1	16	1	63	2
19*s*	A		S-TD	0.008	0.06	2	4	32	0.5	32	0.5	32	4
	B			0.008	0.016	0.016	4	16	2	32	1	>125	8
19*r*	A		S-TET	0.25	4	125	4	16	1	16	2	16	8
	B			0.13	1	16	2	4	1	4	1	16	1

TABLE 5. *In vivo* activity

Compound	Blood levels[a] (minutes after administration) (μg/mL) 15	30	60	PD_{50}[b] (mg/kg)
19*i*	8.9	5.6	<2	0.5
Cephalothin	7.3	2.4	<2	3

[a]Average mouse blood levels after intramuscular administration of 10 mg/kg body weight.
[b]Protective effect after administration in mice experimentally infected with *Streptococcus pyogenes*. PD_{50} is drug dose per treatment protecting 50% of infected mice from death; mice treated 1 and 3.5 h after infection.

All cephalosporins used for comparison were either from the Bristol Laboratories (Syracuse) reference collection or were prepared from 7-ACA or 7-ADCA by the same method as used to prepare the corresponding *O*-2-isocephem.

The following abbreviations are used: THF, tetrahydrofuran; DMF, dimethylformamide.

7-β-Phenoxyacetamido-3-carbomethoxymethyl-Δ³-O-2-isocephem-4-carboxylic Acid **8**h

A solution of benzyl 7-β-(aminophenoxyacetoyl)-3-methyl-Δ³-*O*-2-isocephem-4-carboxylate **10** (2.11 g, 5 mmol) in 100 mL of THF was cooled to −70°C under a slow nitrogen stream. A solution of 1.66 *M* butyllithium (6.34 mL, 10.5 mmol) was slowly added keeping the reaction temperature at −70°C. A slow stream of dry carbon dioxide gas was then introduced into the reaction mixture, the cooling bath was removed, and the carbon dioxide introduction continued until the reaction temperature reached 25°C.

The reaction mixture was poured into 200 mL of 10% hydrochloric acid, saturated with sodium chloride, and extracted three times with diethylether (150 mL portions). The combined extracts were washed three times with brine, dried (anhydrous sodium sulfate), and evaporated *in vacuo* to give 2.09 g of a yellow gum. This gum was partitioned between diethylether and 10% sodium bicarbonate solution three times. The bicarbonate solutions were then washed with diethylether (2 × 50 mL) and with methylene chloride (2 × 50 mL). The bicarbonate solution was then acidified to pH 2 with concentrated hydrochloric acid and extracted three times with methylene chloride (100 mL portions). The methylene chloride extracts were washed twice with brine, dried (anhydrous sodium sulfate), and evaporated *in vacuo* to give 0.31 g of a colorless gum. This gum was used as such in the next step.

A solution of diazomethane in diethylether was slowly added to a solution of benzyl 7-β-(aminophenoxyacetoyl)-3-carboxymethylene-Δ³-*O*-2-isocephem-4-carboxylate (0.88 g) in 100 mL of diethylether, until a permanent yellow color (excess diazomethane) was produced. The reaction mixture was then stirred at room temperature for 10 min. The reaction was acidified with 10% hydrochloric acid and extracted twice with 100 mL portions of diethylether. The extract was washed with 10% sodium bicarbonate solution (2 × 75 mL), with brine (100 mL), dried (anhydrous sodium sulfate), and evaporated *in vacuo* to give 0.72 g of crude product which was dry column chromatographed over 36 g of activity III silica gel. Elution with chloroform gave a fraction containing 240 mg of methyl ester **11**. The nmr and ir spectra are in agreement with the assigned structure. This material was used as such in the next step.

A mixture of benzyl 7-β-(aminophenoxyacetoyl)-3-carbomethoxymethylene-Δ³-*O*-2-isocephem-4-carboxylate **11** (147 mg), 10% Pd–C (100 mg), 25 mL of ethanol (USP), and 15 mL of THF was hydrogenated in a Parr hydrogenator at 17 psig for 1 h. The catalyst was filtered off and the filtrate evaporated to dryness *in vacuo* to give 87 mg of a white foam, **8***h*.

The potassium salt of acid **8***h* was prepared by dissolving the foam in a small amount of methylisobutylketone and adding a saturated solution of potassium 2-ethylhexanoate in butanol. The resultant precipitate was filtered off and washed with methylisobutylketone and then diethylether; mp 139–144°C (dec.) (cor.).

p-Nitrobenzyl 7-β-Azido-3-formyloxymethyl-Δ³-O-2-isocephem-4-carboxylate **15**b

A solution of di-iodide **14***b* (6.6 g, 9.6 mmol) in 100 mL of DMF plus 0.1 mL of water was maintained at 0°C while powdered potassium formate (2.54 g, 30 mmol) was added. The cooling bath was removed and the mixture was stirred vigorously for 5 h. The mixture was added to 100 mL of ice water. The aqueous mixture was extracted with CH_2Cl_2 (100 + 50 mL). The combined organic extracts were washed with dilute aqueous NaCl (5 × 100 mL), dried, and the solvent was evaporated *in vacuo* to give the crude product **15***b* (5.3 g) as a brown oil. The product was used as such in the subsequent reaction. The product could be purified by chromatography on silica gel. Elution with Et_2O/EtOAc 3:1 gave pure **15***b*, mp 104–105°C.

p-*Nitrobenzyl 7-β-Azido-3-hydroxymethyl-Δ³-O-2-isocephem-4-carboxylate* **15**c

A solution of compound **15***b* (5.3 g, 13 mmol), acetone (53 mL), water (26 mL), and 12 *M* HCl (3.2 mL) was stirred at 28°C for 7 h, then mixed with water (100 mL) and extracted with CH_2Cl_2 (60 + 25 + 15 mL). The combined extracts were washed with water containing a little NaCl (4 × 100 mL) dried, and the solvent was evaporated *in vacuo* to give a brown oil, 3.6 g. The product was purified by chromatography on silica gel (90 g). Elution of the column first with Et_2O, then with Et_2O/EtOAc 3:1 gave a product which was recrystallized from acetone/Et_2O to give alcohol **15***c*, 950 mg (17.5% yield from compound **14***b*), mp 147–148°C.

p-*Nitrobenzyl 7-β-Azido-3-carbamoyloxymethyl-Δ³-O-2-isocephem-4-carboxylate* **15**d

A mixture of compound **15***c* (375 mg, 1.0 mmol), benzene (15 mL), sodium cyanate (130 mg, 2.0 mmol), and trifluoroacetic acid (0.16 mL, 2.1 mmol) was stirred for 2 h at 23°C. Water (25 mL) and EtOAc (15 mL) were added to the mixture and it was shaken and separated. The aqueous layer was extracted with another 15 mL of EtOAc. The combined organic phases were washed with water and saturated NaCl (30 mL each), dried, and the solvent was evaporated *in vacuo* to give carbamate **15***d* as an amorphous solid, 400 mg (95% yield).

p-*Nitrobenzyl 7-β-Azido-3-[5-thio(1-methyl)tetrazolyl]-methyl-Δ³-O-2-isocephem-4-carboxylate* **15**e

A solution of methanesulfonyl chloride (0.50 mL, 6.5 mmol) in 10 mL of CH_2Cl_2 was added dropwise to a stirred solution of compound **15***c* (2.41 g, 6.43 mmol), Et_3N (0.97 mL, 7.0 mmol), and CH_2Cl_2 (75 mL) at −10°C. The solution was maintained at −10°C for ½ h and 23°C for 1 h, then washed with 5% HCl, 2% $NaHCO_3$, and water (85 mL each). The solvent was evaporated *in vacuo* to give mesylate **15***e* as an amorphous solid, 2.86 g (98% yield).

p-*Nitrobenzyl 7-β-Azido-3-[5-thio(1-methyl)tetrazolyl]-methyl-Δ³-O-2-isocephem-4-carboxylate* **16**a, p-*Nitrobenzyl 7-β-Azido-3-[2-thio(5-methyl)-1,3,4-thiadiazolyl]methyl-Δ³-O-2-isocephem-4-carboxylate* **16**b, *and* p-*Nitrobenzyl 7-β-Azido-3-[5-oxo(1-methyl)tetrazolyl]methyl-Δ³-O-2-isocephem-4-carboxylate* **16**c

A solution of mesylate **15***e* (4.53 g, 10 mmol), Et_3N (1.4 mL, 10 mmol), CH_2Cl_2 (90 mL), and 10 mmol of 1-methyltetrazole-

Can. J. Chem. Downloaded from www.nrcresearchpress.com by 210.87.254.105 on 09/05/12
For personal use only.

Can. J. Chem. Downloaded from www.nrcresearchpress.com by 210.87.254.105 on 09/05/12
For personal use only.

TABLE 6

Starting material	Product	Reaction time (h)	Yield (%)	Melting point (°C)	Anal.	Purification[a]
17*a*	**18***a*	2	100			
17*a*	**18***b*	16				cc Et_2O/Pet. ether
17*a*[b]	**18***c*	16	30	152–157	CHN	cc Et_2O/Hexane
17*b*	**18***e*	16				cc Et_2O
17*b*	**18***f*	24	56			cc Et_2O/EtOAc
17*d*	**18***h*	18	29	95–98		cc Et_2O/EtOAc
17*e*	**18***i*	2	67			cc Et_2O/CH_2Cl_2
17*e*	**18***j*[c]	16	92			—
17*e*	**18***k*	2	52	165–168		R Et_2O/CH_2Cl_2
17*e*	**18***l*	16	93	132–134	CHN	Trit Et_2O
17*f*	**18***m*	2	55	127–129		cc EtOAc R Et_2O/CH_2Cl_2
17*g*	**18***n*	16	91			—

[a]Either column chromatography (cc) or recrystallization (R).
[b]Preparation of sidechain; ref. 21.
[c]Prepared using **17***e* and mandeloyl carbonate but no EEDQ.

TABLE 7

Product	Starting material	Solvent mixture[a]	Reaction conditions[b]	Catalyst[c]	Yield (%)	Melting point (°C)	Anal.
19*a*	**18***a*	A	A	A	69	197–198	CHN
19*b*	**18***b*	BCD	B	B	100	—	—
19*c*	**18***c*	BC	B	B	100	—	—
19*g*	**18***e*	BCD	B	B	95	—	—
19*h*	**18***f*	B	C	C	73	146–149	CHN
19*n*	**18***h*	CED	D	C	12.5	—	—
19*o*	**18***i*	AB	D	A	37	—	—
19*p*	**18***k*	CED	D	C	18.5	182–184	CHN
19*q*	**18***j*	CED	C	C	45	—	—
19*r*	**18***l*	CED	D	C	67	—	—
19*s*	**18***m*	CED	D	C	39	100–105	CHNS
19*t*	**18***n*	CED	D	C	32	190–192	CHN

[a]Solvents used: A, THF; B, EtOH; C, EtOAc; D, aqueous HCl; E, *n*-BuOH.
[b]A, 1 atm for 10 min; B, 1 atm until uptake completed; C, 3 atm for 1 h; D, 3 atm for 3–4 h.
[c]A, 10% Pd/C.B, 30% Pd/Celite. C, 20% $Pd(OH)_2/C$.

TABLE 8

Product	Procedure	Yield (%)	Melting point (°C)	Anal.
19*d*	Same method as for **19***i* (2*h*)	50	—	CHNS
19*e*	Below	13	—	CHN
19*m*	Below	52	—	—
19*j*	Below	27	—	—
19*h*	Same method as for corresponding cephalosporin (15)	73	115–120 (dec.)	—
19*l*	Same method as for corresponding cephalosporin (15)	38	165–170 (dec.)	—

5-thiol, 2-methylthiadiazole-5-thiol, or 1-methyltetrazole-5-ol was stirred at 23°C for 16 h. In the cases of the first two, the solution was washed with 5% HCl and water (100 mL each), dried, and the solvent was evaporated *in vacuo* to give the product.

The tetrazole **16***a* was recrystallized from EtOAc, 3.70 g (78% yield), mp 150–152°C.

The thiadiazole **16***b* was obtained as an oil, 4.65 g (95% yield).

In the case of **16***c*, the solvent was evaporated *in vacuo*, replaced by $CHCl_3$ (500 mL), Et_3N (10 mmol), 1-methyltetrazole-5-ol (10 mmol), and the solution was heated under reflux for 20 h. The solution was washed and concentrated (in the manner for **16***a* and **16***b*) to give crude **16***c*. This material was purified by chromatography on silica gel (730 g) and was eluted

Can. J. Chem. Downloaded from www.nrcresearchpress.com by 210.87.254.105 on 09/05/12
For personal use only.

from the column with Et_2O/EtOAc 3:1. It was recrystallized from EtOAc to give **16***c*, 1.07 g (22.5% yield), mp 174–176°C (dec.).

p-*Nitrobenzyl 7-β-azido-3[5-thio(1-methyl) tetrazolyl]methyl-* Δ^3*-O-2- isocephem-4-carboxylate* **16***a from* **14**b

The dibromide **14***a* (R^1 = PNB) was prepared in exactly the same manner as the corresponding benzyl ester (2*h*). 1-Methyltetrazole-5-thiol (565 mg, 4.85 mmol) was added to a solution of dibromide **14***a* (2.90 g, 4.85 mmol) in 35 mL of CH_2Cl_2 at 0°C. A solution of Et_3N (0.67 mL, 4.85 mmol) in 7 mL of CH_2Cl_2 was added and the solution was stirred at 23°C for 30 min. The solution was washed with water (2 × 40 mL), dried, treated with charcoal, and filtered. The solvent was evaporated *in vacuo* to give compound **14***c*, 2.70 g, in about 30% purity.

Potassium acetate (835 mg, 8.54 mmol) was added to a solution of **14***c* (2.70 g) in 27 mL of DMF at 0°C. The mixture was stirred at 23°C for 18 h, then diluted with 80 mL of CH_2Cl_2 and washed with 1% NaCl solution (6 × 80 mL). The organic phase was dried and absorbed onto silica gel (7.5 g) which was placed on a silica gel column (30 g). The column was eluted with Et_2O then with Et_2O/CH_2Cl_2 1:1. Evaporation of the solvent from the appropriate fractions gave compound **16***a*, 344 mg (15% yield), identical in all respects to that prepared above.

Azide Reductions using Hydrogen Sulfide – Triethylamine **17**d–g

A solution of equimolar amounts of the azido compound and triethylamine in CH_2Cl_2 (~10% solution) was cooled to 0°C and saturated with H_2S. After 1 to 1.5 h the solution was acidified (10% HCl), the CH_2Cl_2 was evaporated *in vacuo*, and the mixture was extracted with CH_2Cl_2. The CH_2Cl_2 extract was filtered to remove elemental sulfur and the solvent was evaporated *in vacuo* to give product **17***e* (86% yield), **17***f* (85% yield), or **17***g* (61% yield). Compound **17***d* was obtained in 100% yield simply by evaporation of the solvent *in vacuo* after the H_2S addition. These crude products were used as such in subsequent reactions.

EEDQ Coupling Reactions

A solution of equimolar amounts of EEDQ, the acid to be coupled, and the appropriate amine in methylene chloride (from 5–20 wt% solutions) was let stand at room temperature (~23°C) for the specified time (see Table 6). The resulting solution was washed with dilute solutions of HCl, $NaHCO_3$, and NaCl. The organic layers were dried over Na_2SO_4 and the solvent evaporated at reduced pressure.

Ester Removal by Hydrogenolysis

The hydrogenolysis of the various benzyl and *p*-nitrobenzyl esters to yield the desired acids was carried out as follows: a solution of *x* mg of the ester in 100 × mL of solvent was hydrogenated under the conditions shown in Table 7. When the reaction was complete the catalyst was removed by filtration. For those products carrying a phenylglycyl side chain one equivalent of HCl was added to the hydrogenation mixture. The solution was evaporated at reduced pressure to give the product as its hydrochloride salt. For non-basic products the reaction solution was extracted with aqueous sodium bicarbonate. The aqueous extracts were acidified and back extracted into EtOAc. The solvent was evaporated at reduced pressure to yield the product.

Compounds **19**d, e, j, k, l, m

These compounds were prepared from **17***c* or **21** as described in Table 8.

Compound **17***c* and 4-chloromethylphenylacetyl chloride were reacted by the method used to prepare **19***i* (2*h*) to give amide **33**. A solution of **33** (635 mg, 1.5 mmol) in 6 mL of acetone was mixed with a solution of thiourea (120 mg, 1.6 mmol) in 3 mL of acetone and maintained at 23°C for 72 h. The precipitate was collected by filtration and washed with acetone to give **19***m*, 397 mg, in about 80% purity.

To a suspension of potassium 2-(1-carbomethoxypropen-2-ylaminomethyl)phenylacetate (1.2 g, 38 mmol) in 23 mL of tetrahydrofuran was added 3 drops of dimethylbenzylamine. The mixture was cooled to −40°C and isobutyl chloroformate (520 mg, 38 mmol) was added. After 5 min, the solution was added to a cooled (0°C) solution of compound **17***c* or **21** (1.8 mmol) and *N*-methylmorpholine (0.71 mL) in 13 mL of water. The solution was stirred for 1 h at 0°C, then acidified to pH 5.2 with hydrochloric acid. Ethyl acetate was added and the mixture was stirred for 1 h at 23°C. The product was collected by filtration and dried *in vacuo*. Compound **19***e* was obtained analytically pure while **19***j* was obtained in about 80% purity.

Acknowledgements

We would like to thank the following for their technical assistance during the course of this work: J. Meunier and P. Rivest (Candiac) and W. Gottstein (Syracuse).

1. L. D. Cama and B. G. Cristensen. Annu. Rep. Med. Chem. **13**, 149 (1978).
2. (*a*) T. W. Doyle, B. Belleau, B.-y. Luh, C. F. Ferrari, and M. P. Cunningham. Can. J. Chem. **55**, 468 (1977); (*b*) T. W. Doyle, B. Belleau, B.-y. Luh, T. T. Conway, M. Menard, J. L. Douglas, D. T.-w. Chu, G. Lim, L. R. Morris, P. Rivest, and M. Casey. Can. J. Chem. **55**, 484 (1977); (*c*) T. W. Doyle, B.-y. Luh, and A. Martel. Can. J. Chem. **55**, 2700 (1977); (*d*) T. W. Doyle, A. Martel, and B.-y. Luh. Can. J. Chem. **55**, 2708 (1977); (*e*) T. W. Doyle. Can. J. Chem. **55**, 2714 (1977); (*f*) T. W. Doyle, B.-y. Luh, D. T.-w. Chu, and B. Belleau. Can. J. Chem. **55**, 2719 (1977); (*g*) T. W. Doyle, J. L. Douglas, B. Belleau, J. Meunier, and B.-y. Luh. Can. J. Chem. **55**, 2873 (1977); (*h*) T. T. Conway, G. Lim, J. L. Douglas, M. Menard, T. W. Doyle, P. Rivest, D. Horning, L. R. Morris, and D. Cimon. Can. J. Chem. **56**, 1335 (1978); (*i*) J. L. Douglas, D. E. Horning, and T. T. Conway. Can. J. Chem. **56**, 2879 (1978); (*j*) T. W. Doyle, T. T. Conway, M. Casey, and G. Lim. Can. J. Chem. **57**, 222 (1979); (*k*) T. W. Doyle, T. T. Conway, G. Lim, and B.-y. Luh. Can. J. Chem. **57**, 227 (1979); (*l*) A. Martel, T. W. Doyle, and B.-y. Luh. Can. J. Chem. **57**, 614 (1979); (*m*) J. L. Douglas, T. W. Doyle, T. T. Conway, M. Menard, B. Belleau, and M. Misiek. ABSTRACTS: 176th ACS National Meeting, Miami, MEDI II (1978).
3. G. Lowe and J. Parker. Chem. Commun. 577 (1971); D. M. Brunwin and G. Lowe. J. Chem. Soc. Perkin Trans. I, 1321 (1973).
4. D. B. Bryan, R. F. Hall, K. G. Holden, W. F. Huffman, and J. G. Gleason. J. Am. Chem. Soc. **99**, 2353 (1977).
5. J. Finkelstein, K. G. Holden, and C. D. Perchonock. Tetrahedron Lett. 1629 (1978).
6. J. Finkelstein, K. G. Holden, R. Sneed, and C. D. Perchonock. Tetrahedron Lett. 1855 (1977).
7. M. Narisada, H. Onoue, and W. Nagata. Heterocycles, **7**, 839 (1977); Y. Hamashima, M. Narisada, M. Yoshioka, S. Uyeo, T. Tsuji, I. Kikkawa, and W. Nagata. ABSTRACTS, 176th ACS National Meetings, Miami, MEDI 14 (1978).
8. W. F. Huffman, K. G. Holden, T. F.Buckley III, J. G. Gleason, and L. Wu. J. Am. Chem. Soc. **99**, 2352 (1977).
9. W. F. Huffman, R. F. Hall, J. A. Grant, and K. G. Holden. J. Med. Chem. **21**, 413 (1978).

10. P. H. BENTLEY, P. D. BERRY, G. BROOKS, M. L. GILPIN, E. HUNT, and I. I. ZOMAYA. J. Chem. Soc. Chem. Commun. 748 (1977).
11. A. J. EGLINGTON. J. Chem. Soc. Chem. Commun. 720 (1977).
12. I. ERNEST, J. GOSTELI, C. W. GREENGRASS, W. HOLICK, D. E. JACKMAN, H. R. PFAENDLER, and R. B. WOODWARD. J. Am. Chem. Soc. **100**, 8214 (1978).
13. D. B. R. JOHNSTON, S. M. SCHMITT, F. A. BOUFFARD, and B. G. CHRISTENSEN. J. Am. Chem. Soc. **100**, 313 (1978).
14. B. BELLEAU and G. MALEK. J. Am. Chem. Soc. **90**, 1651 (1968).
15. L. B. CRAST, R. G. GRAHAM, and L. C. CHENEY, J. Med. Chem. **16**, 1413 (1973).
16. A. K. MILLER, E. CELOZZI, B. A. PELAK, E. D. STAPLEY, and D. HENDLIN. Antimicrob. Agents Chemother. **2**, 281 (1972); H. C. NEU. Antimicrob. Agents Chemother. **6**, 170 (1974).
17. W. A. SPITZER and T. GOODSON. Tetrahedron Lett. 273 (1973).
18. H. E. APPLEGATE, J. E. DOLFINI, M. S. PUAR, W. A. SLUSARCHYK, B. TOEPLITZ, and J. Z. GOUGOUTAS. J. Org. Chem. **39**, 2794 (1974).
19. T. A. PURSIANO, M. MISIEK, F. LEITNER, and K. E. PRICE. Antimicrob. Agents Chemother. **3**, 33 (1973).
20. E. FLYNN (*Editor*). Cephalosporins and penicillins chemistry and biology. Academic Press, New York. 1972. Chapt. 12.
21. A. P. KRAPCHO, E. G. E. JAHNGEN, and D. S. KASHDAN. Tetrahedron Lett. 2721 (1974); Chem. Abstr. **63**, 13269g (1965).

Can. J. Chem. Downloaded from www.nrcresearchpress.com by 210.87.254.105 on 09/05/12
For personal use only.

Synthesis of camphor-1,4-homoenol (7-hydroxy-1,2-dimethyl[3,3,0,$0^{2,7}$]tricyclooctane)

WILLIAM M. DADSON AND THOMAS MONEY

Chemistry Department, The University of British Columbia, Vancouver, B.C., Canada V6T 1W5

Received April 7, 1980

This paper is dedicated to Prof. Raymond U. Lemieux on the occasion of his 60th birthday

WILLIAM M. DADSON and THOMAS MONEY. Can. J. Chem. **58**, 2524 (1980).

A simple synthesis of camphor-1,4-homoenol has been accomplished by reductive cyclization of 8-bromocamphor.

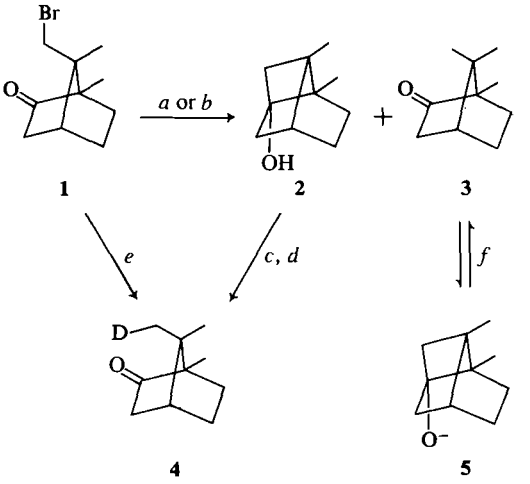
WILLIAM M. DADSON et THOMAS MONEY. Can. J. Chem. **58**, 2524 (1980).

Une synthèse simple du 7-hydroxy-1,2-dimethyl[3,3,0,$0^{2,7}$]tricyclo octane (le camphore-1,4-homoenol) à partir d'une cyclisation reductive est décrite.

[Traduit par le journal]

Can. J. Chem. Downloaded from www.nrcresearchpress.com by 210.87.254.5 on 09/05/12
For personal use only.

During recent attempts to extend the use of camphor in monoterpenoid (1) and sesquiterpenoid synthesis (2) we treated 8-bromocamphor (**1**) (3) with calcium/liquid ammonia at −33°C and obtained a mixture of camphor (**3**) (~33% yield by glc) and a new compound (~56% yield by glc) which was easily isolated as a colorless crystalline solid by column chromatography. The spectroscopic properties (ν_{max} (CCl_4): 3620, 3335 cm^{-1}; δ($CDCl_3$, 270 MHz): 0.90 (3H, s) 1.01 (3H, s)) of the new compound were consistent with those expected for the 1,4-homoenol (**2**) of camphor and this structural assignment was confirmed when treatment with Me_3COK/Me_3COD/80°C/3 h followed by Me_3COK/Me_3COH/80°C/16 h provided 8-deuteriocamphor (**4**) with spectral characteristics[1] (δ($CDCl_3$, 400 MHz): 0.82 (2H, t, J = 1.8 Hz), 0.91 (3H, s), 0.96 (3H, s)) identical to those of an authentic sample prepared by reduction of (+)-8-bromocamphor with tri-*n*-butyltin deuteride (6–8). In more recent experiments it has been shown that treatment of 8-bromocamphor (**1**) with magnesium powder in refluxing THF (9*c*) provides camphor-1,4-homoenol (**2**) in excellent yield (96%) and we recommend this method of synthesis. The formation of camphor-1,4-homoenol (**2**) in the above reactions could involve cleavage of the carbon–bromine bond followed by nucleophilic addition to the carbonyl group (9) or intramolecular alkylation of an intermediate radical anion (10). Treatment of **2** with sodium hydride in HMPA at 80°C for 2 minutes provided camphor (**3**) in 98% yield. It is interesting to note, however, that this homoketonization (11) reaction does not occur at ≤40°C and indeed treatment of **2** with NaH/HMPA/40°C/1 h in the presence of methyl iodide or benzyl chloride provides



(*a*) Ca/NH_3 (liq); (*b*) Mg/THF; (*c*) Me_3COK/Me_3COD/80°C/3 h; (*d*) Me_3COK/Me_3COH/80°C/16 h; (*e*) *n*-Bu_3SnD/C_6H_6; (*f*) Me_3COK/Me_3COH/250°C/sealed tube

the corresponding ethers. The *p*-bromobenzoate of **2** has also been synthesized and its structure confirmed by X-ray crystallographic analysis (12).

During their elegant investigations on homoenolization of bicyclic ketones, Nickon *et al.* (13) noted that the C(3), C(6), C(8), and C(10) hydrogen atoms in camphor (**3**) were exchanged during prolonged treatment with Me_3COK/Me_3COH at 185–250°C (sealed tube) and the intermediacy of the highly strained 1,4-homoenolate ion (**5**) was proposed to account for exchange at the C(8) position.[2] The synthesis of camphor-1,4-homoenol (**2**) and its subsequent conversion to 8-deuteriocamphor (**4**) provides strong support for this mechanism.

[1]Mass spectra of camphor and deuterio derivatives have been reported in ref. 4, and ^{13}C nmr of camphor in ref. 5.

[2]Related investigations by Stothers and co-workers (14) have shown that γ-homoenolization also occurs when 3,3-dimethylbicyclo[3,3,0]octan-2-one is treated under similar reaction conditions.

0008-4042/80/232524-03$01.00/0

©1980 National Research Council of Canada/Conseil national de recherches du Canada

Can. J. Chem. Downloaded from www.nrcresearchpress.com by 210.87.254.5 on 09/05/12
For personal use only.

The potential of reductive cyclization in natural product synthesis has previously been recognised by several research groups (9, 10) and homoketonization of camphor-1,4-homoenol (**2**) could provide a new method of generating nucleophilic activity at the C(8) position in camphor. This aspect of the chemistry of (**2**) is currently being investigated.

Experimental

Melting points were determined on a Thomas Hoover capillary melting point apparatus and are uncorrected. The glc analysis was carried out on a Hewlett-Packard Model 5831-A gas chromatograph using a 6 ft × ⅛ in. column (3% OV-17; Chromosorb W(HP), 80–100 mesh) and nitrogen as carrier gas. The carrier gas flow rate was about 35 mL/min. The 60 MHz nmr spectra were recorded on a Varian Associates Model T-60, 100 MHz spectra on a Varian Associates Model HA-100 or Model XL-100, and 270 MHz spectra on a 270 MHz instrument constructed from a Bruker console, a Nicolet computer Model 293A with a Diablo disk, and a 270 MHz superconducting magnet supplied by Oxford Instruments. The 400 MHz spectra were recorded on a Bruker WH-400 instrument and ^{13}C nmr spectra on a Varian CFT-20 instrument. Signal positions are given in delta (δ) with tetramethylsilane (TMS) as internal reference and signal multiplicity and integrated areas are indicated in parentheses. Infrared spectra were recorded on a Perkin-Elmer 137 spectrophotometer and optical rotations were measured with a Perkin-Elmer Model 241 MC polarimeter. Low resolution mass spectra were recorded on a Varian/Mat Model CH4B mass spectrometer and high resolution mass spectra were determined on the AEI Model MS902 or Model MS 50 instrument. Microanalyses were performed by Mr. P. Borda, Microanalytical Laboratory, University of British Columbia, Vancouver.

Camphor-1,4-homoenol (2)

Method A

A solution of 8-bromocamphor (**1**) (1.0 g) in dry THF (5 mL) was added to magnesium powder (1.05 g) and THF (2 mL) and the reaction mixture refluxed for 16 h. After acidification with HCl (6 *N*) the mixture was extracted with ether and the extract washed with potassium carbonate solution. Removal of dried solvent provided camphor-1,4-homoenol (**2**) as a colorless solid (632 mg, 96% yield, glc purity 99%) which crystallized from petroleum ether (35–60°C) as colorless needles, mp 98–100°C (sealed tube), $[\alpha]_D$ +14.1° (*c* 0.87, $CHCl_3$); ν_{max} (CCl_4): 3620, 3335 cm^{-1}; δ($CDCl_3$, 270 MHz): 0.90 (3H, s), 1.01 (3H, s); *Mol. Wt.* calcd. for $C_{10}H_{16}O$: 152.1201; found (mass spectrometry): 152.1202.

Method B

8-Bromocamphor (**1**) (1.0 g) in dry ether (5 mL) was added to a solution of calcium (850 mg) in liquid ammonia (200 mL) at −33°C. After 30 min methanol was added and the decolorized reaction mixture diluted with water (50 mL) and extracted with ether. Removal of solvent provided a colorless solid (560 mg, 85% yield) which, by glc analysis (3% OV-17 column), was shown to be a mixture of camphor (**3**) (~30%) and its 1,4-homoenol (**2**) (~70%). Column chromatography (alumina, Grade III; elution with ether – petroleum ether (35–60°C) (1:1)) yielded pure camphor 1,4-homoenol (**2**) with spectroscopic properties indicated above.

8-Deuteriocamphor (4)

From 8-Bromocamphor (1)

Tri-*n*-butyltin deuteride (5.0 g) in dry benzene (5 mL) was added under nitrogen to 8-bromocamphor (**1**) (3.2 g) and azobisisobutyronitrile (2.2 g) (8*a*) in dry benzene (10 mL) and the mixture stirred for 3 h at 50°C, then 24 h at room temperature. The ether extract of the reaction mixture was washed with 5% KOH (4 × 25 mL), water, 10% KF (4 × 25 mL), and water (8*b*). Removal of solvent provided impure product which was purified by column chromatography (silica; elution with hexane–ether (5:1)) and sublimed to provide 8-deuteriocamphor (**4**) in 46% yield (glc purity 99%); ν_{max} ($CHCl_3$): 2200, 1745, 1415 cm^{-1}; δ($CDCl_3$, 400 MHz): 0.82 (2H, t, J = 1.8 Hz), 0.91 (3H, s), 0.96 (3H, s); δ(^{13}C) ($CDCl_3$): 9.2, 19.1, 19.4 (t, J = 19 Hz); ms *m/e*: 153 (54%, M^+), 138 (7), 111 (28), 109 (74), 96 (100), 84 (38), 69 (28).

From Camphor-1,4-homoenol (2)

A mixture of camphor-1,4-homoenol (**2**) (250 mg), potassium *tert*-butoxide (1.0 g), and *tert*-butanol-OD (10 mL) was refluxed for 3 h. The reaction mixture was diluted with water (25 mL) and extracted with ether. Removal of solvent provided a solid product (crude 3,3,8-trideuteriocamphor) which was refluxed with potassium *tert*-butoxide (1.0 g) and *tert*-butanol (10 mL) for 16 h. Work-up in the usual way provided a pale yellow solid (157 mg, 62% yield) which, on sublimation, yielded 8-deuteriocamphor (**4**) contaminated with a small amount (ca. 10%) of camphor.[3]

Camphor-1,4-homoenol p-*Bromobenzoate*

A solution of camphor-1,4-homoenol (**2**) (250 mg) and *p*-bromobenzoyl chloride (1.0 g) in dry hexamethylphosphoramide (2 mL) was stirred at room temperature under nitrogen for 24 h. After dilution with water, the mixture was extracted with ether and the extract washed with sodium bicarbonate solution. Removal of solvent provided a pale yellow semisolid (360 mg) which was purified by column chromatography (alumina, Grade III; elution with petroleum ether (35–60°C)). The colorless oil (150 mg) obtained was crystallized from petroleum ether (35–60°C) to give the *p*-bromobenzoate of **2**, mp 85–86°C; ν_{max} (CCl_4): 1725, 1270 cm^{-1}; δ(CCl_4, 100 MHz): 0.92 (3H, s), 1.00 (3H, s); ms *m/e*: 334–336 (9%, M^+), 183–185 (100), 134 (16), 121 (25), 95 (53). *Anal.* calcd. for $C_{17}H_{19}O_2Br$: C 60.89, H 5.67, Br 23.88%; found: C 60.82, H 5.73, Br 23.67%.

Acknowledgement

We thank the Natural Sciences and Engineering Research Council of Canada for generous financial support.

1. (*a*) N. Darby, N. Lamb, and T. Money. Can. J. Chem. **57**, 742 (1979); (*b*) M. S. Allen, N. Darby, P. Salisbury, E. R. Sigurdson, and T. Money. Can. J. Chem. **57**, 733 (1979), and references cited therein; (*c*) M. S. Allen, N. Lamb, and T. Money. J. Chem. Soc. Chem. Commun. 112 (1979).
2. C. R. Eck, G. L. Hodgson, D. F. MacSweeney, R. W. Mills, and T. Money. J. Chem. Soc. Perkin Trans. I, 1938 (1974); cf. G. L. Hodgson, D. F. MacSweeney, and T. Money. J. Chem. Soc. Perkin Trans. I, 2113 (1973).
3. C. R. Eck, R. W. Mills, and T. Money. J. Chem. Soc. Perkin Trans. I, 251 (1975); P. Cachia, N. Darby, C. R.

[3]Neither camphor or 8-deuteriocamphor undergo exchange of C(8)-hydrogen under these conditions and therefore the small amount of unlabelled camphor produced in this reaction may be formed by intramolecular abstraction of C(3)-*exo*-hydrogen by the C(8) carbanion.

ECK, and T. MONEY. J. Chem. Soc. Perkin Trans. I, 359 (1976).
4. D. R. DIMMEL and J. WOLINSKY. J. Org. Chem. **32**, 410 (1967); D. S. WEINBERG and C. DJERASSI. J. Org. Chem. **31**, 115 (1966).
5. J. B. STOTHERS, C. T. TAN, and K. C. TEO. Can. J. Chem. **51**, 2893 (1973); E. LIPPMAA, T. PEHK, J. PAASIVIRTA, N. BELIKOVA, and A. PLATE. Org. Magn. Reson. **2**, 581 (1970); E. WENKERT, A. O. CLOUSE, D. W. COCHRAN, and D. DODDRELL. Chem. Commun. 1433 (1969).
6. W. L. MEYER, C. E. CAPSHAW, J. H. JOHNSON, A. R. KLUSENER, A. P. LOBO, and R. N. MCCARTY. J. Org. Chem. **42**, 527 (1977).
7. H. G. KUIVILA. Synthesis, 499 (1970).
8. (*a*) P. A. GRIECO, C. S. POGONOWSKI, S. D. BURKE, M. N. NISHIZAWA, M. MIYASHITA, Y. MASAKI, C.-L. J. WANG, and G. MAJETICH. J. Am. Chem. Soc. **99**, 4111 (1977); (*b*) J. E. LEIBNER and J. JACOBUS. J. Org. Chem. **44**, 449 (1979).
9. (*a*) S. DANISHEFSKY and D. DUMAS. Chem. Commun. 1287 (1968); (*b*) D. P. G. HAMON and R. W. SINCLAIR. Chem. Commun. 890 (1968); (*c*) Y. LEROUX. Bull. Soc. Chim. Fr. 359 (1968); (*d*) E. J. COREY and I. KUWAJIMA. J. Am. Chem. Soc. **92**, 395 (1970).
10. H. O. HOUSE, J.-J. RIEHL, and C. G. PITT. J. Org. Chem. **30**, 650 (1965), and references cited therein; cf. H. O. HOUSE. Modern synthetic reactions. W. A. Benjamin, Inc., Menlo Park, CA. 1972. pp. 161–162.
11. (*a*) R. HOWE and S. WINSTEIN. J. Am. Chem. Soc. **87**, 915 (1964); (*b*) T. FUKANAGA. J. Am. Chem. Soc. **87**, 916 (1964).
12. R. A. PAUPTIT and J. TROTTER. Can. J. Chem. In press.
13. A. NICKON, J. L. LAMBERT, J. E. OLIVER, D. F. COVEY, and J. MORGAN. J. Am. Chem. Soc. **98**, 2593 (1976), and references cited therein.
14. A. L. JOHNSON, N. W. PETERSEN, M. B. RAMPERSAD, and J. B. STOTHERS. Can. J. Chem. **52**, 4143 (1974); cf. A. L. JOHNSON, J. B. STOTHERS, and C. T. TAN. Can. J. Chem. **53**, 212 (1975).

Can. J. Chem. Downloaded from www.nrcresearchpress.com by 210.87.254.5 on 09/05/12
For personal use only.

Pyrrole chemistry. XXII. A "one-pot" synthesis of some 4-acylpyrrole-2-carboxaldehydes from pyrrole

HUGH J. ANDERSON, CHARLES E. LOADER, AND AIDAN FOSTER

Department of Chemistry, Memorial University of Newfoundland, St. John's, Nfld., Canada A1B 3X7

Received May 29, 1980

This paper is dedicated to Prof. Raymond U. Lemieux on the occasion of his 60th birthday

HUGH J. ANDERSON, CHARLES E. LOADER, and AIDAN FOSTER. Can. J. Chem. **58**, 2527 (1980).

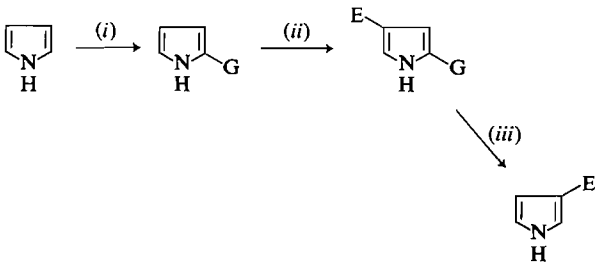
The Vilsmeier–Haack intermediates formed from pyrrole and from 1-methylpyrrole may be acylated under normal Friedel–Crafts conditions. Hydrolytic work-up then gives 4-acylpyrrole-2-carboxaldehydes in good yield. The methoxide/methanol treatment of the 4-trichloroacetylated intermediate leads to methyl 2-formylpyrrole-4-carboxylate. These are all "one-pot" syntheses from pyrrole. The formyl group has been removed from several of the products thus affording some 3-acylpyrroles in two operations.

HUGH J. ANDERSON, CHARLES E. LOADER et AIDAN FOSTER. Can. J. Chem. **58**, 2527 (1980).

Les intermédiaires de Vilsmeier–Haack, formés à partir du pyrrole et du méthyl-1 pyrrole, peuvent être acylés dans les conditions normales de Friedel–Crafts. Par hydrolyse, on obtient alors avec un bon rendement les acyl-4 pyrrole carboxaldéhydes-2. L'intermédiaire trichloroacétyle-4, traité au méthylate dans le méthanol, conduit au formyl-2 pyrrole carboxylate-4 de méthyle. Tous ces produits sont préparés en une seule étape à partir du pyrrole. L'élimination du groupe formyle de plusieurs de ces composés permet alors d'obtenir en deux étapes les acyl-3 pyrroles.

[Traduit par le journal]

The pathway to 3-substituted pyrroles shown in Scheme 1 has been used very widely. However, each of the three steps has its own limitations.



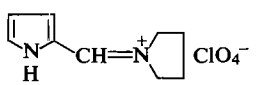
SCHEME 1

It is necessary to introduce an electron-withdrawing group in step (*i*) which can be removed in step (*iii*). Among the groups which may be introduced into position-2 of pyrrole in highest yield are the formyl (1) and trichloroacetyl (2). However, in step (*ii*) we found that yields were low for Friedel–Crafts acylation and related reactions of the 2-aldehyde (3). Others found both yield and isomer problems with nitration (4) of the 2-aldehyde. While the 2-trichloroacetyl derivative gave excellent results in a wide variety of electrophilic 4-substitutions (5) it must be removed by base hydrolysis to the 2-acid followed by decarboxylation. Some authors have been fairly successful in the decarboxylation of 3-substituted-2-acids (6), but we (3) and others (7, 8) found some yields to be poor and others to be good when an electron-withdrawing 4-substituent was present on the 2-acid in the absence of any alkyl group.

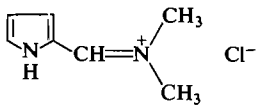
We have reported the satisfactory 4-substitution reactions of the pyrrole 2-thiol ester (9) and of the 2-nitrile (10), together with subsequent removal of these directing groups. However, the preparation of the 2-thiol ester gave only about 50% yield and its eventual removal required quite large amounts of Raney nickel. We have recently (11) improved on earlier preparations of the 2-nitrile, but the final removal of this group involved two steps: first, reduction to the aldehyde, and then decarbonylation. Nevertheless, this approach afforded satisfactory syntheses of 3-acetylpyrrole and methyl pyrrole-3-carboxylate (10).

The easy and efficient removal of the 2-aldehyde group by Raney nickel decarbonylation suggested that a special effort should be made to improve step (*ii*) for the 2-aldehyde. Sonnet (12) has shown how the 2-aldehyde may be converted to an iminium perchlorate **1**, which then undergoes 4-substitution in generally good yield, affording the product of step (*ii*) on hydrolytic work-up.

In the course of our investigation (11) of the preparation of the 2-nitrile through the Vilsmeier–Haack intermediate, we realized that this intermediate, **2**, was a close analogue of Sonnet's



1



2

0008-4042/80/232527-04$01.00/0

©1980 National Research Council of Canada/Conseil national de recherches du Canada

Can. J. Chem. Downloaded from www.nrcresearchpress.com by 210.87.254.6 on 09/05/12
For personal use only.

Can. J. Chem. Downloaded from www.nrcresearchpress.com by 210.87.254.6 on 09/05/12
For personal use only.

substrate, **1**. Consequently, we began to consider the possibility of combining the customary efficient synthesis of the 2-aldehyde with Sonnet's type of electrophilic attack on the iminum salt intermediate in the aldehyde synthesis, to be followed by the usual hydrolytic work-up affording a 4-substituted-2-aldehyde. When the iminum salt **2** was prepared using oxalyl chloride and dimethylformamide in either dichloromethane or 1,2-dichloroethane the clear, pale yellow solution underwent a slight warming and darkening on adding aluminum chloride. Addition of neat acetyl chloride caused some further warming and a color change through red to brown. Nuclear magnetic resonance spectral observation of the neat solution enabled the course of the reaction to be followed. Conversion to a 2,4-disubstituted pyrrole took about two hours of stirring at room temperature. The hydrolytic work-up and separation of the organic layer was followed by continuous ether extraction of the aqueous layer affording, from the combined organic layers, about 80% of pale yellow product which was almost pure 4-acetylpyrrole-2-carboxaldehyde. When combined with the Raney nickel decarbonylation reported before (10), the overall yield of 3-acetylpyrrole from pyrrole was close to 70%. Thus the three steps of Scheme 1 have been accomplished in two fairly simple preparative operations which give excellent results for this synthesis of a useful 3-substituted pyrrole.

Another useful starting material is methyl pyrrole-3-carboxylate which we had prepared previously (10) by the Friedel–Crafts trichloroacetylation of the 2-nitrile, followed by methanolysis of the trichloroacetyl group to the ester, and then removal of the nitrile directing group by reduction to the aldehyde and decarbonylation. Trichloroacetylation of the intermediate **2** was found to be satisfactory, so we proceeded to work up the product by a succession of methanolysis and hydrolysis steps leading, in one continuous sequence of operations, from pyrrole to methyl 2-formylpyrrole-4-carboxylate in about 80% yield of isolated product. Again, the success of the decarbonylation operation (10) means the preparation of methyl pyrrole-3-carboxylate can be accomplished rapidly and easily in two steps affording a 65–70% overall yield from pyrrole.

The Friedel–Crafts benzoylation of the intermediate **2** was not quite so successful, giving only about 55% of 4-benzoylpyrrole-2-carboxaldehyde. This time our earlier method for the removal of the aldehyde grouping by decarbonylation with active Raney nickel was unsatisfactory. The action of Raney nickel on 4-benzoylpyrrole-2-carboxaldehyde gives very poor yields (<25%) of 3-benzolypyrrole and there was some evidence of complex formation between the nickel and the pyrrole. We had found in earlier work (unpublished) that catalytic decarbonylation of 1-methyl-3-acetylpyrrole-2-carboxaldehyde using palladium on charcoal at about 220°C, according to the method reported by Tsuji and Ohno (13) for some other aldehydes, gave a good yield of 1-methyl-3-acetylpyrrole. The yields obtained for decarbonylation of related pyrroles with the 1-H unsubstituted were poorer than obtained from Raney nickel decarbonylation. However, 4-benzoylpyrrole-2-carboxaldehyde gave a 68% yield of 3-benzoylpyrrole.

As Sonnet (12) had already demonstrated the versatility of the iminium salt in a variety of reactions, we have examined some different or less successful types. One interesting reaction is the use of ethyl chlorothiolformate as an acylating agent. This had proved a satisfactory operation on the 2-nitrile (10) and was now found to give good yields with the iminium salt, provided the final hydrolysis was carried out under acidic rather than basic conditions.

The Friedel–Crafts formylation of the iminium salt using either methyl or butyl dichloromethyl ether failed to improve on the modest yield reported by Sonnet (12) for this type of reaction. However, our experience has been that conditions are critical for the formylation and yields often improve with further modifications.

We have found that the use of two moles of the DMF – oxalyl chloride complex does not introduce a second iminium grouping onto the pyrrole ring, even in the presence of aluminum chloride. Nor does the reagent attack furan under the conditions successful for pyrrole. The reagent does substitute the 5-position of 2-methylfuran, but the Friedel–Crafts acylation of the intermediate so formed does not take place, as shown by the absence of further change in the nmr spectrum.

The reagent, chlorosulfonyl isocyanate (CSI), offered the possibility of introducing the cyano group (14) in position-4 of the iminium salt. This is a very powerful reagent and can react with pyrrole to give 2,4-disubstitution when used in excess (11). However, to our surprise, the product isolated from the treatment of intermediate **2** with CSI, followed by DMF, was 4-chloropyrrole-2-carboxaldehyde. The same product was obtained when CSI was added in the presence of aluminum chloride.

We also attempted to carry out a Houben–Hoesch reaction on the complex **2** using ethyl cyanoformate and hydrogen chloride. No change was observed in the nmr spectrum of the reaction

Can. J. Chem. Downloaded from www.nrcresearchpress.com by 210.87.254.6 on 09/05/12
For personal use only.

mixture, nor did aluminum chloride promote the reaction. On work-up the only product was pyrrole-2-carboxaldehyde.

Experimental

Instruments and conditions were as described in ref. 10 except where indicated below.

4-Acetylpyrrole-2-carboxaldehyde

A solution of the pyrrole–Vilsmeier complex **2** was prepared in 1,2-dichloroethane on a five mmol scale as described before (11). To this was added aluminum chloride (11 mmol, Fluka), followed by acetyl chloride (5 mmol), rapidly and at room temperature. A small amount of warming occurred and the solution soon darkened. The ^1H nmr spectrum (neat) of the dark oil that had separated after 2 h indicated complete conversion to a 2,4-disubstituted pyrrole. The mixture was then poured onto about 50 mL of ice and water, 50% aqueous sodium hydroxide (4 mL) was added, and the mixture was stirred rapidly for about 10 min. The mixture was than made slightly acidic with concentrated hydrochloric acid and the organic and aqueous layers were separated. The aqueous layer was continuously extracted with ethyl ether for 8 h. The combined organic layer and ether extract was dried ($MgSO_4$), evaporated, and the solid residue recrystallized from benzene giving 0.55 g (80%) 4-acetylpyrrole-2-carboxaldehyde, mp 141–142°C (lit. (10) mp 141.5–142°C). Mixture mp undepressed.

4-Benzoylpyrrole-2-carboxaldehyde (Prepared by J. Doull)

The procedure above, using 5 mmol benzoyl chloride, gave a black solid. This was dissolved in ethyl acetate and filtered through a short plug of neutral alumina. Crystallization from ethyl acetate – petroleum (bp 60–80°C) gave 0.55 g (55%) of 4-benzoylpyrrole-2-carboxaldehyde, mp 138.5–139°C; ir ν: 1615, 1670 cm^{-1}; nmr ($CDCl_3$) δ: 9.45 (1H, d, J = 1.2 Hz), 7.8–7.2 (7H, m); *m/e*: 199. *Anal.* calcd. for $C_{12}H_9NO_2$: C 72.35, H 4.55, N 7.03; found: C 72.32, H 4.56, N 7.03.

Methyl 2-Formyl-4-pyrrolecarboxylate

Using the acetylation procedure above, the complex **2** (5 mmol) was treated with aluminum chloride (1.47 g, 11 mmol) and trichloroacetyl chloride (0.56 mL, 5 mmol).

The nmr spectrum of the pyrrole–Vilsmeier complex, as prepared in 1,2-dichloroethane, was determined using tetramethylsilane as external standard; δ: 11.36 (1H), 9.37 (1H), 8.08 (1H), 7.74 (1H), 7.12 (1H). Following the addition of aluminum chloride the spectrum was again determined; δ: 10.3 (1H, very broad), 8.61 (1H), 8.11 (1H), 7.80 (1H), 7.20 (1H). Trichloroacetyl chloride was added and, after 2 h at room temperature, the spectrum showed δ: 11.5 (1H, broad), 9.50 (1H, d), 9.19 (1H), 8.90 (1H).

After 2 h at room temperature, methanol (10 mL) was added and, after 5 min stirring, a solution of sodium (0.8 g, 35 mmol) in methanol (10 mL) was added and stirring continued for 2 h. The reaction product was then poured into cold water, stirred 10 min, and acidified with concentrated hydrochloric acid. The entire mixture was continuously extracted with ethyl ether. After drying ($MgSO_4$), the solvent was removed, giving a dark brown solid. The crude material in ethyl acetate was passed through a short plug of alumina and then was recrystallized from benzene–petroleum (60–80°C) to give 0.61 g (80%) of methyl 2-formylpyrrole-4-carboxylate, mp 126–128°C (lit. (10) mp 127–128°C). Mixture mp undepressed.

Pyrrole-2,4-dicarboxaldehyde

A solution of complex **2** (5 mmol) was treated with nitromethane (0.64 mL, 12 mmol) and aluminum chloride (1.47 g, 11 mmol), then cooled to 0°C. Dichloromethyl methyl ether (0.68 mL, 5 mmol) was added all at once and the cooling bath removed shortly after. The solution was stirred for 30 min at room temperature and worked up in the usual manner giving a yellow-brown solid. Recrystallization from toluene–petroleum gave 0.25 g (40%) of pyrrole-2,4-dicarboxaldehyde, mp 149–151°C (lit. (9) mp 151.5–152°C). Mixture mp undepressed.

Ethyl 2-Formylpyrrole-4-thiolcarboxylate

A solution of complex **2** (5 mmol) was treated with aluminum chloride (1.47 g, 11 mmol) and ethyl chlorothiolformate (0.59 mL, 5 mmol) at room temperature and stirred for 2 h. The product was poured into cold water (50 mL) and stirred rapidly for 45 min. The layers were separated and the aqueous layer extracted three times with chloroform. After drying the combined organic extracts ($MgSO_4$), the solvent was removed to give a pale brown solid. Recrystallization from benzene–petroleum (60–80°C) produced 0.57 g (62%) of ethyl 2-formylpyrrole-4-thiolcarboxylate, mp 71–73°C (lit. (10) mp 72.5–74°C). Mixture mp undepressed.

1-Methyl-4-acetylpyrrole-2-carboxaldehyde

(*a*)[1] To a suspension of aluminum chloride (40 g, 0.30 mol) in dichloromethane (250 mL) and acetyl chloride (7.1 mL, 0.10 mol) was added a solution of 1-methylpyrrole-2-carboxaldehyde (8.8 g, 0.08 mol) in dichloromethane (50 mL). The mixture was refluxed for 2 h, then poured on ice and stirred until melted. The layers were separated and the aqueous layer extracted three times with chloroform. The organic layer and the extracts were combined, dried ($MgSO_4$), and the solvent was removed. The crude solid product was dissolved in 1:3 chloroform–benzene, passed through a short column of neutral alumina, and sublimed to give 10.0 g (83%) of 1-methyl-4-acetylpyrrole-2-carboxaldehyde, mp 104–105°C; ir ν: 1657 cm^{-1}; nmr ($CDCl_3$) δ: 9.75 (1H, d), 7.57 (1H, m), 7.40 (1H, m), 4.05 (3H, s), 2.47 (3H, s); *m/e*: 151. *Anal.* calcd. for $C_8H_9NO_2$: C 63.56, H 6.00, N 9.27; found: C 63.55, H 6.03, N 9.25.

(*b*) Following the procedure for acetylation of the pyrrole complex **2**, a 5 mmol solution of the 1-methylpyrrole complex afforded a 78% yield of 1-methyl-4-acetylpyrrole-2-carboxaldehyde, mp 100–103°C. Mixture mp undepressed.

1-Methylpyrrole-2,4-dicarboxaldehyde

Following the procedure for formylation of pyrrole complex **2**, a 5 mmol solution of 1-methylpyrrole gave 0.42 g (61%) of 1-methylpyrrole-2,4-dicarboxaldehyde, mp 93–95°C (lit. (15) mp 95–96°C). Mixture mp undepressed.

Reaction of Pyrrole–Vilsmeier Complex 2 with Chlorosulfonyl Isocyanate

To a solution of **2** (5 mmol) in a bath at −25°C was added chlorosulfonyl isocyanate (0.43 mL, 5 mmol) in 1,2-dichloroethane (5 mL). The mixture was slowly allowed to reach room temperature. The nmr spectrum showed no evidence of reaction, so stirring was continued overnight. The usual work-up gave 0.30 g (50%) of 4-chloropyrrole-2-carboxaldehyde, mp 128.5–129°C (lit. (12*b*) mp 129–129.5°C).

The reaction was also carried out using acetonitrile as solvent giving the same product in 52% yield. The presence of 11 mmol of aluminum chloride in the reaction mixture also gave about the same result.

3-Benzoylpyrrole

4-Benzoylpyrrole-2-carboxaldehyde (100 mg) was mixed with palladized charcoal (10 mg, 5% Pd on C. Matheson, Coleman and Bell). The mixture was placed at the bottom of a long glass tube (normally used for small scale sublimations). The glass tube was connected to an eudiometer system, to measure the volume

[1]Taken from the M.Sc. thesis of H. Nagy, Memorial University of Newfoundland, 1970.

of gas evolved, and to a vacuum system. The tube was evacuated and then filled with nitrogen. The tube was then opened to the eudiometer and was heated to about 210°C in a sublimation apparatus. Gas evolution, apart from that due to expansion, became noticeable at about 180°C and became brisk at 210°C and a small amount of distillate (later indentified as water from the palladized charcoal) appeared on the sides of the tube. When gas evolution ceased (about 97% of the calculated volume of CO was produced), the eudiometer was disconnected and the tube was again evacuated (0.1 Torr). A colorless oily liquid soon began to collect on the cold surface of the tube and slowly crystallized. When distillation ceased the apparatus was allowed to cool and the section containing the distillate was cut from the tube. The distillate was recrystallized from chloroform–petroleum (bp 80–100°C) to give 58 mg, (68%) of 3-benzoylpyrrole mp 99.5–100°C (lit. (6) 96–97°C); ir (Nujol) ν: 1623 cm^{-1}; nmr ($CDCl_3$) δ: 6.66 (2H, m), 7.18 (1H, m), 7.27–7.90 (5H, m).

Using a similar procedure the following were also prepared by this method.

3-Acetylpyrrole

3-Acetylpyrrole was obtained as a pure colorless sublimate (67% yield), mp 113–114.5°C (lit. (10) 115–116°C). Mixture melting point with authentic material was undepressed.

Methyl Pyrrole-3-carboxylate

Methyl pyrrole-3-carboxylate was obtained as a colorless sublimate (44% yield) mp 87–88°C (lit. (10) 87–87.5°C). Mixture melting point with authentic material was undepressed.

1-Methyl-3-acetylpyrrole

1-Methyl-3-acetylpyrrole was obtained as a liquid distillate. The product was redistilled to give a colorless liquid (73% yield), bp 148–150°C/15 Torr; ir (film) ν: 1652 cm^{-1}; nmr δ: 2.30 (3H, s), 3.60 (3H, s), 6.49 (2H, m), 7.16 (1H, m); *m/e*: 171. *Anal.* calcd. for C_7H_9NO: C 68.27, H 7.37; found: C 68.34, H 7.40.

Acknowledgements

The authors gratefully acknowledge the financial assistance of the Memorial University of Newfoundland and the Natural Sciences and Engineering Research Council of Canada.

1. R. M. Silverstein, E. E. Ryskiewicz, and C. Willard. Org. Synth. **36**, 74 (1956).
2. A. Treibs and F. H. Kreutzer. Justus Liebigs Ann. Chem. **721**, 105 (1969); J. W. Harbuck and H. Rapoport. J. Org. Chem. **37**, 3618 (1972).
3. H. J. Anderson and C. W. Huang. Can. J. Chem. **45**, 897 (1967).
4. P. Fournari and J. Tirouflet. Bull. Soc. Chim. Fr. 484 (1963).
5. P. Bélanger. Tetrahedron Lett. 2505 (1979); P. Barker, P. Gendler, and H. Rapoport. J. Org. Chem. **43**, 4849 (1978).
6. M. K. A. Khan, K. J. Morgan, and D. P. Morrey. Tetrahedron, **22**, 2095 (1966).
7. P. Fournari, M. Farnier, and C. Fournier. Bull. Soc. Chim. Fr. 283 (1972).
8. J. Elguero, R. Jacquier, and B. Shimizu. Bull. Soc. Chim. Fr. 1585 (1970).
9. C. E. Loader and H. J. Anderson. Tetrahedron, **25**, 3879 (1969).
10. H. J. Anderson, C. R. Riche, T. G. Costello, C. E. Loader, and G. H. Barnett. Can. J. Chem. **56**, 654 (1978).
11. G. H. Barnett, H. J. Anderson, and C. E. Loader. Can. J. Chem. **58**, 409 (1980).
12. P. E. Sonnet. (*a*) J. Org. Chem. **36**, 1005 (1971); (*b*) J. Org. Chem. **37**, 925 (1972).
13. J. Tsuji and K. Ohno. J. Am. Chem. Soc. **90**, 94 (1968).
14. G. Lohaus. Chem. Ber. **100**, 2719 (1967).
15. H. J. Anderson and H. Nagy. Can. J. Chem. **50**, 1961 (1972).

Can. J. Chem. Downloaded from www.nrcresearchpress.com by 210.87.254.6 on 09/05/12
For personal use only.

Stereoelectronic control in acetal formation

NORMAND BEAULIEU,[1] ROBERT A. DICKINSON,[2] AND PIERRE DESLONGCHAMPS

Laboratoire de Synthèse Organique, Département de Chimie, Faculté des Sciences, Université de Sherbrooke, Sherbrooke (Qué.), Canada J1K 2R1

Received February 26, 1980

This paper is dedicated to Prof. Raymond U. Lemieux on the occasion of his 60th birthday

NORMAND BEAULIEU, ROBERT A. DICKINSON, and PIERRE DESLONGCHAMPS. Can. J. Chem. **58**, 2531 (1980).

The cyclization under acidic conditions of bicyclic and monocyclic hydroxypropyl methoxytetrahydropyrans **1** and **4** is reported. At room temperature, compound **1** gives only *cis* tricyclic acetal **2**. At reflux, compound **2** equilibrates to yield a mixture of *cis* and *trans* tricyclic acetals **2** (45%) and **3** (55%). Compound **4** gives directly the equilibrium mixture of *cis* and *trans* bicyclic acetals **5** (55%) and **6** (45%) at room temperature. The specific formation of **2** from **1** constitutes strong experimental evidence that acetal formation is controlled by stereoelectronic effects. The anomeric effect can be estimated (≃1.5 kcal/mol) from the equilibrium study of **2** and **3**. This value confirms the result previously obtained by Descotes (9).

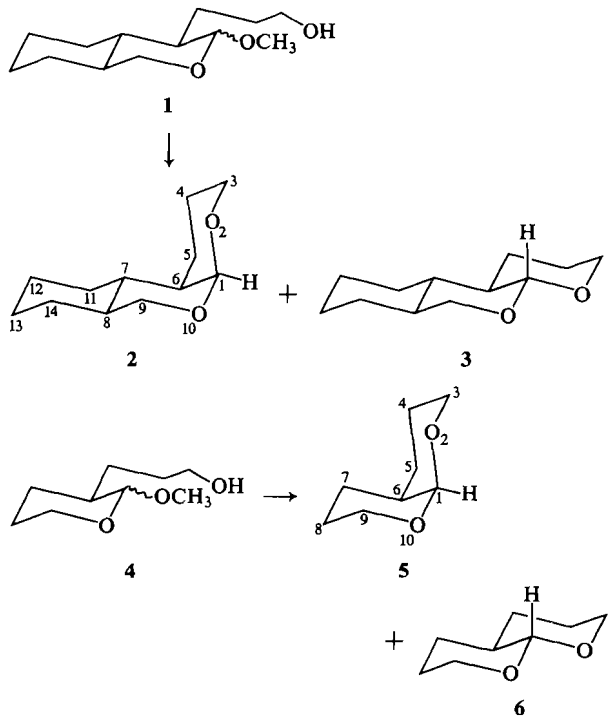
NORMAND BEAULIEU, ROBERT A. DICKINSON et PIERRE DESLONGCHAMPS. Can. J. Chem. **58**, 2531 (1980).

On rapporte la cyclisation, sous conditions acides, des hydroxy-propylméthoxytétrahydropyrannes bicyclique et monocyclique **1** et **4**. A température ambiante, le composé **1** donne uniquement l'acétal tricyclique *cis* **2**. A reflux, le composé **2** forme un mélange des acétals tricycliques *cis* **2** (45%) et *trans* **3** (55%). Le composé **4**, à température ambiante, donne directement le mélange à l'équilibre des acétals bicycliques *cis* **5** (55%) et *trans* **6** (45%). La formation spécifique de **2** à partir de **1** constitue une preuve convaincante démontrant que la formation d'acétal est contrôlée par des effets stéréoélectroniques. L'effet anomère peut être évalué à partir de l'analyse du mélange à l'équilibre de **2** et **3**; la valeur trouvée de ≃1.5 kcal/mol s'accorde bien avec les résultats déjà obtenus par Descotes (9).

The influence of stereoelectronic effects on the configuration and the conformation of the acetal function has been recognized for a long time, particularly in carbohydrates where these effects have been discussed in terms of the anomeric and the *exo*-anomeric effects (1).

A pertinent question which follows is whether or not these stereoelectronic effects have an important influence on the formation or the cleavage of the acetal function. The first experimental evidences that acetal hydrolysis is indeed controlled by stereoelectronic effects have been obtained recently by Kirby and Martin (2, 3). The reverse process, i.e. acetal formation, should therefore be controlled by stereoelectronic effects. We wish to report an experiment which shows that this is indeed the case.

In this work, we describe the study of the cyclization of bicyclic hydroxypropyl methoxytetrahydropyran **1** (Scheme 1) and monocyclic hydroxypropyl methoxytetrahydropyran **4** under mild acidic conditions. Theoretically, compound **1** may yield both *cis* and *trans* tricyclic acetals **2** and **3** or either of them, whereas compound **4** may cyclize to the corresponding *cis* and/or *trans* bicyclic acetals **5** and **6**.



SCHEME 1

Method

Syntheses of Compounds 1 and 4

The syntheses of compounds **1** and **4** are described in Scheme 2. Bicyclic lactone **7** was alky-

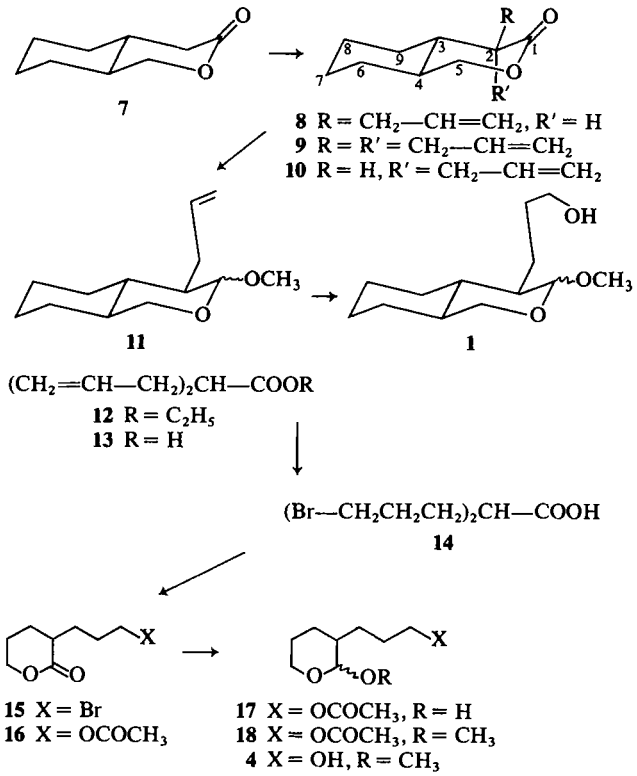
[1]Holder of a Natural Sciences and Engineering Research Council of Canada (NSERCC) Postgraduate Scholarship.

[2]Holder of a National Research Council of Canada Postdoctoral Fellowship (1974).

0008-4042/80/232531-06$01.00/0

©1980 National Research Council of Canada/Conseil national de recherches du Canada

Can. J. Chem. Downloaded from www.nrcresearchpress.com by 210.87.254.6 on 09/05/12
For personal use only.



SCHEME 2

lated (LDA, allyl bromide, HMPT, −78° and −40°C) to produce a mixture of **7** (11%), bicyclic allyl lactone **8** (85%), and bicyclic bis-allyl lactone **9** (4%) which were separated by column chromatography.

Treatment of bicyclic allyl lactone **8** with sodium methoxide in methanol yielded a mixture of **8** (68%) and **10** (33%) which were separated by vpc. Epimerization of compound **8** with *p*-toluenesulfonic acid in benzene yielded a mixture of **8** (64%) and **10** (36%). As compound **8** is the major epimer, the allyl side chain in **8** is therefore oriented equatorially. The ^{13}C nmr spectra of compounds **8** and **10** confirm this assignment.[3]

Reduction of bicyclic allyl lactone **8** (DIBAL in THF, −78°C) followed by methanolysis (CH_3OH, *p*-TsOH, room temperature) resulted in bicyclic allyl methoxytetrahydropyran **11** as a mixture of isomers at the anomeric center (axial/equatorial ratio = 3:1). Hydroboration ($(CH_3)_2S \cdot BH_3$ in THF, 0°C) (5) of **11** gave the desired bicyclic hydroxypropyl methoxytetrahydropyran **1** as a mixture of axial and equatorial isomers (ratio 3:1). This mixture of **1** was used for our study.

[3]In the axial isomer **10** carbon-4 appears at a higher chemical shift (32.8 ppm) than the equatorial isomer **8** (37.9 ppm) due to the γ effect (4).

Basic hydrolysis of ethyl bis-allyl acetate **12** (6) (KOH, C_2H_5OH, reflux, 12 h) gave the corresponding bis-allyl acetic acid **13** which was converted into dibromocarboxylic acid **14** (92% yield) by the photochemically induced addition of hydrogen bromide (*hν*, pentane (7)). Treatment of dibromocarboxylic acid **14** with triethylamine in dichloromethane yielded bromolactone **15** (93% yield) which was further transformed (CH_3COONa, HMPT, room temperature, (8)) into acetate lactone **16** (49% yield).

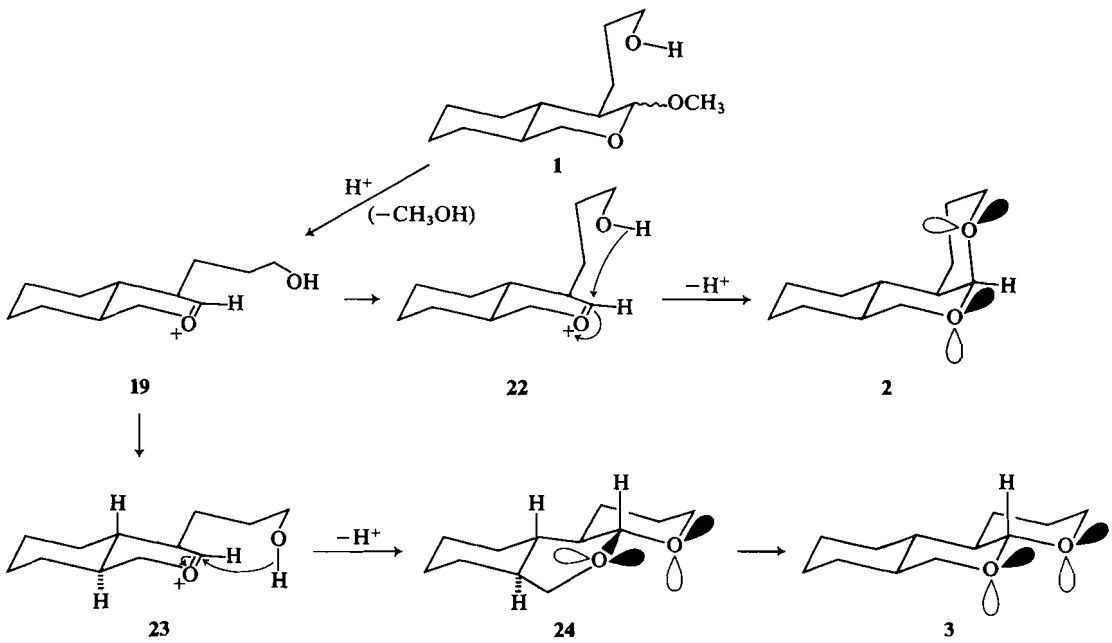
Reduction of acetate lactone **16** with diisobutyl aluminium hydride in tetrahydrofuran produced the corresponding acetate hemiacetal **17**. Treatment of **17** with methanol in the presence of *p*-toluenesulfonic acid gave **18** which was hydrolyzed with potassium carbonate to yield hydroxypropyl methoxytetrahydropyran **4** as a mixture of *cis* and *trans* isomers (1 ≃ 1 ratio, nmr) which produces a single peak on vpc. The isomeric mixture of **4** was used in our study.

Cyclization of Compounds 1 and 4

Methanolysis (CH_3OH, *p*-TsOH (1 equiv.), room temperature, 72 h) of bicyclic hydroxypropyl methoxytetrahydropyran gave the *cis* tricyclic acetal **2** only. The appearance of a small quantity of

Can. J. Chem. Downloaded from www.nrcresearchpress.com by 210.87.254.6 on 09/05/12
For personal use only.

Can. J. Chem. Downloaded from www.nrcresearchpress.com by 210.87.254.6 on 09/05/12
For personal use only.



SCHEME 3

the *trans* tricyclic acetal **3** occurred only after 5 days. When the *cis* tricyclic acetal **2** was refluxed under the above conditions (CH_3OH, *p*-TsOH), isomerization took place to yield an equilibrium mixture of *cis* and *trans* tricyclic acetals **2** (45%) and **3** (55%). *Cis* and *trans* tricyclic acetals **2** and **3** were separated by vpc.

Methanolysis (CH_3OH, *p*-TsOH (1 equiv.), room temperature, 5 days) of hydroxypropyl methoxytetrahydropyran **4** gave an equilibrium mixture of *cis* and *trans* bicyclic acetals **5** (55%) and **6** (45%). This reaction was followed by thin layer chromatography which showed the gradual and simultaneous appearance of **5** and **6**. Compounds **5** and **6** were separated by vpc. They are known compounds and their equilibration under acidic conditions has been previously reported (9).

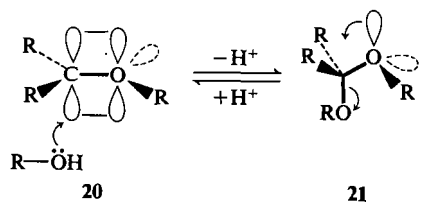
The structures of tricyclic acetals **2** and **3** were established by ^1H and ^{13}C nmr on comparison with the spectra of bicyclic acetals **5** and **6**.

Discussion

The specific conversion of compound **1** into the *cis* tricyclic acetal **2** is clearly the result of a kinetically controlled reaction because under more vigorous conditions the *cis* acetal **2** equilibrates with the slightly more stable *trans* acetal **3** (thermodynamic control). As a consequence, the formation of *trans* acetal **3** must require an energetically higher transition state than that for the formation of *cis* acetal **2**.

The first step during the cyclization reaction must be the formation of the bicyclic hydroxy oxenium ion **19** by the loss of methanol from the starting product **1** (Scheme 3). The hydroxyl group in **19** has then the choice to attack the β or the α face of the oxenium ion which would give the *cis* or the *trans* tricyclic acetals **2** and **3** respectively. However, under kinetically controlled conditions, the α attack cannot compete with the β attack as the *cis* acetal **2** is the only product formed.

These results can be explained if stereoelectronic effects are taken into consideration. Indeed, if we accept that acetal formation will take place with minimum energy, only when the intermediate oxenium ion can develop an electron pair which will become antiperiplanar to the newly formed C—O bond in the final product (stereoelectronic control (10), cf. **20** → **21**), the above results can be easily rationalized.



20 **21**

It can readily be seen that the β attack on **19** (i.e. **22**) can give the *cis* acetal **2** with stereoelectronic control, because the oxygen of ring B in **2** has an electron pair oriented antiperiplanar to the newly

Can. J. Chem. Downloaded from www.nrcresearchpress.com by 210.87.254.6 on 09/05/12
For personal use only.

formed C—O bond. On the other hand, the α attack on **19** with stereoelectronic control cannot yield the *trans* acetal directly in its more stable conformation **3**. The α attack on **19** (i.e. **23**) must first give conformer **24** of *trans* acetal having its ring B twisted; in **24**, the oxygen of ring B has an electron pair oriented antiperiplanar to the newly formed C—O bond. Conformer **24** would then undergo a conformational change to the more stable conformation **3** of *trans* tricyclic acetal. The transition **19** → **23** → **24** requires more energy than the transition **19** → **22** → **2**, so the formation of *trans* acetal **3** should be a higher energy process than the formation of *cis* acetal **2**.

This conclusion is in accord with the above experimental results which clearly show that *trans* tricyclic acetal **3** is produced only when the experimental conditions allow the cyclization process to become thermodynamically controlled. If stereoelectronic effects are neglected, we would have predicted that the formation of **3** would be as facile as that of **2** from **19**. Consequently, the above results constitute strong evidence that acetal formation is stereoelectronically controlled.

The direct conversion of compound **4** into the equilibrium mixture of *cis* and *trans* bicyclic acetals **5** and **6** shows that this reaction is under thermodynamic control even at room temperature. Consequently, this experiment is not valid to either prove or disprove the influence of stereoelectronic effects in acetal formation. In this case, the formation of *trans* acetal can compete with the formation of *cis* acetal. The reason might simply be that it is easier to go through a twisted acetal conformer with the monocyclic compound **4** than with the bicyclic compound **1**.

At equilibrium, there is a larger percentage of the *cis* acetal in the bicyclic series (**5**, 55%) (9) than in the tricyclic series (**2**, 45%). This difference can be explained by the fact that the *cis* bicyclic acetal is conformationally mobile (*cis* decalin system) whereas the *cis* tricyclic acetal **2** is conformationally rigid. There is therefore an entropy factor which favors the *cis* over the *trans* acetal in the bicyclic series only, and this is reflected in the equilibrium value.

Descotes (9) had carried out the equilibration of *cis* and *trans* acetals **5** and **6** in order to evaluate the anomeric effect and obtained a value of 1.4 kcal/mol. Our equilibration study with *cis* and *trans* acetals **2** and **3** confirms his conclusion.

If the same value are taken for the steric interactions in the *cis* acetal **2** (one *gauche* interaction = 0.85 kcal/mol and one interaction for an axial OR group to cyclohexane = 0.8 kcal/mol), the *cis* acetal **2** should be less stable than the *trans* acetal **2** by 1.65 kcal/mol. The equilibration studies show that the *cis* acetal **2** is less stable than the *trans* acetal **3** by 0.14 kcal/mol (65°C, 45%), the anomeric effect is therefore evaluated to be about ≃1.5 kcal/mol from this experiment.

Experimental

Vapor phase chromatographic (vpc) analysis and separations were carried out on a Varian Aerograph instrument, model 2868 with thermal conductivity detector (column 1: SE-30, 15% Chromosorb W, 60–80 mesh, 5 ft × ¼ in.; 2: SE-30, 10% Chromosorb W, 60–80 mesh, 5 ft × ¼ in.; 3: SE-30, 5% Chromosorb W, 100–200 mesh, 5 ft × ¼ in.). The infrared (ir) spectra were taken on a Perkin-Elmer 257 spectrophotometer. Proton nuclear magnetic resonance (nmr) spectra were recorded on a Bruker WP-60 instrument. The ^{13}C nmr spectra were recorded on a Bruker HX-90 spectrometer equipped with a Nicolet 1083 computer (8K memory for data) operating in the Fourier transform mode. Sweep widths of 5000 Hz were used with a line broadening factor of 0.5 Hz. The compounds were studied as approximately 0.7 *M* solutions in $CDCl_3$ with internal TMS as reference, Mass spectral assays were obtained using a Hitachi-Perkin-Elmer RMU-6A and a Vg Micromass ZAB-2F mass spectrometer. Microanalyses were carried out by Schwarzkopf Microanalytical Laboratories, New York and by Guelph Chemical Laboratories Ltd, Guelph, Ont.

Bicyclic lactone **7** was obtained by Baeyer–Villiger oxidation (11) of *trans*-hydrindanone (12).

Bicyclic Equatorial Allyl Lactone **8**

A solution of diisopropylamine (10 mmol) in anhydrous tetrahydrofuran (50 mL) was mixed with *n*-butyllithium (10 mmol, 2.2 *M* in hexane) at room temperature. After 20 min, the solution was cooled at −78°C and a solution of bicyclic lactone **7** (769 mg, 5 mmol) in anhydrous tetrahydrofuran (20 mL) was added dropwise and the mixture was left for 1 h. Allyl bromide (6 mmol) in hexamethylphosphoramide (7 mmol) was then added. The reaction mixture was then left for 3 h at −40°C. A saturated solution (20 mL) of ammonium chloride was added, and the resulting mixture was extracted with ether (100 mL). The organic phase was washed with dilute hydrochloric acid (10%, 2 × 25 mL) and brine. The organic phase was dried with magnesium sulfate, filtered, and evaporated to yield an oil (876 mg). Vapor phase chromatographic analysis indicated a mixture of bicyclic allyl lactone **8** (85%), starting bicyclic lactone **7** (11%), and bicyclic bis-allyl lactone **9** (4%). These compounds were separated by column chromatography with silica gel using ether–hexane (1:4) as eluant.

Bicyclic Allyl Lactone **8**: vpc: retention time, 20.7 min (153°C, column 3); ir (CCl_4); 1744 and 1638 cm^{-1}; nmr ($CDCl_3$) δ: 1.0–2.0 (10H), 2.0–3.0 (3H, multiplet, C=C—CH_2—CH—CO), 3.85 and 4.27 (2H, AB part of an ABX system, J_{AX} = 10.5 Hz, J_{BX} = 4.0 Hz, and J_{AB} = 11.0 Hz, CH_2O), 5.16 (2H, complex doublets, $J_{(trans)} \simeq 16$ Hz, and $J_{(cis)} \simeq 10$ Hz, C=CH_2), and 5.87 (1H, multiplet, —CH=C). Data for ^{13}C nmr ($CDCl_3$): 172.7 (C1), 117.9 (C12), 134.5 (C11), 73.9 (C5), 46.9 (C3), 39.1 (C2), 37.9 (C4), 32.4 (C10), 30.4 (C9), 27.3 (C6), 25.2 (C7), and 24.8 (C8); ms *m/e* (70 eV): 194 (M^+). *Anal.* calcd. for $C_{12}H_{18}O_2$: C 74.23, H 9.28; found: C 73.97, H 9.42.

Bicyclic Bis-allyl Lactone **9**: ir ($CHCl_3$): 1745 and 1638 cm^{-1}; nmr ($CDCl_3$) δ: 1.0–2.0 (10H), 2.0–3.0 (4H, multiplet, two CH_2—C=C), 3.85 and 4.27 (2H, AB part of an ABX system, J_{AX} = 10.5 Hz, J_{BX} = 4.0 Hz, J_{AB} = 11.0 Hz, CH_2O), 5.16 (4H, complex doublets, $J_{(trans)} \simeq 16$ Hz, $J_{(cis)} \simeq 10$ Hz, two C=CH_2), and 5.87 (2H, multiplet, two C—CH=C); ms *m/e* (70 eV): 234 (M^+).

Can. J. Chem. Downloaded from www.nrcresearchpress.com by 210.87.254.6 on 09/05/12
For personal use only.

Bicyclic Axial Allyl Lactone 10

Bicyclic equatorial allyl lactone **8** (42 mg, 0.22 mmol) was added to a solution of sodium methoxide (24 mg, 0.44 mmol) in methanol (4 mL), and the mixture was refluxed under nitrogen for 24 h. The methanol was evaporated, the residue was acidified with dilute hydrochloric acid (2 *N*, 3 mL) and extracted with ether. The organic phase was washed with brine, dried over sodium sulfate, filtered, and evaporated to dryness. The vpc analysis showed a major product (equatorial allyl **8**) and a minor product (axial allyl **10**) which were separated (vpc) yielding pure equatorial allyl lactone **8** (14 mg) and pure axial allyl lactone **10** (7 mg).

Bicyclic Axial Allyl Lactone 10: vpc: retention time, 24.4 min (153°C, column 3); ir (CCl_4): 1748 and 1640 cm^{-1}; nmr ($CDCl_3$) δ: 1.0–2.0 (10H), 2.5 (3H, multiplet, C=C—CH_2—CH—CO), 3.79 and 4.31 (2H, AB part of an ABX system, J_{AX} = 10.5 Hz, J_{BX} = 5.0 Hz, J_{AB} = 11.0 Hz, CH_2O), 5.03 (2H, complex doublets, $J_{(trans)} \simeq 16$ Hz, $J_{(cis)} \simeq 10$ Hz, C=CH_2), and 5.87 (1H, multiplet, —CH=C); ^{13}C nmr ($CDCl_3$): 174.9 (C1), 116.9 (C12), 136.0 (C11), 74.9 (C5), 44.8 (C3), 40.3 (C2), 32.8 (C4 and C10), 28.3 (C9), 28.0 (C6), 25.8 (C7), and 25.1 (C8); ms *m/e* (70 eV): 194 (M^+).

Epimerization of Bicyclic Equatorial Allyl Lactone 8

Bicyclic equatorial allyl lactone **8** (39 mg, 0.20 mmol) was refluxed in benzene (5 mL) containing *p*-toluenesulfonic acid (38 mg, 0.20 mmol) during 14 h. Dilute sodium bicarbonate (5%, 5 mL) was added and the mixure was extracted with ether (3 × 20 mL). The organic extract was dried over sodium sulfate, filtered, and evaporated to yield a product (38 mg, 97%) which was shown by vpc to be a mixture of equatorial (64%) and axial (36%) bicyclic allyl lactones **8** and **10**.

Bicyclic Allyl Methoxytetrahydropyran 11

A solution of bicyclic equatorial allyl lactone **8** (595 mg, 3.07 mmol) in anhydrous tetrahydrofuran (40 mL) was treated at −78°C with diisobutylaluminium hydride (4 mmol, 1 *M* in hexane) during 2 h. The mixture was warmed up to room temperature and was slowly added to aqueous acetic acid (10%, 100 mL); it was then extracted with ether (3 × 50 mL). The organic phase was washed with sodium bicarbonate (5%, 3 × 50 mL), dried over sodium sulfate, filtered, and evaporated. The residue was treated with anhydrous methanol (50 mL) containing trimethyl orthoformate (1 mL) and a catalytic amount of *p*-toluenesulfonic acid. After 15 h at room temperature, potassium carbonate (300 g) was added followed by the addition of water (40 mL). The reaction mixture was extracted with ether (3 × 50 mL), the organic extract was dried over sodium sulfate, filtered, and evaporated to dryness yielding crude bicyclic allyl methoxytetrahydropyran **11** (503 mg, 78%). This product was purified by vpc: retention time, 9 min (160°C, column 2); ir ($CHCl_3$): 1645 cm^{-1}; nmr ($CDCl_3$) δ: 0.8–2.5 (15H), 3.25 and 3.40 (3H, two singlets, ratio 3:1, axial and equatorial OCH_3), 3.2–4.5 (2.25H, CH_2O and axial anomeric hydrogen), 4.45 (0.75H, broad doublet, equatorial anomeric hydrogen), and 4.7–6.1 (3H, multiplet, CH=CH_2); ms *m/e* (70 eV): 210 (M^+), 178 (M^+ − CH_3OH).

Bicyclic Hydroxypropyl Methoxytetrahydropyran 1

A solution of bicyclic allyl methoxytetrahydropyran **11** (183 mg, 0.87 mmol) in anhydrous tetrahydrofuran (5 mL) was treated at 0°C with dimethyl sulfide – borane complex (0.4 mmol) during 2 h. Aqueous sodium hydroxide (3 *N*, 2 mL) followed by hydrogen peroxide (30%, 2 mL) was then added and the mixture was stirred for 90 min at 0°C. Water (20 mL) was added and the mixture was extracted with chloroform (4 × 25 mL). The organic extract was dried over sodium sulfate, filtered, and evaporated to yield crude bicyclic hydroxypropyl methoxytetrahydropyran **1**. Infrared ($CHCl_3$): 3350–3600 and 1200–1250 cm^{-1}; nmr ($CDCl_3$) δ: 0.80–2.30 (15H), 3.38 and 3.52 (3H, two singlets, ratio 3:1, axial and equatorial O—CH_3), 3.3–4.0 (4.25H, two CH_2O and axial anomeric hydrogen), 4.63 (0.75H, broad doublet, equatorial anomeric hydrogen).

cis *Tricyclic Acetal 2*

Bicyclic hydroxypropyl methoxytetrahydropyran **1** (199 mg, 0.87 mmol) was treated with anhydrous methanol (20 mL) containing *p*-toluenesulfonic acid (165 mg, 0.87 mmol) at room temperature during 72 h. Potassium carbonate (300 mg) was added and after 30 min, the mixture was evaporated. The residue was dissolved in water (20 mL) and the aqueous phase was extracted with ether. The organic phase was dried over sodium sulfate, filtered, and evaporated to yield an oil. The vpc and tlc analyses indicated the presence of *cis* tricyclic acetal **2**, and the absence of the *trans* isomer **3**. Purification by thin layer chromatography with silica gel using ether gave pure *cis* tricyclic acetal **2** (106 mg, 62%); vpc: retention time, 20.7 min (150°C, column 2); ir ($CHCl_3$): 1000–1200 cm^{-1}; nmr ($CDCl_3$) δ: 0.5–2.5 (15H), 3.5–4.3 (4H, multiplet, two OCH_2), and 4.75 (1H, broad singlet, anomeric hydrogen); ^{13}C nmr ($CDCl_3$): 98.9 (C1), 67.7 (C9), 66.7 (C3), 40.9 (C8), 40.5 (C6), 35.6 (C7), 28.8 (C11), 27.8 (C14), 26.4 (C13), 25.8 (C12), 23.8 (C4), and 20.5 (C5); ms *m/e* (70 eV): 196 (M^+).

Isomerization of cis *and* trans *Tricyclic Acetals 2 and 3*

Cis tricyclic acetal **2** (40 mg, 0.2 mmol) was dissolved in anhydrous methanol (5 mL) containing *p*-toluenesulfonic acid (0.2 mmol) and the solution was stirred at room temperature. After 24 h, tlc analysis showed the presence of *cis* tricyclic acetal **2** only. The solution was then refluxed during 24 h; analysis by tlc indicated the gradual appearance of a new product. The reaction mixture was evaporated and sodium bicarbonate (5%, 20 mL) was added and the resulting mixture was extracted with dichloromethane (3 × 30 mL). The organic phase was dried over sodium sulfate, filtered, and evaporated. Vapor phase chromatographic analysis indicated a mixture (39 mg, 97%) of *cis* (45%) and *trans* (55%) tricyclic acetals **2** and **3**. These compounds were separated by vpc (retention time, 12.5 min for compound **2** and 19 min for compound **3** (135°C, column 3)).

Trans *Tricyclic Acetal 3*: ir ($CHCl_3$): 1000–1200 cm^{-1}; nmr ($CDCl_3$) δ: 0.5–2.5 (15H), 3.5–4.3 ((5H, multiplet, two OCH_2 and anomeric hydrogen); ^{13}C nmr ($CDCl_3$): 105.1 (C1), 71.9 (C9), 67.3 (C3), 45.1 (C7), 43.9 (C6), 41.6 (C8), 28.2 (C11), 27.6 (C14), 26.1 (C13), 25.6 (C12), 25.1 (C4), and 19.4 (C5); ms *m/e* (70 eV): 196 (M^+).

Bis-allyl Acetic Acid 13

Ethyl bis-allyl acetate **12** (4.23 g, 0.03 mol) (6) was mixed with a solution of potassium hydroxide (2.5 g, 40 mmol) in ethanol (95%, 75 mL) and the mixture was refluxed during 12 h. The solvent was evaporated, water (50 mL) was added, and the aqueous phase was extracted with ether (2 × 25 mL). The aqueous phase was then acidified with concentrated hydrochloric acid and extracted with ether (3 × 50 mL). The organic phase was dried with magnesium sulfate, filtered, and evaporated to yield crude bis-allyl acetic acid **13** (3.25 g, 92%) which was used without further purification. An analytical sample was prepared by vpc; vpc: retention time, 7 min (115°C, column 1); ir ($CHCl_3$): 2400–3400 (broad), 1715 and 1642 cm^{-1}; nmr ($CDCl_3$) δ: 2.1–2.5 (5H), 4.7–6.0 (6H, multiplet, CH=CH_2), and 11.8 (1H, singlet, OH); ms *m/e* (70 eV): 140 (M^+). *Anal.* calcd. for $C_8H_{12}O_2$: C 68.53, H 8.63; found: C 68.40, H 8.64.

Dibromocarboxylic Acid 14

Bis-allyl acetic acid **13** (1.125 g, 8.0 mmol) was dissolved in pentane (300 mL). (The pentane used was treated with concentrated sulfuric acid during 4 days followed by washing with water, drying with magnesium sulfate, and distillation over cal-

Can. J. Chem. Downloaded from www.nrcresearchpress.com by 210.87.254.6 on 09/05/12
For personal use only.

cium hydride.) Nitrogen gas was bubbled through the solution during 5 min. Hydrogen bromide gas was then bubbled through the solution (20 min) which was exposed to the radiation of an ultraviolet lamp (450 W). Nitrogen gas was again bubbled through the solution, ether was added, and the organic phase was washed with sodium thiosulfate (5%, 4 × 50 mL) and brine (50 mL). The organic phase was dried with magnesium sulfate, filtered, and evaporated to yield an oil which was crystallized from hexane (2.21 g, 90%); mp 37–37.5°C; ir ($CHCl_3$): 3400–2400 (broad), 1712 cm^{-1}; nmr ($CDCl_3$) δ: 1.6–2.6 (9H, multiplets), 3.35 (4H, triplet, J = 6 Hz, two CH_2Br), and 11.4 (1H, singlet, OH); ms *m/e* (70 eV): 220 and 221 ($M^+ - Br$). *Anal.* calcd. for $C_8H_{14}Br_2O_2$: C 31.82, H 4.67; found: C 31.92, H 4.84.

Bromolactone 15

Triethylamine (0.6 mmol) was added to a solution of dibromocarboxylic acid **14** (160 mg, 0.53 mmol) in anhydrous dichloromethane (15 mL) and the mixture was left at room temperature during 3 h. The organic solution was washed with dilute hydrochloric acid (10%, 3 × 5 mL), dried with magnesium sulfate, filtered, and evaporated to yield crude bromolactone **15** (109 mg, 93%). An analytical sample was prepared by microdistillation; bp 131°C (0.5 Torr); vpc: retention time, 12 min (175°C, column 2); ir ($CHCl_3$): 1740 cm^{-1}; nmr ($CDCl_3$) δ: 1.5–2.6 (9H, multiplet, 3.35 (2H, triplet, J = 6 Hz, CH_2Br), and 4.2 (2H, triplet, J = 5.5 Hz, CH_2O); ms *m/e* (70 eV): 141 ($M^+ - Br$). *Anal.* calcd. for $C_8H_{13}BrO_2$: C 43.46, H 5.93; found: C 43.26, H 6.31.

Acetate Lactone 16

Sodium acetate (10 mmol) was added to a solution of bromolactone **15** (796 mg, 3.6 mmol) in hexamethylphosphoramide (40 mL) and the mixture was heated at 60°C during 2 h. After cooling to room temperature, ether (75 mL) was added. The organic phase was washed with water (6 × 50 mL), dried over sodium sulfate, filtered, and evaporated. The residue was purified by column chromatography with silica gel using a mixture of ethyl acetate and hexane (1:4) to yield pure acetate lactone **16** (370 mg, 49%), which was found identical with an authentic sample (13). Infrared ($CHCl_3$): 1740 cm^{-1}; nmr ($CDCl_3$) δ: 4.38 (2H, diffuse triplet, J = 6 Hz, CH_2O of the ring), 4.15 (2H, triplet, J = 6 Hz, CH_2OAc), and 2.06 (3H, singlet, CH_3COO).

Hydroxypropyl Methoxytetrahydropyran 4

Diisobutylaluminium hydride (0.9 mmol, 1 *M* in hexane) was added to a solution of acetate lactone **16** (171 mg, 0.85 mmol) in anhydrous tetrahydrofuran under nitrogen atmosphere. After stirring at −78°C during 2 h, dilute hydrochloric acid (0.5 *N*, 40 mL) was added and the mixture was extracted with ether (3 × 50 mL). The organic phase was dried over sodium sulfate, filtered, and evaporated to yield crude **17** (153 mg, 88%) which was used without further purification. Infrared ($CHCl_3$): 3200–3600 and 1735 cm^{-1}; nmr ($CDCl_3$) δ: 0.8–2.0 (9H, multiplet), 2.15 (3H, singlet, CH_3COO), and 3.3–4.0 (6H, multiplet), CH_2OCHOH and CH_2OCO).

Crude product **17** (153 mg, 0.76 mmol) was treated with methanol (4 mL) containing a catalytic amount of *p*-toluenesulfonic acid during 12 h at room temperature. Potassium carbonate (50 mg) was then added and the mixture was stirred during 6 h at room temperature. The reaction mixture was evaporated to dryness *in vacuo*, water (10 mL) was added, and the aqueous mixture was extracted with ether (3 × 25 mL). The organic phase was dried over sodium sulfate, filtered, and evaporated to yield crude product **4** (101 mg, 76%). A sample was obtained pure by vpc. This sample is a 1:1 mixture of *cis* and *trans* isomers; vpc: retention time, 5 min (175°C, column 2); ir ($CHCl_3$): 3200–3600 cm^{-1}; nmr ($CDCl_3$) δ: 1.2–2.0 (9H, multiplets), 3.43 and 3.35 (3H, two singlets, ratio ≃ 1:1, OCH_3 of *cis* and *trans* isomers), 3.5–3.9 (5H, multiplet, two CH_2O and OH), 4.55 and 4.1 (1H, two doublets, anomeric H of *cis* and *trans* isomers).

cis *and* trans *Bicyclic Acetals 5 and 6*

Hydroxypropyl methoxytetrahydropyran **4** (96 mg, 0.47 mmol) dissolved in anhydrous methanol (4 mL) containing *p*-toluenesulfonic acid (89 mg, 0.47 mmol) was left at room temperature during 5 days. (The reaction was followed by tlc and *cis* and *trans* bicyclic acetals **5** and **6** appeared from the beginning to the end of the reaction as a mixture.) Sodium carbonate (100 mg) was added and after stirring for 30 min, the mixture was evaporated. The residue was dissolved in water (15 mL) and extracted with ether (3 × 25 mL). The organic phase was dried over sodium sulfate, filtered, and evaporated to yield a mixture of *cis* bicyclic acetal **5** (56%) and *trans* bicyclic acetal **6** (44%) which were analyzed and separated by vpc (column 2 (130°C)).

Cis *Bicyclic Acetal* **5** *(9)*: vpc: retention time, 5 min (130°C, column 2); ir ($CHCl_3$): no OH or carbonyl absorption and 1000–1200 cm^{-1}; nmr ($CDCl_3$) δ: 1.0–2.0 (9H), 3.25–4.0 (4H, multiplet, two CH_2O), and 4.70 (1H, singlet, anomeric hydrogen); ^{13}C nmr ($CDCl_3$): 98.0 (C1), 64.3 (C3 and C9), 34.6 (C6), 25.3 (C4 and C8), and 23.0 (C5 and C7); ms *m/e* (70 eV): 142 (M^+).

Trans *Bicyclic Acetal 6 (9)*: vpc: retention time, 6.7 min (130°C, column 2); ir ($CHCl_3$): 1000–1200 cm^{-1}; nmr ($CDCl_3$) δ: 0.9–2.2 (9H), 3.28–4.20 (5H, multiplet, two CH_2O and anomeric hydrogen); ^{13}C nmr ($CDCl_3$): 105.4 (C1), 67.5 (C3 and C9), 40.6 (C6), 28.8 (C4 and C8), and 26.1 (C5 and C7); ms *m/e* (70 eV): 142 (M^+).

Acknowledgements

We wish to thank Professor John K. Saunders and Mr. Normand Pothier for the interpretation of ^{13}C nmr spectra.

This research was supported by the Natural Sciences and Engineering Research Council of Canada (NSERCC) and by the Ministère de l'Education du Québec.

1. R. U. Lemieux and S. Koto. Tetrahedron, **30**, 1933 (1974), and references quoted therein.
2. A. J. Kirby and R. J. Martin. J. Chem. Soc. Chem. Commun. 803 (1978).
3. A. J. Kirby and R. J. Martin. J. Chem. Soc. Chem. Commun. 1079 (1979).
4. H. Bierbeck and J. K. Saunders. Can. J. Chem. **54**, 2985 (1976).
5. C. F. Lane. J. Org. Chem. **39**, 1437 (1974).
6. N. Beaulieu and P. Deslongchamps. Can. J. Chem. **58**, 164 (1980).
7. H. O. House, C.-Y. Chu, W. V. Phillips, T. S. B. Sayer, and C.-C. Yau. J. Org. Chem. **42**, 1709 (1977).
8. N. Ikota and B. Ganem. J. Am. Chem. Soc. **100**, 351 (1978).
9. G. Descotes, M. Lissac, J. Delmau, and J. Duplan. C. R. Acad. Sci. Ser. C, **267**, 1240 (1968).
10. P. Deslongchamps. Pure Appl. Chem. **43**, 351 (1975); Tetrahedron, **31**, 2463 (1975); Heterocycles, **7**, 1271 (1977).
11. J. Meinwald and E. Frauenglass. J. Am. Chem. Soc. **82**, 5235 (1960).
12. G. A. Haggis and L. N. Owen. J. Chem. Soc. 389 (1953); E. Ali and L. N. Owen. J. Chem. Soc. 2111 (1958); W. Huckel and W. Egerer. Ann. Chem. **645**, 162 (1961).
13. P. Deslongchamps, P. Atlani, D. Frehel, A. Malaval, and C. Moreau. Can. J. Chem. **52**, 3651 (1974).

Merostabilization in radical ions, triplets, and biradicals. 4. Substituent effects on the half-wave reduction potentials and n,π^* triplet energies of aromatic ketones[1]

WILLIAM J. LEIGH, DONALD R. ARNOLD,[2] ROBERT W. R. HUMPHREYS, AND PO CHEONG WONG
Department of Chemistry, Dalhousie University, Halifax, N.S., Canada B3H 4J3

Received January 16, 1980

This paper is dedicated to Prof. Raymond V. Lemieux on the occasion of his 60th birthday

WILLIAM J. LEIGH, DONALD R. ARNOLD, ROBERT W. R. HUMPHREYS, and PO CHEONG WONG. Can. J. Chem. **58**, 2537 (1980).

The half-wave reduction potentials, measured by cyclic voltammetry, and n,π^* triplet energies, measured by phosphorescence spectroscopy, were determined for a series of eighteen symmetrically and unsymmetrically substituted benzophenones. Attempts are made to correlate the results with Hammett substituent constants. Better correlations are observed when the data are correlated with a two-parameter function consisting of Hammett substituent constants and a set of substituent parameters describing variations in free radical stability. Significant deviations from "normal" behaviour are observed for benzophenones substituted by both electron-donating and electron-withdrawing substituents. These deviations are attributed to merostabilization of the radical-like species, and an empirical approach designed to evaluate the importance of this effect is developed. *Ab initio* calculations of molecular orbital energies in *meta*- and *para*-substituted benzaldehydes are used to evaluate the substituent effects on $E_{1/2}^{red}$ and E_T^{n,π^*} in terms of the effect on the energies of the *n*- and π^*-orbitals.

WILLIAM J. LEIGH, DONALD R. ARNOLD, ROBERT W. R. HUMPHREYS et PO CHEONG WONG. Can. J. Chem. **58**, 2537 (1980).

On a déterminé les potentiels de réduction de demi-vague mesurés par voltamétrie cyclique et les énergies de l'état triplet, n,π^* mesurées par spectroscopie de phosphorescence, pour une série de 18 benzophénones substituées symétriquement et asymétriquement. On a essayé d'établir une corrélation entre les résultats et les constantes de substituant de Hammett. On a observé les meilleures corrélations quand les données sont reliées à une fonction à deux paramètres se composant des constantes de substituant de Hammett et à un ensemble de paramètres de substituant décrivant les variations de stabilité du radical libre. On a observé des déviations importantes par rapport au comportement "normal" dans le cas des benzophénones substituées à la fois avec des substituants donneurs et des substituants accepteurs d'électrons. Ces déviations sont attribuées à une mérostabilisation de l'espèce radicalaire et on a développé une approche empirique pour évaluer l'importance de cet effet. On a utilisé des calculs *ab initio* d'énergies d'orbitales moléculaires dans des benzaldéhydes substitués en *méta* et en *para* pour évaluer les effects de substituants sur $E_{1/2}^{red}$ et E_T^{n,π^*} en fonction de l'effet sur les énergies des orbitales *n* et π^*.

[Traduit par le journal]

Introduction

One of the early successes of molecular orbital theory was the recognition that the half-wave reduction potential of polynuclear aromatic hydrocarbons correlates with the energy calculated for the lowest unoccupied molecular orbital (LUMO; that is, the π^*-orbital) of the aromatic hydrocarbon (1). This correlation was also found to apply for a series of polynuclear aromatic aldehydes, where the LUMO was treated as the corresponding hydrocarbon radical (for example, the benzyl radical was used as the model for the LUMO of benzaldehyde) (1*a*, 2). This reasoning was then more generally extended and it was proposed that the half-wave reduction potential of a substituted aromatic carbonyl compound could be used as an indication of the energy of its π^*-orbital (1*a*, 2, 3). Since it was known that there is a correlation of half-wave reduction potentials of substituted benzophenones with Hammett substituent constants (4, 5), the conclusion was reached that the substituents were, in fact, influencing the energy of the π^*-orbital (3).

It was also found that there is a correlation between the n,π^* triplet energy of a series of substituted aromatic carbonyl compounds and their half-wave reduction potentials (3). This was attributed to the variation in the energy of the π^*-orbital, with the assumption that the energy of the *n*-orbital remained fairly constant within the series. The sequence was completed by the recognition that there is a correlation (albeit, not a particularly good one) between Hammett substituent constants and the n,π^* triplet energy of aromatic carbonyl compounds (5).

Superficially, these results are all consistent. The substituent effect on the half-wave reduction potential and the n,π^* triplet energy of substituted aromatic carbonyl compounds correlates with Hammett substituent constants as a result of the substituent influencing the energy of the π^*-orbital. Electron-withdrawing groups lower, while electron-donating groups raise the energy of the π^*-orbital; the energy of the *n*-orbital is relatively unaffected since it lies in the nodal plane of the π-system (3, 6).

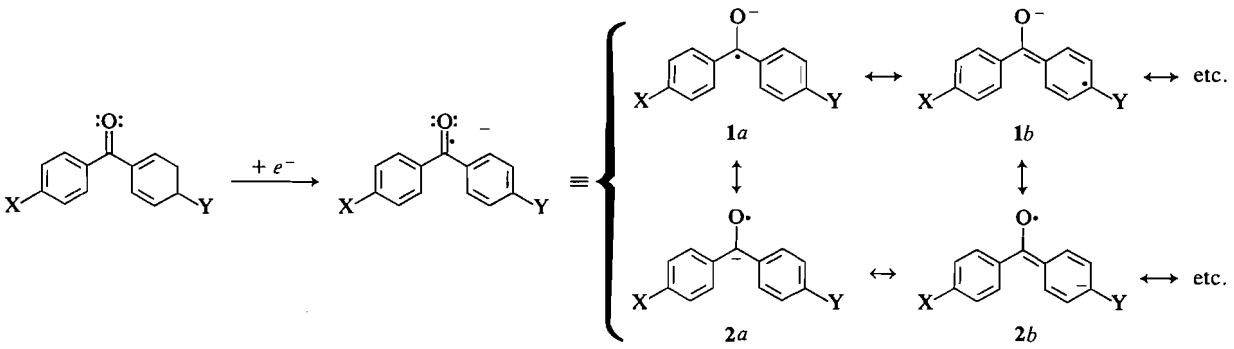
[1]A portion of this work was carried out at the University of Western Ontario.

[2]Author to whom correspondence may be addressed.

0008-4042/80/232537-13$01.00/0

©1980 National Research Council of Canada/Conseil national de recherches du Canada

Can. J. Chem. Downloaded from www.nrcresearchpress.com by 210.87.254.6 on 09/05/12
For personal use only.



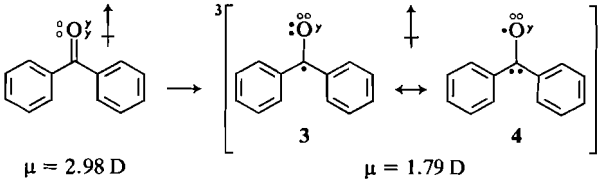
To attribute the effect of substituents entirely to variations in the energy of the π^*-orbital must be an oversimplification and is in fact correct only when the variation in substituent produces little change in electron demand. It is unreasonable to assume that polar substituents should have no effect on the energy of the *n*-orbital. The *n*-orbital in aromatic carbonyl compounds has been shown by spectroscopic studies to be significantly delocalized into the π-system (7).

The use of the benzylic-type radical as a model for the π^*-orbital in aromatic carbonyl compounds implies that the π^*-orbital energy is affected primarily by factors which influence the stability of the free radical. While this may be a valid model in certain cases, it obviously provides a rather poor description of the n,π^* triplet state and radical anion of carbonyl compounds containing polar substituents, since substituent effects on free radical stabilities are normally small and do not correlate well with Hammett σ-values (8). In fact, the observation of a Hammett correlation for the substituent effect on the rate of a free radical reaction is usually taken as evidence that the transition state has appreciable polar character (8). In the series of polynuclear aromatic aldehydes mentioned above (1*a*), the arylmethyl radical satisfactorily represents the π^*-orbital only because the variation in polar factors within the series is small relative to the variation in arylmethyl radical stability.

As a first approximation, it would appear more reasonable to consider the correlation of half-wave reduction potential and the n,π^* triplet energy of substituted aromatic carbonyl compounds with Hammett substituent constants in terms of the variation in charge redistribution between the ground state and the radical anion and the triplet. The rationale for this is obvious in the case of the radical anion, since electron density on the molecule is increased.

We can represent the benzophenone radical anion as the hybrid of two parent valence bond structures **1** and **2**. In benzophenone, structures of type **1** (in which the negative charge is localized on the electronegative oxygen and the unpaired electron is delocalized into the aromatic π-system) are dominant in the hybrid. It is known from esr studies that the spin density in the benzophenone radical anion is largely on the carbonyl carbon (9); further, the spin distribution in the radical anion is very similar to that in the diphenylmethyl radical.[3] The reduction potentials of substituted benzophenones should then correlate with Hammett substituent constants if, and only if, the substituent effect on radical stability is comparatively small, since the negatively charged oxygen is in a position analogous to that in the benzoate anion. Valence bond structures of type **2** (in which the unpaired electron is localized on the oxygen and the negative charge is delocalized into the aromatic π-system) may be more important contributors to the hybrid structure when X and Y are strong electron-withdrawing groups (12), and their stability should of course be subject to an even larger polar substituent effect.

The n,π^* triplet state of benzophenone can be represented as the hybrid of valence bond structures **3** and **4** (13). While the n,π^* triplet is of course



μ = 2.98 D μ = 1.79 D

a neutral species, it is apparent from the measured dipole moments of both the excited state and the ground state that the electron density on the oxygen atom decreases upon excitation (14). The observed substituent effect is again consistent with this shift in electron density, if the variation in radical stability is insignificant.

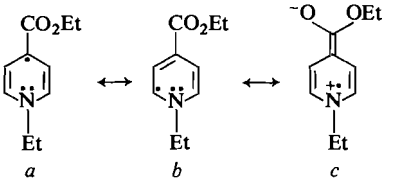
[3]The experimental spin densities for the *ortho*-, *meta*-, and *para*-positions in the benzophenone radical anion are 0.123, −0.042, and 0.157 respectively (Q = 25 G) (10). The corresponding spin densities in the diphenylmethyl radical are 0.127, −0.053, and 0.144 (Q = 25 G) (11).

Can. J. Chem. Downloaded from www.nrcresearchpress.com by 210.87.254.6 on 09/05/12
For personal use only.

Can. J. Chem. Downloaded from www.nrcresearchpress.com by 210.87.254.6 on 09/05/12
For personal use only.

It seems reasonable, in view of the small effect of substituents on benzylic radicals (15), that as an approximation, the contribution to the stability of the radical anion and triplet due to free radical stabilization might be ignored, in which case the relative stability will correlate reasonably well with Hammett substituent constants. However, in the special situation where X and Y have the opposite electron demand (i.e. when X is a strong electron-donating substituent and Y a strong electron-withdrawing substituent), there may be a more significant effect on radical stability. This would then be revealed as a deviation from Hammett behaviour.

It has been recognized for some time that radicals can be stabilized by direct simultaneous substitution with both electron-withdrawing and electron-donating groups (16). This additional stability has been attributed to the contribution of low energy charge-separated valence bond structures to the resonance hybrid. The classic example of Kosower's radical (**5**) serves to illustrate this con-



5

cept (17); there are many others (18). The term merostabilization[4] has been suggested to describe this effect (18*a*). This term, which derives from the similarity of structures of type **5***c* to the electronic situation in merocyanine dyes, emphasizes the importance of the charge-separated valence bond structure in contributing to free radical stabilization and we have accepted it.

While the concept of merostabilization is now firmly established (16–18) in free radical chemistry, there is little evidence of the more general application of this phenomenon to other classes of molecules containing unpaired electrons.[5] We have initiated a program designed to systematically assess the importance of merostabilization as a factor contributing to the stability of radical ions, triplet states, and biradical species. The first reports from this program described electron spin resonance (esr) evidence of merostabilization extending electron delocalization in appropriately substituted diphenylmethylenes (19). The variation in the zero-field splitting parameter (*D*) for a series of 4-substituted and 4,4′-disubstituted (methoxy-, cyano-, dimethylamino-, and nitro-) diphenylmethylenes is consistent with the average separation of the unpaired electrons being greater for the unsymmetrically substituted derivatives.

We have recently described a preliminary account of the effect of merostabilization on the n,π^* triplet energies of a limited series of substituted benzophenones, and developed an approach to quantitatively assess its contribution to the triplet energy as a function of the difference in electron demand between the two substituents (20). In this paper, we provide a further assessment of the importance of merostabilization in benzophenone n,π^* triplets through the inclusion of a broader range of substituents, as well as assess its effect on the stability of the corresponding radical anions. Merostabilization in substituted diphenylmethylenes is also reexamined. As well, we will examine the relative contributions of polar and radical-stabilizing effects to the stability of benzophenone n,π^* triplets and radical anions through the use of a two-parameter linear free energy approach, and rationalize the results in terms of simple valence bond theory. We then provide a more rigorous analysis employing calculated (*ab initio*) molecular orbital energies in a series of substituted benzaldehydes.

Results

The benzophenones **6***a–r* were either synthesized by standard techniques or obtained commercially, and were rigorously purified before use (see Experimental).

Half-wave reduction potentials were measured by cyclic voltammetry in acetonitrile solution using a platinum working electrode and a $Ag/AgNO_3$ (0.1 *M*) reference electrode. All the voltammagrams were typical of reversible or quasi-reversible reductive one-electron transfer. The half-wave potentials, taken as the midpoints of the forward and reverse waves, are therefore thermodynamically significant. These results are summarized in Table 1.

Phosphorescence emission spectra were recorded at 77 K in ethanol–methanol (4:1) and ether–isopentane–alcohol (EPA, 5:5:2). A number of these spectra have been observed previously (5). We chose to remeasure them in order to provide a greater degree of internal consistency in our triplet energy values. The emission spectra in both solvents all showed the five-fingered pattern characteristic of emission from the n,π^* triplet state. Triplet energies were calculated from the positions of the short wavelength 0–0 band maxima and are summarized along with the half-wave reduction

[4]The effect has been alternatively labelled "push-pull substitution" (18*d*) and "capto-dative bonding" (18*k*).

[5]For an example of merostabilization of a 1,4-biradical, see ref. 18*f*.

Can. J. Chem. Downloaded from www.nrcresearchpress.com by 210.87.254.6 on 09/05/12
For personal use only.

TABLE 1. Half-wave reduction potentials ($E_{1/2}^{red}$) and n,π^* triplet energies (E_T) of substituted benzophenones (**6***a–r*)

				E_T (kcal mol^{-1})	
6	X[a]	Y	$-E_{1/2}^{red}$ (eV)[b]	[c]	[d]
a	OMe	OMe	2.39	69.8	69.9
b	Me	Me	2.29	69.5	69.2
c	H	H	2.20	69.2	69.2
d	3-CF_3	3-CF_3	1.90	69.1	69.1
e	CF_3	CF_3	1.83	67.9	67.9
f	3-CN	3-CN	1.83	69.1	69.4
g	CN	CN	1.64	65.9	65.9
h	Br	Br	—	68.4	68.6
i	OMe	H	2.29	69.4	69.0
j	Me	H	2.24	69.4	69.2
k	H	CF_3	1.97	68.2	68.2
l	Me	CF_3	2.01	68.2	68.2
m	OMe	CF_3	2.05	67.7	67.3
n	H	3-CN	1.98	69.0	69.0
o	OMe	3-CN	2.04	68.2	67.9
p	H	CN	1.82	67.0	66.9
q	Me	CN	1.85	66.8	66.8
r	OMe	CN	1.88	66.6	66.4

[a]Substituents in *para*-positions unless noted otherwise.
[b]Versus $Ag/AgNO_3$; 0.1 *M* TEAP/CH_3CN; 23°C; error = ±0.01 eV.
[c]EPA (5:5:2); 77 K; error = ±0.2 kcal mol^{-1}.
[d]Ethanol–methanol (4:1); 77 K; error = ±0.2 kcal mol^{-1}.

potentials in Table 1. The spectra were all measured on the same instrument under identical conditions, were rechecked at various times during the course of the study, and are reproducible to within 1 nm. Thus, although our values may differ slightly from those previously reported (5), the triplet energies reported here can be assumed to be internally consistent and the differences significant in the following discussion.

Ab initio calculations of the *n*-, π- and π*-orbital energies in benzaldehyde, *meta*- and *para*-cyanobenzaldehyde, and *meta*- and *para*-hydroxybenzaldehyde were carried out using the Gaussian 76 program (21) with an STO-3G minimal basis set and standard valence-shell scaling factors on a CDC 6400 computer. Standard bond lengths and angles (22) were employed throughout, and a planar conformation assumed for all derivatives (23). The calculated energies of the lowest unoccupied and the three highest occupied molecular orbitals are compiled in Table 2.

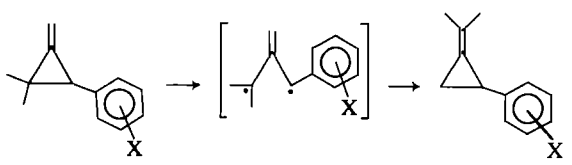
Discussion

The effect of substituents on free radical stability is not nearly as well understood as is the effect on ionic reactions and stabilities, despite the numerous efforts that have been directed to this end. Attempts are traditionally made to correlate the rates of reactions involving radical intermediates, such as hydrogen abstraction from substituted toluenes or radical addition to substituted benzenes, with Hammett substituent constants (8). The acceptable correlations that are often observed are generally considered as evidence for polarization of the transition state, the ρ-value providing a measure of the nucleo- or electrophilicity of the attacking radical. In reactions for which the transition state has predominantly free radical character, poor correlations with Hammett substituent constants and ρ-values close to zero are generally observed. Improved fits are often obtained by using σ^+-values for electron-donating substituents and σ^--values for electron-withdrawing substituents in order to allow for additional resonance interaction between the substituent and the radical site. Obviously, the best approach would be to use a set of parameters that accurately describes the variation in radical stability with substituent, independent of polar factors.

A number of workers have constructed substituent parameter scales specifically for use with free radical reactions (24*a–i*). These are without exception based on the relative rates of reactions proceeding through radical intermediates. Contributions from polar factors are found (or assumed) in all cases, and the radical substituent parameters are evaluated by fitting the data to a two-parameter Hammett equation such as eq. [1].

$$[1] \quad \log k_X/k_H = \rho\sigma + r\sigma^{\cdot}$$

Although it is generally accepted that both electron-donating and accepting substituents are effective in stabilizing a free radical, the rather poor agreement in the relative magnitudes and even in the order of the substituent parameters from series to series exemplifies the difficulty of separating polar from radical-stabilizing effects. The most recent and probably most successful attempt to eradicate polar factors in a free radical reaction is provided by Creary (25), who determined the relative rates of isomerization of a large number of *meta*- and *para*-substituted 2-aryl-3,3-dimethyl methylenecyclopropanes (**7**) in isooctane at 100°C. The small ρ-value (−0.16) obtained from a plot of relative rate vs. σ_m for several *meta*-substituted derivatives demonstrates that the transition state for this isomerization is almost (at least) devoid of polar character. However, Creary made no attempt to construct a $\sigma^{\cdot}$-scale from his data.



7

TABLE 2. Calculated (*ab initio*) orbital energies for substituted benzaldehydes

Compound	$-E_n$ (au)	$-E_{\pi_1}$ (au)	$-E_{\pi_2}$ (au)	E_{π^*} (au)
Benzaldehyde	0.3429	0.2899	0.2666	0.1843
4-Cyanobenzaldehyde	0.3625	0.3137	0.2838	0.1497
3-Cyanobenzaldehyde	0.3599	0.3078	0.2868	0.1626
4-Hydroxybenzaldehyde	0.3361	0.2955	0.2392	0.1925
3-Hydroxybenzaldehyde	0.3466	0.2807	0.2542	0.1804

We have examined the various existing $\sigma^\cdot$-scales (24*b–i*) and a scale constructed from Creary's data (25) ($\sigma^\cdot = \log k_X/k_H$), by plotting them against the hyperfine coupling constants due to the α-protons in the esr spectra of substituted benzyl radicals (15*a*). Actually, had more substituents been investigated, this system in itself could provide a far more accurate substituent parameter scale than those involving relative rates since the hyperfine constants provide a measure of unpaired electron delocalization in the radical itself, and the complicating factors that must be dealt with in the analysis of relative rates of a radical reaction are not present. It has been noted that relative variations in benzyl proton hyperfine constants provide a fairly accurate representation of variations in benzyl radical stability with substituent (26). Also, Afanas'ev (24*a*) incorporated β-proton hyperfine constants in his derivation of a scale of σ^r-values describing substituent effects on methyl radical stabilities. Least squares analysis of plots of $a_{CH_2}^X/a_{CH_2}^H$ (15*a*) vs. $\sigma^\cdot$ reveal that the best fits are obtained with the E_R-values of Yamamoto and Otsu (24*f*) (cc = 0.890) and the log k_X/k_H values calculated from the data of Creary (25) (cc = 0.977). Creary's data thus seem the most suitable indication of substituent effects on radical stabilities.[6]

The term merostabilization has been suggested to describe the additional stabilization imparted to free radicals bearing substituents of opposite electron demand (18*a*). This concept, though recognized as early as 1952 (16), has only recently received any degree of attention in the literature (18*a–n*), and is the subject of a recent review (18*m*). Contributions to the stability of a radical from merostabilization should not be predictable from consideration of $\sigma^\cdot$-values, since one would expect the magnitude of the effect to be proportional to the ability of the substituents to support charge separation in the radical (i.e. σ or $\sigma^\pm$). We have developed the following approach to qualitatively assess (and predict) the importance of merostabilization in radicals and radical-like species (20).

[6] $\sigma^\cdot$-values from the data of Creary (25) are ($\sigma^\cdot = \log k_X/k_H$): 4-OMe, 0.24; 4-Me, 0.11; 4-CF_3, 0.08; 4-CN, 0.46; 4-Br, 0.14; 3-CF_3, −0.07; 3-CN, −0.12.

In the absence of merostabilization, one might expect substitution by one group X in a radical system to cause half the effect of substitution by two symmetrically positioned X-groups. For example, the estimated energy (E_{est}) for a monosubstituted system is the average of the observed energies (E_{obs}) of the symmetrically disubstituted and unsubstituted derivatives. In general then, the energy estimated ($E_{est}^{X,Y}$) for any unsymmetrically substituted radical can be written:

$$[2] \quad E_{est}^{X,Y} = (E_{obs}^{X,X} + E_{obs}^{Y,Y})/2$$

We can now define the *merostabilization energy* ($E_{mero}^{X,Y}$) of such a system as the difference between the estimated and observed values of the energy:

$$[3] \quad E_{mero}^{X,Y} = E_{obs}^{X,Y} - E_{est}^{X,Y}$$

This derivation should of course be equally valid for any measurable quantity which reflects the stability of the radical system.

We expect the merostabilization energy to correlate with some parameter indicating the difference in electron demand between the two substituents. This quantity should increase as X becomes a better electron-donating group and Y a better electron-withdrawing group. A convenient parameter can be defined as:

$$[4] \quad \Delta\sigma_{X,Y}^{\pm} = \sigma_Y^- - \sigma_X^+$$

where X and Y are electron-donating and accepting groups, respectively. $\Delta\sigma_{X,Y}^{\pm}$ will be zero for symmetrically substituted derivatives and positive for unsymmetrically substituted derivatives and thus describes the ability of the substituent pair to enhance charge separation in the free spin system. Our preliminary account (20) revealed the value of this approach in assessing the contribution from merostabilization to the n,π^* triplet energies of a limited series of substituted benzophenones.

We are now in a position to understand the cause and nature of the substituent effects on the half-wave reduction potential and n,π^* triplet energy of benzophenone, and the *D*-value obtained from the esr spectrum of diphenylmethylene. These three systems illustrate the interplay between polar and

Can. J. Chem. Downloaded from www.nrcresearchpress.com by 210.87.254.6 on 09/05/12
For personal use only.

Can. J. Chem. Downloaded from www.nrcresearchpress.com by 210.87.254.6 on 09/05/12
For personal use only.

radical-stabilizing effects on the stability of radical-like systems. We shall see in the following detailed discussion that although the relative contribution from polar and radical-stabilizing factors to the substituent effects on stability varies from one extreme to the other, merostabilization plays a significant role in each. Furthermore, the extent to which it contributes to the stability of these systems can be easily evaluated using the approach outlined above.

Benzophenone Half-wave Reduction Potentials

Half-wave reduction potentials of benzophenones **6***a–r* are plotted versus Hammett substituent constants $\sum\sigma$ in Fig. 1. The line drawn is that obtained from least squares analysis of the points *for the symmetrically substituted derivatives* **6***a–f* (cc = 0.998). The 4,4′-dicyano derivative **6***g* was excluded from this correlation (*vide infra*); if it is included in the analysis, the correlation is somewhat poorer (cc = 0.980), though the slope of the line changes negligibly. The Hammett correlation observed for **6***a–f* can be rationalized through consideration of the expected substituent effects on the relative stability and contributions of **1** and **2** to the valence bond hybrid structure.

In the dominant contributor to the resonance hybrid (**1**) (9), the negative charge resides on the carbonyl oxygen (cf. benzoate anion) and the unpaired electron resides on the carbonyl carbon (cf. diphenylmethyl radical). Substituent effects on the stability of this valence bond structure might therefore be expected to be represented by some blend of σ- and $\sigma^{\cdot}$-values. The excellent correlation of $E_{1/2}^{red}$ with $\sum\sigma$ observed for **6***a–f* demonstrates that the $\sigma^{\cdot}$-contribution is small, since any appreciable contribution to radical anion stability from radical-stabilizing effects should result in marked deviations from linearity in the Hammett plot (all these substituents stabilize the benzyl radical). The pronounced deviation from Hammett behaviour observed for 4,4′-dicyanobenzophenone (**6***g*) may be an indication of the varying contribution from structure **2** to the resonance hybrid. It has been suggested that when X and Y are strong electron-withdrawing groups, the contribution from **2** should increase since delocalization of an electron pair will occur at the expense of unpaired electron delocalization (12). Furthermore, Exner and co-workers (4*b*) observed acceptable correlations with σ^{-} in their investigation of substituent effects on benzophenone half-wave reduction potentials. However, theoretical and experimental (esr) determinations of spin densities in 4,4′-disubstituted benzophenone radical anions (27) indicate that the spin density in the carbonyl group *decreases* with increasing electron-accepting power of the substituents. It would seem therefore that **1** best represents the situation in benzophenone radical anions; the marked deviation observed for **6***g* may then be the result of the very strong radical-stabilizing effect of the *para*-cyano substituent.

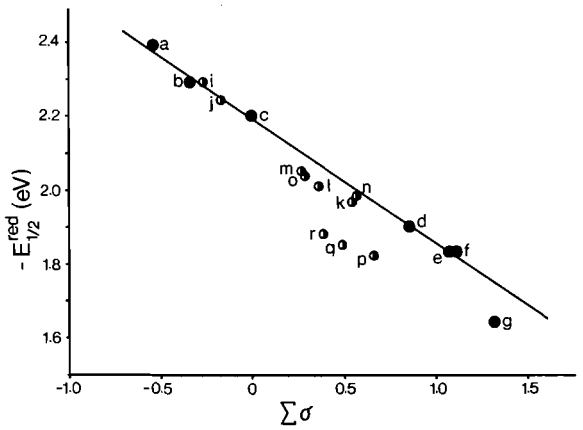


FIG. 1. Hammett correlation: half-wave reduction potentials of benzophenones **6***a–g*, *i–r* vs. $\sum\sigma$.

The half-wave reduction potentials of **6***a–g* were fit by standard regression analysis to a two-parameter Hammett relation employing σ-values and the $\sigma^{\cdot}$-values calculated from Creary's data (25). The relation obtained (eq. [5]) illustrates in a more quantitative fashion the dominance of polar

$$[5]\quad E_{1/2}^{red}(\text{eV}) = -2.21 + 0.363\sum\sigma + 0.086\sum\sigma^{\cdot}(\text{cc} = 0.996)$$

factors in the substituent effect on benzophenone half-wave reduction potentials. The indication that radical-stabilizing effects account for about 20% of the total substituent effect would admittedly be more convincing if the Hammett correlation in Fig. 1 did not appear to be so good. We feel that this figure is reasonable, however, in view of the fact that free radical stabilities are, in general, considerably less sensitive to variations in substituent than are the stabilities of the corresponding ions (8). Equation [5] is represented in graphical form in Fig. 2.

Included in Figs. 1 and 2 are the points for the unsymmetrically substituted benzophenones **6***i–r*. As can be seen, the reduction potentials of the majority of these derivatives deviate significantly from the correlation observed for **6***a–g*. Furthermore, the deviations are seen to increase with increasing electron-donating/withdrawing power of the substituents. We attribute these deviations from "normal" behaviour to merostabilization;

Can. J. Chem. Downloaded from www.nrcresearchpress.com by 210.87.254.6 on 09/05/12
For personal use only.

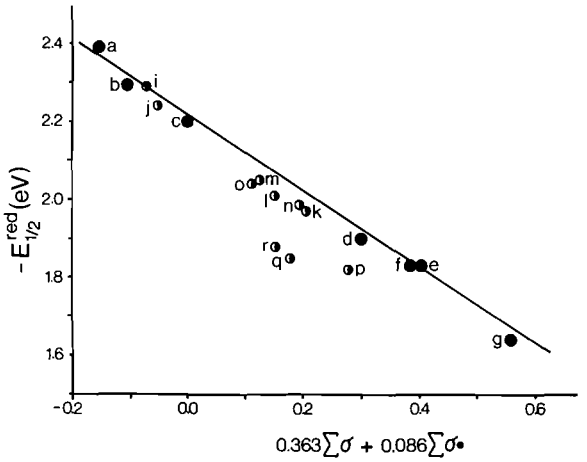


FIG. 2. Two-parameter Hammett correlation: half-wave reduction potentials of benzophenones **6***a–g*, *i–r* vs. $(0.363\sum\sigma + 0.086\sum\sigma^{\bullet})$; $\sigma^{\bullet} = \log k_X/k_H$ from data of Creary (25).

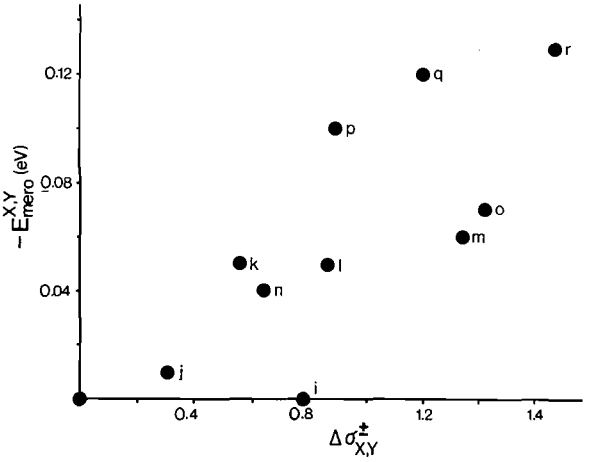
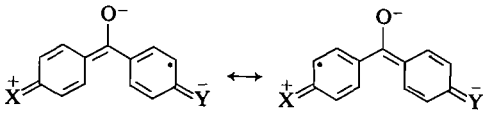


FIG. 3. Merostabilization in benzophenone radical anions: $-E_{mero}{}^{X,Y}$ vs. $\Delta\sigma^{\pm}_{X,Y}$ for half-wave reduction potentials of **6***i–r*.

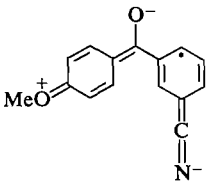
unsymmetric substitution allows for greater delocalization of the unpaired electron due to the increased importance of charge-separated resonance structures such as **1***d*.

Merostabilization energies were calculated for **6***i–r* from eqs. [2] and [3] and are shown plotted vs. $\Delta\sigma^{\pm}_{X,Y}$[7] in Fig. 3 for the benzophenone half-wave



1*d*

reduction potentials. While the correlation is obviously not particularly good (cc = 0.61), the overall trend in the plot illustrates the increasing importance of merostabilization with increasing difference in electron demand between the two substituents X and Y. While the *para*-trifluoromethyl derivatives **6***k–m* do not vary much as the X group changes, the importance of merostabilization is seen to increase quite regularly with increasing electron-donating power of the X-group for the *para*-cyano derivatives **6***p–r*. It is noteworthy that



6*o*′

merostabilization appears to be significant even for the monosubstituted derivatives **6***k* and **6***p*, and for the *meta*-substituted **6***n* and **6***o*. We did not expect merostabilization to be important in **6***n* and *o*, since direct resonance interaction of the type illustrated in **1***d* is not possible with the *meta*-cyano group. However, charge-separated resonance structures (such as **6***o*′) can be drawn for these derivatives. While these structures do not allow delocalization of spin density onto the *meta*-carbon atoms, they should contribute somewhat to the lower reduction potentials observed for **6***n* and *o*.

Benzophenone n,π* *Triplet Energies*

Reasonable agreement is observed between the *n*,π* triplet energies determined in EPA (5:5:2) and ethanol–methanol (4:1) (Table 1). Good agreement is also noted with literature values for those compounds which have been previously studied. We have plotted the triplet energies against Hammett substituent constants $\sum\sigma$ in Fig. 4. The rather severe scatter in the plots has been noted previously (5). As was done in the previous section, we shall first consider the symmetrically substituted derivatives **6***a–h* and attempt to rationalize the observed substituent effect on triplet energy in the absence of complicating factors such as merostabilization.

The measured dipole moments of the ground and *n*,π* states of benzophenone indicate a shift in electron density away from the oxygen atom upon excitation (14). This is reasonable since excitation to these states involves promotion of an electron in an orbital strongly localized on oxygen to one with some component of electron density on both carbon and oxygen. This shift in electron density should be revealed in a polar substituent effect on

[7] σ^{+}- and σ^{-}-values were taken from ref. 28, as were σ_m- and σ_p-values. $\sigma^{-}_{CF_3} = +0.56(29)$; $\sigma^{-}_{3\text{-}CN} = +0.64(30)$.

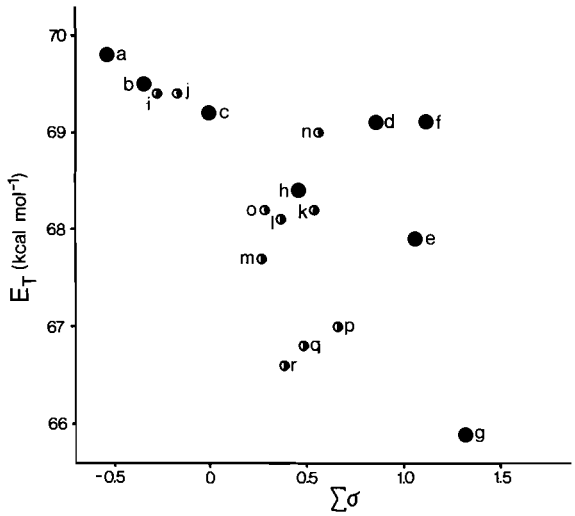


FIG. 4. Hammett correlation: n,π^* triplet energies of substituted benzophenones **6***a–r* vs. $\sum\sigma$ (EPA, 77 K).

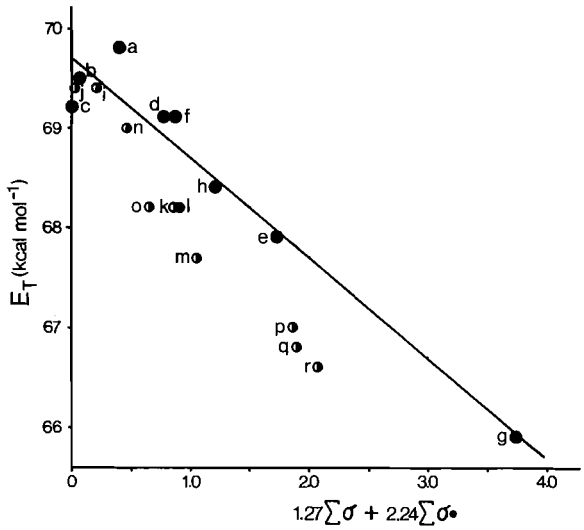


FIG. 5. Two-parameter Hammett correlation: n,π^* triplet energies of substituted benzophenones **6***a–r* vs. ($1.27\sum\sigma + 2.24\sum\sigma^\bullet$); (EPA; 77 K). $\sigma^\bullet = \log k_X/k_H$ from data of Creary (25).

triplet energy; however, this effect is expected to be small since the difference in dipole moments between ground and excited states is rather small. To the extent that the benzylic radical is a reasonable model for the π^*-orbital in aromatic ketones, we would also expect radical-stabilizing factors to contribute to the observed substituent effect on triplet energy. This expected blend of polar and radical-stabilizing factors provides a qualitative rationalization of the observed substituent effect. The triplet energy of 4,4′-dicyanobenzophenone (**6***g*) falls below the line due to the particularly strong radical-stabilizing effect of the cyano group (24, 25), while those of the two *meta,meta′*-disubstituted derivatives (**6***d, f*) are above the line due to the radical-destabilizing effect of *meta*-substitution (25).

This can be expressed more quantitatively in the form of the two-parameter relation employing σ- and σ•-values. Equation [6] was obtained from standard regression analysis of the triplet energies of **6***a–h* in EPA.[8]

$$[6]\quad E_T(\text{kcal mol}^{-1}) = 69.7 - 1.27\sum\sigma - 2.24\sum\sigma^\bullet \quad (\text{cc} = 0.941)$$

The triplet energies of this series (**6***a–r*) are shown plotted against the two-parameter relation (eq. [6]) in Fig. 5. While this equation successfully fits **6***b*, *d–h* to good linear behaviour, it correlates very poorly with benzophenone (**6***c*) and 4,4′-dimethoxybenzophenone (**6***a*).[9] Though the unacceptably low correlation coefficient obtained for the symmetric derivatives precludes attaching a great deal of quantitative significance to eq. [6], the observation that *all* the symmetric derivatives now correlate fairly well with "effective" substituent constants obtained from the two-parameter treatment illustrates the blend of polar and radical-stabilizing effects on the n,π^* triplet state of benzophenone.

The contribution from merostabilization to the n,π^* triplet energy results in the apparently random scatter observed for the unsymmetrically substituted derivatives in Figs. 4 and 5. While certain patterns are evident upon close inspection of these plots, the situation becomes considerably clearer upon examination of Fig. 5. The triplet energies of these derivatives are all lower than what would be expected on the basis of consideration of the "normal" blend of polar and radical-stabilizing factors.

Merostabilization energies were calculated for **6***i–r* using eqs. [2] and [3] and the triplet energies in Table 1. These are shown plotted against $\Delta\sigma^{\pm}_{X,Y}$ in Fig. 6 for the EPA data. The trend in these plots is significant; merostabilization energy increases quite regularly with the ability of the substituents to support charge separation in the free spin system. Again, merostabilization appears to be important

[8]Similar treatment of the ethanol–methanol results yielded

$E_T = 69.7 - 1.18\sum\sigma - 2.34\sum\sigma^\bullet$ (cc = 0.898)

[9]We note in passing that exclusion of **6***a, b* from the analysis yields a considerably better correlation ($E_T = 69.3 - 0.77\sum\sigma - 2.60\sum\sigma^\bullet$; cc = 0.990). We are unable to justify excluding these two derivatives, however.

Can. J. Chem. Downloaded from www.nrcresearchpress.com by 210.87.254.6 on 09/05/12
For personal use only.

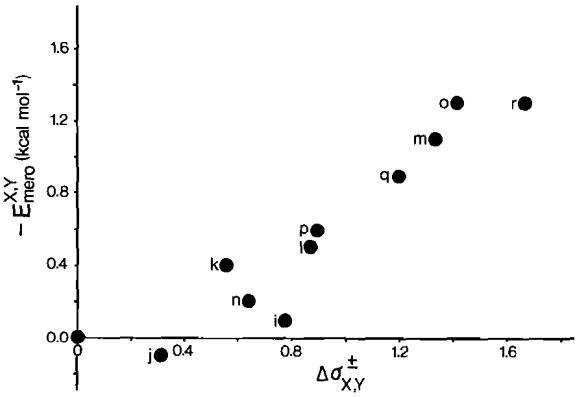


FIG. 6. Merostabilization in benzophenone n,π^* triplets: $-E_{mero}^{X,Y}$ vs. $\Delta\sigma^{\pm}_{X,Y}$ for n,π^* triplet energies (EPA) of **6***i*–*r*.

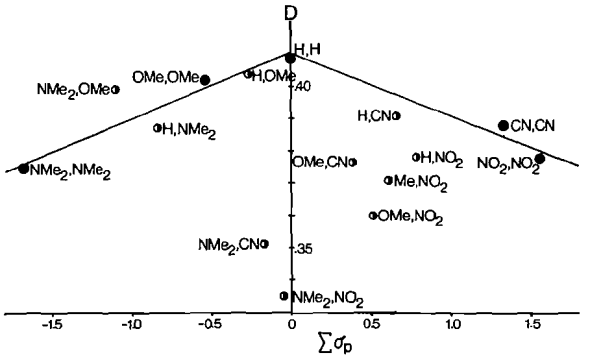


FIG. 7. Hammett correlation: zero-field splitting parameter D of substituted diphenylmethylenes (19*b*) vs. $\sum\sigma_p$.

even for the mono- and *meta*-substituted derivatives.

Diphenylmethylene D-*Values*

In our initial reports in this series (19*a*, *b*), we examined the variation in the zero-field splitting parameter D for a series of *para*-substituted and *para*,*para'*-disubstituted diphenylmethylenes. D is inversely proportional to the cube of the distance between electrons with unpaired spins in a triplet; any increase in electron delocalization is therefore reflected in a decrease in the D-value (31). Our immediate observation was the lack of any correlation between D-values and Hammett substituent constants, a decrease in D-value relative to that of diphenylmethylene being observed for all substituted systems. This is of course in accord with the expected substituent effect on spin density delocalization in the diphenylmethyl radical, the accepted model for diphenylmethylene (19*b*). For diphenylmethylenes simultaneously substituted with electron-donating and withdrawing groups anomalously low D-values were observed, which we attributed to merostabilization. We compared the decrease in D for the merostabilized derivatives relative to diphenylmethylene to the sum of the effects for the two corresponding monosubstituted derivatives. We are now in a position to express the effect of merostabilization in substituted diphenylmethylenes in a more quantitative way using the approach outlined above.

The Hammett plot (D vs. $\sum\sigma_p$) for our series (19*b*) is shown in Fig. 7. The trend in the plot observed for the symmetrically substituted derivatives is consistent with the expected substituent effect on diphenylmethyl radical stability. We would expect the D-values to correlate well with the σ^*-values calculated from Creary's work; unfortunately, nitro- and *N*,*N*-dimethylamino groups were not included in his study, so a meaningful correlation cannot be obtained.[10] It is, however, interesting to note the trends observed for the 4-nitro-4'-X and 4-cyano-4'-X derivatives in Fig. 7. The regular decrease in D which occurs as X becomes a progressively better electron-donating group is indicative of the role of merostabilization in extending electron delocalization in this system. We can calculate the extent to which merostabilization lowers the D-value of an unsymmetrically substituted diphenylmethylene in a manner analogous to the derivation of merostabilization energy in eqs. [2] and [3]. We have plotted $D_{mero}^{X,Y}$ vs. $\Delta\sigma^{\pm}_{X,Y}$ in Fig. 8. Once again the trend in the plot is consistent with the notion that the importance of merostabilization increases with increasing ability of the substituents to support charge separation in the free spin system.

Theoretical Considerations

In correlations between $E_{1/2}^{red}$ and the calculated energy of the π^*-orbital in aromatic carbonyl compounds, the corresponding hydrocarbon radical has been used as a model for the LUMO of the carbonyl compound (i.e. the benzyl radical is the model for the LUMO of benzaldehyde) (1*a*). This model predicts variations in the energy of the π^*-orbital on the basis of changes in free radical stability only, and neglects polar contributions. When the correlation is limited to polynuclear aromatic aldehydes, this may be acceptable since the variation in polar factors should be considerably less than the variation in radical stability within the series. Indeed, the reduction potentials within this

[10] A correlation coefficient of 0.949 is obtained from a four-point plot of D vs. $\sum\sigma^*$ (H, H; H, OMe; OMe, OMe; CN, CN).

Can. J. Chem. Downloaded from www.nrcresearchpress.com by 210.87.254.6 on 09/05/12
For personal use only.

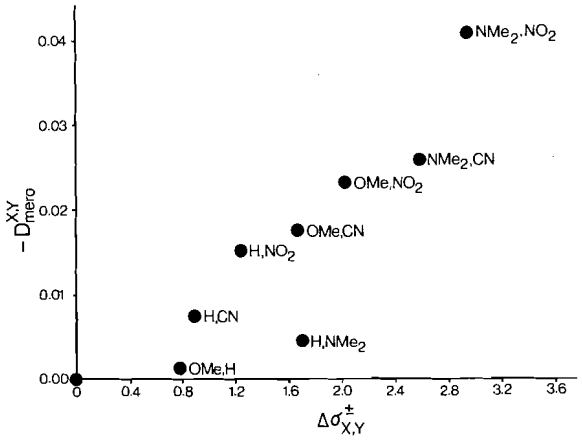


FIG. 8. Merostabilization in diphenylmethylenes: $-D_{mero}^{X,Y}$ vs. $\Delta\sigma^{\pm}_{X,Y}$.

series do not correlate with the strengths of the corresponding carboxylic acids (32).

In contrast to the results of other studies (3*c*), we find no correlation between n,π^* triplet energy and half-wave reduction potential for our extended series of substituted benzophenones. In view of the differing relative contributions from polar and radical-stabilizing factors to the substituent effects on these quantities, we do not find this particularly surprising. The obvious implication is that more is being affected by substitution than simply the energy of the π^*-orbital.

We have carried out *ab initio* calculations of the energies of the *n*-, π-, and π^*-orbitals in a series of substituted benzaldehydes. These minimal basis set calculations incorrectly indicate the π-orbital to be the HOMO. While further refinements are obviously necessary to correct the orbital ordering, we believe the calculated changes in individual orbital energies with substituent are meaningful. The results of the calculations are collected in Table 2.

The most significant thing revealed by these calculations is the indication that the energy of the *n*-orbital is substantially affected by substitution in both the *meta*- and *para*-positions. Furthermore, these calculated *n*-orbital energies correlate respectably with Hammett σ-values (Fig. 9). This is consistent with the conclusions of Goodman and co-workers (7) that the *n*-orbital is significantly delocalized into the aromatic π-system in benzaldehyde. The calculations also reveal the expected variation in the energy of the π^*-orbital, though it does not vary in the same way as the stability of substituted benzyl radicals. The curvature in the plot of $E_{\pi^*}^{calc}$ vs. σ (Fig. 9) is consistent with *both* polar and radical-stabilizing effects contributing to the energy of the π^*-orbital.

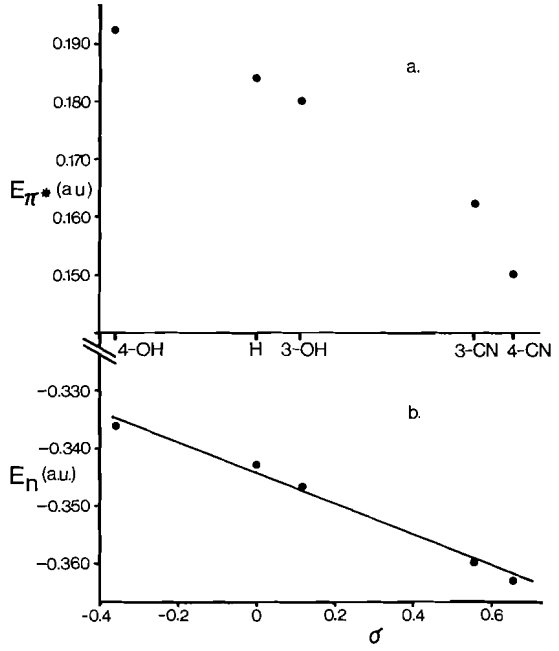


FIG. 9. Hammett correlation: calculated (*ab initio*) orbital energies of substituted benzaldehydes vs. σ; (a) E_{π^*} vs. σ; (b) E_n vs. σ.

The calculated substituent effect on orbital energies in the ground state of benzaldehyde can be used to provide an understanding of that on the n,π^* triplet energy and half-wave reduction potential of benzophenone. The substituent effect on the stabilities of both the triplet and the radical anion is the composite of a polar effect on the energies of the *n*- and π^*-orbitals and a radical-stabilizing effect on the energy of the π^*-orbital. Since the *n*-orbital in the triplet contains one less electron than in the radical anion, we would naively expect the magnitude of the polar effect on the triplet energy to be much smaller than that on the reduction potential. On the other hand, since the population of the π^*-orbital is the same in both states, we would expect the contribution from radical-stabilizing effects on the n,π^* triplet energies to equal that on the reduction potentials. The coefficients obtained from the two-parameter Hammett treatments (eqs. [5] and [6]) are consistent with these expectations. The coefficients describing the σ-dependence are 8.4 kcal mol^{-1} for $E_{1/2}^{red}$ and 1.3 kcal mol^{-1} for E_T^{EPA}, while those describing the σ^*-dependence are 2.0 and 2.2 kcal mol^{-1}, respectively. Also consistent with this are the roughly equal slopes obtained from least squares analysis of the merostabilization energy plots for the reduction potentials (1.6 $\pm$ 0.5 kcal mol^{-1}) and triplet energies (1.2 $\pm$ 0.3 kcal mol^{-1}) (Figs. 3 and 6). Merostabilization

Can. J. Chem. Downloaded from www.nrcresearchpress.com by 210.87.254.6 on 09/05/12
For personal use only.

Can. J. Chem. Downloaded from www.nrcresearchpress.com by 210.87.254.6 on 09/05/12
For personal use only.

produces equal effects on the energies of these two states due to a stabilizing effect on the energy of the π^*-orbital.

Summary and Conclusions

The observed substituent effects on benzophenone half-wave reduction potentials and n,π^* triplet energies can be rationalized in terms of contributions from a polar effect on the energy of the n- and π^*-orbitals and a radical-stabilizing effect on the energy of the π^*-orbital. While polar factors apparently dominate the effect on $E_{1/2}^{red}$, radical-stabilizing factors do contribute somewhat. Furthermore, this contribution is of the same magnitude as that on the n,π^* triplet state, in which radical-stabilizing factors dominate. Although the effect of merostabilization in enhancing the stability of these extended, radical-like systems in which the substituents are rather remote from the radical site is smaller than that in systems in which the substituents are attached directly to the radical site (18), it is by no means insignificant. The roughly equal extent to which it contributes to the stability of benzophenone radical anions and n,π^* triplets provides evidence that merostabilization affects the energy of the π^*-orbital in these systems. Further publications will describe the effects of merostabilization on the ground and excited state properties of aryl ethylenes and cyclopropanes.

Experimental

All melting points are corrected. The ^{1}Hmr spectra were recorded on a Varian T60 spectrometer and are reported in parts per million downfield from TMS. Infrared spectra were recorded on a Perkin-Elmer 180 grating infrared spectrometer and are reported in wave numbers, calibrated against the 1601.8 cm^{-1} polystyrene absorption. Ultraviolet spectra were recorded on a Cary-Varian 210 ultraviolet spectrometer and are reported in nanometers.

Half-wave reduction potentials were measured by cyclic voltammetry with a Princeton Applied Research (PAR) Model 175 universal programmer, PAR Model 173 potentiostat/galvanostat, and a Houston Omnigraphic 2000 X-Y recorder. Electrolytic measurements were carried out using a three electrode cyclic voltammetric cell. The working electrode was a platinum wire. The reference electrode was $Ag/AgNO_3$ (0.1 *M*) with 0.1 *M* TEAP as supporting electrolyte in acetonitrile solution under an atmosphere of dried argon. Substrate concentrations were typically 20 mg/25 mL 0.1 *M* TEAP. The voltammagrams were scanned at 20 mV/s, 100 mV/s, and 200 mV/s. The half-wave reduction potentials were calculated as the average of the midpoints between the forward and reverse waves for the 20 mV/s and 100 mV/s scans. The half-wave reduction potential of benzophenone was measured at various times during the course of the study to check the reproducibility of the measurements, and did not vary by more than 5 mV.

Phosphorescence emission spectra were recorded with an Aminco-Bowman Model 4-8202 spectrophotofluorometer with phosphoroscope attachment and quartz Dewar and a Houston Omnigraphic 2000 X-Y recorder. All spectra were calibrated with a Pen-ray low pressure mercury vapour calibration lamp and were measured repeatedly. The triplet energies were calculated from the position of the short wavelength maximum and are the average of at least four measurements.

Samples were prepared by dissolving the benzophenone (1–2 mg) in 5 mL solvent, placed in evacuable Suprasil tubes, and degassed (four freeze–pump–thaw cycles).

Acetonitrile was refluxed with calcium hydride under dry nitrogen for three days and distilled as required. Absolute ethanol was obtained by refluxing 95% ethanol over magnesium turnings and iodine for 24 h followed by distillation. Methanol was Fisher certified A.C.S. and used as obtained. EPA (5:5:2) was prepared from diethyl ether (500 mL; Anachemia; stirred with sodium for seven days and distilled under dry nitrogen), 2-methylbutane (500 mL; J. T. Baker; passed down an alumina column and distilled slowly), and absolute alcohol (200 mL; as above with one additional distillation from Mg/I_2) and was stored over 4A molecular sieves in the cold under dry nitrogen.

Tetraethylammonium perchlorate (TEAP; Aldrich) was recrystallized three times from 90% ethanol. Silver nitrate (Engelhard A.C.S.) was recrystallized three times from aqueous ethanol and stored in the dark.

4,4'-Dimethoxybenzophenone (**6***a*, Aldrich), 4,4'-dimethylbenzophenone (**6***b*, Fisher), and benzophenone (**6***c*, BDH) were each recrystallized three times from purified ethanol.

3,3'-Bis(trifluoromethyl)benzophenone (**6**d) was prepared by the method of Lichtenberger and Weiss (33), and was purified by recrystallization from ethanol, treatment with Norite in boiling ethanol, and one recrystallization from benzene–hexane (mp 97–98°C (33)).

4,4'-Bis(trifluoromethyl)benzophenone (**6**e) was prepared by the method of Lichtenberger and Weiss (33), recrystallized twice from ethanol, treated with Norite in boiling chloroform, and recrystallized again from ethanol (mp 111–112°C (34)).

4,4'-Dibromobenzophenone (**6**h) was prepared from 4-bromobenzoyl chloride, aluminum trichloride, and bromobenzene (see general Friedel–Crafts procedure below), and was recrystallized three times from 95% ethanol (mp 173–174°C).

4,4'-Dicyanobenzophenone (**6**g) was prepared as described previously (35), treated with Norite in boiling chloroform, and recrystallized twice from methanol (mp 158–159°C).

3,3'-Dicyanobenzophenone (**6**f)

3,3'-Dibromobenzophenone (36) (11.0 g, 0.032 mol) and cuprous cyanide (7.22 g, 0.081 mol) were placed in a 100 mL round-bottom flask fitted with magnetic stirrer, reflux condenser, and calcium chloride drying tube. Anhydrous *N,N*-dimethylformamide (40 mL) was added and the mixture was refluxed for 12 h. The resulting brown-black mixture was allowed to cool, and then poured into 15% aqueous sodium cyanide (400 mL) and heated on the steam bath for 1.5 h. The brown crystalline precipitate was extracted with benzene (5 × 50 mL). The combined benzene extracts were washed with water (4 × 50 mL), dried over anhydrous sodium sulfate, and filtered. Evaporation of the solvent on the rotary evaporator yielded a yellow solid, which was recrystallized from chloroform–methanol (1:1) to give an off-white solid (5.4 g, 0.024 mol, 73%). The nmr spectrum of this crude product was almost identical to that of 3-cyanobenzaldehyde (37); tlc showed it to be contaminated with a small amount of faster moving material (presumably monocyanated product). A portion of this material was chromatographed on a silica gel column with benzene (75%) – hexane. The first few fractions contained mixtures of the two products. Subsequent fractions (pure by tlc) were combined, evaporated, and the resulting white solid was recrystallized once from chloroform–ether (1:4) and once from chloroform–methanol (1:1) to yield colourless prisms (mp 148–148.5°C); λ_{max} (EtOH): 221(47 950), 248(15 140), 286(sh,

Can. J. Chem. Downloaded from www.nrcresearchpress.com by 210.87.254.6 on 09/05/12
For personal use only.

1211), 335(11); ir (KBr): 3070(w), 2235(s), 2224(s), 1667(s), 1601(s), 1429(m), 1290(s), 1163(s), 1009(m), 755(s); ^{1}Hmr ($CDCl_3$) δ: 7.3–8.2(m). *Anal.* calcd. for $C_{15}H_8N_2O$: C 77.57, H 3.47; found: C 77.29, H 3.33.

4-Methoxybenzophenone (6i) was prepared from benzoyl chloride, aluminum trichloride, and anisole and was recrystallized twice from 90% methanol and twice from ether–hexane (7:3) (mp 61–62°C).

4-Methylbenzophenone (6j) was prepared from benzoyl chloride, aluminum trichloride, and toluene, and was recrystallized once from hexane and twice from 85% ethanol (mp 51–52°C).

4-(Trifluoromethyl)benzophenone (6k) was prepared by the addition of 4-(trifluoromethyl)phenylmagnesium bromide to benzoyl chloride (see preparation of **6*l***) and was purified by column chromatography on silica gel with benzene (75%) – hexane, followed by one recrystallization from 95% ethanol and one recrystallization from chloroform (10%) – methanol (mp 116–116.5°C (38)).

4-Methyl-4'-(trifluoromethyl)benzophenone (6l)

4-(Trifluoromethyl)phenylmagnesium bromide (0.04 mol) was prepared in the usual manner from 4-bromobenzotrifluoride (8.76 g, 0.04 mol) and magnesium turnings (1.23 g, 0.05 g-atom) in anhydrous diethyl ether. The deep red solution obtained after stirring for four hours was diluted to 30 mL and transferred by syringe to the dropping funnel of an apparatus consisting of a 100 mL 3-neck round-bottom flask, reflux condenser, magnetic stirrer, and dropping funnel under an atmosphere of dry nitrogen. Toluoyl chloride (15.4 g, 0.1 mol) and anhydrous diethyl ether (30 mL) were placed in the flask and degassed by bubbling nitrogen through for 10 min. The Grignard reagent was then added dropwise over four hours with vigorous stirring, while the reaction mixture was kept at room temperature with a water bath. The mixture was stirred at room temperature overnight, poured into 5% aqueous hydrochloric acid, and heated on the steam bath for two hours, during which time a large amount of solid formed. The mixture was cooled and extracted with ether (4 × 75 mL). The combined ether extracts were washed with 5% aqueous hydroxide (2 × 70 mL), once with water (30 mL), once with saturated brine (30 mL), dried over anhydrous sodium sulfate, and filtered. Evaporation of the solvent on the rotary evaporator yielded a yellow-orange solid which was dissolved in hot 95% ethanol (75 mL), filtered, and refrigerated. The yellow crystals were collected by filtration (3.2 g, 0.012 mol, 30%). Column chromatography (silica gel; benzene (75%) – hexane) followed by two recrystallizations from methanol afforded the product as colourless plates (mp 145–146°C). Ultraviolet λ_{max} (EtOH): 243(21 590), 268(26 130), 332(204); ir (KBr): 1648(s), 1605(s), 1408(s), 1330(s), 1312(s), 1289(m), 1170(br s), 1130(br s), 1068(s); ^{1}Hmr ($CDCl_3$) δ: 2.48(s, 3H), 7.35(d, 2H), 7.75(d, 2H), 7.84 (br s, 4H). *Anal.* calcd. for $C_{15}H_{11}F_3O$: C 68.18, H 4.20; found: C 68.11, H 4.12.

4-Methoxy-4'-(trifluoromethyl)benzophenone (6m) was prepared from 4-(trifluoromethyl)phenylmagnesium bromide and 4-anisoyl chloride (see preparation of **6*l***) and was purified by column chromatography (silica gel; benzene (75%) – hexane) followed by one recrystallization from chloroform–ether and one recrystallization from methanol (mp 123–124°C (38)).

3-Cyanobenzophenone (6n) was prepared from 3-cyanobenzoyl chloride, aluminum trichloride, and benzene, and was recrystallized three times from 90% ethanol (mp 91–92°C (39)).

3-Cyano-4'-methoxybenzophenone (6o) was prepared from 3-cyanobenzoyl chloride, aluminum trichloride, and anisole, and was purified by column chromatography (silica gel; benzene (50 → 80%) – hexane) followed by two recrystallizations from 90% ethanol (mp 95–97°C (40)).

4-Cyanobenzophenone (6p) was prepared from 4-cyanobenzoyl chloride, aluminum trichloride, and benzene, and was purified by recrystallization from 90% ethanol, column chromatography (alumina; benzene), and one further recrystallization from 90% ethanol (mp 114–115°C (40)).

4-Cyano-4'-methylbenzophenone (6q) was prepared from 4-cyanobenzoyl chloride, aluminum trichloride, and toluene, and was recrystallized three times from ethanol (mp 163–164°C (40)).

4-Cyano-4'-methoxybenzophenone (6r) was prepared from 4-cyanobenzoyl chloride, aluminum trichloride, and anisole, and was recrystallized twice from methanol, once from chloroform–methanol, and once more from methanol (mp 129.5–131°C (40)).

General Friedel–Crafts Procedure

The benzoyl chlorides were either commercially available or obtained by refluxing the benzoic acid in thionyl chloride for 12 h, followed by removal of excess thionyl chloride by vacuum distillation.

The chloride (0.1 mol) is dissolved in benzene, toluene, anisole, or bromobenzene (100 mL) and placed in a 250 mL 2-neck round-bottom flask fitted with magnetic stirrer, condenser, and HCl trap. Anhydrous aluminum trichloride (0.11 mol) is then added over 15 min through the side arm with vigorous stirring and occasional cooling. The HCl trap is then replaced with a drying tube and the mixture is stirred at room temperature for 12 h (24 h for the additions of the cyanobenzoyl chlorides). The mixture is poured into ice water (250 mL) and stirred for one hour, during which time the organic layer turns off-white or yellow in colour. Benzene (50 mL) is added, the layers are separated, and the aqueous portion is extracted with benzene (3 × 25 mL). The combined organic portions are washed once with 5% aqueous sodium hydroxide (30 mL), once with water (30 mL), once with saturated brine (15 mL), dried over anhydrous sodium sulfate, and filtered. Solvents are removed on the rotary evaporator, and the resulting solid recrystallized from ethanol or methanol. Yields were generally 50% or better.

Acknowledgements

We wish to express our appreciation to Dr. C. M. Elson, Department of Chemistry, St. Mary's University, Halifax for making available the potentiostat to measure the reduction potentials.

This work was supported by the Natural Sciences and Engineering Research Council of Canada.

1. (*a*) A. Streitwieser, Jr. Molecular orbital theory for organic chemists. J. Wiley and Sons, Inc., New York. 1961. pp. 175–185; (*b*) A. Maccoll. Nature, **163**, 178 (1949).
2. R. W. Schmid and E. Heilbronner. Helv. Chim. Acta, **37**, 1453 (1954).
3. (*a*) R. O. Loutfy and R. O. Loutfy. J. Phys. Chem. **77**, 336 (1973); (*b*) R. O. Loutfy and R. O. Loutfy. Tetrahedron, **29**, 2551 (1973); (*c*) R. O. Loutfy and R. O. Loutfy. J. Phys. Chem. **76**, 1650 (1972).
4. (*a*) L. Nadjo and J. M. Saveant. J. Electroanal. Chem. **30**, 41 (1971); (*b*) P. Zuman, O. Exner, R. F. Rekker, and W. Th. Nauta. Collect. Czech. Chem. Commun. **33**, 3213 (1968).
5. D. R. Arnold. Adv. Photochem. **6**, 301 (1968).
6. S. Nagakura. Bull. Chem. Soc. Jpn. **25**, 164 (1952).
7. (*a*) L. Goodman and R. Zwarich. J. Am. Chem. Soc. **93**, 2068 (1971); (*b*) M. Koyanagi and L. Goodman. J. Chem.

Can. J. Chem. Downloaded from www.nrcresearchpress.com by 210.87.254.6 on 09/05/12
For personal use only.

Phys. **55**, 2959 (1971); (*c*) J. SMOLAREK, R. ZWARICH, and L. GOODMAN. J. Mol. Spectrosc. **43**, 416 (1972); (*d*) E. J. MCALDUFF. Can. J. Chem. **58**, 622 (1980).
8. W. A. PRYOR, T. H. LIN, J. P. STANLEY, and R. W. HENDERSON. J. Am. Chem. Soc. **95**, 6993 (1973), and references therein.
9. P. B. AYSCOUGH and R. WILSON. J. Chem. Soc. 5412 (1963).
10. H. R. FALLE and F. C. ADAM. Can. J. Chem. **44**, 1387 (1966).
11. A. R. BASSINDALE, A. J. BOWLES, A. HUDSON, R. A. JACKSON, K. SCHREINER, and A. BERNDT. Tetrahedron Lett. 3185 (1973).
12. R. I. WALTER. J. Am. Chem. Soc. **88**, 1923 (1966).
13. H. E. ZIMMERMAN and D. I. SCHUSTER. J. Am. Chem. Soc. **84**, 4527 (1962).
14. R. M. HOCHSTRASSER and L. J. NOE. J. Mol. Spectrosc. **38**, 175 (1971).
15. (*a*) P. NETA and R. H. SCHULER. J. Phys. Chem. **77**, 1368 (1973); (*b*) E. GEY and N. E. KRUGLYAK. Z. Phys. Chem. Leipzig, **255**, 915 (1974); (*c*) E. GEY and N. E. KRUGLYAK. Z. Phys. Chem. Leipzig, **256**, 737 (1975).
16. M. J. S. DEWAR. J. Am. Chem. Soc. **74**, 3353 (1952).
17. E. M. KOSOWER and E. J. POZIOMEK. J. Am. Chem. Soc. **86**, 5515 (1964).
18. (*a*) R. W. BALDOCK, P. HUDSON, A. R. KATRITZKY, and F. SOTI. J. Chem. Soc. Perkin Trans. I, 1422 (1974); (*b*) A. R. KATRITZKY and F. SOTI. J. Chem. Soc. Perkin Trans. I, 1427 (1974); (*c*) A. T. BALABAN, P. T. FRANGOPOL, M. FRANGOPOL, and N. NEGOITA. Tetrahedron, **23**, 4661 (1967); (*d*) A. T. BALABAN. Rev. Roum. Chim. **16**, 725 (1971); (*e*) A. T. BALABAN, M. T. CAPROIU, N. NEGOITA, and R. BAICAN. Tetrahedron, **33**, 2249 (1977); (*f*) K. D. GUNDERMANN and E. ROHRL. Justus Liebigs Ann. Chem. 1661 (1974); (*g*) T. H. KOCH, J. A. OLESEN, and J. DENIRO. J. Am. Chem. Soc. **97**, 7285 (1975); (*h*) L. DE VRIES. J. Am. Chem. Soc. **99**, 1982 (1977); (*i*) L. DE VRIES. J. Am. Chem. Soc. **100**, 926 (1978); (*j*) N. HEIMER. J. Org. Chem. **42**, 3767 (1977); (*k*) L. STELLA, Z. JANOUSEK, R. MERENYI, and H. G. VIEHE. Angew. Chem. Int. Ed. Engl. **17**, 691 (1978); (*l*) H. G. AURICH, E. DEUTSCHLE, and W. WEISS. J. Chem. Res. M, 3455 (1977); (*m*) H. G. VIEHE, R. MERENYI, L. STELLA, and Z. JANOUSEK. Angew. Chem. Int. Ed. Engl. **18**, 917 (1979); (*n*) L. STELLA, R. MERENYI, Z. JANOUSEK, H. G. VIEHE, P. TORDO, and A. MUNOZ. J. Phys. Chem. **84**, 304 (1980).
19. (*a*) D. R. ARNOLD and R. W. R. HUMPHREYS. J. Chem. Soc. Chem. Commun. 181 (1978); (*b*) R. W. R. HUMPHREYS and D. R. ARNOLD. Can. J. Chem. **57**, 2652 (1979).
20. W. J. LEIGH and D. R. ARNOLD. J. Chem. Soc. Chem. Commun. 406 (1980).
21. J. S. BINKLEY, R. A. WHITESIDE, P. C. HARIHARAN, R. SEEGER, J. A. POPLE, W. J. HEBRE, and M. D. NEWTON. Gaussian 76. Program No. 368. Quantum Chemistry Program Exchange, Bloomington, IN.
22. J. A. POPLE and D. L. BEVERIDGE. Approximate molecular orbital theory. McGraw-Hill, Inc., New York. 1970.
23. R. HOFFMANN and J. R. SWENSON. J. Phys. Chem. **74**, 415 (1970).
24. (*a*) I. B. AFANAS'EV. Int. J. Chem. Kinet. **7**, 857 (1975); (*b*) T. ALFREY, JR. and C. C. PRICE. J. Polym. Sci. **2**, 101 (1947); (*c*) C. H. BAMFORD and A. D. JENKINS. Trans. Faraday Soc. **59**, 530 (1963); (*d*) R. E. PEARSON and J. C. MARTIN. J. Am. Chem. Soc. **85**, 3142 (1963); (*e*) R. ITO, T. MIGITA, N. MORIKAWA, and O. SIMAMURA. Tetrahedron, **21**, 955 (1965); (*f*) T. YAMAMOTO and T. OTSU. Chem. Ind. 787 (1967); (*g*) H. SAKURAI, S. HAYASHI, and A. HOSOMI. Bull. Chem. Soc. Jpn. **44**, 1945 (1971); (*h*) T. H. FISHER and A. W. MEIERHOEFER. J. Org. Chem. **43**, 224 (1978); (*i*) S. DINCTÜRK, R. A. JACKSON, and M. TOWNSON. J. Chem. Soc. Chem. Commun. 172 (1979).
25. X. CREARY. J. Org. Chem. **45**, 280 (1980).
26. (*a*) E. G. JANZEN. Acc. Chem. Res. **2**, 279 (1969); (*b*) C. RÜCHARDT. Angew. Chem. Int. Ed. Engl. **9**, 830 (1970).
27. V. M. KAZAKOVA, B. I. SHAPIRO, I. D. MOROZOVA, and E. A. POLENOV. J. Struct. Chem. **12**, 14 (1971).
28. E. M. KOSOWER. An introduction to physical organic chemistry. John Wiley and Sons, Inc., New York. 1968. p. 49.
29. C. L. LIOTTA and D. F. SMITH. J. Chem. Soc. Chem. Commun. 416 (1968).
30. H. C. KO, H. W. O'HARA, T. HU, and L. G. HEPLER. J. Am. Chem. Soc. **86**, 1003 (1964).
31. J. E. WERTZ and J. R. BOLTON. Electron spin resonance. McGraw-Hill, Inc., New York. 1972. Chapt. 10.
32. G. KORTUM, W. VOGEL, and K. ANDRUSSOW. Dissociation constants of organic acids in aqueous solution. Butterworths, London. 1961.
33. J. LICHTENBERGER and F. WEISS. Bull. Soc. Chim. Fr. 587 (1962).
34. E. J. SOLOSKI and C. TAMBORSKI. J. Organomet. Chem. **157**, 373 (1978).
35. D. R. ARNOLD and R. W. R. HUMPHREYS. Can. J. Chem. **55**, 2286 (1977).
36. D. E. PEARSON, H. W. POPE, W. E. HARGROVE, and W. E. STAMPER. J. Org. Chem. **23**, 1412 (1958).
37. Aldrich catalogue of nmr spectra. 7, 126B (1974).
38. N. P. BUU-HOI, N. H. NAM, and N. D. XUONG. Recl. Trav. Chim. Pays-Bas, **85**, 367 (1966).
39. V. MYCHAJLYSZYN and M. PROTIVA. Collect. Czech. Chem. Commun. **24**, 3955 (1959).
40. E. WAGNER, B. VOIGT, and K. STEINBRUECK. Pharmazie, **31**, 354 (1976).

The synthesis of 8-aza-3-deazaguanosine [6-amino-1-(β-D-ribofuranosyl)-*v*-triazolo[4,5-*c*]pyridin-4-one] via a novel 1,3-dipolar cycloaddition reaction

ROBERT A. EARL AND LEROY B. TOWNSEND[1]

Department of Medicinal Chemistry, College of Pharmacy, and Department of Chemistry, The University of Michigan, Ann Arbor, MI 48109, U.S.A.

Received March 25, 1980

This paper is dedicated to Prof. Raymond U. Lemieux on the occasion of his 60th birthday

ROBERT A. EARL and LEROY B. TOWNSEND. Can. J. Chem. **58**, 2550 (1980).

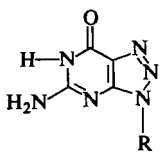
8-Aza-3-deazaguanosine (**2**) has been prepared via a route which used a 1,3-dipolar cycloaddition reaction to provide a key intermediate. The reaction of 2′,3′,5′-tri-*O*-benzoyl-β-D-ribofuranosyl azide (**13**) with methyl 4-hydroxy-2-butynoate (**11**) provided a good yield of crystalline methyl 5-hydroxymethyl-1-(2,3,5-tri-*O*-benzoyl-β-D-ribofuranosyl)-*v*-triazole-4-carboxylate (**14**). A series of functional group transformations were then used to convert **14** into methyl 5-cyanomethyl-1-(2,3,5-tri-*O*-benzoyl-β-D-ribofuranosyl)-*v*-triazolo-4-carboxylate (**19**). Treatment of **19** with liquid ammonia effected not only a smooth removal of the blocking groups, but also an aminolysis of the ester function which was then followed by a ring annulation to provide 8-aza-3-deazaguanosine (**2**). The structures of these nucleosides were established on the basis of proton nmr spectral data and nuclear Overhauser enhancement data. The nucleosides obtained in this study were also converted through a chemical degradation sequence into nucleosides which had been obtained during an earlier work from our laboratory. The present study also provides unequivocal proof of the structures of some triazole nucleosides obtained in the earlier study.

ROBERT A. EARL et LEROY B. TOWNSEND. Can. J. Chem. **58**, 2550 (1980).

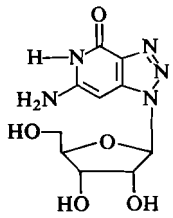
On a préparé l'aza-8 déaza-3 guanosine (**2**) en faisant appel à une réaction de cycloaddition dipolaire-1,3 pour obtenir l'intermédiaire clé. La réaction de l'azoture de tri-*O*-benzoyl-2′,3′,5′ β-D-ribofurannosyle (**13**) avec l'hydroxy-4 butyne-2 oate de méthyle (**11**) conduit avec un bon rendement à l'hydroxyméthyl-5 (tri-*O*-benzoyl-2,3,5 β-D-ribofurannosyle)-1 *v*-triazolecarboxylate-4 de méthyle (**14**). On a utilisé une série de réactions impliquant les groupements fonctionnels pour transformer le composé **14** en cyanométhyl-5 (tri-*O*-benzoyl-2,3,5 β-D-ribofurannosyle)-1 *v*-triazolecarboxylate-4 de méthyle (**19**). Lorsqu'on traite le composé **19** par l'ammoniac liquide, on obtient non seulement une déprotection douce, mais également une aminolyse de la fonction ester suivie d'une annélation du cycle qui conduit à l'aza-8 diaza-3 furannosine (**2**). On a établi la structure de ces nucléosides en se basant sur la rmn du proton et sur des données d'accroissement Overhauser nucléaire. On a également transformé ces nucléosides, par dégradation chimique, en des nucléosides obtenues antérieurement dans notre laboratoire. La présente étude apporte également une preuve univoque de structure de quelques nucléosides triazoles obtenus dans une étude antérieure.

[Traduit par le journal]

The isolation of (1) and characterization of the antibiotic pathocidin as 8-azaguanine (**1***a*) has created considerable interest in the synthesis of other aza, deaza, and aza/deaza guanine and guanosine analogs. Research activity in this area has resulted in the synthesis of 8-azaguanine (2) (**1***a*), 8-azaguanosine (3, 4) (**1***b*), and 2′-deoxy-8-azaguanosine (4); 3-deazaguanine (5) and 3-deazaguanosine (5); 1-deazaguanosine (6); 1-deaza-8-azaguanosine (7), and several (8, 9) guanosine analogs containing a bridgehead nitrogen.



1 *a*, R = H
b, R = β-D-ribofuranosyl



2

Interesting biological and chemotherapeutic activities have been reported for some of the 8-azaguanosine (10) and 3-deazaguanosine (11) derivatives. However, little or no antitumor (*in vitro* or *in vivo*) activity was noted (12) for 1-deaza or 1-deaza-8-azaguanosine or their corresponding bases. Also, to date, only very weak antiviral activity has been reported (9) for one of the bridgehead-nitrogen guanosine analogs.

The interesting biological and chemotherapeutic activities observed in the 8-azaguanosine (10) and 3-deazaguanosine (11) series suggested that similar or enhanced activities might be expected for the guanosine analog 8-aza-3-deazaguanosine **2**. Also, a recent report (12) indicates that there may be a correlation between the biological activity and the pK_a's of certain guanosine analogs. On the basis of this study it was suggested (12) that 8-aza-3-deazaguanosine should possess a pK_a very similar

[1]Author to whom correspondence may be addressed.

0008-4042/80/232550-12$01.00/0

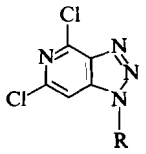
©1980 National Research Council of Canada/Conseil national de recherches du Canada

Can. J. Chem. Downloaded from www.nrcresearchpress.com by 210.87.254.5 on 09/05/12
For personal use only.

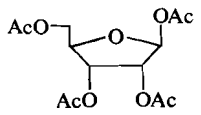
Can. J. Chem. Downloaded from www.nrcresearchpress.com by 210.87.254.5 on 09/05/12
For personal use only.

to that of the naturally occurring compounds (guanosine and 8-azaguanosine) and might be expected to exhibit definite biological and chemotherapeutic activities.

On the basis of the above, we initiated a program designed to synthesize 8-aza-3-deazaguanosine (**2**). In our initial approach, we synthesized (13) 4,6-dichloro-*v*-triazolo[4,5-*c*]pyrimidine (**3***a*) by a diazo ring-closure reaction involving 3,4-diamino-2,6-dichloropyridine (14) and carried out a fusion reaction of **3***a* with 1,2,3,5-tetra-*O*-acetyl-β-D-ribofuranose (**4**). However, this standard pro-



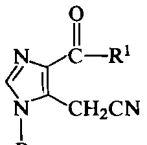
3 *a*, R = H
b, R = 2,3,5-tri-*O*-acetyl-β-D-ribofuranosyl



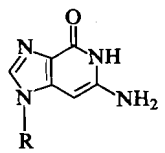
4

cedure for nucleoside synthesis was found (13) to yield a mixture of isomeric, acetylated ribonucleosides from which the 1-isomer (**3***b*) could be isolated in small amounts only after tedious chromatography. Based on these results, this standard approach seemed too cumbersome to be practical since numerous functional group transformations would be required in order to convert **3***b* into 8-aza-3-deazaguanosine (**2**).

Considerable success has been reported (5) in the synthesis of 3-deazaguanosine derivatives via the base-catalyzed ring-closure of imidazole precursors, e.g., **5***c* and **5***d* to **6***a* and **6***b*, respectively.



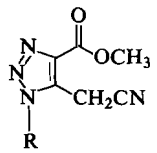
5*a*, R = H, R¹ = OCH_3
b, R = 2,3,5-tri-*O*-acetyl-β-D-ribofuranosyl
R¹ = OCH_3
c, R = H, R¹ = NH_2
d, R = β-D-ribofuranosyl
R¹ = NH_2



6*a*, R = H
b, R = β-D-ribofuranosyl

This report (5) suggested that this approach might be useful[2] for the synthesis of 8-aza-3-deazaguanosine provided that suitable triazole precursors were available.

Unfortunately, a survey of the literature revealed that the *v*-triazole precursor, *per se*, methyl 5(4)-cyanomethyl-*v*-triazole-4(5)-carboxylate (**7***a*) was unknown. To the best of our knowledge, other useful starting materials such as the *v*-triazole analogue of **5***c* were also unknown. Thus we were faced with the task of synthesizing a triazole derivative such as**7***a*. Based on the imidazole work (5), a condensation of **7***a* with 1,2,3,5-tetra-*O*-acetyl-β-D-ribofuranose (**4**) would be expected to yield the triazole nucleoside derivative **7***b*. However, such a condensation using the imidazole derivative was found (5) to give both possible positional isomers. The ratio of these positional isomers could be changed depending on the amount of



7*a*, R = H
b, R = 2,3,5-tri-*O*-acetyl-β-D-ribofuranosyl

catalyst employed. In the case of the proposed triazole series, a third positional isomer is possible and would most likely be formed, based on our experience with 4,6-dichloro-*v*-triazolo[4,5-*c*]-pyridine (13) (**3***a*) and other related compounds (16). This suggested to us that we would again probably encounter serious problems with the separation of isomers possessing very similar chromatographic mobilities.

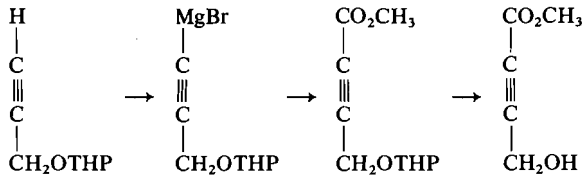
Another more novel approach to the synthesis of a *v*-triazole nucleoside such as **7***b* would be through the 1,3-dipolar cycloaddition of a ribofuranosyl azide derivative to a suitable acetylenic compound. This approach would enjoy the advantage of producing only two positional isomers. Several reports have appeared (17, 18) whereby glycosyl azides have been successfully added to acetylenic compounds to produce *v*-triazole nucleosides with a high degree of regioselectivity (the glycosyl and ester functions being located at the 1- and 4-positions of the triazole ring, respectively). In addition to a high degree of regioselectivity, these reactions (17, 18) also appeared to occur with com-

[2]It is interesting to note, however, that a similar approach has failed to yield 3,7-dideazaguanine from pyrrole precursors (15).

Can. J. Chem. Downloaded from www.nrcresearchpress.com by 210.87.254.5 on 09/05/12
For personal use only.

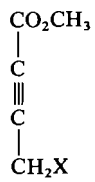
plete retention[3] of configuration at C-1 of the glycosyl moiety.

The 1,3-dipolar cycloaddition route looked very promising as a route for the synthesis of a functionalized triazole nucleoside such as **7***b*. A search of the literature revealed that the highly functionalized acetylenic derivative, methyl 4-hydroxy-2-butynoate (**11**), was a known (20) compound. The compound **11** had been prepared (20) previously, however, we were unable to reproduce the reported (20) yields and also encountered serious problems with emulsion formation during the workup of the carboxylation mixture using this procedure. Therefore, we modified (21) the original procedure, which eliminated the problem with emulsions and provided a 65% yield of **11** (based on **8**).[4]



8 **9** **10** **11**

It had been our intention to convert the hydroxymethyl group of **11** into a cyano methyl group to yield methyl 4-cyano-2-butynoate (**12***b*), since a reaction of **12***b* with a ribofuranosyl azide derivative should furnish a triazole nucleoside of the type represented by **7***b*. However, our attempts to bring about this modification were unsuccessful. Bromination of **11** using a published (20) procedure did not yield a pure product and gplc analysis indicated the presence of at least three new compounds in the reaction mixture. A pmr spectrum of the crude product indicated the presence of allenic compounds. Allenic compounds have been encountered by others (23) when attempting to iodinate certain acetylenic alcohols under very mild conditions. Other methods for bromination (24) and iodination (25) were also unsuccessful in converting **11** into a halo derivative. Similarly, methods (26) for the preparation of mesylates and tosylates from acetylenic alcohols did not give useful products from **11**. Although all of these methods showed evidence of giving some of the desired products, the highly reactive nature of these propargyl compounds ensure a difficult isolation. This isolation problem is due primarily to their tendency to undergo rearrangement (23) to allenic compounds or to react further (26) with bases present in the reaction mixture to give hydrolysis products or quaternary ammonium compounds.



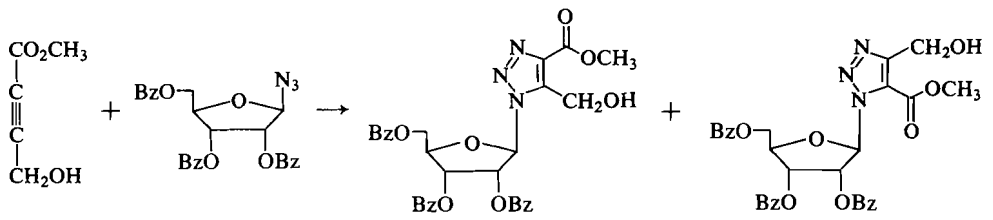
12*a*, X = Br
b, X = CN

In view of the problems we encountered while trying to modify methyl 4-hydroxy-2-butynoate (**11**), we decided to carry out a 1,3-dipolar cycloaddition reaction using **11** as the dipolarophile and to carry out further functional group transformations on the nucleoside rather than the acetylenic precursor. We chose 2,3,5-tri-*O*-benzoyl-β-D-ribofuranosyl azide as a starting material since it has a known β configuration and is available (27) in pure, crystalline form. The reaction between crystalline 2,3,5-tri-*O*-benzoyl-β-D-ribofuranosyl azide (**13**) and methyl 4-hydroxy-2-propynoate (**11**) was found to proceed best when the temperature of the reaction was maintained in the range of 50–70°C with little or no solvent. Under these conditions, the reaction required 5 to 7 days for completion but the reaction was very clean resulting in the production of two close-running (tlc) nucleoside components in a ratio of ca. 4:1 (pmr).

When methanol was added to the hot reaction mixture, the predominant isomer, tentatively (17) assigned structure **14** (methyl 5-hydroxymethyl-1-(2,3,5-tri-*O*-benzoyl-β-D-ribofuranosyl)-*v*-triazole-4-carboxylate), crystallized from solution in a 60% yield. Chromatography of the product obtained from the supernatant yielded an additional 15% of the major isomer (**14**) as well as a 6% yield of the minor, slower running (tlc) nucleoside component. Elemental analysis and proton nmr spectral data indicated that the isolated products were isomeric since both products had the same empirical formula and displayed signals for a carbomethoxy and a hydroxymethyl group as well as the ribose moiety. Both compounds displayed anomeric signals (H-1′) with rather small coupling constants (1.8 Hz for **14** and 1.5 Hz for **15**) indicating (28) that they were both probably β-isomers. Furthermore, the anomeric signal for **15** (δ 7.07) was shifted downfield 0.21 ppm compared to the corresponding signal for **14** (δ 6.86) which sug-

[3]An apparent exception to this observation did not actually involve the cycloaddition of an azide to an acetylenic compound. Instead this reaction involved the reaction of a glycosyl azide with a carbanion followed by a ring closure reaction (see refs. 4 and 19).

[4]After this work was completed, a similar procedure for the removal of the tetrahydropyranyl protecting group was reported (22).



11 13 14 15

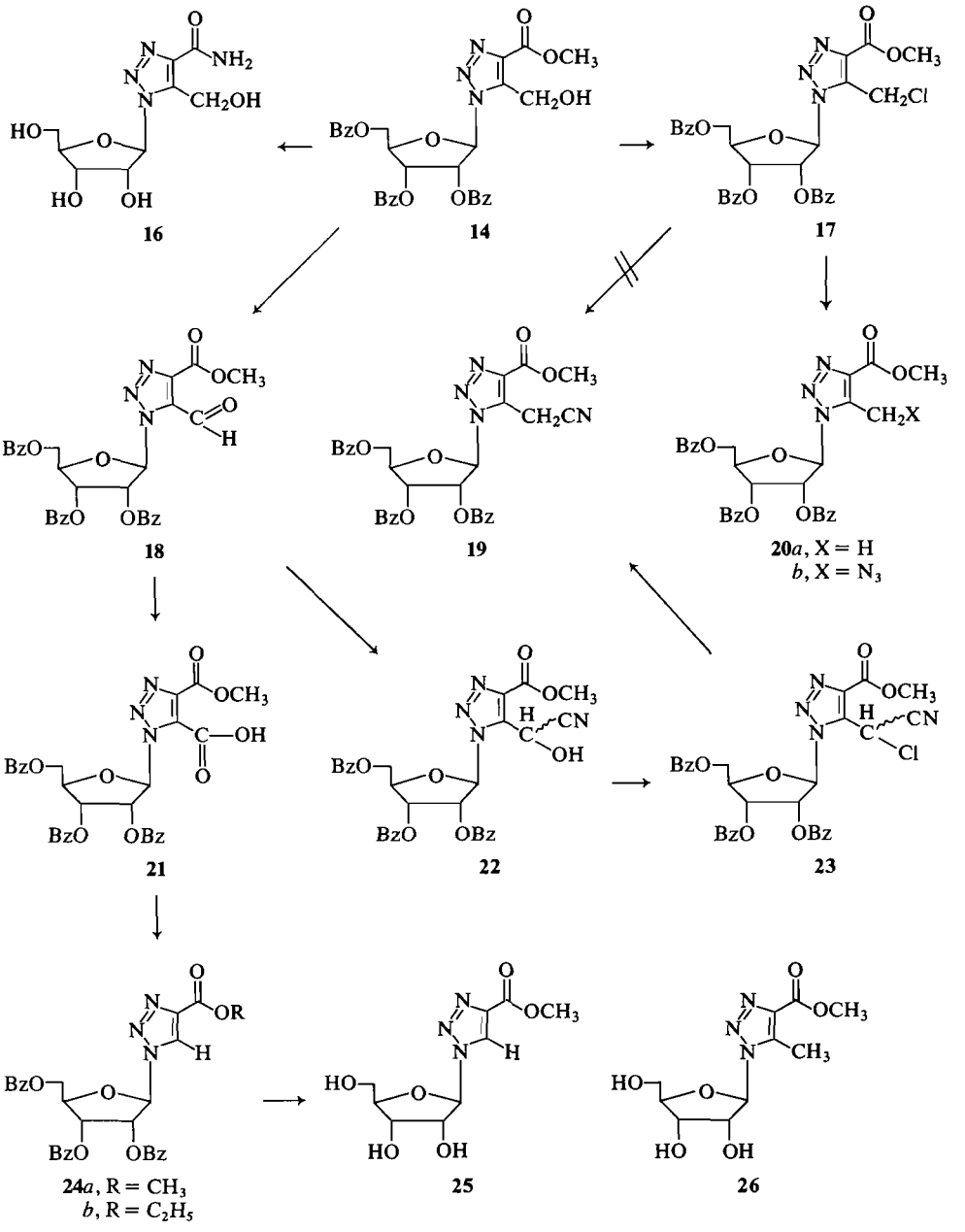
gested that our tentative (17) structural assignments were correct. It has been demonstrated previously in the case of benzimidazole (29*a*), imidazole (5), pyrimidine (29*b*), and 1,2,4-triazole nucleosides (29*c*, *d*) as well as in the case of certain nitrogen bridgehead nucleosides (29*e*) that when a ribosyl moiety is attached to a nitrogen atom α to a carbon atom bearing a carbonyl function (such as an ester group) then the anomeric signal is shifted downfield as compared to the situation where the ribosyl moiety is not adjacent to a carbonyl function. On the basis of this observation, the predominant isomer must have the structure indicated by **14** whereby H-1′ is located away from the carbomethoxy group.

Methanolic ammonia readily converted **14** into the crystalline carboxamide derivative **16**. Chlorination of **14** using thionyl chloride – DMF – methylene chloride provided a quantitative yield of the chloromethyl derivative **17**, isolated as a solid foam. This very reactive chloromethyl derivative (**17**) was readily reduced using catalytic hydrogenation (5% Pd/C) to provide the crystalline methyl derivative **20***a*. The structure of **20***a* was supported by its elemental analysis as well as by the appearance of a new 3-proton singlet in the pmr spectrum at δ 2.64 (methyl group). A reaction of the chloromethyl derivative (**17**) with sodium azide in acetonitrile furnished an 88% yield of the azidomethyl derivative **20***b*. Although the R_f (tlc) values of **17** and **20***b* were nearly identical, the compounds gave different colors when sprayed with 10% sulfuric acid and heated. The tlc indicated that 1 h of reaction at 70°C was probably sufficient for complete reaction. Potassium cyanide in DMSO (25°C) rapidly (3–5 min) converted the chloromethyl derivative **17** into a new product whose R_f was slower than that of the starting material. Although tlc suggested that the product was homogeneous, the pmr spectrum indicated that it was probably a mixture. The spectrum (pmr) was unexpectedly complex showing 5-"singlets" in the region δ 3.4–3.9 where the methoxy singlet should appear. At first, it appeared that the product was perhaps a dimer resulting from a bimolecular condensation of a cyanomethyl group with a carbomethoxy group. However, the mass spectrum was very complex showing peaks with masses much higher than that expected for a dimer. Furthermore, the mass spectrum did not show a molecular ion for the desired monomeric cyanomethyl derivative **19**. The reaction between chloromethyl derivative **17** and "naked" (30) cyanide ion (KCN–acetonitrile – 18-crown-6, 18 h, 45°C) also gave an unidentified product as above.

We, therefore, explored an alternate route for the synthesis of **19** which would not require a nucleophilic displacement with a strong base. During the course of this study, we found that the hydroxymethyl derivative **14** was readily converted (31) (85%) into the corresponding aldehyde **18** by treatment with activated (32) manganese dioxide in toluene at reflux. This compound was readily identified due to the presence of a sharp one-proton singlet in the pmr at δ 10.31 for the formyl proton. The aldehyde **18** could be converted into the cyanohydrin **22** (based on tlc data) using (33) a transcyanohydrination reaction between **18** and acetone cyanohydrin. However, the aldehyde **18** was so reactive that a simple treatment of **18** with 3 to 5 mol of hydrogen cyanide (34) in methylene chloride (25°C) converted it, quantitatively, into the cyanohydrin **22**. The cyanohydrin **22** was isolated as a crisp foam that was stable indefinitely, provided that it was kept dry. Thin layer chromatography resolved the diastereomeric mixture into two spots; however, attempts at column chromatography resulted in partial or complete reversion of **22** into the starting aldehyde **18**. The cyanohydrin was readily converted into the chlorocyanomethyl derivative **23** using thionylchloride–DMF–methylenechloride. Chromatography gave the diastereomeric mixture (**23**) as an analytically pure foam that showed a single spot (tlc) in two different chromatographic solvent systems. Hydrogenation of **23** (5% Pd/C) gave a nearly quantitative yield of the elusive cyanomethyl derivative **19** in the form of an analytically pure white foam. The tlc mobilities for **19** were different from those of the unidentified product(s) obtained from attempted displacement of the chloro group of **17** with cyanide ion. Later experiments demonstrated

Can. J. Chem. Downloaded from www.nrcresearchpress.com by 210.87.254.5 on 09/05/12
For personal use only.

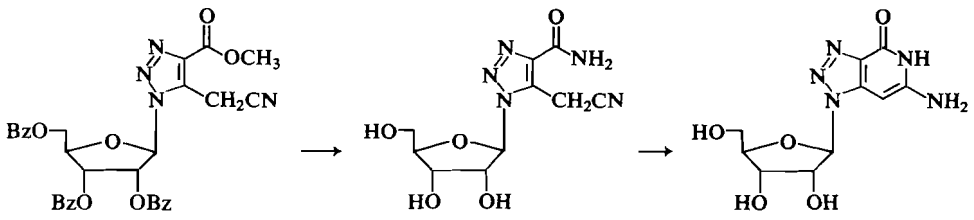
Can. J. Chem. Downloaded from www.nrcresearchpress.com by 210.87.254.5 on 09/05/12
For personal use only.



that the hydroxymethyl derivative **16** could be converted into the cyanomethyl derivative **19** in an overall yield of 57% with only the chlorocyanomethyl derivative requiring purification by chromatography.

Treatment of the cyanomethyl derivative **19** with methanolic ammonia (25°C, 18 h) gave a highly colored reaction mixture from which impure 5-cyanomethyl-1-(β-D-ribofuranosyl)-*v*-triazole-4-carboxamide (**27**) (ca. 25% yield) and 8-aza-3-deazaguanosine (**2**) could be isolated. When **19** was treated[5] with liquid ammonia (25°C) for 5 days, a light purple reaction mixture was obtained. Evaporation of the liquid ammonia followed by tritura-

[5]It should be noted that the ring closure of **19** to give **2** took place under much milder conditions than those required (5) for the corresponding reaction in the imidazole series. This is likely due to the greater electron withdrawing ability of a triazole ring as compared to an imidazole ring which renders the amide protons of **27** more acidic than those in **5***d*. This facilitates abstraction (5) of an amide proton of **27** which is followed by rapid ring closure.



19 27 2

tion with ether and then acetone yielded a yellow-orange colored powder whose pmr spectrum indicated that it was nearly pure 8-aza-3-deazaguanosine (100% crude yield). The crude 8-aza-3-deazaguanosine (**2**) was converted into its sodium salt and absorbed on a Dowex 1 resin (formate form) column. Elution with 0.05 *N* formic acid gave pure 8-aza-3-deazaguanosine, mp 239–241°C in the form of a light, violet colored powder. The pmr spectrum of 8-aza-3-deazaguanosine (**2**) was very similar to that reported (5) for 3-deazaguanosine (**6***b*) showing an anomeric signal at δ 5.83 (δ 5.51 for **6***b*) which was split into a doublet with $J = 5$ Hz (6 Hz for **6***b*). The ring proton (H-7) appeared as a singlet at δ 5.50 (δ 5.52 for **6***a*). The uv spectrum of 8-aza-3-deazaguanosine was also very similar to that reported (5) for 3-deazaguanosine, however, these similarities are not sufficient to allow any conclusions regarding configuration or position of attachment of the ribose moiety in **2**. We had assumed a β-configuration for **2** and its triazole nucleoside precursors on the basis of the known (27) β-configuration of the starting azide **13**. A pmr spectrum (Table 1) of the aldehyde derivative **18** provided conclusive evidence (28) that the cycloaddition had proceeded with retention of configuration at C-1 of the ribose ring since the anomeric signal appeared as a sharp singlet at δ 7.01. The position of attachment of the ribosyl moiety in **2** and **14**, **16–23** remained to be established since we did not feel secure with assignments based on the relative positions of the anomeric signals of the original isomeric cycloadducts (**14** and **15**). We therefore carried out a chemical degradation of the major cycloadduct (**14**) in order to relate it to a nucleoside (**24***a*) of known structure. Oxidation of the hydroxymethyl group of **14** using Jones reagent (35) provided (88%) the carboxylic acid derivative **21**. The pmr spectrum of **21** showed considerable peak broadening suggesting the presence of paramagnetic species. Washing solutions of **21** with dilute mineral acid and even column chromatography did not improve the quality of the spectra. The crude product was triturated with dilute acetic acid, dried, and used without further purification for decarboxylation. Decarboxylation of **21** was carried out in toluene at reflux to give a crude product. This solid was crystallized[6] from methanol to give a 65% yield of methyl 1-(2,3,5-tri-*O*-benzoyl-β-D-ribofuranosyl)-*v*-triazole-4-carboxylate (**24***a*) whose physicochemical data (mp, pmr, and $[\alpha]_D$) were in excellent agreement with the published (17) data for **24***a*. Recrystallization of the crude decarboxylation product from ethanol gave the corresponding ethyl ester **24***b*. However, the published structure of **24***a* was not unequivocal since the assignment of a structure for **24***a* was based only on trends in pmr chemical shifts previously noted (36) for model *N*-methyl derivatives of triazoles. Therefore, compounds **24***a* and **20***a* were deblocked with methanolic sodium methoxide to provide **25** and **26**, respectively. The physicochemical properties of **25** were identical to those previously reported (37) for this compound. These nucleosides (**25** and **26**) were then examined for the presence of nuclear Overhauser enhancements (38, 39). When H-2′ of **25** was irradiated, an nOe of 18.5% was noted for H-5 (Table 2). Similarly, irradiation of H-1′ caused a 10% enhancement of H-5 in **25**. These results could only occur if the ribose moiety of **25** is attached to N-1 of the triazole ring since attachment at N-3 would place H-5 too far away from H-1′ and H-2′ to expect any significant nOe. Furthermore, when the methyl group at C-5 of **26** was irradiated, an enhancement of 16.5% was noted for H-1′ which provided additional evidence that the ribosyl group is in the position indicated. Thus, a combination of pmr and nOe spectral data provided unequivocal proof that **14**, **16–26** possessed the structures as tentatively assigned by us. These data have also provided proof that the cycloaddition reactions reported (17) by earlier workers proceeded with the regioselectivity that they had earlier indicated.

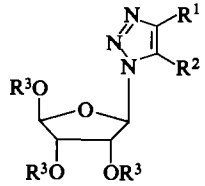
This work has demonstrated once again (40) the

[6]Recrystallization of the crude decarboxylation product from ethanol gave a 65% yield of the corresponding ethyl ester. This behavior is difficult to explain without invoking the presence of some impurity which is acting as a transesterification catalyst.

Can. J. Chem. Downloaded from www.nrcresearchpress.com by 210.87.254.5 on 09/05/12
For personal use only.

Can. J. Chem. Downloaded from www.nrcresearchpress.com by 210.87.254.5 on 09/05/12
For personal use only.

TABLE 1. Proton magnetic resonance spectral data for certain triazole nucleosides[a]



Compound number	R^1	R^2	R^3	H-1′($J_{1',2'}$ in Hz)	H-2′	H-3′	H-4′	H-5′, 5″	OCH_3	Other
14	CO_2CH_3	CO_2H	Bz	6.86 (1.8)	6.46 (dd)	6.26 (t)	5.00 (m)	4.65 (m)	3.86	5.03 (d, CH_2OH), 5.83 (t, CH_2OH)
15	CH_2OH	CO_2CH_3	Bz	7.07 (1.5)	6.57–6.08		5.10	4.60	3.90	4.68 (d, CH_2OH), 5.33 (t, CH_2OH)
17	CO_2CH_3	CH_2Cl	Bz	6.86 (2.0)	6.53 (dd)	6.16 (t)	5.09 (m)	4.67 (m)	3.91	5.26 (s, CH_2Cl)
20*a*	CO_2CH_3	CH_3	Bz	6.46 (5.0)[b]	5.87 (m)	5.87 (m)	5.00–4.32		3.90	2.64 (s, CH_3)
20*b*	CO_2CH_3	CH_2N_3	Bz	6.82 (4.0)	6.54 (dd)	6.22 (t)	4.50–5.20		3.89	5.00 (2, CH_2N_3)
18	CO_2CH_3	CHO	Bz	7.01 (0.0)	6.44 (d)	6.22 (t)	5.06 (m)	4.64 (m)	3.98	10.31 (s, CHO)
22	CO_2CH_3	CHCNOH	Bz	6.97 (1.0)	6.60 (dd)	6.22 (t)	5.11 (m)	4.67 (m)	3.94	6.60 (d, CHOHCN)
23	CO_2CH_3	CHCNCl	Bz	6.95 (1.5)	6.62 (d)	6.20 (t)	5.08 (m)	4.62 (m)	3.96	
19	CO_2CH_3	CH_2CN	Bz	6.93 (2.0)	6.60 (dd)	6.11 (t)	5.07 (m)	4.61 (m)	3.93	4.61 (s, CH_2CN)
21	CO_2CH_3	CO_2H	Bz	6.95 (2.0)	6.52 (dd)	6.25 (t)	5.07 (m)	4.67 (m)	3.92	
24*a*	CO_2CH_3	H	Bz	6.76 (3.2)[c]	6.31 (m)	6.12 (m)	4.99 (m)	4.66 (m)	3.87	9.04 (s, H5)
24*a*	CO_2CH_3	H	Bz	6.45 (3.4)[b,c]	6.23 (m)	6.07 (m)	4.83 (m)	4.83 (m)	3.88	8.37 (s, H5)
16	$CONH_2$	CH_2OH	H	6.06 (3.8)	4.69 (t)	4.25 (t)	3.98 (m)	3.51 (m)	—	4.91 (s, CH_2OH), 7.93 (s), 7.58 (s, $CONH_2$)
26	CO_2CH_3	CH_3	H	5.92 (4.0)	4.78 (t)	4.22 (t)	3.95 (m)	3.48 (m)	3.85	2.56 (s, CH_3)
24*b*	$CO_2C_2H_5$	H	H	6.55 (3.7)	6.20 (m)	6.20 (m)	4.83 (m)	4.83 (m)	—	8.37 (s, H5), 4.43 (q, 2, OCH_2CH_3), 1.37 (t, 3, OCH_2CH_3)
25	CO_2CH_3	H	H	6.03 (4.0)	4.40 (t)	4.32–3.77 (m)		3.62 (m)	3.83	9.03 (s, H5)

[a]Spectra run using DMSO-d_6 as solvent unless otherwise indicated.
[b]Spectrum run using $CDCl_3$ as solvent.
[c]Assigned using JEOL TPJ-PFT 100 instrument.

Can. J. Chem. Downloaded from www.nrcresearchpress.com by 210.87.254.5 on 09/05/12
For personal use only.

TABLE 2. Nuclear Overhauser effects observed for **25** and **26**

Compound	Proton irradiated	Proton observed	Percent enhancement
25	H-1′	H-5	10.0
	H-2′	H-5	18.5
26	CH_3(at C5)	H-1′	16.5

usefulness of the 1,3-dipolar cycloaddition reaction for a quick entry into 5-membered heterocycles with varied functionality. It has also demonstrated that highly functionalized acetylenic derivatives such as methyl 4-hydroxy-2-butynoate (**11**) may be used successfully as dipolarphiles while still obtaining a high degree of regioselectivity in the cycloaddition reactions.

The synthesis of **2** and some closely related derivatives via an alternate route has recently been reported (41).

Experimental

Melting points were determined with a Thomas–Hoover capillary melting point apparatus and are uncorrected. The pmr spectra were recorded on Varian EM-360 and EM-390 spectrophotometers using DMSO-d_6 and $CDCl_3$ as solvents with tetramethylsilane as internal standard. Rotations were obtained with a Perkin–Elmer Model 141 digital readout polarimeter and were determined on samples dissolved in DMSO and having a concentration of 1 g/100 mL, unless otherwise stated. Thin layer chromatography (tlc) was carried out using glass plates precoated with a layer (0.25 mm) of Silicar 7GF silica gel as supplied by Analtech, Inc. ("Uniplate"). Compounds were detected using an ultraviolet lamp (Mineralight, 254 mm) or by spraying the tlc plates with 10% sulfuric acid in water (v/v) followed by heating at 120°C. Column chromatography was carried out using Silica Gel 60 F_{254} (70–230 mesh) as obtained from E. Merck, Darmstadt, West Germany. Columns were packed with dry silica gel and then eluted with one void volume of the eluting solvent before a concentrated solution of impure compound was applied to the top of the column. Elution was carried out using Solvent System A: (SSA) (chloroform–acetone, 19:1 (v/v)) unless otherwise noted. All concentrations of solutions were carried out, *in vacuo*, at 25–35°C unless otherwise noted. Solutions were dried over anhydrous sodium sulfate unless stated otherwise.

Nuclear Overhauser experiments were carried out using a JEOL TPJ-PFT 100 instrument and using an EC-100 data system. Compounds were dissolved in and then freeze dried from deuterium oxide (3 cycles) in order to replace exchangeable protons with deuterium. The deuterated compounds were then dissolved in DMSO-d_6 and deoxygenated by freezing under vacuum and thawing under a nitrogen atmosphere (3 cycles). The solutions (concentration, 5 mg in 0.5 mL DMSO) were then sealed in the nmr tubes while under vacuum.

Methyl 4-Hydroxy-2-butynoate (11)

Caution! Methyl 4-hydroxy-2-butynoate (**11**) is a potent vesicant which causes painful burns on contact with skin. All operations should be carried out in an efficient fume hood and gloves should be worn at all times.

Propargyl alcohol was converted into 1-(tetrahydropyran-2-yloxyprop-2-yne (**8**) in 78% yield using a published (42) general procedure. The THP-propargyl alcohol had a bp of 75–77°C (15–20 Torr), $n_D^{22°}$ = 1.4594 (lit. (20) bp 78°C (25 Torr, $n_D^{20°}$ = 1.4570); pmr (90 MHz, neat) δ: 4.63 (s, 1H, H-1′), 4.03 (d, 2H, C≡C—H, J = 1 Hz), 1.18–1.93 (br m, 6H, H-2′, H-4′).

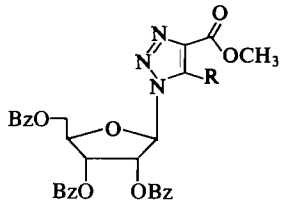
A solution of 280.4 g (2 *M*) of the THP-propargyl alcohol **8** in 2 L of dry tetrahydrofuran was added, dropwise, during 0.75 h to a stirred solution of ethylmagnesium bromide (2 *M*, purchased from Aldrich Chemical Company as a 3 *M* solution in diethyl ether) in diethyl ether (ca. 660 mL). Vigorous boiling and gas (C_2H_4) evolution took place during the addition. The solution was then stirred an additional 1.5 h at 25°C. The acetylenic Grignard reagent, **9**, was then added dropwise under a nitrogen atmosphere, to a vigorously stirred, cold (−10 to −15°C) solution of methyl chloroformate (275.2 g, 2.9 *M*) in 0.5 L of dry tetrahydrofuran during 2 h. The temperature was maintained at −10 to −15°C with continued mechanical stirring for another 0.5 h, and then was stirred at 0°C for an additional 1.5 h. The mixture was stored at +5°C for 18 h and then the supernatant was removed from the magnesium salts by filtration. The salts were washed with cold (0°C) toluene (3 × 300 mL), the filtrates were combined and concentrated, *in vacuo*, to ca. 1-L volume, and the dark-brown solution washed with saturated brine (5 × 200 mL). The solution was dried and concentrated *in vacuo* to remove the toluene. The residue was dissolved in anhydrous methanol (1.25 L), Dowex 50 (50 mL of H^+ form, prewashed with anhydrous methanol) was added, and the mixture stirred for 1.5 h at 25°C. The ion exchange resin was removed by filtration and the resin was then washed with anhydrous methanol (2 × 100 mL). The solvent and by-product (2-methoxytetrahydropyran) were removed by first using a water aspirator and then an oil pump at 0.5 Torr pressure. This residue was then treated a second time with anhydrous methanol (1 L) and Dowex 50 (50 mL) followed by concentration as described above. The dark, oily residue was distilled *in vacuo* through a Claison head to give **11** (147.8 g, 64.8%), bp 66–69°C/0.2 Torr, (lit. (20) bp 70°C/0.5 Torr), $n_D^{22°}$ = 1.4720; ir (neat): 3410 (strong, br, OH), 2240 (strong, C≡C), 1715 (strong, ester) cm^{-1}; pmr (DMSO-d_6) δ: 5.57 (t, 1H, OH), 4.31 (d, 2H, CH_2OH, J = 6 Hz), 3.79 (s, 3H, OCH_3). *Anal.* calcd. for $C_5H_6O_3$: C 52.63, H 5.30; found: C 52.67, H 5.46.

Methyl 5-Hydromethxyl-1-(2,3,5-tri-O-benzoyl-β-D-ribofuranosyl)-v-triazole-4-carboxylate (14) and Methyl 5-Carbomethoxy-4-hydroxymethyl-1-(2,3,5-tri-O-benzoyl-β-D-ribofuranosyl-v-triazole-4-carboxylate (15)

Crystalline 2,3,5-tri-*O*-benzoyl-β-D-ribofuranosyl azide (**27**) (**13**, 58.5 g, 0.12 *M*), methyl 4-hydroxy-2-butynoate (**11**, 13.7 g, 0.12 *M*), and 5 mL of toluene were heated and gently stirred at 50–55°C for 5 days. At the end of days 1, 2, and 3, additional amounts of **11** (1 mL each addition) were added. The temperature was raised to 70°C and heating was continued for an additional 2 days. After seven days, the azide could not be detected in the tlc. Methanol (134 mL) was added, the mixture was heated to boiling, cooled to 25°C, and the product allowed to stand for 3 days. The crystalline product was collected by filtration to give 46.6 g of product (mp 75–79°C). This solid was recrystallized once from ethanol to give the pure product **14** (needles), 43.1 g (59.8%), $[\alpha]_D^{22°}$ 30.2°, mp 87–89.5°C (bubbly, viscous melt). *Anal.* calcd. for $C_{31}H_{27}N_3O_{10}$: C 61.89, H 4.52, N 6.99; found: C 61.73, H 4.43, N 6.79. See Table 1 for pmr spectral data. The supernatants were combined and concentrated to give 38 g of a syrup which was chromatographed over silica gel (270 g) (column, 7 × 35 cm). Elution was carried out with SSA. The first liter of eluent was discarded and then 20-mL fractions were collected. Fractions 30–50 contained additional amounts of pure **14**, 11.05 g (15.3%, total yield 75.1%). Fractions 51–80 (17 g) contained the slower moving isomer **15** and were saved for rechromatography.

A portion (6.18 g) of the concentrates containing the slower moving isomer was rechromatographed over silica gel (270 g of

TABLE 3. Values[a] of R_f for certain 2′,3′,5′-tri-*O*-benzoylated *v*-triazole nucleosides



Compound number	R	SSA[b]		SSB[b]	
		R_f	R_f/R_f Std.	R_f	R_f/R_f Std.
14	CH_2OH	0.26	0.38	0.19	0.31
17	CH_2Cl	0.56	0.84	0.46	0.75
18	CHO	0.50	0.75	0.46	0.75
19	CH_2CN	0.42	0.63	0.30	0.49
20*a*	CH_3	0.49	0.73	0.36	0.59
20*b*	CH_2N_3	0.56	0.84	0.45	0.73
22	CHCNOH	0.25, 0.31	0.37, 0.46	0.22, 0.27	0.36, 0.44
23	CHCNCl	0.59	0.88	0.49	0.80
Standard[c]		0.67	—	0.61	—

[a]Chromatography was carried out using 20 cm × 5 cm glass plates coated with a 250 μm layer of silica gel 7GF as supplied by Analabs. Each spot contained 0.1 mg of compound applied as a solution in chloroform.
[b]SSA = Solvent system composed of chloroform–acetone, 19:1 (v/v). SSB was a mixture of benzene – ethyl acetate, 17:3 (v/v).
[c]1-*O*-Acetyl-2,3,5-tri-*O*-benzoyl-β-D-ribofuranose was used as the standard.

silica gel, column 7 cm × 35 cm). Elution was carried out using SSA and 17 mL fractions were collected. Fractions 35–45 contained the slower moving isomer **15**, 1.55 g, $[\alpha]_D^{25°}$ 20.1°. *Anal.* calcd. for $C_{31}H_{27}N_3O_{10}$: C 61.89, H 4.52, N 6.99; found: C 62.07, H 4.78, N 6.88.

5-Hydroxymethyl-1-(β-D-ribofuranosyl)-v-triazole-4-carboxamide (16)

A solution of **14** (3 g, 5.0 mmol) in 50 mL of methanolic ammonia (saturated at 0°C) was sealed in a pressure bottle at 25°C for 2 days. A single spot (R_f 0.3, $CHCl_3$–CH_3OH, 7:3, v/v) was observed with some difficulty by tlc since it absorbed uv light only very slightly, but the spot charred when it was sprayed with 10% H_2SO_4 and then heated. The solvent was removed *in vacuo* and the residue triturated repeatedly with anhydrous ether (5 × 40 mL) to give a white crystalline solid, 1.15 g (89.3%), mp 136–138°C. The solid was dissolved in 20 mL of boiling ethanol containing a few drops of water and the solution concentrated to 9 mL by boiling. The product (**16**) crystallized out of solution as white spears on cooling to room temperature, 1.08 g, mp 138.5–141°C; $[\alpha]_D^{25°}$ −82.6°. *Anal.* calcd. for $C_9H_{14}N_4O_6$: C 39.42, H 5.15, N 20.43; found: C 39.72, H 5.21, N 20.40.

Methyl 5-Formyl-1-(2,3,5-tri-O-benzoyl-β-D-ribofuranosyl)-v-triazole-4-carboxylate (18)

Activated (32) manganese dioxide (89 g) was suspended in 750 mL of boiling toluene and water was then removed using a Dean–Stark trap. Compound **14** (29.75 g, 49.5 mmol) was added and the mixture stirred and heated at reflux temperature for 3 h while removing water by azeotropic distillation. Another 30 g of manganese dioxide was added, and the mixture stirred and heated an additional 5 h with continued removal of water. The mixture was then filtered, while still hot, through a dry-packed bed of Celite (5 cm × 10 cm), and the filter-cake washed with hot acetone (5 × 100 mL). The filtrates were combined and concentrated *in vacuo* to yield a light yellow colored foam (**18**, 26.1 g, 87%) (one spot, tlc, SSA). A small sample (0.5 g) was chromatographed over silica gel (50 g) using SSA to yield 430 mg of a white foam; $[\alpha]_D^{25°}$ −31.0°. The aldehyde eventually crystallized on standing; white crystals, mp 185–186°C (ethyl acetate – ligroin, 1:5, v/v). *Anal.* calcd. for $C_{31}H_{25}N_3O_{10}$: C 62.10, H 4.20, N 7.01; found: C 61.94, H 4.13, N 6.86.

Methyl 5-(α-Cyano-α-hydroxymethyl)-1-(2,3,5-tri-O-benzoyl-β-D-ribofuranosyl)-v-triazole-4-carboxylate (22)

Unchromatographed methyl 5-formyl-1-(2,3,5-tri-*O*-benzoyl-β-D-ribofuranosyl)-*v*-triazole-4-carboxylate (**18**, 8.15 g, 13.5 mmol) was dissolved in 18 mL of methylene chloride, the solution was cooled to −50°C, and the flask and contents weighed. Liquid (34) hydrogen cyanide was added (ca. 1 mL) and weighing by differences indicated that 1.05 g (38.9 mmol) of HCN was present. The flask was tightly stoppered and allowed to stand at ambient temperature for 6.3 h when tlc indicated that only a trace of aldehyde was present. The cyanohydrin showed two spots (R_f 0.25 and 0.31, SSA) on tlc (diastereoisomeric mixture). The cyanohydrin was unstable on silica gel and if the tlc plates were allowed to stand for more than a few minutes before development, the amount of aldehyde in the mixture increased. Concentration *in vacuo* (**in the hood**) yielded a syrup which readily formed a white foam under oil pump vacuum, 8.47 g (99.4%). A sample was dissolved in chloroform and treated with a small amount of Norite. Filtration through dry-packed Celite and then concentration *in vacuo* yielded a white foam; $[\alpha]_D^{25°}$ 22.7°. *Anal.* calcd. for $C_{32}H_{26}N_4O_{10}$: C 61.34, H 4.18, N 8.94; found: C 61.24, H 4.19, N 8.67.

Methyl 5-(α-Chloro-α-cyanomethyl)-1-(2,3,5-tri-O-benzoyl-β-D-ribofuranosyl)-v-triazole-4-carboxylate (23)

The cyanohydrin **22** (8.26 g, 13.2 mmol) was dissolved in 42 mL of dry methylene chloride and then 1.43 mL of dry dimethylformamide and 1.42 mL of thionyl chloride were added in succession. The reaction mixture was allowed to stand in a sealed flask (25°C) for 4 h. Methanol (0.75 mL) was then added and the mixture allowed to stand for another hour at 25°C. The

Can. J. Chem. Downloaded from www.nrcresearchpress.com by 210.87.254.5 on 09/05/12
For personal use only.

Can. J. Chem. Downloaded from www.nrcresearchpress.com by 210.87.254.5 on 09/05/12
For personal use only.

solution was evaporated *in vacuo* and then co-evaporated twice with toluene (2 × 50 mL) followed by drying overnight, *in vacuo*. This syrup was then dissolved in ethyl acetate (200 mL) and washed in succession with water (50 mL), saturated aqueous sodium bicarbonate solution (2 × 20 mL), water (50 mL), and then saturated brine. The solution was dried and then concentrated *in vacuo* to yield a tan colored foam (8.14 g, 96%). The foam was dissolved in chloroform (12 mL) and applied to the top of a silica gel column (5 cm × 50 cm, 270 g of silica gel). The column was eluted with chloroform–acetone (24:1, v/v) and 18 mL fractions were collected. Fractions 70–85 contained the product (4.79 g, 56%). Concentration of fraction 75 yielded an analytical sample (540 mg) as a colorless foam; $[\alpha]_D^{25°}$ −23.1°. *Anal.* calcd. for $C_{32}H_{25}ClN_4O_9$: C 59.58, H 3.91, N 8.69, Cl 5.50; found: C 59.35, H 3.74, N 8.45, Cl 5.75.

*Methyl 5-Cyanomethyl-1-(2,3,5-tri-*O*-benzoyl-β-*D*-ribofuranosyl)-*v*-triazole-4-carboxylate (19)*

Method 1

The α-chloro-α-cyano derivative **23** (4.23 g, 6.56 mmol), 1.5 g of 5% Pd/C, ethyl acetate (75 mL), and triethylamine (1.0 mL, 7.16 mmol) were added in that order, while purging with nitrogen, to a hydrogenation flask. The mixture was stirred for 4.5 h, under a hydrogen atmosphere at ambient temperature and pressure. The solids were removed by filtration through dry-packed Celite (bed, 1.5 cm × 5 cm) and the filter-cake washed with ethyl acetate (3 × 10 mL). The filtrates were combined and washed in succession with 1% (v/v) aqueous hydrochloric acid (2 × 20 mL), water (15 mL), and then saturated brine (15 mL). After drying, the solvent was removed *in vacuo* to yield a light tan colored syrup, 3.82 g (95.5%). A small sample (500 mg) was chromatographed in the usual manner (SSA, silica gel) to yield a white foam (450 mg). *Anal.* calcd. for $C_{32}H_{26}N_4O_9$: C 63.02, H 4.29, N 9.18; found: C 63.01, H 4.41, N 8.86.

Method 2

Pure methyl 1-(2,3,5-tri-*O*-benzoyl-β-D-ribofuranosyl)-5-hydroxymethyl-*v*-triazole-4-carboxylate (**14**, 29.75 g, 49.5 mmol), 119 g of activated manganese dioxide, and 750 mL of toluene were heated at reflux temperature and with azeotropic removal of water as previously described. Workup as before yielded the aldehyde **18** as a light yellow foam (26.1 g, 87%). The crude aldehyde was treated, as previously described, with liquid hydrogen cyanide (3.6 g, 133 mmol) in methylene chloride for 3 h at 25°C. Concentration, *in vacuo*, gave the cyanohydrin **22** in the form of a pale yellow foam, 26.1 g. The crude cyanohydrin was then treated with 14.9 g (125 mmol) of thionyl chloride and 9 mL of DMF in 250 mL of methylene chloride to yield, after the usual washing and drying operations, 26.6 g of a brown foam. Chromatography over 469 g of silica gel (dry-packed and eluted using SSA) gave the pure α-chloro-α-cyanomethyl derivative (**23**, 18.4 g). This was then subjected to catalytic hydrogenation over 5% Pd/C (6 g) to yield 17.3 g of essentially pure (pmr, tlc) methyl 5-cyanomethyl-1-(2,3,5-tri-*O*-benzoyl-β-D-ribofuranosyl)-*v*-triazole-4-carboxylate (**19**) in an overall yield of 57.6% based on the starting methyl 5-hydroxymethyl-1-(2,3,5-tri-*O*-benzoyl-β-D-ribofuranosyl)-*v*-triazole-4-carboxylate (**14**).

*6-Amino-1-(β-D-ribofuranosyl)-*v*-triazolo[4,5-c]pyridin-4-one(8-aza-3-deazaguanosine) (2)*

Methyl 5-cyanomethyl-1-(2,3,5-tri-*O*-benzoyl-β-D-ribofuranosyl)-*v*-triazole-4-carboxylate (**19**, 16.8 g, 27.5 mmol) was dissolved in liquid ammonia (100 mL). The solution was sealed in a steel reaction vessel and allowed to stand at room temperature for 4 days. The ammonia was then allowed to evaporate and the residue was triturated with anhydrous ether (6 × 200 mL) to give a yellow-orange powder (8.7 g). This powder was triturated with acetone (8 × 50 mL) to give 7.8 g (100%) of crude product. A sample (1 g) of the product was dissolved in 1.03 *N* sodium hydroxide solution (3.90 mL) and the dark, purple solution was applied to the top of a glass column (2 cm × 35 cm) prepacked with Dowex 1 resin (formate form). The column was washed with 200 mL of water. The copumn was then eluted with dilute formic acid (0.05 *N*) with 23 mL fractions being collected. The progress of the chromatography was monitored by uv at 286.5 nm. Fractions 17–40 (550 mL) contained the product and were combined and concentrated, *in vacuo*, to ca. 6 mL of a clear, light violet solution. Ethanol (34 mL) was added to the solution which was then concentrated to ca. 20 mL by boiling. Ethanol (20 mL) was added again and the solution concentrated to 20 mL once more by boiling. The solution was slowly cooled to 25°C and the product separated out as a pale, purple colored powder that was washed with ethanol (4 × 5 mL) and then ethyl ether (2 × 5 mL). The dried solid weighed 283 mg (29.3% recovery), mp 239–241°C (vig. bubbling). Ultraviolet λ_{max} (pH 1): 286.5 nm (ε, 14 700); λ_{min} (pH 1): 245 nm (ε, 1 700); λ_{max} (MeOH): 287.5 nm (ε, 16 700); λ_{min} (MeOH): 245 nm (ε, 900); λ_{max} (pH 11): 230 nm (ε, 19 500), 286 (7 200), 314.5 (7 100); λ_{min} (pH 11): 256.5 nm (ε, 1 900), 298.5 (6 200). Proton magnetic resonance (DMSO-d_6) δ: 10.64 (br s, 1H, N—H), 6.10 (s, 2H, NH_2), 5.83 (d, 1H, H-1′, $J_{H-1',H-2'}$ = 5 Hz), 5.50 (s, 1H, H-7), 4.64 (t, 1H, H-2′), 4.20 (t, 1H, H-3′), 3.97 (q, 1H, H-4′), 3.48 (m, 2H, H-5′, 5″); $[\alpha]_D^{25°}$ −123.2°. *Anal.* calcd. for $C_{10}H_{13}N_5O_5$: C 42.40, H 4.63, N 24.73; found: C 42.64, H 4.54, N 24.76.

*Methyl 1-(2,3,5-Tri-*O*-benzoyl-β-D-ribofuranosyl)-5-chloromethyl-*v*-triazole-4-carboxylate (17)*

Dry DMF (4.0 mL) and thionyl chloride (4.0 mL) were added, in one portion, to a stirred solution of methyl 1-(2,3,5-tri-*O*-benzoyl-β-D-ribofuranosyl)-5-hydroxymethyl-*v*-triazole-4-carboxylate (**14**, 4.0 g, 6.65 mmol) in dry methylene chloride (200 mL). After 20 min, no starting material (R_f 0.2; SSA) was present as determined by tlc, instead a single new faster moving spot (R_f 0.6) had appeared. Methanol (4 mL) was added, dropwise, to the stirred solution (5 min) and the solution allowed to stir another 10 min. The solution was then washed in succession with ice-water (3 × 25 mL), saturated, aqueous sodium carbonate solution (20 mL), water (20 mL), and finally saturated brine (20 mL). The solution was dried (Na_2SO_4) and then concentrated *in vacuo* to afford a syrup (4.12 g, 100%) which did not crystallize even after a sample was purified by chromatography over silica gel (SSA). The compound (chromatographic sample) gave a strongly positive Beilstein test; $[\alpha]_D^{25°}$ −26.6°. *Anal.* calcd. for $C_{31}H_{26}ClN_3O_9$: C 60.05, H 4.23, N 6.78, Cl 5.72; found: C 59.97, H 4.22, N 6.56, Cl 5.91.

*Methyl 5-Methyl-1-(2,3,5-tri-*O*-benzoyl-β-D-ribofuranosyl)-*v*-triazole-4-carboxylate (20a)*

The chloromethyl derivative **17** (182 mg, 0.29 mmol) and triethylamine (100 μL) were added to a suspension of 5% Pd/C (182 mg) in ethyl acetate (5 mL). The mixture was stirred under an atmosphere of hydrogen for 20 h and then filtered through a dry-packed bed of Celite. The filter-cake was washed with small portions of ethyl acetate (3 × 4 mL), the filtrates were then combined and concentrated to give a mass of white needles. These needles were recrystallized from ethanol (4 mL) to give 91 mg (53.6%) of **20***a* as white needles, mp 106–108°C, $[\alpha]_D^{25°}$ −25.4°. *Anal.* calcd. for $C_{31}H_{27}N_3O_9$: C 63.36, H 4.65, N 7.17; found: C 63.16, H 4.43, N 6.99.

*Methyl 5-Methyl-1-(β-D-ribofuranosyl)-*v*-triazole-4-carboxylate (26)*

The tri-*O*-benzoyl derivative **20***a* (900 mg, 1.54 mmol) was suspended in dry methanol (30 mL). A solution of sodium methoxide (2 mL of a 1.0 *N* solution) was added to this suspension and the mixture heated at reflux temperature for 5 min. The

Can. J. Chem. Downloaded from www.nrcresearchpress.com by 210.87.254.5 on 09/05/12
For personal use only.

solution was cooled to room temperature and Dowex 50 (H^+ form, prewashed with methanol) was then added, portionwise (about 1 mL required), until the "pH" was ca. 5. The resin was removed by filtration and washed with methanol (4 mL). The supernatant was concentrated *in vacuo* and the residue triturated with diethyl ether (3 × 20 mL) to remove methyl benzoate. The remaining residue was recrystallized from ethyl acetate (8 mL) to yield pure **26**, 185 mg (44%), mp 125–127°C. *Anal.* calcd. for $C_{10}H_{25}N_3O_6$: C 43.96, H 5.53, N 15.38; found: C 43.77, H 5.56, N 15.45.

*Methyl 5-Azidomethyl-1-(2,3,5-tri-*O*-benzoyl- β-*D*-ribofuranosyl)-*v*-triazole-4-carboxylate (**20**b)*

Powdered sodium azide (1.0 g, dried 18 h/25°C/0.1 Torr) was added to a stirred solution of the chloromethyl derivative **17** (3.2 g, 5.16 mmol) in dry DMF (20 mL) and stirring was continued for an additional 4 h at 25°C. Thin layer chromatography (SSA) indicated that the reaction was probably complete at this time since the grey-black spot of starting material had been replaced by a yellow-orange spot with the same R_f (detection: 10% sulfuric acid, 110°C). The mixture was stirred an additional 1.5 h at 70°C, allowed to stand at room temperature without stirring for 18 h, and then evaporated to dryness. The residue was dissolved in ethyl acetate (50 mL) and washed with saturated brine, dried, and evaporated to dryness to yield 2.82 g (88%) of a yellow syrup. The syrup was chromatographed using SSA (silica gel column, 5 cm × 35 cm) with 23 mL fractions being collected. Fraction 17 contained a single spot (630 mg) and was used to obtain an analytical sample as a pale yellow foam. Fractions 16, 18–23 were combined (to yield 1.14 g) and were nearly as pure as fraction 17. However, these combined fractions did contain a trace of a slower moving spot. *Anal.* calcd. for $C_{31}H_{26}N_6O_9$: C 59.42, H 4.18, N 13.41; found: C 59.60, H 4.27, N 13.17.

*Methyl 1-(2,3,5-Tri-*O*-benzoyl-β-*D*-ribofuranosyl)-5-carboxy-*v*-triazole-4-carboxylate (**21**)*

Methyl 5-hydroxymethyl-1-(2,3,5-tri-*O*-benzoyl-β-D-ribofuranosyl)-*v*-triazole-4-carboxylate (**14**, 1.5 g, 2.5 mmol) was dissolved in acetone (120 mL). This solution was stirred and cooled at 10–15°C while 2.5 mL of Jones reagent (35) was added over a period of 2 h. A small amount of the aldehyde intermediate (**18**) could still be detected so the solution was cooled to 0°C and an additional 0.2 mL of Jones reagent was added and the mixture stirred for another hour at 0°C. Isopropanol (0.5 mL) was then added and stirring was continued until the yellow color of dichromate ion was discharged (about 1 min). Water (150 mL) was added and then the solution was concentrated (25°C) to ca. 150 mL. The product was isolated by extraction with ether (3 × 100 mL). The extracts were combined and washed in succession with 0.1 *N* aqueous hydrochloric acid (2 × 40 mL), water (2 × 40 mL), and then saturated brine (2 × 40 mL). This solution was dried and then evaporated to give a green colored gum. This gum was triturated with 49:1 water – acetic acid (400 mL, v/v) to give a powdery solid. Repetition of this procedure using 97:3 water – acetic acid (400 mL, v/v) furnished 1.34 g (87%) of a white powder. The pmr spectra (see Table 1) of crude and chromatographed samples showed considerable line broadening suggesting the presence of some inorganic (Mn^{2+}) ion. The ir spectrum ($CHCl_3$ smear) displayed a moderate absorption at 2638 cm^{-1} indicating the presence of a carboxylic acid group (OH bonded). This product was not characterized but used without further purification for decarboxylation.

*Ethyl 1-(2,3,5-Tri-*O*-benzoyl-β-*D*-ribofuranosyl)-*v*-triazole-4-carboxylate (**24**b) and Methyl 1-(2,3,5-Tri-*O*-benzoyl-β-*D*-ribofuranosyl)-*v*-triazole-4-carboxylate (**24**a)*

The crude carboxylic acid (**21**, 1.0 g, 1.63 mmol) was dissolved in toluene (50 mL) and heated at reflux temperature for 26 h. The solution was filtered and the filtrate was evaporated to afford a solid residue. This solid was triturated with ethanol (7 mL) and then collected by filtration to afford 602 mg (64.8%) of **24***b*; mp 171–174°C. One recrystallization from ethanol (30 mL) gave pure **24***b* (518 mg); mp 175–176.5°C. *Anal.* calcd. for $C_{31}H_{27}N_3O_9$: C 63.58, H 4.65, N 7.18; found: C 63.30, H 4.60, N 7.22.

Decarboxylation was carried out on a 1.0 g (1.63 mmol) sample of crude **21**. However, the product from this reaction was recrystallized from methanol (50 mL) to give 602 mg (64.8%) of **24***a* as white crystals; mp 191–193.5°C (lit. (17) mp 195°C). Further recrystallization from methanol did not raise the mp; $[\alpha]_D^{25°}$ −74.3° (*c* 1.0, $CHCl_3$) (lit. (17) $[\alpha]_D$ −73.7° (*c* 0.55, $CHCl_3$)); $[\alpha]_D^{25°}$ −58.7° (*c* 1.0, DMSO). The pmr spectral data (Table 1) was nearly identical to that previously reported (17) for **24***a*. *Anal.* calcd. for $C_{30}H_{25}N_3O_9$: C 63.04, H 4.41, N 7.35; found: C 63.06, H 4.54, N 7.25.

*Methyl 1-(β-D-Ribofuranosyl)-v-triazole-4-carboxylate (**25**)*

The tri-*O*-benzoyl derivative **24***a* (493.8 mg, 0.864 mmol) was deblocked with sodium methoxide and methanol using the same procedure as used for the preparation of **26**. The crude product weighed 200 mg (89%) and had a mp of 147–150°C. Recrystallization from ethyl acetate (10 mL) containing a few drops of methanol gave a pure product in the form of white needles, 164 mg (73%); mp 150–151.5°C (lit (37) mp 151–153°C); $[\alpha]_D^{25°}$ −80.5°. *Anal.* calcd. for $C_9H_{13}N_3O_6$: C 41.79, H 5.07, N 16.22; found: C 41.89, H 5.13, N 16.39.

Acknowledgements

The authors wish to thank Drs. C. Whitehead, A. F. Lewis, B. Clough, and J. Kobe for their many useful discussions and suggestions. Indeed, we are particularly indebted to Dr. J. Kobe for his patience and assistance in setting up the nOe experiments. We gratefully acknowledge the support of the NCI for research contract NCI-CM-77142 which supported this work.

1. K. Anzai and S. Suzuki. J. Antibiot. Ser. A, **14**, 253 (1961).
2. G. W. Kidder and V. C. Dewey. J. Biol. Chem. **179**, 181 (1949).
3. J. Davoll. J. Chem. Soc. 1593 (1958).
4. W. Hutzenlaub, R. L. Tolman, and R. K. Robins. J. Med. Chem. **15**, 879 (1972).
5. P. D. Cook, R. J. Rousseau, A. M. Mian, P. Dea, R. B. Meyers, Jr., and R. K. Robins. J. Am. Chem. Soc. **98**, 1492 (1976).
6. (*a*) B. L. Cline, R. P. Panzica, and L. B. Townsend. Proc. Utah Acad. Sci. Arts Lett. **52** (Part 1), 79 (1975); (*b*) B. L. Cline, R. P. Panzica, and L. B. Townsend. J. Heterocycl. Chem. **13**, 1365 (1976); (*b*) B. L. Cline, R. P. Panzica, and L. B. Townsend. J. Heterocycl. Chem. **15**, 839 (1978).
7. (*a*) B. L. Cline, R. P. Panzica, and L. B. Townsend. J. Heterocycl. Chem. **13**, 1365 (1976); (*b*) B. L. Cline, R. P. Panzica, and L. B. Townsend. J. Org. Chem. **43**, 4910 (1978).
8. G. R. Revankar, R. K. Robins, and R. L. Tolman. J. Org. Chem. **39**, 1256 (1974).
9. G. R. Revankar and R. K. Robins. Ann. N.Y. Acad. Sci. **255**, 166 (1975).
10. J. A. Montgomery, R. D. Elliott, and H. J. Thomas.

Ann. N.Y. Acad. Sci. **255**, 292 (1975), and references cited therein.
11. P. D. Cook, L. B. Allen, D. G. Streeter, J. H. Huffman, R. W. Sidwell, and R. K. Robins. J. Med. Chem. **21**, 1212 (1978).
12. L. B. Townsend, B. L. Cline, R. P. Panzica, P. E. Fagerness, L. W. Roti Roti, J. D. Stoeckler, G. W. Crabtree, and R. E. Parks, Jr. *In* Synthesis and studies on the structure–activity relationships of certain aza, deaza and aza/deaza guanine and guanosine analogs. Vol. IV. *Edited by* R. N. Castle and I. Lalezari. Hetero-Corporation, Orem, UT. 1978. p. S-92.
13. R. A. Earl, J. Kobe, and L. B. Townsend. Submitted.
14. R. J. Rousseau and R. K. Robins. J. Heterocycl. Chem. **2**, 196 (1965).
15. S. W. Schneller and R. S. Hosmane. J. Org. Chem. **43**, 4487 (1978).
16. J. A. May and L. B. Townsend. J. Org. Chem. **41**, 1449 (1976).
17. G. Alonso, M. T. Garcia-Lopez, G. Garcia-Munoz, R. Madronero, and M. Rico. J. Heterocycl. Chem. **7**, 1269 (1970).
18. R. E. Harmon, R. A. Earl, and S. K. Gupta. J. Org. Chem. **36**, 2553 (1971).
19. R. L. Tolman, C. W. Smith, and R. K. Robins. J. Am. Chem. Soc. **94**, 2530 (1972).
20. H. B. Henbest, E. R. H. Jones, and I. M. S. Walls. J. Chem. Soc. 3646 (1950).
21. R. A. Earl and L. B. Townsend. Org. Synth. Submitted.
22. R. Beier and B. P. Mundy. Synth. Commun. **9**, 271 (1979).
23. C. S. L. Baker, P. D. Landor, S. R. Landor, and A. N. Patel. J. Chem. Soc. 4348 (1965).
24. (*a*) W. S. Johnson and T. K. Schaff. J. Chem. Soc. Chem. Commun. 611 (1969); (*b*) W. S. Johnson and L. A. Bunes. J. Am. Chem. Soc. **98**, 5600 (1976); (*c*) M. S. Newman and J. H. Wotiz. J. Am. Chem. Soc. **71**, 1292 (1949).
25. (*a*) J. P. H. Verheyden and J. G. Moffatt. J. Org. Chem. **35**, 2319 (1970); (*b*) R. Scheffold and E. Saladin. Angew. Chem. Int. Ed. Engl. **11**, 229 (1972).
26. (*a*) G. Eglinton and M. C. Whiting. J. Chem. Soc. 3650 (1950); (*b*) R. A. Earl and R. E. Harmon. J. Med. Chem. **9**, 776 (1966).
27. J. Baddiley, J. G. Buchanan, R. Hodges, and J. F. Prescott. J. Chem. Soc. 4769 (1957).
28. L. B. Townsend. *In* Synthetic procedures in nucleic acid chemistry. Vol. 2. *Edited by* W. W. Zorbach and R. S. Tipson. Wiley-Interscience, New York. 1973. p. 267.
29. (*a*) G. R. Revankar and L. B. Townsend. J. Heterocycl. Chem. **7**, 1329 (1970); (*b*) M. P. Schweizer, E. B. Banta, J. T. Witkowski, and R. K. Robins. J. Am. Chem. Soc. **95**, 3770 (1973); (*c*) G. P. Kreishman, J. T. Witkowski, R. K. Robins, and M. P. Schweizer. J. Am. Chem. Soc. **94**, 5894 (1972); (*d*) S. R. Naik, J. T. Witkowski, and R. K. Robins. J. Heterocycl. Chem. **11**, 57 (1974); (*e*) P. Dea, G. R. Revankar, R. L. Tolman, M. P. Schweizer, and R. K. Robins. J. Org. Chem. **39**, 3226 (1974).
30. F. L. Cook, C. W. Bowers, and C. L. Liotta. J. Org. Chem. **39**, 3416 (1974).
31. A. J. Fatiadi. Synthesis, 65 (1976), and ref. 30 contained therein.
32. J. Attenburrow, A. F. B. Cameron, J. H. Chapman, R. M. Evans, B. A. Hems, A. B. A. Jansen, and T. Walker. J. Chem. Soc. 1094 (1952).
33. A. Ercoli and P. de Ruggieri. J. Am. Chem. Soc. **75**, 650 (1953).
34. K. Ziegler. *In* Organic syntheses. Coll. Vol. 1. *Edited by* H. Gilman and A. H. Blatt. John Wiley and Sons, Inc., New York. 1941. p. 314.
35. C. Djerassi, R. R. Engle, and A. Bowers. J. Org. Chem. **21**, 1547 (1956), and references therein.
36. J. Elguero, E. Gonzalez, and R. Jacquier. Bull. Soc. Chim. Fr. 2998 (1967).
37. T. C. Thurber and L. B. Townsend. J. Org. Chem. **41**, 1041 (1976).
38. J. H. Noggle and R. E. Schirmer. The nuclear Overhauser effect. Academic Press, New York. 1971.
39. J. Kobe and J. C. Valdes. Carbohydr. Res. **65**, 278 (1978).
40. R. Huisgen. Angew. Chem. Int. Ed. Engl. **2**, 565 (1963).
41. R. B. Meyer, Jr., G. R. Revankar, P. D. Cook, K. W. Ehler, M. P. Schweizer, and R. K. Robins. J. Heterocycl. Chem. **17**, 159 (1980).
42. D. N. Robertson. J. Org. Chem. **25**, 931 (1960).

Can. J. Chem. Downloaded from www.nrcresearchpress.com by 210.87.254.5 on 09/05/12
For personal use only.

A mild, general preparation of *N*-acyl aziridines and 2-substituted 4(*S*)-benzyloxazolines

GORDON S. BATES[1] AND MICHAEL A. VARELAS[2]

Department of Chemistry, University of British Columbia, Vancouver, B.C., Canada V6T 1Y6

Received July 2, 1980

This paper is dedicated to Prof. Raymond U. Lemieux on the occasion of his 60th birthday

GORDON S. BATES and MICHAEL A. VARELAS. Can. J. Chem. **58**, 2562 (1980).

The conversion of a wide range of carboxylic acids into their acyl imidazolides with subsequent addition of an aziridine rapidly gives a quantitative yield of the corresponding *N*-acyl aziridines.

Iodide (or bromide) ion catalysed rearrangement of *N*-acyl 2(*S*)-benzylaziridines **1** to oxazolines **6** proceeds quantitatively.

GORDON S. BATES et MICHAEL A. VARELAS. Can. J. Chem. **58**, 2562 (1980).

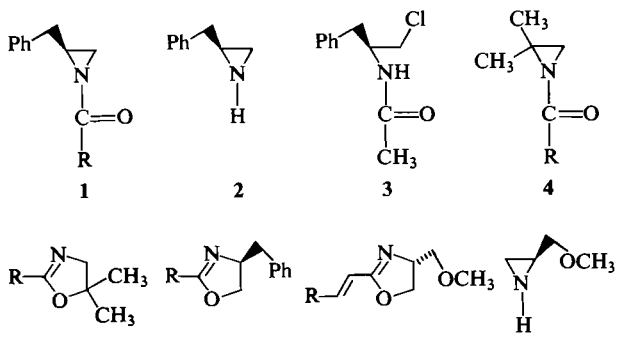
La transformation d'une grande variété d'acides carboxyliques en leurs dérivés imidazolures d'acyles, suivie de l'addition d'une aziridine, donne rapidement et quantitativement les *N*-acyl-aziridines correspondantes. L'ion iodure (ou bromure) catalyse la transposition des *N*-acyl-*S*-benzyl-2 aziridines **1** en oxazolines **6** avec un rendement quantitatif.

[Traduit par le journal]

In connection with another project in our laboratory, we required a convenient, high yielding synthesis of a variety of *N*-acyl 2(*S*)-benzylaziridines (**1**). The reaction of an aziridine with a ketene or an acyl halide (1) and, more recently, condensation with a carboxylic acid in the presence of dicyclohexylcarbodiimide (2) are routes to the formation of *N*-acyl aziridines. However, the lack of generality, potential racemization of centres located α to the carbonyl of the acyl group, and the sluggishness of the reaction in the case of the carbodiimide coupling process are among the drawbacks to the synthetic utility of these existing methods.

We observed while carrying out preliminary investigations of the reaction between the sodium salt of 2(*S*)-benzylaziridine (**2**) and various acetylating agents that in contrast to reactions with acetic anhydride, which cleanly yielded the expected *N*-acetyl aziridine (**1**, R = CH_3), reaction of this salt with acetyl chloride gave a mixture of chlorine-containing compounds. This latter material, which consisted mainly of compound **3**, is presumably derived from nucleophilic opening by chloride of the initially formed *N*-acetyl aziridine. A compound which is at least as reactive as an anhydride but which possesses an essentially neutral, and thus poorly nucleophilic, leaving group appeared to be the desired general acylating reagent. Acyl imidazolides ideally fit both criteria and in addition are readily available from carboxylic acids.

We wish to report that conversion of a carboxylic acid into its acyl imidazolide (3) using 1,1′-carbonyldiimidazole with subsequent addition of one equivalent of an aziridine rapidly gives a quantitative yield of the corresponding *N*-acyl aziridine. This route is general and is applicable to very hindered carboxylic acids as well as to systems for which the acyl chloride is very unstable (e.g. formyl). As mentioned above, our main interest involved derivatives of aziridine **2**. This compound, which is stable for months when stored on a few pellets of potassium hydroxide in a refrigerator, was prepared by a Wenker cyclization (4) of 2(*S*)-amino-3-phenylpropan-1-ol (5). Formation of the desired *N*-acyl aziridines (**1**) proceeded rapidly and quantitatively with a wide variety of carboxylic acids (see Table 1). This method is also applicable to other aziridines. For instance, a quantitative condensation has been carried out between 2,2-dimethylaziridine (6) and the acyl imidazolides of the following carboxylic acids: acetic, propionic, isobutyric, pivalic, and nicotinic. The resulting acyl aziridines **4** may be cleanly rearranged in good yields under acidic conditions to oxazolines **5** using existing methods (2). This new technique is, however, superior to the carbodiimide coupling process



SCHEME 1

[1]Author to whom correspondence should be addressed.

[2]Research Assistant, summer 1979.

0008-4042/80/232562-05$01.00/0

©1980 National Research Council of Canada/Conseil national de recherches du Canada

Can. J. Chem. Downloaded from www.nrcresearchpress.com by 210.87.254.6 on 09/05/12
For personal use only.

Can. J. Chem. Downloaded from www.nrcresearchpress.com by 210.87.254.6 on 09/05/12
For personal use only.

TABLE 1. Optical rotations for compounds **1** and **6**[a,b]

R	$[\alpha]_D^{24}$ ($c \sim 2.0$, $CHCl_3$)	
	Acyl aziridine **1**	Oxazoline **6**
H-	+22.0	−89.4
CH_3-	+59.7	−50.7
C_2H_5-	+61.3	−37.0
$(CH_3)_2CH$-	+66.4	−34.2
$(CH_3)_3C$-	+96.2	−38.2
c-C_6H_{11}-	+39.8	−13.0
C_6H_5-	+49.4	+4.7
3-Pyridyl-	+69.2	−4.3
E-C_3H_5-	+84.6	−52.5
E,E-C_5H_7-	+68.4	−51.8

[a]All compounds had ^{1}H nmr, ir, elemental analysis, and exact parent mass spectrum measurements fully consistent with the proposed structures.
[b]All compounds were formed in >98% yield from the carboxylic acid.

(2) mentioned above, being both faster (2 h vs. 16 h) and higher yielding (100% vs. 50% in the case of the nicotinic derivative).

Our initial observations of a chloride-promoted isomerization suggested that the well-known rearrangement of certain *N*-acyl aziridines (7) should also be possible with the benzylaziridine system **1**. If compound **1** could be isomerized to the corresponding oxazoline **6**, one would have a useful protecting group for carboxylic acids which incorporates a chromophore for use as a chromatographic marker. In addition to many other potential applications (8), such a system may also be useful as a resolving agent for racemic modifications of chiral carboxylic acids (9). Indeed, we found that a quantitative isomerization to the desired oxazoline could be achieved by briefly refluxing a solution of the acyl aziridine in the presence of a catalytic amount of tetrabutylammonium iodide (10) or bromide.

Although the method described above may not be used *directly* for crotonic acid derivatives, since reaction of crotonic acid with 1,1′-carbonyldiimidazole yields a mixture whose ^{1}Hmr spectrum is consistent with the main product being 3-(1-imidazole)-butanoyl imidazolide, the route may be adapted to such compounds. Reaction of crotonyl chloride with one equivalent of **2** at low temperature in the presence of triethylamine gave the *N*-crotonyl aziridine which could be smoothly rearranged to the corresponding oxazoline with no loss of stereochemistry in the side chain. This transformation is important in light of a recent report (11) of the use of chiral oxazolines **7** in the synthesis of highly optically active (~96% ee) 3-substituted alkanoic acids. Since the methodology described in the present paper appears to be general, and as *O*-methyl serine is available in optically pure form (12), we propose our route as a convenient alternative synthesis of compounds **7** via aziridine **8**.

Other workers have shown that hydrolysis of oxazolines to the carboxylic acids (esters) proceeds with little exchange of any protons α to the carboxyl function (13). We have prepared α-deuterated *iso*-butyric acid by repeated quenching of the dianion of this acid with D_2O. A level of 95% deuterium incorporation was achieved after three treatments. The labelled acid was then converted into its chiral oxazoline using the imidazolide route. Mass spectral and ^{1}Hmr measurements showed no loss of deuterium in the product. Thus, the method described in this paper is suitable even for protection of chiral carboxylic acids containing an epimerizable centre since there is little potential for loss of chirality at centres located α to the carbonyl of the original acyl group. The 2(*S*)-amino-3-phenylpropan-1-ol obtained after acidic hydrolysis (13) of oxazolines **6** may be recovered (ca. 85%) and used for recycling to aziridine **2**. There is no difference in the specific rotation of this recovered material and that of the original amino alcohol.

The overall transformation of a carboxylic acid into oxazoline **6** may thus be conveniently carried out in a few hours in a "one pot" reaction to provide an essentially pure product in almost quantitative yield. A variety of solvents including tetrahydrofuran, chloroform, and benzene may be used for the reaction with no change in the yield.

Experimental

General

All reactions were carried out under a nitrogen or argon atmosphere. Stirring was accomplished using Teflon-coated magnetic stirring bars. Tetrahydrofuran was freshly distilled from sodium benzophenone ketyl under a nitrogen atmosphere. All reagents were obtained from the Aldrich Chemical Company, Inc. and were used without further purification.

Melting points were taken on a Gallenkamp melting point apparatus and are uncorrected. Proton magnetic resonance spectra were obtained on Varian Associates T-60 and HA-100 spectrometers. Spectra were run in deuteriochloroform solution with tetramethylsilane as an internal reference. The multiplicity, integrated peak area, and coupling constants (Hz) (if observable) are indicated in parentheses after each signal. Infrared spectra were recorded in chloroform solution using a Perkin-Elmer 700 spectrometer, and were calibrated with the 1601 cm^{-1} band of polystyrene. High resolution mass spectra were obtained using an AEI MS-50 mass spectrometer. Specific rotations were obtained in chloroform solution unless otherwise stated and were determined using a Perkin-Elmer 241 MC polarimeter which was calibrated using a standardized sucrose solution. Elemental analyses were performed at the Microanalytical Laboratory, University of British Columbia.

The following abbreviations are used: THF = tetrahydrofu-

Can. J. Chem. Downloaded from www.nrcresearchpress.com by 210.87.254.6 on 09/05/12
For personal use only.

ran, Et = C_2H_5, EtOAc = ethyl acetate, EtOH = ethanol, Et_2O = ethyl ether, b = broad, s = singlet, d = doublet, t = triplet, q = quartet, s = septet, m = multiplet.

2(S)-Amino-3-phenylpropan-1-ol

To a solution of 33.0 g (200 mmol) of L-phenylalanine ($[\alpha]_D^{24}$ −34.7, *c* 1.9 H_2O) dissolved in 800 mL of absolute EtOH was slowly added 32.7 g (275 mmol) of $SOCl_2$. The solution was then refluxed for 4 h. The reaction mixture was cooled to room temperature and the solvent and excess $SOCl_2$ were then evaporated. The crude ethyl ester hydrochloride was dissolved in 500 mL of 50% aqueous EtOH and added slowly (initial hydrogen evolution) to 37.8 g (1.0 mol) of $NaBH_4$ dissolved in 500 mL of 50% aqueous EtOH. The reaction mixture was then refluxed for 4 h, cooled to room temperature, and the bulk of the EtOH evaporated. The residual aqueous phase was saturated with solid NaCl and extracted with 3 × 500 mL of EtOAc. Occasionally a precipitate of borate ester was observed. Hydrolysis of this ester with aqueous 2 *N* NaOH released the amino alcohol. The aqueous mixture was extracted with additional EtOAc and this extract was combined with the bulk extract above. The organic phase was dried over anhydrous $MgSO_4$ and evaporated to yield 29 g (96%) of essentially pure 2(*S*)-amino-3-phenylpropan-1-ol. Recrystallization from EtOAc–hexane yielded fine white needles, mp 89–91°C; ^{1}Hmr δ: 2.20 (bs, ca. 3), 2.46 (dd, 1, *J* = 8.0, 16.0), 2.75 (dd, 1, *J* = 5.0, 16.0), 2.95–3.20 (m, 1), 3.21–3.50 (m, 1), 3.60 (dd, 1, *J* = 4.0. 12.0), 7.20 (m, 5); $[\alpha]_D^{24}$ −25.8 (*c* 2.2); *Anal.* calcd. for $C_9H_{13}NO$ (151.21): C 71.49, H 8.67, N 9.26; found: C 71.59, H 8.82, N 9.12. *Mol. Wt.* calcd. for $C_9H_{13}NO$: 151.0997; found: 151.0999.

2(S)-Benzylaziridine **2**

A solution of 15.1 g (10.0 mmol) of 2(*S*)-amino-3-phenylpropan-1-ol in 6.0 mL (12 mmol) of aqueous 2 *M* H_2SO_4 was evaporated on a rotary evaporator (50°C, 10 Torr). The salt was then heated at 140°C for 3 h at 0.1 Torr to complete formation of the hydrogen sulphate. The reaction mixture was cooled to room temperature and 25 mL (50 mmol) of aqueous 2 *N* NaOH was added to the crude hydrogen sulphate. The mixture was then distilled at atmospheric pressure. The distillate was collected in an ice-cooled flask containing 50 mL of Et_2O and a few mL of aqueous 2 *N* NaOH. A little water was occasionally added to the distillation flask whenever the residue began to crystallize. When the distillate no longer had a milky appearance, the Et_2O was separated and the aqueous phase was saturated with solid NaCl. The aqueous phase was extracted with 3 × 50 mL of Et_2O. The combined Et_2O extract was dried over anhydrous $MgSO_4$ and evaporated. The residue was subjected to a Kugelrohr distillation (air bath 80°C, 1 Torr) from a pellet of NaOH to yield 9.5 g (73%) of colourless aziridine. The product was stored on a few pellets of KOH in a refrigerator; ir: 3350 cm^{-1}; ^{1}Hmr δ: 1.38 (d, 1, *J* = 3.5), 1.75 (d, 1, *J* = 6.0), 2.04–2.30 (m, 1), 2.62 (dd, 1, *J* = 15.0, 5.0), 2.78 (dd, 1, *J* = 15.0, 6.0), 7.25 (s, 5); $[\alpha]_D^{24}$ −9.8 (*c* 1.95); *Anal.* calcd. for $C_9H_{11}N$ (133.20): C 81.16, H 8.32, N 10.52; found: C 81.11, H 8.45, N 10.22. *Mol. Wt.* calcd. for $C_9H_{11}N$: 133.0891; found: 133.0888.

Acetylation of the Sodium Salt of 2(S)-Benzylaziridine
With Acetic Anhydride

To a suspension of 24 mg (1 mmol) of pentane-washed NaH in 2 mL of THF was added 133 mg (1 mmol) of aziridine **2**. After 10 min at room temperature, 102 mg (1 mmol) of acetic anhydride was added and the reaction mixture was stirred at room temperature for 1 h. The reaction mixture was then poured into Et_2O and washed with H_2O. The Et_2O layer was dried with anhydrous $MgSO_4$ and evaporated to yield 170 mg (97%) of (+)-1-(acetyl)-2(*S*)-benzylaziridine. The spectral data of this compound are described below and are identical to those of the compound prepared via the imidazolide route.

With Acetyl Chloride

A procedure identical to the above was carried out except that acetyl chloride was substituted for acetic anhydride. Workup of the reaction yielded a mixture of several compounds, none of which was the *N*-acetyl aziridine isolated above. Purification of the mixture by thin-layer chromatography yielded the major component (ca. 50%) of the mixture which was identified as compound **3**; ir: 1660 cm^{-1}; ^{1}Hmr δ: 1.90 (s, 3), 2.90 (d, 2, *J* = 8.0), 3.45 (dd, 1, *J* = 4.0, 11.0), 3.58 (dd, 1, *J* = 5.0, 11.0), 4.1–4.6 (m, 1), 5.6–6.0 (bs, 1), 7.25 (s, 5); $[\alpha]_D^{25}$ 3.86 (*c* 1.2); *Anal.* calcd. for $C_{11}H_{14}NOCl$ (211.70): C 62.41, H 6.67, N 6.62, Cl 16.75; found: C 62.13, H 6.50, N 6.44, Cl 16.54. *Mol. Wt.* calcd. for $C_{11}H_{14}NOCl^{35}$: 211.0764; found: 211. 0777.

General Procedure for Preparation of Compounds 1 and 6

To a solution of 10 mmol of carboxylic acid in 10 mL of THF was added 1.62 g (10 mmol) of 1,1′-carbonyldiimidazole in several portions over 5 min. The solution was stirred at room temperature for 30 min (2 h for hindered carboxylic acids) and then 10 mmol of **2** was added. The reaction mixture was then stirred at room temperature for an additional 1 h (2 h for hindered acyl imidazolides). If the *N*-acyl aziridine was the desired product, the reaction mixture was then diluted with Et_2O and the mixture washed with H_2O to remove imidazole. The organic phase was dried over anhydrous $MgSO_4$ and evaporated to yield the *N*-acyl aziridine. If the chiral oxazoline was the desired product, then ca. 180 mg (0.5 mmol) of tetrabutylammonium iodide (or bromide) was added to the *N*-acyl aziridine – imidazole mixture and the reaction mixture was refluxed for 2.5 h. After the reaction mixture had been cooled to room temperature, it was diluted with Et_2O and washed with H_2O. The solvent was dried over anhydrous $MgSO_4$ and was evaporated to provide a 100% yield of material which was generally >98% pure by gas–liquid chromatographic analysis.

(+)-1-(Formyl)-2(S)-benzylaziridine

Infrared: 1690 cm^{-1}; ^{1}Hmr δ: 2.12 (d, 1, *J* = 3.0), 2.46 (d, 1, *J* = 5.0), 2.62–3.05 (m, 3), 7.3 (s, 5), 8.65 (s, 1); $[\alpha]_D^{24}$ 22.0 (*c* 2.13); *Anal.* calcd. for $C_{10}H_{11}NO$ (161.21): C 74.51, H 6.88, N 8.69; found: C 74.40, H 7.00, N 8.70. *Mol. Wt.* calcd. for $C_{10}H_{11}NO$: 161. 0841; found: 161.0844.

(+)-1-(Acetyl)-2(S)-benzylaziridine

Infrared: 1690 cm^{-1}; ^{1}Hmr δ: 1.90 (s, 3), 2.02 (d, 1, *J* = 3.0), 2.35 (d, 1, *J* = 5.4), 2.45–2.70 (m, 1), 2.78 (d, 1, *J* = 6.0), 2.79 (d, 1, *J* = 7.0), 7.25 (s, 5); $[\alpha]_D^{24}$ 59.7 (*c* 2.30); *Anal.* calcd. for $C_{11}H_{13}NO$ (175.23): C 75.40, H 7.48, N 7.99; found: C 75.47, H 7.40, N 7.90. *Mol. Wt.* calcd. for $C_{11}H_{13}NO$: 175.0997; found: 175.0995.

(+)-1-(Propanoyl)-2(S)-benzylaziridine

Infrared: 1690 cm^{-1}; ^{1}Hmr δ: 1.03 (t, 3, *J* = 7.0), 2.0 (d, 1, *J* = 3.0), 2.20 (q, 2, *J* = 7.0), 2.32 (d, 1, *J* = 6.0), 2.45–2.70 (m, 1), 2.78 (d, 1, *J* = 4.0), 2.80 (d, 1, *J* = 8.0), 7.20 (m, 5); $[\alpha]_D^{24}$ 22.0 (*c* 2.13); *Anal.* calcd. for $C_{12}H_{15}NO$ (189.26): C 76.16, H 7.99, N 7.40; found: C 76.46, H 7.88, N 7.59. *Mol. Wt.* calcd. for $C_{12}H_{15}NO$: 189.1153; found: 189.1155.

(+)-1-(iso-Butyryl)-2(S)-benzylaziridine

Infrared: 1680 cm^{-1}; ^{1}Hmr δ: 1.08 (dd, 6, *J* = 5.0, 7.0), 1.96 (d, 1, *J* = 3.0), 2.30 (d, 1, *J* = 6.0), 2.35–2.75 (m, 2), 2.76 (d, 1, *J* = 8.0), 2.85 (d, 1, *J* = 8.0), 7.20 (s, 5); $[\alpha]_D^{24}$ 66.4 (*c* 2.43); *Anal.* calcd. for $C_{13}H_{17}NO$ (203.29): C 76.81, H 8.43, N 6.89; found: C 76.95, H 8.48, N 6.80. *Mol. Wt.* calcd. for $C_{13}H_{17}NO$: 203.1310; found: 203.1308.

Can. J. Chem. Downloaded from www.nrcresearchpress.com by 210.87.254.6 on 09/05/12
For personal use only.

(+)-1-(Pivaloyl)-2(S)-benzylaziridine

Infrared: 1680 cm^{-1}; ^{1}Hmr δ: 1.19 (s, 9), 1.96 (d, 1, J = 3.5), 2.35 (d, 1, J = 5.0), 2.48–2.80 (m, 2), 3.0–3.4 (m, 1), 7.2 (s, 5); $[\alpha]_D^{24}$ 96.2 (c 2.30); *Anal.* calcd. for $C_{14}H_{19}NO$ (217.31): C 77.38, H 8.81, N 6.45; found: C 77.41, H 8.98, N 6.61. *Mol. Wt.* calcd. for $C_{14}H_{19}NO$: 217.1466; found: 217.1465.

(+)-1-(Cyclohexanecarboxyl)-2(S)-benzylaziridine

Infrared: 1680 cm^{-1}; ^{1}Hmr δ: 0.9–2.25 (bm, 11), 1.98 (d, 1, J = 3.0), 2.36 (d, 1, J = 5.5), 2.42–2.75 (m, 1), 2.80 (d, 2, J = 6.0), 7.22 (s, 5); $[\alpha]_D^{24}$ 39.8 (c 2.22); *Anal.* calcd. for $C_{16}H_{21}NO$ (243.37): C 78.98, H 8.70, N 5.76; found: C 78.65, H 8.51, N 5.85. *Mol. Wt.* calcd. for $C_{16}H_{21}NO$: 243.1623; found: 243.1626.

(+)-1-(Benzoyl)-2(S)-benzylaziridine

Infrared: 1670 cm^{-1}; ^{1}Hmr δ: 2.26 (d, 1, J = 3.5), 2.54 (d, 1, J = 6.0), 2.66–2.95 (m, 2), 3.04–3.4 (m, 1), 7.25 (s, 5), 7.35–7.70 (m, 3), 8.05 (dd, 2, J = 2.0, 7.0); $[\alpha]_D^{24}$ 49.4 (c 2.14); *Anal.* calcd. for $C_{16}H_{15}NO$ (237.30): C 80.98, H 6.37, N 5.90; found: C 80.67, H 6.35, N 5.82. *Mol. Wt.* calcd. for $C_{16}H_{15}NO$: 237.1154; found: 237.1164.

(+)-1-(Nicotinyl)-2(S)-benzylaziridine

Infrared: 1670 cm^{-1}; ^{1}Hmr δ: 2.30 (d, 1, J = 3.0), 2.56 (d, 1, J = 6.0), 2.66–2.96 (m, 2), 2.96–3.30 (m, 1), 7.20–7.40 (m, 6), 8.20 (dt, 1, J = 8.0, 2.0), 8.75 (dd, 1, J = 2.0, 5.0), 9.25 (d, 1, J = 2.0); $[\alpha]_D^{24}$ 69.2 (c 2.33); compound too unstable to obtain satisfactory elemental analysis. *Mol. Wt.* calcd. for $C_{15}H_{14}N_2O$: 238.1106; found: 238.1094.

3-(1-Imidazole)-butanoyl Imidazolide

To a solution of 86 mg (1 mmol) of crotonic acid dissolved in 2 mL of THF was added 162 mg (1 mmol) of 1,1′-carbonyldiimidazole. The solution was stirred at room temperature for 1 h and the solvent evaporated to give a mixture of compounds containing predominantly (ca. 90%) 3-(1-imidazole)-butanoyl imidazolide as judged from the ^{1}Hmr spectrum; ^{1}Hmr δ: 1.60 (d, 3, J = 7.0), 3.40 (d, 2, J = 7.0), 4.6–5.1 (m, 1), 6.90 (bs, 2), 6.95 (bs, 2), 7.50 (s, 1), 8.10 (s, 1).

(+)-1-(Crotonyl)-2(S)-benzylaziridine

To a solution of 133 mg (1 mmol) of **2** and 101 mg (1 mmol) of Et_3N in 2 mL of THF at −78°C was added 105 mg (1 mmol) of crotonyl chloride. The reaction mixture was stirred at −78°C for 30 min and then filtered under a nitrogen atmosphere to remove the triethylammonium hydrochloride which had precipitated from the reaction mixture. Evaporation of the solvent gave a quantitative yield of product; ir: 1675, 1640 cm^{-1}; ^{1}Hmr δ: 1.76 (dd, 3, J = 2.0, 7.0), 2.10 (d, 1, J = 3.5), 2.42 (d, 1, J = 5.5), 2.50–2.80 (m, 1), 2.85 (d, 1, J = 4.0), 2.88 (d, 1, J = 7.0), 5.82 (dq, 1, J = 2.0, 16.0), 6.92 (dq, 1, J = 7.0, 16.0), 7.35 (s, 5); $[\alpha]_D^{24}$ 84.6 (c 2.95); *Anal.* calcd. for $C_{13}H_{15}NO$ (201.27): C 77.58, H 7.51, N 6.96; found: C 77.64, H 7.70, N 6.90. *Mol. Wt.* calcd. for $C_{13}H_{15}NO$: 201.1154; found: 201.1153.

(+)-1-(Sorboyl)-2(S)-benzylaziridine

Infrared: 1650 cm^{-1}; ^{1}Hmr δ: 1.85 (d, 3, J = 5.0), 2.14 (d, 1, J = 4.0), 2.45 (d, 1, J = 5.5), 2.54–2.80 (m, 1), 2.88 (d, 1, J = 5.0), 2.92 (d, 1, J = 7.0), 5.75 (d, 1, J = 15.0), 6.0–6.3 (m, 2), 7.0–7.5 (m, 6); $[\alpha]_D^{24}$ 68.4 (c 1.02); *Anal.* calcd. for $C_{15}H_{17}NO$ (227.31): C 79.26, H 7.54, N 6.16; found: C 79.38, H 7.51, N 6.10. *Mol. Wt.* calcd. for $C_{15}H_{17}NO$: 227.1311; found: 227.1300.

(−)-4(S)-Benzyloxazoline

Infrared: 1630 cm^{-1}; ^{1}Hmr δ: 2.70 (dd, 1, J = 7.6, 14.0), 3.15 (dd, 1, J = 5.6, 14.0), 3.96 (t, 1, J = 8.0), 4.22 (t, 1, J = 9.0), 4.3–4.6 (m, 1), 6.86 (d, 1, J = 2.0), 7.2–7.5 (m, 5); $[\alpha]_D^{24}$ −89.4 (c 1.06); *Anal.* calcd. for $C_{10}H_{11}NO$ (161.21): C 74.51, H 6.88, N 8.69; found: C 74.36, H 6.78, N 8.73. *Mol. Wt.* calcd. for $C_{10}H_{11}NO$: 161.0841; found: 161.0849.

(−)-2-Methyl-4(S)-benzyloxazoline

Infrared: 1675 cm^{-1}; ^{1}Hmr δ: 1.90 (d, 3, J = 0.9), 2.60 (dd, 1, J = 8.0, 14.0), 3.05 (dd, 1, J = 5.0, 14.0), 3.85 (t, 1, J = 7.0), 4.10 (t, 1, J = 8.5), 4.1–4.4 (m, 1), 7.1–7.4 (m, 5); $[\alpha]_D^{24}$ −50.7 (c 2.83); *Anal.* calcd. for $C_{11}H_{13}NO$ (175.23): C 75.40, H 7.48, N 7.99; found: C 74.98, H 7.73, N 7.80. *Mol. Wt.* calcd. for $C_{11}H_{13}NO$: 175.0997; found: 175.0998.

(−)-2-Ethyl-4(S)-benzyloxazoline

Infrared: 1670 cm^{-1}; ^{1}Hmr δ: 1.18 (t, 3, J = 7.0), 2.30 (q, 2, J = 7.0), 2.65 (dd, 1, J = 8.0, 14.0), 3.14 (dd, 1, J = 5.0, 14.0), 3.94 (t, 1, J = 7.0), 4.16 (t, 1, J = 9.0), 4.2–4.55 (m, 1), 7.1–7.5 (m, 5); $[\alpha]_D^{24}$ −37.0 (c 2.29); *Anal.* calcd. for $C_{12}H_{15}NO$ (189.26): C 76.16, H. 7.99, N 7.40; found: C 76.01, H 7.88, N 7.28. *Mol. Wt.* calcd. for $C_{12}H_{15}NO$: 189.1154; found: 189.1156.

(−)-2-(Isopropyl)-4(S)-benzyloxazoline

Infrared: 1660 cm^{-1}; ^{1}Hmr δ: 1.15 (d, 6, J = 7.0), 2.5 (sept, 1, J = 7.0), 2.60 (dd, 1, J = 8.0, 13.0), 3.05 (dd, 1, J = 4.8, 13.0), 3.86 (t, 1, J = 7.6), 4.05 (t, 1, J = 8.0), 4.1–4.5 (m, 1), 7.0–7.4 (m, 5); $[\alpha]_D^{24}$ −34.2 (c 1.43); *Anal.* calcd. for $C_{13}H_{17}NO$ (203.29): C 76.81, H 8.43, N 6.89; found: C 76.70, H 8.59, N 6.81. *Mol. Wt.* calcd. for $C_{13}H_{17}NO$: 203.1311; found: 203.1311.

*(−)-2-(*tert*-Butyl)-4(S)-benzyloxazoline*

Infrared: 1655 cm^{-1}; ^{1}Hmr δ: 1.16 (s, 9), 2.60 (dd, 1, J = 7.8, 14.0), 3.04 (dd, 1, J = 4.6, 14.0), 3.90 (t, 1, J = 8.0), 4.06 (t, 1, J = 9.0), 4.15–4.5 (m, 1), 7.1–7.4 (m, 5); $[\alpha]_D^{24}$ −38.2 (c 1.31); *Anal.* calcd. for $C_{14}H_{19}NO$ (217.31): C 77.38, H 8.81, N 6.45; found: C 77.00, H 8.72, N 6.35. *Mol. Wt.* calcd. for $C_{14}H_{19}NO$: 217.1466; found: 217.1464.

(−)-2-(Cyclohexyl)-4(S)-benzyloxazoline

Infrared: 1660 cm^{-1}; ^{1}Hmr δ: 1.0–2.05 (m, 10), 2.05–2.45 (m, 1), 2.60 (dd, 1, J = 8.0, 13.5), 3.06 (dd, 1, J = 4.5, 13.5), 3.85 (t, 1, J = 7.6), 4.06 (t, 1, J = 8.6), 4.15–4.50 (m, 1), 7.0–7.4 (m, 5); $[\alpha]_D^{24}$ −13.0 (c 2.35); *Anal.* calcd. for $C_{16}H_{21}NO$ (243.37): C 78.97, H 8.70, N 5.76; found: C 78.72, H 8.61, N 5.97. *Mol. Wt.* calcd. for $C_{16}H_{21}NO$: 243.1623; found: 243.1624.

(+)-2-(Phenyl)-4(S)-benzyloxazoline

Infrared: 1650 cm^{-1}; ^{1}Hmr δ: 2.75 (dd, 1, J = 8.0, 14.0), 3.26 (dd, 1, J = 5.2, 14.0), 4.12 (t, 1, J = 8.0), 4.35 (t, 1, J = 9.0), 4.4–4.75 (m, 1), 7.2–7.4 (m, 5), 7.4–7.6 (m, 3), 7.9–8.1 (m, 2); $[\alpha]_D^{24}$ 4.7 (c 1.65); *Anal.* calcd. for $C_{16}H_{15}NO$ (237.30): C 80.98, H 6.37, N 5.90; found: C 80.70, H 6.24, N 6.03. *Mol. Wt.* calcd. for $C_{16}H_{15}NO$: 237.1154; found: 237.1149.

(−)-2-(3-Pyridyl)-4(S)-benzyloxazoline

Infrared: 1650 cm^{-1}; ^{1}Hmr δ: 2.75 (dd, 1, J = 8.0, 14.0), 3.22 (dd, 1, J = 5.0, 14.0), 4.15 (t, 1, J = 8.0), 4.38 (t, 1, J = 8.0), 4.5–4.8 (m, 1), 7.15–7.45 (m, 6), 8.22 (dt, 1, J = 8.0, 2.0), 8.70 (dd, 1, J = 2.0, 5.0), 9.18 (d, 1, J = 2.0); $[\alpha]_D^{24}$ −4.3 (c 1.72); *Anal.* calcd. for $C_{15}H_{14}N_2O$ (238.30): C 75.61, H 5.92, N 11.76; found: C 75.23, H 5.83, N 11.61. *Mol. Wt.* calcd. for $C_{15}H_{14}N_2O$: 238.1106; found: 238.1106.

(−)-2-(1-Prop-1(E)-enyl)-4(S)-benzyloxazoline

Infrared: 1675 cm^{-1}; ^{1}Hmr δ: 1.86 (dd, 3, J = 2.0, 7.0), 2.65 (dd, 1, J = 8.0, 14.0), 3.16 (dd, 1, J = 5.0, 14.0), 3.98 (t, 1, J = 8.0), 4.22 (t, I, J = 8.0), 4.25–4.55 (m, 1), 6.05 (dd, 1, J = 2.0, 16.0), 6.64 (dq, 1, J = 7.0, 16.0), 7.1–7.5 (m, 5); $[\alpha]_D^{24}$ −52.5 (c 2.33); *Anal.* calcd. for $C_{13}H_{15}NO$ (201.27): C 77.58, H 7.51, N 6.96; found: C 77.21, H 7.48, N 6.88. *Mol. Wt.* calcd. for $C_{13}H_{15}NO$: 201.1154; found: 201.1149.

(−)-2-(1-Penta-1(E),3(E)-dienyl)-4(S)-benzyloxazoline

Infrared: 1650 cm^{-1}; ^{1}Hmr δ: 1.75 (d, 3, J = 5.6), 2.62 (dd, 1, J = 8.0, 14.0), 3.08 (dd, 1, J = 5.5, 14.0), 3.90 (t, 1, J = 7.6), 4.15 (t, 1, J = 9.0), 4.2–4.6 (m, 1), 5.7–6.3 (m, 3), 6.72–7.06 (m, 1), 7.06–7.4 (m, 5); $[\alpha]_D^{24}$ −51.8 (c 2.60); *Anal.* calcd. for $C_{15}H_{17}NO$

(227.31): C 79.26, H 7.54, N 6.16; found: C 79.03, H 7.43, N 6.21. *Mol. Wt.* calcd. for $C_{15}H_{17}NO$: 227.1311; found: 227.1307.

Preparation of N-*Acyl-2,2-dimethylaziridines* **4**

A similar procedure as is described above for the preparation of compounds **1** was used. 2,2-Dimethylaziridine, which was used in place of **2**, was prepared according to the method described in ref. 6. It is not necessary to break the reaction flask containing the crude hydrogen sulphate; aqueous NaOH may be added directly to the reaction flask in a similar manner to that described above for the preparation of **2**.

1-(Acetyl)-2,2-dimethylaziridine

Infrared: 1690 cm^{-1}; ^{1}Hmr δ: 1.33 (s, 6), 2.1 (s, 5); *Anal.* calcd. for $C_6H_{11}NO$ (113.16): C 63.69, H 9.80, N 12.38; found: C 63.41, H 9.73, N 11.97. *Mol. Wt.* calcd. for $C_6H_{11}NO$: 113.0841; found: 113.0840.

1-(Propanoyl)-2,2-dimethylaziridine

Infrared: 1690 cm^{-1}; ^{1}Hmr δ: 1.16 (t, 3, J = 7.0), 1.33 (s, 6), 2.13 (s, 2), 2.37 (q, 2, J = 7.0); *Anal.* calcd. for $C_7H_{13}NO$ (127.19): C 66.11, H 10.30, N 11.01; found: C 65.91, H 10.36, N 10.88. *Mol. Wt.* calcd. for $C_7H_{13}NO$: 127.0997; found: 127.0997.

*1-(*iso-*Butyryl)-2,2-dimethylaziridine*

Infrared: 1692 cm^{-1}; ^{1}Hmr δ: 1.17 (d, 6, J = 7.0), 1.33 (s, 6), 2.06 (s, 2), 2.40 (sept, 1, J = 7.0); *Anal.* calcd. for $C_8H_{15}NO$ (141.22): C 68.04, H 10.71, N 9.92; found: C 67.88, H 10.53, N 9.80. *Mol. Wt.* calcd. for $C_8H_{15}NO$: 141.1154; found: 141.1150.

1-(Pivaloyl)-2,2-dimethylaziridine

Infrared: 1690 cm^{-1}; ^{1}Hmr δ: 1.23 (s, 9), 1.33 (s, 6), 2.10 (s, 2); *Anal.* calcd. for $C_9H_{17}NO$ (155.24): C 69.63, H 11.04, N 9.02; found: C 69.51, H 10.99, N 8.90. *Mol. Wt.* calcd. for $C_9H_{17}NO$: 155.1310; found: 155.1308.

1-(Nicotinyl)-2,2-dimethylaziridine

Infrared: 1672 cm^{-1}; ^{1}Hmr δ: 1.27 (s, 6), 2.30 (s, 2), 7.27 (dd, 1, J = 5.0, 8.0), 8.10 (dt, 1, J = 8.0, 2.0), 8.60 (dd, 1, J = 2.0, 5.0), 9.0 (d, 1, J = 2.0); compound too unstable to obtain satisfactory elemental analysis. *Mol. Wt.* calcd. for $C_{10}H_{12}N_2O$: 176.0950; found: 176.0948.

α-*Deuterio-*iso-*butyric Acid*

To a mixture of 176 mg (2 mmol) of freshly distilled *iso*-butyric acid and 202 mg (2 mmol) of diisopropylamine in 10 mL of THF was added 3.0 mL (4 mmol) of 1.34 *M n*-butyllithium at −78°C. The reaction was stirred for 30 min at −78°C and was then quenched with 1 *N* DCl in D_2O. The deuterated acid was isolated by a standard workup and the above procedure repeated twice more on the same sample of acid. The ^{1}Hmr and mass spectra of the deuterated *iso*-butyric acid showed a deuterium incorporation level of 95%.

This acid was converted into the chiral oxazoline using the procedure given above. The ^{1}Hmr and mass spectra of the deuterated oxazoline showed a deuterium incorporation level of 93%.

Acknowledgements

This work was supported by the Natural Sciences and Engineering Research Council of Canada and in part by a Cottrell Research Grant provided by Research Corporation.

1. H. BESTIAN. Ann. Chem. **566**, 210 (1950); I. OKADO, T. TAKAHAMA, and R. SUDO. Bull. Chem. Soc. Jpn. **43**, 2591 (1970).
2. D. HAIDUKEWYCH and A. I. MEYERS. Tetrahedron Lett. 3031 (1972).
3. H. A. STAAB. Angew. Chem. Int. Ed. Engl. **1**, 351 (1962).
4. D. V. KASHELIKAR and P. E. FANTA. J. Am. Chem. Soc. **82**, 4930 (1960).
5. H. SEKI, K. KOGA, H. MATSUO, S. OHKI, I. MATSUO, and S. YAMADA. Chem. Pharm. Bull. **13**, 995 (1965).
6. E. C. HORNING (*Editor*). Organic synthesis Coll. Vol. 3. John Wiley and Sons, New York, NY. 1955. p. 148.
7. H. W. HEINE. Angew. Chem. Int. Ed. Engl. **1**, 528 (1962).
8. A. I. MEYERS and E. D. MIHELICH. Angew. Chem. Int. Ed. Engl. **15**, 270 (1976).
9. A. I. MEYERS, J. SLADE, R. K. SMITH, E. D. MIHELICH, F. M. HERSHENSON, and C. D. LIANG. J. Org. Chem. **44**, 2247 (1979).
10. D. A. TOMALIA, N. D. OJHA, and B. P. THILL. J. Org. Chem. **34**, 1401 (1969); T. A. FOGLIA, L. M. GREGORY, and G. MAERKER. J. Org. Chem. **35**, 3779 (1970).
11. A. I. MEYERS, R. K. SMITH, and C. E. WHITTEN. J. Org. Chem. **44**, 2251 (1979).
12. R. S. HODGES and R. B. MERRIFIELD. J. Org. Chem. **39**, 1870 (1974).
13. R. GREENHALGH, R. M. HEGGIE, and M. A. WEINBERGER. Can. J. Chem. **41**, 1662 (1963); A. I. MEYERS, G. KNAUS, and K. KAMATA. J. Am. Chem. Soc. **96**, 268 (1974).

Can. J. Chem. Downloaded from www.nrcresearchpress.com by 210.87.254.6 on 09/05/12
For personal use only.

The rearrangement of isomeric linear decyn-1-ols by reaction with the sodium salt of 1,3-diaminopropane[1]

SUZANNE R. MACAULAY

National Research Council, Prairie Regional Laboratory, Saskatoon, Sask., Canada S7N 0W9

Received March 12, 1980

This paper is dedicated to Prof. Raymond U. Lemieux on the occasion of his 60th birthday

Can. J. Chem. Downloaded from www.nrcresearchpress.com by 210.87.254.42 on 09/05/12
For personal use only.

SUZANNE R. MACAULAY. Can. J. Chem. **58**, 2567 (1980).

Isomerization of straight chain decyn-1-ols mediated by the sodium salt of 1,3-diaminopropane was studied as a function of time, temperature, and the initial position of the triple bond. At 50°C 9-decyn-1-ol, the thermodynamically favoured isomer, was formed rapidly regardless of the initial position of the triple bond. At lower temperatures the appearance of intermediate isomers was observed. The homopropargylic isomer was found to be remarkably stable, and under suitable conditions, conversion of 2- to 3-decyn-1-ol was carried out in 68% isolated yield.

SUZANNE R. MACAULAY. Can. J. Chem. **58**, 2567 (1980).

On a étudié l'isomérisation des décynols-1 à chaîne linéaire en présence d'un sel de sodium du diamino-1,3 propane, en fonction du temps, de la température et de la position initiale de la triple liaison. A 50°C, l'isomère thermodynamiquement favorisé, le décyn-9 ol-1, se forme rapidement indépendamment de la position de la triple liaison. A des températures plus basses on observe la formation d'un isomère intermédiaire. On a trouvé que l'isomère homopropargylique est remarquablement stable et dans des conditions convenables la transformation du décyn-2 ol-1 en décyn-3 ol-1 se fait avec un rendement de 68%.

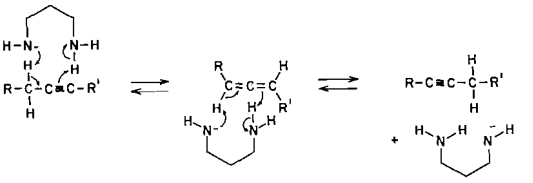
[Traduit par le journal]

Introduction

Since Favorskii's accidental discovery of an acetylene isomerization nearly a century ago (1), base mediated rearrangements of alkynes have been studied extensively (2, 3). Straight chain hydrocarbons containing one triple bond are rearranged by a wide variety of bases generating mixtures of isomeric allenes and acetylenes. In the generally accepted mechanism the base is thought to abstract a proton from a carbon next to the triple bond to give an anion which may be protonated to yield an isomeric allene. Further reversible 1,3-proton shifts lead to new alkynes and allenes. The proportion of products obtained reflects the relative thermodynamic stabilities of the components.

It has been suggested that in cases where the base is the salt of a diamine such as ethylenediamine (4) or 1,3-diaminopropane (5), the base may be able to abstract and donate a proton in a cyclic fashion (Scheme 1). In this postulated mechanism the proton shifts take place without discrete carbanionic intermediates.

Until recently, application of base mediated alkyne isomerizations in synthetic organic chemistry has been limited to a few special cases in which the triple bond is moved to an adjacent position and in which the difference in thermodynamic stability between the starting material and product is marked. For instance, 2-alkynes are significantly more stable than 1-alkynes (2) and several systems have been used to transform the latter into the former (6, 7). The reverse process, which depends upon formation and precipitation from solution of an acetylide salt has also been carried out in good yield (8, 9).



SCHEME 1

The discovery of the "acetylenic zipper" reaction has widened the scope of base mediated alkyne isomerizations (5, 10–12). Using a very strong base, the potassium salt of 1,3-diaminopropane (DAP) in DAP, the migration of a triple bond more than ten carbons along a straight chain has been effected. The product, the salt of the terminal acetylene, is thought to form irreversibly and is obtained in high yield and purity. The reaction is exceptional in that it provides a direct route to terminal acetylenes and acetylenic alcohols which are extremely useful intermediates in the synthesis of many natural products including ω-hydroxy fatty acids and insect pheromones.

In recent work we have modified this reaction to make it safer and more convenient by developing a reagent in which potassium hydride is replaced by

[1]NRCC No. 18495.

0008-4042/80/232567-06$01.00/0

©1980 National Research Council of Canada/Conseil national de recherches du Canada

Can. J. Chem. Downloaded from www.nrcresearchpress.com by 210.87.254.42 on 09/05/12
For personal use only.

sodium hydride (13). Our reagent, sodium aminopropylamide (NaAPA), has been shown to isomerize alkynes[2] and alkyn-1-ols (13) with internal triple bonds to the corresponding terminal acetylenes in good yield. As would be expected, slightly higher temperatures and longer reaction times are required. The present study was undertaken to investigate some of the factors which affect the rate and course of acetylene rearrangements with our modified system.

Results

The system chosen for study was the decyn-1-ol series, as this set of positional isomers is sufficiently large that isolation of acetylenic intermediates from the rearrangement reactions should yield diagnostic information on the course of the isomerizations. All eight isomeric decyn-1-ols were prepared by known procedures, and mixtures of the alkyn-1-ols, as their trimethylsilylethers, were found to be readily resolved using glc (see Experimental). The rearrangements of 2-decyn-1-ol, the isomer with the triple bond furthest removed from the unsubstituted terminus, and 5-decyn-1-ol, the isomer with the acetylenic linkage at an intermediate position in the chain, were followed at several different temperatures.

All isomerizations were performed in the same manner. The reagent was prepared by reaction of sodium hydride with 1,3-diaminopropane, the solvent of the reaction, at 70°C for one hour. After cooling to the desired temperature (50, 0, or −15°C), the substrate in DAP was added, and after the required time reactions were quenched with water. The isolated derivatized product mixtures were analyzed by glc and in every case a minimum of 96% of total peak area was attributable to decyn-1-ols. The same ratio of products was observed on workup of whole reaction mixtures as with aliquots removed from reactions. Results are displayed graphically in Figs 1 to 5. Tabulated data may be obtained from the Depository of Unpublished Data.[3]

The reactions at 50°C show several interesting features. As can be seen from Fig. 1, isomerization of 2-decyn-1-ol results in rapid production of 9-decyn-1-ol, with concomitant decay of the starting material. The terminal acetylene comprises 50% of the mixture in 0.25 h and rises to slightly over 70% of the total decyn-1-ol composition after 2 h. All possible decyn-1-ols are present; those with the triple bond in the 4, 5, 6, 7, or 8 position are formed only in small amounts and level off at about three percent each as the proportion of 9-decyn-1-ol grows. The homopropargylic isomer, 3-decyn-1-ol, rises to 18% of the total mixture by 0.25 h and then decreases to about 8% in the later stages of the

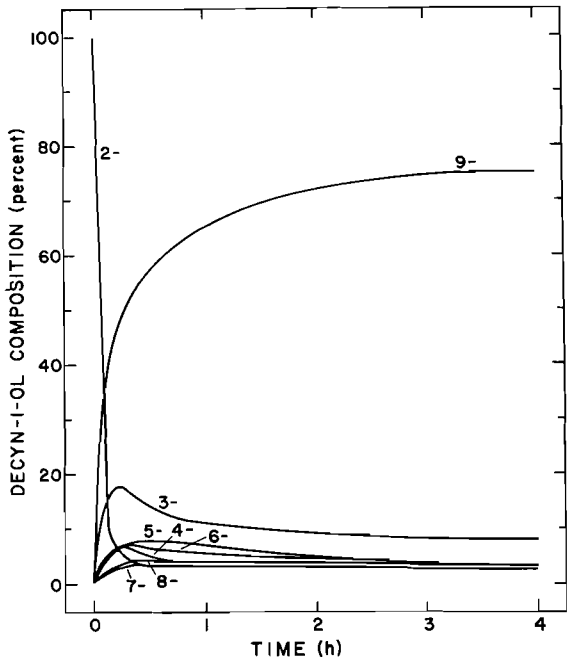


FIG. 1. Isomerization of 2-decyn-1-ol with NaAPA at 50°C.

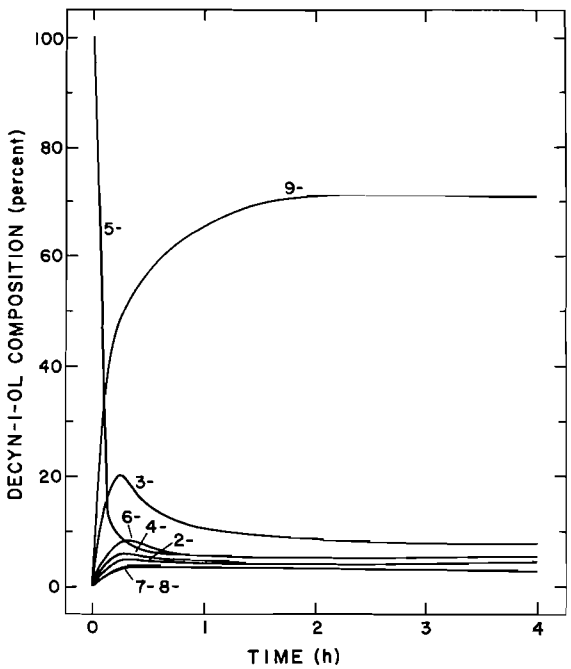


FIG. 2. Isomerization of 5-decyn-1-ol with NaAPA at 50°C.

[2]W. F. Steck, unpublished results.

[3]Photocopies may be obtained at a nominal charge, upon request, from the Depository of Unpublished Data, CISTI, National Research Council of Canada, Ottawa, Ont., Canada K1A 0S2.

Can. J. Chem. Downloaded from www.nrcresearchpress.com by 210.87.254.42 on 09/05/12
For personal use only.

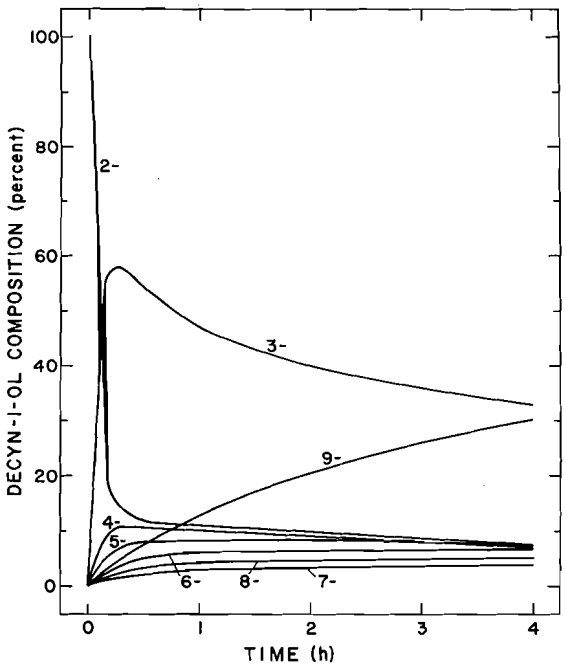


FIG. 3. Isomerization of 2-decyn-1-ol with NaAPA at 0°C.

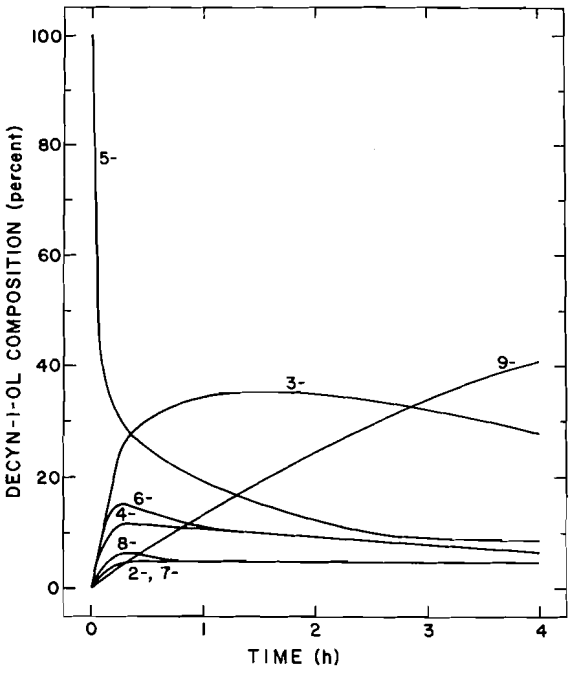


FIG. 4. Isomerization of 5-decyn-1-ol with NaAPA at 0°C.

reaction. The relative proportions of the products change only slightly after 2 h. It is interesting to compare the results obtained for the isomerization of 5-decyn-1-ol (Fig. 2) at the same temperature. The curves are virtually superimposable after 0.25 h reaction time. The terminal acetylene is

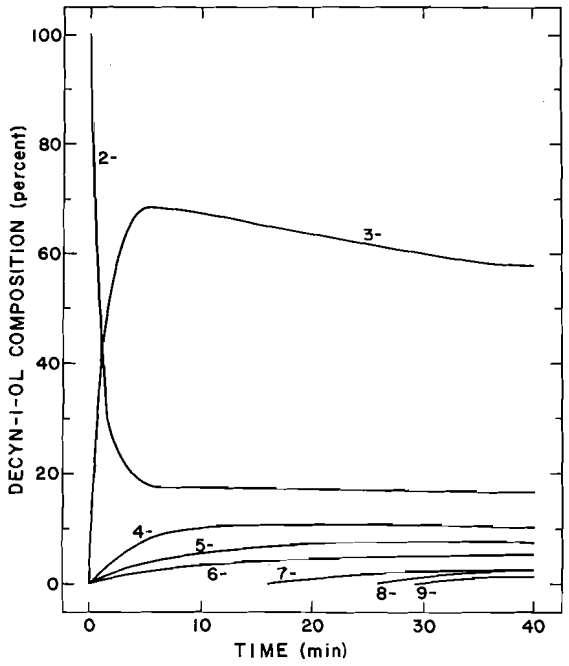


FIG. 5. Isomerization of 2-decyn-1-ol with NaAPA at −15°C.

formed rapidly and 3-decyn-1-ol comprises 20% of the mixture after 0.25 h. The remaining isomers again are formed in relatively low amounts.

The product distribution with time found in the isomerization of 2-decyn-1-ol at 0°C (Fig. 3) shows some similarity to that at 50°C. The relative proportion of terminal acetylene increases steadily, although at a slower rate, and the other isomers, except for the homopropargylic compound, again are present only in small amounts. In contrast, 3-decyn-1-ol is formed to the extent of 58% by 0.25 h. In the reaction of 5-decyn-1-ol at 0°C (Fig. 4) the proportion of starting material does not decrease quite as sharply as in the former cases. The terminal isomer is seen to increase gradually, and the homopropargylic isomer again rises to a higher concentration than do the other internal alkynes.

The rearrangement of 2-decyn-1-ol with NaAPA was carried out just above the freezing point of the mixture, at −15°C, and the reaction was followed at shorter time intervals (Fig. 5). In this case the 3-decyn-1-ols component comprised 68% of the total decyn-1-ols after 5 min, and the composition of the system showed little further change after about 0.5 h.

The rearrangement of 2-decyn-1-ol with NaAPA at −15°C was allowed to proceed for 5 min before quenching; 3-decyn-1-ol was isolated in 68% yield, based upon recovered starting material (54% conversion). Quenching of a similar reaction with

deuterium oxide after the same length of time resulted in no detectable deuterium incorporation in either the isolated product, 3-decyn-1-ol, or in the recovered starting material, 2-decyn-1-ol.

The stability of the terminal 9-decyn-1-ol to the reaction conditions was tested at 50 and 0°C. At the lower temperature no rearrangement was observed after 4 h, but at 50°C after the same length of time, the mixture was composed of 96.4% 9-decyn-1-ol, 1.5% 8-decyn-1-ol, and 2.1% unidentified material.

No allenes or dienes were observed by infrared or proton nmr spectroscopy in any of the product mixtures. No acidic products were detected.

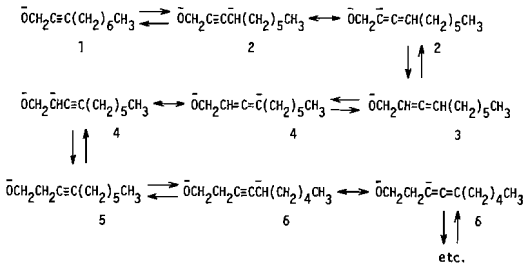
Discussion

At 50°C the reactions of both 2- and 5-decyn-1-ol with NaAPA proceed to give good yields of 9-decyn-1-ol. After about two hours the system appears to reach equilibrium, with both starting materials giving the same distribution of products. At 0°C, however, 9-decyn-1-ol is formed only slowly and after four hours makes up less than half of the total decyn-1-ol mixture. For synthetic purposes raising the temperature is more efficient in driving the reaction to completion than is allowing the isomerization to proceed for a long time. This appears to be so even though the terminal alkyne is not formed irreversibly at the higher temperature.

Our results support the "random walk" mechanism first proposed by Brown and Yamashita (5) for the "acetylenic zipper" reaction. The products from the reaction of 5-decyn-1-ol with NaAPA include alkynes resulting from the migration of the triple bond toward both the oxygen substituted and unsubstituted end of the carbon chain. Although all of the products isolated were acetylenic, the intermediacy of allenes cannot be discounted, and the present results are consistent with the general mechanism in which a series of reversible 1,3-proton shifts effect the migration of the triple bond along the methylene chain.

The most striking finding of this work is the exceptional stability of 3-decyn-1-ol. The homopropargylic isomer was formed in significant proportions in all of the rearrangement reactions studied including those where the triple bond of the starting material was closer to the unsubstituted terminus. This reaction is of synthetic utility; the propargylic isomer was converted to 3-decyn-1-ol in 68% isolated yield.

Scheme 2 shows the possible alkoxides that may be present in the isomerization of 2- to 3-decyn-1-ol with NaAPA. If discrete carbanions are involved then structures **1** through **6** will be intermediates. If, however, the cyclic mechanism is operative then



SCHEME 2

only **1**, **3**, and **5** need be present. Protonation of **1** and **2** would give 2-decyn-1-ol, and of **4**, **5**, and **6** would give 3-decyn-1-ol. The deuterium oxide quenching of the isomerization mixture with 2-decyn-1-ol as the starting material resulted in no detectable incorporation of deuterium into the recovered starting material or into the 3-decyn-1-ol that was produced. This result leads to the conclusion that the predominant species in solution are **1** and **5** and that the anions **2**, **4**, and **6** are not present in large amounts. Either the protonation of the intermediate anions by the solvent of the reaction is rapid so that **2**, **4**, and **6** do not accumulate, or the 1,3 proton shifts take place via the cyclic pathway. As no allenes were found, **3** also must be a minor component.

The extra stability of Δ-3 isomers has been observed previously by other workers in the cases of ethers (14), acetals (15), and acids (16), but the phenomenon is not yet understood.

Further work is being carried out to exploit the synthetic usefulness of the propargyl to homopropargyl transformation, and to investigate the nature of the stability of the Δ-3 isomer.

Experimental

The ^1H nmr spectra were recorded on an HA-100 spectrometer using deuterochloroform with internal tetramethylsilane as reference. The ^{13}C nmr spectra were obtained using an XL-100-15 instrument in the Fourier Transform mode at 25.16 MHz with proton noise decoupling. Deuterochloroform was used as solvent and also provided the internal deuterium lock. Gas chromatographic separations were carried out on a Finnigan 9500 instrument with an SP 2100 capillary column (J and W Scientific, 30 m) with a flame ionization detector, and were run isothermally at 120°C. Mass spectra were recorded on a Finnigan 4000E gc/ms instrument with an Incos 2300 data system, using the same column.

All reactions were performed in flame dried glassware and were carried out under a slight positive pressure of dry nitrogen.

Five of the decyn-1-ols, 2-, 3-, 5-, 7-, and 9-decyn-1-ol, were donated by Dr. W. F. Steck, National Research Council.

4-Decyn-1-ol

According to the method of Struble and Swailes (17), to the tetrahydropyranyl ether of 5-hydroxypent-1-yne (3.36 g, 20 mmol) in dimethoxyethane (distilled from CaH_2, 25 mL) was added lithium amide (0.5 g, 20 mmol). After refluxing for 5 h, the

Can. J. Chem. Downloaded from www.nrcresearchpress.com by 210.87.254.42 on 09/05/12
For personal use only.

Can. J. Chem. Downloaded from www.nrcresearchpress.com by 210.87.254.42 on 09/05/12
For personal use only.

mixture was cooled and *n*-pentyl bromide (3.0 g, 20 mmol) was added. The reaction was refluxed overnight, then cooled, poured onto ice water, and extracted with ether (3×). The combined ethereal extracts were washed with NaCl solution, dried over Na_2SO_4, filtered, and evaporated to yield 4.65 g of crude product. The THP protecting group was removed by refluxing the product in methanol (100 mL) with a catalytic amount of *p*-toluenesulfonic acid for 4 h. Methanol was removed by distillation and the residue partitioned between ether and water. The ether layer was washed with $NaHCO_3$ solution, NaCl solution, and dried over Na_2SO_4. Evaporation of the solvent and distillation at 90–100°C (0.1 Torr) yielded 4-decyn-1-ol 1.8 g (58% yield); ir ν_{max} (neat film): 3450 cm^{-1}; ^1H nmr δ: 3.70 (t, J = 7 Hz, 2H, OCH_2), 2.0–2.4 (m, 4H, $CH_2C{\equiv}C$), 1.70 (m, 2H, $CH_2CH_2C{\equiv}C$), 1.36 (m, 6H, CH_2), 0.90 (t, 3H, CH_3); ^{13}C nmr δ: 79.33 and 80.90 (C4, C5), 61.71 (C1), 31.78 and 31.08 (C2 and C8), 28.79 (C7), 22.19 (C9), 18.68 (C6), 15.38 (C3), 13.92 (C10).

6-Decyn-1-ol

6-Decyn-1-ol was prepared in the same manner as 4-decyn-1-ol starting with the tetrahydropyranyl ether of 7-hydroxyhept-1-yne and *n*-propyl bromide. Distillation afforded 6-decyn-1-ol in 50% yield: bp 90–100°C (0.1 Torr); ir ν_{max} (neat film): 3450 cm^{-1}; ^1H nmr δ: 3.58 (t, J = 7 Hz, 2H, OCH_2), 2.0–2.3 (m, 4H, $CH_2C{\equiv}C$), 1.4–1.8 (CH_2, 8H), 0.94 (t, J = 6 Hz, 3H, CH_3); ^{13}C nmr δ: 80.32, 80.10 (C6, C7), 62.83 (C1), 32.33 (C2), 28.96 (C4), 25.03 (C3), 22.58 (C9), 20.80 (C5), 18.75 (C8), 13.47 (C10).

8-Decyn-1-ol

According to the method of Wojtkowiak and Romanet (6), the tetrahydropyranyl ether of 9-decyn-1-ol (6 g, 25 mmol) was dissolved in a solution of KOH in ethanol (4 *N*, 50 mL) and heated in a sealed metal container at 190°C for 1.5 h. Ethanol was removed by evaporation and the residue partitioned between ether and water. The aqueous phase was washed with ether (2×) and the combined ethereal phases were washed with water until neutral, dried over Na_2SO_4, filtered, and the solvent removed to yield a yellow oil that was treated with methanol and *p*-toluenesulfonic acid to remove the THP group. Distillation (100°C, 0.1 Torr) yielded 8-decyn-1-ol (3.0 g, 70% yield), glc indicated a purity of 92%, with no starting material; ir ν_{max} (neat film): 3350 cm^{-1}, no absorption between 2500–1500 cm^{-1}; ^1H nmr δ: 3.57 (t, J = 7 Hz, 2H, OCH_2), 2.1 (br m, $w_{1/2}$ = 15 Hz, 2H, $CH_2C{\equiv}C$), 1.75 (t, J = 2 Hz, 3H, $C{\equiv}C{-}CH_3$), 1.2–1.7 (m, 10H, CH_2); ^{13}C nmr δ: 79.18 (C8), 75.24 (C9), 62.40 (C1), 32.60 (C2), 28.97 (C6), 28.97 (C5), 28.79 (C4), 25.67 (C3), 18.63 (C7), 3.25 (C10).

Gas–Liquid Chromatographic Separation of the Isomeric Decyn-1-ols

The alcohols were converted to trimethylsilylethers with *N,O*-bis-(trimethylsilyl)acetamide. Retention times relative to the TMS ether of *n*-decanol present in each analysis were: *n*-decanol 1.00, 9-decyn-1-ol 1.07, 4-decyn-1-ol 1.09, 5-decyn-1-ol 1.14, 6-decyn-1-ol 1.16, 3-decyn-1-ol 1.20, 7-decyn-1-ol 1.22, 2-decyn-1-ol 1.29, and 8-decyn-1-ol 1.39.

The response factor for each isomer was determined to be 1.00 ± 0.05. The values obtained by integration were taken without correction.

Isomerization Reactions

Unless otherwise stated, the general procedure used in the isomerization reactions was as follows.

Sodium hydride (NaH, Ventron, 57% in mineral oil, 340 mg; 8 mmol) was placed in a flame dried 50 mL flask fitted with magnetic stirring bar and rubber septum through which a slight positive pressure of dry N_2 was maintained. The NaH was freed of mineral oil by 3 successive washes with petroleum ether. 1,3-Diaminopropane (DAP, corrosive! 6 mL, previously distilled at reduced pressure from BaO and stored over activated molecular sieves 4A) was added by syringe to the flask, and the mixture was stirred in a constant temperature oil bath set at 70 ± 2°C. After 1 h the resultant brown solution was cooled to the desired temperature: (*1*) 50°C, in the constant temperature oil bath; (*2*) 0°C, in an ice/water bath; or (*3*) −15°C in an ethylene glycol/Dry Ice bath. The substrate (304 mg, 2 mmol) in DAP (2 mL) was injected into the flask. At the desired time the reaction, or aliquot, was worked up by pouring the mixture into ice/water and extracting 3 times with ether. The combined ether phases were washed successively with water, HCl solution, water, NaCl solution, and water, then dried over Na_2SO_4, filtered, and the solvent evaporated.

Isomerization of 9-Decyn-1-ol at 0° and 50°C

9-Decyn-1-ol was subjected to the standard reaction conditions at 0°C. The glc analysis of aliquots removed at 0.25 h, 1 h, and 4 h showed no new peaks, only the starting 9-decyn-1-ol.

The preceding reaction was repeated at 50°C. After 4 h glc analysis indicated the mixture consisted of 96.4% 9-decyn-1-ol, 1.5% 8-decyn-1-ol, and 2.1% unidentified material.

Isomerization of 2-Decyn-1-ol at 0°C for 15 Minutes

The standard reaction was carried out with 2-decyn-1-ol. The crude mixture (270 mg) was chromatographed on silica gel (Bio Rad 200–400 mesh, 20 g, 2.5 × 10 cm) eluting with ether/hexane mixtures. A nonpolar fraction (30 mg) was obtained which appeared to consist of mineral oil. A polar fraction (220 mg, 72%) of decyn-1-ols was obtained with 50% ether, 50% hexane. The glc analysis showed the decyn-1-ol mixture to consist of 2- (13%), 3- (60%), 4- (10%), 5- (6%), 6- (4%), 7- (2%), 8- (3%), and 9- (2%): ir ν_{max} (neat film): 3350 cm^{-1} (br s); no absorption between 2600–1500 cm^{-1}.

Preparation of 3-Decyn-1-ol from 2-Decyn-1-ol

To the isomerization reagent (prepared from 680 mg, 16 mmol, NaH and 14 mL DAP; twice normal scale) at −15°C was added 2-decyn-1-ol (616 mg, 4 mmol) in DAP (2 mL). After 5 min the reaction was quenched and worked up as described above to give 650 mg of an oil that was chromatographed on a silica gel column (Bio-Rad 200–400 mesh) eluting with ether/hexane mixtures. Product was collected in 3 fractions: (*1*) recovered starting material 80 mg; (*2*) starting material and 3-decyn-1-ol (1:2) 120 mg; and (*3*) 3-decyn-1-ol 250 mg. The yield of 3-decyn-1-ol was 54%, 68% based on recovered starting material.

Deuterium Oxide Quenching of Isomerization of 2-Decyn-1-ol

The isomerization of 2- to 3-decyn-1-ol (2 mmol scale) at −15°C was repeated and the reaction quenched with D_2O (25 mL). Chromatography yielded pure fractions of 2-decyn-1-ol (40 mg) and 3-decyn-1-ol (100 mg).

Integration of ^1H nmr spectra of both compounds showed no observable deuterium incorporation at the carbons next to the triple bond; 2-decyn-1-ol δ: 4.20 (t, J = 2 Hz, 2H, OCH_2), 2.18 (t of t, J = 2 Hz, 7 Hz, 2H, $C{\equiv}CCH_2$), 1.2 to 1.6 (m, 10H, CH_2), 0.88 (t, J = 7 Hz, 3H, CH_3); 3-decyn-1-ol δ: 3.63 (t, J = 6 Hz, 2H, OCH_2), 2.38 (t of t, J = 2 Hz, 6 Hz, 2H, $OCH_2CH_2C{\equiv}C$), 2.0–2.3 (m, 3H, $C{\equiv}CCH_2$, OH, D_2O exchange 2.0H), 1.2–1.6 (m, 8H, CH_2), 0.88 (t, J = 7 Hz, 3H, CH_3).

Examination of the $(M-15)^+$ peaks of the mass spectra of the TMS derivatives of the recovered 2-decyn-1-ol and 3-decyn-1-ol showed no evidence for D incorporation.

Acknowledgments

I thank W. F. Steck, National Research Council,

for gifts of the decyn-1-ols, J. Mehaffey, University of Saskatchewan for helpful discussions, G. D. Abrams, University of Saskatchewan for critically reading the manuscript, and L. Hogge and D. Olson for performing the gas chromatographic and mass spectral analysis.

1. A. Favorskii. J. Russ. Phys. Chem. Soc. **19**, 414 (1857).
2. R. J. Bushby. Q. Rev. Chem. Soc. **24**, 585 (1970).
3. F. Théron, M. Verny, and R. Vessière. The chemistry of the carbon–carbon triple bond. *Edited by* Saul Patai. John Wiley and Sons, Toronto. 1978. Chapt. 10.
4. J. H. Wotiz, P. M. Barelski, and D. M. Koster. J. Org. Chem. **38**, 489 (1973).
5. C. A. Brown and A. Yamashita. J. Am. Chem. Soc. **97**, 891 (1975).
6. B. Wojtkowiak and R. Romanet. Bull. Soc. Chim. Fr. 805 (1962).
7. J. Klein and E. Gurfinkel. Tetrahedron, **26**, 2127 (1970).
8. D. Caine and F. N. Fuller. J. Org. Chem. **34**, 222 (1969).
9. J. C. Lavalley and J. Saussey. The chemistry of the carbon–carbon triple bond. *Edited by* Saul Patai. John Wiley and Sons, Toronto. 1978. Chapt. 20.
10. J. C. Lindhoudt, G. L. VanMourik, and H. J. J. Pabon. Tetrahedron Lett. 2565 (1976).
11. C. A. Brown and A. Yamashita. J. Chem. Soc. Chem. Commun. 959 (1976).
12. E. Negishi and A. Abramovitch. Tetrahedron Lett. 411 (1977).
13. S. R. Macaulay. J. Org. Chem. **45**, 734 (1980).
14. R. Mantione. C. R. Acad. Sci. **267**, 90 (1968).
15. R. Mantione, M. L. Martin, G. J. Martin, and H. Normant. Bull. Soc. Chim. Fr. 2912 (1967).
16. R. J. Bushby and G. H. Whitham. J. Chem. Soc. B, 67 (1969).
17. D. L. Struble and G. E. Swailes. Environ. Entomol. **4**, 632 (1975).

Can. J. Chem. Downloaded from www.nrcresearchpress.com by 210.87.254.42 on 09/05/12
For personal use only.

Reactions of phthalans with dienophiles.[1] I. Synthesis of naphthalenes from phthalans and activated acetylenes

LUIS CONTRERAS AND DAVID B. MACLEAN

Department of Chemistry, McMaster University, Hamilton, Ont., Canada L8S 4M1

Received June 9, 1980

This paper is dedicated to Prof. Raymond U. Lemieux on the occasion of his 60th birthday

LUIS CONTRERAS and DAVID B. MACLEAN. Can. J. Chem. **58**, 2573 (1980).

Diethoxyphthalans and activated acetylenes react at temperatures of 140–160°C to yield substituted naphthalenes. It is proposed that the reaction occurs through the intermediacy of 1-ethoxyisobenzofurans generated thermally from the phthalans. The transient 1-ethoxyisobenzofurans are postulated to add to the acetylenes in a cycloaddition reaction to yield tricyclic intermediates that are transformed to naphthalenes at the elevated temperature of the reaction. Reactions with unsymmetrical acetylenes provided information on the regioselectivity of the reaction.

LUIS CONTRERAS et DAVID B. MACLEAN. Can. J. Chem. **58**, 2573 (1980).

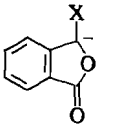
Les diéthoxyphtalannes et les acétylènes activés réagissent à des température allant de 140 à 160°C pour conduire à des naphtalènes substitués. On suggère que la réaction se produit par l'intermédiaire des éthoxy-1 isobenzofurannes produits thermiquement à partir des phtalannes. On propose que les intermédiaires éthoxy-1 isobenzofurannes s'additionnent aux acétylènes selon une réaction de cycloaddition pour conduire à des intermédiaires qui se transforment en naphtalènes à la température élevée de la réaction. Les réactions avec les acétylènes qui ne sont pas substitués d'une façon symétrique fournissent des informations sur la régiosélectivité de la réaction.

[Traduit par le journal]

There have been great strides made recently in synthetic methods leading to the preparation of polysubstituted naphthalenes. The compounds are of interest not only in their own right but also as intermediates in the synthesis of anthracene and naphthacene derivatives. All three classes of compounds contain members that are of pharmacological interest (1, 2).

The traditional route to polynuclear aromatic systems has been through Friedel–Crafts alkylation and acylation reactions but these reactions are often not regiospecific (3, 4). However, the method has been used successfully in recent work reported by Johnson and co-workers (5, 6) in the syntheses of anthraquinones and anthracyclinones.

Nucleophilic condensation reactions, many of which use phthalide anions **1** as key intermediates, have been developed in the past few years for the construction of polynuclear aromatic systems. Thus **1***a* has been condensed with Michael acceptors by Trueb and Eugster (7) and by Sammes and co-workers (8, 9). Hauser and co-workers (10, 11) have used **1***b* as a starting material in several elegant syntheses of natural products and Kraus and Sugimoto (12) have employed **1***c* to yield 1,4-dihydroxynaphthalenes. Other anionic condensations have also been employed. Among these are methods developed by Hauser *et al.* (13, 14, 15), Baldwin and Bair (16),



1*a* X = H
1*b* X = SO_2Ar
1*c* X = CN

Raphael and co-workers (17), Snieckus and co-workers (18, 19), and Wildeman *et al.* (20).

Diels–Alder additions have also played a prominent role in the construction of polynuclear aromatic systems. *o*-Quinodimethides generated in the presence of a dienophile have been employed successfully by several groups (21–26). Similarly isobenzofuran (27) and derivatives of it are highly reactive in cycloaddition reactions. Applications of their use in the construction of linear polycyclic systems have recently appeared (28–30). Other cycloadditions of note in this context are those reported by Sammes and Wallace (31) and by Kraus *et al.* (32).

We describe here a new synthetic method leading to polysubstituted naphthalenes. We have found that activated acetylenes react with phthalans or substituted phthalans when heated for several hours either neat or in solution in a sealed tube. Unsubstituted phthalans and disubstituted acetylenes lead to 1,2,3,4-tetrasubstituted naphthalenes while reaction between a phthalan and a monosubstituted acetylene led to a 1,2,4-trisubstituted naphthalene. By using phthalans substituted in the aromatic ring

[1]A preliminary account of part of this work has been published: L. Contreras, C. E. Slemon, and D. B. MacLean, Tetrahedron Lett. 4237 (1978).

0008-4042/80/232573-07$01.00/0

©1980 National Research Council of Canada/Conseil national de recherches du Canada

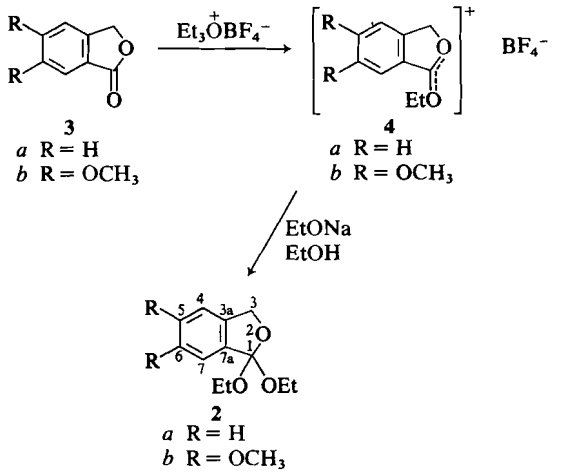
Can. J. Chem. Downloaded from www.nrcresearchpress.com by 210.87.254.42 on 09/05/12
For personal use only.

Can. J. Chem. Downloaded from www.nrcresearchpress.com by 210.87.254.42 on 09/05/12
For personal use only.

more highly substituted naphthalenes have been prepared and others are potentially available.

1,1-Diethoxyphthalan **2***a* (33) was prepared by alkylation of phthalide **3***a* with triethyloxonium fluoroborate (34) followed by treatment of the intermediate **4***a* with sodium ethoxide at 20°C. 5,6-Dimethoxy-1,1-diethoxyphthalan **2***b* was prepared similarly from **3***b* without isolation of the intermediate salt. Instead, the reaction mixture containing **4***b* was treated with sodium ethoxide according to the procedure of Deslongchamps *et al.* (35). The reactions are summarized in Scheme 1. The ^1H and ^{13}C nmr data recorded for **2***a* and **2***b* are in agreement with the assigned structures.

Treatment of **2***a* or **2***b* with dimethyl acetylenedicarboxylate at 140–170°C for 6 h gave compounds **5***a* and **5***b*, respectively. The reactions may be carried out in sealed glass tubes in the presence of solvent or at atmospheric pressure under reflux with a similar outcome in each case. The structures of **5***a* and **5***b* were deduced from their compositions, $C_{16}H_{16}O_6$ and $C_{18}H_{20}O_8$, respectively, from their functionality, and from their spectroscopic properties. It is clear from the following that both compounds are naphthalenes having the structures shown in Scheme 2. The infrared spectra of **5***a* and **5***b* showed two bands in the carbonyl region at 1735 and 1670 cm^{-1} attributed to ester absorption. The lower absorption is assigned to an intramolecularly hydrogen-bonded ester carbonyl group (36). The hydroxyl absorption resulting from intramolecular hydrogen bonding was not clearly visible as it underlay and was obscured by the C—H absorption. The ^1H nmr spectra of **5***a* and **5***b* both showed a peak at 12.1 δ for a hydrogen-bonded hydroxyl proton (37), as well as other peaks consistent with the assigned



3
a R = H
b R = OCH_3

4
a R = H
b R = OCH_3

2
a R = H
b R = OCH_3

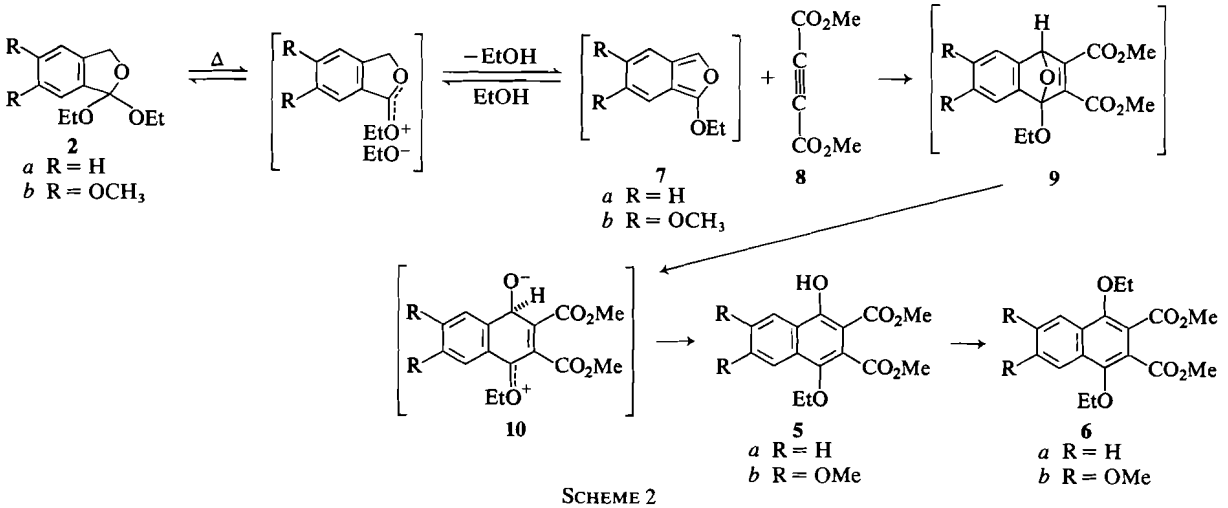
SCHEME 1

structures. Ethylation of **5***a* and **5***b* with ethyl iodide and sodium hydride in tetrahydrofuran (THF) (38) gave the symmetrical compounds **6***a* and **6***b*, each in 60% yield. The infrared spectra of **6***a* and **6***b* show only one absorption attributed to the ester carbonyl group (1735 cm^{-1}). The ^1H nmr spectrum of **6***a* has four aromatic protons forming an AA′BB′ pattern with two multiplets centered at 7.65 and 8.22 δ. The other signals in the spectrum are in accord with the proposed structure. The ^1H nmr spectrum of **6***b* showed a singlet of area 2 attributed to the aromatic protons at 7.46 δ, and signals attributed to the methoxy groups on the aromatic ring and of the ester group at 3.98 and 4.03 δ, each of area 6. Signals attributed to the ethyl groups appear at 1.48 (t) and 4.18 (q) δ associated with the methyl and methylene groups, respectively.

The ^{13}C nmr spectra of **5***a*, **5***b*, **6***a*, and **6***b* were recorded and the data obtained are in accord with the structures but resonances have not been assigned to the aromatic carbon atoms. However, on the basis of the ^{13}C data it is possible to differentiate the hydrogen bonded ester from the nonbonded ester group in **5***a* and **5***b*. The two signals appear at 170.2 and 168.2 in **5***a* and 170.3 and 168.4 in **5***b* for the bonded and nonbonded ester functions, respectively.

The formation of **5***a* and **5***b* can be rationalized as shown in Scheme 2. The reaction is considered to take place through the formation of a transient 1-ethoxyisobenzofuran intermediate **7**, generated *in situ*, which readily undergoes cycloaddition ($4\pi s + 2\pi s$) with ester **8** to yield the tricyclic intermediate **9**. It is proposed that the intermediate **9** undergoes C—O bond cleavage to **10** at the elevated temperature of the reaction and that the latter collapses to **5**. We do not have direct evidence for the generation of the intermediates **7**, **9**, or **10**. However, Hamaguchi and Ibata (39) have proposed the presence of an intermediate similar to **7** when methyl *o*-diazomethylbenzoate was decomposed in the presence of $Cu(acac)_2$. The 1-methoxyisobenzofuran intermediates were considered to form by interaction between a carbene, formed by decomposition of the diazo group, and the carbonyl group. The intermediates were trapped with alcohol (methanol or ethanol) or dienophiles such as *N*-phenylmaleimide, dimethyl fumarate, and dimethyl acetylenedicarboxylate to give phthalide ortho esters and Diels–Alder adducts, respectively.

The question of regioselectivity in Diels–Alder reactions arises when both the diene and dienophile are unsymmetrically substituted. Regioselectivity in the cycloaddition of **7***a* with unsymmetrical acetylenes such as ethyl propiolate **11**, ethyl tetrolate **12**,



SCHEME 2

and phenyl propiolate **13** was studied. It was found that "ortho adducts" (*vide infra*) in these reactions were formed as major products (Scheme 3).

The structures of compounds **14**–**19** are based on their compositions, their functionality, and their spectroscopic properties from which it is evident that all are substituted naphthalenes. It was possible to differentiate between the pairs **14** and **15**, **16** and **17**, and **18** and **19**, by the infrared absorption of the ester group, the chemical shift of the hydroxyl proton in the ^{1}H nmr spectrum, and the chemical shift of the carbonyl group in the ^{13}C nmr spectrum. For example, the infrared spectrum of **14** showed a band for a normal ester carbonyl group. The ^{1}H nmr spectrum showed a peak of 5.90 δ for a free hydroxyl proton and the ^{13}C nmr spectrum showed a signal at 167.3 ppm which is characteristic of a carbonyl carbon in an ester. In contrast, the infrared spectrum of **15** showed a band for an ester carbonyl group at 1655 cm^{-1} consistent with an intramolecularly hydrogen-bonded ester function (36). The ^{1}H nmr spectrum of **15** showed a peak at 11.70 δ for a hydrogen-bonded hydroxyl proton (37) and the ^{13}C nmr spectrum of **15** showed a peak at 171.1 ppm attributed to a hydrogen-bonded ester function. Similar differences were found between **16** and **17** and **18** and **19**, as shown in Table 1.

The preference for "ortho adducts" may be rationalized by using the frontier molecular orbital (FMO) theory (40). In its simplest form the FMO theory predicts that in Diels–Alder reactions between 1-substituted-1,3-butadienes, in which an electron-donating substituent such as NR_2, OMe, Me, etc., is present at C-1, and monosubstituted dienophiles, with an electron-withdrawing substituent such as COOR, CN, NO_2, etc. or a conjugated

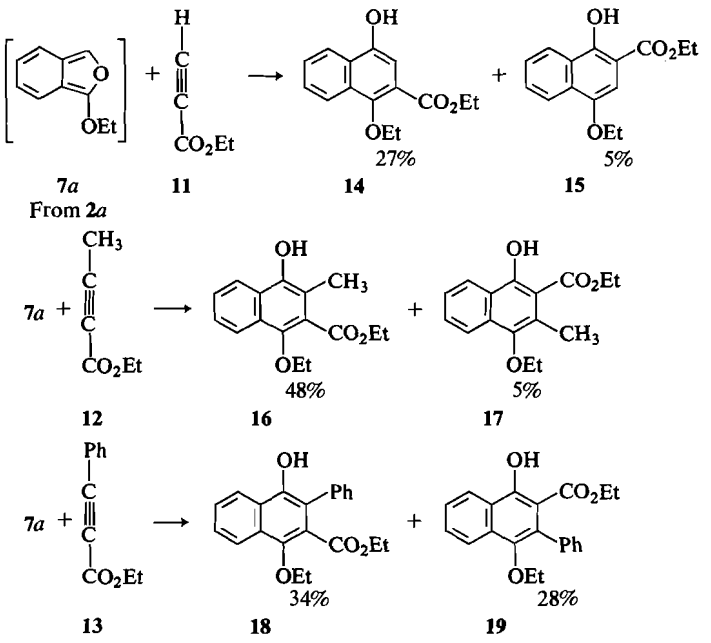
TABLE 1. Infrared, ^{1}H, and ^{13}C nuclear magnetic resonance data for substituted naphthalenes derived from unsymmetrically substituted acetylenes

	Infrared (cm^{-1})		^{1}H nmr	^{13}C nmr
Compound	OH	C=O	OH	C=O
14	3610, 3420	1720	5.90	167.3
15		1655	11.70	171.1
16	3610, 3380	1730	5.50	168.6
17		1655	12.10	172.6
18	3530	1730	5.40	167.4
19		1650	12.10	171.8

substituent such as phenyl, vinyl, etc., the unoccupied molecular orbital of lowest energy (LUMO) of the dienophile will interact strongly with the highest occupied molecular orbital (HOMO) of the diene. The coefficients of these orbitals are largest at C-4 of the diene and at C-2 of the dienophile. Thus, bonding to give "ortho adducts" is favoured. In the present instance 1-ethoxyisobenzofuran **7***a* may be considered analogous to a 1-substituted-1,3-butadiene with an electron-releasing substituent. Thus the reaction of **7***a* with dienophiles **11** and **12** leads to a preponderance of "ortho adduct" in agreement with theory. In the case of reaction with phenyl propiolate, however, there is very little discrimination between the two modes of reaction.

This reaction sequence provides a convenient route to naphthalenes having oxygen substituents at C-1 and C-4 and a variety of substituents at C-2 and C-3, depending on the choice of dienophile. Substitution in the second ring may be controlled by the choice of phthalan. The 1,4-dioxygenated naphthalenes available by this method are potentially useful

Can. J. Chem. Downloaded from www.nrcresearchpress.com by 210.87.254.42 on 09/05/12
For personal use only.



SCHEME 3

intermediates in the syntheses of 1,4-naphthaquinones.

Experimental

Apparatus, Methods, and Materials

Melting points were recorded on a Kofler micro hot stage apparatus and are uncorrected. Infrared spectra (ir) were recorded on a Perkin Elmer 283 spectrophotometer in chloroform solution unless otherwise stated. The ^{1}H nmr spectra were recorded on a Varian EM-390 or Bruker WH-90 Fourier transform spectrometer. Unless otherwise specified, the samples were dissolved in chloroform-d_1 using tetramethylsilane (TMS) as the internal standard. The chemical shifts were measured in relation to TMS and are quoted in δ values. The symbols s = singlet, d = doublet, t = triplet, q = quartet, and m = multiplet are used in reporting spectra. The ^{13}C nmr spectra were recorded on a Bruker WH-90 Fourier transform spectrometer at 22.62 MHz. Some spectra were also recorded on a Bruker WP-80 Fourier transform spectrometer at 20.115 MHz. Mass spectra were routinely run on all samples to check their molecular weight, either on a C.E.C. 21-110B double focussing or a V.G. Micromass 7070 mass spectrometer. Samples were introduced through a direct inlet system and run at 70 eV. High resolution mass spectrometry was used to confirm the composition of several compounds and mass measurements were made by procedures described elsewhere (41). Analytical thin layer chromatography was performed on pre-coated tlc silica gel plates (60F 254, Merck). Preparative thin layer chromatography was performed on pre-coated plc silica gel plates (60F 254, Merck) with layer thickness 2 mm. For column chromatography silica gel (60F 254, Merck), silica gel (Baker, 60–200 mesh), and alumina neutral (Fisher, activity I, 80–200 mesh) were used. Reverse phase chromatography was performed on tlc plates (KC_{18} Whatman) and on a Lobar prepacked column size A (240-10) RP-8 (40–63 μm) for liquid chromatography (Merck).

The microanalyses were performed by Microanalytical Laboratories, Ltd., Toronto, Ontario and Guelph Chemical Laboratories, Ltd., Guelph, Ontario.

1,2-Dichloroethane and methylene chloride were dried and distilled from phosphorus pentoxide. Tetrahydrofuran was dried by refluxing and distilling from sodium and benzophenone under dry nitrogen, and was collected directly from the still just prior to use.

Triethyloxonium Fluoroborate

The title compound was prepared by the method of Meerwein (34). Yield: 92%; mp 91–92°C.

O-Ethylphthalide Fluoroborate **4**a

Phthalide **3***a* (8.8 g, 6.56 mmol) and triethyloxonium fluoroborate (12.5 g, 6.57 mmol) in 15 mL of dry 1,2-dichloroethane were stirred for 48 h at room temperature in a dry box. The solid was separated by filtration (14.3 g, 88%) and washed with 1,2-dichloroethane and dry ether. It melted at 106–108°C (lit. (33) 107–108°C); ^{1}H nmr (CD_3NO_2); 1.20 (t, 3H, OCH_2CH_3, J = 6.0 Hz), 4.76 (q, 2H, OCH_2CH_3, J = 6.0 Hz), 5.83 (s, 2H, Ar—CH_2), and 7.16–7.86 (m, 4H, aromatic).

1,1-Diethoxyphthalan **2**a

O-Ethylphthalide fluoroborate **4***a* (14.3 g, 5.27 mmol) was added at room temperature to a solution of sodium ethoxide in ethanol (prepared from 2.5 g of sodium in 50 mL of absolute ethanol) under a nitrogen atmosphere. The solution was stirred for 1 h, then quenched with 50 mL of 15% aqueous sodium carbonate and extracted thoroughly with ether. The extract was then dried over K_2CO_3, filtered, evaporated, and distilled under vacuum (bp 60°C at 0.1 Torr) to give 11.3 g (94%) of **2***a*; ^{1}H nmr: 1.15 (t, 6H, 2 × OCH_2CH_3, J = 6.0 Hz), 3.25–3.85 (m, 4H, 2 × OCH_2CH_3), 5.03 (s, 2H, $ArCH_2$), and 7.20–7.50 (m, 4H, aromatic); hrms: calcd. for $C_{12}H_{16}O_3$: 208.109; found: 208.110.

5,6-Dimethoxy-1,1-diethoxyphthalan **2**b

5,6-Dimethoxyphthalide **3***b* (42) (14.0 g, 72.1 mmol) and triethyloxonium fluoroborate (15.0, 79.0 mmol) were dissolved in 25 mL of dry 1,2-dichloroethane and stirred at room temperature for two days under an argon atmosphere. The

Can. J. Chem. Downloaded from www.nrcresearchpress.com by 210.87.254.42 on 09/05/12
For personal use only.

Can. J. Chem. Downloaded from www.nrcresearchpress.com by 210.87.254.42 on 09/05/12
For personal use only.

dark solution was transferred to a dropping funnel and added to a solution of sodium ethoxide in ethanol (prepared from 3 g of sodium in 70 mL of absolute ethanol) under a nitrogen atmosphere at −20°C. After completion of the addition the reaction mixture was allowed to warm slowly to room temperature and then was quenched with 100 mL of 15% aqueous sodium carbonate. The resulting solution was extracted with methylene chloride, the extract dried over K_2CO_3, and the solvent evaporated to give a yellow oil which was distilled (bp 121°C at 0.05 Torr) to yield 14 g (72%) of **2***b*; ^{1}H nmr: 1.18 (t, 6H, 2 × OCH_2CH_3, J = 6.0 Hz), 3.30–3.80 (m, 4H, 2 × OCH_2CH_3), 3.92 (s, 6H, 2 × OCH_3), 5.02 (s, 2H, ArCH_2), 6.77 (s, 1H, aromatic), 6.95 (s, 1H, aromatic); hrms: calcd. for $C_{14}H_{20}O_5$: 268:131; found: 268.131. *Anal.* calcd. for $C_{14}H_{20}O_5$: C 62.68, H 7.52%; found: C 62.59, H 7.64%.

Reaction of 1,1-Diethoxyphthalan **2**a *with Dimethyl Acetylenedicarboxylate* **8**

In a Carius tube were placed 500 mg (2.40 mmol) of **2***a* and 434 mg (3.05 mmol) of **8** in 5 mL of chloroform. The tube was cooled and sealed under vacuum, then heated in a furnace for 6 h at 170°C. The tube was cooled, opened, and the contents removed. Upon evaporation of the solvent the oily residue was subjected to high vacuum distillation to remove the more volatile starting material. The product was collected as an oil (560 mg, 76%), crystallized from dry ether, and melted at 85–86°C. It proved to be dimethyl 1-hydroxy-4-ethoxynaphthalene-2,3-dicarboxylate **5***a* and had the following spectroscopic properties: ir ν_{max}: 1735 and 1670 cm^{-1}; ^{1}H nmr: 1.47 (t, 3H, OCH_2CH_3, J = 6.0 Hz), 3.97 (s, 6H, 2 × OCH_3), 4.12 (q, 2H, OCH_2CH_3, J = 6.0 Hz), 7.65 (m, 2H, aromatic), 8.07 (m, 1H, aromatic), 8.47 (m, 1H, aromatic), and 12.13 (s. 1H, ArO*H*); hrms: calcd. for $C_{16}H_{16}O_6$: 304.094; found: 304.097. *Anal.* calcd. for $C_{16}H_{16}O_6$: C 63.15, H 5.30; found: C 63.27, H 5.29%.

Reaction of **2**a *with* **8** *at Atmospheric Pressure*

Compound **2***a* (1.04 g, 5 mmol) and **8** (1.4 g, 10 mmol) were heated together at 145°C for 5 h under an argon atmosphere. The brown oil was subjected to high vacuum distillation to remove the more volatile starting materials. The product (1.17 g, 76%) was collected as a yellow oil. The oil was crystallized from dry ether and identified as **5***a*.

Ethylation of **5**a

Compound **5***a* (304 mg, 1 mmol) was dissolved in 20 mL of dry THF, sodium hydride (2 mmol) was added, followed by the addition of 8 mmol of ethyl iodide. The solution was heated in an oil bath at 80°C for 24 h, the solvent was removed, the residue taken up in benzene, and the benzene extract washed with water, dried over sodium sulfate, and evaporated. The solid residue (205 mg, 62%) was crystallized from pentane and melted at 87–89°C. It proved to be dimethyl 1,4-diethoxynaphthalene-2,3-dicarboxylate **6***a* and had the following spectroscopic properties: ir ν_{max}: 1735 cm^{-1}; ^{1}H nmr: 1.48 (t, 6H, 2 × OCH_2CH_3, J = 6.0 Hz), 3.88 (s, 6H, 2 × OCH_3), 4.20 (m, 4H, 2 × OCH_2CH_3), 7.65 and 8.22 (m, 4H, AA′BB′, aromatic; hrms: calcd. for $C_{18}H_{20}O_6$: 332.125; found: 332.124. *Anal.* calcd. for $C_{18}H_{20}O_6$: C 65.05, H 6.07; found: C 65.31, H 6.21%.

Reaction of 5,6-Dimethoxy-1,1-diethoxyphthalan **2**b *with* **8**

In a Carius tube were placed 564 mg (2.1 mmol) of **2***b* and 298 mg (2.1 mmol) of **8** in 6 mL of chloroform. The tube was cooled and sealed under vacuum, then heated in a furnace for 6 h at 150°C. The tube was cooled, opened, and the contents were removed. Evaporation of the solvent yielded an oil that was subjected to high vacuum distillation. The more volatile starting materials were removed and the product (550 mg, 71%) was crystallized from methanol to give dimethyl 6,7-dimethoxy 1-hydroxy-4-ethoxynaphthalene-2,3-dicarboxylate **5***b*, melting at 149–151°C. Infrared ν_{max}: 1735 and 1670 cm^{-1}; ^{1}H nmr: 1.47 (t, 3H, OCH_2CH_3, J = 7.5 Hz), 3.95 (s, 6H, 2 × OCH_3), 4.03 (s, 6H, 2 × OCH_3), 4.10 (q, 2H, OCH_2CH_3, J = 7.5 Hz), 7.30 (s, 1H, aromatic), 7.68 (s, 1H, aromatic), and 12.10 (s, 1H, ArO*H*); hrms: calcd. for $C_{18}H_{20}O_8$: 364.115; found: 364.113. *Anal.* calcd. for $C_{18}H_{20}O_8$: C 59.33, H 5.53; found: C 59.50, H 5.64%.

Reaction of **2**b *with* **8** *at Atmospheric Pressure*

Compounds **2***b* (1.32 g, 5 mmol) and **8** (1.40 g, 10 mmol) were heated together for 5 h at 155°C under an argon atmosphere. The excess of dienophile was removed under high vacuum distillation. The orange solid was crystallized from methanol to give 1.2 g (67%) of **5***b*.

Ethylation of **5**b

The compound **5***b* (364 mg, 1 mmol) was ethylated in the same way that **5***a* was converted to **6***a*. The resulting product (231 mg, 60%) was crystallized from ether and identified as dimethyl 6,7-dimethoxy-1,4-diethoxynaphthalene-2,3-dicarboxylate. It melted at 152–153°C and had the following spectroscopic properties: ir ν_{max}: 1735 cm^{-1}; ^{1}H nmr: 1.48 (t, 2 × OCH_2CH_3, J = 6.0 Hz), 3.98 (s, 6H, 2 × OCH_3), 4.03 (s, 6H, 2 × OCH_3), 4.18 (q, 4H, 2 × OCH_2CH_3, J = 6.0 Hz), and 7.46 (s, 2H, aromatic); hrms: calcd. for $C_{20}H_{24}O_8$: 392.145; found: 392.147. *Anal.* calcd. for $C_{20}H_{24}O_8$: C 61.22, H 6.17; found: C 61.03, H 6.10%.

Reaction of **2**a *with Ethyl Propiolate* **11**

Ortho ester **2***a* (1.04 g, 5 mmol) and **11** (835 mg, 8.5 mmol) were heated together for 4 h at 115–120°C under an argon atmosphere. The excess of dienophile was then removed by distillation leaving 1.1 g of brown oil that was separated into two components by column chromatography (silica gel, TLC grade, benzene–hexane 50:50). The first component (65 mg, 5%) to be eluted proved to be ethyl 1-hydroxy-4-ethoxynaphthalene-2-carboxylate **15**. It crystallized from hexane and melted at 99–101°C and had the following spectroscopic properties: ir ν_{max}: 1665 cm^{-1}; ^{1}H nmr: 1.45 and 1.53 (overlapping t's 6H, 2 × OCH_2CH_3), 4.18 (q, 2H, OCH_2CH_3, J = 6.0 Hz), 4.46 (q, 2H, OCH_2CH_3, J = 6.0 Hz), 7.04 (s, 1H, aromatic), 7.59 (m, 2H, aromatic), 8.33 (m, 2H, aromatic), and 11.70 (s, 1H, ArO*H*); hrms: calcd. for $C_{15}H_{16}O_4$: 260.104; found: 260.106. *Anal.* calcd. for $C_{15}H_{16}O_4$: C 69.21, H 6.20; found: C 68.74, H 6.28%.

The second component (355 mg, 27%) eluted from the column was an isomer of the previous compound. It proved to be ethyl 1-hydroxy-4-ethoxynaphthalene-3-carboxylate **14**. It melted at 139–141°C after crystallization from acetone–hexane and had the following spectroscopic properties: ir ν_{max}: 3610, 3420, and 1720 cm^{-1}; ^{1}H nmr: 1.49 and 1.53 (overlapping t's, 6H, 2 × OCH_2CH_3), 4.13 (q, 2H, OCH_2CH_3, J = 7.5 Hz), 4.45 (q, 2H, OCH_2CH_3, J = 7.5 Hz), 5.90 (br s, 1H, ArO*H*), 7.33 (s, 1H, aromatic), 7.59 (m, 2H, aromatic), and 8.21 (m, 2H, aromatic); hrms: calcd. for $C_{15}H_{16}O_4$: 260.104; found: 260.108. *Anal.* calcd. for $C_{15}H_{16}O_4$: C 69.21, H 6.20; found: C 68.75, H 6.41%.

Reaction of **2**a *with Ethyl Tetrolate* **12**

Ortho ester **2***a* (1.04 g, 5 mmol) and **12** (1.12 g, 10 mmol) were heated for 4 h at 165–170°C under a nitrogen atmosphere. The excess of dienophile was removed by distillation leaving 1.1 g of brown oil that was separated into two components by column chromatography (silica gel, TLC grade, methylene chloride – petroleum ether 50:50). The first component eluted (73 mg, 5%) proved to be ethyl 1-hydroxy-3-methyl-4-

Can. J. Chem. Downloaded from www.nrcresearchpress.com by 210.87.254.42 on 09/05/12
For personal use only.

ethoxynaphthalene-2-carboxylate **17**. It crystallized from hexane and melted at 82–84°C and had the following spectroscopic properties: ir ν_{max}: 1655 cm^{-1}; ^1H nmr: 1.45 and 1.48 (overlapping t's, 6H, 2 × OCH_2CH_3, J = 6.0 Hz), 2.58 (s, 3H, 1 × CH_3), 3.92 (q, 2H, OCH_2CH_3, J = 6.0 Hz), 4.47 (q, 2H, OCH_2CH_3, J = 6.0 Hz), 7.52 (m, 2H, aromatic), 8.00 (m, 1H, aromatic), 8.40 (m, 1H, aromatic), and 12.10 (s, 1H, ArO*H*); hrms: calcd. for $C_{16}H_{18}O_4$: 274.120; found: 274.123. *Anal.* calcd. for $C_{16}H_{18}O_4$: C 70.05, H 6.62; found: C 70.36, H 6.43%.

The second component (657 mg, 48%) eluted from the column was an isomer of the previous compound. It proved to be ethyl 1-hydroxy-2-methyl-4-ethoxynaphthalene-3-carboxylate **16**. It melted at 91–92°C after crystallization from hexane and had the following spectroscopic properties: ir ν_{max}: 3610, 3380, and 1730 cm^{-1}; ^1H nmr: 1.40 and 1.43 (overlapping t's, 6H, 2 × OCH_2CH_3), 2.25 (s, 3H, 1 × CH_3), 4.08 (q, 2H, OCH_2CH_3, J = 6.0 Hz), 4.46 (q, 2H, OCH_2CH_3, J = 6.0 Hz), 5.50 (s, 1H, ArO*H*), 7.43 (m, 2H, aromatic), and 8.00 (m, 2H, aromatic); hrms: calcd. for $C_{16}H_{18}O_4$: 274.120; found: 274.121. *Anal.* calcd. for $C_{16}H_{18}O_4$: C 70.05, H 6.63; found: C 70.25, H 6.33%.

Reaction of **2***a with Ethyl Phenylpropiolate* ***13***

Ortho ester **2***a* (1.04 g, 5 mmol) and **13** (1.90 g, 11 mmol) were heated together for 4 h at 165–170°C under an argon atmosphere. The solution was cooled, the excess of dienophile was removed by distillation and the residue (1.8 g) of brown oil was chromatographed on silica gel, TLC grade, using benzene–hexane 50:50 as eluant. The first fraction (437 mg, 28%) was crystallized from hexane and melted at 84–85°C. It proved to be ethyl 1-hydroxy-3-phenyl-4-ethoxynaphthalene-2-carboxylate **19** and had the following spectroscopic properties: ir ν_{max}: 1650 cm^{-1}; ^1H nmr: 0.73 (t, 3H, OCH_2CH_3, J = 6.0 Hz), 1.03 (t, 3H, OCH_2CH_3, J = 6.0 Hz), 3.55 (q, 2H, OCH_2CH_3, J = 6.0 Hz), 3.97 (q, 2H, OCH_2CH_3, J = 6.0 Hz), 7.35 (s, 5H, phenyl), 7.40–7.90 (m, 2H, aromatic), 8.10 (m, 1H, aromatic), 8.47 (m, 1H, aromatic), and 12.10 (s, 1H, ArO*H*); hrms: calcd. for $C_{21}H_{20}O_4$: 336.136; found: 336.134. *Anal.* calcd. for $C_{21}H_{20}O_4$: C 74.98, H 5.99; found: C 74.86, H 5.99%.

The second fraction from the column (576 mg, 34%) was an oil that failed to crystallize. The oil was purified by distillation in a Kugelrohr apparatus. It proved to be ethyl 1-hydroxy-2-phenyl-4-ethoxynaphthalene-3-carboxylate **18** which had the following spectroscopic properties: ir (neat) ν_{max}: 3530 and 1730 cm^{-1}; ^1H nmr: 0.93 (t, 3H, OCH_2CH_3, J = 6.0 Hz), 1.45 (t, 3H, OCH_2CH_3, J = 6.0 Hz), 4.00 and 4.17 (overlapping q's, 2 × OCH_2CH_3), 5.43 (br s, 1H, ArO*H*), 7.10–8.40 (m, 4H, aromatic), and 7.42 (s, 5H, phenyl); hrms: calcd. for $C_{21}H_{20}O_4$: 336.136; found: 336.134. *Anal.* calcd. for $C_{21}H_{20}O_4$: C 74.98, H 5.99; found: C 74.80, H 6.01%.

Acknowledgements

We thank the Natural Sciences and Engineering Research Council of Canada for financial support of this work and Consejo de Desarrollo Cientifico y Humanistico de la Universidad Central de Venezuela for a Scholarship to L. Contreras. We wish to acknowledge the contribution of Dr. C. E. Slemon in the early stages of this investigation.

1. R. H. THOMSON. Naturally occurring quinones. Academic Press, New York. 1971.
2. W. A. REMERS. The chemistry of antitumor antibiotics. Vol. 1. Wiley, New York. 1979. Chapt. 2.
3. C. M. WONG, R. SCHWENK, D. POPIEN, and T. L. HO. Can. J. Chem. **51**, 466 (1973).
4. R. H. THOMSON. The chemistry of the quinonoid compounds. Part 1. *Edited by* S. Patai. Wiley, New York. 1974. p. 136.
5. K. S. KIM, M. W. SPATZ, and F. JOHNSON. Tetrahedron Lett. 331 (1979).
6. K. S. KIM, E. VANOTTI, A. SUARATO, and F. JOHNSON. J. Am. Chem. Soc. **101**, 2483 (1979).
7. W. TRUEB and C. H. EUGSTER. Helv. Chim. Acta, **55**, 969 (1972).
8. N. J. P. BROOM and P. G. SAMMES. J. Chem. Soc. Chem. Commun. 162 (1978).
9. P. G. SAMMES and D. J. DODSWORTH. J. Chem. Soc. Chem. Commun. 33 (1979).
10. F. M. HAUSER and R. P. RHEE. J. Am. Chem. Soc. **99**, 4533 (1977).
11. F. M. HAUSER and S. A. POGANY. J. Heterocycl. Chem. **15**, 1535 (1978).
12. G. A. KRAUS and H. SUGIMOTO. Tetrahedron Lett. 2263 (1978).
13. F. M. HAUSER and R. P. RHEE. J. Org. Chem. **42**, 4155 (1977).
14. F. M. HAUSER and R. P. RHEE. J. Org. Chem. **43**, 178 (1978).
15. (*a*) F. M. HAUSER and R. P. RHEE. J. Am. Chem. Soc. **101**, 1628 (1979); (*b*) F. M. HAUSER and S. PRASANNA. J. Org. Chem. **44**, 2596 (1979).
16. J. E. BALDWIN and K. W. BAIR. Tetrahedron Lett. 2559 (1978).
17. I. FORBES, R. A. PRATT, and R. A. RAPHAEL. Tetrahedron Lett. 3965 (1978).
18. S. O. DE SILVA and V. SNIECKUS. Tetrahedron Lett. 5103 (1978).
19. S. O. DE SILVA, M. WATANABE, and V. SNIECKUS. J. Org. Chem. **44**, 4802 (1979).
20. J. WILDEMAN, P. C. BORGEN, H. PLUIM, P. H. F. M. ROUWETTE, and A. M. VAN LEUSEN. Tetrahedron Lett. 2213 (1978).
21. J. F. W. MCOMIE and D. H. PERRY. Synthesis, 416 (1973).
22. F. A. J. KERDESKY and M. P. CAVA. J. Am. Chem. Soc. **100**, 3635 (1978).
23. P. G. SAMMES. Tetrahedron, **32**, 405 (1976).
24. B. J. ARNOLD, S. M. MELLOWS, and P. G. SAMMES. J. Chem. Soc. Perkin Trans. I, 1266 (1973).
25. B. J. ARNOLD, P. G. SAMMES, and T. W. WALLACE. J. Chem. Soc. Perkin Trans. I, 409 (1974).
26. J. R. WISEMAN, J. J. PENDERY, C. A. OTTO, and K. C. CHIONG. J. Org. Chem. **45**, 516 (1980).
27. R. N. WARRENER. J. Am. Chem. Soc. **93**, 2346 (1971).
28. U. E. WIERSUM and W. J. MIJS. J. Chem. Soc. Chem. Commun. 347 (1972).
29. (*a*) J. G. SMITH and R. T. WIKMAN. J. Org. Chem. **39**, 3648 (1974); (*b*) J. G. SMITH, S. S. WELANKIWAR, B. S. SHANTZ, E. H. LAI, and N. G. CHU. J. Org. Chem. **45**, 1817 (1980).
30. A. S. KENDE, D. P. CURRAN, Y. TSAY, and J. E. MILLS. Tetrahedron Lett. 3537 (1977).
31. (*a*) P. G. SAMMES and T. W. WALLACE. J. Chem. Soc. Chem. Commun. 524 (1973); (*b*) P. G. SAMMES and T. W. WALLACE. J. Chem. Soc. Perkin Trans. I, 1377 (1975).
32. G. A. KRAUS, J. O. PEZZANITE, and H. SUGIMOTO. Tetrahedron Lett. 853 (1979).
33. H. MEERWEIN, P. BORNER, O. FUCHS, H. J. SASSE, H. SCHRODT, and J. SPILLE. Chem. Ber. **89**, 2060 (1956).

34. H. MEERWEIN. Org. Synth. **46**, 113 (1966).
35. P. DESLONGCHAMPS, R. CHÊNEVERT, R. J. TAILLEFER, C. MOREAU, and J. K. SAUNDERS. Can. J. Chem. **53**, 1601 (1975).
36. K. NAKANISHI. Infrared absorption spectroscopy. Holden Day, San Francisco. 1962. p. 42.
37. H. HART and K. TAKAGI. J. Org. Chem. **45**, 34 (1980).
38. B. A. STOOCHNOFF and N. L. BENOITON. Tetrahedron Lett. 21 (1973).
39. H. HAMAGUCHI and T. IBATA. Chem. Lett. 287 (1976).
40. I. FLEMING. Frontier orbitals and organic chemical reactions. Wiley, New York. 1976. Chapt. 4.
41. C. K. YU and D. B. MACLEAN. Can. J. Chem. **49**, 3025 (1971).
42. R. H. MANSKE, J. A. MCRAE, and R. Y. MOIR. Can. J. Chem. **29**, 526 (1951).

Can. J. Chem. Downloaded from www.nrcresearchpress.com by 210.87.254.42 on 09/05/12
For personal use only.

Reactions of phthalans with dienophiles.[1] II. Synthesis of naphthalenes and dihydronaphthalenes by reaction of ethyl maleate and maleic anhydride with 1,1-diethoxyphthalan

LUIS CONTRERAS AND DAVID B. MACLEAN

Department of Chemistry, McMaster University, Hamilton, Ont., Canada L8S 4M1

Received July 8, 1980

LUIS CONTRERAS and DAVID B. MACLEAN. Can. J. Chem. **58**, 2580 (1980).

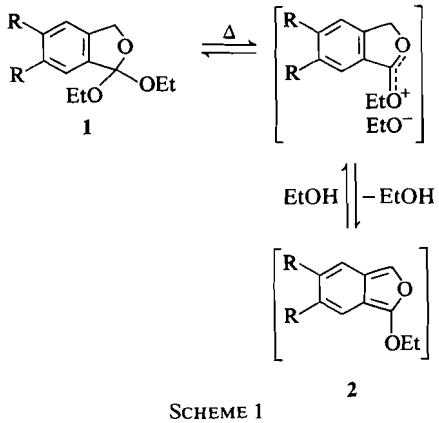
The reactions of 1,1-diethoxyphthalan with diethyl maleate and with maleic anhydride have been studied. The reaction with diethyl maleate in a sealed tube gave a mixture of diethyl 1-hydroxynaphthalene-2,3-dicarboxylate and its *O*-ethyl derivative. The same reactants at atmospheric pressure gave the ethoxy ester above along with a mixture of isomeric diethyl 1,2-dihydro-1-hydroxy-4-ethoxynaphthalene-2,3-dicarboxylates. The reaction with maleic anhydride gave only diethyl-1-ethoxynaphthalene-2,3-dicarboxylic acid anhydride. These reactions provide further insight into the mechanism of the reaction of phthalans with dienophiles.

LUIS CONTRERAS et DAVID B. MACLEAN. Can. J. Chem. **58**, 2580 (1980).

On a étudié les réactions du diéthoxy-1,1 phtalane avec le maléate de diéthyle et l'anhydride maléique. La réaction avec le maléate de diéthyle dans un tube scellé a donné un mélange d'hydroxy-1 naphtalènedicarboxylate-2,3 de diéthyle et de son dérivé *O*-éthyle. A pression atmosphérique, les mêmes réactifs ont conduit au dérivé précédent l'ester éthoxy, accompagné d'un mélange des dihydro-1,2 hydroxyéthoxy-4 naphtalènes dicarboxylate-2,3 de diéthyle isomères. La réaction avec l'anhydride maléique a seulement donné l'anhydride de l'acide éthoxy-1 naphtalène dicarboxylique-2,3. Ces réactions fournissent de plus une conaissance plus approfondie du mécanisme de la réaction des phtalanes avec les diénophyles.

[Traduit par le journal]

The previous paper (1) in this series described the reactions of phthalans with activated acetylenes. It was postulated that 1,1-diethoxyphthalans **1** were converted to transient 1-ethoxyisobenzofurans **2** (Scheme 1) that underwent a 4 + 2 cycloaddition with the dienophiles to give, as final reaction products, polysubstituted naphthalenes. In this communication, we have extended the study to ethylenic dienophiles and describe here the reaction of 1,1-diethoxyphthalan with ethyl maleate and maleic anhydride. Both compounds yield trisubstituted naphthalenes as reaction products but tetrasubstituted dihydronaphthalenes were also obtained from ethyl maleate. Other recently developed routes to substituted naphthalenes have been cited in ref. 1.



SCHEME 1

Treatment of the ortho ester **1** with diethyl maleate **3** in chloroform at 170°C for 72 h in a sealed glass tube gave two products, **4** and **5** (Scheme 2), in approximately 30% and 10% yield, respectively. However, when the reaction was carried out at atmospheric pressure for 6 h at 165°C, the product consisted of three compounds that were separated by column chromatography. The first was the trisubstituted naphthalene **4** (48%). The second (larger R_f) was one of the racemic diastereomers of diethyl-1-hydroxy-4-ethoxy-1,2-dihydronaphthalene-2,3-dicarboxylate **6***a* (18%). The third compound (smaller R_f) **6***b* (34%) was an isomer of **6***a*.

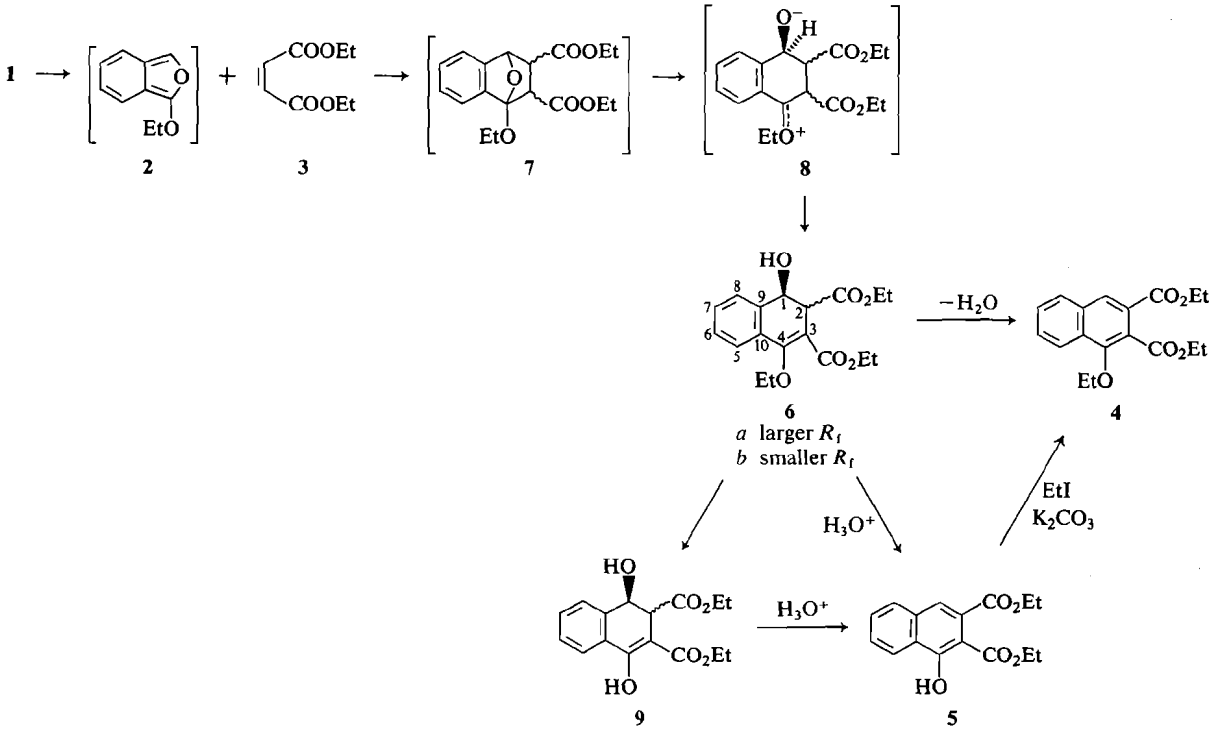
The structures of **4** and **5** are based on a knowledge of their compositions, $C_{16}H_{16}O_5$ and $C_{18}H_{20}O_5$, respectively, and on examination of their spectra. The infrared spectrum of **5** showed two bands in the carbonyl region at 1730 and 1655 cm^{-1} attributed to ester absorptions. The lower field absorption was assigned to an intramolecularly hydrogen-bonded ester carbonyl group (1). The ^1H nmr spectrum of **5** showed a peak at 12.10 δ for a hydrogen-bonded hydroxyl proton. The two methyl groups of the two carboethoxy functions have the same chemical shift and appear as a triplet at 1.40 δ. The methylene protons appear as two

[1]A preliminary account of part of this work has been published. L. Contreras, C. E. Slemon, and D. B. MacLean, Tetrahedron Lett. 4237 (1978).

0008-4042/80/232580-04$01.00/0

©1980 National Research Council of Canada/Conseil national de recherches du Canada

Can. J. Chem. Downloaded from www.nrcresearchpress.com by 210.87.254.5 on 09/05/12
For personal use only.



SCHEME 2

overlapping quartets centred at 4.40 and 4.50 δ. The aromatic region showed two multiplets, one of area 3H centred at 7.68 δ, and the other a multiplet of area 1H centred at 8.43 δ. There was also a singlet for 1H at 7.45 δ, assigned to H-4. Compound **5** has been converted by ethylation into **4**. A multi-step synthesis (2) of **5** has been previously reported, but it was not obtained in crystalline form. In another study, the dimethyl ester of 1-hydroxy-2,3-naphthalene dicarboxylic acid was prepared (3); the spectroscopic properties reported for it are very similar to those of **5**.

The ^{13}C nmr spectrum of **5** showed two signals for the carbonyl carbon atoms of the ester groups. The signal at 170.2 ppm is attributed to the internally hydrogen-bonded ester function and the signal at 169.2 ppm to the nonbonded ester group.

The infrared spectrum of **4** showed only one absorption for the ester carbonyl group at 1730 cm^{-1}. The ^1H nmr spectrum of **4** showed signals attributed to the three ethyl groups at 1.37 (t), 1.38 (t), and 1.43 (t) associated with the methyl groups and at 4.20 (q), 4.38 (q), and 4.47 (q) associated with the methylene groups. The aromatic region consists of 3 multiplets centred at 7.58, 7.92, and 8.12 δ for 2H, 1H, and 1H, respectively. The singlet of the proton at H-4 is deshielded (8.32 δ) relative to that of H-4 in **5**.

The ^{13}C nmr chemical shifts of **4** showed two signals for the ester carbonyl group at 165.6 and 167.9 ppm, respectively.

The enol ethers ***6a*** and ***6b*** were identified on the basis of their spectra. The infrared spectrum of the enol ethers, ***6a*** and ***6b***, showed bands for hydroxyl absorption at 3480 cm^{-1} and for carbonyl absorption at 1730 cm^{-1}. The ^1H nmr spectrum of ***6a*** contains three sets of overlapping ethyl resonances whose peaks are centred at 1.05, 1.38 and 1.42 δ, which are assigned to the methyl groups; the methylene groups appear as two overlapping quartets centred at 4.04 and 4.37 δ. Also overlapping with the methylene peaks is the signal for the proton at C-2 giving a total of 7 hydrogens in this region. The benzylic proton appears as a broad doublet of doublets with a coupling constant, J = 6.0 Hz, due to vicinal coupling to H-2 and to the hydroxyl proton. The latter signal was not located in the spectrum. The broad signal ascribed to H-1 collapsed to a doublet, J = 6.0 Hz, on addition of D_2O. The four aromatic protons form a multiplet over the range 7.20–7.80 δ. When the ^1H nmr spectrum of ***6a*** was run in dimethylsulfoxide

Can. J. Chem. Downloaded from www.nrcresearchpress.com by 210.87.254.5 on 09/05/12
For personal use only.

Can. J. Chem. Downloaded from www.nrcresearchpress.com by 210.87.254.5 on 09/05/12
For personal use only.

(DMSO-d_6), the benzylic proton was shifted to 5.16 δ and appeared as a triplet with $J = 6.0$ Hz. This signal collapsed to a doublet with $J = 6$ Hz when D_2O was added, suggesting a coupling to the hydroxyl proton with the same coupling constant as with H-2. The hydroxyl proton appeared as a doublet with $J = 6.0$ Hz at 5.80 δ in DMSO-d_6. This signal disappeared when D_2O was added. The ^1H nmr spectrum of **6***b* had a spectrum similar to **6***a* except that the vicinal coupling between the benzylic proton on C-1 and H-2 is now 4.5 Hz, indicative of the change in configuration at C-2 and a different dihedral angle between H-1 and H-2.

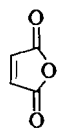
The ^{13}C nmr spectra of **6***a* and **6***b* were also found to be similar. The aliphatic region of both spectra showed the presence of two methine carbon atoms in which C-1 of **6***b* is shielded by −0.5 ppm while C-2 is deshielded by 4.2 ppm relative to the same centres in **6***a*. Also present in this region are other signals corresponding to the carbon atoms of the ethoxy groups. The low field region showed that the carbonyl carbon at C-2 of **6***a* is deshielded by 1.7 ppm with respect to **6***b*. However, it is not possible from these data (^1H nmr and ^{13}C nmr spectra) to assign unequivocally the relative configuration at C-2 in **6***a* and its diastereoisomer **6***b*.

The formation of **4**, **5**, **6***a*, and **6***b* can be rationalized through the intervention of 1-ethoxyisobenzofuran **2** (Scheme 2), which undergoes cycloaddition with **3** to give the intermediate **7**. This intermediate can undergo C—O bond cleavage to the zwitterion **8**, as proposed for the analogous adduct from acetylene addition (1), which then collapses to the enol ethers **6***a* and **6***b*. The isolation of the compounds **6***a* and **6***b* is indirect evidence for the formation of the tricyclic intermediate **7**. From the ratio of **6***a* to **6***b*, one might be tempted to draw conclusions about the *exo–endo* ratio of the addition, but this would be unwise for several reasons, not least of which is that isomerization might have occurred during work-up. Moreover, it has been found that the *exo–endo* ratio of adducts from various cycloaddition reactions of isobenzofurans with dienophiles varies. Whereas Kende *et al.* (4), Wiersum and Mijs (5), and Chacko *et al.* (6) have observed the predominance of *endo* isomers in these reactions, Hamaguchi and Ibata (7) found an *endo–exo* ratio of 1:1 in adducts that they prepared. In all cases, the *endo–exo* ratio was determined by nmr spectral analysis. The geometry in the *exo* adduct prevents the coupling of the protons at the bridge junction and the adjacent protons in the nmr spectrum but coupling is observed in the *endo* adducts (4, 5). Since no general rule can be formulated for such reactions and since the tricyclic compound **7** was not isolated, it is not possible to predict or ascertain the *endo–exo* ratio in the reaction of **1** with **3**.

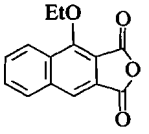
In another experiment the compound **9**, together with **4**, (15%) was isolated from the reaction of **1** with **3** as a mixture of diastereoisomeric enolic forms in 65% yield. The product **9** apparently arises by hydrolysis of **6** in the course of silica gel column chromatography. The infrared spectrum of **9** showed bands for hydroxyl absorption at 3480 cm^{-1} and carbonyl absorption at 1665 and 1735 cm^{-1}. Although the ^1H nmr spectrum of **9** was complex, it showed peaks at 2.80 and 12.80 δ for free and hydrogen-bonded hydroxyl protons, respectively. These signals collapsed when D_2O was added. Treatment of **9** with *p*-toluenesulfonic acid yielded **5** by dehydration in quantitative yield.

It was also found that the enol ethers **6***a* and **6***b* on treatment with acid yielded **5** which indicated that they undergo hydrolysis of the enol ether faster than they undergo dehydration. None of the compound **4** was observed on dehydration of **6***a* or **6***b* with *p*-toluenesulfonic acid in benzene.

When maleic anhydride **10** was used as dienophile, one product **11** was separated by crys-



10



11

tallization in 56% yield. The infrared spectrum of **11** showed two bands in the carbonyl region at 1845 and 1785 cm^{-1}, attributed to the anhydride group (8). The ^1H nmr spectrum of **11** showed peaks for the ethoxy group at 1.55 and 4.82 δ corresponding to methyl and methylene groups, respectively. In the aromatic region, there was a multiplet between 7.50–8.20 δ for 3H, a multiplet centred at 8.47 δ for 1H, and a singlet at 8.07 δ for 1H assigned to H-4.

The ^{13}C nmr spectrum showed signals at 72.9 (t) and 16.0 (q) ppm that can be attributed to the ethoxy group. The low field region showed two signals for the anhydride carbonyl group at 161.5 and 163.5 ppm, respectively. The higher field signal is assigned to the C-2 carbonyl carbon atom, because of the steric effect of the ethoxy group. The resonances of the aromatic carbon atoms are not assigned.

The reactions described above show that phthalans, on reaction with ethylenic dienophiles, may be used to prepare 1,2,3-trisubstituted naphthalenes or 1,2,3,4-tetrasubstituted 1,2-dihydronaphthalenes. The formation of the dihydro compounds provides indirect evidence for the transient formation of the tricyclic intermediate **7**.

Can. J. Chem. Downloaded from www.nrcresearchpress.com by 210.87.254.5 on 09/05/12
For personal use only.

Experimental

Apparatus, Methods, and Materials

The reader is referred to the preceding paper in this series (1).

Reaction of 1 with Diethyl Maleate 3 in a Sealed Tube

Ortho ester **1** (344 mg, 2 mmol), prepared as previously described (1), diethyl maleate (419 mg, 2 mmol), and chloroform (2 mL) were placed in a Carius tube. The tube was cooled and sealed under vacuum. The mixture was heated in a furnace for 72 h at 170°C. The tube was cooled, opened, and the contents were removed. Upon evaporation of the solvent, the yellow oil obtained on vacuum distillation was subjected to preparative tlc (silica gel, benzene) to give two fractions. The first fraction (55 mg, 10%) was a yellow oil that crystallized from hexane and melted at 54–56°C. It was identified as diethyl 1-hydroxynaphthalene-2,3-dicarboxylate **5**. Infrared ν_{max}: 1730 and 1665 cm^{-1}; ^1H nmr: 1.48 (t, 6H, 2 × OCH_2CH_3, J = 6.0 Hz), 4.40 and 4.45 (overlapping q's, 4H, 2 × OCH_2CH_3), 7.45 (s, 1H, aromatic), 7.68 (m, 3H, aromatic), 8.43 (m, 1H, aromatic), and 12.10 (s, 1H, ArO*H*). *Anal.* calcd. for $C_{16}H_{16}O_5$: C 66.66, H 5.55; found: C 66.07, H 5.36%. *Exact Mass* calcd. for $C_{16}H_{16}O_5$: 288.099; found (hrms): 288.099.

The second fraction (214 mg, 30%) was a yellow oil that failed to crystallize. The oil was purified by distillation in a Kugelrohr apparatus and proved to be diethyl-1-ethoxynaphthalene-2,3-dicarboxylate **4**. Infrared (neat liquid) ν_{max}: 1730 cm^{-1}; ^1H nmr: 1.37, 1.38, and 1.43 (overlapping t's, 9H, 3 × OCH_2CH_3), 4.20, 4.38 and 4.47 (overlapping q's, 6H, 3 × OCH_2CH_3), 7.58 (m, 2H, aromatic), 7.92 (m, 1H, aromatic), 8.12 (m, 1H, aromatic), and 8.32 (s, 1H, aromatic). *Anal.* calcd. for $C_{18}H_{20}O_5$: C 68.35, H 6.32, found: C 68.29, H 6.39%. *Exact Mass* calcd. for $C_{18}H_{20}O_5$: 316.131; found (hrms): 316.132.

Ethylation of 5

A mixture of **5** (97 mg, 0.3 mmol), ethyl iodide (2.5 g, 1.6 mmol), and potassium carbonate (2.5 g, 18 mmol) in 20 mL of anhydrous acetone was refluxed for 50 h. The acetone was evaporated and the residue was taken up in benzene. The benzene was washed with 5% aqueous potassium hydroxide, dried over sodium sulfate, and evaporated to give a yellow oil (76.5 mg, 72%) whose spectroscopic properties were identical with those of **4** reported above.

Reaction of 1 with 3 at Atmospheric Pressure

Ortho ester **1** (1.04 g, 5 mmol) and **3** (1.72 g, 10 mmol) were heated together for 6 h at 165–170°C under an atmosphere of argon. The excess of dienophile was removed by distillation under vacuum giving 1.8 g of yellow oily residue. Column chromatography of the oil (silica gel for tlc, benzene–acetone 95:5) yielded three fractions. The first fraction (688 mg, 43%) was the already reported **4**; the second fraction (500 mg) proved to be a mixture of two components that was separated by preparative tlc using the same conditions as in column chromatography. This fraction was comprised of 76 mg (5%) of the compound present in the first fraction and 300 mg (18%) of a second component (larger R_f) that proved to be diethyl-1-hydroxy-4-ethoxy-1,2-dihydronaphthalene **6***a*. Infrared (neat liquid) ν_{max}: 3480 and 1730 cm^{-1}; ^1H nmr: 1.05 (t, 3H, OCH_2CH_3, J = 6.0 Hz), 1.38 and 1.42 (overlapping t's, 6H, 2 × OCH_2CH_3), 4.04 (m, 5H, 2 × OCH_2CH_3 and H-2), 4.31 (q, 2H, OCH_2CH_3, J = 6.0 Hz), 5.08 (d, d, 1H, H-1, J = 6.0 Hz; with added D_2O this signal collapses to a doublet, J = 6.0 Hz), and 7.20–7.80 (m, 4H, aromatic); ^1H nmr (DMSO-d_6): 0.95–1.40 (m, 9H, 3 × OCH_2CH_3), 3.70–4.28 (m, 7H, 3 × OCH_2CH_3 and H-2), 5.16 (t, 1H, H-1, J = 6.0 Hz, with added D_2O this signal collapses to a doublet, J = 6.0 Hz), 5.80 (d, 1H, CO*H*, J = 6.0 Hz, this signal disappears in added D_2O), and 7.36–7.75 (m, 4H, aromatic). *Exact Mass* calcd. for $C_{18}H_{22}O_6$: 334.142; found (hrms): 334.146.

The third fraction (568 mg, 34%) isolated from the column proved to be an isomer, **6***b*, of the previous substance. It was also obtained as an oil and had the following physical properties: ir (neat liquid) ν_{max}: 3480 and 1730 cm^{-1}; ^1H nmr: 1.13, 1.30 and 1.38 (overlapping t's, 9H, 3 × OCH_2CH_3), 2.18 (bs, 1H, CO*H*, disappears in added D_2O), 4.05 (m, 5H, 2 × OCH_2CH_3 and H-2), 5.00 (d, 1H, H-1, J = 4.5 Hz), and 7.30–7.80 (m, 4H, aromatic). *Exact Mass* calcd. for $C_{18}H_{22}O_6$: 334.142; found (hrms): 334.140.

When the reaction was repeated under the same conditions as above, except that a different batch of silica was used, two compounds were isolated. The first fraction (238 mg, 15%), an oil, was identified as **4** and the second fraction (970 mg, 63%), also an oil, was identified as **9**. Infrared (neat liquid) ν_{max}: 3480, 1735 and 1665 cm^{-1}; ^1H nmr: 1.03–1.43 (m, 6H, 2 × OCH_2CH_3), 2.80 (bs, 1H, CO*H*), 3.90–4.36 (m, 5H, 2 × OCH_2CH_3 and H-2), 5.10 (bs, 1H, H-1), 7.43–8.10 (m, 4H, aromatic), and 12.80 (s, 1H, CO*H*). *Exact Mass* calcd. for $C_{16}H_{18}O_6$: 306.107; found (hrms): 306.110.

Conversion of 6a, 6b, and 9 to 5

In each case, the compound was refluxed in benzene in the presence of catalytic quantities of *p*-toluenesulfonic acid for 30 min. The solution was washed with brine and dried over sodium sulfate to give **5** in 92–95% yield, identified by its spectroscopic properties.

Reaction of 1 with Maleic Anhydride 10

Ortho ester **1** (1.04 g, 5 mmol) and **10** (500 mg, 5 mmol) were heated together for 10 min at 165°C under a nitrogen atmosphere. The solution was cooled and the solid residue was crystallized from acetone to give 668 mg (56%) of white crystals that melted at 170–172°C and were identified as 1-ethoxynaphthalene-2,3-dicarboxylic acid anhydride. Infrared ν_{max}: 1845 and 1785 cm^{-1}; ^1H nmr: 1.55 (t, 3H, OCH_2CH_3, J = 7.5 Hz), 4.82 (q, 2H, OCH_2CH_3, J = 7.5 Hz), 7.50–8.20 (m, 3H, aromatic), 8.07 (s, 1H, aromatic), and 8.47 (m, 1H, aromatic). *Anal.* calcd. for $C_{14}H_{10}O_4$: C 69.42, H 4.16; found: C 68.98, H 4.17%. *Exact Mass* calcd. for $C_{14}H_{10}O_4$: 270.057; found (hrms): 270.054.

Acknowledgements

We thank the Natural Sciences and Engineering Research Council of Canada for financial support of this work and Consejo de Desarrollo Cientifico y Humanistica de la Universidad Central de Venezuela for a scholarship to Luis Contreras. We wish to acknowledge the contributions of Dr. C. E. Slemon in the early stages of this work.

1. L. CONTRERAS and D. B. MACLEAN. Can. J. Chem. **58**, 2573 (1980).
2. Z. HORII, T. KATAGI, Y. TAMURA, and T. TANAKA. Chem. Pharm. Bull. **10**, 887 (1962).
3. B. J. ARNOLD, S. M. MELLOWS, P. G. SAMMES, and T. W. WALLACE. J. Chem. Soc. Perkin Trans. I, 401 (1974).
4. A. S. KENDE, D. P. CURRAN, Y. TSAY, and J. E. MILLS. Tetrahedron Lett. 3537 (1977).
5. U. E. WIERSUM and W. J. MIJS. J. Chem. Soc. Chem. Commun. 347 (1972).
6. E. CHACKO, D. J. SARDELLA, and J. BORNSTEIN. Tetrahedron Lett. 2507 (1976).
7. M. HAMAGUCHI and T. IBATA. Chem. Lett. 287 (1976).
8. K. NAKANISHI. Infrared absorption spectroscopy. Holden Day, San Francisco. 1962. p. 42.

The barrier to rotation in 2,2′′-dimethyl-*o*-terphenyl and several 3,3′′-derivatives (rotational isomers of 1,2-di-*o*-tolylbenzene)

REGINALD H. MITCHELL[1] AND JOSEPH SHUE-HEN YAN

Department of Chemistry, University of Victoria, Victoria, B.C., Canada V8W 2Y2

Received June 9, 1980

This paper is dedicated to Prof. Raymond U. Lemieux on the occasion of his 60th birthday

REGINALD H. MITCHELL and JOSEPH SHUE-HEN YAN. Can. J. Chem. **58**, 2584 (1980).

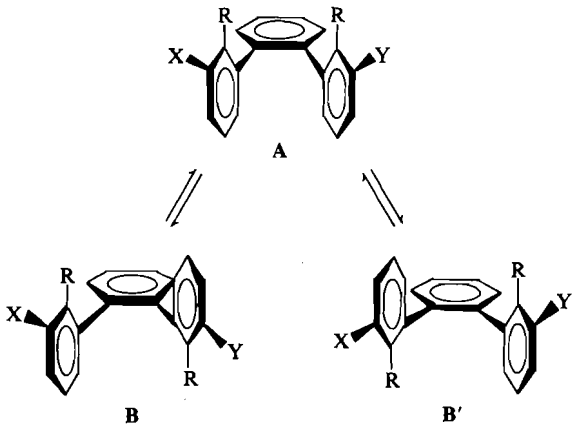
The synthesis and measurement of the barrier to rotation ($\Delta G_c^{\ddagger}$) in 2,2″-dimethyl-*o*-terphenyl (62 kJ/mol) and the following 3,3″-disubstituted derivatives is described (Cl, Cl, 74 kJ/mol), (Cl, CN, 70 kJ/mol), (CN, CN 70 kJ/mol), (CHO, 75 kJ/mol). For 3,3″-bis-CH_2Br, $\Delta\nu$, the separation of the —CH_3 peaks in the ^{1}Hmr spectrum, was too small to obtain $\Delta G_c^{\ddagger}$.

REGINALD H. MITCHELL et JOSEPH SHUE-HEN YAN. Can. J. Chem. **58**, 2584 (1980).

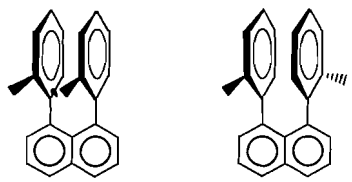
On décrit la synthèse et la mesure de la barrière à la rotation ($\Delta G_c^{\ddagger}$) du diméthyl-2,2″ *o*-terphényle (63 kJ/mol), et des dérivés 3,3″ disubstitués suivants: (Cl, Cl, 74 kJ/mol), Cl, CN, 70 kJ/mol), (CN, CN, 70 kJ/mol), (CHO, CHO, 75 kJ/mol). Dans le cas du composé bis CH_2Br-3,3″, le $\Delta\nu$, la séparation des pics du CH_3 dans le spectre rmn, est trop faible et ne permet pas d'obtenir le $\Delta G_c^{\ddagger}$.
[Traduit par le journal]

Introduction

Adams and Yuan (1), in their review on the stereochemistry of diphenyls in 1933, pointed out that suitably substituted *o*-terphenyls should be capable of existing as isomers. Huang (2) in 1954 synthesized 2,2′′-dimethoxy-*o*-terphenyl **1** and then in 1959 (3), 2,2′′-dichloro- *o*-terphenyl **2**, in an attempt to substantiate this postulate, but was unable to isolate separate isomers **A** and **B**, (**B′**). The



more recent interest in rotational gear or cog-wheel effects, together with the ability to determine thermodynamic parameters by ^{1}Hmr has restimulated investigation of such systems, for example, triptycenes (4), polyarylbenzenes (5) and 1,8-diphenyl- (6) and 1,8-di-*o*-tolylnaphthalenes (7). In the case of the latter, stable *cis*-**3** and *trans*-**4** isomers could be isolated. However, thus far the barrier to rotation



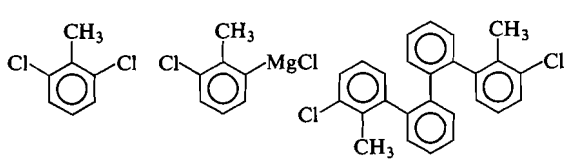
3 4

in simple 2,2′′-disubstituted-*o*-terphenyls appears still not to have been reported. This paper thus reports that measurement for 2,2′′-dimethyl-*o*-terphenyl and a number of 3,3′′-substituted examples.

Results and Discussion

Syntheses

Because of our interest in benzannelated annulenes (8) we required the bis-bromomethyl-*o*-terphenyl **5**. This was synthesized as follows. Reaction of commercial 2,6-dichlorotoluene **6** with magnesium in tetrahydrofuran gave the mono-Grignard reagent **7** which could be coupled with *o*-dibromobenzene in the presence of nickel(II) acetylacetonate as catalyst (9) to give 3,3′′-dichloro-2,2′′-dimethyl-*o*-terphenyl **8** in 60% yield as colourless crystals, mp 102–104°C. These were identified by their ^{1}Hmr spectrum (see below), their mass spectrum molecular ion ($M^{+\cdot}$) at *m/e* 326 (with



6 7 9

[1]Author to whom correspondence should be addressed.

0008-4042/80/232584-04$01.00/0

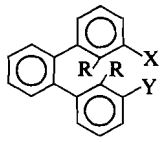
©1980 National Research Council of Canada/Conseil national de recherches du Canada

Can. J. Chem. Downloaded from www.nrcresearchpress.com by 210.87.254.105 on 09/05/12
For personal use only.

Can. J. Chem. Downloaded from www.nrcresearchpress.com by 210.87.254.105 on 09/05/12
For personal use only.

correct isotope pattern for two chlorine atoms) and by elemental analysis. The *quater* phenyl **9**, mp 173–175°C, $M^{+\cdot}$ at *m/e* 402, was also obtained in 3% yield as a minor product from this coupling reaction. This method for the synthesis of *o*-terphenyls appears to be easier than most earlier (10) syntheses.

Conversion of the dichloride **8** to the dinitrile **10** was readily accomplished by the von Braun reaction using cuprous cyanide in *N*-methylpyrrolidin-2-one in 85–95% yield. Compound **10** was obtained as white crystals, mp 151–153°C. The structure was confirmed by its ir band at 2240 cm^{-1} (C≡N) and $M^{+\cdot}$ at *m/e* 308. About 5% of the mono-nitrile **11**, mp 100–102°C, was also obtained, $M^{+\cdot}$ at *m/e* 313. The *o*-cyano group deshields the neighbouring methyl protons in the ^{1}Hmr spectrum of both **10** and **11** by about 0.2 ppm from those in **8**.



	R	X	Y
1	OCH_3	H	H
2	Cl	H	H
5	CH_3	CH_2Br	CH_2Br
8	CH_3	Cl	Cl
10	CH_3	CN	CN
11	CH_3	CN	Cl
12	CH_3	CHO	CHO
13	CH_3	CH_2OH	CH_2OH
14	CH_3	H	H

Reduction of the dinitrile **10** to the dialdehyde **12** was achieved by diisobutyl aluminum hydride in benzene in 86% yield. The dialdehyde **12**, mp 141–143°C, showed the aldehyde protons at δ 10.2 in its ^{1}Hmr spectrum, the —C=O stretch at 1685 cm^{-1} in its ir spectrum, and $M^{+\cdot}$ at *m/e* 314. The dialdehyde **12** was reduced with sodium borohydride in THF in essentially quantitative yield to the diol **13**, mp 135–137°C, ir band at 3250 cm^{-1} (—OH), and —OH proton at δ 1.62 (readily exchangeable with D_2O). Treatment of the diol with PBr_3 in benzene then led to the desired bis(bromomethyl) compound **5**, mp 129–130°C in 74% yield. The mass spectrum of **5** showed the expected 1:2:1 isotope pattern centered at *m/e* 446 for its molecular ion, and the —CH_2Br protons at δ 4.35 in its ^{1}Hmr spectrum.

The parent 2,2′′-dimethyl-*o*-terphenyl **14** was obtained by conversion of dichloride **8** to its Grignard reagent and reaction with water. Compound **14**, mp 84–86°C, gave $M^{+\cdot}$ at *m/e* 258 as the base peak in its mass spectrum. With the syntheses of such compounds achieved, the barrier to rotation could thus be measured.

Proton Magnetic Resonance Results

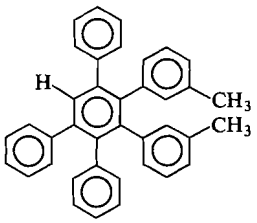
For ^{1}Hmr spectra that are relatively simple, e.g. where the low temperature spectrum consists of two peaks and these collapse to a single peak at higher temperature, the coalescence temperature (T_c) method to estimate $\Delta G_c^{\ddagger}$ (the transition state free energy at coalescence) is most often used (see, for example, ref. 11). This method simply involves measurement of T_c and the frequency separation (Δν) of the peaks concerned at the low temperature limit. Then $\Delta G_c^{\ddagger}$ can be calculated from eq. [1] (12).

$$[1] \quad \Delta G_c^{\ddagger}(\text{kJ/mol}) = 0.01913T_c(9.972 + \log T_c/\Delta\nu)$$

The results for the systems under study here are shown in Table 1.

It is important to note that while this method is simple, it has its limitations, for example, the linewidth of the signals must be small in comparison to Δν. This is reasonably true here.[2] Further, $\Delta G_c^{\ddagger}$ values so obtained should only be compared within similar examples such that $\Delta S^{\ddagger}$ is approximately constant (otherwise a complete lineshape analysis is preferred). This would also seem to be reasonable for the systems under study.

From the data given in Table 1, it can be seen that for the parent **14**, the barrier to rotation is ca. 62 kJ/mol,[3] and that 3,3′′-substituents add a further 8–13 kJ/mol to this barrier. The closest analogies to **14** in the literature appear to be the pentaaryl benzene **15** and the di-*o*-tolylnaphthalene **3**, where



15

the barriers are 65 kJ/mol (5*c*) and 101 kJ/mol (7), respectively. For **3** without the *o*-methyl groups (i.e. for 1,8-diphenylnaphthalene) the barrier is 63 kJ/mol (6). Clearly our results compare favourably with these, and for **14** the change in barrier on adding an *o*-substituent might reasonably be ex-

[2]Except for **5** where $\Delta G_c^{\ddagger}$ was not able to be obtained.

[3]The main error comes from estimation of T_c (±2°C) which gives an error in $\Delta G_c^{\ddagger}$ of about ±0.5 kJ/mol.

Can. J. Chem. Downloaded from www.nrcresearchpress.com by 210.87.254.105 on 09/05/12
For personal use only.

TABLE 1. Thermodynamic data for the barrier to rotation in 3,3''-disubstituted-2,2''-*o*-terphenyls[a]

Compound	X	Y	Δν (Hz)	T_c (°C)	$\Delta G_c^{\ddagger}$ (kJ/mol)
14	H	H	9.0	9	61.9
8	Cl	Cl	7.1	58	73.7
11	Cl		8.0	42	69.7
		CN	7.1	38	69.1
10	CN	CN	7.7	42	69.8
12	CHO	CHO	6.0	62	75.1
5	CH_2Br	CH_2Br	< 1	—	—

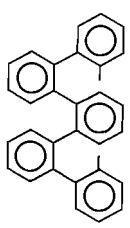
[a]Spectra were determined using ca. 25 mg of sample in 0.5 mL $CDCl_3$ on a Perkin-Elmer R32 (90 MHz) spectrometer: Δν was measured at ca. −40°C.

pected to be smaller than for **3** where the rings are closer to each other.

For the *o*-terphenyl system **14**, the size of the 3,3''-substituent (other than for H) only makes a small difference in the magnitude of the barrier, and follows the order H < CN < Cl, CHO, in fair agreement with other systems (13). It is of interest to note that in the mono-CN, mono-Cl **11**, the barrier is the same as for the di-CN **10**, some 4 kJ/mol less than for the di-Cl **8**. Presumably the linear —C≡N group can slide by more readily than the more spherical —Cl. Some modification of the hybridization at C-2 and 2'' may also be occurring because of the change at C-3,3''.

In the case of **3** and **4** where separate isomers were found to exist, the *trans*-isomer **4** had its methyl protons more shielded. This seems likely also in our system, and for the parent **14** the $-CH_3$ resonances appear at δ 2.0 and δ 2.1 (−40°C); thus the *cis*-isomer **14A** is assigned to δ 2.1 and the *trans*-isomer **14B** to δ 2.0. This is also consistent with previous work on a variety of cyclophanes (14).

Now that we have shown that in simple *o*-terphenyls the barrier to rotation can be measured by the ^{1}Hmr method, we anticipate that this will stimulate work with other 2,2''-substituents. Indeed during the preparation of this manuscript, Hammerschmidt and Vögtle (15) have reported the barrier for bis-*o*-terphenyl **16** to be 71.1 kJ/mol, in



16

excellent agreement with our results, despite the more complicated 2''-substituent which itself has rotational possibilities.

Experimental

All melting points were determined on a Kofler hot stage and are uncorrected. The ^{1}Hmr spectra were determined in $CDCl_3$ (unless otherwise stated) on a Perkin-Elmer R12A (60 MHz) or R32 (90 MHz) spectrometer and are reported in ppm downfield from tetramethylsilane as internal standard. The ir spectra were recorded on a Pye-Unicam SP1000 spectrometer.

Mass spectra were determined on a Hitachi Perkin-Elmer RMU-7 or Finnigan 3300 mass spectrometer at 70 eV. Microanalyses were performed by this department. All evaporations were carried out under reduced pressure on a rotary evaporator at ca. 40°C. Extracts were dried with anhydrous sodium sulfate.

3,3''-Dichloro-2,2''-dimethyl-o-terphenyl ***8***

The Mono-Grignard Reagent ***7***

A solution of 2,6-dichlorotoluene **6** (50.5 g, 0.314 mol) in dry tetrahydrofuran (150 mL) was added dropwise over 30 min to gently warmed Mg (7.63 g, 0.314 mol) under N_2. When the addition was complete the reaction mixture was heated under reflux for 3 h and then diluted with a further portion of THF (50 mL).

The Coupling

A solution of *o*-dibromobenzene (37 g, 0.0157 mol) in dry THF (100 mL) was added dropwise over 30 min to the stirred Grignard **7** held at −70°C under N_2. $Ni(Acac)_2$ (16) (0.8 g, 20 mmol) was then added and the reaction mixture was allowed to warm to ~20°C for 1 h and then refluxed for 12 h. After cooling and addition of ice water, the organic layer was washed with aqueous HCl, water, and then dried and evaporated. The residual brown oil was preabsorbed and chromatographed on silica gel using pentane as eluant to yield firstly the product dichloride **8** (65 g, 60%, individual yields varied between 35–60% over several runs). Recrystallization from cyclohexane yielded colourless crystals, mp 102–104°C; ^{1}Hmr (60 MHz, 25°C) δ: 7.5–6.7 (m, 10H, ArH) and 2.11 and 2.05 (s, 3H each, $-CH_3$); $M^{+\cdot}$ *m/e*: 326 (correct isotope pattern, 57), 291 (17), 256 (18), 166 (17), 165 (61), 126 (59), 125 (32), and 119 (100). *Anal.* calcd. for $C_{20}H_{16}Cl_2$: C 73.61, H 4.94; found: C 73.46, H 4.88.

Eluted subsequently was 3,3'''-dichloro-2,2''''-dimethyl-*o*-quaterphenyl **9** (1.9 g, 3%), colourless crystals from cyclohexane, mp 173–175°C; ^{1}Hmr (60 MHz, 25°C) δ: 7.5–6.3 (m, 14H, ArH), and 1.65 and 1.48 (s, ca. 3H each, $-CH_3$); $M^{+\cdot}$ *m/e*: 402 (100). *Anal.* calcd. for $C_{26}H_{20}Cl_2$: C 77.61, H 4.98; found: C 77.47, H 4.99.

3,3''-Dicyano-2,2''-dimethyl-o-terphenyl ***10***

Cuprous cyanide (25 g, 0.275 mol) was added to a solution of dichloride **8** (20.5 g, 62.9 mmol) in *N*-methyl-2-pyrrolidinone (65 mL) and then the reaction was heated under reflux for 12 h. A further portion of CuCN (25 g) in *N*-methyl-2-pyrrolidinone (65 mL) was then added and reflux continued for a further 12 h. After cooling to ca. 100°C, the reaction mixture was poured onto ice (200 g) and concentrated ammonia ("880", 200 mL). After mixing thoroughly, the precipitate was removed by filtration and washed well with dilute ammonia before extraction with dichloromethane. The organic layer was washed, dried, and evaporated and the residual brown oil was chromatographed over silica gel using pentane–dichloromethane (3:7) as eluant to yield firstly 3-chloro-3''-cyano-2,2''-dimethyl-*o*-terphenyl, **11**, (1.05 g, 5%), mp 100–102°C; ir (KBr): 2240 (—C≡N) cm^{-1}; ^{1}Hmr (60 MHz, 25°C) δ: 7.6–6.7 (m, 10H, ArH), 2.30 and 2.25 (s, total 3H, *o*-NC—ϕ—CH_3), and 2.10 and 2.05 (s, total 3H, *o*-Cl—ϕ—CH_3); $M^{+\cdot}$ *m/e*: 317 (100), 302 (16), and 282 (57). *Anal.* calcd. for $C_{21}H_{16}ClN$: C 79.37, H 5.04, N 4.41; found: C 79.58, H 5.01, N 4.43. Eluted next was the product **10** (18.5 g, 95%), white crystals from ethanol, mp 151–153°C; ir (KBr) 2240 (—C≡N) cm^{-1}; ^{1}Hmr (60 MHz, 25°C) δ: 7.6–7.0 (m, 10H, ArH) and 2.30 and 2.25 (s, 6H total, $-CH_3$); $M^{+\cdot}$ *m/e*: 308 (100), 307 (35), and

Can. J. Chem. Downloaded from www.nrcresearchpress.com by 210.87.254.105 on 09/05/12
For personal use only.

292 (47). *Anal.* calcd. for $C_{22}H_{16}N_2$: C 85.68, H 5.23, N 9.09; found: C 85.48, H 5.19, N 8.67.

2,2''-Dimethyl-o-terphenyl 3,3''-Dicarboxaldehyde **12**

Diisobutylaluminum hydride (113 mmol) in hexane (86 mL) was added dropwise under N_2 to a solution of dinitrile **10** (14.5 g, 47.1 mmol) in dry benzene (140 mL) at 20°C with mechanical stirring. After 12 h, the viscous pale yellow solution was decomposed (with ice bath cooling) by addition of methanol (7 mL), then methanol–water (1:1, 10.5 mL), and then concentrated HCl – water (1:2, 40 mL) such that the resultant solution was slightly acidic. The mixture was extracted with dichloromethane and the organic layer was washed, dried, and evaporated. The resulting brown oil was filtered through a short column of silica gel in pentane–dichloromethane (1:9) to yield the product dialdehyde **12** (12.7 g, 86%). A portion was recrystallized from carbon tetrachloride as white crystals, mp 141–143°C; ir (KBr) 1685 (—CHO) cm^{-1}; ^{1}Hmr (60 MHz, 25°C) δ: 10.2 (s, 2H, —CHO), 7.7–7.0 (m, 10H, ArH), and 2.40 and 2.37 (s, total 6H, —CH_3); $M^{+\cdot}$ *m/e*: 314 (100), 299 (60), and 243 (41). *Anal.* calcd. for $C_{22}H_{18}O_2$: C 84.05, H 5.77; found: C 84.37, H 5.52.

3,3''-Bis(hydroxymethyl)-2,2''-dimethyl-o-terphenyl **13**

A solution of dialdehyde **12** (13.3 g, 42 mmol) in *undried* tetrahydrofuran (95 mL) was added dropwise to a stirred slurry of $NaBH_4$ (1.2 g, 32 mmol) in THF (15 mL) at 20°C. After 12 h the mixture was decomposed with water (5 mL) and concentrated HCl (5 mL). The aqueous layer was saturated with NaCl and extracted with dichloromethane. The organic layers were dried and evaporated to give crude dialcohol **13** (13 g, 98%). A portion was recrystallized from benzene to yield white crystals, mp 135–137°C; ir (KBr): 3240 (—OH) cm^{-1}; ^{1}Hmr (60 MHz, 25°C) δ: 7.5–6.7 (m, 10H, ArH), 4.53 (s, 4H, —CH_2OH), 2.00 (s, 6H, —CH_3), and 1.62 (bs, 2H, —CH_2O*H*, exchanged with D_2O); $M^{+\cdot}$ *m/e*: 318 (100), 300 (63), 285 (69), 282 (86), 270 (84), 296 (88), 267 (85), and 255 (76). *Anal.* calcd. for $C_{22}H_{22}O_2$: C 82.98, H 6.97; found: C 82.88, H 6.95.

3,3''-Bis(bromomethyl)-2,2''-dimethyl-o-terphenyl **5**

A solution of PBr_3 (20 mL, 0.20 mol) in dry benzene (200 mL) was added dropwise over 3 h to a vigorously stirred solution of crude diol **13** (13 g, 41 mmol) in dry benzene (400 mL) containing 5 drops of pyridine at 20°C. After 12 h, ice water was added and the organic layer was washed with aqueous $NaHCO_3$ and water and then dried and evaporated. The resulting brown oil was chromatographed on silica gel using pentane–dichloromethane (7:3) as eluant to yield product bromide **5** (13.5 g, 74%). Recrystallization from cyclohexane gave white crystals, mp 129–130°C; ^{1}Hmr (60 MHz, 25°C) δ: 7.5–6.7 (m, 10H, ArH), 4.35 (s, 4H, —CH_2Br), and 2.07 (s, 6H, —CH_3); $M^{+\cdot}$ *m/e*: 446 (41, correct 1:2:1 isotope pattern), 367 and 365 (48), 366 and 364 (100). *Anal.* calcd. for $C_{22}H_{20}Br_2$: C 59.88, H 4.54; found: C 59.99, H 4.51.

2,2''-Dimethyl-o-terphenyl **14**

A solution of dichloride **8** (3 g, 9.2 mmol) in dry tetrahydrofuran (50 mL) was added dropwise over 30 min to active (17) Mg (2 mmol) in THF and then refluxed for 3 h. After cooling, water was added and the product was extracted into dichloromethane. The organic layer was washed, dried, and evaporated, and the residual oil chromatographed on silica gel using pentane as eluant to yield **14** (1.66 g, 70%) as an oil, which could only be crystallized from pentane with difficulty, mp 84–86°C; ^{1}Hmr (60 MHz, 25°C) δ: 7.15 (s, 4H, central ring ArH), 7.1–6.7 (m, 8H, outer ring ArH), and 1.87 (s, 6H, ArCH); $M^{+\cdot}$ *m/e*: 258 (100), 243 (62), and 228 (35). *Anal.* calcd. for $C_{20}H_{18}$: C 92.98, H 7.02; found: C 92.69, H 7.00.

Acknowledgements

We thank the Natural Sciences and Engineering Research Council of Canada and the University of Victoria for support of this work.

1. R. Adams and H. C. Yuan. Chem. Rev. **12**, 261 (1933).
2. R. L. Huang. J. Chem. Soc. 3655 (1954).
3. R. L. Huang and K. H. Lee. J. Chem. Soc. 923 (1959).
4. G. Yamamoto and M. Oki. Chem. Lett. 1251 (1979); 1255 (1979).
5. (*a*) D. Gust. J. Am. Chem. Soc. **99**, 6980 (1977); (*b*) D. Gust and A. Patton. J. Am. Chem. Soc. **100**, 8175 (1978); (*c*) A. Patton, J. W. Dirks, and D. Gust. J. Org. Chem. **44**, 4749 (1979).
6. R. L. Clough and J. D. Roberts. J. Org. Chem. **43**, 1328 (1978).
7. R. L. Clough and J. D. Roberts. J. Am. Chem. Soc. **98**, 1018 (1976).
8. R. H. Mitchell and J. S.-H. Yan. Can. J. Chem. **55**, 3347 (1977).
9. R. J. P. Corriu and J. P. Masse. J. Chem. Soc. Chem. Commun. 144 (1972).
10. G. R. Ames. Chem. Rev. **58**, 895 (1958).
11. H. H. Hutton, W. E. Hiebert, and V. Mark. Can. J. Chem. **56**, 1261 (1978); I. C. Calder and P. J. Garratt. J. Chem. Soc. B, 660 (1967); R. Gygax, J. Wirz, J. T. Sprague, and N. L. Allinger. Helv. Chim. Acta, **60**, 2522 (1977); H. Kessler. Angew. Chem. Int. Ed. Engl. **9**, 219 (1970).
12. S. Glasstone, K. J. Laidler, and H. Eyring. Theory of rate processes. McGraw-Hill Book Co., New York, NY. 1941; H. S. Gutowsky and C. H. Holm. J. Chem. Phys. **25**, 1228 (1956).
13. H. Förster and F. Vögtle. Angew. Chem. Int. Ed. Engl. **16**, 429 (1977).
14. W. Anker, G. W. Bushnell, and R. H. Mitchell. Can. J. Chem. **57**, 3080 (1979).
15. E. Hammerschmidt and F. Vögtle. Chem. Ber. **113**, 1121 (1980).
16. R. G. Charles and M. A. Pawlikowski. J. Phys. Chem. **62**, 440 (1958).
17. R. D. Rieke and S. E. Bales. J. Am. Chem. Soc. **96**, 1775 (1974).

Use of a bacteriophage to depolymerize a polysaccharide to an oligosaccharide; comparison of the ^1H and ^{13}C nuclear magnetic resonance spectra of the polymer and its hexasaccharide repeating unit[1]

GUY G. S. DUTTON, ANGELA V. SAVAGE, AND MICHEL VIGNON[2]

Department of Chemistry, University of British Columbia, Vancouver, B.C., Canada V6T 1Y6

Received May 1, 1980

This paper is dedicated to Prof. Raymond U. Lemieux on the occasion of his 60th birthday

GUY G. S. DUTTON, ANGELA V. SAVAGE, and MICHEL VIGNON. Can. J. Chem. **58**, 2588 (1980).

A β-D-galactosidase associated with bacteriophage ϕ18 has been used to depolymerize the capsular polysaccharide of *Klebsiella* serotype K18 into the hexasaccharide corresponding to one repeating unit of the polymer. The nmr spectra of the polymer and of the oligosaccharide are comparable, leading to the conclusion that the conformations in solution of the repeating unit of the two substances are similar.

GUY G. S. DUTTON, ANGELA V. SAVAGE et MICHEL VIGNON. Can. J. Chem. **58**, 2588 (1980).

Le bactériophage ϕ18, qui contient une β-D-galactosidase, a été utilisé pour dépolymériser le polyoside capsulaire de *Klebsiella* K18 en hexasaccharide correspondant à une unité répétitive. Les spectres de rmn du polyoside et de l'hexasaccharide sont comparables ce qui nous amène à conclure que les conformations de l'unité répétitive des deux composés en solution sont semblables.

Nuclear magnetic resonance (nmr) spectroscopy may be used to study the solution properties of oligo- and polysaccharides, but a direct comparison of the nmr parameters of a polysaccharide and those of the oligosaccharide, corresponding to one repeating unit of the polysaccharide, is hard to achieve. This difficulty arises since few polysaccharides are known to have regular structures and selective cleavage into one, specific oligosaccharide is often impossible by chemical means.

During the last few years studies (e.g. 1–3) on the structure of the capsular polysaccharides associated with *Klebsiella* bacteria have shown these polymers to be built up of regular repeating units and, incidentally, to exhibit many different structural patterns. Furthermore, for many of these capsular polysaccharides there exists a specific bacterial virus (or bacteriophage) containing an endoglycanase (4). Each enzyme is capable of hydrolyzing a particular capsular polysaccharide into oligosaccharides corresponding to one (or more) repeating units. Since the pure, capsular polysaccharides are readily obtained in gram amounts this technique of using the appropriate bacteriophage also makes available the corresponding oligosaccharide. This paper reports a comparative nmr study on the polysaccharide from *Klebsiella* serotype K18 and the related oligosaccharide.

[1]Presented at the annual meeting of the French Carbohydrate Group, Orléans, France, December 18–20, 1978.

[2]Present address: Centre de Recherches sur les Macromolecules Végétales, C.N.R.S., 53X, 38041 Grenoble, France.

Results and Discussion

Preparation of the Hexasaccharide

The capsular polysaccharide from *Klebsiella* K18 has been shown (5) to be based on a repeating unit having three sugar units in the main chain and a side chain also containing three sugar residues (3 + 3 type); see Figs. 1 and 3, wherein the sugar residues are labelled for convenience **A–F**.

A bacteriophage was isolated from sewage, propagated on *Klebsiella* K18, and purified through isopycnic centrifugation on cesium chloride, according to standard procedures (6). This bacteriophage contains a β-D-galactosidase and thus incubation with the capsular polysaccharide from *Klebsiella* K18, which contains only one β-D-galactopyranosyl unit, yields a linear hexasaccharide corresponding to **F—E—D—C—A—B** (Figs. 2 and 4). The incubation mixture was desalted on Sephadex G-10, dialyzed against distilled water, and the concentrated dialyzate was fractionated on a column of Biogel P-2 to give the pure hexasaccharide.

Proton Nuclear Magnetic Resonance Measurements

The native K18 polysaccharide and the derived hexasaccharide were separately exchanged with D_2O and the proton spectra were run at 250 MHz at a temperature of 80–90°C. The spectra are shown in Figs. 1 and 2 and were compared with respect to the chemical shifts and T_1 relaxation times of the anomeric protons (7). The relevant data are presented in Table 1 from which it may be seen that there is little difference in the chemical shifts of the

0008-4042/80/232588-04$01.00/0

©1980 National Research Council of Canada/Conseil national de recherches du Canada

Can. J. Chem. Downloaded from www.nrcresearchpress.com by 210.87.254.5 on 09/05/12
For personal use only.

Can. J. Chem. Downloaded from www.nrcresearchpress.com by 210.87.254.5 on 09/05/12
For personal use only.

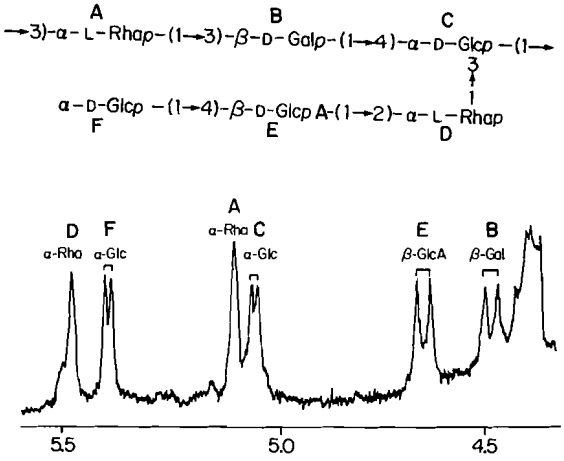


FIG. 1. 250 MHz proton spectrum (anomeric region) of polysaccharide K18.

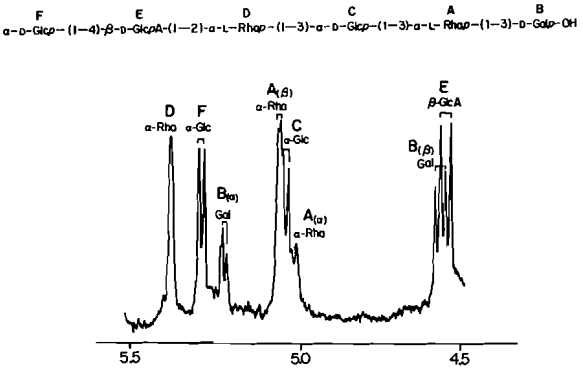


FIG. 2. 250 MHz proton spectrum (anomeric region) of hexasaccharide (for details see text).

anomeric protons in the polysaccharide and the hexasaccharide, except for the β-D-galactopyranosyl residue (unit **B**) which becomes the reducing group in the oligosaccharide; this shift confirms that the phage enzyme is a β-D-galactosidase. It is also clear from Figs. 1 and 2 that the anomeric proton in the α-L-rhamnopyranosyl residue (unit **A**), joined to the reducing galactose residue, is split on account of the mutarotation equilibrium.

The most noteworthy change in T_1 values is that of an α-D-glucopyranosyl residue (unit **C**). This may be attributed to the fact that in the polysaccharide unit **C** represents a branch point whereas the oligosaccharide is linear. It must, however, be pointed out that the T_1 data for unit **C** in the hexasaccharide may not be too accurate due to overlap of the signal from H-1 of unit **C** with that of H-1 from unit **A**. The change in T_1 values for the β-D-galactopyranosyl residue (unit **B**) is to be anticipated since this becomes the reducing terminus of the oligosaccharide (7). It may, however, be observed that the axial H-1 of the β-D-galactose anomer has a significantly shorter relaxation time than the equatorial proton of the α-anomer, due to 1–3 diaxial interactions. The ratio of the α/β times is 1.67 in agreement with the results of Hall and Preston (7).

The polysaccharide contains two sugars that are β-linked; one in the main chain (**B**) and the other in the side chain (**E**). It is of interest that there is no significant difference in their T_1 values. The same is true of the two α-D-glucopyranosyl units, one terminal (**F**) and one constituting a branch point (**C**). For the two α-L-rhamnopyranosyl residues (**A** and **D**) the T_1 values are different, but not greatly so.

^{13}C *Nuclear Magnetic Resonance Measurements*

The anomeric carbons of the polysaccharide K18 and of the hexasaccharide were assigned by selective heteronuclear irradiation of the corresponding anomeric protons; the spectra are shown in Figs. 3 and 4 and the chemical shifts of the anomeric carbon atoms are given in Table 2. The only significant changes are those of the β-D-galactopyranosyl residue (**B**) which becomes the reducing end of the oligosaccharide; two signals corresponding to the mutarotational equilibrium are clearly distinguishable at 97.15 and 93.10 ppm for the anomeric carbon, and at 61.85 and 61.65 ppm for the primary alcohol group (C-6), of unit **B** in the hexasaccharide. Minor shifts are evident for units **D** and **F**. It is of interest that the signal due to the anomeric carbon atom of the α-L-rhamnopyranosyl unit (**A**), glycosidically linked to the reducing D-galactopyranosyl residue (**B**), does not exhibit any splitting as observed in the corresponding proton spectrum.

TABLE 1. Chemical shifts and proton spin–lattice relaxation times for the anomeric protons of polysaccharide K18 and the derived hexasaccharide

Sugar residue[a]	Symbol[b]	Polysaccharide δ[c]	Polysaccharide T_1 (s)	Hexasaccharide δ[c]	Hexasaccharide T_1 (s)
α-Rha	**D**	5.49	0.55	5.41	0.56
α-Glc	**F**	5.40	0.60	5.32	0.63
α-Rha	**A**	5.10	0.63	5.09 (β) 5.03 (α)	0.62 0.66
α-Glc	**C**	5.05	0.61	5.07	0.52
β-GlcA	**E**	4.65	0.48	4.58	0.45
β-Gal	**B**	4.49	0.50	4.59 (β) 5.25 (α)	0.78 1.30

[a]α-Rha = α-rhamnopyranosyl etc.
[b]For the significance of the letters A–E see Figs. 1 and 2.
[c]Chemical shifts are given in ppm relative to internal acetone, δ = 2.23 downfield from sodium 4,4-dimethyl-4-silapentane-1-sulfonate (DSS).

Can. J. Chem. Downloaded from www.nrcresearchpress.com by 210.87.254.5 on 09/05/12
For personal use only.

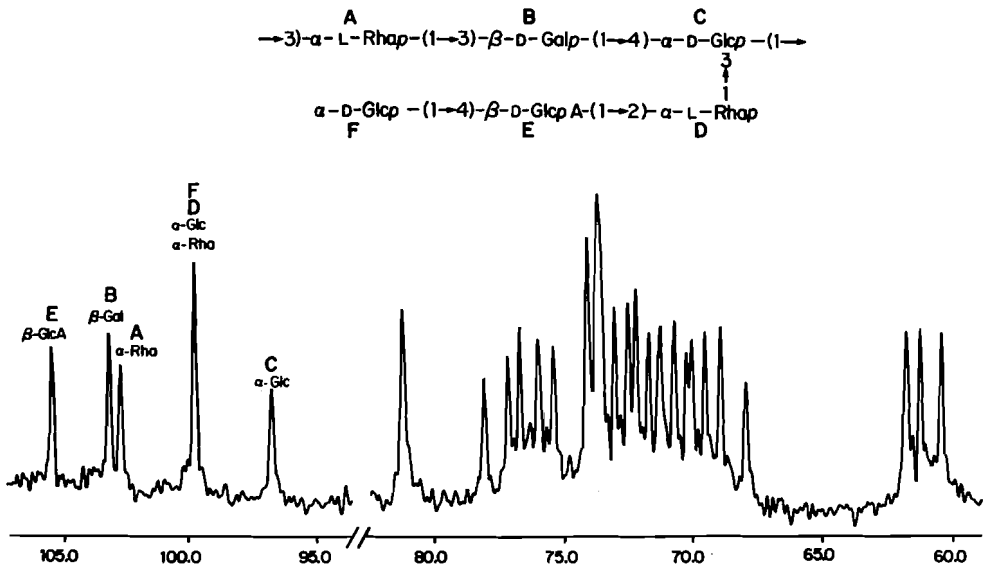


FIG. 3. 62.8 MHz ^{13}C spectrum (60–105 ppm) of polysaccharide K18.

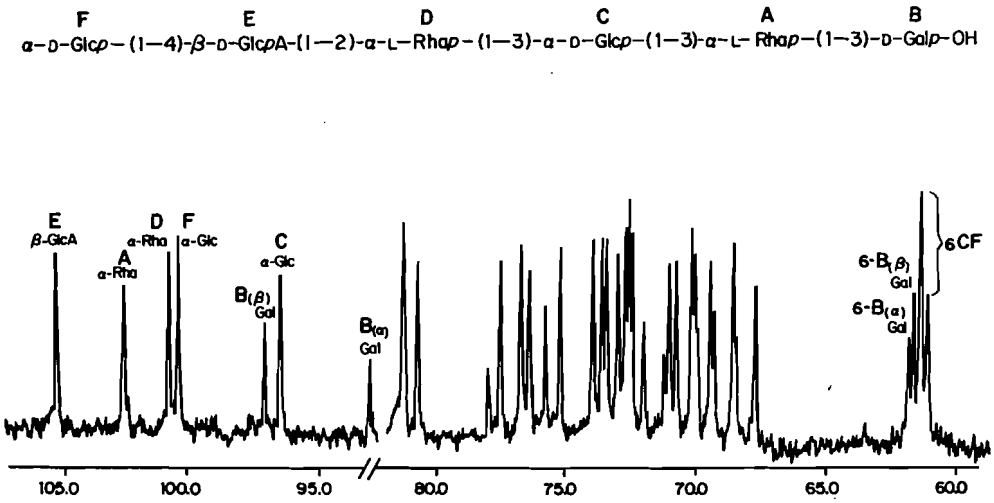


FIG. 4. 62.8 MHz ^{13}C spectrum (60–105 ppm) of hexasaccharide (for details see text).

TABLE 2. Chemical shifts of the anomeric carbon atoms of polysaccharide K18 and the derived hexasaccharide

Sugar residue[a]	Symbol[b]	δ[c] Polysaccharide	δ[c] Hexasaccharide
β-GlcA	E	105.20	105.20
β-Gal	B	103.20	97.15 (β) 93.10 (α)
α-Rha	A	102.60	102.55
α-Rha	D	99.85	100.80
α-Glc	F	99.85	100.40
α-Glc	C	96.80	96.55

[a]As for Table 1.
[b]As for Table 1.
[c]Chemical shifts are given in ppm relative to internal acetone, δ = 31.07 downfield from sodium 4,4-dimethyl-4-silapentane-1-sulfonate (DSS).

Conclusions

This investigation demonstrates that the use of viral enzymes is a convenient method for obtaining oligosaccharides corresponding to one (or more) repeating units of the polysaccharide. In the case of *Klebsiella* capsular polysaccharides, the structures so far reported are based on repeating units of tri- to hepta- saccharides and the derived oligosaccharide may be either linear or branched, depending upon the structure of the original polymer and the nature of the glycosidase. For those polysaccharides that contain acid labile groups, e.g. pyruvic acid acetals (1-carboxyethylidene substituents), it has been demonstrated elsewhere (8) that depolymerization by viral enzymes is the only practical method of

Can. J. Chem. Downloaded from www.nrcresearchpress.com by 210.87.254.5 on 09/05/12
For personal use only.

obtaining an oligosaccharide corresponding to an intact repeating unit.

While it is recognized that changes in chemical shifts, either proton or ^{13}C, represent a relatively unsophisticated basis of comparison, measurement of T_1 values is more sensitive. In either case, the differences reported here for the K18 polysaccharide and the hexasaccharide are minor and lead to the conclusion that the conformations in solution of these two compounds are very similar.

Experimental

Propagation of Bacteriophage

The bacteriophage used was *Klebsiella* phage ϕ18, isolated originally from sewage (6). The host for this phage is *Klebsiella* serotype K18, the structure of whose capsular polysaccharide is known (5). For all phage work the standard procedures given by Adams (9) were used and full details of phage propagation and purification have been given elsewhere (6).

An initial stock of bacteriophage ϕ18 was obtained by the confluent lysis technique (9) and propagation was carried out sequentially in 250, 500, and 1000 mL wash bottles with sintered glass air inlets. *Klebsiella* K18 was grown in these bottles in standard broth (5 g bactopeptone, 3 g bacto-beef extract, and 2 g sodium chloride per L) with strong aeration until the optical density was 1.0–1.2 at 660 nm (1 cm cell) when $\sim 10^9$ colony forming organisms per mL were present. The medium was infected with 3 PFU (plaque forming units) of phage ϕ18 per cell; lysis occurred 30 min later and incubation was continued for a further 1 h.

A total of 1300 mL of medium containing 10^{10} PFU/mL was obtained and the phage were precipitated with polyethylene glycol 6000 (6). Subsequent isopycnic centrifugation (6) through a gradient of cesium chloride gave a total of $\sim 6 \times 10^{12}$ PFU.

Depolymerization of Polysaccharide K18

Capsular polysaccharide from *Klebsiella* K18 (350 mg) was dissolved in 50 mL of phosphate-buffered physiological saline (PBS) and 6×10^{12} PFU of phage ϕ18 in 20 mL of PBS were added. The solution was incubated for 48 h at 37°C and the progress of the reaction was monitored viscometrically (6). The reaction mixture was lyophilized, redissolved in 3 mL of water, and desalted on a column (100 cm × 19.5 cm^2) of Sephadex G-10. The column was eluted with a water–pyridine – glacial acetic acid buffer (500:5:2; pH 4.5) at a flow rate of 25 mL/h and carbohydrate material was localized using the Molisch test.

The desalted material (340 mg) was dialyzed against 3 × 1 L of distilled water and lyophilization yielded 45 mg of nondialyzable material (13%) and 290 mg of oligosaccharides. The dialyzable material was dissolved in 3 mL of the buffer (pH 4.5) applied to the top of a column of Biogel P-2 and was eluted with the same buffer. Fractions (3 mL) were collected and assayed by the phenol – sulfuric acid method (10). A fraction (F-1, 185 mg) was eluted in the void volume, a fraction (F-2, 50 mg) contained a mixture of oligosaccharides, corresponding to two and three repeating units, and a pure fraction (F-3, 30 mg) was the hexasaccharide.

Nuclear Magnetic Resonance Measurements

The capsular polysaccharide K18 and the hexasaccharide obtained by bacteriophage degradation were each exchanged several times with D_2O. The proton spectra were run at 80–90°C and both ^1H and ^{13}C nmr spectra were recorded on a Cameca 250 MHz (62.80 MHz) spectrometer; anomeric carbon atoms were assigned by selective heteronuclear spin decoupling.

The measurements of proton T_1 values were made with WH Bruker (270 MHz) and WM Bruker (250 MHz) instruments on 1% (w/v) solutions in 99.96% D_2O at 87°C. The inversion recovery method was used for T_1 determination (two pulse sequence $(T...180...t...90)_n$) with 10–15 t values. The peak heights of the different anomeric protons were measured as a function of delay times (t) and these data were then used for a computer program.

Acknowledgements

This research was carried out under a Canada–France exchange program. We are grateful to the National Research Council of Canada and le Centre National de la Recherche Scientifique for a Fellowship (to M.R.V.) to spend a year at the University of British Columbia, to MacMillan Bloedel Ltd for a Scholarship (to A.V.S.), and to the Natural Sciences and Engineering Research Council of Canada for continuing financial support (to G.G.S.D.).

We thank Dr. R. Wylde (Montpellier) for her interest in this work, Dr. K. Bock (Lyngby) for measuring T_1 values and the use of his computer program, and Dr. S. Stirm (Giessen) for the bacteriophage ϕ18.

1. H. Niemann and S. Stirm. Carbohydr. Res. **59**, 165 (1977).
2. B. Lindberg, F. Lindh, J. Lönngren, and W. Nimmich. Carbohydr. Res. **70**, 135 (1979).
3. E. H. Merrifield and A. M. Stephen. Carbohydr. Res. **74**, 241 (1979).
4. D. Rieger-Hug and S. Stirm. Virology. In press.
5. G. G. S. Dutton, K. L. Mackie, and M.-T. Yang. Carbohydr. Res. **65**, 251 (1978).
6. H. Thurow, H. Niemann, and S. Stirm. Carbohydr. Res. **41**, 257 (1975).
7. (*a*) L. D. Hall and C. M. Preston. Carbohydr. Res. **49**, 3 (1976); (*b*) C. M. Preston and L. D. Hall. Carbohydr. Res. **37**, 267 (1974).
8. G. G. S. Dutton, K. L. Mackie, A. V. Savage, D. Rieger-Hug, and S. Stirm. Carbohydr. Res. In press.
9. M. Adams. Bacteriophages. Interscience, New York, NY. 1959.
10. M. Dubois, K. A. Gilles, J. K. Hamilton, P. A. Rebers, and F. Smith. Anal. Chem. **28**, 350 (1956).

The mass spectrometric behavior of 3α,5-cyclo-5α-cholestan-6β-yl alkyl ethers[1]

FREDERICK J. BROWN,[2] IAN J. MASSEY, AND CARL DJERASSI[3]
Department of Chemistry, Stanford University, Stanford, CA 94305, U.S.A.

Received May 20, 1980

This paper is dedicated to Prof. Raymond U. Lemieux on the occasion of his 60th birthday

FREDERICK J. BROWN, IAN J. MASSEY, and CARL DJERASSI. Can. J. Chem. **58**, 2592 (1980).

The 3α,5-cyclo-6β-methoxy (*i*-methyl ether) moiety is a common protective grouping in steroid partial synthesis. Therefore, the mass spectrometric behavior of 6β-hydroxy-3α,5-cyclo-5α-cholestane, the corresponding methyl, ethyl, and *tert*-butyl ethers, the analogous ketone, and the parent hydrocarbon has been investigated in order to determine the mechanisms of the characteristic fragmentations of these compounds. Such knowledge is essential for unequivocal structure elucidation by mass spectrometry and also bears on the current interest in the stereospecificity of electron impact induced eliminations. Deuterium labeling of carbon atoms 1,2,3,4,7,8,9, and 19 of 6β-methoxy-3α,5-cyclo-5α-cholestane established the course of methanol extrusion and the identity of the highly diagnostic A ring cleavage ion $M^{+\cdot} - 55$. Mechanisms are proposed for these key fragmentations. The mass spectra of the methyl, ethyl, and *tert*-butyl ethers of cholesterol are analyzed, and the features distinguishing these compounds from the isomeric 3,5-cyclosteroids are noted.

FREDERICK J. BROWN, IAN J. MASSEY et CARL DJERASSI. Can. J. Chem. **58**, 2592 (1980).

La fonction cyclo-3α,5 méthoxy-6β (éther méthylique *i*) est un groupe protecteur courant dans les synthèses partielles de stéroides. Par conséquent, on a étudié le comportement en spectrométrie de masse de l'hydroxy-6β cyclo-3α,5 cholestane-5α, des éthers méthylique, éthylique et *tert*-butylique correspondants, de la cétone analogue et de l'hydrocarbure de base dans le but de déterminer les mécanismes des fragmentations caractéristiques de ces composés. Une telle connaissance est essentielle à la détermination univoque de la structure par spectrométrie de masse et présente également de l'intérêt pour la compréhension de la stéréospécificité des éliminations induites par impact électronique. Le marquage des atomes de carbone-1,2,3,4,7,8,9 et 19 du méthoxy-6β cyclo-3α,5 cholestane-5α par du deutérium a permis d'établir le mode d'élimination du méthanol et l'identité de l'ion caractéristique $M^{+\cdot} - 55$ résultant du clivage du cycle A. On propose des mécanismes pour ces fragmentations fondamentales. On a analysé les spectres de masse des éthers méthylique, éthylique et *tert*-butylique du cholestérol et on a noté les particularités qui distinguent ces composés des cyclo-3,5 stéroïdes isomères.

[Traduit par le journal]

Introduction

The continuing discoveries of new marine sterols possessing unique side chains (2) have spawned a number of intriguing hypotheses concerning the biological origins (2*a*, *c*) and roles of such compounds (3). Investigations directed toward probing these questions, as well as the unequivocal structure proofs of the new sterols themselves, rely on the partial syntheses of these compounds from tetracyclic steroidal precursors. Invariably these syntheses involve protecting the nuclear Δ^5-3β-alcohol moiety as a 3,5-cyclosteroid (4) during elaboration of the side chain (5, 27). In addition, these 3,5-cyclosteroids have proven valuable in recent preparations of plant hormones (6) and A-nor steroids (7). Although mass spectrometry plays a vital role in the structure confirmation of intermediates in these syntheses, a systematic study of the mass spectral behavior of the important 3,5-cyclosteroids has not been published. This fact, in conjunction with a recent report of the stereoselective electron impact induced elimination of methanol from arylcyclohexyl methyl ethers (8), prompted us to investigate the mass spectrometric behavior of 6β-methoxy-3α,5-cyclo-5α-cholestane, some homologous 3,5-cyclocholestanes, and the isomeric cholesterol ethers.

The mass spectra of 6β-hydroxy-3α,5-cyclo-5α-cholestane (**1**) (9) and the corresponding methyl (**2**) (10), ethyl (**3**) (11), and the heretofore unknown *tert*-butyl[4] (**4**) ethers are reproduced in Fig. 1. In each case the elimination of ROH (R = H, CH_3, C_2H_5, and *t*-C_4H_9, respectively) from the molecular ion generates a prominent peak at *m/z* 368. In light of the recent report of stereoselective methanol elimination from cyclohexyl methyl ethers upon electron impact ionization (8), we were interested in determining whether the expulsion of an ROH molecule from these 3,5-cyclosteroids involved a site- and/or stereospecific hydrogen abstraction. To this end 6β-methoxy-3α,5-cyclo-5α-cholestane (**2**; *i*-cholesteryl methyl ether) was labeled with deuterium specifically at carbon atoms 1, 2, 3, 4, 7, 8, 9, and 19 (see Table 1).

In every case the deuterated *i*-cholesteryl methyl ether, **2**, was obtained from the correspondingly labeled cholesterol by tosylation and subsequent solvolysis in anhydrous, potassium acetate-

[1]Paper 256 in the series "Mass Spectrometry in Structural and Stereochemical Problems". For part 255, see ref. 1.

[2]Taken in part from the Ph.D. dissertation of F. J. Brown, Stanford University, 1980.

[3]Author to whom correspondence should be addressed.

[4]The corresponding *n*-butyl ether, 6β-*n*-butoxy-3α,5-cyclo-5α-cholestane, is known (12).

0008-4042/80/232592-08$01.00/0
©1980 National Research Council of Canada/Conseil national de recherches du Canada

Can. J. Chem. Downloaded from www.nrcresearchpress.com by 210.87.254.5 on 09/05/12
For personal use only.

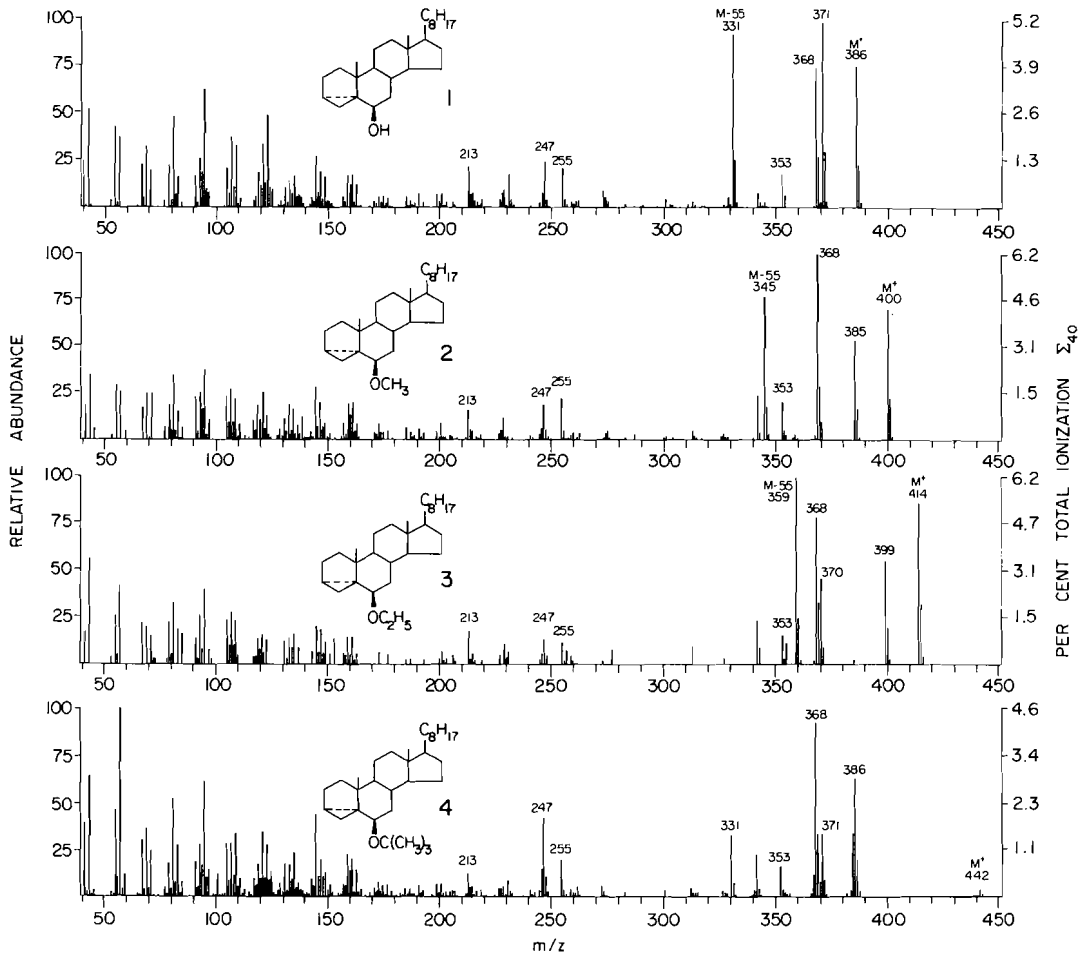


FIG. 1. Electron impact mass spectra of 3α,5-cyclo-5α-cholestanes measured on a Varian-MAT 711 spectrometer at 70 eV. Identities of designated ions (corroborated by labeling data and high resolution mass measurements): *m/z* 213 loss of ring D, H, ROH; *m/z* 255 loss of C_8H_{17}, ROH; *m/z* 247 loss of rings A and B plus one hydrogen atom (deuterium labeling of **2** demonstrated that C-8 (60%) and C-9 (27%) were the origins of the itinerant hydrogen atom, in general agreement with the data for the analogous fragmentation of cholesterol (17)).

buffered methanol (4*a*). The syntheses of 7,7-d_2-, 8β-d_1-, and 9α-d_1-cholesterol have been described in a previous paper from this laboratory (13). The 2,2,4,4-d_4 and 3α-d_1 analogs were prepared via the enol acetate of 4-cholesten-3-one (13) by the procedure of Ockels and Budzikiewicz (14). Cholesterol-4β-d_1 was obtained from 4,6-cholestadien-3-one (13) by the method employed by Fétizon *et al.* (15) in the androstane series, while the 4,4-d_2 compound was synthesized from 4-oxocholesteryl benzoate according to the procedure of Barton *et al.* (16). 1,4-Cholestadien-3-one was converted to cholesterol-1α-d_1 as described by Tökés *et al.* (17). Cholesterol-19,19-d_2 was obtained by electrochemical[5] reduction (18) of 5-cholesten-3β-ol-19-al 3-acetate (19).

[5]We thank Dr. L. Throop (Syntex Research, Palo Alto, CA) for the use of his electrochemical apparatus.

The isotopic composition of each of the labeled 6β-methoxy-3α,5-cyclo-5α-cholestanes is given in Table 1, along with the deuterium-induced shifts observed for two key peaks in the mass spectra. These deuterated compounds were invaluable for defining the mechanisms of some of the diagnostic fragmentations of the 3,5-cyclosteroids as well as for implicating the protons abstracted in the course of methanol extrusion from **2**.

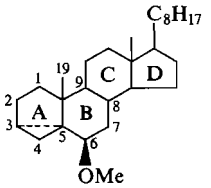
Results and Discussion

m/z *368 Ion*

An intense peak, resulting from the elimination of ROH from the molecular ion, is seen at *m/z* 368 in all of the spectra of Fig. 1. A number of studies of substituted cyclohexanols have established that electron impact induced loss of water occurs predominantly by *cis* 1,3- and 1,4-eliminations in-

Can. J. Chem. Downloaded from www.nrcresearchpress.com by 210.87.254.5 on 09/05/12
For personal use only.

TABLE 1. Peak shifts[a] in the mass spectra of deuterated 6β-methoxy-3α,5-cyclo-5α-cholestane (**2**)



Compound	Isotopic composition, %	*m/z* Values for fragment ions (% shift[b] resulting from labeling) $M^{\ddagger} - CH_3OH$	$M^{\ddagger} - C_4H_7$
2-d_0	—	368	345
-1α-d_1	98d_1	368 (6%)	345
	2d_0	369 (94%)	
-2,2,4,4-d_4	52d_4	371 (32%)	345
	32d_3	372 (68%)	
	8d_2		
	8d_5		
-4,4-d_2	97d_2	369 (10%)	345
	2d_1	370 (90%)	
	1d_3		
-4β-d_1	94d_1	368 (5%)	345
	3d_0	369 (95%)	
	3d_2		
-3-d_1	100d_1	368 (14%)	345
		369 (86%)	
-7,7-d_2	96d_2	369 (18%)	347
	4d_0	370 (82%)	
-8β-d_1	93d_1	368 (9%)	346
	7d_2	369 (91%)	
-9α-d_1	82d_1	368 (9%)	346
	15d_0	369 (91%)	
	3d_2		
-19,19-d_2	99d_2	368 (3%)	347
	1d_3	369 (97%)	
Total % of migrating hydrogen accounted for:		(97%)	

[a]The % shift values have been corrected for natural isotope abundance and deuterium composition.
[b]These figures are reliable to ±5%.

volving abstraction of a proximal proton by the oxygen atom (20). The expulsion of methanol from cyclohexyl methyl ethers has been shown to proceed by an identical process (8, 21). However, one would predict 1,4-elimination from the intact steroid *i*-methyl ether **2** to be precluded since the 9α-proton, being situated on the opposite face of the steroid from the 6β-methoxy group, is prohibited from approaching to within close proximity of the 6β-oxygen atom. *Cis* 1,3-elimination would involve the stereospecific abstraction of either the 4α- or 8β-hydrogen atoms.

Despite these predictions, the labeling data in Table 1 for the 4,4-d_2- and the 4β-d_1-*i*-cholesteryl methyl ethers demonstrate that the proton loss from C-4 is small (10%) and *not* stereospecific. Moreover, the inaccessible 9α-hydrogen atom is abstracted to the same extent as the accessible 8β-proton (9%). Certainly these facts prove that the expulsion of methanol is not occurring by simple elimination from the intact steroid. The multiple origins of the abstracted hydrogen atom (C-7: 18%; C-8: 9%; C-9: 9%; C-4: 10%, C-3: 14%; C-2: 22%; C-1: 12%[6]) demonstrate that fairly extensive cleavage and/or rearrangement of the steroid skeleton must occur prior to the loss of methanol, just as was observed for the extrusion of water from cholesterol under electron impact (17).

The rigidity of the 3,5-cyclosteroid nucleus limits the closest approach of the 6β-oxygen atom to either the 4α- or 8β-proton to approximately 2.6 Å (according to a Dreiding model). This interatomic distance falls considerably outside of the maximum 1.8 Å limit established for hydrogen abstractions by oxygen atoms in alcohols (22) and ketones (23). Thus simple elimination of methanol is disfavored and other initial bond cleavages predominate.

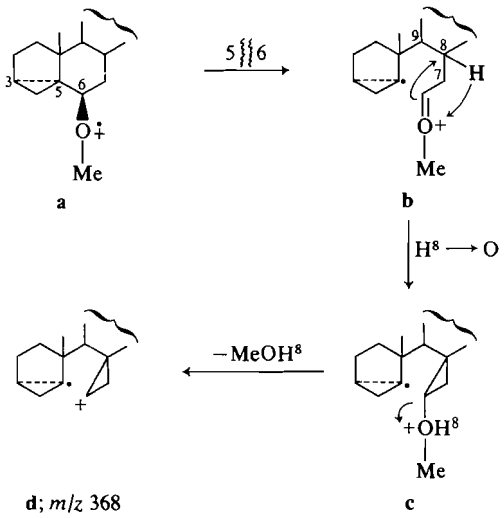
Nonetheless, the eventual expulsion of a hydroxyl-containing moiety from **1** and the related alkyl ethers **2**, **3**, and **4** is a facile process since it gives rise to a pronounced peak in each of the spectra of Fig. 1. Furthermore, this fragmentation is enhanced at low voltages; the *m/z* 368 ion accounts for 20% of the total ion current (Σ_{40}) displayed by **2** at 12 eV. Hydrogen abstraction from carbon atoms 7, 8, and 9 can be accounted for by a common mechanism in which the initial bond cleavage is the well established α-fission of an ether (24). Cleavage of the 5—6 bond of molecular ion **a** generates the relatively stable oxonium ion **b**. Scission of the 5—6 bond, producing a tertiary radical at C-5, should be preferred over the analogous fission of the 6—7 bond which would generate a primary radical. An investigation of acyclic ethers has demonstrated that an oxonium ion such as **b** will rearrange by transferring hydrogen to the oxygen atom via a 4-, 5-, or 6-membered cyclic transition state (25). Thus process **b** → **d**, or a similar mechanism involving hydrogen migration from C-7 or C-9, would explain the loss of protons from carbon atoms 7, 8, and 9 during methanol expulsion. As indicated by the data of Table 1, this mechanism accounts for the generation of approximately 40% of the *m/z* 368 ion.

Inspection of a Dreiding model of species **b** indicates that the oxygen atom cannot come within close proximity of the protons in ring A. Therefore, to explain the abstraction of hydrogen atoms from carbons 1, 2, 3, and 4, a second mechanism is

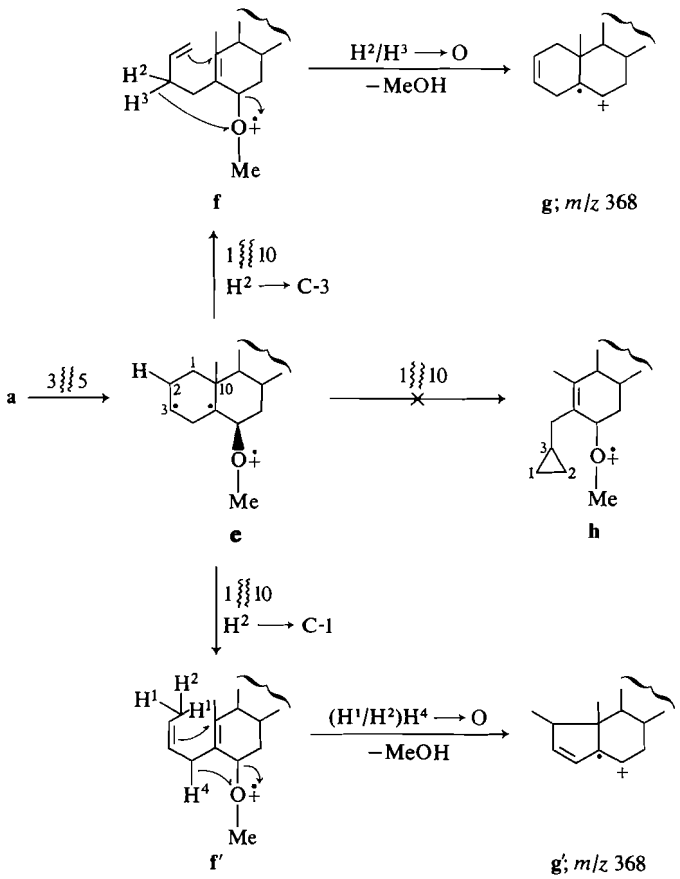
[6]This figure was generated by making the plausible assumption that proton abstraction from C-1 is non-stereospecific.

Can. J. Chem. Downloaded from www.nrcresearchpress.com by 210.87.254.5 on 09/05/12
For personal use only.

Can. J. Chem. Downloaded from www.nrcresearchpress.com by 210.87.254.5 on 09/05/12
For personal use only.



proposed by postulating that initial scission of the cyclopropyl ring of molecular ion **a** is competitive with the α-fission process **a** → **b**. Such a hypothesis is not unreasonable since homolysis of the 3-membered ring relieves much of the excessive strain present in the 3,5-cyclosteroid system. Furthermore, Dias and Djerassi (26) have shown that the mass spectrometric behavior of cyclopropanes can often be explained by invoking preferential rupture of the most highly substituted cyclopropyl bond. Application of this principle to *i*-cholesteryl methyl ether (**2**) suggests that fission of the 3,5-bond to give ion **e** could trigger the subsequent rearrangements leading to the elimination of methanol. Cleavage of the 1—10 bond and migration of a proton from C-2 to the radical site at either C-3 or C-1 yields the more stable dienes **f** or **f′**, respectively. The transfer of an allylic proton from C-3 (H^2 or H^3) of species **f** to the oxygen atom via a 6-membered cyclic transition state followed by expulsion of methanol (**f** → **g**) generates the ionized diene **g**. Alternatively, the migration of an allylic hydrogen atom from C-4 (H^4) or C-1 (H^2 or H^1) in ion **f′** leads to the analogous radical cation **g′**. Since this mechanism migrates the C-2 proton to either C-3 or C-1 prior to methanol expulsion, H^2 should be eliminated from the charge-retaining fragment to the same extent as loss of the C-3 proton plus 1/2



Can. J. Chem. Downloaded from www.nrcresearchpress.com by 210.87.254.5 on 09/05/12
For personal use only.

the loss (statistical correction) of the two C-1 protons. This is indeed the case.

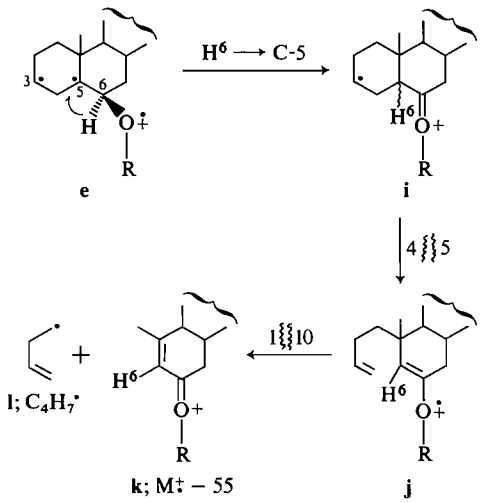
Alternatively, if the possibility of hydrogen migration from C-2 in ion **e** is ignored, 1—10 bond rupture leads to the cyclopropane species **h** in which all of the A ring protons are accessible for participation in the expulsion of methanol. In such a species the proton loss from C-1 and C-2 should be identical. However, Table 1 shows significant differences in the extent of hydrogen loss from C-1 (12%) and C-2 (22%). Hence mechanism **a** → **g** is postulated to explain hydrogen abstraction from carbon atoms 1, 2, 3, and 4, a process which accounts for approximately 60% of the $M^{\ddagger} - CH_3OH$ ion.

Thus the extrusion of methanol from 6β-methoxy-3α,5-cyclo-5α-cholestane is not a simple elimination process, but rather is preceded by cleavages associated with the methoxyl or cyclopropyl substituents. The subsequent hydrogen transfer in intermediates **b** and **f** then proceeds through the usual (25) cyclic transition states. These mechanisms should also be applicable to the loss of water from 6β-hydroxy-3α,5-cyclo-5α-cholestane (**1**) and the expulsion of an alcohol molecule from the corresponding ethyl (**3**) and *tert*-butyl (**4**) ethers.

$M^{\ddagger} - 55$ Ion

A very strong peak at $M^{\ddagger} - 55$, corresponding to the loss of C_4H_7 from the molecular ion, is a ubiquitous feature of the mass spectra of steroids containing the 6β-methoxy-3α,5-cyclo moiety (27). This diagnostic ion is observed in the spectra (Fig. 1) of 6β-hydroxy-3α,5-cyclo-5α-cholestane (**1**, *m/z* 331), the corresponding methyl ether (**2**, *m/z* 345), and the ethyl ether (**3**, *m/z* 359). However, it is conspicuously absent in the spectra of both the parent hydrocarbon, 3α,5-cyclo-5α-cholestane (28) (**5**, spectrum not reproduced), and the *tert*-butyl ether **4**.

The labeling data in Table 1 indicate that the $M^{\ddagger} - 55$ ion arises from the elimination of carbon atoms 1, 2, 3, and 4 without any (reciprocal) hydrogen transfer. The absence of a corresponding peak in the mass spectrum of the hydrocarbon **5** proves that this fragmentation is not characteristic of the isolated 3,5-cyclosteroid functionality, but rather requires the concurrent presence of an oxygen substituent at carbon 6. The further observation that 3α,5-cyclo-5α-cholestan-6-one (29) (**6**, spectrum not reproduced) also fails to produce a $M^{\ddagger} - 55$ ion in the mass spectrometer suggests that a proton at carbon 6, as well as an oxygen atom, is essential. The following mechanism is consistent with these facts and again starts with the molecular



ion **e** in which the cyclopropane ring has suffered homolytic fission.

Migration of the activated C-6 proton to the adjacent radical site at C-5 in molecular ion **e** produces oxonium ion **i**. Subsequent scission of the 4—5 bond gives the ionized enol ether **j**. The even-electron, unsaturated oxonium ion **k**[7] is formed by cleavage of the 1—10 bond and expulsion of the homoallylic radical **l**. This mechanism applies equally well to the alcohol **1** (R = H) or the ethyl ether **3** (R = C_2H_5). 3α,5-Cyclo-5α-cholestan-6-one would not be expected to undergo process **e** → **k** because the proton at C-6 is no longer available, and thus the C-5 radical cannot be saturated by proton transfer (**e** → **i**) to trigger the requisite 4—5 bond scission (**i** → **j**). In the same vein, one would predict that the fragmentation pathway **e** → **k** would not be nearly as favorable for the hydrocarbon 3α,5-cyclo-5α-cholestane since the lack of a C-6 oxygen atom precludes the formation of such stable ions as **i**, **j**, or **k**.

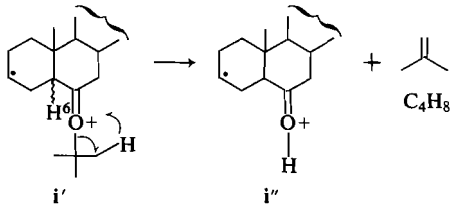
However, the question remains why the mass spectrum of the *tert*-butyl ether **4** does not exhibit a $M^{\ddagger} - 55$ ion. Certainly this compound meets all the prerequisites demanded by the proposed mechanism. The existence of a tertiary carbon atom in the ether substituent must present an alternative fragmentation pathway that is more favorable than the A ring cleavage process **e** → **k**. This hypothesis can, in fact, be documented.

The spectrum of **4** (Fig. 1) contains prominent peaks corresponding to the elimination of isobutylene or its equivalent (*m/z* 386) and isobutylene plus a methyl radical (*m/z* 371). This alkene loss undoubtedly occurs by the well known process of

[7]Djerassi *et al.* (30) have postulated that a species identical to **k** (R = H) is responsible for the $M^{\ddagger} - 55$ ion observed in the mass spectra of 6-keto steroids.

Can. J. Chem. Downloaded from www.nrcresearchpress.com by 210.87.254.5 on 09/05/12
For personal use only.

hydrogen migration and olefin expulsion from an oxonium ion (24, 25). Thus, the *tert*-butyl analog of ion **i** (R = t-C_4H_9) can transfer a proton from the ether substituent to the oxygen atom with subsequent (or concomitant) fission of the carbon–oxygen bond to eliminate isobutylene and regenerate another oxonium ion (**i'** → **i''**). This second oxonium ion **i''** is precisely the intermediate species **i** (R = H) that is formed when *i*-cholesterol (**1**) fragments according to route **e** → **k**. Hence **i''** should undergo further bond fissions to extrude radical **l** (**i**, R = H → **k**). Indeed, this additional fragmentation does occur, as is evidenced by the presence of a

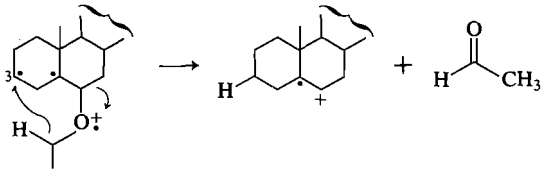


i' i''

peak at *m/z* 331 ($M^+ - (C_4H_8 + C_4H_7)$) in the mass spectrum of **4**.

In contrast to the *tert*-butyl ether **4**, the ethyl ether **3** does not eliminate a simple olefin. Instead the mass spectrum displays an ion at *m/z* 370 due to the loss of C_2H_4O. This fragmentation is most likely precipitated by migration of a heteroatom-activated secondary hydrogen atom from the α-carbon of the ethyl group to the C-3 radical in molecular ion **e**. Heterolytic fission of the carbon–oxygen bond then generates the ionized olefin **m**. The absence of the requisite α-proton prohibits the *tert*-butyl ether **4** from undergoing an analogous fragmentation, while the nonoccurrence of this aldehyde elimination in the *i*-methyl ether **2** is probably associated with the well-documented (25) propensity of secondary (rather than primary) hydrogens to undergo migration.

The elimination of a butene radical, comprised of carbon atoms 1, 2, 3, and 4 of the A ring, constitutes a very diagnostic fragmentation characteristic of 6β-hydroxy-3α,5-cyclo-5α-steranes and the corresponding alkyl ethers. The simultaneous presence of both an oxygen atom and a proton at carbon 6 appears to be a prerequisite for this cleavage. In the case of the *tert*-butyl ether **4** olefin expulsion precedes the A ring fragmentation. Thus all of the



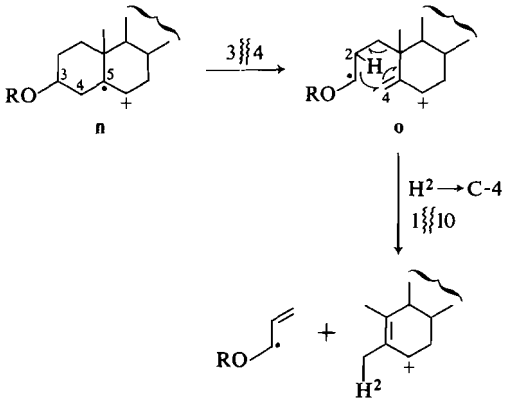
e m; *m/z* 370

experimental observations are nicely explained by a single mechanism.

Alkyl Ethers of Cholesterol

Surprisingly, the mass spectrometric behavior of cholesteryl alkyl ethers has scarcely been investigated (31). For this reason, as well as to allow comparisons with the *i*-cholesteryl ether spectra of Fig. 1, the mass spectra of the methyl (**7**), ethyl (**8**) (11), and *tert*-butyl (**9**) (32) ethers of cholesterol are presented in Fig. 2. The spectra of Figs. 1 and 2 exhibit many similarities in the molecular ion region: $M^+ - 15$ (loss of a methyl radical[8]), *m/z* 368 (loss of ROH), and *m/z* 353 (loss of ROH plus a methyl radical).

However, all of the spectra of Fig. 2 display a significant peak at *m/z* 329 ($M^+ - C_3H_4OR$) which is absent in the spectra of Fig. 1. The analogous cleavage has been observed for cholesteryl trimethylsilyl ether (33) and Δ^5-3-aminosteroids (34). This diagnostic fragmentation is undoubtedly due to cleavage of the A ring, triggered by scission of the doubly activated 3—4 bond.



n o p; *m/z* 329

Hydrogen transfer from C-2 to C-4 and fission of the 1—10 bond completes the process to yield an even-electron allylic cation **p**. The cholesteryl ethers are also distinguished from the isomeric 3,5-cyclosteroidal ethers by the absence of the $M^+ - 55$ ion which is so characteristic of the latter compounds.

Cholesteryl ethyl ether (**8**) loses a molecule of acetaldehyde (or its equivalent) in the mass spectrometer, as did the corresponding 3,5-cyclosteroid **3**. A mechanism similar to **e** → **m** would explain this fragmentation (*m/z* 414 → *m/z* 370). Migration of a hydrogen atom from the α-carbon of the 3β-ether moiety to the ring B olefin would generate a radical cation analogous to **m**. Cholesteryl *tert*-butyl ether

[8]The mass spectrum of **2**-19,19-d_2 proved that 96% of the $M^+ - CH_3$ ion in **2** is due to loss of the C-19 angular methyl.

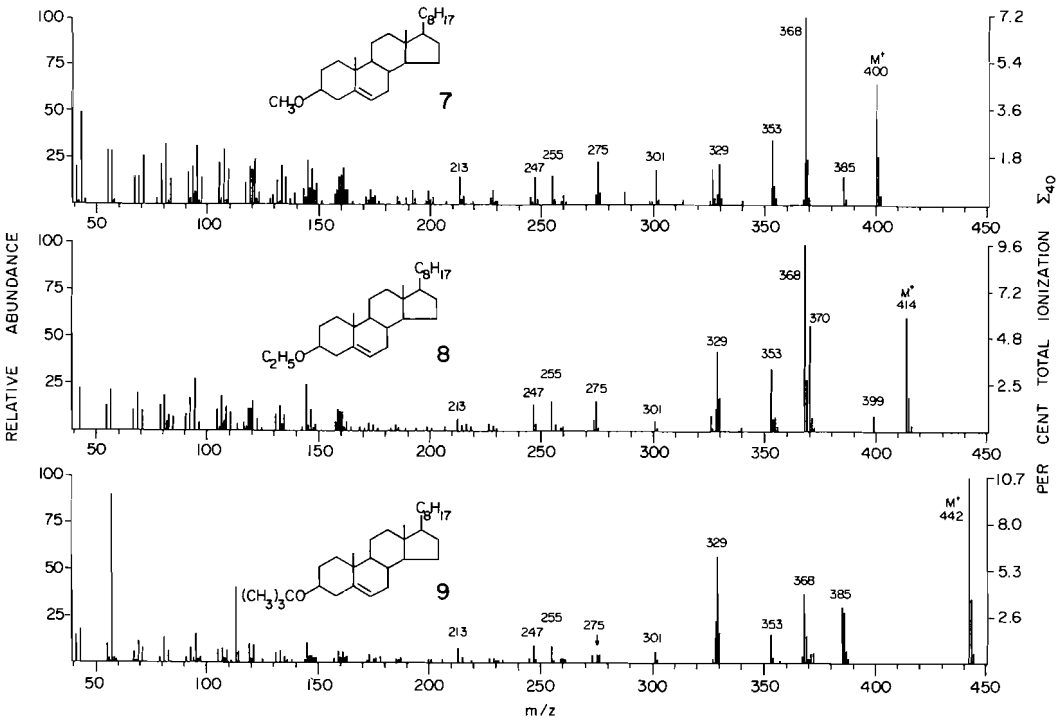


FIG. 2. Electron impact mass spectra of cholesteryl alkyl ethers measured on a Varian-MAT 711 spectrometer at 70 eV. Identities of designated ions (corroborated by labeling data and high resolution mass measurements): *m/z* 213, 247, 255, see Fig. 1; *m/z* 275 loss of C-1 through C-7 (17); *m/z* 301 loss of ring A, C-5, H (17).

(**9**) exhibits the loss of both isobutylene (*m/z* 386) and a *tert*-butyl radical (*m/z* 385), analogous to its 3,5-cyclosteroid counterpart **4**. Again, a similar mechanism is probably operating for both compounds.

Conclusions

Extensive deuterium labeling of 6β-methoxy-3α,5-cyclo-5α-cholestane (**2**) demonstrated that the electron impact induced loss of methanol is not a simple regiospecific elimination but rather is preceded by skeletal bond scissions. The multiple origins (carbons 1, 2, 3, 4, 7, 8, and 9) of the abstracted hydrogen atom are explained by postulating two competing fragmentation mechanisms which are respectively initiated by fission α to the ether substituent or rupture of the 3-membered ring. The prominent $M^+ - 55$ ion, which is highly diagnostic for 6β-hydroxy-3α,5-cyclo-5α-steroids and the corresponding ethers, was shown to result from the loss of carbon atoms 1, 2, 3, and 4 from ring A. A mechanism is proposed which accounts for the observed effects of substituents. The mass spectra of the methyl, ethyl, and *tert*-butyl ethers of cholesterol are analyzed. These compounds can be distinguished mass spectrometrically from the isomeric 3,5-cyclosteroidal ethers by the presence of a prominent ion at *m/z* 329 and the absence of a $M^+ - 55$ ion. The mass spectrometric behavior of more highly substituted analogs of the synthetically important 3,5-cyclosteroids can now be predicted on a mechanistically plausible basis.

Experimental

General Procedures

Mass spectra were obtained on either an AEI MS-9 spectrometer or a Varian-MAT 711 high-resolution mass spectrometer using direct inlet systems. The ^1H nmr spectra were obtained on a Varian XL-100-15 instrument using deuteriochloroform as solvent and tetramethylsilane as an internal standard. Infrared spectra were recorded on a Perkin-Elmer 700A spectrometer. Optical rotations were determined on an Autopol III polarimeter in a thermostated 1.00 dm micro cell. Melting points were taken on a Thomas-Hoover capillary melting point apparatus and are uncorrected.

6β-tert-Butoxy-3α,5-cyclo-5α-cholestane (4)

A solution of 1.4 g cholesteryl tosylate and 2.2 g freshly fused potassium acetate dissolved in 100 mL anhydrous *tert*-butanol (freshly distilled from calcium oxide and stored over 4 Å molecular sieves) was refluxed under nitrogen for 44 h. The *tert*-butanol was removed under vacuum and the resulting residue was partitioned between ether and water. The organic layer was washed with water, dried, and evaporated to yield 1.2 g of an oily yellow solid which was chromatographed on a 60 g tlc-grade silica gel column with 5% ethyl acetate in hexane. An initial fraction yielded 0.16 g (14%) **4** as a clear, colorless oil which resisted all attempts at crystallization: $[\alpha]_D^{20}$ +22° (*c* 0.115, $CHCl_3$); ir (thin film): 3075 (cyclopropyl σ_{C-H}), 1365, 1385

Can. J. Chem. Downloaded from www.nrcresearchpress.com by 210.87.254.5 on 09/05/12
For personal use only.

(*tert*-butyl ν_{C-H}), 1020, 1045 (ν_{C-O-C}) cm^{-1}; nmr δ: 2.97 (bt, 1H, C-6), 1.10 (s, 9H, *tert*-butyl), 0.82 (s, 3H, C-19), 0.72 (s, 3H, C-18), 0.44 (dd, 1H, 4β-H, $J = -5$ and 4 Hz), 0.19 (dd, 1H, 4α-H, $J = -5$ and 8 Hz); ms *m/z*: 442.4188 (M^+, calcd for $C_{31}H_{54}O$: 442.4174).

Subsequent fractions gave (in order of elution) *cholesteryl tert-butyl ether*, **9**: yield, 0.076 g (6%); mp 175–176°C (acetone) (lit. (33) mp 172–173°C); 0.43 g of a mixture of what appeared to be cholesteryl acetate and 3α,5-cyclo-5α-cholestan-6β-yl acetate; *6β-hydroxy-3α,5-cyclo-5α-cholestane*, **1**: yield, 0.13 g (13%); mp 71–74°C (acetone) (lit. (10) mp 73–74°C); and some cholesterol.

Acknowledgements

We thank Dr. Wolfgang Uedelhoven (NATO Research Fellow; German Academic Exchange Service, DAAD) for making the mass spectral measurements. Financial support by the National Institutes of Health (Grant AM-04257) is gratefully acknowledged.

1. D. G. PATTERSON, A. LAVANCHY, and C. DJERASSI. Org. Mass Spectrom. **15**, 41 (1980).
2. (*a*) C. DJERASSI, N. THEOBALD, W. C. M. C. KOKKE, C. S. PAK, and R. M. K. CARLSON. Pure Appl. Chem. **51**, 1815 (1979); (*b*) F. J. SCHMITZ. Marine natural products. Vol. I. *Edited by* P. J. Scheuer. Academic Press, New York, NY. 1970. Chapt. 5; (*c*) L. J. GOAD. Marine natural products. Vol. II. *Edited by* P. J. Scheuer. Academic Press, New York, NY. 1970. Chapt. 2; (*d*) L. MINALE and G. SODANO. Marine natural products chemistry. *Edited by* D. J. Faulkner and W. H. Fenical. Plenum Press, New York, NY. 1977. pp. 87–109.
3. R. M. K. CARLSON, C. TARCHINI, and C. DJERASSI. Frontiers of bio-organic chemistry and molecular biology. *Edited by* S. N. Ananchenko. Pergamon Press, Oxford, England. 1980. pp. 211–224.
4. (*a*) J. A. STEELE and E. MOSETTIG. J. Org. Chem. **28**, 571 (1963); (*b*) C. R. NARAYANAN, S. R. PRAKASH, and B. A. NAGASAMPAGI. Chem. Ind. 966 (1974).
5. (*a*) M. TANABE and K. HAYASHI. J. Am. Chem. Soc. **102**, 862 (1980); (*b*) W. C. M. C. KOKKE, C. TARCHINI, D. B. STIERLE, and C. DJERASSI. J. Org. Chem. **44**, 3385 (1979); (*c*) W. C. M. C. KOKKE, N. W. WITHERS, I. J. MASSEY, W. FENICAL, and C. DJERASSI. Tetrahedron Lett. 3601 (1979); (*d*) I. J. MASSEY and C. DJERASSI. J. Org. Chem. **44**, 2448 (1979); (*e*) C. TARCHINI, M. ROHMER, and C. DJERASSI. Helv. Chim Acta, **62**, 1210 (1979).
6. (*a*) M. J. THOMPSON, N. MANDAVA, J. L. FLIPPEN-ANDERSON, J. F. WORLEY, S. R. DUTKY, W. E. ROBBINS, and W. LUSBY. J. Org. Chem. **44**, 5002 (1979); (*b*) J. R. WIERSIG, N. WAESPE-SARCEVIC, and C. DJERASSI. J. Org. Chem. **44**, 3374 (1979).
7. E.-J. BRUNKE. Chem. Ber. **112**, 1606 (1979).
8. J. SHARVIT and A. MANDELBAUM. Tetrahedron, **33**, 1007 (1977).
9. E. M. KOSOWER and S. WINSTEIN. J. Am. Chem. Soc. **78**, 4347 (1956).
10. (*a*) M. S. PATEL and W. J. PEAL. J. Chem. Soc. 1544 (1963); (*b*) B. RIEGEL, G. P. HAGER, and B. L. ZENITZ. J. Am. Chem. Soc. **68**, 2562 (1946).
11. (*a*) S. WINSTEIN and A. H. SCHLESINGER. J. Am. Chem. Soc. **70**, 3528 (1948); (*b*) J. H. BEYNON, I. M. HEILBRON, and F. S. SPRING. J. Chem. Soc. 907 (1936).
12. A. BERTHO. Justus Liebigs Ann. Chem. **714**, 155 (1968).
13. F. J. BROWN and C. DJERASSI. J. Am. Chem. Soc. **102**, 807 (1980).
14. W. OCKELS and H. BUDZIKIEWICZ. Tetrahedron, **32**, 135 (1976).
15. M. FÉTIZON, H. T. HUY, and P. MOURGUES. Tetrahedron, **34**, 209 (1978).
16. S. ACHMATOWICZ, D. H. R. BARTON, P. D. MAGNUS, G. A. POULTON, and P. J. WEST. J. Chem. Soc. Perkin Trans. I, 1567 (1973).
17. S. G. WYLLIE, B. A. AMOS, and L. TÖKÉS. J. Org. Chem. **42**, 725 (1977).
18. L. TÖKÉS and L. J. THROOP. Organic reactions in steroid chemistry. Vol. I. *Edited by* J. Fried and J. A. Edwards. Van Nostrand Reinhold, New York. 1972. pp. 166–169.
19. R. M. MORIARTY and T. D. D'SILVA. Tetrahedron, **21**, 547 (1965).
20. (*a*) M. M. GREEN. Topics in stereochemistry. Vol. 9. *Edited by* N. Allinger and E. Eliel. Wiley, New York. 1976. pp. 35–110, and references therein; (*b*) J. SHARVIT and A. MANDELBAUM. Org. Mass Spectrom. **11**, 488 (1976).
21. G. W. KLEIN and V. F. SMITH, JR. J. Org. Chem. **35**, 52 (1970).
22. (*a*) M. M. GREEN, R. J. COOK, J. M. SCHWAB, and R. B. ROY. J. Am. Chem. Soc. **92**, 3076 (1970); (*b*) M. M. GREEN, D. BAFUS, and J. L. FRANKLIN. Org. Mass Spectrom. **10**, 679 (1975).
23. H. BUDZIKIEWICZ, C. DJERASSI, and D. H. WILLIAMS. Mass spectrometry of organic compounds. Holden-Day, San Francisco. 1967. p. 157.
24. F. W. MCLAFFERTY. Anal. Chem. **29**, 1782 (1957).
25. C. DJERASSI and C. FENSELAU. J. Am. Chem. Soc. **87**, 5747 (1965).
26. J. R. DIAS and C. DJERASSI. Org. Mass Spectrom. **7**, 753 (1973).
27. (*a*) N. THEOBALD, R. J. WELLS, and C. DJERASSI. J. Am. Chem. Soc. **100**, 7677 (1978); (*b*) E. AYANOGLU, C. DJERASSI, T. R. ERDMAN, and P. J. SCHEUER. Steroids, **31**, 815 (1978); (*c*) D. J. VANDERAH and C. DJERASSI. J. Org. Chem. **43**, 1442 (1978); (*d*) E. STEINER, C. DJERASSI, E. FATTORUSSO, S. MAGNO, L. MAYOL, C. SANTACROCE, and D. SICA. Helv. Chim. Acta, **60**, 475 (1977).
28. A. ROMEO and M. P. PARADISI. J. Org. Chem. **37**, 46 (1972).
29. C. W. SHOPPEE and G. H. R. SUMMERS. J. Chem. Soc. 3361 (1952).
30. C. DJERASSI, R. H. SHAPIRO, and M. VANDEWALLE. J. Am. Chem. Soc. **87**, 4892 (1965).
31. H. BUDZIKIEWICZ. Biochemical applications of mass spectrometry. *Edited by* G. R. Waller. Wiley, New York. 1972. p. 262.
32. H.C. BEYERMAN and G. J. HEISZWOLF. J. Chem. Soc. 755 (1963); Recl. Trav. Chim. Pays-Bas, **84**, 203 (1965).
33. J. DIEKMAN and C. DJERASSI. J. Org. Chem. **32**, 1005 (1967).
34. H. BUDZIKIEWICZ, C. DJERASSI, and D. H. WILLIAMS. Structure elucidation of natural products by mass spectrometry. Holden-Day, San Francisco. 1964. Chapt. 18.

Can. J. Chem. Downloaded from www.nrcresearchpress.com by 210.87.254.5 on 09/05/12
For personal use only.

The nephritogenic glycopeptide from rat glomerular basement membrane: synthesis of α-D-glucopyranosylamine derivatives

TADAHIRO TAKEDA, YOSHIHIRO SUGIURA, YUKIO OGIHARA, AND SEIICHI SHIBATA[1]

Faculty of Pharmaceutical Sciences, Nagoya City University, Nagoya, Japan

Received May 13, 1980

This paper is dedicated to Prof. Raymond U. Lemieux on the occasion of his 60th birthday

TADAHIRO TAKEDA, YOSHIHIRO SUGIURA, YUKIO OGIHARA, and SEIICHI SHIBATA. Can. J. Chem. **58**, 2600 (1980).

N-(L-β-aspartyl)-α-D-glucopyranosylamine has been prepared, as a model of a corresponding derivative possibly present in glomerular basement membrane of rats, by the condensation of α-ethyl benzyloxycarbonyl-L-aspartate with 2,3,4,6-tetra-*O*-acetyl-α-D-glucopyranosylamine in the presence of diethylphosphorocyanidate. This was followed by hydrogenolysis, de-*O*-acetylation, and deethoxylation of the resulting 2,3,4,6-tetra-*O*-acetyl-*N*-(α-ethyl benzyloxycarbonyl-L-β-aspartyl)-α-D-glucopyranosylamine to remove the protecting groups. The ^{13}C nmr spectra of the corresponding glycosylamine derivatives are analyzed and discussed.

TADAHIRO TAKEDA, YOSHIHIRO SUGIURA, YUKIO OGIHARA et SEIICHI SHIBATA. Can. J. Chem. **58**, 2600 (1980).

La *N*-(L-β-aspartyl) α-D-glucopyrannosylamine, un modèle d'un dérivé correspondant qui est probablement présent dans la sous-membrane glomérulaire du rat, est obtenue par condensation du benzyloxycarbonyl L-α-aspartate d'éthyle sur la tétra-*O*-acétyl-2,3,4,6 α-D-glucopyrannosylamine en présence du phosphocyanidate diéthylique. Cette étape est suivie de l'élimination des groupes protecteurs par une hydrogénolyse, une dé-*O*-acétylation et une dééthoxylation de la tétra-*O*-acétyl-2,3,4,6 *N*(α-éthyl benzyloxycarbonyl L-β-aspartyl) α-D-glucopyrannosylamine qui en résulte. On a analysé les spectres rmn du ^{13}C des dérivés correspondants de la glycosylamine.

[Traduit par le journal]

Introduction

Shibata *et al.* (1) isolated from the glomerular basement membrane of rats, and purified, a new glycopeptide that has an activity consisting of induction of glomerulonephritis in homologous animals (nephritogenic activity) (2). The methylation analyses (3, 4), the concanavalin A test, and ^{13}C nmr spectral analyses (5) indicate that the sugar moiety of this glycopeptide has the Glc α-(1→6)Glc β-(1 → 6)Glc structure shown in Fig. 1. This is the first example of a new type of carbohydrate–protein linkage among natural compounds, of a direct, *N*-glycosyl linkage between a glycosyl and an amino acid residue. This paper reports the synthesis of *N*-acylated glycosylamines and studies on the ^{13}C nmr spectra of the above-mentioned glycopeptide and model compounds.

Results and Discussion

Marks and Neuberger (6) have described the synthesis and some properties of *N*-(L-β-aspartyl)-β-D-glucopyranosylamine. The preparation of this compound by a different procedure has also been described by Coutsogeorgopoulos and Zervas (7). Garg and Jeanloz (8) have also described the synthesis of *N*-(L-β- and α-aspartyl)-4-*O*-β-D-galactopyranosyl-β-D-glucopyranosylamines. All these syntheses produced β-D-glucopyranosylamine derivatives.

We now report the synthesis of the *N*-acetyl, *N*-(L-β-aspartyl)-α,β-D-glucopyranosylamine derivatives which were needed for ^{13}C nmr studies. 2,3,4,6-Tetra-*O*-acetyl-β-D-glucopyranosyl azide (**1**) was obtained by the procedure of Bertho (9). The azide was hydrogenated in tetrahydrofuran over Adam's catalyst to give the amino compound (**2**). Compound **2** was acetylated and also condensed with α-ethyl benzyloxycarbonyl-L-aspartate to give **3** and **5**, respectively. These compounds were deblocked in the usual manner to give *N*-acetyl-, *N*-(L-β-aspartyl)-β-D-glucopyranosylamine **4** (mp 255°C) and **7** (mp 253°C), respectively. The basic physical and chemical properties are coincident with those reported earlier (7).

For synthesis of α-D-glucopyranosylamine derivatives, 2,3,4,6-tetra-*O*-acetyl-α-D-glucopyranosyl azide (**9**) was prepared by treating 2,3,4,6-tetra-*O*-acetyl-β-D-glucopyranosyl chloride (**8**) with sodium azide in hexamethylphospholic triamide (HMPT). This S_N2 reaction gave the inverted product in a yield of 65% and neighbouring group participation with retention of configuration is not observed (10). Hydrogenation of **9** in methanol gave the desired key intermediate glycosylamine derivative (**10**).

The α-ethyl benzyloxycarbonyl-L-aspartate was

[1]The Third Department of Internal Medicine, Faculty of Medicine, University of Tokyo, 7-3-1, Hongo, Bunkyo-ku, Tokyo, Japan.

0008-4042/80/232600-04$01.00/0

©1980 National Research Council of Canada/Conseil national de recherches du Canada

Can. J. Chem. Downloaded from www.nrcresearchpress.com by 210.87.254.40 on 09/05/12
For personal use only.

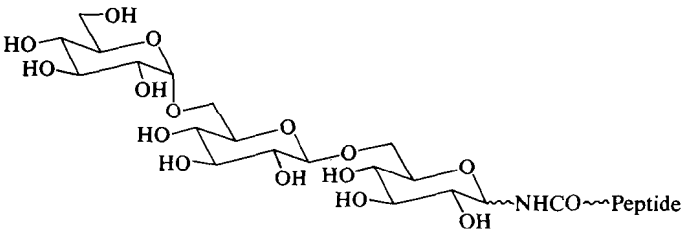
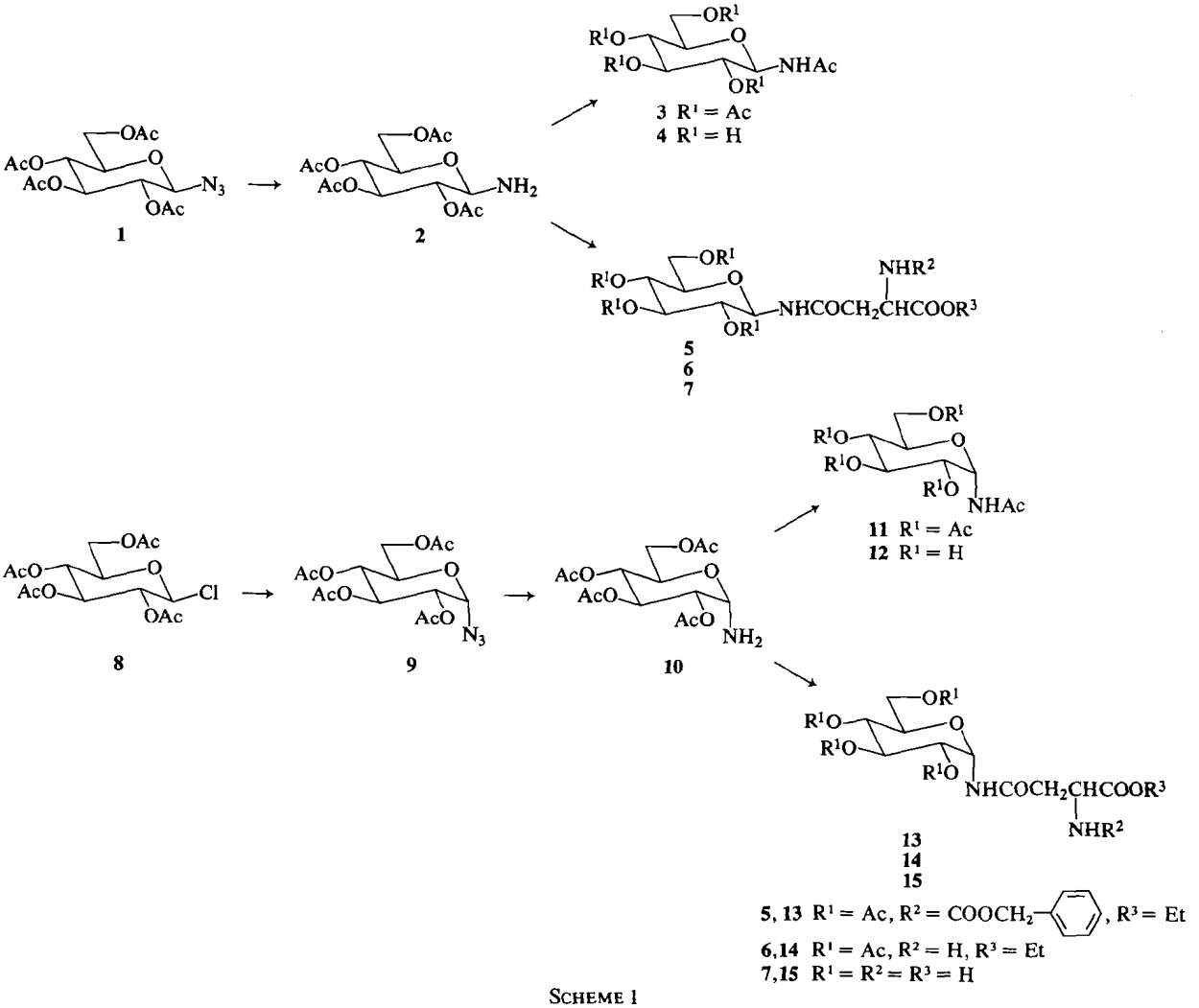


FIG. 1

readily prepared in high yield by the procedure of Wünsch and Zwiek (11) from benzyloxycarbonyl-L-aspartic acid.

The next step involved the condensation of α-ethyl benzyloxycarbonyl-L-aspartate with **10**, which gave the α-aspartyl-glucopyranosylamine derivative (**13**) in 90% yield using the DEPC method of Shioiri *et al.* (12). Removal of the benzyloxycarbonyl group by catalytic hydrogenation afforded the required tetra-*O*-acetyl-*N*-(L-β-aspartyl)-α-D-glucopyranosylamine (**14**). Thus, **14** was deacetylated and deethoxylated with triethylamine in 50% methanolic solution at room temperature to give a *N*-(L-β-aspartyl)-α-D-glucopyranosylamine (**15**) ($[\alpha]_D$ +34.1°). The *N*-acetylation of compound **10** followed by de-*O*-acetylation of the *N*-acetate af-



SCHEME 1

Can. J. Chem. Downloaded from www.nrcresearchpress.com by 210.87.254.40 on 09/05/12
For personal use only.

Can. J. Chem. Downloaded from www.nrcresearchpress.com by 210.87.254.40 on 09/05/12
For personal use only.

forded a *N*-acetyl-α-D-glucopyranosylamine (**12**) ($[\alpha]_D$ +15.0°). The synthetic route is illustrated in Scheme 1. The ^{13}C shifts of the glucosylamine derivatives are listed in Table 1.

The assignment of the α-D-configuration to the azide compound (**9**) was made by comparing its spectrum with that of β-D-azide compound (13). The signal of the anomeric carbon atom is always found at lowest field and normally C-1 of the β-anomer is at lower field than that of the α-anomer. The signals of C-4 and C-6 remain almost constant throughout the series of compounds described here and they are therefore readily assigned in most cases. The assignments of the closely spaced signals of C-3 and C-5 were made by the selective proton decoupling of H-3 and H-5, respectively. The ^{13}C nmr spectra indicate that the chemical shifts of the sugar moiety of compounds **12** and **15** are very similar to each other, and are obviously different from their respective β-isomers (**4**, **7**). A complete similarity of the *N*-glycosyl moieties of the glycopeptide and compound **15** was observed.

Consequently, a glycopeptide that has a nephritogenic activity has its *N*-glycosyl linkage in the α-D-configuration.

Experimental

General Methods

Melting points were determined with a Yanagimoto microapparatus and are uncorrected. The ^1H nmr spectra were recorded on a JNM MH-100 spectrometer with tetramethylsilane as the internal standard; abbreviations used: s, singlet; d, doublet; dd, doublet of doublets; t, triplet; and m, multiplet. The ^{13}C nmr spectra were obtained at 25.0 MHz in the pulsed Fourier transform mode on JEOL FX-100 instruments. Thin-layer chromatography was conducted on precoated silica gel plates (Merck GF-254) and column chromatography on silica gel (Merck Kieselgel 60).

TABLE 1. ^{13}C Chemical shifts of glucosylamine derivatives examined in $CDCl_3$

Compound	δ ppm							
	C-1	C-2	C-3	C-4	C-5	C-6	β (Aspartyl residue)	α (Aspartyl residue)
1	87.9	70.8	72.7	68.0	74.1	61.7		
9	86.1	69.7	69.8	68.1	70.1	61.7		
2	84.9	72.2	72.7	69.0	73.3	62.4		
10	76.7	68.5	68.5	68.1	73.3	62.1		
3	78.2	70.7	73.0	68.3	73.6	61.8		
11	74.5	68.7	68.7	68.2	70.4	62.0		
4	80.1	72.6	77.3	70.1	78.3	61.4		
12	77.4	70.2	73.5	70.2	73.9	61.4		
5	78.0	70.6	72.7	68.1	73.7	61.8	37.8	50.5
13	74.2	68.3	69.1	68.0	70.2	62.3	36.8	50.4
7[a]	80.0	72.7	77.3	70.1	78.4	61.4	36.1	51.9
15[a]	77.4	70.2	73.5	70.2	73.9	61.4	37.3	53.1
Glycopeptide[a] (*N*-glycosyl residue)	77.6	70.8	72.4	70.8	74.1	70.4		

[a]Compounds **7**, **15**, and glycopeptide were measured in D_2O (internal 1,4-dioxane (67.4 ppm)).

Materials

2,3,4,6-Tetra-*O*-acetyl-β-D-glucopyranosyl azide, 2,3,4,6-tetra-*O*-acetyl-β-D-glucopyranosylamine were synthesized by well established procedures (9). α-Ethyl benzyloxycarbonyl-L-aspartate was prepared from benzyloxycarbonyl-L-aspartic acid according to the method of Wünsch and Zwiek (11).

*2,3,4,6-Tetra-*O*-acetyl-α-D-glucopyranosyl Azide (9)*

A solution of 2,3,4,6-tetra-*O*-acetyl-β-D-glucopyranosyl chloride (**8**) (7.2 g), prepared from penta-*O*-acetyl-β-D-glucopyranose according to Mills *et al.* (14), in 75 mL of HMPT was added to 15 g of sodium azide. The mixture was stirred for 3.5 h, then it was filtered and the filtrate concentrated to dryness. The residue was crystallized, and recrystallization from methanol gave 4.77 g (65%), mp 91–92°C; $[\alpha]_D^{24}$ +156.6° (*c* 1.06, $CHCl_3$); R_f 0.77 (benzene–acetone 4:1); ^1H nmr ($CDCl_3$) δ: 1.98, 2.00, 2.04, 2.06 (each s, 3H, CH_3CO), 4.06–4.30 (m, 3H, H-5, 6, 6'), 4.92 (q, J = 4, 8 Hz, 1H, H-2), 5.00 (t, J = 8 Hz, 1H, H-4), 5.33 (t, J = 8 Hz, 1H, H-3), 5.62 (d, J = 4 Hz, 1H, H-1). *Anal.* calcd. for $C_{14}H_{19}O_9N_3$: C 45.04, H 5.13, N 11.26; found: C 45.30, H 5.06, N 10.99.

*2,3,4,6-Tetra-*O*-acetyl-α-D-glucopyranosylamine (10)*

A solution of 3.36 g of azide (**9**) in 15 mL of methanol was hydrogenated at room temperature and atmospheric pressure for 13 h in the presence of Adams' catalyst (0.45 g). After removal of the catalyst by filtration, the filtrate was concentrated to a syrup, which contained (tlc) three components (R_f 0.17, R_f 0.29, R_f 0.4). In this system the α-amine possessed R_f 0.17. The syrup was chromatographed on silica gel using benzene–acetone (4:1) to provide pure **10** (0.63 g, 21% yield), mp 62.5–63°C, $[\alpha]_D^{24}$ +108.7° (*c* 7.5, $CHCl_3$). *Anal.* calcd. for $C_{14}H_{21}O_9N$: C 48.41, H 6.09, N 4.03; found: C 48.50, H 6.19, N 3.83.

*N-Acetyl-2,3,4,6-tetra-*O*-acetyl-α-D-glucopyranosylamine (11)*

A solution of 100 mg of **10** in 2 mL of pyridine and 2 mL of acetic anhydride was allowed to stand at room temperature for 8 h. The solution was poured into ice-water and extracted with $CHCl_3$. The $CHCl_3$ extracts were washed with water, dried, and concentrated to give a syrup; $[\alpha]_D^{20}$ +14.65° (*c* 4.0, $CHCl_3$). *Anal.* calcd. for $C_{16}H_{23}O_{10}N$: C 50.52, H 6.09, N 3.68; found: C 50.48, H 6.12, N 3.59.

N-Acetyl-α-D-glucopyranosylamine (12)

Compound **11** (100 mg) was *O*-deacetylated with triethylamine in 50% MeOH solution. The reaction solution was evaporated to give a syrup; $[\alpha]_D^{20}$ + 15.02° (*c* 0.9, H_2O). *Anal.* calcd. for $C_8H_{15}O_6N$: C 43.44, H 6.83, N 6.33; found: C 43.56, H 6.90, N 6.29.

*2,3,4,6-Tetra-*O*-acetyl-N-(α-ethyl Benzyloxycarbonyl-L-aspartyl)-α-D-glucopyranosylamine (13)*

To a solution of **10** (114 mg) in THF (5 mL) α-ethyl benzyloxycarbonyl-L-aspartate (96.3 mg), DEPC (diethyl phosphorocyanidate) (100 mg), and 0.15 mL of triethylamine were added. The mixture was stirred for 12 h at 0°C. The reaction mixture was diluted with AcOEt (50 mL), and successively washed with 5% HCl, water, saturated $NaHCO_3$, and saturated NaCl. Drying followed by evaporation gave a syrup which contained (tlc) a major (R_f 0.56) and a minor (R_f 0.76) component and some slower-moving components. The syrup was chromatographed on silica gel with the same solvent system as

on tlc (chloroform–methanol 4:1). The eluate of the major component was evaporated and crystallized from ethanol to give pure **13** (185 mg, 90%); $[\alpha]_D^{20}$ +64.6° (*c* 3.2, $CHCl_3$); ^1H nmr ($CDCl_3$) δ: 1.25 (t, 3H, $—CH_2CH_3$), 2.02, 2.03, 2.06, 2.08 (each s, 3H, $COCH_3$), 2.90 (q, 2H, $—CH_2CH_3$), 5.15 (s, 2H, $—CH_2—$ ), 5.65–5.90 (br, 1H, NH), 7.38 (m, 5H, arom. H). *Anal.* calcd. for $C_{28}H_{36}O_{14}N_2 \cdot 2H_2O$: C 50.91, H 6.10, N 4.24; found: C 50.46, H 5.93, N 4.27.

2,3,4,6-Tetra-O-*acetyl*-N-(α-*ethyl*-L-β-*aspartyl*)-α-D-*glucopyranosylamine* (*14*)

A solution of **13** (98 mg) in THF (8 mL) was hydrogenated in the presence of PtO_2 (30 mg) for 12 h at room temperature. The catalyst was filtered off, and the filtrate evaporated to dryness to give **14** (75.4 mg, 98%); $[\alpha]_D^{23}$ +54.1° (*c* 0.8, $CHCl_3$). *Anal.* calcd. for $C_{20}H_{30}O_{12}N_2$: C 48.98, H 6.17, N 5.71; found: C 49.06, H 6.22, N 5.82.

N-(L-β-*Aspartyl*)-α-D-*glucopyranosylamine* (*15*)

To a solution of **14** (18.9 mg) in 50% methanol (2 mL) 0.18 mL of triethylamine was added and kept overnight at room temperature. The solution was concentrated *in vacuo*. A syrup was obtained, yielding 16 mg (99%); $[\alpha]_D^{24}$ +34.1° (*c* 0.9, H_2O). *Anal.* calcd. for $C_{10}H_{18}O_8N_2$: C 40.82, H 6.17, N 9.53; found: C 40.74, H 6.03, N 9.64.

Acknowledgments

We wish to thank Professor R. U. Lemieux for valuable discussions and Miss C. Hamada for technical assistance. We thank Mrs. T. Kumagai for measuring the nmr spectra.

1. S. SHIBATA, Y. MIYAKAWA, T. NARUSE, and T. TAKUMA. J. Immunol. **102**, 593 (1969).
2. S. SHIBATA and T. NAGASAWA. J. Immunol. **106**, 1284 (1971).
3. S. SHIBATA, T. NARUSE, Y. MIYAKAWA, and T. NAGASAWA. J. Immunol. **104**, 215 (1970).
4. S. SHIBATA. Jpn. J. Clin. Chem. **7**, 110 (1978).
5. S. SHIBATA and H. NAKANISHI. Carbohydr. Res. **81**, 345 (1980).
6. G. S. MARKS and A. NEUBERGER. J. Chem. Soc. 4872 (1961).
7. C. COUTSOGEORGOPOULOS and L. ZERVAS. J. Am. Chem. Soc. **83**, 1885 (1961).
8. H. G. GARG and R. W. JEANLOZ. Carbohydr. Res. **43**, 371 (1975).
9. A. BERTHO. Chem. Ber. **63**, 836 (1930).
10. Z. GYÖRGYDEÁK and H. PAULSEN. Ann. Chem. 1987 (1977).
11. E. WÜNSCH and A. ZWIEK. Z. Physiol. Chem. **328**, 235 (1962).
12. T. SHIOIRI, Y. YOKOYAMA, Y. KASAI, and S. YAMADA. Tetrahedron, **32**, 2211 (1976).
13. K. BOCK and C. PEDERSEN. J. Chem. Soc. Perkin Trans. II, 293 (1974).
14. W. KORYTNYK and J. A. MILLS. J. Chem. Soc. 636 (1959).

Can. J. Chem. Downloaded from www.nrcresearchpress.com by 210.87.254.40 on 09/05/12
For personal use only.

Azapropellanes as phase-transfer catalysts. I. Introduction and synthesis of (±)1-azoniatricyclo[4.4.4.0^{1,6}]tetradecane and (±)1-azoniatricyclo[4.4.3.0^{1,6}]tridecane salts[1]

JOHN M. MCINTOSH

Department of Chemistry, University of Windsor, Windsor, Ont., Canada N9B 3P4

Received May 22, 1980

This paper is dedicated to Prof. Raymond U. Lemieux on the occasion of his 60th birthday

JOHN M. MCINTOSH. Can. J. Chem. **58**, 2604 (1980).

The rationale for considering 1-azoniapropellane salts as potential chiral phase-transfer catalysts is presented. The synthesis of two examples of these types of molecules is outlined and their efficacy in phase-transfer catalyzed reactions is established.

JOHN M. MCINTOSH. Can. J. Chem. **58**, 2604 (1980).

On présente une analyse qui permet de considérer les sels de l'azonia-1 propellane comme des catalyseurs chiraux potentiels de transfert de phase. On décrit la synthèse de deux molécules types et on établi leur efficacité dans les réactions catalysées de transfert de phase.

[Traduit par le journal]

Although chemists have used the term biogenetic or biomimetic synthesis with increasing frequency, in fact the use of the central feature of biosynthesis, a catalyst capable of stereospecific transformations of chiral or achiral reactants has rarely been achieved (1). Recently, reports from a variety of sources have told of varying degrees of success in performing absolute asymmetric synthesis using chiral ammonium salts, frequently under phase-transfer conditions (2). The chiral element in these reactions is a catalyst functioning in an achiral bulk medium and thus, in one sense at least, is an approximation of enzyme-catalyzed reactions.

We became interested in this area when we, as well as others (3) recognized that all catalysts reported at that time carry their chirality in the carbon skeleton of an 'onium salt and not at the presumed sites of catalytic activity. Thus, trimethylammonium salts of chiral amines which also contain an adjacent polar group (e.g. ephedrine) have been commonly used. It must be noted that this multifunctionality appears to be necessary for induction in some cases and is similar to the enzyme situation where one group is required for binding before catalytic activity at another site can begin. However, the optical yields using these catalysts have been low. One possible explanation for the disappointing results is the small difference in stability and population of the possible conformations of such small molecules, each of which might lead to a different stereochemical result (2*j*). Some support for this suggestion can be found in the results obtained by Colonna *et al.* (4) using polymer-bound catalysts and in results of Wynberg and Greijdanus (5) using quaternary salts derived from quinine and quinidine. In these larger molecules, conformational preferences would be expected to be larger, leading to higher optical yields. The increased optical yields found in solvents of low dielectric constant (5) may reflect a solvent effect on conformer population. However, Wynberg's catalysts have an additional complicating factor: they possess a chiral nitrogen atom. Since the mechanistic picture of catalysis by 'onium salts involves a tight ion-pair between the site of positive charge and the working anion X^-, chirality at the positive nitrogen atom might be expected to influence strongly the stereochemistry of reactions of X^-. In this context, the solvent dielectric effect (5) would reflect a tighter ion-pair and thus a more effective transfer of chirality.

To separate these effects, it was desirable to use catalysts which contain chiral nitrogen atoms, but as little other chirality which might affect the reacting center as possible. However, as we have pointed out (6), simple quaternary ammonium salts cannot be expected to cause significant asymmetric induction unless three of the four tetrahedral faces of the nitrogen atom are blocked. Thus, we set out to design catalysts which would fulfill the following criteria: (1) they must have a chiral nitrogen atom; (2) they should be as rigid as possible to facilitate interpretation of stereochemical results; (3) three of

[1]Chemical Abstract names: octahydro-5,9a-butanoquinolizinium and octahydro-5,9a-propanoquinolizinium salts.

0008-4042/80/232604-06$01.00/0

©1980 National Research Council of Canada/Conseil national de recherches du Canada

Can. J. Chem. Downloaded from www.nrcresearchpress.com by 210.87.254.105 on 09/05/12
For personal use only.

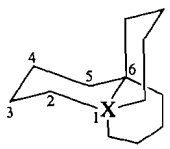
Can. J. Chem. Downloaded from www.nrcresearchpress.com by 210.87.254.105 on 09/05/12
For personal use only.

the faces of the nitrogen atom should be blocked; (4) introduction of various substituents in stereochemically defined ways should be possible.

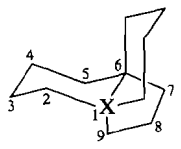
Such molecules are not easy to envisage and unlike the catalysts used heretofore, nature does not supply us with a plentiful source. For example, salts based on the quinuclidine ring system can be modified to satisfy conditions 1, 2, and 4, but not 3. We believe that molecules based on the propellane ring system offer a viable choice. In order to fulfill condition 3, the quaternary nitrogen atom must be located at the bridgehead position.

Molecules possessing the propellane structure, including those incorporating nitrogen atoms, have been known for many years and their chemistry and structural features have been extensively reviewed (7). One example (**4***N*) of a bridgehead nitrogen derivative has been prepared (8) and a closely related system has been derived from lupinine (9). All the carbocyclic compounds **1***C* (10), **2***C* (11), **3***C* (12), and **4***C* (12) are known.

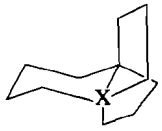
Compound **1***C* possesses D_3 symmetry and is therefore chiral (7). Replacing one bridgehead carbon atom with nitrogen generates an ammonium salt (**1***N*) which possesses C_3 symmetry which is also chiral. Optical inversion of either **1***C* or **1***N* requires chair–chair conformational inversion of all three cyclohexane rings. Similarly **2***C*, **2***N*, **3***C*, and **3***N* are chiral but **4***C* and **4***N* are not. While **1** and **2** are chiral, the exposed *face* of the nitrogen atom is not and another alteration in structure (e.g. appropriate substitution in one of the six-membered rings of **2***N*) would be required to achieve this. Thus the propellane system offers the possibility of examining both types of effects on asymmetric induction. Furthermore, the lack of a "handle" in **1***C* has precluded attempts at its resolution and no direct information as to its optical stability is available (13). On the other hand, **1***N* is ideally suited for attempted resolution via diastereomeric salts.



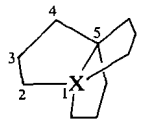
1*C* X = C
1*N* X = N^+



2*C* X = C
2*N* X = N^+



3*C* X = C
3*N* X = N^+



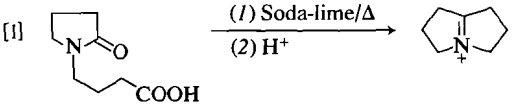
4*C* X = C
4*N* X = N^+

Subsequent introduction of polar substituents should also be possible and the spatial relationships between functionalities should be well-defined, allowing the analysis of substrate–catalyst interactions to a greater degree than in common catalysts.

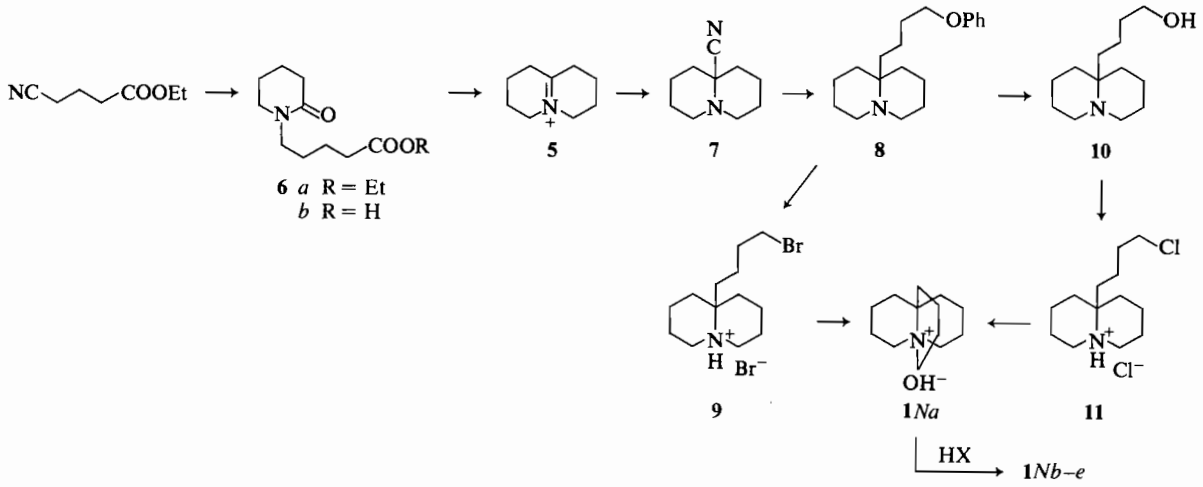
In this paper are reported the syntheses of **1***N* and **2***N*. In subsequent papers, the structures of these molecules as determined by a variety of methods, the preparation of substituted systems, and their utility as phase-transfer catalysts will be reported.

Results and Discussion

Salts **1***N* and **2***N* are bridged quinolizidines. Some question existed as to the feasibility of closing a 9a-substituted quinolizidine because previous work in our laboratory (14) and elsewhere indicated the structure of such compounds to contain a *trans*-fused ring system. However, nitrogen inversion is a facile process and the simplicity of such an approach dictated its investigation. The most attractive feature of this approach is that **1***N*, **2***N*, and a variety of derivatives substituted in one ring can be prepared from a single precursor-5,9a-dehydroquinolizidine (**5**) (15). Previous syntheses of 9a-substituted systems have all started with **5**. However, the preparation of **5** by mercuric acetate oxidation of quinolizidine did not appear attractive for the preparation of the amounts of material we envisaged might be required. After investigating other routes (14), we became aware of the work of Miyano (16) who showed that salts of the desired type were available from cyclization of *N*-substituted lactams (eq. [1])

[1] 

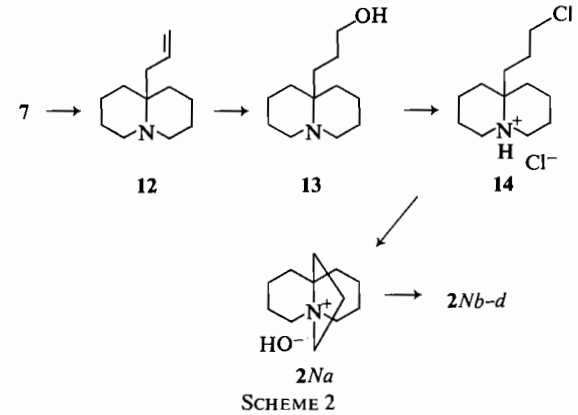
Hydrogenation of ethyl 4-cyanobutanoate afforded a mixture of 2-piperidinone and *N*-(4-carbethoxy)-2-piperidinone (**6***a*) (Scheme 1). Hydrolysis of the ester followed by distillation of the acid **6***b* from soda-lime (16) and neutralization of the distillate with perchloric acid gave **5** in 46% overall yield from **6***a*. Conversion to **7** with potassium cyanide, followed by reaction with the Grignard reagent derived from 4-phenoxybutyl bromide gave **8** which was smoothly cleaved to **9** in hot concentrated hydrobromic acid. Alternatively, **8** could be reduced with sodium in liquid ammonia to alcohol **10** which on treatment with thionyl chloride



SCHEME 1

gave **11**. Treatment of either **9** or **11** with silver oxide gave high yields of **1***N*-hydroxide (**1***Na*). Neutralization of this with a variety of acids gave a series of derivatives (**1***Nb* (X = Br^-), **1***Nc* (X = picrate), **1***Nd* (X = $CF_3CO_2^-$), **1***Ne* (X = $CH_3CO_2^-$)) all of which were solids with the exception of **1***Ne*. In analogy with the reported **4***N*-bromide, **1***Nb* has only limited solubility in water, is insoluble in chloroform, and melts as a temperature in excess of 300°C. However, **1***Nd* can easily be dissolved in chlorinated solvents. The structure of **1***N* is supported by its ^{13}C spectrum which shows only five lines, as well as its field desorption mass spectrum and elemental analysis.

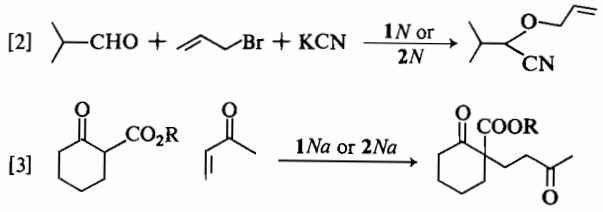
The same starting material **5** led also to **2***N* (Scheme 2). Because the Grignard reagent derived from 3-phenoxypropyl bromide is unstable (17), and that derived from 3-*tert*-butoxypropyl bromide failed to react with **5** or **7**, we resorted to modification of a 3-carbon unit already in place on the quinolizidine ring system. Reaction of **7** with allylmagnesium bromide gave **12** (14) which on hydroboration with disiamylborane (18) gave alcohol **13**. (Hydroboration of **12** with borane gives a mixture of **13** and its secondary alcohol isomer.) Conversion of **13** to **14** with thionyl chloride followed by silver oxide treatment gave **2***Na* which was converted into its bromide (**2***Nb*), picrate (**2***Nc*), and trifluoroacetate (**2***Nd*) salts.



SCHEME 2

The infrared spectra of alcohols **10** and **13** show very broad and weak hydroxyl absorptions in dilute solutions. All the free bases show strong Bohlmann bands (19) and the ^{13}C spectra support trans-fused ring systems. In addition C2 of **1***N*, C2, C7, and C9 of **2***N*, and C2 and C4 of **4***N* show significant carbon–nitrogen coupling as is expected from symmetrical salts such as these. The proton nmr spectra of **1***N* and **2***N* are reported in the Experimental without comment. A detailed analysis of these will appear in a future paper.

Finally, it must be noted that in order for our postulates to be viable, compounds **1***N* and **2***N* must function as phase-transfer catalysts. Using published procedures all of **1***N*, **2***N*, and **4***N* effectively catalyzed the formation of aldehyde cyanohydrin ethers (20) (Eq. [2]) and the reaction of 2-carbethoxycyclohexanone with methyl vinyl ketone (21) (eq. [3]). The latter reaction appears to be much faster using these catalysts than using those derived from cinchona alkaloids.



Can. J. Chem. Downloaded from www.nrcresearchpress.com by 210.87.254.105 on 09/05/12
For personal use only.

Can. J. Chem. Downloaded from www.nrcresearchpress.com by 210.87.254.105 on 09/05/12
For personal use only.

Experimental

Melting points are corrected; boiling points are uncorrected. Infrared spectra were run on Beckman IR-12 or Perkin-Elmer 297 instruments as films or in dilute chloroform solutions. The ^{1}H nmr spectra were run in $CDCl_3$, C_6D_6, or D_2O solutions as 60 or 100 MHz and are reported downfield from Me_4Si as internal standard; ^{13}C nmr spectra were run at 22.64 MHz in the same solvents and are also referenced to internal Me_4Si. Gas chromatographic analyses were performed on 10% SE-30 on Chromosorb W columns, solvents were removed at reduced pressure, and the drying agent was anhydrous sodium sulfate.

N-(4-Carbethoxybutyl)-2-piperidinone (6a)

Ethyl 4-cyanobutanoate (14.5 g, 0.1 mol) was dissolved in 130 mL of 95% ethanol and 0.35 g of platinum oxide was added. The mixture was stirred under one atmosphere of hydrogen for 2 days with periodic catalyst replacement. A total of 1.98 equivalent of hydrogen was absorbed. The solution was filtered, heated at reflux for 3 h, and evaporated. The residue was distilled to give 2.4 g of 2-piperidinone and 6.5 g (56%) of **6a**, bp 142–146°C (0.4 Torr).

N-(4-Carboxybutyl)-2-piperidinone (6b)

Ester **6a** (19.1 g, 0.08 mol) was dissolved in 50 mL of ethanol and 3.7 g (1.1 g) of sodium hydroxide in 10 mL of water was added. The solution was stirred at ambient temperature for 16 h. Most of the ethanol was evaporated, the residue diluted with water and acidified with 10% hydrochloric acid. The aqueous solution was extracted with chloroform (3 × 50 mL), the extracts washed with water, dried, and evaporated. Trituration of the residue with toluene gave 13.6 g (91%) of **6b** as white crystals, mp 83–85°C; ir ($CHCl_3$): 3550–2400, 2940, 2870, 1710, 1620, 1490, 1350 cm^{-1}; ^{1}H nmr ($CDCl_3$): 11.07 (1H, s), 3.60–3.12 (4H, m), 2.68–2.15 (4H, m), 2.02–1.40 (8H, m); ^{13}C nmr ($CDCl_3$); 176.7, 170.7, 47.9, 46.9, 33.8, 31.9, 26.4, 23.1, 22.2, 21.0. *Anal.* calcd. ($C_{10}H_{17}NO_3$): C 60.28, H 8.60, N 7.03; found: C 60.52, H 8.52, N 6.94.

5,9a-Dehydroquinolizidinium Perchlorate (5)

Acid **6b** (5 g, 0.025 mol) was ground with soda-lime (10 g) until an intimate mixture was obtained. The mixture was placed in a 100 mL round bottom flask fitted with a short-path distillation apparatus. The system was purged with nitrogen and the flask heated slowly with a free flame. Vigorous gas evolution occurred, followed by distillation of water (90–105°C) and then organic material (head temperature 160–170°C). After distillation had stopped, the two-phase distillate was diluted with 5 mL of 2% sodium hydroxide solution and extracted with pentane (3 × 25 mL). The combined extracts were dried, evaporated to ca. 5 mL, and poured into a cold solution of 8 mL 70% perchloric acid in 100 mL ethanol. Storage in the freezer overnight followed by filtration gave **5** (1.6 g, 57%) identical to the material reported by Leonard *et al.* (15); ^{13}C nmr ($CDCl_3$): 115.8, 54.2, 32.7, 20.5, 16.6.

Cyanoamine **7** was prepared as described by Leonard and Hay (21). Evaporation of the dried ethereal extract gave a liquid which solidified below −10°C, which was used without further purification. The infrared spectrum of **7** showed extremely weak absorption at 2220 cm^{-1}, a result typical of nitriles carrying oxygen or nitrogen substituents at the α-carbon (22).

9a-(4-Phenoxybutyl)quinolizidine (8)

A solution of 4-phenoxybutyl magnesium bromide in ether was prepared under nitrogen from 0.642 g (0.026 mol) of magnesium and 6.2 g (0.027 mol) of 4-phenoxybutyl bromide (Aldrich) in 50 mL of ether using iodine initiation. To this solution was added a solution of 2.2 g (0.013 mol) of **7** in 10 mL of ether. The addition required 30 min and a thick sludge was formed. The mixture was refluxed overnight, cooled, and treated with saturated aqueous ammonium chloride until effervescence ceased. Water (50 mL) was added, followed by enough concentrated hydrochloric acid to dissolve the precipitate (ca. 75 mL). The solution was extracted with ether (2 × 50 mL), the aqueous phase made basic with 12 *N* sodium hydroxide, and the milky solution extracted with ether (4 × 100 mL). The combined extracts were washed with water, dried, and evaporated to give 2.67 g of a cloudy oil which was shown to consist of 87% **8** and 18% **7** by gc. analysis. Separation of these was achieved using silica gel chromatography with ether as eluant. In this way pure **8** was obtained (1.7 g, 44%); ir ($CHCl_3$): 3010, 2930, 1600, 1583, 1490, 1463, 1450, 1290 cm^{-1}; ^{1}H nmr ($CDCl_3$): 7.42–6.71 (5H, m), 3.48 (2H, t, J = 6 Hz), 2.74–2.07 (4H, m), 2.00–1.00 (18H, m); ^{13}C nmr ($CDCl_3$): 160.3, 129.5, 120.7, 114.8, 67.9, 49.2, 35.5, 26.0, 20.5, 20.2. *Anal.* calcd. ($C_{19}H_{29}NO$): C 79.39, H 10.17, N 4.87; found: C 79.55, H 10.41, N 5.27. The picrate crystallized from ethanol and melted at 129–131°C.

In the normal course of events, the crude material was used directly in subsequent reactions as the products from **7** failed to cyclize in the final step.

9a-(4-Bromobutyl)quinolizidinium Hydrobromide (9)

Ether **8** (0.395 g, 1.38 mmol) was dissolved in 6 mL concentrated hydrobromic acid and the system was purged with nitrogen. The initially heterogeneous mixture became homogeneous when heated. The solution was refluxed for 2 h, the cooled solution diluted with 25 mL of water, and adjusted to pH = 4 with 3 *N* sodium hydroxide. The phenol was extracted with ether (2 × 30 mL) and the aqueous solution evaporated to dryness. The residue was extracted with hot chloroform (3 × 25 mL), the hot solution treated with charcoal, filtered, dried, and evaporated to a volume of 10 mL. Addition of ether caused precipitation of the product (0.395 g, 84%) which melted at 177–178°C; ^{1}H nmr ($CDCl_3$): 3.47 (2H, t, J = 6 Hz), 3.27–2.85 (4H, m), 2.30–1.23 (19H, m).

9a-(4-Hydroxybutyl)quinolizidine (10)

Ether **8** (1.0 g, 3.5 mmol) was dissolved in a mixture of 30 mL liquid ammonia, 15 mL of *tert*-butanol and 15 mL of ether. Sodium (1.6 g, 70 mmol) was added in small pieces over 10 min to give a deep blue solution. After stirring for 2.5 h the solution was colorless. Methanol (8 mL) was added and the ammonia was allowed to evaporate. The residue was diluted with 100 mL of saturated aqueous sodium chloride solution and extracted with ether (3 × 50 mL). The extracts were evaporated, the residue dissolved in 20 mL 10% hydrochloric acid and stirred overnight. Ether extraction removed cyclohexenone. The aqueous solution was made basic with 12 *N* sodium hydroxide solution and extracted with ether (3 × 50 mL). Evaporation of the dried extracts gave an oil which crystallized on trituration with pentane. Alcohol **10** was obtained (0.55 g, 74%) as a white solid, mp 93–94°C; ir ($CHCl_3$): 3550–2500 (weak), 2940, 1450, 1300, 1115, 910 cm^{-1}; ^{1}H nmr ($CDCl_3$): 3.66 (2H, t, J = 5 Hz), 2.90–2.23 (4H, m), 1.90–0.95 (19H, m); ^{13}C nmr ($CDCl_3$): 62.6, 55.5, 49.0, 35.2, 33.9, 25.7, 21.4, 20.0. *Anal.* calcd. ($C_{13}H_{24}NO$): C 73.88, H 11.92, N 6.63; found: C 74.11, H 12.12, N 6.70.

9a-(4-Chlorobutyl)quinolizidinium Hydrochloride (11)

Alcohol **10** (0.2 g, 0.9 mmol) was dissolved in 3 mL of dichloromethane and 0.33 g (2.7 mmol) of thionyl chloride was added. Immediate gas evolution occurred. The solution was stirred at ambient temperature overnight and then evaporated. The residue crystallized on trituration with ether and was purified by treating a hot chloroform solution with charcoal and precipitating the product (0.154 g, 61%) with ether. Compound **11** was a white crystalline material, mp 183–184°C, ir ($CHCl_3$): 2950, 2740–2200, 1460, 1430, 1240 cm^{-1}; ^{1}H nmr ($CDCl_3$): 3.61

Can. J. Chem. Downloaded from www.nrcresearchpress.com by 210.87.254.105 on 09/05/12
For personal use only.

(2H, t, J = 5 Hz), 3.33–2.50 (4H, m), 2.50–1.21 (11H, m); ^{13}C nmr ($CDCl_3$): 62.9, 49.4, 48.1 44.4, 32.5, 22.5, 20.3, 19.8, 17.9. *Anal.* calcd. ($C_{13}H_{25}Cl_2N$): C 58.64, H 9.46, Cl 26.63; found: C 57.94, H 9.03, Cl 27.26.

*1-Azoniatricyclo[4.4.4.0^{1,6}]tetradecane Hydroxide (1*Na*)*

Bromide **9** (500 mg, 1.4 mmol) was dissolved in 2 mL of water and added to 3.6 g (1.03 equiv.) of silver oxide. The slurry was stirred overnight, filtered through Celite, and evaporated to dryness at 20°C. The product was an oil (0.27 g, 91%) which was best purified by conversion to its bromide (see below). Analytically pure **1***Na* was obtained from **1***Nb* by treatment with 1.1 equiv. of silver oxide in water and isolation as described above; ^{1}H nmr (D_2O): 4.00 (3H, m), 3.00 (3H, bd), 2.72–2.32 (3H, m), 2.32–1.55 (12H, m), 1.26 (3H, bd); ^{13}C nmr (D_2O): 65.4, 56.1 (t), 29.3 (t), 19.4, 17.1. *Anal.* calcd. ($C_{13}H_{25}NO$): C 73.88, H 11.92, N 6.63; found: C 73.55, H 12.00, N 6.41.

*Preparation of Salts of 1*N

A solution of **1***Na* in water was treated with enough concentrated hydrobromic acid to bring the pH to 2. The precipitate was filtered and recrystallized from methanol–ether to give **1***Nb*, mp > 300°C. *Anal.* calcd. ($C_{13}H_{24}NBr$): C 56.94, H 8.82, N 5.11; found: C 57.00, H 8.78, N 5.02. The only peak shown in the field desorption mass spectrum (fdms) was at *m/e* 194.

In a similar manner, using solid picric acid, the salt **1***Nc* was prepared, mp > 300°C; ^{1}H nmr (D_2O): 4.05 (3H, m), 2.72 (3H, bd), 2.63–2.30 (3H, m), 2.13–1.54 (12H, m), 1.23 (3H, bd). *Anal.* calcd. ($C_{19}H_{26}N_4O_7$): C 54.02, H 6.20, N 13.26; found: C 54.14, H 6.24, N 13.29.

Treating a chloroform solution of **1***Na* with excess trifluoroacetic acid, followed by evaporation, gave an oil which crystallized on trituration with ether. Salt **1***Nd* was a white solid, mp 118–120°C. Its proton and ^{13}C nmr were identical to **1***Na*. *Anal.* calcd. ($C_{15}H_{24}F_3NO_2$): C 58.62, H 7.87, N 4.56; found: C 58.52, H 7.80, N 4.23.

9a-Allylquinolizidine (12)

To the Grignard reagent prepared from 1.5 g (0.012 mol) of allyl bromide and 0.29 g of magnesium (0.012 mol) in 25 mL of ether was added a solution of 1.0 g (6.1 mmol) of **7** in 10 mL of ether. After the final addition, the solution was refluxed for 3 h and worked up as described for compound **8**. There was obtained 1.00 g (92%) of a clear oil identical to that prepared previously (14).

9a-(3-Hydroxypropyl)quinolizidine (13)

Disiamyl borane was prepared by reaction of 10.0 mL of a 1 *M* borane solution in THF with 1.4 g 2-methyl-2-butene. To this solution was added a solution of 0.461 g (2.6 mmol) of **12** in 10 mL of THF over 10 min. The mixture was stirred at 0°C for 30 min and ambient temperature for 4 h. Water was added dropwise until effervescence ceased. Aqueous sodium hydroxide (8.0 mL of 10% solution) was added, followed by dropwise addition of 2.5 mL of 30% hydrogen peroxide. The mixture was stirred for 1 h, the aqueous phase saturated with potassium carbonate, the phases separated, and the aqueous layer extracted with ether (2 × 30 mL). The combined organic phases were evaporated, dissolved in ether, and extracted with 2 × 10 mL 10% hydrochloric acid and then water (2 × 10 mL). The combined aqueous phases were made basic with 10 *N* sodium hydroxide and extracted with ether (3 × 30 mL). The ether extract was dried and evaporated to give **13** as a colorless solid (0.41 g, 81%) mp 108–110°C; ir ($CHCl_3$): 3500–2400 (weak), 2930, 1450, 1360, 1295 cm^{-1}; ^{1}H nmr ($CDCl_3$); 3.64 (2H, t, J = 6 Hz), 2.90–2.36 (5H, m), 1.86–1.10 (16H, m); ^{13}C nmr ($CDCl_3$): 63.5, 54.7, 48.7, 34.2, 29.5, 24.8, 21.6, 19.9. *Anal.* calcd. ($C_{12}H_{23}NO$): C 73.04, H 11.75, N 7.10; found: C 72.81, H 11.63, N 7.00.

9a-(3-Chloropropyl)quinolizidinium Hydrochloride (14)

To a solution of 100 mg (0.51 mmol) of **13** in 4 mL chloroform was added 2 mL of thionyl chloride. Immediate gas evolution was evident. The solution was refluxed for 3 h, evaporated, and the residual oil was crystallized from acetone solution by addition of ethyl acetate. Chloride **14** was obtained (82 mg, 64%) as a colorless crystalline material, mp 158–160°C; ir ($CHCl_3$): 2950, 2850–2400, 1467, 1430, 1320 cm^{-1}; ^{1}H nmr ($CDCl_3$): 3.65 (2H, t, J = 5 Hz), 3.35–2.83 (4H, m), 2.70–1.40 (17H); ^{13}C nmr ($CDCl_3$): 62.6, 49.4, 44.8, 32.4, 25.7, 22.4, 20.9, 17.7. *Anal.* calcd. ($C_{12}H_{23}Cl_2N$): C 57.14, H 9.19, N 5.55, Cl 28.11; found: C 56.92, H 9.00, N 5.39, Cl 28.41.

*1-Azoniatricyclo[4.4.3.0^{1,6}]tridecane Hydroxide (2*Na*)*

To a solution of 128 mg (0.51 mmol) of **14** in 5 mL of water was added 1.0 g (4 equiv.) of silver oxide. The slurry was stirred for 24 h at ambient temperature, filtered through Celite, and evaporated below 30°C, initially at 15 Torr pressure and finally at 0.05 Torr. The oil which was obtained (85 mg, 85%) was used directly in the test reactions described below.

*Preparation of Salts of 2*N

A portion of hydroxide **2***Na* was neutralized with concentrated hydrobromic acid. The solution was evaporated to dryness, dissolved in absolute ethanol, and reevaporated. The semi-solid residue crystallized from ethanol to give white microcrystals of **2***Nb*, mp > 300°C; *m/e* (fdms) 180. *Anal.* calcd. ($C_{12}H_{22}BrN$): C 55.39, H 8.52, N 5.38, Br 30.71; found: C 55.21, H 8.15, N 4.98, Br 29.98. In a similar manner, using a saturated ethanolic picric acid solution, the picrate **2***Nc* was prepared as a bright yellow powder, mp > 300°C.

The trifluoroacetate **2***Nd* was prepared by adding excess trifluoroacetic acid to **2***Na* and evaporating at 0.05 Torr. The salt was an oil which showed the following spectral characteristics: ^{1}H nmr ($CDCl_3$): 3.80–3.55 (2H, m), 3.55–3.11 (4H, m), 2.20 (4H, bs), 2.05–1.56 (12H, m); ^{13}C nmr ($CDCl_3$): 72.7, 59.0, 55.9, 31.7, 29.4, 19.7, 17.5, 16.9.

Phase-transfer Reactions

Reaction of isobutyraldehyde and allyl bromide in methylene chloride with aqueous potassium cyanide using **1***Nd*, **2***Nd*, or **4***Na* as catalyst as previously described (20) gave the allyl ether of isobutyraldehyde cyanohydrin in yields of 50–60% in 16 h.

Reaction of 2-carboethoxycyclohexanone and methyl vinyl ketone in methylene chloride solution using catalytic amounts of **1***Na*, **2***Na*, or **4***Na* as previously described (2*g*) gave the Michael addition product in yields of 90–95%. The reaction was complete in 1 h at 25°C.

Acknowledgements

Financial support for this work came from the Natural Sciences and Engineering Research Council of Canada and is gratefully acknowledged. Much of this work was performed while the author was on sabbatical leave at the University of Alberta. The help and encouragement of the members of the Chemistry Department are truly appreciated.

1. J. D. Morrison and H. S. Mosher. Asymmetric organic reactions. American Chemical Society, Washington, DC. 1976; H. B. Kagan and J. C. Fiaud. Top. Stereochem. **10**, 175 (1979); J. W. Apsimon and R. P. Seguin. Tetrahedron, **35**, 2797 (1979).
2. (*a*) J. C. Fiaud. Tetrahedron Lett. 3495 (1975); (*b*) T. Hijama, H. Sawada, M. Tsukanaka, and H. Nozaki.

Tetrahedron Lett. 3013 (1975); (*c*) H. WYNBERG and R. HELDER. Tetrahedron Lett. 4057 (1975); (*d*) J. P. MASSE and E. R. PARAYRE. J. Chem. Soc. Chem. Commun. 438 (1976); (*e*) J. BALCELLS, S. COLONNA, and R. FORNASIER. Synthesis, 266 (1976); (*f*) R. HELDER, J. C. HUMMELEN, R. W. P. M. LAANE, J. C. WIERING, and H. WYNBERG. Tetrahedron Lett. 1831 (1976); (*g*) H. HIEMSTRA, W. BOLT, and H. WYNBERG. Tetrahedron Lett. 2181 (1977); (*h*) J. C. HUMMELEN and H. WYNBERG. Tetrahedron Lett. 1089 (1978); (*i*) S. JULIA, A. GINEBREDA, and J. GUIZER. J. Chem. Soc. Chem. Commun. 742 (1978); (*j*) K. HERRMANN and H. WYNBERG. J. Org. Chem. **44**, 2238 (1979).

3. E. V. DEHMLOW. Angew. Chem. Int. Ed. Engl. **16**, 493 (1977).
4. S. COLONNA, R. FORNASIER, and U. PFEIFFER. J. Chem. Soc. Perkins Trans. I, 8 (1978).
5. H. WYNBERG and B. GREIJDANUS. J. Chem. Soc. Chem. Commun. 427 (1978).
6. J. M. MCINTOSH. Tetrahedron Lett. 403 (1979).
7. D. GINSBURG. Acc. Chem. Res. **2**, 121 (1969); D. GINSBURG. Acc. Chem. Res. **7**, 286 (1974); D. GINSBURG. Propellanes-structure and reactions. Verlag Chemie, Weinheim. 1975.
8. F. SORM and J. BERANAK. Collect. Czech. Chem. Commun. **19**, 298 (1954).
9. G. R. CLEMO and J. RUDINGA. J. Chem. Soc. 2714 (1951).
10. J. ALTMAN, E. BABAD, J. PUCKNAT, N. RESCHEF, and D. GINSBURG. Tetrahedron, **24**, 975 (1968).
11. J. ALTMAN, E. BABAD, J. ITZCHAKI, and D. GINSBURG. Tetrahedron Suppl. 8, Part 1, 279 (1966).
12. R. W. WEBER and J. M. COOKE. Can. J. Chem. **56**, 189 (1978).
13. H. GILBOA, J. ALTMAN, and A. LOEWENSTEIN. J. Am. Chem. Soc. **91**, 6062 (1969).
14. J. M. MCINTOSH. Can. J. Chem. **57**, 2114 (1979).
15. N. J. LEONARD, A. S. HAY, R. W. FULMER, and V. W. GASH. J. Am. Chem. Soc. **77**, 439 (1955).
16. S. MIYANO. Synthesis, 701 (1978).
17. N. RABJOHN and M. S. COHEN. J. Am. Chem. Soc. **74**, 6290 (1952).
18. H. C. BROWN and M. K. UNNI. J. Am. Chem. Soc. **90**, 2902 (1968).
19. F. BOHLMANN. Chem. Ber. **92**, 1798 (1959).
20. J. M. MCINTOSH. Can. J. Chem. **55**, 4200 (1977).
21. N. J. LEONARD and A. S. HAY. J. Am. Chem. Soc. **78**, 1984 (1956).
22. L. J. BELLAMY. The infrared spectra of complex molecules. J. Wiley, New York. 1975. p. 297.

Can. J. Chem. Downloaded from www.nrcresearchpress.com by 210.87.254.105 on 09/05/12
For personal use only.

Facile cleavage of some 2-acetamido-2-deoxy-β-D-gluco- and galactopyranosides using aqueous HF[1]

HAROLD J. JENNINGS AND CZESLAW LUGOWSKI[2]

Division of Biological Sciences, National Research Council of Canada, Ottawa, Ont., Canada K1A 0R6

Received June 19, 1980

This paper is dedicated to Prof. Raymond U. Lemieux on the occasion of his 60th birthday

HAROLD J. JENNINGS and CZESLAW LUGOWSKI. Can. J. Chem. **58**, 2610 (1980).

Treatment of pneumococcal C-substance (PnC) with 48% aqueous HF resulted in not only the intended removal of all the phosphate esters but also in the highly specific hydrolysis of the glycosidic bond between the 2-acetamido-2-deoxy-β-D-galactopyranose and ribitol residues. Some of the structural features associated with this facile hydrolysis were elucidated from studies on the treatment of model methyl glycosides and oligosaccharides with the same reagent. These studies indicate that an increase in the rate of hydrolysis is associated with glycosides of 2-acetamidohexapyranoses having a *trans* diequatorial disposition of the aglycon and 2-acetamido groups. These studies also indicate that the nature of the aglycon is also a contributing factor, because although simple alkoxy and terminal open-chain glycitols are readily cleaved from glycosides satisfying the above criteria, hydrolysis does not occur where the aglycon is another cyclized sugar moiety. Thus chitotriose can only be degraded to chitobiose using this reagent following the reduction of its terminal reducing moiety.

HAROLD J. JENNINGS et CZESLAW LUGOWSKI. Can. J. Chem. **58**, 2610 (1980).

L'action d'une solution aqueuse à 48% de HF sur la substance pneumocoque C (PnC) n'enlève pas seulement tous les groupements esters phosphoriques mais hydrolyse également de façon fortement spécifique la liaison glycosidique entre les unités acétamido-2 déoxy-2 β-D-galactopyrannose et le ribitol. On a éclairci quelques aspects structuraux associés à cette hydrolyse facile, en se basant sur les études réalisées en traitant des modèles de glycosides de méthyle et d'oligosaccharides avec le même réactif. Ces études indiquent qu'une augmentation de la vitesse d'hydrolyse se produit avec les glycosides d'acétamido-2 hexapyrannoses ayant les groupements aglycone et acétamido-2 en position *trans* diéquatoriale. Ces études indiquent également que par sa nature l'unité aglycone est un facteur contributif, parce que les groupes alkoxy simples et glycitols terminaux à chaîne ouverte sont facilement enlevés selon les critères ci-dessus mentionnés. L'hydrolyse ne se produit pas quand l'unité aglycone est un noyau de sucre cyclique. Ainsi l'emploi de ce réactif sur le chitotriose suivi de la réduction de son unité terminale permet seulement de la dégrader en chitobiose.

[Traduit par le journal]

Introduction

Aqueous hydrofluoric acid is an extremely specific reagent for the low-temperature cleavage of different types of phosphate esters (1). The specificity is such that it has been used to remove phosphate esters from complex oligosaccharides without cleaving its *O*-glycosidic linkages (2). However, exceptions to this rule have been recently reported. On treatment with aqueous HF at 4°C the terminal erythritol residue of a tetrasaccharide was cleaved from the penultimate α-L-rhamnopyranose residue (3) which can probably be attributed to the general acid-lability of rhamnopyranosides. Perhaps more surprisingly an ethylene glycol residue of a tetrasaccharide, obtained from C-substance (PnC), was also cleaved from the penultimate 2-acetamido-2-deoxy-β-D-galactopyranose residue (4), and the direct treatment of PnC with aqueous HF also resulted in the cleavage of ribitol from an identical residue (4). These latter results prompted further studies on model compounds to determine some of the structural features associated with this facile and highly specific cleavage of a 2-acetamidohexapyranoside and to ascertain the possible general utility of this reagent for the specific degradation of other oligosaccharides and polysaccharides.

Experimental

Materials

C-Substance (PnC) was obtained from *Streptococcus pneumoniae* type 1 and was *N*-acetylated as previously described (4). The phosphocholine-substituted trisaccharide (1) was obtained by the Smith degradation of this *N*-acetylated PnC (4). Tri-*N*-acetylchitotriose was the gift of Dr. Martin Young of this laboratory and the methyl α- and β-D-glycosides of both 2-acetamido-2-deoxygluco- and mannopyranose were prepared and purified by the method of Beychok *et al.* (5). Oligosaccharides were reduced with sodium borohydride and the reduced oligosaccharides were purified by gel-filtration.

Gel-filtration

Gel-filtration was performed on a Sephadex G-25 column (1.6 cm × 90 cm) using a 0.02 *M* pyridine acetate buffer at pH 5.4 and the column was monitored using a Waters Associates differential refractometer (model R403).

Hydrolysis with HF

The glycosides and oligosaccharides were treated with aque-

[1]NRCC No. 18580.

[2]Present address: Institute of Immunology and Experimental Therapy, Polish Academy of Sciences, U1. Czerska 12, 53-114 Wroclaw, Poland.

0008-4042/80/232610-03$01.00/0

©1980 National Research Council of Canada/Conseil national de recherches du Canada

Can. J. Chem. Downloaded from www.nrcresearchpress.com by 210.87.254.42 on 09/05/12
For personal use only.

Can. J. Chem. Downloaded from www.nrcresearchpress.com by 210.87.254.42 on 09/05/12
For personal use only.

ous HF (48%) in a concentration of 5 mg/mL at 4°C in polyethylene tubes. Samples (0.2–2.0 mL) were withdrawn at intervals and the HF was removed from them under reduced pressure in a desiccator over solid NaOH during a period of 2 h. The extent of hydrolysis attained in each case was determined by specific analyses of each of the residues as described below.

Analytical Methods

All hydrolyses of glycosides and oligosaccharides were monitored by the quantification of the release of terminal substituent groups and/or in the case of the breakage of some glycosidic bonds by the estimation of newly formed hemiacetal. The methods employed are listed below. Reducing sugars were determined by the Nelson–Somogyi copper reduction method (6) and D-glucose was specifically determined using "Glucostat" reagent (Worthington Biochemicals Corp., Freehold, NJ). Phosphate was determined by the method of Chen *et al.* (7). Ribitol, glucosaminitol, and galactosaminitol were identified and quantified by gas–liquid chromatographic analysis of their peracetates (8), using the peracetylated derivatives of inositol galactosaminitol and glucosaminitol as internal standards respectively. Gas–liquid chromatography was performed on a Hewlett-Packard 5830A instrument equipped with a flame ionization detector and a model 18850A electronic integrator. The glass column employed contained 3% OV-275 on gas Chrom Q at 200°C for ribitol and 250°C for the hexaminitols.

Results and Discussion

In the treatment of PnC (Fig. 1) with 48% aqueous HF at 4°C to remove phosphocholine residues and backbone phosphodiester groups, an additional hydrolysis of the *O*-glycosidic bond in the 1-*O*-2-acetamido-2-deoxy-β-D-galactopyranosyl-D-ribitol moiety also occurred (4). That the lability of this *O*-glycosidic bond of the 2-acetamidogalactose residue, under the extremely mild conditions employed, was of the same order as that of the P—O bonds of the phosphate esters was rather surprising, but was further substantiated by the monitoring of the release of phosphate and ribitol from PnC on treatment with 48% aqueous HF (Fig. 2). Both moieties were released simultaneously and at 48 h the greater part of both had been removed. Thus using these conditions the preferential release of phosphate from PnC could not be achieved. In order to elucidate some of the structural features associated with this facile and highly specific hydrolysis of the ribitol aglycon from the 2-acetamido-2-deoxygalactose residue, a number of methyl glycosides and oligosaccharides were subjected to identical treatment with aqueous HF. These hydrolyses established some of the individual structural features conducive to this facile cleavage and also demonstrated that the terminal disaccharide of the repeating unit of PnC is a unique combination of all these features.

The hydrolyses of the methyl 2-acetamido-2-deoxyglycopyranosides are shown in Fig. 2 and were monitored by the quantification of the newly-

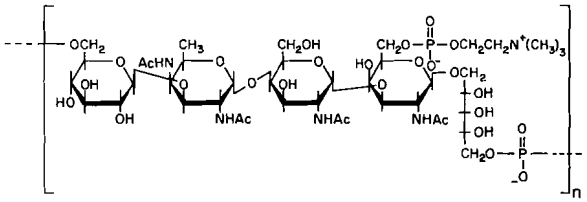


FIG. 1. The repeating unit of *N*-acetylated PnC.

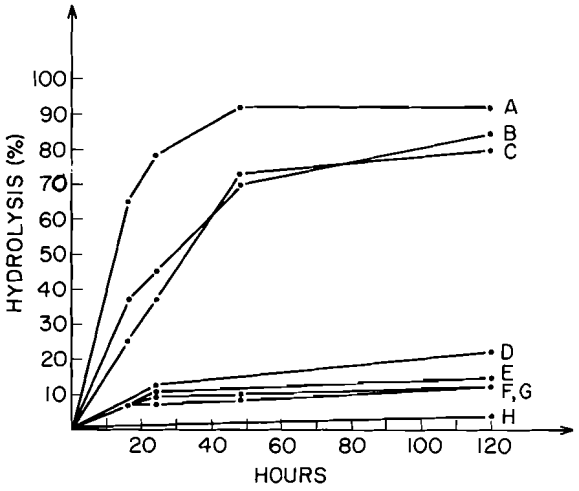


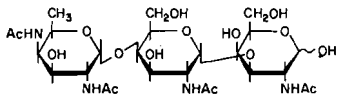
FIG. 2. The rate of hydrolysis of the following substrates using 48% aqueous HF. The expected amounts of released terminal moieties on which these rates were calculated are shown in brackets: A, *N*-acetylated C-substance (phosphate); B, methyl 2-acetamido-2-deoxy-β-D-glucopyranoside (hemiacetal); C, *N*-acetylated C-substance (ribitol); D, methyl 2-acetamido-2-deoxy-α-D-mannopyranoside (hemiacetal); E, methyl 2-acetamido-2-deoxy-β-D-mannopyranoside (hemiacetal); F, methyl 2-acetamido-2-deoxy-α-D-glucopyranoside (hemiacetal); G, methyl β-D-glucopyranoside (hemiacetal); H, methyl α-D-glucopyranoside (hemiacetal).

formed hemiacetal. That the β-D-configuration is more conducive to hydrolysis was ascertained by a comparison of the rates of hydrolysis of methyl-2-acetamido-2-deoxy-α- and β-D-glycopyranosides. Of the two anomers the β-D-anomer was hydrolysed much more rapidly (by approximately eight-fold at 120 h) and in fact proved to be an excellent model for PnC because the hydrolysis of each proceeded at almost identical rates. These experiments on the methyl glycosides also established the contribution of the 2-acetamido group to the ease of hydrolysis when methyl α- and β-D-glucopyranosides (configurational analogues of the formerly treated methyl glycosides minus the 2-acetamido group) were treated with 48% aqueous HF. Even the most labile of these methyl glucopyranosides (β-D-anomer) proved to be less readily hydrolysed than the α-D-anomer of methyl 2-

Can. J. Chem. Downloaded from www.nrcresearchpress.com by 210.87.254.42 on 09/05/12
For personal use only.

acetamido-2-deoxyglucopyranoside. Although the above results using 48% aqueous HF are similar to those obtained on the same methyl glycosides using other mineral acids (9, 10), there are two important differences which would preclude the use of these latter mineral acids to effect the same specific and quantitative cleavage of the β-D-glycosides of 2-acetamidohexoses. These mineral acids are employed at higher temperatures and simultaneously remove *N*-acetyl groups thus stabilizing any remaining unhydrolysed glycosidic bonds (11). By contrast aqueous HF is a very mild hydrolytic reagent and does not break *N*-acyl bonds (1). A further structural feature associated with an increase in the rate of hydrolysis of 2-acetamidohexapyranosides was elucidated by experiments on methyl 2-acetamido-2-deoxy-α- and β-D-mannopyranosides (Fig. 1). In contrast to the D-*gluco* epimers both anomers were found to be relatively stable to aqueous HF and no enhanced sensitivity to hydrolysis of the methyl β-D-glycoside could be detected. Thus the axial orientation of the 2-acetamido group of the D-*manno* epimers ($^4_1$C conformation) retards this enhancing effect of the β-D-orientation of the aglycon. Thus in summary all these experiments of the methyl glycosides indicate that only a *trans* diequatorial disposition of the aglycon and vicinal 2-acetamido group is conducive to an enhanced acid lability of the aglycon.

Because of the highly selective nature of the hydrolyses of the methyl glycosides of 2-acetamido-2-deoxy-β-D-galacto- and glucopyranose it was decided to ascertain whether aqueous HF could be used to selectively cleave the β-D-glycoside bonds of these residues in oligosaccharides or polysaccharides. The model employed was chitotriose which, although having the required terminal β-D-glucosidic bonds of 2-acetamido-2-deoxy-D-glucopyranose, proved to be relatively insensitive to hydrolysis with aqueous HF (Table 1). On reduction of chitotriose, however, prior to treatment with aqueous HF, the newly formed terminal 2-acetamido-2-deoxyglucosaminitol residue could then be easily and selectively removed leaving chitobiose as the other product of hydrolysis. In addition to providing a method for the stepwise degradation of this type of oligosaccharide this experiment also provided evidence that only an open-chain glycitol aglycon of a 2-acetamido-2-deoxy-β-D-gluco- or galactopyranose residue is subject to this facile cleavage. Certainly this is consistent with the facile removal of the terminal ribitol aglycon from the repeating unit of PnC (Fig. 1) (4). It is interesting to note that in cases where the structural features are not conducive to the ease of hydrolysis that the formation of a glycitol aglycon alone does not greatly enhance the rate of hydrolysis. The retarding effect of the α-D-configuration of the penultimate 2-acetamido-2-deoxygalactose of oligosaccharide **1** from PnC remained dominant even after the reduction of **1**, because on treatment with aqueous HF no 2-acetamido-2-deoxygalactosaminitol was released (Table 1). Also the reduction of cellobiose did not result in any significant increase in the poor acid lability of its β-D-glycosidic linkage.



1

TABLE 1. Hydrolysis of oligosaccharides using aqueous HF[a]

Oligosaccharide	Released terminal moiety	Hydrolysis (%)
Chitotriose	Glucosamine[b]	<1
Reduced Chitotriose	Glucosaminitol	44[c]
	Hemiacetal	43
Oligosaccharide **1** from *N*-acetylated C-substance (reduced)	Galactosaminitol	<1
	Hemiacetal	5
Cellobiose	Glucose	1
	Hemiacetal	2
Cellobiitol	Glucose	1
	Hemiacetal	2

[a]All hydrolyses carried out at 4°C for 120 h.
[b]Estimates as glucosaminitol after reduction of the hydrolysis products.
[c]Complete hydrolysis could be attained by prolongation of the period of hydrolysis.

1. D. LIPKIN, B. E. PHILLIPS, and J. W. ABRELL. J. Org. Chem. **34**, 1539 (1969).
2. P. PREHM, S. STIRM, B. JANN, and K. JANN. Eur. J. Biochem. **56**, 41 (1975).
3. L. G. BENNETT and C. P. J. GLAUDEMANS. J. Immunol. **122**, 2356 (1979).
4. H. J. JENNINGS, C. LUGOWSKI, and N. M. YOUNG. Biochemistry. In press.
5. S. BEYCHOK, G. ASHWELL, and E. A. KABAT. Carbohydr. Res. **17**, 13 (1971).
6. R. G. SPIRO. Methods Enzymol. **8**, 7 (1966).
7. P. S. CHEN, J. V. TORIBA, and H. WARNER. Anal. Chem. **28**, 1756 (1956).
8. J. S. SAWARDEKER, J. H. SLONEKER, and A. R. JEANES. Anal. Chem. **37**, 1602 (1965).
9. M. S. FEATHER and J. F. HARRIS. J. Org. Chem. **30**, 153 (1965).
10. K. ONODERA and T. KOMANO. Agric. Biol. Chem. Tokyo, **25**, 932 (1961).
11. A. B. FOSTER, D. HORTON, and M. STACEY. J. Chem. Soc. **81** (1957).

Total synthesis of tetracyclic sesquiterpenoids: (±)-ishwarone

EDWARD PIERS AND TSE-WAI HALL

Department of Chemistry, University of British Columbia, 2036 Main Mall, University Campus, Vancouver, B.C., Canada V6T 1Y6

Received June 9, 1980

This paper is dedicated to Prof. Raymond U. Lemieux on the occasion of his 60th birthday

EDWARD PIERS and TSE-WAI HALL. Can. J. Chem. **58**, 2613 (1980).

A stereoselective total synthesis of the racemic modification of the tetracyclic sesquiterpenoid ishwarone (**2**) is described. Treatment of the known ketal aldehyde **19** with dibromomethylenetriphenylphosphorane gave the dibromo alkene **20**, which was transformed efficiently into the propargylic alcohol **21**. The latter compound was converted via the intermediates **22–24** into the octalone **12**, which in turn was transformed by standard methodology into the corresponding ketal **7**. Treatment of **7** with bromoform – aqueous sodium hydroxide in the presence of a phase-transfer catalyst, followed by acid hydrolysis of the resultant crude product, gave the crystalline keto dibromide **27**. When a solution of the corresponding ketal **26** in tetrahydrofuran–hexamethylphosphoramide containing methyl iodide was treated with *tert*-butyllithium, the monobromo ketals **28** (58%) and **29** (38%) were formed. Compound **28** was converted by means of conventional reactions into the keto alcohol **32**. Attempts to transform the latter substance into (±)-ishwarone (**2**) proved unsuccessful. When the olefinic ketal **7** was allowed to react with dimethyl diazomalonate in the presence of copper bronze, the diester **44** was produced in good yield. The latter intermediate was converted via standard methodology into the keto dimesylate **47** which, upon reaction with lithium chloride in ether – hexamethylphosphoramide, gave the corresponding dichloride **48**. Treatment of **48** with potassium *tert*-butoxide in tetrahydrofuran resulted in an intramolecular alkylation to provide the tetracyclic keto chloride **50**. Reduction of **50** with lithium triethylborohydride in tetrahydrofuran afforded (±)-ishwarol (**51**) which, upon oxidation with pyridinium chlorochromate in dichloromethane, furnished (±)-ishwarone (**2**).

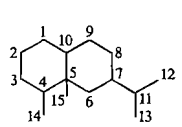
EDWARD PIERS et TSE-WAI HALL. Can. J. Chem. **58**, 2613 (1980).

On décrit la synthèse totale stéréosélective de la modification racémique du sesquiterpène tétracyclique ishwarone (**2**). Le traitement du cétaldéhyde connu **19** par le dibromométhylènetriphénylphosphorane conduit à l'alcène dibromé **20** qui est transformé efficacement en alcool propargylique **21**. Ce dernier conduit par les intermédiaires **22–24** à l'octalone **12** qui a son tour est transformé par des méthodes normales en cétal correspondant **7**. Le composé **7** traité par une solution aqueuse de bromoforme – hydroxyde de sodium en présence d'un catalyseur de transfert de phase, suivi d'une hydrolyse acide du produit brut donne la dibromocétone cristalline **27**. Lorsque l'on traite le cétal correspondant, **26**, en solution dans un mélange de tétrahydrofuranne–hexaméthylphosphoramide contenant de l'iodure de méthyle, par le *tert*-butyllithium il y a formation des cétals monobromés **28** (58%) et **29** (38%). Le composé **28** par des réactions conventionnelles conduit à l'alcool cétonique **32**. On n'a pas réussi à transformer cet alcool en (±)-ishwarone (**2**). Si on fait réagir le cétal oléfinique avec du diazomalonate de méthyle en présence d'un bronze de cuivre, il se forme le diester **44** avec de très bons rendements. Ce dernier intermédiaire, par des méthodes normales, est transformé en céto dimésylate **47** qui, par réaction avec le chlorure de lithium dans le mélange éther–hexaméthylphosphoramide, donne le composé dichloré correspondant **48**. Ce composé, en présence de *tert*-butylate de potassium dans le tétrahydrofuranne, subit une alkylation intramoléculaire qui conduit à la cétone tétracyclique chlorée **50**. Cette dernière est réduite par le triéthylborohydrure de lithium dans le tétrahydrofuranne en (±)-ishwarol **51** qui par oxydation avec le chlorochromate de pyridinium dans le dichlorométhane fournit la (±)-ishwarone (**2**).

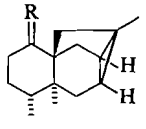
[Traduit par le journal]

Introduction

The natural products belonging to the eremophilane–valencane class of sesquiterpenoids[1] possess the general carbon skeleton shown in **1**.[2] Ishwarone (**2**), a structurally novel member of this general



1



2 R = O
3 R = H_2

class, was first isolated from *Aristolochia indica* in 1935 (2), although the unique tetracyclic structure of this material was not recognized until the structural elucidation was completed some 34 years later (3). Subsequently, the parent hydrocarbon ishwarane (**3**) was also shown to be a natural product, having been isolated from *Aristolochia indica* (4) and *Cymbopetalum penduliforum* (Dunal) Baill (5).

Although the total synthesis of (±)-ishwarane (**3**) has been accomplished independently by two groups (6, 7), the preparation of ishwarone (**2**) had not been reported prior to the completion of our work.[3] We report herein the details of our synthesis of the racemic modification of this interesting natural product.[4]

[1]For a recent review, see ref. 1.

[2]The numbering system shown in **1** is that normally employed for eremophilane–valencane sesquiterpenoids.

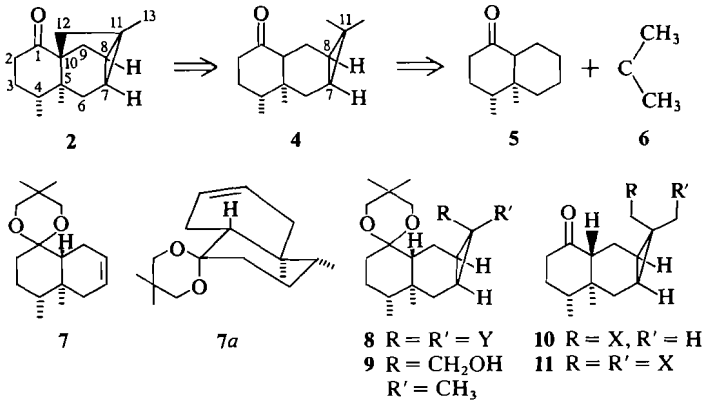
[3]For a preliminary report outlining a portion of the work described herein, see ref. 8. Very recently, a short, elegant synthesis of (±)-ishwarone via a route entirely different from ours was reported (9).

[4]For an excellent general account of sesquiterpenoid syntheses completed prior to approximately the middle of 1970, see ref. 10.

0008-4042/80/232613-11$01.00/0

©1980 National Research Council of Canada/Conseil national de recherches du Canada

Can. J. Chem. Downloaded from www.nrcresearchpress.com by 210.87.254.42 on 09/05/12
For personal use only.



SCHEME 1

Synthetic Plan

An examination of the structure of ishwarone (**2**) makes it quite clear that any plan to effect the synthesis of this material should focus on an efficient construction of the structurally novel feature present in the compound, the tricyclo[3.2.1.$0^{2,7}$]octane ring system. Although retrosynthetic analyses reveal a number of possible "key" reactions which might be employed for this purpose, our synthetic plan was based on the following disconnective analysis (see Scheme 1). Disconnection of the C(10)—C(12) bond of ishwarone (**2**) provides the synthon **4**, which upon further (theoretical) cleavage (C(7)—C(11) and C(8)—C(11)) gives the dimethyldecalone **5** and a three-carbon fragment **6**.

On the basis of this analysis, it was decided to attempt the synthesis of (±)-ishwarone (**2**) via the following general route (Scheme 1). It appeared at the outset that a stereoselective preparation of the bicyclic ketal **7** would be relatively straightforward. Addition of a symmetrical carbene (or carbenoid) $:CY_2$ to this compound would be predicted to take place from the less hindered side of the carbon–carbon double bond, opposite to the angular methyl group (cf. **7***a*). Synthetic differentiation between the two Y groups of the expected product **8** to produce an intermediate **9**, followed by hydrolytic removal of the ketal protecting group, conversion of the hydroxyl functionality into a good leaving group (X), and intramolecular alkylation of the resultant product **10** would provide (±)-ishwarone (**2**). Alternatively, compound **8** might also be converted into an intermediate such as **11**. Alkylative cyclization of the latter material, followed by reductive removal of the second X functionality would also produce the desired final product **2**.

Regarding the nature of Y, two possibilities were considered, bromine and carboalkoxy. The addition of dibromocarbene to alkenes is a well-known process, and recent work has shown that the two bromine atoms in unsymmetrical *gem*-dibromocyclopropanes can be differentiated synthetically (11–14). Similarly, the copper–catalyzed addition of dialkyl diazomalonates to alkenes to provide the corresponding *gem*-dicarboalkoxycyclopropanes has been well documented (15). Therefore, our first synthetic objective became the olefinic ketal **7**. For reasons already mentioned, it was expected that addition of dibromocarbene or dimethyl diazomalonate to this substance would produce the corresponding adducts **8** (Y = Br or CO_2Me), which, in turn, might be transformed into intermediates of the type **10** or **11**, respectively.

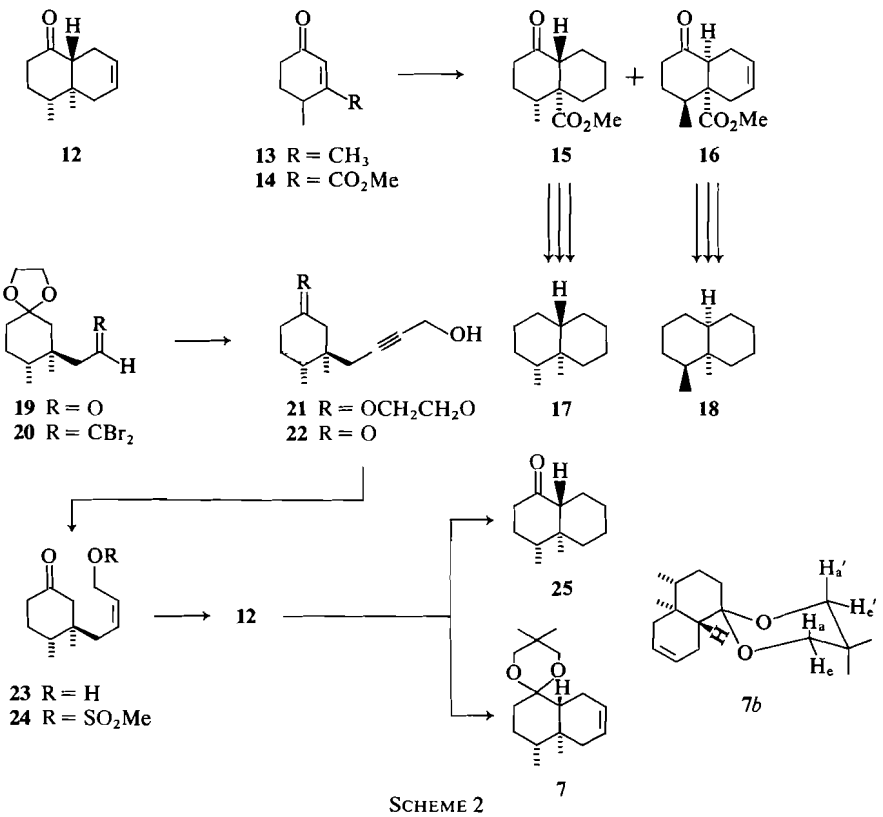
Preparation of the Bicyclic Olefinic Ketal 7 (see Scheme 2)

The synthesis of compound **7** would, presumably, require the prior preparation of the corresponding ketone **12**. At first sight, an obvious method for preparing the latter substance would involve the Diels–Alder reaction of 1,3-butadiene with 3,4-dimethyl-2-cyclohexen-1-one (**13**) (16). However, it is known that Diels–Alder cycloadditions of 2-cyclohexen-1-ones with 1,3-dienes are quite sluggish reactions[5] and that 3-substituted cyclohexenones are even more reluctant to act as dienophiles. Indeed, attempted reaction of 3,4-dimethyl-2-cyclohexen-1-one (**13**) (16) with 1,3-butadiene under a variety of conditions (including the use of Lewis acid catalysts) failed to provide any of the desired octalone adduct.[6] In an attempt to increase the reactivity of the dienophile, 3-carbomethoxy-4-methyl-2-cyclohexen-1-one

[5]For a recent, brief discussion of this problem and for a report regarding the successful Lewis acid catalyzed Diels–Alder reactions of 1,3-butadiene with 2-cyclohexen-1-one and 2-methyl-2-cyclohexen-1-one, see ref. 17.

[6]For details regarding these attempts, see ref. 18.

Can. J. Chem. Downloaded from www.nrcresearchpress.com by 210.87.254.42 on 09/05/12
For personal use only.



SCHEME 2

(**14**) was prepared.[7] Although attempted Diels–Alder reaction of **14** with 1,3-butadiene under purely thermal conditions proved to be unsuccessful,[8] a 1:1 cycloaddition adduct was obtained when a solution of **14** and excess 1,3-butadiene in dichloromethane in the presence of aluminum trichloride was heated at 95–100°C (sealed tube) for 1 day. However, the product, in addition to being obtained in only modest yield (~50% at best), was shown unambiguously to consist of an approximately 1:1 mixture of the two bicyclic keto esters **15** (desired product) and **16**.[9] Separation of these two diastereomers by means of column chromatography on silica gel gave the desired isomer **15**, mp 96–97°C, in approximately 20–25% yield. Thus, the nonstereoselective, low-yielding nature of this Diels–Alder reaction, along with the fact that the ester functionality of the desired product **15** would still have to be transformed into a methyl group, made this approach appear to be quite unattractive. Therefore, an alternative preparation of the keto olefin **12** was devised, employing a route which, although more lengthy, was quite efficient and highly stereoselective.

Recently, in connection with a very elegant synthesis of (±)-eremophilone, Ziegler and co-workers (21) reported the stereoselective conversion of 3,4-dimethyl-2-cyclohexen-1-one (**13**) into the ketal aldehyde **19**. It appeared that the latter compound would serve as a convenient precursor for the keto olefin **12**. This proved to be the case. Thus, treatment of **19** with dibromomethylenetriphenylphosphorane (derived from the reaction of carbon tetrabromide with triphenylphosphine in the presence of zinc dust) (22) gave the dibromo alkene **20**. When the latter substance was allowed to react with two equivalents of *n*-butyllithium at −78°C (22) and the

[7]Hydrogenation (H_2, tris(triphenylphosphine)rhodium chloride, benzene, room temperature, atmospheric pressure) of the less substituted double bond of methyl 6-methyl-1,4-cyclohexadienecarboxylate (19), followed by allylic oxidation (CrO_3, CH_3CO_2H) of the resultant product (methyl 6-methylcyclohexenecarboxylate) afforded the keto ester **14** in 46% overall yield. For further details, see ref. 18.

[8]The successful thermal Diels–Alder reaction of 3-carbomethoxy-2-cyclohexen-1-one with 1,3-butadiene has been reported (20).

[9]The structures of **15** and **16** were established by unambiguous correlations with the known dimethyldecalins **17** and **18**, respectively, which had been prepared previously in our laboratory. For details, see ref. 18. We are very grateful to Dr. P. M. Worster for his assistance in making these correlations possible.

Can. J. Chem. Downloaded from www.nrcresearchpress.com by 210.87.254.42 on 09/05/12
For personal use only.

Can. J. Chem. Downloaded from www.nrcresearchpress.com by 210.87.254.42 on 09/05/12
For personal use only.

resultant lithium acetylide was trapped (23) with gaseous formaldehyde at 0°C, the substituted propargylic alcohol **21** was produced (75% from **19**). Hydrolysis (hydrochloric acid in aqueous methanol) of the ketal functionality afforded (92%) the crystalline keto alcohol **22**, mp 43–45°C, which was smoothly hydrogenated (palladium-on-barium sulfate) in ethanol containing a small amount of *purified* quinoline (24)[10] to yield the *cis* allylic alcohol **23**. Conversion (methanesulfonyl chloride, triethylamine dichloromethane) of this material into the rather unstable allylic mesylate **24**, followed by immediate treatment of the latter compound with 4 equivalents of potassium *tert*-butoxide in *tert*-butyl alcohol at room temperature, gave the desired octalone **12** (60% from the propargylic alcohol **22**). Conformational analysis of **12**, as compared with a similar analysis of the corresponding *cis*-fused diastereomer, would lead one to predict that the *trans*-fused isomer **12** should be the thermodynamically more stable octalone. Therefore, since the intramolecular alkylation was done in the presence of excess base, the expected product was **12**. Further evidence for this stereochemical conclusion was provided as follows. Hydrogenation (palladium-on-carbon, methanol) of **12** gave the corresponding decalone **25**, which was also recovered unchanged from potassium *tert*-butoxide – *tert*-butyl alcohol.

The first stage of the synthetic work was completed by conversion, under standard conditions, of the octalone **12** into the corresponding ketal derivative **7**, mp 100.5–102.5°C. Although the spectral data obtained from this material was largely straightforward and was fully consistent with the structural assignment, one rather unusual feature of the ^{1}H nmr spectrum should be discussed briefly, since this feature was seen in some of the subsequent synthetic intermediates as well. In the ^{1}H nmr spectrum of **7**, the protons of the methylene groups of the ketal functionality gave rise to an interesting pattern of signals consisting of an overlapped pair of doublets and a pair of doublet of doublets. If one considers the more stable chair conformation of the ketal ring (cf. **7***b*), then the signals can be assigned as follows. The overlapped pair of doublets (J = 11 Hz in each case) at δ 3.74 and 3.63 can be attributed to the two axial protons (H_a, H_a') each of which is geminally coupled to the corresponding equatorial proton (H_e, H_e', respectively). On the other hand, the equatorial protons H_e and H_e' each give rise to a doublet of doublets. These signals, which appear at δ 3.32 and 3.27, exhibit coupling constants of 11 Hz and ~2.5 Hz. Thus, in addition to being coupled to the axial protons, H_e and H_e' are mutually coupled (long-range W-type coupling) (26).

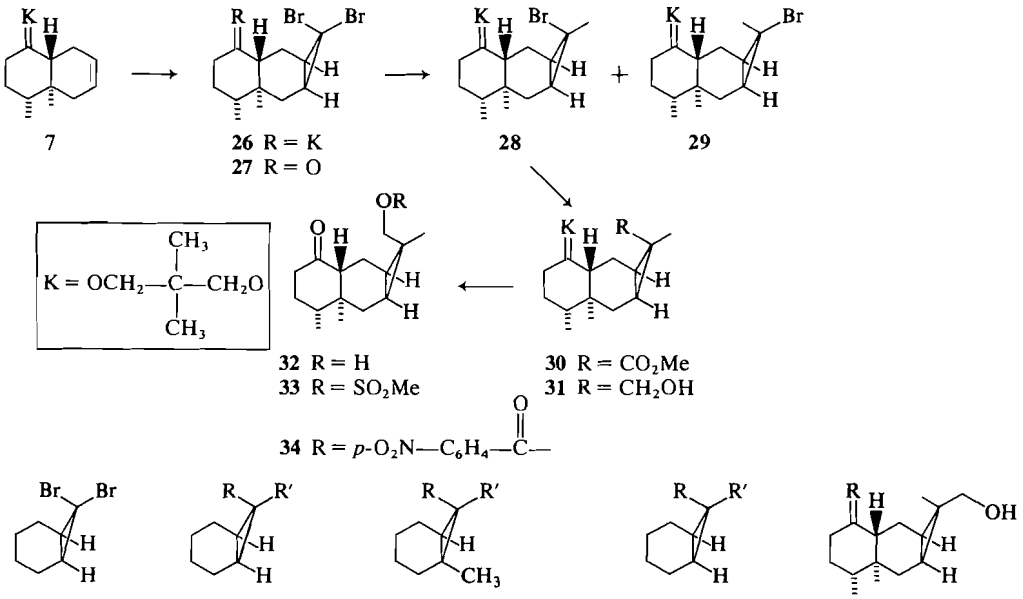
The acquisition of the olefinic ketal **7** set the stage for investigations into the use of this material for the synthesis of (±)-ishwarone (**2**).

Attempted Synthesis of (±)-Ishwarone (2) via the Dibromo Ketal 26 (see Scheme 3)

Treatment of the ketal olefin **7** with bromoform and aqueous sodium hydroxide containing a small amount of ethanol and the phase-transfer catalyst triethylbenzylammonium chloride (27) afforded, in good yield, a crude product which consisted mainly of the desired dibromocarbene adduct **26**. However, the ir spectrum of this material exhibited a weak absorption in the "carbonyl region," indicating that the ketal functionality had been partially lost. Furthermore, allowing this crude material to stand at room temperature, or attempted purification by means of distillation (reduced pressure) or column chromatography (silica gel), led to the acquisition of material which exhibited an increase in the intensity of the carbonyl absorption. In order to avoid these difficulties, the crude product obtained from the carbene addition reaction was hydrolyzed immediately with aqueous hydrochloric acid in methanol, and the resultant product was purified by column chromatography on silica gel. The highly crystalline ketone **27**, mp 130–131.5°C, was thus obtained in 80% yield. Reketalization of **27** under standard conditions gave (93%) the desired synthetic intermediate **26**.

Recently, Kitatani *et al.* (12) have shown that the two bromine atoms of 7,7-dibromobicyclo[4.1.0]heptane (**35**) can be differentiated synthetically by alkylation of the carbenoid (α-bromocyclopropyllithium) species derived from **35** by means of a bromine–lithium exchange reaction. For example, it was reported that treatment of **35** with *n*-butyllithium in tetrahydrofuran at −95°C, followed by addition of methyl iodide and warming of the resultant mixture to room temperature, gave 7-*exo*-bromo-7-methylbicyclo[4.1.0]heptane (**36**) as the sole alkylation product (60% yield). On the other hand, addition of *n*-butyllithium to a cold (−95°C) solution of **35** in tetrahydrofuran–hexamethylphosphoramide *containing methyl iodide*, gave, after subsequent warming of the solution to room temperature, a mixture of **36** and the epimer **37**, in a ratio of approximately 80:20 (86% yield). Therefore, it was decided to attempt a similar differentiation of the two bromine atoms of compound **26**. After a considerable amount of experimentation, it was found that when a pentane solution of 2 equiva-

[10]It was found that this reduction did not proceed well unless the quinoline employed was freshly purified as described by Vogel (25).



SCHEME 3

lents of *tert*-butyllithium was added to a cold (−95°C) solution of 1 equivalent of the dibromide **26** in tetrahydrofuran containing 3.5 equivalents of methyl iodide and 10% by volume of hexamethylphosphoramide, and the resultant solution was stirred at −95°C for 1 hour and at −78°C for 4 hours, a mixture of the two epimeric methylated products **28** and **29** (ratio approximately 3:2, respectively) was produced. Separation of these isomers by means of column chromatography on silica gel gave the two pure substances as oils in yields of 58 and 38%, respectively.

The stereochemical assignments with respect to the alkylation products **28** and **29** were made primarily on the basis of ^{1}H nmr spectroscopy. The C-7 methyl groups of the substituted bicyclo[4.1.0]-heptanes **36–39** have been shown to give rise to singlets at δ 1.70, 1.76, 1.76, and 1.83, respectively (12). Thus, in these substances, the *endo* methyl groups (**36**, δ 1.70; **38**, δ 1.76) resonate at higher field than the corresponding *exo* methyl groups (**37**, δ 1.76 ; **39**, δ 1.83). The ^{1}H nmr spectrum of the major isomer obtained from the reaction described above exhibited the methyl group on the cyclopropane ring as a singlet at δ 1.74, while the corresponding signal in the ^{1}H nmr spectrum of the minor isomer appeared at δ 1.62. Therefore, it seemed to be very reasonable to conclude that the major and minor products possessed the stereo-structures **28** and **29**, respectively. Further evidence in favor of these assignments will be presented later (*vide infra*).

Treatment of compound **28** with 2 equivalents of *tert*-butyllithium in ether at −78°C, followed by trapping of the resultant cyclopropyllithium reagent with freshly distilled methyl chloroformate, afforded the ketal ester **30** in 71% yield. Reduction of the latter substance with lithium aluminum hydride in ether gave the corresponding alcohol **31** which, upon hydrolysis with hydrochloric acid in methanol, was smoothly transformed into the keto alcohol **32** (69% from **30**).

Appropriate ^{1}H nmr data obtained from compounds **31** and **32**, compared with that derived from the related alcohols **40–43**,[11] provided corroborative evidence for the stereochemical assignments made for this series of compounds. Thus, the singlets due to the methylene protons of the hydroxymethyl group of compounds **31** and **32** appeared at δ 3.58 and 3.56, respectively. These chemical shifts are very similar to that of the corresponding signal (singlet, δ 3.65) of 7-*endo*-hydroxymethyl-7-methylbicyclo-[4.1.0]heptane (**40**). On the other hand, the ^{1}H nmr spectra of compounds **42** and **43** exhibited the —C*H*$_2$OH singlet at δ 3.30 and 3.26, respectively, values which compare favorably with the corres-

[11]Compounds **40** and **41** were obtained from **36** (12) and **37** (12), respectively, via a route which paralleled exactly the conversion of **28** into **31**. In similar fashion, the bromo ketal **29** was transformed into the ketal alcohol **42**, which was subsequently hydrolyzed (cf. **31** → **32**) to provide the corresponding ketone **43**. For details regarding these conversions, see ref. 18.

Can. J. Chem. Downloaded from www.nrcresearchpress.com by 210.87.254.42 on 09/05/12
For personal use only.

Can. J. Chem. Downloaded from www.nrcresearchpress.com by 210.87.254.42 on 09/05/12
For personal use only.

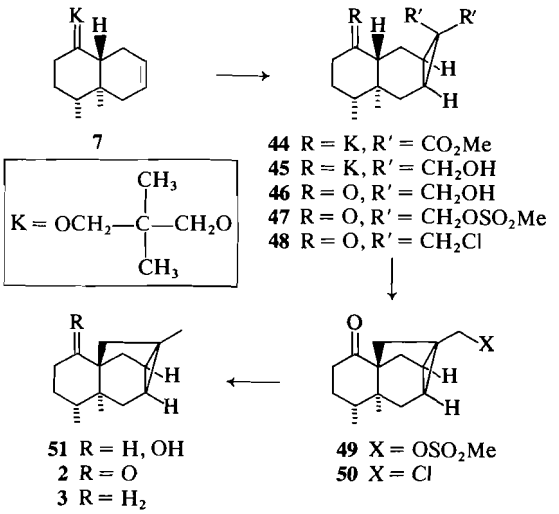
ponding signal (singlet, δ 3.20) of 7-*exo*-hydroxymethyl-7-methylbicyclo[4.1.0]heptane (**41**).

The use of the keto alcohol **32** as an intermediate in the synthesis of (±)-ishwarone (**2**) required bond formation between the carbinol carbon and the bridgehead position adjacent to the carbonyl group. However, conversion of **32** into a derivative in which the hydroxyl group had been transformed into a good leaving group proved to be problematic. For example, attempts to prepare and isolate (even under very mild conditions) the corresponding mesylate **33** were consistently unsuccessful, presumably due to the high propensity of the cyclopropylcarbinyl mesylate system to undergo solvolytic rearrangements.[12] On the other hand, treatment of compound **32** with *p*-nitrobenzoyl chloride in pyridine at 0°C afforded (91%) the *p*-nitrobenzoate **34**, which turned out to be a fairly stable oil. However, all attempts to effect intramolecular alkylation of **34** (*p*-nitrobenzoate anion as a leaving group) failed to produce any (±)-ishwarone (**2**). Use of different bases (e.g. potassium *tert*-butoxide, potassium hydride) in a variety of solvents (e.g. *tert*-butyl alcohol, tetrahydrofuran) resulted either in the recovery of starting material or produced the keto alcohol **32**.

The projected conversion of **32** into (±)ishwarone (**2**) remains an attractive possibility. In fact, it appears to be highly likely that some method which would effect this transformation could be found. However, at this stage of our work, lack of sufficient quantities of compound **32** precluded the possibility of more exhaustive investigations. Furthermore, at the same time at which this possibility was being studied, an alternative synthetic route to (±)-ishwarone (**2**) was also under investigation. This alternative, which is described in the following section of this paper, proved to be successful and, therefore, further efforts to prepare larger quantities of **32** and attempts to effect cyclization of this material were discontinued.

Total Synthesis of (±)-Ishwarone (2) via the Ketal Diester 44 (see Scheme 4)

Treatment of the ketal olefin **7** with excess dimethyl diazomalonate in the presence of copper bronze at 130–140°C (15) gave, in 64% yield, a single, crystalline (mp 132–133.5°C) adduct which, on the basis of steric approach control (*vide supra*), could be confidently assigned structure **44**.[13] Reduction of



SCHEME 4

the latter material with lithium aluminum hydride in ether, followed by treatment of the resultant ketal diol **45** (mp 173–174.5°C) with dilute hydrochloric acid in acetone, afforded the keto diol **46**, mp 138–139.5°C (79% from **44**). The corresponding oily dimesylate **47**, obtained by treatment of **46** with an excess of methanesulfonyl chloride in dichloromethane containing triethylamine, proved to be an isolable material, although it was not very stable. Furthermore, all attempts to effect conversion of the dimesylate into the tetracyclic monomesylate **49** via a base-promoted intramolecular alkylation failed. Although it appears to be highly probable that the required transformation had indeed occurred, the desired product **49** (a cyclopropylcarbinyl mesylate) was, again, apparently not sufficiently stable under the reaction conditions to allow for isolation. In order to overcome this difficulty, it was felt that if the mesylate groups of **47** were replaced by a "poorer" leaving group, such as chloride ion, then the corresponding tetracyclic system (such as **50**) might be stable enough to serve as a suitable synthetic intermediate.

When a solution of the keto dimesylate **47** in ether–hexamethylphosphoramide containing excess lithium chloride was stirred at room temperature, the corresponding dichloride **48** (mp 133–135°C after recrystallization from hexane)[14] was obtained in 91% yield. Treatment of **48** with a slight excess of freshly prepared potassium *tert*-butoxide in tetrahydrofuran at room temperature afforded the desired

[12]Although structurally simple cyclopropylcarbinyl mesylates and arenesulfonates have been isolated, these compounds are quite unstable and undergo solvolysis very readily (see refs. 28 and 29 for examples).

[13]For a recent report which describes the copper bronze-catalyzed addition of dimethyl diazomalonate to *trans*-Δ²-octalin, see ref. 30.

[14]A sample of the keto dichloride **48** which was obtained by means of preparative thin-layer chromatography (silica gel) using 7:3 hexane–ether as developing solvent, and which was not recrystallized, exhibited mp 74–76°C, as reported in our preliminary communication (8).

Can. J. Chem. Downloaded from www.nrcresearchpress.com by 210.87.254.42 on 09/05/12
For personal use only.

tetracyclic keto chloride **50** (91% yield). Although this cyclopropylcarbinyl chloride could be isolated, it was not very stable and, therefore, was used immediately for the next step in the synthetic sequence. Reduction of **50** with lithium triethylborohydride (31) in tetrahydrofuran provided (88% from the keto dichloride **48**) the alcohol **51**.[15] Oxidation of the latter material with pyridinium chlorochromate (32) in dichloromethane gave crystalline (mp 80–81°C) (±)-ishwarone (**2**), which exhibited spectral data which were in excellent agreement with those reported for the natural product itself (3). In order to obtain further confirmation regarding the structure of the synthetic material, (±)-**2** was subjected to Wolff–Kishner reduction, as previously described (3). The product, (±)-ishwarane (**3**) was identical in all respects with an authentic sample of (±)-**3**.[16]

Experimental

General

Melting points, which were determined on a Fisher-Johns melting point apparatus, and distillation temperatures are uncorrected. Infrared spectra were recorded on a Perkin-Elmer model 710 spectrophotometer. Proton magnetic resonance spectra were measured using Varian Associates spectrometers, models T-60 and/or HA-100 or XL-100. Signal positions are given in δ units, with tetramethylsilane as the internal standard; the multiplicity, integrated peak areas, and proton assignments are indicated in parentheses. High resolution mass spectrometric measurements were recorded on an A.E.I. model MS-50 mass spectrometer. Gas–liquid chromatographic analyses were carried out with a Hewlett-Packard model 5832A gas chromatograph containing a 6 ft × 0.125 in. column (10% OV-210 on 100–120 mesh HP Chromosorb W). Microanalyses were performed by Mr. P. Borda, Microanalytical Laboratory, University of British Columbia, Vancouver, B.C.

*Preparation of the Ketal Dibromide **20***

To a suspension of zinc dust (5.35 g) in a solution of triphenylphosphine (21.0 g, 80.2 mmol) in 280 mL of dry dichloromethane was added 26.57 g (80.1 mmol) of carbon tetrabromide, and the resultant mixture was stirred at room temperature under an atmosphere of nitrogen for 27 h. A solution of 8.51 g (40.1 mmol) of the ketal aldehyde **19** (21) in a minimum amount of dry dichloromethane was added. After the reaction mixture had been stirred for an additional 2 h, approximately 200 mL of petroleum ether (bp 30–60°C) was added and the resulting mixture was filtered. The collected solid material was dissolved in 60 mL of dichloromethane, the resultant solution was diluted again with 200 mL of petroleum ether, and filtered. This process was repeated twice and all of the filtrates were combined. Removal of the solvent gave a residue which consisted of a mixture of a light yellow oil and a white solid. This material was diluted with a small amount of ether and filtered. The collected solid material was washed with ether. Removal of the solvent from the filtrate, followed by distillation (air-bath temperature 114–124°C/0.3 Torr) of the residual material gave 11.33 g (77%) of the ketal dibromide **20** as a very pale yellow oil; ir (film): 1615 cm^{-1}; ^1H nmr ($CDCl_3$) δ: 0.86 (d, 3H, secondary methyl, J = 6 Hz), 0.92 (s, 3H, tertiary methyl), 1.86–2.32 (8-line multiplet, AB part of ABX system, 2H, allylic protons, $J_{AX} = J_{BX} \approx 7$ Hz, $J_{AB} \approx 15$ Hz), 3.91 (m, 4H, ethylene ketal protons), 6.43 (overlapped d of d, X part of ABX system, 1H, vinyl proton, $J_{AX} = J_{BX} \approx 7$ Hz). *Exact Mass* calcd. for $C_{13}H_{20}{}^{79}Br^{81}BrO_2$: 367.9840; found: 367.9810.

*Preparation of the Ketal Propargyl Alcohol **21***

To a cold (−78°C) stirred solution of the ketal dibromide **20** (7.86 g, 21.4 mmol) in 100 mL of dry tetrahydrofuran under an atmosphere of nitrogen was added 21 mL of a solution of *n*-butyllithium in hexane (2.37 *M*, 49.8 mmol). The mixture was stirred at −78°C for 1.5 h, and then was allowed to warm to 0°C. Gaseous formaldehyde, obtained by thermolysis of 8 g of paraformaldehyde at 160–190°C (oil bath temperature), was swept into the reaction mixture with a stream of nitrogen. After the reaction mixture had been stirred vigorously for another 30 min, 30 mL of saturated aqueous ammonium chloride was added. The resultant mixture was diluted with water and then extracted thoroughly with ether. The combined extract was washed with water and brine and dried over anhydrous magnesium sulfate. Removal of the solvent gave a viscous yellow oil which, upon distillation (air-bath temperature 135–145°C/0.4 Torr) afforded 5.0 g (98%) of the propargyl alcohol **21** as a colourless oil; ir (film): 3475 (broad), 2325, 2255 cm^{-1}; ^1H nmr ($CDCl_3$) δ: 0.82 (d, 3H, secondary methyl, J = 6 Hz), 0.90 (s, 3H, tertiary methyl), 2.14 (unresolved t, 2H, —$CH_2C{\equiv}C$—), 3.87 (m, 4H, ethylene ketal protons), 4.19 (t, 2H, —CH_2OH, $J \approx 2$ Hz). *Exact Mass* calcd. for $C_{14}H_{22}O_3$: 238.1546; found: 238.1569.

*Preparation of the Keto Propargyl Alcohol **22***

To a solution of the ketal **21** (5.27 g, 22.1 mmol) in 300 mL of methanol was added 22 mL of water and 22 mL of 3 *N* hydrochloric acid. After the solution had been stirred at room temperature for 3 h, most of the methanol was removed under reduced pressure. The residue was diluted with water and thoroughly extracted with ether. The combined ether extract was washed with saturated aqueous sodium bicarbonate, water, and brine, and then dried over anhydrous magnesium sulfate. Removal of the solvent, followed by distillation (air-bath temperature 130–140°C/0.5 Torr) of the residual material gave 3.95 g (92%) of the ketone **22** as a viscous, colourless oil which crystallized on standing. Recrystallization of a small amount of this material from ether – petroleum ether gave an analytical sample which exhibited mp 43–45°C; ir ($CHCl_3$): 3500, 2320, 2260, 1705 cm^{-1}; ^1H nmr ($CDCl_3$) δ: 0.80 (s, 3H, tertiary methyl), 0.93 (d, 3H, secondary methyl, J = 6 Hz), 4.29 (t, 2H, —CH_2OH, $J \approx 2$ Hz). *Anal.* calcd. for $C_{12}H_{18}O_2$: C 74.19, H 9.34; found: C 74.28, H 9.30.

*Preparation of the Keto Allylic Alcohol **23***

To a stirred solution of the keto propargylic alcohol **22** (2.73 g, 14.1 mmol) in 50 mL of ethanol was added 549 mg of 5% palladium-on-barium sulfate and four drops of purified quinoline. After the resultant mixture had been subjected to hydrogenation at room temperature and atmospheric pressure until one equivalent of hydrogen had been absorbed, it was filtered through Celite. Removal of the solvent from the filtrate, followed by distillation (air-bath temperature 132–140°C/

[15]This material, (±)-ishwarol (3), consisted mainly of one isomer, expected to be that with the hydroxyl group in an axial orientation, *cis* to the angular methyl group. In the ^1H nmr spectrum of **51**, the carbinol proton appeared as an unresolved multiplet (δ 3.42) with a width at half-height of about 6 Hz, thus indicating that this proton was equatorially oriented.

[16]We are very grateful to Professor Ronald B. Kelly for a sample of synthetic (±)-ishwarane (**3**).

Can. J. Chem. Downloaded from www.nrcresearchpress.com by 210.87.254.42 on 09/05/12
For personal use only.

0.4 Torr) of the residual material, provided 2.62 g (95%) of the keto alcohol **23** as a colourless oil, which according to glc analysis consisted of one component; ir (film): 3450 (broad), 3050, 1710 cm^{-1}; ^1H nmr ($CDCl_3$) δ: 0.80 (s, 3H, tertiary methyl), 0.93 (d, 3H, secondary methyl, $J = 6$ Hz), 4.12 (d, 2H, $—CH_2OH$, $J = 5.5$ Hz), 5.12–6.00 (m, 2H, vinyl protons). *Exact Mass* calcd. for $C_{12}H_{20}O_2$: 196.1457; found: 196.1463.

Preparation of the Keto Mesylate ***24***

To a cold (0°C) solution of the alcohol **23** (2.71 g, 13.8 mmol) in 50 mL of dry dichloromethane containing 2.1 g (20.8 mmol) of dry triethylamine was added slowly 1.75 g (15.3 mmol) of methanesulfonyl chloride. The solution was stirred at 0°C under an atmosphere of nitrogen for 30 min and was then poured into ice water. The resultant mixture was extracted quickly with cold ether. The combined extract was washed thrice with ice cold water, once with brine, and dried over anhydrous magnesium sulfate. Removal of the solvent (temperature ≤25°C) gave 3.64 g (96%) of the crude keto mesylate **24** as a yellow oil; ir (film): 3060, 1710, 1350, 1170 cm^{-1}; ^1H nmr ($CDCl_3$) δ: 0.90 (s, 3H, tertiary methyl), 1.03 (d, 3H, secondary methyl, $J = 6$ Hz), 3.08 (s, 3H, $—OSO_2CH_3$), 4.78 (d, 2H, $—CH_2OMs$, $J = 6$ Hz), 5.64–5.95 (m, 2H, vinyl protons). Since compound **24** was quite unstable, it was not purified further and was used directly for the next synthetic transformation.

Preparation of the Octalone ***12***

To a solution of potassium *tert*-butoxide (3.2 g, 28.5 mmol) in 175 mL of dry *tert*-butyl alcohol under an atmosphere of nitrogen was added, dropwise, a solution of the crude keto mesylate **24** (3.64 g, 13.3 mmol) in 30 mL of dry *tert*-butyl alcohol. After the orange mixture had been stirred at room temperature for 2.5 h, it was treated with aqueous ammonium chloride and the resultant mixture was extracted thoroughly with ether. The combined ether extract was washed with water and dried over magnesium sulfate. Removal of the solvent, followed by distillation (air-bath temperature 62–75°C/0.2 Torr) of the residual reddish brown oil afforded 1.56 g (63% from the keto alcohol **23**) of the bicyclic keto olefin **12** as a colourless oil which, according to glc analysis, consisted of a single component; ir (film): 3050, 1705, 1660 cm^{-1}; ^1H nmr ($CDCl_3$) δ: 0.68 (s, 3H, tertiary methyl), 0.94 (d, 3H, secondary methyl, $J = 6$ Hz), 5.68 (broad signal, 2H, vinyl protons). *Anal.* calcd. for $C_{12}H_{18}O$: C 80.85, H 10.18; found: C 80.51, H 10.01.

Preparation of the Decalone ***25***

To a stirred solution of the octalone **12** (223 mg, 1.25 mmol) in 10 mL of methanol was added 52 mg of 5% palladium-on-carbon and the resultant mixture was subjected to hydrogenation at room temperature and atmospheric pressure until hydrogen absorption ceased. Successive filtration, evaporation of the solvent from the filtrate, and distillation (air-bath temperature 160–172°C/16–20 Torr) of the residual material gave 186 mg (83%) of the decalone **25** as a colourless oil; ir (film): 1710 cm^{-1}; ^1H nmr ($CDCl_3$) δ: 0.66 (s, 3H, tertiary methyl), 0.88 (d, 3H, secondary methyl, $J = 6$ Hz). *Exact Mass* calcd. for $C_{12}H_{20}O$: 180.1507; found: 180.1514. When a solution of **25** in *tert*-butyl alcohol containing potassium *tert*-butoxide was stirred at room temperature for 22 h, it was recovered unchanged.

Preparation of the Ketal Olefin ***7***

A solution of the octalone **12** (5.2 g, 29.2 mmol), 2,2-dimethyl-1,3-propanediol (4.5 g, 43.3 mmol), and *p*-toluenesulfonic acid (520 mg) in 200 mL of dry benzene was refluxed for 20 h under a Dean–Stark water separator. The cooled solution was diluted with ether, washed with saturated aqueous sodium bicarbonate, water, and brine, and then dried over anhydrous magnesium sulfate. Removal of the solvent provided a pale yellow oil which solidified on standing at 0°C. Recrystallization of this material from hexane furnished 6.52 g (85%) of the desired ketal olefin **7**; mp 100.5–102.5°C; ir ($CHCl_3$): 3030, 1650 cm^{-1}; ^1H nmr ($CDCl_3$) δ: 0.69, 0.80, 1.18 (s, s, s, 3H each, tertiary methyls), 0.84 (d, 3H, secondary methyl, $J = 6$ Hz), 2.86 (m, 2H, allylic protons, $w_{1/2} \approx 10$ Hz), 2.34 (m, 2H, allylic protons, $w_{1/2} \approx 16$ Hz), 2.81 (poorly resolved d of d, 1H, bridgehead proton, $J \approx 4$ Hz, 12 Hz), 3.27, 3.32 (two d of d, 2H, equatorially oriented protons of ketal functionality (cf. **7***b*), $J \approx 11$ Hz, 2.5 Hz in each case), 3.63, 3.74 (overlapped d of d, 2H, axially oriented protons of ketal functionality (cf. **7***b*), $J = 11$ Hz in each case), 5.42–5.86 (m, 2H, vinyl protons). *Anal.* calcd. for $C_{17}H_{28}O_2$: C 77.22, H 10.67; found: C 77.08, H 10.55.

Preparation of the Keto Dibromide ***27***

To a rapidly stirred mixture of 358 mg (1.36 mmol) of the ketal olefin, 82 mg (0.36 mmol) of triethylbenzylammonium chloride, a catalytic amount of ethanol, and 5.0 g (19.8 mmol) of bromoform was added, dropwise, 10 mL of 50% aqueous sodium hydroxide. The heterogeneous mixture was warmed to 40–50°C, kept at this temperature for 3 h, and poured into cold water. The resultant mixture was extracted thoroughly with dichloromethane. The combined organic extract was washed with water and dried over anhydrous magnesium sulfate. Removal of the solvent gave a dark brown oil. This material was dissolved in 20 mL of methanol containing 1 mL of 1 *N* hydrochloric acid, and the resultant solution was stirred at room temperature for 4 h. After most of the methanol had been removed under reduced pressure, the residual material was diluted with saturated aqueous sodium bicarbonate and the resultant mixture was extracted with ether. The combined ether extract was washed with water and dried over anhydrous magnesium sulfate. Removal of the solvent furnished a dark oil which was subjected to column chromatography on 200 g of silica gel. The column was eluted with 1 : 4 ether – petroleum ether (bp 30–60°C). Combination of all of the fractions containing the desired product afforded 378 mg (80%) of the keto dibromide **27** as pale yellow crystals. An analytical sample, obtained by recrystallization of a small amount of this material from ether, exhibited mp 130–131.5°C; ir ($CHCl_3$): 3100, 1710 cm^{-1}; ^1H nmr ($CDCl_3$) δ: 0.57 (s, 3H, tertiary methyl), 0.93 (d, 3H, secondary methyl, $J = 6.0$ Hz), 1.12–1.34 (m, 1H), 2.50–3.45 (diffuse, 11H). *Exact Mass* calcd. for $C_{13}H_{18}{}^{79}Br^{81}BrO$: 349.9474; found: 349.9467.

Preparation of the Ketal Dibromide ***26***

A solution of the keto dibromide **27** (350 mg, 1.0 mmol), 2,2-dimethyl-1,3-propanediol (1.5 g, 14.4 mmol), and *p*-toluenesulfonic acid (10 mg) in 25 mL of dry benzene was refluxed under a Dean–Stark water separator for 20 h. The cooled solution was diluted with ether, washed with saturated aqueous sodium bicarbonate, and dried over anhydrous magnesium sulfate. Removal of the solvent gave a viscous yellow oil which was subjected to column chromatography on 50 g of silica gel. Elution of the column with 1:4 ether – petroleum ether (bp 30–60°C) afforded 405 mg (93%) of the ketal dibromide **26** as a pale yellow oil; ir (film): no carbonyl absorption; ^1H nmr ($CDCl_3$) δ: 0.66, 0.72, 1.16 (s, s, s, 3H each, tertiary methyls), 0.83 (d, 3H, secondary methyl, $J = 5$ Hz), 2.73 (d of d, 1H, bridgehead proton, $J \approx 3$ Hz, 12 Hz), 3.14–3.78 (m, 4H, ketal protons). *Exact Mass* calcd. for $C_{18}H_{28}{}^{79}Br^{81}BrO_2$: 436.0475; found: 436.0456.

Can. J. Chem. Downloaded from www.nrcresearchpress.com by 210.87.254.42 on 09/05/12
For personal use only.

Preparation of the Ketal Monobromides ***28*** *and* ***29***

A solution of the ketal dibromide **26** (268 mg, 0.61 mmol) and methyl iodide (500 mg, 3.52 mmol) in 4 mL of dry tetrahydrofuran containing 0.4 mL of dry hexamethylphosphoramide was cooled, under an atmosphere of nitrogen, to −95°C. A solution of *tert*-butyllithium in pentane (0.7 mL, 1.93 *M*, 1.35 mmol) was added. The mixture was allowed to stir at −95°C for 1 h, was warmed to −78°C, and then left for an additional 4 h. Water (10 mL) was added, and the resultant mixture was extracted with hexane. The combined hexane extract was washed with water and brine and dried over anhydrous magnesium sulfate. Removal of the solvent gave an oil which, on the basis of a glc analysis, appeared to consist mainly of two components, in a ratio of approximately 3 : 2. The crude product was subjected to chromatography on 25 g of silica gel, with 9 : 1 hexane–benzene being employed as the eluting solvent mixture.

The major product **28** (130 mg, 58%), which was the first component to be eluted from the column, was obtained as a pale yellow oil; ^{1}H nmr ($CDCl_3$) δ: 0.64, 0.72, 1.13 (s, s, s, 3H each, tertiary methyls), 0.79 (d, 3H, secondary methyl, J = 6 Hz), 1.74 (s, 3H, cyclopropyl methyl), 2.69 (d of d, 1H, bridgehead proton, $J \approx$ 3 Hz, 12 Hz), 3.06–3.74 (m, 4H, ketal protons). *Exact Mass* calcd. for $C_{19}H_{31}{}^{79}BrO_2$: 370.1552; found: 370.1567.

The minor isomer **29** (85 mg, 38%), was also obtained as a pale yellow oil; ^{1}H nmr ($CDCl_3$) δ: 0.64, 0.71, 1.12 (s, s, s, 3H each, tertiary methyls), 0.77 (d, 3H, secondary methyl, J = 6 Hz), 1.62 (s, 3H, cyclopropyl methyl), 2.69 (unresolved d of d, 1H, bridgehead proton, $J \approx$ 3.5 Hz, 13 Hz), 3.08–3.74 (m, 4H, ketal protons). *Exact Mass* calcd. for $C_{19}H_{31}{}^{79}BrO_2$: 370.1552; found: 370.1537.

Preparation of the Ketal Ester ***30***

To a cold (−78°C) solution of the ketal bromide **28** (144 mg, 0.39 mmol) in 8 mL of anhydrous ether under an atmosphere of nitrogen was added slowly 0.45 mL of a solution of *tert*-butyllithium in pentane (1.93 *M*, 0.87 mmol). After the solution had been stirred at −78°C for 1 h, methyl chloroformate (0.25 mL, 3.23 mmol) and dry hexamethylphosphoramide (0.8 mL) were added successively. The mixture was maintained at −78°C for another 4 h and then was diluted with water. The resultant mixture was extracted with petroleum ether. The combined extract was washed with water and brine and dried over anhydrous magnesium sulfate. Removal of the solvent gave a yellow oil which was subjected to column chromatography on 15 g of silica gel, with 1 : 9 ether – petroleum ether (bp 30–60°C) being used as the eluting solvent mixture. The fractions containing the ketal ester **30** were combined, yielding 97 mg (71%) of the desired material as pale yellow crystals; mp 120–123°C; ir ($CHCl_3$): 1720 cm^{-1}; ^{1}H nmr ($CDCl_3$) δ: 0.66, 0.78, 1.16, 1.24 (s, s, s, s, 3H each, tertiary methyls), 0.80 (d, 3H, secondary methyl, J = 5 Hz), 2.58–2.84 (unresolved d of d, 1H, bridgehead proton), 3.12–3.78 (m, 4H, ketal protons), 3.66 (s, 3H, —CO_2CH_3). *Exact Mass* calcd. for $C_{21}H_{34}O_4$: 350.2432; found: 350.2457.

Preparation of the Ketal Alcohol ***31***

To a solution of lithium aluminum hydride (104 mg, 2.73 mmol) in 5 mL of anhydrous ether was added a solution of the ketal ester **30** (97 mg, 0.28 mmol) in 7 mL of anhydrous ether. The mixture was stirred under an atmosphere of nitrogen for 20 h at room temperature. The excess reducing agent was destroyed by addition of powdered sodium sulfate decahydrate. The resultant mixture was filtered and the collected solid material was washed thoroughly with ether. The combined ethereal filtrate was washed with brine and dried over anhydrous magnesium sulfate. Removal of the solvent gave 63 mg (71%) of the ketal alcohol **31** as a very viscous oil; ir (film): 3400 cm^{-1}; ^{1}H nmr ($CDCl_3$) δ: 0.66, 0.78, 1.10, 1.15 (s, s s, s, 3H each, tertiary methyls), 0.80 (d, 3H, secondary methyl, J = 5 Hz), 2.52–2.90 (unresolved d of d, 1H, bridgehead proton), 3.00–3.84 (m, 4H, ketal protons), 3.60 (s, 2H, —CH_2OH). *Exact Mass* calcd. for $C_{20}H_{34}O_3$: 322.2506; found: 322.2508.

Preparation of the Keto Alcohol ***32***

To a solution of the ketal alcohol **31** (63 mg, 0.20 mmol) in a mixture of acetone (3 mL), methanol (3 mL), and water (1 mL) was added 6 drops of 1 *N* hydrochloric acid. The mixture, under an atmosphere of nitrogen, was stirred at room temperature for 3 h. Most of the solvent was removed under reduced pressure, the residue was diluted with saturated aqueous sodium bicarbonate, and the resultant mixture was extracted with ether. The combined ether extract was washed with water and brine and dried over anhydrous magnesium sulfate. Removal of the solvent, followed by purification of the resultant crude material by means of preparative tlc on silica gel (2 : 1 benzene – ethyl acetate used as developing solvent mixture) gave 46 mg (97%) of the keto alcohol **32** as a colourless oil; ir ($CHCl_3$): 3500, 1705 cm^{-1}; ^{1}H nmr ($CDCl_3$) δ: 0.66, 1.13 (s, s, 3H each, tertiary methyls), 0.86 (d, 3H, secondary methyl, J = 6.0 Hz), 3.56 (s, 2H, —CH_2OH). *Exact Mass* calcd. for $C_{15}H_{24}O_2$: 236.1771; found: 236.1776.

Preparation of the Keto p*-Nitrobenzoate* ***34***

To a solution of the keto alcohol **32** (45 mg, 0.19 mmol) in 5 mL of dry dichloromethane was added dry pyridine (100 mg, 1.27 mmol) and recrystallized *p*-nitrobenzoyl chloride (100 mg, 0.54 mmol). The mixture was allowed to stand at 0°C for 24 h, and then was poured into water. The resultant mixture was extracted with ether. The combined ether extract was washed with water and brine and dried over anhydrous magnesium sulfate. Removal of the solvent, followed by purification of the resultant yellow oil by means of preparative tlc on silica gel (2 : 1 benzene – ethyl acetate used as developing solvent mixture), gave 67 mg (91%) of the expected product **34** as a viscous, clear oil; ir (film): 1720, 1705, 1609, 1525, 1345 cm^{-1}; ^{1}H nmr ($CDCl_3$) δ: 0.66, 1.20 (s, s, 3H each, tertiary methyls), 0.90 (poorly resolved d, 3H, secondary methyl, $J \approx$ 6 Hz), 4.38 (s, 2H, —CH_2OCOAr), 8.28 (m, 4H, aromatic protons). *Exact Mass* calcd. for $C_{22}H_{27}NO_5$: 385.1889; found: 385.1889.

Preparation of the Ketal Diester ***44***

To a stirred mixture of the ketal olefin 7 (786 mg, 2.98 mmol) and copper bronze (64 mg), heated with an external oil bath at 130–140°C under an atmosphere of nitrogen, was added dropwise 2.04 g (12.9 mmol) of dimethyl diazomalonate. After the addition was complete, the mixture was stirred at 130–140°C for an additional 1.5 h, and then was cooled. Dichloromethane was added to the resultant solid material, and the mixture was filtered through a short Florisil column. The column was eluted with further volumes of dichloromethane. Removal of the solvent from the combined eluant gave a crude semi-solid material which was triturated in the presence of ether. The mixture was filtered. Removal of the solvent from the filtrate gave a yellow oil which was subjected to column chromatography on 230 g of silica gel. Elution of the column with 1 : 3 ethyl acetate – petroleum ether (bp 30–60°C), afforded 930 mg (80%) of a colourless oil which crystallized on standing. Recrystallization from hexane produced 750 mg (64%) of the ketal diester **44**; mp 132–133.5°C; ir ($CHCl_3$): 1730 cm^{-1}; ^{1}H nmr ($CDCl_3$) δ: 0.66, 0.82, 1.15 (s, s, s, 3H each, tertiary

Can. J. Chem. Downloaded from www.nrcresearchpress.com by 210.87.254.42 on 09/05/12
For personal use only.

methyls), ~0.81 (poorly resolved d, 3H, secondary methyl), 2.62–2.84 (poorly resolved d of d, 1H, bridgehead proton), 3.12–3.72 (m, 4H, ketal protons), 3.68, 3.74 (s, s, 3H each, $-CO_2CH_3$ groups). *Anal.* calcd. for $C_{22}H_{34}O_6$: C 66.98, H 8.69; found: C 67.09, H 8.50.

Preparation of the Ketal Diol ***45***

To a solution of lithium aluminum hydride (500 mg, 13.2 mmol) in 50 mL of anhydrous ether was added, over a period of 30 min, a solution of the ketal diester **44** (532 mg, 1.35 mmol) in 50 mL of anhydrous ether. The mixture was stirred at room temperature under an atmosphere of nitrogen for 20 h. After the reaction mixture had been diluted with approximately 20 mL of dichloromethane, the excess reducing agent was destroyed by addition of excess powdered sodium sulfate decahydrate. The resultant mixture was filtered through Celite and the collected solid material was washed thoroughly (trituration) with dichloromethane. The combined filtrate was dried over anhydrous magnesium sulfate. Removal of the solvent gave 429 mg (94%) of a crystalline solid which exhibited mp 170–172°C. An analytical sample of the ketal diol **45**, obtained by recrystallization of a small amount of this material from acetone, exhibited mp 173–174.5°C; ir (Nujol): 3300 cm^{-1}; ^1H nmr ($CDCl_3$) δ: 0.63, 0.75, 1.10 (s, s, s, 3H each, tertiary methyls), ~0.78 (d, 3H, secondary methyl), 2.56–2.79 (poorly resolved d of d, 1H, bridgehead proton), 3.04–3.98 (complex m, 8H, $-CH_2OH$ groups and ketal protons). *Anal.* calcd. for $C_{20}H_{34}O_4$: C 70.97, H 10.12; found: C 70.89, H 10.00.

Preparation of the Keto Diol ***46***

To a solution of the ketal diol **45** (371 mg, 1.10 mmol) in 60 mL of reagent grade acetone and 5 mL of water was added 5 drops of 4 *N* hydrochloric acid. The solution was stirred at room temperature under a nitrogen atmosphere for 3 h. Anhydrous sodium bicarbonate was added and most of the solvent was removed under reduced pressure. The residue was diluted with water and the resultant mixture was extracted thoroughly with dichloromethane. The combined organic extract was washed with water and dried over anhydrous magnesium sulfate. Removal of the solvent gave a pale yellow semisolid which was triturated with a small amount of ether. Filtration furnished 147 mg of the desired keto diol **46**. Concentration of the filtrate gave another 85 mg (total yield 232 mg, 84%) of the desired product which exhibited mp 138–139.5°C; ir (Nujol): 3300, 1700 cm^{-1}; ^1H nmr ($CDCl_3$) δ: 0.66 (s, 3H, tertiary methyl), 0.93 (d, 3H, secondary methyl, J = 6 Hz), 3.44, 3.63 (AB pair of d, 2H, $-CH_2OH$, J = 12 Hz), 3.75, 3.91 (AB pair of d, 2H, $-CH_2OH$, J = 12 Hz). *Anal.* calcd. for $C_{15}H_{24}O_3$: C 71.39, H 9.59; found: C 71.00, H 9.52.

Preparation of the Keto Dimesylate ***47***

To a cold (0°C) solution of the keto diol **46** (232 mg, 0.92 mmol) in 20 mL of dry dichloromethane under an atmosphere of nitrogen was added, successively, dry triethylamine (290 mg, 2.87 mmol) and methanesulfonyl chloride (266 mg, 2.32 mmol). The mixture was stirred at 0°C for 30 min, was diluted with ether, washed four times with ice-cold water and once with brine, and dried over anhydrous magnesium sulfate. Removal of the solvent gave 370 mg of a slightly yellow viscous oil; ir (film): 1700, 1355, 1170 cm^{-1}; ^1H nmr ($CDCl_3$) δ: 0.66 (s, 3H, tertiary methyl), 0.90 (unresolved d, 3H, secondary methyl), 3.03, 3.06 (s, s, 3H each, $-OSO_2CH_3$ groups), 3.93, 4.14 (AB pair of d, 2H, $-CH_2OMs$, $J \approx 11$ Hz), 4.32 (s, 2H, $-CH_2OMs$). Since the dimesylate **47** was quite unstable, the crude material was used immediately for the next synthetic step.

Preparation of the Keto Dichloride ***48***

To a solution of the crude dimesylate **47** (370 mg) in 15 mL of anhydrous ether and 30 mL of dry hexamethylphosphoramide was added 2.1 g of anhydrous lithium chloride. The mixture was stirred overnight under an atmosphere of nitrogen and then poured into 150 mL of water. The resultant mixture was extracted thoroughly with ether. The combined ether extract was washed with water and dried over anhydrous magnesium sulfate. Removal of the solvent gave a pale yellow oil which solidified on cooling to 0°C. Recrystallization from hexane gave 242 mg (91% from the keto diol **46**) of the keto dichloride **48**; mp 133–135°C; ir ($CHCl_3$): 1706 cm^{-1}; ^1H nmr ($CDCl_3$) δ: 0.62 (s, 3H, tertiary methyl), 0.92 (d, 3H, secondary methyl, J = 6 Hz), 3.36, 3.67 (AB pair of d, 2H, $-CH_2Cl$, J = 11 Hz), 3.61, 3.83 (AB pair of d, 2H, $-CH_2Cl$, J = 12 Hz). *Anal.* calcd. for $C_{15}H_{22}Cl_2O$: C 62.29, H 7.67; found: C 62.27, H 7.85.

Preparation of the Tetracyclic Keto Chloride ***50***

To a solution of freshly prepared potassium *tert*-butoxide (103 mg, 0.92 mmol) in 10 mL of dry tetrahydrofuran was added a solution of 178 mg (0.62 mmol) of the keto dichloride **48** in 5 mL of dry tetrahydrofuran. The resulting yellow solution was stirred under an atmosphere of nitrogen at room temperature for 1.5 h. Aqueous ammonium chloride was added and the resulting mixture was extracted thoroughly with pentane. The combined extract was washed with water and brine and dried over anhydrous magnesium sulfate. Removal of the solvent gave 141 mg of the crude keto chloride **50**, which, due to its unstable character was used immediately for the next synthetic step. The crude product **50** exhibited ir (film): 1700 cm^{-1}; ^1H nmr ($CDCl_3$) δ: 0.73 (s, 3H, tertiary methyl), 0.87 (d, 3H, secondary methyl, J = 6 Hz), 3.60 (s, 2H, $-CH_2Cl$).

*(±)-Ishwarol (****51****)*

To a cold (0°C) solution of the crude keto chloride **50** (141 mg) in 10 mL of dry tetrahydrofuran was added 2.8 mL (1 *M*, 2.8 mmol) of a solution of lithium triethylborohydride in tetrahydrofuran. The mixture was stirred at room temperature under an atmosphere of nitrogen for 20 h. After the excess reducing agent had been destroyed by addition of 4 mL of water, 3 mL of 3 *N* sodium hydroxide and 3 mL of 30% hydrogen peroxide were added successively. The mixture was stirred at room temperature for 4 h, was diluted with water, and then thoroughly extracted with ether. The combined ether extracts were washed with water and brine and dried over anhydrous magnesium sulfate. Removal of the solvent, followed by distillation (air-bath temperature 100–110°C/0.5 Torr; lit. (3) bp 114°C/1 Torr) of the residual oil gave 119 mg (88% based on the keto dichloride **48**) of (±)-ishwarol (**51**) as a colourless oil; ir (film): 3350 cm^{-1}; ^1H nmr ($CDCl_3$) δ: 0.77 (d, 3H, secondary methyl, J = 5.5 Hz), 1.03, 1.13 (s, s, 3H each, tertiary methyls), 3.42 (m, 1H, —C*H*OH).

*(±)-Ishwarone (****2****)*

To a suspension of chromium trioxide (282 mg, 2.82 mmol) in 20 mL of dichloromethane was added 330 mg (2.86 mmol) of pyridinium hydrochloride. The mixture was stirred for 1 h. To the resultant orange suspension–solution was added a solution of 119 mg (0.54 mmol) of the alcohol **51** in a small amount of dichloromethane. The reaction mixture was stirred at room temperature for 2 h, was diluted with ether, and then filtered through a short column of Florisil. The column was eluted with ether. Removal of the solvents from the combined eluant, followed by distillation (air-bath temperature 120–130°C, water aspirator) of the residual oil, gave 86 mg (73%)

of a colourless oil which solidified on cooling. Recrystallization from pentane gave an analytical sample of (±)-ishwarone (**2**); mp 80–81°C; ir ($CHCl_3$): 1705 cm^{-1}; ^1H nmr ($CDCl_3$) δ: 0.56 (m, 1H, cyclopropyl proton), 0.74, 1.16 (s, s, 3H each, tertiary methyls), 0.87 (d, 3H, secondary methyl, $J = 7$ Hz). *Exact Mass* calcd. for $C_{15}H_{22}O$: 218.1671; found: 218.1679.

(±)-Ishwarane (3)

To 20 mL of diethylene glycol was added 0.5 g of sodium metal and the mixture was warmed (steam bath) until all of the sodium had reacted. To the resultant solution was added 31 mg (0.14 mmol) of (±)-ishwarone (**2**) and 3 mL of hydrazine hydrate. The solution was distilled slowly (the distillate was saved) until the internal temperature reached 180°C, and was then allowed to reflux for 18 h. The solution was again slowly distilled (the distillate was saved) until the internal temperature had reached 210°C, and was then allowed to reflux for an additional 6 h. The cooled solution was combined with the two distillates obtained as described above, and poured into water. The resultant mixture was extracted with ether. The combined ether extract was washed with water and brine and dried over anhydrous magnesium sulfate. Removal of the solvent, followed by distillation (air-bath temperature 90–110°C, water aspirator) of the residual material gave 23 mg (81%) of (±)-ishwarane (**3**) as a colourless oil. This material exhibited ir and ^1H nmr spectra, as well as glc retention time, identical with those of an authentic sample of racemic ishwarane (**3**) (6).

Acknowledgements

Financial support for this work from the Natural Sciences and Engineering Research Council of Canada and an N.S.E.R.C. Scholarship (to T.W.H.) are gratefully acknowledged.

1. A. R. Pinder. Fortschr. Chem. Org. Naturst. **34**, 81 (1977).
2. U. S. K. Rao, B. L. Manjunath, and K. N. Menon. J. Indian Chem. Soc. **12**, 494 (1935).
3. A. K. Ganguly, K. W. Gopinath, T. R. Govindachari, K. Nagarajan, B. R. Pai, and P. C. Parthasarathy. Tetrahedron Lett. 133 (1969); T. R. Govindachari, K. Nagarajan, and P. C. Parthasarathy. Chem. Commun. 823 (1969); H. Fuhrer, A. K. Ganguly, K. W. Gopinath, T. R. Govindachari, K. Nagarajan, B. R. Pai, and P. C. Parthasarathy. Tetrahedron, **26**, 2371 (1970).
4. T. R. Govindachari, P. A. Mohamed, and P. C. Parthasarathy. Tetrahedron, **26**, 615 (1970).
5. L. C. Teng and J. F. De Bardeleben. Experientia, **27**, 14 (1971).
6. R. B. Kelly, J. Zamecnik, and B. A. Beckett. Chem. Commun. 479 (1971); Can. J. Chem. **50**, 3455 (1972); R. B. Kelly and S. J. Alward. Can. J. Chem. **55**, 1786 (1977).
7. R. M. Cory and F. R. McLaren. J. Chem. Soc. Chem. Commun. 587 (1977).
8. E. Piers and T. W. Hall. J. Chem. Soc. Chem. Commun. 881 (1977).
9. R. M. Cory, D. M. T. Chan, F. R. McLaren, M. H. Rasmussen, and R. M. Renneboog. Tetrahedron Lett. 4133 (1979).
10. C. H. Heathcock. The total synthesis of natural products. Vol. 2. *Edited by* J. W. ApSimon. John Wiley & Sons, Inc., New York, NY. 1973. pp. 197–558.
11. D. Seyferth, R. L. Lambert, Jr., and M. Massol. J. Organomet. Chem. **88**, 255 (1975).
12. K. Kitatani, T. Hiyama, and H. Nozaki. J. Am. Chem. Soc. **97**, 949 (1975); Bull. Chem. Soc. Jpn. **50**, 3288 (1977).
13. K. Kitatani, T. Hiyama, and H. Nozaki. J. Am. Chem. Soc. **98**, 2362 (1976); Bull. Chem. Soc. Jpn. **50**, 1600 (1977).
14. K. Kitatani, H. Yamamoto, T. Hiyama, and H. Nozaki. Bull. Chem. Soc. Jpn. **50**, 2158 (1977).
15. B. W. Peace and D. S. Wulfman. Synthesis, 137 (1973).
16. W. G. Dauben, G. W. Shaffer, and N. D. Vietmeyer. J. Org. Chem. **33**, 4060 (1968).
17. F. Fringuelli, F. Pizzo, A. Taticchi, and E. Wenkert. Synth. Commun. **9**, 391 (1979).
18. T. W. Hall. Ph.D. Thesis, University of British Columbia, Vancouver, B.C., 1978.
19. A. A. Petrov and K. B. Rall. J. Gen. Chem. U.S.S.R. **26**, 1779 (1956).
20. S. Torii, T. Kunitomi, and T. Okamoto. Bull. Chem. Soc. Jpn. **47**, 2349 (1974).
21. F. E. Ziegler and P. A. Wender. Tetrahedron Lett. 449 (1974); F. E. Ziegler, G. R. Reid, W. L. Studt, and P. A. Wender. J. Org. Chem. **42**, 1991 (1977).
22. E. J. Corey and P. L. Fuchs. Tetrahedron Lett. 3769 (1972).
23. S. S. Klioze and F. P. Darmory. J. Org. Chem. **35**, 3195 (1970).
24. D. J. Cram and N. L. Allinger. J. Am. Chem. Soc. **78**, 2518 (1956).
25. A. I. Vogel. Practical organic chemistry. 3rd ed. Longmans, Green and Co. Ltd., London. 1956. p. 829.
26. L. M. Jackman and S. Sternhill. Applications of nuclear magnetic resonance spectroscopy in organic chemistry. 2nd ed. Pergamon Press Ltd., Oxford. 1969. pp. 334–341.
27. M. Makosza and M. Fedorynski. Synth. Commun. **3**, 305 (1973).
28. D. D. Roberts. J. Org. Chem. **29**, 294 (1964); **30**, 23 (1965); **31**, 2000 (1966).
29. M. Nikoletić, S. Borčić, and D. E. Sunko. Tetrahedron, **23**, 649 (1967).
30. R. K. Singh and S. Danishefsky. J. Org. Chem. **41**, 1668 (1976).
31. H. C. Brown and S. Krishnamurthy. J. Am. Chem. Soc. **95**, 1669 (1973).
32. E. J. Corey and J. W. Suggs. Tetrahedron Lett. 2647 (1975).

Can. J. Chem. Downloaded from www.nrcresearchpress.com by 210.87.254.42 on 09/05/12
For personal use only.

C-Nucleoside studies. Part XI. *Cine*-substitution in 1,4-dinitropyrazoles; application to the synthesis of formycin via nitropyrazole derivatives

J. GRANT BUCHANAN, ALAN STOBIE, AND RICHARD H. WIGHTMAN

Department of Chemistry, Heriot-Watt University, Riccarton, Currie, Edinburgh EH14 4AS, Scotland

Received May 28, 1980

This paper is dedicated to Prof. Raymond U. Lemieux on the occasion of his 60th birthday

J. GRANT BUCHANAN, ALAN STOBIE, and RICHARD H. WIGHTMAN. Can. J. Chem. **58**, 2624 (1980).

Reaction of 1,4-dinitro-3-methylpyrazole with a variety of nucleophiles led to the formation of 5-substituted 3-methyl-4-nitropyrazoles **11–15** by a process of *cine*-substitution. This reaction has been applied as the key step in a novel synthesis of formycin. Treatment of 1,4-dinitro-3-(2,3,5-tri-*O*-acetyl-β-D-ribofuranosyl)pyrazole (**17**) with cyanide ion produced 3(5)-cyano-4-nitro-5(3)-(2,3,5-tri-*O*-acetyl-β-D-ribofuranosyl)pyrazole (**19**) in 89% yield. Catalytic reduction to the 4-amino compound **20** (84%), and subsequent reaction with formamidine acetate yielded formycin triacetate **21** (79%). Methanolysis of **21** produced formycin (**1**) in 90% yield.

J. GRANT BUCHANAN, ALAN STOBIE et RICHARD H. WIGHTMAN. Can. J. Chem. **58**, 2624 (1980).

La réaction de la dinitro-1,4 méthyl-3 pyrazole avec divers nucléophiles, par une *ciné* substitution conduit à la formation des méthyl-3 nitro-4 pyrazoles substitués en position 5 **11** à **15**. On a utilisé cette réaction comme l'étape fondamentale d'une nouvelle synthèse de la formycine. La dinitro-1,4 (tri-*O*-acétyl-2,3,5, β-D-ribofurannosyl)-3 pyrazole (**17**) traitée par l'ion cyanure fournit la cyano-3 (5) nitro-4 (tri-*O*-acétyl-2,3,5 β-D-ribofurannosyl)-5 (3) pyrazole (**19**) avec un rendement de 89%. Une réduction catalytique conduit, avec un rendement de 84%, au composé amino-4 **20** qui par une réaction subséquente avec l'acétate de formamidine donne le triacétate de formycine **21** (79%). La méthanolyse du composé **21** fournit la formycine (**1**) avec un rendement de 90%.

[Traduit par le journal]

The *C*-nucleoside antibiotic formycin (**1**) (1–3) is a naturally-occurring isomer of adenosine, in which the imidazole ring has been replaced by a pyrazole. Formycin has antiviral and antitumour properties, and is thought to be able to substitute for the adenosine moiety in a variety of enzymic reactions occurring at the nucleotide level (3). The biological activity (3) of formycin and the related metabolite formycin B (**2**) (1) has stimulated interest in the synthesis of these compounds. Acton and co-workers (4) have reported a total synthesis of formycin B, which can be converted into formycin by the method of Townsend and co-workers (5). More recently, Kalvoda (6) has synthesized formycin and formycin B by a different route. We have been interested in developing a general synthetic approach to *C*-nucleoside antibiotics and their analogs proceeding via ribofuranosylalkyne intermediates such as **3** (7), **4** (8), and **5** (9), and in this paper we describe a synthesis of formycin by means of this approach.[1]

We have previously reported the conversion of the ribofuranosylalkyne **5** into 3(5)-β-D-ribofuranosyl-4-nitropyrazole (**6**) (9). Clearly, for the further transformation of this intermediate into formycin (**1**) it is necessary to introduce a carbon-containing substituent at the unsubstituted 3(5)-position of the pyrazole ring. As a means of achieving this, we were attracted by the report by Habraken and Poels (11) that 1,4-dinitropyrazoles such as **7** react readily with secondary amines, for example morpholine, to give 5-substituted pyrazoles typified by **8**. A reasonable mechanism for this interesting "*cine*"-substitution process could involve intermediates of type **9** and **10**. Since 1,4-dinitropyrazoles such as **7** are readily prepared by *N*-nitration, with acetyl nitrate, of the appropriate *C*-nitropyrazole (11, 12), we decided to investigate whether this substitution would also occur with other nucleophiles, and in particular carbanions. Our expectations were fulfilled.

Thus, when an ethereal solution of 3-methyl-1,4-dinitropyrazole (**7**) (11) was added to refluxing liquid ammonia, 3-methyl-4-nitro-5-aminopyrazole (**11**) (13) was produced in near-quantitative yield. Treatment of **7** with potassium hydroxide in ethanol produced the ethyl ether **12** (14) in quantitative yield, whilst reaction of **7** with ethane thiol and potassium hydroxide gave the corresponding sulphide **13**. A phosphorus nucleophile could also be introduced; reaction of **7** and trimethylphosphite gave an Arbusov-type reaction to yield the phosphonate **14** in 77% yield. Finally, and most importantly for our present purposes, when an ethanolic solution of **7** was added to excess potassium cyanide in aqueous ethanol, a rapid reaction ensued to yield 3-methyl-4-nitro-5-cyanopyrazole (**15**) (15)

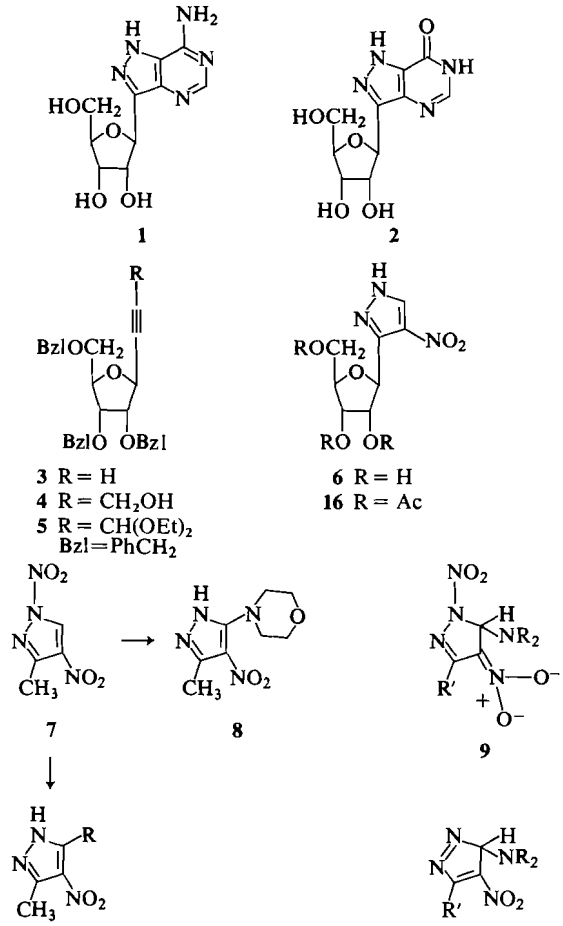
[1]For a preliminary communication of part of this work, see ref. 10.

0008-4042/80/232624-04$01.00/0

©1980 National Research Council of Canada/Conseil national de recherches du Canada

Can. J. Chem. Downloaded from www.nrcresearchpress.com by 210.87.254.6 on 09/05/12
For personal use only.

Can. J. Chem. Downloaded from www.nrcresearchpress.com by 210.87.254.6 on 09/05/12
For personal use only.



in 85% yield.[2] It thus appears that this *cine*-substitution process is a fairly general reaction of 1,4-dinitropyrazoles, and we were hopeful that such a substitution with cyanide ion could be used as the key step in the synthesis of formycin from nitropyrazole **6**.

When 3(5)-β-D-ribofuranosyl-4-nitropyrazole (**6**) (10) was treated with acetic anhydride in pyridine, a tetraacetyl derivative was formed, which could be deacetylated selectively on the pyrazole nitrogen by brief exposure to methanol containing a trace of pyridine. The resultant tri-*O*-acetyl derivative **16** was subjected to *N*-nitration using cupric nitrate trihydrate and acetic anhydride (16) to yield a single isomer **17** in 87% yield. That **17** had the assigned structure, and not the isomeric structure **18**, was clearly indicated (11) by the ^{1}H nmr spectrum; the pyrazole ring proton resonated at 9.11, a downfield shift of 0.9 ppm from the corresponding signal in the precursor **16**. When a solution of dinitropyrazole **17** was added to excess potassium cyanide in aqueous ethanol, the desired *cine*-substitution process occurred readily, and 3(5)-cyano-4-nitro-5(3)-(tri-*O*-acetyl-β-D-ribofuranosyl) pyrazole (**19**) was isolated in 89% yield, as a crystalline benzene solvate. No loss of acetate protecting groups was observed during the short reaction time (10 min) used.

The nitro group in **19** could be reduced cleanly to an amino function by catalytic hydrogenation, and the resultant 4-aminopyrazole **20**, obtained as a syrup in 84% yield, was subjected to cyclization with formamidine acetate in refluxing ethoxyethanol. Reaction was complete (tlc) within 20 min, and isolation by chromatography yielded formycin triacetate (**21**) in 77% yield.

Deacetylation of the triacetate **21** with sodium methoxide in methanol produced formycin (**1**), isolated as its crystalline monohydrate in 90% yield. This material proved identical (melting point and mixture melting point, ir, uv, tlc, optical rotation) with genuine formycin monohydrate.

The synthesis described should be capable of adaptation and extension to the synthesis of a range of analogues of formycin containing specific modifications in either the sugar (17) or heterocyclic rings.

Experimental

The general methods used were as stated in Part II (18). Column chromatography was carried out using Kieselgel H type 60 (Merck); an external pressure was applied to the top of columns. Thin-layer chromatography was carried out on precoated aluminium-backed plates (Kieselgel HF_{254} type 60 (Merck)).

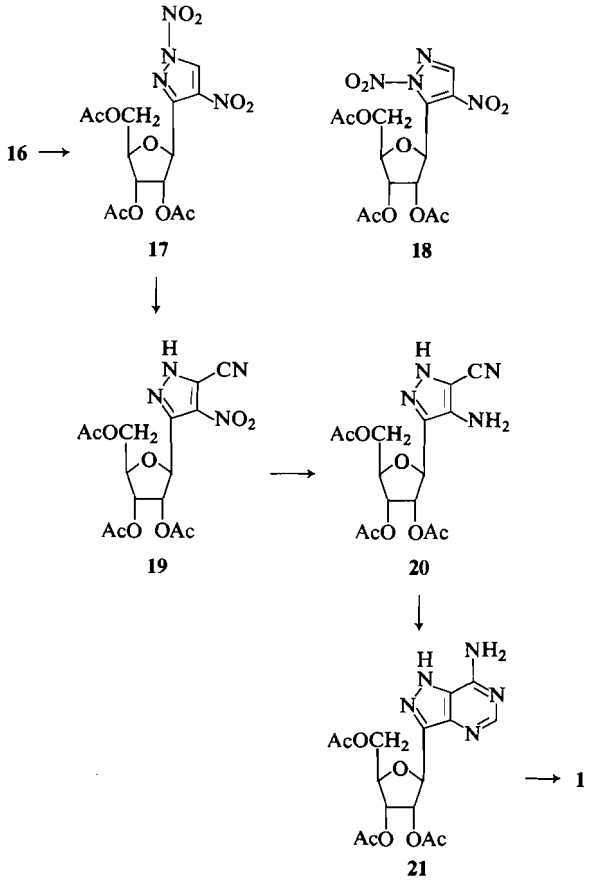
3-Methyl-4-nitro-5-aminopyrazole (11)

1,4-Dinitro-3-methylpyrazole (7) (0.40 g) in ether (5 mL) was slowly added to refluxing liquid ammonia (10 mL). The mixture was stirred at reflux for 0.5 h, and the solvents then allowed to evaporate. The residue was partitioned between ethyl acetate and water; the organic layer was dried ($MgSO_4$) and evaporated to leave a crystalline residue. Recrystallization from ethyl acetate yielded **11** (0.32 g, 97%), mp 230–233°C (lit. (13) mp 228°C); ^{1}Hmr (CF_3CO_2H) δ: 2.80 (s, CH_3); ms (70 eV) *m/e*: 142 (M^+).

3-Methyl-4-nitro-5-ethoxypyrazole (12)

A solution of 1,4-dinitro-3-methylpyrazole (7) (0.10 g) in ethanol (1 mL) was slowly added to a solution of potassium hydroxide (0.50 g) in ethanol (10 mL). After 5 min, the mixture was neutralized with acetic acid, and the solvents evaporated. Partition between ethyl acetate and water, drying and evaporation of the organic layer, and crystallization of the residue from

[2]Analogous reactions can also be achieved with the anions of ethyl acetoacetate and diethyl malonate (D. M. Service and R. H. Wightman, unpublished results).



dichloromethane–petrol gave **12** (0.10 g, 98%); mp 118–121°C (lit (14) mp 126°C); ^{1}Hmr (60 MHz, $CDCl_3$) δ: 1.40 (t, J = 6 Hz, 3H, CH_3), 2.60 (s, 3H, CH_3), 4.40 (q, J = 6 Hz, 2H, CH_2).

Ethyl-5-(3-methyl-4-nitropyrazolyl)sulphide (13)

A solution of **7** (0.20 g) in ether (1 mL) was slowly added to a stirred suspension of powdered potassium hydroxide (0.50 g) in ether (10 mL) and ethanethiol (2 mL). After 1 h, the mixture was neutralized with acetic acid, the solvents evaporated, and the residue partitioned between ethyl acetate and water. Evaporation of the dried organic layer gave pale yellow crystals which were recrystallized from dichloromethane–petrol to give the sulphide **13** (0.21 g, 97%); mp 105–108°C; ^{1}Hmr (60 MHz, $CDCl_3$) δ: 1.40 (t, J = 6 Hz, 3H, CH_3), 2.65 (s, 3H, CH_3), 3.04 (q, J = 6 Hz, 2H, CH_2). *Anal.* calcd. for $C_6H_9N_3O_2S$: C 38.49, H 4.85, N 22.45, S 17.13; found: C 38.50, H 4.81, N 22.27, S 16.96.

Dimethyl-5-(3-methyl-4-nitropyrazolyl)phosphonate (14)

A solution of **7** (0.20 g) in benzene (2 mL) was added to a solution of trimethylphosphite (1 mL) in benzene (10 mL). The mixture was stirred at room temperature for 15 h. The product precipitated from the reaction mixture, and was recrystallized from methanol–ether to yield phosphonate **14** (0.21 g, 77%); mp 180–182°C; ir (KBr) ν_{max}: 1600 (C=N), 1500 (NO_2), 1220 (P=O), 1030 (P—O) cm^{-1}; ^{1}Hmr (60 MHz, DMSO-d_6) δ: 2.55 (s, 3H, CH_3) 3.8 (d, J = 12 Hz, 6H, OCH_3). *Anal.* calcd. for $C_6H_{10}N_3O_5P$: C 30.64, H 4.29, N 17.87, P 13.17; found: C 30.68, H 4.35, N 17.97, P 13.01.

3-Methyl-4-nitro-5-cyanopyrazole (15)

A solution of 1,4-dinitro-3-methylpyrazole **7** (10 g) in ethanol (120 mL) was added slowly to a stirred solution of potassium cyanide (53 g) in water (236 mL) and ethanol (743 mL). After addition was complete, stirring was continued for 5 min, and the solution then neutralized with acetic acid. Solvents were evaporated and the residue extracted with ethyl acetate. The dried extracts were evaporated to give a light yellow solid residue, which was recrystallized from toluene to yield cyano compound **15** (7.5 g, 85%); mp 176–179°C (lit. (15) mp 180–181°C); ir ν_{max}: 2260 (C≡N) cm^{-1}.

3-(2,3,5-Tri-O-acetyl-β-D-ribofuranosyl)-4-nitropyrazole (16)

A solution of triol **6** (2.0 g) in pyridine (100 mL) and acetic anhydride (50 mL) was left to stand for 15 h. Solvents were removed under vacuum, and the residue stirred for 5 min with methanol (20 mL) containing a few drops of pyridine. Evaporation, and chromatography of the residue on silica gel, eluting with light petroleum – ethyl acetate (2:1) yielded triacetate **16** (2.85 g, 94%) as a syrup; $[\alpha]_D$ +107.7° (*c* 0.59, $CHCl_3$); ir (film) ν_{max}: 3300 (NH), 1750 (C=O), 1510 and 1375 (NO_2) cm^{-1}; ^{1}Hmr (100 MHz, $CDCl_3$) δ: 2.12 (s, 3H, $COCH_3$), 2.15 (s, 6H, $2COCH_3$), 4.2–4.5 (m, 3H, H-4′, H-5′), 5.2–5.7 (m, 3H, H-1′ – 3′), 8.21 (s, 1H, H-5). *Anal.* calcd. for $C_{14}H_{17}N_3O_9$: C 45.28, H 4.62, N 11.32; found: C 45.41, H 4.73, N 11.17.

1,4-Dinitro-3-(2,3,5-tri-O-acetyl-β-D-ribofuranosyl)pyrazole (17)

Triacetate **16** (1.0 g) was added to a mixture of cupric nitrate trihydrate (3.0 g) and acetic anhydride (23 mL) which had been prestirred for 1 h. The mixture was stirred overnight, poured into water, and extracted with ethyl acetate. The washed and dried organic layer was evaporated to yield a syrup which was purified by chromatography on silica, eluting with light petroleum – ether (1:1), to yield the dinitro compound **17** (0.97 g, 87%) as a pale yellow syrup; $[\alpha]_D$ +2.5° (*c* 0.8, $CHCl_3$); ir (film) ν_{max}: 1750 (C=O), 1660 and 1280 (N—NO_2), 1520 and 1370 (C—NO_2) cm^{-1}; ^{1}Hmr (100 MHz, $CDCl_3$) δ: 2.11, 2.12, 2.13 (3s, 9H, $COCH_3$), 4.1–4.6 (m, 3H, H-4′, H-5′), 5.3–5.8 (m, 3H, H-1′, H-2′, H-3′), 9.11 (s, 1H, H-5). *Anal.* calcd. for $C_{14}H_{16}N_4O_{11}$: C 40.39, H 3.87, N 13.46; found: C 40.35, H 3.76, N 13.25.

3(5)-Cyano-4-nitro-5(3)-(2,3,5-tri-O-acetyl-β-D-ribofuranosyl)-pyrazole (19)

A solution of dinitro compound **17** (3.40 g) in ethanol (35 mL) and ethyl acetate (35 mL) was added dropwise over 5 min to a stirred solution of potassium cyanide (5.0 g) in water (25 mL) and ethanol (100 mL). After a further 5 min, the mixture was neutralized with acetic acid and diluted with ethyl acetate (500 mL) and water (200 mL). The layers were separated, and the aqueous phase extracted once with more ethyl acetate. The dried organic layers were evaporated to yield a syrup, which crystallized on adding benzene. This material was recrystallized from benzene–petrol. The mother liquors from the crystallization were chromatographed on silica gel, eluting with benzene–acetone (9:1), and the residue after evaporation of product-containing fractions was crystallized from benzene–petrol. The nitrile **19** was obtained in a combined yield of 3.16 g, 89%, as a crystalline benzene solvate; mp 101–110°C (with loss of benzene); $[\alpha]_D$ + 141.0° (*c* 0.59, $CHCl_3$); ir (KBr) ν_{max}: 3300 (N—H), 2250 (C≡N), 1760, 1740 (C=O), 1580 (C=N), 1510 and 1365 (C—NO_2) cm^{-1}; ^{1}Hmr (100 MHz, $CDCl_3$) δ: 2.10, 2.14, 2.18 (each s, 3H, $COCH_3$), 4.1–4.7 (m, 3H, H-4′, H-5′), 5.18 (t, J = 6 Hz, 1H, H-3′), 5.44 (t, J = 5 Hz, 1H, H-2′), 5.66 (d, J = 5 Hz, 1H, H-1′), 7.34 (s, 3H, 0.5 C_6H_6). *Anal.* calcd. for $C_{15}H_{16}N_4O_9 \cdot 0.5C_6H_6$: C 49.65, H 4.40, N 12.87; found: C 50.20, H 4.26, N 12.88.

3(5)-Cyano-4-amino-5(3)-(2,3,5-tri-O-acetyl-β-D-ribofuranosyl)-pyrazole 20

A solution of **19** (0.55 g, as benzene solvate) in ethanol (30 mL) was hydrogenated overnight using 5% palladium on charcoal

Can. J. Chem. Downloaded from www.nrcresearchpress.com by 210.87.254.6 on 09/05/12
For personal use only.

(0.1 g) as catalyst. The mixture was filtered through Celite, which was washed well with ethyl acetate. The residue after evaporation was chromatographed on silica, eluting with benzene–acetone (9:1) to yield the amino compound **20** (0.39 g, 84%) as a syrup; $[\alpha]_D$ −4.8° (*c* 0.42, $CHCl_3$); ir (film) ν_{max}: 3400–3200 (NH), 2230 (CN), 1750 (C=O) cm^{-1}; ^{1}Hmr (100 MHz, $(CD_3)_2CO$) δ: 1.98, 2.00, 2.04 (each s, 3H, $COCH_3$), 4.1–4.6 (m, 4H), 4.8–5.5 (m, 2H). *Exact Mass* calcd. for $C_{15}H_{18}N_4O_7$: 366.1175; found (ms): 366.1159.

2′,3′,5′-Tri-O-acetyl Formycin (21)

A solution of aminonitrile **20** (0.10 g) and formamidine acetate (0.085 g) in ethoxyethanol (2 mL) was heated under reflux for 20 min, when tlc indicated complete reaction. The solvent was removed under vacuum, and the residue chromatographed on silica gel, eluting with benzene–acetone (1:1) to yield formycin triacetate **21** (0.083 g, 77%) as a foam; $[\alpha]_D$ −36.2° (*c* 0.75, acetone); uv (MeOH) λ_{max}: 293.4, 229.6, 206.4 nm; ir (KBr) ν_{max}: 3500–3300 (NH), 1750 (C=O) cm^{-1}; ^{1}Hmr (100 MHz, $(CD_3)_2CO$) δ: 1.94 (s, 6H, $COCH_3$), 2.02 (s, 3H, $COCH_3$), 4.0–4.6 (m, 3H, H-4′, H-5′), 5.26 (d, J = 5 Hz, 1H, H-1′), 5.56 (t, J = 5 Hz, 1H, H-3′), 5.86 (t, J = 5 Hz, 1H, H-2′), 6.4–7.0 (b, 2H, exchangeable, NH_2), 8.08 (s, 1H, H-2). *Anal.* calcd. for $C_{16}H_{19}N_5O_7$: C 48.85, H 4.87, N 17.81; found: C 49.00, H 5.04, N 17.41.

Formycin (1)

A solution of sodium methoxide (5.6 mL of 0.1 *M* solution) was added to formycin triacetate **21** (0.18 g). After 1 h, the mixture was neutralized with acetic acid and evaporated. The residue, dissolved in water, was applied to a column of Dowex 50-X8 (H+ form). This was washed with water and the product was then eluted with dilute ammonia. The product fractions were evaporated and the residue dissolved in water. Some water was evaporated under vacuum and the solution set aside overnight, when the product crystallized. Formycin (**1**) (0.11 g, 90%) was obtained as its monohydrate; mp 148–153°C (lit. (5) mp 148–150°C); mixture mp with authentic material 149–154°C; $[\alpha]_D$ −41.2° (*c* 0.95, 0.1 *M* HCl) (lit. (5), $[\alpha]_D$ −40.0° (*c* 1, 0.1 *M* HCl)); ms (70 eV) *m/e*: 267 (M^+), 164 (heterocycle + 30). The ir and uv spectra of the synthetic material were superimposable on those of authentic material.

Acknowledgements

We thank Professor J. C. Gilbert (Department of Pharmacy, Heriot-Watt University) for a gift of authentic formycin, and the Science Research Council for a studentship (to A.S.).

1. (*a*) G. KOYAMA, K. MAEDA, and H. UMEZAWA. Tetrahedron Lett. 597 (1966); (*b*) R. K. ROBINS, L. B. TOWNSEND, F. CASSIDY, J. F. GERSTER, A. F. LEWIS, and R. L. MILLER. J. Heterocycl. Chem. **3**, 110 (1966).
2. G. D. DAVES, JR. and C. C. CHENG. Prog. Med. Chem. **13**, 303 (1976).
3. R. J. SUHADOLNIK. Prog. Nucleic Acid Res. Mol. Biol. **22**, 193 (1979).
4. E. M. ACTON, K. J. RYAN, D. W. HENRY, and L. GOODMAN. Chem. Commun. 986 (1971); J. FARKAŠ and F. ŠORM. Collect. Czech. Chem. Commun. **37**, 2798 (1972).
5. R. A. LONG, A. F. LEWIS, R. K. ROBINS, and L. B. TOWNSEND. J. Chem. Soc. C, 2443 (1971).
6. L. KALVODA. Collect. Czech. Chem. Commun. **43**, 1431 (1978).
7. (*a*) J. G. BUCHANAN, A. R. EDGAR, and M. J. POWER. J. Chem. Soc. Perkin Trans. I, 1943 (1974); (*b*) J. G. BUCHANAN, A. R. EDGAR, M. J. POWER, and C. T. SHANKS. J. Chem. Soc. Perkin Trans. I, 225 (1979).
8. J. G. BUCHANAN, A. D. DUNN, A. R. EDGAR, R. J. HUTCHISON, M. J. POWER, and G. C. WILLIAMS. J. Chem. Soc. Perkin Trans. I, 1786 (1977).
9. J. G. BUCHANAN, A. R. EDGAR, R. J. HUTCHISON, A. STOBIE, and R. H. WIGHTMAN. J. Chem. Soc. Perkin Trans. I. In press.
10. J. G. BUCHANAN, A. R. EDGAR, R. J. HUTCHISON, A. STOBIE, and R. H. WIGHTMAN. J. Chem. Soc. Chem. Commun. 237 (1980).
11. C. L. HABRAKEN and E. K. POELS. J. Org. Chem. **42**, 2893 (1977).
12. J. W. A. M. JANSSEN, H. J. KOENERS, C. J. KRUSE, and C. L. HABRAKEN. J. Org. Chem. **38**, 1777 (1973).
13. C. MUSANTE. Gazz. Chim. Ital. **72**, 537 (1942).
14. H. J. BACKER and W. MEIJER. Recl. Trav. Chim. Pays-Bas, **45**, 428 (1926).
15. R. A. LONG, J. F. GERSTER, and L. B. TOWNSEND. J. Heterocycl. Chem. **7**, 863 (1970).
16. A. V. TOPCHIEV. Nitration of hydrocarbons and other organic compounds. *Translated by* C. Mathews. Pergamon Press, London. 1959. pp. 291–298.
17. J. G. BUCHANAN, M. E. CHACÓN-FUERTES, and R. H. WIGHTMAN. J. Chem. Soc. Perkin Trans. I, 244 (1979).
18. J. G. BUCHANAN, A. D. DUNN, and A. R. EDGAR. J. Chem. Soc. Perkin Trans. I, 1191 (1975).

Can. J. Chem. Downloaded from www.nrcresearchpress.com by 210.87.254.6 on 09/05/12
For personal use only.

An investigation of the Kishner elimination as a route to dideoxy sugars

L. KIRTHI G. WICKREMESINGHE AND KEITH N. SLESSOR

Department of Chemistry, Simon Fraser University, Burnaby, B.C., Canada V5A 1S6

Received May 30, 1980

This paper is dedicated to Prof. Raymond U. Lemieux on the occasion of his 60th birthday

L. KIRTHI G. WICKREMESINGHE and KEITH N. SLESSOR. Can. J. Chem. **58**, 2628 (1980).

Methyl 4,6-*O*-benzylidene-2-*O*-*p*-toluenesulphonyl-α-D-*ribo*hexopyranosid-3-ulose has been used as a substrate for an investigation of the Kishner elimination as a route to deoxygenated sugars. The conditions of the reaction of the ketotosylate with hydrazine have a large effect on the outcome of the reaction and the products produced. Conditions have been investigated which provide methyl 4,6-*O*-benzylidene-α-D-*erythro*hex-2-enopyranoside (**4**), methyl 4,6-*O*-benzylidene-2,3-dideoxy-α-D-*erythro*hexopyranoside (**3**), methyl 4,6-*O*-benzylidene-3-deoxy-α-D-*ribo*hexopyranoside (**2**), and methyl 4,6-*O*-benzylidene-2-deoxy-α-D-*erythro*hexopyranosid-3-ulose (**8**) in good to moderate yields.

L. KIRTHI G. WICKREMESINGHE et KEITH N. SLESSOR. Can. J. Chem. **58**, 2628 (1980).

On a utilisé le *O*-benzylidène-4,6 *O*-*p*-toluènesulphonyl-2 α-D-*ribo*hexopyrannoside-ulose-3 de méthyle comme substrat pour étudier la réaction de Kishner comme voie d'accès aux sucres désoxygénés. Les conditions de la réaction du cétotosylate avec l'hydrazine influencent grandement le résultat de la réaction et les produits obtenus. On a mis au point des conditions qui conduisent au *O*-benzylidène-4,6 α-D-*érythro*hexéno-2 pyrannoside de méthyle (**4**), au *O*-benzylidène-4,6 didéoxy-2,3 α-D-*érythro*hexopyrannoside de méthyle (**3**), au *O*-benzylidène-4,6 déoxy-3 α-D-*ribo*hexopyrannoside de méthyle (**2**) et au *O*-benzylidène-4,6 déoxy-2 α-D-*érythro*hexopyrannoside ulose-3 (**8**) avec des rendements variables.

[Traduit par le journal]

Introduction

A major feature of the utilization of carbohydrates as chiral precursors to chiral insect pheromones (1) is the removal of several hydroxyl groups in a mild and efficient manner. A method, which could remove two vicinal oxygen functionalities simultaneously, seemed advantageous and thus we chose to investigate the Kishner elimination (2). Leonard and Gelfand (3) had studied the scope of the Kishner reaction and observed that elimination varied with the ability of the α-substituent to assume anionic character. Investigations by Wharton *et al.* (4, 5) indicated the elimination proceeded through an alkenyldiazene and the principal product was an alkene (Fig. 1).

Our choice of substrate for this investigation was methyl 4,6-*O*-benzylidene-2-*O*-toluenesulphonyl-α-D-*ribo*hexopyranosid-3-ulose (**1**) since the sulphonate at position 2 is a good leaving group adjacent to the keto function. The availability of expected products and ease of identification of other species involved favored the choice of this substrate and simplified the undertaking of a thorough study.

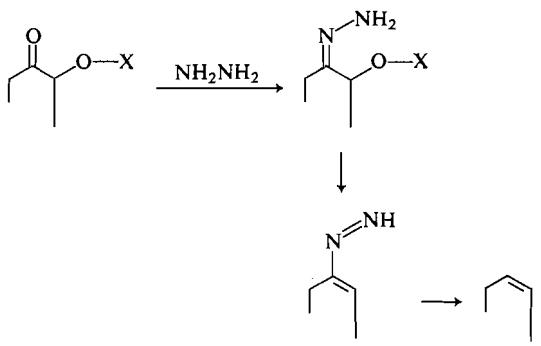


FIG. 1. Mechanism of the Kishner elimination.

Results and Discussion

Treatment of methyl 4,6-*O*-benzylidene-2-*O*-toluenesulphonyl-α-D-*ribo*hexopyranosid-3-ulose (**1**) with hydrazine under reflux conditions for 48 h, gave 3-deoxy-D-*ribo* (**2**)- and 2,3-dideoxy-D-*erythro* (**3**)-hexopyranosides which were isolated in 5% and 50% yields, respectively. When this reaction was carried out under nitrogen,the unsaturated 2-ene (**4**) was produced in place of dideoxy (**3**). If the latter reaction was further refluxed open to the atmosphere for 24 h, the complete conversion of ene (**4**) to dideoxy (**3**) was observed as indicated by tlc. It is likely, therefore, that dideoxy (**3**) is produced by reduction of ene (**4**) with diimide generated *in situ*. Aerial oxidation of hydrazine produces diimide which has a pronounced tendency to transfer hydrogen to nonpolar multiple bonds (6, 7). The major product under these conditions, a 3-deoxy-D-*ribo* sugar (**2**), can be thought to arise from nucleophilic addition of water to the intermediate alkenyldiazene. The susceptibility of alkenyldiazenes to nucleophilic attack has been previously suggested to account for the variation in the yield of alkene in the Kishner elimination (5). The increase

0008-4042/80/232628-05$01.00/0

©1980 National Research Council of Canada/Conseil national de recherches du Canada

Can. J. Chem. Downloaded from www.nrcresearchpress.com by 210.87.254.40 on 09/05/12
For personal use only.

Can. J. Chem. Downloaded from www.nrcresearchpress.com by 210.87.254.40 on 09/05/12
For personal use only.

in yield of this 3-deoxy *ribo* sugar, when the reaction was carried out in hydrazine hydrate, supports this hypothesis.

Two aspects of this nucleophilic attack are worthy of consideration. Of the two modes of addition, 1,2 seems favored since an α-hydroxy hydrazone which must tautomerize to the diazene, a relatively difficult process, is considered to be the rate determining step in the Wolff–Kishner reduction (8). In support of this, the rate of formation of 3-deoxy *ribo* (**2**) from the 2-*O*-*p*-toluenesulphonate (**1**) was much faster than from the 2-hydroxyl (**5**) (Fig. 2). However, when ethanol was used as solvent, hydrolysis gave **5** in 40% yield, a product which may well have arisen via an intermediate produced by 1,4-addition. The formation of the *ribo* isomer (**2**) necessitates the stereoselective α-attack but reasons for this are unclear. Nucleophilic 1,4-additions to a similar system, methyl 4,6-*O*-benzylidene-2,3-dideoxy-3-phenylazo-D-*erythro*hex-2-enopyranoside, have been shown to result in only one isomer (9), the stereochemistry of which is dependent on the nature of the nucleophile.

Treatment of α-keto tosylate (**1**) with hydrazine at room temperature or with hydrazine in ethanol under reflux gave neither the 3-deoxy sugar (**2**) nor

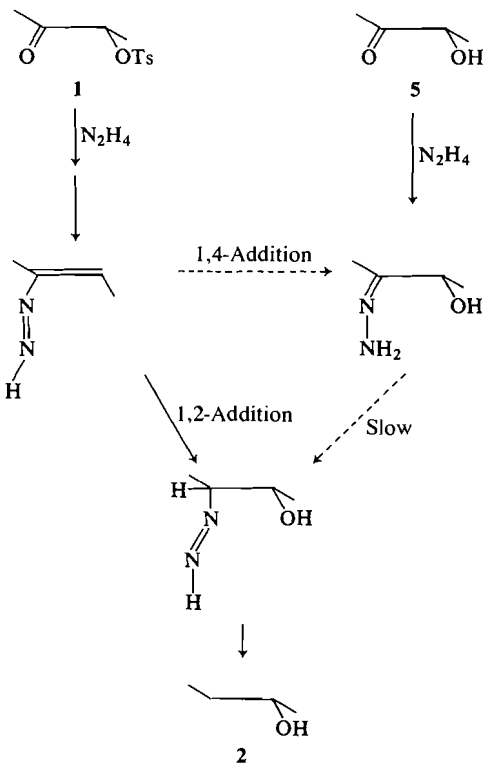


FIG. 2.

the dideoxy sugar (**3**). These observations indicate that high temperature and a large excess of hydrazine are necessary requirements for the formation of these materials. The reaction of **1** with hydrazine in ethanol at room temperature was characterized by the formation of crystalline transient material which on isolation gave results consistent with a carbinol hydrazine. Hydrolysis of this moderately stable substance **9** either during tlc or directly with ethanol led predominantly to the parent compound **1**. No C=O or C=N were apparent in the ir but strong broad NH and/or OH were present. Collins and Overend (10) have reported a similar addition compound of hydroxylamine with a pyranosid-2-ulose. These types of addition compounds are intermediates in Schiff base formation and under acidic conditions addition is rate-determining, whereas under neutral or basic conditions dehydration becomes rate controlling (11).

With the disappearance of the supposed carbinol hydrazine **9** two new products appear. Methyl 2-*O*-*p*-toluenesulphonyl-α-D-allopyranoside (**6**) is presumably formed by diimide reduction of the 3-keto (**1**) by preferred equatorial attack. The second product, an azine (**7**), was characterized by its elemental composition and spectral data. A mass spectrum indicated a dimeric structure due to its molecular peak at *m/e* 524. An infrared spectrum indicated the C=N stretch at 1630 cm^{-1} with no NH or OH absorption. This compound exhibited unusual solubility properties, being sparingly soluble in chloroform and recrystallizable from dimethylsulfoxide. A chloroform solution decomposed to give methyl 4,6-*O*-benzylidene-2-deoxy-α-D-*erythro*hexopyranosid-3-ulose (**8**). Since the immediate precursor of the azine **7** would be its hydrazone, at a low hydrazine concentration hydrazone/azine equilibrium should be favoured towards the azine. In fact, the yield of azine was doubled when the concentration of hydrazine was reduced from ten equivalents to five equivalents. Attempts to isolate pure hydrazone resulted in a mixture which was approximately 60% *syn* hydrazone. Recrystallization resulted in formation of azine **7**. Hydrolysis of the anticipated hydrazone resulted in two routes for the formation of 2 deoxy *erythro* 3-ulose (**8**). From the combined studies a reaction pathway for keto tosylate (**1**) reactions with hydrazine is outlined in Fig. 3. As is clear from the scheme, several of the intermediates were not isolated, in some cases due to the difficulties in purification, others such as the diazenes due to their instability.

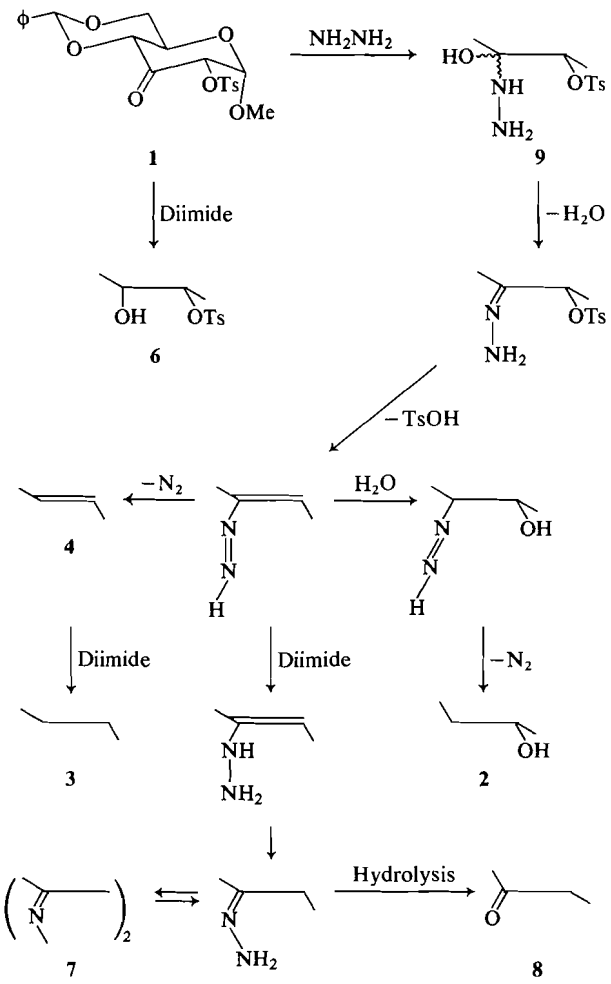


FIG. 3. Proposed routes to products.

Although the Kishner elimination did not provide high yields of dideoxygenated products, i.e., **3** and **4**, this study clearly shows the variety of compounds that can be produced in moderate yield by a small change in experimental conditions. This work provides an alternate explanation to the reported di-Wolff–Kishner reduction of D-galactose (12). An alkenyl diazene produced from D-galactose hydrazone could undergo (*i*) fragmentation, (*ii*) fragmentation–diimide reduction, (*iii*) 1,2-addition of water/fragmentation, illustrating the formation of all three observed products (Fig. 4).

Experimental

Evaporations were conducted on a Büchi rotary evaporator at bath temperatures not exceeding 50°C. Melting points were determined on a Fisher-Johns apparatus and are uncorrected. Optical rotations were measured on a Perkin-Elmer Model P22 spectropolarimeter. The ^{1}H nmr spectra were recorded on a Varian A-56/60A or XL-100. All chemical shift values are given in ppm downfield from internal TMS ($\delta = 0$); coupling constants (J) are given in Hz. Mass spectra were recorded by Mr. G. Owen on a Hitachi-Perkin-Elmer RMU-6E spectrometer using an ionization potential of 80 eV. Infrared spectra were recorded on a Perkin-Elmer 457 grating spectrophotometer. Silica gel G, E. Merck type 60, was used for tlc; toluene – diethyl ether, 1:1, was used as the solvent system. Detection of sugars was accomplished by spraying with sulphuric acid (10%) and heating the plate. Microanalyses were performed by Mr. M. K. Yang. Hydrazine (97%) was obtained from Matheson Coleman and Bell, OH, and kept over Linde molecular sieve Type 4A. Hydrazine hydrate was obtained from Fisher Scientific. Commercial ethanol (95%) was distilled over potassium hydroxide and then kept over Linde molecular sieve Type 4A. The authentic samples of the 3-deoxy sugar (**2**), the dideoxy sugar (**3**), the ene (**4**), and the 2-deoxy ketose (**8**) were prepared by Dr. A. S. Tracey.

Methyl 4,6-O-Benzylidene-2-O-p-toluenesulphonyl-α-D-ribohexopyranosid-3-ulose (1)

Prepared from methyl 4,6-*O*-benzylidene-2-*O*-*p*-toluenesulphonyl-α-D-glucopyranoside (13) by oxidation with dimethyl sulfoxide and phosphorus pentoxide in dimethyl formamide as described by Onodera *et al.* (14); mp 163–164°C, $[\alpha]_D^{25}$ +41° (*c* 0.25, $CHCl_3$) (lit. (15) mp 162–164°C, $[\alpha]_D^{28}$ +44° (*c* 1, $CHCl_3$)).

Reactions of Methyl 4,6-O-Benzylidene-2-O-p-toluenesulphonyl-α-D-ribohexopyranosid-3-ulose (1) with Hydrazine

(a) *Hydrazine in the Presence of Oxygen*

The α-keto tosylate (**1**) (500 mg, 1.15 mmol) was added to hydrazine (10 mL) and heated under reflux open to the atmosphere. With the immediate dissolution of the starting material, the reaction mixture turned greenish-yellow. After 5 min, tlc revealed the complete absence of the starting material and the presence of a new component having R_f 0.28 in addition to the compound(s) at the origin; after 1/2 h, a second component (R_f 0.72) was detected and the greenish-yellow colouration faded during this period. The reaction mixture was maintained at reflux temperature for 2 days, after which an absence of compound(s) at the origin was indicated by tlc. The reaction mixture was allowed to cool, poured into ice-cold water (125 mL) and extracted with chloroform (25 mL × 3). The organic layer was washed with water (25 mL) and evaporated. The residue was partitioned between 75% aqueous methanol – petroleum ether (bp 30–60°C); the petroleum ether layer was washed with 75% aqueous methanol (25 mL), dried over sodium sulphate, filtered, and evaporated to yield the component having R_f 0.28, which was crystallized from hexane (25 mg, 5%). The aqueous methanol layer was mixed with water (100 mL) and then extracted with chloroform (25 mL × 3). The combined chloroform extracts were dried over sodium sulphate, filtered, and evaporated to yield the component having R_f 0.72, which was crystallized from 2-propanol (150 mg, 50%).

The component having R_f 0.28 was identified as methyl 4,6-*O*-benzylidene-3-deoxy-α-D-*ribo*hexopyranoside (**2**); mp 185–186°C (a mixture mp with an authentic sample was undepressed), $[\alpha]_D^{25}$ +125° (*c* 0.28, $CHCl_3$) (lit. (16) mp 186°C, $[\alpha]_D^{24}$ +126° (*c* 1, $CHCl_3$)). The ir, nmr, and mass spectra were identical with an authentic sample.

The component having R_f 0.72 was identified as methyl 4,6-*O*-benzylidene-2,3-dideoxy-α-D-*erythro*hexopyranoside (**3**); mp 82–83°C (a mixture mp with an authentic sample was undepressed), $[\alpha]_D^{25}$ +120° (*c* 0.24, $CHCl_3$) (lit. (17) mp 82–84°C, $[\alpha]_D^{21}$ +118° (*c* 1, $CHCl_3$)). The ir, nmr, and ms were identical with an authentic sample.

When the refluxing was discontinued after 1/2 h and the reac-

Can. J. Chem. Downloaded from www.nrcresearchpress.com by 210.87.254.40 on 09/05/12
For personal use only.

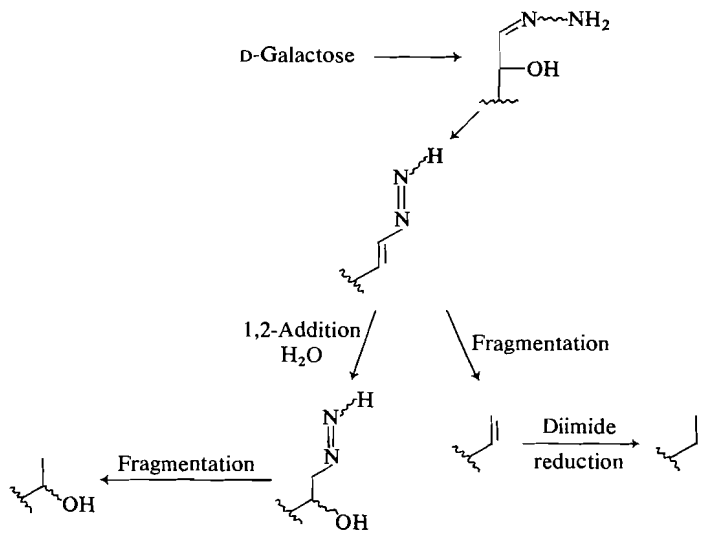


FIG. 4. Possible reaction pathways in the hydrazine reaction of D-galactose (12).

tion mixture was worked up as indicated above, a crude product mixture (300 mg) was obtained. Crystallization using 2-propanol afforded the 3-deoxy sugar (**2**) (90 mg, 30%). Two unidentified components (R_f 0.03, 0.05) and a trace amount of the ene (**4**) were present in the mother liquor (tlc).

(b) *Hydrazine under Nitrogen*

The α-keto tosylate (**1**) (500 mg, 1.15 mmol) was heated at reflux temperature in hydrazine (10 mL) under nitrogen. As in the previous reaction, the progress of the reaction was monitored by tlc, which indicated the appearance of the 3-deoxy sugar (**2**) (R_f 0.28) after 5 min and a new component (R_f 0.76) after 1/2 h. The reaction mixture was refluxed under nitrogen for 2 days and was worked up as in the previous experiment. The presence of a trace of the dideoxy sugar (**3**) (R_f 0.72) was detected by tlc. The 3-deoxy sugar (**2**) was isolated in 53% (165 mg) yield; a mixture mp with an authentic sample was undepressed.

The component having R_f 0.76 was recrystallized from methanol (30 mg, 6%) and was identified as methyl 4,6-*O*-benzylidene-α-D-*erythro*hex-2-enopyranoside (**4**); mp 118–120°C (a mixture mp with an authentic sample was undepressed), $[\alpha]_D^{25}$ +138° (*c* 0.28, $CHCl_3$) (lit. (18) mp 119–120°C, $[\alpha]_D^{22}$ +130° (*c* 0.54, $CHCl_3$)). The ir, nmr, and ms were identical with an authentic sample.

When the reaction (*b*) was repeated with the exception that, after 2 days, the reaction mixture was refluxed in open atmosphere for 24 h, the final product distribution was the same as in (*a*) (tlc).

(c) *Hydrazine Hydrate*

The α-keto tosylate (**1**) (2.5 g, 5.75 mmol) was heated under reflux in hydrazine hydrate (50 mL). Slow dissolution of the starting material gave a light yellow solution after 15 min. The presence of **2** and the complete absence of the starting material were shown by tlc. The reaction mixture was maintained at reflux open to the atmosphere for 48 h and was worked up as in (*a*) to yield the 3-deoxy sugar (**2**) (1.05 g, 70%) and the dideoxy sugar (**3**) (75 mg, 3%). A trace of methyl 4,6-*O*-benzylidene-2-deoxy-*arabino*pyranoside was detected by tlc (R_f 0.32).

(d) *Hydrazine in Ethanol*

The α-keto tosylate (**1**) (500 mg, 1.15 mmol) in ethanol (25 mL) containing hydrazine (368.6 mg, 11.5 mmol) was stirred at room temperature. Dissolution of the sparingly soluble starting material was followed by the appearance of a milky white residue. This residue became thick during the first 1/2 h and then redissolved (~1 h) to give a colourless solution. The presence of a new component (**6**) having R_f 0.55 in addition to the starting material (R_f 0.66) was shown by tlc. After 3.5 h, the presence of starting material could not be detected by tlc; after 1.5 days, the formation of a white residue was observed. This white residue was filtered after 4 days and was recrystallized from dimethyl sulfoxide to give the azine (**7**) (100 mg, 33%). The filtrate was mixed with water (50 mL) and extracted with petroleum ether (30–60°C). The organic fraction was refrigerated to give a white residue (**6**) which was recrystallized from ethanol to yield methyl 4,6-*O*-benzylidene-2-*O*-*p*-toluenesulphonyl-α-D-*allo*pyranoside (**6**) (50 mg, 10%); mp 164°C, $[\alpha]_D^{25}$ +32° (*c* 0.21, $CHCl_3$) (lit. (19) mp 166–167°C, $[\alpha]_D^{25}$ +36°). Infrared, nmr, and ms were consistent with this assignment.

Compound **7** showed no mobility on tlc and was sparingly soluble in chloroform to give solutions which turned yellow, indicating decomposition. Thin-layer chromatography of a chloroform solution indicated that the major decomposition product was methyl 4,6-*O*-benzylidene-2-deoxy-α-D-*erythro*-hexopyranosid-3-ulose (**8**) (R_f 0.37). Compound **7** was identified as methyl 4,6-*O*-benzylidene-2-deoxy-α-D-*erythro*hexopyranosid-3-uloazine; mp >180°C (dec.), $[\alpha]_D^{25}$ +68° (*c* 0.074, DMSO); ir (KBr): 2900 (CH), 1630 (C=N), 700 and 750 (phenyl) cm^{-1}; nmr (DMSO-d_6) δ: 2.3 (dd, 1H, H-2_a, J_{2a-2e} = 16, $J_{1,2}$ = 4.5 Hz), 3.2 (d, 1H, H-2_e), 3.22 (s, 3H, OMe), 3.84 (d, 2H, H-6,6'), 4.2–4.5 (m, 2H, H-4,5), 5.0 (d, 1H, H-1), 5.8 (s, 1H, benzylidene H), 7.4 (s broad, 5H, phenyl); ms (240°C) *m/e*: 525 (M + 1, 1.1), 524 (M, 2.1), 494 (1.9), 493 (4.8), 492 (M − MeOH, 6.1), 462 (3.3), 461 (12.7), 460 (M − 2MeOH, 26.7), 149 (Ph—CH=O=CH_2CHO, 13.9), 107 (33.7), 106 (84.2), 105 (100); *Anal.* calcd. for $C_{28}H_{32}N_2O_8$: C 64.12, H 6.10, H 5.34%; found: C 63.89, H 6.19, N 5.21%.

When the above reaction was repeated with five equivalents of hydrazine (184.3 mg, 5.75 mmol), the azine **7** was obtained in 60% yield. Methyl 4,6-*O*-benzylidene-2-*O*-*p*-toluenesulphonyl-α-D-allopyranoside (**6**) and methyl 4,6-*O*-benzylidene-α-D-*erythro*hex-2-enopyranoside (**4**) were present in trace amounts (tlc).

The α-keto tosylate (**1**) (2.5 g, 5.75 mmol) in ethanol (125 mL) containing hydrazine (461 mg, 14.5 mmol) was stirred at room temperature. Slow dissolution of the starting material gave a colourless solution which assumed a faint yellow colour. After

Can. J. Chem. Downloaded from www.nrcresearchpress.com by 210.87.254.40 on 09/05/12
For personal use only.

Can. J. Chem. Downloaded from www.nrcresearchpress.com by 210.87.254.40 on 09/05/12
For personal use only.

3 h, tlc indicated the appearance of the ene (**4**) (R_f 0.76). After 24 h, the reaction mixture was worked up by adding water (300 mL) and extracting with petroleum ether (bp 30–60°C) (75 mL × 4). The organic fraction was dried over sodium sulphate, filtered, and evaporated. Recrystallization of the crude product with methanol yielded methyl 4,6-*O*-benzylidene-α-D-*erythro*hex-2-enopyranoside (**4**) (600 mg, 40%).

Isolation of the milky white residue observed at the beginning of the ethanolic hydrazine reactions could be achieved by filtration of the reaction mixture to yield small amounts (~10% yield) of **9**. Chromatographic (tlc) behaviour of the compound **9** was similar to the starting material **1** (R_f 0.66). Melting point 110°C (dec.); ir (KBr): 3350 (broad, NH, OH), 2900 (CH), 1350 and 1170 (sulfonate) cm^{-1}; nmr ($CDCl_3$) δ: 2.3 and 2.45 (two broad singlets 1:2, Me-φ), 3.3 and 3.37 (two singlets 1:2, OMe), 3.4–4.2 (~10 H), 5.52 (s, 1H, benzylidene H), 7.0–8.0 (m, ~9H). *Anal.* calcd. for $C_{21}H_{26}N_2O_8S$: C 54.07, H 5.58, N 6.0%; found: C 54.76, H 5.72, N 5.79%.

When the compound **9** (20 mg, 0.064 mmol) was stirred in ethanol (1.5 mL) a clear yellowish solution was formed which, in turn, gave a white residue corresponding to the starting material **1** (tlc). The presence of a trace of methyl 4,6-*O*-benzylidene-α-D-*erythro*hex-2-enopyranoside (**4**) (R_f 0.76) was indicated by tlc.

*Reaction of Methyl 4,6-*O*-benzylidene-α-D-*ribo*hexopyranosid-3-ulose (5) with Hydrazine at Reflux*

The α-hydroxy-keto sugar (**5**) (325 mg, 1.15 mmol) was treated with hydrazine (10 mL) under reflux. Immediate dissolution of the starting material was observed. After 15 min, the absence of starting material was shown by tlc. The reaction mixture was maintained at reflux for 48 h and was worked up as usual to obtain the 3-deoxy sugar (**2**) (40%) and the dideoxy sugar (**3**) (5%).

When the above reaction was worked up after refluxing for 1/2 h a crude product mixture (150 mg) was obtained. Analysis (tlc) of this mixture revealed the presence of a trace of the 3-deoxy sugar (**2**) and two unidentified components (R_f 0.03, 0.05).

*Methyl 4,6-*O*-Benzylidene-2-deoxy-*α*-D-*erythro*hexopyranosid-3-ulose (8)*

(a) The α-keto tosylate (**1**) (2.5 g, 5.75 mmol) in ethanol (100 mL) containing hydrazine (1.85 g, 57.5 mmol) was stirred at room temperature. After 12 h, an aqueous solution of copper(II)sulphate pentahydrate (14 g in 50 mL) was added. Immediate evolution of a gas and formation of a greenish residue were observed. The presence of one major component (R_f 0.37) was indicated by tlc. After stirring for 6 h, the reaction mixture was filtered and washed with ethanol (25 mL). The filtrate was mixed with water (300 mL) and extracted with chloroform (75 mL × 3). The organic fraction was washed with water (100 mL), dried over sodium sulphate, filtered, and evaporated. This residue contained traces of the *allo*-tosylate (**6**) (R_f 0.55) and methyl 4,6-*O*-benzylidene-α-D-*ribo*hexopyranosid-3-ulose (**5**) (R_f 0.20) in addition to the 2-deoxy ketose (**8**). The residue was recrystallized from 2-propanol to yield methyl 4,6-*O*-benzylidene-2-deoxy-α-D-*erythro*hexopyranosid-3-ulose (**8**) (750 mg, 50%); mp 170–171°C (a mixture mp with an authentic sample was undepressed), $[\alpha]_D^{25}$ +160° (*c* 0.25, ethyl acetate) (lit. (20) mp 170–171°C, $[\alpha]_D^{20}$ +153° (*c* 0.5, ethyl acetate)).

(b) The α-keto tosylate (**1**) (500 mg, 1.15 mmol) in ethanol (25 mL) containing hydrazine (368.6 mg, 11.5 mmol) was stirred at room temperature. After 12 h, benzaldehyde (5.0 mL) and acetic acid (0.5 mL) were added. The reaction mixture was stirred (2 h) until there was no apparent increase of the 2-deoxy ketose (**8**) as indicated by tlc. The reaction mixture was mixed with water (100 mL) and extracted with chloroform (25 mL × 3). The organic fraction was washed with water (25 mL), dried over sodium sulphate, and evaporated to a syrup. This was chromatographed on silica (petroleum ether bp 30–60°C/ether 20:1) to yield methyl 4,6-*O*-benzylidene-2-deoxy-α-D-*erythro*-hexopyranosid-3-ulose (**8**) (90 mg, 30%).

*Methyl 4,6-*O*-Benzylidene-α-D-ribo*hexopyranosid-3-ulose (5)*

The α-keto tosylate (**1**) (500 mg, 1.15 mmol) in degassed ethanol (25 mL) containing hydrazine (368.6 mg, 11.5 mmol) was stirred under nitrogen. After 12 h, an aqueous solution of copper(II)sulphate pentahydrate (2.9 g in 10 mL) was added. The reaction mixture was worked up as usual after stirring for 6 h. The crude product mixture indicated the presence of a major component (**5**) (R_f 0.20 tlc) and two minor components, methyl 4,6-*O*-benzylidene-2-deoxy-α-D-*erythro*hexopyranosid-3-ulose (**8**) (R_f 0.37) and methyl 4,6-*O*-benzylidene-α-D-*erythro*hex-2-enopyranoside (**4**) (R_f 0.76). Recrystallization of the crude product mixture from toluene yielded methyl 4,6-*O*-benzylidene-α-D-*ribo*hexopyranosid-3-ulose (130 mg, 40%); mp 194°C (a mixture mp with an authentic sample was undepressed), $[\alpha]_D^{25}$ +120° (*c* 0.20, pyridine) (lit. (21) mp 190–192°C, $[\alpha]_D^{23}$ +113° (*c* 1, pyridine)).

Acknowledgements

We wish to thank the Natural Sciences and Engineering Research Council of Canada for support of this work through operating grant A3785 and Simon Fraser University for an Open Graduate Scholarship to L. K. G. Wickremesinghe.

1. H. R. Schuler and K. N. Slessor. Can. J. Chem. **55**, 3280 (1977).
2. N. Kishner. J. Russ. Phys. Chem. Soc. **45**, 973 (1913).
3. N. J. Leonard and S. Gelfand. J. Am. Chem. Soc. 77, 3272 (1955).
4. P. S. Wharton and D. H. Bohlen. J. Org. Chem. **26**, 3615 (1961).
5. P. S. Wharton, S. Dunny, and L. Soto Krebs. J. Org. Chem. **29**, 958 (1964).
6. F. Aylward and M. Sawistowska. Chem. Ind. 484 (1962).
7. E. E. van Tamelen, R. S. Dewey, M. F. Lease, and W. H. Pirkle. J. Am. Chem. Soc. **83**, 4302 (1961).
8. H. H. Szmant. Angew. Chem. Int. Ed. Engl. 7, 120 (1968).
9. P. M. Collins, D. Gardiner, S. Kumar, and W. G. Overend. J. Chem. Soc. Perkin Trans. I, 2596 (1972).
10. P. M. Collins and W. G. Overend. J. Chem. Soc. 3448 (1965).
11. W. P. Jencks. Prog. Phys. Org. Chem. **2**, 63 (1964).
12. J. K. N. Jones, P. Reid, and J. R. Turvey. Can. J. Chem. **43**, 983 (1965).
13. C. J. Robertson and C. F. Griffith. J. Chem. Soc. 1193 (1935).
14. K. Onodera, S. Hirano, and N. Kashimura. Carbohydr. Res. **6**, 276 (1968).
15. E. Vis and P. Karrer. Helv. Chim. Acta, **37**, 378 (1954).
16. S. Umezawa, T. Tsuchiya, and H. Hineno. Bull. Chem. Soc. Jpn. **43**, 1212 (1970).
17. E. L. Albano and D. Horton. J. Org. Chem. **34**, 3519 (1969).
18. E. Albano, D. Horton, and T. Tsuchiya. Carbohydr. Res. **2**, 349 (1966).
19. B. R. Baker and D. H. Buss. J. Org. Chem. **30**, 2304 (1965).
20. A. Klemer and G. Rodemeyer. Chem. Ber. **107**, 2612 (1974).
21. Y. Kondo and F. Takao. Can. J. Chem. **51**, 1476 (1973).

Effects of organic solvents on immobilized enzyme catalyses.[1] Chymotrypsin immobilized on Sephadex

DIANA H. PLIURA AND J. BRYAN JONES

Department of Chemistry, University of Toronto, Toronto, Ont., Canada M5S 1A1

Received May 5, 1980

This paper is dedicated to Prof. Raymond U. Lemieux on the occasion of his 60th birthday

DIANA H. PLIURA and J. BRYAN JONES. Can. J. Chem. **58**, 2633 (1980).

The esterolytic activities of native chymotrypsin (CT) and immobilized CT-Sephadex have been studied in the presence of up to 20% of the organic solvents methanol, ethanol, 2-propanol, *tert*-butyl alcohol, dioxane, or DMSO. The general cosolvent-induced inhibition of the native enzyme was attenuated for immobilized CT. Most noticeably, the apparent catalytic rate constants for the CT-Sephadex-catalyzed hydrolysis of *N*-acetyl-L-tyrosine ethyl ester were invariant over the 2–20% dioxane concentration range surveyed. In contrast, the activity of the native enzyme in 20% dioxane was only 3% the activity recorded in the absence of cosolvent. Increasing the hydrophobic character of the protic cosolvents destabilized the native enzyme but stabilized CT-Sephadex. Both native and immobilized CT displayed remarkable stability in 20% aqueous DMSO ($t_{\frac{1}{2}} > 200$ days). At least part of the DMSO-induced inhibition of native CT and CT-Sephadex was offset by increasing the apparent pH of the reaction medium. The altered kinetic patterns for CT-Sephadex are best explained by the effects of diffusional limitations on the apparent enzyme activity. The best compromise solvent for preparative applications of CT-Sephadex was found to be *tert*-butyl alcohol.

DIANA H. PLIURA et J. BRYAN JONES. Can. J. Chem. **58**, 2633 (1980).

On a étudié les activités estérolytiques de la chymotrypsine naturelle (CT) et de la CT immobilisée sur du Séphadex dans des solutions contenant jusqu'à 20% des solvants organiques suivants: le méthanol, l'éthanol, le propanol-2, l'alcool *tert*-butylique, le dioxanne ou le DMSO. L'inhibition de l'enzyme naturel généralement induite par le co-solvant est atténuée dans le cas de la CT immobilisée. De façon plus notable, la constante de vitesse catalytique apparente de l'hydrolyse catalysée par la CT-Séphadex du *N*-acétyl L-tyrosinate d'éthyle demeure inchangée dans l'échelle de concentration allant de 2 à 20% en dioxanne. Au contraire, l'activité de l'enzyme naturel dans le dioxanne à 20% représente seulement 3% de l'activité enregistrée en l'absence de co-solvant. L'augmentation du caractère hydrophobe des co-solvants protiques déstabilise l'enzyme naturel mais stabilise la CT-Séphadex. Les deux enzymes montrent une stabilité remarquable dans le DMSO aqueux à 20% ($t_{\frac{1}{2}} > 200$ jours). Une partie de l'inhibition de la CT naturelle et de la CT-Séphadex induite par le DMSO est compensée au moins par l'augmentation du pH apparent du milieu réactionnel. Les modèles du CT-Séphadex modifiés cinétiquement s'expliquent mieux par les effets de limitation de diffusion de l'activité apparente de l'enzyme. On a trouvé que l'alcool *tert*-butylique est le meilleur solvant de compromis pour les applications préparatives de la CT-Séphadex.

[Traduit par le journal]

Introduction

The practical value of utilizing enzymes to effect specific transformations in organic synthesis is being increasingly recognized both in academic and industrial laboratories. Already enzyme uses are well documented in a broad variety of reactions (1*b*,*c*). For many current and future applications of enzymes, the addition of organic cosolvents becomes desirable in order to enhance the limited solubility of the often hydrophobic substrates in aqueous solution. Alternatively, the effects of organic solvents can be exploited to influence the equilibrium of an enzyme-catalyzed reaction. Advantage has been taken of this to induce hydrolytic enzymes to catalyze the synthesis, rather than their usual cleavage, of esters (2) and oligopeptides (3).

Unfortunately, organic cosolvents usually exert deleterious effects on catalysis by enzymes (4) and significant activities in nonaqueous media are the exception rather than the rule. However, recent reports indicate that the adverse effects of organic cosolvents can be reduced by using immobilized enzyme derivatives (5–8). Furthermore, immobilization of enzymes (9–11) extends their utility as catalysts by alleviating problems of separation, cost, and supply, and permits reactors capable of continuous operation to be built. With a view towards identifying the best cosolvents to use in preparative applications of immobilized enzymes, we have initiated a systematic investigation of the effects of common organic solvents on such catalysts. In this paper we report on the behaviour of chymotrypsin immobilized on the organic support Sephadex.

The covalent attachment of CT[2] to cyanogen bromide-activated Sephadex provides CT-Sephadex, a representative immobilized enzyme preparation. Sephadex was chosen as our first sup-

[1]Enzymes in organic synthesis 18. For Part 17, see ref. 1*a*. Abstracted from the Ph.D thesis of D.H.P., University of Toronto, 1977.

[2]Abbreviations used: CT, chymotrypsin; DMSO, dimethyl sulfoxide; NATEE, *N*-acetyl-L-tyrosine ethyl ester; (app), apparent.

0008-4042/80/232633-08$01.00/0

©1980 National Research Council of Canada/Conseil national de recherches du Canada

Can. J. Chem. Downloaded from www.nrcresearchpress.com by 210.87.254.105 on 09/05/12
For personal use only.

Can. J. Chem. Downloaded from www.nrcresearchpress.com by 210.87.254.105 on 09/05/12
For personal use only.

port since it is one of the best studied and documented organic polymers used so far (10). Also, the CT-Sephadex conjugate possesses high residual activity and retains both the intrinsic catalytic properties and substrate specificity of the native enzyme (12, 13). The retention of such properties was an important factor in our choice of support since, by maintaining the same intrinsic rate constants for both free and immobilized enzyme, any cosolvent-induced alterations in the kinetic patterns of the immobilized derivative can be interpreted in terms of the effects of partitioning, diffusion, and of the environment of the matrix surface (5–8). The cosolvents surveyed, methanol, ethanol, 2-propanol, *tert*-butyl alcohol, dioxane, and DMSO are representative of the water-miscible organic solvents tolerated by CT (1*b*).

Experimental

Materials

α-Chymotrypsin (EC 3.4.21.1) from bovine pancreas was obtained as a lyophilized powder from Worthington Biochemical Corp. and was used without further purification. Sephadex G-200 (grade 40-120μ) was purchased from Pharmacia Fine Chemicals and cyanogen bromide from Eastman Chemicals. *N*-acetyl-L-tyrosine ethyl ester (NATEE) was a product of Sigma Chemical Co. All other chemicals were of the highest purity available.

Preparation of CT-Sephadex

The general procedure described by Axen and Ernback (14) was followed for the covalent coupling of CT to cyanogen bromide-activated Sephadex G-200. After completion of the coupling reaction and exhaustive washing of the conjugate under conditions that ensured the removal of all adsorbed protein (14), the product was carefully shrunk by slowly washing with ice-cold water/acetone mixtures of gradually increasing acetone concentration, and finally with cold acetone. The product was dried *in vacuo* over P_2O_5 for 2 days and then stored in closed vessels at 4°C.

The protein content of the conjugate was determined by amino acid analysis of the levels of phenylalanine, leucine, alanine, glycine, and glutamic acid and using the reported amino acid composition of CT of molecular weight 25 000 (15). The CT-Sephadex conjugate had a protein content of 57.3 ± 0.5 mg CT/g dry conjugate and a specific activity towards NATEE of 110 μmol/min/mg enzyme, corresponding to 37% residual activity after immobilization.

Kinetic Studies

The activities of both soluble and immobilized enzyme were measured by the pH-stat method (16). Kinetics of NATEE hydrolysis were monitored at 25°C under N_2 in a 10 mL capacity reaction vessel. In order to minimize external diffusion effects, reaction mixtures were stirred vigorously. Solutions of native CT in 1 m*M* aqueous HCl at 0°C were prepared as required. The powdered CT-Sephadex conjugate was allowed to preswell at 4°C in distilled water for 24 h, and the pH of the aqueous immobilized enzyme suspensions was adjusted to 9.8 prior to kinetic studies.

Specific Activity

The specific activity of immobilized CT was assayed against a solution of NATEE (9 mL, 11 m*M*) in 2% (v/v) aqueous methanol, 0.1 *M* in KCl and of $pH_{(app)}$ 9.8. Samples of CT-Sephadex were introduced by adding 0.25–1.0 mL of a well-stirred aqueous suspension. The total assay volume was adjusted to 10 mL by the addition of doubly distilled water when necessary. Typically, the CT-Sephadex suspension contained 2–4 mg conjugate (dry weight)/mL.

pH–Activity Profiles

The esterolytic activities of native and immobilized CT at different pH values were assayed using a solution of NATEE (10 m*M*, 1.0 *M* in KCl), containing either 2% (v/v) methanol or 20% (v/v) organic solvent. Rates of hydrolysis expressed in μmol/min were measured from the linear portions of the titration curves. When necessary, corrections were made for nonenzymic hydrolysis at high pH.

Determination of Apparent Kinetic Parameters

The apparent rate constants for native CT and CT-Sephadex catalyzed hydrolyses of NATEE were determined at 25°C in 1.0 *M* KCl solutions containing 0–20% (v/v) organic cosolvent. For the native enzyme, the esterolytic activities were monitored at $pH_{(app)}$ 7.8 employing a substrate concentration range of 0.2–20 m*M* NATEE and enzyme concentrations of $2–10 \times 10^{-8}$ *M*. The $Km_{(app)}$ and $k_{c(app)}$ values for CT-Sephadex were determined at $pH_{(app)}$ 9.8. Typical enzyme concentrations were $4–8.4 \times 10^{-7}$ *M*. Substrate concentration ranges from 0.2–12 m*M* NATEE were employed. The rate constants were determined by standard linear regression analyses of Lineweaver–Burk plots.

Determination of Catalyst Stability

Native CT

Solutions of $pH_{(app)}$ 7.8 of chymotrypsin (1 mg enzyme/mL), 0.1 *M* in KCl, both with and without 20% (v/v) organic solvent, were stored in stoppered vessels at 20°C. Aliquots of enzyme solution (10–50 μL) were withdrawn at intervals during a 2 month incubation period and their enzymic activities assayed at 25°C using NATEE (10 m*M*) in 2% (v/v) aqueous methanol, 0.1 *M* in KCl, $pH_{(app)}$ 7.8.

Immobilized CT

Powdered CT-Sephadex was allowed to preswell in distilled water for 24 h. An aliquot was then withdrawn and organic solvent was added to a concentration of 20% (v/v). The ionic strengths of all such CT-Sephadex suspensions were adjusted to 0.1 *M* KCl and the suspensions were then stored at $pH_{(app)}$ 9.8 in closed vessels at 20°C. The activity of each was monitored periodically by withdrawing a 1 mL aliquot (containing ~3 mg of conjugate) from the well-stirred suspension and assaying at 25°C using NATEE (9 mL, 11 m*M*) in 2% (v/v) aqueous MeOH, 0.1 *M* in KCl, $pH_{(app)}$ 9.8. During the 2 month incubation period, periodic pH adjustments were made to maintain $pH_{(app)}$ at 7.8 for native enzyme and 9.8 for CT-Sephadex.

Results

Solvent Effects on Kinetic Parameters

Because electrolytes are known to modify the catalytic properties of CT (1*b*), chymotryptic catalyses are usually carried out at high concentrations of electrolyte in order to minimize complications that arise from fluctuations in ionic strength during hydrolysis. To establish the optimum electrolyte concentration for the kinetic studies, experiments were performed to evaluate the kinetic parameters of native and immobilized CT at different concentrations of KCl. When diffusion restric-

Can. J. Chem. Downloaded from www.nrcresearchpress.com by 210.87.254.105 on 09/05/12
For personal use only.

tions are operating, the observed kinetic constants for an immobilized enzyme depend on the substrate concentration (17). Therefore, a fixed substrate concentration range was maintained as the KCl concentration, or the organic solvent concentration in subsequent experiments, was varied. The results are recorded in Table 1.

For native CT, the catalytic activity, as indicated by the specificity constant k_c/Km, is seen to increase monotonically with added electrolyte over the entire KCl concentration range surveyed. In contrast, the apparent catalytic activity for CT-Sephadex is independent of ionic strength at electrolyte concentrations greater than 0.01 *M* KCl. For CT-Sephadex both $k_{c(app)}$ and Km$_{(app)}$ decrease with increasing KCl concentration in the range 0.01–1.0 *M* KCl. In contrast, for native CT, k_c increases while Km decreases with increasing ionic strength. A 1.0 *M* KCl concentration was used in subsequent kinetic studies since this concentration maximized chymotryptic activity for both the native and immobilized enzyme while remaining compatible with solutions containing up to 20% of the organic cosolvents employed.[3]

The effects of organic solvents on the kinetic parameters of native CT and CT-Sephadex were found to differ significantly for the soluble and immobilized catalysts. The data are summarized in Table 2. For the native CT-catalyzed hydrolysis of specific ester substrates such as NATEE, the observed k_c is equal to the deacylation rate constant (18). Nucleophilic cosolvents, particularly methanol, reduce the hydrolytic rate by transesterification of the acyl enzyme intermediate (19), resulting in a decrease in k_c from 178 s^{-1} in the absence of methanol to 97 s^{-1} in 20% methanol. Contrary to the anticipated effects of transacylation, the low value of the $k_{c(app)}$ for CT-Sephadex increases from 12.2 s^{-1} in 4.5% methanol to 81 s^{-1} in 20% methanol (Table 2). Significantly, the nonlinear Lineweaver–Burk plots for CT-Sephadex in 2% aqueous methanol or 2% aqueous ethanol are symptomatic of immobilized enzyme reactions subject to severe diffusion limitations (17*c*, 20).

At least part of the deleterious effects of the nonnucleophilic solvents *tert*-butyl alcohol and dioxane has been attributed to competitive inhibition (21). Accordingly, over the concentration range surveyed, Km for soluble CT increases 10-fold with *tert*-butyl alcohol, or 30-fold with dioxane, while k_c remains invariant. After immobilization of the enzyme, the diminished $k_{c(app)}$ values remain constant for both solvent systems. In contrast, Km$_{(app)}$ for the immobilized enzyme is remarkably insensitive to changes in *tert*-butyl alcohol or dioxane concentrations.

[3]The 20% limit on the maximum organic solvent concentrations used in this study was dictated by the sluggishness of the pH-stat electrode response beyond this level.

TABLE 1. The effects of KCl concentration on the kinetic parameters of native CT and CT-Sephadex[a]

[KCl] (*M*)	Km$_{(app)}$ (m*M*)	$k_{c(app)}$ (s^{-1})	$k_{c(app)}/K$m$_{(app)}$ (mM^{-1} s^{-1})
	Native CT		
0.0	2.62±0.43	82±12	31±10
0.01	1.84±0.21	126±11	68±14
0.1	1.69±0.16	133±10	79±13
1.0	1.46±0.05	167± 3	114±16
	CT-Sephadex		
0.0	8.9 ±1.7	9.2±1.6	1.0±0.4
0.01	3.16±0.66	44.0±9.0	14 ±6
0.1	1.60±0.14	24.4±1.7	15 ±2
1.0	0.84±0.09	12.2±0.8	15 ±2

[a]Esterolytic activity towards NATEE in 4.5% (v/v) methanol, at 25°C and pH 7.8 for native CT and pH 9.8 for the immobilized derivative.

In general, organic solvent-mediated inhibition of CT is attenuated after immobilization of the enzyme. Compared with the esterolytic activity in aqueous solution, for which k_c/Km = 268 mM^{-1} s^{-1}, native CT retains only 12–17% activity in the presence of 20% DMSO, 2-propanol, or *tert*-butyl alcohol and only 3–7% activity at high concentrations of methanol, ethanol, or dioxane. On the other hand, $k_{c(app)}/K$m$_{(app)}$ constants for CT-Sephadex at high solvent concentrations stay in the range of 35% (for methanol, ethanol) – 70% (for *tert*-butyl alcohol, dioxane) of the values observed at low cosolvent concentrations. Nevertheless, in a given solvent medium $k_{c(app)}/K$m$_{(app)}$ for CT-Sephadex is routinely less than the catalytic activity of the soluble enzyme.

Solvent Effects on pH–Activity Profiles

The solvent effects on the pH–activity profiles of both free and immobilized CT are depicted in Fig. 1. In highly aqueous (2% MeOH) solutions, the pH optimum for the CT-Sephadex-catalyzed hydrolysis of NATEE is displaced approximately 2 pH units toward more alkaline values relative to the 7.8 pH optimum for native CT. In 20% methanolic or 20% ethanolic solutions, the activities of both soluble and immobilized CT are reduced at each pH value but there are no significant effects on the pH optima. In contrast, in 20% aqueous DMSO solution the pH–activity profiles for soluble CT and CT-Sephadex are shifted toward more alkaline pH values. The DMSO-induced inhibition of both CT catalysts can be offset by increasing the apparent pH of the reaction medium by ~0.65 pH units. Whereas a 20% aque-

TABLE 2. Effects of organic solvents on the apparent kinetic parameters[a]

Solvent %(v/v)	Native CT			CT-Sephadex		
	Km (mM)	k_c (s^{-1})	k_c/Km (mM^{-1} s^{-1})	$Km_{(app)}$ (mM)	$k_{c(app)}$ (s^{-1})	$k_{c(app)}/Km_{(app)}$ (mM^{-1} s^{-1})
0	0.66±0.01	178± 2	268± 8			
Methanol						
2				—[b]	—[b]	—[b]
4.5	1.46±0.05	167± 3	114± 6	0.84±0.09	12.2± 0.8	15 ±2
10	3.09±0.21	120± 6	39± 5	2.6 ±0.5	22 ± 4	8.5±3.2
15	3.46±0.22	104± 5	30± 3	6.1 ±0.8	35 ± 4	5.8±1.5
20	8.8 ±1.0	97±10	11± 2	15.5 ±4.5	81 ±21	5.2±2.9
Ethanol						
2				—[b]	—[b]	—[b]
4.5	2.17±0.14	212± 9	98±10	2.25±0.20	40 ± 3	17.8±2.7
10	3.79±0.19	210± 7	55± 5	13.1 ±1.7	140 ±16	10.7±2.6
15	5.17±0.48	196±15	38± 6	11.0 ±2.0	133 ±22	12.1±4.2
20	9.41±0.64	181±10	19± 2	22 ±4	153 ±29	7.0±2.6
2-Propanol						
2				6.45±0.51	80 ± 5	12.4±1.7
4.5	1.66±0.12	216±11	130±16	4.72±0.31	74 ± 4	16.3±1.9
10	2.12±0.13	199± 7	94± 9	6.42±0.31	77 ± 3	12.0±1.0
15	2.66±0.09	193± 5	73± 4	7.8 ±1.1	62 ± 8	7.9±2.1
20	3.75±0.18	168± 5	45± 4	8.11±0.68	56 ± 4	6.9±1.1
tert-Butyl alcohol						
2				7.10±0.55	155 ± 9	16.2±2.5
4.5	1.07±0.05	210± 6	196±15	7.91±0.75	142 ±12	18.0±3.2
10	2.84±0.16	224± 8	79± 7	8.1 ±1.2	101 ±14	12.5±3.5
15	3.60±0.39	238±20	66±13	8.5 ±0.9	104 ± 9	12.3±2.3
20	6.08±0.37	211±10	35± 4	9.5 ±1.4	107 ±15	11.3±3.2
Dioxane						
2				12.6 ±1.2	126 ±11	10 ±2
4.5	3.27±0.20	199± 9	61± 7	10.8 ±1.7	133 ±19	12 ±4
10	8.02±0.61	189±11	24± 3	12.7 ±1.9	113 ±15	9 ±3
15	10.9 ±1.3	173±17	16± 4	11.5 ±1.2	113 ±10	10 ±2
20	20.7 ±1.3	165±11	8± 1	13.6 ±1.4	101 ± 9	7 ±1
DMSO						
2				6.45±0.51	80 ± 5	12.4±1.7
4.5	1.66±0.12	216±11	130±16	4.72±0.31	77 ± 4	16.3±1.9
10	2.12±0.13	199± 7	94± 9	6.42±0.31	77 ± 3	12.0±1.0
15	2.66±0.09	193± 5	73± 4	7.8 ±1.1	62 ± 8	7.9±2.1
20	3.75±0.18	168± 5	45± 4	8.11±0.68	56 ± 4	6.9±1.1

[a]Apparent kinetic constants for the native and immobilized CT-catalyzed hydrolysis of NATEE in aqueous organic solvent solutions, 1.0 M in KCl at 25°C and $pH_{(app)}$ 7.8 for native enzyme or $pH_{(app)}$ 9.8 for CT-Sephadex.
[b]Nonlinear Lineweaver–Burk plots under these conditions.

ous dioxane solution eliminates the pH optima for native CT, the general shape and position of the pH–activity profile for CT-Sephadex remains unchanged in this solvent system.

Solvent Effects on CT-Stability

The stabilities of native CT and CT-Sephadex in water and in 20% organic solvent solutions were monitored at room temperature for 2 months. The half-lives observed are recorded in Table 3. In general, attachment of CT to Sephadex considerably extends the half-life of the enzyme. In the cosolvents methanol, ethanol, 2-propanol, and *tert*-butyl alcohol the half-lives of the native enzyme are 16, 9, 7, and 2.5 days respectively. In marked contrast, the half-life of CT-Sephadex increases from 30 up to 80 days as the carbon moiety of the alcohol becomes increasingly hydrophobic. Both native CT and CT-Sephadex show remarkable stability in aqueous DMSO solutions. The soluble enzyme retains half the original activity after 7 months in 20% aqueous DMSO at $pH_{(app)}$ 7.8 while CT-Sephadex has a half-life of approximately 10 months in the same solvent at $pH_{(app)}$ 9.8.

Can. J. Chem. Downloaded from www.nrcresearchpress.com by 210.87.254.105 on 09/05/12
For personal use only.

Can. J. Chem. Downloaded from www.nrcresearchpress.com by 210.87.254.105 on 09/05/12
For personal use only.

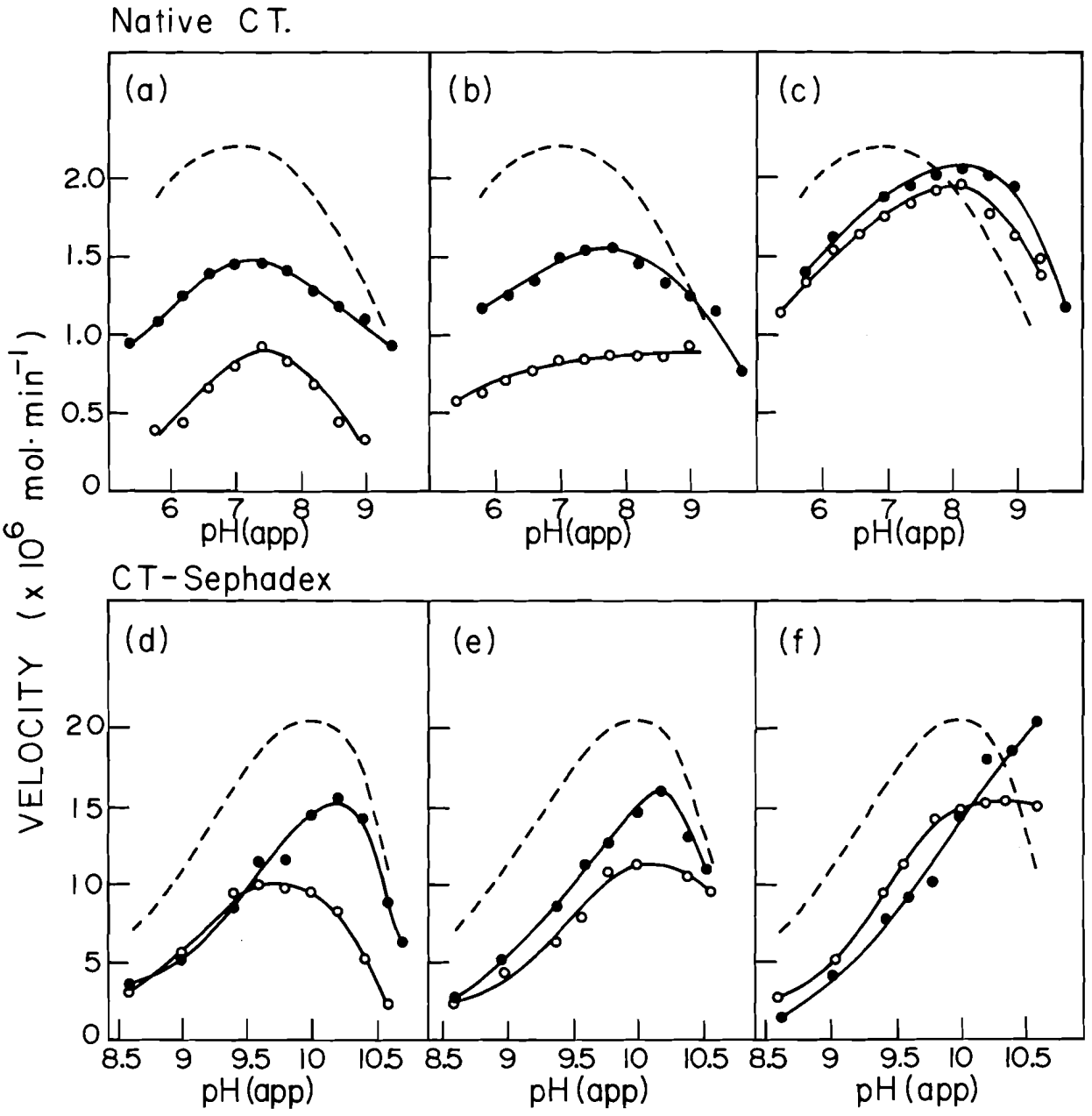


FIG. 1. The effects of 20% organic solvent on the pH–activity profiles for native CT and CT-Sephadex. Activities were assayed using solutions of NATEE (10 m*M*), 1.0 *M* in KCl, at 25°C containing 2% MeOH (----) or 20% organic solvent (——). Enzyme concentrations were 3.3×10^{-8} *M* for native CT (Fig. 1*a–c*) and 8.4×10^{-7} *M* for CT-Sephadex (Fig. 1*d–e*). (a) and (d) ○, MeOH; ●, EtOH. (b) and (e) ○, dioxane; ●, *i*-PrOH. (c) and (f) ○, *t*-BuOH; ●, DMSO.

Solvent Effects on the Configuration of CT-Sephadex

For flexible hydroxylic supports such as Sephadex G-200, changes in the porosity of the matrix can affect the accessibility of the substrate to the enzyme and thereby alter the activity of the immobilized enzyme (12, 22, 23). It was therefore necessary to determine the hydrated volume of CT-Sephadex in the various 20% organic solvent mixtures. Significant (up to 50%) reductions in volume were observed (Table 4). In general, the flexibility of the Sephadex G-200 support is reduced after cyanogen bromide activation and enzyme coupling (12). The Table 4 results support this conclusion. The hydrated volume of the CT-Sephadex conjugate is even further reduced, by 20–30%, in

Can. J. Chem. Downloaded from www.nrcresearchpress.com by 210.87.254.105 on 09/05/12
For personal use only.

TABLE 3. Half-lives of CT catalysts incubated in the absence or presence of 20% (v/v) organic solvent, at 20°C, 0.1 *M* in KCl, $pH_{(app)}$ 7.8 for native CT, or $pH_{(app)}$ 9.8 for CT-Sephadex

Solvent	Half-life (days)	
	Native CT	CT-Sephadex
H_2O	14	36
20% Methanol	16	30
20% Ethanol	9	66
20% 2-Propanol	7	65
20% *tert*-Butyl alcohol	2.5	>80 (est.)
20% Dioxane	13	23
20% DMSO	>200 (est.)	>300 (est.)

TABLE 4. Relative volumes[a] of Sephadex G-200 and CT-Sephadex in the absence or presence of 20% (v/v) organic solvent

Solvent	Sephadex G-200	CT-Sephadex
H_2O	1.04	0.69
20% Methanol	0.76	0.58
20% Ethanol	0.80	0.50
20% 2-Propanol	0.76	0.58
20% *tert*-Butyl alcohol	0.76	0.55
20% Dioxane	0.96	0.64
20% DMSO	0.88	0.62

[a]After 48 h equilibration at 20°C and 1.0 *M* in KCl. Volumes relative to Sephadex G-200 in distilled water (30.2 ± 0.4 mL hydrated gel/g dry support).

alcoholic solutions but it virtually unaffected by the addition of 20% dioxane.

Discussion

Although immobilization of the enzyme as its CT-Sephadex conjugate by the cyanogen bromide technique causes no inherent alteration in the *intrinsic* catalytic parameters (12, 13), our results demonstrate that the effects of organic cosolvents on the *observed* kinetic parameters for native and immobilized CT are significantly different (Table 2). In the absence of changes in specific rate constants due directly to chemical modifications, altered kinetic patterns for immobilized enzymes have been attributed to diffusional inhibition and/or the partitioning of solute molecules (including substrates and products) due to specific interactions with the matrix (17*c*, 20).

For an immobilized enzyme the severity of diffusional restrictions is reflected in the magnitude of the effectiveness factor η (17*a*), defined as V_i/V_f where V_i is the observed rate of reaction for the immobilized enzyme and V_f would be the rate observed for the same amount of enzyme free in solution. At all cosolvent concentrations surveyed, a comparison of the extrapolated values for the k_c/Km ratio for soluble and immobilized enzyme yields first-order effectiveness factors having values of < 0.05 at low organic solvent concentration or ranging from 0.15 in 20% 2-propanol or DMSO to as high as 0.88 in 20% dioxane. In no case does η reach unity. Diffusional inhibition therefore contributes to the observed kinetic parameters for all the systems surveyed. Consequently, effects due to solvent partitioning and/or to stabilization of the enzyme by the microenvironment of the matrix cannot be readily evaluated from this kinetic investigation.

Engasser and Horvath (8) have described quantitatively the case when chemical inhibition by a substance such as an organic cosolvent that is neither substrate nor product, and diffusional inhibition act simultaneously. They found that the combined effect in decreasing the rate of reaction is smaller than the sum of the individual effects. Experimentally, Axen and co-workers (24) have demonstrated that CT-Sephadex acting under diffusional restrictions on a substrate with high turnover number was not influenced by concentrations of *N*-acetyl-D-tryptophan of up to four times the K_I for soluble enzyme. However, by using a substrate with low turnover number, and thereby minimizing diffusional inhibition, the immobilized enzyme derivative showed the same inhibition profiles as the native enzyme. For the CT-Sephadex catalyst used in the present study, the high $Km_{(app)}$ values, the alkaline shifts in pH optima, and the persistently low $k_{c(app)}/Km_{(app)}$ ratios are symptomatic of a catalyst operating under diffusional limitations (8, 17*c*). Therefore, as expected for diffusion-restricted catalysts, the inhibition of catalytic activity by organic solvents is attenuated for the immobilized enzyme. The data of Table 2 show this effect very clearly.

Insoluble polysaccharide supports such as Sephadex undergo configurational changes, due to shrinking or swelling, as the solvent medium is altered (12, 22, 23). For some of the organic solvents surveyed at least part of the observed reduction in catalytic activity for CT-Sephadex can be attributed to the shrinkage of CT-Sephadex (Table 4) and to the concomitant decrease in the accessibility of substrate to enzyme. However, this cannot be the only factor because there is no direct correlation between observed activity and support volume. For instance, the observed $k_{c(app)}/Km_{(app)}$ ratio of 11.3 mM^{-1} s^{-1} in 20% aqueous *tert*-butyl alcohol is twice the value observed in 20% aqueous methanol even though the hydrated volume of CT-Sephadex in these media is effectively the same (Table 4).

The alkaline shifts in the pH activity profiles for CT-Sephadex (Fig. 1), relative to the pH opti-

Can. J. Chem. Downloaded from www.nrcresearchpress.com by 210.87.254.105 on 09/05/12
For personal use only.

mum for the native enzyme, are the result of enzymically generated pH gradients when product diffusion is restricted (17*c*, 20). Such pH gradients can be minimized by reducing the rate of hydrogen ion production and, by increasing the concentration of a suitable competitive inhibitor, the pH optimum for the esterolytic activity of CT-Sephadex can be shifted back toward pH 7.8, the pH optimum for native CT (24). For the six organic cosolvents surveyed in our study the intrinsic activity of the immobilized enzyme was not inhibited sufficiently to effect a shift of this type in the pH optimum toward more acid pH values, even at organic cosolvent concentrations as high as 20%.

The effects of organic solvents on the hydrated volume of CT-Sephadex must also be considered in evaluating solvent effects on the apparent pH optima. In 20% alcoholic solution, the hydrated volume of CT-Sephadex decreases by 20–30% (Table 4). This effective collapse of the flexible, porous support further restricts proton and product diffusion and creates a more pronounced pH gradient. Under these conditions, the attendant alkaline shift in the apparent pH optima counters any displacement of pH optima toward acidic values caused by chemical inhibition (24).

The apparent pH optima for the CT catalysts undergo an alkaline shift in 20% aqueous DMSO (Fig. 1). Similar cosolvent induced shifts in pH–activity profiles have been observed with soluble adenosine triphosphatase (25) and with immobilized acid phosphatase (26). At $pH_{(app)}$ 9.8 the esterolytic activity of CT-Sephadex in 20% DMSO is only 50–60% of that observed at low organic solvent concentration. This inhibition can be negated by increasing, by approximately 0.6 pH units, the apparent pH of the 20% DMSO solution (Fig. 1). Hence, at least part of the DMSO-induced inhibition summarized in Table 2 can be attributed to perturbations in the pK_a's of ionizable groups on the enzyme (27, 28).

The stability of an immobilized enzyme in the presence of organic cosolvents is an important property with respect to the potential utility of the immobilized enzyme. Unfortunately, the inherent stability parameters of immobilized enzymes are difficult to evaluate for catalysts operating under severe diffusional restrictions (17*c*, 20). In the limiting case, when the system is diffusion-controlled, the observed activity of the bound enzyme may remain constant, despite the fact that protein may have undergone considerable denaturation (29) or solvent-induced conformational change (30). In the present study the half-life of CT-Sephadex exceeds that of soluble CT for any given solvent mixture. However, this enhanced stability is purchased at the expense of measurable catalytic activity. In a 20% aqueous 2-propanol medium, the 9-fold increase in half-life after immobilization (Table 3) only marginally offsets the 7-fold decrease in the activity for CT-Sephadex (Table 2). In contrast, for a 20% aqueous *tert*-butyl alcohol solution, the greater than 30-fold increase in the half-life of the enzyme following immobilization more than compensates for the 3-fold decrease in k_c/Km which occurs.

For the protic solvents examined soluble CT becomes increasingly destabilized as the hydrophobic character of the solvent is increased (Table 3). However, CT-Sephadex is more stable in 20% *tert*-butyl alcohol ($t_{\frac{1}{2}} > 80$ days) than in 20% methanol ($t_{\frac{1}{2}} = 30$ days). The preferential exclusion of the more hydrophobic cosolvents such as *tert*-butyl alcohol from the hydrophilic microenvironment of Sephadex accounts for this enhanced stability. Conversely, Johanson and Mosbach (31) demonstrated the preferential absorption of ^{14}C-*n*-butanol within the hydrophobic copolymer methylacrylate-acrylamide, while no partitioning of ethanol was detected. Obviously, the judicious selection of a support matrix makes it possible to exclude or include low molecular weight hydrophobic compounds at will. This could have considerable practical ramifications in the synthetic applications of immobilized enzymes.

Other general solvent effects to which changed enzymic activities have been attributed, including changes in dielectric constant (32), increased substrate solubility (21), and decreased water availability (6), are not discernible under the conditions of the present study.

Of the solvents investigated, DMSO clearly has the most favourable overall properties. The stabilities of both native CT and CT-Sephadex are enhanced in 20% DMSO (Table 3) and the levels of catalytic activities remain high (Table 2). Much higher levels of DMSO are also tolerated well.[3] For example, Khurgin *et al.* (33) have shown that as long as the water of hydration remains >4%, CT continues to catalyze hydrolysis of its ester substrates. For practical applications in general, the use of DMSO may be limited by the fact that the hydrophobic organic compounds of most synthetic interest do not dissolve well in it. In view of this, *tert*-butyl alcohol, for which the transesterification disadvantage of primary and secondary alcohols (19) is precluded, could prove the best compromise choice for enhancing substrate solubility in reactions with enzymes immobilized on hydrophilic organic supports such as Sephadex.

Acknowledgements

We are grateful to the Natural Sciences and Engineering Research Council of Canada for financial support of this work and for the award of a Science Scholarship to one of us (D.H.P.).

1. (*a*) J. B. Jones and D. R. Dodds. Can. J. Chem. **57**, 2533 (1979); (*b*) J. B. Jones and J. F. Beck. Tech. Chem. N.Y. **10**, 107 (1976); (*c*) J. B. Jones. *In* Enzymic and non-enzymic catalysis. *Edited by* P. Dunnill, A. Wiseman, and N. Blakebrough. Ellis Horwood, Chichester, U.K. 1980. pp. 54–83.
2. (*a*) A. Kapune and V. Kasche. Biochem. Biophys. Res. Commun. **80**, 955 (1978); (*b*) A. M. Klibanov, G. P. Samokhin, K. Martinek, and I. V. Berezin. Biotechnol. Bioeng. **19**, 1351 (1977).
3. (*a*) K. Inouye, K. Watanabe, K. Morihara, Y. Tochino, T. Kanaya, J. Emura, and S. Sakakibara. J. Am. Chem. Soc. **101**, 751 (1979); (*b*) P. Kuhl, A. Konnecke, G. Doring, H. Daumer, and H.-D. Jakubke. Tetrahedron Lett. **21**, 893 (1980); (*c*) W. Kullmann. Biochem. Biophys. Res. Commun. **91**, 693 (1979); (*d*) Y. Isowa, M. Ohmori, T. Ichikawa, K. Mori, Y. Nonaka, K-I. Kihara, K. Oyama, H. Satoh, and S. Nishimura. Tetrahedron Lett. 2611 (1979).
4. M. Dixon and E. C. Webb. Enzymes. 2nd ed. Longmans, London. 1964.
5. P. Douzou and C. Balny. Proc. Natl. Acad. Sci. U.S.A. **74**, 2297 (1977).
6. K. Tanizawa and M. L. Bender. J. Biol. Chem. **249**, 2130 (1974).
7. C. R. Lowe. Eur. J. Biochem. **76**, 401 (1977).
8. J.-M. Engasser and C. Horvath. Biochemistry, **13**, 3845 (1974); **13**, 3849 (1974).
9. O. Zaborsky. Immobilized enzymes. CRC Press, Cleveland, OH. 1973.
10. K. Mosbach. Methods Enzymol. 44 (1976).
11. G. G. Guilbault and M. H. Sadar. Acc. Chem. Res. **12**, 344 (1979).
12. R. Axen, P.-A. Myrin, and J. C. Janson. Biopolymers, **9**, 401 (1970).
13. J. Lasch, L. Bessmetnaya, L. V. Kozlov, and V. K. Antonov. Eur. J. Biochem. **63**, 591 (1976).
14. R. Axen and S. Ernback. Eur. J. Biochem. **18**, 351 (1971).
15. P. W. Wilcox, J. Kraut, R. D. Wade, and H. Neurath. Biochim. Biophys. Acta, **24**, 72 (1957).
16. C. F. Jacobsen, J. Leonis, K. Linderstrom-Lang, and M. Ottensen. Methods in biochemical analysis. *Edited by* D. Glick. Wiley-Interscience, NY. 1957. p. 171.
17. (*a*) J.-M. Engasser and C. Horvath. J. Theor. Biol. **42**, 137 (1973); (*b*) J.-M. Engasser and C. Horvath. Biochim. Biophys. Acta, **358**, 178 (1974); (*c*) J.-M. Engasser and C. Horvath. Applied biochemistry and bioengineering. Vol. 1. *Edited by* L. B. Wingard, Jr., E. Katchalski-Katzir, and L. Goldstein. Academic, NY. 1976. pp. 127–200.
18. B. Zerner and M. L. Bender. J. Am. Chem. Soc. **85**, 356 (1963).
19. M. L. Bender and W. A. Glasson. J. Am. Chem. Soc. **82**, 3336 (1960).
20. L. Goldstein. Methods in enzymology. Vol. 44. *Edited by* K. Mosbach. Academic, NY. 1976. pp. 397–443.
21. R. P. Bell, J. F. Critchlow, and M. I. Page. J. Chem. Soc. Perkin Trans. II, 66 (1974).
22. J. F. Kennedy and A. Rosevear. J. Chem. Soc. Perkin Trans. II, 757 (1974).
23. M. A. Mitz and L. J. Sunmaria. Nature, **189**, 576 (1961).
24. J. Carlsson, D. Gabel, and R. Axen. Hoppe-Seyler's Z. Physiol. Chem. **353**, 1850 (1972).
25. S. M. Schuster. Biochemistry, **18**, 1162 (1979).
26. H. Wan and C. Horvath. Biochim. Biophys. Acta, **410**, 135 (1975).
27. G. P. Hess. The enzymes. Vol. 3. 3rd ed. *Edited by* P. D. Boyer. Academic, NY. 1971.
28. D. M. Blow. Acc. Chem. Res. **9**, 145 (1976).
29. D. F. Ollis. Biotechnol. Bioeng. **14**, 871 (1972).
30. T. N. Pattabiraman and W. B. Lawson. Biochem. J. **126**, 645 (1972).
31. A. C. Johansson and K. Mosbach. Biochim. Biophys. Acta, **370**, 339 (1974).
32. A. L. Fink. Biochemistry, **13**, 277 (1974).
33. Y. I. Khurgin, V. Y. Roslyakovc, Y. M. Azizov, and E. D. Kaverzneva. Izv. Akad. Nauk SSSR, Ser. Khim. **12**, 2697 (1968); **12**, 2840 (1968).

Can. J. Chem. Downloaded from www.nrcresearchpress.com by 210.87.254.105 on 09/05/12
For personal use only.

The chemistry of thujone. III. Thujone as a chiral synthon for the preparation of sesquiterpenes. Synthesis of (+)-β-cyperone

JAMES P. KUTNEY,[1] JOHN BALSEVICH, AND PETER GRICE

Department of Chemistry, University of British Columbia, 2036 Main Mall, University Campus, Vancouver, B.C., Canada V6T 1Y6

Received June 26, 1980

This paper is dedicated to Prof. Raymond U. Lemieux on the occasion of his 60th birthday

JAMES P. KUTNEY, JOHN BALSEVICH, and PETER GRICE. Can. J. Chem. **58**, 2641 (1980).

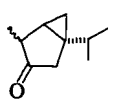
Robinson annelation of thujone (**1**) with methyl and ethyl vinyl ketones proceeds stereospecifically to afford the tricyclic enones **6** and **4** respectively. Enone **4** was converted to the glycol **13** which on treatment with 48% hydrobromic acid gave (+)-9-bromo-β-cyperone (**14**). Reduction with triphenyltin hydride yielded (+)-β-cyperone (**3**). Enone **6** was converted via standard means to the cyclopropyl alcohol **9**, a potential precursor of (+)-junenol (**10**).

JAMES P. KUTNEY, JOHN BALSEVICH et PETER GRICE. Can. J. Chem. **58**, 2641 (1980).

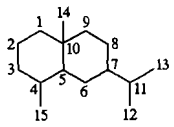
Les annellations de Robinson de la thujone (**1**) avec les méthyle et éthyle vinylcétones sont stéréospécifiques et conduisent respectivement aux énones tricycliques **6** et **4**. On a transformé l'énone **4** en glycol **13** qui, par traitement avec l'acide bromohydrique à 48%, donne la (+)-bromo-9 β-cypérone (**14**) dont la réduction, par l'hydrure de triphénylétain, fournit la (+) β-cypérone (**3**). On a transformé l'énone **6** par des méthodes normales en alcool cyclopropylique **9**, un précurseur potentiel du (+)-junénol (**10**).

[Traduit par le journal]

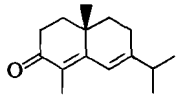
Previous research in this laboratory has shown that thujone[2] (**1**) is a useful starting material in the synthesis of several insect juvenile hormone analogues (1, 2). We have investigated the possibility of employing thujone in the synthesis of optically active sesquiterpenes with the eudesmane carbon skeleton (**2**) and wish to report the synthesis of (+)-β-cyperone (**3**).



1



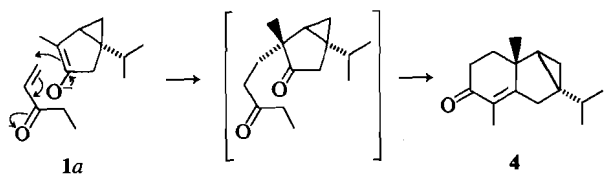
2



3

Earlier synthetic studies (3) in the cyperone series made use of the Robinson annelation with both (+)- and (−)-dihydrocarvone. These reactions, however, led to mixtures of isomers. Consideration of the geometry of the thujone enolate **1***a* led to the conclusion that alkylation should take place from the less hindered face of the enolate with a high degree of selectivity. Hence, annelation of thujone with ethyl vinyl ketone, or an equivalent reagent, was expected to lead to the tricyclic enone **4**, a molecule possessing ample functionality to allow elaboration to a variety of sesquiterpenes.

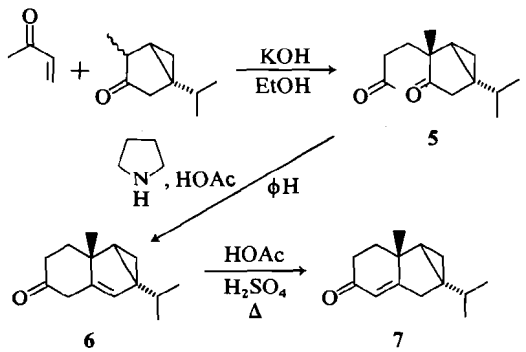
Initially, a study was carried out using methyl vinyl ketone for the Robinson annelation. Reaction



1*a* **4**

of thujone with methyl vinyl ketone in ethanol containing a catalytic amount of potassium hydroxide gave the diketone **5**.[3] This compound, isolated in 61% yield, was established as isomerically pure by means of its carbon-13 and proton magnetic resonance spectra (i.e. no anomalous resonances were present).

It is of interest to note that treatment of diketone **5** in refluxing ethanol with potassium hydroxide failed to effect cyclization to **7** and it was essential



5 **6** **7**

[1]Author to whom correspondence may be addressed.

[2]Thujone is the major component (ca. 80%) of the steam distillate from the slash (waste) of Western red cedar.

[3]The assignment of the absolute stereochemistry was corroborated by the subsequent synthesis of (+)-β-cyperone employing this approach (see **i** →→ **4**).

0008-4042/80/232641-04$01.00/0

©1980 National Research Council of Canada/Conseil national de recherches du Canada

Can. J. Chem. Downloaded from www.nrcresearchpress.com by 210.87.254.42 on 09/05/12
For personal use only.

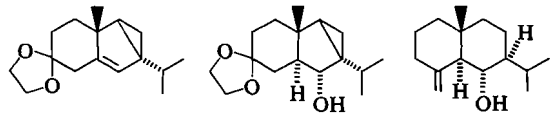
Can. J. Chem. Downloaded from www.nrcresearchpress.com by 210.87.254.42 on 09/05/12
For personal use only.

to achieve this objective by the use of pyrrolidine and acetic acid as shown. In this latter cyclization process the initial product formed is the β,γ-unsaturated ketone **6**. Isolation of **6** is presumably due to the initial formation of the pyrrolidine dienamine intermediate which then undergoes hydrolysis to the product.

The assignment of the double bond in **6** was based on its ultraviolet (λ_{max}: 211 nm, ε = 5 700) and infrared (ν(C=O): 1716 cm^{-1}) spectra, and by its isomerization, in refluxing acetic acid, to the α,β-unsaturated ketone **7** (uv λ_{max}: 234 nm, ε = 13 600; ir ν (C=O, C=C): 1666 cm^{-1}).

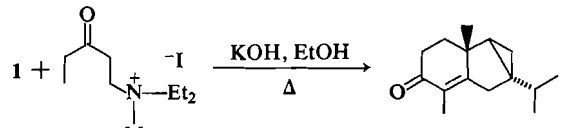
The isomerization of **6** to **7** does not occur readily with acetic acid at room temperature (recovery of starting material after 4 h) but can be achieved in refluxing acetic acid containing a catalytic amount of sulfuric acid.

Ketalisation of **6** by conventional means gave the ketal **8** in almost quantitative yield. Hydroboration of **8** afforded a mixture of alcohols in which the secondary alcohol **9** predominated. The latter compound was isolated in 65% yield by chromatographic purification. The stereochemistry of the 6-hydroxyl function was evident from its proton magnetic resonance spectrum, the large coupling constant (J = 9 Hz) between H-5 and H-6 indicating (4) a diaxial arrangement of these hydrogen atoms. Work is now in progress to convert **9** into (+)-junenol (**10**).

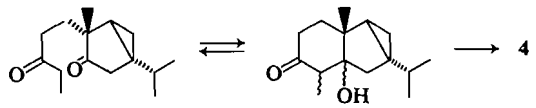


8 **9** **10**

Alternatively, reaction of thujone with ethyl vinyl ketone (generated *in situ* by the action of potassium hydroxide on **11**) in boiling ethanol gave the tricyclic enone **4** in 51% yield. The direct cyclization to **4** under the potassium hydroxide conditions provides an interesting difference from the result obtained in the above-mentioned study where this reagent failed to effect the cyclization of **5**. Presumably the equilibrium between the diketone **i**, formed *in situ* under the conditions employed, and the cyclized aldol product **ii** favors the latter. Furthermore it appears reasonable that the dehydration reaction (**ii** → **4**) is also a facile process, thereby allowing the isolation of **4** directly.

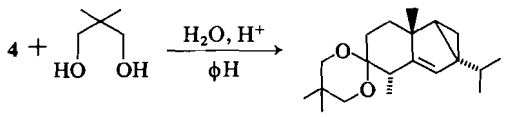


11 **4**



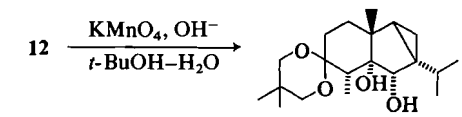
i **ii**

Ketalisation of **4** proceeded with concomitant migration of the double bond to the 5,6 position to give **12** in 89% yield. The latter assignment was evident from the proton magnetic resonance spectrum which exhibited a resonance for a vinyl proton



12

at δ 5.34 (1H, bs). This compound was found to be homogeneous by spectroscopic investigation (270 MHz ^{1}Hmr, ^{13}Cmr) and it was assumed that the 4-methyl group would adopt the more stable α (equatorial) configuration. Treatment of the ketal **12** with potassium permanganate and sodium hydroxide in aqueous *tert*-butyl alcohol (5) gave the diol **13** in 79% yield. Reaction was assumed to have

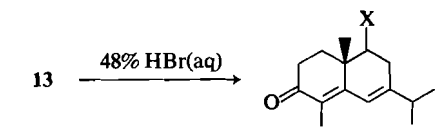


13

taken place from the less hindered (α) face of the molecule. Treatment of **13** with aqueous hydrobromic acid (6) gave the bromodienone **14** in 69% yield. Treatment of the latter with an excess of triphenyltin hydride in benzene gave (+)-β-cyperone (**3**) in 60% yield.

This product gave spectra comparable[4] to those reported in the literature (7, 8) and had an optical rotation of $[\alpha]_{5461}$ +673° (lit. (7) $[\alpha]_{5461}$ +681°) indicating an optical purity of >98.8%.

Hence it has been shown that thujone (**1**) is an extremely efficient chiral synthon and leads to sesquiterpenoids of very high optical purity. Further applications of this approach are under investigation in our laboratory.



14 X = Br
3 X = H)

[4]We differ with R. B. Gammill and T. A. Bryson (8) and assign the ^{13}Cmr resonances at δ 126.47 and 118.34 to C-4 and C-6 respectively on the basis of an off-resonance experiment.

Can. J. Chem. Downloaded from www.nrcresearchpress.com by 210.87.254.42 on 09/05/12
For personal use only.

Experimental

Ultraviolet spectra were recorded on a Cary 15 spectrophotometer using methanol as the solvent. Infrared spectra were recorded on a Perkin-Elmer 457 spectrophotometer. Spectra were obtained with samples as neat films. The ^{1}Hmr spectra were recorded on either a Varian HA- or XL-100 or a 270-MHz spectrometer; ^{13}Cmr spectra were recorded on a Varian CFT-20 instrument. Deuteriochloroform was used as the solvent with TMS as internal standard. Mass spectra were recorded on an Atlas CH-4B or AEI MS-902 instrument. Optical rotations were recorded on a Perkin-Elmer 141 polarimeter. Rotations were obtained using a cell with a pathlength of 10 cm. Microanalyses were carried out by Mr. P. Borda, Microanalytical Laboratory, University of British Columbia. Column chromatography utilized Merck silica gel 60 (70–230 mesh). Preparative and thin layer chromatography utilized Merck silica gel GF_{254}. Petroleum ether refers to the fraction with boiling point 30–60°C.

Diketone 5

A solution of thujone (60 mL, 0.34 mol) and potassium hydroxide (1 g, 0.015 mol) in ethanol (500 mL) under an atmosphere of nitrogen was treated with methyl vinyl ketone (33 mL, 0.41 mol) at a dropwise rate over a period of 8 h. The reaction was stirred for a further 16 h at ambient temperature and then concentrated *in vacuo*. The residue was suction filtered through a short column of silica gel (tlc grade, 80 g) using petroleum ether/ether (3:1 v/v) as eluent (~ 200 mL). The solvent was evaporated and the residue was distilled through a Vigreux column to afford **5** as a pale yellow oil (46 g, 61%); bp 114°C at 0.3 Torr; ir ν_{max}: 3050, 1730, 1716; ^{1}Hmr δ: 2.01 (3H, s), 0.92 (3H, d, J = 7 Hz), 0.85 (3H, s), 0.82 (3H, d, J = 7 Hz), 0.51 (1H, m), −0.11 (1H, dd, J = 4 and 6 Hz); ^{13}Cmr δ: 219.04, 207.25, 50.71, 40.93, 38.25, 32.56, 30.68, 29.87, 27.22, 19.90, 19.79, 18.00, 15.89; ms *m/e*: 222 (M^+), 165, 161, 151, 139, 136, 121 (base peak); $[\alpha]_D$ −46.9° ($CHCl_3$, *c* 3.8). *Anal.* calcd. for $C_{14}H_{22}O_2$: C 75.63, H 9.97; found: C 75.80, H 9.86.

β,γ-Unsaturated Ketone 6

A solution of the diketone **5** (40 g, 0.18 mol) in benzene (400 mL) under an atmosphere of nitrogen was treated with acetic acid (10.5 mL, 0.18 mol) and pyrrolidine (14 mL, 0.17 mol). The reaction mixture was heated at reflux with azeotropic removal of water. After 18 h the reaction was cooled to ambient temperature and treated with sodium acetate (10 g) in aqueous acetic acid (100 mL, 1:1 v/v). After 10 min the reaction mixture was diluted with petroleum ether (200 mL) and separated. The organic portion was washed with hydrochloric acid (3 × 80 mL, 2 *N*), water (2 × 80 mL), sodium bicarbonate solution (1 × 80 mL, 5% w/v), and dried ($MgSO_4$). After evaporation of the solvent, the residue was distilled to afford **6** as a pale yellow oil (29 g, 79%); bp 102°C at 0.4 Torr; uv λ_{max} (ε): 211 (5700), 230 sh (3800), 250 sh (2000) 290 (1300) nm; ir ν_{max}: 3042, 1716, 1650; ^{1}Hmr δ: 5.43 (1H, bs), 1.19 (3H, s), 0.93 (3H, d, J = 7 Hz), 0.81 (3H, d, J = 7 Hz), 0.66 (1H, dd, J = 4 and 8 Hz), 0.28 (1H, t, J = 4 Hz); ^{13}Cmr δ: 207.96, 142.41, 127.57, 46.52, 43.14, 40.41, 38.53, 38.28, 33.58, 30.85, 20.82, 20.60, 19.97, 19.63; ms *m/e*: 204 (M^+), 189, 161, 147, 133, 119, 105 (base peak); $[\alpha]_D$ +313.6° ($CHCl_3$, *c* 2.7). *Anal.* calcd. for $C_{14}H_{20}O$: C 82.30, H 9.87; found: C 82.32, H 9.79.

α,β-Unsaturated Ketone 7

A solution of the ketone **6** (1.0 g, 4.9 mmol) in glacial acetic acid (30 mL) containing sulfuric acid (1 drop) was heated at reflux. After 1 h the reaction was cooled to ambient temperature, diluted with water (100 mL), and extracted with petroleum ether (3 × 30 mL). The combined organic portion was washed with sodium bicarbonate solution (2 × 30 mL, 5% w/v) and dried (Na_2SO_4). After removal of the solvent *in vacuo* the residue was chromatographed on silica gel (80 g) using petroleum ether/ether (3:1 v/v) as eluent. Compound **7** was obtained as a colorless oil (700 mg, 70%); uv λ_{max} (ε): 234 (13 600) nm; ir ν_{max}: 3060, 1666, ^{1}Hmr δ: 5.57 (1H, bs), 1.30 (1H, septet, J = 6.5 Hz), 1.10 (3H, s), 0.90 (3H, d, J = 6.5 Hz), 0.88 (3H, d, J = 6.5 Hz), 0.81 (2H, m); ^{13}Cmr δ: 198.56, 181.04, 119.10, 41.52, 37.84, 37.17, 35.05, 34.87, 33.90, 33,35. 22.47, 20.65; ms *m/e*: 204 (M^+), 189, 176, 161, 147, 133 (base peak), 109; $[\alpha]_D$ +88.4° ($CHCl_3$, *c* 4.3). *Anal.* calcd. for $C_{14}H_{20}O$: C 82.30, H 9.87; found: C 82.60, H 9.71.

Ketal 8

A solution of ketone **6** (37 g, 0.18 mol) in benzene (400 mL) was treated with ethylene glycol (32 mL, 0.57 mol) and *p*-toluenesulfonic acid dihydrate (2 g). The resultant mixture was heated at reflux with azeotropic removal of water. After 4 h the reaction mixture was cooled to ambient temperature, diluted with petroleum ether (200 mL), washed with sodium hydroxide solution (2 × 100 mL, 1 *N*), water (3 × 100 mL), and dried (Na_2SO_4). The solvent was removed *in vacuo* and the residue distilled to give **8** as a pale yellow oil (43 g, 96%); bp 106°C at 0.2 Torr; ir ν_{max}: 3040, 1090; ^{1}Hmr δ: 5.38 (1H, s), 3.92 (4H, m), 1.19 (1H, dd, J = 4 and 8 Hz), 1.08 (3H, s), 0.96 (3H, d, J = 7 Hz), 0.90 (3H, d, J = 7 Hz), 0.61 (1H, dd, J = 4 and 8 Hz), 0.24 (1H, t, J = 4 Hz); ^{13}Cmr δ: 144.58, 126.78, 110.54, 64.34, 64.23, 46.70, 40.11, 37.48, 36.09, 33.70, 31.88, 30.89, 20.82, 20.54, 19.28; ms *m/e*: 248 (M^+, base peak), 233, 203, 186, 171, 161, 147; $[\alpha]_D$ +187.4° ($CHCl_3$, *c* 4.2). *Anal.* calcd. for $C_{16}H_{24}O_2$: C 77.38, H 9.73; found: C 77.60, H 9.83.

Alcohol 9

A 0.5 *M* solution of borane in tetrahydrofuran/1,2-dimethoxyethane (1:1) (400 mL, 0.2 mol) under an atmosphere of nitrogen was treated with a mixture of ketal **8** (20 g, 0.081 mol) and propylene oxide (5 mL). After 1.5 h at ambient temperature the reaction was cooled to 0°C and cautiously treated with aqueous sodium hydroxide (200 mL of 2 *N*) over a period of 30 min. Hydrogen peroxide (200 mL of 30%) was added and the reaction stirred for a further 30 min. Petroleum ether (200 mL) was added and the mixture separated. The organic portion was washed with saturated aqueous sodium bicarbonate (2 × 150 mL) and dried (Na_2SO_4). After removal of the solvent the residue was chromatographed on silica gel (2 × 400 g) using petroleum ether/ethyl acetate (3:1 v/v), then petroleum ether/ethyl acetate/methanol (3:1:0.5 v/v) as eluents. Compound **9** was obtained as a colorless viscous oil (14.1 g, 65%); ir ν_{max}: 3410, 3060, 1102; ^{1}Hmr δ: 4.59 (1H, d, J = 9 Hz), 3.9 (4H, m), 1.01 (3H, d, J = 7 Hz), 0.99 (3H, d, J = 7 Hz), 0.98 (3H, s), 0.63 (1H, t, J = 5 Hz), 0.26 (1H, dd, J = 5 and 7 Hz); ^{13}Cmr δ: 109.31, 75.67, 64.34, 63.62, 48.36, 36.38, 35.41, 34.44, 34.06, 30.96, 30.51, 29.86, 21.90, 20.60, 20.00, 8.13; ms *m/e*: 266 (M^+), 223, 204, 167, 161, 111, 109, 99 (base peak); $[\alpha]_D$ − 14.8° ($CHCl_3$, *c* 1.5). *Anal.* calcd. for $C_{16}H_{26}O_3$: C 72.14, H 9.84; found: C 72.01, H 9.89.

Tricyclic Enone 4

A solution of thujone (60.8 g, 0.4 mol), 1-diethylamino-3-pentanone-methiodide (**11**) (120 g, 0.44 mol), and potassium hydroxide (33 g, 0.5 mol) in ethanol (600 mL) was heated at reflux for 90 min. The solution was cooled and water (1000 mL) and petroleum ether (600 mL) were added. The organic layer was separated and washed with hydrochloric acid (2 × 250 mL, 1 *N*), and water (250 mL), then dried (Na_2SO_4), and evaporated. The residue was distilled collecting the fraction bp 126–128°C at 0.16 Torr. Yield 44 g (51%) of colourless oil; uv λ_{max} (ε): 245 (12 300) nm; ir ν_{max}: 3042, 1678, 1647; ^{1}Hmr δ: 1.65 (3H, d, J = 1.5 Hz), 1.07 (3H, s), 0.91 (3H, d, J = 7 Hz), 0.89 (3H, d, J = 7 Hz), 0.76 (2H, m); ^{13}Cmr δ: 197.84, 174.53, 124.74, 41.97, 36.38, 36.18, 35.93, 35.63, 35.15, 34.15, 33.43, 21.71, 19.87,

Can. J. Chem. Downloaded from www.nrcresearchpress.com by 210.87.254.42 on 09/05/12
For personal use only.

19.69, 11.39; ms *m/e*: 218 (M^+), 203, 175, 161, 147 (base peak); $[\alpha]_D$ +86.8° ($CHCl_3$, *c* 4). *Anal.* calcd. for $C_{15}H_{22}O$: C 82.52, H 10.16; found: C 82.53, H 10.05.

Ketal 12

A solution of enone **4** (14.9 g, 68.3 mmol), 2,2-dimethyl-1,3-propanediol (15 g, 144 mmol), and *p*-toluenesulphonic acid (0.19 g, 1 mmol) in benzene (300 mL) was heated at reflux with azeotropic removal of water for 20 h. The solution was cooled and petroleum ether (200 mL, bp 30–60°C) was added. The solution was washed with saturated aqueous sodium bicarbonate (1 × 200 mL) and water (2 × 200 mL), then dried (Na_2SO_4), and evaporated. The residue was dissolved in a mixture of petroleum ether and ether (200 mL, 9:1 v/v) and filtered through a short column of silica gel (50 g). The filtrate was evaporated to leave the pure ketal as a colourless oil; yield 18.4 g (89%); ir ν_{max}: 3056, 1110; ^{1}Hmr δ: 5.34 (1H, bs), 3.83–3.22 (4H, m), 2.70 (1H, m), 2.18 (1H, q, J = 7 Hz), 1.16 (3H, s), 1.11 (3H, d, J = 7 Hz), 1.07 (3H, s), 0.94 (3H, d, J = 7 Hz), 0.86 (3H, d, J = 7 Hz), 0.69 (3H, s), 0.59 (1H, dd, J = 4 and 8.5 Hz), 0.22 (1H, t, J = 4 Hz); ^{13}Cmr δ: 149.04, 124.74, 100.32, 70.48, 69.69, 47.40, 40.21, 39.72, 36.33, 30.88, 29.77, 23.73, 23.29, 22.25, 20.92, 20.66, 20.56, 19.01, 9.33; ms *m/e*: 304 (M^+), 200, 185, 161, 141 (base peak), 103; $[\alpha]_D$ +149.3° ($CHCl_3$, *c* 2.1). *Anal.* calcd. for $C_{20}H_{32}O_2$: C 78.90, H 10.59; found: C 79.00, H 10.62.

Diol 13

A mixture of ketal **12** (5.3 g, 15.7 mmol), sodium hydroxide (4 g, 100 mmol), and potassium permanganate (5 g, 31.6 mmol) in aqueous *tert*-butanol (1000 mL, 1:1 v/v) was stirred at 0°C for 40 min. Solid sodium metabisulphite was added until a clear solution resulted. The solution was evaporated to ca. half its original volume and then extracted with dichloromethane (3 × 75 mL). The combined extracts were washed with water (2 × 100 mL), dried (Na_2SO_4), and evaporated to leave the diol as a colourless glass, yield 4.67 g (79%); ir ν_{max}: 3470, 1110; ^{1}Hmr δ: 4.81 (1H, s), 3.73 (1H, d, J = 11 Hz), 3.53 (1H, d, J = 11 Hz) 3.30 (2H, dt, J = 11, 2 Hz), 2.51 (2H, dt, J = 13.5, 3 Hz), 1.63 (5H, m), 1.44 (2H, m), 1.33 (1H, t, J = 3 Hz), 1.18 (3H, s), 1.09 (3H, d, J = 7 Hz), 1.06 (3H, s), 1.00 (3H, d, J = 7 Hz), 0.96 (3H, d, J = 7 Hz), 0.95–0.85 (1H, m), 0.75 (3H, s), 0.14 (1H, ddd, J = 8, 5, 1 Hz); ^{13}Cmr δ: 99.12, 80.09, 69.95, 69.14, 47.13, 42.78, 35.52, 35.34, 34.78, 31.75, 29.73, 23.23, 22.25, 20.72, 19.90, 18.37, 11.22, 6.29; ms *m/e*: 338.2447 (M^+, $C_{20}H_{34}O_4$ requires 338.2457); $[\alpha]_D$ +10.4° ($CHCl_3$, *c* 4.64). *Anal.* calcd. for $C_{20}H_{34}O_4$: C 71.01, H 10.01; found: C 71.28, H 10.31.

Bromodienone 14

Diol **13** (1.85 g, 5.48 mmol) was dissolved in petroleum ether (30 mL) and added to ice cold hydrobromic acid (30 mL, 48%). The mixture was rapidly stirred at 0°C for 2 h. The mixture was poured into water (150 mL) and extracted with dichloromethane (3 × 50 mL). The combined extracts were washed with saturated aqueous sodium bicarbonate (2 × 50 mL), dried (Na_2SO_4), and evaporated. The residue was taken up in a mixture of petroleum ether and ether (100 mL of 9:1 v/v) and filtered through a short plug of silica gel (10 g). The filtrate was evaporated to leave the bromodienone as a colourless oil, yield 1.10 g (68%); uv λ_{max} (ε): 293 (24 100) nm; ir ν_{max}: 1660, 1622, 1580; ^{1}Hmr δ: 6.36 (1H, s), 4.2 (1H, t, J = 8 Hz), 2.9–2.1 (7H, m), 1.88 (3H, s), 1.18 (3H, s), 1.16 (6H, d, J = 7 Hz); ^{13}Cmr δ: 198.3, 154.7, 128.6, 119.1, 61.6, 38.69, 36.15, 35.6, 34.8, 33.5, 31.4, 29.9, 16.23, 10.71; ms *m/e*: 296.0768 (M^+, $C_{15}H_{21}OBr^{79}$ requires 296.0775); $[\alpha]_D$ +430° ($CHCl_3$, *c* 1).

(+) β-Cyperone 3

Bromodienone **15** (0.35 g, 1.18 mmol) was dissolved in dry benzene (5 mL) and added to a solution of triphenyltin hydride (0.72 g, 2.05 mmol) in dry benzene. AIBN (16 mg, 0.1 mmol) was added and the mixture heated to 80°C under nitrogen for 2 h. A further portion of AIBN (16 mg) was added and the reaction maintained at 50°C for 16 h. The mixture was evaporated and the residue chromatographed on silica gel to give (+)-β-cyperone as a colourless oil, yield 0.154 g (60%); (ε): 297 (32 970) nm; ir ν_{max}: 1655, 1620, 1580; ^{1}Hmr δ: 6.29 (1H, s), 2.85–2.05 (5H, m), 1.78 (3H, s), 1.75–1.30 (4H, m), 1.2–1.0 (9H, m); ^{13}Cmr δ: 199.15, 156.22, 126.48, 118.35, 37.27, 36.53, 36.19, 33.94, 33.27, 23.77, 21.54, 21.14, 10.12; uv λ_{max} ms *m/e*: 218 (M^+); $[\alpha]_{5461}$ +673° ($CHCl_3$, *c* 0.108).

Acknowledgements

Financial aid from the Science Council of British Columbia is gratefully acknowledged. The authors would also like to thank MacMillan Bloedel Limited for generous supplies of cedar leaf oil.

1. J. P. KUTNEY, J. BALSEVICH, R. CARRUTHERS, A. MARKUS, M. J. MCGRATH, R. N. YOUNG, and B. R. WORTH. Bioorg. Chem. 7, 289 (1979).
2. J. P. KUTNEY, M. J. MCGRATH, R. N. YOUNG, and B. R. WORTH. Can. J. Chem. **57**, 3145 (1979).
3. C. H. HEATHCOCK. *In* The total synthesis of natural products. Vol. 2. *Edited by* J. ApSimon. Wiley-Interscience, New York. 1973. p. 285, and references therein.
4. M. KARPLUS. J. Chem. Phys. **30**, 11 (1959); J. Phys. Chem. **64**, 1793 (1960).
5. K. B. WIBERG and K. A. SAEGEBARTH. J. Am. Chem. Soc. **79**, 2822 (1957).
6. M. JULIA and J. M. PARIS. Tetrahedron Lett. 3445 (1974); M. JULIA, S. JULIA, and R. GUÉGAN. Bull. Soc. Chim. Fr. 1072 (1960).
7. R. HOWE and F. J. MCQUILLIN. J. Chem. Soc. 2423 (1955).
8. R. B. GAMMILL and T. A. BRYSON. Synth. Commun. **6**, 209 (1976).

Direct transformation of carboxylic acids to thiol esters induced by phenyl dichlorophosphate

HSING-JANG LIU AND SUBRAMANIAM IYER SABESAN

Department of Chemistry, University of Alberta, Edmonton, Alta., Canada T6G 2G2

Received July 9, 1980

This paper is dedicated to Prof. Raymond U. Lemieux on the occasion of his 60th birthday

HSING-JANG LIU and SUBRAMANIAM IYER SABESAN. Can. J. Chem. **58**, 2645 (1980).

The condensation of carboxylic acids and thiols is greatly facilitated by the use of phenyl dichlorophosphate as an activating agent giving thiol esters in good yields.

HSING-JANG LIU et SUBRAMANIAM IYER SABESAN. Can. J. Chem. **58**, 2645 (1980).

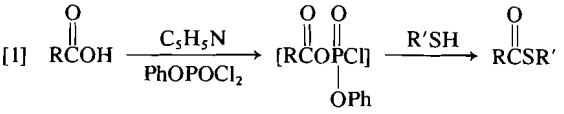
L'emploi du dichlorophosphate de phényle comme agent activant facilite grandement la condensation des acides carboxyliques sur les thiols qui donne les thioesters avec de bons rendements.

[Traduit par le journal]

Can. J. Chem. Downloaded from www.nrcresearchpress.com by 210.87.254.5 on 09/05/12
For personal use only.

The thiol ester is a versatile functional group which facilitates the formation of carbon–carbon bonds and the preparation of a number of important functionalities (1). The growing importance of thiol esters in organic synthesis has stimulated the recent extensive research (1*h*, 2) toward improved methods for their direct preparation from carboxylic acids.[1] A year ago, we described a convenient procedure (2*h*) for the condensation of carboxylic acids and thiols under mild reaction conditions using *N*,*N*-dimethylphosphoramidic dichloride as an activating agent. Further investigation of other phosphorus-containing analogs has revealed that the commercially available[2] (and relatively inexpensive) phenyl dichlorophosphate is a superior reagent which effects the condensation under equally mild conditions giving thiol esters in generally better yields than those obtained using *N*,*N*-dimethylphosphoramidic dichloride. In this article we wish to report these results.

In the presence of phenyl dichlorophosphate and pyridine, the condensation of carboxylic acids and thiols (eq. [1]) occurs smoothly at room temperature. A total of fifteen functionally diverse carboxylic acids were studied using a simple general procedure involving the sequential addition of pyridine (3 equiv.), a thiol (2 equiv.), and phenyl dichlorophosphate (1.5 equiv.) to a solution of a carboxylic acid in 1,2-dimethoxyethane (5 mL/mmol of carboxylic acid). Although in each case the appearance of product on tlc analysis of the reaction mixture was rapid (< 20 min), the reaction was conveniently[3] allowed to continue overnight (15–16 h) to ensure the complete consumption of starting material.



[1] $RCOH \xrightarrow[PhOPOCl_2]{C_5H_5N} [RCOPCl]\ (OPh) \xrightarrow{R'SH} RCSR'$

The generality of the reaction is apparent from the results compiled in Table 1. We wish to emphasize that the reaction conditions employed are near-neutral and sufficiently mild to be widely applicable to acid (entries 7, 8, 12, 13, 17, and 18) and/or base (entries 13, 17, and 18) sensitive compounds. Furthermore, unlike most of the existing methods,[4] the present procedure is applicable to thiols of a broad spectrum of structural types ranging from 1°–3°, as well as phenyl and benzyl ones. The reaction is independent of the steric environment of the thiol; *tert*-butyl mercaptan (entries 6, 10, 15, and 17) gave products in yields comparable with those from sterically less hindered ones.

The utility of the direct transformation of carboxylic acid to thiol ester without the isolation of an active acid derivative is emphasized in the conversion of cyanoacetic acid into the corresponding *tert*-butyl (entry 17) and benzyl (entry 18) thiol esters. The acid chloride of cyanoacetic acid is known to undergo spontaneous polymerization (4) and attempts to prepare thiol ester derivatives via cyanoacetyl chloride (either isolated or generated *in situ*) met with little success.

We have briefly examined the use of chlorophosphates $(PhO)_2POCl$ and $(EtO)_2POCl$ as activating agents under the conditions described above and have found them to be less effective than phenyl dichlorophosphate. For example, when the condensation of cyanoacetic acid and benzyl mercap-

[1]For examples of other methods for thiol ester formation, see refs. 1*a*, 1*b*, 1*h*, 1*i*, 1*u*, and 3.

[2]Since completion of the present studies, *N*,*N*-dimethylphosphoramidic dichloride has been marketed by Fluka.

[3]The disappearance of the starting material is difficult to monitor by conventional means (tlc/gc).

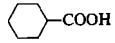
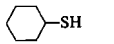
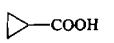
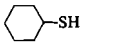
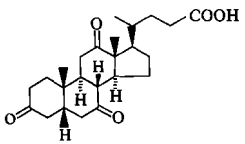
[4]For a relevant discussion, see ref. 3*c*.

0008-4042/80/232645-04$01.00/0

©1980 National Research Council of Canada/Conseil national de recherches du Canada

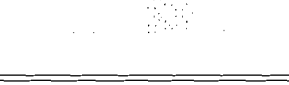
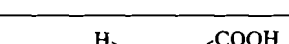
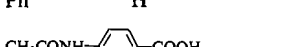
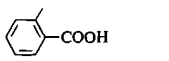
Can. J. Chem. Downloaded from www.nrcresearchpress.com by 210.87.254.5 on 09/05/12
For personal use only.

TABLE 1. Thiol ester formation (RCOOH + R′SH → RCOSR′)

Entry	RCOOH	R′SH	Product: Yield (%)	Infrared (cm^{-1})[e,f]	Nuclear magnetic resonance (δ)[f,j]	Mass spectra[m,n]	Analysis[n]
1	$EtOCH_2COOH$	$PhCH_2SH$	100	1680, 1600, 1585	1.17 (t, 3H, J = 7 Hz), 3.51 (q, 2H, J = 7 Hz), 3.97 (s, 2H), 4.01 (s, 2H), 7.18 (br s, 5H)	210.0713 (210.0714)	C 62.97, H 6.77, S 15.28 (C 62.83, H 6.71, S 15.25)
2	$CH_3(CH_2)_{14}COOH$	PhSH	99[a]	1713, 1585[g]	0.93 (t, 3H, J = 6 Hz), 2.58 (t, 2H, J = 7 Hz), 7.33 (s, 5H)	348.2486 (348.2487)	C 75.81, H 10.31, S 9.16 (C 75.80, H 10.41, S 9.20)
3		$PhCH_2SH$	92	1687, 1605, 1590	3.99 (s, 2H), 7.16 (s, 5H)	234.1080 (234.1078)	C 71.58, H 7.80, S 13.55 (C 71.75, H 7.74, S 13.68)
4		PhSH	100	1700, 1580	7.31 (s, 5H)	220.0919 (220.0922)	C 71.15, H 7.26, S 14.31 (C 70.87, H 7.32, S 14.55)
5	$PhOCH_2COOH$	$PhCH_2SH$	99[b]	1682, 1597, 1589[g]	4.04 (s, 2H), 4.53 (s, 2H), 6.76–6.98 (complex, 3H), 7.11–7.28 (complex, 2H), 7.17 (s, 5H)	258.0710 (258.0715)	C 70.01, H 5.53, S 12.14 (C 69.74, H 5.46, S 12.41)
6		t-BuSH	98	1670, 1595, 1587	1.44 (s, 9H), 4.44 (s, 2H), 6.78–7.31 (complex, 5H)	224.0871 (224.0871)	C 64.51, H 7.19, S 14.32 (C 64.25, H 7.19, S 14.29)
7	$CH_2{=}CH(CH_2)_8COOH$		88	1685, 1640	2.42 (t, 2H, J = 7 Hz), 3.44 (m, 1H), 4.94 (md, 1H, J = 18 J' < 1 Hz), 5.01 (md, 1H, J = 10 J' < 1 Hz), 5.74 (tdd, 1H, J = 18 J' = 10, J'' = 7 Hz)	282.2023 (282.2018)	C 72.13, H 10.42, S 11.08 (C 72.28, H 10.71, S 11.35)
8			97	1675	0.67–1.18 (complex, 4H), 3.49 (m, 1H)	184.0921 (184.0921)	C 65.35, H 8.69, S 17.10 (C 65.17, H 8.75, S 17.40)
9	$PhOCHCOOH$ CH_3	n-BuSH	99	1675, 1597, 1587	0.89 (t, 3H, J = 6 Hz), 1.52 (d, 3H, J = 7 Hz), 2.72 (t, 2H, J = 7 Hz), 4.67 (q, 1H, J = 7 Hz) 6.76–7.31 (complex, 5H)	238.1027 (238.1027)	C 65.62, H 7.55, S 13.38 (C 65.51, H 7.61, S 13.45)
10		t-BuSH	98	1670, 1597, 1585	1.41 (s, 9H), 1.51 (d, 3H, J = 7 Hz), 4.52 (q, 1H, J = 7 Hz), 6.76–7.31 (complex, 5H)	238.1027 (238.1027)	C 65.54, H 7.72, S 13.22 (C 65.51, H 7.61, S 13.45)
11		PhSH	95[c]	1720, 1706, 1580[g]	0.86 (d, 3H, J = 6 Hz), 1.04 (s, 3H), 1.37 (s, 3H), 7.39 (s, 5H)[k]	Base peak 385.2387 (calcd. for $C_{24}H_{33}O_4$: 385.2378)	C 72.64, H 7.61, S 6.53 (C 72.84, H 7.74, S 6.48)

Can. J. Chem. Downloaded from www.nrcresearchpress.com by 210.87.254.5 on 09/05/12
For personal use only.

TABLE 1 (*Concluded*)

Entry	RCOOH	R′SH	Product: Yield (%)	Product: Infrared (cm^{-1})[e,f]	Product: Nuclear magnetic resonance (δ)[f,j]	Product: Mass spectra[m,n]	Product: Analysis[n]
12		*n*-BuSH	100	1654, 1609, 1601, 1590[g]	0.91 (t, 3H, J = 6 Hz), 2.91 (t, 2H, J = 7 Hz), 6.15 (d, 1H, J = 15 Hz), 6.76–7.55 (complex, 8H)	246.1077 (246.1079)	C 73.02, H 7.42, S 12.87 (C 73.13, H 7.37, S 13.01)
13		PhSH	96[d]	3310, 1670, 1605, 1588, 1522[h]	2.15 (s, 3H), 7.45 (s, 5H), 7.72 (d, 2H, J = 9 Hz), 7.99 (d, 2H, J = 9 Hz)[i]	271.0664 (271.0667)	C 66.34, H 4.90, N 5.27, S 11.82 (C 66.40, H 4.83, N 5.16, S 11.82)
14			88	1675	1.17 (s, 9H), 3.33 (m, 1H)	200.1232 (200.1235)	C 65.81, H 10.08, S 16.07 (C 65.95, H 10.06, S 16.00)
15		*t*-BuSH	82	1690, 1665	1.46 (s, 9H), 1.62 (d, 3H, J = 8 Hz), 4.25 (q, 1H, J = 8 Hz)	Base peak 57.0718 (calcd. for C_4H_9 57.0704)	C 46.47, H 7.08, Cl 19.45, S 17.81 (C 46.53, H 7.25, Cl 19.62, S 17.74)
16		PhSH	78	3430, 1705, 1585	0.89 (t, 3H, J = 6 Hz), 2.64 (t, 2H, J = 7 Hz), 3.55 (m, 1H), 7.38 (s, 5H)[k]	392.2751 (392.2748)	C 73.48, H 10.56, S 8.15 (C 73.42, H 10.27, S 8.17)
17	$NCCH_2COOH$	*t*-BuSH	65	2259, 1685[l]	1.45 (s, 9H), 3.48 (s, 2H)	Base peak 57.0725 (calcd. for C_4H_9 57.0704)	C 53.46, H 7.35, N 9.08, S 20.58 (C 53.47, H 7.05, N 8.91, S 20.39)
18		$PhCH_2SH$	89	2250, 1685, 1595, 1575	3.43 (s, 2H), 4.09 (s, 2H), 7.21 (s, 5H)	191.0403 (191.0405)	C 63.02, H 4.72, N 7.15 S 16.84 (C 62.80, H 4.74, N 7.32, S 16.71)
19		PhSH	98	1690, 1600, 1580, 1570	2.45 (s, 3H), 6.89–8.11 (complex, 9H)	228.0605 (228.0609)	C 73.83, H 5.29, S 14.01 (C 73.65, H 5.30, S 14.04)

[a]Melting point 28–29°C (ether–cyclohexane).
[b]Melting point 48–49°C (ether–cyclohexane).
[c]Melting point 207–208°C (chloroform–ether).
[d]Melting point 181–182°C (methanol–ether).
[e]Except where otherwise stated, the ir spectra were obtained on neat liquid.
[f]Only diagnostic signals are cited.
[g]Obtained in chloroform.
[h]Taken in KBr pellet.
[i]Obtained in carbon tetrachloride.
[j]Except where otherwise stated, the nmr spectra were obtained on solutions in carbon tetrachloride with tetramethyl silane as internal reference.
[k]Taken in chloroform-*d*.
[l]Taken in methanol-d_4.
[m]Molecular ions are given with the exception of entries 11, 15, and 17 in which cases molecular ions were not detected.
[n]Calculated values are given in parentheses.

tan was carried out using $(PhO)_2POCl$ or $(EtO)_2POCl$, low yields (<30%) of the desired product were obtained.

Experimental

General and Material

Melting points were determined on a Kofler hot stage apparatus and are uncorrected. Infrared spectra were recorded on a Perkin-Elmer model 457 or Nicolet 7-199 FT-IR spectrophotometer. Nuclear magnetic resonance spectra were recorded on Varian A-60 and 90 MHz Perkin-Elmer 32 spectrometers. Mass spectra were recorded using an A.E.I. Model MS 50 mass spectrometer. Elemental analyses were performed by the microanalytical laboratory of this department. Pyridine was distilled over potassium hydroxide and 1,2-dimethoxyethane was freshly distilled over lithium aluminum hydride. Commercially available carboxylic acids, thiols, and phenyl dichlorophosphate (Aldrich) were used without purification.

Conversion of Carboxylic Acids to Thiol Esters

The conditions used for the transformation of the carboxylic acids studied to the corresponding thiol esters were identical to those illustrated below with ethoxyacetic acid. Physical data and yields of all products are compiled in Table 1.

To a solution of ethoxyacetic acid (208 mg, 2 mmol) in 1,2-dimethoxyethane (10 mL) at 0°C, were added pyridine (475 mg, 6 mmol), benzyl mercaptan (496 mg, 4 mmol), and phenyl dichlorophosphate (633 mg, 3 mmol). After stirring at room temperature under an argon atmosphere for 16 h, the reaction mixture was poured into ice-cold aqueous 1 *N* NaOH (20 mL) and extracted with chloroform. The extracts were washed with aqueous 1 *N* NaOH and saturated aqueous sodium chloride. Drying ($MgSO_4$), filtration, and concentration gave an oily product which was purified by column chromatography on silica gel. Elution with benzene gave benzyl ethoxyethanothioate (420 mg; 100% yield).

Acknowledgments

We are grateful to the Natural Sciences and Engineering Research Council of Canada and the University of Alberta for financial support.

1. (*a*) V. Prelog, J. Norymberski, and O. Jeger. Helv. Chim. Acta, **29**, 360 (1946); (*b*) M. L. Wolfrom and J. V. Karabinos. J. Am. Chem. Soc. **68**, 742 (1946); (*c*) P. A. Bobbio. J. Org. Chem. **26**, 3023 (1961); (*d*) H. J. Bestmann and B. Arnason. Chem. Ber. **95**, 1513 (1962); (*e*) D. E. Bublitz. J. Org. Chem. **32**, 1630 (1967); (*f*) J. Šavrda and D. H. Veyrat. Tetrahedron Lett. 6253 (1968); (*g*) T. Kumamoto and T. Mukaiyama. Bull. Chem. Soc. Jpn. **41**, 2111 (1968); (*h*) K. Lloyd and G. T. Young. J. Chem. Soc. C, 2890 (1971); (*i*) T. Mukaiyama, M. Araki, and H. Takei. J. Am. Chem. Soc. **95**, 4763 (1973); (*j*) R. J. Anderson, C. A. Henrick, and L. D. Rosenblum. J. Am. Chem. Soc. **96**, 3654 (1974); (*k*) J. Wemple. Tetrahedron Lett. 3255 (1975); (*l*) D. J. Dagli, P.-S. Yu, and J. Wemple. J. Org. Chem. **40**, 3173 (1975); (*m*) S. Masamune, Y. Hayase, W. Schilling, W. K. Chan, and G. S. Bates. J. Am. Chem. Soc. **99**, 6756 (1977); (*n*) E. J. Corey and S. Bhattacharyya. Tetrahedron Lett. 3919 (1977); (*o*) Y. Nagao, K. Kawabata, and E. Fujita. Chem. Commun. 330 (1978); (*p*) I. Ernest, J. Gosteli, C. W. Greengrass, W. Holick, D. E. Jackman, H. R. Pfaendler, and R. B. Woodward. J. Am. Chem. Soc. **100**, 8214 (1978); (*q*) M. J. S. Lobo and H. J. Chaves das Neves. Tetrahedron Lett. 2171 (1978); (*r*) Y. Kobuke and J. C. Yoshida. Tetrahedron Lett. 367 (1978); (*s*) H. J. Liu and H. K. Lai. Tetrahedron Lett. 1193 (1979); (*t*) H. J. Liu, H. K. Lai, and S. K. Attah-Poku. Tetrahedron Lett. 4121 (1979); (*u*) H. J. Liu and H. K. Lai. Can. J. Chem. **57**, 2522 (1979), and references cited therein.
2. (*a*) M. V. A. Baig and L. N. Owen. J. Chem. Soc. C, 540 (1966); (*b*) B. I. Stepanov and G. I. Migachev. J. Gen. Chem. USSR, **36**, 1364 (1966); (*c*) A. Pelter, T. Levitt, and K. Smith. Chem. Commun. 435 (1969); (*d*) S. Yamada, Y. Yokoyama, and T. Shioiri. J. Org. Chem. **39**, 3302 (1974); (*e*) F. Souto-Bachiller, G. S. Bates, and S. Masamune. Chem. Commun. 719 (1976); (*f*) K. Horiki. Synth. Commun. **7**, 251 (1977); (*g*) P. A. Grieco, Y. Yokohama, and E. Williams. J. Org. Chem. **43**, 1283 (1978); (*h*) H. J. Liu, S. P. Lee, and W. H. Chan. Synth. Commun. **9**, 91 (1979); (*i*) E. J. Corey and D. A. Clark. Tetrahedron Lett. 2875 (1979).
3. (*a*) T. Mukaiyama, R. Matsued, and H. Maruyama. Bull. Chem. Soc. Jpn. **43**, 1271 (1970); (*b*) T. Mukaiyama. Synth. Commun. **2**, 243 (1972); (*c*) S. Masamune, S. Kamata, J. Diakur, Y. Sugihara, and G. S. Bates. Can. J. Chem. **53**, 3693 (1975); (*d*) S. Masamune, S. Kamata, and W. Schilling. J. Am. Chem. Soc. **97**, 3515 (1975); (*e*) E. J. Corey and D. J. Brunelle. Tetrahedron Lett. 3409 (1976); (*f*) G. S. Bates, J. Diakur, and S. Masamune. Tetrahedron Lett. 4423 (1976); (*g*) T. Cohen and R. E. Gapinski. Tetrahedron Lett. 4319 (1978); (*h*) D. N. Harpp, T. Aida, and T. H. Chan. Tetrahedron Lett. 2853 (1979); (*i*) H. J. Liu, S. K. Attah-Poku, and H. K. Lai. Synth. Commun. **9**, 883 (1979).
4. G. Schroeter and Chr. Seidler. J. Prakt. Chem. **105**, 165 (1922).

Can. J. Chem. Downloaded from www.nrcresearchpress.com by 210.87.254.5 on 09/05/12
For personal use only.

A nuclear Overhauser effect difference study of the solution conformation of (6*R*)-prostaglandin I_1[1]

GEORGE KOTOVYCH[2] AND GERDY H. M. AARTS
Department of Chemistry, University of Alberta, Edmonton, Alta., Canada T6G 2G2

Received June 23, 1980

This paper is dedicated to Prof. Raymond U. Lemieux on the occasion of his 60th birthday

GEORGE KOTOVYCH and GERDY H. M. AARTS. Can. J. Chem. **58**, 2649 (1980).

Proton magnetic resonance studies at 400 MHz allowed the complete assignment of the spectra for (6*R*)-prostaglandin I_1 in phosphate buffer and in $CDCl_3$ solutions. The spectral analysis was based on the nuclear Overhauser effect difference measurements, which also provide accurate chemical shifts and coupling constants. Conformational differences in the two solvents for the ring portion of the molecule are indicated.

GEORGE KOTOVYCH et GERDY H. M. AARTS. Can. J. Chem. **58**, 2649 (1980).

Les études de rmn du ^1H à 400 MHz permettent d'identifier complètement les spectres de la (6*R*)-prostaglandine I_1 en solutions dans un tampon de phosphate et dans le $CDCl_3$. On a analysé les spectres en se basant sur la mesure de la différence d'effet Overhauser nucléaire qui fournit également avec précision les déplacements chimiques et les constantes de couplage. On a indiqué les différences conformationnelles de la partie cyclique de la molécule dans les deux solvants.

[Traduit par le journal]

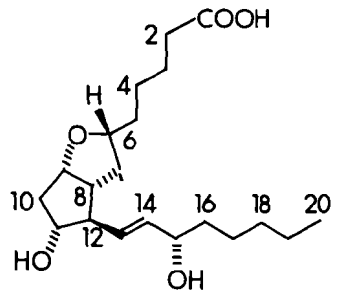
Introduction

Since the discovery of prostacyclin (PGI_2) in 1976 (1), and its structure determination (2), the design of stable prostacyclin analogs has received considerable attention (ref. 3, and references therein). Prostacyclin is extremely important in the cardiovascular system; prostacyclin and chemical analogs may find a use in therapy for states in which excessive platelet aggregation takes place in the circulation (ref. 4, and references therein). Prostacyclin is unstable, and in blood at 37°C it has a half-life of 2–3 minutes, whereas at pH 10.5 at 25°C it has a half-life of 100 hours (4). Because of the PGI_2 instability, and its extreme biological importance, a variety of stable analogs has been prepared, among them 5,6-dihydroprostacyclin, or prostaglandin I_1 (PGI_1) (5–9). The chemical proof of the stereochemistry at C-6 of the PGI_1 isomers was provided by Nelson (7). The stereochemistry at C-5 and C-6 of all products associated with the synthesis of 13,14-dehydroprostacyclin methyl ester has also been assigned (10). The nomenclature for prostacyclin analogs has been discussed (11) and the two epimers (at C-6) are designated (6*R*)-PGI_1, and (6*S*)-PGI_1.

The biological activity of these two epimers has been extensively studied (9, 12–15). Crane *et al.* (12) studied six analogs of PGI_2 and their ability to inhibit platelet aggregation. Their results indicate that the orientation of the α chain may play a key role in explaining the potency of these compounds with respect to PGI_2. The results also indicate that platelets are much more sensitive to structural variations in the PGI_2 molecule than smooth muscle of the gerbil colon or rat uterus. This suggests specificity in the platelet receptor which may prove useful for pharmacological manipulation (12). We have studied the conformation of (6*R*)-PGI_1 (Fig. 1), also referred to as *endo* or α-PGI_1, using high-field proton magnetic resonance techniques. In this way, we hope to correlate the structure and activity of these compounds in solution.

Materials and Methods

The (6*R*)-PGI_1 was a gift from Dr. R. A. Johnson of the Upjohn Co., Kalamazoo, MI. The present measurements were



(6R)-PGI$_1$

FIG. 1. Structure of (6*R*)-PGI_1.

[1]This paper is No. 6 in a series of high-field nmr studies on prostaglandins and vitamins. Paper No. 5 is ref. 21.

[2]Formerly G. Kotowycz.

0008-4042/80/232649-11$01.00/0

©1980 National Research Council of Canada/Conseil national de recherches du Canada

Can. J. Chem. Downloaded from www.nrcresearchpress.com by 210.87.254.6 on 09/05/12
For personal use only.

Can. J. Chem. Downloaded from www.nrcresearchpress.com by 210.87.254.6 on 09/05/12
For personal use only.

carried out both in phosphate buffer (0.2 *M*) in D_2O and in $CDCl_3$. The $CDCl_3$ was purified by treating it with Al_2O_3 (B.D.H. Chemicals) and vacuum degassing it several times using the freeze–pump–thaw technique. The required amount of $CDCl_3$, 0.40 mL, was added to the preweighed (6*R*)-PGI_1, 2.8 mg. The solution was then transferred to an nmr tube, and was vacuum degassed several times. Subsequently, the nmr tube was sealed. Several samples were prepared for the nmr measurements in this manner. In addition, a (6*R*)-PGI_1 solution in $CDCl_3$ was prepared to exchange the —OH and —COOH protons for deuterons. This was accomplished by preparing an additional sample with a drop of D_2O, degassing the sample, and then sealing off the nmr tube. The concentration of (6*R*)-PGI_1 in all samples was ~0.02 *M*. The buffer was made up using 99.96% D_2O (Merck, Sharp and Dohme Canada Ltd.) and KH_2PO_4 (Amachem) and the pH was adjusted to 7.0 (uncorrected meter reading) using 40% (w/w) NaOD in D_2O (Merck, Sharp and Dohme Canada Ltd.). The buffer was then dried by pumping off the solvent, and the exact amount of degassed D_2O was added to the dried buffer *in vacuo*. The final phosphate concentration was 0.2 *M* and the uncorrected pH was 7.0. This procedure was followed to minimize the solvent HDO resonance in the nmr spectrum. The (6*R*)-PGI_1 was weighed out in a container and the required amount of buffer solution was added for a final concentration of 0.02 *M*. The solution was transferred into the nmr tube, vacuum degassed three times, and the nmr tube was sealed. Two samples were prepared in this manner. With the exception of the pH adjustment, all sample preparations were carried out in a dry box under a nitrogen gas atmosphere. All glassware was cleaned extensively to eliminate paramagnetic impurities (16). The reference compounds TSP-d_4 for the buffer solution and TMS for the $CDCl_3$ solution were added to the solutions as reference standards after the completion of all other nmr experiments.

The nmr measurements were carried out in the Fourier transform mode using the Bruker WH-400/DS NMR spectrometer and the Aspect 2000 Data System utilizing 16 or 32K of data memory. All of the experiments were carried out at ambient temperature (298 K). The deuterium resonance of the solvents was used for the lock signal. The homonuclear decoupling experiments were also performed in the pulse mode. The chemical shifts and coupling constants were calculated to first order at 400 MHz and are reported with an accuracy of about ±0.010 ppm and ±0.20 Hz, respectively. For maximum accuracy, spectra were expanded to a width of 2 Hz/cm.

The nuclear Overhauser effect (nOe) difference experiments were carried out at 400 MHz. This involves the measurement of the intensity change of a proton resonance upon saturating another proton. A strong nOe indicates that the two protons are in close proximity. The experimental procedure will be described briefly (17–19). The decoupler, operating in the gated mode, was set on resonance for a time (12 s) greater than 5 times the longest T_1 value for the protons of the molecule to build up the nOe. It was gated off during acquisition. Four free induction decay signals were accumulated. The memory was then negated and the experiment was repeated with the decoupler off-resonance (control spectrum). The off-resonance frequency was placed to high field of TMS. These four free induction decay (FID) signals were thus compared with the original four. In order to achieve steady state, the first 16 scans were eliminated. The cycle was repeated until the required number of transients was accumulated. After collecting the FID's, the signal was Fourier transformed. A 90° pulse (10.7 μs) was used as well as some exponential line broadening. Experiments were carried out as a function of the irradiating field power levels using both the homo and the gated modes of operation. All of the results are self consistent. Very small nOe's of about 1–2% were detected, as can be seen from the spectra. The measurements on (6*R*)-PGI_1 in $CDCl_3$ with a trace of D_2O were carried out at saturating power levels. However, in order not to perturb neighboring multiplets when a given multiplet is irradiated, subsaturating power levels were used for the other measurements. These power levels were sufficiently high so that all nOe's were observed.

Results

Several techniques were used in the assignment of the proton resonances as well as in determining the chemical shifts and coupling constants in both solvents. These include the nOe difference experiments, double resonance, and inversion recovery techniques. The resonances for H-2, H-13 and 14, H-17 to 19, and H-20 were assigned on the basis of their characteristic chemical shifts. In the $CDCl_3$ solution, some of the other proton resonances including H-3, H-8, H-12, and H-15 were assigned on the basis of homonuclear proton decoupling experiments. The multiplets corresponding to the H-7α, H-7β, H-10α, and the H-10β protons were thus also identified, and were definitively assigned using the nOe difference experiments. Several of the decoupling experiments will be briefly described. Decoupling of the multiplet corresponding to H-2, H-8, and H-12, which have nearly equivalent shifts, results in a change in the multiplicity for H-13 and H-11 (decoupling of H-12) and for H-9 (decoupling of H-8). Changes in the high-field region were also observed, where H-3 and H-7α resonate. Further decoupling of either the H-9 or the H-11 multiplets results in a doublet of doublets for both H-10α and H-10β. Decoupling of H-14 results in a triplet for H-15. The triplet is due to the coupling with H-16 and 16*. Finally, decoupling of H-3 results in a singlet for H-2. In this way the H-3 chemical shift was verified.

The H-9 and H-11 multiplets were conclusively assigned on the basis of the nOe experiments. When H-9 is saturated (Fig. 2B), an nOe is observed for H-6, H-8, and H-10β, all of which are in the β configuration with respect to the ring. This proves the assignment of H-9. In Fig. 2C, saturation of H-11 results in an nOe for H-10β, H-8 and /or H-12, and H-13 and H-14. These results confirm the assignment of H-11. In fact, the chemical shifts of H-9, H-15, and H-11 from low to high field, respectively, fall in the same order as was observed for PGI_2 previously (20). The chemical shift for H-10β is obtained from both of these experiments. Saturation of H-6 (Fig. 3B) results in an enhancement for H-9, H-8, H-7β, and for two multiplets at high field. H-7β is assigned since H-6, H-8, and H-9 are all β to the ring. The two high-field multiplets may possibly be assigned to H-3 and H-5 and 5*. Partial

Can. J. Chem. Downloaded from www.nrcresearchpress.com by 210.87.254.6 on 09/05/12
For personal use only.

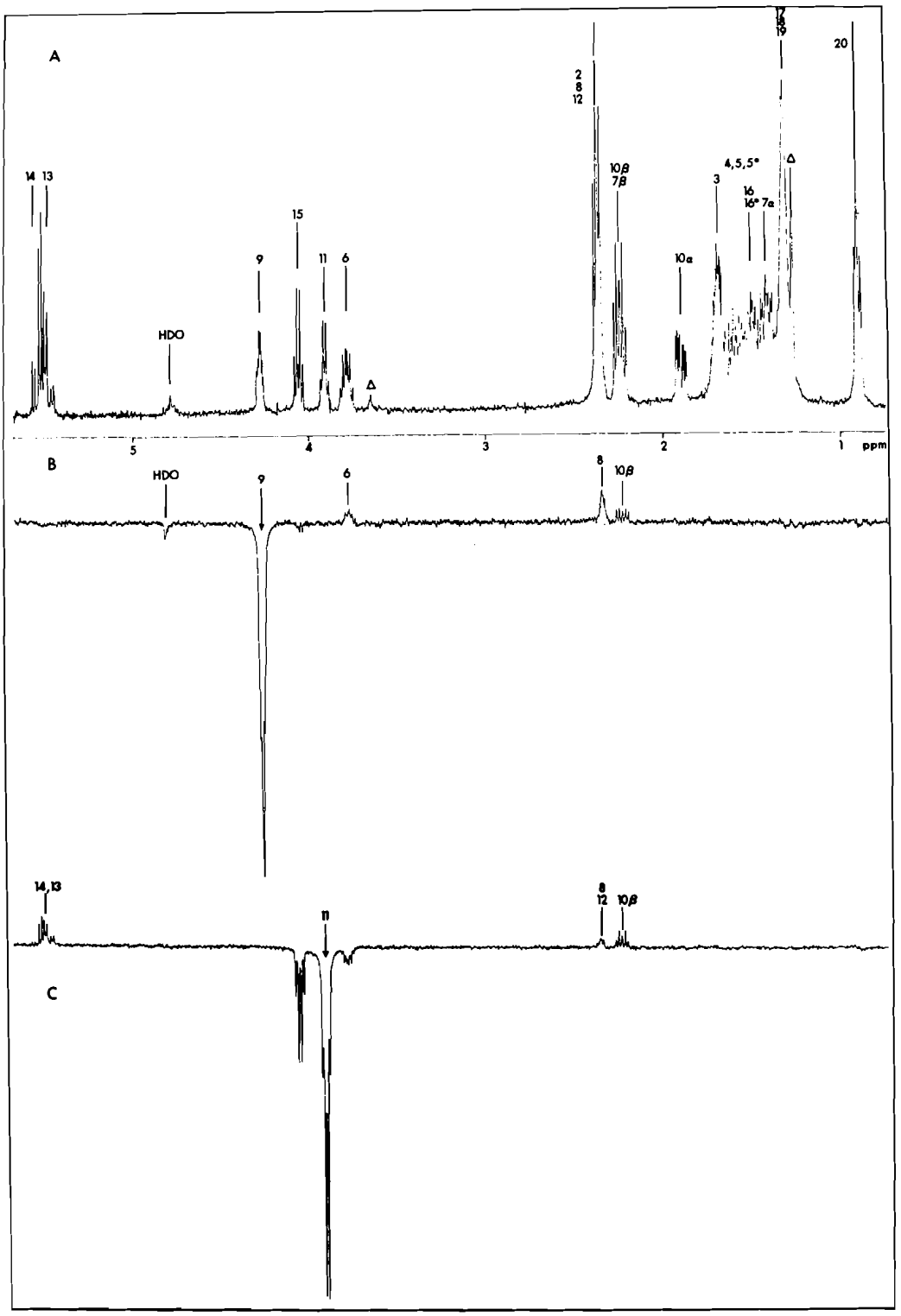


FIG. 2. Results of the nOe difference experiments. (A) General spectrum of (6*R*)-PGI$_1$ in $CDCl_3$ with a trace of D_2O. The protons are assigned as discussed in the text. In (B), H-9 is saturated and in (C), H-11 is saturated. The Δ indicates an impurity picked up during the vacuum degassing.

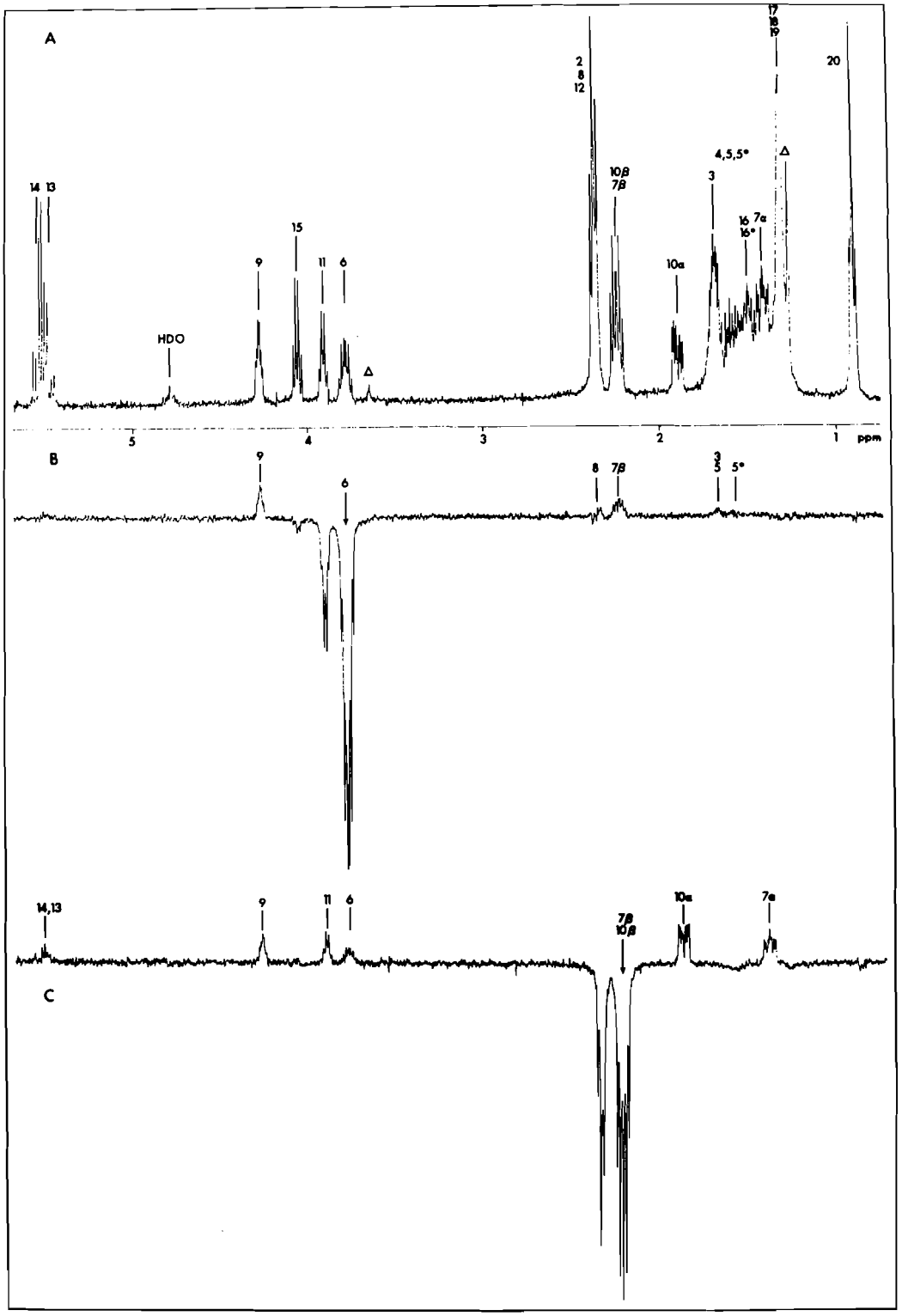


FIG. 3. Results of the nOe difference experiments on a $CDCl_3$ solution with a trace of D_2O. (A) General spectrum of (6*R*)-PGI_1. In (B), H-6 is saturated; in (C), H-7β and H-10β are saturated. The Δ indicates a small impurity.

Can. J. Chem. Downloaded from www.nrcresearchpress.com by 210.87.254.6 on 09/05/12
For personal use only.

Can. J. Chem. Downloaded from www.nrcresearchpress.com by 210.87.254.6 on 09/05/12
For personal use only.

saturation of H-11 may cause a small nOe to H-12 and H-10β. In Fig. 3C, H-7β and H-10β are saturated. An nOe is observed for H-14, H-13, H-9, H-11, H-6, H-10α, and H-7α. All of these enhancements are as expected from the model for (6*R*)-PGI_1. The chemical shift for H-7α is thus obtained. The enhancement to both H-9 and H-11 simultaneously on saturating H-10β confirms the assignment of H-10β to low field of H-10α. This was previously observed for PGI_2 (20), and prostaglandin E_2 (21). This conclusion is in agreement with the torsion angle dependency of chemical shifts for five-membered prostanoid precursors (22). Finally, chemical shifts for H-3 and H-7α were confirmed by an nOe experiment in which the H-2, H-8, and H-12 multiplet was irradiated. The nOe observed for H-7α is mainly due to the close proximity of H-12. As well, irradiation of H-15 results in an nOe for a multiplet at high field, assigned to H-16 and 16*. This assignment was confirmed by a decoupling experiment centered on H-16 and 16*, resulting in a doublet for the H-15 multiplet. On the basis of these experiments, the chemical shifts for the protons were obtained. These are listed in Table 1, together with the coupling constants. The data in Table 1 were prepared on the basis of normal spectra expanded to a sweep width of 2 Hz/cm, as well as from the nOe difference experiments and decoupling experiments. The data are based on at least two independent samples, namely, in $CDCl_3$ with a trace of D_2O, and in dried $CDCl_3$ solutions. Due to the essentially equal chemical shifts for H-8 and H-12 (as well as for H-2), protons H-7α, H-7β, H-9, H-11, H-13, and probably H-14 will be affected by virtual coupling (26–28). For these protons, measured splittings are reported. All of the other coupling constants, as well as the chemical shifts, are reported to first order. A computer fit to H-9 using a five-spin analysis for protons H-8, H-9, H-10α, H-10β, and H-12 was tried. However, the calculated spectra were very sensitive to the chemical shift difference between H-8 and H-12, as expected. As neither multiplet could be observed separately, these calculations were not pursued further. H-10β is also obscured by the overlap with H-7β, making the computer fit difficult.

The nOe experiments in Figs. 2 and 3 were carried out on a sample in $CDCl_3$ with a trace of D_2O. The complete exchange of the —OH protons with D_2O was shown by irradiating the small HDO resonance seen in Figs. 2 and 3. An nOe was not observed for any protons. On the other hand, very small nOe's, arising from the simultaneous irradiation of the very broad OH peak, appear when the nOe experiments were carried out on purified

TABLE 1. Proton chemical shifts and coupling constants for (6*R*)-PGI_1 in $CDCl_3$

Proton	Chemical shift (ppm)	Coupling constants (Hz)
2	2.36	$J(2–3) = 7.3$
3	1.67[a]	
4	—	
5, 5*	~1.68[a], 1.57[a]	
6	3.78	$J(5–6)$, $J(5^*–6)$, $J(6–7\beta) = 6.2$
		$J(6–7\alpha) = 9.2$
7α	1.40[a]	$J(6–7\alpha) = 9.2$[a,c]
		$J(7\alpha–7\beta) = 12.4$[a,b,c]
		$J(7\alpha–8) = 4.2$[a,b,c]
7β	2.23	
8	2.35	
9	4.27	$J(8–9) = 5.9$[c]
10α	1.89	$J(9–10\alpha) = 2.8$
		$J(10\alpha–10\beta) = 13.9$
		$J(10\alpha–11) = 6.2$
10β	2.24[a]	$J(9–10\beta)$, $J(10\beta–11) = 6.2$
11	3.91	$J(10\alpha–11)$, $J(10\beta–11)$, $J(11–12) = 6.2$[c]
12	2.35	
13	5.48	$J(12–13) = 6.7$[c]
		$J(13–14) = 15.4$[c]
14	5.55	$J(14–15) = 6.2$[c]
15	4.06	$J(14–15)$, $J(15–16)$, $J(15–16^*) = 6.4$[c]
16, 16*	~1.52[a]	
17, 18, 19	1.30	
20	0.89	$J(19–20) = 6.7$

[a] Value obtained from nOe difference spectra.
[b] Value obtained from decoupled spectra.
[c] Measured splittings are reported.

$CDCl_3$ samples. This can be seen in Figs. 4B and 4C. When H-9 is saturated (Fig. 4B), very small enhancements are observed for H-14, H-13, H-15, H-10α, and a negative nOe for H-11. When H-6 is irradiated (Fig. 4C), enhancements are also observed for H-14, H-13, H-15, and H-10α. The nOe's experienced by H-15 and H-10α are just above the noise level. In both experiments an enhancement may also be experienced by H-12 but as this proton overlaps the H-8 multiplet, the effect cannot be quantitated. These nOe's are in addition to the expected nOe's observed in Figs. 2 and 3 and are indicated in parentheses in Figs. 4B and 4C. These very small nOe's are experienced by protons in close proximity to the —OH groups at C-11 and C-15. The effects of intra- and intermolecular exchange on nOe measurements have been well documented (23). Caution must be used in interpreting data obtained in this manner.

The assignment of the resonances in buffer solutions was carried out in the same manner as for the

Can. J. Chem. Downloaded from www.nrcresearchpress.com by 210.87.254.6 on 09/05/12
For personal use only.

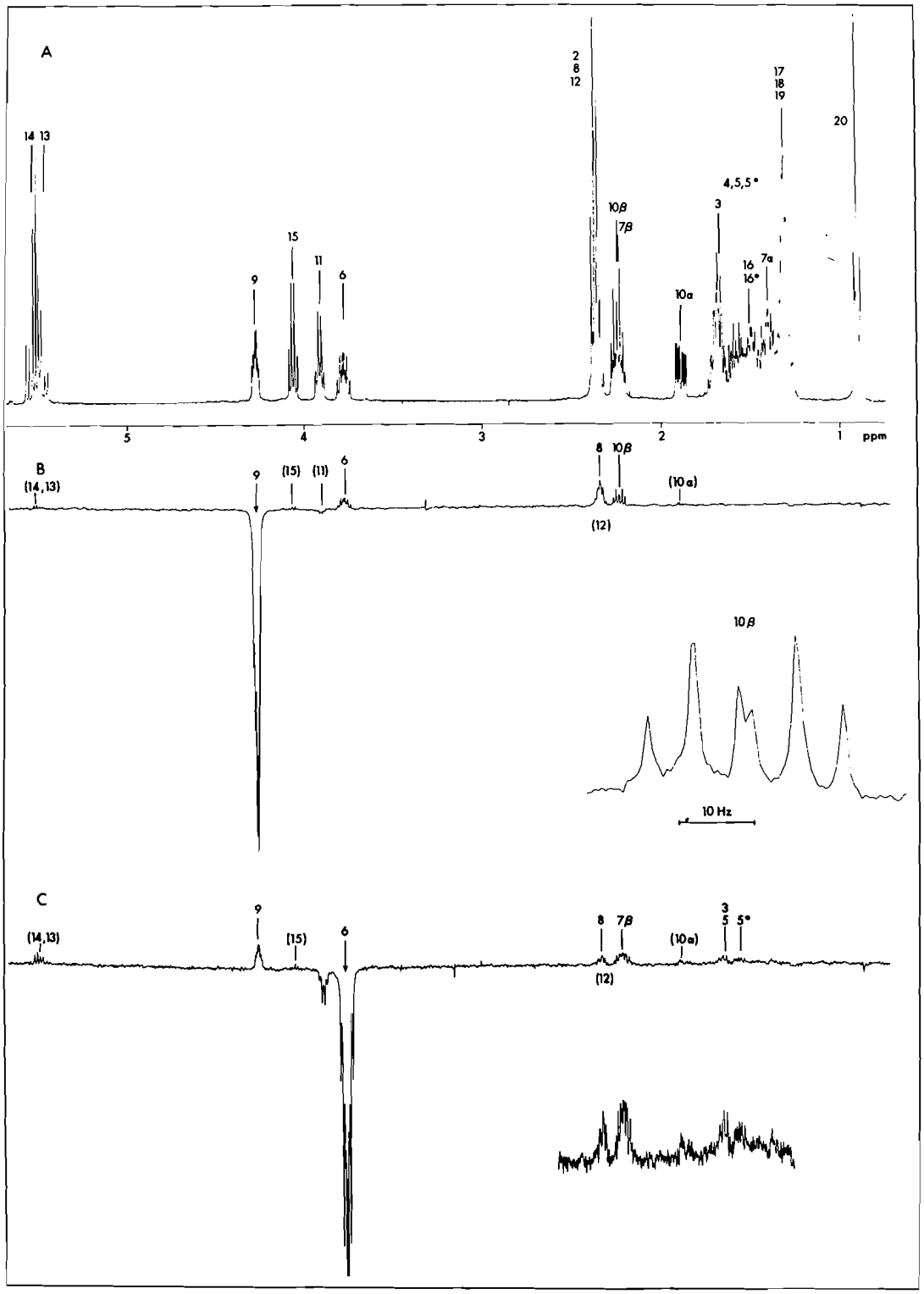


FIG. 4. Results of the nOe difference experiments performed on a sample of (6*R*)-PGI_1 in purified $CDCl_3$. (A) Normal spectrum. (B) H-9 is irradiated and the additional nOe's due to the simultaneous irradiation of the broad OH peak are indicated in parentheses. The expected enhancements as observed in Figs. 2 and 3 are also labelled. An expansion for H-10β is shown. In (C), H-6 is irradiated.

Can. J. Chem. Downloaded from www.nrcresearchpress.com by 210.87.254.6 on 09/05/12
For personal use only.

$CDCl_3$ solutions. Consequently, these experiments will be described in less detail. For example, decoupling of H-3 yields a singlet for H-2, and the H-7β multiplet can be studied more readily. Decoupling of H-13 and H-14 results in a triplet for H-15. From this triplet, the coupling constants $J(15–16) = J(15–16^*)$ were evaluated (Table 2). Finally, the H-4 proton multiplet was assigned on the basis of integration experiments.

The results of the nOe difference experiments in phosphate buffer are shown in Figs. 5 and 6. When H-9 is irradiated (Fig. 5B) an nOe is observed for H-6 (and possibly H-11), H-10β, and H-8. These data are in agreement with the measurements in $CDCl_3$ (Fig. 2B). Irradiation of H-15 (Fig. 5C) produces an enhancement to H-16 and 16*, allowing these chemical shifts to be determined. In Fig. 5D, the H-6 and H-11 multiplets are irradiated, resulting in an nOe for H-14 and H-13, H-9, H-10β, H-8, H-7β (and possibly H-12), and H-5 and H-5*. As in the $CDCl_3$ solutions, it is difficult to distinguish between the overlapping H-3 and the H-5* multiplets. The peak at ~1.36 ppm cannot be definitely assigned, but since this corresponds to the chemical shift for protons H-4 and H-7α, it has been labelled in this manner. Since H-6 and H-11 have almost the same chemical shift, these two protons cannot be irradiated separately. This experiment proves the assignment of H-6 and H-11, which are β to the ring, since an nOe is observed for H-7β, H-8, H-9, and H-10β. The enhancement to H-13 and H-14 confirms the assignment of H-11. Proton H-12α, which has almost the same chemical shift as H-7β, will experience a much smaller nOe due to irradiation of H-11β in comparison to the nOe experienced by H-7β, due to irradiation of H-6.

TABLE 2. Proton chemical shifts and coupling constants for (6*R*)-PGI_1 in phosphate buffer in D_2O (pH 7.0)

Proton	Chemical shift (ppm)	Coupling constants (Hz)
2	2.20	$J(2–3) = 7.4$
3	1.57[a]	
4	~1.36	
5, 5*	1.70[a],1.60[a]	
6β	3.93[b]	$J(5–6)$, $J(5^*–6)$, $J(6–7\beta) = 6.3$[b]; $J(6–7\alpha) = 9.1$[b]
7α	1.36[a]	$J(7\alpha–8) = 5.0$[a]
7β	2.23	$J(7\alpha–7\beta) = 12.0$; $J(7\beta–8) = 9.1$
8	2.38	$J(8–12) = 9.7$[c]
9	4.25	$J(8–9) = 7.2$; $J(9–10\alpha) = 4.4$; $J(9–10\beta) = 7.2$
10α	1.61[a]	$J(9–10\alpha) = 4.4$[a]; $J(10\alpha–10\beta) = 13.6$[a]; $J(10\alpha–11) = 9.3$[a]
10β	2.48	$J(9–10\beta) = 7.2$; $J(10\alpha–10\beta) = 13.6$; $J(10\beta–11) = 7.2$
11	3.95[b]	$J(10\alpha–11) = 9.3$[a,b]; $J(10\beta–11) = 7.2$[a,b]; $J(11–12) = 9.3$[a,b]
12	2.20	
13	5.58	
14	5.58	
15	4.13	$J(15–16) = J(15–16^*) = 6.7$[c]
16, 16*	1.59[a],1.50[a]	
17, 18, 19	1.30	
20	0.87	$J(19–20) = 6.8$

[a] Value obtained from nOe difference spectra.
[b] Value obtained from inversion recovery spectra.
[c] Value obtained from decoupled spectra.

The multiplicity for the H-11 multiplet as well as for the H-10α multiplet is obtained by irradiation of H-10β (Fig. 6B). Enhancements for these protons, together with the nOe to H-9, are as expected since all of these are β to the ring. The expanded spectrum for H-10α shows that accurate coupling constants can be obtained for a multiplet that is buried under many other resonances in the normal spectrum. In addition, this experiment confirms the assignment of H-10β to low field of H-10α, as for the $CDCl_3$ solutions. In Fig. 6C, H-8 is irradiated (with partial saturation of H-10β) resulting in an enhancement for H-13, H-14, H-9, H-11, and possibly H-6, and a very small enhancement to H-10α (due to partial saturation of H-10β). This confirms the assignment for H-8. Finally, irradiation of H-7β (with partial saturation of H-2 and H-12) (Fig. 6D) results in nOe's for H-13, H-14, H-6 (and possibly H-11), H-8, H-3, and H-7α. The chemical shifts for H-3 and H-7α are thus obtained.

In these nOe difference experiments, the overlap of the H-6 and H-11 multiplets causes uncertainty as to which of these protons is experiencing the nOe. In Fig. 6B the enhancement is only to H-11 when H-10β is irradiated, as H-6 is too far removed. In addition to this nOe experiment, the multiplicity and appearance of the H-6 and H-11 multiplets is known from inversion recovery experiments using the 180°—τ—90° two-pulse sequence (24). An attempt was made, on the basis of the splittings observed for the two separate multiplets, to be more specific about the relative nOe's experienced by H-6 and H-11 in experiments shown in Figs. 5B, 6C, and 6D. This proved unsuccessful and hence, in the above description, nOe's to both protons are listed.

Discussion

The nOe difference experiments have been applied previously to a variety of systems including the study of PGI_2 (20), prostaglandin E_2 (21), and

Can. J. Chem. Downloaded from www.nrcresearchpress.com by 210.87.254.6 on 09/05/12
For personal use only.

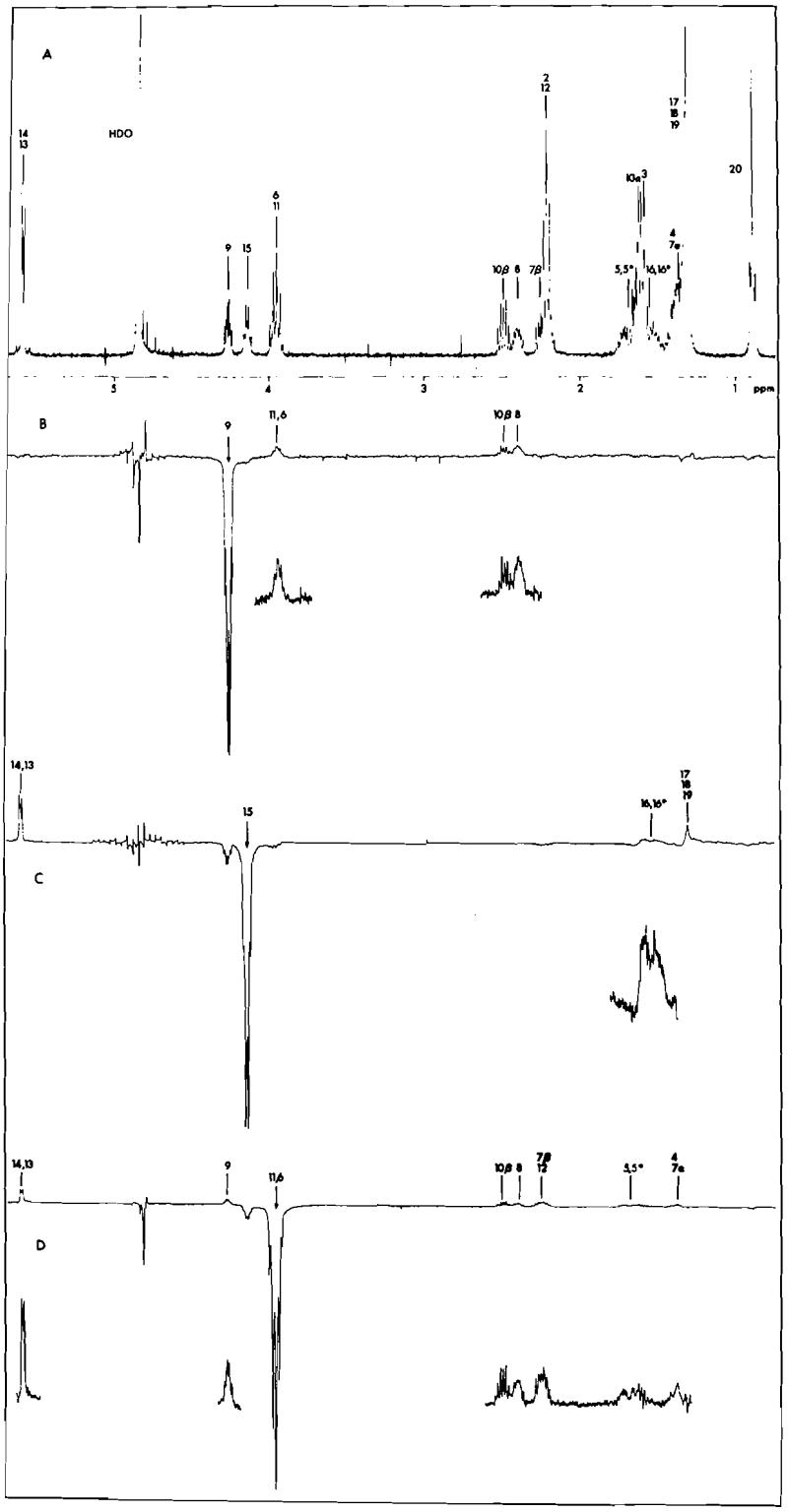


FIG. 5. Results of the nOe difference experiments performed on (6*R*)-PGI$_1$ in phosphate buffer in D_2O, pH 7.0. The normal spectrum is seen in (A), while in (B), H-9 is irradiated. In (C), H-15 is irradiated and in (D), the H-11 and H-6 multiplets are irradiated.

Can. J. Chem. Downloaded from www.nrcresearchpress.com by 210.87.254.6 on 09/05/12
For personal use only.

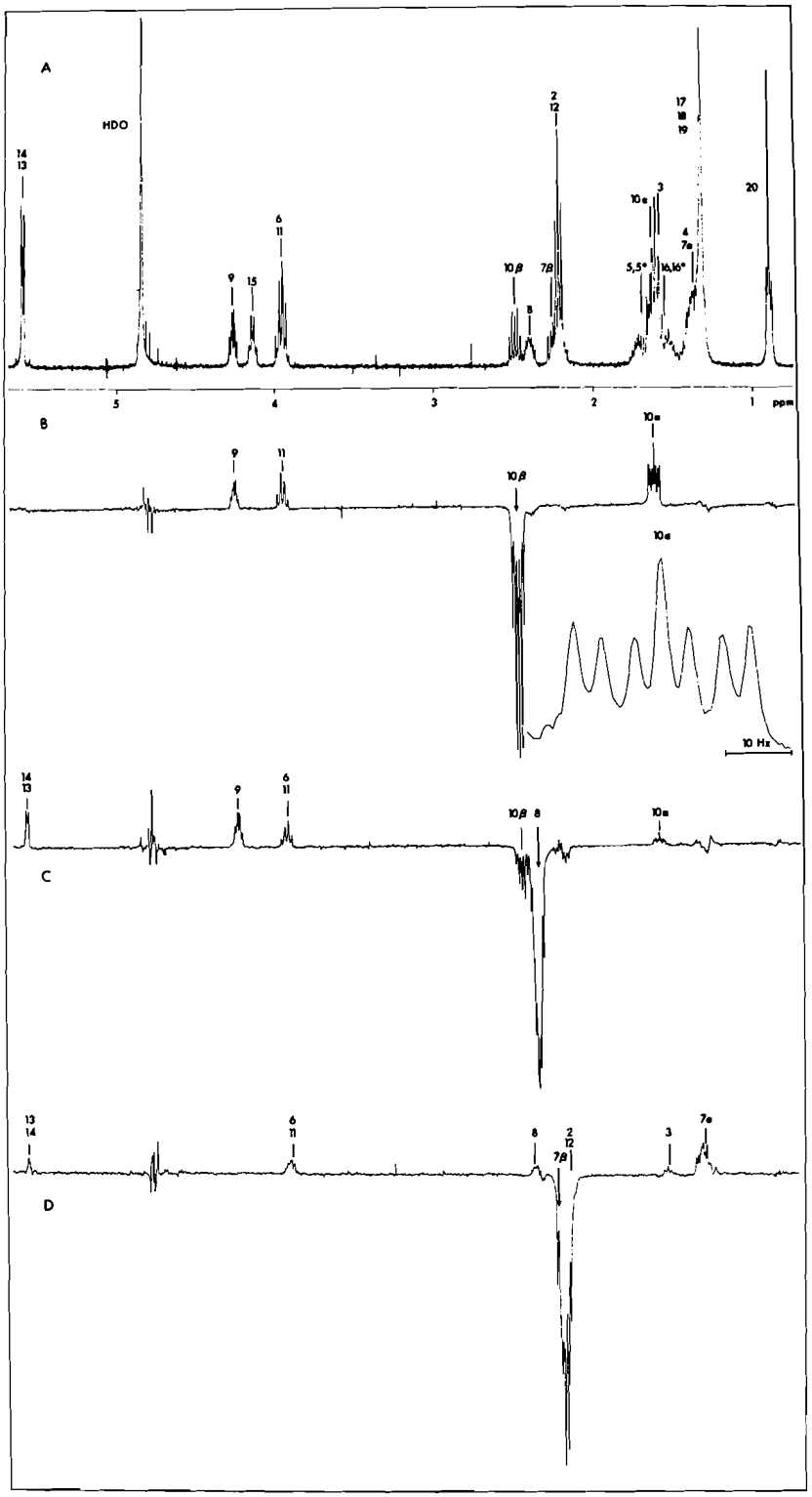


FIG. 6. Results of the nOe difference experiments performed on (6*R*)-PGI$_1$ in phosphate buffer in D_2O, pH 7.0. The normal spectrum is seen in (A) together with the proton assignments. In (B), H-10β is irradiated and an expanded spectrum for H-10α is shown. In (C), H-8 is irradiated whereas in (D), H-7β is irradiated. The protons experiencing the nOe are indicated. In (C), due to the small differences in chemical shift, H-10β was also partially saturated, causing the enhancement to H-10α. In (D), the H-2 and H-12 multiplet was also partially saturated when the irradiation frequency was centered on H-7β.

Can. J. Chem. Downloaded from www.nrcresearchpress.com by 210.87.254.6 on 09/05/12
For personal use only.

carbohydrates (25). Very small effects can be measured since a control spectrum without an nOe is subtracted from the spectrum with an nOe. Instrumental instabilities are corrected for by automation of the experiment so that four FID's are collected with on-resonance saturation and then the four FID's corresponding to the control are subtracted. The choice of four is required to keep the amplitude and phase constant in both channels using quadrature detection. This procedure is followed until the required S/N ratio is obtained.

In the present study, the nOe measurements proved invaluable in the assignment of the proton resonances in both solvents, in the determination of chemical shifts, and in the evaluation of the coupling constants. Changes in the conformation of the two five-membered rings with solvent, however, cannot be verified only on the basis of the nOe measurements because of the overlap of certain multiplets. For example, saturation of H-9 in $CDCl_3$ results in an nOe to H-6, H-8, and H-10β but an nOe is not observed to H-11 (Fig. 2B). However, in buffer solution (Fig. 5B), an nOe is observed for H-8, H-10β, and the overlapping H-6 and H-11 multiplets. Due to the overlap of H-6 and H-11, conformational comparisons concerning the involved protons for both solvents cannot be made. The overlap of H-7β and H-10β in $CDCl_3$ means that both of these protons must be simultaneously irradiated and all of the neighboring protons β to the ring (Fig. 3C) (H-6, H-9, and H-11) experience the nOe. No conclusion can be drawn about H-8 which is too close in chemical shift to the point of irradiation. As well, H-8 overlaps H-2 and H-12. On the other hand, in buffer solution, H-10β, H-8β, and H-7β can all be irradiated separately, with the expected results (Figs. 6B–D), but again the overlap of the H-6 and the H-11 multiplets does not allow conclusions to be drawn about different conformations in the two solvents. However, the nOe measurements are invaluable in the assignment of the proton multiplets.

The proton chemical shifts and coupling constants in $CDCl_3$ solutions are presented in Table 1, whereas these data in phosphate buffer are presented in Table 2. All data are calculated to the first order. Measured splittings are reported for the multiplets which are affected by the virtual coupling arising from the overlap of the H-8 and H-12 multiplets in $CDCl_3$ solutions. The assignment of H-7α and H-7β in buffer solution would have been very difficult, if not impossible, to carry out due to the overlap of the H-6 and H-11 multiplets. As the chemical shifts for these protons should not change with solvent, the chemical shift data in $CDCl_3$ allowed the assignments in buffer solution.

A comparison of the coupling constant data in both solvents (Tables 1 and 2) can be made. The value in brackets is observed in phosphate buffer: $J(9—10\alpha) = 2.8$ (4.4) Hz, $J(9—10\beta) = 6.2$ (7.2) Hz, $J(10\alpha—11) = 6.2$ (9.3) Hz, and $J(10\beta—11) = 6.2$ (7.2) Hz. These coupling constants are obtained from multiplets not affected by virtual coupling. As the C-11 OH group moves further away from the (C-8)—(C-9) bond on changing the solvent from $CDCl_3$ to buffer, these coupling constants increase. Hence these data suggest a conformational change in the C-8 to C-12 five membered ring. The C-11 OH group will be further away from the (C-8)—(C-9) bond in buffer solution than in $CDCl_3$ due to solvation of this OH group by the water. Finally, a comparison of the chemical shift data in phosphate buffer (Table 2) with the data obtained for PGI_2 (20) shows that the highest change is for H-7α (1.36 ppm) and for H-7β (2.23 ppm) since for PGI_2 these chemical shifts are 2.38 ppm and 2.65 ppm, respectively. These high-field shifts, in addition to that for H-5, must be due to the saturation of the (C-5)—(C-6) double bond.

In summary, the nOe difference experiments proved invaluable in assigning the multiplets for (6*R*)-PGI_1 in $CDCl_3$ solutions and in phosphate buffer. Problems associated with interpreting nOe results carried out in dried $CDCl_3$, which has a broad OH peak, are discussed. Changing the solvent from $CDCl_3$ to phosphate buffer appears to change the conformation of the C-8 to C-12 five-membered ring. The C-11 OH group is more accessible to the water, since it is further away from the (C-8)—(C-9) bond in phosphate buffer than in $CDCl_3$ solution.

Acknowledgements

The authors acknowledge valuable discussions with Dr. T. T. Nakashima and Mr. Glen Bigam, Dr. R. A. Johnson of the Upjohn Company in Kalamazoo, MI, for providing the sample of (6*R*)-PGI_1, the Natural Sciences and Engineering Research Council of Canada for a grant towards the purchase of the Bruker WH-400 NMR spectrometer, and the Natural Sciences and Engineering Research Council, the Canadian Heart Foundation, and the University of Alberta for generous financial assistance.

1. S. Moncada, R. Gryglewski, S. Bunting, and J. R. Vane. Nature, **263**, 663 (1976).
2. F. F. Sun, D. R. Morton, J. H. Kinner, R. R. Gorman, J. C. McGuire, R. A. Johnson, N. Whittaker, S. Bunting, J. Salmon, S. Moncada, and J. R. Vane. *In* Biochemical aspects of prostaglandins and thromboxanes. *Edited by* N. Kharasch and J. Fried. Academic Press, New York, NY. 1977. pp. 179–187.
3. K. C. Nicolaou, G. P. Gasic, and W. E. Barnette. Angew. Chem. Int. Ed. Engl. **17**, 293 (1978).

4. S. MONCADA and J. R. VANE. *In* Advances in prostaglandin and thromboxane research. Vol. 6. *Edited by* B. Samuelsson, P. W. Ramwell, and R. Paoletti. Raven Press, New York, NY. 1980. pp. 43–60.
5. E. J. COREY, G. E. KECK, and I. SZÉKELY. J. Am. Chem. Soc. **99**, 2006 (1977).
6. R. A. JOHNSON, F. H. LINCOLN, J. L. THOMPSON, E. G. NIDY, S. A. MIZSAK, and U. AXEN. J. Am. Chem. Soc. **99**, 4182 (1977).
7. N. A. NELSON. J. Am. Chem. Soc. **99**, 7362 (1977).
8. R. A. JOHNSON, F. H. LINCOLN, E. G. NIDY, W. P. SCHNEIDER, J. L. THOMPSON, and U. AXEN. J. Am. Chem. Soc. **100**, 7690 (1978).
9. G. TOGNA, C. GANDOLFI, A. ANDREONI, A. FUMAGALLI, C. PASSAROTTI, F. FAUSTINI, and C. PATRONO. Pharmacol. Res. Commun. **9**, 909 (1977).
10. J. FRIED and J. BARTON. Proc. Natl. Acad. Sci. USA, **74**, 2199 (1977).
11. R. A. JOHNSON, D. R. MORTON, and N. A. NELSON. Prostaglandins, **15**, 737 (1978).
12. B. H. CRANE, T. L. MAISH, Y. T. MADDOX, E. J. COREY, I. SZÉKELY, and P. W. RAMWELL. J. Pharmacol. Exp. Ther. **206**, 132 (1978).
13. N. K. BOUGHTON-SMITH, J. R. VANE, and B. J. R. WHITTLE. Br. J. Pharmacol. **62**, 413P (1978).
14. S. BUNTING, S. MONCADA, P. REED, J. A. SALMON, and J. R. VANE. Prostaglandins, **15**, 565 (1978).
15. K. SCHRÖR. Naunyn-Schmiedeberg's Arch. Pharmacol. **306**, 213 (1979).
16. Y. THERIAULT, Y. MORIO, and G. KOTOWYCZ. Can. J. Biochem. **57**, 165 (1979).
17. R. RICHARZ and K. WÜTHRICH. J. Magn. Reson. **30**, 147 (1978).
18. G. E. CHAPMAN, B. D. ABERCROMBIE, P. D. CARY, and E. M. BRADBURY. J. Magn. Reson. **31**, 459 (1978).
19. G. KOTOVYCH, G. H. M. AARTS, and K. BOCK. Can. J. Chem. **58**, 1206 (1980).
20. G. KOTOVYCH, G. H. M. AARTS, T. T. NAKASHIMA, and G. BIGAM. Can. J. Chem. **58**, 974 (1980).
21. G. KOTOVYCH, G. H. M. AARTS, and G. BIGAM. Can. J. Chem. **58**, 1577 (1980).
22. M. ANTEUNIS and D. DANNEELS. Org. Magn. Reson. **7**, 345 (1975).
23. J. H. NOGGLE and R. E. SCHIRMER. The nuclear Overhauser effect. Academic Press, New York, NY. 1971. Chapt. 7.
24. T. C. FARRAR and E. D. BECKER. Pulse and Fourier transform nmr. Academic Press, New York, NY. 1971.
25. R. U. LEMIEUX, K. BOCK, L. T. J. DELBAERE, S. KOTO, and V. S. RAO. Can. J. Chem. **58**, 631 (1980).
26. F. A. L. ANET. Can. J. Chem. **39**, 2262 (1961).
27. J. I. MUSHER and E. J. COREY. Tetrahedron, **18**, 791 (1962).
28. G. KOTOWYCZ and R. U. LEMIEUX. Chem. Rev. **73**, 669 (1973).

Can. J. Chem. Downloaded from www.nrcresearchpress.com by 210.87.254.6 on 09/05/12
For personal use only.

Photocyclisation des (oxo-3)-butyl glycopyranosides

GEORGES REMY, LOUIS COTTIER ET GÉRARD DESCOTES

Laboratoire de Chimie Organique 2, Université de Lyon 1, 69622 Villeurbanne, France

Reçu le 11 avril 1980

Ce papier est dédié au Prof. Raymond U. Lemieux pour son 60ème anniversaire

GEORGES REMY, LOUIS COTTIER et GÉRARD DESCOTES. Can. J. Chem. **58**, 2660 (1980).

La formation d'hydroxyspirocétals par photocyclisation selon Norrish II des (oxo-3)-butyl glycopyranosides est décrite en fonction de la configuration du carbone anomère, de la nature des substituants en position 2 et des conditions opératoires. La photocyclisation privilégiée des glycosides β avec rétention de configuration s'interprète par la stabilité plus grande du radical résultant de l'arrachement de l'hydrogène anomérique axial.

GEORGES REMY, LOUIS COTTIER, and GÉRARD DESCOTES. Can. J. Chem. **58**, 2660 (1980).

3-Oxo butyl glycopyranosides undergo Norrish type II photocyclization giving hydroxyspiroketals. The influence of the anomeric configuration and of different substituents at C-2 has been studied. The favored photocyclization of various β-glycosides occurs with retention of configuration and is interpreted in terms of the greater stability of the radical formed by abstraction of the axial anomeric hydrogen atom.

Can. J. Chem. Downloaded from www.nrcresearchpress.com by 210.87.254.42 on 09/05/12
For personal use only.

La photocyclisation d'(oxo-3)-butyl-2 tétrahydropyranne selon une réaction de type Norrish II est une voie de synthèse de spirocétal (1) qui peut être éventuellement envisagée pour la synthèse de produits naturels tels que phéromones (2) et polyéthers antibiotiques ionophores (3).

Cependant, la création photolytique du carbone cétalique avec des hétérocycles oxygénés substitués en C-6 s'effectue sans aucune stéréosélectivité. Aussi, la formation de système spirocétalique en série glucidique a été entreprise en vue de préciser l'influence de la configuration au niveau du carbone anomère et d'étudier celle de la nature des substituants situés sur le carbone C-2.

Synthèse des (oxo-3)-butyl glycosides

Les anomères α **6** et β **4** (oxo-3)-butyl tétra-*O*-acétyl-2,3,4,6-D-glucopyranosides sont obtenus par une réaction de type Koenigs–Knorr de l'hydroxy-4 butanone-2 sur les dérivés halogénés **1** (4) ou **2** (5) avec des rendements respectifs de 24 et 40% (Schéma 1). Les configurations anomériques de **6** et **4** sont attribuées grâce aux déplacements et aux constantes de couplage du proton anomère (**6**: δ 5.09, d, $J_{1,2}$ = 4 Hz; **4** δ 4.73, d, $J_{1,2}$ = 8 Hz).

Si le dérivé chloré **2** permet d'obtenir uniquement 1′(oxo-3)-butyl tri-*O*-acétyl-3,4,6-α-D-glucopyranoside **7** avec un rendement de 24%, la substitution effectuée sur le dérivé bromé **3** conduit préférentiellement selon la nature du catalyseur (6, 7) à l'anomère α **7** ou β **5** (rendement 40% avec 80% d'α et 25% avec 90% de β). La configuration de ces composés désacétylés en C-2 est confirmée par rmn (**7** δ H-1 4.93, d, $J_{1,2}$ = 4 Hz; **5**, δ H-1 4.50, d, $J_{1,2}$ = 8 Hz) et par leur acétylation donnant respectivement les glycosides **6** et **4**.

L'application de la réaction de Ferrier et Prasad (8) au tri-*O*-acétyl-3,4,6-D-glucal utilisant l'hydroxy-4 butanone-2 permet d'obtenir principalement le glycoside insaturé α **8** thermodynamiquement le plus stable (Schéma 1). Un abaissement de température (−10°C) diminue la formation de produits secondaires et augmente à 70% le rendement de la réaction.

L'(oxo-3 butyl)di-*O*-acétyl-4,6 didéoxy-2,3-α-D-*érythro* hexopyranoside **9** est obtenu par hydrogénation catalytique de **8** avec un rendement limité à 66% du fait de réactions d'hydrogénolyse précédemment observées (9, 10) dans des séries voisines.

Photolyse des (oxo-3)-butyl glycosides

La photolyse en solution benzénique des composés précédemment synthétisés conduit selon leurs structures à des spiro C-1 sucres **10**, **11**, **12** et **13** avec des rendements n'excédant pas 45%.

Avec les produits tétraacétylés **6** et **4**, si l'anomère α **6** ne se photolyse que très lentement (100 h), sans donner de produits définis, par contre l'anomère β **4** subit en 40 h une transformation complète en spiroglycoside **10** de configuration β confirmée par étude rmn ^{1}H et ^{13}C (Tableau 1) et par cristallographie (11). En effet, la conformation du cycle tétrahydropyrannique est bloquée à l'état cristallin sous la forme $^{1,4}B$ avec la liaison C—O du cycle tétrahydrofurannique en position "mat" démontrant ainsi la configuration β-D des isomères **10**. Cette conformation se retrouve à l'état dissous du fait de la multiplicité des signaux des protons H-2 et H-3 (doublet de doublet au lieu de triplet pour H-3) et de la valeur des constantes de couplage H-2, H-3 ($J_{2,3}$ = 3 Hz pour **10** *cis* et 2 Hz pour **10** *trans*; $J_{3,4}$ = 8 Hz).

La configuration *cis* ou *trans* au niveau du cycle

0008-4042/80/232660-06$01.00/0

©1980 National Research Council of Canada/Conseil national de recherches du Canada

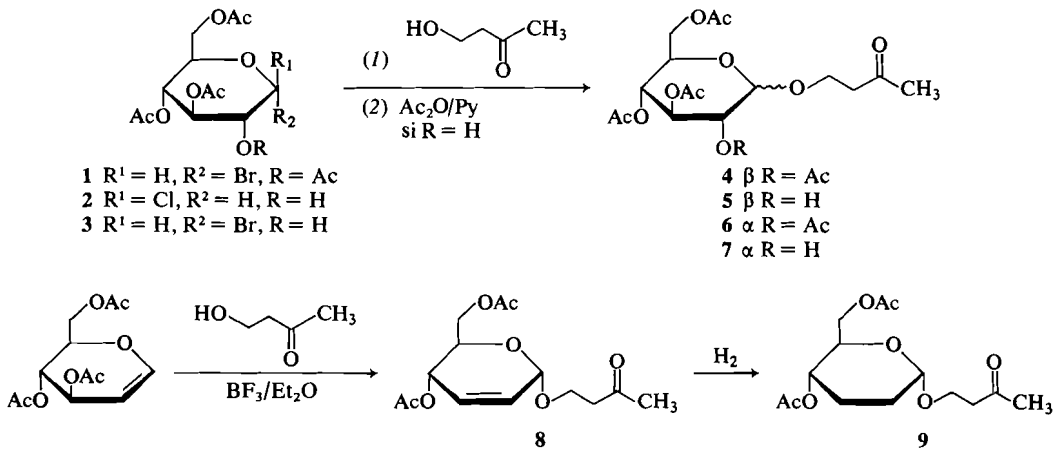


SCHÉMA 1

tétrahydrofurannique découle des données rmn que nous avons précédemment signalées en série hétérocyclique (1, 12) ($\Delta\delta$ CH_3 ($\mathbf{6}_t - \mathbf{6}_c$) = 0.26 ppm; $\Delta\delta$ C-1 ($\mathbf{6}_t - \mathbf{6}_c$) = 3.2 ppm; $\Delta\delta$ CH_3 ($\mathbf{6}_t - \mathbf{6}_c$) = −0.2 ppm).

Comme les composés **6** de configuration α, le dérivé triacétylé **7** de même configuration se dégrade très lentement (80 h) en donnant avec un faible rendement (16%) les mêmes spiro C-1 sucres triacétylés **11** que ceux provenant de la photolyse de l'anomère β **5** (Schéma 2). L'acétylation de chacun des isomères des spiro sucres **11** permet de déterminer leur structure car les produits obtenus correspondent respectivement à **10** *cis* et **10** *trans*. La conformation $^{1,4}B$ n'a été confirmée par rmn que pour l'isomère **11** *trans* du fait de la présence du doublet de doublet pour le proton H-3 ($J_{2,3}$ = 4 Hz; $J_{3,4}$ = 8.5 Hz).

Enfin, l'irradiation photochimique du sucre insaturé **8** et du didéoxy-2,3-α-D-hexopyranoside **9** donne au bout de 24 et 48 h, les quatre stéréoisomères **12** et **13** attendus avec des rendements globaux de 26 et 33%. Seule l'isomérie *cis–trans* a été déterminée par rmn. L'hydrogénation catalytique de chacun des isomères de **12** donnant respectivement les isomères saturés **13** correspondant, l'examen du tableau 1 montre que les produits **12***a*, *b* et **13***a*, *b* ont une configuration *cis* (**13** $\Delta\delta CH_3$

TABLEAU 1. Données physiques et spectrales des spiro C-1 sucres

		Rendement[a] %	$[\alpha]_D$[b] ($CHCl_3$, *c* 1.0)	*F* °C	Résonance magnétique nucléaire ^1H (CD_3COCD_3) δ CH_3	^1H (CD_3COCD_3) δ OH	^{13}C (CCl_4) C-1	^{13}C (CCl_4) C-9	^{13}C (CCl_4) Me
10	*cis*[c]	11	−3	116	1.28	3.70	102.8	79.1	22.0
	trans[c]	33	−16.1	140	1.54	2.80	106.0	80.8	21.8
11	*cis*[c]	12		Liq.					
	trans[c]	26	−63.3	144	1.45	2.90			
	a b *cis*	13		Liq.	1.33	2.72 2.82			
12	*c trans*	7	+18.0	74	1.28	2.20			
	d trans	6	+41	Liq.	1.30	3.05			
	a cis	8	−6.6	68	1.23	2.83	103.2	78.9	21.7
	b cis	4	+67.2 (*c* 0.4)	Liq.	1.23	2.74	102.9	78.6	21.4
13	*c trans*	21	+77	Liq.	1.33	2.43	106.4	80.7	21.0
	d trans		+ 7.5 (*c* 0.9)			2.82	106.2	80.3	21.0

[a]Rendement en produit pur calculé à partir de la quantité de produit mise en jeu.
[b]Les pouvoirs rotatoires ont été pris à des températures différentes 26°C pour **10** et 24°C pour **12**, **13***a* et **13***b*; 25°C pour **13***c* et 20°C pour **13***d*.
[c]L'isomérie *cis–trans* se rapporte à la configuration des carbones acétaliques et carbinolique du cycle tétrahydrofurannique.

Can. J. Chem. Downloaded from www.nrcresearchpress.com by 210.87.254.42 on 09/05/12
For personal use only.

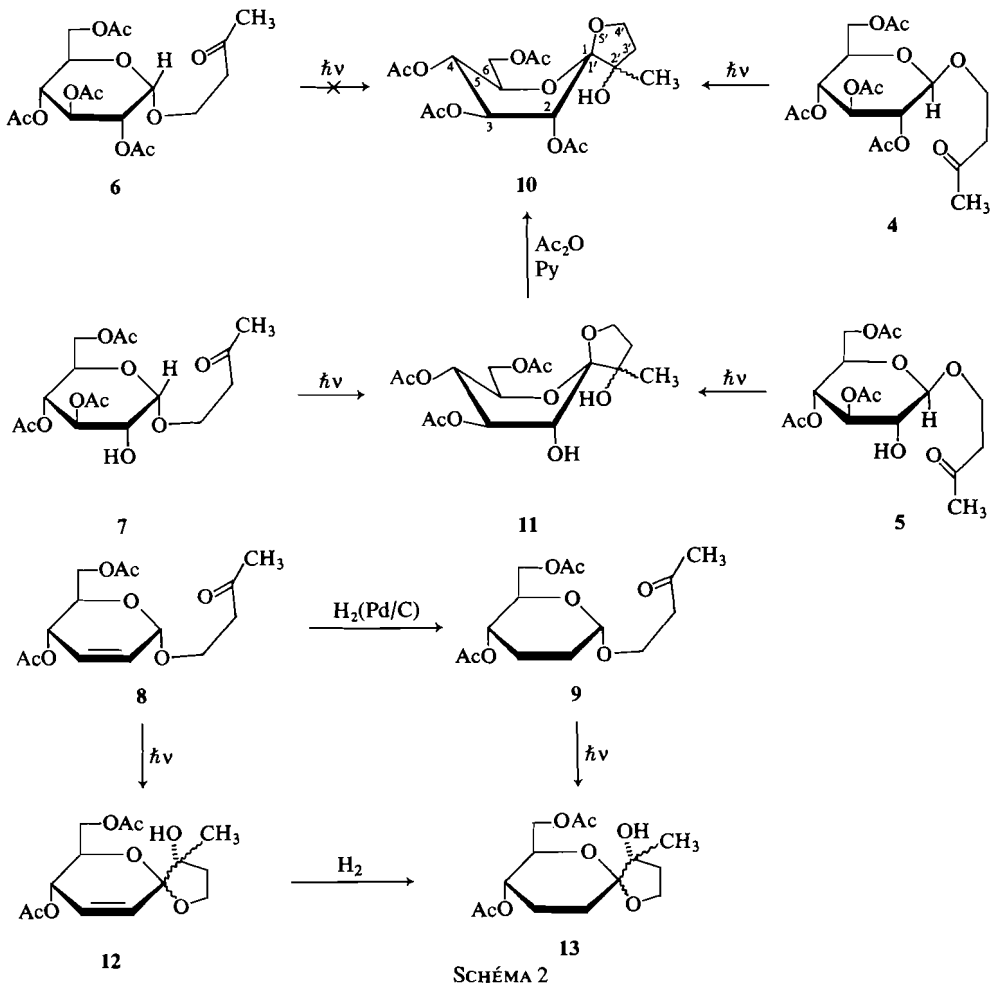


SCHÉMA 2

$(\mathbf{13}_t - \mathbf{13}_c) = 0.10$ ppm; $\Delta\delta$C-1 $(\mathbf{13}_t - \mathbf{13}_c) \geq 3$ ppm; $\Delta\delta CH_3$ $(\mathbf{13}_t - \mathbf{13}_c) \geq -0.4$ ppm). On peut noter que la présence de la double liaison de **12** inverse les déplacements chimiques des groupements méthyles carbinoliques qui sont alors plus déblindés pour les isomères **12***a*, *b cis*.

Discussion

En série hétérocyclique oxygénée, diverses observations montrant les différences de réactivité photochimique d'acétals cycliques diastéréoisomères ont déjà été signalées (1, 13). La photolyse d'hydrogène anomérique équatorial parait plus difficile et diverses études de rpe (14*a*) et des calculs théoriques (14*b*) confirment la plus grande stabilité du radical acétalique orientant son orbitale non liée en position axiale dans une structure non plane.

Les résultats obtenus en série osidique confirment de façon beaucoup plus nette ces premières indications. En effet, la présence d'un groupe hydroxyle en C-2 permet aux (oxo-3)-butyl glycosides **7** et **5** de se photocycliser en spiro C-1 sucres **11** de configuration β selon une réaction stéréosélective. En outre, ce même type de photocyclisation devient stéréospécifique pour les seuls anomères β **4** qui présentent un groupe acétate en C-2. La participation du groupe acétate déjà observée lors de la conversion radicalaire d'acétals en lactones (15) peut donc être envisagée lors de la formation des radicaux intermédiaires de type **A** et **B**, ce qui limiterait les processus d'isomérisation de **B** en **A** et entrainerait diverses réactions secondaires. Ainsi, un effet "antianomère" pour le radical intermédiaire permet d'expliquer les différences de réactivité observées pour les photolyses des anomères α et β **6**, **7** et **4**, **5** (Schéma 3).

Avec le glycoside insaturé **8**, la stabilisation du radical allylique intermédiaire par la délocalisation des électrons π de la double liaison entraine vrai-

Can. J. Chem. Downloaded from www.nrcresearchpress.com by 210.87.254.42 on 09/05/12
For personal use only.

Can. J. Chem. Downloaded from www.nrcresearchpress.com by 210.87.254.42 on 09/05/12
For personal use only.

semblablement une certaine planéité du radical permettant l'attaque de chaque côté du plan pour donner les quatre stéréoisomères **12** en une photocyclisation non stéréosélective.

Enfin, l'isomérisation du biradical intermédiaire correspondant à la photolyse du composé didéoxy **9** ne doit pas être aussi rapide qu'en série tétrahydropyrannique du fait de la formation des quatre diastéréoisomères **13**.

Conclusion

La photocyclisation d'oxo-3-butyl glycosides entrainant la formation de spiro C-1 sucres est fonction de la configuration du carbone anomère et de la nature des substituants du carbone 2. Un effet "anti anomère" semble favoriser la photocyclisation des glycosides β **4** et **5** par arrachement privilégié de l'hydrogène anomérique axial conduisant intermédiairement au biradical **A** de configuration β thermodynamiquement le plus stable. Une participation du groupe acétate en C-2 permet d'expliquer les différences de vitesse de photolyse entre les composés acétylés **6** et **4** et non acétylés **7** et **5**. Si la présence du groupe hydroxyle en C-2 rend stéréosélective la photocyclisation des anomères α **7** et β **5**, celle du groupe acétate entraine la stéréospécificité de la cyclisation du seul anomère β **5** avec rétention de configuration. L'influence de la configuration du substituant en C-2 est actuellement étudiée en vue de généraliser cette photocyclisation.

Partie expérimentale

Synthèse des (oxo-3)-butyl glycosides

Les points de fusion non corrigés ont été déterminés sur un appareil Buchi. Les spectres ir et rmn ont été tracés à température ambiante avec un Perkin-Elmer 237, un Varian A. 60, A. 100 ou XL 100 et un Bruker WP 80 CW. Les séparations chromatographiques ont été réalisées en faisant passer 0.6 à 5 g de produit brut sur 50 à 150 g de silice (Merck 0.040–0.60 mm) contenus dans une colonne de 50 cm (ϕ 3.5 cm).

*Bromure de tétra-*O*-acétyl-2,3,4,6-α-*D*-glucopyranosyle 1*

Il a été obtenu selon Lemieux (4).

*Chlorure de tri-*O*-acétyl-3,4,6-β-*D*-glucopyranosyle 2*

Il a été obtenu selon Birgl et Keppler (5).

*Bromure de tri-*O*-acétyl-3,4,6-α-*D*-glucopyranosyle 3*

A une solution de dichloro-1,2 éthane saturée par de l'acide bromhydrique gazeux est ajoutée sous forte agitation du tétra-*O*-acétyl-1,3,4,6-α-D-glucopyranoside (0.630 g, 1.73×10^{-3} mol) (16). Au bout de 8 min, le mélange est hydrolysé avec de l'eau glacée puis extrait au chloroforme (3 × 20 mL). Après neutralisation, séchage et évaporation de la phase organique, le produit brut est chromatographié (toluène/acétate d'éthyle: 1:1) donnant 0.450 g de **3** (rendement 71%); rmn ($CDCl_3$) δ: 2.00 à 2.15 (9H, 2s, —C(=O)—CH_3), 2.65 (1H, s, OH), 3.67 (1H, dd, H-2), 3.90 à 4.45 (3H, m, H-5, H-6, H-6'), 5.10 (1H, t, $J_{H-4,H-5}$ = 9 Hz, H-4), 5.33 (1H, t, $J_{H-3,H-4} = J_{H-2,H-3}$ = 9Hz, H-3), 6.48 (1H, d, $J_{H-1,H-2}$ = 4 Hz, H-1).

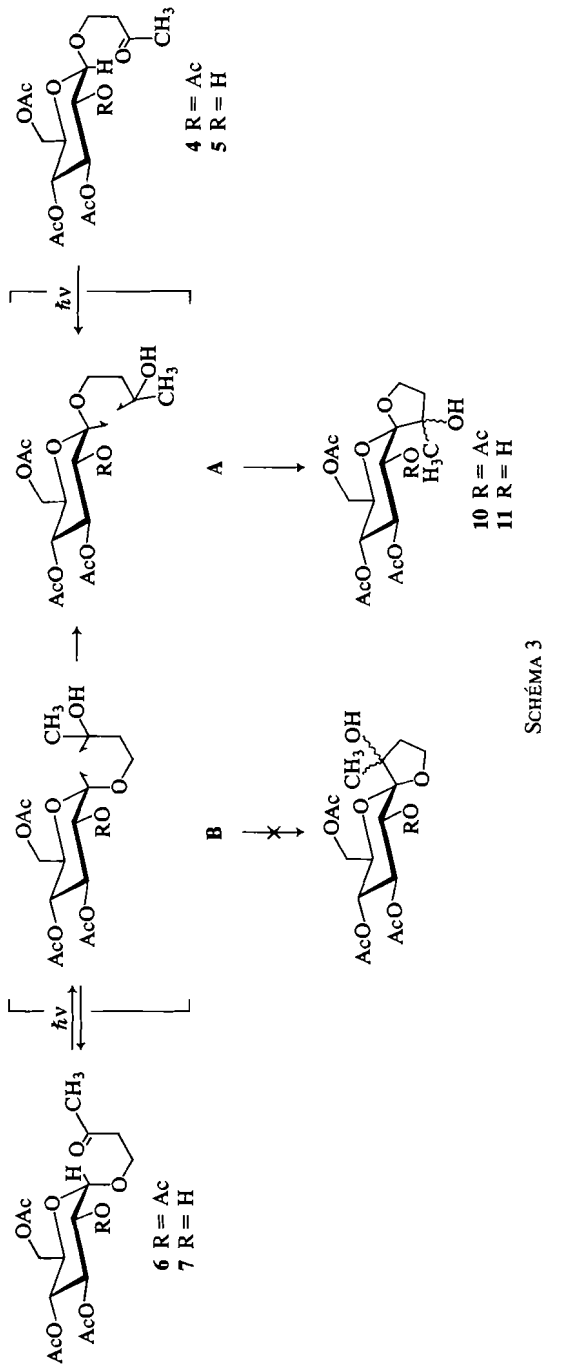


Schéma 3

Can. J. Chem. Downloaded from www.nrcresearchpress.com by 210.87.254.42 on 09/05/12
For personal use only.

Ce composé se dégradant rapidement est utilisé dès son obtention.

*(Oxo-3)-butyl-tétra-*O*-acétyl-2,3,4,6-α-D-glucopyranoside 6*

Le composé **6** a été obtenu soit par isomérisation de l'anomère β **4**, soit par acétylation de **7**.

Isomérisation de **4**. A une solution de **4** (2 g, 4.8 × 10^{-3} mol) dans du dichlorométhane (50 mL) sont ajoutés 2 g de sulfate de calcium puis 1.2 mL (5.6 × 10^{-3} mol) d'une solution de tétrachlorure de titane dans du dichlorométhane. Après 12 h d'agitation, le mélange réactionnel est hydrolysé avec 50 g de glace. Après décantation, lavage, séchage et évaporation de la phase organique le produit résiduel est chromatographié (éther) donnant 550 mg de produit **6** (rendement 28%).

Acétylation de **7**. A la solution froide (0°C) de **7** (100 mg, 0.23 × 10^{-3} mol) dans la pyridine (un millilitre) est ajouté un millilitre d'anhydride acétique. Après deux heures d'agitation à 0°C, le mélange est hydrolysé avec de l'eau (50 mL) puis extrait au chloroforme. Après un lavage acidulé, neutralisation au bicarbonate, décantation et séchage de la phase organique, l'évaporation du solvant laisse un résidu qui, chromatographié (éther), donne 77 mg de **6** (rendement 80%).

Liquide incolore: $[\alpha]_D^1$ 99° (*c* 1.0, $CHCl_3$): ir: 1740 cm^{-1}; rmn 100 MHz (CD_3COCD_3) δ: 1.9 à 2.2 (15H, m, —C(=O)—CH_3), 2.80 (2H, t, *J* = 6.5 Hz, —CH_2—C(=O)—), 3.78 (1H, m, H-5), 3.90 à 4.20 (3H, m, H-6, —O—CH_2—), 4.23 (1H, dd, $J_{H\text{-}6,H\text{-}6'}$ = 5 Hz, $J_{H\text{-}6,H\text{-}5}$ = 12 Hz), 4.78 (1H, dd, H-2), 5.00 (1H, t, $J_{H\text{-}4,H\text{-}5}$ = 9.25 Hz), 5.05 (1H, d, $J_{H\text{-}1,H\text{-}2}$ = 4 Hz, H-1), 5.38 (1H, dd, $J_{H\text{-}3,H\text{-}2}$ = 10 Hz, $J_{H\text{-}3,H\text{-}4}$ = 9.25 Hz, H-3). *Anal.* calc. pour $C_{18}H_{26}O_{11}$: C 51.67, H 6.26; trouvée: C 51.62, H 6.26.

*(Oxo-3)-butyle-tétra-*O*-acétyl-2,3,4,6-β-D-glucopyranoside 4*

Au mélange d'hydroxy-4 butanone-2[1] (7.65 g, 0.087 mol), de cyanure mercureux (7.52 g, 0.03 mol) et de sulfate de calcium (4.08 g, 0.03 mol) dans 80 mL de benzène et 80 mL de nitrométhane est ajouté le bromure **1** (12.3 g, 0.03 mol). Le milieu est porté à 45°C. Lorsque tout le bromure a réagi (ccm, méthanol/éther/dichloro-1,2 éthane 0.5:29.5:70), les produits minéraux sont filtrés et lavés avec du chloroforme. Les phases organiques réunies sont neutralisées avec du bicarbonate de sodium, lavées et séchées. Après évaporation du solvant, le résidu est dilué avec de l'éther (10 mL); puis aprés précipitation au bout de 48 h, la solution éthérée est filtrée donnant 5.11 g de **4** (rendement 43%). Solide; *F* 93°C (litt. (18) *F* 94°C); $[\alpha]_D^1$ − 11.3° (*c* 1.0, $CHCl_3$); ir: 1770 et 1720 cm^{-1}; rmn 100 MHz (CD_3COCD_3) δ: 1.90 à 2.10 (15H, 4s, —C(=O)—CH_3), 2.72 (2H, t, H-8, H-8'), 3.83 (1H, dt, $J_{H\text{-}7,H\text{-}8}$ = 6 Hz, H-7'). 3.95 (1H, ddd, H-5), 4.05 (1H, dt, $J_{H\text{-}7,H\text{-}7'}$ = 10 Hz, $J_{H\text{-}7,H\text{-}8}$ = 6 Hz, H-7), 4.11 (1H, q, $J_{H\text{-}6',H\text{-}5}$ = 2.5 Hz, H-6'), 4.30 (1H, q, $J_{H\text{-}6,H\text{-}6'}$ = 12 Hz, $J_{H\text{-}5,H\text{-}6}$ = 5 Hz, H-6), 4.73 (1H, q, H-1), 4.87 (1H, t, $J_{H\text{-}2,H\text{-}1}$ = 8 Hz, H-2), 5.1 (1H, t, $J_{H\text{-}4,H\text{-}5}$ = 9.5 Hz, H-4), 5.27 (1H, td, $J_{H\text{-}3,H\text{-}1}$ = 1 Hz, $J_{H\text{-}3,H\text{-}4}$ = 9.5 Hz, $J_{H\text{-}3,H\text{-}2}$ = 8 Hz, H-3).

*(Oxo-3)-butyl-tri-*O*-acétyl-3,4,6-α-D-glucopyranoside 7*

Une solution d'hydroxy-4 butanone-2 (5.28 g, 0.96 mol) dans du nitrométhane (25 mL) et du benzène (25 mL) est agitée pendant une heure avec du sulfate de calcium (4 g) et du cyanure mercureux (5 g, 0.06 mol). Après addition du dérivé chloré **2** (6.2 g, 0.019 mol), le mélange est chauffé à 45°C pendant 20 h. Après filtration la phase organique est lavée à l'eau bicarbonatée, séchée, puis évaporée. Le produit brut est chromatographié (éther) donnant 2.68 g de **7** (rendement 36%). Liquide incolore; $[\alpha]_D^{17}$ +1.38° (*c* 1.0, $CHCl_3$); ir: 3450, 1780, 1720 cm^{-1}; rmn (CD_3COCD_3) δ: 1.90 à 2.10 (9H, m, —C(=O)—CH_3), 2.20 (3H, s, —CH_2—C(=O)—CH_3), 2.85 (2H, t, *J* = 7 Hz, —CH_2—C(=O)—), 3.60 à 4.30 (7H, m, H-5, H-6, H-6', H-2, —O—CH_2—, OH), 4.93 (1H, d, $J_{H\text{-}1,H\text{-}2}$ = 4 Hz, H-1), 4.94 (1H, t, $J_{H\text{-}4,H\text{-}5}$ = 9.5 Hz, H-4), 5.23 (1H, t, $J_{H\text{-}3,H\text{-}4}$ = $J_{H\text{-}3,H\text{-}2}$ = 9.5 Hz, H-3). *Anal.* calc. pour $C_{16}H_{24}O_{10}$: C 51.06, H 6.43; trouvée: C 50.83, H 6.53.

Le composé **7** peut être également obtenu à partir du bromure **3** selon les mêmes conditions opératoires qu'avec le dérivé chloré **2**.

*(Oxo-3)-butyl-tri-*O*-acétyl-3,4,6-β-D-glucopyranoside 5*

Le composé a été obtenu selon Reynolds et Evans (7) (rendement 25%). Liquide; $[\alpha]_D^{24}$ +21.5° (*c* 1.0, $CHCl_3$); ir: 3460, 1740 cm^{-1}; rmn 100 MHz (CD_3COCD_3) δ: 1.80 à 2.30 (12H, m, —C(=O)—CH_3), 2.74 (2H, t, *J* = 6 Hz, —CH_2—C(=O)—), 3.40 (1H, d, *J* = 8 Hz, OH), 3.70 à 4.40 (6H, m, H-5, H-6, H-6', H-2, —O—CH_2—), 4.50 (1H, d, $J_{H\text{-}1,H\text{-}2}$ = 8 Hz, H-1), 4.87 (1H, t, $J_{H\text{-}4,H\text{-}5}$ = $J_{H\text{-}3,H\text{-}4}$ = 9.8 Hz, H-4), 5.10 (1H, dd, $J_{H\text{-}3,H\text{-}4}$ = 9.8 Hz, $J_{H\text{-}3,H\text{-}2}$ = 8.5 Hz, H-3). *Anal.* calc. pour $C_{16}H_{24}O_{10}$: C 51.06, H 6.43; trouvée: C 51.44, H 6.47.

*(Oxo-3)-butyl-di-*O*-acétyl-4,6-didéoxy-2,3-α-D-*érythro*-hexeno-2 pyranoside 8*

Dans une solution de dichlorométhane (30 mL) contenant l'hydroxy-4 butanone-2 (0.475 g, 5.4 × 10^{-3} mol) et le sulfate de calcium (200 mg) sont ajoutés à −10°C, le tri-*O*-acétyl-3,4,6-D-glucal (1 g, 3.6 × 10^{-3} mol) et l'éthérate de trifluorure de bore (0.18 mol). Lorsque tout le glucal a réagi (ccm benzène/éther 1:1) la réaction est arrêtée par addition de carbonate de sodium (0.64 g) et d'eau (50 mL). Après filtration, extraction, lavage, séchage et évaporation le produit brut est chromatographié (benzène/éther 1:1) donnant 0.7 g de **8** (rendement: 70%). Huile jaune; $[\alpha]_D^{23}$ +89° (*c* 1.0 $CHCl_3$); ir: 1750 cm^{-1}; rmn ($CDCl_3$) δ: 2.05 à 2.25 (9H, 3s, —C(=O)—CH_3), 2.75 (2H, t, *J* = 6 Hz, —CH_2—C(=O)—), 3.55 à 4.32 (5H, m, H-5, H-6, H-6', —O—CH_2—), 5.05 (1H, s, H-1), 5.30 (1H, d, $J_{H\text{-}4,H\text{-}3}$ = 9 Hz, H-4), 5.83 (2H, s, H-2, H-3). *Anal.* calc. pour $C_{14}H_{20}O_7$: C 55.89, H 6.71; trouvée: C 55.64, H 6.78.

*(Oxo-3)-butyl-di-*O*-acétyl-4,6-didéoxy-2,3-α-D-*érythro*-hexopyranoside 9*

L'hydrogénation de **8** (615 mg) sur charbon palladié (13 mg) dans l'éthanol (20 mL) conduit à un produit brut qui, chromatographié, donne **9** (407 mg, 66%). Liquide incolore: $[\alpha]_D^{23}$ +91° (*c* 1.0, $CHCl_3$); ir: 1740 cm^{-1}; rmn (C_6D_6) δ: 1.4 à 2.9 (13H, m, H-2e, H-2a, H-3e, H-3a, —C(=O)—CH_3), 2.30 (2H, t, *J* = 6 Hz, CH_2—C(=O)—), 3.20 à 4.50 (5H, m, H-5, H-6, H-6', —O—CH_2—), 4.60 (1H, s, H-1). 4.90 (1H, d, $J_{H\text{-}4,H\text{-}5}$ = 8 Hz, H-4). *Anal.* calc. pour $C_{14}H_{22}O_7$: C 55.62, H 7.34; trouvée: C 55.33, H 7.28.

Photolyse des (oxo-3)-butyl glycosides

La photolyse des oxo-3-butyl glycosides a été réalisée selon les conditions opératoires déjà décrites (14) avec un filtre Vycor. La dégradation est suivie par ccm.

Glycoside 4: 10.45 g (25 × 10^{-3} mol) de **4** dans 500 mL de benzène (5 × 10^{-2} mol L^{-1}), sont irradiés pendant 40 h. Après évaporation, le produit brut 10.33 g est chromatographié

[1]Ce cétol nous a été gracieusement donné par la Société BASF que nous remercions vivement.

Can. J. Chem. Downloaded from www.nrcresearchpress.com by 210.87.254.42 on 09/05/12
For personal use only.

(acétate d'éthyle/hexane 70:30) donnant 3.4 g (33%) de **10** *trans* et 1.1 g (11%) de **10** *cis*.

*Spiro[méthyl-2' tétrahydrofurannol-2']-1,1'-tétra-*O*-acétyl-2,3,4,6-β-D-glucopyranoside 10*: *trans*; solide blanc; *F* 140°C; ir (KBr): 3540 cm^{-1}; rmn (100 MHz) (CD_3COCD_3) δ: 1.54 (3H, s, CH_3), 1.80 à 2.30 (14H, m, H-3', —C(=O)—CH_3), 2.80 (1H, s, OH), 3.90 à 4.35 (5H, m, H-5, H-6, H-6', H-4'), 5.05 (1H, q, H-2), 5.12 (1H, dd, $J_{H-3,H-2}$ = 2 Hz, $J_{H-3,H-4}$ = 8 Hz, H-3), 5.5 (1H, q, $J_{H-4,H-5}$ = 9 Hz, H-4). *Anal.* calc. pour $C_{18}H_{26}O_{11}$: C 51.67, H 6.26; trouvée: C 51.78, H 6.41. *Cis*; solide blanc; *F* 116°C; ir (KBr): 3495 cm^{-1}; rmn 100 MHz (CD_3COCD_3) δ: 1.28 (3H, s, CH_3), 1.70 à 2.50 (14H, m, H-3', —C(=O)—CH_3), 3.60 à 4.50 (6H, m, H-5, H-6, H-6', H-4', OH), 4.98 (1H, d, H-2), 5.13 (1H, dd, $J_{H-3,H-2}$ = 3 Hz, $J_{H-3,H-4}$ = 8 Hz, H-3), 5.50 (1H, q, $J_{H-4,H-5}$ = 9 Hz, H-4). *Anal.* calc. pour $C_{18}H_{26}O_{11}$: C 51.67, H 6.26; trouvée: C 51.91, H 6.24.

Glycoside 6: 2 mL d'une solution benzénique de **6** à 5 × 10^{-2} mol L^{-1} sont irradiés pendant 100 h. Après évaporation du solvant, 90% de **6** sont récupérés.

Glycoside 5: 628 mg (1.81 × 10^{-3} mol) de **5** dans 36.3 mL de benzène sont irradiés pendant 30 h. Après évaporation, le produit brut est chromatographié (éther/acétone 9:1) donnant 117 mg (26%) de **11** *trans* et 86 mg (12%) de **11** *cis* impur.

*Spiro[méthyl-2' tétrahydrofurannol-2']-1,1'-tri-*O*-acétyl-3,4,6-β-D-glucopyranoside 11* trans

Solide blanc; *F* 144°C; $[\alpha]_D^1$ − 63.3 (*c* 1.0, $CHCl_3$); ir: 3640 cm^{-1}; rmn 80 MHz (CD_3COCD_3) δ: 1.45 (3H, s, CH_3), 1.90 à 2.25 (11H, m, H-3', —C(=O)—CH_3), 2.90 (1H, s, OH), 3.25 à 4.25 (6H, m, H-5, H-6, H-6', H-4', H-2), 4.65 (1H, d, *J* = 6 Hz, OH), 5.07 (1H, dd, $J_{H-3,H-2}$ = 4 Hz, $J_{H-3,H-4}$ = 8.5 Hz, H-3), 5.40 (1H, t, $J_{H-4,H-5}$ = 8.5 Hz, H-4). *Anal.* calc. pour $C_{16}H_{24}O_{10}$: C 51.06, H 6.43; trouvée: C 50.91, H 6.60.

L'acétylation de **11** *trans* (71 mg) par le mélange anhydride acétique – pyridine donne **10** *trans* (62 mg, 79%). L'acétylation de **11** *cis* (86 mg) donne **10** *cis* (73 mg, 80%).

Glycoside 7: 830 mg (2.2 × 10^{-3} mol) de **7** dans 44 mL de benzène sont irradiés pendant 50 h. Après évaporation, le résidu est chromatographié (éther/acétone 9:1) donnant 79 mg (16%) de **11** *trans* et des traces de **11** *cis*.

Glycoside 8: 7.5 g (2.5 × 10^{-3} mol) de **8** dans 500 mL de benzène sont irradiés pendant 24 h. Après évaporation, le résidu est chromatographié (dichlorométhane/acétone 80:10) donnant **12***a* et **12***b* (1 g, 13%) puis **12***c* (0.528 g, 7%) et **12***d* (0.486 g, 6%).

Composés **12***a* et **12***b*: ir: 3550 cm^{-1}; rmn (CD_3COCD_3) δ: 1.33 (3H, s, CH_3), 2.12 (6H, s, —C(=O)—CH_3), 1.90 à 2.50 (2H, m, H-3'), 2.72 (1H, s, OH de **12***a*), 2.82 (1H, s, OH de **12***b*), 3.80 à 4.32 (5H, m, H-5, H-6, H-6', H-4'), 5.05 (1H, m, H-4 de **12***b*), 5.33 (1H, m, H-4 de **12***a*), 5.70 à 6.30 (2H, m, H-2, H-3). *Anal.* calc. pour $C_{14}H_{20}O_7$: C 55.99, H 6.71; trouvée: C 55.74, H 6.71.

Composé **12***c*: ir: 3580 cm^{-1}; rmn (CD_3COCD_3) δ: 1.28 (1H, s, CH_3), 2.09 et 2.11 (6H, s, —C(=O)—CH_3), 2.20 (1H, s, OH), 1.90 à 2.50 (2H, m, H-3'), 3.80 à 4.50 (5H, m, H-5, H-6, H-6', H-4'), 5.28 (1H, d, $J_{H-4,H-5}$ = 8 Hz, H-4), 6.02 (2H, s, H-2 H-3). *Anal.* calc. pour $C_{14}H_{20}O_7$: C 55.99, H 6.71; trouvée: C 55.98, H 6.70.

Composé **12***d*: ir: 3460 cm^{-1}; rmn (CD_3COCD_3) δ: 1.30 (3H, s, CH_3), 2.10 (6H, s, —C(=O)—CH_3), 1.80 à 2.50 (2H, m, H-3'), 3.05 (1H, m, OH), 3.80 à 4.40 (5H, m, H-5, H-6, H-6', H-4'), 5.05 (1H, d, $J_{H-4,H-5}$ = 4 Hz), 6.20 (2H, m, H-2, H-3). *Anal.* calc. pour $C_{14}H_{20}O_7$: C 55.99, H 6.71; trouvée: C 55.82, H 6.87.

Glycoside 9

7.55 g (25 × 10^{-3} mol) de **9** dans 500 mL de benzène sont irradiés pendant 48 h. Après évaporation du solvant, le résidu est chromatographié donnant **13***a* (0.613 g, 8%), **13***b* (0.356 g, 4%) et **13***c* + *d* (1.656 g, 21%).

Composé **13***a*; ir: 3530 cm^{-1}; rmn (CD_3COCD_3) δ: 1.23 (3H, s, CH_3), 1.50 à 2.20 (2H, m, H-4'), 2.05 et 2.11 (6H, s, —C(=O)—CH_3), 1.65 à 2.30 (4H, m, H-2, H-3), 2.83 (1H, s, OH), 3.60 à 4.50 (5H, m, H-5, H-6, H-6', H-3'), 4.92 (1H, m, H-4). *Anal.* calc. pour $C_{14}H_{22}O_7$: C 55.62, H 7.34; trouvée: C 55.56, H 7.39.

Composé **13***b*; ir: 3500 cm^{-1}; rmn (CD_3COCD_3) δ: 1.23 (3H, s, CH_3), 1.50 à 2.20 (2H, m, H-3), 2.05 et 2.11 (6H, s, —C(=O)—CH_3), 1.65 à 2.30 (4H, m, H-2, H-3), 2.74 (1H, s, OH), 3.65 à 4.30 (5H, m, H-5, H-6, H-6', H-4'), 5.05 (1H, m, H-4). *Anal.* calc. pour $C_{14}H_{22}O_7$: C 55.62, H 7.34; trouvée: C 55.79, H 7.37.

Composés **13***c* + *d*: ir: 3500(c), 3400(d) cm^{-1}; rmn (CD_3COCD_3) δ: 1.33 (3H, s, CH_3), 1.50 à 2.20 (2H, m, H-3'), 2.05 et 2.11 (6H, s, —C(=O)—CH_3), 1.65 à 2.30 (4H, m, H-2, H-3), 2.43 (1H, s, OH de *c*), 2.82 (1H, s, OH de *d*), 3.70 à 4.50 (5H, m, H-5, H-6, H-6', H-4'), 4.70 à 4.90 (1H, m, H-4). *Anal.* calc. pour $C_{14}H_{22}O_7$: C 55.62, H 7.34; trouvée: C 55.61, H 7.41.

1. (*a*) C. Bernasconi, L. Cottier et G. Descotes. Bull. Soc. Chim. Fr. 101 (1977); 107 (1977); (*b*) L. Cottier et G. Descotes. J. Heterocycl. Chem. 1271 (1977).
2. W. Francke, G. Hindorf et W. Reith. Angew. Chem. Int. Ed. Engl. 862 (1978).
3. (*a*) J. W. Westley. Advances in applied microbiology. Vol. 22. Academic Press, New York. 1977. pp. 177–223; (*b*) T. Fukuyama, K. Akasaka, D. S. Karanewsky, C. L. J. Wang, G. Schmid et Y. Kishi. J. Am. Chem. Soc. **101**, 262 (1979).
4. R. U. Lemieux. Methods Carbohydr. Chem. **2**, 221 (1963).
5. P. Brigl et H. Keppler. Ber. **59**, 1588 (1926).
6. (*a*) L. R. Schroeder et J. W. Green. J. Chem. Soc. C, 530 (1966); (*b*) J. E. Wallace et L. R. Schroeder. J. Chem. Soc. Perkin Trans. I, 1938 (1976).
7. D. D. Reynolds et W. L. Evans. J. Am. Chem. Soc. **60**, 2559 (1938).
8. R. J. Ferrier et N. Prasad. J. Chem. Soc. C, 570 (1969).
9. G. R. Gray et R. Barker. J. Org. Chem. **32**, 2764 (1967).
10. R. U. Lemieux et J. C. Martin. Carbohydr. Res. **13**, 139 (1970).
11. G. Remy, L. Cottier, G. Descotes, R. Faure, H. Loiseleur et G. Thomas-David. Acta Crystallogr. Sect. B, **36**, 873 (1980).
12. L. Cottier, G. Descotes, M. F. Grenier et F. Metras. Tetrahedron. A paraître.
13. K. Hayday et R. D. McKelvey. J. Org. Chem. **41**, 2222 (1976).
14. (*a*) V. Malatesta, R. D. McKelvey, B. W. Babcock et R. U. Ingold. J. Org. Chem. **44**, 1872 (1979); (*b*) A. R. Gregory et V. Malatesta. J. Org. Chem. **45**, 122 (1980).
15. C. M. Rynard, C. Thankachan et T. Tidwell. J. Am. Chem. Soc. **101**, 1196 (1979).
16. B. Helferich et J. Zirner. Chem. Ber. **95**, 2604 (1962).
17. C. E. Ballou et K. P. Link. J. Am. Chem. Soc. **72**, 3147 (1950).

Resolution of conflicting migratory reports in ring expansion of 3-keto steroids to oxygen and nitrogen[1]

VINOD DAVE, J. B. STOTHERS, AND E. W. WARNHOFF
Department of Chemistry, University of Western Ontario, London, Ont., Canada N6A 5B7

Received June 27, 1980

This paper is dedicated to Prof. Raymond U. Lemieux on the occasion of his 60th birthday

VINOD DAVE, J. B. STOTHERS, and E. W. WARNHOFF. Can. J. Chem. **58**, 2666 (1980).

The migration of C-2 and/or C-4 to O or N in the Beckmann, Schmidt, and Baeyer–Villiger reactions of 3-keto steroids has been studied with the aid of ^{13}Cmr spectroscopy. Authentic specimens of the eight possible lactone and lactam products from both 5α- and 5β-cholestan-3-one have been prepared; their physical properties and ^{13}Cmr assignments are given. Seven ring expansion reactions reported to give only one product have been found to give both possible migration products. The much studied reactions of 5α-cholestane-3,6-dione and its derivatives have been reexamined. The results emphasize again the necessity of using ^{13}C spectra both as an analytical tool and as the best criterion of purity in work with these molecules.

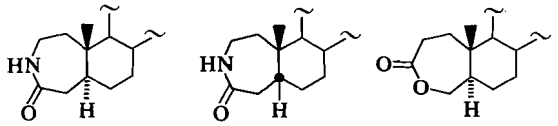
VINOD DAVE, J. B. STOTHERS et E. W. WARNHOFF. Can. J. Chem. **58**, 2666 (1980).

Faisant appel à la spectroscopie de rmn du ^{13}C et opérant sur des céto-3 stéroides, on a étudié la migration des carbones en positions 2 et/ou 4 vers l'oxygène ou l'azote dans les réactions de Beckmann, de Schmidt et de Baeyer–Villiger. On a préparé des échantillons authentiques des 8 lactones et lactames qui pourraient se produire à partir des 5α et 5β cholestanones-3 et on rapporte leurs propriétés physiques ainsi que leurs caractéristiques spectrales en rmn du ^{13}C. On a trouvé que les 7 réactions d'extension de cycle, qui d'après les publications ne donnent qu'un seul produit, donnent deux produits possibles de migration. On a examiné les réactions les plus étudiées de la 5α-cholestanedione-3,6 et de ses dérivés. Les résultats démontrent à nouveau la nécessité des spectres du ^{13}C comme outil d'analyse et comme critère du pureté dans des travaux portant sur ces molécules.

[Traduit par le journal]

In a thorough examination with the aid of ^{13}Cmr spectroscopy, it was shown recently that a number of ring expansion reactions of the cyclohexanone ring of 3-keto steroids to C, N, or O exhibit no migratory preference for either C-2 or C-4, and that product ratios are essentially 1:1 (1). For the ring expansions to N or O, although some workers have recognized that both products are formed (e.g. 2–9), it was pointed out that there are still a number of unsubstantiated reports of a single product resulting from these reactions (e.g. 10–20). Some of these cases (10, 14, 15, 18, 20) involve variations on the standard Beckmann and Baeyer–Villiger conditions and could conceivably give other than ~1:1 ratios of products for unknown reasons. Certainly the Beckmann rearrangement with 3-keto steroids can yield single products provided that configurationally pure oxime isomers are rearranged under mild nonequilibrating conditions (21, 22). Since these ring expansion reactions are being used in the synthesis of alkaloids (4, 7, 21) and some physiologically active steroids (23–25), as well as to prepare authentic samples for structure proof (10, 16, 26), it is essential to be certain of the structure and purity of any ring expansion products. For this purpose, melting point, tlc, and even ^{1}Hmr spectra are unreliable criteria of purity with these compounds. Therefore, we have used ^{13}Cmr absorption to reexamine some of these reports of single products with the object of reconciling them with our earlier conclusions (1).

To enable analysis of the ^{13}Cmr spectra of reaction products, authentic specimens of the pairs of lactam and lactone ring expansion products of both 5α- and 5β-cholestan-3-one were prepared. One lactone **3***a* and two lactams **1***a* and **2***a* had been



1 **2** **3**

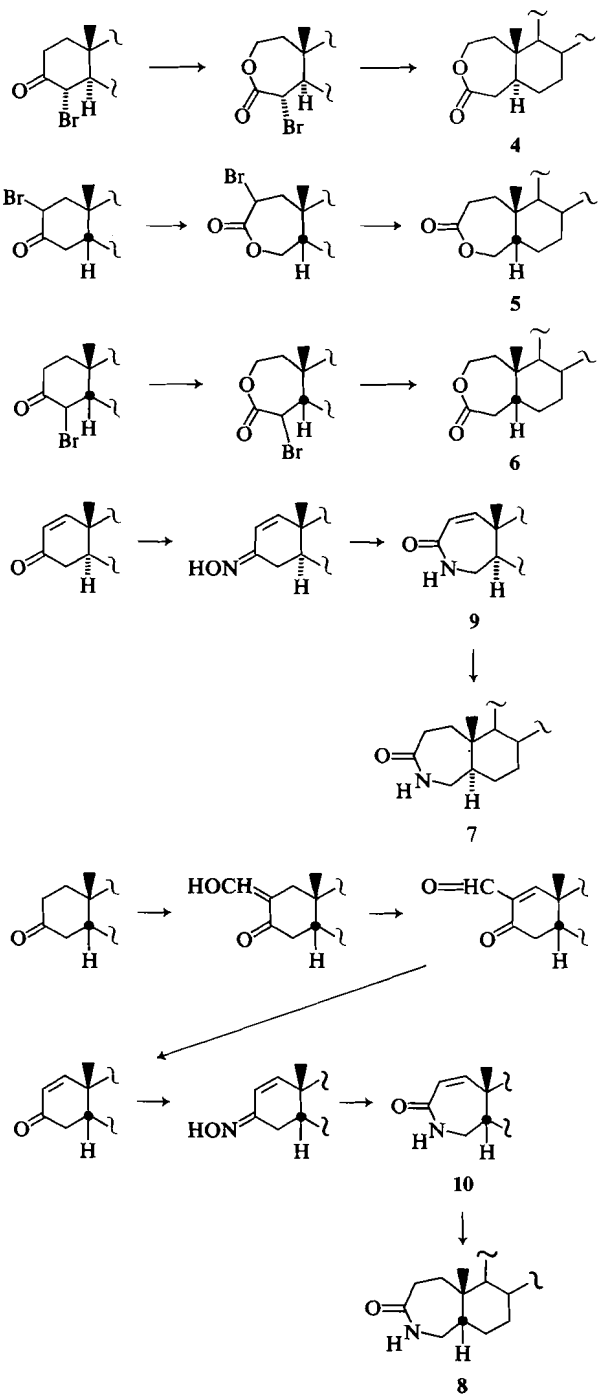
(*a*) Cholestane
(*b*) Pregnan-20-one
(*c*) 17β-Hydroxyandrostane
(*d*) 17β-Acetoxyandrostane
(*e*) Solasodane

made previously for these studies (1). The three new lactones **4***a*, **5***a*, and **6***a* were prepared by Baeyer–Villiger expansion of the appropriate α-bromo ketones as outlined in Scheme 1, in extension of Bolliger and Courtney's finding that migration of the halogenated carbon in 2α-halo-5α-cholestan-3-ones is suppressed (16). The remaining two lactams **7***a* and **8***a* were prepared by known proce-

[1]Part 92 of ^{13}C nuclear magnetic resonance studies of one of us (J.B.S.). For part 91 see ref. 51.

0008-4042/80/232666-13$01.00/0
©1980 National Research Council of Canada/Conseil national de recherches du Canada

Can. J. Chem. Downloaded from www.nrcresearchpress.com by 210.87.254.105 on 09/05/12
For personal use only.



SCHEME 1

dures (8) from the appropriate conjugated ketone (Scheme 1) via the Beckmann rearrangement procedure recently developed for unsaturated oximes (2, 27); migration of the sp^2-α-carbon does not occur under these conditions. The ^{13}Cmr spectra of all eight compounds, grouped in the pairs expected from an expansion reaction, are given in Table 1.

TABLE 1. ^{13}C shieldings of cholestane *A*-homo lactones and lactams[a]

Compound	Series	Functional groups	C-1	C-2	C-3	C-4	C-4a	C-5	C-6	C-7	C-8	C-9	C-10	C-11	C-12	C-13	C-14	C-19
1*a*	5α	3-aza, 4-oxo	37.9	39.7	—	178.8	42.0	**43.3**	31.1	32.1	34.7	**54.1**	**38.8**	**21.3**	40.0	42.3	56.4	12.0
7*a*		3-oxo, 4-aza	31.4	35.3	178.9	—	**44.5**	**49.7**	27.8	31.8	35.1	**53.9**	**38.7**	**21.0**	40.0	42.3	56.5	12.1
4*a*		3-oxa, 4-oxo	37.6	**64.7**	—	178.2	41.8	**43.5**	30.6	31.9	34.7	**53.9**	37.9	**21.3**	39.9	42.4	56.3	12.0
3*a*		3-oxo, 4-oxa	29.7	35.5	178.5	—	**70.1**	**48.6**	26.4	31.6	34.9	**53.6**	37.6	**21.1**	39.8	42.3	56.2	12.3
2*a*	5β	3-aza, 4-oxo	36.9	38.8	—	178.2	40.3	**43.0**	**26.0**	29.9	35.8	39.8	37.2	**21.3**	40.2	42.6	56.3	23.3
8*a*		3-oxo, 4-aza	28.3	34.0	178.7	—	44.3	**45.7**	**27.1**	30.0	35.9	42.3	37.4	**21.0**	40.2	42.7	56.4	23.6
6*a*		3-oxa, 4-oxo	40.1	**63.3**	—	176.3	36.9	41.3	29.7	25.8	35.7	41.3	36.7	**21.3**	39.7	42.7	56.4	24.2
5*a*		3-oxo, 4-oxa	28.3	33.3	176.2	—	**70.5**	45.5	(27.0)	(27.4)	35.8	41.5	36.5	**21.0**	40.1	42.7	56.4	23.9

[a]In ppm from internal TMS for $CDCl_3$ solutions; similar values in parentheses may be interchanged. In these compounds C-15 to C-18 and C-20 to C-27 absorb at 24.2, 28.3, 56.2, 12.1, 35.8, 18.7, 36.2, 23.9, 39.5, 28.0, 22.6, and 22.8 ppm, respectively.

Can. J. Chem. Downloaded from www.nrcresearchpress.com by 210.87.254.105 on 09/05/12
For personal use only.

Can. J. Chem. Downloaded from www.nrcresearchpress.com by 210.87.254.105 on 09/05/12
For personal use only.

The components of each pair are readily identified and analyzed quantitatively by the peaks in bold face type. It is relevant to note here for later reference that the C-19 *proton* signal of each pair has the same chemical shift, and therefore this signal can not be used as a criterion of purity.

The original report of the Beckmann rearrangement of 5α- and 5β-cholestan-3-one oximes by Shoppee and Sly (28) concluded that each reaction gave a single lactam. This claim was revised after Shoppee *et al.* (26) prepared authentic specimens of both 5α-lactams by a different route; it became clear that the 5α Beckmann product was a mixture. We have now confirmed, as Shoppee *et al.* (26) suspected, that the Beckmann rearrangement of 5β-cholestan-3-one also gives both lactams (see Experimental). Concurrently, Doorenbos and Wu (29) had claimed that the Schmidt reaction on 5α- and 5β-cholestan-3-one gave a single lactam in each case, a claim which was discounted by Kobayashi *et al.* (8) and corrected in our earlier paper (1).

In the Beckmann rearrangements described by Shoppee *et al.*, both lactams were to be expected because not only were the *syn*/*anti* isomers not separated,[2] but also the conditions employed may have been vigorous enough to equilibrate the geometrical isomers. However, with the method of Craig and Naik (20), the mild, heterogeneous conditions make expectations less obvious. In this method the oxime of 5α-cholestan-3-one **12***a* (*syn*/*anti* ratio unspecified) was treated with TsCl–pyridine at 0°C, and the resulting sulfonate ester was chromatographed on activity I–II alumina (acid or alkaline). The product was stated to be pure 3-aza-*A*-homo-5α-cholestan-4-one **1***a*. Astonishingly, when this same rearrangement procedure, with substitution of $PhSO_2Cl$ for TsCl, was used by Nace and Watterson (14) on the 3-oxime of 5α-pregnane-3,20-dione **11**, the product obtained in 93% yield was stated to be the opposite rearrangement isomer, pure 4-aza-3-one **7***b* with no evidence in the ^{1}Hmr spectrum (single C-19 ^{1}Hmr peak) of any other product. However, as already pointed out, the appearance of only one C-19 methyl signal in the ^{1}Hmr spectrum is not valid proof of purity with these isomeric ring expansion compounds. This fact together with the improbability of the same reaction on two such closely related compounds giving diametrically opposite results prompted reexamination of both reactions.

The oxime tosylate of **12***a* and the benzenesulfonate of oxime **11** were prepared according to specifications (14, 20); the ^{1}Hmr spectrum of the oxime tosylate of **12***a* was that of a ~ 1:1 mixture of two isomers. Chromatography of both sulfonates on activity I alumina gave crude lactam products whose ^{13}Cmr spectra revealed that in fact the product of each reaction was a ~1:1 mixture of both possible lactams,[3] thus removing the apparent contradiction between the two reports.

In more recent work (13), it was asserted that a mixture of 5α-cholestan-3-one oximes was isomerized to a single oxime (presumably **13***a*) and precipitated almost quantitatively as the hydrochloride by dry HCl gas in ether. Subsequent Beckmann rearrangement of the liberated oxime by $SOCl_2$ was reported to give the 4-aza-*A*-homo-3-one **7***a*. Since there was no obvious reason why either oxime isomer should be favoured over the other, the work was repeated. In our hands, after regeneration at room temperature from its hydrochloride, the oxime was found by ^{13}Cmr spectroscopy to be a ~2:1 mixture of *syn*/*anti* isomers rather than a single isomer. Beckmann rearrangement of this material as specified (13) gave a ~1:2 mixture of both lactams **1***a* and **7***a* in accordance with stereospecific *anti* migration of the oxime mixture.

The most recent report of a single product from Beckmann rearrangement of 5α-cholestan-3-one oxime is that of Kim *et al.* (10) who used the Ph_3P–CCl_4 reagent. The product which precipitated and was recrystallized was stated to be pure 3-aza-*A*-homo-4-one **1***a*, apparently because the melting point was not depressed by the lactam (mixture) from the Schmidt reaction on 5α-cholestan-3-one, erroneously thought to be pure **1***a*. On repetition of the reaction, we find that there is steroidal material both in the precipitate (together with Ph_3P—O and Ph_3P) and in the filtrate. The steroidal material consists of a lactam portion plus an appreciable amount of dimeric substance, $C_{54}H_{92}N_2$, of uninvestigated structure. The ^{13}Cmr spectra of the lactam fraction in both the precipitate and the filtrate revealed each to be a mixture of the two lactams **1***a* and **7***a*. Hence, all four of these Beckmann reactions discussed above give 1–2:1 mixtures of lactams in agreement with our previous findings (1).

Turning to the Baeyer–Villiger reaction, we note that the reports (16, 19) of 5α-3-ketones **12***a* and **12***c* with CF_3CO_3H giving 4-oxa-*A*-homo-5α-3-ones **3***a*

[2]Although it was claimed that a single oxime was obtained (28), in fact a ~ 1:1 mixture of *syn*/*anti* isomers is formed from 5α-cholestan-3-one under various conditions which we have tried.

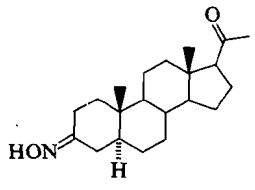
[3]The lactone, which Nace and Watterson (14) obtained by treatment of their lactam product with NO_2–pyridine–CCl_4 must also be a mixture of both isomers **3***b* and **4***b* in spite of its single C-19 ^{1}Hmr signal at δ 0.93.

Can. J. Chem. Downloaded from www.nrcresearchpress.com by 210.87.254.105 on 09/05/12
For personal use only.

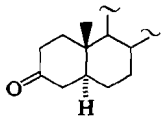
and **3***c* have already been shown to be false; the ^{13}Cmr spectrum of the product from **12***a* shows both lactones **3***a* and **4***a* to be present in ~1:1 ratio (1). Therefore, $LiAlH_4$–$AlCl_3$ reduction of the lactone so prepared must have led to a mixture of cyclic ethers rather than the pure 4-oxa-*A*-homo-5α-cholestane claimed (11).

More subtle is the report (17) that although perbenzoic acid treatment of 17β-acetoxy-5α-androstan-3-one (**12***d*) gave both possible lactones **3***d* and **4***d*, recrystallization of the mixture gave pure 4-oxa-*A*-homo-3-one **3***d*. Repetition of this reaction with *m*-chloroperbenzoic acid under the conditions of Caspi *et al.* (17) gave a ~1:1 mixture of the two lactones **3***d* and **4***d* instead of the 7:3 ratio reported. However, two recrystallizations of this mixture from ethyl acetate did indeed give pure lactone **3***d* as claimed, although the evidence originally presented (17) did not establish this point.

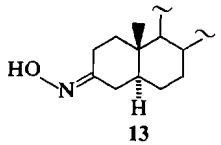
The reported (15) formation of only lactone **3***a* from 5α-cholestan-3-one oxime and CH_3CO_3H–$CHCl_3$ was suspect since the oxime is a mixture of *syn*/*anti* isomers. Not having access to 85% H_2O_2, we were unable to repeat the described experiment, but treatment of the oxime with *m*-ClPBA–$CHCl_3$ gave lactonic material contaminated by two less polar materials (chloronitro steroids?). The ^{13}Cmr spectrum of the product showed it to be mostly a ~1:1 mixture of both lactones **3***a* and **4***a*.



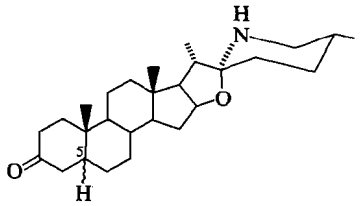
11



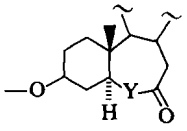
12



13

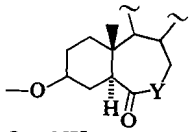


14
(*f*) 5α-H
(*g*) 5β-H

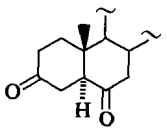


15

Y = O or NH



16



17

Catalytic oxidation of 5α-cholestan-3β-ol with RuO_4–$Pb(OAc)_4$–HOAc was stated to give a lactone which was either **3***a* or **4***a* (18). In our hands, several repetitions of the reaction, both as described and with variations, gave only 5α-cholestan-3-one with no trace of lactone.

The report (12) that steroidal alkaloid derivatives 5α- and 5β-solasodan-3-one **14***f* and **14***g* gave single lactones **3***e* and **5***e* is surprising in view of the fact that the same workers found that the 5α-ketone (and the corresponding Δ^4-unsaturated ketone) gives both possible lactams **1***e* and **7***e* in both the Beckmann and Schmidt reactions (30, 31). Undoubtedly the lactones are actually mixtures of both possible migration products.

The final matter taken up was the ring expansion of 5α-cholestane-3,6-dione **17***a* and its derivatives. Originally it was reported that the Schmidt (32, 33) and Baeyer–Villiger (34, 35) reactions on the 6-oxo group of 3-oxygenated 5α-cholestan-6-one gave a single product **15**. More recently the reactions were actually found to give a mixture of both lactones (36) and both lactams (5) **15** and **16**. In similar manner, the Schmidt reaction on the 3,6-diketone **17***a* was earlier (32) thought to give a single dilactam **18***a*, identical with the lactam from the Schmidt reaction on the 3-oxo-*B*-homo lactam **20***a*. A more recent reexamination (37) of the Schmidt reaction on **20***a* found both dilactams **18***a* and **19***a*. However, specific structural assignments could not be made. Our interest was two-fold: to assign the dilactam structures unambiguously, and to determine the migration ratio for the 3-oxo-*B*-homolactam **20***a* to learn whether the N bonded to C-5 exerts any effect on the migration.

Assignment of the dilactam structures was achieved by separate unequivocal syntheses of each according to Scheme 2. The Schmidt reaction on the lactam Δ^1-enone **22***a* gave both rearrangement products **24***a* and **25***a* which were readily identified from their ^{1}Hmr and ultraviolet spectra.[4] Hydrogenation of **24***a* and **25***a* gave the pure isomeric 5α-lactams **18***a* and **19***a*. However, the amount of **18***a* was small enough that an attempt was made to get more by reduction of **26***a* which was available as one of the products of Beckmann rearrangement of **23***a*. Unfortunately, hydrogenation of **26***a* in the presence of Pt–HOAc or Pd–KOH–MeOH gave ~90% of the 5β-H and only ~10% of 5α-H according to the ^{13}C-19 signals at δ 22.8 and 14.8 ppm. Therefore more **18***a* was eventually obtained by thick layer separation of the

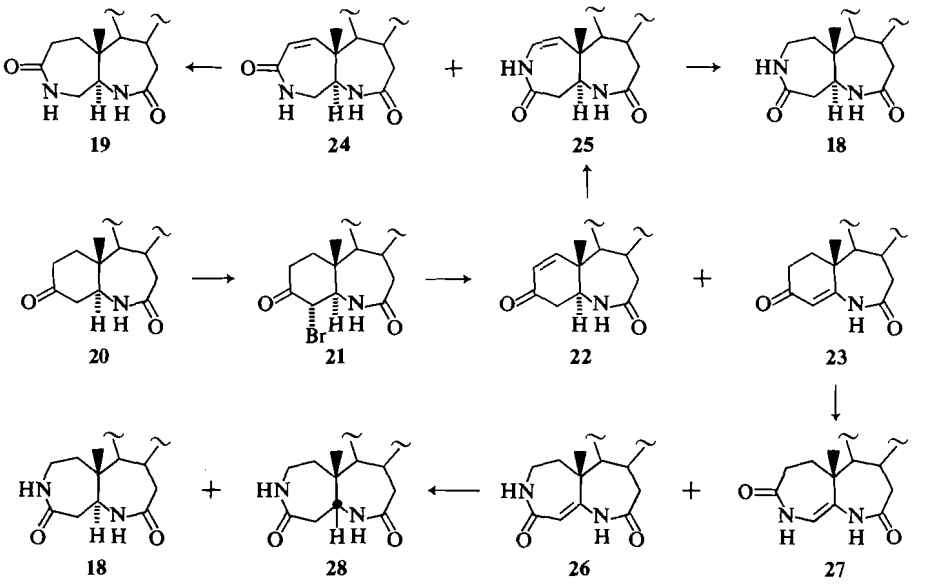
[4]Likewise, the Schmidt reaction on 5α-cholest-4-en-3-one gave both rearrangement products (see Experimental) contrary to an earlier report (50).

Can. J. Chem. Downloaded from www.nrcresearchpress.com by 210.87.254.105 on 09/05/12
For personal use only.

TABLE 2. ^{13}C shieldings of some *A*-homo steroids and two cholestenones[a]

Compound	Series	Functional groups[b]	C-1	C-2	C-3	C-4	C-4a	C-5	C-6	C-7	C-8	C-9	C-10	C-11	C-12	C-13	C-14	C-19
Cholestenones																		
	5α	Δ^1-3-oxo	158.5	127.4	200.2	41.0	—	44.3	27.7	31.3	35.7	50.0	39.0	21.3	39.8	42.7	56.4	13.0
	5β	Δ^1-3-oxo	161.7	126.9	200.8	39.1	—	46.3	(26.0)	(26.5)	35.2	41.1	38.7	22.4	39.9	42.7	55.8	20.9
A-Homo androstanes and cholestanes																		
3*c*	5α	3-oxo, 4-oxa, 17β-OH	29.7	35.6	176.3	—	70.0	48.7	26.2	31.2	35.0	53.7	37.5	20.7	36.6	42.8	50.9	12.3
4*c*	5α	3-oxa, 4-oxo, 17β-OH	35.8	64.7	—	176.0	41.7	43.5	30.4	31.4	34.7	54.0	37.7	20.9	36.6	42.8	50.9	12.1
3*d*	5α	3-oxo, 4-oxa, 17β-OAc	29.6	35.5	176.0	—	69.9	48.5	26.1	31.1	34.7	53.5	37.7	20.5	36.7	42.4	50.6	12.3
7*b*	5α	3-oxo, 4-aza, 17β-Ac	31.8	35.1	178.8	—	44.2	49.7	27.5	31.3	34.9	53.6	38.6	20.9	38.9	43.8	56.4	11.9
1*b*	5α	3-aza, 4-oxo, 17β-Ac	37.7	39.5	—	178.9	41.8	43.1	30.8	31.5	34.5	53.8	38.7	21.2	38.9	43.8	56.5	12.0
	5α	2α-Br, 3-oxo, 4-oxa	48.7	48.0	169.9	—	70.1	44.6	25.9	31.4	34.8	53.1	39.0	21.1	39.6	42.3	56.1	12.6
	5α	3-oxa, 4-oxo, 4aα-Br	42.4	65.9	—	170.5	50.8	51.0	29.0	31.2	35.0	56.0	38.5	21.3	39.9	42.4	56.2	15.4
	5β	2β-Br, 3-oxo, 4-oxa	46.3	42.2	170.0	—	70.7	44.9	26.5	27.4	35.8	41.7	38.5	21.4	39.9	42.7	56.4	21.4
	5β	3-oxa, 4-oxo, 4aβ-Br	42.5	63.1	—	169.4	45.9	51.2	25.8	27.4	35.3	39.8	37.7	21.5	40.0	42.5	56.3	25.4
	—	Δ^{4a}, 3-aza, 4-oxo	36.5	42.0	—	170.6	118.8	161.3	33.7	36.0	35.5	53.3	44.4	21.3	39.7	42.4	55.8	21.3
	—	Δ^{4a}, 3-oxo, 4-aza	33.9	33.9	177.0	—	114.2	131.4	31.5	33.0	35.9	52.3	41.7	21.8	39.9	42.5	56.2	20.6
9	5α	Δ^1, 3-oxo, 4-aza	149.9	121.6	169.4	—	44.2	49.0	27.8	31.7	34.7	51.6	44.9	22.2	39.8	42.4	56.2	15.9
10	5β	Δ^1, 3-oxo, 4-aza	150.8	121.2	169.6	—	44.5	(47.3)	26.9	28.5	35.7	(46.8)	44.2	21.4	40.0	42.4	56.0	21.4

[a]In ppm from internal TMS for $CDCl_3$ solutions; similar values in parentheses may be interchanged. For the remaining shieldings of the cholestane derivatives see footnote *a* of Table 1. The other shieldings for the androstane and pregnane derivatives are listed in Table 3.
[b]Where no 17-substituent is mentioned, it is understood that the cholestane side chain is present.



SCHEME 2

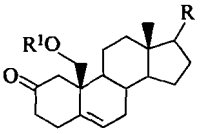
TABLE 3. D-Ring ^{13}C shieldings of the *A*-homo and/or *B*-homo steroids in Tables 2 and 4[a]

Compound	C-15	C-16	C-17	C-18
3*c*	23.3	30.4	81.6	11.1
4*c*	23.3	30.4	81.6	11.1
3*d*[b]	23.4	27.5	82.5	12.0
7*b*[c]	24.2	22.7	63.6	13.3
1*b*[c]	24.2	22.7	63.6	13.3
17*a*	23.8	28.0	56.1	12.0
20*a*	25.6	27.6	56.4	11.8
23*a*	25.4	27.7	56.8	12.0
22*a*	25.5	27.6	56.4	12.0
30*a*	25.4	27.5	56.8	11.9
27*a*	25.4	27.7	56.4	11.8
26*a*	25.2	27.7	56.3	11.9
24*a*	25.5	27.6	56.5	12.0
19*a*	25.6	27.7	56.5	11.9
18*a*	25.5	27.7	56.5	11.9

[a]In ppm from internal TMS for $CDCl_3$ solutions.
[b]Acetoxyl absorption at 21.0 (CH_3) and 171.0 (C=O) ppm.
[c]C-20, 209.4 ppm; C-21, 31.4 ppm.

product mixture from the Schmidt reaction on **20***a*. The ^{13}Cmr assignments for most of the compounds in Scheme 2 are listed in Table 4. The ^{13}Cmr spectrum of the product of the Schmidt reaction on **20***a* contained a number of ill-resolved signals, and therefore the product ratio **18***a*:**19***a* was determined from the ratio of the ^{13}C-19 methyl peaks only and found to be 55:45. This ratio is so slightly different from 1:1 that the effect of the electron-withdrawing lactam N at C-5 on the migratory aptitude of C-4 in **20***a* is apparently negligible.

In conclusion, most of the reported exceptions to a ~1:1 mixture of migration products in ring expansion of 3-keto steroids are seen to vanish when the reaction products are subjected to ^{13}Cmr analysis. However, in the Beckmann rearrangement, if the usual ~1:1 oxime ratio has been altered by some treatment, and if the rearrangement conditions do not equilibrate the *syn*/*anti* oximes, then the product composition will be determined by the oxime ratio in a stereospecific *anti* migration. Of course, exceptions to an equimolar mixture of products can also be caused by a polar substituent too close to the site of reaction as is apparently the case in the Beckmann rearrangement of **29** (23). If



29 R = a variety of substituents
R¹ = H, alkyl, or acyl

the double bond is absent, both migration products are obtained, but with the double bond present only C-3 is reported to migrate.

Experimental

General

Reagents, instruments, procedures, and ^{13}Cmr operating conditions are the same as in ref. 1. Reaction mixtures were stirred with rotating magnetic bars. The following abbreviations are used in describing ^1Hmr spectra: s singlet, d doublet, t triplet, q quartet, b broad, sp split, and m multiplet.

The following C-19 methyl peak chemical shifts in $CDCl_3$ were observed for the authentic cholestane A-ring lactones and lactams: **1***a* 0.90, **7***a* 0.90, **4***a* 0.93, **3***a* 0.93, **2***a* 0.99, **8***a* 1.00, **6***a* 1.01, and **5***a* 1.02 ppm.

The ^{13}Cmr spectra for the pure compounds are collected in Tables 1, 2, 3, and 4. Most spectra were run with 10–20 mg/0.25 mL, but to avoid line broadening from association, two dilactams were run in more dilute solution ~6 mg/0.4 mL.

Can. J. Chem. Downloaded from www.nrcresearchpress.com by 210.87.254.105 on 09/05/12
For personal use only.

Can. J. Chem. Downloaded from www.nrcresearchpress.com by 210.87.254.105 on 09/05/12
For personal use only.

TABLE 4. ^{13}C shieldings of some *A*-homo and/or *B*-homo steroids and their cholestanedione precursors[a]

Compound	Series	Functional groups	C-1	C-2	C-3	C-4	C-4a	C-5	C-6	C-7	C-8	C-9	C-10	C-11	C-12	C-13	C-14	C-19
17*a*	5α	3,6-dioxocholestane	(37.0)	(37.3)	209.0	(38.0)	—	57.4	211.0	46.6	38.0	53.4	41.2	21.7	39.4	43.0	56.6	12.5
									C-7	C-7a								
A-Homo and/or *B*-homo cholestanes																		
20*a*	5α	3,7-dioxo, 6-aza	(35.9)	(36.9)	208.1	43.5	—	58.6	176.7	40.2	34.8	58.0	39.0	23.6	39.9	42.5	55.7	12.3
23*a*	—	Δ^4-3,7-dioxo, 6-aza	(33.2)	(35.8)	198.1	120.8	—	164.2	174.1	41.4	35.0	50.4	41.4	23.8	39.9	42.8	55.8	20.6
22*a*	5α	Δ^1-3,7-dioxo, 6-aza	155.4	127.0	199.0	39.6	—	(54.9)	176.7	39.6	35.0	(55.4)	42.1	23.4	39.8	42.7	55.9	12.7
30*a*	—	Δ^1,Δ^4-3,7-dioxo, 6-aza	154.6	126.5	186.3	121.7	—	160.2	174.7	41.8	35.7	(55.5)	45.7	25.0	39.8	42.3	(55.7)	18.6
27*a*	—	Δ^{4a}-3,7-dioxo, 4,6-diaza	(32.0)	(31.0)	(177.5)	—	121.6	127.6	(176.4)	39.5	34.4	53.0	42.4	21.7	39.7	42.7	55.6	20.6
26*a*	—	Δ^{4a}-4,7-dioxo, 3,6-diaza	42.3	37.4	—	169.5	120.7	154.0	175.4	39.1	34.3	53.3	45.3	22.6	39.7	42.6	55.0	21.6
24*a*	5α	Δ^1-3,7-dioxo, 4,6-diaza	148.9	121.8	169.9	—	44.3	63.5	176.5	(39.9)	34.1	57.5	47.7	24.7	(39.8)	42.6	55.4	16.7
19*a*	5α	3,7-dioxo, 4,6-diaza	(32.3)	(30.1)	176.6	—	43.3	60.2	176.6	39.5	34.7	(56.5)	41.3	23.2	40.0	42.5	(55.9)	14.3
18*a*	5α	4,7-dioxo, 3,6-diaza	37.0	37.4	—	173.9	39.5	(55.1)	176.4	39.5	34.7	(54.9)	41.3	23.5	40.0	42.5	(56.0)	14.8

[a]In ppm from internal TMS for $CDCl_3$ solutions; similar values in parentheses may be interchanged. The shieldings for C-20 to C-27 are given in footnote *a* to Table 1. The shieldings for C-15 to C-18 are listed in Table 3.

*3-Oxa-*A*-homo-5α-cholestan-4-one (**4a**)*

To a stirred suspension of CF_3CO_3H (prepared from 70 mg of 63% aqueous H_2O_2, 360 mg of $(CF_3CO)_2O$, and 1.5 mL of CH_2Cl_2) and 200 mg of Na_2HPO_4 was added a solution of 200 mg of 4α-bromo-5α-cholestan-3-one (38) in 2 mL of CH_2Cl_2. After 4 h at room temperature, the CH_2Cl_2 was evaporated in a stream of nitrogen. The residue was dissolved in ether, washed with 10% aqueous Na_2CO_3 and water, dried, and concentrated to leave 165 mg of colorless solid 4aα-bromo-3-oxa-*A*-homo-5α-cholestan-4-one; ir($CHCl_3$): 1730 cm^{-1}; ^{1}Hmr ($CDCl_3$) δ:4–5 (m, 2- and 4aβ-H's) ppm; M^+ calcd. for $C_{27}H_{45}{}^{79}BrO_2$:480.2602; found: 480.2600. Since tlc and the ^{13}Cmr spectrum indicated it to be a single compound, it was used without further purification.

To a stirred suspension of $CrCl_2$ in water (prepared from 1.5 g of $CrCl_3 \cdot 6H_2O$, 3.0 g of Zn dust, 2.4 g of $HgCl_2$, 0.8 mL of concentrated HCl, and 6 mL of H_2O) under nitrogen was added a solution of 140 mg of the above bromo lactone in 2 mL of $CHCl_3$ and 4 mL of HOAc. After 12 h most of the solvent was evaporated in a stream of air. The residue was extracted with ether, washed with 10% aqueous Na_2CO_3 and water, dried, and concentrated to leave 105 mg of colorless solid. Chromatography on a 10-g silica gel plate developed in benzene–ether (84:16) afforded 64 mg of solid from a band at R_f 0.41. Recrystallization from ether–MeOH and from $CHCl_3$–MeOH gave 44 mg of colorless plates of pure **3-oxa-5α-lactone 4***a*, mp 179.5–180.5°C with previous sintering, $[\alpha]_D^{25}$ +45.5° (*c* 1.55, $CHCl_3$); ir ($CHCl_3$): 1725 cm^{-1}; ^{1}Hmr ($CDCl_3$) δ: 0.93 (C-19 Me), 2.87 (1 H, dd, 4aβ-H), and 4–5 (2 H, m, 2-H's) ppm; M^+ calcd. for $C_{27}H_{46}O_2$: 402.3498; found: 402.3497. *Anal.* calcd. for $C_{27}H_{46}O_2$: C 80.54, H 11.51; found: C 80.62, H 11.29.

*4-Oxa-*A*-homo-5β-cholestan-3-one (**5a**)*

Baeyer–Villiger oxidation of 200 mg of 2β-bromo-5β-cholestan-3-one (39) with CF_3CO_3H as in the preceding experiment gave 190 mg of off-white solid **2β-bromo-4-oxa-A-homo-5β-cholestan-3-one**; ir ($CHCl_3$): 1750 cm^{-1}; ^{1}Hmr ($CDCl_3$) δ:3.99 (1 H, sp d, 4aβ-H), 4.67 (1 H, dd, 4aα-H), and 4.96 (1 H, sp d, 2α-H) ppm; M^+ calcd. for $C_{27}H_{45}{}^{79}BrO_2$: 480.2602; found: 480.2597. Since the tlc and the ^{13}Cmr spectrum indicated it to be almost pure, it was used without further purification.

Chromous chloride reduction of 175 mg of the above bromo lactone was performed as in the preceding experiment. Work-up gave 155 mg of colorless solid which was chromatographed on a 20-g silica gel plate developed in benzene–ether (90:10). A band at R_f 0.40 yielded 96 mg of colorless solid which on two recrystallizations from $CHCl_3$–MeOH gave 77 mg of pure **4-oxa-5β-lactone 5***a*, mp 164–165°C, $[\alpha]_D^{25}$ +48.5° (*c* 1.57, $CHCl_3$); ir ($CHCl_3$): 1730 cm^{-1}; ^{1}Hmr ($CDCl_3$) δ:1.02 (C-19 Me), 3.90 (1 H, dd, 4aβ-H?), and 4.67 (1 H, dd, 4aα-H) ppm; M^+ calcd. for $C_{27}H_{46}O_2$: 402.3498; found: 402.3499. *Anal.* calcd. for $C_{27}H_{46}O_2$: C 80.54, H 11.51; found: C 80.83, H 11.50.

*3-Oxa-*A*-homo-5β-cholestan-4-one (**6a**)*

The Baeyer–Villiger oxidation of 290 mg of 4β-bromo-5β-cholestan-3-one (40) was carried out in 5 mL of $CHCl_3$ with 580 mg of *m*-chloroperbenzoic acid (Aldrich 75%) at room temperature for 4 days. After work-up, the crude product was chromatographed on a column of 10 g of silica gel. Benzene–ether mixtures eluted 160 mg of colorless solid **4aβ-bromo-3-oxa-A-homo-5β-cholestan-4-one**, ir ($CHCl_3$): 1750 (C=O) cm^{-1}, which tlc and ^{13}Cmr absorption indicated was pure enough for direct use; M^+ calcd. for $C_{27}H_{45}{}^{79}BrO_2$: 480.2602; found: 480.2596.

Chromous chloride reduction of 110 mg of the bromo lactone as in the preceding two experiments gave 62 mg of colorless solid. Recrystallization from MeOH gave 30 mg of colorless plates of **3-oxa-5β-lactone 6***a*, mp 164–167°C (capillary), $[\alpha]_D^{20}$ +58° (*c* 1.42, $CHCl_3$); ir ($CHCl_3$): 1730 cm^{-1}; ^{1}Hmr ($CDCl_3$) δ: 1.01 (C-19, Me), 3.21 (1 H, t, 4aβ-H?), and 3.9–4.5 (2 H, m, 2-H's) ppm; M^+ calcd. for $C_{27}H_{46}O_2$: 402.3498; found: 402.3495.

Can. J. Chem. Downloaded from www.nrcresearchpress.com by 210.87.254.105 on 09/05/12
For personal use only.

4-Aza-A-homo-5α-cholestan-3-one (7a)

5α-Cholest-1-en-3-one was prepared by the method of Green and Long (41) from 200 mg of 2α-bromo-5α-cholestan-3-one, 160 mg of $CaCO_3$, and 7 mL of dimethylacetamide and was purified by thick-layer chromatography on a 20-g silica gel plate developed twice in $CHCl_3$–benzene (90:10). The main uv active band at R_f 0.45 yielded 94 mg of the conjugated ketone. One recrystallization from ether–MeOH gave 72 mg of colorless plates, mp 97–98°C (lit.(41) mp 98°C).

A solution of 215 mg of the Δ^1-enone, 215 mg of $HONH_2 \cdot HCl$, and 215 mg of NaOAc in 2 mL of water and 20 mL of MeOH was refluxed for 1.5 h. After distillation of most of the MeOH, the residue was dissolved in ether, washed with water, and concentrated to give 210 mg of viscous oily **oxime**. Thin-layer chromatography (benzene–ether, 92:8) showed the complete absence of Δ^1-enone and the presence of two overlapping more polar spots.

A solution of the 210 mg of oxime, 210 mg of *p*-TsCl, and 5 mL of dry pyridine was stirred at room temperature for 3 h. After evaporation of the pyridine in a stream of nitrogen, ice was added to the residue. After 15 min, extraction with chloroform yielded the oily **Δ^1-oxime *p*-toluenesulfonate** which was used directly for the Beckmann rearrangement by Oka and Hara's procedure (2).

A mixture of the oxime tosylate from above and 0.2 mL of concentrated aqueous HCl in 20 mL of MeOH was refluxed with stirring. Within 0.5 h all solid had dissolved. At the end of 2 h most of the MeOH was distilled, and the residue was neutralized with aqueous NaOH. The product was extracted with $CHCl_3$, washed with water, dried, and concentrated to leave 205 mg of off-white solid. Chromatography on two 20-g silica gel plates developed in EtOAc–MeOH (95:5) afforded 115 mg of solid from the band at R_f 0.31. One recrystallization from $CHCl_3$–MeOH gave 82 mg of colorless needles of **4-aza-A-homo-5α-cholest-1-en-3-one** (**9***a*), mp 224–226°C (lit.(8) mp 232°C), $[\alpha]_D^{8.5}$ +32.8° (*c* 1.51, $CHCl_3$); uv (MeOH): 213 (13 000) nm; ir ($CHCl_3$):3420 (NH), 1650 (C=O), and 1610 (C=C) cm^{-1}; ^{1}Hmr ($CDCl_3$) δ:1.00 (C-19 Me), 2.67 (1 H, q, 4aα-H), 3.36 (1 H, dq, 4aβ-H), 5.73 (1 H, sp d, 2-H), 6.31 (1 H, d, 1-H), and 7.03 (1 H, bd, NH) ppm; M^+ calcd. for $C_{27}H_{45}NO$: 399.3501; found: 399.3502.

A solution of 45 mg of unsaturated lactam **9** in 12 mL of MeOH was hydrogenated at atmospheric pressure and room temperature in the presence of 15 mg of 10% Pd/C catalyst. The crude reduction product was recrystallized twice from MeOH to give 24 mg of colorless granules of the **4-aza-5α-lactam** **7***a*, mp 265–280°C (dec.), mp 270–276°C (dec. sealed capillary), $[\alpha]_D^{19.5}$ +2.7° (*c* 1.52, $CHCl_3$);[5] ir ($CHCl_3$): 3430 (NH) and 1655 (C=O) cm^{-1}; ^{1}Hmr ($CDCl_3$) δ: 0.90 (C-19 Me), 3.1–3.6 (1 H?, bb, 4aβH), and 6.52 (1 H, bs, NH) ppm; M^+ calcd. for $C_{27}H_{47}NO$: 401.3658; found: 401.3659.

4-Aza-A-homo-5β-cholestan-3-one (8a)

The procedure of Clinton *et al.* (42) was used to prepare **2-hydroxymethylene-5β-cholestan-3-one** from 2.0 g of 5β-cholestan-3-one, 2.3 g of HCOOEt, and 562 mg of NaOMe in 27 mL of dry benzene. The crude hydroxymethylene ketone obtained from the Na salt amounted to 1.4 g of colorless solid, mp 80–85°C (lit.(42) mp 90–100°C), which was free of starting ketone and was used without further purification; ir ($CHCl_3$): 1650 (conj. C=O) and 1595 (conj. C=C) cm^{-1}; M^+ calcd. for $C_{28}H_{46}O_2$: 414.3497; found: 414.3497.

The method of Shimizu *et al.* (43) was adapted. A solution of 1.4 g of the above hydroxymethylene ketone, 840 mg of dichlorodicyano quinone and 20 mL of benzene was stirred and refluxed for 1 h. The precipitated solid was filtered and washed with benzene. The filtrate was washed with basified (KOH) aqueous $Na_2S_2O_4$ and water, dried, and concentrated to leave 900 mg of off-white oily solid **unsaturated keto aldehyde**; ir ($CHCl_3$): 1685 (center of fine-structured C=O) and 1610 (conj. C=C) cm^{-1}; ^{1}Hmr ($CDCl_3$) δ: 7.53 (1 H, s, 1-H) and 10.0 (1 H, s, CH=O) ppm; M^+ calcd. for $C_{28}H_{44}O_2$: 412.3341; found 412.3342. The product, which gave a single tlc spot, was used without further purification.

With ref. 43 as guide, a mixture of 900 mg of the above unsaturated aldehyde, 2.2 g of tris(triphenylphosphine)chlororhodium(I), and 25 mL of benzene was stirred and refluxed under nitrogen for 4 h. The solid in the cooled reaction mixture was removed by filtration and washed with benzene. The filtrate was concentrated, dissolved in CCl_4, and chromatographed on a column of 40 g of neutral alumina (activity IV). Hexanes–benzene mixtures eluted 700 mg of colorless solid **5β-cholest-1-en-3-one**. A sample recrystallized from ether–MeOH gave colorless plates, mp 105–105.5°C (lit. (39) mp 106.5°C), $[\alpha]_D^{20.5}$+154° (*c* 0.93, $CHCl_3$) (lit.(8) $[\alpha]_D$ +107°); ir ($CHCl_3$): 1670 (C=O) cm^{-1}; ^{1}Hmr ($CDCl_3$) δ: 1.20 (C-19 Me), 2.79 (1 H, dd, 4β-H), 5.90 (1 H, d, *J* = 10 Hz, 2-H), and 6.85 (1 H, d, *J* = 10 Hz, 1-H) ppm; M^+ calcd. for $C_{27}H_{44}O$: 384.3392; found: 384.3391.

A solution of 275 mg of 5β-cholest-1-en-3-one, 275 mg of $HONH_2 \cdot HCl$, and 275 mg of NaOAc in 3 mL of water and 3 mL of MeOH was refluxed for 2 h. After distillation of the MeOH, the residue was dissolved in ether, washed with water, dried, and concentrated to leave 270 mg of colorless solid oxime, ir ($CHCl_3$): 3580 and 3280 (OH) cm^{-1}, no C=O absorption; M^+ calcd. for $C_{27}H_{45}NO$: 399.3501; found: 399.3499. Thin-layer chromatography (benzene–ether, 95:5) revealed the complete absence of starting ketone and the presence of two overlapping more polar spots.

A mixture of 270 mg of the above oxime, 270 mg of *p*-TsCl, and 6 mL of dry pyridine was stirred at room temperature for 3 h. After removal of most of the pyridine in a stream of nitrogen, the residue was dissolved in $CHCl_3$, washed with water, dried, and concentrated to leave the oily **oxime tosylate**; ir ($CHCl_3$): 1380 and 1180 (sulfonate) cm^{-1}, no OH absorption; ^{1}Hmr ($CDCl_3$) δ: 2.40 and 2.46 (two s, $ArCH_3$ of *syn* and *anti* isomers), 5.86 (1 H, d, *J* = 10 Hz, 2-H), and 6.23 (1 H, d, *J* = 10 Hz, 1-H) ppm, the aromatic H peaks were also doubled because of *syn–anti* isomers; M^+ calcd. for $C_{34}H_{51}NO_3S$: 553.3589; found: 553.3592.

The crude tosylate from above was stirred and refluxed for 2.5 h with 0.7 mL of concentrated aqueous HCl in 40 mL of MeOH. Within 0.5 h all solid had dissolved. After distillation of most of the MeOH, the residue was dissolved in $CHCl_3$, washed with water, dried, and concentrated to leave 245 mg of off-white solid. Two recrystallizations from $CHCl_3$–MeOH gave 140 mg of colorless needles of **4-aza-A-homo-5β-cholest-1-en-3-one** (**10***a*), mp 185–198°C (dec.), $[\alpha]_D^{21}$ +118° (*c* 1.44, $CHCl_3$); uv (MeOH): 213 (13 000) nm; ir ($CHCl_3$): 3410 (NH) 1660 (C=O), and 1610 (C=C) cm^{-1}; ^{1}Hmr ($CDCl_3$) δ: 1.12 (C-19 Me), 2.85 (1 H, dd, 4aα-H), 3.66 (1 H,m, 4aβ-H), 5.72 (1 H, bd, *J* = 13 Hz, 2-H), 6.25 (1 H, d, *J* = 13 Hz, 1-H), and 6.74 (1 H, bm, NH) ppm; M^+ calcd. for $C_{27}H_{45}NO$: 399.3501; found: 399.3502.

A solution of 70 mg of the unsaturated lactam **10** in 35 mL of MeOH was hydrogenated at atmospheric pressure and room temperature in the presence of 30 mg of 10% Pd/C catalyst for 1 h. Two recrystallizations of the reduction product from $CHCl_3$–MeOH gave 60 mg of colorless needles of the **4-aza-5β-lactam** **8***a*, mp 188–190°C, $[\alpha]_D^{21}$ +29.7° (*c* 1.52, $CHCl_3$) (lit. (26) mp 195°C, $[\alpha]_D$ +21°)[6]; ir($CHCl_3$): 3410 (NH) and 1660 (C=O) cm^{-1}; ^{1}Hmr ($CDCl_3$) δ: 1.00 (C-19 Me), 2.72 (1 H, bq, 4aα-H), 3.80 (1 H, m, 4aβ-H), and 6.41 (1 H, bm, NH) ppm; M^+ calcd. for $C_{27}H_{47}NO$: 401.3658; found: 401.3659.

[5] There is no evidence that the compound reported in ref. 26 to be lactam **7***a*, mp 295°C, $[\alpha]_D$ −8°, was a pure compound.

[6] It is by no means clear that the lactam described in ref. 26 was a pure compound.

Can. J. Chem. Downloaded from www.nrcresearchpress.com by 210.87.254.105 on 09/05/12
For personal use only.

Beckmann Rearrangements

(*a*) The procedure of Craig and Naik (20) was followed. To a solution of 150 mg of 5α-cholestan-3-one oxime in 1.5 mL of dry pyridine at 0°C was added 95 mg of *p*-TsCl. After 0.5 h the pyridine was evaporated at 0.1 Torr and room temperature. The residual solid was chromatographed on a 3-g column of Woelm neutral alumina (activity I) packed in benzene. After elution of 6 mg of recovered oxime with benzene–ether mixtures, further elution with benzene–ether (50:50) and EtOAc–MeOH (60:40) afforded 110 mg (73%) of colorless crystalline lactam giving a single tlc spot (EtOAc–MeOH, 95:5). The ^{13}Cmr spectrum showed the presence of both **1***a* and **7***a*. Comparison of peak heights for the following pairs of signals: 54.1 vs. 53.9 (C-9), 43.3 vs. 49.5 (C-5), 38.8 vs. 38.7 (C-10), and 21.3 vs. 21.0 (C-11) ppm revealed a composition slightly richer in **1***a* with a ratio of **1***a*:**7***a* of ~52:48.

(*b*) The 3-monoxime **11** of 5α-pregnane-3,20-dione was prepared according to the directions of Nace and Waterson (14) and then rearranged under both sets of conditions used by these authors; ir ($CHCl_3$): 3580 and 3280 (NOH) and 1705 (C=O) cm^{-1}. The ^{13}Cmr spectrum ($CDCl_3$–DMSO-d_6) showed the presence of both *syn* and *anti* oximes. For a sample recrystallized four times, comparison of peak heights at 46.3 (C-5 of OH *syn* to C-2) and 45.3 (C-5 of OH *anti* to C-2) ppm revealed a *syn*/*anti* ratio of ~43:57.

(*i*) *Benzenesulfonate–Alumina*

To a solution of 62 mg of the monoxime in 1 mL of dry pyridine at 0°C was added a solution of 42 mg of $PhSO_2Cl$ in 0.5 mL of dry pyridine. After 0.5 h, during which the reaction mixture was allowed to warm to room temperature, there was no oxime left (tlc). Solvent was evaporated at 0.1 Torr and room temperature, and the residual colorless solid[7] was chromatographed on a 2.8-g column of Woelm neutral alumina (activity I). Elution with ether and with EtOAc–MeOH (88:12) gave 49 mg (79%) of colorless crystalline lactam (single tlc spot), mp 250–268°C (dec.) with a phase change at 230°C (lit.(14) mp 275–277°C (dec.)); ir ($CHCl_3$): 3420 (NH), 1700 (C=O), and 1660 (N—C=O) cm^{-1}. The mass spectrum indicated about 8% of an impurity corresponding in mass to bis lactam. The ^{13}Cmr spectrum showed the presence of both **1***b* and **7***b*. Comparison of peak heights for the following pairs of signals: 53.8 vs. 53.6 (C-9), 43.1 vs 49.7 (C-5), and 21.2 vs. 21.0 (C-11) ppm , revealed a composition slightly richer in **1***b* with a ratio of **1***b*:**7***b* of ~53:47.

Four recrystallizations of this material from MeOH–CH_2Cl_2 removed the bis lactam and gave 22 mg of colorless granules, mp 278–281°C (with subl. and dec. on the hot stage), mp 260–265°C (dec. in a sealed capillary), (lit. (14) mp 275–277°C (dec.)); M^+ calcd. for $C_{21}H_{33}NO_2$: 331.2511; found: 331.2511.

Comparison of the same sets of peaks in the ^{13}Cmr spectrum showed no change in the **1***b*:**7***b* ratio.

(*ii*) *Thionyl Chloride–Dioxane*

To a stirred solution of 259 mg of monoxime in 30 mL of dry dioxane cooled in an ice bath was added a solution of 2.3 mL of distilled $SOCl_2$ in 6 mL of dry dioxane during 7 min. The reaction was allowed to warm slowly to room temperature over an hour. After addition of water and NH_4OH, the product was extracted with CH_2Cl_2 to yield 218 mg (84%) of off-white solid. Aside from ~8% of starting oxime, tlc (benzene–ether–HOAc, 75:22:3) showed only one spot corresponding to the more polar lactam. Two recrystallizations from MeOH gave 115 mg of crystals of very wide mp 218–280°C which was chromatographed on a 3.5-g column of silica gel. Elution with benzene, benzene–ether, and ether–EtOAc (50:50) gave 17 mg of recovered oxime. Further elution with ether–EtOAc to EtOAc–MeOH (80:20) afforded 70 mg of colorless solid lactam. One recrystallization from CH_2Cl_2–MeOH gave 55 mg of granules, mp 260–295°C (dec. on the hot stage), mp 268–285°C (dec. in a sealed capillary) (lit (14) mp 270–276°C); ir ($CHCl_3$): same as in (*i*); M^+ calcd. for $C_{21}H_{33}NO_2$: 331.2511; found: 331.2511.

The ^{13}Cmr spectrum showed the presence of both **1***b* and **7***b*. Comparison of peak heights for the following pairs of signals: 53.8 vs. 53.6 (C-9), 43.1 vs. 49.4 (C-5), and 21.2 vs. 21.0 (C-11) ppm, revealed a composition richer in **7***b* with a ratio of **1***b*:**7***b* of ~40:60.

(*c*) The procedure of Ogura *et al.* (13) was repeated. A mixture of 1.0 g of 5α-cholestan-3-one, 1.0 g of $HONH_2$·HCl, 1.0 g of NaOAc, 5 mL of water, and 50 mL of MeOH was stirred and refluxed for 3 h. Distillation of MeOH, addition of water, and filtration gave 950 mg (91%) of colorless oxime, mp 192–198°C (lit.(44) mp 199°C).

The ^{13}Cmr spectrum showed the presence of both *syn* (OH and C-2) and *anti* (OH and C-2) oximes. Comparison of peak heights for the following pairs of signals: 46.4 (*syn*) vs. 45.3 (*anti* C-5), 37.2 (*syn*) vs. 38.4 (*anti* C-1), and 34.4 (*syn*) vs. 27.3 (*anti* C-4) ppm, revealed a composition slightly richer in the *anti* isomer with a *syn*/*anti* ratio of ~47:53.

Dry HCl gas was bubbled into a solution of 500 mg of the above oxime in 20 mL of ether. After 0.5 h the precipitated solid was filtered, triturated with aqueous $NaHCO_3$, and extracted with ether. Concentration of the dried ether solution at room temperature left 430 mg of colorless oxime, mp 195–198°C with a phase change at ~175°C (lit.(13) mp 195–196°C).

The ^{13}Cmr spectrum showed the presence of both *syn* (OH and C-2) and *anti* (OH and C-2) oximes. Comparison of peak heights for the following pairs of signals: 46.4 (*syn*) vs. 45.3 (*anti* C-5), 37.2 (*syn*) vs. 38.4 (*anti* C-1), and 34.4 (*syn*) vs. 27.3 (*anti* C-4) ppm, revealed a composition richer in the *syn* isomer with a *syn*/*anti* ratio of ~65:35.

To a solution of 100 mg of the above regenerated oxime in 2.5 mL of dry dioxane at 40°C was added 0.3 mL of redistilled $SOCl_2$. After 10 min at 40°C, the reaction mixture was basified with aqueous $NaHCO_3$ and extracted with $CHCl_3$. Evaporation of the dried $CHCl_3$ solution left 93 mg (93%) of semi-solid lactam which gave a single tlc spot more polar than the starting oxime.

The ^{13}Cmr spectrum showed the presence of both **1***a* and **7***a*. Comparison of peak heights for the following pairs of signals: 54.1 vs. 53.8 (C-9), 43.3 vs. 49.5 (C-5), 38.8 vs. 38.6 (C-10), and 21.1 vs. 21.0 (C-11) ppm, revealed a composition richer in **7***a* with a **1***a*:**7***a* ratio of 35:65 in agreement with stereospecific *anti* rearrangement for the oxime mixture used.

(*d*) The procedure of Kim *et al.* (10) was followed for both oxime preparation and rearrangement. The oxime so prepared was a 50:50 mixture of *syn* and *anti* isomers from comparison of the C-5 ^{13}Cmr signals at 46.5 (*syn*) and 45.3 ppm (*anti*). A solution of 500 mg of 5α-cholestan-3-one oxime and 630 mg of triphenylphosphine in 12 mL of CCl_4 was refluxed for 5 h. After cooling in ice, the reaction mixture was filtered. The gummy solid (~500 mg), containing Ph_3P and Ph_3PO as well as steroidal product, was chromatographed on ten 20-g preparative plates developed thrice in benzene–EtOAc–MeOH (85:5:10). The band (I_2) at R_f 0.67 gave 41 mg of off-white lactam.

The ^{13}Cmr spectrum showed the presence of both **1***a* and **7***a*. Comparison of peak heights for the following pairs of signals: 54.1 vs. 53.9 (C-9), 43.3 vs. 49.5 (C-5), 38.8 vs. 38.7 (C-10), and 21.3 vs. 21.0 (C-11) ppm, revealed a composition slightly richer in **1***a* with a ratio of **1***a*:**7***a* of ~55:45.

The band at R_f 0.33 gave 85 mg of a colorless solid. Two recrystallizations from $CHCl_3$–MeOH afforded 25 mg of granules of dimeric steroid, mp 295–305°C (dec.); ir: 1650 cm^{-1}; *m*/*e*:768.7, $C_{54}H_{94}N_2$ requires 768.7.

[7]The crude oxime tosylate was reported to be a red oil in ref. 14.

Can. J. Chem. Downloaded from www.nrcresearchpress.com by 210.87.254.105 on 09/05/12
For personal use only.

Since most of the steroidal material had remained in the filtrate, a portion of the evaporated filtrate was chromatographed on a 20-g silica gel plate as described above. The lactam isolated in this way was also subjected to ^{13}Cmr analysis which showed the presence of both **1***a* and **7***a*. Comparison of peak heights for the following pairs of signals: 54.1 vs. 53.9 (C-9), 43.3 vs. 49.5 (C-5), 38.8 vs. 38.7 (C-10), and 21.3 vs. 21.0 (C-11) ppm, revealed a composition slightly richer in **7***a* with a ratio of **1***a*:**7***a* of ~45:55.

(*e*) A mixture of 115 mg of 5β-cholestan-3-one, 115 mg of $HONH_2 \cdot HCl$, 115 mg of NaOAc, 3 drops of water, and 4 mL of MeOH was stirred and refluxed for 6 h. The MeOH was distilled and the residue partitioned between water and ether to yield 108 mg of oxime, mp 65–70°C; ir ($CHCl_3$): 3580 and 3300 (OH) cm^{-1}, no C=O absorption. Thin-layer chromatography (benzene–ether, 90:10) showed a single spot more polar than starting ketone.

The procedure of Shoppee and Sly (28) was used for the Beckmann rearrangement. To a solution of the 108 mg of oxime in 4 mL of dry dioxane at 40°C was added 0.23 mL of distilled $SOCl_2$ during 20 s. The solution became yellow and then brown. After 20 min the reaction was quenched by addition of aqueous $NaHCO_3$. Extraction with $CHCl_3$ yielded 97 mg of viscous brown oil. Thick layer chromatography on a 20-g silica gel plate (EtOAc–MeOH, 94:6) to remove a small amount of 5β-cholestan-3-one and colored material afforded, from the band at R_f 0.5, 47 mg of colorless oily solid lactam; ir ($CHCl_3$): 3420 (NH) and 1655 (amide C=O) cm^{-1}; M^+ calcd. for $C_{27}H_{47}NO$: 401.3658; found: 401.3655.

The ^{13}Cmr spectrum showed the presence of both **2***a* and **8***a*. Comparison of peak heights for the following pairs of signals: 43.0 vs. 45.5 (C-5), 26.0 vs. 27.0 (C-6), and 21.3 vs. 20.9 (C-11) ppm, revealed a composition slightly richer in **2***a* with a ratio of **2***a*:**8***a* of ~53:47.

Baeyer–Villiger Rearrangements

(*a*) The rearrangement of 17β-acetoxy-5α-androstan-3-one was carried out according to the directions of Caspi *et al.* (17) except that *m*-chloroperbenzoic acid was substituted for perbenzoic acid. A solution of 150 mg of the steroid and 250 mg of *m*-ClPBA (Aldrich 75%) in 5 mL of $CHCl_3$ was allowed to stand at 0°C for 6 days. Thin-layer chromatography (benzene–ether, 75:25) showed the absence of starting material and the presence of a single more polar spot. The solution was diluted with $CHCl_3$ and washed successively with aqueous Na_2SO_3, aqueous $NaHCO_3$, and water. Evaporation of the dried solution left 150 mg (95%) of colorless solid lactone.

The ^{13}Cmr spectrum showed the presence of both **3***d* and **4***d*. Comparison of peak heights for the following pairs of signals: 64.6 (C-2 of **4***d*) vs. 69.9 (C-4a of **3***d*), 53.7 vs. 53.5 (C-9), and 43.3 vs. 48.5 (C-5) ppm, revealed a composition slightly richer in **3***d* with a ratio of **3***d*:**4***d* of ~55:45.

Two recrystallizations from EtOAc furnished 58 mg of colorless plates, mp 250–252°C (with subl. on the hot stage), mp 235–245°C (in a sealed capillary) (lit. (17) mp 240–242°C); ir ($CHCl_3$): 1730 (lactone + acetate C=O) cm^{-1}; ^{1}Hmr ($CDCl_3$) δ: 0.78 (C-18 Me), 0.94 (C-19 Me), 2.03 (CH_3C=O), 3.67 (1 H, d, J = 13 Hz, 4aαH), 4.29 (1 H, dd, J = 13, 8 Hz, 4aβ-H), and 4.59 (1 H, dd, 17α-H) ppm; M^+ calcd. for $C_{21}H_{32}O_4$: 348.2300; found; 348.2300; ^{13}Cmr analysis revealed this material to be pure **3***d* (see Table 2).

(*b*) The procedure of Bull *et al.* (15) was followed except that *m*-ClPBA was substituted for peracetic acid. To a refluxing solution of 1.10 g of *m*-ClPBA (Aldrich, 75%) in 5 mL of $CHCl_3$ was added a solution of 250 mg of 5α-cholestan-3-one oxime in 2 mL of $CHCl_3$. The reaction mixture immediately turned blue, and by the end of 1 h it was colorless. The cooled solution was washed with aqueous Na_2SO_3, aqueous $NaHCO_3$, and water. Evaporation of the dried solution left 320 mg of a colorless oil. Analysis by tlc (benzene–ether, 90:10) showed the absence of oxime and the presence of a major spot less polar than oxime together with two even less polar spots (chloronitro steroids?). The product was chromatographed on two 20-g preparative plates developed in benzene–ether (85:15). The band at R_f 0.46 (I_2 detection) gave 82 mg of colorless solid lactone; ir ($CHCl_3$): 1725 (lactone C=O) cm^{-1}; M^+ calcd. for $C_{27}H_{46}O_2$: 402.3498; found: 402.3499.

The ^{13}Cmr spectrum showed the presence of both **3***a* and **4***a*. Comparison of peak heights for the following pairs of signals: 70.0 (C-4a of **3***a*) vs. 64.7 (C-2 of **4***a*), 53.6 vs 53.8 (C-9), 48.5 vs. 43.4 (C-5), and 21.1 vs. 21.3 (C-11) ppm, revealed a composition slightly richer in **3***a* with a ratio of **3***a*:**4***a* of ~56:44.

(*c*) When the RuO_4-catalyzed oxidation of 75 mg of 5α-cholestan-3β-ol was carried out at 40°C according to procedure (*b*) of Nakata (18) with 750 mg of $Pb(OAc)_4$, 0.29 mL of 0.056 M RuO_4 in CCl_4, and 7.5 mL of HOAc, there was isolated 60 mg of crude product which did not contain any lactone **3***b* or **4***b* by tlc comparison with authentic specimens. Recrystallization from ether–MeOH gave 48 mg of 5α-cholestan-3-one. When the reaction was done with 2 drops of concentrated H_2SO_4 added, or when the reaction was run in refluxing HOAc, the only product was still 5α-cholestan-3-one. When the reaction was done with double addition of RuO_4 and $Pb(OAc)_4$, 2α-acetoxy-5α-cholestan-3-one was isolated in addition to 5α-cholestan-3-one.

Reactions Related to the Schmidt Reaction on 5α-Cholestane-3,6-dione

*6-Aza-*B*-homo-5α-cholestane-3,7-dione (20a)*

The oxime was prepared from 250 mg of 3β-acetoxy-5α-cholestan-6-one (46–48) by reflux with 250 mg of $HONH_2 \cdot HCl$ and 250 mg of NaOAc in 20 mL of MeOH. To a solution of 264 mg of the oxime in 5 mL of dioxane at 10°C was added 0.3 mL of distilled $SOCl_2$. The bath was allowed to warm to room temperature during 0.5 h. Addition of concentrated NH_4OH and extraction with $CHCl_3$ yielded 233 mg of semi-solid **6-aza-*B*-homo-3β-acetoxy-5α-cholestan-7-one**. This crude product was saponified by reflux with KOH–MeOH to give 163 mg of 3β-hydroxylactam. A solution of 163 mg of the alcohol in 6 mL of HOAc was oxidized at room temperature with a solution of 65 mg of CrO_3 in 0.5 mL of water. Dilution with water and ether extraction gave the crude keto lactam which was chromatographed on a 20-g silica gel plate developed in EtOAc. Extraction of the band at R_f 0.44 gave 73 mg of colorless 6-aza-*B*-homo-5α-cholestane-3,7-dione (**20***a*), mp 231–234°C (lit.(47) mp 236–237°C), $[\alpha]_D^{22}$ +13.5° (*c* 1.36, $CHCl_3$); ir ($CHCl_3$): 3400 (NH), 1720 (C=O), and 1660 (NC=O) cm^{-1}; ^{1}Hmr ($CDCl_3$) δ: 1.06 (C-19 Me), 3.66 (1 H, m, 5α-H), and 6.56 (1 H, bd, NH) ppm; M^+ calcd. for $C_{27}H_{45}NO_2$: 415.3450; found: 415.3452.

*6-Aza-*B*-homocholest-4-ene-3,7-dione (23a) and 6-Aza-*B*-homo-5α-cholest-1-ene-3,7-dione (22a)*

The bromination of **20***a* was carried out with a modification of the procedure of Singh *et al.* (45). To a stirred solution of 375 mg (0.90 mmol) of keto lactam **20***a* in 3 mL of HOAc was added 280 mg (0.88 mmol) of $Py \cdot HBr \cdot Br_2$ during 5 min. All solid dissolved within 10 min, and the orange solution was kept at room temperature for 30 min. The reaction mixture was diluted with water and extracted with ether. The dried organic layer was evaporated and the residual oily **4α-bromo ketone 21***a* was used directly for dehydrobromination, ir ($CHCl_3$): 3380 (NH), 1740 (C=O), and 1670 (NC=O) cm^{-1}; ^{1}Hmr ($CDCl_3$) δ: 4.65 (1 H, d, J = 11 Hz, 4β-H) ppm.

A mixture of the above crude **21***a*, 375 mg of $CaCO_3$, and 6 mL of dimethylacetamide was stirred and refluxed for 1.5 h. After distillation of the solvent *in vacuo*, the residual solid was tritu-

Can. J. Chem. Downloaded from www.nrcresearchpress.com by 210.87.254.105 on 09/05/12
For personal use only.

rated with $CHCl_3$ and filtered. The amber colored concentrated filtrate was chromatographed on two 20-g silica gel plates developed in EtOAc.

The band at R_f 0.59 gave 177 mg (47%) of **6-aza-*B*-homocholest-4-ene-3,7-dione** (**23*a***). Two recrystallizations of 50 mg from MeOH afforded 18 mg of colorless granules, mp 178–180°C with previous sintering, $[\alpha]_D^{0.5}$ +377° (*c* 1.30, $CHCl_3$); uv (MeOH): 275 (12 000) nm; ir ($CHCl_3$): 3380 (NH), 1660 (C=O, NC=O), and 1610 (C=C) cm^{-1}; ^{1}Hmr ($CDCl_3$) δ: 1.18 (C-19 Me), 5.73 (1 H, s, 4-H), and 8.11 (1 H, bs, NH) ppm; M^+ calcd. for $C_{27}H_{43}NO_2$: 413.3293; found 413.3292.

The band at R_f 0.36 from the above plates gave 105 mg of colorless oily solid which was rechromatographed on a 20-g silica gel plate developed twice in ether–MeOH (96:4). A band at R_f 0.45 gave 46 mg (12%) of recovered keto amide **20*a***. A band at R_f 0.59 gave 50 mg (13%) of **6-aza-*B*-homo-5α-cholest-1-ene-3,7-dione** (**22*a***). Two recrystallizations from MeOH gave colorless plates, mp 216.5–218.5°C, $[\alpha]_D^{22}$ +77° (*c* 0.93, $CHCl_3$); uv (MeOH): 225 (13 000) nm; ir ($CHCl_3$): 3400 (NH) and 1670 (conj. C=O + NC=O) cm^{-1}; ^{1}Hmr ($CDCl_3$) δ: 1.07 (C-19 Me), 3.95 (1 H, bdd, 5α-H), 5.92 (1 H, d, J = 10 Hz, 2-H), 7.00 (1 H, bs, NH), and 7.00 (1 H, d, J = 10 Hz, 1-H) ppm; M^+ calcd. for $C_{27}H_{43}NO_2$: 413.3293; found: 413.3290.

If the original bromination was carried out with 1.5 mmol of **20*a*** and 1.6 mmol of Py·HBr·Br_2, and if **20*a*** was added to Py·HBr·Br_2, the Δ^1-keto lactam **22*a*** was not isolated. Instead, the minor product was **6-aza-*B*-homocholest-1,4-diene-3,7-dione** (**30*a***), mp 237–240°C from EtOAc, $[\alpha]_D^{21}$ +526° (*c* 1.47, $CHCl_3$); uv (MeOH): 243 (15 100) and 286 (7130) nm; ir ($CHCl_3$): 3380 (NH), 1660 (conj. C=O, NC=O), 1625 and 1600 (C=C) cm^{-1}; ^{1}Hmr ($CDCl_3$) δ: 1.33 (C-19 Me), 6.02 (1 H, d, J = 1 Hz, 4-H), 6.20 (1 H, dd, J = 1, 10 Hz, 2-H), 7.04 (1 H, d, J = 10 Hz, 1-H), and 9.14 (1 H, s, NH) ppm; M^+ calcd. for $C_{27}H_{41}NO_2$: 411.3137; found: 411.3133.

*Schmidt Reaction on 6-Aza-*B*-homo-5α-cholest-1-ene-3,7-dione (22*a*)*

To a stirred mixture of 50 mg of **22*a***, 5 mL of $CHCl_3$, and 0.2 mL of concentrated H_2SO_4 at 5°C was added 70 mg of powdered NaN_3 during 5 min. The bath was allowed to warm to room temperature while the mixture was stirred for 1 h. After neutralization of the acid with aqueous NaOH, the mixture was diluted with $CHCl_3$ and washed with water. Evaporation of the dried $CHCl_3$ solution left 44 mg of oily solid which was chromatographed on a 10-g silica gel plate developed in EtOAc–MeOH (88:12).

From the band at R_f 0.62 was extracted 6 mg of **3,6-diaza-*A*-homo-*B*-homo-5α-cholest-1-ene-4,7-dione** (**25*a***), mp 280–290°C (dec.); uv (MeOH): 226 (8300) nm; ir ($CHCl_3$): 3400 (NH), 1690 and 1665 (2 NC=O) cm^{-1}; ^{1}Hmr ($CDCl_3$, 50°C) δ: 1.25 (C-19 Me), 2.88 (1 H, dd, 4aα-H), 3.98 (1 H, bt, 5α-H), 5.06 (1 H, d, J = 11 Hz, 1-H), 5.77 (1 H, dd, J = 5, 11 Hz, 2-H), 6.11 (1 H, bd, J = 5 Hz, 3-NH), and 7.21 (1 H, bs, 6-NH) ppm; ^{13}Cmr (CD_3COOD) δ: 12.2 (C-18), 16.6 (C-9), 47.3 (C-10), 58.7 (C-5), 120.5 (C-2), and 125.3 (C-1) ppm; M^+ calcd. for $C_{27}H_{44}N_2O_2$: 428.3402; found: 428.3400.

From the band at R_f 0.24 was extracted 17 mg of colorless solid which after one recrystallization each from EtOAc and EtOAc–MeOH gave 11 mg of granules of **4,6-diaza-*A*-homo-*B*-homo-5α-cholest-1-ene-3,7-dione** (**24*a***), mp 278–290°C (dec.), $[\alpha]_D^{22}$ +37° (*c* 0.84, $CHCl_3$); uv (MeOH): rising end absorption only ε_{205} 15 000; ir ($CHCl_3$): 3400 and 3200 (NH), 1660 (2 NC=O), and 1620 (C=C) cm^{-1}; ^{1}Hmr ($CDCl_3$) δ: 1.00 (C-19 Me), 3–4 (3 H, m, 4aH's, 5α-H), 5.78 (1 H, d, J = 13 Hz, 2-H), 6.33 (1 H, d, J = 13 Hz, 1-H), and 7.56 (2 H, m, 2 NH) ppm; M^+ calcd. for $C_{27}H_{44}N_2O_2$: 428.3402; found: 428.3400.

*3,6-Diaza-*A*-homo-*B*-homo-5α-cholestane-4,7-dione (18*a*)*

A solution of 6 mg of Δ^1-dilactam **25*a*** in 1.5 mL of HOAc was hydrogenated in the presence of 3 mg of PtO_2. Filtration and evaporation left a colorless solid, saturated dilactam **18*a***; M^+ calcd. for $C_{27}H_{46}N_2O_2$: 430.3559; found: 430.3559. The ^{13}Cmr spectrum was identical with that of the less polar dilactam of the Schmidt reaction on keto lactam **20*a***.

*4,6-Diaza-*A*-homo-*B*-homo-5α-cholestane-3,7-dione (19*a*)*

A solution of 17 mg of the unsaturated dilactam **24*a*** in 3 mL of MeOH was hydrogenated in the presence of 10 mg of 10% Pd/C catalyst. Filtration and evaporation left 17 mg of colorless solid. Recrystallization from MeOH gave 6 mg of granules of the saturated dilactam **19*a***, mp 295–305°C (dec.) (lit.(37) mp > 300°C. (dec.)); ir ($CHCl_3$): 3400 (NH) and 1652 (NC=O) cm^{-1}; M^+ calcd. for $C_{27}H_{46}N_2O_2$: 430.3559; found: 430.3559. Thin layer comparison showed this compound to have the same R_f as the more polar dilactam from the Schmidt reaction on **20*a***.

*Beckmann Rearrangement of 6-Aza-*B*-homocholest-4-ene-3,7-dione (23*a*)*

A mixture of 167 mg of **23*a***, 167 mg of $HONH_2$·HCl, 167 mg of NaOAc, and 7 mL of MeOH was refluxed for 4 h. Distillation of MeOH, addition of water, and extraction with ether gave 170 mg of semi-solid oxime. A solution of the oxime and 170 mg of *p*-TsCl in 5 mL of dry pyridine was allowed to stand at room temperature for 1.5 h. After evaporation of the pyridine in a stream of nitrogen, the residue was dissolved in benzene and chromatographed on a column of 8 g of Woelm neutral alumina (grade I). Elution with benzene to benzene–ether (50:50) gave 53 mg of oxime tosylate. Elution with EtOAc gave 111 mg of unsaturated dilactams contaminated with oxime. The 53 mg of recovered oxime tosylate was rechromatographed on 3.8 g of the same alumina. EtOAc eluted 40 mg of unsaturated dilactam which was combined with the 111 mg. Thick-layer chromatography on three 20-g silica gel plates developed thrice in EtOAc–MeOH (90:10) gave three bands. The band at the solvent front gave 72 mg of recovered oxime on extraction.

Extraction of the band at R_f 0.73 yielded 38 mg of colorless **4,6-diaza-*A*-homo-*B*-homocholest-4a-ene-3,7-dione** (**27*a***). Two recrystallizations from MeOH gave 25 mg of granules, mp 265–285°C (dec. on the hot stage), mp 258–290° (dec. in a sealed capillary) (lit.(49) mp 290–296° (dec.)), $[\alpha]_D^{21}$ +111° (*c* 1.05, $CHCl_3$); uv (MeOH): 254 (12 800) nm; ir ($CHCl_3$): 3400 (NH) and 1660 (NC=O) cm^{-1}; ^{1}Hmr ($CDCl_3$) δ: 1.09 (C-19 Me), 5.95 (1 H, bd, J = 7 Hz, 4a-H), 7.86 (1 H, bs, NH), and 8.09 (1 H, bd, J = 7 Hz, NH) ppm; M^+ calcd. for $C_{27}H_{44}N_2O_2$: 428.3402; found: 428.3400.

Extraction of the third band at R_f 0.49 afforded 32 mg of colorless **3,6-diaza-*A*-homo-*B*-homocholest-4a-ene-4,7-dione** (**26*a***). Recrystallization from $CHCl_3$–MeOH gave 21 mg of plates, mp 285–305°C (dec. range), $[\alpha]_D^{21}$ +123° (*c* 1.04, $CHCl_3$); uv (MeOH): 240 (11 600) nm; ir ($CHCl_3$): 3420 and 3395 (NH), 1655 (NC=O), and 1610 (C=C) cm^{-1}; ^{1}Hmr ($CDCl_3$) δ: 1.20 (C-19 Me), 3.25 (2 H, m, 2-H's), 5.83 (1 H, s, 4a-H), 7.41 (1 H, bs, NH), and 8.30 (1 H, bs, NH) ppm; M^+ calcd. for $C_{27}H_{44}N_2O_2$: 428.3402; found: 428.3400.

*3,6-Diaza-*A*-homo-*B*-homo-5β-cholestane-4,7-dione (28*a*)*

(*a*) *Pd/C–MeOH–KOH*: A mixture of 10 mg of 10% Pd/C catalyst, 10 mg of KOH, and 1 mL of MeOH was saturated with hydrogen for 0.5 h. A solution of 10 mg of Δ^{4a}-dilactam **26*a*** in 2.5 mL of MeOH was added and hydrogenated for 24 h.[8] Filtration and evaporation left a residue which was dissolved in $CHCl_3$ and washed with water. Evaporation of the dried solution left 8 mg of colorless solid saturated dilactam, *m/e*: 430; $C_{27}H_{46}N_2O_4$ requires 430. The ^{13}Cmr spectrum revealed that the product was ~90% of the 5β-isomer.

(*b*) *PtO_2–HOAc*: A mixture of 5 mg of PtO_2 and 0.5 mL of

[8]The isomeric Δ^{4a}-dilactam **27*a*** did not absorb hydrogen under either of these sets of conditions.

Can. J. Chem. Downloaded from www.nrcresearchpress.com by 210.87.254.105 on 09/05/12
For personal use only.

HOAc was saturated with hydrogen for 45 min. A solution of 10 mg of Δ^{4a}-dilactam **26***a* in 1.5 mL of HOAc was added and hydrogenated for 8 h.[8] Filtration and concentration left 10 mg of saturated dilactam. Thin-layer chromatography in EtOAc–MeOH (88:12) showed a single spot more polar than **26***a*; *m/e*: 430; $C_{27}H_{46}N_2O_4$ requires 430. The ^{13}Cmr revealed that the product was ~90% of the 5β-isomer.

*Schmidt Reaction on 6-Aza-*B*-homo-5α-cholestane-3,7-dione (20a)*

The keto lactam **20***a* (50 mg) was dissolved in 1.5 g of polyphosphoric acid with the aid of heating at 85°C for 0.5 h. Then 100 mg of NaN_3 was added, and the reaction mixture was kept at 85°C for 15 h with occasional stirring. Ice was added, and the acid was neutralized with KOH pellets. Extraction with $CHCl_3$ yielded 36 mg of oily solid. Chromatography on a 10-g silica gel plate developed in EtOAc–MeOH (80:20) afforded 26 mg of bis lactam product from the band at R_f 0.29; ir ($CHCl_3$): 3400 and 3220 (NH), and 1660 (NC=O) cm^{-1}; *m/e*: 430.

The ^{13}Cmr spectrum showed the presence of both **18***a* and **19***a*, but the only well-resolved signals were those of ^{13}C-19 at 14.8 (**18***a*) and 14.3 (**19***a*) ppm. Comparison of peak heights gave a ratio of **18***a*:**19***a* of ~55:45.

For separation of the isomers, a larger scale reaction was run. To a stirred mixture of 100 mg of **20***a*, 10 mL of $CHCl_3$, and 0.4 mL of concentrated H_2SO_4 at 5°C was added 150 mg of NaN_3 during 10 min. The cooling bath was allowed to warm to room temperature, and the reaction mixture was stirred for 1.5 h. Work-up gave 100 mg of colorless solid. Analytical tlc in $CHCl_3$–MeOH–EtOAc (75:12.5:12.5, four developments) revealed the absence of **20***a* and the presence of two more polar spots, R_f 0.50 and 0.38, in a ~1:1 ratio. The crude product was chromatographed on four 20-g preparative plates developed four times in the same solvent system.

Extraction of the band at R_f 0.45 (I_2 detection) gave 39 mg of colorless solid. Recrystallization from MeOH afforded pure 3-aza dilactam **18***a*, mp 280–285°C (dec.) (lit.(37) mp 283°C (dec.)); ir ($CHCl_3$): 3400 (NH) and 1660 (NC=O) cm^{-1}; ^{1}Hmr ($CDCl_3$, 50°C) δ: 0.90 (C-19 Me), 2.9–3.3 (2H, m, 2-H's), 3.7–3.9 (1H, m, 5α-H), 5.99 (1H, d, NH), and 6.53 (1H, bs, NH) ppm; M^+ calcd. for $C_{27}H_{46}N_2O_2$: 430.3559; found: 430.3559. The ^{13}Cmr spectrum was identical with that of the sample made by hydrogenation of **25***a*.

Extraction of the band at R_f 0.41 (I_2 detection) yielded 34 mg of colorless solid. Recrystallization from MeOH gave pure 4-aza dilactam **19***a* identical with the sample from hydrogenation of **24***a*.

Schmidt Reaction on Cholest-4-en-3-one

To a well-stirred mixture of 500 mg of cholest-4-en-3-one and 5.0 g of polyphosphoric acid at 70°C was added 100 mg of NaN_3. The reaction mixture was stirred occasionally with a spatula during the next 5 h. A second portion of 100 mg of NaN_3 was added, and the reaction was continued for 12 h more. Ice was added and the acid neutralized with KOH pellets. Extraction with $CHCl_3$ yielded 425 mg of oily solid. Since tlc indicated some unreacted starting material, the crude product was recycled as described above to afford 365 mg of oily solid free of starting ketone. Chromatography on two 20-g preparative silica gel plates developed in EtOAc–ether (75:25) separated two bands (uv detection).

Extraction of the band at R_f 0.73 gave 30 mg of solid. Two recrystallizations from benzene–acetone gave 19 mg of colorless granules of **4-aza-A-homocholest-4a-en-3-one**, mp 235–239°C with a phase change at 195°C, $[\alpha]_D^{20}$ −12.3° (*c* 1.50, $CHCl_3$) (lit.(8) mp 236°C, $[\alpha]_D$ −11.5°); uv(MeOH): 244 (11 600) nm; ir ($CHCl_3$): 3400 (NH), 1670 and 1655 (O=CNC=C) cm^{-1}; ^{1}Hmr ($CDCl_3$) δ: 1.09 (C-19 Me), 5.52 (1H, d, J = 6 Hz, 4a-H), and 6.96 (1H, bd, NH) ppm; M^+ calcd. for $C_{27}H_{45}NO$: 399.3501; found: 399.3499.

Extraction of the band at R_f 0.29 yielded 160 mg of off-white solid. One recrystallization from benzene–acetone gave 102 mg of colorless granules of **3-aza-A-homocholest-4a-en-4-one** identical with the specimen prepared by Beckmann rearrangement of the oxime of cholest-4-en-3-one reported earlier (1).

Acknowledgments

We would like to thank the Natural Sciences and Engineering Research Council of Canada for financial support, Heather Schroeder for the 100 MHz ^{1}Hmr spectra, and Doug Hairsine for the mass spectra.

1. V. Dave, J. B. Stothers, and E. W. Warnhoff. Can. J. Chem. **57**, 1557 (1979).
2. K. Oka and S. Hara. J. Org. Chem. **43**, 3790 (1978).
3. D. H. R. Barton, M. J. Day, R. H. Hesse, and M. M. Pechet. J. Chem. Soc. Perkin Trans. I, 1764 (1975).
4. M. Benn and R. Shaw. Can. J. Chem. **52**, 2936 (1974).
5. B. Matkovics and Z. Tegyey. Acta Chim. Budapest, **80**, 211 (1974).
6. G. Zanati and M. E. Wolff. J. Med. Chem. **14**, 958 (1971).
7. G. Habermehl and A. Haaf. Ann. **722**, 155 (1969).
8. M. Kobayashi, Y. Shimizu, and H. Matsuhashi. Chem. Pharm. Bull. **17**, 1255 (1969).
9. S. Hara, N. Matsumoto, and M. Takeuchi. Chem. Ind. London, 2086 (1962).
10. J. C. Kim, S. K. Choi, W. W. Park, and Y. T. Lee. J. Korean Chem. Soc. **22**, 42 (1979).
11. A. M. Maione and M. G. Quaglia. Chem. Ind. London, 230 (1977).
12. V. V. Kuril'skaya, M. P. Irismetov, M. I. Goryaev, V. S. Bazalitskaya, and L. G. Mikhaleva. Izv. Akad. Nauk Kaz. SSR, Ser. Khim. **27**, 46 (1977).
13. H. Ogura, H. Takayanagi, and K. Furuhata. J. Chem. Soc. Perkin Trans. I, 665 (1976).
14. H. R. Nace and A. C. Watterson. J. Org. Chem. **31**, 2109 (1966).
15. J. R. Bull, E. R. H. Jones, and G. D. Meakins. J. Chem. Soc. 2601 (1965).
16. J. E. Bolliger and J. L. Courtney. Aust. J. Chem. **17**, 440 (1964).
17. E. Caspi, Y. Shimizu, and S. N. Balasubramanyam. Tetrahedron, **20**, 1271 (1964).
18. H. Nakata. Tetrahedron, **19**, 1959 (1963).
19. G. R. Pettit, B. Green, T. R. Kasturi, and U. R. Ghatak. Tetrahedron, **18**, 953 (1962).
20. J. C. Craig and A. R. Naik. J. Am. Chem. Soc. **84**, 3410 (1962).
21. K. Oka and S. Hara. J. Am. Chem. Soc. **99**, 3859 (1977).
22. K. Oka and S. Hara. Chem. Ind. London, 168 (1969).
23. O. Jeger and H. U. Wehrli. Swiss Patent No. 537,948 (1973); Chem. Abstr. **79**, 137387g (1973).
24. H. Singh, V. V. Parashar, S. Padmanabhan, and R. B. Mathur. Ind. J. Pharm. Educ. **4**, 2 (1970).
25. H. Singh, V. V. Parashar, and S. Padmanabhan. J. Sci. Ind. Res. India, **25**, 200 (1966).
26. C. W. Shoppee, G. Krüger, and R. N. Mirrington. J. Chem. Soc. 1050 (1962).
27. I. Fleming and R. B. Woodward. J. Chem. Soc. Perkin Trans. I, 1653 (1973).
28. C. W. Shoppee and J. C. P. Sly. J. Chem. Soc. 3458 (1958).

29. N. J. DOORENBOS and M. T. WU. J. Org. Chem. **26**, 2548 (1961).
30. G. N. ROMACHENKO, M. I. GORYAEV, and M. P. IRISMETOV. Izv. Akad. Nauk Kaz. SSR, Ser. Khim. **22**, 67 (1972).
31. M. N. IRISMETOV, G. Y. TSVETKOVA, and M. I. GORYAEV. J. Gen. Chem. **47**, 857 (1977).
32. N. J. DOORENBOS and H. SINGH. J. Pharm. Sci. **50**, 628 (1961).
33. B. MATKOVICS, Z. TEGYEY, M. RESCH, F. SIROKMÁN, and E. BOGA. Acta Chim. Budapest, **66**, 333 (1970).
34. G. J. FONKEN and H. M. MILES. J. Org. Chem. **28**, 2432 (1963).
35. M. S. AHMAD, SHAFIULLAH, M. MUSHFIQ, and M. ASIF. Ind. J. Chem. **8**, 1062 (1970).
36. M. S. AHMAD, G. MOINUDDIN, and I. A. KHAN. J. Org. Chem. **43**, 163 (1978).
37. H. SINGH, R. B. MATHUR, A. K. BOSE, and S. D. SHARMA. Ind. J. Chem. **10**, 240 (1972).
38. I. MALYNOWICZ, J. FARKAS, and F. ŠORM. Collect. Czech. Chem. Commun. **25**, 1359 (1960).
39. J. Y. SATOH, K. MISAWA, T. T. TAKAHASHI, M. HIROSE, C. A. HORIUCHI, S. TSUJII, and A. HAGITANI. Bull. Chem. Soc. Jpn. **46**, 3155 (1973).
40. A. BUTENANDT and A. WOLFE. Chem. Ber. **68**, 2091 (1935).
41. G. F. H. GREEN and A. G. LONG. J. Chem. Soc. 2532 (1961).
42. R. O. CLINTON, R. L. CLARKE, F. W. STONNER, A. J. MANSON, K. F. JENNINGS, and D. K. PHILLIPS. J. Org. Chem. **27**, 2800 (1962).
43. Y. SHIMIZU, H. MITSUHASHI, and E. CASPI. Tetrahedron Lett. 4113 (1966).
44. J. O. RALLS. J. Am. Chem. Soc. **60**, 1744 (1938).
45. H. SINGH, R. B. MATHUR, N. J. DOORENBOS, A. K. BOSE, and S. D. SHARMA. Tetrahedron, **27**, 3993 (1971).
46. A. T. ROWLAND. Steroids, **26**, 251 (1975).
47. R. M. DODSON and B. RIEGEL. J. Org. Chem. **13**, 424 (1948).
48. J. F. BAGLI, P. F. MORAND, and R. GAUDRY. J. Org. Chem. **27**, 2938 (1962).
49. H. SINGH, S. PADMANABHAN, A. K. BOSE, and I. KUGAJEVSKY. J. Chem. Soc. Perkin Trans. I, 993 (1972).
50. N. J. DOORENBOS and H. SINGH. J. Pharm. Sci. **51**, 418 (1962).
51. Y. HOYANO, V. PATEL, and J. B. STOTHERS. Can. J. Chem. **58**, 2730 (1980).

Can. J. Chem. Downloaded from www.nrcresearchpress.com by 210.87.254.105 on 09/05/12
For personal use only.

Chlorosulphation of amino sugars: synthesis of methyl 2-acetamido-4-amino-2,4,6-trideoxy-β-D-glucopyranoside (bacillosamine) from a D-glucosamine derivative[1]

DAVID R. BUNDLE AND STAFFAN JOSEPHSON[2]

Division of Biological Sciences, National Research Council of Canada, Ottawa, Ont., Canada K1A 0R6

Received June 16, 1980

This paper is dedicated to Prof. Raymond U. Lemieux on the occasion of his 60th birthday

DAVID R. BUNDLE and STAFFAN JOSEPHSON. Can. J. Chem. **58**, 2679 (1980).

Chlorosulphation of methyl 2-deoxy-2-phthalimido-β-D-glucopyranoside **3** under controlled conditions provided either methyl 6-chloro-2,6-dideoxy-2-phthalimido-β-D-glucopyranoside **4** or methyl 4,6-dichloro-2,4,6-trideoxy-2-phthalimido-β-D-galactopyranoside **5**. Chlorination at C-4 occurs to the exclusion of that at C-3, in sharp contrast to the chlorosulphation of methyl β-D-glucopyranoside which is known to give both the 4,6-dichloro-*galacto*- and 3,6-dichloro-*allo*-pyranosides. Conversion of the chlorinated phthalimido derivatives **4** and **5** to the corresponding 2-acetamido-2-deoxyhexopyranosides **6** and **7** permitted reduction of the chloro functions by palladium, W-4 Raney nickel, and nickel boride. Reduction of methyl 2-acetamido-6-chloro-2,6-dideoxy-β-D-glucopyranoside **6** by Raney nickel gave methyl 2-acetamido-2,6-dideoxy-β-D-glucopyranoside **8**. Selective dechlorination at C-4 was achieved by palladium catalysed reduction of methyl 2-acetamido-4,6-dichloro-2,4,6-trideoxy-β-D-galactopyranoside **7**. Nickel boride or Raney nickel reduction of **7** effected selective dechlorination at C-6 to give methyl 2-acetamido-4-chloro-2,4,6-trideoxy-β-D-galactopyranoside **9**. Azide displacement of the 4-chloro group of **9** provided a simple route to the 2,4-diamino sugar bacillosamine. A side product of the azide displacement reaction was the unsaturated sugar, methyl 2-acetamido-2,4,6-trideoxy-α-L-*threo*-hex-4-enopyranoside, **14**.

DAVID R. BUNDLE et STAFFAN JOSEPHSON. Can. J. Chem. **58**, 2679 (1980).

La chlorosulfuration du déoxy-2 phtalimido-2 β-D-glucopyrannoside de méthyle **3** dans des conditions contrôlées conduit soit au chloro-6 didéoxy-2,6 phtalimido-2 β-D-glucopyrannoside de méthyle **4** soit au dichloro-4,6 tridéoxy-2,4,6 phtalimido-2 β-D-galactopyrannoside de méthyle **5**. La chloration a lieu en position C-4 à l'exclusion de celle en C-3; ceci contraste nettement avec la chlorosulfuration du β-D-glucopyrannoside de méthyle qui, comme on le sait, conduit aux dichloro-4,6 *galacto* et dichloro-3,6 *allo* pyrannosides de méthyle. La transformation des dérivés phtalimido chlorés en acétamido-2 déoxy-2 hexopyrannosides correspondants permet la réduction subséquente de fonctions chlorées par le palladium, le nickel de Raney W-4 et le borure de nickel. La réduction de l'acétamido-2 chloro-6 didéoxy-2,6 β-D-glucopyrannoside de méthyle **6** par le nickel de Raney donne l'acétamido-2 didéoxy-2,6 β-D-glucopyrannoside de méthyle **8**. La déchloration sélective en position C-4 se fait grâce à la réduction, catalysée par le palladium, de l'acétamido-2 dichloro-4,6 tridéoxy-2,4,6 β-D-galactopyrannoside de méthyle **7**. La réduction du composé **7** par le borure de nickel ou le nickel de Raney enlève sélectivement le chlore au niveau du carbone en position 6 et conduit à l'acétamido-2 chloro-4 tridéoxy-2,4,6 β-D-galactopyrannoside de méthyle **9**. Le déplacement du chlore en position 4 du composé **9** par l'azoture fournit une voie d'accès simple à la bacillosamine un sucre diaminé en 2,4. On obtient comme produit secondaire de cette réaction de déplacement par l'azoture le sucre insaturé, acétamido-2 tridéoxy-2,4,6 α-L-*thréo* hexèno-4 pyrannoside de méthyle **14**.

[Traduit par le journal]

Introduction

Chlorosulphation of neutral sugars has provided a rapid and efficient procedure for synthesis of chloro-deoxy pentoses, hexoses, and their glycosides (1–3). Furthermore, certain hexopyranoside chlorosulphates undergo displacement by nucleophiles such as bromide and azide (4, 5). Reduction (6–9), substitution, and elimination (7) reactions performed on chloro-deoxy sugars have provided ready access to modified pyranosides and furanosides. Despite the ease and synthetic flexibility of the chlorosulphation reaction, it has not previously been applied to amino-sugars. Whereas 2-acetamido-2-deoxy-D-glucopyranose reacts with sulphuryl chloride under standard conditions (1) to yield a black tar, we have shown that 2-deoxy-2-phthalimido-D-glucose yields 6-chloro-2,6-dideoxy-2-phthalimido-α-D-glucopyranosyl chloride 3,4-bischlorosulphate.[3]

Encouraged by this observation and prompted by the need for a sample of the diamino sugar, 2-acetamido-4-amino-2,4,6-trideoxy-D-glucopyranose, we have investigated the chlorosulphation of methyl 2-deoxy-2-phthalimido-β-D-glucopyranoside, with the intention of exploiting the resultant chloro-deoxy derivatives for the introduction of new functionalities (cf. refs. 4–9).

Results and Discussion

Methyl tri-*O*-acetyl-2-deoxy-2-phthalimido-β-D-glucopyranoside (**2**) was prepared from tri-*O*-acetyl-2-deoxy-2-phthalimido-αβ-D-glucopyranosyl bromides (**1**) (10) by reaction with methanol in benzene solution utilizing mercuric cyanide (11) as the promoter. Transesterification (cf. ref. 12) of the triacetate **2** by sodium methoxide provided crys-

[1]Issued as NRCC No. 18550.

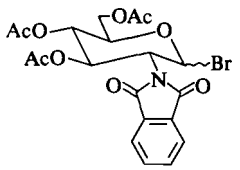
[2]NRCC Research Associate 1977–1979.

[3]D. R. Bundle and S. Josephson, unpublished results.

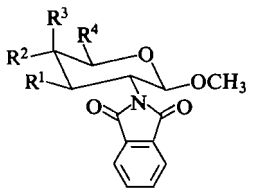
0008-4042/80/232679-07$01.00/0

©1980 National Research Council of Canada/Conseil national de recherches du Canada

Can. J. Chem. Downloaded from www.nrcresearchpress.com by 210.87.254.6 on 09/05/12
For personal use only.



1

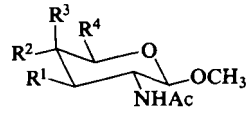


2 $R^1 = R^2 = OAc, R^3 = H, R^4 = CH_2OAc$
3 $R^1 = R^2 = OH, R^3 = H, R^4 = CH_2OH$
4 $R^1 = R^2 = OH, R^3 = H, R^4 = CH_2Cl$
5 $R^1 = OH, R^2 = H, R^3 = Cl, R^4 = CH_2Cl$

talline methyl 2-deoxy-2-phthalimido-β-D-glucopyranoside (**3**) in ~65% yield from tri-*O*-acetyl-2-deoxy-2-phthalimido-D-glucopyranosyl bromide (**1**). Chlorosulphation of glycoside **3** using 3.5 molar equivalents of sulphuryl chloride for 4 hours at −20° to −10°C provided the chlorosulphated 6-chloro-6-deoxy glycoside. Dechlorosulphation yielded the crystalline methyl 6-chloro-2,6-dideoxy-2-phthalimido-β-D-glucopyranoside **4** in 70% yield from **3**. When chlorosulphation of the methyl glycoside **3** was performed with 7.7 molar equivalents of sulphuryl chloride and allowed to reach 20°C an optimum 59% yield of methyl 4,6-dichloro-2,4,6-trideoxy-2-phthalimido-β-D-galactopyranoside (**5**) was obtained after dechlorosulphation. The preparation of **5** could also be achieved by refluxing the crude methyl 6-chloro-2,6-dideoxy-2-phthalimido-β-D-glucopyranoside-3,4-bischlorosulphate with tetraethylammonium chloride in chloroform solution. The exclusive formation in either case of 4,6-dichloro-galactopyranoside **5** may be contrasted with the reaction between sulphuryl chloride and methyl β-D-glucopyranoside (13). In this case both the 4,6-dichloro-*galacto*- and 3,6-dichloro-*allo*-pyranosides were formed. Methyl 2-deoxy-2-phthalimido-β-D-glucopyranoside **3** undergoes the usual (1, 2) displacement at C-6 at temperatures above −30°C and above 0°C a slower displacement with inversion occurs at C-4 but not C-3, leading to the 4,6-dichloro-galactopyranoside **5**. Extended reaction times and the use of undistilled, technical grade sulphuryl chloride result in reduced yields of the 4,6-dichloro-derivative **5**. The absence of detectable quantities of a 3,6-dichloro-*allo*-pyranoside from the reaction products probably relates to the stereochemistry of the C-2 phthalimido function. This argument is based on the fact that the plane of the phthalimido ring systems is perpendicular (10) to the mean plane of the pyranose ring. In this position the carbonyl disposed toward the α-face of the pyranose ring would render unfavourable the transition state leading to a 3-chloro-*allo*-pyranoside derivative.

The object of this work was to use chlorosulphation as a route to the diamino-sugar, 2-acetamido-4-amino-2,4,6-trideoxy-D-glucose. Although previously synthesized (14), this sugar was required as the glycoside, methyl 2-acetamido-4-amino-2,4,6-trideoxy-β-D-glucopyranoside (**15**), to facilitate comparison of ^{13}C and ^1H nmr parameters with those of the 2,4-diamino-6-deoxyhexose identified as a component of pneumococcal C substance (15, 16). As the derivative (**15**), the synthesis may be envisaged as starting from methyl 4,6-dichloro-2,4,6-trideoxy-2-phthalimido-β-D-galactopyranoside (**5**) and proceeding by selective dechlorination at C-6 with W-4 Raney nickel (6, 7, 9). When the phthalimido derivatives **4** and **5** were subjected to these conditions, reduction of the aromatic ring occurred to the exclusion of dechlorination at C-6. Conversion of the phthalimido compounds **4** and **5** to their acetamido analogues **6** and **7** gave derivatives amenable to smooth catalytic reduction.

Methyl 2-acetamido-6-chloro-2,6-dideoxy-β-D-glucopyranoside (**6**) was reduced to the 6-deoxy glucoside **8** (quinovosamine) in 71% yield. Similar conditions, freshly prepared W-4 Raney nickel and triethylamine in ethanol solution, selectively dechlorinated the 4,6-dichloro-galactoside (**7**) to methyl 2-acetamido-4-chloro-2,4,6-trideoxy-β-D-galactopyranoside (**9**) in 80% yield. In repeated experiments nickel boride (17) was found to be a more convenient catalyst for this reduction of **7** to **9**. The ease with which nickel boride is prepared coupled with reproducible selectivity for dechlorination at C-6 indicate this to be the catalyst of choice in this case. No 4,6-dideoxy-*xylo*-hexopyranoside or 4-



6 $R^1 = R^2 = OH, R^3 = H, R^4 = CH_2Cl$
7 $R^1 = OH, R^2 = H, R^3 = Cl, R^4 = CH_2Cl$
8 $R^1 = R^2 = OH, R^3 = H, R^4 = CH_3$
9 $R^1 = OH, R^2 = H, R^3 = Cl, R^4 = CH_3$
10 $R^1 = OH, R^2 = R^3 = H, R^4 = CH_2Cl$
11 $R^1 = R^2 = OH, R^3 = H, R^4 = CH_2N_3$
12 $R^1 = R^2 = OH, R^3 = H, R^4 = CH_2NH_2$
13 $R^1 = OH, R^2 = N_3, R^3 = H, R^4 = CH_3$
15 $R^1 = OH, R^2 = NH_2, R^3 = H, R^4 = CH_3$
16 $R^1 = OAc, R^2 = R^3 = H, R^4 = CH_3$

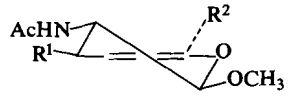
Can. J. Chem. Downloaded from www.nrcresearchpress.com by 210.87.254.6 on 09/05/12
For personal use only.

Can. J. Chem. Downloaded from www.nrcresearchpress.com by 210.87.254.6 on 09/05/12
For personal use only.

deoxy-6-chloro-*xylo*-hexopyranoside **10** were detected in crude hydrogenation mixtures by ^{13}C nmr. However, when **7** was hydrogenated over palladium on charcoal in the presence of sodium hydroxide, dechlorination at C-4 was observed together with some reduction at C-6. The ratio of the two products **10** and **9** was ~4:1. This observation was surprising in view of the fact that chloro-deoxy sugars are usually unreactive to palladium catalysed reduction. One notable exception is the palladium catalysed reduction of methyl 4-*O*-benzoyl-3-bromo-2,6-dichloro-2,3,6-trideoxy-α-D-mannopyranoside to methyl 4-*O*-benzoyl-6-chloro-2,3,6-trideoxy-α-D-*erythro* hexopyranoside, where activation of the 2-chloro group to reduction has been attributed to the presence of a bromo substituent (18). In this case and the conversion of **7** to **10** the chloro substituents were both axial. Selective dechlorination by nickel catalysts at C-6 was expected based on earlier findings (9) but the stereospecificity is in marked contrast to the results with neutral hexosides (7). In this regard Raney nickel dechlorination of the neutral hexoside, methyl 4,6-dichloro-4,6-dideoxy-β-D-galactopyranoside, yields methyl 6-chloro-4,6-dideoxy-β-D-*xylo*-hexopyranoside in addition to the preponderant product, methyl 4-chloro-4,6-dideoxy-β-D-galactopyranoside (9). Chlorosulphation in conjunction with nickel catalysed selective dechlorination, therefore, provides the crucial derivative **9**, for the synthesis of bacillosamine, in three steps from methyl 2-deoxy-2-phthalimido-β-D-glucopyranoside (**3**).

Methyl 2-acetamido-6-chloro-2,6-dideoxy-β-D-glucopyranoside (**6**) was converted to the crystalline 6-azido derivative **11** from which methyl 2-acetamido-6-amino-2,6-dideoxy-β-D-glucopyranoside **12** was obtained in 77% yield. Since both displacement and reduction steps were achieved in high yield a similar reaction sequence was envisaged for the preparation of bacillosamine methyl glycoside **15** from the 4-chloro derivative **9**. In this way a second inversion at C-4 restores the *gluco*-configuration to the pyranose ring (cf. ref. 7). Displacement of the 4-chloro function by azide was expected to provide methyl 2-acetamido-4-azido-2,4,6-trideoxy-β-D-hexopyranoside (**13**). However, when **9** was heated with potassium azide in DMF (dried over molecular sieve) at 120°C no reaction occurred and at 150°C extensive decomposition was observed. Crown ethers have been shown (4, 5) to effectively promote difficult nucleophilic substitutions on the pyranose ring. Reaction of the 4-chloro derivative **9** with potassium azide and 18-crown-6 in DMF at 150°C gave a 1:2 mixture of the desired product **13** and methyl 2-acetamido-2,4,6-trideoxy-β-L-*threo*-hex-4-enopyranoside (**14**). If the solvent, DMF, was first rigorously dried (by distillation from calcium hydride at reduced pressure) the reaction of **9** proceeded in similar fashion but the ratio of products **13** and **14** increased to 2:1. Despite rigorous drying of DMF and the use of activated molecular sieve the proportion of elimination product **14** could not be reduced below 30%, a reflection of the stereochemistry of the 4-chloro derivative, **9**. The optimized yield of **13** from **9** was 59%. By conducting the reaction of **9** with a weak nucleophile such as sodium benzoate a quantitative yield of the 4,5 unsaturated sugar **14** may be secured. A related product, the 6-azido derivative **17** was obtained when methyl 2-acetamido-4,6-dichloro-2,4,6-trideoxy-β-D-galactopyranoside (**7**) was reacted with azide (cf. ref. 7). Reduction of the 4-azido glucoside **13** yielded the desired product, methyl 2-acetamido-4-amino-2,4,6-trideoxy-β-D-glucopyranoside, **15**. Satisfactory elemental analyses were not obtained for this compound despite ^{13}C and ^{1}H nmr indications of high purity. The di-*N*-acetyl derivative was analytically pure, although the substitution pattern of this compound is not pertinent to the native state.

The glycal-like compounds **14** and **17** are interesting compounds for further manipulation but in this paper we report only the reduction of the 6-deoxy derivative **14**. Compound **17** gave multiple products on reduction but the unsaturated sugar **14** was reduced by palladium and hydrogen to a single product which was acetylated to give methyl 3-*O*-acetyl-2,4,6-trideoxy-β-D-*xylo*-hexopyranoside (**16**). The specificity of the hydrogenation reaction was somewhat surprising and in view of this the arguments based upon nmr, which lead to the conclusion that **16** is the product of reduction, are discussed. Reduction of **14** followed by acetylation could be expected to provide both C-5 epimers, methyl 2-acetamido-3-*O*-acetyl-2,4,6-trideoxy-α-L-*arabino*-hexopyranoside and the D-*xylo*-hexopyranoside **16**. However, ^{13}C nmr of the reaction product indicated the presence of one hexoside and in addition, ^{1}H nmr evidence is consistent only with the formation of the *xylo*-hexopyranoside **16**. Methyl 2-acetamido-3-*O*-acetyl-2,4,6-trideoxy-α-L-*arabino*-hexopyranoside could potentially exist in solution as either the $^{4}C_{1}$(L) or $^{1}C_{4}$(L) chair con-



14 $R^1 = OH, R^2 = CH_3$
17 $R^1 = OH, R^2 = CH_2N_3$

Can. J. Chem. Downloaded from www.nrcresearchpress.com by 210.87.254.6 on 09/05/12
For personal use only.

formation. The 400 MHz ^{1}H nmr evidence for reduced **14** includes a large (8.3 Hz) $J_{1,2}$ coupling constant. This excludes the $^1C_4$(L) chair conformation immediately. However, the $^4C_1$(L) conformation requires both $J_{4a,5}$ and $J_{4e,5}$ to have small (< 4–5 Hz) couplings, and since the axial H-4 resonance is a multiplet with large (~10 Hz) coupling constants the data are consistent only with the assigned structure, **16**.

Until very recently the occurrence of 2,4-diamino sugars has been limited to a small number of polysaccharides (15, 16, 19, 20). Extensive synthetic work has provided numerous 2,4-amino-deoxyhexoses of the D and L series (21, 22). Application of recently developed methods of polysaccharide analysis (23, 24) to a pneumococcal polysaccharide (25) and *Shigella sonnei* lipopolysaccharide (26) has revealed two additional examples of 2-acetamido-4-amino-6-deoxyhexopyranoside containing structures. The same substitution pattern (2-acetamido-4-amino-) also occurs in the pneumococcal C substance (16). In view of this recurring feature we have used chlorosulphation to provide an abbreviated route to the 2,4-diamino glucoside derivative **15** bearing the acetamido substituent at C-2 and amino group at C-4. In addition to the novel application of chlorosulphation to amino sugars this approach has also provided valuable ^{13}C nmr parameters for the β-hexopyranoside **15**, which were previously unavailable. Furthermore in the form synthesized here compound **15** provides a valuable comparative model for the degradative methods (nitrous acid deamination) (23, 25, 26) used to confirm the presence in polysaccharides of these rare and labile sugars.

Chlorosulphation of amino-deoxy sugars is of significant potential since it leads directly to amino-chloro-deoxy derivatives which are useful intermediates for further manipulation. As demonstrated here selective dechlorination can be executed at either primary or secondary positions with readily available catalysts. Although the 2-phthalimido function was used to avoid chlorosulphation at the reactive hydrogens of the 2-amino or 2-acetamido function of D-glucosamine, alternate protecting groups such as the di-*N*-benzoyl derivatives reported by Inch and Fletcher (27) would also fulfill this requirement.

Experimental

Thin layer chromatography was performed with Merck precoated silica gel 60F-254 plates and detection of compounds was achieved by quenching of uv fluorescence and by charring after spraying plates with 5% sulphuric acid in ethanol. Column chromatography was performed on silica gel G60 (70–230 mesh) with redistilled solvents. The loading of all columns was 1:100. Separations were also performed using a LC Prep 500 (Waters Associates). In these instances as much as 8–10 g of sample was purified in a single operation using solvent systems similar to those employed for conventional chromatography. Sulphuryl chloride (technical grade) was redistilled through a column containing 5 Å molecular sieve (Linde). W-4 Raney nickel was prepared according to the literature method (28). For the reproducible dechlorination of chloro-deoxy sugars only the most active catalyst was effective and the literature method (28) must be followed closely (cf. ref. 6). Nickel boride was prepared according to Boar *et al.* (17). DMF was dried by heating for 4 h at 90°C with calcium hydride followed by distillation under reduced pressure, or by stirring over phosphorous pentoxide for 1 week, followed by decanting and distillation under reduced pressure (~5 Torr). Until use DMF was stored over activated 3 Å molecular sieve (29). LH20 Gel was prepared and used according to the manufacturer's (Pharmacia) instructions.

Methyl 3,4,6-Tri-O-acetyl-2-deoxy-2-phthalimido-β-D-glucopyranoside (2)

The syrupy anomeric mixture of 3,4,6-tri-*O*-acetyl-2-deoxy-2-phthalimido-D-glucopyranosyl bromides (**1**) (63.9 g) prepared according to Lemieux *et al.* (10) was dried under vacuum and dissolved in dry benzene (145 mL). This solution was added dropwise to a stirred suspension of mercuric cyanide (33.7 g) and Drierite (9.4 g) in dry benzene (195 mL), containing anhydrous methanol (19 mL). After 24 h at room temperature, tlc in the solvent ethyl acetate – Skellysolve B 1:1 showed no starting material and a new component with R_f 0.30. The reaction mixture was filtered and the residue washed with ethyl acetate. Extraction of the combined organic filtrates with 30% potassium iodide (100 mL), 5% sodium thiosulphate (200 mL), and water, followed by concentration, provided a syrup (52 g). Crystallization of the syrup from ethyl acetate and Skellysolve B provided 40.2 g (68%) of crystalline **2** in three successive crops. The crystals had mp 160.5–162.0°C; $[\alpha]_{589}$ +44.7 (*c* 1.1, chloroform) (lit. (30) mp 156–157°C, $[\alpha]_D$ +45.5 (*c* 3.23 chloroform)); R_f 0.30 (ethyl acetate – Skellysolve B 1:1); ^{13}C nmr ($CDCl_3$) δ: 99.1(C1), 71.9(C5), 70.9(C3), 69.1(C4), 62.0(C6), 57.0(OCH_3), 54.6(C2). *Anal.* calcd. for $C_{21}H_{23}NO_{10}$: C 56.12, H 5.16, N 3.12; found: C 56.08, H 5.32, N 3.09.

Methyl 2-Deoxy-2-phthalimido-β-D-glucopyranoside (3)

Sodium (1 g, 43.5 mmol) was dissolved in dry methanol (300 mL) and this solution was added to the tri-*O*-acetate **2** (40.0 g) in 200 mL of dry methanol. After 2 h at room temperature de-*O*-acetylation was complete and the solution was deionized with Rexyn (H^+) resin. Removal of the resin and concentration provided a syrup, which crystallized from methanol – ethyl acetate to give pure **3** (22.7 g 79%) mp 202.5–204.0°C; $[\alpha]_{589}$ −8.62 (*c* 1.0, methanol); R_f 0.45 (ethyl acetate – methanol–water 85:10:5); ^{13}C nmr (CD_3OD) δ: 100.6(C1), 78.2(C5), 72.6(2C, C3 and C4), 62.6(C6), 58.3(C2), 57.0(OCH_3). *Anal.* calcd. for $C_{15}H_{17}NO_7$: C 55.73, H 5.30, N 4.33; found: C 55.87, H 5.46, N 4.33.

Methyl 6-Chloro-2,4-dideoxy-2-phthalimido-β-D-glucopyranoside (4)

Methyl 2-deoxy-2-phthalimido-β-D-glucopyranoside (**3**) (8 g, 25 mmol) was dissolved in dry pyridine (8 mL) to which 15 mL of absolute chloroform was added. This solution was cooled to −70°C and stirred with an overhead stirrer. Freshly distilled sulphuryl chloride (7 mL, 87 mmol) was added dropwise. After 30 min at −70°C the temperature was maintained between −10° and −20°C for 4 h. The reaction mixture was poured into 50 mL of 10% sulphuric acid and chloroform (300 mL) was added. The organic phase was extracted with 5% potassium bicarbonate solution (150 mL) and water. Concentration to a syrup provided

Can. J. Chem. Downloaded from www.nrcresearchpress.com by 210.87.254.6 on 09/05/12
For personal use only.

9.0 g of the chlorosulphated derivative of **4**. The syrup was dissolved in methanol (190 mL) and stirred with solid potassium bicarbonate (12.0 g) and 0.1 g sodium iodide. After 20 min dechlorosulphation was complete and, following evaporation, the solid residue was partitioned between 200 mL of chloroform and 50 mL of saturated sodium chloride. The chloroform solution was washed with 5% sodium thiosulphate (50 mL) and dried. The syrup crystallized from ethanol to give 5.0 g of crystals mp 197.5°–199°C; $[\alpha]_{589}$ −11.5° (*c* 1.0, methanol); ^{13}C nmr (CD_3OD) δ: 100.6(C1), 77.1(C5), 73.4(C3), 72.4(C4), 58.3(C2), 57.0(OCH_3), 45.3(C6). *Anal.* calcd. for $C_{15}H_{16}NO_6Cl$: C 52.72, H 4.72, N 4.10, Cl 10.38; found: C 52.58, H 4.79, N 3.97, Cl 10.22.

Methyl 4,6-Dichloro-2,4,6-trideoxy-2-phthalimido-β-D-galactopyranoside (5)

Methyl 2-deoxy-2-phthalimido-β-D-glucopyranoside **3** (12.0 g, 37 mmol) was dissolved in dry pyridine (45 mL) and 90 mL of absolute chloroform was added. The stirred solution was cooled to −70°C and sulphuryl chloride (freshly distilled, 23 mL 285 mmol) was added dropwise. The resulting solution became very viscous and a further 115 mL of chloroform was added to the reaction mixture. After 1 h at −70°C the reaction was stirred for 5 h at room temperature. The reaction mixture was quenched and worked up in a similar manner to that described for the 6-chloro compound **4**. The dechlorosulphated syrup (12 g) which resulted consisted of two components, as judged by tlc, R_f 0.37 and 0.11 (solvent, ethyl acetate – Skellysolve B, 1:1). The separation of these components was accomplished both by conventional column chromatography and on larger (8 g) scales by hplc with the solvent ethyl acetate – Skellysolve B 1:1. The title compound **5** (7.9 g, 59%) was obtained as a syrup, whilst the slower component (1.9 g, 15%) corresponded to the 6-chloro derivative **4**. The optimum yield of **5** was obtained with reaction times between 4 h and 8 h; longer time resulted in reduced overall yields although the ratio of **5**:**4** increased. Compound **5** crystallized from ethanol mp 149.5–151.5°C; $[\alpha]_{589}$ +20.5° (*c* 1.0, methanol); R_f 0.37 (ethyl acetate – Skellysolve B 1:1); ^{13}C nmr (CD_3OD) δ: 101.2(C1), 75.2(C5), 68.1(C3), 64.2(C4), 57.1(OCH_3), 54.8(C2), 43.7(C6). *Anal.* calcd. for $C_{15}H_{15}NO_5Cl_2$: C 50.02, H 4.20, N 3.89, Cl 19.69; found: C 50.13, H 4.20, N 3.82, Cl 19.54.

Methyl 2-Acetamido-6-chloro-2,6-dideoxy-β-D-glucopyranoside (6)

Compound **4** (5.7 g, 16.7 mmol) was dissolved in ethanol (400 mL) containing hydrazine hydrate (6 mL of an 85% solution in water), the solution was refluxed for 2 h, then filtered, evaporated, dried, and redissolved in methanol–water (3:1, 50 mL); acetic anhydride (5 mL) was added and the solution was stirred overnight. The solid obtained from this solution after solvent removal was dried and then purified on a silica gel column with chloroform–methanol (4:1). The compound obtained from the column was recrystallized from ethanol to give pure **6** (3.0 g, 71% yield) mp 178.5–180.0°C; $[\alpha]_{589}$ −29.5° (*c* 1.0, methanol); R_f 0.38 (same solvent as above); ^{13}C nmr (CD_3OD) δ: 103.4(C1), 76.8(C5), 75.8(C3), 72.9(C4), 57.2(C2), 57.0(OCH_3), 45.4(C6), 23.0($NHCOCH_3$). *Anal.* calcd. for $C_9H_{16}NO_5Cl$: C 42.61, H 6.36, N 5.52, Cl 13.98; found: C 42.76, H 6.54, N 5.63, Cl 13.87.

Methyl 2-Acetamido-4,6-dichloro-2,4,6-trideoxy-β-D-galactopyranoside (7)

Compound **5** (9.5 g, 26.4 mmol) was dissolved in ethanol (600 mL) containing hydrazine hydrate (10 mL of an 85% solution in water). The solution was refluxed for 2 h, filtered, evaporated, and dried. The residue was dissolved in methanol–water (100 mL, 3:1) and acetic anhydride (10 mL) was added. The solution was stirred overnight, evaporated, and dried. Recrystallization from ethanol gave pure **6** (5.6 g, 78%), the mother liquor was evaporated, and the residue was purified on a silica gel column using chloroform–methanol (4:1) as solvent; this gave more of the pure compound **7** (1.2 g), total yield 93%. Melting point 216.0–216.5°C; $[\alpha]_{589}$ +12.7° (*c* 1.0, methanol); R_f 0.56 (solvent as above); ^{13}C nmr (CD_3OD) δ: 104.0(C1), 75.0(C5), 71.7(C3), 63.8(C4), 57.0(OCH_3), 53.8(C2), 43.8(C6), 23.0($NHCOCH_3$). *Anal.* calcd. for $C_9H_{15}NO_4Cl_2$: C 39.72, H 5.56, N 5.15, Cl 26.06; found: C 39.51, H 5.77, N 5.11, Cl 25.96.

Methyl 2-Acetamido-2,6-dideoxy-β-D-glucopyranoside (8)

Compound **6** (0.51 g, 2.0 mmol) in ethanol (40 mL) containing W-4 Raney nickel catalyst (~1 g) and triethylamine (1.0 mL) was hydrogenated at 50 psi for 24 h. Filtration and evaporation gave a solid which was purified on a silica gel column with chloroform–methanol (4:1) as solvent. This gave pure **8** (0.31 g, 71% yield), mp 235–237°C (recrystallized from ethyl acetate – Skellysolve B); $[\alpha]_{589}$ −58.3° (*c* 1.0, methanol); R_f 0.38 (solvent as above); ^{13}C nmr (D_2O) δ: 103.1(C1), 76.4(C5), 74.9(C3), 73.1(C4), 58.3(OCH_3), 56.9(C2), 23.4($NHCOCH_3$), 17.9(C6). *Anal.* calcd. for $C_9H_{17}NO_5$: C 49.31, H 7.82, N 6.39; found: C 49.17, H 7.87, N 6.32.

Methyl 2-Acetamido-4-chloro-2,4,6-trideoxy-β-D-galactopyranoside (9)

Method A, Raney Nickel

Compound **7** (3.0 g, 11.0 mmol) in ethanol (60 mL) containing W-4 Raney nickel catalyst (~3 g) and triethylamine (4 mL) was hydrogenated at 50 psi for 36 h. Filtration and evaporation gave a solid residue, which was purified on a silica gel column with chloroform–methanol (4:1) as solvent. This gave, after recrystallization from ethanol, pure **9** (2.1 g, 80% yield), mp 166.0–167.5°C; $[\alpha]_{589}$ +6.7° (*c* 1.0, methanol); R_f 0.50 (solvent as above); ^{13}C nmr (CD_3OD) δ: 103.9(C1), 73.3(C5), 70.7(C3), 67.9(C4), 57.0(OCH_3), 53.6(C2), 23.1($NHCOCH_3$), 18.3(C6). *Anal.* calcd. for $C_9H_{16}NO_4Cl$: C 45.50, H 6.79, N 5.89, Cl 14.92; found: C 45.66, H 6.94, N 5.97, Cl 14.81.

Method B, Nickel Boride

Nickel chloride (1.3 g, 10 mmol) dissolved in 120 mL of ethanol was stirred under nitrogen and treated dropwise with a solution of sodium borohydride (0.75 g, 19.8 mmol) in water (10 mL) (17). The substrate **7** (1.5 g, 5.5 mmol) in 20 mL of ethanol containing 2 mL of triethylamine was added to the black suspension. The mixture was hydrogenated at 70 psi for 6 h. The reaction products were worked up and purified as described in method A. The yield of **9** after recrystallization from ethanol was 0.95 g, 72%, mp 166–167°C.

Methyl 2-Acetamido-6-chloro-2,4-dideoxy-β-D-xylo-hexapyranoside (10)

The 4,6-dichloro derivative **7** (2.3 g, 9 mmol) in ethanol (50 mL) was hydrogenated over palladium on charcoal at 70 psi for 18 h in the presence of one equivalent of sodium hydroxide. Filtration and evaporation gave a syrup, which was chromatographed on silica gel with chloroform–methanol (4:1). The material eluted as a single component and crystallized from ethanol–Skellysolve B to yield crystals of **10** (1.5 g, 75% yield), mp 185–186°C; $[\alpha]_{589}$ −21.2° (*c* 1.2, methanol); R_f 0.52 chloroform–methanol (4:1). The mother liquors were enriched for the 4-chloro-6-deoxy derivative **9**, which by C-13 was judged to comprise 15% of the reaction product. Compound **10** gave ^{13}C nmr data and a proton spectrum recorded at 400 MHz in full agreement with the assigned structure; ^{1}H nmr (400 MHz) ($CDCl_3$) δ: 1.51(s, 1H, $J_{3,4a} \approx J_{4a,5} = 11.1$ Hz, $J_{4e,4a} = 13.0$ Hz, H-4a), 2.09(s, 3H, $NHCOCH_3$), 2.20(m, 1H, $J_{3,4e} = 5.2$ Hz, $J_{4e,5} = 2.0$ Hz, $J_{4a,4e} = 13.0$ Hz, H-4e), 3.28(m, 1H, $J_{1,2} = 8.2$ Hz, $J_{2,3} = 9.8$ Hz, $J_{NH,2} \approx 4.0$ Hz, H-2), 3.55(s, 3H, OCH_3),

Can. J. Chem. Downloaded from www.nrcresearchpress.com by 210.87.254.6 on 09/05/12
For personal use only.

3.54–3.71(m, 3H, H-5, H-6), 3.86(m, 1H, $J_{2,3}$ = 9.8 Hz, $J_{3,4a}$ = 11.1 Hz, $J_{3,4e}$ = 5.2 Hz, H-3), 4.25(d, 1H, $J_{1,2}$ = 8.2 Hz); ^{13}C nmr (CD_3OD) δ: 103.7(C1), 72.9(C5), 70.3(C3), 58.6(C2), 56.8(OCH_3), 47.2(C6), 38.1(C4), 22.9($NHCOCH_3$). *Anal.* calcd. for $C_9H_{16}NO_4Cl$: C 45.50, H 6.79, N 5.89, Cl 14.92; found: C 45.63, H 6.76, N 5.86, Cl 14.80.

Methyl 2-Acetamido-6-azido-2,6-dideoxy-β-D-glucopyranoside (11)

Compound **6** (0.51 g, 2.0 mmol), potassium azide (0.16 g, 2.0 mmol), and dicyclohexano-18-crown-6 (0.80 g, 2.1 mmol) in dry DMF (30 mL) was refluxed for 45 min. Evaporation followed by purification on a silica gel column with chloroform–methanol (4:1) as solvent gave after recrystallization from ethanol – Skellysolve B pure **10** (0.42 g, 81% yield), mp 204–206°C; $[\alpha]_{589}$ −40.6° (*c* 1.0, methanol); R_f 0.33 (solvent as above); ir (KBr pellet): 2088 (N≡N) cm^{-1}; ^{13}C nmr (CD_3OD) δ: 103.4(C1), 77.2(C5), 75.9(C3), 73.0(C4), 57.2(C2), 56.9(OCH_3), 52.8(C6), 22.9($NHCOCH_3$). *Anal.* calcd. for $C_9H_{16}N_4O_5$: C 41.54, H 6.20, N 21.15; found: C 41.62, H 6.34, N 21.04.

Methyl 2-Acetamido-6-amino-2,6-dideoxy-β-D-glucopyranoside (12)

Compound **11** (100 mg, 0.38 mmol) was dissolved in ethanol (40 mL) containing platinum oxide catalyst. The solution was hydrogenated at atmospheric pressure for 2 h, then filtered and evaporated. The solid residue was purified on a LH20 column with methanol as solvent, followed by recrystallization from propan-2-ol–methanol, to give pure **12** (70 mg, 77% yield), mp 180°C (dec.); $[\alpha]_{589}$ −23.7° (*c* 1.0, methanol); ^{13}C nmr (D_2O) δ: 103.2(C1), 76.7(C5), 75.0(C3), 72.8(C4), 58.3(OCH_3), 56.7(C2), 42.7(C6), 23.4 ($NHCOCH_3$). *Anal.* calcd. for $C_9H_{18}N_2O_5$: C 46.15, H 7.75, N 11.96; found: C 45.98, H 7.84, N 12.05.

Methyl 2-Acetamido-4-azido-2,4,6-trideoxy-β-D-glucopyranoside (13) and Methyl 2-Acetamido-2,4,6-trideoxy-α-L-threo-hex-4-enopyranoside (14)

Compound **6** (350 mg, 1.47 mmol) was added to a cooled solution of dicyclohexano-18-crown-6 (650 mg, 1.24 mmol) and potassium azide (130 mg, 1.6 mmol), which had first been refluxed for 10 min. The solution was refluxed for 1 h, evaporated, and purified on a silica gel column with chloroform–methanol (95:5) as solvent. This gave pure **13** (210 mg, 59% yield) and **14** (100 mg, 34% yield). Compound **13** mp 207–209°C (recrystallized from ethyl acetate – Skellysolve B); $[\alpha]_{589}$ −2.7° (*c* 1.2, methanol); R_f 0.37 (chloroform–methanol 7:1); ir (KBr pellet) 2107 (N≡N) cm^{-1}; ^{13}C nmr (CD_3OD) δ: 103.1(C1), 75.2(C5), 71.8(C3), 70.2(C4), 57.7(C2), 56.8(OCH_3), 22.9($NHCOCH_3$), 18.7(C6). *Anal.* calcd. for $C_9H_{16}N_4O_4$: C 44.26, H 6.60, N 22.94; found: C 44.28, H 6.75, N 23.04.

Compound **14** mp 108–110°C (recrystallized from ethyl acetate – Skellysolve B); $[\alpha]_{589}$ −9.7° (*c* 1.1, methanol); R_f 0.40 (chloroform–methanol 7:1); ^{1}H nmr ($CDCl_3$) δ: 1.82 (t, 3H, $J_{4,6}$ = 1.0 Hz, H-6), 1.97 (s, 3H, CH_3CONH—), 3.43 (s, 3H, CH_3O), 4.90 (m, 2H, H-1 and H-4); ^{13}C nmr ($CDCl_3$) δ: 148.7(C5), 99.6(C1), 99.2(C4), 64.2(C3), 56.3(OCH_3), 50.2(C2), 23.0($NHCOCH_3$), 19.7(C6). *Anal.* calcd. for $C_9H_{15}NO_4$: C 53.72, H 7.51, N 6.96; found: C 53.55, H 7.47, N 7.10.

Methyl 2-Acetamido-4-amino-2,4,6-trideoxy-β-D-glucopyranoside (15)

Compound **13** (200 mg 0.82 mmol) was dissolved in ethanol (50 mL) containing platinum oxide catalyst and the solution was hydrogenated at atmospheric pressure. After 2 h the solution was filtered, evaporated, and the solid residue was purified on a LH20 column with methanol as solvent. This gave pure **15** (130 mg, 73% yield); $[\alpha]_{589}$ −50.1° (*c* 1.0, CH_3OH); ^{1}H nmr (D_2O) δ: 1.24 (d, 3H, $J_{5,6}$ = 6.2 Hz, H-6), 1.95 (s, 3H, $NHCOCH_3$), 2.47 (t, 1H, $J_{3,4}$ = 9.4 Hz, H-4), 3.40 (s, 3H, OCH_3), 4.34 (d, 1H, $J_{1,2}$ = 8.2 Hz, H-1); ^{13}C nmr (D_2O) δ: 103.0(C1), 72.9(C5), 71.6(C3), 58.9(C4), 58.4(OCH_3), 57.3(C2), 23.2($NHCOCH_3$), 18.1(C6). *Anal.* calcd. for $C_9H_{18}N_2O_4$: C 49.53, H 8.31, N 12.84; found: C 48.70, H 8.18, N 11.71. Methyl 2,4-diacetamido-2,4,6-trideoxy-β-D-glucopyranoside prepared from **15** was analytically pure.

Methyl 2-Acetamido-3-O-acetyl-2,4,6-trideoxy-β-D-xylo-hexopyranoside (16)

Compound **14** (400 mg, 2.0 mmol) was dissolved in ethanol (60 mL) containing palladium (10% on charcoal) catalyst and the mixture was hydrogenated at atmospheric pressure for 3 h, filtered, and then evaporated. Purification on a silica gel column gave a compound that was not pure according to ^{13}C nmr. The compound was dissolved in chloroform (30 mL) to which pyridine (2 mL) and acetic acid anhydride (0.5 mL) was added. The reaction was stirred overnight and then evaporated to a syrup which was purified on a silica gel column with the solvent chloroform–methanol (7:1). This gave pure **16** (290 mg, 59%) mp 205–206°C (recrystallized from ethyl acetate – Skellysolve B); $[\alpha]_{589}$ −57.4° (*c* 1.0, methanol); R_f 0.50 (solvent as above); ^{1}H nmr ($CDCl_3$) 400 MHz, δ: 1.28 (d, 3H, $J_{5,6}$ = 6.2 Hz, H-6), 1.51 (m, 1H, $J_{3,4a} \approx J_{4a,5}$ = 11.3 Hz, $J_{4e,4a}$ = 12.6 Hz, H-4a), 1.98 (s, 3H, $OCOCH_3$), 2.02(m, 1H, $J_{3,4e} \approx J_{4e,5}$ = 4.9 Hz, $J_{4e,4a}$ = 12.6 Hz, H-4e), 2.05 (s, 3H, $NHCOCH_3$), 3.77 (m, 1H, $J_{1,2}$ = 8.3 Hz, $J_{2,3}$ = 10.5 Hz, $J_{2,NH}$ = 8.9 Hz, H-2), 3.64 (m, 1H, $J_{4a,5}$ = 11.3 Hz, $J_{4e,5}$ = 4.9 Hz, $J_{5,6}$ = 6.2 Hz, H-5), 3.47 (s, 3H, OCH_3), 4.37 (d, 1H, $J_{1,2}$ = 8.3 Hz, H-1), 5.04 (m, 1H, $J_{2,3}$ = 10.5 Hz, $J_{3,4a}$ = 11.3 Hz, $J_{3,4e}$ = 4.9 Hz, H-3), 5.57 (d, 1H, $J_{2,NH}$ = 8.9 Hz, NH); ^{13}C nmr (CD_3OD) δ: 103.2(C1), 72.4(C5), 68.8(C3), 56.6(OCH_3), 55.5(C2), 39.2(C4), 22.6($NHCOCH_3$), 20.9(C6), 20.6($COCH_3$). *Anal.* calcd. for $C_{11}H_{19}NO_5$: C 53.87, H 7.81, N 5.71; found: C 54.02, H 7.90, N 5.64.

Methyl 2-Acetamido-6-azido-2,4,6-trideoxy-α-L-threo-hex-4-enopyranoside (17)

Compound **6** (400 mg, 1.5 mmol) was added to a cooled solution of dicyclohexano-18-crown-6 (1200 mg, 3.2 mmol) and potassium azide (250 mg, 3.1 mmol) in DMF (30 mL), which had first been refluxed for 10 min. The solution was refluxed for 1 h, evaporated, and purified on a silica gel column with chloroform–methanol (7:1) as solvent. This gave pure **17** (270 mg, 75% yield), mp 92–94°C (recrystallized from ethanol – Skellysolve B); $[\alpha]_{589}$ +10.0° (*c* 1.1, methanol); R_f 0.40 (solvent as above); ^{13}C nmr (CD_3OD) δ: 148.6(C5), 103.7(C1), 101.3(C4), 65.8(C3), 56.8(OCH_3), 53.6(C2), 53.2(C6), 22.6($NHCOCH_3$). *Anal.* calcd. for $C_9H_{14}N_4O_4$: C 44.63, H 5.83, N 23.13; found: C 44.83, H 6.01, N 22.98.

Acknowledgements

We wish to thank Mr. J. Christ for invaluable technical assistance and Mr. H. Seguin for microanalyses. We express our sincere gratitude to Dr. T. Nakashima, University of Alberta Chemistry Department, NMR Centre, for proton spectra recorded at 400 MHz.

1. H. J. Jennings and J. K. N. Jones. Can. J. Chem. **40**, 1408 (1962).
2. H. J. Jennings and J. K. N. Jones. Can. J. Chem. **41**, 1151 (1963).
3. H. J. Jennings and J. K. N. Jones. Can. J. Chem. **43**, 2372 (1965).
4. D. R. Bundle. J. Chem. Soc. Perkin Trans. I, 2751 (1979).
5. N. T. Naidoo and H. Paralis. Carbohydr. Res. **62**, C5 (1978).

6. B. T. LAWTON, D. J. WARD, W. A. SZAREK, and J. K. N. JONES. Can. J. Chem. **47**, 2899 (1969).
7. B. T. LAWTON, W. A. SZAREK, and J. K. N. JONES. Carbohydr. Res. **15**, 397 (1970).
8. E. W. WILLIAMS, W. A. SZAREK, and J. K. N. JONES. Can. J. Chem. **49**, 796 (1971).
9. W. A. SZAREK, A. ZAMOJSKI, A. R. GIBSON, D. M. VYAS, and J. K. N. JONES. Can. J. Chem. **54**, 3783 (1976).
10. R. U. LEMIEUX, T. TAKEDA, and B. Y. CHUNG. Am. Chem. Soc. Symposium Series, **39**, 90 (1976).
11. B. HELFERICH and J. ZIRNER. Chem. Ber. **95**, 2604 (1962).
12. R. B. BAKER, J. P. JOSEPH, R. E. SCHAUB, and J. H. WILLIAMS. J. Org. Chem. **19**, 1786 (1954).
13. D. M. DEAN, W. A. SZAREK, and J. K. N. JONES. Carbohydr. Res. **33**, 383 (1974).
14. A. LIAV, J. HILDESHEIM, U. ZEHAIR, and N. SHARON. Carbohydr. Res. **33**, 217 (1974).
15. D. E. BRUNDISH and J. BADDILEY. Biochem. J. **110**, 103 (1977).
16. I. R. POXTON, E. TARELLI, and J. BADDILEY. Biochem. J. **175**, 1033 (1978).
17. R. B. BOAR, D. W. HAWKINS, J. F. MCGHIE, and D. H. R. BARTON. J. Chem. Soc. Perkin Trans. I, 654 (1973).
18. S. HANESSIAN and N. R. PLESSAS. J. Org. Chem. **34**, 2163 (1969).
19. N. SHARON and R. JEANLOZ. Biochim. Biophys. Acta, **31**, 277 (1959); J. Biol. Chem. **235**, 1 (1960).
20. S. G. WILKINSON. Biochem. J. **161**, 103 (1968).
21. A. LIAU, J. HILDESHEIM, U. ZEHAIR, and N. SHARON. J. Chem. Soc. Chem. Commun. 668 (1973); Carbohydr. Res. **33**, 217 (1974).
22. A. LIAU and N. SHARON. Carbohydr. Res. **30**, 109 (1973); **37**, 248 (1974).
23. B. LINDBERG and J. LÖNNGREN. Methods in enzymology. Vol. 50. Part C. *Edited by* V. Ginsburg. Academic Press, New York. 1978. pp. 3–33.
24. H. J. JENNINGS and I. C. P. SMITH. Methods in enzymology. Vol. 50. Part C. *Edited by* V. Ginsburg. Academic Press, New York. 1978. pp. 39–50.
25. B. LINDBERG, B. LINDQUIST, J. LÖNNGREN, and D. A. POWELL. Carbohydr. Res. **78**, 111 (1980).
26. L. KENNE, B. LINDBERG, K. PETERSSON, E. KATZENELLENBOGEN, and E. ROMANOWSKA, Carbohydr. Res. **78**, 119 (1980).
27. T. D. INCH and H. G. FLETCHER, JR. J. Org. Chem. **31**, 1815 (1966); **31**, 1821 (1966).
28. A. A. PAULIC and H. ADKINS. J. Am. Chem. Soc. **68**, 1471 (1946).
29. D. R. BURFIELD and R. H. SMITHERS. J. Org. Chem. **43**, 3966 (1978).
30. S. AKLYA and T. OSAWA. Chem. Pharm. Bull. Tokyo, **8**, 583 (1960).

Can. J. Chem. Downloaded from www.nrcresearchpress.com by 210.87.254.6 on 09/05/12
For personal use only.

The chemical synthesis of oligoribonucleotides. IX.[1] A comparison of protecting groups in the dichloridite procedure

KELVIN K. OGILVIE, NICOLE Y. THERIAULT, JAN-MARCUS SEIFERT, RICHARD T. PON, AND MONA J. NEMER

Department of Chemistry, McGill University, Montreal, P.Q., Canada H3A 2K6

Received May 6, 1980

This paper is dedicated to Prof. Raymond U. Lemieux on the occasion of his 60th birthday

KELVIN K. OGILVIE, NICOLE Y. THERIAULT, JAN-MARCUS SEIFERT, RICHARD T. PON, and MONA J. NEMER. Can. J. Chem. **58**, 2686 (1980).

A series of phosphorodichloridites has been prepared incorporating the most commonly used phosphate protecting groups in oligonucleotide synthesis. The groups include trichloroethyl, tribromoethyl, cyanoethyl, benzyl, methyl, *p*-chlorophenyl, and nitrophenethyl. The trichloroethyl and the nitrophenethyl appear to be the most stable groups while the cyanoethyl and methyl offer specific advantages. The benzyl and *p*-chlorophenyl groups are subject to limitations on their utility. Condensations can be carried out in a range of solvents including THF, pyridine, and DMF and at temperatures from −78°C to 20°C with a slight drop in yield with increasing temperature, at least for dinucleotide condensations.

KELVIN K. OGILVIE, NICOLE Y. THERIAULT, JAN-MARCUS SEIFERT, RICHARD T. PON et MONA J. NEMER. Can. J. Chem. **58**, 2686 (1980).

On a préparé une série de phosphodichloridures incorporant les groupements protecteurs phosphates les plus fréquemment utilisés dans la synthèse des oligonucléotides. Les groupements comprennent le trichloroéthyle, le tribromoéthyle, le cyanoéthyle, le benzyle, le méthyle, le *p*-chlorophényle et le nitrophenéthyle. Les groupements trichloroéthyle et nitrophenéthyle semblent être les plus stables tandis que le groupements cyanoéthyle et méthyle offrent des avantages spécifiques. Les groupements benzyle et *p*-chlorophényle sont d'une utilisation limitée. Les condensations peuvent être réalisées dans une variété de solvants incluant le THF, la pyridine et le DMF à des températures allant de −78°C à 20°C avec une légère diminution du rendement quand la température augmente au moins lors de condensation impliquant les dinucléotides.

[Traduit par le journal]

Introduction

For the development of a complete procedure for the synthesis of ribonucleotides, three important aspects must be investigated. These include the development of a complete set of protecting groups for the nucleoside units; the determination of an effective method of condensation, and the choice of a compatible phosphate protecting group when necessary (triester approach).

We have been developing a complete and effective method for the synthesis of oligoribonucleotides (1–5). The key feature of the protection of the nucleoside units in our procedure is the use of the *tert*-butyldimethylsilyl (TBDMS) group for the protection of the 2′-oxygen ribonucleosides. We have described in detail the synthesis of protected ribonucleosides having all possible degrees of silylation from A, C, G, and U, the *N*-benzoyl derivatives of C and G, and the methoxytrityl derivatives of A, C, G, U, C^{Bz}, and G^{Bz} for a total of 63 silylated derivatives (2, 3). We have also described (5) the use of the levulinyl group for protecting the 3′-position of 2′-silylated ribonucleosides, and this has completed the development of the first phase of our method.

For the question of condensation of silylated nucleosides to form nucleotide chains we have used the dichloridite procedure (1–5) originally introduced by Letsinger *et al.* (6). The utility of the procedure was established through the stepwise synthesis (4) of the heptanucleotide GCAACCA and the block condensation synthesis (5) of a hexadecauridylic acid. We have shown (7) the TBDMS group to be compatible with nine of the condensing agents currently used in oligonucleotide synthesis. We have concluded from this study (7) that the phosphorodichloridite procedure offers the most rapid and clean procedure for the synthesis of oligoribonucleotides.

During most of the above developmental work, we have been using the trichloroethyl group as the phosphate protecting group. In this report we de-

[1]This article constitutes Part XIII in a series on silyl protecting groups in nucleoside and nucleotide chemistry. For the previous article in both series, see K. K. Ogilvie, M. J. Nemer, N. Theriault, R. Pon, and J.-M. Seifert, Nucleic Acids Research Special Publication No. 7. 1980. p. 147.

0008-4042/80/232686-08$01.00/0

©1980 National Research Council of Canada/Conseil national de recherches du Canada

Can. J. Chem. Downloaded from www.nrcresearchpress.com by 210.87.254.105 on 09/05/12
For personal use only.

Can. J. Chem. Downloaded from www.nrcresearchpress.com by 210.87.254.105 on 09/05/12
For personal use only.

scribe the synthesis of the dichloridites from the most commonly used phosphate protecting groups. We have compared them in the synthesis of ribonucleotides using the dichloridite procedure. We also describe in this report the effects of solvent and temperature on the yields in condensation steps. The ability to remove the phosphate protecting groups from silylated ribonucleotides is also described.

Discussion

Several important phosphate protecting groups have been introduced during the development of the triester synthesis of oligonucleotides. The benzyl group was used during the first successful chemical synthesis (8) of a nucleotide. This original synthesis did not appear to be practical and the benzyl group was considered to be too sensitive to acid hydrolysis (and nucleophilic attack) to be generally useful.

The cyanoethyl group (CE), introduced by Tener (9) for diesters, was used by Letsinger *et al.* (10) as the phosphate protecting group in his discovery of the modern triester synthesis of oligonucleotides. The cyanoethyl group is stable to the usual acid conditions, but is readily eliminated by mild base (e.g. dilute NH_3, 10 min, 20°C).

The β,β,β-trichloroethyl group (TCE) was introduced to nucleotide triester synthesis by Eckstein and Rizk (11). This group is stable to acid and mild base, but can be removed with Zn/Cu in DMF. The β,β,β-tribromoethyl group has also been used (12, 13) and is reported to be more easily removed than the TCE group.

The phenyl (14) and substituted (15, 16) phenyl groups have been described for the synthesis of nucleotide triesters. These groups are stable to acid but are base labile. Until recently, cleavage of the nucleotide chain by the conditions used to remove the phenyl groups has been an undesired complication. However, the introduction of the oximate method of deprotection (17, 18) seems to have significantly reduced this problem.

Pfleiderer and Uhlmann (19) have recently suggested the use of substituted phenethyl groups for the synthesis of nucleotide triesters. These groups are stable to acid and vary in their resistance to base cleavage.

The methyl protecting group has not been widely used, but has gained some recent attention (20, 21). The small size of the group has potential advantages both in synthesis and subsequent biological testing (22).

In order to evaluate these protecting groups in the dichloridite procedure for condensing TBDMS-protected ribonucleosides, the following dichloridites were prepared:

Compound	Number	Abbreviation
$Cl_3CCH_2OPCl_2$	**1***a*	(TCE)$OPCl_2$
$Br_3CCH_2OPCl_2$	**1***b*	(TBE)$OPCl_2$
ϕCH_2OPCl_2	**1***c*	(ϕCH_2)$OPCl_2$
CH_3OPCl_2	**1***d*	CH_3OPCl_2
$NCCH_2CH_2OPCl_2$	**1***e*	(CE)$OPCl_2$
	1*f*	(*p*Clφ)$OPCl_2$
	1*g*	(PE)$OPCl_2$
	**1***h*	(NPE)$OPCl_2$

The dichloridites were all prepared by the reaction of the appropriate alcohol with phosphorus trichloride according to the equation

$$ROH + PCl_3 \rightarrow ROPCl_2 + HCl$$

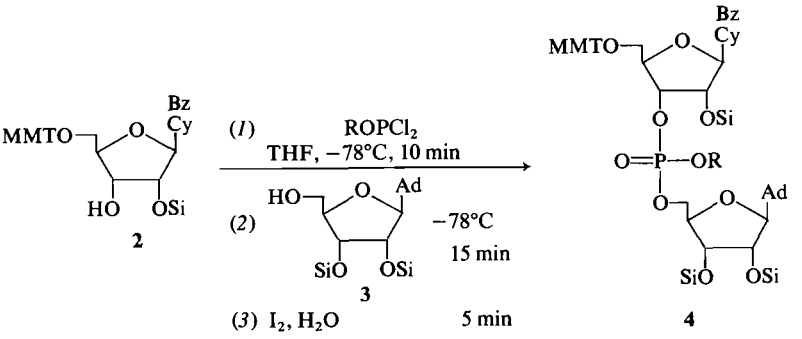
Most of the dichloridites have been reported previously (see Experimental). Preparations of **1***c* are reported (22) to lead to explosions and the reported preparations (23) of **1***e* lead to very low yields. We have modified the general procedures by conducting the reactions in ether as solvent at −78°C and, in the case of **1***e*, adding pyridine to the solution. Products were generally isolated by short-path distillation in a Kugelrohr apparatus. Yields were quite acceptable, being generally 40–80%.

Synthesis of Ribonucleotides

The phosphorodichloridite procedure was first used by Letsinger *et al.* for the synthesis of deoxynucleotides (6) and we have reported extensively on its use in the synthesis of ribonucleotides (1–5, 7). The general procedure is outlined in Scheme 1 for the synthesis of the fully protected CpA. The results of the condensations are collected in Table 1.

From Table 1 it can be seen that the only reagent that did not give satisfactory results was the benzyl phosphorodichloridite (**1***c*). The yield of **4***c* was only 29% while the yields in all the other condensations ranged from 40–80%, being generally in the vicinity of 70%. The benzyl group appears to be quite sensitive to the reaction conditions. We have conducted experiments with **1***c* and deoxynucleosides[2] and find the yields to be very low (~20%). It is clear from the table that the most commonly used protecting groups are all very compatible with the phosphorodichloridite procedure. Compounds

[2]J. M. Seifert and K. K. Ogilvie, unpublished results.



a R = TCE
b R = TBE
c R = $CH_2\phi$
d R = CH_3
e R = CE
f R = *p*Clϕ

SCHEME 1

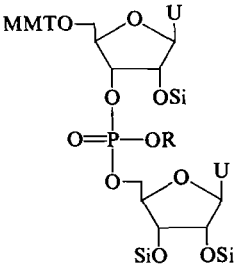
5*a–c* and **6***a–d* were also prepared in the yields indicated (Table 1).

General Reaction Conditions

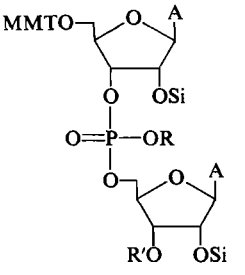
We have previously indicated (2, 3) that the ratio of reactants (e.g. **2**:**1**:**3**) of 1:1.1:0.8 gives the best results for ribonucleotide synthesis. From Table 1, it can be seen that slight variation from this ratio does not have much effect. Most of our experiments have been carried out using longer times than are necessary. For example, we have generally used times of 30–45 min (at −78°C) for step (*1*) (Scheme 1) and 40–60 min (−78°C) followed by 60 min at 20°C for step (*2*). Entries 1 and 2 in Table 1 show that very short reaction times can be used (5 min for *1*, and 15 min for *2*). We now routinely use 5–15 min for step (*1*) and 15–30 min for step (*2*) followed by rapid warming to room temperature and oxidation by iodine–water (5 min).

Solvent

While most condensations have been reported in THF as solvent, other solvents work equally well and may have advantages in specific situations. Entries 2–6 show that reactions carried out at −78°C in THF, DMF, collidine, and pyridine all show similar yields. Collidine has the practical disadvantage that it freezes at −78°C and must occasionally be removed from the cooling bath in order to mobilize the thick sludge by partial warming. Collidine is also difficult to remove in any quantity at the end of the reaction. Pyridine and DMF have the advantage that most nucleosides and their derivatives are soluble in these solvents. This allows the dichloridite procedure to be applied to nucleosides protected with groups other than TBDMS which are less soluble in organic solvents such as THF than are the TBDMS substituted nucleosides. DMF shows a significant decrease in yield for reactions carried out above 0°C as discussed below.



5*a* R = TCE
b R = TBE
c R = CH_3



6*a* R = TBE, R′ = Si
b R = TBE, R′ = Lv
c R = NPE, R′ = Si
d R = CH_3, R′ = Lv

Temperature

The question of the temperature at which the reactions must be carried out is an important one. While the original (6) and subsequent reports (1–4, 20) have used −78°C, such low temperatures are not generally necessary. We have found (5) that block condensations work very well in THF at 0°C. In this report, we have compared reactions at −78°C, 0°C, and 20°C. From Table 1, it is apparent that reactions at 0°C have similar yields to those at −78°C. However, a definite decrease in yield occurs in all solvents at 20°C. For THF and pyridine, the yields (64%) are easily acceptable, but for DMF, the drop to 48% is more severe.

In the DMF reactions, all solutions show color. At −78°C, the solution is a pale yellow, becoming a definitive yellow at 0°C and nearly orange at 20°C. Others (25, 26) have reported that DMF reacts with PCl_3 in a manner shown below (R = Cl).

It is quite probable that in our reactions a reaction between (TCE)$OPCl_2$ and DMF may occur to produce a compound of the type **8***b* which could rearrange to **9***b*. Either of these two species could

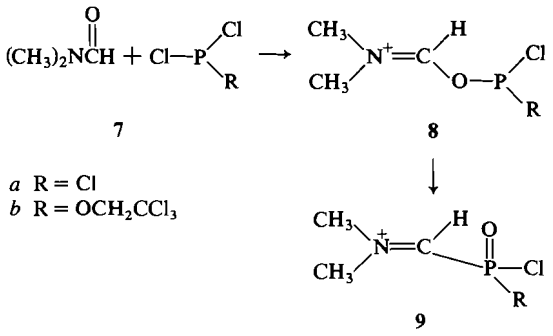
Can. J. Chem. Downloaded from www.nrcresearchpress.com by 210.87.254.105 on 09/05/12
For personal use only.

Can. J. Chem. Downloaded from www.nrcresearchpress.com by 210.87.254.105 on 09/05/12
For personal use only.

TABLE 1. Summary of condensation reactions

Entry No.	1st Nucleoside	$ROPCl_2$	2nd Nucleoside	Reactant ratio (e.g. 2:1:3)	Time (°C) of reaction steps* (1); (2) (min)	Solvent	Product (yield)
1	MMT-C^{Bz}_{OH} (2)	$TCEOPCl_2$	HOA^{Si}_{Si} (3)	1:1.1:0.8	5m(−78); 15m(−78)	THF	4*a* (77%)
2	MMT-C^{Bz}_{OH} (2)	$TCEOPCl_2$	HOA^{Si}_{Si} (3)	1:1.1:0.8	15m(−78); 30m(−78)	THF	4*a* (77%)
3	MMT-C^{Bz}_{OH} (2)	$TCEOPCl_2$	HOA^{Si}_{Si} (3)	1:1.1:0.8	30m(−78); 60m(−78), 60m(20)	DMF†	4*a* (71%)
4	MMT-C^{Bz}_{OH} (2)	$TCEOPCl_2$	HOA^{Si}_{Si} (3)	1:1.1:0.8	30m(−78); 20m(−78), 100 m(20)	2,4,6-Collidine†	4*a* (67%)
5	MMT-C^{Bz}_{OH} (2)	$TCEOPCl_2$	HOA^{Si}_{Si} (3)	1:1.1:0.8	30m(−78); 40m(−78), 75m(20)	Pyridine	4*a* (72%)
6	MMT-C^{Bz}_{OH} (2)	$TCEOPCl_2$	HOA^{Si}_{Si} (3)	1:1.1:0.8	5m(−78); 15m(−78), 15m(20)	DMF†	4*a* (73%)
7	MMT-C^{Bz}_{OH} (2)	$TCEOPCl_2$	HOA^{Si}_{Si} (3)	1:1.1:0.8	5m(0); 15m(0), 15m(20)	DMF	4*a* (75%)
8	MMT-C^{Bz}_{OH} (2)	$TCEOPCl_2$	HOA^{Si}_{Si} (3)	1:1.1:0.8	5m(20); 30m(20)	DMF	4*a* (48%)
9	MMT-C^{Bz}_{OH} (2)	$TCEOPCl_2$	HOA^{Si}_{Si} (3)	1:1.1:0.8	5m(20); 30m(20)	THF	4*a* (64%)
10	MMT-C^{Bz}_{OH} (2)	$TCEOPCl_2$	HOA^{Si}_{Si} (3)	1:1.1:0.8	5m(20); 30m(20)	Pyridine	4*a* (64%)
11	MMT-C^{Bz}_{OH} (2)	$TBEOPCl_2$	HOA^{Si}_{Si} (3)	1:1.1:0.8	30m(−78); 60m(−78), 60m(20)	THF	4*b* (57%)
12	MMT-C^{Bz}_{OH} (2)	$TBEOPCl_2$	HOA^{Si}_{Si} (3)	1:1.1:0.8	30m(−78); 60m(−78), 60m(20)	DMF†	4*b* (55%)
13	MMT-C^{Bz}_{OH} (2)	ϕCH_2OPCl_2	HOA^{Si}_{Si} (3)	1:1.1:0.8	30m(−78); 30m(−78), 60m(20)	THF	4*c* (29%)
14	MMT-C^{Bz}_{OH} (2)	$CEOPCl_2$	HOA^{Si}_{Si} (3)	1:1.1:0.8	30m(−78); 45m(−78), 30m(20)	THF	4*e* (71%)
15	MMT-C^{Bz}_{OH} (2)	$p Cl\phi OPCl_2$	HOA^{Si}_{Si} (3)	1:1.1:0.8	5m(−78); 15m(−78)	THF	4*f* (80%)
16	MMT-C^{Bz}_{OH} (2)	CH_3OPCl_2	HOA^{Si}_{Si} (3)	1:1.1:0.8	10m(−78); 15m(−78), 30m(20)	THF	4*d* (40%)
17	MMT-U^{Si}_{OH}	$TCEOPCl_2$	HOU^{Si}_{Si}	1:1.0:0.8	10m(−78); 20m(−78), 10m(20)	THF	5*a* (74%)
18	MMT-U^{Si}_{OH}	$TBEOPCl_2$	HOU^{Si}_{Si}	1:1.0:0.8	10m(−78); 20m(−78), 10m(20)	THF	5*b* (69%)
19	MMT-U^{Si}_{OH}	CH_3OPCl_2	HOU^{Si}_{Si}	1:1.0:0.8	10m(−78); 20m(−78), 10m(20)	THF	5*d* (75%)
20	MMT-A^{Si}_{OH}	$TBEOPCl_2$	HOA^{Si}_{Si}	1:1.1:1.0	30m(−78); 30m(−78), 60m(20)	THF	6*a* (81%)
21	MMT-A^{Si}_{OH}	$TBEOPCl_2$	HOA^{Si}_{Lv}	1:1.1:0.9	30m(−78); 30m(−78), 60m(20)	THF	6*b* (67%)
22	MMT-A^{Si}_{OH}	$NPEOPCl_2$	HOA^{Si}_{Si}	1:1.1:1.0	30m(−78); 30m(−78), 60m(20)	THF	6*c* (77%)
23	MMT-A^{Si}_{OH}	CH_3OPCl_2	HOA^{Si}_{Lv}	1:1.1:0.9	30m(−78); 30m(−78), 60m(20)	THF	6*d* (40%)

*See Scheme 1.
†Reaction mixture solidifies.



7 8 9

a R = Cl
b R = OCH_2CCl_3

react with nucleosides and thereby reduce the yields of desired products.

Stability of Phosphate Protecting Groups to Acid and Hydrazine

In order to allow chain extension it must be possible to remove the 5′-methoxytrityl group without affecting the phosphate protecting group. All of the compounds **4** were treated with acid to remove the methoxytrityl group.

$$\underset{\mathbf{4}\,a\text{–}f}{\text{MMT-C}^{\text{Bz}^{\text{Si}}_{\text{P}}}\text{(R)A}^{\text{Si}}_{\text{Si}}} \xrightarrow{\text{H}^+} \underset{\mathbf{7}\,a\text{–}f}{\text{HOC}^{\text{Bz}^{\text{Si}}_{\text{P}}}\text{(R)A}^{\text{Si}}_{\text{Si}}}$$

The conditions used were either 80% HOAc at room temperature for 24 h or 2% benzenesulfonic acid in chloroform–methanol (7:3) for 2 h. Yields of **7** were generally 80–85% except for R = benzyl or methyl where yields were 65–70%.

All of the compounds **4** were treated with hydrazine solution (7) for 10 min. None of the phosphate groups were affected. Normally, only 5 min are required to remove the levulinyl group which we use to protect the 3′-position (7)

$$\underset{\mathbf{4}\,a\text{–}f}{\text{MMT-C}^{\text{Bz}^{\text{Si}}_{\text{P}}}\text{(R)A}^{\text{Si}}_{\text{Si}}} \xrightarrow{\text{H}_2\text{NNH}_2} \text{No reaction}$$

Complete Deprotection of MMT-C$^{\text{Bz}^{\text{Si}}_{\text{P}}}$(R)A$^{\text{Si}}_{\text{Si}}$ to CpA (Removal of the Phosphate Protecting Group)

A. Trichloroethyl and Tribromoethyl Derivatives

Compounds **7***a*, *b* were treated with Zn/Cu in DMF at 55°C for 5 h followed by half-saturated methanolic ammonia at 20°C for 48 h and TBAF for 1 h at 20°C.

$$\underset{\mathbf{7}a}{\text{HOC}^{\text{Bz}^{\text{Si}}_{\text{P}}}\text{(R)A}^{\text{Si}}_{\text{Si}}} \xrightarrow[(2)\ \text{NH}_3\ (3)\ \text{TBAF}]{(1)\ \text{Zn/Cu}} \text{CpA}$$

For trichloroethyl protected nucleotides, we have never observed any internucleotide cleavage. Only the desired nucleotide product is observed. For the tribromoethyl compounds, the reaction with zinc is over within 2 h.

The actual yield of fully deprotected nucleotide (e.g. CpA) based on the amount of starting material (e.g. **7***a*) ranges from 40–90% and seems to be most dependent upon the quality of the zinc–copper couple. The nucleotide product in both cases is completely degraded by RNAse A.

B. The Benzyl and Methyl Groups

The benzyl group can be removed from nucleotides using 1-amines such as 3-butylamine as recently described for methyl groups (21). The reaction is very clean. Thus, when **7***c* was treated with *tert*-butylamine at 50°C for 14 h, a quantitative yield of the debenzylated material is obtained. Exactly the same result is obtained for the methyl protecting group. Subsequent treatments with NH_3 and TBAF yield the product CpA.

$$\text{HOC}^{\text{Bz}^{\text{Si}}_{\text{P}}}\text{(R)A}^{\text{Si}}_{\text{Si}} \xrightarrow[(2)\ \text{NH}_3\ (3)\ \text{TBAF}]{(1)\ t\text{-BuNH}_2} \text{CpA}$$

R = ϕCH_2 **7***c*, CH_3 **7***d*

This deprotection sequence is very clean and only the desired nucleotide product CpA is obtained which is completely degradable by RNAse A. Overall yields are generally 80–95%. The only disadvantage of the CH_3 and benzyl protecting groups would appear to be the condensation yields.

C. Cyanoethyl

The cyanoethyl group is a very easy group to remove, requiring only mild ammonia. In the case of **7***e*, the conditions to remove the *N*-benzoyl group also remove the cyanoethyl group. Thus, treatment of **7***e* for 2 days with NH_3 followed by TBAF gives the products CpA as the only nucleotidic product in virtually quantitative yield (> 90% in all cases). The product is completely degradable by enzymes

$$\underset{\mathbf{7}e}{\text{HOC}^{\text{Bz}^{\text{Si}}_{\text{P}}}\text{(CE)A}^{\text{Si}}_{\text{Si}}} \xrightarrow[(2)\ \text{TBAF}]{(1)\ \text{NH}_3} \text{CpA}$$

D. p-*Chlorophenyl*

Recently a method has been described for the removal of chlorophenyl groups from phosphate triesters which involves a minimum of internucleotide cleavage (17, 18). We have found that this procedure does not appear to be compatible with the silyl protecting groups. For example, when **4***f* was treated first with N^1,N^1,N^2,N^2-tetramethylguanidinium pyridine 2′-carboxaldoximate (TGPC) at 20°C for 48 h followed successively by treatment with 2% benzenesulfonic acid in chloroform methanol (7:3) for 90 min at 20°C, half-saturated methanolic ammonia for 48 h at 20°C, and finally TBAF at 20°C for 60 min, three products were obtained and identified as CpA, Cp, and A. In this

Can. J. Chem. Downloaded from www.nrcresearchpress.com by 210.87.254.105 on 09/05/12
For personal use only.

Can. J. Chem. Downloaded from www.nrcresearchpress.com by 210.87.254.105 on 09/05/12
For personal use only.

case, the Cp and A constitute 10–15% of the total uv-absorbing product and must arise by chain cleavage.

$$\text{MMT-C}^{\text{Bz}}{}^{\text{Si}}_{\text{P}}(p\text{Cl}\phi)\text{A}^{\text{Si}}_{\text{Si}} \xrightarrow[(2)\ 2\%\ \text{BSA}\ (3)\ \text{NH}_3, \text{CH}_3\text{OH}\ (4)\ \text{TBAF}]{(1)\ \text{TGPC}} \text{CpA} + \text{Cp} + \text{A}$$

Since purification of products from the above reaction only occurred after the final step, it was possible that the chain degradation occurred as a result of a combination of reagents rather than the action of a single reagent. However, subsequent investigation seemed to indicate that the problem arises at the oximate deprotection step.

When MMT-U^{Si}_{P} (pClϕ)U^{Si}_{Si} was treated with the oximate reagent followed by treatment with 80% HOAc for 30 min at 80°C and the products isolated by tlc, several products were obtained including U and Up (~25%), UpU (~15%), and $U^{Si}_{P}U^{Si}_{Si}$ (~50%). Clearly, loss of the silyl group had occurred during these steps. In addition, the UpU obtained was only 85% degraded by pancreatic RNAse A. Since the material was completely degraded by snake venom, the UpU would appear to be contaminated by about 15% of the 2′–5′ isomer.

In a subsequent reaction U^{Si}_{P} (pClϕ)U^{Si}_{Si} was treated with oximate and the product was isolated on tlc sheets before further deprotection. The product mixture consisted of UpU (~2%), a second band that appeared to be a mixture of partially silylated UpU (~6%) and a third and major band (~92%) which was mostly fully silylated UpU. Band no. 2 after treatment with TBAF gave a product that had the same chromatographic properties as UpU, which was not degraded by RNAse A, but was completely degraded by snake venom. The third band on treatment with TBAF gave a material which was identical to UpU and which was completely degraded to Up and U (1.0:1.0) by pancreatic RNAse A.

When U^{Si}_{P}(pClϕ)U^{Si}_{Si} was treated successively with oximate and TBAF and worked up on paper chromatography, the products isolated were U + Up (~18%) and UpU (82%). Only 93% of the UpU was degraded by RNAse A.

The p*-Nitrophenethyl Group*

This group has recently been proposed as a new phosphate protecting group (19) and we have found it to be compatible both with the phosphodichloridite procedure and the silyl protecting groups. The *p*-nitrophenethyl group was removed from **6***c* in 2 h at room temperature using neat 1,5-diazabicyclo[4.3.0]non-5-ene as has been previously suggested (19*b*).

Conclusion

As a result of this study on the dichloridite procedure for the synthesis of ribonucleotides, we can conclude (*1*) that a variety of solvents may be used and thus accommodate a range of specific needs; (*2*) the procedure works over a range of temperatures from −78°C to 20°C with yields decreasing slightly as temperature increases; (*3*) most commonly used phosphate protecting groups are amenable to the procedure. It is clear that the trichloroethyl group appears to offer the advantage of stability to a variety of reagents. The benzyl group, while easily removed, is not sufficiently stable to the condensation procedure. The methyl and cyanoethyl groups appear to offer advantages with regard to deprotection. The oximate method of removal of the chlorophenyl group would appear to require further investigation to be compatible with the silyl protecting group.

Experimental

General Methods

All general procedures and techniques including chromatography, uv, nmr, elemental analyses, melting points, electrophoresis, and enzyme analyses are as previously described (2, 5). All protected nucleosides were prepared according to the procedures already fully described (2, 3, 5). The preparation of the tetrabutylammonium fluoride (TBAF) in THF reagent has been described (2). The zinc–copper reagent was prepared according to the literature (27) and used in DMF at 50°C for 5 h (28). All alcohols used in the preparation of phosphorodichloridites were obtained commercially with the exception of 4-nitrophenethanol which was prepared according to literature procedures (29, 30). Alcohols were distilled before use as was the phosphorus trichloride used in the preparations of the dichloridites.

Preparation of the Dichloridites **1**a–h

The dichloridites (TCE)$OPCl_2$ (**1***a*), (pClϕ)$OPCl_2$ (**1***f*), CH_3OPCl_2 (**1***d*) were prepared according to their respective literature preparations (31–33) and their properties are listed in Table 2.

The general procedure for the preparation of the other dichloridites can be illustrated by the preparation of β-cyanoethylphosphorodichloridite (**1***e*) which has only been described in very low yields in the literature (24). Hydracrylonitrile (0.5 mol in ether (30 mL)) was added slowly to a cooled solution (−78°C) of pyridine (1 mol, pyridine was not used in any of the other preparations) in ether (30 mL) containing PCl_3 (0.5 mol). After a total of 1 h at −78°C the solution was filtered from pyridinium hydrochloride and the ether was removed under reduced pressure at room temperature to leave a clear liquid. This liquid was carefully distilled in a Kugelrohr apparatus to give a 59% yield of the desired product (**1***e*). Properties are listed in Table 2.

The dichloridites (TBE)$OPCl_2$ (**1***b*), (PE)$OPCl_2$ (**1***g*), and (NPE)$OPCl_2$ (**1***h*) were prepared in a similar fashion except that the addition of alcohol was carried out at 0° to −78°C over a 15 min period followed by warming the solution to room temperature for 30–50 min. Pyridine was not used. The product yields were 56, 45, and 78% respectively.

The benzylphosphodichloridite (**1***c*) was prepared at −78°C but no solvent was used. That is, the benzyl alcohol was added

TABLE 2. Properties of phosphorodichloridites

Dichloridite	Yield (%)	Boiling point (°C)	Density (g/mL)	^{31}P δ rel 85% H_3PO_4	Refractive index	Reference
1*a*, (TCE)$OPCl_2$	50	42 (0.1 Torr)	1.698 (22°C)	−175.40	1.5140 (22°C)	32
1*b*, (TBE)$OPCl_2$	56	65 (0.05 Torr)	2.2795 (26°C)	−174.06	1.5959 (24°C)	37
1*c*, (φCH_2)$OPCl_2$	30	65 (0.2 Torr)	1.2790 (23°C)	−174.80	1.5584 (20°C)	23
1*d*, CH_3OPCl_2	60	93 (76 Torr)	1.406 (4°C)	−178.42		34
1*e*, (CE)$OPCl_2$	59	70 (0.4 Torr)	1.3919 (20°C)	−175.94	1.4908 (28°C)	35
1*f*, (*p*Clφ)$OPCl_2$	50	113 (10 Torr)	1.4714 (20°C)	−174.80	1.5749 (20°C)	33
1*g*, (PE)$OPCl_2$	45	90 (0.25 Torr)	1.2507 (24°C)	−175.53	1.5470 (24°C)	
1*h*, (NPE)$OPCl_2$	78	120 (0.18 Torr)	1.3935 (26°C)	−175.47	1.5755 (24°C)	

directly to PCl_3, maintained at −78°C for 30 min, followed by warming to room temperature for 30 min. The yield of **1***c* was 30%. While this may seem low, it should be noted that previous literature reports (23) indicate that these reactions usually end in explosions. No explosions have occurred during our preparation.

General Procedure for the Synthesis of Dinucleotides

The general procedure can be illustrated by the synthesis of **4***a*. To a solution of 2,4,6-collidine (0.14 mL, 1 mmol) in dry THF (0.35 mL) maintained at −78°C in a small flask equipped with a septum cover was added via a syringe, (TCE)$OPCl_2$ (39 μL, 0.265 mmol). (The pressure inside the flask is maintained via a syringe equipped as a drying tube and inserted through the septum.) To the solution was added **2***a* (174 mg, 0.24 mmol) dissolved in 0.35 mL of dry THF. After a total of 5 min, a solution of **3** (98 mg, 0.19 mmol) in THF (0.65 mL) was added (via syringe). The solution was maintained at −78°C for 15 min. The reaction mixture was warmed to room temperature and to it was added a solution of iodine (114 mg, 0.43 mmol) and a drop of pyridine in THF:H_2O (2:1, 1.5 mL). After 5 min at room temperature, the solvent was evaporated to dryness. The residue was dissolved in chloroform (20 mL) which was washed with 20 mL of water containing 1 mL of a 5% sodium bisulfite solution. The aqueous layer was back-extracted four times with chloroform (10 mL). The combined chloroform solutions were concentrated to a small volume at reduced pressure and applied to three silica gel plates developed three times in ether. The product was eluted with acetone followed by ethyl acetate. After evaporation of the solvent, 216 mg of a product **4***a* (77%) was obtained (**4***a*, mp 129–134°C, λ_{max} (EtOH): 305, 261, 237 nm, R_f(Et_2O) 0.14, R_f(EtOAc) 0.68).

This general procedure was used in all the syntheses listed in Table 1 with the variations of time and temperature noted in the table. For condensations in collidine (as solvent) at low temperatures, the solution solidifies and must occasionally be removed from the bath and shaken vigorously with slight warming to allow the slurry to be stirred.

Removal of Protecting Groups

1. The Methoxytrityl Group

Two procedures are used interchangeably for removal of the methoxytrityl group. (*a*) 80% HOAc at room temperature for 24 h. The temperature is kept at 20–25°C to avoid any debenzamidation of *N*-benzoylcytidine units. We have observed that, on heating, as much as 5–10% of *N*-benzoylcytidine units may be converted to uridine. At room temperature, 80% HOAc usually requires 14–24 h to affect complete demethoxytritylation. At the end of the reaction, the solvents are removed at reduced pressure and the residue applied to tlc plates for product isolation. While only the desired product is observed on analytical tlc, isolated yields are generally 80–85% from preparative tlc plates.

(*b*) 2% Benzenesulfonic acid (34) in chloroform–methanol (7:3) for 2 h at room temperature. At the end of the reaction period, the solution is diluted to 50 mL with $CHCl_3$ and extracted with 5% sodium bicarbonate solution (2 × 40 mL). The bicarbonate wash solutions are back-extracted with chloroform (2 × 30 mL) and the combined chloroform extracts are washed once with water (50 mL). The chloroform is then removed at reduced pressure and the residue is applied to tlc plates. Yields are generally 80–90%.

2. Treatment With Hydrazine Solution

Compounds **4***a–f* (5 mg each) were dissolved in ~70 μL of the standard hydrazine solution (0.25 mL hydrazine–hydrate (1:1)/10 mL pyridine–acetic acid (4:1)). The solution was stirred at room temperature for 10 min and then stopped by the addition of two drops of acetylacetone. Thin-layer chromatography showed that none of the starting compounds had been affected by this treatment.

3. Phosphate, Amine, and Hydroxyl Protecting Groups

A. Trichloroethyl and Tribromoethyl

The detritylated nucleotide (either purified or direct from the detritylation procedure) is treated with Zn/Cu couple in DMF (~20 mg of Zn/Cu per 20 mg of dinucleotide in 2 mL) at 50°C for 2 h. The mixture is cooled to room temperature and is diluted with 2 mL of half-saturated methanolic ammonia and stirred at room temperature for 2 days. At the end of this time, the solution is centrifuged to eliminate metal and salts, the solvent is concentrated at reduced pressure, and the residue is applied to Eastman Chromagram sheets developed in solvent A. The product moves to the solvent front away from salts and other impurities. The product is eluted with methanol which is evaporated and the residue is treated with 2 mL TBAF in THF (0.68 mmol/mL) for 1–2 h at room temperature. The THF is evaporated and the residue dissolved in water (3–5 mL). The cloudy solution is applied to a column of Dowex 50W-X8 (Na^+ form, 1 × 30 cm) which is eluted with 50 mL of water. The combined eluted solvent is evaporated (lyophilized) and the residue is applied to Whatman 3 mm paper developed in solvent A (2). Yields are calculated from the OD units (260 nm) and are generally 40–80% based on the starting fully protected nucleotide.

B. Benzyl and Methyl Groups (20)

These phosphate protecting groups are very easily removed. Immediately after detritylation of the fully protected nucleotide (20 mg) and removal of acetic acid, the residue is dissolved in *tert*-butylamine (10–20 mL) and heated at reflux for 14–20 h. The solvent is removed at reduced pressure (tlc shows complete and clean deprotection for both benzyl and methyl groups) and the residue is then treated directly and successively with methanolic ammonia and TBAF as described above in A. Overall isolated yields are 80–95% and it is worth indicating that a very clean product isolation step is observed.

Can. J. Chem. Downloaded from www.nrcresearchpress.com by 210.87.254.105 on 09/05/12
For personal use only.

C. Cyanoethyl

The cyanoethyl group is removed in the same step that removes *N*-benzoyl groups. Consequently, the detritylated product is treated directly with half-saturated methanolic ammonia for 2 days followed by TBAF. Once again, a very clean product is obtained and the deprotection occurs in > 90% yields.

D. p-Chlorophenyl

The procedure used to remove the *p*-chlorophenyl group was essentially that described by Gilham and co-workers (18) and Reese and Yau (17). The nucleotide (~20 mg) was stirred in 0.36 mL of N^1,N^1,N^2,N^2-tetramethylguanidinium pyridine 2-carboxaldoximate at room temperature and, after 16 h, 5 μL of 1,1,3,3-tetramethylguanidine was added and stirring was continued for an additional 25 h. The product was then isolated on Eastman Chromagram sheets developed in ether–chloroform–methanol (5:4:1). The product remains at the origin while all other reagents move near the solvent front. The product can be eluted with methanol and treated with acid, ammonia, and TBAF as described in A above.

E. p-Nitrophenethyl

Compound **6***c* (50 mg, 36.8 μmol) was dissolved in 1,5-diazabicyclo[4.3.0]non-5-ene (DBN, 400 μL) and stirred at room temperature. Thin-layer chromatography showed the reaction to be complete after 2 h at which point the solution was concentrated at reduced pressure; 80% HOAc (4 mL) was added and after 24 h at room temperature, the solvents were removed at reduced pressure. The residue was dissolved in chloroform (20 mL) which was extracted with saturated aqueous ammonium chloride solution (3 × 15 mL) to remove the DBN. The chloroform was removed at reduced pressure and the residue treated with TBAF solution (3 mL) as described above. The product ApA was isolated cleanly from paper chromatography in overall yields of 50–70%.

Acknowledgements

We gratefully acknowledge financial support from the Natural Sciences and Engineering Research Council of Canada (NSERCC), Gouvernement du Québec-Ministère de l'Education (FCAC), Bio Logicals Inc., and McGill University. We also thank Michael Gillen who prepared the methylphosphodichloridite used in this work.

1. K. K. Ogilvie, N. Theriault, and K. Sadana. J. Am. Chem. Soc. **99**, 7741 (1977).
2. K. K. Ogilvie, S. L. Beaucage, A. L. Schifman, N. Y. Theriault, and K. L. Sadana. Can. J. Chem. **56**, 2768 (1978).
3. K. K. Ogilvie, A. L. Schifman, and C. L. Penney. Can. J. Chem. **57**, 2230 (1979).
4. K. K. Ogilvie and N. Y. Theriault. Can. J. Chem. **57**, 3140 (1979).
5. K. K. Ogilvie and M. J. Nemer. Can. J. Chem. **58**, 1389 (1980).
6. R. L. Letsinger, J. L. Finnan, G. A. Heavner, and W. B. Lunsford. J. Am. Chem. Soc. **97**, 3278 (1975); R. L. Letsinger and W. B. Lunsford. J. Am. Chem. Soc. **98**, 3655 (1976).
7. K. K. Ogilvie and R. T. Pon. Nucleic Acids Res. **8**, 2105 (1980).
8. A. M. Michelson and A. R. Todd. J. Chem. Soc. 2632 (1955).
9. G. M. Tener. J. Am. Chem. Soc. **83**, 159 (1961).
10. R. L. Letsinger and K. K. Ogilvie. J. Am. Chem. Soc. **89**, 4801 (1967); R. L. Letsinger and V. Mahedevan. J. Am. Chem. Soc. **87**, 3526 (1965); **88**, 5319 (1966).
11. F. Eckstein and I. Rizk. Angew. Chem. Int. Ed. Engl. **79**, 939 (1967).
12. K. Itakura, N. Katagiri, C. P. Bahl, R. H. Wightman, and S. A. Narang. J. Am. Chem. Soc. **97**, 7327 (1975).
13. J. H. van Boom, P. M. J. Burgers, R. Crea, G. van der Marel, and G. Wille. Nucleic Acids Res. **4**, 747 (1977).
14. C. B. Reese and R. Saffhill. Chem. Commun. 767 (1968).
15. J. H. van Boom, P. M. J. Burgers, P. H. van Deursen, R. Arentzen, and C. B. Reese. Tetrahedron Lett. 3785 (1974).
16. K. Itakura, N. Katagiri, and S. A. Narang. Can. J. Chem. **52**, 3689 (1974).
17. C. B. Reese and L. Yau. Tetrahedron Lett. 4443 (1978).
18. G. R. Gough, C. K. Singleton, H. L. Weith, and P. T. Gilham. Nucleic Acids Res. **6**, 1557 (1979).
19. (*a*) W. Pfleiderer and E. Uhlmann. Nucleic Acids Res. Special Pub. No. 4, 525 (1978); (*b*) E. Uhlmann and W. Pfleiderer. Tetrahedron Lett. **21**, 1181 (1980).
20. G. W. Daub and E. E. van Tamelen. J. Am. Chem. Soc. **99**, 3526 (1977).
21. D. J. H. Smith, K. K. Ogilvie, and M. F. Gillen. Tetrahedron Lett. **21**, 861 (1980).
22. P. S. Miller, K. N. Fang, N. S. Kondo, and P. O. P. Ts'O. J. Am. Chem. Soc. **93**, 6657 (1971).
23. A. I. Razumov and N. F. Rispolozhenskii. Trans. Kirov. Inst. Chem. Tech. Kazan, **8**, 42 (1940); Chem. Abstr. **35**, 2485 (1941); A. I. Razumov. J. Gen. Chem. USSR, **14**, 464 (1944); Chem. Abstr. **39**, 4586 (1945).
24. E. V. Kusnetsov and R. K. Valetdinov. Tr. Kazan. Khim. Tekhnol. Inst. **23**, 167 (1957); Chem. Abstr. **52**, 8938d (1958).
25. D. R. Hepburn and H. R. Hudson. Chem. Ind. London, 664 (1974).
26. A. G. Anderson, N. E. T. Owen, F. J. Freeman, and D. Erickson. Synthesis, 398 (1976).
27. E. Legoft. J. Org. Chem. **29**, 2048 (1964).
28. E. S. Werstiuk and T. Neilson. Can. J. Chem. **54**, 2689 (1976).
29. M. E. Fourneau and M. Y. de Lestrange. Bull. Soc. Chim. Fr. **53**, 330 (1933).
30. E. Ferber. Chem. Ber. **62**, 183 (1929).
31. W. Gerrard, W. J. Green, and R. J. Phillips. J. Chem. Soc. 1148 (1954).
32. H. Tolkmith. J. Org. Chem. **23**, 1682 (1952).
33. D. R. Martin and P. J. Pizzolato. J. Am. Chem. Soc. **72**, 4584 (1950).
34. J. Stawinski, T. Hozumi, S. A. Narang, C. P. Bahl, and R. Wu. Nucleic Acids Res. **4**, 353 (1927).

Can. J. Chem. Downloaded from www.nrcresearchpress.com by 210.87.254.105 on 09/05/12
For personal use only.

Pillaromycin-A: structural and synthetic studies related to the sugar moiety, pillarose[1]

BERT FRASER-REID AND DAVID LOUIS WALKER[2]

Guelph–Waterloo Centre for Graduate Work in Chemistry, Waterloo Campus, University of Waterloo, Waterloo, Ont., Canada N2L 3G1

Received April 28, 1980

This paper is dedicated to Prof. Raymond U. Lemieux on the occasion of his 60th birthday

BERT FRASER-REID and DAVID LOUIS WALKER. Can. J. Chem. **58**, 2694 (1980).

The photo-induced alkylation of enone **6** with ethylene glycol gave an adduct from which the α-D-*threo* (**16**) and α-D-*erythro* (**17**) modifications of structure **2** have been elaborated. It was thereby shown that **2** is not the structure of pillarose. Addition of vinyl magnesium bromide to the ketone **24***b* gave a slight excess of one allylic alcohol, **25**, which upon treatment with osmium tetroxide and hydrogen peroxide gave directly the α,α′-ketodiol **3***a*. The epimer of the latter **33***b* was available via carboxymethylenation of ketone **24***b*, reduction of ester, and hydroxylation. Benzoylation of these epimers gave **3***b* and **33***c* respectively and it was concluded that the former, methyl 2,3,6-trideoxy-4-*C*-[oxo(benzoyloxymethyl)methyl]-α-D-*threo*-hexopyranoside, **3***b*, is the enantiomer of the "methyl 8-*O*-benzoyl pillaroside" obtained from the antibiotic pillaromycin A.

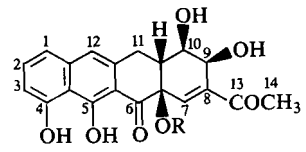
BERT FRASER-REID et DAVID LOUIS WALKER. Can. J. Chem. **58**, 2694 (1980).

L'alkylation photo induite de l'énone **6** par l'éthylèneglycol donne un adduit à partir duquel on a étudié soigneusement les composés α-D-*thréo* (**16**) et α-D-*érythro* (**17**) qui résultent des modifications de la structure du composé **2**. On a ainsi montré que le composé **2** ne représente pas la structure de la pillarose. L'addition du bromure de vinylmagnésium sur la cétone **24***b*, donne un léger excès de l'alcool allylique **25** qui, traité par le tétraoxyde d'osmium et l'eau oxygénée, conduit directement au cétodiol-α,α′ **3***a*. L'épimère de ce dernier **33***b* est préparé par la carboxyméthylénation de la cétone **24***b* et la réduction de l'ester suivie d'une hydroxylation. Par benzoylation, les épimères conduisent respectivement à **3***b* et **33***c* et on a conclu que le premier des deux soit le méthyltridéoxy-2,3,6 *C*-(oxo(benzoyloxyméthyl)-méthyl)-4 α-D-*thréo* hexopyrannoside **3***b* est l'énantiomère du "méthyl-*O*-benzoyl-8 pillaroside" obtenu à partir de l'antibiotique pillaromycine A.

[Traduit par le journal]

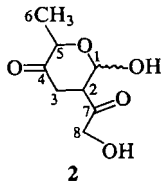
Introduction

Current interest in the anthracycline antibiotics runs very high (1) because of the antitumor activity displayed by many members of this family. Pillaromycin A, **1***a*, isolated from cultures of *Streptomyces flavovirens*, was no exception since it displayed colchicine-like antitumor activity, and relatively low toxicity (2*a*). From the standpoint of structure, considerable interest centres around the differences in the aglycones of **1***a* (2*b*) and those of daunomycin and its analogues. For example in **1***b*, (*a*) the acetyl side chain is at C8 rather than C9, (*b*) the site of unsaturation in ring A is unusual, (*c*) the sugar is attached at the ring junction rather than at C7, and (*d*) the sugar is linked through a tertiary rather than secondary oxygen.

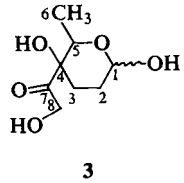


1

a R = Pillarose
b R = H



2



3

The structure originally assigned to the sugar moiety, pillarose, was equally unique in being a tricarbonyl sugar with a two-carbon branch located at C2 (2*c*). We therefore set out to confirm this assignment, in the course of which we showed that the structure was in fact **3** and not **2**, by synthesizing all related structures (3). Since then, other synthetic routes to **3** have been developed in the laboratories of Paulsen (4) and Brimacombe (5).

In this paper, we give details of our synthesis of (+)-**3** and reexamine some of the data used for making the original structure assignments (2).

Some Anomalies in Structural Assignment of 2

At the outset a number of questions could be raised about the assignments leading to structure **2** (2*c*).

1. An equilibrium between the hemiacetal, **2**, and hemiketal, **4**, was clearly possible, although no mention of its occurrence had been made, and no glycosides arising from **4** had been reported.

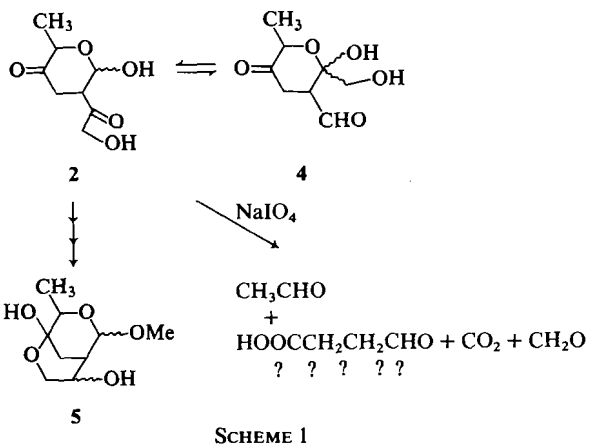
[1]For preliminary accounts of this work see refs. 3 and 10.

[2]Taken in part from the M.Sc. Thesis of D.L.W., University of Waterloo, 1975.

0008-4042/80/232694-09$01.00/0

©1980 National Research Council of Canada/Conseil national de recherches du Canada

Can. J. Chem. Downloaded from www.nrcresearchpress.com by 210.87.254.42 on 09/05/12
For personal use only.



SCHEME 1

2. Treatment of **1***a* with methanolic hydrogen chloride was said to produce methyl glycosides of **2** without any ketalisation at the C7 and C4 carbonyl groups.

3. Sodium borohydride reduction of **2** was said to occur at the "isolated" carbonyl; however, the dihydropillaroside obtained is assigned as **5**, which would have resulted from reduction at the more hindered carbonyl.

4. Since the dihydropillaroside obtained by borohydride reduction did not show a carbonyl group in the ir, the hemiketal form **5** seemed to be suggested. However, such a hemiketal would also have been reduced by borohydride.

5. Sodium periodate oxidation of pillarose was found to give acetaldehyde, carbon dioxide, formaldehyde, and succinaldehydic acid. However, the last-named substance could not have arisen from **2**.

Synthesis of the Proposed Pillarosides 18 and 19 Related to 2

The original structural studies (2) did not assign configurations at C2 and C5; hence a synthesis of structures **18** and **19**, which represent the possible *relative* stereochemistries, was devised.

The photochemically-induced addition of alcohols to enones had been developed in our laboratory as a valuable and simple method of alkylation (6), and we had found that the addition of ethanol to enone **6** (8) led to the epimeric mixture of alcohols **7** from which diketone **8** could be obtained by oxidation with Collin's reagent (9). Alternatively **8** may be obtained by photo-induced addition of acetaldehyde to **6** (7).

Compound **8** was therefore a convenient substance for studying the epimerization at C2. Sodium methoxide in methanol failed to epimerize **8** at room temperature, and at elevated temperatures decomposition occurred. However 1,5-diazabicyclo[4.3.0]-non-5-ene (DBN) in tetrahydrofuran at room temperature led after 1 hour to a 3:2 mixture of **8** and **9** judging from the H1 signals at 5.25 and 5.45 ppm. Prolonged treatment with the base, or use of elevated temperatures, did not affect the proportions of **8** and **9**.

The information obtained in these studies was now applied towards the synthesis of analogues of **2**. Photoaddition of ethylene glycol to enone **6** (7) and acetylation of the resulting diol afforded **10***b* in 80% yield. Deoxygenation at C6 was carried out using standard procedure leading to the diacetate **11**. The latter was then deacetylated and the diol **12** was tritylated giving **13**. Compounds **10–13** are epimeric mixtures at C7 and hence did not crystallize. Fortunately the transformations could be readily monitored by nmr and mass spectroscopy. Thus when the difference was removed by oxidation of the epimeric alcohols **13**, the ketone **14** crystallized readily.

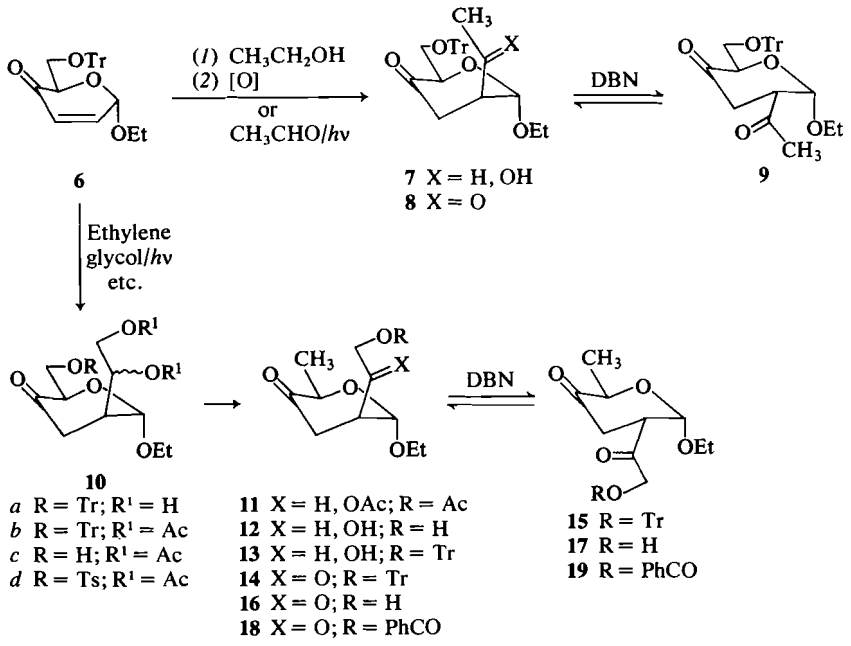
As with the prototype **8**, treatment of **14** with DBN gave the equatorial isomer **15**, judging from the nmr spectra. Unfortunately the epimers **14** and **15** were not resolved on tlc; however, when the mixture was detritylated the two alcohols **16** and **17** were resolved on tlc. However, these substances proved to be very sensitive and did not survive prolonged contact on a silica column during chromatographic fractionation. Hence upon completion of the detritylation, and removal of the triphenylmethanol on a short column, the mixture of **16** + **17** was benzoylated giving **18** + **19**. These were also resolved on tlc and were stable to column chromatography, which therefore afforded each diketone as a crystalline substance. The identity of **18** as the axial C2 epimer was verified by independent preparation from crystalline **14**.

Some Differences between Methyl 8-O-Benzoyl Pillaroside and 18 and 19

Asai (2) had reported the isolation of a crystalline methyl glycoside of 8-*O*-benzoyl pillarose. Our compounds **18** and **19** are in the α-D series, but one of them had to be the same as his with the possible exceptions that (*i*) ours is an ethyl glycoside, (*ii*) his could be an L-sugar, or (*iii*) his could be a β-anomer. None of these differences would be expected to affect grossly the ^{1}Hmr spectra of these analogues. However the data assembled in Table 1 show some striking differences in the entries in the first three rows. Particularly noteworthy are the differences in the chemical shifts for H1, H2, and CH_3.

From the standpoint of chemical behaviour, our experience (*vide supra*) had shown that **16** and **17**

Can. J. Chem. Downloaded from www.nrcresearchpress.com by 210.87.254.42 on 09/05/12
For personal use only.



SCHEME 2

were decomposed by attempted fractionation on a column of silica gel. It therefore seemed unlikely that such delicate structures would have survived the highly acidic conditions used for the cleavage of pillaromycin A (*2a*) or for the glycosidation of pillarose (*2c*).

Spectroscopic Analysis of Pillaromycin A

In the original investigations an X-ray study had been made of the aglycone pillaromycinone, **1***b*, by itself (11); but in view of the discrepancies noted in Table 1 and the anomalies discussed above, it was decided to obtain an X-ray study of the entire antibiotic, pillaromycin A, **1***a*.[3] It was thereby found that the structure of pillarose was **3** and not **2**, and from the absolute stereochemistry which had been established for the aglycon pillaromycinone **1***b* (11), it was possible to further establish that pillarose was the L-*threo* modification of **3** (10).

Structure **2** is two mass units less than **3**, hence the

TABLE 1. Some physical data for pillaroside analogues

Compound	Chemical shifts in ppm; *J* values in Hertz							Melting point (°C)	$[\alpha]_D^{23}$
	H1	H2	H3a	H3e	H5	H8,8′	CH_3		
Methyl 8-*O*-benzoyl pillaroside (ref. 2*c*)	4.6 $J_{1,2}=3$ Doublet	1.9 Multiplet	1.7–2.3		4.29 Quartet	5.21 Singlet	1.14 Doublet	103–105	−98.8
18	5.15 $J_{1,2}=5.2$ Doublet	3.24 Multiplet	2.81 Multiplet	2.94 Multiplet	4.23 Quartet	5.0 Quartet	1.32 Doublet	85.5–86	+219
19	5.38 $J_{1,2}=4.6$ Doublet	3.58 Multiplet	2.50 Multiplet	2.54 Multiplet	4.26 Quartet	4.97 Singlet	1.29 Doublet	85.5–86	+77.2
33*c*	4.82 Triplet	~2.0			3.98 Quartet	5.18 Singlet	1.22 Doublet	(syrup)	+74.8
3*b*	4.7 Broad Singlet	1.6–2.3			4.22 Quartet	5.22 Singlet	1.15 Doublet	107–108	+94.6

Can. J. Chem. Downloaded from www.nrcresearchpress.com by 210.87.254.42 on 09/05/12
For personal use only.

Can. J. Chem. Downloaded from www.nrcresearchpress.com by 210.87.254.42 on 09/05/12
For personal use only.

TABLE 2. Cmr and ^{1}Hmr data of pillaromycin-A in pyridine-d_5 (TMS)[a,b]

Carbon	δ (ppm)	Proton	δ (ppm)	Multiplicity (*J*)
		Aglycon		
1	118.6	1	7.18	d (7.7)
2	133.3	2	7.53	dd (7.7, 7.8)
3	113.3	3	7.18	d (7.8)
4	158.9	7	7.12	s
4a	135.9			
		9	5.22	d (3.6)
5	167.2			
5a	113.3	10	3.76	d (bs)
		10a	3.76	
6	200.0			
		11	3.48	ddd (12, 2.2, 2.2)
7	118.6			
		11	3.88	dd (12, 3.7)
8	110.2			
		12	7.84	s
9	64.2			
		14	2.48	s
10	67.8			
11	25.2			
11a	140.6			
12	139.6			
12a	142.2			
13	198.2			
14	26.4			
		Sugar		
1	92.6	1	5.88	
2	25.0	2 ax	2.77	dddd (14, 14, 4, 4)
3	29.1	2 eq	1.61	bd (14)
4	97.5	3 ax	1.80	bd (14)
5	69.0	3 eq	2.61	ddd (14, 14, 4)
6	14.9	5	4.80	q (6.3)
		6	0.94	d (6.3)
		8	5.07	d (22)
		8	5.06	d (22)

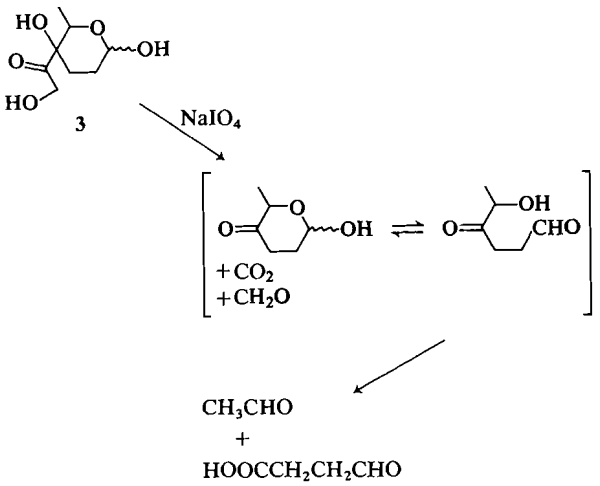
[a]Obtained on PS-100 and HR-220 spectrometers by Dr. I. Miura of Columbia University, New York.
[b]The numbering of the aglycon, *1b*, is typical for the anthracyclines (1), and is different from that used in the original publications on pillaromycin-A (2).

crystalline antibiotic[3] was examined by Field Desorption Mass Spectroscopy[4]; *m/e* 543 (29%), 542 (100), 526 (2), 370 (2), 336 (2), 173 (1). The *m/e* 370 peak represents the aglycon + H, the corresponding glycosyl portion (i.e., 3 minus the anomeric OH) appearing at *m/e* 173. The molecular weight of the complete sugar is therefore confirmed at 190.

Carbon and proton magnetic resonance data for the antibiotic in pyridine-d_5 are shown in Table 2.

Periodate Oxidation

The periodate oxidation results which were called into question in Scheme 1, since they could not be reconciled with structure **2**, may now be reinterpreted in the light of the revised structure **3**. The origin of the key fragment succinaldehydic acid is now apparent.



Synthesis of Methyl 8-O-Benzoyl-α-D-pillarose, 3b, and its C4 Epimer, 33c

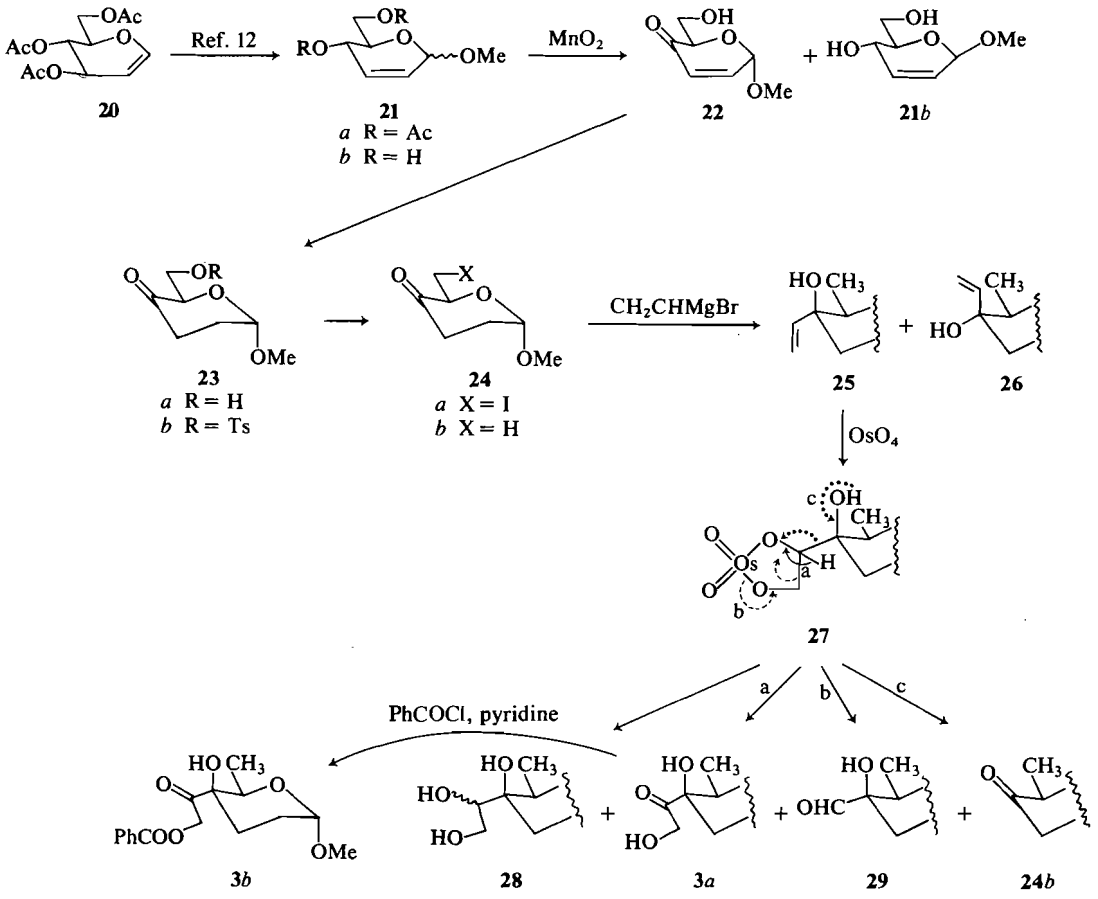
For the purposes of verifying the structure, it was decided to prepare the D-enantiomer of the crystalline methyl 8-*O*-benzoyl-α-D-pillaroside obtained by Asai (*2c*). The starting material for our studies was the enone **22**, the crystalline benzoate of which has been prepared in our laboratory by a lengthy route (8). The Ferrier reaction of **20** with methanol gives **21***a*αβ as an inseparable mixture, unlike the corresponding ethyl glycosides where the α-anomer crystallizes out (12). Actually **21***a*α can be obtained pure via precipitation as the di *p*-nitrobenzoate (12); however, this route proved to be very time consuming and costly in *p*-nitrobenzoyl chloride.

Earlier work in our laboratory had reported the surprising result that certain β-D-hex-2-enopyranosides were not oxidized by manganese dioxide (13). Accordingly the anomeric mixture of diols **21***b*αβ was treated with manganese dioxide, whereupon only the α-anomer responded. The product mixture, **22** and **21***b*β, was then freed of the latter by extraction into water. The overall yield of **22** from **20** by this route was 45% and its authenticity could be verified by comparison with our previously reported material (8).

The conversion of **22** into the 6-deoxy ketone **24***b* in 62% overall yield utilized the standard protocol. The physical constants of **24***b* compared well with those of the enantiomer prepared by Paulsen *et al.* (4) and Brimacombe *et al.* (5).

Inspection of models did not indicate any over-

[3]We are grateful to Dr. M. Asai of Takeda Industries Ltd., Osaka, for a 10 mg sample of pillaromycin A.
[4]The source was 68°C anode 10 kV, 20 MA.



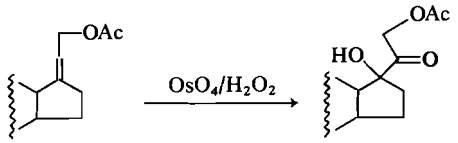
SCHEME 3

whelming preference for α or β approach of a reagent to the trigonal centre at C4. We therefore prepared the ester **31***a* (Scheme 4) in the expectation that the desired stereochemistry at C4 could be generated either by addition of a two-carbon nucleophile to ketone **24***b*, or by hydroxylation of the double bond of **31**.

Addition of vinyl magnesium bromide to **24***b* gave two alcohols which were isolated chromatographically in yields of 47 and 35%. Their spectra did not permit an unambiguous assignment of stereochemistry, but the major isomer was chosen for further processing because the H1 signal appeared as a triplet. Subsequent transformations confirmed that the major isomer was **25** and the minor **26**.

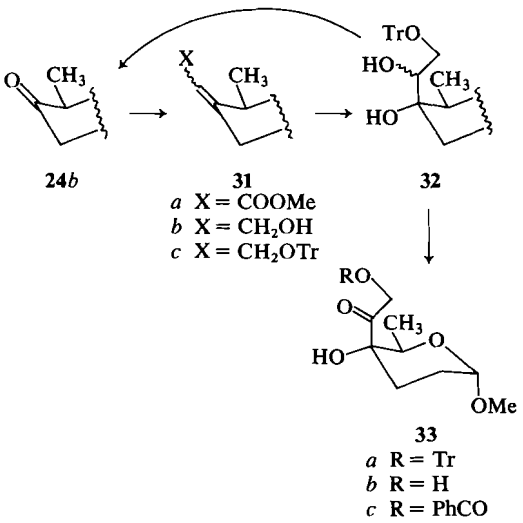
With regard to the hydroxylation of the double bond we knew that hydroxylation of Δ^{17}-sterols with osmium tetroxide/hydrogen peroxide led to α ketols such as **30** (14). Although the mechanism of the reaction is not known it was decided to treat **25** in the hope that the secondary position would be oxidized before the primary. In the event, osymylation of **25** gave a complex mixture from which the triol **28**, actually a mixture of epimers, was isolated as an oil whichdecomposed rapidly. However, overoxidation products included the desired ketodiol **3***a* as well as compounds **29** and **24***b*. Pathways a, b, and c leading to **3***a*, **29**, and **24***b* from the intermediate osmate ester **27** are suggested in Scheme 3.

The alternative approach to the carbon skeleton of **3** involving addition of oxygen to the trigonal centre at C4 was now examined (Scheme 4). A Wadsworth–Emmons–Wittig reaction on **24***b* afforded the *E,Z* mixture **31***a* which was reduced to the alcohols and protected with trityl chloride *E,Z*



30

Can. J. Chem. Downloaded from www.nrcresearchpress.com by 210.87.254.42 on 09/05/12
For personal use only.



SCHEME 4

31*c*. Because of the insolubility of the latter in *tert*-butanol it was not possible to carry out a catalytic hydroxylation. However, reaction with osmium tetroxide in pyridine and chromatographic isolation afforded **32** in 27% overall yield from **24***b*.

The stereochemistry of this diol was not known until subsequent transformations confirmed it to be **32**. Oxidation of **32** with Collin's reagent (9) regenerated ketone **24***b*. However, the Pfitzner–Moffat reagent (15) did oxidize **32**, judging from tlc, although ketol **33***a* could not be separated from the noncarbohydrate by-products until it had been detritylated. The overall yield of **33***b* from **32** was 27%.

Conclusion

The epimers **3***a* and **33***b* were now benzoylated so as to enable comparisons with methyl 8-*O*-benzoyl pillaroside. As indicated in Table 1, the benzoate **3***b* was obtained as a crystalline substance, but **33***c* failed to crystallize. Further comparison of the data in Table 1 indicate that methyl 4-*C*-(2-benzoyloxy-1-oxoethyl)-2,3,6-trideoxy-α-D-*threo*-hexopyranoside, **3***b*, is the enantiomer of Asai's methyl 8-*O*-benzoyl pillaroside (2*c*).

Experimental

Melting points were determined in capillary tubes in a Mel-Temp block and are uncorrected. Elemental analyses were performed by Micro-analyses Laboratory, Toronto, Ontario. The nmr spectra ($CDCl_3$, TMS) were determined on a Varian T-60, a Varian HA 100, or a Varian HR-220 spectrometer, the *J* values quoted being the spacing measured directly from the spectra. Infrared spectra were determined on a Beckman model IR-10 spectrometer using 0.1 mm sodium chloride solution cells (chloroform as solvent). Optical rotations were determined on a Carl Zeiss model LEP nür 370740 Lichtelektrishes Prazision polarimeter at 23°C.

Thin-layer chromatography was performed on glass plates coated with silica gel (HF-254, E. Merck) to a thickness of 0.3 mm. The following solvent systems were used to develop the plates: ethyl acetate – petroleum ether (30–60°C) (1:4); ethyl acetate – petroleum ether (30–60°C) (1:1); ethyl acetate; or benzene. For column chromatography E. Merck silica gel (0.063–0.20 mm, 70–230 mesh A.S.T.M.) was used.

The general procedure for detritylation was to dissolve the tritylated compound in chloroform, lower the temperature to −30°C, and add a −30°C solution of hydrogen chloride in chloroform to this. The hydrogen chloride/chloroform solution was prepared by bubbling hydrogen chloride into the chloroform for approximately 0.5 min. This addition would not, in most cases, be enough to complete the reaction (tlc was run 15 min after addition). One further addition of the same volume of hydrogen chloride/chloroform, however, normally was sufficient to complete the reaction. Throughout the reaction the temperature was maintained at −30°C.

Ethyl 2-C-Acetyl-2,3-dideoxy-6-O-triphenylmethyl-α-D-threo-hexapyranosid-4-ulose, **8**

The enone **6** (8) (1.0 g; 2.42×10^{-3} mol) was irradiated in ethanol (400 mL) and benzophenone (0.12 g; 6.38×10^{-4} mol) for 5 h at which time tlc showed completion of the reaction. Column chromatography (petroleum ether (30–60°C) – ethyl acetate (13:7)) afforded **7** (0.858 g; 75%) as an epimeric mixture at C7. This photoproduct was oxidized in methylene chloride (25 mL) with Collin's reagent (9) (5.0 g; 1.94×10^{-2} mol) for 0.5 h. The solution was diluted with diethyl ether (75 mL), stirred for an additional 5 min, and then filtered through Celite. The filtrate was washed with a 5% solution of hydrochloric acid, a saturated solution of sodium bicarbonate, and then dried over anhydrous sodium sulphate. Evaporation under reduced pressure yielded **8** (0.82 g; 96%) which crystallized on standing. Recrystallization from diethyl ether afforded needles, mp 107.5–108°C; $[\alpha]_D^{23}$ +152.6° (*c* 1.25, chloroform); nmr (HR-220) δ: 2.23 (s, 3, H_3C—CO), 2.47 (dd, 1, $J_{2,3e}$ = 4.4 Hz, $J_{3e,3a}$ = 15.5 Hz, H-3e), 2.79 (dd, 1, $J_{2,3a}$ = 12.0 Hz, H-3a), 3.03 (m, 1, H-2), 3.40 (dd, 1, $J_{5,6'}$ = 6.0 Hz, $J_{6,6'}$ = 10.0 Hz, H-6′), 3.49 (dd, 1, $J_{5,6}$ = 2.7 Hz, H-6′), 4.23 (dd, 1, H-5), 5.25 (d, 1, $J_{1,2}$ = 5.2 Hz, H-1). *Anal.* calcd. for $C_{29}H_{30}O_5$: C 75.96, H 6.59; found: C 75.91, H 6.44.

Ethyl 2,3-Dideoxy-2-C-acetyl-6-O-triphenylmethyl-α-D-erythro-hexopyranosid-4-ulose, **9**

The diketone **8** (0.68 g; 1.48×10^{-3} mol) was dissolved in dry tetrahydrofuran (40 mL) and a solution of diazabicyclononene (0.20 g; 1.62×10^{-3} mol) in tetrahydrofuran (10 mL) was added to this. After 1 h the solution was poured into ice-water (60 mL) and extracted twice with chloroform (100 mL). The chloroform layer was washed with 5% hydrochloric acid and then with a saturated solution of sodium bicarbonate, dried over anhydrous sodium sulphate, and finally evaporated under reduced pressure. The resulting oil (0.64 g; 94%) showed two products on tlc (petroleum ether (30–60°C) – ethyl acetate (4:1)). The more polar component, R_f 0.19, was **9** and the less, R_f 0.21, was **8**. Column chromatography afforded **8** (0.28 g), a mixture of **8** and **9** (0.11 g), and **9** (0.15 g). Attempts to crystallize **9** failed.

Nuclear magnetic resonance (HR-220) δ: 2.18 (s, 3, H_3C—CO), 2.54 (dd, 1, $J_{2,3e}$ = 6.7 Hz, $J_{3e,3a}$ = 17 Hz, H-3e), 2.92 (dd, 1, $J_{2,3a}$ = 10.0 Hz, H-3a), 3.35 (m, 1, H-2), 3.42 (dd, 1, $J_{5,6'}$ = 6.0 Hz, $J_{6,6'}$ = 10.0 Hz, H-6), 3.54 (dd, 1, $J_{5,6}$ = 2.6 Hz, H-6), 4.19 (dd, 1, H-5), 5.45 (d, 1, $J_{1,2}$ = 3.9, H-1).

Can. J. Chem. Downloaded from www.nrcresearchpress.com by 210.87.254.42 on 09/05/12
For personal use only.

Can. J. Chem. Downloaded from www.nrcresearchpress.com by 210.87.254.42 on 09/05/12
For personal use only.

*Ethyl 2,3,6-Trideoxy-2-C-[1-oxo-2-(triphenylmethoxy)ethyl]-α-D-*threo-*hexopyranosid-4-ulose*, ***14***

The intermediates **10**, **11**, **12**, and **13** were all epimeric mixtures at C7 and hence did not crystallize. The course of the transformations was monitored by nmr.

Crystalline enone **6** (8) (6.0 g; 1.45×10^{-2} mol) and benzophenone (0.45 g; 2.48×10^{-3} mol) were dissolved in acetonitrile (300 mL) and ethylene glycol (1500 mL) was then added. The solution was irradiated under a stream of nitrogen for 5 h. The acetonitrile and ethylene glycol were evaporated under reduced pressure, 0.01 Torr and a bath temperature of 80°C being required to remove ethylene glycol. Subsequent column chromatography (diethyl ether–benzene (1:1)) of the residue yielded photoproduct diol, **10***a*, (5.02 g; 72%) which was acetylated in pyridine (60 mL) with acetic anhydride (5 mL) at 0°C over 18 h. Normal workup yielded **10***b* (5.57 g; 94%) as a thick oil; ir: 1730 cm^{-1} (saturated ketone). The nmr spectrum of the oil showed two doublets for H1 at 5.28 ppm ($J_{1,2}$ = 4.1 Hz) and 5.08 ppm ($J_{1,2}$ = 5.0 Hz) in 2:1 ratio.

This material was dissolved in chloroform (160 mL) and detritylated with HCl as described in "General Methods" above. Chromatographic purification afforded the alcohol **10***c* (2.66 g) which was tosylated (pyridine (60 mL); TsCl (3.2 g)) at 0°C for 24 h. Normal workup gave **10***d* as a thick yellow oil (3.71 g) showing the required nmr signal for the *p*-toluenesulfonyl group (δ = 2.44 ppm).

The sulphonate ester **10***d* (3.71 g; 7.88×10^{-3} mol) was dissolved in methyl ethyl ketone (180 mL) and sodium iodide (2.3 g; 1.57×10^{-2} mol) was added with stirring and the solution brought to reflux. Thin-layer chromatography (diethyl ether – benzene (1:1)) after 1.5 h showed one new product (R_f 0.56 as compared to 0.52 for **10***d*). At 2 h the reaction mixture was poured into ice-water and extracted three times with chloroform (300 mL). The combined chloroform layers were washed once with a 2% solution of sodium thiosulphate and then a saturated sodium bicarbonate solution. After drying over anhydrous sodium sulphate, evaporation under reduced pressure gave a product, presumed to be the desired 6-iodide, since the nmr spectrum no longer showed the 2.44 ppm signal for the toluenesulphonyl group.

The oil (3.142 g) was dissolved in reagent acetone and treated with Raney nickel under reflux for 12 h. The solution was filtered through Celite and the Raney nickel washed with reagent acetone. Evaporation of the filtrate gave **11** (2.16 g; 97%) as a pale yellow mobile oil. Its nmr spectrum showed a doublet (3H) at δ 1.28 ppm for the C6 hydrogens, and the mass spectrum gave a peak at *m/e* 257 corresponding to the loss of the aglycon (OEt) from the molecular ion.

The 6-deoxy sugar **11** (2.16 g; 7.14×10^{-3} mol) was deacetylated by treatment with a mixture of methanol (70 mL), water (25 mL), and triethylamine (5 mL) for 4 h (R_f 0.27, EtOAc). The reaction mixture was evaporated to dryness under reduced pressure and final traces of water were azeotroped with benzene. The orange oil **12** (1.53 g; 7.02×10^{-3} mol; 98%) was dissolved in pyridine (40 mL) and trityl chloride (4.0 g; 1.44×10^{-2} mol) was added. The tritylation was complete after 48 h. Normal work-up gave a thick orange oil which after column chromatography (diethyl ether – benzene (1:9)) afforded **13** (2.42 g; 75%). This material was oxidized with Collin's reagent (8.25 g) as described for **7** above. The customary workup gave **14** (2.32 g; 93%) which crystallized from its oil on standing. Recrystallization from diethyl ether gave needles, mp 108–109°C; $[\alpha]_D^{23}$ +108.0° (*c* 1.80, chloroform); nmr (HR-220) δ: 1.24 (d, 3, $J_{5,6}$ = 6.8 Hz H_3C—C), 2.45 (dd, 1, $J_{2,3e}$ = 5.1 Hz, $J_{3e,3a}$ = 16.2 Hz, H-3e), 2.61 (dd, 1, $J_{2,3a}$ = 8.6 Hz, H-3a), 3.44 (m, 1, H-2), 3.90 (ABq, 2, $J_{8,8'}$ = 17.8 Hz, H-8,8′), 4.14 (q, 1, H-5), 5.11 (d, 1, $J_{1,2}$ = 4.5 Hz, H-1). *Anal.* calcd. for $C_{29}H_{30}O_5$: C 75.96, H 6.59; found: C 76.04, H 6.72.

*Ethyl 2-*C*-(2-Benzoyloxy-1-oxoethyl)-2,3,6-trideoxy-α-D-*threo-*hexopyranosid-4-ulose*, ***18***

Compound **14** (1.25 g; 2.72×10^{-3} mol) was dissolved in chloroform (80 mL) and detritylated as described in the "General Methods" above. Column chromatography (diethyl ether – benzene (1:1)) yielded **16** (0.30 g; 51%) as a mobile oil, $[\alpha]_D^{23}$ +174.0° (*c* 2.79, chloroform); ir (chloroform) ν_{max}: 3510, 1726 cm^{-1}; nmr (HR-220) δ: 1.32 (d, 3, $J_{5,6}$ = 6.8 Hz, H_3C—C), 2.49 (dd, 1, $J_{2,3e}$ = 4.5 Hz, $J_{3e,3a}$ = 16.5 Hz, H-3e), 2.77 (dd, 1, $J_{2,3a}$ = 10.4 Hz, H-3a), 3.14 (m, 1, H-2), 4.22 (q, 1, H-5), 4.37 (ABq, 2, $J_{8,8'}$ = 19.6 Hz, H-8, 8′), 5.04 (d, 1, $J_{1,2}$ = 5.5 Hz, H-1).

The alcohol **16** (0.22 g; 1.02×10^{-3} mol) was benzoylated in pyridine (10 mL) with benzoyl chloride (0.5 mL) at 0°C over 12 h. Normal work-up yielded **18** (0.29 g, 89%) which crystallized from its oil on standing. Recrystallization from diethyl ether – hexane (1:1) at 0°C afforded white flaky crystals, mp 85.5–86°C; $[\alpha]_D^{23}$ +219.0° (*c* 1.34, chloroform); nmr (HR-220) δ: 1.32 (d, 3, $J_{5,6}$ = 6.8 Hz, H_3C—C), 2.50 (dd, 1, $J_{2,3e}$ = 4.4 Hz, $J_{3e,3a}$ = 16.3 Hz, H-3e), 2.81 (dd, 1, $J_{2,3a}$ = 11.2 Hz, H-3a), 3.24 (m, 1, H-2), 4.23 (q, 1, H-5), 5.00 (ABq, 2, $J_{8,8'}$ = 17.0 Hz, H-8,8′), 5.15 (d, 1, $J_{1,2}$ = 5.2 Hz, H-1). *Anal.* calcd. for $C_{17}H_{20}O_6$: C 63.74, H 6.29; found: C 63.78, H 6.31.

*Ethyl 2-*C*-(2-Benzoyloxy-1-oxoethyl)-2,3,6-trideoxy-α-D-*erythro-*hexopyranosid-4-ulose*, ***19***

Compound **14** (2.96 g, 6.45×10^{-3} mol) was treated with diazabicyclononene in tetrahydrofuran as described above for **8**. The resulting mixture of epimers **14** + **15** (2.78 g) was detritylated with hydrogen chloride as described in "General Methods" above. Column chromatography (diethyl ether – benzene (1:1)) gave a substance (0.49 g) which was benzoylated at 0°C in pyridine (20 mL) with benzoyl chloride (2 mL) over 12 h. Normal work-up afforded a two component mixture (0.66 g; 91%) as visualized by tlc (diethyl ether – benzene (1:9)). Column chromatography gave the above described **18** (0.41 g; R_f 0.19) and **19** (0.17 g; R_f 0.13). The latter crystallized from ether to give white fibers, mp 85.5–87°C; $[\alpha]_D^{23}$ +77.2° (*c* 0.93, chloroform); nmr (HR-220) δ: 1.29 (d, 3, $J_{5,6}$ = 6.8 Hz, H_3C—C), 2.54 (dd, 1, $J_{2,3e}$ = 5.9 Hz, $J_{3e,3a}$ = 16.0 Hz, H-3e), 2.94 (dd, 1, $J_{2,3a}$ = 9.2 Hz, H-3a), 3.58 (m, 1, H-2), 4.26 (q, 1, H-5), 4.97 (s, 2, H-8, 8′), 5.38 (d, 1, $J_{1,2}$ = 4.6 Hz, H-1). *Anal.* calcd. for $C_{17}H_{20}O_6$: C 63.74, H 6.29; found: C 63.85, H 6.53.

*Methyl 2,3-Dideoxy-α-D-*glycero-*hex-2-enopyranosid-4-ulose*, ***22***

Triacetyl glucal **20** (25.0 g; 9.2×10^{-2} mol) in benzene (85 mL), dry methanol (8.5 mL), and boron trifluoride-etherate (6.5 mL) was stirred for 0.75 h (12). The solution was neutralized with saturated aqueous sodium bicarbonate, dried over anhydrous sodium sulphate, and evaporated. The resulting oil **21***aαβ* was deacetylated in methanol (340 mL), water (210 mL), and triethylamine (17 mL) during 3.5 h. Customary work-up (see above) gave **21***bαβ* which in turn was treated with active manganese dioxide (95.0 g) in chloroform (4000 mL) for 18 h. The chloroform was filtered and concentrated to a volume of approximately 200 mL, and then washed with water (2 × 50 mL) to remove unreacted **21***bβ*. Evaporation of the remaining chloroform solution afforded **22** (6.5 g; 45% from **20**). Recrystallization from cold diethyl ether gave **22** as white fibers, mp 82.5°C; $[\alpha]_D^{23}$ +36.1° (*c* 2.66, chloro-

Can. J. Chem. Downloaded from www.nrcresearchpress.com by 210.87.254.42 on 09/05/12
For personal use only.

form); nmr (T-60) δ: 3.52 (s, 3, OMe), 3.95 (d, 2, $J_{5,6} = J_{5,6'} = 4.6$ Hz, H-6,6′), 4.46 (t, 1, H-5), 5.20 (d, 1, $J_{1,2} = 4.0$ Hz, H-1), 6.12 (d, 1, $J_{2,3} = 11.0$ Hz, H-3), 6.90 (dd, 1, H-2). *Anal.* calcd. for $C_7H_{10}O_4$: C 53.16, H 6.37; found: C 53.09, H 6.28.

*Methyl 2,3,6-Trideoxy-α-D-*glycero-*hexopyranosid-4-ulose*, **24**b

The enone **22** (6.5 g; 4.12×10^{-2} mol) in ethyl acetate (240 mL) was hydrogenated in the presence of 5% palladium/carbon (0.24 g). After 2 h, uptake of hydrogen (950 mL) was complete. The solution was filtered through Celite and evaporated to give **23***a* (6.5 g) as a mobile oil (ir: 3600, 1726 cm^{-1}) which was dissolved in pyridine (45 mL) and methylene chloride (20 mL), and treated with *p*-toluenesulfonyl chloride (16.0 g; 8.14×10^{-2} mol) for 18 h, at which time tlc showed that formation of the ester **23***b* was complete. The syrupy material (11.5 g; 3.65×10^{-2} mol), which had an extremely irritating odour, was dissolved in methyl ethyl ketone (290 mL), and stirred at room temperature with sodium iodide (30.0 g; 2.0×10^{-1} mol) for 17 h. Thin-layer chromatography (diethyl ether – benzene (1:1)) at this time showed that the tosylate **23***b* (R_f 0.42) had been converted to the iodide **24***a* (R_f 0.63). The solution was poured into ice-water and extracted twice with chloroform (300 mL) and the combined chloroform layers were washed with a dilute solution of sodium thiosulphate, dried over anhydrous sodium sulphate, and evaporated to give a mobile oil (7.7 g; 78%). This oil, **24***a*, (2.85×10^{-2} mol) was immediately refluxed in reagent grade acetone (600 mL) with Raney nickel (80 g) for 18 h at which time tlc (diethyl ether – benzene (1:1)) showed a single component (R_f 0.55). The solution was filtered through Celite and evaporated to give **24***b* (3.76 g; 92%) as a mobile oil, *m/e* 113 ($M^+ - OMe$); $[\alpha]_D^{23}$ −225° (*c* 0.7, chloroform) (lit. (4) $[\alpha]_D^{23}$ −232°; (5) −254°).

Grignard Addition of Vinyl Magnesium Bromide to **24**b

Dry tetrahydrofuran (140 mL) and magnesium turnings (1.65 g; 6.95×10^{-2} mol) were introduced into a 500 mL 3-necked round bottom flask fitted with a dry ice/isopropanol condenser and drying tube, an atmosphere of nitrogen being maintained. A few crystals of iodine were added with stirring, followed by vinyl bromide (8.5 mL; 1.20×10^{-1} mol), and the solution brought to reflux. The iodine colour disappeared after 5 min and the magnesium had completely reacted after 30 min. The Grignard solution was then cooled to 0°C and a tetrahydrofuran (20 mL) solution of the ketone **24***b* (2.0 g; 1.39×10^{-2} mol) was added dropwise. Thin-layer chromatography (diethyl ether – benzene (1:1)) showed the absence of ketone **24***b* (R_f 0.55) and the appearance of two products (R_f 0.40, 0.33) after 15 min. At 45 min a saturated ammonium chloride solution was added and the resultant solution extracted with chloroform (2 × 100 mL). The combined chloroform layers were washed with water, dried over anhydrous sodium sulphate, and evaporated. Subsequent column chromatography of the residue gave **26** (R_f 0.40; 0.85 g; 35% from **24***b*), and **25** (R_f 0.33; 1.11 g; 47% from **24***b*) as mobile oils.

For **25**, nmr (T-60) δ: 1.06 (d, 3, $J_{5,6} = 6.8$ Hz, H_3C—C), 1.4–2.1 (m, 4, H-2a, 2e, 3a, 3e), 2.4 (s, 1, OH), 3.34 (s, 3, OMe), 3.82 (q, 1, H-5), 4.68 (d, 1, $J_{1,2e} = 0$ Hz, $J_{1,2a} = 2.5$ Hz, H-1), 5.14 (dd, 1, $J_{7,8'} = 10.0$ Hz, $J_{8,8'} = 2.5$ Hz, H-8′) 5.35 (dd, 1, $J_{7,8} = 15.2$ Hz, H-8), 5.80 (dd, 1, H-7).

For **26**, nmr (T-60) δ: 1.06 (d, 3, $J_{5,6} = 6.8$ Hz, H_3C—C), 1.5–2.0 (m, 4, H-2a, 2e, 3a, 3e), 2.43 (s, 1, OH), 3.35 (s, 3, OMe), 3.84 (q, 1, H-5), 4.72 (t, 1, H-1), 5.31 (dd, 1, $J_{7,8'} = 11.0$ Hz, $J_{8,8'} = 2.5$ Hz, H-8′), 5.41 (dd, 1, $J_{7,8} = 18.5$ Hz, H-8), 6.37 (dd, 1, H-7).

Hydroxylation of **25**

The olefin **25** (1.02 g; 5.9×10^{-3} mol) was dissolved in dry *tert*-butanol (15 mL). Osmium tetroxide (0.03 g; 1.18×10^{-4} mol) in *tert*-butanol (30 mL) and a 6% solution (15 mL) of dry hydrogen peroxide in *tert*-butanol were added with stirring. After 18 h, tlc (diethyl ether – benzene (1:1)) showed no olefin (R_f 0.33) and four products (R_f 0.54, 0.26, 0.16, and 0.03). The osmium tetroxide was destroyed with excess sodium bisulphite and the solution was evaporated, taken up in water (75 mL), and extracted with chloroform (4 × 60 mL). The chloroform layer was dried and evaporated and the resulting residue chromatographed to give **24***b* (0.085 g; 10%; R_f 0.54); **29** (0.090 g; 8.7%; R_f 0.26), and **3** (0.255 g; 21%; R_f 0.155). The water layer was evaporated to dryness and the residue extracted with ethyl acetate. Evaporation of the ethyl acetate gave the epimeric mixture **28** (0.61 g; 50%; R_f 0.027); *m/e* 175 ($M^+ - OMe$). This substance decomposed on standing.

For **29**, nmr (T-60) δ: 1.1 (d, 3, $J_{5,6} = 6.8$ Hz, H_3C—C), 1.2–2.3 (m, 4, H-2a, 2e, 3a, 3e), 2.9 (broad singlet, 1, OH), 3.38 (s, 3, OMe), 4.20 (q, 1, H-5), 4.77 (d, 1, $J_{1,2e} = 0$ Hz, $J_{1,2a} = 2.0$ Hz, H-1), 9.55 (s, 1, H-7); *m/e*: 143 ($M^+ - OMe$).

For **3**, nmr (T-60) δ: 1.0 (d, 3, $J_{5,6} = 6.8$ Hz, H_3C—C), 1.4–2.3 (m, 4, H-2a, 2e, 3a, 3e), 3.1 (broad singlet, 1, OH), 3.38 (s, 3, OMe), 4.18 (q, 1, H-5), 4.50 (s, 2, H-8,8′), 4.68 (broad singlet, 1, H-1); *m/e*: 173 ($M^+ - OMe$), 160, 155, 145, 142, 113, and 85.

*Methyl 8-*O*-Benzoyl-α-D-pillaroside*, **3***b*

Methyl pillaroside **3***a* (0.24 g; 1.2×10^{-3} mol) was benzoylated in pyridine (10 mL) with benzoyl chloride (0.5 mL) at 0°C for 8 h. Normal work-up gave **3***b* (0.305 g; 83%) which crystallized on standing. Recrystallization from cold diethyl ether – hexane (1:1) gave plates, mp 107–108°C; $[\alpha]_D^{23}$ +94.6° (*c* 0.45, chloroform); nmr (T-60) δ: 1.15 (d, 3, $J_{5,6} = 6.8$ Hz, H_3C—C), 1.6–2.3 (m, 4, H-2a, 2e, 3a, 3e), 2.79 (broad singlet, 1, OH), 3.34 (s, 3, OMe), 4.22 (q, 1, H-5), 4.7 (broad singlet, 1, H-1), 5.22 (s, 2, H-8,8′), 7.3–8.2 (m, 5, aromatic). *Anal.* calcd. for $C_{16}H_{20}O_6$: C 62.33, H 6.54; found: C 62.40, H 6.42.

*Methyl 4-*C*-(2-Benzoyloxy-1-oxoethyl)-2,3,6-trideoxy-α-D-*erythro-*hexopyranoside*, **33**c

The entire sequence was carried out without chromatographic isolation of the intermediates **31** and **32** since these were geometric and epimeric mixtures respectively.

An ice-cold solution of potassium *tert*-butoxide (0.95 g; 9.3×10^{-3} mol) and trimethyl phosphonacetate (4.1 mL) in dry dimethylformamide (15 mL) was added dropwise to a 0°C solution of the ketone **24***b* (1.13 g; 7.84×10^{-3} mol) in dry dimethylformamide (25 mL). Thin-layer chromatography (diethyl ether – benzene (1:1)) after 1 h showed only one product of higher R_f (0.62). The dimethylformamide was then distilled (0.01 Torr and external temperature of 40°C). The resulting residue was taken up in water (20 mL) and extracted with diethyl ether (3 × 25 mL). The combined ether layers were dried over anhydrous sodium sulphate and evaporated to give a crude oil (1.4 g), whose nmr spectrum showed considerable contamination of the desired product **31***a*. The material was dissolved in dry diethyl ether (100 mL) and the solution cooled to 0°C. Excess lithium aluminum hydride (0.840 g) was added to this solution with stirring. Thin-layer chromatography (diethyl ether – benzene (1:1)) showed absence of **31***a* with one product of lower R_f after 0.5 h. The excess lithium aluminum hydride was destroyed with ethyl acetate and the solution filtered through Celite. Evaporation gave the cor-

Can. J. Chem. Downloaded from www.nrcresearchpress.com by 210.87.254.42 on 09/05/12
For personal use only.

responding alcohol **31***b* (0.94 g) as a crude oil, which was treated with trityl chloride (2.5 g) in pyridine (10 mL) and methylene chloride (4 mL) over 18 h. Normal work-up and column chromatography (diethyl ether – benzene (1:9)) gave **31***c* (1.80 g), contaminated heavily, however, with trityl alcohol.

The crude olefin **31***c* (0.95 g) was dissolved in dry pyridine (15 mL) and osmium tetroxide (0.50 g) in pyridine was added with stirring. After 24 h (tlc showing completion) the osmium tetroxide was destroyed by addition of sodium bisulphite (0.9 g) in water (15 mL) and pyridine (10 mL). The solution was then extracted with chloroform (2 × 50 mL) and the combined chloroform layers were washed with a 5% solution of hydrochloric acid (until the aqueous layer remained acidic), a saturated solution of sodium bicarbonate, dried over anhydrous sodium sulphate, and evaporated. Column chromatography of the resultant residue (0.97 g) gave the diol **32** (0.46 g; 27% from **24***b*).

A portion of the diol **32** (0.28 g; 6.40×10^{-4} mol) was dissolved in benzene (20 mL) and dimethyl sulphoxide (0.6 mL); pyridine (0.5 mL), trifluoroacetic acid (0.25 mL), and *N,N'*-dicyclohexylcarbodiimide (1.0 g; 4.85×10^{-3} mol) were added with stirring. At 2.5 h oxalic acid dihydrate (0.70 g) was added and the stirring continued for 0.5 h. The reaction mixture was then diluted with chloroform (50 mL) and water (50 mL), the two layers separated, and the organic layer washed with a saturated solution of sodium bicarbonate, dried and concentrated to ~30 mL, and cooled to −30°C. Detritylation of **33***a* with hydrogen chloride in chloroform was effected as described in "General Methods". Column chromatography afforded the corresponding alcohol **33***b* (0.029 g; 23% from **32**) which was benzoylated in pyridine (3 mL) with benzoyl chloride (0.2 mL) at 0°C for 10 h. Normal work-up gave the title compound **33***c* (0.040 g; 91%) as an oil, $[\alpha]_D^{23}$ +74.8 (*c* 1.54, chloroform); nmr (T-60) δ: 1.22 (d, 3, $J_{5,6}$ = 6.8 Hz, H_3C—C), 2.0 (broad singlet, 4, H-2a, 2e, 3a, 3e), 3.39 (s, 3, OMe), 3.98 (q, 2, H-5, OH), 4.82 (t, 1, H-1), 5.18 (s, 2, H-8,8′), 7.3–8.2 (m, 5, aromatic).

Acknowledgements

This study was supported by grants from the National Research Council of Canada and Bristol Laboratories (Syracuse) and we express our gratitude to these bodies. We are grateful to Professor K. Nakanishi and Dr. I. Miura of Columbia University for determining the cmr and ^{1}Hmr spectra reported in Table 2.

1. F. ARCAMONE. Top. Antibiot. Chem. **2**, 98 (1978); T. R. KELLY. Annu. Rep. Med. Chem. **14**, 288 (1979).
2. M. ASAI. Chem. Pharm. Bull. (Jpn.), (*a*) **18**, 1699 (1970); (*b*) **18**, 1706 (1970); (*c*) **18**, 1713 (1970).
3. D. L. WALKER and B. FRASER-REID. J. Am. Chem. Soc. **97**, 6251 (1975).
4. H. PAULSEN, K. RODEN, and V. SINNWELL. Chem. Ber. **110**, 2146 (1977); H. PAULSEN, K. RODEN, V. SINNWELL, and W. KOEBERNICK. Angew. Chem. Int. Ed. Engl. **15**, 439 (1976).
5. J. S. BRIMACOMBE, A. M. MATHER, and R. HANNA. Tetrahedron Lett. 1171 (1978).
6. B. FRASER-REID, N. L. HOLDER, D. R. HICKS, and D. L. WALKER. Can. J. Chem. **55**, 3978 (1977).
7. B. FRASER-REID, R. C. ANDERSON, D. R. HICKS, and D. L. WALKER. Can. J. Chem. **55**, 3986 (1977).
8. B. FRASER-REID, A. MCLEAN, E. W. USHERWOOD, and M. YUNKER. Can. J. Chem. **48**, 2877 (1970).
9. J. C. COLLINS, W. W. HESS, and F. J. FRANK. Tetrahedron Lett. 3363 (1968).
10. J. O. PEZZANITE, J. CLARDY, P-Y. LAU, G. WOOD, D. L. WALKER, and B. FRASER-REID. J. Am. Chem. Soc. **97**, 6250 (1975).
11. K. KAMIYA, M. ASAI, M. NISHIKAWA, K. MIZUNO, Y. TOMIIE, and I. NITTA. Chem. Pharm. Bull. (Jpn.), **18**, 1724 (1970).
12. R. J. FERRIER and N. PRASAD. J. Chem. Soc. C, 570 (1969).
13. B. FRASER-REID, B. J. CARTHY, N. L. HOLDER, and M. YUNKER. Can. J. Chem. **49**, 3038 (1971).
14. B. MAGERLEIN and J. HOGG. J. Am. Chem. Soc. **80**, 2226 (1958); J. HOGG, P. BEAL, A. NATHAN, F. LINCOLN, W. SCHNEIDER, B. MAGERLEIN, A. HANZE, and R. JACKSON. J. Am. Chem. Soc. **77**, 4436 (1955).
15. A. F. COOK and J. G. MOFFATT. J. Am. Chem. Soc. **89**, 2697 (1967); **90**, 740 (1968).

Marine organic chemistry. IV.[1] Isolation of (20*R*)-5α-pregn-9(11)-ene-3β,6α,20-triol from the saponins of the starfish, *Asterias forbesi* and *Asterias vulgaris*, and its synthesis

JOHN W. APSIMON, SATYANAND BADRIPERSAUD, JOHN A. BUCCINI, AND JOOP EENKHOORN
Department of Chemistry, Carleton University, Ottawa, Ont., Canada K1S 5B6
AND
MICHAEL W. GILGAN
Fisheries and Marine Service, Department of the Environment, P.O. Box 429, Halifax, N.S., Canada B3J 2R3

Received July 24, 1980

This paper is dedicated to Prof. Raymond U. Lemieux on the occasion of his 60th birthday

JOHN W. APSIMON, SATYANAND BADRIPERSAUD, JOHN A. BUCCINI, JOOP EENKHOORN, and MICHAEL W. GILGAN. Can. J. Chem. **58**, 2703 (1980).

A minor constituent of the saponin hydrolysate of the starfishes *Asterias forbesi* and *Asterias vulgaris* is shown to be (20*R*)-5α-pregn-9(11)-ene-3β,6α,20-triol by synthesis from 11-oxoprogesterone. The occurrence of the reduced progesterone side chain could have implications concerning the origins of progesterone-type compounds in saponin hydrolysates from starfish.

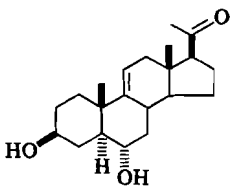
JOHN W. APSIMON, SATYANAND BADRIPERSAUD, JOHN A. BUCCINI, JOOP EENKHOORN et MICHAEL W. GILGAN. Can. J. Chem. **58**, 2703 (1980).

En se basant sur une synthèse réalisée à partir de l'oxo-11 progestérone, on a montré que le constituant secondaire du produit d'hydrolyse de la saponine des étoiles de mer *Asterias forbesi* et *Asterias vulgaris* est le 5α-pregnène-9(11) triol-3β,6α,20(*R*). La présence de la chaîne latérale réduite de la progestérone pourrait avoir des implications en ce qui a trait aux origines des composés du type progestérone contenus dans les hydrolysats de la saponine de l'étoile de mer.

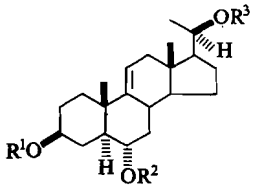
[Traduit par le journal]

During our studies of the steroids from the saponins of the starfish *Asterias forbesi* we have reported the isolation and characterization, from the acid hydrolysate of the saponin mixture, of the dihydroxypregnane derivative **1** (1), a compound also detected by others in the same and related species (2–6). The conversion of this material into possible corticosteroid precursors has also been reported (7).

Column chromatography on silica gel or preparative thin layer chromatography also led to the isolation of a small amount of a new material that we now assign as the title compound **2**.[2] This material, mp 263–266°C, showed a molecular ion in its high resolution mass spectrum at 334.2500 indicating a molecular formula of $C_{21}H_{34}O_3$; this observation plus all other spectral data were in accord with the structure shown (see Experimental), only the question of stereochemical assignment at C-20 remaining. In separate experiments larger amounts of **2** have been isolated by high performance liquid chromatography (hplc) from the saponins of *Asterias vulgaris*.



1



	R¹	R²	R³
2	H	H	H
3	Ac	Ac	Ac
9	H	H	Ac

The structural assignment was confirmed and the stereochemistry at C-20 shown to be the *R*-configuration by an unequivocal synthesis of its triacetate **3** from **1** by sodium borohydride reduction in ethanol followed by acetylation. All spectral data of the synthetic and natural materials were identical. Literature precedent (8) and the coincidence of observed nuclear magnetic resonance (nmr) chemical shifts for the angular C-18 and C-19 methyl group signals with those calculated for a number of compounds by the use of Zurcher's tables (9) strongly support the assignment of the *R*-configuration at C-20 (see Table 1).

A further synthesis of **2** as its triacetate **3** was carried out as outlined in Scheme 1. This route not only provided further samples of **2** but also provided a number of compounds of use for the as-

[1]For part III see ref. 7*b*.

[2]Our trivial name for the major aglycone **1** is asterone. In some experiments, the herein described triol **2** appeared by gc to have about one half the retention time of asterone. This observation engendered the familiar term "half-asterone". The more logical trivial name asterogenol will be used in this article!

0008-4042/80/232703-06$01.00/0
©1980 National Research Council of Canada/Conseil national de recherches du Canada

Can. J. Chem. Downloaded from www.nrcresearchpress.com by 210.87.254.105 on 09/05/12
For personal use only.

Can. J. Chem. Downloaded from www.nrcresearchpress.com by 210.87.254.105 on 09/05/12
For personal use only.

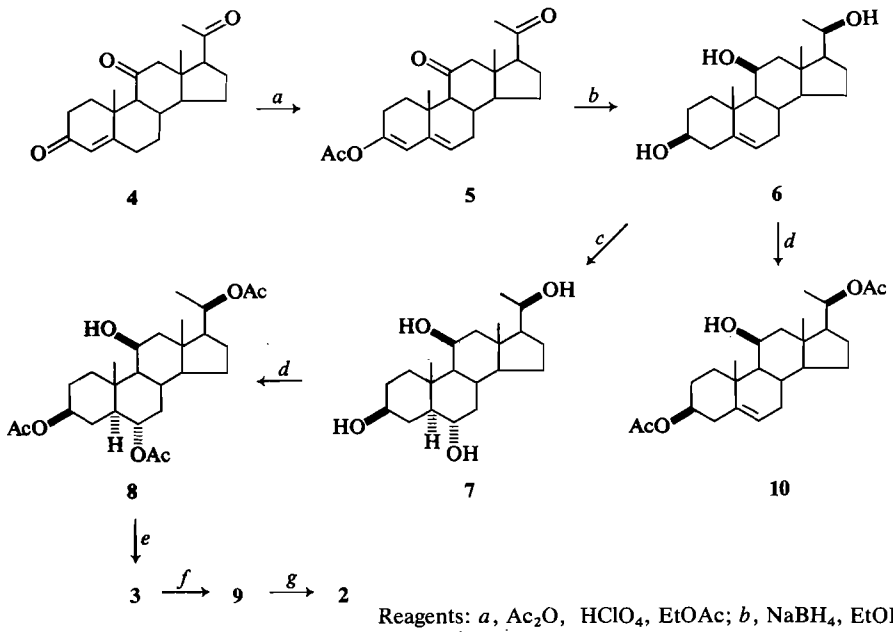
TABLE 1. Proton chemical shifts (δ values) in ppm of angular methyl groups for a variety of hydroxy pregnanes studied[a]

	Experimental values		Calculated values		
			C-19	C-18	
Compound	C-19	C-18	*R* and *S*	*R*	(*S*)
3	1.02	0.56	1.018	0.558	(0.608)
8	1.13	0.86	1.134	0.857	(0.917)
9	0.95	0.57	0.951	0.558	(0.608)
10	1.29	0.89	1.292	0.893	(0.943)
11	0.89	0.64	0.884	0.625	(0.675)
12	1.03	0.65	1.034	0.651	(0.701)
13	1.02	0.65	1.025	0.651	(0.701)

[a]All values determined on a Varian XL-100 nmr spectrometer using TMS as an internal standard with $CDCl_3$ as a solvent.

signment of ^1H and ^{13}C nmr signals. Thus, 11-oxoprogesterone **4** was converted into the known dienolacetate **5** (10) which upon treatment with sodium borohydride in ethanol afforded the pregnene triol **6**. Hydroboration–oxidation of this material led to tetra-ol **7** which (after acetylation to **8**) was dehydrated with perchloric acid in acetic acid at steambath temperature, providing asterogenol triacetate **3**. This compound could be partially hydrolysed to the monoacetate **9** with sodium hydroxide in methanol at room temperature for 1 h. Hydrolysis at reflux temperature in methanol led to asterogenol **2**. Acetylation of triol **6** gave the diacetate **10**, of use in the nmr signal assignments. Three pregnane derivatives (**11**, **12**, and **13**) available in our laboratory were also of use in this study.

A summary of the observed proton nmr chemical shifts of the angular methyl groups of a number of compounds studied are presented in Table 1 together with the values calculated from Zurcher's tables for both the 20*R* and 20*S* configurations. Because of the poor solubility of 20-hydroxy compounds these studies were performed on the corresponding 20-acetoxy derivatives. The close agreement between the experimental and observed values for the C-18 methyl group signals confirms the assignment of the *R* configuration at C-20. The ^{13}C nmr chemical shifts for these compounds are presented in Table 2 and are assigned using the data of Djerassi and



Reagents: *a*, Ac_2O, $HClO_4$, EtOAc; *b*, $NaBH_4$, EtOH; *c*, B_2H_6, H_2O_2, NaOH; *d*, Ac_2O, pyridine; *e*, HOAc, $HClO_4$; *f*, MeOH, aq. NaOH, room temp.; *g*, MeOH, aq. NaOH, reflux.

SCHEME 1

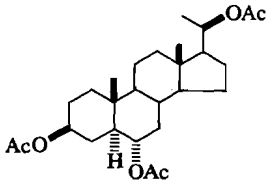
Can. J. Chem. Downloaded from www.nrcresearchpress.com by 210.87.254.105 on 09/05/12
For personal use only.

TABLE 2. ^{13}C nmr chemical shifts of a variety of steroids studied (δ values) in ppm determined in $CDCl_3$ using TMS as an internal standard

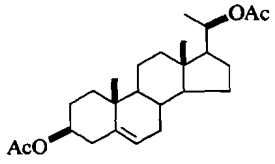
	Compounds						
	3	**8**	**9**	**10**	**11**	**12**	**13**
C-1	35.3	36.6	35.5	36.9	37.0	37.1	37.3
2	27.3	26.9	30.9	27.7	27.2	27.8	31.8[c]
3	72.1	72.0	70.9	73.6	72.3	74.0	71.7
4	28.9	28.1	32.7	37.3	28.5	38.2	42.4[d]
5	46.7	49.4	49.8	140.8	48.7	139.8	140.9
6	72.9	73.0	69.1	121.3	73.2	122.5	121.4
7	38.4	37.9	42.2	32.2	37.7	31.8[b]	31.7[c]
8	28.9	30.3	30.9	28.2	34.1	31.9[b]	31.7[c]
9	143.9	57.5	145.4	53.9	53.8	50.2	50.3
10	38.4	36.6	38.2	36.4	36.7	36.7	36.6
11	117.6	68.0	116.8	68.2	20.9	21.0	21.0
12	38.4	48.6	38.2	49.0	39.2	39.2	39.3
13	41.0	41.6	41.0	41.2	42.5	42.2	42.2[d]
14	52.9	57.2	52.9	58.0	55.6	56.1	56.2
15	25.6	24.1	25.4[a]	24.2	24.2	24.4	24.3
16	25.6	25.0	25.6[a]	25.0	25.4	25.5	25.5
17	55.3	55.6	55.2	55.6	55.1	55.1	55.1
18	12.1	15.1	12.0	14.8	12.5	12.4	12.4
19	19.1	16.1	19.3	22.3	13.3	19.3	19.3
20	72.9	72.8	72.9	72.9	72.8	72.9	72.9
21	20.0	19.8	19.9	19.8	19.9	19.8	19.9
C=O		170.2			170.3	170.4	
	170.5	170.5	170.5	170.5	170.5	170.5	170.3
		170.7			170.7		
CH_3COO[e]		21.3			21.1		
	21.4	21.5	21.5	21.3	21.3	21.4	21.5
					21.4		

[a,b,c,d] These assignments could be interchanged.
[e] A coincidence of some signals noted.

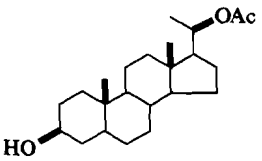
co-workers (11) for substituent effects in monohydroxy androstanes and pregnanes and their corresponding acetyl derivatives together with the data for pregn-5-en-3β-ol and its acetyl derivative (12) except for compounds **3** and **9**. However, introduction of the 9(11) double bond changes the relative conformational relationships of positions α and β to the double bond. The work of Enzell and co-workers (13) was of particular use here in the assignments for unsaturated species. Of particular note in these data is the invariance of the signals for C-20 (72.8–72.9) and C-21 (19.9 ± 0.1 ppm), supporting the fact that the configuration at C-20 for all these compounds is identical. At the same time the same data for the ring A and B carbon atoms confirm the stereochemistry assigned for the oxygen functions at positions 3 and 6.



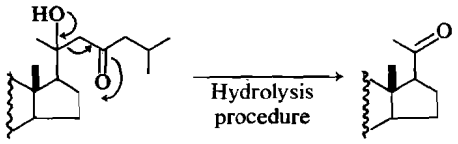
11



12



13



SCHEME 2

The occurrence of asterogenol (**2**) in the saponin mixtures of *Asterias forbesi* and *A. vulgaris* is worthy of note since it has been suggested that asterone **1** is not a true aglycone (6, 14), but rather it occurs from a retroaldol decomposition of the side chain of the true saponin during hydrolysis as outlined in Scheme 2. The appearance of species possessing a 20-hydroxyl group in a hydrolysis mixture cannot be accounted for on this basis, suggesting

Can. J. Chem. Downloaded from www.nrcresearchpress.com by 210.87.254.105 on 09/05/12
For personal use only.

that at least some of the saponins present in the starfish species studied exist with the progesterone side chain as its reduced form. Furthermore we have treated crude saponin mixtures with sodium borohydride in ethanol followed by hydrolysis and hplc analysis. In these cases the yield of asterogenol is significantly increased, suggesting that, in fact, the progesterone side chain is present in the original saponin mixture, and thus that the aglycone **1** is not wholly an artefact.

Experimental

Melting points were determined on a Fisher-Johns melting point apparatus and are uncorrected. The nmr spectra were obtained on a Varian T-60 (^{1}H) or a Varian XL 100 (^{1}H and ^{13}C) spectrometer with tetramethylsilane as internal standard and deuteriochloroform as solvent. Chemical shifts are expressed in the δ scale and the following abbreviations apply: s, singlet; d, doublet; t, triplet; m, multiplet. Infrared spectra were determined on a Perkin-Elmer 237 B ir spectrophotometer and were run in methylene chloride unless otherwise stated. Ultraviolet spectra were obtained on a Perkin-Elmer 202 uv–visible spectrophotometer and were run in 95% ethanol. Mass spectra were determined on an A.E.I. M.S. 12 instrument at Trent University, Peterborough.

*Isolation of (20*R*)-5α-Pregn-9(11)ene-3β,6α,20-triol (2) from the Saponins of* Asterias forbesi

Preparative thin layer chromatography of the *Asterias forbesi* aglycones (from 4.3 g of saponin mixture) (2 mm silica gel plates) developing twice with ethyl acetate – methanol 20:1 allowed for ready separation of asterone (3β,6α-dihydroxy-5α-pregn-9(11)- en-20-one (**1**)). Those aglycones with an R_f less than 0.2 were eluted and rechromatographed, eluting with ethyl acetate – methanol 15:1. Elution of the band with an R_f less than 0.3 with methanol followed by recrystallization from methanol provided a crystalline aglycone (4 mg), mp. 263–266°C; $[\alpha]_D^{20}$ +8° (*c* 0.124 g/100 mL ethanol); ν_{max} (Nujol): 3360, 1033 cm^{-1}. *Exact Mass* calcd. for $C_{21}H_{34}O_3$: 334.2507; found (ms): M^+ 334.2500. Low resolution mass spectrum: 334 (M^+), 319 (*M*-15), 316 (*M*-18), 301 (*M*-15-18), 298 (*M*-(2 × 18)), 283 (301-18), 265 (283-18). *Anal.* calcd. for $C_{21}H_{34}O_3$: C 75.41, H 10.25%; found: C 75.13, H 10.11%.

*The Isolation of Asterogenol Acetate 3 from an Extract of the Common Starfish (*Asterias Vulgaris*)*

Live starfish (*Asterias vulgaris*, 18.9 kg) obtained off Halifax were cleaned of solid debris and then "milked" (1) by immersing them three times in fresh water (ca. 1 L/kg starfish at each immersion). The combined "milks" were filtered through four layers of cheese cloth, passed down a column of Amberlite XAD-2 (Rohm and Haas Company, 330 × 50 mm id), and washed in a procedure similar to that of Hori (15). The solution was passed through the column twice at 50–75 mL/min. The column was washed with two bed volumes of distilled water and eluted with 1.5 bed volumes each of 50% methanol/water and methanol. The solvents were evaporated *in vacuo* (residues: 50% methanol saponins, 1.4 g; 100% methanol saponins, 2.9 g).

The dried residues were suspended in 1 L redistilled ethyl acetate per g of residue. Immediately before heating 10 μL 60% perchloric acid were added per mL of ethyl acetate. The mixture was refluxed for 30 min, cooled, and extracted with water (2 × 100 mL), 1 *N* NaOH (2 × 100 mL), and water (2 × 100 mL). The solvent was evaporated and the brown residues thoroughly dried. The residues were acetylated with pyridine – acetic anhydride (20°C for 30 min), the acetates partitioned between 70% methanol/water and chloroform (2 × 1 vol.), and the chloroform-extractable material recovered (from the 50% methanol fraction, saponin, 1.03 g; 100% methanol fraction, saponin, 2.36 g).

Fractions and recoveries were monitored by gas–liquid chromatography (glc) on a Hewlett-Packard model 402 (column: 3% OV-101 on Chromsorb W-HP (Pierce Chemical Company) 122 cm × 4 mm id, 260°C, helium flow rate 60 mL/min); chromatography (tlc) on Silica Gel-F 254 plates (E. Merck, solvent system: chloroform–hexane – ethyl acetate (15:3:2). The steroids gave visible or uv fluorescent (360 nm) spots when sprayed with sulfuric acid and heated to 110°C for 2–5 min.

Column Fractionation of Aglycone Acetates

Alumina III (Woelm, for dry-column chromatography) columns (150 g, 18 cm long) were packed in 50 mm (flat width) nylon casing. A 5 cm layer of Celite 545 (Johns Manville) was added to protect the alumina origin. The aglycone acetate sample in chloroform was added to a similar amount of Celite, mixed, dried, and added to the top of the column. The column was irrigated with 100 mL chloroform–hexane – ethyl acetate (15:3:2). The appropriate parts of the column were extracted with ethyl acetate (aglycone acetates from 50% methanol fraction, saponins 0.30 g; 100% methanol fraction, 1.15 g).

Liquid Chromatography

The aglycone acetates from the 50% methanol fraction of saponins, which contained the bulk of the asterogenol acetate (**3**) as indicated by glc analysis, were applied as several small samples (up to 300 mg in chloroform solution) to a Porasil A 60 column (Waters Assoc., 1830 × 7.7 mm id) and the column was irrigated with hexane–chloroform – ethyl acetate (10:5:1) at 3 mL/min. The 100% methanol saponin aglycones, with asterogenol acetate as a minor constituent, were fractionated in a similar manner but with uv (Chromatronix model 200) and refractive index detectors (Laboratory Data Control, model 1107). The combination of the appropriate fractions yielded asterogenol acetate (**3**) (oil, 50 mg) which appeared pure by glc and tlc.

*(20*R*)-5α-Pregn-9(11)-ene-3β,6α,20-triol (2)*

Asterone (**1**) (2.0 g, 6.0 mmol) was dissolved in 200 mL of ethanol and was stirred at room temperature for 41 h with sodium borohydride (1 g). Water (100 mL) was added and the reaction mixture was stirred one more hour. The solvent was removed *in vacuo* and to the residue was added 0.5 L of water. The solids were filtered, washed with water, and dried by ethanol–benzene azeotropic removal of the water. A solid white residue (2 g) was obtained, the ir spectrum of which did not indicate any carbonyl absorption peak. For full characterization of this compound, see hydrolysis of asterogenol triacetate (**3**) below.

*(20*R*)-5α-Pregn-9(11)-ene-3β,6α,20-triol Triacetate (3)*

The above crude reaction product (1 g) was dissolved in pyridine (5 mL), acetic anhydride (50 mL) was added, and the reaction mixture was stirred at room temperature for 19 h after which the mixture was poured into water (100 mL). After stirring the mixture for 1 h, the aqueous solution was extracted with ether and the extracts were washed with 2 *N* aqueous HCl solution, saturated NaCl solution, saturated $NaHCO_3$ solution, and saturated NaCl solution. After drying over Na_2SO_4 the ether was removed *in vacuo* to give 1.5 g of a white foam. Pure asterogenol triacetate (**3**) was obtained by column chromatography (silica gel (45 g) prepared in petroleum ether containing 5% diethyl ether). The column was eluted with petroleum ether 30–60°C containing increasing amounts of ether to provide a

Can. J. Chem. Downloaded from www.nrcresearchpress.com by 210.87.254.105 on 09/05/12
For personal use only.

colourless oil (1.1 g) (i.e. 80% over two steps). Infrared (neat) ν_{max}: 1730 (C=O) cm^{-1}; nmr δ: 0.56 (s, 3, CH_3-18 H), 1.02 (s, 3, CH_3-19 H), 1.17 (d, 3, CH_3-21 H, J = 3 Hz), 2.04 (s, 9, CH_3COO), 4.8 (m, 3, H-C-OAc), 5.4 (6.5, 1, vinyl H); mass spectrum: 460 (1%, M^+), 400 (20, M − HOAc), 340 (48, M − 2HOAc), 280 (64, M − 3HOAc), 265 (43, M − 3HOAc − CH_3). *Anal.* not submitted due to instability of the compound. *Exact Mass* calcd. for $C_{27}H_{40}O_6$: 460.2825; found (high resolution mass spectrum): M^+ 460.2787.

11-Oxoprogesterone (4)

Material obtained from the Upjohn Co. was recrystallized from methanol, mp 178–179°C; uv λ_{max}: 238 (14 900); ir ν_{max}: 1701 (CO), 1667 (α,β-unsaturated CO) cm^{-1}; nmr δ: 0.65 (s, 3, CH_3-18 H), 1.42 (s, 3, CH_3-19 H), 2.12 (s, 3, CH_3CO), 5.72 (s, 1, vinyl H).

3-Acetoxypregna-3,5-diene-11,20-dione (5)

To a solution of 11-oxoprogesterone (**4**) (10.0 g, 30.5 mmol), dissolved in ethyl acetate (300 mL), was added a mixture of acetic anhydride (40 mL) and ethyl acetate (120 mL), followed by a solution of perchloric acid (0.04 mL) in ethyl acetate (40 mL). The resulting yellow solution was stirred for 20 min at room temperature. The reaction was stopped by addition of saturated sodium bicarbonate solution (100 mL). The mixture was added to a slurry of sodium bicarbonate (100 g) in water (200 mL) which was stirred until carbon dioxide evolution had ceased. The organic layer was separated and the aqueous layer was extracted with ether. The combined organic layers were washed with saturated sodium bicarbonate solution and with water, and were dried (Na_2SO_4). The solvent was removed *in vacuo* and the solid residue was recrystallized from methanol containing some pyridine to give 9.6 g of a colorless crystalline product (85%), mp 145–147°C (lit. (10) mp 143–145°C); uv λ_{max}: 233 (19 100) nm; ir ν_{max}: 1751 (acetate CO), 1708 and 1701 (CO) cm^{-1}; nmr δ: 0.64 (s, 3, CH_3-18 H), 1.20 (s, 3, CH_3-19 H), 2.12 (s, 3, CH_3CO), 2.14 (s, CH_3CO), 5.35 (m,1, vinyl H-6), 5.67 (s, 1, vinyl H-4).

(20R)-Pregn-5-ene-3β,11β,20-triol (6)

3-Acetoxy-pregna-3,5-diene-11,20-dione (**5**) (9.4 g, 25.4 mmol) was dissolved in ethanol (900 mL) and was stirred with sodium borohydride (4 × 1.5 g added over 12 days) at room temperature. Water (200 mL) was added and the reaction mixture was stirred for 2 h. The solvent was removed *in vacuo* and the residue was stirred with water (500 mL). The solids were collected by filtration and washed with water. Recrystallization from acetone gave 4.5 g of a crystalline product, mp 200–205°C. Three recrystallizations from methanol gave **6** (3.7 g, 43.5%), mp 227–228°C; ir (Nujol) ν_{max}: 3330 (OH) cm^{-1}; nmr (pyridine-d_5) δ: 1.32 (d, 3, CH_3-21H, J = 6 Hz), 1.42 (s, 3, CH_3-18H), 1.70 (s, 3, CH_3-19H), 3.88 (m, 2, C*H*OH-3H and 20H), 4.60 (m, 1, C*H*OH-11H), ~ 5 (vinyl H, under H_2O peak); ms *m/e*: 334 (28%, M^+), 316 (100, M − H_2O), 301 (14, M − H_2O − CH_3), 298 (11, M − $2H_2O$), 283 (15, M − $2H_2O$ − CH_3), 265 (7, M − $3H_2O$ − CH_3). *Anal.* calcd. for $C_{21}H_{34}O_3 \cdot 1H_2O$: C 71.56, H 10.29%; found: C 71.56, H 10.27%.

(20R)-Pregn-5-ene-3β,11β,20-triol-(3,20-diacetate) (10)

(20*R*)-Pregn-5-ene-3β,11β,20-triol(**6**)(1.9 g, 5.7 mmol) was dissolved in pyridine (10 mL). Acetic anhydride (100 mL) was added and the solution was left at room temperature for 3 days. The solution was poured into water and extracted with ether. The ether extracts were washed with saturated sodium bicarbonate solution, then with saturated sodium chloride solution, and were dried (Na_2SO_4). The solvent was removed *in vacuo* to give 1.9 g of a semi-solid residue. Recrystallization from methanol gave 1.2 g (51%) of crystalline product, mp 163–165°C. Two more recrystallizations from methanol afforded a product, mp 165–166°C; ir ν_{max}: 3600 (OH), 1722 (CO), 1650 (C=C) cm^{-1}; nmr δ: 0.89 (s, 3, CH_3-18H), 1.15 (d, 3, CH_3-21H, J = 6 Hz), 1.29 (s, 3, CH_3-19H), 2.05 (s, 6, CH_3CO), 4.3 (m, 1, *H*COH-11H), 4.7 (m, 2, HCOAc), 5.25 (m, 1, vinyl-H); ms *m/e*: 4.18 (0.3% M^+), 358 (100, M − HOAc), 340 (6, M − HOAc − H_2O), 325 (19, M − HOAc − H_2O − CH_3), 265 (6, M − 2HOAc − H_2O − CH_3). *Anal.* calcd. for $C_{25}H_{38}O_5$: C 71.74, H 9.15%; found: C 71.83, H 9.14%.

(20R)-5α-Pregna-3β,6α,11β,20-tetraol (7)

In a nitrogen atmosphere (20*R*)-pregn-5-ene-3β,11β,20-triol (**6**) (334 mg, 1 mmol) was dissolved into 20 mL of dry tetrahydrofuran. Sodium borohydride (0.15 g) was added and the mixture was cooled to 0°C. A solution of boron trifluoride etherate (0.70 g) in tetrahydrofuran (10 mL) was added dropwise within 15 min to the stirred mixture, which was allowed to come to room temperature and was then stirred for 3.5 h. At 0°C were added, in order, 3 mL 3 *N* aqueous sodium hydroxide solution and 3 mL of a 30% hydrogen peroxide solution. The reaction mixture was stirred overnight at room temperature. Saturated sodium chloride solution (20 mL) was added and after stirring one hour at room temperature, the layers were separated. The aqueous layer was further extracted with ether. The organic layers were combined and washed with saturated sodium chloride solution and dried (Na_2SO_4). The solvent was evaporated *in vacuo*. The residue (0.3 g) was recrystallized from chloroform to give 181 mg (52%) of colorless crystalline material, mp 250–252°C. A further recrystallization from acetone afforded material with mp 253–255°C; ir (Nujol) ν_{max}: 3600, 3300 (OH) cm^{-1}; nmr (pyridine-d_5) δ: 1.31 (d, 3, CH_3-21H, J = 6 Hz), 1.40 (s, 3, CH_3-18H), 1.47 (s, 3, CH_3-19H), 3.9 (m, 3, *H*COH), 4.5 (m, 1, *H*COH-11H); ms *m/e*: 352 (7%, M^+), 334 (57, M − H_2O), 316 (100, M − $2H_2O$), 301 (16, M − $2H_2O$ − CH_3), 298 (17, M − $3H_2O$), 283 (9, M − $3H_2O$ − CH_3), 265 (36, M − $4H_2O$ − CH_3). *Anal.* calcd. for $C_{21}H_{36}O_4$: C 71.56, H 10.29%; found: C 71.67, H 10.20%.

(20R)-5α-Pregna-3β,6α,11β,20-tetraol 3,6,20-Triacetate (8)

(20*R*)-5α-Pregna-3β,6α,11β,20-tetraol (**7**) (9.3 g, 26.7 mmol of crude product) was suspended in 30 mL of pyridine and 300 mL of acetic anhydride and stirred at room temperature for 20 h. The solution was poured into 1 L of ice water containing 50 mL of 2 *N* hydrochloric acid. After stirring for 1 h, the mixture was extracted with ether. The extracts were stirred with a slurry of water and sodium bicarbonate until carbon dioxide evolution had stopped, were washed with saturated sodium chloride solution, and were dried (Na_2SO_4). The solvent was evaporated *in vacuo* and the solid residue was recrystallized from a 1:1 mixture of diethyl ether – hexane to give 5.6 g (44%) of crystalline product, mp 204–206°C. Repeated recrystallization from ether afforded a product of mp 210–212°C; ir ν_{max}: 3600, 3500 (OH), 1722 (CO), 1655 (C=CH) cm^{-1}; nmr δ: 0.86 (s, 3, CH_3 − 18H), 1.13 (s, 3, CH_3-19H), 1.14 (d, 3, CH_3-21H, J = 6 Hz), 2.04 (s, 9, CH_3COO), 4.26 (m, 1, C*H*OH-11H), 4.7 (m, 3, CHOAc); ms *m/e*: 478 (< 1%, M^+), 418 (19, M − HOAc), 400 (16, M − HOAc − H_2O), 358 (55, M − 2HOAc), 340 (26, M − 2HOAc − H_2O), 298 (9, M − 3HOAc), 280 (11, M − 3HOAc − H_2O), 265 (14, M − 3HOAc − H_2O − CH_3). *Anal.* calcd. for $C_{27}H_{42}O_7$: C 67.76, H 8.85%; found: C 67.56, H 8.89%.

(20R)-5α-Pregn-9(11)-ene-3β,6α,20β-triol Triacetate (3)

(20*R*)-5α-Pregna-3β,6α,11β,20-tetraol 3,6,20-triacetate (**8**) (3.0 g, 6.3 mmol) was dissolved into 60 mL of glacial acetic acid containing 0.3 mL of perchloric acid. The solution was heated on a steambath for 1 h and was poured into a slurry of 300 g of sodium bicarbonate in 1 L of water. The mixture was extracted with ether. The ether extracts were washed with saturated

sodium chloride solution and were dried (Na_2SO_4). Evaporation of the solvent *in vacuo* gave 2.8 g of yellow oil. Column chromatography (120 g of silica gel, petroleum ether – methylene chloride) afforded 2.1 g (80%) of a colourless oil. The compound was identical in all respects to compound **3** prepared by the shorter synthesis as described above.

(20R)-5α-Pregn-9(11)ene-3β,6α,20-triol-(20-acetate) (9)

The above triacetate **3** (1.0 g, 2.2 mmol) was dissolved into 20 mL of methanol. A solution of 0.33 g of sodium hydroxide in 2 mL of water was added and the resulting yellow solution was stirred at room temperature for 3 h, after which it was acidified with acetic acid. The solvent was removed *in vacuo*. The residue was dissolved in methylene chloride and the solution was washed with saturated sodium bicarbonate solution and with water, and was dried (Na_2SO_4). Evaporation of the solvent gave 0.7 g of yellow oil which was purified by column chromatography (21 g of silica gel, methylene chloride – methanol) followed by recrystallization from acetone to give 0.40 g (50%) of a colorless crystalline product, mp 224–226°C; ir ν_{max}: 3590, 3420 (OH), 1730 (CO) cm^{-1}; nmr δ: 0.57 (s, 3, CH_3-18H), 0.95 (s, 3, CH_3-19H), 2.17 (d, 3, CH_3-21H, J = 6 Hz), 3.55 (m, 2, C*H*OH), 4.8 (m, 1, C*H*OAc), 8.60 (m, 1, vinyl-H); ms *m/e*: 376 (3%, M^+) 316 (100 – M – HOAc), 298 (7, M – HOAc – H_2O), 283 (19, M – HOAc – H_2O – CH_3), 265 (23, M – HOAc – $2H_2O$ – CH_3). *Anal.* calcd. for $C_{23}H_{36}O_4$: C 73.37, H 9.64%; found: C 73.33, H 9.73%.

(20R)-5α-Pregn-9(11)-ene-3β,6α,20-triol (Asterogenol)

(20*R*)-5α-Pregn-9(11)-ene3β,6α,20-triol-(20-acetate) (**9**) (0.10 g, 0.27 mmol) was dissolved into a mixture of methanol (8 mL) and a solution of sodium hydroxide (0.2 g) in water (1.0 mL). The solution was left at room temperature for 5 days, then it was diluted with water to a volume of 200 mL. The mixture was extracted with methylene chloride. The extracts were washed with water and dried (Na_2SO_4). The solvent was evaporated *in vacuo* and the solid residue was recrystallized from aqueous methanol to give 0.08 g (90%) of crystalline material, which on recrystallization afforded a product with mp 263–264°C; $[\alpha]_D^{20}$ +8.2 (*c* 0.242 g/100 mL ethanol); ir (Nujol) ν_{max}: 3360 (OH) cm^{-1}; ms *m/e*: 334 (52%, M^+), 316 (63%, M – H_2O), 301 (48%, H – H_2O – CH_3), 283 (30%, M – $2H_2O$ – CH_3), 265 (26%, M – $3H_2O$ – CH_3). *Anal.* calcd. for $C_{21}H_{34}O_3$: C 75.41, H 10.25%; found: C 75.25, H 10.20%. This material was identical in all respects to the naturally isolated material.

Acknowledgements

We thank the Natural Sciences and Engineering Research Council of Canada for generous support of this work.

1. J. W. ApSimon, J. A. Buccini, and S. Badripersaud. Can. J. Chem. **51**, 850 (1973); J. W. ApSimon and J. A. Eenkhoorn. Can. J. Chem. **52**, 4113 (1974).
2. Y. Shimizu. J. Am. Chem. Soc. **94**, 4051 (1972).
3. Y. M. Sheikh, B. M. Tursch, and C. Djerassi. J. Am. Chem. Soc. **94**, 3278 (1972).
4. S. Ikegami, Y. Kamiya, and S. Tamura. Agric. Biol. Chem. **36**, 1777 (1972).
5. D. S. H. Smith and A. B. Turner. Tetrahedron Lett. 5263 (1972).
6. W. J. Fleming, R. Salathe, S. G. Wyllie, and M. E. H. Howden. Comp. Biochem. Physiol. **53B**, 267 (1976).
7. (*a*) J. E. Gurst, Y. M. Sheikh, and C. Djerassi. J. Am. Chem. Soc. **95**, 628 (1973); (*b*) J. W. ApSimon, J. Burnell, and J. Eenkhoorn. Synth. Commun. **9**, 215 (1979).
8. W. Klyne and E. Miller. J. Chem. Soc. 1972 (1950).
9. R. F. Zurcher. Helv. Chim. Acta, **44**, 1380 (1961); **46**, 2054 (1963).
10. J. J. Schmeider. Tetrahedron, **28**, 2717 (1972).
11. H. Eggert, C. L. van Antwerp, N. S. Bhacca, and C. Djerassi. J. Org. Chem. **41**, 1 (1976).
12. H. J. Leich, M. Jautelat, M. T. Messe, F. J. Weigert, and J. D. Roberts. J. Am. Chem. Soc. **91**, 7445 (1969).
13. J. Wahlberg, S-O. Almguist, T. Nishida, and C. Enzell. Acta Chim. Scand. Ser. B, **29**, 1047 (1975).
14. I. Kitagawa, M. Kobayashi, and T. Sugawa. Chem. Pharm. Bull. **26**, 1852 (1978).
15. M. Hori. Steroids, **14**, 33 (1969).

Can. J. Chem. Downloaded from www.nrcresearchpress.com by 210.87.254.105 on 09/05/12
For personal use only.

The conformational equilibrium in [^{13}C-1-*methyl*]-*cis*-1,4-dimethylcyclohexane

HAROLD BOOTH AND JEREMY RAMSEY EVERETT[1]

Department of Chemistry, University of Nottingham, Nottingham, England NG7 2RD

Received June 16, 1980

This paper is dedicated to Prof. Raymond U. Lemieux on the occasion of his 60th birthday

HAROLD BOOTH and JEREMY RAMSEY EVERETT. Can. J. Chem. **58**, 2709 (1980).

The conformational equilibrium in [^{13}C-1-*methyl*]-*cis*-1,4-dimethylcyclohexane has been assessed by (*a*) direct integration of signals due to equatorial and axial methyl carbons in the ^{13}C nmr spectrum at 172 K and (*b*) by measurement of the ^{13}C chemical shifts of C-1 and C-4 in the spectrum at 300 K. It is concluded that a ^{13}C isotope effect on the position of the degenerate equilibrium in *cis*-1,4-dimethylcyclohexane is either nonexistent, or is too small to be detected by methods of analyses employed. The ^{13}C nmr data incidental to the study (chemical shifts, coupling constants, spin–lattice relaxation times, nuclear Overhauser enhancements, and 1-bond isotope shifts) are recorded for the title compound and its *trans*-isomer.

HAROLD BOOTH et JEREMY RAMSEY EVERETT. Can. J. Chem. **58**, 2709 (1980).

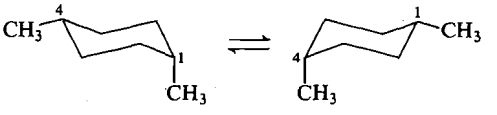
On a déterminé l'équilibre conformationnel du [^{13}C *méthyl*-1]-diméthyl-1,4 cyclohexane *cis* par: (*a*) l'intégration directe des signaux des carbones de méthyles en positions axiale et équatoriale dans le spectre rmn du ^{13}C à 172 K et (*b*) par la mesure des déplacements chimiques du ^{13}C des carbones en position 1 et 4 dans le spectre à 300 K. On a conclu que l'effet de l'isotope ^{13}C sur la position de l'équilibre dégénérée du diméthyl-1,4 cyclohexane *cis* est inexistant ou trop faible pour être décelé par les méthodes d'analyse utilisées. On a enregistré les données de la rmn du ^{13}C inhérentes à l'étude du composé étudié et de son isomère *trans* (déplacements chimiques, constantes de couplage, temps de relaxation spin–réseau, effets Overhauser nucléaire et déplacements isotopiques de la liaison-1).

[Traduit par le journal]

Introduction

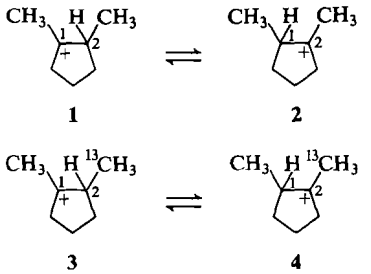
A number of recent papers (1, 2) have described isotope effects on equilibrium processes. Using chemical shift measurements, Baldry and Robinson (1) were able to detect small changes in the position of chair–chair equilibria in cyclohexanes when a CH_3 substituent was replaced by a CD_3 substituent. Saunders *et al.* (2) using ^{13}C chemical shifts, found it relatively easy to detect changes in the position of tautomeric equilibria of degenerate cations (e.g. **1** ⇌ **2**) caused by replacement of CH_3 by CD_3, and of 3-CH_2 by 3-CD_2. Of considerable interest was the change in the position of equilibrium **1** ⇌ **2** caused by replacement of $^{12}CH_3$ by $^{13}CH_3$, a change detected by the slight difference in chemical shift between C-1 and C-2. The ion **4**, with the charge adjacent to ^{13}C, was preferred to the ion **3**. On the other hand, Wehrli *et al.* (3) recently examined cyclodecanone and measured the movements in ^{13}C chemical shifts which accompanied deuteration; effects were detected over distances of up to 6 bonds and were attributed to a direct, or intrinsic, isotope effect, rather than to any perturbation of a conformational equilibrium (4). Chertkov and Sergeyev (5) failed to detect (within 2%) any change in the conformational equilibrium of cyclohexane when eleven hydrogen atoms were replaced by deuterium atoms. However, the preference, in cyclohexanones, for axial deuterium over axial hydrogen, has been demonstrated by ORD measurements (6, 7).

We considered it worthwhile to attempt to determine the effect on the degenerate chair–chair equilibrium in *cis*-1,4-dimethylcyclohexane **5** ⇌ **6**



5 **6**

which would result from substitution of a $^{12}CH_3$ by a $^{13}CH_3$. The occurrence of *syn*-axial nonbonded interactions in cyclohexanes is thought to be a major factor in determining conformational enthalpies and, therefore, conformational equilibria. Furthermore, the CH_3/H *syn*-axial interactions may be considered to consist of both H/H and C/H interactions. The overall effect on the equilibrium **5** ⇌ **6** due to the isotopic replacement may have two



1 **2**

3 **4**

[1]Present address: Department of Chemistry, McGill University, Montreal, P.Q.

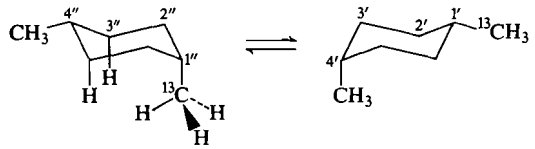
0008-4042/80/232709-05$01.00/0

©1980 National Research Council of Canada/Conseil national de recherches du Canada

Can. J. Chem. Downloaded from www.nrcresearchpress.com by 210.87.254.6 on 09/05/12
For personal use only.

Can. J. Chem. Downloaded from www.nrcresearchpress.com by 210.87.254.6 on 09/05/12
For personal use only.

contributions: a *direct* one due to the difference in interaction energy, at the same distance, between $^{12}C/H$ and $^{13}C/H$ interactions, and an *indirect* one, due to the different geometry induced in (**7** ⇌ **8**) by

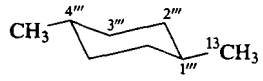


7 **8**
x $(1-x)$

the isotopic substitution. Neither effect is predictable. With regard to the geometry of **7**, compared to that of **5**, it seems likely (cf. ref. 8) that both ^{13}C—H and ^{13}C—C bond lengths are less than the corresponding bond lengths for ^{12}C. The relatively shorter ^{13}C—H bond length in **7** should result in reduced *syn*-axial repulsive interactions of the H/H variety. On the other hand a shortening of the $^{13}CH_3$—C bond causes a reduction in H/H and CH_3/H distances, leading to increased repulsive interactions.

Results and Discussion

The syntheses of *cis*-1,4-dimethylcyclohexane **7** ⇌ **8** and *trans*-1,4-dimethylcyclohexane **9**, each enriched to the extent of 90.6% with ^{13}C at one of the methyl carbons, employed well established methods which require no comment (see Experimental).



9

Two methods were used to measure the equilibrium constant for **7** ⇌ **8**. The first method involved the measurement of the relative areas of the well-separated signals due to equatorial methyl (1′-CH_3, 23.3 ppm) and axial methyl (1″-CH_3, 17.4 ppm) carbons in the ^{13}C nmr spectrum recorded at 173 K. This method is relatively inaccurate, whether instrumental integration or the preferred method of hand planimetry is employed. Whilst the planimeter is very accurate and capable of good reproducibility, the overall accuracy is limited by the uncertainty in choosing a straight line for the base of the signals. This uncertainty is obviously related to noise level and, therefore, to sample size and computer capability. The advantage of the method of relative areas is that it is direct and involves no assumptions, provided that the experimental parameters are chosen sensibly. In a multi-pulse Fourier transform ^{13}C experiment, recorded with ^{1}H decoupling, the relative signal areas are dependent on spin–lattice relaxation times and nuclear Overhauser enhancements. Table 1 shows that the T_1 values of 172 K are little different for carbons of axial and equatorial methyl groups. Table 1 also includes the nuclear Overhauser enhancements for equatorial and axial carbons at 172 K; again the difference is insignificant. We conclude that the signal areas for equatorial and axial carbons reflect accurately the molecular proportions of **8** and **7** respectively. The relatively small nuclear Overhauser enhancements (98–99%) for the methyl carbons are noteworthy since they imply that only about 50% of the total spin–lattice relaxation is due to dipole–dipole interaction. Since samples were not degassed, there is the expected contribution to relaxation from dissolved oxygen. Nevertheless, it seems that there must be an appreciable contribution from relaxation by spin rotation. From the low temperature area method, the equilibrium constant K (= **8**/**7**) was determined to be 1.00. As a precaution, the same method was applied to the degenerate system **5** ⇌ **6**. In this case the equilibrium constant was found to be 1.01 by instrumental integration and 0.97 from hand planimetry, giving an average of 0.99. We conclude that the $^{13}C/^{12}C$ isotope effect on the position of equilibrium **5** ⇌ **6** is nonexistent, or is too small to be detectable by the low temperature area method.

The second method used to measure the position of equilibrium in **7** ⇌ **8** involved chemical shift determinations and is, in principle, a more accurate method than the first. The basis of the method is the fact that the room-temperature averaged ^{13}C chemical shifts of the methine carbons C-4″ and C-4′ is different from the room-temperature averaged chemical shifts of the methine carbons C-1″ and C-1′. These averaged chemical shifts are, of course, identical in the degenerate equilibrium **5** ⇌ **6**. The general theory is as follows. Let x and $(1-x)$ be the mole fractions of **7** and **8** respectively; let δ_1 and δ_4 be the observed, averaged chemical shifts of C-1 and C-4, respectively, at room temperature. If $\delta_{1'}$ and $\delta_{4'}$ are the chemical shifts of C-1′ and C-4′, respectively, in **8**, whilst $\delta_{1''}$ and $\delta_{4''}$ are the corresponding shifts in **7**, we may write

$$\delta_4 = x\delta_{4''} + (1-x)\delta_{4'}$$
$$\delta_1 = x\delta_{1''} + (1-x)\delta_{1'}$$

Let the intrinsic 1-bond isotope shifts which accompany the replacement of a $^{12}CH_3$ by a $^{13}CH_3$ be I_e for ring carbon substituted by CH_3 (equatorial), and I_a for ring carbon substituted by CH_3 (axial). Then

$$I_e = \delta_{1'} - \delta_{4''}$$
$$I_a = \delta_{1''} - \delta_{4'}$$

TABLE 1. ^{13}C relaxation times (T_1), $^{13}C[^1H]$ nuclear Overhauser enhancements, and the equilibrium constant for **7** ⇌ **8** (solvent $CDCl_3/CFCl_3$)

	CH_3 axial	CH_3 equatorial
T_1 (s)	1.07±0.05[a]	1.00±0.05[a]
T_1 (s)	8.60±0.48[b]	8.60±0.48[b]
Nuclear Overhauser enhancement (%)	99[a]	98[a]
Equilibrium constant **8**/**7**	1.035 (instrumental integration)	
	1.028 (hand planimetry)	
	1.031 (average)	
	1.00[c] (corrected)	

[a]172 K.
[b]302 K.
[c]After correction for presence of **9**.

It is assumed that intrinsic isotope shifts over 4-bonds are negligible (cf. ref. 8). From the above relationships, it can easily be shown that

$$[1] \quad x = \frac{(\delta_{4''} - \delta_{4'}) + (\delta_4 - \delta_1) + I_e}{2(\delta_{4''} - \delta_{4'}) + (I_e - I_a)}$$

Now the observed signal for C-1 arises largely from molecules which are effectively doubly labelled (in ^{13}C) at C-1 and the adjacent methyl carbon, and is therefore the low-field doublet part of an AB spin system ($J_{AB} = {}^1J_{CC}$). The high-field doublet part of this system is a pair of satellites to the intense singlet due to the methyl carbon of singly labelled molecules. Analysis of the AB spectrum yields the chemical shift δ_1 and also the chemical shift of the methyl carbon in doubly labelled species. The observed signal for C-4 also arises largely from molecules containing a ^{13}C-enriched methyl carbon attached to C-1, but since the coupling ${}^4J_{CC}$ is very small, this signal is a single line, the position of which yields δ_4 directly.

The ^{13}C nmr spectrum of **7** ⇌ **8** recorded at temperatures below 195 K includes distinct resonances for CH_3 (equatorial) in **8**, CH_3 (axial) in **7**, C-1′ (low-field half of AB quartet), C-4′ (singlet), C-1″ (low-field half of AB quartet), and C-4″ (singlet). The chemical shifts $\delta_{1'}$, $\delta_{4'}$, $\delta_{1''}$, and $\delta_{4''}$ are readily obtained from this spectrum. Thus all the parameters required for the calculation of x through eq. [1] are available.

The most attractive feature of this method of assessing the position of equilibrium in **7** ⇌ **8** is that it involves the measurement of chemical shift differences in the spectrum of a *single* sample of a *single* compound. Most methods of determining conformational equilibria through measurement of chemical shifts utilize conformationally biased compounds as standards for chemical shift parameters. A basic weakness of such methods is that the validity of the models is always questionable; furthermore, chemical shift data are required from at least three compounds and are often recorded in separate solutions. The present method, although free from most of these objections, suffers from the drawback that the parameters $\delta_{1'}$, $\delta_{4'}$, $\delta_{1''}$, and $\delta_{4''}$ are derived from a low-temperature spectrum whereas δ_1 and δ_4 come from a room-temperature spectrum.

Spectral data for [^{13}C-1-*methyl*]-*cis*-1,4-dimethylcyclohexane are summarized in Table 2. Fourier transform spectra at 62.901 MHz employed 32 K data points over a spectral width of 2500 Hz, equivalent to digital resolution of 0.1526 Hz (0.002426 ppm), and corresponding to a possible error due to digitization of ±0.0763 Hz (±0.001213 ppm). The spectrum at 180 K includes a "triplet" at 31.67 ppm, comprising a singlet due to C-2″,6″ and a doublet (${}^3J_{CC}$ = 3.42 Hz) due to C-3′,5′ which is coupled to the equatorial methyl carbon. Since the combined signal due to C-2′,6′ and C-3″,5″ is an unresolved singlet at 29.20 ppm, it is evident that the 3-bond coupling between C-3″,5″ and the *axial* methyl carbon is less than 1.0 Hz. Table 2 indicates that the intrinsic 1-bond isotope effects for the *substituted ring carbons* are −0.011510 ppm for I_e and −0.011875 ppm for I_a. The corresponding isotope effects for the *methyl carbons* are −0.0075833 ppm for equatorial methyl and −0.0002067 ppm for axial methyl.

The directions of these intrinsic isotope effects, to high field, are in agreement with the usual finding, that substitution of a nucleus by a heavier isotope produces greater shielding for all nuclei involved (9). Whereas I_e and I_a are identical, within experimental error, the isotope effects for the methyl carbons appear to show a dependence on the orientation of the methyl group. In the spectrum of **7** ⇌ **8** at 300 K the "triplet" observed at 31.13 ppm consists of a singlet due to C-2,6 (${}^2J_{CC} = 0$) and a doublet (${}^3J_{CC}$ = 2.29 Hz) due to C-3,5. The doublet splitting represents the average of the ${}^3J_{CC}$ values for conformations **7** (< 1 Hz) and **8** (3.42 Hz), obtained from the spectrum at 180 K.

Before application of eq. [1], it was necessary to justify the assumption, implicit in [1], that the variation in ^{13}C chemical shifts with temperature is

Can. J. Chem. Downloaded from www.nrcresearchpress.com by 210.87.254.6 on 09/05/12
For personal use only.

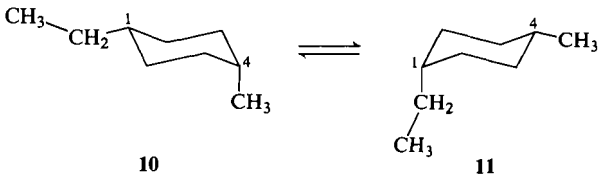
Can. J. Chem. Downloaded from www.nrcresearchpress.com by 210.87.254.6 on 09/05/12
For personal use only.

TABLE 2. ^{13}C chemical shifts[a] at 62.901 MHz (δ values, ppm downfield from Me_4Si) for carbons in [^{13}C-1-*methyl*]-*cis*-1,4-dimethylcyclohexane **7** ⇌ **8**

Carbon	Chemical shift	
	300 K[b]	180 K
1″	30.488609[c]	26.619020[e]
1′	30.488609[c]	33.379008[f]
4″	30.500119	33.391711
4′	30.500119	26.630896
2″,6″	31.133257	31.666937
2′,6′	31.133257	29.195005
3″,5″	31.134473[d]	29.195005[g]
3′,5′	31.134473[d]	31.666937[h]
CH_3-1″	20.366735[c]	17.414938[e]
CH_3-1′	20.366735[c]	23.312110[f]
CH_3-4″	20.369803	23.319693
CH_3-4′	20.369803	17.415144

[a]Measured using 32K data points over 2500 Hz, a possible error due to digitization of ±0.001213 ppm.
[b]Averaged shifts observed, i.e. $\delta_1 = \delta_{1'} = \delta_{1''}$ etc.
[c]Doublet, $^1J_{CC}$ 35.55 Hz.
[d]Doublet, $^3J_{CC}$ 2.29 Hz.
[e]Doublet, $^1J_{CC}$ 34.64 Hz.
[f]Doublet, $^1J_{CC}$ 35.40 Hz.
[g]Singlet, $^3J_{CC} \lesssim 1$ Hz.
[h]Doublet, $^3J_{CC}$ 3.42 Hz.

approximately the same for cyclohexane carbon substituted by equatorial Me, as that substituted by axial Me. The temperature dependence of the ^{13}C chemical shifts for *cis*-1-ethyl-4-methylcyclohexane **10** ⇌ **11** were recorded over a range of 36 K



10 **11**

below the slow exchange limit (10). The results confirm the work of Schneider and Freitag (11), which demonstrated a linear deshielding, with increasing temperature, of ring carbons in cycloalkanes. In our case the plots of chemical shift against temperature indicated an approximately linear relationship for C-4 in both **10** and **11**. In **10**, C-4 was deshielded, with increasing temperature, by 3.18×10^{-3} ppm K^{-1}; the corresponding shift/temperature gradient for C-4 in **11** was 3.63×10^{-3} ppm K^{-1}. If we assume that similar ^{13}C shift/temperature gradients hold for C-4′ in **8** and C-4″ in **7**, then the discrepancy arising from the use of $(\delta_{4''} - \delta_{4'})$ at 180 K, rather than at 300 K, amounts to only 0.054 ppm. The entries in Table 2 yield the following chemical shift differences:

$$\delta_{4''} - \delta_{4'} = 6.760815 \text{ ppm}$$

$$\delta_4 - \delta_1 = 0.011510 \text{ ppm}$$

Application of these to eq. [1] leads to a value for x of 0.4999424, i.e. 0.500, within experimental error. We conclude that any isotope effect (caused by replacement of $^{12}CH_3$ by $^{13}CH_3$) on the position of equilibrium in **5** ⇌ **6** is either nonexistent, or is too small to be detected by the technique employed.

The ^{13}C nmr spectrum of the conformationally homogeneous [^{13}C-1-*methyl*]-*trans*-1,4-dimethylcyclohexane **9** was also measured and the relevant details appear in Table 3. As for the *cis*-isomer, chemical shifts for C-1‴ and CH_3-1‴ were obtained by analysis of the AB spin system arising from doubly labelled molecules. Table 3 indicates that the intrinsic 1-bond isotope effect for C-1‴ is $(\delta_{1'''} - \delta_{4'''} =) -0.01603$ ppm and for CH_3-1‴ is −0.00796 ppm. Encouragingly, these values are close to those determined for C-1′ and CH_3-1′ in conformation **8** of the *cis*-isomer **7** ⇌ **8**.

The ^{13}C—^{13}C coupling constants of Tables 2 and 3 are of interest in suggesting a tentative correlation of J values with stereochemistry. Thus ^1J(C-1′, CH_3) in **8** (i.e. *equatorial* methyl) is 35.40 Hz, significantly greater than ^1J(C-1″, CH_3) in **7** (i.e. *axial* methyl), which is 34.64 Hz. A larger effect, in the same sense, was noted by Barna and Robinson (12) for 4-*tert*-butyl-2-methylpiperidines and 4-*tert*-butyl-2-methylcyclohexanones, but was attributed to the proximity of nonbonding electrons or unsaturation. The coupling constant ^1J(C-1‴, CH_3) in *trans*-1,4-dimethylcyclohexane **9** is 35.89 Hz at 301 K and 35.64 Hz at 173 K, values which are close to the 36.0 (±0.3) Hz reported earlier for the comparable coupling in the major conformation of methylcyclohexane at 172 K (13). It is noteworthy that ^3J(C-3, CH_3) is 3.4–4.5 Hz for equatorial methyl, corresponding to a dihedral angle of 180°, whereas ^3J(C-3, CH_3) is ≲ 1 Hz for axial methyl, corresponding to a dihedral angle of 60°. A

TABLE 3. ^{13}C chemical shifts[a] at 25.15 MHz (δ values, ppm downfield from Me_4Si) and 301 K for carbons in [^{13}C-1-*methyl*]-*trans*-1,4-dimethylcyclohexane **9**

Carbon	Shift
1‴	32.96110[b]
2‴,6‴	35.85105
3‴,5‴	35.84862[c]
4‴	32.97713
CH_3-1‴	22.83280[b]
CH_3-4‴	22.84076

[a]Measured using 16K data points over 1000 Hz, a possible error due to digitization of ±0.00243 ppm.
[b]Doublet, $^1J_{CC}$ 35.89 Hz (35.64 Hz at 173 K).
[c]Doublet, $^3J_{CC}$ 4.52 Hz.

Can. J. Chem. Downloaded from www.nrcresearchpress.com by 210.87.254.6 on 09/05/12
For personal use only.

Karplus-type correlation of vicinal coupling ($^3J_{CC}$) with dihedral angle is now well established (14, 15). Of greater interest is the significant difference between ^3J(C-3‴, CH_3) in **9** (4.5 Hz) and ^3J(C-3′, CH_3) in **8** (3.4 Hz). (The former compares well with the value of 4.3 Hz recorded for methylcyclohexane, ref. 13.) One or both of two factors may contribute to an explanation of the difference: the remote axial methyl in **8** causes a slight flattening of the ring, relative to the effect of equatorial methyl (16–20), leading to a loss of coplanarity of the coupling pathway CH_3—C1—C2—C3. At the same time the change of the 4-methyl substituent from an equatorial orientation in **9** to an axial orientation in **8** may affect $^3J_{CC}$ because the electronegativity effect of methyl will depend on orientation (21).

Experimental

^{13}C spectra were recorded for solutions in $CFCl_3$–$CDCl_3$ (9:1 v/v) at 25.15 MHz on a JEOL JNM-PS-100 spectrometer interfaced to a Nicolet 1085 20 K computer, and at 62.90 MHz on a Bruker WM-250 spectrometer. General instructions for the preparation of 1,4-dialkylcyclohexanes have been given elsewhere (22).

*[^{13}C-1-*Methyl*]-1,4-dimethylcyclohexane*

4-Methylcyclohexanone (1.442 g, 0.0129 mol) was reacted with the Grignard reagent formed from magnesium turnings (0.34 g, 0.014 mol) and [^{13}C] iodomethane (2.0 g, 0.014 mol, 91.0 ^{13}C at.%). [1-*Me*-^{13}*C*]-1,4-Dimethylcyclohexanol (2.48 g, > 100%) was isolated as a pale yellow oil still containing some ether. The alcohol was dehydrated using 4-methylbenzenesulfonic acid (0.3838 g) to give [1-*Me*-^{13}*C*]-1,4-dimethylcyclohex-1-ene (0.9574 g, 0.0862 mol) as a colourless oil. The alkene (neat) was hydrogenated over PtO_2 (0.1026 g) to yield a mixture of *cis*- and *trans*-[1-*Me*-^{13}*C*]-1,4-dimethylcyclohexane (0.5432 g, 0.00481 mol) as a colourless oil (M^+: 113.1298, $C_7{}^{13}C_1H_{16}$ requires 113.1282). The mixture was completely separated using a 12 ft × ¾ in. aluminium column packed with 30% SE-30 coated on a support of acid-washed siliconized 60–80 mesh Chromosorb W. At a column temperature of 65°C and a flow rate of 30 cm^3 min^{-1}, the *trans*- and *cis*-isomers had retention times of 45.6 min and 57.0 min respectively. In the ^1H nmr spectrum ($CDCl_3$), the methyl proton of the *trans*-isomer, at δ 0.86 ppm, gave a doublet of doublets with separations of 122.5 Hz ($^1J_{CH}$) and 5.5 Hz ($^3J_{HH}$). The methyl protons of the *cis*-isomer, at δ 0.94 ppm, gave a doublet of doublets with separations of 122 Hz ($^1J_{CH}$) and 6.2 Hz ($^3J_{HH}$).

1. K. W. Baldry and M. J. T. Robinson. Tetrahedron, **33**, 1663 (1977).
2. M. Saunders, L. Telkowski, and M. R. Kates. J. Am. Chem. Soc. **99**, 8070 (1977).
3. F. W. Wehrli, D. Jeremic, M. Mihailovic, and S. Milosavljevic. J. Chem. Soc. Chem. Commun. 302 (1978).
4. F. A. L. Anet, A. K. Cheng, and J. Krane. J. Am. Chem. Soc. **95**, 7877 (1973).
5. V. A. Chertkov and N. M. Sergeyev. J. Am. Chem. Soc. **99**, 6750 (1977).
6. S.-F. Lee, G. Barth, K. Kieslich, and C. Djerassi. J. Am. Chem. Soc. **100**, 3965 (1978).
7. S.-F. Lee, G. Barth, and C. Djerassi. J. Am. Chem. Soc. **100**, 8010 (1978).
8. H. Batiz-Hernandez and R. A. Bernheim. *In* Progress in nmr spectroscopy. Vol. 3. *Edited by* J. Emsley, J. Feeney, and L. H. Sutcliffe. Pergamon Press, Oxford. 1967. p. 63.
9. W. T. Raynes. *In* Nuclear magnetic resonance specialist periodical report. Vol. 3. (R. K. Harris, Senior Reporter), The Chemical Society, London. 1974. p. 34.
10. H. Booth and J. R. Everett. J. Chem. Soc. Perkin Trans. II, 255 (1980).
11. H.-J. Schneider and W. Freitag. J. Am. Chem. Soc. **98**, 478 (1976).
12. J. C. J. Barna and M. J. T. Robinson. Tetrahedron Lett. 1459 (1979).
13. H. Booth and J. R. Everett. J. Chem. Soc. Chem. Commun. 278 (1976).
14. J. L. Marshall, S. A. Conn, and M. Barfield. Org. Magn. Reson. **9**, 404 (1977).
15. P. E. Hansen. Org. Magn. Reson. **11**, 215 (1978).
16. H. Booth and P. R. Thornburrow. J. Chem. Soc. B, 1051 (1971).
17. J. D. Remijnse, H. Van Bekkum, and B. W. Wepster. Recl. Trav. Chim. **89**, 658 (1970).
18. H. J. Geise, H. R. Buys, and F. G. Mijlhoff. J. Mol. Struct. **9**, 447 (1971).
19. H. J. Geise, F. G. Mijlhoff, and C. Altona. J. Mol. Struct. **13**, 211 (1972).
20. E. Osawa, J. B. Collins, and P. v. R. Schleyer. Tetrahedron, **33**, 2667 (1977).
21. H. Booth and P. R. Thornburrow. Chem. Ind. 685 (1968).
22. H. Booth, J. R. Everett, and R. A. Fleming. Org. Magn. Reson. **12**, 63 (1979).

The conformational free energy difference for the trideuteromethyl substituent in cyclohexane

HAROLD BOOTH AND JEREMY RAMSEY EVERETT[1]

Department of Chemistry, University of Nottingham, Nottingham, England NG7 2RD

Received June 16, 1980

This paper is dedicated to Prof. Raymond U. Lemieux on the occasion of his 60th birthday

HAROLD BOOTH and JEREMY RAMSEY EVERETT. Can. J. Chem. **58**, 2714 (1980).

Studies at 169 K to 194 K of the ^{13}C nmr spectrum of *cis*-1-ethyl-[4-*Me*-$^2H_3$]-4-methylcyclohexane show that the conformational enthalpy difference $-\Delta H°(C^2H_3)$ is 1.82 ± 0.07 kcal mol^{-1} and the conformational entropy difference $\Delta S°(C^2H_3)$ is -0.28 ± 0.4 cal K^{-1} mol^{-1}, values which do not differ significantly from the values for CH_3. However, analysis of the room temperature ^{13}C nmr spectrum of a mixture of *cis*-1-ethyl-4-methylcyclohexane and *cis*-1-ethyl-[4-*Me*-$^2H_3$]-4-methylcyclohexane showed that $-\Delta G°(C^2H_3)$ at 298 K is 11.89 ± 1.46 cal mol^{-1} *less* than that for CH_3, i.e. C^2H_3 has a slightly greater preference than CH_3 for the axial orientation. The ^{13}C nmr spectrum of a mixture of *trans*-1-ethyl-4-methylcyclohexane and *trans*-1-ethyl-[4-*Me*-$^2H_3$]-4-methylcyclohexane indicates that deuterium-induced ^{13}C nmr isotope shifts, all upfield, occur across 1, 2, 3, and 5 bonds.

HAROLD BOOTH et JEREMY RAMSEY EVERETT. Can. J. Chem. **58**, 2714 (1980).

Une étude des spectres de rmn du ^{13}C de l'éthyl-1 [*Me*-4-$^2H_3$]-méthyl-4 cyclohexane *cis*, mesurées entre 169 et 194 K, montrent que la différence d'enthalpie conformationnelle $-\Delta H°(C^2H_3)$ est de $1,82 \pm 0,07$ kcal mol^{-1} et la différence d'entropie conformationnelle $\Delta S°(C^2H_3)$ est de $-0,28 \pm 0,4$ cal K^{-1} mol^{-1}. Ces valeurs ne different pas de façon significative de celles de CH_3. Cependant l'analyse du spectre de rmn du ^{13}C à la température ambiante d'un mélange d'éthyl-1 méthyl-4 cyclohexane *cis* et d'éthyl-1 [*Me*-4-$^2H_3$] méthyl-4 cyclohexane *cis* a montré que le $\Delta G°(C^2H_3)$ à 298 K est de $11,89 \pm 1,46$ cal mol^{-1} plus faible que celle du CH_3 i.e. la préférence du C^2H_3 pour une orientation axiale est légèrement plus grande que celle du CH_3. Le spectre rmn du ^{13}C d'un mélange d'éthyl-1 méthyl-4 cyclohexane *trans* et d'éthyl-1 [*Me*-4-$^2H_3$] méthyl-4 cyclohexane *trans* indique que tous les déplacements chimiques vers les champs forts du ^{13}C induits par le deutérium se produisent à travers 1, 2, 3 et 5 liaisons.

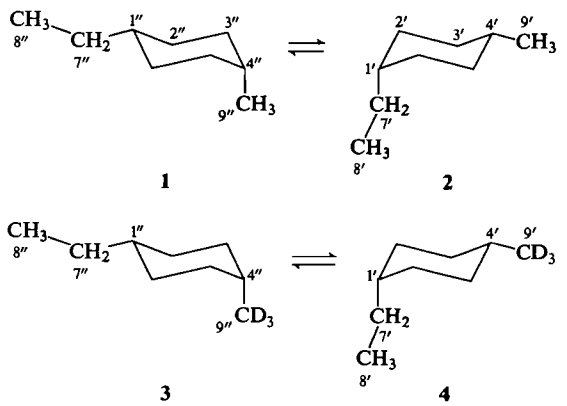
[Traduit par le journal]

Introduction

There is a growing interest in the effects of isotopic replacement of nuclei on the position of conformational equilibria. As recently reported, we failed to detect, by nmr methods, a change in the conformational equilibrium in *cis*-1,4-dimethylcyclohexane after replacement of a methyl group by a ^{13}C-methyl group (1). However, a change resulting from the replacement of CH_3 by C^2H_3 should be detected with greater ease. For example, using chemical shift measurements, Baldry and Robinson (2) succeeded in showing that the conformational equilibrium in *trans*-[1-*Me*-$^2H_3$]-1,3-dimethylcyclohexane favours that conformation with C^2H_3 axial by about 11.0 cal mol^{-1}. Moreover, circular dichroism studies have established that axial deuterium is preferred to axial hydrogen at the 3- and 4-positions of 2,2-dimethylcyclohexanone (3, 4); the shorter bond length of C—^{2}H (as against C—^{1}H), and the smaller vibrational amplitudes may well provide sufficient explanation.

Results and Discussion

We chose to study the effect on the equilibrium in *cis*-1-ethyl-4- methylcyclohexane **1** ⇌ **2** caused by the replacement of CH_3 by C^2H_3. The ^{13}C nmr chemical shifts for carbons in **1** and **2**, and molecular proportions, are already available from a previous study in the temperature range 141 K to 177 K (5). As the difference between the chemical shifts of C-7″ and C-7′ is as much as 7 ppm, the room-temperature averaged shift of C-7 should be particularly sensitive to any change in the position of equilibrium, i.e. the averaged shift of C-7 in **3** ⇌ **4**



should differ significantly from that of C-7 in **1** ⇌ **2**. Moreover, a direct or *intrinsic* isotope effect on the chemical shift of C-7 is unlikely to occur across the

[1]Present address: Department of Chemistry, McGill University, Montreal, P.Q.

0008-4042/80/232714-06$01.00/0

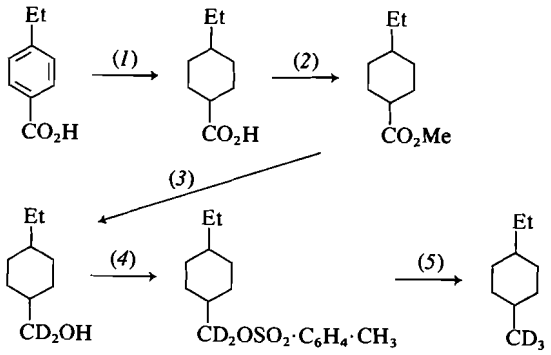
©1980 National Research Council of Canada/Conseil national de recherches du Canada

Can. J. Chem. Downloaded from www.nrcresearchpress.com by 210.87.254.5 on 09/05/12
For personal use only.

Can. J. Chem. Downloaded from www.nrcresearchpress.com by 210.87.254.5 on 09/05/12
For personal use only.

intervening six bonds. Initially, however, we analyzed the equilibrium **3** $\rightleftharpoons$ **4** by the low-temperature area method, followed by a comparison of the derived thermodynamic parameters $\Delta H°$ (C^2H_3) and $\Delta S°$ (C^2H_3) with those previously determined for C^1H_3 (5).

The syntheses of *cis*- and *trans*-1-ethyl-4-methylcyclohexane have already been reported (6). A second synthesis also proved satisfactory and as illustrated in Scheme 1 was readily adapted to the preparation of molecules specifically trideuterated at the 4-methyl positions. The complete separation of *cis*- and *trans*-isomers was carried out by preparative gas–liquid chromatography after the final stage. Examination of the *cis*- and *trans*-1-ethyl-[4-*Me*-$^2H_3$]-4-methylcyclohexane by ^2H nmr spectroscopy proved conclusively that no scrambling of the deuterium had occurred during the synthesis.



Reagents:
(*1*) H_2, PtO_2 (*4*) $CH_3{\cdot}C_6H_4SO_2Cl$
(*2*) MeOH, H_2SO_4 (*5*) $LiAlD_4$, ether
(*3*) $LiAlD_4$, ether

SCHEME 1

The ^{13}C nmr spectrum of *cis*-1-ethyl-[4-*Me*-$^2H_3$]-4-methylcyclohexane **3** $\rightleftharpoons$ **4** was recorded within the range 169 K to 194 K, where ring inversion is slow compared to differences in chemical shifts between structurally identical nuclei in the two conformations. The proportions of **3** and **4** were obtained from the relative areas of well separated signals due to C-1′ and C-1″; signals due to C-8′ and C-8″ were similarly employed and the two equilibrium constants were averaged. The results were analysed as reported earlier (5) for *cis*-1-ethyl-4-methylcyclohexane and the thermodynamic parameters for C^2H_3 were 1.82 ± 0.07 kcal mol^{-1} for $-\Delta H°$ and −0.28 ± 0.4 cal K^{-1} mol^{-1} for $\Delta S°$. Since the comparable parameters for CH_3 are 1.75 ± 0.04 for $-\Delta H°$ and −0.03 ± 0.2 for $\Delta S°$, it is obvious that the *low temperature area method* is insufficiently accurate to distinguish C^2H_3 from CH_3.

The theoretical background to the *room-temperature chemical shift method* is given below.

Let the mole fractions of **1** and **3** be x and y respectively. Let δ_7(H) and δ_7(D) be the observed chemical shifts of C-7 in **1** $\rightleftharpoons$ **2** and **3** $\rightleftharpoons$ **4**, respectively, at room temperature. Let $\delta_{7''}$ and $\delta_{7'}$ be the chemical shifts of C-7 in **1** and **2** respectively. In the absence of intrinsic isotope shifts, $\delta_{7''}$ and $\delta_{7'}$ are also the chemical shifts of C-7 in **3** and **4** respectively. Then

$$\delta_7(\mathrm{H}) = x\delta_{7''} + (1 - x)\delta_{7'}$$

and

$$\delta_7(\mathrm{D}) = y\delta_{7''} + (1 - y)\delta_{7'}$$

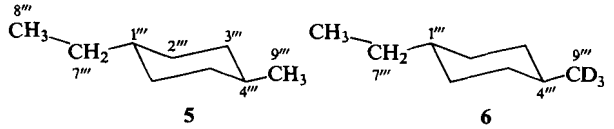
These equations give rise to

$$[1] \quad x - y = \frac{\delta_7(\mathrm{H}) - \delta_7(\mathrm{D})}{\delta_{7''} - \delta_{7'}}$$

Now the mole fraction x can be calculated for any temperature from the thermodynamic parameters previously determined (5) for Me and Et. The shifts $\delta_{7''}$ and $\delta_{7'}$ are known at eight temperatures between 160 and 194 K, and extrapolation of the two linear plots yields theoretical values for $\delta_{7''}$ and $\delta_{7'}$ at room temperature (298 K). Thus, provided that δ_7(H) − δ_7(D) can be measured, the mole fraction y can be calculated.

Equation [1] shows, as expected, that the sensitivity of the method of determining $(x - y)$ is a function of $(\delta_{7''} - \delta_{7'})$ i.e. of the ^{13}C nmr chemical shift difference, for the chosen carbon, between conformation **1** and conformation **2**. Carbon 7 was chosen for reasons already indicated, but two other carbons were considered, at C-1 and C-8. Carbon 8 was not useful because $(\delta_{8''} - \delta_{8'})$ is only 0.8 ppm, and although $(\delta_{1''} - \delta_{1'})$ is as great as 5.9 ppm, there is in this case the possibility of a direct isotope shift across 5 bonds.

The chemical shift difference δ_7(H) − δ_7(D) was determined from the ^{13}C nmr spectrum of a solution containing a *mixture* of *cis*-1-ethyl-4-methylcyclohexane **1** $\rightleftharpoons$ **2** and *cis*-1-ethyl-[4-*Me*-$^2H_3$]-4-methylcyclohexane **3** $\rightleftharpoons$ **4**. It was also essential to incorporate in this mixture the *trans*-isomers **5** and **6**. This allowed us to establish, under identical experimental conditions and for a similar structure,



5 **6**

Can. J. Chem. Downloaded from www.nrcresearchpress.com by 210.87.254.5 on 09/05/12
For personal use only.

that intrinsic isotope shifts do not extend across 6 bonds, and also to measure accurately the intrinsic isotope shifts observed across a smaller number of bonds.

In the mixture containing **1** ⇌ **2**, **3** ⇌ **4**, **5** and **6**, the ratio of *cis*-molecules to *trans*-molecules was approximately 2:1 for both nondeuterated and deuterated species, whereas the ratio of nondeuterated to deuterated species was 1:1 for both *cis*- and *trans*-molecules, i.e.

$$([\mathbf{1}] + [\mathbf{2}])/[\mathbf{5}] = ([\mathbf{3}] + [\mathbf{4}])/[\mathbf{6}] \simeq 2$$

$$([\mathbf{1}] + [\mathbf{2}])/([\mathbf{3}] + [\mathbf{4}]) = [\mathbf{5}]/[\mathbf{6}] = 1$$

Although the use of a molar ratio of 1:1 for nondeuterated to deuterated species optimized the conditions for resolution of signals separated by small isotope shifts, it prevented *assignment* of the signals. Consequently the crucial experiment was exactly repeated after increasing the proportion of deuterated species from 50% to 55%.

In the ^{13}C nmr spectrum of the mixture, recorded at 62.901 MHz, the signals for C-7 in **1** ⇌ **2**, and for C-7 in **3** ⇌ **4**, were well resolved; the separation was 2.21 Hz (0.035 ppm), the signal for the deuterated molecule **3** ⇌ **4** being at *lower* field. On the other hand the signals for C-7‴ in the *trans*-molecules **5** and **6** were not resolved. Therefore we attribute the difference in chemical shift for C-7 in **1** ⇌ **2** and **3** ⇌ **4** as arising solely from an alteration in the position of conformational equilibrium caused by replacement of CH_3 by C^2H_3. ^{13}C Chemical shifts for carbons in **1** ⇌ **2**, **3** ⇌ **4**, **5** and **6** are recorded in Tables 1 and 2. Direct, or intrinsic isotope effects accompanying the change **5** → **6** were observed for carbons 9, 4, 3(5), and 1. It is important to note that all the intrinsic isotope shifts accompanying the change $^1H \rightarrow {}^2H$ are *upfield*. Consequently it was particularly reassuring that the observed shift for C-7 in **3** ⇌ **4** was *downfield* of that in **1** ⇌ **2**. In fact this downfield shift, indicating that $\delta_7(4) - \delta_7(D)$ is negative, establishes conclusively that mole fraction y is greater than mole fraction x, for $(\delta_{7''} - \delta_{7'})$ is positive. Consequently, it is clear that the substituent C^2H_3 has a greater preference for the axial orientation than CH_3. The extent of this preference was expressed as an energy difference between $\Delta G°(C^2H_3)$ and $\Delta G°(CH_3)$ of 11.89 ± 1.46 cal mol^{-1} (49.79 ± 6.11 J mol^{-1}). The principal errors arise from the extrapolation needed to determine $(\delta_{7''} - \delta_{7'})$ at room temperature, and from the digitization of the spectrum (±0.092 Hz). It was estimated that the possible error in the extrapolation was ±15.725 Hz. However, since $(\delta_{7''} - \delta_{7'})$ is 441.635 Hz, the proportional error arising from the extrapolation is rather less than that in $\delta_7(H) - \delta_7(D)$ due to digitization.

The determined value of $\Delta G°(C^2H_3) - \Delta G°(CH_3)$ is very close to the value of 46 J mol^{-1} obtained by Baldry and Robinson (2) from ^{13}C nmr shifts in *trans*-[1-*Me*-$^2H_3$]1,3-dimethylcyclohexane, although these workers neglected intrinsic isotope effects across 5 bonds. The intrinsic isotope effects measured in the present study are given in Table 2. Wehrli *et al.* (7) claimed that intrinsic isotope shifts for ^{13}C occurred over as many as 6 bonds in [2-$^2H_1$] cyclodecanone. However, it is possible that these effects are due in part to the perturbation of a conformational equilibrium (8, 9). In this connection it is perhaps significant that whereas all the isotope-induced ^{13}C shifts of the present study are upfield, several of those observed by Wehrli *et al.* are downfield. Anet and Dekmezian (9) have observed deuterium-induced ^1H shifts over 5 bonds when an axial hydrogen and an axial CD_3 were *syn*-diaxial in a substituted 1,3-

TABLE 1. ^{13}C chemical shifts[a] at 62.901 MHz (δ values, ppm downfield from Me_4Si) for carbons in **1** ⇌ **2** and **3** ⇌ **4**

Carbons	**1** ⇌ **2**	**3** ⇌ **4**
1	37.580	37.612
2,6	28.718	28.718
3,5	31.209	31.153
4	30.519	30.259
7	27.231	27.266
8	11.930	11.930
9	20.298	19.342[b]

[a]Measured at 298 K on a mixture of **1** ⇌ **2**, **3** ⇌ **4**, **5** and **6** using 32K data points over 3012 Hz, giving a possible error due to digitization of ±0.092 Hz or ±0.001463 ppm.
[b]Septet, with $^1J(^{13}C—^2H) = 18.94$ Hz.

TABLE 2. ^{13}C chemical shifts[a] at 62.901 MHz (δ values, ppm downfield from Me_4Si) for carbons in **5** and **6**, and intrinsic isotope-induced shifts *I*

Carbons	**5**	**6**	*I* (ppm)
1‴	39.644	39.632	−0.012
2‴, 6‴	33.313	33.313	0[c]
3‴, 5‴	35.762	35.686	−0.076
4‴	33.275	33.038	−0.237
7‴	30.291	30.291	0[c]
8‴	11.527	11.527	0[c]
9‴	22.803	21.876[b]	−0.927

[a]Measured at 298 K on a mixture of **1** ⇌ **2**, **3** ⇌ **4**, **5** and **6** using 32K data points over 3012 Hz, giving a possible error due to digitization of ±0.092 Hz or ±0.001463 ppm.
[b]Septet, with $^1J(^{13}C—^2H) = 18.94$ Hz.
[c]No separation observed.

Can. J. Chem. Downloaded from www.nrcresearchpress.com by 210.87.254.5 on 09/05/12
For personal use only.

dioxane. However, the same compound did not reveal deuterium-induced 4-bond or 5-bond ^{13}C shifts.

The solvents used in this study were $CDCl_3$ and $CFCl_3$–$CDCl_3$ (9:1 v/v). The addition of $CFCl_3$ to $CDCl_3$ is required to allow measurements at temperatures below 200 K, but the volatility of $CFCl_3$ poses problems when accumulations are made over long periods at room temperature. Consequently low temperature spectra were determined in $CFCl_3$–$CDCl_3$ whereas room temperature spectra employed neat $CDCl_3$. Chemical shift data for several alkylcyclohexanes have shown that only small changes (generally deshielding) accompany the change from $CFCl_3$–$CDCl_3$ to $CDCl_3$. For example, the ^{13}C nmr chemical shifts (at 302 K) for carbons in *trans*-1-ethyl-4-methylcyclohexane, **5**, measured on the same instrument, are listed in Table 3 for the two solvents. As anticipated, the largest solvent-induced changes are for carbons on the periphery of the molecule; the changes for ring carbons are insignificant. Bearing in mind that ($\delta_{7''} - \delta_{7'}$) for the system **1** ⇌ **2** is as great as 7.02 ppm, the error for this parameter in using a value taken from a determination in $CFCl_3$–$CDCl_3$ (rather than $CDCl_3$) is negligible.

Experimental

Spectra

The ^1H nmr spectra were measured at 99.8 MHz on a JEOL JNM-MH-100 spectrometer; ^2H nmr spectra were measured in $CHCl_3$ on a JEOL JNM-PS-100 spectrometer interfaced to a Nicolet 1085 20 K computer; the reference was $CDCl_3$ (δ = 7.17 ppm). The ^{13}C nmr spectra were recorded on the JEOL JNM-PS-100 instrument at 25.15 MHz and on a Bruker WM 250 spectrometer at 62.901 MHz. Low temperature ^{13}C nmr spectra were recorded as described previously (5).

Materials

The preparations of *cis*- and *trans*-1-ethyl-4-methylcyclohexane have been reported elsewhere (6).

TABLE 3. ^{13}C chemical shifts[a] at 25.147 MHz (δ values, ppm downfield from Me_4Si) for carbons in **5**

	Solvent	
Carbons	$CFCl_3/CDCl_3$[b]	$CDCl_3$
1‴	39.490	39.490
2‴, 6‴	33.179	33.176
3‴, 5‴	35.607	35.613
4‴	33.179	33.176
7‴	30.218	30.229
8‴	11.408	11.578
9‴	22.815	22.831

[a]Measured at 302 K using 8K data points over 2500 Hz.
[b]Proportions 9:1 by volume.

Methyl cis- *and* trans-*4-Ethylcyclohexanecarboxylate*

4-Ethylbenzoic acid (4.4723 g) was hydrogenated over platinum oxide (0.203 g) in glacial acetic acid (25 cm^3) at room temperature and atmospheric pressure. After 18 h the uptake of hydrogen was 2133 cm^3 (theoretical 2000 cm^3). The mixture was filtered and acetic acid was removed under vacuum. Distillation of the residue gave a mixture of *cis*- and *trans*-4-ethylcyclohexanecarboxylic acid (3.5714 g, 79%) as a colourless oil, bp 88–94°C at 0.3 Torr (ref. 10 gives *cis*-, bp 127°C at 5 Torr and *trans*-, mp 49–49.8°C). Thin-layer chromatography on silica gel with $CHCl_3$–MeOH 95:5 gave 2 spots with R_f values 0.24 (major) and 0.06. The ^1H nmr spectrum in $CDCl_3$ showed signals for the 1-hydrogen at δ 2.64 (*cis*, quintet with separations of about 5 Hz) and δ 2.30 (*trans*, triplet of triplets with separations of 12 Hz and 3.5 Hz). Mass spectrometry gave M^+ 156.1120 ($C_9H_{16}O_2$ requires 156.1150).

The above mixture (2.50 g) was refluxed for 4 h with dry methanol (2.3 cm^3, 1.80 g) and concentrated sulphuric acid (0.15 cm^3). After addition of water (10 cm^3) the mixture was extracted several times with ether. The combined ether extracts were washed successively with saturated aqueous $NaHCO_3$ solution and saturated aqueous NaCl solution. Finally the ether was dried ($MgSO_4$), filtered, and distilled, leaving a residue of *cis*- and *trans*-4-ethylcyclohexanecarboxylate (2.418 g, 89%). A small sample was distilled as a pale yellow oil with an aniseed-like odour, bp 50°C (bath temp) at 14 Torr; tlc showed two spots, R_f 0.69 (major) and 0.06. The ^1H nmr spectrum showed the methoxy protons as singlets at δ 3.78 (*cis*-, major) and δ 3.76 (*trans*-), and the 1-hydrogen at δ 2.56 (*cis*-, quintet with separations of about 5 Hz) and δ 2.26 (*trans*-, triplet of triplets with separations of 12 Hz and 3.5 Hz). Mass spectrometry gave M^+ 170.1286 ($C_{10}H_{18}O_2$ requires 170.1307). Microanalysis yielded C 70.25, H 10.35; $C_{10}H_{18}O_2$ requires C 70.55, H 10.65%.

cis- *and* trans-*4-Ethylcyclohexane[α,α-$^2H_2$]methanol*

Lithium aluminium deuteride (0.9741 g, 0.0232 mol) was stirred in dry redistilled ether (40 cm^3) under argon. A solution of methyl *cis*- and *trans*-4-ethylcyclohexanecarboxylate (5.4107 g, 0.0318 mol) in dry ether (35 cm^3) was added to the slurry of $LiAl^2H_4$ at a rate sufficient to maintain boiling. After completion of the addition, the mixture was stirred for 10 min, cooled in ice, and quenched by addition of iced water (9 cm^3). Two molar H_2SO_4 (45 cm^3) was added and the mixture was extracted several times with ether. Distillation of the dried (K_2CO_3) extracts gave a mixture of *cis*- and *trans*-4-ethylcyclohexane[α,α-$^2H_2$]methanol (4.12 g, 0.0286 mol, 90%) as a colourless oil, bp 100°C (bath temp) at 0.1 Torr. The ^2H nmr spectrum showed a singlet at δ 3.27. Mass spectrometry gave $M^+ - H_2O$ at 126.1366 ($C_9{}^1H_{14}{}^2H_2$ requires 126.1378). Microanalysis gave C 74.7, H 13.65; $C_9{}^1H_{16}{}^2H_2O$ requires C 74.95, H 13.95%.

cis- *and* trans-*4-Ethylcyclohexanemethanol*

A similar experiment to the above, using a mixture of methyl *cis*- and *trans*-4-ethylcyclohexanecarboxylate (1.70 g) and lithium aluminium hydride (0.3008 g) gave *cis*- and *trans*-4-ethylcyclohexanemethanol (1.3805 g, 97%), bp 50°C (bath temp) at 0.005 Torr. The ^1H nmr spectrum showed the protons of —CH_2—O as doublets (with separations of 6.5 and 5.8 Hz) at δ 3.56 (*cis*-, major) and δ 3.45 (*trans*-), respectively. The mass spectrum gave $M^+ - H_2O$ at 124.1241 (C_9H_{16} requires 124.1252). Microanalysis yielded C 75.7, H 12.35; $C_9H_{18}O$ requires C 76.0, H 12.75%.

cis- *and* trans-*4-Ethylcyclohexane[α,α-$^2H_2$]methanol 4′-Methylbenzenesulphonate*

4-Methylbenzenesulphonyl chloride was purified by dissolution in ether and repeated washing with aqueous sodium carbo-

Can. J. Chem. Downloaded from www.nrcresearchpress.com by 210.87.254.5 on 09/05/12
For personal use only.

nate (1 *M*) until the pH of the ether exceeded 6.0. The ether solution was dried over anhydrous Na_2SO_4, filtered, and evaporated. The crystals of pure sulphonyl chloride were crushed and dried under high vacuum.

The mixture of *cis*- and *trans*-4-ethylcyclohexane [α,α-$^2H_2$]methanol (7.009 g, 0.0486 mol) was dissolved in dry (KOH), redistilled pyridine (15.36 g) at 0°C. To the stirred mixture was added 4-methylbenzenesulphonyl chloride (10.2011 g, 0.0535 mol) in portions during 30 min. The mixture was stirred for 2 h at 2°C and then for a further 1.5 h as the temperature was allowed to rise to 14°C. A mixture of concentrated hydrochloric acid (30 cm^3) and ice water (100 g) was added to the white, pasty reaction mixture. Several extracts with ether were combined, dried ($MgSO_4$), filtered, and evaporated. The residue of *cis*- and *trans*-4-ethylcyclohexane [α,α-$^2H_2$]methanol 4′-methyl benzenesulphonate (14.71 g, 102%) was a colourless oil contaminated with ether. An attempted distillation of a small portion at 1 Torr caused decomposition. The ^2H nmr spectrum gave signals at δ 3.88 (—CD_2O—, *cis*-) and δ 3.65 (—CD_2O—, *trans*-). The mass spectrum gave M^+ at 298.1594 ($C_{16}{}^1H_{22}{}^2H_2O_3S$ requires 298.1572). Microanalysis yielded C 64.05, H 9.0; $C_{16}{}^1H_{22}{}^2H_2O_3S$ requires C 64.4, H 8.8%.

cis- *and* trans-*4-Ethylcyclohexanemethanol 4′-Methylbenzenesulphonate*

An experiment similar to the above, using a mixture of *cis*- and *trans*-4-ethylcyclohexanemethanol (1.33 g, 0.00937 mol) and 4-methylbenzenesulphonyl chloride (1.98 g, 0.0103 mol) gave *cis*- and *trans*-4-ethylcyclohexanemethanol 4′-methylbenzenesulphonate (2.5992 g, 0.00878 mol, 94%) as a colourless oil. The ^1H nmr spectrum included doublets (separations 7 and 6 Hz) at δ 4.00 (—CH_2O—, *cis*-) and δ 3.88 (—CH_2O—, *trans*-), respectively. The mass spectrum gave M^+ as 296.1429 ($C_{16}H_{24}O_3S$ requires 296.1446). Microanalysis yielded C 64.4, H 8.0; $C_{16}H_{24}O_3S$ requires C 64.85, H 8.15%.

cis- *and* trans-*1-Ethyl-4[*Me-$^2H_3$*]methylcyclohexane*

Lithium aluminium deuteride (2.4618 g, 0.0568 mol) was stirred in dry, redistilled ether (56 cm^3) under argon. The mixture of *cis*- and *trans*-4-ethylcyclohexane [α,α-$^2H_2$]methanol 4′-methylbenzenesulphonate (14.30 g, 0.0480 mol), dissolved in dry, redistilled ether (140 cm^3) was added to the slurry of $LiAl^2H_4$ at 20°C. The mixture was heated under reflux, with stirring, for 2.5 h during which time a precipitate appeared. The reaction mixture was poured into ice water (24 cm^3) and aqueous sulphuric acid (210 cm^3, 2 *M*) was added. Several ether extracts were combined, dried ($MgSO_4$), filtered, and distilled, giving a mixture of *cis*- and *trans*-1-ethyl-4[*Me*-$^2H_3$] methylcyclohexane (4.2642 g, 0.0331 mol, 78%) as a colourless oil, bp 140–144°C. Mass spectrometry gave M^+ at 129.1574 ($C_9{}^1H_{15}{}^2H_3$ requires 129.1597). A complete separation was achieved by preparative gas–liquid chromatography, as described earlier (6). In the ^1H nmr spectrum, *cis*-1-ethyl-4[*Me*-$^2H_3$]methylcyclohexane gave a triplet, separations 6 Hz, at δ 0.88 (CH_3); the *trans*-1-ethyl-4[*Me*-$^2H_3$]methylcyclohexane gave a triplet, separations 6 Hz, at δ 0.86 (CH_3). The ^2H nmr spectra gave singlets at δ 0.96 (C^2H_3, *cis*-) and δ 0.90 (C^2H_3, *trans*-).

Calculation of Thermodynamic Parameters

(a) Low Temperature Area Method

Low temperature ^{13}C nmr spectra were recorded for *cis*-1-ethyl-4[*Me*-$^2H_3$] methylcyclohexane **3** ⇌ **4** as indicated previously (5) for the corresponding nondeuterated compound. The results are summarized below (equilibrium constant K = [**4**]/[**3**]).

T (K)	T^{-1} (K^{-1})	K	ln K
169	0.005912	1.218	0.1968
173	0.005775	1.219	0.1976
177	0.005645	1.179	0.1647
182	0.005505	1.164	0.1515
186	0.005386	1.147	0.1368
190	0.005273	1.142	0.1327

The data were analyzed as described elsewhere (5). Bearing in mind the following experimentally derived parameters for the ethyl group: 1.60 ± 0.06 kcal mol^{-1} for $-\Delta H°$ and 0.64 ± 0.35 cal K^{-1} mol^{-1} for $\Delta S°$, and on the reasonable assumption of additivity, we obtain the following:

$$-\Delta H°(C^2H_3) = 1.79 \pm 0.07 \text{ kcal mol}^{-1}$$

(plot method)

$$-\Delta H°(C^2H_3) = 1.85 \pm 0.07 \text{ kcal mol}^{-1}$$

(curve fit method)

Averaged value for $-\Delta H°(C^2H_3) = 1.82 \pm 0.07$ kcal mol^{-1}.

$$\Delta S°(C^2H_3) = -0.10 \pm 0.32 \text{ cal K}^{-1} \text{ mol}^{-1}$$

(plot)

$$\Delta S°(C^2H_3) = -0.45 \pm 0.39 \text{ cal K}^{-1} \text{ mol}^{-1}$$

(curve fit)

Averaged value for $\Delta S°(C^2H_3) = -0.28 \pm 0.40$ cal K^{-1} mol^{-1}.

(b) Room Temperature Chemical Shift Method

Measurements gave

$$\nu_7(H) - \nu_7(D) = -2.21 \text{ Hz}$$

at 62.901 MHz and 298 K. Thus

$$\delta_7(H) - \delta_7(D) = -0.035134 \text{ ppm}$$

Graph extrapolation gave

$$\delta_{7''} - \delta_{7'} = 7.0211125 \text{ ppm}$$

at 298 K. From [1], $x - y = -0.0050041$. From the previously determined (5) values of $\Delta G°(CH_3)$, $\Delta S°(CH_3)$, $\Delta G°(Et)$, and $\Delta S°(Et)$, we deduce that mole fraction $x = 0.5209961$ at 298 K, and equilibrium constant K for **1** ⇌ **2** is 0.91940 at 298 K.

Hence mole fraction $y = 0.5260002$ at 298 K and equilibrium constant K for **3** ⇌ **4** is 0.90114 at 298 K. Thus

$$\Delta G°(C^2H_3) - \Delta G°(Et) = RT \ln 0.90114$$
$$= 61.554181 \text{ cal mol}^{-1}$$

at 298 K

Now

$$\Delta G°(CH_3) - \Delta G°(Et) = 49.660000 \text{ cal mol}^{-1} \text{ at 298 K}$$

Hence

$$\Delta G°(C^2H_3) - \Delta G°(CH_3) = 11.894181 \text{ cal mol}^{-1} \text{ at 298 K}$$

Since possible errors are ±0.001463 ppm in digitization and ±0.25 ppm in the extrapolation to find $(\delta_{7''} - \delta_{7'})$, the final result may be expressed as

$$\Delta G°(C^2H_3) - \Delta G°(CH_3) = 11.89 \pm 1.46 \text{ cal mol}^{-1} \text{ or } 49.79 \pm 6.11 \text{ J mol}^{-1}$$

1. H. Booth and J. R. Everett. Can. J. Chem. **58**, 2709 (1980).
2. K. W. Baldry and M. J. T. Robinson. Tetrahedron, **33**, 1663 (1977).
3. S.-F. Lee, G. Barth, K. Kieslich, and C. Djerassi. J. Am. Chem. Soc. **100**, 3965 (1978).
4. S.-F. Lee, G. Barth, and C. Djerassi. J. Am. Chem. Soc. **100**, 8010 (1978).
5. H. Booth and J. R. Everett. J. Chem. Soc. Perkin Trans. II, 255 (1980).
6. H. Booth, J. R. Everett, and R. A. Fleming. Org. Magn. Reson. **12**, 63 (1979).
7. F. W. Wehrli, D. Jeremic, M. Mihailovic, and S. Milosavljevic. J. Chem. Soc. Chem. Commun. 302 (1978).
8. F. A. L. Anet, A. K. Cheng, and D. Krane. J. Am. Chem. Soc. **95**, 7877 (1973).
9. F. A. L. Anet and A. H. Dekmezian. J. Am. Chem. Soc. **101**, 5449 (1979).
10. N. L. Allinger and C. A. Freiburg. J. Org. Chem. **31**, 894 (1979).

Can. J. Chem. Downloaded from www.nrcresearchpress.com by 210.87.254.5 on 09/05/12
For personal use only.

Catalytic reduction of dimeric acetylated 2-deoxy-2-nitroso-α-D-glycopyranosyl chlorides

T. L. NAGABHUSHAN

Schering-Plough Corporation, 60 Orange Street, Bloomfield, NJ 07003, U.S.A.

Received July 7, 1980

This paper is dedicated to Prof. Raymond U. Lemieux on the occasion of his 60th birthday

T. L. NAGABHUSHAN. Can. J. Chem. **58**, 2720 (1980).

Reduction of tri-*O*-acetyl-2-deoxy-2-nitroso-α-D-glucopyranosyl chloride dimer with hydrogen and platinum oxide in the presence of methanol or ethanol afforded the corresponding alkyl tri-*O*-acetyl-2-amino-2-deoxy-β-D-glucopyranoside hydrochloride. In the absence of an alcohol the product was tri-*O*-acetyl-2-amino-1,5-anhydro-2-deoxy-D-glucitol hydrochloride. The glycosylation/reduction process gave similar results with the *galacto* isomer.

A method is described for the ready and large-scale synthesis of D-galactosamine hydrochloride.

T. L. NAGABHUSHAN. Can. J. Chem. **58**, 2720 (1980).

La réduction du dimère du chlorure de tri-*O*-acétyl déoxy-2 nitroso-2 α-D-glucopyrannosyle par l'hydrogène et l-oxyde de platine en présence de méthanol ou d'éthanol conduit au chlorhydrate du tri-*O*-acétyl amino-2 déoxy-2 β-D-glucopyrannoside d'alkyle. En l'absence d'un alcool, le produit de la réduction est le chlorhydrate du tri-*O*-acétyl amino-2 anhydro-1,5 déoxy-2 D-glucitol. La réaction de glycosylation/réduction a donné des résultats analogues avec l'isomère de la série *galacto*.

On décrit une méthode simple de synthèse du chlorhydrate de D-galactosamine appropriée à l'échelle industrielle.

[Traduit par le journal]

Reactions of dimeric acetylated 2-deoxy-2-nitroso-α-D-glycopyranosyl chlorides reported here are new and render syntheses of methyl (and ethyl) β-D-glycosaminides and 2-amino-1,5-anhydro-2-deoxy-D-glycitols readily accomplished. The former reaction is particularly useful for large-scale production of D-galactosamine hydrochloride.

Hydrogenation of 3,4,6-tri-*O*-acetyl-2-deoxy-2-nitroso-α-D-glucopyranosyl chloride (**1**) (1) in a mixture of tetrahydrofuran and methanol or dioxane and methanol using platinum oxide as the catalyst afforded methyl 3,4,6-tri-*O*-acetyl-2-amino-2-deoxy-β-D-glucopyranoside hydrochloride (**2**) as a crystalline compound in 70% yield. Evidence for its structure was obtained by the preparation of known crystalline derivatives **3**–**6**, using standard procedures (Table 1). Similarly, reduction of 3,4,6-tri-*O*-acetyl-2-deoxy-2-nitroso-α-D-galactopyranosyl chloride (**7**) (1) provided methyl 3,4,6-tri-*O*-acetyl-2-amino-2-deoxy-β-D-galactopyranoside hydrochloride (**8**), also in 70% yield. Structure of **8** was, likewise, proved by conversion to the crystalline derivatives **9**–**12** (Table 1).

When the reductions of **1** and **7** were carried out in the presence of ethanol instead of methanol, the ethyl 3,4,6-tri-*O*-acetyl-2-amino-2-deoxy-β-D-glucopyranoside hydrochloride (**15**) and its *galacto* isomer **16** were obtained, respectively, in reasonably good yields (50%) (Table 1). With higher alcohols, however, the yields dropped drastically.

Catalytic hydrogenation of **1** in the absence of an alcohol afforded a crystalline compound in 40% yield which was shown to be 3,4,6-tri-*O*-acetyl-2-amino-1,5-anhydro-2-deoxy-D-glucitol hydrochloride (**13**) by proton magnetic resonance spectroscopy and conversion to the known tetraacetate **14** (Table 1). Thus, in the ^{1}Hmr spectrum the three *O*-acetyl groups appeared as singlets at δ 2.17 and δ 2.13 in the ratio 1:2. H-3 and H-4 showed triplets at δ 5.35 ($J_{2,3}$ = 9.0 Hz) and δ 5.03 ($J_{3,4}$ = 9.0 Hz), respectively. The remainder of the protons appeared as superimposed multiplets between δ 4.4 and δ 3.6.

The ease of reduction, retention of the equatorial stereochemistry at the 2-position, and the exclusive formation of the β-glycosidic linkage preclude isomerization of the nitroso dimer to the oxime form prior to reduction (2). It is thought that the observed stereoselective β-glycosaminide formation in the current work proceeds in three stages. First, the nitroso dimer is rapidly reduced to the azoxy structure. There is precedence for this, as shown by Lemieux *et al.* (3), who actually isolated the azoxy chlorides following careful hydrogenation of the dimeric forms of acetylated 2-deoxy-2-nitroso-α-D-glycopyranosyl chlorides in dioxane using a weak hydrogenation catalyst. It is recalled that, under proper conditions, dimeric nitrosyl chloride adducts of acetylated glycals react with alcohols by way of the nitroso-glycal intermediates formed through a series of reactions involving dissociation to the monomeric form, isomerization to the oximinochloride, and elimination of hydrogen chloride (2). In the second stage, the α-chloride reacts with the alcohol in the presence of the

0008-4042/80/232720-04$01.00/0

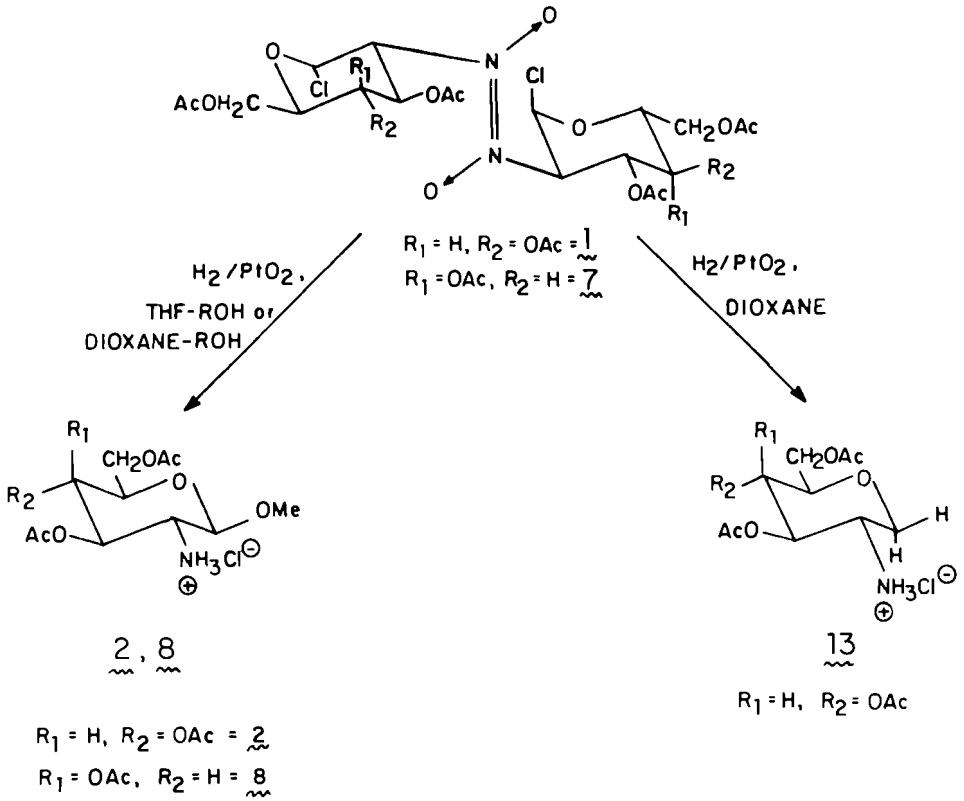
©1980 National Research Council of Canada/Conseil national de recherches du Canada

Can. J. Chem. Downloaded from www.nrcresearchpress.com by 210.87.254.40 on 09/05/12
For personal use only.

Can. J. Chem. Downloaded from www.nrcresearchpress.com by 210.87.254.40 on 09/05/12
For personal use only.

TABLE 1. Derivatives of D-glucosamine and D-galactosamine hydrochlorides

Compound	Structure	Melting point °C		$[\alpha]_D°$ (c, Solvent)		Analysis %							
						Calculated				Found			
		Determined	Literature (reference)	Determined	Literature (reference)	C	H	Cl	N	C	H	Cl	N
Methyl 3,4,6-tri-*O*-acetyl-2-amino-2-deoxy-β-D-glucopyranoside hydrochloride	2	222–223	233(12)	+19.6 (1.33, Methanol)	+17 (Methanol)(12)	43.90	6.18	9.96	3.93	43.75	6.05		4.08
Methyl 2-acetamido-3,4,6-tri-*O*-acetyl-2-deoxy-β-D-glucopyranoside	3	160–162	163(5)	−18.06 (1.55, Methanol)	−22 (Methanol)(5)	49.84	6.37		3.87	50.15	6.30		4.04
D-Glucosamine hydrochloride	4	190–212	190–210(6)	+71.4 (1, Water, final)	+72 (Water, final)(6)								
Methyl 2-acetamido-2-deoxy-β-D-glucopyranoside	5	200–202	204(5)	−46.9 (2, Water)	−47.1 (Water)(7)	45.97	7.35		5.95	46.05	7.16		6.15
Methyl 2-amino-2-deoxy-β-D-glucopyranoside hydrochloride	6	190–191	190(7)	−28.4 (0.92, Water)	−24.2 (Water)(7)	36.63	6.97	15.44	6.10	36.60	6.82	15.14	6.00
Methyl 3,4,6-tri-*O*-acetyl-2-amino-2-deoxy-β-D-galactopyranoside hydrochloride	8	232–238(dec.)		+25.9 (2.91, Water)		43.90	6.18	9.96	3.93	44.09	6.21	10.10	4.05
Methyl 2-acetamido-3,4,6-tri-*O*-acetyl-2-deoxy-β-D-galactopyranoside	9	211–213	216–217(8)	−17.5 (2.86, Chloroform)	−17 (Chloroform)(8)	49.84	6.37		3.87	49.54	6.85		3.28
D-Galactosamine hydrochloride	10	183(dec.)	Near 178(dec.)(9)	+91 (1.14, Water, final)	+93 (Water, final)(9)								
Methyl 2-acetamido-2-deoxy-β-D-galactopyranoside	11	223–224(dec.)	191–193(8)	−11.71 (2.29, Methanol)	−12 (Methanol)(8)	45.97	7.35		5.95	45.65	7.21		5.90
Methyl 2-amino-2-deoxy-β-D-galactopyranoside hydrochloride	12	195(dec.)		±0 (1.36, Water)		36.63	6.97	15.44	6.10	36.91	6.81	15.12	6.29
3,4,6-Tri-*O*-acetyl-2-amino-1,5-anhydro-2-deoxy-D-glucitol hydrochloride	13	235–240(dec.)				44.23	6.14	10.90	4.30	44.13	6.34	11.08	4.22
2-Acetamido-3,4,6-tri-*O*-acetyl-1,5-anhydro-2-deoxy-D-glucitol	14	165	164(10)	±0 (0.9, Chloroform)	±0 (Chloroform)(10)	50.75	6.34		4.22	50.69	6.14		4.01
Ethyl 3,4,6-tri-*O*-acetyl-2-amino-2-deoxy-β-D-glucopyranoside hydrochloride	15	237–238(dec.)		+14.4 (1.04, Water)		45.49	6.49	9.59	3.78	45.85	6.27	9.86	3.97
Ethyl 3,4,6-tri-*O*-acetyl-2-amino-2-deoxy-β-D-galactopyranoside hydrochloride	16	243–244(dec.)		+20.9 (1.0, Water)		45.49	6.49	9.59	3.78	45.40	6.61	9.70	3.96
Ethyl 2-acetamido-3,4,6-tri-*O*-acetyl-2-deoxy-β-D-glucopyranoside	17	169–171	167(11)	−24.4 (2.4, Methanol)	−25 (Methanol)(11)	51.20	6.66		3.73	51.35	6.94		3.71
Ethyl 2-acetamido-3,4,6-tri-*O*-acetyl-2-deoxy-β-D-galactopyranoside	18	224–226	225–226(8)	−19.9 (2.4, Methanol)	−19 (Methanol)(8)	51.20	6.66		3.73	51.28	6.82		3.70



catalyst with inversion of configuration and liberation of hydrogen chloride. Finally, the azoxy β-glycoside is reduced in the presence of the acid to give β-glycosaminide hydrochlorides. In the absence of a nucleophile, however, the azoxychlorides undergo hydrogenolysis at the anomeric center and further reduction to give 2-amino-1,5-anhydro-2-deoxy-glycitol hydrochlorides. The mechanisms of these reactions are under study with the hope that a general method can be developed for syntheses of β-glycosaminides from glycals.

Experimental

All melting points are uncorrected. Infrared spectra were measured with a Perkin-Elmer Model 137 "Infracord" spectrophotometer. Optical rotations were determined using a Carl Zeiss circular polarimeter Model 0.01°. Elemental analyses were performed by Dr. G. Weiler and Dr. F. B. Strauss, Microanalytical Laboratory, Oxford, England. Solvents were removed *in vacuo* at 45°C.

Physical constants and elemental analyses of the following compounds are given in Table 1.

Methyl 3,4,5-Tri-O-acetyl-2-amino-2-deoxy-β-D-glucopyranoside Hydrochloride (2) and its galacto *Isomer 8*

To a solution of freshly prepared dimeric 3,4,6-tri-*O*-acetyl-2-deoxy-2-nitroso-α-D-glucopyranosyl chloride (**1**, 3 g) (1) in dry tetrahydrofuran (17 mL) was added anhydrous methanol (20 mL) with vigorous swirling of the flask to prevent crystallization of **1**. (If the solution is not clear, a few drops of tetrahydrofuran are added. In no case should the mixture be warmed to get a clear solution.) The mixture was hydrogenated in the presence of platinum oxide catalyst (0.2 g, Engelhard Industries of Canada Ltd., Toronto, Canada) at atmospheric pressure and room temperature until the consumption of hydrogen ceased (12–15 h). The catalyst was removed by filtration through a bed of Celite and washed with water. The combined filtrates were concentrated and the residue dried. Crystallization of the product from methanol–ether provided 2.2 g (70%) of pure **2**.

In a similar manner the *galacto* isomer **8** was obtained in 70% yield by the hydrogenation of a solution of **7** (3 g) (1) in a mixture of tetrahydrofuran (10 mL) and methanol (20 mL).

Methyl 2-Acetamido-3,4,6-tri-O-acetyl-2-deoxy-β-D-glucopyranoside (3) and its galacto *Isomer 9*

To a stirred solution of **2** (or **8**) (7.08 g) in water (16 mL) was added methanol (8 mL). The solution was cooled to 5°C and acetic anhydride (6.0 mL) was added followed by sodium carbonate (2.12 g). After 1 h, the cooling bath was removed and the mixture stirred for an additional 0.5 h. The mixture was concentrated and partitioned between chloroform (30 mL) and water. The organic layer was dried over sodium sulfate, evaporated to dryness, and crystallized from isopropanol to give 6.0 g (83.3%) of pure **3**. The *galacto* isomer **9** was crystallized in 89% yield from ethanol.

Methyl 2-Acetamido-2-deoxy-β-D-glucopyranoside (5) and its galacto *Isomer 11*

Triethylamine (3 mL) was added to a solution of **3** (or **9**) (1 g) in methanol (6 mL) and water (5 mL). The mixture was set aside for 18 h at room temperature. The solvents were removed and the residue dried and crystallized from methanol–ether to afford 0.6 g (94%) of pure **5**. The yield of the crystalline *galacto* isomer **11** (from methanol–ether) was 0.59 g (90.8%).

Can. J. Chem. Downloaded from www.nrcresearchpress.com by 210.87.254.40 on 09/05/12
For personal use only.

D-Glucosamine (4) and D-Galactosamine (10) Hydrochlorides

These were prepared by acid hydrolysis of **3** and **9** respectively (4).

Methyl 2-Amino-2-deoxy-β-D-glucopyranoside Hydrochloride (6) and its galacto *Isomer 12*

O-Deacetylation of **2** (or **8**) (0.711 g) with triethylamine (2 mL) in methanol (2 mL) and water (2 mL), as above, afforded a syrup which was dissolved in a little methanol and acidified with 1 *N* methanolic hydrogen chloride. Removal of the solvent and crystallization of the residue from ethanol–acetone provided pure **6**, 0.348 g (76%) or **12**, 0.4 g (87.3%).

3,4,6-Tri-O-acetyl-2-amino-1,5-anhydro-2-deoxy-D-glucitol Hydrochloride (13)

A solution of **1** (1.35 g) (1) in dioxane (15 mL) was hydrogenated in the presence of platinum oxide catalyst (0.5 g) at 60 psi for 18 h. The catalyst was removed by filtration through a bed of Celite and washed with a little dioxane. The filtrate was discarded. The filter cake was next washed thoroughly with water and removal of water afforded a white crystalline compound. The compound was dried and recrystallized from methanol–ether to yield 0.49 g (37.7%) of pure **13**.

2-Acetamido-3,4,6-tri-O-acetyl-1,5-anhydro-2-deoxy-D-glucitol (14)

N-Acetylation of **13** in a manner similar to the one described above for the preparation of **3** afforded **14** in 90% yield.

Ethyl 3,4-6-Tri-O-acetyl-2-amino-2-deoxy-β-D-glucopyranoside Hydrochloride (15) and its galacto *Isomer 16*

These were prepared in essentially the same manner as **2** except that dioxane (10 mL) and absolute ethanol (20 mL) were used as cosolvents. The products **15** and **16** obtained in 50% yield from **1** and **8**, respectively, crystallized from methanol – excess ether on standing for a prolonged period of time at 4°C.

Ethyl 2-Acetamido-3,4,6-tri-O-acetyl-2-deoxy-β-D-glucopyranoside (17) and its galacto *Isomer 18*

N-Acetylations of **15** and **16** were performed as mentioned earlier. The yields of **17** and **18** were 85% and 82%, respectively. Acid hydrolysis of these compounds (4) and paper chromatographic analysis of the hydrolysates using butanol, pyridine, and water (6:4:3) as the mobile phase showed single ninhydrin and $AgNO_3$–NaOH positive spots which were indistinguishable from those of authentic **4** and **10**, respectively.

1. R. U. LEMIEUX and T. L. NAGABHUSHAN. Methods in carbohydrate chemistry. Vol. VI. *Edited by* R. L. Whistler and J. N. BeMiller. Academic Press, New York. 1972. p. 487.
2. R. U. LEMIEUX, Y. ITO, K. JAMES, and T. L. NAGABHUSHAN. Can. J. Chem. **51**, 7 (1973).
3. R. U. LEMIEUX, T. L. NAGABHUSHAN, and I. K. O'NEILL. Can. J. Chem. **46**, 413 (1967).
4. A. THOMPSON and M. L. WOLFROM. Methods in carbohydrate chemistry. Vol. II. *Edited by* R. L. Whistler and M. L. Wolfrom. Academic Press, New York. 1963. p. 219.
5. D. M. LEABACK and P. G. WALKER. J. Chem. Soc. 4754 (1957).
6. R. KUHN, W. BISTER, and H. FISCHER. Ann. **617**, 109 (1958).
7. J. C. IRVINE and H. C. HYND. J. Chem. Soc. **103**, 41 (1913).
8. Z. TARASIEJSKA and R. W. JEANLOZ. J. Am. Chem. Soc. **80**, 6325 (1958).
9. R. W. JEANLOZ and P. J. STOFFYN. Methods in carbohydrate chemistry. Vol. II. *Edited by* R. L. Whistler and M. L. Wolfrom. Academic Press, New York. 1962. p. 227.
10. D. HORTON and M. L. WOLFROM. J. Org. Chem. **27**, 1794 (1962).
11. F. MICHEEL, F. P. VAN DE KAMP, and H. PETERSEN. Chem. Ber. **90**, 521 (1957).
12. G. FODOR and L. OTVOS. Acta Chim. Acad. Sci. Hung. **5**, 205 (1954).

Can. J. Chem. Downloaded from www.nrcresearchpress.com by 210.87.254.40 on 09/05/12
For personal use only.

Structure of the type XXXIII *Streptococcus pneumoniae* (pneumococcal) capsular polysaccharide[1]

LARRY G. BENNETT[2] AND CLAUDE T. BISHOP

Division of Biological Sciences, National Research Council of Canada, Ottawa, Ont., Canada K1A 0R6

Received July 10, 1980

This paper is dedicated to Prof. Raymond U. Lemieux on the occasion of his 60th birthday

LARRY G. BENNETT and CLAUDE T. BISHOP. Can. J. Chem. **58**, 2724 (1980).

The type XXXIII *Streptococcus pneumoniae* (pneumococcal) capsular polysaccharide contains D-glucose (2 mol), D-galactose (1 mol), D-glucuronic acid (1 mol), and 2-acetamido-2-deoxy-D-mannose (1 mol). Structural investigations by methylation analysis, specific degradations, and nmr spectroscopy showed that the repeating unit was a linear pentasaccharide of the following structure: →3)-α-D-Gal*p*-(1→3)-β-D-Man*p*NAc-(1→4)-α-D-Glc*p*-(1→4)-β-D-Glc*p*-(1→4)-α-D-Glc*p*A-(1→.

LARRY G. BENNETT et CLAUDE T. BISHOP. Can. J. Chem. **58**, 2724 (1980).

Le polysaccharide capsulaire du *Streptococcus pneumonial* (pneumocoque) de type XXXIII contient du D-glucose (2 mol), du D-galactose (1 mol), de l'acide D-glucoronique (1 mol) et l'acétamido-2 déoxy-2 D-mannose (1 mol). Les études de structures réalisées par l'anaylse des méthylations, par des dégradations spécifiques et par la spectroscopie de rmn montrent que le motif monomère est un pentasaccharide linéaire ayant la structure suivante: →3)-α-D-Gal*p*-(1→3)-β-D-Man*p*NAc-(1→4)-α-D-Glc*p*-(1→4)-β-D-Glc*p*-(1→4)-α-D-Glc*p*A-(1→.

[Traduit par le journal]

Introduction

Capsular polysaccharides constitute the major, type-specific immunological determinants of *Streptococcus pneumoniae* and studies of their serological properties have contributed greatly to our knowledge of immunochemistry (1). About 80 types of *S. pneumoniae* have been identified serologically but structural studies have been reported for only some 25 of the type-specific polysaccharides (2). Some serotypes of *S. pneumoniae* are more prevalent than others in clinical infections but the distribution of serotypes varies with time and the whole range may be implicated as potential sources of public health problems (3, 4).

S. pneumoniae type XXXIII has been found in a relatively low but persistent number of pneumococcal infections for more than 40 years (3, 4). One previous report indicated that the type XXXIII polysaccharide contained glucose, galactose, and galacturonic acid in unspecified proportions (5) and an earlier report stated that this polysaccharide contained 1.65% N and 11.24% acetyl groups but no amino sugars (6); neither of these reports presented any structural information. The present paper describes structural studies that permit definition of the repeating unit of *S. pneumoniae* type XXXIII capsular polysaccharide.

Results and Discussion

The polysaccharide as received gave one peak on elution from DEAE cellulose and from Sephadex G-200, showed no absorption in the uv at 260 or 280 nm, and gave a single precipitin band on immunodiffusion against homologous antiserum. There was therefore little if any contamination with other cellular components and the structural studies were performed on the polysaccharide as supplied.

Analysis of hydrolysates of the type XXXIII polysaccharide on an amino acid autoanalyzer revealed that 2-amino-2-deoxy-D-mannose was present in substantial amounts. Graded hydrolysis of the polysaccharide showed a maximum release of amino sugar after 18 h at 100°C in 2 *N* hydrochloric acid and colorimetric estimation (7) gave an amino sugar content of 19.7%. The nitrogen content (1.40%) of the native polysaccharide would correspond to an amino sugar content of 17.9% if all of the nitrogen was contributed by the 2-amino-2-deoxy-D-mannose. Proton and ^{13}C nmr spectra of the native polysaccharide and of a slightly depolymerized sample (mild acid hydrolysis) showed the presence of *N*-acetyl groups. Integration of the peak areas of the *N*-acetyl signal and the signal of a single anomeric proton gave a ratio of 3:1 showing that the amino sugar was fully *N*-acetylated. The nmr spectra also showed the presence of one *O*-acetyl group for every two *N*-acetyls; the location of the *O*-acetyl was not investigated.

The presence of uronic acid was confirmed by the carbazole test (8) and quantitative estimation (9) showed that it constituted 20.7% of the polysaccharide. However, as reduction of the uronic acid yielded D-glucose it must have been D-glucuronic

[1]Issued as NRCC No. 18648,
[2]NRCC Research Associate, 1975–1977.

0008-4042/80/232724-04$01.00/0

©1980 National Research Council of Canada/Conseil national de recherches du Canada

Can. J. Chem. Downloaded from www.nrcresearchpress.com by 210.87.254.42 on 09/05/12
For personal use only.

Can. J. Chem. Downloaded from www.nrcresearchpress.com by 210.87.254.42 on 09/05/12
For personal use only.

acid and not galacturonic acid as previously reported (5).

Accurate quantitative analysis of the neutral sugars in the polysaccharide was difficult because of the acid stability of the uronosyl and aminoglycosyl linkages. Hydrolysates of the native polysaccharide contained 8% D-galactose and 33% D-glucose. However, when the polysaccharide was reduced by carbodiimide-borohydride (10), subsequent hydrolysis yielded 17.1% D-galactose and 52.3% D-glucose. This is a ratio of 1:3 with one of the three glucoses coming from the uronic acid. These results, together with the quantitative data for uronic acid and amino sugar, were consistent with a pentasaccharide repeating unit; two D-glucoses, and one each of D-galactose, D-glucuronic acid, and 2-acetamido-2-deoxy-D-mannose. The enantiomeric forms of these components were established by glc of the trimethylsilylated (−)2-butyl glycosides (11, 12).

Methylation analysis of the native polysaccharide gave 2,4,6-tri-*O*-methyl-D-galactose and 2,3,6-tri-*O*-methyl-D-glucose in a ratio of 1:2.5 as determined by gas chromatography – mass spectrometry of their alditol acetates (13). The low recovery of the tri-*O*-methyl-D-galactose was attributed to its probable linkage to the stable uronosyl unit, a conclusion that was subsequently confirmed. The presence of 2-deoxy-4,6-di-*O*-methyl-2-(*N*-methylacetamido)-D-mannose was also observed as the sole amino sugar derivative. Quantitation of this latter component was not attempted because of uncertainties about complete hydrolysis and response factors on glc. When the methylated, native polysaccharide was reduced before hydrolysis, an extra component was found, 2,3-di-*O*-methyl-D-glucose, that must have arisen from the uronic acid. This was confirmed by reduction of the native polysaccharide before methylation when the same products were obtained as from the methylated native polysaccharide but the ratio of 2,4,6-tri-*O*-methyl-D-galactose to 2,3,6-tri-*O*-methyl-D-glucose was 1:3, one of the three moles of the glucose derivative having arisen from the reduced uronic acid.

The results of the methylation analyses showed that the pentasaccharide repeating unit was linear and contained two D-glucose residues both linked through *O*-4, one D-glucuronic acid also linked through *O*-4, one D-galactose linked through *O*-3, and one 2-acetamido-2-deoxy-D-mannose linked through *O*-3. The methylation results in conjunction with the nmr results showed that all of the residues were in the pyranose ring form.

Partial hydrolysis studies and periodate degradations provided information about the sequence of the residues in the pentasaccharide repeating unit. Acid hydrolysis of the native polysaccharide yielded two disaccharides isolated by chromatography on Bio-Gel P-2 and on thin layer plates. One disaccharide contained equimolar amounts of 2-acetamido-2-deoxy-D-mannose and D-glucose. Periodate oxidation of this disaccharide, followed by reduction and hydrolysis, yielded glycerol and erythritol. Since it was known that the 2-acetamido-2-deoxy-D-mannose was *O*-3 linked and that D-glucose was *O*-4 linked in the polysaccharide, the results of periodate oxidation indicated the partial structure, D-Man*p*NAc-1→4-D-Glc*p*, for this disaccharide. The other disaccharide contained equal amounts of D-glucuronic acid and D-galactose. Lyxitol was identified as a product of periodate oxidation, reduction, and hydrolysis of this disaccharide which could therefore be assigned the partial structure D-Glc*p*A-1→3-D-Gal*p*.

Periodate oxidation of the native polysaccharide gave results that were initially confusing and difficult to interpret. Despite prolonged exposure to periodate only 75 to 80% of the glucose content was oxidized. As expected, the D-glucuronic acid was oxidized while the D-galactose and 2-acetamido-2-deoxy-D-mannose were completely resistant to oxidation. When the periodate oxidized polysaccharide was reduced, subjected to mild acid hydrolysis, and the products were chromatographed on Bio-Gel P-2, an oligosaccharide was obtained that contained equimolar amounts of D-galactose, D-glucose, 2-acetamido-2-deoxy-D-mannose, and erythritol. Methylation analysis of this oligosaccharide gave 2,3,4,6-tetra-*O*-methyl-D-galactose and 2,3,6-tri-*O*-methyl-D-glucose; no attempt was made to characterize the methylation products from the amino sugar or from erythritol because that information was not necessary. These results showed that D-galactose was in the nonreducing terminal position and that D-glucose was linked through *O*-4. Given the known sequence of D-Man*p*NAc-1→4-D-Glc*p* from the previously characterized disaccharide and the isolation of D-Gal*p*-1→3-D-Man*p*NAc-1→erythritol from the twice oxidized polysaccharide (see below), it was clear that this oligosaccharide had the partial structure D-Gal*p*-(1→3)-D-Man*p*NAc-(1→4)-D-Glc*p*-(1→erythritol). Since the erythritol could only have come from the other *O*-4 linked glucose and since D-glucuronic acid was found to be 1→3 linked to galactose in the other disaccharide previously characterized, the full sequence of the pen-

Can. J. Chem. Downloaded from www.nrcresearchpress.com by 210.87.254.42 on 09/05/12
For personal use only.

tasaccharide is defined as: →4)-D-Glc*p*A-(1→3)-D-Gal*p*-(1→3)-D-Man*p*NAc-(1→4)-D-Glc*p*-(1→4)-D-Glc*p*-(1→. The reason for the periodate resistance, in the native polysaccharide, of the 4-*O*-linked D-glucose residue found in this oligosaccharide was not investigated. It could have been due to partial substitution of the 2- or 3-hydroxyl groups by the unlocated *O*-acetyl groups, or that D-glucose residue could have been protected by hemiacetal formation with the aldehydo groups generated by oxidation of the neighbouring D-glucose residue (14, 15).

The assignments of anomeric configurations to the glycosidic linkages in the pentasaccharide were based upon nmr spectra and optical rotations of some degradation products. The carbodiimide-borohydride reduced polysaccharide was subjected to periodate oxidation and borohydride reduction. Following this initial reduction of any hemiacetals or aldehydo functions, the product was again oxidized by periodate and reduced. The ^{13}C nmr spectrum of this polymer showed four signals in the region 100 to 105 ppm characteristic of anomeric or acetal carbons. A resonance at 103.3 ppm represented two carbons and together with the single carbon resonances at 100.5, 101.4, and 104.8 ppm provided clear evidence of the five-residue repeating unit.

When this twice-oxidized and reduced polysaccharide was hydrolysed with 0.5 *N* sulphuric acid at room temperature for 18 h, a single oligosaccharide was obtained by chromatography on Bio-Gel P-2. This oligosaccharide contained D-galactose, 2-acetamido-2-deoxy-D-mannose and erythritol and after periodate oxidation and borohydride reduction it yielded 2-acetamido-2-deoxy-D-mannosyl glycerol. The oligosaccharide was therefore D-Gal*p*-1→3-D-Man*p*NAc-1→erythritol, the major product to be expected after complete periodate oxidation of the proposed repeating unit. The proton nmr spectrum of this disaccharide erythritol glycoside showed anomeric signals at δ 5.35 ($J_{1,2}$ = 2.7 Hz) and δ 4.96 ($J_{1,2}$ = 1.4 Hz), and an apparent doublet at δ 4.70 (J = 3.3 Hz) that was attributed to a slowly exchanging *N*-acetamido proton. It was only present in fragments containing the *N*-acetamido groups and was absent after Hakomori methylations of the same fragments. Sequential periodate oxidation, reduction, and hydrolysis (16) removed the D-galactose residue and its anomeric proton signal at δ 5.35. The coupling constant of that signal ($J_{1,2}$ = 2.7 Hz) clearly showed that the D-galactosyl linkage was in the α-configuration. The product from this degradation was 2-acetamido-2-deoxy-D-mannosyl glycerol that had $[\alpha]_D^{25}$ −52.5° in water showing that this glycosidic linkage was β (cf. methyl α-D-mannopyranoside, $[\alpha]_D$ +80°; methyl β-D-mannopyranoside, $[\alpha]_D$ −49°).

The anomeric configuration of the glucuronosyl residue was established by the proton nmr spectrum of the aldobiouronic acid (D-Glc*p*A-1→3-D-Gal) described earlier. The spectrum showed a strong anomeric signal at δ 5.12 assignable to the uronosyl residue and two smaller signals at δ 5.2 and 4.6 assignable to the galactose residue. The chemical shift and coupling constant ($J_{1,2}$ = 3.0 Hz) of the uronosyl anomeric proton showed that it was the α-anomer.

The anomeric configurations of the two glucosyl residues were established by proton nmr of the polysaccharide and subsequent disappearance of one of the anomeric signals by β-elimination. Based upon the spectra of the oligosaccharides described above, the signals in the anomeric region of the spectrum of the native polysaccharide could be assigned as follows: a doublet at δ 5.20 ($J_{1,2}$ = 3.4 Hz) was from the α-D-galactosyl residue, a doublet at δ 4.92 ($J_{1,2}$ = 1.0 Hz) was from the 2-acetamido-2-deoxy-β-D-mannosyl residue, and a doublet at δ 4.66 ($J_{1,2}$ = 3.3 Hz) was the *N*-acetamido proton. A doublet at δ 5.37 ($J_{1,2}$ = 3.2 Hz) was assigned to the α-D-glucuronosyl proton. Two doublets remained and must then represent the two D-glucosyl units. It was clear from their coupling constants that one, δ 5.45 ($J_{1,2}$ = 3.3 Hz), represented an α-anomer and the other, δ 4.57 ($J_{1,2}$ = 7.4 Hz) a β-anomer. Since it was known from sequence studies that one of the D-glucosyl units was linked to *O*-4 of the glucuronosyl residue, a β-elimination reaction was the most direct way to determine which anomer was in that position (17, 18). The proton nmr spectrum of the β-elimination product showed the expected absence of three doublets in the anomeric region: the *N*-acetamido proton, the α-D-glucuronosyl proton, and the high field β-D-glucosyl proton. The remaining three doublets had appropriate chemical shifts and coupling constants for α-D-glucosyl, α-D-galactosyl, and 2-acetamido-2-deoxy-β-D-mannosyl anomeric protons. This was conclusive evidence that the β-D-glucosyl residue was located next to the glucuronosyl residue and the complete sequence could therefore be defined as: →3)-α-D-Gal*p*-(1→3)-β-D-Man*p*NAc-(1→4)-α-D-Glc*p*-(1→4)-β-D-Glc*p*-(1→4)-α-D-Glc*p*A-(1→.

Experimental

Biological Materials

The *S. pneumoniae* type XXXIII polysaccharide was from the collection of Dr. R. Brown (6) and was generously provided by Dr. K. Amiraian, New York State Department of Health, Albany, NY. Type XXXIII specific rabbit antiserum was a gift

Can. J. Chem. Downloaded from www.nrcresearchpress.com by 210.87.254.42 on 09/05/12
For personal use only.

from Dr. J. Henrichsen, Pneumococcus Laboratory, Statens Seruminstitut, Copenhagen, Denmark. The polysaccharide as received was eluted as a single peak from Sephadex G-200 and from DEAE cellulose (19). On double diffusion (20) in 1% agarose gel the polysaccharide showed a single precipitin band against the specific type XXXIII antiserum. A 1% solution of the polysaccharide showed no absorbance at 260 or 280 nm.

Analytical Methods

Neutral sugars in hydrolysates were analysed by glc of their alditol acetates (20). The material to be analysed (1 mg sample) and inositol (200 μg, internal standard) were hydrolysed in 0.25 *M* sulphuric acid (0.5 mL) in a sealed vial at 100°C for 20 h. The hydrolysate was neutralized with barium carbonate and sugars in the aqueous solution were reduced by sodium borohydride. The resultant alditols were acetylated in acetic anhydride – pyridine and then analysed on a Hewlett-Packard 5830 A gas–liquid chromatograph. Separations were obtained on glass columns packed with either 3% ECNSS-M or 3% OV-275 on Gas-chrom Q. Peak areas were integrated automatically.

The uronic acid content of the polysaccharide was estimated colorimetrically (8) and by decarboxylation (9) with the latter method giving the more reproducible results. Amino sugars were analysed by an automatic amino acid analyser using an elution system previously described (21). A colorimetric method (7) was used to follow the release of amino sugar in graded hydrolyses.

General Methods

Carboxylate reduction of uronic acid residues in the polysaccharide was achieved by the carbodiimide-borohydride method (10). The various degradations based upon sequential periodate oxidation, reduction, and hydrolysis were done according to standard procedures (16). All methylations were done by the Hakomori procedure (22) and *O*-methylated sugars in hydrolysates were characterized by retention times and mass fragmentation patterns of their alditol acetates on glc–ms (13). Enantiomeric forms of the monosaccharides were established by glc of their trimethylsilylated (−)2-butyl glycosides (11, 12). The glc separations for this analysis were done at 220°C on glass capillary columns (50 m × 0.2 mm) wall-coated with OV-101. Peaks with the following retention times relative to trimethylsilylated methyl α-D-galactopyranoside corresponded to the indicated reference sugars: 1.10, 1.85, 1.88 (D-glucuronic acid); 1.12, 1.23, 1.30 (D-galactose); 1.32, 1.48 (D-glucose); 1.52, 1.76 (2-amino-2-deoxy-D-mannose).

Carbon-13 and proton magnetic resonance spectra were obtained on a Varian CFT-20 spectrometer at 20 MHz and 80 MHz respectively using a pulsed Fourier transform mode. ^{13}C spectra were obtained at 30°C with complete proton decoupling and the ^{2}H resonance of the deuterium oxide solvent providing a field frequency lock. Chemical shifts are reported as parts per million downfield relative to an external tetramethylsilane standard. Proton spectra were obtained at 85–90°C to shift the ^{1}H resonance of the water peak upfield from the anomeric proton signals. Chemical shifts are reported as parts per million downfield (δ) relative to internal sodium 3-trimethylsilyl propionate-2,2,3,3-d_2 or tetramethylsilane standard.

Isolation of Oligosaccharides

The type XXXIII polysaccharide (20 mg) was hydrolysed in *N* hydrochloric acid at 100°C for 3 h. The hydrolysate was evaporated to dryness under diminished pressure at 40°C. The residue was chromatographed on Bio-Gel P-2 (minus 400 mesh; 120 × 1.2 cm) in 0.1 *M* pyridine–acetate buffer, pH 5.0. A drop-counter was used to collect fractions (15 drops) and a clean separation of disaccharides (fractions 97–107) from monosaccharides (fractions 110–117) was obtained. Eluate was monitored by refractive index and by the phenol – sulphuric acid colorimetric assay (23). Two disaccharides were isolated from the disaccharide fraction by thin-layer chromatography on silica gel plates using ethyl acetate/acetic acid/methanol/water 12:3:3:2. These disaccharides were found to be Glc*p*A-1→3-Gal and Man*p*NAc-1→4-Glc as described in the results. Oligosaccharides resulting from periodate degradations were isolated by chromatography on Bio-Gel P-2 as described above and were characterized as reported in the results and discussion.

β-*Elimination Reaction*

The native polysaccharide (15 mg) was methylated (22) and the product (13.4 mg) was degraded with sodium methoxide (17). The proton magnetic resonance spectrum of the degraded material in deuterochloroform showed doublets at δ 6.05 ($J_{1,2}$ = ~3.4 Hz), δ 5.43 ($J_{1,2}$ = ~3.0 Hz), and δ 5.22 ($J_{1,2}$ = ~1.0 Hz). Permethylated trisaccharide α-D-Gal*p*-(1→3)-β-D-Man*p*NAc-1→erythritol gave a spectrum with doublets at δ 5.35 ($J_{1,2}$ = ~3.0 Hz) and δ 5.20 ($J_{1,2}$ = ~1.0 Hz).

Acknowledgments

The authors gratefully acknowledge the skillful technical assistance of F. P. Cooper and D. W. Griffith.

1. M. Heidelberger. Fortschr. Chem. Org. Naturst. **18**, 501 (1960).
2. O. Larm and B. Lindberg. Adv. Carbohydr. Chem. Biochem. **33**, 295 (1976).
3. M. Finland and M. W. Barnes. J. Clin. Microbiol. **5**, 154 (1977).
4. R. Austrian, V. M. Howie, and J. H. Ploussard. Johns Hopkins Med. J. **141**, 104 (1977).
5. G. T. Mills, E. E. B. Smith, H. P. Bernheimer, R. Austrian, and B. Galloway. Biochem. J. **76**, 31P (1960).
6. R. Brown and L. K. Robinson. J. Immunol. **47**, 7 (1943).
7. R. Gatt and E. R. Berman. Anal. Biochem. **15**, 167 (1965).
8. T. Bitter and H. M. Muir. Anal. Biochem. **4**, 330 (1962).
9. A. E. Castagne and I. R. Siddiqui. Carbohydr. Res. **42**, 382 (1975).
10. R. L. Taylor and H. E. Conrad. Biochemistry, **11**, 1383 (1972).
11. G. J. Gerwig, J. P. Kamerling, and J. F. G. Vliegenthart. Carbohydr. Res. **62**, 349 (1978).
12. G. J. Gerwig, J. P. Kamerling, and J. F. G. Vliegenthart. Carbohydr. Res. **77**, 1 (1979).
13. H. Bjorndal, C. G. Hellerqvist, B. Lindberg, and S. Svensson. Angew. Chem. Intl. Ed. Engl. **9**, 610 (1970).
14. M. F. Ishak and T. Painter. Acta Chem. Scand. **27**, 1268 (1973).
15. J. H. Pazur and L. Scott. Carbohydr. Res. **58**, 222 (1977).
16. I. J. Goldstein, G. W. Hay, B. A. Lewis, and F. Smith. Meth. Carbohydr. Chem. **5**, 361 (1965).
17. B. Lindberg, J. Lönngren, and J. L. Thompson. Carbohydr. Res. **28**, 351 (1973).
18. G. O. Aspinall and K-G. Rosell. Carbohydr. Res. **57**, C23 (1977).
19. H. Neukom, H. Deuel, W. J. Heri, and W. Kündig. Helv. Chim. Acta, **43**, 64 (1960).
20. J. S. Sawardeker, J. H. Sloneker, and A. R. Jeanes. Anal. Chem. **37**, 1602 (1965).
21. M. Yaguchi and M. B. Perry. Can. J. Biochem. **48**, 386 (1970).
22. S. Hakomori. J. Biochem. Tokyo, **55**, 205 (1964).
23. M. Dubois, K. A. Gilles, J. K. Hamilton, R. A. Rebers, and F. Smith. Anal. Chem. **28**, 350 (1956).

Can. J. Chem. Downloaded from www.nrcresearchpress.com by 210.87.254.5 on 09/05/12
For personal use only.

Evidence for cyclopropoxide intermediates in α-methyl H/D exchange of cyclic ketones under homoenolization conditions[1]

VIJAY PATEL AND J. B. STOTHERS
Department of Chemistry, University of Western Ontario, London, Ont., Canada N6A 5B7

Received June 18, 1980

This paper is dedicated to Prof. Raymond U. Lemieux on the occasion of his 60th birthday

VIJAY PATEL and J. B. STOTHERS. Can. J. Chem. **58**, 2728 (1980).

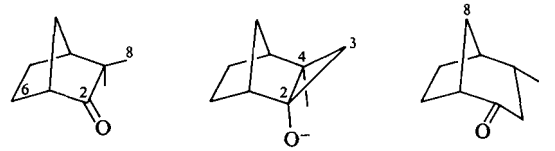
Base-catalyzed homoketonization of a series of polycyclic cyclopropanols provides strong evidence for the intermediacy of their anions for H/D exchange at α-methyl carbons in polycyclic ketones under homoenolization conditions.

VIJAY PATEL et J. B. STOTHERS. Can. J. Chem. **58**, 2728 (1980).

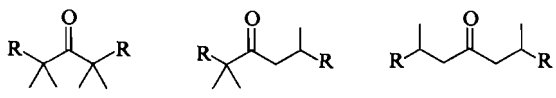
L'homocétonisation, catalysée par une base, d'une série de cyclopropanols polycycliques fournit la preuve formelle de l'existence intermédiaire de leurs anions lors de l'échange H/D, au niveau des méthyles des carbones en position α des cétones polycycliques, dans des conditions d'homocétonisation.

[Traduit par le journal]

After their original discovery of homoenolization in camphenilone (**1**) through proton abstraction from C-6 (1), Nickon and Lambert also established that β-proton abstraction occurred at the α-methyl carbons (2). By implication, a homoenolate anion such as **2** was suggested for the intermediate species but experimental verification was not pursued. Subsequently, a variety of mono- and bicyclic ketones, each having *gem*-dimethyl substitution at the α-methylene positions, has been found to exhibit α-methyl H/D exchange in deuteriated base under homoenolization conditions (3–7). These examples include the tetramethylcycloalkanones with 4- to 8- and 10-membered rings (3, 4), fenchone (5), 3,3-dimethylbicyclo[3.2.1]octan-2-one (6), 3,3-dimethylbicyclo[2.2.2]octan-2-one (4) and its Δ^5 analog (7) as well as the isomeric 7,7-dimethylbicyclo[3.2.1]octan-6-one (4) and its corresponding unsaturated analogs (7). Although **2** can undergo cleavage in two ways, to regenerate **1** or to form **3**, a ring-expanded product was not detected (2) indicating that **2** → **3** is a minor process in *t*-BuO$^-$/*t*-BuOH at 185°C. Analogous results were found for the other examples and, in all cases, the recovery of starting material and/or rearranged products arising through homoenolization at skeletal carbons was high. One can conclude, therefore, that either bonding is not fully developed between C-2 and C-8 in the intermediate, or **2** is the intermediate and its opening to an incipient primary carbanion at C-3 is favored over formation of a tertiary carbanionic centre at C-4, i.e. toward the carbon more able to stabilize the negative charge (8). While the regioselectivity of α-methyl exchange found for several bicyclic ketones (5–7) pointed to the intermediacy of cyclopropoxide ions, the first direct evidence that a fully formed cyclopropoxide ion may indeed be involved was the finding that acyclic ketones such as **4** slowly rearrange to **5** (9). In fact with **4***b*, traces of **6***b* were detected after very long reaction times demonstrating that a second rearrangement can occur; this was more clearly illustrated with **4***c* and **5***c*, both of which furnish **6***c* in significant amounts (10). However, the balance between the factors determining the regioselectivity of cleavage of cyclopropoxide **7** may differ from

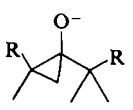


1 **2** **3**



4 **5** **6**

a = *n*-Bu, *b* = Me, *c* = Ph



7

[1]Part 90 in the series ^{13}Cmr Studies; for Part 89 see ref. 17.

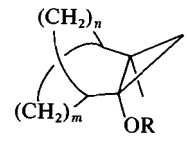
0008-4042/80/232728-03$01.00/0

©1980 National Research Council of Canada/Conseil national de recherches du Canada

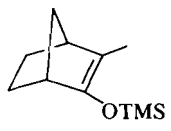
Can. J. Chem. Downloaded from www.nrcresearchpress.com by 210.87.254.5 on 09/05/12
For personal use only.

those governing ring opening of **2** and its polycyclic analogs, as has been suggested (9, 10). To date there is no evidence for the existence of cyclopropoxides such as **2** under homoenolization conditions. In this communication we wish to present results from an examination of base-catalyzed homoketonization of a series of substituted cyclopropanols **8** (R = H) which strongly support the intermediacy of cyclopropoxide ions for α-methyl exchange in polycyclic systems.

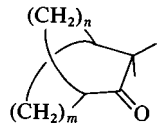
The requisite cyclopropanols were prepared employing the general sequence described by Girard and Conia for simpler systems (11). For **2**, methylation of norcamphor with lithium diisopropylamide (LDA) and methyl iodide gave 3-methylnorcamphor which was converted to the enolate with LDA and reacted with trimethylsilyl chloride and triethylamine in THF (12) to furnish **9**. Cyclopropanation (zinc–silver couple and methylene iodide) gave **8** (R = Me_3Si; $n = 1$, $m = 2$)[2] in 58% yield, isolated by bulb-to-bulb distillation. Cleavage of this ether with dilute HCl in THF afforded the corresponding alcohol, and its homoketonization via **2** was accomplished by rapid addition to a solution of t-BuO^-K^+ in anhydrous t-BuOH at 25°C. After 10 min, the solution was diluted with water and the ketonic products isolated by pentane extraction. Gas–liquid chromatography (glc) on 10% Carbowax or 6% FFAP revealed two products in a 63:37 ratio; pure samples of each were obtained by preparative glc. The same products in an 81:19 ratio resulted with the base solution at reflux (82°C). The major product in each case was easily shown by nmr to be **1**. The second, an isomeric ketone by ms, exhibited a ^{13}Cmr spectrum ($CDCl_3$) δ: 19.4 (CH_3); 22.4, 28.1, 38.6, 43.4 (CH_2's); 37.2, 40.4, 50.3 (CH's) and 213.8 (C=O) which is entirely consistent with **3** upon comparison with the



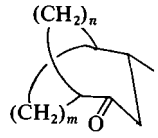
8



9



10



11

[2]For all new compounds, the spectra (ir, ^{1}Hmr, ^{13}Cmr) were in agreement with the assigned structures. Precise mass measurements were obtained for each.

TABLE 1. Base-catalyzed homoketonizations of **8**

Starting material **8**		Temperature (°C)	Products (%)[a] **10**	**11**
n	*m*			
1	2	25	63	37
		82	81	19
2	2	25	>99	<1
2 (Δ[6])	2	25	78	22
		82	81	19
3	1	25	90	10

[a]Product proportions determined by glc analysis, ±2%.

^{13}C data for the parent ketone (13) with due allowance for the usual shielding effects of the methyl substituent. The methylene signal at 38.6 ppm is readily assigned to the methano bridge carbon (C-8) from the off-resonance spectrum (14). Its position is particularly significant since this is essentially the same as that for C-8 in the parent (38.3 ppm), strongly indicating an *endo* orientation for the methyl group in **3**. Thus, ring opening of **2** by cleavage of the C-2—C-4 bond proceeds with inversion of configuration at C-4, as generally observed for related systems with oxygen on tertiary carbon (15). In any event, these results establish that **2** opens preferentially via a primary carbanion (cleavage of the C-2—C-3 bond) to form **1**. The observed temperature dependency of the regioselectivity of homoketonization indicates that **2** → **1** will be even more highly favored at 185°C, the temperature of the homoenolization studies of **1**. Thus, **2** is a very reasonable intermediate for H/D exchange at the methyl sites in **1** under homoenolization conditions.

Results for some homologs of **2** are collected in Table 1. In each case, the substituted cyclopropanol **8** (R = H) was found to open preferentially to the corresponding dimethyl ketone **10**, with minor amounts of the ring-expanded product **11**. Similarly, **8** (R = H) from 3-methylbicyclo[2.2.2]oct-5-enone gave the dimethylbicyclooctenone as the major product.

Each of these cyclopropanol derivatives is a model intermediate for α-methyl exchange in the corresponding bicyclic ketone known to undergo H/D exchange at the methyl sites (2, 4–7). Our earlier work established that *exo*-methyl groups in these systems undergo exchange most readily and the present study was designed to test cyclopropoxides as potential intermediates for *exo*-methyl exchange. From the results it is apparent that **8** is a reasonable intermediate for the process. The ear-

lier studies (4–7) provided crude kinetic data showing methyl exchange to be very slow ($k \sim 10^{-7}$ s^{-1}). Consequently, small amounts of ring-expanded products, generated by the less-favored cleavage of **8**, may have escaped detection since presumably these would undergo aldol condensation readily. It may be noted that homoketonization of the 1-hydroxybicyclo[n.1.0]alkanes, n = 3–6, was reported earlier (16) and found to give >90% yields of the corresponding 2-methylcycloalkanones. Thus, one can conclude that α-methyl exchange in α,α,α′,α′-tetramethylcycloalkanones under homoenolization conditions (3, 4) also involves cyclopropoxide intermediates, although the precise model systems have not been examined.

Acknowledgement

We are grateful for the financial support provided by the Natural Sciences and Engineering Research Council of Canada.

1. A. NICKON and J. L. LAMBERT. J. Am. Chem. Soc. **84**, 4604 (1962).
2. A. NICKON, J. L. LAMBERT, and J. E. OLIVER. J. Am. Chem. Soc. **88**, 2787 (1966).
3. A. NICKON, J. L. LAMBERT, J. E. OLIVER, D. F. COVEY, and J. MORGAN. J. Am. Chem. Soc. **98**, 2593 (1976).
4. A. K. CHENG, J. B. STOTHERS, and C. T. TAN. Can. J. Chem. **55**, 447 (1977).
5. A. L. JOHNSON, J. B. STOTHERS, and C. T. TAN. Can. J. Chem. **53**, 212 (1975).
6. A. L. JOHNSON, N. O. PETERSEN, M. B. RAMPERSAD, and J. B. STOTHERS. Can. J. Chem. **52**, 4143 (1974).
7. A. K. CHENG and J. B. STOTHERS. Can. J. Chem. **56**, 1342 (1978).
8. D. H. GIBSON and C. H. DEPUY. Chem. Rev. **74**, 605 (1974).
9. M. B. RAMPERSAD and J. B. STOTHERS. J. Chem. Soc. Chem. Commun. 709 (1976).
10. R. A. DYLLICK-BRENZINGER and J. B. STOTHERS. J. Chem. Soc. Chem. Commun. 108 (1979).
11. C. GIRARD and J-M. CONIA. J. Chem. Res. (M) 2346 (1978).
12. H. O. HOUSE, L. J. CZUBA, M. GALL, and H. D. OLMSTEAD. J. Org. Chem. **34**, 2324 (1969).
13. S. H. GROVER, D. H. MARR, J. B. STOTHERS, and C. T. TAN. Can. J. Chem. **53**, 1351 (1975).
14. J. B. GRUTZNER. J. Chem. Soc. Chem. Commun. 64 (1974).
15. D. H. HUNTER, J. B. STOTHERS, and E. W. WARNHOFF. *In* Rearrangements in ground and excited states. *Edited by* P. de Mayo. Academic Press, New York. 1980. Chapt. 6, pp. 430–433.
16. J. M. CONIA and C. GIRARD. Tetrahedron Lett. 2767 (1973).
17. A. STOESSL and J. B. STOTHERS. Can. J. Chem. **58**, 2069 (1980).

A new preparative ring expansion for bicyclic ketones. Homoketonization of cyclopropoxide analogs[1]

YUMIKO HOYANO,[2] VIJAY PATEL, AND J. B. STOTHERS

Department of Chemistry, University of Western Ontario, London, Ont., Canada N6A 5B7

Received June 18, 1980

This paper is dedicated to Prof. Raymond U. Lemieux on the occasion of his 60th birthday

YUMIKO HOYANO, VIJAY PATEL, and J. B. STOTHERS. Can. J. Chem. **58**, 2730 (1980).

Homoketonization of some readily prepared cyclopropoxides affords a new synthetic method for ring expansion of the [2.2.1] and [2.2.2] ring systems.

YUMIKO HOYANO, VIJAY PATEL et J. B. STOTHERS. Can. J. Chem. **58**, 2730 (1980).

L'homocétonisation de quelques oxydes cyclopropaniques facilement accessibles fournit une nouvelle méthode d'extension de systèmes cycliques [2.2.1] et [2.2.2].

[Traduit par le journal]

In the preceding communication (1) we have described the base-catalyzed homoketonization of some tricyclic systems containing a cyclopropanol moiety as model intermediates for α-methyl exchange in bicyclic ketones under homoenolization conditions. In the development of our experimental procedures, the 4-normethyl derivatives **1** were prepared and their cleavage via homoketonization was also examined. Significantly different regioselectivities were encountered such that a synthetic route to a variety of bicyclic ketones was revealed. We wish to present the results of these experiments to illustrate a new ring expansion procedure for some polycyclic systems.

[1]Part 91 in the series ^{13}Cmr Studies; for Part 90 see preceding communication.

[2]Present address: Department of Chemistry, University of Alberta, Edmonton, Alta., Canada T6G 2G2.

0008-4042/80/232730-03$01.00/0

©1980 National Research Council of Canada/Conseil national de recherches du Canada

Can. J. Chem. Downloaded from www.nrcresearchpress.com by 210.87.254.5 on 09/05/12
For personal use only.

lier studies (4–7) provided crude kinetic data showing methyl exchange to be very slow ($k \sim 10^{-7}$ s^{-1}). Consequently, small amounts of ring-expanded products, generated by the less-favored cleavage of **8**, may have escaped detection since presumably these would undergo aldol condensation readily. It may be noted that homoketonization of the 1-hydroxybicyclo[n.1.0]alkanes, n = 3–6, was reported earlier (16) and found to give >90% yields of the corresponding 2-methylcycloalkanones. Thus, one can conclude that α-methyl exchange in α,α,α′,α′-tetramethylcycloalkanones under homoenolization conditions (3, 4) also involves cyclopropoxide intermediates, although the precise model systems have not been examined.

Acknowledgement

We are grateful for the financial support provided by the Natural Sciences and Engineering Research Council of Canada.

1. A. NICKON and J. L. LAMBERT. J. Am. Chem. Soc. **84**, 4604 (1962).
2. A. NICKON, J. L. LAMBERT, and J. E. OLIVER. J. Am. Chem. Soc. **88**, 2787 (1966).
3. A. NICKON, J. L. LAMBERT, J. E. OLIVER, D. F. COVEY, and J. MORGAN. J. Am. Chem. Soc. **98**, 2593 (1976).
4. A. K. CHENG, J. B. STOTHERS, and C. T. TAN. Can. J. Chem. **55**, 447 (1977).
5. A. L. JOHNSON, J. B. STOTHERS, and C. T. TAN. Can. J. Chem. **53**, 212 (1975).
6. A. L. JOHNSON, N. O. PETERSEN, M. B. RAMPERSAD, and J. B. STOTHERS. Can. J. Chem. **52**, 4143 (1974).
7. A. K. CHENG and J. B. STOTHERS. Can. J. Chem. **56**, 1342 (1978).
8. D. H. GIBSON and C. H. DEPUY. Chem. Rev. **74**, 605 (1974).
9. M. B. RAMPERSAD and J. B. STOTHERS. J. Chem. Soc. Chem. Commun. 709 (1976).
10. R. A. DYLLICK-BRENZINGER and J. B. STOTHERS. J. Chem. Soc. Chem. Commun. 108 (1979).
11. C. GIRARD and J-M. CONIA. J. Chem. Res. (M) 2346 (1978).
12. H. O. HOUSE, L. J. CZUBA, M. GALL, and H. D. OLMSTEAD. J. Org. Chem. **34**, 2324 (1969).
13. S. H. GROVER, D. H. MARR, J. B. STOTHERS, and C. T. TAN. Can. J. Chem. **53**, 1351 (1975).
14. J. B. GRUTZNER. J. Chem. Soc. Chem. Commun. 64 (1974).
15. D. H. HUNTER, J. B. STOTHERS, and E. W. WARNHOFF. *In* Rearrangements in ground and excited states. *Edited by* P. de Mayo. Academic Press, New York. 1980. Chapt. 6, pp. 430–433.
16. J. M. CONIA and C. GIRARD. Tetrahedron Lett. 2767 (1973).
17. A. STOESSL and J. B. STOTHERS. Can. J. Chem. **58**, 2069 (1980).

A new preparative ring expansion for bicyclic ketones. Homoketonization of cyclopropoxide analogs[1]

YUMIKO HOYANO,[2] VIJAY PATEL, AND J. B. STOTHERS

Department of Chemistry, University of Western Ontario, London, Ont., Canada N6A 5B7

Received June 18, 1980

This paper is dedicated to Prof. Raymond U. Lemieux on the occasion of his 60th birthday

YUMIKO HOYANO, VIJAY PATEL, and J. B. STOTHERS. Can. J. Chem. **58**, 2730 (1980).

Homoketonization of some readily prepared cyclopropoxides affords a new synthetic method for ring expansion of the [2.2.1] and [2.2.2] ring systems.

YUMIKO HOYANO, VIJAY PATEL et J. B. STOTHERS. Can. J. Chem. **58**, 2730 (1980).

L'homocétonisation de quelques oxydes cyclopropaniques facilement accessibles fournit une nouvelle méthode d'extension de systèmes cycliques [2.2.1] et [2.2.2].

[Traduit par le journal]

In the preceding communication (1) we have described the base-catalyzed homoketonization of some tricyclic systems containing a cyclopropanol moiety as model intermediates for α-methyl exchange in bicyclic ketones under homoenolization conditions. In the development of our experimental procedures, the 4-normethyl derivatives **1** were prepared and their cleavage via homoketonization was also examined. Significantly different regioselectivities were encountered such that a synthetic route to a variety of bicyclic ketones was revealed. We wish to present the results of these experiments to illustrate a new ring expansion procedure for some polycyclic systems.

[1]Part 91 in the series ^{13}Cmr Studies; for Part 90 see preceding communication.

[2]Present address: Department of Chemistry, University of Alberta, Edmonton, Alta., Canada T6G 2G2.

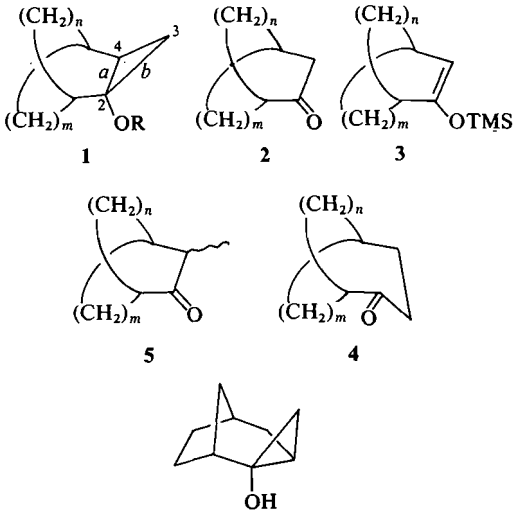
0008-4042/80/232730-03$01.00/0

©1980 National Research Council of Canada/Conseil national de recherches du Canada

Can. J. Chem. Downloaded from www.nrcresearchpress.com by 210.87.254.6 on 09/05/12
For personal use only.

Can. J. Chem. Downloaded from www.nrcresearchpress.com by 210.87.254.6 on 09/05/12
For personal use only.

Following the sequence developed by Girard and Conia (2) for several acyclic and monocyclic ketones, we have prepared a series of derivatives of general formula **1** (R = Me_3Si)[3] from the parent ketones **2**. Treatment of each ketone with lithium diisopropylamide followed by reaction with trimethylsilyl chloride and triethylamine afforded the trimethylsilyl enol ethers **3**; this procedure is a modification of that reported by House *et al.* (3). Cyclopropanation using a zinc–silver couple and methylene iodide gave **1** (R = Me_3Si) in reasonable yields, isolated by bulb-to-bulb distillation. In each case a single cyclopropyl ether was formed and the orientation of the cyclopropyl methylene carbon



relative to the other bridges in the ring system assigned from its ^{13}C shielding.[4] Cleavage of these ethers with dilute HCl in THF produced the corresponding cyclopropanol derivatives **1** (R = H).

Homoketonization of each cyclopropanol was carried out by its rapid addition to a solution of potassium *tert*-butoxide in anhydrous *tert*-BuOH at 25°C or at reflux (82°C). After 10 min, the reaction solution was diluted with water, the ketonic products isolated by pentane extraction, and analyzed by gas–liquid chromatography (glc) using 10% Carbowax or 6% FFAP columns. The cyclopropoxides, immediately formed in base, open rapidly by cleavage of bond *a* or *b* (see **1**) to give **4** or **5**, respectively, and subsequent enolization will epimerize the α-methyl group in **5**. Thus, the product mixtures were expected to contain two or three isomeric ketones depending on the carbon skeleton. The results for the six cyclopropanols studied are collected in Table 1. The ring-expanded ketones **4** were shown to be isomeric by ms and their ^{13}Cmr spectra lacked methyl absorption; the ^{13}C spectra for some of these ketones have been published (4, 5). The α-methyl ketones **5** were readily identified by their ^{13}C spectra, all of which have been reported previously (4, 6). Mixtures of *exo* and *endo* isomers were obtained in four cases while a single α-methyl ketone resulted in two systems. Because of the short reaction times, the mixtures are not necessarily at equilibrium. It may be noted that we have previously reported that *exo*-3-methylbicyclo[3.2.1]octan-2-one (**7**) cannot be epimerized under normal conditions (4), contrary to an earlier claim (7). In the present study, therefore, it was not surprising to find that **6** gave the single α-methyl isomer **7**.

From the data in Table 1 it is apparent that there is a delicate balance between the two modes of ring opening for these cyclopropoxides with the ratio of bond cleavage *a*:*b* varying between 95:5 and 5:95. Two opposing major factors governing the regioselectivity for a given system can be envisaged. Opening by cleavage of bond *b* may be inherently favored because the primary carbanion thereby generated (at C-3) is more stable and less hindered for protonation than the secondary carbanion formed (at C-4) by cleavage of bond *a* (8). However, the relief of ring strain resulting by cleavage of *a* may, in some systems, render it the favored mode, i.e. a dependence on product stability. The influence of the latter factor will be reflected in the proportion of ring-expanded product and will diminish as the size of the bridges in the ring system

TABLE 1. Base-catalyzed homoketonizations of **1** and **6**

Starting material		Temperature	Products (%)[a]	
1				
n	*m*	(°C)	**4**	**5** (*exo*/*endo*)
1	2	25	90	10 (1.6)
		82	85	15 (1.3)
2	2	25	73	27
		82	47	53
2 (Δ^6)	2	25	95	5 (0.5)[b]
3	1	25	30	70 (0.8)
3	2	25	~5[b]	~95[b] (0.7)[b]
6		25	23[c]	77[d,e]

[a]Unless otherwise indicated, the relative proportions (**4** and **5**) and the *exo*/*endo* ratios were determined by glc analysis; estimated precision ±2%.
[b]From ^{13}Cmr spectra, ±10%.
[c]Bicyclo[4.2.1]nonan-2-one.
[d]3-Methylbicyclo[3.2.1]octan-2-one.
[e]*Exo* isomer only, see text.

[3]For each new compound, the spectra (ir, ^1Hmr, ^{13}Cmr) were in agreement with the assigned structures. Precise mass measurements were obtained for each compound.

[4]The complete ^{13}C data will be presented in the full report.

increases. It can be seen that ring expansion is decreasingly favored in the saturated series in the order: [2.2.1], [2.2.2], [3.2.1], [3.2.2], with the unsaturated [2.2.2] skeleton exhibiting the greatest tendency for ring expansion; this is in qualitative agreement with expectations. For three of the systems, homoketonization is potentially useful for preparative purposes. Although **6** opens preferentially to the α-methyl ketone, its 3,3-dichloro derivative undergoes reductive fragmentation to the ring-expanded [4.2.1] skeleton (9). Hence, the two types of cyclopropyl derivatives provide many interesting synthetic possibilities. The temperature dependence of regioselectivity for homoketonization of **1** is similar to that found for the 4-methyl analogs (1), with lower temperatures favoring ring expansion.

The predominance of ring expansion in three of these homoketonizations provides a new synthetic method for these and closely related systems. Extensions to other systems are in hand to define the scope of the method more precisely, to establish the stereochemistry of bond *a* cleavage, and to investigate the reaction at lower temperatures. As an example of the synthetic utility of homoketonization for ring expansion, we have found that homologation of tricyclo[5.2.1.$0^{2,6}$]decan-8-one, as well as its Δ^3 and Δ^4 derivatives, to the corresponding tricyclo[5.3.1.$0^{2,6}$]undecan-8-ones is straightforward and the product is essentially free of the unexpanded α-methyl isomers.[5]

Acknowledgement

We are grateful for the financial support provided by the Natural Sciences and Engineering Research Council of Canada.

1. V. PATEL and J. B. STOTHERS. Can. J. Chem. **58**, 2728 (1980).
2. C. GIRARD and J-M. CONIA. J. Chem. Res. (M), 2346 (1978).
3. H. O. HOUSE, L. J. CZUBA, M. GALL, and H. D. OLMSTEAD. J. Org. Chem. **34**, 2324 (1969).
4. S. H. GROVER, D. H. MARR, J. B. STOTHERS, and C. T. TAN. Can. J. Chem. **53**, 1351 (1975).
5. K. YAMADA, S. MANABE, Y. KYOTANI, M. SUZUKI, and Y. HIRATA. Bull. Chem. Soc. Jpn. **52**, 186 (1979).
6. K. R. STEPHENS, J. B. STOTHERS, and C. T. TAN. *In* Mass spectrometry and nmr in pesticide chemistry. *Edited by* R. Haque and J. F. Boros. Plenum Press, New York, NY. 1974. pp. 179–196; J. B. STOTHERS, C. T. TAN, and K. C. TEO. Can. J. Chem. **51**, 2893 (1973).
7. M. A. MCKINNEY and P. P. PATEL. J. Org. Chem. **38**, 4064 (1973).
8. D. H. GIBSON and C. H. DEPUY. Chem. Rev. **74**, 605 (1974).
9. W. KRAUS, W. ROTHENWÖHRER, H. SADLO, and G. KLEIN. Angew. Chem. Int. Ed. Engl. **11**, 641 (1972).

[5]B. A. Dawson and J. B. Stothers, unpublished results.

A synthesis of (+) and (−) methyl nonactate from a derivative of D-ribose

KING MO SUN AND BERT FRASER-REID

Guelph–Waterloo Centre for Graduate Work in Chemistry, Waterloo Campus, University of Waterloo, Waterloo, Ont., Canada N2L 3G1

Received April 28, 1980

This paper is dedicated to Prof. Raymond U. Lemieux on the occasion of his 60th birthday

KING MO SUN and BERT FRASER-REID. Can. J. Chem. **58**, 2732 (1980).

C-Glycofuranosides with an activated methylene group at C1 of the glycosyl residue are amenable to epimerisation via a retro-Michael–Michael addition sequence. Advantage is taken of this phenomenon by converting methyl 2,3-*O*-isopropylidene-β,D-*ribo*-octofuranosid-6-ulose (**8**) into the corresponding α,L-*lyxo* isomer (**15**) by treatment with base. Both **8** and **15** are then converted into the (−) and (+) enantiomers of methyl nonactate (**14**) respectively, in ~ 45 percent yield.

KING MO SUN et BERT FRASER-REID. Can. J. Chem. **58**, 2732 (1980).

Les *C*-glycofurannosides ayant un groupement méthylène activé au niveau du carbone en position 1 de la portion glycosyle sont susceptibles d'être épimérisés par l'intermédiaire d'une addition de type rétro-Michael. On profite de ce fait pour transformer, au moyen d'une base, le *O*-isopropylidène-2,3 β-D-*ribo*-octofurannoside-6 ulose de méthyle (**8**) en son isomère le α,L-*lyxo* (**15**). Les deux composés **8** et **15** sont alors transformés respectivement en des énantiomères (−) et (+) du nonactate de méthyle avec un rendement de 45%.

[Traduit par le journal]

Moffatt and co-workers have shown that the reaction of 2,3-*O*-isopropylidene furanoses, e.g. **1**, with stabilized Wittig reagents **2** gives unsaturated adducts **3** from which *C*-glycosides such as **4** and **5** may be obtained as the products of kinetic and thermodynamic control respectively (1) (Scheme

0008-4042/80/232732-04$01.00/0
©1980 National Research Council of Canada/Conseil national de recherches du Canada

Can. J. Chem. Downloaded from www.nrcresearchpress.com by 210.87.254.6 on 09/05/12
For personal use only.

increases. It can be seen that ring expansion is decreasingly favored in the saturated series in the order: [2.2.1], [2.2.2], [3.2.1], [3.2.2], with the unsaturated [2.2.2] skeleton exhibiting the greatest tendency for ring expansion; this is in qualitative agreement with expectations. For three of the systems, homoketonization is potentially useful for preparative purposes. Although **6** opens preferentially to the α-methyl ketone, its 3,3-dichloro derivative undergoes reductive fragmentation to the ring-expanded [4.2.1] skeleton (9). Hence, the two types of cyclopropyl derivatives provide many interesting synthetic possibilities. The temperature dependence of regioselectivity for homoketonization of **1** is similar to that found for the 4-methyl analogs (1), with lower temperatures favoring ring expansion.

The predominance of ring expansion in three of these homoketonizations provides a new synthetic method for these and closely related systems. Extensions to other systems are in hand to define the scope of the method more precisely, to establish the stereochemistry of bond *a* cleavage, and to investigate the reaction at lower temperatures. As an example of the synthetic utility of homoketonization for ring expansion, we have found that homologation of tricyclo[5.2.1.$0^{2,6}$]decan-8-one, as well as its Δ^3 and Δ^4 derivatives, to the corresponding tricyclo[5.3.1.$0^{2,6}$]undecan-8-ones is straightforward and the product is essentially free of the unexpanded α-methyl isomers.[5]

Acknowledgement

We are grateful for the financial support provided by the Natural Sciences and Engineering Research Council of Canada.

1. V. PATEL and J. B. STOTHERS. Can. J. Chem. **58**, 2728 (1980).
2. C. GIRARD and J-M. CONIA. J. Chem. Res. (M), 2346 (1978).
3. H. O. HOUSE, L. J. CZUBA, M. GALL, and H. D. OLMSTEAD. J. Org. Chem. **34**, 2324 (1969).
4. S. H. GROVER, D. H. MARR, J. B. STOTHERS, and C. T. TAN. Can. J. Chem. **53**, 1351 (1975).
5. K. YAMADA, S. MANABE, Y. KYOTANI, M. SUZUKI, and Y. HIRATA. Bull. Chem. Soc. Jpn. **52**, 186 (1979).
6. K. R. STEPHENS, J. B. STOTHERS, and C. T. TAN. *In* Mass spectrometry and nmr in pesticide chemistry. *Edited by* R. Haque and J. F. Boros. Plenum Press, New York, NY. 1974. pp. 179–196; J. B. STOTHERS, C. T. TAN, and K. C. TEO. Can. J. Chem. **51**, 2893 (1973).
7. M. A. MCKINNEY and P. P. PATEL. J. Org. Chem. **38**, 4064 (1973).
8. D. H. GIBSON and C. H. DEPUY. Chem. Rev. **74**, 605 (1974).
9. W. KRAUS, W. ROTHENWÖHRER, H. SADLO, and G. KLEIN. Angew. Chem. Int. Ed. Engl. **11**, 641 (1972).

[5]B. A. Dawson and J. B. Stothers, unpublished results.

A synthesis of (+) and (−) methyl nonactate from a derivative of D-ribose

KING MO SUN AND BERT FRASER-REID

Guelph–Waterloo Centre for Graduate Work in Chemistry, Waterloo Campus, University of Waterloo, Waterloo, Ont., Canada N2L 3G1

Received April 28, 1980

This paper is dedicated to Prof. Raymond U. Lemieux on the occasion of his 60th birthday

KING MO SUN and BERT FRASER-REID. Can. J. Chem. **58**, 2732 (1980).

C-Glycofuranosides with an activated methylene group at C1 of the glycosyl residue are amenable to epimerisation via a retro-Michael–Michael addition sequence. Advantage is taken of this phenomenon by converting methyl 2,3-*O*-isopropylidene-β,D-*ribo*-octofuranosid-6-ulose (**8**) into the corresponding α,L-*lyxo* isomer (**15**) by treatment with base. Both **8** and **15** are then converted into the (−) and (+) enantiomers of methyl nonactate (**14**) respectively, in ~ 45 percent yield.

KING MO SUN et BERT FRASER-REID. Can. J. Chem. **58**, 2732 (1980).

Les *C*-glycofurannosides ayant un groupement méthylène activé au niveau du carbone en position 1 de la portion glycosyle sont susceptibles d'être épimérisés par l'intermédiaire d'une addition de type rétro-Michael. On profite de ce fait pour transformer, au moyen d'une base, le *O*-isopropylidène-2,3 β-D-*ribo*-octofurannoside-6 ulose de méthyle (**8**) en son isomère le α,L-*lyxo* (**15**). Les deux composés **8** et **15** sont alors transformés respectivement en des énantiomères (−) et (+) du nonactate de méthyle avec un rendement de 45%.

[Traduit par le journal]

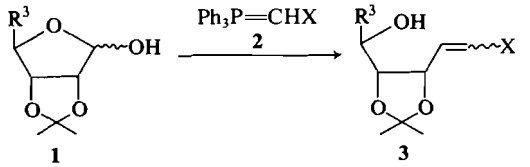
Moffatt and co-workers have shown that the reaction of 2,3-*O*-isopropylidene furanoses, e.g. **1**, with stabilized Wittig reagents **2** gives unsaturated adducts **3** from which *C*-glycosides such as **4** and **5** may be obtained as the products of kinetic and thermodynamic control respectively (1) (Scheme

0008-4042/80/232732-04$01.00/0
©1980 National Research Council of Canada/Conseil national de recherches du Canada

Can. J. Chem. Downloaded from www.nrcresearchpress.com by 210.87.254.6 on 09/05/12
For personal use only.

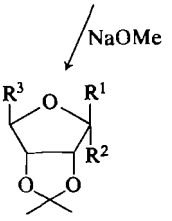
Can. J. Chem. Downloaded from www.nrcresearchpress.com by 210.87.254.6 on 09/05/12
For personal use only.

1). This principle should facilitate asymmetric syntheses of *cis* and *trans* 2,5-dialkyltetrahydrofuran systems by "cyclic transfer"[1] from **4** and **5** respectively. In this communication we utilize this principle for a synthesis[2] of the (+) and (−) enantiomers of nonactic acid (**14**) from the same derivative of D-ribose.



1 **3**

X = CN, CO_2R, COR etc.



	R^1	R^2	
4	CH_2X	H	(kinetic product)
5	H	CH_2X	(thermodynamic product)

	R^1	R^2	R^3
6	OMe	H	CHO
7	OMe	H	$CH{=}C(OMe){-}CH_3$
8	OMe	H	CH_2COCH_3

SCHEME 1

The known aldehyde, **6**, prepared readily from D-ribose (5), was converted into the syrupy ketone **8**[3] in 62% overall yield via a Wittig reaction to give the enol ether **7**, followed by hydrolysis (0.03*N* HCl, 15 min). Inspection of models suggested that chelation of the C8 carbonyl, dioxolane, and ring oxygens by Raney nickel (6) should lead to the desired (*S*) alcohol **9** upon hydrogenation. Indeed the ratio of **9** and **10** was 9:1, and the fact that these epimers were well resolved (R_f[4] 0.43 and 0.48 respectively) meant that the minor component could be separated on a silica column and transformed into **9** via sulfonation followed by solvolysis with sodium benzoate.

With the configuration of the C8 hydroxyl group secured, compound **9** was transformed into the aldose **11** which was subjected to the Moffatt two-step procedure (1) depicted in Scheme 1, whereupon the epimers **12** and **13** were obtained *exclusively* under conditions of kinetic control. The initial ratio of **12** and **13** was 1:3, but this could be raised to 3:2 by refluxing with sodium methoxide for 3 h (*vide infra*). Hence after three cycles of equilibration and separation, 90% of **13** had been converted into **12**[3] (R_f[4] 0.50 and 0.43, respectively).

The final steps leading from **12** to (−) methyl nonactate (−)-**14**, in 78% overall yield, employed the Eastwood deoxygenation (7) as outlined in Scheme 3. Thus the benzoate of **12** was deacetonated, and the resulting diol converted into the amide acetal (**22**) which upon boiling in acetic anhydride afforded the alkene (**23**). Hydrogenation over palladium then afforded (−)-**14**, $[\alpha]_D^{20}$ −16.0° (lit. (4) value −17.8°). Identification of the product was established by comparison with an authentic sample.[5]

For the synthesis of the dextrorotatory enantiomer (+)-**14** we made use of the phenomenological observation (Scheme 1) which predicted that treatment of **8** with base would give **15** as the thermodynamically favoured isomer; indeed the ratio of **15** to **8** at equilibrium was 9:1. The sequences leading to **16**,[3] and thence to **18**, were identical with those used for **8** → **11**.

Our strategy now required the addition of a Wittig reagent to **18** and prolonged treatment with base in order to bring C1 into *syn* relationship with the acetonide. Our earlier studies with **12** and **13** (*vide supra*) had revealed that these α-alkylated esters were reluctant to move "down" into *syn*-relationship with the acetonide. However, in a model study the corresponding nitriles had been found to behave "normally." Hence compound **18** was converted in 93% yield into the epimeric mixture **19**. This mixture was then subjected to sodium ethoxide in refluxing ethanol, whereupon 80% epimerisation occurred giving **20** and **21** in equal amounts. Subjecting **21** and recovered **19** to a few cycles of epimerisation and separation afforded **20** in ~ 84% yield from **19**.

Deoxygenation of **20** was carried out as described for **12** (Scheme 3), and the nitrile was converted into the methyl ester (+)-**14** by treatment with hydrogen peroxide (8) and nitrosyl chloride (9). The identity of (+)-**14** ($[\alpha]_D^{20}$ +16.2° (lit. (4)

[1]For definition of this term see ref. 2.

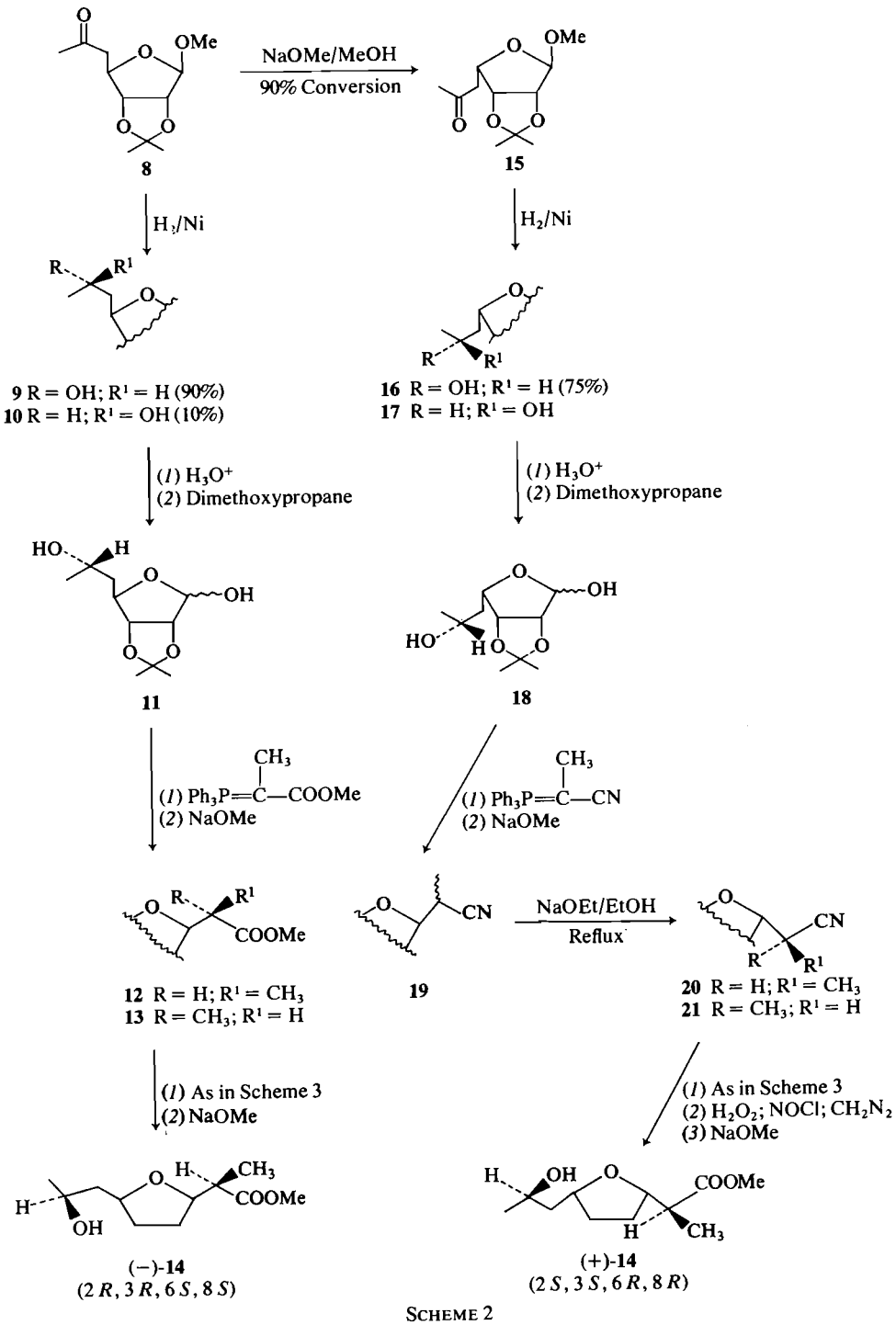
[2]For racemic and asymmetric syntheses of nonactin, see refs. 3 and 4 respectively.

[3]This compound gave satisfactory hrms, 220 MHz ^{1}Hmr and ^{13}Cmr spectra.

[4]All R_f's in diethyl ether with the exception of **20** and **21** which were in $MeOH/CH_2Cl_2$ (1:23).

[5]We are indebted to Professor Ulrich Schmidt of the Universität Wien for authentic samples of nonactic acid derivatives (4).

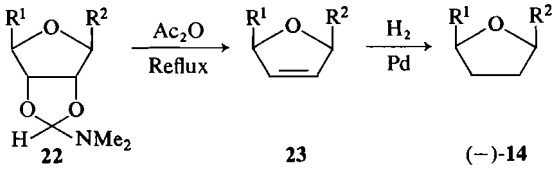
Can. J. Chem. Downloaded from www.nrcresearchpress.com by 210.87.254.6 on 09/05/12
For personal use only.



SCHEME 2

value +16.2°)) was established by comparison with the previously prepared levorotatory enantiomer (−)-**14**.

Assuming virtually quantitative interconversion of the epimers (e.g. **10** → **9**, **13** → **12**, etc.) it is seen that the transformation of **8** into (−)-**14** and **15** into (+)-**14** may be carried out in ~45 percent overall yields. The synthetic plan can obviously be utilized to obtain specifically the C2 and/or C8 epimers of nonactic acid by accumulating the "other" compo-



22 **23** (−)-**14**

$R^1 = CH_2CHOCOPhCH_3$, $R^2 = CH(CH_3)COOMe$

SCHEME 3

nent of each epimeric pair shown in Scheme 2. Furthermore, the general synthetic plan should be applicable to the other building units of the higher analogues of the nactin family (10).

Acknowledgements

We are grateful to the Natural Sciences and Engineering Research Council and to Merck, Sharp & Dohme (Rahway) for financial support.

1. H. OHRUI, G. H. JONES, J. G. MOFFATT, M. L. MADOX, A. T. CHRISTENSEN, and S. K. BYRAM. J. Am. Chem. Soc. **97**, 4602 (1975).
2. B. FRASER-REID and R. C. ANDERSON. Prog. Chem. Org. Nat. Prod. **39**, 1 (1980).
3. H. GERLACH and H. WETTER. Helv. Chim. Acta, **57**, 250 (1974); H. ZAK and U. SCHMIDT. Angew Chem. Int. Ed. Engl. **14**, 432 (1975); M. J. ARCO, M. H. TRAMMELL, and J. D. WHITE. J. Org. Chem. **41**, 2075 (1976); G. BECK and E. HENSELEIT. Chem. Ber. **104**, 21 (1971).
4. J. GOMBOS, E. HASLINGER, H. ZAK, and U. SCHMIDT. Monatsh. Chem. **106**, 219 (1975); U. SCHMIDT, J. GOMBOS, E. HASLINGER, and H. ZAK. Chem. Ber. **109**, 2628 (1976).
5. R. E. ARVICK, D. S. BAKER, and D. HORTON. Carbohydr. Res. **26**, 411 (1973).
6. S. NITSUI, Y. SENDA, and H. SAITO. Bull. Chem. Soc. Jpn. **39**, 694 (1966).
7. F. W. EASTWOOD, K. J. HARRINGTON, J. S. JOSAN, and J. L. PURA. Tetrahedron Lett. 5223 (1970).
8. ALFRED HASSNER, THOMAS K. MORGAN, JR., and A. R. MCLAUGHLIN. J. Org. Chem. **44**, 1999 (1979).
9. M. L. WOLFROM, M. KONIGSBERG, and D. I. WEISBLAT. J. Am. Chem. Soc. **61**, 574 (1939).
10. W. KELLER-SCHIERLEIN and H. GERLACH. Prog. Chem. Org. Nat. Prod. **26**, 161 (1968); K. ANDO, H. OISHI, T. OKUTOMI, K. SUZUKI, H. OKAZAKI, M. SAWADA, and T. SAGAWA. J. Antibiot. (Tokyo), **24**, 347 (1971).

Can. J. Chem. Downloaded from www.nrcresearchpress.com by 210.87.254.6 on 09/05/12
For personal use only.

Canadian Journal of Chemistry
Published by
THE NATIONAL RESEARCH COUNCIL OF CANADA

Journal canadien de chimie
Publié par
LE CONSEIL NATIONAL DE RECHERCHES DU CANADA

Volume 58 Number 24 December 15, 1980 Volume 58 numéro 24 15 décembre 1980

Electrophilic additions to allenes. VI. The role of steric versus electronic effects in the reactions of arenesulphenyl halides with allenes[1]

DENNIS G. GARRATT[2] AND PIERRE L. BEAULIEU[3]
Department of Chemistry, University of Ottawa, Ottawa, Ont., Canada K1N 9B4

Received June 4, 1980

DENNIS G. GARRATT and PIERRE L. BEAULIEU. Can. J. Chem. **58**, 2737 (1980).

The role of steric and electronic effects during the rate and product determining steps for the addition of arenesulphenyl chlorides to 1,3-disubstituted allenes has been briefly examined. Both effects appear to be generally of minimal importance during the rate determining step. The available rate data indicate the presence of little, if any, build up of positive charge on sulphur. These results are interpreted in terms of an S_N2 attack on bivalent sulphur leading to an alkylidenethiiranium ion intermediate. Steric effects are of greater importance in the product determining step, particularly when the sulphenyl chlorides possess two bulky *ortho* substituents, as in the case of 2,4,6-triisopropylbenzenesulphenyl chloride.

DENNIS G. GARRATT et PIERRE L. BEAULIEU. Can. J. Chem. **58**, 2737 (1980).

On a examiné brièvement le rôle des effets stérique et électronique dans les étapes déterminant la vitesse de la réaction et la valeur des produits d'addition des chlorures d'arène-sulphényle sur les allènes disubstitués en positions 1,3. Les deux effets semblent n'avoir qu'une faible importance sur l'étape déterminant la vitesse de la réaction. Les données cinétiques disponibles indiquent la présence d'une faible charge positive sur le soufre. On interprète ces résultats en termes d'une attaque S_N2 sur le soufre bivalent conduisant à un ion alkylidènethiiranium intermédiaire. Les effets stériques jouent un rôle important dans l'étape déterminant la nature des produits formés en particulier quand le chlorure de sulphényle possède deux substituants encombrants en position *ortho* comme dans le cas du chlorure de triisopropyl-2,4,6 benzènesulphényle.

[Traduit par le journal]

In previous papers of this series we have reported the reactions of benzenesulphenyl chloride and some derivatives thereof with a series of 1,3-disubstituted allenes (1–3). In all cases studied the arylthio moiety was observed to attack regiospecifically on the central allenic carbon, with the *E* isomer formed preferentially or exclusively under conditions of kinetic control. The ratio of products was interpreted as corresponding to the percentage of attack on each face of the respective π systems, and therefore reflecting the direction of approach of the electrophile towards the allenic system. The preponderance of the *E* isomer led us to propose that one observes *steric approach control*, wherein the steric interactions in the product determining transition state are of the long range type between attacking reagent, *ArSCl*, and substrate molecule, *allene*, which is in its ground state geometry (2, 4).

[1] $R''SCl + RCH=C=CHR' \longrightarrow \left[RHC(-S^+R'')-C(Cl^-)=CHR' \right]^{\ddagger} \longrightarrow R''S-C(RHC(Cl))=CHR'$

In order to further ascertain the degree and nature of involvement of steric factors and/or electronic effects during the course of these reactions, we have carried out a series of kinetic and stereochemical investigations, the results of which we report herein.

[1]Issued as NRCC No. 18627.

[2]Author to whom correspondence may be addressed at the Division of Chemistry, National Research Council of Canada, Ottawa, Ont., Canada K1A 0R6.

[3]Current address: Department of Chemistry, University of Alberta, Edmonton, Alta., Canada T6G 2G2.

0008-4042/80/242737-08$01.00/0
©1980 National Research Council of Canada/Conseil national de recherches du Canada

Can. J. Chem. Downloaded from www.nrcresearchpress.com by 210.87.254.6 on 09/05/12
For personal use only.

Can. J. Chem. Downloaded from www.nrcresearchpress.com by 210.87.254.6 on 09/05/12
For personal use only.

Results and Discussion

Kinetic Studies

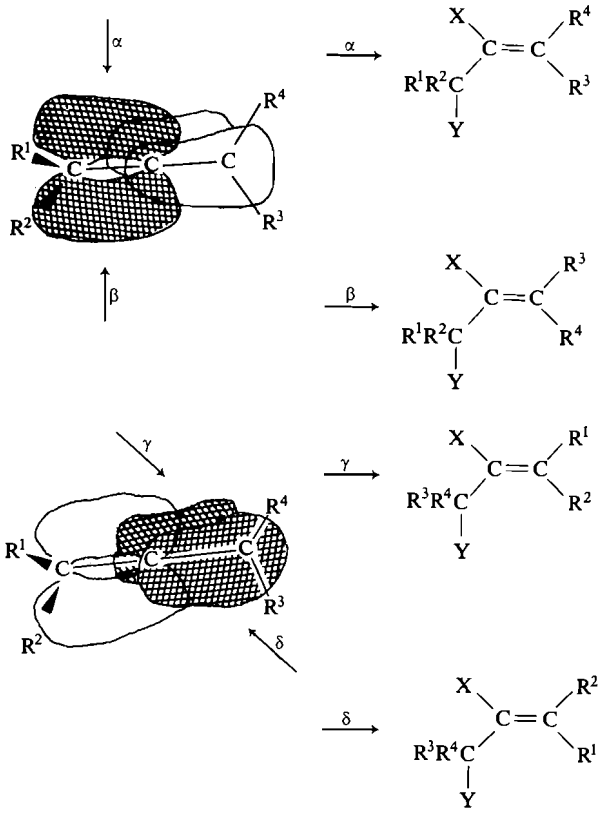
The rates of addition of benzenesulphenyl chloride to nine 1,3-disubstituted allenes at 24.5°C in methylene chloride solution were determined using the stopped-flow technique. The rate of disappearance of sulphenyl chloride was followed by measuring the decrease in its absorption at 392 nm. The additions are found to exhibit normal second order kinetics, first order in allene, and first order in sulphenyl chloride, to at least 85% completion of the reaction (5). Specific rate constants are given in Table 1.

Of particular note upon examining Table 1 is the observation that benzenesulphenyl chloride shows only minor variations in rate of addition as the 1,3 alkyl groups are changed. Steric and polar effects of the alkyl substituents are apparently quite minimal. Considering only the first three entries, the effect of substituting two ethyl groups or two isopropyl groups for the methyl groups in 2,3-pentadiene (1,3-dimethylallene) is to cause minor decreases in rate of 17 and 46%, respectively. If only one methyl group from 2,3-pentadiene is changed to ethyl, isopropyl, or *tert*-butyl, one observes initially a slight increase in rate of 9% followed by slow decreases. Such variations are also seen if one holds, for example, the isopropyl group on 5-methyl-2,3-hexadiene constant and varies the methyl group from ethyl to isopropyl to *tert*-butyl. In fact such variations are typical of those previously observed for the analogously substituted *trans*-1,2-disubstituted ethylenes (6). These data thus tend to support our earlier hypothesis (5) that the rate determining transition state in the arenesulphenylation of allenes is stabilized equally well by a methyl group as by an ethylidene (=$CHCH_3$) group, and allows us to extend the comparison to ethyl, isopropyl, and *tert*-butyl in terms of, respectively, *n*-propylidene (=$CHCH_2CH_3$), isobutylidene (=$CHCH(CH_3)_2$), and neopentylidene (=$CHC(CH_3)_3$).

The real situation is, however, somewhat more complex. As noted in the first paper of this series (2), when the two substituents on a given terminal allenic carbon atom are different, there exist two possible directions of approach by the electrophile as shown in Scheme 1. If our hypothesis of steric approach control is correct the values of k_2 given in Table 1 may be partitioned into four terms, $k_2 = k_\alpha^E + k_\alpha^Z + k_\beta^E + k_\beta^Z$, each term reflecting the relative propensity for attack upon a given π orbital-lobe of the allenic system. Such a partition has been carried out and the values listed in Table 2. This partitioning was accomplished using the previously determined kinetically controlled product distributions as partition factors (3, 7).[4]

TABLE 1. Specific rate constants for the addition of benzenesulphenyl chloride to a series of 1,3-disubstituted allenes, RCH=C=CHR', in methylene chloride at 24.5°C

Allene		
R	R'	k_2 (dm^3 mol^{-1} s^{-1})
CH_3	CH_3	151
C_2H_5	C_2H_5	126
i-C_3H_7	*i*-C_3H_7	82.0
CH_3	C_2H_5	165
CH_3	*i*-C_3H_7	125
CH_3	*t*-C_4H_9	104
C_2H_5	*i*-C_3H_7	99.8
C_2H_5	*t*-C_4H_9	106
i-C_3H_7	*t*-C_4H_9	56.0



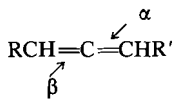
SCHEME I

An analysis of these substituent effects allows one to draw some further insights into the nature of the polar and steric effects during the rate determining step. These effects are perhaps most easily evaluated by regrouping the partitioned rate data of Table 2 into a series of subsets as shown in Table 3.

[4]See Table 5 this paper.

Can. J. Chem. Downloaded from www.nrcresearchpress.com by 210.87.254.6 on 09/05/12
For personal use only.

TABLE 2. Partitioned rate coefficients ($dm^3\ mol^{-1}\ s^{-1}$) for the reaction of benzenesulphenyl chloride with a series of 1,3-disubstituted allenes



R	R′	k_2	k_α^E	k_α^Z	k_β^E	k_β^Z
CH_3	CH_3	151	41.5	34.0	41.5	34.0
C_2H_5	C_2H_5	126	45.4	17.6	45.4	17.6
i-C_3H_7	i-C_3H_7	82.0	32.8	8.2	32.8	8.2
CH_3	C_2H_5	165	49.0	38.5	54.3	23.2
CH_3	i-C_3H_7	125	39.2	29.6	45.0	11.3
CH_3	t-C_4H_9	104	35.6	25.8	37.5	5.11
C_2H_5	i-C_3H_7	99.8	30.0	16.9	38.6	14.2
C_2H_5	t-C_4H_9	106	39.1	19.2	47.7	—
i-C_3H_7	t-C_4H_9	56.0	24.1	7.2	21.7	3.0

Subsets 1–4, for example, demonstrate the effect of varying a remote substituent on the allene, which is oriented *anti* with respect to the incoming electrophile,[5] while the substituent, R, on the double bond being attacked is held constant. Similarly, subsets 5–8 demonstrate the analogous effect wherein the remote substituent is oriented *syn* relative to the incoming electrophile.[5]

Regarding first of all subsets 1–4, we observe that varying the remote substituent from methyl to ethyl, isopropyl, and *tert*-butyl leads to only marginal rate enhancements or retardations when the substituent group is oriented *anti* with respect to the approaching electrophile. Somewhat surprisingly, perhaps, in view of the orthogonality of the π systems, the effect of the remote substituent appears to be coupled to the substituent group which is on the double bond undergoing attack. Thus, for example, a remote isopropyl group in the *anti* orientation relative to the approaching electrophile leads to a slight rate enhancement, 8%, over methyl when the group on the double bond being attacked is methyl, but gives a retarding effect relative to a remote methyl when the group on the double bond being attacked is ethyl, isopropyl, or *tert*-butyl. Transmission of substituent effects across both double bonds of the allenic system as observed above has been previously reported (5).

When the remote substituent group is oriented *syn* with respect to the incoming electrophile the results are more dramatic as can be seen from an examination of subsets 5–8. Replacing a *syn* methyl group by ethyl uniformly leads to a rate decrease. Similar decreases are observed upon substituting isopropyl for ethyl or *tert*-butyl for isopropyl, in accord with the relative spatial volume or steric bulk of each substituent. Once again we observe an apparent coupling between the magnitude of the effect and the nature of the substituent on the double bond being attacked. For example, when the remote substituent is *tert*-butyl and the group on the double bond undergoing attack is methyl, we observe a rate retardation of 85% relative to a remote methyl group. If, however, the group on the double bond being attacked is isopropyl the analogous substitution of *tert*-butyl for methyl on the remote terminus leads to a 91% rate retardation. This increase in steric retardation can be accounted for in terms of an additional steric effect caused by the isopropyl group on the double bond being attacked.

Subsets 9–12 and 13–16 allow us to evaluate the effect of changing a substituent on the double bond which is under attack while holding the remote substituents constant. From these data it is apparent that replacing methyl by either isopropyl or *tert*-butyl will lead to a rate retardation. The ethyl group, however, shows ambivalent behaviour giving rise to either rate enhancement or retardation depending upon the nature and orientation, i.e. *syn* or *anti*, of the remote substituent.

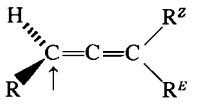
An alternative method of gaining information on the nature of the rate determining transition state is to vary substituents on the electrophile itself thus changing the bridging ability or degree of neighbouring group participation of the arylthio moiety while holding the allenic functionality constant (8). In a previous article (3) we noted that such variations had little effect on either the chemoselectivity or configurational-selectivity of the reaction except for a minor steric effect when the sulphenyl chloride has an *ortho*-nitro or *ortho*-methyl substituent. In Table 4 are given the specific rate constants for the reactions of nine arenesulphenyl chlorides with 3-methyl-1,2-butadiene (1,1-dimethylallene) and 2,3-pentadiene at 24.5°C in methylene chloride solution. From these data it is clear that varying the electron-donating or electron-withdrawing ability of a remote substituent on the sulphenyl chloride leads to only minor changes in the rate of addition. In terms of linear free energy relationships of, for example, the Hammett type, a plot of log k_2 versus σ or σ^+ is essentially linear with a ρ value very close to unity or slightly positive.[6] Such a result is best interpreted in terms of little, if any, build up of positive

[5]This orientation of approach leads specifically to the adduct of *E* configuration. *Syn* attack conversely gives an adduct of *Z* configuration.

[6]For the purposes of these plots the data for 2,5-dichlorobenzenesulphenyl chloride, 2-methylbenzenesulphenyl chloride, and 2,4,6-trimethylbenzenesulphenyl chloride have been omitted.

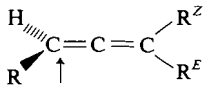
Can. J. Chem. Downloaded from www.nrcresearchpress.com by 210.87.254.6 on 09/05/12
For personal use only.

TABLE 3. Variation of partitioned rate constants as a function of alkyl group and substitution pattern



R	R^Z	R^E	k	k_{rel}
Subset 1				
CH_3	H	CH_3	41.5	1.00
CH_3	H	C_2H_5	54.3	1.31
CH_3	H	i-C_3H_7	45.0	1.08
CH_3	H	t-C_4H_9	37.5	0.90
Subset 2				
C_2H_5	H	CH_3	49.0	1.00
C_2H_5	H	C_2H_5	45.4	0.93
C_2H_5	H	i-C_3H_7	38.6	0.79
C_2H_5	H	t-C_4H_9	47.7	0.97
Subset 3				
i-C_3H_7	H	CH_3	39.2	1.00
i-C_3H_7	H	C_2H_5	30.0	0.77
i-C_3H_7	H	i-C_3H_7	32.8	0.84
i-C_3H_7	H	t-C_4H_9	21.7	0.55
Subset 4				
t-C_4H_9	H	CH_3	35.6	1.00
t-C_4H_9	H	C_2H_5	39.1	1.10
t-C_4H_9	H	i-C_3H_7	24.1	0.68
Subset 5				
CH_3	CH_3	H	34.0	1.00
CH_3	C_2H_5	H	23.2	0.68
CH_3	i-C_3H_7	H	11.3	0.33
CH_3	t-C_4H_9	H	5.11	0.15
Subset 6				
C_2H_5	CH_3	H	38.5	1.00
C_2H_5	C_2H_5	H	17.6	0.46
C_2H_5	i-C_3H_7	H	14.2	0.37
C_2H_5	t-C_4H_9	H	—	—
Subset 7				
i-C_3H_7	CH_3	H	29.6	1.00
i-C_3H_7	C_2H_5	H	16.9	0.57
i-C_3H_7	i-C_3H_7	H	8.2	0.28
i-C_3H_7	t-C_4H_9	H	3.0	0.10
Subset 8				
t-C_4H_9	CH_3	H	25.8	1.00
t-C_4H_9	C_2H_5	H	19.2	0.74
t-C_4H_9	i-C_3H_7	H	7.2	0.28
Subset 9				
CH_3	H	CH_3	41.5	1.00
C_2H_5	H	CH_3	49.0	1.18
i-C_3H_7	H	CH_3	39.2	0.94
t-C_4H_9	H	CH_3	35.6	0.86
Subset 10				
CH_3	H	C_2H_5	54.3	1.00
C_2H_5	H	C_2H_5	45.4	0.84
i-C_3H_7	H	C_2H_5	30.0	0.55
t-C_4H_9	H	C_2H_5	39.1	0.72
Subset 11				
CH_3	H	i-C_3H_7	45.0	1.00
C_2H_5	H	i-C_3H_7	38.6	0.86
i-C_3H_7	H	i-C_3H_7	32.8	0.73
t-C_4H_9	H	i-C_3H_7	24.1	0.54

TABLE 3 (*Concluded*)



R	R^Z	R^E	k	k_{rel}
Subset 12				
CH_3	H	t-C_4H_9	37.5	1.00
C_2H_5	H	t-C_4H_9	47.7	1.27
i-C_3H_7	H	t-C_4H_9	21.7	0.58
Subset 13				
CH_3	CH_3	H	34.0	1.00
C_2H_5	CH_3	H	38.5	1.13
i-C_3H_7	CH_3	H	29.6	0.87
t-C_4H_9	CH_3	H	25.8	0.76
Subset 14				
CH_3	C_2H_5	H	23.2	1.00
C_2H_5	C_2H_5	H	17.6	0.76
i-C_3H_7	C_2H_5	H	16.9	0.73
t-C_4H_9	C_2H_5	H	19.2	0.83
Subset 15				
CH_3	i-C_3H_7	H	11.3	1.00
C_2H_5	i-C_3H_7	H	14.2	1.26
i-C_3H_7	i-C_3H_7	H	8.2	0.73
t-C_4H_9	i-C_3H_7	H	7.2	0.64
Subset 16				
CH_3	t-C_4H_9	H	5.11	1.00
C_2H_5	t-C_4H_9	H	—	—
i-C_3H_7	t-C_4H_9	H	3.0	0.59

or negative charge on sulphur during the rate determining step.

To appreciate the significance of this result it is necessary to consider the possible modes of interaction for an olefinic double bond with a sulphenyl halide,[7] as shown in Scheme 2. This scheme has been discussed previously and will not be further elaborated in detail at this time (9, 10). The results presented herein are in agreement with our previously proposed mechanism (2) and appear to be most consistent with path 'a' of Scheme 2. We note that for path 'a' a rate determining transition state structure of the S_N2 sort is anticipated to have a charge distribution leading to a ρ value which is zero or slightly positive or negative in analogy to S_N2 displacement at carbon. If path 'b' is to be of importance, one would anticipate a ρ value of moderate magnitude, ± 2–4, the sign being dependent upon whether or not formation or collapse of the episulphurane species is rate determining. A zero ρ value as found during this study thus tends to rule out path 'b'.

Upon further examination of Table 4 the following additional points may be made. Firstly, while

[7]The following scenarios are valid irrespective of whether one is dealing with an isolated, conjugative, or cumulative double bond.

Can. J. Chem. Downloaded from www.nrcresearchpress.com by 210.87.254.6 on 09/05/12
For personal use only.

TABLE 4. Specific rate constants for the addition of various arenesulphenyl chlorides to 3-methyl-1,2-butadiene and 2,3-pentadiene in methylene chloride solution at 24.5°C

Arenesulphenyl chloride substituents	k_2 (dm^3 mol^{-1} s^{-1}) Allene	
	3-Methyl-1,2-butadiene	2,3-Pentadiene
3-Cl, 4-Cl	200	200
2-Cl, 5-Cl	150	100
4-Cl	170	150
4-Br	220	220
4-F	170	150
None	200	151
4-CH_3	150	130
2-CH_3	160	85
4-CH_3O	120	90
2-CH_3, 4-CH_3, 6-CH_3	155	37

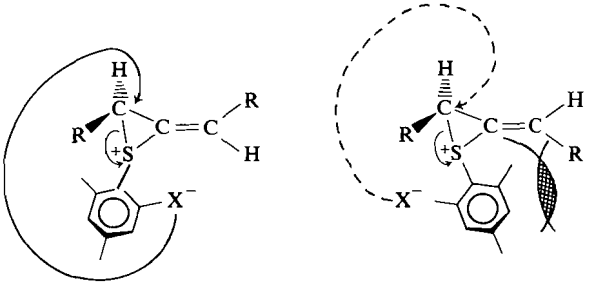
the *ortho*-chloro and *ortho*-methyl substituted arenesulphenyl chlorides are found to react somewhat slower than their *para* substituted analogues, there does not appear to be substantial steric retardation from these substituents in the rate determining step. The only anomalous result appears, at first sight, to be the rate constant for the reaction of 2,4,6-trimethylbenzenesulphenyl chloride with 2,3-pentadiene. The rate retardation found in this case is, however, easily explained. Using the configurational-selectivity data in Table 5, it is found that 40% of the product distribution results from attack by the sulphenyl chloride *syn* with respect to the remote methyl group on the allene. The presence of two *ortho* methyl groups on the sulphenyl chloride in this case leads to a rather sterically congested rate determining transition state and thus to a slower rate of addition. The absence of a rate retardation upon reaction of 2,4,6-trimethylbenzenesulphenyl chloride with 3-methyl-1,2-butadiene is seen to reflect the 90:10 chemoselectivity in favour of attack upon the most substituted double bond of this allenic system. In this case there is only a hydrogen atom in the same plane as the π orbital which is interacting with the sulphenyl chloride. Therefore, no steric effect is anticipated to be observable.

Product Studies

In order to further evaluate the nature of polar and steric effects in the product determining transition state,[8] we have investigated the reactions of a series of thirteen arenesulphenyl chlorides with ten 1,3-disubstituted allenes. Our hypothesis during this portion of our work is based upon the premise that the presence of *ortho* substituents on the phenyl ring of these electrophiles will lead to greater configurational-selectivity in the formation of adducts under conditions of kinetic control. Although the reactions of some of these sulphenyl chlorides have previously been reported (3), their product distributions are given here for purposes of comparison and completeness.

All reactions were carried out at ambient temperature using methylene chloride as solvent. The kinetically controlled product distributions, as given in Table 5, were determined by immediate ^{1}H nmr analysis of the reaction mixture. Reaction end-points were determined by the disappearance of the S—Cl chromophore (λ_{max} 392 nm) and/or a negative starch iodide test (12). Analysis of the spectral data, using the criteria previously established (2, 3), indicates that the 1:1 adducts are formed via regiospecific attack of the arylthio moieties on the central allenic carbons as shown in eq. [1].

In accord with our initial hypothesis (2, 3) the substitution of an *ortho* hydrogen by a larger group such as methyl, trifluoromethyl, or nitro leads to an increase in the configurational-selectivity as is reflected in the $\alpha(E{:}Z)$ and $\beta(E{:}Z)$ ratios. The substitution of both *ortho* hydrogens by alkyl groups, such as methyl or isopropyl, demonstrates this effect more dramatically. The *E* isomers in these latter two examples are formed with configurational-specificity in eleven out of sixteen of the cases investigated. This configurational-specificity is interpreted as the result of severe steric interactions between the two *ortho* groups and the remote *syn* oriented substituent on the allenic system which by virtue of the orthogonality of the two allenic π systems must lie in the same plane as the π orbital which is interacting with the sulphenyl chloride as is shown below.

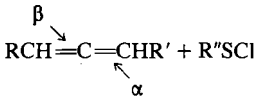


E Favored *Z*

Data for two of the sulphenyl chlorides listed in Table 5 appear, at first sight, to be anomalous. Both 1-naphthalenesulphenyl chloride and 9-phenanthracenesulphenyl chloride show a lesser degree of configurational-selectivity towards favouring the *E* isomer under conditions of kinetic control than would have been expected upon replacing an *ortho*

[8]See ref. 3 for a preliminary discussion of this concept.

TABLE 5. Kinetically controlled product distributions for the reactions of arenesulphenyl



	R	R′	C_6H_5	4-$CH_3C_6H_4$	2-$CH_3C_6H_4$	2,4-$(CH_3)_2C_6H_3$	2,4,6-$(CH_3)_3C_6H_2$
	Symmetrically substituted allenes						
$E:Z^a$	CH_3	CH_3	55:45	55:45	56:44	55:45	60:40
	C_2H_5	C_2H_5	72:28	—	72:28	68:32	83:17
	i-C_3H_7	i-C_3H_7	80:20	79:21	81:19	83:17	100: 0
	t-C_4H_9	t-C_4H_9	97: 3	100: 0	100: 0	100: 0	100: 0
	Unsymmetrically substituted allenes						
$\alpha:\beta^b$	CH_3	C_2H_5	53:47	—	—	—	50:50
	CH_3	i-C_3H_7	55:45	63:37	66:34	—	65:35
	CH_3	t-C_4H_9	59:41	55:45	48:52	38:62	82:18
	C_2H_5	i-C_3H_7	47:53	49:51	47:53	59:41	62:38
	C_2H_5	t-C_4H_9	55:45	53:47	43:57	65:35	83:17
	i-C_3H_7	t-C_4H_9	56:44	60:40	34:66	53:47	80:20
$\alpha(E:Z)^c$	CH_3	C_2H_5	56:44	—	—	—	69:31
	CH_3	i-C_3H_7	57:43	55:45	67:33	—	85:15
	CH_3	t-C_4H_9	58:42	55:45	69:31	58:42	100: 0
	C_2H_5	i-C_3H_7	64:36	64:36	68:32	80:20	100: 0
	C_2H_5	t-C_4H_9	67:33	64:36	63:37	62:38	100: 0
	i-C_3H_7	t-C_4H_9	77:23	66:34	87:13	83:17	100: 0
$\beta(E:Z)^c$	CH_3	C_2H_5	70:30	—	—	—	83:17
	CH_3	i-C_3H_7	80:20	81:19	85:15	—	100: 0
	CH_3	t-C_4H_9	88:12	100: 0	100: 0	100: 0	100: 0
	C_2H_5	i-C_3H_7	73:27	73:27	77:23	83:17	100: 0
	C_2H_5	t-C_4H_9	100: 0	100: 0	100: 0	100: 0	100: 0
	i-C_3H_7	t-C_4H_9	88:12	100: 0	100: 0	100: 0	100: 0

[a]Configurational-selectivity.
[b]Chemoselectivity.
[c]Configurational-selectivity for the α and β double bonds, respectively.
[d]1-$C_{10}H_7$ = 1-naphthyl; 9-$C_{14}H_9$ = phenanthryl.

and a *meta* hydrogen by the benzo moiety. For example, the *E*:*Z* ratios of 40:60 and 42:58 observed for these sulphenyl chlorides upon reaction with 2,3-pentadiene are the only examples, to our knowledge, of the addition of sulphenyl halides to 1,3-disubstituted allenes wherein the *Z* isomer is formed preferentially under conditions of kinetic control. In view of these latter results it is surprising that normal *E*:*Z* ratios are observed for attack on 2,3-hexadiene, 5-methyl-2,3-hexadiene, and 5,5-dimethyl-2,3-hexadiene. While we do not completely understand the reasons for this anomalous behaviour it seems likely that the lower configurational-selectivity observed must reflect in part the planar configuration of these aryl groups compared to, for example, 2,4,6-trimethyl- or 2,4,6-triisopropylbenzenesulphenyl chloride, where the alkyl groups in the *ortho* positions occupy a larger volume in space close to the reaction center and thus present a bulkier local environment during the product determining step.

In summary, the data presented here and in earlier segments of this series allow us to define the reaction hypersurface for the interaction of sulphenyl chlorides with allenes as one which follows an Ad_E2 mechanism (13) similar to that first proposed by Kharasch and Buess for simple alkenes (14). The first step appears to be rate determining formation of an alkylidenethiiranium ion by S_N2 attack on sulphur. This intermediate subsequently undergoes nucleophilic attack by the halide ion in a fast step.

Experimental

General

The allenes used during this study were prepared by standard literature procedures as previously described (1–3). 2,3-pentadiene and 3-methyl-1,2-butadiene were purchased from Chemical Samples Co. The ^1H nmr spectra were recorded as $CDCl_3$ solutions using a Varian HA-100 spectrometer. All melting points and boiling points are uncorrected.

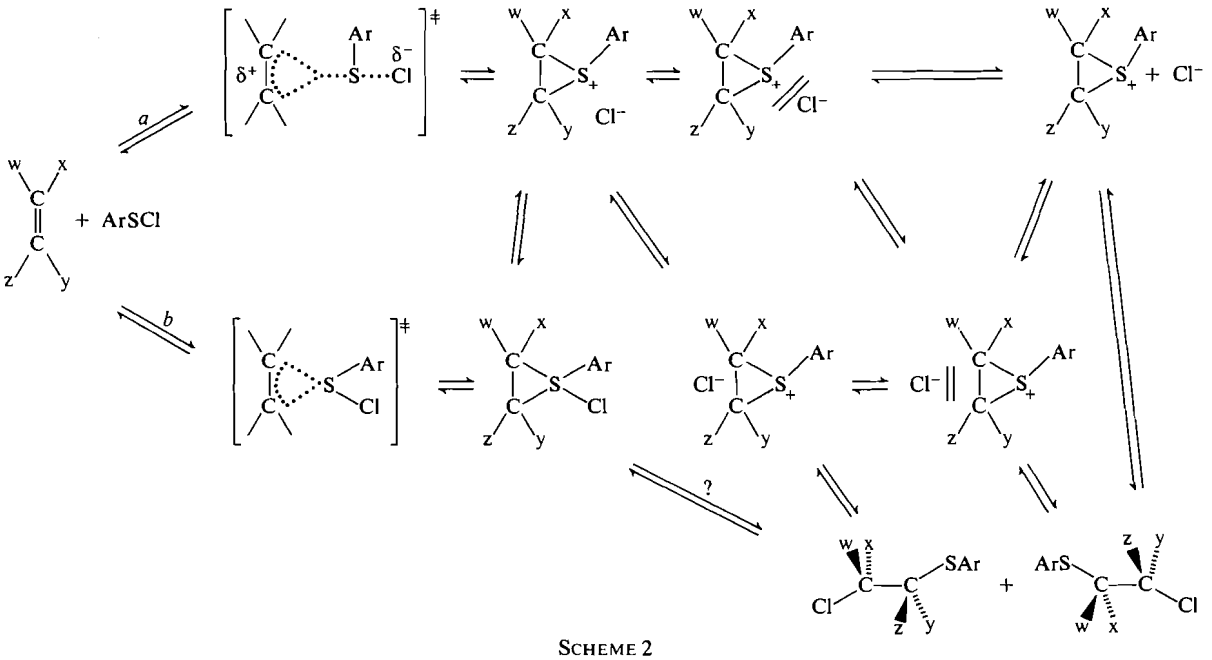
Sulphenyl Chlorides

4-Methyl-, 2-methyl-, 4-chloro-, 2,5-dichloro-, 3,4-dichloro-, 4-nitro-, 2,4-dimethyl-, 2,4,6-trimethyl-, 2,4,6-triisopropyl-, 2-trifluoromethyl-, 4-trifluoromethyl-, and benzenesulphenyl chloride were prepared by the direct chlorination, chlorine gas

Can. J. Chem. Downloaded from www.nrcresearchpress.com by 210.87.254.6 on 09/05/12
For personal use only.

chlorides with some 1,3-disubstituted allenes at 23–25°C in methylene chloride solution

R″							
2,4,6-$(CH(CH_3)_2)_3C_6H_2$	4-$NO_2C_6H_4$	2-$NO_2C_6H_4$	2,4-$(NO_2)_2C_6H_3$	4-$CF_3C_6H_4$	2-$CF_3C_6H_4$	1-$C_{10}H_7$[d]	9-$C_{14}H_9$[d]
76:24	50:50	59:41	64:36	53:47	55:45	40:60	42:58
98: 2	69:31	72:28	80:20	70:30	78:22	60:40	71:29
100: 0	82:18	82:18	92: 8	82:18	95: 5	71:29	65:35
100: 0	100: 0	100: 0	100: 0	100: 0	100: 0	—	—
49:51	55:45	53:47	53:47	57:43	50:50	—	60:40
66:34	62:38	48:52	52:48	57:43	50:50	73:27	58:42
84:16	65:35	33:67	42:58	62:38	36:64	60:40	48:52
60:40	51:49	46:54	46:54	57:43	45:55	48:52	47:53
85:15	50:50	31:69	33:67	62:38	40:60	45:55	46:54
75:25	50:50	31:69	38:62	50:50	38:62	25:75	24:76
76:24	53:47	60:40	66:34	58:42	58:42	—	53:47
79:21	53:47	65:35	65:35	54:46	55:45	53:47	55:45
100: 0	54:46	73:27	69:31	52:48	53:47	57:43	56:44
100: 0	73:27	85:15	76:24	65:35	65:35	65:35	66:34
100: 0	70:30	84:16	76:24	61:39	63:37	71:29	72:28
100: 0	82:18	84:16	100: 0	72:28	70:30	73:27	100: 0
86:14	71:29	77:23	86:14	79:21	80:20	82:18	81:19
100: 0	84:16	87:13	95: 5	86:14	83:17	85:15	79:21
100: 0	100: 0	100: 0	100: 0	100: 0	100: 0	100: 0	100: 0
100: 0	90:10	91: 9	100: 0	79:21	83:17	77:23	80:20
100: 0	92: 8	100: 0	100: 0	100: 0	100: 0	100: 0	100: 0
100: 0	100: 0	100: 0	100: 0	100: 0	100: 0	100: 0	100: 0



SCHEME 2

Can. J. Chem. Downloaded from www.nrcresearchpress.com by 210.87.254.6 on 09/05/12
For personal use only.

bubbled through CCl_4, of the corresponding thiols at 0°C. 2,4-Dinitrobenzenesulphenyl chloride was prepared as previously described (2), mp 96–96.5°C, recrystallized from CCl_4. 2-Nitrobenzenesulphenyl chloride was purchased from Aldrich Chemicals, recrystallized from CCl_4, mp 76–76.8°C; 2-methylbenzenesulphenyl chloride, bp 89–95°C/0.5 Torr; 4-methylbenzenesulphenyl chloride, bp 85°C/1 Torr; 4-chlorobenzenesulphenyl chloride, bp 71–72°C/0.12 Torr; 2,4,6-triisopropylbenzenesulphenyl chloride, bp 130–136°C/0.45 Torr; ^{13}C nmr ($CDCl_3$): 155.8(s), 154.6(s), 122.5(d), 34.8 (d, $C_pCH(CH_3)_2$), 31.9 (d, $C_oCH(CH_3)_2$), 24.6 (q, $C_pCH(CH_3)_2$), 24.2 and 23.8 (q, $C_oCH(CH_3)_2$). 1-Naphthalenesulphenyl chloride and 9-phenanthracenesulphenyl chlorides were prepared via chlorination of the respective thiols with *N*-chlorosuccinimide in CH_2Cl_2 at room temperature.

Thiols

2-Trifluoromethyl-, 4-trifluoromethyl-, 2-methyl-, 2,4-dimethyl-, 2,4,6-trimethyl-, and 4-bromobenzenethiols were prepared from the commercially available bromides by the reaction of the analogous Grignard reagents with elemental sulphur in Et_2O. 1-Naphthyl and 9-phenanthrylthiols were prepared in a similar fashion; 1-naphthylthiol in 84% yield as a brownish oil, 9-phenanthrylthiol in 88% yield as light yellow crystals, mp 175–176°C. 2,4,6-Triisopropylbenzenethiol was prepared by the Zn/HCl reduction of the commercially available sulphonyl chloride followed by steam distillation, extraction, and high vacuum distillation in 70–85% yields along with some triisopropylbenzene as by-product. 4-Chloro-, 4-methyl-, 4-fluoro-, 4-methoxy-, 2,5-dichloro-, 3,4-dichloro-, and benzenethiol were the commercial products.

General Procedure

As previously described (2), to a solution of the sulphenyl chloride (1–2 mmol) in 10–15 mL of anhydrous CH_2Cl_2 was added an equivalent (1–2 mmol) of the respective allene. The mixture was stirred at room temperature until the reaction was observed to be complete (disappearance of the red-orange color S—Cl, or a negative starch-iodide test). The solvent was evaporated and the residual oil analyzed by ^1H nmr. Control experiments run in nmr tubes gave the same kinetically controlled product distributions. Satisfactory elemental analyses for C, H, S, and Cl were obtained for a representative sample of the new adducts (≅ 15% of the compounds prepared). In each case the analytical samples were mixtures of isomers, except in the case of adducts derived from 2,4,6-trimethylbenzenesulphenyl chloride and 2,4-6-triisopropylbenzenesulphenyl chloride.

Kinetics were carried out as previously described (5, 6, 8, 10).

Spectral parameters, Tables 7–19, are available from the authors upon request.

Acknowledgements

Continued financial support from the Natural Sciences and Engineering Research Council of Canada during the course of this work is gratefully acknowledged. We are also indebted to the Province of Ontario for a scholarship to P.L.B. (1978–1980) and to Professor K. Laidler of the University of Ottawa for allowing us to use his stopped-flow apparatus.

1. D. G. GARRATT, P. L. BEAULIEU, and G. H. SCHMID. Chem. Scr. In press.
2. D. G. GARRATT and P. L. BEAULIEU. Can. J. Chem. **57**, 119 (1979).
3. D. G. GARRATT and P. L. BEAULIEU. Can. J. Chem. **58**, 1275 (1980).
4. D. J. PASTO and B. LEPESKA. J. Am. Chem. Soc. **98**, 1091 (1976); W. G. DAUBEN, G. J. FAUKEN, and D. S. NOYCE. J. Am. Chem. Soc. **78**, 2579 (1956); E. C. ASHLY and S. A. NODING. J. Org. Chem. **42**, 264 (1977).
5. G. H. SCHMID, D. G. GARRATT, and S. YEROUSHALMI. J. Org. Chem. **43**, 3764 (1978).
6. D. G. GARRATT. Ph.D thesis, University of Toronto, Toronto, Ontario, Canada, 1975; Chem. Abstr. **91**, 174 (1979); **91**, 420 (1979); Diss. Abstr. Int. B, **39**, 2804 (1978); G. H. SCHMID, C. L. DEAN, and D. G. GARRATT. Can. J. Chem. **54**, 1253 (1976).
7. D. G. GARRATT, P. L. BEAULIEU, and M. D. RYAN. Tetrahedron, **36**, 1507 (1980).
8. D. G. GARRATT and P. L. BEAULIEU. J. Org. Chem. **44**, 3555 (1979); D. G. GARRATT, P. L. BEAULIEU, and V. M. MORISSET. Can. J. Chem. **58**, 1021 (1980); P. L. BEAULIEU, A. KABO, and D. G. GARRATT. Can. J. Chem. **58**, 1014 (1980); C. BROWN and D. R. HOGG. J. Chem. Soc. B, 1262 (1968).
9. G. H. SCHMID and D. G. GARRATT. *In* The chemistry of functional groups, Supplement A: The chemistry of double-bonded functional groups. *Edited by* S. Patai. Wiley and Sons, London. 1977. pp. 828–854; G. H. SCHMID. *In* Topics in sulphur chemistry. *Edited by* A. Senning and P. S. Magee. Georg Thieme Publishers, Stuttgart. 1977. p. 103.
10. (*a*) G. H. SCHMID and T. T. TIDWELL. J. Org. Chem. **43**, 460 (1978); (*b*) W. A. SMIT, A. S. GYBIN, V. S. BOGDANOV, M. Z. KRIMER, and E. A. VOROBIEVA. Tetrahedron Lett. 1085 (1978); (*c*) G. H. SCHMID and V. M. CSIZMADIA. Can. J. Chem. **44**, 1338 (1966); (*d*) G. H. SCHMID and P. H. FITZGERALD. J. Am. Chem. Soc. **93**, 2547 (1971); (*e*) G. H. SCHMID and V. M. CSIZMADIA. Can. J. Chem. **50**, 2465 (1972); (*f*) G. H. SCHMID and V. J. NOWLAN. J. Org. Chem. **37**, 3086 (1972); (*g*) K. IZAWA, T. OKUYAMA, and T. FUENO. Bull. Chem. Soc. Jpn. **47**, 1480 (1974); (*h*) E. DUNKELBLUM. Tetrahedron, **30**, 3991 (1974); (*i*) M. OKI, W. NAKANISHI, M. FUKUNAGA, G. D. SMITH, W. L. DUAX, and Y. OSAWA. Chem. Lett. 1277 (1975); (*j*) G. M. BEVERLY and D. R. HOGG. J. Chem. Soc. Chem. Commun. 138 (1966); (*k*) W. H. MUELLER and P. E. BUTLER. J. Am. Chem. Soc. **90**, 2075 (1968); (*l*) W. A. THALER, W. H. MUELLER, and P. E. BUTLER. J. Am. Chem. Soc. **90**, 2069 (1968); (*m*) G. H. SCHMID and D. G. GARRATT. Can. J. Chem. **52**, 1807 (1974); (*n*) G. H. SCHMID and D. G. GARRATT. Can. J. Chem. **52**, 2463 (1974); (*o*) G. H. SCHMID, D. G. GARRATT, and S. YEROUSHALMI. J. Org. Chem. **43**, 3764 (1978); (*p*) D. G. GARRATT and P. BEAULIEU. Can. J. Chem. **57**, 119 (1979).
11. J. L. KICE. *In* Sulfur in organic and inorganic chemistry. Vol. 1. *Edited by* A. Senning. Marcel Dekker, New York. 1971. Chapt. 6. p. 176.
12. N. KHARASCH. J. Chem. Educ. **33**, 858 (1956).
13. C. K. INGOLD. Structure and mechanism in organic chemistry. 2nd ed. Cornell University Press, Ithaca, NY. 1969.
14. N. KHARASCH and C. M. BUESS. J. Am. Chem. Soc. **71**, 2724 (1949).

Can. J. Chem. Downloaded from www.nrcresearchpress.com by 210.87.254.6 on 09/05/12
For personal use only.

Electrophilic additions to allenes. VII. The role of steric versus electronic effects in the reactions of areneselenenyl halides with allenes[1]

DENNIS G. GARRATT,[2] PIERRE L. BEAULIEU, VERONIQUE M. MORISSET, AND MARK UJJAINWALLA

Department of Chemistry, University of Ottawa, Ottawa, Ont., Canada K1N 9B4

Received June 4, 1980

DENNIS G. GARRATT, PIERRE L. BEAULIEU, VERONIQUE M. MORISSET, and MARK UJJAINWALLA. Can. J. Chem. **58**, 2745 (1980).

The reactions of benzeneselenenyl chloride, bromide, and 2,4,6-trimethylbenzeneselenenyl bromide with alkyl 1,3-disubstituted allenes in methylene chloride solution have been investigated. While kinetic data are in accord with similar rate determining transition states, exhibiting strong steric effects for all three species, the product distributions show changes in both chemoselectivity and configurational-selectivity in accord with two different types of steric interaction mechanisms during the product determining transition states. A mechanism involving rate limiting formation of alkylideneseleniranium ions and/or alkylideneepiselenuranes, followed by isomerization between the alkylideneseleniranium ions by a path not involving allylic ions, prior to the product determining transition states, is proposed.

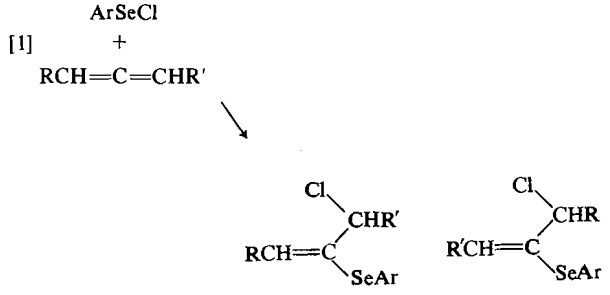
DENNIS G. GARRATT, PIERRE L. BEAULIEU, VERONIQUE M. MORISSET et MARK UJJAINWALLA. Can. J. Chem. **58**, 2745 (1980).

On a étudié les réactions, dans le chlorure de méthylène, des chlorure et bromure de benzènesélényles et du bromure de triméthyl-2,4,6 benzènesélényle avec les allènes disubstitués par des groupements alkyles en positions 1 et 3. Bien que les données cinétiques soient en accord avec des états de transition semblables, déterminants la vitesse et montrant des effets stériques importants pour les trois espèces, la distribution des produits révèle des variations à la fois dans la sélectivité chimique et dans la sélectivité configurationnelle; ces résultats impliquent l'existence de types différents de mécanismes d'interactions stériques pendant les états de transition déterminant la formation des produits. On propose un mécanisme dans lequel la vitesse de la réaction est limitée par la formation des ions alkylidèneséléniranium et/ou des alkylidèneépisélénuranes, comportant aussi une isomérisation des ions alkylidèneséléniranium par un processus n'impliquant pas les ions allyliques avant des états de transition qui déterminent la formation des produits.

[Traduit par le journal]

In a previous paper of this series we have reported the reactions of benzeneselenenyl chloride with a series of 1,3-disubstituted allenes (1). In all cases the phenylseleno moiety was observed to attack regiospecifically on the central allenic carbon, with the *Z* isomer formed preferentially or exclusively under conditions of kinetic control. Furthermore, chemoselectivity was observed in additions to unsymmetrically substituted allenes, in that the double bond with the most electron-donating and bulky substituent is preferentially attacked, the percentage of attack increasing as the electron-donating ability and bulk increases: $t\text{-}C_4H_9 > i\text{-}C_3H_7 > C_2H_5 > CH_3$.

In particular, attack on a double bond with a *tert*-butyl substituent appears to favour formation of the thermodynamically more stable *Z* alkenes. Thus attack on the double bond with a *tert*-butyl substituent gives an *E*:*Z* isomer ratio[3] of 9:91 for 5,5-dimethyl-2,3-hexadiene, 12:88 for 2,2-dimethyl-3,4-heptadiene, 11:89 for 2,2,6-trimethyl-3,4-heptadiene, and 0:100 for 2,2,6,6-tetramethyl-3,4-heptadiene. The directing effect, with respect to the *E*:*Z* configuration, of methyl, ethyl, or isopropyl groups appears to be essentially constant when the remote substituent is methyl, whereas some fluctuations are apparent when the remote group is changed to ethyl, isopropyl, or *tert*-butyl.



Assuming a stereospecificity at least as large as that for arenesulphenylation (2), we proposed a mechanism involving the preequilibration formation of alkylideneseleniranium ions **1** and/or alkylideneepiselenuranes **2** which in the product determining step collapse to the adducts via an *anti*

[1]Issued as NRCC No. 18626.

[2]Author to whom correspondence should be addressed at the Division of Chemistry, National Research Council of Canada, 100 Sussex Dr., Ottawa, Ont., Canada K1A 0R6.

[3]The term configurational-selectivity has been coined to describe the preference for attack upon one face of the olefinic double bond relative to the other. In an allenic system such as is described in this article, preferential attack upon one such π lobe will lead to a predominance of either the *E* or *Z* alkene adduct.

0008-4042/80/242745-09$01.00/0

©1980 National Research Council of Canada/Conseil national de recherches du Canada

Can. J. Chem. Downloaded from www.nrcresearchpress.com by 210.87.254.105 on 09/05/12
For personal use only.

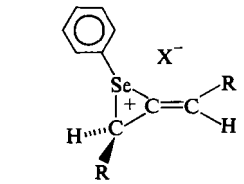
attack of chloride at the methine carbon of the ring, leading to the preferential formation of the *Z* isomer. This pathway is consistent with the observed second order kinetics, first order in selenenyl chloride and first order in allene, which serve to define the composition of the rate determining transition state in terms of one molecule of each species (3). Subsequent studies (4) were able to establish that the addition process is stereospecific.

This mechanistic scenario requires a somewhat larger preference for the *Z* isomer if the nucleophile is changed from chloride to, for example, bromide or iodide. Alternatively, it appears possible to force the preferential formation of the *E* isomer by destabilizing the *Z*-alkylideneseleniranium ion or *Z*-alkylideneepiselenurane through steric effects from suitable *ortho*-substituents placed on the phenyl group of the electrophile. We report herein experimental evidence which has a direct bearing upon these hypotheses.

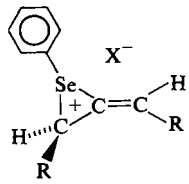
Results

In order to ascertain the degree and type of involvement of steric factors in the rate and product determining transition states, we have examined the reactions of ten 1,3-disubstituted allenes with three areneselenenyl halides, **3–5**. All reactions were carried out at ambient temperature, 25°C, using methylene chloride as solvent. The kinetically controlled product distributions (Table 1) were determined by immediate ^{1}H nmr analysis of the reaction mixture. In every case it was possible to find at least one nonoverlapping signal from which the initial (kinetically controlled) isomer distribution could be calculated. It should be noted that an immediate *in situ* determination of the adduct isomer ratio is necessary because of the tendency of many of the adducts to isomerize. If the reaction mixtures are allowed to stand at 25°C for several hours or days, an equilibrium mixture is obtained. Assignment of product configurations is based upon previously established criteria (1, 5).

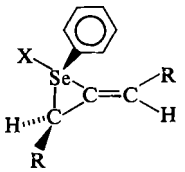
The rates of addition were determined using a Durrum-Gibson stopped-flow spectrophotometer. The rate of disappearance of benzeneselenenyl chloride, benzeneselenenyl bromide, and 2,4,6-trimethylbenzeneselenenyl bromide was followed by measuring the decrease in their respective absorptions at 433, 468, and 497 nm. The additions are found to exhibit second order kinetics, first order in allene and first order in selenenyl halide, to at least 90% completion of the reaction. Specific rate constants are given in Table 2. For purposes of comparison the analogous rate data for benzenesulphenyl chloride are also given in Table 2.

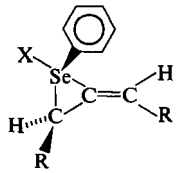


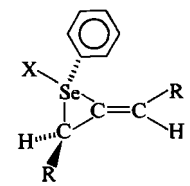
Z-1



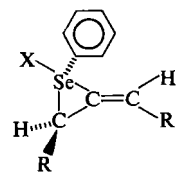
E-1







Z-2



E-2

Discussion

An examination of Table 1 shows a number of trends. In particular, benzeneselenenyl chloride and benzeneselenenyl bromide show very similar product distributions, the configurational-selectivity of the additions[3] favouring the *Z* alkene under conditions of kinetic control. 2,4,6-Trimethylbenzeneselenenyl bromide, on the other hand, shows a configurational-selectivity which favours the *E* alkene! The most dramatic example of this change in selectivity is found in the product distributions for 2,2,6,6-tetramethyl-3,4-heptadiene (1,3-di-*tert*-butylallene) where the *E*:*Z* ratio changes from 0:100 for benzeneselenenyl chloride and bromide to a value of 100:0 for 2,4,6-trimethylbenzeneselenenyl bromide. Large reversals, but of a smaller magnitude, are also observed for 5,5-dimethyl-2,3-hexadiene, 2,2-dimethyl-3,4-heptadiene, 2,6-dimethyl-3,4-heptadiene, and 2,2,6-trimethyl-3,4-heptadiene. While the tendency may exist at this point to attribute the configurational-selectivity, i.e. the preferential formation of the *E*-isomer observed with 2,4,6-trimethylbenzeneselenenyl bromide, in terms of "steric approach control" as we have previously done for the analogous arenesulphenylations (5, 6), further study is warranted.

The kinetic data in Table 2, for example, are quite informative. The specific rate constants for

Can. J. Chem. Downloaded from www.nrcresearchpress.com by 210.87.254.105 on 09/05/12
For personal use only.

Can. J. Chem. Downloaded from www.nrcresearchpress.com by 210.87.254.105 on 09/05/12
For personal use only.

TABLE 1. The kinetically controlled product distributions for the reactions of benzeneselenenyl chloride, benzeneselenenyl bromide, and 2,4,6-trimethylbenzeneselenenyl bromide with a series of 1,3-disubstituted allenes in methylene chloride solution at 25°C

$$RCH\overset{\beta}{=}C\overset{\alpha}{=}CHR'$$

		% Composition		
		C_6H_5SeCl	C_6H_5SeBr	2,4,6-$(CH_3)_3C_6H_2SeBr$
Symmetrically substituted allenes (R = R')			*E*:*Z*	
CH_3		26:74	28:72	55:45
C_2H_5		40:60	37:63	54:46
i-C_3H_7		36:64	30:70	80:20
t-C_4H_9		0:100	0:100	100:0
—$(CH_2)_6$—		100:0	100:0	100:0
—$(CH_2)_{10}$—		36:64	32:68	100:0
Unsymmetrically substituted allenes			α:β	
R = CH_3	R' = C_2H_5	33:67	65:35	55:45
CH_3	*i*-C_3H_7	56:44	62:38	67:33
CH_3	*t*-C_4H_9	76:24	89:11	65:35
C_2H_5	*i*-C_3H_7	44:56	48:52	52:48
C_2H_5	*t*-C_4H_9	80:20	78:22	71:29
i-C_3H_7	*t*-C_4H_9	75:25	79:21	64:36
			α(*E*:*Z*)	
CH_3	C_2H_5	27:73	28:72	47:53
CH_3	*i*-C_3H_7	30:70	26:74	61:39
CH_3	*t*-C_4H_9	9:91	12:88	55:45
C_2H_5	*i*-C_3H_7	27:73	27:73	71:29
C_2H_5	*t*-C_4H_9	12:88	13:87	73:27
i-C_3H_7	*t*-C_4H_9	11:89	14:86	81:19
			β(*E*:*Z*)	
CH_3	C_2H_5	30:70	31:69	62:38
CH_3	*i*-C_3H_7	43:57	50:50	85:15
CH_3	*t*-C_4H_9	39:61	27:73	100:0
C_2H_5	*i*-C_3H_7	46:54	42:58	83:17
C_2H_5	*t*-C_4H_9	27:73	27:73	100:0
i-C_3H_7	*t*-C_4H_9	16:84	14:86	100:0

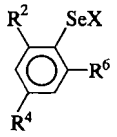
TABLE 2. Specific rate constants for the additions of benzenesulphenyl chloride, benzeneselenenyl chloride, benzeneselenenyl bromide, and 2,4,6-trimethylbenzeneselenenyl bromide to a series of 1,3-disubstituted allenes, RHC=C=CHR', in methylene chloride solution at 24.5°C

Allene		k_2 (dm^3 mol^{-1} s^{-1})			
R	R'	C_6H_5SCl	C_6H_5SeCl	C_6H_5SeBr	2,4,6-$(CH_3)_3C_6H_2SeBr$
CH_3	CH_3	151	19 700	4 420	153
C_2H_5	C_2H_5	126	6 740	1 180	40.8
i-C_3H_7	*i*-C_3H_7	82.0	1 870	567	18.2
CH_3	C_2H_5	165	18 000	4 890	140
CH_3	*i*-C_3H_7	125	3 410	646	35.4
CH_3	*t*-C_4H_9	104	342	79.8	3.15
C_2H_5	*i*-C_3H_7	99.8	2 000	316	13.7
C_2H_5	*t*-C_4H_9	106	233	44.5	1.63
i-C_3H_7	*t*-C_4H_9	56.0	62.0	16.3	0.394

TABLE 3. Relative rates of addition for the reactions of benzenesulphenyl chloride, benzeneselenenyl chloride, benzeneselenenyl bromide, and 2,4,6-trimethylbenzeneselenenyl bromide with some 1,3-disubstituted allenes, RCH=C=CHR′, in methylene chloride solution at 24.5°C

Allene		k_{rel}			
R	R′	C_6H_5SCl	C_6H_5SeCl	C_6H_5SeBr	2,4,6-$(CH_3)_3C_6H_2SeBr$
CH_3	CH_3	1.00	1.00	1.00	1.00
C_2H_5	C_2H_5	0.83	0.34	0.27	0.27
i-C_3H_7	i-C_3H_7	0.54	0.095	0.13	0.12
CH_3	C_2H_5	1.09	0.91	1.11	0.92
CH_3	i-C_3H_7	0.83	0.17	0.15	0.23
CH_3	t-C_4H_9	0.69	0.017	0.018	0.021
C_2H_5	i-C_3H_7	0.66	0.10	0.071	0.090
C_2H_5	t-C_4H_9	0.70	0.012	0.010	0.011
i-C_3H_7	t-C_4H_9	0.37	0.0031	0.0037	0.0026

benzenesulphenyl chloride and benzeneselenenyl chloride show a number of trends. Perhaps most notable is the large rate decrease upon substituting sulphur for selenium. On closer examination, however, one observes that whereas benzenesulphenyl chloride shows only minor variations in k_2 as the 1,3 alkyl groups are changed, benzeneselenenyl chloride exhibits very large fluctuations. In particular, k_2 is seen to decrease quite dramatically as



R^2	R^4	R^6	X
H	H	H	Cl
H	H	H	Br
CH_3	CH_3	CH_3	Br

the alkyl substituents increase in steric bulk and, interestingly enough, electron-donating ability. These variations in k_2, as a function of the alkyl substituents on the allenes, are more readily seen in Table 3, where relative reactivities derived from the k_2's, in Table 2, are tabulated for each electrophile.

In the case of benzenesulphenyl chloride the steric and electronic effects of the alkyl substituents are clearly minimal. Considering only the first three entries in this column, the effect of substituting two ethyl groups or two isopropyl groups for the methyl groups in 2,3-pentadiene is to cause minor decreases in the rate of 17 and 46%, respectively. If only one methyl group from 2,3-pentadiene is changed to ethyl, isopropyl, or *tert*-butyl, one observes initially a slight increase in rate (9%) followed by slow decreases. Such variations are also seen if one holds, for example, the isopropyl group on 5-methyl-2,3-hexadiene constant and varies the methyl group from ethyl to isopropyl to *tert*-butyl. In fact, such variations are typical of those previously observed for the analogously substituted *trans*-1,2-disubstituted ethylenes (7). These data thus tend to support our initial arguments (8) that the rate determining transition state in arenesulphenylations of allenes is stabilized equally well by a methyl as by an ethylidene (=$CHCH_3$) group, and allow us to extend the comparison to ethyl, isopropyl, and *tert*-butyl in terms of, respectively, *n*-propylidene (=$CHCH_2CH_3$), isobutylidene (=$CHCH(CH_3)_2$), and neopentylidene (=$CHC(CH_3)_3$).

The data for benzeneselenenyl chloride, in contrast, are interpreted in terms of a much larger steric effect. Thus in substituting two ethyl groups for the methyls in 2,3-pentadiene the rate is decreased by two-thirds, the analogous substitution of two isopropyl groups leading to a decrease of 90%! While substitution of only one methyl group by ethyl gives rise to only a very small rate decrease (9%), the subsequent substitution of either an isopropyl or a *tert*-butyl group leads to relatively large rate retardations. For example, 5,5-dimethyl-2,3-hexadiene has a rate which is only 1.7% of that observed for 2,3-pentadiene, and 2,2,6-trimethyl-3,4-heptadiene exhibits a rate constant which is smaller still at only 0.31% of that observed for 2,3-pentadiene. In contrast to the above, the rate of benzenesulphenylation of 2,2,6-trimethyl-3,4-heptadiene is 37% of that observed for 2,3-pentadiene under equivalent conditions! Quite clearly the steric and electronic factors governing the nature of the rate determining transition states for the, on the surface, similar addition reactions (9) of benzenesulphenyl and benzeneselenenyl chlorides, are very different.

While these observations are quite instructive, the most significant aspect of the observations to be made from the data in Table 3 is the very similar structure–reactivity effects exhibited by the three

Can. J. Chem. Downloaded from www.nrcresearchpress.com by 210.87.254.105 on 09/05/12
For personal use only.

TABLE 4. Rate ratios as a function of changes in the nature of the electrophilic species

Allene RCH=C=CHR'				
R	R'	$k_{C_6H_5SCl}/k_{C_6H_5SeCl}$	$k_{C_6H_5SeCl}/k_{C_6H_5SeBr}$	$k_{C_6H_5SeBr}/k_{2,4,6\text{-}(CH_3)_3C_6H_2SeBr}$
CH_3	CH_3	0.0077	4.46	28.9
C_2H_5	C_2H_5	0.019	5.71	28.9
i-C_3H_7	i-C_3H_7	0.044	3.30	31.2
CH_3	C_2H_5	0.0092	3.68	34.9
CH_3	i-C_3H_7	0.037	5.28	18.2
CH_3	t-C_4H_9	0.30	4.29	25.3
C_2H_5	i-C_3H_7	0.050	6.33	23.1
C_2H_5	t-C_4H_9	0.46	5.24	27.3
i-C_3H_7	t-C_4H_9	0.90	3.80	41.4
			avg. 4.68	avg. 28.8

selenenyl halides. Such a correlation is perhaps more readily demonstrated by taking the ratios of k_2's as we have done in Table 4. Thus we see that the ratio of k_2's for benzeneselenenyl chloride and benzeneselenenyl bromide, $k_{C_6H_5SeCl}/k_{C_6H_5SeBr}$, is essentially constant; the mean being 4.68 ± 0.86. Similarly the ratio $k_{C_6H_5SeBr}/k_{2,4,6\text{-}(CH_3)_3C_6H_2SeBr}$, is relatively constant at 28.8 ± 4.7. Although some values fall outside the standard deviation, these most likely reflect experimental error in the determination of the k_2's, which normally falls in the range of $\pm$ 5–10% for the stopped-flow technique. In contrast the ratio of k_2's for benzenesulphenyl chloride and benzeneselenenyl chloride has a mean value of 0.203 ± 0.250; clearly showing no correlation of value between the rate determining steps for the two reactions.

The value of these kinetic data is two-fold. Firstly we have demonstrated that benzenesulphenyl chloride and benzeneselenenyl chloride have different rate determining transition state structures. Secondly we have determined that, in all probability, benzeneselenenyl chloride, benzeneselenenyl bromide, and 2,4,6-trimethylbenzeneselenenyl bromide have similar, if not identical, rate determining transition state structures. This latter point is very significant since this conclusion, in conjunction with the observation of different substituent effects upon the product determining transition states for benzeneselenenyl chloride and benzeneselenenyl bromide compared to 2,4,6-trimethylbenzeneselenenyl bromide, leads us to the further conclusion that the rate and product determining transition states are quite distinct from each other and thus must be separated from each other by at least one intermediate species. Our data therefore rule out the possibility of steric approach control as a rationalization of the product distributions obtained for the reactions of 2,4,6-trimethylbenzeneselenenyl bromide, despite the reversal of configurational-selectivities in favour of E:Z values which are greater than one.

Further support for this scenario is to be found in Table 5 wherein we compare the product distributions obtained from 2,4,6-trimethylbenzeneselenenyl bromide with those obtained from 2,4,6-trimethylbenzenesulphenyl bromide, 2,4,6-trimethylbenzenesulphenyl chloride, and benzenesulphenyl chloride. Although the data given for 2,4,6-trimethylbenzenesulphenyl bromide are most likely of little utility because of experimental difficulties in determining the chemoselectivity and configurational-selectivity under conditions of kinetic control, the comparisons to be made between the remaining data for the selenenyl bromide and the sulphenyl chlorides are indicative of different factors of both a steric and electronic origin as being important in the transition states for selenenylation vs. sulphenylation.

A comparison of the specific rate constants for the addition of benzeneselenenyl chloride to some 1,3-disubstituted allenes and the analogous E,Z isomeric 1,2-disubstituted ethylenes (11) (see Table 6) leads us to the conclusion that while steric effects are of importance to both reactions, there is no strong indication of the type of similar steric–electronic interaction mechanisms previously observed for the arenesulphenylation of these species.

The available data support a mechanism where the activation energy of the reaction is large compared with the barrier to interconversion between intermediates of opposite configuration (for example, the E and Z alkylideneseleniranium ions); the proportion of products will in no way, therefore, reflect the relative populations of the ground state configurations but will depend only on the activation energies of the processes leading to these products. Stated somewhat differently, this implies

Can. J. Chem. Downloaded from www.nrcresearchpress.com by 210.87.254.105 on 09/05/12
For personal use only.

TABLE 5. A comparison of the initial product distributions for the reactions of 2,4,6-trimethylbenzeneselenenyl bromide, 2,4,6-trimethylbenzenesulphenyl bromide, 2,4,6-trimethylbenzenesulphenyl chloride, and benzenesulphenyl chloride to some 1,3-disubstituted allenes in methylene chloride solution at 23–25°C

$$RCH\overset{\beta}{=}C\overset{\alpha}{=}CHR'$$

		% Composition			
		ArSeBr[a]	ArSBr[b]	ArSCl[c]	C_6H_5SCl[c]
Symmetrically substituted allenes (R = R′)			*E*:*Z*		
CH_3		55:45	60:40	60:40	55:45
C_2H_5		54:46	35:65	98:2	72:28
i-C_3H_7		80:20	45:55	100:0	80:20
t-C_4H_9		100:0	100:0	100:0	97:3
Unsymmetrically substituted allenes			α:β		
R = CH_3	R′ = C_2H_5	55:45	45:55	60:40	53:47
CH_3	*i*-C_3H_7	67:33	40:60	70:30	55:45
CH_3	*t*-C_4H_9	65:35	60:40	82:18	59:41
C_2H_5	*i*-C_3H_7	52:48	45:55	62:38	47:53
C_2H_5	*t*-C_4H_9	71:29	56:44	83:17	55:45
i-C_3H_7	*t*-C_4H_9	64:36	65:35	80:20	56:44
			α(*E*:*Z*)		
CH_3	C_2H_5	47:53	18:82	60:40	56:44
CH_3	*i*-C_3H_7	61:39	35:65	80:20	57:43
CH_3	*t*-C_4H_9	55:45	57:43	100:0	58:42
C_2H_5	*i*-C_3H_7	71:29	51:49	100:0	64:36
C_2H_5	*t*-C_4H_9	73:27	29:71	100:0	67:33
i-C_3H_7	*t*-C_4H_9	81:19	5:95	100:0	77:23
			β(*E*:*Z*)		
CH_3	C_2H_5	62:38	38:62	100:0	70:30
CH_3	*i*-C_3H_7	85:15	33:67	100:0	80:20
CH_3	*t*-C_4H_9	100:0	78:22	100:0	88:12
C_2H_5	*i*-C_3H_7	83:17	31:69	100:0	73:27
C_2H_5	*t*-C_4H_9	100:0	89:11	100:0	100:0
i-C_3H_7	*t*-C_4H_9	100:0	100:0	100:0	88:12

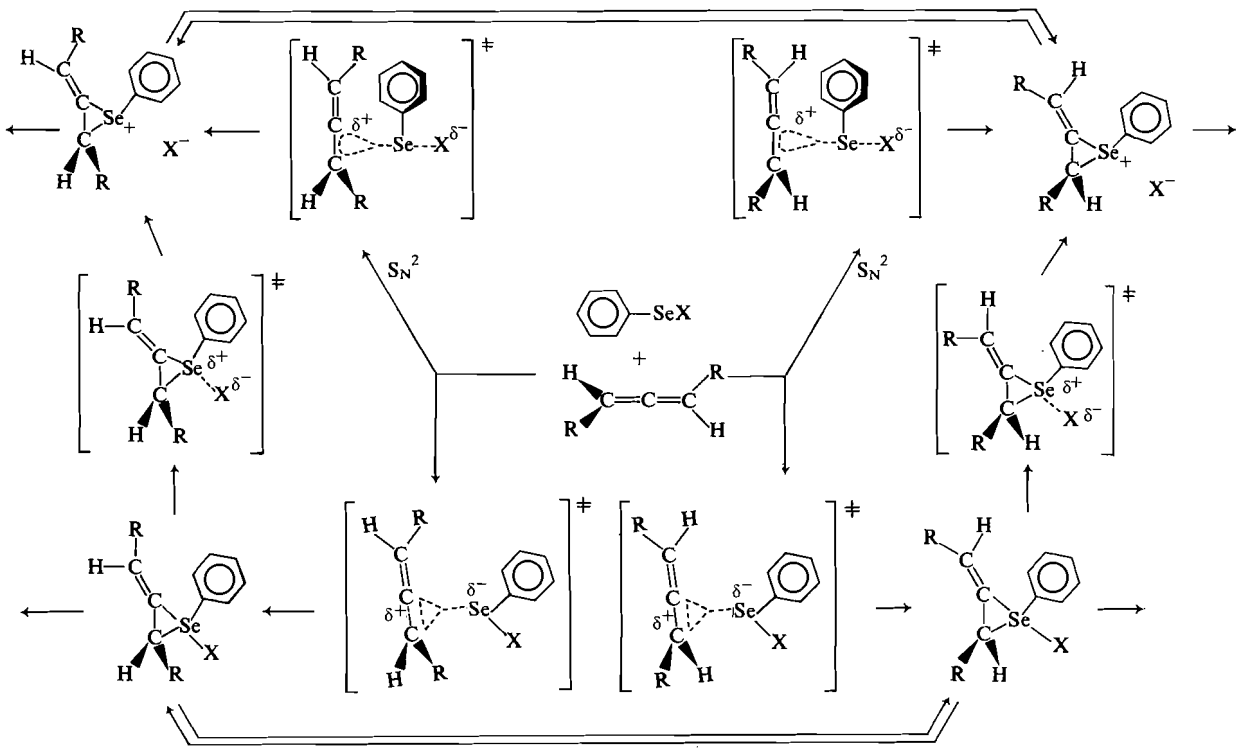
[a]Ar = 2,4,6-trimethylphenyl.
[b]The adducts derived from 2,4,6-trimethylbenzenesulphenyl bromide were found to isomerize very rapidly even at −78°C. Values given in this column thus do *not* necessarily reflect kinetic control.
[c]See ref. 6.

that the ratio of two or more products formed from one starting material depends only upon the difference in the free energy levels of the product determining transition states (10).

A mechanistic scheme compatible with our observations is given in Scheme 1. Of particular note in considering the mode of interaction between a selenenyl halide and an allenic double bond is the direction of approach. Two scenarios are of obvious importance. The first might be considered the selenium analogue of the classic S_N2 class of substitution reactions. In this case the allenic π orbitals would be considered as nucleophiles and the halogen atom as the leaving group. During the rate determining transition state the trigonal bipyramidal geometry about selenium is considered to be characterized by two lone-pair electron pairs and the aryl group in the equatorial positions, with the entering and leaving groups occupying the remaining apical sites. Upon completion of bond breaking and bond formation, one obtains as the intermediate species an alkylideneseleniranium cation–halide ion ion-pair. If the entering and leaving groups do *not* form a collinear arrangement with the selenium atom, the second scenario becomes important.

In the second scenario, one makes the hypothesis that a tetracovalent selenium species, i.e. an

Can. J. Chem. Downloaded from www.nrcresearchpress.com by 210.87.254.105 on 09/05/12
For personal use only.



SCHEME 1

TABLE 6. A comparison of the specific rate constants for the addition of benzeneselenenyl chloride to some 1,3-disubstituted allenes, RCH=C=CHR′, and the analogous *E*,*Z* isomeric 1,2-disubstituted ethylenes in methylene chloride solution at 24.5°C and 25.0°C, respectively

Substituents		k_2 (dm^3 mol^{-1} s^{-1})		
R	R′	Allene	*Z*-Alkene[a]	*E*-Alkene[a]
CH_3	CH_3	19 700	1 868	1 036
C_2H_5	C_2H_5	6 740	2 610	1 390
i-C_3H_7	*i*-C_3H_7	1 870	18.08	15.24
CH_3	C_2H_5	18 000	4 116	1 851
CH_3	*i*-C_3H_7	3 410	755.1	609.9
CH_3	*t*-C_4H_9	342	910	13.5
C_2H_5	*i*-C_3H_7	2 000	641.4	375.2
C_2H_5	*t*-C_4H_9	233	871.8	4.500

[a]See refs. 3*b* and 11.

alkylideneepiselenurane, **2**, is the first formed intermediate. This species may dissociate, forming upon fission of the selenium–halogen bond an alkylideneseleniranium ion. Alternatively, an alkylideneepiselenurane may collapse to product directly in a concerted manner. Data compatible with both of these scenarios and both of these species have been previously (12, 13) presented with respect to the related reaction with simple alkenes. The existence of episelenuranes and related species is, however, controversial (14–21). In accord with our previous discussion we postulate that the product determining transition states arise from the alkylideneseleniranium ion ion-pairs after partial or perhaps total equilibration of the various configurational types.

Using this scheme the configurational-selectivity is seen to be a function of two competitive steric effects. Our observations with benzeneselenenyl chloride and bromide ($E:Z < 1$) may be interpreted in terms of a repulsive steric interaction between the attacking nucleophile, Cl^- or Br^-, and the alkyl substituent on the olefinic carbon of the alkylideneseleniranium ion which is situated in the *E* configuration. All else being equal, one anticipates attack by Cl^- or Br^- upon the *Z*-alkylideneseleniranium ion to be preferred. However, we note that in the case of 2,4,6-trimethylbenzeneselenenyl bromide a second type of steric interaction must be present. Here the *Z*-alkylideneseleniranium ion is destabilized relative to its *E* isomer because of steric repulsions between the *ortho* methyl groups on the selenenyl bromide and the olefinic alkyl group situated *cis* with respect to the selenium atom.

An interpretation of the structure of the rate determining transition state is a more difficult problem. The available kinetic evidence defines the

Can. J. Chem. Downloaded from www.nrcresearchpress.com by 210.87.254.105 on 09/05/12
For personal use only.

Can. J. Chem. Downloaded from www.nrcresearchpress.com by 210.87.254.105 on 09/05/12
For personal use only.

composition of this transition state as containing one molecule of selenenyl halide and one molecule of allene. A large steric effect is observed with respect to alkyl substituents on the allenes but no change in the structure–reactivity profile is apparent upon substitution of *ortho* methyl groups for the *ortho* hydrogens on the electrophile. Also of note is the observation that the steric effect of an alkyl group on the allene is of major importance only when that group is isopropyl or *tert*-butyl. Indeed earlier studies, in this laboratory and elsewhere (3*a*), concerned with the kinetics of addition of benzeneselenenyl chloride to allene and all of its methyl substituted derivatives gave no evidence of a steric effect in the rate determining step, a linear correlation between log k_2 and $\Sigma\sigma^*$ being found.

The effect of a single ethyl group also appears to be predominantly electronic in nature, as can be seen by a comparison of the k_2's for 2,3-pentadiene and 2,3-hexadiene. Similar small variations between methyl and ethyl substituted allenes are noted on comparison of 5-methyl-2,3-hexadiene and 2-methyl-3,4-heptadiene, or 5,5-dimethyl-2,3-hexadiene and 2,2-dimethyl-3,4-heptadiene. The presence of a second ethyl group does, however, lead to a significant rate retardation as is seen upon comparing 2,3-hexadiene and 3,4-heptadiene. Such a result may be interpreted in terms of some type of very specific configurational interactions in the rate determining transition state which involves only the alkyl group on one terminus of the allenic functionality.

While conclusive evidence is lacking at this time, we tend to favour rate determining formation, or perhaps dissociation, of an episelenurane-like species over the alternative S_N2 type of attack. Our reasons for this are as follows. Firstly the appearance of large steric interactions would appear to reflect the congested environment about a tetracovalent selenium atom more readily than the anticipated 'loose' trigonal bipyramid arrangement in an S_N2 like transition state. The increased atomic radius of bromine relative to chlorine would then account for the approximately five-fold decrease in reactivity between benzeneselenenyl chloride and benzeneselenenyl bromide. The analogous 29-fold decrease in reactivity between benzeneselenenyl bromide and 2,4,6-trimethylbenzeneselenenyl bromide may be accounted for in a similar fashion, the increased congestion of the larger aryl moiety leading to the rate retardation.

Experimental

General

Melting points were determined on a Fisher-Johns block, and are reported uncorrected. The ^{1}H nmr spectra were run on Varian T-60 and HA-100 spectrometers. All spectral parameters are referenced to tetramethylsilane as an internal standard while using $CDCl_3$ or CD_2Cl_2 as solvent. The ^{1}H nmr parameters for the adducts are given in Tables 7 and 8 (C_6H_5SeBr and 2,4,6-$(CH_3)_3C_6H_2SeBr$ adducts only);[4] the analogous data for the C_6H_5SeCl adducts have been previously reported (1). Elemental analyses were performed by Scandinavian Microanalysis Laboratories, Herlev, Denmark. Mass spectra were run on an MS-9.

Allenes

2,3-Pentadiene was commercially available from Chemical Samples. 2,3-Hexadiene, 5-methyl-2,3-hexadiene, 5,5-dimethyl-2,3-hexadiene, 3,4-heptadiene, 2,6-dimethyl-3,4-heptadiene, 1,2-cyclononadiene, and 1,2-cyclotridecadiene were prepared by standard literature procedures from the commercially available alkenes (Chemical Samples) (22–24). 2,2,6,6-Tetramethyl-3,4-heptadiene, 2,2,6-trimethyl-3,4-heptadiene, 2,2-dimethyl-3,4- heptadiene, and 2-methyl-3,4-heptadiene were prepared by the method of Vermeer and co-workers (25, 26).

Diphenyl diselenide was prepared from bromobenzene by the method of Taboury (27) and Wuyts and Cosyne (28), as modified by Foster (29); mp 62.5–63°C (lit. (29) mp 63°C); ^{13}C nmr ($CDCl_3$) δ: 131.4, 129.0, 127.5, and 130.9; ms *m/e* [$\%\sum_{30}$]:314 (25.6), 234 (6.93), 154 (4.04), 157 (23.3), 77 (13.4).

Bis(2,4,6-trimethylphenyl)diselenide was prepared from 2-bromomesitylene (Aldrich) as above; mp 113.5–115°C, crystallized from 95% ethanol; ^{13}C nmr ($CDCl_3$) δ: 20.9 q, 24.0 q, 129.2 s, 143.6 s, 128.2 d, 139.0 s; ms *m/e*: 398 ($M^{+\cdot}$), 318 ($M^+ - Se$), 279 ($M^+ - Ar$), 368 ($M^+ - (CH_3)_2$), 199 ($M^+/2$), 183 ($M^+/2 - CH_3$), 119 ($Ar^{+\cdot}$). *Anal.* calcd. for $C_{18}H_{22}Se_2$ (mol wt. 396.2551$_4$): C 54.56, H 5.60; found: C 54.68, H 5.62.

Benzeneselenenyl chloride was the commercial product (Aldrich), recrystallized from CCl_4, mp 64.5°C; uv ($n \rightarrow \pi^*$ Se-Cl) λ_{max}: 433 nm, ε 264 dm^3 mol^{-1} cm^{-1}.

Benzeneselenenyl bromide was prepared from the diselenide by the dropwise addition of an equivalent of molecular bromine in CCl_4 solution at room temperature. Recrystallized from CCl_4, mp 56–57°C (lit. (30, 31) mp 61°C); uv ($n \rightarrow \pi^*$ Se-Br) λ_{max}: 468 nm, ε 238 dm^3 mol^{-1} cm^{-1}.

2,4,6-Trimethylbenzeneselenenyl bromide was prepared as above. Recrystallized from CCl_4, mp 66–67°C; uv ($n \rightarrow \pi^*$ Se-Br) λ_{max}: 497 nm, ε 183 dm^3 mol^{-1} cm^{-1}. *Anal.* calcd. for $C_9H_{11}SeBr$ (mol. wt. 278.056): C 38.59, H 3.99, Br 28.74; found: C 38.94, H 4.03, Br 29.34.

General Procedure

This procedure for the product studies was as previously described (1,5).

Kinetic Studies

All kinetic runs were carried out on a Durrum-Gibson stopped-flow spectrophotometer. Prior to any set of runs the instrument was allowed to stabilize for at least two hours. A constant temperature bath was maintained at 24.50 ± 0.03°C. The instrument was checked out and calibrated prior to each set of runs. Zero and 100% transmittance lines were determined by running pure solvent vs. the allene solution. Kinetic runs with each solution were carried out until a reproducible trace was stored on the oscilloscope. Measurements and calculations of k_2 were carried out in the standard way (3, 32).

Acknowledgements

The continued financial support, in the form of an annual operating grant, from the Natural Sciences

[4]Tables 7 and 8 are on deposit and may be obtained, at a nominal charge, from the Depository of Unpublished Data, CISTI, National Research Council of Canada, Ottawa, Ont., Canada K1A 0S2.

and Engineering Research Council of Canada is gratefully acknowledged, as is a Province of Ontario Scholarship, 1978–1980, to one of us (P.L.B.).

1. D. R. GARRATT, P. L. BEAULIEU, and M. D. RYAN. Tetrahedron, **36**, 1507 (1980).
2. T. L. JACOBS, R. MACOMBER, and D. ZUCKER. J. Am. Chem. Soc. **89**, 7001 (1967).
3. (*a*) G. H. SCHMID, D. G. GARRATT, and P. L. BEAULIEU. Chem. Scr. In press; (*b*) D. G. GARRATT. Ph.D. thesis, University of Toronto, Toronto, Ont., Canada, 1975; (*c*) P. L. BEAULIEU, V. M. MORISSET, and D. G. GARRATT. Tetrahedron Lett. **21**, 129 (1980).
4. D. G. GARRATT, P. L. BEAULIEU, and V. M. MORISSET. Can. J. Chem. To be published.
5. D. G. GARRATT and P. BEAULIEU. Can. J. Chem. **57**, 119 (1979).
6. D. G. GARRATT and P. L. BEAULIEU. Can. J. Chem. **58**, 1275 (1980).
7. G. H. SCHMID, C. L. DEAN, and D. G. GARRATT. Can. J. Chem. **54**, 1253 (1976).
8. G. H. SCHMID, D. G. GARRATT, and S. YEROUSHALMI. J. Org. Chem. **43**, 3764 (1978).
9. G. H. SCHMID and D. G. GARRATT. Tetrahedron, **34**, 2869 (1978).
10. E. L. ELIEL. *In* Stereochemistry of carbon compounds. McGraw-Hill, New York, NY. 1962. pp. 149–151, 237–239.
11. G. H. SCHMID and D. G. GARRATT. *In* The chemistry of double-bonded functional groups. Supplement A. Part 2. *Edited by* S. Patai. Wiley & Sons, London. 1977. p. 856.
12. G. H. SCHMID and D. G. GARRATT. Tetrahedron Lett. 3991 (1975).
13. (*a*) D. G. GARRATT and G. H. SCHMID. Can. J. Chem. **52**, 1027 (1974); (*b*) D. G. GARRATT. Tetrahedron Lett. 1915 (1978).
14. H. G. REICH and J. E. TREND. Can. J. Chem. **53**, 1922 (1975).
15. G. H. SCHMID. *In* Topics in sulfur chemistry. Vol. 3. *Edited by* A. Senning and P. S. Magee. Georg Thieme, Stuttgart. 1977. pp. 101–117.
16. W. A. SMIT, N. S. ZEFIROV, I. V. BODRIKOV, and M. Z. KRIMER. Acc. Chem. Res. **12**, 282 (1979).
17. (*a*) N. S. ZEFIROV, N. K. SADOVAJA, A. M. MAGNERRAMOV, I. V. BODRIKOV, and V. E. KARTASHOV. Tetrahedron, **31**, 2948 (1975); (*b*) N. S. ZEFIROV, N. K. SADOVAJA, L. A. NOVGORODTSEVA, and I. V. BODRIKOV. Zh. Org. Khim. **14**, 1806 (1978); (*c*) K. A. POTECHIN, E. N. KURKUTOVA, M. YU. ANTIPIN, YU. T. STRUCHKOV, A. M. MAGERRAMOV, N. K. SADOVAYA, and N. S. ZEFIROV. Zh. Org. Khim. **13**, 2093 (1977).
18. P. L. BEAULIEU, V. M. MORISSET, and D. G. GARRATT. Can. J. Chem. **58**, 1005 (1980).
19. D. G. GARRATT and A. KABO. Can. J. Chem. **58**, 1030 (1980).
20. (*a*) D. G. GARRATT and P. L. BEAULIEU. J. Org. Chem. **44**, 3555 (1979); (*b*) D. G. GARRATT, P. L. BEAULIEU, and V. M. MORISSET. Can. J. Chem. **58**, 1021 (1980).
21. P. L. BEAULIEU, A. KABO, and D. G. GARRATT. Can. J. Chem. **58**, 1014 (1980).
22. W. VON DOERING and P. M. LAFLAMME. Tetrahedron, **2**, 75 (1958).
23. L. SKATTEBOL. Acta Chem. Scand. **17**, 1683 (1963).
24. W. R. MOORE and H. R. WARD. J. Org. Chem. **27**, 4179 (1962).
25. P. VERMEER, H. WESTMIJZE, H. KLEIGIN, and L. A. VAN DIJCK. Recl. J. Royal Netherlands Chem. Soc. **97**, 56 (1978).
26. P. VERMEER, J. MEIJER, and L. BRANDSMA. Recl. Trav. Chim. Pays-Bas, **94**, 112 (1975).
27. F. TABOURY. Bull. Soc. Chim. Fr. **29**, 761 (1903).
28. H. WUYTS and G. COSYNE. Bull. Soc. Chim. Fr. **29**, 689 (1903).
29. D. G. FOSTER and S. F. BROWN. J. Am. Chem. Soc. **50**, 1182 (1928).
30. D. G. FOSTER. J. Am. Chem. Soc. **55**, 822 (1933).
31. O. K. EDWARDS, W. R. GAYTHWAITE, J. KENYON, and H. PHILLIPS. J. Chem. Soc. 2302 (1928).
32. (*a*) G. H. SCHMID, V. M. CSIZMADIA, V. J. NOWLAN, and D. G. GARRATT. Can. J. Chem. **50**, 2457 (1972); (*b*) G. H. SCHMID and D. G. GARRATT. Can. J. Chem. **51**, 2463 (1973); (*c*) G. H. SCHMID, A. MODRO, F. LENZ, D. G. GARRATT, and K. YATES. J. Org. Chem. **41**, 2331 (1976); (*d*) G. H. SCHMID and D. G. GARRATT. Chem. Scr. **10**, 76 (1976).

Can. J. Chem. Downloaded from www.nrcresearchpress.com by 210.87.254.105 on 09/05/12
For personal use only.

Substituent effects in some autoxidation and hydrogen abstraction reactions in terms of their field (F) and resonance (R) components inclusive of unique positional weighting factors

LALIT N. PATNAIK, NIGAMANANDA MALLICK, AND M. K. ROUT

Department of Chemistry, Ravenshaw College, Cuttack 753003, India

AND

SWOYAM P. ROUT

Center for Macromolecular Science, University of Florida, Gainesville, FL 32611, U.S.A.

Received February 19, 1979[1]

LALIT N. PATNAIK, NIGAMANANDA MALLICK, M. K. ROUT, and SWOYAM P. ROUT. Can. J. Chem. **58**, 2754 (1980).

Substituent effects in some autoxidation and hydrogen abstraction reactions have been studied in terms of the field (F_k) and resonance (R_k) components proposed by Swain and Lupton and the unique positional weighting factors f_j and r_j incorporated by Williams and Norrington with the aid of the following equation:

$$P_i = \alpha_i f_j F_k + \beta_i r_j R_k + e_i + P_i^0$$

where P_i's are the rate parameters, P_i^0 being that for a standard reference compound. The correlations are found to be quite satisfactory, showing the general validity of the above equation for the types of reactions considered. From the information obtained from the present correlation studies, an attempt has been made to resolve the conflict with regard to the nature of the transition state involved in the hydrogen abstraction reactions — that is, whether or not there is charge separation in the transition state. The results of the present studies seem to suggest that both the differences in the resonance stabilization energies of the ring-substituted benzyl radical and the contribution of polar structures to the transition state are to be invoked to explain the observed data.

LALIT N. PATNAIK, NIGAMANANDA MALLICK, M. K. ROUT et SWOYAM P. ROUT. Can. J. Chem. **58**, 2754 (1980).

On a étudié les effets des substituants, dans quelques réactions d'autoxydation et d'élimination d'hydrogène, en fonction des composants de champ (F_k) et de résonance (R_k) proposés par Swain et Lupton et en fonction des facteurs uniques d'appréciation de position f_j et r_j incorporés par William et Norrington à l'aide de l'équation suivante:

$$P_i = \alpha_i f_j F_k + \beta_i r_j R_k + e_i + P_i^0$$

où les P_i sont des paramètres de vitesse, P_i^0 est celui d'un composé étalon de référence. On a trouvé que les corrélations sont satisfaisantes, montrant ainsi la validité générale de l'équation ci-dessus, pour le genre de réactions considérées. A partir des informations obtenues au cours des présente études de corrélation, on a essayé de résoudre le conflit en ce qui concerne la nature de l'état de transition impliquée dans les réactions d'élimination d'hydrogène, soit de savoir s'il est exact ou pas qu'il y a une séparation de charges dans l'état de transition. Les résultats de la présente étude semblent suggérer qu'il faut faire appel à la fois aux différences entre les énergies de stabilisation par résonance du radical benzyle substitué sur le cycle à la contribution des structures polaires à l'état de transition pour expliquer les données observées.

[Traduit par le journal]

Introduction

The present report deals with studies on correlation of the rate parameters of some autoxidation and hydrogen abstraction reactions with Swain and Lupton's (1) substituent parameters F_k and R_k involving the unique positional weighting factors f_j and r_j, suggested by Williams and Norrington (2).

Use of multiparameter equations for correlation studies in radical reactions has also been proposed by Yamamoto and Otsu (3) and Streitwieser and Perrin (4), following the suggestion of Timberlake *et al.* (5), that no single substituent parameter like $\sigma, \sigma^+, \sigma^-, \sigma_R$, etc. would give the desired Hammett plot for such reactions. Yukawa and Tsuno (6) had first suggested multiparameter equations for ionic reactions. Afanas'ev (7) has proposed a two-parameter equation for radical reactions of compounds, in which the reaction centres are not sterically hindered, similar to the one suggested by Taft for aliphatic compounds (8). Afanas'ev's equation is based on the relationship between the spin density in free radicals and the rate constants of radical substitution reactions with $CH_3\cdot$. The data correlated in the present work will also be treated by means of the models mentioned above to bring out the relative merits of each of the models and the results will be reported in future communications.

Swain and Lupton's (1) approach towards the problem of structure-reactivity relationships, with regard to substituent effects, consists of expressing the Hammett substituent constants, σ_k, as a linear combination of their two components, the field (F_k)

[1]Revision received December 3, 1979.

0008-4042/80/242754-07$01.00/0

©1980 National Research Council of Canada/Conseil national de recherches du Canada

Can. J. Chem. Downloaded from www.nrcresearchpress.com by 210.87.254.40 on 09/05/12
For personal use only.

Can. J. Chem. Downloaded from www.nrcresearchpress.com by 210.87.254.40 on 09/05/12
For personal use only.

and resonance (R_k) effects, i.e.,

[1] $\sigma_k = aF_k + bR_k$

where a and b are the empirical sensitivities or weighting factors independent of the substituents but different for each set of substituent constants (σ_m, σ_p, etc.). The constants F_k and R_k have been claimed to be better defined and physically more significant parameters for correlating or predicting substituent effects on a variety of free energy dependent processes than any other pair $\sigma_m, \sigma_p, \sigma_p^+$, etc.

The scope and significance of Swain and Lupton's work were greatly enhanced and refined by the work of Williams and Norrington (2), who proposed unique values for the positional weighting factors f and r in place of Swain and Lupton's empirical sensitivities a and b, which can be applied to *ortho-*, *meta-*, and *para-* positions of the benzene ring simultaneously. The values suggested are:

$$f_o = 1.248;\ f_m = 0.980;\ f_p = 1.000$$

$$r_o = 0.863;\ r_m = 0.347;\ r_p = 1.000$$

For a data set consisting of only *meta-* and *para-* derivatives, the suggested values are:

$$f_m = 1.002,\ f_p = 1.000,\ r_m = 0.424,$$

$$\text{and } r_p = 1.000$$

These values were found to give good correlation between physico-chemical properties of the side chain and substituent parameters of mixed or multiply substituted benzene derivatives.

The original Hammett equation, which is of the form

[2] $P_i = \rho_i\sigma_k + P_i^0$

(where P_i's are some free energy related property, P_i^0 being that for some standard reference state for the ith reaction set), now becomes, with Swain–Lupton and Williams–Norrington's modifications,

[3] $P_i = \alpha_i f_j F_k + \beta_i r_j R_k + P_i^0$

where f_j and r_j are the Williams–Norrington positional weighting factors for the position j and where F_k and R_k are the field and resonance components of the substituent k (Swain–Lupton). As a further refinement, Williams and Norrington (2) introduced a normally distributed error term, e_i, independent of the nature and position of the substituent in eq. [3], so that the final form of the Swain–Lupton–Williams–Norrington (SLWN) equation becomes:

[4] $P_i = \alpha_i f_j F_k + \beta_i r_j R_k + e_i + P_i^0$

Results and Discussion

The kinetic data of two types of oxidation reactions, namely, autoxidation, and hydrogen abstraction from hydrocarbons by radicals, already reported in the literature, have been chosen for investigation in the present study with a view to assessing their amenability to the above model eq. [4], proposed for the study of substituent effects, and to reexamining the conclusions of the earlier workers in the light of results obtained therefrom. The present work forms a part of our general programme on studies of substituent effects in polymerization reactions. In view of the close relationship between autoxidation and hydrogen abstraction reactions on one hand, and processes of polymerization on the other, these two particular types of oxidation reactions have been chosen for the present correlation studies. It is quite well known that most of the familiar autoxidations like drying of linseed oil paint, or the deterioration of rubber or plastics, or the autoxidation of styrene involve the process of polymerization in some way or other. The competitive kinetics of the autoxidation of substituted benzaldehydes are identical with those of copolymerizations (9). The abstraction of hydrogen atoms by alkoxy radicals from substrates in the liquid phase is of particular interest in relation to autoxidation phenomena (10). These radicals are produced in the chain branching decomposition of the initially formed hydroperoxides and are, therefore, responsible for the autocatalytic nature of most autoxidations. Hydrogen atom abstraction by radicals may also be important in the autoxidations in yet another way in being involved in the inhibition of autoxidations by substrates like phenols, amines, and toluenes.

The reaction dependent parameters α_i and β_i and the error term e_i of eq. [4] were evaluated by a method of multiple regression. The statistical parameters, standard deviation (S), correlation coefficient (C), the F-distribution, and the significance levels were calculated by the method suggested by Shorter (11).

(A) Autoxidation Reactions

(i) Autoxidation of Ring Substituted Styrenes

Correlation studies have been undertaken with three types of rate parameters reported by Howard and Ingold (12), for the autoxidation of the ring substituted styrenes. The data are summarised in Table 1, where k_p and k_t's are the rate constants for

Can. J. Chem. Downloaded from www.nrcresearchpress.com by 210.87.254.40 on 09/05/12
For personal use only.

TABLE 1. Absolute rate constants for the autoxidation of substituted styrenes at 40°C (12)

Substituent	Relative rate of thermal oxidation	k_p (M^{-1} s^{-1})	k_t (M^{-1} s^{-1})
p-OMe	1.97	123	2.2
p-Me	1.29	83	2.8
None	1.00	70	3.6
p-Cl	1.37	123	4.9
m-Cl	1.24	101	5.4
p-CN	1.30	91	4.4
m-NO_2	1.14	—	—
p-NO_2	1.25	—	—

TABLE 2. Correlation parameters

Rate parameter	*e*	α	β	*S*	*C*
Oxidation	0.0838	0.0358	−0.3148	0.049	0.89
k_p	0.0356	0.1726	−0.3076	0.034	0.98
k_t	−0.0591	0.2305	0.3311	0.14	0.92

the propagation and the bimolecular termination respectively. The correlation parameters are described in Table 2.

The results confirm the earlier view (12) that there is no good correlation between the relative rates of oxidation and polar properties of the substituents and that the second order termination (k_t) should be facilitated by electron attracting substituents (positive α and β).

The lack of correlation of the propagation rate constants k_p with a Hammett substituent parameter was rationalised (12) by invoking a dual action of the substituents in the reaction mechanism. The substituent in the styrene can affect the reactivity of either the styrene itself or the styryl peroxy radical. Electron attracting groups increase the reactivity of the styryl peroxy radical and decrease the reactivity of styrene, while the electron donating groups will have little contribution towards radical stability. The excellent correlation of k_p, obtained in the present study, with opposite signs of the regression parameters α and β clearly point to the dual mode of the substituent action. If the substituent effect in the peroxy radical is governed mainly by the inductive effect and that in the styrene by the resonance effect, then electron attracting groups should enhance the reactivity of the radical (positive α), while electron donating groups should facilitate the reactivity of styrene (negative β). We have earlier seen in connection with the polymerization reactions that different signs of α and β suggest weak contribution of polar structures to the transition state. This, in this particular case, would mean that structure **III** plays a more important role than structure **II** in stabilizing the transition state.

$$\underset{\mathbf{I}}{XC_6H_4CH{=}CH_2{\cdot}OOR} \leftrightarrow \underset{\mathbf{II}}{XC_6H_4\overset{+}{C}H{-}\dot{C}H_2\bar{O}OR} \leftrightarrow \underset{\mathbf{III}}{XC_6\dot{H}_4CH{-}CH_2{-}OOR}$$

The same conclusion was reached by Howard and Ingold (12) by considering substituent effects from a different angle.

(B) Hydrogen Abstraction Reactions

The rate data for the hydrogen abstraction reactions from toluenes by different attacking radicals as reported in the literature and used for the present correlation studies are described in Table 3, along with their sources.

The mechanism of hydrogen abstraction reactions, particularly with respect to the nature of the transition states involved, has, for sometime, been a subject of controversy.

The applicability of Hammett ρσ correlation in free radical abstraction of hydrogen from substituted toluenes has been one of the reasons for the formulation of the theory of polar effects in these reactions (13–15, 21, 22). The course of these reactions is described as follows:

$$X{\cdot} + RH \rightarrow \underset{\mathbf{I}}{[X{:}H{\cdot}R} \leftrightarrow \underset{\mathbf{II}}{\bar{X}{:}\,H^{+}{\cdot}R} \leftrightarrow \underset{\mathbf{III}}{X^{+}{:}H\,{:}\bar{R}]} \rightarrow XH + R{\cdot}$$

where X· is the attacking radical and RH is the generalised hydrogen donor or substituted toluene. A Hammett correlation implies that structures **II** or **III** contribute to the transition state. A common feature in all these correlations, till recently, has been a negative value for the reaction parameter ρ. Since all the reactions studied were with electrophilic radicals, a negative ρ suggests that structure **II** is more important than **III**. Recently, however, Pryor *et al.* (21) have, for the first time, reported a positive ρ value for the reaction of *tert*-butyl radicals with toluenes, which indicated a greater contribution of structure **III** to the transition state. A better correlation of these reactions with σ^+ rather than σ has also been advanced as additional evidence to prove charge separation in the transition state.

Zavitsas and Pinto (22), on the other hand, have proposed from an observed linear correlation of ρ and ΔH for hydrogen abstraction reactions from toluenes that a charge separation in the transition state either does not occur or is an "unnecessary" assumption. The observed ρ–ΔH relationship

TABLE 3. Rate data for hydrogen abstraction from substituted toluenes

Substituent in toluene	Relative rate toward						
	$Cl_3C\cdot$ (17)	Br·[a] (18)	Br·[b] (18)	$HCOOCH_2\cdot$ (16)	*t*-BuO· (19)	Cl· (14)	*t*-BuO· (20)
H	1	1	1	1	1	1	1
p-F	—	—	—	1.11	—	—	0.99 (17)
p-Cl	0.73	0.679	0.728	0.89	0.89	0.79	0.67
p-CH_3	2.76	3.02	2.415	1.66	1.47	1.57	1.52
p-OCH_3	14.1	9.55	9.036	3.64	2.2	—	—
p-Ph	—	—	—	1.60	—	1.55	—
p-OPh	—	—	—	—	2.13	2.50	1.42
p-NO_2	—	—	—	—	0.25	0.32	—
p-CN	—	0.143	0.122	—	0.36	—	0.29
p-iPr	—	2.523	2.472	—	—	—	—
m-Br	0.25	0.242	0.224	0.58	—	—	—
m-CH_3	1.58	—	—	1.19	1.07	1.30	1.14
m-OCH_3	0.87	—	—	0.92	—	—	—
m-OPh	—	—	—	—	—	0.86	—
m-Cl	—	—	—	—	0.59	0.595	0.52
m-NO_2	—	—	—	—	0.29	—	—
p-Br	0.70	—	—	0.87	—	—	—
Solvent	Chlorobenzene	Benzene	Benzene	Acetic acid	CCl_4	CCl_4	Benzene
T (°C)	50	80	80	130	40	40	40

[a]Br· from *N*-bromotetramethyl succinimide (NBTMS).
[b]Br· from Br_2. These two sets of data have been recalculated in the present work from the logarithms of relative rates.

would mean that the differences in the reactivities of a series of substituted toluenes toward any given radical are due to differences in the bond dissociation energies of the benzyl C—H bonds in each of these substrates and that these Bond Dissociation Energy (BDE) values are dependent on the electron donating or electron withdrawing characteristics of the substituents. The reported "better" correlation with σ^+ have also been challenged on the grounds that most of these reactions give better, or at least as good, correlation with σ^-. We also find in the literature quite a few reports on the excellent correlations with σ (20, 21, 23).

Zavitsas and Pinto's (22) proposition has been refuted by the exponents of the polar effect theory on the grounds that the observed linear correlation between ρ and ΔH for only five radicals (Br·, $Cl_3C\cdot$, Cl·, *t*-BuO·, $\cdot C_6H_5$) could be fortuitous and a reported positive ρ value by Pryor *et al.* (21) should be impossible according to Zavitsas's treatment.

Afanas'ev (7) applied his two parameter equation to the hydrogen abstraction reactions of free radicals with toluenes. The results show that the apparent polar effect of substituents as stipulated by Howard and Chenier (15*c*) and Pryor *et al.* (21) can result from the resonance interaction of electron-withdrawing and electron-donating substituents with π-electrons of the aromatic ring.

With this background of conflicting opinions about the mechanism of hydrogen abstraction reactions, it was considered worthwhile to reexamine some of the data reported in the literature, in the light of eq. [4]. Since the substituent constants employed in this equation (F and R) are of a more generalised nature than either σ or σ^+ and since eq. [4] enables one to find out the sensitivity of the reaction to the inductive and resonance effects separately, it was expected that the additional information obtained from the present studies would be helpful in deciding in favour of one of these two conflicting postulates. The correlation parameters and the regression line constants are described in Table 4.

Before attempting any critical discussion pertaining to hydrogen atom abstraction reactions from toluene in general, it is necessary to discuss certain characteristics of some of the individual systems to clarify certain points:

(*i*) Reactions of substituted toluenes toward Br· were studied by Pearson and Martin (18) using two widely differing brominating agents, *N*-bromotetramethyl succinimide (NBTMS), and molecular bromine, respectively. They obtained identical ρ values under identical reaction conditions and at temperatures as high as 80°C and as low as 19°C. From this, they concluded that the same reaction mechanism was operating for both the brominating agents.

It is indeed very interesting that the present correlation studies with the two differing reaction systems give identical α and β values, both in sign and magnitude, indicating the operation of the same reaction mechanism.

(*ii*) Hydrogen abstraction from substituted tol-

Can. J. Chem. Downloaded from www.nrcresearchpress.com by 210.87.254.40 on 09/05/12
For personal use only.

TABLE 4. Correlation parameters and regression constants for hydrogen abstraction from toluenes by different radicals

Attacking radical	e	α	β	S	C	Significance level (%)	%R
Cl_3·	−0.092	−0.964	−3.208	0.146	0.983	98	17.0
Br·[a]	0.072	−0.818	−2.244	0.205	0.983	95	22.9
Br·[b]	0.009	−0.778	−2.336	0.191	0.971	95	22.9
$HOOCH_2$·	0.024	−0.494	−1.341	0.096	0.951	99	38.2
t-BuO·[c]	−0.033	−0.329	−1.274	0.062	0.993	99.9	48.2
Cl·	0.076	−0.4396	−0.823	0.069	0.983	99	37.9
t-BuO·[d]	0.025	−0.484	−0.719	0.051	0.990	99.5	64.6

[a]From *N*-bromotetramethyl succinimide.
[b]From bromine.
[c]Data from Kennedy and Ingold (19).
[d]Data from Gilliom and Ward (20).

uenes by *tert*-butoxy radicals was studied by two groups of workers, using the same radical source, *tert*-butyl hypochlorite and at the same temperature, but in different solvents (Table 3). The rate constants were reasonably expected to be different. But while Gilliom and Ward (20), who performed the reaction in benzene, report an excellent correlation of their data with the Hammett σ constants, Kennedy and Ingold (19), using carbon tetrachloride as the solvent, report even a better correlation of their data with σ^+. The latter workers have questioned the validity of Gilliom and Ward's correlation on the grounds that the hypochlorite–toluene reactions are more complex in benzene than in carbon tetrachloride, because of the likely participation of benzene in the reaction. In a subsequent paper, Gilliom and Howles (23) reaffirmed their earlier contention and expressed doubt about the genuineness of the rate data of *p*-phenoxy toluene reported by Kennedy and Ingold (19). In the present correlation study, Kennedy and Ingold's data gave good results with the exception of *p*-phenoxy toluene which showed a large deviation. Exclusion of this substituent from the data set markedly improved the correlation. Equally good results were also obtained with Gilliom and Ward's data, but with α and β values differing widely in magnitude, but with the same sign.

(*i*) All substituents, from Kennedy and Ingold (19)

$$\log k/k_0 = 0.082 - 0.338 f_j F_k - 1.395 r_j R_k$$

$$S = 0.173$$

$$C = 0.937$$

(*ii*) Excluding *p*-phenoxy, from Kennedy and Ingold (19)

$$\log k/k_0 = -0.033 - 0.329 f_j F_k - 1.274 r_j R_k$$

$$S = 0.062$$

$$C = 0.993$$

Significance = 99.9%

(*iii*) From Gilliom and Ward (20)

$$\log k/k_0 = 0.025 - 0.484 f_j F_k - 0.719 r_j R_k$$

$$S = 0.051$$

$$C = 0.990$$

Significance = 99.5%

Thus we find that so far as the present correlation is concerned, but for the *p*-phenoxy toluene, both sets of data are equally good. We have included the second and the third correlations in Table 4 (rows 5 and 7).

Particular attention has been drawn to these two reaction systems to emphasize two points:

(*a*) The magnitudes of α and β, like those of ρ, are solvent and temperature dependent. Attempts to make any generalizations from the magnitudes of α and β from reactions carried out under widely differing conditions of temperature and solvent such as those described in the tables may, therefore, be misleading.

(*b*) The sign of α and β, also that of ρ, apparently, is free from this short-coming. Pryor *et al.* (24) have critically discussed these points with regard to ρ. They have emphasized that it is only the sign, and not the magnitude of the reaction parameter, which has any mechanistic significance in drawing conclusions from the ρ values of a series of similar reactions. Since α and β are also reaction parameters related to ρ, it is also suggested that the sign, and not the magnitude, should be the critical factor for making generalisations.

Can. J. Chem. Downloaded from www.nrcresearchpress.com by 210.87.254.40 on 09/05/12
For personal use only.

Can. J. Chem. Downloaded from www.nrcresearchpress.com by 210.87.254.40 on 09/05/12
For personal use only.

A common feature of all the present correlations is the negative signs of both α and β. This perhaps means that the reactions in general are facilitated by electron donating groups. The magnitude of this effect is also in accord with the rate data. Reaction of $Cl_3C\cdot$ radical (17) which has the largest α and β values, shows the most pronounced sensitivity towards the presence of electron donating groups while that of *t*-BuO· (in benzene) (20) which has the lowest β value, and a low α value, shows the least sensitivity.

The discussion above does not tell *a priori* what bearing the signs and/or magnitudes of α and β of the reactions under study have on the nature of the transition state. It may be desirable to examine, if it is possible to determine with the help of these factors, whether the substituent effect is due to (*a*) differences in the resonance stabilization energies of the ring substituted benzyl radicals, or (*b*) polar contributions to the transition state, or (*c*) both. For this, again we draw attention to two particular pairs of reactions in Table 3, which have been carried out under identical (reactions 5 and 6, carbon tetrachloride, 40°C) or near identical (reactions 2 or 3, and 7, benzene, 80°C and 40°C respectively) conditions.

Taking the BDE ($D(PhCH_2—H) = 85$ kcal mol^{-1} (15*c*) and D(Cl—H) = 103.3 kcal mol^{-1} (25)), the exothermicity of the hydrogen abstraction by Cl· should be about 18.2 kcal mol^{-1}, a value comparable to that of the *t*-BuO· radical (22), 21 kcal mol^{-1}. According to Zavitsas and Pinto's argument (22), the α and β values for these two reactions should be nearly the same, that for the *t*-butoxy being a little higher. The total polar effect, as measured by both α and β, seems to point to this (compare reactions 5 and 6), despite large electronegativity differences between Cl· and *t*-BuO·. This observation is even more clearly manifested in the reverse direction, when one considers reactions 2 (or 3) and 7. Taking the (D(Br—H) = 87.5 kcal mol^{-1} (25)), the exothermicity of the hydrogen abstraction reaction by Br· should be about 2.5 kcal mol^{-1}. Although the electronegativity difference between Br· and *t*-BuO· is less than that between Cl· and *t*-BuO·, there is a large difference in the α and β value of the reactions of Br· and *t*-BuO·, those for Br· being much higher than those for *t*-BuO·. Such contradicatory observations can only be explained by considering both the electronegativity of the attacking radical and the extent of bond breaking and thus by invoking polar contributions to the transition state. The reported linear correlation by Zavitsas and Pinto (22) has obviously been a result of not taking into account the different reaction conditions.

More conclusive evidence (1) for the above suggestion is perhaps brought out by the magnitudes of the "Percent Resonance" (%R, sensitivity to resonance effects) of the different reaction series. This has been calculated by the following expression:

$$\%R = \frac{100\psi|\beta|}{\Phi|fF| + \psi|rR|}$$

where

$$\phi = \Sigma|fF - \overline{fF}|/n$$

and

$$\psi = \Sigma|rR - \overline{rR}|/n$$

Except for *t*-butoxy, the resonance percent for all the reactions is low, suggesting that resonance contributions to the stability of the transition state is not very significant, which, in turn, means that the transition state is predominantly formed by the polar structures. The high resonance contribution in case of *t*-butoxy is perhaps because of a lower degree of bond breaking the transition state and a smaller contribution from the dipolar structures **II** or **III**.

1. C. G. Swain and E. C. Lupton. J. Am. Chem. Soc. **90**, 4328 (1968).
2. S. G. Williams and F. E. Norrington. J. Am. Chem. Soc. **98**, 508 (1976).
3. T. Yamamoto and T. Otsu. Chem. Ind. London, 787 (1967).
4. A. Streitwieser and C. Perrin. J. Am. Chem. Soc. **86**, 4938 (1964).
5. (*a*) J. W. Timberlake and M. L. Hodges. Tetrahedron Lett. 4147 (1970); (*b*) J. W. Timberlake, A. W. Garner, and M. L. Hodges. Tetrahedron Lett. 309 (1973); (*c*) B. K. Bandlish, A. W. Garner, M. L. Hodges, and J. W. Timberlake. J. Am. Chem. Soc. **97**, 5856 (1975).
6. Y. Yukawa and Y. Tsuno. Bull. Chem. Soc. Jpn. **32**, 960 (1959); **32**, 965 (1959); **32**, 971 (1959).
7. I. B. Afanas'ev. Int. J. Chem. Kinet. **7**, 857 (1975).
8. R. W. Taft. Steric effects in organic chemistry. *Edited by* M. S. Newman. Wiley, New York. 1956. p. 587.
9. C. Walling. Free radicals in solutions. John Wiley and Sons Inc., New York. 1957. p. 417.
10. (*a*) K. U. Ingold. Can. J. Chem. **43**, 2737 (1965); (*b*) **41**, 2807 (1963).
11. J. Shorter. Correlation analysis in organic chemistry. Clarendon Press, Oxford. 1973. p. 103.
12. J. A. Howard and K. U. Ingold. Can. J. Chem. **43**, 2737 (1965).
13. J. A. Howard and K. U. Ingold. Can. J. Chem. **41**, 1744 (1963).
14. G. A. Russell and R. C. Williamsons, Jr. J. Am. Chem. Soc. **86**, 2357 (1964).
15. (*a*) G. A. Russell and H. C. Brown. J. Am. Chem. Soc. **77**, 4578 (1955); (*b*) C. Walling. Free radicals in solutions.

John Wiley and Sons Inc., New York. 1957. pp. 132, 365, 375, 474; (*c*) J. A .HOWARD and J. H. B. CHENIER. J. Am. Chem. Soc. **95**, 3054 (1973).
16. E. I. HEIBA, R. M. DESSAU, and W. J. KOEHL, JR. J. Am. Chem. Soc. **91**, 138 (1969).
17. E. S. HUYSER. J. Am. Chem. Soc. **82**, 394 (1960).
18. R. E. PEARSON and J. C. MARTIN. J. Am. Chem. Soc. **85**, 354 (1963).
19. B. R. KENNEDY and K. U. INGOLD. Can. J. Chem. **44**, 2381 (1966).
20. R. D. GILLIOM and B. F. WARD, JR. J. Am. Chem. Soc. **87**, 3944 (1965).
21. W. A. PRYOR, W. H. DAVIS, and J. P. STANLEY. J. Am. Chem. Soc. **95**, 4754 (1973).
22. A. A. ZAVITSAS and J. A. PINTO. J. Am. Chem. Soc. **94**, 7390 (1972).
23. R. D. GILLIOM and J. R. HOWLES. Can. J. Chem. **46**, 2752 (1968).
24. W. A. PRYOR, T. H. LIN, J. P. STANLEY, and R. W. HENDERSON. J. Am. Chem. Soc. **95**, 6993 (1973).
25. L. PAULING. The nature of the chemical bond. Indian ed. Oxford and IBH Publishing, New Delhi. 1969. p. 85.

Can. J. Chem. Downloaded from www.nrcresearchpress.com by 210.87.254.40 on 09/05/12
For personal use only.

Acyl transfer in *o*-hydroxybenzenethiol

DAVID M. MCKINNON

Chemistry Department, University of Manitoba, Winnipeg, Man., Canada R3T 2N2

Received March 31, 1980

DAVID M. MCKINNON. Can. J. Chem. **58**, 2761 (1980).

o-Hydroxybenzenethiol reacts with one equivalent of acetic anhydride to give a mixture of starting material, diacylated material, and *O*- or *S*-monoacylated products as determined by nmr. The same products are obtained by equilibration of a mixture of *o*-hydroxybenzenethiol and its diacetate. The mixture does not contain detectable amounts of 2-methylbenzothioxolan-2-ol.

DAVID M. MCKINNON. Can. J. Chem. **58**, 2761 (1980).

En se basant sur des données de la rmn, on conclut que le *o*-hydroxybenzènethiol réagit avec un équivalent d'anhydride acétique pour donner un mélange de produits de départ, de produits diacétylés et des produits *S*- ou *O*-monoacétylés. On obtient les mêmes résultats en équilibrant un mélange de *o*-hydroxybenzènethiol et de son diacétate. Le mélange des produits obtenus ne contient pas des quantités décelables de méthyl-2 benzothioxolanol-2.

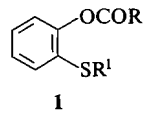
[Traduit par le journal]

Can. J. Chem. Downloaded from www.nrcresearchpress.com by 210.87.254.6 on 09/05/12
For personal use only.

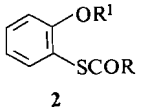
Introduction

In connection with another investigation it was desired to prepare *o*-mercaptophenyl acetate (**1***a*). Examination of the structure, however, suggested the likelihood of isomerism of this with *o*-hydroxyphenyl thiolacetate (**2***a*) via the cyclic orthoester form **3***a* and that, even more, these three compounds could possibly exist in some equilibrium mixture with *o*-hydroxybenzenethiol (**4**) and its diacetate (**5***a*). It is reported that 2-arylbenzoxathiolium salts, which may be made from *o*-mercaptophenol and an acyl equivalent (1–3), undergo hydrolysis to give materials of the type **1–5**. The pseudo base **3***b*, formed by attack of water on 2-phenylbenzoxathiolium perchlorate, underwent fast conversion to *o*-mercaptophenyl benzoate (**1***b*) which then slowly converted to *o*-hydroxyphenyl thiolbenzoate (**2***b*) (2). In addition, *o*-hydroxybenzenethiol dibenzoate (**5***b*) was isolated. These last two products must have arisen by intra- and intermolecular acyl transfer reactions.

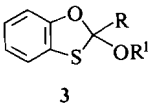
Since the corresponding acetate analogs (**1***a*, **2***a*, **3***a*, **5***a*) would be more amenable to study by nmr spectroscopy, and, being more aliphatic, more related to studies on thiolester hydrolyses (4) or other acyl displacements from thiolesters (5), it seemed desirable to examine this sytem to determine the exact species present in the equilibrium mixture.



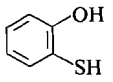
1



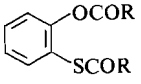
2



3



4

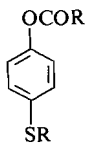


5

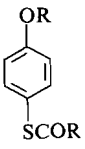
$PhSCO_2CH_3$

6

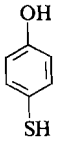
1–3, 5, 7, 8, 10
a R = CH_3, R^1 = H
b R = Ph, R^1 = H
c R = R^1 = CH_3
d R = OMe



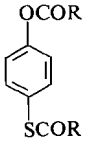
7



8



9



10

Results and Discussion

When *o*-hydroxybenzenethiol was treated with an equimolar quantity of acetic anhydride in the presence of triethylamine, and the reaction mixture worked up, the ^1H nmr of the product exhibited three peaks at 2.16 δ, 2.22 δ, and 2.26 δ, with a broad peak at 5.35 δ. These must be due, respectively, to three different types of methyl groups and an acidic proton bonded to oxygen and/or sulfur. The aromatic protons were evident as a complicated group of peaks between 6.7 and 7.5 δ. An identical spectrum was obtained from an equimolar mixture of **4** and **5***a* when treatedwith a trace of triethylamine. With more added triethylamine the acidic proton absorption shifted to 8.22 δ, characteristic of the triethylammonium ion proton.

Examination of the spectrum of an equimolar mixture of **4** and **5***a* without added triethylamine revealed at first that only a mixture of the two components was present, with the two peaks due to the methyl protons at 2.20 and 2.30 δ. These are tentatively assigned to the methyl protons of the *O*-ester and the *S*-ester in **5***a* on the following basis.

0008-4042/80/242761-04$01.00/0

©1980 National Research Council of Canada/Conseil national de recherches du Canada

Can. J. Chem. Downloaded from www.nrcresearchpress.com by 210.87.254.6 on 09/05/12
For personal use only.

The spectrum of 2-methoxyphenyl thiolacetate **2***c* exhibited the acetate methyl peak at 2.27 δ. In 2-(methylthio)phenyl acetate (**1***c*) two peaks were evident in this range at 2.20 δ and 2.28 δ. The latter of these was slightly broadened and was therefore assigned to the *S*-methyl protons which are expected to exhibit through-space coupling with a ring proton[1] by analogy with some other methylthio compounds and, to some extent, with 2-methoxyphenol (6). Thus the peak at 2.20 δ is assigned to the acetate protons. For more information on chemical shifts in these compounds the *para* analogs were studied. *p*-Methoxyphenyl thiolacetate (**8***c*) exhibited the acetate methyl absorption at 2.26 δ and the *o*-methyl at 3.64 δ. Likewise *p*-(methylthio)phenyl acetate (**7***c*) exhibited two absorptions at 2.17 and 2.36 δ. The latter was slightly broadened and was therefore assigned to the *S*-methyl group. The absorptions in *p*-hydroxybenzenethiol diacetate (**10***c*), at 2.23 and 2.38 δ, were therefore assigned respectively to the *O*-acetyl and *S*-acetyl groups. These differences in δ values between *O*-acetyl and *S*-acetyl compounds are consistent with known differences in aliphatic thiolesters (7) and ordinary esters. Hence it appears that the thiolacetates absorb at a slightly lower field than acetates.

Examination of this mixture of **4** and **5***a* at selected intervals indicated the appearance of two new peaks at 2.18 and 2.21 δ until after 5 h there was no further change in the spectrum. Four methyl peaks were now evident. When this mixture was treated with a trace of triethylamine its spectrum changed immediately to that of the *o*-hydroxybenzenethiol/acetic anhydride/triethylamine experiment product, i.e. it had only three methyl peaks. Over the temperature range 30° to 100°C there was little effect on the spectrum of the mixture of **4** and **5***a*, but at 150°C the spectrum was identical to when triethylamine was present. On cooling, the single centre peak split into two to reproduce the original spectrum. This is consistent with there being a high energy barrier to interconversion of the two compounds. These peaks at 2.18 and 2.21 δ are assigned to the methyl protons in **1***a* and **2***a* respectively.

The proportions of the components of the mixture, as estimated by integration, were for the equilibrated mixture at room temperature **4**:**5***a*:**1***a*:**2***a*, 2:3:3:3; for **4**:**5***a*:(**1***a* + **2***a*) at 150°C, 1:1:4; and 1:1:2 when triethylamine was present.

It is possible that one of these peaks at 2.18 and 2.15 might be due to the intermediate "pseudo base" or orthoacetate structure **3***a* since the spectrum of this might be expected to have an approximately equal chemical shift. Data from acyclic compounds (8) suggest that this is at least a possibility and a closely related orthoester (**3**, R = Ph, R^1 = Et) absorbs in this region (9). Comparison of the ^{13}C nmr spectrum of the equilibrated mixture of **4** and **5***a* and the mixture of pure **4** and **5***a* demonstrated no increase in the number of methyl carbon absorptions. Evidently the chemical shifts of the acetate methyl carbons are rather insensitive to groups more than a few carbon atoms distant. Nevertheless it did reveal the presence of four types of carbonyl groups, two in the region 193 ppm, assigned to *S*-acyl, and two in the region 169 ppm, assigned to *O*-acyl. Comparable differences in values are found for coumarin and benzothiopyran-2-one (10). In addition, four tertiary carbons bonded to oxygen, i.e. the  type and four tertiary carbons bonded to sulfur, i.e. the  type were evident at around 152 and 119 ppm respectively. In all, the spectrum of the equilibrated mixture was consistent with a mixture of only compounds **1***a*, **2***a*, **4**, and **5***a*. There were no absorptions in a range suitable to justify the presence of the orthoacetate **3***a*. These orthoesters or equivalents must be intermediates in the formation of benzoxathiolium salts, but under acidic conditions only the salts are obtained (1, 2).

Likewise the mixture of **4** and **5***a* treated with triethylamine indicated no extra absorptions other than those of added triethylamine and **1***a* and **2***a*. However, the relative heights of the carbonyloxy and the carbonylthio absorptions from **1***a* and **2***a* respectively shifted in favor of the latter, probably because of enhanced nucleophilicity of the thiolate group. These results are interesting in that thiolate esters hydrolyse more readily than ordinary esters (4), usually attributed to a greater mesomeric effect of oxygen over sulfur, affecting coordination of the nucleophile at the carbonyl carbon. Also, this effect has been used to explain bond distance differences in thiolacetic acid (11). Hence in the system above, the production of **1***a* would be favored in the equilibrium mixture. However, the phenyl mercaptide ion would be a stronger nucleophile than phenoxide ion, which should favor the formation of **2***a*. Evidently in this system the two effects are closely balanced.

The ir spectrum of the equilibrated mixture was of little use on deciding its components. The only main features evident were two absorptions at 1725 and 1779 cm^{-1} assigned to thiolacetate and acetate

[1]T. Schaefer, unpublished results.

Can. J. Chem. Downloaded from www.nrcresearchpress.com by 210.87.254.6 on 09/05/12
For personal use only.

carbonyl groups respectively. The effect of sulfur is to reduce the frequency of this carbonyl absorption (12). Attempts to separate these components by extraction with mild base failed, probably because of facile hydrolysis of the phenolic esters. Attempted separation by gas chromatography failed.

It is interesting to compare the results above with the *para* analog, where intermolecular reaction is impossible. *p*-Hydroxybenzenethiol (**9**) mixed with its diacetate (**10***c*) gave, by ^1H and ^{13}C nmr, additive spectra which exhibited little change, even after several days. Treatment of the mixture with triethylamine gave at first a rather complicated spectrum but over several hours this simplified until only one large methyl absorption at 2.235 was evident. The ^{13}C spectrum of the mixture showed a large absorption at 159.4 ppm assigned to *p*-mercaptophenyl acetate (**7***a*). This is further indicated by the ir spectrum, which showed only one large carbonyl absorption, at 1768 cm^{-1}. In this case then it appears that thiolester cleavage is the main reaction, implying that the phenolic group is a stronger nucleophile than with the *ortho* case. Possibly this reflects differences in hydrogen bonding (13).

It is reported that *o*-hydroxybenzenethiol may be made by treatment of *o*-hydroxybenzenediazonium chloride with potassium ethylxanthate, followed by hydrolysis of the crude product (14), presumably *o*-hydroxyphenyl ethylxanthate. In review of its similarity to the above, it was decided to investigate this and related systems also. Because of side reactions occuring in the diazotization reaction these were approached via the treatment of *o*-hydroxybenzenethiol with the methyl esters of chloroformic acid or chlorothionoformic acid in the presence of triethylamine. The products were obtained as colorless or pale yellow oils.

For the reaction of methylchloroformate with the equivalent quantity of *o*-hydroxybenzenethiol, work-up afforded an oil whose ^1H nmr exhibited only two methyl signals at 3.80 and 3.91 δ . Substantially similar spectra were obtained from an equimolar mixture of the diesters **5***d* and **4**, either on treatment with triethylamine, or on standing for 16 h. Since these two absorptions were at the same δ value as in **5***d*, the ^{13}C spectra of the three reactions were examined. Again all were similar in the number of peaks exhibited apart from added triethylamine, although absorption intensities varied. Absorptions corresponding to compounds **4** and **5***d* could be seen and four different methyl groups were evident. Also evident were two thiolcarbonate absorptions, around 169 ppm, but carbonate absorptions could not be differentiated properly from tertiary carbons bonded to oxygen, and tertiary carbons bonded to sulfur could not be differentiated from aromatic carbons despite Overhauser effects. Positions of absorption were assigned by comparison of spectra with methyl phenyl carbonate and methyl *S*-phenyl thiolcarbonate **6**. The ir spectra of the reactions exhibited two absorptions at 1735 and 1770 cm^{-1} respectively, assigned to thiolcarbonate and carbonate groups respectively.

Although in the ^1H nmr spectrum of the reaction product of *o*-hydroxybenzenethiol with methyl chlorothionoformate the only peak was evident in the region of methoxy groups, the ^{13}C nmr spectrum showed three such groups, at least two thiocarbonyl groups, and three aromatic carbons bonded to oxygen. Unfortunately, apart from *o*-hydroxybenzenethiol, it has not been possible to identify the actual components.

Experimental

Solutions were made up as approximately 60% mixtures in deuteriochloroform using tetramethylsilane as an internal standard. The ^1H nmr spectra were determined on a Varian model 56/60A spectrometer. The ^{13}C nmr spectra were obtained in the Fourier transform mode on a Bruker WH-90DS spectrometer (22.63 MHz), equipped with a Nicolet-1180 computer, the N.T.C.-FT-1180 software package, and quadrature phase detection. Normally spectra were recorded with complete proton noise decoupling; ir spectra were obtained on a Perkin-Elmer model 337 spectrophotometer using neat samples of reaction products.

o-*Hydroxybenzenethiol*

This was commercially available (Parish) or was synthesized according to Leukart (14).

p-*Hydroxybenzenethiol* (*9*)

The commercially available material (Parish) was purified by careful distillation *in vacuo*.

o-*Hydroxybenzenethiol Diacetate* (*5c*)

o-Hydroxybenzenethiol (3.78 g, 0.03 mol) and excess acetic anhydride (10 g) in benzene (10 mL) were treated with triethylamine (2 mL). The volatile materials were removed under reduced pressure and the mixture was fractionally distilled *in vacuo*. The volatile fraction boiling at 108–110°C at 0.4 Torr was collected. A colorless rather viscous liquid was obtained (63%). *Anal.* calcd. for $C_{10}H_{10}O_3S$: C 57.14, H 4.76, S 15.26; found: C 56.93, H 4.72, S 15.31.

o-*Hydroxybenzenethiol Bis(methyl) Carbonate* (*5d*)

o-Hydroxybenzenethiol (2.52 g, 0.02 mol) and methyl chloroformate (3.68 g, 0.04 mol) in anhydrous ether (25 mol) were treated with triethylamine (2 mL). The mixture was washed with 0.1 *N* hydrochloric acid and the ether dried over anhydrous magnesium sulfate. The solution was evaporated under reduced pressure and distilled *in vacuo*. The fraction bp 121–123°C at 0.4 Torr was collected (50%). *Anal.* calcd. for $C_{10}H_{10}O_5S$: C 49.58, H 4.14, S 13.22; found: C 49.63, H 4.21, S 12.98.

2-Methoxyphenyl Thiolacetate (*2c*)

This was made by a published procedure (15) from 2-

methoxybenzenethiol (Fluka) except that triethylamine was used as a basic catalyst.

2-(Methylthio)phenyl Acetate (1c)

2-(Methylthio)phenol (7 g, 0.05 mol) (16) was treated with an excess of acetic anhydride and triethylamine (5 mL). The mixture was warmed briefly and distilled *in vacuo*. The fraction bp 65°C at 0.4 Torr was collected (91%). *Anal.* calcd. for $C_9H_{10}O_2S$: C 59.34, H 5.49, S 17.58; found: C 59.21, H 5.69, S 17.43.

p-*Hydroxybenzenethiol Diacetate (10c)*

This was prepared according to a literature procedure (17).

O-*Methyl*-S-*phenyl Thiolcarbonate (6)*

Benzenethiol (5.5 g, 0.05 mol) was treated with excess methyl chloroformate in anhydrous ether (25 mL). Addition of triethylamine gave a vigorous reaction. The mixture was washed with 0.1 *N* hydrochloric acid and dried over anhydrous magnesium sulfate. Evaporation and distillation *in vacuo* afforded a colorless oil. The fraction bp 71–72°C at 0.4 Torr was collected (83%). *Anal.* calcd. for $C_8H_8O_2S$: C 57.14, H 4.77, S 19.04; found: C 57.26, H 4.83, S 18.99.

Reaction of o-*Hydroxybenzenethiol with One Equivalent of Acetic Anhydride*

The thiol (2.52 g, 0.02 mol) and acetic anhydride (2.02 g, 0.02 mol) were mixed together, and triethylamine (1 mL) added. The mixture warmed immediately. After 30 min the mixture was fractionally distilled at 0.4 Torr to remove acetic acid and triethylamine.

Reaction of o-*Hydroxybenzenethiol with Methyl Chloroformate*

The thiol (2.48 g, 0.02 mol) and methyl chloroformate (1.88 g, 0.02 mol) were mixed in ether (25 mL) and treated with triethylamine (2 mL). After the vigorous reaction the ether was washed with 0.1 *M* hydrochloric acid, dried, and evaporated. The mixture was then fractionally distilled at 0.1 Torr to remove traces of volatile impurities.

Acknowledgements

Grateful thanks are due to the Natural Sciences and Engineering Research Council of Canada for financial support, to Mr. K. Marat for preparation of spectra, and to Drs. T. Schaefer and F. Hruska for helpful discussion.

1. I. Degani and R. Fochi. J. Chem. Soc. Perkin Trans I, 323 (1975).
2. L. Costa, I. Regani, R. Fochi, and P. Tundo. J. Heterocycl. Chem. **11**, 507 (1974).
3. I. Degani, R. Fochi, and P. Tundo. Ann. Chim. Rome, **62**, 570 (1972).
4. J. P. Idoux, P. T. R. Hwang, and C. K. Hancock. J. Org. Chem. **38**, 4239 (1973).
5. T. C. Bruice. *In* Organic sulfur chemistry. Vol. I. *Edited by* N. Kharasch. Pergamon Press, New York. 1961.
6. T. Schaefer and T. Wildman. Can. J. Chem. **57**, 450 (1979).
7. Eric Block. *In* Reactions of organosulfur compounds. Academic Press, New York. 1978. Table B-4.
8. C. W. N. Cumper, A. Melnikoff, E. F. Mooney, and A. I. Vogel. J. Chem. Soc. B, 874 (1966).
9. S. Cabiddu and S. Melis. Snythesis, **10**, 660 (1975).
10. I. W. J. Still, N. Plavac, D. M. McKinnon, and M. S. Chauhan. Can. J. Chem. **54**, 280 (1976).
11. C. C. Price and S. Oae. Sulfur bonding. Ronald Press, New York. 1962.
12. (*a*) R. A. Nyquist and W. T. Potts. Spectrochim. Acta, **15**, 514 (1959); (*b*) A. W. Baker and G. H. Harris. J. Am. Chem. Soc. **82**, 1923 (1960).
13. T. Schaefer, T. A. Wildman, and S. R. Salman. J. Am. Chem. Soc. **102**, 107 (1980).
14. R. Leuckart. J. Prakt. Chem. **41**, 192 (1890).
15. G. Cilento. J. Org. Chem. **24**, 413 (1959).
16. H. S. Holt and E. E. Reid. J. Am. Chem. Soc. **46**, 2333 (1924).
17. T. Zincke and C. Ebel. Ber. **47**, 1100 (1914).

Can. J. Chem. Downloaded from www.nrcresearchpress.com by 210.87.254.6 on 09/05/12
For personal use only.

ERRATA

The hydroxyl groups in structure 1 should be cis (cf. ref. 6).

The action of hypochlorite on *m*-cresol. Part 2.[1] Muconic acid derivatives[2,3]

GEORGE M. STRUNZ, MASATOSHI KAKUSHIMA, AND ALAN D. GIBSON
Canadian Forestry Service, P.O. Box 4000, Fredericton, N.B., Canada E3B 5P7
ARCHIBALD W. MCCULLOCH
Atlantic Regional Laboratory, National Research Council of Canada, Halifax, N.S., Canada B3H 3Z1
AND
PETER S. WHITE
Department of Chemistry, University of New Brunswick, Fredericton, N.B., Canada E3B 6E2
Received June 23, 1980

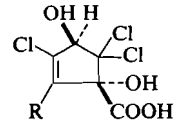
GEORGE M. STRUNZ, MASATOSHI KAKUSHIMA, ALAN D. GIBSON, ARCHIBALD W. MCCULLOCH, and PETER S. WHITE. Can. J. Chem. **58**, 2765 (1980).

Two new crystalline products were isolated from the chlorination of *m*-cresol in cold alkaline solution. These products have been identified as *E*,*Z*-2-chloro-5-methyl muconic acid and 5*Z*-carboxymethylene-3-chloro-4-methyl-2(5*H*) furanone.

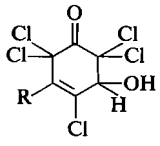
GEORGE M. STRUNZ, MASATOSHI KAKUSHIMA, ALAN D. GIBSON, ARCHIBALD W. MCCULLOCH et PETER S. WHITE. Can. J. Chem. **58**, 2765 (1980).

Deux nouveaux produits cristallins ont été isolés de la réaction du *m*-cresol avec chlore en milieu alkalin froid. On a identifié ces produits comme l'acide *E*,*Z*-2-chloro-5-méthyle muconique et la furfuranone-2(5*H*)-5*Z*-carboxyméthylène-3-chloro-4-méthyle.

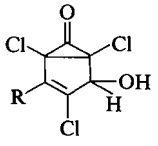
The reaction of phenol with hypochlorite in alkaline solution gives rise, *inter alia*, to 3,5,5-trichloro-1,4-dihydroxy-2-cyclopentene-1-carboxylic acid (**1**, R=H) (2–4). Mechanisms advanced for this transformation invoked Favorskii-type ring contraction, involving intermediates such as **2** (3) or **3** (4). It was demonstrated that *meta* alkyl substituted phenols afforded the corresponding 2-alkyl derivatives (**1**, R = methyl or *n*-propyl) under similar conditions (1, 5), and the reaction was exploited as the key step in the total synthesis of the fungal metabolite[4] cryptosporiopsin (5).



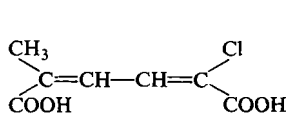
1



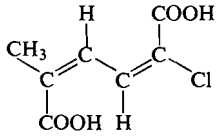
2



3



4



5

The capricious nature of the reaction, resulting from its sensitivity to minor variations in experimental conditions, has been noted (3, 4). In the course of studies with *m*-cresol aimed at optimization of yields of **1** (R = methyl), cf. ref. 1, the effects of variations in temperature, pH, chlorine flow rate, etc. were explored. Under certain conditions (see Experimental), two additional crystalline compounds were obtained as minor products.

We report here on the structures of these compounds, $C_7H_7O_4Cl$ and $C_7H_5O_4Cl$, which are products of oxidative cleavage of the aromatic ring.

The substance with the greater hydrogen complement displayed in its mass spectrum isotope peaks at *m/e* 190 and 192, corresponding to the molecular ion; the base peak at *m/e* 155 resulted from loss of chlorine.

In the infrared spectrum (KBr), a carbonyl band at 1695 cm^{-1} and broad absorption between 3600 and 2100 cm^{-1} are indicative of a conjugated carboxylic acid. The presence of an extended chromophore was manifested by an ultraviolet absorption maximum at 281 nm (ε 20 300).

The 100 MHz ^1H nmr spectrum, recorded in tetrahydrofuran-d_8, shows an AB system centred at δ 7.76 for two vicinally-coupled olefinic protons (J_{AB} = 11.7 Hz; $\Delta\nu_{AB}$ = 53.8 Hz). The high-field and

[1]For part 1, see ref. 1.
[2]NRCC No. 18672.
[3]This paper is dedicated to Professor Karel Wiesner on the occasion of his 60th birthday.

[4]The phenol-hypochlorite product, **1** (R=H), was also elaborated into a fungal metabolite, caldariomycin (4), and has recently been used to prepare a chiral intermediate for prostanoid synthesis (6).

0008-4042/80/242765-05$01.00/0
©1980 National Research Council of Canada/Conseil national de recherches du Canada

FOR ERRATA SEE v 59 1981 p 3161

Can. J. Chem. Downloaded from www.nrcresearchpress.com by 210.87.254.105 on 09/05/12
For personal use only.

Can. J. Chem. Downloaded from www.nrcresearchpress.com by 210.87.254.105 on 09/05/12
For personal use only.

TABLE 1. ^{13}C nmr data for **5** (in tetrahydrofuran-d_8)

Carbon	δ_C (ppm)	Multiplicity*†	$^nJ_{CH}$ (Hz)
C-1	163.74	d	^3J 10.0
C-2	127.01	ddq	^3J 6.5, ^2J 3.0, ^5J 1.5
C-3	137.00	d	^1J 164.1
C-4	132.51	ddq	^1J 162.4, ^2J 2.3, ^3J 6.6
C-5	135.32	dq	^3J 3.5, ^2J 7.0
C-6	168.21	dq	^3J 12.3, ^3J 4.0
C-7 (Methyl)	21.64	qd	^1J 128.5, ^3J 6.7

*Abbreviations: d = doublet, q = quartet
†All quartet spacings were removed on irradiation of H-7, while the C-3 doublet was sharpened.

low-field protons of this system show, in addition, coupling (J = 1.5 and 0.5 Hz respectively) to the hydrogens of an allylic methyl group at δ 2.02. A broad peak at δ 10.55 is attributable to two acidic protons. The structure **4**, 2-chloro-5-methyl muconic acid is consistent with these spectra.

The proton noise decoupled ^{13}C nmr spectrum, as expected, shows resonances for one methyl, two carboxyl, and four olefinic carbons. The high resolution ^{13}C nmr spectrum (Table 1), recorded without decoupling and then with selective decoupling of the methyl hydrogens, provided unequivocal evidence for formulation **4** and in addition allowed assignment of the *EZ* geometry depicted in **5**.

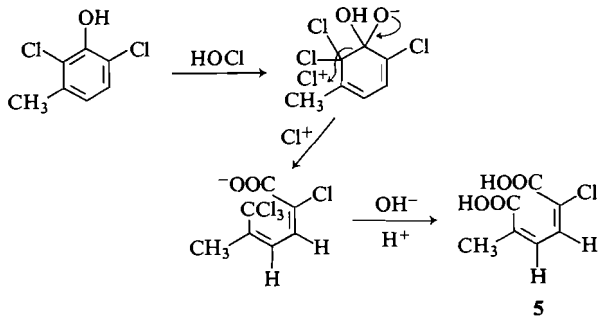
The magnitude of the coupling between the carboxyl carbon at δ 168.21 and the methyl hydrogens (^3J = 4.0 Hz) indicates that this carboxyl must be geminal with the methyl group, while the magnitude of the doublet coupling (^3J = 12.3 Hz) establishes that it is also oriented *trans* to an olefinic hydrogen (7). This stereochemistry is further confirmed by the characteristic *cis* coupling (^3J = 6.7 Hz) observed between the methyl carbon and the vicinal olefinic proton.

Since the two olefinic hydrogens are vicinal, the chlorine must be located α to the second carboxyl carbon. This is reflected by the chemical shift (δ 163.74) of the latter (8). Chlorine substitution at this centre would also be expected to reduce the magnitude of the coupling between the adjacent carboxyl and the β olefinic hydrogen (7). Thus, the magnitude of the observed coupling (^3J = 10.0 Hz) is compatible again only with a *trans* relationship of these atoms. The combined evidence therefore establishes structure **5**.

The selective decoupling experiment showed that the methyl hydrogens are also coupled to the α-(^2J = 7.0 Hz), β-($^3J \simeq$ 6.6 Hz), and δ-($^5J \simeq$ 1.5 Hz) olefinic carbons. These, and all other couplings observed, are entirely compatible with **5**.

The presence of another isomer (up to 25% of the 2-chloro-5-methyl muconic acid) was evident in the product from most runs. This was tentatively assigned the *ZZ* geometry on the basis of the signals for the vinyl protons in the ^1H nmr spectrum (AB system centred at δ 7.68, J_{AB} = 11.3 Hz, $\Delta\nu_{AB}$ = 163.8 Hz; high-field and low-field protons coupled to hydrogens of allylic methyl group at δ 2.09 (J = 1.6 and 0.6 Hz respectively).

A mechanism for the formation of **5** (from 2,6-dichloro-*m*-cresol) is suggested in Scheme 1. The presence of the minor, *ZZ* isomer may be rationalized in several ways. One facile mechanism for isomerization of a *cis–cis* muconic acid to the *cis–trans* form involves the formation of a lactone intermediate, cf. ref. 9.

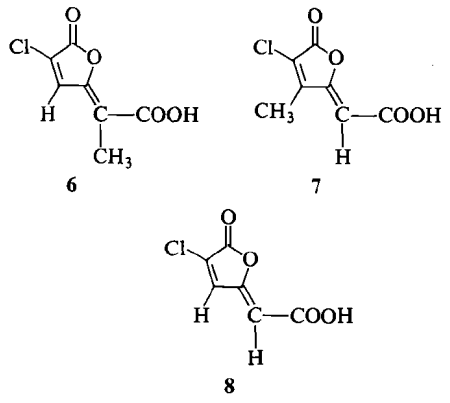


SCHEME 1

Like its congener, the other crystalline by-product, $C_7H_5ClO_4$, also shows infrared absorption characteristic of a conjugated carboxylic acid (1695 and 3650–2250 cm^{-1}). An extended chromophore is again manifested in the ultraviolet spectrum (λ_{max} 281 nm (ε 20 000)). Besides the broad absorption associated with the acid proton (exchangeable), the 60 MHz ^1H nmr spectrum in acetone-d_6 solution consists of two sharp singlets: one, at δ 5.83 due to a vinyl proton, and the other, at δ 2.30, attributable to the hydrogens of an allylic methyl group. These features, together with a strong, sharp band at 1805 cm^{-1} in the infrared spectrum, cf. ref. 10, suggest an enol-lactone structure such as **6** or **7** (geometry not implied).

The structure **7** was firmly established by a single crystal X-ray analysis. Figure 1 is a perspective

Can. J. Chem. Downloaded from www.nrcresearchpress.com by 210.87.254.105 on 09/05/12
For personal use only.



view of the molecule with bond distances and angles shown in Table 2. Details relevant to the X-ray analysis are presented in the Experimental.

The mechanism in Scheme 2 could account for the formation of 7. This scheme bears a formal resemblance to the latter part of the pathway whereby the herbicide 2,4-D is metabolized by *Pseudomonas* spp. (10). The lactone 8 has been recognized as an intermediate in this pathway (10).

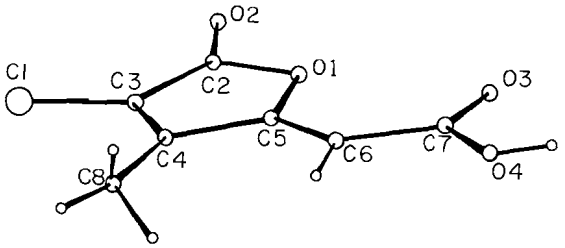


FIG. 1. Perspective view of molecule 7, showing numbering scheme used.

TABLE 2. Bond lengths and angles*

Bond	Length (Å)	Bond	Length (Å)
O1—C2	1.390(4)	C4—C8	1.479(5)
C2—O2	1.190(4)	C5—O1	1.375(3)
C2—C3	1.455(4)	C5—C6	1.319(4)
Cl—C3	1.705(3)	C6—C7	1.477(4)
C3—C4	1.334(4)	C7—O3	1.221(4)
C4—C5	1.478(4)	C7—O4	1.311(4)

Bonds	Angle (°)	Bonds	Angle (°)
C2—O1—C5	108.3(2)	C5—C4—C8	124.7(3)
O1—C2—O2	121.5(3)	O1—C5—C4	109.2(3)
O1—C2—C3	106.4(2)	O1—C5—C6	123.2(3)
O2—C2—C3	132.1(3)	C4—C5—C6	127.6(3)
Cl—C3—C2	121.6(2)	C5—C6—C7	125.7(3)
C2—C3—C4	110.9(3)	C6—C7—O3	123.4(3)
Cl—C3—C4	127.5(3)	C6—C7—O4	113.2(3)
C3—C4—C5	105.2(3)	O3—C7—O4	123.4(3)
C3—C4—C8	130.1(3)		

*Estimated standard deviations in parentheses.

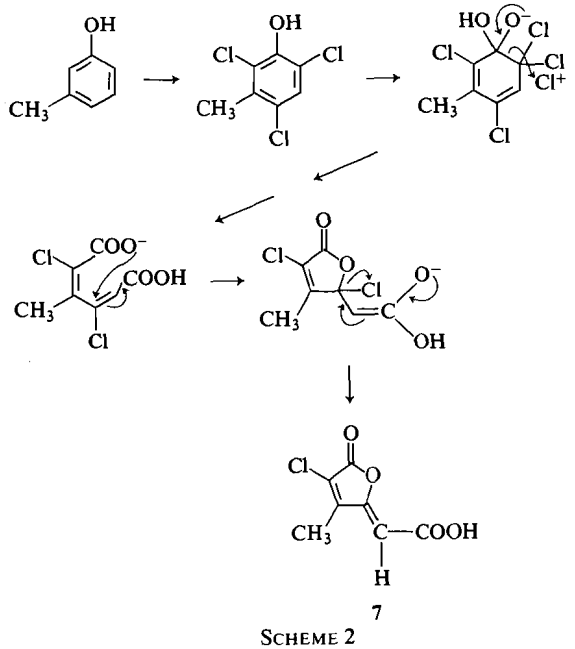
Experimental

Melting points were determined on a hot-stage apparatus and are uncorrected. Infrared and ultraviolet spectra were recorded on Beckman Acculab 2 and DK-2A spectrophotometers respectively. Mass spectra were obtained with an Hitachi Perkin-Elmer RMU-6D mass spectrometer. The 60 MHz ^{1}H nmr spectra were recorded using a Varian T-60 instrument with tetramethylsilane as internal standard; the 100 MHz spectrum of 5 in tetrahydrofuran-d_8 was measured on a Varian HA-100 spectrometer using the tetramethylsilane resonance to provide the field-frequency lock. The ^{13}C nmr spectra were recorded in tetrahydrofuran-d_8 (90 mg/0.3 mL) on a Varian FT-80 spectrometer under the following conditions: frequency 20 MHz; acquisition time 0.99 or 1.98 s (data accuracy ±0.5 or ±0.25 Hz); spectral width 4132 Hz; flip angle 25° or 50°; internal ^{2}H lock to solvent; temperature about 35°C; ^{1}H irradiation at 80 MHz (*a*) $\gamma H_2/2\pi$ ca. 4000 Hz, bandwidth 2000 Hz (broadband decoupling); (*b*) $\gamma H_2/2\pi$ ca. 2900 Hz, bandwidth 1000 Hz, field applied for 2 s between data acquisitions to retain nOe (high-resolution spectrum); (*c*) as for (*b*), but with additional constant ^{1}H irradiation $\gamma H_2/2\pi$ 196 Hz at frequency of methyl ^{1}H resonance (single-frequency decoupling with nOe retained at all resonances).

Microanalyses were performed by Spang Microanalytical Laboratory, Eagle Harbor, MI.

Reaction of m-*Cresol with Alkaline Hypochlorite*

A solution of *m*-cresol (50 g, 0.46 mol) in 2.5 *M* aqueous sodium hydroxide (435 mL) was cooled to −2°C. Chlorine was passed slowly into the stirred mixture through a gas dispersion tube while the temperature was maintained around −2°C by judicious application of the cooling bath. During the first hour of this treatment, six 85 mL portions of cold 5 *M* sodium hydroxide solution were added, at roughly 10 min intervals; the chlorine flow was then continued for a second hour while the temperature



SCHEME 2

Can. J. Chem. Downloaded from www.nrcresearchpress.com by 210.87.254.105 on 09/05/12
For personal use only.

was maintained at 10–15°C. At the end of this period the solution was still alkaline. The mixture was made acidic by addition of 12 *M* hydrochloric acid (30 mL), and was then filtered through a bed of Celite. The filtrate was extracted successively with eight portions of ether (total volume 1200 mL). The extracts were dried over magnesium sulfate and evaporated to dryness *in vacuo*. The residue (22.1 g) formed a semicrystalline mass on being set aside in a refrigerator. The product was partially dissolved in boiling chloroform (100 mL), and after standing at 23°C for 3 h, insoluble material was collected by vacuum filtration. In this manner 465 mg (0.53% from *m*-cresol) of **5** was obtained as almost colorless crystals. Recrystallization from chloroform yielded colorless crystals, mp 156–176°C; ir (KBr) *inter alia*: 3600–2100, 1695, 1560, 1405, 1310, 1245, 970, and 910 cm^{-1}; uv λ_{max} (EtOH): 281 nm (ε 20 300); λ_{max} (alkaline EtOH): 272 nm (ε 19 200); ^1H and ^{13}C nmr spectra described in text; mass spectrum *m/e*: 190 (M^+), (($M + 2$)$^+$ 34% of M^+), 155 (base peak) ($M - Cl$)$^+$. *Anal.* calcd. for $C_7H_7ClO_4$: C 44.12, H 3.70, Cl 18.60, O 33.58; found: C 44.26, H 3.21, Cl 18.61, O 33.80.

The filtrate from above was concentrated, and on standing further crystals separated and were filtered at the pump. Crystalline **7** (548 mg, 0.63%) was thus obtained. Recrystallized from chloroform, the material sublimed at ca. 192°C and was completely molten at 206°C. Recrystallization from acetone–cyclohexane gave colorless needles which began to sublime around 200°C and melted at 225–235°C (dec.). Spectral characteristics of **7** are as follows: ir (KBr) *inter alia*: 3650–2250, 1805, 1695, 1645, 1420, 1260, 1195, and 975 cm^{-1}; uv λ_{max} (EtOH): 281 nm (ε 19 800); 60 MHz ^1H nmr spectrum described in text; mass spectrum *m/e*: 188 (M^+); (($M + 2$)$^+$ 35% of M^+). *Anal.* calcd. for $C_7H_5ClO_4$: C 44.58, H 2.67, Cl 18.80; found: C 44.42, H 2.83, Cl 18.71.

Evaporation of the filtrate gave an oil (17.6 g), which on redissolving in hot chloroform deposited 2.36 g (2%) of "Hantzsch acid" (**1**, R = CH_3), mp 148–152°C (1). Additional Hantzsch acid could be obtained from the mother liquors.

X-ray Diffraction Study of 7

A preliminary photographic investigation was used to obtain approximate cell dimensions and determine the space group as $P2_1/n$. Final unit cell dimensions were obtained by centering 12 reflections and their Friedel opposites on a Picker FACS-I diffractometer, and fitting the cell parameters and an orientation matrix to the coordinates by a least-squares routine. Graphite monochromated Mo K_α radiation was used, and throughout the investigation the diffractometer was controlled by the NRC FORTRAN control routines of Larson and Gabe (11). The relevant crystallographic data are:

$C_7H_5O_4Cl$ fw = 188.6
Monoclinic, $P2_1/n$, a = 5.0640(7), b = 13.312(3), c = 11.561(2) Å, β = 99.94(1)°, V = 767.7 Å^3, D_c = 1.63 Mg m^{-3}, Z = 4, (20°C, Mo K_α, λ = 0.71069 Å). Crystal size = 0.02 × 0.02 × 0.05 cm, μ = 0.47 mm^{-1}.

Intensities were measured on the diffractometer using an ω–2θ scan at a rate of 2 deg (2θ) min^{-1} over a range of 2° (2θ) corrected for dispersion of the K_α doublet. The background was estimated by an analysis of the profile of each peak measured by the computer during each scan. Three reference reflections, monitored every 50 reflections, showed no significant variation in intensity throughout the data collection. Data were collected for $2\theta \leq 45°$ which resulted in 1006 unique reflections of which 178 (17.6%) were considered unobserved ($I \leq 1.5\sigma(I)$) and were not included in the subsequent refinement.

Structure Determination and Refinement

The structure was solved by multiple solution direct methods using a version of the computer program MULTAN modified for use on the PDP8/E computer. The set of phases with the highest figure of merit was used to phase an *E*-map which revealed the positions of all the nonhydrogen atoms. The oxygen positions were assigned using chemical considerations and later confirmed by the geometry of the structure.

The structure was refined by least-squares methods, minimizing the function $\Sigma w(|F_o| - |F_c|)^2$. The weighting scheme was of the form $w = 1/\sigma^2(F)$, with σ estimated from the measured intensity. After initial refinement of the positions of the nonhydrogen atoms a difference synthesis was calculated which revealed the positions of the hydrogen atoms. The final cycles of least squares included the positional parameters of all atoms, isotropic thermal parameters for the hydrogens, and anisotropic thermal parameters for all other atoms. The final agreement indices were R = 0.071 and R_w = 0.085 (0.085 and 0.090 respectively including the unobserved reflections). Table 3 contains the final atomic positional parameters.[5]

All computations were performed on a Digital Equipment PDP8/A computer, equipped with a floating point processor, using the NRC PDP-8e Crystal Structure System (11) and locally written programs.

TABLE 3. Fractional coordinates (esd's) × 10^4

Atom	*x*	*y*	*z*
Cl	1066(1)	3771(0)	545(0)
O(1)	7368(4)	4925(1)	2530(1)
C(2)	5061(6)	5008(2)	1688(2)
O(2)	4334(5)	5797(1)	1263(2)
C(3)	3942(5)	4002(2)	1515(2)
C(4)	5453(5)	3340(2)	2200(2)
C(5)	7683(6)	3934(2)	2860(2)
C(6)	9701(6)	3605(2)	3646(2)
C(7)	11956(6)	4221(2)	4245(2)
O(3)	12227(5)	5111(1)	4040(2)
O(4)	13676(4)	3708(1)	4997(2)
C(8)	5115(7)	2244(2)	2322(3)
H(4)	14925(102)	4067(41)	5314(34)
H(6)	9865(57)	2953(24)	3800(22)
H(8a)	4194(98)	2001(49)	1732(41)
H(8b)	4925(137)	2117(53)	3005(48)
H(8c)	6968(119)	1821(81)	2496(45)

Acknowledgement

The authors thank D. G. Smith for assistance with the selective decoupling experiment.

1. G. M. STRUNZ, A. S. COURT, and J. KOMLOSSY. Tetrahedron Lett. 3613 (1969).
2. A. HANTZSCH. Chem. Ber. **20**, 2780 (1887); **22**, 1238 (1889).
3. C. J. MOYE and S. STERNHELL. Tetrahedron Lett. 2411 (1964); Aust. J. Chem. **19**, 2107 (1966).
4. A. W. BURGSTAHLER, T. B. LEWIS, and M. O. ABDEL-RAHMEN. J. Org. Chem. **31**, 3516 (1966).
5. G. M. STRUNZ and A. S. COURT. J. Am. Chem. Soc. **95**, 3000 (1973).

[5]Tables of thermal parameters and structure factors are available, at a nominal charge, from the Depository of Unpublished Data, CISTI, National Research Council of Canada, Ottawa, Ont., Canada K1A 0S2.

6. M. GILL and R. W. RICKARDS. Tetrahedron Lett. 1539 (1979).
7. U. VOGELI and W. VON PHILIPSBORN. Org. Magn. Reson. **7**, 617 (1975).
8. E. LIPPMAA, T. PEHK, K. ANDERSON, and C. RAPPE. Org. Magn. Reson. **2**, 109 (1970).
9. J. A. ELVIDGE, R. P. LINSTEAD, and P. SIMS. J. Chem. Soc. 3386 (1951); J. A. ELVIDGE, R. P. LINSTEAD, and J. F. SMITH. J. Chem. Soc. 1026 (1952).
10. W. C. EVANS, B. S. W. SMITH, H. N. FERNLEY, and J. I. DAVIES. Biochem. J. **122**, 543 (1971).
11. A. C. LARSON and E. J. GABE. Minimum computer system for complete crystal structure determination. *In* Computing in crystallography. *Edited by* H. Schenk, R. Olthof-Hazekamp, H. van Koningsveld, and G. C. Bassi. Delft University Press, The Netherlands. 1978. pp. 81–89.

Can. J. Chem. Downloaded from www.nrcresearchpress.com by 210.87.254.105 on 09/05/12
For personal use only.

A regiospecific synthesis of protoberberine alkaloids

ZINOVIA KIPARISSIDES, ROBERT H. FICHTNER, JANUSZ POPLAWSKI, BALA C. NALLIAH, AND DAVID B. MACLEAN

Department of Chemistry, McMaster University, Hamilton, Ont., Canada L8S 4M1

Received June 9, 1980

ZINOVIA KIPARISSIDES, ROBERT H. FICHTNER, JANUSZ POPLAWSKI, BALA C. NALLIAH, and DAVID B. MACLEAN. Can. J. Chem. **58**, 2770 (1980).

The protoberberine skeleton has been prepared in two steps from *N*-benzyl-3,4-dihydroisoquinolinium salts. Treatment of the salts with the anion of methyl methylthiomethylsulfoxide yields mixtures of diastereomeric adducts that cyclize on heating with concentrated hydrochloric acid to dihydroprotoberberines. The latter compounds may be reduced to their tetrahydro analogues with sodium borohydride, oxidized to protoberberinium salts with iodine, or converted to 13-methyltetrahydroprotoberberines by treatment with formaldehyde according to an established procedure. The method has been applied successfully to the synthesis of (±)-tetrahydropalmatine, palmatine iodide, (±)-xylopinine, (±)-sinactine, and (±)-corydaline. *N*-Benzylisoquinolinium salts may be used in place of their dihydro analogues as starting materials in this synthesis, thereby extending the range of substitution patterns potentially available.

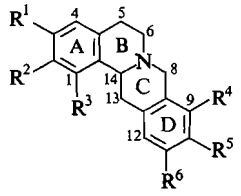
ZINOVIA KIPARISSIDES, ROBERT H. FICHTNER, JANUSZ POPLAWSKI, BALA C. NALLIAH et DAVID B. MACLEAN. Can. J. Chem. **58**, 2770 (1980).

On a préparé en deux étapes le squelette de la protoberbérine à partir des sels de *N*-benzyldihydro-3,4 isoquinolinium. Les sels traités par l'anion du méthylthiométhylsulfoxyde de méthyle donnent un mélange d'adduits diastéréoisomères qui, par chauffage dans de l'acide chlorohydrique concentré, se cyclisent en donnant les dihydroprotoberbérines. Ces derniers peuvent être soit réduits en leurs analogues tétrahydro par le borohydrure de sodium, soit oxydés par l'iode en sels de protoberbérinium, soit transformés en méthyl-13 tétrahydroprotoberbérines par réaction avec le formol selon une méthode connue. On a utilisé cette méthode avec succès pour la synthèse des composés suivants: la (±)-tétrahydropalmatine, l'iodure de palmatine, la (±)-xylopinine, la (±)-sinactine et la (±)-corydaline. Dans cette synthèse, on peut utiliser comme produit de départ le sels de *N*-benzylisoquinolinium au lieu de leurs analogues dihydro ce qui augmente le nombre potentiel de modèles de substitution disponibles.

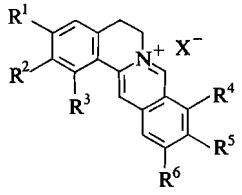
[Traduit par le journal]

The protoberberine alkaloids exist in nature as tetrahydroprotoberberines or quaternary protoberberine salts as shown in structures **1** and **2**, respectively. The R groups are present as hydroxy, methoxy, or methylenedioxy. The substitution pattern most commonly encountered is 2, 3, 9, 10 but other substitution patterns are found in the aromatic rings and in some cases methyl groups are also present at C-8 or at C-13 and hydroxy groups at C-5 or at C-13. Many methods have been described for the construction of this ring system and excellent reviews are available not only on the synthesis of the protoberberines but also on other aspects of their chemistry (1–6). However, many of the methods of synthesis are not regiospecific, and many are multistep or require intermediates that are not readily accessible. The new method described here is regiospecific and uses starting materials that are easily prepared. It has been applied to the synthesis of 2,3,9,10- and 2,3,10,11-tetrasubstituted alkaloids, and in principle is adaptable to the preparation of other alkaloids of the series differently substituted in the aromatic rings.

Appropriately substituted *N*-benzyl-3,4-dihydroisoquinolinium salts such as **3** were used initially as starting materials in this work. They were prepared from substituted benzyl halides and substituted 3,4-dihydroisoquinolines, both of which are accessible by standard procedures. The objective of the work was to insert a one-carbon unit between C-1 and C-6′ of **3** (eventually to become C-13 of the protoberberine) and in this way to generate the protoberberine skeleton. Carbon atom 1 of **3** is a reactive centre amenable to attack by one-carbon nucleophiles while C-6′ is an activated site amenable to electrophilic attack. Thus a one-carbon nucleophile that, once introduced, might be converted into an electrophilic centre was required. The reagent of choice proved to be lithio methyl methylthiomethylsulfoxide (7), a reagent already known to add to iminium salts (8). This reagent, generated from methyl methylthiomethylsulfoxide (MMTS), added readily to the



1



2

a $R^1 = R^2 = R^4 = R^5 = OCH_3$; $R^3 = R^6 = H$
b $R^1 = R^2 = R^5 = R^6 = OCH_3$; $R^3 = R^4 = H$
c $R^1 = R^2 = OCH_3$; $R^4 + R^5 = OCH_2O$; $R^3 = R^6 = H$

0008-4042/80/242770-10$01.00/0
©1980 National Research Council of Canada/Conseil national de recherches du Canada

Can. J. Chem. Downloaded from www.nrcresearchpress.com by 210.87.254.105 on 09/05/12
For personal use only.

Can. J. Chem. Downloaded from www.nrcresearchpress.com by 210.87.254.105 on 09/05/12
For personal use only.

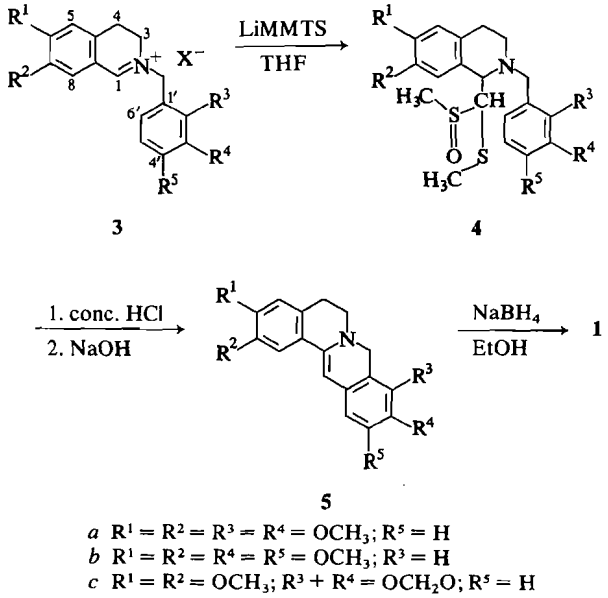
dihydroisoquinolinium salts **3**. The reagent, generated at −35°C in anhydrous tetrahydrofuran (THF), was added by a syringe to a suspension of the dihydroisoquinolinium salt in THF at a temperature of ca. −30°C and the mixture was held at this temperature for 3 h during which time the suspended solids had entered solution. The reaction mixtures were worked up in a conventional manner yielding crude residues that were purified by chromatography or in some cases used directly in the next reaction step. The products were obtained as oils in yields of 90% and their nmr spectra indicated that they were mixtures of isomers (see Scheme 1).

A detailed chromatographic examination was carried out on the adduct **4***a* in an attempt to ascertain its composition. Initially the crude residue was chromatographed over alumina and in this way a product was obtained as an oil in yields in excess of 90%. The ^{1}H nmr spectrum showed a multiplicity of signals in the S—Me region suggesting that the compound was a mixture of diastereomers. Examination of the crude adduct by tlc on silica using ether–ethanol (absolute) 8:1 as eluent showed three components at R_f 0.16, 0.20, and 0.33. By using flash chromatography (9) on silica and the same solvent system used for tlc it was possible to separate the crude reaction product into the three fractions obtained on tlc. ^{1}H nuclear magnetic resonance examination showed that the middle fraction contained two S—Me signals in its spectrum and was apparently pure, while the other two fractions contained four S—Me signals each in their spectra and were mixtures. Two S—Me peaks in the fraction R_f 0.16 were found to be coincident with the corresponding peaks of MMTS. Unused MMTS from the condensation must therefore have been carried through the purification procedure and chromatographic conditions were not found for its separation from this isomer. A more complex solvent system (hexane–ethanol–THF 6:3:1) proved effective in resolving the fraction, R_f 0.33, into two components. Variable temperature nmr studies showed that the two components of this fraction were not rotamers since the four peaks failed to coalesce to two even at 90°C. Mass spectrometric examination of the three fractions obtained by flash chromatography showed only slight differences in their spectra (taking into account the presence of MMTS in the R_f 0.16 fraction). The chromatographic work combined with the nmr and ms studies suggests that the adduct is a mixture of four racemic diastereomers as expected of a compound having three chiral centres.

Further attempts were not made to characterize the diastereomers since it was found that the crude reaction mixture derived from alumina chromatography, or any of the three fractions obtained from silica chromatography, were all suitable starting materials in the next synthetic step. In all cases the same product was obtained on treatment with concentrated hydrochloric acid, for 5–10 min, at steam bath temperatures under a nitrogen atmosphere.

Two methods were used to work up the product of the reaction with concentrated HCl. In the first method the reaction mixture was cooled and carefully basified with sodium hydroxide solution. The products were not the expected 1-carboxaldehydes but instead the dihydroprotoberberines **5**. Only in one case, that of **5***b*, was the product characterized by spectroscopic examination. In other cases the dihydro compounds **5**, because of their sensitivity to aerial oxidation, were treated directly with sodium borohydride in ethanol to give the tetrahydroprotoberberines, **1***a*, **1***b*, and **1***c*. The synthetic sequence is outlined in Scheme 1.

In this way (±)-tetrahydropalmatine **1***a*, (±)-xylopinine **1***b*, and (±)-sinactine **1***c*, were prepared beginning with **3***a*, **3***b*, and **3***c*, respectively, in overall yields of ca. 45% based on the dihydroisoquinolinium salts. In all cases the spectral properties, ir and nmr, of the synthetic alkaloids in solution were identical with those of the naturally occurring bases. Their mass spectra were also identical.



3 **4** **5**

a $R^1 = R^2 = R^3 = R^4 = OCH_3$; $R^5 = H$
b $R^1 = R^2 = R^4 = R^5 = OCH_3$; $R^3 = H$
c $R^1 = R^2 = OCH_3$; $R^3 + R^4 = OCH_2O$; $R^5 = H$

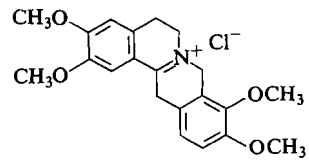
SCHEME 1

Can. J. Chem. Downloaded from www.nrcresearchpress.com by 210.87.254.105 on 09/05/12
For personal use only.

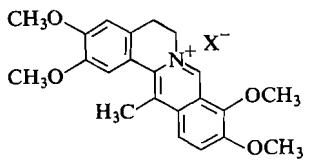
The second method of work-up was based on the observation that fine yellow crystalline needles separated in yields of 70–90% from the reaction mixture of **4***a* and concentrated HCl when the mixture was cooled and allowed to stand. The iminium salt structure **6** has been assigned to this product. Unfortunately good analytical data were not obtained on this compound, presumably because it was highly solvated. Moreover it appeared to suffer decomposition on heating in a drying pistol. However, the ^{1}H nmr spectrum in trifluoroacetic acid (TFA) supported this structure. Besides the methoxyl and the aromatic protons there were signals attributed to 8 aliphatic protons in the spectrum. Two of these hydrogens appeared upfield from the methoxyl signals as a multiplet at 3.40 δ and were assigned to the hydrogen atoms at C-5, and two other hydrogens in the region 4.16–4.35 δ to those at C-6. The latter were partially obscured by the methoxyl resonances. At lower field from the methoxyl resonances there were two broad absorptions each of area 2 at 4.64 δ and 5.30 δ that were assigned to hydrogen atoms at C-13 and C-8, respectively. The infrared spectrum of **6** in $CDCl_3$ showed a peak at 1634 cm^{-1} characteristic of a $C{=}N^+$ function. The mass spectrum had peaks at *m/e* 355 (35), 354 (35), 353 (100), and 352 (45). The dihydro palmatinium ion would be expected at *m/e* 354. It is possible that the ions at *m/e* 355 and *m/e* 353 may arise by disproportionation of the sample at the source temperatures required for volatilization of the sample. Ions at *m/e* 190 (25) and *m/e* 164 (50) present in the spectrum are characteristic of protoberberine systems (10). Compound **6** was readily reduced with sodium borohydride in ethanol to **1***a*, thus lending further support to the assigned structure.

Compound **6** was a convenient starting material for the synthesis of corydaline. Bersch (11) reported that the reaction of formaldehyde with dihydroprotoberberines yielded quaternary protoberberinium salts methylated at C-13. When **6** was heated with formaldehyde in aqueous acetic acid containing sodium acetate, and then with sodium iodide it was converted into dehydrocorydaline iodide **7**. Reaction of **7** with sodium borohydride yielded (±)-corydaline **8** and none of its isomer, in agreement with the work of Kondo (12). This total synthesis of corydaline proceeds in 46% yield from **6** and is shorter by several steps than a recently reported route (13). In principle this method should be applicable to other protoberberines methylated at C-13.

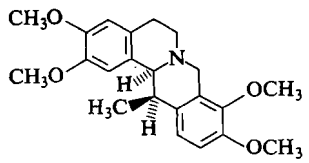
The syntheses reported to this point all involve dihydroisoquinoline intermediates prepared by



6



7

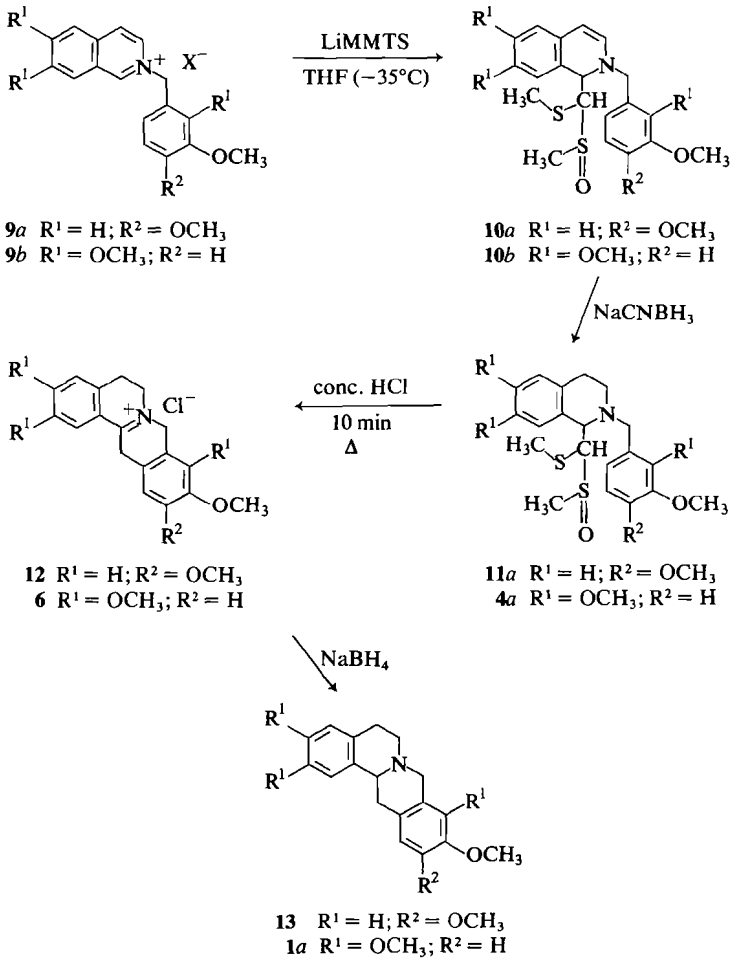


8

Bischler–Napieralski cyclization (14). In order to extend this synthetic approach to substituted protoberberines not available by the Bischler–Napieralski reaction we have investigated the applicability of isoquinolines in place of 3,4-dihydroisoquinolines as starting materials in this synthesis. Through the use of isoquinolines a full range of substituted compounds is available by making use of the other synthetic pathways to this ring system. In preliminary studies we have found that isoquinoline itself and 6,7-dimethoxyisoquinoline are suitable starting materials and we plan in the future to extend the reaction to other isoquinolines.

Treatment of isoquinoline with 3,4-dimethoxybenzyl chloride yielded the salt **9***a* that was treated with the anion of MMTS at −35°C (Scheme 2). Structure **10***a* has been assigned to the product of this reaction. Like the analogues discussed previously this compound was a mixture as shown by tlc and by its nmr spectrum. Unlike the compounds of structure **4**, compound **10***a* was unstable and decomposed on attempted column chromatography.[1] It also failed to give recognizable products on attempted cyclization in concentrated HCl or on treatment with sodium borohydride in ethanol. It did, however, undergo reduction with sodium cyanoborohydride in methanolic acetic acid, a reaction accompanied by spectacular color

[1]Other workers (ref. 15, and references therein) have noted that 2-alkyl-1,2-dihydroisoquinolines are unstable and undergo disproportionation to isoquinolines and tetrahydroisoquinolines. This and other reactions may be occurring here.



9a $R^1 = H; R^2 = OCH_3$
9b $R^1 = OCH_3; R^2 = H$

10a $R^1 = H; R^2 = OCH_3$
10b $R^1 = OCH_3; R^2 = H$

12 $R^1 = H; R^2 = OCH_3$
6 $R^1 = OCH_3; R^2 = H$

11a $R^1 = H; R^2 = OCH_3$
4a $R^1 = OCH_3; R^2 = H$

13 $R^1 = H; R^2 = OCH_3$
1a $R^1 = OCH_3; R^2 = H$

SCHEME 2

changes. The product, to which structure **11a** was assigned, was a mixture of isomers as evidenced by its tlc behaviour and by its nmr spectrum. In its properties **11a** resembled compounds **4**. It was formed in 60% overall yield from **9a**. Without further purification the yellow oil **11a** was heated with concentrated HCl for 10 min on the steam bath. A yellow solid, assigned structure **12**, crystallized from the reaction mixture in 62% yield. The spectroscopic properties of this compound were very similar to those of **6**. In particular, in the ^1H nmr spectrum in TFA, there were four signals attributed to methylene signals as follows. There were two apparent triplets at 3.40 and 4.30 δ assigned to hydrogens at C-5 and C-6, respectively, and two broad singlets at 4.65 and 5.20 δ attributed to hydrogens at C-13 and C-8, respectively. The ir and ms were also in accord with the assigned structure and were similar to those of **6**. Reduction of **12** with sodium borohydride afforded **13**, a compound previously described in the literature (16. 17). The mass spectrum of this compound was typical of the protoberberine group in that it showed a molecular ion at *m/e* 295 (90) and a typical fragment ion at *m/e* 164 (100).

In a second series of experiments to test this new route to the tetrahydroprotoberberines, the quaternary salt **9b** was prepared and converted to the mercaptal **10b**. Like its analogue **10a**, this compound was relatively unstable and decomposed on attempted chromatography. When it was treated with $NaCNBH_3$ under the same conditions that led to the conversion of **10a** to **11a**, it did not give the expected product but instead *N*-(2,3-dimethoxybenzyl)-6,7-dimethoxy-1,2,3,4-tetrahydroisoquinoline was obtained. Apparently in this medium **10b** must exist in equilibrium with **9b** and MMTS anion and suffers reduction to the observed product. Conversion to **4a** was achieved by changing the solvent system by replacing methanol with

Can. J. Chem. Downloaded from www.nrcresearchpress.com by 210.87.254.105 on 09/05/12
For personal use only.

Can. J. Chem. Downloaded from www.nrcresearchpress.com by 210.87.254.105 on 09/05/12
For personal use only.

THF. Under these conditions **10***b* was converted into **4***a* again accompanied by spectacular color changes. The overall yield of **4***a* from **9***b* was 43%. The chromatographic behaviour of this reaction sequence was identical with that reported in the derivation of **4***a* from a dihydroisoquinoline. Nevertheless the product **4***a* from this sequence was carried through the sequence **4***a* → **6** → **1***a* to verify its structure.

The conversion of **9***a* and **9***b* to the tetrahydroprotoberberine system demonstrates that isoquinolines may be substituted for dihydroisoquinolines in this synthetic route although the yields are not as high. Nevertheless the fact that isoquinolines may be used as starting materials greatly broadens the range of substitution patterns available using this synthetic approach.

The synthetic strategy used here is similar to that of Bradsher *et al.* (18) in that ring C is formed in the final step of the synthesis by introduction of a one-carbon unit that becomes C-13 of the protoberberine system. This procedure is however more direct than its earlier counterpart.

The manner in which compounds of structure **4** cyclize to compounds of structure **5** has not been investigated in detail. Previous investigators (19) have studied the hydrolysis of mercaptal sulfoxides to aldehydes and it is possible that an aldehyde intermediate may be involved in the cyclization step in this instance, although our attempts to intercept an aldehyde were unsuccessful. It is more likely that the cyclization proceeds through the cation generated in the acidic medium by loss of CH_3SOH from the mercaptal sulfoxide. This cation would be stabilized not only by the adjacent sulfur atom but also by the neighboring nitrogen (20). The cyclized product would then lose CH_3SH to form the dihydroprotoberberines, isolated as compounds **5** or **6**, depending upon the procedure employed.

Trost *et al.* (21) have reported similar cyclizations of mercaptals and mercaptal sulfoxides in which they isolated the cyclized product still containing an S—CH_3 group. They noted that CH_3SH was expelled when the initial cyclization product was heated in a more strongly acidic medium. We have not observed a sulfur-containing cyclization product in these studies but, in view of the results of Trost *et al.*, one would not be expected under the strongly acidic reaction conditions that were used.

Oikawa and Yonemitsu (ref. 22, and references therein) have reported on the cyclization of β-ketosulfoxides in the presence of acids and have used this reaction in the synthesis of a variety of carbocyclic and heterocyclic systems. They too have isolated S—CH_3 compounds as primary products of cyclization and have proposed a similar cyclization process.

Experimental

Apparatus, Materials, and Methods

The continuous wave ^1H nmr spectra were run on a Varian EM 390 or T-60 spectrometer. The Fourier transform spectra were run on either a Bruker WP 80 or WH 90 spectrometer. Unless otherwise specified, the samples were dissolved in chloroform-*d* using tetramethylsilane (TMS) as the internal standard. Chemical shifts, quoted as δ values, were measured in relation to TMS. The symbols s singlet, d doublet, t triplet, q quartet, and m multiplet are used in reporting spectra.

Mass spectra were recorded on either a Consolidated Electrodynamics Corporation Model #21-110B mass spectrometer or a V.G. Micromass 7070 F mass spectrometer, at 70 eV.

Infrared spectra were recorded on a Perkin Elmer 283 spectrometer in chloroform solution. Melting points were determined on a Kofler micro hot stage and are uncorrected. The microanalyses were performed by the Guelph Chemical Laboratories Ltd., Guelph, Ontario or by Microanalysis Laboratories Ltd., Toronto, Ontario.

Column and thin-layer chromatography (tlc) were performed using silica gel 60 as the adsorbent. Gravity columns were run using Baker 60–200 mesh silica, and "flash" columns prepared as described in the literature (9). Lobar columns were run using a prepacked Merck silica gel 60, size B column.

Tetrahydrofuran (THF) was dried by distillation from sodium in a nitrogen atmosphere, just prior to use. The following compounds were prepared by standard methods and gave satisfactory physical and spectral data: 6,7-dimethoxy-3,4-dihydroisoquinoline (23), 2,3-dimethoxybenzyl chloride (24), 2,3-dimethoxybenzyl bromide (25), 3,4-dimethoxybenzyl chloride (26), and 6,7-dimethoxyisoquinoline (27).

*3,4-Dihydro-6,7-dimethoxy-*N*-(2,3-dimethoxybenzyl)isoquinolinium Bromide 3*a

To a solution of 3,4-dihydro-6,7-dimethoxyisoquinoline (5.6 g) in benzene (40 mL), 2,3-dimethoxybenzyl bromide (6.7 g) was added slowly. The mixture was stirred for 24 h at room temperature, and the yellow precipitate was filtered and recrystallized from ethanol (11 g, 89%) yielding pale yellow crystals melting at 202–205°C; ^1H nmr (CD_3OD): 3.0–4.0 (m, 4H, $-CH_2-CH_2-N^+$), 3.83 (6H, s, 2 × OCH_3), 3.86 (3H, s, OCH_3), 3.93 (3H, s, OCH_3), 5.10 (2H, s, N^+-CH_2-Ar), 7.03 (1H, s, aromatic), 7.08 (3H, s, aromatic), 7.43 (1H, s, aromatic), and 9.01 (1H, s, $H-C=N^+$). *Anal.* calcd. for $C_{20}H_{24}O_4NBr$: C 56.91, H 5.68, N 3.31, Br 18.93%; found: C 56.57, H 5.72, N 3.21, Br 18.78%.

*3,4-Dihydro-6,7-dimethoxy-*N*-(2,3-dimethoxybenzyl)isoquinolinium Chloride*

To a stirring solution of the 3,4-dihydro-6,7-dimethoxyisoquinoline (2.0 g, 10.5 mmol) in benzene (50 mL) was added the 2,3-dimethoxybenzyl chloride (2.0 g, 10.7 mmol) dropwise. The solvent was removed under vacuum after 24 h, and the oily residue crystallized from benzene–ethanol 20:1 to yield yellow prisms (3.87 g, 10.2 mmol, 97%), mp 187–189°C; ^1H nmr: 3.16 (2H, t, $-CH_2-CH_2-N^+$, J = 7.5 Hz), 3.8–4.0 (2H, m, $CH_2-CH_2-N^+$), 3.88 (3H, s, OCH_3), 3.94 (3H, s, OCH_3), 3.96 (3H, s, OCH_3), 4.00 (3H, s, OCH_3), 5.44 (2H, s, N^+-CH_2-Ar), 6.94–7.34 (4H, m, arom.), 7.74 (1H, s, arom.), 10.46 (1H, s, $-CH=N^+$).

*Condensation of Iminium Salt 3*a *with MMTS Anion*

To a solution of methyl methylthiomethylsulfoxide (MMTS)

Can. J. Chem. Downloaded from www.nrcresearchpress.com by 210.87.254.105 on 09/05/12
For personal use only.

(700 mg) in anhydrous tetrahydrofuran (30 mL), 2.5 mL *n*-BuLi (2.2 *M* in hexane, a stoichiometric quantity) was added under an atmosphere of nitrogen. The temperature was maintained at −35°C during the addition and for 30 min afterwards. This cold solution was added dropwise via a syringe to a stirred suspension of iminium bromide **3***a* (1.5 g) in anhydrous tetrahydrofuran (50 mL). The suspension was cooled in Dry Ice – acetonitrile and the reaction was conducted under nitrogen. The mixture was stirred at −30°C for 3 h and during this period the solution became clear. Finally, 100 mL methylene chloride was added followed by 30 mL of water to hydrolyse excess LiMMTS. The organic phase was separated, dried over Na_2SO_4, and evaporated. The residue showed one major spot and two minor spots on tlc (alumina), (eluent, chloroform – ethyl acetate 4:1). The product (2 g) was separated by column chromatography on alumina (neutral) (80 g of Brockmann activity 1, mixed with 4.8 mL water). The solvents used as eluents were benzene, benzene–chloroform 9:1, 4:1, 1:1, and chloroform in that order. The pale yellow oil **4***a* (1.4 g, 98%) was a mixture (*vide infra*) that was used directly in the next step. ^{1}H nuclear magnetic resonance: 2.05, 2.23 (3H, 2s, SCH_3), 2.63, 2.70 (3H, 2s, $S(O)CH_3$), 3.78 (3H, s, OCH_3), 3.86 (9H, s, 3 × OCH_3), 2.3–4.8 (8H, m, 3 × CH_2 and N—C*H*—C*H*—S), and 6.6–7.3 (5H, m, arom.).

(±)-Tetrahydropalmatine **1***a from Mercaptal* **4***a*

(*a*) A mixture of **4***a* (370 mg) and concentrated HCl (7 mL) was heated on a steam bath for 5 min under nitrogen. The reaction mixture was cooled rapidly to 0°C, diluted with water (20 mL), and extracted three times with ether (50 mL) and the extract discarded. The aqueous phase was made basic by adding NaOH pellets slowly and then extracted three times with ether (50 mL). The combined ethereal extract was dried over K_2CO_3 and the solvent evaporated to dryness giving a yellow solid (216 mg, 66%) which was very air-sensitive. From its spectral properties (nmr and ir) the presence of the cyclized product **5***a* was indicated. The next step was carried out without purification.

(*b*) The cyclized yellow product **5***a* (216 mg) was dissolved in ethanol (25 mL) and an excess of $NaBH_4$ was added. The mixture was stirred at room temperature under nitrogen for one hour or until the color disappeared. After the solvent had been removed on the rotary evaporator, water was added to the reaction mixture and the excess hydride destroyed by careful addition of glacial acetic acid. The aqueous mixture was basified to pH 10 with NaOH pellets and extracted with ether (3 × 50 mL). The organic phase was shaken twice with 10% HCl to take up the basic material into the aqueous phase. Basification of the aqueous phase followed by extraction with ether (3 × 50 mL) and removal of the solvent gave a product, which did not need further purification. The compound was a white solid (167 mg, 76.7%), which melted at 147°C (lit. (28) mp 148°C); ^{1}H nmr: 2.7–4.0 (8H, m, two hydrogens each at C-5, C-6, C-13, and one each at C-8 and C-14), 3.90 (12H, s, 4 × OCH_3), 4.41 (1H, low field proton of AB quartet from hydrogens at C-8, J = 15 Hz), 6.70 (1H, s, arom.), 6.80 (1H, s, arom.), and 6.86 (2H, d, arom.).

The free base, tetrahydropalmatine, is air and light sensitive and the compound was converted to palmatine iodide to confirm the identity of the product.

Palmatine Iodide **2***a*

A solution of iodine (100 mg) in methanol (20 mL) was added dropwise to a refluxing solution of tetrahydropalmatine **1***a* (100 mg) prepared above and potassium acetate (100 mg) in methanol (15 mL) over a period of 4 h. Refluxing was continued for another two hours, and the mixture was cooled. The orange needle-shaped crystals were separated by filtration (128 mg, 95%), mp 237–238°C (authentic sample mp 239°C).

The ir and nmr spectra of the synthetic sample and of an authentic sample were superimposable, ^{1}H nmr (CF_3CO_2H); 3.35 (2H, t, hydrogens at C-5), 3.98 (3H, s, OCH_3), 4.05 (6H, s, 2 × OCH_3), 4.22 (3H, s, OCH_3), 5.00 (2H, t, hydrogens at C-6), 6.92 (1H, s, arom.), 7.52 (1H, s, arom.), 7.90 and 8.08 (2H, AB quartet, H-11 and H-12, J = 9 Hz), 8.65 (1H, s, H-13), 9.76 (1H, s, H-8).

*3,4-Dihydro-6,7-dimethoxy-*N*-(3,4-dimethoxybenzyl)isoquinolinium Chloride* **3***b*

To a solution of 3,4-dihydro-6,7-dimethoxyisoquinoline (3 g) in benzene (30 mL), 3,4-dimethoxybenzylchloride (3 g) was added slowly. The mixture was stirred for 24 h at room temperature, the yellow precipitate was separated by filtration and crystallized from 6:3:1 benzene–acetone–ethanol yielding 5.3 g (89.8%) of yellow hygroscopic prisms, melting at 123–127°C; ^{1}H nmr (CD_3OD): 2.9–3.5 (4H, m, H's at C-5 and C-6), 3.81 (3H, s, OCH_3), 3.83 (3H, s, OCH_3), 3.85 (3H, s, OCH_3), 3.95 (3H, s, OCH_3), 5.06 (2H, s, Ar—CH_2—N^+), 6.8–7.2 (4H, m, arom.), 7.40 (1H, s, arom.), and 9.01 (1H, s, H-1).

Condensation of Iminium Salt **3***b with MMTS Anion*

The solution of the MMTS anion, generated from MMTS (700 mg) and *n*-BuLi 2.2 *M* (2.5 mL) in dry THF, as previously described, was added dropwise via a syringe to a stirred suspension of the iminium chloride **3***b* (1.5 g) in anhydrous THF (50 mL). The system was cooled in Dry Ice – acetonitrile and kept under nitrogen. The mixture was stirred at −35°C for 3 h and during this period the solution became clear. In the work-up methylene chloride was added and then water. The organic phase was separated, dried (Na_2SO_4), and evaporated. The crude residue, a brownish oil (~2 g), was separated by column chromatography using the same stationary phase and eluents as before. The pale yellow oil **4***b* (1.5 g, 94%) was examined by nmr; ^{1}H nmr: 2.00 and 2.20 (3H, 2s, SCH_3), 2.63 and 2.73 (3H, 2, $S(O)CH_3$), 3.85 (12H, s, 4 × OCH_3), 2.9–4.7 (8H, m, other nonarom. H's), 6.6–7.4 (5H, m, arom.).

(±)-Xylopinine **1***b from Mercaptal* **4***b*

(*a*) A mixture of **4***b* (600 mg) and concentrated HCl (7 mL) was heated on a steam bath for 5 min under nitrogen. Following the same work-up as with (±)-tetrahydropalmatine, a bright yellow solid was obtained (350 mg, 66%) which was recrystallized from CH_2Cl_2–ether–methanol 7:2:1 yielding **5***b* as yellow square crystals melting at 173–176°C with decomposition; ^{1}H nmr: 2.7–3.4 (4H, m, H's at C-5 and C-6), 3.83 (9H, s, 3 × OCH_3), 3.90 (3H, s, OCH_3), 4.13 (2H, s, H's at C-8), 5.92 (1H, s, H-13), 6.55 (3H, s, arom.), and 7.15 (1H, s, arom.). The cyclized product **5***b* was air sensitive and the next step followed immediately.

(*b*) The $NaBH_4$ reduction of the cyclized product **5***b* (350 mg) in ethanol was carried out at room temperature under nitrogen until the color disappeared. The reduction product was obtained following the same work-up as before, yielding a white flaky solid (270 mg, 77%) which was recrystallized from ethanol (mp 156–157°C). The nmr spectrum is identical with the published spectrum (10); ^{1}H nmr: 2.56–4.32 (9H, m, H's at C-5, C-6, C-8, C-13, and C-14) 3.82 (9H, s, 3 × OCH_3), 3.83 (3H, s, OCH_3), 6.54–6.71 (4H, m, arom.).

2,3-Methylenedioxybenzyl Chloride

To 2,3-methylenedioxybenzyl alcohol (2 g) (29), thionyl chloride (3 mL) was added dropwise and the mixture was stirred at room temperature for 2 h. The excess thionyl chloride was removed on the rotary evaporator and the dark brown oil distilled under vacuum. The product was a colorless oil (bp 52°C/0.05 Torr) (1.5 g, 68%); ^{1}H nmr: 4.50 (2H, s, CH_2Cl), 5.85 (2H, s, O—CH_2—O), and 6.72 (3H, s, arom.).

*3,4-Dihydro-6,7-dimethoxy-*N*-(2,3-methylenedioxybenzyl)isoquinolinium Chloride* **3***c*

To a solution of 3,4-dihydro-6,7-dimethoxyisoquinoline

TABLE 1. ^{1}H nmr data of fractions from chromatography of mercaptal **4***a*

Component (R_f on silica gel, Et_2O/EtOH = 8:1)	Wt. recovered from column (mg)	^{1}H nmr chemical shifts: —S—CH_3 and —S(=O)—CH_3	^{1}H nmr chemical shifts: —OCH_3	^{1}H nmr chemical shifts: Aromatic
0.33[a]	360	2.16(s), 2.22(s) 2.36(s), 2.62(s)	3.78(3H, s), 3.88(3H, s) 3.89(3H, s), 3.91(3H, s).	6.60–7.16(5H, m)
0.20	120	2.22(s), 2.64(s)	3.87(9H, s), 3.78(3H, s).	6.61–7.06(5H, m)
0.16[b]	280	2.02(s), 2.30(s) 2.68(s), 2.70(s)	3.78(3H, s), 3.85(6H, s), 3.88(3H, s).	6.62–7.24(5H, m)

[a]This fraction was later resolved into two components by tlc using hexane–ethanol–THF 6:3:1.
[b]This fraction contains MMTS.

(1.5 g) in benzene (30 mL), 2,3-methylenedioxybenzyl chloride (1.5 g) was added slowly. The mixture was stirred for 24 h at room temperature. The yellow solid was filtered and recrystallized from methylene chloride – ether 4:6 yielding yellow crystals melting at 164–166°C. Yield: 2.5 g, 80%, ^{1}H nmr: 3.0–3.7 (4H, m, 2 × CH_2), 3.88 (3H, s, OCH_3), 3.95 (3H, s, OCH_3), 5.38 (2H, s, Ar—CH_2—N^+), 5.95 (2H, s, O—CH_2—O), 6.7–7.2 (4H, m, arom.), 7.68 (1H, s, arom.), and 10.05 (1H, s, H-1).

Condensation of Iminium Salt **3***c with MMTS Anion*

The solution of the MMTS anion, generated from MMTS (680 mg) and 2.2 *M* *n*-BuLi (2.4 mL) in anhydrous THF, was added dropwise via a syringe to a stirred suspension of the iminium chloride **3***c* (1.3 g) in anhydrous THF (50 mL). The mixture was cooled in Dry Ice – acetonitrile and kept under N_2 during the addition and was stirred at −35°C for an additional 3 h. Methylene chloride was added and then water. The organic phase was separated, dried (Na_2SO_4), and evaporated. The crude oily residue (~1.7 g) was separated by column chromatography as in the previous cases. The pale yellow oil, **4***c* (1.2 g, 92%), gave an ^{1}H nmr spectrum with the characteristic peaks present. Because of the complexity of the spectrum, probably because of impurities, assignment of the chemical shifts is not given.

(±)-Sinactine **1***c from Mercaptal* **4***c*

(*a*) The cyclization of **4***c* (310 mg) was carried out as before yielding a bright yellow solid, which was the cyclized product **5***c* (200 mg, 73%).

(*b*) The $NaBH_4$ reduction of **5***c* (200 mg) was carried out at room temperature and for 24 h under nitrogen. After work-up the product was obtained as a white solid (160 mg, 79%) melting at 166°C, lit. (30) mp 170°C. The ir spectrum and the nmr spectrum were superimposable on those of an authentic sample of sinactine; ^{1}H nmr: 2.4–4.4 (8H, m, two H's each at C-5, C-6, and C-13 and 1H each at C-8 and C-14), 3.81 (3H, s, OCH_3), 3.83 (3H, s, OCH_3), 4.08 (1H at C-8, lower field portion of an AB quartet, J = 15 Hz), 5.85 (2H, m, O—CH_2—O), and 6.5–6.8 (4H, m, arom.).

Chromatography of Adduct **4***a*

The yellow oily residue **4***a*, obtained by condensation of **3***a* with MMTS anion, showed a mixture of components by tlc on silica. Using ether–ethanol (abs.) 8:1, three components were visible at R_f 0.16, 0.20, and 0.33. Large scale (1.0 g) chromatography of the crude oil by the method of Still *et al.* (9) using the same solvent system used for tlc gave three fractions corresponding in R_f value to the three components found on tlc. Each of these fractions was examined by ^{1}H nmr and the data are summarized in Table 1.

The three fractions were also examined by ms. Apart from differences in intensity of the peaks, the 3 spectra were similar, as expected of diastereomers. Major peaks in the spectrum of the fraction, R_f 0.20, are given expressed as *m/e* values with intensities in brackets: 447(10), 432(20), 401(80), 386(40), 370(40), 354(100), 342(40), 340(15), 338(10), 325(40), 324(100), 323(50), 322(60), 308(15), 250(15).

Cyclization of Mercaptals **4***a to Dihydropalmatine Chloride* **6**

Each of the three fractions (Table 1) isolated from the column was subjected to cyclization by the following procedure. The yellow oil (75 mg) was dissolved in concentrated HCl (3.5 mL) and heated in a flask equipped with a reflux condenser on a steam bath in an atmosphere of N_2. The flask was allowed to cool to room temperature and was then placed in an ice–salt bath. Bright yellow crystals of **6** were obtained in 70 to 90% yield, which were recrystallized from concentrated HCl and washed with cold acetone and ether. The melting points observed for the cyclized materials obtained from the R_f 0.33, 0.20, and 0.16 mercaptals were 152–157°C (dec.), 153–162°C (dec.), and 157–165°C (dec.), respectively. The differences in the melting points of the three products are probably due to varying degrees of solvation of the crystals. The samples were examined spectroscopically as follows. In the ms the three products of cyclization gave similar fragmentation patterns, including a base peak at *m/e* 353, corresponding to the loss of H from the iminium cation. The intensities of the peaks in the three spectra varied, probably because of decomposition of the samples at the probe temperatures necessary to volatilize the chloride salts. The spectrum of the cyclization product of the mercaptal R_f 0.33 is given, where only peaks ≥ 20% of the base peak are recorded: 355(35), 354(35), 353(100), 352(45), 338(35), 190(25), 164(50), 149(35).

The ir spectrum of the samples were also similar and that of the sample obtained from the fraction R_f 0.33 is ir $\nu_{max}(CHCl_3)$: 1634, 1602, and 1564 cm^{-1}.

The ^{1}H nmr spectrum of the sample in TFA is: 3.40 (2H, m, C-5), 4.04 (3H, s, —OCH_3), 4.15 (9H, s, 3 × OCH_3), 4.16–4.35 (2H, m, C-6), 4.64 (2H, s(broad), C-13), 5.30 (2H, s(broad), C-8), 6.94–7.78 (4H, m, arom.).

Can. J. Chem. Downloaded from www.nrcresearchpress.com by 210.87.254.105 on 09/05/12
For personal use only.

Can. J. Chem. Downloaded from www.nrcresearchpress.com by 210.87.254.105 on 09/05/12
For personal use only.

Reduction of Dihydropalmatine Chloride **6** *to (±)-Tetrahydropalmatine* ***1****a*

Each of the cyclized products was subjected to borohydride reduction by the following method. To a solution of the chloride (14 mg, 0.04 mmol) in absolute EtOH (10 mL) was added sodium borohydride in excess. The mixture was stirred mechanically under N_2 for 45 min, at which time the reaction appeared complete by tlc (ether). Solvent was removed under vacuum, H_2O added (15 mL), and glacial acetic acid added dropwise with cooling to remove unreacted $NaBH_4$. Basification with a saturated solution of NaOH to pH > 10 was followed by extraction with ether (4 × 15 mL). The organic phase was shaken with 10% HCl (3 × 10 mL) after which the aqueous layer was basified to pH > 10 with NaOH (saturated solution). Extraction of the basic solution with ether (3 × 15 mL), followed by drying over Na_2SO_4 and concentration under vacuum, yielded a pale white crystalline product (11.7 mg, 90%) mp 146–148°C (lit (28) mp 148°C), whose spectroscopic properties were identical with those of (±)-tetrahydropalmatine.

All three reduction products were identical.

Dehydrocorydaline Iodide **7**

Dihydropalmatine chloride **6** (288 mg, 0.74 mmol) was treated with 10% acetic acid (10 mL), 30% formaldehyde (1 mL), and sodium acetate (124 mg). The mixture was heated on a steam bath for 15 min under N_2, after which 2.5 mL of a saturated solution of NaI was added. The flask was cooled to room temperature, then placed in the refrigerator. The fine yellow needles which formed (247 mg, 68%) were recrystallized from 47–51% HI to yield bright yellow square prisms, mp 139–143°C (dec.). ^{1}H nmr: 3.00 (3H, s, CH_3), 3.30 (2H, m, CH_2—CH_2—N^+), 3.96 (3H, s, OCH_3), 4.02 (3H, s, OCH_3), 4.08 (3H, s, OCH_3), 4.32 (3H, s, OCH_3), 5.12 (2H, m, CH_2—CH_2—N^+), 7.00 (1H, s, arom.), 7.25 (1H, s, arom.), 8.02 (2H, s, arom.), 10.25 (1H, s, arom.).

(±)-Corydaline ***8***

To a solution of the iodide (65 mg, 0.13 mmol) in 95% EtOH (10 mL) was added $NaBH_4$ (10 mg, 0.26 mmol). The mixture was stirred mechanically under N_2 for 1 h, at which time the reaction mixture was still deep orange in color. A further 10 mg of borohydride were then added along with one drop of glacial acetic acid. The color of the reaction mixture changed immediately to pale yellow, and tlc (ether – petroleum ether 9:1) showed one major component present at R_f 0.4. Solvent was removed under vacuum, H_2O added (15 mL), and excess $NaBH_4$ was destroyed by the careful addition of glacial acetic acid. Basification to pH > 10 with a saturated solution of NaOH was followed by extraction with ether (3 × 20 mL). This extract was shaken with 10% HCl (2 × 25 mL) and the aqueous layer basified to pH > 10 as before. This alkaline solution was extracted with ether (3 × 25 mL), and the organic extract dried over Na_2SO_4 and concentrated under vacuum to yield a yellow solid (29 mg, 60%). Recrystallization from absolute EtOH yielded deep yellow prisms, mp 135–136°C (lit. (20) mp 135°C); ^{1}H nmr (identical with that of natural corydaline): 0.90 (3H, d, CH_3, J = 6 Hz), 2.40–4.45 (8H, m, H's at C-5, C-6, C-8, C-13, and C-14), 3.88 (12H, s, 4 × OCH_3), 6.59 (1H, s, arom.), 6.68 (1H, s, arom.), 6.82 (1H, s, arom.), 6.86 (1H, s, arom.). ms: The mass spectrum showed a parent peak at m/e 369 (intensity 30%) and a base peak at m/e 178 corresponding to $C_{11}H_{14}O_2$ (21).

N-*(3,4-Dimethoxybenzyl)isoquinolinium Chloride* ***9****a*

Isoquinoline (3.22 g, 25 mmol, freshly distilled from zinc dust (224°C/760 Torr)) was dissolved in benzene (30 mL). 3,4-Dimethoxybenzylchloride (4.41 g, 23.6 mmol) was added slowly, and the mixture refluxed gently for 24 h. At this time, the yellow crystals which had formed were filtered off and washed. The solid was dried on filter paper to yield 3.92 g (12.4 mmol, 50%) of product. The mother liquor was heated under reflux for a further 3 h producing 0.30 g of yellow crystals (total yield 54%); ^{1}H nmr (CD_3OD): 3.81 (3H, s, OCH_3), 3.85 (3H, s, OCH_3), 5.95 (2H, s, N—CH_2—Ar), 6.98–7.30 (3H, m, arom.), 7.96–8.30 (4H, m, arom.), 8.48–8.82 (2H, m, —CH=CH—N), 10.20 (1H, s, HC=N). *Anal.* calcd. for $C_{18}H_{18}O_2NCl$: C 68.52, H 5.75, N 4.44, Cl 11.24%; found: C 68.53, H 5.69, N 4.14, Cl 11.15%.

Condensation of MMTS Anion with Quaternary Salt ***9****a*

(a) Anion Generation

To 1.10 g of freshly distilled MMTS was added THF (50 mL), and the solution was stirred mechanically under dry argon and cooled to −35°C. To this solution was added 4.2 mL of *N*-BuLi (2.14 *M* in hexane, 1 equiv.) dropwise via a syringe. The solution was stirred under dry argon for 45 min at −35°C.

(b) Condensation

The cold solution from (*a*) was added dropwise via a syringe needle to a cold (−35°C) stirred suspension of isoquinolinium chloride **9***a* (1.57 g, 5.0 mmol) in THF (75 mL). The suspension was stirred mechanically under argon and its temperature maintained at −35°C for a further 3.5 h, during which time the solution became red in color. At this time, 150 mL of CH_2Cl_2 were added, followed by 40 mL H_2O to hydrolyse unreacted LiMMTS. The organic layer was drained off, and the aqueous fraction washed with CH_2Cl_2 (20 mL). The organic layers were combined, dried over Na_2SO_4, and concentrated under vacuum to yield 2.66 g (6.6 mmol, > 100%) of brown oil (crude **10***a*) which showed four components present by tlc (THF–hexane 6:1). The ^{1}H nmr of the crude material was very complex, showing at least six S—CH_3 peaks. Attempts to chromatograph the mixture on silica gel resulted in rapid decomposition to very polar material.

Reduction of Enamine ***10****a*

A stirred solution of **10***a* (2.62 g), in methanol (20 mL) and glacial acetic acid (50 mL), was treated with $NaCNBH_3$ (419 mg). Within two minutes of the addition of the cyanoborohydride, the deep purple solution turned clear yellow. Since the tlc of the solution (THF–hexane 6:4) was not conclusive, and no further changes were noted in the reaction flask, the solvent was removed under vacuum, 0.1 *N* NaOH added (30 mL), and the solution extracted with ether (3 × 40 mL). During the course of the extraction, 2 *M* NaOH was added to maintain pH > 10. The ethereal layers were combined and shaken with 10% HCl (4 × 20 mL) to take the basic material into the aqueous phase. Basification of the aqueous extract to pH > 10 with saturated NaOH solution was followed by extraction with ether (3 × 50 mL). The extract was dried over Na_2SO_4 and concentrated under vacuum to yield a yellow oil **11***a* (1.23 g, 60% based on quaternary salt **9***a* used in the MMTS condensation). The tlc of the oil (THF–hexane 6:4) showed three components present at R_f 0.12, 0.21, and 0.24, whereas the starting material showed four spots from R_f 0.14 to 0.29; ^{1}H nmr: 1.94 (3H, s, S—CH_3), 2.18 (3H, s, S—CH_3), 2.50 (3H, s, S(O)CH_3), 2.76 (3H, s, S(O)CH_3), 2.62–4.75 (4H, m, N—CH_2—Ar and N—CH—CH—S), 3.56 (2H, t, —CH_2—CH_2—N, J = 4.5 Hz), 3.72 (2H, t, —CH_2—CH_2—N, J = 4.5 Hz), 6.72–7.34 (7H, m, arom.).

Cyclization of **11***a to Iminium Salt* **12**

The reduction product above, **11***a* (1.23 g, 3.04 mmol as pure compound), was dissolved in concentrated HCl (15 mL) and heated in a steam bath in a flask equipped with a reflux condenser under N_2 for 10 min. The flask was placed in the refrigerator overnight, after which the crystals were filtered off, washed, and dried on the vacuum line over P_2O_5. The yield of

Can. J. Chem. Downloaded from www.nrcresearchpress.com by 210.87.254.105 on 09/05/12
For personal use only.

yellow crystals was 617 mg (1.87 mmol, 62% in this step, 37% relative to the *N*-benzyl isoquinolinium salt **9***a*); ir $\nu_{max}(CHCl_3)$: 1631, 1610 and 1576 cm^{-1}; ^1H nmr (TFA): 3.40 (2H, t, C-5, J = 7.5 Hz), 4.04 (6H, s, 2 × OCH_3), 4.30 (2H, t, C-6, J = 7.5 Hz), 4.65 (2H, s(broad), C-13), 5.20 (2H, s(broad), C-8), 6.98 (1H, s, arom.), 7.08 (1H, s, arom.), 7.50–8.20 (4H, m, arom.). The mass spectrum showed a peak at *m/e* 295 ($M^+ + 1$) and the expected peaks at *m/e* 132 and 164 (base peak).

10,11-Dimethoxy-5,6,13,13a-tetrahydro-8H-dibenzo[a,g]-quinolizine **13**

To an ice cold solution of the iminium salt **12** (100 mg, 0.30 mmol) in 95% EtOH (10 mL) was added excess $NaBH_4$. The mixture was allowed to warm to room temperature and was stirred under N_2 for 1 h. At this time the reaction appeared complete by tlc (ether) so the solvent was removed under vacuum, H_2O added (10 mL), and unreacted $NaBH_4$ destroyed by adding glacial acetic acid with cooling in ice. Basification to pH > 10 with a saturated solution of NaOH was followed by extraction with ether (4 × 20 mL). The ethereal extract was shaken with HCl (3 × 25 mL) and the aqueous extract basified to pH > 10 as above. Extraction with ether (4 × 25 mL) followed by drying over Na_2SO_4 and concentration under vacuum yielded white crystals (75 mg, 0.25 mmol, 83%) which were recrystallized from EtOH (abs.)/$CHCl_3$, mp 124–125°C; ^1H nmr: 2.62–3.85 (9H, m, H's at C-5, C-6, C-8, C-13, and C-14), 3.85 (6H, s, 2 × OCH_3), 6.55 (1H, s, arom.), 6.60 (1H, s, arom.), 7.10–7.20 (4H, m, arom.). The mass spectrum showed a molecular ion at *m/e* 295(90) corresponding to $C_{19}H_{21}N$ and a base peak at 164 corresponding to $C_{10}H_{12}O_2$. *Anal.* calcd. for $C_{19}H_{21}O_2N$: C 77.29, H 7.12, N 4.74%; found: C 77.60, H 7.55, N 4.73%.

6,7-Dimethoxy-N-(2,3-dimethoxybenzyl)isoquinolinium Chloride **9**b

To a solution of 6,7-dimethoxyisoquinoline (1.5 g, 7.9 mmol) in benzene (30 mL, freshly distilled from $CaCl_2$) was added 2,3-dimethoxybenzyl chloride **41** (1.5 g, 8.0 mmol) dropwise with mechanical stirring. The mixture was gently refluxed under a $CaCl_2$ drying tube for 24 h. At this time the fine white needles which had formed were filtered off, washed with fresh benzene, and dried. Since the yield of crystals was only 1.37 g (3.6 mmol, 46%), the mother liquor was stirred under reflux for a further 48 h. A further 1.22 g of crystals were obtained (3.2 mmol, total yield 86%). The solid was recrystallized from benzene–chloroform producing white rods mp 109–112°C; ^1H nmr: 3.82 (3H, s, OCH_3), 3.94 (3H, s, OCH_3), 4.08 (3H, s, OCH_3), 4.15 (3H, s, OCH_3), 6.10 (2H, s, N^+—CH_2—Ar), 6.92–7.58 (4H, m, arom.), 7.98 (1H, s, arom.), 8.14, 8.48 (2H, AB quartet, N^+—CH=CH, $J_{3,4}$ = 7.5 Hz), 10.72 (1H, s, HC=H^+).

Reaction of **9**b *with the Anion of MMTS*

A solution of MMTS anion generated from MMTS (445 mg) as previously described was added dropwise to a stirring suspension of the chloride **9***b* (735 mg, 1.96 mmol, dried overnight over P_2O_5, 0.01 Torr at 82°C) in 30 mL freshly distilled THF. The suspension was stirred mechanically under argon at −35°C for 3 h.

To the flask was then added 80 mL CH_2Cl_2, followed by 20 mL H_2O to hydrolyse excess LiMMTS. The organic layer was drained off and the aqueous layer washed with 10 mL CH_2Cl_2 which was then combined with the organic extract. This organic solution was dried over Na_2SO_4 and concentrated under vacuum to yield 1.09 g (2.4 mmol, > 100%) of brown oil (crude **10***b*).

Reduction of **10**b

To the enamine **10***b* (1.06 g, 2.3 mmol as pure material) was added THF (15 mL) and glacial acetic acid (25 mL). The deep purple mixture was stirred mechanically under N_2. To this solution was added $NaCNBH_3$ (239 mg, 3.8 mmol) and within 15 min, the color of the solution had changed from deep purple through red and orange, to yellow. At this time, tlc (ether–EtOH 8:1) showed that the reaction was complete. The solvent was removed under vacuum, H_2O (20 mL) added, then 2 *M* NaOH (20 mL) to make the solution strongly alkaline. This solution was extracted with ether and the organic extracts filtered on paper to remove an oily precipitate. The ethereal solution was shaken with 10% HCl (3 × 30 mL) and the ether layer was discarded. The aqueous solution was rendered strongly alkaline with a saturated NaOH solution. Extraction with ether (3 × 30 mL), followed again by filtration of the organic layer on paper, yielded a clear yellow ethereal solution which was dried over Na_2SO_4 and concentrated under vacuum. The product (crude **4***a*) was a yellow-green oil (383 mg, 0.824 mmol, 43% relative to quaternary salt **9***b*).

To remove both the polar and fast-moving contaminants, 200 mg of the crude oil were chromatographed on a flash column (ether–EtOH 8:1) which yielded 140 mg (70% recovery) of clear yellow oil. Thin-layer chromatography in this solvent system showed only the characteristic three components of **4***a* to be present. In order to confirm its identity the product was cyclized to **6** with concentrated HCl and the latter reduced to (±)-tetrahydropalmatine, identical with an authentic sample (28).

Acknowledgement

We thank the Natural Sciences and Engineering Research Council of Canada for financial support of this work.

1. M. SHAMMA. The isoquinoline alkaloids, chemistry and pharmacology. Academic Press, New York. 1972. p. 268.
2. M. SHAMMA and J. L. MONIOT. Isoquinoline alkaloid research 1972–1977. Plenum Press, New York. 1978. p. 209.
3. T. KAMETANI, M. IHARA, and T. HONDA. Heterocycles, **4**, 483 (1976).
4. B. R. PAI, K. NAGARAJAN, H. SUGUNA, and S. NATARAJAN. Heterocycles, **6**, 1377 (1977).
5. T. KAMETANI. The total synthesis of natural products. Vol. 3. *Edited by* J. ApSimon. Wiley-Interscience, New York. 1977. p. 1.
6. R. H. F. MANSKE and W. R. ASHFORD. The alkaloids. Vol. 4. *Edited by* R. H. F. Manske. Academic Press, New York. 1954. p. 77; P. W. JEFFS. The alkaloids. Vol. 9. *Edited by* R. H. F. Manske. Academic Press, New York. 1968. p. 41.
7. K. OGURA and G. TSUCHIHASHI. Tetrahedron Lett. 3151 (1971).
8. L. DUHAMEL, P. DUHAMEL, and N. MANCELLE. Bull. Soc. Chim. Fr. 331 (1974).
9. W. C. STILL, M. KAHN, and A. MITRA. J. Org. Chem. **43**, 2923 (1978).
10. C. Y. CHEN and D. B. MACLEAN. Can. J. Chem. **46**, 2501 (1968).
11. H. W. BERSCH. Arch. Pharm. **283**, 192 (1950).
12. Y. KONDO. Yakugaku Zasshi, **83**, 1017 (1963).
13. M. CUSHMAN and F. W. DEKOW. Tetrahedron, **34**, 1435 (1978).
14. W. M. WHALEY and T. R. GOVINDACHARI. Org. React. **6**, 74 (1951).
15. R. T. DEAN and H. RAPOPORT. J. Org. Chem. **43**, 4183 (1978).
16. S. TEITEL and J. P. O'BRIEN. Heterocycles, **2**, 625 (1974).
17. British Patent No. 1,004,077 (Cl.A 61k 3/00) assigned to Smith, Kline and French Laboratories, Sept. 8, 1965. U.S. Appl. Sept. 21, 1962.

18. C. K. BRADSHER and N. L. DUTTA. J. Org. Chem. **26**, 2231 (1961); **27**, 2213 (1962); W. AUGSTEIN and C. K. BRADSHER. J. Org. Chem. **34**, 1349 (1969); H. F. ANDREW and C. K. BRADSHER. Tetrahedron Lett. 3069 (1966).
19. R. KUHN and W. BASCHANG-BISTER. Justus Liebigs Ann. Chem. **641**, 160 (1961); R. KUHN and F. A. NEUGEBAUER. Chem. Ber. **94**, 2629 (1961).
20. R. T. LALONDE. Acc. Chem. Res. **13**, 39 (1980).
21. B. M. TROST, M. REIFFEN, and M. CRIMMIN. J. Am. Chem. Soc. **101**, 257 (1979).
22. Y. OIKAWA and O. YONEMITSU. J. Org. Chem. **41**, 1118 (1976).
23. W. M. WHALEY and M. MEADOW. J. Chem. Soc. 1067 (1953).
24. A. KAUFMANN and H. MULLER. Ber. **51**, 123 (1918).
25. R. D. HAWORTH and W. H. PERKIN. J. Chem. Soc. **127**, 1434 (1925).
26. K. KINDLER and E. GEHLHAAR. Arch. Pharm. **274**, 377 (1936).
27. F. D. POPP and W. E. MCEWEN. J. Am. Chem. Soc. **79**, 3773 (1957).
28. C. K. YU, D. B. MACLEAN, R. G. A. RODRIGO, and R. H. F. MANSKE. Can. J. Chem. **48**, 3673 (1970).
29. T. STEVENS. J. Chem. Soc. 725 (1935).
30. T. KAMETANI. The chemistry of the isoquinoline alkaloids. Elsevier Publishing Company, Amsterdam. 1969.

Can. J. Chem. Downloaded from www.nrcresearchpress.com by 210.87.254.105 on 09/05/12
For personal use only.

3-Diethylphosphonoacrolein diethylthioacetal anion (6*), a reagent for the conversion of aldehydes to α,β-unsaturated ketene dithioacetals and three-carbon homologated α,β-unsaturated aldehydes

GEORGE JUST,[1] PIERRE POTVIN, AND GHOLAM HOSEIN HAKIMELAHI
Department of Chemistry, McGill University, Montreal, P.Q., Canada H3A 2K6

Received July 21, 1980

GEORGE JUST, PIERRE POTVIN, and GHOLAM HOSEIN HAKIMELAHI. Can. J. Chem. **58**, 2780 (1980).

A short synthesis of the title compound is reported. It can be used to transform aldehydes to the corresponding α,β-unsaturated ketene dithioacetals, the sulfoxides of which can be converted to α,β-unsaturated aldehydes.

GEORGE JUST, PIERRE POTVIN et GHOLAM HOSEIN HAKIMELAHI. Can. J. Chem. **58**, 2780 (1980).

On décrit une courte synthèse du composé du titre, qui peut transformer les aldéhydes en dithioacétals de cétenes α,β-insaturés, dont les sulfoxides conduisent aux aldéhydes α,β-insaturées correspondantes.

Can. J. Chem. Downloaded from www.nrcresearchpress.com by 210.87.254.105 on 09/05/12
For personal use only.

No synthesis of the title compound (**6***) has hitherto been described. We felt that its chemistry should be useful and interesting, since the anion is stabilized and could be used as a three-carbon homologating agent for base-sensitive aldehydes (10).[2] We describe here the synthesis of **6***, and some of its applications.

Diethyl 2,3-epoxyprop-1-ylphosphonate **1** (2) was treated with sodium methoxide in methanol, and the resulting allylic alcohol **2** oxidized with pyridinium chlorochromate (4) to give the phosphonoacrolein **4**. Both **2** and **4** were characterized as their *p*-nitrobenzoate **3** and 2,4-dinitrophenylhydrazone **5** respectively. Reaction of phosphonoacrolein **4** with ethanethiol and zinc chloride (6) gave the dithioacetal **6**, which could be oxidized with *m*-chloroperbenzoic acid to give sulfoxide **9** as a mixture of geometric isomers. In the oxidation, the double bond of α,β-unsaturated phosphonate **6** was shifted into conjugation with the sulfoxide, providing a ketene dithioacetal *S*-oxide **9**.

Reaction of **6** with potassium *tert*-butoxide in tetrahydrofuran at −23°C for 15 minutes, followed by addition of either benzaldehyde **7***a*, diisopropylidene-L-arabinose **7***b*, or *tert*-butyl glyoxalate **7***c*, gave in nearly quantitative yield the corresponding α,β-unsaturated ketene dithioacetals **8***a–c*. Their oxidation with *m*-chloroperbenzoic acid gave the corresponding *S*-oxides **10***a–c*. Whereas ketene dithioacetals **8** were quite stable, the corresponding *S*-oxides had to be kept at low T (~−20°C) to ensure survival for a few days. *S*-oxide **10***b* was also obtained by reaction of **7***b* with ketene dithioacetal sulfoxide **9**, albeit in lower yield.

All attempts to hydrolyse either compounds **8***a,b* with mercuric chloride – mercuric oxide or red mercuric oxide – boron trifluoride (8), or **10***a,b* with perchloric acid (9), iodine, or mercuric chloride – mercuric oxide failed, or gave mixtures which were not identified. However, reaction of sulfoxides **10***a–c* with lithium triethylborohydride proceeded smoothly to provide a mixture of olefins **11** and **12**. Reaction of **11***a*/**12***a* with mercuric chloride – mercuric oxide in aqueous acetonitrile gave aldehyde **13***a*, which was extremely unstable. Similarly, **11***b*/**12***b* was converted to **13***b*; **13***c* could not be obtained by this method.

In pursuing the chemistry of aldehyde **4**, we reacted it with trimethylsilyl cyanide (12), and obtained an approx. 1:1 mixture of olefins **14** and **15**,[3] in quantitative yield. This mixture, when treated successively with potassium *tert*-butoxide and benzaldehyde in tetrahydrofuran at room temperature, did not give the Wittig-type product. The sole product obtained still contained the phosphonate grouping as well as a phenyl ring, by nmr analysis. Therefore, **14**/**15** cannot be used as a three-carbon homologating agent.

Experimental

For general procedures, see ref. 13. Although ir spectra were recorded for all compounds, only characteristic, assignable peaks are reported.

3-Diethylphosphonylallyl Alcohol (2) and its p-*Nitrobenzoate 3 (1)*

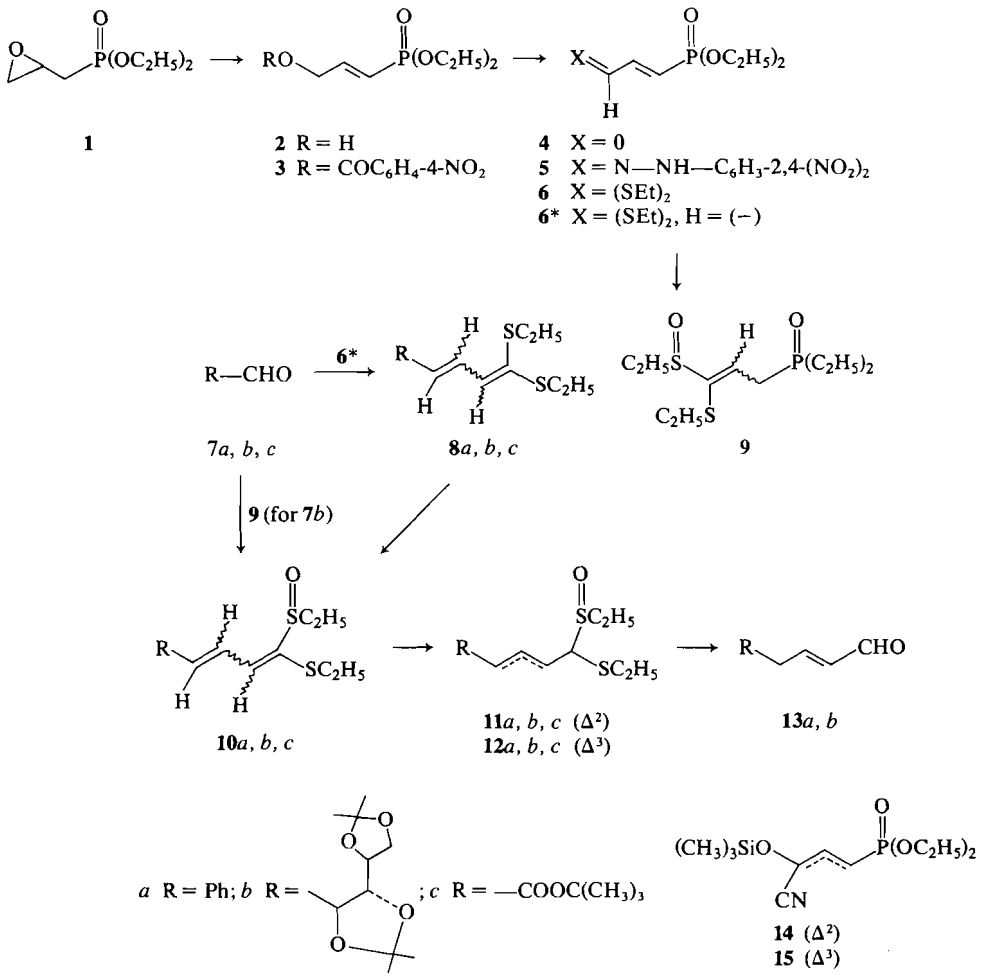
Diethyl 2,3-epoxyprop-1-ylphosphonate **1** (2) (9.71 g, 50 mmol) was treated with sodium methoxide in methanol (0.1 equiv.) dropwise, slowly, at 0°C, with stirring. After the addition, the

[1]Author to whom correspondence may be addressed.

[2]Reagents now available are either unstabilized or cannot be used with carbonyl compounds containing acid-labile groups (see ref. 11).

[3]Mixture **14**/**15**: nmr ($CDCl_3$) δ: 0.23, 0.37 (2s, 9H, $(CH_3)_3Si$), 1.37 (t, 6H, J = 7 Hz, CH_3CH_2O—), 2.74 (2d, ~1H, J = 8, 23 Hz, P—CH_2), 4.18 (2q, 4H, J = 7 Hz, CH_3CH_2O—), 5.13 (3d, ~0.5H, J = 2, 3 Hz, CH(CN)OSi), 5.58 (2t, ~0.5H, J = 8 Hz, PCH_2CH=C), 5.90–7.10 (m, ~1H, P—CH=CH).

0008-4042/80/242780-04$01.00/0
©1980 National Research Council of Canada/Conseil national de recherches du Canada



reaction was stirred a further 0.5 h at room temperature. Then 2 g of Dowex 50W-X8 (H^+) resin, previously washed with methanol, was added and the mixture was stirred for 15 min, at which time the resin was filtered off, washed with methanol, and the combined filtrate and washing were evaporated to dryness to give 9.71 g of crude allylic alcohol (100%), suitable for the next step, and characterized as its *p*-nitrobenzoate, prepared by standard means, and purified by flash chromatography (3) using ethyl acetate as eluent.

Compound **2**: ir (neat): 3450 (OH), 1630 (CH=CH) cm^{-1}; nmr ($CDCl_3$) δ: 1.32 (t, 6H, J = 7 Hz, OCH_2CH_3), 4.06 (2q, 4H, J = 7, 8 Hz, OCH_2CH_3), 4.28 (m, 2H, CH_2OH), 4.74 (b, 1H, OH, D_2O exch.), 5.96 (4t, 1H, J = 2, 17.5, 23 Hz, P—CH=CH), 6.84 (4t, 1H, J = 3, 17.5, 22 Hz, P—CH=CH); mass spectrum (70 eV, E.I.) *m/e*: 193 (M^+ − 1), 177 (M^+ − OH), 166, 165 (M^+ − Et), 163 (M^+ − CH_2OH), 149 (M^+ − OEt).

Compound **3**: ir (neat): 1727 (COOAr), 1640, 1608, 1525 (NO_2) cm^{-1}; nmr ($CDCl_3$) δ: 1.27 and 1.37 (2t, 6H, J = 7.5 Hz, OCH_2CH_3), 4.17 (2q, 4H, J = 7.5, 7.5 Hz, OCH_2CH_3), 5.01 (m, 2H, J = 1.5, 4.5 Hz, CH_2OBz), 6.01 (ABq of t, 1H, J = 1.5, 17, 18 Hz, P—CH=CH), 6.96 (ABq of t, 1H, J = 4.5, 18, 22 Hz, P—CH=CH), 8.33 (s, 4H, Ar); mass spectrum (70 eV, E.I.) *m/e*: 344 (M^+ + 1, base peak). *Anal.* calcd. for $C_{14}H_{18}NO_7P$: C 48.98, H 5.29, N 4.08; found: C 48.62, H 5.45, N 4.09.

3-Diethylphosphonoacrolein 4 and its 2,4-DNPH 5[4]

3-Diethylphosphoallyl alcohol **2** (1.94 g, 10 mmol) in 5 mL of dry methylene chloride was added dropwise to a stirred mixture of 2.59 g of pyridinium chlorochromate (4) (12 mmol) and 3 g of Celite in 30 mL of dry methylene chloride. The mixture was stirred for 2 h at room temperature, at which time it was filtered through Celite. The Celite pad was washed several times with methylene chloride, and the combined filtrate and washings were evaporated to dryness. The residue was triturated with ether and the solution was filtered through a Florisil pad, which was then washed several times with ether. The combined ethereal solutions were evaporated to dryness, giving 1.12 g of crude aldehyde containing some inorganic matter. This was distilled in a Kugelrohr apparatus (0.05 Torr, 100°C) to afford 1.00 g of pure aldehyde **4** (52%), bp 85–87°C (0.1 Torr). Its 2,4-dinitrophenylhydrazone **5** was prepared by the method of Parrick and Rasburn (5) and recrystallized from ethanol, mp 155–156°C.[4]

Compound **4**: ir (neat): 1710 (CHO), 1610 (CH=CH) cm^{-1};

[4]The aldehyde prepared here is of *trans*-geometry. The *cis*-isomer has been prepared by another, lengthier route, and it gives a *trans*- 2,4-dinitrophenylhydrazone, mp 160.5–161.5°C (see ref. 7).

Can. J. Chem. Downloaded from www.nrcresearchpress.com by 210.87.254.105 on 09/05/12
For personal use only.

Can. J. Chem. Downloaded from www.nrcresearchpress.com by 210.87.254.105 on 09/05/12
For personal use only.

nmr ($CDCl_3$) δ: 1.37 (t, 6H, J = 7 Hz, OCH_2CH_3), 4.15 (2q, 4H, J = 7, 8.5 Hz, OCH_2CH_3), 6.77 (m, 2H, CH=CH), 10.93 (t, 1H, J = 3.5 Hz, CHO); mass spectrum (70 eV, E.I.) m/e: 193 ($M^+ + 1$), 191 ($M^+ - 1$), 163 (M^+ − CHO), 147 (M^+ − OEt), 137 (M^+ − CHO—HC≡CH).

Compound **5**: *Anal.* calcd. for $C_{13}H_{17}N_4O_7P$: C 41.94, H 4.60, N 15.05; found: C 41.73, H 4.62, N 14.82.

3-Diethylphosphonoacrolein Diethyldithioacetal 6

Using a modification of the procedure of Barry and Craig (6), dithioacetal **4** was prepared as follows.

In an ice-salt bath, 1.08 g of 3-diethylphosphonoacrolein **4** (5.62 mmol) in 9.8 mL of ethanethiol were treated with 0.5 g of anhydrous zinc chloride, and the mixture was stored in the freezer (−15°C) for 18 h, at which time a further 0.5 g of zinc chloride was added. After a further 6 h in the cold, the ethanethiol was blown away through a copper sulphate solution with a nitrogen stream, and the thick residue was taken up in ethyl acetate (10 mL). The solution was washed with water (2 × 10 mL) and saturated sodium bicarbonate solution (2 × 10 mL). After standing exposed to bicarbonate for a few minutes, some precipitate formed, and was filtered off. The precipitate was washed with ethyl acetate, and the combined filtrate and washings were dried ($MgSO_4$) and evaporated to afford 1.39 g of crude dithioacetal (83%) suitable for further transformations. An analytical sample was obtained by purification through flash chromatography, using 60% ethyl acetate in petroleum ether as eluent. Infrared (neat): 1620 (CH=CH) cm^{-1}; nmr ($CDCl_3$) δ: 1.26 (t, 6H, J = 7.5 Hz, SCH_2CH_3), 1.33 (t, 6H, J = 7.5 Hz, OCH_2CH_3), 2.63 (q, 4H, J = 7.5 Hz, SCH_2CH_3), 4.11 (2q, 4H, J = 7.5, 7.5 Hz, OCH_2CH_3), 4.43 (dd, J = 1, 8 Hz, C*H*—CH=CH), 5.80 (A portion of ABq of dd, 1H, J = 2, 17, 19 Hz, P—C*H*=CH), 6.69 (B portion of ABq of dd, 1H, J = 7.5, 16.5, 20.5 Hz, P—CH=C*H*); mass spectrum (70 eV, E.I.) m/e: 298 (M^+, S_2-cluster), 269 (M^+ − Et, S_2-cluster), 237 (M^+ − SEt, S-cluster). *Anal.* calcd. for $C_{11}H_{23}O_3PS_2$: C 44.27, H 7.77, S 21.49; found: C 44.63, H 7.75, S 21.60.

3-Diethylphosphono-1,1-di(thioethyl)but-1-ene Mono-S-oxide 9

A solution of dithioacetal **6** (1.00 g, 3.35 mmol) in 35 mL of dry methylene chloride cooled to 0°C (ice bath) was treated dropwise with a solution of 0.68 g of *m*-chloroperbenzoic acid (85% pure, 3.95 mmol, 1.18 equiv.) in 35 mL of dry methylene chloride, under an N_2 atmosphere. The mixture was stirred 0.5 h after the addition, and then transferred to a separating funnel, where it was washed with saturated sodium bicarbonate solution (3 × 20 mL) and water (20 mL), dried ($MgSO_4$), and evaporated to dryness. Flash chromatography of the product using ethyl acetate as eluent afforded 0.85 g of pure *S*-oxide **9** (81%). Nuclear magnetic resonance ($CDCl_3$) δ: 1.18 (t, 3H, J = 7 Hz, SCH_2CH_3), 1.27 (t, 3H, J = 7.5 Hz, $S(O)CH_2CH_3$), 1.33 (t, 6H, J = 7 Hz, OCH_2CH_3), 2.61–3.41 (m, 6H, P—CH_2CH=C, SCH_2CH_3, $S(O)CH_2CH_3$), 4.13 (2q, 4H, J = 7, 7 Hz, OCH_2CH_3), 6.84 (dt, 1H, J = 6, 8 Hz, P—CH_2C*H*=C); mass spectrum (70 eV, E.I.) m/e: 315 ($M^+ + 1$), 299 ($M^+ - CH_3$), 269 (M^+ − OEt), 237 (M^+ − S(O)Et, S-cluster), 181 (S-cluster).

Ketene-S,S-acetals 8: General Procedure

A 1 *M* THF solution of 3-diethylphosphonoacrolein diethyldithioacetal **6** was added dropwise to a cooled (dry ice/CCl_4) and stirred suspension of potassium *tert*-butoxide (1.05 equiv.) in dry THF (2 mL/mmol), under an inert atmosphere. Fifteen minutes after the addition, a 1 *M* THF solution of the aldehyde **7** was added dropwise, and the mixture was allowed to stir a further 30 min. Water and ether were then added, and the separated aqueous layer was reextracted with ether. The combined ether layers were washed with water, dried ($MgSO_4$), and evaporated to give crude product, which was purified by flash chromatography. Crude product may be used directly for the next step.

Compound **8***a*: this compound was obtained in 75% yield, and chromatographed using 0.5% ethyl acetate – petroleum ether (30–60°C); nmr ($CDCl_3$) δ: 1.27 (t, 6H, J = 7 Hz, SCH_2CH_3), 2.81 and 2.83 (2q, 4H, J = 7 Hz, SCH_2CH_3), 6.43–7.70 (m, 8H, PhC*H*=C*H*—C*H*); mass spectrum (70 eV, E.I.) m/e: 250 (M^+, S_2-cluster). *Anal.* calcd. for $C_{14}H_{18}S_2$: C 67.15, H 7.25, S 25.61; found: C 66.68, H 7.52, S 25.71.

Compound **8***b*: this compound was obtained in 72% yield, and chromatographed using 5% ethyl acetate – petroleum ether; $[\alpha]_D^{22}$ −1.17° (*c* 4.88, $CHCl_3$); nmr ($CDCl_3$) δ: 1.10–1.40 (m, 18H, CH_3), 2.78 (q, 4H, SCH_2), 3.58–4.93 (m, 5H), 5.28–7.18 (m, 3H, C*H*=C*H*—C*H*); mass spectrum (70 eV, E.I.) m/e: 374 (M^+, S_2-cluster), 345 (M^+ − Et, S_2-cluster), 313 (M^+ − SEt, S-cluster).

Compound **8***c*: the *cis–trans* mixture was obtained in 60% yield, and purified by normal chromatography on silica gel, using CH_2Cl_2 as eluent. The *trans*-isomer was obtained by refluxing the *cis–trans* mixture in benzene for 24 h. Infrared (CH_2Cl_2): 1705 (COOR) cm^{-1}; nmr ($CDCl_3$) δ: 1.10–1.60 (m, 15H, CH_3), 2.61–3.20 (m, 4H, SCH_2), 5.40–5.90 (q, 1H, J = 14, 16 Hz, CH=C(SEt)$_2$), 6.40–8.00 (m, 2H, C*H*=C*H*—CH=C); nmr of *trans*-isomer ($CDCl_3$) δ: 1.10–1.60 (m, 15H, CH_3), 2.61–3.10 (q, 4H, J = 6 Hz, SCH_2), 5.71 (d, 1H, J = 14 Hz, C*H*=C(SEt)$_2$), 6.51 (d, 1H, J = 11 Hz, C*H*—COOC$(CH_3)_3$), 7.58–8.00 (2d, 1H, J = 11, 14 Hz, C*H*—CH=C(SEt)$_2$); mass spectra (70 eV, E.I.) m/e: 274 (M^+, S_2-cluster), 245 (M^+ − Et, S_2-cluster), 173 (M^+ − COOC$(CH_3)_3$, S_2-cluster); (70 eV, C.I.) m/e: 275 ($M^+ + 1$, S_2-cluster), 219 ($M^+ + 1 - CH_2$=C$(CH_3)_2$, S_2-cluster). *Anal.* calcd. for $C_{13}H_{22}O_2S_2$: C 56.93, H 8.03, S 23.35; found: C 56.81, H 8.10, S 23.09.

Ketene-S,S(O)-acetals 10

(a) Compound 10b, from Aldehyde 7b and 9

Using the same procedure as for **8***b*, the oxide **10***b* was obtained directly from **7***b* in 43% yield, after flash chromatography using 60% ethyl acetate in petroleum ether; $[\alpha]_D^{22}$ +5.66° (*c* 2.21, $CHCl_3$); nmr ($CDCl_3$) δ: 1.08–1.44 (m, 18H, CH_3), 2.59–3.17 (m, 4H, CH_2), 3.53–5.01 (m, 5H), 5.65–7.87 (m, 3H, CH=CH—CH=C(SEt)(S(O)Et)); mass spectrum (70 eV, E.I.) m/e: 390 M^+, S_2-cluster), 375 ($M^+ - CH_3$, S_2-cluster), 361 (M^+ − Et, S_2-cluster). *Anal.* calcd. for $C_{18}H_{30}O_5S_2$: C 55.35, H 7.74, S 16.42; found: C 55.44, H 8.00, S 16.53.

(b) From Ketene-S,S-acetals 8

To a stirred and cooled (ice bath) 0.1 *M* CH_2Cl_2 solution of ketene-*S,S*-acetal **8** was added 1.18 equiv. of a 0.16 *M* CH_2Cl_2 solution of technical grade *m*-chloroperbenzoic acid (85% pure), under an atmosphere of N_2. The solution was stirred an additional 30 min, then washed with saturated $NaHCO_3$ solution (2×) and water, dried ($MgSO_4$), and evaporated. All compounds were purified by flash chromatography, using 60% ethyl acetate in petroleum ether.

Compound **10***a*: this compound was obtained in 80% yield using crude **8***a*; nmr ($CDCl_3$) δ: 1.17 and 1.28 (2t, 6H, J = 7 Hz, CH_3), 2.78 and 3.38 (2q, ~3.2H and 0.8H, J = 7 Hz, CH_2), 6.47–8.00 (m, 8H, Ph—CH=CH—CH); mass spectrum (70 eV, E.I.) m/e: 266 (M^+, S_2-cluster), 237 (M^+ − Et, S_2-cluster), 205 (M^+ − SEt, S-cluster), 189 (M^+ − S(O)Et, S-cluster), 128. *Anal.* calcd. for $C_{14}H_{18}OS_2$: C 63.11, H 6.81, S 24.07; found: C 63.18, H 6.77, S 24.05.

Compound **10***b*: obtained by this method in 75% yield from crude **8***b* (60% overall from **7***b*). The product has identical physical data as that prepared previously using **9** on **7***b*.

Compound **10***c*: the *cis–trans* mixture was obtained in 85% yield. The *trans*-isomer was obtained by refluxing for 24 h a benzene solution of the *cis–trans* mixture. Infrared (CH_2Cl_2):

Can. J. Chem. Downloaded from www.nrcresearchpress.com by 210.87.254.105 on 09/05/12
For personal use only.

1690 (COOR) cm^{-1}; nmr ($CDCl_3$) δ: 1.10–1.60 (m, 15H, CH_3), 2.70–3.30 (m, 4H, SCH_2—), 5.80–6.38 (2d, 1H, J = 14, 16 Hz, C*H*=C(SEt)(S(O)Et)), 7.00–8.60 (m, 2H, C*H*=C*H*—CH=C); nmr of *trans*-isomer ($CDCl_3$) δ: 1.10–1.60 (m, 15H, CH_3), 2.70–3.10 (m, 4H, SCH_2—), 6.28 (d, 1H, J = 14 Hz, C*H*=C(SEt)(S(O)Et)), 7.11 (d, 1H, J = 10 Hz, C*H*—COOC$(CH_3)_3$), 7.80–8.60 (2d, 1H, J = 10, 14 Hz, CH=C*H*—CH=C); mass spectrum (70 eV, C.I.) *m/e*: 291 ($M^+ + 1$, S_2-cluster), 261 ($M^+ - Et$, S_2-cluster), 229 ($M^+ - SEt$, S-cluster), 152.

Olefins 11 and 12

Oxide **10** is dissolved in dry THF (3 mL/mmol) and 1.5 equiv. of a 1 *M* THF solution of lithium triethylborohydride were added at 0°C. After stirring for 1 h, the solution was evaporated and treated with water. This was then extracted with ether, and the ether solution was dried ($MgSO_4$) and evaporated to give crude product which was chromatographed on silica gel, using first CH_2Cl_2 to remove impurities, then $CHCl_3$ to elute the mixture of olefins.

Mixture **11***a*/**12***a*: this mixture was obtained in 80% yield. Compound **12***a* was fractionated by chromatography in 10% yield. Nuclear magnetic resonance ($CDCl_3$) δ: 1.02–1.60 (m, 6H, CH_3), 2.30–3.40 (m, 6H, CH_2—, SCH_2—), 3.50–4.40 (m, 1H, C*H*(SEt)(S(O)Et)), 5.40–6.80 (m, 2H, CH=CH), 7.3 (2s, 5H, Ph); nmr of **12***a* ($CDCl_3$) δ: 1.31, 1.45 (2t, 6H, CH_3), 2.41–3.21 (m, 6H, CH_2— and SCH_2—), 3.70, 3.81 (2t, 1H, CH(SEt)-(S(O)Et)), 6.00–6.80 (m, 2H, CH=CH), 7.4 (s, 5H, Ph); mass spectra (70 eV, E.I.) *m/e*: 268 (M^+, S_2-cluster); (70 eV, C.I.) *m/e*: 269 ($M^+ + 1$, S_2-cluster), 191 ($M^+ - Ph$). *Anal.* calcd. for $C_{14}H_{20}OS_2$: C 62.68, H 7.46, S 23.88; found: C 62.49, H 7.41, S 24.01.

Mixture **11***b*/**12***b*: the isomeric mixture was obtained in 75% yield; $[\alpha]_D^{22}$ −10.4° (*c* 1.25, $CHCl_3$); nmr ($CDCl_3$) δ: 1.20–1.42 (m, 18H, CH_3), 2.40–3.00 (m, 6H, CH_2— and SCH_2—), 3.80–4.21 (m, 5H), 5.40–6.60 (m, 2H, CH=CH); mass spectra (70 eV, E.I.) *m/e*: 392 (M^+, S_2-cluster); (70 eV, C.I.) *m/e*: 393 ($M^+ + 1$, S_2-cluster), 316 ($M^+ + 1 - S(O)Et$, S-cluster). *Anal.* calcd. for $C_{18}H_{32}O_5S_2$: C 55.10, H 8.16, S 16.32; found: C 55.31, H 8.09, S 16.61.

Mixture **11***c*/**12***c*: this mixture was obtained in 65% yield. Infrared (CH_2Cl_2): 1700 (COOR) cm^{-1}; nmr ($CDCl_3$) δ: 1.10–1.58 (m, 15H, CH_3), 2.30–3.10 (m, 6H, CH_2— and SCH_2—), 4.00–4.30 (m, 1H, CH(SEt)(S(O)Et)), 5.40–7.40 (m, 2H, CH=CH); mass spectrum (70 eV, C.I.) *m/e*: 293 ($M^+ + 1$, S_2-cluster), 236 ($M^+ + 1 - C(CH_3)_3$, S_2-cluster), 232 ($M^+ + 1 -$ SEt, S-cluster), 216 ($M^+ + 1 - S(O)Et$, S-cluster). *Anal.* calcd. for $C_{13}H_{24}O_3S_2$: C 53.42, H 8.21, S 21.91; found: C 53.61, H 7.99, S 22.17.

Aldehydes 13

Olefins **11**/**12** were dissolved in 95% aqueous CH_3CN (3 mL/mmol). Mercuric oxide (2.2 equiv.) and mercuric chloride (2.2 equiv.) were added, and the mixture was gently refluxed for 10 h. The whole was then evaporated, redissolved in CH_2Cl_2, and filtered. The filtrate was washed with water, dried ($MgSO_4$), and evaporated to give crude product, which was chromatographed on silica gel, using CH_2Cl_2 as eluent.

Compound **13***a*: this compound was obtained in 60% yield. Infrared (CH_2Cl_2): 1690 cm^{-1}; nmr ($CDCl_3$) δ: 3.50–3.70 (m, 2H, CH_2), 6.10 (2d, 1H, J = 8 Hz, C*H*CHO), 6.70–7.60 (m, 6H, Ph and C*H*=CHCHO), 11.12 (d, 1H, J = 8 Hz, CHO); mass spectra (70 eV, E.I.) *m/e*: 146 (M^+), 118 ($M^+ - CO$), 91 ($PhCH_2^+$); (70 eV, C.I.) *m/e*: 147 ($M^+ + 1$).

Compound **13***b*: this was obtained in 50% yield; $[\alpha]_D^{22}$ −13.3° (*c* 0.89, $CHCl_3$); ir (CH_2Cl_2): 1690 cm^{-1}; nmr ($CDCl_3$) δ: 1.10–1.30 (m, 12H, CH_3), 2.30–2.80 (m, 2H, CH_2—), 3.60–4.20 (m, 5H), 6.12 (2d, 1H, J = 8 Hz, C*H*CHO), 6.85 (2t, 1H, C*H*=CHCHO), 11.13 (d, 1H, J = 8 Hz, CHO); mass spectra (70 eV, E.I.) *m/e*: 270 (M^+); (70 eV, C.I.) *m/e*: 271 ($M^+ + 1$), 213 ($M^+ + 1 - (CH_3)_2CO$), 155 ($M^+ + 1 - 2(CH_3)_2CO$), 185 ($M^+ + 1 - CO - (CH_3)_2CO$).

Acknowledgements

We wish to thank the Natural Sciences and Engineering Research Council of Canada for financial support and a scholarship (P.P.), the Ministry of Science and Higher Education of Iran and the University of Shiraz for a scholarship (G.H.H.), and Dr. O. Mamer and V. Y. Taguchi for recording the mass spectra.

1. A. P. Rakov and A. V. Alekseev. Zh. Obshch. Khim. **43**, 276 (1973); Chem. Abstr. **78**, 159756 (1973).
2. C. E. Griffin and S. K. Kundu. J. Org. Chem. **34**, 1532 (1969).
3. W. C. Still, M. Kahn, and A. Mitra. J. Org. Chem. **43**, 2923 (1978).
4. E. J. Corey and J. W. Suggs. Tetrahedron Lett. 2647 (1975).
5. J. Parrick and J. W. Rasburn. Can. J. Chem. **43**, 3453 (1965).
6. P. J. Barry and B. M. Craig. Can. J. Chem. **33**, 716 (1955).
7. A. J. Rudinskas and T. L. Hullar. J. Org. Chem. **41**, 2411 (1976).
8. E. J. Corey and D. J. Beames. J. Am. Chem. Soc. **95**, 5829 (1973).
9. J. E. Richman, J. L. Herrmann, and R. H. Schlessinger. Tetrahedron Lett. 3267 (1973).
10. Yu. A. Zhdanov, Yu. E. Alexeev, and V. G. Alexeeva. Adv. Carbohydr. Chem. Biochem. **27**, 227 (1972).
11. (*a*) H. S. Corey, Jr., J. R. D. McCormick, and W. E. Swensen. J. Am. Chem. Soc. **86**, 1884 (1964); (*b*) S. F. Martin and P. J. Garrison. Tetrahedron Lett. 3875 (1977); (*c*) G. Lavielle and G. Sturtz. Bull. Soc. Chim. Fr. 1369 (1970); (*d*) J. C. Stowell and P. R. Keith. Synthesis, 132 (1979); (*e*) H. P. Cristau, J.-P. Vors, and H. Christol. Synthesis, 538 (1979).
12. (*a*) D. A. Evans, L. K. Truesdale, and G. L. Carroll. J. Chem. Soc. Chem. Commun. 55 (1973); (*b*) W. Lidy and W. Sundermeyer. Chem. Ber. **106**, 587 (1973).
13. G. H. Hakimelahi and G. Just. Can. J. Chem. **57**, 1932 (1979).

The reactions of ethyl-, vinyl-, and ethynyl(trichloromethyl)carbinols with aqueous and methanolic potassium hydroxide, thiourea, and cyanamide[1]

WILKINS REEVE AND THOMAS F. STECKEL

Department of Chemistry, University of Maryland, College Park, MD 20742, U.S.A.

Received May 12, 1980

WILKINS REEVE and THOMAS F. STECKEL. Can. J. Chem. **58**, 2784 (1980).

The reactions of ethyl(trichloromethyl)carbinol, dimethyl(trichloromethyl)carbinol, (trichloromethyl)vinylcarbinol, ethynyl (trichloromethyl)carbinol, and 1,1,1,-trichloro-3-nonyn-2-ol have been studied with the following reagents. *Methanolic potassium hydroxide*: α-methoxy acids are formed in 70 and 79% yields with the ethyl- and vinylcarbinols respectively. Double bond migration to the conjugated position was observed with the vinylcarbinol. *Thiourea*: substituted 2-imino-4-thiazolidinones are formed in 27 to 66% yield with the first three carbinols with double bond migration in the case of the vinylcarbinol. *Cyanamide*: the saturated carbinols were converted to substituted ethyl 2-imino-4-oxo-1-imidazolidinecarboximidates in 30 to 60% yield. *Aqueous potassium hydroxide*: α-chloro acids were formed from the ethyl- and vinylcarbinols in 23 and 24% yields respectively, again with double bond migration in the case of the vinylcarbinol.

The results are discussed in terms of the known parallel reactions with phenyl (trichloromethyl)carbinol, and provide information which illustrates the usefulness and defines the limits of certain known synthetic reactions when applied to the alkyl, alkenyl, and alkynyl trichloromethylcarbinols.

WILKINS REEVE et THOMAS F. STECKEL. Can. J. Chem. **58**, 2784 (1980).

On a étudié les réactions des alcools éthyl(trichlorométhyl)carbinol, diméthyl(trichlorométhyl)carbinol, (trichlorométhyl)vinylcarbinol, éthynyl(trichlorométhyl)carbinol et trichloro-1,1,1 nonyne-3 ol-2 avec divers réactifs. Par réaction avec une solution méthanolique d'hydroxyde de potassium, on obtient les α-méthoxy acides avec des rendements respectifs de 70 et 79% dans le cas des alcools éthylique et vinylique. On a observé une migration de la double liaison vers la position conjuguée avec le carbinol vinylique. Avec la thiourée, il se forme des imino-2 thiazolidinones-4 substituées avec des rendements allant de 27 à 66% pour les trois premiers carbinols et une migration de la double liaison dans le cas du vinylcarbinol. Avec la cyanamide, les carbinols saturés se transforment en imino-2 oxa-4 imidazolidinecarboximidates-1 substitués avec des rendements allant de 30 à 60%. Avec l'hydroxyde de potassium aqueux il y a formation des acides α-chlorés avec des rendements respectifs de 23 et 24% dans les cas des carbinols éthylique et vinylique. On observe également une migration de la double liaison dans le cas du carbinol vinylique.

On discute des résultats en fonction des réactions paralèlles connues du phényl(trichlorométhyl)carbinol. Ces résultats fournissent des informations qui illustrent l'utilité et définissent les limites de certaines réactions connues quand on les applique aux alkyl, alkényl et alkynyl trichlorométhylcarbinols.

[Traduit par le journal]

Phenyl(trichloromethyl)carbinol has been shown to be a valuable reagent for the synthesis of α-alkoxy acids (1), α-chloro acids (2, 3), α-amino acids (4), as well as many heterocyclic compounds such as substituted thiadiazinones (5, 7), hydroxythiazoles (5), thiazolones (6, 7), and imidazolidinecarboximidates (8). Almost nothing is known about how well alkyl-, alkenyl-, and alkynyl-(trichloromethyl) carbinols undergo these reactions. Accordingly, we report here on the reactions of these carbinols with methanolic potassium hydroxide, thiourea, cyanamide, and cold aqueous potassium hydroxide solution. We have previously reported on the reactions of the aliphatic-(trichloromethyl)carbinols with phosphorus pentachloride and shown that a wide variety of compounds are formed (9).

Most of the various reactions summarized above can occur by either of two possible mechanisms (10). In both of the mechanisms the (trichloromethyl)carbinol is first converted *in situ* into epoxide **2**. In pathway one, the epoxide ring is opened by attack of a nucleophile to give **3** which is closely related to the final product. In contrast, the conversion of **2** to **4** via pathway two is a slower reaction which involves a chlorine migration at the epoxide stage to give alkyl or aryl substituted α-chloroacetate **4**. These compounds undergo further reaction in the usual way with nucleophiles to give α-substituted alkyl- or arylacetates. This second mechanism accounts for the conversion of secondary (trichloromethyl)carbinols into α-chloro acids (3) and is also a minor pathway in the formation of α-methoxyphenylacetic acid (10).

Reaction with Methanolic Potassium Hydroxide

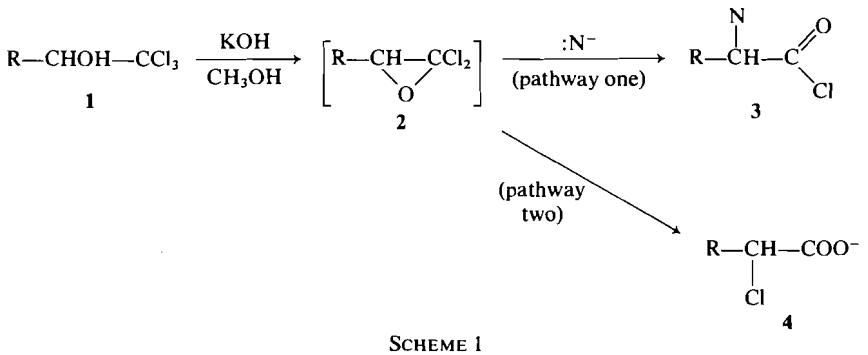
Phenyl(trichloromethyl)carbinol is known to react with methanolic potassium hydroxide at 50°C by pathway one to form α-methoxyphenylacetic acid in 70 to 80% yield (10); and dimethyl(trichloromethyl)carbinol (chloretone) is known to react with sodium ethoxide in ethanol to form ethyl α-ethoxyisobutyrate in 72% yield (11), and with

[1]Taken in part from the doctoral thesis of Thomas F. Steckel, University of Maryland, 1970.

0008-4042/80/242784-05$01.00/0

©1980 National Research Council of Canada/Conseil national de recherches du Canada

Can. J. Chem. Downloaded from www.nrcresearchpress.com by 210.87.254.40 on 09/05/12
For personal use only.



SCHEME 1

potassium hydroxide in methanol to form α-methoxyisobutyric acid in 71% yield (1).

In this work we have studied the reaction of methanolic potassium hydroxide with ethyl(trichloromethyl)carbinol as an example of a saturated alkyl(trichloromethyl)carbinol, and also with the unsaturated carbinols (trichloromethyl)vinylcarbinol, ethynyl(trichloromethyl)carbinol, and 1,1,1-trichloro-3-nonyn-2-ol.

Ethyl(trichloromethyl)carbinol gave α-methoxybutyric acid in 79% yield. (Trichloromethyl)vinylcarbinol gave a 70% yield of α-methoxycrotonic acid. In all reactions of this carbinol under basic conditions, the migration of the terminal double bond to the conjugated position was observed.

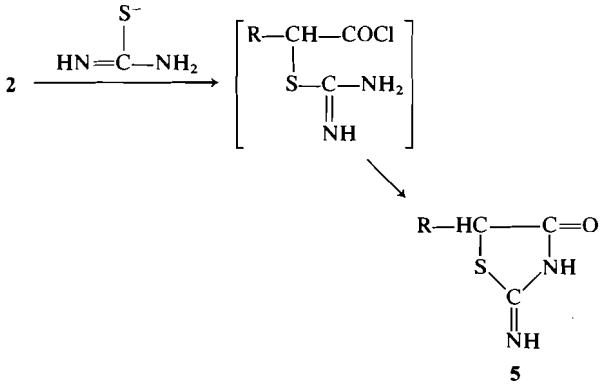
No α-methoxy acid could be isolated from reactions with ethynyl (trichloromethyl)carbinol or with 1,1,1-trichloro-3-nonyn-2-ol. The acid fraction from the former was a black tar with no ir absorption bands corresponding to the triple bond or the acetylenic proton. The latter acetylenic carbinol formed an intractable black oil, and part must also have undergone a reverse Claisen reaction to 2-octynal, for a crude acid having the ^{1}H nmr and ir spectra of 2-octynoic acid was isolated.[2]

In conclusion, substituted (trichloromethyl)carbinols react with methanolic potassium hydroxide to form substituted α-methoxyacetic acids in excellent yield if the substituent group in **1** is aryl, alkyl or dialkyl, or vinyl. The reaction fails with ethynylcarbinols. The reaction works equally well if the methanol is replaced by ethanol or other alcohols (1, 13).

Reaction with Thiourea

Phenyl(trichloromethyl)carbinol is known to react with thiourea in methanolic potassium hydroxide solution at 50°C to form 2-imino-5-phenyl-4-thiazolidinone in 55% yield (6). By analogy with the reaction of **1** (R = Ph) with methoxide, the reaction is believed to involve the attack of the thioenolate anion of thiourea on epoxide **2** (R = Ph) followed by ring closure to give **5**.

We have studied the reaction of thiourea in methanolic potassium hydroxide with ethyl(trichloromethyl)carbinol, dimethyl(trichloromethyl)carbinol, (trichloromethyl)vinylcarbinol, ethynyl(trichloromethyl)carbinol, and 1,1,1-trichloro-3-nonyn-2-ol. As in the case of the reaction of these carbinols with methanolic potassium hydroxide alone, the reaction works well with the alkyl-, dialkyl-, and vinylcarbinols; it fails with the two acetylenic carbinols. 5-Ethyl-2-imino-4-thiazolidinone[3] was formed in 57% yield from ethyl(trichloromethyl)carbinol. With dimethyl(trichloromethyl)carbinol, the yield of 5,5-dimethyl-2-



imino-4-thiazolidinone was reduced to 27%, but 40% of α-methoxyisobutyric acid was formed. This suggests the smaller methoxide nucleophile is more

[2]Dichloroacetic acid was also detected (ir and ^{1}H nmr spectra); this could be formed from chloral by preliminary epoxide formation followed by cleavage to dichloroacetic acid. Dichloroacetic acid is known to be formed from chloral in the presence of potassium cyanide (12).

[3]The traditional thiazolidinone names are used here. The ^{1}H nmr spectra indicate the 5-ethyl- and 5-ethylidene-2-imino-4-thiazolidinones to be 2-amino-4(5*H*)-thiazolones in the inner-salt form. See ref. 7.

Can. J. Chem. Downloaded from www.nrcresearchpress.com by 210.87.254.40 on 09/05/12
For personal use only.

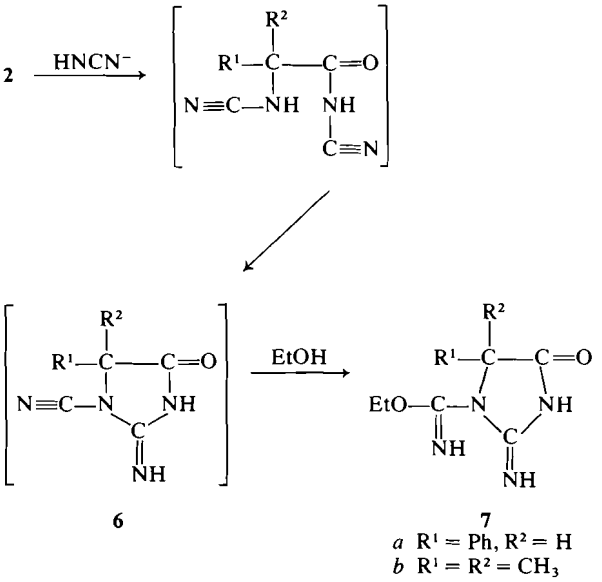
effective than the more bulky thioenolate of thiourea in opening the tertiary epoxide ring. 5-Ethylidene-2-imino-4-thiazolidinone was formed in 66% yield from (trichloromethyl)vinyl carbinol; again, migration of the terminal double bond to the conjugated position had occurred. The only products obtained from ethynyl(trichloromethyl)carbinol and 1,1,1-trichloro-3-nonyn-2-ol were high melting, dark-colored polymeric materials. These contained sulfur and nitrogen, showing thiourea had been incorporated into the final product.

Reaction with Cyanamide

Phenyl(trichloromethyl)carbinol has been shown to react with cyanamide in ethanolic potassium hydroxide solution at 2°C to form ethyl 5-phenyl-2-imino-4-oxo-1-imidazolidinecarboximidate (*7a*) in 50% yield (8). The reaction involves the attack of two cyanamide anions on epoxide **2** followed by ring closure and alcoholysis of a nitrile group.

We have found that dimethyl(trichloromethyl)carbinol reacts with cyanamide in ethanolic potassium hydroxide solution in the same manner to give a 60% yield of ethyl 5,5-dimethyl-2-imino-4-oxo-1-imidazolidinecarboximidate (*7b*). On hydrolysis with 20% sulfuric acid, *7b* gave the known ethyl 5,5-dimethyl-2,4-dioxo-1-imidazolidinecarboxylate, thus establishing that the carboximidate group is in the one position, as would be predicted from the earlier work on *7a* (8). Ethyl(trichloromethyl)carbinol appeared to react in the same way, but the product, obtained in approximately 30% yield, was impure and could not be purified by repeated crystallization. Partial hydrolysis with 3 *N* hydrochloric acid substituted a keto group for one of the imino groups, and complete hydrolysis with 20% sulfuric acid gave ethyl 2,4-dioxo-5-ethyl-1-imidazolidinecarboxylate. (Trichloromethyl)vinylcarbinol reacted with cyanamide under the same conditions, but only a 3% yield of 1- or 3-cyano-5-ethylidene-2-imino-4-imidazolidinone could be isolated. The major fraction was an ether-insoluble, brown oil which slowly became a tar. The reactions of ethynyl(trichloromethyl)carbinol and of 1,1,1-trichloro-3-nonyn-2-ol with cyanamide were not studied because of their instability to base (*vide supra*).

Cyanamide is not as good a nucleophile as is methoxide or thiourea, and this probably accounts for the unsatifactory reactions of ethyl(trichloromethyl)carbinol and (trichloromethyl)vinyl carbinol. The successful reaction of dimethyl(trichloromethyl)carbinol with cyanamide demonstrates that two alkyl groups have no adverse effect on the reaction. This reaction must be occurring by



6

7
a $R^1 = Ph, R^2 = H$
b $R^1 = R^2 = CH_3$

pathway one in Scheme 1 since pathway two with tertiary carbinols gives only small yields of α-chloro acids.

Reaction with Aqueous Potassium Hydroxide at 0°C

Phenyl(trichloromethyl)carbinol is converted into α-chlorophenylacetic acid in 60% yield on stirring with 10% aqueous potassium hydroxide solution at 0°C for 30 h (2, 3). This unusual reaction (pathway two in Scheme 1) has been shown to be 83% intramolecular and therefore must involve a migration of chlorine from the terminal to the α position; the mechanism of the rearrangement is uncertain (3).

All available evidence indicates that an α-hydrogen is necessary for the formation of more than traces of the α-chloro acid. Thus, dimethyl(trichloromethyl)carbinol gave at most a 3% yield of crude 2-chloro-2-methylpropanoic acid. In contrast ethyl(trichloromethyl)carbinol gave a 23% yield of α-chlorobutyric acid. More was probably formed, but hydrolysis to the hydroxy acid was a troublesome competing reaction. (Trichloromethyl)vinyl carbinol gave a 24% yield of crude *Z*-2-chloro-2-butenoic acid, the double bond again shifting to the conjugated position. This reaction could be carried out at room temperature since the final chloro acid was stable to base.

Again, the reactions of ethynyl(trichloromethyl)carbinol and of 1,1,1-trichloro-3-nonyn-2-ol were unsatisfactory. Dichloroacetic acid could be detected in both reaction mixtures and 2-octynoic acid was isolated from the latter reaction mixture.

Can. J. Chem. Downloaded from www.nrcresearchpress.com by 210.87.254.40 on 09/05/12
For personal use only.

Can. J. Chem. Downloaded from www.nrcresearchpress.com by 210.87.254.40 on 09/05/12
For personal use only.

Experimental

Ethynyl(trichloromethyl)carbinol, 1,1,1-trichloro-3-nonyn-2-ol, (trichloromethyl)vinylcarbinol, and ethyl(trichloromethyl)carbinol were synthesized as previously described (9). Dimethyl(trichloromethyl)carbinol is commercially available (as Chloretone). Elemental microanalyses were performed by Dr. Franz J. Kasler.

α-Methoxy-n-butyric Acid

This follows our standard procedure for the conversion of (trichloromethyl)carbinols to α-methoxy acids. To 8.9 g (0.05 mol) of ethyl(trichloromethyl)carbinol in 15 mL of methanol was added over a 1 h period a filtered solution of 16.3 g (0.25 mol) of potassium hydroxide in 60 mL of methanol. The reaction mixture was stirred and maintained at 50°C during the addition and for an additional two hours, and then allowed to stand while cooling to room temperature overnight. The potassium chloride was filtered off (94% of theory), and the filtrate was diluted with an equal volume of water and extracted with ether to remove traces of neutral materials. The aqueous solution was acidified to pH 1.7, and extracted with ether. Evaporation yielded 4.7 g (79% of theory) of α-methoxy-*n*-butyric acid; the ^{1}H nmr spectrum indicated the material to be pure except for a trace of water; bp 114–120°C/26 Torr (lit. (14) bp 94–95°C/15 Torr); ir (film): 3600–2800, 1730, 1450, 1200, 1135, 1110, 1085, and 950 cm^{-1}; ^{1}H nmr ($CDCl_3$) δ: 9.0 (s, 1.5, COO*H* plus 3.5% H_2O), 3.8 (t, 1, J = 5.7 Hz, CH), 3.46 (s, 3, OCH_3), 2.1 to 1.6 (m, 2, —CH_2—), and 1.0 (t, 3, J = 7.2 Hz, CH_3).

The *p*-phenylphenacyl ester was also prepared and melted at 81°C in agreement with the literature value (14).

α-Methoxycrotonic Acid

This was prepared from 8.8 g of (trichloromethyl)vinylcarbinol by the above procedure. There was obtained 4.1 g of crude product (70% of theory). It distilled at 113–115°C/14 Torr and crystallized in the receiving flask. After recrystallization from cyclohexane it melted at 60–61°C (lit. (14) bp 117°C/16 Torr, lit. (14, 15) mp 58°C and 60–62°C); ir (KBr): 3400–2500, 1695, 1640, 1445, 1410, 1320, 1275, 1195, 1135, 1085, 1020, 955, 895, 840, 800, and 770 cm^{-1}; ^{1}H nmr ($CDCl_3$) δ: 10.2 (s, 1, COOH), 6.5 (q, 1, J = 7.2 Hz, —CH=), 3.7 (s, 3, OCH_3), and 1.8 (d, 3, J = 7.2 Hz, CH_3).

5-Ethyl-2-imino-4-thiazolidinone (5, R = Et)

This followed the same procedure used with phenyl(trichloromethyl)carbinol (6). From 8.9 g of ethyl(trichloromethyl)carbinol, there was obtained 3.7 of product (57% of theory), mp 190–193°C (dec.). Recrystallization from water gave white crystals, mp 195–197°C (dec.) (lit. (16, 17) mp 195–196°C (dec.) and 198–200°C (dec.)); ir (KBr): 3250, 3050, 1690, 1650, 1500, 1360, 1280, 1130, and 740 cm^{-1}; ^{1}H nmr (DMSO-d_6) δ: 8.8 (broad s, 2, —NH—), 4.23 (m, 1, —CH_2—C*H*=), 2.15 to 1.1 (m, 2, CH_3—CH_2—), and 0.9 (t, 3, J = 7.2 Hz, CH_3). From the filtrate, 0.9 g (15% of theory) of crude α-methoxy-*n*-butyric acid was isolated and identified by ir.

5,5-Dimethyl-2-imino-4-thiazolidinone

This was prepared as above; from 9.8 g of dimethyl(trichloromethyl)carbinol there was obtained 2.1 g of product (27% of theory), mp 247°C. After recrystallization from water, it melted at 249–251°C (lit, (18, 19) mp 242°C and 245°C); ir (KBr): 3230, 2960–2600, 1670, 1500, 1440, 1390, 1350, 1270, 1185, 1125, 770, and 710 cm^{-1}; ^{1}H nmr (DMSO-d_6) δ: 8.8 (broad s, 1, NH), 3.44 (broad s, 1, NH), and 1.5 (s, 6, CH_3). From the filtrate, 2.6 g of crude 2-methoxy-2- methylpropanoic acid (40% of theory) was isolated and identified by ir and nmr.

5-Ethylidene-2-imino-4-thiazolidinone

This was prepared as above; from 4.4 g of (trichloromethyl)-vinylcarbinol there was obtained 2.35 g of product (66% of theory). Three recrystallizations from ethanol (decolorizing carbon) raised the mp to 233–235°C (dec.) (lit. (16, 20) mp 240–241°C and 250°C (dec.)); ir (KBr): 3200, 3000–2700, 1675, 1500, 1360, 1270, 1245, and 1145 cm^{-1}; ^{1}H nmr (DMSO-d_6) δ: 8.2 (broad s, 2, —NH—), 5.85 (q, 1, J = 7.1 Hz, —CH=), and 1.0 (d, 3, J = 7.1 Hz, CH_3).

Hydrolysis of 0.3 g of the above with 9 mL of 20% sulfuric acid for 3 h gave the known 5-ethylidene-2,4-thiazolidinedione, mp 119.5–121.5°C in agreement with literature values (16, 20); ^{1}H nmr ($CDCl_3$) δ; 9.6 (broad s, 1, NH), 7.14 (q, 1, J = 7.3 Hz, —CH=), and 1.95 (d, 3, J = 7.3 Hz, CH_3).

Ethyl 5,5-Dimethyl-2-imino-4-oxo-1-imidazolidinecarboximidate (7b)

This followed Barron's procedure (8) using ethanol as a solvent. From 17.8 g of dimethyl(trichloromethyl)carbinol there was obtained at pH 7.5, after concentrating and chilling the aqueous alcoholic reaction mixture, 10.6 g of product, mp 149–162°C (dec.). Another 1.3 g was obtained from ether extractions making a total of 11.9 g, 60% of theory. Recrystallization from water and from ethanol raised the mp to 165–166°C (dec.); ir (KBr): 3330, 3220, 2980, 1730, 1660, 1470, 1420, 1390, 1355, 1295, 1235, 1150, 1120, 1075, 770, 745, and 675 cm^{-1}; ^{1}H nmr (DMSO-d_6) δ: 9.64 (broad s, 1, NH), 8.86 (broad s, 1, NH), 7.48 (broad s, 1, NH), 4.15 (q, 2, J = 7 Hz, —CH_2—O—), and 1.35 (s) and 1.30 (t) with combined area of 9, J = 7 Hz, 3 CH_3). *Anal.* calcd. for $C_8H_{14}N_4O_2$: C 48.48, H 7.12, N 28.26; found: C 48.59, H 7.08, N 28.54.

From an ether extraction of the filtrate was obtained 0.5 g of *N*-cyano-*O*-ethylpseudourea ($H_2N(EtO)C$=N—CN), mp 117–117.5°C after crystallization from water. This agrees with the literature value (21); C,H,N analysis, ir, and ^{1}H nmr confirmed the structure.

The above carboximidate was hydrolyzed to the known ethyl 5,5-dimethyl-2,4-dioxo-1-imidazolidinecarboxylate by refluxing 2.5 g for 1.6 h with 25 mL of 20% sulfuric acid to establish the position of the carboximidate group as at the one position. On chilling, 1.5 g white platelets (60% of theory) was obtained which melted at 173.5–174°C after crystallization from water (lit. (22) mp 174–175°C); ir (KBr): 3240, 1830, 1815, 1770, 1700, 1420, 1390, 1360, 1340, 1145, 1130, 1110, 1100, 1020, 945, and 770 cm^{-1}; ^{1}H nmr (DMSO-d_6) δ: 4.25 (q, 2, J = 7.1 Hz, —CH_2O—), 3.4 (broad s, 1, NH), 1.53 (s, 6, CH_3), and 1.26 (t, 3, J = 7.1 Hz, CH_3CH_2—). *Anal.* calcd. for $C_8H_{12}N_2O_4$: C 48.00, H 6.04, N 14.00; found: C 47.93, H 5.98, N 14.20.

Reaction of Ethyl(trichloromethyl)carbinol with Cyanamide

This was carried out as above starting with 8.9 g of ethyl(trichloromethyl)carbinol, but the 5.0 g of product which precipitated at pH 6.1, mp 137–141°C after crystallization from ethanol, could not be further purified. The carbon analysis was 3% low.

One gram of the above product was refluxed for 1 h with 6 mL of 20% sulfuric acid and the reaction mixture extracted with ether. There was obtained 0.35 g of *ethyl 2,4-dioxo-5-ethyl-1-imidazolidinecarboxylate*, mp 73–74°C (dec.) after crystallization from water. The carboxylate group is assigned to the 1-nitrogen by analogy with the reaction of cyanamide with dimethyl(trichloromethyl)carbinol and with phenyl(trichloromethyl)carbinol, and also by the fact that it dissolves easily in cold 5% sodium hydroxide. Infrared (KBr): 3200, 1800, 1730, 1380, 1300, 1180, 1170, 1110, 1045, and 765 cm^{-1}; ^{1}H nmr ($CDCl_3$) δ: 8.23 (broad s, 1, NH), 4.4 (m, 3, —CH_2O— and —CH=), 2.2 (m, 2, CH_3—C*H*$_2$—CH=), 1.35 (t, 3, J = 7.1 Hz, CH_3), and 0.9 (t, 3, J = 7.5 Hz, CH_3). *Anal.* calcd. for $C_8H_{12}N_2O_4$: C 48.00, H 6.04, N 14.00; found: C 48.27, H 5.86, N 14.70.

1- or 3-Cyano-5-ethylidene-2-imino-4-imidazolidinone

This was prepared starting with 8.8 g of (trichloromethyl)vinylcarbinol. Ether extraction of the acidified aqueous reaction mixture gave 1.8 g of a mixture of oil and solid. The solid (0.26 g) was recrystallized from ethanol. It did not melt below 360°C. Infrared (KBr): 3180, 2940, 2700, 2200, 1740, 1650, 1460, 1380, 1340, 1270, 1130, 980, 830, and 630 cm^{-1}; ^1H nmr (DMSO-d_6) δ: 5.93 (q, 1, J = 7.7 Hz, CH_3—CH=), 4.1 (broad s, 2.5, NH + H_2O), and 1.96 (d, 3, J = 7.7 Hz, CH_3). *Anal.* calcd. for $C_6H_6N_4O$: C 48.00, H 4.03, N 37.32; found: C 48.14, H 4.16, N 37.60.

α-*Chlorobutyric Acid*

This was prepared by stirring 13.3 g (0.075 mol) of ethyl(trichloromethyl)carbinol with 18.8 g (0.284 mol) of potassium hydroxide in 150 mL of water at −5°C for 12 h followed by ether extraction of first the basic and then the acidified reaction mixture. The crude acid (23%) was redistilled to give 1.1 g of α-chlorobutyric acid; bp 99–101°C/16 Torr (lit. (23) bp 98–99°C/15 Torr); ir identical with Sadtler prism spectra number 21372; ^1H nmr ($CDCl_3$) identical with Sadtler nmr spectra number 23254 M.

Z-2-Chloro-2-butenoic Acid

This was prepared by stirring 8.8 g (0.05 mol) of (trichloromethyl)vinylcarbinol with 20 g (0.3 mol) of potassium hydroxide in 200 mL of water at room temperature for 7 h. After extraction with ether as above, 1.45 g (24%) of brown crystalline *Z*-2-chloro-2-butenoic acid was obtained; bp 110–119°C/19 Torr (lit. (24) bp 111–112°C/14 Torr); mp (from cyclohexane) 98–99°C (lit. (24) mp 98–99°C); ir (film): 3100–2400, 1670, 1610, 1420, 1315, 1280, 1110, 950, 895, 840, and 735 cm^{-1}; ^1H nmr ($CDCl_3$) δ: 11.6 (s, 1, COOH), 7.35 (q, 1, J = 6.9 Hz, —CH=), and 2.16 (d, 3, J = 6.9 Hz, CH_3).

1. CH. WEIZMANN, M. SULZBACHER, and E. BERGMANN. J. Am. Chem. Soc. **70**, 1153 (1948).
2. Z. JOCIC. Zh. Russ. Fiz.-Khim. Ova. **29**, 97 (1897); W. REEVE. Synthesis, 131 (1971).
3. W. REEVE, J. R. MCKEE, R. BROWN, S. LAKSHMANAN, and G. A. MCKEE. Can. J. Chem. **58**, 485 (1980).
4. W. REEVE and L. W. FINE. J. Org. Chem. **29**, 1148 (1964).
5. W. REEVE and E. R. BARRON. J. Org. Chem. **40**, 1917 (1975).
6. W. REEVE and M. NEES. J. Am. Chem. Soc. **89**, 647 (1967).
7. W. REEVE and W. R. COLEY. Can. J. Chem. **57**, 444 (1979).
8. W. REEVE and E. BARRON. J. Org. Chem. **34**, 1005 (1969).
9. E. W. REEVE and T. F. STECKEL. Can. J. Chem. **51**, 2017 (1973).
10. W. REEVE, R. J. BIANCHI, and J. R. MCKEE. J. Org. Chem. **40**, 339 (1975).
11. S. M. MCELVAIN and C. L. STEVENS. J. Am. Chem. Soc. **69**, 2667 (1947).
12. M. DELEPINE. Bull Soc. Chim. Fr. **45**, 827 (1929).
13. P. ALUOTTO. Ph.D. Thesis, University of Maryland, College Park, MD. 1967.
14. L. N. OWEN. J. Chem. Soc. 385 (1945).
15. K. PFISTER, C. A. ROBINSON, and M. TISHLER. J. Am. Chem. Soc. **67**, 2269 (1945).
16. A. S. U. CHOUGHULEY and M. S. CHADHA. Indian J. Chem. **1**, 437 (1963).
17. A. E. KRETOV and A. S. BESPALYI. Zh. Obshch. Khim. **33**, 3323 (1963); Chem. Abstr. **60**, 5475 (1964).
18. R. HAZAD, J. CHEYMOL, P. CHABRIER, and K. SMARZEWSKA. C. R. Acad. Sci. **226**, 1850 (1948).
19. H. ASPELUND and L. SJOBLOM. Acta Acad. Abo. Ser. B, **24** (1964); Chem. Abstr. **64**, 6634 (1966).
20. J. A. DURDEN, JR., H. A. STANSBURY, JR., and W. H. CATLETTE. J. Am. Chem. Soc. **81**, 1943 (1959).
21. E. ALLENSTEIN and R. FUCHS. Chem. Ber. **100**, 2604 (1967).
22. S. UMEMOTO. Yakugaku Zasshi, **84**, 504 (1964); Chem. Abstr. **61**, 8296 (1964).
23. G. STEINBRUNN. Ger. Patent No. 1,014,092, Aug. 22, 1957; Chem. Abstr. **53**, 15981 (1959).
24. R. RAMBAUD. Bull. Soc. Chim. Fr. 1352 (1934).

Can. J. Chem. Downloaded from www.nrcresearchpress.com by 210.87.254.40 on 09/05/12
For personal use only.

The adsorption of lower trialkylphosphates at the dodecane–water interface[1,2]

NORMAN H. SAGERT AND WOON LEE

Research Chemistry Branch, Atomic Energy of Canada Research Company, Whiteshell Nuclear Research Establishment, Pinawa, Man., Canada R0E 1L0

Received June 3, 1980

NORMAN H. SAGERT and WOON LEE. Can. J. Chem. **58**, 2789 (1980).

The adsorption of tripropylphosphate, triethylphosphate, and trimethylphosphate at the dodecane–water interface has been studied at temperatures from 293 to 313 K. Standard free energies of adsorption were obtained from the lowering of interfacial tensions in the low ($< 10^{-4}$) solute mole fraction region. Standard enthalpies and entropies of adsorption were then obtained from the temperature variation of the standard free energies of adsorption.

Standard free energies of adsorption from dodecane showed little variation with solute chain length, with the exception of trimethylphosphate. On the other hand, free energies of adsorption from water decreased by 3.45 kJ/mol for each methylene group added, again with the exception of trimethylphosphate. Enthalpies of adsorption increased linearly with increasing solute chain length for adsorption from either phase. For each methylene group added, the enthalpy of adsorption from dodecane increased by 2.9 kJ/mol, while that from water increased by 2.4 kJ/mol.

Results for tripropylphosphate adsorption and for triethylphosphate adsorption at higher temperatures could be adequately described by the Schofield–Rideal equation of state, but not by simple two-dimensional solution models. Results for trimethylphosphate adsorption and for triethylphosphate adsorption at lower temperatures could not be fitted adequately by either type of equation of state.

NORMAN H. SAGERT et WOON LEE. Can. J. Chem. **58**, 2789 (1980).

On a étudié l'adsorption des phosphates de tripropyle, de triéthyle et de triméthyle à l'interface dodécane–eau, à des températures variant de 293 K à 313 K. On a obtenu les énergies libres d'absorption à partir de l'abaissement des tensions interfaciales dans la région ou la fraction molaire du soluté est faible ($< 10^{-4}$). On a alors obtenu les enthalpies et entropies normales d'absorption à partir de la variation, en fonction de la température, des énergies libres normales d'adsorption.

A l'exception du phosphate de triméthyle, les énergies libres normales d'absorption des autres phosphates à partir du dodécane varient peu avec la longueur de la chaîne de soluté. D'autre part, les énergies libres d'adsorption à partir de l'eau décroissent de 3,45 kJ/mol avec l'addition de chaque groupe méthylénique, la encore le phosphate de triméthyle fait exception. Les enthalpies d'adsorption augmentent linéairement avec la longueur de la chaîne du soluté lors de l'adsorption dans l'une ou l'autre phase. Pour chaque addition de groupes méthylènes, l'enthalpie d'adsorption à partir du dodécane augmente de 2,9 kJ/mol alors que celle provenant de l'eau augmente de 2,4 kJ/mol.

Les résultats de l'adsorption des phosphates tripropyle et de triéthyle à des températures plus élevées peuvent être décrits adéquatement par l'équation d'état de Schofield–Rideal et non pas par de simples modèles de solution en deux dimensions. Les résultats de l'adsorption des phosphates de triméthyle et de triéthyle à des températures plus basses ne s'accordent pas adéquatement à un type quelconque d'équation d'état.

[Traduit par le journal]

Introduction

We have reported previously on our study (1) of the adsorption of tributylphosphate (TBP) at the dodecane–water interface. Our work was done as part of a program to study the interfacial properties of those solvent extraction systems used for separating the components of irradiated nuclear fuel. The work reported here extends the study to three other trialkylphosphate solutes, tripropylphosphate (TPP), triethylphosphate (TEP), and trimethylphosphate (TMP).

Adsorption of nonionic alkylphosphates at alkane–water interfaces has not been studied as thoroughly as adsorption of alcohols at the same surfaces (2–4), although some studies have been done on the adsorption of TBP at benzene–water interfaces (5, 6). Our studies of TBP adsorption from dodecane to the dodecane–water interface (1) concentrated on determining the thermodynamic parameters of the adsorption process. The free energy change was large and negative, since adsorption was strong, and a high negative enthalpy of adsorption was also obtained. Since available thermodynamic data (7–9) were not sufficient to allow an accurate calculation of solute distribution coefficients as a function of temperature and thus calculation of the thermodynamics of adsorption from both phases, distribution coefficients of TBP, TPP, TEP, and TMP were measured in our laboratory (10). Then in a related study, which we are reporting here, the adsorption of the three lower trialkylphosphates at the dodecane–water interface was examined. Both the thermodynamics of adsorption and equations of state for the adsorbed layer could then be compared with those for TPB adsorption.

[1]AECL No. 6919.

[2]Presented in part at the 3rd International Conference on Surface and Colloid Science, Stockholm, Sweden, August 1979.

0008-4042/80/242789-07$01.00/0

©1980 National Research Council of Canada/Conseil national de recherches du Canada

Can. J. Chem. Downloaded from www.nrcresearchpress.com by 210.87.254.6 on 09/05/12
For personal use only.

Can. J. Chem. Downloaded from www.nrcresearchpress.com by 210.87.254.6 on 09/05/12
For personal use only.

Experimental

Interfacial tensions were measured using the drop-volume method. The apparatus and general procedures have been described (1). Drops were formed on a stainless steel tip of radius 3.166 mm, and were aged at least 5 min. The cell was a Ramé–Hart thermostatted chamber with temperature control to ±0.002 K. Temperatures were known to ±0.05 K. Interfacial tensions were calculated using the Harkins and Brown correction curve (11), and were reproducible to ±50 μN/m.

The sources and purification of the water and dodecane have been described previously (1). The three lower trialkylphosphates were obtained from Aldrich, and their purification has also been described (10).

For experiments using TPP as solute, a stock solution of TPP in dodecane was prepared and appropriate amounts of the stock solution were added to 50 cm^3 dodecane plus 50 cm^3 water in the cell to make up the required mole fraction of TPP in dodecane. For experiments using TEP and TMP as solutes, the procedure was similar except that stock solutions were made up in water and were freshly prepared for each solute mole fraction. Our measured distribution coefficients (10) were used to calculate solute mole fractions in both phases.

Densities were measured to within ±0.2 mg/cm^3 using a 25 cm^3 pycnometer flask.

Two preliminary experiments were done to test for possible hydrolysis of the trialkylphosphates in water. Stock solutions were allowed to stand for several weeks and during this period there was no detectable change in pH. Furthermore, interfacial tensions remained constant over the period. Thus, it was concluded that hydrolysis of the trialkylphosphates would not seriously affect our results.

Adsorption of each of the three trialkylphosphates at the dodecane–water interface was studied at 293.2, 298.2, 303.2, 308.2, and 313.2 K by measuring interfacial tensions. At these five temperatures, interfacial tensions were measured over an "extended" concentration range which meant that to the system of 50 cm^3 water and 50 cm^3 dodecane, we added up to 150 μmol TEP, or up to 20 μmol TMP. In addition, interfacial tensions were measured in the "dilute" region for four intermediate temperatures of 295.7, 300.7, 305.7, and 310.7 K. For these studies up to 5 μmol solute were added to the system.

Results

Adsorption of Trialkylphosphates

Typical results[3] for TEP at 298.2 K are shown in Fig. 1. For computational purposes, it was convenient to express the interfacial data by eq. [1].

$$[1] \quad \gamma = C_1 + C_2 \ln X + C_3 (\ln X)^2 + C_4 (\ln X)^3$$

In eq. [1], γ is the interfacial tension in N/m and X is the mole fraction of trialkylphosphate in the phase being considered. The values of the constants, C_i, obtained by the third-order least-squares fit to eq. [1] are given in Table 1. For the TEP and TMP, the constants give the interfacial tensions as a function of solute mole fraction in the water phase whereas for TPP they give the interfacial tensions as a function of TPP mole fraction in dodecane. Dodecane was used as the reference phase merely for convenience since the distribution coefficient is such that most of the TPP stays in the dodecane. The fits are reasonably good, as indicated by the standard deviations obtained. At this point, it is necessary to note two incorrect entries in a recently published table of constants for expressing these interfacial tensions with TBP as the solute. In Table 1 of ref. 1, C_3 should be -1.617146×10^{-4} and -1.730985×10^{-4} at 293.15 K and 298.15 K respectively.

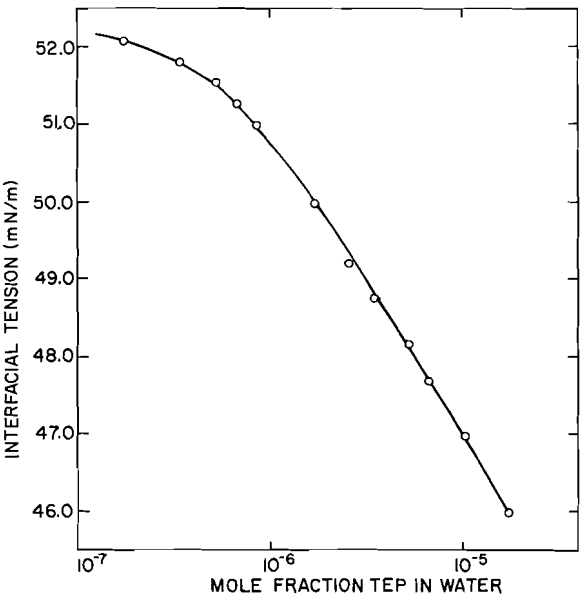


FIG. 1. Interfacial tensions at the dodecane–water interface as a function of TEP mole fraction in the aqueous phase. T = 298.2 K.

Molecular Areas

The simple form of the Gibbs adsorption equation (eq. [2]) was used to calculate the area available to each molecule at the interface, A.

$$[2] \quad A = -kT(\partial\gamma/\partial \ln fX)^{-1}$$

where f is the activity coefficient of the solute in the solvent from which it is being adsorbed. The activity coefficient is chosen as approaching unity when the solution becomes infinitely dilute. In this work, activity coefficients will be taken as unity. Previous work has shown (12, 13) that this is a reasonable assumption for the mole fractions used here. Equations [1] and [2] may be combined to yield eq. [3], giving the area available per molecule in terms of the constants of eq. [1].

$$[3] \quad A = -kT(C_2 + 2C_3 \ln X + 3C_4 (\ln X)^2)^{-1}$$

[3]All the measured data on interfacial tensions are available, at a nominal charge, from the Depository of Unpublished Data, CISTI, National Research Council of Canada, Ottawa, Ont., Canada K1A 0S2.

Can. J. Chem. Downloaded from www.nrcresearchpress.com by 210.87.254.6 on 09/05/12
For personal use only.

TABLE 1. Coefficients of eq. [1] for the adsorption of lower trialkylphosphates at the dodecane–water interface

Solute	T (K)	10^2C_1	10^2C_2	10^3C_3	10^5C_4	10^4 standard deviation of fit
TPP	293.2	−2.084275	−1.005506	−0.351317	−0.021837	2.346
TPP	298.2	−3.161725	−1.367235	−0.710028	−1.128799	1.743
TPP	303.2	−4.836083	−1.876105	−1.190453	−2.562256	0.657
TPP	308.2	−5.091138	−2.003542	−1.335684	−3.040396	0.537
TPP	313.2	−4.383312	−1.830397	−1.190522	−2.611088	2.571
TEP	293.2	15.49139	2.904801	2.455505	6.503382	0.818
TEP	298.2	9.307837	1.497574	1.406753	3.943156	0.705
TEP	303.2	2.475973	−0.076426	0.218758	1.006443	0.784
TEP	308.2	−1.527526	−0.990037	−0.459649	−0.632334	0.531
TEP	313.2	−6.407654	−2.113797	−1.304521	−2.705754	0.481
TMP	293.2	22.02018	3.712125	2.644707	3.939210	0.394
TMP	298.2	13.94923	1.979814	1.416629	3.257475	0.422
TMP	303.2	14.78284	2.157399	1.544135	3.572754	0.371
TMP	308.2	19.78134	3.225432	2.303209	5.372505	0.609
TMP	313.2	22.44065	3.773422	2.670953	6.238312	0.685

Discussion

Thermodynamics of Adsorption

The standard free energies of adsorption, $\Delta_a\mu^\theta$, were calculated from the initial slopes of the plots of interfacial pressure against solute mole fraction where interfacial pressure is, of course, the difference between the interfacial tension in the absence of solute and that in its presence. Such plots were linear in the low mole fraction region and Fig. 2 shows some typical results with the solute TEP. From the slopes of the lines in Fig. 2, free energies of adsorption were calculated using eq. [4],

$$[4]\quad \Delta_a\mu^\theta = -RT \ln \{(\pi/X)_0(X_s/\pi_s)\}$$

where $(\pi/X)_0$ is the initial slope of the plot of surface pressure against mole fraction of solute. The standard states, denoted X_s and π_s were those used previously by us (1) and by Aveyard and Briscoe (3, 14). The surface standard state is simply a surface pressure of 1 μN/m, and the bulk standard state is that hypothetical standard state where the solute mole fraction is unity, but the solute activity coefficient is also unity.

Standard free energies of adsorption for the three solutes, TMP, TEP, and TPP at all temperatures used are shown in Table 2 for adsorption from both phases. All these standard free energies are large and negative, being considerably larger in the negative sense than the standard free energies of adsorption of alcohols at the same interface (3, 14). Thus strong adsorption of these solutes is noted from both phases. The TMP results at the highest temperatures are not reported since the plots did not go through the origin, although the nonlinearity was just within the claimed reproducibility

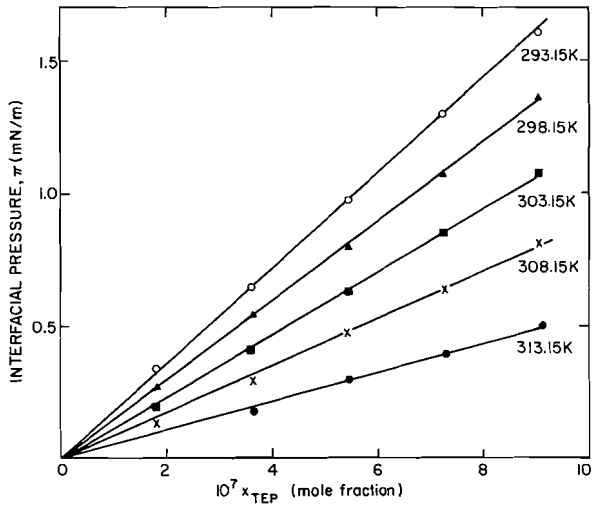


FIG. 2. Interfacial pressures at the dodecane–water interface as functions of TEP mole fraction in the aqueous phases.

of the surface pressures (±100 μN/m). Possibly at higher temperatures there is some reversible sorption of TMP in the seals of the cell.

Figure 3 shows standard free energies of adsorption at 298.2 K from both the aqueous phase and the dodecane phase plotted as a function of the number of carbon atoms in the trialkylphosphate solution. Also shown on the same figure are previously reported standard free energies of transfer of the trialkylphosphates from water to dodecane (10), as well as standard free energies for the adsorption of tributylphosphate (1). These three standard free energies add algebraically to zero.

Apart from the results for TMP adsorption, which may well be atypical since TMP is the first

TABLE 2. Standard free energies of adsorption of trialkylphosphates at the dodecane–water interface from the aqueous (aq) phase and from the dodecane (dod) phase

	$-\Delta_a\mu^\theta$ (kJ/mol)					
T (K)	TMP(aq)	TMP(dod)	TEP(aq)	TEP(dod)	TPP(aq)	TPP(dod)
293.2	37.21	45.73	35.19	36.52	43.35	34.08
295.7	37.11	45.44	35.29	36.42	43.60	34.08
298.2	37.14	45.27	35.35	36.30	43.67	33.91
300.7	37.06	45.05	35.39	36.05	43.91	33.82
303.2	37.01	44.79	35.41	35.80	44.12	33.74
305.7	37.00	44.64	35.33	35.52	44.31	33.60
308.2	36.90	44.37	35.40	35.42	44.47	33.44
310.7	—	—	35.37	35.04	44.57	33.32

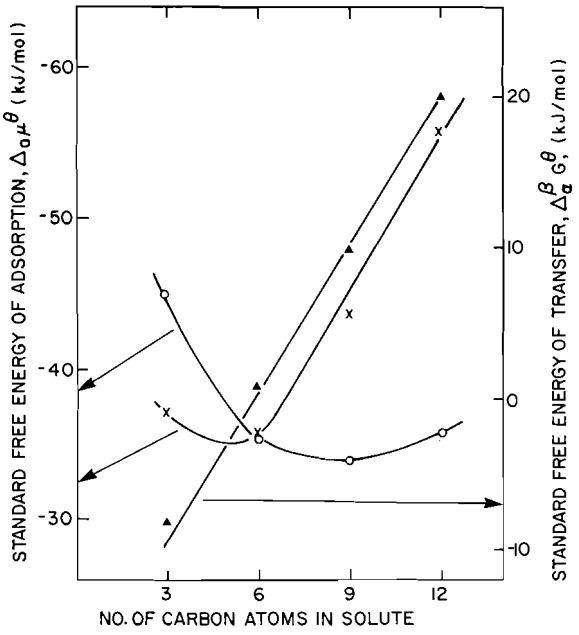


FIG. 3. Comparison of standard free energies of adsorption from water to the interface (×), dodecane to the interface (○), and of transfer from water to dodecane (▲). T = 298.2 K.

member of the series, the standard free energies of adsorption from dodecane do not change greatly with increasing chain length. If the hydrophilic phosphate group is attracted to the water phase, while the alkyl chains remain in the dodecane, then this constant free energy change can be associated with the transfer of the phosphate group into the water from the dodecane.

On the other hand, the standard free energy of adsorption from water to the interface becomes about 3.45 kJ/mol more negative for each CH_2 group added to the chain, again omitting the result for TMP adsorption. This value is very close to the 3.5 kJ/mol decrease in standard free energy change per CH_2 group for complete transfer of the solute from water into the dodecane (10), which in turn is very similar to the value quoted for transfer of CH_2 groups from water to oil for many classes of organic compounds (15, 16). It is therefore tempting to interpret the close correspondence of the changes in the standard free energies of transfer to the changes in the standard free energy of adsorption from water as evidence that the alkyl groups exist entirely in the dodecane when equilibrium is achieved during adsorption. This is certainly a reasonable interpretation. However, Aveyard and Briscoe (3) have pointed out that the free energies of adhesion are such that the possibility that some methylene groups may be in contact with water at the interface cannot be excluded.

The TMP seems to be adsorbed more strongly from both media than would be predicted by extrapolating the standard free energies of adsorption of the trialkylphosphates with longer chain lengths. The reasons for this seem to lie with specific enthalpic and entropic effects which will be discussed later.

Standard enthalpies of adsorption, $\Delta_a h^\theta$, were obtained from the temperature variation of the standard free energies of adsorption using eq. [5].

$$[5] \quad \Delta_a h^\theta = \partial(\Delta_a\mu^\theta/T)/\partial(1/T)$$

Over the temperature range investigated, straight lines were obtained, of comparable precision to those obtained for TBP (1). Having determined the standard enthalpies of adsorption, and knowing the standard free energies of adsorption, the standard entropies of adsorption were calculated directly. These enthalpies and entropies of adsorption calculated at 298.2 K are shown in Table 3 for the three solutes studied.

In Fig. 4, the standard enthalpies of adsorption are plotted as a function of the number of carbon atoms in the solute. These enthalpies decrease linearly as the chain length is increased, the change

Can. J. Chem. Downloaded from www.nrcresearchpress.com by 210.87.254.6 on 09/05/12
For personal use only.

TABLE 3. Standard enthalpies, $\Delta_a h^\theta$, and entropies, $\Delta_a S^\theta$, of adsorption at 298.2 K

Solute adsorbed	Phase from which adsorbed	$-\Delta_a h^\theta$ (kJ/mol)	$\Delta_a S^\theta$ (J/mol K)
TMP	Aqueous	40.0	−9.6
TMP	Dodecane	71.6	−87.7
TEP	Aqueous	33.0	7.9
TEP	Dodecane	62.4	−87.5
TPP	Aqueous	23.6	67.3
TPP	Dodecane	52.3	−61.7

being about 2.9 kJ/mol per CH_2 group for adsorption from the dodecane and 2.4 kJ/mol per CH_2 group for adsorption from the water.

Adsorption from the dodecane phase is, to a first approximation, the hydration of the hydrophilic phosphate group while the alkane chain remains in the dodecane, perhaps in contact with the interface. In principle, the phosphoryl oxygen is capable of forming two hydrogen bonds and the bridging internal oxygens one each for a potential total of five. The standard enthalpy of adsorption of TMP from water is −71.6 kJ/mol, which corresponds to the enthalpy of formation of four to five hydrogen bonds (17), close to the maximum possible. The small methyl groups must allow the TMP molecule good access to the water near the interface. As the length of the alkyl chain increases the relative attraction of the solute molecules to the dodecane increases, and the phosphate groups will not penetrate as far into the water. For TBP the enthalpy of adsorption increases to −45.5 kJ/mol, which is equivalent to between only two or three hydrogen bonds. As an alternative to this steric model, it is also possible that the larger alkyl groups decrease the basicity of the oxygen, leading to weaker hydrogen bonds (18). However, Karyakin and Muradova (17) found no spectroscopic evidence for much weaker hydrogen bonds between water and TEP as compared with TBP.

When trialkylphosphates are dissolved in water, from 12 to 25 kJ/mol of heat is evolved (7, 9) and these exothermic heats of solution have been attributed to the hydrophobic effect (9, 15, 19). The hydrophobic effect is characterized by a large increase in the order of the hydrogen-bonded structure close to the hydrophobic solute molecule. The entropy change is large, and while the enthalpy change for dissolution of trialkylphosphates is also large (7, 9), it is very much less than that associated with the formation of five hydrogen bonds. It seems that the cooperative hydration envelope, formed by the hydrophobic interactions and thought by Lindenbaum *et al.* (9) to involve some 30 water molecules, shields at least some of the oxygens of the solute from hydrogen-bonding with water. Of course trialkylphosphates are highly associated in the liquid state (20, 21) so this simple explanation is not sufficient. Since we are dealing with the dodecane–water system, it is perhaps useful to note that the enthalpy of transfer of trialkylphosphates from dodecane to water is −27 to −30 kJ/mol (1), again equivalent to about two hydrogen bonds rather than five. Again, there is association with water molecules in the dodecane phase so again this simple explanation of the shielding of some oxygen atoms by the hydration envelope cannot be entirely sufficient.

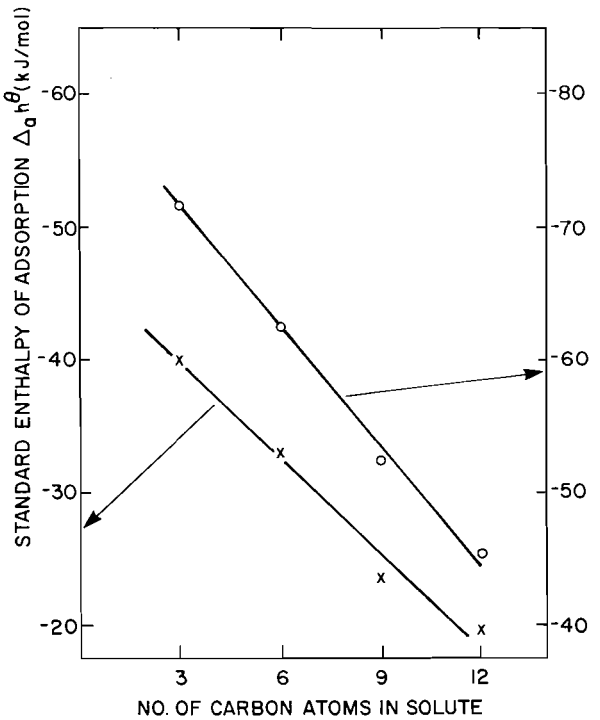


FIG. 4. Standard enthalpies of adsorption from water (×) and from dodecane (○) to the interface.

Adsorption from water to the interface is accompanied by another sizable enthalpy release. This release is expected when we note that the cooperative hydration envelope associated with the alkyl groups in water is destroyed when they are taken up by the dodecane, freeing the hydrophilic phosphate to hydrogen-bond more strongly with the water. On the other hand, the enthalpy change on adsorption from water per CH_2 group is very close to the negative of that for solution in water (9). This suggests, enthalpically at least, some similarity in the changes of environment per CH_2 group for the hy-

Can. J. Chem. Downloaded from www.nrcresearchpress.com by 210.87.254.6 on 09/05/12
For personal use only.

Can. J. Chem. Downloaded from www.nrcresearchpress.com by 210.87.254.6 on 09/05/12
For personal use only.

drocarbon chain in the adsorbed state and in liquid trialkylphosphate.

Using the standard states described above, entropies of adsorption from water become very large and positive for the longer-chain trialkylphosphates, reflecting increasing loss of water structure during the adsorption process as the chain length is increased (Fig. 5). The TMP results aside, the entropy increase is 19.3 J/mol K for each CH_2 group added to the solute. Similarly, there is also a gain in entropy with increasing chain length for adsorption from the dodecane, but in this case, the increase is only 9.3 J/mol K for each CH_2 group added, again omitting the TMP results.

A comparison of Figs. 4 and 5 shows that the high adsorption of TMP at the dodecane–water interface is the result of high entropies of adsorption, rather than anomalies in the enthalpies of adsorption. While we believe that these entropic effects are real, nevertheless the possibility exists that TMP hydrolysis products (23) play some role in the anomalous behaviour of this system. Our results showed no detectable hydrolysis in the aqueous phase, but increased hydrolysis in the surface phase is possible and the extent of hydrolysis necessary to affect the results is unknown. The hydrolysis of TMP is known to be about five times faster than that of TEP (24).

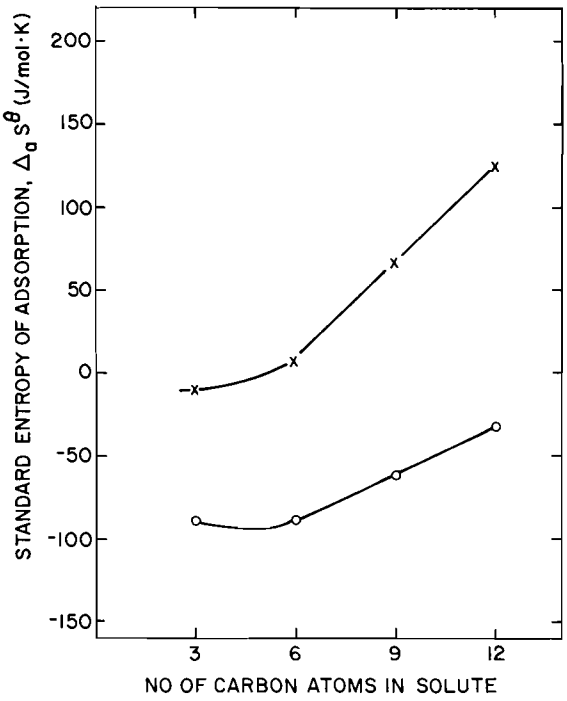


FIG. 5. Standard entropies of adsorption from water (×) and from dodecane (○) to the interface.

Surface Equation of State

Attempts were made to fit the measured values of π and A to a two-dimensional equation of state known as the Schofield–Rideal equation (22), shown here as eq. [6], where i and A_0 are fitting constants.

$$[6] \quad \pi(A - A_0) = ikT$$

To obtain values of i and A_0, eq. [6] was combined with eq. [3], eq. [1], and the constants listed in Table 1. The interfacial tension – solute mole fraction data were then fitted using a non-linear, least-squares fitting routine based on Marquardt's method employing the algorithm of Brown and Dennis (25) (Chalk River Nuclear Laboratories CDC Fortran program MLSQQ). The results obtained are shown in Table 4 and the errors listed are the standard deviation of the fit, as returned by the program. Fits could not be obtained to the TMP data and to the TEP data at the two lower temperatures. In all these cases, an inflection was noted in the curve of interfacial tension against the logarithm of the solute mole fraction. Activity coefficient corrections in the aqueous and organic phases may be large enough that they can no longer be neglected at the higher mole fractions used here.

The values of A_0 obtained for TPP and for TEP at 313.2 K are only about one half those obtained for TBP under the same conditions (1). Although A_0 is, strictly speaking, only a fitting constant, it is generally associated with the static geometric area of the molecule at the interface (3). Thus it is tempting to rationalize the values obtained in terms of geometric areas. From its geometry, the cross-sectional area of the TPP molecule is about 0.6 nm² and that of the TEP molecule is about 0.5 nm². Thus, the A_0's obtained for TPP are only slightly smaller than the static geometric area. The A_0 for TEP is about equal to the geometric area at 313.2 K, but appears to rise enormously as the temperature is lowered. This is most likely apparent, due to changes in activity coefficients in the solvent.

As with TBP (1), the best fit of eq. [6] is not with $i = 1.0$, the Volmer equation, but with i substantially

TABLE 4. Constants of Schofield–Rideal Equation

Solute	T (K)	A_0 (nm²)	i
TPP	293.2	0.50 ± 0.03	1.36 ± 0.07
TPP	298.2	0.43 ± 0.03	1.56 ± 0.07
TPP	303.2	0.34 ± 0.03	1.75 ± 0.06
TPP	308.2	0.33 ± 0.06	1.41 ± 0.06
TPP	313.2	0.39 ± 0.04	1.38 ± 0.08
TEP	303.2	1.50 ± 0.02	0.89 ± 0.03
TEP	308.2	0.86 ± 0.05	1.31 ± 0.06
TEP	313.2	0.56 ± 0.04	1.32 ± 0.04

greater than unity. The deviations from the Volmer equation are in a direction suggesting extra repulsions in the monolayer, rather than the increased cohesion observed at vapor–liquid interfaces (26). Previously, we suggested (1) that some of this repulsion could be accounted for by dipole–diple repulsions in the adsorbed layer, or alternatively, by variations of A_0 with coverage. It should also be noted that relatively small errors in the interfacial tension can give rise to fairly large errors in the area, A. Thus, the Volmer equation, with $A_0 \sim 0.8\ nm^2$, while not the best fit of the data is not an unreasonable one.

Attempts were made to use a two-dimensional solution model for the surface (27, 28), employing the simplifying assumptions that the solute is located entirely in the dodecane (3). However, it was not possible to fit our data in this way using any reasonable values of the surface areas of the trialkylphosphates and dodecane.

Acknowledgements

We thank our colleagues at the Whiteshell Nuclear Research Establishment, especially R. J. Lemire and P. R. Tremaine, for helpful advice.

1. N. H. SAGERT, W. LEE, and M. J. QUINN. Can. J. Chem. **57**, 1218 (1979).
2. S. ROSS and E. S. CHEN. Ind. Eng. Chem. **57** (7), 40 (1965).
3. R. AVEYARD and B. J. BRISCOE. J. Chem. Soc. Faraday I, **68**, 478 (1972).
4. M. LIN, J-L. FIRPO, P. MANSOURA, and J. F. BARET. J. Chem. Phys. **71**, 2202 (1979).
5. E. CHIFU, Z. ANDREI, and M. TOMOAIA. Ann. Chim. **64**, 869 (1974).
6. Z. ANDREI and E. CHIFU. Stud. Univ. Babes-Bolyai Ser. Chem. **21**, 10 (1976).
7. A. S. KERTES and L. TSIMERING. J. Phys. Chem. **81**, 120 (1977).
8. A. S. KERTES, L. TSIMERING, and F. GRAUER. J. Inorg. Nucl. Chem. **38**, 867 (1976).
9. S. LINDENBAUM, D. STEVENSON, and J. H. RYTTING. J. Solution Chem. **4**, 893 (1975).
10. N. H. SAGERT and W. LEE. Can. J. Chem. **58**, 1463 (1980).
11. W. D. HARKINS and F. E. BROWN. J. Am. Chem. Soc. **41**, 499 (1919).
12. Y. MARCUS. Critical evaluation of some equilibrium constants involving organophosphorus extractants. Butterworths, London. 1974. p. 27.
13. Y. MARCUS. J. Phys. Chem. **65**, 1647 (1961).
14. R. AVEYARD and B. J. BRISCOE. Trans. Faraday Soc. **66**, 2911 (1970).
15. C. TANFORD. The hydrophobic effect: formation of micelles and biological membranes. John Wiley, New York. 1973. pp. 4–15.
16. C. TANFORD. J. Phys. Chem. **83**, 1802 (1979).
17. A. V. KARYAKIN and G. A. MURADOVA. Zh. Fiz. Khim. **45**, 1054 (1971) (Russ J. Phys. Chem. **45**, 591 (1971)).
18. Y. MARCUS and A. S. KERTES. Ion exchange and solvent extraction of metal complexes. John Wiley, New York. 1969. p. 652.
19. A. BEN-NAIM. Hydrophobic interactions. Plenum Press, New York. 1980. pp. 185-209.
20. D. DYRSSEN and D. M. PETKOVIĆ. J. Inorg. Nucl. Chem. **27**, 1381 (1965).
21. D. M. PETKOVIĆ. *In* Solvent extraction chemistry. *Edited by* D. Dyrssen, J. O. Liljenzin, and J. Rydberg. North Holland, Amsterdam. 1967. pp. 305–308.
22. R. K. SCHOFIELD and E. K. RIDEAL. Proc. R. Soc. London, A**109**, 57 (1925).
23. P. W. C. BARNARD, C. A. BUNTON, D. R. LLEWELLYN, C. A. VERNON, and V. A. WELCH. J. Chem. Soc. 2670 (1961).
24. E. P. LYZNICKI, K. OYAMA, and T. T. TIDWELL. Can. J. Chem. **52**, 1066 (1974).
25. K. M. BROWN and J. E. DENNIS. Numerische Math. **18**, 289 (1972).
26. R. AVEYARD and B. VINCENT. Prog. Surf. Sci. **8**, 59 (1977).
27. F. M. FOWKES. J. Phys. Chem. **66**, 1863 (1962).
28. E. H. LUCASSEN-REYNDERS. *In* Progress in surface and membrane science. Vol. 10. *Edited by* D. A. Cadenhead and J. F. Danielli. Academic Press, New York. 1976. pp. 253–360.

Can. J. Chem. Downloaded from www.nrcresearchpress.com by 210.87.254.6 on 09/05/12
For personal use only.

Heats of vaporization of esters by the gas chromatography–calorimetry method[1]

RICHARD FUCHS AND L. ALAN PEACOCK
Department of Chemistry, University of Houston, Houston, TX 77004, U.S.A.
Received May 27, 1980

RICHARD FUCHS and L. ALAN PEACOCK. Can. J. Chem. **58**, 2796 (1980).

A recently developed gc–calorimetry procedure involving a combination of gas chromatography and heat of solution measurements has been used to measure heats of vaporization of 17 esters, including methyl 2,2-dimethylpropanoate, butyl acetate, glyceryl triacetate, diethyl phthalate, methyl 9-octadecenoate, and 12 methyl esters of C_3- to C_{15}-fatty acids. Comparison with measurements of ΔH_v reported in the literature indicates that the gc–calorimetry method often has smaller uncertainties in measurements (0.25 to 1.00 kJ mol^{-1}) and more consistent methylene increments for the series of fatty acid methyl esters. Two of the experimental ΔH_v measurements which differ appreciably from recent literature values have been verified by vaporization calorimetry.

RICHARD FUCHS et L. ALAN PEACOCK. Can. J. Chem. **58**, 2796 (1980).

Pour mesurer les chaleurs de vaporisation de 17 esters comprenant le diméthyl-2,2 propionate de méthyle, l'acétate de butyle, le triacétate de glycéryle, le phtalate de diéthyle, l'octadécène-9 oate de méthyle et 12 esters méthyliques d'acides gras allant de C_3 à C_{15}, on a utilisé un procédé récemment mis au point (cpg/calorimétrie) qui fait intervenir une combinaison de la chromatographie en phase gazeuse et de mesures des chaleurs de solutions. Une comparaison avec les valeurs de ΔH_v rapportées dans la littérature indique que la méthode cpg/calorimétrie a souvent de plus faibles incertitudes (0,25 à 1,00 kJ/mol^{-1}) et des incréments pour les méthylènes qui sont plus réguliers pour la série d'esters méthyliques des acides gras. On a vérifié par calorimétrie de vaporisation deux des mesures expérimentales de ΔH_v qui diffèrent de façon appréciable de celles de la littérature.

[Traduit par le journal]

The determination of enthalpies of formation in the gaseous state (from enthalpies of combustion or hydrogenation in solution), and comparisons of acidities, basicities, and reactivities in the gaseous state and in solution require a knowledge of the enthalpies of vaporization (ΔH_v) of the involved species (1–3). The available body of good experimental data is far more limited than is generally recognized. Much of the ΔH_v literature (4) consists of estimates based on various schemes and experimental values using methods with large uncertainties.

We have recently developed the gc–calorimetry technique for measuring ΔH_v by a combination of gas chromatography and solution calorimetry (5, 6). Excellent results have been obtained for low boiling compounds ($< \sim 425$ K), but the method is especially useful for high boiling compounds. Partial sample decomposition, which leads to serious problems with other methods, does not affect the gc–calorimetry results.

In view of the biological importance of fatty acids, the common use of the methyl esters in gc analysis of the acids, and the incomplete and inconsistent nature of the ΔH_v data available at the time this work was started, it appeared that the fatty acid methyl esters would constitute an appropriate series of compounds for determination of ΔH_v values by the gc–calorimetry method. In the interim new values for these compounds have been published (7), which furnish useful comparisons and contrasts with the present values. Several additional esters have been examined (Tables 1 and 2), although for only two, butyl acetate and glyceryl triacetate (triacetin), have ΔH_v values with reasonable uncertainties been previously determined.

Values for methyl propanoate and methyl butanoate based on vapor pressure measurements (8) are available, but it was necessary to correct the resulting ΔH_v values to 298.15 K using calculated heat capacities (9, 10). Calorimetric values have recently been determined (11). Enthalpies of vaporization of the remaining esters in Table 1 have been calculated from more recent vapor pressure measurements (4, 12–15) or estimated (4). Two values of ΔH_v originally reported at higher temperatures have been corrected to 298.15 K using calculated values of C_p(l) and C_p(g) (9, 10): glyceryl triacetate (12) ((94.40 ± 0.21) kJ mol^{-1} at 301.1 K) and methyl 9-octadecenoate (13) (methyl oleate) ((84.5 ± 4.2) kJ mol^{-1} at 427 K). Direct vaporization calorimetry has been used to obtain enthalpies of vaporization for several acetates (16).

Recently, enthalpies of vaporization for the methly esters of C_5–C_{15} fatty acids have been measured (7) using the Wadsö calorimeter (16) for the methyl esters of C_5–C_7 fatty acids and the

[1]This study was supported by the Robert A. Welch Foundation Grant E-136.

0008-4042/80/242796-04$01.00/0
©1980 National Research Council of Canada/Conseil national de recherches du Canada

Can. J. Chem. Downloaded from www.nrcresearchpress.com by 210.87.254.40 on 09/05/12
For personal use only.

Can. J. Chem. Downloaded from www.nrcresearchpress.com by 210.87.254.40 on 09/05/12
For personal use only.

TABLE 1. Gas chromatographic data for esters on DC-200 silicone fluid

Compound	ΔH_{soln}[a] / kJ mol^{-1}	ΔC_p[b] / J mol^{-1} K^{-1}	ΔT/K[c]	Slope[d]	$-\Delta H(v \rightarrow S)$[e] / kJ mol^{-1}
Methyl propanoate	3.35	60.7	35.0	3339.71	29.92
Methyl butanoate	2.80	66.5	35.0	3799.53	33.93
Methyl pentanoate	2.51	72.4	33.9	4348.71	38.62
Methyl hexanoate	2.68	79.9	36.7	4868.71[g]	43.39
Methyl heptanoate	2.51	87.4	59.7	5119.08	47.78
Methyl octanoate	2.55	95.0	51.2	5705.20[g]	52.30
Methyl nonanoate	2.72	102.5	65.1	6045.20[g]	56.90
Methyl decanoate	2.89	110.0	79.5	6300.76[g]	61.13
Methyl dodecanoate	3.22	125.1	99.4	7076.44[g]	71.25
Methyl tridecanoate	3.47	132.6	108.9	7394.50[g]	75.90
Methyl tetradecanoate	3.97	140.2	128.9	7498.77[g]	80.42
Methyl pentadecanoate	4.31	147.7	129.3	7992.15[g]	85.52
Methyl 2,2-dimethylpropanoate	1.67	67.4[f]	3.5	3937.58	34.98
Butyl acetate	2.59	72.4[f]	59.7	4068.61	38.07
Glyceryl triacetate	14.06	146.4[f]	80.2	6693.98[g]	67.40
Diethyl phthalate	10.88	104.2[f]	108.4	6853.30[g]	68.16
Methyl *cis*-9-octadecenoate	4.39	192.9	154.2	8575.21[g]	101.04

[a] Enthalpies of solution in DC-200 silicone fluid at 298 K. Uncertainty is (±0.08 to ±0.13) kJ mol^{-1}, except glyceryl triacetate (±0.33 kJ mol^{-1}) and diethyl phthalate (±0.29 kJ mol^{-1}).
[b] $\Delta C_p = C_p(l) - C_p(g)$ at 298.15 K. $C_p(l)$ from ref. 9, with the exception of the following group values (20) derived from experimental values: (O)—CH_2— (24.7 J mol^{-1} K^{-1}), (C)—CO—O— (70.3 J mol^{-1} K^{-1}), —CH_2— (28.9 J mol^{-1} K^{-1} in straight chains of seven or fewer carbon and oxygen atoms, 30.5 J mol^{-1} K^{-1} for additional CH_2 groups in longer chains). $C_p(g)$ from ref. 10.
[c] (Mean temperature of gc measurements) − 298.15 K.
[d] Slope of plot of ln (gc corrected retention time) vs. $1/T$.
[e] From eq. [2] corrected to 298.15 K using eq. [3].
[f] ΔC_p from experimental values of $C_p(l)$ (20).
[g] Gas chromatographic retention times measured on DC-200 capillary column I (ref. 6). Others measured using column II.

Morawetz calorimeter (17) for the others. These values show considerably smaller uncertainties than previous data.

The recently developed gc–calorimetry method for determining enthalpies of vaporization (5, 6) relies upon calorimetric enthalpies of solution at infinite dilution, ΔH_s, and solvation enthalpies, $\Delta H(v \rightarrow S)$, obtained by gas chromatography.

$$[1] \quad \Delta H_v = \Delta H_s - \Delta H(v \rightarrow S)$$

Solvation enthalpies are obtained from the temperature coefficient of the corrected retention times (Δt) (which are linearly related to retention volumes),

$$[2] \quad \Delta H(v \rightarrow S) = R\mathrm{d}(\ln \Delta t)/\mathrm{d}(1/T)$$

and are corrected to 298.15 K using calculated heat capacity values,

$$[3] \quad \Delta H^{0\ 298.15\ K}(v \rightarrow S) = \Delta H^{T}(v \rightarrow S) + \int_{T}^{298.15\ K} [C_p^{0}(l) - C_p^{0}(g)]\,\mathrm{d}T$$

The solvent in which enthalpies of solution are obtained is the same as the gc stationary phase, DC-200 silicone fluid.

Experimental

Ester sample (Fluka, Aldrich, and Fisher Companies) were of 99 mass% or greater purity (by gas chromatography) or brought to this purity by preparative gc. The samples used for vaporization calorimetry were distilled just before use through a Vigreux column, and a center fraction with a boiling point range < 0.1°C was collected in each case.

Gas chromatographic retention times were determined three times at each of six temperatures over a 50°C range using 30 m × 0.5 mm id stainless steel capillary columns, and corrected for the dead volume time which was assumed to be equal to the retention time of methane at each temperature. The stationary phase was DC-200 silicone fluid of 100 cSt viscosity. Heats of solution of the esters in the silicone fluid were determined in a vacuum jacketed isoperibol (isothermal environment) solution calorimeter at 25°C. $\Delta H(v \rightarrow$ DC-200) was calculated (eq. [2]) from the slope of the plot of ln Δt vs. $1/T$. From this quantity at the mean temperature of the Δt measurements $\Delta H(v \rightarrow$ DC-200) at 25°C can be calculated (eq. [3]) by making appropriate ΔC_p corrections. Apparent ΔH_v^{25} values were calculated from the 25°C values of ΔH_s and $\Delta H(v \rightarrow$ DC-200), and corrected by a calibration equation determined from a series of calibration compounds of known ΔH_v. The detailed gas chromatographic and calorimetric procedures, analysis of the data, and calibration method have been previously reported (6).

Calorimetric heats of vaporization were determined by evaporating 100 μL samples inside a coiled copper tube 15 cm in length and 0.3 cm id, imbedded in a copper disc 4 cm in diameter and 2.5 cm high. A thermistor and a metal-film electronic resistor (heater) are mounted in small wells in the copper disc. The entire assembly is contained in a vacuum jacketed solution calorimeter. The copper coil is connected to the outside by Teflon tubing. The block is thermally equilibrated with a nitrogen flow of 4 cm^3/min, with appropriate vacuum drawn on the outlet. A sample of 100 μL is introduced (microliter syringe, 30 cm Teflon needle) through a stopcock, down the Teflon con-

Can. J. Chem. Downloaded from www.nrcresearchpress.com by 210.87.254.40 on 09/05/12
For personal use only.

TABLE 2. Enthalpies of vaporization of esters (kJ mol^{-1})

Expl ΔH_v^{0a}	Δ/CH_2^b	Lit ΔH_v^{0c}	Δ/CH_2^d	Lit ΔH_v^{0e}	Δ/CH_2^f
Methyl propanoate					
36.32 ± 0.25	3.43	35.82 ± 0.09[g]	3.46	36.8[h]	3.8
Methyl butanoate					
39.75 ± 0.25	4.31	39.28 ± 0.22[g]	3.82	40.6[h]	2.1
Methyl pentanoate					
44.06 ± 0.29	4.64	43.10 ± 0.04	4.94	42.7 ± 1.3[j]	3.8
44.10 ± 0.08[i]					
Methyl hexanoate					
48.74 ± 0.33	4.35	48.03 ± 0.13	3.60	46.4 ± 1.3[j]	3.8
Methyl heptanoate					
53.05 ± 0.42	4.27	51.63 ± 0.46	4.77	50.2 ± 1.3[j]	6.7
53.07 ± 0.12[i]					
Methyl octanoate					
57.32 ± 0.42	4.64	56.40 ± 0.50	5.61	56.9 ± 1.7	6.3
Methyl nonanoate					
61.97 ± 0.46	4.31	62.01 ± 0.42	4.73	63.2 ± 2.1	5.9
Methyl decanoate					
66.27 ± 0.50	5.15	66.73 ± 0.59	5.23	69.0 ± 2.1	5.9
Methyl dodecanoate					
76.53 ± 0.71	4.77	77.15 ± 0.54	5.52	80.8 ± 2.1	0.8
Methyl tridecanoate					
81.30 ± 0.71	4.94	82.68 ± 0.84	4.31	81.6 ± 4.2	7.5
Methyl tetradecanoate					
86.23 ± 0.96	5.31	86.99 ± 0.92	6.49	89.1 ± 4.2	−1.3
Methyl pentadecanoate					
91.55 ± 0.92		93.47 ± 0.92		87.9 ± 1.3	
Methyl 2,2-dimethylpropanoate					
39.66 ± 0.25				38.5 ± 1.3[j]	
Butyl acetate					
43.64 ± 0.54		43.60 ± 0.21[k]			
43.68 ± 0.23[i]					
Glyceryl triacetate					
83.35 ± 1.00				82.51 ± 0.21[l]	
Diethyl phthalate					
81.09 ± 0.75				88.3 ± 2.1	
Methyl *cis*-9-octadecenoate					
106.82 ± 0.96				109.2 ± 4.2[m]	

[a] Experimental values at 298.15 K, corrected by calibration curve as discussed in ref. 6.
[b] Methylene increments in ΔH_v^0. The average from methyl pentanoate to methyl pentadecanoate is (4.73 ± 0.33) kJ mol^{-1}.
[c] Literature values of ΔH_v^0 measured calorimetrically (7).
[d] Methylene increment in ΔH_v^0. The average is (5.02 ± 0.79) kJ mol^{-1}.
[e] Literature values of ΔH_v^0 measured via vapor pressure, from ref. 4, except where noted.
[f] Methylene increment in ΔH_v^0. The average is (4.10 ± 2.59) kJ mol^{-1}.
[g] Reference 11.
[h] Values of ΔH_v^0 calculated from vapor pressure measurements (8) and corrected to 298.15 K.
[i] By vaporization calorimetry (see Experimental). Indicated uncertainty intervals are twice the standard deviation.
[j] Estimated values of ΔH_v^0 (4).
[k] Reference 15.
[l] Value of ΔH_v^0 (11) corrected to 298.15 K (see text).
[m] Value of ΔH_v^0 (12) corrected to 298.15 K (see text).

necting tubing, and well into the copper coil. Nitrogen flow is then reestablished, and evaporation of the sample begins. The cooling effect is compensated by short periods of heating from a timed constant current source. When no further evaporation cooling occurs (12–20 min) the block is brought to the original temperature (±1 × 10^{-4} K). Heat capacity corrections are made for the sample and needle which are introduced at 22.0°C. The sample mass is established by weighing several 100 μL samples. The heat of vaporization (J mol^{-1}) is calculated from the equation

$$[4] \quad \Delta H_v = I^2R(\mathrm{MW})t/m$$

where I is the heater current (A), R is the heater resistance (Ω), MW is the molar mass, t is the total heating period (s), and m is the sample mass.

Operation of the vaporization calorimeter was verified by measurements of compounds with well established values of ΔH_v (4): pentane, 26.87 ± 0.38 kJ mol^{-1} (reported, 26.74 ± 0.21); heptane, 36.61 ± 0.12 (36.57 ± 0.04); nonane, 46.42 ± 0.16 (46.44 ± 0.04); 1-butanol, 52.34 ± 0.16 (52.30 ± 0.08); and 2-heptanone 47.53 ± 0.20 (47.45 ± 0.29 (18), 47.24 ± 0.04 (11)). The indicated uncertainties are twice the standard deviations from the mean. Details of the calorimeter design may be obtained from the senior author.

Results and Discussion

Enthalpies of vaporization from the gc–calorimetry method, and literature values (4, 7, 8) are listed in Table 2. For the methyl esters of the C_8–C_{15} fatty acids the gc–calorimetry values and the recent literature values (7) measured with the

Can. J. Chem. Downloaded from www.nrcresearchpress.com by 210.87.254.40 on 09/05/12
For personal use only.

Morawetz calorimeter (17) have comparable uncertainties, and generally agree within the combined uncertainties. For the esters of the C_5–C_7 acids measured (7) using the Wadsö calorimeter (16), ΔH_v values are lower than by the gc–calorimetry method. However, the gc–calorimetry value for butyl acetate is in excellent agreement with the value measured by Wadsö (16).

Because of the considerable differences (1–1.5 kJ mol^{-1}) between several gc–calorimetry values of ΔH_v and the reported calorimetric values (7), we have remeasured several ester heats of vaporization by vaporization calorimetry. Values for methyl pentanoate, methyl heptanoate, and butyl acetate obtained this way are in excellent agreement with the gc–calorimetry results.

In the methyl ester series of the C_5–C_{15} acids the gc–calorimetry method shows methylene increments of 4.27–5.31 kJ mol^{-1} and a mean (4.73 ± 0.33), compared with literature values (7) varying from 3.60 to 6.49, with a mean value of (5.02 ± 0.79). The gc–calorimetry method therefore appears to be capable of somewhat higher self-consistency within the set of values.

The highly branched ester, methyl 2,2-dimethylpropanoate (methyl pivalate), has an enthalpy of vaporization 4.27 kJ mol^{-1} lower than that of the straight chain isomer, methyl pentanoate. This is consistent with the behavior of hydrocarbons (18) and ketones (19) for which each quaternary carbon atom lowers ΔH_v by 3.8 to 4.8 kJ mol^{-1}. The ΔH_v value for the isomers methyl pentanoate and butyl acetate agree within 0.42 kJ mol^{-1} implying that ΔH_v for linear esters is not highly dependent on the location of the ester linkage.

A comparison of the unsaturated ester methyl *cis*-9-octadecenoate (methyl oleate) and methyl pentadecanoate indicates a difference of 15.27 kJ mol^{-1}. The effect of the double bond mush be taken into consideration. The literature ΔH_v values for *n*-hexane (4) and *cis*-3-hexene (4) are (31.55 ± 0.04) and (31.34 ± 0.21) kJ mol^{-1}, respectively. Assuming this double bond contribution to be representative of higher alkenes, a value of 107.03 kJ mol^{-1} would be calculated for the saturated ester, methyl octadecanoate. The ΔH_v difference between methyl pentadecanoate and methyl octadecanoate would be 15.48 kJ mol^{-1}, corresponding to a methylene increment of 5.16 kJ mol^{-1} CH_2^{-1}. This is consistent with the methylene increments of the higher members of the methyl ester sequence.

1. N. Adriaanse, H. Dekker, and J. Coops. Recl. Trav. Chim. Pays-Bas, **84**, 393 (1965).
2. M. Mansson. J. Chem. Thermodyn. **4**, 865 (1972).
3. J. O. Fenwick, D. Harrop, and A. J. Head. J. Chem. Thermodyn. **10**, 687 (1978).
4. J. D. Cox and G. Pilcher. Thermochemistry of organic and organometallic compounds. Academic Press, New York, NY. 1970.
5. L. A. Peacock and R. Fuchs. J. Am. Chem. Soc. **99**, 5524 (1977).
6. R. Fuchs and L. A. Peacock. Can. J. Chem. **56**, 2493 (1978).
7. M. Mansson, P. Sellers, G. Stridh, and S. Sunner. J. Chem. Thermodyn. **9**, 91 (1977).
8. S. Young and G. L. Thomas. J. Chem. Soc. **63**, 1191 (1893).
9. R. Shaw. J. Chem. Eng. Data, **14**, 461 (1969).
10. S. W. Benson. Thermochemical kinetics. 2nd ed. Wiley, New York, NY. 1976.
11. S. Sunner, C. Svensson, and A. S. Zelepuga. J. Chem. Thermodyn. **11**, 491 (1979).
12. A. L. Woodman and A. Adicoff. J. Chem. Eng. Data, **8**, 241 (1963).
13. T. A. Scott, D. MacMillan, and E. H. Melvin. Ind. Eng. Chem. **44**, 172 (1952).
14. H. Hoyer and W. Peperle. Z. Electrochem. **62**, 61 (1958).
15. D. P. Baccanari, J. A. Novinski, Y.-C. Pan, M. M. Yevitz, and H. A. Swain, Jr. Trans. Faraday Soc. **64**, 1201 (1968).
16. I. Wadsö. Acta Chem. Scand. **20**, 544 (1966).
17. E. Morawetz. J. Chem. Thermodyn. **4**, 139 (1972).
18. P. P. S. Saluja, T. M. Young, R. F. Rodewald, F. H. Fuchs, D. Kohli, and R. Fuchs. J. Am. Chem. Soc. **99**, 2949 (1977).
19. P. P. S. Saluja, L. A. Peacock, and R. Fuchs. J. Am. Chem. Soc. **101**, 1958 (1979).
20. R. Fuchs. J. Chem. Thermodyn. **11**, 959 (1979).

Assignment of anomeric configuration and identification of carbohydrate residues by ^{13}C nmr. 1. Galacto- and glucopyranosides and furanosides[1]

ROSS C. BEIER AND BRADFORD P. MUNDY
Department of Chemistry, Montana State University, Bozeman, MT 59717, U.S.A.
AND
GARY A. STROBEL
Department of Plant Pathology, Montana State University, Bozeman, MT 59717, U.S.A.
Received June 24, 1980

ROSS C. BEIER, BRADFORD P. MUNDY, and GARY A. STROBEL. Can. J. Chem. **58**, 2800 (1980).

A ^{13}C nmr analysis method is described for the identification of carbohydrate residues in galactosides and glucosides. This method reveals the capability of ^{13}C nmr to distinguish the difference in structural configuration of these carbohydrate residues. Not only can the anomeric configuration be assigned, the furanyl and pyranyl nature of the ring is concomitantly determined. This method is consistent for all reported ^{13}C nmr spectra of nonaromatic galactosides and glucosides.

ROSS C. BEIER, BRADFORD P. MUNDY et GARY A. STROBEL. Can. J. Chem. **58**, 2800 (1980).

On décrit une méthode d'analyse par rmn du ^{13}C permettant d'identifier les unités d'hydrate de carbone contenues dans des galactosides et dans des glucosides. Cette méthode met en évidence la capacité de la rmn du ^{13}C de distinguer les différences de configuration de ces unités d'hydrates de carbone. On peut déterminer à la fois la configuration du carbone anomère ainsi que la nature furannyle ou pyrannyle du cycle. Cette méthode est en accord avec tous les spectres de rmn du ^{13}C des galactosides et glucosides non aromatiques qui ont déjà été publiée dans la littérature.

[Traduit par le journal]

The structural characteristics of carbohydrates have been a general theme intertwined throughout our investigations of naturally occurring plant toxins. As a consequence of this program, we have been concerned with assignment of anomeric configuration, also the concern of many other research groups. Proton nmr spectroscopy has been used extensively, and this technique has been reviewed by Bundle and Lemieux (1) who suggest that it is not a totally reliable method. Carbon nmr spectroscopy has also been used as a tool for carbohydrate structural analysis (2–4). It has been suggested (1) that, like ^{1}H nmr, the assignment of anomeric configuration by ^{13}C requires more input data than just a single parameter, i.e., the resonance of the anomeric carbon.

Coupling constants have been used for evaluating the anomeric configuration of glycopyranosides. The two-bond $^{13}C—^{1}H$ coupling constant has an opposite sign for the α (+) than for the β (−) anomer (5). This sign difference would seem to be a most definitive way of assigning configuration; however, there are problems associated with the technique, and improvements are needed to afford a generally applicable method. Two- and three-bond $^{13}C—^{1}H$ coupling constants have now been obtained from natural abundance ^{13}C nmr spectra (6); however, the three-bond coupling constant is more difficult to obtain.

In our investigation of naturally occurring disaccharides containing galactose and glucose residues, assignment of the linkage position between these residues by ^{13}C nmr was required (7, 8). Before the linkage assignment could be made, the configuration of the individual residues had to be determined. An approach to this problem is described below, where chemical shift relationships enable the identification of eight isomeric glycosides.

Results and Discussion

We evaluated all the carbon nmr data published for galactosides and glucosides. When all six carbons are considered simultaneously, a useful correlation is observed, which can be likened to a fingerprint for each isomer.

All ^{13}C nmr values for the carbohydrate residues in α- and β-D-galactopyranosides are presented in Table 1; for α- and β-D-glucopyranosides, Table 2; for α- and β-D-galactofuranosides, Table 3; and for α- and β-D-glucofuranosides, Table 4. For each reported compound a value was tabulated for every carbon of the carbohydrate moiety (C-1 through C-6). The mean values and standard deviations, where applicable, are included in these tables. Since large downfield shifts (7–10 ppm) can be expected for carbons with *O*-methylation or *O*-glycosylation (7), the carbons (C-4 through C-6)

[1]This is paper no. 1089 of the Montana Agricultural Experiment Station.

0008-4042/80/242800-05$01.00/0
©1980 National Research Council of Canada/Conseil national de recherches du Canada

Can. J. Chem. Downloaded from www.nrcresearchpress.com by 210.87.254.40 on 09/05/12
For personal use only.

TABLE 1. Reported ^{13}C nmr values for the carbohydrate residues in α- and β-D-galactopyranosides

Compound (reference)	Chemical shift[a] C1	C2	C3	C4	C5	C6
α-D-Galactopyranosides						
Methyl α-D-galactopyranoside (9)	100.5	69.4	70.6	70.4	71.8	62.3
Terminal galactose in raffinose (10)	99.5	69.6[b]	70.6[c]	70.6	71.9	62.2
Terminal galactose in stachyose (10)	99.1	69.6[b]	70.7[c]	70.7	72.0	62.2
Internal galactose in stachyose (10)	99.4	69.8[b]	70.7[c]	69.8	70.7	67.5[d]
Mean	99.6	69.6	70.6	70.4	71.6	62.2
Standard deviation	0.6	0.2	0.1	0.4	0.6	0.1
β-D-Galactopyranosides						
Methyl β-D-galactopyranoside (9)	104.9	71.8	73.9	69.8	76.2	62.1
Terminal galactose linked (1→4) to rhamnose (11)	104.9	72.9	74.0	69.8	76.4	62.1
Terminal galactose linked (1→3) to rhamnose (11)	105.5	72.4	73.8	69.9	76.3	62.3
Terminal galactose in lactose (12)	104.0	72.2	73.9	69.8	76.3	62.1
Terminal galactose in lactose (13)	103.0	71.05	72.6	68.6	75.4	61.1
Terminal galactose in methyl β-lactose (12)	104.1	72.1	73.9	69.8	76.4	62.1
Terminal galactose in methyl β-lactose (13)	104.14	72.2	73.8	69.8	76.55	62.55
Mean	104.4	72.1	73.7	69.6	76.2	62.1
Standard deviation	0.8	0.6	0.5	0.5	0.4	0.5

[a]Relative to external TMS.
[b]These numbers have been interchanged with those designated *c* to conform with assignments by Gorin (9).
[d]The downfield shift of this resonance is due to substitution.

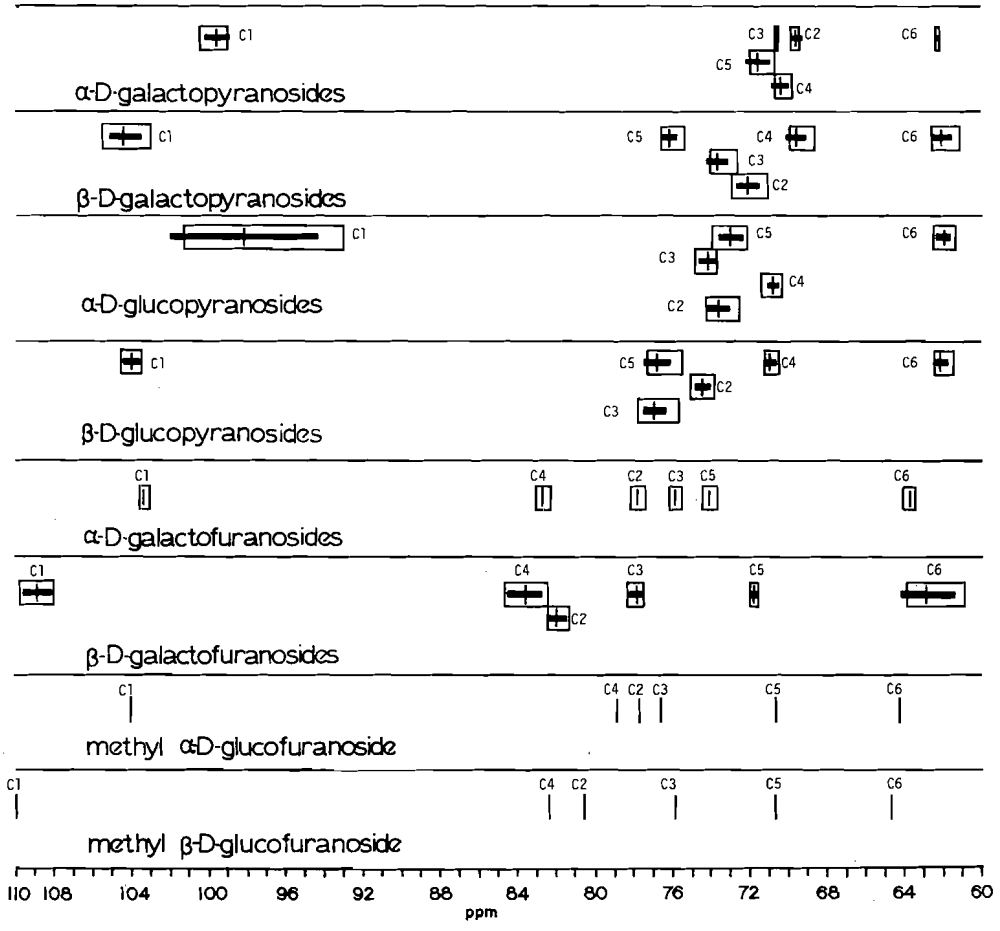


FIG. 1. Fingerprint diagrams of eight isomeric forms of the D-galactosides and D-glucosides.

Can. J. Chem. Downloaded from www.nrcresearchpress.com by 210.87.254.40 on 09/05/12
For personal use only.

TABLE 2. Reported ^{13}C nmr values for the carbohydrate residues in α- and β-D-glucopyranosides

Compound (reference)	Chemical shift[a] C1	C2	C3	C4	C5	C6
α-D-Glucopyranosides						
Methyl α-D-glucopyranoside (9)	100.3	72.5	74.2	70.6	72.7	61.7
Methyl α-D-glucopyranoside (14)	100.1	72.5	74.2	70.7	72.3	61.7
Methyl α-D-glucopyranoside (15)	100.5	73.1	74.8	71.4	72.8	62.3
Terminal glucose in α-maltose (12)	100.9	73.8	73.8	70.7	73.0	61.9
Terminal glucose in α-maltose (15)	101.0	74.3	74.6	71.0	73.4	62.5
Terminal glucose in β-maltose (15)	101.0	74.3	74.6	71.0	73.4	62.5
Terminal glucose in methyl β-maltoside (12)	100.8	74.1	74.1	70.6	72.9	61.9
Terminal glucose in methyl β-maltoside (15)	101.1	74.3	74.6	70.9	73.4	62.3
Glucose in sucrose (12)	93.1	73.4	73.9	70.5	72.2	61.6
Glucose in sucrose (10)	93.0	73.3	73.7	70.3	72.1	61.3
Ring B glucose in stachyose (10)	93.1	73.9	73.9	70.7	73.9	67.1[b]
Ring B glucose in raffinose (10)	93.0	73.9	73.9	70.6	73.9	67.2[b]
Mean	98.2	73.6	74.2	70.8	73.0	61.97
Standard deviation	3.8	0.7	0.4	0.3	0.6	0.4
β-D-Glucopyranosides						
Methyl β-D-glucopyranoside (9)	104.3	74.2	76.9	70.8	76.9	61.9
Methyl β-D-glucopyranoside (14)	104.2	74.1	76.9	70.7	76.8	61.9
Methyl β-D-glucopyranoside (15)	104.5	74.6	77.3	71.2	77.3	62.4
Terminal glucose in α-cellobiose (12)	103.5	74.3	76.9	70.7	76.9	61.8
Terminal glucose in α-cellobiose (15)	103.9	74.7	77.2	71.1	77.2	62.4
Terminal glucose in β-cellobiose (12)	103.5	74.3	76.6	70.7	76.9	61.8
Terminal glucose in β-cellobiose (15)	103.9	74.7	77.2	71.1	77.2	62.4
Terminal glucose in methyl β-cellobioside (12)	103.7	74.3	77.0	70.7	76.9	61.9
Terminal glucose in methyl β-cellobioside (15)	103.9	74.6	77.5	71.2	77.2	62.4
Internal glucose in methyl β-cellobioside (12)	104.2	74.0	75.7	80.1[b]	75.5	61.4
Internal glucose in methyl β-cellobioside (15)	104.5	74.2	76.4	80.3[b]	75.9	61.8
Internal glucose in methyl β-maltoside (12)	104.1	73.8	75.7	78.4[b]	77.3	61.7
Internal glucose in methyl β-maltoside (15)	104.4	74.6	77.8	78.7[b]	76.1	62.3
Internal glucose in methyl β-lactose (12)	104.1	73.9	75.8	79.8[b]	75.6	61.4
Terminal glucose in α-laminaribiose (15)	103.9	74.8	77.1	71.2	77.1	62.4
Terminal glucose in β-laminaribiose (15)	103.9	74.8	77.1	71.2	77.1	62.4
Terminal glucose in α-gentiobiose (15)	103.8	74.5	77.1	71.1	77.1	62.5
Terminal glucose in β-gentiobiose (15)	103.8	74.5	77.1	71.1	77.1	62.5
Terminal glucose in methyl β-gentiobiose (15)	104.0	74.0	77.2	71.0	77.2	62.5
Internal glucose in α-gentiotriose (15)	103.7	74.6	77.1	71.2	76.1	70.0[b]
Terminal glucose in α-gentiotriose (15)	103.7	74.6	77.1	71.0	77.1	62.4
Internal glucose in β-gentiotriose (15)	103.7	74.6	77.1	71.0	76.1	70.0[b]
Terminal glucose in β-gentiotriose (15)	103.7	74.6	77.1	71.0	77.1	62.4
Terminal glucose (1 → 3) to rhamnose (11)	105.0	74.7	76.9	70.8	76.9	61.9
Terminal glucose (1 → 4) to rhamnose (11)	104.4	75.1	77.2	70.8	77.0	61.9
Terminal glucose (1 → 2) to rhamnose (11)	104.6	74.5	77.0	70.5	76.7	61.7
Mean	104.0	74.4	76.9	71.0	76.8	62.1
Standard deviation	0.4	0.3	0.5	0.2	0.5	0.4

[a]Relative to external TMS.
[b]This downfield shift of this resonance is due to substitution.

involved in these substitutions were not evaluated.

In Fig. 1 are presented the data of Table 1–4. A rectangular box is drawn enclosing the maximum and minimum values for each carbon atom. A vertical line within that box shows the position of the mean values, and a horizontal bar delineates the standard deviation. It is clear from Fig. 1 that each isomer has a definite set of intervals or fingerprint, each one being different from the other. Therefore, by using these intervals one can, in principle, not only determine the anomeric configuration, but also predict the nature of the carbohydrate moiety.

We have synthesized a number of α-D-galactopyranosides, and their ^{13}C nmr spectra are listed in Table 5. A plot of these resonance values is compared to the α- and β-D-galacto- and glucopyranoside intervals, shown in Fig. 2. It is clear that these α-D-galactopyranosides correlate only with

Can. J. Chem. Downloaded from www.nrcresearchpress.com by 210.87.254.40 on 09/05/12
For personal use only.

TABLE 3. Reported ^{13}C nmr values for the carbohydrate residues in α- and β-D-galactofuranosides

Compound (reference)	Chemical shift[a] C1	C2	C3	C4	C5	C6
α-Anomers						
Methyl α-D-galactofuranoside (16)	103.1	77.4	75.5	82.3	73.7	63.4
Methyl α-D-galactofuranoside (17)	103.8	78.2	76.2	83.1	74.5	64.1
Mean	103.4	77.8	75.8	82.7	74.1	63.7
β-Anomers						
Methyl β-D-galactofuranoside (16)	109.2	81.9	77.8	84.0	72.0	63.9
Methyl β-D-galactofuranoside (17)	109.9	81.3	78.4	84.7	71.7	63.6
Galactofuranotetraose, terminal residue (7)	108.2	82.4	77.5	83.7	71.6	63.8
Galactofuranotetraose, internal residue (7)	108.0	82.4	77.5	82.4	76.6[b]	62.1
Methyl 5-methyl-β-D-galactofuranoside (7)	109.0	81.8	77.8	83.4	81.8[b]	60.9
Mean	108.9	82.0	77.8	83.6	71.8	62.9
Standard deviation	0.8	0.5	0.4	0.8	0.2	1.3

[a]Relative to external TMS.
[b]The downfield shift of this resonance is due to substitution.

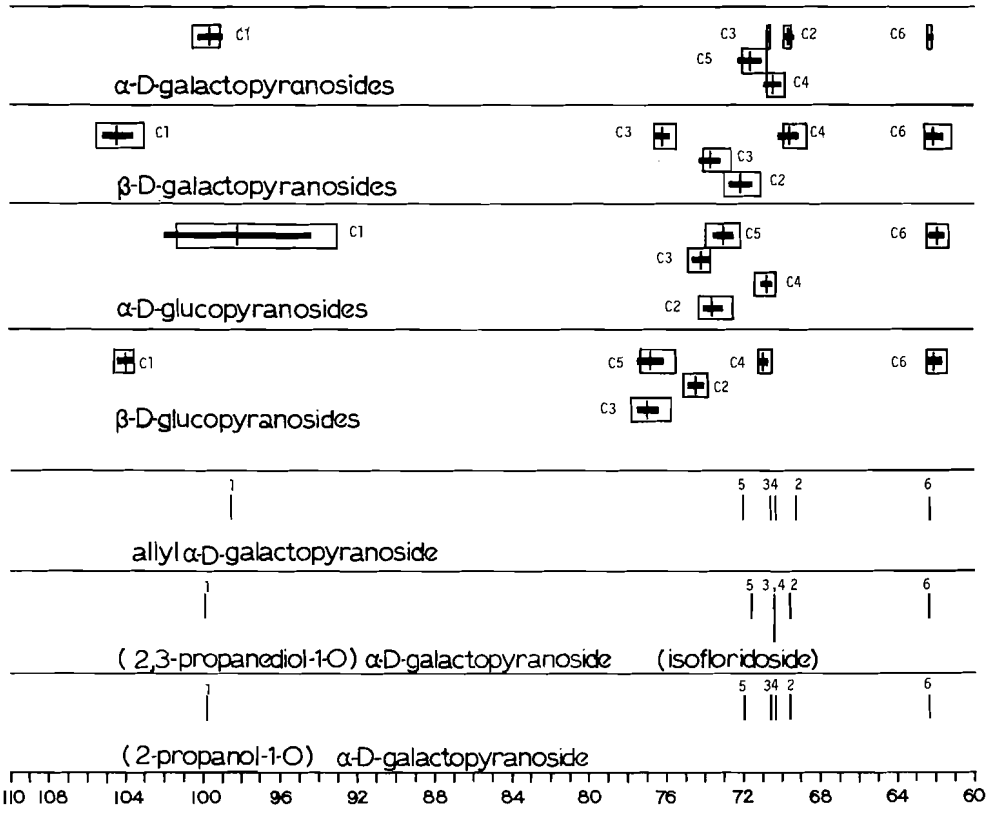


FIG. 2. Comparison of some α-D-galactopyranosides to the fingerprint diagrams of the galactosides and glucopyranosides.

the intervals for α-D-galactopyranosides. We were also able to predict a terminal β-D-galactofuranosyl residue of a plant toxin, which was also shown to be present by methylation – mass spectroscopy studies (paper in preparation).

In conclusion, the ^{13}C nmr method described here appears to be simple and useful. The resonance values obtained in the totally decoupled experiment are sufficient to determine the difference between galacto- and glucosides, including the na-

Can. J. Chem. Downloaded from www.nrcresearchpress.com by 210.87.254.40 on 09/05/12
For personal use only.

TABLE 4. Reported ^{13}C nmr values for the carbohydrate residues in α- and β-D-glucofuranosides

Compound (reference)	Chemical shift[a] C1	C2	C3	C4	C5	C6
α-Anomers						
Methyl α-D-glucofuranoside (17)	104.0	77.7	76.6	78.8	70.7	64.2
β-Anomers						
Methyl β-D-glucofuranoside (17)	110.0	80.6	75.8	82.3	70.7	64.7

[a]Relative to external TMS.

TABLE 5. ^{13}C nmr values for some α-D-galactopyranosides

Compound (reference)	Chemical shift[a] C1	C2	C3	C4	C5	C6
Allyl α-D-galactopyranoside (18)	98.5	69.2	70.6	70.3	72.0	62.3
(2,3-Propanediol-1-*O*) α-D-galactopyranoside (18)	99.9	69.6	70.4[b]	70.4[b]	71.6	62.4
(2-Propanol-1-*O*) α-D-galactopyranoside (18)	99.8[c] 99.2	69.6	70.6	70.4	72.0	62.3

[a]Relative to external TMS.
[b]These signals were not resolved.
[c]These values resulted from diastereomers, at carbon-2 of the aglycone.

ture of the carbohydrate moiety, furanyl or pyranyl, and their anomeric configuration, α or β.

This method is useful to both natural product and carbohydrate chemists. *Note*: A plastic overlay of these intervals can be made to match graph paper (20 × 20 to the inch) where resonances of unknowns may be plotted.

Acknowledgements

This work was supported in part by a Herman Frasch Foundation Grant to G. A. Strobel and by NSF grant PCM-78-22517.

1. D. R. BUNDLE and R. U. LEMIEUX. Methods in carbohydrate chemistry. Vol. VII. Academic Press, New York, NY. 1976. pp. 79–86.
2. R. U. LEMIEUX and S. KOTO. Tetrahedron, **30**, 1933 (1974).
3. A. S. PERLIN. Organic chemistry. Series 2. Buterworths, London. 1975–1976. p. 1.
4. H. A. NUNEZ, T. E. WALKER, R. FUENTES, J. O'CONNOR, A. SERIANNI, and R. BARKER. J. Supramol. Struct. **6**, 535 (1977).
5. J. A. SCHWARCZ, N. CYR, and A. S. PERLIN. Can. J. Chem. **53**, 1872 (1975).
6. K. BOCK and C. PEDERSEN. Acta Chem. Scand. Ser. B, **31**, 354 (1977).
7. P. A. J. GORIN and M. MAZUREK. Carbohydr. Res. **48**, 171 (1976).
8. A. M. NGUYEN PHUOC DU, F. WINTERNITZ, R. WYLDE, and F. PRATVIEL-SOSA. Carbohydr. Res. **67**, 105 (1978).
9. P. A. J. GORIN. Can. J. Chem. **52**, 458 (1974).
10. A. ALLERHAND and D. DODDRELL. J. Am. Chem. Soc. **93**, 2777 (1971).
11. P. COLSON and R. R. KING. Carbohydr. Res. **47**, 1 (1976).
12. D. E. DORMAN and J. D. ROBERTS. J. Am. Chem. Soc. **93**, 4463 (1971).
13. W. VOELTER, U. BILIK, and E. BREITMAIER. Collect. Czech. Chem. Commun. **38**, 2054 (1973).
14. J. B. STOTHERS. Carbon-13 nmr spectroscopy. Academic Press, New York, NY. 1972.
15. T. USUI, N. YAMAOKA, K. MATSUDA, K. TUZIMURA, H. SUGIYAMA, and S. SETO. J. Chem. Soc. Perkin Trans. I, 2425 (1973).
16. P. A. J. GORIN and M. MAZUREK. Can. J. Chem. **53**, 1212 (1975).
17. R. G. S. RITCHIE, N. CYR, B. KORSCH, H. J. KOCH, and A. S. PERLIN. Can. J. Chem. **53**, 1424 (1975).
18. R. C. BEIER. Ph. D. Thesis. Montana State University, Bozeman, MT. 1980.

Can. J. Chem. Downloaded from www.nrcresearchpress.com by 210.87.254.40 on 09/05/12
For personal use only.

Crystal structure of camphor-1,4-homoenol *p*-bromobenzoate

RICHARD A. PAUPTIT AND JAMES TROTTER

Department of Chemistry, University of British Columbia, Vancouver, B.C., Canada V6T 1Y6

Received July 2, 1980

RICHARD A. PAUPTIT and JAMES TROTTER. Can. J. Chem. **58**, 2805 (1980).

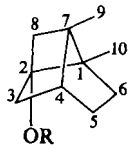
Crystals of the title compound, $C_{17}H_{19}BrO_2$, are orthorhombic, $P2_12_12_1$, $a = 6.875(1)$, $b = 8.522(2)$, $c = 26.658(6)$ Å, $Z = 4$. The structure was determined by Patterson and Fourier methods, and refined to $R = 0.045$ for 697 reflections with $I \geq 3\sigma(I)$; the absolute configuration was established. The four-membered ring is tightly folded, and bond angles in the vicinity of this ring indicate considerable strain.

RICHARD A. PAUPTIT et JAMES TROTTER. Can. J. Chem. **58**, 2805 (1980).

Les cristaux du composé du titre, $C_{17}H_{19}BrO_2$, sont orthorhombiques, $P2_12_12_1$, $a = 6,875(1)$, $b = 8,522(2)$, $c = 26,658(6)$ Å, $Z = 4$. La structure a été determinée par les méthodes de Patterson et de Fourier, et a été affinée jusqu'à $R = 0,045$ pour 697 réflexions avec $I \geq 3\sigma(I)$; la configuration absolue a été établie. Le cycle de quatres membres est bien plié, et les angles de liaison à proximité de ce cycle indiquent une tension considérable.

Introduction

In investigations of homoenolization of bicyclic ketones (1), intermediacy of a highly strained 1,4-homoenol was proposed to account for hydrogen exchange at the C(8) position of camphor. Support for this mechanism was provided by synthesis of material with properties which suggest the 1,4-homoenol structure (**1**, R = H). The present X-ray study was undertaken to verify the structure (**1**, R = $OCOC_6H_4Br$, camphor-1,4-homoenol *p*-bromobenzoate, 7-*p*-bromobenzoyloxy-1,2-dimethyltricyclo[3,3,0,$0^{2,7}$]octane).



1

Experimental

Crystal data are as follows:

$C_{17}H_{19}BrO_2$ fw = 335.2
Orthorhombic, $P2_12_12_1$, $a = 6.875(1)$, $b = 8.522(2)$, $c = 26.658(6)$ Å, $V = 1562$ Å^3, $Z = 4$, $\rho_c = 1.43$ g cm^{-3}, MoKα, $\lambda = 0.71073$ Å, $\mu = 25.5$ cm^{-1}.

Intensity data were measured on an Enraf-Nonius CAD-4 Diffractometer with monochromatic MoKα radiation and an ω–(4/3)θ scan, with an ω scan angle of $(0.80 + 0.35 \tan\theta)°$. The horizontal aperture width was $(2.5 + \tan\theta)$ mm and the vertical aperture width was 4 mm. Three intensity control reflections were measured every 1 h and used to scale the data, although variations were small. Three other reflections were used as orientation controls and were measured every 100 reflections. Reorientation occurred if the difference between the observed and calculated scattering vectors was greater than 0.050°.

700 out of 1645 (42.6%) reflections in the range $0 < \theta \leq 25°$ had $I/\sigma(I) \geq 3.0$ (where $\sigma^2(I) = S + B + (0.04S)^2$ and S and B are the scan and background counts), and were classified as observed. In the refinement the range $0 < \theta \leq 23°$ was used where 697 out of 1300 (53.6%) reflections were observed. Unobserved reflections were not included in the refinement.

The crystal shape was approximated by 11 faces for an absorption correction. In the correction 184 sampling points with an average spacing of 5.0×10^{-3} cm were used for the crystal (volume = 0.0205 mm^3). Transmission factors ranged from 0.450 to 0.633. Lorentz and polarization corrections were also applied.

A Patterson map revealed the position of the Br atom. Three successive difference maps interspersed with least-squares refinement cycles revealed all non-hydrogen atoms. After three more least-squares cycles with all atoms anisotropic R had dropped to 0.062. All the hydrogens could be located on a difference map but best results were obtained when the hydrogens were kept fixed in calculated positions with fixed isotropic temperature factors.

To determine the absolute configuration, the two enantiomers were each refined in three equivalent least-squares cycles, with scattering factors of ref. 2 for non-hydrogen atoms, those of ref. 3 for hydrogen atoms, with anomalous dispersion corrections (4) applied to Br, O, and C, and with a Hughes weighting scheme: $\sqrt{w} = 1.0$ for $|F_o| \leq 23.5$ and $\sqrt{w} = 23.5/|F_o|$ for $|F_o| > 23.5$. For the enantiomer originally chosen, the three cycles refined to $R = 0.056$ and $R_w = 0.070$; for the enantiomer obtained by changing signs of x, y, z, the three cycles refined to $R = 0.046$ and $R_w = 0.056$. The latter is therefore the correct enantiomorph and was refined until convergence, with the weighting scheme modified such that $\sqrt{w} = 1.0$ for $11.5 \leq |F_o| < 17.8$, $\sqrt{w} = |F_o| / 11.5$ for $|F_o| < 11.5$, and $\sqrt{w} = 17.8 / |F_o|$ for $|F_o| > 17.8$. In the final refinement the mean and maximum shifts were 0.001σ and 0.005σ, and R and R_w had dropped to 0.045 and 0.054, respectively (0.123 and 0.054 for all reflections).[1] The atomic positional parameters are given in Table 1.[1]

Discussion

The structure and atomic labelling scheme are shown in Fig. 1. All bond distances (Table 2) agree with accepted values. The *p*-bromobenzoate group is not far from planar (there is an angle of 5° be-

[1]The structure factor table, non-hydrogen thermal parameters, hydrogen positional parameters, and packing diagram are available, at a nominal charge, from the Depository of Unpublished Data, CISTI, National Research Council of Canada, Ottawa, Ont., Canada K1A 0S2.

0008-4042/80/242805-03$01.00/0

©1980 National Research Council of Canada/Conseil national de recherches du Canada

Can. J. Chem. Downloaded from www.nrcresearchpress.com by 210.87.254.40 on 09/05/12
For personal use only.

TABLE 1. Positional parameters of the non-hydrogen atoms ($\times 10^4$)*

Atom	x	y	z	Atom	x	y	z
Br	−3868(3)	−6066(2)	−94.4(5)	O(1)	893(12)	−268(9)	−1329(3)
O(2)	3485(13)	−1335(11)	−954(4)	C(1)	931(17)	2325(12)	−1793(4)
C(2)	2068(17)	907(15)	−1558(4)	C(3)	3478(20)	436(13)	−1966(4)
C(4)	3889(19)	2120(16)	−2165(4)	C(5)	2471(25)	2396(16)	−2602(5)
C(6)	509(20)	2183(17)	−2346(4)	C(7)	2988(20)	3074(14)	−1739(4)
C(8)	3288(17)	2100(16)	−1259(4)	C(9)	3309(26)	4843(17)	−1747(6)
C(10)	−706(20)	2914(17)	−1480(6)	C(11)	1762(19)	−1316(16)	−1019(5)
C(12)	339(17)	−2411(13)	−794(4)	C(13)	−1595(17)	−2434(14)	−923(4)
C(14)	−2878(21)	−3488(15)	−719(5)	C(15)	−2136(21)	−4566(13)	−373(5)
C(16)	−228(22)	−4572(14)	−236(4)	C(17)	1055(21)	−3482(13)	−445(4)

*Estimated standard deviations are given in parentheses and correspond to the least significant digits.

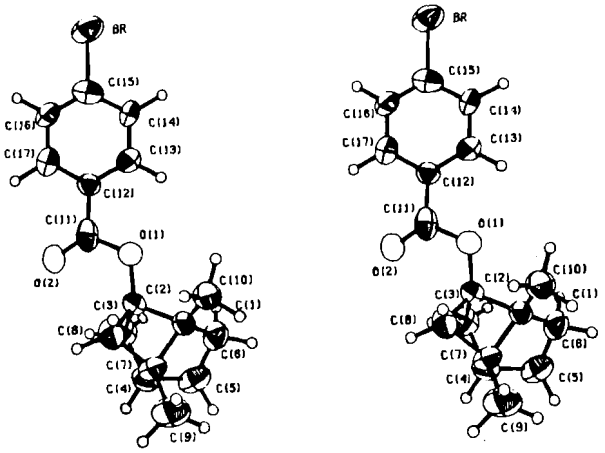


FIG. 1. A stereoview of the molecule.

tween the bromophenyl and carboxyl planes), with normal bond angles (Table 2). The C—C—C angles in the four-membered ring are 80, 88, 81, and 89(1)°, i.e. two opposite angles are significantly smaller than the free cyclobutane C—C—C angle, 89.3° (5). These two angles C(2)—C(1)—C(7) and C(2)—C(8)—C(7) also form envelopes of two five-membered rings whose conformations are adapted to allow for the four-membered ring. The C—C—C angles in the five-membered rings are lower than normal (97, 99, 101, 81, 106 and 97, 99, 104, 95, 80°) and the dihedral angles between the envelopes and the remainder of the rings are 117 and 110° (Fig. 2), i.e. quite small.[2] The envelope of the C(1)C(2)C(3)C(4)C(7) ring has shifted from C(7) in the free camphor to C(1) in the title compound.

The four-membered ring is fairly tightly folded; the dihedral angles are 133 and 129° (Fig. 2) which are significantly smaller than the 162.6° for free cyclobutane (5). Further away from the four-membered ring the deviations from ideal bond angles are less pronounced.

The crystal is held together by van der Waals forces.[1]

[2]Plane C(2)—C(3)—C(4)—C(7) has equation $-0.7953X + 0.0525Y - 0.6039Z = 1.3643$, with atom displacements C(2) 0.05, C(3) −0.08, C(4) 0.09, C(7) −0.06, C(1) 1.12, C(8) −1.04(1) Å.

TABLE 2. Bond distances (Å, σ = 0.02 Å for C—C, 0.01 Å for Br—C and O—C) and angles (deg, σ = 1°) for non-hydrogen atoms

Bond	Distance	Bond	Distance
C(1)—C(2)	1.57	C(11)—C(12)	1.48
C(1)—C(6)	1.51	C(12)—C(13)	1.37
C(1)—C(7)	1.56	C(12)—C(17)	1.39
C(1)—C(10)	1.49	C(13)—C(14)	1.37
C(2)—C(3)	1.51	C(14)—C(15)	1.40
C(2)—C(8)	1.54	C(15)—C(16)	1.36
C(3)—C(4)	1.56	C(16)—C(17)	1.40
C(4)—C(5)	1.53		
C(4)—C(7)	1.53	Br—C(15)	1.90
C(5)—C(6)	1.52	O(1)—C(2)	1.42
C(7)—C(8)	1.54	O(1)—C(11)	1.35
C(7)—C(9)	1.52	O(2)—C(11)	1.20

Bonds	Angle	Bonds	Angle
C(2)—O(1)—C(11)	118	C(1)—C(7)—C(4)	95
C(2)—C(1)—C(6)	115	C(1)—C(7)—C(8)	89*
C(2)—C(1)—C(7)	80*	C(1)—C(7)—C(9)	122
C(2)—C(1)—C(10)	114	C(4)—C(7)—C(8)	106
C(6)—C(1)—C(10)	115	C(4)—C(7)—C(9)	117
C(6)—C(1)—C(7)	107	C(8)—C(7)—C(9)	122
C(7)—C(1)—C(10)	120	C(2)—C(8)—C(7)	81*
O(1)—C(2)—C(1)	115	O(1)—C(11)—O(2)	122
O(1)—C(2)—C(3)	119	O(1)—C(11)—C(12)	112
O(1)—C(2)—C(8)	123	O(2)—C(11)—C(12)	126
C(1)—C(2)—C(3)	104	C(11)—C(12)—C(13)	123
C(1)—C(2)—C(8)	88*	C(11)—C(12)—C(17)	117
C(3)—C(2)—C(8)	101	C(13)—C(12)—C(17)	120
C(2)—C(3)—C(4)	97	C(12)—C(13)—C(14)	122
C(3)—C(4)—C(5)	107	C(13)—C(14)—C(15)	117
C(3)—C(4)—C(7)	99	C(14)—C(15)—C(16)	122
C(5)—C(4)—C(7)	103	C(14)—C(15)—Br	118
C(4)—C(5)—C(6)	102	C(16)—C(15)—Br	120
C(1)—C(6)—C(5)	105	C(15)—C(16)—C(17)	120
		C(12)—C(17)—C(16)	119

*Cyclobutane ring angles.

Can. J. Chem. Downloaded from www.nrcresearchpress.com by 210.87.254.40 on 09/05/12
For personal use only.

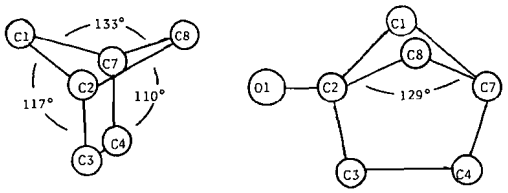


FIG. 2. Dihedral angles involving the cyclobutane ring.

Acknowledgements

We thank the Natural Sciences and Engineering Research Council of Canada and the Natural, Applied and Health Sciences Committee, University of British Columbia for financial support, the University of British Columbia Computing Centre for assistance, and Drs. W. M. Dadson and T. Money for crystals and discussion.

1. W. M. DADSON and T. MONEY. Can. J. Chem. In press.
2. D. T. CROMER and J. B. MANN. Acta Crystallogr. **22**, 457 (1967).
3. R. F. STEWART, E. R. DAVIDSON, and W. T. SIMPSON. J. Chem. Phys. **42**, 3175 (1965).
4. D. T. CROMER and D. LIBERMAN. J. Chem. Phys. **53**, 1891 (1970).
5. C.-H. CHANG, R. F. PORTER, and S. H. BAUER. J. Molec. Struct. **7**, 89 (1971).

Can. J. Chem. Downloaded from www.nrcresearchpress.com by 210.87.254.40 on 09/05/12
For personal use only.

Absolute rate constants for hydrocarbon autoxidation. 29. Rate constants for abstraction of primary aliphatic hydrogens from 2,2-dimethylbutane by the *tert*-butylperoxy radical[1]

J. A. HOWARD AND J. H. B. CHENIER

Division of Chemistry, National Research Council of Canada, Ottawa, Ont., Canada K1A 0R9

Received April 16, 1980

J. A. HOWARD and J. H. B. CHENIER. Can. J. Chem. **58**, 2808 (1980).

Rate constants for abstraction of primary and secondary hydrogens from 2,2-dimethylbutane by the *tert*-butylperoxy radical at temperatures from 323 to 353 K have been determined from autoxidations and co-autoxidations in the presence of *tert*-butyl hydroperoxide. At 333 K the rate constant for abstraction of a secondary hydrogen is $\sim 1.5 \times 10^{-3}$ M^{-1} s^{-1} and the rate constants for abstraction of a primary hydrogen from the *tert*-butyl and methyl groups of 2,2-dimethylbutane are $\sim 4 \times 10^{-5}$ and $\sim 6 \times 10^{-5}$ M^{-1} s^{-1} respectively.

J. A. HOWARD et J. H. B. CHENIER. Can. J. Chem. **58**, 2808 (1980).

On a déterminé, à partir des autoxydation et co-autoxydations en présence de l'hydroperoxyde de *tert*-butyle, la vitesse d'élimination des hydrogènes primaire et secondaire du diméthyl-2,2 butane par le radical *tert*-butylpéroxy à des températures allant de 323 à 353 K. A 333 K, la constante de vitesse d'élimination d'un hydrogène secondaire est d'environ $1,5 \times 10^{-3}$ M^{-1} s^{-1} et les constantes de vitesse de l'élimination d'un hydrogène primaire des groupes *tert*-butyle et méthyle du diméthyl-2,2 butane sont respectivement d'environ 5×10^{-5} et 6×10^{-5} M^{-1} s^{-1}.

[Traduit par le journal]

Introduction

We have recently reported absolute rate constants for abstraction of secondary and tertiary aliphatic hydrogens by the *tert*-butylperoxy radical in solution at temperatures from 303 to 353 K (1, 2). These rate constants were obtained from the concentrations of propagation products produced by competitive co-oxidations in the presence of *tert*-butyl hydroperoxide under conditions where *t*-$BuO_2^{\bullet}$ was the principal radical involved in rate controlling propagation and termination reactions.

We have since discovered that autoxidation of 2,2-dimethylbutane under these conditions gives significant yields of oxidation products derived from abstraction of the primary hydrogens. Consequently we are able to report here the first reasonably accurate rate constants for abstraction of a primary aliphatic hydrogen by an alkylperoxy radical.

Experimental

Materials

Cyclohexane and 2,2-dimethylbutane (Phillips Research Grade) were used without further purification. *tert*-Butyl hydroperoxide (Aldrich Chemical Co., Inc., 70%) was purified by the method of Hiatt, Clipsham, and Visser (3) and triphenylphosphine (Aldrich) was purified by the method of Hiatt, Smythe, and McColeman (4). 2,2,3,3-Tetraphenylbutane was obtained from L. R. Mahoney (Ford Motor Co., Dearborn, MI). Cyclohexyl hydroperoxide was a gift from V. Malatesta (N.R.C.) and had been prepared by the method of Caglioti, Gasparrini, and Palmieri (5). Di-*tert*-butyl peroxide, 3,3-dimethylbutan-2-one (Matheson, Coleman and Bell), 3,3-dimethylbutan-2-ol (J. T. Baker), 3,3-dimethylbutan-1-ol (Aldrich), 2,2-dimethylbutan-1-ol (Chem. Samples Co.), cyclohexanone (Aldrich), and cyclohexanol (Fischer) were commercially available.

Procedure

Co-autoxidations were carried out in the presence of *tert*-butyl hydroperoxide (1 *M*). Reactions conducted below 323 K were initiated by thermolysis of 2,2,3,3-tetraphenylbutane while at and above 323 K this initiator was not needed because homolysis of *t*-BuOOH provided adequate initiation. Oxidized samples were reduced with enough Ph_3P to convert all hydroperoxides to the corresponding alcohol. They were then pumped into a trap maintained at the temperature of liquid nitrogen and analyzed by gas chromatography (Varian 2800 chromatograph equipped with 12 ft × 1/8 in. columns packed with FFAP or FC-431 stationary phases). It is well known that hydroperoxides are quantitatively reduced to alcohol. Consequently the concentration of an alcohol found by glc was equal to the concentration of the corresponding hydroperoxide formed in propagation.

Oxidized samples were also reduced with lithium aluminum hydride (6) and analyzed by glc.

Results and Discussion

2,2-Dimethylbutane

We can assume from our previous work on autoxidation of hydrocarbons in the presence of *tert*-butyl hydroperoxide (1, 2) that autoxidation of 2,2-dimethylbutane in the presence of *t*-BuOOH can be described by the elementary reactions shown in Scheme 1.

The yields of the major autoxidation products at temperatures from 323 to 353 K (after reduction with Ph_3P) are given in Table 1 and it is apparent that di-*tert*-butyl peroxide (**1**) and 3,3-dimethylbutan-2-one (**2**) were the major products while 3,3-dimethyl-2-hydroperoxybutane (**3**), 2,2-dimethyl-1-hydroperoxybutane (**4**), and 3,3-di-

[1]NRCC No. 18676.

0008-4042/80/242808-05$01.00/0

©1980 National Research Council of Canada/Conseil national de recherches du Canada

Can. J. Chem. Downloaded from www.nrcresearchpress.com by 210.87.254.105 on 09/05/12
For personal use only.

Can. J. Chem. Downloaded from www.nrcresearchpress.com by 210.87.254.105 on 09/05/12
For personal use only.

Initiation

[1] $2t\text{-BuOOH} \longrightarrow t\text{-BuO}_2^{\cdot} + t\text{-BuOH} + H_2O$

Propagation

[2] $t\text{-BuO}_2^{\cdot} + (CH_3)_3CCH_2CH_3 \xrightarrow{k_{2a}} (CH_3)_3CC(CH_3)H^{\cdot} + t\text{-BuOOH}$

$\xrightarrow{k_{2b}} CH_3CH_2C(CH_3)_2CH_2^{\cdot} + t\text{-BuOOH}$

$\xrightarrow{k_{2c}} (CH_3)_3CCH_2CH_2^{\cdot} + t\text{-BuOOH}$

$(CH_3)_3CC(CH_3)H^{\cdot} \xrightarrow{O_2} (CH_3)_3CC(CH_3)HO_2^{\cdot}$

[3] $CH_3CH_2C(CH_3)_2CH_2^{\cdot} \xrightarrow{O_2} CH_3CH_2C(CH_3)_2CH_2O_2^{\cdot}$

$(CH_3)_3CCH_2CH_2^{\cdot} \xrightarrow{O_2} (CH_3)_3CCH_2CH_2O_2^{\cdot}$

Chain transfer

$(CH_3)_3CC(CH_3)HO_2^{\cdot} \xrightarrow{t\text{-BuOOH}} (CH_3)_3CC(CH_3)HOOH + t\text{-BuO}_2^{\cdot}$

3

[4] $CH_3CH_2C(CH_3)_2CH_2O_2^{\cdot} \xrightarrow{t\text{-BuOOH}} CH_3CH_2C(CH_3)_2CH_2OOH + t\text{-BuO}_2^{\cdot}$

4

$(CH_3)_3CCH_2CH_2O_2^{\cdot} \xrightarrow{t\text{-BuOOH}} (CH_3)_3CCH_2CH_2OOH + t\text{-BuO}_2^{\cdot}$

5

[5] $2t\text{-BuO}_2^{\cdot} \longrightarrow 2t\text{-BuO}^{\cdot} + O_2$

[6] $t\text{-BuO}^{\cdot} + t\text{-BuOOH} \longrightarrow t\text{-BuOH} + t\text{-BuO}_2^{\cdot}$

Termination

[7] $2t\text{-BuO}_2^{\cdot} \xrightarrow{2k_t} t\text{-BuOOBu-}t + O_2$

1

SCHEME 1. k_{2a}, k_{2b}, and k_{2c} are overall rate constants for reaction of $t\text{-BuO}_2^{\cdot}$ with 2,2-dimethylbutane and $2k_t$ is the termination rate constant for $t\text{-BuO}_2^{\cdot}$.

methyl-1-hydroperoxybutane (**5**) were formed in significant but lower yields.

Kinetic chain lengths for this autoxidation must have been quite short because concentrations of the termination product **1** were greater than the combined concentrations of the propagation products **3** + **4** + **5**. They were, however, almost certainly greater than 2[**1**]/[**3**] + [**4**] + [**5**] because the substantial yields of 2,2-dimethylbutan-2-one were probably formed by induced decomposition of **3** (reaction [8]) rather than in the cross termination reaction [9]. This is because the termination rate constant was equal, within experimental error, to the rate constant for reaction [7] ($2k_t$ at 303 K = $1.2 \times 10^3\ M^{-1}\ s^{-1}$ (7)).

[8] $t\text{-BuO}_2^{\cdot} + (CH_3)_3CC(CH_3)HOOH \rightarrow t\text{-BuOOH} + (CH_3)_3CC(O)CH_3 + OH^{\cdot}$

[9] $t\text{-BuO}_2^{\cdot} + (CH_3)_3CC(CH_3)HO_2^{\cdot} \rightarrow t\text{-BuOH} + (CH_3)_3CC(O)CH_3 + OH^{\cdot}$

2

We can, therefore, make the reasonable assumption that the total concentration of **3** produced was equal to [**3**] + [**2**].

It has been suggested by a referee that the yields of **4** and **5** may also have been influenced by the following reactions

$t\text{-BuO}_2^{\cdot} + CH_3CH_2C(CH_3)_2CH_2OOH \rightarrow t\text{-BuOOH} + CH_3CH_2C(CH_3)_2CHO + OH^{\cdot}$

$t\text{-BuO}_2^{\cdot} + (CH_3)_3CCH_2CH_2OOH \rightarrow t\text{-BuOOH} + (CH_3)_3CCH_2CHO + OH^{\cdot}$

2,2-Dimethylbutan-1-al, 3,3-dimethylbutan-1-al, and the corresponding acids were, however, not formed in significant yields after reduction with Ph_3P. Furthermore, the ratios of [**2**] + [**3**]/[**4**] and [**2**] + [**3**]/[**5**] after reduction with Ph_3P were equal, within experimental error to the ratios [**3**]/[**4**] and [**3**]/[**5**] after reduction with $LiAlH_4$ — confirming that a significant fraction of **4** and **5** had not been oxidized to aldehyde. Thus the aldehydes would have been reduced by $LiAlH_4$ and the ratios obtained from the two reducing agents would not have been equal.

Can. J. Chem. Downloaded from www.nrcresearchpress.com by 210.87.254.105 on 09/05/12
For personal use only.

TABLE 1. Product yields from autoxidation of 2,2-dimethylbutane in the presence of *tert*-butyl hydroperoxide (1 *M*)

Temperature/K	Reaction time/day	Product/m*M*				
		1	**2**	**3**	**4**	**5**
323	60	58	33	3.0	1.45	1.05
333	17	33	32.5	1.15	0.53	0.83
343	10	31	37	2	0.65	0.7
353	14	29	44	1.2	0.72	0.34

TABLE 2. Product yields and overall relative rate constants from co-oxidations of 2,2-dimethylbutane (R_1H) and cyclohexane (R_2H) in the presence of *tert*-butyl hydroperoxide (1 *M*)

Temperature/K	$[R_1H]_0/M$	$[R_2H]_0/M$	Yield/m*M*							k_{2a}/k_{10}	k_{2b}/k_{10}	k_{2c}/k_{10}
			1	**2**	**3**	**4**	**5**	**6**	**7**			
303	2.26	5.5	1.5	—	2.5	—	—	52	1.1	0.11	—	—
303	4.52	2.75	1.9	—	2.7	—	—	13.8	—	0.12	—	—
323	4.52	2.75	35	4.9	4.3	0.79	0.6	53.7	33.2	0.064	0.0055	0.004
323	5.65	1.37	13	7.5	5.4	0.54	0.31	26	14	0.08	0.0033	0.002
333	4.52	2.75	0.1	5.2	4.7	1.34	0.63	51.8	34.2	0.07	0.009	0.004
333	5.65	1.37	20.3	8.7	6.2	1.2	0.73	35	24.4	0.06	0.005	0.003
343	4.52	2.75	7.6	3.6	7	0.66	0.64	64	27.5	0.07	0.004	0.004
343	5.65	1.37	12.2	6.6	8.2	0.9	0.7	40.3	19.1	0.06	0.004	0.003
353	4.52	2.75	2.9	1.5	6.8	0.75	0.33	54.3	13.7	0.074	0.007	0.003
353	5.65	1.37	7.2	4.5	8.75	1.2	0.87	36.5	13.1	0.065	0.006	0.004

A comparison of [**3**] + [**2**] with [**4**] indicates that a secondary C—H in 2,2-dimethylbutane is about 300 times more reactive than a primary hydrogen of the *tert*-butyl group in this alkane. More interestingly, it would appear, from the relative concentrations of **4** and **5**, that a primary hydrogen of the *tert*-butyl group is somewhat less reactive than a primary hydrogen of the methyl group, i.e. $3k_{2c} > k_{2b}$.

2,2-Dimethylbutane–Cyclohexane

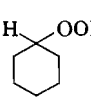
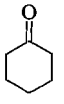
In order to estimate absolute rate constants for abstraction of primary aliphatic hydrogens from 2,2-dimethylbutane we co-autoxidized this substrate with cyclohexane in the presence of *tert*-butyl hydroperoxide because rate constants for reaction of cyclohexane with *t*-$BuO_2^{\cdot}$ from 303 to 353 K are known (2). This co-autoxidation produced cyclohexyl hydroperoxide (**6**) and cyclohexanone (**7**) as well as **1**, **2**, **3**, **4**, and **5** in the yields given in Table 2.

Cyclohexyl hydroperoxide must have been formed by the propagation reaction [10]

[10] *t*-$BuO_2^{\cdot}$ +  $\xrightarrow{k_{10}}$ *t*-BuOOH + 

and total product yields indicated that kinetic chain lengths were of the order of 2–15, i.e. they were substantially longer than chain lengths for autoxidation of 2,2-dimethylbutane in the presence of *t*-BuOOH.

Cyclohexanone was almost certainly produced by autoxidation of cyclohexyl hydroperoxide, reaction [11],

[11] *t*-$BuO_2^{\cdot}$ +  $\longrightarrow$ *t*-BuOOH +  + $HO^{\cdot}$

7

because co-autoxidation of 2,2-dimethylbutane and **6** (using concentrations of **6** similar to those produced by co-autoxidation of 2,2-dimethylbutane and cyclohexane) gave significant yields of **7**. For instance, 2,2-dimethylbutane (6.78 *M*), **6** (0.02 *M*), and *t*-BuOOH (1 *M*) under oxygen at 353 K for 24 h gave [**2**] + [**3**] = 0.014 *M* and [**7**] = 0.004 *M* which suggests that at this temperature the *t*-C—H in cyclohexyl hydroperoxide is about 225 times more reactive than a *s*-C—H in 2,2-dimethylbutane towards *t*-$BuO_2^{\cdot}$.

As was found from autoxidations of neat 2,2-dimethylbutane yields of **4** and **5** were not influenced to any significant extent by autoxidation. We have, therefore, concluded that the reactivities of the secondary and primary hydrogens in 2,2-dimethylbutane relative to cyclohexane, k_{2a}/k_{10}, k_{2b}/k_{10}, and k_{2c}/k_{10} are proportional to ([**2**] + [**3**])/([**6**] + [**7**]), [**4**]/([**6**] + [**7**]), and [**5**]/([**6**] + [**7**]).

TABLE 3. Rate constants per active H (in M^{-1} s^{-1}) for abstraction of primary and secondary H-atoms from 2,2-dimethylbutane and cyclohexane by t-BuO_2·

	Rate constants			
Temperature/K		$(CH_3)_3CCH_2CH_3$	$(CH_3)_3CCH_2CH_3$	$(CH_3)_3CH_2CH_3$
303	0.0002	0.00013	—	—
323	0.0016	0.0007	0.00001	0.00002
333	0.0040	0.0015	0.00004	0.00006
343	0.0095	0.004	0.00005	0.0001
353	0.021	0.009	0.0002	0.0003

Values of these relative rate constants at different ratios of 2,2-dimethylbutane and cyclohexane are given in Table 2 and absolute values of k_{2a}, k_{2b}, and k_{2c} per active H relative to absolute rate constants for cyclohexane are given in Table 3.

A comparison of these rate constants indicates that a secondary hydrogen in 2,2-dimethylbutane is about one half as reactive as a hydrogen in cyclohexane. This difference is due to a difference in both activation parameters since $\log (k_{2a}/k_{10}) = (-2.6 \pm 0.5) + (2.3 \pm 0.8)/\theta$, where $\theta = 2.303RT$ kcal mol^{-1} confirming our previous conclusions regarding the relative reactivities of cyclic and acyclic secondary aliphatic hydrogens towards t-BuO_2· (2). A secondary hydrogen in 2,2-dimethylbutane is also slightly less reactive than a secondary hydrogen in 3-methylpentane (1) which is consistent with our previous conclusions regarding the influence of steric effects on H-atom abstraction from alkanes by t-BuO_2· (2).

It should be pointed out that ratios of **2** to **3** were much lower in the co-autoxidations than they were in autoxidation of 2,2-dimethylbutane, a difference that can probably be attributed to the lower chain lengths in the latter case. Furthermore co-autoxidations always gave [**2**]/[**3**] > [**7**]/[**6**] probably because **3** is more susceptible to induced decomposition than **6**.

The yields of the primary alcohols **4** and **5** relative to [**6**] + [**7**] indicate that at 323 K $k_{2b} = 0.0045k_{10}$ and $k_{2c} = 0.003k_{10}$, i.e. a primary H in the *tert*-butyl and methyl groups of 2,2-dimethylbutane are ~170 and 80 times less reactive than a H atom in cyclohexane.

In addition the relative yields of **4** and **5** support our suggestion that the primary hydrogens of the *tert*-butyl group are slightly less reactive than the primary hydrogens of the methyl group in 2,2-dimethylbutane. This conclusion must, however, be very tentative because of the extremely low yields of **4** and **5**.

Mill, Mayo, Richardson, Irwin, and Allara (8) have previously concluded that the secondary hydrogens in *n*-butane are ~45 times more reactive than the primary hydrogens at 373 K while Van Sickle, Mill, Mayo, and Richardson (9) have reported a relative selectivity of 38 for the primary and secondary hydrogens in pentane towards the *t*-butylperoxy. Our work suggests a similar selectivity bearing in mind, however, that the reactivity of an aliphatic *s*-C—H bond to t-BuO_2· can vary by a factor of about 10 depending on its environment (2).

Our rate constants for reaction of t-BuO_2· with cyclohexane and cyclohexyl hydroperoxide, $k_{10} = 0.25$ M^{-1} s^{-1} and k_{11}/t-C—H = 2 M^{-1} s^{-1} at 353 K are in reasonable agreement with the rate constants reported by Hendry, Gould, Schuetzle, Syz, and Mayo (10), $k_{10} = 0.175$ M^{-1} s^{-1} and k_{11}(overall) = 9.8 M^{-1} s^{-1} at this temperature.

We can conclude from the present work and our previous work on alkane autoxidation (1, 2) that the relative reactivities of 1°, 2°, and 3° hydrogens in acyclic alkanes towards t-BuO_2 at 323 K are 1:35–70:325–3000 which can be compared with relative reactivities towards Br· at 380 K (1:220:19400) and t-BuO· at 323 K (1:12:44) (11). Clearly t-BuO_2· is more selective than t-BuO· which is consistent with the relative strengths of the t-BuO—H and t-BuOO—H bonds (12, 13). It is, however, less selective than Br· which is not entirely consistent with the conclusion that $D_{ROO-H} \sim D_{Br-H}$ (12–14).

Finally Roberts (15) has very recently discovered that the primary hydrogens of the ethyl group in isopentane are about twice as reactive (on a per hydrogen basis) to $(Me_3Si)_2N$· as the primary hydrogens of the isopropyl group in this alkane. This observation makes our finding regarding the relative reactivity of the primary hydrogens of 2,2-dimethylbutane towards t-BuO_2 more credible.

1. J. A. HOWARD, J. H. B. CHENIER, and D. A. HOLDEN. Can. J. Chem. **56**, 170 (1978).
2. J. H. B. CHENIER, S.-B. TONG, and J. A. HOWARD. Can. J. Chem. **56**, 3047 (1978).

Can. J. Chem. Downloaded from www.nrcresearchpress.com by 210.87.254.105 on 09/05/12
For personal use only.

3. R. HIATT, J. CLIPSHAM, and T. VISSER. Can. J. Chem. **42**, 2754 (1964).
4. R. HIATT, R. J. SMYTHE, and C. MCCOLEMAN. Can. J. Chem. **49**, 1707 (1971).
5. L. CAGLIOTI, F. GASPARRINI, and G. PALMIERI. Tetrahedron Lett. 3987 (1976).
6. R. K. JENSEN, S. KORCEK, L. R. MAHONEY, and M. ZINBO. J. Am. Chem. Soc. **101**, 7574 (1979).
7. S. KORCEK, J. H. B. CHENIER, J. A. HOWARD, and K. U. INGOLD. Can. J. Chem. **50**, 2285 (1972).
8. T. MILL, F. MAYO, H. RICHARDSON, K. IRWIN, and D. L. ALLARA. J. Am. Chem. Soc. **94**, 6802 (1972).
9. D. E. VAN SICKLE, T. MILL, F. R. MAYO, H. RICHARDSON, and C. W. GOULD. J. Org. Chem. **38**, 4435 (1973).
10. D. G. HENDRY, C. W. GOULD, D. SCHUETZLE, M. G. SYZ, and F. R. MAYO. J. Org. Chem. **41**, 1 (1976).
11. G. A. RUSSELL. *In* Free radicals. Vol. 1. *Edited by* J. K. Kochi. Wiley, New York, NY. 1973. Chapt. 7.
12. L. R. MAHONEY and M. A. DAROOGE. J. Am. Chem. Soc. **92**, 4063 (1970).
13. J. A. KERR, M. J. PARSONAGE, and A. F. TROTMAN-DICKENSON. C.R.C. handbook of chemistry and physics. 56th ed.
14. J. A. HOWARD and J. H. B. CHENIER. J. Am. Chem. Soc. **95**, 3054 (1973).
15. B. P. ROBERTS. Private communication.

Can. J. Chem. Downloaded from www.nrcresearchpress.com by 210.87.254.105 on 09/05/12
For personal use only.

Polymérisation du norbornène par des amorceurs au ruthénium. Etude cinétique de la réaction

CHARLES TANIELIAN, ALAIN KIENNEMANN[1] ET TEMEL ÖSPARPUCU
Laboratoire de Chimie Organique Appliquée, 1, rue Blaise Pascal, 67008 Strasbourg, France
Reçu le 13 mai 1980

CHARLES TANIELIAN, ALAIN KIENNEMANN et TEMEL ÖSPARPUCU. Can. J. Chem. **58**, 2813 (1980).

La détermination des paramètres cinétiques de la réaction de polymérisation du norbornène avec $RuCl_3,3H_2O$ et $RuCl_2(P\Phi_3)_3$ en catalyse homogène (ordre un par rapport aux deux amorceurs, ordre zéro par rapport au monomère avec $RuCl_3,3H_2O$, ordre variable avec $RuCl_2(P\Phi_3)_3$, E_a de 6,2 kcal/mol pour $RuCl_2(P\Phi_3)_3$ et 22,8 pour $RuCl_3,3H_2O$) nous permet de conclure à une interprétation différente du schéma réactionnel de la polymérisation à partir de ces deux amorceurs tout au moins en ce qui concerne l'étape d'amorçage. Avec $RuCl_2(P\Phi_3)_3$ l'étape lente de la réaction serait la métathèse alors que pour $RuCl_3,3H_2O$, celle-ci serait un échange de ligand au niveau de l'amorceur faisant intervenir le solvant (alcool) suivant un mécanisme dissociatif ou associatif. Cette étape lente est confirmée par une étude en fonction de la concentration en alcool et du vieillissement du amorceur.

CHARLES TANIELIAN, ALAIN KIENNEMANN, and TEMEL ÖSPARPUCU. Can. J. Chem. **58**, 2813 (1980).

The kinetic parameters for the polymerisation reaction of norbornene with $RuCl_3 \cdot 3H_2O$, and $RuCl_2(P\Phi_3)_3$ using homogeneous catalysis have been determined (first-order with respect to two initiators, zero-order with respect to the monomer with $RuCl_3 \cdot 3H_2O$, and variable order with $RuCl_2(P\Phi_3)_3$: E_a 6.2 kcal/mol for $RuCl_2(P\Phi_3)_3$ and 22.8 for $RuCl_3 \cdot 3H_2O$) and leads us to propose different reaction mechanisms for the polymerisation starting from the two initiators, at least for the initiation step. With $RuCl_2(P\Phi_3)_3$ the slow step of the reaction is the metathesis whereas with $RuCl_3 \cdot 3H_2O$ the slow step is a ligand exchange at the initiator involving solvent (alcohol) by a dissociative or associative mechanism. This slow step is confirmed by a study of varying alcohol concentration and initiator aging.

[Journal translation]

Introduction

Depuis les premiers exemples de la réaction de métathèse d'oléfines en catalyse hétérogène ou homogène (1, 2), les travaux sur cette réaction sont exposés périodiquement dans un certain nombre de mises au point (3–10). Les alcènes cycliques présentent un intérêt particulier et l'étude, en catalyse homogène, du mécanisme de la polymérisation est toujours d'actualité (11–15). Nous étudions ici une cycloléfine, le norbornène, pour laquelle les sels ou les complexes de métaux du groupe VIII (Ru, Ir, Os) (11, 16–19) et d'autres éléments de métaux de transition (14, 20), permettent une polymérisation par ouverture de cycle. Avec les amorceurs $RuCl_2(P\Phi_3)_3$ et $RuCl_3,3H_2O$, nous avons pu montrer (21), comme le suggérait Hiraki et coll. (11), une participation du solvant alcool voisine de celle montrée pour l'eau (14). L'effet des alcools (EtOH, *n*BuOH et *t*-BuOH) ne se traduit pas d'une manière identique pour les deux amorceurs ce qui permet de supposer un schéma réactionnel différent tout au moins pour l'étape d'amorçage de la réaction de polymérisation. Ceci nous a conduit dans ce travail, à étudier pour ces deux amorceurs, en milieu alcool, les paramètres cinétiques de la réaction afin de pouvoir d'une part confirmer le rôle de l'alcool et d'autre part traduire les différences de comportement des deux amorceurs au niveau d'un schéma réactionnel.

Partie expérimentale[2]

Toutes les réactions sont effectuées en utilisant l'argon comme gaz protecteur. Les alcools utilisés (puriss Fluka) ont été séchés et distillés selon la méthode au phtalate (22). Le norbornène (purum Fluka) a été distillé puis contrôlé par chromatographie en phase gazeuse et rmn. Les amorceurs $RuCl_3,3H_2O$ et $RuCl_2(P\Phi_3)_3$ (purum Fluka) ont été utilisés sans autre purification.

Conduite d'une réaction de cinétique: dans un ballon de 100 mL, on dissout l'amorceur $RuCl_3,3H_2O$ ou $RuCl_2(P\Phi_3)_3$ ($3{,}94 \times 10^{-3}$ mol/L) dans EtOH puis on ajoute le monomère (3,94 mol/L) dans EtOH. La consommation de norbornène est mesurée en chromatographie en phase vapeur par la méthode de l'étalon interne: octane (2×10^{-4} mol/L). Des prélèvements du milieu réactionnel (0,1 mL) sont effectués à intervalles réguliers (10 min). Du dicyclopentadiène (0,3 mL) est ajouté de suite pour bloquer la réaction et le mélange est injecté immédiatement en chromatographie en phase gazeuse. Pour chaque essai, la courbe de conversion en fonction du temps présente deux parties distinctes: une partie linéaire donc à vitesse de polymérisation constante, tant que le milieu reste homogène (~ 1 h 30 min), et une partie où la vitesse décroît lentement à partir du moment où le milieu devient hérérogène par précipitation du polymère formé. Le système devient ensuite progressivement inactif.

Différentes raisons peuvent être évoquées pour expliquer ce phénomène: hétérogénéité du milieu, diminution de la quantité d'amorceur par entraînement lors de la précipitation du polymère, ou établissement d'un équilibre entre norbornène, oligomère et polymère comme montré pour le cyclopentène ou le cyclooctène (23–25). Pour notre part, nous n'avons pu montrer

[1] A qui toute correspondance doit être adressée.

[2] Avec la collaboration de Madame S. Libs pour la partie chromatographique.

0008-4042/80/242813-06$01.00/0
©1980 National Research Council of Canada/Conseil national de recherches du Canada

un tel équilibre. Lors de la détermination de tous nos paramètres cinétiques, nous nous limiterons à la partie linéaire de la courbe.

Les conditions chromatographiques sont les suivantes: appareil Varian 202, détecteur catharomètre, gaz vecteur He 30 mL/min, colonne SE 30, 10% sur chromosorb W (80–100 mesh), longueur 2 m, diamètre, 3,2 mm, isotherme 75°C, t injecteur 150°C, t détecteur 150°C.

Le polymère obtenu en fin de réaction est soigneusement lavé au méthanol, séché et pesé ce qui permet en fin de réaction de contrôler les résultats obtenus par chromatographie. Bien que l'action des deux amorceurs conduise à des paramètres cinétiques différents, nous obtenons, avec $RuCl_3,3H_2O$ et $RuCl_2(P\Phi_3)_3$, un polymère de même type: ouverture de cycle *trans* (21).

Résultats

I. Détermination des paramètres cinétiques

Il est d'usage, lors de l'étude cinétique des réactions de polymérisation de distinguer la cinétique en fonction des concentrations initiales ou des paramètres courants, c'est la première qui sera considérée ici. La vitesse de polymérisation peut s'exprimer par:

$$V = V_a + V_p = -d[M]/dt$$

où V, V_p et V_a sont les vitesses de polymérisation, de propagation et d'amorçage et [M] la concentration en monomère. Si la chaîne cinétique est longue $V = V_p$. Si de plus, nous supposons que toutes les molécules d'amorceur donnent naissance à autant de chaînes actives, la loi de vitesse pourra s'exprimer par $v = k[\text{amorceur}]^{\alpha}[\text{monomère}]^{\beta}$.

(1) Ordre par rapport à l'amorceur

Les figs 1 et 2 représentent les variations du taux de conversion en fonction du temps pour différentes concentrations en $RuCl_3,3H_2O$ et $RuCl_2(P\Phi_3)_3$. Pour chaque concentration en amorceur, la pente de la partie linéaire (taux de conversion <20–25%) donne directement la valeur de chaque vitesse. Celle-ci, reportée en fonction de [Co], concentration initiale en amorceur, conduit à une droite. L'ordre de la réaction est donc un par rapport à l'amorceur pour $RuCl_3,3H_2O$ et $RuCl_2(P\Phi_3)_3$.

(2) Ordre par rapport au monomère

(a) Cas de $RuCl_2(P\Phi_3)_3$. Pour des concentrations en monomère allant de 7,6 mol/L à 0,13 mol/L la vitesse de polymérisation reste constante alors que pour des concentrations plus faibles 0,13 mol/L à 0,023 mol/L, la vitesse de polymérisation décroît avec la concentration initiale en monomère (fig. 3). L'ordre par rapport au monomère est variable: proche de zéro pour les concentrations importantes et proche de un pour de faibles concentrations.

(b) Cas de $RuCl_3,3H_2O$. La réaction est d'ordre zéro par rapport au monomère car la vitesse de polymérisation reste constante pour un domaine de

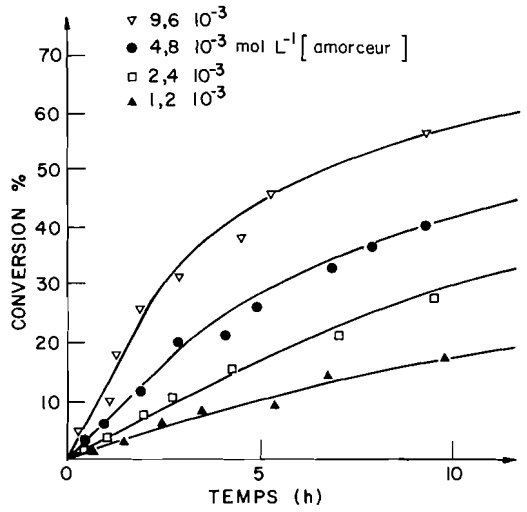


FIG. 1. Influence de la concentration de l'amorceur $RuCl_3,3H_2O$ sur la conversion du norbornène. Solvant EtOH; T = 60°C; [monomère] = 2,5 mol/L.

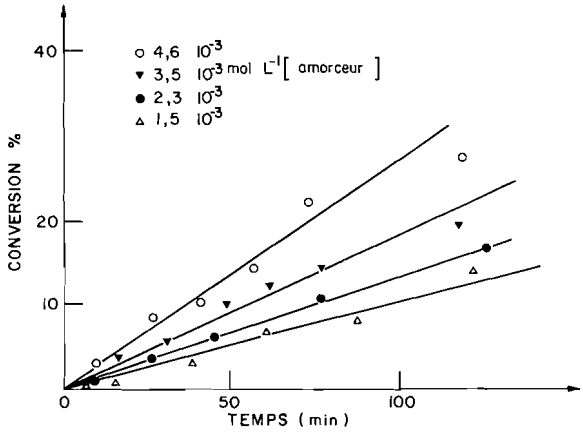


FIG. 2. Influence de la concentration de l'amorceur $RuCl_2(P\Phi_3)_3$ sur la conversion du norbornène. Solvant EtOH; T = 55°C; [monomère] = 2,5 mol/L.

concentration initiale de 0,011 à 5,25 mol/L de norbornène (fig. 4).

Pour $RuCl_3,3H_2O$ et pour $RuCl_2(P\Phi_3)_3$ à partir d'une certaine concentration en monomère, la loi de vitesse peut s'écrire $v = k[\text{Co}]^1[\text{Mo}]^0 = k[\text{Co}]$. Pour la détermination des constantes de vitesse de la réaction et des paramètres thermodynamiques d'activation, la concentration en monomère sera toujours telle que cette loi de vitesse reste vérifiée.

(3) Constante de vitesse et paramètre thermodynamique d'activation

L'étude de la vitesse de réaction en fonction de la température (figs 5 et 6) permet de calculer les constantes de vitesse k (L mol^{-1} s^{-1}): 3,7; 9,7; 21 et 88 × 10^{-6} respectivement à 40, 50, 60 et 68°C avec

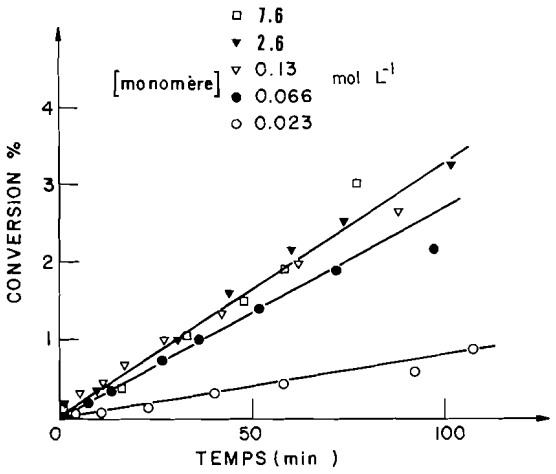


FIG. 3. Influence de la concentration en monomère sur la conversion du norbornène. Solvant EtOH; $T = 60°C$; amorceur: $[RuCl_2(P\Phi_3)_3] = 3{,}95 \times 10^{-3}$ mol/L.

$RuCl_3,3H_2O$. 1,4; 1,75 et 2,1 $\times 10^{-4}$ respectivement à 60, 68 et 76°C pour $RuCl_2(P\Phi_3)_3$. Ces valeurs, à l'aide de la représentation $\log k = f(1/T)$ déterminent les différents paramètres thermodynamiques d'activation (tableau 1).

Discussion

De nombreux essais ont été tentés en catalyse hétérogène afin d'approcher le mécanisme réactionnel par l'étude cinétique (8). Cependant la mauvaise fiabilité des résultats, due, soit à des catalyseurs non reproductibles, soit à une variation du nombre de sites actifs, fait que les énergies d'activation et les chaleurs d'adsorption calculées sont très relatives. Cependant, Clark et Cook (26) pour la métathèse hétérogène du propène et Ramain et Trambouze (27) pour le 2-pentène en homogène concluent que la réaction est du premier ordre par rapport à l'alcène et du premier ordre par rapport à l'amorceur dans le second cas. Davie et coll. (28) pour sa part indique qu'il est impossible de distinguer entre premier et deuxième ordre pour une réaction réversible. Si l'on développe le modèle de Langmuir–Hinshelwood vérifié par Moffat et Clark (29) et Lewis et Wills (30) pour la métathèse hétérogène du propène et par Hughes (31) pour la métathèse homogène du 2-pentène, cette expression laisse prévoir que la réaction doit être du premier ordre par rapport au catalyseur et d'ordre variable par rapport à l'oléfine ce qui est le cas pour $RuCl_2(P\Phi_3)_3$.

(1) Cas de $RuCl_2(P\Phi_3)_3$

Nous pensons que le type de schéma réactionnel pouvant le mieux rendre compte de nos résultats peut se résumer ainsi:

[1] $RuCl_2(P\Phi_3)_3 + M \rightleftharpoons C(M)$

[2] $C(M) \rightleftharpoons CM_D$

[3] $CM_D + M \rightleftharpoons CM_D(M)$

[4] $CM_D(M) \rightleftharpoons CM_{D+1}$

[5] $CM_{D+1} + M \rightleftharpoons CM_{D+1}(M)$

[6] $CM_{D+1}(M) \rightleftharpoons CM_{D+2}$

. . . . . .

. . . . . .

[7] $CM_{Dn} + M \rightleftharpoons CM_{Dn}(M)$

[8] $CM_{Dn}(M) \rightleftharpoons CM_{Dn+1}$

L'étape [1] consiste en la formation d'une espèce C(M) dans laquelle le norbornène M se trouve

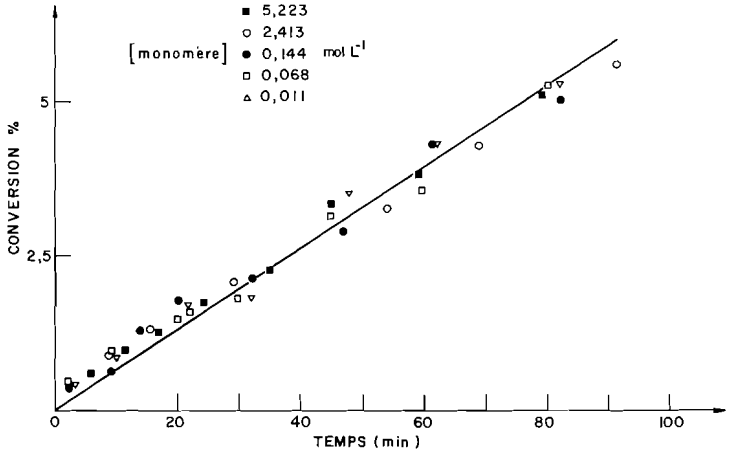


FIG. 4. Influence de la concentration en monomère sur la conversion du norbornène. Solvant EtOH; $T = 60°C$; amorceur: $[RuCl_3,3H_2O] = 3{,}94 \times 10^{-3}$ mol/L.

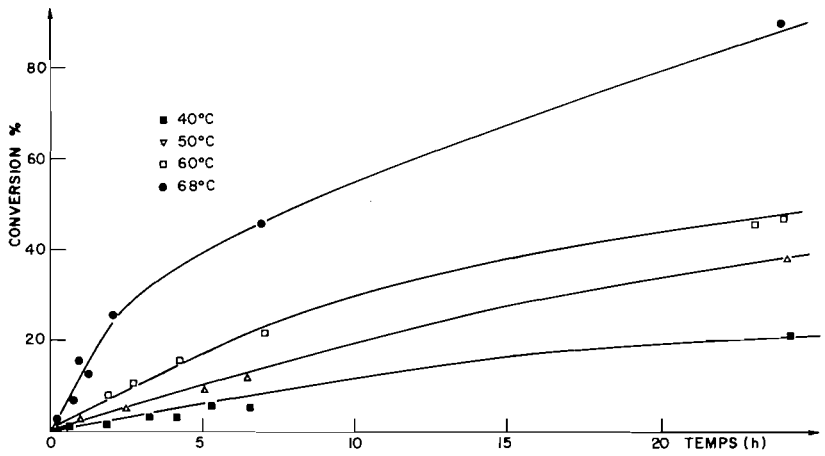


FIG. 5. Influence de la température sur la conversion du norbornène. Solvant EtOH; amorceur: [$RuCl_3,3H_2O$] = 3,94 × 10^{-3} mol/L; [monomère] = 3,95 mol/L.

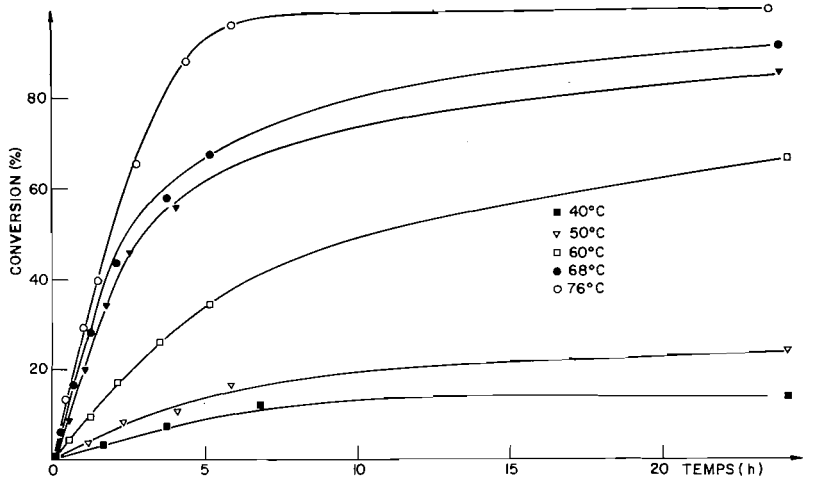


FIG. 6. Influence de la température sur la conversion du norbornène. Solvant EtOH; amorceur: [$RuCl_2(P\Phi_3)_3$] = 3,94 × 10^{-3} mol/L; [monomère] = 3,94 mol/L.

TABLEAU 1. Paramètres thermodynamiques d'activation

	A (L mol s^{-1})	E (kcal/mol)	$\Delta S^{\neq}$ (ue) (60°C)	$\Delta H^{\neq}$ (kcal) (60°C)	$\Delta G^{\neq}$ (kcal) (60°C)
$RuCl_3,3H_2O$	$2,8 \times 10^{10}$	22,8	−10,9	22,1	25,7
$RuCl_2(P\Phi_3)_3$	1,6	6,2	−57,7	5,5	24,7

coordiné au ruthénium par complexe π. L'ensemble de nos résultats étant en accord avec un mécanisme par métathèse faisant intervenir des espèces métallocarbéniques, l'étape [2] représente la formation d'un métallocarbène CM_D à partir de C(M), conformément au schéma réactionnel de Hérisson et Chauvin (32). Le stade [3] correspond à la complexation d'une molécule d'oléfine avec le métallocarbène et la réaction [4] au premier processus de métathèse (constante de vitesse k_p). On a ensuite, de nouveau, la coordination d'une molécule de monomère (étape [5], constante d'équilibre K) suivie d'une métathèse (stade [6], constante k_p) et ainsi de suite [7], [8].

La réaction de métathèse serait l'étape lente de l'ensemble du phénomène et l'expression de la vitesse est alors donnée par:

$$v = -\frac{d[M]}{dt} = k_p \sum_n [CM_{Dn}(M)]$$

or:

$$\sum_n [CM_{Dn}(M)] = K[M] \sum_n [CM_{Dn}]$$

et:

$$[Co] \simeq \sum_n [CM_{Dn}] + \sum_n [CM_{Dn}(M)]$$

où [Co] est la concentration initiale en catalyseur, puisque la chaîne cinétique est longue, d'où:

$$\sum_n [CM_{Dn}(M)] = K[M]\left\{Co - \sum_n [CM_{Dn}(M)]\right\}$$

et:

$$\sum_n [CM_{Dn}(M)] = \frac{K[M][Co]}{1 + K[M]}$$

la vitesse de la polymérisation devient alors:

$$v = k_p \frac{K[M][Co]}{1 + K[M]}$$

Cette expression laisse bien prévoir que la réaction doit être du premier ordre par rapport à l'amorceur, à concentration constante en oléfine, et d'ordre variable par rapport au norbornène, à teneur fixe en amorceur.

Dans le cas de la polymérisation du norbornène par ouverture de cycle les valeurs trouvées des paramètres d'activation sont proches de celles de la littérature. L'énergie d'activation 6,2 kcal/mol est voisine de celles données par Hughes (31) 6,6 et 7,2 kcal/mol pour le 2-pentène et le 4-nonène, par Kranz et Beck (33) 4,17 et 3,23 kcal/mol pour le *trans* et le *cis* polypentenamère, 7,3 (26) et 7,3 kcal/mol (28) pour le propène et même 12,1 kcal/mol (34) pour le 1,4 polybutadiène. L'entropie d'activation 57,7 ue est aussi proche de celle trouvée par Hughes (31). Cette concordance semble bien indiquer la réaction procède bien par un mécanisme de métathèse avec $RuCl_2(P\Phi_3)_3$. La valeur de 6 kcal/mol pour E_a est vraisemblablement inférieure à l'énergie de dissociation des liaisons les plus faibles mises en jeu ce qui indique l'établissement d'un processus concerté faisant intervenir simultanément des ruptures et des formations de liaisons. La valeur très fortement négative de $\Delta S^{\neq}$ est l'indice d'une réduction des degrés de liberté du système et confirme la formation d'un état de transition cyclique.

(2) Cas de $RuCl_3,3H_2O$

Avec $RuCl_3,3H_2O$, les données cinétiques très différentes de celles obtenues pour $RuCl_2(P\Phi_3)_3$ excluent une interprétation analogue venant ainsi confirmer une étude de la réaction en présence de différents alcools (21). Nos résultats s'expliquent si l'étape lente de la réaction n'est plus la réaction de métathèse mais est un échange de ligands au niveau de l'amorceur. Cette étape ne fait pas intervenir le monomère mais le solvant suivant un mécanisme dissociatif ou associatif.

Le mécanisme dissociatif représenté par les deux équations:

$$L_3MX_3 \xrightarrow{\text{lent}} L_2MX_3 + L$$

$$L_2MX_3 + L' \xrightarrow{\text{rapide}} L_2L'MX_3$$

suppose une cinétique d'ordre un par rapport à l'amorceur et zéro par rapport au solvant. Par contre, la deuxième possibilité:

$$L_3MX_3 + ROH \rightarrow L_2(ROH)MX_3 + L$$

suppose un ordre un par rapport à l'alcool. Une étude en fonction de la concentration en alcool en milieu hexane (de $3{,}4 \times 10^{-3}$ à 0,274 mol de EtOH) montre que l'ordre de la réaction est nul par rapport à l'alcool donc nous avons un mécanisme dissociatif. La valeur très élevée de l'énergie d'activation (22,8 kcal/mol) montre aussi que l'étape lente ne se situe pas au niveau de la réaction de métathèse mais lors de la formation de l'espèce active initiale. Ceci est confirmé par une étude du vieillissement de l'amorceur. Si l'on chauffe une solution alcoolique de $RuCl_3,3H_2O$ pendant 4, 24 et 72 h ($T = 60°C$) avant d'additionner le monomère nous constatons une augmentation très nette de la vitesse initiale de polymérisation: 3×10^{-4} pour les essais à 24 et 72 h; (sans vieillissement: $0{,}2 \times 10^{-4}$) suivie d'une vitesse voisine pour les quatres essais après cette période initiale (10 min).

Les vitesses initiales identiques pour les essais à 24 et 72 h indiquent l'établissement d'un équilibre entre espèce initiale et dissociée. Les vitesses initiales ainsi obtenues sont proches de celles avec $RuCl_2(P\Phi_3)_3$ à la même température mais sans vieillissement: (3×10^{-4} mol L^{-1} s^{-1} comparé à $1{,}4 \times 10^{-4}$). Nous pouvons donc conclure que d'après cette étude, l'étape lente de la réaction avec $RuCl_3,3H_2O$ est la formation de l'espèce active obtenue par un mécanisme dissociatif.

(3) Mécanismes relatifs aux systèmes $RuCl_3,3H_2O$ et $RuCl_2(P\Phi_3)_3$

(a) $RuCl_2(P\Phi_3)_3$. Différents mécanismes (11, 16, 17) ont été suggérés pour la polymérisation du norbornène par les amorceurs au ruthénium. Nous avons montré la participation de l'alcool (21) selon un schéma voisin de celui de Laverty et coll. (14, 35). L'étude cinétique confirme la possibilité de ce schéma en mettant en évidence les différences existant entre $RuCl_2(P\Phi_3)_3$ et $RuCl_3,3H_2O$, mais ne permet pas de trancher entre différentes propositions mécanistiques (réfs 10, 36, 37, par exemple).

Cependant nous pensons que pour $RuCl_2(P\Phi_3)_3$, la polymérisation débute par la formation d'un complexe de coordination π ruthénium–norbornène, formation d'un métallocarbène, complexation d'une deuxième molécule d'oléfine suivie de la réaction de métathèse faisant intervenir un état de transition cyclique à quatre centres. La coordination d'une nouvelle molécule de norbornène permet la poursuite de la réaction par métathèses successives.

(b) $RuCl_3,3H_2O$. Il semble logique de supposer que la phase de propagation reste analogue à celle proposée pour $RuCl_2(P\Phi_3)_3$. La différence essentielle se situerait au niveau de l'amorceur comme le montre l'étude en fonction de l'alcool utilisé et du vieillissement. La réaction débuterait par une dissociation du complexe

$$RuX_3L_3 \rightarrow RuX_3L_2 + L$$

suivie d'une fixation de l'alcool pour former un complexe

$$\begin{matrix} & Y_1 & Y_1 = H \\ Ru & \diagup & \\ & \diagdown & \\ & Y_2 & Y_2 = OR, OH \end{matrix}$$

qui en présence de norbornène conduit à la coordination de celui-ci et formation d'un métallocarbène.

Remerciements

Les auteurs remercient très vivement le Docteur Raoul Fonseca pour ses fructueuses discussions et Madame Louise Méchin pour la frappe du manuscrit.

1. R. L. Banks et G. C. Bailey. Ind. Eng. Chem. Proc. Res. Develop. **3**, 170 (1964).
2. N. Calderon, H. Y. Chen et K. W. Scott. Tetrahedron Lett. 3327 (1967).
3. G. Dall'asta et G. Motroni. Angew. Makromol. Chem. **16/17**, 51 (1971).
4. K. W. Scott, N. Calderon, E. A. Ofstead, W. A. Judy et J. P. Ward. Rubber Chem. Technol. **44**, 1341 (1971).
5. K. W. Scott. Polym. Prepr. **13**, 874 (1972).
6. N. Calderon. J. Macromol. Sci. Rev. Macromol. Chem. C**7**, 105 (1972).
7. G. Dall'asta. Rubber Chem. Technol. **47**, 511 (1974).
8. J. C. Mol et J. A. Moulijn. Adv. Catal. **10**, 131 (1974).
9. N. Calderon, J. P. Lawrence et E. A. Ofstead. Adv. Organomet. Chem. **17**, 449 (1979).
10. J. J. Rooney et A. Stewart. Catalysis, **1**, 277 (1979).
11. H. Hiraki, A. Kuroiwa et H. Hirai. J. Polym. Sci., Part A-1, **9**, 2323 (1971).
12. Y. Chauvin et D. Commereuc. Rev. Inst. Franc. Pétrole, **29**, 73 (1974).
13. N. Calderon. Acc. Chem. Res. **5**, 127 (1972).
14. T. Laverty, M. A. McKervey, J. J. Rooney et A. Stewart. Chem. Commun. 193 (1976).
15. K. J. Ivin, J. J. Rooney et C. D. Stewart. Chem. Commun. 603 (1978).
16. F. W. Michelotti et W. P. Keaveney. J. Polym. Sci., Part I, **3**, 895 (1965).
17. L. Porri, R. Rossi, P. Diversi et A. Lucherini. Polym. Prepr. **13**, 897 (1972).
18. L. Porri, R. Rossi, P. Diversi et A. Lucherini. Makromol. Chem. **175**, 3097 (1974).
19. L. Porri, R. Rossi, P. Diversi et A. Lucherini. Makromol. Chem. **176**, 3121 (1975).
20. T. Oskika et H. Tabuchi. Bull. Soc. Chim. Jpn. **41**, 211 (1968).
21. C. Tanielian, A. Kiennemann et T. Ösparpucu. Can. J. Chem. **57**, 2022 (1979).
22. A. I. Vogel. Practical organic chemistry. 3rd ed. Longman. 1970. pp. 168, 170.
23. E. A. Ofstead et N. Calderon. Makromol. Chem. **154**, 21 (1972).
24. H. Höcker, W. Reimann, K. Reibel et Z. Szentivanyi. Makromol. Chem. **177**, 1707 (1976).
25. J. P. Soufflet. C.R. Acad. Sci. C**276**, 169 (1973).
26. A. Clark et C. Cook. J. Catal. **15**, 420 (1969).
27. L. Ramain et Y. Trambouze. C.R. Acad. Sci. C**273**, 1409 (1971).
28. E. S. Davie, D. A. Whan et C. Kemball. J. Catal. **24**, 272 (1972).
29. A. J. Moffat et A. Clark. J. Catal. **17**, 264 (1970).
30. M. J. Lewis et G. B. Wills. J. Catal. **15**, 140 (1969).
31. W. B. Hughes. J. Am. Chem. Soc. **92**, 532 (1970).
32. J. L. Hérisson et J. Chauvin. Makromol. Chem. **141**, 161 (1970).
33. D. Kranz et M. Beck. Angew. Makromol. Chem. **27**, 29 (1972).
34. F. Stelzer, R. Thummer et K. Hummel. Colloid. Polym. Sci. **255**, 664 (1977).
35. D. T. Laverty, J. J. Rooney et A. Stewart. J. Catal. **45**, 110 (1976).
36. P. Chevalier, D. Sinou, G. Descotes, R. Mutin et J. Basset. J. Organomet. Chem. **113**, 1 (1976).
37. J. Levisalles, H. Rudler et D. Villemin. J. Organomet. Chem. **87**, C_7 (1975).

The photolysis of tetrahydrofuran and of some of its methyl derivatives at 185 nm[1]

NURAY KIZILKILIC, HEINZ-PETER SCHUCHMANN, AND CLEMENS VON SONNTAG

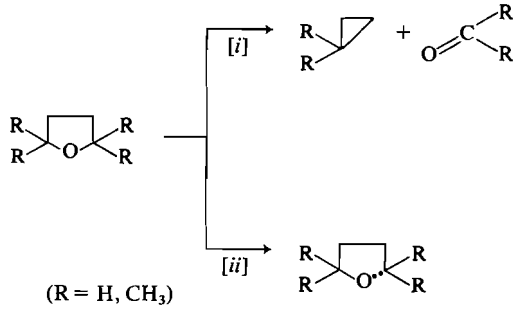
Institut für Strahlenchemie im Max-Planck-Institut für Kohlenforschung, Stiftstr. 34-36, D-4330 Mülheim a.d. Ruhr, West Germany

Received March 5, 1980

This paper is dedicated to Prof. K. J. Laidler on the occasion of his 65th birthday

NURAY KIZILKILIC, HEINZ-PETER SCHUCHMANN, and CLEMENS VON SONNTAG. Can. J. Chem. **58**, 2819 (1980).

The uv photolysis of tetrahydrofuran, **1**, 2-methyltetrahydrofuran, **2**, *cis*-2,5-dimethyltetrahydrofuran, **3**, *trans*-2,5-dimethyltetrahydrofuran, **4**, and 2,2,5,5-tetramethyltetrahydrofuran, **5**, has been investigated by product analysis in the liquid phase, and quantum yields have been determined. The photolysis of tetrahydrofuran itself was also studied in the gas phase at pressures ranging from 1 to 120 atm (pressurizing gas N_2); and very little difference was found between the photolytic behaviour of the vapour at 120 atm and that of the liquid. The major products are in all cases the cyclopropanes and the corresponding carbonyl compounds, as well as the olefinic alcohols and the carbonyl compounds that are isomeric with the starting material. These products are considered to be formed by the two major primary processes [*i*] and [*ii*].



The cyclopropanes formed in reaction [*i*] retain some excess energy (apparently more than is needed to realize the trimethylene form), and in the photolysis of tetrahydrofuran vapour the hot cyclopropane rearranges to a considerable extent into propene. The propene to cyclopropane yield ratio falls strongly with increasing pressure, to a value of 0.065 at 120 atm. A similar value is observed in the liquid phase photolysis.

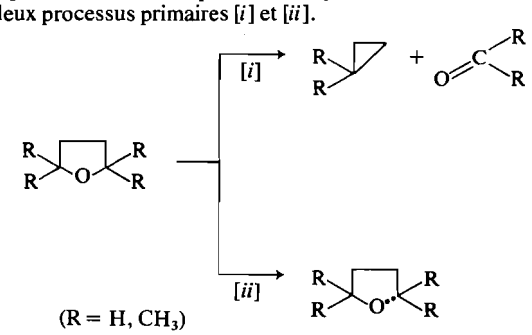
The five-membered oxyl alkyl diradical from reaction [*ii*] is the likely intermediate in the *cis–trans* photoisomerization that is observable with the 2,5-dimethyltetrahydrofurans ($\phi(cis \rightarrow trans) \approx \phi(trans \rightarrow cis) \approx 0.2$). The photolysis of these compounds also demonstrates that steric factors have a strong bearing on the course of the reaction, e.g. the quantum yield of methylcyclopropane from the *cis* compound is 0.22, vs. 0.08 from the *trans* compound.

Molecular hydrogen is produced if the tetrahydrofurans carry hydrogen in α-position. Its production is enhanced if the α-position is shared with a methyl group (**1** gives a hydrogen quantum yield of 0.07, **2** of 0.17, **3** of 0.27, **4** of 0.29, and **5** of zero).

NURAY KIZILKILIC, HEINZ-PETER SCHUCHMANN et CLEMENS VON SONNTAG. Can. J. Chem. **58**, 2819 (1980).

La photolyse à 185 nm du tétrahydrofuranne et de quelques-uns de ses dérivés méthylés à l'état liquide a été étudiée par l'analyse des produits; les rendements quantiques des produits ont été déterminés.

De même, la photolyse du tétrahydrofuranne fut étudiée, à l'état gazeux sous des pressions variant d'une à 120 atm, N_2 servant à soutenir la pression. On trouve que les comportements photolytiques à l'état gazeux à 120 atm, et à l'état liquide, sont presque identiques. Dans tous les cas, les produits majeurs sont les cyclopropanes et les composés carbonylés qui leur sont complémentaires, ainsi que des alcools oléfiniques et d'autres composés carbonylés isomères des tétrahydrofurannes originaux. Ces produits résultent vraisemblablement des deux processus primaires [*i*] et [*ii*].



[1]Part XII of the series "Strahlenchemie von Ethern". For Part XI see ref. 10.

0008-4042/80/242819-08$01.00/0

©1980 National Research Council of Canada/Conseil national de recherches du Canada

Can. J. Chem. Downloaded from www.nrcresearchpress.com by 210.87.254.40 on 09/05/12
For personal use only.

La génération de la molécule de cyclopropane à la forme chaude, voire triméthylénique, paraît établie par le fait que, dans la photolyse du tétrahydrofuranne gazeux, la proportion de propylène par rapport au cyclopropane décroît fortement quand la pression croît, et atteint la valeur de 0.065 quand la pression s'élève à 120 atm. Une valeur similaire est trouvée lors de la photolyse en phase liquide. Le diradical oxyle alkyle à cinq chaînons est l'intermédiaire fort probable de la réaction de photoisomérisation *cis–trans* que l'on observe chez les tétrahydrofurannes diméthylés en 2,5 ($\phi(cis \rightarrow trans) \approx \phi(trans \rightarrow cis) \approx 0.2$). En plus, la photolyse des ces derniers montre que des facteurs stériques peuvent influer puissamment sur le cours de la réaction photochimique. Le rendement quantique du méthylcyclopropane provenant du composé *cis* égale 0.22 alors que, à partir du composé *trans*, il atteint 0.08 seulement. De l'hydrogène est produit quand le composé original porte des atomes d'hydrogène en position α. Sa production est augmentée quand un atome d'hydrogène partage la position α avec un groupement méthyle.

Can. J. Chem. Downloaded from www.nrcresearchpress.com by 210.87.254.40 on 09/05/12
For personal use only.

Introduction

In saturated ethers photolyzed at 185 nm the C—O bond is cleaved with high quantum yields, through homolytic and molecular primary processes (1). In cyclic ethers the first of these paths leads to a diradical. The second kind of pathway is not easily distinguished from the first because in principle reactions of the diradical as well as concerted rearrangements may lead to the same products. In the gas phase, tetrahydrofuran (2–4) as well as oxetane (5) and 1,4-dioxane (6) are known to undergo extensive fragmentation into products of molecular weight below that of the starting material. The same is true of liquid 1,4-dioxane (7, 8), whereas liquid tetrahydropyran (9) and oxepane (10) mainly yield unsaturated alcohols $CH_2{=}CH{-}(CH_2)_n{-}OH$ and aldehydes $CH_3{-}(CH_2)_n{-}CHO$ that are isomeric with the starting material. One does expect a high degree of fragmentation from non-thermalized intermediates in the gas phase compared to in the liquid phase. Even so, ring size appears to emerge as an influencing factor in the photolytic behaviour of the homologous monooxacyclanes.

The present work addresses itself to the question whether the products cyclopropane, propene, formaldehyde, hydrogen, and carbon monoxide that are observed besides other minor products in the tetrahydrofuran gas phase photolysis (2–4) are due to the fragmentation of non-thermalized larger intermediates, or rather formed primarily. The influence that is exercised by non-chromophoric substituents such as methyl groups has also been studied.

Experimental

Tetrahydrofuran (Merck), 2-methyltetrahydrofuran (Aldrich), and 2,2,5,5-tetramethyltetrahydrofuran (11) were fractionated from sodium under argon to a gc purity of better than 99.9% (the former two) and 99.6%. 2,5-Dimethyltetrahydrofuran (Aldrich) was separated by preparative gc into the *cis* and *trans* isomers, assigned as such according to their ^1H nmr spectra (12). After subsequent distillation under argon they showed a gc purity of better than 99.6% (*cis*) and 98.3% (*trans*). The latter still contained some *cis*-2,5-dimethyltetrahydrofuran.

Samples (2 mL) were deaerated by purging with argon for 20 min. Deaeration by this procedure is sufficient since longer purging does not change the product distribution, and oxydation products otherwise present are not formed in measurable amounts. Irradiation was carried out with a low pressure Hg arc at 15°C in a Suprasil QS cell with an exposed area of 2 cm². Only the 185 nm light is photoactive in pure tetrahydrofuran as shown by the fact that on interposition of a Vycor quartz plate, which absorbs at 185 nm but passes 254 nm radiation, the decomposition yield is negligible ($\leq 10^{-3}$) compared to that at 185 nm. For this reason the light could be used unfiltered. Dose rates of 185 nm light were near 5×10^{17} quanta/min. Dosimetry was done by means of the ethanol actinometer (1). In the kinetic runs, doses totalled up to 3×10^{19} quanta, corresponding roughly to a conversion of 0.25%. The products (except formaldehyde) were identified by gc with the help of reference materials and/or gc–ms, and determined by gc using a suitable alkane as an internal standard. Formaldehyde was determined photometrically by the acetylacetone – ammonium acetate method (13). In general, procedures employed were similar to those previously described (14, 15).

The photolysis of tetrahydrofuran vapour was also studied. Relative quantum yields were determined at different pressures. A cell (Beckman Instruments, type RIK F 076) that could be pressurized up to 150 atm was charged by passing through it a stream of argon saturated with tetrahydrofuran at 0°C. Then the sample was brought to the desired pressure with N_2. The optical path length of the cell was 5 cm, its window size 3 cm². There is total absorption of the 185 nm light under these conditions. Conversions were kept below 20%. After photolysis the contents of the cell were expanded through a sampling device where part of the gas mixture was retained for gc analysis. A complicating feature in these vapour phase photolyses was the gradual formation of a polyformaldehyde deposit on the cell window whereby the effective light intensity was diminished somewhat from one run to the next. No attempt was made to determine formaldehyde in these experiments because of its poor gc flame ionization response.

The molar extinction coefficients of the substituted tetrahydrofurans studied were determined in the region from 185 nm to near 200 nm on a Cary model 17 spectrophotometer (Figs. 1 and 2). The procedure was similar to that described previously (16).

Results

Ultraviolet absorption of the methylated tetrahydrofurans sets in near 200 nm, ε(185 nm, gas phase) reaching about $10^3\ M^{-1}\ cm^{-1}$ (Figs. 1 and 2). The molar extinction coefficient of tetrahydrofuran itself at that wavelength is between 600 and $700\ M^{-1}\ cm^{-1}$, cf. ref. 17.

The products of the liquid tetrahydrofuran photolysis, and the quantum yields, are given in Table 1. The results from the photolysis of the substituted tetrahydrofurans in the liquid phase are summarized in the subsequent tables (2-methyltetrahydrofuran, Table 2; *cis*- and *trans*-2,5-dimethyltetrahydrofuran, Table 3; 2,2,5,5-tetra-

Can. J. Chem. Downloaded from www.nrcresearchpress.com by 210.87.254.40 on 09/05/12
For personal use only.

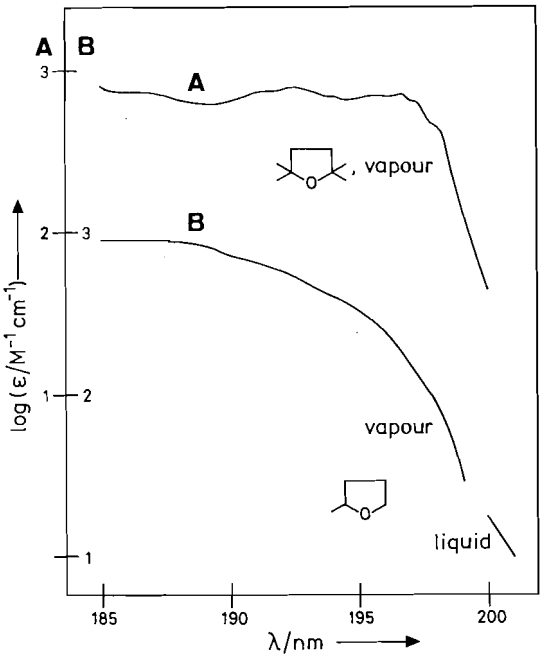


FIG. 1. The molar extinction coefficients of 2-methyltetrahydrofuran (*B*) and 2,2,5,5-tetramethyltetrahydrofuran (*A*) between 185 and 201 nm.

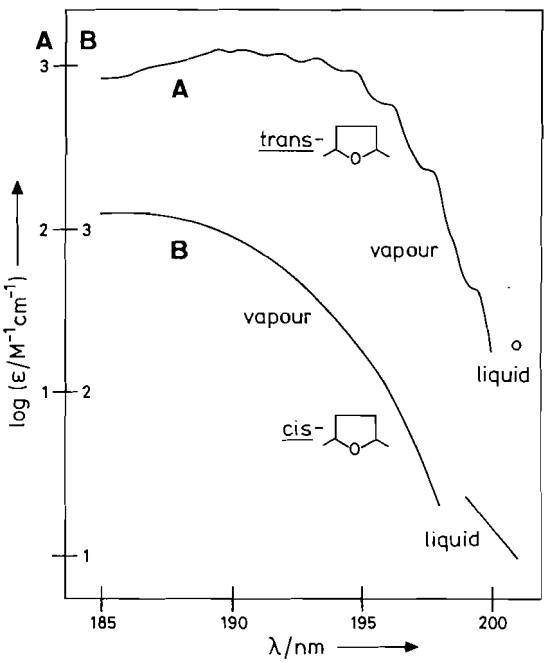


FIG. 2. The molar extinction coefficients of *trans*- (*A*) and *cis*- (*B*) -2,5-dimethyltetrahydrofuran between 185 and 201 nm.

methyltetrahydrofuran, Table 4). The quantum yields of the major products from the liquid phase photolysis are considered accurate within ±10%. Product formation was linear with dose in the dose range employed. The combined yield of unidentified products as seen by gc amounted to less than 5% of the starting material consumed. The quantum yields of cyclopropane, ethylene, and propylene appear to slightly decrease with temperature, whereas that of propane increases.

The cyclopropanes and the corresponding carbonyl compounds are major products in all cases. A remarkable feature is the large difference between

TABLE 1. Photolysis (185 nm) of deaerated liquid tetrahydrofuran at 15°C: products and quantum yields

Product	φ	Product	φ
Hydrogen	0.07	Ethylene oxide	0.016
Carbon monoxide	$< 10^{-3}$	2,3-Dihydrofuran	0.04
Methane	0.001	2,5-Dihydrofuran	$< 10^{-3}$
Ethane	$< 10^{-4}$	Butyraldehyde	0.06
Ethylene	0.025	But-3-en-1-ol	0.02
Propylene	0.007	1-Butanol	0.005
Cyclopropane	0.19	Octahydrobifuryl	0.01
Propane	4×10^{-4}	Dimer[a]	0.03
Formaldehyde	0.14	1,8-Octanediol	Nil ($\leq 10^{-3}$)
Acetaldehyde	0.008		

[a]Gc–ms analysis suggests a molecular weight of 144, with base peak *m/e* 71. Relatively large retention volume suggests presence of hydroxyl function. By analogy with findings in the photolysis of tetrahydropyran (9) its structure is believed to be

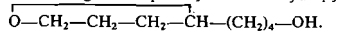


TABLE 2. Photolysis (185 nm) of deaerated liquid 2-methyltetrahydrofuran at 15°C: products and quantum yields

Product	φ	Product	φ
Hydrogen	0.17	Acetone	0.015
Carbon monoxide	$< 10^{-3}$	Propylene oxide	0.015
Methane	0.005	Pent-4-en-2-ol	0.003
Ethylene	0.021	1-Pentanol	0.005
Ethane	$< 10^{-4}$	Pent-3-en-1-ol	0.001
Propene	0.014	Pentan-2-one	0.05
But-1-ene	5×10^{-4}	Pentanal	0.02
Cyclopropane	0.20	4,5-Dihydro-2-methylfuran	~0.1[a]
Methylcyclopropane	0.026	Dehydrodimer[b]	0.03
Formaldehyde	0.028	Dimer[c]	0.01
Acetaldehyde	0.21	Decanediols	$< 10^{-3}$
Ethylene oxide	0.003		

[a]Difficult to determine quantitatively because of incomplete gc separation from the starting material.
[b]Gc–ms indicates probable molecular weight of 170, with base peak *m/e* 85.
[c]Gc–ms suggests molecular weight of 172, with base peak *m/e* 85. Relatively large retention volume suggests presence of hydroxyl function.

cis- and *trans*-2,5-dimethyltetrahydrofuran with respect to this mode of fragmentation, cf. Table 5. Another fragmentation path, leading to oxirans and their isomeric carbonyl compounds as well as the corresponding small olefins, is of lesser importance. The sum of the quantum yields of the carbonyl compounds and the olefinic alcohols that are isomeric with the starting material (ring-opened isomers) is around 0.1 except for 2,2,5,5-tetramethyltetrahydrofuran where it reaches a value of 0.27. $\phi(H_2)$ strongly depends on the degree of

Can. J. Chem. Downloaded from www.nrcresearchpress.com by 210.87.254.40 on 09/05/12
For personal use only.

TABLE 3. Photolysis (185 nm) of deaerated liquid *cis*- and *trans*-2,5-dimethyltetrahydrofuran at 15°C: products and quantum yields

Product	ϕ	
	cis-	*trans*-
Hydrogen	0.27	0.29
Carbon monoxide	$< 10^{-3}$	$< 10^{-3}$
Methane	0.007	0.005
Ethane	$< 10^{-4}$	$< 10^{-4}$
Ethylene	$< 10^{-4}$	$< 10^{-4}$
Propene	0.015	0.011
But-1-ene	4×10^{-3}	0.6×10^{-3}
Methylcyclopropane	0.22	0.08
Acetaldehyde	0.22	0.09
Acetone	0.01	0.04
Propylene oxide	0.01	0.01
Hexan-2-one	0.03	0.02
Hex-1-en-5-ol / Hex-2-en-5-ols	0.06	0.06
Hexan-2-ol	0.03	0.03
2,5-Dimethyl-2,3-dihydrofuran[a]	0.2	0.2
cis-2,5-Dimethyltetrahydrofuran	—	0.2
trans-2,5-Dimethyltetrahydrofuran	0.22	—
Dehydrodimer[b]	Not determined	0.02
Dimers[c]	Not determined	0.02

[a]Separation from starting material difficult.
[b]Gc–ms indicates a molecular weight of 198. Base peak *m/e* 99.
[c]Gc–ms suggests a molecular weight of 200. Base peak *m/e* 99. Relatively large retention volume suggests presence of hydroxyl function.

methyl substitution. Hydrogen in α-position appears to be a prerequisite for H_2 formation. Otherwise $\phi(H_2)$ rises with the number of methyl substituents in α-position. With the 2,5-dimethyltetrahydrofurans a *cis* ⇄ *trans* isomerization with a quantum yield of ~ 0.2 is observed. In principle the same type of reaction should occur with the other compounds but cannot be detected there.

From the vapour phase photolysis of tetrahydrofuran, only products more volatile than the starting material were measured. Since it was impractical to determine quantum yields from these runs, the product yields are expressed in terms relative to the sum of the cyclopropane and propylene yields at different pressures (Fig. 3 and Table 6). Beside the products shown there, acetaldehyde and ethylene oxide, some methane, but-1-ene, and pent-1-ene as well as traces of butane, *cis*- and *trans*-pent-2-ene, hex-1-ene, and allyl methyl ether were observed at the lower pressures employed. There were also traces of a further few unidentified products. At the highest pressures where a proportionally greater part of the sample cannot be brought to analysis owing to the procedure employed, conversions needed to be higher for easy product measurement. In these cases, the relative yield of butyraldehyde after the longer photolysis times tended to fall below the value reached after a shorter time. Within experimental error, which is estimated at about ±10%, such behaviour was not observed in the other products measured.

Discussion

In the liquid phase, vibrationally excited intermediates formed subsequent to the primary act of photolysis are for the most part thermalized if their lifetime with respect to fragmentation is not very short. In this way, species can be trapped which would undergo fragmentation at low pressures. Vapour phase photolysis at high pressure provides a transition between these extreme regimes. In the case of tetrahydrofuran it appears that the high pressure limits of certain quantities can be taken to be identical with their values obtained from the liquid phase photolysis (Table 1, Fig. 3). The present work indicates that the tetrahydrofurans studied essentially obey, if structurally possible, the same photolysis mechanism represented in Scheme 1 where the case of *cis*-2,5-dimethyltetrahydrofuran is shown as an example.

The Oxyl Alkyl Diradical

In general, the cleavage of a C—O bond is the most important process in the photolysis of ethers (1). In the cyclic ethers such as the tetrahydrofurans such a process would lead to an oxyl alkyl diradical (reaction [3], Scheme 1). The assumption of oxyl alkyl diradical intermediates in the photolysis of cyclic ethers is supported by results from the oxepane system (10). If the lifetime of the oxyl alkyl diradical with respect to reclosure is long

TABLE 4. Photolysis (185 nm) of deaerated liquid 2,2,5,5-tetramethyltetrahydrofuran at 15°C: products and quantum yields

Product	ϕ	Product	ϕ
Hydrogen	$< 10^{-3}$	1,1-Dimethylcyclopropane	0.39
Carbon monoxide	$< 10^{-3}$	Acetone	0.40
Methane	0.035	Isobutene oxide	0.05
Ethylene	$< 10^{-4}$	2,5-Dimethylhex-4-en-2-ol[a] (?)	0.21
Ethane	0.002	2,5-Dimethylhex-en-2-ol[a] (?)	0.06
Isobutene	0.043	Dehydrodimer	≤0.001
2-Methylbut-2-ene	0.004		

[a]Gc–ms analysis suggests a molecular weight of 128. Base peak *m/e* 59. Gc behaviour indicates the presence of a hydroxyl function.

TABLE 5. Photolysis of some neat liquid tetrahydrofurans: quantum yields grouped by reaction type

Compound	Quantum yield 		Ring-opened isomers	Dehydro-genation	*cis–trans*-Rearrangement
THF	0.20	0.02	0.08	0.07	
2-MeTHF	0.24	0.03	0.07	0.17	
cis-2,5-Me_2THF	0.22	0.02	0.09	0.27	0.22
trans-2,5-Me_2THF	0.08	0.05	0.08	0.29	0.2
2,2,5,5-Me_4THF	0.39	0.05	0.27	0.00	

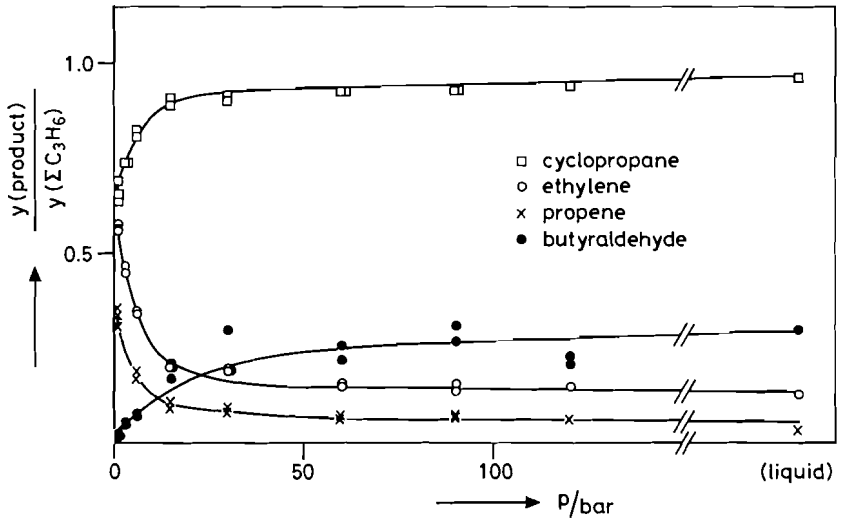


FIG. 3. Yields of cyclopropane □, butyraldehyde ●, ethylene ○, and propylene × relative to the sum of the C_3H_6 yields, from the vapour phase 185 nm photolysis of tetrahydrofuran at different N_2 pressures (30°C). Conversions up to 20%.

TABLE 6. The 185 nm vapour phase photolysis of tetrahydrofuran in the absence of oxygen: yields of some products relative to the sum of the cyclopropane and propylene yields between 1 and 120 atm, conversions up to 20%, temperature 30°C, pressurizing gas N_2

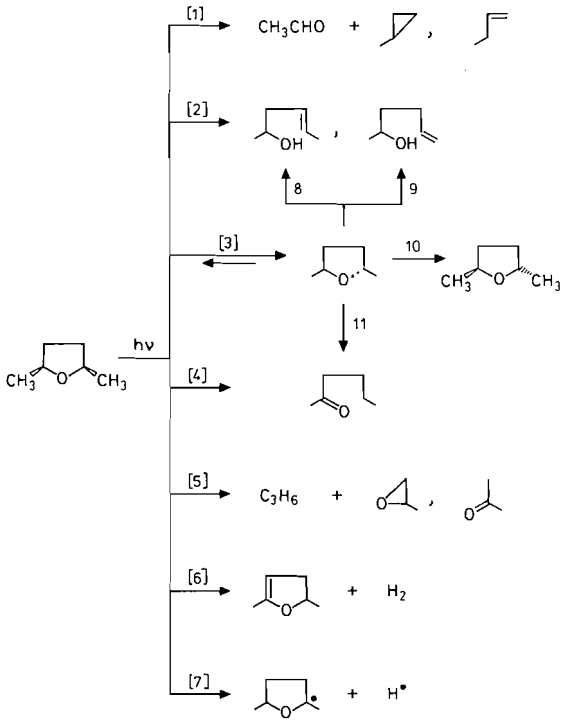
	Yield				
p (atm)	C_2H_4	C_3H_6	*c*-C_3H_6	C_3H_8	*n*-C_3H_7CHO
1	0.57	0.31	0.69	0.076	0.015
1	0.58	0.34	0.66	0.053	0.013
1	0.56	0.36	0.64	—	—
3	0.45	0.26	0.74	0.024	0.047
3	0.47	0.26	0.74	0.040	0.054
6	0.35	0.19	0.81	—	0.076
6	0.34	0.17	0.83	—	0.079
15	0.20	0.11	0.89	—	0.21
15	0.20	0.09	0.91	0.031	0.17
30	0.19	0.095	0.91	—	0.30
30	0.20	0.080	0.92	0.024	0.19
60	0.16	0.072	0.93	0.022	0.26
60	0.15	0.068	0.93	0.035	0.22
90	0.15	0.071	0.93	—	0.27
90	0.14	0.075	0.93	—	0.31
120	—	—	—	—	0.23
120	0.15	0.065	0.94	—	0.21
Liquid	0.127	0.036	0.964	0.02	0.30

enough, rotation around an adjacent bond can lead to an isomerization which will be detected in the case of suitably substituted compounds such as the *cis*- and *trans*-2,5-dimethyltetrahydrofurans. One might consider that the observed *cis* ⇄ *trans* isomerization of these compounds is due to a process like reaction [10]. With quantum yields of about 0.2 in the forward direction this process appears to be of major importance. The reverse of reaction [3] which must also occur cannot be measured. It is probably of similar importance and constitutes a major path of deactivation applicable to all systems examined.

In principle, a *cis* ⇄ *trans* isomerization would also occur if a C(α)—C(β) bond were broken in the primary step. We consider this process unlikely because C—C bond cleavage has been found to be insignificant in the ethers investigated except when highly branched (1). The following discussion rests upon the assumption that the oxyl alkyl diradical is indeed an intermediate.

In competition with reclosure the oxyl alkyl diradical may disproportionate to give the ring-

Can. J. Chem. Downloaded from www.nrcresearchpress.com by 210.87.254.40 on 09/05/12
For personal use only.



SCHEME 1. Primary processes in the photolysis (185 nm) of liquid *cis*-2,5-dimethyltetrahydrofuran.

opened isomers, carbonyl compounds (reaction [11]) and olefinic alcohols (reactions [8] and [9]). However, the same products could be formed via true molecular processes (reactions [2] and [4]). It is difficult to distinguish between such processes and the disproportionation reactions of the oxyl alkyl diradical (a similar difficulty is encountered in open-chain ethers with respect to cage disproportionation reactions (1)). Nevertheless, the approach taken in the following suggests that one of the reaction modes is favoured over the other. To this end we consider the formation of butyraldehyde which could be formed either directly (reaction type [4]) or through the oxyl alkyl diradical (reaction type [3] followed by reaction type [11]).

The rate constant (classical) for the unimolecular decay of a molecule containing an energy $E - E_0$ in excess of its decomposition threshold E_0 is assumed at $k_{dec} = A(1 - E_0/E)^{s-1}$ (where A is the frequency factor; s, the number of oscillators in the molecule, cf. ref. 18*a*). The original energy input at 185 nm is 640 kJ mol^{-1}. The initial hotness (E) of the alkyl oxyl diradical equals the energy input minus the C—O bond dissociation energy, plus release of ring strain (19), i.e. about 280 kJ mol^{-1}. The initial hotness of a directly formed butyraldehyde molecule (reaction type [4]) equals the energy input minus the ground state energy difference between butyraldehyde and tetrahydrofuran, i.e. about 660 kJ mol^{-1} (for heats of formation, see e.g. ref. 20). These estimates give upper limits for the initial hotness E, because energy loss through vibrational thermalization of the electronically excited tetrahydrofurans has been neglected. The critical energy E_0 for bond cleavage of the diradical is estimated at about 60 kJ mol^{-1}; it equals the endothermicity of reaction [13] (28 kJ mol^{-1} as estimated according to (21)) plus the activation energy of the back reaction [−13] which is assumed at ~30 kJ mol^{-1} (for similar reactions cf. ref. 19). This estimate is based on the assumption that in the bond-breaking process [13] the electrons of the trimethylene species neither effectively interact nor that the diradical decomposes concertedly into cyclopropane and formaldehyde, a process which is likely to require a rather strained transition state. For butyraldehyde E_0 is probably near 340 kJ mol^{-1}

[13] $\cdot CH_2—CH_2—CH_2—CH_2—O\cdot$
$\rightarrow \cdot CH_2—CH_2—CH\cdot_2 + CH_2O$

(cf. 341 kJ mol^{-1} for acetaldehyde (22) and 343 kJ mol^{-1} for propionaldehyde (23)). It thus appears that the probability of the thermalization of the hot diradical before decomposition should be considerably smaller (hotness $E = 280$ kJ mol^{-1}, $E_0 = 60$ kJ mol^{-1}) than for the hot butyraldehyde molecule (hotness $E = 660$ kJ mol^{-1}, $E_0 = 340$ kJ mol^{-1}). On the other hand, the rate constant for deactivation, $k_{deact} \approx Z\Delta E/(E - E_0)$, cf. ref. 18*b*, should be roughly the same for both species (Z, collision number; ΔE, energy loss per collision: for N_2 as the medium perhaps 25 kJ mol^{-1}, cf. ref. 24). While the energy quantities appear accessible, it does not seem feasible to assign proper values to the other parameters that appear in k_{dec}, i.e. A and s. The assumption that these parameters do not differ from one species to the other leads to the conclusion that the excited butyraldehyde is much more easily thermalized than the oxyl alkyl diradical. If there were two precursors of butyraldehyde, one of them readily thermalized (hot butyraldehyde), the other more difficult to thermalize (oxyl alkyl diradical), one would expect to distinguish two pressure regions, in the lower of which the hot butyraldehyde is stabilized whereas the oxyl alkyl radical is thermalized only at higher pressures.

Figure 3 shows that there is only one thermalization range, and that at low pressure (1 atm) virtually no butyraldehyde is formed. It may thus be inferred that the butyraldehyde yield curve (Fig. 3) essentially reflects the thermalization of the oxyl alkyl diradical, suggesting that the aldehyde is formed in reaction type [11]. This leaves little room for reaction type [4].

Can. J. Chem. Downloaded from www.nrcresearchpress.com by 210.87.254.40 on 09/05/12
For personal use only.

Can. J. Chem. Downloaded from www.nrcresearchpress.com by 210.87.254.40 on 09/05/12
For personal use only.

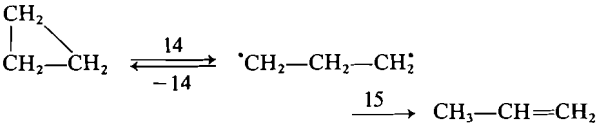
The rearrangement of an α-oxolanyl radical such as might be generated in reaction [7], followed by hydrogen abstraction from the starting material, is not expected to furnish butyraldehyde at room temperature (25).

The Path to the Cyclopropanes

A major reaction in all cases is the formation of the cyclopropane and the conjugate carbonyl compound. It appears likely that this is a molecular process (reaction [1]) rather than the fragmentation of the oxyl alkyl diradical (reaction [13]) and closure of the trimethylene species. As discussed above, in the liquid the oxyl alkyl diradical is largely thermalized before it enters into most of its reactions, and one therefore expects reaction [13] to be unimportant. The remarkable difference between the methylcyclopropane quantum yields (and those of the complementary product acetone) from the isomeric *cis*- and *trans*-2,5-dimethyltetrahydrofurans (ϕ(methylcyclopropane) = 0.22 vs. 0.08, Table 3), both of which would generate the same alkyl oxyl diradical, lends strong support to the occurrence of reaction [1] rather than type [13]. This result again proves the influence of configurational factors on molecular fragmentation processes (cf. also ref. 26). In the present case the two 2,5-dimethyltetrahydrofurans are not only of different symmetry but also of different ring conformation (half-chair (*trans*) vs. envelope (*cis*)). The fragments formed in reaction type [1] will, between themselves, retain an excess energy of almost 600 kJ mol^{-1}. The cyclopropanes and the corresponding carbonyl compounds are therefore hot. Hot cyclopropanes are known to rearrange into the corresponding olefins (cf. refs. 27, 28). In accordance with this there is a considerable yield of propene at low pressures in the gas phase photolysis of tetrahydrofuran (Fig. 3; refs. 2–4). The increase of $\phi(\Delta)/[\phi(\Delta) + \phi(\diagup\!\diagdown)]$ is considered to be due to the thermalization of the hot cyclopropane. The high pressure limit of the above ratio is 0.94, near to the value of 0.96 found for the liquid phase. It is much higher than had earlier been believed (2, 3) and similar to the yield ratio obtained after chemical activation at high pressures (29) and thermolysis of liquid 1-pyrazoline (30).

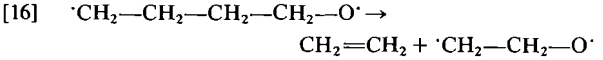
It has been postulated that the rearrangement of cyclopropane into propene occurs via the trimethylene diradical (reactions [14] and [15], e.g. ref. 21; for reviews see refs. 27, 28). There might be an activation barrier with respect to the closure of this diradical (reaction [−14]), although this point is controversial (cf. refs. 19, 31–34). It is noted that such an activation barrier has also been observed with cyclobutane systems (19, 35).

With the assumption that propene is formed via reactions [14] and [15] with the intermediacy of a thermalized trimethylene, the ratio of the rate constants for reactions [−14] and [15] may be estimated: $k_{-14}/k_{15} = \phi(\diagup\!\diagdown)/\phi(\triangle) = 0.037$ at room temperature, whereas from transition state estimates (19) a value of 0.008 is obtained.



The Path to the Oxirans

A further set of interrelated products are, in the case of tetrahydrofuran, ethylene and acetaldehyde/ethylene oxide. The fragmentation of the thermalized oxyl alkyl diradical according to reaction [16] appears precluded near room temperature on account of its relatively high endothermicity of about 80 kJ mol^{-1}, estimated according to ref. 21.



It has been argued above that, owing to the rapid thermalization of the hot cyclopropanes, rearrangement to the corresponding olefins occurs to only a very small extent in the liquid phase. A similarly rapid thermalization of the hot oxirans is expected if they are formed in similar true molecular processes. However, comparable amounts of the rearranged carbonyl compounds are found. This suggests a somewhat different mechanism, possibly the intermediacy of ·O—CH_2—CH_2· diradicals. A considerable effort has been made (36–40) to produce such species both in the triplet and in the singlet state by reacting olefins with $O(^3P)$ and $O(^1D)$ atoms, respectively. In each of these cases, comparable amounts of oxirans and rearranged carbonyl compounds were observed. Owing to the complex nature of these systems firm conclusions with respect to the details of the mechanism are difficult to draw.

In Scheme 1 the formation of the oxirans and the corresponding carbonyl compounds is therefore only given summarily (reaction [5]) and the question as to the nature of the precursor must remain open. In particular, it cannot be decided yet whether these products result from singlet or triplet excited tetrahydrofurans. The latter might be formed to some extent by intersystem crossing from the primarily generated excited singlet state.

If one admits, as appears plausible on the basis of the present results, that all the tetrahydrofurans investigated here decompose in a like manner, the ethylene molecule can be said to comprise an α and

a β carbon atom from the tetrahydrofuran molecule but not both β, since from the 2,5-dimethyl- and 2,2,5,5-tetramethyltetrahydrofurans no ethylene is produced. In the gas phase photolysis of tetrahydrofuran at 147 nm (4), the ethylene seems to be both of the kind α–β and β–β in the above sense.

The Path to Hydrogen

The degree of hydrogen production varies within wide limits. In tetrahydrofuran itself as well as in the mono- and dimethyl-substituted compounds its quantity is found to exceed what can easily be explained via homolytic processes such as [7] (Scheme 1) since $\phi(H_2)$ outweighs that of the products stemming from radicals, such as the dehydrodimers, unless one accepts rather high ratios of α-oxolanyl radical disproportionation vs. combination. For the 1-ethoxyethyl radical which has structural analogies, $k_d/k_c \sim 0.42$ (cf. ref. 41). From this, and the fact that $\phi(H_2)$ from 2,2,5,5-tetramethyltetrahydrofuran is nil, i.e. 3,4-hydrogen elimination is unimportant, reaction [6] is chosen to explain most of the hydrogen. It should be pointed out that while a hydrogen atom in α position seems to be needed for the formation of H_2, $\phi(H_2)$ strongly increases with methyl substitution at this position (see Table 5).

Minor Products

Products so far not discussed include the saturated alcohols and the products termed "dimers" (see Tables 1–4). All these are formed in comparatively small yields. In the tetrahydropyran (9) and oxepane (10) systems such "dimers", to which the structure of 2-(ω-hydroxyalkyl)oxacycloalkanes can be assigned, are also found, with a particularly high quantum yield in the former case (9). Arguments have been put forward (10) which point to their formation in the excited state without free radicals intervening. As well, saturated alcohols are produced in the photolysis of tetrahydropyran and oxepane. It has been suggested (10) that a disproportionation reaction occurring in the excited state might lead to this kind of product.

Acknowledgements

We want to thank Drs. G. Schomburg and D. Henneberg of this Institute, as well as their staff, for aiding us with the gc and ms analyses.

1. C. VON SONNTAG and H.-P. SCHUCHMANN. Adv. Photochem. **10**, 59 (1977).
2. B. C. ROQUITTE. J. Phys. Chem. **70**, 1334 (1966).
3. B. C. ROQUITTE. J. Am. Chem. Soc. **91**, 7664 (1969).
4. Z. DIAZ and R. D. DOEPKER. J. Phys. Chem. **82**, 10 (1978).
5. J. MARGERUM, J. N. PITTS, JR., J. R. RUTGERS, and S. SEARLES. J. Am. Chem. Soc. **81**, 1549 (1959).
6. R. R. HENTZ and C. F. PARRISH. J. Phys. Chem. **75**, 3899 (1971).
7. J. KIWI. J. Photochem. **7**, 237 (1977).
8. H.-P. SCHUCHMANN, H. BANDMANN, and C. VON SONNTAG. Z. Naturforsch. **34b**, 327 (1979).
9. H.-P. SCHUCHMANN, P. NADERWITZ, and C. VON SONNTAG. Z. Naturforsch. **33b**, 942 (1978).
10. H.-P. SCHUCHMANN and C. VON SONNTAG. J. Photochem. **13**, 347 (1980).
11. L. HENRY. C. R. Acad. Sci. **143**, 498 (1906).
12. D. GAGNAIRE and P. MONZEGLIO. Bull. Soc. Chim. Fr. 474 (1965).
13. B. KAKAĆ and Z. J. VEJDELEK. Handbuch der photometrischen Analyse organischer Verbindungen, Verlag Chemie, Weinheim. 1974. p. 257.
14. H.-P. SCHUCHMANN and C. VON SONNTAG. Tetrahedron, **29**, 3351 (1973).
15. F. WEEKE, E. BASTIAN, and G. SCHOMBURG. Chromatographia, **7**, 163 (1974).
16. H.-P. SCHUCHMANN and C. VON SONNTAG. J. Chem. Soc. Perkin Trans. II, 1408 (1976).
17. J. DOUCET, P. SAUVAGEAU, and C. SANDORFY. Chem. Phys. Lett. **17**, 316 (1972).
18. P. J. ROBINSON and K. A. HOLBROOK. Unimolecular reactions. Wiley, London. 1972. (*a*) p. 53; (*b*) p. 318.
19. S. W. BENSON and H. E. O'NEAL. NSRDS-NBS 21, U.S. Dept. of Commerce, Washington, DC. 1970.
20. J. D. COX and G. PILCHER. Thermochemistry of organic and organometallic compounds. Academic Press, London. 1970. p. 204.
21. S. W. BENSON. Thermochemical kinetics. 2nd ed. Wiley, New York. 1976.
22. M. T. H. LIU and K. J. LAIDLER. Can. J. Chem. **46**, 479 (1968).
23. T. BÉRCES. *In* Comprehensive chemical kinetics. Vol. 5. *Edited by* C. H. Bamford and C. F. H. Tipper. Elsevier, Amsterdam. 1972. p. 234.
24. J. W. SIMONS, B. S. RABINOVITCH, and D. W. SETSER. J. Chem. Phys. **41**, 800 (1964).
25. T. J. WALLACE and R. J. GRITTER. J. Org. Chem. **26**, 5256 (1961).
26. C. VON SONNTAG and D. SÄNGER. Tetrahedron Lett. 4515 (1968).
27. K. J. LAIDLER and L. F. LOUCKS. *In* Comprehensive chemical kinetics. Vol. 5. *Edited by* C. H. Bamford and C. F. H. Tipper. Elsevier, Amsterdam. 1972. p. 1.
28. R. G. BERGMAN. *In* Free radicals. Vol. 1. *Edited by* J. K. Kochi. Wiley, New York. 1973. p. 191.
29. B. S. RABINOVITCH, E. TSCHUIKOW-ROUX, and E. W. SCHLAG. J. Am. Chem. Soc. **81**, 1081 (1959).
30. B. H. AL-SADER and R. J. CRAWFORD. Can. J. Chem. **46**, 3301 (1968).
31. G. R. FREEMAN. Can. J. Chem. **44**, 245 (1966).
32. W. VON E. DOERING and K. SACHDEV. J. Am. Chem. Soc. **96**, 1168 (1974).
33. R. HOFFMANN. J. Am. Chem. Soc. **90**, 1475 (1968).
34. P. J. HAY, W. J. HUNT, and W. A. GODDARD III. J. Am. Chem. Soc. **94**, 638 (1972).
35. J. L. EKMANIS. Doctoral thesis. Harvard University. 1976. p. 70.
36. R. J. CVETANOVIĆ. Adv. Photochem. **1**, 115 (1963).
37. R. J. CVETANOVIĆ. J. Chem. Phys. **23**, 1375 (1955).
38. K. F. PRESTON and R. J. CVETANOVIĆ. Ber. Bunsenges. Phys. Chem. **72**, 177 (1968).
39. C. CANOSA, R.-D. PENZHORN, and C. VON SONNTAG. Ber. Bunsenges. Phys. Chem. **83**, 217 (1979).
40. O. KAJIMOTO, H. YAMASAKI, and T. FUENO. Chem. Phys. Lett. **68**, 127 (1979).
41. C. VON SONNTAG, H.-P. SCHUCHMANN, and G. SCHOMBURG. Tetrahedron, **28**, 4333 (1972).

Can. J. Chem. Downloaded from www.nrcresearchpress.com by 210.87.254.40 on 09/05/12
For personal use only.

Can. J. Chem. Downloaded from www.nrcresearchpress.com by 210.87.254.6 on 09/05/12
For personal use only.

COMMUNICATION

Total synthesis of (−)-phytuberin

JOHN A. FINDLAY, DIXIT N. DESAI, GREG C. LONERGAN, AND PETER S. WHITE
Department of Chemistry, University of New Brunswick, Fredericton, N.B., Canada E3B 6E2

Received August 11, 1980

JOHN A. FINDLAY, DIXIT N. DESAI, GREG C. LONERGAN, and PETER S. WHITE. Can. J. Chem. **58**, 2827 (1980).
An efficient, total synthesis of the phytoalexin (−)-phytuberin **10** is described starting from (−)-carvone **1**.

JOHN A. FINDLAY, DIXIT N. DESAI, GREG C. LONERGAN et PETER S. WHITE. Can. J. Chem. **58**, 2827 (1980).
Une synthèse totale du (−)-phytuberin **10** est décrite à partir de les (−)-carvone **1**.

[Traduit par le journal]

The structure of phytuberin, a novel sesquiterpenoid phytoalexin originating in potato tubers and tobacco, was established as **10** by the X-ray crystallographic studies of Hughes and Coxon (1). The only synthesis of this stress metabolite reported (2) to date contains a fourteen-step sequence from (+)-α-cyperone which, in turn, is available via a choice of multistage pathways from commercially available (−)-carvone **1**. The overall yield from (−)-carvone is ~1.5% at best. We report here a total synthesis of (−)-phytuberin **10** from (−)-carvone **1** with very substantial economies both in number of steps and overall yield (~10%).

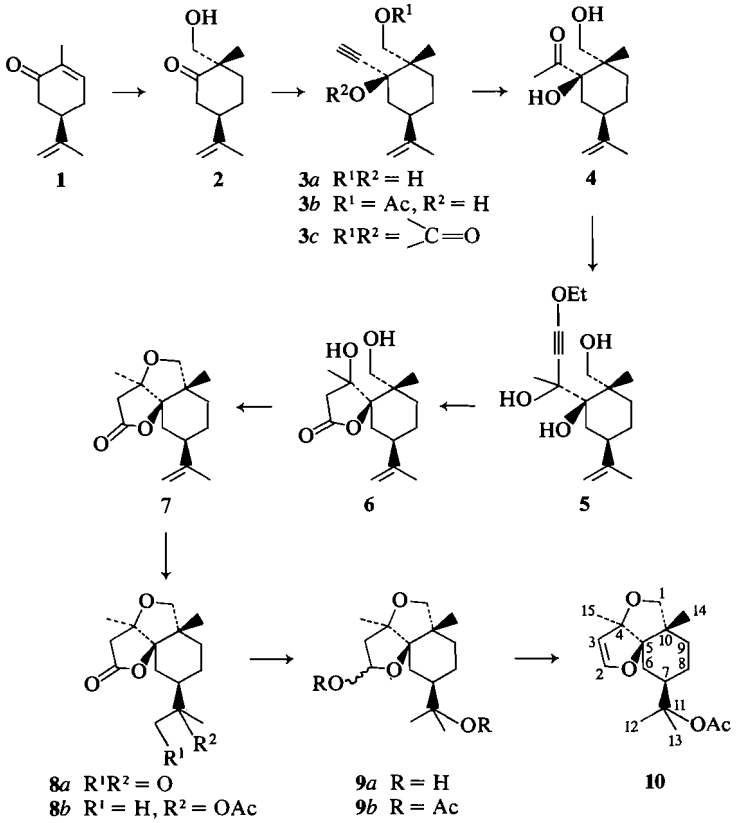
Alkylation of the lithium enolate of (−)-carvone with formaldehyde at −78°C under N_2 afforded a mixture of **2** plus its C10 (phytuberin numbering system) epimer (2:3) in 98% yield, readily separable by short column silica gel G chromatography. The undesired C10 epimer of **2** can be equilibrated to a mixture with **2** (5:4) by pyrolysis at 185°C for 15 min, the equilibration apparently proceeding via a dealdolization/aldolization mechanism currently being investigated. Thus the yield of the desired diastereomer **2** can be augmented substantially.

Ethynylation of the hydroxy ketone **2** with lithium acetylide in THF at −78°C gave, after chromatography, the crystalline diol **3***a* in 64% yield, mp 88–91°C, separated from its C5 epimer (9%). X-ray crystallographic examination[1] of the carbonate **3***c* of **3***a* confirmed the structure and stereochemistry of this series in every detail as portrayed. Acetylation of the acetylenic diol **3***a* through the agency of acetic anhydride/pyridine at room temperature for 6 h furnished, in quantitative yield, the corresponding monoacetate **3***b* which was hydrated to the methyl ketone **4** using $HgSO_4$ catalyst in aqueous methanol at room temperature for 30 h. Treatment of **4** with ethoxyacetylene/*n*-butyllithium in THF at 0°C under N_2 gave a mixture of C4 diastereomers **5**. The latter, obtained in 91% yield, were separated by preparative tlc on silica gel and fully characterized individually. Hydration of either isomer of **5** using dilute methanolic oxalic acid at room temperature for 4 h gave directly the corresponding lactone **6** in quantitative yield, each of which was quantitatively converted into the same furano lactone **7** possessing the appropriate tricyclic skeleton, correctly substituted and with all chiral centres correctly generated for transformation into (−)-phytuberin. The structure of the key intermediate **7** was fully substantiated by spectroscopic data. The ir spectrum ($CHCl_3$) ν_{max}: 1740 cm^{-1} (lactone). The ^1H nmr spectrum ($CDCl_3$) δ_{TMS}: 1.13 (s, 3H, 14 Me), 1.60 (s, 3H, 15 Me), 1.71 (s, 3H, C11 Me), 2.71 (s, 2H, C3 methylene), 3.68 (s, 2H, C1 methylene) ppm. Mass spectrum *m/e* 250 (M^+, $C_{15}H_{22}O_3$). The synthetic product **7** was identical in all respects with the compound obtained quantitatively by pyrolysis (3) of phytuberin lactone (4) **8***b* at 310°C for 0.5 h in an evacuated sealed tube.

Treatment of the key synthetic intermediate **7** with *m*-chloroperbenzoic acid (1 equiv.) in CH_2Cl_2 at room temperature for 4.5 h effected complete conversion to the epoxy lactone **8***a* whose ^1H nmr spectrum displayed a broad singlet at δ 2.68 ppm for the new ethereal hydrogens. Reduction of **8***a* with $LiAlH_4$/ether at room temperature for 1 h gave the epimeric mixture of diols **9***a* (~65% yield after chromatography) whose diacetate (**9***b*)

[1]Details to be disclosed in a forthcoming full paper on phytuberin synthesis by the authors of the present communication.

0008-4042/80/242827-02$01.00/0
©1980 National Research Council of Canada/Conseil national de recherches du Canada



(Ac_2O/pyridine at 80°C) was pyrolyzed in a sealed tube at 150°C for 0.5 h affording **10** (66% yield from **9***a*), indistinguishable in all spectroscopic properties and chromatographic behaviour from natural (−)-phytuberin (4).

Acknowledgements

We are grateful to David T. Coxon, A.R.C. Food Research Institute, Norwich, England for supplying a sample of natural (−)-phytuberin and to the Natural Sciences and Engineering Research Council of Canada for financial assistance.

1. D. L. Hughes and D. T. Coxon. J. Chem. Soc. Chem. Commun. 822 (1974).
2. A. Murai, M. Ono, A. Abiko, and T. Masamune. J. Am. Chem. Soc. **100**, 7751 (1978).
3. G. C. Lonergan. Ph.D. Thesis, University of New Brunswick, Fredericton, N.B. 1978.
4. D. T. Coxon, K. R. Price, B. Howard, and R. F. Curtis. J. Chem. Soc. Perkin Trans. I, 53 (1977).

Can. J. Chem. Downloaded from www.nrcresearchpress.com by 210.87.254.6 on 09/05/12
For personal use only.